



Petroleum Engineers



Handbook

Petroleum Engineering Handbook

Editor-in-Chief

Howard B. Bradley
Professional/Technical Training Consultant

Associate Editors

Fred W. Gipson
Senior Engineering Professional (retired)
Conoco Inc.

Aziz S. Odeh
Senior Scientist
Mobil R&D Corp.

Phillip S. Sizer
Senior Vice President/Technical Director
Otis Engineering Corp.

Mohamed Mortada
President
Mortada Intl. Inc.

Lewis L. Raymer
President
Lewis L. Raymer Enterprises

Gerry L. Smith
Engineering Consultant
(deceased)

Third Printing
Society of Petroleum Engineers
Richardson, TX, U.S.A.

©Copyright 1987 by the Society of Petroleum Engineers. Printed in the United States of America. All rights reserved. This book, or parts thereof, cannot be reproduced in any form without written consent of the publisher.

Third printing, Feb. 1992, incorporating minor changes on Pages 22-3, 30-3, 30-4, 33-2, and 51-52.

ISBN 1-55563-010-3

Preface

The 1962 edition of the *Petroleum Production Handbook* filled a need at that time for a comprehensive compilation of practical information and data covering production equipment and reservoir engineering. This 1987 edition updates the original 48 chapters and adds 11 new ones. New technology, developed over the past 25 years, resulted in improved equipment, materials, and methods. They are described and discussed in the revised original chapters and in the new ones. The 11 new chapters are the following:

- Chapter 7—Electric Submersible Pumps
- Chapter 18—Offshore Operations
- Chapter 19—Crude-Oil Emulsions
- Chapter 45—Miscible Displacement
- Chapter 46—Thermal Recovery
- Chapter 47—Chemical Flooding
- Chapter 48—Reservoir Simulation
- Chapter 51—Acoustic Well Logging
- Chapter 52—Mud Logging
- Chapter 58—SI Metric System of Units and SPE Metric Standard
- Chapter 59—SPE Letter and Computer Symbols Standard

This 1987 edition, now called the *Petroleum Engineering Handbook*, provides a current and worthwhile addition to the industry's literature for students and experienced professionals working in the petroleum industry.

The handbook is again divided into three sections: Sec. 1, Mathematics (one chapter); Sec. 2, Production Engineering (18 chapters); and Sec. 3, Reservoir Engineering (40 chapters). There are 57 chapters written by professionals who are recognized as authorities in their fields of expertise. Chap. 58 is a revised version of the 1982 SI Metric System of Units and SPE Metric Standard, and Chap. 59 is the 1986 revision of the 1984 Standard SPE Letter and Computer Symbols for Economics, Formation Evaluation and Well Logging, Natural Gas Engineering, and Petroleum Reservoir Engineering.

The Mathematics section presents the basic tables and calculation procedures required by persons engaged in petroleum production. The Production Engineering section covers basic types of materials, methods, and tools available for use in petroleum operations, including their capabilities and proper applications. The Reservoir Engineering section treats gas, oil, condensate, and formation water properties and correlations; reservoir rocks and traps; primary, secondary, and tertiary recovery data and methods; oil and gas reserves; formation evaluation, including well logging methods; and well treating methods. The what, why, how, and now-what aspects of each topic are emphasized. Also, at the end of the appropriate chapters, key equations are presented with SI metric units.

Special acknowledgment is due the SPE staff for their immeasurable help and advice, the associate editors for their avid dedication to the technical-editing task, and all the authors who contributed much time and effort to provide the timely and excellent information included within each chapter. We are much indebted to the editor-in-chief of the 1962 edition, Thomas C. Fricke, and to the original group of authors for their arduous 3-year job of developing the original edition of the *Petroleum Production Handbook*. Special thanks are due Ed Mayer of THUMS and B.J. Dotson of Mobil Oil Corp. (now retired) for their advice and helpful discussions on the proper use of the 1986 SPE standard letter symbols throughout the handbook and for their editing of Chap. 59, the SPE Letter and Computer Symbols Standard.

Our hope is that by proper application of the updated information contained within the second edition of this handbook, the petroleum-industry professional will be led to more efficient production and use of the world's petroleum-energy resources.

Howard B. Bradley
Editor-in-Chief

Acknowledgments

The Society of Petroleum Engineers sincerely thanks the following organizations and individuals for permission to use the cited material.

Chap. 2

Figs. 2.1 through 2.3 and 2.6 through 2.8, from *Casing, Tubing, and Drill Pipe*, API Spec. 5A, 38th edition, API, Dallas (1985).

Fig. 2.9, from *Line Pipe*, API Spec. 5L, 35th edition, API, Dallas (1985).

Figs. 2.10A, 2.10B, 2.11, 2.12, and 2.14 through 2.18, from *Threading, Gaging, and Thread Inspection*, API Spec. 5B, 11th edition, API, Dallas (1985).

Table 2.1, modified from *Casing, Tubing, and Drill Pipe*, API Spec. 5A, 37th edition, API, Dallas (1984).

Tables 2.2, 2.5 through 2.7, and 2.25 through 2.27, "Casing, Tubing, and Drill Pipe," *Bull.*, USS, Pittsburgh, PA (1972).

Tables 2.3, 2.4, and 2.24, modified from "Performance Properties of Casing, Tubing, and Drill Pipe," *API Bull. 5C2*, API, Dallas (1983).

Tables 2.8 through 2.11 and 2.28, from "USS Seamless Casing, Tubing, and Drill Pipe," *Bull.*, USS, Pittsburgh, PA (1972).

Table 2.14, *Bull. 664*, National Supply Co., Houston.

Tables 2.31 through 2.33, 2.36, and 2.37, from *Line Pipe*, API Spec. 5L, 34th edition, API, Dallas (1984).

Tables 2.38 through 2.43, from "Formulas and Calculations for Casing, Tubing, Drill Pipe, and Line Pipe Properties," *API Bull. 5C3*, third edition with Supplement No. 1, API, Dallas (1983).

Tables 2.44 through 2.54, from *Threading, Gaging, and Thread Inspection*, API Spec. 5B, 10th edition with Supplement No. 4, API, Dallas (1983).

Chap. 3

Figs. 3.1 and 3.3, and Tables 3.1 through 3.33, from *Specifications for Wellhead and Christmas Tree Equipment*, API Spec. 6A, 14th and 15th editions, API, Dallas (April 1, 1986).

Fig. 3.2, courtesy McEvoy Co., General Catalog 58-59 (Jan. 1959).

Fig. 3.5, from Eichenberg, R., "Design Consideration for AWHM 15,000 psi Flanges," ASME Paper 57-PET-23, Sept. 22, 1957.

Figs. 3.6 through 3.17, courtesy Otis Engineering Corp., Dallas.

Chap. 4

Figs. 4.1 through 4.11, from Patton, L.D. and Abbott, W.A.: *Well Completions and Workovers: The Systems Approach*, second edition, Energy Publications, Dallas (1985) 57-67.

Tables 4.1 and 4.2, from *Packer Calculations Handbook*, Baker Oil Tool Div. (1971).

Chap. 5

Fig. 5.1, from Winkler, H.W.: "How to Design a Closed Rotative Gas Lift System—Part I: Procedure," *World Oil* (July 1960) 116-19.

Figs. 5.2, 5.5, 5.6, and 5.18, from *Gas Lift*, Book 6 of API Vocational Training Series, revised edition, API, Dallas (1984) 65.

Fig. 5.3, from Winkler, H.W.: "Here's How to Improve Your Gas Lift Installations—Part 1: Pressure at Depth Determinations," *World Oil* (Aug. 1959) 63-67.

Figs. 5.4 and 5.29, from Winkler, H.W. and Smith, S.S.: *Camco Gas Lift Manual*, Camco Inc., Houston (1962) A2-001.

Fig. 5.7, from King, W.R.: "Time and Volume Control for Gas Intermitters," U.S. Patent No. 2,339,487 (Jan. 1944).

Fig. 5.21, from Kirkpatrick, C.V.: "Advances in Gas-Lift Technology," *API Drill. and Prod. Prac.* (1959) 24-60.

Fig. 5.25, from *Gas Lift*, Book 6 of API Vocational Training Series, API, Dallas (1965) 109.

Fig. 5.33, from *Camco Complete Service Catalog*, Camco Inc. (1962) 42.

Chap. 6

Figs. 6.1, 6.5, 6.7, 6.12, 6.13, 6.31, 6.40, 6.44, 6.47, 6.49, and 6.51, and Table 6.18, courtesy Trico Industries, Gardena, CA.

Figs. 6.2, 6.3, 6.6, 6.8, 6.11, 6.14, 6.15, 6.19 through 6.24, 6.26 through 6.29, 6.32 through 6.39, 6.41 through 6.45, 6.48, 6.50, 6.52, 6.53, and 6.55, and Table 6.1, from National-Oilwell, Los Nietos, CA.

Fig. 6.9, courtesy Otis Engineering Corp., Dallas.

Figs. 6.17 and 6.52, and Tables 6.3, 6.12, and 6.17, courtesy Dresser Industries, Dallas.

Fig. 6.18 and Table 6.4, courtesy of Highland Pump Co. Inc., Midland, TX.

Fig. 6.56, from *Sizing and Selection of Electric Submersible Pump Installations*, API RP 11U, second edition, API, Dallas (May 30, 1986).

Table 6.2, courtesy Kobe Inc., Huntington Park, CA.

Chap. 7

Figs. 7.1 through 7.18 and 7.20 through 7.32, and Table 7.1, courtesy TRW Energy Products Group, Reda Pump Div., Bartlesville, OK.

Chap. 8

Fig. 8.1, from *Subsurface Pumps and Fittings*, API Spec. 11AX, seventh edition, API, Dallas (June 1979).

Figs. 8.3, 8.5, and 8.7, courtesy Oilwell Div. of U.S. Steel Corp., Garland, TX.

Chap. 9

Figs. 9.2 and 9.3, and Tables 9.1 through 9.4, from *Sucker Rods*, API Spec. 11B, 21st edition, API, Dallas (May 1985).
Figs. 9.5 and 9.9, and Table 9.9, from *Care and Handling of Sucker Rods*, API RP 11BR, seventh edition, API, Dallas (May 30, 1986).

Fig. 9.10 and Tables 9.10 and 9.11, from *Reinforced Plastic Sucker Rods*, API Spec. 11C, first edition, API, Dallas (Jan. 1, 1986).

Table 9.7, from *Design Calculations for Sucker Rod Pumping Systems*, API RP 11L, third edition, API, Dallas (Feb. 1977).

Chap. 10

Figs. 10.1, 10.3, 10.6, 10.7, 10.9 through 10.12, and 10.14 (pumping unit), courtesy Lufkin Industries Inc., Lufkin, TX.
Fig. 10.8, from *Design Calculations for Sucker Rod Pumping Systems (Conventional Units)*, API RP 11L, third edition, API, Dallas (Feb. 1977).

Figs. 10.13, 10.16 through 10.20, and 10.24 through 10.28, and Tables 10.5, 10.7, and 10.9, from Sargent Oil Well Equipment Co., Odessa, TX.

Fig. 10.14 (engine), from Arrow Specialty Co., Tulsa, OK.

Fig. 10.15, from Waukesha Engine Div., Dresser Industries Inc., Waukesha, WI.

Fig. 10.21, from *Motors and Generators*, MG 1-1978, Natl. Electrical Manufacturers Assn., Washington, DC (1978).

Figs. 10.29 through 10.31, from Ronk Electrical Industries Inc., Nokomis, IL.

Figs. 10.32 and 10.33, from *Classification of Areas for Electrical Installations at Drilling Rigs and Production Facilities on Land and on Marine Fixed and Mobile Platforms*, API RP 500B, second edition, API, Dallas (July 1973) 8.

Tables 10.2 and 10.3, from *Installation and Lubrication of Pumping Units*, API RP 11G, second edition, API, Dallas (Feb. 1959) and Supplement (Jan. 1980).

Tables 10.6 and 10.10, from *Motor Application and Maintenance Handbook*, second edition, R.W. Smeaton (ed.), McGraw-Hill Book Co. Inc., New York City, Table 1 on Page 3-7 and Table 3 on Page 11-3.

Chap. 11

Figs. 11.1 and 11.3, from C-E Natco, Tulsa, OK.

Fig. 11.4, from *Design and Fabrication of Galvanized Products*, American Hot Dip Galvanizer Assn. and the Zinc Inst. (Nov. 1983).

Fig. 11.7, from CBI Industries Inc. (Chicago Bridge and Iron Co.), Oak Brook, IL.

Figs. 11.9 and 11.10, from Fenix & Scisson Inc., Tulsa, OK.

Table 11.1, from *Bolted Production Tanks*, API Spec. 12B, 12th edition, API Div. of Production, Dallas (Jan. 1977).

Tables 11.3 and 11.4, from *Venting Atmospheric and Low-Pressure Storage Tanks*, API Std. 2000, third edition, API, Dallas (Jan. 1982).

Chap. 12

Fig. 12.2, courtesy Jaragua S.A. Industrias Mecanicas, São Paulo, Brazil.

Figs. 12.7 and 12.8, courtesy Fisher Controls Co., Marshalltown, IA.

Figs. 12.16 and 12.19, courtesy ACS Industries Inc., Woonsocket, RI.

Fig. 12.18, courtesy Peerless Mfg. Co., Dallas.

Fig. 12.20, courtesy Plenty Metrol, Newbury, England.

Fig. 12.21, courtesy Vortec, Inc., Woodside, CA.

Fig. 12.22, courtesy Porta-Test Systems, Ltd., Edmonton, Alta., Canada.

Figs. 12.24, 12.26, and 12.40, courtesy C-E Natco, Tulsa, OK.

Tables 12.9 and 12.10, courtesy Comsign Computer Program, Ellis Engineering Inc., Houston.

Tables 12.11 and 12.17, from KWIC Index of Intl. Standards, Intl. Organization for Standardization, Geneva.

Tables 12.12, 12.18, and 12.19, from *ASME Boiler and Pressure Vessel Code*, Sec. VIII, Div. 1, New York City (1984).

Tables 12.13 and 12.14, from Megyesy, E.F.: *Pressure Vessel Handbook*, Pressure Vessel Handbook Publishing Inc., Tulsa, OK.

Table 12.15, from Kimmell, G.O.: "Stage Separation," paper 48-PET-15 presented at the ASME Annual Meeting, Oklahoma City, Oct. 1949.

Table 12.16, "Separation Flash Calculations, Process Version 0882," Simulation Sciences Inc., Houston.

Chap. 13

Fig. 13.2, courtesy The Bristol Co.

Fig. 13.3, from *Orifice Constant Tables*, American Gas Assn., Report No. 3, revised (1969). Also, ANSI/API 2530.

Fig. 13.4 and Tables 13.2a, 13.2b, and 13.4, from *GPSA Engineering Databook*, Gas Processors Suppliers Assn., Tulsa, OK (1972).

Figs. 13.20 through 13.22, courtesy Fischer Governor Co.

Table 13.1, courtesy American Meter Co., Inc.

Chap. 14

Fig. 14.5, from *GPSA Engineering Databook*, ninth edition, fifth revision, Gas Processors Suppliers Assn., Tulsa, OK (1981).

Fig. 14.14, from *NGSMA Handbook*.

Figs. 14.19 through 14.21, and Tables 14.1 and 14.2 from Campbell, J.M.: "J.M. Campbell Gas Conditioning and Processing," Campbell Petroleum Series, Norman, OK (1962) 2.

Chap. 15

Figs. 15.1 through 15.3, and Table 15.9, from *Design and Installation of Offshore Production Platform Piping Systems*, API RP 14E, third edition, API, Dallas (1981) 22.

Figs. 15.4 through 15.6, and Tables 15.2 through 15.5, from *GPSA Engineering Databook*, Gas Processors Suppliers Assn., Tulsa, OK (1980).

Fig. 15.8, courtesy Paragon Engineering Services Inc., Houston.

Fig. 15.11 and Table 15.10, courtesy Perry Equipment Co., Mineral Wells, TX.

Fig. 15.12, courtesy C-E Natco, Tulsa, OK.

Fig. 15.13, courtesy U.S. Filter, Fluid System Corp., Whittier, CA.

Figs. 15.15 and 15.19, from "Oil-Water Separator Process Design," API Manual on Disposal of Refinery Wastes, Volume on Liquid Wastes, API, Dallas (1975) Chap. 5.

Fig. 15.20, Engineering Specialties Inc., Covington, LA.

Tables 15.6 and 15.7, from *American National Standard, Pipe Flanges and Flanged Fittings*, ANSI B26.5, ASME, New York City (1981).

Chap. 18

Fig. 18.32, courtesy CanOcean Resources Ltd., New Westminster, B.C., Canada.

Fig. 18.36, courtesy Fluor Subsea Services, Irvine, CA.

Fig. 18.38, courtesy Hamilton Bros. Oil Co., Denver.

Fig. 18.40, from Lagers, G.H.C., Gusto, B.V., and Bell, C.R.: "The Third Generation Lay Barge," *Proc.*, Offshore Technology Conference (1974) 1, 35-46.

Fig. 18.41, courtesy Apache, Santa Fe Intl. Corp., Alhambra, CA.

Fig. 18.43, courtesy Swan Wooster Engineering Ltd., Vancouver, B.C., Canada.

Fig. 18.44, from Willits, K.L.: "Well Completions in the Prudhoe Bay Field," *Pet. Eng.* (Feb. 1976).

Fig. 18.45, courtesy Brian Watt Assocs., Houston.

Chap. 19

Figs. 19.1, 19.3, and 19.6 through 19.8, courtesy Shell Development Co., Houston.

Figs. 19.4, 19.5, 19.9, and 19.10, courtesy Baker Performance Chemicals Inc., Santa Fe Springs, CA.

Fig. 19.12, courtesy ASTM, Philadelphia, PA.

Fig. 19.17, courtesy Chemineer-Kenics, Dayton, OH.

Fig. 19.18, courtesy Modular Production Equipment Inc., Houston.

Figs. 19.19, 19.29, and 19.30, courtesy C-E Natco Inc., Tulsa, OK.

Figs. 19.20 and 19.32, courtesy Hydrocarbon Research Inc., Long Beach, CA.

Figs. 19.21, 19.22, and 19.28, courtesy Energy Recovery Div., Daniel Industries Inc.

Chap. 20

Figs. 20.2A and 20.3, from Katz, D.L. *et al.*: *Handbook of Natural Gas Engineering*, McGraw-Hill Book Co. Inc., New York City (1959).

Figs. 20.2B and 20.2C, from Brown, G.G. *et al.*: "Natural Gasoline and the Volatile Hydrocarbons," Natural Gas Assn. of America, Tulsa OK (1948).

Fig. 20.4, from Wichert, E. and Aziz, K.: "Compressibility Factor for Sour Natural Gases," *Cdn. J. Chem. Eng.* (1972) 49, 269-75.

Figs. 20.8 and 20.9, from Stiel, L.I. and Thodos, G.: "The Viscosity of Non-Polar Gases at Normal Pressures," *AIChE J.* (1961) 7, 611-20.

Fig. 20.10, from Matthews, T.A., Roland, C.H., and Katz, D.L.: "High Pressure Gas Measurement," *Proc.*, Natural Gas Assn. of America (1942) 41-51.

Fig. 20.14 and Table 20.1, from Perry, R.H. and Chilton, C.H.: *Chemical Engineers Handbook*, fifth edition, McGraw-Hill Book Co. Inc., New York City (1975).

Table 20.2, from *GPSA Engineering Databook*, ninth edition, fifth revision, Gas Processors Suppliers Assn., Tulsa, OK.

Chap. 21

Fig. 21.1, from *Encyclopedia of Chemical Technology*, The Interscience Encyclopedia Inc. (1953) 10, 117.

Fig. 21.3, after Nelson, W.L.: *Petroleum Refinery Engineering*, fourth edition, McGraw-Hill Book Co. Inc., New York City (1958) 910-37.

Fig. 21.4, courtesy Hansen, D.N. and Hurd, C.O., Shell Development Co., *Petroleum Refiner* (April 1945).

Figs. 21.7 through 21.21, from *ASTM Standards on Petroleum Products and Lubricants*, Part 24, ASTM, Philadelphia (1975) 796.

Fig. 21.22, from Matthews, T.A., Roland, C.H., and Katz, D.L.: "High Pressure Gas Measurements," *Proc.*, Natural Gas Assn. of America (1942) 41.

Figs. 21.23 and 21.24, from Standing, M.B.: *Volumetric and Phase Behavior of Oil Field Hydrocarbon Systems*, Reinhold Publishing Corp., New York City (1952).

Fig. 21.25, from Standing, M.B.: "A Pressure-Volume-Temperature Correlation for Mixtures of California Oil and Gases," *Drill. and Prod. Prac.*, API (1947) 275.

Fig. 21.26, courtesy California Research Corp., 1947.

Table 21.7, from Nelson, W.L.: *Petroleum Refinery Engineering*, fourth edition, McGraw-Hill Book Co. Inc., New York City (1958) 910-37.

Table 21.10, from "A Guide to World Export Crudes," *Oil & Gas J.* (1976).

Table 21.11, courtesy Bartlesville Energy Technology Center, Bartlesville, OK.

Chap. 22

Figs. 22.1 through 22.3, from Standing, M.B.: *Volumetric and Phase Behavior of Oil Field Hydrocarbon Systems*, Reinhold Publishing Corp., New York City (1952).

Fig. 22.4, from Katz, D.L.: "Prediction of the Shrinkage of Crude Oils," *Drill. and Prod. Prac.*, API (1942).

Figs. 22.5, 22.9, and 22.13, courtesy California Research Corp.

Figs. 22.19 and 22.20, from Baker, O. and Swerdloff, W.: "Finding Surface Tension of Hydrocarbon Liquids," *Oil & Gas J.* (Jan. 2, 1956).

Chap. 23

Fig. 23.9 from *GPSA Engineering Databook*, Gas Processors Suppliers Assn., ninth edition, Tulsa, OK (1972).

Figs. 23.12 and 23.13 from Reamer, H.H., Fiskin, J.M., and Sage, B.H.: "Phase Equilibria in Hydrocarbon Systems," *Ind. Eng. Chem.* (Dec. 1949) **41**, 2871.

Chap. 24

Fig. 24.3, from Hoke, S.H. and Collins, A.G.: *Mobile Wellhead Analyzer for the Determination of Unstable Constituents in Oil-Field Waters*, ASTM STP 735 (1981) 34-48.

Fig. 24.9, from Burcik: *Properties of Petroleum Reservoir Fluids*, John Wiley & Sons Inc., New York City (1957).

Figs. 24.11 and 24.12, from PI-Petroleum Information.

Chap. 25

Figs. 25.3 and 25.4, from Kobayashi, R.: "Vapor-Liquid Equilibria in Binary Hydrocarbon-Water Systems," PhD dissertation, U. of Michigan, Ann Arbor (1951).

Figs. 25.5, 25.10, 25.21, 25.23, and 25.24, and Table 25.4, from Katz, D.L. *et al.*: "Water-Hydrocarbon Systems," *Handbook of Natural Gas Engineering*, McGraw-Hill Book Co. Inc., New York City (1959) 189-221.

Figs. 25.6, 25.8, and 25.33, from Kobayashi, R. and Katz, D.L.: "Vapor-Liquid Equilibria for Binary Hydrocarbon-Water Systems," *Ind. Eng. Chem.* (1953) **45**, 440-51.

Fig. 25.7, from Alder, S.B. and Spencer, C.F.: "Case Studies of Industrial Problems, Phase Equilibria and Fluid Properties in the Chemical Industry," *Proc.*, Equilibrium Fluid Properties in the Chemical Industry (1980) 465-95.

Fig. 25.14, from von Stackelberg, M.: "Solid Gas Hydrates," *Naturwissenschaften* (1949) **36**, 327-33, 359-62.

Figs. 25.17 through 25.20, from Sloan, E.D.: "Phase Equilibria of Natural Gas Hydrates," paper 67f presented at the 1983 AIChE Summer Natl. Meeting, Denver, Aug. 28-31.

Fig. 25.22, from Song, K.Y. and Kobayashi, R.: "Measurement and Interpretation of the Water Content of a Methane-Propane Mixture in the Gaseous State in Equilibrium with Hydrate," *Ind. Eng. Chem. Fund.* (1982) **21**, No. 4, 391-95.

Fig. 25.25, from Deaton, W.J. and Frost, E.M.: *Gas Hydrates and Their Relation to the Operation of Natural Gas Pipe Lines*, Monograph 8, USBM, Washington, DC (1946).

Fig. 25.30, from Saito, S., Marshall, D.R., and Kobayashi, R.L.: "Hydrates at High Pressures: Part II. Application of Statistical Mechanics to the Study of the Hydrates of Methane, Argon, and Nitrogen," *AIChE J.* (1964) **10**, No. 5, 734-40.

Fig. 25.32, from Dodson, C.R. and Standing, M.B.: "Pressure-Volume-Temperature and Solubility Relations for Natural Gas-Water Mixtures," *Drill. and Prod. Prac.*, API, Dallas (1944) 173-79.

Figs. 25.34 through 25.36, from Peng, D.-Y. and Robinson, D.B.: "Two- and Three-Phase Equilibrium Calculations for Coal Gasification and Related Process," *Thermodynamics of Aqueous Systems with Industrial Applications*, S.A. Newman (ed.), Symposium Series 133, ACS (1980) 393-414.

Figs. 25.37 and 25.41, from Scauzillo, F.R.: "Inhibiting Hydrate Formations in Hydrocarbon Gases," *Chem. Eng. Progr.* (1956) **52**, No. 8, 324-28.

Figs. 25.38 through 25.40, from *Gas Conditioning Fact Book*, Dow Chemical Co., Midland, MI (1962) 69-71.

Table 25.5, from Dharmawardhand, P.B.: "The Measurement of the Thermodynamic Parameters of the Hydrate Structure and Application of Them in the Prediction of Natural Gas Hydrates," PhD dissertation, Colorado School of Mines, Golden (1980).

Chap. 26

Fig. 26.1, from Fraser, H.J. and Gratton, L.C.: "Systematic Packing of Spheres—With Particular Relation to Porosity and Permeability," *J. Geol.* (Nov.-Dec. 1935) 785-909.

Figs. 26.3 and 26.30, courtesy Core Laboratories Inc., Dallas.

Fig. 26.5, 26.24, and 26.25, from Stevens, A.B.: *A Laboratory Manual for Petroleum Engineering 308*, Texas A&M U., College Station (1954).

Fig. 26.7, from Krumbein, W.C. and Sloss, L.L.: *Stratigraphy and Sedimentation*, Appleton-Century-Crofts Inc., New York City (1951) 218.

Fig. 26.27, from Klinkenberg, L.J.: "The Permeability of Porous Media to Liquids and Gases," *Drill. and Prod. Prac.*, API, Dallas (1941) 200-13.

Fig. 26.29, from Kennedy, H.T., VanMeter, O.E., and Jones, R.G.: "Saturation Determination of Rotary Cores," *Pet. Eng.* (Jan. 1954) B.52-B.64.

Chap. 27

Table 27.12, courtesy Alaska Oil & Gas Conservation Commission, Anchorage.

Tables 27.13 through 27.15 and 27.17, courtesy Core Laboratories Inc., Dallas.

Table 27.16, from *European Continental Shelf Guide*, Oilfield Publications Ltd., Ledbury, Herefordshire, England (1982).

Chap. 28

Figs. 28.3 and 28.4, from Rose, W.: U.S. Patent No. 4,506,542 (1985).

Fig. 28.7, from Rose, W.: "Permeability and Gas Slippage Phenomena," *Drill. and Prod. Prac.*, API, Dallas (1948) 127-35.

Fig. 28.8, from Stone, H.L.: "Probability Model for Estimating Three-Phase Relative Permeability," *J. Cdn. Pet. Tech.* (Oct. 1973) 53-59.

Fig. 28.12, from Panteleev, V.G. *et al.*: "Influence of Carbon Dioxide on Three Phase Permeability by Oil and Water," *Neftepromyslovoe delo* (1973) No. 6, 11-13.

Fig. 28.16, from Ashford, F.E.: "Determination of Two Phase and Multiphase Relative Permeability for Drainage and Imbibition Cycles Based on Capillary Pressure Measurement," *Revista Tecnica Intevep* (1981) 1, 77-94.

Fig. 28.19, from Lin, C. and Slattery, J.C.: "Three-Dimensional, Randomized, Network Model for Two-Phase Flow Through Porous Media," *AIChE J.* (1982) 28, No. 2, 311-24.

Chap. 29

Figs. 29.1 through 29.3, from Galloway, T.J.: *Bull. 118*, California Div. of Mines, Sacramento (Aug. 1957).

Fig. 29.6, from Sams, H.: "Atkinson Field, Good Example of 'Subtle Stratigraphic Trap,'" *Oil & Gas J.* (Aug. 12, 1974) 145-63.

Fig. 29.7, from Hoyt, W.V.: "Erosional Channel in the Middle Wilcox Near Yoakum, Lavaca County, Texas," *Trans., Gulf Coast Assn. of Geological Societies* (Nov. 1959) 9, 41-50.

Fig. 29.8, from Pirson, S.J.: *Oil Reservoir Engineering*, second edition, McGraw-Hill Book Co. Inc., New York City (1958).

Figs. 29.9 and 29.10, from "Occurrence of Oil and Gas in Northeast Texas," F.A. Herald (ed.), Bureau of Economic Geology and East Texas Geological Soc. (April 1951).

Fig. 29.11, from *An Introduction to Gulf Coast Oil Fields*, Houston Geological Soc., Houston (1941).

Fig. 29.12, from *A Guide Book*, Houston Geological Soc., Houston (1953).

Chap. 30

Tables 30.1 through 30.4, from Bergman, J.C., Guimard, A., and Hagenar, D.S.: "High Performance Pressure Measurement Systems," Schlumberger Well Services, Houston (1980) 10.

Chap. 31

Fig. 31.1, from *Climatological Data in the United States*, U.S. Weather Bureau, Washington, DC.

Chap. 32

Fig. 32.1, from the Railroad Commission of Texas, Austin.

Figs. 32.2 and 32.3, from Calhoun, J.C. Jr.: *Fundamentals of Reservoir Engineering*, revised edition, U. of Oklahoma Press, Norman (1953).

Figs. 32.10 and 32.11, from "Turbine Meters," *API Manual of Petroleum Measurement Standards*, Chap. 5, Sec. 3.

Fig. 32.12, from *API Measurement of Petroleum Liquid Hydrocarbons by Positive Displacement Meter*, API Std. 1101, first edition (Aug. 1960).

Chap. 33

Table 33.7, from Rawlins, E.L. and Schellhardt, M.A.: "Back-pressure Data on Natural Gas Wells and Their Application to Production Practices," USBM Monograph, Washington, DC (1935).

Chap. 34

Fig. 34.2, from Moody, L.F.: "Friction Factors for Pipe Flow," *Trans., ASME* (1944) 66, 671.

Fig. 34.3, from Brown, G.G. *et al.*: *Natural Gasoline and the Volatile Hydrocarbons*, Natural Gas Assn. of America (1948).

Fig. 34.4, from Nisle, R.G. and Poettmann, F.H.: "Calculation of the Flow and Storage of Natural Gas in Pipe," *Pet Eng.* (1955) 27, No. 1, D-14; No. 2, C-36; No. 3, D-37.

Figs. 34.8 and 34.9, from Griffith, P. and Wallis, G.B.: "Two-Phase Slug Flow," *J. Heat Transfer* (Aug. 1961) 307-20; *Trans., ASME*.

Figs. 34.11 and 34.12, from Poettmann, F.H. and Carpenter, P.G.: "Multiphase Flow of Gas, Oil, and Water Through Vertical Flow Strings with Application to the Design of Gas-Lift Installations," *Drill. and Prod. Prac.*, API (1952) 257-317.

Figs. 34.13 through 34.17, from Davis, G.J. and Weidner, C.R.: "Investigation of the Air Lift Pump," *Bull., Eng. Series*, U. of Wisconsin (1911) 6, No. 7.

Figs. 34.23 through 34.25, from Poettmann, F.H. and Beck, R.L.: "New Charts Developed to Predict Gas-Liquid Flow Through Chokes," *World Oil* (March 1963) 95-101.

Table 34.7, from Rawlins, E.L. and Schellhardt, M.A.: "Back-Pressure Data on Natural Gas Wells and Their Application to Production Practices," Monograph Series, USBM (1936) 7.

Chap. 36

Fig. 36.9, from Dahm, C.G. and Graebner, R.J.: "Field Development With Three-Dimensional Seismic Methods in the Gulf of Thailand—A Case History," *Geophysics* (Feb. 1982) 149-76.

Chap. 37

Fig. 37.6 and 37.7, from Turner, J.: "How Different Size Gas Caps and Pressure Maintenance Programs Affect Amount of Recoverable Oil," *Oil Weekly* (June 12, 1944) 32-44.

Figs. 37.16 through 37.24, and Tables 37.1 and 37.2, from Singh, D. and Guerrero, E.T.: "Material Balance Equation Sensitivity," *Oil & Gas J.* (Oct. 20, 1969) 95-102.

Figs. 37.29 and 37.30, from Cronquist, C.: "Evaluating Producing Volatile Oil Reservoirs," *World Oil* (April 1979) 159-66 and 246.

Chap. 39

Figs. 39.1 through 39.3, and Table 39.1, after Eilerts, K.C. *et al.*: *Phase Relations of Gas-Condensate Fluids*, American Gas Assn., New York City (1957).

Figs. 39.4 through 39.6, and Tables 39.2 through 39.10, courtesy Core Laboratories Inc., Dallas (1985).

Fig. 39.7, after Marshall, D.L. and Oliver, L.R.: "Some Uses and Limitations of Model Studies in Cycling," *Trans.*, AIME (1948) 174, 67-87.

Fig. 39.8, after Stelzer, R.B.: "Model Study vs. Field Performance, Cycling the Paluxy Condensate Reservoir," *Drill. and Prod. Prac.*, API (1956) 336-42.

Fig. 39.9, data derived from Stelzer, R.B.: "Model Study vs. Field Performance, Cycling the Paluxy Condensate Reservoir," *Drill. and Prod. Prac.*, API (1956) 336-42.

Table 39.12, from Miller, M.G. and Lents, M.R.: "Performance of Bodcaw Reservoir, Cotton Valley Field Cycling Project, New Methods of Predicting Gas-Condensate Reservoir Performance Under Cycling Operations," *Drill. and Prod. Prac.*, API (1946) 128-49.

Chap. 41

Table 41.11, courtesy Republic Bank of Dallas.

Table 41.14, from Wilson, W.W. and Boyd, W.L.: "Simplified Calculations Determine Loan Payout," *World Oil* (May 1958).

Chap. 44

Figs. 44.6 through 44.8 and Table 44.2, from Craft, B.C. and Hawkins, M.J. Jr.: *Applied Petroleum Reservoir Engineering*, Prentice-Hall Inc., Englewood Cliffs, NJ (1959) 107, 357, 412-13.

Figs. 44.58 through 44.61, from Guerrero, E.T. and Earlougher, R.C.: "Analysis and Comparison of Five Methods Used to Predict Waterflooding Reserves and Performance," *Drill. and Prod. Prac.*, API, Dallas (1961) 78-95.

Fig. 44.62, from Higgins, R.V. and Leighton, A.J.: "Computer Techniques for Predicting Three-Phase Flow in Five-Spot Waterfloods," RI 7011, USBM (Aug. 1967).

Chap. 45

Fig. 45.4, from Brown, G.G. *et al.*: "Natural Gasoline and the Volatile Hydrocarbons," Natural Gasoline Assn. of America (1948).

Fig. 45.5, from Hutchinson, C.A. Jr. and Braun, P.H.: "Phase Relations of Miscible Displacement in Oil Recovery," *AIChE J.* (1961) 7, 64.

Fig. 45.7, modified from Slobod, R.L. and Koch, H.A. Jr.: "High Pressure Gas Injection—Mechanism of Recovery Increase," *Drill. and Prod. Prac.*, API, Dallas (1953) 82.

Fig. 45.8, modified from Sage B.H. and Lacey, W.N.: *Some Properties of the Lighter Hydrocarbons, Hydrogen Sulfide, and Carbon Dioxide*, Monograph Research Project 37, API, Dallas (1955).

Chap. 46

Fig. 46.1, from Farouq Ali, S.M.: "Steam Injection, Secondary and Tertiary Oil Recovery Processes," *Interstate Oil Compact Commission*, Oklahoma City (Sept. 1974) 148.

Fig. 46.2, from McNeil, M.S. and Moss, J.T.: "Oil Recovery by In-Situ Combustion," *Pet. Eng.* (July 1958) B-29-B-42.

Fig. 46.5, from Smith, R.W. and Perkins, T.K.: "Experimental and Numerical Simulation Studies of the Wet Combustion Recovery Process," *J. Cdn. Pet. Tech.* (July-Sept. 1973) 44-54.

Fig. 46.34, from Mace, C.: "Deepest Combustion Project Proceeding Successfully," *Oil & Gas J.* (Nov. 17, 1975) 74-81.

Fig. 46.59, from Poettmann, F.H. and Mayland, B.J.: "Equilibrium Constants for High Boiling Hydrocarbon Fractures of Varying Characterization Factors," *Pet. Refiner* (July 1949) 101-12.

Tables 46.1 through 46.6, from "Steam Dominates Enhanced Oil Recovery," *Oil & Gas J.* (April 5, 1982) 139-59.

Table 46.31, from "1967 ASTM Steam Tables," ASME, New York City (1967).

Chap. 47

Figs. 47.1, 47.12, and 47.26, from U.S. DOE; drawing by J. Lindley, Bartlesville, OK.

Fig. 47.3, from Mungan, N.: *Rev. Inst. Fr. Pet.*, Editions Technip, Paris (1969) 24, 232.

Fig. 47.4, from Tsaur, K.: "A Study of Polymer/Surfactant Interactions for Micellar/Polymer Flooding Applications," MS thesis, U. of Texas, Austin (1978).

Fig. 47.5, from Martin, F.D., Donaruma, L.G., and Hatch, M.J.: "Development of Improved Mobility Control Agents for Surfactant/Polymer Flooding," second annual report, Contract No. DOE/BC/00047-13, U.S. DOE (Oct. 1980).

Fig. 47.8, from Overbeck, J.Th.G.: "Colloids and Surface Chemistry, A Self-Study Subject Guide. Part 2, Lyophobic Colloids," *Bull.*, Center for Advanced Engineering, Massachusetts Inst. of Technology, Cambridge, MA (1972).

Fig. 47.9, from Khan, S.A.: "The Flow of Foam Through Porous Media," MS thesis, Stanford U., Stanford, CA (1965).

- Fig. 47.19**, from Reed, R.L. and Healy, R.N.: "Some Physico-Chemical Aspects of Microemulsion Flooding: A Review," *Improved Oil Recovery by Surfactant and Polymer Flooding*, D.O. Shah and R.S. Schechter (eds.), Academic Press, New York City (1977) 383-438.
- Fig. 47.20**, from Harwell, J.H.: "Surfactant Adsorption and Chromatographic Movement with Application in Enhanced Oil Recovery," PhD dissertation, U. of Texas, Austin (1983).
- Fig. 47.23**, from Lake, L.W. and Pope, G.A.: "Status of Micellar-Polymer Field Tests," *Pet. Eng. Intl.* (Nov. 1979) **51**, 38-60.
- Fig. 47.27**, from Minssieux, L.: "Waterflood Improvement by Means of Alkaline Water," *Enhanced Oil Recovery by Displacement with Saline Solutions*, Kogan Page Ltd., London (1979) 75-90; courtesy BP Trading Co. Ltd.
- Table 47.1**, from Manning, R.K., Pope, G.A., and Lake, L.W.: "A Technical Survey of Polymer Flooding Projects," Contract No. DOE/BETC/10327-19, U.S. DOE (Sept. 1983).
- Table 47.2**, from Akstinat, M.H.: "Surfactants for WOR Process in High-salinity Systems: Product selection and evaluation," *Enhanced Oil Recovery*, Elsevier Scientific Publishing Co., New York City (1981).

Chap. 49

- Figs. 49.9, 49.10, 49.19 through 49.22, 49.25 through 49.30, and 49.34**, from *Log Interpretation Principles*, Vol. 1, Schlumberger Well Services, Houston.
- Figs. 49.42 through 49.44 and Table 49.2**, from Calver, J.C., Rau, R., and Wells, L.: "Electromagnetic Propagation—A New Dimension in Logging," Schlumberger Well Services, Houston.
- Figs. 49.46 and 49.47**, from Best, D.L., Gardner, J.S., and Dumanoir, J.L.: "A Computer-Processed Wellsite Log Computation," paper presented at the 1978 SPWLA Annual Logging Symposium, June 13-16.
- Fig. 49.48**, from Coates, G.R., Schulze, R.P., and Throop, W.H.: "VOLAN*—An Advanced Computational Log Analysis," paper presented at the 1982 SPWLA Annual Logging Symposium, July 6-9.
- Tables 49.1 and 49.3 through 49.6**, from Bateman, R.M., *Log Quality Control*, IHRDC, Boston, 1984.

Chap. 50

- Figs. 50.5 and 50.6**, from Evans, R.D.: *The Atomic Nucleus*, McGraw-Hill Book Co. Inc., New York City (1967) 426-38.
- Figs. 50.9, 50.21, 50.30, 50.32 through 50.34, 50.40, 50.43, 50.50, and 50.51**, courtesy Schlumberger Well Services, Houston.
- Fig. 50.18**, from Tidman, J.: "Geophysical Well Logging," excerpts from *Methods in Experimental Physics: Physics*, Academic Press (1986) 24.
- Figs. 50.22 and 50.36**, from Schlumberger Log Interpretation Charts, Schlumberger Well Services, Houston, 1984.
- Figs. 50.23, 50.24, and 50.26**, from Edmundson, H. and Raymer, L.L.: "Radioactive Logging Parameters for Common Minerals," paper presented at the 1979 SPWLA Annual Logging Symposium, Tulsa, June 3-6.
- Fig. 50.29**, from Hertzog, R.C. and Plasek, R.E.: "Neutron-Excited Gamma-Ray Spectrometry for Well Logging," *IEEE Trans. Nuc. Sci.* (Feb. 1979) NS-26, No. 1.
- Fig. 50.46**, Arnold, D.M. and Smith, H.D. Jr.: "Experimental Determination of Environmental Corrections for a Dual-Spaced Neutron Porosity Log," paper W presented at the 1981 SPWLA Annual Logging Symposium, Mexico City, June 23-26.
- Fig. 50.47**, from Schlumberger Chart Book, Schlumberger Well Services, Houston (1977).
- Table 50.3**, from Bertuzzi, W., Ellis, D.V., and Wahl, J.S.: "The Physical Foundation of Formation Lithology Logging with Gamma Rays," *Geophysics* (Oct. 1981) **46**, No. 10.

Chap. 51

- Fig. 51.2**, from Sears, F.W. and Zemansky, M.W.: *University Physics*, Addison-Wesley Publishing Co. Inc., Reading, MA (1955) 1031.
- Figs. 51.3 and 51.4**, from Krautkramer, J. and Krautkramer, H.: *Ultrasonic Testing of Materials*, Springer-Verlag, New York City (1969) 521.
- Figs. 51.6 and 51.71**, from Timur, A.: "Rock Physics," *The Arabian J. Sci. Eng. Special Issue* (1978) 5-30.
- Figs. 51.7 and 51.15**, from Timur, A.: "Temperature Dependence of Compressional and Shear Wave Velocities in Rocks," *Geophysics* (1977) **42**, 950-56.
- Figs. 51.8 and 51.9 and Table 51.2**, from Jones, S.B., Thompson, D.D., and Timur, A.: "A Unified Investigation of Elastic Wave Propagation in Crustal Rocks," paper presented at the Rock Mechanics Conference, Vail, CO (1976).
- Fig. 51.10**, from Johnston, D.H., Toksoz, M.N., and Timur, A.: "Attenuation of Seismic Waves in Dry and Saturated Rocks: Part II: Theoretical Models and Mechanism," *Geophysics* (1979) **44**, 691-711.
- Fig. 51.11**, from Wyllie, M.R.J., Gardner, G.H.F., and Gregory, A.R.: "Studies of Elastic Wave Attenuation in Porous Media," *Geophysics* (1962) **27**, 269.
- Figs. 51.12 through 51.14**, from Gardner, G.H.F., Gardner, L.W.R., and Gregory, A.R.: "Formation Velocity and Density—The Diagnostic Basics for Stratigraphic Traps," *Geophysics* (1974) **39**, 770-80.
- Fig. 51.16**, from Timur, A.: "Velocities of Compressional Waves in Porous Media at Permafrost Temperatures," *Geophysics* (1968) **33**, 584-96.
- Figs. 51.17, 51.19, and 51.21**, from Toksoz, M.N., Cheng, C.H., and Timur, A.: "Velocities of Seismic Waves in Porous Rocks," *Geophysics* (1976) **41**, 621-45.
- Fig. 51.17**, from King, M.S.: "Wave Velocities in Rocks as a Function of Changes in Overburden Pressure and Pore Fluid Saturants," *Geophysics* (1966) **31**, 50-73.
- Fig. 51.18**, Gregory, A.R.: "Fluid Saturation Effects on Dynamic Elastic Properties of Sedimentary Rocks," *Geophysics* (1976) **41**, 895-921.
- Fig. 51.20**, from Timur, A., Hemphkins, W.B., and Weinbrandt, R.M.: "Scanning Electron Microscope Study of Pore Systems in Rocks," *J. Geophys. Res.* (1971) **76**, No. 20, 4932-48.

Figs. 51.22, 51.37, 51.50, and 51.94, from Geyer, R.L. and Myung, J.I.: "The 3-D Velocity Log: a Tool for In-Situ Determination of the Elastic Moduli of Rocks," *Dynamic Rock Mechanics, Proc.*, Twelfth Symposium on Rock Mechanics (1971) 71-107.

Figs. 51.23 and 51.24, from Minear, J.W. and Fletcher, C.R.: "Full-Wave Acoustic Logging," *Trans.*, SPWLA (1983) paper EE.

Fig. 51.25, from Cheng, C.H. and Toksoz, M.N.: "Elastic Wave Propagation in a Fluid-Filled Borehole and Synthetic Acoustic Logs," *Geophysics* (1981) **46**, 1042-53.

Fig. 51.26, from Cheng, C.H. and Toksoz, M.N.: "Generation, Propagation and Analysis of Tube Waves in a Borehole," *Trans.*, SPWLA (1982) paper P.

Figs. 51.27, 51.28, 51.31, and 51.46, from Thomas, D.H.: "Seismic Applications of Sonic Logs," *The Log Analyst* (Jan.-Feb. 1977) 23-32.

Figs. 51.29 and 51.33, from Lynch, E.J.: *Formation Evaluation*, Harper and Row, New York City (1962) 422.

Figs. 51.36 and 51.77, from Ausburn, J.R.: "Well Log Editing in Support of Detailed Seismic Studies," *Trans.*, SPWLA (1977) paper F.

Figs. 51.39 and 51.42, from Goetz, J.F., Dupal, L., and Bowler, J.: "An Investigation into Discrepancies Between Sonic Log and Seismic Check Shot Velocities, Part I," *APEA J.* (1979) **19**, 131-41.

Fig. 51.40, from Ransom, R.C.: "Methods Based on Density and Neutron Well-Logging Responses to Distinguish Characteristics of Shaly Sandstone Reservoir Rock," *The Log Analyst* (May-June 1977) **18**, 47-62.

Figs. 51.41, 51.43, 51.44, and 51.48, from "The Long Spacing Sonic," Schlumberger technical pamphlet (1980).

Fig. 51.45, from Misk, A. *et al.*: "Effects of Hole Conditions on Log Measurements and Formation Evaluation," *SAID*, Third Annual Logging Symposium (June 1976).

Figs. 51.47 and 51.49, from "The Long Spacing Sonic," Schlumberger technical pamphlet (1982).

Fig. 51.56, from Parks, T.W., McClellan, J.H., and Morris, C.F.: "Algorithms for Full-Waveform Sonic Logging," paper presented at the 1983 IEEE-ASSP Workshop on Spectral Estimation.

Fig. 51.58, from Wiley, R.: "Borehole Televiwer—Revisited," *Trans.*, SPWLA (1980) **21**, paper HH.

Fig. 51.60, from "Seisviewer Logging," Birdwell, Div. of Seismograph Service Corp., technical pamphlet (1981).

Fig. 51.61, from Broding, R.A.: "Volumetric Scanning Well Logging," *Trans.*, SPWLA (1981) **22**, paper B.

Fig. 51.63, from "Log Interpretation Charts," Schlumberger (1979).

Fig. 51.65, from "Evaluación de Formaciones en la Argentina," Schlumberger (1973) 9495.

Fig. 51.66, from Raymer, L.L., Hunt, E.R., and Gardner, J.S.: "An Improved Sonic Transit Time-To-Porosity Transform," *Trans.*, SPWLA (1980) paper P.

Fig. 51.67, from Hartley, K.B.: "Factors Affecting Sandstone Acoustic Compressional Velocities and An Examination of Empirical Correlations Between Velocities and Porosities," *Trans.*, SPWLA (1981) paper PP.

Figs. 51.70 and 51.72, from Nations, J.F.: "Lithology and Porosity from Acoustic Shear and Compressional Wave Transit Time Relationships," *Trans.*, SPWLA 18th Annual Logging Symposium (June 1974).

Fig. 51.73 and 51.74, from Gardner, G.H.F. and Harris, M.H.: "Velocity and Attenuation of Elastic Waves in Sands," *Trans.*, SPWLA (1968) **9**, paper M.

Fig. 51.75, from Arditty, P.C., Ahrens, G., and Staron, Ph.: "EVA: A Long Spacing Sonic Tool for Evaluation of Velocities and Attenuation," paper presented at the 1981 SEG Annual Meeting, Los Angeles.

Fig. 51.76, from Domenico, S.N.: "Effect of Brine-Gas Mixture on Velocity in an Unconsolidated Sand Reservoir," *The Log Analyst* (1977) **18**, 38-46.

Figs. 51.78 and 51.79, from Kithas, B.A.: "Lithology, Gas Detection, and Rock Properties from Acoustic Logging Systems," *Trans.*, SPWLA (1976) **17**, paper R.

Figs. 51.80 and 51.81, from Laws, W.R., Edwards, C.A.M., and Wichmann, P.A.: "A Study of the Acoustic and Density Changes Associated with High-Amplitude Events on Seismic Data," *Trans.*, SPWLA (1974) **15**, paper D.

Figs. 51.83 and 51.84, from Herring, E.A.: "North Sea Abnormal Pressures Determined from Logs," *Pet. Eng.* (1973) **45**, 72-84.

Figs. 51.85 through 51.89, from "Acoustic Cement Bond Log," Dresser Atlas technical pamphlet (1979) 20.

Figs. 51.90 and 51.92, from "Cement Bond Evaluation in Cased Holes Through 3-D Velocity Logging," Birdwell technical pamphlet (1978) 12.

Fig. 51.91, from "Cement Evaluation Tool," Schlumberger technical pamphlet (1983).

Fig. 51.96, from Walker, T.: "Acoustic Character of Unconsolidated Sand," Welex paper (1971).

Fig. 51.97, from Myung, J.I. and Baltosser, R.W.: "Fracture Evaluation by the Borehole Logging Method," *Stability Rock Slopes*, Thirteenth Symposium on Rock Mechanics (1972) 31-56.

Figs. 51.98 and 51.99, from Taylor, T.J.: "Interpretation and Application of Borehole Televiwer Surveys," *Trans.*, SPWLA (1983) **24**, paper QQ.

Fig. 51.100, from Williams, D.M. *et al.*: "The Long Spacing Acoustic Logging Tool," *Trans.*, SPWLA (1984) **25**, paper T.

Table 51.1, from Timur, A.: "Application of Acoustic Wave Propagation Methods to Evaluation and Production of Hydrocarbon Reservoirs," *Proc.*, IEEE Ultrasonic Symposium, Dallas (1984).

Table 51.3, from Guyod, H. and Shane, L.E.: *Geophysical Well Logging*, Hubert Guyod, Houston (1969) 1, 256; and Wyllic, M.R.J., Gregory, A.R., and Gardner, G.H.F.: "Elastic Wave Velocities in Heterogeneous and Porous Media," *Geophysics* (1956) **21**, 41-70.

Chap. 52

Figs. 52.1 and 52.2, from MS-196, Exploration Logging Inc., Sacramento, CA (1979).

Figs. 52.3 through 52.12 and 52.22 and Table 52.1, courtesy Exploration Logging Inc., Sacramento, CA.

Figs. 52.13, 52.14, 52.16, 52.17, and 52.19 through 52.21, from MS-156, Exploration Logging Inc., Sacramento, CA (1981).

Figs. 52.15 and 52.18, from AV-6, Exploration Logging Inc., Sacramento, CA (1980).

Fig. 52.23, from AV-13, Exploration Logging Inc., Sacramento, CA (1982).

Chap. 53

Fig. 53.3, from "Measurement While Drilling, Technical Specifications," Anadrill Logging Unit, Schlumberger.
Fig. 53.7 and Table 53.2, from *Log Quality Control Manual*, Vizilog Inc., Houston.
Figs. 53.9 through 53.11, from *Dipmeter Interpretation—Vol. 1, Fundamentals*, Schlumberger, Houston (1981).
Fig. 53.12 and 53.15, from Gilbreath, J.A.: "Dipmeter Interpretation Rules," Schlumberger Offshore Services. New Orleans.
Figs. 53.13 and 53.14, from "Open Hole Log Analysis and Formation Evaluation," Vizilog Inc., Houston.
Figs. 53.16 through 53.18, from *The Log Analyst* (March-April 1979) 20.
Fig. 53.20, from "Well Evaluation Developments" Schlumberger, Houston (1982).
Fig. 53.23 through 53.25, from *Dresser Atlas Production Services Catalog*, Dresser Atlas.
Fig. 53.26, from *The Log Analyst* (March-April 1984) 25–28.
Fig. 53.27 through 53.32, from "Well Evaluation Developments 1982," Schlumberger.
Table 53.1 and Fig. 53.5, from EXLOG Flyer GA 817-A, EXLOG (June 1983).
Table 53.3 and Figs. 53.21 and 53.22, from Dia-Log flyer, The Dia-Log Co., Houston.

Chap. 54

Figs. 54.6 through 54.9, courtesy Dowell Schlumberger Technical Brochure TSL-2038, "Acidizing—State-of-the-Art," Tulsa, OK (1981).

Chap. 56

Figs. 56.1 through 56.8, courtesy Dowell Schlumberger Technical Brochure TSL-4519, "Dowell Sand Control Techniques and Equipment Catalog" (Sept. 1982). Tulsa, OK.

Contents

Preface	iii
Acknowledgments	v
1. Mathematical Tables and Units and Systems of Weights and Measures	
Mathematical Tables	1-2
Units and Systems of Weights and Measures	1-68
2. Casing, Tubing, and Line Pipe	
Casing	2-1
Tubing	2-38
Line Pipe	2-46
Equations for Calculating Performance Properties of Casing, Tubing, and Line Pipe	2-46
API Threading Data	2-64
3. Wellhead Equipment and Flow Control Devices	
Introduction	3-1
API Flanged or Clamped Wellhead Equipment	3-1
Flow Control Devices: Safety Shut-In Systems	3-18
Other Flow-Control Devices	3-34
Corrosion	3-35
Special Application	3-36
Independent Screwed Wellhead	3-39
4. Production Packers	
Production Packers Classification and Objectives	4-1
Tubing-to-Packer Connections	4-1
Packer Utilization and Constraints	4-1
Considerations for Packer Selection	4-4
Tubing/Packer System	4-6
Tubing Response Characteristics	4-8
Combination Tubing/Packer Systems	4-11
Tubing/Packer Forces on Intermediate Packers	4-11
5. Gas Lift	
Introduction	5-1
Gas Fundamentals as Applied to Gas Lift	5-3
Gas Lift Valve Mechanics	5-12
Continuous-Flow Gas Lift	5-21
Intermittent Gas Lift	5-38
Unloading Procedures and Proper Adjustment of Injection Gas Rate	5-53
6. Hydraulic Pumping	
Introduction	6-1
Downhole Pumps	6-2
Principles of Operation—Reciprocating Pumps	6-8
Jet Pumps	6-34
Surface Equipment	6-49
Appendix A—Fluid Properties	6-66
Appendix B—Friction Relationships	6-69
7. Electric Submersible Pumps	
Introduction	7-1
ESP System	7-1
Applications	7-1
ESP System Components	7-3
Selection Data and Methods	7-9
Handling, Installation, and Operation	7-12
Troubleshooting	7-14

8. Subsurface Sucker-Rod Pumps	
Introduction	8-1
Pump Selection	8-2
Plungers	8-4
Slippage Past Plungers	8-5
Soft-Packed Plungers	8-6
Balls and Seats	8-7
Double Valves	8-7
Bottom-Discharge Valve	8-8
Three-Tube Pump	8-8
Gas Anchors	8-9
Special Pumps	8-9
Corrosion	8-9
Effect of Gases and Vapors	8-10
Conclusions	8-10
9. Sucker Rods	
Introduction	9-1
Steel Sucker Rods	9-1
Fiberglass Sucker Rods	9-10
10. Pumping Units and Prime Movers for Pumping Units: Part 1—Pumping Units	
Introduction	10-1
Pumping Units	10-1
Component Parts	10-4
Pumping Unit Loading	10-5
Counterbalance	10-6
Sizing	10-7
Installation	10-7
Lubrication	10-12
Changing the Oil	10-13
Pumping Units and Prime Movers for Pumping Units: Part 2—Prime Movers for Pumping Units	
Introduction	10-14
Internal-Combustion Engines	10-14
Electric Motors for Oilwell Pumping	10-19
11. Oil Storage	
Types of Storage Tanks	11-1
Tank Corrosion Protection	11-4
Appurtenances	11-6
Venting Atmospheric and Low-Pressure Storage Tanks	11-6
Materials of Construction	11-9
Production Equipment	11-9
Vapor Losses	11-11
Vapor Control and Gravity Conservation With Storage Tanks	11-12
Underground Storage	11-13
12. Oil and Gas Separators	
Summary	12-1
Introduction	12-1
Primary Functions of Oil and Gas Separators	12-3
Secondary Functions of Oil and Gas Separators	12-4
Special Problems in Oil and Gas Separation	12-6
Methods Used To Remove Oil From Gas in Separators	12-8
Mist Extractors Used in Oil and Gas Separators	12-11
Methods Used To Remove Gas From Oil in Separators	12-13
Estimated Quality of Separated Fluids	12-13
Classification of Oil and Gas Separators	12-16
Centrifugal Oil and Gas Separators and Gas Scrubbers	12-20
Illustrations of Oil and Gas Separators	12-21
Comparison of Oil and Gas Separators	12-21
Estimating the Sizes and Capacities of Oil and Gas Separators	12-21

Computer Sizing of Oil and Gas Separators	12-25
Capacity Curves for Vertical and Horizontal Oil and Gas Separators	12-27
Practical Considerations in Sizing Oil and Gas Separators	12-32
Stage Separation of Oil and Gas	12-32
Selection and Application of Separators and Scrubbers	12-35
Construction Codes for Oil and Gas Separators	12-38
Controls, Valves, Accessories, and Safety Features for Oil and Gas Separators	12-39
Operation and Maintenance Considerations for Oil and Gas Separators	12-40
 13. Gas Measurement and Regulation	
Introduction	13-1
Gas Measurement	13-1
Regulation	13-49
 14. Lease-Operated Hydrocarbon Recovery Systems	
Introduction	14-1
Low-Temperature Separation (LTS) Systems	14-1
Gas-Treating Systems for Removal of Water Vapor, CO ₂ , and H ₂ S	14-17
 15. Surface Facilities for Waterflooding and Saltwater Disposal	
Introduction	15-1
Piping System Design	15-1
Selecting Pumps and Drivers	15-14
Separating Suspended Solids From Heater	15-18
Treating Hydrocarbons From Water	15-21
Dissolved Gas Removal	15-28
Dissolved Solids Removal	15-29
Removing Hydrocarbons From Solids	15-30
Process Selection and Project Management	15-30
Project Control	15-32
 16. Automation of Lease Equipment	
Introduction	16-1
Automatic Production-Control Equipment	16-2
Production Safety Controls	16-4
Automatic Quantitative Measurement	16-5
Gas Measurement	16-6
Temperature Measurement	16-7
Automatic Sampler	16-7
BS&W Monitor	16-7
Net-Oil Computer	16-7
Supervisory Control and Data Acquisition (SCADA) Systems	16-8
Typical Automatic-Control Installations	16-10
Automatic Well Testing	16-12
LACT	16-12
 17. Measuring, Sampling, and Testing Crude Oil	
Introduction	17-1
Procedure for Typical Measuring, Sampling, and Testing	17-1
Abstract of API Manual	17-3
 18. Offshore Operations	
Introduction	18-1
Historical Review	18-1
Offshore Drilling	18-3
Field Operations	18-17
Special Considerations	18-20
Structures	18-22
Offshore Production Operations	18-27
Arctic	18-38
Electrical, Instrumentation and Control Systems	18-43
Control of Subsea Production Facilities	18-48

19. Crude Oil Emulsions	
Introduction	19-1
Theories of Emulsions	19-1
Sampling and Analyzing Crude Oil Emulsions	19-6
Methods Used in Treating Crude Oil Emulsions	19-6
Emulsion-Treating Equipment and Systems	19-15
Description of Equipment Used in Treating Crude Oil Emulsions	19-16
Operational Considerations for Emulsion-Treating Equipment	19-28
Economics of Treating Crude Oil Emulsions	19-32
20. Gas Properties and Correlations	
Molecular Weight	20-1
Ideal Gas	20-1
Critical Temperature and Pressure	20-2
Specific Gravity (Relative Density)	20-4
Mole Fraction and Apparent Molecular Weight of Gas Mixtures	20-4
Specific Gravity of Gas Mixtures	20-4
Dalton's Law	20-4
Amagat's Law	20-4
Real Gases	20-4
Principle of Corresponding States	20-4
Equations of State	20-6
Van der Waals' Equation	20-7
Viscosity	20-9
Viscosity Correlations	20-9
Natural Gasoline Content of Gas	20-10
Formation Volume Factor	20-11
Coefficient of Isothermal Compressibility	20-11
Vapor Pressure	20-11
Cox Chart	20-12
Calingeart and Davis Equation	20-13
Lee-Kesler	20-13
Example Problems	20-13
21. Crude Oil Properties and Condensate Properties and Correlations	
Introduction	21-1
Base of Crude Oil	21-1
Physical Properties	21-3
True-Boiling-Point Crude-Oil Analyses	21-8
Bubblepoint-Pressure Correlations	21-9
Dewpoint-Pressure Correlations	21-10
Sage and Olds' Correlation	21-11
Total Formation Volume Correlations	21-15
22. Oil System Correlations	
Introduction	22-1
Oil Density Determination	22-2
Bubblepoint-Pressure Correlations	22-5
Solution GOR for Saturated Oils	22-9
Oil FVF Correlations	22-10
Total FVF's	22-13
Oil Viscosity Correlations	22-13
Gas/Oil IFT	22-16
Glossary	22-20
23. Phase Diagrams	
Introduction	23-1
Single-Component Phase Diagrams	23-1
Phase Rule	23-2
Types of Diagrams	23-2
Calculation of Phase Compositions	23-10

24. Properties of Produced Waters	
Introduction and History	24-1
Sampling	24-3
Analysis Methods for Oilfield Waters	24-5
Chemical Properties of Oilfield Waters	24-5
Inorganic Constituents	24-9
Physical Properties of Oilfield Waters	24-12
Interpretation of Chemical Analyses	24-18
Occurrence, Origin, and Evolution of Oilfield Waters	24-19
Recovery of Minerals From Brines	24-20
25. Phase Behavior of Water/Hydrocarbon Systems	
Introduction	25-1
General Hydrocarbon/Water Phase Diagrams and Equilibrium Data Sources	25-1
Hydrate Stability Conditions	25-4
Determining the Water Content of Gas (or Hydrocarbon-Rich Liquid) in Equilibrium With Hydrates	25-10
Definition of the Saturated Water Content of Natural Gases in Equilibrium With Aqueous Phases	25-11
Quantitative Prediction of Water Content in Light Hydrocarbon Systems	25-16
Quantitative Predictions of Solute Concentrations in the Aqueous Phase	25-16
Sour Water Stripper Correlations	25-17
Oil and Gas Reservoirs That Exist in the Gas Hydrate Region	25-18
Hydrate Inhibition	25-19
26. Properties of Reservoir Rocks	
Introduction	26-1
Porosity	26-1
Permeability	26-10
Fluid Saturations	26-20
Electrical Conductivity of Fluid-Saturated Rocks	26-27
Empirical Correlation of Electrical Properties	26-29
27. Typical Core Analysis of Different Formations	
Introduction	27-1
Porosity	27-1
Permeability	27-1
Liquid Saturations	27-8
Percussion Sidewall Core Data	27-9
Data From U.S. Areas	27-9
Data From Non-U.S. Areas	27-9
28. Relative Permeability	
Introduction	28-1
Historical Background	28-2
Framework Ideas	28-2
Measurement Methodologies	28-3
Recent Literature	28-9
Critique of Recent Work	28-10
Ramifications Needing Attention	28-12
Conclusions	28-13
29. Petroleum Reservoir Traps	
Introduction	29-1
Trap Classification	29-1
Characteristics of Reservoir Rocks	29-6
Glossary	29-8
30. Bottomhole Pressures	
Introduction	30-1
BHP Instruments	30-1
Pressure Transducer Technology	30-6
Calculated BHP	30-7
Application of BHP	30-8

31. Temperature in Wells	
Introduction	31-1
Thermometers	31-1
Thermometry	31-2
Summary	31-7
32. Potential Tests of Oil Wells	
Texas Allowable Rule	32-1
Productivity Index (PI)	32-2
Specific PI	32-4
Theoretical PI	32-4
Pseudosteady-State Flow	32-5
Stock-Tank Measurement	32-6
Portable Well Testers	32-7
GOR	32-14
GOR as a Criterion of Reservoir Performance	32-15
33. Open Flow of Gas Wells	
Introduction	33-1
Pitot-Tube Gauging of Low-Pressure Wells	33-1
Backpressure Testing	33-3
Gas Well Inflow Equation, Pseudosteady State	33-5
Multipoint Test and Example	33-7
Isochronal Test and Example	33-10
Comparison of Multipoint With Isochronal Test	33-11
Gas Measurement	33-13
Calculation of Subsurface Pressures	33-13
Application of Backpressure Tests to Producing Problems	33-20
Production Rate	33-20
Causes of Deterioration in Performance	33-20
Examples of Remedial Operations	33-22
34. Wellbore Hydraulics	
Introduction	34-1
Theoretical Basis	34-1
Producing Wells	34-3
Injection Wells	34-28
Oil Wells	34-30
Multiphase Flow	34-35
Flow Through Chokes	34-45
Liquid Loading in Wells	34-46
35. Well Performance Equations	
Introduction	35-1
Diffusivity Equation	35-1
Multiphase Flow	35-2
Oil Well Performance	35-2
Gas Well Performance	35-10
Transient Well Test Analysis	35-14
36. Development Plan for Oil and Gas Reservoirs	
Introduction	36-1
Oil and Gas Differences	36-2
Characterization of the Reservoir	36-3
Prediction of Reservoir Performance	36-9
37. Solution-Gas-Drive Reservoirs	
Introduction	37-1
Definitions	37-1
Typical Performance	37-1
Types of Models Used	37-2
Basic Assumptions of Tank-Type Material Balance	37-2
Basic Data Required	37-3
Material-Balance Equation	37-5

Material Balance as Equation of Straight Line for Determination of OIP and of Gas-Cap Size	37-6
Material-Balance Calculations Using Tracy's Method	37-7
Comparison of Tarner's and Tracy's Methods	37-10
Material-Balance Calculations Using Muskat and Taylor's Method	37-10
Sensitivity of Material-Balance Results	37-13
Production Rate and Time Calculations	37-17
Insights From Simulator Studies	37-21
Volatile Oil Reservoir Performance Predictions	37-22
38. Water Drive Oil Reservoirs	
Introduction	38-1
Definitions	38-1
Mathematical Analysis	38-1
39. Gas-Condensate Reservoirs	
Introduction	39-1
Properties and Behavior of Gas-Condensate Fluids	39-1
Gas-Condensate Well Tests and Sampling	39-4
Sample Collection and Evaluation	39-6
Operation by Pressure Depletion	39-10
Operation by Pressure Maintenance or Cycling	39-15
General Operating Problems: Well Characteristics and Requirements	39-24
Economics of Gas-Condensate Reservoir Operation	39-26
40. Estimation of Oil and Gas Reserves	
Estimating Reserves	40-1
Petroleum Reserves—Definitions and Nomenclature	40-2
Glossary of Terms	40-3
Computation of Reservoir Volume	40-4
Computation of Oil or Gas in Place	40-5
Saturated Depletion-Type Oil Reservoirs—Volumetric Methods	40-8
API Estimation of Oil and Gas Reserves	40-12
Undersaturated Oil Reservoirs Without Water Drive Above the Bubblepoint—Volumetric Method	40-12
Volatile Oil Reservoirs—Volumetric Methods	40-13
Oil Reservoirs With Gas-Cap Drive—Volumetric Unit Recovery Computed by Frontal-Drive Method	40-13
Oil Reservoirs Under Gravity Drainage	40-14
Oil Reservoirs With Water Drive—Volumetric Methods	40-15
Volumetric Recovery Estimates for Nonassociated Gas Reservoirs	40-21
Production-Decline Curves	40-26
Other Performance Curves	40-32
41. Valuation of Oil and Gas Reserves	
Types of Oil and Gas Property Ownership	41-1
Valuation	41-2
Forecast of Future Rate of Production	41-9
Development and Operating Costs	41-11
Federal Taxes	41-12
Different Concepts of Valuation	41-16
Interest Tables and Deferment Factors	41-25
42. Injection Operations	
Introduction	42-1
Important Factors in the Design of Injection Operations	42-2
Analysis of a Reservoir for Injection Operations	42-3
43. Gas-Injection Pressure Maintenance in Oil Reservoirs	
Introduction	43-1
Types of Gas-Injection Operations	43-2
Optimal Time To Initiate Gas Pressure-Maintenance Operations	43-3
Efficiencies of Oil Recovery by Gas Displacement	43-3
Methods of Evaluating Unit-Displacement Efficiency	43-3
Methods of Evaluating Conformance Efficiency	43-6
Methods of Evaluating Areal Sweep Efficiency	43-7
Calculation of Gas Pressure-Maintenance Performance	43-8

Appendix A—Example Calculations of Future Performance	43-10
Appendix B—Selected References Containing Equations, Calculation Procedures, and Example Calculations Related to Gas-Injection Performance Predictions	43-16
Appendix C—Data Requirements for Engineering Analysis of Gas-Injection Operations	43-17
44. Water-Injection Pressure Maintenance and Waterflood Processes	
Introduction	44-1
Important Factors in Waterflooding or Water-Injection Pressure Maintenance	44-2
Determination of Residual Oil After Waterflooding	44-5
Predicting Water Injection Oil Recovery and Performance	44-7
Water-Injection Well Behavior	44-32
Water-Injection Case Histories	44-36
Pilot Floods	44-37
Surface-Active Agents in Waterflooding	44-39
Water Source and Requirements	44-41
Water Treating	44-43
Selection and Sizing of Waterflood Plants	44-45
45. Miscible Displacement	
Introduction	45-1
Theoretical Aspects of Miscible-Phase Displacement	45-1
Factors Affecting Displacement Efficiency	45-6
Engineering Study	45-8
Appendix—Engineering Examples	45-10
46. Thermal Recovery	
Introduction	46-1
Two Forms of Steam Injection Processes	46-1
Three Forms of In-Situ Combustion	46-1
Historical Development	46-3
Current Status	46-3
Theoretical Considerations	46-4
Analytical Models for Steam Injection	46-7
Numerical Simulation	46-11
Laboratory Experimentation	46-12
Field Projects	46-13
Project Design	46-17
Well Completion	46-19
Field Facilities	46-19
Monitoring and Coring Programs	46-20
Operational Problems and Remedies	46-21
Case Histories	46-22
Thermal Properties	46-31
47. Chemical Flooding	
Introduction	47-1
Mobility Control Processes	47-1
Low-IFT Processes	47-9
High-pH Processes	47-18
Summary	47-22
48. Reservoir Simulation	
Introduction	48-1
A Brief History	48-1
General Description of Simulation Models	48-2
Purpose of Reservoir Simulation	48-6
Considerations in Practical Application of Simulation Models	48-7
Validity of Simulation Results	48-9
Simulation Technology	48-13
49. Electrical Logging	
Fundamentals	49-1
Spontaneous Potential (SP) Log	49-7
Resistivity Logging Devices	49-11

Induction Logging	49-14
Focused-Electrode Logs	49-18
Microresistivity Devices	49-22
Uses and Interpretation of Well Logs	49-25
The Digital Age	49-36
50. Nuclear Logging Techniques	
Introduction	50-1
Nuclear Physics for Logging Applications	50-3
Nuclear Radiation Logging Devices	50-15
Interpretation of Nuclear Logs	50-23
51. Acoustic Logging	
Introduction	51-1
Elasticity	51-1
Acoustic Wave Propagation in Rocks	51-4
Acoustic Wave Propagation Methods	51-11
Methods of Recording Acoustic Data	51-14
Applications	51-28
Conclusions	51-47
Appendix—Theory of Elastic Wave Propagation in Rocks	51-49
52. Mud Logging	
Introduction	52-1
Service Types	52-1
Formation Evaluation Services	52-2
The Modern Mud Logging Unit	52-11
The Mud Log	52-11
Petroleum Engineering Services	52-16
Drilling Engineering Services	52-27
Selecting a Mud Logging Service	52-28
Standards for and Status of Services	52-30
53. Other Well Logs	
Introduction	53-1
MWD	53-1
Directional Surveys	53-3
Dipmeter Logging	53-7
Caliper Logs	53-16
Casing Inspection Logs	53-17
54. Acidizing	
Introduction	54-1
General Principles	54-1
Acid Reaction Rates	54-4
Acid Additives	54-6
Acidizing Techniques	54-8
Laboratory Testing	54-9
Acid Treatment Design	54-10
Critical Wells	54-11
Summary	54-12
55. Formation Fracturing	
Introduction	55-1
Hydraulic Fracturing Theory	55-1
Formations Fractured	55-2
Fracture Planes	55-2
Fracture Area	55-2
Reservoir-Controlled Fluids	55-2
Viscosity-Controlled Fluids	55-4
Fluid-Loss-Controlled Fluids	55-4
Stimulation Results	55-4
Fracturing Materials	55-5
Fracturing Techniques	55-8

Multiple-Zone Fracturing	55-9
Fracturing Equipment	55-9
Treatment Planning and Design	55-9
56. Remedial Cleanup, Sand Control, and Other Stimulation Treatments	
Introduction	56-1
Reperforation	56-1
Abrasive Jet Cleaning	56-1
Mud Removal	56-1
Water Blocks and Emulsions	56-2
Scale Deposits	56-2
Paraffin Removal	56-2
Large-Volume Injection Treatments	56-2
Steam Injection	56-2
General Comments	56-2
Sand Control	56-2
57. Oil and Gas Leases	
The Landowner's Interest	57-1
The Oil and Gas Lease	57-3
Assignments by the Landowner	57-6
Assignments by the Lessee	57-7
Unit Operations	57-7
Getting the Well Drilled	57-8
Lease Problems During Development	57-10
Taxation	57-11
Offshore Leasing	57-11
58. The SI Metric System of Units and SPE Metric Standard	
Preface	58-2
Part 1: SI—The International System of Units	58-2
Introduction	58-2
SI Units and Unit Symbols	58-2
Application of the Metric System	58-3
Rules for Conversion and Rounding	58-5
Special Terms and Quantities Involving Mass and Amount of Substance	58-7
Mental Guides for Using Metric Units	58-8
Appendix A—Terminology	58-8
Appendix B—SI Units	58-9
Appendix C—Style Guide for Metric Usage	58-11
Appendix D—General Conversion Factors	58-14
Appendix E—Conversion Factors for the Vara	58-20
Part 2: Discussion of Metric Unit Standards	58-21
Introduction	58-21
Review of Selected Units	58-22
Unit Standards Under Discussion	58-24
Notes for Table 2.2	58-25
Notes for Table 2.3	58-25
59. SPE Letter and Computer Symbols Standard	
Symbols in Alphabetical Order	59-2
Quantities in Alphabetical Order	59-18
Subscript Definitions in Alphabetical Order	59-52
Subscript Symbols in Alphabetical Order	59-63
Index	1
Author	1
Subject	15

Chapter 1

Mathematical Tables and Units and Systems of Weights and Measures

Philip Franklin, Massachusetts Inst. of Technology*
L.E. Barbrow, U.S. Natl. Bureau of Standards

Contents

Mathematical Tables By Philip Franklin

Numbers

Table 1.1—Squares	1-2
Table 1.2—Cubes	1-7
Table 1.3—Square Roots	1-11
Table 1.4—Cube Roots	1-14
Table 1.5—Three-Halves Powers	1-19
Table 1.6—Reciprocals	1-21

Circles

Table 1.7—Circumferences by Hundredths	1-24
Table 1.8—Areas by Hundredths	1-26
Table 1.9—Circumferences and Areas by Eighths	1-28
Table 1.10—Areas in Square Feet	1-30
Table 1.11—Segments, Given h/c	1-31
Table 1.12—Segments, Given h/d	1-32

Spheres

Table 1.13—Segments	1-33
Table 1.14—Volumes by Hundredths	1-34
Table 1.15—Regular Polygons	1-36
Table 1.16—Binomial Coefficients	1-37
Table 1.17—Common Logarithms (1.00 to 2.00)	1-38
Table 1.18—Common Logarithms	1-40
Table 1.19—Degrees and Minutes in Radians	1-42
Table 1.20—Radians in Degrees	1-43
Table 1.21—Natural Sines and Cosines	1-44
Table 1.22—Natural Tangents and Cotangents	1-46
Table 1.23—Natural Secants and Cosecants	1-48
Table 1.24—Trigonometric Functions	1-50
Table 1.25—Exponentials	1-55
Table 1.26—Natural Logarithms	1-56
Table 1.27—Hyperbolic Sines	1-58
Table 1.28—Hyperbolic Cosines	1-59
Table 1.29—Hyperbolic Tangents	1-60
Table 1.30—Multiples of 0.4343	1-60
Table 1.31—Multiples of 2.3026	1-60
Table 1.32—Standard Distribution of Residuals	1-61
Table 1.33—Factors for Computing Probable Error	1-61

Compound Interest

Table 1.34—Amount of a Given Principal	1-62
Table 1.35—Amount of an Annuity	1-63
Table 1.36—Principal Amounting to a Given Sum	1-64

Annuities

Table 1.37—Amounting to a Given Sum (Sinking Fund)	1-65
Table 1.38—Present Worth	1-66
Table 1.39—Provided for by a Given Capital	1-66
Table 1.40—Decimal Equivalents	1-67

Units and Systems of Weights and Measures by L.E. Barbrow

Conversion Tables

Table 1.41—Length Equivalents	1-71
Table 1.42—Conversion of Lengths	1-71
Table 1.43—Common Fractions of an Inch to Millimeters	1-72
Table 1.44—Decimals of an Inch to Millimeters	1-72
Table 1.45—Millimeters to Decimals of an Inch	1-72
Table 1.46—Area Equivalents	1-73
Table 1.47—Volume and Capacity Equivalents	1-73
Table 1.48—Areas	1-74
Table 1.49—Volumes or Cubic Meters	1-74
Table 1.50—Volumes or Capacities	1-74
Table 1.51—Mass Equivalents	1-75
Table 1.52—Masses	1-75
Table 1.53—Velocity Equivalents	1-76
Table 1.54—Linear and Angular Velocities	1-76
Table 1.55—Pressures	1-76
Table 1.56—Pressure Equivalents	1-77
Table 1.57—Energy or Work Equivalents	1-77
Table 1.58—Energy, Work, Heat	1-78
Table 1.59—Power Equivalents	1-78
Table 1.60—Power	1-78
Table 1.61—Density Equivalents	1-79
Table 1.62—Thermal Conductivity	1-79
Table 1.63—Thermal Conductance	1-79
Table 1.64—Heat Flow	1-79
Table 1.65—Relative Densities Corresponding to °API and Weights per U.S. Gallon	1-80

* This chapter in the 1962 edition was written by Philip Franklin and Lewis V. Judson (both deceased).

TABLE 1.1—SQUARES OF NUMBERS

<i>N</i>	0	1	2	3	4	5	6	7	8	9	Average Difference
1.00	1.000	1.002	1.004	1.006	1.008	1.010	1.012	1.014	1.016	1.018	2
1.01	1.020	1.022	1.024	1.026	1.028	1.030	1.032	1.034	1.036	1.038	
1.02	1.040	1.042	1.044	1.047	1.049	1.051	1.053	1.055	1.057	1.059	
1.03	1.061	1.063	1.065	1.067	1.069	1.071	1.073	1.075	1.077	1.080	
1.04	1.082	1.084	1.086	1.088	1.090	1.092	1.094	1.096	1.098	1.100	
1.05	1.102	1.105	1.107	1.109	1.111	1.113	1.115	1.117	1.119	1.121	
1.06	1.124	1.126	1.128	1.130	1.132	1.134	1.136	1.138	1.141	1.143	
1.07	1.145	1.147	1.149	1.151	1.153	1.156	1.158	1.160	1.162	1.164	
1.08	1.166	1.169	1.171	1.173	1.175	1.177	1.179	1.182	1.184	1.186	
1.09	1.188	1.190	1.192	1.195	1.197	1.199	1.201	1.203	1.206	1.208	
1.10	1.210	1.212	1.214	1.217	1.219	1.221	1.223	1.225	1.228	1.230	
1.11	1.232	1.234	1.237	1.239	1.241	1.243	1.245	1.248	1.250	1.252	
1.12	1.254	1.257	1.259	1.261	1.263	1.266	1.268	1.270	1.272	1.275	
1.13	1.277	1.279	1.281	1.284	1.286	1.288	1.290	1.293	1.295	1.297	
1.14	1.300	1.302	1.304	1.306	1.309	1.311	1.313	1.316	1.318	1.320	
1.15	1.322	1.325	1.327	1.329	1.332	1.334	1.336	1.339	1.341	1.343	
1.16	1.346	1.348	1.350	1.353	1.355	1.357	1.360	1.362	1.364	1.367	
1.17	1.369	1.371	1.374	1.376	1.378	1.381	1.383	1.385	1.388	1.390	
1.18	1.392	1.395	1.397	1.399	1.402	1.404	1.407	1.409	1.411	1.414	
1.19	1.416	1.418	1.421	1.423	1.426	1.428	1.430	1.433	1.435	1.438	
1.20	1.440	1.442	1.445	1.447	1.450	1.452	1.454	1.457	1.459	1.462	3
1.21	1.464	1.467	1.469	1.471	1.474	1.476	1.479	1.481	1.484	1.486	
1.22	1.488	1.491	1.493	1.496	1.498	1.501	1.503	1.506	1.508	1.510	
1.23	1.513	1.515	1.518	1.520	1.523	1.525	1.528	1.530	1.533	1.535	
1.24	1.538	1.540	1.543	1.545	1.548	1.550	1.553	1.555	1.558	1.560	
1.25	1.562	1.565	1.568	1.570	1.573	1.575	1.578	1.580	1.583	1.585	
1.26	1.588	1.590	1.593	1.595	1.598	1.600	1.603	1.605	1.608	1.610	
1.27	1.613	1.615	1.618	1.621	1.623	1.626	1.628	1.631	1.633	1.636	
1.28	1.638	1.641	1.644	1.646	1.649	1.651	1.654	1.656	1.659	1.662	
1.29	1.664	1.667	1.669	1.672	1.674	1.677	1.680	1.682	1.685	1.687	
1.30	1.690	1.693	1.695	1.698	1.700	1.703	1.706	1.708	1.711	1.713	
1.31	1.716	1.719	1.721	1.724	1.727	1.729	1.732	1.734	1.737	1.740	
1.32	1.742	1.745	1.748	1.750	1.753	1.756	1.758	1.761	1.764	1.766	
1.33	1.769	1.772	1.774	1.777	1.780	1.782	1.785	1.788	1.790	1.793	
1.34	1.796	1.798	1.801	1.804	1.806	1.809	1.812	1.814	1.817	1.820	
1.35	1.822	1.825	1.828	1.831	1.833	1.836	1.839	1.841	1.844	1.847	
1.36	1.850	1.852	1.855	1.858	1.860	1.863	1.866	1.869	1.871	1.874	
1.37	1.877	1.880	1.882	1.885	1.888	1.891	1.893	1.896	1.899	1.902	
1.38	1.904	1.907	1.910	1.913	1.915	1.918	1.921	1.924	1.927	1.929	
1.39	1.932	1.935	1.938	1.940	1.943	1.946	1.949	1.952	1.954	1.957	
1.40	1.960	1.963	1.966	1.968	1.971	1.974	1.977	1.980	1.982	1.985	
1.41	1.988	1.991	1.994	1.997	1.999	2.002	2.005	2.008	2.011	2.014	
1.42	2.016	2.019	2.022	2.025	2.028	2.031	2.033	2.036	2.039	2.042	
1.43	2.045	2.048	2.051	2.053	2.056	2.059	2.062	2.065	2.068	2.071	
1.44	2.074	2.076	2.079	2.082	2.085	2.088	2.091	2.094	2.097	2.100	
1.45	2.102	2.105	2.108	2.111	2.114	2.117	2.120	2.123	2.126	2.129	
1.46	2.132	2.135	2.137	2.140	2.143	2.146	2.149	2.152	2.155	2.158	
1.47	2.161	2.164	2.167	2.170	2.173	2.176	2.179	2.182	2.184	2.187	
1.48	2.190	2.193	2.196	2.199	2.202	2.205	2.208	2.211	2.214	2.217	
1.49	2.220	2.223	2.226	2.229	2.232	2.235	2.238	2.241	2.244	2.247	
1.50	2.250	2.253	2.256	2.259	2.262	2.265	2.268	2.271	2.274	2.277	
1.51	2.280	2.283	2.286	2.289	2.292	2.295	2.298	2.301	2.304	2.307	
1.52	2.310	2.313	2.316	2.320	2.323	2.326	2.329	2.332	2.335	2.338	
1.53	2.341	2.344	2.347	2.350	2.353	2.356	2.359	2.362	2.365	2.369	
1.54	2.372	2.375	2.378	2.381	2.384	2.387	2.390	2.393	2.396	2.399	
1.55	2.402	2.406	2.409	2.412	2.415	2.418	2.421	2.424	2.427	2.430	
1.56	2.434	2.437	2.440	2.443	2.446	2.449	2.452	2.455	2.459	2.462	
1.57	2.465	2.468	2.471	2.474	2.477	2.481	2.484	2.487	2.490	2.493	
1.58	2.496	2.500	2.503	2.506	2.509	2.512	2.515	2.519	2.522	2.525	
1.59	2.528	2.531	2.534	2.538	2.541	2.544	2.547	2.550	2.554	2.557	

Explanation of Table of Squares

This table gives the value of N^2 for values of N from 1 to 10, correct to four figures. (Interpolated values may be in error by 1 in the fourth figure.)

To find the square of a number N outside the range from 1 to 10, note that moving the decimal point one place in Column N is equivalent to moving it two places in the body of the table. For example, $(3.217)^2 = 10.35$, $(0.03217)^2 = 0.001035$, and $(3,217)^2 = 10,035,000$.

This table also can be used inversely to give square roots.

TABLE 1.1—SQUARES OF NUMBERS (continued)

<i>N</i>	0	1	2	3	4	5	6	7	8	9	Average Difference
1.60	2.560	2.563	2.566	2.570	2.573	2.576	2.579	2.582	2.586	2.589	3
1.61	2.592	2.595	2.599	2.602	2.605	2.608	2.611	2.615	2.618	2.621	
1.62	2.624	2.628	2.631	2.634	2.637	2.641	2.644	2.647	2.650	2.654	
1.63	2.657	2.660	2.663	2.667	2.670	2.673	2.676	2.680	2.683	2.686	
1.64	2.690	2.693	2.696	2.699	2.703	2.706	2.709	2.713	2.716	2.719	
1.65	2.722	2.726	2.729	2.732	2.736	2.739	2.742	2.746	2.749	2.752	
1.66	2.756	2.759	2.762	2.766	2.769	2.772	2.776	2.779	2.782	2.786	
1.67	2.789	2.792	2.796	2.799	2.802	2.806	2.809	2.812	2.816	2.819	
1.68	2.822	2.826	2.829	2.832	2.836	2.839	2.843	2.846	2.849	2.853	
1.69	2.856	2.859	2.863	2.866	2.870	2.873	2.876	2.880	2.883	2.887	
1.70	2.890	2.893	2.897	2.900	2.904	2.907	2.910	2.914	2.917	2.921	4
1.71	2.924	2.928	2.931	2.934	2.938	2.941	2.945	2.948	2.952	2.955	
1.72	2.958	2.962	2.965	2.969	2.972	2.976	2.979	2.983	2.986	2.989	
1.73	2.993	2.996	3.000	3.003	3.007	3.010	3.014	3.017	3.021	3.024	
1.74	3.028	3.031	3.035	3.038	3.042	3.045	3.049	3.052	3.056	3.059	
1.75	3.062	3.066	3.070	3.073	3.077	3.080	3.084	3.087	3.091	3.094	
1.76	3.098	3.101	3.105	3.108	3.112	3.115	3.119	3.122	3.126	3.129	
1.77	3.133	3.136	3.140	3.144	3.147	3.151	3.154	3.158	3.161	3.165	
1.78	3.168	3.172	3.176	3.179	3.183	3.186	3.190	3.193	3.197	3.201	
1.79	3.204	3.208	3.211	3.215	3.218	3.222	3.226	3.229	3.233	3.236	
1.80	3.240	3.244	3.247	3.251	3.254	3.258	3.262	3.265	3.269	3.272	
1.81	3.276	3.280	3.283	3.287	3.291	3.294	3.298	3.301	3.305	3.309	
1.82	3.312	3.316	3.320	3.323	3.327	3.331	3.334	3.338	3.342	3.345	
1.83	3.349	3.353	3.356	3.360	3.364	3.367	3.371	3.375	3.378	3.382	
1.84	3.386	3.389	3.393	3.397	3.400	3.404	3.408	3.411	3.415	3.419	
1.85	3.422	3.426	3.430	3.434	3.437	3.441	3.445	3.448	3.452	3.456	
1.86	3.460	3.463	3.467	3.471	3.474	3.478	3.482	3.486	3.489	3.493	
1.87	3.497	3.501	3.504	3.508	3.512	3.516	3.519	3.523	3.527	3.531	
1.88	3.534	3.538	3.542	3.546	3.549	3.553	3.557	3.561	3.565	3.568	
1.89	3.572	3.576	3.580	3.583	3.587	3.591	3.595	3.599	3.602	3.606	
1.90	3.610	3.614	3.618	3.621	3.625	3.629	3.633	3.637	3.640	3.644	
1.91	3.648	3.652	3.656	3.660	3.663	3.667	3.671	3.675	3.679	3.683	
1.92	3.686	3.690	3.694	3.698	3.702	3.706	3.709	3.713	3.717	3.721	
1.93	3.725	3.729	3.733	3.736	3.740	3.744	3.748	3.752	3.756	3.760	
1.94	3.764	3.767	3.771	3.775	3.779	3.783	3.787	3.791	3.795	3.799	
1.95	3.802	3.806	3.810	3.814	3.818	3.822	3.826	3.830	3.834	3.838	
1.96	3.842	3.846	3.849	3.853	3.857	3.861	3.865	3.869	3.873	3.877	
1.97	3.881	3.885	3.889	3.893	3.897	3.901	3.905	3.909	3.912	3.916	
1.98	3.920	3.924	3.928	3.932	3.936	3.940	3.944	3.948	3.952	3.956	
1.99	3.960	3.964	3.968	3.972	3.976	3.980	3.984	3.988	3.992	3.996	
2.00	4.000	4.004	4.008	4.012	4.016	4.020	4.024	4.028	4.032	4.036	
2.01	4.040	4.044	4.048	4.052	4.056	4.060	4.064	4.068	4.072	4.076	
2.02	4.080	4.084	4.088	4.093	4.097	4.101	4.105	4.109	4.113	4.117	
2.03	4.121	4.125	4.129	4.133	4.137	4.141	4.145	4.149	4.153	4.158	
2.04	4.162	4.166	4.170	4.174	4.178	4.182	4.186	4.190	4.194	4.198	
2.05	4.202	4.207	4.211	4.215	4.219	4.223	4.227	4.231	4.235	4.239	
2.06	4.244	4.248	4.252	4.256	4.260	4.264	4.268	4.272	4.277	4.281	
2.07	4.285	4.289	4.293	4.297	4.301	4.306	4.310	4.314	4.318	4.322	
2.08	4.326	4.331	4.335	4.339	4.343	4.347	4.351	4.356	4.360	4.364	
2.09	4.368	4.372	4.376	4.381	4.385	4.389	4.393	4.397	4.402	4.406	
2.10	4.410	4.414	4.418	4.423	4.427	4.431	4.435	4.439	4.444	4.448	
2.11	4.452	4.456	4.461	4.465	4.469	4.473	4.477	4.482	4.486	4.490	
2.12	4.494	4.499	4.503	4.507	4.511	4.516	4.520	4.524	4.528	4.533	
2.13	4.537	4.541	4.545	4.550	4.554	4.558	4.562	4.567	4.571	4.575	
2.14	4.580	4.584	4.588	4.592	4.597	4.601	4.605	4.610	4.614	4.618	
2.15	4.622	4.627	4.631	4.635	4.640	4.644	4.648	4.653	4.657	4.661	
2.16	4.666	4.670	4.674	4.679	4.683	4.687	4.692	4.696	4.700	4.705	
2.17	4.709	4.713	4.718	4.722	4.726	4.731	4.735	4.739	4.744	4.748	
2.18	4.752	4.757	4.761	4.765	4.770	4.774	4.779	4.783	4.787	4.792	
2.19	4.796	4.800	4.805	4.809	4.814	4.818	4.822	4.827	4.831	4.836	

$$\pi^2 = 9.86960; 1/\pi^2 = 0.101321; e^2 = 7.38906. \quad \pi^2 = 9.86960; (\pi/2)^2 = 2.46740; 1/\pi^2 = 0.101321.$$

(continued on next page)

TABLE 1.1—SQUARES OF NUMBERS (continued)

<i>N</i>	0	1	2	3	4	5	6	7	8	9	Average Difference
2.20	4.840	4.844	4.849	4.853	4.858	4.862	4.866	4.871	4.875	4.880	4
2.21	4.884	4.889	4.893	4.897	4.902	4.906	4.911	4.915	4.920	4.924	
2.22	4.928	4.933	4.937	4.942	4.946	4.951	4.955	4.960	4.964	4.968	
2.23	4.973	4.977	4.982	4.986	4.991	4.995	5.000	5.004	5.009	5.013	
2.24	5.018	5.022	5.027	5.031	5.036	5.040	5.045	5.049	5.054	5.058	
2.25	5.062	5.067	5.072	5.076	5.081	5.085	5.090	5.094	5.099	5.103	5
2.26	5.108	5.112	5.117	5.121	5.126	5.130	5.135	5.139	5.144	5.148	
2.27	5.153	5.157	5.162	5.167	5.171	5.176	5.180	5.185	5.189	5.194	
2.28	5.198	5.203	5.208	5.212	5.217	5.221	5.226	5.230	5.235	5.240	
2.29	5.244	5.249	5.253	5.258	5.262	5.267	5.272	5.276	5.281	5.285	
2.30	5.290	5.295	5.299	5.304	5.308	5.313	5.318	5.322	5.327	5.331	
2.31	5.336	5.341	5.345	5.350	5.355	5.359	5.364	5.368	5.373	5.378	
2.32	5.382	5.387	5.392	5.396	5.401	5.406	5.410	5.415	5.420	5.424	
2.33	5.429	5.434	5.438	5.443	5.448	5.452	5.457	5.462	5.466	5.471	
2.34	5.476	5.480	5.485	5.490	5.494	5.499	5.504	5.508	5.513	5.518	
2.35	5.522	5.527	5.532	5.537	5.541	5.546	5.551	5.555	5.560	5.565	
2.36	5.570	5.574	5.579	5.584	5.588	5.593	5.598	5.603	5.607	5.612	
2.37	5.671	5.622	5.626	5.631	5.636	5.641	5.645	5.650	5.655	5.660	
2.38	5.664	5.669	5.674	5.679	5.683	5.688	5.693	5.698	5.703	5.707	
2.39	5.712	5.717	5.722	5.726	5.731	5.736	5.741	5.746	5.750	5.755	
2.40	5.760	5.765	5.770	5.774	5.779	5.784	5.789	5.794	5.798	5.803	
2.41	5.808	5.813	5.818	5.823	5.827	5.832	5.837	5.842	5.847	5.852	
2.42	5.856	5.861	5.866	5.871	5.876	5.881	5.885	5.890	5.895	5.900	
2.43	5.905	5.910	5.915	5.919	5.924	5.929	5.934	5.939	5.944	5.949	
2.44	5.954	5.958	5.963	5.968	5.973	5.978	5.983	5.988	5.993	5.998	
2.45	6.002	6.007	6.012	6.017	6.022	6.027	6.032	6.037	6.042	6.047	
2.46	6.502	6.057	6.061	6.066	6.071	6.076	6.081	6.086	6.091	6.096	
2.47	6.101	6.106	6.111	6.116	6.121	6.126	6.131	6.136	6.140	6.145	
2.48	6.150	6.155	6.160	6.165	6.170	6.175	6.180	6.185	6.190	6.195	
2.49	6.200	6.205	6.210	6.215	6.220	6.225	6.230	6.235	6.240	6.245	
2.50	6.250	6.255	6.260	6.265	6.270	6.275	6.280	6.285	6.290	6.295	5
2.51	6.300	6.305	6.310	6.315	6.320	6.325	6.330	6.335	6.340	6.345	
2.52	6.350	6.355	6.360	6.366	6.371	6.376	6.381	6.386	6.391	6.396	
2.53	6.401	6.406	6.411	6.416	6.421	6.426	6.431	6.436	6.441	6.447	
2.54	6.452	6.457	6.462	6.467	6.472	6.477	6.482	6.487	6.492	6.497	
2.55	6.502	6.508	6.513	6.518	6.523	6.528	6.533	6.538	6.543	6.548	
2.56	6.554	6.559	6.564	6.569	6.574	6.579	6.584	6.589	6.595	6.600	
2.57	6.605	6.610	6.615	6.620	6.625	6.631	6.636	6.641	6.646	6.651	
2.58	6.656	6.662	6.667	6.672	6.677	6.682	6.687	6.693	6.698	6.703	
2.59	6.708	6.713	6.718	6.724	6.729	6.734	6.739	6.744	6.750	6.755	
2.60	6.760	6.765	6.770	6.776	6.781	6.786	6.791	6.796	6.802	6.807	
2.61	6.812	6.817	6.823	6.828	6.833	6.838	6.843	6.849	6.854	6.859	
2.62	6.864	6.870	6.875	6.880	6.885	6.891	6.896	6.901	6.906	6.912	
2.63	6.917	6.922	6.927	6.933	6.938	6.943	6.948	6.954	6.959	6.964	
2.64	6.970	6.975	6.980	6.985	6.991	6.996	7.001	7.007	7.012	7.017	
2.65	7.022	7.028	7.033	7.038	7.044	7.049	7.054	7.060	7.065	7.070	
2.66	7.076	7.081	7.086	7.092	7.097	7.102	7.108	7.113	7.118	7.124	
2.67	7.129	7.134	7.140	7.145	7.150	7.156	7.161	7.166	7.172	7.177	
2.68	7.182	7.188	7.193	7.198	7.204	7.209	7.215	7.220	7.225	7.231	
2.69	7.236	7.241	7.247	7.252	7.258	7.263	7.268	7.274	7.279	7.285	
2.70	7.290	7.295	7.301	7.306	7.312	7.317	7.322	7.328	7.333	7.339	
2.71	7.344	7.350	7.355	7.360	7.366	7.371	7.377	7.382	7.388	7.393	
2.72	7.398	7.404	7.409	7.415	7.420	7.426	7.431	7.437	7.442	7.447	
2.73	7.453	7.458	7.464	7.469	7.475	7.480	7.486	7.491	7.497	7.502	
2.74	7.508	7.513	7.519	7.524	7.530	7.535	7.541	7.546	7.552	7.557	
2.75	7.562	7.568	7.574	7.579	7.585	7.590	7.596	7.601	7.607	7.612	6
2.76	7.618	7.623	7.629	7.634	7.640	7.645	7.651	7.656	7.662	7.667	
2.77	7.673	7.678	7.684	7.690	7.695	7.701	7.706	7.712	7.717	7.723	
2.78	7.728	7.734	7.740	7.745	7.751	7.756	7.762	7.767	7.773	7.779	
2.79	7.784	7.790	7.795	7.801	7.806	7.812	7.818	7.823	7.829	7.834	

$$\pi^2 = 9.86960; 1/\pi^2 = 0.101321; e^2 = 7.38906. \quad \pi^2 = 9.86960; (\pi/2)^2 = 2.46740; 1/\pi^2 = 0.101321.$$

TABLE 1.1—SQUARES OF NUMBERS (continued)

<i>N</i>	0	1	2	3	4	5	6	7	8	9	Average Difference
2.80	7.840	7.846	7.851	7.857	7.862	7.868	7.874	7.879	7.885	7.890	6
2.81	7.896	7.902	7.907	7.913	7.919	7.924	7.930	7.935	7.941	7.947	
2.82	7.952	7.958	7.964	7.969	7.975	7.981	7.986	7.992	7.998	8.003	
2.83	8.009	8.015	8.020	8.026	8.032	8.037	8.043	8.049	8.054	8.060	
2.84	8.066	8.071	8.077	8.083	8.088	8.094	8.100	8.105	8.111	8.117	
2.85	8.122	8.128	8.134	8.140	8.145	8.151	8.157	8.162	8.168	8.174	
2.86	8.180	8.185	8.191	8.197	8.202	8.208	8.214	8.220	8.225	8.231	
2.87	8.237	8.243	8.248	8.254	8.260	8.266	8.271	8.277	8.283	8.289	
2.88	8.294	8.300	8.306	8.312	8.317	8.323	8.329	8.335	8.341	8.346	
2.89	8.352	8.358	8.364	8.369	8.375	8.381	8.387	8.393	8.398	8.404	
2.90	8.410	8.416	8.422	8.427	8.433	8.439	8.445	8.451	8.456	8.462	
2.91	8.468	8.474	8.480	8.486	8.491	8.497	8.503	8.509	8.515	8.521	
2.92	8.526	8.532	8.538	8.544	8.550	8.556	8.561	8.567	8.573	8.579	
2.93	8.585	8.591	8.597	8.602	8.608	8.614	8.620	8.626	8.632	8.638	
2.94	8.644	8.649	8.655	8.661	8.667	8.673	8.679	8.685	8.691	8.697	
2.95	8.702	8.708	8.714	8.720	8.726	8.732	8.738	8.744	8.750	8.756	
2.96	8.762	8.768	8.773	8.779	8.785	8.791	8.797	8.803	8.809	8.815	
2.97	8.821	8.827	8.833	8.839	8.845	8.851	8.857	8.863	8.868	8.874	
2.98	8.880	8.886	8.892	8.898	8.904	8.910	8.916	8.922	8.928	8.934	
2.99	8.940	8.946	8.952	8.958	8.964	8.970	8.976	8.982	8.988	8.994	
3.00	9.000	9.006	9.012	9.018	9.024	9.030	9.036	9.042	9.048	9.054	
3.01	9.060	9.066	9.072	9.078	9.084	9.090	9.096	9.102	9.108	9.114	
3.02	9.120	9.126	9.132	9.139	9.145	9.151	9.157	9.163	9.169	9.175	
3.03	9.181	9.187	9.193	9.199	9.205	9.211	9.217	9.223	9.229	9.236	
3.04	9.242	9.248	9.254	9.260	9.266	9.272	9.278	9.284	9.290	9.296	
3.05	9.302	9.309	9.315	9.321	9.327	9.333	9.339	9.345	9.351	9.357	
3.06	9.364	9.370	9.376	9.382	9.388	9.394	9.400	9.406	9.413	9.419	
3.07	9.425	9.431	9.437	9.443	9.449	9.456	9.462	9.468	9.474	9.480	
3.08	9.486	9.493	9.499	9.505	9.511	9.517	9.523	9.530	9.536	9.542	
3.09	9.548	9.554	9.560	9.567	9.573	9.579	9.585	9.591	9.598	9.604	
3.10	9.610	9.616	9.622	9.629	9.635	9.641	9.647	9.653	9.660	9.666	
3.11	9.672	9.678	9.685	9.691	9.697	9.703	9.709	9.716	9.722	9.728	
3.12	9.734	9.741	9.747	9.753	9.759	9.766	9.772	9.778	9.784	9.791	
3.13	9.797	9.803	9.809	9.816	9.822	9.828	9.834	9.841	9.847	9.853	
3.14	9.860	9.866	9.872	9.878	9.885	9.891	9.897	9.904	9.910	9.916	
3.15	9.922	9.929	9.935	9.941	9.948	9.954	9.960	9.967	9.973	9.979	
3.16	9.986	9.992	9.998	10.005							
3.1							9.99	10.05	10.11	10.18	6
3.2	10.24	10.30	10.37	10.43	10.50	10.56	10.63	10.69	10.76	10.82	
3.3	10.89	10.96	11.02	11.09	11.16	11.22	11.29	11.36	11.42	11.49	
3.4	11.56	11.63	11.70	11.76	11.83	11.90	11.97	12.04	12.11	12.18	
3.5	12.25	12.32	12.39	12.46	12.53	12.60	12.67	12.74	12.82	12.89	
3.6	12.96	13.03	13.10	13.18	13.25	13.32	13.40	13.47	13.54	13.62	
3.7	13.69	13.76	13.84	13.91	13.99	14.06	14.14	14.21	14.29	14.36	
3.8	14.44	14.52	14.59	14.67	14.75	14.82	14.90	14.98	15.05	15.13	
3.9	15.21	15.29	15.37	15.44	15.52	15.60	15.68	15.76	15.84	15.92	
4.0	16.00	16.08	16.16	16.24	16.32	16.40	16.48	16.56	16.65	16.73	
4.1	16.81	16.89	16.97	17.06	17.14	17.22	17.31	17.39	17.47	17.56	9
4.2	17.64	17.72	17.81	17.89	17.98	18.06	18.15	18.23	18.32	18.40	
4.3	18.49	18.58	18.66	18.75	18.84	18.92	19.01	19.10	19.18	19.27	
4.4	19.36	19.45	19.54	19.62	19.71	19.80	19.89	19.98	20.07	20.16	
4.5	20.25	20.34	20.43	20.52	20.61	20.70	20.79	20.88	20.98	21.07	
4.6	21.16	21.25	21.34	21.44	21.53	21.62	21.72	21.81	21.90	22.00	
4.7	22.09	22.18	22.28	22.37	22.47	22.56	22.66	22.75	22.85	22.94	
4.8	23.04	23.14	23.23	23.33	23.43	23.52	23.62	23.72	23.81	23.91	
4.9	24.01	24.11	24.21	24.30	24.40	24.50	24.60	24.70	24.80	24.90	
5.0	25.00	25.10	25.20	25.30	25.40	25.50	25.60	25.70	25.81	25.91	10
5.1	26.01	26.11	26.21	26.32	26.42	26.52	26.63	26.73	26.83	26.94	
5.2	27.04	27.14	27.25	27.35	27.46	27.56	27.67	27.77	27.88	27.98	
5.3	28.09	28.20	28.30	28.41	28.52	28.62	28.73	28.84	28.94	29.05	
5.4	29.16	29.27	29.38	29.48	29.59	29.70	29.81	29.92	30.03	30.14	

$$\pi^2 = 9.86960; 1/\pi^2 = 0.101321; e^2 = 7.38906; \quad \pi^2 = 9.86960; (\pi/2)^2 = 2.46740; 1/\pi^2 = 0.101321.$$

(continued on next page)

TABLE 1.1—SQUARES OF NUMBERS (continued)

<i>N</i>	0	1	2	3	4	5	6	7	8	9	Average Difference
5.5	30.25	30.36	30.47	30.58	30.69	30.80	30.91	31.02	31.14	31.25	11
5.6	31.36	31.47	31.58	31.70	31.81	31.92	32.04	32.15	32.26	32.38	
5.7	32.49	32.60	32.72	32.83	32.95	33.06	33.18	33.29	33.41	33.52	
5.8	33.64	33.76	33.87	33.99	34.11	34.22	34.34	34.46	34.57	34.69	
5.9	34.81	34.93	35.05	35.16	35.28	35.40	35.52	35.64	35.76	35.88	12
6.0	36.00	36.12	36.24	36.36	36.48	36.60	36.72	36.84	36.97	37.09	
6.1	37.21	37.33	37.45	37.58	37.70	37.82	37.95	38.07	38.19	38.32	
6.2	38.44	38.56	38.69	38.81	38.94	39.06	39.19	39.31	39.44	39.56	
6.3	39.69	39.82	39.94	40.07	40.20	40.32	40.45	40.58	40.70	40.83	13
6.4	40.96	41.09	41.22	41.34	41.47	41.60	41.73	41.86	41.99	42.12	
6.5	42.25	42.38	42.51	42.64	42.77	42.90	43.03	43.16	43.30	43.43	
6.6	43.56	43.69	43.82	43.96	44.09	44.22	44.36	44.49	44.62	44.76	
6.7	44.89	45.02	45.16	45.29	45.43	45.56	45.70	45.83	45.97	46.10	14
6.8	46.24	46.38	46.51	46.65	46.79	46.92	47.06	47.20	47.33	47.47	
6.9	47.61	47.75	47.89	48.02	48.16	48.30	48.44	48.58	48.72	48.86	
7.0	49.00	49.14	49.28	49.42	49.56	49.70	49.84	49.98	50.13	50.27	
7.1	50.41	50.55	50.69	50.84	50.98	51.12	51.27	51.41	51.55	51.70	15
7.2	51.84	51.98	52.13	52.27	52.42	52.56	52.71	52.85	53.00	53.14	
7.3	53.29	53.44	53.58	53.73	53.88	54.02	54.17	54.32	54.46	54.61	
7.4	54.76	54.91	55.06	55.20	55.35	55.50	55.65	55.80	55.95	56.10	
7.5	56.25	56.40	56.55	56.70	56.85	57.00	57.15	57.30	57.46	57.61	16
7.6	57.76	57.91	58.06	58.22	58.37	58.52	58.68	58.83	58.98	59.14	
7.7	59.29	59.44	59.60	59.75	59.91	60.06	60.22	60.37	60.53	60.68	
7.8	60.84	61.00	61.15	61.31	61.47	61.62	61.78	61.94	62.09	62.25	
7.9	62.41	62.57	62.73	62.88	63.04	63.20	63.36	63.52	63.68	63.84	17
8.0	64.00	64.16	64.32	64.48	64.64	64.80	64.96	65.12	65.29	65.45	
8.1	65.61	65.77	65.93	66.10	66.26	66.42	66.59	66.75	66.91	67.08	
8.2	67.24	67.40	67.57	67.73	67.90	68.06	68.23	68.39	68.56	68.72	
8.3	68.89	69.06	69.22	69.39	69.56	69.72	69.89	70.06	70.22	70.39	18
8.4	70.56	70.73	70.90	71.06	71.23	71.40	71.57	71.74	71.91	72.08	
8.5	72.25	72.42	72.59	72.76	72.93	73.10	73.27	73.44	73.62	73.79	
8.6	73.96	74.13	74.30	74.48	74.65	74.82	75.00	75.17	75.34	75.52	
8.7	75.69	75.86	76.04	76.21	76.39	76.56	76.74	76.91	77.09	77.26	19
8.8	77.44	77.62	77.79	77.97	78.15	78.32	78.50	78.68	78.85	79.03	
8.9	79.21	79.39	79.57	79.74	79.92	80.10	80.28	80.46	80.64	80.82	
9.0	81.00	81.18	81.36	81.54	81.72	81.90	82.08	82.26	82.45	82.63	
9.1	82.81	82.99	83.17	83.36	83.54	83.72	83.91	84.09	84.27	84.46	20
9.2	84.64	84.82	85.01	85.19	85.38	85.56	85.75	85.93	86.12	86.30	
9.3	86.49	86.68	86.86	87.05	87.24	87.42	87.61	87.80	87.98	88.17	
9.4	88.36	88.55	88.74	88.92	89.11	89.30	89.49	89.68	89.87	90.06	
9.5	90.25	90.44	90.63	90.82	91.01	91.20	91.39	91.58	91.78	91.97	20
9.6	92.16	92.35	92.54	92.74	92.93	93.12	93.32	93.51	93.70	93.90	
9.7	94.09	94.28	94.48	94.67	94.87	95.06	95.26	95.45	95.65	95.84	
9.8	96.04	96.24	96.43	96.63	96.83	97.02	97.22	97.42	97.61	97.81	
9.9	98.01	98.21	98.41	98.60	98.80	99.00	99.20	99.40	99.60	99.80	
10.0	100.0										

$$\pi^2 = 9.86960, 1/\pi^2 = 0.101321, e^2 = 7.38906.$$

$$\pi^2 = 9.86960, (\pi/2)^2 = 2.46740, 1/\pi^2 = 0.101321.$$

TABLE 1.2—CUBES OF NUMBERS

<i>N</i>	0	1	2	3	4	5	6	7	8	9	Average Difference
1.00	1.000	1.003	1.006	1.009	1.012	1.015	1.018	1.021	1.024	1.027	3
1.01	1.030	1.033	1.036	1.040	1.043	1.046	1.049	1.052	1.055	1.058	
1.02	1.061	1.064	1.067	1.071	1.074	1.077	1.080	1.083	1.086	1.090	
1.03	1.093	1.096	1.099	1.102	1.106	1.109	1.112	1.115	1.118	1.122	
1.04	1.125	1.128	1.131	1.135	1.138	1.141	1.144	1.148	1.151	1.154	
1.05	1.158	1.161	1.164	1.168	1.171	1.174	1.178	1.181	1.184	1.188	
1.06	1.191	1.194	1.198	1.201	1.205	1.208	1.211	1.215	1.218	1.222	4
1.07	1.225	1.228	1.232	1.235	1.239	1.242	1.246	1.249	1.253	1.256	
1.08	1.260	1.263	1.267	1.270	1.274	1.277	1.281	1.284	1.288	1.291	
1.09	1.295	1.299	1.302	1.306	1.309	1.313	1.317	1.320	1.324	1.327	
1.10	1.331	1.335	1.338	1.342	1.346	1.349	1.353	1.357	1.360	1.364	
1.11	1.368	1.371	1.375	1.379	1.382	1.386	1.390	1.394	1.397	1.401	
1.12	1.405	1.409	1.412	1.416	1.420	1.424	1.428	1.431	1.435	1.439	
1.13	1.443	1.447	1.451	1.454	1.458	1.462	1.466	1.470	1.474	1.478	
1.14	1.482	1.485	1.489	1.493	1.497	1.501	1.505	1.509	1.513	1.517	
1.15	1.521	1.525	1.529	1.533	1.537	1.541	1.545	1.549	1.553	1.557	
1.16	1.561	1.565	1.569	1.573	1.577	1.581	1.585	1.589	1.593	1.598	
1.17	1.602	1.606	1.610	1.614	1.618	1.622	1.626	1.631	1.635	1.639	
1.18	1.643	1.647	1.651	1.656	1.660	1.664	1.668	1.672	1.677	1.681	
1.19	1.685	1.689	1.694	1.698	1.702	1.706	1.711	1.715	1.719	1.724	
1.20	1.728	1.732	1.737	1.741	1.745	1.750	1.754	1.758	1.763	1.767	
1.21	1.772	1.776	1.780	1.785	1.789	1.794	1.798	1.802	1.807	1.811	
1.22	1.816	1.820	1.825	1.829	1.834	1.838	1.843	1.847	1.852	1.856	
1.23	1.861	1.865	1.870	1.875	1.879	1.884	1.888	1.893	1.897	1.902	
1.24	1.907	1.911	1.916	1.920	1.925	1.930	1.934	1.939	1.944	1.948	5
1.25	1.953	1.958	1.963	1.967	1.972	1.977	1.981	1.986	1.991	1.996	
1.26	2.000	2.005	2.010	2.015	2.019	2.024	2.029	2.034	2.039	2.044	
1.27	2.048	2.053	2.058	2.063	2.068	2.073	2.078	2.082	2.087	2.092	
1.28	2.097	2.102	2.107	2.112	2.117	2.122	2.127	2.132	2.137	2.142	
1.29	2.147	2.152	2.157	2.162	2.167	2.172	2.177	2.182	2.187	2.192	
1.30	2.197	2.202	2.207	2.212	2.217	2.222	2.228	2.233	2.238	2.243	
1.31	2.248	2.253	2.258	2.264	2.269	2.274	2.279	2.284	2.290	2.295	
1.32	2.300	2.305	2.310	2.316	2.321	2.326	2.331	2.337	2.342	2.347	
1.33	2.353	2.358	2.363	2.369	2.374	2.379	2.385	2.390	2.395	2.401	
1.34	2.406	2.411	2.417	2.422	2.428	2.433	2.439	2.444	2.449	2.455	
1.35	2.460	2.466	2.471	2.477	2.482	2.488	2.493	2.499	2.504	2.510	
1.36	2.515	2.521	2.527	2.532	2.538	2.543	2.549	2.554	2.560	2.566	6
1.37	2.571	2.577	2.583	2.588	2.594	2.600	2.605	2.611	2.617	2.622	
1.38	2.628	2.634	2.640	2.645	2.651	2.657	2.663	2.668	2.674	2.680	
1.39	2.686	2.691	2.697	2.703	2.709	2.715	2.721	2.726	2.732	2.738	
1.40	2.744	2.750	2.756	2.762	2.768	2.774	2.779	2.785	2.791	2.797	
1.41	2.803	2.809	2.815	2.821	2.827	2.833	2.839	2.845	2.851	2.857	
1.42	2.863	2.869	2.875	2.881	2.888	2.894	2.900	2.906	2.912	2.918	
1.43	2.924	2.930	2.936	2.943	2.949	2.955	2.961	2.967	2.974	2.980	
1.44	2.986	2.992	2.998	3.005	3.011	3.017	3.023	3.030	3.036	3.042	
1.45	3.049	3.055	3.061	3.068	3.074	3.080	3.087	3.093	3.099	3.106	
1.46	3.112	3.119	3.125	3.131	3.138	3.144	3.151	3.157	3.164	3.170	
1.47	3.177	3.183	3.190	3.196	3.203	3.209	3.216	3.222	3.229	3.235	
1.48	3.242	3.248	3.255	3.262	3.268	3.275	3.281	3.288	3.295	3.301	7
1.49	3.308	3.315	3.321	3.328	3.335	3.341	3.348	3.355	3.362	3.368	
1.50	3.375	3.382	3.389	3.395	3.402	3.409	3.416	3.422	3.429	3.436	
1.51	3.443	3.450	3.457	3.464	3.470	3.477	3.484	3.491	3.498	3.505	
1.52	3.512	3.519	3.526	3.533	3.540	3.547	3.554	3.561	3.568	3.575	
1.53	3.582	3.589	3.596	3.603	3.610	3.617	3.624	3.631	3.638	3.645	
1.54	3.652	3.659	3.667	3.674	3.681	3.688	3.695	3.702	3.709	3.717	
1.55	3.724	3.731	3.738	3.746	3.753	3.760	3.767	3.775	3.782	3.789	
1.56	3.796	3.804	3.811	3.818	3.826	3.833	3.840	3.848	3.855	3.863	
1.57	3.870	3.877	3.885	3.892	3.900	3.907	3.914	3.922	3.929	3.937	8
1.58	3.944	3.952	3.959	3.967	3.974	3.982	3.989	3.997	4.005	4.012	
1.59	4.020	4.027	4.035	4.042	4.050	4.058	4.065	4.073	4.081	4.088	

Explanation of Table of Cubes

This table gives the value of N^3 for values of N from 1 to 10, correct to four figures. (Interpolated values may be in error by 1 in the fourth figure.)

To find the cube of a number N outside the range from 1 to 10, note that moving the decimal point *one* place in Column N is equivalent to moving it *three* places in the body of the table. For example, $(4.852)^3 = 114.2$, $(0.4852)^3 = 0.1142$, and $(485.2)^3 = 114,200,000$.

This table also can be used inversely to give cube roots.

(continued on next page)

TABLE 1.2—CUBES OF NUMBERS (continued)

N	0	1	2	3	4	5	6	7	8	9	Average Difference
1.60	4.096	4.104	4.111	4.119	4.127	4.135	4.142	4.150	4.158	4.166	8
1.61	4.173	4.181	4.189	4.197	4.204	4.212	4.220	4.228	4.236	4.244	
1.62	4.252	4.259	4.267	4.275	4.283	4.291	4.299	4.307	4.315	4.323	
1.63	4.331	4.339	4.347	4.355	4.363	4.371	4.379	4.387	4.395	4.403	
1.64	4.411	4.419	4.427	4.435	4.443	4.451	4.460	4.468	4.476	4.484	
1.65	4.492	4.500	4.508	4.517	4.525	4.533	4.541	4.550	4.558	4.566	9
1.66	4.574	4.583	4.591	4.599	4.607	4.616	4.624	4.632	4.641	4.649	
1.67	4.657	4.666	4.674	4.683	4.691	4.699	4.708	4.716	4.725	4.733	
1.68	4.742	4.750	4.759	4.767	4.776	4.784	4.793	4.801	4.810	4.818	
1.69	4.827	4.835	4.844	4.853	4.861	4.870	4.878	4.887	4.896	4.904	
1.70	4.913	4.922	4.930	4.939	4.948	4.956	4.965	4.974	4.983	4.991	10
1.71	5.000	5.009	5.018	5.027	5.035	5.044	5.053	5.062	5.071	5.080	
1.72	5.088	5.097	5.106	5.115	5.124	5.133	5.142	5.151	5.160	5.169	
1.73	5.178	5.187	5.196	5.205	5.214	5.223	5.232	5.241	5.250	5.259	
1.74	5.268	5.277	5.286	5.295	5.304	5.314	5.323	5.332	5.341	5.350	
1.75	5.359	5.369	5.378	5.387	5.396	5.405	5.415	5.424	5.433	5.442	11
1.76	5.452	5.461	5.470	5.480	5.489	5.498	5.508	5.517	5.526	5.536	
1.77	5.545	5.555	5.564	5.573	5.583	5.592	5.602	5.611	5.621	5.630	
1.78	5.640	5.649	5.659	5.668	5.678	5.687	5.697	5.707	5.716	5.726	
1.79	5.735	5.745	5.755	5.764	5.774	5.784	5.793	5.803	5.813	5.822	
1.80	5.832	5.842	5.851	5.861	5.871	5.881	5.891	5.900	5.910	5.920	12
1.81	5.930	5.940	5.949	5.959	5.969	5.979	5.989	5.999	6.009	6.019	
1.82	6.029	6.039	6.048	6.058	6.068	6.078	6.088	6.098	6.108	6.118	
1.83	6.128	6.139	6.149	6.159	6.169	6.179	6.189	6.199	6.209	6.219	
1.84	6.230	6.240	6.250	6.260	6.270	6.280	6.291	6.301	6.311	6.321	
1.85	6.332	6.342	6.352	6.362	6.373	6.383	6.393	6.404	6.414	6.424	13
1.86	6.435	6.445	6.456	6.466	6.476	6.487	6.497	6.508	6.518	6.529	
1.87	6.539	6.550	6.560	6.571	6.581	6.592	6.602	6.613	6.623	6.634	
1.88	6.645	6.655	6.666	6.677	6.687	6.698	6.708	6.719	6.730	6.741	
1.89	6.751	6.762	6.773	6.783	6.794	6.805	6.816	6.827	6.837	6.848	
1.90	6.859	6.870	6.881	6.892	6.902	6.913	6.924	6.935	6.946	6.957	14
1.91	6.968	6.979	6.990	7.001	7.012	7.023	7.034	7.045	7.056	7.067	
1.92	7.078	7.089	7.100	7.111	7.122	7.133	7.144	7.156	7.167	7.178	
1.93	7.189	7.200	7.211	7.223	7.234	7.245	7.256	7.268	7.279	7.290	
1.94	7.301	7.313	7.324	7.335	7.347	7.358	7.369	7.381	7.392	7.403	
1.95	7.415	7.426	7.438	7.449	7.461	7.472	7.484	7.495	7.507	7.518	15
1.96	7.530	7.541	7.553	7.564	7.576	7.587	7.599	7.610	7.622	7.634	
1.97	7.645	7.657	7.669	7.680	7.692	7.704	7.715	7.727	7.739	7.751	
1.98	7.762	7.774	7.786	7.798	7.810	7.821	7.833	7.845	7.857	7.869	
1.99	7.881	7.892	7.904	7.916	7.928	7.940	7.952	7.964	7.976	7.988	
2.00	8.000	8.012	8.024	8.036	8.048	8.060	8.072	8.084	8.096	8.108	16
2.01	8.121	8.133	8.145	8.157	8.169	8.181	8.194	8.206	8.218	8.230	
2.02	8.242	8.255	8.267	8.279	8.291	8.304	8.316	8.328	8.341	8.353	
2.03	8.365	8.378	8.390	8.403	8.415	8.427	8.440	8.452	8.465	8.477	
2.04	8.490	8.502	8.515	8.527	8.540	8.552	8.565	8.577	8.590	8.603	
2.05	8.615	8.628	8.640	8.653	8.666	8.678	8.691	8.704	8.716	8.729	17
2.06	8.742	8.755	8.767	8.780	8.793	8.806	8.818	8.831	8.844	8.857	
2.07	8.870	8.883	8.895	8.908	8.921	8.934	8.947	8.960	8.973	8.986	
2.08	8.999	9.012	9.025	9.038	9.051	9.064	9.077	9.090	9.103	9.116	
2.09	9.129	9.142	9.156	9.169	9.182	9.195	9.208	9.221	9.235	9.248	
2.10	9.261	9.274	9.287	9.301	9.314	9.327	9.341	9.354	9.367	9.381	18
2.11	9.394	9.407	9.421	9.434	9.447	9.461	9.474	9.488	9.501	9.515	
2.12	9.528	9.542	9.555	9.569	9.582	9.596	9.609	9.623	9.636	9.650	
2.13	9.664	9.677	9.691	9.704	9.718	9.732	9.745	9.759	9.773	9.787	
2.14	9.800	9.814	9.828	9.842	9.855	9.869	9.883	9.897	9.911	9.925	
2.15	9.938	9.952	9.966	9.980	9.994	10.008					14
2.1						9.94	10.08	10.22	10.36	10.50	14
2.2	10.65	10.79	10.94	11.09	11.24	11.39	11.54	11.70	11.85	12.01	15
2.3	12.17	12.33	12.49	12.65	12.81	12.98	13.14	13.31	13.48	13.65	16
2.4	13.82	14.00	14.17	14.35	14.53	14.71	14.89	15.07	15.25	15.44	18

$$\pi^3 = 31.0063 \text{ and } 1/\pi^3 = 0.0322515 +$$

TABLE 1.2—CUBES OF NUMBERS (continued)

<i>N</i>	0	1	2	3	4	5	6	7	8	9	Average Difference
2.5	15.62	15.81	16.00	16.19	16.39	16.58	16.78	16.97	17.17	17.37	20
2.6	17.58	17.78	17.98	18.19	18.40	18.61	18.82	19.03	19.25	19.47	21
2.7	19.68	19.90	20.12	20.35	20.57	20.80	21.02	21.25	21.48	21.72	23
2.8	21.95	22.19	22.43	22.67	22.91	23.15	23.39	23.64	23.89	24.14	24
2.9	24.39	24.64	24.90	25.15	25.41	25.67	25.93	26.20	26.46	26.73	26
3.0	27.00	27.27	27.54	27.82	28.09	28.37	28.65	28.93	29.22	29.50	28
3.1	29.79	30.08	30.37	30.66	30.96	31.26	31.55	31.86	32.16	32.46	30
3.2	32.77	33.08	33.39	33.70	34.01	34.33	34.65	34.97	35.29	35.61	32
3.3	35.94	36.26	36.59	36.93	37.26	37.60	37.93	38.27	38.61	38.96	34
3.4	39.30	39.65	40.00	40.35	40.71	41.06	41.42	41.78	42.14	42.51	36
3.5	42.88	43.24	43.61	43.99	44.36	44.74	45.12	45.50	45.88	46.27	39
3.6	46.66	47.05	47.44	47.83	48.23	48.63	49.03	49.43	49.84	50.24	40
3.7	50.65	51.06	51.48	51.90	52.31	52.73	53.16	53.58	54.01	54.44	42
3.8	54.87	55.31	55.74	56.18	56.62	57.07	57.51	57.96	58.41	58.86	44
3.9	59.32	59.78	60.24	60.70	61.16	61.63	62.10	62.57	63.04	63.52	47
4.0	64.00	64.48	64.96	65.45	65.94	66.43	66.92	67.42	67.92	68.42	49
4.1	68.92	69.43	69.93	70.44	70.96	71.47	71.99	72.51	73.03	73.56	52
4.2	74.09	74.62	75.15	75.69	76.23	76.77	77.31	77.85	78.40	78.95	54
4.3	79.51	80.06	80.62	81.18	81.75	82.31	82.88	83.45	84.03	84.60	58
4.4	85.18	85.77	86.35	86.94	87.53	88.12	88.72	89.31	89.92	90.52	59
4.5	91.12	91.73	92.35	92.96	93.58	94.20	94.82	95.44	96.07	96.70	62
4.6	97.34	97.97	98.61	99.25	99.90	100.54					64
4.6						100.5	101.2	101.8	102.5	103.2	7
4.7	103.8	104.5	105.2	105.8	106.5	107.2	107.9	108.5	109.2	109.9	7
4.8	110.6	111.3	112.0	112.7	113.4	114.1	114.8	115.5	116.2	116.9	7
4.9	117.6	118.4	119.1	119.8	120.6	121.3	122.0	122.8	123.5	124.3	7
5.0	125.0	125.8	126.5	127.3	128.0	128.8	129.6	130.3	131.1	131.9	8
5.1	132.7	133.4	134.2	135.0	135.8	136.6	137.4	138.2	139.0	139.8	
5.2	140.6	141.4	142.2	143.1	143.9	144.7	145.5	146.4	147.2	148.0	
5.3	148.9	149.7	150.6	151.4	152.3	153.1	154.0	154.9	155.7	156.6	9
5.4	157.5	158.3	159.2	160.1	161.0	161.9	162.8	163.7	164.6	165.5	
5.5	166.4	167.3	168.2	169.1	170.0	171.0	171.9	172.8	173.7	174.7	
5.6	175.6	176.6	177.5	178.5	179.4	180.4	181.3	182.3	183.3	184.2	10
5.7	185.2	186.2	187.1	188.1	189.1	190.1	191.1	192.1	193.1	194.1	
5.8	195.1	196.1	197.1	198.2	199.2	200.2	201.2	202.3	203.3	204.3	
5.9	205.4	206.4	207.5	208.5	209.6	210.6	211.7	212.8	213.8	214.9	
6.0	216.0	217.1	218.2	219.3	220.3	221.4	222.5	223.6	224.8	225.9	11
6.1	227.0	228.1	229.2	230.3	231.5	232.6	233.7	234.9	236.0	237.2	
6.2	238.3	239.5	240.6	241.8	243.0	244.1	245.3	246.5	247.7	248.9	12
6.3	250.0	251.2	252.4	253.6	254.8	256.0	257.3	258.5	259.7	260.9	
6.4	262.1	263.4	264.6	265.8	267.1	268.3	269.6	270.8	272.1	273.4	
6.5	274.6	275.9	277.2	278.4	279.7	281.0	282.3	283.6	284.9	286.2	13
6.6	287.5	288.8	290.1	291.4	292.8	294.1	295.4	296.7	298.1	299.4	
6.7	300.8	302.1	303.5	304.8	306.2	307.5	308.9	310.3	311.7	313.0	14
6.8	314.4	315.8	317.2	318.6	320.0	321.4	322.8	324.2	325.7	327.1	
6.9	328.5	329.9	331.4	332.8	334.3	335.7	337.2	338.6	340.1	341.5	
7.0	343.0	344.5	345.9	347.4	348.9	350.4	351.9	353.4	354.9	356.4	15
7.1	357.9	359.4	360.9	362.5	364.0	365.5	367.1	368.6	370.1	371.7	
7.2	373.2	374.8	376.4	377.9	379.5	381.1	382.7	384.2	385.8	387.4	16
7.3	389.0	390.6	392.2	393.8	395.4	397.1	398.7	400.3	401.9	403.6	
7.4	405.2	406.9	408.5	410.2	411.8	413.5	415.2	416.8	418.5	420.2	17
7.5	421.9	423.6	425.3	427.0	428.7	430.4	432.1	433.8	435.5	437.2	
7.6	439.0	440.7	442.5	444.2	445.9	447.7	449.5	451.2	453.0	454.8	18
7.7	456.5	458.3	460.1	461.9	463.7	465.5	467.3	469.1	470.9	472.7	
7.8	474.6	476.4	478.2	480.0	481.9	483.7	485.6	487.4	489.3	491.2	
7.9	493.0	494.9	496.8	498.7	500.6	502.5	504.4	506.3	508.2	510.1	19
8.0	512.0	513.9	515.8	517.8	519.7	521.7	523.6	525.6	527.5	529.5	
8.1	531.4	533.4	535.4	537.4	539.4	541.3	543.3	545.3	547.3	549.4	20
8.2	551.4	553.4	555.4	557.4	559.5	561.5	563.6	565.6	567.7	569.7	
8.3	571.8	573.9	575.9	578.0	580.1	582.2	584.3	586.4	588.5	590.6	21
8.4	592.7	594.8	596.9	599.1	601.2	603.4	605.5	607.6	609.8	612.0	

$$\pi^3 = 31.0063 \text{ and } 1/\pi^3 = 0.0322515 +$$

(continued on next page)

TABLE 1.2—CUBES OF NUMBERS (continued)

<i>N</i>	0	1	2	3	4	5	6	7	8	9	Average Difference
8.5	614.1	616.3	618.5	620.7	622.8	625.0	627.2	629.4	631.6	633.8	22
8.6	636.1	638.3	640.5	642.7	645.0	647.2	649.5	651.7	654.0	656.2	
8.7	658.5	660.8	663.1	665.3	667.6	669.9	672.2	674.5	676.8	679.2	23
8.8	681.5	683.8	686.1	688.5	690.8	693.2	695.5	697.9	700.2	702.6	24
8.9	705.0	707.3	709.7	712.1	714.5	716.9	719.3	721.7	724.2	726.6	
9.0	729.0	731.4	733.9	736.3	738.8	741.2	743.7	746.1	748.6	751.1	25
9.1	753.6	756.1	758.6	761.0	763.6	766.1	768.6	771.1	773.6	776.2	
9.2	778.7	781.2	783.8	786.3	788.9	791.5	794.0	796.6	799.2	801.8	26
9.3	804.4	807.0	809.6	812.2	814.8	817.4	820.0	822.7	825.3	827.9	
9.4	830.6	833.2	835.9	838.6	841.2	843.9	846.6	849.3	852.0	854.7	27
9.5	857.4	860.1	862.8	865.5	868.3	871.0	873.7	876.5	879.2	882.0	
9.6	884.7	887.5	890.3	893.1	895.8	898.6	901.4	904.2	907.0	909.9	28
9.7	912.7	915.5	918.3	921.2	924.0	926.9	929.7	932.6	935.4	938.3	
9.8	941.2	944.1	947.0	949.9	952.8	955.7	958.6	961.5	964.4	967.4	29
9.9	970.3	973.2	976.2	979.1	982.1	985.1	988.0	991.0	994.0	997.0	
10.0	1000.0										

$$\pi^3 = 31.0063 \text{ and } 1/\pi^3 = 0.0322515 + .$$

TABLE 1.3—SQUARE ROOTS OF NUMBERS

<i>N</i>	0	1	2	3	4	5	6	7	8	9	Average Difference
1.0	1.000	1.005	1.010	1.015	1.020	1.025	1.030	1.034	1.039	1.044	5
1.1	1.049	1.054	1.058	1.063	1.068	1.072	1.077	1.082	1.086	1.091	4
1.2	1.095	1.100	1.105	1.109	1.114	1.118	1.122	1.127	1.131	1.136	
1.3	1.140	1.145	1.149	1.153	1.158	1.162	1.166	1.170	1.175	1.179	
1.4	1.183	1.187	1.192	1.196	1.200	1.204	1.208	1.212	1.217	1.221	
1.5	1.255	1.229	1.233	1.237	1.241	1.245	1.249	1.253	1.257	1.261	
1.6	1.265	1.269	1.273	1.277	1.281	1.285	1.288	1.292	1.296	1.300	
1.7	1.304	1.308	1.311	1.315	1.319	1.323	1.327	1.330	1.334	1.338	
1.8	1.342	1.345	1.349	1.353	1.356	1.360	1.364	1.367	1.371	1.375	
1.9	1.378	1.382	1.386	1.389	1.393	1.396	1.400	1.404	1.407	1.411	
2.0	1.414	1.418	1.421	1.425	1.428	1.432	1.435	1.439	1.442	1.446	
2.1	1.449	1.453	1.456	1.459	1.463	1.466	1.470	1.473	1.476	1.480	
2.2	1.483	1.487	1.490	1.493	1.497	1.500	1.503	1.507	1.510	1.513	
2.3	1.517	1.520	1.523	1.526	1.530	1.533	1.536	1.539	1.543	1.546	3
2.4	1.549	1.552	1.556	1.559	1.562	1.565	1.568	1.572	1.575	1.578	
2.5	1.581	1.584	1.587	1.591	1.594	1.597	1.600	1.603	1.606	1.609	
2.6	1.612	1.616	1.619	1.622	1.625	1.628	1.631	1.634	1.637	1.640	
2.7	1.643	1.646	1.649	1.652	1.655	1.658	1.661	1.664	1.667	1.670	
2.8	1.673	1.676	1.679	1.682	1.685	1.688	1.691	1.694	1.697	1.700	
2.9	1.703	1.706	1.709	1.712	1.715	1.718	1.720	1.723	1.726	1.729	
3.0	1.732	1.735	1.738	1.741	1.744	1.746	1.749	1.752	1.755	1.758	
3.1	1.761	1.764	1.766	1.769	1.772	1.775	1.778	1.780	1.783	1.786	
3.2	1.789	1.792	1.794	1.797	1.800	1.803	1.806	1.808	1.811	1.814	
3.3	1.817	1.819	1.822	1.825	1.828	1.830	1.833	1.836	1.838	1.841	
3.4	1.844	1.847	1.849	1.852	1.855	1.857	1.860	1.863	1.865	1.868	
3.5	1.871	1.873	1.876	1.879	1.881	1.884	1.887	1.889	1.892	1.895	
3.6	1.897	1.900	1.903	1.905	1.908	1.910	1.913	1.916	1.918	1.921	
3.7	1.924	1.926	1.929	1.931	1.934	1.936	1.939	1.942	1.944	1.947	
3.8	1.949	1.952	1.954	1.957	1.960	1.962	1.965	1.967	1.970	1.972	
3.9	1.975	1.977	1.980	1.982	1.985	1.987	1.990	1.992	1.995	1.997	
4.0	2.000	2.002	2.005	2.007	2.010	2.012	2.015	2.017	2.020	2.022	
4.1	2.025	2.027	2.030	2.032	2.035	2.037	2.040	2.042	2.045	2.047	
4.2	2.049	2.052	2.054	2.057	2.059	2.062	2.064	2.066	2.069	2.071	
4.3	2.074	2.076	2.078	2.081	2.083	2.086	2.088	2.090	2.093	2.095	2
4.4	2.098	2.100	2.102	2.105	2.107	2.110	2.112	2.114	2.117	2.119	
4.5	2.121	2.124	2.126	2.128	2.131	2.133	2.135	2.138	2.140	2.142	
4.6	2.145	2.147	2.149	2.152	2.154	2.156	2.159	2.161	2.163	2.166	
4.7	2.168	2.170	2.173	2.175	2.177	2.179	2.182	2.184	2.186	2.189	
4.8	2.191	2.193	2.195	2.198	2.200	2.202	2.205	2.207	2.209	2.211	
4.9	2.214	2.216	2.218	2.220	2.223	2.225	2.227	2.229	2.232	2.234	
5.0	2.236	2.238	2.241	2.243	2.245	2.247	2.249	2.252	2.254	2.256	
5.1	2.258	2.261	2.263	2.265	2.267	2.269	2.272	2.274	2.276	2.278	
5.2	2.280	2.283	2.285	2.287	2.289	2.291	2.293	2.296	2.298	2.300	
5.3	2.302	2.304	2.307	2.309	2.311	2.313	2.315	2.317	2.319	2.322	
5.4	2.324	2.326	2.328	2.330	2.332	2.335	2.337	2.339	2.341	2.343	
5.5	2.345	2.347	2.349	2.352	2.354	2.356	2.358	2.360	2.362	2.364	
5.6	2.366	2.369	2.371	2.373	2.375	2.377	2.379	2.381	2.383	2.385	
5.7	2.387	2.390	2.392	2.394	2.396	2.398	2.400	2.402	2.404	2.406	
5.8	2.408	2.410	2.412	2.415	2.417	2.419	2.421	2.423	2.425	2.427	
5.9	2.429	2.431	2.433	2.435	2.437	2.439	2.441	2.443	2.445	2.447	
6.0	2.449	2.452	2.454	2.456	2.458	2.460	2.462	2.464	2.466	2.468	
6.1	2.470	2.472	2.474	2.476	2.478	2.480	2.482	2.484	2.486	2.488	
6.2	2.490	2.492	2.494	2.496	2.498	2.500	2.502	2.504	2.506	2.508	
6.3	2.510	2.512	2.514	2.516	2.518	2.520	2.522	2.524	2.526	2.528	
6.4	2.530	2.532	2.534	2.536	2.538	2.540	2.542	2.544	2.546	2.548	
6.5	2.550	2.551	2.553	2.555	2.557	2.559	2.561	2.563	2.565	2.567	
6.6	2.569	2.571	2.573	2.575	2.577	2.579	2.581	2.583	2.585	2.587	
6.7	2.588	2.590	2.592	2.594	2.596	2.598	2.600	2.602	2.604	2.606	
6.8	2.608	2.610	2.612	2.613	2.615	2.617	2.619	2.621	2.623	2.625	
6.9	2.627	2.629	2.631	2.632	2.634	2.636	2.638	2.640	2.642	2.644	

Explanation of Table of Square Roots

This table gives the value of \sqrt{N} for values of N from 1 to 100, correct to four figures. (Interpolated values may be in error by 1 in the fourth figure).

To find the square root of a number N outside the range from 1 to 100, divide the digits of the number into blocks of two (beginning with the decimal point), and note that moving the decimal point two places in N is equivalent to moving it one place in the square root of N . For example, $\sqrt{2.718} = 1.648$, $\sqrt{27.18} = 5.213$, $\sqrt{271.8} = 16.48$, $\sqrt{2,718} = 52.13$, $\sqrt{0.002718} = 0.01648$, and $\sqrt{0.002718} = 0.05213$.

(continued on next page)

TABLE 1.3—SQUARE ROOTS OF NUMBERS (continued)

<i>N</i>	0	1	2	3	4	5	6	7	8	9	Average Difference
7.0	2.646	2.648	2.650	2.651	2.653	2.655	2.657	2.659	2.661	2.663	2
7.1	2.665	2.666	2.668	2.670	2.672	2.674	2.676	2.678	2.680	2.681	
7.2	2.683	2.685	2.687	2.689	2.691	2.693	2.694	2.696	2.698	2.700	
7.3	2.702	2.704	2.706	2.707	2.709	2.711	2.713	2.715	2.717	2.718	
7.4	2.720	2.722	2.724	2.726	2.728	2.729	2.731	2.733	2.735	2.737	
7.5	2.739	2.740	2.742	2.744	2.746	2.748	2.750	2.751	2.753	2.755	
7.6	2.757	2.759	2.760	2.762	2.764	2.766	2.768	2.769	2.771	2.773	
7.7	2.775	2.777	2.778	2.780	2.782	2.784	2.786	2.787	2.789	2.791	
7.8	2.793	2.795	2.796	2.798	2.800	2.802	2.804	2.805	2.807	2.809	
7.9	2.811	2.812	2.814	2.816	2.818	2.820	2.821	2.823	2.825	2.827	
8.0	2.828	2.830	2.832	2.834	2.835	2.837	2.839	2.841	2.843	2.844	
8.1	2.846	2.848	2.850	2.851	2.853	2.855	2.857	2.858	2.860	2.862	
8.2	2.864	2.865	2.867	2.869	2.871	2.872	2.874	2.876	2.877	2.879	
8.3	2.881	2.883	2.884	2.886	2.888	2.890	2.891	2.893	2.895	2.897	
8.4	2.898	2.900	2.902	2.903	2.905	2.907	2.909	2.910	2.912	2.914	
8.5	2.915	2.917	2.919	2.921	2.922	2.924	2.926	2.927	2.929	2.931	
8.6	2.933	2.934	2.936	2.938	2.939	2.941	2.943	2.944	2.946	2.948	
8.7	2.950	2.951	2.953	2.955	2.956	2.958	2.960	2.961	2.963	2.965	
8.8	2.966	2.968	2.970	2.972	2.973	2.975	2.977	2.978	2.980	2.982	
8.9	2.983	2.985	2.987	2.988	2.990	2.992	2.993	2.995	2.997	2.998	
9.0	3.000	3.002	3.003	3.005	3.007	3.008	3.010	3.012	3.013	3.015	16
9.1	3.017	3.018	3.020	3.022	3.023	3.025	3.027	3.028	3.030	3.032	
9.2	3.033	3.035	3.036	3.038	3.040	3.041	3.043	3.045	3.046	3.048	
9.3	3.050	3.051	3.053	3.055	3.056	3.058	3.059	3.061	3.063	3.064	
9.4	3.066	3.068	3.069	3.071	3.072	3.074	3.076	3.077	3.079	3.081	
9.5	3.082	3.084	3.085	3.087	3.089	3.090	3.092	3.094	3.095	3.097	
9.6	3.098	3.100	3.102	3.103	3.105	3.106	3.108	3.110	3.111	3.113	
9.7	3.114	3.116	3.118	3.119	3.121	3.122	3.124	3.126	3.127	3.129	
9.8	3.130	3.132	3.134	3.135	3.137	3.138	3.140	3.142	3.143	3.145	
9.9	3.146	3.148	3.150	3.151	3.153	3.154	3.156	3.158	3.159	3.161	
10.0	3.162	3.178	3.194	3.209	3.225	3.240	3.256	3.271	3.286	3.302	
11.0	3.317	3.332	3.347	3.362	3.376	3.391	3.406	3.421	3.435	3.450	
12.0	3.464	3.479	3.493	3.507	3.521	3.536	3.550	3.564	3.578	3.592	
13.0	3.606	3.619	3.633	3.647	3.661	3.674	3.688	3.701	3.715	3.728	
14.0	3.742	3.755	3.768	3.782	3.795	3.808	3.821	3.834	3.847	3.860	
15.0	3.873	3.886	3.899	3.912	3.924	3.937	3.950	3.962	3.975	3.987	12
16.0	4.000	4.012	4.025	4.037	4.050	4.062	4.074	4.087	4.099	4.111	
17.0	4.123	4.135	4.147	4.159	4.171	4.183	4.195	4.207	4.219	4.231	
18.0	4.243	4.254	4.266	4.278	4.290	4.301	4.313	4.324	4.336	4.347	
19.0	4.359	4.370	4.382	4.393	4.405	4.416	4.427	4.438	4.450	4.461	
20.0	4.472	4.483	4.494	4.506	4.517	4.528	4.539	4.550	4.561	4.572	
21.0	4.583	4.593	4.604	4.615	4.626	4.637	4.648	4.658	4.669	4.680	
22.0	4.690	4.701	4.712	4.722	4.733	4.743	4.754	4.764	4.775	4.785	
23.0	4.796	4.806	4.817	4.827	4.837	4.848	4.858	4.868	4.879	4.889	
24.0	4.899	4.909	4.919	4.930	4.940	4.950	4.960	4.970	4.980	4.990	
25.0	5.000	5.010	5.020	5.030	5.040	5.050	5.060	5.070	5.079	5.089	
26.0	5.099	5.109	5.119	5.128	5.138	5.148	5.158	5.167	5.177	5.187	
27.0	5.196	5.206	5.215	5.225	5.235	5.244	5.254	5.263	5.273	5.282	
28.0	5.292	5.301	5.310	5.320	5.329	5.339	5.348	5.357	5.367	5.376	
29.0	5.385	5.394	5.404	5.413	5.422	5.431	5.441	5.450	5.459	5.468	
30.0	5.477	5.486	5.495	5.505	5.514	5.523	5.532	5.541	5.550	5.559	9
31.0	5.568	5.577	5.586	5.595	5.604	5.612	5.621	5.630	5.639	5.648	
32.0	5.657	5.666	5.675	5.683	5.692	5.701	5.710	5.718	5.727	5.736	
33.0	5.745	5.753	5.762	5.771	5.779	5.788	5.797	5.805	5.814	5.822	
34.0	5.831	5.840	5.848	5.857	5.865	5.874	5.882	5.891	5.899	5.908	
35.0	5.916	5.925	5.933	5.941	5.950	5.958	5.967	5.975	5.983	5.992	
36.0	6.000	6.008	6.017	6.025	6.033	6.042	6.050	6.058	6.066	6.075	
37.0	6.083	6.091	6.099	6.107	6.116	6.124	6.132	6.140	6.148	6.156	
38.0	6.164	6.173	6.181	6.189	6.197	6.205	6.213	6.221	6.229	6.237	
39.0	6.245	6.253	6.261	6.269	6.277	6.285	6.293	6.301	6.309	6.317	

$$\sqrt{\pi} = 1.77245 +, 1/\sqrt{\pi} = 0.56419, \sqrt{\pi/2} = 1.25331, \text{ and } \sqrt{e} = 1.64872$$

TABLE 1.3—SQUARE ROOTS OF NUMBERS (continued)

<i>N</i>	0	1	2	3	4	5	6	7	8	9	Average Difference
40.0	6.325	6.332	6.340	6.348	6.356	6.364	6.372	6.380	6.387	6.395	8
41.0	6.403	6.411	6.419	6.427	6.434	6.442	6.450	6.458	6.465	6.473	
42.0	6.481	6.488	6.496	6.504	6.512	6.519	6.527	6.535	6.542	6.550	
43.0	6.557	6.565	6.573	6.580	6.588	6.595	6.603	6.611	6.618	6.626	
44.0	6.633	6.641	6.648	6.656	6.663	6.671	6.678	6.686	6.693	6.701	
45.0	6.708	6.716	6.723	6.731	6.738	6.745	6.753	6.760	6.768	6.775	7
46.0	6.782	6.790	6.797	6.804	6.812	6.819	6.826	6.834	6.841	6.848	
47.0	6.856	6.863	6.870	6.877	6.885	6.892	6.899	6.907	6.914	6.921	
48.0	6.928	6.935	6.943	6.950	6.957	6.964	6.971	6.979	6.986	6.993	
49.0	7.000	7.007	7.014	7.021	7.029	7.036	7.043	7.050	7.057	7.064	
50.0	7.071	7.078	7.085	7.092	7.099	7.106	7.113	7.120	7.127	7.134	7
51.0	7.141	7.148	7.155	7.162	7.169	7.176	7.183	7.190	7.197	7.204	
52.0	7.211	7.218	7.225	7.232	7.239	7.246	7.253	7.259	7.266	7.273	
53.0	7.280	7.287	7.294	7.301	7.308	7.314	7.321	7.328	7.335	7.342	
54.0	7.348	7.355	7.362	7.369	7.376	7.382	7.389	7.396	7.403	7.409	
55.0	7.416	7.423	7.430	7.436	7.443	7.450	7.457	7.463	7.470	7.477	6
56.0	7.483	7.490	7.497	7.503	7.510	7.517	7.523	7.530	7.537	7.543	
57.0	7.550	7.556	7.563	7.570	7.576	7.583	7.589	7.596	7.603	7.609	
58.0	7.616	7.622	7.629	7.635	7.642	7.649	7.655	7.662	7.668	7.675	
59.0	7.681	7.688	7.694	7.701	7.707	7.714	7.720	7.727	7.733	7.740	
60.0	7.746	7.752	7.759	7.765	7.772	7.778	7.785	7.791	7.797	7.804	
61.0	7.810	7.817	7.823	7.829	7.836	7.842	7.849	7.855	7.861	7.868	
62.0	7.874	7.880	7.887	7.893	7.899	7.906	7.912	7.918	7.925	7.931	
63.0	7.937	7.944	7.950	7.956	7.962	7.969	7.975	7.981	7.987	7.994	
64.0	8.000	8.006	8.012	8.019	8.025	8.031	8.037	8.044	8.050	8.056	
65.0	8.062	8.068	8.075	8.081	8.087	8.093	8.099	8.106	8.112	8.118	
66.0	8.124	8.130	8.136	8.142	8.149	8.155	8.161	8.167	8.173	8.179	
67.0	8.185	8.191	8.198	8.204	8.210	8.216	8.222	8.228	8.234	8.240	
68.0	8.246	8.252	8.258	8.264	8.270	8.276	8.283	8.289	8.295	8.301	
69.0	8.307	8.313	8.319	8.325	8.331	8.337	8.343	8.349	8.355	8.361	
70.0	8.367	8.373	8.379	8.385	8.390	8.396	8.402	8.408	8.414	8.420	
71.0	8.426	8.432	8.438	8.444	8.450	8.456	8.462	8.468	8.473	8.479	
72.0	8.485	8.491	8.497	8.503	8.509	8.515	8.521	8.526	8.532	8.538	
73.0	8.544	8.550	8.556	8.562	8.567	8.573	8.579	8.585	8.591	8.597	
74.0	8.602	8.608	8.614	8.620	8.626	8.631	8.637	8.643	8.649	8.654	
75.0	8.660	8.666	8.672	8.678	8.683	8.689	8.695	8.701	8.706	8.712	
76.0	8.718	8.724	8.729	8.735	8.741	8.746	8.752	8.758	8.764	8.769	
77.0	8.775	8.781	8.786	8.792	8.798	8.803	8.809	8.815	8.820	8.826	
78.0	8.832	8.837	8.843	8.849	8.854	8.860	8.866	8.871	8.877	8.883	
79.0	8.888	8.894	8.899	8.905	8.911	8.916	8.922	8.927	8.933	8.939	
80.0	8.944	8.950	8.955	8.961	8.967	8.972	8.978	8.983	8.989	8.994	5
81.0	9.000	9.006	9.011	9.017	9.022	9.028	9.033	9.039	9.044	9.050	
82.0	9.055	9.061	9.066	9.072	9.077	9.083	9.088	9.094	9.099	9.105	
83.0	9.110	9.116	9.121	9.127	9.132	9.138	9.143	9.149	9.154	9.160	
84.0	9.165	9.171	9.176	9.182	9.187	9.192	9.198	9.203	9.209	9.214	
85.0	9.220	9.225	9.230	9.236	9.241	9.247	9.252	9.257	9.263	9.268	
86.0	9.274	9.279	9.284	9.290	9.295	9.301	9.306	9.311	9.317	9.322	
87.0	9.327	9.333	9.338	9.343	9.349	9.354	9.359	9.365	9.370	9.375	
88.0	9.381	9.386	9.391	9.397	9.402	9.407	9.413	9.418	9.423	9.429	
89.0	9.434	9.439	9.445	9.450	9.455	9.460	9.466	9.471	9.476	9.482	
90.0	9.487	9.492	9.497	9.503	9.508	9.513	9.518	9.524	9.529	9.534	
91.0	9.539	9.545	9.550	9.555	9.560	9.566	9.571	9.576	9.581	9.586	
92.0	9.592	9.597	9.602	9.607	9.612	9.618	9.623	9.628	9.633	9.638	
93.0	9.644	9.649	9.654	9.659	9.664	9.670	9.675	9.680	9.685	9.690	
94.0	9.695	9.701	9.706	9.711	9.716	9.721	9.726	9.731	9.737	9.742	
95.0	9.747	9.752	9.757	9.762	9.767	9.772	9.778	9.783	9.788	9.793	
96.0	9.798	9.803	9.808	9.813	9.818	9.823	9.829	9.834	9.839	9.844	
97.0	9.849	9.854	9.859	9.864	9.869	9.874	9.879	9.884	9.889	9.894	
98.0	9.899	9.905	9.910	9.915	9.920	9.925	9.930	9.935	9.940	9.945	
99.0	9.950	9.955	9.960	9.965	9.970	9.975	9.980	9.985	9.990	9.995	

SQUARE ROOTS OF CERTAIN FRACTIONS

<i>N</i>	\sqrt{N}	<i>N</i>	\sqrt{N}	<i>N</i>	\sqrt{N}	<i>N</i>	\sqrt{N}	<i>N</i>	\sqrt{N}	<i>N</i>	\sqrt{N}
$\frac{1}{2}$	0.7071	$\frac{3}{5}$	0.7746	$\frac{4}{7}$	0.7559	$\frac{1}{9}$	0.3333	$\frac{5}{12}$	0.6455	$\frac{9}{16}$	0.7500
$\frac{1}{3}$	0.5774	$\frac{4}{5}$	0.8944	$\frac{5}{7}$	0.8452	$\frac{2}{9}$	0.4714	$\frac{7}{12}$	0.7638	$\frac{11}{16}$	0.8292
$\frac{2}{3}$	0.8165	$\frac{1}{6}$	0.4082	$\frac{6}{7}$	0.9258	$\frac{4}{9}$	0.6667	$\frac{11}{12}$	0.9574	$\frac{13}{16}$	0.9014
$\frac{1}{4}$	0.5000	$\frac{5}{6}$	0.9129	$\frac{1}{8}$	0.3536	$\frac{5}{9}$	0.7454	$\frac{1}{16}$	0.2500	$\frac{15}{16}$	0.9682
$\frac{3}{4}$	0.8660	$\frac{1}{7}$	0.3780	$\frac{3}{8}$	0.6124	$\frac{7}{9}$	0.8819	$\frac{3}{16}$	0.4330	$\frac{1}{32}$	0.1768
$\frac{1}{5}$	0.4472	$\frac{2}{7}$	0.5345	$\frac{5}{8}$	0.7906	$\frac{8}{9}$	0.9428	$\frac{5}{16}$	0.5590	$\frac{1}{64}$	0.1250
$\frac{2}{5}$	0.6325	$\frac{3}{7}$	0.6547	$\frac{7}{8}$	0.9354	$\frac{1}{12}$	0.2887	$\frac{7}{16}$	0.6614	$\frac{1}{50}$	0.1414

TABLE 1.4—CUBE ROOTS OF NUMBERS

<i>N</i>	0	1	2	3	4	5	6	7	8	9	Average Difference
1.0	1.000	1.003	1.007	1.010	1.013	1.016	1.020	1.023	1.026	1.029	3
1.1	1.032	1.035	1.038	1.042	1.045	1.048	1.051	1.054	1.057	1.060	
1.2	1.063	1.066	1.069	1.071	1.074	1.077	1.080	1.083	1.086	1.089	
1.3	1.091	1.094	1.097	1.100	1.102	1.105	1.108	1.111	1.113	1.116	
1.4	1.119	1.121	1.124	1.127	1.129	1.132	1.134	1.137	1.140	1.142	
1.5	1.145	1.147	1.150	1.152	1.155	1.157	1.160	1.162	1.165	1.167	2
1.6	1.170	1.172	1.174	1.177	1.179	1.182	1.184	1.186	1.189	1.191	
1.7	1.193	1.196	1.198	1.200	1.203	1.205	1.207	1.210	1.212	1.214	
1.8	1.216	1.219	1.221	1.223	1.225	1.228	1.230	1.232	1.234	1.236	
1.9	1.239	1.241	1.243	1.245	1.247	1.249	1.251	1.254	1.256	1.258	
2.0	1.260	1.262	1.264	1.266	1.268	1.270	1.272	1.274	1.277	1.279	
2.1	1.281	1.283	1.285	1.287	1.289	1.291	1.293	1.295	1.297	1.299	
2.2	1.301	1.303	1.305	1.306	1.308	1.310	1.312	1.314	1.316	1.318	
2.3	1.320	1.322	1.324	1.326	1.328	1.330	1.331	1.333	1.335	1.337	
2.4	1.339	1.341	1.343	1.344	1.346	1.348	1.350	1.352	1.354	1.355	
2.5	1.357	1.359	1.361	1.363	1.364	1.366	1.368	1.370	1.372	1.373	
2.6	1.375	1.377	1.379	1.380	1.382	1.384	1.386	1.387	1.389	1.391	
2.7	1.392	1.394	1.396	1.398	1.399	1.401	1.403	1.404	1.406	1.408	
2.8	1.409	1.411	1.413	1.414	1.416	1.418	1.419	1.421	1.423	1.424	
2.9	1.426	1.428	1.429	1.431	1.433	1.434	1.436	1.437	1.439	1.441	
3.0	1.442	1.444	1.445	1.447	1.449	1.450	1.452	1.453	1.455	1.457	
3.1	1.458	1.460	1.461	1.463	1.464	1.466	1.467	1.469	1.471	1.472	
3.2	1.474	1.475	1.477	1.478	1.480	1.481	1.483	1.484	1.486	1.487	
3.3	1.489	1.490	1.492	1.493	1.495	1.496	1.498	1.499	1.501	1.502	
3.4	1.504	1.505	1.507	1.508	1.510	1.511	1.512	1.514	1.515	1.517	
3.5	1.518	1.520	1.521	1.523	1.524	1.525	1.527	1.528	1.530	1.531	1
3.6	1.533	1.534	1.535	1.537	1.538	1.540	1.541	1.542	1.544	1.545	
3.7	1.547	1.548	1.549	1.551	1.552	1.554	1.555	1.556	1.558	1.559	
3.8	1.560	1.562	1.563	1.565	1.566	1.567	1.569	1.570	1.571	1.573	
3.9	1.574	1.575	1.577	1.578	1.579	1.581	1.582	1.583	1.585	1.586	
4.0	1.587	1.589	1.590	1.591	1.593	1.594	1.595	1.597	1.598	1.599	
4.1	1.601	1.602	1.603	1.604	1.606	1.607	1.608	1.610	1.611	1.612	
4.2	1.613	1.615	1.616	1.617	1.619	1.620	1.621	1.622	1.624	1.625	
4.3	1.626	1.627	1.629	1.630	1.631	1.632	1.634	1.635	1.636	1.637	
4.4	1.639	1.640	1.641	1.642	1.644	1.645	1.646	1.647	1.649	1.650	
4.5	1.651	1.652	1.653	1.655	1.656	1.657	1.658	1.659	1.661	1.662	
4.6	1.663	1.664	1.666	1.667	1.668	1.669	1.670	1.671	1.673	1.674	
4.7	1.675	1.676	1.677	1.679	1.680	1.681	1.682	1.683	1.685	1.686	
4.8	1.687	1.688	1.689	1.690	1.692	1.693	1.694	1.695	1.696	1.697	
4.9	1.698	1.700	1.701	1.702	1.703	1.704	1.705	1.707	1.708	1.709	
5.0	1.710	1.711	1.712	1.713	1.715	1.716	1.717	1.718	1.719	1.720	
5.1	1.721	1.722	1.724	1.725	1.726	1.727	1.728	1.729	1.730	1.731	
5.2	1.732	1.734	1.735	1.736	1.737	1.738	1.739	1.740	1.741	1.742	
5.3	1.744	1.745	1.746	1.747	1.748	1.749	1.750	1.751	1.752	1.753	
5.4	1.754	1.755	1.757	1.758	1.759	1.760	1.761	1.762	1.763	1.764	
5.5	1.765	1.766	1.767	1.768	1.769	1.771	1.772	1.773	1.774	1.775	
5.6	1.776	1.777	1.778	1.779	1.780	1.781	1.782	1.783	1.784	1.785	
5.7	1.786	1.787	1.788	1.789	1.790	1.792	1.793	1.794	1.795	1.796	
5.8	1.797	1.798	1.799	1.800	1.801	1.802	1.803	1.804	1.805	1.806	
5.9	1.807	1.808	1.809	1.810	1.811	1.812	1.813	1.814	1.815	1.816	
6.0	1.817	1.818	1.819	1.820	1.821	1.822	1.823	1.824	1.825	1.826	
6.1	1.827	1.828	1.829	1.830	1.831	1.832	1.833	1.834	1.835	1.836	
6.2	1.837	1.838	1.839	1.840	1.841	1.842	1.843	1.844	1.845	1.846	
6.3	1.847	1.848	1.849	1.850	1.851	1.852	1.853	1.854	1.855	1.856	
6.4	1.857	1.858	1.859	1.860	1.860	1.861	1.862	1.863	1.864	1.865	
6.5	1.866	1.867	1.868	1.869	1.870	1.871	1.872	1.873	1.874	1.875	
6.6	1.876	1.877	1.878	1.879	1.880	1.881	1.881	1.882	1.883	1.884	
6.7	1.885	1.886	1.887	1.888	1.889	1.890	1.891	1.892	1.893	1.894	
6.8	1.895	1.895	1.896	1.897	1.898	1.899	1.900	1.901	1.902	1.903	
6.9	1.904	1.905	1.906	1.907	1.907	1.908	1.909	1.910	1.911	1.912	

Explanation of Table of Cube Roots

This table gives the value of $\sqrt[3]{N}$ for values of N from 1 to 1,000, correct to four figures. (Interpolated values may be in error by 1 in the fourth figure).

To find the square root of a number N outside the range from 1 to 1,000, divide the digits of the number into blocks of three (beginning with the decimal point), and note that moving the decimal point *three* places in column N is equivalent to moving it *one* place in the cube root of N . For example, $\sqrt[3]{2.718} = 1.396$, $\sqrt[3]{27.18} = 3.007$, $\sqrt[3]{271.8} = 6.477$, $\sqrt[3]{2,718} = 13.96$, $\sqrt[3]{27,180} = 30.07$, $\sqrt[3]{271,800} = 64.77$, $\sqrt[3]{0.00002718} = 0.01396$, $\sqrt[3]{0.0002718} = 0.03007$, and $\sqrt[3]{0.0002718} = 0.06477$.

TABLE 1.4—CUBE ROOTS OF NUMBERS (continued)

<i>N</i>	0	1	2	3	4	5	6	7	8	9	Average Difference
7.0	1.913	1.914	1.915	1.916	1.917	1.917	1.918	1.919	1.920	1.921	1
7.1	1.922	1.923	1.924	1.925	1.926	1.926	1.927	1.928	1.929	1.930	
7.2	1.931	1.932	1.933	1.934	1.935	1.935	1.936	1.937	1.938	1.939	
7.3	1.940	1.941	1.942	1.943	1.943	1.944	1.945	1.946	1.947	1.948	
7.4	1.949	1.950	1.950	1.951	1.952	1.953	1.954	1.955	1.956	1.957	
7.5	1.957	1.958	1.959	1.960	1.961	1.962	1.963	1.964	1.964	1.965	
7.6	1.966	1.967	1.968	1.969	1.970	1.970	1.971	1.972	1.973	1.974	
7.7	1.975	1.976	1.976	1.977	1.978	1.979	1.980	1.981	1.981	1.982	
7.8	1.983	1.984	1.985	1.986	1.987	1.987	1.988	1.989	1.990	1.991	
7.9	1.992	1.992	1.993	1.994	1.995	1.996	1.997	1.997	1.998	1.999	
8.0	2.000	2.001	2.002	2.002	2.003	2.004	2.005	2.006	2.007	2.007	
8.1	2.008	2.009	2.010	2.011	2.012	2.012	2.013	2.014	2.015	2.016	
8.2	2.017	2.017	2.018	2.019	2.020	2.021	2.021	2.022	2.023	2.024	
8.3	2.025	2.026	2.026	2.027	2.028	2.029	2.030	2.030	2.031	2.032	
8.4	2.033	2.034	2.034	2.035	2.036	2.037	2.038	2.038	2.039	2.040	
8.5	2.041	2.042	2.042	2.043	2.044	2.045	2.046	2.046	2.047	2.048	
8.6	2.049	2.050	2.050	2.051	2.052	2.053	2.054	2.054	2.055	2.056	
8.7	2.057	2.057	2.058	2.059	2.060	2.061	2.061	2.062	2.063	2.064	
8.8	2.065	2.065	2.066	2.067	2.068	2.068	2.069	2.070	2.071	2.072	
8.9	2.072	2.073	2.074	2.075	2.075	2.076	2.077	2.078	2.079	2.079	
9.0	2.080	2.081	2.082	2.082	2.083	2.084	2.085	2.085	2.086	2.087	
9.1	2.088	2.089	2.089	2.090	2.091	2.092	2.092	2.093	2.094	2.095	
9.2	2.095	2.096	2.097	2.098	2.098	2.099	2.100	2.101	2.101	2.102	
9.3	2.103	2.104	2.104	2.105	2.106	2.107	2.107	2.108	2.109	2.110	
9.4	2.110	2.111	2.112	2.113	2.113	2.114	2.115	2.116	2.116	2.117	
9.5	2.118	2.119	2.119	2.120	2.121	2.122	2.122	2.123	2.124	2.125	
9.6	2.125	2.126	2.127	2.128	2.128	2.129	2.130	2.130	2.131	2.132	
9.7	2.133	2.133	2.134	2.135	2.136	2.136	2.137	2.138	2.139	2.139	
9.8	2.140	2.141	2.141	2.142	2.143	2.144	2.144	2.145	2.146	2.147	
9.9	2.147	2.148	2.149	2.149	2.150	2.151	2.152	2.152	2.153	2.154	
10.0	2.154	2.162	2.169	2.176	2.183	2.190	2.197	2.204	2.210	2.217	7
11.0	2.224	2.231	2.237	2.244	2.251	2.257	2.264	2.270	2.277	2.283	6
12.0	2.289	2.296	2.302	2.308	2.315	2.321	2.327	2.333	2.339	2.345	
13.0	2.351	2.357	2.363	2.369	2.375	2.381	2.387	2.393	2.399	2.404	
14.0	2.410	2.416	2.422	2.427	2.433	2.438	2.444	2.450	2.455	2.461	
15.0	2.466	2.472	2.477	2.483	2.488	2.493	2.499	2.504	2.509	2.515	5
16.0	2.520	2.525	2.530	2.535	2.541	2.546	2.551	2.556	2.561	2.566	
17.0	2.571	2.576	2.581	2.586	2.591	2.596	2.601	2.606	2.611	2.616	
18.0	2.621	2.626	2.630	2.635	2.640	2.645	2.650	2.654	2.659	2.664	
19.0	2.668	2.673	2.678	2.682	2.687	2.692	2.696	2.701	2.705	2.710	
20.0	2.714	2.719	2.723	2.728	2.732	2.737	2.741	2.746	2.750	2.755	4
21.0	2.759	2.763	2.768	2.772	2.776	2.781	2.785	2.789	2.794	2.798	
22.0	2.802	2.806	2.811	2.815	2.819	2.823	2.827	2.831	2.836	2.840	
23.0	2.844	2.848	2.852	2.856	2.860	2.864	2.868	2.872	2.876	2.880	
24.0	2.884	2.888	2.892	2.896	2.900	2.904	2.908	2.912	2.916	2.920	
25.0	2.924	2.928	2.932	2.936	2.940	2.943	2.947	2.951	2.955	2.959	
26.0	2.962	2.966	2.970	2.974	2.978	2.981	2.985	2.989	2.993	2.996	
27.0	3.000	3.004	3.007	3.011	3.015	3.018	3.022	3.026	3.029	3.033	
28.0	3.037	3.040	3.044	3.047	3.051	3.055	3.058	3.062	3.065	3.069	
29.0	3.072	3.076	3.079	3.083	3.086	3.090	3.093	3.097	3.100	3.104	
30.0	3.107	3.111	3.114	3.118	3.121	3.124	3.128	3.131	3.135	3.138	3
31.0	3.141	3.145	3.148	3.151	3.155	3.158	3.162	3.165	3.168	3.171	
32.0	3.175	3.178	3.181	3.185	3.188	3.191	3.195	3.198	3.201	3.204	
33.0	3.208	3.211	3.214	3.217	3.220	3.224	3.227	3.230	3.233	3.236	
34.0	3.240	3.243	3.246	3.249	3.252	3.255	3.259	3.262	3.265	3.268	
35.0	3.271	3.274	3.277	3.280	3.283	3.287	3.290	3.293	3.296	3.299	
36.0	3.302	3.305	3.308	3.311	3.314	3.317	3.320	3.323	3.326	3.329	
37.0	3.332	3.335	3.338	3.341	3.344	3.347	3.350	3.353	3.356	3.359	
38.0	3.362	3.365	3.368	3.371	3.374	3.377	3.380	3.382	3.385	3.388	
39.0	3.391	3.394	3.397	3.400	3.403	3.406	3.409	3.411	3.414	3.417	

$$\sqrt[3]{\pi} = 1.46459 \text{ and } 1/\sqrt[3]{\pi} = 0.682784.$$

(continued on next page)

TABLE 1.4—CUBE ROOTS OF NUMBERS (continued)

<i>N</i>	0	1	2	3	4	5	6	7	8	9	Average Difference
40.0	3.420	3.423	3.426	3.428	3.431	3.434	3.437	3.440	3.443	3.445	3
41.0	3.448	3.451	3.454	3.457	3.459	3.462	3.465	3.468	3.471	3.473	
42.0	3.476	3.479	3.482	3.484	3.487	3.490	3.493	3.495	3.498	3.501	
43.0	3.503	3.506	3.509	3.512	3.514	3.517	3.520	3.522	3.525	3.528	
44.0	3.530	3.533	3.536	3.538	3.541	3.544	3.546	3.549	3.552	3.554	
45.0	3.557	3.560	3.562	3.565	3.567	3.570	3.573	3.575	3.578	3.580	2
46.0	3.583	3.586	3.588	3.591	3.593	3.596	3.599	3.601	3.604	3.606	
47.0	3.609	3.611	3.614	3.616	3.619	3.622	3.624	3.627	3.629	3.632	
48.0	3.634	3.637	3.639	3.642	3.644	3.647	3.649	3.652	3.654	3.657	
49.0	3.659	3.662	3.664	3.667	3.669	3.672	3.674	3.677	3.679	3.682	
50.0	3.684	3.686	3.689	3.691	3.694	3.696	3.699	3.701	3.704	3.706	
51.0	3.708	3.711	3.713	3.716	3.718	3.721	3.723	3.725	3.728	3.730	
52.0	3.733	3.735	3.737	3.740	3.742	3.744	3.747	3.749	3.752	3.754	
53.0	3.756	3.759	3.761	3.763	3.766	3.768	3.770	3.773	3.775	3.777	
54.0	3.780	3.782	3.784	3.787	3.789	3.791	3.794	3.796	3.798	3.801	
55.0	3.803	3.805	3.808	3.810	3.812	3.814	3.817	3.819	3.821	3.824	
56.0	3.826	3.828	3.830	3.833	3.835	3.837	3.839	3.842	3.844	3.846	
57.0	3.849	3.851	3.853	3.855	3.857	3.860	3.862	3.864	3.866	3.869	
58.0	3.871	3.873	3.875	3.878	3.880	3.882	3.884	3.886	3.889	3.891	
59.0	3.893	3.895	3.897	3.900	3.902	3.904	3.906	3.908	3.911	3.913	
60.0	3.915	3.917	3.919	3.921	3.924	3.926	3.928	3.930	3.932	3.934	
61.0	3.936	3.939	3.941	3.943	3.945	3.947	3.949	3.951	3.954	3.956	
62.0	3.958	3.960	3.962	3.964	3.966	3.968	3.971	3.973	3.975	3.977	
63.0	3.979	3.981	3.983	3.985	3.987	3.990	3.992	3.994	3.996	3.998	
64.0	4.000	4.002	4.004	4.006	4.008	4.010	4.012	4.015	4.017	4.019	
65.0	4.021	4.023	4.025	4.027	4.029	4.031	4.033	4.035	4.037	4.039	
66.0	4.041	4.043	4.045	4.047	4.049	4.051	4.053	4.055	4.058	4.060	
67.0	4.062	4.064	4.066	4.068	4.070	4.072	4.074	4.076	4.078	4.080	
68.0	4.082	4.084	4.086	4.088	4.090	4.092	4.094	4.096	4.098	4.100	
69.0	4.102	4.104	4.106	4.108	4.109	4.111	4.113	4.115	4.117	4.119	
70.0	4.121	4.123	4.125	4.127	4.129	4.131	4.133	4.135	4.137	4.139	
71.0	4.141	4.143	4.145	4.147	4.149	4.151	4.152	4.154	4.156	4.158	
72.0	4.160	4.162	4.164	4.166	4.168	4.170	4.172	4.174	4.176	4.177	
73.0	4.179	4.181	4.183	4.185	4.187	4.189	4.191	4.193	4.195	4.196	
74.0	4.198	4.200	4.202	4.204	4.206	4.208	4.210	4.212	4.213	4.215	
75.0	4.217	4.219	4.221	4.223	4.225	4.227	4.228	4.230	4.232	4.234	
76.0	4.236	4.238	4.240	4.241	4.243	4.245	4.247	4.249	4.251	4.252	
77.0	4.254	4.256	4.258	4.260	4.262	4.264	4.265	4.267	4.269	4.271	
78.0	4.273	4.274	4.276	4.278	4.280	4.282	4.284	4.285	4.287	4.289	
79.0	4.291	4.293	4.294	4.296	4.298	4.300	4.302	4.303	4.305	4.307	
80.0	4.309	4.311	4.312	4.314	4.316	4.318	4.320	4.321	4.323	4.325	
81.0	4.327	4.329	4.330	4.332	4.334	4.336	4.337	4.339	4.341	4.343	
82.0	4.344	4.346	4.348	4.350	4.352	4.353	4.355	4.357	4.359	4.360	
83.0	4.362	4.364	4.366	4.367	4.369	4.371	4.373	4.374	4.376	4.378	
84.0	4.380	4.381	4.383	4.385	4.386	4.388	4.390	4.392	4.393	4.395	
85.0	4.397	4.399	4.400	4.402	4.404	4.405	4.407	4.409	4.411	4.412	
86.0	4.414	4.416	4.417	4.419	4.421	4.423	4.424	4.426	4.428	4.429	
87.0	4.431	4.433	4.434	4.436	4.438	4.440	4.441	4.443	4.445	4.446	
88.0	4.448	4.450	4.451	4.453	4.455	4.456	4.458	4.460	4.461	4.463	
89.0	4.465	4.466	4.468	4.470	4.471	4.473	4.475	4.476	4.478	4.480	
90.0	4.481	4.483	4.485	4.486	4.488	4.490	4.491	4.493	4.495	4.496	
91.0	4.498	4.500	4.501	4.503	4.505	4.506	4.508	4.509	4.511	4.513	
92.0	4.514	4.516	4.518	4.519	4.521	4.523	4.524	4.526	4.527	4.529	
93.0	4.531	4.532	4.534	4.536	4.537	4.539	4.540	4.542	4.544	4.545	
94.0	4.547	4.548	4.550	4.552	4.553	4.555	4.556	4.558	4.560	4.561	
95.0	4.563	4.565	4.566	4.568	4.569	4.571	4.572	4.574	4.576	4.577	
96.0	4.579	4.580	4.582	4.584	4.585	4.587	4.588	4.590	4.592	4.593	
97.0	4.595	4.596	4.598	4.599	4.601	4.603	4.604	4.606	4.607	4.609	
98.0	4.610	4.612	4.614	4.615	4.617	4.618	4.620	4.621	4.623	4.625	
99.0	4.626	4.628	4.629	4.631	4.632	4.634	4.635	4.637	4.638	4.640	

$$\sqrt[3]{\pi} = 1.46459 \text{ and } 1/\sqrt[3]{\pi} = 0.682784.$$

TABLE 1.4—CUBE ROOTS OF NUMBERS (continued)

N	0	1	2	3	4	5	6	7	8	9	Average Difference
Cube roots of numbers from 100.0 to 499.0											
10	4.642	4.657	4.672	4.688	4.703	4.718	4.733	4.747	4.762	4.777	15
11	4.791	4.806	4.820	4.835	4.849	4.863	4.877	4.891	4.905	4.919	14
12	4.932	4.946	4.960	4.973	4.987	5.000	5.013	5.027	5.040	5.053	13
13	5.066	5.079	5.092	5.104	5.117	5.130	5.143	5.155	5.168	5.180	
14	5.192	5.205	5.217	5.229	5.241	5.254	5.266	5.278	5.290	5.301	12
15	5.313	5.325	5.337	5.348	5.360	5.372	5.383	5.395	5.406	5.418	
16	5.429	5.440	5.451	5.463	5.474	5.485	5.496	5.507	5.518	5.529	11
17	5.540	5.550	5.561	5.572	5.583	5.593	5.604	5.615	5.625	5.636	
18	5.646	5.657	5.667	5.677	5.688	5.698	5.708	5.718	5.729	5.739	10
19	5.749	5.759	5.769	5.779	5.789	5.799	5.809	5.819	5.829	5.838	
20	5.848	5.858	5.867	5.877	5.887	5.896	5.906	5.915	5.925	5.934	
21	5.944	5.953	5.963	5.972	5.981	5.991	6.000	6.009	6.018	6.028	9
22	6.037	6.046	6.055	6.064	6.073	6.082	6.091	6.100	6.109	6.118	
23	6.127	6.136	6.145	6.153	6.162	6.171	6.180	6.188	6.197	6.206	
24	6.214	6.223	6.232	6.240	6.249	6.257	6.266	6.274	6.283	6.291	
25	6.300	6.308	6.316	6.325	6.333	6.341	6.350	6.358	6.366	6.374	8
26	6.383	6.391	6.399	6.407	6.415	6.423	6.431	6.439	6.447	6.455	
27	6.463	6.471	6.479	6.487	6.495	6.503	6.511	6.519	6.527	6.534	
28	6.542	6.550	6.558	6.565	6.573	6.581	6.589	6.596	6.604	6.611	
29	6.619	6.627	6.634	6.642	6.649	6.657	6.664	6.672	6.679	6.687	
30	6.694	6.702	6.709	6.717	6.724	6.731	6.739	6.746	6.753	6.761	7
31	6.768	6.775	6.782	6.790	6.797	6.804	6.811	6.818	6.826	6.833	
32	6.840	6.847	6.854	6.861	6.868	6.875	6.882	6.889	6.896	6.903	
33	6.901	6.917	6.924	6.931	6.938	6.945	6.952	6.959	6.966	6.973	
34	6.980	6.986	6.993	7.000	7.007	7.014	7.020	7.027	7.034	7.041	
35	7.047	7.054	7.061	7.067	7.074	7.081	7.087	7.094	7.101	7.107	
36	7.114	7.120	7.127	7.133	7.140	7.147	7.153	7.160	7.166	7.173	6
37	7.179	7.186	7.192	7.198	7.205	7.211	7.218	7.224	7.230	7.237	
38	7.243	7.250	7.256	7.262	7.268	7.275	7.281	7.287	7.294	7.300	
39	7.306	7.312	7.319	7.325	7.331	7.337	7.343	7.350	7.356	7.362	
40	7.368	7.374	7.380	7.386	7.393	7.399	7.405	7.411	7.417	7.423	
41	7.429	7.435	7.441	7.447	7.453	7.459	7.465	7.471	7.477	7.483	
42	7.489	7.495	7.501	7.507	7.513	7.518	7.524	7.530	7.536	7.542	
43	7.548	7.554	7.560	7.565	7.571	7.577	7.583	7.589	7.594	7.600	
44	7.606	7.612	7.617	7.623	7.629	7.635	7.640	7.646	7.652	7.657	
45	7.663	7.669	7.674	7.680	7.686	7.691	7.697	7.703	7.708	7.714	5
46	7.719	7.725	7.731	7.736	7.742	7.747	7.753	7.758	7.764	7.769	
47	7.775	7.780	7.786	7.791	7.797	7.802	7.808	7.813	7.819	7.824	
48	7.830	7.835	7.841	7.846	7.851	7.857	7.862	7.868	7.873	7.878	
49	7.884	7.889	7.894	7.900	7.905	7.910	7.916	7.921	7.926	7.932	
Cube roots of numbers from 500.0 to 1,000.0											
50	7.937	7.942	7.948	7.953	7.958	7.963	7.969	7.974	7.979	7.984	5
51	7.990	7.995	8.000	8.005	8.010	8.016	8.021	8.026	8.031	8.036	
52	8.041	8.047	8.052	8.057	8.062	8.067	8.072	8.077	8.082	8.088	
53	8.093	8.098	8.103	8.108	8.113	8.118	8.123	8.128	8.133	8.138	
54	8.143	8.148	8.153	8.158	8.163	8.168	8.173	8.178	8.183	8.188	
55	8.193	8.198	8.203	8.208	8.213	8.218	8.223	8.228	8.233	8.238	
56	8.243	8.247	8.252	8.257	8.262	8.267	8.272	8.277	8.282	8.286	
57	8.291	8.296	8.301	8.306	8.311	8.316	8.320	8.325	8.330	8.335	
58	8.340	8.344	8.349	8.354	8.359	8.363	8.368	8.373	8.378	8.382	
59	8.387	8.392	8.397	8.401	8.406	8.411	8.416	8.420	8.425	8.430	
60	8.434	8.439	8.444	8.448	8.453	8.458	8.462	8.467	8.472	8.476	
61	8.481	8.486	8.490	8.495	8.499	8.504	8.509	8.513	8.518	8.522	
62	8.527	8.532	8.536	8.541	8.545	8.550	8.554	8.559	8.564	8.568	
63	8.573	8.577	8.582	8.586	8.591	8.595	8.600	8.604	8.609	8.613	4
64	8.618	8.622	8.627	8.631	8.636	8.640	8.645	8.649	8.653	8.658	
65	8.662	8.667	8.671	8.676	8.680	8.685	8.689	8.693	8.698	8.702	
66	8.707	8.711	8.715	8.720	8.724	8.729	8.733	8.737	8.742	8.746	
67	8.750	8.755	8.759	8.763	8.768	8.772	8.776	8.781	8.785	8.789	
68	8.794	8.798	8.802	8.807	8.811	8.815	8.819	8.824	8.828	8.832	
69	8.837	8.841	8.845	8.849	8.854	8.858	8.862	8.866	8.871	8.875	

$$\sqrt[3]{x} = 1.46459 \text{ and } 1/\sqrt[3]{x} = 0.682784.$$

(continued on next page)

TABLE 1.4—CUBE ROOTS OF NUMBERS (continued)

<i>N</i>	0	1	2	3	4	5	6	7	8	9	Average Difference
70	8.879	8.883	8.887	8.892	8.896	8.900	8.904	8.909	8.913	8.917	4
71	8.921	8.925	8.929	8.934	8.938	8.942	8.946	8.950	8.955	8.959	
72	8.963	8.967	8.971	8.975	8.979	8.984	8.988	8.992	8.996	9.000	
73	9.004	9.008	9.012	9.016	9.021	9.025	9.029	9.033	9.037	9.041	
74	9.045	9.049	9.053	9.057	9.061	9.065	9.069	9.073	9.078	9.082	
75	9.086	9.090	9.094	9.098	9.102	9.106	9.110	9.114	9.118	9.122	
76	9.126	9.130	9.134	9.138	9.142	9.146	9.150	9.154	9.158	9.162	
77	9.166	9.170	9.174	9.178	9.182	9.185	9.189	9.193	9.197	9.201	
78	9.205	9.209	9.213	9.217	9.221	9.225	9.229	9.233	9.237	9.240	
79	9.244	9.248	9.252	9.256	9.260	9.264	9.268	9.272	9.275	9.279	
80	9.283	9.287	9.291	9.295	9.299	9.302	9.306	9.310	9.314	9.318	
81	9.322	9.326	9.329	9.333	9.337	9.341	9.345	9.348	9.352	9.356	
82	9.360	9.364	9.368	9.371	9.375	9.379	9.383	9.386	9.390	9.394	
83	9.398	9.402	9.405	9.409	9.413	9.417	9.420	9.424	9.428	9.432	
84	9.435	9.439	9.443	9.447	9.450	9.454	9.458	9.462	9.465	9.469	
85	9.473	9.476	9.480	9.484	9.488	9.491	9.495	9.499	9.502	9.506	
86	9.510	9.513	9.517	9.521	9.524	9.528	9.532	9.535	9.539	9.543	
87	9.546	9.550	9.554	9.557	9.561	9.565	9.568	9.572	9.576	9.579	
88	9.583	9.586	9.590	9.594	9.597	9.601	9.605	9.608	9.612	9.615	
89	9.619	9.623	9.626	9.630	9.633	9.637	9.641	9.644	9.648	9.651	
90	9.655	9.658	9.662	9.666	9.669	9.673	9.676	9.680	9.683	9.687	
91	9.691	9.694	9.698	9.701	9.705	9.708	9.712	9.715	9.719	9.722	
92	9.726	9.729	9.733	9.736	9.740	9.743	9.747	9.750	9.754	9.758	
93	9.761	9.764	9.768	9.771	9.775	9.778	9.782	9.785	9.789	9.792	
94	9.796	9.799	9.803	9.806	9.810	9.813	9.817	9.820	9.824	9.827	
95	9.830	9.834	9.837	9.841	9.844	9.848	9.851	9.855	9.858	9.861	
96	9.865	9.868	9.872	9.875	9.879	9.882	9.885	9.889	9.892	9.896	
97	9.899	9.902	9.906	9.909	9.913	9.916	9.919	9.923	9.926	9.930	
98	9.933	9.936	9.940	9.943	9.946	9.950	9.953	9.956	9.960	9.963	
99	9.967	9.970	9.973	9.977	9.980	9.983	9.987	9.990	9.993	9.997	
100	10.00										

CUBE ROOTS OF CERTAIN FRACTIONS

<i>N</i>	$\sqrt[3]{N}$	<i>N</i>	$\sqrt[3]{N}$	<i>N</i>	$\sqrt[3]{N}$	<i>N</i>	$\sqrt[3]{N}$	<i>N</i>	$\sqrt[3]{N}$	<i>N</i>	$\sqrt[3]{N}$
1/2	0.7937	3/5	0.8434	4/7	0.8298	1/9	0.4807	5/12	0.7469	9/16	0.8255
1/3	0.6934	4/5	0.9283	5/7	0.8939	2/9	0.6057	7/12	0.8355	11/16	0.8826
2/3	0.8736	1/6	0.5503	6/7	0.9499	4/9	0.7631	1 1/12	0.9714	13/16	0.9331
1/4	0.6300	5/6	0.9410	1/8	0.5000	5/9	0.8221	1/16	0.3969	15/16	0.9787
3/4	0.9086	1/7	0.5228	3/8	0.7211	7/9	0.9196	3/16	0.5724	1/32	0.3150
1/5	0.5848	2/7	0.6586	5/8	0.8550	8/9	0.9615	5/16	0.6786	1/64	0.2500
2/5	0.7368	3/7	0.7539	7/8	0.9565	1/12	0.4368	7/16	0.7591	1/60	0.2714

$$\sqrt[3]{\pi} = 1.46459 \text{ and } 1/\sqrt[3]{\pi} = 0.682784.$$

TABLE 1.5—THREE-HALVES POWERS OF NUMBERS

<i>N</i>	0	1	2	3	4	5	6	7	8	9	Average Difference
1.0	1.000	1.154	1.315	1.482	1.657	1.837	2.024	2.217	2.415	2.619	183
2.0	2.828	3.043	3.263	3.488	3.718	3.953	4.192	4.437	4.685	4.939	237
3.0	5.196	5.458	5.724	5.995	6.269	6.548	6.831	7.117	7.408	7.702	280
4.0	8.000	8.302	8.607	8.917	9.230	9.546	9.866	10.190			313
4.0								10.19	10.52	10.85	33
5.0	11.18	11.52	11.86	12.20	12.55	12.90	13.25	13.61	13.97	14.33	35
6.0	14.70	15.07	15.44	15.81	16.19	16.57	16.96	17.34	17.73	18.12	38
7.0	18.52	18.92	19.32	19.72	20.13	20.54	20.95	21.37	21.78	22.20	41
8.0	22.63	23.05	23.48	23.91	24.35	24.78	25.22	25.66	26.11	26.55	44
9.0	27.00	27.45	27.90	28.36	28.82	29.28	29.74	30.21	30.68	31.15	46
10.0	31.62	32.10	32.58	33.06	33.54	34.02	34.51	35.00	35.49	35.99	49
11.0	36.48	36.98	37.48	37.99	38.49	39.00	39.51	40.02	40.53	41.05	51
12.0	41.57	42.09	42.61	43.14	43.66	44.19	44.73	45.26	45.79	46.33	53
13.0	46.87	47.41	47.96	48.50	49.05	49.60	50.15	50.71	51.26	51.82	55
14.0	52.38	52.95	53.51	54.08	54.64	55.21	55.79	56.36	56.94	57.51	57
15.0	58.09	58.68	59.26	59.85	60.43	61.02	61.62	62.21	62.80	63.40	59
16.0	64.00	64.60	65.20	65.81	66.41	67.02	67.63	68.25	68.86	69.48	61
17.0	70.09	70.71	71.33	71.96	72.58	73.21	73.84	74.47	75.10	75.73	63
18.0	76.37	77.00	77.64	78.28	78.93	79.57	80.22	80.87	81.51	82.17	65
19.0	82.82	83.47	84.13	84.79	85.45	86.11	86.77	87.44	88.10	88.77	66
20.0	89.44	90.11	90.79	91.46	92.14	92.82	93.50	94.18	94.86	95.55	68
21.0	96.23	96.92	97.61	98.30	99.00	99.69	100.38				69
21.0							100.4	101.1	101.8	102.5	7
22.0	103.2	103.9	104.6	105.3	106.0	106.7	107.4	108.2	108.9	109.6	7
23.0	110.3	111.0	111.7	112.5	113.2	113.9	114.6	115.4	116.1	116.8	7
24.0	117.6	118.3	119.0	119.8	120.5	121.3	122.0	122.8	123.5	124.3	7
25.0	125.0	125.8	126.5	127.3	128.0	128.8	129.5	130.3	131.0	131.8	8
26.0	132.6	133.3	134.1	134.9	135.6	136.4	137.2	138.0	138.7	139.5	8
27.0	140.3	141.1	141.9	142.6	143.4	144.2	145.0	145.8	146.6	147.4	8
28.0	148.2	149.0	149.8	150.5	151.3	152.1	153.0	153.8	154.6	155.4	8
29.0	156.2	157.0	157.8	158.6	159.4	160.2	161.9	161.9	162.7	163.5	8
30.0	164.3	165.1	166.0	166.8	167.6	168.4	169.3	170.1	170.9	171.8	8
31.0	172.6	173.4	174.3	175.1	176.0	176.8	177.6	178.5	179.3	180.2	8
32.0	181.0	181.9	182.7	183.6	184.4	185.3	186.1	187.0	187.9	188.7	9
33.0	189.6	190.4	191.3	192.2	193.0	193.9	194.8	195.6	196.5	197.4	9
34.0	198.3	199.1	200.0	200.9	201.8	202.6	203.5	204.4	205.3	206.2	9
35.0	207.1	208.0	208.8	209.7	210.6	211.5	212.4	213.3	214.2	215.1	9
36.0	216.0	216.9	217.8	218.7	219.6	220.5	221.4	222.3	223.2	224.2	9
37.0	225.1	226.0	226.9	227.8	228.7	229.6	230.6	231.5	232.4	233.3	9
38.0	234.2	235.2	236.1	237.0	238.0	238.9	239.8	240.8	241.7	242.6	9
39.0	243.6	244.5	245.4	246.4	247.3	248.3	249.2	250.1	251.1	252.0	9
40.0	253.0	253.9	254.9	255.8	256.8	257.7	258.7	259.7	260.6	261.6	10
41.0	262.5	263.5	264.5	265.4	266.4	267.3	268.3	269.3	270.2	271.2	10
42.0	272.2	273.2	274.1	275.1	276.1	277.1	278.0	279.0	280.0	281.0	10
43.0	282.0	283.0	283.9	284.9	285.9	286.9	287.9	288.9	289.9	290.9	10
44.0	291.9	292.9	293.9	294.9	295.9	296.9	297.9	298.9	299.9	300.9	10
45.0	301.9	302.9	303.9	304.9	305.9	306.9	307.9	308.9	310.0	311.0	10
46.0	312.0	313.0	314.0	315.0	316.1	317.1	318.1	319.1	320.2	321.2	10
47.0	322.2	323.2	324.3	325.3	326.3	327.4	328.4	329.4	330.5	331.5	10
48.0	332.6	333.6	334.6	335.7	336.7	337.8	338.8	339.9	340.9	342.0	10
49.0	343.0	344.0	345.1	346.2	347.2	348.3	349.3	350.4	351.4	352.5	11
50.0	353.6	354.6	355.7	356.7	357.8	358.9	359.9	361.0	362.1	363.1	11
51.0	364.2	365.3	366.4	367.4	368.5	369.6	370.7	371.7	372.8	373.9	11
52.0	375.0	376.1	377.1	378.2	379.3	380.4	381.5	382.6	383.7	384.8	11
53.0	385.8	386.9	388.0	389.1	390.2	391.3	392.4	393.5	394.6	395.7	11
54.0	396.8	397.9	399.0	400.1	401.2	402.3	403.4	404.6	405.7	406.8	11
55.0	407.9	409.0	410.1	411.2	412.3	413.5	414.6	415.7	416.8	418.0	11
56.0	419.1	420.2	421.3	422.4	423.6	424.7	425.8	426.9	428.1	429.2	11
57.0	430.3	431.5	432.6	433.7	434.9	436.0	437.1	438.3	439.4	440.6	11
58.0	441.7	442.9	444.0	445.1	446.3	447.4	448.6	449.7	450.9	452.0	11
59.0	453.2	454.3	455.5	456.6	457.8	459.0	460.1	461.3	462.4	463.6	12

Explanation of Table

This table gives $N^{3/2}$ from $N = 1$ to $N = 100$. Moving the decimal point *two* places in N requires moving it *three* places in body of table. For example, $(7.23)^{3/2} = 19.44$, $(723)^{3/2} = 19,440$, $(0.0723)^{3/2} = 0.01944$, $(72.3)^{3/2} = 614.8$, $(7,230)^{3/2} = 614,800$, and $(0.723)^{3/2} = 0.6148$.

Used inversely, this table gives $M^{2/3}$ from $M = 1$ to $M = 1,000$. For example, $(0.6148)^{2/3} = 0.7230$.

(continued on next page)

TABLE 1.5—THREE-HALVES POWERS OF NUMBERS (continued)

<i>N</i>	0	1	2	3	4	5	6	7	8	9	Average Difference
60.0	464.8	465.9	467.1	468.2	469.4	470.6	471.7	472.9	474.1	475.3	12
61.0	476.4	477.6	478.7	479.9	481.1	482.3	483.5	484.6	485.8	487.0	12
62.0	488.2	489.4	490.6	491.7	492.9	494.1	495.3	496.5	497.7	498.9	12
63.0	500.0	501.2	502.4	503.6	504.8	506.0	507.2	508.4	509.6	510.8	12
64.0	512.0	513.2	514.4	515.6	516.8	518.0	519.2	520.4	521.6	522.8	12
65.0	524.0	525.3	526.5	527.7	528.9	530.1	531.3	532.5	533.8	535.0	12
66.0	536.2	537.4	538.6	539.8	541.1	542.3	543.5	544.7	546.0	547.2	12
67.0	548.4	549.6	550.9	552.1	553.3	554.6	555.8	557.0	558.3	559.5	12
68.0	560.7	562.0	563.2	564.5	565.7	566.9	568.2	569.4	570.7	571.9	12
69.0	573.2	574.4	575.7	576.9	578.1	579.4	580.6	581.9	583.2	584.4	13
70.0	585.7	586.9	588.2	589.4	590.7	591.9	593.2	594.5	595.7	597.0	13
71.0	598.3	599.5	600.8	602.1	603.3	604.6	605.9	607.1	608.4	609.7	13
72.0	610.9	612.2	613.5	614.8	616.0	617.3	618.6	619.9	621.2	622.4	13
73.0	623.7	625.0	626.3	627.6	628.8	630.1	631.4	632.7	634.0	635.3	13
74.0	636.6	637.9	639.2	640.4	641.7	643.0	644.3	645.6	646.9	648.2	13
75.0	649.5	650.8	652.1	653.4	654.7	656.0	657.3	658.6	659.9	661.2	13
76.0	662.6	663.9	665.2	666.5	667.8	669.1	670.4	671.7	673.0	674.4	13
77.0	675.7	677.0	678.3	679.6	680.9	682.3	683.6	684.9	686.2	687.6	13
78.0	688.9	690.2	691.5	692.9	694.2	695.5	696.8	698.2	699.5	700.8	13
79.0	702.2	703.5	704.8	706.2	707.5	708.8	710.2	711.5	712.9	714.2	13
80.0	715.5	716.9	718.2	719.6	720.9	722.3	723.6	725.0	726.3	727.7	13
81.0	729.0	730.4	731.7	733.1	734.4	735.8	737.1	738.5	739.8	741.2	14
82.0	742.5	743.9	745.3	746.6	748.0	749.3	750.7	752.1	753.4	754.8	14
83.0	756.2	757.5	758.9	760.3	761.6	763.0	764.4	765.8	767.1	768.5	14
84.0	769.9	771.2	772.6	774.0	775.4	776.8	778.1	779.5	780.9	782.3	14
85.0	783.7	785.0	786.4	787.8	789.2	790.6	792.0	793.4	794.8	796.1	14
86.0	797.5	798.9	800.3	801.7	803.1	804.5	805.9	807.3	808.7	810.1	14
87.0	811.5	812.9	814.3	815.7	817.1	818.5	819.9	821.3	822.7	824.1	14
88.0	825.5	826.9	828.3	829.7	831.1	832.6	834.0	835.4	836.8	838.2	14
89.0	839.6	841.0	842.5	843.9	845.3	846.7	848.1	849.5	851.0	852.4	14
90.0	853.8	855.2	856.7	858.1	859.5	860.9	862.4	863.8	865.2	866.7	14
91.0	868.1	869.5	870.9	872.4	873.8	875.2	876.7	878.1	879.6	881.0	14
92.0	882.4	883.9	885.3	886.8	888.2	889.6	891.1	892.5	894.0	895.4	14
93.0	896.9	898.3	899.8	901.2	902.7	904.1	905.6	907.0	908.5	909.9	15
94.0	911.4	912.8	914.3	915.7	917.2	918.6	920.1	921.6	923.0	924.5	15
95.0	925.9	927.4	928.9	930.3	931.8	933.3	934.7	936.2	937.7	939.1	15
96.0	940.6	942.1	943.5	945.0	946.5	948.0	949.4	950.9	952.4	953.9	15
97.0	955.3	956.8	958.3	959.8	961.3	962.7	964.2	965.7	967.2	968.7	15
98.0	970.2	971.6	973.1	974.6	976.1	977.6	979.1	980.6	982.1	983.5	15
99.0	985.0	986.5	988.0	989.5	991.0	992.5	994.0	995.5	997.0	998.5	15
100.0	1,000.0										

**AUXILIARY TABLE OF TWO-THIRDS POWERS
AND THREE-HALVES POWERS
(to assist in locating the decimal point)**

For complete table of three-halves powers, see preceding. That table, used inversely, provides a complete table of two-thirds powers.

<i>N</i>	$N^{2/3} (= \sqrt[3]{N^2})$	$N^{3/2} (= \sqrt{N^3})$
0.0001	0.002154	0.000001
0.001	0.01	0.00003162
0.01	0.0464	0.001
0.1	0.2154	0.03162278
1.0	1.0	1.0
10.0	4.64	31.62278
100.0	21.54	1,000.0
1,000.0	100.0	31,622.78
10,000.0	464.16	1,000,000.0

TABLE 1.6—RECIPROCAL OF NUMBERS

N^{**}	0	1	2	3	4	5	6	7	8	9	Average Difference
1.00		0.9990	0.9980	0.9970	0.9960	0.9950	0.9940	0.9930	0.9921	0.9911	- 10
1.01	0.9901	0.9891	0.9881	0.9872	0.9862	0.9852	0.9843	0.9833	0.9823	0.9814	
1.02	0.9804	0.9794	0.9785	0.9775	0.9766	0.9756	0.9747	0.9737	0.9728	0.9718	
1.03	0.9709	0.9699	0.9690	0.9681	0.9671	0.9662	0.9653	0.9643	0.9634	0.9625	
1.04	0.9615	0.9606	0.9597	0.9588	0.9579	0.9569	0.9560	0.9551	0.9542	0.9533	- 9
1.05	0.9524	0.9515	0.9506	0.9497	0.9488	0.9479	0.9470	0.9461	0.9452	0.9443	
1.06	0.9434	0.9425	0.9416	0.9407	0.9398	0.9390	0.9381	0.9372	0.9363	0.9355	
1.07	0.9346	0.9337	0.9328	0.9320	0.9311	0.9302	0.9294	0.9285	0.9276	0.9268	
1.08	0.9259	0.9251	0.9242	0.9234	0.9225	0.9217	0.9208	0.9200	0.9191	0.9183	- 8
1.09	0.9174	0.9166	0.9158	0.9149	0.9141	0.9132	0.9124	0.9116	0.9107	0.9099	
1.10	0.9091	0.9083	0.9074	0.9066	0.9058	0.9050	0.9042	0.9033	0.9025	0.9017	
1.11	0.9009	0.9001	0.8993	0.8985	0.8977	0.8969	0.8961	0.8953	0.8945	0.8937	
1.12	0.8929	0.8921	0.8913	0.8905	0.8897	0.8889	0.8881	0.8873	0.8865	0.8857	- 7
1.13	0.8850	0.8842	0.8834	0.8826	0.8818	0.8811	0.8803	0.8795	0.8787	0.8780	
1.14	0.8772	0.8764	0.8757	0.8749	0.8741	0.8734	0.8726	0.8718	0.8711	0.8703	
1.15	0.8696	0.8688	0.8681	0.8673	0.8666	0.8658	0.8651	0.8643	0.8636	0.8628	
1.16	0.8621	0.8613	0.8606	0.8598	0.8591	0.8584	0.8576	0.8569	0.8562	0.8554	- 6
1.17	0.8547	0.8540	0.8532	0.8525	0.8518	0.8511	0.8503	0.8496	0.8489	0.8482	
1.18	0.8475	0.8467	0.8460	0.8453	0.8446	0.8439	0.8432	0.8425	0.8418	0.8410	
1.19	0.8403	0.8396	0.8389	0.8382	0.8375	0.8368	0.8361	0.8354	0.8347	0.8340	
1.20	0.8333	0.8326	0.8319	0.8313	0.8306	0.8299	0.8292	0.8285	0.8278	0.8271	- 5
1.21	0.8264	0.8258	0.8251	0.8244	0.8237	0.8230	0.8224	0.8217	0.8210	0.8203	
1.22	0.8197	0.8190	0.8183	0.8177	0.8170	0.8163	0.8157	0.8150	0.8143	0.8137	
1.23	0.8130	0.8123	0.8117	0.8110	0.8104	0.8097	0.8091	0.8084	0.8078	0.8071	
1.24	0.8065	0.8058	0.8052	0.8045	0.8039	0.8032	0.8026	0.8019	0.8013	0.8006	- 4
1.25	0.8000	0.7994	0.7987	0.7981	0.7974	0.7968	0.7962	0.7955	0.7949	0.7943	
1.26	0.7937	0.7930	0.7924	0.7918	0.7911	0.7905	0.7899	0.7893	0.7886	0.7880	
1.27	0.7874	0.7868	0.7862	0.7855	0.7849	0.7843	0.7837	0.7831	0.7825	0.7819	
1.28	0.7812	0.7806	0.7800	0.7794	0.7788	0.7782	0.7776	0.7770	0.7764	0.7758	- 3
1.29	0.7752	0.7746	0.7740	0.7734	0.7728	0.7722	0.7716	0.7710	0.7704	0.7698	
1.30	0.7692	0.7686	0.7680	0.7675	0.7669	0.7663	0.7657	0.7651	0.7645	0.7639	
1.31	0.7634	0.7628	0.7622	0.7616	0.7610	0.7605	0.7599	0.7593	0.7587	0.7582	
1.32	0.7576	0.7570	0.7564	0.7559	0.7553	0.7547	0.7541	0.7536	0.7530	0.7524	- 2
1.33	0.7519	0.7513	0.7508	0.7502	0.7496	0.7491	0.7485	0.7479	0.7474	0.7468	
1.34	0.7463	0.7457	0.7452	0.7446	0.7440	0.7435	0.7429	0.7424	0.7418	0.7413	
1.35	0.7407	0.7402	0.7396	0.7391	0.7386	0.7380	0.7375	0.7369	0.7364	0.7358	
1.36	0.7353	0.7348	0.7342	0.7337	0.7331	0.7326	0.7321	0.7315	0.7310	0.7305	- 1
1.37	0.7299	0.7294	0.7289	0.7283	0.7278	0.7273	0.7267	0.7262	0.7257	0.7252	
1.38	0.7246	0.7241	0.7236	0.7231	0.7225	0.7220	0.7215	0.7210	0.7205	0.7199	
1.39	0.7194	0.7189	0.7184	0.7179	0.7174	0.7168	0.7163	0.7158	0.7153	0.7148	
1.40	0.7143	0.7138	0.7133	0.7128	0.7123	0.7117	0.7112	0.7107	0.7102	0.7097	0
1.41	0.7092	0.7087	0.7082	0.7077	0.7072	0.7067	0.7062	0.7057	0.7052	0.7047	
1.42	0.7042	0.7037	0.7032	0.7027	0.7022	0.7018	0.7013	0.7008	0.7003	0.6998	
1.43	0.6993	0.6988	0.6983	0.6978	0.6974	0.6969	0.6964	0.6959	0.6954	0.6949	
1.44	0.6944	0.6940	0.6935	0.6930	0.6925	0.6920	0.6916	0.6911	0.6906	0.6901	1
1.45	0.6897	0.6892	0.6887	0.6882	0.6878	0.6873	0.6868	0.6863	0.6859	0.6854	
1.46	0.6849	0.6845	0.6840	0.6835	0.6831	0.6826	0.6821	0.6817	0.6812	0.6807	
1.47	0.6803	0.6798	0.6793	0.6789	0.6784	0.6780	0.6775	0.6770	0.6766	0.6761	
1.48	0.6757	0.6752	0.6748	0.6743	0.6739	0.6734	0.6729	0.6725	0.6720	0.6716	2
1.49	0.6711	0.6707	0.6702	0.6698	0.6693	0.6689	0.6684	0.6680	0.6676	0.6671	
1.50	0.6667	0.6662	0.6658	0.6653	0.6649	0.6645	0.6640	0.6636	0.6631	0.6627	
1.51	0.6623	0.6618	0.6614	0.6609	0.6605	0.6601	0.6596	0.6592	0.6588	0.6583	
1.52	0.6579	0.6575	0.6570	0.6566	0.6562	0.6557	0.6553	0.6549	0.6545	0.6540	3
1.53	0.6536	0.6532	0.6527	0.6523	0.6519	0.6515	0.6510	0.6506	0.6502	0.6498	
1.54	0.6494	0.6489	0.6485	0.6481	0.6477	0.6472	0.6468	0.6464	0.6460	0.6456	

Explanation of Table of Reciprocals

This table gives the values of $1/N$ for values of N from 1 to 10, correct to four figures. (Interpolated values may be in error by 1 in the fourth figure.)

To find the reciprocal of a number N outside the range from 1 to 10, note that moving the decimal point any number of places in either direction in Column N is equivalent to moving it the same number of places in the *opposite* direction in the body of the table. For example, $1/3.217 = 0.3109$, $1/3,217 = 0.0003109$, and $1/0.003217 = 310.9$.

(continued on next page)

TABLE 1.6—RECIPROCAL OF NUMBERS (continued)

<i>N</i>	0	1	2	3	4	5	6	7	8	9	Average Difference
1.55	0.6452	0.6447	0.6443	0.6439	0.6435	0.6431	0.6427	0.6423	0.6418	0.6414	- 4
1.56	0.6410	0.6406	0.6402	0.6398	0.6394	0.6390	0.6386	0.6382	0.6378	0.6373	
1.57	0.6369	0.6365	0.6361	0.6357	0.6353	0.6349	0.6345	0.6341	0.6337	0.6333	
1.58	0.6329	0.6325	0.6321	0.6317	0.6313	0.6309	0.6305	0.6301	0.6297	0.6293	
1.59	0.6289	0.6285	0.6281	0.6277	0.6274	0.6270	0.6266	0.6262	0.6258	0.6254	
1.60	0.6250	0.6246	0.6242	0.6238	0.6234	0.6231	0.6227	0.6223	0.6219	0.6215	
1.61	0.6211	0.6207	0.6203	0.6200	0.6196	0.6192	0.6188	0.6184	0.6180	0.6177	
1.62	0.6173	0.6169	0.6165	0.6161	0.6158	0.6154	0.6150	0.6146	0.6143	0.6139	
1.63	0.6135	0.6131	0.6127	0.6124	0.6120	0.6116	0.6112	0.6109	0.6105	0.6101	
1.64	0.6098	0.6094	0.6090	0.6086	0.6083	0.6079	0.6075	0.6072	0.6068	0.6064	
1.65	0.6061	0.6057	0.6053	0.6050	0.6046	0.6042	0.6039	0.6035	0.6031	0.6028	- 3
1.66	0.6024	0.6020	0.6017	0.6013	0.6010	0.6006	0.6002	0.5999	0.5995	0.5992	
1.67	0.5988	0.5984	0.5981	0.5977	0.5974	0.5970	0.5967	0.5963	0.5959	0.5956	
1.68	0.5952	0.5949	0.5945	0.5942	0.5938	0.5935	0.5931	0.5928	0.5924	0.5921	
1.69	0.5917	0.5914	0.5910	0.5907	0.5903	0.5900	0.5896	0.5893	0.5889	0.5886	
1.70	0.5882	0.5879	0.5875	0.5872	0.5869	0.5865	0.5862	0.5858	0.5855	0.5851	
1.71	0.5848	0.5845	0.5841	0.5838	0.5834	0.5831	0.5828	0.5824	0.5821	0.5817	
1.72	0.5814	0.5811	0.5807	0.5804	0.5800	0.5797	0.5794	0.5790	0.5787	0.5784	
1.73	0.5780	0.5777	0.5774	0.5770	0.5767	0.5764	0.5760	0.5757	0.5754	0.5750	
1.74	0.5747	0.5744	0.5741	0.5737	0.5734	0.5731	0.5727	0.5724	0.5721	0.5718	
1.75	0.5714	0.5711	0.5708	0.5705	0.5701	0.5698	0.5695	0.5692	0.5688	0.5685	- 2
1.76	0.5682	0.5679	0.5675	0.5672	0.5669	0.5666	0.5663	0.5659	0.5656	0.5653	
1.77	0.5650	0.5647	0.5643	0.5640	0.5637	0.5634	0.5631	0.5627	0.5624	0.5621	
1.78	0.5618	0.5615	0.5612	0.5609	0.5605	0.5602	0.5599	0.5596	0.5593	0.5590	
1.79	0.5587	0.5583	0.5580	0.5577	0.5574	0.5571	0.5568	0.5565	0.5562	0.5559	
1.80	0.5556	0.5552	0.5549	0.5546	0.5543	0.5540	0.5537	0.5534	0.5531	0.5528	
1.81	0.5525	0.5522	0.5519	0.5516	0.5513	0.5510	0.5507	0.5504	0.5501	0.5498	
1.82	0.5495	0.5491	0.5488	0.5485	0.5482	0.5479	0.5476	0.5473	0.5470	0.5467	
1.83	0.5464	0.5461	0.5459	0.5456	0.5453	0.5450	0.5447	0.5444	0.5441	0.5438	
1.84	0.5435	0.5432	0.5429	0.5426	0.5423	0.5420	0.5417	0.5414	0.5411	0.5408	
1.85	0.5405	0.5402	0.5400	0.5397	0.5394	0.5391	0.5388	0.5385	0.5382	0.5379	- 24
1.86	0.5376	0.5373	0.5371	0.5368	0.5365	0.5362	0.5359	0.5356	0.5353	0.5350	
1.87	0.5348	0.5345	0.5342	0.5339	0.5336	0.5333	0.5330	0.5328	0.5325	0.5322	
1.88	0.5319	0.5316	0.5313	0.5311	0.5308	0.5305	0.5302	0.5299	0.5297	0.5294	
1.89	0.5291	0.5288	0.5285	0.5283	0.5280	0.5277	0.5274	0.5271	0.5269	0.5266	
1.90	0.5263	0.5260	0.5258	0.5255	0.5252	0.5249	0.5247	0.5244	0.5241	0.5238	
1.91	0.5236	0.5233	0.5230	0.5227	0.5225	0.5222	0.5219	0.5216	0.5214	0.5211	
1.92	0.5208	0.5206	0.5203	0.5200	0.5198	0.5195	0.5192	0.5189	0.5187	0.5184	
1.93	0.5181	0.5179	0.5176	0.5173	0.5171	0.5168	0.5165	0.5163	0.5160	0.5157	
1.94	0.5155	0.5152	0.5149	0.5147	0.5144	0.5141	0.5139	0.5136	0.5133	0.5131	
1.95	0.5128	0.5126	0.5123	0.5120	0.5118	0.5115	0.5112	0.5110	0.5107	0.5105	- 15
1.96	0.5102	0.5099	0.5097	0.5094	0.5092	0.5089	0.5086	0.5084	0.5081	0.5079	
1.97	0.5076	0.5074	0.5071	0.5068	0.5066	0.5063	0.5061	0.5058	0.5056	0.5053	
1.98	0.5051	0.5048	0.5045	0.5043	0.5040	0.5038	0.5035	0.5033	0.5030	0.5028	
1.99	0.5025	0.5023	0.5020	0.5018	0.5015	0.5013	0.5010	0.5008	0.5005	0.5003	
2.0	0.5000	0.4975	0.4950	0.4926	0.4902	0.4878	0.4854	0.4831	0.4808	0.4785	
2.1	0.4762	0.4739	0.4717	0.4695	0.4673	0.4651	0.4630	0.4608	0.4587	0.4566	
2.2	0.4545	0.4525	0.4505	0.4484	0.4464	0.4444	0.4425	0.4405	0.4386	0.4367	
2.3	0.4348	0.4329	0.4310	0.4292	0.4274	0.4255	0.4237	0.4219	0.4202	0.4184	
2.4	0.4167	0.4149	0.4132	0.4115	0.4098	0.4082	0.4065	0.4049	0.4032	0.4016	
2.5	0.4000	0.3984	0.3968	0.3953	0.3937	0.3922	0.3906	0.3891	0.3876	0.3861	- 14
2.6	0.3846	0.3831	0.3817	0.3802	0.3788	0.3774	0.3759	0.3745	0.3731	0.3717	
2.7	0.3704	0.3690	0.3676	0.3663	0.3650	0.3636	0.3623	0.3610	0.3597	0.3584	
2.8	0.3571	0.3559	0.3546	0.3534	0.3521	0.3509	0.3497	0.3484	0.3472	0.3460	
2.9	0.3448	0.3436	0.3425	0.3413	0.3401	0.3390	0.3378	0.3367	0.3356	0.3344	
3.0	0.3333	0.3322	0.3311	0.3300	0.3289	0.3279	0.3268	0.3257	0.3247	0.3236	
3.1	0.3226	0.3215	0.3205	0.3195	0.3185	0.3175	0.3165	0.3155	0.3145	0.3135	
3.2	0.3125	0.3115	0.3106	0.3096	0.3086	0.3077	0.3067	0.3058	0.3049	0.3040	
3.3	0.3030	0.3021	0.3012	0.3003	0.2994	0.2985	0.2976	0.2967	0.2959	0.2950	
3.4	0.2941	0.2933	0.2924	0.2915	0.2907	0.2899	0.2890	0.2882	0.2874	0.2865	

TABLE 1.6—RECIPROCAL OF NUMBERS (continued)

<i>N</i>	0	1	2	3	4	5	6	7	8	9	Average Difference
3.5	0.2857	0.2849	0.2841	0.2833	0.2825	0.2817	0.2809	0.2801	0.2793	0.2786	– 8
3.6	0.2778	0.2770	0.2762	0.2755	0.2747	0.2740	0.2732	0.2725	0.2717	0.2710	– 8
3.7	0.2703	0.2695	0.2688	0.2681	0.2674	0.2667	0.2660	0.2653	0.2646	0.2639	– 7
3.8	0.2632	0.2625	0.2618	0.2611	0.2604	0.2597	0.2591	0.2584	0.2577	0.2571	– 7
3.9	0.2564	0.2558	0.2551	0.2545	0.2538	0.2532	0.2525	0.2519	0.2513	0.2506	– 6
4.0	0.2500	0.2494	0.2488	0.2481	0.2475	0.2469	0.2463	0.2457	0.2451	0.2445	– 6
4.1	0.2439	0.2433	0.2427	0.2421	0.2415	0.2410	0.2404	0.2398	0.2392	0.2387	– 6
4.2	0.2381	0.2375	0.2370	0.2364	0.2358	0.2353	0.2347	0.2342	0.2336	0.2331	– 6
4.3	0.2326	0.2320	0.2315	0.2309	0.2304	0.2299	0.2294	0.2288	0.2283	0.2278	– 5
4.4	0.2273	0.2268	0.2262	0.2257	0.2252	0.2247	0.2242	0.2237	0.2232	0.2227	– 5
4.5	0.2222	0.2217	0.2212	0.2208	0.2203	0.2198	0.2193	0.2188	0.2183	0.2179	– 5
4.6	0.2174	0.2169	0.2165	0.2160	0.2155	0.2151	0.2146	0.2141	0.2137	0.2132	– 5
4.7	0.2128	0.2123	0.2119	0.2114	0.2110	0.2105	0.2101	0.2096	0.2092	0.2088	– 4
4.8	0.2083	0.2079	0.2075	0.2070	0.2066	0.2062	0.2058	0.2053	0.2049	0.2045	– 4
4.9	0.2041	0.2037	0.2033	0.2028	0.2024	0.2020	0.2016	0.2012	0.2008	0.2004	– 4
5.0	0.2000	0.1996	0.1992	0.1988	0.1984	0.1980	0.1976	0.1972	0.1969	0.1965	– 4
5.1	0.1961	0.1957	0.1953	0.1949	0.1946	0.1942	0.1938	0.1934	0.1931	0.1927	
5.2	0.1923	0.1919	0.1916	0.1912	0.1908	0.1905	0.1901	0.1898	0.1894	0.1890	
5.3	0.1887	0.1883	0.1880	0.1876	0.1873	0.1869	0.1866	0.1862	0.1859	0.1855	
5.4	0.1852	0.1848	0.1845	0.1842	0.1838	0.1835	0.1832	0.1828	0.1825	0.1821	– 3
5.5	0.1818	0.1815	0.1812	0.1808	0.1805	0.1802	0.1799	0.1795	0.1792	0.1789	
5.6	0.1786	0.1783	0.1779	0.1776	0.1773	0.1770	0.1767	0.1764	0.1761	0.1757	
5.7	0.1754	0.1751	0.1748	0.1745	0.1742	0.1739	0.1736	0.1733	0.1730	0.1727	
5.8	0.1724	0.1721	0.1718	0.1715	0.1712	0.1709	0.1706	0.1704	0.1701	0.1698	
5.9	0.1695	0.1692	0.1689	0.1686	0.1684	0.1681	0.1678	0.1675	0.1672	0.1669	
6.0	0.1667	0.1664	0.1661	0.1658	0.1656	0.1653	0.1650	0.1647	0.1645	0.1642	
6.1	0.1639	0.1637	0.1634	0.1631	0.1629	0.1626	0.1623	0.1621	0.1618	0.1616	
6.2	0.1613	0.1610	0.1608	0.1605	0.1603	0.1600	0.1597	0.1595	0.1592	0.1590	
6.3	0.1587	0.1585	0.1582	0.1580	0.1577	0.1575	0.1572	0.1570	0.1567	0.1565	– 2
6.4	0.1563	0.1560	0.1558	0.1555	0.1553	0.1550	0.1548	0.1546	0.1543	0.1541	
6.5	0.1538	0.1536	0.1534	0.1531	0.1529	0.1527	0.1524	0.1522	0.1520	0.1517	
6.6	0.1515	0.1513	0.1511	0.1508	0.1506	0.1504	0.1502	0.1499	0.1497	0.1495	
6.7	0.1493	0.1490	0.1488	0.1486	0.1484	0.1481	0.1479	0.1477	0.1475	0.1473	
6.8	0.1471	0.1468	0.1466	0.1464	0.1462	0.1460	0.1458	0.1456	0.1453	0.1451	
6.9	0.1449	0.1447	0.1445	0.1443	0.1441	0.1439	0.1437	0.1435	0.1433	0.1431	
7.0	0.1429	0.1427	0.1425	0.1422	0.1420	0.1418	0.1416	0.1414	0.1412	0.1410	
7.1	0.1408	0.1406	0.1404	0.1403	0.1401	0.1399	0.1397	0.1395	0.1393	0.1391	
7.2	0.1389	0.1387	0.1385	0.1383	0.1381	0.1379	0.1377	0.1376	0.1374	0.1372	
7.3	0.1370	0.1368	0.1366	0.1364	0.1362	0.1361	0.1359	0.1357	0.1355	0.1353	
7.4	0.1351	0.1350	0.1348	0.1346	0.1344	0.1342	0.1340	0.1339	0.1337	0.1335	
7.5	0.1333	0.1332	0.1330	0.1328	0.1326	0.1325	0.1323	0.1321	0.1319	0.1318	
7.6	0.1316	0.1314	0.1312	0.1311	0.1309	0.1307	0.1305	0.1304	0.1302	0.1300	
7.7	0.1299	0.1297	0.1295	0.1294	0.1292	0.1290	0.1289	0.1287	0.1285	0.1284	
7.8	0.1282	0.1280	0.1279	0.1277	0.1276	0.1274	0.1272	0.1271	0.1269	0.1267	
7.9	0.1266	0.1264	0.1263	0.1261	0.1259	0.1258	0.1256	0.1255	0.1253	0.1252	
8.0	0.1250	0.1248	0.1247	0.1245	0.1244	0.1242	0.1241	0.1239	0.1238	0.1236	
8.1	0.1235	0.1233	0.1232	0.1230	0.1229	0.1227	0.1225	0.1224	0.1222	0.1221	
8.2	0.1220	0.1218	0.1217	0.1215	0.1214	0.1212	0.1211	0.1209	0.1208	0.1206	
8.3	0.1205	0.1203	0.1202	0.1200	0.1199	0.1198	0.1196	0.1195	0.1193	0.1192	
8.4	0.1190	0.1189	0.1188	0.1186	0.1185	0.1183	0.1182	0.1181	0.1179	0.1178	– 1
8.5	0.1176	0.1175	0.1174	0.1172	0.1171	0.1170	0.1168	0.1167	0.1166	0.1164	
8.6	0.1163	0.1161	0.1160	0.1159	0.1157	0.1156	0.1155	0.1153	0.1152	0.1151	
8.7	0.1149	0.1148	0.1147	0.1145	0.1144	0.1143	0.1142	0.1140	0.1139	0.1138	
8.8	0.1136	0.1135	0.1134	0.1133	0.1131	0.1130	0.1129	0.1127	0.1126	0.1125	
8.9	0.1124	0.1122	0.1121	0.1120	0.1119	0.1117	0.1116	0.1115	0.1114	0.1112	
9.0	0.1111	0.1110	0.1109	0.1107	0.1106	0.1105	0.1104	0.1103	0.1101	0.1100	
9.1	0.1099	0.1098	0.1096	0.1095	0.1094	0.1093	0.1092	0.1091	0.1089	0.1088	
9.2	0.1087	0.1086	0.1085	0.1083	0.1082	0.1081	0.1080	0.1079	0.1078	0.1076	
9.3	0.1075	0.1074	0.1073	0.1072	0.1071	0.1070	0.1068	0.1067	0.1066	0.1065	
9.4	0.1064	0.1063	0.1062	0.1060	0.1059	0.1058	0.1057	0.1056	0.1055	0.1054	
9.5	0.1053	0.1052	0.1050	0.1049	0.1048	0.1047	0.1046	0.1045	0.1044	0.1043	
9.6	0.1042	0.1041	0.1040	0.1038	0.1037	0.1036	0.1035	0.1034	0.1033	0.1032	
9.7	0.1031	0.1030	0.1029	0.1028	0.1027	0.1026	0.1025	0.1024	0.1022	0.1021	
9.8	0.1020	0.1019	0.1018	0.1017	0.1016	0.1015	0.1014	0.1013	0.1012	0.1011	
9.9	0.1010	0.1009	0.1008	0.1007	0.1006	0.1005	0.1004	0.1003	0.1002	0.1001	

TABLE 1.7—CIRCUMFERENCES OF CIRCLES BY HUNDREDTHS

<i>d</i>	0	1	2	3	4	5	6	7	8	9	Average Difference
1.0	3.142	3.173	3.204	3.236	3.267	3.299	3.330	3.362	3.393	3.424	31
1.1	3.456	3.487	3.519	3.550	3.581	3.613	3.644	3.676	3.707	3.738	
1.2	3.770	3.801	3.833	3.864	3.896	3.927	3.958	3.990	4.021	4.053	
1.3	4.084	4.115	4.147	4.178	4.210	4.241	4.273	4.304	4.335	4.367	
1.4	4.398	4.430	4.461	4.492	4.524	4.555	4.587	4.618	4.650	4.681	
1.5	4.712	4.744	4.775	4.807	4.838	4.869	4.901	4.932	4.964	4.995	
1.6	5.027	5.058	5.089	5.121	5.152	5.184	5.215	5.246	5.278	5.309	
1.7	5.341	5.372	5.404	5.435	5.466	5.498	5.529	5.561	5.592	5.623	
1.8	5.655	5.686	5.718	5.749	5.781	5.812	5.843	5.875	5.906	5.938	
1.9	5.969	6.000	6.032	6.063	6.095	6.126	6.158	6.189	6.220	6.252	
2.0	6.283	6.315	6.346	6.377	6.409	6.440	6.472	6.503	6.535	6.566	
2.1	6.597	6.629	6.660	6.692	6.723	6.754	6.786	6.817	6.849	6.880	
2.2	6.912	6.943	6.974	7.006	7.037	7.069	7.100	7.131	7.163	7.194	
2.3	7.226	7.257	7.288	7.320	7.351	7.383	7.414	7.446	7.477	7.508	
2.4	7.540	7.571	7.603	7.634	7.665	7.697	7.728	7.760	7.791	7.823	
2.5	7.854	7.885	7.917	7.948	7.980	8.011	8.042	8.074	8.105	8.137	
2.6	8.168	8.200	8.231	8.262	8.294	8.325	8.357	8.388	8.419	8.451	
2.7	8.482	8.514	8.545	8.577	8.608	8.639	8.671	8.702	8.734	8.765	
2.8	8.796	8.828	8.859	8.891	8.922	8.954	8.985	9.016	9.048	9.079	
2.9	9.111	9.142	9.173	9.205	9.236	9.268	9.299	9.331	9.362	9.393	
3.0	9.425	9.456	9.488	9.519	9.550	9.582	9.613	9.645	9.676	9.708	31
3.1	9.739	9.770	9.802	9.833	9.865	9.896	9.927	9.959	9.990	10.022	
3.1										10.02	
3.2	10.05	10.08	10.12	10.15	10.18	10.21	10.24	10.27	10.30	10.34	
3.3	10.37	10.40	10.43	10.46	10.49	10.52	10.56	10.59	10.62	10.65	
3.4	10.68	10.71	10.74	10.78	10.81	10.84	10.87	10.90	10.93	10.96	
3.5	11.00	11.03	11.06	11.09	11.12	11.15	11.18	11.22	11.25	11.28	
3.6	11.31	11.34	11.37	11.40	11.44	11.47	11.50	11.53	11.56	11.59	
3.7	11.62	11.66	11.69	11.72	11.75	11.78	11.81	11.84	11.88	11.91	
3.8	11.94	11.97	12.00	12.03	12.06	12.10	12.13	12.16	12.19	12.22	
3.9	12.25	12.28	12.32	12.35	12.38	12.41	12.44	12.47	12.50	12.53	
4.0	12.57	12.60	12.63	12.66	12.69	12.72	12.75	12.79	12.82	12.85	
4.1	12.88	12.91	12.94	12.97	13.01	13.04	13.07	13.10	13.13	13.16	
4.2	13.19	13.23	13.26	13.29	13.32	13.35	13.38	13.41	13.45	13.48	
4.3	13.51	13.54	13.57	13.60	13.63	13.67	13.70	13.73	13.76	13.79	
4.4	13.82	13.85	13.89	13.92	13.95	13.98	14.01	14.04	14.07	14.11	
4.5	14.14	14.17	14.20	14.23	14.26	14.29	14.33	14.36	14.39	14.42	
4.6	14.45	14.48	14.51	14.55	14.58	14.61	14.64	14.67	14.70	14.73	
4.7	14.77	14.80	14.83	14.86	14.89	14.92	14.95	14.99	15.02	15.05	
4.8	15.08	15.11	15.14	15.17	15.21	15.24	15.27	15.30	15.33	15.36	
4.9	15.39	15.43	15.46	15.49	15.52	15.55	15.58	15.61	15.65	15.68	
5.0	15.71	15.74	15.77	15.80	15.83	15.87	15.90	15.93	15.96	15.99	3
5.1	16.02	16.05	16.08	16.12	16.15	16.18	16.21	16.24	16.27	16.30	
5.2	16.34	16.37	16.40	16.43	16.46	16.49	16.52	16.56	16.59	16.62	
5.3	16.65	16.68	16.71	16.74	16.78	16.81	16.84	16.87	16.90	16.93	
5.4	16.96	17.00	17.03	17.06	17.09	17.12	17.15	17.18	17.22	17.25	

Explanation of Table of Circumferences

This table gives the product of π times any number d (diameter) from 1 to 10; i.e., it is a table of multiples of π .

Moving the decimal point *one* place in Column d is equivalent to moving it *one* place in the body of the table.

Circumference = $\pi \times d = 3.141593 \times d$. Conversely, $d = 1/\pi \times \text{circumference} = 0.31831 \times \text{circumference}$.

TABLE 1.7—CIRCUMFERENCES OF CIRCLES BY HUNDREDTHS (continued)

<i>d</i>	0	1	2	3	4	5	6	7	8	9	Average Difference
5.5	17.28	17.31	17.34	17.37	17.40	17.44	17.47	17.50	17.53	17.56	3
5.6	17.59	17.62	17.66	17.69	17.72	17.75	17.78	17.81	17.84	17.88	
5.7	17.91	17.94	17.97	18.00	18.03	18.06	18.10	18.13	18.16	18.19	
5.8	18.22	18.25	18.28	18.32	18.35	18.38	18.41	18.44	18.47	18.50	
5.9	18.54	18.57	18.60	18.63	18.66	18.69	18.72	18.76	18.79	18.82	
6.0	18.85	18.88	18.91	18.94	18.98	19.01	19.04	19.07	19.10	19.13	
6.1	19.16	19.20	19.23	19.26	19.29	19.32	19.35	19.38	19.42	19.45	
6.2	19.48	19.51	19.54	19.57	19.60	19.63	19.67	19.70	19.73	19.76	
6.3	19.79	19.82	19.85	19.89	19.92	19.95	19.98	20.01	20.04	20.07	
6.4	20.11	20.14	20.17	20.20	20.23	20.26	20.29	20.33	20.36	20.39	
6.5	20.42	20.45	20.48	20.51	20.55	20.58	20.61	20.64	20.67	20.70	
6.6	20.73	20.77	20.80	20.83	20.86	20.89	20.92	20.95	20.99	21.02	
6.7	21.05	21.08	21.11	21.14	21.17	21.21	21.24	21.27	21.30	21.33	
6.8	21.36	21.39	21.43	21.46	21.49	21.52	21.55	21.58	21.61	21.65	
6.9	21.68	21.71	21.74	21.77	21.80	21.83	21.87	21.90	21.93	21.96	
7.0	21.99	22.02	22.05	22.09	22.12	22.15	22.18	22.21	22.24	22.27	
7.1	22.31	22.34	22.37	22.40	22.43	22.46	22.49	22.53	22.56	22.59	
7.2	22.62	22.65	22.68	22.71	22.75	22.78	22.81	22.84	22.87	22.90	
7.3	22.93	22.97	23.00	23.03	23.06	23.09	23.12	23.15	23.18	23.22	
7.4	23.25	23.28	23.31	23.34	23.37	23.40	23.44	23.47	23.50	23.53	
7.5	23.56	23.59	23.62	23.66	23.69	23.72	23.75	23.78	23.81	23.84	
7.6	23.88	23.91	23.94	23.97	24.00	24.03	24.06	24.10	24.13	24.16	
7.7	24.19	24.22	24.25	24.28	24.32	24.35	24.38	24.41	24.44	24.47	
7.8	24.50	24.54	24.57	24.60	24.63	24.66	24.69	24.72	24.76	24.79	
7.9	24.82	24.85	24.88	24.91	24.94	24.98	25.01	25.04	25.07	25.10	
8.0	25.13	25.16	25.20	25.23	25.26	25.29	25.32	25.35	25.38	25.42	
8.1	25.45	25.48	25.51	25.54	25.57	25.60	25.64	25.67	25.70	25.73	
8.2	25.76	25.79	25.82	25.86	25.89	25.92	25.95	25.98	26.01	26.04	
8.3	26.08	26.11	26.14	26.17	26.20	26.23	26.26	26.30	26.33	26.36	
8.4	26.39	26.42	26.45	26.48	26.52	26.55	26.58	26.61	26.64	26.67	
8.5	26.70	26.73	26.77	26.80	26.83	26.86	26.89	26.92	26.95	26.99	
8.6	27.02	27.05	27.08	27.11	27.14	27.17	27.21	27.24	27.27	27.30	
8.7	27.33	27.36	27.39	27.43	27.46	27.49	27.52	27.55	27.58	27.61	
8.8	27.65	27.68	27.71	27.74	27.77	27.80	27.83	27.87	27.90	27.93	
8.9	27.96	27.99	28.02	28.05	28.09	28.12	28.15	28.18	28.21	28.24	
9.0	28.27	28.31	28.34	28.37	28.40	28.43	28.46	28.49	28.53	28.56	
9.1	28.59	28.62	28.65	28.68	28.71	28.75	28.78	28.81	28.84	28.87	
9.2	28.90	28.93	28.97	29.00	29.03	29.06	29.09	29.12	29.15	29.19	
9.3	29.22	29.25	29.28	29.31	29.34	29.37	29.41	29.44	29.47	29.50	
9.4	29.53	29.56	29.59	29.63	29.66	29.69	29.72	29.75	29.78	29.81	
9.5	29.85	29.88	29.91	29.94	29.97	30.00	30.03	30.07	30.10	30.13	
9.6	30.16	30.19	30.22	30.25	30.28	30.32	30.35	30.38	30.41	30.44	
9.7	30.47	30.50	30.54	30.57	30.60	30.63	30.66	30.69	30.72	30.76	
9.8	30.79	30.82	30.85	30.88	30.91	30.94	30.98	31.01	31.04	31.07	
9.9	31.10	31.13	31.16	31.20	31.23	31.26	31.29	31.32	31.35	31.38	
10.0	31.42										

TABLE 1.8—AREAS OF CIRCLES BY HUNDREDTHS

<i>d</i>	0	1	2	3	4	5	6	7	8	9	Average Difference
1.0	0.785	0.801	0.817	0.833	0.849	0.866	0.882	0.899	0.916	0.933	16
1.1	0.950	0.968	0.985	1.003	1.021	1.039	1.057	1.075	1.094	1.112	18
1.2	1.131	1.150	1.169	1.188	1.208	1.227	1.247	1.267	1.287	1.307	20
1.3	1.327	1.348	1.368	1.389	1.410	1.431	1.453	1.474	1.496	1.517	21
1.4	1.539	1.561	1.584	1.606	1.629	1.651	1.674	1.697	1.720	1.744	23
1.5	1.767	1.791	1.815	1.839	1.863	1.887	1.911	1.936	1.961	1.986	24
1.6	2.011	2.036	2.061	2.087	2.112	2.138	2.164	2.190	2.217	2.243	26
1.7	2.270	2.297	2.324	2.351	2.378	2.405	2.433	2.461	2.488	2.516	27
1.8	2.545	2.573	2.602	2.630	2.659	2.688	2.717	2.746	2.776	2.806	29
1.9	2.835	2.865	2.895	2.926	2.956	2.986	3.017	3.048	3.079	3.110	31
2.0	3.142	3.173	3.205	3.237	3.269	3.301	3.333	3.365	3.398	3.431	32
2.1	3.464	3.497	3.530	3.563	3.597	3.631	3.664	3.698	3.733	3.767	34
2.2	3.801	3.836	3.871	3.906	3.941	3.976	4.011	4.047	4.083	4.119	35
2.3	4.155	4.191	4.227	4.264	4.301	4.337	4.374	4.412	4.449	4.486	37
2.4	4.524	4.562	4.600	4.638	4.676	4.714	4.753	4.792	4.831	4.870	38
2.5	4.909	4.948	4.988	5.027	5.067	5.107	5.147	5.187	5.228	5.269	40
2.6	5.309	5.350	5.391	5.433	5.474	5.515	5.557	5.599	5.641	5.683	42
2.7	5.726	5.768	5.811	5.853	5.896	5.940	5.983	6.026	6.070	6.114	43
2.8	6.158	6.202	6.246	6.290	6.335	6.379	6.424	6.469	6.514	6.560	45
2.9	6.605	6.651	6.697	6.743	6.789	6.835	6.881	6.928	6.975	7.022	46
3.0	7.069	7.116	7.163	7.211	7.258	7.306	7.354	7.402	7.451	7.499	48
3.1	7.548	7.596	7.645	7.694	7.744	7.793	7.843	7.892	7.942	7.992	49
3.2	8.042	8.093	8.143	8.194	8.245	8.296	8.347	8.398	8.450	8.501	51
3.3	8.553	8.605	8.657	8.709	8.762	8.814	8.867	8.920	8.973	9.026	53
3.4	9.079	9.133	9.186	9.240	9.294	9.348	9.402	9.457	9.511	9.566	54
3.5	9.621	9.676	9.731	9.787	9.842	9.898	9.954	10.010			56
								10.01	10.07	10.12	6
3.6	10.18	10.24	10.29	10.35	10.41	10.46	10.52	10.58	10.64	10.69	6
3.7	10.75	10.81	10.87	10.93	10.99	11.04	11.10	11.16	11.22	11.28	
3.8	11.34	11.40	11.46	11.52	11.58	11.64	11.70	11.76	11.82	11.88	
3.9	11.95	12.01	12.07	12.13	12.19	12.25	12.32	12.38	12.44	12.50	
4.0	12.57	12.63	12.69	12.76	12.82	12.88	12.95	13.01	13.07	13.14	7
4.1	13.20	13.27	13.33	13.40	13.46	13.53	13.59	13.66	13.72	13.79	
4.2	13.85	13.92	13.99	14.05	14.12	14.19	14.25	14.32	14.39	14.45	
4.3	14.52	14.59	14.66	14.73	14.79	14.86	14.93	15.00	15.07	15.14	
4.4	15.21	15.27	15.34	15.41	15.48	15.55	15.62	15.69	15.76	15.83	
4.5	15.90	15.98	16.05	16.12	16.19	16.26	16.33	16.40	16.47	16.55	
4.6	16.62	16.69	16.76	16.84	16.91	16.98	17.06	17.13	17.20	17.28	
4.7	17.35	17.42	17.50	17.57	17.65	17.72	17.80	17.87	17.95	18.02	
4.8	18.10	18.17	18.25	18.32	18.40	18.47	18.55	18.63	18.70	18.78	8
4.9	18.86	18.93	19.01	19.09	19.17	19.24	19.32	19.40	19.48	19.56	
5.0	19.63	19.71	19.79	19.87	19.95	20.03	20.11	20.19	20.27	20.35	
5.1	20.43	20.51	20.59	20.67	20.75	20.83	20.91	20.99	21.07	21.16	
5.2	21.24	21.32	21.40	21.48	21.57	21.65	21.73	21.81	21.90	21.98	
5.3	22.06	22.15	22.23	22.31	22.40	22.48	22.56	22.65	22.73	22.82	
5.4	22.90	22.99	23.07	23.16	23.24	23.33	23.41	23.50	23.59	23.67	9

Explanation of Table of Areas of Circles

Moving the decimal point one place in Column *d* (diameter) is equivalent to moving it two places in the body of the table. For example, area of circle = $\pi/4 \times d^2 = 0.785398 \times (d^2)$.

Conversely, diameter of circle = $\sqrt{4/\pi \times \text{area}} = 1.128379 \times \sqrt{\text{area}}$.

TABLE 1.8—AREAS OF CIRCLES BY HUNDREDTHS (continued)

<i>d</i>	0	1	2	3	4	5	6	7	8	9	Average Difference
5.5	23.76	23.84	23.93	24.02	24.11	24.19	24.28	24.37	24.45	24.54	9
5.6	24.63	24.72	24.81	24.89	24.96	25.07	25.16	25.25	25.34	25.43	
5.7	25.52	25.61	25.70	25.79	25.88	25.97	26.06	26.15	26.24	26.33	
5.8	26.42	26.51	26.60	26.69	26.79	26.88	26.97	27.06	27.15	27.25	
5.9	27.34	27.43	27.53	27.62	27.71	27.81	27.90	27.99	28.09	28.18	
6.0	28.27	28.37	28.46	28.56	28.65	28.75	28.84	28.94	29.03	29.13	10
6.1	29.22	29.32	29.42	29.51	29.61	29.71	29.80	29.90	30.00	30.09	
6.2	30.19	30.29	30.39	30.48	30.58	30.68	30.78	30.88	30.97	31.07	
6.3	31.17	31.27	31.37	31.47	31.57	31.67	31.77	31.87	31.97	32.07	
6.4	32.17	32.27	32.37	32.47	32.57	32.67	32.78	32.88	32.98	33.08	
6.5	33.18	33.29	33.39	33.49	33.59	33.70	33.80	33.90	34.00	34.11	11
6.6	34.21	34.32	34.42	34.52	34.63	34.73	34.84	34.94	35.05	35.15	
6.7	35.26	35.36	35.47	35.57	35.68	35.78	35.89	36.00	36.10	36.21	
6.8	36.32	36.42	36.53	36.64	36.75	36.85	36.96	37.07	37.18	37.28	
6.9	37.39	37.50	37.61	37.72	37.83	37.94	38.05	38.16	38.26	38.37	
7.0	38.48	38.59	38.70	38.82	38.93	39.04	39.15	39.26	39.37	39.48	12
7.1	39.59	39.70	39.82	39.93	40.04	40.15	40.26	40.38	40.49	40.60	
7.2	40.72	40.83	40.94	41.06	41.17	41.28	41.40	41.51	41.62	41.74	
7.3	41.85	41.97	42.08	42.20	42.31	42.43	42.54	42.66	42.78	42.89	
7.4	43.01	43.12	43.24	43.36	43.47	43.59	43.71	43.83	43.94	44.06	
7.5	44.18	44.30	44.41	44.53	44.65	44.77	44.89	45.01	45.13	45.25	13
7.6	45.36	45.48	45.60	45.72	45.84	45.96	46.08	46.20	46.32	46.45	
7.7	46.57	46.69	46.81	46.93	47.05	47.17	47.29	47.42	47.54	47.66	
7.8	47.78	47.91	48.03	48.15	48.27	48.40	48.52	48.65	48.77	48.89	
7.9	49.02	49.14	49.27	49.39	49.51	49.64	49.76	49.89	50.01	50.14	
8.0	50.27	50.39	50.52	50.64	50.77	50.90	51.02	51.15	51.28	51.40	14
8.1	51.53	51.66	51.78	51.91	52.04	52.17	52.30	52.42	52.55	52.68	
8.2	52.81	52.94	53.07	53.20	53.33	53.46	53.59	53.72	53.85	53.98	
8.3	54.11	54.24	54.37	54.50	54.63	54.76	54.89	55.02	55.15	55.29	
8.4	55.42	55.55	55.68	55.81	55.95	56.08	56.21	56.35	56.48	56.61	
8.5	56.75	56.88	57.01	57.15	57.28	57.41	57.55	57.68	57.82	57.95	15
8.6	58.09	58.22	58.36	58.49	58.63	58.77	58.90	59.04	59.17	59.31	
8.7	59.45	59.58	59.72	59.86	59.99	60.13	60.27	60.41	60.55	60.68	
8.8	60.82	60.96	61.10	61.24	61.38	61.51	61.65	61.79	61.93	62.07	
8.9	62.21	62.35	62.49	62.63	62.77	62.91	63.05	63.19	63.33	63.48	
9.0	63.62	63.76	63.90	64.04	64.18	64.33	64.47	64.61	64.75	64.90	16
9.1	65.04	65.18	65.33	65.47	65.61	65.76	65.90	66.04	66.19	66.33	
9.2	66.48	66.62	66.77	66.91	67.06	67.20	67.35	67.49	67.64	67.78	
9.3	67.93	68.08	68.22	68.37	68.51	68.66	68.81	68.96	69.10	69.25	
9.4	69.40	69.55	69.69	69.84	69.99	70.14	70.29	70.44	70.58	70.73	
9.5	70.88	71.03	71.18	71.33	71.48	71.63	71.78	71.93	72.08	72.23	16
9.6	72.38	72.53	72.68	72.84	72.99	73.14	73.29	73.44	73.59	73.75	
9.7	73.90	74.05	74.20	74.36	74.51	74.66	74.82	74.97	75.12	75.28	
9.8	75.43	75.58	75.74	75.89	76.05	76.20	76.36	76.51	76.67	76.82	
9.9	76.98	77.13	77.29	77.44	77.60	77.76	77.91	78.07	78.23	78.38	

TABLE 1.9—CIRCUMFERENCES AND AREAS OF CIRCLES BY EIGHTHS

Diameter	Circumference	Area	Diameter	Circumference	Area	Diameter	Circumference	Area
			$\frac{7}{8}$	2.749	0.6013	4	12.57	12.57
$\frac{1}{64}$	0.04909	0.00019	$\frac{57}{64}$	2.798	0.6230	$\frac{1}{16}$	12.76	12.96
$\frac{1}{32}$	0.09817	0.00077	$\frac{29}{32}$	2.847	0.6450	$\frac{1}{8}$	12.96	13.36
$\frac{3}{64}$	0.1473	0.00173	$\frac{59}{64}$	2.896	0.6675	$\frac{3}{16}$	13.16	13.77
$\frac{1}{16}$	0.1963	0.00307	$\frac{15}{16}$	2.945	0.6903	$\frac{1}{4}$	13.35	14.19
$\frac{5}{64}$	0.2454	0.00479	$\frac{61}{64}$	2.994	0.7135	$\frac{5}{16}$	13.55	14.61
$\frac{3}{32}$	0.2945	0.00690	$\frac{31}{32}$	3.043	0.7371	$\frac{3}{8}$	13.74	15.03
$\frac{7}{64}$	0.3436	0.00940	$\frac{63}{64}$	3.093	0.7610	$\frac{7}{16}$	13.94	15.47
$\frac{1}{8}$	0.3927	0.01227	1	3.142	0.7854	$\frac{1}{2}$	14.14	15.90
$\frac{9}{64}$	0.4418	0.01553	$\frac{1}{16}$	3.338	0.8866	$\frac{9}{16}$	14.33	16.35
$\frac{5}{32}$	0.4909	0.01917	$\frac{1}{8}$	3.534	0.9940	$\frac{5}{8}$	14.53	16.80
$\frac{11}{64}$	0.5400	0.02320	$\frac{3}{16}$	3.731	1.108	$\frac{11}{16}$	14.73	17.26
$\frac{3}{16}$	0.5890	0.02761	$\frac{1}{4}$	3.927	1.227	$\frac{3}{4}$	14.92	17.72
$\frac{13}{64}$	0.6381	0.03241	$\frac{5}{16}$	4.123	1.353	$\frac{13}{16}$	15.12	18.19
$\frac{7}{32}$	0.6872	0.03758	$\frac{3}{8}$	4.320	1.485	$\frac{7}{8}$	15.32	18.67
$\frac{15}{64}$	0.7363	0.04314	$\frac{7}{16}$	4.516	1.623	$\frac{15}{16}$	15.51	19.15
$\frac{1}{4}$	0.7854	0.04909	$\frac{1}{2}$	4.712	1.767	5	15.71	19.63
$\frac{17}{64}$	0.8345	0.05542	$\frac{9}{16}$	4.909	1.917	$\frac{1}{16}$	15.90	20.13
$\frac{9}{32}$	0.8836	0.06213	$\frac{5}{8}$	5.105	2.074	$\frac{1}{8}$	16.10	20.63
$\frac{19}{64}$	0.9327	0.06922	$\frac{11}{16}$	5.301	2.237	$\frac{3}{16}$	16.30	21.14
$\frac{5}{16}$	0.9817	0.07670	$\frac{3}{4}$	5.498	2.405	$\frac{1}{4}$	16.49	21.65
$\frac{21}{64}$	1.031	0.08456	$\frac{13}{16}$	5.694	2.580	$\frac{5}{16}$	16.69	22.17
$\frac{11}{32}$	1.080	0.09281	$\frac{7}{8}$	5.890	2.761	$\frac{3}{8}$	16.89	22.69
$\frac{23}{64}$	1.129	0.1014	$\frac{15}{16}$	6.087	2.948	$\frac{7}{16}$	17.08	23.22
$\frac{3}{8}$	1.178	0.1104	2	6.283	3.142	$\frac{1}{2}$	17.28	23.76
$\frac{25}{64}$	1.227	0.1198	$\frac{1}{16}$	6.480	3.341	$\frac{9}{16}$	17.48	24.30
$\frac{13}{32}$	1.276	0.1296	$\frac{1}{8}$	6.676	3.547	$\frac{5}{8}$	17.67	24.85
$\frac{27}{64}$	1.325	0.1398	$\frac{3}{16}$	6.872	3.758	$\frac{11}{16}$	17.87	25.41
$\frac{7}{16}$	1.374	0.1503	$\frac{1}{4}$	7.069	3.976	$\frac{3}{4}$	18.06	25.97
$\frac{29}{64}$	1.424	0.1613	$\frac{5}{16}$	7.265	4.200	$\frac{13}{16}$	18.26	26.53
$\frac{15}{32}$	1.473	0.1726	$\frac{3}{8}$	7.461	4.430	$\frac{7}{8}$	18.46	27.11
$\frac{31}{64}$	1.522	0.1843	$\frac{7}{16}$	7.658	4.666	$\frac{15}{16}$	18.65	27.69
$\frac{1}{2}$	1.571	0.1963	$\frac{1}{2}$	7.854	4.909	6	18.85	28.27
$\frac{33}{64}$	1.620	0.2088	$\frac{9}{16}$	8.050	5.157	$\frac{1}{8}$	19.24	29.46
$\frac{17}{32}$	1.669	0.2217	$\frac{5}{8}$	8.247	5.412	$\frac{1}{4}$	19.63	30.68
$\frac{35}{64}$	1.718	0.2349	$\frac{11}{16}$	8.443	5.673	$\frac{3}{8}$	20.03	31.92
$\frac{9}{16}$	1.767	0.2485	$\frac{3}{4}$	8.639	5.940	$\frac{1}{2}$	20.42	33.18
$\frac{37}{64}$	1.816	0.2625	$\frac{13}{16}$	8.836	6.213	$\frac{5}{16}$	20.81	34.47
$\frac{19}{32}$	1.865	0.2769	$\frac{7}{8}$	9.032	6.492	$\frac{3}{4}$	21.21	35.78
$\frac{39}{64}$	1.914	0.2916	$\frac{15}{16}$	9.228	6.777	$\frac{7}{8}$	21.60	37.12
$\frac{5}{8}$	1.963	0.3068	3	9.425	7.069	7	21.99	38.48
$\frac{41}{64}$	2.013	0.3223	$\frac{1}{16}$	9.621	7.366	$\frac{1}{8}$	22.38	39.87
$\frac{21}{32}$	2.062	0.3382	$\frac{1}{8}$	9.817	7.670	$\frac{1}{4}$	22.78	41.28
$\frac{43}{64}$	2.111	0.3545	$\frac{3}{16}$	10.01	7.980	$\frac{3}{8}$	23.17	42.72
$\frac{11}{16}$	2.160	0.3712	$\frac{1}{4}$	10.21	8.296	$\frac{1}{2}$	23.56	44.18
$\frac{45}{64}$	2.209	0.3883	$\frac{5}{16}$	10.41	8.618	$\frac{5}{8}$	23.95	45.66
$\frac{23}{32}$	2.258	0.4057	$\frac{3}{8}$	10.60	8.946	$\frac{3}{4}$	24.35	47.17
$\frac{47}{64}$	2.307	0.4236	$\frac{7}{16}$	10.80	9.281	$\frac{7}{8}$	24.74	48.71
$\frac{3}{4}$	2.356	0.4418	$\frac{1}{2}$	11.00	9.621	8	25.13	50.27
$\frac{49}{64}$	2.405	0.4604	$\frac{9}{16}$	11.19	9.968	$\frac{1}{8}$	25.53	51.85
$\frac{25}{32}$	2.454	0.4794	$\frac{5}{8}$	11.39	10.32	$\frac{1}{4}$	25.92	53.46
$\frac{51}{64}$	2.503	0.4987	$\frac{11}{16}$	11.58	10.68	$\frac{3}{8}$	26.31	55.09
$\frac{13}{16}$	2.553	0.5185	$\frac{3}{4}$	11.78	11.04	$\frac{1}{2}$	26.70	56.75
$\frac{53}{64}$	2.602	0.5386	$\frac{13}{16}$	11.98	11.42	$\frac{5}{8}$	27.10	58.43
$\frac{27}{32}$	2.651	0.5591	$\frac{7}{8}$	12.17	11.79	$\frac{3}{4}$	27.49	60.13
$\frac{55}{64}$	2.700	0.5800	$\frac{15}{16}$	12.37	12.18	$\frac{7}{8}$	27.88	61.86

TABLE 1.9—CIRCUMFERENCES AND AREAS OF CIRCLES BY EIGHTHS (continued)

Diameter	Circumference	Area	Diameter	Circumference	Area	Diameter	Circumference	Area
9	28.27	63.62	16	50.27	201.1	23	72.26	415.5
$\frac{1}{8}$	28.67	65.40	$\frac{1}{8}$	50.66	204.2	$\frac{1}{8}$	72.65	420.0
$\frac{1}{4}$	29.06	67.20	$\frac{1}{4}$	51.05	207.4	$\frac{1}{4}$	73.04	424.6
$\frac{3}{8}$	29.45	69.03	$\frac{3}{8}$	51.44	210.6	$\frac{1}{2}$	73.43	429.1
$\frac{1}{2}$	29.85	70.88	$\frac{1}{2}$	51.84	213.8	$\frac{1}{2}$	73.83	433.7
$\frac{5}{8}$	30.24	72.76	$\frac{5}{8}$	52.23	217.1	$\frac{5}{8}$	74.22	438.4
$\frac{3}{4}$	30.63	74.66	$\frac{3}{4}$	52.62	220.4	$\frac{3}{4}$	74.61	443.0
$\frac{7}{8}$	31.02	76.59	$\frac{7}{8}$	53.01	223.7	$\frac{7}{8}$	75.01	447.7
10	31.42	78.54	17	53.41	227.0	24	75.40	452.4
$\frac{1}{8}$	31.81	80.52	$\frac{1}{8}$	53.80	230.3	$\frac{1}{4}$	76.18	461.9
$\frac{1}{4}$	32.20	82.52	$\frac{1}{4}$	54.19	233.7	$\frac{1}{2}$	76.97	471.4
$\frac{3}{8}$	32.59	84.54	$\frac{3}{8}$	54.59	237.1	$\frac{3}{4}$	77.75	481.1
$\frac{1}{2}$	32.99	86.59	$\frac{1}{2}$	54.98	240.5	25	78.54	490.9
$\frac{5}{8}$	33.38	88.66	$\frac{5}{8}$	55.37	244.0	$\frac{1}{4}$	79.33	500.7
$\frac{3}{4}$	33.77	90.76	$\frac{3}{4}$	55.76	247.4	$\frac{1}{2}$	80.11	510.7
$\frac{7}{8}$	34.16	92.89	$\frac{7}{8}$	56.16	250.9	$\frac{3}{4}$	80.90	520.8
11	34.56	95.03	18	56.55	254.5	26	81.68	530.9
$\frac{1}{8}$	34.95	97.21	$\frac{1}{8}$	56.94	258.0	$\frac{1}{2}$	82.47	541.2
$\frac{1}{4}$	35.34	99.40	$\frac{1}{4}$	57.33	261.6	$\frac{1}{2}$	83.25	551.5
$\frac{3}{8}$	35.74	101.6	$\frac{3}{8}$	57.73	265.2	$\frac{3}{4}$	84.04	562.0
$\frac{1}{2}$	36.13	103.9	$\frac{1}{2}$	58.12	268.8	27	84.82	572.6
$\frac{5}{8}$	36.52	106.1	$\frac{5}{8}$	58.51	272.4	$\frac{1}{4}$	85.61	583.2
$\frac{3}{4}$	36.91	108.4	$\frac{3}{4}$	58.90	276.1	$\frac{1}{2}$	86.39	594.0
$\frac{7}{8}$	37.31	110.8	$\frac{7}{8}$	59.30	279.8	$\frac{3}{4}$	87.18	604.8
12	37.70	113.1	19	59.69	283.5	28	87.96	615.8
$\frac{1}{8}$	38.09	115.5	$\frac{1}{8}$	60.08	287.3	$\frac{1}{4}$	88.75	626.8
$\frac{1}{4}$	38.48	117.9	$\frac{1}{4}$	60.48	291.0	$\frac{1}{2}$	89.54	637.9
$\frac{3}{8}$	38.88	120.3	$\frac{3}{8}$	60.87	294.8	$\frac{3}{4}$	90.32	649.2
$\frac{1}{2}$	39.27	122.7	$\frac{1}{2}$	61.26	298.6	29	91.11	660.5
$\frac{5}{8}$	39.66	125.2	$\frac{5}{8}$	61.65	302.5	$\frac{1}{4}$	91.89	672.0
$\frac{3}{4}$	40.06	127.7	$\frac{3}{4}$	62.05	306.4	$\frac{1}{2}$	92.68	683.5
$\frac{7}{8}$	40.45	130.2	$\frac{7}{8}$	62.44	310.2	$\frac{3}{4}$	93.46	695.1
13	40.84	132.7	20	62.83	314.2	30	94.25	706.9
$\frac{1}{8}$	41.23	135.3	$\frac{1}{8}$	63.22	318.1	$\frac{1}{4}$	95.03	718.7
$\frac{1}{4}$	41.63	137.9	$\frac{1}{4}$	63.62	322.1	$\frac{1}{2}$	95.82	730.6
$\frac{3}{8}$	42.02	140.5	$\frac{3}{8}$	64.01	326.1	$\frac{3}{4}$	96.60	742.6
$\frac{1}{2}$	42.41	143.1	$\frac{1}{2}$	64.40	330.1	31	97.39	754.8
$\frac{5}{8}$	42.80	145.8	$\frac{5}{8}$	64.80	334.1	$\frac{1}{4}$	98.17	767.0
$\frac{3}{4}$	43.20	148.5	$\frac{3}{4}$	65.19	338.2	$\frac{1}{2}$	98.96	779.3
$\frac{7}{8}$	43.59	151.2	$\frac{7}{8}$	65.58	342.2	$\frac{3}{4}$	99.75	791.7
14	43.98	153.9	21	65.97	346.4	32	100.5	804.2
$\frac{1}{8}$	44.37	156.7	$\frac{1}{8}$	66.37	350.5	$\frac{1}{4}$	101.3	816.9
$\frac{1}{4}$	44.77	159.5	$\frac{1}{4}$	66.76	354.7	$\frac{1}{2}$	102.1	829.6
$\frac{3}{8}$	45.16	162.3	$\frac{3}{8}$	67.15	358.8	$\frac{3}{4}$	102.9	842.4
$\frac{1}{2}$	45.55	165.1	$\frac{1}{2}$	67.54	363.1	33	103.7	855.3
$\frac{5}{8}$	45.95	168.0	$\frac{5}{8}$	67.94	367.3	$\frac{1}{4}$	104.5	868.3
$\frac{3}{4}$	46.34	170.9	$\frac{3}{4}$	68.33	371.5	$\frac{1}{2}$	105.2	881.4
$\frac{7}{8}$	46.73	173.8	$\frac{7}{8}$	68.72	375.8	$\frac{3}{4}$	106.0	894.6
15	47.12	176.7	22	69.12	380.1	34	106.8	907.9
$\frac{1}{8}$	47.52	179.7	$\frac{1}{8}$	69.51	384.5	$\frac{1}{4}$	107.6	921.3
$\frac{1}{4}$	47.91	182.7	$\frac{1}{4}$	69.90	388.8	$\frac{1}{2}$	108.4	934.8
$\frac{3}{8}$	48.30	185.7	$\frac{3}{8}$	70.29	393.2	$\frac{3}{4}$	109.2	948.4
$\frac{1}{2}$	48.69	188.7	$\frac{1}{2}$	70.69	397.6	35	110.0	962.1
$\frac{5}{8}$	49.09	191.7	$\frac{5}{8}$	71.08	402.0	$\frac{1}{4}$	110.7	975.9
$\frac{3}{4}$	49.48	194.8	$\frac{3}{4}$	71.47	406.5	$\frac{1}{2}$	111.5	989.8
$\frac{7}{8}$	49.87	197.9	$\frac{7}{8}$	71.86	411.0	$\frac{3}{4}$	112.3	1003.8

TABLE 1.10—AREAS OF CIRCLES—DIAMETERS IN FEET AND INCHES, AREAS IN SQUARE FEET

Feet	Inches										
	0	1	2	3	4	5	6	7	8	9	10
0	0.0000	0.0055	0.0218	0.0491	0.0873	0.1364	0.1963	0.2673	0.3491	0.4418	0.5454
1	0.7854	0.9218	1.069	1.227	1.396	1.576	1.767	1.969	2.182	2.405	2.640
2	3.142	3.409	3.687	3.976	4.276	4.587	4.909	5.241	5.585	5.940	6.305
3	7.069	7.467	7.876	8.296	8.727	9.168	9.621	10.08	10.56	11.04	11.54
4	12.57	13.10	13.64	14.19	14.75	15.32	15.90	16.50	17.10	17.72	18.35
5	19.63	20.29	20.97	21.65	22.34	23.04	23.76	24.48	25.22	25.97	26.73
6	28.27	29.07	29.87	30.68	31.50	32.34	33.18	34.04	34.91	35.78	36.67
7	38.48	39.41	40.34	41.28	42.24	43.20	44.18	45.17	46.16	47.17	48.19
8	50.27	51.32	52.38	53.46	54.54	55.64	56.75	57.86	58.99	60.13	61.28
9	63.62	64.80	66.00	67.20	68.42	69.64	70.88	72.13	73.39	74.66	75.94
10	78.54	79.85	81.18	82.52	83.86	85.22	86.59	87.97	89.36	90.76	92.18
11	95.03	96.48	97.93	99.40	100.9	102.4	103.9	105.4	106.9	108.4	110.0
12	113.1	114.7	116.3	117.9	119.5	121.1	122.7	124.4	126.0	127.7	129.4
13	132.7	134.4	136.2	137.9	139.6	141.4	143.1	144.9	146.7	148.5	150.3
14	153.9	155.8	157.6	159.5	161.4	163.2	165.1	167.0	168.9	170.9	172.8

*If given diameter is not found in this table, reduce diameter to feet and decimals of a foot by aid of the following auxiliary table and use Table 1.8

From Inches and Fractions of an Inch to Decimals of a Foot**

Inches	1	2	3	4	5	6	7	8	9	10	11
Feet	0.0833	0.1667	0.2500	0.3333	0.4167	0.5000	0.5833	0.6667	0.7500	0.8333	0.9167
Inches	$\frac{1}{8}$	$\frac{1}{4}$	$\frac{3}{8}$	$\frac{1}{2}$	$\frac{5}{8}$	$\frac{3}{4}$	$\frac{7}{8}$				
Feet	0.0104	0.0208	0.0313	0.0417	0.0521	0.0625	0.0729				

**For example, 5 ft $7\frac{3}{8}$ in. = 5.0 + 0.5833 + 0.0313 = 5.6146 ft

TABLE 1.11—SEGMENTS OF CIRCLES, GIVEN h/c

h/c	d/c	Difference	Arc/c	Difference	Area/ $h \times c$	Difference	Central Angle, α (degrees)	Difference	h/d	Difference
0.00			1.000	0	0.6667	0	0.00	458	0.0000	4
0.01	25.010		1.000	1	0.6667	2	4.58	458	0.0004	12
0.02	12.520	12,490	1.001	1	0.6669	2	9.16	457	0.0016	20
0.03	8.363	4,157*	1.002	2	0.6671	4	13.73	457	0.0036	28
0.04	6.290	2,073*	1.004	3	0.6675	5	18.30	454	0.0064	35
		1,240*								
0.05	5.050	823*	1.007	3	0.6680	6	22.84	453	0.0099	43
0.06	4.227	586*	1.010	3	0.6686	7	27.37	451	0.0142	50
0.07	3.641	436*	1.013	4	0.6693	8	31.88	448	0.0192	58
0.08	3.205	337*	1.017	4	0.6701	9	36.36	446	0.0250	64
0.09	2.868	268*	1.021	5	0.6710	10	40.82	442	0.0314	71
0.10	2.600	217*	1.026	6	0.6720	11	45.24	439	0.0385	77
0.11	2.383	180*	1.032	6	0.6731	12	49.63	435	0.0462	83
0.12	2.203	150*	1.038	6	0.6743	13	53.98	432	0.0545	88
0.13	2.053	127*	1.044	7	0.6756	14	58.30	427	0.0633	94
0.14	1.926	109*	1.051	8	0.6770	15	62.57	423	0.0727	99
0.15	1.817	94*	1.059	8	0.6785	16	66.80	418	0.0826	103
0.16	1.723	82*	1.067	8	0.6801	17	70.98	413	0.0929	107
0.17	1.641	72*	1.075	9	0.6818	18	75.11	409	0.1036	111
0.18	1.569	63*	1.084	10	0.6836	19	79.20	403	0.1147	116
0.19	1.506	56	1.094	9	0.6855	20	83.23	399	0.1263	116
0.20	1.450	50	1.103	11	0.6875	21	87.21	392	0.1379	120
0.21	1.400	44	1.114	10	0.6896	22	91.13	387	0.1499	123
0.22	1.356	39	1.124	12	0.6918	23	95.00	381	0.1622	124
0.23	1.317	35	1.136	11	0.6941	24	98.81	375	0.1746	127
0.24	1.282	32	1.147	12	0.6965	24	102.56	370	0.1873	127
0.25	1.250	28	1.159	12	0.6989	25	106.26	364	0.2000	128
0.26	1.222	26	1.171	13	0.7014	27	109.90	358	0.2128	130
0.27	1.196	23	1.184	13	0.7041	27	113.48	352	0.2258	129
0.28	1.173	21	1.197	14	0.7068	28	117.00	345	0.2387	130
0.29	1.152	19	1.211	14	0.7096	29	120.45	341	0.2517	130
0.30	1.133	17	1.225	14	0.7125	29	123.86	334	0.2647	130
0.31	1.116	15	1.239	15	0.7154	31	127.20	328	0.2777	129
0.32	1.101	13	1.254	15	0.7185	31	130.48	322	0.2906	128
0.33	1.088	13	1.269	15	0.7216	32	133.70	316	0.3034	128
0.34	1.075	11	1.284	16	0.7248	32	136.86	311	0.3162	127
0.35	1.064	10	1.300	16	0.7280	34	139.97	305	0.3289	125
0.36	1.054	8	1.316	16	0.7314	34	143.02	299	0.3414	124
0.37	1.046	8	1.332	17	0.7348	35	146.01	293	0.3538	123
0.38	1.038	7	1.349	17	0.7383	36	148.94	288	0.3661	122
0.39	1.031	6	1.366	17	0.7419	36	151.82	282	0.3783	119
0.40	1.025	5	1.383	18	0.7455	37	154.64	277	0.3902	119
0.41	1.020	5	1.401	18	0.7492	38	157.41	271	0.4021	116
0.42	1.015	4	1.419	18	0.7530	38	160.12	266	0.4137	115
0.43	1.011	3	1.437	18	0.7568	39	162.78	261	0.4252	112
0.44	1.008	2	1.455	19	0.7607	40	165.39	256	0.4364	111
0.45	1.006	3	1.474	19	0.7647	40	167.95	251	0.4475	109
0.46	1.003	1	1.493	19	0.7687	41	170.46	245	0.4584	107
0.47	1.002	1	1.512	19	0.7728	41	172.91	241	0.4691	105
0.48	1.001	1	1.531	20	0.7769	42	175.32	237	0.4796	103
0.49	1.000	0	1.551	20	0.7811	43	177.69	231	0.4899	101
0.50	1.000		1.571		0.7854		180.00		0.5000	

*Interpolation may be inaccurate at these points.

Explanation of Table of Segments of Circles, Given h/c

Given: h = height of segment and c = chord, to find the diameter, d , of the circle, the length of the arc, or the area of the segment, form the ratio h/c , and find from the table the value of d/c , arc/ c , or area/ hc ; then, by a simple multiplication, $d = c \times (d/c)$, arc = $c \times (\text{arc}/c)$, and area = $h \times c \times (\text{area}/hc)$.

The table also gives the angle subtended at the center, and the ratio of h to d .

TABLE 1.12—SEGMENTS OF CIRCLES, GIVEN h/d

h/d	arc/d	Difference	$Area/d^2$	Difference	Central Angle, α (degrees)	Difference	c/d	Difference	Arc Circumference	Difference	Area Circle	Difference
0.00	0.000		0.0000		0.00	2296	0.0000		0.0000		0.0000	
0.01	0.2003	2003	0.0013	13	22.96	956*	0.1990	1990	0.0638	638*	0.0017	17
0.02	0.2838	835*	0.0037	24	32.52	738*	0.2800	810*	0.0903	265*	0.0048	31
0.03	0.3482	644*	0.0069	32	39.90	625*	0.3412	612*	0.1108	205*	0.0087	39
0.04	0.4027	545*	0.0105	36	46.15	553*	0.3919	507*	0.1282	174*	0.0134	47
		483*		42				440*		154*		53
0.05	0.4510		0.0147	45	51.68	504*	0.4359	391*	0.1436	139*	0.0187	58
0.06	0.4949	439*	0.0192	50	56.72	465*	0.4750	353*	0.1575	130*	0.0245	63
0.07	0.5355	406*	0.0242	52	61.37	435*	0.5103	323*	0.1705	121	0.0308	67
0.08	0.5735	380*	0.0294	56	65.72	411*	0.5426	298*	0.1826	114	0.0375	71
0.09	0.6094	359*	0.0350	59	69.83	391*	0.5724	276*	0.1940	108	0.0446	74
		341*										
0.10	0.6435		0.0409	61	73.74	374*	0.6000	258*	0.2048	104	0.0520	78
0.11	0.6761	326*	0.0470	64	77.48	359*	0.6258	241*	0.2152	100	0.0598	82
0.12	0.7075	314*	0.0534	66	81.07	347*	0.6499	227*	0.2252	96	0.0680	84
0.13	0.7377	302*	0.0600	68	84.54	335*	0.6726	214*	0.2348	93	0.0764	87
0.14	0.7670	293*	0.0668	71	87.89	326*	0.6940	201*	0.2441	91	0.0851	90
		284*										
0.15	0.7954		0.0739	72	91.15	316	0.7141	191*	0.2532	88	0.0941	92
0.16	0.8230	276	0.0811	74	94.31	309	0.7332	181*	0.2620	86	0.1033	94
0.17	0.8500	270	0.0885	76	97.40	302	0.7513	171*	0.2706	83	0.1127	97
0.18	0.8763	263	0.0961	78	100.42	295	0.7684	162	0.2789	82	0.1224	99
0.19	0.9021	258	0.1039	79	103.37	289	0.7846	154	0.2871	81	0.1323	101
		252										
0.20	0.9273		0.1118	81	106.26	284	0.8000	146	0.2952	79	0.1424	103
0.21	0.9521	248	0.1199	82	109.10	279	0.8146	139	0.3031	77	0.1527	104
0.22	0.9764	243	0.1281	84	111.89	274	0.8285	132	0.3108	76	0.1631	107
0.23	1.0004	240	0.1365	84	114.63	271	0.8417	125	0.3184	75	0.1738	108
0.24	1.0239	235	0.1449	86	117.34	266	0.8542	118	0.3259	74	0.1846	109
		233										
0.25	1.0472		0.1535	88	120.00	263	0.8660	113	0.3333	73	0.1955	111
0.26	1.0701	229	0.1623	88	122.63	260	0.8773	106	0.3406	72	0.2066	112
0.27	1.0928	227	0.1711	89	125.23	256	0.8879	101	0.3478	72	0.2178	114
0.28	1.1152	224	0.1800	90	127.79	254	0.8980	95	0.3550	70	0.2292	115
0.29	1.1374	222	0.1890	92	130.33	251	0.9075	90	0.3620	70	0.2407	116
		219										
0.30	1.1593		0.1982	92	132.84	249	0.9165	85	0.3690	69	0.2523	117
0.31	1.1810	217	0.2074	93	135.33	247	0.9250	80	0.3759	69	0.2640	119
0.32	1.2025	215	0.2167	93	137.80	245	0.9330	74	0.3828	68	0.2759	119
0.33	1.2239	214	0.2260	95	140.25	242	0.9404	70	0.3896	67	0.2878	120
0.34	1.2451	212	0.2355	95	142.67	241	0.9474	65	0.3963	67	0.2998	121
		210										
0.35	1.2661		0.2450	96	145.08	240	0.9539	61	0.4030	67	0.3119	122
0.36	1.2870	209	0.2546	96	147.48	238	0.9600	56	0.4097	66	0.3241	123
0.37	1.3078	208	0.2642	97	149.86	237	0.9656	52	0.4163	66	0.3364	123
0.38	1.3284	206	0.2739	97	152.23	235	0.9708	47	0.4229	65	0.3487	124
0.39	1.3490	206	0.2836	98	154.58	235	0.9755	43	0.4294	65	0.3611	124
		204										
0.40	1.3694		0.2934	98	156.93	233	0.9798	39	0.4359	65	0.3735	125
0.41	1.3898	204	0.3032	98	159.26	233	0.9837	34	0.4424	65	0.3860	126
0.42	1.4101	203	0.3130	99	161.59	231	0.9871	31	0.4489	64	0.3986	126
0.43	1.4303	202	0.3229	99	163.90	232	0.9902	26	0.4553	64	0.4112	126
0.44	1.4505	202	0.3328	100	166.22	230	0.9928	22	0.4617	64	0.4238	126
		201										
0.45	1.4706		0.3428	99	168.52	230	0.9950	18	0.4681	64	0.4364	127
0.46	1.4907	201	0.3527	100	170.82	230	0.9968	14	0.4745	64	0.4491	127
0.47	1.5108	201	0.3627	100	173.12	229	0.9982	10	0.4809	64	0.4618	127
0.48	1.5308	200	0.3727	100	175.41	229	0.9992	6	0.4873	63	0.4745	128
0.49	1.5508	200	0.3827	100	177.71	229	0.9998	2	0.4936	64	0.4873	127
0.50	1.5708		0.3927		180.00		1.0000		0.5000		0.5000	

*Interpolation may be inaccurate at these points

Explanation of Table of Segments of Circles, Given h/d

Given: h = height of segment and d = diameter of circle, to find the chord, the length of arc, or the area of the segment, form the ratio h/d and find from the table the value of (c/d) , (arc/d) , or $(area/d^2)$; then by a simple multiplication, $c = d \times (c/d)$, $arc = d \times (arc/d)$, and $area = d^2 \times (area/d^2)$.

The table also gives the angle subtended at the center, the ratio of the arc of the segment to the whole circumference, and the ratio of the area of the segment to the area of the whole circle.

TABLE 1.13—SEGMENTS OF SPHERES

h/d	Volume segment	Difference	Volume segment	Difference
	d^3		Volume sphere	
0.00	0.0000		0.0000	
0.01	0.0002	2	0.0003	3
0.02	0.0006	4	0.0012	9
0.03	0.0014	8	0.0026	14
0.04	0.0024	10	0.0047	21
		14		26
0.05	0.0038	16	0.0073	31
0.06	0.0054	19	0.0104	36
0.07	0.0073	22	0.0140	42
0.08	0.0095	25	0.0182	46
0.09	0.0120	27	0.0228	52
0.10	0.0147	29	0.0280	56
0.11	0.0176	32	0.0336	61
0.12	0.0208	34	0.0397	66
0.13	0.0242	37	0.0463	70
0.14	0.0279	39	0.0533	74
0.15	0.0318	41	0.0607	79
0.16	0.0359	44	0.0686	83
0.17	0.0403	45	0.0769	86
0.18	0.0448	47	0.0855	91
0.19	0.0495	50	0.0946	94
0.20	0.0545	51	0.1040	98
0.21	0.0596	53	0.1138	101
0.22	0.0649	55	0.1239	105
0.23	0.0704	56	0.1344	108
0.24	0.0760	58	0.1452	110
0.25	0.0818	60	0.1562	114
0.26	0.0878	61	0.1676	117
0.27	0.0939	63	0.1793	120
0.28	0.1002	64	0.1913	122
0.29	0.1066	65	0.2035	125
0.30	0.1131	67	0.2160	127
0.31	0.1198	67	0.2287	130
0.32	0.1265	69	0.2417	131
0.33	0.1334	70	0.2548	134
0.34	0.1404	71	0.2682	135
0.35	0.1475	72	0.2817	138
0.36	0.1547	73	0.2955	139
0.37	0.1620	74	0.3094	141
0.38	0.1694	74	0.3235	142
0.39	0.1768	75	0.3377	143
0.40	0.1843	76	0.3520	145
0.41	0.1919	76	0.3665	145
0.42	0.1995	77	0.3810	147
0.43	0.2072	77	0.3957	147
0.44	0.2149	78	0.4104	148
0.45	0.2227	78	0.4252	149
0.46	0.2305	78	0.4401	150
0.47	0.2383	78	0.4551	149
0.48	0.2461	78	0.4700	150
0.49	0.2539	79	0.4850	150
0.50	0.2618		0.5000	

*Volume segment = $\frac{1}{6}\pi h^2(3d - 2h)$.

Explanation of Table of Segments of Spheres

Given: h = height of segment and d = diameter of sphere, to find the volume of the segment, form the ratio h/d and find from the table the value of (volume/ d^3): then, by a simple multiplication, volume segment = $d^3 \times$ (volume/ d^3).

The table also gives the ratio of the volume of the segment to the entire volume of the sphere. Note that the area of zone = $\pi \times h \times d$.

TABLE 1.14—VOLUMES OF SPHERES BY HUNDREDTHS

<i>d</i>	0	1	2	3	4	5	6	7	8	9	Difference
1.0	0.5236	0.5395	0.5556	0.5722	0.5890	0.6061	0.6236	0.6414	0.6596	0.6781	173
1.1	0.6969	0.7161	0.7356	0.7555	0.7757	0.7963	0.8173	0.8386	0.8603	0.8823	208
1.2	0.9048	0.9276	0.9508	0.9743	0.9983	1.0227					236
1.2						1.023	1.047	1.073	1.098	1.124	25
1.3	1.150	1.177	1.204	1.232	1.260	1.288	1.317	1.346	1.376	1.406	29
1.4	1.437	1.468	1.499	1.531	1.563	1.596	1.630	1.663	1.697	1.732	33
1.5	1.767	1.803	1.839	1.875	1.912	1.950	1.988	2.026	2.065	2.105	38
1.6	2.145	2.185	2.226	2.268	2.310	2.352	2.395	2.439	2.483	2.527	43
1.7	2.572	2.618	2.664	2.711	2.758	2.806	2.855	2.903	2.953	3.003	48
1.8	3.054	3.105	3.157	3.209	3.262	3.315	3.369	3.424	3.479	3.535	54
1.9	3.591	3.648	3.706	3.764	3.823	3.882	3.942	4.003	4.064	4.126	60
2.0	4.189	4.252	4.316	4.380	4.445	4.511	4.577	4.644	4.712	4.780	66
2.1	4.849	4.919	4.989	5.060	5.131	5.204	5.277	5.350	5.425	5.500	73
2.2	5.575	5.652	5.729	5.806	5.885	5.964	6.044	6.125	6.206	6.288	80
2.3	6.371	6.454	6.538	6.623	6.709	6.795	6.882	6.970	7.059	7.148	87
2.4	7.238	7.329	7.421	7.513	7.606	7.700	7.795	7.890	7.986	8.083	94
2.5	8.181	8.280	8.379	8.478	8.580	8.682	8.785	8.888	8.992	9.097	102
2.6	9.203	9.309	9.417	9.525	9.634	9.744	9.855	9.966	10.079		110
2.6									10.08	10.19	11
2.7	10.31	10.42	10.54	10.65	10.77	10.89	11.01	11.13	11.25	11.37	12
2.8	11.49	11.62	11.74	11.87	11.99	12.12	12.25	12.38	12.51	12.64	13
2.9	12.77	12.90	13.04	13.17	13.31	13.44	13.58	13.72	13.86	14.00	14
3.0	14.14	14.28	14.42	14.57	14.71	14.86	15.00	15.15	15.30	15.45	15
3.1	15.60	15.75	15.90	16.06	16.21	16.37	16.52	16.68	16.84	17.00	16
3.2	17.16	17.32	17.48	17.64	17.81	17.97	18.14	18.31	18.48	18.65	17
3.3	18.82	18.99	19.16	19.33	19.51	19.68	19.86	20.04	20.22	20.40	18
3.4	20.58	20.76	20.94	21.13	21.31	21.50	21.69	21.88	22.07	22.26	19
3.5	22.45	22.64	22.84	23.03	23.23	23.43	23.62	23.82	24.02	24.23	20
3.6	24.43	24.63	24.84	25.04	25.25	25.46	25.67	25.88	26.09	26.31	21
3.7	26.52	26.74	26.95	27.17	27.39	27.61	27.83	28.06	28.28	28.50	22
3.8	28.73	28.96	29.19	29.42	29.65	29.88	30.11	30.35	30.58	30.82	23
3.9	31.06	31.30	31.54	31.78	32.02	32.27	32.52	32.76	33.01	33.26	25
4.0	33.51	33.76	34.02	34.27	34.53	34.78	35.04	35.30	35.56	35.82	26
4.1	36.09	36.35	36.62	36.88	37.15	37.42	37.69	37.97	38.24	38.52	27
4.2	38.79	39.07	39.35	39.63	39.91	40.19	40.48	40.76	41.05	41.34	28
4.3	41.63	41.92	42.21	42.51	42.80	43.10	43.40	43.70	44.00	44.30	30
4.4	44.60	44.91	45.21	45.52	45.83	46.14	46.45	46.77	47.08	47.40	31
4.5	47.71	48.03	48.35	48.67	49.00	49.32	49.65	49.97	50.30	50.63	33
4.6	50.97	51.30	51.63	51.97	52.31	52.65	52.99	53.33	53.67	54.02	34
4.7	54.36	54.71	55.06	55.41	55.76	56.12	56.47	56.83	57.19	57.54	35
4.8	57.91	58.27	58.63	59.00	59.37	59.73	60.10	60.48	60.85	61.22	37
4.9	61.60	61.98	62.36	62.74	63.12	63.51	63.89	64.28	64.67	65.06	38
5.0	65.45	65.84	66.24	66.64	67.03	67.43	67.83	68.24	68.64	69.05	40
5.1	69.46	69.87	70.28	70.69	71.10	71.52	71.94	72.36	72.78	73.20	42
5.2	73.62	74.05	74.47	74.90	75.33	75.77	76.20	76.64	77.07	77.51	43
5.3	77.95	78.39	78.84	79.28	79.73	80.18	80.63	81.08	81.54	81.99	45
5.4	82.45	82.91	83.37	83.83	84.29	84.76	85.23	85.70	86.17	86.64	47

Explanation of Table of Volumes of Spheres

Moving the decimal point *one* place in Column *d* (diameter) is equivalent to moving it *three* places in the body of the table.

For example, volume of sphere = $\pi/6 \times (d^3) = 0.523599 \times (d^3)$. Conversely, $d = \sqrt[3]{6/\pi \times \text{volume}} = 1.240701 \times \sqrt[3]{\text{volume}}$.

TABLE 1.14—VOLUMES OF SPHERES BY HUNDREDTHS (continued)

d	0	1	2	3	4	5	6	7	8	9	Difference
5.5	87.11	87.59	88.07	88.55	89.03	89.51	90.00	90.48	90.97	91.49	48
5.6	91.95	92.45	92.94	93.44	93.94	94.44	94.94	95.44	95.95	96.46	50
5.7	96.97	97.48	97.99	98.51	99.02	99.54	100.06				52
5.7							100.1	100.6	101.1	101.6	5
5.8	102.2	102.7	103.2	103.8	104.3	104.8	105.4	105.9	106.4	107.0	5
5.9	107.5	108.1	108.6	109.2	109.7	110.3	110.9	111.4	112.0	112.5	6
6.0	113.1	113.7	114.2	114.8	115.4	115.9	116.5	117.7	117.1	118.3	6
6.1	118.8	119.4	120.0	120.6	121.2	121.8	122.4	123.6	123.0	124.2	
6.2	124.8	125.4	126.0	126.6	127.2	127.8	128.4	129.1	129.7	130.3	
6.3	130.9	131.5	132.2	132.8	133.4	134.1	134.7	135.3	136.0	136.6	
6.4	137.3	137.9	138.5	139.2	139.8	140.5	141.2	141.8	142.5	143.1	7
6.5	143.8	144.5	145.1	145.8	146.5	147.1	147.8	148.5	149.2	149.8	
6.6	150.5	151.2	151.9	152.6	153.3	154.0	154.7	155.4	156.1	156.8	
6.7	157.5	158.2	158.9	159.6	160.3	161.0	161.7	162.5	163.2	163.9	
6.8	164.6	165.4	166.1	166.8	167.6	168.3	169.0	169.8	170.5	171.3	
6.9	172.0	172.8	173.5	174.3	175.0	175.8	176.5	177.3	178.1	178.8	8
7.0	179.6	180.4	181.1	181.9	182.7	183.5	184.3	185.0	185.8	186.6	
7.1	187.4	188.2	189.0	189.8	190.6	191.4	192.2	193.0	193.8	194.6	
7.2	195.4	196.2	197.1	197.9	198.7	199.5	200.4	201.2	202.0	202.9	
7.3	203.7	204.5	205.4	206.2	207.1	207.9	208.8	209.6	210.5	211.3	
7.4	212.2	213.0	213.9	214.8	215.6	216.5	217.4	218.3	219.1	220.0	9
7.5	220.9	221.8	222.7	223.6	224.4	225.3	226.2	227.1	228.0	228.9	
7.6	229.8	230.8	231.7	232.6	233.5	234.4	235.3	236.3	237.2	238.1	
7.7	239.0	240.0	240.9	241.8	242.8	243.7	244.7	245.6	246.6	247.5	
7.8	248.5	249.4	250.4	251.4	252.3	253.3	254.3	255.2	256.2	257.2	10
7.9	258.2	259.1	260.1	261.1	262.1	263.1	264.1	265.1	266.1	267.1	
8.0	268.1	269.1	270.1	271.1	272.1	273.1	274.2	275.2	276.2	277.2	
8.1	278.3	279.3	280.3	281.4	282.4	283.4	284.5	285.5	286.6	287.6	11
8.2	288.7	289.8	290.8	291.9	292.9	294.0	295.1	296.2	297.2	298.3	
8.3	299.4	300.5	301.6	302.6	303.7	304.8	305.9	307.0	308.1	309.2	
8.4	310.3	311.4	312.6	313.7	314.8	315.9	317.0	318.2	319.3	320.4	
8.5	321.6	322.7	323.8	325.0	326.1	327.3	328.4	329.6	330.7	331.9	
8.6	333.0	334.2	335.4	336.5	337.7	338.9	340.1	341.2	342.4	343.6	12
8.7	344.8	346.0	347.2	348.4	349.6	350.8	352.0	353.2	354.4	355.6	
8.8	356.8	358.0	359.3	360.5	361.7	362.9	364.2	365.4	366.6	367.9	
8.9	369.1	370.4	371.6	372.9	374.1	375.4	376.6	377.9	379.2	380.4	13
9.0	381.7	383.0	384.3	385.5	386.8	388.1	389.4	390.7	392.0	393.3	
9.1	394.6	395.9	397.2	398.5	399.8	401.1	402.4	403.7	405.1	406.4	
9.2	407.7	409.1	410.4	411.7	413.1	414.4	415.7	417.1	418.4	419.8	14
9.3	421.2	422.5	423.9	425.2	426.6	428.0	429.4	430.7	432.1	433.5	
9.4	434.9	436.3	437.7	439.1	440.5	441.9	443.3	444.7	446.1	447.5	
9.5	448.9	450.3	451.8	453.2	454.6	456.0	457.5	458.9	460.4	461.8	
9.6	463.2	464.7	466.1	467.6	469.1	470.5	472.0	473.5	474.9	476.4	15
9.7	477.9	479.4	480.8	482.3	483.8	485.3	486.8	488.3	489.8	491.3	
9.8	492.8	494.3	495.8	497.3	498.9	500.4	501.9	503.4	505.0	506.5	16
9.9	508.0	509.6	511.1	512.7	514.2	515.8	517.3	518.9	520.5	522.0	
10.0	523.6										

TABLE 1.15—REGULAR POLYGONS

n	α	Area $\frac{L^2}{4}$	Area $\frac{R^2}{4}$	Area $\frac{r^2}{4}$	$\frac{R}{L}$	$\frac{R}{r}$	$\frac{L}{R}$	$\frac{L}{r}$	$\frac{r}{R}$	$\frac{r}{L}$
3	120°	0.4330	1.299	5.196	0.5774	2.000	1.732	3.464	0.5000	0.2887
4	90°	1.000	2.000	4.000	0.7071	1.414	1.414	2.000	0.7071	0.5000
5	72°	1.721	2.378	3.633	0.8507	1.236	1.176	1.453	0.8090	0.6882
6	60°	2.598	2.598	3.464	1.000	1.155	1.000	1.155	0.8660	0.8660
7	51°.43	3.634	2.736	3.371	1.152	1.110	0.8678	0.9631	0.9010	1.038
8	45°	4.828	2.828	3.314	1.307	1.082	0.7654	0.8284	0.9239	1.207
9	40°	6.182	2.893	3.276	1.462	1.064	0.6840	0.7279	0.9397	1.374
10	36°	7.694	2.939	3.249	1.618	1.052	0.6180	0.6498	0.9511	1.539
12	30°	11.20	3.000	3.215	1.932	1.035	0.5176	0.5359	0.9659	1.866
15	24°	17.64	3.051	3.188	2.405	1.022	0.4158	0.4251	0.9781	2.352
16	22°.50	20.11	3.062	3.183	2.563	1.020	0.3902	0.3978	0.9808	2.514
20	18°	31.57	3.090	3.168	3.196	1.013	0.3129	0.3168	0.9877	3.157
24	15°	45.58	3.106	3.160	3.831	1.009	0.2611	0.2633	0.9914	3.798
32	11°.25	81.23	3.121	3.152	5.101	1.005	0.1960	0.1970	0.9952	5.077
48	7°.50	183.1	3.133	3.146	7.645	1.002	0.1308	0.1311	0.9979	7.629
64	5°.625	325.7	3.137	3.144	10.19	1.001	0.0981	0.0983	0.9968	10.18

n = number of sides,

α = $360^\circ/n$ = angle subtended at the center by one side,

L = length of one side = $R(2 \sin \alpha/2) = r(2 \tan \alpha/2)$,

R = radius of circumscribed circle = $L(1/2 \csc \alpha/2) = r(\sec \alpha/2)$,

r = radius of inscribed circle = $R(\cos \alpha/2) = L(1/2 \cot \alpha/2)$, and

area = $L^2 (1/4 n \cot \alpha/2) = R^2 (1/2 n \sin \alpha) = r^2 (n \tan \alpha/2)$.

TABLE 1.16—BINOMIAL COEFFICIENTS

$(n)_0 = 1$, $(n)_1 = n$, $(n)_2 = [n(n-1)]/(1 \times 2)$, $(n)_3 = [n(n-1)(n-2)]/(1 \times 2 \times 3)$, etc.; in general, $(n)_r = n(n-1)(n-2) \dots [n-(r-1)]/(1 \times 2 \times 3 \dots r)$. Other notations: $nCr = (n/r) = (n)_r$.

n	$(n)_0$	$(n)_1$	$(n)_2$	$(n)_3$	$(n)_4$	$(n)_5$	$(n)_6$	$(n)_7$	$(n)_8$	$(n)_9$	$(n)_{10}$	$(n)_{11}$	$(n)_{12}$	$(n)_{13}$
1	1	1												
2	1	2	1											
3	1	3	3	1										
4	1	4	6	4	1									
5	1	5	10	10	5	1								
6	1	6	15	20	15	6	1							
7	1	7	21	35	35	21	7	1						
8	1	8	28	56	70	56	28	8	1					
9	1	9	36	84	126	126	84	36	9	1				
10	1	10	45	120	210	252	210	120	45	10	1			
11	1	11	55	165	330	462	462	330	165	55	11	1		
12	1	12	66	220	495	792	924	792	495	220	66	12	1	
13	1	13	78	286	715	1,287	1,716	1,716	1,287	715	286	78	13	1
14	1	14	91	364	1,001	2,002	3,003	3,432	3,003	2,002	1,001	364	91	14
15	1	15	105	455	1,365	3,003	5,005	6,435	6,435	5,005	3,003	1,365	455	105

* For $n = 14$, $(n)_{14} = 1$; for $n = 15$, $(n)_{15} = 1$; and $(n)_{15} = 1$.

TABLE 1.17—COMMON LOGARITHMS (1.00 TO 2.00)

Number	0	1	2	3	4	5	6	7	8	9	Average Difference
1.00	0.0000	0.0004	0.0009	0.0013	0.0017	0.0022	0.0026	0.0030	0.0035	0.0039	4
1.01	0.0043	0.0048	0.0052	0.0056	0.0060	0.0065	0.0069	0.0073	0.0077	0.0082	
1.02	0.0086	0.0090	0.0095	0.0099	0.0103	0.0107	0.0111	0.0116	0.0120	0.0124	
1.03	0.0128	0.0133	0.0137	0.0141	0.0145	0.0149	0.0154	0.0158	0.0162	0.0166	
1.04	0.0170	0.0175	0.0179	0.0183	0.0187	0.0191	0.0195	0.0199	0.0204	0.0208	
1.05	0.0212	0.0216	0.0220	0.0224	0.0228	0.0233	0.0237	0.0241	0.0245	0.0249	
1.06	0.0253	0.0257	0.0261	0.0265	0.0269	0.0273	0.0278	0.0282	0.0286	0.0290	
1.07	0.0294	0.0298	0.0302	0.0306	0.0310	0.0314	0.0318	0.0322	0.0326	0.0330	
1.08	0.0334	0.0338	0.0342	0.0346	0.0350	0.0354	0.0358	0.0362	0.0366	0.0370	
1.09	0.0374	0.0378	0.0382	0.0386	0.0390	0.0394	0.0398	0.0402	0.0406	0.0410	
1.10	0.0414	0.0418	0.0422	0.0426	0.0430	0.0434	0.0438	0.0441	0.0445	0.0449	
1.11	0.0453	0.0457	0.0461	0.0465	0.0469	0.0473	0.0477	0.0481	0.0484	0.0488	
1.12	0.0492	0.0496	0.0500	0.0504	0.0508	0.0512	0.0515	0.0519	0.0523	0.0527	
1.13	0.0531	0.0535	0.0538	0.0542	0.0546	0.0550	0.0554	0.0558	0.0561	0.0565	
1.14	0.0569	0.0573	0.0577	0.0580	0.0584	0.0588	0.0592	0.0596	0.0599	0.0603	
1.15	0.0607	0.0611	0.0615	0.0618	0.0622	0.0626	0.0630	0.0633	0.0637	0.0641	
1.16	0.0645	0.0648	0.0652	0.0656	0.0660	0.0663	0.0667	0.0671	0.0674	0.0678	
1.17	0.0682	0.0686	0.0689	0.0693	0.0697	0.0700	0.0704	0.0708	0.0711	0.0715	
1.18	0.0719	0.0722	0.0726	0.0730	0.0734	0.0737	0.0741	0.0745	0.0748	0.0752	
1.19	0.0755	0.0759	0.0763	0.0766	0.0770	0.0774	0.0777	0.0781	0.0785	0.0788	
1.20	0.0792	0.0795	0.0799	0.0803	0.0806	0.0810	0.0813	0.0817	0.0821	0.0824	3
1.21	0.0828	0.0831	0.0835	0.0839	0.0842	0.0846	0.0849	0.0853	0.0856	0.0860	
1.22	0.0864	0.0867	0.0871	0.0874	0.0878	0.0881	0.0885	0.0888	0.0892	0.0896	
1.23	0.0899	0.0903	0.0906	0.0910	0.0913	0.0917	0.0920	0.0924	0.0927	0.0931	
1.24	0.0934	0.0938	0.0941	0.0945	0.0948	0.0952	0.0955	0.0959	0.0962	0.0966	
1.25	0.0969	0.0973	0.0976	0.0980	0.0983	0.0986	0.0990	0.0993	0.0997	0.1000	
1.26	0.1004	0.1007	0.1011	0.1014	0.1017	0.1021	0.1024	0.1028	0.1031	0.1035	
1.27	0.1038	0.1041	0.1045	0.1048	0.1052	0.1055	0.1059	0.1062	0.1065	0.1069	
1.28	0.1072	0.1075	0.1079	0.1082	0.1086	0.1089	0.1092	0.1096	0.1099	0.1103	
1.29	0.1106	0.1109	0.1113	0.1116	0.1119	0.1123	0.1126	0.1129	0.1133	0.1136	
1.30	0.1139	0.1143	0.1146	0.1149	0.1153	0.1156	0.1159	0.1163	0.1166	0.1169	
1.31	0.1173	0.1176	0.1179	0.1183	0.1186	0.1189	0.1193	0.1196	0.1199	0.1202	
1.32	0.1206	0.1209	0.1212	0.1216	0.1219	0.1222	0.1225	0.1229	0.1232	0.1235	
1.33	0.1239	0.1242	0.1245	0.1248	0.1252	0.1255	0.1258	0.1261	0.1265	0.1268	
1.34	0.1271	0.1274	0.1278	0.1281	0.1284	0.1287	0.1290	0.1294	0.1297	0.1300	
1.35	0.1303	0.1307	0.1310	0.1313	0.1316	0.1319	0.1323	0.1326	0.1329	0.1332	
1.36	0.1335	0.1339	0.1342	0.1345	0.1348	0.1351	0.1355	0.1358	0.1361	0.1364	
1.37	0.1367	0.1370	0.1374	0.1377	0.1380	0.1383	0.1386	0.1389	0.1392	0.1396	
1.38	0.1399	0.1402	0.1405	0.1408	0.1411	0.1414	0.1418	0.1421	0.1424	0.1427	
1.39	0.1430	0.1433	0.1436	0.1440	0.1443	0.1446	0.1449	0.1452	0.1455	0.1458	
1.40	0.1461	0.1464	0.1467	0.1471	0.1474	0.1477	0.1480	0.1483	0.1486	0.1489	
1.41	0.1492	0.1495	0.1498	0.1501	0.1504	0.1508	0.1511	0.1514	0.1517	0.1520	
1.42	0.1523	0.1526	0.1529	0.1532	0.1535	0.1538	0.1541	0.1544	0.1547	0.1550	
1.43	0.1553	0.1556	0.1559	0.1562	0.1565	0.1569	0.1572	0.1575	0.1578	0.1581	
1.44	0.1584	0.1587	0.1590	0.1593	0.1596	0.1599	0.1602	0.1605	0.1608	0.1611	
1.45	0.1614	0.1617	0.1620	0.1623	0.1626	0.1629	0.1632	0.1635	0.1638	0.1641	
1.46	0.1644	0.1647	0.1649	0.1652	0.1655	0.1658	0.1661	0.1664	0.1667	0.1670	
1.47	0.1673	0.1676	0.1679	0.1682	0.1685	0.1688	0.1691	0.1694	0.1697	0.1700	
1.48	0.1703	0.1706	0.1708	0.1711	0.1714	0.1717	0.1720	0.1723	0.1726	0.1729	
1.49	0.1732	0.1735	0.1738	0.1741	0.1744	0.1746	0.1749	0.1752	0.1755	0.1758	

Moving the decimal point n places to the right (or left) in the number requires adding $+n$ (or $-n$) in the body of the table. See Table 1.18.

TABLE 1.17—COMMON LOGARITHMS (1.00 TO 2.00) (continued)

Number	0	1	2	3	4	5	6	7	8	9	Average Difference
1.50	0.1761	0.1764	0.1767	0.1770	0.1772	0.1775	0.1778	0.1781	0.1784	0.1787	3
1.51	0.1790	0.1793	0.1796	0.1798	0.1801	0.1804	0.1807	0.1810	0.1813	0.1816	
1.52	0.1818	0.1821	0.1824	0.1827	0.1830	0.1833	0.1836	0.1838	0.1841	0.1844	
1.53	0.1847	0.1850	0.1853	0.1855	0.1858	0.1861	0.1864	0.1867	0.1870	0.1872	
1.54	0.1875	0.1878	0.1881	0.1884	0.1886	0.1889	0.1892	0.1895	0.1898	0.1901	
1.55	0.1903	0.1906	0.1909	0.1912	0.1915	0.1917	0.1920	0.1923	0.1926	0.1928	
1.56	0.1931	0.1934	0.1937	0.1940	0.1942	0.1945	0.1948	0.1951	0.1953	0.1956	
1.57	0.1959	0.1962	0.1965	0.1967	0.1970	0.1973	0.1976	0.1978	0.1981	0.1984	
1.58	0.1987	0.1989	0.1992	0.1995	0.1998	0.2000	0.2003	0.2006	0.2009	0.2011	
1.59	0.2014	0.2017	0.2019	0.2022	0.2025	0.2028	0.2030	0.2033	0.2036	0.2038	
1.60	0.2041	0.2044	0.2047	0.2049	0.2052	0.2055	0.2057	0.2060	0.2063	0.2066	2
1.61	0.2068	0.2071	0.2074	0.2076	0.2079	0.2082	0.2084	0.2087	0.2090	0.2092	
1.62	0.2095	0.2098	0.2101	0.2103	0.2106	0.2109	0.2111	0.2114	0.2117	0.2119	
1.63	0.2122	0.2125	0.2127	0.2130	0.2133	0.2135	0.2138	0.2140	0.2143	0.2146	
1.64	0.2148	0.2151	0.2154	0.2156	0.2159	0.2162	0.2164	0.2167	0.2170	0.2172	
1.65	0.2175	0.2177	0.2180	0.2183	0.2185	0.2188	0.2191	0.2193	0.2196	0.2198	
1.66	0.2201	0.2204	0.2206	0.2209	0.2212	0.2214	0.2217	0.2219	0.2222	0.2225	
1.67	0.2227	0.2230	0.2232	0.2235	0.2238	0.2240	0.2243	0.2245	0.2248	0.2251	
1.68	0.2253	0.2256	0.2258	0.2261	0.2263	0.2266	0.2269	0.2271	0.2274	0.2276	
1.69	0.2279	0.2281	0.2284	0.2287	0.2289	0.2292	0.2294	0.2297	0.2299	0.2302	
1.70	0.2304	0.2307	0.2310	0.2312	0.2315	0.2317	0.2320	0.2322	0.2325	0.2327	2
1.71	0.2330	0.2333	0.2335	0.2338	0.2340	0.2343	0.2345	0.2348	0.2350	0.2353	
1.72	0.2355	0.2358	0.2360	0.2363	0.2365	0.2368	0.2370	0.2373	0.2375	0.2378	
1.73	0.2380	0.2383	0.2385	0.2388	0.2390	0.2393	0.2395	0.2398	0.2400	0.2403	
1.74	0.2405	0.2408	0.2410	0.2413	0.2415	0.2418	0.2420	0.2423	0.2425	0.2428	
1.75	0.2430	0.2433	0.2435	0.2438	0.2440	0.2443	0.2445	0.2448	0.2450	0.2453	
1.76	0.2455	0.2458	0.2460	0.2463	0.2465	0.2467	0.2470	0.2472	0.2475	0.2477	
1.77	0.2480	0.2482	0.2485	0.2487	0.2490	0.2492	0.2494	0.2497	0.2499	0.2502	
1.78	0.2504	0.2507	0.2509	0.2512	0.2514	0.2516	0.2519	0.2521	0.2524	0.2526	
1.79	0.2529	0.2531	0.2533	0.2536	0.2538	0.2541	0.2543	0.2545	0.2548	0.2550	
1.80	0.2553	0.2555	0.2558	0.2560	0.2562	0.2565	0.2567	0.2570	0.2572	0.2574	2
1.81	0.2577	0.2579	0.2582	0.2584	0.2586	0.2589	0.2591	0.2594	0.2596	0.2598	
1.82	0.2601	0.2603	0.2605	0.2608	0.2610	0.2613	0.2615	0.2617	0.2620	0.2622	
1.83	0.2625	0.2627	0.2629	0.2632	0.2634	0.2636	0.2639	0.2641	0.2643	0.2646	
1.84	0.2648	0.2651	0.2653	0.2655	0.2658	0.2660	0.2662	0.2665	0.2667	0.2669	
1.85	0.2672	0.2674	0.2676	0.2679	0.2681	0.2683	0.2686	0.2688	0.2690	0.2693	
1.86	0.2695	0.2697	0.2700	0.2702	0.2704	0.2707	0.2709	0.2711	0.2714	0.2716	
1.87	0.2718	0.2721	0.2723	0.2725	0.2728	0.2730	0.2732	0.2735	0.2737	0.2739	
1.88	0.2742	0.2744	0.2746	0.2749	0.2751	0.2753	0.2755	0.2758	0.2760	0.2762	
1.89	0.2765	0.2767	0.2769	0.2772	0.2774	0.2776	0.2778	0.2781	0.2783	0.2785	
1.90	0.2788	0.2790	0.2792	0.2794	0.2797	0.2799	0.2801	0.2804	0.2806	0.2808	2
1.91	0.2810	0.2813	0.2815	0.2817	0.2819	0.2822	0.2824	0.2826	0.2828	0.2831	
1.92	0.2833	0.2835	0.2838	0.2840	0.2842	0.2844	0.2847	0.2849	0.2851	0.2853	
1.93	0.2856	0.2858	0.2860	0.2862	0.2865	0.2867	0.2869	0.2871	0.2874	0.2876	
1.94	0.2878	0.2880	0.2882	0.2885	0.2887	0.2889	0.2891	0.2894	0.2896	0.2898	
1.95	0.2900	0.2903	0.2905	0.2907	0.2909	0.2911	0.2914	0.2916	0.2918	0.2920	
1.96	0.2923	0.2925	0.2927	0.2929	0.2931	0.2934	0.2936	0.2938	0.2940	0.2942	
1.97	0.2945	0.2947	0.2949	0.2951	0.2953	0.2956	0.2958	0.2960	0.2962	0.2964	
1.98	0.2967	0.2969	0.2971	0.2973	0.2975	0.2978	0.2980	0.2982	0.2984	0.2986	
1.99	0.2989	0.2991	0.2993	0.2995	0.2997	0.2999	0.3002	0.3004	0.3006	0.3008	

Moving the decimal point n places to the right (or left) in the number requires adding $+n$ (or $-n$) in the body of the table. See Table 1.18.

TABLE 1.18—COMMON LOGARITHMS

Number	0	1	2	3	4	5	6	7	8	9	Average Difference
1.0	0.0000	0.0043	0.0086	0.0128	0.0170	0.0212	0.0253	0.0294	0.0334	0.0374	See Table 1.17
1.1	0.0414	0.0453	0.0492	0.0531	0.0569	0.0607	0.0645	0.0682	0.0719	0.0755	See Table 1.17
1.2	0.0792	0.0828	0.0864	0.0899	0.0934	0.0969	0.1004	0.1038	0.1072	0.1106	See Table 1.17
1.3	0.1139	0.1173	0.1206	0.1239	0.1271	0.1303	0.1335	0.1367	0.1399	0.1430	See Table 1.17
1.4	0.1461	0.1492	0.1523	0.1553	0.1584	0.1614	0.1644	0.1673	0.1703	0.1732	See Table 1.17
1.5	0.1761	0.1790	0.1818	0.1847	0.1875	0.1903	0.1931	0.1959	0.1987	0.2014	See Table 1.17
1.6	0.2041	0.2068	0.2095	0.2122	0.2148	0.2175	0.2201	0.2227	0.2253	0.2279	See Table 1.17
1.7	0.2304	0.2330	0.2355	0.2380	0.2405	0.2430	0.2455	0.2480	0.2504	0.2529	See Table 1.17
1.8	0.2553	0.2577	0.2601	0.2625	0.2648	0.2672	0.2695	0.2718	0.2742	0.2765	See Table 1.17
1.9	0.2788	0.2810	0.2833	0.2856	0.2878	0.2900	0.2923	0.2945	0.2967	0.2989	See Table 1.17
2.0	0.3010	0.3032	0.3054	0.3075	0.3096	0.3118	0.3139	0.3160	0.3181	0.3201	21
2.1	0.3222	0.3243	0.3263	0.3284	0.3304	0.3324	0.3345	0.3365	0.3385	0.3404	20
2.2	0.3424	0.3444	0.3464	0.3483	0.3502	0.3522	0.3541	0.3560	0.3579	0.3598	19
2.3	0.3617	0.3636	0.3655	0.3674	0.3692	0.3711	0.3729	0.3747	0.3766	0.3784	18
2.4	0.3802	0.3820	0.3838	0.3856	0.3874	0.3892	0.3909	0.3927	0.3945	0.3962	17
2.5	0.3979	0.3997	0.4014	0.4031	0.4048	0.4065	0.4082	0.4099	0.4116	0.4133	17
2.6	0.4150	0.4166	0.4183	0.4200	0.4216	0.4232	0.4249	0.4265	0.4281	0.4298	16
2.7	0.4314	0.4330	0.4346	0.4362	0.4378	0.4393	0.4409	0.4425	0.4440	0.4456	16
2.8	0.4472	0.4487	0.4502	0.4518	0.4533	0.4548	0.4564	0.4579	0.4594	0.4609	15
2.9	0.4624	0.4639	0.4654	0.4669	0.4683	0.4698	0.4713	0.4728	0.4742	0.4757	15
3.0	0.4771	0.4786	0.4800	0.4814	0.4829	0.4843	0.4857	0.4871	0.4886	0.4900	14
3.1	0.4914	0.4928	0.4942	0.4955	0.4969	0.4983	0.4997	0.5011	0.5024	0.5038	14
3.2	0.5051	0.5065	0.5079	0.5092	0.5105	0.5119	0.5132	0.5145	0.5159	0.5172	13
3.3	0.5185	0.5198	0.5211	0.5224	0.5237	0.5250	0.5263	0.5276	0.5289	0.5302	13
3.4	0.5315	0.5328	0.5340	0.5353	0.5366	0.5378	0.5391	0.5403	0.5416	0.5428	13
3.5	0.5441	0.5453	0.5465	0.5478	0.5490	0.5502	0.5514	0.5527	0.5539	0.5551	12
3.6	0.5563	0.5575	0.5587	0.5599	0.5611	0.5623	0.5635	0.5647	0.5658	0.5670	12
3.7	0.5682	0.5694	0.5705	0.5717	0.5729	0.5740	0.5752	0.5763	0.5775	0.5786	12
3.8	0.5798	0.5809	0.5821	0.5832	0.5843	0.5855	0.5866	0.5877	0.5888	0.5899	11
3.9	0.5911	0.5922	0.5933	0.5944	0.5955	0.5966	0.5977	0.5988	0.5999	0.6010	11
4.0	0.6021	0.6031	0.6042	0.6053	0.6064	0.6075	0.6085	0.6096	0.6107	0.6117	11
4.1	0.6128	0.6138	0.6149	0.6160	0.6170	0.6180	0.6191	0.6201	0.6212	0.6222	10
4.2	0.6232	0.6243	0.6253	0.6263	0.6274	0.6284	0.6294	0.6304	0.6314	0.6325	10
4.3	0.6335	0.6345	0.6355	0.6365	0.6375	0.6385	0.6395	0.6405	0.6415	0.6425	10
4.4	0.6435	0.6444	0.6454	0.6464	0.6474	0.6484	0.6493	0.6503	0.6513	0.6522	10
4.5	0.6532	0.6542	0.6551	0.6561	0.6571	0.6580	0.6590	0.6599	0.6609	0.6618	10
4.6	0.6628	0.6637	0.6646	0.6656	0.6665	0.6675	0.6684	0.6693	0.6702	0.6712	10
4.7	0.6721	0.6730	0.6739	0.6749	0.6758	0.6767	0.6776	0.6785	0.6794	0.6803	9
4.8	0.6812	0.6812	0.6830	0.6839	0.6848	0.6857	0.6866	0.6875	0.6884	0.6893	9
4.9	0.6902	0.6911	0.6920	0.6928	0.6937	0.6946	0.6955	0.6964	0.6972	0.6981	9
5.0	0.6990	0.6998	0.7007	0.7016	0.7024	0.7033	0.7042	0.7050	0.7059	0.7067	9
5.1	0.7076	0.7084	0.7093	0.7101	0.7110	0.7118	0.7126	0.7135	0.7143	0.7152	8
5.2	0.7160	0.7168	0.7177	0.7185	0.7193	0.7202	0.7210	0.7218	0.7226	0.7235	8
5.3	0.7243	0.7251	0.7259	0.7267	0.7275	0.7284	0.7292	0.7300	0.7308	0.7316	8
5.4	0.7324	0.7332	0.7340	0.7348	0.7356	0.7364	0.7372	0.7380	0.7388	0.7396	8
5.5	0.7404	0.7412	0.7419	0.7427	0.7435	0.7443	0.7451	0.7459	0.7466	0.7474	8
5.6	0.7482	0.7490	0.7497	0.7505	0.7513	0.7520	0.7528	0.7536	0.7543	0.7551	8
5.7	0.7559	0.7566	0.7574	0.7582	0.7589	0.7597	0.7604	0.7612	0.7619	0.7627	8
5.8	0.7634	0.7642	0.7649	0.7657	0.7664	0.7672	0.7679	0.7686	0.7694	0.7701	7
5.9	0.7709	0.7716	0.7723	0.7731	0.7738	0.7745	0.7752	0.7760	0.7767	0.7774	7

This table gives the common logarithms of numbers between 1 and 10, correct to four places. Moving the decimal point n places to the right (or left) in the number is equivalent to adding n (or $-n$) to the logarithm. Thus, $\log 0.017453 = 0.2419 - 2$, which may also be written 2.2419 or $8.2419 - 10$.

For example, $\log(ab) = \log a + \log b$, $\log(a^N) = N \log a$, $\log(a/b) = \log a - \log b$, and $\log(\sqrt[N]{a}) = 1/N \log a$.

TABLE 1.18—COMMON LOGARITHMS (continued)

Number	0	1	2	3	4	5	6	7	8	9	Average Difference
6.0	0.7782	0.7789	0.7796	0.7803	0.7810	0.7818	0.7825	0.7832	0.7839	0.7846	7
6.1	0.7853	0.7860	0.7868	0.7875	0.7882	0.7889	0.7896	0.7903	0.7910	0.7917	7
6.2	0.7924	0.7931	0.7938	0.7945	0.7952	0.7959	0.7966	0.7973	0.7980	0.7987	7
6.3	0.7993	0.8000	0.8007	0.8014	0.8021	0.8028	0.8035	0.8041	0.8048	0.8055	7
6.4	0.8062	0.8069	0.8075	0.8082	0.8089	0.8096	0.8102	0.8109	0.8116	0.8122	7
6.5	0.8129	0.8136	0.8142	0.8149	0.8156	0.8162	0.8169	0.8176	0.8182	0.8189	7
6.6	0.8195	0.8202	0.8209	0.8215	0.8222	0.8228	0.8235	0.8241	0.8248	0.8254	7
6.7	0.8261	0.8267	0.8274	0.8280	0.8287	0.8293	0.8299	0.8306	0.8312	0.8319	6
6.8	0.8325	0.8331	0.8338	0.8344	0.8351	0.8357	0.8363	0.8370	0.8376	0.8382	6
6.9	0.8388	0.8395	0.8401	0.8407	0.8414	0.8420	0.8426	0.8432	0.8439	0.8445	6
7.0	0.8451	0.8457	0.8463	0.8470	0.8476	0.8482	0.8488	0.8494	0.8500	0.8506	6
7.1	0.8513	0.8519	0.8525	0.8531	0.8537	0.8543	0.8549	0.8555	0.8561	0.8567	6
7.2	0.8573	0.8579	0.8585	0.8591	0.8597	0.8603	0.8609	0.8615	0.8621	0.8627	6
7.3	0.8633	0.8639	0.8645	0.8651	0.8657	0.8663	0.8669	0.8675	0.8681	0.8686	6
7.4	0.8692	0.8698	0.8704	0.8710	0.8716	0.8722	0.8727	0.8733	0.8739	0.8745	6
7.5	0.8751	0.8756	0.8762	0.8768	0.8774	0.8779	0.8785	0.8791	0.8797	0.8802	6
7.6	0.8808	0.8814	0.8820	0.8825	0.8831	0.8837	0.8842	0.8848	0.8854	0.8859	6
7.7	0.8865	0.8871	0.8876	0.8882	0.8887	0.8893	0.8899	0.8904	0.8910	0.8915	6
7.8	0.8921	0.8927	0.8932	0.8938	0.8943	0.8949	0.8954	0.8960	0.8965	0.8971	6
7.9	0.8976	0.8982	0.8987	0.8993	0.8998	0.9004	0.9009	0.9015	0.9020	0.9025	5
8.0	0.9031	0.9036	0.9042	0.9047	0.9053	0.9058	0.9063	0.9069	0.9074	0.9079	5
8.1	0.9085	0.9090	0.9096	0.9101	0.9106	0.9112	0.9117	0.9122	0.9128	0.9133	5
8.2	0.9138	0.9143	0.9149	0.9154	0.9159	0.9165	0.9170	0.9175	0.9180	0.9186	5
8.3	0.9191	0.9196	0.9201	0.9206	0.9212	0.9217	0.9222	0.9227	0.9232	0.9238	5
8.4	0.9243	0.9248	0.9253	0.9258	0.9263	0.9269	0.9274	0.9279	0.9284	0.9289	5
8.5	0.9294	0.9299	0.9304	0.9309	0.9315	0.9320	0.9325	0.9330	0.9335	0.9340	5
8.6	0.9345	0.9350	0.9355	0.9360	0.9365	0.9370	0.9375	0.9380	0.9385	0.9390	5
8.7	0.9395	0.9400	0.9405	0.9410	0.9415	0.9420	0.9425	0.9430	0.9435	0.9440	5
8.8	0.9445	0.9450	0.9455	0.9460	0.9465	0.9469	0.9474	0.9479	0.9484	0.9489	5
8.9	0.9494	0.9499	0.9504	0.9509	0.9513	0.9518	0.9523	0.9528	0.9533	0.9538	5
9.0	0.9542	0.9547	0.9552	0.9557	0.9562	0.9566	0.9571	0.9576	0.9581	0.9586	5
9.1	0.9590	0.9595	0.9600	0.9605	0.9609	0.9614	0.9619	0.9624	0.9628	0.9633	5
9.2	0.9638	0.9643	0.9647	0.9652	0.9657	0.9661	0.9666	0.9671	0.9675	0.9680	5
9.3	0.9685	0.9689	0.9694	0.9699	0.9703	0.9708	0.9713	0.9717	0.9722	0.9727	5
9.4	0.9731	0.9736	0.9741	0.9745	0.9750	0.9754	0.9759	0.9763	0.9768	0.9773	5
9.5	0.9777	0.9782	0.9786	0.9791	0.9795	0.9800	0.9805	0.9809	0.9814	0.9818	5
9.6	0.9823	0.9827	0.9832	0.9836	0.9841	0.9845	0.9850	0.9854	0.9859	0.9863	4
9.7	0.9868	0.9872	0.9877	0.9881	0.9886	0.9890	0.9894	0.9899	0.9903	0.9908	4
9.8	0.9912	0.9917	0.9921	0.9926	0.9930	0.9934	0.9939	0.9943	0.9948	0.9952	4
9.9	0.9956	0.9961	0.9965	0.9969	0.9974	0.9978	0.9983	0.9987	0.9991	0.9996	4

$\log \mu = 0.4971$, $\log \mu/2 = 0.1961$, $\log \mu^2 = 0.9943$, $\log \sqrt{\mu} = 0.2486$, $\log e = 0.4343$, and $\log (0.4343) = 0.6378 - 1$.

TABLE 1.19—DEGREES AND MINUTES EXPRESSED IN RADIAN*^a

Degrees				Hundredths				Minutes	
1	0.0175	61	1.0647	121	2.1118	0°.01	0.0002	0°.51	0.0089
2	0.0349	62	1.0821	122	2.1293	0°.02	0.0003	0°.52	0.0091
3	0.0524	63	1.0996	123	2.1468	0°.03	0.0005	0°.53	0.0093
4	0.0698	64	1.1170	124	2.1642	0°.04	0.0007	0°.54	0.0094
5	0.0873	65	1.1345	125	2.1817	0°.05	0.0009	0°.55	0.0096
6	0.1047	66	1.1519	126	2.1991	0°.06	0.0010	0°.56	0.0098
7	0.1222	67	1.1694	127	2.2166	0°.07	0.0012	0°.57	0.0099
8	0.1396	68	1.1868	128	2.2340	0°.08	0.0014	0°.58	0.0101
9	0.1571	69	1.2043	129	2.2515	0°.09	0.0016	0°.59	0.0103
10	0.1745	70	1.2217	130	2.2689	0°.10	0.0017	0°.60	0.0105
11	0.1920	71	1.2392	131	2.2864	0°.11	0.0019	0°.61	0.0106
12	0.2094	72	1.2566	132	2.3038	0°.12	0.0021	0°.62	0.0108
13	0.2269	73	1.2741	133	2.3213	0°.13	0.0023	0°.63	0.0110
14	0.2443	74	1.2915	134	2.3387	0°.14	0.0024	0°.64	0.0112
15	0.2618	75	1.3090	135	2.3562	0°.15	0.0026	0°.65	0.0113
16	0.2793	76	1.3265	136	2.3736	0°.16	0.0028	0°.66	0.0115
17	0.2967	77	1.3439	137	2.3911	0°.17	0.0030	0°.67	0.0117
18	0.3142	78	1.3614	138	2.4086	0°.18	0.0031	0°.68	0.0119
19	0.3316	79	1.3788	139	2.4260	0°.19	0.0033	0°.69	0.0120
20	0.3491	80	1.3963	140	2.4435	0°.20	0.0035	0°.70	0.0122
21	0.3665	81	1.4137	141	2.4609	0°.21	0.0037	0°.71	0.0124
22	0.3840	82	1.4312	142	2.4784	0°.22	0.0038	0°.72	0.0126
23	0.4014	83	1.4486	143	2.4958	0°.23	0.0040	0°.73	0.0127
24	0.4189	84	1.4661	144	2.5133	0°.24	0.0042	0°.74	0.0129
25	0.4363	85	1.4835	145	2.5307	0°.25	0.0044	0°.75	0.0131
26	0.4538	86	1.5010	146	2.5482	0°.26	0.0045	0°.76	0.0133
27	0.4712	87	1.5184	147	2.5656	0°.27	0.0047	0°.77	0.0134
28	0.4887	88	1.5359	148	2.5831	0°.28	0.0049	0°.78	0.0136
29	0.5061	89	1.5533	149	2.6005	0°.29	0.0051	0°.79	0.0138
30	0.5236	90	1.5708	150	2.6180	0°.30	0.0052	0°.80	0.0140
31	0.5411	91	1.5882	151	2.6354	0°.31	0.0054	0°.81	0.0141
32	0.5585	92	1.6057	152	2.6529	0°.32	0.0056	0°.82	0.0143
33	0.5760	93	1.6232	153	2.6704	0°.33	0.0058	0°.83	0.0145
34	0.5934	94	1.6406	154	2.6878	0°.34	0.0059	0°.84	0.0147
35	0.6109	95	1.6581	155	2.7053	0°.35	0.0061	0°.85	0.0148
36	0.6283	96	1.6755	156	2.7227	0°.36	0.0063	0°.86	0.0150
37	0.6458	97	1.6930	157	2.7402	0°.37	0.0065	0°.87	0.0152
38	0.6632	98	1.7104	158	2.7576	0°.38	0.0066	0°.88	0.0154
39	0.6807	99	1.7279	159	2.7751	0°.39	0.0068	0°.89	0.0155
40	0.6981	100	1.7453	160	2.7925	0°.40	0.0070	0°.90	0.0157
41	0.7156	101	1.7628	161	2.8100	0°.41	0.0072	0°.91	0.0159
42	0.7330	102	1.7802	162	2.8274	0°.42	0.0073	0°.92	0.0161
43	0.7505	103	1.7977	163	2.8449	0°.43	0.0075	0°.93	0.0162
44	0.7679	104	1.8151	164	2.8623	0°.44	0.0077	0°.94	0.0164
45	0.7854	105	1.8326	165	2.8798	0°.45	0.0079	0°.95	0.0166
46	0.8029	106	1.8500	166	2.8972	0°.46	0.0080	0°.96	0.0168
47	0.8203	107	1.8675	167	2.9147	0°.47	0.0082	0°.97	0.0169
48	0.8378	108	1.8850	168	2.9322	0°.48	0.0084	0°.98	0.0171
49	0.8552	109	1.9024	169	2.9496	0°.49	0.0086	0°.99	0.0173
50	0.8727	110	1.9199	170	2.9671	0°.50	0.0087	1°.00	0.0175
51	0.8901	111	1.9373	171	2.9845				
52	0.9076	112	1.9548	172	3.0020				
53	0.9250	113	1.9722	173	3.0194				
54	0.9425	114	1.9897	174	3.0369				
55	0.9599	115	2.0071	175	3.0543				
56	0.9774	116	2.0246	176	3.0718				
57	0.9948	117	2.0420	177	3.0892				
58	1.0123	118	2.0595	178	3.1067				
59	1.0297	119	2.0769	179	3.1241				
60	1.0472	120	2.0944	180	3.1416				

Arc 1° = 0.0174533, Arc 1' = 0.000290888, Arc 1" = 0.00000484814; 1 radian = 57°0.295780 = 57°17'0.7466 = 57°17'44"0.806.
^aSee also Table 1.40.

TABLE 1.20—RADIAN EXPRESSED IN DEGREES

										Interpolation	
0.01	0° 57	0.64	36° 67	1.27	72° 77	1.90	108° 86	2.53	144° 96		
0.02	1° 15	0.65	37° 24	1.28	73° 34	1.91	109° 43	2.54	145° 53	0.0002	0° 01
0.03	1° 72	0.66	37° 82	1.29	73° 91	1.92	110° 01	2.55	146° 10	0.0004	0° 02
0.04	2° 29	0.67	38° 39	1.30	74° 48	1.93	110° 48	2.56	146° 68	0.0006	0° 03
0.05	2° 86	0.68	38° 96	1.31	75° 06	1.94	111° 15	2.57	147° 25	0.0008	0° 05
0.06	3° 44	0.69	39° 53	1.32	75° 63	1.95	111° 73	2.58	147° 82	0.0010	0° 06
0.07	4° 01	0.70	40° 11	1.33	76° 20	1.96	112° 30	2.59	148° 40	0.0012	0° 07
0.08	4° 58	0.71	40° 68	1.34	76° 78	1.97	112° 87	2.60	148° 97	0.0014	0° 08
0.09	5° 16	0.72	41° 25	1.35	77° 35	1.98	113° 45	2.61	149° 54	0.0016	0° 09
0.10	5° 73	0.73	41° 83	1.36	77° 92	1.99	114° 02	2.62	150° 11	0.0018	0° 10
0.11	6° 30	0.74	42° 40	1.37	78° 50	2.00	114° 59	2.63	150° 69	0.0020	0° 11
0.12	6° 88	0.75	42° 97	1.38	79° 07	2.01	115° 16	2.64	151° 26	0.0022	0° 13
0.13	7° 45	0.76	43° 54	1.39	79° 64	2.02	115° 74	2.65	151° 83	0.0024	0° 14
0.14	8° 02	0.77	44° 12	1.40	80° 21	2.03	116° 31	2.66	152° 41	0.0026	0° 15
0.15	8° 59	0.78	44° 69	1.41	80° 79	2.04	116° 88	2.67	152° 98	0.0028	0° 16
0.16	9° 17	0.79	45° 26	1.42	81° 36	2.05	117° 46	2.68	153° 55	0.0030	0° 17
0.17	9° 74	0.80	45° 84	1.43	81° 93	2.06	118° 03	2.69	154° 13	0.0032	0° 18
0.18	10° 31	0.81	46° 41	1.44	82° 51	2.07	118° 60	2.70	154° 70	0.0034	0° 19
0.19	10° 89	0.82	46° 98	1.45	83° 08	2.08	119° 18	2.71	155° 27	0.0036	0° 21
0.20	11° 46	0.83	47° 56	1.46	83° 65	2.09	119° 75	2.72	155° 84	0.0038	0° 22
0.21	12° 03	0.84	48° 13	1.47	84° 22	2.10	120° 32	2.73	156° 42	0.0040	0° 23
0.22	12° 61	0.85	48° 70	1.48	84° 80	2.11	120° 89	2.74	156° 99	0.0042	0° 24
0.23	13° 18	0.86	49° 27	1.49	85° 37	2.12	121° 47	2.75	157° 56	0.0044	0° 25
0.24	13° 75	0.87	49° 85	1.50	85° 94	2.13	122° 04	2.76	158° 14	0.0046	0° 26
0.25	14° 32	0.88	50° 42	1.51	86° 52	2.14	122° 61	2.77	158° 71	0.0048	0° 28
0.26	14° 90	0.89	50° 99	1.52	87° 09	2.15	123° 19	2.78	159° 28	0.0050	0° 29
0.27	15° 47	0.90	51° 57	1.53	87° 66	2.16	123° 76	2.79	159° 86	0.0052	0° 30
0.28	16° 04	0.91	52° 14	1.54	88° 24	2.17	124° 33	2.80	160° 43	0.0054	0° 31
0.29	16° 62	0.92	52° 71	1.55	88° 81	2.18	124° 90	2.81	161° 00	0.0056	0° 32
0.30	17° 19	0.93	53° 29	1.56	89° 38	2.19	125° 48	2.82	161° 57	0.0058	0° 33
0.31	17° 76	0.94	53° 86	1.57	89° 95	2.20	126° 05	2.83	162° 15	0.0060	0° 34
0.32	18° 33	0.95	54° 43	1.58	90° 53	2.21	126° 62	2.84	162° 72	0.0062	0° 36
0.33	18° 91	0.96	55° 00	1.59	91° 10	2.22	127° 20	2.85	163° 29	0.0064	0° 37
0.34	19° 48	0.97	55° 58	1.60	91° 67	2.23	127° 77	2.86	163° 87	0.0066	0° 38
0.35	20° 05	0.98	56° 15	1.61	92° 25	2.24	128° 34	2.87	164° 44	0.0068	0° 39
0.36	20° 63	0.99	56° 72	1.62	92° 82	2.25	128° 92	2.88	165° 01	0.0070	0° 40
0.37	21° 20	1.00	57° 30	1.63	93° 39	2.26	129° 49	2.89	165° 58	0.0072	0° 41
0.38	21° 77	1.01	57° 87	1.64	93° 97	2.27	130° 06	2.90	166° 16	0.0074	0° 42
0.39	22° 35	1.02	58° 44	1.65	94° 54	2.28	130° 63	2.91	166° 73	0.0076	0° 44
0.40	22° 92	1.03	59° 01	1.66	95° 11	2.29	131° 21	2.92	167° 30	0.0078	0° 45
0.41	23° 49	1.04	59° 59	1.67	95° 68	2.30	131° 78	2.93	167° 88	0.0080	0° 46
0.42	24° 06	1.05	60° 16	1.68	96° 26	2.31	132° 35	2.94	168° 45	0.0082	0° 47
0.43	24° 64	1.06	60° 73	1.69	96° 83	2.32	132° 93	2.95	169° 02	0.0084	0° 48
0.44	25° 21	1.07	61° 31	1.70	97° 40	2.33	133° 50	2.96	169° 60	0.0086	0° 49
0.45	25° 78	1.08	61° 88	1.71	97° 98	2.34	134° 07	2.97	170° 17	0.0088	0° 50
0.46	26° 36	1.09	62° 45	1.72	98° 55	2.35	134° 65	2.98	170° 74	0.0090	0° 52
0.47	26° 93	1.10	63° 03	1.73	99° 12	2.36	135° 22	2.99	171° 31	0.0092	0° 53
0.48	27° 50	1.11	63° 60	1.74	99° 69	2.37	135° 79	3.00	171° 89	0.0094	0° 54
0.49	28° 07	1.12	64° 17	1.75	100° 27	2.38	136° 36	3.01	172° 46	0.0096	0° 55
0.50	28° 65	1.13	64° 74	1.76	100° 84	2.39	136° 94	3.02	173° 03	0.0098	0° 56
0.51	29° 22	1.14	65° 32	1.77	101° 41	2.40	137° 51	3.03	173° 61		
0.52	29° 79	1.15	65° 89	1.78	101° 99	2.41	138° 08	3.04	174° 18		
0.53	30° 37	1.16	66° 46	1.79	102° 56	2.42	138° 66	3.05	174° 75		
0.54	30° 94	1.17	67° 04	1.80	103° 13	2.43	139° 23	3.06	175° 33	1	3.1416 180°
0.55	31° 51	1.18	67° 61	1.81	103° 71	2.44	139° 80	3.07	175° 90	2	6.2832 360°
0.56	32° 09	1.19	68° 18	1.82	104° 28	2.45	140° 37	3.08	176° 47	3	9.4248 540°
0.57	32° 66	1.20	68° 75	1.83	104° 85	2.46	140° 95	3.09	177° 04	4	12.5664 720°
0.58	33° 23	1.21	69° 33	1.84	105° 42	2.47	141° 52	3.10	177° 62	5	15.7080 900°
0.59	33° 80	1.22	69° 90	1.85	106° 00	2.48	142° 09	3.11	178° 19	6	18.8496 1,080°
0.60	34° 38	1.23	70° 47	1.86	106° 57	2.49	142° 67	3.12	178° 76	7	21.9911 1,260°
0.61	34° 95	1.24	71° 05	1.87	107° 14	2.50	143° 24	3.13	179° 34	8	25.1327 1,440°
0.62	35° 52	1.25	71° 62	1.88	107° 72	2.51	144° 81	3.14	179° 91	9	28.2743 1,620°
0.63	36° 10	1.26	72° 19	1.89	108° 29	2.52	144° 39	3.15	180° 48	10	31.4159 1,800°

Multiples of π

TABLE 1.21—NATURAL SINES AND COSINES

Natural Sines at Intervals of 0° 01 or 6''

Degrees	° 0 (0')	° 1 (6')	° 2 (12')	° 3 (18')	° 4 (24')	° 5 (30')	° 6 (36')	° 7 (42')	° 8 (48')	° 9 (54')	° 10 (60')	Degrees	Average Difference
											0.0000	90	
0	0.0000	0.0017	0.0035	0.0052	0.0070	0.0087	0.0105	0.0122	0.0140	0.0157	0.0175	89	17
1	0.0175	0.0192	0.0209	0.0227	0.0244	0.0262	0.0279	0.0297	0.0314	0.0332	0.0349	88	17
2	0.0349	0.0366	0.0384	0.0401	0.0419	0.0436	0.0454	0.0471	0.0488	0.0506	0.0523	87	17
3	0.0523	0.0541	0.0558	0.0576	0.0593	0.0610	0.0628	0.0645	0.0663	0.0680	0.0698	86	17
4	0.0698	0.0715	0.0732	0.0750	0.0767	0.0785	0.0802	0.0819	0.0837	0.0854	0.0872	85	17
5	0.0872	0.0889	0.0906	0.0924	0.0941	0.0958	0.0976	0.0993	0.1011	0.1028	0.1045	84	17
6	0.1045	0.1063	0.1080	0.1097	0.1115	0.1132	0.1149	0.1167	0.1184	0.1201	0.1219	83	17
7	0.1219	0.1236	0.1253	0.1271	0.1288	0.1305	0.1323	0.1340	0.1357	0.1374	0.1392	82	17
8	0.1392	0.1409	0.1426	0.1444	0.1461	0.1478	0.1495	0.1513	0.1530	0.1547	0.1564	81	17
9	0.1564	0.1582	0.1599	0.1616	0.1633	0.1650	0.1668	0.1685	0.1702	0.1719	0.1736	80	17
10	0.1736	0.1754	0.1771	0.1788	0.1805	0.1822	0.1840	0.1857	0.1874	0.1891	0.1908	79	17
11	0.1908	0.1925	0.1942	0.1959	0.1977	0.1994	0.2011	0.2028	0.2045	0.2062	0.2079	78	17
12	0.2079	0.2096	0.2113	0.2130	0.2147	0.2164	0.2181	0.2198	0.2215	0.2233	0.2250	77	17
13	0.2250	0.2267	0.2284	0.2300	0.2317	0.2334	0.2351	0.2368	0.2385	0.2402	0.2419	76	17
14	0.2419	0.2436	0.2453	0.2470	0.2487	0.2504	0.2521	0.2538	0.2554	0.2571	0.2588	75	17
15	0.2588	0.2605	0.2622	0.2639	0.2656	0.2672	0.2689	0.2706	0.2723	0.2740	0.2756	74	17
16	0.2756	0.2773	0.2790	0.2807	0.2823	0.2840	0.2857	0.2874	0.2890	0.2907	0.2924	73	17
17	0.2924	0.2940	0.2957	0.2974	0.2990	0.3007	0.3024	0.3040	0.3057	0.3074	0.3090	72	17
18	0.3090	0.3107	0.3123	0.3140	0.3156	0.3173	0.3190	0.3206	0.3223	0.3239	0.3256	71	17
19	0.3256	0.3272	0.3289	0.3305	0.3322	0.3338	0.3355	0.3371	0.3387	0.3404	0.3420	70	16
20	0.3420	0.3437	0.3453	0.3469	0.3486	0.3502	0.3518	0.3535	0.3551	0.3567	0.3584	69	16
21	0.3584	0.3600	0.3616	0.3633	0.3649	0.3665	0.3681	0.3697	0.3714	0.3730	0.3746	68	16
22	0.3746	0.3762	0.3778	0.3795	0.3811	0.3827	0.3843	0.3859	0.3875	0.3891	0.3907	67	16
23	0.3907	0.3923	0.3939	0.3955	0.3971	0.3987	0.4003	0.4019	0.4035	0.4051	0.4067	66	16
24	0.4067	0.4083	0.4099	0.4115	0.4131	0.4147	0.4163	0.4179	0.4195	0.4210	0.4226	65	16
25	0.4226	0.4242	0.4258	0.4274	0.4289	0.4305	0.4321	0.4337	0.4352	0.4368	0.4384	64	16
26	0.4384	0.4399	0.4415	0.4431	0.4446	0.4462	0.4478	0.4493	0.4509	0.4524	0.4540	63	16
27	0.4540	0.4555	0.4571	0.4586	0.4602	0.4617	0.4633	0.4648	0.4664	0.4679	0.4695	62	16
28	0.4695	0.4710	0.4726	0.4741	0.4756	0.4772	0.4787	0.4802	0.4818	0.4833	0.4848	61	15
29	0.4848	0.4863	0.4879	0.4894	0.4909	0.4924	0.4939	0.4955	0.4970	0.4985	0.5000	60	15
30	0.5000	0.5015	0.5030	0.5045	0.5060	0.5075	0.5090	0.5105	0.5120	0.5135	0.5150	59	15
31	0.5150	0.5165	0.5180	0.5195	0.5210	0.5225	0.5240	0.5255	0.5270	0.5284	0.5299	58	15
32	0.5299	0.5314	0.5329	0.5344	0.5358	0.5373	0.5388	0.5402	0.5417	0.5432	0.5446	57	15
33	0.5446	0.5461	0.5476	0.5490	0.5505	0.5519	0.5534	0.5548	0.5563	0.5577	0.5592	56	15
34	0.5592	0.5606	0.5621	0.5635	0.5650	0.5664	0.5678	0.5693	0.5707	0.5721	0.5736	55	14
35	0.5736	0.5750	0.5764	0.5779	0.5793	0.5807	0.5821	0.5835	0.5850	0.5864	0.5878	54	14
36	0.5878	0.5892	0.5906	0.5920	0.5934	0.5948	0.5962	0.5976	0.5990	0.6004	0.6018	53	14
37	0.6018	0.6032	0.6046	0.6060	0.6074	0.6088	0.6101	0.6115	0.6129	0.6143	0.6157	52	14
38	0.6157	0.6170	0.6184	0.6198	0.6211	0.6225	0.6239	0.6252	0.6266	0.6280	0.6293	51	14
39	0.6293	0.6307	0.6320	0.6334	0.6347	0.6361	0.6374	0.6388	0.6401	0.6414	0.6428	50	13
40	0.6428	0.6441	0.6455	0.6468	0.6481	0.6494	0.6508	0.6521	0.6534	0.6547	0.6561	49	13
41	0.6561	0.6574	0.6587	0.6600	0.6613	0.6626	0.6639	0.6652	0.6665	0.6678	0.6691	48	13
42	0.6691	0.6704	0.6717	0.6730	0.6743	0.6756	0.6769	0.6782	0.6794	0.6807	0.6820	47	13
43	0.6820	0.6833	0.6845	0.6858	0.6871	0.6884	0.6896	0.6909	0.6921	0.6934	0.6947	46	13
44	0.6947	0.6959	0.6972	0.6984	0.6997	0.7009	0.7022	0.7034	0.7046	0.7059	0.7071	45	12
45	0.7071	0.7083	0.7096	0.7108	0.7120	0.7133	0.7145	0.7157	0.7169	0.7181	0.7193	44	12
46	0.7193	0.7206	0.7218	0.7230	0.7242	0.7254	0.7266	0.7278	0.7290	0.7302	0.7314	43	12
47	0.7314	0.7325	0.7337	0.7349	0.7361	0.7373	0.7385	0.7396	0.7408	0.7420	0.7431	42	12
48	0.7431	0.7443	0.7455	0.7466	0.7478	0.7490	0.7501	0.7513	0.7524	0.7536	0.7547	41	12
49	0.7547	0.7559	0.7570	0.7581	0.7593	0.7604	0.7615	0.7627	0.7638	0.7649	0.7660	40	11
		° 9 (54')	° 8 (48')	° 7 (42')	° 6 (36')	° 5 (30')	° 4 (24')	° 3 (18')	° 2 (12')	° 1 (6')	° 0 (0')		
		Natural Cosines											

* For 10' intervals, see Table 1.24.

TABLE 1.21—NATURAL SINES AND COSINES (continued)

Natural Sines at Intervals of 0° 01 or 6''

Degrees	° 0 (0')	° 1 (6')	° 2 (12')	° 3 (18')	° 4 (24')	° 5 (30')	° 6 (36')	° 7 (42')	° 8 (48')	° 9 (54')	° 10 (60')	Degrees	Average Difference
50	0.7660	0.7672	0.7683	0.7694	0.7705	0.7716	0.7727	0.7738	0.7749	0.7760	0.7771	39	11
51	0.7771	0.7782	0.7793	0.7804	0.7815	0.7826	0.7837	0.7848	0.7859	0.7869	0.7880	38	11
52	0.7880	0.7891	0.7902	0.7912	0.7923	0.7934	0.7944	0.7955	0.7965	0.7976	0.7986	37	11
53	0.7986	0.7997	0.8007	0.8018	0.8028	0.8039	0.8049	0.8059	0.8070	0.8080	0.8090	36	10
54	0.8090	0.8100	0.8111	0.8121	0.8131	0.8141	0.8151	0.8161	0.8171	0.8181	0.8192	35	10
55	0.8192	0.8202	0.8211	0.8221	0.8231	0.8241	0.8251	0.8261	0.8271	0.8281	0.8290	34	10
56	0.8290	0.8300	0.8310	0.8320	0.8329	0.8339	0.8348	0.8358	0.8368	0.8377	0.8387	33	10
57	0.8387	0.8396	0.8406	0.8415	0.8425	0.8434	0.8443	0.8453	0.8462	0.8471	0.8480	32	9
58	0.8480	0.8490	0.8499	0.8508	0.8517	0.8526	0.8536	0.8545	0.8554	0.8563	0.8572	31	9
59	0.8572	0.8581	0.8590	0.8599	0.8607	0.8616	0.8625	0.8634	0.8643	0.8652	0.8660	30	9
60	0.8660	0.8669	0.8678	0.8686	0.8695	0.8704	0.8712	0.8721	0.8729	0.8738	0.8746	29	9
61	0.8746	0.8755	0.8763	0.8771	0.8780	0.8788	0.8796	0.8805	0.8813	0.8821	0.8829	28	8
62	0.8829	0.8838	0.8846	0.8854	0.8862	0.8870	0.8878	0.8886	0.8894	0.8902	0.8910	27	8
63	0.8910	0.8918	0.8926	0.8934	0.8942	0.8949	0.8957	0.8965	0.8973	0.8980	0.8988	26	8
64	0.8988	0.8996	0.9003	0.9011	0.9018	0.9026	0.9033	0.9041	0.9048	0.9056	0.9063	25	7
65	0.9063	0.9070	0.9078	0.9085	0.9092	0.9100	0.9107	0.9114	0.9121	0.9128	0.9135	24	7
66	0.9135	0.9143	0.9150	0.9157	0.9164	0.9171	0.9178	0.9184	0.9191	0.9198	0.9205	23	7
67	0.9205	0.9212	0.9219	0.9225	0.9232	0.9239	0.9245	0.9252	0.9259	0.9265	0.9272	22	7
68	0.9272	0.9278	0.9285	0.9291	0.9298	0.9304	0.9311	0.9317	0.9323	0.9330	0.9336	21	6
69	0.9336	0.9342	0.9348	0.9354	0.9361	0.9367	0.9373	0.9379	0.9385	0.9391	0.9397	20	6
70	0.9397	0.9403	0.9409	0.9415	0.9421	0.9426	0.9432	0.9438	0.9444	0.9449	0.9455	19	6
71	0.9455	0.9461	0.9466	0.9472	0.9478	0.9483	0.9489	0.9494	0.9500	0.9505	0.9511	18	6
72	0.9511	0.9516	0.9521	0.9527	0.9532	0.9537	0.9542	0.9548	0.9553	0.9558	0.9563	17	5
73	0.9563	0.9568	0.9573	0.9578	0.9583	0.9588	0.9593	0.9598	0.9603	0.9608	0.9613	16	5
74	0.9613	0.9617	0.9622	0.9627	0.9632	0.9636	0.9641	0.9646	0.9650	0.9655	0.9659	15	5
75	0.9659	0.9664	0.9668	0.9673	0.9677	0.9681	0.9686	0.9690	0.9694	0.9699	0.9703	14	4
76	0.9703	0.9707	0.9711	0.9715	0.9720	0.9724	0.9728	0.9732	0.9736	0.9740	0.9744	13	4
77	0.9744	0.9748	0.9751	0.9755	0.9759	0.9763	0.9767	0.9770	0.9774	0.9778	0.9781	12	4
78	0.9781	0.9785	0.9789	0.9792	0.9796	0.9799	0.9803	0.9806	0.9810	0.9813	0.9816	11	3
79	0.9816	0.9820	0.9823	0.9826	0.9829	0.9833	0.9836	0.9839	0.9842	0.9845	0.9848	10	3
80	0.9848	0.9851	0.9854	0.9857	0.9860	0.9863	0.9866	0.9869	0.9871	0.9874	0.9877	9	3
81	0.9877	0.9880	0.9882	0.9885	0.9888	0.9890	0.9893	0.9895	0.9898	0.9900	0.9903	8	3
82	0.9903	0.9905	0.9907	0.9910	0.9912	0.9914	0.9917	0.9919	0.9921	0.9923	0.9925	7	2
83	0.9925	0.9928	0.9930	0.9932	0.9934	0.9936	0.9938	0.9940	0.9942	0.9943	0.9945	6	2
84	0.9945	0.9947	0.9949	0.9951	0.9952	0.9954	0.9956	0.9957	0.9959	0.9960	0.9962	5	2
85	0.9962	0.9963	0.9965	0.9966	0.9968	0.9969	0.9971	0.9972	0.9973	0.9974	0.9976	4	1
86	0.9976	0.9977	0.9978	0.9979	0.9980	0.9981	0.9982	0.9983	0.9984	0.9985	0.9986	3	1
87	0.9986	0.9987	0.9988	0.9989	0.9990	0.9990	0.9991	0.9992	0.9993	0.9993	0.9994	2	1
88	0.9994	0.9995	0.9995	0.9996	0.9996	0.9997	0.9997	0.9997	0.9998	0.9998	0.9998	1	0
89	0.9998	0.9999	0.9999	0.9999	0.9999	1.0000	1.0000	1.0000	1.0000	1.0000	1.0000	0	0
90	1.0000												
		° 9 (54')	° 8 (48')	° 7 (42')	° 6 (36')	° 5 (30')	° 4 (24')	° 3 (18')	° 2 (12')	° 1 (6')	° 0 (0')		
		Natural Cosines											

*For 10' intervals, see Table 1.24.

TABLE 1.22—NATURAL TANGENTS AND COTANGENTS

Natural Tangents at Intervals of 0°.1 or 6''

Degrees	° 0 (0')	° 1 (6')	° 2 (12')	° 3 (18')	° 4 (24')	° 5 (30')	° 6 (36')	° 7 (42')	° 8 (48')	° 9 (54')	° 10 (60')	Degrees	Average Difference
	0.0000	0.0017	0.0035	0.0052	0.0070	0.0087	0.0105	0.0122	0.0140	0.0157	0.0175	90	
0	0.0000	0.0017	0.0035	0.0052	0.0070	0.0087	0.0105	0.0122	0.0140	0.0157	0.0175	89	17
1	0.0175	0.0192	0.0209	0.0227	0.0244	0.0262	0.0279	0.0297	0.0314	0.0332	0.0349	88	17
2	0.0349	0.0367	0.0384	0.0402	0.0419	0.0437	0.0454	0.0472	0.0489	0.0507	0.0524	87	17
3	0.0524	0.0542	0.0559	0.0577	0.0594	0.0612	0.0629	0.0647	0.0664	0.0682	0.0699	86	18
4	0.0699	0.0717	0.0734	0.0752	0.0769	0.0787	0.0805	0.0822	0.0840	0.0857	0.0875	85	18
5	0.0875	0.0892	0.0910	0.0928	0.0945	0.0963	0.0981	0.0998	0.1016	0.1033	0.1051	84	18
6	0.1051	0.1069	0.1086	0.1104	0.1122	0.1139	0.1157	0.1175	0.1192	0.1210	0.1228	83	18
7	0.1228	0.1246	0.1263	0.1281	0.1299	0.1317	0.1334	0.1352	0.1370	0.1388	0.1405	82	18
8	0.1405	0.1423	0.1441	0.1459	0.1477	0.1495	0.1512	0.1530	0.1548	0.1566	0.1584	81	18
9	0.1584	0.1602	0.1620	0.1638	0.1655	0.1673	0.1691	0.1709	0.1727	0.1745	0.1763	80	18
10	0.1763	0.1781	0.1799	0.1817	0.1835	0.1853	0.1871	0.1890	0.1908	0.1926	0.1944	79	18
11	0.1944	0.1962	0.1980	0.1998	0.2016	0.2035	0.2053	0.2071	0.2089	0.2107	0.2126	78	18
12	0.2126	0.2144	0.2162	0.2180	0.2199	0.2217	0.2235	0.2254	0.2272	0.2290	0.2309	77	18
13	0.2309	0.2327	0.2345	0.2364	0.2382	0.2401	0.2419	0.2438	0.2456	0.2475	0.2493	76	19
14	0.2493	0.2512	0.2530	0.2549	0.2568	0.2586	0.2605	0.2623	0.2642	0.2661	0.2679	75	19
15	0.2679	0.2698	0.2717	0.2736	0.2754	0.2773	0.2792	0.2811	0.2830	0.2849	0.2867	74	19
16	0.2867	0.2886	0.2905	0.2924	0.2943	0.2962	0.2981	0.3000	0.3019	0.3038	0.3057	73	19
17	0.3057	0.3076	0.3096	0.3115	0.3134	0.3153	0.3172	0.3191	0.3211	0.3230	0.3249	72	19
18	0.3249	0.3269	0.3288	0.3307	0.3327	0.3346	0.3365	0.3385	0.3404	0.3424	0.3443	71	19
19	0.3443	0.3463	0.3482	0.3502	0.3522	0.3541	0.3561	0.3581	0.3600	0.3620	0.3640	70	20
20	0.3640	0.3659	0.3679	0.3699	0.3719	0.3739	0.3759	0.3779	0.3799	0.3819	0.3839	69	20
21	0.3839	0.3859	0.3879	0.3899	0.3919	0.3939	0.3959	0.3979	0.4000	0.4020	0.4040	68	20
22	0.4040	0.4061	0.4081	0.4101	0.4122	0.4142	0.4163	0.4183	0.4204	0.4224	0.4245	67	21
23	0.4245	0.4265	0.4286	0.4307	0.4327	0.4348	0.4369	0.4390	0.4411	0.4431	0.4452	66	21
24	0.4452	0.4473	0.4494	0.4515	0.4536	0.4557	0.4578	0.4599	0.4621	0.4642	0.4663	65	21
25	0.4663	0.4684	0.4706	0.4727	0.4748	0.4770	0.4791	0.4813	0.4834	0.4856	0.4877	64	21
26	0.4877	0.4899	0.4921	0.4942	0.4964	0.4986	0.5008	0.5029	0.5051	0.5073	0.5095	63	22
27	0.5095	0.5117	0.5139	0.5161	0.5184	0.5206	0.5228	0.5250	0.5272	0.5295	0.5317	62	22
28	0.5317	0.5340	0.5362	0.5384	0.5407	0.5430	0.5452	0.5475	0.5498	0.5520	0.5543	61	23
29	0.5543	0.5566	0.5589	0.5612	0.5635	0.5658	0.5681	0.5704	0.5727	0.5750	0.5774	60	23
30	0.5774	0.5797	0.5820	0.5844	0.5867	0.5890	0.5914	0.5938	0.5961	0.5985	0.6009	59	24
31	0.6009	0.6032	0.6056	0.6080	0.6104	0.6128	0.6152	0.6176	0.6200	0.6224	0.6249	58	24
32	0.6249	0.6273	0.6297	0.6322	0.6346	0.6371	0.6395	0.6420	0.6445	0.6469	0.6494	57	25
33	0.6494	0.6519	0.6544	0.6569	0.6594	0.6619	0.6644	0.6669	0.6694	0.6720	0.6745	56	25
34	0.6745	0.6771	0.6796	0.6822	0.6847	0.6873	0.6899	0.6924	0.6950	0.6976	0.7002	55	26
35	0.7002	0.7028	0.7054	0.7080	0.7107	0.7133	0.7159	0.7186	0.7212	0.7239	0.7265	54	26
36	0.7265	0.7292	0.7319	0.7346	0.7373	0.7400	0.7427	0.7454	0.7481	0.7508	0.7536	53	27
37	0.7536	0.7563	0.7590	0.7618	0.7646	0.7673	0.7701	0.7729	0.7757	0.7785	0.7813	52	28
38	0.7813	0.7841	0.7869	0.7898	0.7926	0.7954	0.7983	0.8012	0.8040	0.8069	0.8098	51	28
39	0.8098	0.8127	0.8156	0.8185	0.8214	0.8243	0.8273	0.8302	0.8332	0.8361	0.8391	50	29
40	0.8391	0.8421	0.8451	0.8481	0.8511	0.8541	0.8571	0.8601	0.8632	0.8662	0.8693	49	30
41	0.8693	0.8724	0.8754	0.8785	0.8816	0.8847	0.8878	0.8910	0.8941	0.8972	0.9004	48	31
42	0.9004	0.9036	0.9067	0.9099	0.9131	0.9163	0.9195	0.9228	0.9260	0.9293	0.9325	47	32
43	0.9325	0.9358	0.9391	0.9424	0.9457	0.9490	0.9523	0.9556	0.9590	0.9623	0.9657	46	33
44	0.9657	0.9691	0.9725	0.9759	0.9793	0.9827	0.9861	0.9896	0.9930	0.9965	1.0000	45	34
		° 9 (54')	° 8 (48')	° 7 (42')	° 6 (36')	° 5 (30')	° 4 (24')	° 3 (18')	° 2 (12')	° 1 (6')	° 0 (0')		

Natural Cotangents

*For 10' intervals, see Table 1.24.

TABLE 1.22—NATURAL TANGENTS AND COTANGENTS (continued)

Natural Tangents at Intervals of 0° 1 or 6 "

Degrees	° 0 (0)	° 1 (6)	° 2 (12)	° 3 (18)	° 4 (24)	° 5 (30)	° 6 (36)	° 7 (42)	° 8 (48)	° 9 (54)	° 10 (60)	Degrees	Average Difference
45	1.0000	1.0035	1.0070	1.0105	1.0141	1.0176	1.0212	1.0247	1.0283	1.0319	1.0355	44	35
46	1.0355	1.0392	1.0428	1.0464	1.0501	1.0538	1.0575	1.0612	1.0649	1.0686	1.0724	43	37
47	1.0724	1.0761	1.0799	1.0837	1.0875	1.0913	1.0951	1.0990	1.1028	1.1067	1.1106	42	38
48	1.1106	1.1145	1.1184	1.1224	1.1263	1.1303	1.1343	1.1383	1.1423	1.1463	1.1504	41	40
49	1.1504	1.1544	1.1585	1.1626	1.1667	1.1708	1.1750	1.1792	1.1833	1.1875	1.1918	40	41
50	1.1918	1.1960	1.2002	1.2045	1.2088	1.2131	1.2174	1.2218	1.2261	1.2305	1.2349	39	43
51	1.2349	1.2393	1.2437	1.2482	1.2527	1.2572	1.2617	1.2662	1.2708	1.2753	1.2799	38	45
52	1.2799	1.2846	1.2892	1.2938	1.2985	1.3032	1.3079	1.3127	1.3175	1.3222	1.3270	37	47
53	1.3270	1.3319	1.3367	1.3416	1.3465	1.3514	1.3564	1.3613	1.3663	1.3713	1.3764	36	49
54	1.3764	1.3814	1.3865	1.3916	1.3968	1.4019	1.4071	1.4124	1.4176	1.4229	1.4281	35	52
55	1.4281	1.4335	1.4388	1.4442	1.4496	1.4550	1.4605	1.4659	1.4715	1.4770	1.4826	34	55
56	1.4826	1.4882	1.4938	1.4994	1.5051	1.5108	1.5166	1.5224	1.5282	1.5340	1.5399	33	57
57	1.5399	1.5458	1.5517	1.5577	1.5637	1.5697	1.5757	1.5818	1.5880	1.5941	1.6003	32	60
58	1.6003	1.6066	1.6128	1.6191	1.6255	1.6319	1.6383	1.6447	1.6512	1.6577	1.6643	31	64
59	1.6643	1.6709	1.6775	1.6842	1.6909	1.6977	1.7045	1.7113	1.7182	1.7251	1.7321	30	67
60	1.732	1.739	1.746	1.753	1.760	1.767	1.775	1.782	1.789	1.797	1.804	29	7
61	1.804	1.811	1.819	1.827	1.834	1.842	1.849	1.857	1.865	1.873	1.881	28	8
62	1.881	1.889	1.897	1.905	1.913	1.921	1.929	1.937	1.946	1.954	1.963	27	8
63	1.963	1.971	1.980	1.988	1.997	2.006	2.014	2.023	2.032	2.041	2.050	26	9
64	2.050	2.059	2.069	2.078	2.087	2.097	2.106	2.116	2.125	2.135	2.145	25	9
65	2.145	2.154	2.164	2.174	2.184	2.194	2.204	2.215	2.225	2.236	2.246	24	10
66	2.246	2.257	2.267	2.278	2.289	2.300	2.311	2.322	2.333	2.344	2.356	23	11
67	2.356	2.367	2.379	2.391	2.402	2.414	2.426	2.438	2.450	2.463	2.475	22	12
68	2.475	2.488	2.500	2.513	2.526	2.539	2.552	2.565	2.578	2.592	2.605	21	13
69	2.605	2.619	2.633	2.646	2.660	2.675	2.689	2.703	2.718	2.733	2.747	20	14
70	2.747	2.762	2.778	2.793	2.808	2.824	2.840	2.856	2.872	2.888	2.904	19	16
71	2.904	2.921	2.937	2.954	2.971	2.989	3.006	3.024	3.042	3.060	3.078	18	17
72	3.078	3.096	3.115	3.133	3.152	3.172	3.191	3.211	3.230	3.251	3.271	17	19
73	3.271	3.291	3.312	3.333	3.354	3.376	3.398	3.420	3.442	3.465	3.487	16	22
74	3.487	3.511	3.534	3.558	3.582	3.606	3.630	3.655	3.681	3.706	3.732	15	24
75	3.732	3.758	3.785	3.812	3.839	3.867	3.895	3.923	3.952	3.981	4.011	14	28
76	4.011	4.041	4.071	4.102	4.134	4.165	4.198	4.230	4.264	4.297	4.331	13	32
77	4.331	4.366	4.402	4.437	4.474	4.511	4.548	4.586	4.625	4.665	4.705	12	37
78	4.705	4.745	4.787	4.829	4.872	4.915	4.959	5.005	5.050	5.097	5.145	11	44
79	5.145	5.193	5.242	5.292	5.343	5.396	5.449	5.503	5.558	5.614	5.671	10	53
80	5.671	5.730	5.789	5.850	5.912	5.976	6.041	6.107	6.174	6.243	6.314	9	
81	6.314	6.386	6.460	6.535	6.612	6.691	6.772	6.855	6.940	7.026	7.115	8	
82	7.115	7.207	7.300	7.396	7.495	7.596	7.700	7.806	7.916	8.028	8.144	7	
83	8.144	8.264	8.386	8.513	8.643	8.777	8.915	9.058	9.205	9.357	9.514	6	
84	9.514	9.677	9.845	10.02	10.20	10.39	10.58	10.78	10.99	11.20	11.43	5	
85	11.43	11.66	11.91	12.16	12.43	12.71	13.00	13.30	13.62	13.95	14.30	4	
86	14.30	14.67	15.06	15.46	15.90	16.35	16.83	17.34	17.89	18.46	19.08	3	
87	19.08	19.74	20.45	21.20	22.02	22.90	23.86	24.90	26.03	27.27	28.64	2	
88	28.64	30.14	31.82	33.69	35.80	38.19	40.92	44.07	47.74	52.08	57.29	1	
89	57.29	63.66	71.62	81.85	95.49	114.6	143.2	191.0	286.5	573.0	∞	0	
90	∞												
	° 9 (54)	° 8 (48)	° 7 (42)	° 6 (36)	° 5 (30)	° 4 (24)	° 3 (18)	° 2 (12)	° 1 (6)	° 0 (0)			
	Natural Cotangents												

*For 10' intervals, see Table 1.24.

TABLE 1.23—NATURAL SECANTS AND COSECANTS

Natural Secants at Intervals of 0°.1 or 6''

Degrees	° 0 (0')	° 1 (6')	° 2 (12')	° 3 (18')	° 4 (24')	° 5 (30')	° 6 (36')	° 7 (42')	° 8 (48')	° 9 (54')	° 1.0 (60')	Degrees	Average Difference
0	1.0000	1.0000	1.0000	1.0000	1.0000	1.0000	1.0001	1.0001	1.0001	1.0001	1.0000	90	
1	1.0002	1.0002	1.0002	1.0003	1.0003	1.0003	1.0004	1.0004	1.0005	1.0006	1.0006	89	0
2	1.0006	1.0007	1.0007	1.0008	1.0009	1.0010	1.0010	1.0011	1.0012	1.0013	1.0014	88	0
3	1.0014	1.0015	1.0016	1.0017	1.0018	1.0019	1.0020	1.0021	1.0022	1.0023	1.0024	87	1
4	1.0024	1.0026	1.0027	1.0028	1.0030	1.0031	1.0032	1.0034	1.0035	1.0037	1.0038	86	1
5	1.0038	1.0040	1.0041	1.0043	1.0045	1.0046	1.0048	1.0050	1.0051	1.0053	1.0055	85	1
6	1.0055	1.0057	1.0059	1.0061	1.0063	1.0065	1.0067	1.0069	1.0071	1.0073	1.0075	84	2
7	1.0075	1.0077	1.0079	1.0082	1.0084	1.0086	1.0089	1.0091	1.0093	1.0096	1.0098	83	2
8	1.0098	1.0101	1.0103	1.0106	1.0108	1.0111	1.0114	1.0116	1.0119	1.0122	1.0125	82	2
9	1.0125	1.0127	1.0130	1.0133	1.0136	1.0139	1.0142	1.0145	1.0148	1.0151	1.0154	81	3
10	1.0154	1.0157	1.0161	1.0164	1.0167	1.0170	1.0174	1.0177	1.0180	1.0184	1.0187	80	3
11	1.0187	1.0191	1.0194	1.0198	1.0201	1.0205	1.0209	1.0212	1.0216	1.0220	1.0223	79	3
12	1.0223	1.0227	1.0231	1.0235	1.0239	1.0243	1.0247	1.0251	1.0255	1.0259	1.0263	78	4
13	1.0263	1.0267	1.0271	1.0276	1.0280	1.0284	1.0288	1.0293	1.0297	1.0302	1.0306	77	4
14	1.0306	1.0311	1.0315	1.0320	1.0324	1.0329	1.0334	1.0338	1.0343	1.0348	1.0353	76	4
15	1.0353	1.0358	1.0363	1.0367	1.0372	1.0377	1.0382	1.0388	1.0393	1.0398	1.0403	75	5
16	1.0403	1.0408	1.0413	1.0419	1.0424	1.0429	1.0435	1.0440	1.0446	1.0451	1.0457	74	5
17	1.0457	1.0463	1.0468	1.0474	1.0480	1.0485	1.0491	1.0497	1.0503	1.0509	1.0515	73	5
18	1.0515	1.0521	1.0527	1.0533	1.0539	1.0545	1.0551	1.0557	1.0564	1.0570	1.0576	72	6
19	1.0576	1.0583	1.0589	1.0595	1.0602	1.0608	1.0615	1.0622	1.0628	1.0635	1.0642	71	6
20	1.0642	1.0649	1.0655	1.0662	1.0669	1.0676	1.0683	1.0690	1.0697	1.0704	1.0711	70	7
21	1.0711	1.0719	1.0726	1.0733	1.0740	1.0748	1.0755	1.0763	1.0770	1.0778	1.0785	69	7
22	1.0785	1.0793	1.0801	1.0808	1.0816	1.0824	1.0832	1.0840	1.0848	1.0856	1.0864	68	7
23	1.0864	1.0872	1.0880	1.0888	1.0896	1.0904	1.0913	1.0921	1.0929	1.0938	1.0946	67	8
24	1.0946	1.0955	1.0963	1.0972	1.0981	1.0989	1.0998	1.1007	1.1016	1.1025	1.1034	66	8
25	1.1034	1.1043	1.1052	1.1061	1.1070	1.1079	1.1089	1.1098	1.1107	1.1117	1.1126	65	9
26	1.1126	1.1136	1.1145	1.1155	1.1164	1.1174	1.1184	1.1194	1.1203	1.1213	1.1223	64	9
27	1.1223	1.1233	1.1243	1.1253	1.1264	1.1274	1.1284	1.1294	1.1305	1.1315	1.1326	63	10
28	1.1326	1.1336	1.1347	1.1357	1.1368	1.1379	1.1390	1.1401	1.1412	1.1423	1.1434	62	10
29	1.1434	1.1445	1.1456	1.1467	1.1478	1.1490	1.1501	1.1512	1.1524	1.1535	1.1547	61	11
30	1.1547	1.1559	1.1570	1.1582	1.1594	1.1606	1.1618	1.1630	1.1642	1.1654	1.1666	60	11
31	1.1666	1.1679	1.1691	1.1703	1.1716	1.1728	1.1741	1.1753	1.1766	1.1779	1.1792	59	12
32	1.1792	1.1805	1.1818	1.1831	1.1844	1.1857	1.1870	1.1883	1.1897	1.1910	1.1924	58	13
33	1.1924	1.1937	1.1951	1.1964	1.1978	1.1992	1.2006	1.2020	1.2034	1.2048	1.2062	57	13
34	1.2062	1.2076	1.2091	1.2105	1.2120	1.2134	1.2149	1.2163	1.2178	1.2193	1.2208	56	14
35	1.2208	1.2223	1.2238	1.2253	1.2268	1.2283	1.2299	1.2314	1.2329	1.2345	1.2361	55	15
36	1.2361	1.2376	1.2392	1.2408	1.2424	1.2440	1.2456	1.2472	1.2489	1.2505	1.2521	54	15
37	1.2521	1.2538	1.2554	1.2571	1.2588	1.2605	1.2622	1.2639	1.2656	1.2673	1.2690	53	16
38	1.2690	1.2708	1.2725	1.2742	1.2760	1.2778	1.2796	1.2813	1.2831	1.2849	1.2868	52	17
39	1.2868	1.2886	1.2904	1.2923	1.2941	1.2960	1.2978	1.2997	1.3016	1.3035	1.3054	51	18
40	1.3054	1.3073	1.3093	1.3112	1.3131	1.3151	1.3171	1.3190	1.3210	1.3230	1.3250	50	19
41	1.3250	1.3270	1.3291	1.3311	1.3331	1.3352	1.3373	1.3393	1.3414	1.3435	1.3456	49	20
42	1.3456	1.3478	1.3499	1.3520	1.3542	1.3563	1.3585	1.3607	1.3629	1.3651	1.3673	48	21
43	1.3673	1.3696	1.3718	1.3741	1.3763	1.3786	1.3809	1.3832	1.3855	1.3878	1.3902	47	22
44	1.3902	1.3925	1.3949	1.3972	1.3996	1.4020	1.4044	1.4069	1.4093	1.4118	1.4142	46	23
												45	24
	° 9 (54')	° 8 (48')	° 7 (42')	° 6 (36')	° 5 (30')	° 4 (24')	° 3 (18')	° 2 (12')	° 1 (6')	° 0 (0')			
	Natural Cotangents												

* For 10' intervals, see Table 1.24.

TABLE 1.23—NATURAL SECANTS AND COSECANTS (continued)

Natural Secants at Intervals of 0°.1 or 6''

Degrees	° 0 (0°)	° 1 (6')	° 2 (12')	° 3 (18')	° 4 (24')	° 5 (30')	° 6 (36')	° 7 (42')	° 8 (48')	° 9 (54')	° 10 (60')	Degrees	Average Difference
45	1.4142	1.4167	1.4192	1.4217	1.4242	1.4267	1.4293	1.4318	1.4344	1.4370	1.4396	44	25
46	1.4396	1.4422	1.4448	1.4474	1.4501	1.4527	1.4554	1.4581	1.4608	1.4635	1.4663	43	27
47	1.4663	1.4690	1.4718	1.4746	1.4774	1.4802	1.4830	1.4859	1.4887	1.4916	1.4945	42	28
48	1.4945	1.4974	1.5003	1.5032	1.5062	1.5092	1.5121	1.5151	1.5182	1.5212	1.5243	41	30
49	1.5243	1.5273	1.5304	1.5335	1.5366	1.5398	1.5429	1.5461	1.5493	1.5525	1.5557	40	31
50	1.5557	1.5590	1.5622	1.5655	1.5688	1.5721	1.5755	1.5788	1.5822	1.5856	1.5890	39	33
51	1.5890	1.5925	1.5959	1.5994	1.6029	1.6064	1.6099	1.6135	1.6171	1.6207	1.6243	38	35
52	1.6243	1.6279	1.6316	1.6353	1.6390	1.6427	1.6464	1.6502	1.6540	1.6578	1.6616	37	37
53	1.6616	1.6655	1.6694	1.6733	1.6772	1.6812	1.6852	1.6892	1.6932	1.6972	1.7013	36	40
54	1.7013	1.7054	1.7095	1.7137	1.7179	1.7221	1.7263	1.7305	1.7348	1.7391	1.7434	35	42
55	1.7434	1.7478	1.7522	1.7566	1.7610	1.7655	1.7700	1.7745	1.7791	1.7837	1.7883	34	45
56	1.7883	1.7929	1.7976	1.8023	1.8070	1.8118	1.8166	1.8214	1.8263	1.8312	1.8361	33	48
57	1.8361	1.8410	1.8460	1.8510	1.8561	1.8612	1.8663	1.8714	1.8766	1.8818	1.8871	32	51
58	1.8871	1.8924	1.8977	1.9031	1.9084	1.9139	1.9194	1.9249	1.9304	1.9360	1.9416	31	54
59	1.9416	1.9473	1.9530	1.9587	1.9645	1.9703	1.9762	1.9821	1.9880	1.9940	2.0000	30	58
60	2.000	2.006	2.012	2.018	2.025	2.031	2.037	2.043	2.050	2.056	2.063	29	6
61	2.063	2.069	2.076	2.082	2.089	2.096	2.103	2.109	2.116	2.123	2.130	28	7
62	2.130	2.137	2.144	2.151	2.158	2.166	2.173	2.180	2.188	2.195	2.203	27	7
63	2.203	2.210	2.218	2.226	2.233	2.241	2.249	2.257	2.265	2.273	2.281	26	8
64	2.281	2.289	2.298	2.306	2.314	2.323	2.331	2.340	2.349	2.357	2.366	25	8
65	2.366	2.375	2.384	2.393	2.402	2.411	2.421	2.430	2.439	2.449	2.459	24	9
66	2.459	2.468	2.478	2.488	2.498	2.508	2.518	2.528	2.538	2.549	2.559	23	10
67	2.559	2.570	2.581	2.591	2.602	2.613	2.624	2.635	2.647	2.658	2.669	22	11
68	2.669	2.681	2.693	2.705	2.716	2.729	2.741	2.753	2.765	2.778	2.790	21	12
69	2.790	2.803	2.816	2.829	2.842	2.855	2.869	2.882	2.896	2.910	2.924	20	13
70	2.924	2.938	2.952	2.967	2.981	2.996	3.011	3.026	3.041	3.056	3.072	19	15
71	3.072	3.087	3.103	3.119	3.135	3.152	3.168	3.185	3.202	3.219	3.236	18	16
72	3.236	3.254	3.271	3.289	3.307	3.326	3.344	3.363	3.382	3.401	3.420	17	18
73	3.420	3.440	3.460	3.480	3.500	3.521	3.542	3.563	3.584	3.606	3.628	16	21
74	3.628	3.650	3.673	3.695	3.719	3.742	3.766	3.790	3.814	3.839	3.864	15	24
75	3.864	3.889	3.915	3.941	3.967	3.994	4.021	4.049	4.077	4.105	4.134	14	27
76	4.134	4.163	4.192	4.222	4.253	4.284	4.315	4.347	4.379	4.412	4.445	13	31
77	4.445	4.479	4.514	4.549	4.584	4.620	4.657	4.694	4.732	4.771	4.810	12	36
78	4.810	4.850	4.890	4.931	4.973	5.016	5.059	5.103	5.148	5.194	5.241	11	43
79	5.241	5.288	5.337	5.386	5.436	5.487	5.540	5.593	5.647	5.702	5.759	10	52
80	5.759	5.816	5.875	5.935	5.996	6.059	6.123	6.188	6.255	6.323	6.392	9	
81	6.392	6.464	6.537	6.611	6.687	6.765	6.845	6.927	7.011	7.097	7.185	8	
82	7.185	7.276	7.368	7.463	7.561	7.661	7.764	7.870	7.979	8.091	8.206	7	
83	8.206	8.324	8.446	8.571	8.700	8.834	8.971	9.113	9.259	9.411	9.567	6	
84	9.567	9.728	9.895	10.07	10.25	10.43	10.63	10.83	11.03	11.25	11.47	5	
85	11.47	11.71	11.95	12.20	12.47	12.75	13.03	13.34	13.65	13.99	14.34	4	
86	14.34	14.70	15.09	15.50	15.93	16.38	16.86	17.37	17.91	18.49	19.11	3	
87	19.11	19.77	20.47	21.23	22.04	22.93	23.88	24.92	26.05	27.29	28.65	2	
88	28.65	30.16	31.84	33.71	35.81	38.20	40.93	44.08	47.75	52.09	57.30	1	
89	57.30	63.66	71.62	81.85	95.49	114.6	143.2	191.0	286.5	573.0	∞	0	
90	∞												
	° 9 (54')	° 8 (48')	° 7 (42')	° 6 (36')	° 5 (30')	° 4 (24')	° 3 (18')	° 2 (12')	° 1 (6')	° 0 (0')			
	Natural Cotangents												

*For 10' intervals, see Table 1.24.

TABLE 1.24—TRIGONOMETRIC FUNCTIONS (AT INTERVALS OF 10')*

Degrees	Radians	Sines		Cosines		Tangents		Cotangents			
		Natural	Log**	Natural	Log**	Natural	Log**	Natural	Log**		
0° 00'	0.0000	0.0000	∞	1.0000	0.0000	0.0000	∞	∞	∞	1.5708	90° 00'
0° 10'	0.0029	0.0029	7.4637	1.0000	0.0000	0.0029	7.4637	343.77	2.5363	1.5679	90° 50'
0° 20'	0.0058	0.0058	7.7648	1.0000	0.0000	0.0058	7.7648	171.89	2.2352	1.5650	90° 40'
0° 30'	0.0087	0.0087	7.9408	1.0000	0.0000	0.0087	7.9409	114.59	2.0591	1.5621	90° 30'
0° 40'	0.0116	0.0116	8.0658	0.9999	0.0000	0.0116	8.0658	85.940	1.9342	1.5592	90° 20'
0° 50'	0.0145	0.0145	8.1627	0.9999	0.0000	0.0145	8.1627	68.750	1.8373	1.5563	90° 10'
1° 00'	0.0175	0.0175	8.2419	0.9998	9.9999	0.0175	8.2419	57.290	1.7581	1.5533	89° 00'
1° 10'	0.0204	0.0204	8.3088	0.9998	9.9999	0.0204	8.3089	49.104	1.6911	1.5504	89° 50'
1° 20'	0.0233	0.0233	8.3668	0.9997	9.9999	0.0233	8.3669	42.964	1.6331	1.5475	89° 40'
1° 30'	0.0262	0.0262	8.4179	0.9997	9.9999	0.0262	8.4181	38.188	1.5819	1.5446	89° 30'
1° 40'	0.0291	0.0291	8.4637	0.9996	9.9998	0.0291	8.4638	34.368	1.5362	1.5417	89° 20'
1° 50'	0.0320	0.0320	8.5050	0.9995	9.9998	0.0320	8.5053	31.242	1.4947	1.5388	89° 10'
2° 00'	0.0349	0.0349	8.5428	0.9994	9.9997	0.0349	8.5431	28.636	1.4569	1.5359	88° 00'
2° 10'	0.0378	0.0378	8.5776	0.9993	9.9997	0.0378	8.5779	26.432	1.4221	1.5330	88° 50'
2° 20'	0.0407	0.0407	8.6097	0.9992	9.9996	0.0407	8.6101	24.542	1.3899	1.5301	88° 40'
2° 30'	0.0436	0.0436	8.6397	0.9990	9.9996	0.0437	8.6401	22.904	1.3599	1.5272	88° 30'
2° 40'	0.0465	0.0465	8.6677	0.9989	9.9995	0.0466	8.6682	21.470	1.3318	1.5243	88° 20'
2° 50'	0.0495	0.0494	8.6940	0.9988	9.9995	0.0495	8.6945	20.206	1.3055	1.5213	88° 10'
3° 00'	0.0524	0.0523	8.7188	0.9986	9.9994	0.0524	8.7194	19.081	1.2806	1.5184	87° 00'
3° 10'	0.0553	0.0552	8.7423	0.9985	9.9993	0.0553	8.7429	18.075	1.2571	1.5155	87° 50'
3° 20'	0.0582	0.0581	8.7645	0.9983	9.9993	0.0582	8.7652	17.169	1.2348	1.5126	87° 40'
3° 30'	0.0611	0.0610	8.7857	0.9981	9.9992	0.0612	8.7865	16.350	1.2135	1.5097	87° 30'
3° 40'	0.0640	0.0640	8.8059	0.9980	9.9991	0.0641	8.8067	15.605	1.1933	1.5068	87° 20'
3° 50'	0.0669	0.0669	8.8251	0.9978	9.9990	0.0670	8.8261	14.924	1.1739	1.5039	87° 10'
4° 00'	0.0698	0.0698	8.8436	0.9976	9.9989	0.0699	8.8446	14.301	1.1554	1.5010	86° 00'
4° 10'	0.0727	0.0727	8.8613	0.9974	9.9989	0.0729	8.8624	13.727	1.1376	1.4981	86° 50'
4° 20'	0.0756	0.0756	8.8783	0.9971	9.9988	0.0758	8.8795	13.197	1.1205	1.4952	86° 40'
4° 30'	0.0785	0.0785	8.8946	0.9969	9.9987	0.0787	8.8960	12.706	1.1040	1.4923	86° 30'
4° 40'	0.0814	0.0814	8.9104	0.9967	9.9986	0.0816	8.9118	12.251	1.0882	1.4893	86° 20'
4° 50'	0.0844	0.0843	8.9256	0.9964	9.9985	0.0846	8.9272	11.826	1.0728	1.4864	86° 10'
5° 00'	0.0873	0.0872	8.9403	0.9962	9.9983	0.0875	8.9420	11.430	1.0580	1.4835	85° 00'
5° 10'	0.0902	0.0901	8.9545	0.9959	9.9982	0.0904	8.9563	11.059	1.0437	1.4806	85° 50'
5° 20'	0.0931	0.0929	8.9682	0.9957	9.9981	0.0934	8.9701	10.712	1.0299	1.4777	85° 40'
5° 30'	0.0960	0.0958	8.9816	0.9954	9.9980	0.0963	8.9836	10.385	1.0164	1.4748	85° 30'
5° 40'	0.0989	0.0987	8.9945	0.9951	9.9979	0.0992	8.9966	10.078	1.0034	1.4719	85° 20'
5° 50'	0.1018	0.1016	9.0070	0.9948	9.9977	0.1022	9.0093	9.7882	0.9907	1.4690	85° 10'
6° 00'	0.1047	0.1045	9.0192	0.9945	9.9976	0.1051	9.0216	9.5144	0.9784	1.4661	84° 00'
6° 10'	0.1076	0.1074	9.0311	0.9942	9.9975	0.1080	9.0336	9.2553	0.9664	1.4632	84° 50'
6° 20'	0.1105	0.1103	9.0426	0.9939	9.9973	0.1110	9.0453	9.0098	0.9547	1.4603	84° 40'
6° 30'	0.1134	0.1132	9.0539	0.9936	9.9972	0.1139	9.0567	8.7769	0.9433	1.4574	84° 30'
6° 40'	0.1164	0.1161	9.0648	0.9932	9.9971	0.1169	9.0678	8.5555	0.9322	1.4544	84° 20'
6° 50'	0.1193	0.1190	9.0755	0.9929	9.9969	0.1198	9.0786	8.3450	0.9214	1.4515	84° 10'
7° 00'	0.1222	0.1219	9.0859	0.9925	9.9968	0.1228	9.0891	8.1443	0.9109	1.4486	83° 00'
7° 10'	0.1251	0.1248	9.0961	0.9922	9.9966	0.1257	9.0995	7.9530	0.9005	1.4457	83° 50'
7° 20'	0.1280	0.1276	9.1060	0.9918	9.9964	0.1287	9.1096	7.7704	0.8904	1.4428	83° 40'
7° 30'	0.1309	0.1305	9.1157	0.9914	9.9963	0.1317	9.1194	7.5958	0.8806	1.4399	83° 30'
7° 40'	0.1338	0.1334	9.1252	0.9911	9.9961	0.1346	9.1291	7.4287	0.8709	1.4370	83° 20'
7° 50'	0.1367	0.1363	9.1345	0.9907	9.9959	0.1376	9.1385	7.2687	0.8615	1.4341	83° 10'
8° 00'	0.1396	0.1392	9.1436	0.9903	9.9958	0.1405	9.1478	7.1154	0.8522	1.4312	82° 00'
8° 10'	0.1425	0.1421	9.1525	0.9899	9.9956	0.1435	9.1569	6.9682	0.8431	1.4283	82° 50'
8° 20'	0.1454	0.1449	9.1612	0.9894	9.9954	0.1465	9.1658	6.8269	0.8342	1.4254	82° 40'
8° 30'	0.1484	0.1478	9.1697	0.9890	9.9952	0.1495	9.1745	6.6912	0.8255	1.4224	82° 30'
8° 40'	0.1513	0.1507	9.1781	0.9886	9.9950	0.1524	9.1831	6.5606	0.8169	1.4195	82° 20'
8° 50'	0.1542	0.1536	9.1863	0.9881	9.9948	0.1554	9.1915	6.4348	0.8085	1.4166	82° 10'
9° 00'	0.1571	0.1564	9.1943	0.9877	9.9946	0.1584	9.1997	6.3138	0.8003	1.4137	81° 00'
9° 10'	0.1600	0.1593	9.2022	0.9872	9.9944	0.1614	9.2078	6.1970	0.7922	1.4108	81° 50'
9° 20'	0.1629	0.1622	9.2100	0.9868	9.9942	0.1644	9.2158	6.0844	0.7842	1.4079	81° 40'
9° 30'	0.1658	0.1650	9.2176	0.9863	9.9940	0.1673	9.2236	5.9758	0.7764	1.4050	81° 30'
9° 40'	0.1687	0.1679	9.2251	0.9858	9.9938	0.1703	9.2313	5.8708	0.7687	1.4021	81° 20'
9° 50'	0.1716	0.1708	9.2324	0.9853	9.9936	0.1733	9.2389	5.7694	0.7611	1.3992	81° 10'
		Natural	Log**	Natural	Log**	Natural	Log**	Natural	Log**		
		Cosines		Sines		Cotangents		Tangents		Radians	Degrees

*For 0° 1 intervals, see Tables 1.21, 1.22, and 1.23.

**Add 10 in these columns.

TABLE 1.24—TRIGONOMETRIC FUNCTIONS (AT INTERVALS OF 10')* (continued)

Degrees	Radians	Sines		Cosines		Tangents		Cotangents			
		Natural	Log**	Natural	Log**	Natural	Log**	Natural	Log**		
10° 00'	0.1745	0.1736	9.2397	0.9848	9.9934	0.1763	9.2463	5.6713	0.7537	1.3963	80° 00'
10° 10'	0.1774	0.1765	9.2468	0.9843	9.9931	0.1793	9.2536	5.5764	0.7464	1.3934	80° 50'
10° 20'	0.1804	0.1794	9.2538	0.9838	9.9929	0.1823	9.2609	5.4845	0.7391	1.3904	80° 40'
10° 30'	0.1833	0.1822	9.2606	0.9833	9.9927	0.1853	9.2680	5.3955	0.7320	1.3875	80° 30'
10° 40'	0.1862	0.1851	9.2674	0.9827	9.9924	0.1883	9.2750	5.3093	0.7250	1.3846	80° 20'
10° 50'	0.1891	0.1880	9.2740	0.9822	9.9922	0.1914	9.2819	5.2257	0.7181	1.3817	80° 10'
11° 00'	0.1920	0.1908	9.2806	0.9816	9.9919	0.1944	9.2887	5.1446	0.7113	1.3788	79° 00'
11° 10'	0.1949	0.1937	9.2870	0.9811	9.9917	0.1974	9.2953	5.0658	0.7047	1.3759	79° 50'
11° 20'	0.1978	0.1965	9.2934	0.9805	9.9914	0.2004	9.3020	4.9894	0.6980	1.3730	79° 40'
11° 30'	0.2007	0.1994	9.2997	0.9799	9.9912	0.2035	9.3085	4.9152	0.6915	1.3701	79° 30'
11° 40'	0.2036	0.2022	9.3058	0.9793	9.9909	0.2065	9.3149	4.8430	0.6851	1.3672	79° 20'
11° 50'	0.2065	0.2051	9.3119	0.9787	9.9907	0.2095	9.3212	4.7729	0.6788	1.3643	79° 10'
12° 00'	0.2094	0.2079	9.3179	0.9781	9.9904	0.2126	9.3275	4.7046	0.6725	1.3614	78° 00'
12° 10'	0.2123	0.2108	9.3238	0.9775	9.9901	0.2156	9.3336	4.6382	0.6664	1.3584	78° 50'
12° 20'	0.2153	0.2136	9.3296	0.9769	9.9899	0.2186	9.3397	4.5736	0.6603	1.3555	78° 40'
12° 30'	0.2182	0.2164	9.3353	0.9763	9.9896	0.2217	9.3458	4.5107	0.6542	1.3526	78° 30'
12° 40'	0.2211	0.2193	9.3410	0.9757	9.9893	0.2247	9.3517	4.4494	0.6483	1.3497	78° 20'
12° 50'	0.2240	0.2221	9.3466	0.9750	9.9890	0.2278	9.3576	4.3897	0.6424	1.3468	78° 10'
13° 00'	0.2269	0.2250	9.3521	0.9744	9.9887	0.2309	9.3634	4.3315	0.6366	1.3439	77° 00'
13° 10'	0.2298	0.2278	9.3575	0.9737	9.9884	0.2339	9.3691	4.2747	0.6309	1.3410	77° 50'
13° 20'	0.2327	0.2306	9.3629	0.9730	9.9881	0.2370	9.3748	4.2193	0.6252	1.3381	77° 40'
13° 30'	0.2356	0.2334	9.3682	0.9724	9.9878	0.2401	9.3804	4.1653	0.6196	1.3352	77° 30'
13° 40'	0.2385	0.2363	9.3734	0.9717	9.9875	0.2432	9.3859	4.1126	0.6141	1.3323	77° 20'
13° 50'	0.2414	0.2391	9.3786	0.9710	9.9872	0.2462	9.3914	4.0611	0.6086	1.3294	77° 10'
14° 00'	0.2443	0.2419	9.3837	0.9703	9.9869	0.2493	9.3968	4.0108	0.6032	1.3265	76° 00'
14° 10'	0.2473	0.2447	9.3887	0.9696	9.9866	0.2524	9.4021	3.9617	0.5979	1.3235	76° 50'
14° 20'	0.2502	0.2476	9.3937	0.9689	9.9863	0.2555	9.4074	3.9136	0.5926	1.3206	76° 40'
14° 30'	0.2531	0.2504	9.3986	0.9681	9.9859	0.2586	9.4127	3.8667	0.5873	1.3177	76° 30'
14° 40'	0.2560	0.2532	9.4035	0.9674	9.9856	0.2617	9.4178	3.8208	0.5822	1.3148	76° 20'
14° 50'	0.2589	0.2560	9.4083	0.9667	9.9853	0.2648	9.4230	3.7760	0.5770	1.3119	76° 10'
15° 00'	0.2618	0.2588	9.4130	0.9659	9.9849	0.2679	9.4281	3.7321	0.5719	1.3090	75° 00'
15° 10'	0.2647	0.2616	9.4177	0.9652	9.9846	0.2711	9.4331	3.6891	0.5669	1.3061	75° 50'
15° 20'	0.2676	0.2644	9.4223	0.9644	9.9843	0.2742	9.4381	3.6470	0.5619	1.3032	75° 40'
15° 30'	0.2705	0.2672	9.4269	0.9636	9.9839	0.2773	9.4430	3.6059	0.5570	1.3003	75° 30'
15° 40'	0.2734	0.2700	9.4314	0.9628	9.9836	0.2805	9.4479	3.5656	0.5521	1.2974	75° 20'
15° 50'	0.2763	0.2728	9.4359	0.9621	9.9832	0.2836	9.4527	3.5261	0.5473	1.2945	75° 10'
16° 00'	0.2793	0.2756	9.4403	0.9613	9.9828	0.2867	9.4575	3.4874	0.5425	1.2915	74° 00'
16° 10'	0.2822	0.2784	9.4447	0.9605	9.9825	0.2899	9.4622	3.4495	0.5378	1.2886	74° 50'
16° 20'	0.2851	0.2812	9.4491	0.9596	9.9821	0.2931	9.4669	3.4124	0.5331	1.2857	74° 40'
16° 30'	0.2880	0.2840	9.4533	0.9588	9.9817	0.2962	9.4716	3.3759	0.5284	1.2828	74° 30'
16° 40'	0.2909	0.2868	9.4576	0.9580	9.9814	0.2994	9.4762	3.3402	0.5238	1.2799	74° 20'
16° 50'	0.2938	0.2896	9.4618	0.9572	9.9810	0.3026	9.4808	3.3052	0.5192	1.2770	74° 10'
17° 00'	0.2967	0.2924	9.4659	0.9563	9.9806	0.3057	9.4853	3.2709	0.5147	1.2741	73° 00'
17° 10'	0.2996	0.2952	9.4700	0.9555	9.9802	0.3089	9.4898	3.2371	0.5102	1.2712	73° 50'
17° 20'	0.3025	0.2979	9.4741	0.9546	9.9798	0.3121	9.4943	3.2041	0.5057	1.2683	73° 40'
17° 30'	0.3054	0.3007	9.4781	0.9537	9.9794	0.3153	9.4987	3.1716	0.5013	1.2654	73° 30'
17° 40'	0.3083	0.3035	9.4821	0.9528	9.9790	0.3185	9.5031	3.1397	0.4969	1.2625	73° 20'
17° 50'	0.3113	0.3062	9.4861	0.9520	9.9786	0.3217	9.5075	3.1084	0.4925	1.2595	73° 10'
18° 00'	0.3142	0.3090	9.4900	0.9511	9.9782	0.3249	9.5118	3.0777	0.4882	1.2566	72° 00'
18° 10'	0.3171	0.3118	9.4939	0.9502	9.9778	0.3281	9.5161	3.0475	0.4839	1.2537	72° 50'
18° 20'	0.3200	0.3145	9.4977	0.9492	9.9774	0.3314	9.5203	3.0178	0.4797	1.2508	72° 40'
18° 30'	0.3229	0.3173	9.5015	0.9483	9.9770	0.3346	9.5245	2.9887	0.4755	1.2479	72° 30'
18° 40'	0.3258	0.3201	9.5052	0.9474	9.9765	0.3378	9.5287	2.9600	0.4713	1.2450	72° 20'
18° 50'	0.3287	0.3228	9.5090	0.9465	9.9761	0.3411	9.5329	2.9319	0.4671	1.2421	72° 10'
19° 00'	0.3316	0.3256	9.5126	0.9455	9.9757	0.3443	9.5370	2.9042	0.4630	1.2392	71° 00'
19° 10'	0.3345	0.3283	9.5163	0.9446	9.9752	0.3476	9.5411	2.8770	0.4589	1.2363	71° 50'
19° 20'	0.3374	0.3311	9.5199	0.9436	9.9748	0.3508	9.5451	2.8502	0.4549	1.2334	71° 40'
19° 30'	0.3403	0.3338	9.5235	0.9426	9.9743	0.3541	9.5491	2.8239	0.4509	1.2305	71° 30'
19° 40'	0.3432	0.3365	9.5270	0.9417	9.9739	0.3574	9.5531	2.7980	0.4469	1.2275	71° 20'
19° 50'	0.3462	0.3393	9.5306	0.9407	9.9734	0.3607	9.5571	2.7725	0.4429	1.2246	71° 10'
		Natural	Log**	Natural	Log**	Natural	Log**	Natural	Log**	Radians	Degrees
		Cosines		Sines		Cotangents		Tangents			

*For 0°.1 intervals, see Tables 1.21, 1.22, and 1.23.

**Add 10 in these columns.

(continued on next page)

TABLE 1.24—TRIGONOMETRIC FUNCTIONS (AT INTERVALS OF 10')* (continued)

Degrees	Radians	Sines		Cosines		Tangents		Cotangents			
		Natural	Log**	Natural	Log**	Natural	Log**	Natural	Log**		
20° 00'	0.3491	0.3420	9.5341	0.9397	9.9730	0.3640	9.5611	2.7475	0.4389	1.2217	70° 00'
20° 10'	0.3520	0.3448	9.5375	0.9387	9.9725	0.3673	9.5650	2.7228	0.4350	1.2188	70° 50'
20° 20'	0.3549	0.3475	9.5409	0.9377	9.9721	0.3706	9.5689	2.6985	0.4311	1.2159	70° 40'
20° 30'	0.3578	0.3502	9.5443	0.9367	9.9716	0.3739	9.5727	2.6746	0.4273	1.2130	70° 30'
20° 40'	0.3607	0.3529	9.5477	0.9356	9.9711	0.3772	9.5766	2.6511	0.4234	1.2101	70° 20'
20° 50'	0.3636	0.3557	9.5510	0.9346	9.9706	0.3805	9.5804	2.6279	0.4196	1.2072	70° 10'
21° 00'	0.3665	0.3584	9.5543	0.9336	9.9702	0.3839	9.5842	2.6051	0.4158	1.2043	69° 00'
21° 10'	0.3694	0.3611	9.5576	0.9325	9.9697	0.3872	9.5879	2.5826	0.4121	1.2014	69° 50'
21° 20'	0.3723	0.3638	9.5609	0.9315	9.9692	0.3906	9.5917	2.5605	0.4083	1.1985	69° 40'
21° 30'	0.3752	0.3665	9.5641	0.9304	9.9687	0.3939	9.5954	2.5386	0.4046	1.1956	69° 30'
21° 40'	0.3782	0.3692	9.5673	0.9293	9.9682	0.3973	9.5991	2.5172	0.4009	1.1926	69° 20'
21° 50'	0.3811	0.3719	9.5704	0.9283	9.9677	0.4006	9.6028	2.4960	0.3972	1.1897	69° 10'
22° 00'	0.3840	0.3746	9.5736	0.9272	9.9672	0.4040	9.6064	2.4751	0.3936	1.1868	68° 00'
22° 10'	0.3869	0.3773	9.5767	0.9261	9.9667	0.4074	9.6100	2.4545	0.3900	1.1839	68° 50'
22° 20'	0.3898	0.3800	9.5798	0.9250	9.9661	0.4108	9.6136	2.4342	0.3864	1.1810	68° 40'
22° 30'	0.3927	0.3827	9.5828	0.9239	9.9656	0.4142	9.6172	2.4142	0.3828	1.1781	68° 30'
22° 40'	0.3956	0.3854	9.5859	0.9228	9.9651	0.4176	9.6208	2.3945	0.3792	1.1752	68° 20'
22° 50'	0.3985	0.3881	9.5889	0.9216	9.9646	0.4210	9.6243	2.3750	0.3757	1.1723	68° 10'
23° 00'	0.4014	0.3907	9.5919	0.9205	9.9640	0.4245	9.6279	2.3559	0.3721	1.1694	67° 00'
23° 10'	0.4043	0.3934	9.5948	0.9194	9.9635	0.4279	9.6314	2.3369	0.3686	1.1665	67° 50'
23° 20'	0.4072	0.3961	9.5978	0.9182	9.9629	0.4314	9.6348	2.3183	0.3652	1.1636	67° 40'
23° 30'	0.4102	0.3987	9.6007	0.9171	9.9624	0.4348	9.6383	2.2998	0.3617	1.1606	67° 30'
23° 40'	0.4131	0.4014	9.6036	0.9159	9.9618	0.4383	9.6417	2.2817	0.3583	1.1577	67° 20'
23° 50'	0.4160	0.4041	9.6065	0.9147	9.9613	0.4417	9.6452	2.2637	0.3548	1.1548	67° 10'
24° 00'	0.4189	0.4067	9.6093	0.9135	9.9607	0.4452	9.6486	2.2460	0.3514	1.1519	66° 00'
24° 10'	0.4218	0.4094	9.6121	0.9124	9.9602	0.4487	9.6520	2.2286	0.3480	1.1490	66° 50'
24° 20'	0.4247	0.4120	9.6149	0.9112	9.9596	0.4522	9.6553	2.2113	0.3447	1.1461	66° 40'
24° 30'	0.4276	0.4147	9.6177	0.9100	9.9590	0.4557	9.6587	2.1943	0.3413	1.1432	66° 30'
24° 40'	0.4305	0.4173	9.6205	0.9088	9.9584	0.4592	9.6620	2.1775	0.3380	1.1403	66° 20'
24° 50'	0.4334	0.4200	9.6232	0.9075	9.9579	0.4628	9.6654	2.1609	0.3346	1.1374	66° 10'
25° 00'	0.4363	0.4226	9.6259	0.9063	9.9573	0.4663	9.6687	2.1445	0.3313	1.1345	65° 00'
25° 10'	0.4392	0.4253	9.6286	0.9051	9.9567	0.4699	9.6720	2.1283	0.3280	1.1316	65° 50'
25° 20'	0.4422	0.4279	9.6313	0.9038	9.9561	0.4734	9.6752	2.1123	0.3248	1.1286	65° 40'
25° 30'	0.4451	0.4305	9.6340	0.9026	9.9555	0.4770	9.6785	2.0965	0.3215	1.1257	65° 30'
25° 40'	0.4480	0.4331	9.6366	0.9013	9.9549	0.4806	9.6817	2.0809	0.3183	1.1228	65° 20'
25° 50'	0.4509	0.4358	9.6392	0.9001	9.9543	0.4841	9.6850	2.0655	0.3150	1.1199	65° 10'
26° 00'	0.4538	0.4384	9.6418	0.8988	9.9537	0.4877	9.6882	2.0503	0.3118	1.1170	64° 00'
26° 10'	0.4567	0.4410	9.6444	0.8975	9.9530	0.4913	9.6914	2.0353	0.3086	1.1141	64° 50'
26° 20'	0.4596	0.4436	9.6470	0.8962	9.9524	0.4950	9.6946	2.0204	0.3054	1.1112	64° 40'
26° 30'	0.4625	0.4462	9.6495	0.8949	9.9518	0.4986	9.6977	2.0057	0.3023	1.1083	64° 30'
26° 40'	0.4654	0.4488	9.6521	0.8936	9.9512	0.5022	9.7009	1.9912	0.2991	1.1054	64° 20'
26° 50'	0.4683	0.4514	9.6546	0.8923	9.9505	0.5059	9.7040	1.9768	0.2960	1.1025	64° 10'
27° 00'	0.4712	0.4540	9.6570	0.8910	9.9499	0.5095	9.7072	1.9626	0.2928	1.0996	63° 00'
27° 10'	0.4741	0.4566	9.6595	0.8897	9.9492	0.5132	9.7103	1.9486	0.2897	1.0966	63° 50'
27° 20'	0.4771	0.4592	9.6620	0.8884	9.9486	0.5169	9.7134	1.9347	0.2866	1.0937	63° 40'
27° 30'	0.4800	0.4617	9.6644	0.8870	9.9479	0.5206	9.7165	1.9210	0.2835	1.0908	63° 30'
27° 40'	0.4829	0.4643	9.6668	0.8857	9.9473	0.5243	9.7196	1.9074	0.2804	1.0879	63° 20'
27° 50'	0.4858	0.4669	9.6692	0.8843	9.9466	0.5280	9.7226	1.8940	0.2774	1.0850	63° 10'
28° 00'	0.4887	0.4695	9.6716	0.8829	9.9459	0.5317	9.7257	1.8807	0.2743	1.0821	62° 00'
28° 10'	0.4916	0.4720	9.6740	0.8816	9.9453	0.5354	9.7287	1.8676	0.2713	1.0792	62° 50'
28° 20'	0.4945	0.4746	9.6763	0.8802	9.9446	0.5392	9.7317	1.8546	0.2683	1.0763	62° 40'
28° 30'	0.4974	0.4772	9.6787	0.8788	9.9439	0.5430	9.7348	1.8418	0.2652	1.0734	62° 30'
28° 40'	0.5003	0.4797	9.6810	0.8774	9.9432	0.5467	9.7378	1.8291	0.2622	1.0705	62° 20'
28° 50'	0.5032	0.4823	9.6833	0.8760	9.9425	0.5505	9.7408	1.8165	0.2592	1.0676	62° 10'
29° 00'	0.5061	0.4848	9.6856	0.8746	9.9418	0.5543	9.7438	1.8040	0.2562	1.0647	61° 00'
29° 10'	0.5091	0.4874	9.6878	0.8732	9.9411	0.5581	9.7467	1.7917	0.2533	1.0617	61° 50'
29° 20'	0.5120	0.4899	9.6901	0.8718	9.9404	0.5619	9.7497	1.7796	0.2503	1.0588	61° 40'
29° 30'	0.5149	0.4924	9.6923	0.8704	9.9397	0.5658	9.7526	1.7675	0.2474	1.0559	61° 30'
29° 40'	0.5178	0.4950	9.6946	0.8689	9.9390	0.5696	9.7556	1.7556	0.2444	1.0530	61° 20'
29° 50'	0.5207	0.4975	9.6968	0.8675	9.9383	0.5735	9.7585	1.7437	0.2415	1.0501	61° 10'
		Natural	Log**	Natural	Log**	Natural	Log**	Natural	Log**	Radians	Degrees
		Cosines		Sines		Cotangents		Tangents			

*For 0° intervals, see Tables 1.21, 1.22, and 1.23.
 **Add 10 in these columns.

TABLE 1.24—TRIGONOMETRIC FUNCTIONS (AT INTERVALS OF 10')* (continued)

Degrees	Radians	Sines		Cosines		Tangents		Cotangents			
		Natural	Log**	Natural	Log**	Natural	Log**	Natural	Log**		
30° 00'	0.5236	0.5000	9.6990	0.8660	9.9375	0.5774	9.7614	1.7321	0.2386	1.0472	60° 00'
30° 10'	0.5265	0.5025	9.7012	0.8646	9.9368	0.5812	9.7644	1.7205	0.2356	1.0443	60° 50'
30° 20'	0.5294	0.5050	9.7033	0.8631	9.9361	0.5851	9.7673	1.7090	0.2327	1.0414	60° 40'
30° 30'	0.5323	0.5075	9.7055	0.8616	9.9353	0.5890	9.7701	1.6977	0.2299	1.0385	60° 30'
30° 40'	0.5352	0.5100	9.7076	0.8601	9.9346	0.5930	9.7730	1.6864	0.2270	1.0356	60° 20'
30° 50'	0.5381	0.5125	9.7097	0.8587	9.9338	0.5969	9.7759	1.6753	0.2241	1.0327	60° 10'
31° 00'	0.5411	0.5150	9.7118	0.8572	9.9331	0.6009	9.7788	1.6643	0.2212	1.0297	59° 00'
31° 10'	0.5440	0.5175	9.7139	0.8557	9.9323	0.6048	9.7816	1.6534	0.2184	1.0268	59° 50'
31° 20'	0.5469	0.5200	9.7160	0.8542	9.9315	0.6088	9.7845	1.6426	0.2155	1.0239	59° 40'
31° 30'	0.5498	0.5225	9.7181	0.8526	9.9308	0.6128	9.7873	1.6319	0.2127	1.0210	59° 30'
31° 40'	0.5527	0.5250	9.7201	0.8511	9.9300	0.6168	9.7902	1.6212	0.2098	1.0181	59° 20'
31° 50'	0.5556	0.5275	9.7222	0.8496	9.9292	0.6208	9.7930	1.6107	0.2070	1.0152	59° 10'
32° 00'	0.5585	0.5299	9.7742	0.8480	9.9284	0.6249	9.7958	1.6003	0.2042	1.0123	58° 00'
32° 10'	0.5614	0.5324	9.7262	0.8465	9.9276	0.6289	9.7986	1.5900	0.2014	1.0094	58° 50'
32° 20'	0.5643	0.5348	9.7282	0.8450	9.9268	0.6330	9.8014	1.5798	0.1986	1.0065	58° 40'
32° 30'	0.5672	0.5373	9.7302	0.8434	9.9260	0.6371	9.8042	1.5697	0.1958	1.0036	58° 30'
32° 40'	0.5701	0.5398	9.7322	0.8418	9.9252	0.6412	9.8070	1.5597	0.1930	1.0007	58° 20'
32° 50'	0.5730	0.5422	9.7342	0.8403	9.9244	0.6453	9.8097	1.5497	0.1903	0.9977	58° 10'
33° 00'	0.5760	0.5446	9.7361	0.8387	9.9236	0.6494	9.8125	1.5399	0.1875	0.9948	57° 00'
33° 10'	0.5789	0.5471	9.7380	0.8371	9.9228	0.6536	9.8153	1.5301	0.1847	0.9919	57° 50'
33° 20'	0.5818	0.5495	9.7400	0.8355	9.9219	0.6577	9.8180	1.5204	0.1820	0.9890	57° 40'
33° 30'	0.5847	0.5519	9.7419	0.8339	9.9211	0.6619	9.8208	1.5108	0.1792	0.9861	57° 30'
33° 40'	0.5876	0.5544	9.7438	0.8323	9.9203	0.6661	9.8235	1.5013	0.1765	0.9832	57° 20'
33° 50'	0.5905	0.5568	9.7457	0.8307	9.9194	0.6703	9.8263	1.4919	0.1737	0.9803	57° 10'
34° 00'	0.5934	0.5592	9.7476	0.8290	9.9186	0.6745	9.8290	1.4826	0.1710	0.9774	56° 00'
34° 10'	0.5963	0.5616	9.7494	0.8274	9.9177	0.6787	9.8317	1.4733	0.1683	0.9745	56° 50'
34° 20'	0.5992	0.5640	9.7513	0.8258	9.9169	0.6830	9.8344	1.4641	0.1656	0.9716	56° 40'
34° 30'	0.6021	0.5664	9.7531	0.8241	9.9160	0.6873	9.8371	1.4550	0.1629	0.9687	56° 30'
34° 40'	0.6050	0.5688	9.7550	0.8225	9.9151	0.6916	9.8398	1.4460	0.1602	0.9657	56° 20'
34° 50'	0.6080	0.5712	9.7568	0.8208	9.9142	0.6959	9.8425	1.4370	0.1575	0.9628	56° 10'
35° 00'	0.6109	0.5736	9.7586	0.8192	9.9134	0.7002	9.8452	1.4281	0.1548	0.9599	55° 00'
35° 10'	0.6138	0.5760	9.7604	0.8175	9.9125	0.7046	9.8479	1.4193	0.1521	0.9570	55° 50'
35° 20'	0.6167	0.5783	9.7622	0.8158	9.9116	0.7089	9.8506	1.4106	0.1494	0.9541	55° 40'
35° 30'	0.6196	0.5807	9.7640	0.8141	9.9107	0.7133	0.8533	1.4019	0.1467	0.9512	55° 30'
35° 40'	0.6225	0.5831	9.7657	0.8124	9.9098	0.7177	9.8559	1.3934	0.1441	0.9483	55° 20'
35° 50'	0.6254	0.5854	9.7675	0.8107	9.9089	0.7221	9.8586	1.3848	0.1414	0.9454	55° 10'
36° 00'	0.6283	0.5878	9.7692	0.8090	9.9080	0.7265	9.8613	1.3764	0.1387	0.9425	54° 00'
36° 10'	0.6312	0.5901	9.7710	0.8073	9.9070	0.7310	9.8639	1.3680	0.1361	0.9396	54° 50'
36° 20'	0.6341	0.5925	9.7727	0.8056	9.9061	0.7355	9.8666	1.3597	0.1334	0.9367	54° 40'
36° 30'	0.6370	0.5948	9.7744	0.8039	9.9052	0.7400	9.8692	1.3514	0.1308	0.9338	54° 30'
36° 40'	0.6400	0.5972	9.7761	0.8021	9.9042	0.7445	9.8718	1.3432	0.1282	0.9308	54° 20'
36° 50'	0.6429	0.5995	9.7778	0.8004	9.9033	0.7490	9.8745	1.3351	0.1255	0.9279	54° 10'
37° 00'	0.6458	0.6018	9.7795	0.7986	9.9023	0.7536	9.8771	1.3270	0.1229	0.9250	53° 00'
37° 10'	0.6487	0.6041	9.7811	0.7969	9.9014	0.7581	9.8797	1.3190	0.1203	0.9221	53° 50'
37° 20'	0.6516	0.6065	9.7828	0.7951	9.9004	0.7627	9.8824	1.3111	0.1176	0.9192	53° 40'
37° 30'	0.6545	0.6088	9.7844	0.7934	9.8995	0.7673	9.8850	1.3032	0.1150	0.9163	53° 30'
37° 40'	0.6574	0.6111	9.7861	0.7916	9.8985	0.7720	9.8876	1.2954	0.1124	0.9134	53° 20'
37° 50'	0.6603	0.6134	9.7877	0.7898	9.8975	0.7766	9.8902	1.2876	0.1098	0.9105	53° 10'
38° 00'	0.6632	0.6157	9.7893	0.7880	9.8965	0.7813	9.8928	1.2799	0.1072	0.9076	52° 00'
38° 10'	0.6661	0.6180	9.7910	0.7862	9.8955	0.7860	9.8954	1.2723	0.1046	0.9047	52° 50'
38° 20'	0.6690	0.6202	9.7926	0.7844	9.8945	0.7907	9.8980	1.2647	0.1020	0.9018	52° 40'
38° 30'	0.6720	0.6225	9.7941	0.7826	9.8935	0.7954	9.9006	1.2572	0.0994	0.8988	52° 30'
38° 40'	0.6749	0.6248	9.7957	0.7808	9.8925	0.8002	9.9032	1.2497	0.0968	0.8959	52° 20'
38° 50'	0.6778	0.6271	9.7973	0.7790	9.8915	0.8050	9.9058	1.2423	0.0942	0.8930	52° 10'
39° 00'	0.6807	0.6293	9.7989	0.7771	9.8905	0.8098	9.9084	1.2349	0.0916	0.8901	51° 00'
39° 10'	0.6836	0.6316	9.8004	0.7753	9.8895	0.8146	9.9110	1.2276	0.0890	0.8872	51° 50'
39° 20'	0.6865	0.6338	9.8020	0.7735	9.8884	0.8195	9.9135	1.2203	0.0865	0.8843	51° 40'
39° 30'	0.6894	0.6361	9.8035	0.7716	9.8874	0.8243	9.9161	1.2131	0.0839	0.8814	51° 30'
39° 40'	0.6923	0.6383	9.8050	0.7698	9.8864	0.8292	9.9187	1.2059	0.0813	0.8785	51° 20'
39° 50'	0.6952	0.6406	9.8066	0.7679	9.8853	0.8342	9.9212	1.1988	0.0788	0.8756	51° 10'
		Natural	Log**	Natural	Log**	Natural	Log**	Natural	Log**		
		Cosines		Sines		Cotangents		Tangents		Radians	Degrees

*For 0°.1 intervals, see Tables 1.21, 1.22, and 1.23.

**Add 10 in these columns.

(continued on next page)

TABLE 1.24—TRIGONOMETRIC FUNCTIONS (AT INTERVALS OF 10')* (continued)

		Sines		Cosines		Tangents		Cotangents			
Degrees	Radians	Natural	Log**	Natural	Log**	Natural	Log**	Natural	Log**		
40° 00'	0.6981	0.6428	9.8081	0.7660	9.8843	0.8391	9.9238	1.1918	0.0762	0.8727	50° 00'
40° 10'	0.7010	0.6450	9.8096	0.7642	9.8832	0.8441	9.9264	1.1847	0.0736	0.8698	50° 50'
40° 20'	0.7039	0.6472	9.8111	0.7623	9.8821	0.8491	9.9289	1.1778	0.0711	0.8668	50° 40'
40° 30'	0.7069	0.6494	9.8125	0.7604	9.8810	0.8541	9.9315	1.1708	0.0685	0.8639	50° 30'
40° 40'	0.7098	0.6517	9.8140	0.7585	9.8800	0.8591	9.9341	1.1640	0.0659	0.8610	50° 20'
40° 50'	0.7127	0.6539	9.8155	0.7566	9.8789	0.8642	9.9366	1.1571	0.0634	0.8581	50° 10'
41° 00'	0.7156	0.6561	9.8169	0.7547	9.8778	0.8693	9.9392	1.1504	0.0608	0.8552	49° 00'
41° 10'	0.7185	0.6583	9.8184	0.7528	9.8767	0.8744	9.9417	1.1436	0.0583	0.8523	49° 50'
41° 20'	0.7214	0.6604	9.8198	0.7509	9.8756	0.8796	9.9443	1.1369	0.0557	0.8494	49° 40'
41° 30'	0.7243	0.6626	9.8213	0.7490	9.8745	0.8847	9.9468	1.1303	0.0532	0.8465	49° 30'
41° 40'	0.7272	0.6648	9.8227	0.7470	9.8733	0.8899	9.9494	1.1237	0.0506	0.8436	49° 20'
41° 50'	0.7301	0.6670	9.8241	0.7451	9.8722	0.8952	9.9519	1.1171	0.0481	0.8407	49° 10'
42° 00'	0.7330	0.6691	9.8255	0.7431	9.8711	0.9004	9.9544	1.1106	0.0456	0.8378	48° 00'
42° 10'	0.7359	0.6713	9.8269	0.7412	9.8699	0.9057	9.9570	1.1041	0.0430	0.8348	48° 50'
42° 20'	0.7389	0.6734	9.8283	0.7392	9.8688	0.9110	9.9595	1.0977	0.0405	0.8319	48° 40'
42° 30'	0.7418	0.6756	9.8297	0.7373	9.8676	0.9163	9.9621	1.0913	0.0379	0.8290	48° 30'
42° 40'	0.7447	0.6777	9.8311	0.7353	9.8665	0.9217	9.9646	1.0850	0.0354	0.8261	48° 20'
42° 50'	0.7476	0.6799	9.8324	0.7333	9.8653	0.9271	9.9671	1.0786	0.0329	0.8232	48° 10'
43° 00'	0.7505	0.6820	9.8338	0.7314	9.8641	0.9325	9.9697	1.0724	0.0303	0.8203	47° 00'
43° 10'	0.7534	0.6841	9.8351	0.7294	9.8629	0.9380	9.9722	1.0661	0.0278	0.8174	47° 50'
43° 20'	0.7563	0.6862	9.8365	0.7274	9.8618	0.9435	9.9747	1.0599	0.0253	0.8145	47° 40'
43° 30'	0.7592	0.6884	9.8378	0.7254	9.8606	0.9490	9.9772	1.0538	0.0228	0.8116	47° 30'
43° 40'	0.7621	0.6905	9.8391	0.7234	9.8594	0.9545	9.9798	1.0477	0.0202	0.8087	47° 20'
43° 50'	0.7650	0.6926	9.8405	0.7214	9.8582	0.9601	9.9823	1.0416	0.0177	0.8058	47° 10'
44° 00'	0.7679	0.6947	9.8418	0.7193	9.8569	0.9657	9.9848	1.0355	0.0152	0.8029	46° 00'
44° 10'	0.7709	0.6967	9.8431	0.7173	9.8557	0.9713	9.9874	1.0295	0.0126	0.7999	46° 50'
44° 20'	0.7738	0.6988	9.8444	0.7153	9.8545	0.9770	9.9899	1.0235	0.0101	0.7970	46° 40'
44° 30'	0.7767	0.7009	9.8457	0.7133	9.8532	0.9827	9.9924	1.0176	0.0076	0.7941	46° 30'
44° 40'	0.7796	0.7030	9.8469	0.7112	9.8520	0.9884	9.9949	1.0117	0.0051	0.7912	46° 20'
44° 50'	0.7825	0.7050	9.8482	0.7092	9.8507	0.9942	9.9975	1.0058	0.0025	0.7883	46° 10'
45° 00'	0.7854	0.7071	9.8495	0.7071	9.8495	1.0000	0.0000	1.0000	0.0000	0.7854	45° 00'
		Natural	Log**	Natural	Log**	Natural	Log**	Natural	Log**		
		Cosines		Sines		Cotangents		Tangents		Radians	Degrees

*For 0° 1 intervals see Tables 1.21, 1.22, and 1.23

**Add 10 in these columns

TABLE 1.25—EXPONENTIALS (e^n and e^{-n})*

n	e^n	Difference	n	e^n	Difference	n	e^n	n	e^{-n}	Difference	n	e^{-n}	n	e^{-n}
0.00	1.000		0.50	1.649	16	1.0	2.718*	0.00	1.000	-10	0.50	0.607	1.0	0.368**
0.01	1.010	10	0.51	1.665	17	1.1	3.004	0.01	0.990	-10	0.51	0.600	1.1	0.333
0.02	1.020	10	0.52	1.682	17	1.2	3.320	0.02	0.980	-10	0.52	0.595	1.2	0.301
0.03	1.030	10	0.53	1.699	17	1.3	3.669	0.03	0.970	-9	0.53	0.589	1.3	0.273
0.04	1.041	11	0.54	1.716	17	1.4	4.055	0.04	0.961	-10	0.54	0.583	1.4	0.247
0.05	1.051	10	0.55	1.733	18	1.5	4.482	0.05	0.951	-9	0.55	0.577	1.5	0.223
0.06	1.062	11	0.56	1.751	17	1.6	4.953	0.06	0.942	-10	0.56	0.571	1.6	0.202
0.07	1.073	11	0.57	1.768	18	1.7	5.474	0.07	0.932	-9	0.57	0.566	1.7	0.183
0.08	1.083	10	0.58	1.786	18	1.8	6.050	0.08	0.923	-9	0.58	0.560	1.8	0.165
0.09	1.094	11	0.59	1.804	18	1.9	6.686	0.09	0.914	-9	0.59	0.554	1.9	0.150
0.10	1.105	11	0.60	1.822	18	2.0	7.389	0.10	0.905	-9	0.60	0.549	2.0	0.135
0.11	1.116	11	0.61	1.840	19	2.1	8.166	0.11	0.896	-9	0.61	0.543	2.1	0.122
0.12	1.127	11	0.62	1.859	19	2.2	9.025	0.12	0.887	-9	0.62	0.538	2.2	0.111
0.13	1.139	12	0.63	1.878	19	2.3	9.974	0.13	0.878	-9	0.63	0.533	2.3	0.100
0.14	1.150	11	0.64	1.896	18	2.4	11.02	0.14	0.869	-8	0.64	0.527	2.4	0.0907
0.15	1.162	12	0.65	1.916	20	2.5	12.18	0.15	0.861	-9	0.65	0.522	2.5	0.0821
0.16	1.174	12	0.66	1.935	19	2.6	13.46	0.16	0.852	-8	0.66	0.517	2.6	0.0743
0.17	1.185	11	0.67	1.954	19	2.7	14.88	0.17	0.844	-8	0.67	0.512	2.7	0.0672
0.18	1.197	12	0.68	1.974	20	2.8	16.44	0.18	0.835	-9	0.68	0.507	2.8	0.0608
0.19	1.209	12	0.69	1.994	20	2.9	18.17	0.19	0.827	-8	0.69	0.502	2.9	0.0550
0.20	1.221	12	0.70	2.014	20	3.0	20.09	0.20	0.819	-8	0.70	0.497	3.0	0.0498
0.21	1.234	13	0.71	2.034	20	3.1	22.20	0.21	0.811	-8	0.71	0.492	3.1	0.0450
0.22	1.246	12	0.72	2.054	21	3.2	24.53	0.22	0.803	-8	0.72	0.487	3.2	0.0408
0.23	1.259	13	0.73	2.075	21	3.3	27.11	0.23	0.795	-8	0.73	0.482	3.3	0.0369
0.24	1.271	13	0.74	2.096	21	3.4	29.96	0.24	0.787	-8	0.74	0.477	3.4	0.0334
0.25	1.284	13	0.75	2.117	21	3.5	33.12	0.25	0.779	-8	0.75	0.472	3.5	0.0302
0.26	1.297	13	0.76	2.138	22	3.6	36.60	0.26	0.771	-8	0.76	0.468	3.6	0.0273
0.27	1.310	13	0.77	2.160	21	3.7	40.45	0.27	0.763	-7	0.77	0.463	3.7	0.0247
0.28	1.323	13	0.78	2.181	22	3.8	44.70	0.28	0.756	-8	0.78	0.458	3.8	0.0224
0.29	1.336	14	0.79	2.203	23	3.9	49.40	0.29	0.748	-7	0.79	0.454	3.9	0.0202
0.30	1.350	13	0.80	2.226	22	4.0	54.60	0.30	0.741	-8	0.80	0.449	4.0	0.0183
0.31	1.363	14	0.81	2.248	22	4.1	60.34	0.31	0.733	-7	0.81	0.445	4.1	0.0166
0.32	1.377	14	0.82	2.270	23	4.2	66.69	0.32	0.726	-7	0.82	0.440	4.2	0.0150
0.33	1.391	14	0.83	2.293	23	4.3	73.70	0.33	0.719	-7	0.83	0.436	4.3	0.0136
0.34	1.405	14	0.84	2.316	24	4.4	81.45	0.34	0.712	-7	0.84	0.432	4.4	0.0123
0.35	1.419	14	0.85	2.340	23	4.5	90.02	0.35	0.705	-7	0.85	0.427	4.5	0.0111
0.36	1.433	15	0.86	2.363	24	5.0	148.4	0.36	0.698	-7	0.86	0.423	5.0	0.00674
0.37	1.448	14	0.87	2.387	24	6.0	403.4	0.37	0.691	-7	0.87	0.419	6.0	0.00248
0.38	1.462	15	0.88	2.411	24	7.0	1 097	0.38	0.684	-7	0.88	0.415	7.0	0.000912
0.39	1.477	14	0.89	2.435	25	8.0	2.981	0.39	0.677	-7	0.89	0.411	8.0	0.000335
0.40	1.492	15	0.90	2.460	24	9.0	8.103	0.40	0.670	-6	0.90	0.407	9.0	0.000123
0.41	1.507	15	0.91	2.484	25	10.0	22.026	0.41	0.664	-7	0.91	0.403	10.0	0.000045
0.42	1.522	15	0.92	2.509	26	$\pi/2$	4.810	0.42	0.657	-6	0.92	0.399	$\pi/2$	0.208
0.43	1.537	16	0.93	2.535	25	$2\pi/2$	23.14	0.43	0.651	-7	0.93	0.395	$2\pi/2$	0.0432
0.44	1.553	15	0.94	2.560	26	$3\pi/2$	111.3	0.44	0.644	-6	0.94	0.391	$3\pi/2$	0.00898
0.45	1.568	16	0.95	2.586	26	$4\pi/2$	535.5	0.45	0.638	-7	0.95	0.387	$4\pi/2$	0.00187
0.46	1.584	16	0.96	2.612	26	$5\pi/2$	2 576.0	0.46	0.631	-6	0.96	0.383	$5\pi/2$	0.000388
0.47	1.600	16	0.97	2.638	26	$6\pi/2$	12 392.0	0.47	0.625	-6	0.97	0.379	$6\pi/2$	0.000081
0.48	1.616	16	0.98	2.664	27	$7\pi/2$	59 610.0	0.48	0.619	-6	0.98	0.375	$7\pi/2$	0.000017
0.49	1.632	17	0.99	2.691	27	$7\pi/2$	286.751.0	0.49	0.613	-6	0.99	0.372	$8\pi/2$	0.000003
0.50	1.649		1.00	2.718				0.50	0.607		1.00	0.368		

* $e = 2.71828$, $1/e = 0.367879$, $\log_{10} e = 0.4343$, $1/(0.4343) = 2.3026$, $\log_{10}(0.4343) = 1.6378$, $\log_{10} e^n = n(0.4343)$. For tables of multiples of 0.4343, see Table 1.30.

**Do not interpolate in this column.

TABLE 1.26—NATURAL LOGARITHMS*

	<i>n</i>	<i>n</i> (2.3026)	<i>n</i> (0.6974 - 3)
	1	2.3026	0.6974 - 3
	2	4.6052	0.3948 - 5
	3	6.9078	0.0922 - 7
	4	9.2103	0.7897 - 10
	5	11.5129	0.4871 - 12
	6	13.8155	0.1845 - 14
	7	16.1181	0.8819 - 17
	8	18.4207	0.5793 - 19
	9	20.7233	0.2767 - 21

Number	0	1	2	3	4	5	6	7	8	9	Average Difference
1.0	0.0000	0.0100	0.0198	0.0296	0.0392	0.0488	0.0583	0.0677	0.0770	0.0862	95
1.1	0.0953	0.1044	0.1133	0.1222	0.1310	0.1398	0.1484	0.1570	0.1655	0.1740	87
1.2	0.1823	0.1906	0.1989	0.2070	0.2151	0.2231	0.2311	0.2390	0.2469	0.2546	80
1.3	0.2624	0.2700	0.2776	0.2852	0.2927	0.3001	0.3075	0.3148	0.3221	0.3293	74
1.4	0.3365	0.3436	0.3507	0.3577	0.3646	0.3716	0.3784	0.3853	0.3920	0.3988	69
1.5	0.4055	0.4121	0.4187	0.4253	0.4318	0.4383	0.4447	0.4511	0.4574	0.4637	65
1.6	0.4700	0.4762	0.4824	0.4886	0.4947	0.5008	0.5068	0.5128	0.5188	0.5247	61
1.7	0.5306	0.5365	0.5423	0.5481	0.5539	0.5596	0.5653	0.5710	0.5766	0.5822	57
1.8	0.5878	0.5933	0.5988	0.6043	0.6098	0.6152	0.6206	0.6259	0.6313	0.6366	54
1.9	0.6419	0.6471	0.6523	0.6575	0.6627	0.6678	0.6729	0.6780	0.6831	0.6881	51
2.0	0.6931	0.6981	0.7031	0.7080	0.7129	0.7178	0.7227	0.7275	0.7324	0.7372	49
2.1	0.7419	0.7467	0.7514	0.7561	0.7608	0.7655	0.7701	0.7747	0.7793	0.7839	47
2.2	0.7885	0.7930	0.7975	0.8020	0.8065	0.8109	0.8154	0.8198	0.8242	0.8286	44
2.3	0.8329	0.8372	0.8416	0.8459	0.8502	0.8544	0.8587	0.8629	0.8671	0.8713	43
2.4	0.8755	0.8796	0.8838	0.8879	0.8920	0.8961	0.9002	0.9042	0.9083	0.9123	41
2.5	0.9163	0.9203	0.9243	0.9282	0.9322	0.9361	0.9400	0.9439	0.9478	0.9517	39
2.6	0.9555	0.9594	0.9632	0.9670	0.9708	0.9746	0.9783	0.9821	0.9858	0.9895	38
2.7	0.9933	0.9969	1.0006	1.0043	1.0080	1.0116	1.0152	1.0188	1.0225	1.0260	36
2.8	1.0296	1.0332	1.0367	1.0403	1.0438	1.0473	1.0508	1.0543	1.0578	1.0613	35
2.9	1.0647	1.0682	1.0716	1.0750	1.0784	1.0818	1.0852	1.0886	1.0919	1.0953	34
3.0	1.0986	1.1019	1.1053	1.1086	1.1119	1.1151	1.1184	1.1217	1.1249	1.1282	33
3.1	1.1314	1.1346	1.1378	1.1410	1.1442	1.1474	1.1506	1.1537	1.1569	1.1600	32
3.2	1.1632	1.1663	1.1694	1.1725	1.1756	1.1787	1.1817	1.1848	1.1878	1.1909	31
3.3	1.1939	1.1969	1.2000	1.2030	1.2060	1.2090	1.2119	1.2149	1.2179	1.2208	30
3.4	1.2238	1.2267	1.2296	1.2326	1.2355	1.2384	1.2413	1.2442	1.2470	1.2499	29
3.5	1.2528	1.2556	1.2585	1.2613	1.2641	1.2669	1.2698	1.2726	1.2754	1.2782	28
3.6	1.2809	1.2837	1.2865	1.2892	1.2920	1.2947	1.2975	1.3002	1.3029	1.3056	27
3.7	1.3083	1.3110	1.3137	1.3164	1.3191	1.3218	1.3244	1.3271	1.3297	1.3324	27
3.8	1.3350	1.3376	1.3403	1.3429	1.3455	1.3481	1.3507	1.3533	1.3558	1.3584	26
3.9	1.3610	1.3635	1.3661	1.3686	1.3712	1.3737	1.3762	1.3788	1.3813	1.3838	25
4.0	1.3863	1.3888	1.3913	1.3938	1.3962	1.3987	1.4012	1.4036	1.4061	1.4085	25
4.1	1.4110	1.4134	1.4159	1.4183	1.4207	1.4231	1.4255	1.4279	1.4303	1.4327	24
4.2	1.4351	1.4375	1.4398	1.4422	1.4446	1.4469	1.4493	1.4516	1.4540	1.4563	23
4.3	1.4586	1.4609	1.4633	1.4656	1.4679	1.4702	1.4725	1.4748	1.4770	1.4793	23
4.4	1.4816	1.4839	1.4861	1.4884	1.4907	1.4929	1.4951	1.4974	1.4996	1.5019	22
4.5	1.5041	1.5063	1.5085	1.5107	1.5129	1.5151	1.5173	1.5195	1.5217	1.5239	22
4.6	1.5261	1.5282	1.5304	1.5326	1.5347	1.5369	1.5390	1.5412	1.5433	1.5454	21
4.7	1.5476	1.5497	1.5518	1.5539	1.5560	1.5581	1.5602	1.5623	1.5644	1.5665	21
4.8	1.5686	1.5707	1.5728	1.5748	1.5769	1.5790	1.5810	1.5831	1.5851	1.5872	20
4.9	1.5892	1.5913	1.5933	1.5953	1.5974	1.5994	1.6014	1.6034	1.6054	1.6074	20
5.0	1.6094	1.6114	1.6134	1.6154	1.6174	1.6194	1.6214	1.6233	1.6253	1.6273	20
5.1	1.6292	1.6312	1.6332	1.6351	1.6371	1.6390	1.6409	1.6429	1.6448	1.6467	19
5.2	1.6487	1.6506	1.6525	1.6544	1.6563	1.6582	1.6601	1.6620	1.6639	1.6658	19
5.3	1.6677	1.6696	1.6715	1.6734	1.6752	1.6771	1.6790	1.6808	1.6827	1.6845	18
5.4	1.6864	1.6882	1.6901	1.6919	1.6938	1.6956	1.6974	1.6993	1.7011	1.7029	18

This table gives the natural or Napierian logarithms (ln) of numbers between 1 and 10, correct to four places. Moving the decimal point *n* places to the right (or left) in the number is equivalent to adding *n* times 2.3026 (or *n* times 3.6974) to the logarithm. Base *e* = 2.71828 + .

*ln *x* = (2.3026) log₁₀ *x*, log₁₀ *x* = (0.4343) ln *x*, where 2.3026 = ln 10 and 0.4343 = log₁₀ *e*.

TABLE 1.26—NATURAL LOGARITHMS* (continued)

	<i>n</i>	<i>n</i> (2.3026)	<i>n</i> (0.6974 – 3)
	1	2.3026	0.6974 – 3
	2	4.6052	0.3948 – 5
	3	6.9078	0.0922 – 7
	4	9.2103	0.7897 – 10
	5	11.5129	0.4871 – 12
	6	13.8155	0.1845 – 14
	7	16.1181	0.8819 – 17
	8	18.4207	0.5793 – 19
	9	20.7233	0.2767 – 21

Number	0	1	2	3	4	5	6	7	8	9	Average Difference
5.5	1.7047	1.7066	1.7084	1.7102	1.7120	1.7138	1.7156	1.7174	1.7192	1.7210	18
5.6	1.7228	1.7246	1.7263	1.7281	1.7299	1.7317	1.7334	1.7352	1.7370	1.7387	18
5.7	1.7405	1.7422	1.7440	1.7457	1.7475	1.7492	1.7509	1.7527	1.7544	1.7561	17
5.8	1.7579	1.7596	1.7613	1.7630	1.7647	1.7664	1.7681	1.7699	1.7716	1.7733	17
5.9	1.7750	1.7766	1.7783	1.7800	1.7817	1.7834	1.7851	1.7867	1.7884	1.7901	17
6.0	1.7918	1.7934	1.7951	1.7967	1.7984	1.8001	1.8017	1.8034	1.8050	1.8066	16
6.1	1.8083	1.8099	1.8116	1.8132	1.8148	1.8165	1.8181	1.8197	1.8213	1.8229	16
6.2	1.8245	1.8262	1.8278	1.8294	1.8310	1.8326	1.8342	1.8358	1.8374	1.8390	16
6.3	1.8405	1.8421	1.8437	1.8453	1.8469	1.8485	1.8500	1.8516	1.8532	1.8547	16
6.4	1.8563	1.8579	1.8594	1.8610	1.8625	1.8641	1.8656	1.8672	1.8687	1.8703	15
6.5	1.8718	1.8733	1.8749	1.8764	1.8779	1.8795	1.8810	1.8825	1.8840	1.8856	15
6.6	1.8871	1.8886	1.8901	1.8916	1.8931	1.8946	1.8961	1.8976	1.8991	1.9006	15
6.7	1.9021	1.9036	1.9051	1.9066	1.9081	1.9095	1.9110	1.9125	1.9140	1.9155	15
6.8	1.9169	1.9184	1.9199	1.9213	1.9228	1.9242	1.9257	1.9272	1.9286	1.9301	15
6.9	1.9315	1.9330	1.9344	1.9359	1.9373	1.9387	1.9402	1.9416	1.9430	1.9445	14
7.0	1.9459	1.9473	1.9488	1.9502	1.9516	1.9530	1.9544	1.9559	1.9573	1.9587	14
7.1	1.9601	1.9615	1.9629	1.9643	1.9657	1.9671	1.9685	1.9699	1.9713	1.9727	14
7.2	1.9741	1.9755	1.9769	1.9782	1.9796	1.9810	1.9824	1.9838	1.9851	1.9865	14
7.3	1.9879	1.9892	1.9906	1.9920	1.9933	1.9947	1.9961	1.9974	1.9988	2.0001	13
7.4	2.0015	2.0028	2.0042	2.0055	2.0069	2.0082	2.0096	2.0109	2.0122	2.0136	13
7.5	2.0149	2.0162	2.0176	2.0189	2.0202	2.0215	2.0229	2.0242	2.0255	2.0268	13
7.6	2.0281	2.0295	2.0308	2.0321	2.0334	2.0347	2.0360	2.0373	2.0386	2.0399	13
7.7	2.0412	2.0425	2.0438	2.0451	2.0464	2.0477	2.0490	2.0503	2.0516	2.0528	13
7.8	2.0541	2.0554	2.0567	2.0580	2.0592	2.0605	2.0618	2.0631	2.0643	2.0656	13
7.9	2.0669	2.0681	2.0694	2.0707	2.0719	2.0732	2.0744	2.0757	2.0769	2.0782	12
8.0	2.0794	2.0807	2.0819	2.0832	2.0844	2.0857	2.0869	2.0882	2.0894	2.0906	12
8.1	2.0919	2.0931	2.0943	2.0956	2.0968	2.0980	2.0992	2.1005	2.1017	2.1029	12
8.2	2.1041	2.1054	2.1066	2.1078	2.1090	2.1102	2.1114	2.1126	2.1138	2.1150	12
8.3	2.1163	2.1175	2.1187	2.1199	2.1211	2.1223	2.1235	2.1247	2.1258	2.1270	12
8.4	2.1282	2.1294	2.1306	2.1318	2.1330	2.1342	2.1353	2.1365	2.1377	2.1389	12
8.5	2.1401	2.1412	2.1424	2.1436	2.1448	2.1459	2.1471	2.1483	2.1494	2.1506	12
8.6	2.1518	2.1529	2.1541	2.1552	2.1564	2.1576	2.1587	2.1599	2.1610	2.1622	12
8.7	2.1633	2.1645	2.1656	2.1668	2.1679	2.1691	2.1702	2.1713	2.1725	2.1736	11
8.8	2.1748	2.1759	2.1770	2.1782	2.1793	2.1804	2.1815	2.1827	2.1838	2.1849	11
8.9	2.1861	2.1872	2.1883	2.1894	2.1905	2.1917	2.1928	2.1939	2.1950	2.1961	11
9.0	2.1972	2.1983	2.1994	2.2006	2.2017	2.2028	2.2039	2.2050	2.2061	2.2072	11
9.1	2.2083	2.2094	2.2105	2.2116	2.2127	2.2138	2.2148	2.2159	2.2170	2.2181	11
9.2	2.2192	2.2203	2.2214	2.2225	2.2235	2.2246	2.2257	2.2268	2.2279	2.2289	11
9.3	2.2300	2.2311	2.2322	2.2332	2.2343	2.2354	2.2364	2.2375	2.2386	2.2396	11
9.4	2.2407	2.2418	2.2428	2.2439	2.2450	2.2460	2.2471	2.2481	2.2492	2.2502	11
9.5	2.2513	2.2523	2.2534	2.2544	2.2555	2.2565	2.2576	2.2586	2.2597	2.2607	10
9.6	2.2618	2.2628	2.2638	2.2649	2.2659	2.2670	2.2680	2.2690	2.2701	2.2711	10
9.7	2.2721	2.2732	2.2742	2.2752	2.2762	2.2773	2.2783	2.2793	2.2803	2.2814	10
9.8	2.2824	2.2834	2.2844	2.2854	2.2865	2.2875	2.2885	2.2895	2.2905	2.2915	10
9.9	2.2925	2.2935	2.2946	2.2956	2.2966	2.2976	2.2986	2.2996	2.3006	2.3016	10
10.0	2.3026										

This table gives the natural or Napierian logarithms (ln) of numbers between 1 and 10, correct to four places. Moving the decimal point *n* places to the right (or left) in the number is equivalent to adding *n* times 2.3026 (or *n* times 3.6974) to the logarithm. Base *e* = 2.71828 + .

* $\ln x = (2.3026) \log_{10} x$, $\log_{10} x = (0.4343) \ln x$, where $2.3026 = \ln 10$ and $0.4343 = \log_{10} e$.

TABLE 1.27—HYPERBOLIC SINES [$\sinh x = \frac{1}{2}(e^x - e^{-x})$]*

x	0	1	2	3	4	5	6	7	8	9	Average Difference
0.0	0.0000	0.0100	0.0200	0.0300	0.0400	0.0500	0.0600	0.0701	0.0801	0.0901	100
0.1	0.1002	0.1102	0.1203	0.1304	0.1405	0.1506	0.1607	0.1708	0.1810	0.1911	101
0.2	0.2013	0.2115	0.2218	0.2320	0.2423	0.2526	0.2629	0.2733	0.2837	0.2941	103
0.3	0.3045	0.3150	0.3255	0.3360	0.3466	0.3572	0.3678	0.3785	0.3892	0.4000	106
0.4	0.4108	0.4216	0.4325	0.4434	0.4543	0.4653	0.4764	0.4875	0.4986	0.5098	110
0.5	0.5211	0.5324	0.5438	0.5552	0.5666	0.5782	0.5897	0.6014	0.6131	0.6248	116
0.6	0.6367	0.6485	0.6605	0.6725	0.6846	0.6967	0.7090	0.7213	0.7336	0.7461	122
0.7	0.7586	0.7712	0.7838	0.7966	0.8094	0.8223	0.8353	0.8484	0.8615	0.8748	130
0.8	0.8881	0.9015	0.9150	0.9286	0.9423	0.9561	0.9700	0.9840	0.9981	1.012	138
0.9	1.027	1.041	1.055	1.070	1.085	1.099	1.114	1.129	1.145	1.160	15
1.0	1.175	1.191	1.206	1.222	1.238	1.254	1.270	1.286	1.303	1.319	16
1.1	1.336	1.352	1.369	1.386	1.403	1.421	1.438	1.456	1.474	1.491	17
1.2	1.509	1.528	1.546	1.564	1.583	1.602	1.621	1.640	1.659	1.679	19
1.3	1.698	1.718	1.738	1.758	1.779	1.799	1.820	1.841	1.862	1.883	21
1.4	1.904	1.926	1.948	1.970	1.992	2.014	2.037	2.060	2.083	2.106	22
1.5	2.129	2.153	2.177	2.201	2.225	2.250	2.274	2.299	2.324	2.350	25
1.6	2.376	2.401	2.428	2.454	2.481	2.507	2.535	2.562	2.590	2.617	27
1.7	2.646	2.674	2.703	2.732	2.761	2.790	2.820	2.850	2.881	2.911	30
1.8	2.942	2.973	3.005	3.037	3.069	3.101	3.134	3.167	3.200	3.234	33
1.9	3.268	3.303	3.337	3.372	3.408	3.443	3.479	3.516	3.552	3.589	36
2.0	3.627	3.665	3.703	3.741	3.780	3.820	3.859	3.899	3.940	3.981	39
2.1	4.022	4.064	4.106	4.148	4.191	4.234	4.278	4.322	4.367	4.412	44
2.2	4.457	4.503	4.549	4.596	4.643	4.691	4.739	4.788	4.837	4.887	48
2.3	4.937	4.988	5.039	5.090	5.142	5.195	5.248	5.302	5.356	5.411	53
2.4	5.466	5.522	5.578	5.635	5.693	5.751	5.810	5.869	5.929	5.989	58
2.5	6.050	6.112	6.174	6.237	6.300	6.365	6.429	6.495	6.561	6.627	64
2.6	6.695	6.763	6.831	6.901	6.971	7.042	7.113	7.185	7.258	7.332	71
2.7	7.406	7.481	7.557	7.634	7.711	7.789	7.868	7.948	8.028	8.110	79
2.8	8.192	8.275	8.359	8.443	8.529	8.615	8.702	8.790	8.879	8.969	87
2.9	9.060	9.151	9.244	9.337	9.431	9.527	9.623	9.720	9.819	9.918	96
3.0	10.02	10.12	10.22	10.32	10.43	10.53	10.64	10.75	10.86	10.97	11
3.1	11.08	11.19	11.30	11.42	11.53	11.65	11.76	11.88	12.00	12.12	12
3.2	12.25	12.37	12.49	12.62	12.75	12.88	13.01	13.14	13.27	13.40	13
3.3	13.54	13.67	13.81	13.95	14.09	14.23	14.38	14.52	14.67	14.82	14
3.4	14.97	15.12	15.27	15.42	15.58	15.73	15.89	16.05	16.21	16.38	16
3.5	16.54	16.71	16.88	17.05	17.22	17.39	17.57	17.74	17.92	18.10	17
3.6	18.29	18.47	18.66	18.84	19.03	19.22	19.42	19.61	19.81	20.01	19
3.7	20.21	20.41	20.62	20.83	21.04	21.25	21.46	21.68	21.90	22.12	21
3.8	22.34	22.56	22.79	23.02	23.25	23.49	23.72	23.96	24.20	24.45	24
3.9	24.69	24.94	25.19	25.44	25.70	25.96	26.22	26.48	26.75	27.02	26
4.0	27.29	27.56	27.84	28.12	28.40	28.69	28.98	29.27	29.56	29.86	29
4.1	30.16	30.47	30.77	31.08	31.39	31.71	32.03	32.35	32.68	33.00	32
4.2	33.34	33.67	34.01	34.35	34.70	35.05	35.40	35.75	36.11	36.48	35
4.3	36.84	37.21	37.59	37.97	38.35	38.73	39.12	39.52	39.91	40.31	39
4.4	40.72	41.13	41.54	41.96	42.38	42.81	43.24	43.67	44.11	44.56	43
4.5	45.00	45.46	45.91	46.37	46.84	47.31	47.79	48.27	48.75	49.24	47
4.6	49.74	50.24	50.74	51.25	51.77	52.29	52.81	53.34	53.88	54.42	52
4.7	54.97	55.52	56.08	56.64	57.21	57.79	58.37	58.96	59.55	60.15	58
4.8	60.75	61.36	61.98	62.60	63.23	63.87	64.51	65.16	65.81	67.47	64
4.9	67.14	67.82	68.50	69.19	69.88	70.58	71.29	72.01	72.73	73.46	71
5.0	74.20										

*If $x > 5$, $\sinh x = \frac{1}{2}(e^x)$ and $\log_{10} \sinh x = (0.4343)x + 0.6990 - 1$, correct to four significant figures. For tables of multiples of 0.4343, see Table 1.30.

TABLE 1.28—HYPERBOLIC COSINES [$\cosh x = \frac{1}{2}(e^x + e^{-x})$]*

x	0	1	2	3	4	5	6	7	8	9	Average Difference
0.0	1.000	1.000	1.000	1.000	1.001	1.001	1.002	1.002	1.003	1.004	1
0.1	1.005	1.006	1.007	1.008	1.010	1.011	1.013	1.014	1.016	1.018	2
0.2	1.020	1.022	1.024	1.027	1.029	1.031	1.034	1.037	1.039	1.042	3
0.3	1.045	1.048	1.052	1.055	1.058	1.062	1.066	1.069	1.073	1.077	4
0.4	1.081	1.085	1.090	1.094	1.098	1.103	1.108	1.112	1.117	1.122	5
0.5	1.128	1.133	1.138	1.144	1.149	1.155	1.161	1.167	1.173	1.179	6
0.6	1.185	1.192	1.198	1.205	1.212	1.219	1.226	1.233	1.240	1.248	7
0.7	1.255	1.263	1.271	1.278	1.287	1.295	1.303	1.311	1.320	1.329	8
0.8	1.337	1.346	1.355	1.365	1.374	1.384	1.393	1.403	1.413	1.423	10
0.9	1.433	1.443	1.454	1.465	1.475	1.486	1.497	1.509	1.520	1.531	11
1.0	1.543	1.555	1.567	1.579	1.591	1.604	1.616	1.629	1.642	1.655	13
1.1	1.669	1.682	1.696	1.709	1.723	1.737	1.752	1.766	1.781	1.796	14
1.2	1.811	1.826	1.841	1.857	1.872	1.888	1.905	1.921	1.937	1.954	16
1.3	1.971	1.988	2.005	2.023	2.040	2.058	2.076	2.095	2.113	2.132	18
1.4	2.151	2.170	2.189	2.209	2.229	2.249	2.269	2.290	2.310	2.331	20
1.5	2.352	2.374	2.395	2.417	2.439	2.462	2.484	2.507	2.530	2.554	23
1.6	2.577	2.601	2.625	2.650	2.675	2.700	2.725	2.750	2.776	2.802	25
1.7	2.828	2.855	2.882	2.909	2.936	2.964	2.992	3.021	3.049	3.078	28
1.8	3.107	3.137	3.167	3.197	3.228	3.259	3.290	3.321	3.353	3.385	31
1.9	3.418	3.451	3.484	3.517	3.551	3.585	3.620	3.655	3.690	3.726	34
2.0	3.762	3.799	3.835	3.873	3.910	3.948	3.987	4.026	4.065	4.104	38
2.1	4.144	4.185	4.226	4.267	4.309	4.351	4.393	4.436	4.480	4.524	42
2.2	4.568	4.613	4.658	4.704	4.750	4.797	4.844	4.891	4.939	4.988	47
2.3	5.037	5.087	5.137	5.188	5.239	5.290	5.343	5.395	5.449	5.503	52
2.4	5.557	5.612	5.667	5.723	5.780	5.837	5.895	5.954	6.013	6.072	58
2.5	6.132	6.193	6.255	6.317	6.379	6.443	6.507	6.571	6.636	6.702	64
2.6	6.769	6.836	6.904	6.973	7.042	7.112	7.183	7.255	7.327	7.400	70
2.7	7.473	7.548	7.623	7.699	7.776	7.853	7.932	8.011	8.091	8.171	78
2.8	8.253	8.335	8.418	8.502	8.587	8.673	8.759	8.847	8.935	9.024	86
2.9	9.115	9.206	9.298	9.391	9.484	9.579	9.675	9.772	9.869	9.968	95
3.0	10.07	10.17	10.27	10.37	10.48	10.58	10.69	10.79	10.90	11.01	11
3.1	11.12	11.23	11.35	11.46	11.57	11.69	11.81	11.92	12.04	12.16	12
3.2	12.29	12.41	12.53	12.66	12.79	12.91	13.04	13.17	13.31	13.44	13
3.3	13.57	13.71	13.85	13.99	14.13	14.27	14.41	14.56	14.70	14.85	14
3.4	15.00	15.15	15.30	15.45	15.61	15.77	15.92	16.08	16.25	16.41	16
3.5	16.57	16.74	16.91	17.08	17.25	17.42	17.60	17.77	17.95	18.13	17
3.6	18.31	18.50	18.68	18.87	19.06	19.25	19.44	19.64	19.84	20.03	19
3.7	20.24	20.44	20.64	20.85	21.06	21.27	21.49	21.70	21.92	22.14	21
3.8	22.36	22.59	22.81	23.04	23.27	23.51	23.74	23.98	24.22	24.47	23
3.9	24.71	24.96	25.21	25.46	25.72	25.98	26.24	26.50	26.77	27.04	26
4.0	27.31	27.58	27.86	28.14	28.42	28.71	29.00	29.29	29.58	29.88	29
4.1	30.18	30.48	30.79	31.10	31.41	31.72	32.04	32.37	32.69	33.02	32
4.2	33.35	33.69	34.02	34.37	34.71	35.06	35.41	35.77	36.13	36.49	35
4.3	36.86	37.23	37.60	37.98	38.36	38.75	39.13	39.53	39.93	40.33	39
4.4	40.73	41.14	41.55	41.97	42.39	42.82	43.25	43.68	44.12	44.57	43
4.5	45.01	45.47	45.92	46.38	46.85	47.32	47.80	48.28	48.76	49.25	47
4.6	49.75	50.25	50.75	51.26	51.78	52.30	52.82	53.35	53.89	54.43	52
4.7	54.98	55.53	56.09	56.65	57.22	57.80	58.38	58.96	59.56	60.15	58
4.8	60.76	61.37	61.99	62.61	63.24	63.87	64.52	65.16	65.82	66.48	64
4.9	67.15	67.82	68.50	69.19	69.89	70.59	71.30	72.02	72.74	73.47	71
5.0	74.21										

*If $x > 5$, $\cosh x = \frac{1}{2}(e^x)$ and $\log_{10} \cosh x = (0.4343)x + 0.6990 - 1$, correct to four significant figures. For table of multiples of 0.4343, see Table 1.30.

TABLE 1.29—HYPERBOLIC TANGENTS [$\tanh x = (e^x - e^{-x})/(e^x + e^{-x}) = \sinh x / \cosh x$]

x	0	1	2	3	4	5	6	7	8	9	Average Difference
0.0	0.0000	0.0100	0.0200	0.0300	0.0400	0.0500	0.0599	0.0699	0.0798	0.0898	100
0.1	0.0997	0.1096	0.1194	0.1293	0.1391	0.1489	0.1587	0.1684	0.1781	0.1878	98
0.2	0.1974	0.2070	0.2165	0.2260	0.2355	0.2449	0.2543	0.2636	0.2729	0.2821	94
0.3	0.2913	0.3004	0.3095	0.3185	0.3275	0.3364	0.3452	0.3540	0.3627	0.3714	89
0.4	0.3800	0.3885	0.3969	0.4053	0.4137	0.4219	0.4301	0.4382	0.4462	0.4542	82
0.5	0.4621	0.4700	0.4777	0.4854	0.4930	0.5005	0.5080	0.5154	0.5227	0.5299	75
0.6	0.5370	0.5441	0.5511	0.5581	0.5649	0.5717	0.5784	0.5850	0.5915	0.5980	67
0.7	0.6044	0.6107	0.6169	0.6231	0.6291	0.6352	0.6411	0.6469	0.6527	0.6584	60
0.8	0.6640	0.6696	0.6751	0.6805	0.6858	0.6911	0.6963	0.7014	0.7064	0.7114	52
0.9	0.7163	0.7211	0.7259	0.7306	0.7352	0.7398	0.7443	0.7487	0.7531	0.7574	45
1.0	0.7616	0.7658	0.7699	0.7739	0.7779	0.7818	0.7857	0.7895	0.7932	0.7969	39
1.1	0.8005	0.8041	0.8076	0.8110	0.8144	0.8178	0.8210	0.8243	0.8275	0.8306	33
1.2	0.8337	0.8367	0.8397	0.8426	0.8455	0.8483	0.8511	0.8538	0.8565	0.8591	28
1.3	0.8617	0.8643	0.8668	0.8693	0.8717	0.8741	0.8764	0.8787	0.8810	0.8832	24
1.4	0.8854	0.8875	0.8896	0.8917	0.8937	0.8957	0.8977	0.8996	0.9015	0.9033	20
1.5	0.9052	0.9069	0.9087	0.9104	0.9121	0.9138	0.9154	0.9170	0.9186	0.9202	17
1.6	0.9217	0.9232	0.9246	0.9261	0.9275	0.9289	0.9302	0.9316	0.9329	0.9342	14
1.7	0.9354	0.9367	0.9379	0.9391	0.9402	0.9414	0.9425	0.9436	0.9447	0.9458	11
1.8	0.9468	0.9478	0.9488	0.9498	0.9508	0.9518	0.9527	0.9536	0.9545	0.9554	9
1.9	0.9562	0.9571	0.9579	0.9587	0.9595	0.9603	0.9611	0.9619	0.9626	0.9633	8
2.0	0.9640	0.9647	0.9654	0.9661	0.9668	0.9674	0.9680	0.9687	0.9693	0.9699	6
2.1	0.9705	0.9710	0.9716	0.9722	0.9727	0.9732	0.9738	0.9743	0.9748	0.9753	5
2.2	0.9757	0.9762	0.9767	0.9771	0.9776	0.9780	0.9785	0.9789	0.9793	0.9797	4
2.3	0.9801	0.9805	0.9809	0.9812	0.9816	0.9820	0.9823	0.9827	0.9830	0.9834	4
2.4	0.9837	0.9840	0.9843	0.9846	0.9849	0.9852	0.9855	0.9858	0.9861	0.9863	3
2.5	0.9866	0.9869	0.9871	0.9874	0.9876	0.9879	0.9881	0.9884	0.9886	0.9888	2
2.6	0.9890	0.9892	0.9895	0.9897	0.9899	0.9901	0.9903	0.9905	0.9906	0.9908	2
2.7	0.9910	0.9912	0.9914	0.9915	0.9917	0.9919	0.9920	0.9922	0.9923	0.9925	2
2.8	0.9926	0.9928	0.9929	0.9931	0.9932	0.9933	0.9935	0.9936	0.9937	0.9938	1
2.9	0.9940	0.9941	0.9942	0.9943	0.9944	0.9945	0.9946	0.9947	0.9949	0.9950	1
3.0	0.9951	0.9959	0.9967	0.9973	0.9978	0.9982	0.9985	0.9988	0.9990	0.9992	4
4.0	0.9993	0.9995	0.9996	0.9996	0.9997	0.9998	0.9998	0.9998	0.9999	0.9999	1
5.0	0.9999										

If $x > 5$, $\tanh x = 1.0000$ to four decimal places.TABLE 1.30—MULTIPLES OF 0.4343 ($0.43429448 = \log_{10} e$)

x	0	1	2	3	4	5	6	7	8	9
0.0	0.0000	0.0434	0.0869	0.1303	0.1737	0.2171	0.2606	0.3040	0.3474	0.3909
1.0	0.4343	0.4777	0.5212	0.5646	0.6080	0.6514	0.6949	0.7383	0.7817	0.8252
2.0	0.8686	0.9120	0.9554	0.9989	1.0423	1.0857	1.1292	1.1726	1.2160	1.2595
3.0	1.3029	1.3463	1.3897	1.4332	1.4766	1.5200	1.5635	1.6069	1.6503	1.6937
4.0	1.7372	1.7806	1.8240	1.8675	1.9109	1.9543	1.9978	2.0412	2.0846	2.1280
5.0	2.1715	2.2149	2.2583	2.3018	2.3452	2.3886	2.4320	2.4755	2.5189	2.5623
6.0	2.6058	2.6492	2.6926	2.7361	2.7795	2.8229	2.8663	2.9098	2.9532	2.9966
7.0	3.0401	3.0835	3.1269	3.1703	3.2138	3.2572	3.3006	3.3441	3.3875	3.4309
8.0	3.4744	3.5178	3.5612	3.6046	3.6481	3.6915	3.7349	3.7784	3.8218	3.8652
9.0	3.9087	3.9521	3.9955	4.0389	4.0824	4.1258	4.1692	4.2127	4.2561	4.2995

TABLE 1.31—MULTIPLES OF 2.3026 ($2.3025851 = \ln_{10} = 1/0.4343$)

x	0	1	2	3	4	5	6	7	8	9
0.0	0.0000	0.2303	0.4605	0.6908	0.9210	1.1513	1.3816	1.6118	1.8421	2.0723
1.0	2.3026	2.5328	2.7631	2.9934	3.2236	3.4539	3.6841	3.9144	4.1447	4.3749
2.0	4.6052	4.8354	5.0657	5.2959	5.5262	5.7565	5.9867	6.2170	6.4472	6.6775
3.0	6.9078	7.1380	7.3683	7.5985	7.8288	8.0590	8.2893	8.5196	8.7498	8.9801
4.0	9.2103	9.4406	9.6709	9.9011	10.131	10.362	10.592	10.822	11.052	11.283
5.0	11.513	11.743	11.973	12.204	12.434	12.664	12.894	13.125	13.355	13.585
6.0	13.816	14.046	14.276	14.506	14.737	14.967	15.197	15.427	15.658	15.888
7.0	16.118	16.348	16.579	16.809	17.039	17.269	17.500	17.730	17.960	18.190
8.0	18.421	18.651	18.881	19.111	19.342	19.572	19.802	20.032	20.263	20.493
9.0	20.723	20.954	21.184	21.414	21.644	21.875	22.105	22.335	22.565	22.796

TABLE 1.32—STANDARD DISTRIBUTION
OF RESIDUALS

a/r	y/n	Difference
0.0	0.000	54
0.1	0.054	53
0.2	0.107	53
0.3	0.160	53
0.4	0.213	51
0.5	0.264	50
0.6	0.314	49
0.7	0.363	48
0.8	0.411	45
0.9	0.456	44
1.0	0.500	42
1.1	0.542	40
1.2	0.582	37
1.3	0.619	36
1.4	0.655	33
1.5	0.688	31
1.6	0.719	29
1.7	0.748	27
1.8	0.775	25
1.9	0.800	23
2.0	0.823	20
2.1	0.843	19
2.2	0.862	17
2.3	0.879	16
2.4	0.895	13
2.5	0.908	13
2.6	0.921	10
2.7	0.931	10
2.8	0.941	9
2.9	0.950	7
3.0	0.957	6
3.1	0.963	6
3.2	0.969	5
3.3	0.974	4
3.4	0.978	4
3.5	0.982	3
3.6	0.985	2
3.7	0.987	3
3.8	0.990	1
3.9	0.991	2
4.0	0.993	6
5.0	0.999	

a = any positive quantity,
 y = number of residuals that are
numerically smaller than 1,
 r = probable error of a single
observation, and
 n = number of observations.

TABLE 1.33—FACTORS FOR COMPUTING
PROBABLE ERROR

$n/2$	Bessel		Peters	
	$\frac{0.6745}{\sqrt{n-1}}$	$\frac{0.6745}{\sqrt{n(n-1)}}$	$\frac{0.8453}{\sqrt{n(n-1)}}$	$\frac{0.8453}{n\sqrt{n-1}}$
2	0.6745	0.4769	0.5978	0.4227
3	0.4769	0.2754	0.3451	0.1993
4	0.3894	0.1947	0.2440	0.1220
5	0.3372	0.1508	0.1890	0.0845
6	0.3016	0.1231	0.1543	0.0630
7	0.2754	0.1041	0.1304	0.0493
8	0.2549	0.0901	0.1130	0.0399
9	0.2385	0.0795	0.0996	0.0332
10	0.2248	0.0711	0.0891	0.0282
11	0.2133	0.0643	0.0806	0.0243
12	0.2034	0.0587	0.0736	0.0212
13	0.1947	0.0540	0.0677	0.0188
14	0.1871	0.0500	0.0627	0.0167
15	0.1803	0.0465	0.0583	0.0151
16	0.1742	0.0435	0.0546	0.0136
17	0.1686	0.0409	0.0513	0.0124
18	0.1636	0.0386	0.0483	0.0114
19	0.1590	0.0365	0.0457	0.0105
20	0.1547	0.0346	0.0434	0.0097
21	0.1508	0.0329	0.0412	0.0090
22	0.1472	0.0314	0.0393	0.0084
23	0.1438	0.0300	0.0376	0.0078
24	0.1406	0.0287	0.0360	0.0073
25	0.1377	0.0275	0.0345	0.0069
26	0.1349	0.0265	0.0332	0.0065
27	0.1323	0.0255	0.0319	0.0061
28	0.1298	0.0245	0.0307	0.0058
29	0.1275	0.0237	0.0297	0.0055
30	0.1252	0.0229	0.0287	0.0052
31	0.1231	0.0221	0.0277	0.0050
32	0.1211	0.0214	0.0268	0.0047
33	0.1192	0.0208	0.0260	0.0045
34	0.1174	0.0201	0.0252	0.0043
35	0.1157	0.0196	0.0245	0.0041
36	0.1140	0.0190	0.0238	0.0040
37	0.1124	0.0185	0.0232	0.0038
38	0.1109	0.0180	0.0225	0.0037
39	0.1094	0.0175	0.0220	0.0035
40	0.1080	0.0171	0.0214	0.0034
45	0.1017	0.0152	0.0190	0.0028
50	0.0964	0.0136	0.0171	0.0024
55	0.0918	0.0124	0.0155	0.0021
60	0.0878	0.0113	0.0142	0.0018
65	0.0843	0.0105	0.0131	0.0016
70	0.0812	0.0097	0.0122	0.0015
75	0.0784	0.0091	0.0113	0.0013
80	0.0759	0.0085	0.0106	0.0012
85	0.0736	0.0080	0.0100	0.0011
90	0.0715	0.0075	0.0094	0.0010
95	0.0696	0.0071	0.0089	0.0009
100	0.0678	0.0068	0.0085	0.0008

TABLE 1.34—COMPOUND INTEREST—AMOUNT OF A GIVEN PRINCIPAL

The amount A at the end of n years of a given principal P placed at compound interest today is $A = P \times x$ or $A = P \times y$ or $A = P \times z$, according as the interest (at the rate of i percent per annum) is compounded annually, semiannually, or quarterly; the factor x or y or z being taken from the following tables.

Values of x —Interest Compounded Annually: $A = P \times x^*$

Years	$i = 2$	$2\frac{1}{2}$	3	$3\frac{1}{2}$	4	$4\frac{1}{2}$	5	6	7
1	1.0200	1.0250	1.0300	1.0350	1.0400	1.0450	1.0500	1.0600	1.0700
2	1.0404	1.0506	1.0609	1.0712	1.0816	1.0920	1.1025	1.1236	1.1449
3	1.0612	1.0769	1.0927	1.1087	1.1249	1.1412	1.1576	1.1910	1.2250
4	1.0824	1.1038	1.1255	1.1475	1.1699	1.1925	1.2155	1.2625	1.3108
5	1.1041	1.1314	1.1593	1.1877	1.2167	1.2462	1.2763	1.3382	1.4026
6	1.1262	1.1597	1.1941	1.2293	1.2653	1.3023	1.3401	1.4185	1.5007
7	1.1487	1.1887	1.2299	1.2723	1.3159	1.3609	1.4071	1.5036	1.6058
8	1.1717	1.2184	1.2668	1.3168	1.3686	1.4221	1.4775	1.5938	1.7182
9	1.1951	1.2489	1.3048	1.3629	1.4233	1.4861	1.5513	1.6895	1.8385
10	1.2190	1.2801	1.3439	1.4106	1.4802	1.5530	1.6289	1.7908	1.9672
11	1.2434	1.3121	1.3842	1.4600	1.5395	1.6229	1.7103	1.8983	2.1049
12	1.2682	1.3449	1.4258	1.5111	1.6010	1.6959	1.7959	2.0122	2.2522
13	1.2936	1.3785	1.4685	1.5640	1.6651	1.7722	1.8856	2.1329	2.4098
14	1.3195	1.4130	1.5126	1.6187	1.7317	1.8519	1.9799	2.2609	2.5785
15	1.3459	1.4483	1.5580	1.6753	1.8009	1.9353	2.0789	2.3966	2.7590
16	1.3728	1.4845	1.6047	1.7340	1.8730	2.0224	2.1829	2.5404	2.9522
17	1.4002	1.5216	1.6528	1.7947	1.9479	2.1134	2.2920	2.6928	3.1588
18	1.4282	1.5597	1.7024	1.8575	2.0258	2.2085	2.4066	2.8543	3.3799
19	1.4568	1.5987	1.7535	1.9225	2.1068	2.3079	2.5270	3.0256	3.6165
20	1.4859	1.6386	1.8061	1.9898	2.1911	2.4117	2.6533	3.2071	3.8697
25	1.6406	1.8539	2.0938	2.3632	2.6658	3.0054	3.3864	4.2919	5.4274
30	1.8114	2.0976	2.4273	2.8068	3.2434	3.7453	4.3219	5.7435	7.6123
40	2.2080	2.6851	3.2620	3.9593	4.8010	5.8164	7.0400	10.286	14.974
50	2.6916	3.4371	4.3839	5.5849	7.1067	9.0326	11.467	18.420	29.457
60	3.2810	4.3998	5.8916	7.8781	10.520	14.027	18.679	32.988	57.946

*This table is computed from the formula $x = 1 + (i/100)^n$.

Values of y —Interest Compounded Semiannually: $A = P \times y^*$

Years	$i = 2$	$2\frac{1}{2}$	3	$3\frac{1}{2}$	4	$4\frac{1}{2}$	5	6	7
1	1.0201	1.0252	1.0302	1.0353	1.0404	1.0455	1.0506	1.0609	1.0712
2	1.0406	1.0509	1.0614	1.0719	1.0824	1.0931	1.1038	1.1255	1.1475
3	1.0615	1.0774	1.0934	1.1097	1.1262	1.1428	1.1597	1.1941	1.2293
4	1.0829	1.1045	1.1265	1.1489	1.1717	1.1948	1.2184	1.2668	1.3168
5	1.1046	1.1323	1.1605	1.1894	1.2190	1.2492	1.2801	1.3439	1.4106
6	1.1268	1.1608	1.1956	1.2314	1.2682	1.3060	1.3449	1.4258	1.5111
7	1.1495	1.1900	1.2318	1.2749	1.3195	1.3655	1.4130	1.5126	1.6187
8	1.1726	1.2199	1.2690	1.3199	1.3728	1.4276	1.4845	1.6047	1.7340
9	1.1961	1.2506	1.3073	1.3665	1.4282	1.4926	1.5597	1.7024	1.8575
10	1.2202	1.2820	1.3469	1.4148	1.4859	1.5605	1.6386	1.8061	1.9898
11	1.2447	1.3143	1.3876	1.4647	1.5460	1.6315	1.7216	1.9161	2.1315
12	2.2697	1.3474	1.4295	1.5164	1.6084	1.7058	1.8087	2.0328	2.2833
13	1.2953	1.3812	1.4727	1.5700	1.6734	1.7834	1.9003	2.1566	2.4460
14	1.3213	1.4160	1.5172	1.6254	1.7410	1.8645	1.9965	2.2879	2.6202
15	1.3478	1.4516	1.5631	1.6828	1.8114	1.9494	2.0976	2.4273	2.8068
16	1.3749	1.4881	1.6103	1.7422	1.8845	2.0381	2.2038	2.5751	3.0067
17	1.4026	1.5256	1.6590	1.8037	1.9607	2.1308	2.3153	2.7319	3.2209
18	1.4308	1.5639	1.7091	1.8674	2.0399	2.2278	2.4325	2.8983	3.4503
19	1.4595	1.6033	1.7608	1.9333	2.1223	2.3292	2.5557	3.0748	3.6960
20	1.4889	1.6436	1.8140	2.0016	2.2080	2.4352	2.6851	3.2620	3.9593
25	1.6446	1.8610	2.1052	2.3808	2.6916	3.0420	3.4371	4.3839	5.5849
30	1.8167	2.1072	2.4432	2.8318	3.2810	3.8001	4.3998	5.8916	7.8781
40	2.2167	2.7015	3.2907	4.0064	4.8754	5.9301	7.2096	10.641	15.676
50	2.7048	3.4634	4.4320	5.6682	7.2446	9.2540	11.814	19.219	31.191
60	3.3004	4.4402	5.9693	8.0192	10.765	14.441	19.358	34.711	62.064

*This table is computed from the formula $y = 1 + (i/200)^{2n}$.

TABLE 1.34—COMPOUND INTEREST—AMOUNT OF A GIVEN PRINCIPAL (continued)Values of z —Interest Compounded Quarterly: $A = P \times z^*$

Years	$i = 2$	$2\frac{1}{2}$	3	$3\frac{1}{2}$	4	$4\frac{1}{2}$	5	6	7
1	1.0202	1.0252	1.0303	1.0355	1.0406	1.0458	1.0509	1.0614	1.0719
2	1.0407	1.0511	1.0616	1.0722	1.0829	1.0936	1.1045	1.1265	1.1489
3	1.0617	1.0776	1.0938	1.1102	1.1268	1.1437	1.1608	1.1956	1.2314
4	1.0831	1.1048	1.1270	1.1496	1.1726	1.1960	1.2199	1.2690	1.3199
5	1.1049	1.1327	1.1612	1.1903	1.2202	1.2508	1.2820	1.3469	1.4148
6	1.1272	1.1613	1.1964	1.2326	1.2697	1.3080	1.3474	1.4295	1.5164
7	1.1499	1.1906	1.2327	1.2763	1.3213	1.3679	1.4160	1.5172	1.6254
8	1.1730	1.2206	1.2701	1.3215	1.3749	1.4305	1.4881	1.6103	1.7422
9	1.1967	1.2514	1.3086	1.3684	1.4308	1.4959	1.5639	1.7091	1.8674
10	1.2208	1.2830	1.3483	1.4169	1.4889	1.5644	1.6436	1.8140	2.0016
11	1.2454	1.3154	1.3893	1.4672	1.5493	1.6360	1.7274	1.9253	2.1454
12	1.2705	1.3486	1.4314	1.5192	1.6122	1.7108	1.8154	2.0435	2.2996
13	1.2961	1.3826	1.4748	1.5731	1.6777	1.7891	1.9078	2.1689	2.4648
14	1.3222	1.4175	1.5196	1.6288	1.7458	1.8710	2.0050	2.3020	2.6420
15	1.3489	1.4533	1.5657	1.6866	1.8167	1.9566	2.1072	2.4432	2.8318
16	1.3760	1.4900	1.6132	1.7464	1.8905	2.0462	2.2145	2.5931	3.0353
17	1.4038	1.5276	1.6621	1.8083	1.9672	2.1398	2.3274	2.7523	3.2534
18	1.4320	1.5661	1.7126	1.8725	2.0471	2.2378	2.4459	2.9212	3.4872
19	1.4609	1.6056	1.7645	1.9389	2.1302	2.3402	2.5705	3.1004	3.7378
20	1.4903	1.6462	1.8180	2.0076	2.2167	2.4473	2.7015	3.2907	4.0064
25	1.6467	1.8646	2.1111	2.3898	2.7048	3.0609	3.4634	4.4320	5.6682
30	1.8194	2.1121	2.4514	2.8446	3.3004	3.8285	4.4402	5.9693	8.0192
40	2.2211	2.7098	3.3053	4.0306	4.9138	5.9892	7.2980	10.828	16.051
50	2.7115	3.4768	4.4567	5.7110	7.3160	9.3693	11.995	19.643	32.128
60	3.3102	4.4608	6.0092	8.0919	10.893	14.657	19.715	35.633	64.307

*This table is computed from the formula $z = 1 + (i/400)^{100}$.**TABLE 1.35—AMOUNT OF AN ANNUITY**

The amount S accumulated at the end of n years by a given annual payment Y set aside at the end of each year is $S = Y \times v$, where the factor v is taken from the following table. (Interest at i percent per annum, compounded annually.)

Values of v^*

Years	$i = 2$	$2\frac{1}{2}$	3	$3\frac{1}{2}$	4	$4\frac{1}{2}$	5	6	7
1	1.0000	1.0000	1.0000	1.0000	1.0000	1.0000	1.0000	1.0000	1.0000
2	2.0200	2.0250	2.0300	2.0350	2.0400	2.0450	2.0500	2.0600	2.0700
3	3.0604	3.0756	3.0909	3.1062	3.1216	3.1370	3.1525	3.1836	3.2149
4	4.1216	4.1525	4.1836	4.2149	4.2465	4.2782	4.3101	4.3746	4.4399
5	5.2040	5.2563	5.3091	5.3625	5.4163	5.4707	5.5256	5.6371	5.7507
6	6.3081	6.3877	6.4684	6.5502	6.6330	6.7169	6.8019	6.9753	7.1533
7	7.4343	7.5474	7.6625	7.7794	7.8983	8.0192	8.1420	8.3938	8.6540
8	8.5830	8.7361	8.8923	9.0517	9.2142	9.3800	9.5491	9.8975	10.260
9	9.7546	9.9545	10.159	10.368	10.583	10.802	11.027	11.491	11.978
10	10.950	11.203	11.464	11.731	12.006	12.288	12.578	13.181	13.816
11	12.169	12.483	12.808	13.142	13.486	13.841	14.207	14.972	15.784
12	13.412	13.796	14.192	14.602	15.026	15.464	15.917	16.870	17.888
13	14.680	15.140	15.618	16.113	16.627	17.160	17.713	18.882	20.141
14	15.974	16.519	17.086	17.677	18.292	18.932	19.599	21.015	22.550
15	17.293	17.932	18.599	19.296	20.024	20.784	21.579	23.276	25.129
16	18.639	19.380	20.157	20.971	21.825	22.719	23.657	25.673	27.888
17	20.012	20.865	21.762	22.705	23.698	24.742	25.840	28.213	30.840
18	21.412	22.386	23.414	24.500	25.645	26.855	28.132	30.906	33.999
19	22.841	23.946	25.117	26.357	27.671	29.064	30.539	33.760	37.379
20	24.297	25.545	26.870	28.280	29.778	31.371	33.066	36.786	40.995
25	32.030	34.158	36.459	38.950	41.646	44.565	47.727	54.865	63.249
30	40.568	43.903	47.575	51.623	56.085	61.007	66.439	79.058	94.461
40	60.402	67.403	75.401	84.550	95.026	107.03	120.80	154.76	199.64
50	84.579	97.484	112.80	131.00	152.67	178.50	209.35	290.34	406.53
60	114.05	135.99	163.05	196.52	237.99	289.50	353.58	533.13	813.52

*The formula used for this table is $v = \{[1 + (i/100)]^n - 1\} / (i/100) = (x - 1) / (i/100)$.

TABLE 1.36—PRINCIPAL AMOUNTING TO A GIVEN SUM

The principal P which, if placed at compound interest today, will amount to a given sum A at the end of n years is $P = A \times x'$ or $P = A \times y'$ or $P = A \times z'$, according as the interest (at the rate of i percent per annum) is compounded annually, semiannually, or quarterly; the factor x' or y' or z' being taken from the following tables.

Values of x' —Interest Compounded Annually: $P = A \times x'$ *

Years	$i = 2$	$2\frac{1}{2}$	3	$3\frac{1}{2}$	4	$4\frac{1}{2}$	5	6	7
1	0.98039	0.97561	0.97087	0.96618	0.96154	0.95694	0.95238	0.94340	0.93458
2	0.96117	0.95181	0.94260	0.93351	0.92456	0.91573	0.90703	0.89000	0.87344
3	0.94232	0.92860	0.91514	0.90194	0.88900	0.87630	0.86384	0.83962	0.81630
4	0.92385	0.90595	0.88849	0.87144	0.85480	0.83856	0.82270	0.79209	0.76290
5	0.90573	0.88385	0.86261	0.84197	0.82193	0.80245	0.78353	0.74726	0.71299
6	0.88797	0.86230	0.83748	0.81350	0.79031	0.76790	0.74622	0.70496	0.66634
7	0.87056	0.84127	0.81309	0.78599	0.75992	0.73483	0.71068	0.66506	0.62275
8	0.85349	0.82075	0.78941	0.75941	0.73069	0.70319	0.67684	0.62741	0.58201
9	0.83676	0.80073	0.76642	0.73373	0.70259	0.67290	0.64461	0.59190	0.54393
10	0.82035	0.78120	0.74409	0.70892	0.67556	0.64393	0.61391	0.55839	0.50835
11	0.80426	0.76214	0.72242	0.68495	0.64958	0.61620	0.58468	0.52679	0.47509
12	0.78849	0.74356	0.70138	0.66178	0.62460	0.58966	0.55684	0.49697	0.44401
13	0.77303	0.72542	0.68095	0.63940	0.60057	0.56427	0.53032	0.46884	0.41496
14	0.75788	0.70773	0.66112	0.61778	0.57748	0.53997	0.50507	0.44230	0.38783
15	0.74301	0.69047	0.64186	0.59689	0.55526	0.51672	0.48102	0.41727	0.36245
16	0.72845	0.67362	0.62317	0.57671	0.53391	0.49447	0.45811	0.39365	0.33873
17	0.71416	0.65720	0.60502	0.55720	0.51337	0.47318	0.43630	0.37136	0.31657
18	0.70016	0.64117	0.58739	0.53839	0.49363	0.45280	0.41552	0.35034	0.29586
19	0.68643	0.62553	0.57029	0.52016	0.47464	0.43330	0.39573	0.33051	0.27651
20	0.67297	0.61027	0.55368	0.50257	0.45639	0.41464	0.37689	0.31180	0.25842
25	0.60953	0.53939	0.47761	0.42315	0.37512	0.33273	0.29530	0.23300	0.18425
30	0.55207	0.47674	0.41199	0.35628	0.30832	0.26700	0.23138	0.17411	0.13137
40	0.45289	0.37243	0.30656	0.25257	0.20829	0.17193	0.14205	0.09722	0.06678
50	0.37153	0.29094	0.22811	0.17905	0.14071	0.11071	0.08720	0.05429	0.03395
60	0.30478	0.22728	0.16973	0.12693	0.09506	0.07129	0.05354	0.03031	0.01726

*The formula used for this table is $x' = [1 + (i/100)]^{-n} = 1/x$.

Values of y' —Interest Compounded Semiannually: $P = A \times y'$ *

Years	$i = 2$	$2\frac{1}{2}$	3	$3\frac{1}{2}$	4	$4\frac{1}{2}$	5	6	7
1	0.98030	0.97546	0.97066	0.96590	0.96117	0.95647	0.95181	0.94260	0.93351
2	0.96098	0.95152	0.94218	0.93296	0.92385	0.91484	0.90595	0.88849	0.87144
3	0.94205	0.92817	0.91454	0.90114	0.88797	0.87502	0.86230	0.83748	0.81350
4	0.92348	0.90540	0.88771	0.87041	0.85349	0.83694	0.82075	0.78941	0.75941
5	0.90529	0.88318	0.86167	0.84073	0.82035	0.80051	0.78120	0.74409	0.70892
6	0.88745	0.86151	0.83639	0.81206	0.77849	0.76567	0.74356	0.70138	0.66178
7	0.86996	0.84037	0.81185	0.78436	0.75788	0.73234	0.70773	0.66112	0.61778
8	0.85282	0.81975	0.78803	0.75762	0.72845	0.70047	0.67362	0.62317	0.57671
9	0.83602	0.79963	0.76491	0.73178	0.70016	0.66998	0.64117	0.58739	0.53836
10	0.81954	0.78001	0.74247	0.70682	0.67297	0.64082	0.61027	0.55368	0.50257
11	0.80340	0.76087	0.72069	0.68272	0.64684	0.61292	0.58086	0.52189	0.46915
12	0.78757	0.74220	0.69954	0.65944	0.62172	0.58625	0.55288	0.49193	0.43796
13	0.77205	0.72398	0.67902	0.63695	0.59758	0.56073	0.52623	0.46369	0.40884
14	0.75684	0.70622	0.65910	0.61523	0.57437	0.53632	0.50088	0.43708	0.38165
15	0.74192	0.68889	0.63976	0.59425	0.55207	0.51298	0.47674	0.41199	0.35628
16	0.72730	0.67198	0.62099	0.57398	0.53063	0.49065	0.45377	0.38834	0.33259
17	0.71297	0.65549	0.60277	0.55441	0.51003	0.46930	0.43191	0.36604	0.31048
18	0.69892	0.63941	0.58509	0.53550	0.49022	0.44887	0.41109	0.34503	0.28983
19	0.68515	0.62372	0.56792	0.51724	0.47119	0.42933	0.39128	0.32523	0.27056
20	0.67165	0.60841	0.55126	0.49960	0.45289	0.41065	0.37243	0.30656	0.25257
25	0.60804	0.53734	0.47500	0.42003	0.37153	0.32873	0.29094	0.22811	0.17905
30	0.55045	0.47457	0.40930	0.35313	0.30478	0.26315	0.22728	0.16973	0.12693
40	0.45112	0.37017	0.30389	0.24960	0.20511	0.16863	0.13870	0.09398	0.06379
50	0.36971	0.28873	0.22563	0.17642	0.13803	0.10806	0.08465	0.05203	0.03206
60	0.30299	0.22521	0.16752	0.12470	0.09289	0.06925	0.05166	0.02881	0.01611

*The formula used for this table is $y' = [1 + (i/200)]^{-2n} = 1/y$.

TABLE 1.36—PRINCIPAL AMOUNTING TO A GIVEN SUM (continued)

Values of z' —Interest Compounded Quarterly: $P = A \times z'$ *

Years	$i = 2$	$2\frac{1}{2}$	3	$3\frac{1}{2}$	4	$4\frac{1}{2}$	5	6	7
1	0.98025	0.97539	0.97055	0.96575	0.96098	0.95624	0.95152	0.94218	0.93296
2	0.96089	0.95138	0.94198	0.93268	0.92348	0.91439	0.90540	0.88771	0.87041
3	0.94191	0.92796	0.91424	0.90074	0.88745	0.87437	0.86151	0.83639	0.81206
4	0.92330	0.90512	0.88732	0.86989	0.85282	0.83611	0.81975	0.78803	0.75762
5	0.90506	0.88284	0.86119	0.84010	0.81954	0.79952	0.78001	0.74247	0.70682
6	0.88719	0.86111	0.83583	0.81132	0.78757	0.76453	0.74220	0.69954	0.65944
7	0.86966	0.83991	0.81122	0.78354	0.75684	0.73107	0.70622	0.65910	0.61523
8	0.85248	0.81924	0.78733	0.75670	0.72730	0.69908	0.67198	0.62099	0.57390
9	0.83564	0.79908	0.76415	0.73079	0.69892	0.66849	0.63941	0.58509	0.53550
10	0.81914	0.77941	0.74165	0.70576	0.67165	0.63923	0.60841	0.55126	0.49960
11	0.80296	0.76022	0.71981	0.68159	0.64545	0.61126	0.57892	0.51939	0.46611
12	0.78710	0.74151	0.69861	0.65825	0.62026	0.58451	0.55086	0.48936	0.43486
13	0.77155	0.72326	0.67804	0.63570	0.59606	0.55893	0.52415	0.46107	0.40570
14	0.75631	0.70546	0.65808	0.61393	0.57280	0.53447	0.49874	0.43441	0.37851
15	0.74137	0.68809	0.63870	0.59291	0.55045	0.51108	0.47457	0.40930	0.35313
16	0.72673	0.67115	0.61989	0.57260	0.52897	0.48871	0.45156	0.38563	0.32946
17	0.71237	0.65464	0.60164	0.55299	0.50833	0.46733	0.42967	0.36334	0.30737
18	0.69830	0.63852	0.58392	0.53405	0.48850	0.44687	0.40884	0.34233	0.28676
19	0.68451	0.62281	0.56673	0.51576	0.46944	0.42732	0.38903	0.32254	0.26754
20	0.67099	0.60748	0.55004	0.49810	0.45112	0.40862	0.37017	0.30389	0.24960
25	0.60729	0.53630	0.47369	0.41845	0.36971	0.32670	0.28873	0.22563	0.17642
30	0.54963	0.47347	0.40794	0.35154	0.30299	0.26120	0.22521	0.16752	0.12470
40	0.45023	0.36903	0.30255	0.24810	0.20351	0.16697	0.13702	0.09235	0.06230
50	0.36880	0.28762	0.22438	0.17510	0.13669	0.10673	0.08337	0.05091	0.03113
60	0.30210	0.22417	0.16641	0.12358	0.09181	0.06823	0.05072	0.02806	0.01555

*The formula used for this table is $z' = [1 + (i/100)]^{-4n} = 1/z$.

TABLE 1.37—ANNUITY AMOUNTING TO A GIVEN SUM (SINKING FUND)

The annual payment, Y , which, if set aside at the end of each year, will amount with accumulated interest to a given sum S at the end of n years is $Y = S \times v'$, where the factor v' is given below. Interest is i percent per annum, compounded annually.)

Values of v' *

Years	$i = 2$	$2\frac{1}{2}$	3	$3\frac{1}{2}$	4	$4\frac{1}{2}$	5	6	7
2	0.49505	0.49383	0.49261	0.49140	0.49020	0.48900	0.48780	0.48544	0.48309
3	0.32675	0.32514	0.32353	0.32193	0.32035	0.31877	0.31721	0.31411	0.31105
4	0.24262	0.24082	0.23903	0.23725	0.23549	0.23374	0.23201	0.22859	0.22523
5	0.19216	0.19025	0.18835	0.18648	0.18463	0.18279	0.18097	0.17740	0.17389
6	0.15853	0.15655	0.15460	0.15267	0.15076	0.14888	0.14702	0.14336	0.13980
7	0.13451	0.13250	0.13051	0.12854	0.12661	0.12470	0.12282	0.11914	0.11555
8	0.11651	0.11447	0.11246	0.11048	0.10853	0.10661	0.10472	0.10104	0.09747
9	0.10252	0.10046	0.09843	0.09645	0.09449	0.09257	0.09069	0.08702	0.08349
10	0.09133	0.08926	0.08723	0.08524	0.08329	0.08138	0.07950	0.07587	0.07238
11	0.08218	0.08011	0.07808	0.07609	0.07415	0.07225	0.07039	0.06679	0.06336
12	0.07456	0.07249	0.07046	0.06848	0.06655	0.06467	0.06283	0.05928	0.05590
13	0.06812	0.06605	0.06403	0.06206	0.06014	0.05828	0.05646	0.05296	0.04965
14	0.06260	0.06054	0.05853	0.05657	0.05467	0.05282	0.05102	0.04758	0.04434
15	0.05783	0.05577	0.05377	0.05183	0.04994	0.04811	0.04634	0.04296	0.03979
16	0.05365	0.05160	0.04961	0.04768	0.04582	0.04402	0.04227	0.03895	0.03586
17	0.04997	0.04793	0.04595	0.04404	0.04220	0.04042	0.03870	0.03544	0.03243
18	0.04670	0.04467	0.04271	0.04082	0.03899	0.03724	0.03555	0.03236	0.02941
19	0.04378	0.04176	0.03981	0.03794	0.03614	0.03441	0.03275	0.02962	0.02675
20	0.04116	0.03915	0.03722	0.03536	0.03358	0.03188	0.03024	0.02718	0.02439
25	0.03122	0.02928	0.02743	0.02567	0.02401	0.02244	0.02095	0.01823	0.01581
30	0.02465	0.02278	0.02102	0.01937	0.01783	0.01639	0.01505	0.01265	0.01059
40	0.01656	0.01484	0.01326	0.01183	0.01052	0.00934	0.00828	0.00646	0.00467
50	0.01182	0.01026	0.00887	0.00763	0.00655	0.00560	0.00478	0.00344	0.00238
60	0.00877	0.00735	0.00613	0.00509	0.00420	0.00345	0.00283	0.00188	0.00121

*The formula used for this table is $v' = (i/100)/[1 + (i/100)]^n - 1 = 1/v$.

TABLE 1.38—PRESENT WORTH OF AN ANNUITY

The capital C , which, if placed at interest today, will provide for a given annual payment Y for a term of n years before it is exhausted is $C = Y \times w$, where the factor w is given below. (Interest at i percent per annum, compounded annually.)

Values of w^*

Years	$i = 2$	$2\frac{1}{2}$	3	$3\frac{1}{2}$	4	$4\frac{1}{2}$	5	6	7
1	0.9804	0.9756	0.9709	0.9662	0.9615	0.9569	0.9524	0.9434	0.9346
2	1.9416	1.9274	1.9135	1.8997	1.8861	1.8727	1.8594	1.8334	1.8080
3	2.8839	2.8560	2.8286	2.8016	2.7751	2.7490	2.7232	2.6730	2.6243
4	3.8077	3.7620	3.7171	3.6731	3.6299	3.5875	3.5460	3.4651	3.3872
5	4.7135	4.6458	4.5797	4.5151	4.4518	4.3900	4.3295	4.2124	4.1002
6	5.6014	5.5081	5.4172	5.3286	5.2421	5.1579	5.0757	4.9173	4.7665
7	6.4720	6.3494	6.2303	6.1145	6.0021	5.8927	5.7864	5.5824	5.3893
8	7.3255	7.1701	7.0197	6.8740	6.7327	6.5959	6.4632	6.2098	5.9713
9	8.1622	7.9709	7.7861	7.6077	7.4353	7.2688	7.1078	6.8017	6.5152
10	8.9826	8.7521	8.5302	8.3166	8.1109	7.9127	7.7217	7.3601	7.0236
11	9.7868	9.5142	9.2526	9.0016	8.7605	8.5289	8.3064	7.8869	7.4987
12	10.575	10.258	9.9540	9.6633	9.3851	9.1186	8.8633	8.3838	7.9427
13	11.348	10.983	10.635	10.303	9.9856	9.6829	9.3936	8.8527	8.3577
14	12.106	11.691	11.296	10.921	10.563	10.223	9.8986	9.2950	8.7455
15	12.849	12.381	11.938	11.517	11.118	10.740	10.380	9.7122	9.1079
16	13.578	13.055	12.561	12.094	11.652	11.234	10.838	10.106	9.4466
17	14.292	13.712	13.166	12.651	12.166	11.707	11.274	10.477	9.7632
18	14.992	14.353	13.754	13.190	12.659	12.160	11.690	10.828	10.059
19	15.678	14.979	14.324	13.710	13.134	12.593	12.085	11.158	10.336
20	16.351	15.589	14.877	14.212	13.590	13.008	12.462	11.470	10.594
25	19.523	18.424	17.413	16.482	15.622	14.828	14.094	12.783	11.654
30	22.396	20.930	19.600	18.392	17.292	16.289	15.372	13.765	12.409
40	27.355	25.103	23.115	21.355	19.793	18.402	17.159	15.046	13.332
50	31.424	28.362	25.730	23.456	21.482	19.762	18.256	15.762	13.801
60	34.761	30.909	27.676	24.945	22.623	20.638	18.929	16.161	14.039

* The formula used for this table is $w = \{1 - [1 + (i/100)]^{-n}\} / (i/100) = v/i$.

TABLE 1.39—ANNUITY PROVIDED FOR BY A GIVEN CAPITAL

The annual payment Y provided for for a term of n years by a given capital C placed at interest today is $Y = C \times w'$. Interest at i percent per annum, compounded annually; the fund is supposed to be exhausted at the end of the term.

Values of w'^*

Years	$i = 2$	$2\frac{1}{2}$	3	$3\frac{1}{2}$	4	$4\frac{1}{2}$	5	6	7
2	0.51505	0.51883	0.52261	0.52640	0.53020	0.53400	0.53780	0.54544	0.55309
3	0.34675	0.35014	0.35353	0.35693	0.36035	0.36377	0.36721	0.37411	0.38105
4	0.26262	0.26582	0.26903	0.27225	0.27549	0.27874	0.28201	0.28859	0.29523
5	0.21216	0.21525	0.21835	0.22148	0.22463	0.22779	0.23097	0.23740	0.24389
6	0.17853	0.18155	0.18460	0.18767	0.19076	0.19388	0.19702	0.20336	0.20980
7	0.15451	0.15750	0.16051	0.16354	0.16661	0.16970	0.17282	0.17914	0.18555
8	0.13651	0.13947	0.14246	0.14548	0.14853	0.15161	0.15472	0.16104	0.16747
9	0.12252	0.12546	0.12843	0.13145	0.13449	0.13757	0.14069	0.14702	0.15349
10	0.11133	0.11426	0.11723	0.12024	0.12329	0.12638	0.12950	0.13587	0.14238
11	0.10218	0.10511	0.10808	0.11109	0.11415	0.11725	0.12039	0.12679	0.13336
12	0.09456	0.09749	0.10046	0.10348	0.10655	0.10967	0.11283	0.11928	0.12590
13	0.08812	0.09105	0.09403	0.09706	0.10014	0.10328	0.10646	0.11296	0.11965
14	0.08260	0.08554	0.08853	0.09157	0.09467	0.09782	0.10102	0.10758	0.11434
15	0.07783	0.08077	0.08377	0.08683	0.08994	0.09311	0.09634	0.10296	0.10979
16	0.07365	0.07660	0.07961	0.08268	0.08582	0.08902	0.09227	0.09895	0.10586
17	0.06997	0.07293	0.07595	0.07904	0.08220	0.08542	0.08870	0.09544	0.10243
18	0.06670	0.06967	0.07271	0.07582	0.07899	0.08224	0.08555	0.09236	0.09941
19	0.06378	0.06676	0.06981	0.07294	0.07614	0.07941	0.08275	0.08962	0.09675
20	0.06116	0.06415	0.06722	0.07036	0.07358	0.07688	0.08024	0.08718	0.09439
25	0.05122	0.05428	0.05743	0.06067	0.06401	0.06744	0.07095	0.07823	0.08581
30	0.04465	0.04778	0.05102	0.05437	0.05783	0.06139	0.06505	0.07265	0.08059
40	0.03656	0.03984	0.04326	0.04683	0.05052	0.05434	0.05828	0.06646	0.07467
50	0.03182	0.03526	0.03887	0.04263	0.04655	0.05060	0.05478	0.06344	0.07238
60	0.02877	0.03235	0.03613	0.04009	0.04420	0.04845	0.05283	0.06188	0.07121

* The formula for this table is $w' = (i/100) / \{1 - [1 + (i/100)]^{-n}\} = 1/w = v' + (i/100)$.

Common Fractions

From Minutes and Seconds into Decimal Parts of a Degree				From Decimal Parts of a Degree into Minutes and Seconds (exact values)				Exact				Exact Decimal Values	
								8ths	16ths	32nds	64ths		
0'	0°.0000	0'	0°.0000	0°.00	0'	0°.50	30'					1	0.01 5625
1'	0°.0167	1"	0°.0003	0°.01	0' 36"	0°.51	30' 36"			1	2	0.03 125	
2'	0°.0333	2"	0°.0006	0°.02	1' 12"	0°.52	31' 12"				3	0.04 6875	
3'	0°.05	3"	0°.0008	0°.03	1' 48"	0°.53	31' 48"			2	4	0.06 25	
4'	0°.0667	4"	0°.0011	0°.04	2' 24"	0°.54	32' 24"		1		5	0.07 8125	
5'	0°.0833	5"	0°.0014	0°.05	3'	0°.55	33'				6	0.09 375	
6'	0°.10	6"	0°.0017	0°.06	3' 36"	0°.56	33' 36"				7	0.10 9375	
7'	0°.1167	7"	0°.0019	0°.07	4' 12"	0°.57	34' 12"	1	2	4	8	0.12 5	
8'	0°.1333	8"	0°.0022	0°.08	4' 48"	0°.58	34' 48"				9	0.14 0625	
9'	0°.15	9"	0°.0025	0°.09	5' 24"	0°.59	35' 24"			5	10	0.15 625	
10'	0°.1667	10"	0°.0028	0°.10	6'	0°.60	36'				11	0.17 1875	
11'	0°.1833	11"	0°.0031	0°.11	6' 36"	0°.61	36' 36"			3	12	0.18 75	
12'	0°.20	12"	0°.0033	0°.12	7' 12"	0°.62	37' 12"				13	0.20 3125	
13'	0°.2167	13"	0°.0036	0°.13	7' 48"	0°.63	37' 48"				14	0.21 875	
14'	0°.2333	14"	0°.0039	0°.14	8' 24"	0°.64	38' 24"				15	0.23 4375	
15'	0°.25	15"	0°.0042	0°.15	9'	0°.65	39'	2	4	8	16	0.25	
16'	0°.2667	16"	0°.0044	0°.16	9' 36"	0°.66	39' 36"				17	0.26 5625	
17'	0°.2833	17"	0°.0047	0°.17	10' 12"	0°.67	40' 12"				18	0.28 125	
18'	0°.30	18"	0°.005	0°.18	10' 48"	0°.68	40' 48"			9	19	0.29 6875	
19'	0°.3167	19"	0°.0053	0°.19	11' 24"	0°.69	41' 24"		5	10	20	0.31 25	
20'	0°.3333	20"	0°.0056	0°.20	12'	0°.70	42'				21	0.32 8125	
21'	0°.35	21"	0°.0058	0°.21	12' 36"	0°.71	42' 36"				22	0.34 375	
22'	0°.3667	22"	0°.0061	0°.22	13' 12"	0°.72	43' 12"			11	23	0.35 9375	
23'	0°.3833	23"	0°.0064	0°.23	13' 48"	0°.73	43' 48"	3	6	12	24	0.37 5	
24'	0°.40	24"	0°.0067	0°.24	14' 24"	0°.74	44' 24"				25	0.39 0625	
25'	0°.4167	25"	0°.0069	0°.25	15'	0°.75	45'				26	0.40 625	
26'	0°.4333	26"	0°.0072	0°.26	15' 36"	0°.76	45' 36"			13	27	0.42 1875	
27'	0°.45	27"	0°.0075	0°.27	16' 12"	0°.77	46' 12"				28	0.43 75	
28'	0°.4667	28"	0°.0078	0°.28	16' 48"	0°.78	46' 48"		7	14	29	0.45 3125	
29'	0°.4833	29"	0°.0081	0°.29	17' 24"	0°.79	47' 24"				30	0.46 875	
30'	0°.50	30"	0°.0083	0°.30	18'	0°.80	48'			15	31	0.48 4375	
31'	0°.5167	31"	0°.0086	0°.31	18' 36"	0°.81	48' 36"	4	8	16	32	0.50	
32'	0°.5333	32"	0°.0089	0°.32	19' 12"	0°.82	49' 12"				33	0.51 5625	
33'	0°.55	33"	0°.0092	0°.33	19' 48"	0°.83	49' 48"			17	34	0.53 125	
34'	0°.5667	34"	0°.0094	0°.34	20' 24"	0°.84	50' 24"				35	0.54 6875	
35'	0°.5833	35"	0°.0097	0°.35	21'	0°.85	51'				36	0.56 25	
36'	0°.60	36"	0°.01	0°.36	21' 36"	0°.86	51' 36"			9	37	0.57 8125	
37'	0°.6167	37"	0°.0103	0°.37	22' 12"	0°.87	52' 12"				38	0.59 375	
38'	0°.6333	38"	0°.0106	0°.38	22' 48"	0°.88	52' 48"				39	0.60 9375	
39'	0°.65	39"	0°.0108	0°.39	23' 24"	0°.89	53' 24"	5	10	20	40	0.62 5	
40'	0°.6667	40"	0°.0111	0°.40	24'	0°.90	54'				41	0.64 0625	
41'	0°.6833	41"	0°.0114	0°.41	24' 36"	0°.91	54' 36"				42	0.65 625	
42'	0°.70	42"	0°.0117	0°.42	25' 12"	0°.92	55' 12"			21	43	0.67 1875	
43'	0°.7167	43"	0°.0119	0°.43	25' 48"	0°.93	55' 48"				44	0.68 /5	
44'	0°.7333	44"	0°.0122	0°.44	26' 24"	0°.94	56' 24"				45	0.70 3125	
45'	0°.75	45"	0°.0125	0°.45	27'	0°.95	57'			23	46	0.71 875	
46'	0°.7667	46"	0°.0128	0°.46	27' 36"	0°.96	57' 36"				47	0.73 4375	
47'	0°.7833	47"	0°.0131	0°.47	28' 12"	0°.97	58' 12"	6	12	24	48	0.75	
48'	0°.80	48"	0°.0133	0°.48	28' 48"	0°.98	58' 48"				49	0.76 5625	
49'	0°.8167	49"	0°.0136	0°.49	29' 24"	0°.99	59' 24"				50	0.78 125	
50'	0°.8333	50"	0°.0139	0°.50	30'	1°.00	60'			25	51	0.79 6875	
51'	0°.85	51"	0°.0142								52	0.81 25	
52'	0°.8667	52"	0°.0144		0°.000	0" .0				13	26	0.82 8125	
53'	0°.8833	53"	0°.0147		0°.001	3" .6					27	0.84 375	
54'	0°.90	54"	0°.015		0°.002	7" .2					28	0.85 9375	
55'	0°.9167	55"	0°.0153		0°.003	10" .8		7	14		56	0.87 5	
56'	0°.9333	56"	0°.0156		0°.004	14" .4					57	0.89 0625	
57'	0°.95	57"	0°.0158		0°.005	18" .					58	0.90 625	
58'	0°.9667	58"	0°.0161		0°.006	21" .6				29	59	0.92 1875	
59'	0°.9833	59"	0°.0164		0°.007	25" .2					60	0.93 75	
60'	1°.00	60"	0°.0167		0°.008	28" .8				15	30	0.95 3125	
					0°.009	32" .4					31	0.96 875	
					0°.010	36" .					62	0.98 4375	
											63		

Units and Systems of Weights and Measures

L.E. Barrow, U.S. Natl. Bureau of Standards

The U.S. Natl. Bureau of Standards was established by act of congress in 1901 to serve as a national scientific laboratory in the physical sciences and to provide fundamental measurement standards for science and industry. In carrying out these related functions the bureau conducts research and development in many fields of physics, mathematics, chemistry, and engineering. At the time of its founding, the bureau had custody of two primary standards—the meter bar for length and the kilogram cylinder for mass (or weight). With the phenomenal growth of science and technology over the past half century, the bureau has become a major research institution concerned not only with everyday weights and measures but also with hundreds of other scientific and engineering standards that have become necessary to the industrial progress of the U.S. Nevertheless, the U.S. still looks to the bureau for information on the units of weights and measures, particularly their definitions and equivalents.

The subject of weights and measures can be treated from several different standpoints. Scientists and engineers are interested in the methods by which precision measurements are made, general knowledge of weights and measures, the present status of units and standards, and miscellaneous facts that will be useful in their everyday professional life.

The expression “weights and measures” is used here in its basic sense of referring to measurements of length, mass, and capacity, thus excluding such topics as electrical and time measurements and thermometry. This section on units and systems of weights and measures presents some fundamental information to clarify thinking on this subject and to eliminate erroneous and misleading use of terms.

Unit and Standard Definitions

It is essential that there be established and kept in mind the distinction between the terms “units” and “standards” of weights and measures.

A *unit* is a value, quantity, or magnitude in terms of which other values, quantities, or magnitudes are expressed. In general, a unit is fixed by definition and is independent of such physical conditions as temperature. Examples include the yard, the pound, the gallon, the meter, the liter, the gram.

A *standard* is a physical embodiment of a unit. In general it is not independent of physical conditions, and it is a true embodiment of the unit only under specified conditions. For example, a yard standard has a length of one yard when at some definite temperature and supported in a certain manner. If supported in a different manner, it might have to be at a different temperature in order to have a length of 1 yard.

The Metric System

Definition, Origin, and Development

The metric system* is the international system of weights and measures based on the meter and the kilogram. The essential features of the system were embodied in a report made to the French Natl. Assembly by the Paris Academy of Sciences in 1791. The definitive action taken in 1791 was the outgrowth of recommendations along similar lines dating back to 1670. The adoption of the system in France was slow, but its desirability as an international system was recognized by geodesists and others. On May 20, 1875, an international treaty known as the Intl. Metric Convention was signed providing for an Intl. Bureau of Weights and Measures, thus ensuring “the international unification and improvement of the metric system.” The metric system is now either obligatory or permissible throughout the world.

Although the metric system is a decimal system, the words “metric” and “decimal” are not synonymous, and care should be taken not to confuse the two terms.

*See also Chap. 58

Units and Standards of the Metric System

In the metric system, the fundamental units of length and mass are the meter and the kilogram. The other units of length and mass, as well as all units of area, volume, and compound units such as density, are derived from these two fundamental units.

From 1960 to 1983, the meter was defined as the length equal to 1 650 763.73 wavelengths in vacuum of the radiation corresponding to the transition between the levels $2p_{10}$ and $5d_5$ of the krypton 86 atom. Since 1983, the meter has been defined as the length of the path travelled by light in a vacuum during a time interval of $1/299\,792\,458$ of a second. The kilogram previously defined as the mass of 1 cubic decimeter of water at the temperature of maximum density was known as the Kilogram of the Archives. It was replaced after the Intl. Metric Convention in 1875 by the Intl. Prototype Kilogram, which became the unit of mass without reference to the mass of a cubic decimeter of water or to the Kilogram of the Archives.

The liter is a unit of capacity. In 1964 the 12th General Conference on Weights and Measures redefined the liter as being 1 cubic decimeter. By its previous definition—the volume occupied, under standard conditions, by a quantity of pure water having a mass of 1 kilogram—the liter was larger than the cubic decimeter by 28 parts in 1 000 000; except for determinations of high precision, this difference is so small as to be of no consequence.

The modernized metric system includes "base" units such as units of temperature and time, as well as many "derived" units such as units of force and work. For details, see Chap. 58.

The Intl. Bureau of Weights and Measures

The Intl. Bureau of Weights and Measures was established at Sèvres, a suburb of Paris, in accordance with the Intl. Metric Convention of May 20, 1875. At the bureau are kept the Intl. Prototype kilogram, many secondary standards of all sorts, and equipment for comparing standards and making precision measurements. The Bureau, maintained by assessed contributions of the signatory governments, is truly international.

In recent years the scope of the work at the Intl. Bureau has been considerably broadened. It now carries on research in the fields of electricity and photometry in addition to its former work in weights and measures, which included such allied fields as thermometry and the measurement of barometric pressures.

Present Status of the Metric System in the U.S.

The use of the metric system in this country was legalized by act of congress in 1866, but was not made obligatory.

The speed of light in a vacuum and U.S. Prototype Kilogram No. 20 are recognized as the primary standards of length and mass for both the metric and the inch-pound (customary) systems of measurement in this country because these standards are the most precise and reliable standards available. Since 1893 in the U.S. the yard has been defined in terms of the meter and the pound in terms of the kilogram. There is in the U.S. no primary standard either of length or mass in the inch-pound system.

From 1893 until 1959, the yard was defined as being equal exactly to 3600/3937 m. In 1959 a small change was made in the definition of the yard to resolve discrepancies both in the U.S. and abroad. Since 1959, the yard is defined as being equal exactly to 0.9144 m; the new yard is shorter than the old yard by exactly two parts in a million. At the same time, it was decided that any data expressed in feet derived from geodetic surveys within the U.S. would continue to bear the relationship as defined in 1893 (1 ft equals 1200/3937 m). This foot is called the U.S. survey foot, while the foot defined in 1959 is called the international foot. Measurements expressed in statute miles, survey feet, rods, chains, links, or the squares thereof, and also acres should therefore be converted to the corresponding metric values by using pre-1959 conversion factors where more than five-significant-figure accuracy is involved.

In 1971 the Natl. Bureau of Standards completed a 3-year study of the impact of increasing worldwide metric use on the U.S. The study ended with a report to the Congress entitled *A Metric America—A Decision Whose Time Has Come*. In the last few years metric use has been increasing rapidly in the U.S., principally in the manufacturing and educational sectors. Public Law 93-380, enacted Aug. 21, 1974, states that it is the policy of the U.S. to encourage educational agencies and institutions to prepare students to use the metric system of measurement with ease and facility as a part of the regular education program. On Dec. 23, 1975, President Gerald Ford signed Public Law 94-168, the Metric Conversion Act of 1975. This act declares a national policy of coordinating the increasing use of the metric system in the U.S. It established a U.S. Metric Board, whose functions as of Oct. 1, 1982 were transferred to the Dept. of Commerce, Office of Metric Programs, to coordinate the voluntary conversion to the metric system.

British and U.S. Systems

The implication is sometimes made that the inch/pound system of weights and measures in the British Commonwealth countries and the U.S. system are identical. It is true that the U.S. and the British inch are defined identically for scientific work, that they are practically identical in commercial usage, that a similar situation exists for the U.S. and the British pound, and that many tables, such as 12 in. = 1 ft, 3 ft = 1 yd, and 1,760 yd = 1 international mile, are the same in both countries; but there are some very important differences.

First, the U.S. bushel, the U.S. gallon, and their subdivisions differ from the corresponding British units. Also, the British ton is 2,240 lbm, whereas the ton generally used in the U.S. is the short ton of 2,000 lbm. The American colonists adopted the English wine gallon of 231 cu in. The English of that period used this wine gallon, but they also had another gallon, the ale gallon of 282 cu in. In 1824 these two gallons were abandoned by the British when they adopted the British imperial gallon, which is defined as the volume of 10 lbm of water, at a temperature of 62°F, which, by calculation, is equivalent to 277.42 cu in. At the same time, the bushel was redefined as 8 gal. In the British system, the units of dry measure are the same as those of liquid measure. In the U.S. these two are not the same, the gallon and its subdivisions being

used in the measurement of liquids, while the bushel, with its subdivisions, is used in the measurement of certain dry commodities. The U.S. gallon is divided into 4 liquid quarts and the U.S. bushel into 32 dry quarts. All the units of capacity mentioned thus far are larger in the British system than in the U.S. system. But the British fluid ounce is smaller than the U.S. fluid ounce, because the British quart is divided into 40 fluid ounces, whereas the U.S. quart is divided into 32 fluid ounces.

From the foregoing it is seen that in the British system an avoirdupois ounce of water at 62°F has a volume of 1 fluid oz, because 10 lbm is equivalent to 160 avoirdupois oz, and 1 gal is equivalent to 4 quarts, or 160 fluid oz. This convenient relation does not exist in the U.S. system because a U.S. gallon of water at 62°F weighs about $8\frac{1}{8}$ lbm, or $133\frac{1}{8}$ avoirdupois oz, and the U.S. gallon is equivalent to 4×32 , or 128 fluid oz. In comparison, 1 U.S. fluid oz = 1.041 British fluid oz; 1 British fluid oz = 0.961 U.S. fluid oz; 1 U.S. gal = 0.833 British imperial gal; and 1 British imperial gal = 1.201 U.S. gal.

Subdivision of Units

In general, units are subdivided by one of three systems: (1) decimal, i.e., into tenths; (2) duodecimal, into twelfths; or (3) binary, into halves. Usually the subdivision is continued by use of the same system. Each method has advantages for certain purposes, and it cannot properly be said that any one method is "best" unless the use to which the unit and its subdivisions are to be put is known.

For example, if we are concerned only with measurements of length to moderate precision, it is convenient to measure and to express these lengths in feet, inches, and binary fractions of an inch, thus 9 ft $4\frac{3}{8}$ in. If, however, these measured lengths are to be used subsequently in calculations of area or volume, that method of subdivision at once becomes extremely inconvenient. For that reason, engineers, instead of dividing the foot into inches and binary subdivisions of the inch, divide it decimally; that is, into tenths, hundredths, and thousandths of a foot.

The method of subdivision of a unit is thus made largely on the basis of convenience to the user. The fact that units have commonly been subdivided into certain subunits for centuries does not preclude their also having another mode of subdivision in some frequently used cases where convenience indicates the value of such other method. Thus the gallon is usually subdivided into quarts and pints, but the majority of gasoline-measuring pumps of the price-computing type are graduated to show tenths of a gallon. Although the mile has for centuries been divided into rods, yards, feet, and inches, the odometer part of an automobile speedometer indicates tenths of a mile. Although our dollar is divided into 100 parts, we habitually use and speak of halves and quarters.

Standards

Length

A specified spectral line emitted by krypton 86 is the international standard on which all length measurements are based. To obtain a constant and uniform wavelength, krypton lamps are operated at the temperature of the triple point of nitrogen.

One yard is defined as 0.9144 m. The inch is therefore exactly equal to 25.4 mm.

Mass

The primary standard of mass for this country is U.S. Prototype Kilogram 20, which is a platinum-iridium cylinder kept at the Natl. Bureau of Standards. The value of this mass standard is known in terms of the Intl. Prototype Kilogram, a platinum-iridium standard, which is kept at the Intl. Bureau of Weights and Measures.

The avoirdupois pound is defined in terms of the kilogram by the relation 1 avoirdupois lbm = 0.453 592 37 kg.

Mass vs. Weight. The mass of a body is a measure of its inertial property. The *weight* of a body has in the past been used at times to designate its mass and at other times to designate a force that is related to gravitational attraction. Because these two concepts of weight are incompatible, and have therefore resulted in confusion, the term "weight" should be avoided in technical practice except under circumstances in which its meaning is completely clear. When the term is used, it is important to know whether *mass* or *force* is intended and to use SI units properly by using kilograms for mass and newtons for force. See also Chapter 58.

As weighing and measuring are important factors in our everyday lives, it is quite natural that questions arise about the use of various units and terms and about the magnitude of quantities involved.

The ton is used as a unit of measure in two distinct senses: (1) as a unit of weight, and (2) as a unit of capacity or volume.

In the weight sense the term means: (1) the *short*, or *net* ton of 2,000 lbm; (2) the *long*, *gross*, or *shipper's* ton of 2,240 lbm; (3) the *metric* ton of 1,000 kg, or 2,204.6 lbm. In the capacity sense "ton" is restricted to uses related to ships.

In the U.S. and Canada the ton (weight) most commonly used is the *short* ton, in Great Britain it is the *long* ton, and in countries using the metric system it is the *metric* ton.

Effect of Air Buoyancy. Another point to consider in the calibration and use of standards of mass is the buoyancy or lifting effect of the air. A body immersed in any fluid is buoyed up by a force equal to the force of gravity on the displaced fluid. Two bodies of equal mass, if placed one on each pan of an equal-arm balance, will balance each other in a vacuum. A comparison in a vacuum against a known mass standard gives "true mass." If compared in air, however, they will not balance each other unless they are of equal volume. If of unequal volume, the larger body will displace the greater volume of air and will be buoyed up by a greater force than will the smaller body, and the larger body will appear to be of less mass than the smaller body. The greater the difference in volume, and the greater the density of the air in which the comparison weighing is made, the greater will be the apparent difference in mass. For that reason, in assigning a precise numerical value of mass to a standard, it is necessary to base this value on definite values for the air density and the density of the mass standard of reference.

TABLE 1.41—LENGTH EQUIVALENTS

Meters	Centimeters	Inches	Feet	Yards	Chains	Kilometers	Miles
1	100	39.37	3.281	1.0936	0.04971	0.001	0.0₅6214
	2.00000	1.59517	0.51598	0.03886	2.69644	3.00000	6.79335
0.01	1	0.3937	0.03281	0.01094	0.0₃4971	10⁻⁵	0.0₅6214
2.00000		1.59517	2.51598	2.03886	4.69644	5.00000	4.79335
0.0254	2.540	1	0.08333	0.02778	0.001263	0.0₄254	0.0₄1578
2.40483	0.40483		2.92082	2.44370	3.10127	5.40483	5.19818
0.3048	30.48	12	1	0.3333	0.01515	0.0₃3048	0.0₃1894
1.48402	1.48402	1.07918		1.52288	2.18046	4.48402	4.27736
0.9144	91.44	36	3	1	0.04545	0.0₃9144	0.0₃5682
1.96114	1.96114	1.55630	0.47712		2.65758	4.96114	4.75449
20.12	2012	792	66	22	1	0.02012	0.0125
1.30356	3.30356	2.89873	1.81954	1.34242		2.30356	2.09691
1000	100 000	39,370	3,281	1,093.6	49.71	1	0.6214
3.00000	5.00000	4.59517	3.51598	3.03886	1.69644		1.79335
1609	160 935	63,360	5,280	1,760	80	1.609	1
3.20665	5.20665	4.80182	3.72263	3.24551	1.90309	0.20665	

The equivalents are given in the bold-faced type. Logarithms of the equivalents are given immediately below with the characteristic of the logarithm (i.e., 1.59517 = 0.59517). In some cases, the equivalents have been rounded off, while the logarithm corresponds to the equivalent carried to a greater number of decimal places. Subscripts after any figure—0₃, 9₄—mean that that figure is to be repeated the indicated number of times.

TABLE 1.42—CONVERSION OF LENGTHS*

	Inches to Millimeters	Millimeters to Inches	Feet to Meters	Meters to Feet	Yards to Meters	Meters to Yards	Miles to Kilometers	Kilometers to Miles
1	25.40	0.03937	0.3048	3.281	0.9144	1.094	1.609	0.6214
2	50.80	0.07874	0.6096	6.562	1.829	2.187	3.219	1.243
3	76.20	0.1181	0.9144	9.842	2.743	3.281	4.828	1.864
4	101.60	0.1575	1.219	13.12	3.658	4.374	6.437	2.485
5	127.00	0.1968	1.524	16.40	4.572	5.468	8.047	3.107
6	152.40	0.2362	1.829	19.68	5.486	6.562	9.656	3.728
7	177.80	0.2756	2.134	22.97	6.401	7.655	11.27	4.350
8	203.20	0.3150	2.438	26.25	7.315	8.749	12.87	4.971
9	228.60	0.3543	2.743	29.53	8.230	9.842	14.48	5.592

*For example, 1 in. = 25.40 mm.

The corrections furnished by the U.S. Natl. Bureau of Standards (NBS) for the more precise mass standards are given on two bases: comparison in vacuum and comparison against normal brass standards in air under standard conditions, with no correction applied for the buoyant effect of the air. By definition, brass standards have a density of 8400 kg per m³ at 0°C and a coefficient of cubical thermal expansion of 0.000 054 per °C. Standard conditions are defined as air of 1.2 kg per m³ and temperature of 20°C. The corrections to be used with precise analytical weights are ordinarily given only in terms of apparent mass against normal brass standards.

A full discussion of this topic is given in NBS Monograph 133, Mass and Mass Values, by Paul E. Pontius (Natl. Technical Information Service, 5285 Port Royal Road, Springfield, VA 22161; COM 7450309).

Capacity

Units of capacity, being derived units, are defined in the U.S. in terms of linear units and are not represented by fundamental standards. Laboratory standards have been constructed and are maintained at NBS. These have validity only by calibration with reference either directly or indirectly to the linear standards.

TABLE 1.43—COMMON FRACTIONS OF AN INCH TO MILLIMETERS (FROM $\frac{1}{64}$ to 1 in.)

64ths	Millimeters	64ths	Millimeters	64ths	Millimeters	64ths	Millimeters	64ths	Millimeters	64ths	Millimeters
1	0.397	13	5.159	25	9.922	37	14.684	49	19.447	57	22.622
2	0.794	14	5.556	26	10.319	38	15.081	50	19.844	58	23.019
3	1.191	15	5.953	27	10.716	39	15.478	51	20.241	59	23.416
4	1.588	16	6.350	28	11.113	40	15.875	52	20.638	60	23.813
5	1.984	17	6.747	29	11.509	41	16.272	53	21.034	61	24.209
6	2.381	18	7.144	30	11.906	42	16.669	54	21.431	62	24.606
7	2.778	19	7.541	31	12.303	43	17.066	55	21.828	63	25.003
8	3.175	20	7.938	32	12.700	44	17.463	56	22.225	64	25.400
9	3.572	21	8.334	33	13.097	45	17.859				
10	3.969	22	8.731	34	13.494	46	18.256				
11	4.366	23	9.128	35	13.891	47	18.653				
12	4.763	24	9.525	36	14.288	48	19.050				

TABLE 1.44—DECIMALS OF AN INCH TO MILLIMETERS (FROM 0.01 in. TO 0.99 in.)

	0	1	2	3	4	5	6	7	8	9
0.0		0.254	0.508	0.762	1.016	1.270	1.524	1.778	2.032	2.286
0.1	2.540	2.794	3.048	3.302	3.556	3.810	4.064	4.318	4.572	4.826
0.2	5.080	5.334	5.588	5.842	6.096	6.350	6.604	6.858	7.112	7.366
0.3	7.620	7.874	8.128	8.382	8.636	8.890	9.144	9.398	9.652	9.906
0.4	10.160	10.414	10.668	10.922	11.176	11.430	11.684	11.938	12.192	12.446
0.5	12.700	12.954	13.208	13.462	13.716	13.970	14.224	14.478	14.732	14.986
0.6	15.240	15.494	15.748	16.002	16.256	16.510	16.764	17.018	17.272	17.526
0.7	17.780	18.034	18.288	18.542	18.796	19.050	19.304	19.558	19.812	20.066
0.8	20.320	20.574	20.828	21.082	21.336	21.590	21.844	22.098	22.352	22.606
0.9	22.860	23.114	23.368	23.622	23.876	24.130	24.384	24.638	24.892	25.146

TABLE 1.45—MILLIMETERS TO DECIMALS OF AN INCH (FROM 1 TO 99 mm)

	0.	1.	2.	3.	4.	5.	6.	7.	8.	9.
0		0.0394	0.0787	0.1181	0.1575	0.1968	0.2362	0.2756	0.3150	0.3543
1	0.3937	0.4331	0.4724	0.5118	0.5512	0.5906	0.6299	0.6693	0.7087	0.7480
2	0.7874	0.8268	0.8661	0.9055	0.9449	0.9842	1.0236	1.0630	1.1024	1.1417
3	1.1811	1.2205	1.2598	1.2992	1.3386	1.3780	1.4173	1.4567	1.4961	1.5354
4	1.5748	1.6142	1.6535	1.6929	1.7323	1.7716	1.8110	1.8504	1.8898	1.9291
5	1.9685	2.0079	2.0472	2.0866	2.1260	2.1654	2.2047	2.2441	2.2835	2.3228
6	2.3622	2.4016	2.4409	2.4803	2.5197	2.5590	2.5984	2.6378	2.6772	2.7165
7	2.7559	2.7953	2.8346	2.8740	2.9134	2.9528	2.9921	3.0315	3.0709	3.1102
8	3.1496	3.1890	3.2283	3.2677	3.3071	3.3464	3.3858	3.4252	3.4646	3.5039
9	3.5433	3.5827	3.6220	3.6614	3.7008	3.7402	3.7795	3.8189	3.8583	3.8976

TABLE 1.46—AREA EQUIVALENTS*

Square Meters	Square Inches	Square Feet	Square Yards	Square Rods	Square Chains	Roods	Acres	Square Miles or Sections
1 4.80967	1,550 3.19033	10.76 1.03197	1.196 0.07773	0.0395 2.59699	0.002471 3.39288	0.0₃9884 4.99494	0.0₃2471 4.39288	0.0₆3861 7.58670
0.0₃6452 4.80967	1	0.006944 3.84164	0.0₃7716 4.88740	0.0₄2551 5.40667	0.0₅1594 6.20255	0.0₆6377 7.80461	0.0₆1594 7.20255	0.0₉2491 10.39637
0.09290 2.96803	144 2.15836	1	0.1111 1.04576	0.003673 3.56503	0.0₃2296 4.36091	0.0₄9184 5.96297	0.0₄2296 5.36091	0.0₇3587 8.55473
0.8361 1.92227	1,296 3.11260	9 0.95424	1	0.03306 2.51927	0.002066 3.31515	0.0₃8264 4.91721	0.0002066 4.31515	0.0₆3228 7.50898
25.29 1.40300	39,204 4.59333	272.25 2.43497	30.25 1.48072	1	0.0625 2.79588	0.02500 2.39794	0.00625 3.79588	0.0₅9766 6.98970
404.7 2.60712	627,264 5.79745	4,356 3.63909	484 2.68484	16 1.20412	1	0.4 1.60206	0.1 1.00000	0.0001562 4.19382
1012 3.00506	1,568,160 6.19539	10,890 4.03703	1,210 3.08278	40 1.60206	2.5 0.39794	1	0.25 1.39794	0.0₃3906 4.59176
4047 3.60712	6,272,640 6.79745	43,560 4.63909	4,840 3.68484	160 2.20412	10 1.00000	4 0.60206	1	0.001562 3.19382
2 589 998 6.41330		27,878,400 7.44527	3,097,600 6.49102	102,400 5.01030	6,400 3.80618	2,560 3.40824	640 2.80618	1

The equivalents are given in the bold-faced type. Logarithms of the equivalents are given immediately below with the characteristic of the logarithm (i.e., 2.59699 = 0.059699). In some cases, the equivalents have been rounded off, while the logarithm corresponds to the equivalent carried to a greater number of decimal places. Subscripts after any figure—0₃, 9₄, etc.—mean that the figure is to be repeated the indicated number of times.

*1 hectare = 100 acres = 10 000 m².

TABLE 1.47—VOLUME AND CAPACITY EQUIVALENTS

Liters	Cubic Inches	Cubic Feet	Cubic Yards	U.S. Apothecary Fluid Ounces	U.S. Quarts		U.S. Gallons	U.S. Bushels
					Liquid	Dry		
1	61.03 1.78551	0.03532 2.54796	0.001308 3.11659	33.81 1.52909	1.057 0.02394	0.9081 1.95812	0.2642 1.42188	0.02838 2.45297
0.01639 2.21450	1	0.0₃5787 4.76246	0.0₄2143 5.33109	0.5541 1.74360	0.01732 2.23845	0.01488 2.17263	0.0₂4329 3.63639	0.0₃4650 4.66748
28.32 1.45205	1728 3.23754	1	0.03704 2.56864	957.5 2.98114	29.92 1.47599	25.71 1.41017	7.481 0.87393	0.8036 1.90502
764.5 2.88340	46656 4.66891	27 1.43136	1	25853 4.41251	807.9 2.90736	694.3 2.84153	202.2 2.30530	21.70 1.33638
0.02957 2.47091	1.805 0.25640	0.001044 3.01886	0.0₄3868 5.58749	1	0.03125 2.49485	0.02686 2.42903	0.007812 3.89279	0.0₃8392 4.92388
0.9463 1.97604	57.75 1.76155	0.03342 2.52401	0.001238 3.09264	32 1.50515	1	0.8594 1.93418	0.25 1.39794	0.02686 2.42903
1.101 0.04188	67.20 1.82737	0.03889 2.58983	0.001440 3.15847	37.24 1.57097	1.164 0.06582	1	0.2909 1.46376	0.03125 2.49485
3.785 0.57812	231 2.36361	0.1337 1.12607	0.004951 3.69470	128 2.10721	4 0.60206	3.437 0.53624	1	0.1074 1.03109
35.24 1.54703	2150 3.33252	1.244 0.09498	0.04609 2.66362	1192 3.07612	37.24 1.57097	32 1.50515	9.309 0.96891	1

The equivalents are given in the bold-faced type. Logarithms of the equivalents are given immediately below with the characteristic of the logarithm (i.e., 2.54796 = 0.054796). In some cases, the equivalents have been rounded off, while the logarithm corresponds to the equivalent carried to a greater number of decimal places. Subscripts after any figure—0₃, 9₄, etc.—mean that the figure is to be repeated the indicated number of times.

TABLE 1.48—CONVERSION OF AREAS*

	sq in. to cm ²	cm ² to sq in.	sq ft to m ²	m ² to sq ft	sq yd to m ²	m ² to sq yd	acres to hectares	hectares to acres	sq miles to km ²	km ² to sq miles
1	6.452	0.1550	0.0929	10.76	0.8361	1.196	0.4047	2.471	2.590	0.3861
2	12.90	0.3100	0.1858	21.53	1.672	2.392	0.8094	4.942	5.180	0.7722
3	19.35	0.4650	0.2787	32.29	2.508	3.588	1.214	7.413	7.770	1.158
4	25.81	0.6200	0.3716	43.06	3.345	4.784	1.619	9.884	10.360	1.544
5	32.26	0.7750	0.4645	53.82	4.181	5.980	2.023	12.355	12.950	1.931
6	38.71	0.9300	0.5574	64.58	5.017	7.176	2.428	14.826	15.540	2.317
7	45.16	1.085	0.6503	75.35	5.853	8.372	2.833	17.297	18.130	2.703
8	51.61	1.240	0.7432	86.11	6.689	9.568	3.237	19.768	20.720	3.089
9	58.06	1.395	0.8361	96.87	7.525	10.764	3.642	22.239	23.310	3.475

*For example, 1 sq in. = 6.452 cm².

TABLE 1.49—CONVERSION OF VOLUMES OR CUBIC MEASURES

	cu in. to cm ³	cm ³ to cu in.	cu ft to m ³	m ³ to cu ft	cu yd to m ³	m ³ to cu yd	gal to cu ft	cu ft to gal
1	16.39	0.06102	0.02832	35.31	0.7646	1.308	0.1337	7.481
2	32.77	0.1220	0.05663	70.63	1.529	2.616	0.2674	14.96
3	49.16	0.1831	0.08495	105.9	2.294	3.924	0.4010	22.44
4	65.55	0.2441	0.1133	141.3	3.058	5.232	0.5347	29.92
5	81.94	0.3051	0.1416	176.6	3.823	6.540	0.6684	37.40
6	98.32	0.3661	0.1699	211.9	4.587	7.848	0.8021	44.88
7	114.7	0.4272	0.1982	247.2	5.352	9.156	0.9358	52.36
8	131.1	0.4882	0.2265	282.5	6.116	10.46	1.069	59.84
9	147.5	0.5492	0.2549	317.8	6.881	11.77	1.203	67.32

TABLE 1.50—CONVERSION OF VOLUMES OR CAPACITIES

	Fluid oz to cm ³	cm ³ to fluid oz	liquid pints to liters	liters to liquid pints	liquid quarts to liters	liters to liquid quarts	gal to liters	liters to gal	bushels to hectoliters	hectoliters to bushels
1	29.57	0.03381	0.4732	2.113	0.9463	1.057	3.785	0.2642	0.3524	2.838
2	59.15	0.06763	0.9463	4.227	1.893	2.113	7.571	0.5284	0.7048	5.676
3	88.72	0.1014	1.420	6.340	2.839	3.170	11.36	0.7925	1.057	8.513
4	118.3	0.1353	1.893	8.454	3.785	4.227	15.14	1.057	1.410	11.35
5	147.9	0.1691	2.366	10.57	4.732	5.284	18.93	1.321	1.762	14.19
6	177.4	0.2092	2.839	12.68	5.678	6.340	22.71	1.585	2.114	17.03
7	207.0	0.2367	3.312	14.79	6.624	7.397	26.50	1.849	2.467	19.86
8	236.6	0.2705	3.785	16.91	7.571	8.454	30.28	2.113	2.819	22.70
9	266.2	0.3043	4.259	19.02	8.517	9.510	34.07	2.378	3.171	25.54

TABLE 1.51—MASS EQUIVALENTS

kg	grains	oz		lbm		tons		
		troy and apothecary	avoirdupois	troy and apothecary	avoirdupois	short	long	metric
1	15,432 4.18843	32.15 1.50719	35.27 1.54745	2.6792 0.42801	2.205 0.34333	0.0₂1102 3.04230	0.0₃9842 4.99309	0.001 3.00000
0.0₄6480 5.81157	1	0.0₂2083 3.31876	0.0₂2286 3.35902	0.0₃1736 4.23958	0.0₃1429 4.15490	0.0₇7143 8.85387	0.0₇6378 8.80465	0.0₇6480 8.81157
0.03110 2.49281	480 2.68124	1	1.09714 0.04026	0.08333 2.92082	0.06857 2.83614	0.0₄3429 5.53511	0.0₄3061 5.48590	0.0₄3110 5.49281
0.02835 2.45255	437.5 2.64098	0.9115 1.95974	1	0.07595 2.88056	0.0625 2.79588	0.0₄3125 5.49485	0.0₄2790 5.44563	0.0₄2835 5.45255
0.3732 1.57199	5,760 3.76042	12 1.07918	13.17 1.11944	1	0.8229 1.91532	0.0₃4114 4.61429	0.0₃3673 4.56508	0.0₃3732 4.57199
0.4536 1.65667	7,000 3.84510	14.58 1.16386	16 1.20412	1.215 0.08468	1	0.0005 4.69897	0.0₃4464 4.64975	0.0₃4536 4.65667
907.2 2.95770	140₆ 7.14613	29,167 4.46489	320₃ 4.50515	2431 3.38571	2,000 3.30103	1	0.8929 1.95078	0.9072 1.95770
1016 3.00691	15680₄ 7.19535	32,667 4.51411	35,840 4.55437	2722 3.43492	2,240 3.35025	1.12 0.04922	1	1.016 0.00691
1000 3.00000	15,432,356 7.18843	32,151 4.50719	35,274 4.54745	2679 3.42801	2,205 3.34333	1.102 0.04230	0.9842 1.99309	1

The equivalents are given in the bold-faced type. Logarithms of the equivalents are given immediately below with the characteristic of the logarithm (i.e., 3.04230 = 0.0004230). In some cases, the equivalents have been rounded off, while the logarithm corresponds to the equivalent carried to a greater number of decimal places. Subscripts after any figure—0₃, 9₄, etc.—mean that the figure is to be repeated the indicated number of times.

TABLE 1.52—CONVERSION OF MASSES

	lbm (avoirdupois) to kg	kg to lbm (avoirdupois)	grains to grams	grams to grains	oz (avoirdupois) to grams	grams to oz (avoirdupois)	short tons (2,000 lbm)	metric tons (1,000 kg)	long tons (2,240 lbm)	metric tons
							to metric tons	to short tons	to metric tons	to long tons
1	0.4536	2.205	0.06480	15.43	28.35	0.03527	0.907	1.102	1.016	0.984
2	0.9072	4.409	0.1296	30.86	56.70	0.07055	1.814	2.205	2.032	1.968
3	1.361	6.614	0.1944	46.30	85.05	0.1058	2.722	3.307	3.048	2.953
4	1.814	8.818	0.2592	61.73	113.40	0.1411	3.629	4.409	4.064	3.937
5	2.268	11.02	0.3240	77.16	141.75	0.1764	4.536	5.512	5.080	4.921
6	2.722	13.23	0.3888	92.59	170.10	0.2116	5.443	6.614	6.096	5.905
7	3.175	15.43	0.4536	108.03	198.45	0.2469	6.350	7.716	7.112	6.889
8	3.629	17.64	0.5184	123.46	226.80	0.2822	7.257	8.818	8.128	7.874
9	4.082	19.84	0.5832	138.89	255.15	0.3175	8.165	9.921	9.144	8.858

TABLE 1.53—VELOCITY EQUIVALENTS

m/sec	m/min	km/hr	cm/sec	ft/sec	ft/min	mph	knots
1	60	3.6	100	3.281	196.85	2.237	1.943
	1.77815	0.55630	2.00000	0.51598	2.29414	0.34965	0.28836
0.01667	1	0.06	1.667	0.05468	3.281	0.03728	0.03238
2.22184		2.77815	0.22184	2.73783	0.51598	2.57150	2.51022
0.2778	16.67	1	27.78	0.9113	54.68	0.6214	0.53959
1.44370	1.22184		1.44370	1.95908	1.73783	1.79335	1.73205
0.01	0.6	0.036	1	0.03281	1.9685	0.02237	0.01943
	1.77815	2.55630		2.51598	0.29414	2.34965	2.28836
0.3048	18.29	1.097	30.48	1	60	0.6818	0.59209
1.48402	1.26217	0.04032	1.48402		1.77815	1.83367	1.77238
0.005080	0.3048	0.01829	0.5080	0.01667	1	0.01136	0.00987
3.70586	1.48402	2.26217	1.70586	2.22185		2.05553	3.99423
0.4470	26.82	1.609	44.70	1.467	88	1	0.86839
1.65035	1.42850	0.20670	1.65035	0.16633	1.94448		1.93871
0.51479	30.887	1.8532	51.479	1.68894	101.337	1.15155	1
1.71163	1.48978	0.26793	1.71163	0.22761	2.00577	0.06128	

TABLE 1.54—CONVERSION OF LINEAR AND ANGULAR VELOCITIES

	rev/min to rads/sec	rads/sec to rev/min	cm/s to ft/min	ft/min to cm/s	cm/s to mph	mph to cm/s	ft/s to mph	mph to ft/s
1	0.1047	9.55	1.97	0.508	0.0224	44.70	0.682	1.47
2	0.2094	19.10	3.94	1.016	0.0447	89.41	1.364	2.93
3	0.3142	28.65	5.91	1.524	0.0671	134.1	2.045	4.40
4	0.4189	38.20	7.87	2.032	0.0895	178.8	2.727	5.87
5	0.5236	47.75	9.84	2.540	0.1118	223.5	3.409	7.33
6	0.6283	57.30	11.81	3.048	0.1342	268.2	4.091	8.80
7	0.7330	66.84	13.78	3.556	0.1566	312.9	4.773	10.27
8	0.8378	76.39	15.75	4.064	0.1790	357.6	5.455	11.73
9	0.9425	85.94	17.72	4.572	0.2013	402.3	6.136	13.20

TABLE 1.55—CONVERSION OF PRESSURES*

	lbm per sq in. to kilopascals	kilopascals to lbm per sq in.	atmospheres to lbm per sq in.	lbm per sq in. to atmospheres	atmospheres to kilopascals	kilopascals to atmospheres
1	6.8948	0.1450	14.70	0.0680	101.3	0.00987
2	13.789	0.2901	29.39	0.1361	202.6	0.01974
3	20.684	0.4351	44.09	0.2041	304.0	0.02961
4	27.579	0.5802	58.78	0.2722	405.3	0.03947
5	34.474	0.7252	73.48	0.3402	506.6	0.04935
6	41.369	0.8702	88.18	0.4083	608.0	0.05922
7	48.263	1.0153	102.9	0.4763	709.3	0.06908
8	55.158	1.1603	117.6	0.5444	810.6	0.07895
9	62.053	1.3053	132.3	0.6124	911.9	0.08882

*For example, 1 lbm/sq in. = 6.8948 kilopascals.

TABLE 1.56—PRESSURE EQUIVALENTS

kilopascals	kg/cm ² (metric atmospheres)	lbm/sq in.	short tons per sq ft	atmospheres	columns of mercury at temperature 0°C and $g = 9.80665 \text{ m/s}^2$		columns of water at temperature 15°C and $g = 9.80665 \text{ m/s}^2$		
					(m)	(in.)	(m)	(in.)	(ft)
1	0.010197 2.00848	0.14504 1.16148	0.010443 2.01862	0.009869 3.87510	0.007501 3.99427	0.2953 1.47025	0.1021 1.00886	4.018 0.60402	0.3349 1.52485
98.066 1.99152	1	14.22 1.15300	1.024 0.01034	0.9678 1.98579	0.7356 1.86662	28.96 1.46177	10.01 1.00038	394.1 2.59556	32.84 1.51636
6.8948 0.83852	0.07031 2.84700	1	0.072 2.85733	0.06805 2.83280	0.05171 2.71360	2.036 0.30876	0.7037 1.84738	27.70 1.44254	2.309 0.36336
95.760 1.98119	0.9765 1.98966	13.89 1.14267	1	0.9451 1.97547	0.7183 1.85628	28.28 1.45143	9.774 0.99006	384.8 2.58521	32.07 1.50604
101.325 2.00573	1.0332 0.01420	14.70 1.16722	1.058 0.02453	1	0.76 1.88081	29.92 1.47598	10.34 1.01459	407.1 2.60975	33.93 1.53058
133.322 2.12490	1.3595 0.13338	19.34 1.28640	1.392 0.14373	1.316 0.11919	1	39.37 1.59517	13.61 1.13378	535.7 2.72894	44.64 1.64976
3.386 0.52975	0.03453 2.53823	0.4912 1.69124	0.03536 2.51857	0.03342 2.52402	0.02540 2.40484	1	0.3456 1.53861	13.61 1.13378	1.134 0.05460
9.798 0.99114	0.09991 2.99962	1.421 0.15262	0.1023 1.00996	0.09670 2.98541	0.07349 2.86622	2.893 0.46139	1	39.37 1.59517	3.281 0.51598
0.2489 1.39598	0.002538 3.40446	0.03609 2.55745	0.002599 3.41479	0.002456 3.39024	0.001867 3.27106	0.07349 2.86622	0.02540 2.40484	1	0.08333 2.92082
2.926 0.47516	0.03045 2.48364	0.4331 1.63663	0.03119 2.49397	0.02947 2.46942	0.02240 2.35024	0.8819 1.94540	0.3048 1.48402	12 1.07918	1

TABLE 1.57—ENERGY OR WORK EQUIVALENTS

J	kg-m	ft-lbf	kW hours	metric hp hours	hp hours	L-atm	kilocalories	Btu's
1	0.10197 1.00848	0.7376 1.86780	0.0₆2778 7.44370	0.0₆3777 7.57711	0.0₆3725 7.57113	0.009869 3.99427	0.0₃2388 4.37809	0.0₃9478 4.97670
9.80665 0.9915207	1	7.233 0.85932	0.0₅2724 6.43521	0.0₅37037 6.56863	0.0₅3653 6.56265	0.09678 2.98579	0.002342 3.36961	0.009295 3.96825
1.356 0.13220	0.1383 1.14068	1	0.0₆3766 7.57590	0.0₆51206 7.70932	0.0₆50505 7.70333	0.01338 2.12647	0.0₃3238 4.51029	0.001285 3.10890
3.600 × 10⁶ 6.55630	3.671 × 10⁵ 5.56478	2.655 × 10⁶ 6.42410	1	1.3596 0.13342	1.341 0.12743	35 528 4.55057	859.9 2.93443	3,412 3.53303
2.648 × 10⁶ 6.42288	270 000 5.43136	1.9529 × 10⁶ 6.29068	0.7355 1.86658	1	0.9863 1.99401	26 131 4.41715	632.4 2.80098	2,510 3.39961
2.6845 × 10⁶ 6.42887	2.7375 × 10⁵ 5.43735	1.98 × 10⁶ 6.29667	0.7457 1.87356	1.0139 0.00598	1	26 493 4.42314	641.2 2.80699	2,544 3.40557
101.33 2.00573	10.333 1.01421	74.74 1.87353	0.0₄2815 5.44952	0.0₄3827 5.58284	0.0₄3775 5.57686	1	0.02420 2.38382	0.09604 2.98246
4187 3.62191	426.9 2.63036	3,088 3.48971	0.001163 3.06558	0.001581 3.19902	0.001560 3.19304	41.32 1.61618	1	3.968 0.59861
1055 3.02360	107.6 2.03178	778.2 2.89110	0.0₃2931 4.46697	0.0₃3985 4.60042	0.0₃3930 4.59444	10.41 1.01757	0.25200 1.40139	1

The equivalents are given in bold-faced type. Logarithms of the equivalents are given immediately below with the characteristic of the logarithm (i.e., 1.00848 = 0.00848). In some cases, the equivalents have been rounded off, although the logarithm corresponds to the equivalent carried to a greater number of decimal places. Subscripts after any figure—0₃, 9₄, etc.—mean that the figure is to be repeated the indicated number of times.

TABLE 1.58—CONVERSION OF ENERGY, WORK, HEAT

	calories to J	J to calories	ft-lbf to kg-m	kg-m to ft-lbf	ft-lbf to Btu	Btu to ft-lbf	kg-m to kilocalories	kilocalories to kg-m
1	4.187	0.2388	0.1383	7.233	0.001285	778.2	0.002342	426.9
2	8.374	0.4777	0.2765	14.47	0.002570	1,556.	0.004685	853.9
3	12.56	0.7165	0.4148	21.70	0.003855	2,334.	0.007027	1,281.
4	16.75	0.9554	0.5530	28.93	0.005140	3,113.	0.009369	1,708.
5	20.93	1.194	0.6913	36.16	0.006425	3,891.	0.01172	2,135.
6	25.12	1.433	0.8295	43.40	0.007710	4,669.	0.01405	2,562.
7	29.31	1.672	0.9678	50.63	0.008995	5,447.	0.01640	2,989.
8	33.49	1.911	1.106	57.86	0.01028	6,225.	0.01874	3,415.
9	37.68	2.150	1.244	65.10	0.01156	7,003.	0.02108	3,842.

TABLE 1.59—POWER EQUIVALENTS*

kW	hp	metric hp	poucelets	kg-m/s	ft-lbf/sec	kilocalories/s	Btu/sec
1	1.341	1.360	1.020	102.0	737.6	0.2388	0.9478
	0.12743	0.13343	0.00848	2.00848	2.86780	1.37813	1.97673
0.7457	1	1.014	0.7604	76.04	550	0.1781	0.7068
1.87256		0.00599	1.88105	1.88105	2.74036	1.25066	1.84936
0.7355	0.9863	1	0.75	75	542.5	0.1757	0.6971
1.86658	1.99402		1.87506	1.87506	2.73438	1.24467	1.84328
0.9807	1.315	1.333	1	100	723.3	0.2342	0.9295
1.99152	0.11896	0.12493		2.00000	2.85932	1.36961	1.96825
0.009807	0.01315	0.01333	0.01	1	7.233	0.002342	0.009295
3.99152	2.11896	2.12493	2.00000		0.85932	3.36961	3.96825
0.001356	0.00182	0.00184	0.00138	0.1383	1	0.03238	0.001285
3.13220	3.25946	3.26562	3.14067	1.14067		4.51029	3.10890
4.187	5.615	5.692	4.269	426.9	3,088	1	3.968
0.62187	0.74934	0.75530	0.63036	2.63036	3.48971		0.59861
1.055	1.415	1.434	1.076	107.6	778.2	0.2520	1
0.02320	0.15074	0.15668	0.03178	2.03178	2.89110	1.40138	

*For example, 1 hp = 0.7457 kW.

TABLE 1.60—CONVERSION OF POWER

	hp to kW	kW to hp	metric hp to kW	kW to metric hp	hp to metric hp	metric hp to hp
1	0.7457	1.341	0.7355	1.360	1.014	0.9863
2	1.491	2.682	1.471	2.719	2.028	1.973
3	2.237	4.023	2.206	4.079	3.042	2.959
4	2.983	5.364	2.942	5.438	4.055	3.945
5	3.729	6.705	3.677	6.798	5.069	4.932
6	4.474	8.046	4.412	8.158	6.083	5.918
7	5.220	9.387	5.147	9.520	7.097	6.904
8	5.966	10.73	5.883	10.88	8.111	7.891
9	6.711	12.07	6.618	12.24	9.125	8.877

TABLE 1.61—DENSITY EQUIVALENTS AND CONVERSION FACTORS*

Equivalents					Conversion Factors				
kg/m ³	g/cm ³	lbm/cu in.	lbm/cu ft	lbm/U.S. gal		lbm/cu ft to kg/m ³	kg/m ³ to lbm/cu ft	g/cm ³ to kg/m ³	kg/m ³ to g/cm ³
1	0.001	0.03613	0.0624	0.00835	1	16.019	0.0624	1000	0.001
		5.55787	2.79539	3.92143	2	32.037	0.1249	2000	0.002
1000	1	0.03613	62.43	8.345	3	48.055	0.1873	3000	0.003
		2.55787	1.79539	0.92143	4	64.074	0.2497	4000	0.004
27680	27.68	1	1,728	231	5	80.092	0.3121	5000	0.005
4.44217	1.44217		3.23754	2.36361	6	96.111	0.3746	6000	0.006
16.019	0.01602	0.035787	1	0.1337	7	112.129	0.4370	7000	0.007
1.20466	2.20466	4.76245		1.12613	8	128.148	0.4994	8000	0.008
119.83	0.1198	0.004329	7.481	1	9	144.166	0.5619	9000	0.009
2.07855	1.07855	3.63639	0.87396		10	160.185	0.6243	10 000	0.010

*For example, 1 kg/m³ = 0.0624 lbm/cu ft.

TABLE 1.62—THERMAL CONDUCTIVITY

W/m·°C	Cal/[s(cm ² /cm)°C]	W/[(cm ² /cm)°C]	Cal/[h(cm ² /cm)°C]	Btu/[hr(sq ft/ft)°F]
1	0.002388	0.0100	8.598	0.5778
418.7	1	4.187	3600.	241.9
100.0	0.2388	1	860	57.78
0.1163	0.0002778	0.001163	1	0.0672
1.731	0.004134	0.01731	14.88	1

TABLE 1.63—THERMAL CONDUCTANCE

W/m ² ·°C	Cal/[s·cm ² ·°C]	W/cm ² ·°C	Cal/[h·cm ² ·°C]	Btu/hr-sq ft-°F
1	0.042388	0.0001	0.08598	0.1761
41868	1	4.187	3600	7373
10000	0.2388	1	860	1761
11.63	0.032778	0.001163	1	2.048
5.678	0.031355	0.035678	0.4862	1

TABLE 1.64—HEAT FLOW

W/m ²	Cal/s·cm ²	W/cm ²	Cal/h·cm ²	Btu/hr-sq ft
1	0.042388	0.0001	0.08598	0.3170
41868	1	4.187	3600	13272
10000	0.2388	1	860	3170
11.63	0.032778	0.001163	1	3.687
3.155	0.047535	0.03154	0.2712	1

TABLE 1.65—RELATIVE DENSITIES CORRESPONDING TO °API AND WEIGHTS PER U.S. GALLON

°API	Relative Density	lbm/U.S. gal	°API	Relative Density	lbm/U.S. gal	°API	Relative Density	lbm/U.S. gal	°API	Relative Density	lbm/U.S. gal
10	1.0000	8.328	33	0.8602	7.163	56	0.7547	6.283	79	0.6722	5.595
11	0.9930	8.270	34	0.8550	7.119	57	0.7507	6.249	80	0.6690	5.568
12	0.9861	8.212	35	0.8498	7.076	58	0.7467	6.216	81	0.6659	5.542
13	0.9792	8.155	36	0.8448	7.034	59	0.7428	6.184	82	0.6628	5.516
14	0.9725	8.099	37	0.8398	6.993	60	0.7389	6.151	83	0.6597	5.491
15	0.9659	8.044	38	0.8348	6.951	61	0.7351	6.119	84	0.6566	5.465
16	0.9593	7.989	39	0.8299	6.910	62	0.7313	6.087	85	0.6536	5.440
17	0.9529	7.935	40	0.8251	6.870	63	0.7275	6.056	86	0.6506	5.415
18	0.9465	7.882	41	0.8203	6.830	64	0.7238	6.025	87	0.6476	5.390
19	0.9402	7.830	42	0.8155	6.790	65	0.7201	5.994	88	0.6446	5.365
20	0.9340	7.778	43	0.8109	6.752	66	0.7165	5.964	89	0.6417	5.341
21	0.9279	7.727	44	0.8063	6.713	67	0.7128	5.934	90	0.6388	5.316
22	0.9218	7.676	45	0.8017	6.675	68	0.7093	5.904	91	0.6360	5.293
23	0.9159	7.627	46	0.7972	6.637	69	0.7057	5.874	92	0.6331	5.269
24	0.9100	7.578	47	0.7927	6.600	70	0.7022	5.845	93	0.6303	5.246
25	0.9042	7.529	48	0.7883	6.563	71	0.6988	5.817	94	0.6275	5.222
26	0.8984	7.481	49	0.7839	6.526	72	0.6953	5.788	95	0.6247	5.199
27	0.8927	7.434	50	0.7796	6.490	73	0.6919	5.759	96	0.6220	5.176
28	0.8871	7.387	51	0.7753	6.455	74	0.6886	5.731	97	0.6193	5.154
29	0.8816	7.341	52	0.7711	6.420	75	0.6852	5.703	98	0.6166	5.131
30	0.8762	7.296	53	0.7669	6.385	76	0.6819	5.676	99	0.6139	5.109
31	0.8708	7.251	54	0.7628	6.350	77	0.6787	5.649	100	0.6112	5.086
32	0.8654	7.206	55	0.7587	6.316	78	0.6754	5.622			

* Calculated from the formula relative density = $(141.5)/(131.5 + \gamma_{API})$. The weights in this table are weights in air at 60°F with humidity 50% and pressure 760 mm Hg.

Relative Density and Density

The relative density of a solid or liquid is the ratio of the mass of the body to the mass of an equal volume of water at some standard temperature. At the present time, a temperature of 4°C [39°F] is commonly used by physicists, but the engineer uses 60°F. The relative density of gases is usually expressed in terms of hydrogen or air.

The density of a body is its mass per unit volume. If the gram is used as the unit of mass and the millimeter as the unit of volume, or if the kilogram is used as the unit of mass and the liter as the unit of volume, the figures representing the density are the same as the relative density of the body. The inch-pound unit is pounds per cubic foot.

The relative density of liquids is usually measured by a hydrometer, and different special arbitrary hydrometer

scales are used in various trades and industries. The most common of these are the API and Baumé. The API scale is approved by the American Petroleum Inst., the ASTM, the U.S. Bureau of Mines, and the Natl. Bureau of Standards and is recommended for exclusive use in the U.S. petroleum industry, superseding the Baumé scale for liquids lighter than water. The relation between API degrees and relative density is expressed by the following equation.

$$\gamma_{API} = (141.5)/(\rho_{60/60^{\circ}F}) - 131.5.$$

The relative densities corresponding to °API and weights per U.S. gallon are given in Table 1.65.

Chapter 2

Casing, Tubing, and Line Pipe

William O. Clinedinst, Consultant

Casing

The successful production of oil and gas depends on the proper performance of casing, which serves as a structural retainer in the well, excludes undesirable fluids, and confines and conducts oil or gas from subsurface strata to ground level. Casing must be capable of withstanding external collapsing pressure from fluid surrounding the casing, internal pressure encountered in conducting oil or gas from the producing formation, and tension loads resulting from its own suspended weight. It also must be equipped with threaded joints that can be made up easily and that provide leakproof connections.

API Casing

API developed specifications for casing that meet the major needs of the oil and gas industry and published these in API specifications and bulletins.¹⁻⁶ These provide standard dimensions, strength and performance properties, and the required thread-gauging practice to ensure complete interchangeability.

In addition to the API strength grades, the following tables include information on higher-strength casing developed to meet the needs of unusually deep wells. Tables 2.1 and 2.2 give the tensile requirements and range lengths of API casing and liner casing. Table 2.3 lists the minimum performance properties of casing. Table 2.4 lists the minimum collapse resistance under axial loads for various API casing grades. Tables 2.5 through 2.7 give the dimensions, weights, and tolerances of round-thread and buttress-thread coupling and length of upset for extreme-line API casing (see also Figs. 2.1 through 2.3). Factors for conversion of gross linear footage to net footage of API short-thread, long-thread, buttress-thread, and extreme-line casings are shown in Tables 2.8 through 2.11, respectively. Equations for calculating performance properties of casing are given in a later section.

Special Casing Joints

A number of special casing joints are available that are useful where higher strength, leak resistance, or clearance is needed than that provided by the standard API round-thread, buttress-thread, or extreme-line casing joints. These special joints obtain their improved properties by various means, such as (1) couplings or box ends with seal rings of teflon, etc.; (2) special thread profiles, such as Acme; (3) torque shoulders; (4) metal-to-metal seals; (5) internal upsets; (6) external upsets; (7) integral joints; and (8) flush joints.

API Liner Casing

Table 2.12 shows the minimum performance properties of API Grade J-55 plain-end liner casing. Table 2.13 shows the minimum collapse resistance under axial loads of API Grade J-55 liner casing.

Design of Casing Strings

Oil, Water, and Mud-Weight Factors. Table 2.14 gives the oil, water, and mud weight factors used in casing string design.

Safety factors commonly used in the design of casing strings are the following: collapse strength, 1.125; joint strength, 1.80; plain-end yield strength, 1.25; and internal yield pressure, 1.00. These safety factors will be used in the following casing string designs. However, it is the responsibility of the designer to select safety factors to suit particular needs.

Single Weight and Grade Casing String. Collapse Safety Factor. The collapse pressure for a single weight and grade casing string is determined by multiplying the height of the head of mud by the factor for the mud weight found

TABLE 2.1—API CASING AND LINER CASING
TENSILE REQUIREMENTS

Casing Grade	Yield Strength (psi)		Minimum Tensile Strength (psi)	Maximum Hardness		Minimum Elongation in 2 in. ** (%)
	Minimum	Maximum		HRC*	BHN*	
H-40	40,000	80,000	60,000			
J-55	55,000	80,000	75,000			
K-55	55,000	80,000	95,000			
C-75 [†]	75,000	90,000	95,000			
L-80	80,000	95,000	95,000	23	241	
N-80	80,000	110,000	100,000			
C-90 [†]	90,000	105,000	100,000	25.4	255	
C-95 [†]	95,000	110,000	105,000			
HC-95 ^{‡§}	95,000	—	110,000			
P-110	110,000	140,000	125,000			
Q-125 [‡]	125,000	150,000	135,000			
V-150 [‡]	150,000	180,000	160,000			
Liner Casing						
J-55	55,000	80,000	75,000			

*HRC is Rockwell hardness C scale; BHN is Brinell hardness.

**In customary units,

$$\Delta L = 625,000 \frac{A_s^{0.2}}{\sigma_T^{0.9}}$$

and in metric units,

$$\Delta L = 1942.57 \frac{A_s^{0.2}}{\sigma_T^{0.9}}$$

where

 ΔL = minimum elongation in 2 in. in percent to nearest 1/2%, A_s = cross-sectional area of the tensile test specimen in square inches based on specified OD or nominal specimen width and specified wall thickness rounded to the nearest 0.01 or 0.75 sq in., whichever is smaller, and σ_T = specified minimum ultimate tensile strength, psi.[†]Restricted yield strength intended for use in sour gas service.[‡]Non-API.[§]Special requirements on toughness, uniform hardness, and mill testing.

in Table 2.14. Thus the collapse pressure for an 11,000-ft head of mud with a weight of 9.625 lbm/gal is 5,500 psi (11,000 ft × 0.5 psi/ft = 5,500 psi). To meet the 1.125 collapse safety factor, a collapse resistance of at least 6,188 psi (1.125 × 5,500) is required.

In Table 2.3, the lightest weight of 7-in. casing with a collapse resistance of at least 6,188 psi is 29-lbm N-80 with a collapse resistance of 7,020 psi. (The designer should select the most economical weight and grade that meets the performance property requirements.) By dividing the 7,020-psi collapse resistance by the 5,500-psi collapse pressure, the collapse safety factor is found to be 1.276 (see Table 2.15).

Joint Strength Safety Factor. For the same string, the total load on the joint at the top of the well (ignoring buoyancy effects) is the product of the length of the string (11,000 ft) and the 29-lbm/ft weight of the casing or 319,000 lbm. Dividing the 597,000-lbm minimum joint strength of 7-in., 29-lbm, N-80 long-thread casing given in Table 2.3 on minimum performance properties by the 319,000-lbm weight of casing yields a 1.87 safety factor for joint strength.

Pipe Body Yield Safety Factor. In Table 2.3, the pipe body yield strength is found to be 676,000 lbm. The 676,000-lbm pipe body yield strength divided by the 319,000-lbm weight of the casing string yields the 2.12 safety factor.

Internal Yield Pressure Safety Factor. The bottomhole pressure (BHP) given is 5,500 psi. The internal yield pressure (pressure resistance) for 7-in., 29-lbm, N-80 long-thread casing is 8,160 psi (Table 2.3). The 8,160-psi internal yield pressure divided by the 5,500-psi BHP yields a 1.48 safety factor.

Combination Casing Strings

Collapse Safety Factors. In designing a combination casing string, first determine the casing required to resist the collapse pressure at the bottom of the well (Table 2.16). Then, determine how far this weight and grade must be run before a weight and grade with a lower collapse resistance can be used. The procedure is repeated until the weight with the lowest possible collapse resistance has been used, or until a higher-weight casing is chosen because the advantages of a lower-cost material are offset by increased identification and handling problems. The collapse resistance of casing is affected by any axial load applied to it. Only the bottom section is not affected by axial loading. Sections above the bottom section will have their collapse resistance reduced by the weight of the casing below. Because the axial load acting on the casing and the collapse pressure are both dependent on the depth at which the new casing item is introduced, the changeover point must be determined by

successive approximation or trial-and-error calculations.

When design calculations are made with a computer, the collapse resistance under axial loading can be calculated by use of the method described in the section on equations. Take the depth to which the weight and grade being considered will set with the desired safety factor without axial load as a starting point. Then decrease the depth by suitable increments (perhaps 50 ft), calculating the axial load, the collapse resistance, the collapse pressure, and the safety factor for each increment until the desired safety factor value is obtained.

When design calculations are made without a computer, collapse resistance values can be obtained from Table 2.4 (minimum collapse resistance under axial loading). This table lists collapse resistance under axial stress increments of 5,000 psi. For stresses intermediate to the 5,000-psi increments, collapse resistance can be determined by interpolation. The following collapse calculations for the design of the 7-in., 11,000-ft string were made from Table 2.4.

29-lbm N-80 Bottom-Section Collapse Safety Factor. The method for selection of 29-lbm N-80 for the bottom section and the determination of the 1.276 collapse safety factor is identical to that shown for the 11,000-ft single weight and grade string.

26-lbm N-80 Intermediate-Section Collapse Safety Factor. Determination of the length of the bottom section and the changeover point to 26 lbm, the next lower weight, is facilitated by constructing Table 2.17.

In this table, starting with the tabulated values of axial stress and the corresponding collapse resistance for 26-lbm N-80 casing, the lengths of the 29-lbm casing required to cause the stress and the corresponding collapse safety factors are calculated.

Col. 1 gives the axial stress values in 5,000-psi increments. Col. 3 gives collapse resistance under axial load for the cross-sectional area obtained from Table 2.4 for Grades L-80 and N-80. Col. 2 is the product of Col. 1 and the cross-sectional area. Col. 4 is determined by calculating the weight of casing below the section for which the length is being determined. (This is the general format of the table for use with all sections. In this case, the weight of casing below the section is zero because there is no casing below the 29-lbm N-80.) Col. 5 is the difference between Cols. 2 and 4. Col. 6 is Col. 5 divided by 29. Col. 7 is the depth to the bottom of the 26-lbm section—the changeover point—in this case 11,000 ft minus Col. 6. Col. 8 is Col. 7 multiplied by the mud factor (0.5), and Col. 9 is Col. 3 divided by Col. 8.

The 1,600-ft length of the 29-lbm section found in Col. 6 and the 1.126 safety factor for the 26-lbm section at the changeover point were determined by interpolation according to the following method. The length of the 29-lbm section found in Col. 6 was estimated by calculating

$$1,302 + [(1.125 - 1.095)/(1.238 - 1.095)]$$

$$\times (2,605 - 1,302) = 1,575 \text{ ft,}$$

which is rounded to the next 50-ft multiple to yield 1,600 ft. Cols. 1, 2, 5, 7, and 8 were back-calculated from Col. 6. For instance, the axial stress found in Col. 1 equals $(1,600 \times 29)/7.549$, which equals 6,147 psi.

TABLE 2.2—API CASING AND LINER CASING RANGE LENGTHS

Casing	16 to 25	25 to 34	34 to 48
Total range length, inclusive			
Range length for 95% or more of carload			
Permissible variation, maximum	6	5	6
Permissible length, minimum	18	28	36
Liners			
Same requirements as for casing in Ranges 2 and 3.			

The collapse resistance for the 26-lbm section that corresponds to the 6,147-psi axial stress is estimated by calculating

$$5,310 - [(6,147 - 5,000)/(10,000 - 5,000)]$$

$$\times (5,310 - 5,200) = 5,285 \text{ psi,}$$

which is rounded to the nearest 10 psi according to API procedures to yield 5,290 psi. The collapse safety factor at the 26-lbm section bottom that is shown in Col. 9 is obtained by dividing Col. 3 by Col. 8.

23-lbm N-80 Top Section Collapse Safety Factor. The length of the 26-lbm intermediate section and the changeover point to the next lower weight are calculated with Table 2.18. In Table 2.18, Cols. 5 through 9 cannot be calculated until Col. 2 exceeds Col. 4. The 2,900-ft length of the 26-lbm section that is shown in Col. 6 and the 1.120 safety factor of the 23-lbm section at the changeover point were determined by interpolation.

The length of the 26-lbm section listed in Col. 6 was estimated by calculating

$$2,055 + [(1.125 - 1.005)/(1.194 - 1.005)]$$

$$\times (3,335 - 2,055) = 2,868 \text{ ft,}$$

which is rounded to the next 50-ft multiple to yield 2,900 ft. Cols. 1, 2, 5, 7, and 8 were back-calculated from Col. 6. The collapse resistance of the 23-lbm section that corresponds to the 18,299-psi axial stress is estimated by calculating

$$3,690 - [(18,299 - 15,000)/(20,000 - 15,000)]$$

$$\times (3,690 - 3,620) = 3,644 \text{ psi,}$$

which is rounded to the nearest 10 psi according to API procedures to yield 3,640 psi. The 1.120 collapse safety factor at the 23-lbm section bottom that is listed in Col. 9 is obtained by dividing Col. 3 by Col. 8. By increasing the length of the 29-lbm intermediate section to 2,950 ft and by repeating the calculations for collapse resistance, we obtain a safety factor of 1.129.

(continued on page 32)

TABLE 2.3—MINIMUM PERFORMANCE PROPERTIES OF CASING

1	2	3	4	5	6	7	8	9	10	11	12
OD (in.)	Nominal Weight, Threads and Coupling (lbm/ft)	Grade	Wall Thickness (in.)	ID (in.)	Threaded and Coupled			Extreme Line			Pipe-Body Yield Strength (1,000 lbf)
					Drift Diameter (in.)	OD of Coupling (in.)	OD Special Clearance Coupling (in.)	Drift Diameter (in.)	OD of Box Powertight (in.)	Collapse Resistance (psi)	
4½	9.50	H-40	0.205	4.090	3.965	5.000	—	—	—	2,760	111
	9.50	J-55	0.205	4.090	3.965	5.000	—	—	—	3,310	152
	10.50	J-55	0.224	4.052	3.927	5.000	4.875	—	—	4,010	165
	11.60	J-55	0.250	4.000	3.875	5.000	4.875	—	—	4,960	184
	9.50	K-55	0.205	4.090	3.965	5.000	—	—	—	3,310	152
	10.50	K-55	0.224	4.052	3.927	5.000	4.875	—	—	4,010	165
	11.60	K-55	0.250	4.000	3.875	5.000	4.875	—	—	4,960	184
	11.60	C-75	0.250	4.000	3.875	5.000	4.875	—	—	6,100	250
	13.50	C-75	0.290	3.920	3.795	5.000	4.875	—	—	8,140	288
	11.60	L-80	0.250	4.000	3.875	5.000	4.875	—	—	6,350	267
	13.50	L-80	0.290	3.920	3.795	5.000	4.875	—	—	8,540	307
	11.60	N-80	0.250	4.000	3.875	5.000	4.875	—	—	6,350	267
	13.50	N-80	0.290	3.920	3.795	5.000	4.875	—	—	8,540	307
	11.60	C-90	0.250	4.000	3.875	5.000	4.875	—	—	6,820	300
	13.50	C-90	0.290	3.920	3.795	5.000	4.875	—	—	9,300	345
	11.60	C-95	0.250	4.000	3.875	5.000	4.875	—	—	7,030	317
	13.50	C-95	0.290	3.920	3.795	5.000	4.875	—	—	9,660	364
*	11.60	HC-95	0.250	4.000	3.875	5.000	4.875	—	—	8,650	317
*	13.50	HC-95	0.290	3.920	3.795	5.000	4.875	—	—	10,380	364
*	15.10	HC-95	0.337	3.826	3.701	5.000	4.875	—	—	12,330	419
	11.60	P-110	0.250	4.000	3.875	5.000	4.875	—	—	7,580	367
	13.50	P-110	0.290	3.920	3.795	5.000	4.875	—	—	10,680	422
	15.10	P-110	0.337	3.826	3.701	5.000	4.875	—	—	14,350	485
	15.10	Q-125	0.337	3.826	3.701	5.000	4.875	—	—	15,840	551
*	16.60	Q-125	0.375	3.750	3.625	5.000	4.875	—	—	19,100	608
*	19.10	Q-125	0.437	3.626	3.501	5.000	4.875	—	—	21,920	697
*	15.10	V-150	0.337	3.826	3.701	5.000	4.875	—	—	18,110	661
*	16.60	V-150	0.375	3.750	3.625	5.000	4.875	—	—	22,330	729
*	19.10	V-150	0.437	3.626	3.501	5.000	4.875	—	—	26,300	837
5	11.50	J-55	0.220	4.560	4.435	5.563	—	—	—	3,060	182
	13.00	J-55	0.253	4.494	4.369	5.563	5.375	—	—	4,140	208
	15.00	J-55	0.296	4.408	4.283	5.563	5.375	4.151	5.360	5,560	241
	11.50	K-55	0.220	4.560	4.435	5.563	—	—	—	3,060	182
	13.00	K-55	0.253	4.494	4.369	5.563	5.375	—	—	4,140	208
	15.00	K-55	0.296	4.408	4.283	5.563	5.375	4.151	5.360	5,560	241
	15.00	C-75	0.296	4.408	4.283	5.563	5.375	4.151	5.360	6,940	328
	18.00	C-75	0.362	4.276	4.151	5.563	5.375	4.151	5.360	9,960	396
	21.40	C-75	0.437	4.126	4.001	5.563	5.375	—	—	11,970	470
	23.20	C-75	0.478	4.044	3.919	5.563	5.375	—	—	12,970	509
	24.10	C-75	0.500	4.000	3.875	5.563	5.375	—	—	13,500	530
	15.00	L-80	0.296	4.408	4.283	5.563	5.375	4.151	5.360	7,250	350
	18.00	L-80	0.362	4.276	4.151	5.563	5.375	4.151	5.360	10,500	422
	21.40	L-80	0.437	4.126	4.001	5.563	5.375	—	—	12,760	501
	23.20	L-80	0.478	4.044	3.919	5.563	5.375	—	—	13,830	543
	24.10	L-80	0.500	4.000	3.875	5.563	5.375	—	—	14,400	566
	15.00	N-80	0.296	4.408	4.283	5.563	5.375	4.151	5.360	7,250	350
	18.00	N-80	0.362	4.276	4.151	5.563	5.375	4.151	5.360	10,500	422
	21.40	N-80	0.437	4.126	4.001	5.563	5.375	—	—	12,760	501
	23.20	N-80	0.478	4.044	3.919	5.563	5.375	—	—	13,830	543
	24.10	N-80	0.500	4.000	3.875	5.563	5.375	—	—	14,400	566
	15.00	C-90	0.296	4.408	4.283	5.563	5.375	4.151	5.366	7,840	394
	18.00	C-90	0.362	4.276	4.151	5.563	5.375	4.151	5.366	11,530	475
	21.40	C-90	0.437	4.126	4.001	5.563	5.375	—	—	14,360	564
	23.20	C-90	0.478	4.044	3.919	5.563	5.375	—	—	15,560	611
	24.10	C-90	0.500	4.000	3.875	5.563	5.375	—	—	16,200	636

*Non-API weights and grades.

TABLE 2.3—MINIMUM PERFORMANCE PROPERTIES OF CASING (continued)

13	14	15	16	17	18	19	20	21	22	23	24	25	26	27
Joint Strength** (1,000 lbf)														
Internal Pressure Resistance† (psi)														
Threaded and Coupled														
Buttress Thread														
Plain End or Extreme Line	Round Thread		Regular Coupling		Special Clearance Coupling		Round Thread		Regular Coupling	Buttress Thread		Special Clearance Coupling	Extreme Line	
	Short	Long	Same Grade	Higher Grade	Same Grade	Higher Grade	Short	Long		Regular Coupling	Higher Grade†	Higher Grade†	Standard Joint	Optional Joint
3.190	3.190	—	—	—	—	—	77	—	—	—	—	—	—	—
4.380	4.380	—	—	—	—	—	101	—	—	—	—	—	—	—
4.790	4.790	—	4.790	4.790	4.790	4.790	132	—	203	203	203	203	—	—
5.350	5.350	5.350	5.350	5.350	5.350	5.350	154	162	225	225	225	225	—	—
4.380	4.380	—	—	—	—	—	112	—	—	—	—	—	—	—
4.790	4.790	—	4.790	4.790	4.790	4.790	146	—	249	249	249	249	—	—
5.350	5.350	5.350	5.350	5.350	5.350	5.350	170	180	277	277	277	277	—	—
7.290	—	7.290	7.290	—	7.290	—	—	212	288	—	288	—	—	—
8.460	—	8.460	8.460	—	7.490	—	—	257	331	—	320	—	—	—
7.780	—	7.780	7.780	7.780	7.780	7.780	—	212	291	—	291	—	—	—
9.020	—	9.020	9.020	9.020	7.990	9.020	—	257	334	—	320	—	—	—
7.780	—	7.780	7.780	7.780	7.780	7.780	—	223	304	304	304	304	—	—
9.020	—	9.020	9.020	9.020	7.990	9.020	—	270	349	349	337	349	—	—
8.750	—	8.750	8.750	—	8.750	—	—	223	309	—	309	—	—	—
10.150	—	10.150	10.150	—	9.000	—	—	270	355	—	337	—	—	—
9.240	—	9.240	9.240	—	9.240	—	—	234	325	325	325	—	—	—
10.710	—	10.710	10.710	—	9.490	—	—	284	374	374	353	—	—	—
9.240	—	9.240	9.240	9.240	9.240	9.240	—	245	338	338	338	338	—	—
10.710	—	10.710	10.710	10.710	9.500	10.710	—	297	388	388	370	388	—	—
12.450	—	12.450	11.630	12.450	9.500	11.000	—	357	446	446	370	421	—	—
10.690	—	10.690	10.690	10.690	10.690	10.690	—	279	385	385	385	385	—	—
12.410	—	12.410	12.410	12.410	10.990	12.410	—	338	443	443	421	443	—	—
14.420	—	14.420	13.460	14.420	10.990	13.910	—	406	509	509	421	509	—	—
16.380	—	16.380	15.300	—	12.490	—	—	438	554	—	—	—	—	—
18.230	—	16.650	15.300	18.230	12.490	14.980	—	496	579	611	454	539	—	—
21.240	—	16.650	15.300	18.370	12.490	14.980	—	588	579	686	454	539	—	—
19.660	—	19.660	18.360	—	14.980	—	—	519	658	—	539	—	—	—
21.880	—	19.980	18.360	—	14.980	—	—	588	686	—	539	—	—	—
25.490	—	19.980	18.360	—	14.980	—	—	697	686	—	539	—	—	—
4.240	4.240	—	—	—	—	—	133	—	—	—	—	—	—	—
4.870	4.870	4.870	4.870	4.870	4.870	4.870	169	182	252	252	252	252	—	—
5.700	5.700	5.700	5.700	5.700	5.130	5.700	207	223	293	293	287	293	328	—
4.240	4.240	—	—	—	—	—	147	—	—	—	—	—	—	—
4.870	4.870	4.870	4.870	4.870	4.870	4.870	186	201	309	309	309	309	—	—
5.700	5.700	5.700	5.700	5.700	5.130	5.700	228	246	359	359	359	359	416	—
7.770	—	7.770	7.770	—	6.990	—	—	295	375	—	364	—	416	—
9.500	—	9.500	9.290	—	6.990	—	—	376	452	—	364	—	446	—
11.470	—	10.140	9.290	—	6.990	—	—	466	510	—	364	—	—	—
12.550	—	10.140	9.290	—	7.000	—	—	513	510	—	364	—	—	—
13.130	—	10.140	9.290	—	6.990	—	—	538	510	—	364	—	—	—
8.290	—	8.290	8.290	8.290	7.460	8.290	—	295	379	—	364	—	416	—
10.140	—	10.140	9.910	10.140	7.460	10.140	—	376	457	—	364	—	446	—
12.240	—	10.810	9.910	—	7.460	—	—	466	510	—	364	—	—	—
13.380	—	10.810	9.910	—	7.460	—	—	513	510	—	364	—	—	—
14.000	—	10.810	9.910	—	7.460	—	—	538	510	—	364	—	—	—
8.290	—	8.290	8.290	8.290	7.460	8.290	—	311	396	396	383	396	437	—
10.140	—	10.140	9.910	10.140	7.460	10.140	—	396	477	477	383	477	469	—
12.240	—	10.810	9.910	12.240	7.460	10.250	—	490	537	566	383	479	—	—
13.380	—	10.810	9.910	13.380	7.460	10.250	—	540	537	614	383	479	—	—
14.000	—	10.810	9.910	13.620	7.460	10.250	—	567	537	639	383	479	—	—
9.320	—	9.320	9.320	—	8.400	—	—	311	404	—	383	—	430	—
11.400	—	11.400	11.150	—	8.400	—	—	396	487	—	383	—	469	—
13.770	—	12.170	11.150	—	8.400	—	—	490	537	—	383	—	—	—
15.060	—	12.170	11.150	—	8.400	—	—	540	537	—	383	—	—	—
15.750	—	12.170	11.150	—	8.400	—	—	567	537	—	383	—	—	—

* Some joint strengths listed in Col. 20 through 27 are greater than the corresponding pipe body yield strength listed in Col. 12.

† Internal pressure resistance is the lowest of the internal yield pressure of the pipe, the internal yield pressure of the coupling, or the internal pressure leak resistance at the E or E₁ plane.

‡ For P-110 casing the next higher grade is 150YS, a non-API steel grade having a minimum yield strength of 150,000 psi.

TABLE 2.3—MINIMUM PERFORMANCE PROPERTIES OF CASING (continued)

1	2	3	4	5	6	7	8	9	10	11	12
OD (in.)	Nominal Weight, Threads and Coupling (lbm/ft)	Grade	Wall Thickness (in.)	ID (in.)	Threaded and Coupled			Extreme Line			Pipe-Body Yield Strength (1,000 lbf)
					Drift Diameter (in.)	OD of Coupling (in.)	OD Special Clearance Coupling (in.)	Drift Diameter (in.)	OD of Box Powertight (in.)	Collapse Resistance (psi)	
5	15.00	C-95	0.296	4.408	4.283	5.563	5.375	4.151	5.360	8,110	416
	18.00	C-95	0.362	4.276	4.151	5.563	5.375	4.151	5.360	12,030	501
	21.40	C-95	0.437	4.126	4.001	5.563	5.375	—	—	15,160	595
	23.20	C-95	0.478	4.044	3.919	5.563	5.375	—	—	16,430	645
	24.10	C-95	0.500	4.000	3.875	5.563	5.375	—	—	17,100	672
	15.00	HC-95	0.296	4.408	4.283	5.563	5.375	—	—	9,380	416
	18.00	HC-95	0.362	4.276	4.151	5.563	5.375	—	—	11,880	501
	23.20	HC-95	0.478	4.044	3.919	5.563	5.375	—	—	15,820	645
	15.00	P-110	0.296	4.408	4.283	5.563	5.375	4.151	5.360	8,850	481
	18.00	P-110	0.362	4.276	4.151	5.563	5.375	4.151	5.360	13,470	580
	21.40	P-110	0.437	4.126	4.001	5.563	5.375	—	—	17,550	689
	23.20	P-110	0.478	4.044	3.919	5.563	5.375	—	—	19,020	747
	24.10	P-110	0.500	4.000	3.875	5.563	5.375	—	—	19,800	778
	15.00	Q-125	0.296	4.408	4.283	5.563	5.375	—	—	9,480	547
	18.00	Q-125	0.362	4.276	4.151	5.563	5.375	—	—	14,830	659
	23.20	Q-125	0.478	4.044	3.919	5.563	5.375	—	—	21,620	849
	24.10	Q-125	0.500	4.000	3.875	5.563	—	—	—	22,500	884
	15.00	V-150	0.296	4.408	4.283	5.563	5.375	—	—	10,250	656
	18.00	V-150	0.362	4.276	4.151	5.563	5.375	—	—	16,860	791
	23.20	V-150	0.478	4.044	3.919	5.563	5.375	—	—	25,940	1,019
5½	14.00	H-40	0.244	5.012	4.887	6.050	—	—	—	2,620	161
	14.00	J-55	0.244	5.012	4.887	6.050	—	—	—	3,120	222
	15.50	J-55	0.275	4.950	4.825	6.050	5.875	4.653	5.860	4,040	248
	17.00	J-55	0.304	4.892	4.767	6.050	5.875	4.653	5.860	4,910	273
	14.00	K-55	0.244	5.012	4.887	6.050	—	—	—	3,120	222
	15.50	K-55	0.275	4.950	4.825	6.050	5.875	4.653	5.860	4,040	248
	17.00	K-55	0.304	4.892	4.767	6.050	5.875	4.653	5.860	4,910	273
	17.00	C-75	0.304	4.892	4.767	6.050	5.875	4.653	5.860	6,040	372
	20.00	C-75	0.361	4.778	4.653	6.050	5.875	4.653	5.860	8,410	437
	23.00	C-75	0.415	4.670	4.545	6.050	5.875	4.545	5.860	10,470	497
	17.00	L-80	0.304	4.892	4.767	6.050	5.875	4.653	5.860	6,280	397
	20.00	L-80	0.361	4.778	4.653	6.050	5.875	4.653	5.860	8,830	466
	23.00	L-80	0.415	4.670	4.545	6.050	5.875	4.545	5.860	11,160	530
	17.00	N-80	0.304	4.892	4.767	6.050	5.875	4.653	5.860	6,280	397
	20.00	N-80	0.361	4.778	4.653	6.050	5.875	4.653	5.860	8,830	466
	23.00	N-80	0.415	4.670	4.545	6.050	5.875	4.545	5.860	11,160	530
	17.00	C-90	0.304	4.892	4.767	6.050	5.875	4.653	5.860	6,740	447
	20.00	C-90	0.361	4.778	4.653	6.050	5.875	4.653	5.860	9,630	525
	23.00	C-90	0.415	4.670	4.545	6.050	5.875	4.545	5.860	12,380	597
	26.00	C-90	0.476	4.548	4.423	6.050	5.875	—	—	14,240	676
	35.00	C-90	0.650	4.200	4.075	6.050	5.875	—	—	18,760	891
	17.00	C-95	0.304	4.892	4.767	6.050	5.875	4.653	5.860	6,940	471
	20.00	C-95	0.361	4.778	4.653	6.050	5.875	4.653	5.860	10,010	554
	23.00	C-95	0.415	4.670	4.545	6.050	5.875	4.545	5.860	12,940	630
	17.00	HC-95	0.304	4.892	4.767	6.050	5.875	—	—	8,580	471
	20.00	HC-95	0.361	4.778	4.653	6.050	5.875	—	—	10,630	554
	23.00	HC-95	0.415	4.670	4.545	6.050	5.875	—	—	12,450	630
	17.00	P-110	0.304	4.892	4.767	6.050	5.875	4.653	5.860	7,480	546
	20.00	P-110	0.361	4.778	4.653	6.050	5.875	4.653	5.860	11,100	641
	23.00	P-110	0.415	4.670	4.545	6.050	5.875	4.545	5.860	14,540	729
	17.00	Q-125	0.304	4.892	4.767	6.050	5.875	—	—	7,890	620
	20.00	Q-125	0.360	4.778	4.653	6.050	5.875	—	—	12,080	729
	23.00	Q-125	0.415	4.670	4.545	6.050	5.875	—	—	16,070	829
	26.80	Q-125	0.500	4.500	4.375	6.050	5.875	—	—	20,660	982
	20.00	V-150	0.361	4.778	4.653	6.050	5.875	—	—	13,460	874
	23.00	V-150	0.415	4.670	4.545	6.050	5.875	—	—	18,390	995
	26.80	V-150	0.500	4.500	4.375	6.050	5.875	—	—	24,790	1,178

* Non-API weights or grades

TABLE 2.3—MINIMUM PERFORMANCE PROPERTIES OF CASING (continued)

13	14	15	16	17	18	19	20	21	22	23	24	25	26	27
Joint Strength** (1,000 lbf)														
Internal Pressure Resistance† (psi)							Threaded and Coupled							
Plain End or Extreme Line	Round Thread		Buttress Thread				Buttress Thread							
			Regular Coupling		Special Clearance Coupling		Round Thread		Regular Coupling		Special Clearance Coupling		Extreme Line	
	Short	Long	Same Grade	Higher Grade	Same Grade	Higher Grade	Short	Long	Regular Coupling	Higher Grade [‡]	Clearance Coupling	Higher Grade [‡]	Standard Joint	Optional Joint
9.840	—	9.840	9.840	—	8.850	—	—	326	424	—	402	—	459	—
12.040	—	12.040	11.770	—	8.850	—	—	416	512	—	402	—	493	—
14.530	—	12.840	11.770	—	8.850	—	—	515	563	—	402	—	—	—
15.890	—	12.850	11.770	—	8.860	—	—	567	563	—	402	—	—	—
16.630	—	12.850	11.770	—	8.850	—	—	595	563	—	402	—	—	—
9.840	—	9.840	9.840	9.840	8.860	9.840	—	342	441	441	422	441	—	—
12.040	—	12.040	11.770	12.040	8.860	10.260	—	436	532	532	422	479	—	—
15.890	—	12.850	11.770	13.630	8.860	10.260	—	594	591	671	422	479	—	—
11.400	—	11.400	11.400	11.400	10.250	11.400	—	388	503	503	479	503	547	—
13.940	—	13.940	13.620	13.940	10.250	13.940	—	495	606	606	479	606	587	—
16.820	—	14.870	13.620	16.820	10.250	13.980	—	613	671	720	479	613	—	—
18.400	—	14.880	13.630	18.400	10.260	13.990	—	675	671	780	479	613	—	—
19.250	—	14.870	13.620	18.580	10.250	13.980	—	708	671	812	479	613	—	—
12.950	—	12.950	12.950	—	—	—	—	420	548	—	—	—	—	—
15.840	—	15.840	15.490	—	—	—	—	535	661	—	—	—	—	—
20.910	—	16.000	15.490	—	—	—	—	729	725	—	—	—	—	—
21.880	—	16.000	15.490	—	—	—	—	765	725	—	—	—	—	—
15.540	—	15.540	15.540	—	13.990	—	—	497	651	—	613	—	—	—
19.010	—	16.000	18.590	—	13.990	—	—	634	785	—	613	—	—	—
25.090	—	16.000	18.590	—	13.990	—	—	864	859	—	613	—	—	—
3.110	3.110	—	—	—	—	—	130	—	—	—	—	—	—	—
4.270	4.270	—	—	—	—	—	172	—	—	—	—	—	—	—
4.810	4.810	4.810	4.810	4.810	4.730	4.810	202	217	300	300	300	300	339	339
5.320	5.320	5.320	5.320	5.320	4.730	5.320	229	247	329	329	318	329	372	372
4.270	4.270	—	—	—	—	—	189	—	—	—	—	—	—	—
4.810	4.810	4.810	4.810	4.810	4.730	4.810	222	239	366	366	366	366	429	429
5.320	5.320	5.320	5.320	5.320	4.730	5.320	252	272	402	402	402	402	471	471
7.250	—	7.250	7.250	—	6.450	—	—	327	423	—	403	—	471	471
8.610	—	8.610	8.430	—	6.450	—	—	403	497	—	403	—	497	479
9.900	—	9.260	8.430	—	6.450	—	—	473	550	—	403	—	549	479
7.740	—	7.740	7.740	7.740	6.880	7.740	—	338	428	—	403	—	471	471
9.190	—	9.190	8.990	9.190	6.880	9.190	—	416	503	—	403	—	497	479
10.560	—	9.880	8.990	10.560	6.880	9.460	—	489	550	—	403	—	549	479
7.740	—	7.740	7.740	7.740	6.880	7.740	—	348	446	446	424	446	496	496
9.190	—	9.190	8.990	9.190	6.880	9.190	—	428	524	524	424	524	523	504
10.560	—	9.880	8.990	10.560	6.880	9.460	—	502	579	596	424	530	577	504
8.710	—	8.710	8.710	—	7.740	—	—	356	456	—	424	—	496	496
10.340	—	10.340	10.120	—	7.740	—	—	438	536	—	424	—	523	504
11.880	—	11.110	10.120	—	7.740	—	—	514	580	—	424	—	577	504
13.630	—	11.110	10.120	—	7.740	—	—	598	580	—	424	—	—	—
18.610	—	11.110	10.120	—	7.740	—	—	614	580	—	424	—	—	—
9.190	—	9.190	9.190	—	8.170	—	—	374	480	—	445	—	521	521
10.910	—	10.910	10.680	—	8.170	—	—	460	563	—	445	—	549	530
12.540	—	11.730	10.680	—	8.170	—	—	540	608	—	445	—	606	530
9.190	—	9.190	9.190	9.190	8.170	9.190	—	392	498	498	466	498	—	—
10.910	—	10.910	10.680	10.910	8.170	9.460	—	482	585	585	466	530	—	—
12.540	—	11.730	10.680	12.370	8.170	9.460	—	566	638	665	466	530	—	—
10.640	—	10.640	10.640	10.640	9.460	10.640	—	445	568	568	530	568	620	620
12.640	—	12.640	12.360	12.640	9.460	11.880	—	548	667	667	530	667	654	630
14.520	—	13.160	12.360	14.520	9.460	11.880	—	643	724	759	530	668	722	630
12.090	—	12.090	12.090	12.090	10.770	12.090	—	481	620	620	573	620	—	—
14.360	—	14.360	14.360	14.070	10.770	12.920	—	592	728	728	573	679	—	—
16.510	—	16.510	15.210	14.070	10.770	12.920	—	694	783	828	573	679	—	—
19.890	—	19.890	15.210	14.070	10.770	12.920	—	842	783	928	573	679	—	—
17.230	—	17.230	16.880	—	12.920	—	—	701	865	—	678	—	—	—
19.810	—	18.250	16.880	—	12.920	—	—	823	928	—	678	—	—	—
23.860	—	18.250	16.880	—	12.920	—	—	998	928	—	678	—	—	—

** Some joint strengths listed in Col. 20 through 27 are greater than the corresponding pipe body yield strength listed in Col. 12.

† Internal pressure resistance is the lowest of the internal yield pressure of the pipe, the internal yield pressure of the coupling, or the internal pressure leak resistance at the E₁ or E₂ plane.

‡ For P-110 casing the next higher grade is 150YS, a non-API steel grade having a minimum yield strength of 150,000 psi.

TABLE 2.3—MINIMUM PERFORMANCE PROPERTIES OF CASING (continued)

1	2	3	4	5	6	7	8	9	10	11	12
OD (in.)	Nominal Weight, Threads and Coupling (lbm/ft)	Grade	Wall Thickness (in.)	ID (in.)	Threaded and Coupled			Extreme Line			Pipe-Body Yield Strength (1,000 lbf)
					Drift Diameter (in.)	OD of Coupling (in.)	OD Special Clearance Coupling (in.)	Drift Diameter (in.)	OD of Box Powertight (in.)	Collapse Resistance (psi)	
6 $\frac{5}{8}$	20.00	H-40	0.288	6.049	5.924	7.390	—	—	—	2,520	229
	20.00	J-55	0.288	6.049	5.924	7.390	7.000	—	—	2,970	315
	24.00	J-55	0.352	5.921	5.796	7.390	7.000	5.730	7.000	4,560	382
	20.00	K-55	0.288	6.049	5.924	7.390	7.000	—	—	2,970	315
	24.00	K-55	0.352	5.921	5.796	7.390	7.000	5.730	7.000	4,560	382
	24.00	C-75	0.352	5.921	5.796	7.390	7.000	5.730	7.000	5,550	520
	28.00	C-75	0.417	5.791	5.666	7.390	7.000	5.666	7.000	7,790	610
	32.00	C-75	0.475	5.675	5.550	7.390	7.000	5.550	7.000	9,800	688
	24.00	L-80	0.352	5.921	5.796	7.390	7.000	5.730	7.000	5,760	555
	28.00	L-80	0.417	5.791	5.666	7.390	7.000	5.666	7.000	8,170	651
	32.00	L-80	0.475	5.675	5.550	7.390	7.000	5.550	7.000	10,320	734
	24.00	N-80	0.352	5.921	5.796	7.390	7.000	5.730	7.000	5,760	555
	28.00	N-80	0.417	5.791	5.666	7.390	7.000	5.666	7.000	8,170	651
	32.00	N-80	0.475	5.675	5.550	7.390	7.000	5.550	7.000	10,320	734
	24.00	C-90	0.352	5.921	5.796	7.390	7.000	5.730	7.000	6,140	624
	28.00	C-90	0.417	5.791	5.666	7.390	7.000	5.666	7.000	8,880	732
	32.00	C-90	0.475	5.675	5.550	7.390	7.000	5.550	7.000	11,330	826
	24.00	C-95	0.352	5.921	5.796	7.390	7.000	5.730	7.000	6,310	659
	28.00	C-95	0.417	5.791	5.666	7.390	7.000	5.666	7.000	9,220	773
	32.00	C-95	0.475	5.675	5.550	7.390	7.000	5.550	7.000	11,810	872
	24.00	P-110	0.352	5.921	5.796	7.390	7.000	5.730	7.000	6,730	763
	28.00	P-110	0.417	5.791	5.666	7.390	7.000	5.666	7.000	10,160	895
	32.00	P-110	0.475	5.675	5.550	7.390	7.000	5.550	7.000	13,220	1,009
*	24.00	Q-125	0.352	5.921	5.796	7.390	7.000	—	—	7,020	867
*	28.00	Q-125	0.417	5.791	5.666	7.390	7.000	—	—	10,990	1,017
*	32.00	Q-125	0.475	5.675	5.550	7.390	7.000	—	—	14,530	1,147
*	24.00	V-150	0.352	5.921	5.796	7.390	7.000	—	—	7,340	1,041
*	28.00	V-150	0.417	5.791	5.666	7.390	7.000	—	—	12,120	1,220
*	32.00	V-150	0.475	5.675	5.550	7.390	7.000	—	—	16,500	1,317
7	17.00	H-40	0.231	6.538	6.413	7.656	—	—	—	1,420	196
	20.00	H-40	0.272	6.456	6.331	7.656	—	—	—	1,970	230
	20.00	J-55	0.272	6.456	6.331	7.656	—	—	—	2,270	316
	23.00	J-55	0.317	6.366	6.241	7.656	7.375	6.151	7.390	3,270	366
	26.00	J-55	0.362	6.276	6.151	7.656	7.375	6.151	7.390	4,320	415
	20.00	K-55	0.272	6.456	6.331	7.656	—	—	—	2,270	316
	23.00	K-55	0.317	6.366	6.241	7.656	7.375	6.151	7.390	3,270	366
	26.00	K-55	0.362	6.276	6.151	7.656	7.375	6.151	7.390	4,320	415
	23.00	C-75	0.317	6.366	6.241	7.656	7.375	6.151	7.390	3,750	499
	26.00	C-75	0.362	6.276	6.151	7.656	7.375	6.151	7.390	5,220	566
	29.00	C-75	0.408	6.184	6.059	7.656	7.375	6.059	7.390	6,730	634
	32.00	C-75	0.453	6.094	5.969	7.656	7.375	5.969	7.390	8,200	699
	35.00	C-75	0.498	6.004	5.879	7.656	7.375	5.879	7.530	9,670	763
	38.00	C-75	0.540	5.920	5.795	7.656	7.375	5.795	7.530	10,680	822
	23.00	L-80	0.317	6.366	6.241	7.656	7.375	6.151	7.390	3,830	532
	26.00	L-80	0.362	6.276	6.151	7.656	7.375	6.151	7.390	5,410	604
	29.00	L-80	0.408	6.184	6.059	7.656	7.375	6.059	7.390	7,020	676
	32.00	L-80	0.453	6.094	5.969	7.656	7.375	5.969	7.390	8,610	745
	35.00	L-80	0.498	6.004	5.879	7.656	7.375	5.879	7.530	10,180	814
	38.00	L-80	0.540	5.920	5.795	7.656	7.375	5.795	7.530	11,390	877
	23.00	N-80	0.317	6.366	6.241	7.656	7.375	6.151	7.390	3,830	532
	26.00	N-80	0.362	6.276	6.151	7.656	7.375	6.151	7.390	5,410	604
	29.00	N-80	0.408	6.184	6.059	7.656	7.375	6.059	7.390	7,020	676
	32.00	N-80	0.453	6.094	5.969	7.656	7.375	5.969	7.390	8,610	745
	35.00	N-80	0.498	6.004	5.879	7.656	7.375	5.879	7.530	10,180	814
	38.00	N-80	0.540	5.920	5.795	7.656	7.375	5.795	7.530	11,390	877

*Non-API weights or grades

TABLE 2.3—MINIMUM PERFORMANCE PROPERTIES OF CASING (continued)

13	14	15	16	17	18	19	20	21	22	23	24	25	26	27
Joint Strength** (1,000 lbf)														
Internal Pressure Resistance† (psi)							Threaded and Coupled							
Plain End or Extreme Line	Buttress Thread						Buttress Thread							
	Round Thread		Regular Coupling		Special Clearance Coupling		Round Thread		Regular Coupling		Special Clearance Coupling		Extreme Line	
	Short	Long	Same Grade	Higher Grade	Same Grade	Higher Grade	Short	Long	Regular Coupling	Higher Grade [‡]	Special Clearance Coupling	Higher Grade [‡]	Standard Joint	Optional Joint
3.040	3.040	—	—	—	—	—	184	—	—	—	—	—	—	—
4.180	4.180	4.180	4.180	4.180	4.060	4.180	245	266	374	374	—	374	—	—
5.110	5.110	5.110	5.110	5.110	4.060	5.110	314	340	453	453	390	453	477	477
4.180	4.180	4.180	4.180	4.180	4.060	4.180	267	290	453	453	453	453	—	—
5.110	5.110	5.110	5.110	5.110	4.060	5.110	342	372	548	548	494	520	605	605
6.970	—	6.970	6.970	—	5.540	—	—	453	583	—	494	—	605	605
8.260	—	8.260	8.260	—	5.540	—	—	552	683	—	494	—	648	644
9.410	—	9.410	9.200	—	5.540	—	—	638	771	—	494	—	717	644
7.440	—	7.440	7.440	—	5.910	—	—	473	592	—	494	—	605	605
8.810	—	8.810	8.810	—	5.910	—	—	576	693	—	494	—	648	644
10.040	—	10.040	9.820	—	5.910	—	—	666	783	—	494	—	717	644
7.440	—	7.440	7.440	7.440	5.910	7.440	—	481	615	615	520	615	637	637
8.810	—	8.810	8.810	8.810	5.910	8.120	—	586	721	721	520	650	682	678
10.040	—	10.040	9.820	10.040	5.910	8.120	—	677	814	814	520	650	755	678
8.370	—	8.370	8.370	—	6.650	—	—	520	633	—	520	—	637	637
9.910	—	9.910	9.910	—	6.650	—	—	633	742	—	520	—	682	678
11.290	—	11.290	11.050	—	6.650	—	—	732	837	—	520	—	755	678
8.830	—	8.830	8.830	—	7.020	—	—	546	665	—	546	—	668	668
10.460	—	10.460	10.460	—	7.020	—	—	665	780	—	546	—	716	712
11.920	—	11.830	11.660	—	7.020	—	—	769	880	—	546	—	793	712
10.230	—	10.230	10.230	10.230	8.120	8.310	—	641	786	786	650	786	796	796
12.120	—	11.830	12.120	12.120	8.120	8.310	—	781	992	922	650	832	852	848
13.800	—	11.830	13.500	13.800	8.120	8.310	—	904	1,040	1,040	650	832	944	848
11.620	—	11.620	11.620	—	8.310	—	—	702	860	—	702	—	—	—
13.770	—	11.830	13.770	—	8.310	—	—	855	1,008	—	702	—	—	—
15.680	—	11.830	14.780	—	8.310	—	—	989	1,138	—	—	—	—	—
13.950	—	11.830	13.950	—	8.310	—	—	831	1,023	—	832	—	—	—
16.520	—	11.830	14.780	—	8.310	—	—	1,013	1,199	—	832	—	—	—
18.820	—	11.830	14.780	—	8.310	—	—	1,172	1,353	—	832	—	—	—
2.310	2.310	—	—	—	—	—	122	—	—	—	—	—	—	—
2.720	2.720	—	—	—	—	—	176	—	—	—	—	—	—	—
3.740	3.740	—	—	—	—	—	234	—	—	—	—	—	—	—
4.360	4.360	4.360	4.360	4.360	3.950	4.360	284	313	432	432	421	432	499	499
4.980	4.980	4.980	4.980	4.980	3.950	4.980	334	367	490	490	421	490	506	506
3.740	3.740	—	—	—	—	—	254	—	—	—	—	—	—	—
4.360	4.360	4.360	4.360	4.360	3.950	4.360	309	341	522	522	522	522	632	632
4.980	4.980	4.980	4.980	4.980	3.950	4.980	364	401	592	592	533	561	641	641
5.940	—	5.940	5.940	—	5.380	—	—	416	557	—	533	—	632	632
6.790	—	6.790	6.790	—	5.380	—	—	489	631	—	533	—	641	641
7.650	—	7.650	7.650	—	5.380	—	—	562	707	—	533	—	685	674
8.490	—	8.490	7.930	—	5.380	—	—	633	779	—	533	—	761	674
9.340	—	8.660	7.930	—	5.380	—	—	703	833	—	533	—	850	761
10.120	—	8.660	7.930	—	5.380	—	—	767	833	—	533	—	917	761
6.340	—	6.340	6.340	6.340	5.740	6.340	—	435	565	—	533	—	632	632
7.240	—	7.240	7.240	7.240	5.740	7.240	—	511	641	—	533	—	641	641
8.160	—	8.160	8.160	8.160	5.740	7.890	—	587	718	—	533	—	685	674
9.060	—	9.060	8.460	9.060	5.740	7.890	—	661	791	—	533	—	761	674
9.960	—	9.240	8.460	9.960	5.740	7.890	—	734	833	—	533	—	850	761
10.800	—	9.240	8.460	10.800	5.740	7.890	—	801	833	—	533	—	917	761
6.340	—	6.340	6.340	6.340	5.740	6.340	—	442	588	588	561	588	666	666
7.240	—	7.240	7.240	7.240	5.740	7.240	—	519	667	667	561	667	675	675
8.160	—	8.160	8.160	8.160	5.740	7.890	—	597	746	746	561	702	721	709
9.060	—	9.060	8.460	9.060	5.740	7.890	—	672	823	823	561	702	801	709
9.960	—	9.240	8.460	9.960	5.740	7.890	—	746	876	898	561	702	895	801
10.800	—	9.240	8.460	10.800	5.740	7.890	—	814	876	968	561	702	965	801

**Some joint strengths listed in Col. 20 through 27 are greater than the corresponding pipe body yield strength listed in Col. 12.

†Internal pressure resistance is the lowest of the internal yield pressure of the pipe, the internal yield pressure of the coupling, or the internal pressure leak resistance at the E or E₁ plane.

‡For P-110 casing the next higher grade is 150YS, a non-API steel grade having a minimum yield strength of 150,000 psi.

TABLE 2.3—MINIMUM PERFORMANCE PROPERTIES OF CASING (continued)

1	2	3	4	5	6	7	8	9	10	11	12
OD (in.)	Nominal Weight, Threads and Coupling (lbm/ft)	Grade	Wall Thickness (in.)	ID (in.)	Threaded and Coupled			Extreme Line			Pipe-Body Yield Strength (1,000 lbf)
					Drift Diameter (in.)	OD of Coupling (in.)	OD Special Clearance Coupling (in.)	Drift Diameter (in.)	OD of Box Powertight (in.)	Collapse Resistance (psi)	
7	23.00	C-90	0.317	6.366	6.241	7.656	7.375	6.151	7.390	4,030	599
	26.00	C-90	0.362	6.276	6.151	7.656	7.375	6.151	7.390	5,740	679
	29.00	C-90	0.408	6.184	6.059	7.656	7.375	6.059	7.390	7,580	760
	32.00	C-90	0.453	6.094	5.969	7.656	7.375	5.969	7.390	9,380	839
	35.00	C-90	0.498	6.004	5.879	7.656	7.375	5.879	7.530	11,170	915
	38.00	C-90	0.540	5.920	5.795	7.656	7.375	5.795	7.530	12,820	986
	23.00	C-95	0.317	6.366	6.241	7.656	7.375	6.151	7.390	4,140	632
	26.00	C-95	0.362	6.276	6.151	7.656	7.375	6.151	7.390	5,880	717
	29.00	C-95	0.408	6.184	6.059	7.656	7.375	6.059	7.390	7,830	803
	32.00	C-95	0.453	6.094	5.969	7.656	7.375	5.969	7.390	9,750	885
	35.00	C-95	0.498	6.004	5.879	7.656	7.375	5.879	7.530	11,650	966
	38.00	C-95	0.540	5.920	5.795	7.656	7.375	5.795	7.530	13,440	1,041
	23.00	HC-95	0.317	6.366	6.241	7.656	7.375	—	—	5,650	632
	26.00	HC-95	0.362	6.276	6.151	7.656	7.375	—	—	7,800	717
	29.00	HC-95	0.408	6.184	6.059	7.656	7.375	—	—	9,200	803
	32.00	HC-95	0.453	6.094	5.969	7.656	7.375	—	—	10,400	885
	35.00	HC-95	0.498	6.004	5.879	7.656	7.375	—	—	11,600	966
	38.00	HC-95	0.540	5.920	5.795	7.656	7.375	—	—	12,700	1,041
	26.00	P-110	0.362	6.276	6.151	7.656	7.375	6.151	7.390	6,230	830
	29.00	P-110	0.408	6.184	6.059	7.656	7.375	6.059	7.390	8,530	929
	32.00	P-110	0.453	6.094	5.969	7.656	7.375	5.969	7.390	10,780	1,025
	35.00	P-110	0.498	6.004	5.879	7.656	7.375	5.879	7.530	13,020	1,119
	38.00	P-110	0.540	5.920	5.795	7.656	7.375	5.795	7.530	15,140	1,205
	29.00	Q-125	0.408	6.184	6.059	7.656	7.375	—	—	9,100	1,056
	32.00	Q-125	0.453	6.094	5.969	7.656	7.375	—	—	11,720	1,165
	35.00	Q-125	0.498	6.004	5.879	7.656	7.375	—	—	14,310	1,272
	38.00	Q-125	0.540	5.920	5.795	7.656	7.375	—	—	16,750	1,370
	42.70	Q-125	0.625	5.750	5.625	7.656	7.375	—	—	20,330	1,565
	29.00	V-150	0.408	6.184	6.059	7.656	7.375	—	—	9,790	1,267
	32.00	V-150	0.453	6.094	5.969	7.656	7.375	—	—	13,020	1,388
	35.00	V-150	0.498	6.004	5.879	7.656	7.375	—	—	16,220	1,526
	38.00	V-150	0.540	5.920	5.795	7.656	7.375	—	—	19,240	1,644
	42.70	V-150	0.625	5.750	5.625	7.656	7.375	—	—	24,390	1,878
7 $\frac{5}{8}$	24.00	H-40	0.300	7.025	6.900	8.500	—	—	—	2,030	276
	26.40	J-55	0.328	6.969	6.844	8.500	8.125	6.750	8.010	2,890	414
	26.40	K-55	0.328	6.969	6.844	8.500	8.125	6.750	8.010	2,890	414
	26.40	C-75	0.328	6.969	6.844	8.500	8.125	6.750	8.010	3,280	564
	29.70	C-75	0.375	6.875	6.750	8.500	8.125	6.750	8.010	4,650	641
	33.70	C-75	0.430	6.765	6.640	8.500	8.125	6.640	8.010	6,300	729
	39.00	C-75	0.500	6.625	6.500	8.500	8.125	6.500	8.010	8,400	839
	42.80	C-75	0.562	6.501	6.376	8.500	8.125	—	—	10,240	935
	45.30	C-75	0.595	6.435	6.310	8.500	8.125	—	—	10,790	986
	47.10	C-75	0.625	6.375	6.250	8.500	8.125	—	—	11,290	1,031
	26.40	L-80	0.328	6.969	6.844	8.500	8.125	6.750	8.010	3,400	602
	29.70	L-80	0.375	6.875	6.750	8.500	8.125	6.750	8.010	4,790	683
	33.70	L-80	0.430	6.765	6.640	8.500	8.125	6.640	8.010	6,560	778
	39.00	L-80	0.500	6.625	6.500	8.500	8.125	6.500	8.010	8,820	895
	42.80	L-80	0.562	6.501	6.376	8.500	8.125	—	—	10,810	998
	45.30	L-80	0.595	6.435	6.310	8.500	8.125	—	—	11,510	1,051
	47.10	L-80	0.625	6.375	6.250	8.500	8.125	—	—	12,040	1,100
	26.40	N-80	0.328	6.969	6.844	8.500	8.125	6.750	8.010	3,400	602
	29.70	N-80	0.375	6.875	6.750	8.500	8.125	6.750	8.010	4,790	683
	33.70	N-80	0.430	6.765	6.640	8.500	8.125	6.640	8.010	6,560	778
	39.00	N-80	0.500	6.625	6.500	8.500	8.125	6.500	8.010	8,820	895
	42.80	N-80	0.562	6.501	6.376	8.500	8.125	—	—	10,810	998
	45.30	N-80	0.595	6.435	6.310	8.500	8.125	—	—	11,510	1,051
	47.10	N-80	0.625	6.375	6.250	8.500	8.125	—	—	12,040	1,100

*Non-API weights or grades

TABLE 2.3—MINIMUM PERFORMANCE PROPERTIES OF CASING (continued)

13	14	15	16	17	18	19	20	21	22	23	24	25	26	27
Internal Pressure Resistance† (psi)													Joint Strength** (1,000 lbf)	
Plain End or Extreme Line	Buttress Thread						Threaded and Coupled						Extreme Line Standard Joint Optional Joint	
	Round Thread	Regular Coupling		Special Clearance Coupling		Round Thread	Regular Coupling		Special Clearance Coupling					
		Same Grade	Higher Grade	Same Grade	Higher Grade		Same Grade	Higher Grade¹	Same Grade	Higher Grade¹				
7.130	—	7.130	7.130	—	6.450	—	—	447	605	—	561	—	666	666
8.150	—	8.150	8.150	—	6.450	—	—	563	687	—	561	—	675	675
9.180	—	9.180	9.180	—	6.450	—	—	648	768	—	561	—	721	709
10.190	—	9.520	9.520	—	6.450	—	—	729	847	—	561	—	801	709
11.210	—	9.520	9.520	—	6.450	—	—	809	876	—	561	—	895	801
12.150	—	9.520	9.520	—	6.450	—	—	883	876	—	561	—	965	801
7.530	—	7.530	7.530	—	6.810	—	—	505	636	—	589	—	699	699
8.600	—	8.600	8.600	—	6.810	—	—	593	722	—	589	—	709	709
9.690	—	9.520	9.690	—	6.810	—	—	683	808	—	589	—	757	744
10.760	—	9.520	10.050	—	6.810	—	—	768	891	—	589	—	841	744
11.830	—	9.520	10.050	—	6.810	—	—	853	920	—	589	—	940	841
12.820	—	9.520	10.050	—	6.810	—	—	931	920	—	589	—	1,013	841
7.530	—	7.530	7.530	7.530	6.810	7.480	—	512	659	659	617	659	—	—
8.600	—	8.600	8.600	8.600	6.810	7.480	—	602	747	747	617	701	—	—
9.690	—	9.520	9.690	9.690	6.810	7.480	—	692	836	836	617	701	—	—
10.760	—	9.520	10.050	10.760	6.810	7.480	—	779	922	922	617	701	—	—
11.830	—	9.520	10.050	11.630	6.810	7.480	—	865	964	1,007	617	701	—	—
12.830	—	9.520	10.050	11.630	6.810	7.480	—	944	964	1,085	617	701	—	—
9.960	—	9.520	9.960	9.960	7.480	7.480	—	693	853	853	702	853	844	844
11.220	—	9.520	11.220	11.220	7.480	7.480	—	797	955	955	702	898	902	886
12.460	—	9.520	11.640	11.790	7.480	7.480	—	897	1,053	1,053	702	898	1,002	886
13.700	—	9.520	11.640	11.790	7.480	7.480	—	996	1,096	1,150	702	898	1,118	1,002
14.850	—	9.520	11.640	11.790	7.480	7.480	—	1,087	1,096	1,239	702	898	1,207	1,002
12.750	—	9.520	11.790	—	7.480	—	—	885	1,045	—	757	—	—	—
14.160	—	9.520	11.790	—	7.480	—	—	996	1,183	—	757	—	—	—
15.560	—	9.520	11.790	—	7.480	—	—	1,106	1,183	—	757	—	—	—
16.880	—	9.520	11.790	—	7.480	—	—	1,207	1,183	—	757	—	—	—
19.530	—	9.520	11.790	—	7.480	—	—	1,277	1,183	—	757	—	—	—
15.300	—	9.520	11.790	—	7.480	—	—	1,049	1,243	—	898	—	—	—
16.990	—	9.520	11.790	—	7.480	—	—	1,180	1,402	—	898	—	—	—
18.680	—	9.520	11.790	—	7.480	—	—	1,310	1,402	—	898	—	—	—
20.250	—	9.520	11.790	—	7.480	—	—	1,430	1,402	—	898	—	—	—
23.440	—	9.520	11.790	—	7.480	—	—	1,514	1,402	—	898	—	—	—
2.750	2.750	—	—	—	—	—	212	—	—	—	—	—	—	—
4.140	4.140	4.140	4.140	4.140	4.140	4.140	315	346	483	483	483	483	553	553
4.140	4.140	4.140	4.140	4.140	4.140	4.140	342	377	581	581	581	581	700	700
5.650	—	5.650	5.650	—	5.650	—	—	461	624	—	624	—	700	700
6.450	—	6.450	6.450	—	6.140	—	—	542	709	—	709	—	700	700
7.400	—	7.400	7.400	—	6.140	—	—	635	806	—	735	—	766	744
8.610	—	8.610	8.610	—	6.140	—	—	751	929	—	735	—	851	744
9.670	—	9.670	9.190	—	6.140	—	—	852	1,035	—	735	—	—	—
10.240	—	9.840	9.180	—	6.140	—	—	905	1,090	—	764	—	—	—
10.760	—	9.840	9.190	—	6.140	—	—	953	1,140	—	735	—	—	—
6.020	—	6.020	6.020	6.020	6.020	6.020	—	482	635	—	635	—	700	700
6.890	—	6.890	6.890	6.890	6.550	6.890	—	566	721	—	721	—	700	700
7.900	—	7.900	7.900	7.900	6.550	7.900	—	664	820	—	735	—	766	744
9.180	—	9.180	9.180	9.180	6.550	9.000	—	786	945	—	735	—	851	744
10.320	—	10.320	9.790	—	6.550	—	—	892	1,053	—	735	—	—	—
10.920	—	10.500	9.790	—	6.550	—	—	947	1,109	—	764	—	—	—
11.480	—	10.490	9.790	—	6.550	—	—	997	1,160	—	735	—	—	—
6.020	—	6.020	6.020	6.020	6.020	6.020	—	490	659	659	659	659	737	737
6.890	—	6.890	6.890	6.890	6.550	6.890	—	575	749	749	749	749	737	737
7.900	—	7.900	7.900	7.900	6.550	7.900	—	674	852	852	773	852	806	784
9.180	—	9.180	9.180	9.180	6.550	9.000	—	798	981	981	773	967	896	784
10.320	—	10.320	9.790	10.320	6.550	9.000	—	905	1,093	1,093	773	967	—	—
10.920	—	10.500	9.790	10.920	6.550	8.030	—	962	1,152	1,152	804	1,005	—	—
11.480	—	10.490	9.790	11.480	6.550	9.000	—	1,013	1,205	1,204	773	967	—	—

** Some joint strengths listed in Col. 20 through 27 are greater than the corresponding pipe body yield strength listed in Col. 12.

† Internal pressure resistance is the lowest of the internal yield pressure of the pipe, the internal yield pressure of the coupling, or the internal pressure leak resistance at the E or E₁ plane.

¹ For P-110 casing the next higher grade is 150YS, a non-API steel grade having a minimum yield strength of 150,000 psi.

TABLE 2.3—MINIMUM PERFORMANCE PROPERTIES OF CASING (continued)

1	2	3	4	5	6	7	8	9	10	11	12
OD (in.)	Nominal Weight, Threads and Coupling (lbm/ft)	Grade	Threaded and Coupled					Extreme Line			Pipe-Body Yield Strength (1,000 lbf)
			Wall Thickness (in.)	ID (in.)	Drift Diameter (in.)	OD of Coupling (in.)	OD Special Clearance Coupling (in.)	Drift Diameter (in.)	OD of Box Powertight (in.)	Collapse Resistance (psi)	
7 $\frac{5}{8}$	26.40	C-90	0.328	6.969	6.844	8.500	8.125	6.750	8.010	3,610	677
	29.70	C-90	0.375	6.875	6.750	8.500	8.125	6.750	8.010	5,040	769
	33.70	C-90	0.430	6.765	6.640	8.500	8.125	6.640	8.010	7,050	875
	39.00	C-90	0.500	6.625	6.500	8.500	8.125	6.500	8.010	9,620	1,007
	42.80	C-90	0.562	6.501	6.376	8.500	8.125	—	—	11,890	1,122
	45.30	C-90	0.595	6.435	6.310	8.500	8.125	—	—	12,950	1,183
	47.10	C-90	0.625	6.375	6.250	8.500	8.125	—	—	13,540	1,237
	26.40	C-95	0.328	6.969	6.844	8.500	8.125	6.750	8.010	3,710	714
	29.70	C-95	0.375	6.875	6.750	8.500	8.125	6.750	8.010	5,140	811
	33.70	C-95	0.430	6.765	6.640	8.500	8.125	6.640	8.010	7,280	923
	39.00	C-95	0.500	6.625	6.500	8.500	8.125	6.500	8.010	10,000	1,063
	42.80	C-95	0.562	6.501	6.376	8.500	8.125	—	—	12,410	1,185
	45.30	C-95	0.595	6.435	6.310	8.500	8.125	—	—	13,660	1,248
	47.10	C-95	0.625	6.375	6.250	8.500	8.125	—	—	14,300	1,306
	* 26.40	HC-95	0.328	6.969	6.844	8.500	8.125	—	—	4,850	714
	* 29.70	HC-95	0.375	6.875	6.750	8.500	8.125	—	—	7,150	811
	* 33.70	HC-95	0.430	6.765	6.640	8.500	8.125	—	—	8,800	923
	* 39.00	HC-95	0.500	6.625	6.500	8.500	8.125	—	—	10,600	1,063
	* 45.30	HC-95	0.595	6.435	6.310	8.500	8.125	—	—	12,900	1,248
	29.70	P-110	0.375	6.875	6.750	8.500	8.125	6.750	8.010	5,350	940
	33.70	P-110	0.430	6.765	6.640	8.500	8.125	6.640	8.010	7,870	1,069
	39.00	P-110	0.500	6.625	6.500	8.500	8.125	6.500	8.010	11,080	1,231
	42.80	P-110	0.562	6.501	6.376	8.500	8.125	—	—	13,920	1,372
	45.30	P-110	0.595	6.435	6.310	8.500	8.125	—	—	15,430	1,446
	47.10	P-110	0.625	6.375	6.250	8.500	8.125	—	—	16,550	1,512
	* 29.70	Q-125	0.375	6.875	6.750	8.500	8.125	—	—	5,670	1,068
	* 33.70	Q-125	0.430	6.765	6.640	8.500	8.125	—	—	8,350	1,215
	39.00	Q-125	0.500	6.625	6.500	8.500	8.125	—	—	12,060	1,399
	42.80	Q-125	0.562	6.501	6.376	8.500	8.125	—	—	15,350	1,559
	45.30	Q-125	0.595	6.435	6.310	8.500	8.125	—	—	17,090	1,643
	47.10	Q-125	0.625	6.375	6.250	8.500	—	—	—	18,700	1,718
	* 29.70	V-150	0.375	6.875	6.750	8.500	8.125	—	—	6,060	1,282
	* 33.70	V-150	0.430	6.765	6.640	8.500	8.125	—	—	8,850	1,458
	* 39.00	V-150	0.500	6.625	6.500	8.500	8.125	—	—	13,440	1,679
	* 45.30	V-150	0.595	6.435	6.310	8.500	8.125	—	—	19,660	1,971
8 $\frac{5}{8}$	28.00	H-40	0.304	8.017	7.892	9.625	—	—	—	1,610	318
	32.00	H-40	0.352	7.921	7.796	9.625	—	—	—	2,200	366
	24.00	J-55	0.264	8.097	7.972	9.625	—	—	—	1,370	381
	32.00	J-55	0.352	7.921	7.796	9.625	9.125	7.700	9.120	2,530	503
	36.00	J-55	0.400	7.825	7.700	9.625	9.125	7.700	9.120	3,450	568
	24.00	K-55	0.264	8.097	7.972	9.625	—	—	—	1,370	381
	32.00	K-55	0.352	7.921	7.796	9.625	9.125	7.700	9.120	2,530	503
	36.00	K-55	0.400	7.825	7.700	9.625	9.125	7.700	9.120	3,450	568
	36.00	C-75	0.400	7.825	7.700	9.625	9.125	7.700	9.120	4,000	775
	40.00	C-75	0.450	7.725	7.600	9.625	9.125	7.600	9.120	5,330	867
	44.00	C-75	0.500	7.625	7.500	9.625	9.125	7.500	9.120	6,660	957
	49.00	C-75	0.557	7.511	7.386	9.625	9.125	7.386	9.120	8,180	1,059
	36.00	L-80	0.400	7.825	7.700	9.625	9.125	7.700	9.120	4,100	827
	40.00	L-80	0.450	7.725	7.600	9.625	9.125	7.600	9.120	5,520	925
	44.00	L-80	0.500	7.625	7.500	9.625	9.125	7.500	9.120	6,950	1,021
	49.00	L-80	0.557	7.511	7.386	9.625	9.125	7.386	9.120	8,580	1,129

* Non-API weights or grades.

TABLE 2.3—MINIMUM PERFORMANCE PROPERTIES OF CASING (continued)

13	14	15	16	17	18	19	20	21	22	23	24	25	26	27
Joint Strength** (1,000 lbf)														
Internal Pressure Resistance† (psi)							Threaded and Coupled							
Plain End or Extreme Line	Buttress Thread						Buttress Thread						Extreme Line	
	Round Thread		Regular Coupling		Special Clearance Coupling		Round Thread		Regular Coupling		Special Clearance Coupling		Extreme Line	
	Short	Long	Same Grade	Higher Grade	Same Grade	Higher Grade	Short	Long	Same Grade	Higher Grade†	Same Grade	Higher Grade†	Standard Joint	Optional Joint
6.780	—	6.780	6.780	—	6.780	—	—	532	681	—	681	—	737	737
7.750	—	7.750	7.750	—	7.750	—	—	625	773	—	773	—	737	737
8.880	—	8.880	8.880	—	7.370	—	—	733	880	—	804	—	806	784
10.330	—	10.330	10.330	—	7.370	—	—	867	1,013	—	804	—	896	784
11.610	—	11.610	11,020	—	7.370	—	—	984	1,129	—	804	—	—	—
12.290	—	11.800	11,020	—	7.370	—	—	1,045	1,189	—	804	—	—	—
12.910	—	11.800	11,020	—	7.370	—	—	1,100	1,239	—	804	—	—	—
7.150	—	7.150	7.150	—	7.150	—	—	560	716	—	716	—	774	774
8.180	—	8.180	8.180	—	7.780	—	—	659	813	—	812	—	774	774
9.380	—	9.380	9.380	—	7.780	—	—	772	925	—	812	—	846	823
10.900	—	10.900	10.900	—	7.780	—	—	914	1,065	—	812	—	941	823
12.250	—	11.800	11,620	—	7.780	—	—	1,037	1,187	—	812	—	—	—
12.970	—	11.800	11,630	—	7.780	—	—	1,101	1,251	—	854	—	—	—
13.630	—	11.800	11,620	—	7.780	—	—	1,159	1,300	—	812	—	—	—
7.150	—	7.150	7.150	7.150	7.150	—	—	568	740	740	740	740	—	—
8.180	—	8.180	8.180	8.180	7.780	8.030	—	668	841	841	841	841	—	—
9.380	—	9.380	9.380	9.380	7.780	8.030	—	783	957	957	885	957	—	—
10.900	—	10.900	10.900	10.900	7.780	8.030	—	926	1,101	1,101	885	1,005	—	—
12.970	—	11.800	11,630	12,680	7.780	8.030	—	1,116	1,293	1,293	885	1,005	—	—
9.470	—	9.470	9.470	9.470	9,000	9,470	—	769	960	960	960	960	922	922
10.860	—	10.860	10.860	10.860	9,000	10.860	—	901	1,093	1,093	967	1,093	1,008	979
12.620	—	11.800	12,620	12,620	8,030	8,030	—	1,066	1,258	1,258	967	1,237	1,120	979
14.190	—	11.800	12,680	12,680	8,030	8,030	—	1,210	1,402	1,402	967	1,237	—	—
15.020	—	11.800	12,680	12,680	8,030	8,030	—	1,285	1,477	1,477	1,005	1,287	—	—
15.780	—	11.800	12,680	12,680	8,030	8,030	—	1,353	1,545	1,545	967	1,237	—	—
10.760	—	10.760	10.760	—	8,030	—	—	861	1,052	—	1,052	—	—	—
12.340	—	11.800	12,340	—	8,030	—	—	1,009	1,197	—	1,086	—	—	—
14.340	—	11.800	12,680	—	8,030	—	—	1,194	1,379	—	1,086	—	—	—
16.120	—	11.800	12,680	—	—	—	—	1,355	1,536	—	—	—	—	—
17.070	—	11.800	12,680	—	8,030	—	—	1,439	1,619	—	1,086	—	—	—
17.930	—	11.800	12,680	—	—	—	—	1,515	1,673	—	—	—	—	—
12.910	—	11.800	12,680	—	8,030	—	—	1,030	1,252	—	1,252	—	—	—
14.800	—	11.800	12,680	—	8,030	—	—	1,207	1,424	—	1,287	—	—	—
17.210	—	11.800	12,680	—	8,030	—	—	1,428	1,640	—	1,287	—	—	—
20.480	—	11.800	12,680	—	8,030	—	—	1,721	1,926	—	1,287	—	—	—
2.470	2.470	—	—	—	—	—	233	—	—	—	—	—	—	—
2.860	2.860	—	—	—	—	—	279	—	—	—	—	—	—	—
2.950	2.950	—	—	—	—	—	244	—	—	—	—	—	—	—
3.930	3.930	3.930	3.930	3.930	3.930	3.930	372	417	579	579	579	579	686	686
4.460	4.460	4.460	4.460	4.460	4.060	4.460	434	486	654	654	654	654	688	688
2.950	2.950	—	—	—	—	—	263	—	—	—	—	—	—	—
3.930	3.930	3.930	3.930	3.930	3.930	3.930	402	452	690	690	690	690	869	869
4.460	4.460	4.460	4.460	4.460	4.060	4.460	468	526	780	780	780	780	871	871
6.090	—	6.090	6.090	—	5.530	—	—	648	847	—	839	—	871	871
6.850	—	6.850	6.850	—	5.530	—	—	742	947	—	839	—	942	886
7.610	—	7.610	—	—	5.530	—	—	834	1,046	—	839	—	1,007	886
8.480	—	8.480	8.480	—	5.530	—	—	939	1,157	—	839	—	1,007	886
6.490	—	6.490	6.490	6.490	5.900	6.490	—	678	864	—	839	—	871	871
7.300	—	7.300	7.300	7.300	5.900	7.300	—	776	966	—	839	—	942	886
8.120	—	8.120	8.120	8.120	5.900	8.110	—	874	1,066	—	839	—	1,007	886
9.040	—	9.040	9.040	9.040	5.900	8.110	—	983	1,180	—	839	—	1,007	886
6.490	—	6.490	6.490	6.490	5.900	6.340	—	688	895	895	883	895	917	917
7.300	—	7.300	7.300	7.300	5.900	6.340	—	788	1,001	1,001	883	1,001	992	932
8.120	—	8.120	8.120	8.120	5.900	6.340	—	887	1,105	1,105	883	1,103	1,060	932
9.040	—	9.040	9.040	9.040	5.900	6.340	—	997	1,222	1,222	883	1,103	1,060	932

** Some joint strengths listed in Col. 20 through 27 are greater than the corresponding pipe body yield strength listed in Col. 12.

† Internal pressure resistance is the lowest of the internal yield pressure of the pipe, the internal yield pressure of the coupling, or the internal pressure leak resistance at the E₁ or E₂ plane.

‡ For P-110 casing the next higher grade is 150Y5, a non-API steel grade having a minimum yield strength of 150,000 psi.

TABLE 2.3—MINIMUM PERFORMANCE PROPERTIES OF CASING (continued)

1	2	3	4	5	6	7	8	9	10	11	12
OD (in.)	Nominal Weight, Threads and Coupling (lbm/ft)	Grade	Wall Thickness (in.)	ID (in.)	Threaded and Coupled			Extreme Line			Pipe-Body Yield Strength (1,000 lb/ft)
					Drift Diameter (in.)	OD of Coupling (in.)	OD Special Clearance Coupling (in.)	Drift Diameter (in.)	OD of Box Powertight (in.)	Collapse Resistance (psi)	
8 $\frac{5}{8}$	36.00	N-80	0.400	7.825	7.700	9.625	9.125	7.700	9.120	4,100	827
	40.00	N-80	0.450	7.725	7.600	9.625	9.125	7.600	9.120	5,520	925
	44.00	N-80	0.500	7.625	7.500	9.625	9.125	7.500	9.120	6,950	1,021
	49.00	N-80	0.557	7.511	7.386	9.625	9.125	7.386	9.120	8,580	1,129
	36.00	C-90	0.400	7.825	7.700	9.625	9.125	7.700	9.120	4,250	930
	40.00	C-90	0.450	7.725	7.600	9.625	9.125	7.600	9.120	5,870	1,040
	44.00	C-90	0.500	7.625	7.500	9.625	9.125	7.500	9.120	7,490	1,149
	49.00	C-90	0.557	7.511	7.386	9.625	9.125	7.386	9.120	9,340	1,271
	36.00	C-95	0.400	7.825	7.700	9.625	9.125	7.700	9.120	4,350	982
	40.00	C-95	0.450	7.725	7.600	9.625	9.125	7.600	9.120	6,020	1,098
	44.00	C-95	0.500	7.625	7.500	9.625	9.125	7.500	9.120	7,740	1,212
	49.00	C-95	0.557	7.511	7.386	9.625	9.125	7.386	9.120	9,710	1,341
	36.00	HC-95	0.400	7.825	7.700	9.625	9.125	—	—	6,060	982
	40.00	HC-95	0.450	7.725	7.600	9.625	9.125	—	—	7,900	1,098
	44.00	HC-95	0.500	7.625	7.500	9.625	9.125	—	—	9,100	1,212
	49.00	HC-95	0.557	7.511	7.386	9.625	9.125	—	—	10,400	1,341
	40.00	P-110	0.450	7.725	7.600	9.625	9.125	7.600	9.120	6,390	1,271
	44.00	P-110	0.500	7.625	7.500	9.625	9.125	7.500	9.120	8,420	1,404
	49.00	P-110	0.557	7.511	7.386	9.625	9.125	7.386	9.120	10,740	1,553
	40.00	Q-125	0.450	7.725	7.600	9.625	9.125	—	—	6,630	1,445
	44.00	Q-125	0.500	7.625	7.500	9.625	9.125	—	—	8,980	1,595
	49.00	Q-125	0.557	7.511	7.386	9.625	9.125	—	—	11,660	1,765
	44.00	V-150	0.500	7.625	7.500	9.625	9.125	—	—	9,640	1,914
	49.00	V-150	0.557	7.511	7.386	9.625	9.125	—	—	12,950	2,118
9 $\frac{5}{8}$	32.30	H-40	0.312	9.001	8.845	10.625	—	—	—	1,370	365
	36.00	H-40	0.352	8.921	8.765	10.625	—	—	—	1,720	410
	36.00	J-55	0.352	8.921	8.765	10.625	10.125	—	—	2,020	564
	40.00	J-55	0.395	8.835	8.679	10.625	10.125	8.599	10.100	2,570	630
	36.00	K-55	0.352	8.921	8.765	10.625	10.125	—	—	2,020	564
	40.00	K-55	0.395	8.835	8.679	10.625	10.125	8.599	10.100	2,570	630
	40.00	C-75	0.395	8.835	8.679	10.625	10.125	8.599	10.100	2,990	859
	43.50	C-75	0.435	8.755	8.599	10.625	10.125	8.599	10.100	3,730	942
	47.00	C-75	0.472	8.681	8.525	10.625	10.125	8.525	10.100	4,610	1,018
	53.50	C-75	0.545	8.535	8.379	10.625	10.125	8.379	10.100	6,350	1,166
	40.00	L-80	0.395	8.835	8.679	10.625	10.125	8.599	10.100	3,090	916
	43.50	L-80	0.435	8.755	8.599	10.625	10.125	8.599	10.100	3,810	1,005
	47.00	L-80	0.472	8.681	8.525	10.625	10.125	8.525	10.100	4,760	1,086
	53.50	L-80	0.545	8.535	8.379	10.625	10.125	8.379	10.100	6,620	1,244
	40.00	N-80	0.395	8.835	8.679	10.625	10.125	8.599	10.100	3,090	916
	43.50	N-80	0.435	8.755	8.599	10.625	10.125	8.599	10.100	3,810	1,005
	47.00	N-80	0.472	8.681	8.525	10.625	10.125	8.525	10.100	4,760	1,086
	53.50	N-80	0.545	8.535	8.379	10.625	10.125	8.379	10.100	6,620	1,244
	40.00	C-90	0.395	8.835	8.679	10.625	10.125	8.599	10.100	3,250	1,031
	43.50	C-90	0.435	8.755	8.599	10.625	10.125	8.599	10.100	4,010	1,130
	47.00	C-90	0.472	8.681	8.525	10.625	10.125	8.525	10.100	5,000	1,221
	53.50	C-90	0.545	8.535	8.379	10.625	10.125	8.379	10.100	7,120	1,399
	40.00	C-95	0.395	8.835	8.679	10.625	10.125	8.599	10.100	3,320	1,088
	43.50	C-95	0.435	8.755	8.599	10.625	10.125	8.599	10.100	4,120	1,193
	47.00	C-95	0.472	8.681	8.525	10.625	10.125	8.525	10.100	5,090	1,289
	53.50	C-95	0.545	8.535	8.379	10.625	10.125	8.379	10.100	7,340	1,477
	40.00	HC-95	0.395	8.835	8.679	10.625	10.125	—	—	4,230	1,088
	43.50	HC-95	0.435	8.755	8.599	10.625	10.125	—	—	5,600	1,193
	47.00	HC-95	0.472	8.681	8.525	10.625	10.125	—	—	7,100	1,289
	53.50	HC-95	0.545	8.535	8.379	10.625	10.125	—	—	8,850	1,477
	58.40	HC-95	0.595	8.435	8.279	10.625	10.125	—	—	9,950	1,604
	61.10	HC-95	0.625	8.375	8.219	10.625	10.125	—	—	10,500	1,679
	43.50	P-110	0.435	8.755	8.599	10.625	10.125	8.599	10.100	4,420	1,381
	47.00	P-110	0.472	8.681	8.525	10.625	10.125	8.525	10.100	5,300	1,493
	53.50	P-110	0.545	8.535	8.379	10.625	10.125	8.379	10.100	7,950	1,710

*Non-API weights or grades.

TABLE 2.3—MINIMUM PERFORMANCE PROPERTIES OF CASING (continued)

13	14	15	16	17	18	19	20	21	22	23	24	25	26	27
Joint Strength** (1,000 lbf)														
Internal Pressure Resistance† (psi)							Threaded and Coupled							
Plain End or Extreme Line	Buttress Thread						Buttress Thread							
	Round Thread		Regular Coupling		Special Clearance Coupling		Round Thread		Regular Coupling		Special Clearance Coupling		Extreme Line	
	Short	Long	Same Grade	Higher Grade	Same Grade	Higher Grade	Short	Long	Regular Coupling	Higher Grade†	Special Clearance Coupling	Higher Grade†	Standard Joint	Optional Joint
7.300	—	7.300	7.300	—	6.340	—	—	749	928	—	883	—	917	917
8.220	—	8.220	8.220	—	6.340	—	—	858	1.038	—	883	—	992	992
9.130	—	9.130	9.130	—	6.340	—	—	965	1.146	—	883	—	1.060	932
10.170	—	10.170	10.170	—	6.340	—	—	1.085	1.268	—	883	—	1.060	932
7.710	—	7.710	7.710	—	6.340	—	—	789	976	—	927	—	963	963
8.670	—	8.670	8.670	—	6.340	—	—	904	1.092	—	927	—	1.042	979
9.640	—	9.640	9.640	—	6.340	—	—	1.017	1.206	—	927	—	1.113	979
10.740	—	10.380	10.740	—	6.340	—	—	1.114	1.334	—	927	—	1.113	979
7.710	—	7.710	7.710	7.710	6.340	6.340	—	800	1.008	1.008	971	1.008	—	—
8.670	—	8.670	8.670	8.670	6.340	6.340	—	916	1.127	1.127	971	1.104	—	—
9.640	—	9.640	9.640	9.640	6.340	6.340	—	1.030	1.244	1.244	971	1.104	—	—
10.740	—	10.380	10.740	10.740	6.340	6.340	—	1.159	1.377	1.377	971	1.104	—	—
10.040	—	10.040	10.040	10.040	6.340	6.340	—	1.055	1.288	1.288	1.103	1.288	1.240	1.165
11.160	—	10.380	11.160	11.160	6.340	6.340	—	1.186	1.423	1.423	1.103	1.412	1.326	1.165
12.430	—	10.380	11.230	11.230	6.340	6.340	—	1.335	1.574	1.574	1.103	1.412	1.326	1.165
11.410	—	10.380	11.230	—	6.340	—	—	1.182	1.415	—	1.192	—	—	—
12.680	—	10.380	11.230	—	6.340	—	—	1.330	1.562	—	1.192	—	—	—
14.130	—	10.380	11.230	—	6.340	—	—	1.496	1.728	—	—	—	—	—
15.220	—	10.380	11.230	—	6.340	—	—	1.591	1.859	—	1.413	—	—	—
16.950	—	10.380	11.230	—	6.340	—	—	1.789	2.056	—	1.413	—	—	—
2.270	2.270	—	—	—	—	—	254	—	—	—	—	—	—	—
2.560	2.560	—	—	—	—	—	294	—	—	—	—	—	—	—
3.520	3.520	3.520	3.520	3.520	3.520	3.520	394	453	639	639	639	639	—	—
3.950	3.950	3.950	3.950	3.950	3.660	3.950	452	520	714	714	714	714	770	770
3.520	3.520	3.520	3.520	3.520	3.520	3.520	423	489	755	755	755	755	—	—
3.950	3.950	3.950	3.950	3.950	3.660	3.950	486	561	843	843	843	843	975	975
5.390	—	5.390	5.390	—	4.990	—	—	694	926	—	926	—	975	975
5.930	—	5.930	5.930	—	4.990	—	—	776	1.016	—	934	—	975	975
6.440	—	6.440	6.440	—	4.990	—	—	852	1.098	—	934	—	1.032	1.032
7.430	—	7.430	7.430	—	4.990	—	—	999	1.257	—	934	—	1.173	1.053
5.750	—	5.750	5.750	—	5.140	—	—	727	947	—	934	—	975	975
6.330	—	6.330	6.330	—	5.140	—	—	813	1.038	—	934	—	975	975
6.870	—	6.870	6.870	—	5.140	—	—	893	1.122	—	934	—	1.032	1.032
7.930	—	7.930	7.930	—	5.140	—	—	1.047	1.286	—	934	—	1.173	1.053
5.750	—	5.750	5.750	5.750	5.140	5.140	—	737	979	979	979	979	1.027	1.027
6.330	—	6.330	6.330	6.330	5.140	5.140	—	825	1.074	1.074	983	1.074	1.027	1.027
6.870	—	6.870	6.870	6.870	5.140	5.140	—	905	1.161	1.161	983	1.161	1.086	1.086
7.930	—	7.930	7.930	7.930	5.140	5.140	—	1.062	1.329	1.329	983	1.229	1.235	1.109
6.460	—	6.460	6.460	—	5.140	—	—	804	1.021	—	983	—	1.027	1.027
7.120	—	7.120	7.120	—	5.140	—	—	899	1.119	—	983	—	1.027	1.027
7.720	—	7.720	7.720	—	5.140	—	—	987	1.210	—	983	—	1.086	1.086
8.920	—	8.460	8.920	—	5.140	—	—	1.157	1.386	—	983	—	1.235	1.109
6.820	—	6.820	6.820	—	5.140	—	—	847	1.074	—	1.032	—	1.078	1.078
7.510	—	7.510	7.510	—	5.140	—	—	948	1.178	—	1.032	—	1.078	1.078
8.150	—	8.150	8.150	—	5.140	—	—	1.040	1.273	—	1.032	—	1.141	1.141
9.410	—	8.460	8.460	—	5.140	—	—	1.220	1.458	—	1.032	—	1.297	1.164
6.820	—	6.820	6.820	6.820	5.140	5.140	—	858	1.106	1.106	1.082	1.106	—	—
7.510	—	7.510	7.510	7.510	5.140	5.140	—	959	1.213	1.213	1.082	1.213	—	—
8.150	—	8.150	8.150	8.150	5.140	5.140	—	1.053	1.311	1.311	1.082	1.229	—	—
9.410	—	8.460	9.160	9.160	5.140	5.140	—	1.235	1.502	1.502	1.082	1.229	—	—
10.280	—	8.460	9.160	9.160	5.140	5.140	—	1.357	1.631	1.631	1.082	1.229	—	—
10.800	—	8.460	9.160	9.160	5.140	5.140	—	1.430	1.707	1.707	1.082	1.229	—	—
8.700	—	8.700	8.700	8.700	5.140	5.140	—	1.106	1.388	1.388	1.229	1.388	1.283	1.283
9.440	—	9.440	9.160	9.160	5.140	5.140	—	1.213	1.500	1.500	1.229	1.500	1.358	1.358
10.900	—	9.670	9.160	9.160	5.140	5.140	—	1.422	1.718	1.718	1.229	1.573	1.544	1.386

** Some joint strengths listed in Col. 20 through 27 are greater than the corresponding pipe body yield strength listed in Col. 12.

† Internal pressure resistance is the lowest of the internal yield pressure of the pipe, the internal yield pressure of the coupling, or the internal pressure leak resistance at the E₁ or E₂ plane.

‡ For P-110 casing the next higher grade is 150YS, a non-API steel grade having a minimum yield strength of 150,000 psi.

TABLE 2.3—MINIMUM PERFORMANCE PROPERTIES OF CASING (continued)

1	2	3	4	5	6	7	8	9	10	11	12
OD (in.)	Nominal Weight, Threads and Coupling (lbm/ft)	Grade	Wall Thickness (in.)	ID (in.)	Threaded and Coupled			Extreme Line		Collapse Resistance (psi)	Pipe-Body Yield Strength (1,000 lbf)
					Drift Diameter (in.)	OD of Coupling (in.)	OD Special Clearance Coupling (in.)	Drift Diameter (in.)	OD of Box Powertight (in.)		
9 $\frac{5}{8}$	47.00	Q-125	0.472	8.681	8.525	10.625	—	—	—	5,640	1,697
	53.50	Q-125	0.545	8.535	8.379	10.625	—	—	—	8,440	1,943
	* 58.40	Q-125	0.595	8.435	8.279	10.625	10.125	—	—	10,530	2,110
	* 61.10	Q-125	0.625	8.375	8.219	10.625	10.125	—	—	11,800	2,209
	* 53.50	V-150	0.545	8.535	8.379	10.625	10.125	—	—	8,960	2,332
	* 58.40	V-150	0.595	8.435	8.279	10.625	10.125	—	—	11,560	2,532
	* 61.10	V-150	0.625	8.375	8.219	10.625	10.125	—	—	13,120	2,651
	* 70.30	V-150	0.734	8.157	8.001	10.625	10.125	—	—	18,800	3,075
10 $\frac{3}{4}$	32.75	H-40	0.279	10.192	10.036	11.750	—	—	—	840	367
	40.50	H-40	0.350	10.050	9.894	11.750	—	—	—	1,390	457
	40.50	J-55	0.350	10.050	9.894	11.750	11.250	—	—	1,580	629
	45.50	J-55	0.400	9.950	9.794	11.750	11.250	9.794	11.460	2,090	715
	51.00	J-55	0.450	9.850	9.694	11.750	11.250	9.694	11.460	2,700	801
	40.50	K-55	0.350	10.050	9.894	11.750	11.250	—	—	1,580	629
	45.50	K-55	0.400	9.950	9.794	11.750	11.250	9.794	11.430	2,090	715
	51.00	K-55	0.450	9.850	9.694	11.750	11.250	9.694	11.460	2,700	801
	51.00	C-75	0.450	9.850	9.694	11.750	11.250	9.694	11.460	3,110	1,092
	55.50	C-75	0.495	9.760	9.604	11.750	11.250	9.604	11.460	3,920	1,196
	51.00	L-80	0.450	9.850	9.694	11.750	11.250	9.694	11.460	3,220	1,165
	55.50	L-80	0.495	9.760	9.604	11.750	11.250	9.604	11.460	4,020	1,276
	51.00	N-80	0.450	9.850	9.694	11.750	11.250	9.694	11.460	3,220	1,165
	55.50	N-80	0.495	9.760	9.604	11.750	11.250	9.604	11.460	4,020	1,276
	51.00	C-90	0.450	9.850	9.694	11.750	11.250	9.694	11.460	3,400	1,310
	55.50	C-90	0.495	9.760	9.604	11.750	11.250	9.604	11.460	4,160	1,435
	51.00	C-95	0.450	9.850	9.694	11.750	11.250	9.694	11.460	3,480	1,383
	55.50	C-95	0.495	9.760	9.604	11.750	11.250	9.604	11.460	4,290	1,515
	* 51.00	HC-95	0.450	9.850	9.694	11.750	11.250	—	—	4,460	1,383
	* 55.50	HC-95	0.495	9.760	9.604	11.750	11.250	—	—	5,950	1,515
	* 60.70	HC-95	0.545	9.660	9.504	11.750	11.250	—	—	7,550	1,660
	* 65.70	HC-95	0.595	9.560	9.404	11.750	11.250	—	—	8,640	1,803
	* 71.10	HC-95	0.650	9.450	9.294	11.750	11.250	—	—	9,600	1,959
	51.00	P-110	0.450	9.850	9.694	11.750	11.250	9.694	11.460	3,660	1,602
	55.50	P-110	0.495	9.760	9.604	11.750	11.250	9.604	11.460	4,610	1,754
	60.70	P-110	0.545	9.660	9.504	11.750	11.250	9.504	11.460	5,880	1,922
	65.70	P-110	0.595	9.560	9.404	11.750	11.250	—	—	7,500	2,088
	* 55.50	Q-125	0.495	9.760	9.604	11.750	11.250	—	—	4,850	1,993
	60.70	Q-125	0.545	9.660	9.504	11.750	11.250	—	—	6,070	2,184
	65.70	Q-125	0.595	9.560	9.404	11.750	11.250	—	—	7,920	2,373
	* 71.10	Q-125	0.650	9.450	9.294	11.750	11.250	—	—	9,990	2,573
	* 73.20	Q-125	0.672	9.406	9.250	11.750	11.250	—	—	10,810	2,660
	* 79.20	Q-125	0.734	9.282	9.126	11.750	11.250	—	—	13,150	2,887
	60.70	V-150	0.545	9.660	9.504	11.750	11.250	—	—	6,550	2,621
	* 65.70	V-150	0.595	9.560	9.404	11.750	11.250	—	—	8,320	2,847
	* 71.10	V-150	0.650	9.450	9.294	11.750	11.250	—	—	10,880	3,094
	* 73.20	V-150	0.672	9.406	9.250	11.750	11.250	—	—	11,900	3,191
	* 79.20	V-150	0.734	9.282	9.126	11.750	11.250	—	—	14,790	3,464
11 $\frac{3}{4}$	42.00	H-40	0.333	11.084	10.928	12.750	—	—	—	1,070	478
	47.00	J-55	0.375	11.000	10.844	12.750	—	—	—	1,510	737
	54.00	J-55	0.435	10.880	10.724	12.750	—	—	—	2,070	850
	60.00	J-55	0.489	10.772	10.616	12.750	—	—	—	2,660	952
	47.00	K-55	0.375	11.000	10.844	12.750	—	—	—	1,510	737
	54.00	K-55	0.435	10.880	10.724	12.750	—	—	—	2,070	850
	60.00	K-55	0.489	10.772	10.616	12.750	—	—	—	2,660	952

*Non-API weights or grades.

TABLE 2.3—MINIMUM PERFORMANCE PROPERTIES OF CASING (continued)

13	14	15	16	17	18	19	20	21	22	23	24	25	26	27
Internal Pressure Resistance† (psi)							Joint Strength** (1 000 lbf)							
Plain End or Extreme Line	Threaded and Coupled						Threaded and Coupled							
	Buttress Thread						Buttress Thread							
	Round Thread		Regular Coupling		Special Clearance Coupling		Round Thread		Regular Coupling		Special Clearance Coupling		Special Clearance Coupling	
	Same Grade	Higher Grade	Same Grade	Higher Grade	Same Grade	Higher Grade	Short	Long	Regular Coupling	Higher Grade†	Clearance Coupling	Higher Grade†	Standard Joint	Optional Joint
10,730	—	9,670	9,160	—	5,140	—	—	1,361	1,650	—	—	—	—	—
12,390	—	9,670	9,160	—	5,140	—	—	1,595	1,890	—	—	—	—	—
13,520	—	9,670	9,160	—	5,140	—	—	1,754	2,052	—	1,328	—	—	—
14,200	—	9,670	9,160	—	5,140	—	—	1,848	2,149	—	1,328	—	—	—
12,390	—	9,670	9,160	—	5,140	—	—	1,595	2,251	—	1,574	—	—	—
13,520	—	9,670	9,160	—	5,140	—	—	1,754	2,444	—	1,574	—	—	—
14,200	—	9,670	9,160	—	5,140	—	—	1,848	2,559	—	1,574	—	—	—
16,680	—	9,670	9,160	—	5,140	—	—	2,185	2,812	—	1,574	—	—	—
1,820	1,820	—	—	—	—	—	205	—	—	—	—	—	—	—
2,280	2,280	—	—	—	—	—	314	—	—	—	—	—	—	—
3,130	3,130	—	3,130	3,130	3,130	3,130	420	—	700	700	700	700	—	—
3,580	3,580	—	3,580	3,580	3,290	3,580	493	—	796	796	796	796	975	—
4,030	4,030	—	4,030	4,030	3,290	4,030	565	—	891	891	822	891	1,092	—
3,130	3,130	—	3,130	3,130	3,130	3,130	450	—	819	819	819	819	—	—
3,580	3,580	—	3,580	3,580	3,290	3,580	528	—	931	931	931	931	1,236	—
4,030	4,030	—	4,030	4,030	3,290	4,030	606	—	1,043	1,043	1,041	1,043	1,383	—
5,490	5,490	—	5,490	—	4,150	—	756	—	1,160	—	1,041	—	1,383	—
6,040	6,040	—	6,040	—	4,150	—	843	—	1,271	—	1,041	—	1,515	—
5,860	5,860	—	5,860	—	4,150	—	794	—	1,190	—	1,041	—	1,383	—
6,450	6,450	—	6,450	—	4,150	—	884	—	1,303	—	1,041	—	1,515	—
5,860	5,860	—	5,860	5,860	4,150	4,150	804	—	1,228	1,228	1,096	1,228	1,456	—
6,450	6,450	—	6,450	6,450	4,150	4,150	895	—	1,345	1,345	1,096	1,345	1,595	—
6,590	6,590	—	6,590	—	4,150	—	692	—	1,287	—	1,112	—	1,456	—
7,250	6,880	—	7,250	—	4,150	—	771	—	1,409	—	1,112	—	1,595	—
6,960	6,880	—	6,960	—	4,150	—	927	—	1,354	—	1,151	—	1,529	—
7,660	6,880	—	7,450	—	4,150	—	1,032	—	1,483	—	1,151	—	1,675	—
6,960	6,880	—	6,960	6,960	4,150	4,150	737	—	1,392	1,392	1,223	1,389	—	—
7,660	6,880	—	7,450	7,450	4,150	4,150	821	—	1,524	1,524	1,223	1,389	—	—
8,430	6,880	—	7,450	7,450	4,150	4,150	914	—	1,670	1,670	1,223	1,389	—	—
9,200	6,880	—	7,450	7,450	4,150	4,150	1,005	—	1,814	1,814	1,223	1,389	—	—
10,050	6,880	—	7,450	7,450	4,150	4,150	1,105	—	1,971	1,971	1,223	1,389	—	—
8,060	7,860	—	7,450	7,450	4,150	4,150	1,080	—	1,594	1,594	1,370	1,594	1,820	—
8,860	7,860	—	7,450	7,450	4,150	4,150	1,203	—	1,745	1,745	1,370	1,745	1,993	—
9,760	7,860	—	7,450	7,450	4,150	4,150	1,338	—	1,912	1,912	1,370	1,754	2,000	—
10,650	7,860	—	7,450	7,450	4,150	4,150	1,472	—	2,077	2,077	1,370	1,754	—	—
10,070	7,860	—	7,450	—	4,150	—	1,351	—	1,925	—	1,501	—	—	—
11,090	7,860	—	7,450	—	—	—	1,503	—	2,109	—	1,501	—	—	—
12,110	7,860	—	7,450	—	—	—	1,653	—	2,291	—	1,501	—	—	—
13,230	7,860	—	7,450	—	4,150	—	1,817	—	2,489	—	1,501	—	—	—
13,670	7,860	—	7,450	—	4,150	—	1,882	—	2,568	—	1,501	—	—	—
14,940	7,860	—	7,450	—	4,150	—	2,063	—	2,639	—	1,501	—	—	—
13,310	7,860	—	7,450	—	4,150	—	1,798	—	2,513	—	1,779	—	—	—
14,530	7,860	—	7,450	—	4,150	—	1,918	—	2,730	—	1,779	—	—	—
15,870	7,860	—	7,450	—	4,150	—	2,174	—	2,966	—	1,779	—	—	—
16,410	7,860	—	7,450	—	4,150	—	2,252	—	3,060	—	1,779	—	—	—
17,920	7,860	—	7,450	—	4,150	—	2,469	—	3,127	—	1,779	—	—	—
1,980	1,980	—	—	—	—	—	307	—	—	—	—	—	—	—
3,070	3,070	—	3,070	3,070	—	—	477	—	807	807	—	—	—	—
3,560	3,560	—	3,560	3,560	—	—	568	—	931	931	—	—	—	—
4,010	4,010	—	4,010	4,010	—	—	649	—	1,042	1,042	—	—	—	—
3,070	3,070	—	3,070	3,070	—	—	509	—	935	935	—	—	—	—
3,560	3,560	—	3,560	3,560	—	—	606	—	1,079	1,079	—	—	—	—
4,010	4,010	—	4,010	4,010	—	—	693	—	1,208	1,208	—	—	—	—

**Some joint strengths listed in Col. 20 through 27 are greater than the corresponding pipe body yield strength listed in Col. 12.

† Internal pressure resistance is the lowest of the internal yield pressure of the pipe, the internal yield pressure of the coupling, or the internal pressure leak resistance at the E₁ or E₂ plane.

‡ For P-110 casing the next higher grade is 150YS—a non-API steel grade having a minimum yield strength of 150,000 psi.

TABLE 2.3—MINIMUM PERFORMANCE PROPERTIES OF CASING (continued)

1	2	3	4	5	6	7	8	9	10	11	12
OD (in.)	Nominal Weight, Threads and Coupling (lbm/ft)	Grade	Wall Thickness (in.)	ID (in.)	Threaded and Coupled			Extreme Line			Pipe-Body Yield Strength (1,000 lbf)
					Drift Diameter (in.)	OD of Coupling (in.)	OD Special Clearance Coupling (in.)	Drift Diameter (in.)	OD of Box Powertight (in.)	Collapse Resistance (psi)	
11¾	60.00	C-75	0.489	10.772	10.616	12.750	—	—	—	3,070	1,298
	60.00	L-80	0.489	10.772	10.616	12.750	—	—	—	3,180	1,384
	60.00	N-80	0.489	10.772	10.616	12.750	—	—	—	3,180	1,384
	60.00	C-90	0.489	10.772	10.616	12.750	—	—	—	3,360	1,557
	60.00	C-95	0.489	10.772	10.616	12.750	—	—	—	3,440	1,644
*	60.00	HC-95	0.489	10.772	10.616	12.750	—	—	—	4,410	1,644
	60.00	P-110	0.489	10.772	10.616	12.750	—	—	—	3,610	1,903
	60.00	Q-125	0.489	10.772	10.616	12.750	—	—	—	3,680	2,162
*	66.70	Q-125	0.547	10.656	10.500	12.750	—	—	—	4,980	2,407
*	66.70	V-150	0.547	10.656	10.500	12.750	—	—	—	5,200	2,888
13¾	48.00	H-40	0.330	12.715	12.559	14.375	—	—	—	740	541
	54.50	J-55	0.380	12.615	12.459	14.375	—	—	—	1,130	853
	61.00	J-55	0.430	12.515	12.359	14.375	—	—	—	1,540	962
	68.00	J-55	0.480	12.415	12.259	14.375	—	—	—	1,950	1,069
	54.50	K-55	0.380	12.615	12.459	14.375	—	—	—	1,130	853
	61.00	K-55	0.430	12.515	12.359	14.375	—	—	—	1,640	962
	68.00	K-55	0.480	12.415	12.259	14.375	—	—	—	1,950	1,069
	68.00	C-75	0.480	12.415	12.259	14.375	—	—	—	2,220	1,458
	72.00	C-75	0.514	12.347	12.191	14.375	—	—	—	2,600	1,558
	68.00	L-80	0.480	12.415	12.259	14.375	—	—	—	2,260	1,556
	72.00	L-80	0.514	12.347	12.191	14.375	—	—	—	2,670	1,661
	68.00	N-80	0.480	12.415	12.259	14.375	—	—	—	2,260	1,556
	72.00	N-80	0.514	12.347	12.191	14.375	—	—	—	2,670	1,661
	68.00	C-90	0.480	12.415	12.259	14.375	—	—	—	2,320	1,750
	72.00	C-90	0.514	12.347	12.191	14.375	—	—	—	2,780	1,869
	68.00	C-95	0.480	12.415	12.259	14.375	—	—	—	2,330	1,847
	72.00	C-95	0.514	12.347	12.191	14.375	—	—	—	2,820	1,973
*	72.00	HC-95	0.514	12.347	12.191	14.375	—	—	—	3,470	1,973
*	86.00	HC-95	0.625	12.125	11.969	14.375	—	—	—	6,240	2,378
	68.00	P-110	0.480	12.415	12.259	14.375	—	—	—	2,330	2,139
	72.00	P-110	0.514	12.347	12.191	14.375	—	—	—	2,880	2,284
	72.00	Q-125	0.514	12.347	12.191	14.375	—	—	—	2,800	2,596
*	76.60	Q-125	0.547	12.281	12.125	14.375	—	—	—	3,490	2,756
*	92.50	Q-125	0.672	12.031	11.875	14.375	—	—	—	5,950	3,352
*	92.50	V-150	0.672	12.031	11.875	14.375	—	—	—	6,400	4,023
*	100.30	V-150	0.734	11.907	11.751	14.375	—	—	—	8,090	4,373
16	65.00	H-40	0.375	15.250	15.062	17.000	—	—	—	630	736
	75.00	J-55	0.438	15.124	14.936	17.000	—	—	—	1,020	1,178
	84.00	J-55	0.495	15.010	14.822	17.000	—	—	—	1,410	1,326
	75.00	K-55	0.438	15.124	14.936	17.000	—	—	—	1,020	1,178
	84.00	K-55	0.495	15.010	14.822	17.000	—	—	—	1,410	1,326
18½	87.50	H-40	0.435	17.755	17.567	20.000	—	—	—	630*	994
	87.50	J-55	0.435	17.755	17.567	20.000	—	—	—	630*	1,367
	87.50	K-55	0.435	17.755	17.567	20.000	—	—	—	630*	1,367
20	94.00	H-40	0.438	19.124	18.936	21.000	—	—	—	520*	1,077
	94.00	J-55	0.438	19.124	18.936	21.000	—	—	—	520*	1,480
	106.50	J-55	0.500	19.000	18.812	21.000	—	—	—	770*	1,685
	133.00	J-55	0.635	18.730	18.542	21.000	—	—	—	1,500	2,125
	94.00	K-55	0.438	19.124	18.936	21.000	—	—	—	520*	1,480
	106.50	K-55	0.500	19.000	18.812	21.000	—	—	—	770*	1,685
	133.00	K-55	0.635	18.730	18.542	21.000	—	—	—	1,500	2,125

*Non-API weights or grades.

TABLE 2.3—MINIMUM PERFORMANCE PROPERTIES OF CASING (continued)

13	14	15	16	17	18	19	20	21	22	23	24	25	26	27
Joint Strength** (1,000 lbf)														
Internal Pressure Resistance† (psi)							Threaded and Coupled							
Plain End or Extreme Line	Round Thread		Buttress Thread				Buttress Thread							
			Regular Coupling		Special Clearance Coupling		Round Thread		Regular Coupling		Special Clearance Coupling		Extreme Line	
	Short	Long	Same Grade	Higher Grade	Same Grade	Higher Grade	Short	Long	Regular Coupling	Higher Grade‡	Special Clearance Coupling	Higher Grade‡	Standard Joint	Optional Joint
5.460	5.460	—	5.460	—	—	—	869	—	1,361	—	—	—	—	—
5.830	5.820	—	5.830	—	—	—	913	—	1,399	—	—	—	—	—
5.830	5.820	—	5.830	—	—	—	924	—	1,440	1,440	—	—	—	—
6.550	5.820	—	6,300	—	—	—	1,011	—	1,517	—	—	—	—	—
6.920	5.820	—	6,300	—	—	—	1,066	—	1,596	—	—	—	—	—
6.920	5.820	—	6,300	—	—	—	1,078	—	1,638	—	—	—	—	—
8.010	5.820	—	6,300	6,300	—	—	1,242	—	1,877	1,877	—	—	—	—
9.100	6.650	—	6,300	—	—	—	1,395	—	2,074	—	—	—	—	—
10.180	6.650	—	6,300	—	—	—	1,582	—	2,308	—	—	—	—	—
12.220	6.650	—	6,300	—	—	—	1,893	—	2,752	—	—	—	—	—
1.730	1.730	—	—	—	—	—	322	—	—	—	—	—	—	—
2.730	2.730	—	2,730	2,730	—	—	514	—	909	909	—	—	—	—
3.090	3.090	—	3,090	3,090	—	—	595	—	1,025	1,025	—	—	—	—
3.450	3.450	—	3,450	3,450	—	—	675	—	1,140	1,140	—	—	—	—
2.730	2.730	—	2,730	2,730	—	—	547	—	1,038	1,038	—	—	—	—
3.090	3.090	—	3,090	3,090	—	—	633	—	1,169	1,169	—	—	—	—
3.450	3.450	—	3,450	3,450	—	—	718	—	1,300	1,300	—	—	—	—
4.710	4.550	—	4,710	—	—	—	905	—	1,496	—	—	—	—	—
5.040	4.550	—	4,930	—	—	—	978	—	1,598	—	—	—	—	—
5.020	4.550	—	4,930	—	—	—	952	—	1,545	—	—	—	—	—
5.380	4.550	—	4,930	—	—	—	1,029	—	1,650	—	—	—	—	—
5.020	4.550	—	4,930	4,930	—	—	963	—	1,585	1,585	—	—	—	—
5.380	4.550	—	4,930	4,930	—	—	1,040	—	1,693	1,693	—	—	—	—
5.650	4.550	—	4,930	—	—	—	1,057	—	1,683	—	—	—	—	—
6.050	4.550	—	4,930	—	—	—	1,142	—	1,797	—	—	—	—	—
5.970	4.550	—	4,930	—	—	—	1,114	—	1,772	—	—	—	—	—
6.390	4.550	—	4,930	—	—	—	1,204	—	1,893	—	—	—	—	—
6.390	4.550	—	4,930	—	—	—	1,215	—	1,935	—	—	—	—	—
7.770	4.550	—	4,930	—	—	—	1,507	—	2,333	—	—	—	—	—
6.910	4.550	—	4,930	4,930	—	—	1,297	—	2,079	2,079	—	—	—	—
7.400	4.550	—	4,930	4,930	—	—	1,402	—	2,221	2,221	—	—	—	—
8.400	4.550	—	4,930	—	—	—	1,576	—	2,463	—	—	—	—	—
8.950	4.550	—	4,930	—	—	—	1,690	—	2,615	—	—	—	—	—
10.990	4.550	—	4,930	—	—	—	2,113	—	3,181	—	—	—	—	—
13.190	4.550	—	4,930	—	—	—	2,529	—	3,795	—	—	—	—	—
14.410	4.550	—	4,930	—	—	—	2,776	—	3,863	—	—	—	—	—
1.640	1.640	—	—	—	—	—	439	—	—	—	—	—	—	—
2.630	2.630	—	2,630	2,630	—	—	710	—	1,200	1,200	—	—	—	—
2.980	2.980	—	2,980	2,980	—	—	817	—	1,351	1,351	—	—	—	—
2.630	2.630	—	2,630	2,630	—	—	752	—	1,331	1,331	—	—	—	—
2.980	2.980	—	2,980	2,980	—	—	865	—	1,499	1,499	—	—	—	—
1.630	1.630	—	—	—	—	—	559	—	—	—	—	—	—	—
2.250	2.250	—	2,250	2,250	—	—	754	—	1,329	1,329	—	—	—	—
2.250	2.250	—	2,250	2,250	—	—	794	—	1,427	1,427	—	—	—	—
1.530	1.530	1,530	—	—	—	—	581	—	—	—	—	—	—	—
2.110	2.110	2,110	2,110	2,110	—	—	784	907	1,402	1,402	—	—	—	—
2.410	2.400	2,400	2,320	2,320	—	—	913	1,057	1,596	1,596	—	—	—	—
3.060	2.400	2,400	2,320	2,320	—	—	1,192	1,380	2,012	2,012	—	—	—	—
2.110	2.110	2,110	2,110	2,110	—	—	824	955	1,479	1,479	—	—	—	—
2.410	2.400	2,400	2,320	2,320	—	—	960	1,113	1,683	1,683	—	—	—	—
3.060	2.400	2,400	2,320	2,320	—	—	1,253	1,453	2,123	2,123	—	—	—	—

**Some joint strengths listed in Col. 20 through 27 are greater than the corresponding pipe body yield strength listed in Col. 12.

† Internal pressure resistance is the lowest of the internal yield pressure of the pipe, the internal yield pressure of the coupling, or the internal pressure leak resistance at the E or E₁ plane.

‡ For P-110 casing the next higher grade is 150YS, a non-API steel grade having a minimum yield strength of 150,000 psi.

TABLE 2.4a—MINIMUM COLLAPSE RESISTANCE UNDER AXIAL LOAD, GRADE H-40

d_o (in.)	Weight (lbm/ft)	d_o/e	Area (sq in.)	Axial Stress, psi												
				-10,000	-5,000	0	5,000	10,000	15,000	20,000	25,000	30,000	35,000	40,000	45,000	50,000
				Collapse Pressure, psi												
4½	9.5	21.95	2.766	2,930	2,860	2,760	2,640	2,500	2,320	2,100	1,840	—	—	—	—	—
5½	14	22.54	4.029	2,770	2,710	2,620	2,510	2,380	2,220	2,010	1,760	—	—	—	—	—
6½	20	23	5.734	2,650	2,600	2,502	2,420	2,290	2,140	1,950	1,710	—	—	—	—	—
7	17	30.3	4.912	1,490	1,460	1,420	1,380	1,320	1,260	1,170	1,080	—	—	—	—	—
7	20	25.74	5.749	2,050	2,020	1,970	1,910	1,830	1,730	1,590	1,420	—	—	—	—	—
7½	24	25.42	6.904	2,120	2,080	2,030	1,960	1,880	1,770	1,630	1,450	—	—	—	—	—
8½	28	28.37	7.947	1,690	1,650	1,610	1,550	1,490	1,410	1,320	1,200	—	—	—	—	—
8½	32	24.5	9.149	2,310	2,260	2,200	2,120	2,020	1,900	1,740	1,550	—	—	—	—	—
9½	32.3	30.85	9.128	1,430	1,410	1,370	1,330	1,280	1,220	1,140	1,050	—	—	—	—	—
9½	36	27.34	10.254	1,810	1,770	1,720	1,660	1,600	1,520	1,420	1,290	—	—	—	—	—
10¾	32.75	38.53	9.178	860	850	840	830	810	780	750	700	—	—	—	—	—
10¾	40.5	30.71	11.435	1,450	1,420	1,390	1,340	1,290	1,230	1,150	1,050	—	—	—	—	—
11¾	42	35.29	11.944	1,070	1,060	1,040	1,010	980	940	890	830	—	—	—	—	—
13¾	48	40.53	13.524	740	740	740	730	720	700	670	640	—	—	—	—	—
16	65	42.67	18.408	630	630	630	630	630	620	600	570	—	—	—	—	—
18½	87.5	42.82	24.858	630	630	630	630	620	610	590	570	—	—	—	—	—
20	94	45.66	26.918	520	520	520	520	520	510	510	490	—	—	—	—	—

TABLE 2.4b—MINIMUM COLLAPSE RESISTANCE UNDER AXIAL LOAD, GRADES J-55 AND K-55

d_o (in.)	Weight (lbm/ft)	d_o/e	Area (sq in.)	Axial Stress, psi												
				10,000	5,000	0	5,000	10,000	15,000	20,000	25,000	30,000	35,000	40,000	45,000	50,000
				Collapse Pressure, psi												
4½	9.5	21.95	2.766	3,440	3,390	3,310	3,230	3,120	3,000	2,850	2,680	2,470	2,220	1,930	1,420	—
4½	10.5	20.09	3.009	4,200	4,110	4,010	3,880	3,740	3,570	3,380	3,150	2,890	2,570	2,150	1,540	—
4½	11.6	18	3.338	5,220	5,100	4,960	4,790	4,590	4,360	4,100	3,800	3,450	2,980	2,380	1,710	—
5	11.5	22.73	3.304	3,170	3,120	3,060	2,980	2,890	2,790	2,660	2,500	2,320	2,090	1,820	1,370	—
5	13	19.76	3.773	4,340	4,250	4,140	4,010	3,860	3,690	3,480	3,240	2,970	2,640	2,180	1,570	—
5	15	16.89	4.374	5,880	5,730	5,560	5,360	5,120	4,860	4,550	4,210	3,730	3,160	2,530	1,820	—
5½	14	22.54	4.029	3,230	3,180	3,120	3,040	2,950	2,840	2,700	2,550	2,350	2,130	1,850	1,380	—
5½	15.5	20	4.514	4,230	4,150	4,040	3,920	3,770	3,600	3,410	3,180	2,910	2,590	2,160	1,550	—
5½	17	18.09	4.962	5,180	5,060	4,910	4,740	4,550	4,320	4,060	3,770	3,430	2,970	2,370	1,700	—
6½	20	23	5.734	3,070	3,030	2,970	2,900	2,820	2,720	2,590	2,450	2,270	2,050	1,790	1,360	—
6½	24	18.82	6.937	4,790	4,690	4,560	4,410	4,230	4,030	3,800	3,530	3,220	2,850	2,290	1,640	—
7	20	25.74	5.749	2,370	2,320	2,270	2,210	2,140	2,090	2,020	1,930	1,810	1,670	1,480	1,220	—
7	23	22.08	6.656	3,400	3,340	3,270	3,180	3,080	2,960	2,820	2,650	2,450	2,200	1,910	1,410	—
7	26	19.34	7.549	4,540	4,440	4,320	4,190	4,020	3,840	3,620	3,370	3,080	2,730	2,230	1,600	—
7¾	26.4	23.25	7.519	2,990	2,950	2,890	2,830	2,750	2,650	2,530	2,390	2,220	2,010	1,760	1,340	—
8½	24	32.67	6.934	1,400	1,390	1,370	1,350	1,320	1,290	1,250	1,200	1,140	1,070	980	870	—
8½	32	24.5	9.149	2,600	2,570	2,530	2,490	2,430	2,350	2,260	2,150	2,010	1,830	1,610	1,280	—
8½	36	21.56	10.336	3,590	3,530	3,450	3,360	3,240	3,110	2,960	2,770	2,550	2,290	1,980	1,440	—
9½	36	27.34	10.254	2,100	2,070	2,020	1,970	1,920	1,850	1,770	1,670	1,590	1,480	1,330	1,150	—
9½	40	24.37	11.454	2,640	2,610	2,570	2,520	2,460	2,380	2,290	2,170	2,030	1,850	1,630	1,280	—
10¾	40.5	30.71	11.435	1,630	1,610	1,580	1,550	1,520	1,470	1,420	1,360	1,280	1,190	1,090	960	—
10¾	45.5	26.88	13.006	2,170	2,140	2,090	2,040	1,980	1,900	1,820	1,740	1,650	1,530	1,370	1,180	—
10¾	51	23.89	14.561	2,780	2,750	2,700	2,650	2,580	2,500	2,390	2,260	2,110	1,920	1,680	1,310	—
11¾	47	31.33	13.401	1,550	1,540	1,510	1,490	1,450	1,410	1,360	1,310	1,230	1,150	1,050	930	—
11¾	54	27.01	15.463	2,150	2,120	2,070	2,020	1,960	1,890	1,810	1,720	1,630	1,520	1,360	1,170	—
11¾	60	24.03	17.3	2,740	2,710	2,660	2,610	2,540	2,460	2,360	2,240	2,080	1,900	1,660	1,300	—
13¾	54.5	35.2	15.514	1,140	1,140	1,130	1,120	1,110	1,090	1,060	1,030	980	930	860	770	—
13¾	61	31.1	17.487	1,580	1,560	1,540	1,510	1,480	1,440	1,380	1,320	1,250	1,160	1,060	940	—
13¾	68	27.86	19.445	2,020	1,990	1,950	1,900	1,850	1,780	1,710	1,620	1,520	1,420	1,290	1,120	—
16	75	36.53	21.414	1,020	1,020	1,020	1,010	1,010	990	970	950	910	860	800	720	—
16	84	32.32	24.112	1,440	1,420	1,410	1,390	1,360	1,320	1,280	1,230	1,160	1,090	1,000	890	—
18½	87.5	42.82	24.858	630	630	630	630	630	630	630	630	620	600	580	530	—
20	94	45.66	26.918	520	520	520	520	520	520	520	520	520	510	490	470	—
20	106.5	40	30.631	770	770	770	770	770	770	770	760	740	710	670	610	—
20	133	31.5	38.632	1,530	1,520	1,500	1,470	1,440	1,400	1,350	1,290	1,220	1,140	1,040	920	—

TABLE 2.4c—MINIMUM COLLAPSE RESISTANCE UNDER AXIAL LOAD, GRADE C-75

d _o (in.)	Weight (lbm/ft)	d _o /e	Area (sq in.)	Axial Stress, psi												
				-10,000	-5,000	0	5,000	10,000	15,000	20,000	25,000	30,000	35,000	40,000	45,000	50,000
				Collapse Pressure, psi												
4½	11.6	18	3.338	6,330	6,220	6,100	5,970	5,810	5,640	5,440	5,220	4,980	4,710	4,400	4,060	3,660
4½	13.5	15.52	3.836	8,500	8,330	8,140	7,920	7,680	7,420	7,130	6,810	6,450	6,060	5,610	5,010	4,370
5	15	16.89	4.374	7,220	7,090	6,940	6,770	6,580	6,370	6,140	5,870	5,580	5,260	4,900	4,500	4,040
5	18	13.81	5.275	10,440	10,220	9,960	9,680	9,340	8,920	8,460	7,970	7,440	6,860	6,250	5,590	4,870
5	21.4	11.44	6.264	12,680	12,340	11,970	11,550	11,090	10,590	10,050	9,460	8,830	8,150	7,420	6,630	5,780
5	23.2	10.46	6.791	13,750	13,380	12,970	12,520	12,020	11,480	10,890	10,260	9,570	8,840	8,040	7,190	6,270
5	24.1	10	7.069	14,310	13,930	13,500	13,030	12,510	11,950	11,340	10,680	9,960	9,200	8,370	7,480	6,520
5½	17	18.09	4.962	6,260	6,160	6,040	5,910	5,750	5,580	5,390	5,170	4,930	4,670	4,360	4,020	3,630
5½	20	15.24	5.828	8,790	8,610	8,410	8,180	7,930	7,660	7,350	7,020	6,650	6,240	5,700	5,100	4,440
5½	23	13.25	6.63	11,090	10,800	10,470	10,100	9,700	9,260	8,790	8,280	7,730	7,130	6,490	5,800	5,060
6⅝	24	18.82	6.937	5,740	5,650	5,550	5,430	5,300	5,150	4,980	4,790	4,580	4,340	4,070	3,760	3,410
6⅝	28	15.89	8.133	8,130	7,970	7,790	7,590	7,370	7,120	6,840	6,540	6,200	5,830	5,420	4,900	4,270
6⅝	32	13.95	9.177	10,270	10,050	9,800	9,520	9,210	8,830	8,380	7,890	7,370	6,800	6,190	5,530	4,820
7	23	22.08	6.656	3,830	3,790	3,750	3,700	3,650	3,580	3,490	3,400	3,280	3,140	2,980	2,790	2,570
7	26	19.34	7.549	5,390	5,310	5,220	5,120	5,000	4,860	4,710	4,540	4,340	4,120	3,870	3,580	3,250
7	29	17.16	8.449	6,990	6,870	6,730	6,570	6,390	6,180	5,960	5,710	5,430	5,120	4,780	4,390	3,950
7	32	15.45	9.317	8,570	8,400	8,200	7,990	7,750	7,480	7,180	6,860	6,500	6,100	5,630	5,030	4,390
7	35	14.06	10.172	10,130	9,910	9,670	9,400	9,100	8,760	8,320	7,840	7,310	6,750	6,150	5,490	4,790
7	38	12.96	10.959	11,320	11,020	10,680	10,310	9,900	9,450	8,970	8,450	7,880	7,280	6,630	5,920	5,160
7⅞	26.4	23.25	7.519	3,390	3,340	3,280	3,220	3,160	3,120	3,060	2,990	2,900	2,800	2,670	2,510	2,330
7⅞	29.7	20.33	8.541	4,780	4,720	4,650	4,560	4,470	4,360	4,230	4,090	3,930	3,740	3,520	3,270	2,990
7⅞	33.7	17.73	9.72	6,540	6,430	6,300	6,150	5,990	5,810	5,600	5,370	5,120	4,840	4,520	4,160	3,750
7⅞	39	15.25	11.192	8,770	8,600	8,400	8,170	7,920	7,650	7,340	7,010	6,640	6,230	5,700	5,100	4,440
7⅞	42.8	13.57	12.47	10,760	10,520	10,240	9,880	9,490	9,060	8,600	8,100	7,560	6,980	6,350	5,680	4,950
7⅞	45.3	12.82	13.141	11,430	11,130	10,790	10,410	10,000	9,550	9,060	8,530	7,960	7,350	6,690	5,980	5,210
7⅞	47.1	12.2	13.745	11,960	11,640	11,290	10,890	10,460	9,990	9,480	8,930	8,330	7,690	7,000	6,260	5,450
8⅝	36	21.56	10.336	4,090	4,050	4,000	3,940	3,880	3,800	3,700	3,590	3,460	3,310	3,130	2,930	2,690
8⅝	40	19.17	11.557	5,500	5,420	5,330	5,220	5,100	4,960	4,800	4,620	4,420	4,190	3,930	3,640	3,300
8⅝	44	17.25	12.763	6,920	6,800	6,660	6,500	6,320	6,120	5,900	5,650	5,380	5,070	4,730	4,350	3,920
8⅝	49	15.48	14.118	8,540	8,370	8,180	7,960	7,720	7,450	7,160	6,840	6,480	6,080	5,620	5,030	4,380
9⅝	40	24.37	11.454	3,080	3,030	2,990	2,930	2,870	2,800	2,720	2,640	2,580	2,500	2,400	2,270	2,120
9⅝	43.5	22.13	12.559	3,800	3,770	3,730	3,680	3,620	3,560	3,470	3,380	3,260	3,130	2,970	2,780	2,560
9⅝	47	20.39	13.572	4,740	4,680	4,610	4,530	4,440	4,330	4,210	4,060	3,900	3,720	3,500	3,260	2,970
9⅝	53.5	17.66	15.547	6,590	6,480	6,350	6,200	6,040	5,850	5,650	5,410	5,160	4,870	4,550	4,190	3,780
10¾	51	23.89	14.561	3,210	3,160	3,110	3,050	2,980	2,910	2,840	2,780	2,710	2,620	2,510	2,370	2,200
10¾	55.5	21.72	15.947	4,010	3,970	3,920	3,870	3,800	3,730	3,640	3,530	3,400	3,260	3,090	2,890	2,650
11¾	60	24.03	17.3	3,170	3,120	3,070	3,020	2,950	2,870	2,800	2,740	2,670	2,580	2,480	2,340	2,180
13⅜	68	27.66	19.445	2,260	2,240	2,220	2,190	2,160	2,120	2,070	2,020	1,960	1,880	1,790	1,690	1,580
13⅜	72	26.02	20.768	2,660	2,630	2,600	2,560	2,510	2,450	2,390	2,320	2,230	2,140	2,040	1,950	1,840

TABLE 2.4d—MINIMUM COLLAPSE RESISTANCE UNDER AXIAL LOAD, GRADES L-80 AND N-80

d_o (in.)	Weight (lbm/ft)	d_o/e	Area (sq in.)	Axial Stress, psi												
				-10,000	-5,000	0	5,000	10,000	15,000	20,000	25,000	30,000	35,000	40,000	45,000	50,000
				Collapse Pressure, psi												
4 1/2	11.6	18	3.338	6,570	6,470	6,350	6,230	6,080	5,920	5,730	5,530	5,310	5,050	4,770	4,460	4,100
4 1/2	13.5	15.52	3.836	8,890	8,720	8,540	8,330	8,100	7,850	7,570	7,260	6,930	6,560	6,150	5,710	5,100
5	15	16.89	4.374	7,520	7,400	7,250	7,090	6,910	6,710	6,490	6,240	5,970	5,670	5,340	4,970	4,560
5	18	13.81	5.275	10,970	10,750	10,500	10,220	9,910	9,580	9,150	8,670	8,150	7,590	7,000	6,360	5,680
5	21.4	11.44	6.264	13,490	13,140	12,760	12,350	11,890	11,400	10,870	10,290	9,680	9,020	8,310	7,560	6,740
5	23.2	10.46	6.791	14,620	14,250	13,830	13,380	12,890	12,350	11,780	11,160	10,490	9,780	9,010	8,190	7,310
5	24.1	10	7.069	15,220	14,830	14,400	13,930	13,420	12,860	12,260	11,610	10,920	10,180	9,380	8,530	7,610
5 1/2	17	18.09	4.962	6,500	6,400	6,290	6,160	6,020	5,860	5,680	5,480	5,260	5,010	4,730	4,420	4,070
5 1/2	20	15.24	5.828	9,200	9,020	8,830	8,610	8,370	8,100	7,810	7,490	7,140	6,760	6,340	5,810	5,180
5 1/2	23	13.25	6.63	11,770	11,500	11,160	10,800	10,400	9,970	9,500	9,000	8,470	7,890	7,270	6,610	5,900
6 5/8	24	18.82	6.937	5,940	5,860	5,760	5,650	5,530	5,390	5,230	5,060	4,860	4,640	4,400	4,120	3,800
6 5/8	28	15.89	8.133	8,500	8,340	8,170	7,970	7,760	7,520	7,260	6,970	6,650	6,300	5,920	5,500	4,990
6 5/8	32	13.95	9.177	10,780	10,560	10,320	10,050	9,750	9,420	9,060	8,590	8,070	7,520	6,940	6,300	5,630
7	23	22.08	6.656	3,890	3,870	3,830	3,790	3,740	3,690	3,620	3,530	3,430	3,320	3,180	3,010	2,820
7	26	19.34	7.549	5,570	5,490	5,410	5,310	5,200	5,080	4,940	4,780	4,600	4,400	4,170	3,920	3,620
7	29	17.16	8.449	7,280	7,160	7,020	6,870	6,700	6,510	6,300	6,060	5,800	5,510	5,200	4,840	4,440
7	32	15.45	9.317	8,960	8,800	8,610	8,400	8,170	7,910	7,630	7,320	6,980	6,610	6,200	5,730	5,120
7	35	14.06	10.172	10,630	10,420	10,180	9,910	9,620	9,300	8,950	8,520	8,020	7,470	6,890	6,260	5,580
7	38	12.96	10.959	12,040	11,730	11,390	11,020	10,610	10,170	9,700	9,190	8,640	8,050	7,420	6,750	6,020
7 3/8	26.4	23.25	7.519	3,500	3,450	3,400	3,340	3,270	3,190	3,150	3,090	3,020	2,930	2,820	2,690	2,540
7 3/8	29.7	20.33	8.541	4,910	4,850	4,790	4,720	4,630	4,530	4,420	4,290	4,140	3,980	3,780	3,560	3,310
7 3/8	33.7	17.73	9.72	6,790	6,680	6,560	6,430	6,270	6,100	5,910	5,700	5,460	5,200	4,900	4,580	4,210
7 3/8	39	15.25	11.192	9,180	9,010	8,820	8,600	8,360	8,090	7,800	7,480	7,130	6,750	6,330	5,800	5,180
7 3/8	42.8	13.57	12.47	11,300	11,070	10,810	10,520	10,180	9,750	9,300	8,810	8,280	7,720	7,110	6,470	5,770
7 3/8	45.3	12.82	13.141	12,160	11,850	11,510	11,130	10,720	10,280	9,800	9,280	8,730	8,130	7,500	6,810	6,080
7 3/8	47.1	12.2	13.745	12,720	12,400	12,040	11,650	11,220	10,750	10,250	9,710	9,130	8,510	7,840	7,130	6,360
8 5/8	36	21.56	10.336	4,180	4,140	4,100	4,050	3,990	3,920	3,840	3,740	3,630	3,500	3,350	3,170	2,960
8 5/8	40	19.17	11.557	5,690	5,610	5,520	5,420	5,310	5,180	5,030	4,870	4,690	4,480	4,250	3,980	3,680
8 5/8	44	17.25	12.763	7,200	7,080	6,950	6,800	6,630	6,440	6,230	6,000	5,750	5,460	5,150	4,800	4,410
8 5/8	49	15.48	14.118	8,930	8,760	8,580	8,370	8,140	7,880	7,600	7,290	6,960	6,590	6,180	5,720	5,110
9 5/8	40	24.37	11.454	3,170	3,130	3,090	3,030	2,980	2,910	2,840	2,750	2,660	2,560	2,520	2,420	2,290
9 5/8	43.5	22.13	12.559	3,870	3,840	3,810	3,770	3,720	3,660	3,590	3,510	3,410	3,300	3,160	3,000	2,810
9 5/8	47	20.39	13.572	4,870	4,820	4,760	4,680	4,600	4,500	4,390	4,260	4,120	3,950	3,760	3,540	3,290
9 5/8	53.5	17.66	15.547	6,850	6,740	6,620	6,480	6,320	6,150	5,960	5,740	5,500	5,240	4,940	4,610	4,240
10 3/4	51	23.89	14.561	3,310	3,260	3,220	3,160	3,100	3,030	2,950	2,860	2,810	2,730	2,640	2,530	2,390
10 3/4	55.5	21.72	15.947	4,090	4,060	4,020	3,970	3,920	3,850	3,770	3,680	3,570	3,440	3,290	3,120	2,920
11 3/4	60	24.03	17.3	3,260	3,220	3,180	3,120	3,060	2,990	2,920	2,830	2,760	2,690	2,610	2,500	2,360
13 3/8	68	27.86	19.445	2,290	2,280	2,260	2,240	2,220	2,180	2,140	2,100	2,040	1,970	1,900	1,810	1,710
13 3/8	72	26.02	20.768	2,730	2,700	2,670	2,630	2,590	2,540	2,490	2,420	2,350	2,260	2,160	2,050	1,970

TABLE 2.4e—MINIMUM COLLAPSE RESISTANCE UNDER AXIAL LOAD, GRADE C-90

d _o (in.)	Weight (lbm/ft)	d _o /e	Area (sq in.)	Axial Stress, psi													
				-10,000	-5,000	0	5,000	10,000	15,000	20,000	25,000	30,000	35,000	40,000	45,000	50,000	
				Collapse Pressure, psi													
4½	11.6	18	3.338	7,010	6,920	6,820	6,700	6,570	6,430	6,270	6,100	5,900	5,690	5,450	5,180	4,890	
4½	13.5	15.52	3.836	9,630	9,470	9,300	9,100	8,890	8,660	8,400	8,130	7,820	7,490	7,140	6,740	6,320	
5	15	16.89	4.374	8,090	7,970	7,840	7,690	7,530	7,350	7,150	6,930	6,690	6,430	6,140	5,830	5,480	
5	18	13.81	5.275	11,990	11,770	11,530	11,260	10,970	10,660	10,320	9,950	9,550	9,030	8,470	7,880	7,240	
5	21.4	11.44	6.264	15,090	14,740	14,360	13,940	13,490	13,010	12,500	11,940	11,350	10,730	10,060	9,350	8,600	
5	23.2	10.46	6.791	16,360	15,980	15,560	15,110	14,630	14,100	13,540	12,940	12,310	11,630	10,910	10,140	9,320	
5	24.1	10	7.069	17,020	16,630	16,200	15,730	15,220	14,680	14,100	13,470	12,810	12,100	11,350	10,550	9,700	
5½	17	18.09	4.962	6,930	6,840	6,740	6,630	6,500	6,360	6,210	6,030	5,840	5,630	5,400	5,130	4,840	
5½	20	15.24	5.828	9,980	9,810	9,630	9,420	9,200	8,950	8,690	8,400	8,080	7,740	7,360	6,950	6,510	
5½	23	13.25	6.63	12,690	12,650	12,360	12,090	11,770	11,380	10,930	10,450	9,930	9,380	8,800	8,180	7,520	
5½	26	11.55	7.513	14,960	14,610	14,240	13,820	13,380	12,900	12,390	11,840	11,260	10,640	9,980	9,270	8,530	
5½	35	8.46	9.904	19,720	19,260	18,760	18,220	17,630	17,000	16,330	15,600	14,840	14,020	13,150	12,220	11,240	
6½	24	18.82	6.937	6,290	6,220	6,140	6,050	5,940	5,820	5,690	5,540	5,380	5,190	4,990	4,760	4,500	
6½	28	15.89	8.133	9,190	9,040	8,880	8,700	8,500	8,280	8,040	7,780	7,500	7,190	6,850	6,480	6,080	
6½	32	13.95	9.177	11,770	11,560	11,330	11,070	10,780	10,480	10,140	9,780	9,390	8,950	8,390	7,800	7,170	
7	23	22.08	6.656	4,130	4,080	4,030	3,960	3,890	3,850	3,810	3,750	3,680	3,600	3,500	3,380	3,230	
7	26	19.34	7.549	5,870	5,810	5,740	5,660	5,570	5,460	5,350	5,220	5,070	4,900	4,720	4,510	4,270	
7	29	17.16	8.449	7,810	7,700	7,580	7,440	7,280	7,110	6,920	6,720	6,490	6,240	5,960	5,660	5,330	
7	32	15.45	9.317	9,720	9,560	9,380	9,180	8,970	8,730	8,470	8,190	7,890	7,550	7,190	6,800	6,360	
7	35	14.06	10.172	11,610	11,400	11,170	10,910	10,640	10,340	10,010	9,650	9,270	8,860	8,330	7,750	7,120	
7	38	12.96	10.959	13,390	13,140	12,820	12,450	12,050	11,610	11,150	10,660	10,140	9,580	8,980	8,350	7,680	
7	41	11.66	11.881	14,600	14,270	13,900	13,500	13,060	12,590	12,090	11,560	10,990	10,380	9,740	9,050	8,320	
7	46	10.45	13.324	16,370	15,990	15,580	15,130	14,640	14,120	13,550	12,960	12,320	11,640	10,920	10,150	9,330	
7	49.5	9.59	14.379	17,670	17,250	16,810	16,330	15,800	15,240	14,630	13,980	13,290	12,560	11,780	10,950	10,070	
7	57.5	7.95	16.919	20,800	20,320	19,790	19,220	18,600	17,940	17,220	16,460	15,650	14,790	13,870	12,890	11,850	
7½	26.4	23.25	7.519	3,700	3,660	3,610	3,560	3,500	3,440	3,360	3,280	3,190	3,130	3,060	2,980	2,870	
7½	29.7	20.33	8.541	5,130	5,090	5,040	4,980	4,910	4,830	4,740	4,640	4,520	4,390	4,240	4,060	3,860	
7½	33.7	17.73	9.72	7,260	7,160	7,050	6,930	6,790	6,640	6,480	6,290	6,090	5,860	5,610	5,330	5,020	
7½	39	15.25	11.192	9,970	9,800	9,620	9,410	9,190	8,940	8,680	8,390	8,070	7,730	7,350	6,950	6,500	
7½	42.8	13.57	12.47	12,370	12,140	11,890	11,610	11,310	10,980	10,630	10,220	9,720	9,180	8,610	8,000	7,360	
7½	45.3	12.82	13.141	13,600	13,290	12,950	12,570	12,170	11,730	11,260	10,770	10,240	9,670	9,070	8,430	7,750	
7½	47.1	12.2	13.745	14,230	13,910	13,540	13,150	12,730	12,270	11,790	11,270	10,710	10,120	9,490	8,820	8,110	
7½	53.58	10.45	15.813	16,370	15,990	15,580	15,130	14,640	14,120	13,550	12,960	12,320	11,640	10,920	10,150	9,330	
7¾	44.7	13.48	12.961	12,510	12,280	12,020	11,740	11,440	11,100	10,740	10,280	9,780	9,240	8,660	8,050	7,400	
7¾	46.1	13.03	13.374	13,270	13,020	12,740	12,390	11,990	11,560	11,100	10,610	10,090	9,530	8,940	8,310	7,640	
8½	36	21.56	10.336	4,340	4,290	4,250	4,220	4,180	4,130	4,070	4,000	3,920	3,820	3,700	3,570	3,410	
8½	40	19.17	11.557	6,010	5,940	5,870	5,780	5,690	5,580	5,460	5,320	5,170	5,000	4,800	4,590	4,340	
8½	44	17.25	12.763	7,720	7,610	7,490	7,350	7,200	7,040	6,850	6,650	6,420	6,180	5,910	5,610	5,280	
8½	49	15.48	14.118	9,680	9,520	9,340	9,150	8,930	8,700	8,440	8,160	7,860	7,530	7,170	6,770	6,340	
9½	40	24.37	11.454	3,320	3,290	3,250	3,210	3,170	3,110	3,050	2,980	2,910	2,820	2,720	2,630	2,550	
9½	43.5	22.13	12.559	4,120	4,070	4,010	3,940	3,870	3,830	3,780	3,730	3,660	3,580	3,480	3,360	3,220	
9½	47	20.39	13.572	5,090	5,040	5,000	4,940	4,870	4,800	4,710	4,610	4,490	4,360	4,210	4,040	3,840	
9½	53.5	17.66	15.547	7,330	7,230	7,120	6,990	6,850	6,700	6,530	6,340	6,130	5,900	5,650	5,370	5,060	
9½	58.4	16.18	16.879	8,860	8,720	8,560	8,390	8,200	8,000	7,770	7,520	7,250	6,960	6,640	6,290	5,890	
9½	60.7	15.4	17.671	9,780	9,620	9,440	9,240	9,020	8,780	8,520	8,240	7,930	7,600	7,230	6,830	6,400	
10¾	51	23.89	14.561	3,480	3,440	3,400	3,360	3,310	3,250	3,180	3,110	3,020	2,930	2,840	2,770	2,680	
10¾	55.5	21.72	15.947	4,280	4,220	4,160	4,130	4,090	4,040	3,990	3,920	3,840	3,750	3,640	3,510	3,360	
10¾	82	14.33	23.562	11,210	11,010	10,790	10,550	10,290	10,000	9,690	9,350	8,980	8,580	8,150	7,610	7,000	
11¾	60	24.03	17.3	3,430	3,400	3,360	3,320	3,270	3,210	3,140	3,070	2,990	2,890	2,800	2,730	2,640	
13¾	68	27.86	19.445	2,330	2,330	2,320	2,310	2,300	2,280	2,250	2,220	2,180	2,130	2,080	2,010	1,930	
13¾	72	26.02	20.768	2,820	2,800	2,780	2,760	2,730	2,690	2,650	2,600	2,540	2,470	2,390	2,300	2,200	

TABLE 2.4f—MINIMUM COLLAPSE RESISTANCE UNDER AXIAL LOAD, GRADE C-95

d _o (in.)	Weight (lbm/ft)	d _e /e	Area (sq. in.)	Axial Stress, psi												
				-10,000	-5,000	0	5,000	10,000	15,000	20,000	25,000	30,000	35,000	40,000	45,000	50,000
				Collapse Pressure, psi												
4½	11.6	18	3.338	7,210	7,120	7,030	6,920	6,800	6,670	6,520	6,350	6,170	5,970	5,750	5,510	5,240
4½	13.5	15.52	3.836	9,990	9,830	9,660	9,470	9,270	9,040	8,800	8,540	8,250	7,940	7,600	7,230	6,830
5	15	16.89	4.374	8,350	8,240	8,110	7,970	7,810	7,640	7,460	7,250	7,030	6,780	6,510	6,220	5,890
5	18	13.81	5.275	12,480	12,270	12,030	11,770	11,490	11,180	10,850	10,500	10,110	9,700	9,200	8,620	8,000
5	21.4	11.44	6.264	15,890	15,540	15,160	14,740	14,300	13,820	13,310	12,760	12,190	11,570	10,920	10,230	9,500
5	23.2	10.46	6.791	17,220	16,840	16,430	15,980	15,490	14,980	14,420	13,830	13,210	12,540	11,840	11,090	10,300
5	24.1	10	7.069	17,930	17,530	17,100	16,630	16,130	15,590	15,010	14,400	13,750	13,060	12,320	11,540	10,720
5½	17	18.09	4.962	7,120	7,040	6,940	6,840	6,720	6,590	6,450	6,290	6,110	5,910	5,700	5,460	5,190
5½	20	15.24	5.828	10,360	10,190	10,010	9,810	9,600	9,360	9,110	8,830	8,520	8,200	7,840	7,460	7,040
5½	23	13.25	6.63	13,440	13,200	12,940	12,650	12,340	12,000	11,640	11,160	10,660	10,120	9,550	8,950	8,310
6¾	24	18.82	6.937	6,450	6,380	6,310	6,220	6,130	6,020	5,900	5,760	5,610	5,440	5,250	5,040	4,810
6¾	28	15.89	8.133	9,520	9,370	9,220	9,040	8,850	8,640	8,410	8,170	7,900	7,600	7,290	6,940	6,560
6¾	32	13.95	9.177	12,250	12,040	11,810	11,560	11,290	10,990	10,670	10,320	9,940	9,540	9,100	8,540	7,930
7	23	22.08	6.656	4,240	4,200	4,140	4,080	4,020	3,940	3,880	3,830	3,780	3,710	3,620	3,520	3,400
7	26	19.34	7.549	6,000	5,950	5,880	5,810	5,730	5,630	5,530	5,410	5,280	5,120	4,960	4,760	4,550
7	29	17.16	8.449	8,060	7,950	7,830	7,700	7,560	7,390	7,220	7,020	6,810	6,580	6,320	6,040	5,730
7	32	15.45	9.317	10,080	9,920	9,750	9,560	9,350	9,120	8,880	8,610	8,320	8,000	7,660	7,290	6,880
7	35	14.06	10.172	12,080	11,870	11,650	11,400	11,130	10,840	10,520	10,180	9,810	9,410	8,990	8,470	7,870
7	38	12.96	10.959	13,970	13,720	13,440	13,140	12,760	12,330	11,880	11,390	10,880	10,330	9,750	9,130	8,480
7¾	26.4	23.25	7.519	3,780	3,750	3,710	3,660	3,610	3,550	3,480	3,400	3,320	3,220	3,150	3,080	2,990
7¾	29.7	20.33	8.541	5,220	5,180	5,140	5,090	5,030	4,960	4,880	4,790	4,690	4,570	4,430	4,280	4,100
7¾	33.7	17.73	9.72	7,470	7,380	7,280	7,160	7,030	6,890	6,740	6,560	6,370	6,160	5,930	5,670	5,390
7¾	39	15.25	11.192	10,340	10,180	10,000	9,800	9,590	9,350	9,090	8,820	8,510	8,190	7,830	7,450	7,030
7¾	42.8	13.57	12.47	12,880	12,660	12,410	12,140	11,840	11,530	11,180	10,810	10,410	9,900	9,350	8,760	8,130
7¾	45.3	12.82	13.141	14,230	13,970	13,660	13,290	12,890	12,460	12,000	11,510	10,990	10,430	9,850	9,230	8,570
7¾	47.1	12.2	13.745	14,990	14,660	14,300	13,910	13,490	13,030	12,550	12,040	11,490	10,920	10,300	9,650	8,960
8¾	36	21.56	10.336	4,470	4,410	4,350	4,290	4,250	4,210	4,160	4,100	4,030	3,950	3,850	3,730	3,600
8¾	40	19.17	11.557	6,150	6,090	6,020	5,940	5,860	5,760	5,650	5,520	5,380	5,230	5,050	4,850	4,630
8¾	44	17.25	12.763	7,960	7,860	7,740	7,610	7,470	7,310	7,140	6,950	6,740	6,510	6,260	5,980	5,670
8¾	49	15.48	14.118	10,040	9,880	9,710	9,520	9,310	9,090	8,840	8,580	8,290	7,970	7,630	7,260	6,860
9¾	40	24.37	11.454	3,380	3,350	3,320	3,290	3,250	3,200	3,150	3,090	3,010	2,940	2,850	2,740	2,640
9¾	43.5	22.13	12.559	4,220	4,180	4,120	4,070	4,000	3,920	3,850	3,810	3,750	3,680	3,600	3,500	3,380
9¾	47	20.39	13.572	5,170	5,140	5,090	5,040	4,990	4,920	4,840	4,760	4,650	4,540	4,400	4,250	4,070
9¾	53.5	17.66	15.547	7,540	7,450	7,340	7,230	7,100	6,950	6,790	6,620	6,420	6,210	5,980	5,720	5,430
10¾	51	23.89	14.561	3,550	3,520	3,480	3,440	3,400	3,340	3,280	3,220	3,140	3,050	2,960	2,860	2,790
10¾	55.5	21.72	15.947	4,400	4,350	4,290	4,220	4,150	4,120	4,070	4,020	3,950	3,870	3,780	3,670	3,540
11¾	60	24.03	17.3	3,500	3,470	3,440	3,400	3,350	3,300	3,240	3,180	3,100	3,020	2,920	2,820	2,750
13¾	68	27.86	19.445	2,340	2,340	2,330	2,330	2,320	2,310	2,290	2,260	2,230	2,190	2,150	2,090	2,020
13¾	72	26.02	20.768	2,850	2,840	2,820	2,800	2,780	2,750	2,710	2,670	2,620	2,560	2,490	2,410	2,320

TABLE 2.4g—MINIMUM COLLAPSE RESISTANCE UNDER AXIAL LOAD, GRADE HC-95*

d_o (in.)	Weight (lbm/ft)	d_o/e	Area (sq in.)	Axial Stress, psi												
				-10,000	-5,000	0	5,000	10,000	15,000	20,000	25,000	30,000	35,000	40,000	45,000	50,000
				Collapse Pressure, psi												
4½	11.6	18	3.338	8,840	8,760	8,650	8,520	8,370	8,190	8,000	7,770	7,530	7,260	6,960	6,630	6,270
4½	13.5	15.52	3.836	10,610	10,510	10,380	10,220	10,040	9,830	9,600	9,330	9,030	8,710	8,350	7,950	7,520
4½	15.1	13.35	4.407	12,600	12,480	12,330	12,150	11,930	11,660	11,400	11,080	10,730	10,340	9,920	9,450	8,930
5	15	16.89	4.374	9,590	9,500	9,380	9,240	9,070	8,890	8,670	8,430	8,160	7,870	7,540	7,190	6,800
5	18	13.81	5.275	12,140	12,030	11,880	11,700	11,490	11,250	10,980	10,680	10,340	9,970	9,550	9,100	8,610
5	23	10.46	6.791	16,170	16,020	15,820	15,580	15,310	14,990	14,620	14,220	13,770	13,270	12,720	12,120	11,460
5½	17	18.09	4.962	8,770	8,690	8,580	8,450	8,300	8,130	7,930	7,710	7,470	7,200	6,900	6,570	6,220
5½	20	15.24	5.828	10,870	10,760	10,630	10,470	10,280	10,070	9,830	9,550	9,250	8,920	8,550	8,140	7,700
5½	23	13.25	6.63	12,730	12,600	12,450	12,260	12,040	11,790	11,510	11,190	10,840	10,440	10,010	9,540	9,020
7	23	22.08	6.656	5,780	5,720	5,650	5,570	5,470	5,350	5,220	5,080	4,920	4,740	4,540	4,330	4,090
7	26	19.34	7.549	7,970	7,900	7,800	7,680	7,550	7,390	7,210	7,010	6,790	6,540	6,270	5,980	5,650
7	29	17.16	8.449	9,400	9,310	9,200	9,060	8,900	8,710	8,500	8,270	8,010	7,720	7,400	7,050	6,660
7	32	15.45	9.317	10,630	10,530	10,400	10,240	10,060	9,850	9,610	9,350	9,050	8,720	8,360	7,970	7,530
7	35	14.06	10.172	11,860	11,740	11,600	11,430	11,220	10,990	10,720	10,430	10,100	9,730	9,330	8,890	8,400
7	38	12.96	10.959	12,980	12,860	12,700	12,510	12,290	12,030	11,740	11,410	11,050	10,650	10,210	9,730	9,200
7⅞	26.4	23.25	7.519	4,960	4,910	4,850	4,780	4,690	4,590	4,480	4,360	4,220	4,070	3,900	3,720	3,510
7⅞	29.7	20.33	8.541	7,310	7,240	7,150	7,040	6,920	6,770	6,610	6,430	6,220	6,000	5,750	5,480	5,180
7⅞	33.7	17.73	9.72	9,000	8,910	8,800	8,670	8,510	8,340	8,130	7,910	7,660	7,380	7,080	6,740	6,370
7⅞	39	15.25	11.192	10,840	10,730	10,600	10,440	10,260	10,040	9,800	9,530	9,220	8,890	8,520	8,120	7,680
7⅞	45.3	12.82	13.141	13,190	13,060	12,900	12,710	12,480	12,220	11,920	11,590	11,230	10,820	10,370	9,880	9,350
8⅝	36	21.56	10.336	6,190	6,140	6,060	5,970	5,860	5,740	5,600	5,450	5,270	5,080	4,870	4,640	4,390
8⅝	40	19.17	11.557	8,080	8,000	7,900	7,780	7,640	7,480	7,300	7,100	6,880	6,630	6,350	6,050	5,720
8⅝	44	17.25	12.763	9,300	9,210	9,100	8,960	8,800	8,620	8,410	8,180	7,920	7,630	7,320	6,970	6,590
8⅝	49	15.48	14.118	10,630	10,530	10,400	10,240	10,060	9,850	9,610	9,350	9,050	8,720	8,360	7,970	7,530
9⅝	40	24.37	11.454	4,320	4,280	4,230	4,170	4,090	4,010	3,910	3,800	3,680	3,550	3,400	3,240	3,060
9⅝	43.5	22.13	12.559	5,720	5,670	5,600	5,520	5,420	5,300	5,180	5,030	4,870	4,700	4,500	4,290	4,060
9⅝	47	20.39	13.572	7,260	7,190	7,100	6,990	6,870	6,730	6,560	6,380	6,180	5,960	5,710	5,440	5,140
9⅝	53.5	17.66	15.547	9,050	8,960	8,850	8,720	8,560	8,380	8,180	7,950	7,700	7,420	7,120	6,780	6,410
9⅝	58.4	16.18	16.879	10,170	10,070	9,950	9,800	9,630	9,430	9,200	8,940	8,660	8,350	8,000	7,620	7,210
9⅝	61.1	13.8	15.708	10,730	10,630	10,500	10,340	10,160	9,950	9,710	9,440	9,140	8,810	8,440	8,040	7,610
10¾	51	23.89	14.561	4,560	4,520	4,460	4,390	4,310	4,220	4,120	4,010	3,880	3,740	3,590	3,420	3,230
10¾	55.5	21.72	15.947	6,080	6,020	5,950	5,860	5,760	5,640	5,500	5,350	5,180	4,990	4,780	4,560	4,310
10¾	60.7	19.72	17.473	7,720	7,640	7,550	7,440	7,300	7,150	6,980	6,790	6,570	6,330	6,070	5,780	5,470
10¾	65.7	18.07	18.982	8,830	8,750	8,640	8,510	8,360	8,180	7,990	7,770	7,520	7,250	6,950	6,620	6,260
10¾	71.1	16.54	20.625	9,810	9,720	9,600	9,460	9,290	9,090	8,870	8,630	8,350	8,050	7,720	7,350	6,950
11¾	60	24.03	17.3	4,510	4,460	4,410	4,340	4,270	4,180	4,080	3,960	3,840	3,700	3,550	3,380	3,190
13⅜	72	26.02	20.768	3,550	3,510	3,470	3,420	3,360	3,290	3,210	3,120	3,020	2,910	2,790	2,660	2,510
13⅜	86	21.4	25.035	6,380	6,320	6,240	6,150	6,040	5,910	5,770	5,610	5,430	5,230	5,020	4,780	4,520

*Non-API grade

TABLE 2.4h—MINIMUM COLLAPSE RESISTANCE UNDER AXIAL LOAD, GRADE P-110

d _o (in.)	Weight (lbm/ft)	d _o /e	Area (sq. in.)	Axial Stress, psi												
				-10,000	-5,000	0	5,000	10,000	15,000	20,000	25,000	30,000	35,000	40,000	45,000	50,000
				Collapse Pressure, psi												
4½	11.6	18	3.338	7,720	7,650	7,580	7,490	7,390	7,290	7,170	7,040	6,900	6,740	6,560	6,370	6,160
4½	13.5	15.52	3.836	10,980	10,840	10,680	10,510	10,330	10,130	9,920	9,690	9,440	9,170	8,880	8,560	8,230
5	15	16.89	4.374	9,060	8,960	8,850	8,730	8,600	8,460	8,300	8,130	7,940	7,740	7,520	7,270	7,010
5	18	13.81	5.275	13,900	13,700	13,470	13,230	12,970	12,690	12,390	12,060	11,720	11,350	10,960	10,530	10,080
5	21.4	11.44	6.264	18,290	17,940	17,550	17,140	16,700	16,230	15,740	15,210	14,660	14,080	13,470	12,820	12,140
5	23.2	10.46	6.791	19,830	19,440	19,020	18,570	18,100	17,590	17,060	16,490	15,890	15,260	14,600	13,900	13,160
5	24.1	10	7.069	20,640	20,230	19,800	19,330	18,840	18,310	17,750	17,160	16,540	15,880	15,190	14,470	13,700
5½	17	18.09	4.962	7,620	7,550	7,480	7,400	7,300	7,200	7,090	6,960	6,820	6,660	6,490	6,300	6,100
5½	20	15.24	5.828	11,410	11,260	11,100	10,920	10,720	10,510	10,280	10,040	9,780	9,490	9,190	8,860	8,500
5½	23	13.25	6.63	15,030	14,800	14,540	14,270	13,980	13,670	13,330	12,980	12,590	12,190	11,750	11,220	10,620
6⅝	24	18.82	6.937	6,830	6,790	6,730	6,670	6,590	6,510	6,420	6,320	6,200	6,080	5,930	5,780	5,600
6⅝	28	15.89	8.133	10,430	10,300	10,160	10,000	9,830	9,650	9,450	9,240	9,010	8,760	8,490	8,190	7,880
6⅝	32	13.95	9.177	13,640	13,440	13,220	12,980	12,730	12,460	12,160	11,850	11,510	11,150	10,770	10,350	9,910
7	26	19.34	7.549	6,310	6,270	6,230	6,180	6,120	6,050	5,980	5,890	5,800	5,690	5,560	5,420	5,270
7	29	17.16	8.449	8,720	8,630	8,530	8,420	8,290	8,160	8,010	7,850	7,680	7,480	7,270	7,040	6,790
7	32	15.45	9.317	11,090	10,940	10,780	10,610	10,430	10,230	10,010	9,770	9,520	9,250	8,950	8,640	8,300
7	35	14.06	10.172	13,430	13,240	13,020	12,790	12,540	12,280	11,990	11,680	11,350	11,000	10,620	10,220	9,780
7	38	12.96	10.959	15,650	15,400	15,140	14,850	14,540	14,210	13,860	13,480	13,080	12,570	12,020	11,450	10,840
7⅝	26.4	23.25	7.519	3,970	3,950	3,920	3,890	3,860	3,810	3,770	3,710	3,650	3,580	3,500	3,410	3,310
7⅝	29.7	20.33	8.541	5,440	5,390	5,350	5,320	5,290	5,250	5,200	5,140	5,080	5,000	4,910	4,800	4,680
7⅝	33.7	17.73	9.72	8,030	7,960	7,870	7,780	7,760	7,560	7,430	7,290	7,140	6,970	6,790	6,580	6,360
7⅝	39	15.25	11.192	11,400	11,250	11,080	10,900	10,710	10,500	10,270	10,030	9,760	9,480	9,170	8,850	8,490
7⅝	42.8	13.57	12.47	14,370	14,160	13,920	13,670	13,390	13,100	12,780	12,450	12,080	11,700	11,290	10,850	10,380
7⅝	45.3	12.82	13.141	15,950	15,700	15,430	15,140	14,820	14,480	14,120	13,710	13,220	12,690	12,140	11,560	10,950
7⅝	47.1	12.2	13.745	17,260	16,920	16,550	16,170	15,750	15,310	14,840	14,350	13,830	13,280	12,700	12,090	11,460
8⅝	40	19.17	11.557	6,480	6,440	6,390	6,340	6,270	6,200	6,120	6,030	5,930	5,810	5,680	5,540	5,370
8⅝	44	17.25	12.763	8,610	8,520	8,420	8,310	8,190	8,060	7,920	7,760	7,590	7,400	7,190	6,970	6,720
8⅝	49	15.48	14.118	11,040	10,900	10,740	10,570	10,390	10,190	9,970	9,740	9,480	9,210	8,920	8,610	8,270
9⅝	43.5	22.13	12.559	4,490	4,460	4,420	4,370	4,320	4,270	4,200	4,130	4,050	3,970	3,870	3,810	3,750
9⅝	47	20.39	13.572	5,410	5,350	5,300	5,270	5,240	5,200	5,160	5,100	5,030	4,960	4,870	4,770	4,650
9⅝	53.5	17.66	15.547	8,110	8,040	7,950	7,850	7,750	7,630	7,500	7,360	7,200	7,030	6,840	6,640	6,410
10¾	51	23.89	14.561	3,700	3,680	3,660	3,640	3,610	3,570	3,530	3,490	3,430	3,370	3,300	3,220	3,130
10¾	55.5	21.72	15.947	4,690	4,650	4,610	4,560	4,510	4,440	4,370	4,300	4,210	4,140	4,090	4,020	3,950
10¾	60.7	19.72	17.473	5,950	5,920	5,880	5,840	5,790	5,740	5,670	5,600	5,510	5,410	5,300	5,180	5,030
10¾	65.7	18.07	18.982	7,640	7,580	7,500	7,420	7,320	7,220	7,100	6,980	6,840	6,680	6,510	6,320	6,110
11¾	60	24.03	17.3	3,640	3,620	3,610	3,580	3,560	3,520	3,490	3,440	3,390	3,330	3,260	3,190	3,100
13⅜	68	27.86	19.445	2,340	2,340	2,340	2,340	2,340	2,340	2,340	2,330	2,330	2,310	2,290	2,270	2,230
13⅜	72	26.02	20.766	2,680	2,680	2,680	2,680	2,670	2,660	2,650	2,630	2,600	2,570	2,540	2,510	2,470

TABLE 2.4i—MINIMUM COLLAPSE RESISTANCE UNDER AXIAL LOAD, GRADE Q-125

d_o (in.)	Weight (lbm/ft)	d_o/e	Area (sq in.)	Axial Stress, psi												
				-10,000	-5,000	0	5,000	10,000	15,000	20,000	25,000	30,000	35,000	40,000	45,000	50,000
				Collapse Pressure, psi												
4½	15.1	13.35	4.407	16,290	16,070	15,840	15,590	15,320	15,040	14,730	14,410	14,070	13,700	13,320	12,910	12,470
4½*	16.1	12	4.86	19,820	19,470	19,100	18,700	18,290	17,850	17,390	16,900	16,390	15,850	15,290	14,710	14,100
4½*	19.1	10.3	5.578	22,740	22,340	21,920	21,460	20,990	20,480	19,950	19,390	18,810	18,190	17,550	16,880	16,180
5	15	16.89	4.374	9,650	9,570	9,480	9,380	9,270	9,150	9,020	8,880	8,730	8,560	8,380	8,180	7,960
5*	18	13.81	5.275	15,230	15,040	14,830	14,600	14,360	14,100	13,820	13,530	13,220	12,880	12,530	12,160	11,760
5*	21.4	11.44	6.264	20,690	20,330	19,940	19,530	19,100	18,640	18,160	17,650	17,110	16,560	15,970	15,360	14,720
5	23.2	10.46	6.791	22,430	22,030	21,620	21,170	20,700	20,200	19,680	19,130	18,550	17,940	17,310	16,650	15,950
5*	24.1	10	7.069	23,350	22,940	22,500	22,040	21,550	21,030	20,480	19,910	19,310	18,680	18,020	17,330	16,610
5½*	17	18.09	4.962	7,990	7,950	7,890	7,830	7,760	7,680	7,600	7,500	7,390	7,270	7,140	6,990	6,830
5½*	20	15.24	5.828	12,360	12,230	12,080	11,920	11,740	11,560	11,350	11,140	10,910	10,660	10,390	10,110	9,800
5½	23	13.25	6.63	16,520	16,300	16,070	15,810	15,540	15,250	14,940	14,610	14,260	13,890	13,490	13,080	12,640
5½*	26.8	11	7.854	21,440	21,060	20,660	20,240	19,790	19,310	18,810	18,280	17,730	17,150	16,550	15,910	15,250
6½*	24	18.82	6.937	7,090	7,060	7,020	6,980	6,930	6,880	6,820	6,740	6,660	6,570	6,470	6,350	6,220
6½*	28	15.89	8.133	11,230	11,110	10,990	10,860	10,710	10,550	10,380	10,190	9,990	9,780	9,550	9,300	9,030
6½	32	13.95	9.177	14,930	14,740	14,530	14,310	14,080	13,830	13,560	13,270	12,970	12,650	12,300	11,940	11,550
7*	29	17.16	8.449	9,260	9,190	9,100	9,010	8,910	8,810	8,690	8,550	8,410	8,250	8,080	7,900	7,690
7*	32	15.45	9.317	11,990	11,860	11,720	11,560	11,400	11,220	11,030	10,820	10,600	10,370	10,110	9,840	9,550
7	35	14.06	10.172	14,690	14,500	14,310	14,090	13,860	13,620	13,360	13,080	12,780	12,460	12,130	11,770	11,390
7	38	12.96	10.959	17,240	17,000	16,750	16,480	16,190	15,880	15,550	15,200	14,830	14,440	14,030	13,590	13,120
7*	42.7	11.2	12.517	21,090	20,720	20,330	19,910	19,470	19,000	18,510	17,990	17,450	16,880	16,280	15,660	15,000
7½*	29.7	20.33	8.541	5,760	5,720	5,670	5,620	5,560	5,490	5,420	5,350	5,320	5,280	5,220	5,160	5,080
7½*	33.7	17.73	9.72	8,470	8,410	8,350	8,270	8,190	8,100	8,000	7,890	7,770	7,640	7,490	7,330	7,160
7½	39	15.25	11.192	12,340	12,210	12,060	11,900	11,730	11,540	11,340	11,120	10,890	10,640	10,380	10,100	9,790
7½	42.8	13.57	12.47	15,770	15,570	15,350	15,110	14,850	14,580	14,290	13,980	13,650	13,300	12,930	12,540	12,120
7½*	45.3	12.82	13.141	17,590	17,350	17,090	16,810	16,510	16,200	15,860	15,500	15,120	14,720	14,290	13,840	13,270
7½	47.1	12.2	13.745	19,270	18,990	18,700	18,380	18,010	17,580	17,130	16,650	16,140	15,620	15,070	14,490	13,880
8½*	40	19.17	11.557	6,680	6,660	6,630	6,600	6,560	6,520	6,460	6,400	6,330	6,250	6,160	6,060	5,940
8½*	44	17.25	12.763	9,130	9,060	8,980	8,890	8,800	8,690	8,570	8,450	8,310	8,150	7,990	7,810	7,610
8½	49	15.48	14.118	11,930	11,800	11,660	11,510	11,350	11,170	10,980	10,780	10,560	10,330	10,070	9,800	9,510
9½	47	20.39	13.572	5,720	5,680	5,640	5,580	5,520	5,460	5,390	5,310	5,270	5,230	5,180	5,120	5,040
9½	53.5	17.66	15.547	8,560	8,500	8,440	8,360	8,280	8,190	8,090	7,970	7,850	7,710	7,560	7,400	7,220
9½*	58.4	16.18	16.879	10,750	10,650	10,530	10,410	10,270	10,130	9,970	9,800	9,610	9,410	9,190	8,960	8,710
9½*	61.1	15.4	17.671	12,070	11,940	11,800	11,650	11,480	11,300	11,110	10,900	10,680	10,440	10,180	9,900	9,610
10¾*	55.5	21.72	15.947	4,900	4,870	4,850	4,810	4,770	4,730	4,680	4,620	4,560	4,490	4,410	4,320	4,220
10¾	60.7	19.72	17.473	6,180	6,130	6,070	6,020	6,000	5,970	5,930	5,890	5,840	5,780	5,700	5,620	5,520
10¾	65.7	18.07	18.982	8,020	7,970	7,920	7,850	7,780	7,710	7,620	7,520	7,410	7,290	7,160	7,010	6,850
10¾*	71.1	16.54	20.625	10,180	10,090	9,990	9,880	9,760	9,620	9,480	9,320	9,150	8,970	8,770	8,550	8,320
10¾*	73.2	16	21.276	11,050	10,940	10,810	10,680	10,540	10,390	10,220	10,040	9,850	9,640	9,410	9,170	8,910
10¾*	79.2	14.65	23.096	13,480	13,320	13,150	12,960	12,760	12,550	12,320	12,070	11,810	11,520	11,220	10,900	10,560
11¾	60	24.03	17.3	3,680	3,680	3,680	3,670	3,660	3,650	3,630	3,610	3,580	3,550	3,500	3,450	3,400
11¾*	66.7	21.48	19.252	5,040	5,010	4,980	4,940	4,900	4,850	4,800	4,740	4,670	4,600	4,510	4,420	4,330
13¾	72	26.02	20.768	2,880	2,880	2,880	2,880	2,880	2,880	2,880	2,880	2,880	2,870	2,850	2,830	2,800
13¾*	76.6	24.45	22.044	3,490	3,490	3,490	3,490	3,490	3,480	3,460	3,450	3,420	3,390	3,360	3,310	3,260
13¾*	92.5	19.9	26.818	6,060	6,010	5,950	5,890	5,830	5,800	5,770	5,730	5,680	5,630	5,560	5,480	5,390

* Non-API grade

TABLE 2.4j—MINIMUM COLLAPSE RESISTANCE UNDER AXIAL LOAD, GRADE V-150*

d_o (in.)	Weight (lbm/ft)	d_o/e	Area (sq in.)	Axial Stress, psi												
				-10,000	-5,000	0	5,000	10,000	15,000	20,000	25,000	30,000	35,000	40,000	45,000	50,000
				Collapse Pressure, psi												
4½	15.1	13.35	4.407	18,510	18,320	18,110	17,890	17,660	17,410	17,150	16,870	16,570	16,260	15,930	15,580	15,210
4½	16.6	12	4.86	22,890	22,620	22,330	22,020	21,700	21,360	21,000	20,630	20,230	19,770	19,240	18,690	18,120
4½	19.1	10.3	5.576	27,130	26,730	26,300	25,850	25,380	24,880	24,370	23,830	23,270	22,690	22,080	21,450	20,800
5	15	16.89	4.374	10,360	10,310	10,250	10,190	10,120	10,040	9,960	9,860	9,760	9,640	9,520	9,380	9,230
5	18	13.81	5.275	17,220	17,050	16,860	16,670	16,460	16,240	16,000	15,750	15,490	15,210	14,910	14,600	14,260
5	23.2	10.46	6.791	26,760	26,360	25,940	25,500	25,030	24,540	24,040	23,510	22,950	22,380	21,780	21,160	20,510
5½	20	15.24	5.828	13,690	13,580	13,460	13,340	13,200	13,050	12,890	12,720	12,540	12,340	12,130	11,910	11,670
5½	23	13.25	6.63	18,800	18,610	18,390	18,170	17,930	17,670	17,400	17,120	16,820	16,500	16,160	15,800	15,430
5½	26.8	11	7.854	25,580	25,200	24,790	24,370	23,930	23,460	22,970	22,470	21,940	21,390	20,820	20,220	19,610
6½	24	18.82	6.937	7,440	7,360	7,340	7,290	7,230	7,200	7,180	7,160	7,120	7,090	7,040	6,980	6,910
6½	28	15.89	8.133	12,290	12,210	12,120	12,020	11,910	11,790	11,660	11,530	11,380	11,210	11,040	10,850	10,650
6½	32	13.95	9.177	16,840	16,670	16,500	16,310	16,110	15,900	15,670	15,430	15,170	14,900	14,610	14,310	13,990
7	29	17.16	8.449	9,880	9,840	9,790	9,740	9,680	9,610	9,530	9,450	9,350	9,250	9,140	9,010	8,870
7	32	15.45	9.317	13,220	13,130	13,020	12,900	12,770	12,630	12,480	12,320	12,150	11,970	11,770	11,560	11,330
7	35	11.86	11.881	23,400	23,120	22,820	22,510	22,180	21,820	21,450	20,990	20,500	19,980	19,450	18,890	18,320
7	38	12.96	10.959	19,680	19,470	19,240	19,000	18,740	18,470	18,180	17,870	17,550	17,210	16,850	16,470	16,070
7	42.7	11.2	12.517	25,170	24,790	24,390	23,980	23,540	23,080	22,600	22,110	21,590	21,040	20,480	19,900	19,290
7½	29.7	20.33	8.541	6,100	6,080	6,050	6,030	6,000	5,960	5,920	5,870	5,820	5,760	5,690	5,620	5,540
7½	33.7	17.73	9.72	8,900	8,880	8,850	8,820	8,780	8,730	8,670	8,610	8,540	8,460	8,370	8,270	8,160
7½	39	15.25	11.192	13,670	13,560	13,440	13,320	13,180	13,030	12,870	12,700	12,520	12,330	12,120	11,890	11,660
7½	45.3	12.82	13.141	20,120	19,900	19,660	19,410	19,140	18,860	18,560	18,250	17,910	17,560	17,190	16,800	16,390
8½	44	17.25	12.763	9,720	9,680	9,640	9,590	9,530	9,470	9,390	9,310	9,220	9,120	9,010	8,890	8,760
8½	49	15.48	14.118	13,160	13,060	12,950	12,840	12,710	12,570	12,430	12,270	12,100	11,920	11,720	11,510	11,280
9½	53.5	17.66	15.547	9,020	8,990	8,960	8,930	8,880	8,830	8,780	8,710	8,640	8,560	8,460	8,360	8,240
9½	58.4	16.18	16.879	11,710	11,640	11,560	11,470	11,370	11,260	11,150	11,020	10,890	10,740	10,580	10,410	10,220
9½	61.1	15.4	17.671	13,330	13,230	13,120	13,000	12,870	12,730	12,580	12,420	12,240	12,060	11,860	11,640	11,410
9½	70.3	13.11	20.502	19,220	19,020	18,800	18,560	18,320	18,050	17,770	17,480	17,170	16,840	16,490	16,120	15,740
10¾	60.7	19.72	17.473	6,620	6,590	6,550	6,510	6,470	6,430	6,370	6,310	6,250	6,180	6,100	6,020	5,990
10¾	65.7	18.07	18.982	8,350	8,340	8,320	8,300	8,270	8,230	8,190	8,140	8,090	8,010	7,940	7,850	7,750
10¾	71.1	16.54	20.625	11,010	10,950	10,880	10,810	10,720	10,630	10,530	10,420	10,300	10,170	10,030	9,870	9,710
10¾	79.2	14.65	23.096	15,060	14,930	14,790	14,630	14,470	14,290	14,100	13,900	13,690	13,460	13,210	12,960	12,680
11¾	66.7	21.48	19.252	5,210	5,200	5,200	5,190	5,170	5,160	5,130	5,110	5,080	5,040	4,990	4,940	4,880
13¾	92.5	19.9	26.818	6,460	6,430	6,400	6,370	6,330	6,290	6,240	6,180	6,120	6,050	5,970	5,890	5,810
13¾	100.3	18.22	29.149	8,120	8,110	8,090	8,070	8,050	8,020	7,980	7,940	7,880	7,820	7,750	7,670	7,580

*Non-API grade

TABLE 2.5—ROUND-THREAD CASING COUPLING DIMENSIONS, WEIGHTS, AND TOLERANCES (FIG. 2.1)

Size* (in.)	OD** d_{oc} (in.)	Minimum Length, L_{min} , in.		Diameter of Recess d_r (in.)	Width of Bearing Face b (in.)	Weight, lbm	
		Short	Long			Short	Long
4½	5.000	6¼	7	419/32	5/32	8.05	9.07
5	5.563	6½	7¾	53/32	3/16	10.18	12.56
5½	6.050	6¾	8	519/32	1/8	11.44	14.03
6½	7.390	7¼	8¾	623/32	1/4	19.97	24.82
7	7.656	7¼	9	73/32	3/16	18.34	23.67
7½	8.500	7½	9¼	723/32	1/4	26.93	34.23
8½	9.625	7¾	10	823/32	3/32	35.58	47.48
9½	10.625	7¾	10½	923/32	9/32	39.51	55.77
10¾	11.750	8	—	1027/32	9/32	45.53	—
11¾	12.750	8	—	1127/32	9/32	49.61	—
13¾	14.375	8	—	1315/32	5/16	56.23	—
16	17.000	9	—	163/32	5/16	78.98	—
18½	20.000	9	—	1823/32	5/16	118.94	—
20	21.000	9	11½	203/32	5/16	98.25	126.74

*The size of the coupling is the same as the corresponding pipe size.

**Tolerance on OD d_{oc} $\pm 1\%$, but not greater than $\pm 1/16$ in.

TABLE 2.6—BUTTRESS-THREAD CASING COUPLING DIMENSIONS, WEIGHTS, AND TOLERANCES (FIG. 2.2)

Size* (in.)	OD, in.		Minimum Length L_{min} (in.)	Diameter of Chamfer d_c (in.)	Width of Bearing Face b (in.)	Weight, lbm	
	Regular** d_{oc}	Special Clearance† d_{ocs} (in.)				Regular	Special Clearance
4½	5.000	4.875	8⅞	4.640	⅛	10.11	7.67
5	5.563	5.375	9⅛	5.140	⅝ ₃₂	12.99	8.81
5½	6.050	5.875	9¼	5.640	⅝ ₃₂	14.14	9.84
6⅝	7.390	7.000	9⅝	6.765	¼	24.46	12.44
7	7.656	7.375	10	7.140	⅞ ₃₂	23.22	13.82
7⅝	8.500	8.125	10⅜	7.765	⅝ ₁₆	34.84	20.45
8⅝	9.625	9.125	10⅝	8.765	⅜	45.94	23.77
9⅝	10.625	10.125	10⅝	9.765	⅜	50.99	26.47
10¾	11.750	11.250	10⅝	10.890	⅜	56.68	29.49
11¾	12.750	—	10⅝	11.890	⅜	61.74	—
13¾	14.375	—	10⅝	13.515	⅜	69.95	—
16	17.000	—	10⅝	16.154	⅜	87.56	—
18⅝	20.000	—	10⅝	18.779	⅜	138.03	—
20	21.000	—	10⅝	20.154	⅜	110.33	—

*The size of the coupling is the same as the corresponding pipe size.

Tolerance on OD d_{oc} , $\pm 1\%$, but not greater than $\pm \frac{1}{16}$ in.†Tolerance on OD d_{ocs} , $+\frac{1}{32}$, $-\frac{1}{64}$ in.TABLE 2.7—EXTREME-LINE API CASING SIZE AND LENGTH OF UPSET (FIG. 2.3)**

OD (in.)	Length of Upset, in.		
	Pin Minimum (L_p) _{min}	Box Minimum (L_b) _{min}	Pin or Box Maximum (L_{bp}) _{max}
5	6⅝	7	8
5½	6⅝	7	8
6⅝	6⅝	7	8
7	6⅝	7	8*
7⅝	6⅝	7	8
8⅝	8	8¾	11
9⅝	8	8¾	11
10¾	8	8¾	12¾

 L_p = minimum length from end of pipe of the machined diameter d_{mp} on pin. L_b = the machined diameter d_{mb} plus length of thread on box, to the beginning of the internal upset runout.* L_{bp} = 9 in. (228.6 mm) maximum for 7 in.—35 lb/ft and 7 in.—38 lb/ft casing.**TABLE 2.8—GROSS LINEAR FOOTAGE FROM NET FOOTAGE, API SHORT-THREAD CASING**

OD (in.)	Nominal Weight per Foot (lbm)	Number of Threads per inch	Make-Up Loss per Joint (in.)	Multiplication Factor* for Average Joint Length		
				20 ft	30 ft	40 ft
4½	9.50	8	2.000	1.0084	1.0056	1.0042
4½	others	8	2.625	1.0111	1.0073	1.0055
5	11.50	8	2.500	1.0105	1.0070	1.0052
5	others	8	2.750	1.0116	1.0077	1.0058
5½	all	8	2.875	1.0121	1.0081	1.0060
6⅝	all	8	3.125	1.0132	1.0088	1.0066
7	17.00	8	2.375	1.0100	1.0066	1.0050
7	others	8	3.125	1.0132	1.0088	1.0066
7⅝	all	8	3.250	1.0137	1.0091	1.0068
8⅝	24.00	8	3.000	1.0127	1.0084	1.0063
8⅝	others	8	3.375	1.0143	1.0095	1.0071
9⅝	all	8	3.375	1.0143	1.0095	1.0071
10¾	32.75	8	2.750	1.0116	1.0077	1.0058
10¾	others	8	3.500	1.0148	1.0098	1.0073
11¾	all	8	3.500	1.0148	1.0098	1.0073
13¾	all	8	3.500	1.0148	1.0098	1.0073
16	all	8	4.000	1.0169	1.0112	1.0084
18⅝	all	8	4.000	1.0169	1.0112	1.0084
20	all	8	4.000	1.0169	1.0112	1.0084

*To obtain the gross shipping length, multiply net length in feet by the multiplication factor.

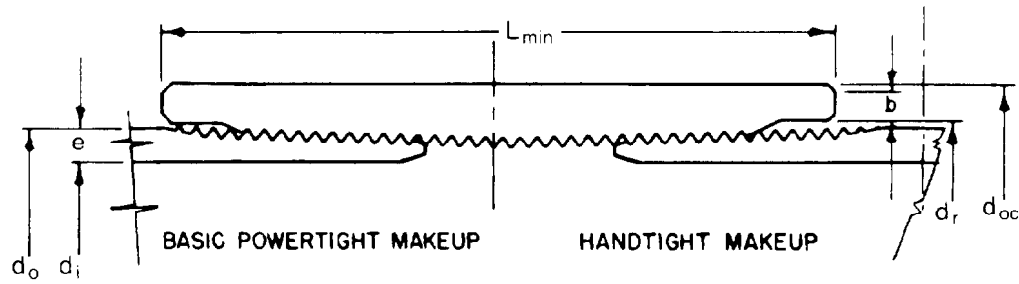


Fig. 2.1—Round-thread casing and coupling.

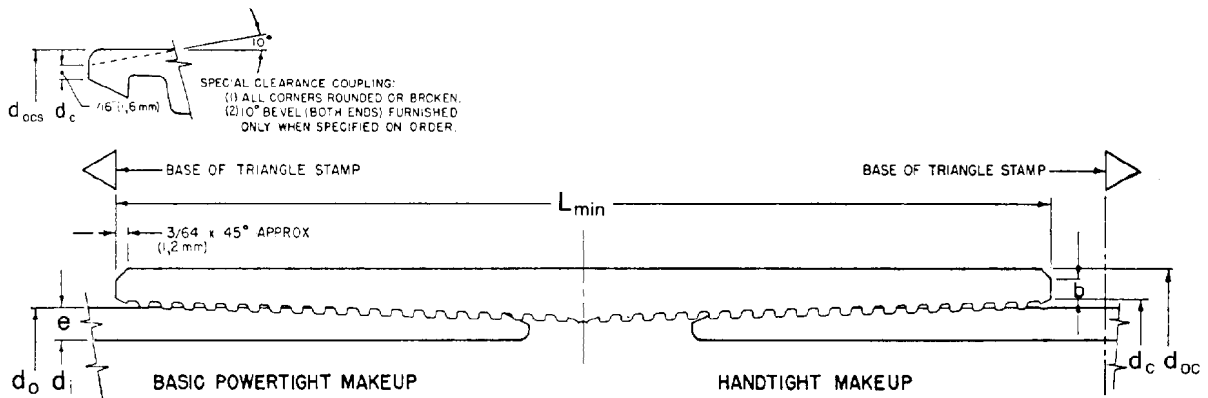


Fig. 2.2—Buttress-thread casing and coupling.

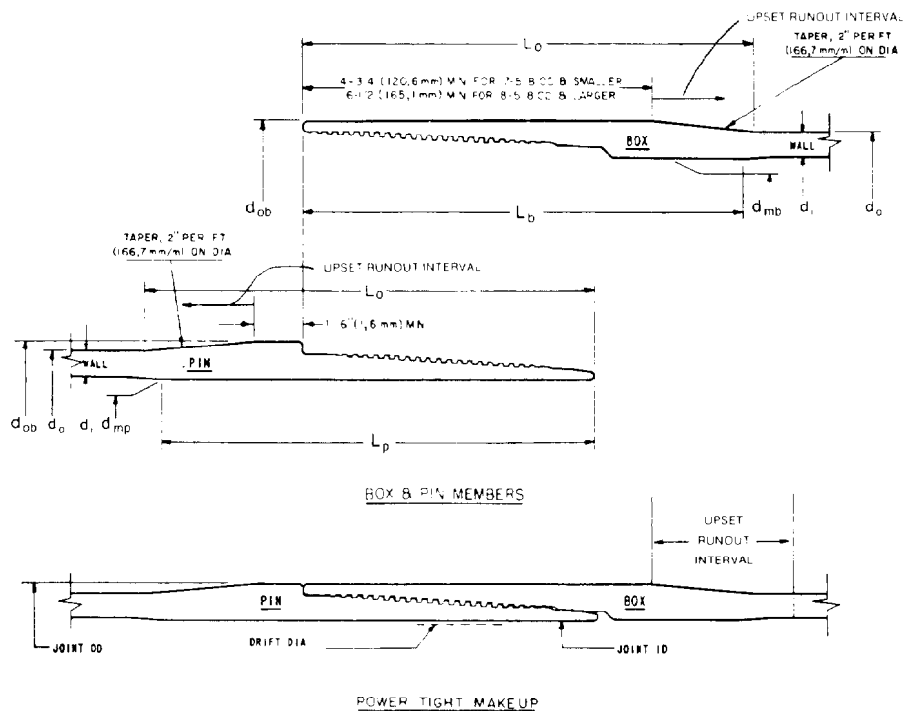


Fig. 2.3—Extreme-line casing.

TABLE 2.9—GROSS LINEAR FOOTAGE FROM NET FOOTAGE, API LONG-THREAD CASING

OD (in.)	Nominal Weight per Foot (lbm)	Number of Threads per inch	Make-Up Loss per Joint (in.)	Multiplication Factor* for Average Joint Length		
				20 ft	30 ft	40 ft
4½	all	8	3.000	1.0127	1.0084	1.0063
5	all	8	3.375	1.0143	1.0095	1.0071
5½	all	8	3.500	1.0148	1.0098	1.0073
6⅝	all	8	3.875	1.0164	1.0109	1.0081
7	all	8	4.000	1.0169	1.0112	1.0084
7⅝	all	8	4.125	1.0175	1.0116	1.0087
8⅝	all	8	4.500	1.0191	1.0127	1.0095
9⅝	all	8	4.755	1.0202	1.0134	1.0100
20	all	8	5.250	1.0224	1.0148	1.0111

*To obtain the gross shipping length, multiply net length in feet by the multiplication factor.

TABLE 2.10—GROSS LINEAR FOOTAGE FROM NET FOOTAGE, API BUTTRESS-THREAD CASING

OD (in.)	Nominal Weight per Foot (lbm)	Number of Threads per inch	Make-Up Loss per Joint (in.)	Multiplication Factor* for Average Joint Length		
				20 ft	30 ft	40 ft
4½	all	5	3.9375	1.0167	1.0111	1.0083
5	all	5	4.0625	1.0172	1.0114	1.0085
5½	all	5	4.1250	1.0175	1.0116	1.0087
6⅝	all	5	4.3125	1.0183	1.0121	1.0091
7	all	5	4.5000	1.0191	1.0127	1.0095
7⅝	all	5	4.6875	1.0199	1.0132	1.0099
8⅝	all	5	4.8125	1.0205	1.0135	1.0101
9⅝	all	5	4.8125	1.0205	1.0135	1.0101
10¾	all	5	4.8125	1.0205	1.0135	1.0101
11¾	all	5	4.8125	1.0205	1.0135	1.0101
13⅝	all	5	4.8125	1.0205	1.0135	1.0101
16	all	5	4.8125	1.0205	1.0135	1.0101
18⅝	all	5	4.8125	1.0205	1.0135	1.0101
20			4.8125	1.0205	1.0135	1.0101

*To obtain the gross shipping length, multiply net length in feet by the multiplication factor.

TABLE 2.11—GROSS LINEAR FOOTAGE FROM NET FOOTAGE, API EXTREME-THREAD CASING

OD (in.)	Nominal Weight per Foot (lbm)	Number of Threads per inch	Make-Up Loss per Joint (in.)	Multiplication Factor* for Average Joint Length		
				20 ft	30 ft	40 ft
5	all	6	4.590	1.0195	1.0129	1.0097
5½	all	6	4.590	1.0195	1.0129	1.0097
6⅝	all	6	4.590	1.0195	1.0129	1.0097
7	all	6	4.590	1.0195	1.0129	1.0097
7⅝	all	6	4.590	1.0195	1.0129	1.0097
8⅝	all	6	6.0625	1.0259	1.0171	1.0128
9⅝	all	6	6.0625	1.0259	1.0171	1.0128
10¾	all	6	6.0615	1.0259	1.0171	1.0128

*To obtain the gross shipping length, multiply net length in feet by the multiplication factor.

**TABLE 2.12—MINIMUM PERFORMANCE PROPERTIES,
PLAIN-END LINER CASING, GRADE J-55**

OD (in.)	Weight per Foot (lbm)	Wall (in.)	ID (in.)	Minimum Collapse Resistance (psi)	Minimum Internal Yield Pressure (psi)	Minimum Pipe-Body Yield (1,000 lbm)
3½	9.91	0.289	2.922	8,330	7,950	160
4	11.34	0.286	3.428	7,300	6,880	184
4½	13.04	0.290	3.920	6,420	6,200	211
5	17.93	0.362	4.276	7,390	6,970	290
5½	19.81	0.361	4.778	6,610	6,320	321
6⅝	27.65	0.417	5.791	6,170	6,060	447

Joint Strength Safety Factor. To calculate the joint strength safety factor, the weight below each section of the string is calculated and multiplied by the safety factor (1.8 has been used in this design), the joint strength that equals or exceeds the value for the particular section selected, and the actual safety factor calculated. If the joint required is not the short or long thread, that section of the string should be evaluated to determine how much of the section requires the higher-strength joint. The weight per foot and length of each section required to meet the collapse safety factor requirements are listed in Table 2.19.

Joint Required for 23-lbm At Top of String. Table 2.19 shows that the total weight of the string is 271,450 lbm. Multiplying by 1.8 yields a required minimum joint strength of 488,610 lbm. In Table 2.3 we find that the long-thread joint with a joint strength of 442,000 lbm will not provide the required 1.8 minimum safety factor and that the buttress thread with a joint strength of 588,000 lbm is required. Dividing the 588,000-lbm strength of the buttress joint by the 271,450-lbm total weight of the casing yields a safety factor of 2.17.

Joint for the Lower Part of 23-lbm Section. The depth at which the 23-lbm round-thread joint with a strength of 442,000 lbm can be set with a safety factor of 1.8 is

$$(271,450 - 442,000 / 1.8) / 23 = 1,126 \text{ ft,}$$

which is rounded to 1,150 ft. At a depth of 1,150 ft, the weight of the string is $271,450 - 1,150 \times 23$, or 245,000 lbm. Dividing the 442,000-lbm joint strength by the 245,000-lbm load yields a safety factor of 1.804.

Joint for 26-lbm Section. Table 2.19 shows the weight acting on the top of the 26-lbm section to be 123,100 lbm. Multiplying 123,100 lbm by 1.8 requires that the joint strength be equal to or greater than 221,580 lbm. Referring to Table 2.3, we find that the long-thread joint has a strength of 519,000 lbm and can be used. Dividing the 519,000-lbm joint strength by the 221,580-lbm load at the top of the 26-lbm section yields the safety factor 2.34.

Joint for 29-lbm Section. Table 2.19 shows the weight of the string acting on the top of the 29-lbm section to be 46,400 lbm. Multiplying 46,400 lbm by the safety factor, 1.8, requires that the joint strength be equal to or greater than 83,520 lbm. Table 2.3 shows that a long-thread joint has a joint strength of 597,000 lbm and can be used. Dividing the 597,000-lbm joint strength by the 46,400-lbm load at the top of the 29-lbm section gives a safety factor of 12.87.

Pipe-Body Yield-Strength Safety Factors. Values of pipe-body yield strength are determined from Table 2.3 and the string weight at the top of each casing weight from Table 2.19. Pipe-body yield-strength safety factors are determined by dividing the pipe-body yield strengths by the casing weights at the top of the casing string sections (Table 2.20).

Internal-Yield-Pressure Safety Factors. The entire string can be subjected to an internal yield pressure equal to the BHP, which is 5,500 psi. Values of internal yield pressures for the casing joints are obtained from Tables 2.2 and 2.3. Safety factors are determined by dividing the internal yield pressures by 5,500 psi (Table 2.21).

TABLE 2.13—MINIMUM COLLAPSE PRESSURE UNDER AXIAL LOAD, GRADE J-55 LINER CASING

d_o (in.)	Weight (lbm/ft)	d_o/e	Area (sq in.)	Axial Stress, psi												
				- 10,000	- 5,000	0	5,000	10,000	15,000	20,000	25,000	30,000	35,000	40,000	45,000	50,000
				Collapse Pressure, psi												
3.5	9.91	12.11	2.915	8.990	8.690	8.330	7.930	7.470	6.960	6.390	5.770	5.070	4.300	3.440	2.470	—
4	11.34	13.99	3.337	7.870	7.610	7.300	6.950	6.550	6.100	5.600	5.050	4.440	3.770	3.020	2.170	—
4.5	13.04	15.52	3.836	6.810	6.630	6.420	6.170	5.890	5.540	5.090	4.590	4.040	3.420	2.740	1.970	—
5	17.93	13.81	5.275	7.970	7.700	7.390	7.030	6.620	6.170	5.670	5.110	4.500	3.810	3.050	2.190	—
5.5	19.81	15.24	5.828	7.020	6.830	6.610	6.360	6.050	5.630	5.170	4.670	4.110	3.480	2.790	2.000	—
6.625	27.65	15.89	8.133	6.540	6.370	6.170	5.940	5.670	5.370	4.980	4.490	3.950	3.350	2.680	1.920	—

TABLE 2.14—OIL, WATER, AND MUD WEIGHT FACTORS

Degrees API	Specific Gravity	Weight (Density)			Fluid Head		Buoyancy Factor* Totally Immersed
		(lbm/gal)	(lbm/ft ³)	(lbm/bbl)	(psi/ft)	(ft/psi)	
10							
API	1.00	8.34	62.4	350	0.433	2.31	0.873
or	1.01	8.4	62.8	353	0.436	2.29	0.872
Pure	1.03	8.6	64.3	361	0.447	2.24	0.869
Water	1.06	8.8	65.8	370	0.457	2.19	0.866
	1.08	9.0	67.3	378	0.468	2.14	0.862
	1.10	9.2	68.8	386	0.478	2.09	0.860
	1.13	9.4	70.3	395	0.488	2.05	0.856
	1.15	9.6	71.8	403	0.499	2.00	0.853
Salt Water }	1.154	9.625	72.0	404	0.500	2.00	0.853
	1.18	9.8	73.3	412	0.509	1.96	0.850
	1.20	10.0	74.8	420	0.519	1.93	0.847
	1.22	10.2	76.3	428	0.530	1.89	0.844
	1.25	10.4	77.8	437	0.540	1.85	0.841
	1.27	10.6	79.3	445	0.551	1.81	0.838
	1.29	10.8	80.8	454	0.561	1.78	0.835
	1.32	11.0	82.3	462	0.571	1.75	0.832
	1.34	11.2	83.8	470	0.582	1.72	0.829
	1.37	11.4	85.3	479	0.592	1.69	0.826
	1.39	11.6	86.8	487	0.603	1.66	0.823
	1.41	11.8	88.3	496	0.613	1.63	0.820
	1.44	12.0	89.8	504	0.623	1.61	0.817
	1.46	12.2	91.3	512	0.634	1.58	0.814
	1.49	12.4	92.8	521	0.644	1.55	0.810
	1.51	12.6	94.3	529	0.655	1.53	0.808
	1.53	12.8	95.8	538	0.665	1.50	0.804
	1.56	13.0	97.2	546	0.675	1.48	0.801
	1.58	13.2	98.7	554	0.686	1.46	0.798
	1.61	13.4	100	563	0.696	1.44	0.795
	1.63	13.6	102	571	0.706	1.42	0.792
	1.65	13.8	103	580	0.717	1.39	0.789
	1.68	14.0	105	588	0.727	1.38	0.786
	1.70	14.2	106	596	0.738	1.36	0.783
	1.73	14.4	108	605	0.748	1.34	0.780
	1.75	14.6	109	613	0.758	1.32	0.777
	1.77	14.8	111	622	0.769	1.30	0.774
	1.80	15.0	112	630	0.779	1.28	0.771
	1.82	15.2	114	638	0.790	1.27	0.768
	1.85	15.4	115	647	0.800	1.25	0.765
	1.87	15.6	117	655	0.810	1.23	0.762
	1.89	15.8	118	664	0.821	1.22	0.759
Common Cement Slurry** }	1.92	16.0	120	672	0.831	1.20	0.755
	1.94	16.2	121	680	0.842	1.19	0.753
	1.97	16.4	123	689	0.852	1.17	0.749
	1.99	16.6	124	697	0.862	1.16	0.746
	2.01	16.8	126	706	0.873	1.15	0.743
	2.04	17.0	127	714	0.883	1.13	0.740
	2.06	17.2	129	722	0.894	1.12	0.737
	2.09	17.4	130	731	0.904	1.11	0.734
	2.11	17.6	132	739	0.914	1.09	0.731
	2.13	17.8	133	748	0.925	1.08	0.728
	2.16	18.0	135	756	0.935	1.07	0.725
	2.18	18.2	136	764	0.945	1.06	0.722
	2.21	18.4	138	773	0.956	1.05	0.719
	2.23	18.6	139	781	0.966	1.04	0.716
	2.25	18.8	141	790	0.977	1.02	0.713
	2.28	19.0	142	798	0.987	1.01	0.710
	2.30	19.2	144	806	0.997	1.00	0.707
	2.33	19.4	145	815	1.01	0.992	0.704
	2.35	19.6	147	823	1.02	0.982	0.701
	2.37	19.8	148	832	1.03	0.972	0.698
	2.40	20.0	150	840	1.04	0.962	0.694
	2.42	20.2	151	848	1.05	0.953	0.692
	2.45	20.4	153	857	1.06	0.943	0.688
	2.47	20.6	154	865	1.07	0.935	0.685
	2.49	20.8	156	874	1.08	0.925	0.682
	2.52	21.0	157	882	1.09	0.917	0.679
	2.54	21.2	159	890	1.10	0.908	0.676
	2.57	21.4	160	899	1.11	0.899	0.673
	2.59	21.6	162	907	1.12	0.891	0.670
	2.61	21.8	163	916	1.13	0.883	0.667

*Buoyancy factor is for converting weight of steel in air to weight in liquid, for checking dead weight on hook. Actual load = length of string times weight per foot times buoyancy factor.

**Slurry giving 11.1 cu ft per sack of cement after setting.

Rough temperature correction (for oil): For temperatures close to 60°F, an approximate correction to 60°F may be made by deducting 1° API for each 13°F that the observed temperature is above 60°F or adding 1° API for each 13°F below.

Calculations based on 11.1 cu ft per sack of cement after setting.

TABLE 2.15—DESIGN SAFETY FACTORS FOR A SINGLE WEIGHT AND GRADE CASING STRING

Nominal Weight per Foot (lbm/ft)	Grade	Type Thread	Amount (ft)	Safety Factor			
				Collapse Bottom of Section	Joint Strength Top of Section	Pipe-Body Yield Strength Top of Section	Internal Yield Pressure Bottom of Section
29.00	N-80	Long	11,000	1.276	1.87	2.12	1.48

TABLE 2.16—DESIGN SAFETY FACTORS FOR COMBINATION CASING STRING

Nominal Weight per Foot (lbm/ft)	Grade	Type Thread	Section Length (ft)	Safety Factor			
				Collapse Bottom of Section	Joint Strength Top of Section	Pipe-Body Yield Strength Top of Section	Internal Yield Pressure Bottom of Section
23.00	N-80	Buttress	1,150	> 1.129	2.17	1.96	1.15
23.00	N-80	Long	5,500	1.129	1.80	2.17	1.15
26.00	N-80	Long	2,300	1.126	2.34	4.91	1.32
29.00	N-80	Long	2,050	1.160	12.87	14.57	1.48

TABLE 2.17—INTERMEDIATE SECTION COLLAPSE SAFETY FACTORS

7-in., 26-lbm, N-80 Axial Load Collapse			Net 26-lbm Load Availability for 29-lbm Weight			26-lbm Section Bottom		
Stress (psi)	Load (lbm)	Collapse Resistance (psi)	Weight Below 29 lbm (lbm)	Weight (lbm)	Equivalent 29-lbm Length (ft)	Depth (ft)	Collapse Pressure (psi)	Safety Factor
0	0	5,410	0	0	0	11,000	5,500	0.984
5,000	37,745	5,310	0	37,745	1,302	9,698	4,849	1.095
10,000	75,490	5,200	0	75,490	2,603	8,397	4,199	1.238
6,147	46,400	5,290	0	46,400	1,600	9,400	4,700	1.126

7-in., 26-lbm cross-sectional area = 7.549 sq in.

TABLE 2.18—TOP SECTION COLLAPSE SAFETY FACTORS

7-in., 23 lbm, N-80 Axial Load Collapse			Net 23-lbm Load			23-lbm Section Bottom		
Stress (psi)	Load (lbm)	Collapse Resistance (psi)	Weight Below 26 lbm (lbm)	Availability for 26-lbm Weight (lbm)	Equivalent 26-lbm Length (ft)	Depth (ft)	Collapse Pressure (psi)	Safety Factor
0	0	3,830	46,400	—	—	—	—	—
5,000	33,280	3,790	46,400	—	—	—	—	—
10,000	66,560	3,740	46,400	20,160	775	8,625	4,313	0.867
15,000	99,840	3,690	46,400	53,440	2,055	7,345	3,673	1.005
20,000	133,120	3,620	46,400	86,720	3,335	6,065	3,033	1.194
18,299	121,800	3,640	46,400	75,400	2,900	6,500	3,250	1.120
18,495	123,100	3,640	46,400	76,700	2,950	6,450	3,225	1.129

7-in., 23-lbm cross-sectional area = 6.656 sq in.
Length of 29-lbm intermediate section = 9,400 ft

Stretch in Casing When Freely Suspended in Fluid Media (Also Applicable to Tubing)

When pipe is subjected to an axial stress, either tension or compression, that does not exceed the elastic limit of the material, the stretch or contraction may be determined by use of Young's modulus of elasticity (30 million psi for steel pipe).

$$E = \frac{\sigma}{\Delta L_u} \text{ or } E = \frac{W_u/A_m}{\Delta L_t/L_p}, \dots\dots\dots (1)$$

where

- E = Young's modulus of elasticity, psi,
- σ = unit stress, psi,
- ΔL_u = unit axial stretch or contraction, in.,
- W_u = superimposed tension or compression axial load, lbm,
- A_m = cross-sectional metal area of pipe, sq in.,
- ΔL_t = total axial stretch or contraction, in., and
- L_p = length of pipe, in.

The unit tension or compression stress in pipe, when lateral deflection is prevented, is $\sigma = W_u/A_m$, unit axial stretch or contraction being $\Delta L_u = \Delta L_t/L_p$.

Fig. 2.4 gives stretch in single-weight strings of pipe of one grade, or in combination strings of more than one weight or grade. The equations from which these charts

were developed are based on a modified form of Eq. 1 with the lateral contraction of the pipe taken into consideration.

$$\Delta L_t = \Delta L_1 + \Delta L_2 + \Delta L_3 + F_1 \frac{W_2 + W_3}{W_1} + F_2 \frac{W_3}{W_2} + C_1 [L_{s1} \times L_{s2} + (L_{s1} + L_{s2}) L_{s3}] - C_2 \left(L_{s2}^2 \frac{W_1}{W_2} + L_{s3}^2 \frac{W_1 + W_2}{W_3} \right) \dots\dots\dots (2)$$

From Fig. 2.4 we get the values of ΔL_1 and F_1 (Free Stretch Factor 1) corresponding to length L_{s1} ; ΔL_2 and F_2 (Free Stretch Factor 2) from L_{s2} ; and ΔL_3 from L_{s3} .

TABLE 2.20—PIPE-BODY YIELD STRENGTH SAFETY FACTORS

Section Weight per Foot (lbm/ft)	Pipe-Body Yield Strength (lbm)	Weight Below Section (lbm)	Safety Factor
23	532,000	271,450	1.96
26	604,000	123,100	4.91
29	676,000	46,400	14.57

TABLE 2.19—WEIGHT AND LENGTH TO MEET JOINT-STRENGTH SAFETY FACTORS

Section Weight per Foot (lbm/ft)	Length (ft)	Weight (lbm)	Weight Below Top of Section, lbm		
			29 lbm	26 lbm	29 lbm
23	6,450	148,350			271,450
26	2,950	76,700		123,100	
29	1,600	46,400	46,400		
	11,000				

TABLE 2.21—INTERNAL YIELD PRESSURE SAFETY FACTORS

Nominal Weight per Foot (lbm/ft)	Joint	Internal Yield Pressure (psi)	Safety Factor
23	Buttress	6,340	1.15
23	Long	6,340	1.15
26	Long	7,240	1.32
29	Long	8,160	1.48

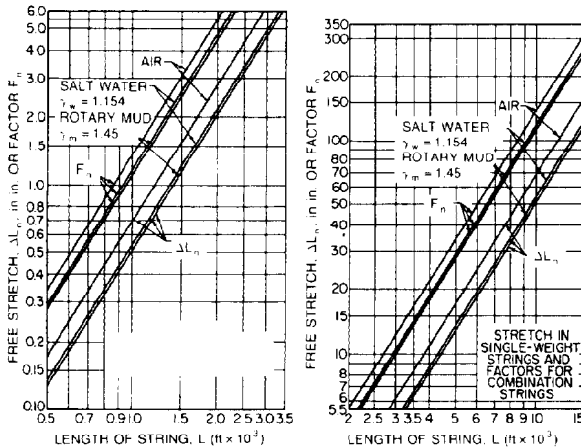


Fig. 2.4—Relieving stresses in suspended casing strings.

Example Problem 1. Assume a 10,000-ft, three-weight combination string is freely suspended in salt water. The weight of the 5,000-ft, 23-lbm/ft top section is $5,000 \times 23 = 115,000$ lbm. The weight of the 3,000-ft, 26-lbm/ft middle section is $3,000 \times 26 = 78,000$ lbm. The weight of the 2,000-ft, 29-lbm/ft bottom section is $2,000 \times 29 = 58,000$ lbm. Determine the casing stretch.

Solution.

$$\begin{aligned} \Delta L_t &= 13.5 + 4.86 + 2.16 + 29 \frac{78,000 + 58,000}{115,000} \\ &+ 10.4 \frac{58,000}{78,000} + 0.000000120177[5,000 \times 3,000 \\ &+ (5,000 + 3,000)2,000] - 0.000000200294 \left[(3,000)^2 \right. \\ &\times \frac{115,000}{78,000} + (2,000)^2 \frac{115,000 + 78,000}{58,000} \left. \right] \\ &= 20.52 + 29 \times 1.183 + 10.4 \times 0.744 + 0.000000120177 \\ &\times 31,000,000 - 0.000000200294 \times 26,578,000 \\ &= 20.52 + 34.31 + 7.74 + 3.73 - 5.32 \\ &= 60.98 \text{ in.} \end{aligned}$$

To determine tension stresses in casing strings after they are set and cemented, the following equations are used.

$$W_t = C_3(w'_1 L'_1 + w'_2 L'_2 + \dots + w'_n L'_n),$$

$$L_0 = C_4 W_t (L_1/w_1 + L_2/w_2 + \dots + L_n/w_n),$$

and

$$L_s = C_5 \sigma_t L,$$

where

$$L = (L_1 + L_2 + \dots + L_n),$$

$$L_d = L_0 - L_s,$$

$$C_3 = (1 - \rho_f/\rho_s),$$

$$C_4 = 40.8/E, \text{ and}$$

$$C_5 = 12/E.$$

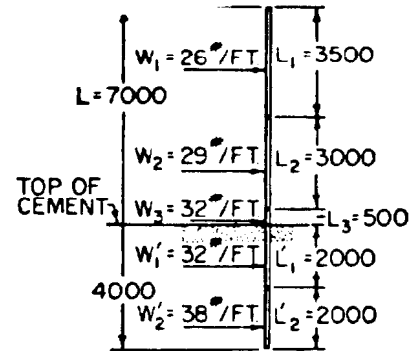


Fig. 2.5—Example string.

In these equations,

L_1, L_2, \dots

L_n = lengths above top of cement of single-weight Sections 1, 2, ..., n of combination string, ft,

L'_1, L'_2, \dots

L'_n = lengths below top of cement of single-weight Sections 1, 2, ..., n of combination string, ft,

w_1, w_2, \dots

w_n = weights of single-weight Sections 1, 2, ..., n of combination string above top of cement, lbm/ft,

w'_1, w'_2, \dots

w'_n = weights of single-weight Sections 1, 2, ..., n of combination strings below top of cement, lbm/ft,

C_1 = constant (for salt water, 0.000000120177; for rotary mud, 0.000000150869; and for air, zero),

C_2 = constant (for salt water, 0.000000200294; for rotary mud, 0.000000251448; and for air, zero),

C_3 = constant (for salt water, 0.8527; for rotary mud, 0.8151; for air, 1.0),*

C_4 = constant, 0.00000136,

C_5 = constant, 0.0000004,

L_d = distance to lower top of casing for a desired stress at top of cement, in.,

L_s = stretch corresponding to σ_t , in.,

L_0 = distance required to lower top of casing for zero stress at top of cement, in.,

W_t = total load below top of cement, lbm,

σ_t = tension stress desired to be left at top of cement, psi.

ρ_f = density of floatant, lbm/cu in. (for salt water, 0.041728; for rotary mud, 0.052385),* and

ρ_s = density of steel, 0.2833 lbm/cu in.

*Based on salt water and rotary mud having specific gravities of 1.155 and 1.45, respectively.

TABLE 2.22—API TUBING TENSILE REQUIREMENTS

Tubing Grade	Yield Strength, psi		Minimum Tensile Strength (psi)	Maximum Hardness		Minimum Elongation in 2 in.* (%)
	Minimum	Maximum		HRC	BHN	
H-40	40,000	80,000	60,000			
J-55	55,000	80,000	75,000			
C-75	75,000	90,000	95,000			
L-80	80,000	95,000	95,000	23	241	
N-80	80,000	110,000	100,000			
C-90	90,000	105,000	100,000	25.4	255	
P-105	105,000	135,000	120,000			

*The minimum elongation in 2 in. is determined by the equation in Table 2.1

Example Problem 2. Assume that an 11,000-ft combination string of 7-in.-OD casing is suspended freely in salt water, then cemented 4,000 ft up. The weight and length of the sections are shown in Fig. 2.5. We must find L_0 for zero stress at the top of the cement and L_d for a 5,000-lbm tension at the top of the cement.

Solution.

$$\begin{aligned}
 W_t &= C_3(w_1' L_1' + w_2' L_2') \\
 &= 0.8527[(32 \times 2,000) + (38 \times 2,000)] \\
 &= 0.8527(64,000 + 76,000) \\
 &= 0.8527 \times 140,000 \\
 &= 119,378 \text{ lbm.}
 \end{aligned}$$

$$\begin{aligned}
 L_0 &= C_4 W_t \left(\frac{L_1}{w_1} + \frac{L_2}{w_2} + \frac{L_3}{w_3} \right) \\
 &= 0.00000136 \times 119,378 \left(\frac{3,500}{26} + \frac{3,000}{29} + \frac{500}{32} \right) \\
 &= 0.16235(134.62 + 103.45 + 15.63) \\
 &= 0.16235 \times 253.70 \\
 &= 41.19 \text{ in.}
 \end{aligned}$$

$$\begin{aligned}
 L_s &= C_5 \sigma_t L \\
 &= 0.0000004 \times 5,000(3,500 + 3,000 + 500) \\
 &= 0.002 \times 7,000 \\
 &= 14 \text{ in.}
 \end{aligned}$$

$$\begin{aligned}
 L_d &= L_0 - L_s \\
 &= 41.19 - 14 \\
 &= 27.19 \text{ in.}
 \end{aligned}$$

For any variation in temperature after cementing, the corresponding expansion or contraction for the part of the string above the cement must be considered.

Single-Weight String Suspended in Rotary Mud

For a single-weight string suspended in rotary mud, the distance required to lower the top of the casing for a zero stress at the top of the cement is determined by

$$L_0 = C_6(D - L')L'$$

where

$$C_6 = C_3 C_4,$$

D = total depth of the well or length of string, ft, and

L' = length of casing below top of cement, ft.

Example Problem 3. Assume an 8,000-ft-long single-weight string of any OD and weight suspended freely in rotary mud with a specific gravity of 1.45, then cemented 2,100 ft up. Determine the amount the top of the casing has to be lowered for a zero stress at the top of the cement. For rotary mud with this specific gravity, $C_3 = 0.8151$, $D = 8,000$ ft, and $L' = 2,100$ ft.

Solution.

$$\begin{aligned}
 L_0 &= C_6(D - L')L' \\
 &= 0.8151 \times 0.00000136(8,000 - 2,100)2,100 \\
 &= 0.0000011085 \times 5,900 \times 2,100 \\
 &= 13.7 \text{ in.}
 \end{aligned}$$

TABLE 2.23—API TUBING RANGE LENGTHS

	Range	
	1	2
Total range length, inclusive, ft	20 to 24	28 to 32
Range length for 95% or more of carload		
Permissible variation, maximum ft	2	2
Permissible length, minimum ft	20	28

TABLE 2.24—MINIMUM PERFORMANCE PROPERTIES OF TUBING

1	2	3	4	5	6	7	8	9	10	11
OD d_o (in.)	Nominal Weight (lbm/ft)				Wall Thickness e (in.)	ID d_i (in.)	Drift Diameter (in.)	Threaded and Coupled		
	Threads and Coupling		Integral Joint	Grade				OD of Coupling (in.)		
	Nonupset	Upset						Nonupset d_{oc}	Regular d_{oc}	Upset Special Clearance d_{ocs}
1.050	1.14	1.20	—	H-40	0.113	0.824	0.730	1.313	1.660	—
	1.14	1.20	—	J-55	0.113	0.824	0.730	1.313	1.660	—
	1.14	1.20	—	C-75	0.113	0.824	0.730	1.313	1.660	—
	1.14	1.20	—	L-80,N-80	0.113	0.824	0.730	1.313	1.660	—
	1.14	1.20	—	C-90	0.113	0.824	0.730	1.313	1.660	—
1.315	1.70	1.80	1.72	H-40	0.133	1.049	0.955	1.660	1.900	—
	1.70	1.80	1.72	J-55	0.133	1.049	0.955	1.660	1.900	—
	1.70	1.80	1.72	C-75	0.133	1.049	0.955	1.660	1.900	—
	1.70	1.80	1.72	L-80,N-80	0.133	1.049	0.955	1.660	1.900	—
	1.70	1.80	1.72	C-90	0.133	1.049	0.955	1.660	1.900	—
1.660	—	—	2.10	H-40	0.125	1.410	—	—	—	—
	2.30	2.40	2.33	H-40	0.140	1.380	1.286	2.054	2.200	—
	—	—	2.10	J-55	0.125	1.410	—	—	—	—
	2.30	2.40	2.33	J-55	0.140	1.380	1.286	2.054	2.200	—
	2.30	2.40	2.33	C-75	0.140	1.380	1.286	2.054	2.200	—
	2.30	2.40	2.33	L-80, N-80	0.140	1.380	1.286	2.054	2.200	—
	2.30	2.40	2.33	C-90	0.140	1.380	1.286	2.054	2.200	—
1.900	—	—	2.40	H-40	0.125	1.650	—	—	—	—
	2.75	2.90	2.76	H-40	0.145	1.610	1.516	2.200	2.500	—
	—	—	2.40	J-55	0.125	1.650	—	—	—	—
	2.75	2.90	2.76	J-55	0.145	1.610	1.516	2.200	2.500	—
	2.75	2.90	2.76	C-75	0.145	1.610	1.516	2.200	2.500	—
	2.75	2.90	2.76	L-80, N-80	0.145	1.610	1.516	2.200	2.500	—
	2.75	2.90	2.76	C-90	0.145	1.610	1.516	2.200	2.500	—

Tubing

The performance of the tubing that is run inside the casing to conduct oil or gas to ground level is important. Tubing not only must withstand the same stresses to which casing is subjected, but also must resist the corrosive action of well fluids that in some areas is severe.

API has developed specifications that meet the major needs of the oil and gas industry.^{1,2,4-7} API specifications and bulletins provide standard dimensions, strength and performance properties, and the required gauging practice to ensure complete interchangeability.

Tables 2.22 and 2.23 give the tensile requirements and range lengths of API tubing. Listed in Table 2.24 are the minimum performance properties of tubing. Tables 2.25 through 2.27 give the dimensions, weights, and tolerances of nonupset and external-upset tubing, couplings, and integral-joint tubing upsets (see also Figs. 2.6 through 2.8). Multiplication factors for converting net footage to gross linear footage are given in Table 2.28. Equations for calculating performance properties of tubing are found in the section on equations.

Special Tubing Joints

A number of special tubing joints are useful when more strength, leak resistance, or clearance is needed than that provided by the standard API nonupset, upset, or integral joints. These special joints obtain their improved properties by various means, such as couplings or box ends with seal rings of teflon, etc.; special thread profiles, such as Acme or buttress; torque shoulders; metal-to-metal seals; internal upsets; external upsets; integral joints; and flush joints.

Design of Tubing Strings: Oil, Water, and Mud-Weight Factors

For information on oil, water, and mud weight factors needed in the design of tubing strings, refer to Table 2.14, which lists these factors for casing. The same table also will apply to tubing design.

Safety Factors

The following safety factors are commonly used in the design of tubing strings. These safety factors will be used

TABLE 2.24—MINIMUM PERFORMANCE PROPERTIES OF TUBING (continued)

12	13	14	15	16	17	18
Integral Joint				Joint Yield Strength (lbf)		
Drift Diameter (in.)	OD of Box d_{ob} (in.)	Collapse Resistance (psi)	Internal Yield Pressure (psi)	Threaded and Coupled		Integral Joint
				Nonupset	Upset	
—	—	7,680	7,530	6,360	13,310	—
—	—	10,560	10,360	8,740	18,290	—
—	—	14,410	14,130	11,920	24,950	—
—	—	15,370	15,070	12,710	26,610	—
—	—	17,290	16,950	14,300	29,940	—
0.955	1.550	7,270	7,080	10,960	19,760	15,970
0.955	1.550	10,000	9,730	15,060	27,160	21,960
0.955	1.550	13,640	13,270	20,540	37,040	29,940
0.955	1.550	14,550	14,160	21,910	39,510	31,940
0.955	1.550	16,360	15,930	24,650	44,450	35,930
1.286	1.880	5,570	5,270	—	—	22,180
1.286	1.880	6,180	5,900	15,530	26,740	22,180
1.286	1.880	7,660	7,250	—	—	30,500
1.286	1.880	8,490	8,120	21,360	36,770	30,500
1.286	1.880	11,580	11,070	29,120	50,140	41,600
1.286	1.880	12,360	11,810	31,060	53,480	44,370
1.286	1.880	13,900	13,280	34,950	60,170	49,920
1.516	2.110	4,920	4,610	—	—	26,890
1.516	2.110	5,640	5,340	19,090	31,980	26,890
1.516	2.110	6,640	6,330	—	—	36,970
1.516	2.110	7,750	7,350	26,250	43,970	36,970
1.516	2.110	10,570	10,020	35,800	59,960	50,420
1.516	2.110	11,280	10,680	38,180	63,960	53,780
1.516	2.110	12,630	12,020	42,960	71,950	60,500

in the example tubing string design. The designer has the responsibility to select safety factors to suit particular needs: collapse strength, 1.125; joint yield strength, 1.80; and internal yield pressure, 1.00.

Single Weight and Grade Tubing String. Table 2.29 includes design data and safety factors for an 11,000-ft single weight and grade upset tubing string with an OD of 2 $\frac{7}{8}$ in.

Selection of Nominal Weight and Grade. Formulating a table similar to Table 2.30 is convenient when the nominal weight and grade of tubing are selected to meet the adopted safety factor requirements. Table 2.30 is based on the safety factor requirements, collapse resistance, joint yield strengths, and internal yield pressures that can be found in Table 2.24.

Cols. 1 through 4 and 7 were obtained directly from Table 2.24. Grades C-95 and L-80, which have restricted yield-strength ranges, were eliminated from consid-

eration because the well conditions did not warrant the use of such premium grades of tubing. The collapse setting depths in Col. 5 were obtained by dividing collapse resistance (Col. 3) by the 0.5-psi pressure gradient and 1.125, the safety factor. The joint yield-strength setting depths (Col. 6) were obtained by dividing the joint yield-strength values in Col. 4 by the nominal weight per foot (Col. 1) and 1.80, the safety factor. Col. 7 was obtained directly from Table 2.24 and required no modification because the entire string may be subjected to an internal pressure equal to the BHP.

It is apparent from Table 2.30 that 2 $\frac{7}{8}$ -in., 6.5-lbm N-80 upset tubing will be required because it is the lowest grade that provides adequate collapse resistance, joint yield strength, and internal yield pressure strength.

Collapse Safety Factor. The collapse safety factor of 2.029 in Table 2.29 was determined by dividing the 11,160-psi collapse resistance in Col. 3 of Table 2.30 by the 0.5-psi/ft pressure gradient and the 11,000-ft length of the string.

TABLE 2.24—MINIMUM PERFORMANCE PROPERTIES OF TUBING (continued)

1	2	3	4	5	6	7	8	9	10	11
OD d_o (in.)	Nominal Weight (lbm/ft)				Wall Thickness e (in.)	ID d_i (in.)	Drift Diameter (in.)	Threaded and Coupled		
	Threads and Coupling		Integral Joint	Grade				OD of Coupling (in.)		
	Nonupset	Upset						Nonupset d_{oc}	Regular d_{oc}	Special Clearance d_{ocs}
2.063	—	—	3.25	H-40	0.156	1.751	—	—	—	—
	—	—	3.25	J-55	0.156	1.751	—	—	—	—
	—	—	3.25	C-75	0.156	1.751	—	—	—	—
	—	—	3.25	L-80, N-80	0.156	1.751	—	—	—	—
	—	—	3.25	C-90	0.156	1.751	—	—	—	—
2 $\frac{3}{8}$	4.00	—	—	H-40	0.167	2.041	1.947	2.875	—	—
	4.60	4.70	—	H-40	0.190	1.995	1.901	2.875	3.063	2.910
	4.00	—	—	J-55	0.167	2.041	1.947	2.875	—	—
	4.60	4.70	—	J-55	0.190	1.995	1.901	2.875	3.063	2.910
	4.00	—	—	C-75	0.167	2.041	1.947	2.875	—	—
	4.60	4.70	—	C-75	0.190	1.995	1.901	2.875	3.063	2.910
	5.80	5.95	—	C-75	0.254	1.867	1.773	2.875	3.063	2.910
	4.00	—	—	L-80, N-80	0.167	2.041	1.947	2.875	—	—
	4.60	4.70	—	L-80, N-80	0.190	1.995	1.901	2.875	3.063	2.910
	5.80	5.95	—	L-80, N-80	0.254	1.867	1.773	2.875	3.063	2.910
	4.60	4.70	—	P-105	0.190	1.995	1.901	2.875	3.063	2.910
	5.80	5.95	—	P-105	0.254	1.867	1.773	2.875	3.063	2.910
	4.00	—	—	C-90	0.167	2.041	1.947	2.875	—	—
	4.60	4.70	—	C-90	0.190	1.995	1.901	2.875	3.063	2.910
	5.80	5.95	—	C-90	0.254	1.867	1.773	2.875	3.063	2.910
2 $\frac{7}{8}$	6.40	6.50	—	H-40	0.217	2.441	2.347	3.500	3.668	3.460
	6.40	6.50	—	J-55	0.217	2.441	2.347	3.500	3.668	3.460
	6.40	6.50	—	C-75	0.217	2.441	2.347	3.500	3.668	3.460
	7.80	7.90	—	C-75	0.276	2.323	2.229	3.500	3.668	3.460
	8.60	8.70	—	C-75	0.308	2.259	2.165	3.500	3.668	3.460
	6.40	6.50	—	L-80, N-80	0.217	2.441	2.347	3.500	3.668	3.460
	7.80	7.90	—	L-80, N-80	0.276	2.323	2.229	3.500	3.668	3.460
	8.60	8.70	—	L-80, N-80	0.308	2.259	2.165	3.500	3.668	3.460
	6.40	6.50	—	P-105	0.217	2.441	2.347	3.500	3.668	3.460
	7.80	7.90	—	P-105	0.276	2.323	2.229	3.500	3.668	3.460
	8.60	8.70	—	P-105	0.308	2.259	2.165	3.500	3.668	3.460
	6.40	6.50	—	C-90	0.217	2.441	2.347	3.500	3.668	3.460
	7.80	7.90	—	C-90	0.276	2.323	2.229	3.500	3.668	3.460
	8.60	8.70	—	C-90	0.308	2.259	2.165	3.500	3.668	3.460

TABLE 2.24—MINIMUM PERFORMANCE PROPERTIES OF TUBING (continued)

12	13	14	15	16	17	18	19	20
			Internal					
Integral Joint			Upset			Joint Yield Strength (lbf)		
Drift Diameter (in.)	OD of Box d_{ob} (in.)	Collapse Resistance (psi)	Plain-end and Nonupset (psi)	Regular	Special	Threaded and		Integral
				Coupling (psi)	Clearance Coupling (psi)	Coupled	Upset	
						Nonupset	Upset	
1.657	2.325	5,590	5,290	—	—	—	—	35,700
1.657	2.325	7,690	7,280	—	—	—	—	49,000
1.657	2.325	10,480	9,920	—	—	—	—	66,900
1.657	2.325	11,180	10,590	—	—	—	—	71,400
1.657	2.325	12,430	11,910	—	—	—	—	80,300
—	—	5,230	4,920	—	—	30,100	—	—
—	—	5,890	5,600	5,600	5,600	36,000	52,000	—
—	—	7,190	6,770	—	—	41,400	—	—
—	—	8,100	7,700	7,700	7,700	49,500	71,700	—
—	—	9,520	9,230	—	—	56,500	—	—
—	—	11,040	10,500	10,500	10,500	67,400	97,800	—
—	—	14,330	14,040	13,960	10,720	96,600	126,900	—
—	—	9,980	9,840	—	—	60,300	—	—
—	—	11,780	11,200	11,200	11,200	71,900	104,300	—
—	—	15,280	14,970	14,890	11,440	103,000	135,400	—
—	—	15,460	14,700	14,700	14,700	94,400	136,900	—
—	—	20,060	19,650	19,540	15,010	135,200	177,700	—
—	—	10,940	11,070	—	—	67,800	—	—
—	—	13,250	12,600	12,600	12,600	80,900	117,400	—
—	—	17,190	16,840	16,710	12,860	115,900	152,300	—
—	—	5,580	5,280	5,280	5,510	52,800	72,500	—
—	—	7,680	7,260	7,260	7,260	72,600	99,700	—
—	—	10,470	9,910	9,910	9,910	99,000	135,900	—
—	—	13,020	12,600	12,600	10,340	132,100	169,000	—
—	—	14,350	14,060	14,010	10,340	149,400	186,300	—
—	—	11,160	10,570	10,570	10,570	105,600	145,000	—
—	—	13,890	13,440	13,440	11,030	140,900	180,300	—
—	—	15,300	15,000	14,940	11,030	159,300	198,700	—
—	—	14,010	13,870	13,870	13,870	138,600	190,300	—
—	—	18,220	17,640	17,640	14,480	184,900	236,600	—
—	—	20,090	19,690	19,610	14,480	209,100	260,800	—
—	—	12,380	11,890	11,890	11,890	118,800	163,100	—
—	—	15,620	15,120	15,120	12,420	158,500	202,800	—
—	—	17,220	16,870	16,820	12,420	179,200	223,500	—

TABLE 2.24—MINIMUM PERFORMANCE PROPERTIES OF TUBING (continued)

1	2	3	4	5	6	7	8	9	10	11
								Threaded and Coupled		
OD d_o (in.)	Nominal Weight (lbm/ft)			Grade	Wall Thickness e (in.)	ID d_i (in.)	Drift Diameter (in.)	OD of Coupling (in.)		
	Threads and Coupling		Integral Joint					Upset		
	Nonupset	Upset						Nonupset d_{oc}	Regular d_{oc}	Special Clearance d_{ocs}
3½	7.70	—	—	H-40	0.216	3.068	2.943	4.250	—	—
	9.20	9.30	—	H-40	0.254	2.992	2.867	4.250	4.500	4.180
	10.20	—	—	H-40	0.289	2.922	2.797	4.250	—	—
	7.70	—	—	J-55	0.216	3.068	2.943	4.250	—	—
	9.20	9.30	—	J-55	0.254	2.992	2.867	4.250	4.500	4.180
	10.20	—	—	J-55	0.289	2.922	2.797	4.250	—	—
	7.70	—	—	C-75	0.216	3.068	2.943	4.250	—	—
	9.20	9.30	—	C-75	0.254	2.992	2.867	4.250	4.500	4.180
	10.20	—	—	C-75	0.289	2.922	2.797	4.250	—	—
	12.70	12.95	—	C-75	0.375	2.750	2.625	4.250	4.500	4.180
	7.70	—	—	L-80, N-80	0.216	3.068	2.943	4.250	—	—
	9.20	9.30	—	L-80, N-80	0.254	2.992	2.867	4.250	4.500	4.180
	10.20	—	—	L-80, N-80	0.289	2.922	2.797	4.250	—	—
	12.70	12.95	—	L-80, N-80	0.375	2.750	2.625	4.250	4.500	4.180
	7.70	—	—	C-90	0.216	3.068	2.943	4.250	—	—
	9.20	9.30	—	C-90	0.254	2.992	2.867	4.250	4.500	4.180
	10.20	—	—	C-90	0.289	2.922	2.797	4.250	—	—
	12.70	12.95	—	C-90	0.375	2.750	2.625	4.250	4.500	4.180
	9.20	9.30	—	P-105	0.254	2.992	2.867	4.250	4.500	4.180
	12.70	12.95	—	P-105	0.375	2.750	2.625	4.250	4.500	4.180
4	9.50	—	—	H-40	0.226	3.548	3.423	4.750	—	—
	—	11.00	—	H-40	0.262	3.476	3.351	—	5.000	—
	9.50	—	—	J-55	0.226	3.548	3.423	4.750	—	—
	—	11.00	—	J-55	0.262	3.476	3.351	—	5.000	—
	9.50	—	—	C-75	0.226	3.548	3.423	4.750	—	—
	—	11.00	—	C-75	0.262	3.476	3.351	—	5.000	—
	9.50	—	—	L-80, N-80	0.226	3.548	3.423	4.750	—	—
	—	11.00	—	L-80, N-80	0.262	3.476	3.351	—	5.000	—
	9.50	—	—	C-90	0.226	3.548	3.423	4.750	—	—
	—	11.00	—	C-90	0.262	3.476	3.351	—	5.000	—
4½	12.60	12.75	—	H-40	0.271	3.958	3.833	5.200	5.563	—
	12.60	12.75	—	J-55	0.271	3.958	3.833	5.200	5.563	—
	12.60	12.75	—	C-75	0.271	3.958	3.833	5.200	5.563	—
	12.60	12.75	—	L-80, N-80	0.271	3.958	3.833	5.200	5.563	—
	12.60	12.75	—	C-90	0.271	3.958	3.833	5.200	5.563	—

TABLE 2.25—NONUPSET TUBING COUPLING DIMENSIONS, WEIGHTS, AND TOLERANCES (FIG. 2.6)

Size (in.)	OD** d_{oc} (in.)	Minimum Length L_{min} (in.)	Diameter of Recess d_r (in.)	Width of Bearing Face b (in.)	Maximum Bearing Face Diameter Special Bevel $(d_{bf})_{max}$ (in.)	Weight (lbm)
1.050	1.313	3⅜	1.113	⅜	1.181	0.51
1.315	1.660	3¼	1.378	⅜	1.488	0.84
1.660	2.054	3½	1.723	⅜	1.857	1.29
1.900	2.200	3¾	1.963	⅜	2.050	1.23
2⅜	2.875	4¼	2.438	⅜	2.625	2.82
2⅞	3.500	5⅞	2.938	⅜	3.188	5.15
3½	4.250	5⅞	3.563	⅜	3.875	8.17
4	4.750	5¾	4.063	⅜	4.375	9.57
4½	5.200	6⅞	4.563	⅜	4.850	10.76

*The size of the coupling is the same as the corresponding pipe size.

**Tolerance on OD d_{oc} , $\pm 1\%$.

TABLE 2.24—MINIMUM PERFORMANCE PROPERTIES OF TUBING (continued)

12	13	14	15	16	17	18	19	20
Integral Joint			Internal			Joint Yield Strength (lbf)		
Drift Diameter (in.)	OD of Box d_{ob} (in.)	Collapse Resistance (psi)	Plain-end and Nonupset (psi)	Upset		Threaded and Coupled		Integral Joint
				Regular Coupling (psi)	Special Clearance Coupling (psi)	Nonupset	Upset	
—	—	4,630	4,320	—	—	65,100	—	—
—	—	5,380	5,080	5,080	5,080	79,500	103,600	—
—	—	6,060	5,780	—	—	92,600	—	—
—	—	5,970	5,940	—	—	89,500	—	—
—	—	7,400	6,990	6,990	6,990	109,400	142,500	—
—	—	8,330	7,950	—	—	127,300	—	—
—	—	7,540	8,100	—	—	122,000	—	—
—	—	10,040	9,530	9,530	9,530	149,100	194,300	—
—	—	11,360	10,840	—	—	173,500	—	—
—	—	14,350	14,060	14,060	9,990	231,000	276,100	—
—	—	7,870	8,640	—	—	130,100	—	—
—	—	10,530	10,160	10,160	10,160	159,100	207,200	—
—	—	12,120	11,560	—	—	185,100	—	—
—	—	15,310	15,000	15,000	10,660	246,400	294,500	—
—	—	8,540	9,720	—	—	146,400	—	—
—	—	11,570	11,430	11,430	11,430	179,000	233,100	—
—	—	13,640	13,010	—	—	208,200	—	—
—	—	17,220	16,880	16,880	11,990	277,200	331,300	—
—	—	13,050	13,340	13,340	13,340	208,900	272,000	—
—	—	20,090	19,690	19,690	13,990	323,400	386,600	—
—	—	4,060	3,960	—	—	72,000	—	—
—	—	4,900	4,590	4,590	—	—	123,100	—
—	—	5,110	5,440	—	—	99,000	—	—
—	—	6,590	6,300	6,300	—	—	169,200	—
—	—	6,350	7,420	—	—	135,000	—	—
—	—	8,410	8,600	8,600	—	—	230,800	—
—	—	6,590	7,910	—	—	144,000	—	—
—	—	8,800	9,170	9,170	—	—	246,100	—
—	—	7,080	8,900	—	—	162,000	—	—
—	—	9,590	10,320	10,320	—	—	276,900	—
—	—	4,590	4,220	4,220	—	104,400	144,000	—
—	—	5,720	5,800	5,800	—	143,500	198,000	—
—	—	7,200	7,900	7,900	—	195,700	270,000	—
—	—	7,500	8,430	8,430	—	208,700	288,000	—
—	—	8,120	9,480	9,480	—	234,800	324,000	—

TABLE 2.26—EXTERNAL-UPSET TUBING COUPLING DIMENSIONS, WEIGHTS, AND TOLERANCES (FIG. 2.7)

Size* (in.)	OD		Minimum Length L_{min} (in.)	Diameter of Recess d_r (in.)	Width of Bearing Face Regular b (in.)	Maximum Bearing Face Diameter (d_{bf}) _{max} (in.)		Weight (lbm)	
	Regular and Special Bevel**	Special Clearance†				Special Bevel	Special Clearance	Regular	Special Clearance
	d_{oc} (in.)	d_{ocs} (in.)							
1.050	1.660	—	3¼	1.378	¾ ₃₂	1.488	—	0.84	—
1.315	1.900	—	3½	1.531	¾ ₃₂	1.684	—	1.26	—
1.660	2.200	—	3¾	1.875	⅞	2.006	—	1.49	—
1.900	2.500	—	3⅞	2.156	⅞	2.297	—	1.85	—
2⅜	3.063	2.910	4⅞	2.656	⅞ ₃₂	2.828	2.752	3.42	2.38
2⅞	3.668	3.460	5¼	3.156	⅞ ₃₂	3.381	3.277	5.29	3.45
3½	4.500	4.180	5¾	3.813	⅞	4.125	3.965	9.02	5.22
4	5.000	—	6	4.313	⅞	4.625	—	10.62	—
4½	5.563	—	6¼	4.813	⅞	5.156	—	13.31	—

*The size of the coupling is the same as the corresponding pipe size.

**Tolerance on OD d_{oc} , $\pm 1\%$.†Tolerance on OD d_{ocs} , ± 0.015 in.

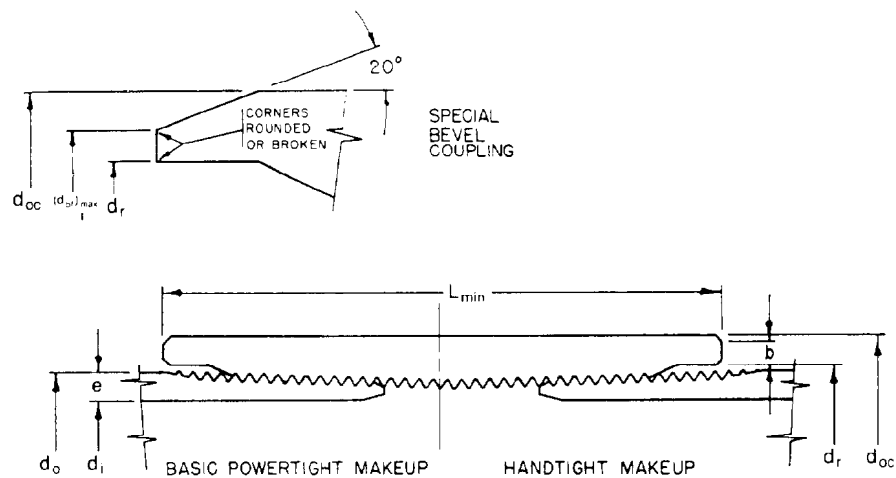


Fig. 2.6—Nonupset tubing and coupling.

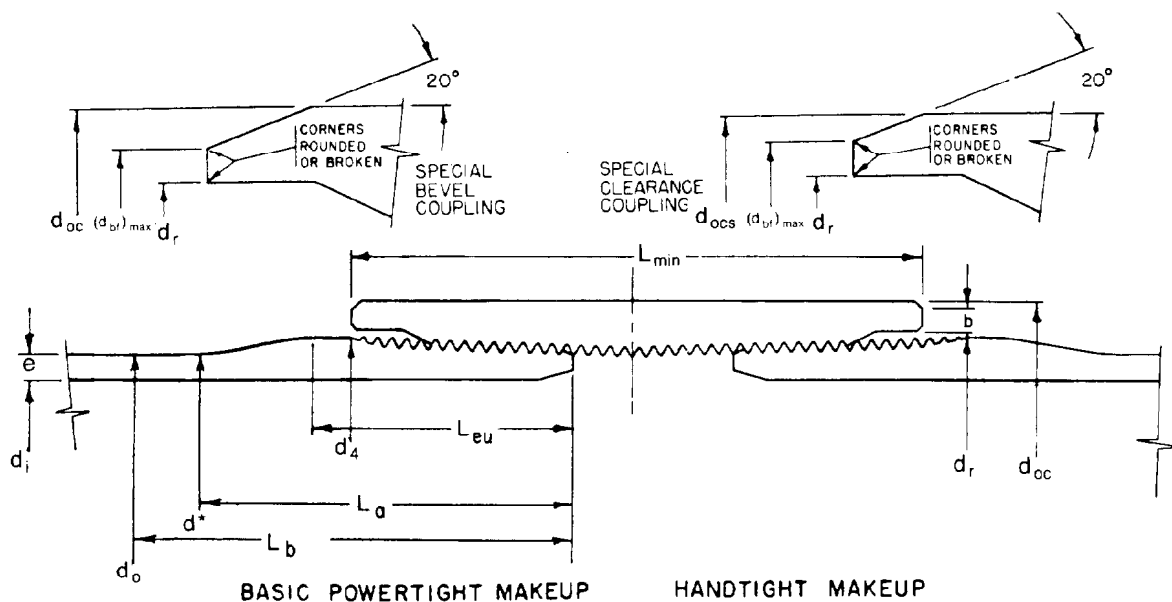


Fig. 2.7—External-upset tubing and coupling.

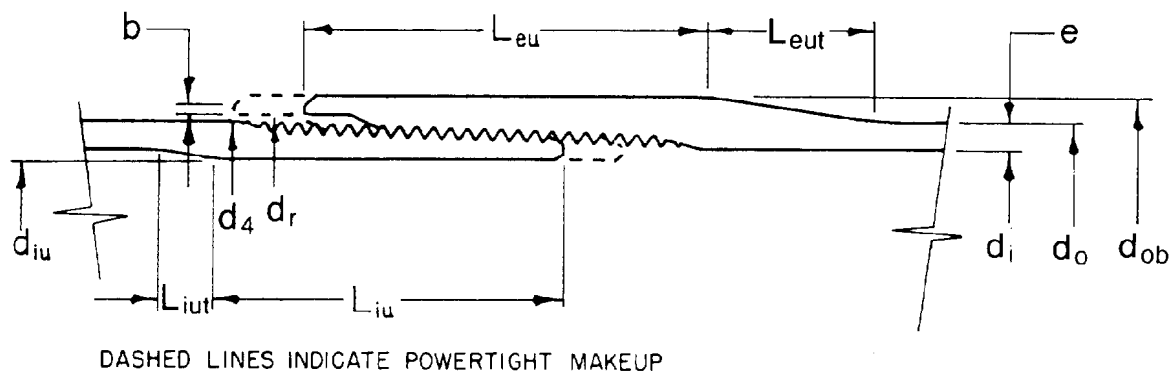


Fig. 2.8—Integral-joint tubing.

TABLE 2.27—INTEGRAL-JOINT TUBING UPSET DIMENSIONS, WEIGHTS, AND TOLERANCES (FIG. 2.8)

OD d_o (in.)	Nominal Weight; Upset and Threaded* (lbm/ft)	Upset Dimensions (in.)								
		Pin				Box				
		OD** + 0.0625 d_a	ID† + 0.015 d_{iu}	Minimum Length L_{iu}	Length of Taper Minimum L_{iut}	OD + 0.005 − 0.025 d_{ob}	Minimum Length, L_{eu}	Length of Taper L_{eut}	Diameter of Recess d_r	Width of Face Minimum b
1.315	1.72	—	0.970	1 $\frac{3}{8}$	$\frac{1}{4}$	1.550	1.750	1	1.378	$\frac{1}{32}$
1.660	2.10	—	1.301	1 $\frac{1}{2}$	$\frac{1}{4}$	1.880	1.875	1	1.723	$\frac{1}{32}$
1.660	2.33	—	1.301	1 $\frac{1}{2}$	$\frac{1}{4}$	1.880	1.875	1	1.723	$\frac{1}{32}$
1.900	2.40	—	1.531	1 $\frac{5}{8}$	$\frac{1}{4}$	2.110	2.000	1	1.963	$\frac{1}{32}$
1.900	2.76	—	1.531	1 $\frac{5}{8}$	$\frac{1}{4}$	2.110	2.000	1	1.963	$\frac{1}{32}$
2.063	3.25	2.094	1.672	1 $\frac{11}{16}$	$\frac{1}{4}$	2.325	2.125	1	2.156	$\frac{1}{32}$

*Nominal weights, upset, and threaded, are shown for the purpose of identification in ordering.

**The minimum OD, d_a , is limited by the minimum length of fullcrest threads (see Table 2.46).†The minimum ID, d_{iu} , is limited by the drift test.

TABLE 2.28—GROSS LINEAR FOOTAGE FROM NET FOOTAGE, API TUBING

OD (in.)	Nominal Weight per Foot (lbm/ft)	Number of Threads per inch	Make-Up Loss Per Joint (in.)	Multiplication Factor for Average Joint Length	
				20 ft	30 ft
Nonupset Tubing					
2⅜	all	10	1.625	1.0068	1.0045
2⅞	all	10	2.063	1.0087	1.0058
3½	all	10	2.313	1.0097	1.0065
4	9.50	8	2.375	1.0100	1.0066
4½	12.60	8	2.563	1.0108	1.0072
External Upset Tubing					
2⅜	all	8	1.938	1.0081	1.0054
2⅞	all	8	2.125	1.0089	1.0059
3½	all	8	2.375	1.0100	1.0066
4	11.00	8	2.500	1.0105	1.0070
4½	12.75	8	2.625	1.0111	1.0074
Integral Joint Tubing					
1.315	1.72	10	1.125	1.0047	1.0031
1.660	all	10	1.250	1.0052	1.0035
1.900	all	10	1.375	1.0058	1.0038
2.063	3.25	10	1.438	1.0060	1.0040

TABLE 2.29—DESIGN SAFETY FACTORS FOR SINGLE WEIGHT AND GRADE TUBING STRING
Design data for an 11,000-ft string of 2 $\frac{7}{8}$ -in.-OD upset tubing with 9.625-lbm/gal
mud weight and 5,500-psi BHP

Nominal Weight per Foot (lbm/ft)	Grade	Type Thread	Amount (ft)	Safety Factor		
				Collapse	Joint Yield Strength	Internal Yield Pressure (psi)
6.50	6,680	API	11,000	2.029	2.03	1.92

TABLE 2.30—2 7/8-in.-OD UPSET TUBING SETTING DEPTHS IN COLLAPSE, TENSION, AND INTERNAL PRESSURE RESISTANCE, INCLUDING SAFETY FACTORS

Nominal Weight per Foot (lbm/ft)	Grade	Collapse Resistance (psi)	Joint Yield Strength (lbf)	Setting Depth (ft)		Internal Yield Pressure (psi)
				Collapse	Joint Yield Strength	
					Safety Factors	
				1.125	1.80	1.00
				6.50	H-40	5,580
6.50	J-55	7,680	99,700	13,653	8,521	7,260
6.50	N-80	11,160	145,000	19,840	12,393	10,570

Joint Yield Strength Safety Factor. The joint yield strength safety factor of 2.03 was determined by dividing the 145,000-lbm joint yield strength in Col. 4 by 6.50 lbm, the nominal weight per foot, and the 11,000-ft length of the string.

Internal Yield Pressure Safety Factor. The internal yield pressure safety factor of 1.92 was determined by dividing the 10,570-psi internal yield pressure in Col. 7 by 5,500 psi, the BHP.

Stretch in Tubing When Freely Suspended in Fluid Media

When tubing is subjected to an axial stress, either tension or compression, that does not exceed the elastic limit of the material, the stretch or contraction may be determined by Eqs. 1 and 2 for casing. These equations also are applicable to tubing.

Line Pipe

Line pipe is used by the oil and gas industry to transport oil, gas, and water. API has developed specifications for line pipe⁶⁻⁸ to meet the needs of the oil and gas industry. These provide standard dimensions, strength and performance properties, and the required thread gauging practice to ensure complete interchangeability. Tables 2.31 through 2.37 include dimensional and strength data of API line pipe.

Tables 2.31 and 2.32 give the tensile requirements and tolerances on lengths of API line pipe. Performance property data applicable to standard-weight, threaded line pipe are given in Tables 2.33 through 2.35 and Fig. 2.9. Table 2.36 gives the dimensions, weights, and test pressures of extra-strong threaded line pipe. Table 2.37 lists the dimensions, weights, and test pressures of plain-end line pipe. Equations for calculating performance properties of line pipe are found in the following section.

Equations for Calculating Performance Properties of Casing, Tubing, and Line Pipe

API developed equations for calculating the performance properties of API casing, tubing, and line pipe.⁷ These equations were used to calculate the performance properties for non-API grades of casing and tubing, except for the collapse resistance of HC-95 casing. The collapse resistance of HC-95 casing is assumed to be the same as that published by Lone Star Steel⁹ for their proprietary S-95 grade. This proprietary grade is offered by other manufacturers under various 95 designations.

Collapse Pressure Equations

The minimum collapse pressures given in API Bull. 5C2 are calculated by means of Eqs. 3, 5, 7, and 9, adopted at the API 1968 Standardization Conference and reported in API Circular PS-1360, Sept. 1968.¹⁰ Eqs. 4, 6, and 8 for the intersections between the four collapse pressure equations have been determined algebraically and are included for use in calculating the applicable d_o/e range (OD/wall thickness) for each collapse pressure equation. Factors F_A , F_B , F_C , F_F , and F_G are calculated by Eqs. 12 through 16.

The collapse pressures for Tables 2.3 and 2.4 are calculated with the specified values for d_o and e . The calculated d_o/e was rounded to two decimals. The collapse pressure calculations were carried to eight or more digits and rounded to the nearest 10 psi to produce the final values in the tables.

TABLE 2.31—TENSILE REQUIREMENTS OF LINE PIPE

Grade	Minimum Yield Strength (psi)	Minimum Ultimate Tensile Strength (psi)	Minimum Elongation in 2 in.* (%)
A25	25,000	45,000	
A	30,000	48,000	
B	35,000	60,000	
X42	42,000	60,000	
X46	46,000	63,000	
X52	52,000	66,000**	
		72,000†	
X56	56,000	71,000**	
		75,000†	
X60‡	60,000	75,000**	
		78,000†	
X65	65,000	77,000**	
		80,000†	
X70	70,000	82,000	

*The minimum elongation in 2 in. shall be that determined by the equation in Table 2.1.

**For pipe less than 20 in. OD with any wall thickness and for pipe 20 in. OD and larger with wall thickness greater than 0.375 in.

†For pipe with a 20-in. OD and larger with a wall thickness of 0.375 in. and less.

‡The minimum ultimate tensile strength for Grade X60 Electric-Resistance Welded Pipe in all sizes and wall thicknesses shall be 75,000 psi.

TABLE 2.32—TOLERANCES ON LENGTHS OF LINE PIPE*

	Shortest Length in Entire Shipment (ft)	Shortest Length in 95% of Entire Shipment (ft)	Shortest Length in 90% of Entire Shipment (ft)	Minimum Average Length Entire Shipment (ft)
Threaded-and-Coupled Pipe				
Single random lengths	16.0	8.0	—	
Double random lengths	22.0	—	—	35.0
Plain-End Pipe				
Single random lengths	9.0	—	—	17.5
Double random lengths	14.0	—	26.3	35.0
As agreed upon lengths in excess of 20 ft*	40% of average agreed upon	—	75% of average agreed upon	

*By agreement between the purchaser and the manufacturer, these tolerances shall apply to each carload.

TABLE 2.33—STANDARD-WEIGHT THREADED LINE PIPE DIMENSIONS, WEIGHTS, AND TEST PRESSURES (FIG. 2.9)

Nominal Size (in.)	OD d_o (in.)	Nominal Weight: Threads and Coupling* (lbm/ft)	Wall Thickness e (in.)	ID d_i (in.)	Calculated Weight		Test Pressure (psi)		
					Plain End W_{pe} (lbm/ft)	Threads and Coupling** W_{tc} (lbm)	Grade A25	Grade A	Grade B
1/8	0.405	0.25	0.068	0.269	0.24	0.20	700	700	700
1/4	0.540	0.43	0.088	0.364	0.42	0.20	700	700	700
3/8	0.675	0.57	0.091	0.493	0.57	0.00	700	700	700
1/2	0.840	0.86	0.109	0.622	0.85	0.20	700	700	700
3/4	1.050	1.14	0.113	0.824	1.13	0.20	700	700	700
1	1.315	1.70	0.133	1.049	1.68	0.20	700	700	700
1 1/4	1.660	2.30	0.140	1.380	2.27	0.60	1,000	1,000	1,100
1 1/2	1.900	2.75	0.145	1.610	2.72	0.40	1,000	1,000	1,100
2	2.375	3.75	0.154	2.067	3.65	1.20	1,000	1,000	1,100
2 1/2	2.875	5.90	0.203	2.469	5.79	1.80	1,000	1,000	1,100
3	3.500	7.70	0.216	3.068	7.58	1.80	1,000	1,000	1,100
3 1/2	4.000	9.25	0.226	3.548	9.11	3.20	1,200	1,200	1,300
4	4.500	11.00	0.237	4.026	10.79	4.40	1,200	1,200	1,300
5	5.563	15.00	0.258	5.047	14.62	5.60	1,200	1,200	1,300
5	6.625	19.45	0.280	6.065	18.97	7.20	—	1,200	1,300
8	8.625	25.55	0.277	8.071	24.70	14.80	—	1,160	1,350
8	8.625	29.35	0.322	7.981	28.55	14.00	—	1,340	1,570
10	10.750	32.75	0.279	10.192	31.20	20.00	—	930	1,090
10	10.750	35.75	0.307	10.136	34.24	19.20	—	1,030	1,200
10	10.750	41.85	0.365	10.020	40.48	17.40	—	1,220	1,430
12	12.750	45.45	0.330	12.090	43.77	32.60	—	960	1,090
12	12.750	51.15	0.375	12.000	49.56	30.80	—	1,060	1,240
14D	14.000	57.00	0.375	13.250	54.57	24.60	—	960	1,120
16D	16.000	65.30	0.375	15.250	62.58	30.00	—	840	980
18D	18.000	73.00	0.375	17.250	70.59	35.60	—	750	880
20D	20.000	81.00	0.375	19.250	78.60	42.00	—	680	790

*Nominal weights, threads, and coupling are shown for the purpose of identification in ordering.

**Weight gain resulting from end finishing.

TABLE 2.34—MINIMUM COLLAPSE RESISTANCE AND JOINT STRENGTH OF STANDARD-WEIGHT THREADED LINE PIPE

Nominal Size (in.)	OD d_o (in.)	Nominal Weight per Foot (lbm/ft)	Collapse Resistance (psi)			Joint Strength (1,000 lbf)		
			Grade			Grade		
			A25	A	B	A25	A	B
1/8	0.405	0.25	6,980	8,380	9,770	1.65	1.77	2.21
1/4	0.540	0.43	6,820	8,180	9,540	2.52	2.69	2.36
3/8	0.675	0.57	5,830	7,000	8,160	3.55	3.79	4.73
1/2	0.840	0.86	5,640	6,770	7,900	4.97	5.30	6.63
3/4	1.050	1.14	4,800	5,760	6,720	9.12	9.73	12.2
1	1.315	1.70	4,540	5,450	6,360	10.0	10.7	13.4
1 1/4	1.660	2.30	3,860	4,630	5,400	14.4	15.4	19.2
1 1/2	1.900	2.75	3,530	4,230	4,940	16.8	18.9	22.9
2	2.375	3.75	3,030	3,640	4,240	20.5	23.2	28.0
2 1/2	2.875	5.90	3,280	3,940	4,590	33.2	37.4	45.3
3	3.500	7.70	2,900	3,480	4,050	41.3	46.7	56.4
3 1/2	4.000	9.25	2,670	3,200	3,670	47.9	54.3	65.5
4	4.500	11.00	2,490	2,930	3,270	54.5	61.9	74.5
5	5.563	15.00	2,110	2,380	2,630	69.4	79.2	95.1
6	6.626	19.45	—	2,020	2,200	—	95.8	115
8	8.625	25.55	—	1,190	1,270	—	107	128
8	8.625	29.35	—	1,580	1,700	—	133	159
10	10.750	32.75	—	780	820	—	122	146
10	10.750	35.75	—	950	1,010	—	141	168
10	10.750	41.85	—	1,310	1,410	—	178	213
12	12.750	45.45	—	780	810	—	173	206
12	12.750	51.15	—	1,010	1,070	—	205	244
10D	14.000	57.00	—	840	880	—	226	283
16D	16.000	65.30	—	620	630	—	253	301
18D	18.000	73.00	—	440	440	—	376	238
20D	20.000	81.00	—	320	320	—	294	349

TABLE 2.35a—MINIMUM COLLAPSE RESISTANCE UNDER AXIAL LOAD, GRADE A

d _o (in.)	Weight per Foot (lbm/ft)	Area (sq in.)	Axial Stress (psi)												
			-10,000	-5,000	0	5,000	10,000	15,000	20,000	25,000	30,000	35,000	40,000	45,000	50,000
			Collapse Pressure (psi)												
0.405	0.25	5.96	0.072	9,420	8,990	8,380	7,590	6,620	5,460	—	—	—	—	—	—
0.54	0.43	6.14	0.125	9,200	8,780	8,180	7,410	6,470	5,330	—	—	—	—	—	—
0.675	0.57	7.42	0.167	7,860	7,510	7,000	6,340	5,530	4,560	—	—	—	—	—	—
0.84	0.86	7.71	0.25	7,610	7,270	6,770	6,140	5,360	4,410	—	—	—	—	—	—
1.05	1.14	9.29	0.333	6,480	6,180	5,760	5,220	4,560	3,750	—	—	—	—	—	—
1.315	1.7	9.89	0.494	6,130	5,850	5,450	4,940	4,310	3,550	—	—	—	—	—	—
1.66	2.3	11.86	0.669	5,210	4,970	4,630	4,200	3,660	3,020	—	—	—	—	—	—
1.9	2.75	13.1	0.799	4,760	4,540	4,230	3,830	3,350	2,760	—	—	—	—	—	—
2.375	3.75	15.42	1.075	4,090	3,900	3,640	3,300	2,880	2,370	—	—	—	—	—	—
2.875	5.9	14.16	1.704	4,430	4,220	3,940	3,570	3,110	2,570	—	—	—	—	—	—
3.5	7.7	16.2	2.228	3,910	3,730	3,480	3,150	2,750	2,260	—	—	—	—	—	—
4	9.25	17.7	2.68	3,570	3,430	3,200	2,900	2,530	2,080	—	—	—	—	—	—
4.5	11	18.99	3.174	3,190	3,080	2,930	2,710	2,370	1,950	—	—	—	—	—	—
5.563	15	21.56	4.3	2,570	2,490	2,380	2,230	2,040	1,730	—	—	—	—	—	—
6.625	19.45	23.66	5.581	2,160	2,100	2,020	1,900	1,750	1,560	—	—	—	—	—	—
8.625	25.55	31.14	7.265	1,250	1,230	1,190	1,140	1,080	1,000	—	—	—	—	—	—
8.625	29.35	26.79	8.399	1,670	1,630	1,580	1,510	1,410	1,280	—	—	—	—	—	—
10.75	32.75	38.53	9.178	810	800	780	760	730	690	—	—	—	—	—	—
10.75	35.75	35.02	10.072	1,000	980	950	920	880	820	—	—	—	—	—	—
10.75	41.85	29.45	11.908	1,390	1,360	1,310	1,260	1,180	1,100	—	—	—	—	—	—
12.75	45.45	38.64	12.876	800	790	780	750	720	680	—	—	—	—	—	—
12.75	51.15	34	14.579	1,060	1,040	1,010	970	930	860	—	—	—	—	—	—
14	57	37.33	16.052	870	860	840	810	780	730	—	—	—	—	—	—
16	65.3	42.67	18.408	630	620	620	600	590	560	—	—	—	—	—	—
18	73	48	20.764	440	440	440	440	440	430	—	—	—	—	—	—
20	81	53.33	23.12	320	320	320	320	320	320	—	—	—	—	—	—

TABLE 2.35b—MINIMUM COLLAPSE RESISTANCE UNDER AXIAL LOAD, GRADE A25

d_o (in.)	Weight per Foot (lbm/ft)	d_o/e	Area (sq in.)	Axial Stress (psi)													
				- 10,000	- 5,000	0	5,000	10,000	15,000	20,000	25,000	30,000	35,000	40,000	45,000	50,000	
				Collapse Pressure (psi)													
0.405	0.25	5.96	0.072	7,950	7,570	6,980	6,180	5,150	—	—	—	—	—	—	—		
0.54	0.43	6.14	0.125	7,760	7,400	6,820	6,030	5,030	—	—	—	—	—	—	—		
0.675	0.57	7.42	0.167	6,640	6,330	5,830	5,160	4,300	—	—	—	—	—	—	—		
0.84	0.86	7.71	0.25	6,420	6,120	5,640	4,990	4,170	—	—	—	—	—	—	—		
1.05	1.14	9.29	0.333	5,470	5,210	4,800	4,250	3,540	—	—	—	—	—	—	—		
1.315	1.7	9.89	0.494	5,170	4,930	4,540	4,020	3,350	—	—	—	—	—	—	—		
1.66	2.3	11.86	0.669	4,390	4,190	3,860	3,420	2,850	—	—	—	—	—	—	—		
1.9	2.75	13.1	0.799	4,010	3,820	3,530	3,120	2,600	—	—	—	—	—	—	—		
2.375	3.75	15.42	1.075	3,450	3,290	3,030	2,680	2,240	—	—	—	—	—	—	—		
2.875	5.9	14.16	1.704	3,730	3,560	3,280	2,900	2,420	—	—	—	—	—	—	—		
3.5	7.7	16.2	2.228	3,300	3,140	2,900	2,560	2,140	—	—	—	—	—	—	—		
4	9.25	17.7	2.68	3,030	2,890	2,670	2,360	1,970	—	—	—	—	—	—	—		
4.5	11	18.99	3.174	2,820	2,710	2,490	2,210	1,840	—	—	—	—	—	—	—		
5.563	15	21.56	4.3	2,300	2,220	2,110	1,950	1,630	—	—	—	—	—	—	—		

TABLE 2.35c—MINIMUM COLLAPSE RESISTANCE UNDER AXIAL LOAD, GRADE B

d_o (in.)	Weight per Foot (lbm/ft)	d_o/e	Area (sq in.)	Axial Stress (psi)													
				- 10,000	- 5,000	0	5,000	10,000	15,000	20,000	25,000	30,000	35,000	40,000	45,000	50,000	
				Collapse Pressure (psi)													
0.405	0.25	5.96	0.072	10,870	10,400	9,770	9,000	8,070	6,980	5,700	—	—	—	—	—	—	
0.54	0.43	6.14	0.125	10,610	10,150	9,540	8,790	7,880	6,820	5,570	—	—	—	—	—	—	
0.675	0.57	7.42	0.167	9,070	8,680	8,160	7,520	6,740	5,830	4,760	—	—	—	—	—	—	
0.84	0.86	7.71	0.25	8,780	8,410	7,900	7,280	6,530	5,640	4,610	—	—	—	—	—	—	
1.05	1.14	9.29	0.333	7,480	7,150	6,720	6,190	5,550	4,800	3,920	—	—	—	—	—	—	
1.315	1.7	9.89	0.494	7,070	6,770	6,360	5,860	5,260	4,540	3,710	—	—	—	—	—	—	
1.66	2.3	11.86	0.669	6,010	5,750	5,400	4,980	4,460	3,860	3,150	—	—	—	—	—	—	
1.9	2.75	13.1	0.799	5,490	5,250	4,940	4,550	4,080	3,530	2,880	—	—	—	—	—	—	
2.375	3.75	15.42	1.075	4,720	4,520	4,250	3,910	3,510	3,030	2,480	—	—	—	—	—	—	
2.875	5.9	14.16	1.704	5,110	4,890	4,590	4,230	3,800	3,280	2,680	—	—	—	—	—	—	
3.5	7.7	16.2	2.228	4,510	4,310	4,050	3,730	3,350	2,900	2,360	—	—	—	—	—	—	
4	9.25	17.7	2.68	3,970	3,840	3,670	3,440	3,080	2,670	2,180	—	—	—	—	—	—	
4.5	11	18.99	3.174	3,530	3,420	3,270	3,080	2,850	2,490	2,040	—	—	—	—	—	—	
5.563	15	21.56	4.3	2,810	2,730	2,630	2,490	2,320	2,110	1,810	—	—	—	—	—	—	
6.625	19.45	23.66	5.581	2,340	2,280	2,200	2,100	1,970	1,810	1,600	—	—	—	—	—	—	
8.625	25.55	31.14	7.265	1,330	1,310	1,270	1,230	1,170	1,100	1,020	—	—	—	—	—	—	
8.625	29.35	26.79	8.399	1,770	1,740	1,700	1,640	1,560	1,450	1,310	—	—	—	—	—	—	
10.75	32.75	38.53	9.178	840	830	820	800	770	740	700	—	—	—	—	—	—	
10.75	35.75	35.02	10.072	1,050	1,030	1,010	980	940	890	830	—	—	—	—	—	—	
10.75	41.85	29.45	11.908	1,480	1,450	1,410	1,360	1,290	1,210	1,110	—	—	—	—	—	—	
12.75	45.45	38.64	12.876	830	820	810	790	770	740	690	—	—	—	—	—	—	
12.75	51.15	34	14.579	1,120	1,100	1,070	1,040	1,000	940	880	—	—	—	—	—	—	
14	57	37.33	16.052	900	890	880	860	830	790	740	—	—	—	—	—	—	
16	65.3	42.67	18.408	630	630	630	620	610	590	570	—	—	—	—	—	—	
18	73	48	20.764	440	440	440	440	440	440	430	—	—	—	—	—	—	
20	81	53.33	23.12	320	320	320	320	320	320	320	—	—	—	—	—	—	

TABLE 2.36—EXTRA-STRONG THREADED LINE PIPE DIMENSIONS, WEIGHTS, AND TEST PRESSURES

Nominal Size (in.)	OD d_o (in.)	Nominal Weight: Threads and Coupling* (lbm/ft)	Wall Thickness e (in.)	Test Pressure Grade (psi)		
				Grade A25	Grade A	Grade B
1/8	0.405	0.31	0.095	850	850	850
1/4	0.540	0.54	0.119	850	850	850
3/8	0.675	0.74	0.126	850	850	850
1/2	0.840	1.09	0.147	850	850	850
3/4	1.050	1.48	0.154	850	850	850
1	1.315	2.18	0.179	850	850	850
1 1/4	1.660	3.02	0.191	1,300	1,500	1,600
1 1/2	1.900	3.66	0.200	1,300	1,500	1,600
2	2.375	5.07	0.218	1,300	2,500	2,500
2 1/2	2.875	7.73	0.276	1,300	2,500	2,500
3	3.500	10.33	0.300	1,300	2,500	2,500
3 1/2	4.000	12.63	0.318	1,700	2,800	2,800
4	4.500	15.17	0.337	1,700	2,700	2,800
5	5.563	21.09	0.375	1,700	2,400	2,800
6	6.625	28.89	0.432	—	2,300	2,700
8	8.625	43.90	0.500	—	2,100	2,400
10	10.75	55.82	0.500	—	1,700	2,000
12	12.75	66.71	0.500	—	1,400	1,600

*Nominal weights, threads, and coupling are shown for the purpose of identification in ordering.

TABLE 2.37a—PLAIN-END LINE PIPE DIMENSIONS, WEIGHTS, AND TEST PRESSURES, 1/8 to 1 1/2 in.

Size		Plain- End Weight (lbm/ft)	Wall Thickness (in.)	ID (in.)	Minimum Test Pressure (psi)					
Nominal (in.)	Designation				OD (in.)	Grade A		Grade B		Grade A25
					Standard	Alternative	Standard	Alternative		
1/8	Standard	0.405	0.24	0.068	0.269	700	—	700	—	700
1/8	XS	0.405	0.31	0.095	0.215	850	—	850	—	850
1/4	Standard	0.540	0.42	0.088	0.364	700	—	700	—	700
1/4	XS	0.540	0.54	0.119	0.302	850	—	850	—	850
3/8	Standard	0.675	0.57	0.091	0.493	700	—	700	—	700
3/8	XS	0.675	0.74	0.126	0.423	850	—	850	—	850
1/2	Standard	0.840	0.85	0.109	0.622	700	—	700	—	700
1/2	XS	0.840	1.09	0.147	0.546	850	—	850	—	850
1/2	XXS	0.840	1.71	0.294	0.252	1,000	—	1,000	—	1,000
3/4	Standard	1.050	1.13	0.113	0.824	700	—	700	—	700
3/4	XS	1.050	1.47	0.154	0.742	850	—	850	—	850
3/4	XXS	1.050	2.44	0.308	0.434	1,000	—	1,000	—	1,000
1	Standard	1.315	1.68	0.133	1.049	700	—	700	—	700
1	XS	1.315	2.17	0.179	0.957	850	—	850	—	850
1	XXS	1.315	3.66	0.358	0.599	1,000	—	1,000	—	1,000
1 1/4	Standard	1.660	2.27	0.140	1.380	1,200	—	1,300	—	1,000
1 1/4	XS	1.660	3.00	0.191	1.278	1,800	—	1,900	—	1,300
1 1/4	XXS	1.660	5.21	0.382	0.896	2,200	—	2,300	—	1,400
1 1/2	Standard	1.900	2.72	0.145	1.610	1,200	—	1,300	—	1,000
1 1/2	XS	1.900	3.63	0.200	1.500	1,800	—	1,900	—	1,300
1 1/2	XXS	1.900	6.41	0.400	1.100	2,200	—	2,300	—	1,400

TABLE 2.37b—PLAIN-END LINE PIPE DIMENSIONS, WEIGHTS, AND TEST PRESSURES, 2³/₈ to 5⁹/₁₆ in.

OD <i>d_o</i> (in.)	Weight <i>W_{pe}</i> (lbm/ft)	Wall Thickness <i>e</i> (in.)	ID <i>d_i</i> (in.)	Minimum Text Pressure (psi)										
					Grade A25	Grade A	Grade B	Grade X42	Grade X46	Grade X52	Grade X56	Grade X60	Grade X65	Grade X70
2 3/8	2.03	0.083	2.209	Standard	600	1,260	1,470	1,760	1,930	2,180	2,350	2,520	2,730	2,940
2 3/8	2.64	0.109	2.157	Alternative	—	—	—	2,200	2,410	2,730	2,940	3,000	3,000	3,000
				Standard	800	—	—	2,310	2,530	2,860	3,000	3,000	3,000	3,000
				Alternative	—	—	—	2,890	3,000	3,000	3,000	3,000	3,000	3,000
2 3/8	3.00	0.125	2.125	Standard	1,000	—	—	2,650	2,910	3,000	3,000	3,000	3,000	
				Alternative	—	—	—	3,000	3,000	3,000	3,000	3,000	3,000	3,000
2 3/8	3.36	0.141	2.093	Standard	1,000	—	—	2,990	3,000	3,000	3,000	3,000	3,000	3,000
				Alternative	—	—	—	3,000	3,000	3,000	3,000	3,000	3,000	3,000
2 3/8	3.65	0.154	2.067	Standard	1,000	2,330	2,500	3,000	3,000	3,000	3,000	3,000	3,000	3,000
				Alternative	—	—	—	3,000	3,000	3,000	3,000	3,000	3,000	3,000
2 3/8	4.05	0.172	2.031	Standard	1,100	2,500	2,500	3,000	3,000	3,000	3,000	3,000	3,000	3,000
				Alternative	—	—	—	3,000	3,000	3,000	3,000	3,000	3,000	3,000
2 3/8	4.39	0.188	1.999	Standard	1,200	2,500	2,500	3,000	3,000	3,000	3,000	3,000	3,000	3,000
				Alternative	—	—	—	3,000	3,000	3,000	3,000	3,000	3,000	3,000
2 3/8	5.02	0.218	1.939	Standard	1,300	2,500	2,500	3,000	3,000	3,000	3,000	3,000	3,000	3,000
				Alternative	—	—	—	3,000	3,000	3,000	3,000	3,000	3,000	3,000
2 3/8	5.67	0.250	1.875	Standard	1,400	2,500	2,500	3,000	3,000	3,000	3,000	3,000	3,000	3,000
				Alternative	—	—	—	3,000	3,000	3,000	3,000	3,000	3,000	3,000
2 3/8	6.28	0.281	1.813	Standard	1,400	2,500	2,500	3,000	3,000	3,000	3,000	3,000	3,000	3,000
				Alternative	—	—	—	3,000	3,000	3,000	3,000	3,000	3,000	3,000
2 3/8	9.03	0.436	1.503	Standard	1,400	2,500	2,500	3,000	3,000	3,000	3,000	3,000	3,000	3,000
				Alternative	—	—	—	3,000	3,000	3,000	3,000	3,000	3,000	3,000
2 7/8	2.47	0.083	2.709	Standard	600	1,040	1,210	1,460	1,590	1,800	1,940	2,080	2,250	2,430
				Alternative	—	—	—	1,820	1,990	2,250	2,430	2,600	2,810	3,000
2 7/8	3.22	0.109	2.657	Standard	800	—	—	1,910	2,090	2,370	2,550	2,730	2,960	3,000
				Alternative	—	—	—	2,390	2,620	2,960	3,000	3,000	3,000	3,000
2 7/8	3.67	0.125	2.625	Standard	1,000	—	—	2,190	2,400	2,710	2,920	3,000	3,000	3,000
				Alternative	—	—	—	2,740	3,000	3,000	3,000	3,000	3,000	3,000
2 7/8	4.12	0.141	2.593	Standard	1,000	—	—	2,470	2,710	3,000	3,000	3,000	3,000	3,000
				Alternative	—	—	—	3,000	3,000	3,000	3,000	3,000	3,000	3,000
2 7/8	4.53	0.156	2.563	Standard	1,000	1,950	2,280	2,730	3,000	3,000	3,000	3,000	3,000	3,000
				Alternative	—	—	—	3,000	3,000	3,000	3,000	3,000	3,000	3,000
2 7/8	4.97	0.172	2.531	Standard	1,000	2,150	2,500	3,000	3,000	3,000	3,000	3,000	3,000	3,000
				Alternative	—	—	—	3,000	3,000	3,000	3,000	3,000	3,000	3,000
2 7/8	5.40	0.188	2.499	Standard	1,000	2,350	2,500	3,000	3,000	3,000	3,000	3,000	3,000	3,000
				Alternative	—	—	—	3,000	3,000	3,000	3,000	3,000	3,000	3,000
2 7/8	5.79	0.203	2.469	Standard	1,000	2,500	2,500	3,000	3,000	3,000	3,000	3,000	3,000	3,000
				Alternative	—	—	—	3,000	3,000	3,000	3,000	3,000	3,000	3,000
2 7/8	6.13	0.216	2.443	Standard	1,100	2,500	2,500	3,000	3,000	3,000	3,000	3,000	3,000	3,000
				Alternative	—	—	—	3,000	3,000	3,000	3,000	3,000	3,000	3,000
2 7/8	7.01	0.250	2.375	Standard	1,200	2,500	2,500	3,000	3,000	3,000	3,000	3,000	3,000	3,000
				Alternative	—	—	—	3,000	3,000	3,000	3,000	3,000	3,000	3,000
2 7/8	7.66	0.276	2.323	Standard	1,300	2,500	2,500	3,000	3,000	3,000	3,000	3,000	3,000	3,000
				Alternative	—	—	—	3,000	3,000	3,000	3,000	3,000	3,000	3,000
2 7/8	13.69	0.552	1.771	Standard	1,400	2,500	2,500	3,000	3,000	3,000	3,000	3,000	3,000	3,000
				Alternative	—	—	—	3,000	3,000	3,000	3,000	3,000	3,000	3,000
3 1/2	3.03	0.083	3.334	Standard	600	850	1,000	1,200	1,310	1,480	1,590	1,710	1,850	1,990
				Alternative	—	—	—	1,490	1,640	1,850	1,990	2,130	2,310	2,490
3 1/2	3.95	0.109	3.282	Standard	800	—	—	1,570	1,720	1,940	2,090	2,240	2,430	2,620
				Alternative	—	—	—	1,960	2,150	2,430	2,620	2,800	3,000	3,000
3 1/2	4.51	0.125	3.250	Standard	1,000	1,290	1,500	1,800	1,970	2,230	2,400	2,570	2,790	3,000
				Alternative	—	—	—	2,250	2,460	2,790	3,000	3,000	3,000	3,000
3 1/2	5.06	0.141	3.218	Standard	1,000	—	—	2,030	2,220	2,510	2,710	2,900	3,000	3,000
				Alternative	—	—	—	2,540	2,780	3,000	3,000	3,000	3,000	3,000
3 1/2	5.57	0.156	3.188	Standard	1,000	1,600	1,870	2,250	2,460	2,780	3,000	3,000	3,000	3,000
				Alternative	—	—	—	2,810	3,000	3,000	3,000	3,000	3,000	3,000
3 1/2	6.11	0.172	3.156	Standard	1,000	1,770	2,060	2,480	2,710	3,000	3,000	3,000	3,000	3,000
				Alternative	—	—	—	3,000	3,000	3,000	3,000	3,000	3,000	3,000
3 1/2	6.65	0.188	3.124	Standard	1,000	1,930	2,260	2,710	2,970	3,000	3,000	3,000	3,000	3,000
				Alternative	—	—	—	3,000	3,000	3,000	3,000	3,000	3,000	3,000
3 1/2	7.58	0.216	3.068	Standard	1,000	2,220	2,500	3,000	3,000	3,000	3,000	3,000	3,000	3,000
				Alternative	—	—	—	3,000	3,000	3,000	3,000	3,000	3,000	3,000
3 1/2	8.68	0.250	3.000	Standard	—	2,500	2,500	3,000	3,000	3,000	3,000	3,000	3,000	3,000
				Alternative	—	—	—	3,000	3,000	3,000	3,000	3,000	3,000	3,000
3 1/2	9.66	0.281	2.938	Standard	—	2,500	2,500	3,000	3,000	3,000	3,000	3,000	3,000	3,000
				Alternative	—	—	—	3,000	3,000	3,000	3,000	3,000	3,000	3,000
3 1/2	10.25	0.300	2.900	Standard	1,300	2,500	2,500	3,000	3,000	3,000	3,000	3,000	3,000	3,000
				Alternative	—	—	—	3,000	3,000	3,000	3,000	3,000	3,000	3,000
3 1/2	18.58	0.600	2.300	Standard	—	2,500	2,500	3,000	3,000	3,000	3,000	3,000	3,000	3,000
				Alternative	—	—	—	3,000	3,000	3,000	3,000	3,000	3,000	3,000

TABLE 2.37b—PLAIN-END LINE PIPE DIMENSIONS, WEIGHTS, AND TEST PRESSURES, 2 $\frac{3}{8}$ to 5 $\frac{9}{16}$ in. (continued)

OD d_o (in.)	Weight W_{pe} (lbm/ft)	Wall Thickness e (in.)	ID d_i (in.)		Minimum Test Pressure (psi)									
					Grade A25	Grade A	Grade B	Grade X42	Grade X46	Grade X56	Grade X60	Grade X65	Grade X70	Grade
4	3.47	0.083	3.834	Standard	—	750	870	1,050	1,150	1,290	1,390	1,490	1,620	1,740
				Alternative	—	—	—	1,310	1,430	1,620	1,740	1,870	2,020	2,180
4	4.53	0.109	3.782	Standard	600	980	1,140	1,370	1,500	1,700	1,830	1,960	2,130	2,290
				Alternative	—	—	—	1,720	1,880	2,130	2,290	2,450	2,660	2,860
4	5.17	0.125	3.750	Standard	—	1,120	1,310	1,580	1,730	1,950	2,100	2,250	2,440	2,630
				Alternative	—	—	—	1,970	2,160	2,440	2,630	2,810	3,000	3,000
4	5.81	0.141	3.718	Standard	800	1,270	1,480	1,780	1,950	2,200	2,370	2,540	2,750	2,960
				Alternative	—	—	—	2,220	2,430	2,750	2,960	3,000	3,000	3,000
4	6.40	0.156	3.688	Standard	—	1,400	1,640	1,970	2,150	2,430	2,620	2,810	3,000	3,000
				Alternative	—	—	—	2,460	2,690	3,000	3,000	3,000	3,000	3,000
4	7.03	0.172	3.656	Standard	1,000	1,550	1,810	2,170	2,370	2,680	2,890	3,000	3,000	3,000
				Alternative	—	—	—	2,710	2,970	3,000	3,000	3,000	3,000	3,000
4	7.65	0.188	3.624	Standard	1,200	1,690	1,970	2,370	2,590	2,930	3,000	3,000	3,000	3,000
				Alternative	—	—	—	2,960	3,000	3,000	3,000	3,000	3,000	3,000
4	9.11	0.226	3.548	Standard	1,200	2,030	2,370	2,850	3,000	3,000	3,000	3,000	3,000	3,000
				Alternative	—	—	—	3,000	3,000	3,000	3,000	3,000	3,000	3,000
4	10.01	0.250	3.500	Standard	—	2,250	2,620	3,000	3,000	3,000	3,000	3,000	3,000	3,000
				Alternative	—	—	—	3,000	3,000	3,000	3,000	3,000	3,000	3,000
4	11.16	0.281	3.438	Standard	—	2,530	2,800	3,000	3,000	3,000	3,000	3,000	3,000	3,000
				Alternative	—	—	—	3,000	3,000	3,000	3,000	3,000	3,000	3,000
4	12.50	0.318	3.364	Standard	1,700	2,800	2,800	3,000	3,000	3,000	3,000	3,000	3,000	3,000
				Alternative	—	—	—	3,000	3,000	3,000	3,000	3,000	3,000	3,000
4 $\frac{1}{2}$	3.92	0.083	4.334	Standard	—	660	770	930	1,020	1,150	1,240	1,330	1,440	1,550
				Alternative	—	—	—	1,160	1,270	1,440	1,550	1,660	1,800	1,940
4 $\frac{1}{2}$	5.84	0.125	4.250	Standard	800	1,000	1,170	1,400	1,530	1,730	1,870	2,000	2,170	2,330
				Alternative	—	—	—	1,750	1,920	2,170	2,330	2,500	2,710	2,920
4 $\frac{1}{2}$	6.56	0.141	4.218	Standard	—	1,130	1,320	1,580	1,730	1,960	2,110	2,260	2,440	2,630
				Alternative	—	—	—	1,970	2,160	2,440	2,630	2,820	3,000	3,000
4 $\frac{1}{2}$	7.24	0.156	4.188	Standard	1,000	1,250	1,460	1,750	1,910	2,160	2,330	2,500	2,700	2,910
				Alternative	—	—	—	2,180	2,390	2,700	2,910	3,000	3,000	3,000
4 $\frac{1}{2}$	7.95	0.172	4.156	Standard	—	1,380	1,610	1,930	2,110	2,390	2,570	2,750	2,980	3,000
				Alternative	—	—	—	2,410	2,640	2,980	3,000	3,000	3,000	3,000
4 $\frac{1}{2}$	8.66	0.188	4.124	Standard	1,200	1,500	1,750	2,110	2,310	2,610	2,810	3,000	3,000	3,000
				Alternative	—	—	—	2,630	2,880	3,000	3,000	3,000	3,000	3,000
4 $\frac{1}{2}$	9.32	0.203	4.094	Standard	—	1,620	1,890	2,270	2,490	2,810	3,000	3,000	3,000	3,000
				Alternative	—	—	—	2,840	3,000	3,000	3,000	3,000	3,000	3,000
4 $\frac{1}{2}$	10.01	0.219	4.062	Standard	1,200	1,750	2,040	2,450	2,690	3,000	3,000	3,000	3,000	3,000
				Alternative	—	—	—	3,000	3,000	3,000	3,000	3,000	3,000	3,000
4 $\frac{1}{2}$	10.79	0.237	4.026	Standard	1,200	1,900	2,210	2,650	2,910	3,000	3,000	3,000	3,000	3,000
				Alternative	—	—	—	3,000	3,000	3,000	3,000	3,000	3,000	3,000
4 $\frac{1}{2}$	11.35	0.250	4.000	Standard	—	2,000	2,330	2,800	3,000	3,000	3,000	3,000	3,000	3,000
				Alternative	—	—	—	3,000	3,000	3,000	3,000	3,000	3,000	3,000
4 $\frac{1}{2}$	12.66	0.281	3.938	Standard	—	2,250	2,620	3,000	3,000	3,000	3,000	3,000	3,000	3,000
				Alternative	—	—	—	3,000	3,000	3,000	3,000	3,000	3,000	3,000
4 $\frac{1}{2}$	13.96	0.312	3.876	Standard	—	2,500	2,800	3,000	3,000	3,000	3,000	3,000	3,000	3,000
				Alternative	—	—	—	3,000	3,000	3,000	3,000	3,000	3,000	3,000
4 $\frac{1}{2}$	14.98	0.337	3.826	Standard	1,700	2,700	2,800	3,000	3,000	3,000	3,000	3,000	3,000	3,000
				Alternative	—	—	—	3,000	3,000	3,000	3,000	3,000	3,000	3,000
4 $\frac{1}{2}$	19.00	0.438	3.624	Standard	—	2,800	2,800	3,000	3,000	3,000	3,000	3,000	3,000	3,000
				Alternative	—	—	—	3,000	3,000	3,000	3,000	3,000	3,000	3,000
4 $\frac{1}{2}$	22.51	0.531	3.438	Standard	—	2,800	2,800	3,000	3,000	3,000	3,000	3,000	3,000	3,000
				Alternative	—	—	—	3,000	3,000	3,000	3,000	3,000	3,000	3,000
4 $\frac{1}{2}$	27.54	0.674	3.152	Standard	—	2,800	2,800	3,000	3,000	3,000	3,000	3,000	3,000	3,000
				Alternative	—	—	—	3,000	3,000	3,000	3,000	3,000	3,000	3,000
*5 $\frac{9}{16}$	4.86	0.083	5.397	Standard	—	540	630	750	820	930	1,000	1,040	1,160	1,250
*5 $\frac{9}{16}$	7.26	0.125	5.312	Standard	670	810	940	1,130	1,240	1,400	1,500	1,630	1,750	1,890
*5 $\frac{9}{16}$	9.01	0.156	5.251	Standard	840	1,010	1,180	1,410	1,550	1,750	1,910	2,020	2,120	2,360
*5 $\frac{9}{16}$	10.79	0.188	5.187	Standard	1,010	1,220	1,420	1,700	1,870	2,110	2,270	2,430	2,640	2,840
*5 $\frac{9}{16}$	12.50	0.219	5.125	Standard	1,180	1,420	1,650	1,990	2,170	2,460	2,650	2,830	3,000	3,000
*5 $\frac{9}{16}$	14.62	0.258	5.047	Standard	1,200	1,670	1,950	2,340	2,560	2,890	3,000	3,000	3,000	3,000
*5 $\frac{9}{16}$	15.85	0.281	5.001	Standard	1,520	1,820	2,120	2,550	2,790	3,000	3,000	3,000	3,000	3,000
*5 $\frac{9}{16}$	17.50	0.312	4.939	Standard	1,680	2,020	2,360	3,000	3,000	3,000	3,000	3,000	3,000	3,000
*5 $\frac{9}{16}$	19.17	0.344	4.875	Standard	1,860	2,230	2,600	3,000	3,000	3,000	3,000	3,000	3,000	3,000
*5 $\frac{9}{16}$	20.78	0.375	4.813	Standard	2,020	2,430	2,800	3,000	3,000	3,000	3,000	3,000	3,000	3,000
*5 $\frac{9}{16}$	27.04	0.500	4.563	Standard	2,700	2,800	2,800	3,000	3,000	3,000	3,000	3,000	3,000	3,000
*5 $\frac{9}{16}$	32.96	0.625	4.313	Standard	2,800	2,800	2,800	3,000	3,000	3,000	3,000	3,000	3,000	3,000
*5 $\frac{9}{16}$	38.55	0.750	4.063	Standard	2,800	2,800	2,800	3,000	3,000	3,000	3,000	3,000	3,000	3,000

*The decimal equivalent to 5 $\frac{9}{16}$, shall be taken as 5.563

TABLE 2.37c—PLAIN-END LINE PIPE DIMENSIONS, WEIGHTS, AND TEST PRESSURES, 6 $\frac{5}{8}$ to 12 $\frac{3}{4}$ in.

OD d_o (in.)	Weight W_{pe} (lbm/ft)	Wall Thickness e (in.)	ID d_i (in.)	Minimum Test Pressure (psi)										
				Grade A		Grade B		Grade X42	Grade X46	Grade X52	Grade X56	Grade X60	Grade X65	Grade X70
				Standard	Alternative	Standard	Alternative							
6 $\frac{5}{8}$	5.80	0.083	6.459	450	560	530	660	790	860	980	1,050	1,130	1,220	1,320
6 $\frac{5}{8}$	7.59	0.109	6.407	590	740	690	860	1,040	1,140	1,280	1,380	1,480	1,600	1,730
6 $\frac{5}{8}$	8.68	0.125	6.375	680	850	790	990	1,190	1,300	1,470	1,580	1,700	1,840	1,980
6 $\frac{5}{8}$	9.76	0.141	6.343	770	960	890	1,120	1,340	1,470	1,660	1,790	1,920	2,080	2,230
6 $\frac{5}{8}$	10.78	0.156	6.313	850	1,060	990	1,240	1,480	1,620	1,840	1,980	2,120	2,300	2,470
6 $\frac{5}{8}$	11.85	0.172	6.281	930	1,170	1,090	1,360	1,640	1,790	2,030	2,180	2,340	2,530	2,730
6 $\frac{5}{8}$	12.92	0.188	6.249	1,020	1,280	1,190	1,490	1,790	1,960	2,210	2,380	2,550	2,770	2,980
6 $\frac{5}{8}$	13.92	0.203	6.219	1,100	1,380	1,290	1,610	1,930	2,110	2,390	2,570	2,760	2,990	3,000
6 $\frac{5}{8}$	14.98	0.219	6.187	1,190	1,490	1,390	1,740	2,080	2,280	2,580	2,780	2,980	3,000	3,000
6 $\frac{5}{8}$	17.02	0.250	6.125	1,360	1,700	1,580	1,980	2,380	2,600	2,940	3,000	3,000	3,000	3,000
6 $\frac{5}{8}$	18.97	0.280	6.065	1,520	1,900	1,780	2,220	2,660	2,920	3,000	3,000	3,000	3,000	3,000
6 $\frac{5}{8}$	21.04	0.312	6.001	1,700	2,120	1,980	2,470	2,970	3,000	3,000	3,000	3,000	3,000	3,000
6 $\frac{5}{8}$	23.08	0.344	5.937	1,870	2,340	2,180	2,500	3,000	3,000	3,000	3,000	3,000	3,000	3,000
6 $\frac{5}{8}$	25.03	0.375	5.875	2,040	2,550	2,380	2,730	3,000	3,000	3,000	3,000	3,000	3,000	3,000
6 $\frac{5}{8}$	28.57	0.432	5.761	—	—	—	—	3,000	3,000	3,000	3,000	3,000	3,000	3,000
6 $\frac{5}{8}$	32.71	0.500	5.625	2,720	2,800	2,800	2,800	3,000	3,000	3,000	3,000	3,000	3,000	3,000
6 $\frac{5}{8}$	36.39	0.562	5.501	2,800	2,800	2,800	2,800	3,000	3,000	3,000	3,000	3,000	3,000	3,000
6 $\frac{5}{8}$	40.05	0.625	5.375	2,800	2,800	2,800	2,800	3,000	3,000	3,000	3,000	3,000	3,000	3,000
6 $\frac{5}{8}$	45.35	0.719	5.187	2,800	2,800	2,800	2,800	3,000	3,000	3,000	3,000	3,000	3,000	3,000
6 $\frac{5}{8}$	47.06	0.750	5.125	2,800	2,800	2,800	2,800	3,000	3,000	3,000	3,000	3,000	3,000	3,000
6 $\frac{5}{8}$	63.73	0.875	4.875	2,800	2,800	2,800	2,800	3,000	3,000	3,000	3,000	3,000	3,000	3,000
8 $\frac{5}{8}$	11.35	0.125	8.375	520	650	610	760	910	1,000	1,130	1,220	1,300	1,410	1,520
8 $\frac{5}{8}$	14.11	0.156	8.313	650	810	760	950	1,140	1,250	1,410	1,520	1,630	1,760	1,900
8 $\frac{5}{8}$	16.94	0.188	8.249	780	890	920	1,140	1,370	1,500	1,700	1,830	1,960	2,130	2,290
8 $\frac{5}{8}$	18.26	0.203	8.219	—	—	—	—	1,480	1,620	1,840	2,000	2,120	2,290	2,470
8 $\frac{5}{8}$	19.66	0.219	8.187	910	1,140	1,070	1,330	1,600	1,750	1,980	2,130	2,290	2,480	2,670
8 $\frac{5}{8}$	22.36	0.250	8.125	1,040	1,300	1,220	1,520	1,830	2,000	2,260	2,430	2,610	2,830	3,000
8 $\frac{5}{8}$	24.70	0.277	8.071	1,160	1,450	1,350	1,690	2,020	2,220	2,510	2,700	2,890	3,000	3,000
8 $\frac{5}{8}$	27.70	0.312	8.001	1,300	1,630	1,520	1,900	2,280	2,500	2,820	3,000	3,000	3,000	3,000
8 $\frac{5}{8}$	28.55	0.322	7.981	1,340	1,680	1,570	1,960	2,350	2,580	2,910	3,000	3,000	3,000	3,000
8 $\frac{5}{8}$	30.42	0.344	7.937	1,440	1,790	1,680	2,090	2,510	2,750	3,000	3,000	3,000	3,000	3,000
8 $\frac{5}{8}$	33.04	0.375	7.875	1,570	1,960	1,830	2,280	2,740	3,000	3,000	3,000	3,000	3,000	3,000
8 $\frac{5}{8}$	38.30	0.438	7.749	1,830	2,290	2,130	2,670	3,000	3,000	3,000	3,000	3,000	3,000	3,000
8 $\frac{5}{8}$	43.39	0.500	7.625	—	—	—	—	3,000	3,000	3,000	3,000	3,000	3,000	3,000
8 $\frac{5}{8}$	48.40	0.562	7.501	2,350	2,800	2,740	2,800	3,000	3,000	3,000	3,000	3,000	3,000	3,000
8 $\frac{5}{8}$	53.40	0.625	7.375	2,610	2,800	2,800	2,800	3,000	3,000	3,000	3,000	3,000	3,000	3,000
8 $\frac{5}{8}$	60.71	0.719	7.187	2,800	2,800	2,800	2,800	3,000	3,000	3,000	3,000	3,000	3,000	3,000
8 $\frac{5}{8}$	63.08	0.750	7.125	2,800	2,800	2,800	2,800	3,000	3,000	3,000	3,000	3,000	3,000	3,000
8 $\frac{5}{8}$	67.76	0.812	7.001	2,800	2,800	2,800	2,800	3,000	3,000	3,000	3,000	3,000	3,000	3,000
8 $\frac{5}{8}$	72.42	0.875	6.875	2,800	2,800	2,800	2,800	3,000	3,000	3,000	3,000	3,000	3,000	3,000
8 $\frac{5}{8}$	81.44	1.000	6.625	2,800	2,800	2,800	2,800	3,000	3,000	3,000	3,000	3,000	3,000	3,000
10 $\frac{3}{4}$	17.65	0.156	10.438	520	650	610	760	1,040	1,130	1,280	1,380	1,480	1,600	1,730
10 $\frac{3}{4}$	21.21	0.188	10.374	630	790	730	920	1,250	1,370	1,550	1,660	1,780	1,930	2,080
10 $\frac{3}{4}$	22.87	0.203	10.344	—	—	—	—	1,350	1,480	1,670	1,800	1,930	2,090	2,250
10 $\frac{3}{4}$	24.63	0.219	10.312	730	920	860	1,070	1,450	1,590	1,800	1,940	2,080	2,250	2,420
10 $\frac{3}{4}$	28.04	0.250	10.250	840	1,050	980	1,220	1,660	1,820	2,060	2,210	2,370	2,570	2,770
10 $\frac{3}{4}$	31.20	0.279	10.192	930	1,170	1,090	1,360	1,850	2,030	2,290	2,470	2,650	2,870	3,000
10 $\frac{3}{4}$	34.24	0.307	10.136	1,030	1,290	1,200	1,500	2,040	2,230	2,520	2,720	2,910	3,000	3,000
10 $\frac{3}{4}$	38.23	0.344	10.062	1,150	1,440	1,340	1,680	2,280	2,500	2,830	3,000	3,000	3,000	3,000
10 $\frac{3}{4}$	40.48	0.365	10.020	1,220	1,530	1,430	1,780	2,420	2,660	3,000	3,000	3,000	3,000	3,000
10 $\frac{3}{4}$	48.24	0.438	9.874	1,470	1,830	1,710	2,140	2,910	3,000	3,000	3,000	3,000	3,000	3,000
10 $\frac{3}{4}$	54.74	0.500	9.750	—	—	—	—	3,000	3,000	3,000	3,000	3,000	3,000	3,000
10 $\frac{3}{4}$	61.15	0.562	9.626	1,880	2,350	2,200	2,740	3,000	3,000	3,000	3,000	3,000	3,000	3,000
10 $\frac{3}{4}$	67.58	0.625	9.500	2,090	2,620	2,440	2,800	3,000	3,000	3,000	3,000	3,000	3,000	3,000
10 $\frac{3}{4}$	77.03	0.719	9.312	2,410	2,800	2,800	2,800	3,000	3,000	3,000	3,000	3,000	3,000	3,000
10 $\frac{3}{4}$	86.18	0.812	9.126	2,720	2,800	2,800	2,800	3,000	3,000	3,000	3,000	3,000	3,000	3,000
10 $\frac{3}{4}$	92.28	0.875	9.000	2,800	2,800	2,800	2,800	3,000	3,000	3,000	3,000	3,000	3,000	3,000
10 $\frac{3}{4}$	98.30	0.938	8.874	2,800	2,800	2,800	2,800	3,000	3,000	3,000	3,000	3,000	3,000	3,000
10 $\frac{3}{4}$	104.13	1.000	8.750	2,800	2,800	2,800	2,800	3,000	3,000	3,000	3,000	3,000	3,000	3,000
10 $\frac{3}{4}$	126.83	1.250	8.250	2,800	2,800	2,800	2,800	3,000	3,000	3,000	3,000	3,000	3,000	3,000
12 $\frac{3}{4}$	23.11	0.172	12.406	490	610	570	710	960	1,050	1,190	1,280	1,380	1,490	1,610
12 $\frac{3}{4}$	25.22	0.188	12.374	530	660	620	770	1,050	1,150	1,300	1,400	1,500	1,630	1,750
12 $\frac{3}{4}$	27.20	0.203	12.344	—	—	—	—	1,140	1,250	1,410	1,520	1,620	1,760	1,890
12 $\frac{3}{4}$	29.31	0.219	12.312	620	770	720	900	1,230	1,340	1,520	1,640	1,750	1,900	2,040
12 $\frac{3}{4}$	33.38	0.250	12.250	710	880	820	1,030	1,400	1,530	1,730	1,870	2,000	2,170	2,330
12 $\frac{3}{4}$	37.42	0.281	12.188	790	990	930	1,160	1,570	1,720	1,950	2,100	2,250	2,440	2,620

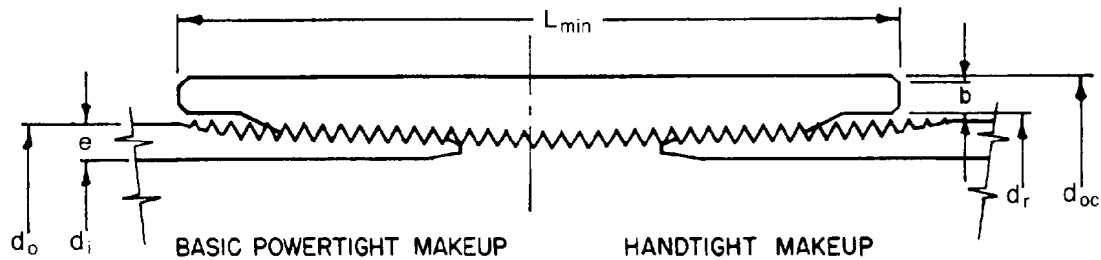


Fig. 2.9—Line pipe and coupling. See Table 2.33 for pipe dimensions.

Yield-Strength Collapse-Pressure Equation. The yield-strength collapse pressure is not a true collapse pressure, but rather the external pressure, p_y , that generates minimum yield stress, σ_y , on the inside wall of a tube as calculated by Eq. 3.

$$p_y = 2\sigma_y \left[\frac{d_o/e - 1}{(d_o/e)^2} \right] \quad \dots \dots \dots (3)$$

Eq. 3 for yield strength collapse pressure is applicable for d_o/e values up to the value corresponding to the intersection with the plastic collapse (Eq. 5). This intersection is calculated by Eq. 4. Applicable d_o/e ratios for yield-strength collapse are shown in Table 2.38.

$$(d_o/e)_{yp} = \frac{\sqrt{(F_A - 2)^2 + 8(F_B + F_C/\sigma_y)} + (F_A - 2)}{2(F_B + F_C/\sigma_y)} \quad \dots \dots \dots (4)$$

TABLE 2.38—YIELD COLLAPSE PRESSURE EQUATION RANGE

Grade*	d_o/e Range**
H-40	16.40 and less
-50	15.24 and less
J-K-55, D	14.81 and less
-60	14.44 and less
-70	13.85 and less
C-75, E	13.60 and less
L-80, N-80	13.38 and less
-90	13.01 and less
C-95	12.85 and less
-100	12.70 and less
P-105	12.57 and less
P-110	12.44 and less
-120	12.21 and less
Q-125	12.11 and less
-130	12.02 and less
-135	11.92 and less
-140	11.84 and less
-150	11.67 and less
-155	11.59 and less
-160	11.52 and less
-170	11.37 and less
-180	11.23 and less

*Grades indicated without letter designation are not API grades but are grades in use or grades being considered for use.

**The d_o/e range values were calculated from Eqs. 4 and 12 through 14 to eight or more digits.

where F_A , F_B , and F_C are equation factors established by the API task group on performance properties (Table 2.39) and σ_y is yield pressure.

Plastic Collapse-Pressure Equation. The minimum collapse pressure for the plastic range of collapse is

$$p_p = \sigma_y \left(\frac{F_A}{d_o/e} - F_B \right) - F_C \quad \dots \dots \dots (5)$$

The equation for minimum plastic collapse pressure is applicable for d_o/e values ranging from $(d_o/e)_{yp}$ (Eq. 4 for yield-point collapse pressure) to the intersection with Eq. 7 for transition collapse pressure, $(d_o/e)_{pT}$. Values for $(d_o/e)_{pT}$ are calculated by

$$(d_o/e)_{pT} = \frac{\sigma_y(F_A - F_F)}{F_C + \sigma_y(F_B - F_G)} \quad \dots \dots \dots (6)$$

TABLE 2.39—EQUATION FACTORS AND d_o/e RANGES FOR PLASTIC COLLAPSE

Grade**	Equation Factors*			d_o/e Range*
	F_A	F_B	F_C	
H-40	2.950	0.0465	754	16.40 to 27.01
-50	2.976	0.0515	1,056	15.24 to 25.63
J-K-55, D	2.991	0.0541	1,206	14.81 to 25.01
-60	3.005	0.0566	1,356	14.44 to 24.42
-70	3.037	0.0617	1,656	13.85 to 23.38
C-75, E	3.054	0.0642	1,806	13.60 to 22.91
L-80, N-80	3.071	0.0667	1,955	13.38 to 22.47
-90	3.106	0.0718	2,254	13.01 to 21.69
C-95	3.124	0.0743	2,404	12.85 to 21.33
-100	3.143	0.0768	2,553	12.70 to 21.00
P-105	3.162	0.0794	2,702	12.57 to 20.70
P-110	3.181	0.0819	2,852	12.44 to 20.41
-120	3.219	0.0870	3,151	12.21 to 19.88
Q-125	3.239	0.0895	3,301	12.11 to 19.63
-130	3.258	0.0920	3,451	12.02 to 19.40
-135	3.278	0.0946	3,601	11.92 to 19.18
-140	3.297	0.0971	3,751	11.84 to 18.97
-150	3.336	0.1021	4,053	11.67 to 18.57
-155	3.356	0.1047	4,204	11.59 to 18.37
-160	3.375	0.1072	4,356	11.52 to 18.19
-170	3.412	0.1123	4,660	11.37 to 17.82
-180	3.449	0.1173	4,966	11.23 to 17.47

*The d_o/e range values and equation factors were calculated from Eqs. 4, 6, and 12 through 16 to eight or more digits.

**Grades indicated without letter designation are not API grades but are grades in use or grades being considered for use.

where F_F and F_G are equation factors (Table 2.40), and the subscript pT denotes transition pressure.

The factors and applicable d_o/e range for the plastic collapse equation are shown in Table 2.39.

Transition Collapse-Pressure Equation. The minimum collapse pressure for the plastic to elastic transition zone is calculated with

$$p_T = \sigma_y \left(\frac{F_F}{d_o/e} - F_G \right) \quad \dots \dots \dots (7)$$

Eq. 7 for p_T is applicable for d_o/e values from $(d_o/e)_{pT}$ (Eq. 6 for plastic collapse pressure) to the intersection $(d_o/e)_{TE}$ with Eq. 9 for elastic collapse. Values for $(d_o/e)_{TE}$ are calculated with

$$(d_o/e)_{TE} = \frac{2 + F_B/F_A}{3F_B/F_A} \quad \dots \dots \dots (8)$$

where the subscript TE denotes elastic transition.

The factors and applicable d_o/e range for the transition collapse-pressure equation are shown in Table 2.40.

Elastic Collapse-Pressure Equation. The minimum collapse pressure for the elastic range of collapse is calculated with

$$p_E = \frac{46.95}{(d_o/e)[(d_o/e) - 1]^2} \quad \dots \dots \dots (9)$$

The applicable d_o/e range for elastic collapse is shown in Table 2.41.

Collapse Pressure Under Axial-Tension Stress. The collapse resistance of casing in the presence of an axial stress is calculated by modifying the yield stress to an axial stress equivalent grade according to Eq. 10.⁵

$$\sigma_{ya} = [\sqrt{1 - 0.75(\sigma_a/\sigma_y)^2} - 0.5\sigma_a/\sigma_y]\sigma_y \quad \dots \dots (10)$$

where

σ_a = axial stress (tension is positive), psi,

σ_y = minimum yield strength of pipe, psi, and

σ_{ya} = yield strength of axial-stress equivalent grade, psi.

Collapse-resistance equation factors and d_o/e ranges for the axial-stress equivalent grade are then calculated with Eqs. 4, 6, 8, and 12 through 16. With the equation factors for the axial-stress equivalent grade, collapse resistance under axial load is calculated with Eqs. 3, 5, 7, and 9, with d_o/e rounded to two decimals. The reduced collapse-pressure calculations are carried to eight digits in all intermediate steps, and the final answer is rounded to the nearest 10 psi.

Eq. 10 is based on the Hencky-von Mises maximum strain energy of distortion theory of yielding.

Example Problem 4. Calculate the collapse pressure of 7-in., 26-lbm P-110 casing with an axial stress of 11,000 psi. The wall thickness is 0.362 in.; $\sigma_a = 11,000$ psi, and $\sigma_y = 110,000$ psi.

TABLE 2.40—EQUATION FACTORS AND d_o/e RANGE FOR TRANSITION COLLAPSE

Grade**	Equation Factors*		d_o/e Range*
	F_F	F_G	
H-40	2.063	0.0325	27.01 to 42.64
-50	2.003	0.0347	25.63 to 38.83
J-K-55, D	1.989	0.0360	25.01 to 37.21
-60	1.983	0.0373	24.42 to 35.73
-70	1.984	0.0403	23.38 to 33.17
C-75, E	1.990	0.0418	22.91 to 32.05
L-80, N-80	1.998	0.0434	22.47 to 31.02
C-90	2.017	0.0466	21.69 to 29.18
C-95	2.029	0.0482	21.33 to 28.36
-100	2.040	0.0499	21.00 to 27.60
P-105	2.053	0.0515	20.70 to 26.89
P-110	2.066	0.0532	20.41 to 26.22
-120	2.092	0.0565	19.88 to 25.01
Q-125	2.106	0.0582	19.63 to 24.46
-130	2.119	0.0599	19.40 to 23.94
-135	2.133	0.0615	19.18 to 23.44
-140	2.146	0.0632	18.97 to 22.98
-150	2.174	0.0666	18.57 to 22.11
-155	2.188	0.06825	18.37 to 21.70
-160	2.202	0.0700	18.19 to 21.32
-170	2.231	0.0734	17.82 to 20.60
-180	2.261	0.0769	17.47 to 19.93

*The d_o/e range values and equation factors were calculated from Eqs. 6, 8, and 12 through 16 to eight or more digits.

**Grades indicated without letter designation are not API grades but are grades in use or grades being considered for use.

TABLE 2.41— d_o/e RANGE FOR ELASTIC COLLAPSE

Grade*	d_o/e Range**
H-40	42.64 and greater
-50	38.83 and greater
J-K-55, D	37.21 and greater
-60	35.73 and greater
-70	33.17 and greater
C-75, E	32.05 and greater
L-80, N-80	31.02 and greater
C-90	29.18 and greater
C-95	28.36 and greater
-100	27.60 and greater
P-105	26.89 and greater
P-110	26.22 and greater
-120	25.01 and greater
Q-125	24.46 and greater
-130	23.94 and greater
-135	23.44 and greater
-140	22.98 and greater
-150	22.11 and greater
-155	21.70 and greater
-160	21.32 and greater
-170	20.60 and greater
-180	19.93 and greater

*Grades indicated without letter designation are not API grades but are grades in use or grades being considered for use.

**The d_o/e range values were calculated from Eqs. 8, 12, and 13 to eight or more digits.

Solution. Substitution into Eq. 10 gives

$$\sigma_{yu} = [\sqrt{1 - 0.75(11,000/110,000)^2} - 0.5(11,000/110,000)]110,000 = 104,087 \text{ psi.}$$

Substitution of σ_{yu} for σ_y in Eqs. 4, 6, 8, and 12 through 16 results in the following values.

$$\begin{aligned} F_A &= 3.158, \\ F_B &= 0.0789, \\ F_C &= 2.675, \\ F_F &= 2.051, \\ F_G &= 0.0512, \\ (d_o/e)_{yp} &= 12.59, \\ (d_o/e)_{pT} &= 20.75, \text{ and} \\ (d_o/e)_{TE} &= 27.02. \end{aligned}$$

The d_o/e range for yield collapse is 12.59 or less; for plastic collapse, 12.59 to 20.75; for transition collapse, 20.75 to 27.02; and for elastic collapse, 27.02 or greater. The d_o/e is 7/0.362, or 19.34, indicating that collapse is in the plastic range. Substitution of F_A (3.158), F_B (0.0789), and F_C (2.675) into Eq. 5 for plastic collapse yields

$$\begin{aligned} p_p &= \sigma_{yu}[F_A/(d_o/e) - F_B] - F_C \\ &= 104,087(3.158/19.34 - 0.0789) - 2.675 \\ &= 6,110 \text{ psi.} \end{aligned}$$

HC-95 Casing. The collapse resistance of casing in the presence of an axial stress is calculated with Eq. 11, which is based on the total strain energy theory of yielding.⁹

$$p_{ca} = [\sqrt{1 - 0.9324(\sigma_a/\sigma_y)^2} - 6.26(\sigma_a/\sigma_y)]p_{co}, \quad (11)$$

where p_{ca} is the minimum collapse pressure under axial stress, psi, and p_{co} is the minimum collapse pressure without axial stress, psi.

Collapse Equation Factors. Collapse equation factors for plastic and transition collapse are calculated by the following equations:

$$\begin{aligned} F_A &= 2.8762 + 0.10679 \times 10^{-5} \sigma_y \\ &\quad + 0.21301 \times 10^{-10} \sigma_y^2 - 0.53132 \times 10^{-16} \sigma_y^3, \end{aligned} \quad (12)$$

$$F_B = 0.026233 + 0.50609 \times 10^{-6} \sigma_y, \quad (13)$$

$$\begin{aligned} F_C &= -465.93 + 0.030867 \sigma_y - 0.10483 \times 10^{-7} \sigma_y^2 \\ &\quad + 0.36989 \times 10^{-13} \sigma_y^3, \end{aligned} \quad (14)$$

and

$$F_F = \frac{46.95 \times 10^6 \left(\frac{3F_B/F_A}{2 + F_B/F_A} \right)^3}{\sigma_y \left(\frac{3F_B/F_A}{2 + F_B/F_A} - F_B/F_A \right) \left(1 - \frac{3F_B/F_A}{2 + F_B/F_A} \right)^2}, \quad (15)$$

Expressed in metric units, Eqs. 12 through 15 become, respectively,

$$\begin{aligned} F_A &= 2.8762 + 1.5488 \times 10^{-4} \sigma_y + 4.4806 \times 10^{-7} \sigma_y^2 \\ &\quad - 1.6209 \times 10^{-3} \sigma_y^3, \end{aligned}$$

$$F_B = 0.026233 + 7.33995 \times 10^{-6} \sigma_y,$$

$$\begin{aligned} F_C &= -3.2126 + 0.030867 \sigma_y - 1.5204 \times 10^{-6} \sigma_y^2 \\ &\quad + 7.7804 \times 10^{-10} \sigma_y^3, \end{aligned}$$

and

$$\begin{aligned} F_F &= \frac{323.7 \times 10^3 \left(\frac{3F_B/F_A}{2 + F_B/F_A} \right)^3}{\sigma_y \left(\frac{3F_B/F_A}{2 + F_B/F_A} - F_B/F_A \right) \left(1 - \frac{3F_B/F_A}{2 + F_B/F_A} \right)^2}, \\ F_G &= \frac{F_F F_B}{F_A}. \end{aligned} \quad (16)$$

Pipe-Body Yield Strength

Pipe-body yield strength is the axial load required to yield the pipe. It is taken as the product of the cross-sectional area and the specified minimum yield strength for the particular grade of pipe.

Values for pipe-body yield strength were calculated with Eq. 17.

$$W_p = 0.7854(d_o^2 - d_i^2)\sigma_y, \quad (17)$$

where

$$\begin{aligned} W_p &= \text{pipe-body yield strength, lbf (rounded to} \\ &\quad \text{the nearest 1,000), and} \\ d_i &= \text{specified inside diameter, in.} \end{aligned}$$

Internal Pressure Resistance

Internal pressure resistance is the lowest of the internal yield pressure of the pipe, the internal yield pressure of the coupling, or the internal pressure leak resistance at the d_{p1} or d_p plane calculated with Eqs. 18, 19, and 22.

Internal Yield Pressure for Pipe. Internal yield pressure for pipe is calculated from Eq. 18. The factor 0.875 appearing in Eq. 18 allows for minimum wall.

$$p_{yi} = 0.875 \left(\frac{2\sigma_y e}{d_o} \right). \quad (18)$$

TABLE 2.42—CASING SHORT-THREAD DIMENSIONS (FIG. 2.10A)

OD d_o (in.)	Major Diameter d_1 (in.)	Nominal Weight: Threads and Coupling (lbm/ft)	Numer of Threads Per Inch	Length, in.			Pitch Diameter at Hand- Tight Plane d_p (in.)	End of Pipe to Center of Coupling, Power Tight Make-Up L_{pc} (in.)	Length: Face of Coupling to Hand- Tight Plane L_m (in.)	Diameter of Coupling Recess d_{cr} (in.)	Depth of Coupling Recess D_{cr} (in.)	Hand- Tight Standoff Thread Turns n_{so}	Minimum Length, Full Crest Threads From End Of Pipe L_c (in.)
				End of Pipe to Hand- Tight Plane L_1	Effective Threads L_2	Total End of Pipe to Vanish Point L_4							
4½	4.500	9.50	8	0.921	1.715	2.000	4.40337	1.125	0.704	4½/32	½	3	0.875
4½	4.500	others	8	1.546	2.340	2.625	4.40337	0.500	0.704	4½/32	½	3	1.500
5	5.000	11.50	8	1.421	2.215	2.500	4.90337	0.750	0.704	5½/32	½	3	1.375
5	5.000	others	8	1.671	2.465	2.750	4.90337	0.500	0.704	5½/32	½	3	1.625
5½	5.500	all	8	1.796	2.590	2.875	5.40337	0.500	0.704	5½/32	½	3	1.750
6¾	6.625	all	8	2.046	2.840	3.125	6.52837	0.500	0.704	6½/32	½	3	2.000
7	7.000	17.00	8	1.296	2.090	2.375	6.90337	1.250	0.704	7½/32	½	3	1.250
7	7.000	others	8	2.046	2.840	3.125	6.90337	0.500	0.704	7½/32	½	3	2.000
7¾	7.625	all	8	2.104	2.965	3.250	7.52418	0.500	0.709	7½/32	½	3½	2.125
8¾	8.625	24.00	8	1.854	2.715	3.000	8.52418	0.875	0.709	8½/32	½	3½	1.875
8¾	8.625	others	8	2.229	3.090	3.375	8.52418	0.500	0.709	8½/32	½	3½	2.250
9¾	9.625	all	8	2.229	3.090	3.375	9.52418	0.500	0.709	9½/32	½	3½**	2.250
10¾	10.750	32.75	8	1.604	2.465	2.750	10.64918	1.250	0.709	10½/32	½	3½**	1.625
10¾	10.750	others	8	2.354	3.215	3.500	10.64918	0.500	0.709	10½/32	½	3½**	2.375
11¾	11.750	all	8	2.354	3.215	3.500	11.64918	0.500	0.709	11½/32	½	3½	2.375
13¾	13.375	all	8	2.354	3.215	3.500	13.27418	0.500	0.709	13½/32	½	3½	2.375
16	16.000	all	8	2.854	3.715	4.000	15.89918	0.500	0.709	16½/32	½	3½	2.875
18¾	18.625	87.50	8	2.854	3.715	4.000	18.52418	0.500	0.709	18½/32	½	3½	2.875
20	20.000	all	8	2.854	3.715	4.000	19.89918	0.500	0.709	20½/32	½	3½**	2.875

Included taper on diameter, all sizes, 0.0625 in./in.

* $L_c = L_4 - 1.125$ in. for eight round thread casing.

**For 10¾-in. Grade P-110 casing, and 20-in. Grade J-55 and K-55 casing, the hand-tight standoff "A" is four thread turns.

Internal Yield Pressure for Couplings. Internal yield pressure for threaded and coupled pipe is the same as for plain-end pipe, except where a lower pressure is required to avoid leakage because of insufficient coupling strength. The lower pressure is based on Eq. 19 and is rounded to the nearest 10 psi.

$$p_{yi} = \sigma_{yc} \left(\frac{d_{oc} - d_1}{d_{oc}} \right), \quad (19)$$

where

σ_{yc} = minimum yield strength of coupling, psi.

d_{oc} = nominal OD of coupling, rounded to the nearest 0.001, in., and

d_1 = diameter at the root of the coupling thread at the end of the pipe in the power-tight position, rounded to the nearest 0.001, in.

For round-thread casing and tubing,

$$d_1 = d_p - (L_1 + L_{so})F_T + h_{tc} - 2S_m, \quad (20)$$

where

d_p = pitch diameter at hand-tight plane (Table 2.42), in.,

L_1 = length from end of pipe to hand-tight plane (Table 2.43), in.,

L_{so} = hand-tight standoff, in. (L_{so} in API Standard 5B is given in turns),

F_T = taper, in./in. ($F_T = 0.0625$ for 4½- through 13¾-in. casing and 0.0833 for casing larger than 13¾ in.),

h_{tc} = thread height (0.08660 for 10 threads/in.; 0.10825 for 8 threads/in.), in., and

S_m = thread root truncation (0.014 for 10 threads/in.; 0.017 for 8 threads/in.), in.

For buttress-thread casing,

$$d_1 = d_p' - (L_7 + I)F_T + 0.062, \quad (21)$$

where

d_p' = pitch diameter, in.,

L_7 = length of perfect threads, in., and

I = length from the end of the coupling to the base of the triangle in the hand-tight position (Fig. 2.10), in. ($I = 0.400$ for 4½-in. casing; 0.500 for 5- through 13¾-in. casing; and 0.375 for casing larger than 13¾ in.)

Internal-Pressure Leak Resistance at Plane d_{p1} or d_p

The internal-pressure leak resistance at Plane d_{p1} or d_p is calculated with Eq. 22 and rounded to the nearest 10 psi. Eq. 22 is based on the assumption that the seal is at

TABLE 2.43—CASING LONG-THREAD DIMENSIONS (FIG. 2.10A)

OD d_o (in.)	Major Diameter d_4 (in.)	Number of Threads Per Inch	Length (in.)			Pitch Diameter at Hand- Tight Plane d_p (in.)	End of Pipe to Center of Coupling, Power- Tight Make-Up L_{pc} (in.)	Length: Face of Coupling to Hand- Tight Plane L_m (in.)	Diameter of Coupling Recess d_{cr} (in.)	Depth of Coupling Recess D_{cr} (in.)	Hand- Tight Standoff Thread Turns n_{so}	Minimum Length Full Crest Threads From End of Pipe* L_c (in.)
			End of Pipe to Hand- Tight Plane L_1	Effective Threads L_2	Total End of Pipe to Vanish Point L_4							
4½	4.500	8	1.921	2.715	3.000	4.40337	0.500	0.704	41⅜/32	½	3	1.875
5	5.000	8	2.296	3.090	3.375	4.90337	0.500	0.704	5⅜/32	½	3	2.250
5½	5.500	8	2.421	3.215	3.500	5.40337	0.500	0.704	5⅞/32	½	3	2.375
6⅝	6.625	8	2.796	3.590	3.875	6.52837	0.500	0.704	6⅜/32	½	3	2.750
7	7.000	8	2.921	3.715	4.000	6.90337	0.500	0.704	7⅜/32	½	3	2.875
7⅝	7.625	8	2.979	3.840	4.125	7.52418	0.500	0.709	7⅜/32	½	3½	3.000
8⅝	8.625	8	3.354	4.215	4.500	8.52418	0.500	0.709	8⅜/32	½	3½	3.375
9⅝	9.625	8	3.604	4.465	4.750	9.52418	0.500	0.709	9⅜/32	½	3½**	3.625
20	20.00	8	4.104	4.965	5.250	19.89918	0.500	0.709	20⅜/32	½	3½**	4.125

Included taper on diameter, all sizes, 0.0625 in./in.

* $L_c = L_4 - 1.125$ in. for eight round thread casing.

**For 9⅝-in. Grade P-110 casing, and 20-in. Grade J-55 and K-55 casing, the hand-tight standoff "A" is four thread turns.

Plane d_{p1} for round threads and at Plane d_p for buttress threads where the coupling is the weakest and the internal-pressure leak resistance is the lowest. Eq. 22 is based on the assumption that the internal leak resistance is equal to pressure between the pipe and coupling threads resulting from makeup and the internal pressure with stresses in the elastic range.

$$p_{il} = EF_T n L_{tp} (r_b^2 - r_c^2) / 4 r_c r_b^2, \quad (22)$$

where

p_{il} = internal-pressure leak resistance, psi,

E = modulus of elasticity (30×10^6)

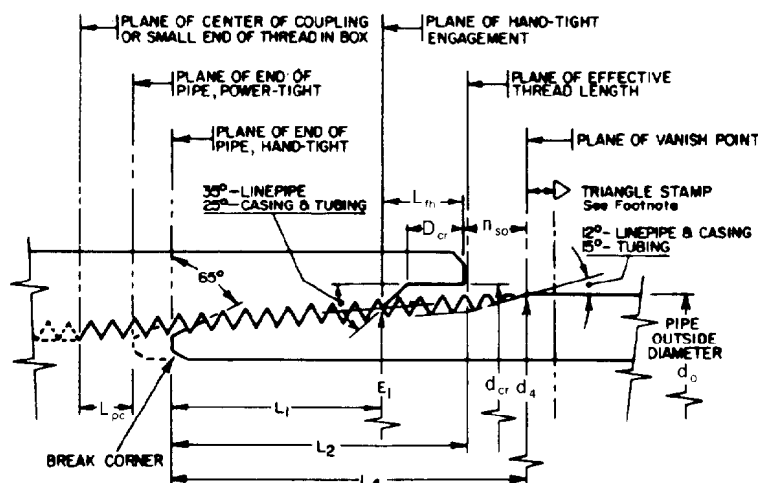
n = number of thread turns makeup ($n = r_i$ for round-thread casing, $r_i + 1\frac{1}{2}$ for buttress-thread casing 13⅝ in. and smaller, and $r_i + 1$ for buttress-thread casing 16 in. and larger, Tables 2.42 through 2.44),

L_{tp} = thread pitch (0.125 for round thread, 0.200 for buttress thread), in.,

r_b = external box radius, $d_{oc}/2$, in.,

r_c = contact radius, $d_{p1}/2$ for round-thread casing, $d_p/2$ for buttress-thread casing, in., and

r_i = pipe internal radius, in.



FOR 16, 18½ AND 20 IN. GRADES H, J AND K CASING A ¼ IN. (9.5 mm) EQUILATERAL TRIANGLE SHALL BE DIE STAMPED AT A DISTANCE OF $L_2 - 1\frac{1}{2}$ IN. ($L_2 + 1.5$ mm) FROM EACH END

THE VANISH CONE ANGLE IS OPTIONAL FOR ROUND THREADS ON DOWNHOLE TOOLS

FOR BASIC POWER-TIGHT MAKE-UP FACE OF COUPLING OR BOX ADVANCES TO PLANE OF VANISH POINT

THE VANISH CONE ANGLE APPLIES TO THE ROOTS OF THE INCOMPLETE THREADS PRODUCED BY EITHER MULTIPLE POINT OR SINGLE POINT TOOLS

Fig. 2.10A—Basic dimensions of line-pipe threads and casing and tubing round thread, hand-tight makeup.

TABLE 2.44—BUTTRESS CASING THREAD DIMENSIONS (FIG. 2.10B)

OD d_o (in.)	Major Diameter d_4 (in.)	Number of Threads Per Inch	Length (in.)			Pitch Diameter* d_p (in.)	End of Pipe to Center of Coupling, Power-Tight Make-Up L_{pc} (in.)	End of Pipe to Center of Coupling, Hand- Tight Make-Up L_{hc} (in.)	Length: Face of Coupling to Plane E ₇ (in.)	Length: End of Pipe to Triangle Stamp L_{ps} (in.)	Hand- Tight Standoff, Thread Turns n_{so}	Diameter of Counterbore in Coupling d_{cc} (in.)	Minimum Length, Full Crest Threads From End of Pipe** L_c (in.)
			Imperfect Threads L_H	Perfect Threads L_7	Total End of Pipe to Vanish Point L_4								
4½	4.516	5	1.984	1.6535	3.6375	4.454	0.500	0.900	1.884	3⅞ ₁₆	½	4.640	1.2535
5	5.016	5	1.984	1.7785	3.7625	4.954	0.500	1.000	1.784	4⅞ ₁₆	1	5.140	1.3785
5½	5.516	5	1.984	1.8410	3.8250	5.454	0.500	1.000	1.784	4⅞ ₁₆	1	5.640	1.4410
6⅞	6.641	5	1.984	2.0285	4.0125	6.579	0.500	1.000	1.784	4⅞ ₁₆	1	6.765	1.6285
7	7.016	5	1.984	2.2160	4.2000	6.954	0.500	1.000	1.784	4½ ₂	1	7.140	1.8160
7⅞	7.641	5	1.984	2.4035	4.3875	7.579	0.500	1.000	1.784	4⅞ ₁₆	1	7.765	2.0035
8⅞	8.641	5	1.984	2.5285	4.5125	8.579	0.500	1.000	1.784	4⅞ ₁₆	1	8.765	2.1285
9⅞	9.641	5	1.984	2.5285	4.5125	9.579	0.500	1.000	1.784	4⅞ ₁₆	1	9.765	2.1285
10¾	10.766	5	1.984	2.5285	4.5125	10.704	0.500	1.000	1.784	4⅞ ₁₆	1	10.890	2.1285
11¾	11.766	5	1.984	2.5285	4.5125	11.704	0.500	1.000	1.784	4⅞ ₁₆	1	11.890	2.1285
13⅞	13.391	5	1.984	2.5285	4.5125	13.329	0.500	1.000	1.784	4⅞ ₁₆	1	13.515	2.1285
16	16.000	5	1.488	3.1245	4.6125	15.938	0.500	0.875	1.313	4⅞ ₁₆	⅞	16.154	2.7245
18⅞	18.625	5	1.488	3.1245	4.6125	18.563	0.500	0.875	1.313	4⅞ ₁₆	⅞	18.779	2.7245
20	20.000	5	1.488	3.1245	4.6125	19.938	0.500	0.875	1.313	4⅞ ₁₆	⅞	20.154	2.7245

Included taper on diameter: Sizes 13 $\frac{3}{8}$ in. and smaller—0.0625 in./in.
 Sizes 16 in. and larger—0.0833 in./in.

* $L_c = L_7 - 0.400$ for buttress casing. Within the L_c length, as many as 2 threads showing the original outside surface of the pipe on their crests for a circumferential distance not exceeding 25% of the pipe circumference is permissible. The remaining threads in the L_c thread length shall be full crested threads.

NOTE: At plane of perfect thread length L_7 , the basic major diameter of the pipe thread and plug gauge thread is 0.016 in. greater than nominal pipe diameter d_o for sizes 13 3/8 in. and smaller, and is equal to the nominal pipe diameter for sizes 16 in. and larger.

The interface pressure between the pin and box as a result of makeup is

$$p_{ij} = EF_T n L_{ip} (r_b^2 - r_c^2)(r_c^2 - r_i^2) / 4 r_c^2 (r_b^2 - r_i^2), \quad \dots \dots \dots (23)$$

where r_i is the pipe radius in inches.

After makeup, internal pressure, p_i , causes a change in the interface pressure by an amount Δp_{if} :

$$\Delta p_{if} = p_i r_i^2 (r_b^2 - r_c^2) / r_c^2 (r_b^2 - r_i^2). \quad \dots\dots\dots (24)$$

Because $r_b > r_c > r_i$, $\Delta p_{if} < p_i$. Therefore, when $p_{if} + \Delta p_{if} = p_i$, the connection has reached the leak resistance limit, p_H . In other words, if $p_i > p_{if} + \Delta p_{if}$, leakage would occur.

$$p_{if} + \Delta p_{if} = p_i = p_{il}, \quad \dots \dots \dots (25)$$

Substituting the appropriate values of $p_{ij} + \Delta p_{ij}$ into Eq. 25 and simplifying produces Eq. 22. Note that the dimension r_i no longer remains a variable.

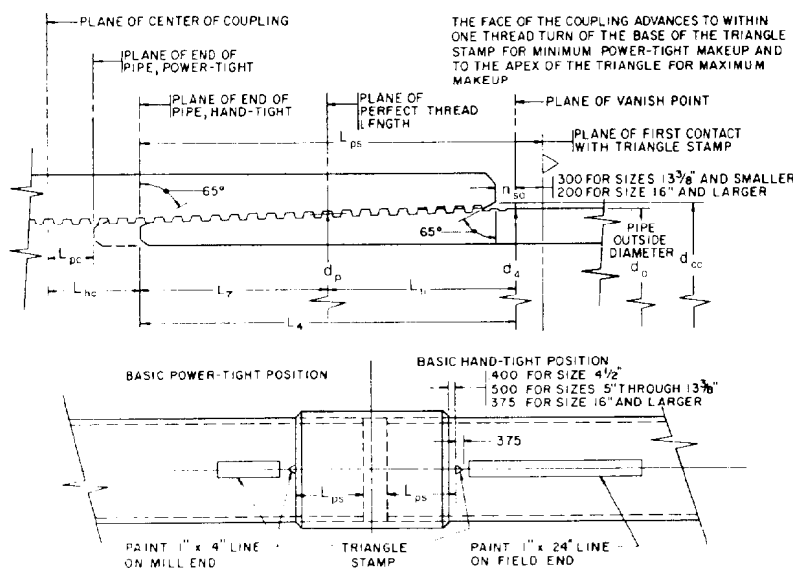


Fig. 2.10B—Basic dimensions of buttress casing threads, hand-tight makeup.

Joint Strength

Round-Thread Casing Joint Strength. Round-thread casing joint strength is calculated with Eqs. 26 and 27. The lesser of the values obtained from these two equations governs. Eqs. 26 and 27 apply to both short and long threads and couplings. Eq. 26 is for minimum strength of a joint failing by fracture, and Eq. 27 is for minimum strength of a joint failing by thread jumpout or pullout.

$$W_j = 0.95 A_{ip} \sigma_{up} \quad (26)$$

and

$$W_j = 0.95 A_{ip} L_e \left(\frac{0.74 d_o^{-0.59} \sigma_{up}}{0.5 L_e + 0.141 d_o} + \frac{\sigma_y}{L_e + 0.14 d_o} \right), \quad (27)$$

where

W_j = minimum joint strength, lbf,

A_{ip} = cross-sectional area of the pipe wall under the last perfect thread,
 $0.7854[(d_o - 0.1425)^2 - d_i^2]$ for eight round threads, sq in.,

L_e = engaged thread length ($L_4 - L_{ph}$ for nominal makeup, API Standard 5B), in.,

L_{ph} = length face of coupling to hand-tight plane, Col. 10 of Table 2.42 or Col. 9 of Table 2.43,

σ_{up} = minimum ultimate strength of pipe, psi, and

σ_y = minimum yield strength of pipe, psi.

Joint strengths of round-thread casing given in API Bull. 5C2⁵ were calculated with tabulated values of diameter and thickness and API-listed values of L_4 and L_{ph} . Pipe area was calculated to three decimals, $d_o^{-0.59}$ was calculated to five digits from a seven-place logarithm table, and remaining calculations used six digits. Listed values were rounded to 1,000 lbf.

Eqs. 26 and 27 were adopted at the 1963 API Standardization Conference.¹¹ Clinedinst¹² covers the derivation of the equations. They are based on the results of an API-sponsored test program consisting of tension tests of 162 joints of round-thread casing in Grades K-55, N-80, and P-110 covering a range of wall thicknesses in 4½-, 5-, 5½-, 6¾-, 7-, 9¾-, and 10¾-in. diameters using both short and long threads where called for by the size and grade tested. Fourteen tests failed by fracture of the pipe, and 148 tests failed by pullout. Eq. 26 agrees satisfactorily with the 14 test fractures. Eq. 27 is based on analytical considerations and was adjusted to fit the data by statistical methods. The analytical procedure included coupling properties, but analysis of the current group of tests showed that the coupling was noncritical for standard coupling dimensions. Subsequent testing established that these equations are also applicable to J-55 casing.

The factor 0.95 in Eqs. 26 and 27 originates in the statistical error of a multiple-regression equation with adjustment to permit the use of minimum properties in place of average properties.

Buttress-Thread Casing Joint Strength. Buttress-thread casing joint strength is calculated from Eqs. 28 and 29. The lesser of the values obtained from the two equations governs.

For pipe thread strength,

$$W_j = 0.95 A_p \sigma_{up} [1.008 - 0.0396(1.083 - \sigma_y/\sigma_{up})d_o], \quad (28)$$

and for coupling thread strength,

$$W_j = 0.95 A_c \sigma_{uc}, \quad (29)$$

where

A_p = cross-sectional area of plain-end pipe
 $(0.7854 \text{ or } d_o^2 - d_i^2)$, sq in.,

A_c = cross-sectional area of coupling $(0.7854 \text{ or } d_{oc}^2 - d_i^2)$, sq in., and

σ_{uc} = minimum ultimate strength of coupling, psi.

Joint strengths were calculated to six-digit accuracy with cross-sectional areas of the pipe and the coupling rounded to three decimals. Final values were rounded to the nearest 1,000 lbf for listing in Table 2.3.

The equations, adopted at the June 1970 API Standardization Conference,¹³ were based on a regression analysis of 151 tests of buttress-thread casing ranging in size from 4½- to 20-in. OD and in strength levels from 40,000- to 150,000-psi minimum yield. Derivation of the equations is covered by Clinedinst.¹⁴

Extreme-Line Casing Joint Strength. Extreme-line casing joint strength is calculated from Eq. 30:

$$W_j = A_{cr} \sigma_{up}, \quad (30)$$

where

A_{cr} = critical section area of box, pin, or pipe, whichever is least $[0.7854(d_{oj}^2 - d_b^2)$ if box is critical, $0.7854(d_p^2 - d_j^2)$ if pin is critical, $0.7854(d_o^2 - d_i^2)$ if pipe is critical],

d_{oj} = nominal joint OD, made up, in.,

d_b = box critical section ID
 $(d_{bc} + 2h_{tb} - \delta_{Td} + \theta_{th})$, in.,

d_p = pin critical section OD $(d_{pp} + \delta_{Tr} - \theta_s)$, in.,

d_j = nominal joint ID, made up, in.,

h_{tb} = minimum box thread height (0.060 for 6 threads/in. and 0.080 for 5 threads/in.), in.,

δ_{Td} = taper drop in pin perfect thread length (0.253 for 6 threads/in. and 0.228 for 5 threads/in.), in.,

θ_{th} = one-half maximum thread interference
 $(d_{pp} - d_{bc})/2$, in.,

d_{pp} = maximum root diameter at last perfect pin thread, in.,

d_{bc} = minimum crest diameter of box thread at Plane H, in.,

- δ_{Tr} = taper rise between Plane H and Plane J
(0.035 for 6 threads/in. and 0.032 for 5
threads/in.), in.,
 θ_s = one-half maximum seal interference
($d_{ps} - d_{bs}$)/2, in.,
 d_{ps} = maximum diameter at pin seal tangent
point, in., and
 d_{bs} = minimum diameter at box seal tangent
point, in.

With the values listed in API standards, critical areas were calculated to three decimals, and the joint strengths were rounded to 1,000 lbf.

Tubing Joint Strength. Tubing joint strength is calculated from Eqs. 31 and 32 as the product of the specified minimum yield strength for the steel grade and the area of section under the root of the last perfect pipe thread or of the area of the pipe body, whichever is smaller. The areas of the critical sections of regular tubing couplings, special-clearance couplings, and the box of integral-joint tubing are, in all instances, greater than the governing critical areas of the pipe part of the joint and do not affect the strength of the joint.

For calculations that are based on the thread root area,

$$W_j = \sigma_y \times 0.7854[(d_o - 2h_{ij})^2 - d_i^2], \quad (31)$$

and for calculations that are based on area of the body of the pipe,

$$W_j = \sigma_y \times 0.7854(d_o^2 - d_i^2), \quad (32)$$

where

$$h_{ij} = \text{height of thread (0.05560 for 10 threads/in. and 0.07125 for 8 threads/in.)}, \text{ in.}$$

Joint strength was calculated to an accuracy of at least six digits and rounded to 100 lbf.

Joint Strength of Round-Thread Casing with Combined Bending and Internal Pressure. Joint strength of round-thread casing subjected to combined bending and internal pressure is calculated from Eqs. 33 through 39 on a total load basis and is expressed in pounds. These equations were based on Clinedinst's paper.¹⁵ Tables of joint strength of API round-thread casing with combined bending and internal pressure are given in API Bull. 5C4.¹⁶

Full Fracture Strength.

$$W_{fu} = 0.95A_{jp}\sigma_{up}, \quad (33)$$

Jumpout and Reduced Fracture Strength.

$$W_{jo} = 0.95A_{jp}L_e \left[\frac{0.74d_o^{-0.59}\sigma_{up}}{0.5L_e + 0.14d_o} + \frac{(1 + 0.5F_{sy})\sigma_y}{L + 0.14d_o} \right], \quad (34)$$

Bending Load Failure Strength. For $W_b/A_{jp} \geq \sigma_y$,

$$W_b = 0.95A_{jp} \left\{ \sigma_{up} - \left[\frac{140.5\delta d_o}{(\sigma_{up} - \sigma_y)^{0.8}} \right]^5 \right\}, \quad (35)$$

For $W_b/A_{jp} < \sigma_y$,

$$W_b = 0.95A_{jp} \left(\frac{\sigma_{up} - \sigma_y}{0.644} + \sigma_y - 218.15r_b d_o \right), \quad (36)$$

Relationship Between Total and External Load.

$$W_t = W_{ex} + W_{sh}, \quad (37)$$

where

$$W_{sh} = p_i A_{id}, \quad (38)$$

Relationship Between Bending and Curvature Radius.

$$\delta = 5730/r_{bc}, \quad (39)$$

In Eqs. 33 through 39,

A_{id} = area corresponding to ID, sq in.,

A_{jp} = cross-sectional area of the pipe wall under the last perfect thread $[0.7854 \text{ or } (d_o - 0.1425)^2 - (d_o - 2e)^2]$, sq in.,

δ = bending, degrees/100 ft,

F_{sy} = ratio of internal pressure stress to yield strength, or $p_i d_o / 2\sigma_y e$,

W_b = total tensile failure load with bending, lbf,

W_{ex} = external load, lbf,

W_{jo} = total tensile load at jumpout or reduced fracture, lbf,

W_{fu} = total tensile load at fracture, lbf,

W_{sh} = head load, lbf,

W_t = total load, the least of W_b , W_s , or W_{fu} , lbf, and

r_{bc} = bending radius of curvature, ft.

Calculations were made to six or more digits accuracy without intermediate rounding of areas. The final joint strength values were rounded to the nearest 1,000 lbf.

The equations for joint strength on a total load basis are based on a work by Clinedinst,¹⁵ who covers the development of combined loading joint strength equations and the determination of material constants and equation coefficients based on the results of an API-sponsored research project where 26 tests were made on 5½-in., 17-lbm/ft K-55 short round-thread casing.

Line-Pipe Joint Strength

The following equations for the fractured strength and the pullout or jumpout strength of API threaded line-pipe joints have been adapted from Clinedinst's¹² equations:

Minimum fracture strength is

$$W_f = 0.95A_{jp}\sigma_{up}, \quad (40)$$

TABLE 2.45—LINE-PIPE THREAD HEIGHT DIMENSIONS, in. (FIG. 2.11)

Thread Element	27 Threads Per Inch $p = 0.0370$	18 Threads Per Inch $p = 0.0556$	14 Threads Per Inch $p = 0.0714$	11½ Threads Per Inch $p = 0.0870$	8 Threads Per Inch $p = 0.1250$
$h_{tc} =$	$0.866p$	0.0321	0.0481	0.0619	0.0753
$h_{ij} = h_n =$	$0.760p$	0.0281	0.0422	0.0543	0.0661
$f_{rs} = f_{rn} =$	$0.033p$	0.0012	0.0018	0.0024	0.0029
$f_{cs} = f_{cn} =$	$0.073p$	0.0027	0.0041	0.0052	0.0063

h_{tc} = sharp thread height
 h_{ij} = thread height of pipe
 h_n = thread height of coupling
 L_{tp} = thread pitch
 f_{rs} = thread root truncation of pipe
 f_{rn} = thread root truncation of coupling
 f_{cs} = thread crest truncation of pipe
 f_{cn} = thread crest truncation of coupling

and minimum pullout strength is

$$W_{po} = 0.95 A_{jp} L_e \left[\frac{2.39(2h)^{0.59} d_o^{-0.59} \sigma_{up}}{0.5L_e + 0.14d_o} + \frac{\sigma_{yc}}{L_e + 0.14d_o} \right], \dots (41)$$

where

$$A_{jp} = 0.7854[(d_o - 2h_{ij})^2 - (d_o - 2e)^2], \text{ sq in.},$$

W_f = minimum joint fracture strength, lbf

W_{po} = minimum joint pullout strength, lbf,

h_{ij} = thread height (0.0950 for 8 threads/in.; 0.0661 for 11½ threads/in.; 0.0543 for 14 threads/in.; 0.0422 for 18 threads/in.; 0.0281 for 27 threads/in.), in.,

h = engaged height of thread or $h_{ij} - (f_{cs} + f_{cn})$ (0.0900 for 8 threads/in.; 0.0627 for 11½ threads/in.; 0.0515 for 14 threads/in.; 0.0399 for 18 threads/in.; 0.0267 for 27 threads/in.), in.,⁷

f_{cs} = crest truncation of pipe (Table 2.45), and

f_{cn} = crest truncation of coupling (Table 2.45).

Hydrostatic Test Pressures for Plain-End Pipe, Extreme-Line Casing, and Integral-Joint Tubing. The hydrostatic test pressures for plain-end pipe, extreme-line casing, and integral-joint tubing are calculated with Eq. 42 except for Grade A25 line pipe, Grades A and B line pipe in sizes less than 2½-in. OD, and threaded and coupled line pipe in sizes 6½-in. OD and less, which were determined arbitrarily.

$$p_H = \frac{2\sigma_f e}{d_o}, \dots (42)$$

where

p_H = hydrostatic test pressure rounded to the nearest 10 psi for line pipe and to the nearest 100 psi for casing and tubing, psi, and

σ_f = fiber stress corresponding to the percent of specified yield strength as given in Table 2.46, psi.

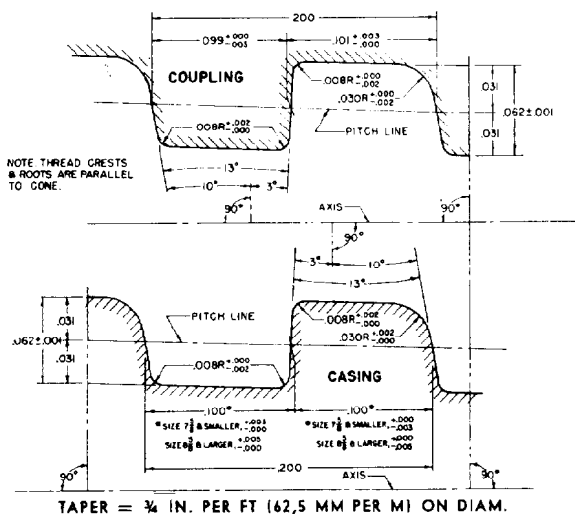


Fig. 2.11—Line pipe thread form. Buttress casing thread form and dimensions for casing sizes 4½ to 13½ in.

Hydrostatic Test Pressure for Threaded and Coupled Pipe. The hydrostatic test pressure for threaded and coupled pipe is the same as for plain-end pipe except where a lower pressure is required to avoid leakage caused by

TABLE 2.46—FACTORS FOR TEST PRESSURE EQUATIONS

Grade	Size (in.)	Fiber Stress as Percent of Specified Minimum Yield Strength		Test Pressure Rounding	Maximum Test Pressure, psi*	
		Standard Test Pressures	Alternative Test Pressures		Standard	Alternative
A, B	2⅜ through 3½	60	75	10	2,500	2,500
A, B	over 3½	60	75	10	2,800	2,800
X, U	4½ and smaller	60	75	10	3,000	3,000
X, U	6⅝ and 8⅝	75	—	10	3,000	—
X, U	10¾ through 18	85	—	10	3,000	—
X, U	20 and larger	90	—	10	3,000	—
H-40, J-55, K-55	9⅝ and smaller	80	80	100	3,000	10,000
H-40, J-55, K-55	10¾ and larger	60	80	100	3,000	10,000
L-80, N-80	all sizes	80	—	100	10,000**	—
C-75	all sizes	80	—	100	10,000**	—
C-95	all sizes	80	—	100	10,000**	—
P-105	all sizes	80	80	100	10,000**	†
P-110	all sizes	80	80	100	10,000**	†

*Higher test pressures are permissible by agreement between purchaser and manufacturer.

**Plain-end pipe is tested to 3,000 psi maximum unless a higher pressure is agreed upon by the purchaser and manufacturer.

†No maximum test pressure, except that plain-end pipe is tested to 3,000 psi maximum unless a higher pressure is agreed upon by the purchaser and manufacturer.

insufficient internal yield pressure of the coupling or insufficient internal pressure leak resistance at Plane d_{p1} or d_p calculated with Eqs. 19 and 43, respectively.

Internal Yield Pressure for Couplings. The internal yield pressure for the coupling is calculated with Eq. 19 and rounded to the nearest 100 psi. For round-thread casing and tubing, d_1 is calculated with Eq. 20. For line pipe,

$$d_1 = d_p - (L_1 + L_{so})F_t + h_{tc} - 2f_{rn}, \quad (43)$$

where $h_{tc} = 0.0321$ for 27 threads/in.; 0.0481 for 18

threads/in.; 0.0619 for 14 threads/in.; 0.0753 for 11½ threads/in.; 0.10825 for 8 threads/in., and $f_{rn} =$ thread root truncation (Table 2.47), 0.0012 for 27 threads/in.; 0.0018 for 18 threads/in.; 0.0024 for 14 threads/in.; 0.0029 for 11½ threads/in.; and 0.0041 for 8 threads/in.

For buttress-thread casing, d_1 is calculated with Eq. 21. Eq. 19 bases the coupling hydrostatic pressure on the assumption that the coupling is stressed to 80% of minimum yield strength at the root of the coupling thread at the end of the pipe in the power-tight position. The basis of this equation was adopted at the 1968 API Standardization Conference.¹⁷

TABLE 2.47—EXTREME-LINE CASING THREADING AND MACHINING DIMENSIONS—SIZES 5 THROUGH 7⅝ in. (FIGS. 2.13, 2.15, AND 2.17)

1	2	3	4	5	6	7	8	9	10	11	12	13			
Threading and Machining Dimensions (in.)															
OD (in.)	Nominal Weight (lbm/ft)	Made-Up Joint ID	Drift Diameter for Bored Upset	A		B	C	D	E	G	H		I		J
				Maximum	Minimum						Minimum	Maximum	Minimum	Maximum	
5	15.00	4.198	4.183	4.504	4.506	4.208	4.545	4.235	4.575	4.938	4.827	4.829	4.819	4.821	4.975
	18.00	4.198	4.183	4.504	4.506	4.208	4.545	4.235	4.575	4.938	4.827	4.829	4.819	4.821	4.975
5½	15.50	4.736	4.721	5.008	5.010	4.746	5.048	4.773	5.079	5.442	5.331	5.333	5.323	5.325	5.479
	17.00	4.701	4.686	5.008	5.010	4.711	5.048	4.738	5.079	5.442	5.331	5.333	5.323	5.325	5.479
	20.00	4.701	4.686	5.008	5.010	4.711	5.048	4.738	5.079	5.442	5.331	5.333	5.323	5.325	5.479
	23.00	4.610	4.595	5.007	5.009	4.619	5.048	4.647	5.079	5.441	5.330	5.332	5.323	5.325	5.479
6⅝	24.00	5.781	5.766	6.089	6.091	5.792	6.130	5.818	6.160	6.523	6.412	6.414	6.403	6.405	6.559
	28.00	5.731	5.716	6.088	6.090	5.741	6.129	5.768	6.160	6.522	6.411	6.413	6.403	6.405	6.559
	32.00	5.615	5.600	6.088	6.090	5.624	6.129	5.652	6.159	6.522	6.411	6.413	6.404	6.406	6.560
7	23.00	6.171	6.156	6.477	6.479	6.182	6.518	6.208	6.549	6.912	6.801	6.803	6.792	6.794	6.948
	26.00	6.171	6.156	6.477	6.479	6.182	6.518	6.208	6.549	6.912	6.801	6.803	6.792	6.794	6.948
	29.00	6.123	6.108	6.477	6.479	6.134	6.518	6.160	6.549	6.912	6.801	6.803	6.792	6.794	6.948
	32.00	6.032	6.017	6.477	6.479	6.042	6.518	6.069	6.548	6.911	6.800	6.802	6.792	6.794	6.948
	35.00	5.940	5.925	6.476	6.478	5.949	6.517	5.977	6.548	6.911	6.800	6.802	6.793	6.795	6.949
	38.00	5.860	5.845	6.476	6.478	5.869	6.517	5.897	6.548	6.911	6.800	6.802	6.793	6.795	6.949
7⅝	26.40	6.770	6.755	7.072	7.074	6.782	7.113	6.807	7.148	7.511	7.400	7.402	7.390	7.392	7.546
	29.70	6.770	6.755	7.072	7.074	6.782	7.113	6.807	7.148	7.511	7.400	7.402	7.390	7.392	7.546
	33.70	6.705	6.690	7.072	7.074	6.716	7.112	6.742	7.147	7.510	7.399	7.401	7.390	7.392	7.548
	39.00	6.565	6.550	7.071	7.073	6.575	7.112	6.602	7.147	7.510	7.399	7.401	7.391	7.393	7.549

TABLE 2.47—EXTREME-LINE CASING THREADING AND MACHINING DIMENSIONS—SIZES 5 THROUGH 7 $\frac{5}{8}$ in. (continued)

1	2	14	15	16	17	18	19	20	21	22	23	24						
Threading and Machining Dimensions (in.)													Gauge To Product Standoff (in.)					
OD (in.)	Nominal Weight (lbm/ft)	M								Ring to Pin				Plug to Box				
		Standard Joint		Optional Joint	N	O		P	X	Y	Seal		Thread		Seal		Thread	
		K			Minimum	Maximum		Minimum	Maximum	Minimum	Maximum	Minimum	Maximum	Minimum	Maximum	Minimum	Maximum	
5	15.00	4.612	5.360	---	4.534	4.496	4.498	4.461	0.151	0.140	0.144	0.156	0.326	0.342	1.042	1.054	0.072	0.088
	18.00	4.612	5.360	---	4.534	4.496	4.498	4.461	0.151	0.140	0.144	0.156	0.326	0.342	1.042	1.054	0.072	0.088
5 1/2	15.50	5.116	5.860	5.780	5.037	5.000	5.002	4.964	0.134	0.122	0.139	0.151	0.310	0.326	1.039	1.051	0.060	0.076
	17.00	5.116	5.860	5.780	5.037	5.000	5.002	4.964	0.151	0.140	0.139	0.151	0.310	0.326	1.039	1.051	0.060	0.076
	20.00	5.116	5.860	5.780	5.037	5.000	5.002	4.964	0.151	0.140	0.139	0.151	0.310	0.326	1.039	1.051	0.060	0.076
	23.00	5.116	5.860	5.780	5.038	5.000	5.002	4.964	0.187	0.166	0.136	0.148	0.306	0.322	1.036	1.048	0.056	0.072
6 1/8	24.00	6.196	7.000	6.930	6.117	6.080	6.082	6.044	0.151	0.140	0.148	0.160	0.358	0.374	1.048	1.060	0.108	0.124
	28.00	6.196	7.000	6.930	6.118	6.080	6.082	6.045	0.177	0.165	0.145	0.157	0.354	0.370	1.045	1.057	0.104	0.120
	32.00	6.197	7.000	6.930	6.118	6.081	6.083	6.045	0.235	0.223	0.142	0.154	0.350	0.366	1.042	1.054	0.100	0.116
7	23.00	6.585	7.390	7.310	6.506	6.468	6.470	6.433	0.151	0.139	0.151	0.163	0.364	0.380	1.051	1.063	0.112	0.128
	26.00	6.585	7.390	7.310	6.506	6.468	6.470	6.433	0.151	0.139	0.151	0.163	0.364	0.380	1.051	1.063	0.112	0.128
	29.00	6.585	7.390	7.310	6.506	6.468	6.470	6.433	0.175	0.163	0.151	0.163	0.364	0.380	1.051	1.063	0.112	0.128
	32.00	6.585	7.390	7.310	6.506	6.469	6.471	6.433	0.220	0.209	0.148	0.160	0.350	0.376	1.048	1.060	0.108	0.124
	35.00	6.586	7.530	7.390	6.507	6.469	6.471	6.434	0.267	0.255	0.145	0.157	0.356	0.372	1.045	1.057	0.104	0.120
	38.00	6.586	7.530	7.390	6.507	6.469	6.471	6.434	0.307	0.295	0.145	0.157	0.356	0.372	1.045	1.057	0.104	0.120
7 5/8	26.40	7.183	8.010	7.920	7.100	7.062	7.064	7.026	0.148	0.137	0.157	0.169	0.350	0.366	1.057	1.069	0.104	0.120
	29.70	7.183	8.010	7.920	7.100	7.062	7.064	7.026	0.148	0.137	0.157	0.169	0.350	0.366	1.057	1.069	0.104	0.120
	33.70	7.183	8.010	7.920	7.100	7.062	7.064	7.027	0.181	0.169	0.154	0.166	0.346	0.362	1.054	1.066	0.100	0.116
	39.00	7.184	8.010	7.920	7.100	7.063	7.065	7.028	0.251	0.240	0.151	0.163	0.342	0.358	1.051	1.063	0.096	0.112

Internal-Pressure Leak Resistance at Plane d_{p1} or d_p . The internal pressure leak resistance at Plane d_{p1} or d_p is calculated with Eq. 22 and rounded to the nearest 100 psi.

API Threading Data

Dimensional data on API threads were taken from API Specification 5B for threading, gauging, and thread inspection of casing, tubing, and line-pipe threads. For information on gauges and gauging, and thread inspection equipment and inspection, refer to Ref. 6.

Fig. 2.10A shows the basic dimensions of line-pipe threads and casing and tubing round-thread hand-tight makeup. Tables 2.42, 2.43, and 2.48 give the tabulated data for casing short-thread, casing long-thread, and line-pipe thread dimensions. Fig. 2.10B shows and Table 2.44 lists the basic dimensions of buttress casing threads, hand-tight makeup. Thread dimensions of nonupset tubing,

external-upset tubing, and integral joint tubing are listed in Tables 2.49 through 2.51.

Thread height dimensions for line pipe are given in Table 2.45 and for casing and tubing in Table 2.52. The respective thread forms are shown in Figs. 2.11 and 2.12. Buttress casing thread forms and dimensions for 4 $\frac{1}{2}$ - through 12-in. sizes are shown in Fig. 2.11 and for 16-in. and larger are shown in Fig. 2.12.

Machining details for 5- through 7 $\frac{5}{8}$ -in. casing are given in Fig. 2.13 and for 8 $\frac{5}{8}$ - through 10 $\frac{3}{4}$ -in. casing in Fig. 2.14 and the tabulated data are given in Tables 2.47 and 2.53, respectively. The box and pin entrance threads are given in Figs. 2.15 and 2.16. Also, the product thread form for 5- through 7 $\frac{5}{8}$ -in. sizes, 6 threads/in., 1 $\frac{1}{2}$ -in. taper/ft on diameter is shown in Fig. 2.17, and for 8 $\frac{5}{8}$ - through 10 $\frac{3}{4}$ -in. sizes, 5 threads/in., 1 $\frac{1}{4}$ -in. taper/ft on diameter is shown in Fig. 2.18.

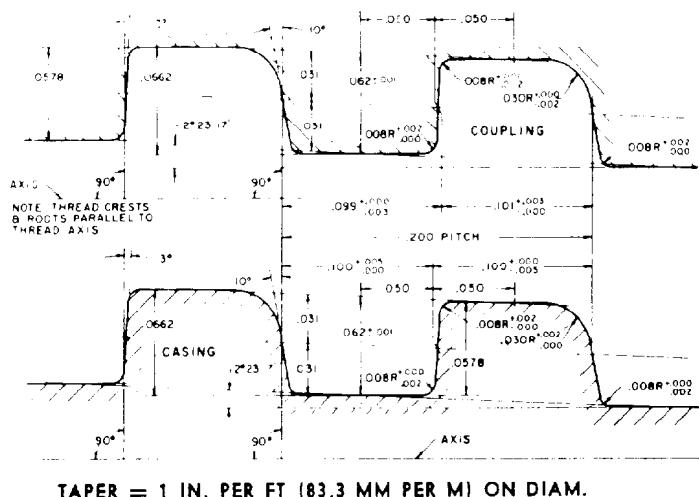


Fig. 2.12—Casing and tubing round-thread form. Buttress casing thread form and dimensions for sizes 16 in. and larger.

TABLE 2.48—LINE-PIPE THREAD DIMENSIONS (FIG. 2.10A)

Nominal Size d_o (in.)	Major Diameter d_4 (in.)	Number of Threads Per Inch	Length (in.)			Pitch Diameter at Hand- Tight Plane d_p (in.)	End of Pipe to Center of Coupling, Power- Tight Make-Up L_{pc} (in.)	Length: Face of Coupling to Hand- Tight Plane L_{th} (in.)	Diameter of Coupling Recess d_{cr} (in.)	Depth of Coupling Recess D_{cr} (in.)	Hand- Tight Standoff Thread Turns n_{so}	Minimum Length, Full Crest Threads From End of Pipe* L_c (in.)
			End of Pipe to Hand- Tight Plane L_1	Effective Threads L_2	Total End of Pipe to Vanish Point L_4							
1/8	0.405	27	0.1615	0.2639	0.3924	0.37360	0.1389	0.1198	0.468	0.0524	3	—
1/4	0.540	18	0.2278	0.4018	0.5946	0.49163	0.2179	0.2001	0.603	0.1206	3	—
3/8	0.675	18	0.240	0.4078	0.6006	0.62701	0.2119	0.1938	0.738	0.1147	3	—
1/2	0.840	14	0.320	0.5337	0.7815	0.77843	0.2810	0.2473	0.903	0.1582	3	—
3/4	1.050	14	0.339	0.5457	0.7935	0.98887	0.2690	0.2403	1.113	0.1516	3	—
1	1.315	11 1/2	0.400	0.6828	0.9845	1.23863	0.3280	0.3235	1.378	0.2241	3	0.3325
1 1/4	1.660	11 1/2	0.420	0.7068	1.0085	1.58338	0.3665	0.3275	1.723	0.2279	3	0.3565
1 1/2	1.900	11 1/2	0.420	0.7235	1.0252	1.82234	0.3498	0.3442	1.963	0.2439	3	0.3732
2	2.375	11 1/2	0.436	0.7565	1.0582	2.29627	0.3793	0.3611	2.469	0.2379	3	0.4062
2 1/2	2.875	8	0.682	1.1375	1.5712	2.76216	0.4913	0.6392	2.969	0.4915	2	0.6342
3	3.500	8	0.766	1.2000	1.6337	3.38850	0.4913	0.6177	3.594	0.4710	2	0.6967
3 1/2	4.000	8	0.821	1.2500	1.6837	3.88881	0.5038	0.6127	4.094	0.4662	2	0.7467
4	4.500	8	0.844	1.3000	1.7337	4.38712	0.5163	0.6397	4.584	0.4920	2	0.7967
5	5.563	8	0.937	1.4063	1.8400	5.44929	0.4725	0.6530	5.657	0.5047	2	0.9030
6	6.625	8	0.958	1.5125	1.9462	6.50597	0.4913	0.7382	6.719	0.5861	2	1.0092
8	8.625	8	1.063	1.7125	2.1462	8.50003	0.4788	0.8332	8.719	0.6768	2	1.2092
10	10.750	8	1.210	1.9250	2.3587	10.62094	0.5163	0.8987	10.844	0.7394	2	1.4217
12	12.750	8	1.360	2.1250	2.5587	12.61781	0.5038	0.9487	12.844	0.7872	2	1.6217
14D	14.000	8	1.562	2.2500	2.6837	13.87263	0.5038	0.8717	14.094	0.7136	2	1.7467
16D	16.000	8	1.812	2.4500	2.8837	15.87575	0.4913	0.8217	16.094	0.6658	2	1.9467
18D	18.000	8	2.000	2.6500	3.0837	17.87500	0.4788	0.8337	18.094	0.6773	2	2.1467
20D	20.000	8	2.125	2.8500	3.2837	19.87031	0.5288	0.9087	20.094	0.7490	2	2.3467

Included taper on diameter, all sizes, 0.0625 in./in.

* $L_c = L_4 - 0.652$ in. for 11 1/2-thread line pipe. $L_c = L_4 - 0.937$ in. for 8-thread line pipe.

TABLE 2.49—INTEGRAL-JOINT TUBING THREAD DIMENSIONS (FIG. 2.10A)

OD d_o (in.)	Major Diameter d_4 (in.)	Number of Threads Per Inch	Length (in.)			Pitch Diameter at Hand- Tight Plane d_p (in.)	End of Pipe to Thread Run-out in Box Power- Tight Make-Up L_{pt} (in.)	Length: Face of Box to Hand- Tight Plane L_{th} (in.)	Diameter of Box Recess d_{cr} (in.)	Depth of Box Recess D_{cr} (in.)	Hand- Tight Standoff Thread Turns n_{so}	Minimum Length, Full Crest Threads, From End of Pipe* L_c (in.)
			End of Pipe to Hand- Tight Plane L_1	Effective Threads L_2	Total End of Pipe to Vanish Point L_4							
1.315	1.315	10	0.479	0.956	1.125	1.25328	0.500	0.446	1.378	5/32	2	0.225
1.660	1.660	10	0.604	1.081	1.250	1.59826	0.500	0.446	1.723	3/16	2	0.350
1.900	1.900	10	0.729	1.206	1.375	1.83826	0.500	0.446	1.963	3/16	2	0.475
2.063	2.094	10	0.792	1.269	1.438	2.03206	0.500	0.446	2.156	5/16	2	0.538

Included taper on diameter, all sizes, 0.0625 in./in.

* $L_c = L_4 - 0.900$ in. for 10-thread tubing.

TABLE 2.50—NONUPSET TUBING THREAD DIMENSIONS (FIG. 2.10A)

OD d_o (in.)	Major Diameter d_4 (in.)	Number of Threads Per Inch	Length (in.)			Pitch Diameter at Hand- Tight Plane d_p (in.)	End of Pipe to Center of Coupling, Power- Tight Make-Up L_{pc} (in.)	Length: Face of Coupling to Hand- Tight Plane L_{th} (in.)	Diameter of Coupling Recess d_{cr} (in.)	Depth of Coupling Recess D_{cr} (in.)	Hand- Tight Standoff Thread Turns n_{so}	Minimum Length, Full Crest Threads From End of Pipe* L_c (in.)
			End of Pipe to Hand- Tight Plane L_1	Effective Threads L_2	Total End of Pipe to Vanish Point L_4							
1.050	1.050	10	0.448	0.925	1.094	0.98826	0.500	0.446	1.113	$\frac{5}{16}$	2	0.300
1.315	1.315	10	0.479	0.956	1.125	1.25328	0.500	0.446	1.378	$\frac{5}{16}$	2	0.300
1.660	1.660	10	0.604	1.081	1.250	1.59826	0.500	0.446	1.723	$\frac{5}{16}$	2	0.350
1.900	1.900	10	0.729	1.206	1.375	1.83826	0.500	0.446	1.963	$\frac{5}{16}$	2	0.475
$2\frac{3}{8}$	2.375	10	0.979	1.456	1.625	2.31326	0.500	0.446	2.438	$\frac{5}{16}$	2	0.725
$2\frac{7}{8}$	2.875	10	1.417	1.894	2.063	2.81326	0.500	0.446	2.938	$\frac{5}{16}$	2	1.163
$3\frac{1}{2}$	3.500	10	1.667	2.144	2.313	3.43826	0.500	0.446	3.563	$\frac{5}{16}$	2	1.413
4	4.000	8	1.591	2.140	2.375	3.91395	0.500	0.534	4.063	$\frac{3}{8}$	2	1.375
$4\frac{1}{2}$	4.500	8	1.779	2.328	2.563	4.41395	0.500	0.534	4.563	$\frac{3}{8}$	2	1.563

Included taper on diameter, all sizes, 0.0625 in./in.

* $L_c = L_4 - 0.900$ in. for 10-thread tubing, but not less than 0.300 in. $L_c = L_4 - 1.000$ in. for 8-thread tubing.

TABLE 2.51—EXTERNAL-UPSET TUBING THREAD DIMENSIONS (FIG. 2.10A)

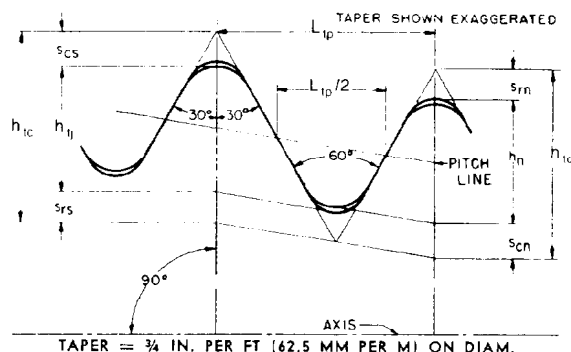
OD d_o (in.)	Major Diameter d_4 (in.)	Number of Threads Per Inch	Length (in.)			Pitch Diameter at Hand- Tight Plane d_p (in.)	End of Pipe to Center of Coupling, Power- Tight Make-Up L_{pc} (in.)	Length: Face of Coupling to Hand- Tight Plane L_{th} (in.)	Diameter of Coupling Recess d_{cr} (in.)	Depth of Coupling Recess D_{cr} (in.)	Hand- Tight Standoff Thread Turns n_{so}	Minimum Length, Full Crest Threads From End of Pipe* L_c (in.)
			End of Pipe to Hand- Tight Plane L_1	Effective Threads L_2	Total End of Pipe to Vanish Point L_4							
1.050	1.315	10	0.479	0.956	1.125	1.25328	0.500	0.446	1.378	$\frac{5}{16}$	2	0.300
1.315	1.469	10	0.604	1.081	1.250	1.40706	0.500	0.446	1.531	$\frac{5}{16}$	2	0.350
1.660	1.812	10	0.729	1.206	1.375	1.75079	0.500	0.446	1.875	$\frac{5}{16}$	2	0.475
1.900	2.094	10	0.792	1.269	1.438	2.03206	0.500	0.446	2.156	$\frac{5}{16}$	2	0.538
$2\frac{3}{8}$	2.594	8	1.154	1.703	1.938	2.50775	0.500	0.534	2.656	$\frac{3}{8}$	2	0.938
$2\frac{7}{8}$	3.094	8	1.341	1.890	2.125	3.00775	0.500	0.534	3.156	$\frac{3}{8}$	2	1.125
$3\frac{1}{2}$	3.750	8	1.591	2.140	2.375	3.66395	0.500	0.534	3.813	$\frac{3}{8}$	2	1.375
4	4.250	8	1.716	2.265	2.500	4.16395	0.500	0.534	4.313	$\frac{3}{8}$	2	1.500
$4\frac{1}{2}$	4.750	8	1.841	2.625	2.390	4.66395	0.500	0.534	4.813	$\frac{3}{8}$	2	1.625

Included taper on diameter, all sizes, 0.0625 in./in.

* $L_c = L_4 - 0.900$ in. for 10-thread tubing, but not less than 0.300 in. $L_c = L_4 - 1.000$ in. for 8-thread tubing.

TABLE 2.52—CASING AND TUBING ROUND THREAD HEIGHT DIMENSIONS, in. (FIG. 2.12)

Thread Element	10 Threads Per Inch $p = 0.1000$	8 Threads Per Inch $p = 0.1250$
$h_{tc} = 0.866p$	0.8660	0.10825
$h_{tr} = h_n = 0.626p - 0.007$	0.05560	0.07125
$s_{rs} = s_{rn} = 0.120p + 0.002$	0.01400	0.01700
$s_{cs} = s_{cn} = 0.120p + 0.005$	0.01700	0.02000



s_{rs} = thread root truncation of pipe
 s_{rc} = thread root truncation of coupling
 s_{cs} = thread crest truncation of pipe
 s_{cn} = thread crest truncation of coupling
 L_p = thread pitch

**TABLE 2.53—EXTREME-LINE CASING THREADING AND MACHINING DIMENSIONS—SIZES 8 $\frac{5}{8}$ THROUGH 10 $\frac{3}{4}$ in.
(FIGS. 2.14, 2.16, AND 2.18)**

1	2	3	4	5	6	7	8	9	10	11	12	13			
Threading and Machining Dimensions (in.)															
OD (in.)	Nominal Weight (lbm/ft)	Made-Up Joint ID	Drift Diameter for Bored Upset	A		B	C	D	E	G	H		I		J
				Maximum	Minimum						Minimum	Maximum	Minimum	Maximum	
8 $\frac{5}{8}$	32.00	7.725	7.710	8.100	8.102	7.737	8.148	7.762	8.192	8.569	8.418	8.420	8.408	8.410	8.601
	36.00	7.725	7.710	8.100	8.102	7.737	8.148	7.762	8.192	8.569	8.418	8.420	8.408	8.410	8.601
	40.00	7.663	7.648	8.100	8.102	7.674	8.148	7.700	8.192	8.569	8.418	8.420	8.409	8.411	8.602
	44.00	7.565	7.550	8.100	8.102	7.575	8.147	7.602	8.191	8.568	8.417	8.419	8.409	8.411	8.602
	49.00	7.451	7.436	8.099	8.101	7.460	8.147	7.488	8.191	8.568	8.417	8.419	8.410	8.412	8.603
9 $\frac{5}{8}$	40.00	8.665	8.650	9.041	9.043	8.677	9.089	8.702	9.134	9.512	9.361	9.363	9.351	9.353	9.544
	43.50	8.665	8.650	9.041	9.043	8.677	9.089	8.702	9.134	9.512	9.361	9.363	9.351	9.353	9.544
	47.00	8.621	8.606	9.041	9.043	8.633	9.089	8.658	9.134	9.512	9.361	9.363	9.351	9.353	9.544
	53.50	8.475	8.460	9.040	9.042	8.485	9.088	8.512	9.133	9.511	9.360	9.362	9.352	9.354	9.545
10 $\frac{3}{4}$	45.50	9.819	9.804	10.286	10.288	9.829	10.334	9.854	10.378	10.756	10.605	10.607	10.597	10.599	10.790
	51.00	9.719	9.704	10.286	10.288	9.729	10.334	9.754	10.378	10.756	10.605	10.607	10.597	10.599	10.790
	55.50	9.629	9.614	10.286	10.288	9.639	10.334	9.664	10.378	10.756	10.605	10.607	10.597	10.599	10.790
	60.70	9.529	9.514	10.286	10.288	9.539	10.334	9.564	10.378	10.756	10.605	10.607	10.597	10.599	10.790

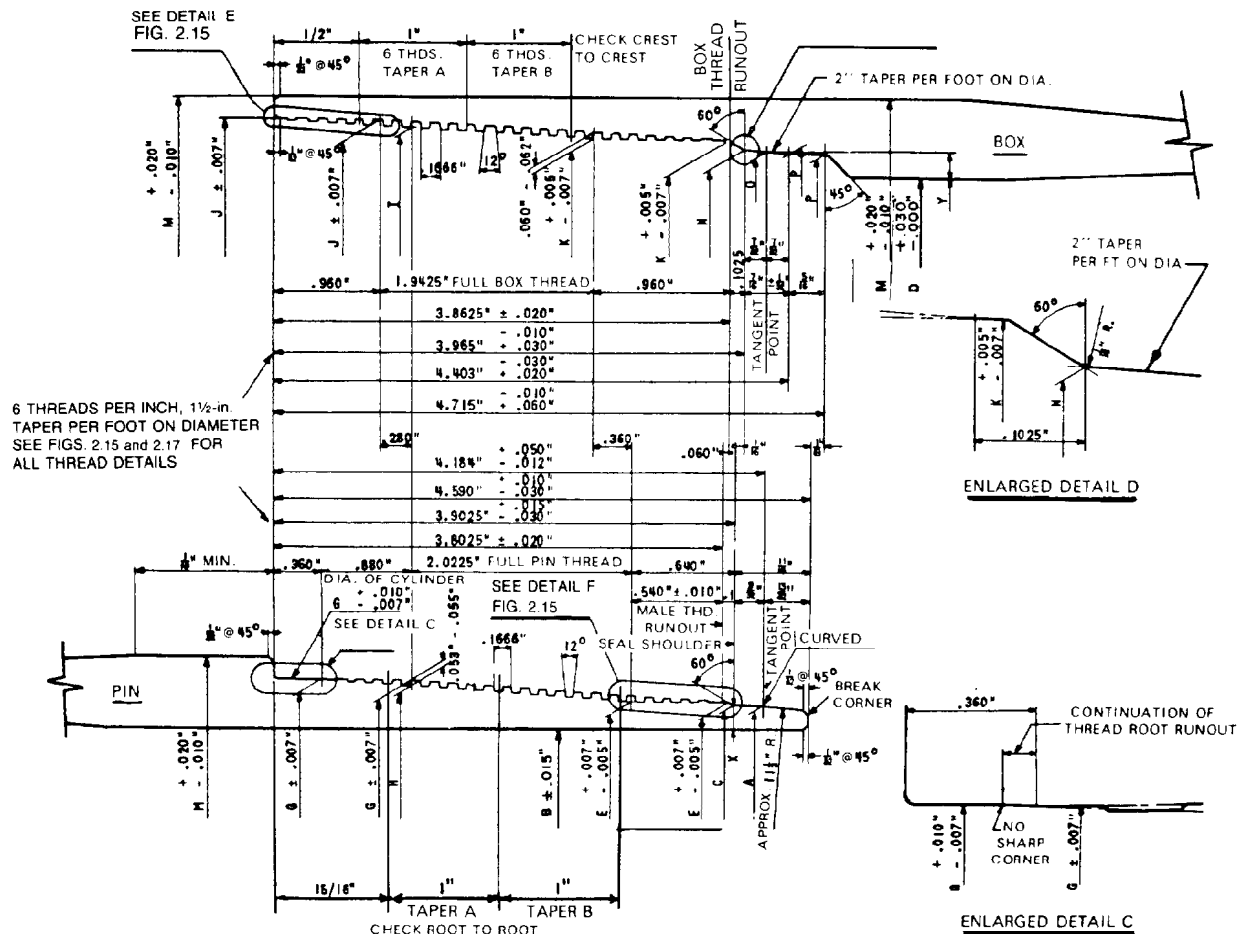


Fig. 2.13—Machining details, extreme-line casing joint sizes 5 through 7 $\frac{5}{8}$ in.

TABLE 2.53—EXTREME-LINE CASING THREADING AND MACHINING DIMENSIONS—SIZES 8 $\frac{5}{8}$ THROUGH 10 $\frac{3}{4}$ in.
(continued)

		2	14	15	16	17	18	19	20	21	22	23	24					
Threaded and Machining Dimensions, in.										Ring to Pin				Plug to Box				
OD (in.)	Nominal Weight (lbm/ft)	M								Seal		Thread		Seal		Thread		
		K	Standard Joint	Optional Joint	N	O		P	X	Y	Minimum	Maximum	Minimum	Maximum	Minimum	Maximum	Minimum	Maximum
8 ⁵ / ₈	32.00	8.224	9.120	9.030	8.133	8.090	8.092	8.050	188	173	160	172	355	374	1.060	1.072	1.06	1.25
	36.00	8.224	9.120	9.030	8.133	8.090	8.092	8.050	188	173	160	172	355	374	1.060	1.072	1.06	1.25
	40.00	8.224	9.120	9.030	8.134	8.091	8.093	8.050	219	205	157	169	350	370	1.057	1.069	1.01	1.20
	44.00	8.225	9.120	9.030	8.134	8.092	8.094	8.051	269	253	154	166	346	365	1.054	1.066	0.96	1.15
	49.00	8.225	9.120	9.030	8.135	8.092	8.094	8.051	326	311	151	163	341	360	1.051	1.063	0.91	1.10
9 ¹ / ₂	40.00	9.167	10.100	10.020	9.074	9.031	9.033	8.991	189	174	160	172	355	374	1.060	1.072	1.06	1.25
	43.50	9.167	10.100	10.020	9.074	9.031	9.033	8.991	189	174	160	172	355	374	1.060	1.072	1.06	1.25
	47.00	9.167	10.100	10.020	9.074	9.031	9.033	8.991	211	196	160	172	355	374	1.060	1.072	1.06	1.25
	53.50	9.168	10.100	10.020	9.075	9.032	9.034	8.992	284	269	154	166	346	365	1.054	1.066	0.96	1.15
10 ³ / ₄	45.50	10.413	11.460	—	10.321	10.278	10.280	10.237	236	220	154	166	346	365	1.054	1.066	0.96	1.15
	51.00	10.413	11.460	—	10.321	10.278	10.280	10.237	286	270	154	166	346	365	1.054	1.066	0.96	1.15
	55.50	10.413	11.460	—	10.321	10.278	10.280	10.237	331	315	154	166	346	365	1.054	1.066	0.96	1.15
	60.70	10.413	11.460	—	10.321	10.278	10.280	10.237	381	365	154	166	346	365	1.054	1.066	0.96	1.15

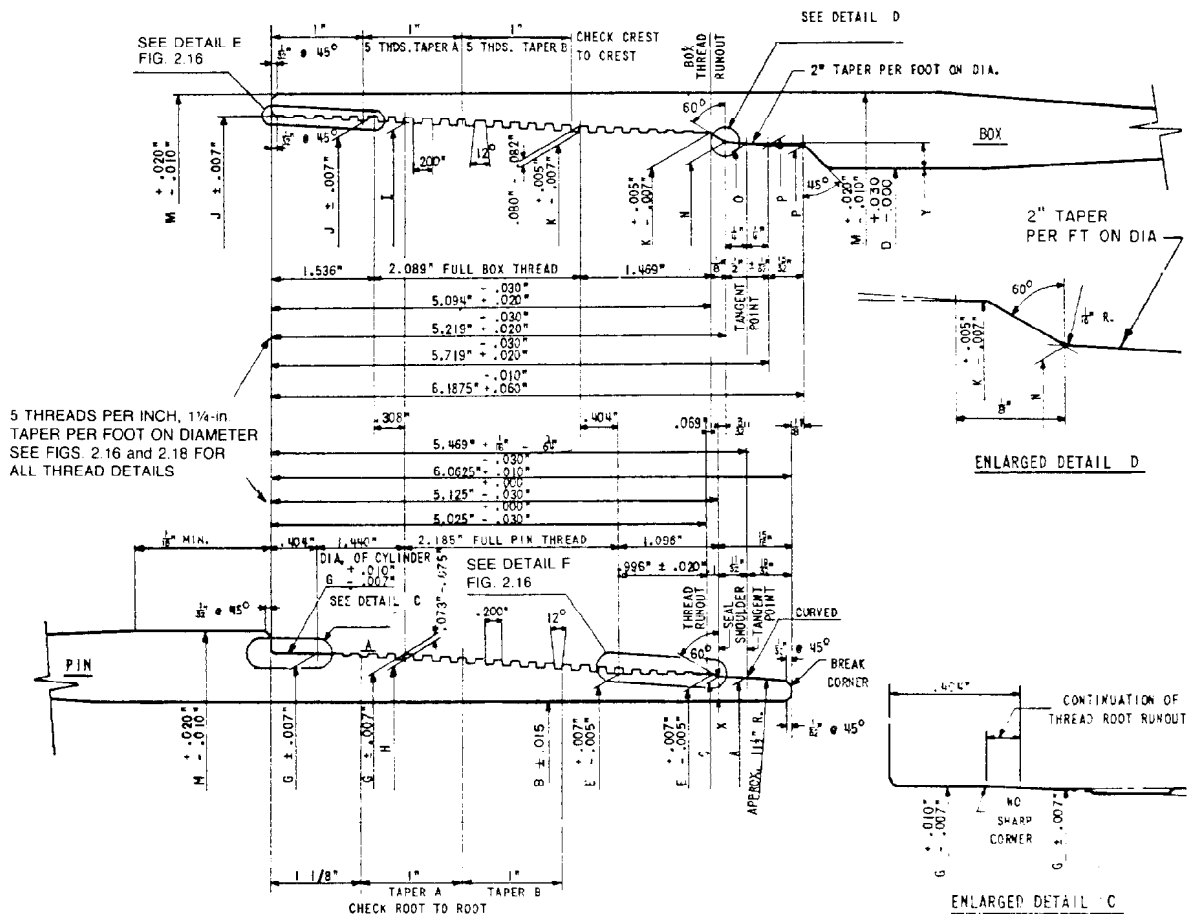


Fig. 2.14—Machining details, extreme-line casing joint sizes 8 $\frac{5}{8}$ through 10 $\frac{3}{4}$ in. (see Table 2.53).

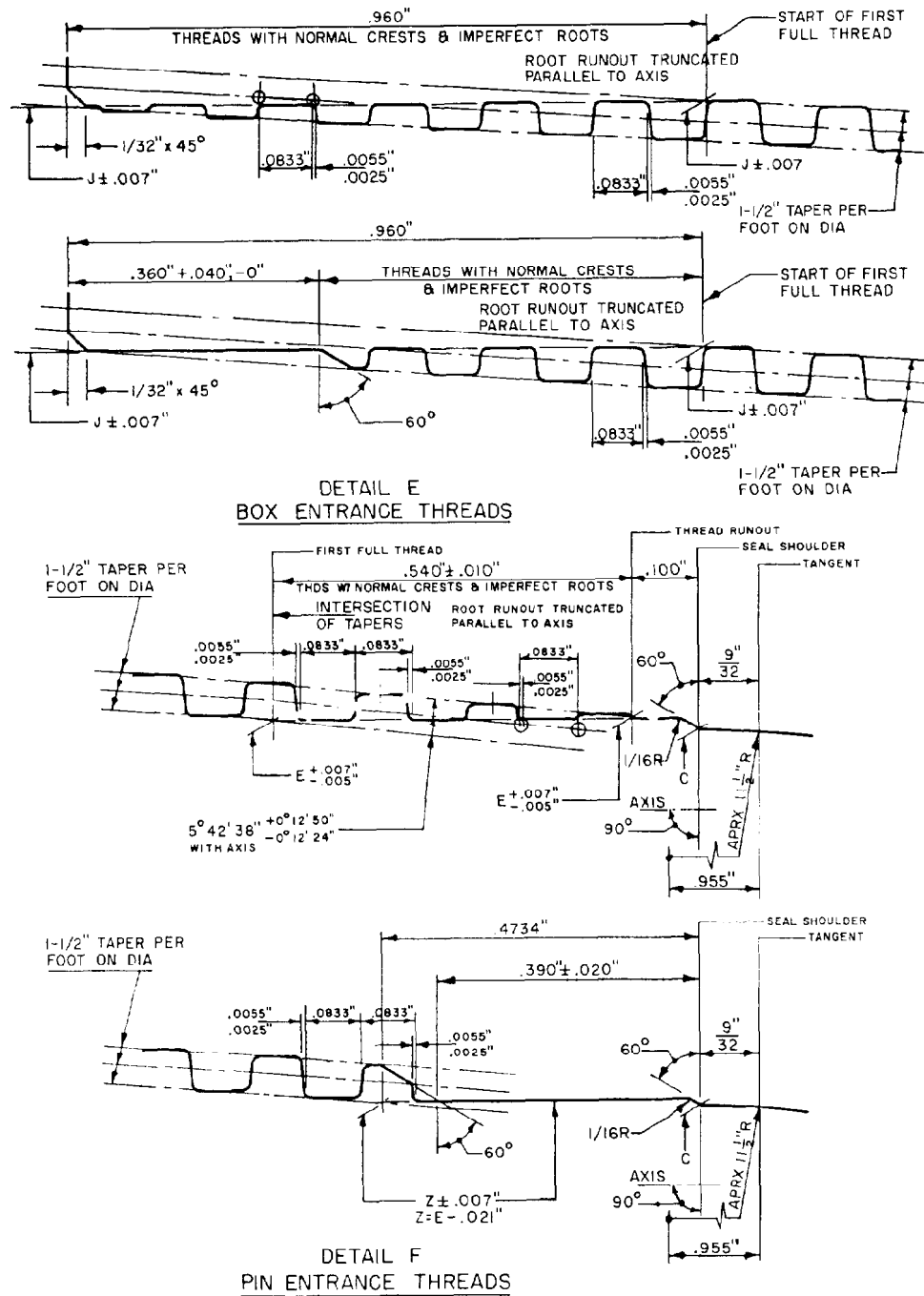


Fig. 2.15—Box-and-pin entrance threads, extreme-line casing joint sizes 5 through 7 $\frac{5}{8}$ in.

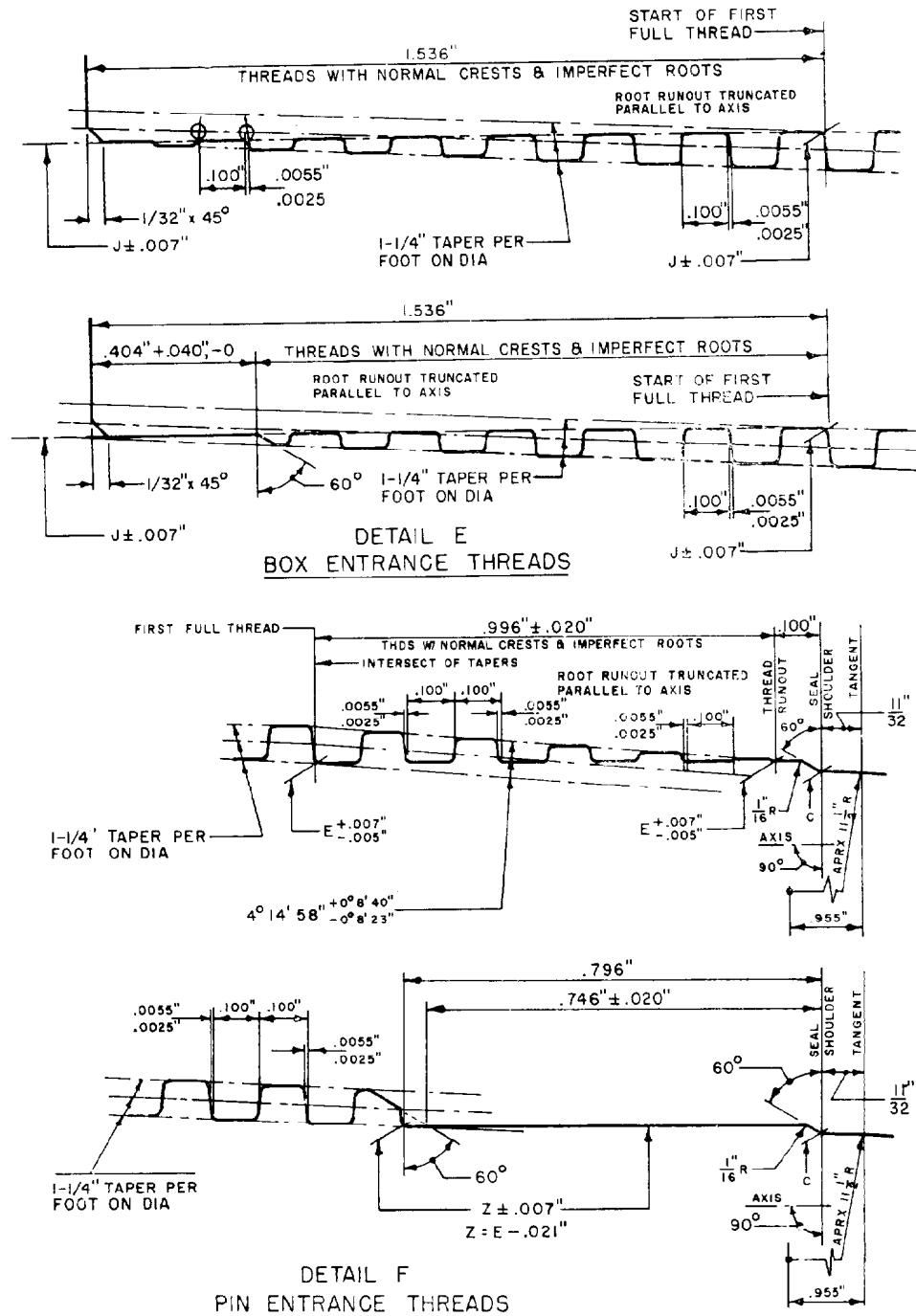
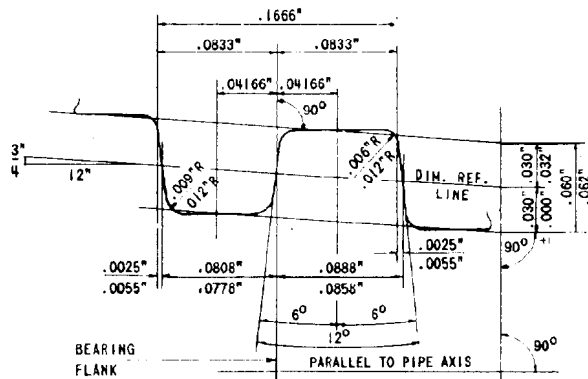
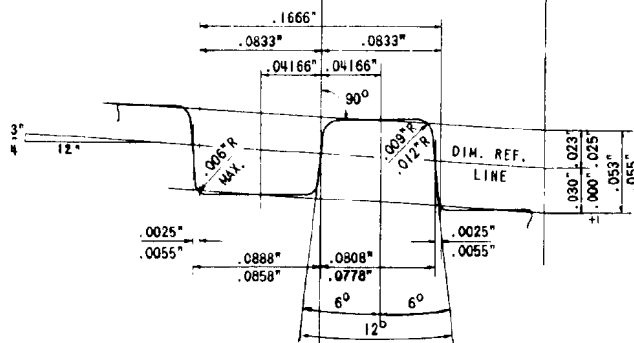


Fig. 2.16—Box-and-pin entrance threads, extreme-line casing joint sizes 8⁵/₈ through 10³/₄ in.

BOX THREAD
FORM



PIN THREAD
FORM



BOX PIN
THREAD
ASSEMBLY

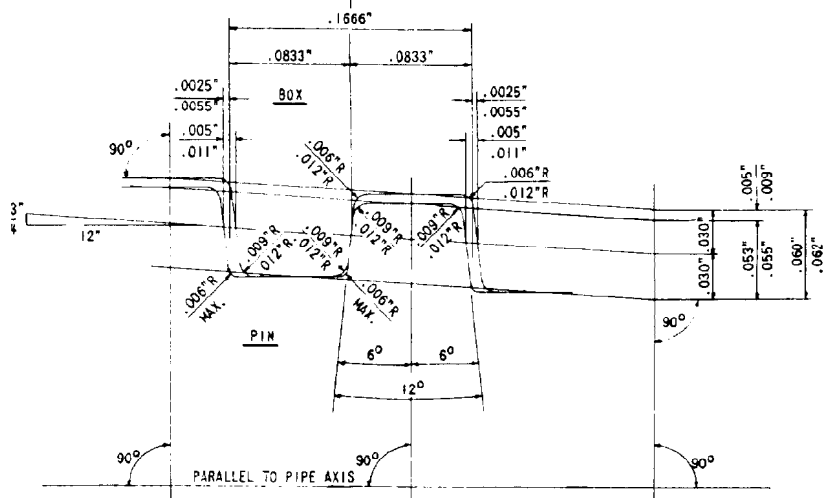


Fig. 2.17—Product thread form, extreme-line casing joint sizes 5 through 7 $\frac{7}{8}$ in., 6 threads/in., 1 $\frac{1}{2}$ -in. taper/ft on diameter.

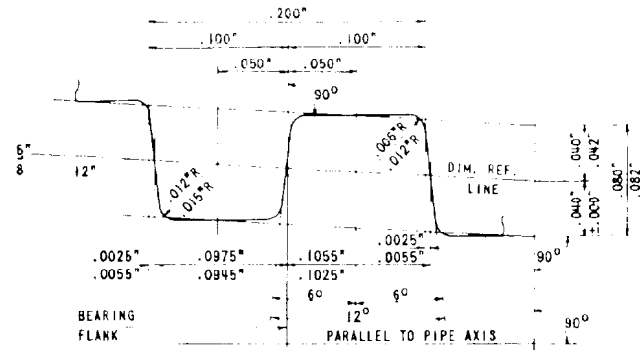
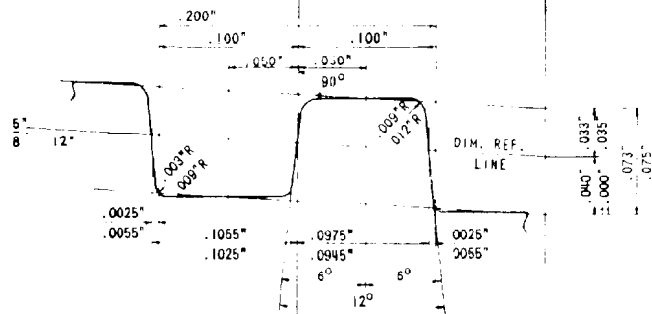
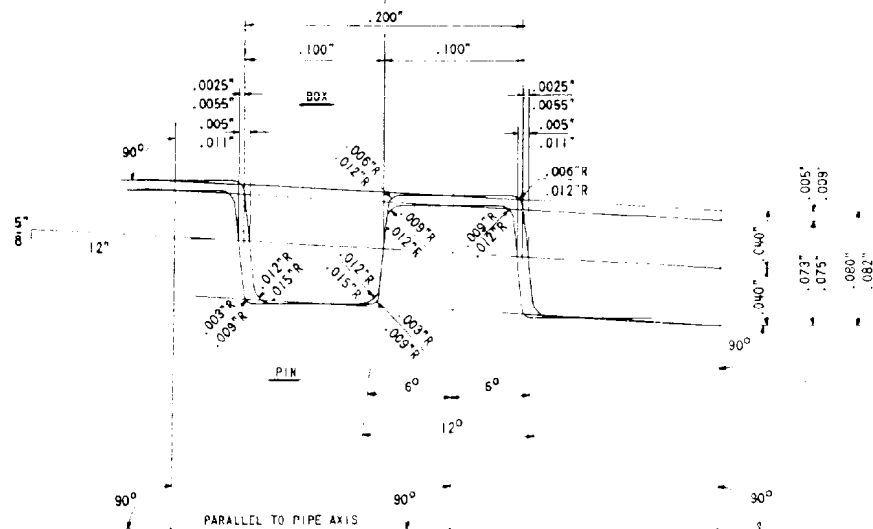
BOX THREAD
FORMPIN THREAD
FORMBOX PIN
THREAD
ASSEMBLY

Fig. 2.18—Product thread form, extreme-line casing joint sizes $8\frac{5}{8}$ through $10\frac{3}{4}$ in., 5 threads/in., $1\frac{1}{4}$ -in. taper/ft on diameter.

Nomenclature

A_c = cross-sectional area of coupling, sq in.
 A_{cr} = critical section area of box, pin, or pipe, whichever is least, sq in.
 A_{id} = area corresponding to ID, sq in.
 A_{jp} = cross-sectional area of the pipe wall under the last perfect thread, sq in.
 A_m = cross-sectional metal area of pipe, sq in.
 A_p = cross-sectional area of plain-end pipe, sq in.
 b = width of bearing face, in.
 C_3 = constant (0.8527 for salt water; 0.8151 for rotary mud; and 1.0 for air)
 C_4 = constant, 0.00000136
 C_5 = constant, 0.0000004
 d_b = box critical section ID, in.
 d_{bc} = minimum crest diameter of box thread at Plane H, in.
 $(d_{bf})_{\max}$ = maximum bearing face diameter bevel, in.
 d_{bs} = minimum diameter at box seal tangent point, in.
 d_c = diameter of chamfer, in.
 d_{cr} = diameter of coupling recess, in.
 d_i = inside diameter, in.
 d_j = nominal joint ID made up, in.
 d_o = OD, in.
 d_{ob} = integral joint OD of box, in.
 $(d_o/e)_{yp}$ = d_o/e intersection between yield-strength collapse and plastic collapse
 $(d_o/e)_{pT}$ = d_o/e intersection between plastic collapse and transition collapse
 $(d_o/e)_{TE}$ = d_o/e intersection between transition collapse and elastic collapse
 d_{oc} = coupling OD, in.
 d_{ocs} = coupling OD, special clearance, in.
 d_{oj} = nominal joint OD made up, in.
 d_p = pitch diameter at hand-tight plane, in.
 d_{p1} = pitch diameter at hand-tight plane for round threads, in.
 d_{ps} = maximum diameter at pin seal tangent point, in.
 d_r = diameter of recess, in.
 d_{rp} = maximum root diameter at last perfect pin thread, in.
 d_1 = diameter at the root of the coupling thread at the end of the pipe in the power tight position, in.
 D_{cr} = depth of coupling recess, in.
 e = wall thickness, in.
 E = Young's modulus of elasticity, psi
 f_{ch} = crest truncation of coupling (Table 2.45)
 f_{cs} = crest truncation of pipe (Table 2.45)
 f_m = thread root truncation of coupling (Table 2.45)
 $F_A, F_B, F_C,$
 F_F, F_6 = equation factors for calculating collapse pressure

F_{sy} = ratio of internal pressure stress to yield strength
 F_T = taper
 F_1 = free stretch factor corresponding to L_{s1}
 F_2 = free stretch factor corresponding to L_{s2}
 h = engaged height of thread, in.
 h_{so} = hand-tight standoff, thread turns
 h_{tb} = minimum box thread height, in.
 h_{tc} = thread height of coupling, in.
 h_{ij} = height of thread, in.
 I = length from end of coupling to base of triangle in hand-tight position (Fig. 2.2), in.
 L_c = minimum length, full crest threads, from end of pipe, in.
 L_d = distance to lower top of casing for desired stress at top of cement, in.
 L_e = engaged thread length, in.
 L_{cut} = length of external upset taper, in.
 L_{fh} = length face of coupling to hand-tight plane, in.
 L_{hc} = end of pipe to center of coupling, hand-tight makeup, in.
 L_{iut} = length of internal upset taper, in.
 L_{\min} = minimum length, in.
 L_p = length of pipe, in.
 L_{pc} = length from end of pipe to center of coupling, power-lift makeup, in.
 L_{ps} = length from end of pipe to triangle stamp, in.
 L_s = stretch, in.
 L_{so} = hand-tight standoff, in.
 ΔL_t = total axial stretch or contraction, in.
 L_{ti} = length from face of coupling to plane of perfect thread, in.
 L_{tp} = thread pitch, in.
 ΔL_u = unit axial stretch or contraction, in.
 L_0 = distance required to lower top of casing for zero stress at top of cement, in.
 L_1 = length from end of pipe to hand-tight plane, in.
 $L_1, L_2 \dots$
 L_n = lengths above top of cement on single-weight Sections 1, 2... n of combination string, ft
 L_4 = total thread length
 L_7 = length of perfect threads, in.
 $L'_1, L'_2 \dots$
 L'_n = lengths below top of cement of single-weight Sections 1, 2... n of combination string, ft
 n = number of thread turns makeup
 p = pressure, psi
 p_{ca} = minimum collapse pressure under axial stress, psi
 p_{co} = minimum collapse pressure without axial stress, psi
 p_E = minimum collapse pressure for elastic range of collapse, psi

- p_H = hydrostatic test pressure, psi
 p_i = internal pressure, psi
 p_{if} = interface pressure, psi
 Δp_{if} = change in interface pressure, psi
 p_{il} = internal-pressure leak resistance, psi
 p_p = minimum collapse pressure for plastic range of collapse, psi
 p_T = minimum collapse pressure for plastic to elastic transition zone, psi
 p_y = yield-strength collapse pressure, psi
 p_{yi} = internal yield pressure, psi
 r_b = external box radius, in.
 r_{bc} = bending radius of curvature
 r_c = contact radius, in.
 r_i = pipe internal radius, in.
 $w_1, w_2 \dots$
 w_n = weights of single-weight Sections 1, 2... n of combination string above cement, lbm/ft
 $w'_1, w'_2 \dots$
 w'_n = weights of single-weight Sections 1, 2... n of combination string below top of cement, lbm/ft
 W_a = superimposed tension or compression, axial load, lbf
 W_b = total tensile failure load with bending, lbf
 W_f = minimum joint fracture strength, lbf
 W_{fu} = total tensile load at fracture, lbf
 W_{fo} = total tensile load at jumpout or reduced fracture strength, lbf
 W_j = minimum joint strength, lbf
 W_p = pipe-body yield strength, lbf
 W_{po} = minimum joint pullout strength, lbf
 W_t = total load below the top of cement, lbf
 γ_m = specific gravity of rotary mud
 γ_w = specific gravity of water
 δ = bending, degrees/100 ft
 δ_{Td} = taper drop in pin perfect thread length, in.
 δ_{Tr} = taper rise between Planes H and J, in.
 θ_s = one-half maximum seal interference, in.
 θ_{th} = one-half maximum thread interference, in.
 σ = unit stress, psi
 σ_a = axial stress, psi
 σ_f = fiber stress corresponding to the percent of specified yield strength given in Table 2.46, psi
 σ_i = tension stress desired to be left at top of cement, psi
 σ_{uc} = minimum ultimate strength of coupling, psi
 σ_{up} = minimum ultimate strength of pipe, psi
 σ_y = minimum yield stress or strength of pipe, psi
 σ_{ya} = yield strength of axial stress equivalent grade, psi
 σ_{yc} = minimum yield strength of coupling, psi

Key Equations in SI Metric Units

$$p_E = \frac{323.7 \times 10^3}{(d_o/e)[(d_o/e) - 1]^2}, \dots \dots \dots (9)$$

where p_E is in kPa.

$$d_1 = d'_p - (L_7 + I)F_T + 1.578, \dots \dots \dots (21)$$

where d_1 , d'_p , and L_7 are in cm.

$$W_j = 0.95 A_{ip} L_e \left(\frac{5d_o^{-0.59} \sigma_{up}}{0.5L_e + 0.14d_o} + \frac{\sigma_y}{L_e + 0.14d_o} \right), \dots \dots \dots (27)$$

where

- W_j is in N,
 A_{ip} is in cm^2 ,
 L_e is in cm,
 d_o is in cm,
 σ_{up} is in kPa, and
 σ_y is in kPa.

References

1. "Casing, Tubing, and Drill Pipe," 37th edition, API Specification 5A, Dallas (May 31, 1984).
2. "Restricted Yield Strength Casing and Tubing," 14th edition, API Specification 5AC, Dallas (May 31, 1984).
3. "Q-125 Casing," first edition, API Specification 5AQ, Dallas (May 31, 1985).
4. "High-Strength Casing, Tubing, and Drill Pipe," 13th edition, API Specification 5AX, Dallas (May 31, 1984).
5. "Performance Properties of Casing, Tubing, and Drill Pipe," 18th edition with Supplement No. 1, API Bull. 5C2, Dallas (April 1983).
6. "Specification for Threading, Gauging, and Thread Inspection of Casing, Tubing, and Line Pipe Threads," tenth edition with Supplement No. 4, API Specification 5B, Dallas (Nov. 1983).
7. "Formulas and Calculations for Casing, Tubing, Drill Pipe, and Line Pipe Properties," third edition with Supplement No. 1, API Bull. 5C3, Dallas (April 1983).
8. "Line Pipe," 34th edition, API Specification 5L, Dallas (May 31, 1984).
9. *Casing and Tubing Technical Data*, Lone Star Steel Co., Dallas (1983).
10. "Collapse Pressure Formulas," API Circular PS-1360, API Standardization Conference, Dallas (Sept. 1968).
11. Clinedinst, W.O.: "Tensile Strength of Casing Joints," API circular PS 1255 presented at the 1963 API Standardization Conference, Dallas, Appendix C.
12. Clinedinst, W.O.: "Strength of Threaded Joints for Steel Pipe," paper 64-Pet-1 presented at the 1964 ASME Petroleum Div. Conference, Los Angeles, Sept.
13. Clinedinst, W.O.: "Buttress Thread Joint Strength Equations," API Circular PS-1398, 1970 API Standardization Conference, API, Dallas (1970).
14. Clinedinst, W.O.: "Buttress Thread Joint Strength," API Circular PS-1398 presented at the 1970 API Standardization Conference, Dallas, Appendix 2-k-9.
15. Clinedinst, W.O.: "The Effect of Internal Pressure and Bending on Tensile Strength of API Casing," paper presented at the Symposium on Mechanical Properties of Pipe, API Standardization Conference, Dallas (June 1967).
16. "Round Thread Casing Joint Strength with Combined Internal Pressure and Bending," API Bull. 5C4, Dallas (April 1972).

Chapter 3

Wellhead Equipment and Flow Control Devices

James H. Foster, Foster Oil Field Equipment Co.*

John Beson, Foster Oil Field Equipment Co.

W.G. Boyle, Otis Engineering Corp.**

Introduction

Wellhead equipment is a general term used to describe equipment attached to the top of the tubular goods used in a well—to support the tubular strings, provide seals between strings, and control production from the well.

Since the American Petroleum Inst. (API) is an active organization set up to establish standards in sizes, grades, designs, dimensions, and quality, to provide safe interchangeable equipment for the industry, this section is confined to equipment covered by API Spec. 6A for wellhead equipment.¹

API Flanged or Clamped Wellhead Equipment

Fig. 3.1 shows a typical wellhead assembly.

Working- and Test-Pressure Terminology

The maximum working pressure is the maximum operating pressure at which the equipment should be used. The hydrostatic test pressure is the static-body test pressure for ensuring a margin of safety above the rated working pressure. It is the test pressure imposed by the manufacturer to prove adequacy in design, materials, and workmanship of the body or shell member and should not be applied as a differential pressure across internal hanger-packer mechanisms or closure mechanisms.

Occasionally wellhead equipment and valves are accidentally or purposely subjected to pressures in excess of design working pressures during high-pressure remedial work. Although the equipment often withstands the mistreatment, such practices should be avoided.

All manufacturers build safety factors into their product based on sound engineering and past experience, but stresses caused by vibration, impact loads, and temperature variations are impossible to predict. Equipment should never be subjected to pressures above the recommended working pressure. If, for any reason, the equipment is to be used at unusually high or extreme working pressure, manufacturers will insist that a disclaimer clause be written and properly worded to relieve them of legal responsibility. The disclaimer should state possible results that are expected because of equipment failure.

Table 3.1 shows the standard API working pressure ratings and their respective body test pressures.

Thread Limitation

In view of the complex mechanics involved in sealing high-pressure threaded connections, it is recommended that field installations be adequately supervised and that API RP 5C1 be followed with regard to lubricants, makeup, etc., of API threads.²

The working pressure of a properly assembled threaded connection joining a wellhead or flowline component and a tubular member often is determined by the rating of the tubular element. In such a case, the maximum working pressure rating of the connection is taken as the internal yield pressure at minimum yield as stipulated in API Bull. 5C2 for the particular size and type of thread and weight and grade of tubing or casing, reduced by a suitable factor of safety.³ However, this pressure rating shall not exceed the maximum working pressure rating shown in Table 3.2. In-plant hydrostatic test pressures of components using tubing or casing threads are shown in Table 3.1

*James H. Foster wrote the original chapter on this topic in the 1962 edition.

**W.G. Boyle is author of the Safety Shut-In Systems section of this chapter.

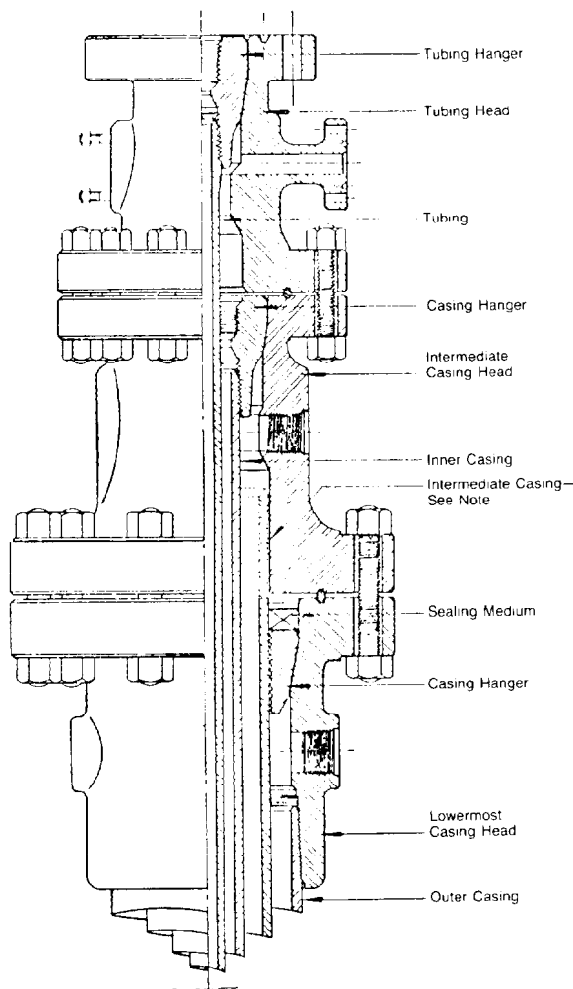


Fig. 3.1—Typical wellhead assembly.

When line pipe threads are used as end or outlet connections of wellhead or flowline components, the maximum working pressure rating of the assembled joint is stipulated in Table 3.2. The in-plant hydrostatic test pressure of components using line pipe threads is shown in Table 3.1.

In many cases the OD of these female threaded members will be greater than API-tabulated coupling or joint diameter to ensure that the structural integrity of the threaded member will not be less than that of the compatible mating API male tubular member.

In addition to the API threads listed in Specs. 5A and 5L, there are a number of proprietary threads available in the same sizes as the API tubing and casing threads.^{4,5} Some of the proprietary threads offer advantages over the API threads, such as maximum clearance for multiple completions, special corrosion protection from internal fluids, low torque requirements, superior internal and external pressure integrity, and high joint strength.

Physical Properties

API body and bonnet members are made from steel with properties equal to or exceeding these specified in Tables 3.3 and 3.4.

Lowermost Casing Heads

The lowermost casing head is a unit or housing attached to the top end of the surface pipe to provide a means for supporting the other strings of pipe, and sealing the annular space between the two strings of casing. It is composed of a casing-hanger bowl to receive the casing hanger necessary to support the next string of casing, a top flange for attaching blowout preventers (BOP's), other intermediate casing heads or tubing heads, and a lower connection.

TABLE 3.1—TEST PRESSURE

Working Pressure		Flanges (14 in. [355.6 mm] and smaller)		Flanges (16¾ in. [425.5 mm] and larger)		Clamp-Type Connectors		Line Pipe and Tubing Threads	
(psi)	(bar)	(psi)	(bar)	(psi)	(bar)	(psi)	(bar)	(psi)	(bar)
1,000	69	2,000	138	1,500	103	—	—	2,000	138
1,500*	103	—	—	—	—	—	—	—	—
2,000	138	4,000	276	3,000	207	4,000	276	4,000**	276
3,000	207	6,000	414	4,500	310	6,000	414	6,000**	414
5,000	345	10,000	690	10,000	690	10,000	690	10,000**	690
10,000	690	15,000	1,035	15,000	1,035	15,000	1,035	15,000**	1,035
15,000	1,035	22,500	1,551	—	—	—	—	—	—
20,000	1,380	30,000	2,070	—	—	—	—	—	—
Casing Threads**									
4½- to 10¾-in. [114.3- to 273.1-mm]		11¾- to 13¾-in. [298.5- to 339.7-mm]		16- to 20-in. [406.4- to 508.0-mm]					
(psi)	(bar)	(psi)	(bar)	(psi)	(bar)				
2,000	138	2,000	138	2,000	138				
—	—	—	—	2,250	155				
4,000	276	4,000	276	—	—				
6,000	414	4,500	310	—	—				
7,500	517	—	—	—	—				

*Working pressure of thread.

**When threads are used as end or outlet connections of wellhead or flowline components, the maximum working pressure of the assembled joint shall be stipulated in Table 3.2 and the test pressure shall be as tabulated in Table 3.1.

**TABLE 3.2—API MAXIMUM WORKING PRESSURE RATINGS
FOR WELLHEAD MEMBERS HAVING FEMALE THREADED END
OR OUTLET CONNECTIONS**

Thread Type	Size		Maximum Working Pressure Rating	
	(in.)	[mm]	(psi)	(bar)
Line Pipe (nominal sizes)	1/2	12.7	10,000	690
	3/4 to 2	19.1 to 50.8	5,000	345
	2 1/2 to 6	63.5 to 152.4	3,000	207
Tubing, nonupset and external upset (API round thread)	1,050 to 4 1/2	26.7 to 114.3	5,000	345
Casing (eight round, buttress and extreme line)	4 1/2 to 10 3/4	114.3 to 273.1	5,000	345
	11 3/4 to 13 3/8	298.5 to 339.7	3,000	207
	16 to 20	406.4 to 508.0	1,500	103

The lower connection may be a female or male thread or a slip-on socket for welding. Most common is the female-threaded lower connection, although the slip-on socket connection provides the strongest joint unless the surface casing is of such composition that welding causes serious weakening. The male lower thread is the weakest of the three connections because of the thin cross section necessary to provide full opening. It is used in most cases only to prevent removing the coupling on the surface pipe. The welded connection is most frequently used on deep wells to give the additional strength needed to suspend heavy casing loads without overstressing the threads on the surface pipe.

A landing base is sometimes used with the lowermost casing head to provide additional support for extremely heavy casing strings. The landing base is a separate unit welded to the lowermost casing head and to the surface pipe with a lower flange or skirt to transfer part of the weight to conductor strings, pilings, or a concrete foundation.

The lower connection is usually the weakest vertical load-supporting connection in an API wellhead assembly. The body-wall thickness of the lowest-working-pressure lowermost casing head is sufficient to support the most extreme casing loads. Therefore, it is not necessary to increase the working pressure of the head because heavy casing loads are anticipated.

Most lowermost casing heads are furnished with two 2-in. line-pipe threaded side outlets, although studded or extended flanged outlets are sometimes used to provide additional strength for attaching valves. Internal valve-removal threads should be included in the studded or extended flanged outlets to provide a means for seating a valve-removal plug to seal the outlet while installing or removing a valve under pressure.

In the event a valve on the side outlet of a casing head cuts out or it is desirable to install or remove a valve under pressure, after the well is completed a special tool can be attached to the outlet or the valve and a valve-removal plug can be inserted into the valve-removal thread to seal the pressure while necessary adjustments are made. A full-opening valve must be used for this application to provide clearance for the plug.

In case threaded outlets are used, a valve-removal nipple may be used to provide the same facility. Internal threads inside the valve-removal nipple provide a receptacle to seat the plug for removing, installing, or replacing the valve.

Lowermost casing heads are available with or without lock screws in the top flange. Lock screws usually are used only to hold the casing hanger down against pressures that may occur during nipple-up operations or when casing-string weights are too light to effect an automatic seal and require a lockscrew to effect the seal.

TABLE 3.3—PHYSICAL AND CHEMICAL PROPERTIES*

	Type 1	Type 2	Type 3	Type 4**
Tensile strength, minimum, psi [MPa]	70,000 [483]	90,000 [621]	100,000 [690]	70,000 [483]
Yield strength, minimum, psi [MPa]	36,000 [248]	60,000 [414]	75,000 [517]	45,000 [310]
Elongation in 2 in., minimum, %	22	18	17	19
Reduction in area, minimum, %	30	35	35	32
Carbon, maximum, %	†	†	†	0.35
Manganese, maximum, %	†	†	†	0.90
Sulfur, maximum, %	†	†	†	0.05
Phosphorus, maximum, %	†	†	†	0.05

* The designation Type 1, Type 2, Type 3, and Type 4 is a nomenclature selected by the API Committee on Standardization of Valves and Wellhead Equipment to identify material falling within the ranges of tensile requirements listed above.

** Flanges made from Type 4 steel are recognized as readily weldable; however, experience indicates that a moderate preheating is desirable under all conditions and is necessary if welding is done at ambient temperatures below 40°F (4°C).

† Chemical analyses of Types 1, 2, and 3 materials are purposely omitted from this specification in order to provide the manufacturer with complete freedom to develop steels most suitable for the multiplicity of requirements encountered in this critical service.

**TABLE 3.4—MATERIAL APPLICATION,
API MATERIAL TYPES SHOWN (1, 2, 3, or 4)**

	Pressure Ratings, psi (bar)						
	1,000 [69]	2,000 [138]	3,000 [207]	5,000 [345]	10,000 [690]	15,000 [1035]	20,000 [1380]
Body (valve, Christmas tree or wellhead equipment)	—	2 or 1*	2 or 1*	2 or 1*	2 or 1*	3	3
Integral end connection							
flanged	—	2	2	2	2	3	3
threaded	—	2	2	2	—	—	—
clamp type	—	—	—	2	2	—	—
Bonnets	—	1,2 3,4	1,2 3,4	1,2 3,4	1,2 3,4	1,2 3,4	1,2 3,4
Independently screwed equipment	1,2 3,4	1,2 3,4	—	—	—	—	—
Loose pieces							
weld-neck flange	—	4	4	4	2	3	—
blind flange	—	2	2	2	2	3	3
threaded flange	—	2	2	2	—	—	—

*Providing end connections are Type 2 and welding is done according to generally accepted welding practices.

The bowl surface can be protected by the use of a bowl protector during the drilling operations. The bowl protector is then removed before the hanger is set.

Sizes and Working Pressures. Lowermost casing heads range in size from 7¹/₁₆ in. to nominal 21 ¹/₄ in. to support casing in sizes from 4 ¹/₂ to 16 in. (Table 3.5). Table 3.5 shows the various casinghead sizes needed for common surface, intermediate, and production string sizes. The sizes of lowermost casing heads are designated by the nominal size of the API flanged-end connection and the nominal size of the lower connection.

Since the wellhead equipment attached above tubular materials should be full-opening to pass full-sized downhole tools, the bore of the tubular materials below an equipment component determines the minimum nominal size of the flange providing access to that tube.

A wellhead component must have a minimum internal diameter approximately ¹/₃₂ in. larger than the drift diameter of the tube over which it is used in order to be considered full-opening. Tables 3.6 and 3.7 give the minimum nominal flange size to give full-opening access to each standard tube size.

Because of the problems encountered in sealing large threaded connections at high pressures in field makeup, Table 3.2 gives the maximum recommended thread pressure ratings for various pipe sizes.

Selection. In selecting a lowermost casing head for a particular application, the following factors should be considered.

Design. The casing head should be designed to receive a casing hanger that will not damage the casing string to be suspended when supporting a full-joint-strength cas-

TABLE 3.5—API CASINGHEAD AND TUBING-HEAD FLANGES (in.)

Surface Pipe Size	To Support Pipe Size	API Flange Size, Lower Casinghead	Nominal Size	First Intermediate Casinghead Flange Size		To Support Pipe Size	Second Intermediate Casing**		To Support Pipe Size	Tubing-Head Flange Size	
				Bottom	Top		Bottom	Top		Bottom	Top*
7	4 ¹ / ₂ , 5	7 ¹ / ₁₆	7 ¹ / ₁₆	—	—	—	—	—	—	7 ¹ / ₁₆	7 ¹ / ₁₆
8 ⁵ / ₈	4 ¹ / ₂ , 5, 5 ¹ / ₂	9	9	—	—	—	—	—	—	9	7 ¹ / ₁₆
9 ⁵ / ₈	4 ¹ / ₂ , 5, 5 ¹ / ₂ , 6 ⁵ / ₈ , 7	11	11	—	—	—	—	—	—	11	7 ¹ / ₁₆
10 ³ / ₄	5 ¹ / ₂ , 6 ⁵ / ₈ , 7, 7 ⁵ / ₈	11	11	—	—	—	—	—	—	11	7 ¹ / ₁₆
11 ³ / ₄	5 ¹ / ₂ , 6 ⁵ / ₈ , 7, 7 ⁵ / ₈	13 ⁵ / ₈	13 ⁵ / ₈	—	—	—	—	—	—	13 ⁵ / ₈	7 ¹ / ₁₆
11 ³ / ₄	7 ⁵ / ₈	13 ⁵ / ₈	13 ⁵ / ₈	13 ⁵ / ₈	11 or 9	4 ¹ / ₂ , 5	—	—	—	11 or 9	7 ¹ / ₁₆
11 ³ / ₄	8 ⁵ / ₈	13 ⁵ / ₈	13 ⁵ / ₈	13 ⁵ / ₈	11 or 9	4 ¹ / ₂ , 5, 5 ¹ / ₂	—	—	—	11 or 9	7 ¹ / ₁₆
13 ³ / ₈	8 ⁵ / ₈	13 ⁵ / ₈	13 ⁵ / ₈	13 ⁵ / ₈	11 or 9	4 ¹ / ₂ , 5, 5 ¹ / ₂	—	—	—	11 or 9	7 ¹ / ₁₆
13 ³ / ₈	9 ⁵ / ₈	13 ⁵ / ₈	13 ⁵ / ₈	13 ⁵ / ₈	11	5 ¹ / ₂ , 6 ⁵ / ₈ , 7	—	—	—	11	7 ¹ / ₁₆
16	8 ⁵ / ₈	16 ³ / ₄	16 ³ / ₄	16 ³ / ₄	11 or 9	4 ¹ / ₂ , 5 ¹ / ₂	—	—	—	11 or 9	7 ¹ / ₁₆
16	9 ⁵ / ₈	16 ³ / ₄	16 ³ / ₄	16 ³ / ₄	11	5 ¹ / ₂ , 6 ⁵ / ₈ , 7	—	—	—	11	7 ¹ / ₁₆
16	10 ³ / ₄	16 ³ / ₄	16 ³ / ₄	16 ³ / ₄	13 ⁵ / ₈ or 11	5 ¹ / ₂ , 6 ⁵ / ₈ , 7, 7 ⁵ / ₈	—	—	—	13 ⁵ / ₈ or 11	7 ¹ / ₁₆
16	10 ³ / ₄	16 ³ / ₄	16 ³ / ₄	16 ³ / ₄	13 ⁵ / ₈ or 11	7 ⁵ / ₈	13 ⁵ / ₈ or 11	11 or 9	4 ¹ / ₂ , 5	11 or 9	7 ¹ / ₁₆
16	13 ³ / ₈	16 ³ / ₄	16 ³ / ₄	16 ³ / ₄	13 ⁵ / ₈	8 ⁵ / ₈	13 ⁵ / ₈	11 or 9	4 ¹ / ₂ , 5 ¹ / ₂	11 or 9	7 ¹ / ₁₆
16	13 ³ / ₈	16 ³ / ₄	16 ³ / ₄	16 ³ / ₄	13 ⁵ / ₈	9 ⁵ / ₈	13 ⁵ / ₈	11	4 ¹ / ₂ , 5 ¹ / ₂ , 7	11	7 ¹ / ₁₆
20	13 ³ / ₈	21 ¹ / ₄	21 ¹ / ₄	21 ¹ / ₄	13 ⁵ / ₈	8 ⁵ / ₈	13 ⁵ / ₈	11	4 ¹ / ₂ , 5 ¹ / ₂	11	7 ¹ / ₁₆
20	13 ³ / ₈	21 ¹ / ₄	21 ¹ / ₄	21 ¹ / ₄	13 ⁵ / ₈	9 ⁵ / ₈	13 ⁵ / ₈	11	4 ¹ / ₂ , 5 ¹ / ₂ , 7	11	7 ¹ / ₁₆
20	16	21 ¹ / ₄	21 ¹ / ₄	21 ¹ / ₄	16 ³ / ₄	10 ³ / ₄	16 ³ / ₄	11	5 ¹ / ₂ , 7	11	7 ¹ / ₁₆
20	16	21 ¹ / ₄	21 ¹ / ₄	21 ¹ / ₄	21 ¹ / ₄	13 ⁵ / ₈	21 ¹ / ₄	13 ⁵ / ₈	8 ⁵ / ₈ , 9 ⁵ / ₈ **	13 ⁵ / ₈	11

*Top tubing-head flange sized for single-tubing-string completions.

**Third intermediate head can be used with 13⁵/₈-in. bottom flange and 11-in. top flange to support 5¹/₂-in. in 8⁵/₈-in. with 11- by 7¹/₁₆-in. tubing head; 5¹/₂ or 7 in. in 9⁵/₈-in. with 11- by 7¹/₁₆-in. tubing head.

TABLE 3.6—MATCHING TUBULAR GOODS SIZES FOR USE WITH 2,000-, 3,000-, and 5,000-psi FLANGES OR 5,000-psi CLAMP-TYPE CONNECTORS

Nominal Size and Bore of Flange** or Clamp Hub	Nominal Flange Size	Size of Tubular Material					
		Line Pipe, Nominal	Tubing OD		Casing OD		
			(in.)	[mm]	(in.)	[mm]	
1 ³ / ₁₆	46.0*	1 ¹ / ₂	1 ¹ / ₂	1.660 and 1.900	42.2 and 48.3	—	—
2 ¹ / ₁₆	52.4	2	2	1.600 through 2 ³ / ₈	42.2 through 60.3	—	—
2 ⁹ / ₁₆	65.1	2 ¹ / ₂	2 ¹ / ₂	2 ⁷ / ₈	73.0	—	—
3 ¹ / ₁₆	79.4	3	3	3 ¹ / ₂	88.9	—	—
4 ¹ / ₁₆	103.2	4	4	4 and 4 ¹ / ₂	101.6 and 114.3	4 ¹ / ₂	114.3
7 ¹ / ₁₆	179.4	6	6	—	—	4 ¹ / ₂ through 7	114.3 through 177.8
9	228.6	8	8	—	—	7 ⁷ / ₈ and 8 ⁵ / ₈	193.7 and 219.1
11	279.4	10	10	—	—	9 ⁵ / ₈ and 10 ³ / ₄	244.5 and 273.1
13 ⁵ / ₈	346.1†	12	12	—	—	11 ³ / ₄ and 13 ³ / ₈	298.5 and 339.7
13 ³ / ₈	346.1‡	13 ⁵ / ₈	—	—	—	11 ³ / ₄ and 13 ³ / ₈	298.5 and 339.7
16 ³ / ₄	425.5	16	16	—	—	16	406.4
16 ³ / ₄	425.5‡	16 ³ / ₄	—	—	—	16	406.4
21 ¹ / ₄	539.8‡	20	20	—	—	20	508.0
20 ³ / ₄	527.1	20	20	—	—	20	508.0

*Generally nonstock size.

**Beginning with the eleventh edition of API Spec. 6A, the traditional 6B flange nominal size designation was changed to a through-bore designation. "Old" nominal sizes will be retained for information until industry becomes accustomed to the new through-bore designations. New nominal sizes 1³/₁₆ in. [46.0 mm] through 11 in. [279.4 mm] replace "old" nominal sizes 1¹/₂ in. through 10 in. The 5,000 psi (345 bar) flanges in the larger sizes are 6BX flanges, and the new 6B flange designations for the larger sizes apply only to 2,000 and 3,000 psi (138 and 207 bar) 6B flanges. The new 20³/₄-in. [527.1-mm] designation applies only to 3,000 psi (207 bar) 6B flanges, and the new 21¹/₄-in. [539.8-mm] designation applies only to 2,000-psi (138-bar) 6B flanges.

†This 6B flange is limited to a maximum working-pressure rating of 3,000 psi (207 bar) when used over 11³/₄-in. [298.5-mm] and 13³/₈-in. [339.7-mm] casing.

‡Type 6BX flanges are required for 5,000-psi (345-bar) maximum working pressure in these sizes.

ing load with a packoff pressure equal to the minimum yield of the supported casing or the working pressure of the casing head, whichever is smaller.

Working Pressure. The minimum working pressure should be at least equal to the anticipated formation breakdown pressure at the bottom of the surface pipe, or equal to or greater than the internal pressure rating of the surface pipe. Maximum working pressure should be at least equal to the formation pressure at the bottom of the next smaller casing string.

Lock Screws. Lock screws in the casinghead flange may be used as an added safety precaution if the annulus pressures are expected during nipple-up or if a very light casing load is to be suspended.

Size. Nominal flange size should normally be the smallest permissible size to provide full-opening access to the surface pipe (Tables 3.6 and 3.7) and should fit a standard out-of-stock intermediate head or tubing head and BOP. It should have the necessary size and type of lower connection to fit the surface pipe.

Casing Hangers

A casing hanger is a device that seats in the bowl of a lowermost casing head or an intermediate casing head to suspend the next smaller casing string securely and provide a seal between the suspended casing and the casinghead bowl.

TABLE 3.7—MATCHING TUBULAR GOODS SIZES FOR USE WITH 10,000-, 15,000-, AND 20,000-psi FLANGES AND 10,000-psi CLAMP-TYPE CONNECTORS

Nominal Flange or Clamp Hub Size	Size of Tubular Material			
	Tubing OD		Casing OD	
	(in.)	[mm]	(in.)	[mm]
1 ¹ / ₁₆ *	42.9	1.900	48.3	—
1 ³ / ₁₆	46.0	2.063	52.4	—
2 ¹ / ₁₆	52.4	2 ³ / ₈	60.3	—
2 ⁹ / ₁₆	65.1	2 ⁷ / ₈	73.0	—
3 ¹ / ₁₆	77.8	3 ¹ / ₂	88.9	—
4 ¹ / ₁₆	103.2	4 and 4 ¹ / ₂	101.6 and 114.3	4 ¹ / ₂
7 ¹ / ₁₆	179.4	—	—	114.3
9**	228.6	—	—	4 ¹ / ₂ through 7
11**	279.4	—	—	7 ⁷ / ₈ and 8 ⁵ / ₈
13 ⁵ / ₈ †	346.1	—	—	8 ⁵ / ₈ and 9 ⁵ / ₈
16 ³ / ₄ †	425.5	—	—	10 ³ / ₄ and 11 ³ / ₄
18 ³ / ₄	476.3	—	—	16
21 ¹ / ₄	539.8	—	—	18
				20

*This flange is inactive; available on special order only.

**Available in 10,000 and 15,000-psi (690- and 1,035-bar) rated flanges only.

†Available in 10,000-psi (690-bar) rated flanges only.

Sizes and Sizing. The size of a casing hanger is determined by the nominal OD, which is the same as the nominal size of the mating casinghead flange. The nominal inside diameter is the same as the nominal outside diameter of the casing it is designed to suspend. Sizes range from nominal $7\frac{1}{16}$ through $21\frac{1}{4}$ in. to support $4\frac{1}{2}$ - through 16-in. casing. Popular sizes are nominal 9 in. for $4\frac{1}{2}$ - through $5\frac{1}{2}$ -in. casing; nominal 11 in. for $4\frac{1}{2}$ - through $7\frac{3}{8}$ -in. casing; nominal $13\frac{3}{8}$ in. for $5\frac{1}{2}$ - through $9\frac{3}{8}$ -in. casing, as indicated in Table 3.5.

Casing hangers are generally available for all casing sizes in the following types.

Automatic (most popular type). The automatic casing hanger is a unitized assembly composed of a set of slips and a sealing mechanism. It can be latched around the casing and dropped through the BOP's to set and seal automatically when the casing is slacked off to set. This type is normally used when annulus pressures are expected during nipple-up operations.

Manual. The manual casing hanger is normally used in preference to the automatic type only as a matter of economics when pressure is not expected in the annulus during nipple-up. It is composed of a set of slips and a separate packoff element. The slips can usually be latched around the casing and dropped through the BOP's, but the packoff is installed after the preventers have been removed and the casing cut off.

Slip-Weld. The slip-weld hanger usually is composed of a set of slips to support the casing weight and a spider or ring that can be welded to the casing to seal the hanger to the casing. The hanger usually is sealed in the head by a resilient compression-type seal. The hanger can be dropped through the BOP's to support casing weight, but the final seal is made by welding after the preventers have been removed and the casing cut off. Particular care must be taken in preheating the casing and the casing head to ensure an adequate weld. Some casing is permanently damaged by improper welding.

Boll-Weevil. The boll-weevil casing hanger is a simple mandrel-type hanger which screws onto the casing to be supported and seats in the casinghead bowl. This type of hanger is not recommended if there is any question about getting the casing to bottom and obtaining the accurate spacing required.

Casing hangers are rated by their capacity to support casing weight rather than by working pressure. Some manufacturers furnish actual pull curves showing the deformation that can be expected in the slip area, for any casing load, up to joint strength, for all standard casing sizes, weights, and grades. Fig. 3.2 shows acceptable pull curves for a heavy-duty casing hanger with a 5,000-psi pressure on the packoff.

Selection. In selecting a casing hanger, after establishing which type of hanger is most practical, the following factors should be considered.

1. The hanger should be capable of hanging the full joint strength of the casing to be used without sufficient reduction in diameter to obstruct full-sized downhole tools.

2. The packoff or primary seal should be of such construction that well pressure, flange test pressure, or fracture pressure cannot force the packoff down and reduce the casing-hanger capacity.

3. The hanger should be of the proper design and size to fit the mating casinghead bowl, and properly sized to support the casing to be used.

Intermediate Casing Heads

An intermediate casing head is a spool-type unit or housing attached to the top flange of the underlying casing head to provide a means of supporting the next smaller casing string and sealing the annular space between the two casing strings. It is composed of a lower flange, one or two side outlets, and a top flange with an internal casing-hanger bowl.

The lower flange of an intermediate casing head is counterbored with a recess to accommodate a removable bit guide, or a bit guide and secondary-seal assembly. The purpose of the bit guide is to protect the top end of the intermediate casing string from damage by bits and tools going into the hole. The counterbore is usually constructed to provide a fixed internal bit guide for the largest-sized intermediate casing string that can be suspended beneath that particular flange size. A removable bit guide must be used to protect smaller-sized intermediate casing.

A removable bit guide and secondary-seal assembly may also be used in place of a removable bit guide to seal the annular space between the intermediate casing and the lower flange of the intermediate casing head. By using a secondary seal, well fluids are confined to the body of the intermediate casing head and not allowed to contact the ring gasket or the packoff on the casing hanger below. If the well fluids are corrosive, use of a dependable secondary seal is particularly important to protect the ring gasket.

Use of a secondary seal and confining well fluids to a diameter approximately equal to the intermediate casing OD greatly reduces piston load or thrust on the flanges and flange studs. This permits use of an intermediate casing head with a top flange one working pressure rating higher than the lower flange. Of course, the body, the top flange, and the outlets must be sized for the higher pressure rating.

Available secondary seals are generally of three types: (1) unitized pressure-energized, (2) plastic-packed, and (3) externally adjustable. The externally adjustable type offers the advantage of being adjustable to stop a leak at any time during the life of a well. A leak in the pressure-energized type or the plastic-packed type may be sealed by injecting a plugging material into the seal under pressure or by replacement.

Intermediate casing heads are available with one or two side outlets, which may be threaded, studded, or extended flanged, depending on the working pressure and particular application. The side outlets should be equipped with valve-removal provisions as discussed in connection with the lowermost casing heads. Like a lowermost casing head, the top flange of an intermediate casing head may be equipped with lock screws if needed because of expected annulus pressures during nipple-up or very light suspended casing loads.

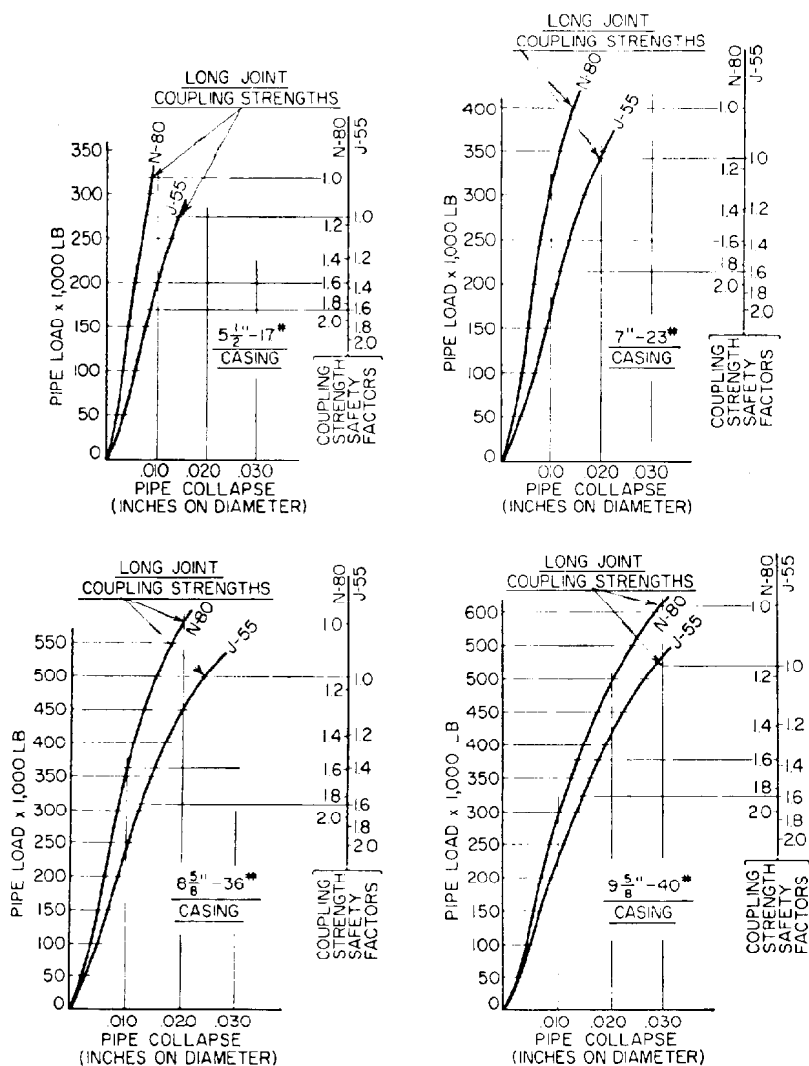


Fig. 3.2—Casing-hanger pull curves.

The design features for an intermediate casinghead bowl are identical to those discussed for a lowermost casinghead bowl. The bowl should be designed to receive a casing hanger which will suspend the next smaller casing string without damage to the pipe. When a relatively short intermediate casing string is used, it is sometimes desirable to use a less-expensive casing hanger with a lower load capacity for support, but a high-capacity casing hanger may be required to suspend the next smaller casing string.

Sizes and Working Pressures. The lower and upper flanges on intermediate casing heads may range in size from nominal 7 1/4 in. to nominal 21 1/4 in. to support casing in sizes from 4 1/2 to 13 3/8 in. Table 3.5 shows the various intermediate head sizes required for standard casing sizes. Tables 3.6 and 3.7 give the minimum nominal flange size to give full-opening access to standard casing.

Intermediate casing heads are available in working pressures of 1,000, 2,000, 3,000, 5,000, and 10,000 psi. Generally, the minimum working pressure of the intermediate head should be equal to or greater than the

maximum surface pressure required to break down the formation at the bottom of the intermediate casing string suspended below the intermediate casing head. The maximum working pressure should at least equal the shut-in formation pressure at the bottom of the casing string to be suspended in the intermediate casing head.

Selection. In selecting an intermediate casing head, the following factors should be considered.

1. Lower flange must be of the proper size and working pressure to fit the uppermost flange on the casing head below, or the crossover flange attached to the casinghead flange if one is used (Tables 3.5 through 3.7).
2. It must have a properly sized bit guide, or bit guide and secondary-seal assembly, to fit the casing suspended beneath it.
3. Top flange must be of the proper size and working pressure to suspend the next smaller casing string and fit the mating flange to be installed above (see working-pressure discussion and Tables 3.5 through 3.7).
4. It should have the proper size, type, and working pressure side outlets.

5. It must include a casing-hanger bowl designed to receive a casing hanger with an effective packoff mechanism that will support joint strength of the casing to be suspended without damage to the casing.

Intermediate Casing Hangers

Intermediate casing hangers are identical in every respect to casing hangers used in lowermost casing heads and are used to suspend the next smaller casing string in the intermediate casing head. These hangers are selected on the same basis as casing hangers used in lowermost casing heads, as previously discussed. Sizes are specified by the nominal diameter of the flange in which the hanger is to be used and the nominal size of the casing to be supported.

Tubing Heads

A tubing head is a spool-type unit or housing attached to the top flange of the uppermost casing head to provide a support for the tubing string and to seal the annular space between the tubing string and production casing string. It also provides access to the casing/tubing annulus through side outlets. It is composed of a lower flange, one or two side outlets, and a top flange with an internal tubing hanger bowl.

Tubing heads are generally of two types: (1) a unit with flanged top and bottom and (2) one with flanged top and threaded bottom. The unit with the threaded bottom is usually screwed directly on the production casing string, and the top flange is used for the same purpose as the double-flanged head. The lower flange, on the double-flanged type, is constructed in much the same way as the lower flange on an intermediate casing head in that a recess is provided to accommodate a bit guide or a bit guide and secondary seal. The design, purpose, types, and application of bit guides and secondary seals are explained in the discussion of the intermediate casing head. Lock screws normally are included in the top flange to hold the tubing hanger in place and/or to compress the tubing hanger seal, which seals the annular space between the tubing and the casing.

Tubing heads are available with one or two side outlets, which may be threaded, studded, or extended flanged. Usually studded-side outlets are used on units with a body working pressure of 3,000 psi and higher. Threaded side outlets are commonly used on units of 2,000-psi working pressure and lower. Extended flanged outlets are used when large-size side outlets are desired. All outlets should be equipped for valve-removal service, as explained in the discussion of the lowermost casing head. The top flange of a tubing head must be equipped with an internal bowl of the proper design to receive the required tubing hanger.

Most available tubing heads will receive any of the various types of single-completion tubing hangers of the same manufacturer. If multiple tubing strings are to be installed, a tubing head with a special bowl may be required. This subject is explained in greater detail under the discussion on multiple completion.

Sizes and Working Pressures. The lower flange on a tubing head may range in size from a nominal $7\frac{1}{16}$ in. to 13 $\frac{3}{4}$ in. The upper flange may vary from nominal $7\frac{1}{16}$

in. to 11 in. for installation over production strings varying in size from $4\frac{1}{2}$ to $9\frac{5}{8}$ in. Table 3.5 gives the various standard tubing-head sizes used over common casing sizes.

Tubing heads are available in working pressures of 1,000, 2,000, 3,000, 5,000, 10,000, 15,000, and 20,000 psi. By using a secondary seal in the lower flange to reduce the piston area exposed to well pressure, a top flange may be used with a working pressure one rating above the lower flange, provided the body and outlet dimensions also correspond to the higher rating.

The working pressure of a tubing head for particular application should be at least equal to the anticipated surface shut-in pressure of the well. In most cases, it is considered more economical to install a tubing head with a working pressure equal to the formation breakdown rather than to replace the tubing head with higher-pressure equipment during high-pressure treatment.

A standard tubing head with a $7\frac{1}{16}$ -in. top flange has a minimum bore of approximately $6\frac{1}{16}$ in., which is considered full-opening for a 7-in. or smaller production string. If a $7\frac{1}{8}$ -in. production string is used, special care should be taken to select a full-opening tubing head for $7\frac{1}{8}$ -in. casing. Special tubing heads are available for this purpose.

Backpressure Valves

Selection. In selecting a tubing head, the following factors should be considered to maintain positive control over the well at all times.

1. The lower flange must be of the proper size and working pressure to fit the uppermost flange on the casing head below or the crossover flange attached to the casinghead flange, if one is used (Table 3.5).

2. The bit guide, or bit guide and secondary-seal assembly, must be sized to fit the production casing string.

3. The size outlets must be of the proper design, size, and working pressure.

4. The working pressure of the unit must be equal to or greater than the anticipated shut-in surface pressure.

5. The top flange must be sized to receive the required tubing hanger, and of the correct working pressure to fit the adapter flange on the Christmas-tree assembly. Lock screws should also be included in the top flange.

6. The tubing head should be full-opening to provide full-sized access to the production casing string below and be adaptable to future remedial operations as well as to artificial lift.

Tubing Hangers

A tubing hanger is a device used to provide a seal between the tubing and the tubing head, or to support the tubing and to seal between the tubing and tubing head.

Types. Several types of tubing hangers are available, and each has a particular application. A brief discussion of the most popular types follows.

Wrap-Around. The popular wrap-around hanger is composed of two hinged halves, which include a resilient sealing element between two steel mandrels or plates. The hanger can be latched around the tubing, dropped into the tubing-head bowl, and secured in place

by the tubing-head lock screws. The lock screws force the top steel mandrel or plate down to compress the sealing element and form a seal between the tubing and tubing head. Full tubing weight can be temporarily supported on the tubing hanger, but permanent support is provided by threading the top tubing thread into the adapter flange on top of the tubing head. The hanger then acts as a seal only.

The tubing can be stripped through the hanger, between upsets, under pressure. After the Christmas-tree assembly has been attached to the adapter flange, the well can be circulated and a packer set under full control. This type of hanger is frequently used as a BOP when running tubing in a low-pressure well loaded with mud. If the well kicks, the tubing hanger can be latched around the tubing and lowered into the tubing-head bowl. A seal is made by tubing weight and by use of the lock screws. After circulation, it can be lifted out of the bowl with the first upset below the hanger.

Polished-Joint. This type of hanger is slipped over or assembled around the top tubing joint, and the internal seals are adjusted to provide a seal on the tubing body. The hanger is sealed against the tubing head with a resilient seal. After the hanger is set, the Christmas tree can be attached to the top tubing thread and the well circulated under full control. The top tubing joint can be stripped through the hanger, between upsets, under pressure.

Boll-Weevil. This is a doughnut- or mandrel-type hanger attached to the top tubing thread and supported in the tubing-head bowl. A seal between the mandrel and tubing head is provided by hydraulic packing or O rings. It is the only hanger designed to support the tubing weight permanently.

Stripper Rubber. A stripper rubber is a pressure-actuated sealing element used to control annulus pressures while running or pulling tubing in a low-pressure well. Tubing weight is supported by the adapter flange, a boll-weevil hanger, or slips located above the stripper rubber. In most cases, the stripper rubber should be used in conjunction with a BOP and is not intended to replace the BOP.

Selection. In selecting a tubing hanger, the particular application should dictate the type required. In general, the hanger should provide an adequate seal between the tubing and tubing head and should be of standard size suitable for lowering through full-opening drilling equipment.

A backpressure valve is a check valve that is installed in the vertical run of the Christmas tree, usually in the tubing hanger or tubing head adapter. A backpressure valve serves two main purposes: (1) to seal the bore of the tubing when removing the BOP and installing the Christmas tree when completing a well and (2) to seal the bore of the tubing when removing the Christmas tree or doing remedial work on the lower master valve. For the backpressure to pass through the Christmas tree the valves and other vertical-run fittings must be full-opening.

Available backpressure valves are generally of two types. One type is secured in place with threads, the other is secured in place with an expanding-lock mechanism.

Adapter

An adapter is a unit used to join connections of different dimensions. The adapter may be used to connect two flanges of different dimensions or connect a flange to a thread. An adapter used to connect two flanges with different dimensions may be studded and grooved on one side for a certain flange size, and studded and grooved on the other side for a different flange size. A unit of this type is called a "double-studded adapter."

Crossover Flange

A crossover flange is an intermediate flange used to connect flanges of different working pressures. Crossover flanges are usually available in two types.

1. A double-studded crossover flange is studded and grooved on one side for one working pressure, and studded and grooved on the other side for the next higher working-pressure rating. The flange must also include a seal around the inner string of pipe to prevent pressure from the higher-working-pressure side reaching the lower-working-pressure side. The seal may be of the resilient type, plastic-packed type, or welded type.

2. Another type of crossover flange includes a restricted-ring groove in the top side of the flange to fit a corresponding restricted-ring groove in the mating head. The restricted-ring groove and the seal between the flange and the inner casing string act to restrict the pressure to a smaller area, thereby allowing a higher pressure rating.

Christmas-Tree Assembly

A Christmas tree is an assembly of valves and fittings used to control production and provide access to the producing tubing string. It includes all equipment above the tubing-head top flange. A typical Christmas tree is shown in Fig. 3.3. Many variations in arrangement of wellhead and Christmas-tree assemblies are available to satisfy the needs of any particular application. Fig. 3.4 shows several typical assemblies.

Tubing-Head Adapter Flange

The tubing-head adapter flange is an intermediate flange used to connect the top tubing-head flange to the master valve and provide a support for the tubing. Standard adapter flanges of the following three types are available.

Studded Type. This unit consists of a lower flange with a ring groove and bolt holes to fit the top tubing-head flange, an internal thread in the bottom of the flange to receive and support the tubing weight, and a studded top connection to accommodate a flanged master valve.

Spool Type. This type is similar to the studded type except that the top connection is a flange to accommodate the master valve, and a top internal thread may be provided to act as a tubing landing or lift thread. It is also available with internal provisions for a backpressure-valve mandrel.

Threaded Adapter Flange. This type of adapter flange is used to connect the top tubing-head flange to a threaded master valve. It is composed of a lower flange with a

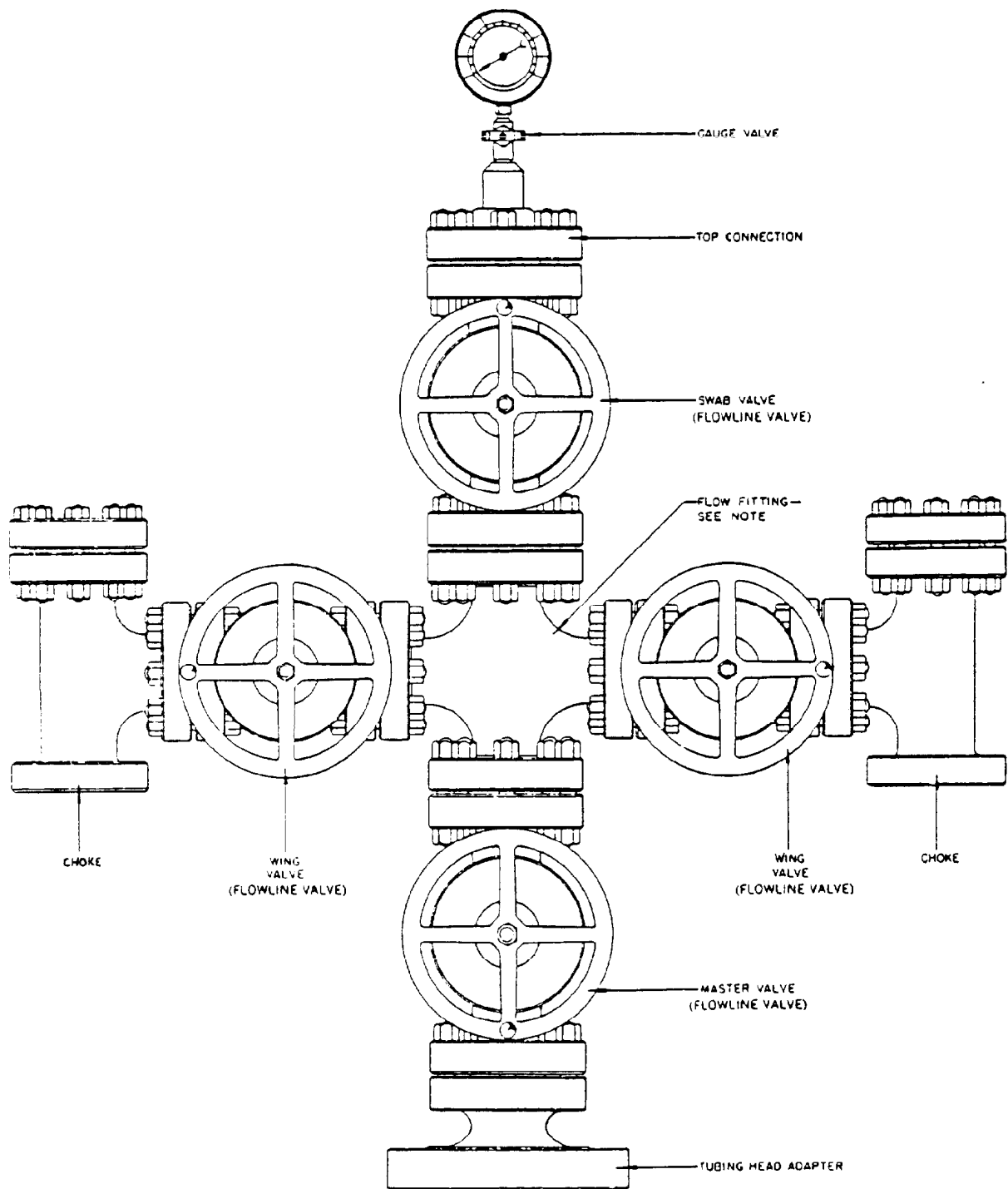


Fig. 3.3—Typical Christmas tree.

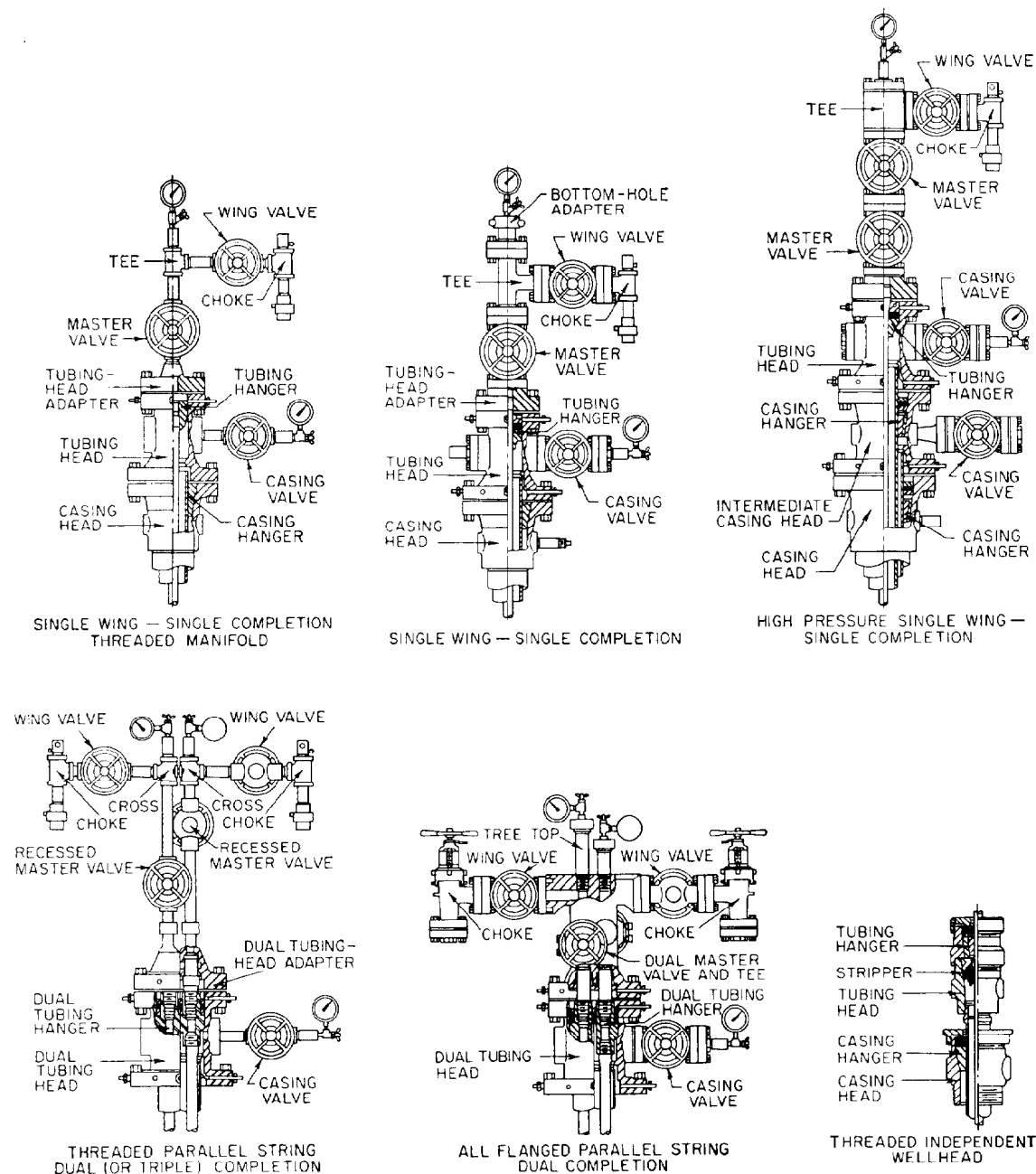


Fig. 3.4—Typical Christmas tree assemblies.

ring groove and bolt holes to fit the top tubing-head flange, an internal thread in the bottom to support the tubing string, and a male thread on top to connect the threaded master valve. The top male thread is usually an upset thread to give added strength.

A tubing-head adapter flange is described by specifying the lower flange size and working pressure, the bottom internal thread size and type, and the top-connection type, size, and working pressure. The lower flange must be of the same size and working pressure as the tubing-head top flange. The top connection must be of the same size and working pressure as the master valve. The top

flange on the adapter and the vertical run of the Christmas tree must be sized to provide full-opening access to the tubing. Tables 3.6 and 3.7 show the flange sizes that will provide full-opening bores for tubular goods.

Valves

API valves, like API wellhead equipment, are made of high-strength alloy steels to give safe dependable service. ASA valves are made of carbon steel and should not be used for wellhead service. Valves used on wellheads are basically of two types—gate valves and plug valves.

**TABLE 3.8—FLANGED AND CLAMPED PLUG AND GATE VALVES,
2,000-psi* MAXIMUM WORKING PRESSURE**

Nominal Size		"Old" Nominal Size	Full-Bore Flowline Valves				End-to-End, Flowline Valves, (± 1/16 in.) [± 1.6 mm]					
			Bore (+ 1/32, - 0) [+ 0.80, - 0]		Drift Diameter		Full-Bore Gate Valves		Plug Valves		Reg. and Venturi	
			(in.)	[mm]	(in.)	[mm]	(in.)	[mm]	(in.)	[mm]	(in.)	[mm]
2 1/16 × 1 13/16	52.4 × 46.0	2 × 1 3/4	1 13/16	46.0	1 25/32	45.20	1 15/8	295.3	—	—	1 15/8	295.3
2 1/16	52.4	2	2 1/16	52.4	2 1/32	51.60	1 15/8	295.3	1 3/8	333.4	1 15/8	295.3
2 9/16	65.1	2 1/2	2 9/16	65.1	2 17/32	64.30	1 3/8	333.4	1 5/8	384.2	1 3/8	333.4
3 1/8**	79.4	3	3 1/8	79.4	3 3/32	78.60	1 4/8	358.8	1 7/8	447.7	1 4/8	358.8
4 1/16**	103.2	4	4 1/16	103.2	4 1/32	102.40	1 7/8	435.0	2 0/8	511.2	1 7/8	435.0
5 1/8	130.2	5	5 1/8	130.2	5 3/32	129.40	2 2/8	562.0	2 5/8	638.2	—	—
7 1/16 × 6**	179.4 × 152.4	6	6	152.4	5 31/32	151.60	2 2/8	562.0	2 8/8	727.1	2 2/8	562.0
7 1/16**	179.4	6 × 7	7 1/16	179.4	7 1/32	178.60	2 6/8	663.6	2 9/8	739.8	—	—

*138 bar maximum working pressure.

**Maximum through bores of 3 3/16, 4 1/4, and 7 1/8 in. [81.0, 108.0, and 181.0 mm] are permissible for nominal sizes 3 1/8, 4 1/16, and 7 1/16 in. [79.4, 103.2, and 179.4 mm]—flanged end connections only.

**TABLE 3.9—FLANGED AND CLAMPED PLUG AND GATE VALVES,
3,000-psi* MAXIMUM WORKING PRESSURE**

Nominal Size		"Old" Nominal Size	Full-Bore Flowline Valves				End-to-End, Flowline Valves, (± 1/16 in.) [± 1.6 mm]					
			Bore (+ 1/32, - 0) [+ 0.80, - 0]		Drift Diameter		Full-Bore Gate Valves		Plug Valves		Reg. and Venturi	
			(in.)	[mm]	(in.)	[mm]	(in.)	[mm]	(in.)	[mm]	(in.)	[mm]
2 1/16 × 1 13/16	52.4 × 46.0	2 × 1 3/4	1 13/16	46.0	1 25/32	45.20	1 4/8	371.5	—	—	1 4/8	371.5
2 1/16	52.4	2	2 1/16	52.4	2 1/32	51.60	1 4/8	371.5	1 5/8	384.2	1 4/8	371.5
2 9/16	65.1	2 1/2	2 9/16	65.1	2 17/32	64.30	1 6/8	422.3	1 7/8	435.0	1 6/8	422.3
3 1/8**	79.4	3	3 1/8	79.4	3 3/32	78.60	1 7/8	435.0	1 8/8	473.1	1 5/8	384.2
4 1/16**	103.2	4	4 1/16	103.2	4 1/32	102.40	2 0/8	511.2	2 2/8	562.0	1 8/8	460.4
5 1/8	130.2	5	5 1/8	130.2	5 3/32	129.40	2 4/8	612.8	2 6/8	663.6	—	—
7 1/16 × 6**	179.4 × 152.4	6	6	152.4	5 31/32	151.60	2 4/8	612.8	3 0/8	765.2	2 4/8	612.8
7 1/16**	179.4	6 × 7	7 1/16	179.4	7 1/32	178.60	2 8/8	714.4	3 1/8	803.3	—	—

*207 bar.

**Maximum through bores of 3 3/16, 4 1/4, and 7 1/8 in. [81.0, 108.0, and 181.0 mm] are permissible for nominal sizes 3 1/8, 4 1/16, and 7 1/16 in. [79.4, 103.2, and 179.4 mm]—flanged end connections only.

**TABLE 3.10—FLANGED AND CLAMPED PLUG AND GATE VALVES,
5,000-psi* MAXIMUM WORKING PRESSURE**

Nominal Size		"Old" Nominal Size	Full-Bore Flowline Valves				End-to-End, Flowline Valves, (± 1/16 in.) [± 1.6 mm]					
			Bore (+ 1/32, - 0) [+ 0.80, - 0]		Drift Diameter		Full-Bore Gate Valves		Plug Valves		Reg. and Venturi	
			(in.)	[mm]	(in.)	[mm]	(in.)	[mm]	(in.)	[mm]	(in.)	[mm]
2 1/16 × 1 13/16	52.4 × 46.0	2 × 1 3/4	1 13/16	46.0	1 25/32	45.20	1 4/8	371.5	—	—	1 4/8	371.5
2 1/16	52.4	2	2 1/16	52.4	2 1/32	51.60	1 4/8	371.5	1 5/2	393.7	1 4/8	371.5
2 9/16	65.1	2 1/2	2 9/16	65.1	2 17/32	64.30	1 6/8	422.3	18	457.2	1 6/8	422.3
3 1/8**	79.4	3	3 1/8	79.4	3 3/32	78.60	1 8/8	473.1	20 3/4	527.1	1 8/8	473.1
4 1/16**	103.2	4	4 1/16	103.2	4 1/32	102.40	2 1/8	549.3	24 3/4	628.7	2 1/8	549.3
5 1/8	130.2	5	5 1/8	130.2	5 3/32	129.40	2 8/8	727.1	31 1/8	790.6	—	—
7 1/16 × 6**	179.4 × 152.4	6	6	152.4	5 31/32	151.60	28	711.2	36 1/8	917.6	28	711.2
7 1/16**	179.4	6 × 7	7 1/16	179.4	7 1/32	178.60	32	812.8	38 1/8	968.4	—	—

*345 bar.

**Maximum through bores of 3 3/16, 4 1/4, and 7 1/8 in. [81.0, 108.0, and 181.0 mm] are permissible for nominal sizes 3 1/8, 4 1/16, and 7 1/16 in. [79.4, 103.2, and 179.4 mm]—flanged and connections only.

Both are available with flanged end connections. Gate valves can be divided into lubricated and nonlubricated, wedging and nonwedging types.

Full-opening valves must be used in the vertical run of the Christmas-tree assembly to provide access to the tubing. Full-opening valves must also be used on tubing-head outlets and casing-head outlets equipped for valve-removal service. Restricted-opening valves are sometimes used as wing valves, without loss of efficiency or utility, to effect an economic saving.

Threaded valves are available in sizes from 1 1/4 to 4 in., with working pressures from 1,000 through 5,000 psi. Upset tubing threads are usually used on valves in the vertical run of a Christmas tree to provide maximum strength. Valves with line-pipe threads are used on tubing wings, threaded tubing-head side outlets, and threaded casinghead side outlets. Most users prefer flanged valves on applications of 3,000-psi working pressure and above. Flanged valves are available in sizes from 1 1/16 through 7 1/16 in. with working pressure ratings from 2,000 to 20,000 psi as shown in Tables 3.8 through 3.14.

Christmas-Tree Fittings

Other Christmas-tree fittings include tees, crosses, and other connections necessary to provide the most desirable arrangement for the particular application.

The size of the vertical run may vary from 2 1/16 to 4 1/16 in. but must be consistent with the master-valve and tubing-head adapter-flange size to give full-opening access to the tubing for wireline tools and instruments. The outlet on the tee or cross and wing assembly must be of sufficient size to handle the production requirements without undue restriction. Outlets vary in size from 1 1/16 to 4 1/16 in., although the 2 1/16-in. size is normally adequate and is most commonly used in the U.S.

All Christmas-tree assemblies should be assembled, pressure-tested to hydrostatic test pressure, and checked with a drift mandrel to ensure full opening before installation. Table 3.15 shows the through-bores and drift diameter for each standard tubing size.

Bottomhole Test Adapter

A bottomhole test adapter is a device attached to the top of a Christmas-tree assembly to provide fast and safe adaptation of a lubricator for swabbing or testing. It may also include an internal thread to act as a lift thread for

TABLE 3.11—FLANGED AND CLAMPED PLUG AND GATE VALVES, 10,000-psi* MAXIMUM WORKING PRESSURE

Full-Bore Flow Line Valves							
Nominal Size		Bore (+ 1/32, - 0) [+ 0.80, - 0]		Drift Diameter		End-to-End (± 1/16)[± 1.6]	
		(in.)	[mm]	(in.)	[mm]	(in.)	[mm]
1 13/16	46.0	1 13/16	46.0	1 25/32	45.20	18 1/4	463.6
2 1/16	52.4	2 1/16	52.4	2 1/32	51.60	20 1/2	520.7
2 9/16	65.1	2 9/16	65.1	2 17/32	64.30	22 1/4	565.2
3 1/16	77.8	3 1/16	77.8	3 1/32	77.00	24 3/8	619.1
4 1/16	103.2	4 1/16	103.2	4 1/32	102.20	26 3/8	669.9

*690 bar.

setting or raising the Christmas tree and tubing. It is available in sizes from 2 1/16 to 4 1/16 in. and in working pressures from 1,000 to 20,000 psi.

Multiple-Completion Equipment

Multiple completions or multiple-tubing-string completions require the same lowermost casing head, intermediate casing head, and tubing-head equipment as single-tubing-string completions with one exception. The tubing-head bowl must be designed and sized to accommodate the required size and number of tubing strings and provide a means for properly orienting the tubing strings. Fig. 3.4 illustrates two types of dual parallel-string installations, and Tables 3.16 and 3.17 give a listing of common multiple-string applications and specifications. The following equations, used with Fig. 3.5, may be used to determine the minimum casing size necessary for any combination of multiple-parallel-tubing-string completions.

Duals and quadruples:

$$d_{c(min)} = A + d_t \quad \dots \dots \dots (1)$$

Triples:

$$d_{c(min)} = 2 \left(L + \frac{d_t}{2} \right), \quad \dots \dots \dots (2)$$

where

$d_{c(min)}$ = minimum casing size,

d_t = tubing diameter,

L = distance (A, B, or C, whichever is greatest, see Fig. 3.5).

TABLE 3.12—FLANGED PLUG AND GATE VALVES, 15,000-psi* MAXIMUM WORKING PRESSURE

Full-Bore Flow Line Valves							
Nominal Size		Bore (+ 1/32, - 0) [+ 0.80, - 0]		Drift Diameter		End-to-End (± 1/16)[± 1.6]	
		(in.)	[mm]	(in.)	[mm]	Short Pattern	Long Pattern
1 13/16	46.0	1 13/16	46.0	1 25/32	45.20	18	457.2
2 1/16	52.4	2 1/16	52.4	2 1/32	51.60	19	482.6
2 9/16	65.1	2 9/16	65.1	2 17/32	64.30	21	533.4
						25	635.0

*1,035 bar.

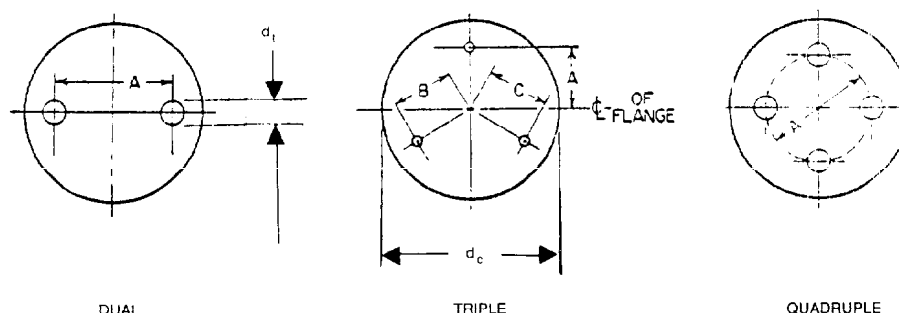


Fig. 3.5—Multiple-parallel tubing strings (see Eqs. 1 and 2).

TABLE 3.13—FLANGED GATE VALVES,
15,000-psi* MAXIMUM WORKING PRESSURE RATING

Full-Bore Flowline Valves							
Nominal Size		Bore (+ 1/32, -0) [+0.80, -0]		Drift Diameter		End-to-End (± 1/16) [± 1.6]	
		(in.)	[mm]	(in.)	[mm]	(in.)	[mm]
3 1/16	77.8	3 1/16	77.8	3 1/32	77.00	23 3/16	598.5
4 1/16	103.2	4 1/16	103.2	4 1/32	102.4	29	736.6

*1,035 bar. All dimensions in in. [mm].

TABLE 3.14—FLANGED GATE VALVES,
20,000-psi* MAXIMUM WORKING PRESSURE RATING

Full-Bore Flowline Valves							
Nominal Size		Bore (+ 1/32, -0) [+0.80, -0]		Drift Diameter		End-to-End (± 1/16) [± 1.6]	
		(in.)	[mm]	(in.)	[mm]	(in.)	[mm]
1 3/16	46.0	1 3/16	46.0	1 25/32	45.20	21	533.4
2 1/16	52.4	2 1/16	52.4	2 1/32	51.60	23	584.2
2 9/16	65.1	2 9/16	65.1	2 1 7/32	64.30	26 1/2	673.1
3 1/16	77.8	3 1/16	77.8	3 1/32	77.00	30 1/2	774.7

*1,380 bar.

Tubing Heads. In selecting a tubing head for multiple parallel-tubing-string service, the same factors should be considered as previously suggested for selecting a single-completion tubing head, with the following additions. The tubing-head bowl should (1) be of the required size and internal design to receive the desired tubing hanger, (2) have the necessary nonrestrictive positioning or indexing devices to orient the tubing hanger accurately, (3) be designed to receive an available tubing hanger, which will suspend the desired number of tubing strings or a single tubing string, and (4) be so designed that removal of the BOP's is not necessary until all tubing strings have been landed and sealed.

Tubing Hangers. Multiple-completion tubing hangers perform the same function as single-completion tubing hangers, and as many types and variations in design are available. A brief description of common available types and designs follows.

Multiple-Bore Mandrel. This type of hanger consists of a large mandrel or doughnut with a separate bore for each tubing string. The individual tubing strings are landed in the large mandrel on landing collars. Backpressure valves can be installed in the individual

TABLE 3.15—THROUGH-BORES AND MANDREL SIZE
OF CHRISTMAS-TREE EQUIPMENT

End Flange or Clamp Hub					Minimum Vertical Through- Bore		Tubing Size			Drift Mandrel Diameter* * (in.) [mm]	
Nominal Size and Bore		"Old" Nominal Size	Working-Pressure Rating				OD		Weight		
(in.)	[mm]	(in.)	(psi)	(bar)	(in.)	[mm]	(in.)	[mm]	(lb/ft)		
—	—	—	—	—	—	—	1.660	42.2	2.4	1.286	32.72
1 13⁄16	46.0	1 1⁄2	2-, 3-, and 5,000	138, 207, and 345	1 11⁄16	42.9	1.900	48.3	2.9	1.516	38.52
2 1⁄16	52.4	2	2-, 3-, and 5,000	138, 207, and 345	2 1⁄16	52.4	2 3⁄8	60.3	4.7	1.901	48.22
2 9⁄16	65.1	2 1⁄2	2-, 3-, and 5,000	138, 207, and 345	2 9⁄16	65.1	2 7⁄8	73.0	6.5	2.347	59.62
3 1⁄8	79.4	3	2-, 3-, and 5,000	138, 207, and 345	3 1⁄8	79.4	3 1⁄2	88.9	9.3	2.867	72.82
—	—	—	—	—	—	—	4	101.6	11.0	3.351	85.12
4 1⁄16	103.2	4	2-, 3-, and 5,000	138, 207, and 345	4 1⁄16	103.2	4 1⁄2	114.3	12.75	3.833	97.32
1 11⁄16	42.9	1 11⁄16	10- and 15,000	690 and 1035	1 11⁄16	42.9	1.900	48.3	2.9	1.516	38.52
1 13⁄16	46.0	1 13⁄16	10- and 15,000	690 and 1035	1 13⁄16	46.0	2.063	52.4	3.25	1.657	42.12
2 1⁄16	52.4	2 1⁄16	10- and 15,000	690 and 1035	2 1⁄16	52.4	2 3⁄8	60.3	4.7	1.901	48.22
2 9⁄16	65.1	2 9⁄16	10- and 15,000	690 and 1035	2 9⁄16	65.1	2 7⁄8	73.0	6.5	2.347	59.62
3 1⁄16	77.8	3 1⁄16	10- and 15,000	690 and 1035	3 1⁄16	77.8	3 1⁄2	88.9	9.3	2.867	72.82
4 1⁄16	103.2	4 1⁄16	10,000	690	4 1⁄16	103.2	4 1⁄2	114.3	12.75	3.833	97.32

*Bar = 100 kPa.

**Drift mandrel diameters conform to the requirements for drift mandrels for external upset tubing as specified in API Spec. 5A: Casing Tubing and Drill Pipe, except 2.063 in. [52.4 mm] tubing, which is integral-joint, internal upset with 1 1/2 EUE threads.

**TABLE 3.16—CENTER DISTANCES OF CONDUIT BORES
FOR DUAL PARALLEL BORE VALVES**

Nominal Size and Minimum Bore		Basic Casing Size†						Large Bore to Flange Center		Small Bore to Flange Center		Nominal* Basic End Flange Size and Bore	
		OD		Weight (lbm/ft)	Bore to Bore								
		(in.)	[mm]		(in.)	[mm]	(in.)	[mm]	(in.)	[mm]	(in.)		
2,000-, 3,000-, and 5,000-psi [138-, 207-, and 345-bar] Maximum Working Preure													
1 1⁄16	42.9	5 1⁄2	139.7	23	2 25⁄32	70.64	1.3905	35.319	1.3905	35.319	7 1⁄16	179.4	
1 13⁄16**	46.0	5 1⁄2	139.7	17	1 25⁄32	70.64	1.3905	35.319	1.3905	35.319	7 1⁄16	179.4	
2 1⁄16	52.4	7	177.8	38	3 35⁄64	90.09	1.7735	45.047	1.7735	45.047	7 1⁄16	179.4	
2 9⁄16 × 2 1⁄16	65.1 × 52.4	7	177.8	29	3 35⁄64	90.09	1.650	41.910	1.897	48.184	7 1⁄16	179.4	
2 9⁄16 × 2 1⁄16	65.1 × 52.4	7 5⁄8	193.7	39	4	101.60	1.875	47.625	2.125	53.975	9	228.6	
2 3⁄16	65.1	7 5⁄8	193.7	29.7	4	101.60	2.000	50.800	2.000	50.800	9	228.6	
2 9⁄16	65.1	8 5⁄8	219.1	49	4 1⁄2	114.30	2.250	57.150	2.250	57.150	9	228.6	
3 1⁄8 × 2 1⁄16	79.4 × 52.4	8 5⁄8	219.1	49	4 37⁄64	116.28	2.008	51.003	2.570	65.278	9	228.6	
3 1⁄8 × 2 9⁄16	79.4 × 65.1	9 5⁄8	244.5	53.5	5 3⁄64	128.19	2.5235	64.097	2.5235	64.097	11	279.4	
3 1⁄8	79.4	9 5⁄8	244.5	53.5	5 3⁄64	128.19	2.5235	64.097	2.5235	64.097	11	279.4	
10,000-psi [690-bar] Maximum Working Pressure													
1 13⁄16**	46.0	5 1⁄2	139.7	17	2 25⁄32	70.64	1.3905	35.319	1.3905	35.319	7 1⁄16	179.4	
2 1⁄16	52.4	7	177.8	38	3 35⁄64	90.09	1.7735	45.047	1.7735	45.047	7 1⁄16	179.4	
2 9⁄16 × 2 1⁄16	65.1 × 52.4	7	177.8	29	3 35⁄64	90.09	1.650	41.910	1.897	48.184	7 1⁄16	179.4	
2 9⁄16 × 2 1⁄16	65.1 × 52.4	7 5⁄8	193.7	39	4	101.60	1.875	47.625	2.125	53.975	9	228.6	
2 9⁄16	65.1	7 5⁄8	193.7	29.7	4	101.60	2.000	50.800	2.000	50.800	9	228.6	
2 3⁄16	65.1	8 5⁄8	219.1	49	4 1⁄2	114.30	2.250	57.150	2.250	57.150	9	228.6	
3 1⁄16	77.8	9 5⁄8	244.5	53.5	5 3⁄64	128.19	2.5235	64.097	2.5235	64.097	11	279.4	

*Basic end connection size is determined by the size of tubing-head top connection, which suspends the several tubing strings. If an adapter flange is used, a smaller valve end flange is sometimes permitted.

**Center distances based on 2 1/16 [52.4 mm] OD tubing.

†CAUTION: Due to the permissible tolerance on the OD immediately behind the tubing upset, the user is cautioned that difficulties may occur. It is recommended that the user select the joint of tubing to be installed at the top of the tubing string.

Note: Drift size for the 1 1/16 in. [42.9 mm] nominal size is 1 1/32 in. [42.1 mm].

**TABLE 3.17—CENTER DISTANCES OF CONDUIT BORES
FOR TRIPLE, QUADRUPLE, AND QUINTUPLE PARALLEL BORE VALVES**

	Nominal Size and Minimum Bore		Basic Casing Size†			Radii to Bores		Nominal Basic* End Flange Size and Bore	
			OD		Weight				
	(in.)	[mm]	(in.)	[mm]	(lbm/ft)	(in.)	[mm]	(in.)	[mm]
	2,000-, 3,000-, and 5,000-psi [138-, 207-, and 345-bar] Maximum Working Pressure								
Triple Valve	1 ³ / ₁₆ **	46.0	6 ⁵ / ₈	168.3	24	1 ⁷ / ₈	47.63	7 ¹ / ₁₆	179.4
	2 ¹ / ₁₆	52.4	7	177.8	26	1 ⁵ / ₁₆	49.21	9	228.6
	2 ¹ / ₁₆	52.4	7 ⁷ / ₈	193.7	39	2 ¹ / ₈	53.98	9	228.6
	2 ⁹ / ₁₆	65.1	9 ⁵ / ₈	244.5	53.5	2 ³ / ₁₆	71.44	11	279.4
Quadruple Valve	1 ³ / ₁₆ **	46.0	8 ⁵ / ₈	219.1	36	2 ⁷ / ₈	73.03	11	279.4
	1 ³ / ₁₆	46.0	9 ⁵ / ₈	244.5	All	3 ¹ / ₁₆	77.79	11	279.4
	2 ¹ / ₁₆	52.4	9 ⁵ / ₈	244.5	53.5	3 ¹ / ₁₆	77.79	11	279.4
	2 ⁹ / ₁₆	65.1	10 ³ / ₄	273.1	55.5	3 ⁷ / ₁₆	87.31	11	279.4
	2 ⁹ / ₁₆	65.1	11 ³ / ₄	298.5	54	4	101.60	13 ⁵ / ₈	346.1
Quintuple Valve	2 ¹ / ₁₆	52.4	9 ⁵ / ₈	244.5	53.5	3 ¹ / ₁₆	77.79	11	279.4
10,000-psi [690-bar] Maximum Working Pressure									
Triple Valve	1 ³ / ₁₆ **	46.0	6 ⁵ / ₈	168.3	24	1 ⁷ / ₈	47.63	7 ¹ / ₁₆	179.4
	2 ¹ / ₁₆	52.4	7	177.8	26	1 ⁵ / ₁₆	49.21	9	228.6
	2 ¹ / ₁₆	52.4	7 ⁷ / ₈	193.7	39	2 ¹ / ₈	53.98	9	228.6
	2 ⁹ / ₁₆	65.1	9 ⁵ / ₈	244.5	53.5	2 ³ / ₁₆	71.44	11	279.4
Quadruple Valve	2 ⁹ / ₁₆	65.1	10 ³ / ₄	273.1	55.5	3 ⁷ / ₁₆	87.31	11	279.4

*Basic end connection size is determined by the size of tubing-head top connection, which suspends the several tubing strings. If an adapter flange is used, a smaller valve end flange is sometimes permitted.

**Center distances based on 2 1/16-in. [52.4-mm] OD tubing.

†CAUTION: Due to the permissible tolerance on the OD immediately behind the tubing upset, the user is cautioned that difficulties may occur. It is recommended that the user select the joint of tubing to be installed at the top of the tubing string.

TABLE 3.18—API TYPE 6B FLANGES FOR 2,000-psi* MAXIMUM WORKING PRESSURE

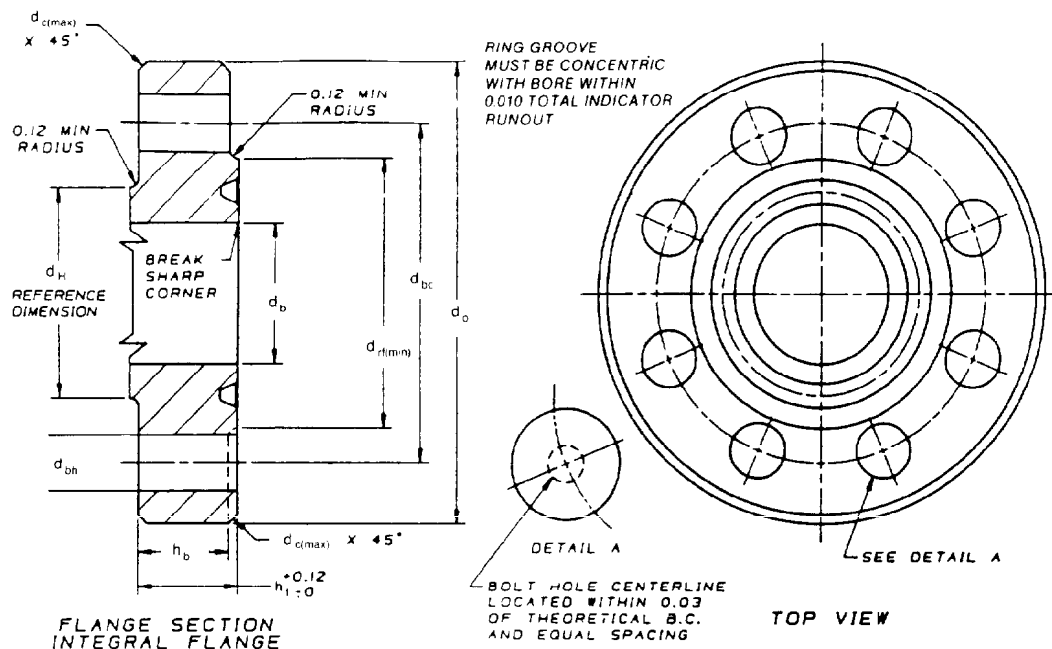
Basic Flange Dimensions										Bolting Dimensions							
Nominal Size and Bore of Flange	"Old" Nominal Size of Flange	OD of Flange		Total Thickness of Flange		Basic Thickness of Flange		Diameter of Hub		Diameter of Bolt Circle	Number of Bolts	Diameter of Bolts	Diameter of Bolt Holes		Length of Stud Bolts	Ring Number R or RX	
(in.) [mm]	(in.)	(in.)	[mm]	(in.)	[mm]	(in.)	[mm]	(in.)	[mm]	(in.) [mm]			(in.)	[mm]	(in.) [mm]		
** 1 1/16	46.0	1 1/2	6 1/8	156	1 1/8	28.6	7/8	22.2	2 3/4	69.9	4	3/4	0.88	23	4 1/4	108	20
2 1/16	52.4	2	6 1/2	165	1 1/16	33.3	1	25.4	3 1/16	84.1	8	5/8	0.75	20	4 1/2	114	23
2 3/16	65.1	2 1/2	7 1/2	191	1 1/8	36.5	1 1/8	28.6	3 1/8	100.0	8	5/8	0.88	23	5	127	26
3 1/8	79.4	3	8 3/4	210	1 1/8	39.7	1 1/4	31.8	4 5/8	117.5	8	3/4	0.88	23	5 1/4	133	31
4 1/8	103.2	4	10 3/4	273	1 1/16	46.0	1 1/2	38.1	6	152.4	8	7/8	1.00	26	6	152	37
** 5 1/8	130.2	5	13	330	2 1/16	52.4	1 3/4	44.5	7 1/16	188.9	8	1	1.12	29	6 3/4	171	41
7 1/16	179.4	6	14	356	2 3/16	55.6	1 7/8	47.6	8 3/4	222.3	12	1	1.12	29	7	178	45
9	228.6	8	16 1/2	419	2 1/2	63.5	2 3/16	55.6	10 3/4	273.1	12	1 1/8	1.25	32	8	203	49
11	279.4	10	20	508	2 13/16	71.4	2 1/2	63.5	13 1/2	342.9	16	1 1/4	1.38	35	8 3/4	222	53
13 3/8	346.1	12	22	559	2 15/16	74.6	2 5/8	66.7	15 3/4	400.1	20	1 1/4	1.38	35	9	229	57
16 3/4	425.5	16	27	686	3 1/16	84.1	3	76.2	19 1/2	495.3	20	1 1/2	1.62	42	10 1/4	260	65
** 17 3/4	450.9	18	29 1/4	743	3 1/8	90.5	3 1/4	82.6	21 1/2	546.1	20	1 5/8	1.75	45	11	279	69
21 1/4	539.8	20	32	813	3 7/8	98.4	3 1/2	88.9	24	609.6	24	1 5/8	1.75	45	11 3/4	298	73

*138 bar.

**These sizes available on special order only.

Notes: Maximum through bores of 3 1/16 in. [81.0 mm], 4 1/8 in. [108.0 mm], and 7 1/8 in. [181.0 mm] are permissible for nominal sizes 3 1/8, 4 1/8, and 7 1/8 in. [79.4, 103.2, and 179.4 mm], respectively.

Flanged end connections of some casing and tubing heads may have entry bevel recesses and/or counterbores greater than "B" maximum to receive a packer mechanism. The sizes and shapes of these bevels, recesses, and/or counterbores are proprietary and are not covered by this specification.



landing collars. This is the most simple and easily installed hanger but is limited to applications where gas-lift valves or tubing accessories with external diameters greater than tubing-joint diameters are not needed.

Multiple-Segment. This type of hanger is composed of an individual hanger segment for each tubing string. Each segment seats in and occupies a part of the bowl when landed. Gas-lift valves and other tubing accessories may be installed on the tubing string. Each hanger segment may be equipped with provisions for backpressure valves.

Combination Mandrel and Boll-Weevil. This type of hanger is similar to the multiple-bore mandrel hanger except that one string of tubing is supported by threading into the large mandrel.

Tension-Type. This type of hanger is constructed similar to the multiple-bore mandrel hanger and consists of a landing collar for each individual tubing string. The individual landing collars may be lowered through and lifted back up into the hanger mandrel, enabling the tubing strings to be set in tension through the BOP's. Backpressure valves may be installed in the landing collars.

Selection. In selecting a multiple-completion tubing hanger, the following factors should be considered.

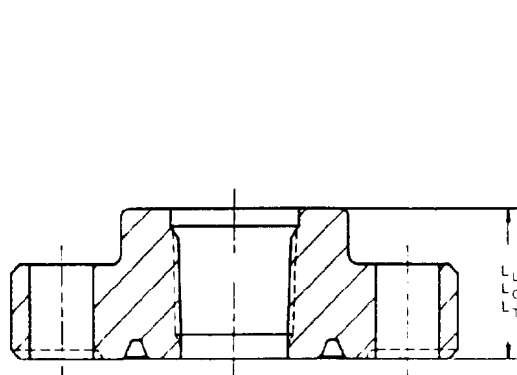
1. Seals on the individual hangers should not be exposed to damage by successive running of remaining tubing strings.

TABLE 3.18—API TYPE 6B FLANGES FOR 2,000-psi* MAXIMUM WORKING PRESSURE (continued)

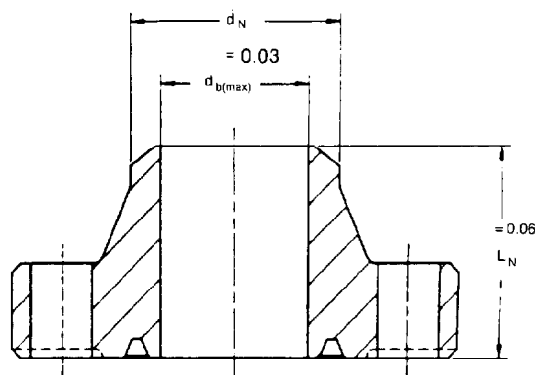
Ring-Joint Groove and Flange Facing Dimensions								Hub and Bore Dimensions												
Nominal Size and Bore of Flange	Pitch Diameter of Type R Ring and Groove		Width of Groove		Depth of Groove		Diameter of Raised Face	Hub Length Threaded Line-Pipe Flange	Hub Length Threaded Casing Flange	Hub Length Welding-Neck Line-Pipe Flange	Neck Diameter Welding-Neck Line-Pipe Flange	Maximum Bore of Welding Neck Flange								
	(in.)	[mm]	(in.)	[mm]	(in.)	[mm]							(in.)	[mm]	(in.)	[mm]	(in.)	[mm]		
**	1 ¹³ / ₁₆	46.0	2 ¹¹ / ₁₆	68.26	1 ¹³ / ₃₂	8.73	1/4	6.35	3 ⁹ / ₁₆	90	1 ¹ / ₂	38	—	—	3	76.2	1.90	48.3	1.610	40.89
	2 ¹ / ₁₆	52.4	3 ¹ / ₄	82.55	1 ⁵ / ₃₂	11.91	5/16	7.94	4 ¹ / ₄	108	1 ³ / ₄	44	—	—	3 ¹ / ₁₆	81.0	2.38	60.5	2.067	52.50
	2 ⁹ / ₁₆	65.1	4	101.60	1 ⁵ / ₃₂	11.91	5/16	7.94	5	127	1 ¹⁵ / ₁₆	49	—	—	3 ⁷ / ₁₆	87.3	2.88	73.2	2.469	62.71
	3 ¹ / ₈	79.4	4 ⁷ / ₈	123.83	1 ⁵ / ₃₂	11.91	5/16	7.94	5 ³ / ₄	146	2 ¹ / ₈	54	—	—	3 ⁹ / ₁₆	90.5	3.50	88.9	3.068	77.93
**	4 ¹ / ₈	103.2	5 ⁷ / ₈	149.23	1 ⁵ / ₃₂	11.91	5/16	7.94	6 ⁷ / ₈	175	2 ⁷ / ₁₆	62	3 ¹ / ₂	89	4 ⁹ / ₁₆	109.5	4.50	114.3	4.026	102.26
	5 ¹ / ₈	130.2	7 ¹ / ₈	180.98	1 ⁵ / ₃₂	11.91	5/16	7.94	8 ¹ / ₄	210	2 ¹¹ / ₁₆	68	4	102	4 ¹ / ₁₆	122.2	5.56	141.2	4.813	122.25
	7 ¹ / ₁₆	179.4	8 ⁵ / ₁₆	211.14	1 ⁵ / ₃₂	11.91	5/16	7.94	9 ¹ / ₂	241	2 ¹⁵ / ₁₆	75	4 ¹ / ₂	114	4 ¹⁵ / ₁₆	125.4	6.63	168.4	5.761	146.33
	9	228.6	10 ⁵ / ₈	269.88	1 ⁵ / ₃₂	11.91	5/16	7.94	11 ⁷ / ₈	302	3 ⁵ / ₁₆	84	5	127	5 ⁹ / ₁₆	141.3	8.63	219.2	7.813	198.45
11	279.4	12 ³ / ₄	323.85	1 ⁵ / ₃₂	11.91	5/16	7.94	14	356	3 ¹¹ / ₁₆	94	5 ¹ / ₄	133	6 ⁵ / ₁₆	160.3	10.75	273.1	9.750	247.65	
13 ³ / ₈	346.1	15	381.00	1 ⁵ / ₃₂	11.91	5/16	7.94	16 ¹ / ₄	413	3 ¹⁵ / ₁₆	100	3 ¹⁵ / ₁₆	100	—	—	—	—	—	—	—
16 ³ / ₄	425.5	18 ¹ / ₂	469.90	1 ⁵ / ₃₂	11.91	5/16	7.94	20	508	4 ¹ / ₂	114	4 ¹ / ₂	114	—	—	—	—	—	—	—
**	17 ³ / ₄	450.9	21	533.40	1 ⁵ / ₃₂	11.91	5/16	7.94	22 ³ / ₈	575	4 ¹⁵ / ₁₆	125	4 ¹⁵ / ₁₆	125	—	—	—	—	—	—
	21 ¹ / ₄	539.8	23	584.20	1 ⁷ / ₃₂	13.49	3/8	9.53	25	635	5 ³ / ₈	137	5 ³ / ₈	137	—	—	—	—	—	—

* 138 bar.

** These sizes available on special order only.



THREADED FLANGE

WELD NECK
LINE PIPE FLANGE

REQUIREMENTS FOR TABLE 3.18

- The contour of the flange face outside the d_N diameter is optional with the manufacturer unless raised or full face is specified on the purchase order.
- Ring-groove radius r_{fg} shall be $1/32$ in. [0.79 mm] for groove widths $1/32$ [8.73 mm] and $1/16$ [11.91 mm]; $1/16$ in. [1.59 mm] for width $1/32$ [13.49 mm].
- The bore d_B of welding-neck flanges shall be as specified on the purchase order.
NOTE: Bore diameter should be the same as ID of pipe to be used; but, because these flanges are constructed of Type 4 material, the bore shall not exceed values of d_B .
- The wall thickness of welding-neck flanges shall be not less than 87½% of the nominal wall thickness of the pipe to which the flange is to be attached.
- The welding end of welding-neck flanges shall be cylindrical or shall have a maximum draft of 7°. The length shall be sufficient to ensure a sound weld, but in no case shall be less than ¼ in. [6.4 mm].

2. Positive packoff elements or seals should be provided.

3. Design should allow passage of gas-lift valves if needed.

4. Center lines should be provided to suspend tubing in the casing without spreading at the top.

5. The hanger should be constructed to accommodate positive seating of backpressure valves that do not require an oversize vertical run.

6. The hanger should be constructed for accurate, dependable pressure testing after tubing strings have been landed and sealed.

Christmas-Tree Assembly. The Christmas-tree assembly for a multiple-parallel-string wellhead includes

all fittings above the tubing-head top flange. Threaded, welded, independently flanged, and integrally flanged Christmas-tree assemblies are available for the installation of multiple tubing strings.

Threaded, welded, and independently flanged assemblies are furnished in working pressures of 2,000 and 3,000 psi, although threaded assemblies are rarely recommended for 3,000-psi applications. Welded assemblies are recommended for 3,000-psi service only on noncorrosive applications when pressures are expected to decline rapidly and economy is of great importance. Integrally flanged assemblies are available in 2,000-, 3,000-, 5,000-, and 10,000-psi working pressures. These assemblies are preferred on severe or corrosive 2,000- and 3,000-psi service, and recommended for 5,000- and 10,000-psi applications.

TABLE 3.19—API TYPE 6B FLANGES FOR 3,000-psi* MAXIMUM WORKING PRESSURE

Basic Flange Dimensions**										Bolting Dimensions**									
Nominal Size and Bore of Flange		"Old" Nominal Size of Flange	Outside Diameter of Flange		Total Thickness of Flange		Basic Thickness of Flange		Diameter of Hub		Diameter of Bolt Circle		Number of Bolts	Diameter of Bolts	Diameter of Bolt Holes		Length of Stud Bolts		Ring Number R or RX
(in.)	[mm]		(in.)	[mm]	(in.)	[mm]	(in.)	[mm]	(in.)	[mm]	(in.)	[mm]			(in.)	[mm]	(in.)	[mm]	
† 1 ³ / ₁₆	46.0	1½	7	178	1½	38.1	1¼	31.8	2¾	69.9	4 ⁷ / ₈	123.8	4	1	1.12	29	5½	140	20
2 ¹ / ₁₆	52.4	2	8½	216	1 ¹³ / ₁₆	46.0	1½	38.1	4½	104.8	6½	165.1	8	7⁄8	1.00	26	6	152	24
2 ³ / ₁₆	65.1	2½	9 ⁵ / ₈	244	1 ¹⁵ / ₁₆	49.2	1 ⁵ / ₈	41.3	4 ⁷ / ₈	123.8	7½	190.5	8	1	1.12	29	6½	165	27
3⁄8	79.4	3	9½	241	1 ¹³ / ₁₆	46.0	1½	38.1	5	127.0	7½	190.5	8	7⁄8	1.00	26	6	152	31
4 ¹ / ₁₆	103.2	4	11½	292	2 ¹ / ₁₆	52.4	1¾	44.5	6¼	158.8	9¼	235.0	8	1 ¹ / ₈	1.25	32	7	178	37
† 5⁄8	130.2	5	13¾	349	2 ³ / ₁₆	58.7	2	50.8	7½	190.5	11	279.4	8	1¼	.38	35	7¾	197	41
7 ¹ / ₁₆	179.4	6	15	381	2½	63.5	2 ³ / ₁₆	55.6	9¼	235.0	12½	317.5	12	1 ¹ / ₈	1.25	32	8	203	45
9	228.6	8	18½	470	2 ¹³ / ₁₆	71.4	2½	63.5	11¾	298.5	15½	393.7	12	1 ³ / ₈	1.50	39	9	229	49
11	279.4	10	21½	546	3 ¹ / ₁₆	77.8	2¾	69.9	14½	368.3	18½	469.9	16	1 ³ / ₈	1.50	39	9½	241	53
13 ⁵ / ₈	346.1	12	24	610	3 ⁷ / ₁₆	87.3	3 ¹ / ₈	79.4	16½	419.1	21	533.4	20	1 ³ / ₈	1.50	39	10¼	260	57
16¾	425.5	16	27¾	705	3 ¹⁵ / ₁₆	100.0	3½	88.9	20	508.0	24¼	616.0	20	1 ⁵ / ₈	1.75	45	11¾	298	66
† 17¾	450.9	18	31	787	4½	114.3	4	101.6	22¼	565.2	27	685.8	20	1 ⁷ / ₈	2.00	51	13¾	349	70
20¾	527.1	20	33¾	857	4¾	120.7	4¼	108.0	24½	622.3	29½	749.3	20	2	2.12	54	14½	368	74

*207 bar.

**See Table 3.18 sketch.

†These sizes inactive; available on special order only.

Nomenclature for Tables 3.18 through 3.29

b_f	= width of flat of octagonal ring, in.
b_g	= width of groove, in.
b_r	= width of ring, in.
d_{bc}	= diameter of bolt circle, in.
d_{bh}	= diameter of bolt holes, in.
$d_{b(max)}$	= maximum bore of welding-neck flange, in.
d_f	= diameter of flat, in.
d_g	= pitch diameter of groove, in.
d_h	= hole size, in.
d_H	= diameter of hub, in.
d_{Hl}	= large diameter of hub, in.
d_{Hs}	= small diameter of hub, in.
d_N	= neck diameter of welding-neck line-pipe flange, in.
d_o	= OD of flange, in.
d_{og}	= groove OD, in.
d_r	= OD of ring, in.
d_{rf}	= diameter of raised face, in.
d_{rg}	= pitch diameter of ring and groove, in.
D_g	= depth of groove, in.
h_o	= height of outside bevel, in., or basic thickness of flange, in.
h_r	= height of ring, in.
h_t	= total thickness of flange, in.
L_C	= hub length of threaded casing flange, in.
L_H	= length of hub, in.
L_L	= hub length of threaded line-pipe flange, in.
L_N	= hub length of welding-neck line-pipe flange, in.
L_{sb}	= length of stud bolts, in.
L_T	= hub length of tubing flange, in.
r_g	= radius in groove, in.
r_H	= radius of hub or radius at hub, in.
r_r	= radius in octagonal ring, in.

Flange Data

Tables 3.18 through 3.26 show API standard flanges and are reproduced with permission of API. These tables cover working pressures of 2,000 to 20,000 psi. API is

presently standardizing flanges for 30,000-psi working pressure. API has recently standardized a line of clamp-type connectors in sizes 2¹/₁₆ through 21¹/₄ in. in the 5,000 and 10,000-psi working pressure ranges. The design criteria and detailed dimensional data for these clamp-type connectors are given in API Spec. 6A.¹ Details for API ring-joint gaskets for API flanges and clamp-type connectors are shown in Tables 3.27 through 3.29.¹

Flow Control Devices: Safety Shut-In Systems

Since the consequences of uncontrolled well flow are so severe, especially offshore, automatic well shut-in safety systems are important enough that they are sometimes mandated by law.⁶ Safety systems must be failsafe. Failure of the energy source or any component must cause the system to go to the safe mode. Usually safe mode means the wells are shut in at one or more points.

Safety systems sense conditions on the lease or platform and shut in the well or wells when conditions deviate from the preset limits. Shutting in the well averts further danger due to (1) uncontrolled flow from ruptured pressure vessels, (2) fueling any fire that has started or may start, or (3) overfilling vessels with fluid and/or pressure.

The systems consist of fail-safe valves (safety valves), sensors, logic control valving and indicators, and a power source. Some systems may be contained in a single valve or they may be very large multiwell, multivalve, multiparameter, multilogic systems integrated into a production control system with telemetry. Severity of consequences usually dictates how elaborate the safety system should be.

Safety valves may be located in the tubing string [sub-surface safety valve (SSSV)], on the Christmas tree, or downstream of the well in the process train (surface safety valve) (Figs. 3.6 and 3.7). Most safety valves are controlled with externally applied fluid pressure. Release of the control pressure allows the valve to close.

TABLE 3.19—API TYPE 6B FLANGES FOR 3,000-psi* MAXIMUM WORKING PRESSURE (continued)

Ring-Joint Groove and Flange Facing Dimensions**										Hub and Bore Dimensions**									
Nominal Size and Bore of Flange	Pitch Diameter of Type R Ring and Groove		Width of Groove		Depth of Groove		Diameter of Raised Face		Hub Length Threaded Line-Pipe Flange	Hub Length Threaded Casing Flange		Hub Length Tubing Flange		Hub Length Welding Neck Line-Pipe Flange		Neck Diameter Welding Neck Line-Pipe Flange		Maximum Bore of Welding Neck Flange	
	(in.)	[mm]	(in.)	[mm]	(in.)	[mm]	(in.)	[mm]		(in.)	[mm]	(in.)	[mm]	(in.)	[mm]	(in.)	[mm]	(in.)	[mm]
** 1 13/16	46.0	21 1/16	68.26	1 1/32	8.73	1/4	6.35	3 3/8	92	2	51	—	—	2	51	3 1/2	88.9	1.90	48.3
2 1/16	52.4	3 3/4	95.25	1 5/32	11.91	5/16	7.94	4 7/8	124	2 9/16	65	—	—	2 9/16	65	4 1/16	109.5	2.38	60.5
2 9/16	65.1	4 1/4	107.95	1 5/32	11.91	5/16	7.94	5 3/8	137	2 13/16	71	—	—	2 13/16	71	4 7/16	112.7	2.88	73.2
3 1/8	79.4	4 7/8	123.83	1 5/32	11.91	5/16	7.94	6 1/8	156	2 17/16	62	—	—	2 15/16	75	4 5/16	109.5	3.50	88.9
4 1/16	103.2	5 7/8	149.23	1 5/32	11.91	5/16	7.94	7 1/8	181	3 1/16	78	3 1/2	89	3 1/2	89	4 13/16	122.2	4.50	114.3
** 5 1/8	130.2	7 1/8	180.98	1 5/32	11.91	5/16	7.94	8 1/2	216	3 15/16	87	4	102	—	—	5 5/16	134.9	5.56	141.2
7 1/16	179.4	8 5/16	211.14	1 5/32	11.91	5/16	7.94	9 1/2	241	3 11/16	94	4 1/2	114	—	—	5 3/16	147.9	6.63	168.4
9	228.6	10 5/8	269.88	1 5/32	11.91	5/16	7.94	12 1/8	308	4 3/16	110	5	127	—	—	6 1/16	169.9	8.63	219.2
11	279.4	12 3/4	323.85	1 5/32	11.91	5/16	7.94	14 1/4	362	4 9/16	116	5 1/4	133	—	—	7 9/16	192.1	10.75	273.1
13 3/8	346.1	15	381.00	1 5/32	11.91	5/16	7.94	16 1/2	419	4 15/16	125	4 15/16	125	—	—	—	—	—	—
16 3/4	425.5	18 1/2	469.90	2 1/32	16.67	7/16	11.11	20 3/8	524	5 11/16	144	5 11/16	144	—	—	—	—	—	—
** 17 3/4	450.9	21	533.40	2 5/32	19.84	1/2	12.70	23 3/8	594	6 1/2	165	6 1/2	165	—	—	—	—	—	—
20 3/4	527.1	23	584.20	2 3/32	19.84	1/2	12.70	25 1/2	648	6 3/4	171	6 3/4	171	—	—	—	—	—	—

*207 bar.

** See Table 3.18 sketch.

†These sizes inactive; available on special order only.

REQUIREMENTS FOR TABLE 3.19

- 1, 3, 4, and 5. See Table 3.18.
2. Ring-groove radius r_g shall be 1/32 in. [0.79 mm] for groove widths 1 1/32 and 1 5/32 [8.73 and 11.91 mm] and 1/16 in. [1.59 mm] for widths 2 1/32 and 2 5/32 [16.67 and 19.84 mm].
6. Except for bore of welding neck flanges, dimensions for sizes 1 1/16 to 2 9/16 in. [46.0 to 65.1 mm], inclusive, are identical with 5,000-psi [345-bar] flanges in Table 3.20.
7. Maximum through bores of 3 1/8, 4 1/4, and 7 1/8 in. [81.0, 108.0, and 181.0 mm] are permissible for nominal sizes 3 1/8, 4 1/16, and 7 1/16 [79.4, 103.2, and 179.4 mm], respectively.
8. Flanged end connections of some casing and tubing heads may have entry bevel recesses and/or counterbores greater than d_b maximum to receive a packer mechanism. The sizes and shapes of these bevels, recesses, and/or counterbores are proprietary and are not covered by this specification.

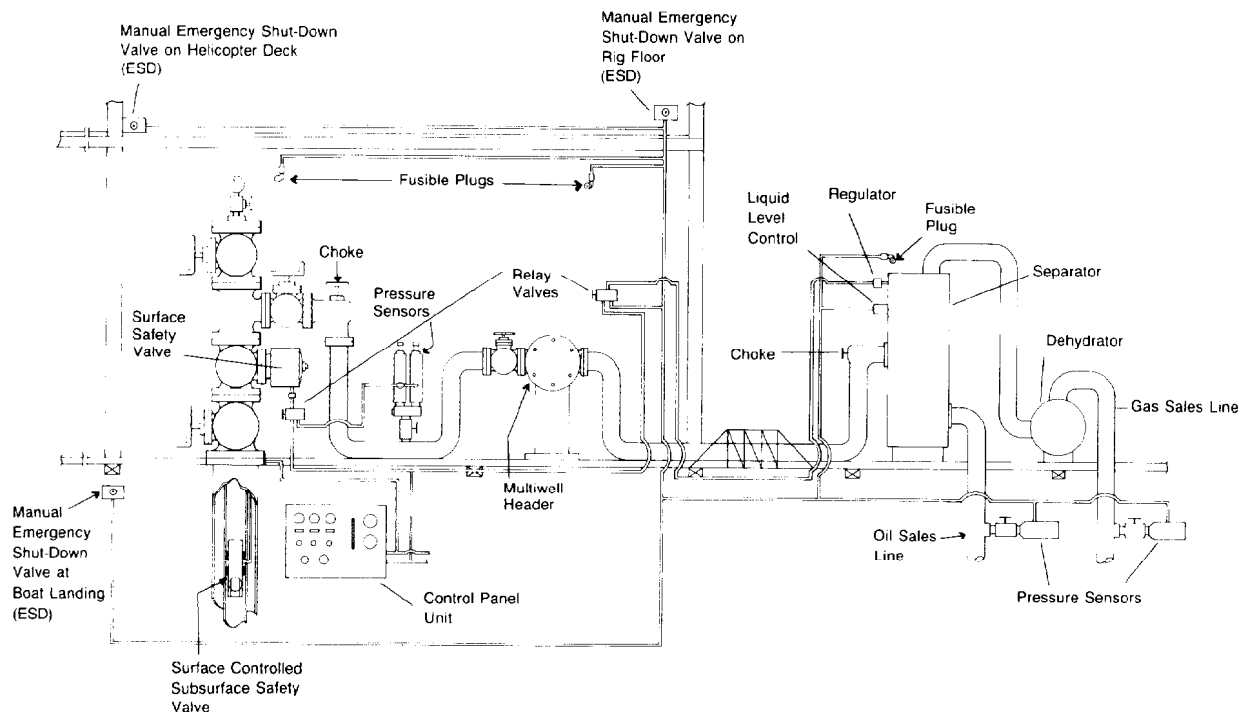
**Fig. 3.6—Production platform safety shut-in system.**

TABLE 3.20—API TYPE 6B FLANGES FOR 5,000-psi * MAXIMUM WORKING PRESSURE

Basic Flange Dimensions* *										Bolting Dimensions* *									
Nominal Size and Bore of Flange		"Old" Nominal Size of Flange	Outside Diameter of Flange		Total Thickness of Flange		Basic Thickness of Flange		Diameter of Hub		Diameter of Bolt Circle		Number of Bolts	Diameter of Bolts	Diameter of Bolt Holes		Length of Stud Bolts		Ring Number R or RX
(in.)	[mm]	(in.)	(in.)	[mm]	(in.)	[mm]	(in.)	[mm]	(in.)	[mm]	(in.)	[mm]		(in.)	(in.)	[mm]	(in.)	[mm]	
† 1 ¹ / ₁₆	46.0	1 ¹ / ₂	7	178	1 ¹ / ₂	38.1	1 ¹ / ₄	31.8	2 ³ / ₄	69.9	4 ⁷ / ₈	123.8	4	1	1.12	29	5 ¹ / ₂	140	20
2 ¹ / ₁₆	52.4	2	8 ¹ / ₂	216	1 ¹ / ₁₆	46.0	1 ¹ / ₂	38.1	4 ¹ / ₈	104.3	6 ¹ / ₂	165.1	8	7/8	1.00	26	6	152	24
2 ⁹ / ₁₆	65.1	2 ¹ / ₂	9 ⁵ / ₈	244	1 ¹ / ₁₆	49.2	1 ⁵ / ₈	41.3	4 ⁷ / ₈	123.8	7 ¹ / ₂	190.5	8	1	1.12	29	6 ¹ / ₂	165	27
3 ¹ / ₈	79.4	3	10 ¹ / ₂	267	2 ³ / ₁₆	55.6	1 ⁷ / ₈	47.6	5 ¹ / ₈	133.4	8	203.2	8	1 ¹ / ₈	1.25	32	7 ¹ / ₄	184	35
4 ¹ / ₈	103.2	4	12 ¹ / ₄	311	2 ⁷ / ₁₆	61.9	2 ¹ / ₈	54.0	6 ³ / ₈	161.9	9 ¹ / ₂	241.3	8	1 ¹ / ₄	1.38	35	8	203	39
† 5 ¹ / ₈	130.2	5	14 ³ / ₄	375	3 ³ / ₁₆	81.0	2 ⁷ / ₈	73.0	7 ³ / ₄	196.9	11 ¹ / ₂	292.1	8	1 ¹ / ₂	1.62	42	10	254	44
7 ¹ / ₁₆	179.4	6	15 ¹ / ₂	394	3 ⁵ / ₈	92.1	3 ¹ / ₄	82.6	9	228.6	12 ¹ / ₂	317.5	12	1 ³ / ₈	1.50	39	10 ³ / ₄	273	46
9	228.6	8	19	483	4 ¹ / ₁₆	103.2	3 ⁵ / ₈	92.1	11 ¹ / ₂	292.1	15 ¹ / ₂	393.7	12	1 ⁵ / ₈	1.75	45	12	305	50
11	279.4	10	23	584	4 ¹ / ₁₆	119.1	4 ¹ / ₄	108.0	14 ¹ / ₂	368.3	19	482.6	12	1 ⁷ / ₈	2.00	51	13 ³ / ₄	349	54
‡ 13 ⁵ / ₈	346.1	* 13 ⁵ / ₈	—	—	—	—	—	—	—	—	—	—	—	—	—	—	—	—	—
‡ 16 ³ / ₄	425.5	16 ³ / ₄	—	—	—	—	—	—	—	—	—	—	—	—	—	—	—	—	—

*345 bar.

**See Table 3.18 sketch.

†These sizes inactive; available on special order only.

‡See Table 3.22 for dimension details on these sizes.

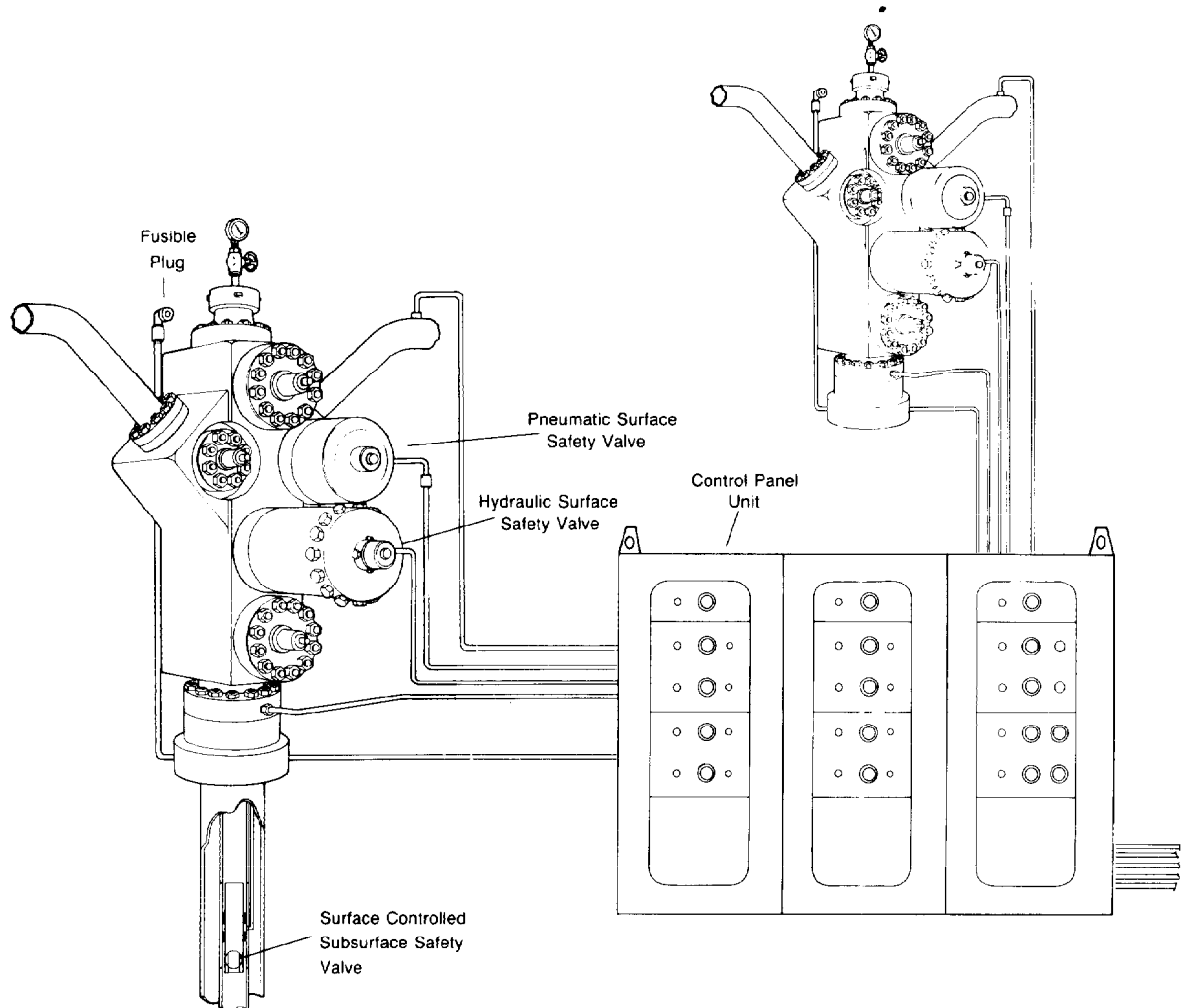


Fig. 3.7—Safety shut-in system with hydraulic valves and pneumatic valves.

TABLE 3.20—API TYPE 6B FLANGES FOR 5,000-psi* MAXIMUM WORKING PRESSURE (continued)

Ring-Joint Groove and Flange Facing Dimensions*										'Hub and Bore Dimensions**												
Nominal Size and Bore of Flange	Pitch Diameter of Type R Ring and Groove		Width of Groove	Depth of Groove	Diameter of Raised Face		Hub Length Threaded Line-Pipe Flange	Hub Length Threaded Casing Flange	Hub Length Tubing Flange	Hub Length Welding Neck Line-Pipe Flange	Neck Diameter Welding Neck Line-Pipe Flange	Maximum Bore of Welding Neck Flange										
	(in.)	[mm]			(in.)	[mm]							(in.)	[mm]	(in.)	[mm]	(in.)	[mm]	(in.)	[mm]		
t 1 13/16	46.0	2 11/16	68.26	1 1/32	8.73	3/4	6.35	3 %	92	2	51	—	—	2	51	3 1/2	88.9	1.90	48.3	1.337	33.96	
2 1/4	52.4	3 3/4	95.25	1 9/16	11.91	5/8	7.94	4 %	124	2 9/16	65	—	—	2 9/16	65	4 5/16	109.5	2.38	60.5	1.689	42.90	
2 9/16	65.1	4 1/4	107.95	1 5/8	11.91	3/4	7.94	5 3/8	137	2 3/16	71	—	—	2 3/16	71	4 7/16	112.7	2.88	73.2	2.125	53.98	
3 %	79.4	5 3/8	136.53	1 5/8	11.91	3/4	7.94	6 3/8	168	3 3/16	81	—	—	3 3/16	81	4 15/16	125.4	3	50	889	2624	66.65
4 1/16	103.2	6 %	161.93	1 5/8	11.91	3/4	7.94	7 3/8	194	3 %	98	3 %	98	5 3/16	131.8	4.50	114.3	3.438	87.33			
† 5 1/8	130.2	7 %	193.68	1 5/8	11.91	3/4	7.94	9	229	4 7/16	113	—	—	6 1/16	163.5	5.56	141.2	4.313	109.55			
7 1/16	179.4	8 5/16	211.14	1 7/8	13.49	3/4	9.53	9 %	248	5 1/16	129	5 1/16	129	—	—	7 1/8	181.0	6.63	168.4	518.9	131.80	
9	228.6	10 %	269.88	2 1/32	16.67	7/8	11.11	12 1/2	318	6 1/16	154	6 1/16	154	—	—	8 3/16	223.8	8.63	219.2	6.813	173.05	
11	279.4	12 %	323.85	2 1/32	16.67	7/8	11.11	14 5/8	371	6 11/16	170	6 11/16	170	—	—	10 7/16	265.1	10.75	273.1	8.500	215.90	
† 13 5/8	346.1	—	—	—	—	—	—	—	—	—	—	—	—	—	—	—	—	—	—	—	—	
† 16 3/4	425.5	—	—	—	—	—	—	—	—	—	—	—	—	—	—	—	—	—	—	—	—	

*345 bar

† See Table 3.18 sketch

‡ These sizes inactive; available on special order only

§ See Table 3.22 for dimension details on these sizes.

REQUIREMENTS FOR TABLE 3.20

1, 3, 4, and 5 See Table 3.18

2 Ring-groove radius, $r_{1/2}$, shall be $1/32$ in [0.79 mm] for groove widths $1 1/32$ and $1 5/16$ in [8.73 and 11.91 mm], $1/16$ in [1.59 mm] for widths $1 7/8$ and $2 1/8$ in [13.49 and 16.67 mm]6 Except for bore of welding-neck flanges, dimensions for sizes $1 13/16$ in to $2 9/16$ in [46.0 to 65.1 mm], inclusive, are identical with 3,000-psi [207-bar] flanges in Table 3.19

7 and 8 See Table 3.19

Surface Safety Valves (SSV's)

An SSV on the Christmas tree is usually the second valve in the flow stream. Hence it is the second master valve, if it is in the vertical run, otherwise it is a wing valve. SSV's can be located downstream of the well in the process train at such places as (1) flowline headers, (2) suction, discharge, and bypass on a compressor (the bypass safety valve safe mode is open instead of closed), or (3) at the entrance to the sales pipeline or the pipeline leaving a platform.

Most SSV's are reverse-acting production-gate valves with piston-type actuators (Fig. 3.8). Valve-body pressure against the lower stem area moves the gate to the up/closed position. Control pressure applied to the piston pushes the gate to the down/open position. Usual-

ly a spring is used to close the valve if valve-body pressure is not present. Valve-body pressure and piston/stem area ratio determine the control pressure required.

Large-ratio pneumatic actuators are used because the larger ratio permits use of lower control pressure. Lower-pressure control-system valves can be simpler and more reliable. Compressed air or produced gas are the usual control fluids. Control pressures are generally 250 psi or less.

Low-ratio hydraulic actuators are used where the SSV is to be controlled by the same system that controls the SSSV, or where limited space is available on the Christmas tree (Fig. 3.9). Control pressures are generally slightly greater than the shut-in pressure of the well.

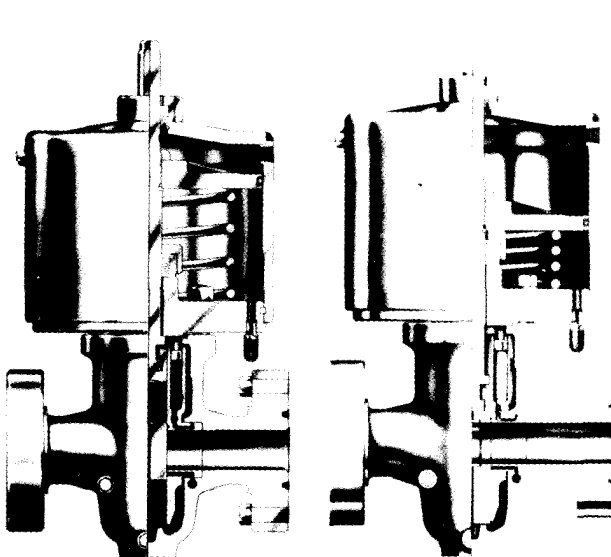


Fig. 3.8—Pneumatic-powered ratio-piston surface safety valve.

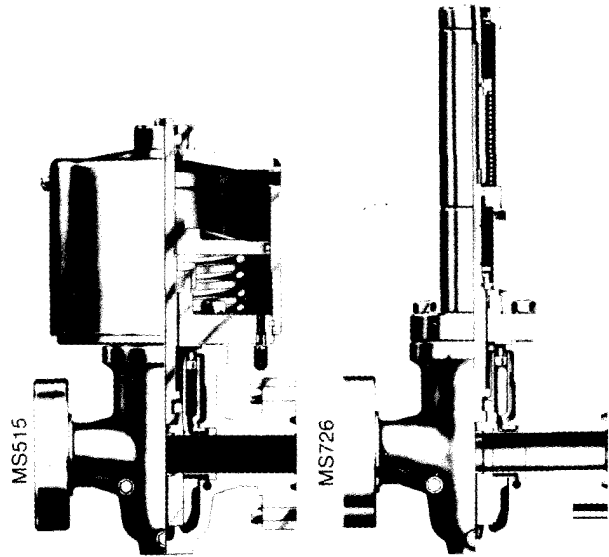


Fig. 3.9—Pneumatic and hydraulic surface safety valves

TABLE 3.21—API TYPE 6BX INTEGRAL FLANGES FOR 5,000- AND 10,000-psi* MAXIMUM WORKING PRESSURE

Basic Flange Dimensions																				
	Nominal Size and Bore		Outside Diameter		Total Thickness		Large Diameter of Hub		Small Diameter of Hub		Length of Hub		Radius at Hub							
	(in.)	[mm]	(in.)	[mm]	(in.)	[mm]	(in.)	[mm]	(in.)	[mm]	(in.)	[mm]	(in.)	[mm]						
2,000 psi (138 bar)	26¾	679.5	41	1041	4 ³¹ / ₃₂	126.2	32 ²⁹ / ₃₂	835.8	29¼	743.0	7 ⁵ / ₁₆	186	5⁄8	15.9						
3,000 psi (207 bar)	26¾	679.5	43¾	1102	6 ¹¹ / ₃₂	161.1	34¼	870.0	30 ⁹ / ₁₆	776.3	7 ⁵ / ₁₆	186	5⁄8	15.9						
5,000 psi (345 bar)	13¾	346.1	26½	673	4 ⁷ / ₁₆	112.7	18 ¹⁵ / ₁₆	481.0	16 ¹¹ / ₁₆	423.9	4½	114	5⁄8	15.9						
	†16¾	425.5	30¾	772	5½	130.2	21 ⁷ / ₈	555.6	20¾	527.1	3	76	¾	19.1						
	18¾	476.3	35½	905	6 ¹⁷ / ₃₂	165.9	26 ⁹ / ₁₆	674.7	23 ⁹ / ₁₆	598.5	6	152	5⁄8	15.9						
	21¼	539.8	39	991	7 ¹ / ₈	181.0	29 ⁷ / ₈	758.8	26¾	679.5	6½	165	1 ¹ / ₁₆	17.5						
10,000 psi (690 bar)	**1 ¹¹ / ₁₆	42.9	7 ³ / ₁₆	183	1 ²¹ / ₃₂	42.1	3 ³ / ₁₆	84.1	2 ¹³ / ₃₂	61.1	1 ²⁷ / ₃₂	47	3⁄8	9.5						
	1 ¹³ / ₁₆	46.0	7¾	187	1 ²¹ / ₃₂	42.1	3½	88.9	2 ⁹ / ₁₆	65.1	1 ²⁹ / ₃₂	48	3⁄8	9.5						
	2 ¹ / ₁₆	52.4	7⁄8	200	1 ⁴⁷ / ₆₄	44.1	3 ¹⁵ / ₁₆	100.0	2 ⁵ / ₁₆	74.6	2 ¹ / ₃₂	52	3⁄8	9.5						
	2 ⁹ / ₁₆	65.1	9½	232	2 ¹ / ₆₄	51.2	4¾	120.7	3¾	92.1	2½	57	3⁄8	9.5						
	3 ¹ / ₁₆	77.8	10½	270	2 ¹⁹ / ₆₄	58.3	5 ¹⁹ / ₃₂	142.1	4 ¹¹ / ₃₂	110.3	2½	64	3⁄8	9.5						
	4 ¹ / ₁₆	103.2	12 ¹ / ₈	316	2 ⁴⁹ / ₆₄	70.2	7 ³ / ₁₆	182.6	5¾	146.1	2¾	73	3⁄8	9.5						
	5½	130.2	14 ¹ / ₁₆	357	3 ¹ / ₈	79.4	8 ¹ / ₁₆	223.8	7 ³ / ₁₆	182.6	3 ³ / ₁₆	81	3⁄8	9.5						
	7 ¹ / ₁₆	179.4	18¾	479	4 ¹ / ₁₆	103.2	11 ⁷ / ₈	301.6	10	254.0	3¾	95	5⁄8	15.9						
	9	228.6	21¾	552	4 ⁷ / ₈	123.8	14¾	374.7	12 ⁷ / ₈	327.0	3 ¹¹ / ₁₆	94	5⁄8	15.9						
	11	279.4	25¾	654	5 ³ / ₁₆	141.3	17¾	450.9	15¾	400.1	4 ¹ / ₁₆	103	5⁄8	15.9						
	13¾	346.1	30¼	768	6½	168.3	21¾	552.5	19½	495.3	4½	114	5⁄8	15.9						
	16¾	425.5	34 ³ / ₁₆	872	6½	168.3	25 ¹³ / ₁₆	655.6	23 ¹¹ / ₁₆	601.7	3	76	¾	19.1						
	18¾	476.3	40 ¹⁵ / ₁₆	1040	8 ²⁵ / ₃₂	223.0	29 ⁵ / ₈	752.5	26 ⁹ / ₁₆	674.7	6	156	5⁄8	15.9						
	21¼	539.8	45	1143	9½	241.3	33¾	847.7	30	762.0	6½	165	1 ¹ / ₁₆	20.6						
Bolting Dimensions																				
	Nominal Size and Bore		Diameter of Bolt Circle		Number of Bolts	Diameter of Bolts		Diameter of Bolt Holes		Length of Stud Bolts		Raised Face Diameter		Groove OD		Width of Groove		Depth of Groove		Ring Number
	(in.)	[mm]	(in.)	[mm]		(in.)	[mm]	(in.)	[mm]	(in.)	[mm]	(in.)	[mm]	(in.)	[mm]	(in.)	[mm]	(in.)	[mm]	
2,000 psi (138 bar)	26¾	679.5	37½	952.5	20	1¾	1.88	48	13¾	349	31 ¹¹ / ₁₆	804.9	30.249	768.32	0.902	22.91	2 ⁷ / ₃₂	21.43	BX-167	
3,000 psi (207 bar)	26¾	679.5	39¾	1000.1	24	2	2.12	54	17	432	32¾	831.9	30.481	774.22	1.018	25.86	2 ⁷ / ₃₂	21.43	BX-168	
5,000 psi (345 bar)	13¾	346.1	23¼	590.6	16	1½	1.75	45	12½	318	18	457.2	16.063	408.00	0.786	19.96	9⁄16	14.29	BX-160	
	†16¾	425.5	26½	676.3	16	1 ⁷ / ₈	2.00	51	14½	368	21 ¹ / ₁₆	535.0	18.832	478.33	0.705	17.91	2 ¹ / ₆₄	8.33	BX-162	
	18¾	476.3	31½	803.3	20	2	2.12	54	17½	445	24 ¹¹ / ₁₆	627.1	22.185	563.50	1.006	25.55	2 ³ / ₃₂	18.26	BX-163	
	21¼	539.8	34 ⁷ / ₈	885.8	24	2	2.12	54	18¾	476	27 ⁷ / ₈	701.7	24.904	632.56	1.071	27.20	¾	19.05	BX-165	
10,000 psi (690 bar)	**1 ¹¹ / ₁₆	42.9	5 ⁹ / ₁₆	141.3	8	¾	0.88	23	5	127	4	101.6	2.893	73.48	0.450	11.43	7⁄32	5.56	BX-150	
	1 ¹³ / ₁₆	46.0	5¾	146.1	8	¾	0.88	23	5	127	4 ¹ / ₈	104.8	3.062	77.77	0.466	11.84	7⁄32	5.56	BX-151	
	2 ¹ / ₁₆	52.4	6¼	158.8	8	¾	0.88	23	5¼	133	4¾	111.1	3.395	86.28	0.498	12.65	1 ¹ / ₆₄	5.95	BX-152	
	2 ⁹ / ₁₆	65.1	7¼	184.2	8	7⁄8	1.00	26	6	152	5 ³ / ₁₆	131.8	4.046	102.77	0.554	14.07	1 ¹ / ₆₄	6.75	BX-153	
	3 ¹ / ₁₆	77.8	8½	215.9	8	1	1.12	29	6¾	171	6	152.4	4.685	119.00	0.606	15.39	1 ¹ / ₆₄	7.54	BX-154	
	4 ¹ / ₁₆	103.2	10 ³ / ₁₆	258.8	8	1 ¹ / ₈	1.25	32	8	203	7 ⁹ / ₃₂	184.9	5.930	150.62	0.698	17.73	2 ¹ / ₆₄	8.33	BX-155	
	5½	130.2	11 ¹³ / ₁₆	300.0	12	1 ¹ / ₈	1.25	32	8¾	222	8 ¹¹ / ₁₆	220.7	6.955	176.66	0.666	16.92	¾	9.53	BX-169	
	7 ¹ / ₁₆	179.4	15¾	403.2	12	1½	1.62	42	11	286	11 ⁷ / ₈	301.6	9.521	241.83	0.921	23.39	7⁄16	11.11	BX-156	
	9	228.6	18¾	476.3	16	1½	1.62	42	13	330	14¾	358.8	11.774	299.06	1.039	26.39	1/2	12.70	BX-157	
	11	279.4	22¼	565.2	16	1¾	1.88	48	15	381	16 ⁷ / ₈	428.6	14.064	357.23	1.149	29.18	9⁄16	14.29	BX-158	
	13¾	346.1	26½	673.1	20	1 ⁷ / ₈	2.00	51	17¼	438	20¾	517.5	17.033	432.64	1.279	32.49	5⁄8	15.88	BX-159	
	16¾	425.5	30 ³ / ₁₆	776.3	24	1 ⁷ / ₈	2.00	51	17½	445	22 ¹¹ / ₁₆	576.3	18.832	478.33	0.705	17.91	2 ¹ / ₆₄	8.33	BX-162	
	18¾	476.3	36 ¹ / ₁₆	925.5	24	2¼	2.38	61	22½	572	27 ⁷ / ₁₆	696.9	22.752	577.90	1.290	32.77	2 ³ / ₃₂	18.26	BX-164	
	21¼	539.8	40¼	1022.4	24	2½	2.62	67	24½	622	30¾	781.1	25.507	647.88	1.373	34.87	¾	19.05	BX-166	

*345 and 690 bar

**This flange is inactive; available on special order only.

†This flange was adopted June 1969 and shall be marked with both the working pressure (5000 WP) and the test pressure (10,000 TP) in addition to other marking requirements.

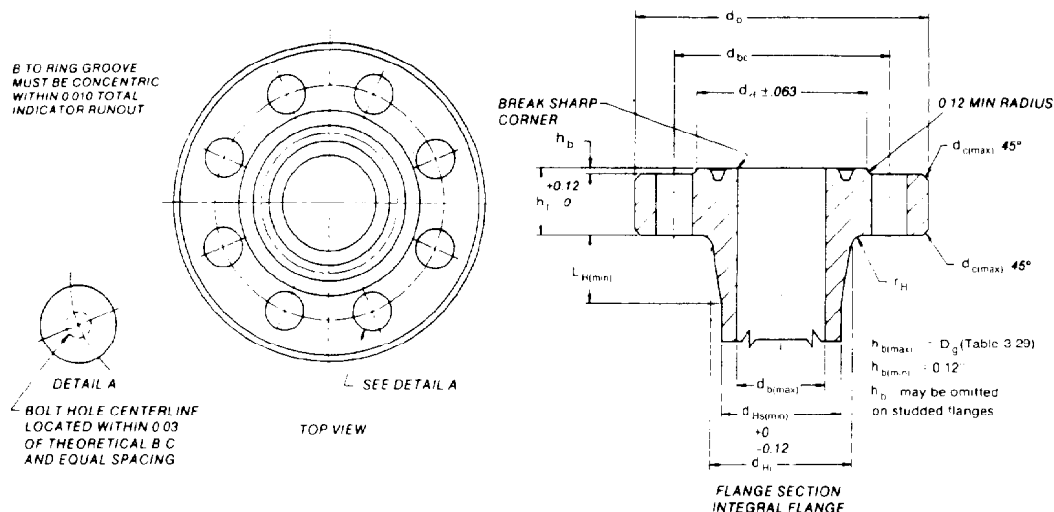
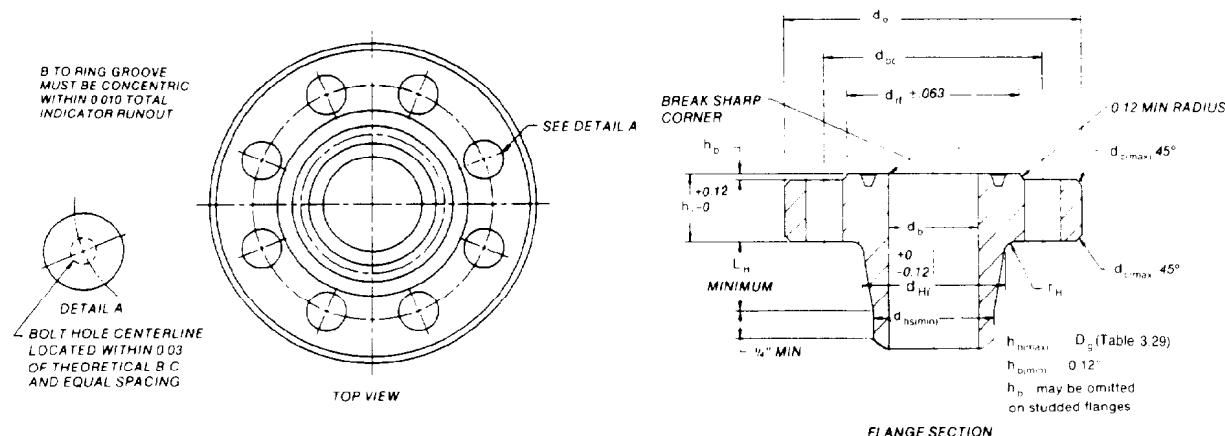


TABLE 3.22—API TYPE 6BX WELDING-NECK FLANGES FOR 10,000- AND 15,000-psi* MAXIMUM WORKING PRESSURE

		Basic Flange Dimensions																	
		Nominal Size and Bore		Outside Diameter		Total Thickness		Large Diameter of Hub		Small Diameter of Hub		Length of Hub		Radius at Hub					
		(in.)	[mm]	(in.)	[mm]	(in.)	[mm]	(in.)	[mm]	(in.)	[mm]	(in.)	[mm]	(in.)	[mm]				
10,000 psi (690 bar)	** 1 1/16	42.9	7 3/16	183	1 21/32	42.1	3 5/16	84.1	2 13/32	61.1	1 27/32	47	3/8	9.5					
	1 13/16	46.0	7 3/8	187	1 21/32	42.1	3 1/2	88.9	2 9/16	65.1	1 29/32	48	3/8	9.5					
	2 1/16	52.4	7 7/8	200	1 47/64	44.1	3 5/16	100.0	2 15/16	74.6	2 1/32	52	3/8	9.5					
	2 5/8	65.1	9 1/8	232	2 1/64	51.2	4 3/4	120.7	3 5/8	92.1	2 1/4	57	3/8	9.5					
	3 1/16	77.8	10 5/8	270	2 15/64	58.3	5 13/32	142.1	4 11/32	110.3	2 1/2	64	3/8	9.5					
	4 1/16	103.2	12 7/16	316	2 49/64	70.2	7 3/16	182.6	5 3/4	146.1	2 7/8	73	3/8	9.5					
	5 1/8	130.2	14 1/16	357	3 3/8	79.4	8 1/16	223.8	7 3/16	182.6	3 3/16	81	3/8	9.5					
	7 1/16	179.4	18 7/8	479	4 1/16	103.2	11 7/8	301.6	10	254.0	3 3/4	95	5/8	15.9					
	9	228.6	21 3/4	552	4 7/8	123.8	14 3/4	374.7	12 7/8	327.0	3 11/16	94	5/8	15.9					
	11	279.4	25 3/4	654	5 5/16	141.3	17 3/4	450.9	15 3/4	400.1	4 1/16	108	5/8	15.9					
	13 5/8	346.1	30 1/4	768	6 5/8	168.3	21 3/4	552.5	19 1/2	495.3	4 1/2	114	5/8	15.9					
	16 3/4	425.5	34 5/16	872	6 5/8	168.3	25 13/16	655.6	23 11/16	601.7	3	76	3/4	19.1					
15,000 psi (1035 bar)	** 1 1/16	42.9	7 5/8	194	1 3/4	44.5	3 11/16	93.7	2 11/16	68.3	1 5/8	48	3/8	9.5					
	1 13/16	46.0	8 3/16	208	1 25/32	45.2	3 27/32	97.6	2 13/16	71.4	1 5/8	48	3/8	9.5					
	2 1/16	52.4	8 3/4	222	2	50.8	4 3/8	111.1	3 1/4	82.6	2 1/8	54	3/8	9.5					
	2 5/8	65.1	10	254	2 1/4	57.2	5 1/16	128.6	3 15/16	100.0	2 1/4	57	3/8	9.5					
	3 1/16	77.8	11 5/16	287	2 17/32	64.3	6 1/16	154.0	4 13/16	122.2	2 1/2	64	3/8	9.5					
	4 1/16	103.2	14 3/16	360	3 3/32	78.6	7 11/16	195.3	6 1/4	158.8	2 7/8	73	3/8	9.5					
	7 1/16	179.4	19 7/8	505	4 11/16	119.1	12 13/16	325.4	10 7/8	276.2	3 5/8	92	5/8	15.9					
Bolting Dimensions														Facing and Groove Dimensions					
	Nominal Size and Bore	Diameter of Bolt Circle		Number of Bolts	Diameter of Bolts	Diameter of Bolt Holes		Length of Stud Bolts		Raised Face Diameter	Groove OD		Width of Groove		Depth of Groove		Ring Number		
		(in.)	[mm]			(in.)	[mm]	(in.)	[mm]		(in.)	[mm]	(in.)	[mm]	(in.)	[mm]			
10,000 psi (690 bar)	** 1 1/16	42.9	5 9/16	141.3	8	3/4	0.88	23	5	127	4	101.6	2.893	73.48	0.450	11.43	7/32	5.56	BX-150
	1 13/16	46.0	5 3/4	146.1	8	3/4	0.88	23	5	127	4 1/8	104.8	3.062	77.77	0.466	11.84	7/32	5.56	BX-151
	2 1/16	52.4	6 1/4	158.8	8	3/4	0.88	23	5 1/4	133	4 3/8	111.1	3.395	86.23	0.498	12.65	15/64	5.95	BX-152
	2 5/8	65.1	7 1/4	184.2	8	7/8	1.00	26	6	152	5 3/16	131.8	4.046	102.77	0.554	14.07	17/64	6.75	BX-153
	3 1/16	77.8	8 1/2	215.9	8	1	1.12	29	6 3/4	171	6	152.4	4.685	119.00	0.606	15.39	19/64	7.54	BX-154
	4 1/16	103.2	10 3/16	258.8	8	1 1/8	1.25	32	8	203	7 9/32	184.9	5.930	150.62	0.698	17.73	21/64	8.33	BX-155
	5 1/8	130.2	11 13/16	300.0	12	1 1/8	1.25	32	8 3/4	222	8 11/16	220.7	6.955	176.66	0.666	16.92	3/8	9.53	BX-169
	7 1/16	179.4	15 7/8	403.2	12	1 1/2	1.62	42	11 1/4	286	11 7/8	301.6	9.521	241.83	0.921	23.39	7/16	11.11	BX-156
	9	228.6	18 3/4	476.3	16	1 1/2	1.62	42	13	330	14 1/8	358.8	11.774	299.06	1.039	26.39	1/2	12.70	BX-157
	11	279.4	22 1/4	565.2	16	1 3/4	1.88	48	15	381	16 7/8	428.6	14.064	357.23	1.149	29.18	9/16	14.29	BX-158
	13 5/8	346.1	26 1/2	673.1	20	1 7/8	2.00	51	17 1/4	438	20 3/8	517.5	17.033	432.64	1.279	32.49	5/8	15.88	BX-159
	16 3/4	425.5	30 5/16	776.3	24	1 7/8	2.00	51	17 1/2	445	22 11/16	576.3	18.832	478.33	0.705	17.91	21/64	8.33	BX-162
15,000 psi (1035 bar)	** 1 1/16	42.9	6	152.4	8	3/4	0.88	23	5 1/4	133	3 13/16	96.8	2.893	73.48	0.450	11.43	7/32	5.56	BX-150
	1 13/16	46.0	6 5/16	160.3	8	7/8	1.00	26	5 1/2	140	4 3/16	106.4	3.062	77.77	0.466	11.84	7/32	5.56	BX-151
	2 1/16	52.4	6 7/8	174.6	8	7/8	1.00	26	6	152	4 1/2	114.3	3.395	86.23	0.498	12.65	15/64	5.95	BX-152
	2 5/8	65.1	7 7/8	200.0	8	1	1.12	29	6 3/4	171	5 1/4	133.4	4.046	102.77	0.554	14.07	17/64	6.75	BX-153
	3 1/16	77.8	8 1/16	230.2	8	1 1/8	1.25	32	7 1/2	191	6 1/16	154.0	4.685	119.00	0.606	15.39	19/64	7.54	BX-154
	4 1/16	103.2	11 7/16	290.5	8	1 3/8	1.50	39	9 1/4	235	7 5/8	193.7	5.930	150.62	0.698	17.73	21/64	8.33	BX-155
	7 1/16	179.4	16 7/8	428.6	16	1 1/2	1.62	42	12 3/4	324	12	304.8	9.521	241.83	0.921	23.39	7/16	11.11	BX-156

*690 and 1035 bar.

**This flange is inactive; available on special order only.



- Due to the difficulty of field welding API Types 2 and 3 material, from which these flanges are made, a transition piece may be shop welded to the basic flange and the weld properly heat treated. This transition piece shall be made from the same or similar material as the pipe to which it is to be welded by the customer. Transition piece ID and OD at the field welding end, and its material, shall be specified on the purchase order.
- The length of the transition piece shall be great enough that the heat from field welding will not affect the metallurgical properties of the shop weld.
- The API monogram shall be applied to the welding-neck flange (solid outline). The API monogram does not apply to the shop weld or the transition piece.
- Dimension h_p may be omitted on studded connections.

TABLE 3.23—API TYPE 6BX INTEGRAL FLANGES FOR 15,000- AND 20,000-psi* MAXIMUM WORKING PRESSURE

Basic Flange Dimensions **																			
	Nominal Size and Bore		Outside Diameter		Total Thickness		Large Diameter of Hub		Small Diameter of Hub		Length of Hub		Radius at Hub						
	(in.)	[mm]	(in.)	[mm]	(in.)	[mm]	(in.)	[mm]	(in.)	[mm]	(in.)	[mm]	(in.)	[mm]					
15,000 psi (1035 bar)	†1 ¹¹ / ₁₆	42.9	7 ⁵ / ₈	194	1 ³ / ₄	44.5	3 ¹¹ / ₁₆	93.7	2 ¹¹ / ₁₆	68.3	1 ⁷ / ₈	48	3 ⁵ / ₈	9.5					
	1 ¹³ / ₁₆	46.0	8 ³ / ₁₆	208	1 ²⁹ / ₃₂	45.2	3 ²⁷ / ₃₂	97.6	2 ¹³ / ₁₆	71.4	1 ⁷ / ₈	48	3 ⁵ / ₈	9.5					
	2 ¹ / ₁₆	52.4	8 ³ / ₄	222	2	50.8	4 ³ / ₈	111.1	3 ¹ / ₄	82.6	2 ¹ / ₂	54	3 ⁵ / ₈	9.5					
	2 ³ / ₁₆	55.1	10	254	2 ¹ / ₄	57.2	5 ¹ / ₁₆	128.6	3 ¹ / ₁₆	100.0	2 ¹ / ₄	57	3 ⁵ / ₈	9.5					
	3 ¹ / ₁₆	77.8	11 ⁵ / ₁₆	287	2 ¹⁷ / ₃₂	64.3	6 ¹ / ₁₆	154.0	4 ¹ / ₁₆	122.2	2 ¹ / ₂	64	3 ⁵ / ₈	9.5					
	4 ¹ / ₁₆	103.2	14 ³ / ₁₆	360	3 ³ / ₃₂	78.6	7 ¹ / ₁₆	195.3	6 ¹ / ₁₆	158.8	2 ³ / ₈	73	3 ⁵ / ₈	9.5					
	7 ¹ / ₁₆	179.4	19 ⁷ / ₁₆	505	4 ¹ / ₁₆	119.1	12 ¹ / ₁₆	325.4	10 ⁷ / ₁₆	276.2	3 ³ / ₈	92	5 ⁵ / ₈	15.9					
	9	228.6	25 ¹ / ₂	648	5 ³ / ₄	146.1	17	431.8	13 ³ / ₄	349.3	4 ⁷ / ₈	124	5 ⁵ / ₈	15.9					
	11	279.4	32	813	7 ³ / ₈	187.3	23	584.2	16 ¹ / ₁₆	427.0	9 ⁹ / ₃₂	236	5 ⁵ / ₈	15.9					
20,000 psi (1380 bar)	1 ¹³ / ₁₆	46.0	10 ¹ / ₈	257	2 ¹ / ₂	63.5	5 ¹ / ₄	133.4	4 ⁵ / ₁₆	109.5	1 ¹⁵ / ₁₆	49	3 ⁵ / ₈	9.5					
	2 ¹ / ₁₆	52.4	11 ¹ / ₁₆	287	2 ¹ / ₁₆	71.4	6 ¹ / ₁₆	154.0	5	127.0	2 ¹ / ₁₆	52	3 ⁵ / ₈	9.5					
	2 ³ / ₁₆	55.1	12 ¹ / ₁₆	325	3 ¹ / ₈	79.4	6 ¹ / ₁₆	173.0	5 ¹ / ₁₆	144.5	2 ⁵ / ₁₆	59	3 ⁵ / ₈	9.5					
	3 ¹ / ₁₆	77.8	14 ¹ / ₁₆	357	3 ³ / ₈	85.7	7 ¹ / ₁₆	192.1	6 ⁵ / ₁₆	160.3	2 ¹ / ₂	64	3 ⁵ / ₈	9.5					
	4 ¹ / ₁₆	103.2	17 ¹ / ₁₆	446	4 ³ / ₁₆	106.4	9 ¹ / ₁₆	242.9	8 ¹ / ₈	206.4	2 ³ / ₈	73	3 ⁵ / ₈	9.5					
	7 ¹ / ₁₆	179.4	25 ¹ / ₁₆	656	6 ¹ / ₂	165.1	15 ¹ / ₁₆	385.8	13 ¹ / ₁₆	338.1	3 ¹ / ₁₆	97	5 ⁵ / ₈	15.9					
Bolting Dimensions **																			
	Nominal Size and Bore		Diameter of Bolt Circle		Number of Bolts	Diameter of Bolts	Diameter of Bolt Holes		Length of Stud Bolts		Raised Face Diameter		Groove OD		Width of Groove		Depth of Groove		Ring Number
	(in.)	[mm]	(in.)	[mm]			(in.)	[mm]	(in.)	[mm]	(in.)	[mm]	(in.)	[mm]	(in.)	[mm]	(in.)	[mm]	
15,000 psi (1035 bar)	†1 ¹¹ / ₁₆	42.9	6	152.4	8	3 ⁴ / ₈	0.88	23	5 ¹ / ₄	133	3 ¹ / ₁₆	96.8	2.893	73.48	0.450	11.43	7 ¹ / ₃₂	5.56	BX-150
	1 ¹³ / ₁₆	46.0	6 ⁵ / ₁₆	160.3	8	7 ⁸ / ₁₆	1.00	26	5 ¹ / ₂	140	4 ³ / ₁₆	106.4	3.062	77.77	0.466	11.84	7 ¹ / ₃₂	5.56	BX-151
	2 ¹ / ₁₆	52.4	6 ³ / ₈	174.6	8	7 ⁸ / ₁₆	1.00	26	6	152	4 ¹ / ₂	114.3	3.395	86.23	0.498	12.65	1 ⁹ / ₆₄	5.95	BX-152
	2 ³ / ₁₆	55.1	7 ⁷ / ₈	200.0	8	1	1.12	29	6 ³ / ₄	171	5 ¹ / ₄	133.4	4.046	102.77	0.554	14.07	1 ⁷ / ₆₄	6.75	BX-153
	3 ¹ / ₁₆	77.8	9 ¹ / ₁₆	230.2	8	1 ¹ / ₈	1.25	32	7 ¹ / ₂	191	6 ¹ / ₁₆	154.0	4.685	119.00	0.606	15.39	1 ⁹ / ₆₄	7.54	BX-154
	4 ¹ / ₁₆	103.2	11 ¹ / ₁₆	290.5	8	1 ³ / ₈	1.50	39	9 ¹ / ₄	235	7 ⁵ / ₁₆	193.7	5.930	150.62	0.698	17.73	2 ¹ / ₆₄	8.33	BX-155
	7 ¹ / ₁₆	179.4	16 ⁷ / ₈	428.6	16	1 ¹ / ₂	1.62	42	12 ³ / ₄	324	12	304.8	9.521	241.83	0.921	23.39	7 ¹ / ₁₆	11.11	BX-156
	9	228.6	21 ³ / ₄	552.5	16	1 ⁷ / ₈	2.00	51	15 ³ / ₄	400	15	381.0	11.774	299.06	1.039	26.39	1 ¹ / ₂	12.70	BX-157
	11	279.4	28	711.2	20	2	2.12	54	19 ¹ / ₄	489	17 ⁷ / ₈	454.0	14.064	357.23	1.149	29.18	9 ¹ / ₁₆	14.29	BX-158
20,000 psi (1380 bar)	1 ¹³ / ₁₆	46.0	8	203.2	8	1	1.12	29	7 ¹ / ₂	191	4 ⁵ / ₁₆	117.5	3.062	77.77	0.466	11.84	7 ¹ / ₃₂	5.56	BX-151
	2 ¹ / ₁₆	52.4	9 ¹ / ₁₆	230.2	8	1 ¹ / ₈	1.25	32	8 ¹ / ₄	210	5 ³ / ₁₆	131.8	3.395	86.23	0.498	12.65	1 ⁹ / ₆₄	5.95	BX-152
	2 ³ / ₁₆	55.1	10 ⁵ / ₁₆	261.9	8	1 ¹ / ₄	1.38	35	9 ¹ / ₄	235	5 ¹ / ₁₆	150.8	4.046	102.77	0.554	14.07	1 ⁷ / ₆₄	6.75	BX-153
	3 ¹ / ₁₆	77.8	11 ¹ / ₁₆	287.3	8	1 ³ / ₈	1.50	39	10	254	6 ³ / ₄	171.5	4.685	119.00	0.606	15.39	1 ⁹ / ₆₄	7.54	BX-154
	4 ¹ / ₁₆	103.2	14 ¹ / ₁₆	357.2	8	1 ³ / ₄	1.88	48	12 ¹ / ₄	311	8 ⁵ / ₁₆	219.1	5.930	150.62	0.698	17.73	2 ¹ / ₆₄	8.33	BX-155
	7 ¹ / ₁₆	179.4	21 ¹ / ₁₆	554.0	16	2	2.12	54	17 ¹ / ₂	445	13 ³ / ₈	352.4	9.521	241.83	0.921	23.39	7 ¹ / ₁₆	11.11	BX-156

*1035 and 1380 bar.

**See Table 3.21 sketch.

†This flange is inactive; available on special order only.

TABLE 3.24—API TYPE 6BX WELDING-NECK FLANGES FOR 20,000-psi* MAXIMUM WORKING PRESSURE

Basic Flange Dimensions**														
Nominal Size and Bore		Outside Diameter		Total Thickness		Large Diameter of Hub		Small Diameter of Hub		Length of Hub		Radius at Hub		
(in.)	[mm]	(in.)	[mm]	(in.)	[mm]	(in.)	[mm]	(in.)	[mm]	(in.)	[mm]	(in.)	[mm]	
1 ¹³ / ₁₆	46.0	10 ¹ / ₈	257	2 ¹ / ₂	63.5	5 ¹ / ₄	133.4	4 ⁵ / ₁₆	109.5	1 ¹⁵ / ₁₆	49	3 ⁵ / ₈	9.5	
2 ¹ / ₁₆	52.4	11 ¹ / ₁₆	287	2 ¹³ / ₁₆	71.4	6 ¹ / ₁₆	154.0	5	127.0	2 ¹ / ₁₆	52	3 ⁵ / ₈	9.5	
2 ³ / ₁₆	55.1	12 ¹ / ₁₆	325	3 ¹ / ₈	79.4	6 ¹³ / ₁₆	173.0	5 ¹¹ / ₁₆	144.5	2 ⁵ / ₁₆	59	3 ⁵ / ₈	9.5	
3 ¹ / ₁₆	77.8	14 ¹ / ₁₆	357	3 ³ / ₈	85.7	7 ¹ / ₁₆	192.1	6 ⁵ / ₁₆	160.3	2 ¹ / ₂	64	3 ⁵ / ₈	9.5	
4 ¹ / ₁₆	103.2	17 ¹ / ₁₆	446	4 ³ / ₁₆	106.4	9 ¹ / ₁₆	242.9	8 ¹ / ₈	206.4	2 ³ / ₈	73	3 ⁵ / ₈	9.5	
7 ¹ / ₁₆	179.4	25 ¹ / ₁₆	656	6 ¹ / ₂	165.1	15 ¹ / ₁₆	385.8	13 ⁵ / ₁₆	338.1	3 ¹ / ₁₆	97	5 ⁵ / ₈	15.9	

Bolting Dimensions**										Facing and Groove Dimensions**								
Nominal Size and Bore		Diameter of Bolt Circle		Number of Bolts	Diameter of Bolts	Diameter of Bolt Holes		Length of Stud Bolts		Raised Face Diameter		Groove OD		Width of Groove		Depth of Groove		Ring Number
(in.)	[mm]	(in.)	[mm]			(in.)	[mm]	(in.)	[mm]	(in.)	[mm]	(in.)	[mm]	(in.)	[mm]	(in.)	[mm]	
1 ¹³ / ₁₆	46.0	8	203.2	8	1	1.12	29	7 ¹ / ₂	191	4 ⁵ / ₁₆	117.5	3.062	77.77	0.466	11.84	7 ¹ / ₃₂	5.56	BX-151
2 ¹ / ₁₆	52.4	9 ¹ / ₁₆	230.2	8	1 ¹ / ₈	1.25	32	8 ¹ / ₄	210	5 ³ / ₁₆	131.8	3.395	86.23	0.498	12.65	1 ⁵ / ₆₄	5.95	BX-152
2 ³ / ₁₆	55.1	10 ⁵ / ₁₆	261.9	8	1 ¹ / ₄	1.38	35	9 ¹ / ₄	235	5 ¹ / ₁₆	150.8	4.046	102.77	0.554	14.07	1 ⁷ / ₆₄	6.75	BX-153
3 ¹ / ₁₆	77.8	11 ¹ / ₁₆	287.3	8	1 ³ / ₈	1.50	39	10	254	6 ³ / ₄	171.5	4.685	119.00	0.606	15.39	1 ⁹ / ₆₄	7.54	BX-154
4 ¹ / ₁₆	103.2	14 ¹ / ₁₆	357.2	8	1 ³ / ₄	1.88	48	12 ¹ / ₄	311	8 ⁵ / ₁₆	219.1	5.930	150.62	0.698	17.73	2 ¹ / ₆₄	8.33	BX-155
7 ¹ / ₁₆	179.4	21 ¹ / ₁₆	554.0	16	2	2.12	54	17 ¹ / ₂	445	13 ³ / ₈	352.4	9.521	241.83	0.921	23.39	7 ¹ / ₁₆	11.11	BX-156

*1380 bar.

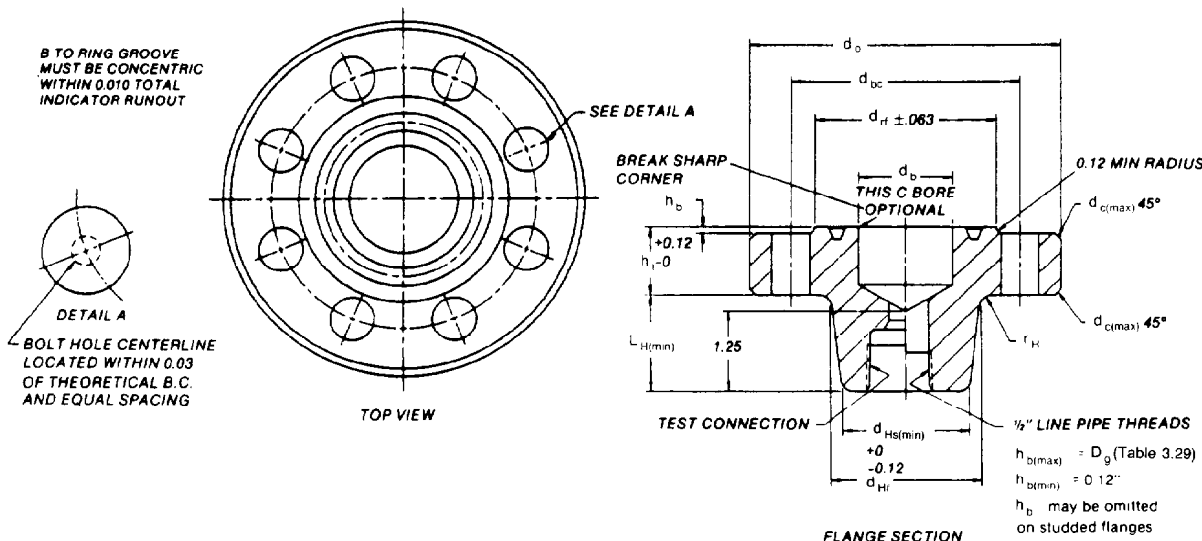
**See Table 3.22 sketch.

TABLE 3.25—API TYPE 6BX BLIND AND TEST FLANGES FOR 10,000- AND 15,000-psi* MAXIMUM WORKING PRESSURE

Basic Flange Dimensions																			
	Nominal Size and Bore		Outside Diameter		Total Thickness		Large Diameter** of Hub		Small Diameter** of Hub		Length** of Hub		Radius at Hub						
	(in.)	[mm]	(in.)	[mm]	(in.)	[mm]	(in.)	[mm]	(in.)	[mm]	(in.)	[mm]	(in.)	[mm]					
10,000 psi (690 bar)	1 ¹¹ / ₁₆	42.9	7 ³ / ₁₆	183	1 ²¹ / ₃₂	42.1	3 ⁹ / ₁₆	84.1	2 ¹³ / ₃₂	61.1	1 ²⁷ / ₃₂	47	3/8	9.5					
	1 ¹³ / ₁₆	46.0	7 ³ / ₁₆	187	1 ²¹ / ₃₂	42.1	3 ¹ / ₂	88.9	2 ⁹ / ₁₆	65.1	1 ²⁹ / ₃₂	48	3/8	9.5					
	2 ¹ / ₁₆	52.4	7 ⁷ / ₁₆	200	1 ⁴⁷ / ₆₄	44.1	3 ¹⁵ / ₁₆	100.0	2 ⁵ / ₁₆	74.6	2 ¹ / ₃₂	52	3/8	9.5					
	2 ⁹ / ₁₆	65.1	9 ⁹ / ₁₆	232	2 ¹ / ₆₄	51.2	4 ³ / ₄	120.7	3 ³ / ₈	92.1	2 ¹ / ₄	57	3/8	9.5					
	3 ¹ / ₁₆	77.8	10 ⁹ / ₁₆	270	2 ¹⁹ / ₆₄	58.3	5 ¹⁹ / ₃₂	142.1	4 ¹¹ / ₃₂	110.3	2 ¹ / ₂	64	3/8	9.5					
	4 ¹ / ₁₆	103.2	12 ⁷ / ₁₆	316	2 ⁴⁹ / ₆₄	70.2	7 ⁷ / ₁₆	182.6	5 ³ / ₄	146.1	2 ⁷ / ₈	73	3/8	9.5					
15,000 psi (1035 bar)	1 ¹¹ / ₁₆	42.9	7 ⁵ / ₁₆	194	1 ³ / ₄	44.5	3 ¹¹ / ₁₆	93.7	2 ¹¹ / ₁₆	68.3	1 ⁷ / ₈	48	3/8	9.5					
	1 ¹³ / ₁₆	46.0	8 ³ / ₁₆	208	1 ²⁵ / ₃₂	45.2	3 ²⁷ / ₃₂	97.6	2 ¹³ / ₁₆	71.4	1 ⁷ / ₈	48	3/8	9.5					
	2 ¹ / ₁₆	52.4	8 ³ / ₄	222	2	50.8	4 ³ / ₈	111.1	3 ¹ / ₄	82.6	2 ¹ / ₈	54	3/8	9.5					
	2 ⁹ / ₁₆	65.1	10	254	2 ¹ / ₄	57.2	5 ¹ / ₁₆	128.6	3 ³ / ₁₆	100.0	2 ¹ / ₄	57	3/8	9.5					
	3 ¹ / ₁₆	77.8	11 ⁵ / ₁₆	287	2 ¹⁷ / ₃₂	64.3	6 ¹ / ₁₆	154.0	4 ¹³ / ₁₆	120.7	2 ¹ / ₂	64	3/8	9.5					
	4 ¹ / ₁₆	103.2	14 ³ / ₁₆	360	3 ³ / ₃₂	78.6	7 ¹¹ / ₁₆	195.3	6 ¹ / ₄	158.8	2 ⁷ / ₈	73	3/8	9.5					
Bolting Dimensions										Facing and Groove Dimensions									
	Nominal Size and Bore		Diameter of Bolt Circle		Number of Bolts	Diameter of Bolt Holes		Length of Stud Bolts		Raised Face Diameter		Groove OD		Width of Groove		Depth of Groove		Ring Number	
	(in.)	[mm]	(in.)	[mm]		(in.)	[mm]	(in.)	[mm]	(in.)	[mm]	(in.)	[mm]	(in.)	[mm]	(in.)	[mm]		
10,000 psi (690 bar)	1 ¹¹ / ₁₆	42.9	5 ⁹ / ₁₆	141.3	8	3/4	0.88	23	5	127	4	101.6	2.893	73.48	0.450	11.43	7/32	5.56	BX-150
	1 ¹³ / ₁₆	46.0	5 ³ / ₄	146.1	8	3/4	0.88	23	5	127	4 ¹ / ₈	104.8	3.062	77.77	0.466	11.84	7/32	5.56	BX-151
	2 ¹ / ₁₆	52.4	6 ¹ / ₄	158.8	8	3/4	0.88	23	5 ¹ / ₄	133	4 ¹ / ₈	111.1	3.395	86.23	0.498	12.65	1/64	5.95	BX-152
	2 ⁹ / ₁₆	65.1	7 ¹ / ₄	184.2	8	7/8	1.00	26	6	152	5 ³ / ₁₆	131.8	4.046	102.77	0.554	14.07	1/64	6.75	BX-153
	3 ¹ / ₁₆	77.8	8 ¹ / ₂	215.9	8	1	1.12	29	6 ³ / ₄	171	6	152.4	4.685	119.00	0.606	15.39	1/64	7.54	BX-154
	4 ¹ / ₁₆	103.2	10 ³ / ₁₆	258.8	8	1 ¹ / ₈	1.25	32	8	203	7 ⁷ / ₃₂	184.9	5.930	150.62	0.698	17.73	2/64	8.33	BX-155
15,000 psi (1035 bar)	1 ¹¹ / ₁₆	42.9	6	152.4	8	3/4	0.88	23	5 ¹ / ₄	133	3 ¹³ / ₁₆	96.8	2.893	73.48	0.450	11.43	7/32	5.56	BX-150
	1 ¹³ / ₁₆	46.0	6 ⁹ / ₁₆	160.3	8	7/8	1.00	26	5 ¹ / ₂	140	4 ³ / ₁₆	106.4	3.062	77.77	0.466	11.84	7/32	5.56	BX-151
	2 ¹ / ₁₆	52.4	6 ⁷ / ₈	174.6	8	7/8	1.00	26	6	152	4 ¹ / ₂	114.3	3.395	86.23	0.498	12.65	1/64	5.95	BX-152
	2 ⁹ / ₁₆	65.1	7 ⁷ / ₈	200.0	8	1	1.12	29	6 ³ / ₄	171	5 ¹ / ₄	133.4	4.046	102.77	0.554	14.07	1/64	6.75	BX-153
	3 ¹ / ₁₆	77.8	9 ¹ / ₁₆	230.2	8	1 ¹ / ₈	1.25	32	7 ¹ / ₂	191	6 ¹ / ₁₆	154.0	4.685	119.00	0.606	15.39	1/64	7.54	BX-154
	4 ¹ / ₁₆	103.2	11 ¹ / ₁₆	290.5	8	1 ³ / ₈	1.50	39	9 ¹ / ₄	235	7 ³ / ₈	193.7	5.930	150.62	0.698	17.73	2/64	8.33	BX-155

* 690 and 1035 bar.

** Type BX blind flanges must be provided with a prolong on the rear face, described by the large and small diameters and length of the hub.



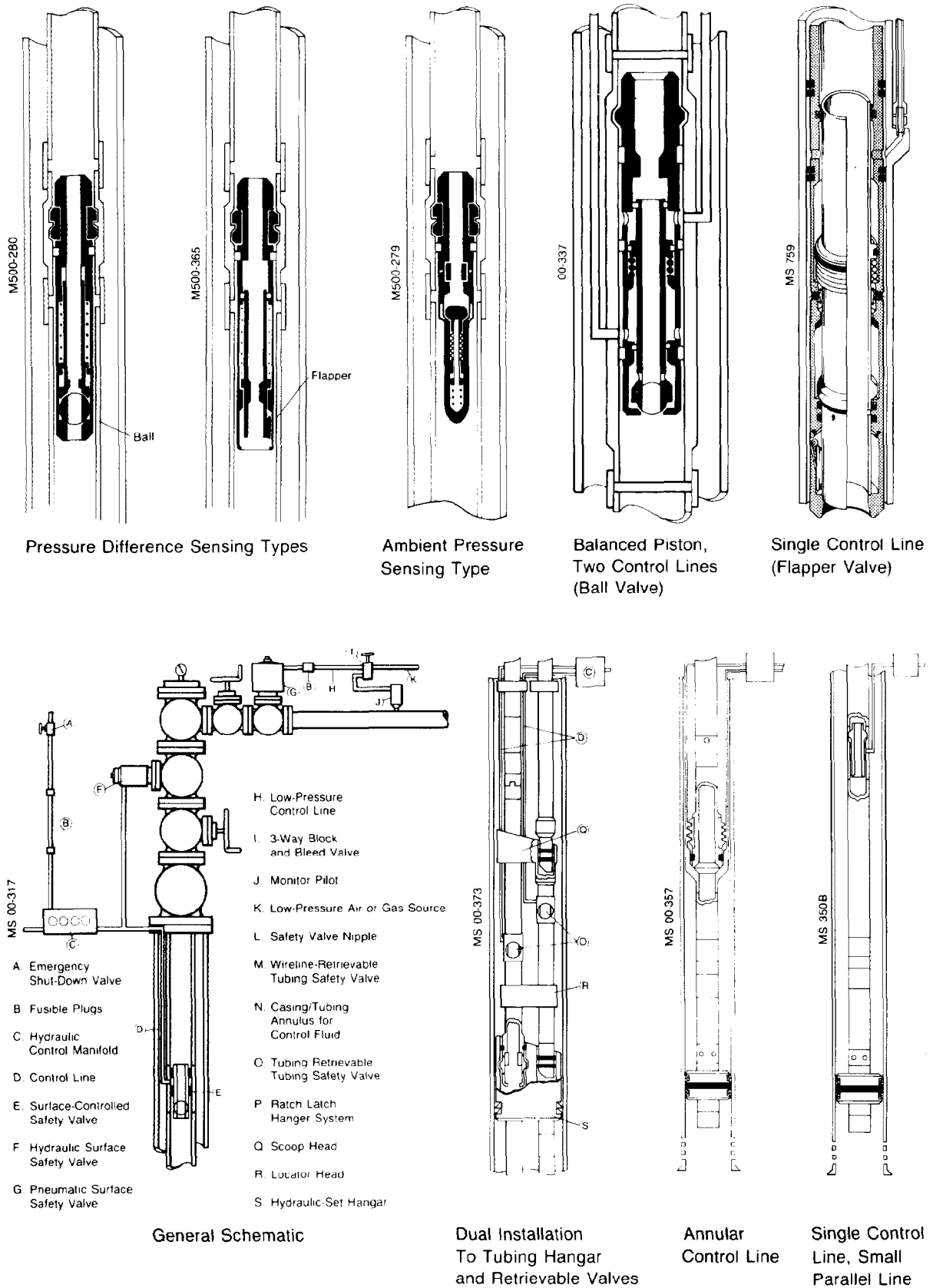


Fig. 3.10—Types of subsurface safety valves and completions.

TABLE 3.26—API TYPE 6BX BLIND AND TEST FLANGES FOR 20,000-psi* MAXIMUM WORKING PRESSURE

Basic Flange Dimensions**													
Nominal Size and Bore		Outside Diameter		Total Thickness		Large Diameter† of Hub		Small Diameter† of Hub		Length† of Hub		Radius at Hub	
(in.)	[mm]	(in.)	[mm]	(in.)	[mm]	(in.)	[mm]	(in.)	[mm]	(in.)	[mm]	(in.)	[mm]
1 ³ / ₁₆	46.0	10 ⁷ / ₈	257	2 ¹ / ₂	63.5	5 ¹ / ₄	133.4	4 ⁵ / ₁₆	109.5	1 ¹⁵ / ₁₆	49	³ / ₈	9.5
2 ¹ / ₁₆	52.4	11 ⁵ / ₁₆	287	2 ¹³ / ₁₆	71.4	6 ¹ / ₁₆	154.0	5	127.0	2 ¹ / ₁₆	52	³ / ₈	9.5
2 ⁹ / ₁₆	65.1	12 ¹³ / ₁₆	325	3 ¹ / ₈	79.4	6 ¹³ / ₁₆	173.0	5 ¹¹ / ₁₆	144.5	2 ⁹ / ₁₆	59	³ / ₈	9.5
3 ¹ / ₁₆	77.8	14 ¹ / ₁₆	357	3 ³ / ₈	85.7	7 ⁹ / ₁₆	192.1	6 ⁵ / ₁₆	160.3	2 ¹ / ₂	64	³ / ₈	9.5
4 ¹ / ₁₆	103.2	17 ⁹ / ₁₆	446	4 ³ / ₁₆	106.4	9 ¹ / ₁₆	242.9	8 ⁷ / ₁₆	206.4	2 ⁷ / ₈	73	³ / ₈	9.5

Bolting Dimensions**								Basic Flange Dimensions**										
Nominal Size and Bore		Diameter of Bolt Circle		Number of Bolts	Diameter of Bolts	Diameter of Bolt Holes		Length of Stud Bolts		Raised Face Diameter		Groove OD		Width of Groove		Depth of Groove		Ring Number
(in.)	[mm]	(in.)	[mm]			(in.)	[mm]	(in.)	[mm]	(in.)	[mm]	(in.)	[mm]	(in.)	[mm]	(in.)	[mm]	
1 ³ / ₁₆	46.0	8	203.2	8	1	1.12	29	7 ¹ / ₂	191	4 ⁵ / ₁₆	117.5	3.062	77.77	0.466	11.84	⁷ / ₃₂	5.56	BX-151
2 ¹ / ₁₆	52.4	9 ¹ / ₁₆	230.2	8	1 ¹ / ₈	1.25	32	8 ¹ / ₄	210	5 ³ / ₁₆	131.8	3.395	86.23	0.498	12.65	¹⁹ / ₆₄	5.95	BX-152
2 ⁹ / ₁₆	65.1	10 ⁹ / ₁₆	261.9	8	1 ¹ / ₄	1.38	35	9 ¹ / ₄	235	5 ¹⁹ / ₁₆	150.8	4.046	102.77	0.554	14.07	¹⁷ / ₆₄	6.75	BX-153
3 ¹ / ₁₆	77.8	11 ⁵ / ₁₆	287.3	8	1 ³ / ₈	1.50	39	10	254	6 ³ / ₄	171.5	4.685	119.00	0.606	15.39	¹⁹ / ₆₄	7.54	BX-154
4 ¹ / ₁₆	103.2	14 ¹ / ₁₆	357.2	8	1 ³ / ₄	1.88	48	12 ¹ / ₄	311	8 ⁵ / ₁₆	219.1	5.930	150.62	0.698	17.73	²¹ / ₆₄	8.33	BX-155

* 1380 bar.

** See Table 3.25 sketch.

† Type 6BX blind flanges must be provided with a prolong on the rear face, described by the large and small diameters and length of the hub.

SSV's usually have a stem protruding from a threaded boss on the actuator cylinder head for several reasons.

1. Stem position gives a visual position indication.
2. A position-indicator switch can be attached to provide telemetry feedback information.
3. A manually operated mechanical or hydraulic jack can be attached to open a closed safety valve where the control pressure source is downstream of the safety valve or where system failure makes control pressure unavailable.

4. A lockout cap, or heat-sensitive lockout cap, can be attached to hold the valve open while wireline work is being done through the valve or when the control system is out of service for maintenance.⁷

Special Designs. Special designs of SSV's may have various modifications.

1. Extra-strong springs for cutting wireline, should an emergency occur while wireline work is in progress. Special hardened gates are used for these valves.
2. Extra extension of the cylinder from the valve for nesting of two pneumatic actuators on a dual valve or tree where there is not enough space for the large cylinders to be mounted side-by-side.
3. Cover sleeve or cylinder over the bonnet bolting to protect the bolts from fire.
4. Integral pressure sensors to monitor flowline pressure and control the safety valve.

Selection. When ordering an SSV the entire system should be considered. The size of the valve is determined by the flowstream in which it is installed. If it is to be in the vertical run of the tree, it should be the same size as the lower master valve. Pressure, temperature, and service ratings should be the same as for the lower master valve. Actuator specifications should consider control system pressure that is available. Valve body pressure, ratio, and control pressure are related by

$$p_{cl} = \frac{2(p_{vb})}{F_{ac}}, \dots \dots \dots (3)$$

where

p_{cl} = control pressure,

p_{vb} = valve body pressure, and

F_{ac} = actuator ratio.

Materials for the actuator parts that contact flowline fluids should be consistent with the service and valve body.

Subsurface Safety Valves (SSSV's)

SSSV's are used because they are located in the wellbore and isolated from possible damage by fire, collision, or sabotage. They are designed to be operational when needed most—in catastrophies, but they are more difficult to maintain. SSSV's are recommended for use with an SSV. Control circuit logic should be designed to close the SSV for routine alarm conditions. Under catastrophic conditions both valves close. SSSV's are either subsurface- or surface-controlled (Fig. 3.10).

Selection. Various features should be considered in selecting an SSSV (Fig. 3.11).

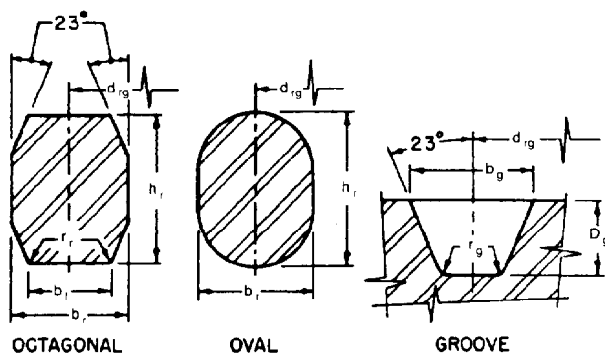
Tubing-Retrievable vs. Wireline-Retrievable. Tubing-retrievable valves have larger bores through the valve for less flowing pressure drop and allow wireline work through the valve without having to retrieve the valve. Since the tubing-retrievable valve is a part of the tubing string and requires a workover rig for retrieval, maintenance is more expensive. Wireline-retrievable valves are located in special landing nipples that are part of the tubing string, and they can be retrieved for maintenance with lower cost wireline methods (Fig. 3.12).

Valve Type. The most common type of valves are rotating ball and flapper.

Single-Control Line vs. Balance Line. Permafrost, paraffin problems or other equipment such as centrifugal or hydraulic pumps may require setting the safety valve deep, and thus require a balance line (two-control-line system).

TABLE 3.27—API TYPE R RING-JOINT GASKET

Ring Number	Pitch Diameter of Ring and Groove		Width of Ring		Height of Ring				Width of Flat of Octagonal Ring	
					Oval		Octagonal			
	(in.)	[mm]	(in.)	[mm]	(in.)	[mm]	(in.)	[mm]	(in.)	[mm]
R20	2 ¹¹ / ₁₆	68.26	⁵ / ₁₆	7.94	⁹ / ₁₆	14.29	¹ / ₂	12.70	0.206	5.23
R23	3 ¹ / ₄	82.55	⁷ / ₁₆	11.11	¹¹ / ₁₆	17.46	⁵ / ₈	15.88	0.305	7.75
R24	3 ³ / ₄	95.25	⁷ / ₁₆	11.11	¹¹ / ₁₆	17.46	⁵ / ₈	15.88	0.305	7.75
R26	4	101.60	⁷ / ₁₆	11.11	¹¹ / ₁₆	17.46	⁵ / ₈	15.88	0.305	7.75
R27	4 ¹ / ₄	107.95	⁷ / ₁₆	11.11	¹¹ / ₁₆	17.46	⁵ / ₈	15.88	0.305	7.75
R31	4 ⁷ / ₈	123.83	⁷ / ₁₆	11.11	¹¹ / ₁₆	17.46	⁵ / ₈	15.88	0.305	7.75
R35	5 ³ / ₈	136.53	⁷ / ₁₆	11.11	¹¹ / ₁₆	17.46	⁵ / ₈	15.88	0.305	7.75
R37	5 ⁷ / ₈	149.23	⁷ / ₁₆	11.11	¹¹ / ₁₆	17.46	⁵ / ₈	15.88	0.305	7.75
R39	6 ³ / ₈	161.93	⁷ / ₁₆	11.11	¹¹ / ₁₆	17.46	⁵ / ₈	15.88	0.305	7.75
R41	7 ¹ / ₈	180.98	⁷ / ₁₆	11.11	¹¹ / ₁₆	17.46	⁵ / ₈	15.88	0.305	7.75
R44	7 ⁵ / ₈	193.68	⁷ / ₁₆	11.11	¹¹ / ₁₆	17.46	⁵ / ₈	15.88	0.305	7.75
R45	8 ⁵ / ₁₆	211.14	⁷ / ₁₆	11.11	¹¹ / ₁₆	17.46	⁵ / ₈	15.88	0.305	7.75
R46	8 ⁵ / ₁₆	211.14	¹ / ₂	12.70	³ / ₄	19.05	¹¹ / ₁₆	17.46	0.341	8.66
R47	9	228.60	³ / ₄	19.05	1	25.40	¹⁵ / ₁₆	23.81	0.485	12.32
R49	10 ⁵ / ₈	269.88	⁷ / ₁₆	11.11	¹¹ / ₁₆	17.46	⁵ / ₈	15.88	0.305	7.75
R50	10 ⁵ / ₈	269.88	⁵ / ₈	15.88	⁷ / ₈	22.23	¹³ / ₁₆	20.64	0.413	10.49
R53	12 ³ / ₄	323.85	⁷ / ₁₆	11.11	¹¹ / ₁₆	17.46	⁵ / ₈	15.88	0.305	7.75
R54	12 ³ / ₄	323.85	⁵ / ₈	15.88	⁷ / ₈	22.23	¹³ / ₁₆	20.64	0.413	10.49
R57	15	381.00	⁷ / ₁₆	11.11	¹¹ / ₁₆	17.46	⁵ / ₈	15.88	0.305	7.75
R63	16 ¹ / ₂	419.10	1	25.40	¹⁵ / ₁₆	33.34	1 ¹ / ₄	31.75	0.681	17.30
R65	18 ¹ / ₂	469.90	⁷ / ₁₆	11.11	¹¹ / ₁₆	17.46	⁵ / ₈	15.88	0.305	7.75
R66	18 ¹ / ₂	469.90	⁵ / ₈	15.88	⁷ / ₈	22.23	¹³ / ₁₆	20.64	0.413	10.49
R69	21	533.40	⁷ / ₁₆	11.11	¹¹ / ₁₆	17.46	⁵ / ₈	15.88	0.305	7.75
R70	21	533.40	³ / ₄	19.05	1	25.40	¹⁵ / ₁₆	23.81	0.485	12.32
R73	23	584.20	¹ / ₂	12.70	³ / ₄	19.05	¹¹ / ₁₆	17.46	0.341	8.66
R74	23	584.20	³ / ₄	19.05	1	25.40	¹⁵ / ₁₆	23.81	0.485	12.32
R82	2 ¹ / ₄	57.15	⁷ / ₁₆	11.11	—	—	⁵ / ₈	15.88	0.305	7.75
R84	2 ¹ / ₂	63.50	⁷ / ₁₆	11.11	—	—	⁵ / ₈	15.88	0.305	7.75
R85	3 ¹ / ₈	79.38	¹ / ₂	12.70	—	—	¹¹ / ₁₆	17.46	0.341	8.66
R86	3 ⁹ / ₁₆	90.49	⁵ / ₈	15.88	—	—	¹³ / ₁₆	20.64	0.413	10.49
R87	3 ¹⁵ / ₁₆	100.01	⁵ / ₈	15.88	—	—	¹³ / ₁₆	20.64	0.413	10.49
R88	4 ⁷ / ₈	123.83	³ / ₄	19.05	—	—	¹⁵ / ₁₆	23.81	0.485	12.32
R89	4 ¹ / ₂	114.30	³ / ₄	19.05	—	—	¹⁵ / ₁₆	23.81	0.485	12.32
R90	6 ¹ / ₈	155.58	⁷ / ₈	22.23	—	—	¹¹ / ₁₆	26.99	0.583	14.81
R91	10 ¹ / ₄	260.35	1 ¹ / ₄	31.75	—	—	1 ¹ / ₂	38.10	0.879	22.33
R99	9 ¹ / ₄	234.95	⁷ / ₁₆	11.11	—	—	⁵ / ₈	15.88	0.305	7.75



TOLERANCES

		(in.)	[mm]
b_r	(width of ring, see Note 3)	± 0.008	± 0.20
h_r	(height of ring)	± 1/64	± 0.39
b_f	(width of flat on octagonal ring)	± 0.008	± 0.20
D_g	(depth of groove)	+ 1/64, - 0	+ 0.39, - 0
b_g	(width of groove)	± 0.008	± 0.20
d_{rg}	(average pitch diameter of ring)	± 0.007	± 0.17
d_{rg}	(average pitch diameter of groove)	± 0.005	± 0.12
r_r	(radius in rings)	± 1/64	± 0.39
r_g	(radius in groove)	—	max
23°	(angle)	—	± 1/2°

- The 23° surfaces on both grooves and octagonal rings shall have a surface finish no rougher than 63 RMS.
- A small bead on the center of either oval or octagonal rings, located so that it will not enter the groove, is permissible.
- A plus tolerance of $3/64$ in. [1.19 mm] on ring height is permitted, provided the variation in height of any given ring does not exceed $1/64$ in. [0.39 mm] throughout the entire circumference.

TABLE 3.27—API TYPE R RING-JOINT GASKET (continued)

Ring Number	Radius in Octagonal Ring		Depth of Groove		Width of Groove		Radius in Groove		Approximate Distance Between Made Up Flanges	
	(in.)	[mm]	(in.)	[mm]	(in.)	[mm]	(in.)	[mm]	(in.)	[mm]
R20	1/16	1.59	1/4	6.35	11/32	8.73	1/32	0.79	5/32	4.0
R23	1/16	1.59	5/16	7.94	15/32	11.91	1/32	0.79	3/16	4.8
R24	1/16	1.59	5/16	7.94	15/32	11.91	1/32	0.79	3/16	4.8
R26	1/16	1.59	5/16	7.94	15/32	11.91	1/32	0.79	3/16	4.8
R27	1/16	1.59	5/16	7.94	15/32	11.91	1/32	0.79	3/16	4.8
R31	1/16	1.59	5/16	7.94	15/32	11.91	1/32	0.79	3/16	4.8
R35	1/16	1.59	5/16	7.94	15/32	11.91	1/32	0.79	3/16	4.8
R37	1/16	1.59	5/16	7.94	15/32	11.91	1/32	0.79	3/16	4.8
R39	1/16	1.59	5/16	7.94	15/32	11.91	1/32	0.79	3/16	4.8
R41	1/16	1.59	5/16	7.94	15/32	11.91	1/32	0.79	3/16	4.8
R44	1/16	1.59	5/16	7.94	15/32	11.91	1/32	0.79	3/16	4.8
R45	1/16	1.59	5/16	7.94	15/32	11.91	1/32	0.79	3/16	4.8
R46	1/16	1.59	3/8	9.53	17/32	13.49	1/16	1.59	1/8	3.2
R47	1/16	1.59	1/2	12.70	25/32	19.84	1/16	1.59	5/32	4.0
R49	1/16	1.59	5/16	7.94	15/32	11.91	1/32	0.79	3/16	4.8
R50	1/16	1.59	7/16	11.11	21/32	16.67	1/16	1.59	5/32	4.0
R53	1/16	1.59	5/16	7.94	15/32	11.91	1/32	0.79	3/16	4.8
R54	1/16	1.59	7/16	11.11	21/32	16.67	1/16	1.59	5/32	4.0
R57	1/16	1.59	5/16	7.94	15/32	11.91	1/32	0.79	3/16	4.8
R63	3/32	2.38	5/8	15.88	11/16	26.99	3/32	2.38	7/32	5.6
R65	1/16	1.59	5/16	7.94	15/32	11.91	1/32	0.79	3/16	4.8
R66	1/16	1.59	7/16	11.11	21/32	16.67	1/16	1.59	5/32	4.0
R69	1/16	1.59	5/16	7.94	15/32	11.91	1/32	0.79	3/16	4.8
R70	1/16	1.59	1/2	12.70	25/32	19.84	1/16	1.59	3/16	4.8
R73	1/16	1.59	3/8	9.53	17/32	13.49	1/16	1.59	1/8	3.2
R74	1/16	1.59	1/2	12.70	25/32	19.84	1/16	1.59	3/16	4.8
R82	1/16	1.59	5/16	7.94	15/32	11.91	1/32	0.79	3/16	4.8
R84	1/16	1.59	5/16	7.94	15/32	11.91	1/32	0.79	3/16	4.8
R85	1/16	1.59	3/8	9.53	17/32	13.49	1/16	1.59	1/8	3.2
R86	1/16	1.59	7/16	11.11	21/32	16.67	1/16	1.59	5/32	4.0
R87	1/16	1.59	7/16	11.11	21/32	16.67	1/16	1.59	5/32	4.0
R88	1/16	1.59	1/2	12.70	25/32	19.84	1/16	1.59	3/16	4.8
R89	1/16	1.59	1/2	12.70	25/32	19.84	1/16	1.59	3/16	4.8
R90	1/16	1.59	9/16	14.29	29/32	23.02	1/16	1.59	3/16	4.8
R91	3/32	2.38	11/16	17.46	15/16	33.34	3/32	2.38	5/16	7.9
R99	1/16	1.59	5/16	7.94	15/32	11.91	1/32	0.79	3/16	4.8

Equalizing Valves. For equalizing pressure differentials across the closed valve rather than equalizing from an external source.

Soft Seat vs. Lapped-Metal Seat. Soft seats can have less minor leakage, but are more susceptible to damage, especially at higher pressure.

Subsurface-Controlled Subsurface Safety Valves (SSCSV's). These valves sense flow conditions in the well at the valve and close when the flow exceeds a preset limit. They are usually located in a landing nipple in the tubing. There are two main types.

Excess flow valves sense the pressure drop across an orifice in the valve and close the valve when the increased flow rate causes the pressure drop to increase past a preset limit.

Low-pressure valves have a stored reference pressure in the valve. The valve closes when tubing pressure at the valve draws down below the reference pressure due to restriction of the formation.

Both types of valves depend on a flow rate substantially in excess of normal maximum. The presumption is that essentially a complete structural failure (opening) of

the Christmas tree exists ahead of the choke. Caution must be exercised that the well is capable of closing the valve at the setting used.

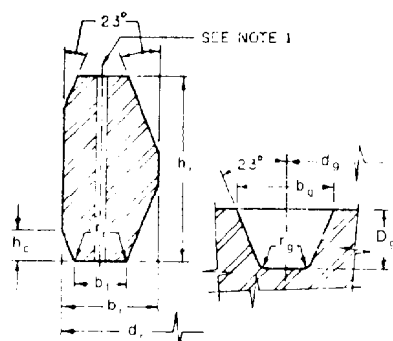
Surface-Controlled Subsurface Safety Valves (SCSSV's). These valves are normally controlled by pressure maintained by a unit at the surface in response to a pilot system. Pressure is transmitted to the safety valve through a small-diameter parallel-tube control line in the annulus or through the tubing/casing annulus in conjunction with a packer below the safety valve (Fig. 3.10). Volumetric compression and expansion of the control fluid usually makes the small tubing system preferable to the annulus conduit even though it is not as rugged. However, the small tubing will convey higher control pressures more economically.

When the control pressure is released, a spring and well pressure on the control piston will close the valve. Since well pressure is not always assumed dependable, some valves have a second line, or balance line, to the surface, which is filled with control liquid. This provides a hydrostatic pressure to the back side of the piston for closure. Single control-line valves have depth failsafe

TABLE 3.28—API TYPE RX PRESSURE ENERGIZED RING-JOINT GASKETS

Ring Number	Outside Diameter of Ring		Total Width of Ring		Width of Flat		Height of Outside Bevel		Height of Ring	
	(in.)	[mm]	(in.)	[mm]	(in.)	[mm]	(in.)	[mm]	(in.)	[mm]
RX20	3	76.20	1 ¹ / ₃₂	8.73	0.182	4.62	0.125	3.18	3/4	19.05
RX23	3 ⁴³ / ₆₄	93.27	1 ⁵ / ₃₂	11.91	0.254	6.45	0.167	4.24	1	25.40
RX24	4 ¹¹ / ₆₄	105.97	1 ⁵ / ₃₂	11.91	0.254	6.45	0.167	4.24	1	25.40
RX25	4 ⁵ / ₁₆	109.54	1 ¹ / ₃₂	8.73	0.182	4.62	0.125	3.18	3/4	19.05
RX26	4 ¹³ / ₃₂	111.92	1 ⁵ / ₃₂	11.91	0.254	6.45	0.167	4.24	1	25.40
RX27	4 ²¹ / ₃₂	118.27	1 ⁵ / ₃₂	11.91	0.254	6.45	0.167	4.24	1	25.40
RX31	5 ¹⁹ / ₆₄	134.54	1 ⁵ / ₃₂	11.91	0.254	6.45	0.167	4.24	1	25.40
RX35	5 ⁵ / ₁₆	147.24	1 ⁵ / ₃₂	11.91	0.254	6.45	0.167	4.24	1	25.40
RX37	6 ¹⁹ / ₆₄	159.94	1 ⁵ / ₃₂	11.91	0.254	6.45	0.167	4.24	1	25.40
RX39	6 ⁵ / ₁₆	172.64	1 ⁵ / ₃₂	11.91	0.254	6.45	0.167	4.24	1	25.40
RX41	7 ³ / ₁₆	191.69	1 ⁵ / ₃₂	11.91	0.254	6.45	0.167	4.24	1	25.40
RX44	8 ³ / ₁₆	204.39	1 ⁵ / ₃₂	11.91	0.254	6.45	0.167	4.24	1	25.40
RX45	8 ⁴ / ₁₆	221.85	1 ⁵ / ₃₂	11.91	0.254	6.45	0.167	4.24	1	25.40
RX46	8 ³ / ₄	222.25	1 ⁷ / ₃₂	13.49	0.263	6.68	0.188	4.78	1 ¹ / ₈	28.58
RX47	9 ²¹ / ₃₂	245.27	2 ⁵ / ₃₂	19.84	0.407	10.34	0.271	6.88	1 ⁵ / ₈	41.28
RX49	11 ¹³ / ₆₄	280.59	1 ⁵ / ₃₂	11.91	0.254	6.45	0.167	4.24	1	25.40
RX50	11 ⁵ / ₃₂	283.37	2 ¹ / ₃₂	16.67	0.335	8.51	0.208	5.28	1 ¹ / ₄	31.75
RX53	13 ¹ / ₁₆	334.57	1 ⁵ / ₃₂	11.91	0.254	6.45	0.167	4.24	1	25.40
RX54	13 ⁹ / ₃₂	337.34	2 ¹ / ₃₂	16.67	0.335	8.51	0.208	5.28	1 ¹ / ₄	31.75
RX57	15 ²⁷ / ₆₄	391.72	1 ⁵ / ₃₂	11.91	0.254	6.45	0.167	4.24	1	25.40
RX63	17 ²⁵ / ₆₄	441.72	1 ¹ / ₁₆	26.99	0.582	14.78	0.333	8.46	2	50.80
RX65	18 ⁵⁹ / ₆₄	480.62	1 ⁵ / ₃₂	11.91	0.254	6.45	0.167	4.24	1	25.40
RX66	19 ¹ / ₃₂	483.39	2 ¹ / ₃₂	16.67	0.335	8.51	0.208	5.28	1 ¹ / ₄	31.75
RX69	21 ²⁷ / ₆₄	544.12	1 ⁵ / ₃₂	11.91	0.254	6.45	0.167	4.24	1	25.40
RX70	21 ³¹ / ₃₂	550.07	2 ⁵ / ₃₂	19.84	0.407	10.34	0.271	6.88	1 ⁵ / ₈	41.28
RX73	23 ¹⁹ / ₃₂	596.11	1 ⁷ / ₃₂	13.49	0.263	6.68	0.208	5.28	1 ¹ / ₄	31.75
RX74	23 ²¹ / ₃₂	600.87	2 ⁵ / ₃₂	19.84	0.407	10.34	0.271	6.88	1 ⁵ / ₈	41.28
RX82	2 ⁴³ / ₆₄	67.87	1 ⁵ / ₃₂	11.91	0.254	6.45	0.167	4.24	1	25.40
RX84	2 ⁵⁹ / ₆₄	74.22	1 ⁵ / ₃₂	11.91	0.254	6.45	0.167	4.24	1	25.40
RX85	3 ³⁵ / ₆₄	90.09	1 ⁷ / ₃₂	13.49	0.263	6.68	0.167	4.24	1	25.40
RX86	4 ⁵ / ₁₆	103.58	1 ⁹ / ₃₂	15.08	0.335	8.51	0.188	4.78	1 ¹ / ₈	28.58
RX87	4 ²⁹ / ₆₄	113.11	1 ⁹ / ₃₂	15.08	0.335	8.51	0.188	4.78	1 ¹ / ₈	28.58
RX88	5 ³¹ / ₆₄	139.30	1 ¹ / ₁₆	17.46	0.407	10.34	0.208	5.28	1 ¹ / ₄	31.75
RX89	5 ⁷ / ₁₆	129.78	2 ³ / ₃₂	18.26	0.407	10.34	0.208	5.28	1 ¹ / ₄	31.75
RX90	6 ⁷ / ₁₆	174.63	2 ⁵ / ₃₂	19.84	0.479	12.17	0.292	7.42	1 ³ / ₄	44.45
RX91	11 ¹⁹ / ₆₄	286.94	1 ³ / ₁₆	30.16	0.780	19.81	0.297	7.54	1 ²⁵ / ₃₂	45.24
RX99	9 ⁴³ / ₆₄	245.67	1 ⁵ / ₃₂	11.91	0.254	6.45	0.167	4.24	1	25.40
RX201	2.026	51.46	0.226	5.74	0.126	3.20	0.057	1.45*	0.445	11.30
RX205	2 ²⁹ / ₆₄	62.31	7/32	5.56	0.120	3.05	0.072	1.83*	0.437	11.10
RX210	3 ²⁷ / ₃₂	97.63	3/8	9.53	0.213	5.41	0.125	3.18*	0.750	19.05
RX215	5 ³⁵ / ₆₄	140.89	1 ⁵ / ₃₂	11.91	0.210	5.33	0.167	4.24*	1.000	25.40

*Tolerance on these dimensions is +0. -0.015 in. [+0. -0.38 mm].



TOLERANCES

	(in.)	[mm]
b_1 (width of ring)	+0.008, -0.000	+0.20, -0.00
b_2 (width of flat)	+0.006, -0.000	+0.15, -0.00
h_1 (height of chamfer)	+0.000, -0.03	+0.00, -0.79
D_g (depth of groove)	+0.02, -0	+0.39, -0
b_g (width of groove)	±0.008	±0.20
h_g (height of ring)	+0.008, -0.000	+0.20, -0.00
d_g (OD of ring)	+0.020, -0.000	+0.50, -0.00
d_g (average pitch diameter of groove)	±0.005	±0.12
r_g (radius in ring)	±0.02	±0.39
r_g (radius in groove)	max	max
23° (angle)	±1/2°	±1/2°

*A plus tolerance of 0.008 in. for b_1 and h_1 is permitted, provided the variation in width or height of any ring does not exceed 0.004 in. throughout its entire circumference.NOTE 1: The pressure passage hole illustrated in the RX ring cross section is required in rings RX-82 through RX-91 only. Centerline of hole shall be located at midpoint of dimension b_1 . Hole diameter shall be 1/16 in. [1.6 mm] for rings RX-82 through RX-85, 3/32 in. [2.4 mm] for rings RX-86 and RX-87, and 1/8 in. [3.2 mm] for rings RX-88 through RX-91.

NOTE 2: The 23° surfaces on both rings and grooves shall have a surface finish no rougher than 63 RMS.

TABLE 3.28—API TYPE RX PRESSURE ENERGIZED RING-JOINT GASKETS (continued)

Ring Number	Radius in Ring		Depth of Groove		Width of Groove		Pitch Diameter of Groove		Radius in Groove		Approximate Distance Between Made Up Flanges	
	(in.)	[mm]	(in.)	[mm]	(in.)	[mm]	(in.)	[mm]	(in.)	[mm]	(in.)	[mm]
RX20	1/16	1.59	1/4	6.35	1 1/32	8.73	2 1/16	68.26	1/32	0.79	3/8	9.5
RX23	1/16	1.59	5/16	7.94	1 5/32	11.91	3 1/4	82.55	1/32	0.79	1 5/32	11.9
RX24	1/16	1.59	5/16	7.94	1 5/32	11.91	3 3/4	95.25	1/32	0.79	1 5/32	11.9
RX25	1/16	1.59	1/4	6.35	1 1/32	8.73	—	—	1/32	0.79	—	—
RX26	1/16	1.59	5/16	7.94	1 5/32	11.91	4	101.60	1/32	0.79	1 5/32	11.9
RX27	1/16	1.59	5/16	7.94	1 5/32	11.91	4 1/4	107.95	1/32	0.79	1 5/32	11.9
RX31	1/16	1.59	5/16	7.94	1 5/32	11.91	4 7/8	123.83	1/32	0.79	1 5/32	11.9
RX35	1/16	1.59	5/16	7.94	1 5/32	11.91	5 3/8	136.53	1/32	0.79	1 5/32	11.9
RX37	1/16	1.59	5/16	7.94	1 5/32	11.91	5 7/8	149.23	1/32	0.79	1 5/32	11.9
RX39	1/16	1.59	5/16	7.94	1 5/32	11.91	6 3/8	161.93	1/32	0.79	1 5/32	11.9
RX41	1/16	1.59	5/16	7.94	1 5/16	11.91	7 1/8	180.98	1/32	0.79	1 5/32	11.9
RX44	1/16	1.59	5/16	7.94	1 5/16	11.91	7 5/8	193.68	1/32	0.79	1 5/32	11.9
RX45	1/16	1.59	5/16	7.94	1 5/32	11.91	8 5/16	211.14	1/32	0.79	1 5/32	11.9
RX46	1/16	1.59	3/8	9.53	1 7/32	13.49	8 5/16	211.14	1/16	1.59	1 5/32	11.9
RX47	3/32	2.38	1/2	12.70	2 5/32	19.84	9	228.60	1/16	1.59	2 9/32	18.3
RX49	1/16	1.59	5/16	7.94	1 5/32	11.91	10 5/8	269.88	1/32	0.79	1 5/32	11.9
RX50	1/16	1.59	7/16	11.11	2 1/32	16.67	10 5/8	269.88	1/16	1.59	1 5/32	11.9
RX53	1/16	1.59	5/16	7.94	1 5/32	11.91	12 3/4	323.85	1/32	0.79	1 5/32	11.9
RX54	1/16	1.59	7/16	11.11	2 1/32	16.67	12 3/4	323.85	1/16	1.59	1 5/32	11.9
RX57	1/16	1.59	5/16	7.94	1 5/32	11.91	15	381.00	1/32	0.79	1 5/32	11.9
RX63	3/32	2.38	5/8	15.88	1 1/16	26.99	16 1/2	419.10	3/32	2.38	2 7/32	21.4
RX65	1/16	1.59	5/16	7.94	1 5/32	11.91	18 1/2	469.90	1/32	0.79	1 5/32	11.9
RX66	1/16	1.59	7/16	11.11	2 1/32	16.67	18 1/2	469.90	1/16	1.59	1 5/32	11.9
RX69	1/16	1.59	5/16	7.94	1 5/32	11.91	21	533.40	1/32	0.79	1 5/32	11.9
RX70	3/32	2.38	1/2	12.70	2 5/32	19.84	21	533.40	1/16	1.59	2 3/32	18.3
RX73	1/16	1.59	3/8	9.53	1 7/32	13.49	23	584.20	1/16	1.59	1 9/32	15.1
RX74	3/32	2.38	1/2	12.70	2 5/32	19.84	23	584.20	1/16	1.59	2 3/32	18.3
RX82	1/16	1.59	5/16	7.94	1 5/32	11.91	2 1/4	57.15	1/32	0.79	1 5/32	11.9
RX84	1/16	1.59	5/16	7.94	1 5/32	11.91	2 1/2	63.50	1/32	0.79	1 5/32	11.9
RX85	1/16	1.59	3/8	9.53	1 7/32	13.49	3 1/8	79.38	1/16	1.59	3/8	9.5
RX86	1/16	1.59	7/16	11.11	2 1/32	16.67	3 9/16	90.49	1/16	1.59	3/8	9.5
RX87	1/16	1.59	7/16	11.11	2 1/32	16.67	3 1 5/16	100.01	1/16	1.59	3/8	9.5
RX88	1/16	1.59	1/2	12.70	2 5/32	19.84	4 7/8	123.83	1/16	1.59	3/8	9.5
RX89	1/16	1.59	1/2	12.70	2 5/32	19.84	4 1/2	114.30	1/16	1.59	3/8	9.5
RX90	3/32	2.38	9/16	14.29	2 9/32	23.02	6 1/8	155.58	1/16	1.59	2 3/32	18.3
RX91	3/32	2.38	1 1/16	17.46	1 5/16	33.34	10 1/4	260.35	3/32	2.38	3/4	19.1
RX99	1/16	1.59	5/16	7.94	1 5/32	11.91	9 1/4	234.95	1/32	0.79	1 5/32	11.9
RX201	1/64	0.40**	5/32	3.97	7/32	5.56	—	—	1/32	0.79	—	—
RX205	1/64	0.40**	5/32	3.97	7/32	5.56	—	—	1/64	0.40	—	—
RX210	1/32	0.79**	1/4	6.35	3/8	9.53	—	—	1/32	0.79	—	—
RX215	1/16	1.59**	5/16	7.94	1 5/32	11.91	—	—	1/32	0.79	—	—

** Tolerance on these dimensions is + 1/64, - 0 in. [+ 0.39, - 0 mm].

limitations. The limit is determined by the ability of the spring to overcome friction and the force of the hydrostatic pressure against the piston without help from well pressure. A depth limitation of the two-control-line system may be the time for closure due to control liquid expansion and flow restriction in the small-diameter long control line.

Control System

The control system is the interface system between the power source, the sensors, and the safety valves. The design of the control system depends on several factors: (1) type of power source available—compressed air, produced gas, or electricity; (2) pressure and volume requirements of the safety valves; (3) number and types of sensors (pneumatic—two- or three-way valves—or electric); (4) power requirements and limitations of the pilots; (5) number and type of indicators (position status,

pressure status, first-out sensor); (6) telemetry interface; and (7) logic required. (Will any pilot shut all the safety valves or should certain sensors close certain valves or combinations of valves?) We recommend a time delay after SSV's close before the SSSV's close, and that SSSV's open first.

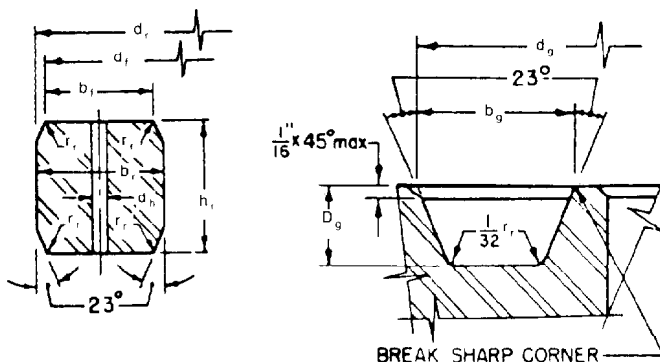
Most systems are pneumatically powered because compressed air or gas is usually available. The power needed by most pilots and safety valves is pneumatic or hydraulic. Power is consumed only when a valve is being opened; most of the time the system is static. Most electrically powered sensors continuously consume power and are sensitive to short-duration power transients. Electro-hydraulic systems are well suited to cold environments.

The air or gas supply should be kept clean and dry. Electrical power should be protected from transient disruptions, especially in the sensor circuitry. Such precautions greatly enhance reliability.

TABLE 3.29—API TYPE BX PRESSURE ENERGIZED RING-JOINT GASKETS

Ring Number	Nominal Size		Outside Diameter of Ring		Height of Ring		Total Width of Ring		Diameter of Flat	
	(in.)	[mm]	(in.)	[mm]	(in.)	[mm]	(in.)	[mm]	(in.)	[mm]
BX-150	1 ¹¹ / ₁₆	42.9	2.842	72.19	0.366	9.30	0.366	9.30	2.790	70.87
BX-151	1 ¹³ / ₁₆	46.0	3.008	76.40	0.379	9.63	0.379	9.63	2.954	75.03
BX-152	2 ¹ / ₁₆	52.4	3.334	84.68	0.403	10.24	0.403	10.24	3.277	83.24
BX-153	2 ⁹ / ₁₆	65.1	3.974	100.94	0.448	11.38	0.448	11.38	3.910	99.31
BX-154	3 ¹ / ₁₆	77.8	4.600	116.84	0.488	12.40	0.488	12.40	4.531	115.09
BX-155	4 ¹ / ₁₆	103.2	5.825	147.96	0.560	14.22	0.560	14.22	5.746	145.95
BX-156	7 ¹ / ₁₆	179.4	9.367	237.92	0.733	18.62	0.733	18.62	9.263	235.28
BX-157	9	228.6	11.593	294.46	0.826	20.98	0.826	20.98	11.476	291.49
BX-158	11	279.4	13.860	352.04	0.911	23.14	0.911	23.14	13.731	348.77
BX-159	13 ⁵ / ₈	346.1	16.800	426.72	1.012	25.70	1.012	25.70	16.657	423.09
BX-160	13 ⁵ / ₈	346.1	15.850	402.59	0.938	23.83	0.541	13.74	15.717	399.21
BX-161	16 ³ / ₄	425.5	19.347	491.41	1.105	28.07	0.638	16.21	19.191	487.45
BX-162	16 ³ / ₄	425.5	18.720	475.49	0.560	14.22	0.560	14.22	18.641	473.48
BX-163	18 ³ / ₄	476.3	21.896	556.16	1.185	30.10	0.684	17.37	21.728	551.89
BX-164	18 ³ / ₄	476.3	22.463	570.56	1.185	30.10	0.968	24.59	22.295	566.29
BX-165	21 ¹ / ₄	539.8	24.595	624.71	1.261	32.03	0.728	18.49	24.417	620.19
BX-166	21 ¹ / ₄	539.8	25.198	640.03	1.261	32.03	1.029	26.14	25.020	635.51
BX-167	26 ³ / ₄	679.5	29.896	759.36	1.412	35.86	0.516	13.11	29.696	754.28
BX-168	26 ³ / ₄	679.5	30.128	765.25	1.412	35.86	0.632	16.05	29.928	760.17
BX-169	5 ¹ / ₈	130.2	6.831	173.52	0.624	15.84	0.509	12.93	6.743	171.27
BX-170	9	228.6	8.584	218.03	0.560	14.22	0.560	14.22	8.505	216.03
BX-171	11	279.4	10.529	267.44	0.560	14.22	0.560	14.22	10.450	265.43
BX-172	13 ⁵ / ₈	346.1	13.113	333.07	0.560	14.22	0.560	14.22	13.034	331.06

Ring Number	Width of Flat		Hole Size		Depth of Groove		Outside Diameter of Groove		Width of Groove	
	(in.)	[mm]	(in.)	[mm]	(in.)	[mm]	(in.)	[mm]	(in.)	[mm]
BX-150	0.314	7.98	¹ / ₁₆	1.6	⁷ / ₃₂	5.56	2.893	73.48	0.450	11.43
BX-151	0.325	8.26	¹ / ₁₆	1.6	⁷ / ₃₂	5.56	3.062	77.77	0.466	11.84
BX-152	0.346	8.79	¹ / ₁₆	1.6	¹⁵ / ₆₄	5.95	3.395	86.23	0.498	12.65
BX-153	0.385	9.78	¹ / ₁₆	1.6	¹⁷ / ₆₄	6.75	4.046	102.77	0.554	14.07
BX-154	0.419	10.64	¹ / ₁₆	1.6	¹⁹ / ₆₄	7.54	4.685	119.00	0.606	15.39
BX-155	0.481	12.22	¹ / ₁₆	1.6	²¹ / ₆₄	8.33	5.930	150.62	0.698	17.73
BX-156	0.629	15.98	¹ / ₈	3.2	⁷ / ₁₆	11.11	9.521	241.83	0.921	23.39
BX-157	0.709	18.01	¹ / ₈	3.2	¹ / ₂	12.70	11.774	299.06	1.039	26.39
BX-158	0.782	19.86	¹ / ₈	3.2	⁹ / ₁₆	14.29	14.064	357.23	1.149	29.18
BX-159	0.869	22.07	¹ / ₈	3.2	⁵ / ₈	15.88	17.033	432.64	1.279	32.49
BX-160	0.408	10.36	¹ / ₈	3.2	⁹ / ₁₆	14.29	16.063	408.00	0.786	19.96
BX-161	0.482	12.24	¹ / ₈	3.2	⁴³ / ₆₄	17.07	19.604	497.94	0.930	23.62
BX-162	0.481	12.22	¹ / ₁₆	1.6	²¹ / ₆₄	8.33	18.832	478.33	0.705	17.91
BX-163	0.516	13.11	¹ / ₈	3.2	²³ / ₃₂	18.26	22.185	563.50	1.006	25.55
BX-164	0.800	20.32	¹ / ₈	3.2	²³ / ₃₂	18.26	22.752	577.90	1.290	32.77
BX-165	0.550	13.97	¹ / ₈	3.2	³ / ₄	19.05	24.904	632.56	1.071	27.20
BX-166	0.851	21.62	¹ / ₈	3.2	³ / ₄	19.05	25.507	647.88	1.373	34.87
BX-167	0.316	8.03	¹ / ₁₆	1.6	²⁷ / ₃₂	21.43	30.249	768.32	0.902	22.91
BX-168	0.432	10.97	¹ / ₁₆	1.6	²⁷ / ₃₂	21.43	30.481	774.22	1.018	25.86
BX-169	0.421	10.69	¹ / ₁₆	1.6	³ / ₈	9.5	6.955	176.66	0.666	16.92
BX-170	0.481	12.22	¹ / ₁₆	1.6	²¹ / ₆₄	8.33	8.926	220.88	0.705	17.91
BX-171	0.481	12.22	¹ / ₁₆	1.6	²¹ / ₆₄	8.33	10.641	270.28	0.705	17.91
BX-172	0.481	12.22	¹ / ₁₆	1.6	²¹ / ₆₄	8.33	13.225	335.92	0.705	17.91



TOLERANCES

	(in.)	[mm]
b_f (width of ring)	+ 0.008, - 0.000	+ 0.20, - 0.00
b_f (width of flat)	+ 0.006, - 0.000	+ 0.15, - 0.00
d_g (hole size)	none	none
d_g (depth of groove)	+ 0.004, - 0	+ 0.39, - 0
d_g (OD of groove)	+ 0.004, - 0.000	+ 0.10, - 0.00
h_r (height of ring)	+ 0.008, - 0.000	+ 0.20, - 0.00
h_r (width of groove)	+ 0.004, - 0.000	+ 0.10, - 0.00
d_f (OD of ring)	+ 0.000, - 0.006	+ 0.00, - 0.15
d_f (OD of flat)	± 0.002	± 0.05
r_r (radius in ring)	see note	see note
23° (angle)	± 1/4°	± 1/4°

* A plus tolerance of 0.008 in. for b_f and h_r is permitted, provided the variation in width or height of any ring does not exceed 0.004 in. throughout its entire circumference.

NOTE: r_r shall be 8 to 12% of the gasket h_r .

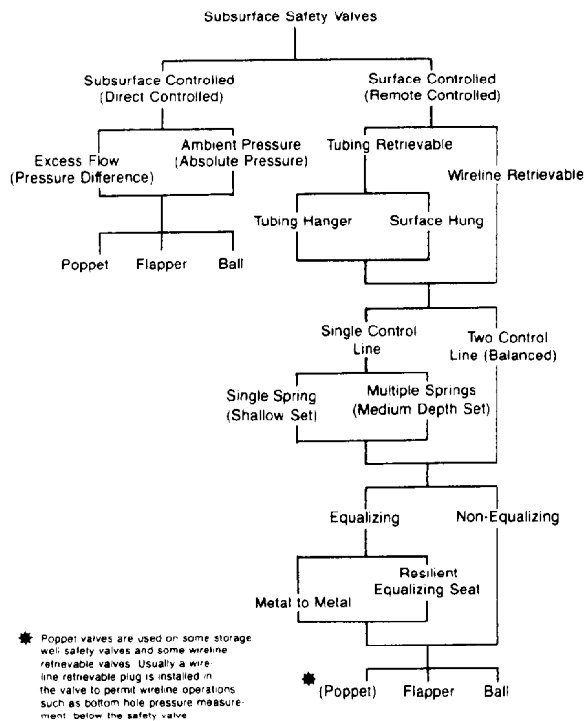


Fig. 3.11—Subsurface safety valve design options.

Hydraulically powered safety valves require a pump/control unit in the system (Fig. 3.13). The preferred type of pump is the ratio-piston pneumatic-over-hydraulic pump. These pumps have pneumatic pressure operating on a relatively large piston to push a relatively small pump plunger. Low pneumatic pressure can thus develop high hydraulic pressure. The output pressure is easily controlled by the pressure of the input power gas, which can be controlled by a simple demand-pressure regulator. Pressure maintenance is automatic and continuous. Care should be taken to select a pump that is free of continuous bleeding of gas and that will not stall in its reciprocating motion at the end of a stroke.

Valve control and system logic is performed by pneumatic/hydraulic or pneumatic/pneumatic relays. These relays permit the use of either bleed (two-way) or block and bleed (three-way) sensors (Figs. 3.14 and 3.15). Relays are reset manually to put the system back in service after a closure. This safety feature ensures that a person is present to determine that the cause for closure has been corrected and that reopening would not be hazardous.

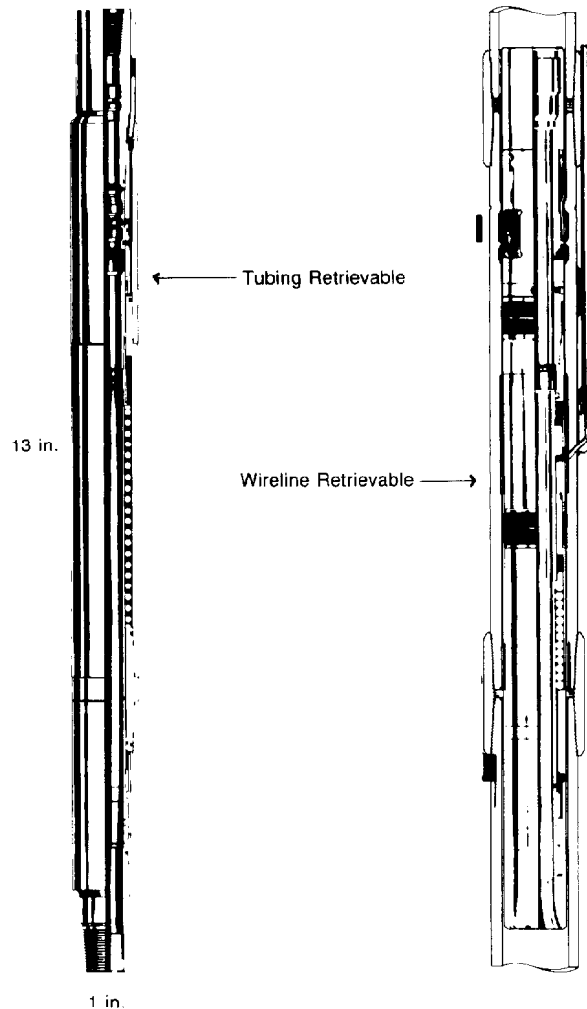


Fig. 3.12—Tubing-retrievable and wireline-retrievable surface-controlled subsurface safety valves.

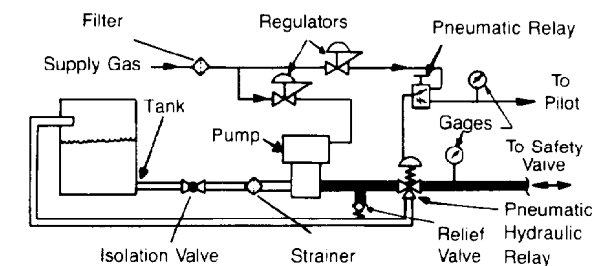


Fig 3.13—Basic hydraulic control circuit.

Circuit design determines the hierarchy of closure. All surface and subsurface safety valves should close in case of fire, collision, and manual actuation of the emergency shutdown system (ESD). Many systems close only the SSV of a single well when sensors on a single well actuate because of high liquid level, high pressure resulting from freezing or valve malfunction downstream, or low pressure resulting from flowline rupture or backpressure

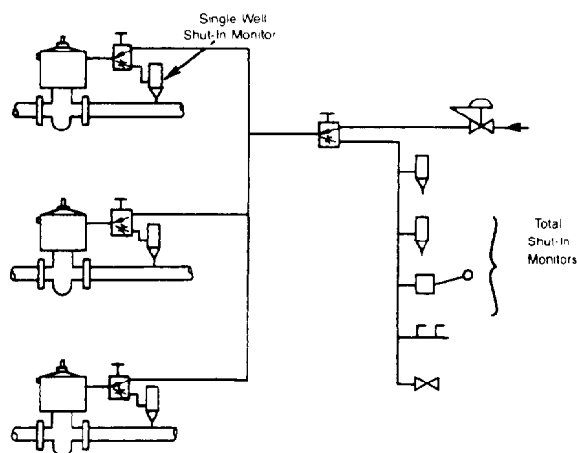


Fig. 3.14—Single branched system for two hierarchies of control (bleed-type sensors).

valve failure. Sometimes several wells on a platform or lease will be closed as a group if they are high vs. low pressure, oil vs. gas wells, etc. Every system should be designed to suit the characteristics of the wells and the severity of consequences of malfunctions.

Platforms and compact land leases may have all the control system in a cabinet or console. Communication between the cabinet and well should be with control system media. If well pressure is piped to sensors in the cabinet, the well fluids may freeze and prevent proper operation. There is also the danger of high-pressure, high-volume flow from a ruptured line and leakage of toxic or flammable fluids to an enclosed area. Electric devices and lines usually need to be explosion proof. Requirements for the designation "explosion proof" are explained in the Natl. Electrical Code.⁸ API RP14F⁹ defines which installation areas require explosion-proof equipment.

Sensors

Sensors monitor conditions that indicate production system hazards or malfunctions. The sensor then actuates an integral pilot valve or switch to activate a control valve. The pilot valve and/or control valve may

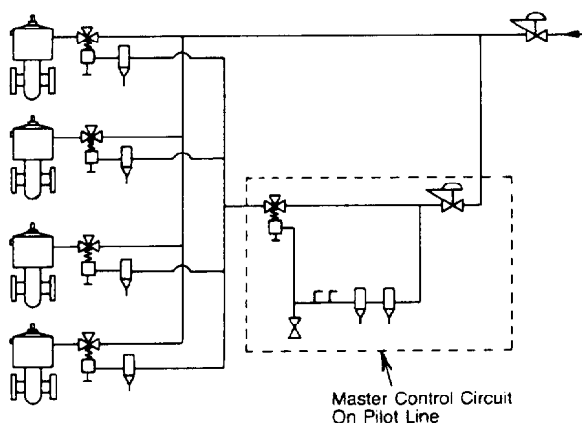


Fig. 3.15—Single branched system for two hierarchies of control (block-and-bleed-type sensors).

bleed (two-way) or block-and-bleed (three-way). Electric sensors interface with pneumatic systems with solenoid valves. Conditions that are usually monitored include (Fig. 3.16): (1) pressure—high or low because of flowline or pressure vessel blockage or rupture; (2) level—high or low in separator or storage tank resulting from control valve system malfunction; (3) fire—heat is sensed by fusible plugs or fusible control line, flames are sensed by ultraviolet detectors, and temperature is detected by infrared detectors; (4) toxic or flammable gas mixtures—detectors located at four or more locations around the perimeter or in enclosures; (5) manual control—ESD system valves at boat landings, living quarters, and other critical locations.

Pressure sensors should be located at any point in the production system where sections of the system can be isolated by a check valve or block valve, or where there is a change in pressure due to a choke or pressure reducing valve.¹⁰ Pressure sensors may have a moving-seal sensing element or an elastic element such as a Bourdon tube. Moving-seal sensors have poorer repeatability but are considerably less susceptible to damage by abuse and overpressure.

Regulations

Governmental regulations control the design and operation of some safety shut-in systems. For example, the Minerals Management Service of the U.S. government controls installations in the outer continental shelf (OCS) waters of the U.S. The rules are published in the OCS Order No. 5.⁶ The OCS orders require that safety valves installed in or on wells in the federally controlled waters be made according to the ANSI/ASME SPPE-1¹¹ specification and API Specs. 14A¹² and 14D.⁷ ANSI/ASME SPPE-1 is an extensive quality-assurance specification. API Specs. 14A and 14D are performance and design specifications for SSSV's and SSV's.

Other Flow-Control Devices

Most flow-control functions are described in this chapter in the sections on Wellheads and Safety Shut-In Systems, and in Chaps. 11 through 16. Some valves and controls are discussed in Chaps. 4 (Production Packers) and 5 (Gas Lift). Other flow-control devices are discussed in the following.

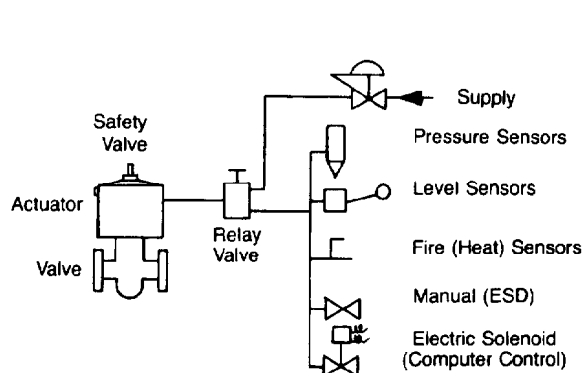


Fig. 3.16—Remote controlled SSV system.

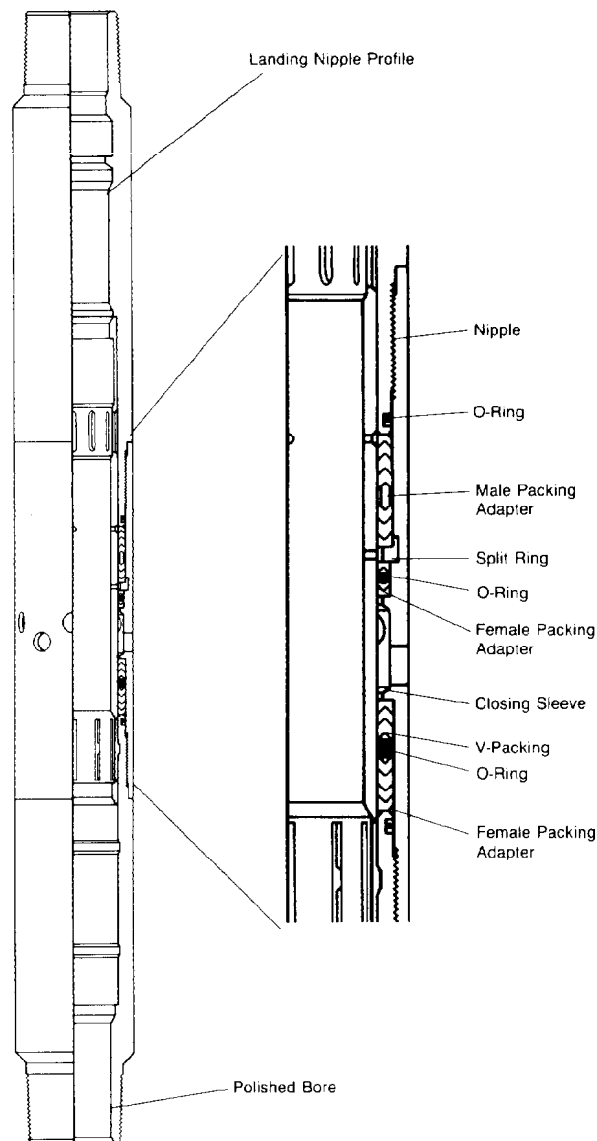


Fig. 3.17—Sliding sleeve valve.

Input Safety Valves (ISV's)

Injection wells can be protected by the safety shut-in systems discussed earlier in this chapter. The ISV is a lower-cost safety valve that can be used for wells where there is only flow downward into the well. It is basically a check valve mounted on a wireline-retrievable mandrel located in a landing nipple. Upward flow closes the valve.

Circulating Devices

Circulating devices are wireline-operable valves or devices used to permit selective communication between the tubing and the tubing/casing annulus. Variations include (1) sliding-sleeve valve (Fig. 3.17), (2) side-pocket mandrel and inserted "dummy" valve (Fig. 3.18), and (3) ported nipple and lock mandrel.

Sliding-sleeve valves and side-pocket mandrels permit wireline operations to be performed through them, and

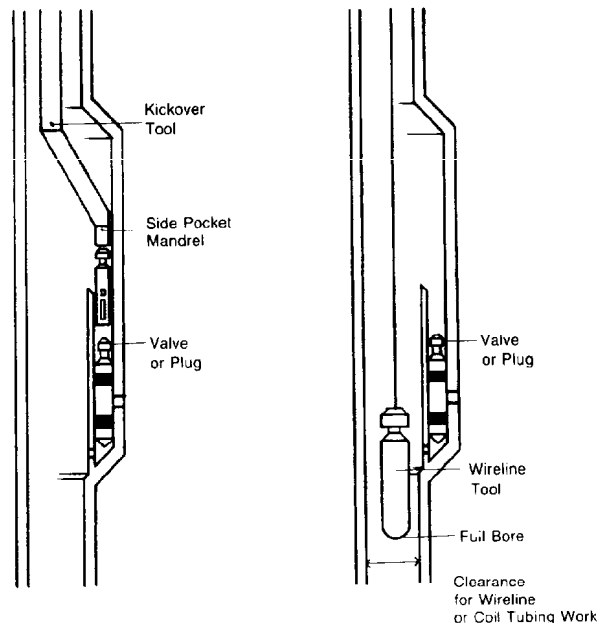


Fig. 3.18—Side pocket mandrel.

they do not obstruct flow up through the tubing. Side-pocket-mandrel valves can be removed by wireline for redressing the seals, which are subject to damage when the circulation path is first opened. Sliding-sleeve valves can be provided with landing-nipple profiles for isolation with a wireline lock mandrel in case of sealing failure. Sliding-sleeve valves can be incorporated in safety-valve nipples to isolate the control line when the safety valve is removed.

Tubing Plug

The tubing should be plugged to prevent flow or loss of control when the tree and/or master valve is to be removed. Plugs are available for landing nipples in the wellhead and for nipples in the tubing string. Tubing plugs are set and retrieved with wireline methods.

Chemical Injection Valves

Some wells require frequent or continuous injection of small quantities of chemicals, such as methanol, for protection from freezing or as inhibitors for corrosion control. The chemicals can be injected down through a small-diameter parallel tubing or through the tubing/casing annulus. Chemical injection valves can be installed in a circulating device to better control the injection rate and to provide backflow protection.

Corrosion

Wellhead Corrosion Aspects

Corrosion has often been defined as the destruction of a metal by reactions with its environment. The attack may be internal or external and may result from chemical or electrochemical action.

Internal attack usually results from weight loss corrosion ("sweet corrosion") caused by the presence of CO₂ and organic acids, or sulfide or chloride stress cracking

corrosion ("sour corrosion") caused by the presence of H_2S , chlorides, or a combination of these elements. External attack usually results from "oxygen corrosion" caused by exposure to atmospheric oxygen, "electrochemical corrosion" caused by the flow of electric currents, or a combination of the two.

One or more methods may be employed to control corrosion in wellhead equipment, depending on the type of corrosion present and the economics involved: (1) use of special corrosion-resistant alloys, (2) injection of an effective inhibitor, (3) application of effective coatings, and/or (4) properly applied and maintained cathodic protection. Although a detailed discussion of corrosion is not the purpose of this section, it is necessary to describe briefly the various types of corrosion encountered in wellhead equipment to explain the various methods of control. Internal and external corrosion are controlled differently and are discussed separately.

Internal Corrosion

Weight Loss Corrosion. Weight loss corrosion is usually defined as corrosion occurring in oil or gas wells where no iron sulfide corrosion product or H_2S odor exists. Corrosion of this type in gas-condensate wells is often attributed to CO_2 and organic acids. Although noncorrosive in the absence of moisture, when moisture is present, CO_2 dissolves and forms carbonic acid. Carbonic acid with the organic acids contributes to corrosion. The quantity of CO_2 dissolved in the corroding fluid determines the severity of corrosion.

Generally, corrosion can be expected when the partial pressure of the CO_2 , at bottomhole conditions, exceeds 30 psi. The partial pressure of CO_2 can be easily determined: partial pressure equals (total pressure) times (percent CO_2).

Wellhead Protection Methods. Wellhead protection methods for weight loss corrosion may take two forms.

1. An effective inhibitor, protective coatings, or special-alloy equipment is generally required when the CO_2 partial pressure, at bottomhole conditions, exceeds 30 psi.

2. Special-alloy equipment is generally required when the CO_2 partial pressure, at bottomhole conditions, exceeds 100 psi.

Sulfide or Chloride Stress Cracking Corrosion. Sulfide or chloride stress cracking corrosion is defined as corrosion occurring in oil or gas wells when hydrogen sulfide or chlorides are present. Iron sulfide appears as a black powder or scale. Hydrogen sulfide, like CO_2 , is not corrosive in the absence of moisture. If moisture is present, the gas becomes corrosive. If CO_2 is also present, the gas is more severely corrosive.

Attack by H_2S causes the formation of iron sulfide, and the adherence of the iron sulfide to steel surfaces creates an electrolytic cell. The iron sulfide is cathodic to the steel and accelerates local corrosion. Hydrogen sulfide also causes hydrogen embrittlement by releasing hydrogen into the steel grain structure to reduce ductility and cause extreme brittleness.

Wellhead Protection Methods for Sulfide or Chloride Stress Cracking. These protection methods take three forms.

1. Special alloy equipment is generally required when pressures exceed 65 psia and the partial pressure of H_2S exceeds 0.05 psia.

2. Proper injection of an effective inhibitor.

3. Carbon and low alloy steels that should not exceed a hardness level of HRC 22.

Extreme Sour Service. This is sometimes referred to as critical service. An extreme sour condition exists when both CO_2 and H_2S are present in the well fluids. In this case, protection is required for both sulfide stress cracking and metal loss. In general, stainless steel, Monel®, or other nonferrous materials are used for this service. API Spec. 6A refers to NACE Standard MR-01-75 as the governing standard for materials to resist sulfide stress cracking.¹³

External Corrosion

Oxygen Corrosion. Oxygen corrosion is caused by the oxidation or rusting of steel due to exposure to atmospheric oxygen or a corrosive atmosphere. The severity of corrosion depends on temperature, erosion of the metal surface, property of corrosion product, surface films, and the availability and type of electrolyte. Salt water causes a very rapid increase in corrosion rate.

On offshore installations, wellhead equipment is often subjected to one or more of three zones of attack: (1) the underwater or submerged zone, (2) the splash zone (most severe), and (3) the spray zone.

Wellhead Protection Methods for Oxygen Corrosion.

The protection methods for oxygen corrosion include (1) use of special-alloy equipment, (2) application of effective external protective coatings of metallic or nonmetallic materials, and (3) use of cathodic protection for the underwater zone.

Electrochemical Corrosion. There are two major types of electrochemical corrosion. One type is somewhat of a reverse plating reaction caused by stray direct electric currents flowing from the steel anode to a cathode. Another type of electrochemical corrosion occurs when pipe or a wellhead is exposed to certain types of moist soil.

Bimetallic corrosion, another form of electrochemical corrosion aggravated by use of dissimilar metals, is often called galvanic corrosion.

Wellhead Protection Methods for Electrochemical Corrosion.

There are four protection methods for electrochemical corrosion: (1) use of properly applied and maintained cathodic protection, (2) application of effective external surface coatings, (3) avoiding use of dissimilar metals, and (4) use of electrical insulation of surface lines from wellhead assembly.

Material Selection

Table 3.30 shows the general accepted materials for various wellhead services.

Special Application

High Pressure Seals

Flange connections for pressures through 20,000 psi have been standardized by API and the specifications for these flanges are given in API Spec. 6A.¹ However, other pressure-sealing elements in wellhead equipment

TABLE 3.30—ENVIRONMENTS AND APPLICATIONS

		Gas/Gas-Condensate Wells								
		General Service	H ₂ S	CO ₂	H ₂ S/ CO ₂	Low-Temperature				Waterflood
Part						General Service	H ₂ S	CO ₂	H ₂ S/ CO ₂	
1. Casing heads	body	A1	A3	A3	A3	A1,A2	A3	A1,A2	A3	—
2. Casing hangers	housing	A	A	A	A	A	A	A	A	—
	slips	J	J	J	J	J	J	J	J	—
	pack-off	K	K	K	K	K,L	K,L	K,L	K,L	—
	gasket	H	H	F,G	F,G	H	H	F,G	F,G	F,G
3. None										
4. None	bolts*	M	M,M1,M2	M	M1,M2	M,M2,M3	M,M1	M,M3	M,M1	M
							M2,M3		M2,M3	
5. None	nuts*	N,N2	N,N1,N2	N,N2	N1,N2	N3	N1,N2	N3	N1,N2	N,N2
6. Intermediate casing heads	body	A1	A3	A3	A3	A1,A2	A3	A1,A2	A3	—
7. Casing hangers	see Item 2	—	—	—	—	—	—	—	—	—
8. Gaskets	see Item 3	—	—	—	—	—	—	—	—	—
9. Bolts	see Item 4	—	—	—	—	—	—	—	—	—
10. Nuts	see Item 5	—	—	—	—	—	—	—	—	—
11. Tubing heads	see Item 1	—	—	—	—	—	—	—	—	—
12. Tubing hangers	housing	A1,B1	A1,B1	A1,B1	A1,B1	A1,B1	A1,B1	A1,B1	A1,B1	—
	top	A1	A3	A1	A3	A1	A3	A1	A3	—
	bottom	A1	A3	A1	A3	A1	A3	A1	A3	—
	pack-off	K	K	K	K	K,L	K,L	K,L	K,L	—
13. Tubing head adapters	body	A1	A3	C1	C2	A1,A2	A3,P	P	P	—
14. Tees and crosses	body	A1	A3	C1	C2	A1,A2	A3,P	P	P	—
15. Valves	body	A1	A3	C1	C2	A1,A2	A3,P	P	P	A1
	bonnet	A1	A3	C1	C2	A1,A2	A3,P	P	P	A1
	bonnet gasket	H	H,G	F,G	F,G	H	H,G	F,G	F,G	G
	bonnet bolts	M	M1,M2	M	M1,M2	M3	M,M1	M,M3	M,M1	M
							M2,M3		M2,M3	
	gates	A,B1	A3,B2	C1	C2	A1	A3	C1	C2	F
	seats	A,B1	A3,B2	C1	C2	A1	A3	C1	C2	F
	stems	R	D	E	D	R	D	E	D	E
	body	A1	A3	C2	C2	A1	A3	C2	C2	A1
	bonnet	A1	A3	C2	C2	A1	A3	C2	C2	A1
16. Adjustable chokes	stem	R	S	S	S	R	S	S	S	S
	seat	R	T	T	T	R	T	T	T	T
	body	A1	A3	C2	C2	A1	A3	C2	C2	—
	bull plug	B1	B2	B1	B2	R	R	R	R	—
17. Positive chokes										

- A AISI 4130 or ASTM A487-9 (normalized)
A1 AISI 4130 or ASTM A487-9Q (quenched & tempered)
A2 AISI 4130 or ASTM A487-9Q modified by nickel
A3 AISI 4130 or ASTM A487-9Q or 9Q modified controlled hardness HRC 22
B1 Carbon steel such as AISI 1020, 1030, 1040
B2 Carbon steel, controlled hardness HRC 22 max.
C1 AISI 410 S.S. or ASTM A217-CA15
C2 AISI 410 S.S. or ASTM A217-CA15 controlled hardness HRC 22 max.
D K-500 Monel, HRC 35 max.
E 17-4 PH, Condition H1150 (final heat-treating temperature)
F AISI 316 S.S., annealed
G AISI 304 S.S., annealed
H Soft iron
J AISI 8620 carbonitrided
K Elastomer, Hycar
L Elastomer, Hydrin
M Bolts, ASTM A193-B7
M1 Bolts, ASTM A193-B7M (HRC 22 max.)
M2 Bolts, ASTM A453-grade 660
M3 Bolts, A320-L7
N Nuts, ASTM A194-2H
N1 Nuts, ASTM A194-2HM (HRC 22 max.)
N2 Nuts, ASTM A194-2
N3 Nuts, ASTM A194, grade 4 or 7
P ASTM A487-CA6NM S.S.
R AISI 4140 low alloy
S K-500 Monel with carbide trim
T AISI 4140 with carbide trim

*Bolts and nuts must not be buried or covered in accordance with NACE MR 01-75.

TABLE 3.31—CHARPY V NOTCH IMPACT REQUIREMENTS

Size of Specimen		Minimum Impact Value Required for Average of Each Set of Three Specimens		Minimum Impact Value Permitted for One Specimen Only Per Set	
		(ft-lbm)	[J]	(ft-lbm)	[J]
3.93	100	15.0	20	10.0	14
2.95	75	12.5	17	8.5	12
1.97	50	10.0	14	7.0	9
0.98	25	5.0	7	3.5	5

NOTE: Purchasers are cautioned that the energy values tabulated above have been selected to cover a broad range of possible physical properties, and care should be exercised in energy value interpretations for the higher strength Types 2 and 3 materials where minimum energy values have not been clearly established.

such as valve seat, valve stem, fittings, hanger-packer, casing secondary seals, lockscrews, etc., have not been standardized and are subject to agreement between purchaser and manufacturer.

Seals other than flange seals for 20,000 psi and higher working pressures require special consideration because of the difficulty in sealing these high pressures, which are usually encountered in combination with hostile fluids and are subject to agreement between purchaser and manufacturer.

Low- and High-Temperature Application

Unless otherwise specified, API Spec. 6A for wellhead equipment is designed to operate in temperatures from -20 to 250°F .

Low Temperature. API Spec. 6A also provides specifications for materials to operate in temperatures below -20°F . Materials operating in extremely low temperatures become brittle and have low impact resistance. API Spec. 6A specifies minimum impact values at -25°F , -50°F , and -75°F test temperatures. The specified impact values are shown in Table 3.31.

High Temperature. As the temperature rises, the strength of steel decreases. Table 3.32 shows the working pressure-temperature relationship of wellhead steel pressure containing parts at temperatures from -20 to 650°F .

There are some applications where valves with fire-resistance capability are required, particularly on offshore platforms where a fire on one well endangers the other wells. API provides API RP 6F, a recommended

practice fire test for valves.¹⁴ The fire test is conducted in a flame with a temperature of $1,400$ to $1,600^{\circ}\text{F}$ for a 30-minute test period.

Subsea Applications

Although subsea wellhead and Christmas-tree equipment has been available for a number of years and a number of installations have been made, most of the installations have been made in relatively shallow water. Equipment is now being designed for use in water depths of several thousand feet. Various methods for installing, operating, repairing, or replacing subsea equipment are being utilized such as by remote operation, the use of divers, or the use of submarines or robots.

At this time, subsea equipment is proprietary, with each manufacturer providing his own design. Subsea installations are designed for specific projects and are agreed on by the manufacturer and the customer.

Offshore wells can be broadly classified as those drilled from a fixed or bottom-supported platform or from a floating platform. Floating platforms are either of the semisubmersible or floating-ship type.

Fixed Platform Drilling. Offshore wells drilled from a fixed platform normally are drilled with the wellhead and the BOP's on the platform. The well is completed with the Christmas tree attached to the wellhead on the platform. Wells drilled using a bottom-supported drilling rig (jackup rig) normally utilize mudline-suspension wellheads. The wellhead is installed on the ocean floor, with riser pipe extending from the wellhead to the rig floor. The well is drilled with BOP's attached to the riser

TABLE 3.32—PRESSURE/TEMPERATURE RATINGS OF STEEL PARTS

Temperature		Maximum Working Pressure					
($^{\circ}\text{F}$)	($^{\circ}\text{C}$)	(psi)	(bar)	(psi)	(bar)	(psi)	(bar)
-20 to 250	-29 to 121	2000	138	3000	207	5000	345
300	149	1955	134.8	2930	202	4880	336.5
350	177	1905	131.4	2860	197.2	4765	328.5
400	204	1860	128.2	2785	192	4645	320.3
450	232	1810	124.8	2715	187.2	4525	312
500	260	1735	119.6	2605	179.5	4340	299.2
550	228	1635	112.7	2455	169.3	4090	282
600	316	1540	106.2	2310	159.3	3850	265.5
650	343	1430	98.6	2145	147.9	3575	246.5

pipe and the completion is made at the top of the riser pipe, above water, usually on a fixed platform that is installed for the completion.

Floating Drilling Vessels. Wells drilled utilizing floating drilling vessels normally utilize remote subsea equipment. The wellhead equipment is installed on the ocean floor. The BOP's are installed on the wellhead on the ocean floor. Riser pipes connect the equipment on the ocean floor with the vessel. Guidelines extending from the wellhead to the vessel are used for guiding equipment to the wellhead. For water depths too deep to utilize guidelines, guidelineless drilling systems are available. The guidelineless systems are normally used with dynamically positioned vessels. Guidance is accomplished by the use of acoustics, sonar, or TV.

The completion (installation of the Christmas tree) on remote subsea equipment can be made either on the ocean floor or on a platform by utilizing tieback equipment.

A variety of completion systems can be utilized for the production of oil and gas in various subsea environments. Some of these include single-well (diver-assisted or diverless) satellite, platform, template, production riser, caisson or capsule (wet or dry), or combinations of the various basic systems.

SPPE/OCS Equipment. The U.S. Geological Survey (USGS), in cooperation with API and ASME, has established rules and regulations for safety and pollution prevention equipment (SPPE) used in offshore oil and gas operations.¹¹

As described under Surface Safety Valve, the USGS rules and regulations require an SSV on each Christmas tree installed in federal offshore waters. The specification governing SSV's is API Spec. 14D.⁷ To qualify as a manufacturer and/or an assembler of SPPE equipment, a company must become an SPPE certificate holder. To become an SPPE certificate holder, a company must be qualified by ASME to certify compliance with ANSI/ASME SPPE-1 standard on quality assurance and certification of safety and pollution prevention equipment used in offshore oil and gas operations.¹¹ An SPPE certificate holder certifies his equipment by marking it with an authorized OCS symbol.

Independent Screwed Wellhead

API Independently Screwed Wellhead Equipment

This section covers casing and tubing heads having upper-body connections other than API flanges or clamps, in 1,000- and 2,000-psi working pressures. A typical arrangement of this equipment is shown in Fig. 3.4.

Lowermost Casing Heads. Lowermost casing heads are furnished with a lower thread, which is threaded onto the surface pipe. Usually the top of the casing head is equipped with an external thread to receive a threaded cap used to compress the packing to make a seal and hold the slips down. The top thread can also be used to support a companion flange with an API ring groove and bolt holes for attaching standard BOP's.

Casing Hanger. The casing-hanger slip segments are wrap-around type with a lower capacity than API casing hangers. The slips can be dropped through the BOP's to support the casing, but the seal must be placed around the suspended casing after the cutoff has been made.

Intermediate Casing Heads. Intermediate casing heads in this class are identical in design to lowermost casing heads. If an intermediate-casing string is used, it is usually suspended in the lower-casing head with a thread positioned just above the lower-casing head to permit easy installation of the intermediate-casing head. If proper spacing is impractical, the intermediate casing may be cut off a few inches above the lower-casing head and a socket-type nipple with a top thread welded to the intermediate casing. Then the intermediate casing head can be attached to the thread.

Tubing Heads. A tubing head threads onto the top thread of the production string to support and seal the tubing string. The tubing may be supported with a set of slips and sealed with a sealing element compressed with a cap screwed down on top of the tubing head. Maximum capacity of the slip-type tubing hanger is about 125,000 lbm of tubing weight. A mandrel or doughnut tubing hanger may be used to support the tubing if desirable. Maximum weight-supporting capacity of this type of tubing hanger is limited only to the weight-supporting strength of the tubing head.

A BOP can be attached to the tubing head with a companion flange for protection while running tubing.

A stripper rubber may also be used to strip the tubing in or out of the hole under pressure, if needed. If a stripper rubber is used, it can be placed in the tubing-head bowl and a separate bowl can be attached to the tubing head to support the slip assembly or mandrel hanger.

Casing heads are available in all standard sizes with working pressures of 1,000 psi and lower. Tubing heads are available in working pressures of 1,000 and 2,000 psi. Both units are usually furnished with two 2-in. line-pipe outlets, although 3-in. outlets are available.

Christmas-Tree Assembly. Christmas-tree assemblies for this type of equipment are usually very simple. If the well is expected to flow, a master valve is screwed onto the top tubing thread, a nipple and tee are screwed into the master valve, and a wing valve and choke are screwed into the tee.

Selection. In selecting this class of equipment, the following factors should be considered.

1. Casinghead and tubing-head components should be constructed of cast steel or forged steel and should be full-opening.

2. Casing-hanger slips should be of drop-through type.

3. Caps used to hold down the suspension members and provide a seal should have hammer lugs for easy effective installation.

4. Both casing heads and tubing heads should be easily adaptable, with a full-opening adapter, to a standard BOP.

References

1. *Specifications for Wellhead and Christmas Tree Equipment*, API Spec. 6A, 15th edition, API, Dallas (April 1, 1986).
2. *Recommended Practice for Care and Use of Casing and Tubing*, API RP 5C1, 12th edition, API, Dallas (March 1981).
3. "Bulletin on Performance Properties of Casing, Tubing and Drill Pipe," 18th edition, *API Bull. 5C2*, API, Dallas (March 1982).
4. *Specifications for Casing Tubing and Drill Pipe*, API Spec. 5A, 36th edition, API, Dallas (March 1982).
5. *Specifications for Line Pipe*, API Spec. 5L, 33rd edition, API, Dallas (March 1983).
6. *Production Safety Systems*, OCS Order No. 5, U.S. Dept. of the Interior (Jan. 1975).
7. *Specifications for Wellhead Surface Safety Valves and Underwater Safety Valves for Offshore Service*, API Spec. 14D, fifth edition, API, Dallas (Feb. 1983).
8. *National Electrical Code*, Natl. Fire Protection Assn., Quincy, MA (1981).
9. *Recommended Practice for Design and Installation of Electrical Systems for Offshore Platforms*, API RP 14F, first edition, API, Dallas (July 1978).
10. *Recommended Practice for Analysis, Design, Installation, and Testing of Basic Surface Safety Systems on Offshore Platforms*, API RP 14C, second edition, API, Dallas (Jan. 1978).
11. "Quality Assurance and Certification of Safety and Pollution Prevention Equipment Used in Offshore Oil and Gas Operations," ANSI/ASME SPPE-1-82 and Addendum SPPE-1b-1983, ANSI/ASME, New York City.
12. *Specification for Subsurface Safety Valve Equipment*, API Spec. 14A, fifth edition, API, Dallas (March 1981).
13. *Material Requirements, Sulfide Stress Cracking Resistant Metallic Material for Oilfield Equipment*, NACE Standard MR-01-75, NACE, Houston (1978).
14. *Recommended Practice for Fire Test for Valves*, API RP 6F, third edition, API, Dallas (Jan. 1982).
15. Fowler, E.D. and Rhodes, A.E.: "Checklist Can Help Specify Proper Wellhead Material," *Oil and Gas J.* (Jan. 1977) 59-61.

General References

- Recommended Practice for Design, Installation and Operation of Subsurface Safety Valve Systems*, API RP 14B, second edition, API, Dallas (Nov. 1981).
- Recommended Practice for Use of Surface Safety Valves Offshore*, API RP 14H, first edition, API, Dallas (April 1982).
- Boyle, W.G.: *Designing Production Safety Systems*, PennWell Publishing Co., Tulsa (1979).

Chapter 4

Production Packers

L. Douglas Patton, L.D. Patton & Assocs.*

Production Packers Classification and Objectives

Production packers generally are classified as either retrievable or permanent types. Packer innovations include the retrievable seal nipple packers or semipermanent type.

The packer isolates and aids in the control of producing fluids and pressures to protect the casing and other formations above or below the producing zone. All packers will attain one or more of the following objectives when they are functioning properly.

1. Isolate well fluids and pressures.
2. Keep gas mixed with liquids, by using gas energy for natural flow.
3. Separate producing zones, preventing fluid and pressure contamination.
4. Aid in forming the annular volume (casing/tubing/packer) required for gas lift or subsurface hydraulic pumping systems.
5. Limit well control to the tubing at the surface, for safety purposes.
6. Hold well servicing fluids (kill fluids, packer fluids) in casing annulus.

Once a tubing-packer system has been selected, designed, and installed in a well there are four modes of operation: shut-in, producing, injection, and treating. These operational modes with their respective temperature and pressure profiles have considerable impact on the length and force changes on the tubing-to-packer connections.

Tubing-To-Packer Connections

There are three methods of connecting a packer and a tubing string, and the tubing can be set in tension, compression, or left in neutral (no load on the packer, tension nor compression).

1. Tubing is latched or fixed on the packer, allowing no movement (retrievable packers). Tubing can be set either in tension, compression, or neutral.

2. Tubing is landed with a seal assembly and locator sub that allows limited movement (permanent or semipermanent packers only). Tubing can be set only in compression or neutral.

3. Tubing is stung into the packer with a long seal assembly that allows essentially unlimited movement (permanent packers only). Tubing is left in neutral and it cannot be set in tension or compression.

A retrievable packer is run and pulled on the tubing string on which it was installed. No special tubing trips are required. It has only one method of connection to the tubing — latched or fixed. The tubing can be set in tension, compression, or left in neutral. Tubing-length changes will result in force changes on the packer and tubing. In deep or high-temperature wells the rubber element may “vulcanize” and take on a permanent set, making release very difficult.

Permanent and semipermanent packers can be run on wireline or tubing. They have three methods of tubing connection: latched (fixed), landed (limited movement), or stung in with a long seal assembly (free movement). Special tools plus milling are needed to recover it from the well. When left for long periods of time without movement, the seal assembly and polished bore (in the packer) may stick together.

Packer Utilization And Constraints

Understanding uses and constraints of the different types of packers will clarify the factors to consider before selecting the best packer and will illustrate how they achieve their specific objectives.

*Author of the chapter on this topic in the 1962 edition was W.B. Bleakley.

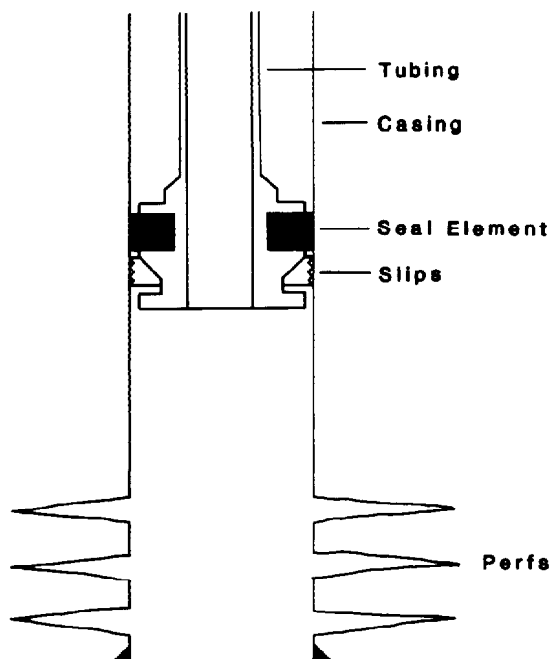


Fig. 4.1—Solid-head retrievable compression packer.

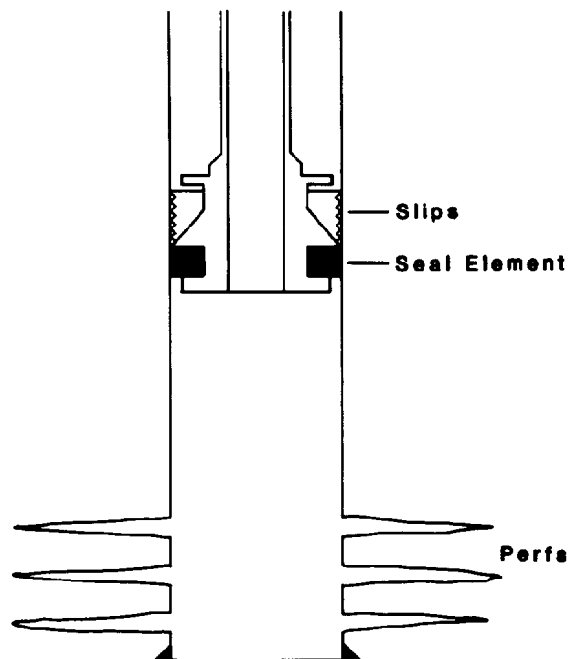


Fig. 4.2—Solid-head retrievable tension packer.

Retrievable Packers

Solid-Head Compression Packer. Retrievable compression (weight-set solid-head) packers are applied when annulus pressure above the packer exceeds pressure below the packer, as in a producing well with a full annulus. This situation precludes gas lift. Fig. 4.1 shows this type of packer.¹

The constraints of a solid-head compression packer are:

1. Packer release can be hampered by high differential pressure across packer.
2. Packer may unseat if a change in the operational mode results in a tubing temperature decrease (tubing shortens).
3. Tubing may corkscrew permanently if a change in the operational mode results in a tubing temperature increase (tubing lengthens).

Solid-Head Tension Packer. Retrievable tension packers generally are used when pressure below the packer is greater than the annulus pressure above the packer, such as in an injection well or low-pressure and -volume treating (Fig. 4.2). These packers also are used in shallow wells where the tubing weight is insufficient to set a compression packer properly.

Constraints of the solid-head retrievable tension packer are:

1. Release is difficult with high differential pressure across the packer.
2. Tubing could part if a change in the operational mode results in a temperature decrease.
3. Packer could release if a change in the operational mode results in a temperature increase.

Isolation Packer. A retrievable isolation packer (Fig. 4.3)

is used when two mechanically set packers are to be set simultaneously. It requires anchor pipe on the plugged back depth below it to use tubing weight to shear the pins that hold the packer in the unset mode. It can be used to isolate old perforations or a damaged spot in the casing temporarily. This packer is for temporary use only and should be retrieved as soon as its purpose is accomplished.

Control-Head Compression Packer. The control-head retrievable compression packer (Fig. 4.4) has a bypass valve to alleviate the packer release problem resulting from excessive differential pressure. The valve is on top of the packer. It is opened, equalizing the pressure across the packer, by picking up the tubing without moving the packer. As with the solid-head packer, using tubing weight, this packer holds pressure from above only. It is not suitable for injection wells or low-volume and -pressure treating.

Constraints are: (1) the bypass or equalizing valve could open if an operational mode change results in a tubing temperature decrease, and (2) tubing could corkscrew permanently if an operational mode change results in a tubing temperature increase.

A control-head retrievable compression packer run with an anchor is basically a treating packer. It holds pressure from below without tubing weight because the anchor holds the packer and constrains its movement. Pressure across the packer is equalized through a valve operated by picking up on the tubing (Fig. 4.5). Temperature changes have the same effect as they have with the control-head compression packer without an anchor.

Control-Head Tension Packer. The control-head retrievable tension packer is released easily even if high

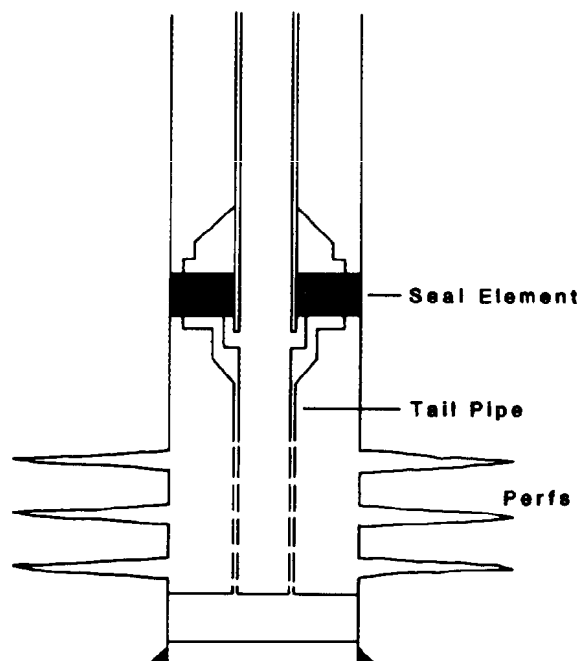


Fig. 4.3—Isolation packer is held in place with shear pins.

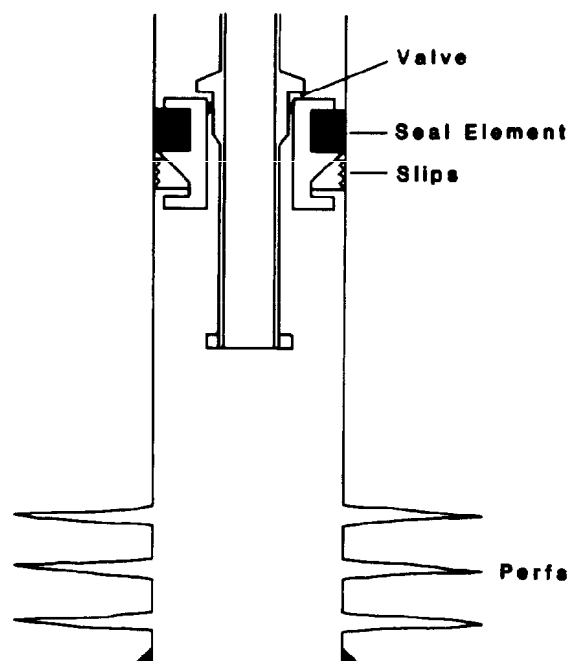


Fig. 4.4—Control-head compression packer employs a top equalizing valve.

differential pressure exists across the packer during normal operations. This pressure is equalized by a valve on top of the packer that is opened by lowering the tubing without moving the packer. This type packer holds pressure from below only, with tubing in tension, and is not suitable for wells with well servicing fluid in the annulus.

Constraints of a control-head tension packer are: (1) premature bypass valve opening could occur with a tubing temperature increase as the tubing elongates, and (2) tubing could part with a tubing temperature decrease as the tubing contracts.

Mechanically Set Packer. Mechanically set retrievable packers (Fig. 4.6) have slips above and below the seal element and can be set with either tension, compression, or rotation. Once the packer is set, the tubing can be left in tension, compression, or neutral mode. How the tubing is left is dictated by future operations to be performed. Careful planning of these subsequent operations is needed to neutralize temperature and pressure effects on the tubing and the equalizing valve.

The mechanically set retrievable packer is suitable for almost universal application, the only constraint being found in deep deviated wells where transmitting tubing movement will be a problem.

Hydraulic-Set Packer. The retrievable hydraulic-set packer (Fig. 4.7) also has slips above and below the packing element. It is set by applying the hydraulic pressure in the tubing to some preset level above hydrostatic pressure. Once the packer is set, the tubing may be put in limited tension, compression, or left neutral. The packer generally is released with tension-actuated shear pins. It is universally applicable, the only constraint being its high cost.

Common Constraint — All Latched Packers. Severe tubing length changes resulting from changing temperatures can develop sufficient forces to move the packer in the casing. This can happen in old corroded casing or in the harder grades of new casing such as P-110. The teeth on the slips “shave” the pipe, thus loosening their grip.

Permanent Packers

The polished sealbore packer (Fig. 4.8) is a permanent-type or semipermanent packer that can be set with precision depth control on conductor wireline. It also can be set mechanically or hydraulically on the tubing. A locator sub and seal assembly is attached to the bottom of the tubing and is stung into the polished bore receptacle of the packer. Isolation is achieved by the fit of the seals inside the polished bore.

This packer allows all three connection methods—fixed, limited movement, or free movement—that subsequent operations will dictate. It is ideal for wells subject to frequent workover because the tubing is retrieved easily.

Permanent packers are especially useful where tubing temperature may vary widely because the seals slide up and down in the polished bore. They can be retrieved by using a special tool on the end of the tubing in place of the seal assembly, but a round trip with the tubing is required.

There is one important constraint with this packer—if the tubing remains in a place for a long time at the same temperature and no movement occurs between the seals and the polished bore, the seals may stick to the polished bore surface, creating a tubing-retrieval problem.

The seal assembly length (Fig. 4.8) should allow sufficient free upward tubing movement during stimulation treatments and permit tubing weight slackoff to eliminate seal movements during the producing life of the well.

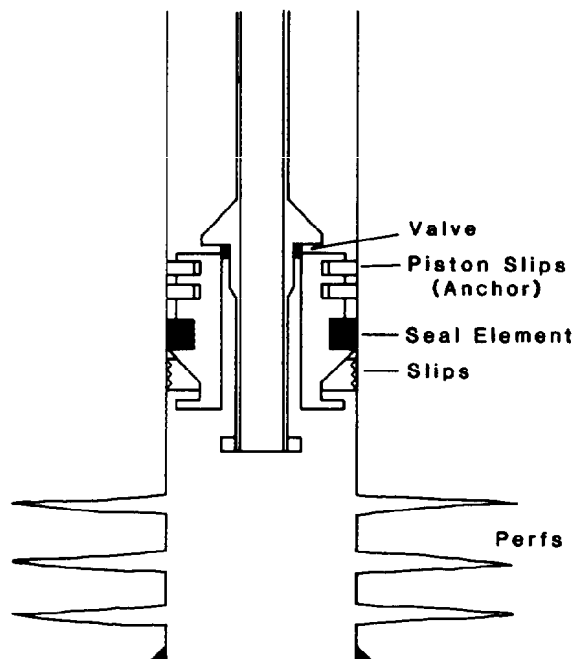


Fig. 4.5—Treating compression packer is held by an anchor containing piston slips.

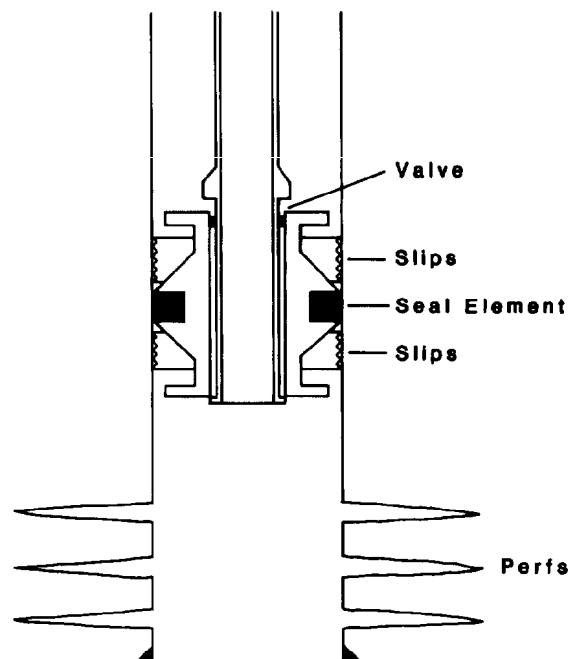


Fig. 4.6—Mechanically set dual-slip packer has slips above and below rubber element.

Considerations For Packer Selection

Packer selection requires an analysis of packer objectives for the anticipated well operations, such as initial completions, production stimulation, and workover procedures. Considering both current and future well conditions, the packer with the minimum overall cost that will accomplish the objectives should be selected. Initial investment and installation costs should not be the only criteria. Overall packer cost is related directly not only to retrievability and failure rate but to such diverse factors as formation damage during subsequent well operations or replacement of corkscrewed tubing.

Retrievability will be enhanced greatly by using oil or solid-free water rather than mud for the packer fluid. Frequency of packer failures may be minimized by using the proper packer for the well condition and by anticipating future conditions when setting the packer. Permanent packers are by far the most reliable and, when properly equipped and set, are excellent for resisting the high pressure differentials imposed during stimulation. They are used widely when reservoir pressures vary significantly between zones in multiple completions.

Weight-set tension types of retrievable packers will perform satisfactorily when the force on the packer is in one direction only and is not excessive.

Surface/Downhole Equipment Coordination

Setting a packer always requires surface action and in most cases either vertical or rotational movement of the tubing. Selection of the packer must be related to wellhead equipment. The well completion must be considered as a coordinated operation. The surface and downhole equipment must be selected to work together as a system to ensure a safe completion. This is especially true in high-pressure well applications.

Packer Mechanics

The end result of most packer setting mechanisms is to (1) drive a cone behind a tapered slip to force the slip into the casing wall and prevent packer movement, and (2) compress a packing element to effect a seal. Although the end result is relatively simple, the means of accomplishing it and subsequent packer retrieval varies markedly between the several types of packers.

Some packers involve two or more round trips, some require wireline time, and some eliminate trips by hydraulic setting. The time cost should be examined carefully, especially on deep wells using high cost rigs. In some cases higher initial packer costs may be more than offset by the saving in rig time, especially offshore.

Corrosive Well Fluids

Materials used in the packer construction must be considered where well fluids contain CO_2 or H_2S in the presence of water or water vapor.

Sour Corrosion (Sulfide or Chloride Stress Cracking Corrosion). Even small amounts of H_2S with water produce iron sulfide corrosion and hydrogen embrittlement. The Natl. Assn. of Corrosion Engineers specifies that materials for H_2S conditions be heat-treated to only a maximum hardness of 22 Rockwell C to alleviate embrittlement. Hardness has no effect on iron sulfide corrosion, however. For critical parts where high strength is required, K-Monel® is resistant to both embrittlement and iron sulfide corrosion. Corrosion inhibitors may be required to protect exposed surfaces.

Sweet Corrosion ("Weight Loss" Corrosion). CO_2 and water cause iron carbonate corrosion, resulting in deep pitting. For ferrous materials, low-strength steels or cast

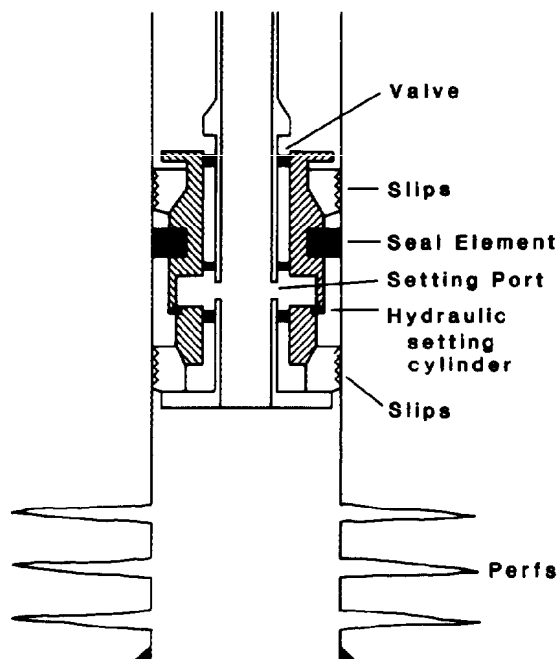


Fig. 4.7—Hydraulic packer is set by tubing pressure.

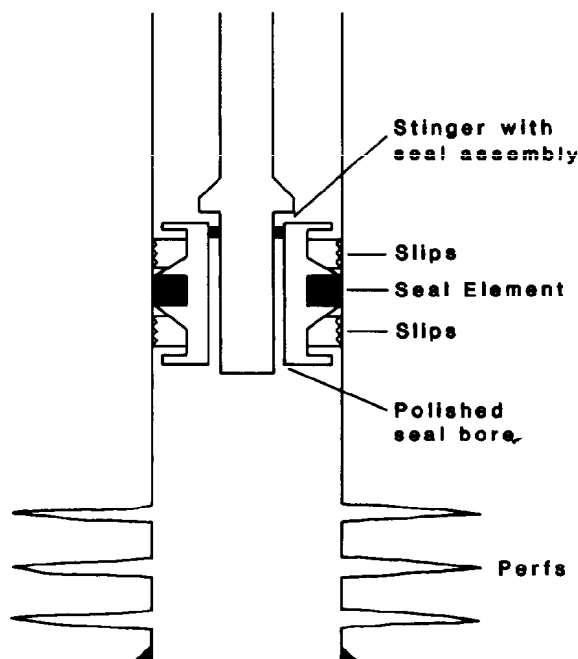


Fig. 4.8—Retrievable, permanent-type packer is made with polished sealbore.

iron are desirable to resist stress concentrations from pitting. Critical parts of production equipment can be made of stainless steel with 9% or higher chromium. Corrosion inhibitors may be required to protect exposed surfaces.

Bimetallic or galvanic corrosion resulting from contact of dissimilar metals should be considered. Usually this is not a problem, since steel is the anode, or sacrificial member, and the resulting damage is negligible because of the massive area of the steel compared with the less-active stainless or K-Monel.

Sealing Element

The ability of a seal to hold differential pressure is a function of the elastomer pressure, or stress developed in the seal. The seal stress must be greater than the differential pressure. In a packer sealing element, the stress developed depends on the packer setting force and the backup provided to limit seal extrusion.

The sealing element may consist of one piece or may be composed of multiple elements of different hardnesses. In a three-element packer, for example, the upper and lowermost elements are usually harder (abrasion resistant) than the center element. The center element seals off against imperfections in the casing, while the harder outside elements restrict extrusion and seal with high temperature and pressure differentials. Many packers also include metallic backup rings to limit extrusion.

Where H_2S or CO_2 is present, seal materials and temperature and pressure conditions must be considered carefully. Teflon® resists H_2S or chemical attack up to 450°F; but Teflon seal extrusion can be a problem. With controlled clearance and suitable metallic backup to prevent extrusion, glass-filled Teflon has performed satisfac-

torily to 450°F with a 15,000-psi differential pressure. Because of seal rigidity it may not perform well below 300°F. With temperatures below 250°F, Nitrile® rubber can be used with metallic backup for static seals. The performance of Viton® seals becomes marginal at 300°F. A tubing-to-packer seal consisting of vee-type rings of Kalrez®, Teflon®, and Rylon® in sequence with metallic backup have been satisfactory (under limited movement) up to 300°F and 10,000-psi differential pressure.

Retrievability

Consideration of retrievability must combine several factors, relative to packer design and use. Retrievable packers are released by either straight pull or rotation. In a deviated hole, applied torque usually can develop more downhole releasing force than pull, although sometimes it also is necessary to manipulate the tubing up and down to transmit the torque to bottom.

The packer sealing element should prevent solids from settling around the slips. Usually the bypass on a control-head packer opens before the seal is released; this allows circulation to remove sand or foreign material.

High setting force is needed to provide a reliable seal under high differential pressures, but it should be recognized that the resulting seal extrusion can contribute to the retrieval problem. A jar stroke between release and pickup positions is an aid in packer removal.

The method of retracting and retaining slip segments is a factor in retrievability. Bypass area around the packer is also important. Where external clearance is minimized to promote sealing, the internal bypass area must be sufficiently large to prevent swabbing by the sealing element when pulling out of the hole.

Fishing Characteristics

A permanent packer must be drilled out to effect removal. This usually presents little problem because all material is millable. Some expensive variations of permanent packers provide for retrieval but retain the removable seal tube feature. Removal of stuck retrievable packers usually results in an expensive fishing operation because components are nondrillable and require washover milling. When selecting packers, consider the volume and type of metal that must be removed if drilled and the presence of rings or hold-down buttons that may act as ball bearings to milling tools.

Through-Tubing Operations

Packers with internal diameters equal to that of the tubing should be used to facilitate through-tubing operations. Also, tubing should be set to minimize or alleviate buckling where through-tubing operations are anticipated.

Purchase Price

Table 4.1 presents a range of packer cost indices. The most economical types are weight-set and tension packers. However, inclusion of a hydraulic hold-down with a compression packer will increase the initial cost from 20 to 100%. Multistring hydraulic-set packers are usually the most expensive and also require many accessories.

Tubing/Packer System

Advantages

By using a properly selected packer, well operations will be more efficient. Wireline pressure and logging operations will proceed faster and smoother. Longer flowing life will be achieved with the use of a packer through the optimal use of the gas energy.

The use of a packer in a gas well, with a tailpipe run below the perforations, will alleviate the problem of gas wells heading, loading up with water, and dying prematurely. (The water is produced continuously as a mist and is not allowed to build up over the perforations.)

This use of a packer and tail pipe will not control the natural water influx, but will keep the water moving along until such time as the available pressure is less than the pressure required to flow.

Where Packers Are Not Used

Packers are not run in rod-pumped wells, unless extraordinary circumstances such as dual completion call for one. Electric submersible pumped wells would not have a packer, except when used with uphole subsurface safety valves required by government safety regulations for off-shore wells. Many naturally flowing, high-volume, sweet-crude wells are produced up the annulus without packers; a small tubing string is run to be used to kill (circulate) the well or for running certain logs or pressure gauges. Dry, sweet-gas wells often are produced up both the tubing and the annulus and have no packers.

Operational Well Modes

There are four modes of operation that any given well might experience: (1) shut-in; (2) producing (either liquids, gas, or a combination); (3) injecting (hot or cold

TABLE 4.1—COST COMPARISON OF PRODUCTION PACKERS

Packer Type	Tubing-Casing size (in.)	Typical Cost Index**
Compression	2 × 5½	1.00
Tension set	2 × 5½	0.925
Mechanical set	2 × 5½	1.54
Hydraulic set	2 × 5½	2.30
Dual	2 × 2 × 7	5.85
Permanent*	2 × 5½	1.85
Semipermanent*	2 × 5½	2.30

*Electric-line setting charge not included.

**Cost of simple compression packer = 1.00.

liquids, or gases); or (4) treating (high, low, or intermediate pressures and volumes).

The usual mode of operation is only one of the factors that need to be considered when selecting a particular type of packer to be used in a well. Subsequent operations and their pressures and temperature changes are likely to be extremely important to packer utilization success.^{2,3} Typical temperature-vs.-depth profiles are illustrated in Fig. 4.9. These profiles are similar to those measured in wells operating in one of four modes: shut-in, production, injection, or treatment.

Fig. 4.9a depicts a typical geothermal gradient, with the temperature increasing with depth to the bottomhole temperature (BHT). Every time a well is shut in, the operating temperature profile will begin to move toward the shape of the natural geothermal profile.

Producing well temperature profiles for both gas and oil are shown in Fig. 4.9b. The wellhead temperature of an oil well will be somewhat less than BHT. The amount of cooling as crude flows to the surface will depend on several factors: (1) the relative amount of oil and water, (2) the specific heats of the oil and water, (3) the flow rate, (4) the gas/liquid ratio, and (5) the vertical flow pressure drop that controls gas liberated and attendant cooling effect.

The temperature profile of a gas well may have a wellhead temperature lower than ambient. In any case the wellhead temperature of a gas well will depend on the BHT, the flow rate, the pressure drop in the tubing, the specific heat of the gas, and other factors.

Injection temperature profiles can be quite varied (Fig. 4.9c). The profile will depend on such factors as the nature of the injection fluid (liquid or gas), the rate of injection, and the injected fluid temperature (cold liquid or gas, hot gas or liquid, or even steam). The liquids injected will tend to have little heat loss down the tubing, while the gas injected will tend to pick up or lose heat to approach the BHT.

While treating is simply a special case of the injection mode, and it is temporary in nature, it is considered important enough to be discussed separately. As with the liquid injection profile, the treating liquid will not pick up any appreciable amount of heat as it moves down the tubing and the treating temperature profile is essentially vertical (Fig. 4.9d).

As illustrated in some examples later, the important thing about these profiles is not their shape but how much the shape and temperature change from one operational

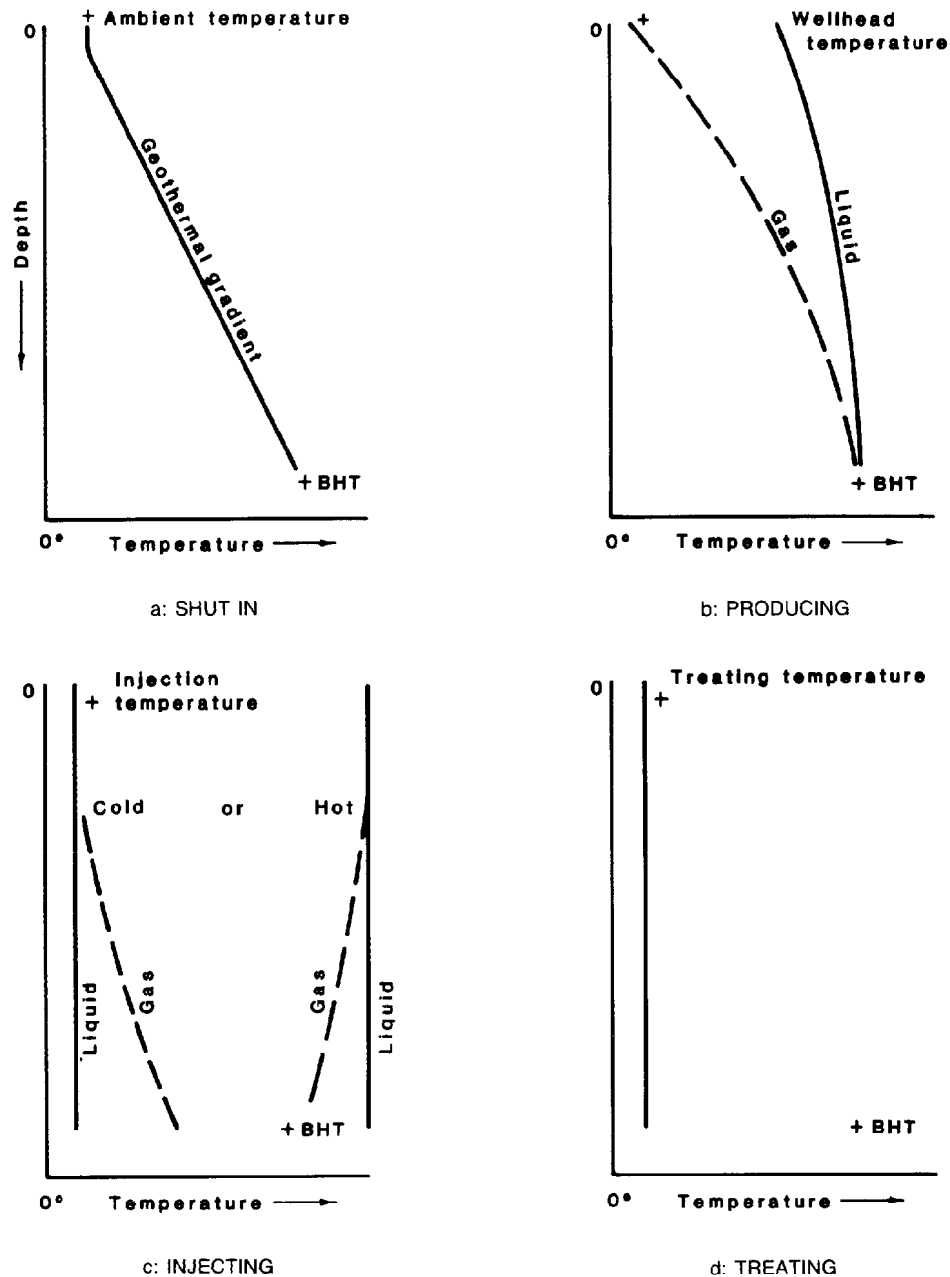


Fig. 4.9—Temperature profiles for four possible modes of oil and gas wells: a. Shut-in, b. Producing, c. Injecting, d. Treating.

mode to another, and how those temperature changes affect the tubing and packer system. It is strongly recommended that anticipated temperature profiles of each operational mode be drawn accurately when planning various steps of any completion or major workover.

Fig. 4.10 shows the pressure profiles of the four modes of well operation. Fig. 4.10a illustrates a typical shut-in well with well servicing fluid in the wellbore. The slope of the profile and the height to which the fluid level rises on the depth scale (and in the wellbore) will depend on the average reservoir pressure, \bar{p}_R , and the gradient of the well servicing fluid. Fig. 4.10b shows the profiles of typical producing oil and gas wells. A liquid injection pro-

file (Fig. 4.10c) is similar to the shut-in profile, the difference being that the bottomhole injection pressure, $(p_i)_{bh}$, is greater than the average reservoir pressure, \bar{p}_R . The wellhead pressure, p_{wh} , can have any value, from a vacuum to several thousand psi. The gas injection profile may have a reverse slope on it or may have a normal but steep slope, depending on the rate, tubing size, and bottomhole injection pressure.

The treating pressure (Fig. 4.10d) is a special temporary case of the injection profile. The bottomhole treating pressure, $(p_t)_{bh}$, often will be greater than the injection pressure, especially in a fracturing job. The surface pressure will be constrained by the burst strength of the

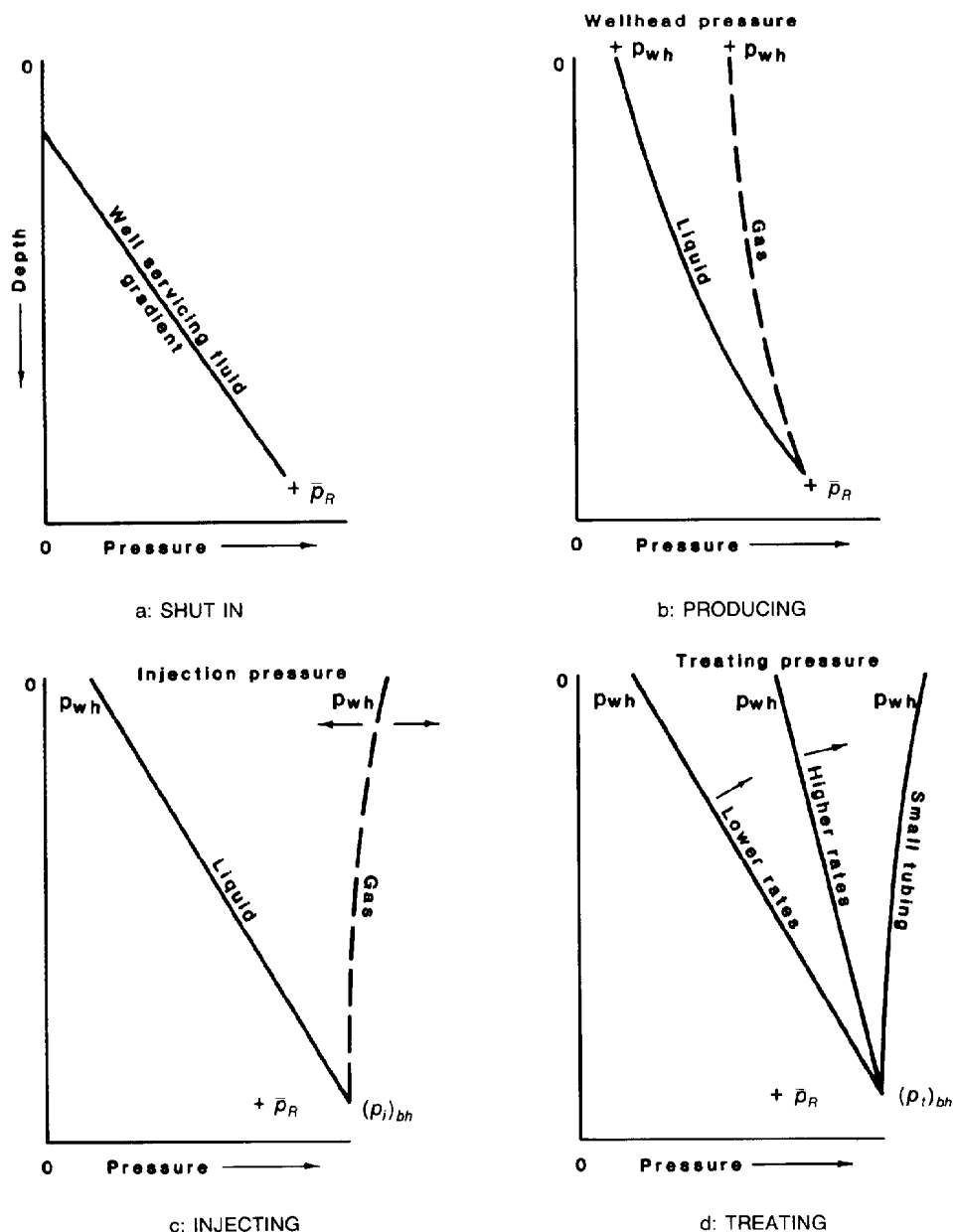


Fig. 4.10—Pressure profiles for four possible operational modes of oil and gas wells: a. Shut-in b. Producing c. Injecting d. Treating.

tubing and casing, and safety considerations. The slope of the pressure profile will depend on the tubing size, the treating rates, and the treating pressure downhole, $(p_t)_{bh}$.

It is recommended that pressure profiles of each operational mode be drawn for each step of a completion or major workover. As the examples will point out, the importance of pressure changes from one well mode to another and their effects on the tubing and packer system cannot be overemphasized.

Tubing Response Characteristics

Changing the mode of a well (producer, injector, shut-in) causes changes in temperature and pressures inside and outside the tubing. Depending on (1) how the tubing

is connected to the packer, (2) the type of packer, and (3) how the packer is set, temperature and pressure changes will effect the following.

1. Length variation in the tubing string will result if the seals are permitted to move inside a permanent polished seal-bore packer.

2. Tensile or compressive forces will be induced in the tubing and packer system if tubing motion is not permitted (latched connection).

3. A permanent packer will be unsealed if motion is permitted (tubing contraction) and the seal assembly section is not long enough.

4. Unseating of a solid-head tension (or compression) packer will occur if it is not set with sufficient strain (or weight) to compensate for tubing movement.

5. The equalizing valve will open prematurely on control-head packers (tension or compression).

The net result of any of these five events could reduce the effectiveness of the downhole tools and/or damage the tubing, casing, or even the formations open to the well. Failure to consider length and force changes may result in costly failures of such operations as squeeze cementing, acidizing, fracturing, and other remedial operations. Formation damage may result. In addition, the tubing string could be corkscrewed or parted.

Potential length changes under extreme conditions determine the length of seals necessary to remain packed-off with a polished seal-bore packer. Potential induced forces need to be calculated to prevent tubing damage, unseating packers, or opening equalizing valves.

The two major factors that tend to lengthen or shorten the string (movement permitted) are^{4,5} (1) temperature effect and (2) pressure effects—piston, ballooning, and buckling effects.

Buckling will only shorten the tubing string. The other factors may shorten or lengthen the tubing string. If motion is prevented, tension or compression forces are induced. It is important to understand and remember the direction of action of the length and force changes. It is equally important to remember that a string of tubing landed in any packer is initially in a neutral condition, except for any subsequent mechanical strain or set-down weight applied by the rig operator. After the tubing is landed, the factors that cause changes in length or force are always the result of a change in temperature and pressure.

Temperature Effect

Thermal expansion or contraction causes the major length change in the tubing.

$$\Delta L_t = 8.28 \times 10^{-5} \times L_t \times \Delta \bar{T}, \quad \dots \dots \dots (1)$$

where

$$\begin{aligned} \Delta L_t &= \text{change in tubing length, ft,} \\ L_t &= \text{tubing length, ft, and} \\ \Delta \bar{T} &= \text{change in average temperature, } ^\circ\text{F.} \end{aligned}$$

Length changes are calculated readily if the average temperature of the tubing can be determined for the initial condition and then again for the next operation and the next, etc. The average string temperature in any given operating mode is one-half the sum of the temperatures at the top and at the bottom of the tubing. The $\Delta \bar{T}$ is the difference between the average temperatures of any two subsequent operating modes.

If the motion is constrained, forces will be induced as a result of the temperature change. The temperature-induced force is

$$F = 207 \times A_{tw} \times \Delta \bar{T}, \quad \dots \dots \dots (2)$$

where

$$\begin{aligned} F &= \text{force (tensile or compressive, depending on} \\ &\quad \text{direction of } T), \text{ lbf, and} \\ A_{tw} &= \text{cross-sectional area of the tubing wall,} \\ &\quad \text{sq in.} \end{aligned}$$

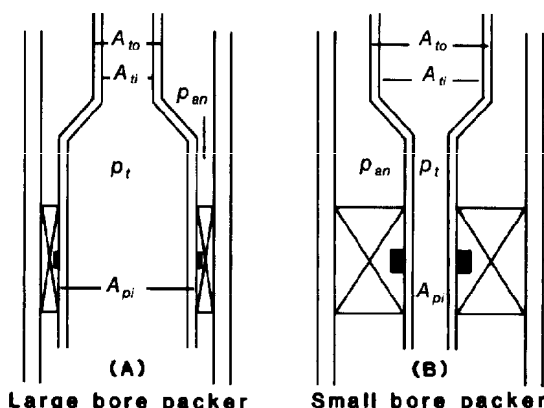


Fig. 4.11—Tubing and packer systems, illustrating various areas and pressures necessary for movement or force calculations.

In most cases, the temperature effect provides the major length or force change when changing from one operational mode to another.

Piston Effect

The length change or force induced by the piston effect is caused by pressure changes inside the annulus and tubing at the packer, acting on different areas (Fig. 4.11). The force and length changes can be calculated as follows.

$$F = \Delta p_t (A_{pi} - A_{ti}) - \Delta p_{an} (A_{pi} - A_{to}) \quad \dots \dots \dots (3)$$

(tubing) (annulus)

and

$$\Delta L_t = \frac{12L_t}{EA_{tw}} [\Delta p_t (A_{pi} - A_{ti}) - \Delta p_{an} (A_{pi} - A_{to})], \quad \dots \dots (4)$$

(pressure acting on differential area)

where

$$\begin{aligned} E &= \text{modulus of elasticity, psi (30} \times 10^6 \text{ for} \\ &\quad \text{steel),} \\ A_{pi} &= \text{area of packer ID, sq in.,} \\ A_{ti} &= \text{area of tubing ID, sq in.,} \\ A_{to} &= \text{area of tubing OD, sq in.,} \\ \Delta p_t &= \text{change in tubing pressure at packer, psi,} \\ &\quad \text{and} \\ \Delta p_{an} &= \text{change in annulus pressure at packer, psi.} \end{aligned}$$

Note that the length change, ΔL_t , is a product of L/EA_{tw} and the piston force (Eq. 3). The piston force is the sum of two pressures acting on two areas—one for the tubing and one for the annulus. Fig. 4.11a shows that for a large bore packer, annulus pressure causes downward force while tubing pressure causes an upward force. For a small bore packer this situation is reversed (Fig. 4.11b). The force greatest in magnitude will determine the resulting direction of action. An accurate schematic of the tubing and packer bore for each case should be made for proper determination of areas, forces, and the resulting direction of action.

**TABLE 4.2—TUBING CONSTANTS FOR USE IN DETERMINING
BUCKLING MOVEMENT CAUSED BY PRESSURE
DIFFERENTIALS**

OD (in.)	W_t (lbm/ft)	A_{to} (sq in.)	A_{ti} (sq in.)	A_{tw} (sq in.)	I (in. ⁴)	F_{oi}^2
1.660	2.40	2.164	1.496	0.668	0.195	1.448
1.900	2.90	2.835	2.036	0.799	0.310	1.393
2.000	3.40	3.142	2.190	0.952	0.404	1.434
2 ¹ / ₁₆	3.40	3.341	2.405	0.936	0.428	1.389
2 ³ / ₈	4.70	4.430	3.126	1.304	0.784	1.417
2 ⁷ / ₈	6.50	6.492	4.680	1.812	1.611	1.387
3 ¹ / ₂	9.20	9.621	7.031	2.590	3.885	1.368

Tubing OD (in.)	Weight (lbm/in.)	W_{ft} and W_{fd} (lbm/in.)	$W_t + W_{ft} - W_{fd}$											
			7.0* 52.3**	8.0 59.8	9.0 67.3	10.0 74.8	11.0 82.3	12.0 89.8	13.0 97.2	14.0 104.7	15.0 112.2	16.0 119.7	17.0 127.2	18.0 134.6
1.660	$W_t = 0.200$	W_{ft}	0.045	0.052	0.058	0.065	0.071	0.078	0.084	0.091	0.097	0.104	0.110	0.116
		W_{fd}	0.065	0.075	0.084	0.094	0.103	0.112	0.122	0.131	0.140	0.150	0.159	0.169
1.900	$W_t = 0.242$	W_{ft}	0.062	0.070	0.079	0.088	0.097	0.106	0.115	0.123	0.132	0.141	0.150	0.159
		W_{fd}	0.086	0.098	0.110	0.123	0.135	0.147	0.159	0.172	0.184	0.196	0.209	0.221
2.000	$W_t = 0.283$	W_{ft}	0.066	0.076	0.085	0.095	0.104	0.114	0.123	0.133	0.142	0.152	0.161	0.171
		W_{fd}	0.095	0.109	0.122	0.136	0.150	0.163	0.177	0.190	0.204	0.218	0.231	0.245
2 ¹ / ₁₆	$W_t = 0.283$	W_{ft}	0.073	0.083	0.094	0.104	0.114	0.125	0.135	0.146	0.156	0.167	0.177	0.187
		W_{fd}	0.101	0.116	0.130	0.145	0.159	0.174	0.188	0.202	0.217	0.231	0.246	0.260
2 ³ / ₈	$W_t = 0.392$	W_{ft}	0.095	0.108	0.122	0.135	0.149	0.162	0.176	0.189	0.203	0.217	0.230	0.243
		W_{fd}	0.134	0.153	0.172	0.192	0.211	0.230	0.249	0.268	0.288	0.307	0.326	0.345
2 ⁷ / ₈	$W_t = 0.542$	W_{ft}	0.142	0.162	0.182	0.203	0.223	0.243	0.263	0.284	0.304	0.324	0.344	0.364
		W_{fd}	0.196	0.225	0.253	0.281	0.309	0.337	0.365	0.393	0.421	0.450	0.478	0.506
3 ¹ / ₂	$W_t = 0.767$	W_{ft}	0.213	0.243	0.274	0.304	0.335	0.365	0.395	0.426	0.456	0.487	0.517	0.548
		W_{fd}	0.291	0.333	0.365	0.416	0.458	0.500	0.541	0.583	0.625	0.666	0.708	0.749

*lbm/gal.

**lbm/cu ft.

Ballooning and Reverse Ballooning

Internal pressure swells or balloons the tubing and causes it to shorten. Likewise, pressure in the annulus squeezes the tubing, causing it to elongate. This effect is called "reverse ballooning." The ballooning and reverse ballooning length change and force are given by

$$\Delta L_t = 2.4 \times 10^{-7} \times L_t \frac{\Delta p_t - F_{oi}^2 \Delta p_{an}}{F_{oi}^2 - 1} \quad (5)$$

and

$$F = 0.6(\Delta \bar{p}_t A_{ti} - \Delta \bar{p}_{an} A_{to}), \quad (6)$$

where

$\Delta \bar{p}_t$ = change in average tubing pressure from one mode to another, psi,

$\Delta \bar{p}_{an}$ = change in average annulus pressure from one mode to another, psi, and

F_{oi} = ratio of tubing OD to ID (Ref. 5 uses R).

Buckling Effects

Tubing strings tend to buckle only when p_t is greater than p_{an} . The result is a shortening of the tubing; the force exerted is negligible. The tubing length change is calculated using

$$\Delta L_t = \frac{r^2 A_{pi}^2 (\Delta p_t - \Delta p_{an})^2}{8EI(W_t + W_{ft} - W_{fd})}, \quad (7)$$

where

r = radial clearance between tubing OD, d_{to} , and casing ID, d_{ci} , $= (d_{ci} - d_{to})/2$, in.,

I = movement of inertia of tubing about its diameter $= \pi/64(d_{to}^4 - d_{ti}^4)$, in.⁴,

W_t = weight of tubing, lbm/in.,

W_{ft} = weight of fluid in tubing, lbm/in., and

W_{fd} = weight of displaced fluid, lbm/in.

Buckling only shortens the tubing and in most wells it will be the smallest constraint. For use with the radial and inertia calculations, values for A_{to} , A_{ti} , A_{tw} , I , F_{oi} , and $(W_t + W_{ft} - W_{fd})$ can be found, for most tubing sizes, in Table 4.2.

The net or overall length change (or force) is the sum of the length change (or forces) caused by the piston, ballooning, and temperature effects. The direction of the length change for each effect (or action of the force) must be considered when summing them. It follows that for a change in conditions, the motion (or force) created by one effect can be offset, or enhanced, by the motion (or force) developed by some other effect.

Moseley⁶ presented a method for graphically determining the length and force changes (Eqs. 5 through 7). This method is particularly useful on a fieldwide basis where wells have the same size tubing, casing and packers.

When planning the sequential steps of a completion or workover, care should be taken to consider the temperatures and pressures in each step, once the tubing

and packer system becomes involved. By careful selection of packer bore and use of annulus pressures, one or a combination of pressure effects could be employed to offset the adverse length or force change of another effect.

Combination Tubing/Packer Systems

Uniform completions have been discussed previously (i.e., a single tubing and casing size). Hammerlindl⁷ presented a method for solving problems with combination completions. His paper in particular covered two items not covered by Lubinski *et al.*⁴ He includes a direct mathematical method for calculating forces in uniform completions where tubing movement is not permitted and a method for handling hydraulic packers set with the wellhead in place. A combination completion consists of (1) more than one size of tubing, (2) more than one size of casing, (3) two or more fluids in the tubing and/or annulus, or (4) one or more of these.

Tubing/Packer Forces on Intermediate Packers

Intermediate packers are an integral part of the tubing string. Examples are dual packers in the long string or selective completion packers. The packer-to-tubing force on the intermediate packer is needed so that wells can be treated through the completion system. Without proper design, it is possible to shear the release mechanism in the intermediate packer(s), which could result in an expensive failure of the completion or workover.

Hammerlindl⁸ wrote an extension on his⁷ and Lubinski's⁴ earlier works that developed a theory required to solve for the intermediate packer-to-tubing forces. The calculation procedure regarding pressure effects requires working the problem from the lowest packer to the surface in stages. The first stage is the tubing between the bottom and second packer. The second stage is the tubing between the second and third packer (or the surface, if there are only two packers). The procedures are the standard ones for uniform completions. The only changes are those to determine the changes in length as a result of applied forces on the intermediate packers; also the actual and fictitious force calculation procedure is modified. Interested readers are referred to Hammerlindl's 1980 paper⁹ for additional information on the nebulous fictitious force of Lubinski *et al.*⁴

Key Equations in SI Metric Units

$$\Delta L_t = 1.4935 \times 10^{-5} L_t \times \Delta \bar{T} \quad \dots \dots \dots (1)$$

$$F = 741.934 A_{pw} \times \Delta \bar{T} \quad \dots \dots \dots (2)$$

$$\Delta L_t = \frac{3.6576 L_t}{E A_{pw}} [\Delta \bar{p}_t (A_{pi} - A_{ti}) - \Delta p_{an} (A_{pi} - A_{to})] \quad \dots \dots \dots (4)$$

$$\Delta L_t = 7.3 \times 10^{-8} \times L_t \frac{\Delta \bar{p}_t - F_{oi}^2 \Delta \bar{p}_{an}}{F_{oi}^2 - 1} \quad \dots \dots \dots (5)$$

Since Table 4.2 is not available in SI metric units, Eq. 7 is solved in English units (inches) and the result is converted to SI metric units (meters).

where

ΔL_t and L_t are

in m,

ΔT is in °C,

F is in N,

A 's are in m²,

p 's are in kPa, and

E is in 30×10^6 psi.

References

1. Patton, L.D. and Abbott, W.A.: *Well Completions and Workovers: The Systems Approach*, second edition, Energy Publications, Dallas (1985) 57-67.
2. Eichmeier, J.R., Ersoy, D., and Ramey, H.J. Jr.: "Wellbore Temperatures and Heat Losses During Production Operations," paper CIM 7016 presented at the 1976 CIM Soc. Meeting, Calgary, Alta. (May 6-7).
3. Arnold, R.B., Sandmeyer, D.J., and Eichmeier, J.R.: "Production Problems of a High-Pressure, High-Temperature Reservoir," paper CIM 7232.
4. Lubinski, A., Althouse, W.H., and Logan, J.L.: "Helical Buckling of Tubing Sealed in Packers," *J. Pet. Tech.* (June 1962) 655-70; *Trans., AIME*, 225.
5. *Packer Calculations Handbook*, Baker Oil Tool Div. (1971).
6. Moseley, Neal F.: "Graphic Solutions to Tubing Movement in Deep Wells," *Pet. Eng. Intl.* (March 1973) 59-66.
7. Hammerlindl, D.J.: "Movement, Forces, and Stresses Associated With Combination Tubing Strings Sealed in Packers," *J. Pet. Tech.* (Feb. 1977) 195-208.
8. Hammerlindl, D.J.: "Packer-to-Tubing Forces for Intermediate Packers," *J. Pet. Tech.* (March 1980) 515-27.
9. Hammerlindl, D.J.: "Basic Fluid and Pressure Forces on Oilwell Tubulars," *J. Pet. Tech.* (Jan. 1980) 153-59.

Chapter 5

Gas Lift

Herald W. Winkler, consultant *

Introduction

Description of Gas Lift Operations

Gas lift is the method of artificial lift that uses an external source of high-pressure gas for supplementing formation gas to lift the well fluids. The primary consideration in the selection of a gas-lift system to lift a well, a group of wells, or an entire field is the availability and compression cost of gas.

Continuous-flow gas lift is the only method of artificial lift that fully utilizes the energy in the formation gas production. Most wells are gas lifted by continuous flow, which can be considered an extension of natural flow by supplementing the formation gas with additional high-pressure gas from an outside source. Gas is injected continuously into the production conduit at a maximum depth on the basis of the available injection gas pressure. The injection gas mixes with the produced well fluids and decreases the flowing pressure gradient of the mixture from the point of gas injection to the surface. The lower flowing pressure gradient reduces the flowing bottomhole pressure (BHFP) to establish the drawdown required for attaining a design production rate from the well. If sufficient drawdown in the bottomhole pressure (BHP) is not possible by continuous flow, intermittent gas lift operation may be used.

Intermittent gas lift requires high instantaneous gas volumes to displace liquid slugs to the surface. The disadvantage of intermittent lift is an "on-off" need for high-pressure gas, which presents a gas handling problem at the surface and surging in the BHFP that cannot be tolerated in many wells producing sand.

Most high-pressure gas lift systems are designed to recirculate the lift gas. The low-pressure gas from the production separator is compressed and reinjected into the

well to lift the fluids from the well. This closed loop, as illustrated in Fig. 5.1, is referred to as a closed rotative gas-lift system.[†] Continuous-flow gas lift operations are preferable with a closed rotative system. Intermittent gas lift operations are particularly difficult to regulate and to operate efficiently in smaller closed rotative systems with limited gas storage capacities in the low- and high-pressure lines.

Applications

Gas lift is particularly applicable for lifting wells where high-pressure gas is available. Gas compressors may have been installed for gas injection, or high-pressure gas wells may be nearby. Since the cost of compression far exceeds the cost of downhole gas lift equipment, gas lift always should be considered when an adequate volume of high-pressure gas is available for wells requiring artificial lift. Most wells can be depleted by gas lift, which is particularly true since the implementation of reservoir pressure maintenance programs in most major oil fields.

Advantages and Limitations

The flexibility of gas lift in terms of production rates and depth of lift cannot be matched by other methods of artificial lift if adequate injection-gas pressure and volume are available. Gas lift is one of the most forgiving forms of artificial lift, since a poorly designed installation will normally gas lift some fluid. Many efficient gas lift installations with wireline-retrievable gas lift valve mandrels are designed with minimal well information for locating the mandrel depths on initial well completion.

Highly deviated wells that produce sand and have a high formation gas/liquid ratio are excellent candidates for gas lift when artificial lift is needed. Many gas lift installations are designed to increase the daily production from

*Original chapter in 1962 edition written by C.V. Kirkpatrick.

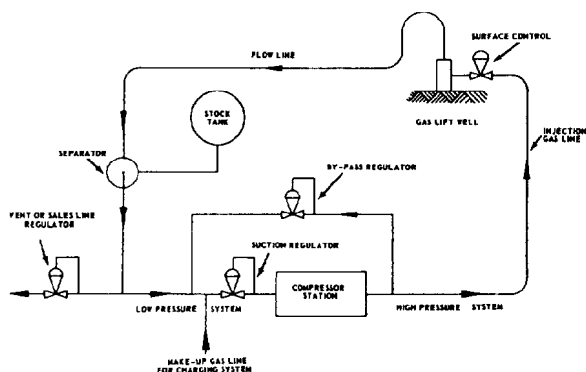


Fig. 5.1—Simplified flow diagram of a closed rotative gas lift system.

flowing wells. No other method is as ideally suited for through-flowline (TFL) ocean floor completions as a gas lift system. Maximum production is possible by gas lift from a well with small casing and high deliverability.

Wireline-retrievable gas lift valves can be replaced without killing a well or pulling the tubing. The gas lift valve is a simple device with few moving parts, and sand-laden well fluids do not have to pass through the valve to be lifted. The individual well in-hole equipment is relatively inexpensive. The surface equipment for injection gas control is simple and requires little maintenance and practically no space for installation. The reported overall reliability and operating costs for a gas lift system are lower than for other methods of lift.

The primary limitations for gas lift operations are the lack of formation gas or of an outside source of gas, wide well spacing, and available space for compressors on off-shore platforms. Generally, gas lift is not applicable to single-well installations and widely spaced wells that are not suited for a centrally located power system. Gas lift can intensify the problems associated with production of a viscous crude, a super-saturated brine, or an emulsion. Old casing, sour gas, and long, small-ID flowlines can rule out gas lift operations. Wet gas without dehydration will reduce the reliability of gas lift operations.

Conventional and Wireline-Retrieval Equipment

The early gas lift valves were the conventional type whereby the tubing mandrel that held the gas lift valve and reverse check valve was part of the tubing string. It was necessary to pull the tubing to replace a conventional gas lift valve. The first selectively retrievable gas lift valve and mandrel were introduced around 1950. The retrievable valve mandrel was designed with a pocket, or receiver, within the mandrel. A gas lift valve could be removed or installed by simple wireline operations without pulling the tubing. The wireline primary device for locating the mandrel pocket and selectively removing or installing a gas lift valve is a kickover tool. The mandrel is called a sidepocket mandrel because the pocket is offset from the centerline of the tubing. Most sidepocket-type retrievable valve mandrels have a full-bore ID equal to the tubing ID. These mandrels permit normal wireline operations, such as pressure surveys. This wireline-retrievable system for gas lift valves revolutionized the

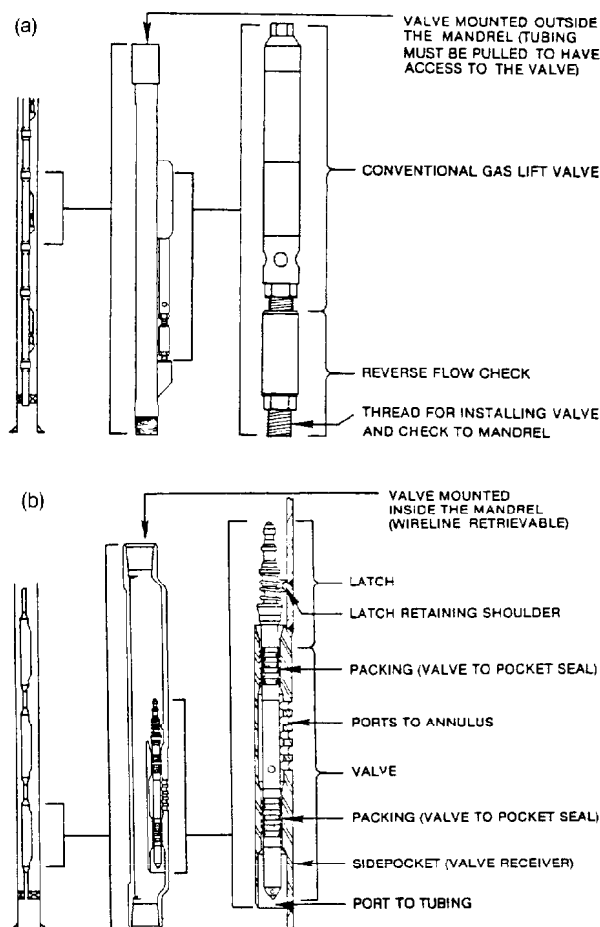


Fig. 5.2—Conventional and wireline-retrievable gas lift valves and mandrels. (a) Conventional gas lift valve and mandrel. (b) Wireline-retrievable gas lift valve and mandrel.

application of gas lift for inaccessible wells. The newer generation of retrievable valve mandrels have orienting devices to assure successful wireline operation in highly deviated wells.

The operating principles for a given type of conventional and wireline-retrievable gas lift valves are the same. Although the performance characteristics may vary between the same type of conventional and wireline-retrievable valve, the installation design calculations outlined in this chapter do not change. The choice between conventional and wireline-retrievable equipment depends primarily on the costs associated with pulling the tubing and on whether a workover fluid may damage the deliverability of a well.

Wireline-retrievable equipment is used in most offshore wells and in wells located inaccessibly where workover operations are extremely expensive. Conventional and wireline-retrievable gas lift valves and mandrels are illustrated in Fig. 5.2.²

Open and Closed Installations

Most tubing-flow gas lift installations will include a packer to stabilize the fluid level in the casing annulus and to prevent injection gas from blowing around the lower end of

the tubing in wells with a low BHFP. A closed gas lift installation implies that the installation includes a packer and a standing valve. An installation without a standing valve may be referred to as semiclosed, which is widely used for continuous flow operations. An installation without a packer or standing valve is called an open installation. An open installation seldom is recommended unless the well has a BHFP that significantly exceeds the injection gas pressure and unless normal packer removal may be difficult or impossible because of sand, scale, etc.

A packer is required for gas lifting low-BHP wells to isolate the injection gas in the casing annulus and to allow surface control of the injection-gas volumetric rate to the well. Intermittent gas lift installations will include a packer and possibly a standing valve. Although most illustrations of an intermittent gas lift installation will show a standing valve, many actual installations do not include this valve. If the permeability of the well is very low, the need for a standing valve is questionable.

The advantages of a packer are particularly important for gas lift installations in an area where the injection gas-line pressure varies or the injection gas supply is interrupted periodically. If the installation does not include a packer, the well must be unloaded after each shutdown. More damage to gas lift valves occurs during unloading operations than during any other time in the life of a gas lift installation. If the injection gas-line pressure varies, the working fluid level changes. The result is a liquid washing action through all valves below the working fluid level, and this continuing fluid transfer can eventually fluid-cut the seat assemblies of these gas lift valves. A packer stabilizes the working fluid level and eliminates the need for unloading after a shutdown and the fluid washing action from a varying injection gas-line pressure.

Considerations for Selecting the Proper Installation and Equipment

If a well can be gas lifted by continuous flow, this form of gas lift should be used to ensure a constant injection-gas circulation rate within the closed rotative gas lift system. Continuous flow reduces the possibility of pressure surges in the BHFP, flowline, and the low- and high-pressure surface facilities that are associated with intermittent gas lift operations. Overdesign rather than underdesign of a gas lift installation always is recommended when the well data are questionable. The gas lift equipment in the wells is the least expensive portion of a closed rotative gas lift system. The larger-OD gas lift valve should be selected for lifting high-rate wells. The superior injection-gas volumetric throughput performance for the 1½-in.-OD gas lift valve as compared to the 1-in.-OD valve is an important consideration for gas lift installations requiring a high injection gas requirement.

The gas lift installation designs outlined in this chapter include several safety factors to compensate for errors in well information and to allow an increase in the injection gas pressure to open the unloading and operating gas lift valves. If an installation is properly designed, all gas lift valves above an operating gas lift valve should be closed and all valves below will be open. The installation methods presented in this chapter are based on this premise. Gas lift valve operation is discussed in detail because it is difficult to design or to analyze a gas lift installation prop-

erly without understanding the mechanics of a gas lift valve.

A large-bore seating nipple, which is designed to receive a lock, is recommended for many gas lift installations. This seating nipple should be installed at the lower end of the tubing. Applications for a seating nipple include installation of a standing valve for testing the tubing or for intermittent gas lift operation, a means to secure and to pack off a BHP gauge for conducting pressure transient tests, etc. The lock should have an equalizing valve if the tubing will be blanked off. The pressure across the lock can be equalized before the lock is disengaged from the nipple to prevent the wireline tool string from being blown up the hole.

Gas Fundamentals as Applied to Gas Lift

Introduction

Only the gas fundamentals essential to the design and analysis of gas lift installations and operations will be discussed in this section. The more important gas calculations related to gas lift wells and systems can be divided into these topics: (1) gas pressure at depth, (2) temperature effect on the confined bellows-charged dome pressure, (3) volumetric gas throughput of a choke or gas lift valve port, and (4) gas volume stored within a conduit.

All gas equations are based on pressure in pounds per square inch absolute (psia), temperature in degrees Rankine (°R), and volume or capacity in cubic feet (cu ft). An exception is pressure difference in pounds per square inch (psi), which may be a difference in gauge or absolute units since the calculated pressure difference would be the same.

Generally, field measurements of pressure are in gauge readings; therefore, the volumetric-gas-throughput and gas-pressure-at-depth charts are in units of psig. The gas lift valve equations and calculations for bellows-charge and operating pressures in this chapter use gauge pressure.

Gas Pressure at Depth

Accurate prediction of injection gas pressure at depth is essential for proper gas lift installation design and for analyzing or trouble-shooting gas lift operations. Most gas-pressure-at-depth calculations are based on a static gas column. Pressure loss because of friction from the flow of injection gas through a typical casing/tubing annulus is negligible. The gas velocity in the annulus is practically nil since the cross-sectional area of the annulus is so much larger than the port area of a gas lift valve. The maximum gas flow rate is limited by the valve port size.

Calculating Static Injection Gas Pressure at Depth. Static injection gas pressure at depth can be calculated using Eq. 1.

$$p_{ioD} = p_{io} e^{(\gamma_g D)/(53.34 T_z)}, \dots \dots \dots (1)$$

where

p_{ioD} = operating injection gas pressure at depth D ,
psia,
 p_{io} = operating injection gas pressure at surface,
psia,

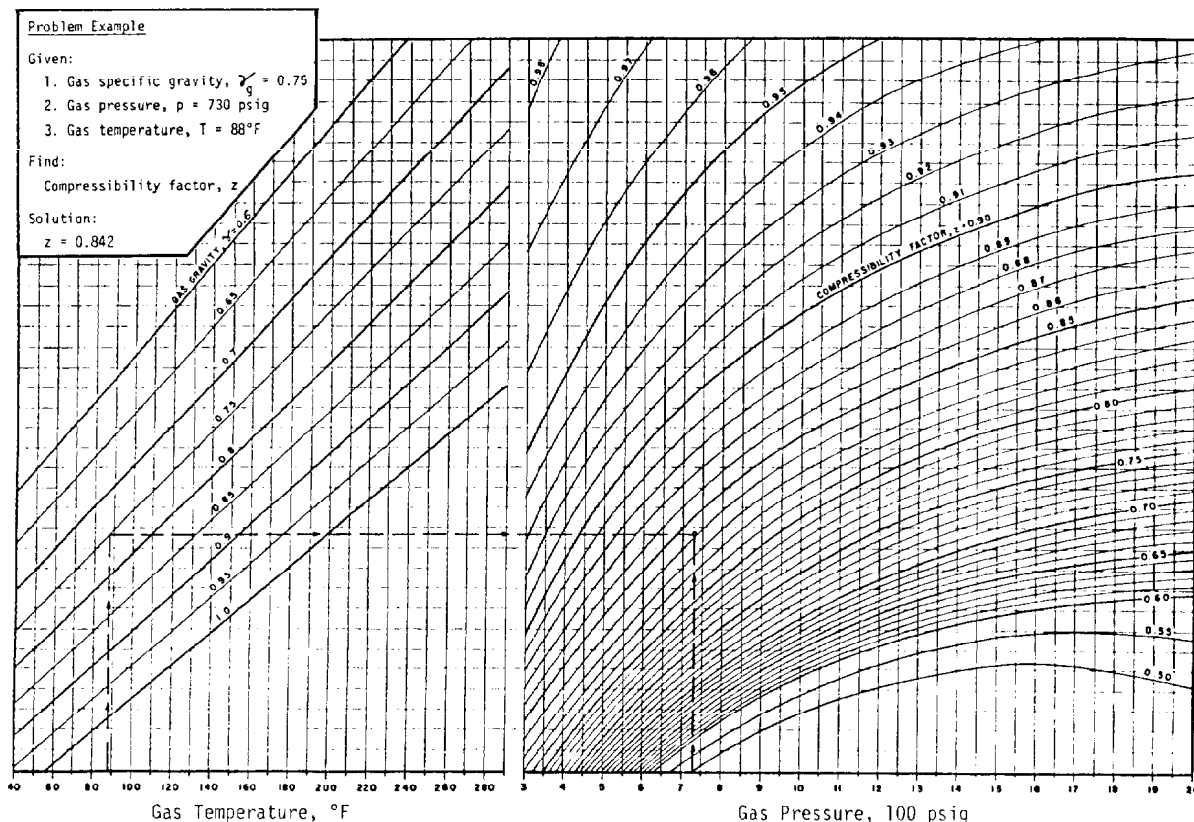


Fig. 5.3—Simplified compressibility factor chart for natural gases.

e = Napierian logarithm base=2.718
 γ_g = gas specific gravity (air=1.0),
 dimensionless,
 D = true vertical depth, ft,
 T = average gas temperature, $^\circ\text{R}$, and
 \bar{z} = compressibility factor based on average
 pressure p and temperature T ,
 dimensionless.

The depth used in the equation is the true vertical depth of the gas column. Since the gas compressibility factor is a function of the average pressure and temperature, the solution to this equation is trial-and-error. A simplified compressibility chart³ is illustrated in Fig. 5.3. Generally, the average pressure and temperature are assumed to be the arithmetic mean of the wellhead and bottom-hole values. This assumption is reasonable because the increase in well temperature with depth tends to result in a constant gas density with depth. A straight-line traverse will approximate an actual static-injection-gas-pressure-at-depth traverse and is used for the design of most gas lift installations.

Example Problem 1.

Given:

1. Gas specific gravity, $\gamma_g=0.70$ (air=1.0).
2. Atmospheric pressure=14.7 psia.
3. Injection gas pressure at surface, $p_{io}=1,000$ psig=1,014.7 psia.

4. True vertical depth of gas column, $D=8,000$ ft.
5. Gas temperature at wellhead, $T_{wh}=80^\circ\text{F}$.
6. Gas temperature at depth, $T_{gD}=200^\circ\text{F}$ at 8,000 ft.

Calculate the static gas pressure at the depth of 8,000 ft.

$$1. \bar{T} = \frac{T_{wh} + T_{gD}}{2} = \frac{80 + 200}{2} = 140^\circ\text{F} + 460 = 600^\circ\text{R}.$$

$$2. \frac{\gamma_g D}{53.34 \bar{T}} = \frac{0.70(8,000)}{53.34(600)} = 0.175 \text{ (constant).}$$

3. First assumption: $p_{ioD} = p_{io} + 2.5 \times 10^{-5} (p_{io}) D$.
 $p_{ioD} = 1,000 + 2.5 \times 10^{-5} (1,000) 8,000 = 1,200$ psig at 8,000 ft.

Note: Gauge pressure can be used for approximate calculations.

$$\bar{p} = \frac{p_{io} + p_{ioD}}{2} = \frac{1,000 + 1,200}{2} = 1,100 \text{ psig,}$$

$\bar{z} = 0.865$ from Fig. 5.3 for 1,100 psig and 140°F , and

$$p_{ioD} = 1,014.7 e^{(0.175/0.865)} = 1,242.2 \text{ psia}$$

$$= 1,227.5 \text{ psig at 8,000 ft.}$$

Chart Basis:

1. Gas specific gravity (air = 1.0) = 0.65
2. Gas temperature at surface = 100°F
3. Gas temperature at depth = 70°F + 1.6°F/100 ft

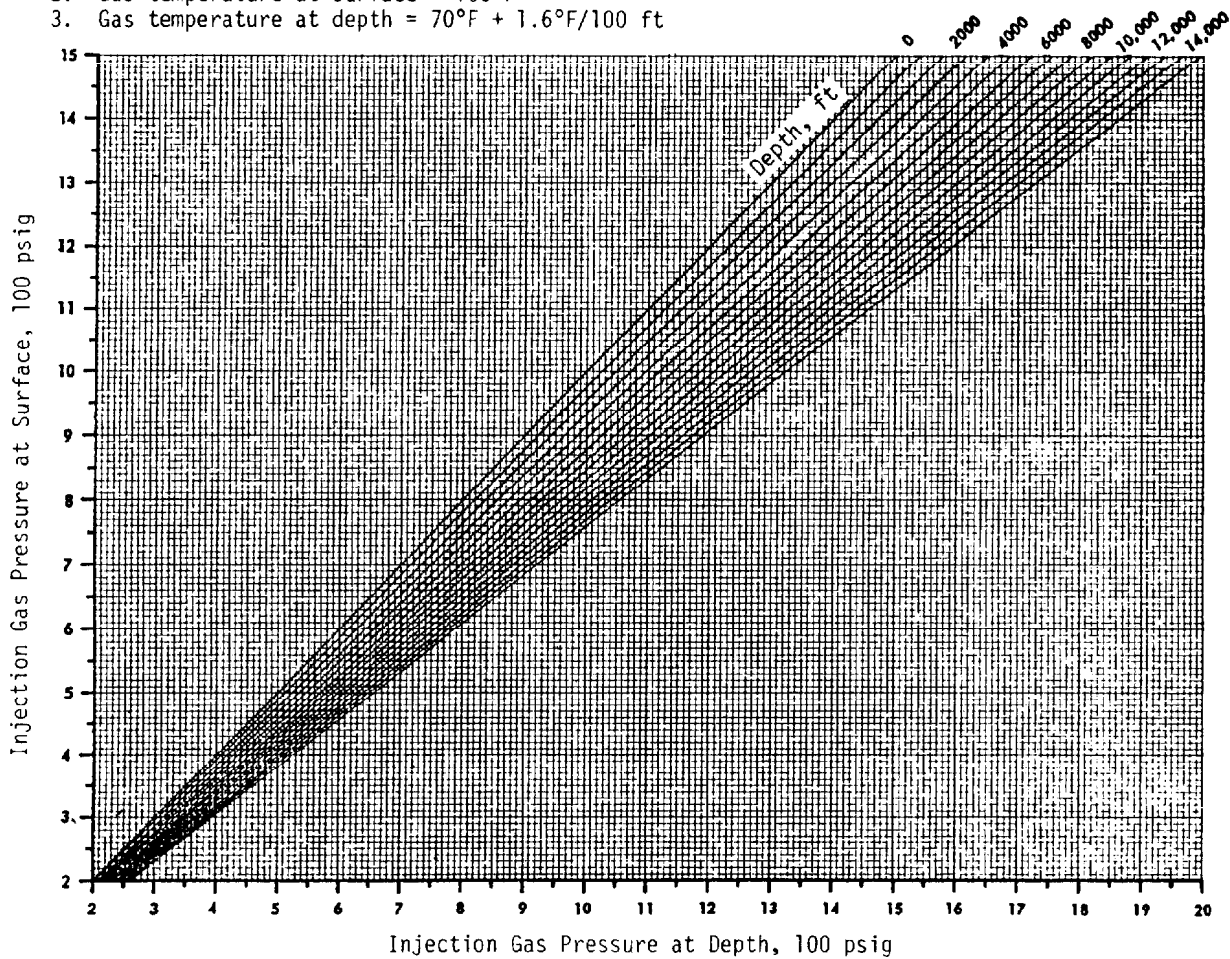


Fig. 5.4—Static injection-gas pressure at depth curve.

4. Repeat Step 3 using the previously calculated p_{ioD} .

$$\bar{p} = \frac{1,000 + 1,227.5}{2} = 1,113.8 \text{ psig,}$$

$\bar{z} = 0.864$ from Fig. 5.3 for 1,114 psig and 140°F, and

$$p_{ioD} = 1,014.7e^{(0.175/0.864)} = 1,242.5 \text{ psia}$$

$$= 1,227.8 \text{ psig at 8,000 ft.}$$

Since the calculated p_{ioD} is approximately equal to the assumed p_{ioD} , let $p_{ioD} = 1,228$ psig at 8,000 ft.

The first assumption in Step 3, using a coefficient of 2.5×10^{-5} to estimate the initial gas pressure at depth, is based on a hydrocarbon gas that is primarily methane. After the initial assumption, the computations are continued as outlined in Step 4 by assuming the previously calculated p_{ioD} until the assumed and calculated values are approximately equal.

Injection-Gas-Pressure-at-Depth Curves. Since the injection gas pressure at depth is based on the injection gas gravity and the geothermal temperature at depth gradient, gas-pressure-at-depth curves should be based on the properties of the injection gas and the actual average temperature of the gas column in the well. There is no one set of gas-pressure-at-depth curves that are suited for gas lift installation design and analysis for all wells. Gas pressures at depth should be calculated on the basis of the actual field data, and should be plotted with an expanded scale for the anticipated range of kick-off and operating injection gas pressures and the well depths for the field. Static injection gas-pressure-at-depth curves are illustrated in Fig. 5.4.⁴ These curves are based on a geothermal gradient of 1.6°F/100 ft of depth and a gas gravity of 0.65. The basis for the injection gas-pressure-at-depth curves must represent actual field conditions. Indiscriminate use of just any gas-pressure-at-depth chart may result in an installation design that will not unload or in an erroneous analysis of the operation of an existing gas lift installation.

Factor for Approximating Gas Pressure at Depth. A convenient and accurate method for estimating static in-

jection gas pressure at depth is to develop a factor for gas pressure at depth on the basis of the available surface operating injection gas pressure, average well depth, the injection gas gravity, and the actual geothermal temperature gradient. The equation for calculating gas pressure at depth with the proper factor is

$$p_{ioD} = p_{io} + F_g \times 10^{-5} (p_{io})D, \quad \dots \quad (2)$$

where F_g is the gas-pressure-at-depth factor, psi/100 psi/1,000 ft.

A factor for gas pressure at depth should be calculated for a particular field on the basis of the actual operating injection gas pressure at the wellsite, the well depth, the injection gas gravity, and the geothermal temperature in the wells. Static gas pressure at true vertical depth can be calculated for the design operating surface injection gas pressure using Eq. 1. Then a gas-pressure-at-depth factor can be calculated with Eq. 3:

$$F_g = 10^5 \left[\frac{p_{ioD} - p_{io}}{p_{io}(D)} \right], \quad \dots \quad (3)$$

Eq. 3 will ensure reasonably accurate gas-pressure-at-depth calculations over the range of surface injection gas pressure associated with gas lift operations in most wells. The slope of the injection gas-pressure-at-depth curve based on Eq. 2 will increase with surface pressure, as it should.

Example Problem 2.

Given (data from previous Example Problem 1):

1. $p_{io} = 1,000$ psig at surface.
2. $p_{ioD} = 1,228$ psig at 8,000 ft.
3. $D = 8,000$ ft.

Calculate:

1. Static gas-pressure-at-depth factor from Eq. 3:

$$F_g = 10^5 \left[\frac{p_{ioD} - p_{io}}{p_{io}(D)} \right] = 10^5 \left[\frac{1,228 - 1,000}{1,000(8,000)} \right]$$

$$= 2.85 \text{ psi/100 psi/1,000 ft.}$$

2. Static gas pressure at 6,000 ft from Eq. 2:

$$p_{ioD} = p_{io} + F_g \times 10^{-5} (p_{io})D = 1,000 + 2.85 \times 10^{-5}$$

$$\times (1,000)6,000 = 1,171 \text{ psig at 6,000 ft.}$$

3. Static gas pressure at 6,000 ft from Eq. 2 for a surface pressure of 800 psig. Compare the calculated value with the chart reading for the proper gas-pressure-at-depth curve in Fig. 5.4. F_g from Fig. 5.4 is approximately 2.3 psi/100 psi/1,000 ft.

$$p_{ioD} = 800 + 2.3 \times 10^{-5} (800)6,000$$

$$= 910 \text{ psig at 6,000 ft.}$$

From Fig. 5.4, $p_{ioD} = 910$ psig at 6,000 ft.

Temperature Effect on the Confined Bellows-Charged Dome Pressure

There are more bellows-charged than spring-loaded gas lift valves in service. Most of these valves have nitrogen gas in the dome. Since it is impractical to set each gas lift valve at its operating well temperature, the test rack opening or closing pressure is set at a standard base temperature. Most manufacturers set their bellows-charged gas lift valves with the nitrogen gas charge in the dome at 60°F. Nitrogen was selected as the charge gas for these reasons: (1) the compressibility factors for nitrogen at various pressures and temperatures are known, (2) nitrogen is noncorrosive and safe to handle, and (3) nitrogen is readily available throughout the world and is inexpensive.

The temperature correction factors for nitrogen based on 60°F are given in Table 5.1. These factors are used to calculate the nitrogen-charged dome pressure at 60°F for a given valve operating temperature (T_{vD}) or unloading temperature (T_{uD}) at valve depth in a well.

$$p_b = F_T (p_{bvD}), \quad \dots \quad (4)$$

where

F_T = temperature correction factor for nitrogen from T_{vD} or T_{uD} to 60°F, dimensionless,

p_b = bellows-charged dome pressure at 60°F, psig, and

p_{bvD} = bellows-charged dome pressure at T_{vD} or T_{uD} , psig.

Although Table 5.1 is based on 60°F, a test rack opening or closing pressure can be calculated for another temperature base, or the temperature correction factors can be used to calculate the test rack opening pressure at a temperature other than 60°F when a valve has been set at 60°F.

$$p_{vos} = \frac{p_{vo}}{F_{Ts}}, \quad \dots \quad (5)$$

where

p_{vo} = test rack valve opening pressure at 60°F, psig,

p_{vos} = test rack valve opening pressure at T_{vs} , psig,

T_{vs} = test rack valve setting temperature (other than 60°F), °F, and

F_{Ts} = temperature correction factor for nitrogen at T_{vs} , dimensionless.

This is a particularly useful equation for testing or setting gas lift valves in a field where a cooler is unavailable. The most important consideration during the test rack setting procedure is that all bellows-charged gas lift valves for a given installation be set exactly at the same temperature. To ensure that the valves are at the same temperature, all gas lift valves for a given well can be stored in the same water bath. The valves remain submerged in the container of water with the exception of the short interval of time that a valve is in the tester. The tester-set tem-

**TABLE 5.1—TEMPERATURE CORRECTION FACTORS FOR NITROGEN
BASED ON 60°F**

°F	F_T^*	°F	F_T^*	°F	F_T^*	°F	F_T^*	°F	F_T^*	°F	F_T^*
61	0.998	101	0.919	141	0.852	181	0.794	221	0.743	261	0.698
62	0.996	102	0.917	142	0.850	182	0.792	222	0.742	262	0.697
63	0.994	103	0.915	143	0.849	183	0.791	223	0.740	263	0.696
64	0.991	104	0.914	144	0.847	184	0.790	224	0.739	264	0.695
65	0.989	105	0.912	145	0.845	185	0.788	225	0.738	265	0.694
66	0.987	106	0.910	146	0.844	186	0.787	226	0.737	266	0.693
67	0.985	107	0.908	147	0.842	187	0.786	227	0.736	267	0.692
68	0.983	108	0.906	148	0.841	188	0.784	228	0.735	268	0.691
69	0.981	109	0.905	149	0.839	189	0.783	229	0.733	269	0.690
70	0.979	110	0.903	150	0.838	190	0.782	230	0.732	270	0.689
71	0.977	111	0.901	151	0.836	191	0.780	231	0.731	271	0.688
72	0.975	112	0.899	152	0.835	192	0.779	232	0.730	272	0.687
73	0.973	113	0.898	153	0.833	193	0.778	233	0.729	273	0.686
74	0.971	114	0.896	154	0.832	194	0.776	234	0.728	274	0.685
75	0.969	115	0.894	155	0.830	195	0.775	235	0.727	275	0.684
76	0.967	116	0.893	156	0.829	196	0.774	236	0.725	276	0.683
77	0.965	117	0.891	157	0.827	197	0.772	237	0.724	277	0.682
78	0.963	118	0.889	158	0.826	198	0.771	238	0.723	278	0.681
79	0.961	119	0.887	159	0.825	199	0.770	239	0.722	279	0.680
80	0.959	120	0.886	160	0.823	200	0.769	240	0.721	280	0.679
81	0.957	121	0.884	161	0.822	201	0.767	241	0.720	281	0.678
82	0.955	122	0.882	162	0.820	202	0.766	242	0.719	282	0.677
83	0.953	123	0.881	163	0.819	203	0.765	243	0.718	283	0.676
84	0.951	124	0.879	164	0.817	204	0.764	244	0.717	284	0.675
85	0.949	125	0.877	165	0.816	205	0.762	245	0.715	285	0.674
86	0.947	126	0.876	166	0.814	206	0.761	246	0.714	286	0.673
87	0.945	127	0.874	167	0.813	207	0.760	247	0.713	287	0.672
88	0.943	128	0.872	168	0.812	208	0.759	248	0.712	288	0.671
89	0.941	129	0.871	169	0.810	209	0.757	249	0.711	289	0.670
90	0.939	130	0.869	170	0.809	210	0.756	250	0.710	290	0.669
91	0.938	131	0.868	171	0.807	211	0.755	251	0.709	291	0.668
92	0.936	132	0.866	172	0.806	212	0.754	252	0.708	292	0.667
93	0.934	133	0.864	173	0.805	213	0.752	253	0.707	293	0.666
94	0.932	134	0.863	174	0.803	214	0.751	254	0.706	294	0.665
95	0.930	135	0.861	175	0.802	215	0.750	255	0.705	295	0.664
96	0.928	136	0.860	176	0.800	216	0.749	256	0.704	296	0.663
97	0.926	137	0.858	177	0.799	217	0.748	257	0.702	297	0.662
98	0.924	138	0.856	178	0.798	218	0.746	258	0.701	298	0.662
99	0.923	139	0.855	179	0.796	219	0.745	259	0.700	299	0.661
100	0.921	140	0.853	180	0.795	220	0.744	260	0.699	300	0.660

$$*F_T = \frac{\text{Gas lift valve dome pressure at 60°F}}{\text{Gas lift valve dome pressure at well temperature}}$$

perature will be the temperature of the water, and the nitrogen-charged dome pressure can be calculated for any setting temperature as follows:

$$p_{bvs} = \frac{F_T(p_{bvD})}{F_{Ts}}, \dots\dots\dots (6)$$

where p_{bvs} is the bellows-charged dome pressure at T_{vs} , psig.

The reciprocal of the temperature correction factors for nitrogen in Table 5.1 is published by some companies. These factors will be greater rather than less than one. If the published factors are greater than one, simply divide instead of multiplying, or multiply rather than dividing when using Eqs. 5 and 6.

Example Problem 3.

Given:

1. Gas lift valve with ratio of valve port ball-seat contact area to effective bellows area $A_p/A_b=0.11$.
2. Valve temperature in the well, $T_{vD}=142^\circ\text{F}$.
3. Calculated bellows-charge pressure of valve at well temperature, $p_{bvD}=800$ psig at 142°F .

Refer to Table 5.2 and Eqs. 16 and 21 in the valve mechanics discussion for explanation of the port-to-bellows-area ratio terms and the equations used in the following calculations.

Calculate the test-rack valve opening pressure at 60°F .

1. $F_T=0.850$ for 142°F from Table 5.1
2. $p_b=F_T(p_{bvD})=0.850(800)=680$ psig at 60°F .

$$3. p_{vo} = \frac{p_b}{(1 - A_p/A_b)} = \frac{680}{(1 - 0.11)}$$

$$= 764 \text{ psig at } 60^\circ\text{F.}$$

Calculate the test-rack valve opening pressure at 90°F .

1. $F_{Ts} = 0.939$ for 90°F from Table 5.1.

$$2. p_{bvs} = \frac{F_T(p_{bD})}{F_{Ts}} = \frac{0.850(800)}{0.939}$$

$$= 724 \text{ psig at } 90^\circ\text{F.}$$

$$3. p_{vos} = \frac{p_{bvs}}{(1 - A_p/A_b)} = \frac{764}{(1 - 0.11)}$$

$$= 814 \text{ psig at } 90^\circ\text{F.}$$

or

$$p_{vos} = \frac{p_{vo}}{F_{Ts}} = \frac{764}{0.939} = 814 \text{ psig at } 90^\circ\text{F}$$

The previous equations using F_{Ts} are recommended when checking tester opening pressures of a string of gas lift valves at a temperature other than the base temperature of 60°F .

Volumetric Gas Throughput of a Choke or Gas Lift Valve Port

The injection gas throughput of a valve can affect the gas-lift installation design and operation. A high-rate installation will not unload if the choke or port size is too small. The volumetric gas rate required to uncover a lower valve by gas injection through the valve above is greater than the injection gas required to lift from the same lower valve for a given production rate.

The volumetric gas throughput of an orifice is calculated on the basis of an equation for flow through a converging nozzle. This equation is complex and lengthy for noncritical flow. For this reason, gas passage charts generally are used for estimating the volumetric gas rate through an orifice or valve port. One of the more widely used equations for gas throughput was published by Thornhill-Craver.⁵

Gas flow through most gas lift valves occurs in the noncritical flow range. The calculation of volumetric gas rate through a choke for noncritical flow is lengthy, as can be seen by the following basic gas flow equation.

$$q_{gsc} = \frac{155.5 C_d(A) p_1 \sqrt{2(g) \left(\frac{k}{k-1} \right) [(F_{du})^{2/k} - (F_{du})^{(k+1)/k}]} }{\sqrt{\gamma_g(T_1)}} \quad (7)$$

where

q_{gsc} = gas flow rate at standard conditions (14.7 psia and 60°F), Mscf/D,

C_d = discharge coefficient (determined experimentally), dimensionless,

A = area of opening, sq in.,

p_1 = upstream pressure, psia,

p_2 = downstream pressure, psia,

g = acceleration of gravity, ft/sec²,

k = ratio of specific heats, dimensionless,

T_1 = upstream temperature, $^\circ\text{R}$,

F_{cf} = critical flow pressure ratio = $\left(\frac{2}{k+1} \right)^{k/(k-1)}$
and

F_{du} = ratio of downstream pressure/upstream pressure, consistent units, $F_{du} = F_{cf}$ if $F_{du} < F_{cf}$ and $F_{du} = p_2/p_1 \geq F_{cf}$.

It is apparent from Eq. 7 that injection gas throughput charts are desirable for installation design and analysis purposes. The gas compressibility factor is not included in Eq. 7; therefore, most published gas passage charts do not include a gas-compressibility-factor correction. Since the compressibility factor would enter the equation as a square root term in the denominator, the chart values will be lower than actual values for most injection gas gravities and pressures.

One type of choke capacity chart is illustrated in Figs. 5.5 and 5.6. The advantages of this type of display are the number of orifice sizes on a single chart for a full range of upstream and downstream pressures, and an orifice size can be determined for a given gas throughput and the given upstream and downstream pressures. The gas throughput capacity of the different orifice sizes is based on 14.65 psia and 60°F for a gas gravity of 0.65 and an orifice discharge coefficient of 0.865. Since gas flow through a gas lift valve occurs in a gas lift installation at the well temperature at valve depth, a correction for temperature improves the prediction for the volumetric gas rate. If the actual gravity differs from 0.65, a second correction should be applied. An approximate correction for gas passage can be calculated using the following equations.

$$C_{gT} = 0.0544 \sqrt{\gamma_g(T_{gD})} \quad (8)$$

and

$$q_{ga} = \frac{q_{gc}}{C_{gT}}, \quad (9)$$

where

C_{gT} = approximate correction factor for gas gravity and temperature, dimensionless,

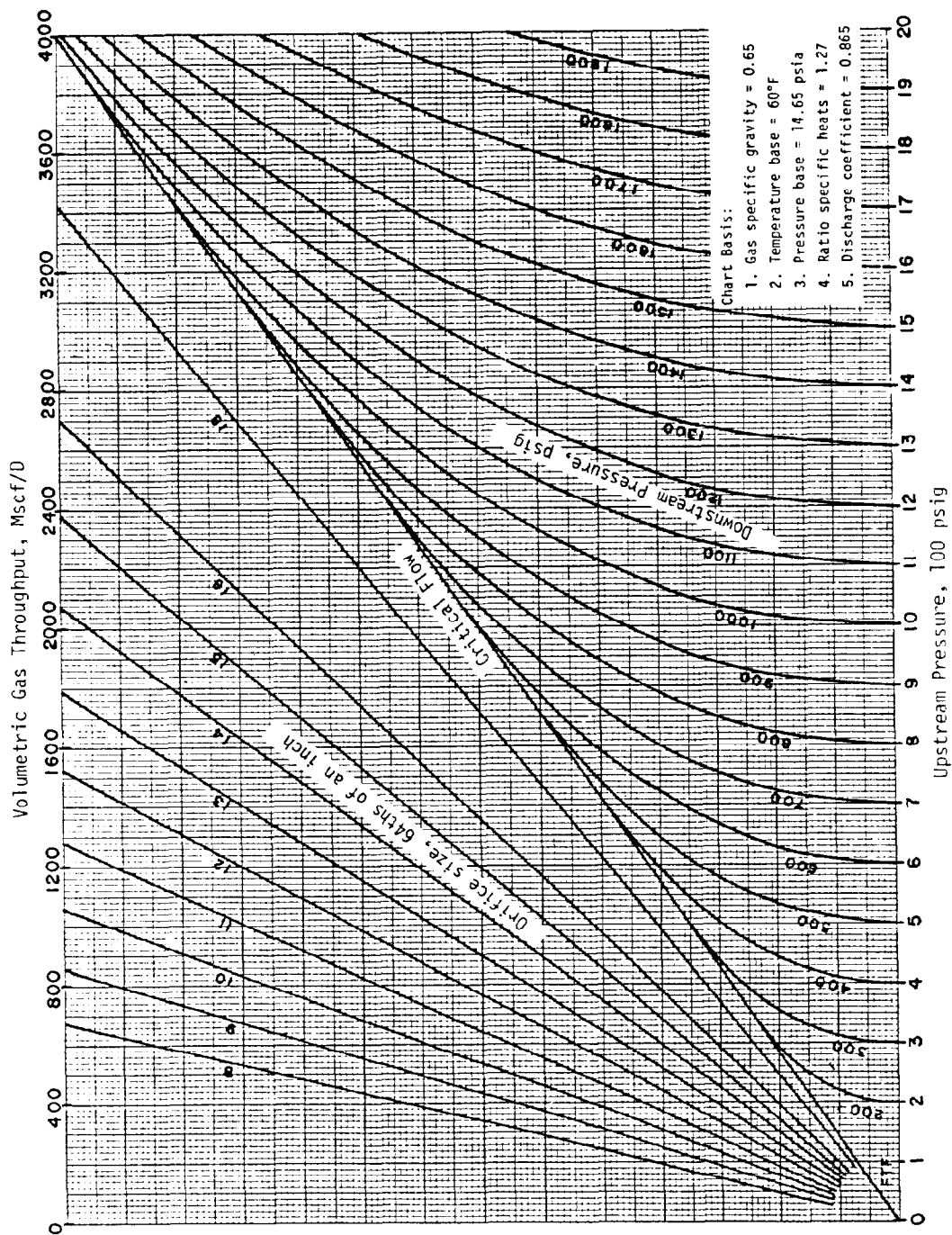
T_{gD} = gas temperature at valve depth, $^\circ\text{R}$,

q_{ga} = actual volumetric gas rate, Mscf/D, and

q_{gc} = chart volumetric gas rate, Mscf/D.

Although most gas lift manuals will include gas capacity charts for every conceivable gas-lift valve port and choke size, numerous charts are unnecessary. The gas capacity for any choke size can be calculated from a known gas capacity for a given choke size because the volumetric gas throughput rate is directly proportional to the area of the orifice.

$$q_{g2} = q_{g1} \left(\frac{d_2}{d_1} \right)^2, \quad (10)$$

Fig. 5.5—Gas passage chart for $\frac{1}{64}$ - through $\frac{1}{64}$ -in. orifices.

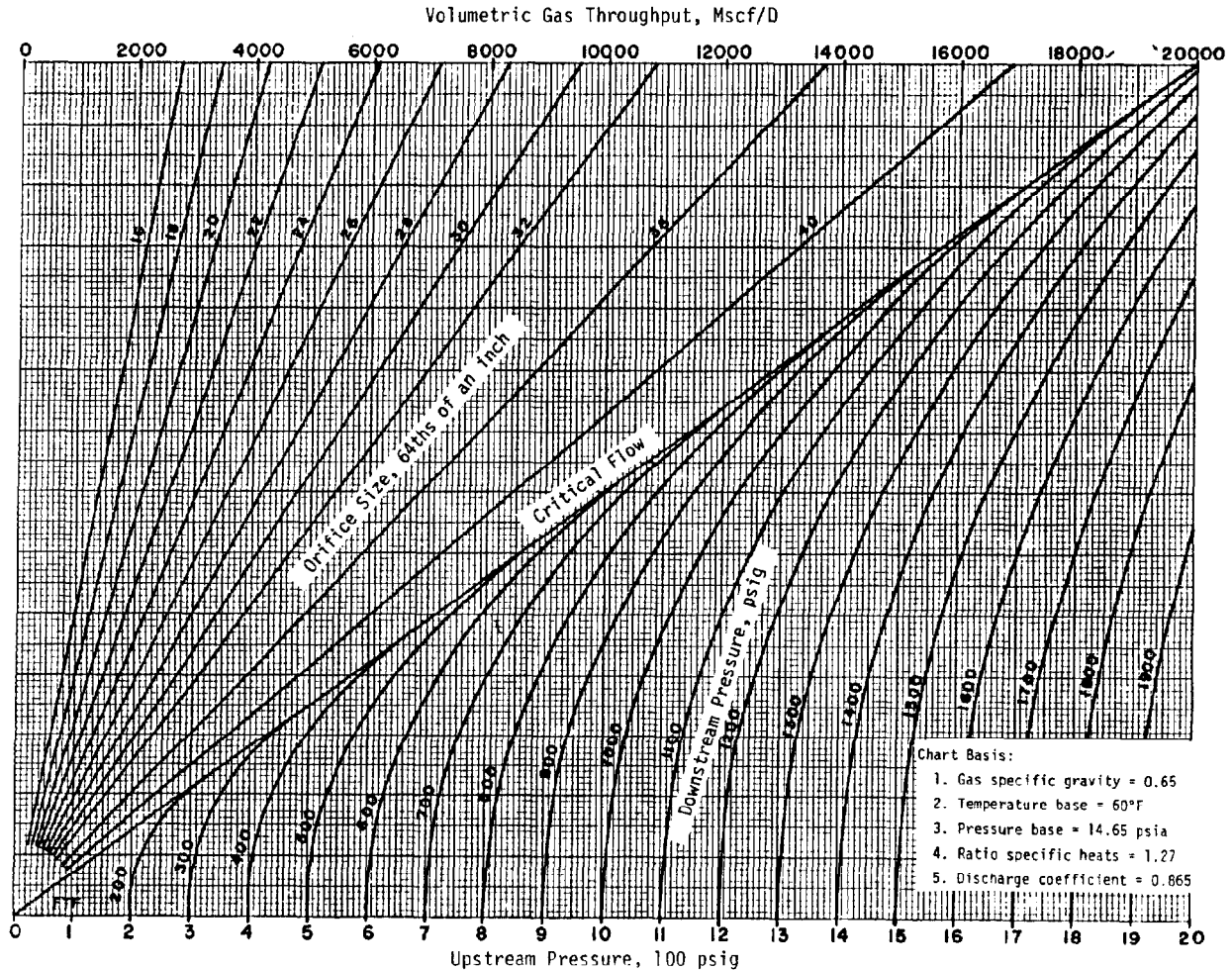


Fig. 5.6—Gas passage chart for $\frac{1}{64}$ -in. through $\frac{40}{64}$ -in. orifices.

where

q_{g1} = known volumetric gas rate, Mscf/D,

d_1 = orifice ID for known volumetric gas rate, in.,

q_{g2} = unknown volumetric gas rate, Mscf/D, and

d_2 = orifice ID for unknown volumetric gas rate, in.

Orifice sizes can be in 64ths of an inch. The denominator of the fraction for both terms must remain consistent.

Example Problem 4.

Given:

1. Injection gas gravity, $\gamma_g = 0.7$ (air = 1.0).
2. Orifice-check valve port size = $\frac{1}{4}$ in.
3. Operating injection gas pressure at valve depth (upstream pressure), $p_{iOD} = 1,100$ psig.
4. Flowing production pressure at valve depth (downstream pressure), $p_{pFD} = 900$ psig.
5. Injection gas temperature at valve depth, $T_{gD} = 140^\circ\text{F}$.

Determine the actual volumetric gas throughput of the orifice-check valve.

$$C_{gT} = 0.0544\sqrt{0.7(140+460)} = 1.115.$$

$$q_{gc} = 1,210 \text{ Mscf/D from Fig. 5.5 (chart value).}$$

$$q_{ga} = 1,210/1.115 = 1,085 \text{ Mscf/D (actual value).}$$

Calculate volumetric gas throughput of a $\frac{1}{2}$ -in. orifice ($\frac{32}{64}$ -in.) on the basis of the capacity of a $\frac{1}{4}$ -in. orifice and compare the calculated and chart values.

$$q_{gc} = 1,210 \left(\frac{0.5}{0.25} \right)^2 = 4,840 \text{ Mscf/D}$$

$$(1,210 \text{ Mscf/D for } \frac{1}{4}\text{-in. orifice}),$$

or

$$\begin{aligned} q_{gc} &= 1,210 \left(\frac{32}{16} \right)^2 \\ &= 4,840 \text{ Mscf/D, and} \end{aligned}$$

$$q_{gc} = 4,850 \text{ Mscf/D from Fig. 5.6 for } \frac{1}{2}\text{-in. orifice.}$$

Gas Volume Stored Within a Conduit

Typical applications for gas volume calculations are (1) the volume of injection gas required to fill the production conduit and to displace a liquid slug to the surface for intermittent gas lift operations; (2) the volume of injection gas available, or removed, from a casing annulus on the basis of a change in the casing pressure during an intermittent injection gas cycle—particularly important for design calculations using choke control of the injection gas; and (3) design calculations for the low- and high-pressure systems in a closed, rotative gas lift system when a minimum capacity is required for storage or retention of the injection gas within the system.

The gas capacity and volume calculations are based on an equation of state for real gases.

$$pV = znRT, \dots\dots\dots (11)$$

where

- p = pressure, psia,
- V = volume or capacity, cu ft,
- z = compressibility factor based on p and T , dimensionless,
- n = number of pound-moles, lbm-mol,
- R = gas constant = 10.73 psia-cu ft/lbm-mol-°R, and
- T = temperature, °R.

Most gas volume and capacity problems can be solved using Eq. 11 and Avogadro's principle, which states that 1 lbm-mol of any gas occupies approximately 379 scf at 14.7 psia and 60°F.

The volume of gas required to fill a conduit can be calculated with the following equation:

$$V_g = V_c \left(\frac{p T_{sc}}{z p_{sc} T} \right), \dots\dots\dots (12)$$

where

- V_g = gas volume at standard conditions, scf,
- V_c = capacity of conduit, cu ft,
- p = average gas pressure, psia,
- p_{sc} = standard pressure base, psia,
- T = average gas temperature, °R, and
- T_{sc} = standard temperature base, °R.

Also, the volume of gas can be calculated by solving for the number of pound-moles in Eq. 11 and by converting the pound-moles to standard cubic feet using Avogadro's principle. Average values for pressure and temperature based on surface and bottomhole values and the corresponding z -value must be used in the equation for inclined conduits.

A gas volume equation for pressure difference can be written as

$$V_g = \frac{V_c T_{sc}}{T p_{sc}} \left(\frac{p_1}{z_1} - \frac{p_2}{z_2} \right), \dots\dots\dots (13)$$

where Subscripts 1 and 2 refer to the high and the low average pressure and the corresponding compressibility factor, respectively, and the average temperature does not change. If the conduit is horizontal, average pressures and

temperature are the surface values in Eqs. 12 and 13. The average temperature of a gas column in the casing is assumed to be the same at the instant a gas lift valve opens or closes. Eq. 13 may be simplified by using one compressibility factor for an average of the average pressures. This assumption is particularly applicable for very little change in pressure.

Approximate estimations and questionable field data do not warrant detailed calculations. The approximate volume of gas required for a given change in pressure within a conduit can be calculated using the following equation:

$$V_{gx} = \left(\frac{\bar{p}_1 - \bar{p}_2}{p_{sc}} \right) V_c, \dots\dots\dots (14)$$

where V_{gx} is the approximate gas volume, scf.

The ratio of the standard to the average temperature, which is less than one, tends to offset the reciprocal of the compressibility factor that is greater than one. This compensation decreases the error made when not including these variables in the approximate equation.

Example Problem 5.

Given:

1. Capacity of casing annulus = 0.10 cu ft/ft (2 7/8-in.-OD tubing × 5 1/2-in.-OD casing).
2. Depth of operating valve, D_{ov} = 6,000 ft.
3. Surface closing pressure of operating valve, p_{vc} = 600 psig.
4. Surface opening pressure of operating valve, p_o = 660 psig.
5. Average temperature of gas column, T = 120°F = 580°R.
6. Standard conditions: 14.7 psia and 60°F (520°R).
7. Gas gravity γ_g = 0.65, (air = 1.0).
8. Gas-pressure-at-depth factor, F_g = 2.4 psi/100 psi/1,000 ft.
9. Atmospheric pressure = 14.7 psia.

Calculate the volume of gas stored in the casing annulus between surface pressures of 660 and 600 psig by using Eq. 13.

$$\begin{aligned} V_c &= 6,000(0.10) = 600 \text{ cu ft,} \\ \bar{p}_1 &= 660 + 2.4 \times 10^{-5} (660) 3,000 \\ &= 707.5 \text{ psig} + 14.7 = 722.2 \text{ psia,} \\ \bar{z}_1 &= 0.911 \text{ from Fig. 5.3 for } T \\ &= 120^\circ\text{F, } \gamma_g = 0.65, \text{ and } p = 707.5 \text{ psig,} \\ \bar{p}_2 &= 600 + 2.4 \times 10^{-5} (600) 3,000 \\ &= 643.2 \text{ psig} + 14.7 = 657.9 \text{ psia, and} \\ \bar{z}_2 &= 0.918 \text{ from Fig. 5.3 for } T \\ &= 120^\circ\text{F, } \gamma_g = 0.65, \text{ and } p = 643.2 \text{ psig.} \end{aligned}$$

$$\begin{aligned} V_g &= \frac{V_c T_{sc}}{T p_{sc}} \left(\frac{p_1}{z_1} - \frac{p_2}{z_2} \right) \\ &= \frac{600(520)}{580(14.7)} \left(\frac{722.2}{0.911} - \frac{657.9}{0.918} \right) \\ &= 2,784 \text{ scf at 14.7 psia and } 60^\circ\text{F.} \end{aligned}$$

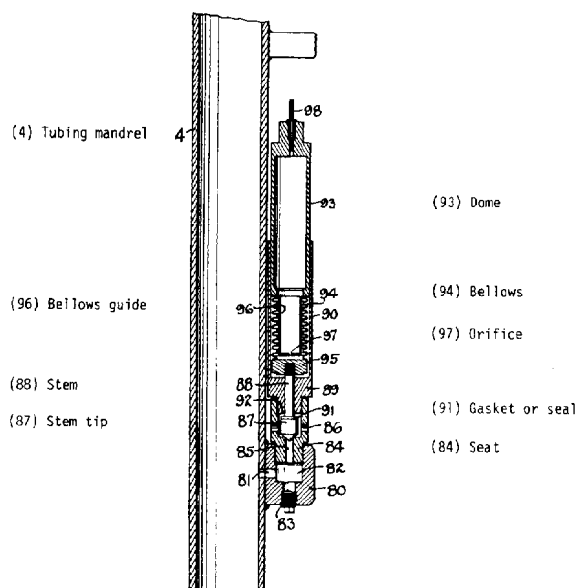


Fig. 5.7—Original King unbalanced, single-element, bellows-charged, gas lift valve on a conventional tubing mandrel.

Calculate the approximate volume of gas stored in the casing annulus between average pressures of 722.2 and 657.9 psia by using Eq. 14:

$$V_{gv} = \left(\frac{p_1 - p_2}{p_{sc}} \right) V_c = \left(\frac{722.2 - 657.9}{14.7} \right) 600$$

$$= 2,624 \text{ scf at } 14.7 \text{ psia.}$$

Calculate the percentage difference between the detailed and approximate solutions:

$$\% \text{ difference} = \left(\frac{2,784 - 2,624}{2,784} \right) 100 = 5.8\%.$$

Gas Lift Valve Mechanics

Introduction

The advent of the single-element, unbalanced, bellows-charged gas lift valve (as illustrated on Sheet 1 of the King patent in Fig. 5.7) revolutionized gas lift application and installation design methods. Before the bellows-charged gas lift valve, there were differential valves and numerous types of unique devices used for gas lifting wells. These devices, or valves, were operated by rotating or vertically moving the tubing and by means of a sinker bar on a wireline.

Single-element implies that the gas lift valve consists of a bellows and dome assembly, a stem with a tip that generally is a carbide ball, and a metal seat housed in a valve body that is attached to a mandrel in the tubing string, as illustrated in Fig. 5.7. The original patent for this type of gas lift valve was filed in 1940 by W.R. King; currently, the unbalanced single-element bellows valve

remains the most widely used type of gas lift valve for gas lifting wells. The original King valve had most of the protective design features of the present gas lift valves. The bellows was protected from high hydrostatic fluid pressure by a gasket that sealed the bellows chamber from well fluids after full stem travel. A small orifice was drilled in a bellows guide tube. The orifice was designed to be an anti-chatter mechanism and the bellows guide provided bellows support.

Purposes of Gas Lift Valves

The gas lift valve is the heart of most gas lift installations and the predictable performance of this valve is essential for successful gas lift design and operations. The gas lift valve performs several functions in a typical gas lift installation.

The primary function of a string of gas lift valves is to unload a well with the available injection gas pressure to a maximum depth of lift that uses fully the energy of expansion on the basis of the injection gas pressure. Gas lift valves provide the flexibility to allow for a changing depth in the point of gas injection to compensate for a varying BHFP, water cut, daily production rate allowable, and well deliverability. The operating gas lift valve in an intermittent gas lift installation prevents an excessive injection gas pressure bleed-down following an injection gas cycle. The gas lift valve provides the means to control the injection gas volume per cycle.

Another important function of gas lift valves is the ability to maintain an excessive BHFP drawdown in a temporarily damaged well until the well cleans up. This operation is accomplished by lifting from near total depth (TD) until reservoir deliverability returns to normal. The final operating point of gas injection for the stabilized production rate in certain deep wells with a high reservoir pressure can be nearer the surface than the point of gas injection to establish initial BHP drawdown during unloading if the load fluid is salt water. Again, gas lift valves must be installed below the depth of the operating gas lift valve to clean up the well.

When the injection gas-line pressure significantly exceeds the BHFP at the maximum valve depth, freezing can occur across the surface controls for the injection gas if the operating valve is a large orifice. The orifice valve can be replaced by an injection-pressure-operated gas lift valve to transfer the pressure drop to the gas lift valve at well temperature where hydrates will not form.

The reverse check in a gas lift valve is important for valves below the working fluid level. The check prevents backflow from the tubing to the casing, which is particularly important if the well produces sand and has a packer.

Unbalanced, Single-Element Valves

The unbalanced, single-element gas lift valve is an unbalanced pressure regulator. The analogy between these two devices is apparent in Fig. 5.8. Unbalanced implies that the pressure applied over the port area exerts an opening force, whereas this same pressure has no effect on the opening pressure of a balanced backpressure or pressure-reducing regulator. The closing force for a gas lift valve can be a gas pressure charge in the bellows exerted over the effective bellows area or a spring force, or a combination of both. The closing force for the regulator or gas lift valve can be adjusted to maintain a desired

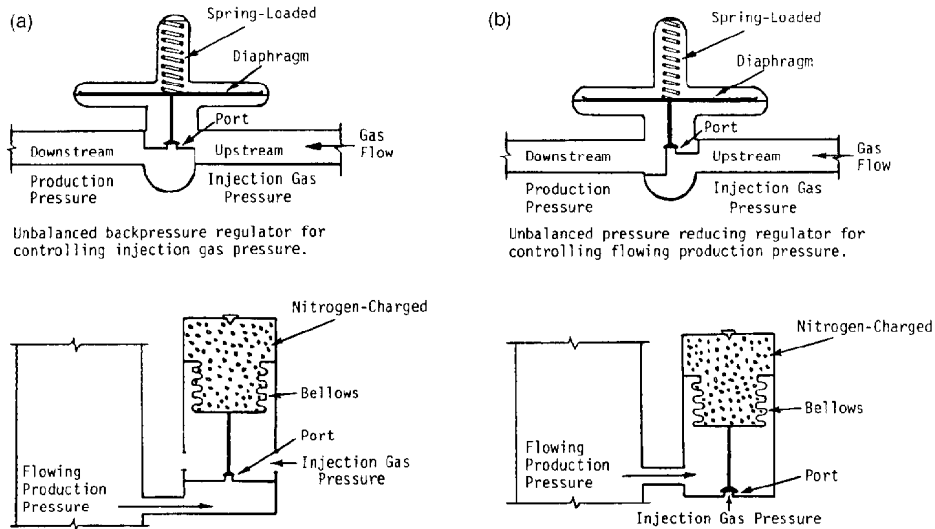


Fig. 5.8—Analogy of unbalanced, single-element, bellows-charged, gas lift valves to unbalanced pressure regulators. (a) Injection-pressure-operated gas lift valve responds to injection-gas pressure. (b) Production-pressure-(fluid)-operated gas lift valve responds to flowing production pressure.

backpressure for injection pressure operation or a design downstream pressure for production pressure operation. The regulator or valve will remain closed until this set closing force is exceeded.

Generally, the major initial opening force for a gas lift valve is the pressure exerted over the effective bellows area less the port area, and the lesser opening force is the pressure acting over the port area. In like manner, the major opening pressure is applied over an area equal to the diaphragm area less the port area for a regulator. The effect of the unbalanced opening force is far less significant for most unbalanced backpressure and pressure-reducing regulators than for gas lift valves because the ratio of the port area to the total effective bellows area of a gas lift valve is much greater than the ratio of the port area to the total diaphragm area for most regulators. The operating principle remains identical for the gas lift valve and regulator, but the pressure applied over the port area has greater effect on the initial opening pressure of most gas lift valves.

Pilot and Differential-Opening, Injection-Pressure-Operated Valves

There are numerous special-application gas lift valves available. The operation of many of these unique valves can be analyzed using the force balance equations for the simple single-element, unbalanced, gas lift valve. The many different types of gas lift valves and the variation in calculations will not be discussed in this chapter because of their limited application. Two special-purpose valves of particular importance are the pilot and the differential-opening, injection-pressure-operated gas lift valves. The construction of the differential-opening valve may vary between manufacturers but the operating principle remains the same.

The pilot-operated gas lift valve in Fig. 5.9a has operating characteristics that are ideally suited for chamber

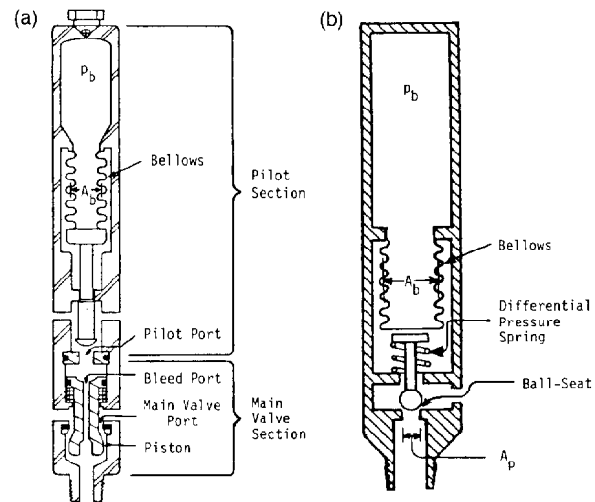


Fig. 5.9—Pilot-operated and differential-pressure opening injection pressure-operated gas lift valves. (a) Pilot-operated gas lift valve. (b) Pressure differential opening, constant closing gas lift valve.

installations and deep intermittent gas lift operations with low injection gas pressure and large casing. The pilot valve offers a very large main port with controlled spread and a predictable constant closing pressure. This type of valve will function properly on time cycle or choke control of the injection gas. The pilot section operates in the same manner as a single-element gas lift valve, with a small choke located downstream of the valve seat. The production pressure at valve depth is exerted over the ball-seat contact area of the pilot section as an initial opening force. When the pilot section begins to open, an increase in pressure occurs between the pilot valve seat and the

TABLE 5.2—VALVE SPECIFICATIONS FOR STEM WITH BALL AND SHARP-EDGED SEAT

Port Size (ID) (in.)	Area of Port (sq in.)	A_p/A_b	$1 - A_p/A_b$	F_p Production Pressure Factor	Full-Open Stem Travel* (in.)
1-in.-OD Gas Lift Valves With $A_b = 0.31$ sq in.					
1/8	0.0123	0.040	0.960	0.041	0.0440
3/16	0.0276	0.089	0.911	0.098	0.0714
1/4	0.0491	0.158	0.842	0.188	0.1002
5/16	0.0767	0.247	0.753	0.329	0.1302
3/8	0.1104	0.356	0.644	0.553	0.1610
1 1/2-in.-OD Gas Lift Valves With $A_b = 0.77$ sq in.					
3/16	0.0276	0.036	0.964	0.037	0.0714
1/4	0.0491	0.064	0.936	0.068	0.1002
5/16	0.0767	0.100	0.900	0.111	0.1302
3/8	0.1104	0.143	0.857	0.167	0.1610
7/16	0.1503	0.195	0.805	0.243	0.1925
1/2	0.1963	0.255	0.745	0.342	0.2246

*Full-open stem travel is on the basis of a stem ball OD that is 1/16 in. larger than the port ID.

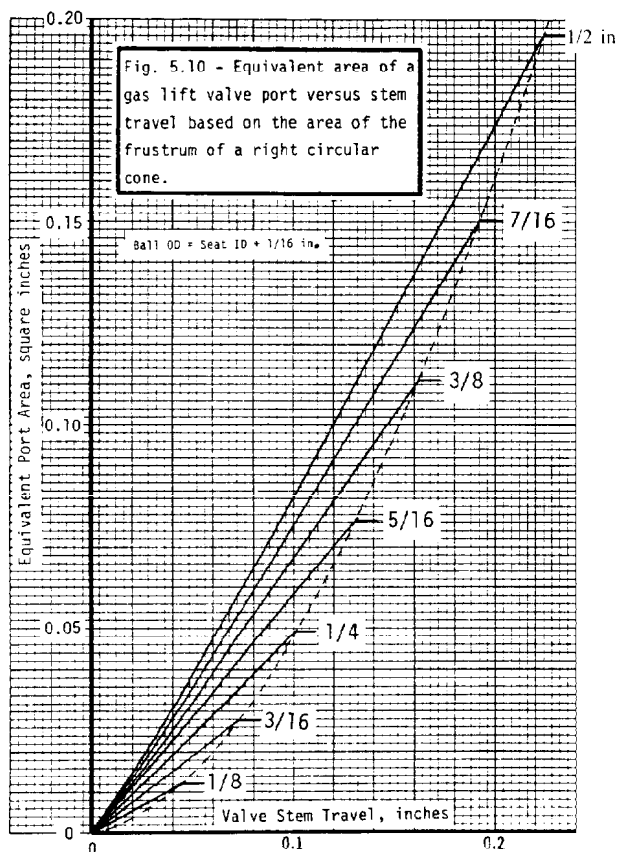


Fig. 5.10—Equivalent area of a gas lift valve port vs. stem travel on the basis of the lateral area of the frustum of a right circular cone.

piston on the main valve. This increase in pressure above the piston results in compression of the spring under the piston, and the main valve snaps open. An exceedingly high, instantaneous, injection gas rate enters the tubing

TABLE 5.3—OPERATING CHARACTERISTICS OF DIFFERENTIAL OPENING AND CONSTANT CLOSING PRESSURE VALVE

p_{oD} (psig)	p_{pID} (psig)	Spread* (psi)
650	450	50
700	500	100
750	550	150

*Based on constant closing pressure = 600 psig.

through the large main valve port. As the injection gas pressure in the casing decreases from gas passage through the large port, the pilot section begins to close. The pressure downstream of the pilot port remains equal to the injection gas pressure until the pilot port area open to flow is less than the bleed-hole area in the main valve piston. When the pressure equalizes across the piston, the spring returns the main valve to its seat. The closing pressure of a pilot valve is predictable and near the theoretical closing pressure of a single-element, unbalanced gas lift valve because the pressure upstream and downstream of the pilot port are approximately equal at the instant the pilot section closes. The spread of a pilot valve can be controlled by selecting the proper pilot port size without altering the high injection-gas throughput capacity of the large main valve port.

The differential-opening, injection-pressure-operated gas lift valve in Fig. 5.9b has operating characteristics that differ from a pilot valve. The differential-opening pressure valve has the unique feature of requiring a constant difference between the injection gas and the production pressure to open the valve when the injection gas pressure exceeds its constant closing pressure. This operating principle is illustrated for a valve with a constant closing pressure of 600 psig and a differential spring setting of 200 psi in Table 5.3.

For example, the valve will snap open when the production pressure exceeds 500 psig with an injection gas pressure of 700 psig and will close after the injection gas pressure decreases to 600 psig. The resulting spread is 100 psi for these operating conditions. The differential-opening, injection-pressure-operated valve is designed for choke control of the injection gas into the well.

The pilot valve does not operate with a constant pressure differential between the injection gas and production pressures at valve depth. The injection-gas opening pressure and spread decrease as the production pressure increases at the depth of a pilot valve. The differential-opening pressure valve cannot be opened by an increase in only the injection gas pressure, whereas the pilot valve can be opened by increasing the injection gas pressure. The similarity in these two valves is that both types have a predictable constant closing pressure and can have large ports.

Valve Specifications and Stem Travel

Gas lift valve specifications are published by each manufacturer for their valves. Some manufacturers assume a sharp-edged seat for the ball-seat contact and others arbitrarily add a small increase to the port ID to account for a slight bevel for the ball-seat contact. Since most

manufacturers use the same source for their supply of bellows and the bellows areas are relatively standard, the specifications in Table 5.2 are representative of many actual single-element, unbalanced, gas lift valves. The theoretical full-open stem travel is not included in the valve specifications published by most manufacturers.

The stem travel required to open an unbalanced, single-element, gas lift valve fully increases with the larger port sizes, as illustrated in Fig. 5.10. The curves were calculated for gas lift valves with a sharp-edged seat and a ball on the stem that is $\frac{1}{16}$ in. larger in diameter than the inside diameter of the port. The equivalent port area before a valve is full-open is based on the lateral area of the frustum of a right circular cone. The major area of the frustum is the port area, which remains constant, and the minor area decreases with an increase in stem travel as the ball moves away from its seat.

There is an important gas-lift-valve performance consideration that is not noted in the published literature and will not be discussed completely in this section. The problem needs to be recognized by operators with high-rate wells being gas lifted through large tubing or through the casing annulus. An injection gas throughput rate based on a full-open port size should not be assumed for the larger port sizes in most single-element, unbalanced, gas lift valves. For nearly all these gas lift valves with a large port area relative to the bellows area, the maximum equivalent port area open to flow of the injection gas will be less than an area based on the reported port size for an actual range in the injection gas pressure during typical gas lift operations. The necessary increase in the injection gas pressure to open fully a 1-in.-OD gas lift valve with a large port can approach 200 psi—assuming this required stem travel is possible. Maximum stem travel may be limited by a mechanical stop or bellows stacking before a full-open port area is achieved.

Gas-Lift-Valve Port Configurations

The port geometry and the maximum stem travel will affect the volumetric gas throughput of a gas lift valve. Most gas lift valves have a carbide ball silver-soldered to the stem. The valve seat can have a sharp-edged port or a taper. The chamfer may be very slight for breaking the seat line or may be of sufficient depth to assure that the ball remains in the taper for full stem travel. A sharp-edged and a tapered seat with a 45° chamfer are illustrated in Fig. 5.11. Most of the example calculations in this chapter are based on the sharp-edged seat since the majority of gas lift valves in service have a sharp-edged seat or a very shallow chamfer for breaking the seat line. The calculations are basically the same for a sharp-edged seat and a seat with a shallow taper. The calculations for an equivalent area open to the injection gas flow differ for a seat with a deep chamfer (Fig. 5.11b).

There has been no standard angle adopted for a taper of a gas-lift-valve seat. Certain manufacturers use the same tapered seat for different stem-ball sizes. The area of the port used in the port-to-bellows area ratio must be redefined for tapered seat when the ball-seat contact area is larger than the bore area through the seat, as shown in Fig. 5.11b. The port area for the ratio A_p/A_b is based on the ball-seat contact area and not on the bore area through the seat, which can be the same for more than one ball size. The specifications for the gas lift valve are

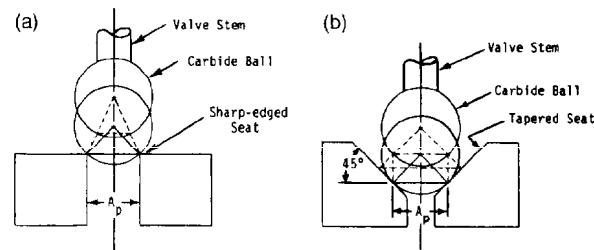


Fig. 5.11—Typical gas lift valve port configurations. (a) Sharp-edged seats have an effective A_p equal to the bore area through the seat. The A_p may be based on a diameter slightly greater than the seat bore ID if the port has a minor taper to eliminate a sharp-edged ball-seat contact. (b) Tapered seat with a 45° chamfer measured from the horizontal (90° included angle). The effective A_p in the A_p/A_b ratio is the ball-seat contact area and not the bore area through the seat.

controlled by changing the ball size and the angle of the taper, because the ball-seat contact area depends on the ball size and the angle of the chamfer for valves with a port similar to Fig. 5.11b. The selection of an angle for the taper, ball size, and the bore area through the seat can result in a ball-seat contact at the base of the taper. For this geometry, the bore area of the port would be used in the A_p/A_b term. The maximum stem travel in many gas lift valves with a deep taper is limited to prevent the ball from pulling out of the taper.

The equivalent port area open to flow for a sharp-edged seat in the throttling mode is based on the frustum of a right circular cone. A throttling mode implies that the generated area open to flow for the injection gas is less than the bore area through the valve seat. Typical curves of equivalent port area vs. stem travel for different sharp-edged port sizes are illustrated in Fig. 5.10. The calculations for an equivalent port area based on stem travel are more complex for valves with deep tapered seats. Certain types of gas lift valves with a deep tapered seat are designed to operate only in the throttling mode for continuous flow application.

Example Problem 6.

Given:

1. Seat angle = 45° (deep chamfer with ball-seat contact on taper).
2. Bore diameter through seat = 0.25 in.
3. Effective bellows area = 0.31 sq in.

Calculate the ball-seat contact diameter and area and the effective A_p/A_b ratio for a $\frac{3}{8}$ -in.-OD ball.

$$\text{Ball-seat contact ID} = (0.375) \sin 45^\circ = 0.265 \text{ in.}$$

$$\text{Ball-seat contact area} = \pi/4(0.265)^2 = 0.055 \text{ sq in.}$$

$$\text{Effective } A_p/A_b = 0.055/0.31 = 0.178.$$

Calculate the ball-seat contact diameter and area and the effective A_p/A_b ratio for a $\frac{1}{2}$ -in.-OD ball.

$$\text{Ball-seat contact ID} = (0.50) \sin 45^\circ = 0.354 \text{ in.}$$

$$\text{Ball-seat contact area} = \pi/4(0.354)^2 = 0.098 \text{ sq in.}$$

$$\text{Effective } A_p/A_b = 0.098/0.31 = 0.316.$$

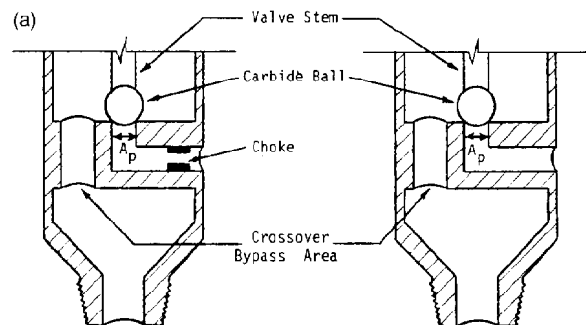


Fig. 5.12—Schematic of crossover seats with and without a choke upstream of the valve port. (a) Choke upstream of port to control injection-gas volume and to ensure downstream pressure being applied to bellows area after valve opens. (b) Crossover bypass area should significantly exceed port area without choke upstream of port.

Crossover Seat

Several types of gas lift valves have a crossover seat for a particular application. The crossover seat is designed to direct the downstream pressure into the valve body, where this pressure is exerted over the area of the bellows less the port area. The upstream pressure is applied to the port area. The crossover seat in Fig. 5.12 is a schematic illustrating the principle of a crossover. An actual crossover seat will have a group of bypass openings around the main port, and the summation of these bypass areas must exceed the port area.

An example of the need for a crossover seat would be a production-pressure-operated gas lift valve in an injection-pressure-operated gas lift valve mandrel. Another application would be a casing (annulus) flow gas lift valve in a tubing flow mandrel. In both examples the gas lift valve is modified rather than the gas lift valve mandrel. For example, wireline-retrievable gas lift valve mandrels with pockets designed for injection-pressure-operated gas lift valves and tubing flow have been installed in a well. The operator desires production pressure operation. The solution is production-pressure-operated gas lift valves with a crossover seat.

Gas lift valves with a crossover seat are not recommended if the proper mandrels can be installed to utilize gas lift valves without this type of seat. The maximum port size is limited for valves with a crossover seat. This limitation can be very serious in wells requiring a high injection gas rate. Another problem with a crossover seat is the possible partial plugging of the crossover bypass area. The physical bypass area should be at least 50% greater than the valve port area because the bypass openings usually are smaller and more likely to plug than a valve port, which can be opened and closed. A production-pressure-operated gas lift valve will not close at the design closing pressure if the crossover area becomes less than the port area, because the injection gas rather than the flowing production pressure is exerted over the bellows area.

Most production-pressure-operated gas lift valves with crossover seats can be choked upstream of the ball-seat contact area. The same port size may be used in all valves,

and the volumetric injection-gas throughput for the upper unloading gas lift valves is limited by a choke size that is smaller than the port area. The small inlet chokes tend to reduce the valve closing pressure problem associated with production pressure operation.

Bellows Protection

All reputable manufacturers of gas lift valves have provided bellows protection in the design of their valves. A bellows should be protected from a high pressure differential between the bellows-charge and the well pressures and from the possibility of a resonance condition that can result in a high-frequency valve stem chatter. The bellows-charge pressure will be atmospheric pressure for a typical spring-loaded valve. The highest pressure differential will occur in most installations during initial unloading operations when the lower gas lift valves are subjected to exceedingly high hydrostatic-load fluid pressures in deep wells.

Gas lift valve bellows are protected from high hydrostatic pressures by four methods: (1) high pressure differential (hydraulically preformed), (2) support rings within the convolutions, (3) confined liquid seal with full stem travel, and (4) isolation of bellows from outside pressure with full stem travel. The primary purpose of these methods for protecting the bellows is to prevent a permanent change in the radii of the convolutions, which in turn can affect the operating pressure of a gas lift valve.

The possibility of a chatter condition is not predictable or fully understood. The evidence of valve stem chatter will be a bellows failure and a dished-out seat if the valve seat is not manufactured from an extremely hard material. Most gas lift valves will have some form of dampening mechanism, and the majority of these devices will operate hydraulically. The bellows will be partially filled with a liquid, and restricted liquid flow rate or fluid shear prevent instantaneous undamped stem movement.

Bellows-Assembly Load Rate

Bellows-assembly load rate is defined as the psi increase exerted over the bellows area per unit travel of the valve stem or unit travel per psi increase. It may be reported in either manner. The controlled pressure is applied over the entire effective bellows area, and the valve stem travel is measured by means of a depth micrometer. The bellows-assembly load rate is the slope of the pressure vs. stem travel curve and the choice of units depends on the manner in which these data are displayed. The increase in nitrogen-charged dome pressure with stem travel is generally negligible as compared with the load rate of a bellows in most bellows-charged gas lift valves. The load rate of a bellows, which is analogous to the load rate of a helical spring, is far greater than the effect of the increase in dome pressure resulting from the decrease in dome volume with the stem travel required to open a typical gas lift valve.

The measured bellows-assembly load rate is not identical for all gas lift valves with the same size of bellows. The typical three-ply monel bellows that is used in many 1½-in.-OD gas lift valves has a reported effective bellows area of 0.77 sq in. The bellows-assembly load rate for a valve with a nitrogen-charged dome will range from 400 to 500 psi/in. in the linear portion of the curve for a valve with a test-rack opening pressure between 600 and

1,000 psig. The three-ply monel bellows in the 1-in.-OD valve has a reported effective area of 0.31 sq in. and a bellows-assembly load-rate range of 1,000 to 1,200 psi/in. for a valve with a nitrogen-charged dome and a test-rack opening pressure between 600 and 1,000 psig. The bellows-assembly load rate for a spring-loaded 1-in.-OD valve can range from near 2,000 to more than 3,500 psi/in. depending on the wire size and number of free coils in the spring.

The purpose in noting the magnitude of the bellows-assembly load rate for typical gas lift valves is to emphasize the fact that a single-element, unbalanced, gas lift valve will not "snap" open. An increase in injection gas pressure, or in flowing production pressure, or a combination of an increase in both pressures, is necessary to stroke the valve stem. The larger gas lift valves should be selected for installations requiring high injection-gas rates since the smaller valves do not have the same gas throughput performance of the larger valve with the same port size. Valves with the smaller bellows assembly are not recommended for low-pressure injection gas systems that may be used to gas lift shallow wells. The low closing force and bellows stiffness can result in leaking valve seats because of poor stem seating characteristics at low injection-gas operating pressures.

Static-Force Balance Equations for Unbalanced, Single-Element, Bellows-Charged Valves

Most gas lift equipment manufacturers use a valve setting temperature based on 60°F for nitrogen-charged gas lift valves. The valve is submerged in a 60°F water bath to assure a constant nitrogen temperature in the dome of each valve during the test-rack setting procedure, whether the valve is set at test-rack opening or closing pressure. The initial tester-set opening pressure is measured with the tester pressure applied over the bellows area less the stem-seat contact area while atmospheric pressure (0 psig) is exerted over the stem-seat contact area. The valve actually is closed and begins to open from an opening force that is slightly greater than the closing force, thus allowing an extremely low tester gas leakage rate through the valve seat. Although most gas lift valves are set with an initial opening pressure, certain types of valves with very high production pressure factors and other valves with unique construction use test-rack closing pressures.

The test-rack closing pressure is obtained by bleeding the tester gas from the downstream side of the gas lift valve. This theoretical closing pressure is obtained only when the downstream and upstream tester pressures are equal at the instant the gas lift valve closes. An accurate closing pressure is more difficult to observe than an initial opening pressure and can be affected by the rate of decrease in the tester pressure during bleed-off of the tester gas. An encapsulating tester with gas capacity rather than a ring-type tester is recommended so that small leaks in the tester piping will not prevent observation of the true closing pressure. The pressure should be bled off of the downstream side of the valve through a small orifice.

The equations for initial opening pressure in a tester and well and a tester closing pressure are based on static-force balance equations and would apply to spring-loaded gas lift valves. The spring pressure effect would replace the bellows-charged pressure of the valve for the closing force. Several manufacturers with spring-loaded gas lift

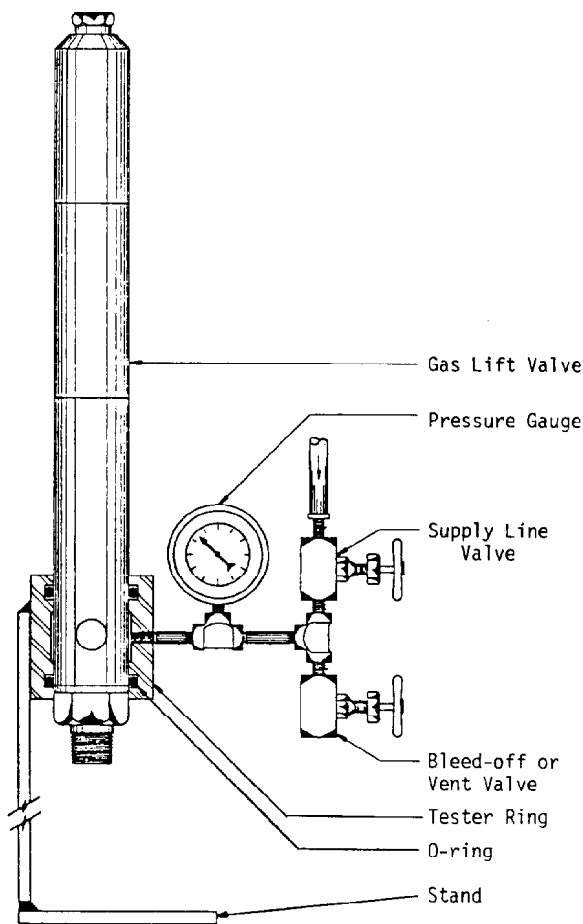


Fig. 5.13—Standard ring-type gas lift valve tester. Insert sleeves are available that fit in this tester for testing smaller-OD gas lift valves.

valves report a test-rack closing pressure. The spring is adjusted until the force exerted by the spring is equal to the desired test-rack closing pressure. Since there is no nitrogen gas charge pressure in the dome, there is no need to set a spring-loaded gas lift valve at a base tester temperature. Spring-loaded valves are considered temperature insensitive. If the total closing force for a gas lift valve is a combination of a bellows-charged pressure and a spring-load, the spring-load effect must be subtracted from the total closing force to obtain the bellows-charged pressure portion of this closing force. The temperature correction factor is applied to the nitrogen-charged dome pressure before calculating the test-rack-set opening pressure of the valve. A typical ring-type tester and piping manifold are illustrated in Fig. 5.13.

The following equations for the initial gas-lift-valve opening pressures in a tester and in a well are derived for an injection-pressure-operated gas lift valve since most gas lift installations use this type of valve. The injection gas pressure and flowing production pressures are interchanged for production-pressure-(fluid)-operated gas lift valves. The flowing production pressure becomes the major opening force by being applied over the effective bellows less port area as an initial opening force.

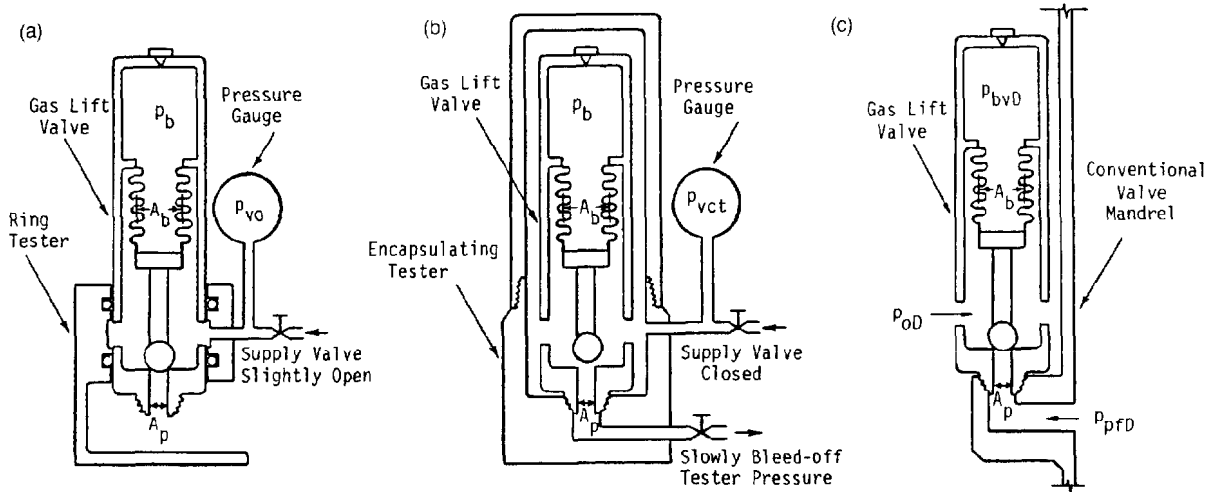


Fig. 5.14—Illustration of nomenclature used in static-force balance equations for gas lift valves in tester and well. (a) Test-rack opening pressure (p_{vo}) obtained by flowing supply gas at a low rate into a ring-type tester with atmospheric pressure applied to the port area. (b) Test-rack closing pressure (p_{vct}) obtained by opening the gas lift valve, closing the supply valve, and slowly bleeding off the encapsulating tester pressure downstream of the port. (c) Initial valve opening pressure in well (p_{oD}) based on the flowing production pressure (p_{pFD}) at valve depth.

1. Initial opening pressure in a tester (Fig. 5.14a):
Closing force=opening force,

$$p_b(A_b) = p_{vo}(A_b - A_p).$$

Dividing by A_b ,

$$p_b = p_{vo}(1 - A_p/A_b). \quad (15)$$

Solving for test-rack initial valve opening pressure (p_{vo}) at the test-rack-setting bellows-charged pressure at 60°F,

$$p_{vo} = \frac{p_b}{(1 - A_p/A_b)}, \quad (16)$$

where

- A_b = effective bellows area, sq in.,
- A_p = valve port ball-seat contact area, sq in.,
- and
- p_b = bellows-charged dome pressure at 60°F, psig.

2. Closing pressure in a tester (Fig. 5.14b):
Closing force=opening forces,

$$p_b(A_b) = p_{vct}(A_b - A_p) + p_{vct}(A_p),$$

$$p_b(A_b) = p_{vct}(A_b).$$

Dividing by A_b ,

$$p_b = p_{vct} \text{ (when } p_o = p_{vct} = p_{pft}), \quad (17)$$

where

- p_o = initial valve opening pressure, psig,
- p_{vct} = test-rack valve closing pressure at 60°F, if, and only if, the upstream and downstream pressures across the valve port are equal at the instant the valve closes, psig, and

p_{pft} = test-rack downstream flowing production pressure, psig.

3. Initial opening pressure in a well (Fig. 5.14c):
Closing force=opening forces,

$$p_{bvD}(A_b) = p_{oD}(A_b - A_p) + p_{pFD}(A_p).$$

Dividing by A_b ,

$$p_{bvD} = p_{oD}(1 - A_p/A_b) + p_{pFD}(A_p/A_b), \quad (18)$$

where

- p_{bvD} = the bellows-charged dome pressure at well temperature, psig,
- p_{pFD} = the flowing production pressure at valve depth, psig, and
- p_{oD} = the initial valve opening pressure at valve depth, psig.

Solving for the initial injection-gas opening pressure for injection-pressure-operated gas lift valves,

$$p_{oD} = \frac{p_{bvD}}{(1 - A_p/A_b)} - p_{pFD} \left(\frac{A_p/A_b}{1 - A_p/A_b} \right), \quad (19a)$$

$$p_{oD} = p_{voD} - p_{pFD}(F_p), \quad (19b)$$

or

$$p_{oD} = \frac{p_{vo}}{F_T} - p_{pe}, \quad (19c)$$

where

- p_{voD} = initial valve opening pressure at T_{vD} when p_{pFD} equals zero, psig,
- F_p = production-pressure factor, dimensionless, and
- p_{pe} = production-pressure effect, psi.

Additional equations used in initial valve opening pressure calculations are the following:

$$F_p = \frac{A_p/A_b}{(1 - A_p/A_b)} = \frac{A_p}{A_b - A_p}, \dots (20)$$

$$p_{voD} = \frac{p_{bvD}}{(1 - A_p/A_b)}, \dots (21a)$$

OR

$$p_{voD} = \frac{p_{vo}}{F_T}, \dots (21b)$$

$$p_{pc} = F_p(p_{pfd}), \dots (22)$$

Initial Opening and Closing Pressures of a Single-Element, Unbalanced Valve

An understanding of the relationship between the initial opening and closing pressures of a single-element, unbalanced, gas lift valve is important for calculating gas lift installation designs and analyzing gas lift operations. A single-element, unbalanced, gas lift valve does not have a constant closing pressure as noted in many publications, and the valve does not "snap" full open at the initial injection-gas opening pressure. This type of gas lift valve is a simple, unbalanced, backpressure regulator. The gas lift valve opens and closes at the same injection pressure if the flowing production pressure remains constant. In like manner, an unbalanced backpressure regulator opens and closes at the same upstream pressure if the downstream pressure remains constant.

Fig. 5.15 shows a plot of the initial injection-gas opening pressure vs. the flowing production pressure for a $\frac{3}{8}$ -in.-ID sharp-edged port in a 1-in.-OD gas lift valve with an effective bellows area of 0.31 sq in. This bellows size is used by most manufacturers in the 1-in.-OD gas lift valve. A $\frac{3}{8}$ -in.-ID port is the largest port size available from several manufacturers for the 1-in.-OD, single-element, unbalanced, gas lift valve. The larger port size was selected because of the higher production pressure factor.

The closing force for a single-element, unbalanced, gas lift valve is assumed to remain constant for this analysis. The slight increase in a bellows-charged dome pressure with stem travel (or the increase in the spring force for a spring-loaded gas lift valve) is neglected in this simplified force-balance discussion. The gas lift valve actually is closed on the line that represents a balance between the opening and closing forces in Fig. 5.15. The valve is open above the line and closed below the line. The valve can be opened by (1) increasing the injection gas pressure with a constant flowing production pressure; (2) increasing the injection gas and flowing production pressures simultaneously; and (3) increasing the flowing production pressure with a constant injection-gas pressure. All three means of opening a valve are illustrated by vectors based on a 100-psi increase in the injection-gas pressure and in the flowing production pressure. The resultant vector is based on both of the other vectors. The bellows-assembly load rate for a valve and the distance from the force-balance line to the tip of the vector would control the actual stem travel. The valve in Fig. 5.15 is an injection-

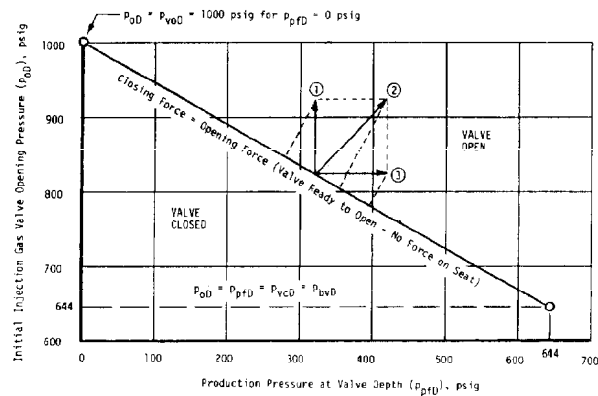


Fig. 5.15—Initial injection-gas opening pressure vs. production pressure at valve depth for 1-in.-OD, unbalanced, single-element, gas lift valve with a $\frac{3}{8}$ -in. sharp-edged port and 0.31-sq-in. bellows area.

pressure-operated gas lift valve since the production-pressure factor is less than one. It is apparent from the slope of the force-balance line in Fig. 5.15 that an increase in the injection-gas pressure will result in a force and resultant stem travel greater than that from the same incremental increase in flowing production pressure because the production factor is less than one. The maximum stem travel is attained by increasing both pressures.

Production-Pressure Factor and Valve Spread

The production-pressure factor (F_p) is a relationship based on the effective bellows and port areas for an unbalanced gas lift valve. Unbalanced implies that the flowing production pressure is exerted over the entire ball-seat contact area as a portion of the initial opening force for a valve. In terms of gas lift valve operation, the production-pressure factor is the ratio of the incremental difference in the initial injection-gas opening pressure to a difference in the flowing production pressure. If the flowing production pressure increases, the initial injection-gas opening pressure decreases, and vice versa. The production-pressure factor can be obtained from the slope of the force-balance line in Fig. 5.15 or can be calculated from the specifications for the valve.

Valve spread is defined as the difference between the initial injection-gas opening and the injection-gas closing pressures of a gas lift valve. The valve spread is zero for a constant flowing production pressure because a valve initially opens and closes at the same injection-gas pressure. This concept is used in several continuous-flow installation design methods. The valve spread observed in intermittent gas lift operations results from a change in the flowing production pressure at the depth of the operating gas lift valve during an injection gas cycle. The production pressure at valve depth approaches the injection gas pressure beneath a liquid slug during gas injection, thus decreasing the valve closing pressure (also the initial opening pressure), which results in a spread between the initial opening and closing pressures of the operating valve. This can be a very important consideration for a chamber lift installation where the initial opening pressure of the operating gas lift valve will be based on a very low tubing pressure because the operating gas lift valve is located above the chamber.

Example Problem 7.

Given:

1. Effective bellows area = 0.31 sq in.
2. Port area = 0.11 sq in. (sharp-edged seat).
3. $p_{voD} = 1,000$ psig for $p_{pfD} = 0$ psig.
4. $p_{oD} = 644$ psig when $p_{pfD} = p_{oD} = 644$ psig.

Calculate the production-pressure factor on the basis of the areas in the valve specifications:

$$F_p = \frac{A_p}{A_b - A_p} = \frac{0.11}{0.31 - 0.11} = 0.55.$$

Calculate the production-pressure factor on the basis of the force-balance curve in Fig. 5.15:

$$F_p = -\left(\frac{\Delta p_{oD}}{\Delta p_{pfD}}\right) = -\left(\frac{1,000 - 644}{0 - 644}\right) = 0.55,$$

where Δp_{oD} is the difference in p_{oD} based on a change in p_{pfD} , psi, and Δp_{pfD} is the difference in p_{pfD} exerted over A_p , psi.

Calculate the initial injection-gas valve opening pressure for $p_{pfD} = 400$ psig:

$$p_{oD} = p_{voD} - F_p(p_{pfD}) = 1,000 - 0.55(400) = 780 \text{ psig}.$$

The same value for p_{oD} can be determined from Fig. 5.15. The valve would close at 780 psig if the flowing production pressure did not change.

Calculate the valve spread (Δp_s) in psi for an initial injection-gas valve opening pressure on the basis of

$p_{pfD} = 400$ psig and a $p_{pfD} = 600$ psig at the instant the valve closes.

$$\Delta p_s = F_p(\Delta p_{pfD}) = 0.55(600 - 400) = 110 \text{ psi},$$

where Δp_{pfD} is the difference in p_{pfD} exerted over A_p at the initial injection-gas opening and closing pressures, psi.

Injection-Gas Volumetric Throughput Profiles for Single-Element, Unbalanced Valves

The injection-gas throughput performance of a single-element, unbalanced, gas lift valve is controlled by the effective area of the bellows, the bellows-assembly load rate, and the stem-seat configuration. The performance profiles of two types of unbalanced, single-element, gas lift valves are illustrated in Fig. 5.16. The injection-pressure-operated gas lift valve in Fig. 5.16a is a bellows-charged valve with a large effective bellows area, and the stem-seat configuration may be considered as having a ball and sharp-edged seat. The seat line is broken by a very shallow chamfer but the valve would perform in the same manner as a valve with a sharp-edged seat. The performance profile for a single-element, unbalanced, spring-loaded gas lift valve with a small effective bellows area and a large ball-seat contact area relative to the bellows area is illustrated in Fig. 5.16b. These injection-gas volumetric throughput profiles are established by measuring the gas passage through the valve while maintaining a constant injection-gas upstream pressure and varying the flowing production downstream pressure. The purpose of this form of performance test is to establish the slope of the linear portion of the gas throughput curve in the throttling range for a given type of gas lift valve and stem-seat configuration.

The performance profiles in Fig. 5.16 are based on actual valve tests. The spring-loaded gas lift valve with a small bellows has a very high bellows-assembly load rate as compared to the bellows-charged valve with a large

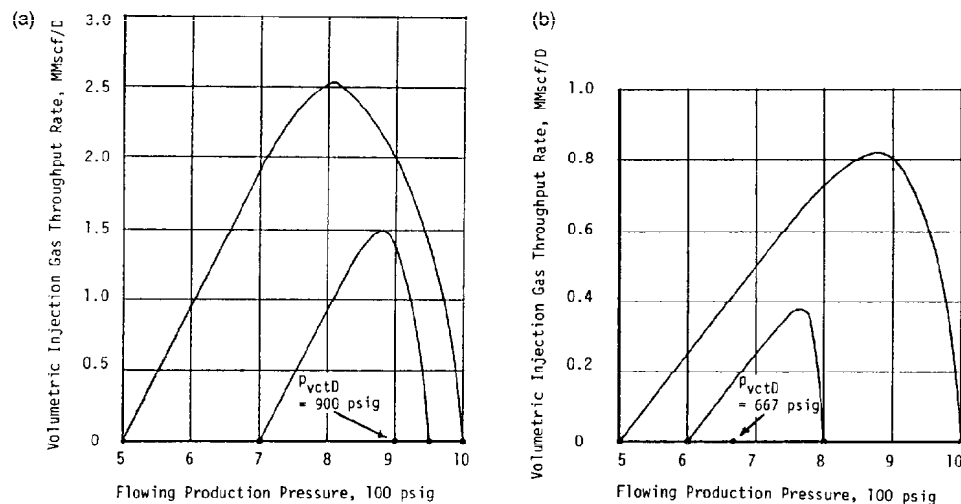


Fig. 5.16—Injection-gas volumetric throughput profiles for unbalanced, single-element, gas lift valves. (a) 1 1/2-in.-OD, bellows-charged gas lift valve. $A_b = 0.77$ sq in. and ball OD = 5/8-in. Seat taper = 45° and $A_p = 0.153$ sq in. Test-rack closing pressure $p_{vctD} = 900$ psig. Constant operating pressure $p_{ioD} = 950$ and 1,000 psig. Throttling range slope = 9.3 Mscf/D-psi. (b) 1-in.-OD, spring-loaded gas lift valve. $A_b = 0.23$ sq in. and ball OD = 5/8-in. Seat taper = 45° and $A_p = 0.153$ sq in. Test-rack closing pressure $p_{vctD} = 667$ psig. Constant operating pressure $p_{ioD} = 800$ and 1,000 psig. Throttling range slope = 2.5 Mscf/D-psi.

bellows. The spring-loaded valve is installed in a well in the same manner as an injection-pressure-operated gas lift valve, with the injection-gas pressure exerted over an area equal to the bellows area less the ball-seat contact area. Since the ball-seat contact area in the spring-loaded valve is larger than the area exposed to the injection-gas pressure, the valve is operated primarily by flowing production pressure. The production-pressure factor for the valve is approximately 2.5. The stem travel for the spring-loaded valve is limited to keep the ball on the stem within the taper of the seat; thus, the flowing production pressure is applied over a relatively constant area as an opening force throughout the operating pressure range of the valve. This type of valve is recommended for a continuous-flow installation design using its throttling range and represents one form of a flowing-production-pressure installation design.

The performance profile in Fig. 5.16a reveals that an unbalanced, bellows-charged, injection-pressure-operated gas lift valve with a sharp-edged seat and a production-pressure factor less than 0.25 will perform in a manner similar to a spring-loaded, unbalanced valve with a large production-pressure factor and a deep chamfered seat. This bellows-charged valve is not recommended for a continuous-flow installation design using the throttling range of the valve for valve spacing because of the steep slope of the throttling portion of the injection-gas throughput performance curve. A minor change in the injection-gas pressure results in a major change in the injection-gas throughput for a valve with a low production-pressure factor.

The differing operating characteristics of injection-gas and flowing production-pressure-operated gas lift valves can be observed from the performance profiles in Fig. 5.16. These operating characteristics are apparent from differences in injection-gas pressures and their corresponding closing flowing-production pressures. If the pressure difference in the constant operating injection-gas pressures is less than the corresponding flowing-production closing pressures, the valve is classified as an injection-pressure-operated valve. The valve is classified as production-pressure-operated when the difference in the constant operating injection-gas pressures exceeds the difference in the corresponding flowing-production closing pressures. The bellows-charged gas lift valve in Fig. 5.16a is an injection-pressure-operated valve, and the spring-loaded valve in Fig. 5.16b is production-pressure-operated.

Continuous-Flow Gas Lift

Introduction

Continuous-flow gas lift is analogous to natural flow, but there are generally two distinct flowing-pressure traverses. The traverse below the point of gas injection includes only formation gas, whereas the traverse above the point of gas injection includes both the formation and injection gases. These flowing-pressure traverses and corresponding gas/liquid ratios are illustrated in Fig. 5.17.

The advent of reliable multiphase flowing pressure-gradient curves provided the means to design a continuous flow installation properly. These gradient curves completely changed the design techniques used by gas lift design engineers. Maximum production rates can be estimated for the available injection-gas volume and pres-

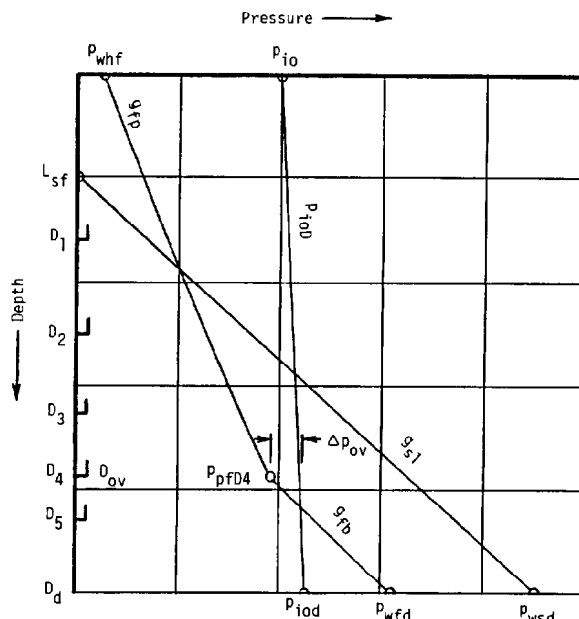


Fig. 5.17—Principles of continuous flow operation illustrated by a pressure-depth diagram. The datum depth (D_d) for the BHP is the lower end of the production conduit. Injection gas is entering the production conduit through the fourth gas lift valve and the three upper unloading gas lift valves are closed. Although the bottom gas lift valve is open, no injection gas can enter this valve at depth (D_5) because the flowing production pressure exceeds the injection-gas pressure at this depth. The flowing pressure at depth traverse (g_{fb}) above the operating gas lift valve depth (D_{ov}) includes the injection plus the formation gas, and the traverse (g_{fb}) below D_{ov} contains only formation gas (see also nomenclature list at the end of the chapter).

sure, and the valve depths can be calculated accurately with reliable gradient curves.

There are numerous gas-lift installation design methods offered by different manufacturers. Several installation designs require unique valve construction or known gas-lift-valve injection-gas throughput performance. Only two installation design techniques will be illustrated in this section. These installations are designed to use the simplest type of single-element, unbalanced, gas lift valve with a bellows-charged dome. This type of valve is the most widely used in the industry and is manufactured by all major gas lift companies.

Gas-lift installation design calculations are divided into two parts. The first part is the determination of the gas lift valve depths, and the second part is the calculation of the test-rack opening pressures of the gas lift valves. The test-rack set opening pressures are calculated after the valve depths because the operating pressures and temperatures during unloading are based on these valve depths.

The primary objective of this section is to outline in detail installation design methods for calculating the valve depths and the test-rack opening pressures of the gas lift valves that will unload a well to a maximum depth of lift for the available injection-gas volume and pressure. The unloading operations, as illustrated by the two-pen pressure recorder chart in Fig. 5.18, should be automatic. As each lower gas lift valve is uncovered, the valve immediately above closes and the point of gas injection transfers

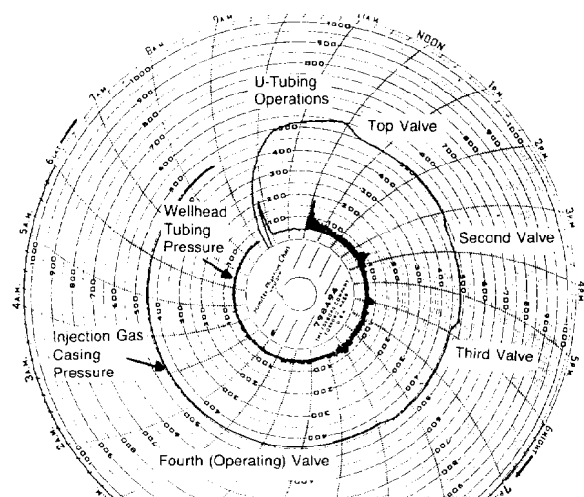


Fig. 5.18—Two-pen pressure recorder chart illustrating continuous-flow gas lift unloading operations with choke control of the injection gas. The static load fluid level was at the surface in the casing and tubing before the well was unloaded, which explains the first wellhead tubing pressure surge immediately after initial gas injection into the casing annulus. The wellhead pressure remains relatively constant during U-tubing operations before injection gas enters the tubing for the first time through the top gas lift valve. A surge in wellhead tubing pressure and a decrease in the injection gas casing pressure occur as the depth of gas injection transfers to each lower gas lift valve.

from the upper to the lower valve. All gas lift valves above an operating valve should be closed and the valves below should be open in a properly designed gas lift installation.

Initial Installation Design Considerations

Continuous-flow installation designs vary depending on whether complete and precise well data are known or unavailable. Reliable inflow well performance and an accurate multiphase flow correlation are required to establish the exact point of gas injection in deep wells. When the well data are limited or questionable, the point of gas injection cannot be calculated. A known point of gas injection is an unrealistic consideration for most wells because the reservoir pressure and water cut change as the reservoir is depleted. An exception will be wells where the maximum depth of lift can be reached initially with the available operating injection-gas pressure. The point of gas injection remains at this maximum depth for the life of the gas lift installation.

Retrievable gas lift valve mandrels are installed in many wells before little, if any, well production information is available. The engineer must locate these mandrels in wells before gas lift is required. The design considerations are similar for wells with a changing point of gas injection. In general, most gas lift installations will be in this category, where accurate well data are unknown or limited and the point of gas injection is unknown and/or changing as the reservoir is depleted. For this reason, the installation designs outlined in this section do not require complete well data. These continuous-flow gas lift installations are designed to lift a given daily production rate

from all valve depths. An orifice-check valve is recommended for the bottom valve in most installations. If a gas lift valve will be run, the test-rack opening pressure is set lower than the valves above so that the gas lift installation will produce at an actual daily production rate that is much less than the design rate without the valve closing.

Installation Design Methods

The two installation design methods outlined here can be classified as (1) the decreasing injection gas pressure design, and (2) the variable flowing pressure gradient method. Injection-pressure-operated gas lift valves with a small production-pressure factor (F_p) are recommended for the decreasing-injection-gas-pressure installation design method. Valves with a small F_p are sensitive primarily to a change in the injection-gas pressure. A decrease in the injection-gas pressure for each lower gas lift valve is essential to ensure the closure of upper unloading valves after gas injection has been established through a lower operating gas lift valve. This decreasing-injection-gas-pressure design is particularly applicable when the available injection-gas pressure is high relative to the required depth of lift, and an incremental decrease in injection-gas pressure can be added to the production-pressure effect for the top valve.

If a small-OD, injection-pressure-operated gas lift valve with a large port (high production-pressure factor) is required for ample gas passage to unload and to gas lift a well, the variable-gradient-valve-spacing design-line method should be used. The injection-pressure gas lift valves should have a production-pressure factor of at least 20 to 25% because a change in the flowing production pressure at valve depth rather than the injection-gas pressure establishes whether a gas lift valve is open or closed. Production-pressure-(fluid)-operated gas lift valves are applicable for the variable flowing-pressure-gradient gas lift installation design method. This design is considered to be particularly applicable for systems with low available injection-gas pressure since a constant surface operating injection-gas pressure is used to locate the valve depths in most installations. When the injection-gas pressure is high relative to the required depth of lift, the variable gradient design can be modified to include an incremental decrease in the operating injection-gas pressure with each succeeding lower gas lift valve. Decreasing the operating injection-gas pressure between valves will reduce the probability of multipoint gas injection, which could result in possible surging or heading conditions.

Although the continuous-flow installation designs outlined here do not require complete well data, these designs can be modified for a known point of gas injection. Generally, the calculated point of gas injection will be bracketed by installing at least one valve below the calculated valve depth in the event there is a slight error in the well information.

Safety Factors in the Simplified Continuous-Flow Installation Design Methods Without Gas Lift Valve Performance

The following safety factors are used for continuous-flow gas lift installation design with unbalanced, single-element, gas lift valves when the load rate and the gas throughput performance of the valve are not considered

in the calculations. The initial gas-lift-valve opening pressures are based on the static-force balance equations and represent the condition of no force applied by the valve stem onto the seat line of the port. Essentially, the valve is closed. These safety factors allow the injection-gas or flowing production pressure increase at valve depth needed to stroke the valve stem for generating an equivalent port area required to pass the injection-gas volume necessary for unloading and gas lifting most wells and to compensate for the actual locations of gas lift valves that are not to the nearest foot. Many operators will not break a stand to install a gas lift mandrel in the tubing string; therefore, the actual depth of the gas lift valve for a thribble (three tubing joints) may be to the nearest 45 to 50 ft of the calculated depth.

1. The operating injection-gas pressure used for the installation design calculations should be at least 50 psi less than the minimum injection-gas pressure available at the wellsite for most wells.

2. The unloading daily production rate is assumed equal to the design daily production rate. Generally, the actual unloading daily production rate will be less than the design production rate and can be controlled at the surface by the injection-gas volume.

3. No formation gas is assumed to be produced during the unloading operations. The total gas/liquid ratio is based on the daily injection-gas volume available for unloading the well.

4. The flowing-pressure-at-depth traverses above the unloading gas lift valves are assumed to be straight rather than curved lines.

5. The unloading flowing-temperature-at-depth traverse is assumed to be a straight rather than a curved line between an assigned unloading flowing wellhead temperature (T_{whu}) and the bottomhole temperature (BHT). The design unloading flowing temperature generally is between the static geothermal surface temperature and the final operating flowing temperature. A final flowing temperature that is higher than the design temperature increases the initial opening pressure of a bellows-charged gas lift valve and aids in keeping the upper valves closed while lifting from a lower gas lift valve.

6. An assigned valve-spacing pressure differential (Δp_v) of 50 psi across a valve for unloading is used commonly by many gas lift design engineers. The actual minimum flowing production pressure required to uncover the next lower unloading gas lift valve is greater by the assigned Δp_v .

7. The flowing-pressure traverse below the point of gas injection for locating the valve depths is assumed to be the static-load fluid gradient. No formation-produced fluids, including free gas, are considered in the valve spacing calculations.

An Orifice-Check Valve for the Operating Gas Lift Valve in Continuous-Flow Installations

An orifice being used for gas lifting a well should include a reverse-flow check valve. The check disk, or dart, should be closed by gravity or should be spring loaded for most applications. If a well with a packer produces sand, the check portion should be closed to prevent sand from accumulating on top of the packer when this valve is below the working fluid level and is not the operating valve. An inlet screen is recommended for orifice-check

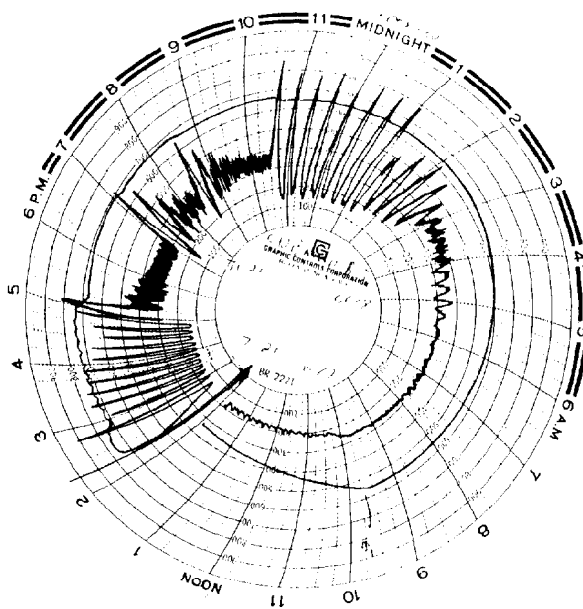


Fig. 5.19—Two-pen pressure recording unloading chart from a continuous flow installation with an orifice-check valve. The heading of the flowing wellhead tubing pressure results from the opening and closing of the unloading gas lift valves because of a $2\frac{3}{4}$ -in. choke in the flowline and a frictional drag mechanism in the valve to prevent stem shatter. When the orifice-check valve is uncovered around 3:00 a.m., heading and the operating injection-gas pressure decrease. The problem is reservoir deliverability and not the gas lift installation.

valves with a small choke to prevent possible plugging. The individual openings in the inlet screen should be smaller than the choke in the orifice-check valve.

A properly designed continuous-flow gas lift installation with an orifice-check valve will not have a higher injection-gas requirement than the same well with an injection-pressure-operated gas lift valve, if the orifice is not too large. The injection-gas volume for lifting a well is controlled by the metering device on the injection gas line at the surface. An orifice-check valve rather than a more expensive and complicated pressure-operated gas lift valve should be considered for the bottom valve in most continuous-flow installations.

Advantages of the Orifice-Check Valve.

1. The construction of an orifice-check valve is the simplest of all types of valves. The cost and the possibility of a malfunction are less for the orifice-check valve than for a pressure-operated gas lift valve.

2. The orifice-check valve is a "flag" because of the change in operating injection-gas-line pressure downstream of the metering device on the injection gas line when this valve is uncovered and becomes the point of gas injection. If the operating injection-gas pressure decreases significantly after the orifice-check valve is uncovered during initial unloading operations, the problem is reservoir deliverability and not the gas lift installation, as illustrated in Fig. 5.19.

3. An orifice-check valve can prevent severe heading or surging in a continuous-flow gas lift installation by assuring a constant port size for injection-gas passage. The equivalent port area in an injection-pressure-operated gas lift valve with a high production-pressure factor or a production-pressure-operated gas lift valve will change with a varying flowing production pressure. A gas lift valve tending to cyclic opening and closing results in heading from a change in the injection-gas throughput of the valve. Note the decrease in heading when lifting from the orifice valve in Fig. 5.19.

4. No injection-gas pressure increase is required to stroke an orifice-check valve. The port size is always known and is equal to the choke size in the valve.

5. When the injection-gas-line pressure decreases below the minimum pressure required to hold an injection-pressure-operated gas lift valve open, this valve will close. An orifice-check valve will remain open and gas lift operations may continue as long as the injection-gas pressure at valve depth exceeds the flowing production pressure at the same depth.

6. An orifice-check valve is recommended as the bottom valve in most production-pressure-(fluid)-operated installations and in other continuous-flow installations with injection-pressure-operated gas lift valves having a high production-pressure factor. If the actual flowing production pressure at the depth of the bottom valve is less than predicted, a gas lift valve may close or restrict the injection-gas rate, whereas an orifice-check valve will remain fully open.

7. A properly sized orifice is required to control the injection-gas volume for gas lifting some wells. One application is gas lifting one zone of a dual gas lift installation with a common injection-gas source in the casing annulus. A design pressure differential of at least 100 to 150 psi across the orifice is necessary to assure a reasonably accurate gas-passage prediction.

8. The orifice-check valve is an excellent annular fluid transfer valve for differential gas lift valve installations with a packer. A differential valve will tend to close during initial U-tubing operations.

Disadvantages of the Orifice-Check Valve.

1. When the injection-gas-line pressure is high, relative to the flowing production pressure at the depth of the orifice-check valve, a high pressure differential occurs across the surface injection-gas metering device. Hydrates may form and shut off the injection gas. The orifice-check valve can be replaced with an injection-pressure-operated gas lift valve. The pressure loss is transferred to the gas lift valve in the well at BHT where hydrates cannot form.

2. The weak wells with an orifice-check operating valve will consume injection gas at lower injection-gas-line pressure than stronger wells with higher flowing production pressures at the depth of the operating orifice-check valve.

3. A hole in the tubing cannot be distinguished from an orifice-check valve during normal, uninterrupted, continuous-flow gas lift operation. The production conduit can be pressured up with injection gas to observe whether flow can be established from the production conduit to the injection-gas conduit. Reverse flow indicates that there is a hole in the production conduit or that the check is not holding.

4. An orifice-check valve generally is not recommended

for a small, closed, rotative, gas lift system when costly makeup gas is required to charge the system after a shut-down. A properly set injection-pressure-operated gas lift valve will close after a slight decrease in the injection-gas pressure and will prevent the unnecessary loss of injection gas from the small high-pressure system.

Depth of the Top Gas Lift Valve

The top gas lift valve should be located at the maximum depth that will permit U-tubing the load fluid from this depth with the available injection-gas pressure. If the well is loaded to the surface with a kill fluid, the depth of the top valve can be calculated using one of the following equations:

$$D_1 = \frac{p_{ko} - p_{whu}}{g_{sl}}, \quad \dots \dots \dots (23)$$

$$D_1 = \frac{p_{ko} - p_{whu}}{(g_{sl} - g_g)}, \quad \dots \dots \dots (24)$$

or

$$D_1 = \frac{p_{ko} - p_{whu} - \Delta p_a}{(g_{sl} - g_g)}, \quad \dots \dots \dots (25)$$

where

D_1 = depth of top valve, ft,

p_{ko} = surface kick-off injection gas pressure, psig,

p_{whu} = surface wellhead U-tubing pressure, psig,

g_{sl} = static-load fluid gradient, psi/ft,

g_g = gas gradient based on p_{ko} and p_{kod} , psi/ft,

p_{kod} = kick-off injection gas pressure at D_d , psig,

D_d = vertical reference datum depth (lower end of production conduit), ft, and

Δp_a = assigned pressure differential for valve spacing, psi.

Eq. 23 does not include the increase in the injection-gas pressure to the depth D_1 . This equation is widely used because of a slight safety factor from neglecting this increase in gas pressure. Eq. 24 yields the same depth as a graphical solution without any pressure drop across the top gas lift valve at the instant this valve is uncovered. In other words, the top valve will not be uncovered if the actual kick-off injection-gas pressure is less than the design value or if the U-tubing wellhead pressure is higher than assumed. Eq. 25 includes injection-gas column weight and an assigned pressure drop at the instant the top valve is uncovered.

The surface U-tubing wellhead pressure is less than the flowing wellhead pressure for most installations. The difference between these two pressures will increase for longer flowlines and higher production rates. The wellhead U-tubing pressure is approximately equal to the separator, or production header, pressure because the rate of load fluid transfer is very low during the U-tubing operation and no injection gas can enter the flowline until the top gas lift valve is uncovered. Gas lift operations do not begin until injection gas enters the production conduit

through the top valve. Flowing wellhead pressure should be used to locate the depths of the remaining gas lift valves.

A load fluid traverse g_{sl} can be drawn from the wellhead U-tubing pressure to the intersection of the kick-off injection-gas-pressure-at-depth curve (p_{koD} traverse) on a pressure-depth worksheet. The top valve may be located at this intersection, which would be the same depth as calculated with Eq. 24. An arbitrary pressure drop across the top gas lift valve can be assumed in conjunction with the graphical method and this technique is the same as Eq. 25. If a pressure drop is assumed, this method becomes similar to the calculation of D_1 with Eq. 23. For this reason, Eq. 23 is recommended for most calculations.

If the depth to the static fluid level exceeds the calculated depth of the top gas lift valve and the well is not loaded, the top valve may be located at the static fluid level. This procedure is not recommended when a well may be loaded in the future or when the elevation of a well is lower than the tank battery, which is not located near the well. A check in the flowline may fail and fluid in the flowline will fill the tubing when a well is shut in. Theoretically, the top valve could be located below a static fluid level on the basis of the ratio of the capacity of the casing annulus to the capacity of the tubing. The primary application for this calculation would be in a casing flow installation, but this procedure is not recommended for typical tubing-casing sizes when the well is being gas lifted through the tubing.

Establishing Slope of Static-Load Fluid Traverse

There are several methods for establishing the slope of a static-load fluid traverse on the pressure-depth worksheet. This load fluid traverse is assumed to be the unloading pressure traverse below the point of gas injection for locating the depths of the gas lift valves. The static fluid level can be calculated on the basis of the static BHP and the load fluid gradient with the following equation:

$$L_{sf} = D_d - \frac{p_{wsd}}{g_{sl}}, \quad \dots \quad (26)$$

where L_{sf} is the static fluid level from surface for zero wellhead pressure, ft, and p_{wsd} is the static BHP at depth D_d , psig.

Plot the static BHP, p_{wsd} , at the datum depth and the L_{sf} at zero pressure and connect these points with a straight line. This line represents a pressure gradient traverse with a slope equal to the load fluid gradient. All unloading traverses below the point of gas injection for locating the gas lift valves are drawn parallel to this static-load fluid traverse.

Another procedure for establishing this static-load fluid traverse below each gas lift valve is to assume a pressure, p_{as} , greater than the operating injection-gas pressure at the lower end of the production conduit p_{iod} and to calculate the depth of this assumed pressure point on the basis of the static-load fluid gradient g_{sl} . Calculated D_c for p_{as} is

$$D_c = D_{uv} + \frac{p_{as} - p_{uvD}}{g_{sl}}, \quad \dots \quad (27)$$

where

D_c = calculated depth for assumed p_{as} , ft,

D_{uv} = depth of unloading valve, ft,

p_{as} = assumed pressure, psig, and

p_{uvD} = minimum flowing or production transfer pressure at D_{uv} , psig.

Plot p_{as} at D_c for this pressure point and draw a straight line between p_{uvD} at D_{uv} and p_{as} at D_c . The load fluid traverse may be terminated at the p_{iod} curve. The slope of this line is the load fluid gradient.

Example Problem 8.

Given:

1. p_{uvD} = 420 psig at 2,310 ft (D_{uv} = 2,310 ft).

2. p_{iod} = 1,140 psig at 6,000 ft.

3. g_{sl} = 0.45 psi/ft.

Find D_c for p_{as} = 1,200 psig (exceeds p_{iod}):

$$D_c = 2,310 + \frac{1,200 - 420}{0.45} = 4,043 \text{ ft.}$$

Draw a straight line originating at the point (420 psig at 2,310 ft) and extending to the point (1,200 psig at 4,043 ft) or the p_{iod} curve. This traverse below the valve at 2,310 ft will have a slope equal to the load fluid gradient g_{sl} .

Multiphase Flow Correlations and Flowing Pressure Gradient Curves

Accurate flowing-pressure-at-depth predictions are essential to good continuous-flow gas lift installation design and analysis. When computer programs for gas lift installation design and analysis are unavailable for daily routine calculations, the gas lift engineers and technicians must rely on published gradient curves to determine flowing pressures at depth. Many oil producing companies have their own multiphase flow correlations and publish in-house gradient curves. Gradient curves are available from the gas lift manufacturers and are published in books that can be purchased. It is not the purpose of this chapter to rank the various multiphase flow correlations or published gradient curves.

The widely accepted multiphase flow correlations are based on pseudosteady-state flow without serious heading through a clean production conduit with an unrestricted cross-sectional area. Accurate pressures cannot be obtained from gradient curves based on these correlations if the conduit is partially plugged with paraffin or scale. Emulsions prevent the application of gradient curves. The applicability of a particular set of gradient curves for a given well can be established only by comparing a measured flowing pressure to a pressure determined from the gradient curves. The measured production data must be accurate and repeatable before discounting the published gradient curves.

A set of typical gradient curves is given in Fig. 5.20. These gradient curves are used in the example installation design calculations in this section. Gas/liquid ratio (GLR) and not gas/oil ratio (GOR) is used for these installation design calculations. Most gradient curves for all oil are identified by GLR rather than GOR, although the values are the same. For this reason, the first step in

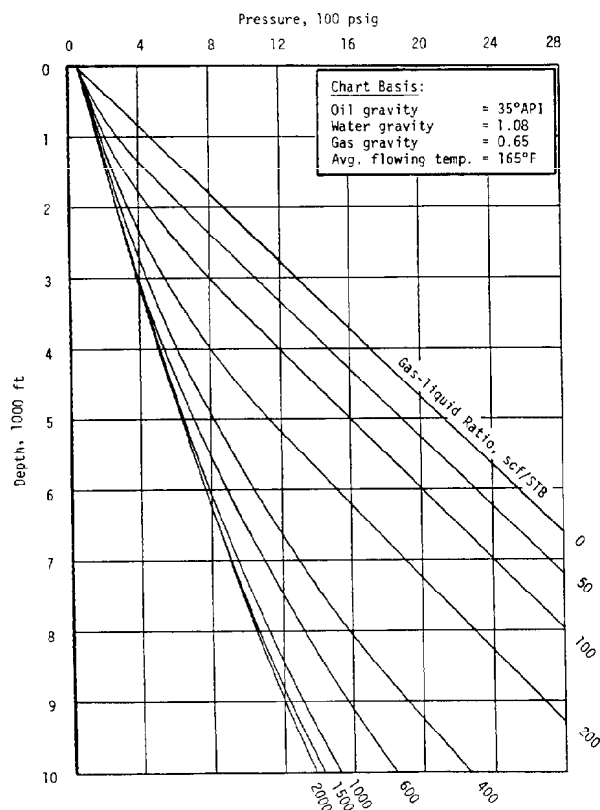


Fig. 5.20—Flowing pressure at depth gradient curves for 800 B/D (65% water) through 2 7/8-in.-OD tubing.

the application of gradient curves is to convert GOR to GLR if only GOR is reported and the well produces water. The GLR can be calculated for a given GOR and water cut with the following equation:

$$R_{glf} = f_o(R), \quad (28)$$

where

$$\begin{aligned} R_{glf} &= \text{formation GLR, scf/STB,} \\ f_o &= \text{oil cut (1 - water cut fraction), fraction,} \\ &\text{and} \\ R &= \text{GOR, scf/STB.} \end{aligned}$$

When gradient curves are used, depth is shifted and *never* pressure. If a flowing-pressure-at-depth traverse is being traced, the pressures on the pressure-depth worksheet must always overlie the same pressures on the gradient curves.

Example Problem 9.

Given:

1. Formation GOR = 500 scf/STB.
2. Water cut = 60%.

Calculate the formation GLR:

$$R_{glf} = (1 - 0.6)500 = 200 \text{ scf/STB.}$$

Flowing Temperature at Depth

The accurate prediction of the flowing-production-fluid temperature at valve depth is important in the design and

analysis of many gas lift installations with nitrogen-charged gas lift valves. The temperature of a wireline-retrievable valve is assumed to be the same as the temperature of the flowing fluids at the valve depth. A retrievable gas lift valve is located in a mandrel pocket inside the tubing and is in contact with the production from the well. The temperature of a conventional valve will be between the flowing fluid temperature and the geothermal temperature for the well.

One of the most widely used flowing temperature gradient correlations was published by Kirkpatrick⁶ in 1959. The family of flowing-temperature-gradient curves in Fig. 5.21 is based on data from high-water-cut wells being produced by gas lift through 2 7/8-in.-OD tubing over a wide range of production rates. Although the correlation does not include several important parameters, such as GLR and fluid properties, the estimated surface temperature and temperatures at depth have proven to be reasonably accurate for many gas lift operations.

Another flowing temperature correlation was published by Shiu and Beggs⁷ on the basis of a study by Shiu. This empirical method for calculating flowing temperature profiles is far more rigorous and is based on well data from several areas. The calculation procedure can be programmed easily for predicting surface flowing temperatures in vertical and inclined wells.

Considerations for Selecting the Bottom Gas Lift Valve

An orifice-check valve is recommended for the bottom valve in most continuous-flow installations. If a gas lift valve is used, the initial injection-gas opening pressure should be at least an additional 25 to 50 psi less than the calculated decrease in injection-gas pressure and a flowing production pressure equal to 50% of the design pressure. This procedure assures that the upper gas lift valves will remain closed after the point of gas injection transfers to the bottom gas lift valve and allows continued operation when the daily production rate and corresponding BHFP are much less than predicted. In addition, this decrease in the injection-gas operating pressure for the bottom gas lift valve indicates that the installation has unloaded to this valve and is being gas lifted from this depth.

Continuous-Flow Installation Design Based on a Constant Decrease in the Operating Injection-Gas Pressure for Each Succeedingly Lower Gas Lift Valve

This installation design method is based on all gas lift valves having the same port size and a constant decrease in the operating injection-gas pressure for each succeeding lower gas lift valve. Many continuous-flow installations use the same type of gas lift valve with one port size. This is particularly true for moderate-rate wells being gas lifted through 2 7/8- and 2 1/2-in.-OD tubing with 1 1/2-in.-OD gas lift valves having a 1/4-in. port. The gas lift valve selection must be based on a port size that will allow the injection gas throughput required for unloading and gas lifting the well. This installation design method is recommended for gas lift valves with a small production pressure factor. When the ratio of the port area to the bellows area is low, the decrease in the injection pressure between gas lift valves based on the production pressure effect for

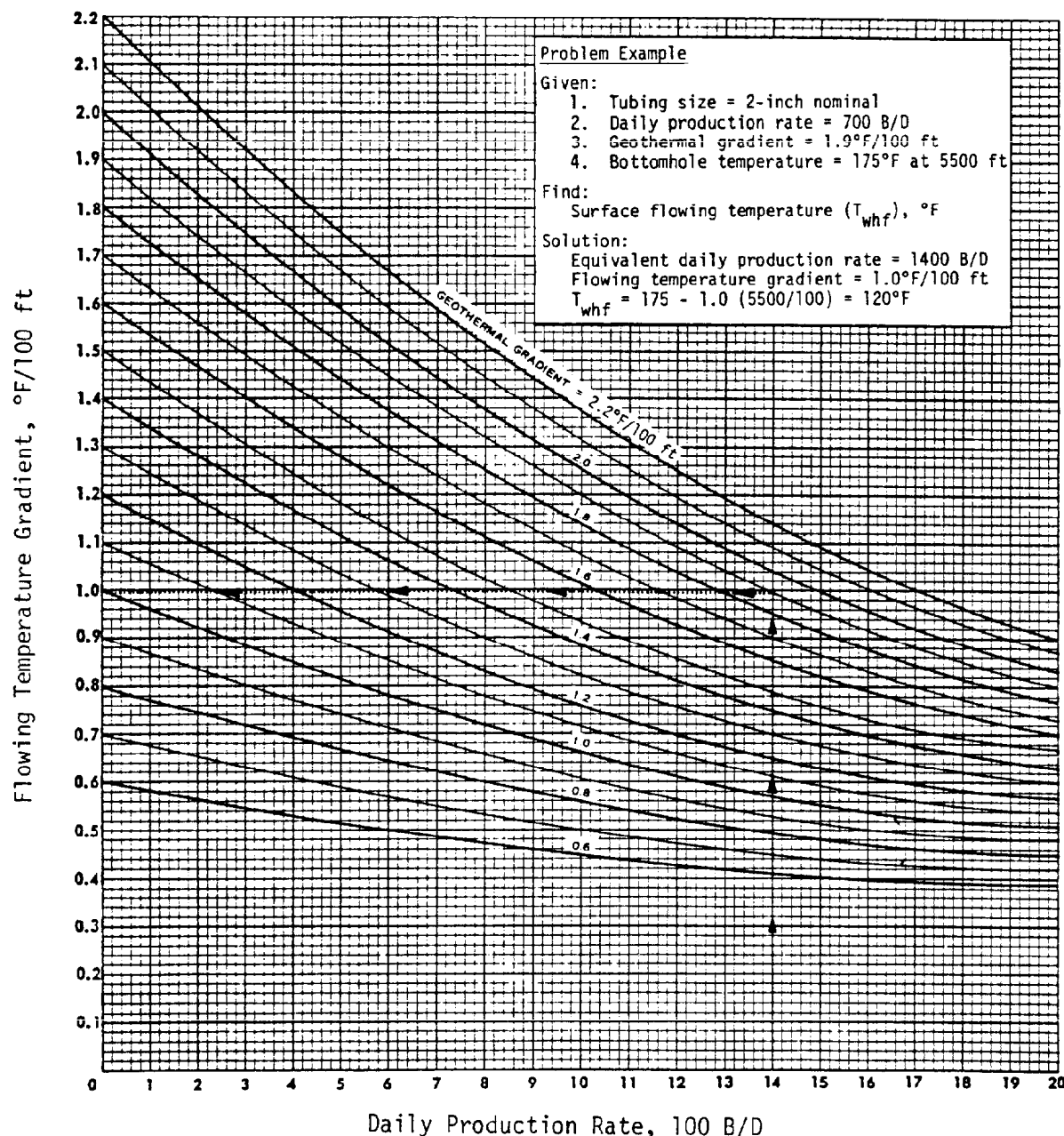


Fig. 5.21—Flowing temperature gradient for different flow rates, geothermal gradients, and tubing sizes. Chart to be used directly for 2½-in. nominal tubing. For 2-in. nominal tubing multiply actual production rate by 2. For 3-in. nominal tubing divide actual production rate by 1.5.

the top valve will not be excessive. The effect of bellows-assembly load rate on the performance of the gas lift valves is not considered in the installation design calculations. Safety factors included in these design calculations should allow sufficient increase in the operating injection-gas pressure necessary to provide the valve stem travel for adequate gas passage through each succeeding lower unloading gas lift valve without excessive interference from upper valves.

Selection of a constant pressure decrease, or drop, in the operating injection-gas pressure for each succeeding lower gas lift valve should not be arbitrary, as proposed in some design methods. The pressure decrease

should be based on the gas lift valve specifications to minimize the possibility of upper valves remaining open while lifting from a lower valve. The production-pressure effect for the top gas lift valve would be a logical choice for this decrease in the operating injection-gas pressure between valves. Closing, or reopening, of an injection-pressure-operated gas lift valve is partially controlled by the production-pressure effect, which is equal to the production-pressure factor for the valve times the flowing production pressure at the valve depth. As the gas lift valve depths increase, the distance between valves and the change in the production-pressure effect decrease but the injection-gas requirement for unloading increases. An

increased stem travel, or stroke, is needed for the lower valves to generate the larger equivalent port area necessary for the higher injection-gas requirements with the lower pressure differentials that occur across these deeper valves. A constant decrease in the operating injection-gas pressure equal to the production pressure effect for the top valve allows a greater increase in the injection-gas pressure above the initial opening pressure for a lower gas lift valve before the valve above begins to open.

Another application for this simplified design method depends on the relationship between the available injection-gas pressure and the flowing production pressure at the maximum depth of lift. When the injection-gas pressure significantly exceeds this flowing production pressure, an arbitrary Δp_{io} decrease in the injection-gas pressure can be added to the additional production-pressure effect for the top valve for calculating the spacing and opening pressures of the unloading gas lift valves. The total decrease in the injection-gas pressure is distributed equally between each succeeding lower unloading gas lift valve rather than having a sizable injection pressure drop across the operating gas lift or orifice-check valve. This procedure eliminates the possibility of multipoint gas injection through upper unloading gas lift valves by ensuring that these valves will remain closed after the point of gas injection has transferred to the next lower gas lift valve.

Selection of Port Size. In many fields where gas lift is the artificial lift method, there has been a standardization of port size that performs successfully in those wells. When a port size must be selected, the first step is to estimate the maximum depth of lift. The final operating injection-gas pressure is based on the number of gas lift valves and on the decrease in the injection-gas pressure between each succeeding lower valve. Since this final injection-gas pressure is unknown until the installation is designed, an assumed pressure difference of approximately 200 psi between the unloading g_{fp} traverse and the p_{ioD} curve is assumed for locating the deepest gas lift valve depth. The operating injection-gas rate and a pressure drop across the deepest valve of 100 psi ($p_{ioD} = p_{pfd} + 100$ psi) should ensure the selection of the proper port size for most wells, which is Step 5 in the procedure for determination of the gas lift valve depths. The last unloading gas lift valve is above the bottom valve and will have a higher injection-gas capacity because of a greater gas pressure differential and higher available injection-gas pressure.

Determination of Valve Depths. The BHP's and BHT generally are referenced to the same depth, which is the lower end of the production conduit (D_d). The steps for establishing the gas lift valve depths are as follows.

1. Determine the unloading flowing production pressure at the lower end of the production conduit (p_{pfd}).

2. Plot the flowing wellhead pressure (p_{whf}) and the p_{pfd} on the pressure-depth worksheet and connect these two pressures with a straight line, which represents the unloading flowing-pressure traverse above the point of gas injection g_{fp} .

3. Determine the operating injection-gas pressure at the lower end of the production conduit (p_{iod}) and draw a straight line between the surface operating pressure (p_{io}) and p_{iod} to establish the p_{ioD} traverse.

4. Draw the unloading gas lift valve temperature-at-depth traverse (T_{uvD}) by assuming a straight-line traverse between the surface unloading flowing wellhead temperature (T_{whu}) and the bottomhole temperature (T_{vd}).

5. Select the port size for the type of gas lift valves to be installed in the installation on the basis of the unloading and operating injection-gas requirements.

6. Record the gas lift valve specifications, which include the effective bellows area (A_b), port area (A_p), A_p/A_b ratio, production-pressure factor (F_p), and the seat angle and ball size for valves with a tapered seat.

7. Calculate the depth of the top gas lift valve (D_1) on the basis of the kick-off injection-gas pressure (p_{ko}), load fluid gradient (g_{sl}), and the wellhead U-tubing pressure (p_{whu}) with Eq. 23.

$$D_1 = \frac{p_{ko} - p_{whu}}{g_{sl}}$$

The top valve may be located graphically or at the static fluid level if this depth exceeds the calculated D_1 .

8. Draw a horizontal line between the g_{fp} traverse and the p_{ioD} curve at the depth D_1 and record the $(p_{pfd1})_{min}$ at the intersection of the g_{fp} traverse, the p_{ioD1} , and the T_{uvD1} at depth (D_1) on the unloading temperature traverse.

9. Calculate the initial injection-gas opening pressure at depth of the top gas lift valve (p_{oD1}).

$$p_{oD1} = p_{ioD1} \quad \dots \dots \dots (29)$$

10. Draw the static-load fluid traverse (g_{sl}) below the depth of the top gas lift valve with the traverse originating at $(p_{pfd1})_{min}$ and extending to the p_{ioD} curve.

11. Locate the depth of the second gas lift valve (D_2) on the basis of the assigned pressure differential (Δp_a) for spacing the gas lift valves and the p_{ioD} curve.

$$\Delta p_{sD2} = \Delta p_a, \quad \dots \dots \dots (30)$$

where Δp_{sD2} is the valve spacing pressure differential at depth of the second gas lift valve.

12. Draw a horizontal line between the g_{fp} traverse and the p_{ioD} curve at the depth D_2 and record the $(p_{pfd2})_{min}$, p_{ioD2} , and T_{uvD2} .

13. Determine the maximum flowing production pressure at the depth of the top gas lift valve ($p_{pfd1})_{max}$ immediately after the second valve is uncovered by drawing a straight line between p_{whf} and a p_{pfd2} equal to $(p_{ioD2} - \Delta p_a)$.

14. Calculate the additional production-pressure effect for the top gas lift valve Δp_{pe1} that represents the decrease in the operating injection-gas pressure for each succeeding lower gas lift valve without an arbitrary decrease in the injection-gas pressure between valves (Δp_{io}).

$$\Delta p_{pe1} = [(p_{pfd1})_{max} - (p_{pfd1})_{min}] F_p \quad \dots \dots \dots (31)$$

15. Calculate the initial injection-gas opening pressure at the depth of the second gas lift valve (p_{oD2}).

$$p_{oD2} = p_{ioD2} - \Delta p_{pe1} - \Delta p_{io} \quad \dots \dots \dots (32)$$

TABLE 5.4—CALCULATION OF THE TEST-RACK-SET OPENING PRESSURES OF THE GAS LIFT VALVES*

Valve Number	D (ft)	p_{oD} (psig)	$(p_{pfD})_{\min}$ (psig)	p_{bvD} (psig)	T_{uvD} (°F)	F_T	p_{vo} (psig)
1	2,311	1,054	420	1,014	127	0.874	947
2	3,679	1,067	598	1,037	143	0.849	940
3	4,660	1,071	726	1,049	154	0.832	931
4	5,351	1,068	816	1,052	162	0.820	921
5	5,825	1,010	439	974	168	0.812	844

*Valve description: 1½-in. OD gas lift valve. Valve specifications: $A_b = 0.77$ sq in. Port ID = ¼ in. $A_p/A_b = 0.064$. $(1 - A_p/A_b) = 0.936$.

16. Draw the static-load fluid traverse (g_M) below the depth of the second gas lift valve with the traverse originating at $(p_{pfD2})_{\min}$ and extending to the p_{ioD} curve.

17. Calculate the spacing pressure differential for the third gas lift valve (Δp_{sD3}).

$$\Delta p_{sD3} = \Delta p_{sD2} + \Delta p_{pe1} + \Delta p_{io}. \quad (33)$$

18. Locate the depth of the third gas lift valve (D_3) on the basis of Δp_{sD3} and the p_{ioD} curve.

19. Draw a horizontal line between the g_{fp} traverse and the p_{ioD} curve at the depth D_3 and record the $(p_{pfD3})_{\min}$, p_{ioD3} , and T_{uvD3} .

20. Calculate the initial injection-gas opening pressure at the depth of the third gas lift valve.

$$p_{oD3} = p_{ioD3} - 2(\Delta p_{pe1} + \Delta p_{io}). \quad (34)$$

21. Draw the static-load fluid traverse below the depth of the third valve.

22. Calculate the spacing pressure differential for the fourth valve.

$$\Delta p_{sD4} = \Delta p_{sD3} + \Delta p_{pe1} + \Delta p_{io}. \quad (35)$$

23. Locate the depth of the fourth valve.

24. Record $(p_{pfD4})_{\min}$, p_{ioD4} , and T_{uvD4} .

25. Calculate the initial injection-gas opening pressure at the depth of the fourth valve.

$$p_{oD4} = p_{ioD4} - 3(\Delta p_{pe1} + \Delta p_{io}). \quad (36)$$

Repeat Steps 21 through 25 until the maximum desired gas lift valve depth is attained or the calculated distance between gas lift valves is less than an assigned minimum distance between valves.

Calculation of the Test-Rack-Set Opening Pressures of the Gas Lift Valves. A tabulation form for these calculations is illustrated in Table 5.4. The equations that are needed to perform the calculations are as follows:

$$p_{bvD} = p_{oD}(1 - A_p/A_b) + (p_{pfD})_{\min}(A_p/A_b) \quad (37)$$

and

$$p_{vo} = \frac{F_T(p_{bvD})}{(1 - A_p/A_b)} \quad (38)$$

The unloading gas lift valve temperature at depth can be

read from the pressure-depth worksheet or calculated using the following equation:

$$T_{uvD} = T_{whu} + D[(T_{vd} - T_{whu})/D_d] \quad (39)$$

This temperature is used to obtain a value for F_T from Table 5.1.

If the test-rack opening pressures of the gas lift valves will be set at a tester temperature (T_{vs}) other than the chart base temperature of 60°F for Table 5.1, the following equation for p_{vos} must be used:

$$p_{vos} = \frac{F_T(p_{bvD})}{F_{Ts}(1 - A_p/A_b)} \quad (40)$$

where F_{Ts} is found in Table 5.1 for T_{vs} .

Example Problem 10.

Well information for installation design calculations :

1. Tubing size = 2⅞-in. OD.
2. Tubing length = 6,000 ft.
3. Maximum valve depth = 5,970 ft.
4. Daily production rate = 800 STB/D.
5. Water cut = 60%.
6. Formation GOR = 500 scf/STB.
7. Oil gravity = 35° API.
8. Gas gravity = 0.65.
9. Water specific gravity = 1.04.
10. BHT = 170°F at 6,000 ft.
11. Design unloading wellhead temperature = 100°F.
12. Load fluid gradient = 0.45 psi/ft.
13. U-tubing wellhead pressure = 60 psig.
14. Flowing wellhead pressure = 120 psig.
15. Static fluid level = 0 ft (loaded).
16. Surface kick-off injection-gas pressure = 1,100 psig.
17. Surface operating injection-gas pressure = 1,000 psig.
18. Kick-off injection-gas rate = 800 Mscf/D.
19. Operating injection-gas rate = 500 Mscf/D.
20. Injection-gas wellhead temperature = 80°F.
21. Gas lift valve bellows area = 0.77 sq in. (1½-in.-OD valve).
22. Gas lift valve with sharp-edged seat.
23. Test-rack-set temperature = 60°F.
24. Assigned pressure drop across valves = 50 psi.
25. Additional decrease in injection-gas pressure between valves = 0 psi.
26. Minimum distance between valves = 200 ft.

13. From the straight-line traverse between $p_{whf} = 120$ psig and $p_{pfD2} = 1,036$ psig,

$$(p_{pfD1})_{\max} = 695 \text{ psig at } 2,311 \text{ ft (Refer to Fig. 5.22).}$$

14. $\Delta p_{pe1} = [(p_{pfD1})_{\max} - (p_{pfD1})_{\min}] F_p = (695 \text{ psig} - 420 \text{ psig}) 0.068 = 19 \text{ psi}$.

15. $p_{oD2} = p_{ioD2} - \Delta p_{pe1} = 1,086 \text{ psig} - 19 \text{ psig} = 1,067 \text{ psig at } 3,680 \text{ ft}$.

16. Draw the g_{sl} traverse originating at 598 psig at 3,680 ft and extending to the p_{ioD} curve.

$$17. \Delta p_{sD3} = \Delta p_{sD2} + \Delta p_{pe1} = 50 \text{ psi} + 19 \text{ psi} = 69 \text{ psi.}$$

$$18. D_3 = 4,660 \text{ ft for } \Delta p_{sD3} = 69 \text{ psi.}$$

19. From the pressure-depth worksheet for $D_3 = 4,660 \text{ ft}$,

$$(p_{pfD3})_{\min} = 726 \text{ psig, } p_{ioD3} = 1,109 \text{ psig.}$$

$$T_{uvD3} = 154^\circ\text{F.}$$

$$20. p_{oD3} = p_{ioD3} - 2(\Delta p_{pe1}) = 1,109 \text{ psig} - 2(19 \text{ psi}) \\ = 1,071 \text{ psig at } 4,660 \text{ ft.}$$

21. Draw the g_{sl} traverse originating at 726 psig at 4,660 ft and extending to the p_{ioD} curve.

$$22. \Delta p_{sD4} = \Delta p_{sD3} + \Delta p_{pe1} = 69 \text{ psi} + 19 \text{ psi} = 88 \text{ psi.}$$

$$23. D_4 = 5,350 \text{ ft for } \Delta p_{sD4} = 88 \text{ psi.}$$

24. From the pressure-depth worksheet for $D_4 = 5,350 \text{ ft}$,

$$(p_{pfD4})_{\min} = 816 \text{ psig, } p_{ioD4} = 1,125 \text{ psig,}$$

$$T_{uvD4} = 162^\circ\text{F.}$$

25. $p_{oD4} = p_{ioD4} - 3(\Delta p_{pe1}) = 1,125 \text{ psig} - 3(19 \text{ psi}) = 1,068 \text{ psig at } 5,350 \text{ ft}$.

Repeat Steps 21 through 25 for Valve No. 5:

21. Draw the g_{sl} traverse originating at 816 psig at 5,350 ft and extending to the p_{ioD} curve.

$$22. \Delta p_{sD5} = \Delta p_{sD4} + \Delta p_{pe1} = 88 \text{ psi} + 19 \text{ psi} = 107 \text{ psi.}$$

$$23. D_5 = 5,825 \text{ ft for } \Delta p_{sD5} = 107 \text{ psi.}$$

24. From the pressure-depth worksheet for $D_5 = 5,825 \text{ ft}$,

$$(p_{pfD5})_{\min} = 877 \text{ psig, } p_{ioD5} = 1,136 \text{ psig,}$$

$$T_{uvD5} = 168^\circ\text{F.}$$

Note: The distance between the fifth gas lift valve and the maximum valve depth is only 145 ft, which is less

than the assigned 200-ft minimum distance between valves. In all probability, a sixth valve near 5,970 ft could not be justified on the basis of an increase in oil production from this well. An orifice-check valve with a $\frac{1}{4}$ -in. port could be installed near 5,970 ft to assure maximum production if the actual productivity of this well is less than predicted.

25. An orifice-check valve with a $\frac{1}{4}$ -in. port is recommended at 5,825 ft if an orifice-check valve will not be run near 5,970 ft. For a gas lift valve at 5,825 ft, assume a 50-psi additional decrease in the injection-gas pressure and a $(p_{pfD5})_{\min}$ based on 50% of the design value.

$$p_{oD5} = p_{ioD5} - 4(\Delta p_{pe1}) - 50 \text{ psi} = 1,136 \text{ psig} - 4(19 \text{ psi}) - 50 \text{ psi} = 1,010 \text{ psig at } 5,825 \text{ ft.}$$

$(p_{pfD5})_{\min} = 0.5(877 \text{ psig}) = 439 \text{ psig at } 5,825 \text{ ft}$ for calculating the test-rack-set opening pressure of the bottom gas lift valve.

The test-rack opening pressure for gas lift valve No. 5 (Table 5.4) is based on the additional production-pressure effect for the top gas lift valve plus an extra 50-psi decrease in the operating-injection pressure and a flowing production pressure equal to 50% of $(p_{pfD5})_{\min}$ for the design production rate. An orifice-check valve with a $\frac{1}{4}$ -in. orifice would be recommended for most installations.

Continuous-Flow Installation Design When Injection-Gas Pressure is High Relative to Depth of Lift

An additional incremental decrease in the injection-gas pressure can be added to the calculated decrease to ensure unloading a gas lift installation when the injection-gas pressure is high relative to the required depth of lift. The flowing production pressure at the depth of lift limits the maximum injection-gas pressure that can be used in terms of contributing to the lift process. An excessive injection-gas pressure drop across the operating gas lift valve represents an inefficient energy loss. Distributing the decrease in the injection-gas pressure between each succeeding lower unloading gas lift valve prevents multipoint gas injection through upper gas lift valves after the point of gas injection transfers to a lower valve. In other words, the gas lift installation can be unloaded without valve interference and the unloading process is apparent from the injection-gas pressure recording at the surface. A high available injection-gas pressure relative to the depth of lift may exist in areas where both shallow and deep wells are being gas lifted with injection gas from the same system, and the flowing production pressure in the shallow wells will limit the injection-gas pressure that can be used to gas lift these wells.

Example Problem 11. The same well information as given in the previous installation design (Example Problem 10), with the exception of the well depth and temperature and an assumed additional decrease in the injection-gas pressure between each succeeding lower gas lift valve, will be used to illustrate the advantage of this design method when the injection-gas pressure is high relative to the required depth of lift. The valve test-rack-set opening pressures are calculated in Table 5.5.

TABLE 5.5—TEST-RACK-SET OPENING PRESSURES FOR VALVES IN AN INSTALLATION WITH ADDITIONAL DECREASE IN INJECTION-GAS PRESSURE BETWEEN VALVES*

Valve Number	D (ft)	p_{iod} (psig)	p_{oD} (psig)	$(p_{pfd})_{min}$ (psig)	T_{uvD} (°F)	p_{bvD} (psig)	p_{vo} (psig)
1	2,311	1,054	1,054	409	123	1,013	953
2	3,706	1,087	1,008	583	137	981	899
3	4,584	1,107	949	693	146	933	841
4	4,970	1,116	829	370	150	800	716

*Additional decrease in injection-gas pressure = 60 psi.

Changes in well information:

2. Tubing length = 5,000 ft.
3. Maximum valve depth = 4,970 ft.
10. BHT = 150°F at 5,000 ft.
24. Additional decrease in injection-gas pressure between valves = 60 psi.

The g_{fp} traverse is based on a $p_{pfd} = 745$ psig at 5,000 ft and the p_{iod} traverse on $p_{iod} = 1117$ psig at 5,000 ft. Test-rack opening pressure for the bottom gas lift valve is based on an additional 50-psi decrease in the injection-gas pressure and a $(p_{pfd})_{min}$ equal to 50% of the design value. An orifice-check valve with a 1/4-in. orifice would be recommended for most wells.

Continuous-Flow Installation Design With Valve Depths Based on a Variable-Gradient Valve Spacing Design Line

The increasing-flowing-pressure-gradient-with-depth installation design is applicable for production-pressure-(fluid)-operated gas lift valves and injection-gas-pressure-operated gas lift valves with a high production-pressure factor (20 to 30% or greater). One advantage of the design is that there is no required decrease in the injection-gas pressure for each succeeding lower valve. The valves are opened (or closed) as a result of a change in the flowing production pressure at valve depth rather than a change in the injection-gas pressure. For this reason, the gas lift valves must be extremely sensitive to the flowing production pressure to operate properly.

The specifications for the gas lift valves do not affect the valve depths but are used to calculate the test-rack opening pressures. The distance between gas lift valves is controlled by several assumed design factors and the unloading flowing pressure traverse above the point of gas injection. The unloading traverse is based on the conduit size, design daily production rate, available injection gas volume for unloading, etc. The assumed percentage factor for calculating the surface pressure and the assigned design operating pressure differential for the lower gas lift valves locate the valve spacing design line that represents the transfer pressures for the upper unloading gas lift valves. The distance between the upper unloading valves will be less (more valves required) for a higher assumed percentage factor for calculating the valve spacing design line surface pressure; that is, the change in the flowing pressure gradient required to transfer from an upper to the next lower gas lift valve will be less. A lower design percentage factor requires fewer gas lift valves, but the chances of inefficient multipoint gas injection and not unloading to the optimal point of gas injection are increased. The percentage factor for calculating the pressure increase to be added to the flowing wellhead pressure

can be multiplied by the operating injection-gas pressure or by the difference between the operating injection gas and the flowing wellhead pressures. The basic concept is the same. Typically, a 20% factor is applied to the operating injection-gas pressure and a 25% factor to the pressure difference term.

The actual gas throughput performance of the gas lift valves is not included in these design calculations. Multipoint gas injection occurs during unloading operations. After the operating gas lift valve depth is attained, the upper gas lift valves should remain closed. The maximum flowing production pressure exists at the depth of the operating gas lift valve, and the flowing production pressure at the depths of the upper gas lift valves should be less than the production pressure required to open these valves.

Since the injection-gas pressure is not decreased for each succeeding lower gas lift valve and no spacing pressure differential is assumed in this design method, the design operating injection-gas pressure for valve spacing and test-rack opening pressure calculations should be at least 50 psi less than the minimum available injection-gas-line pressure at the wellsite. The lower design pressure allows a range in the injection-gas pressure to provide stem travel for the injection- and production-pressure-operated gas lift valves. If the available range of injection-gas pressure is 50 psi from design to full line pressure, a maximum increase of 50 psi above the initial opening pressure should assure ample stem travel for most injection-pressure-operated gas lift valves. Since the actual flowing production transfer pressure could be as much as 50 psi higher than the design transfer pressure for production-pressure-operated gas lift valves, the necessary stem travel to open these valves should present no problem during unloading operations.

If an operator prefers to design a production-pressure-(fluid)-operated installation on the basis of the injection-gas pressure at the wellsite, an assigned spacing pressure differential (Δp_a) should be used for locating the depths of this type of gas lift valve. The actual maximum transfer pressure will be equal to the design flowing production transfer pressure plus the assigned spacing pressure differential. The end result is similar to using a lower design operating injection-gas pressure, as noted above. Applying a spacing pressure differential of 50 psi rather than decreasing the design operating injection-gas pressure 50 psi does not provide the same additional opening force for stroking an injection-pressure-operated gas lift valve.

Determination of the Gas Lift Valve Depths. The BHP's and BHT usually are referenced to the same depth, which is the lower end of the production conduit (D_d). The steps

for establishing the gas lift valve depths on a pressure-depth worksheet are as follows.

1-4. Follow the same four steps as described for the installation design based on a constant decrease in the operating injection-gas pressure for each succeeding lower valve.

5. Calculate the surface pressure (p_{dl}), for the variable-gradient valve spacing design line on the basis of the assigned spacing design line percent factor F_{dl} , surface operating injection-gas pressure (p_{io}), and the flowing wellhead pressure (p_{whf}).

6. Determine the maximum depth for the variable-gradient valve spacing design line (D_{dl}) on the basis of the assigned design operating pressure differential (Δp_{ao}), the g_{fp} traverse, and the p_{ioD} curve or the maximum depth for a gas lift valve. Record the depth D_{dl} and the variable-gradient valve spacing design line pressure (p_{dlD}) at D_{dl} .

$$p_{dl} = p_{whf} + F_{dl}(p_{io})/100. \quad (41)$$

7. Draw the variable-gradient valve spacing design line by connecting the surface spacing design line pressure (p_{dl}) with the design line pressure at maximum depth (p_{dlD}). The design line represents the flowing production transfer pressure (p_{tD}) at depth for each gas lift valve.

8. Draw a continuation of the flowing production transfer pressure (p_{tD}) curve originating at p_{dlD} and paralleling the p_{ioD} curve to the datum depth D_d when additional gas lift valves will be run below D_{dl} .

9. Using Eq. 23, calculate the depth of the top gas lift valve (D_1) on the basis of the surface kick-off injection-gas pressure (p_{ko}), load fluid gradient (g_{sl}), and the wellhead U-tubing pressure (p_{whu}).

$$D_1 = \frac{p_{ko} - p_{whu}}{g_{sl}}.$$

10. Draw a horizontal line between the valve spacing design line and the p_{ioD} curve at the depth D_1 . Record the p_{tD1} at the intersection of the spacing design line, p_{ioD1} , and the T_{uvD1} at depth D_1 on the unloading temperature traverse.

11. Record the initial injection-gas opening pressure at the depth of the top gas lift valve (p_{oD1}), which is the operating injection-gas pressure at D_1 (Eq. 29).

$$p_{oD1} = p_{oiD1}.$$

The initial injection-gas opening pressure for all valves is equal to the operating injection-gas pressure at depth if there is no decrease in the injection-gas pressure between valves.

12. Draw the static-load fluid traverse (g_{sl}) below the depth of the top gas lift valve with the traverse originating at p_{tD1} and extending to the p_{ioD} curve.

13. Locate the depth of the second gas lift valve (D_2) at the intersection of the static-load fluid traverse with the p_{ioD} curve if there is no pressure differential used for locating the valve depths.

14. Continue to determine the unloading gas lift valve depths graphically by repeating Steps 10 through 13 un-

til the maximum depth D_{dl} for the variable-gradient valve spacing design line is reached or exceeded.

15. Calculate the distance between the remaining gas lift valves (L_{bv}) on the basis of the assigned design operating pressure differential (Δp_{ao}) and the static-load fluid gradient (g_{sl}).

$$L_{bv} = \frac{\Delta p_{ao}}{g_{sl}}. \quad (42)$$

16. Calculate the remaining gas lift valve depths by assuming the previous constant distance between all remaining valves until the maximum depth of lift is attained.

17. Record p_{tD} , p_{ioD} , and T_{uvD} at the depth of each gas lift valve.

18. Record the initial injection-gas opening pressure at the depth of the gas lift valve, which is equal to the operating injection-gas pressure at the valve depth.

$$p_{oD} = p_{ioD}. \quad (43)$$

19. Determine the minimum equivalent port size for injection-pressure-operated gas lift valves on the basis of the corrected daily unloading injection gas volume, p_{ioD} and p_{tD} . The minimum port size for production-pressure-operated gas lift valves is based on the injection-gas requirement to establish p_{tD} for each valve depth.

20. Select the port size for the gas lift valves and record the effective bellows area (A_b), port area (A_p), A_p/A_b ratio and $(1 - A_p/A_b)$, the production-pressure factor (F_p), and the seat angle and stem-ball size for valves with a tapered seat. A port size larger than theoretically required for injection-pressure-operated gas lift valves may be advisable for greater production-pressure effect.

Calculation of the Test-Rack-Set Opening Pressures of the Gas Lift Valves. A tabulation form for these calculations is illustrated in Table 5.6. The equation for calculating the bellows-charged pressure at the design unloading valve temperature (p_{bvD}) is

$$p_{bvD} = p_{oD}(1 - A_p/A_b) + p_{tD}(A_p/A_b), \quad (44)$$

where p_{tD} is the flowing production transfer pressure at valve depth, psig.

The unloading temperature at the valve depth can be obtained from a T_{uvD} traverse on the pressure-depth worksheet or calculated with Eq. 39. The test-rack opening pressure is calculated with Eq. 38 for a tester setting temperature of 60°F and Eq. 40 for a tester temperature (T_{ts}) other than 60°F.

Example Problem 12. Well information for installation design calculations:

1. Tubing size = 2 7/8-in. OD.
2. Tubing length = 5,500 ft.
3. Maximum valve depth = 5,470 ft.
4. Daily production rate = 800 STB/D.
5. Water cut = 60%.
6. Formation GOR = 500 scf/STB.
7. Oil gravity = 35° API.
8. Gas gravity = 0.65.
9. Water specific gravity = 1.04.

TABLE 5.6—CALCULATION OF THE TEST-RACK-SET OPENING PRESSURES OF THE RETRIEVABLE GAS LIFT VALVES*

Valve Number	D (ft)	p_{ioD} (psig)	$(p_{io})_{min}$ (psig)	p_{bvD} (psig)	T_{uvD} (°F)	F_T	p_{vo} (psig)
1	1,756	832	446	736	119	0.887	868
2	2,650	848	530	769	129	0.871	890
3	3,387	862	600	797	137	0.858	908
4	3,994	873	657	819	144	0.847	923
5	4,494	882	704	838	149	0.839	934
6	4,905	889	739	852	154	0.832	943
7	5,238	895	745	858	157	0.827	943
8	5,470	849	375	732	160	0.823	800

*Valve description: 1-in.-OD gas lift valves. Valve specifications: $A_b = 0.31$ sq in. Port ID = $5/16$ in. $A_p/A_b = 0.247$. $(1 - A_p/A_b) = 0.753$.

10. BHT = 160°F at 5,500 ft.
11. Design unloading wellhead temperature = 100°F.
12. Load fluid gradient = 0.45 psi/ft.
13. U-tubing wellhead pressure = 60 psig.
14. Flowing wellhead pressure = 120 psig.
15. Static fluid level = 0 ft (loaded).
16. Surface kick-off and operating injection-gas pressure = 850 psig.
17. Surface design operating injection-gas pressure = 800 psig.
18. Kick-off injection-gas rate = 800 Mscf/D.
19. Operating injection-gas rate = 500 Mscf/D.
20. Injection-gas wellhead temperature = 80°F.
21. Gas lift valve bellows area = 0.31 sq in. (1-in.-OD valve).
22. Gas lift valve with sharp-edged seat.
23. Test-rack-set temperature = 60°F.
24. Design operating pressure differential = 150 psi.
25. Percent factor for valve spacing design line = 20%.

Solution—Valve Depths. The traverses for the pressures and temperatures used for calculating the gas lift installation design are drawn on a pressure-depth worksheet in Fig. 5.24.

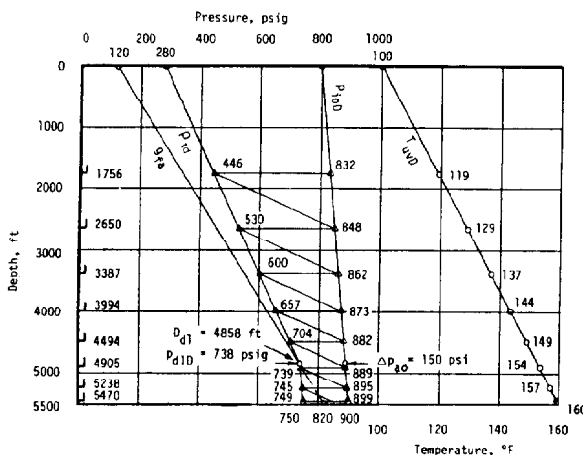


Fig. 5.24—Continuous flow installation design with the valve depths based on a variable-gradient valve spacing design line.

$$1. \text{ Total GLR} = \text{injection GLR} = \frac{800,000 \text{ scf/D}}{800 \text{ STB/D}} = 1,000 \text{ scf/STB.}$$

From the appropriate gradient curves in Fig. 5.20 we obtain the following information.

Actual Depth (ft)	Chart Depth (ft)	Pressure (psig)
0	700	120
5,500	6,200	820

$$p_{pfd} = 820 \text{ psig at 5,500 ft.}$$

2. Draw the g_{fp} traverse by connecting 120 psig at the surface to 820 psig at 5,500 ft with a straight line.

3. p_{io} at surface of 800 psig increases to 900 psig at 5,500 ft (p_{iod}). Draw the p_{ioD} curve by connecting 800 psig at the surface to 900 psig at 5,500 ft with a straight line.

4. Plot the unloading temperature of 100°F at the surface and 160°F at 5,500 ft, and draw the T_{uvD} traverse by connecting 100°F at the surface to 160°F at 5,500 ft with a straight line.

5. From the pressure-depth worksheet for $\Delta p_{ao} = 150$ psi,

$$D_{dl} = 4,858 \text{ ft and } p_{dlD} = 738 \text{ psig at 4,858 ft.}$$

$$6. p_{dl} = p_{whf} + \frac{F_{dl}(p_{io})}{100} = 120 + \frac{20(800)}{100} = 280 \text{ psig at surface.}$$

7. Draw the variable-gradient valve spacing design line by connecting 280 psig at the surface to 738 psig at 4,858 ft with a straight line. This traverse represents the flowing production transfer pressures at valve depth (p_{TD}).

8. For locating valves below D_{dl} , draw a straight line originating at 738 psig at 4,858 ft and paralleling p_{ioD} curve to 750 psig at 5,500 ft (900 psig - 150 psi = 750 psig).

$$9. D_1 = \frac{p_{ko} - p_{whu}}{g_{sl}} = \frac{850 - 60}{0.45} = 1,756 \text{ ft.}$$

10. From the pressure-depth worksheet for $D_1 = 1,756$ ft,

$$p_{tD1} = 446 \text{ psig}, p_{ioD1} = 832 \text{ psig}, \text{ and } T_{uvD1} = 119^\circ\text{F}.$$

11. $p_{oD1} = p_{ioD1} = 832$ psig at 1,756 ft.

12. Draw the g_{sl} traverse (0.45 psi/ft) below the top valve originating at 446 psig at 1,756 ft and extending to the p_{ioD} curve.

13. $D_2 = 2,650$ ft at the intersection of the p_{ioD} curve.

Repeat Steps 10 through 13 until the calculated valve depth exceeds D_{dl} . Calculations for the third gas lift valve are as follows.

10. From the pressure-depth worksheet for $D_2 = 2,650$ ft,

$$p_{tD2} = 530 \text{ psig}, p_{ioD2} = 848 \text{ psig}, \text{ and } T_{uvD2} = 129^\circ\text{F}.$$

11. $p_{oD2} = p_{ioD2} = 848$ psig at 2,650 ft.

12. Draw the g_{sl} traverse below the second valve.

13. $D_3 = 3,387$ ft.

Repeat Steps 10 through 13 for the fourth gas lift valve.

10. $p_{tD3} = 600$ psig, $p_{ioD3} = 862$ psig, and $T_{uvD3} = 137^\circ\text{F}$.

11. $p_{oD3} = p_{ioD3} = 862$ psig at 3,387 ft.

12. Draw the g_{sl} traverse below the third valve.

13. $D_4 = 3,994$ ft.

Repeat Steps 10 through 13 for the fifth gas lift valve.

10. $p_{tD4} = 657$ psig, $p_{ioD4} = 873$ psig, and $T_{uvD4} = 144^\circ\text{F}$.

11. $p_{oD4} = p_{ioD4} = 873$ psig at 3,994 ft.

12. Draw the g_{sl} traverse below the fourth valve.

13. $D_5 = 4,994$ ft.

Repeat Steps 10 through 13 for the sixth gas lift valve.

10. $p_{tD5} = 704$ psig, $p_{ioD5} = 882$ psig, and $T_{uvD5} = 149^\circ\text{F}$.

11. $p_{oD5} = p_{ioD5} = 882$ psig at 4,994 ft.

12. Draw the g_{sl} traverse below the fifth valve.

13. $D_6 = 4,905$ ft ($D_6 > D_{dl}$).

14. Since $D_6 > D_{dl}$, the p_{tD} traverse parallels the p_{ioD} curve ($p_{tD} = p_{ioD} - \Delta p_{ao}$), repeat Steps 10 and 11.

10. $p_{tD6} = 739$ psig, $p_{ioD6} = 889$ psig, and $T_{uvD6} = 154^\circ\text{F}$.

11. $p_{oD6} = p_{ioD6} = 889$ psig.

Remaining gas lift valve depths and pressures.

$$15. L_{bv} = \frac{\Delta p_{ao}}{g_{sl}} = \frac{150}{0.45} = 333 \text{ ft.}$$

16. $D_7 = D_6 + L_{bv} = 4,905 + 333 = 5,238$ ft.

17. From the pressure-depth worksheet for $D_7 = 5,238$ ft,

$$p_{tD7} = 745 \text{ psig}, p_{ioD7} = 895 \text{ psig}, \text{ and } T_{uvD7} = 157^\circ\text{F}.$$

18. $p_{oD7} = p_{ioD7} = 895$ psig at 5,238 ft.

Repeat Steps 16 and 18 until maximum valve depth is at-

tained. Calculations for the eighth gas lift valve are as follow:

16. $D_8 = D_7 + L_{bv} = 5,238 + 333 = 5,571$ ft $> 5,470$ ft, $D_8 = 5,470$ ft (maximum valve depth).

17. $p_{tD8} = 749$ psig, $p_{ioD8} = 899$ psig, and $T_{uvD8} = 160^\circ\text{F}$.

18. If a gas lift valve rather than an orifice-check valve will be installed as the bottom valve, assume that

$$p_{oD8} = p_{ioD8} - 50 \text{ psi} = 899 - 50 = 849 \text{ psig at } 5,470 \text{ ft,}$$

$$p_{tD8} = 0.5(749) = 375 \text{ psig at } 5,470 \text{ ft.}$$

19. $q_{ga} = 800$ Mscf/D (given),

$$T_{gD} = 80^\circ\text{F} + 4,858 \text{ ft} \left(\frac{160^\circ\text{F} - 80^\circ\text{F}}{5,500 \text{ ft}} \right) \\ = 151^\circ\text{F at } 4,858 \text{ ft,}$$

$$C_{gT} = 0.0544 \sqrt{0.65(151^\circ\text{F} + 460)} = 1.084, \text{ and}$$

$$q_{gc} = C_{gT}(q_{ga}) = 1.084(800 \text{ Mscf/D}) \\ = 867 \text{ Mscf/D.}$$

For $p_{ioD} = 888$ psig and $p_{dlD} = 738$ psig at 4,858 ft, equivalent port size = $1\frac{1}{4}$ to $1\frac{3}{4}$ in. for 867 Mscf/D from Fig. 5.5.

20. Minimum standard port size = $\frac{1}{4}$ -in. Select a $\frac{5}{16}$ -in. port for a greater production-pressure factor. For $\frac{5}{16}$ -in. OD port with a sharp-edged seat and $A_b = 0.31$ sq in.,

$$A_p/A_b = 0.247, (1 - A_p/A_b) = 0.753, \text{ and}$$

$$F_p = 0.329 \text{ from Table 5.2.}$$

The test-rack opening pressure for gas lift valve No. 8 (Table 5.6) is based on a 50-psi decrease in the operating injection-gas pressure and a flowing production-transfer pressure equal to 50% of the flowing production-transfer pressure at the depth of this bottom valve. An orifice-check valve with a $\frac{1}{4}$ -in. orifice would be recommended for most installations.

Production-Pressure-(Fluid)-Operated Gas Lift Valves for a Variable Gradient Valve Spacing Continuous-Flow Installation

As previously noted in the discussion of a variable gradient valve spacing continuous-flow installation, production-pressure-(fluid)-operated gas lift valves are particularly applicable for this type of design. The depths of the valves remain the same for production-pressure and injection-pressure operation. The recommended port sizes and the test-rack setting pressures are different.

The flowing production pressure at valve depth during unloading operations varies significantly as compared to the injection-gas pressure. The effective bellows area less the port area is exposed to this changing flowing production pressure for production-pressure-operated gas lift valves. Since the flowing production pressure provides

TABLE 5.7—FLOWING PRODUCTION PRESSURE AT VALVE DEPTH FROM GRADIENT CURVES

Assume Total Gas/Liquid Ratio (scf/STB)	Actual Depth (ft)	Chart Depth (ft)	Pressure (psig)
100	0	500	120
	1,756	2,256	540 > p_{iD1}
200	0	600	120
	1,756	2,356	402 < p_{iD1}

the primary opening force to open a production-pressure-operated valve, the upper valves will open fully during unloading operations because of the wide range in the flowing production pressure at the upper valve depths. The smallest possible port or choke size based on the injection-gas requirement for unloading and operating is recommended to limit the maximum injection-gas throughput of the upper valves. A large port or choke size in the upper unloading gas lift valves may prevent valve closure without a drastic decrease in the operating injection-gas pressure. The test-rack opening pressures of the upper valves are considerably lower than the opening pressures for the deeper valves, since the primary opening force for these valves is based on the flowing production-transfer-pressure traverse rather than the injection-gas-pressure-at-depth traverse. Inefficient gas lift operations result from multipoint gas injection and the inability to unload to a lower valve with single-point gas injection when upper valves will not close.

Since the depths of the valves remain the same for injection-pressure and production-pressure operation, the previous continuous-flow installation design with a graphical pressure-depth display in Fig. 5.24 will be used to illustrate the calculations for production-pressure-operated valves.

The injection-gas requirement to unload and to lift a well increases with the depth of lift for an assumed constant production rate. After the valve depths are determined as outlined in the previous example problem, the first step before calculating the test-rack opening pressure of production-pressure-operated gas lift valves is to establish the necessary port size. The gradient curves in Fig. 5.20 will be used to establish the injection-gas requirement for each gas lift valve. The object is to determine the approximate total gas-liquid ratio (TGLR) curve that will pass through a flowing wellhead pressure of 120

psig at the surface and 446 psig at 1,756 ft. The TGLR curves that bracket 446 psig at 1,765 ft are given in Table 5.7.

Example Problem 13. Installation Design Calculations. The TGLR is between 100 and 200 scf/STB since the flowing production pressures for these GLR's bracket the design flowing-production-transfer pressure of 446 psig. An approximate TGLR can be calculated by proportional interpolation, and this TGLR can be obtained for each valve depth and flowing-production-transfer pressure as outlined for the top gas lift valve. A tabulation of these values for the unloading TGLR are given in Table 5.8. After the TGLR is established, an equivalent port size can be obtained from Fig. 5.5 on the basis of the daily injection-gas throughput rates that have been corrected to chart basis. This information completes Table 5.8.

The smallest standard port size based on the daily injection-gas requirement in Table 5.8 is assumed for the valve opening pressure calculations in a tester. Since the flowing production pressure rather than the injection-gas pressure at valve depth is exerted over the effective bellows area less the port area for a production-pressure-operated gas lift valve, the equation for the bellows-charged pressure at valve temperature differs from the equation for an injection-pressure-operated gas lift valve. The equation for a production-pressure-operated gas lift valve is

$$p_{bvD} = p_{iD}(1 - A_p/A_b) + p_{ioD}(A_p/A_b). \quad (45)$$

The test-rack-set opening pressure is calculated using Eq. 38 or Eq. 40, which is the same for injection-pressure-operated gas lift valves. A summary of the calculations for production-pressure-operated gas lift valves in this installation is tabulated in Table 5.9. An orifice-check valve or injection-pressure-operated gas lift valve is recommended for the bottom valve in a production-pressure-operated valve installation. If the BHFP is lower than predicted, maximum production is not possible with a production-pressure-operated gas lift valve because this type of valve will not remain open for a low BHFP.

If an injection-pressure-operated gas lift valve will be run instead of an orifice-check valve with a ¼-in. choke, the tester-set opening pressure should be based on an operating pressure less than the design operating injection-gas pressure. One recommendation is to assume a 50-psi lower operating injection-gas pressure and the flowing production pressure at valve depth equal to the flowing wellhead

TABLE 5.8—INJECTION-GAS REQUIREMENT AND MINIMUM VALVE PORT AREA FOR PRODUCTION-PRESSURE-OPERATED GAS LIFT VALVES*

Valve Number	D (ft)	p_{ioD} (psig)	p_{iD} (psig)	T_{gD} (°F)	Total Gas/Liquid Ratio (scf/STB)	Actual Injection q_{ga} (Mscf/D)	C_{gT}	Chart Injection q_{gc} (Mscf/D)	Minimum Port Area	
									(sq in.)	Nearest 64th in.
1	1,756	832	446	106	170	136	1.043	141.9	0.0061	5
2	2,650	848	530	119	325	260	1.055	274.4	0.0118	7
3	3,387	862	600	129	440	352	1.064	374.7	0.0165	9
4	3,994	873	657	138	565	452	1.073	484.8	0.0223	10
5	4,494	882	704	145	750	600	1.079	647.3	0.0315	12

*Injection-gas gravity = 0.65 and surface injection gas temperature = 80°F.

**TABLE 5.9—PRODUCTION-PRESSURE-OPERATED GAS LIFT VALVE
TEST-RACK-SET OPENING PRESSURE CALCULATIONS***

Valve Number	D (ft)	p_{ioD} (psig)	p_{iD} (psig)	T_{uvD} (°F)	Port ID (in.)	p_{ovD} (psig)	F_T	p_{vo} (psig)
1	1,756	832	446	119	0.125	461	0.887	420
2	2,650	848	530	129	0.125	543	0.871	492
3	3,387	862	600	137	0.1875	623	0.858	587
4	3,994	873	657	144	0.1875	676	0.847	629
5	4,494	882	704	149	0.1875	720	0.839	663
6	4,905	889	739	154	0.25	763	0.832	754
7	5,239	895	745	157	0.25	769	0.827	756
8**	5,470	849	120	160	0.25	734	0.823	717

*Valve description: 1-in.-OD, retrievable, unbalanced, bellows-charged, single-element valve with $A_p = 0.31$ sq in.

**Injection-pressure-operated, single-element, unbalanced gas lift valve.

pressure. The tester-set opening pressure of the bottom injection-pressure-operated gas lift valve No. 8 is based on these assumptions.

The design daily production rate of 800 STB/D was assumed for calculating the injection-gas requirement for the upper five gas lift valves. This design production rate cannot be gas lifted from the sixth or deeper valve depths on the basis of the gradient curves in Fig. 5.20. The maximum production rate from the well decreases as the required depth of lift increases. The three valves below the valve at 4,494 ft in Table 5.9 were arbitrarily assumed to have a 1/4-in. port, since this port size should assure adequate injection-gas throughput. A 3/16-in. port size may provide ample injection-gas passage. If the smaller port sizes assigned in Table 5.9 are unavailable, chokes can be installed upstream of the port, as illustrated in Fig. 5.12, for valves with a crossover seat or downstream of the port for valves without a crossover seat.

Casing (Annular) Flow Installation Design

The design calculations for an annular flow installation are similar to those for a continuous flow installation through the tubing. Intermittent gas lift is not recommended for casing flow. Since the gross liquid production is generally thousands of barrels per day, selecting valve port sizes for adequate gas passage is very important for annular flow installations. Actual gas lift valve performance based on bellows-assembly load rate is an important factor in the design calculations for casing flow installations because of the high injection-gas requirements. The increase in the injection-gas pressure to overcome the bellows-assembly load rate and to attain the needed equivalent port area for a required injection-gas throughput should be considered.

Selection of the proper size of gas-injection tubing string that will deliver the required daily injection-gas requirement for unloading and operating is absolutely essential. An initial assumption can be an injection tubing size that will deliver the maximum daily injection-gas requirement with no pressure loss—i.e., the increase in the injection-gas pressure with depth as a result of gas column density is offset by the flowing frictional pressure loss. This should be the smallest nominal tubing size considered for the gas-injection string. Charts for static injection-gas pressure at depth cannot be used for the valve spacing calculations.

The Cullender and Smith⁸ correlation is recommended

for calculating the pressure loss in the injection-gas tubing string. This method for calculating the flowing injection-gas pressure at depth was derived for a gas producing well and not for gas injection. The only difference in the calculations is the friction term. When gas is being injected rather than being produced, the sign for the friction term changes—i.e., the friction term becomes negative in the Cullender and Smith equation for gas injection.

The depth of the top valve in a casing flow installation can be deeper than that in a tubing flow installation if the fluid level is not at the surface and if this fluid level is known. The top valve can be located below the fluid level by taking advantage of the ratio of the tubing to the annular capacities. The fluid level in the casing annulus will rise only a few feet when depressing the fluid level in the tubing many feet. The following equation can be used to calculate the top valve depth if the static fluid level is not near the surface.

$$D_1 = L_{sf} + \frac{p_{ko} - p_{whu} - \Delta p_a}{g_{sl}(F_{tc} + 1)}, \dots \dots \dots (46)$$

where F_{tc} is the ratio of capacities of tubing/casing annulus, consistent units.

The check disk in the reverse flow check valve seats in the opposite direction for casing flow as compared to a tubing flow installation and allows gas passage from the injection-gas tubing to the casing. In the retrievable series the valve is similar to a production-pressure-operated valve, except the integral check valve is reversed (for gas flow from gas-injection tubing to casing).

Since bellows-charged gas lift valves have a lower bellows-assembly load rate than a spring-loaded valve, a bellows-charged valve is recommended for high injection-gas volumetric throughput as required for most casing flow installations. Fortunately, the valve temperature at depth is not difficult to predict accurately in high-volume wells. The flowing surface temperature will be near the BHFT; therefore, the operating temperature of all valves in a high-volume, casing-flow, gas lift installation will be approximately the same. An important caution: never use the surface injection-gas temperature to estimate the valve temperature at depth. The injection gas will attain the flowing fluid temperature within about a thousand feet from the surface. The flowing wellhead temperature of

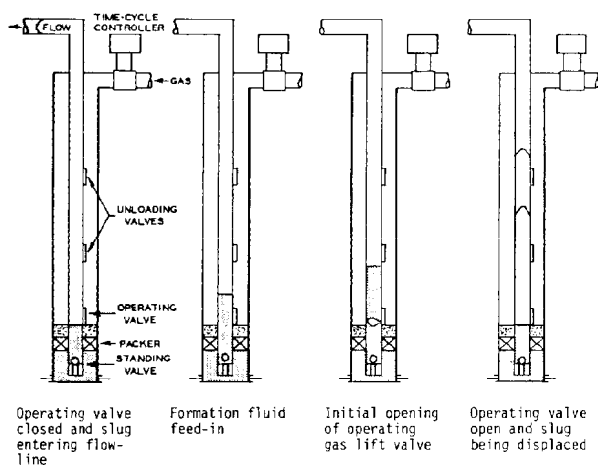


Fig. 5.25—Intermittent gas lift cycle of operation. (a) Operating valve closed and slug entering flowline. (b) Formation fluid feed-in. (c) Initial opening of operating gas lift valve. (d) Operating valve open and slug being displaced.

the fluid production should be used to establish the operating valve temperature at depth. This same consideration is applicable to the Cullender and Smith injection-gas-pressure-at-depth calculations.

Intermittent Gas Lift

Introduction

Intermittent gas lift is applicable to low-productivity wells and to high-productivity wells with a very low reservoir pressure. Chamber installations may be required to gas lift the low-BHP wells with a high productivity index. Occasionally, high-cycle-frequency intermittent gas lift operation has proven more efficient than continuous flow for lifting a viscous crude or for an emulsion condition. Gas lift normally is not recommended for lifting a highly viscous crude. Emulsion-breaking chemical injected into the injection gas line to individual wells has solved the emulsion problem in many gas lift installations.

As the name implies, the reservoir fluid is produced intermittently by displacing liquid slugs with high-pressure injection gas, as illustrated in Fig. 5.25.⁹ The injection gas can be controlled by a time-cycle controller or a choke. Electronic timers are replacing the older clock-driven intermitter pilots. Not all gas lift valves will operate on choke control. The number of intermittent gas lift installations on time-cycle control far exceeds the number of choke-controlled installations.

Disadvantages of Intermittent Gas Lift

Intermittent gas lift has several disadvantages compared to continuous flow operations. If the desired production can be gas lifted by continuous flow, this method is preferable. It is difficult to handle the high instantaneous gas volumes properly in the low- and high-pressure sides of a closed rotative gas lift system. Choke control of the injection gas into a well eliminates the removal of injection gas at high instantaneous rates from the high-pressure system but does not solve the problem of the large gas volume beneath the slug that enters the low-pressure system fol-

lowing displacement of the liquid slug to the surface. Gas volume storage requires pressure difference and physical capacity. The difference between the compressor discharge pressure and the operating injection-gas casing pressure usually will exceed the difference between the separator and compressor suction pressures. For this reason, retaining the needed injection-gas volume in the low-pressure side of a small, closed rotative gas lift system can be difficult unless the injection gas cycles are staggered properly. Staggering of the injection-gas cycles is less precise on choke control than with a time-cycle controller. The electronic timers have improved the accuracy of controlled injection, whereby the injection cycles can be scheduled to prevent more than one well receiving injection gas at the same time. Therefore, total injection plus formation gas can be scheduled to enter the low-pressure system at a more constant rate with accurate time cycle than with choke control of the injection gas.

Severe surging in the BHP can present a serious production problem in unconsolidated sand wells where sand production cannot be controlled properly. Sand bridging can plug off production and result in cleanout costs. Pressure surges in a chamber installation may be far more severe than in a regular intermittent installation. A wireline-release type of lock with an equalizing valve is recommended for the standing valve in a chamber to prevent the standing valve from being blown out of its seating nipple following blowdown after an injection-gas cycle. Some companies have resorted to increasing the operating injection-gas pressures to lift by continuous flow from near TD rather than intermittent-lift wells that produce sand.

The total energy in the formation and injection gas is not fully utilized with intermittent gas lift. The high-pressure gas under the slug is spent in the flowline and does not contribute to the lift process. This is one reason for using continuous-flow operations for a high-GLR well if possible. Plunger lift may be the best method for lifting certain high-GLR wells.

The injection-gas requirements are usually higher for intermittent than for continuous-flow gas lift operations. The tubing beneath the slug must be filled with injection gas to displace the liquid slug to the surface. The tubing under the liquid slug cannot be half or two-thirds filled with high-pressure gas. For this reason, the gas requirements for intermittent lift of low-GLR wells that will not partially flow can be estimated with a reasonable accuracy. Unfortunately, articles have been published that imply that a well, or group of wells, is being lifted with a certain type of gas lift valve that results in an injection-gas requirement of only a fraction of the gas volume needed to fill the tubing beneath the liquid slug. Although gas orifice meter charts are published to prove these claims, the truth is that these wells are partially flowing. Only minimal agitation and displacement of the liquid slug is required to lift these wells. Most of the energy needed to lift the well is being furnished by the formation and not the gas lift system.

The injection-gas requirements for intermittent and continuous-flow gas lift should be compared before eliminating continuous flow operations. With the advent of several reliable multiphase flow correlations, the predictable range of continuous flow has been extended to much lower daily production rates. A careful investigation of

the proper production conduit size for lifting a well by continuous flow may permit this type of gas lift in place of intermittent gas lift, where intermittent lift can result in operational problems.

Types of Intermittent Gas Lift Installations

Intermittent gas lift is used for tubing and not annular flow. Most installations will have a packer and some will include a standing valve in the tubing. Although illustrations of most intermittent gas lift installations will show a standing valve, many actual installations with very low productivity indices will not have a standing valve. The injectivity of a well is less than the productivity; therefore, very little fluid will be pushed back into a tight formation during the injection-gas cycle. If a well produces sand, a standing valve is recommended only if it is essential. A seating nipple should be installed at the lower end of the tubing string in intermittent installations where a standing valve may be needed.

When the working fluid level in a well does not result in a minimum starting slug length that results in a production pressure at the depth of the operating gas lift valve equal to 50 to 60% of the operating injection-gas pressure at depth, a chamber installation or plunger should be considered. The calculated depths of the unloading gas lift valves is the same as a regular intermittent-lift installation. The chamber design converts a few feet of fluid above the formation into many feet of fluid in the tubing above the standing valve before injection gas enters the production conduit. The standing valve is required for efficient chamber operation to ensure U-tubing all fluid from the chamber into the tubing rather than allowing fluid to be pushed into the formation. If a chamber is not installed, a plunger downhole stop and bumper spring can be set by wireline immediately above the operating gas lift valve. The plunger will reduce the injection-gas slippage through the liquid slug and decrease the liquid fallback. Smaller starting liquid slugs can be gas lifted efficiently with the plunger acting as a sealing interface between the liquid slug and injection gas.

Effect of Installation Design Methods on Unloading Injection-Gas Pressure

The intermittent gas lift installation design methods outlined here differ from designs presented in earlier gas lift literature. When the first single-element, bellows-charged gas lift valves were installed for intermittent gas lift service, the valve opening pressures were decreased at least 25 psi, and in some instances as much as 50 psi, for each succeeding lower valve to ensure unloading the well. The surface casing pressure would decrease as each lower gas lift valve was uncovered. A typical two-pen pressure recorder unloading chart from this type of design is displayed in Fig. 5.26.

A 25- to 50-psi decrease in the surface operating injection-gas pressure is required for a balanced type of gas lift valve to unload a well. The term "balance" implies that the production pressure at valve depth has no effect on the initial injection-gas opening pressure of the valve. When the depth of lift is deep and the maximum available injection-gas pressure for lifting the well is low, balanced-type gas lift valves are a poor choice for intermittent gas lift installations. An installation with 10 gas lift valves will have a 270-psi loss in the available

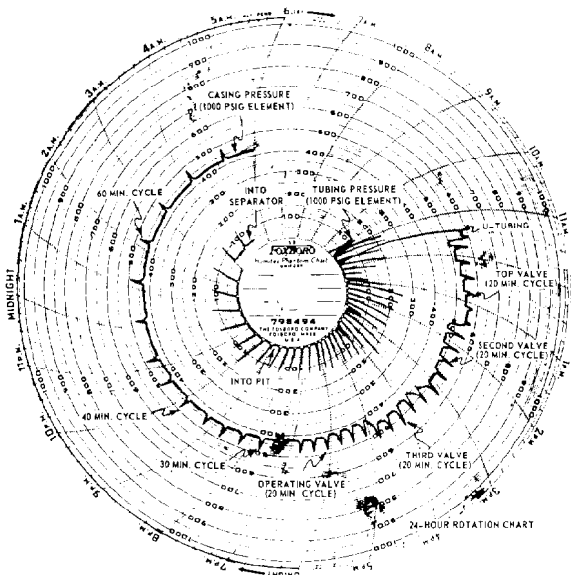


Fig. 5.26—Two-pen pressure recording chart illustrating intermittent gas lift unloading operations with valves having decreasing opening pressures.

injection-gas pressure on the basis of a decrease of 30 psi for each valve, and this does not include the pressure drop below line pressure for the top valve.

Most of the current design methods for an intermittent gas lift installation do not require any decrease in surface operating injection-gas pressure for each succeeding lower valve. Unbalanced gas lift valves with a high production-pressure factor are used in these intermittent installation designs. The operating gas lift valve will always be the valve with the highest production pressure at valve depth that is less than the injection-gas pressure at the same depth. The valve with the highest production pressure will have the lowest initial injection-gas opening pressure, as can be noted from Fig. 5.15, for a valve with a high production-pressure factor. Rather than using a decrease in the injection-gas pressure to control the initial opening pressure of a valve, the production pressure at valve depth provides the difference in the initial opening pressures between gas lift valves. The operating principles for this design method are illustrated in Table 5.10.

TABLE 5.10—GAS LIFT VALVE INITIAL SURFACE OPENING PRESSURES AFTER CONTROLLER OPENS ON THE BASIS OF PRODUCTION PRESSURE AT VALVE DEPTH*

D (ft)	p_{vcD}^{**} (psig)	$p_{p/D}$ (psig)	p_{pe} (psi)	p_{oD} (psig)	Surface p_o^{\dagger} (psig)
4,600	663	60	21	830	751
5,400	675	380	130	776	690
6,000	683	620	212	705	620
6,500	690	820	N/A	N/A	N/A

* Surface closing pressure for all gas lift valves: $p_{vc} = 600$ psig. Gas pressure at depth factor: $F_g = 2.3$ psi/100 psi/1,000 ft. Gas lift valve: 1 1/2-in. OD with 1/2-in. ID sharp-edged seat.

** Valve closing pressure at valve depth.

[†] Initial valve opening pressure at surface.

The 1½-in.-OD valves with a ½-in.-ID sharp-edged seat has a production-pressure factor of 0.342 from Table 5.2. The working fluid level in the tubing for Table 5.10 is assumed to be at 4,600 ft at the instant the time-cycle controller on the injection-gas line opens. The wellhead tubing gas pressure is 60 psig at 4,600 ft, and the production fluid gradient is 0.40 psi/ft for this example.

Since the production pressure at valve depth exceeds the calculated injection-gas pressure at the same depth, the valve at 6,500 ft cannot be the operating valve. The bottom valve at 6,500 ft is open with the check closed, and the valve is under the fluid level in the casing annulus. The gas lift valve at 6,000 ft is the operating valve because this valve has the lowest surface initial opening pressure of all valves above the fluid level in the casing annulus with the highest production pressure at valve depth that is less than the injection-gas pressure at the same depth. There will be no interference from opening of the upper gas lift valves before the valve at 6,000 ft opens since the initial injection-gas opening pressure of this valve is 70 psi less than the next upper gas lift valve. This type of design is ideal for dual intermittent gas lift installations with a common injection-gas source. The surface closing injection-gas pressure is constant and does not change with the depth of lift.

The point of gas injection will adjust automatically to the BHFP. The principles of operation based on using the production-pressure effect rather than decreasing the injection-gas pressure for each succeeding lower valve are apparent in Table 5.10.

This design concept is better than installations with production-pressure-operated gas lift valves because the closing pressure of the injection-pressure-operated gas lift valves is controllable. The closing pressure of production-pressure-operated valves depends on a decrease in the production pressure at valve depth after a slug surfaces, which may or may not occur for a high injection-gas cycle frequency. The actual closing pressure of production-pressure-operated gas lift valves can approach their set pressures if the backpressure is excessive and the production pressure at valve depth does not decrease until the valves close.

Prediction of Daily Production Rates

Two basic factors control the maximum production from a high-rate intermittent gas lift installation: (1) the total liquid production per cycle, and (2) the maximum number of injection-gas cycles per day. An intermittent gas lift installation should be designed to maximize the liquid recovery per cycle on low- and high-capacity wells. All restrictions in and near the wellhead should be eliminated. For this reason, streamlined wellheads are recommended. If the wellhead cannot be streamlined, all unnecessary elbows and tees should be removed to reduce the number of bends between the tubing and flowline. If the velocity of the liquid slug is reduced before the entire column of liquid can be displaced into the horizontal flowline, additional injection-gas breakthrough, or gas slippage, will occur and decrease the liquid recovery per cycle. Performance of the operating gas lift valve, or valves, is important for efficient liquid-slug displacement. The operating gas lift valve should have a large port that will open quickly to ensure ample injection-gas volumetric throughput for efficiently displacing the liquid slug.

The gas lift valve should not open slowly and meter a small injection-gas volume into the production conduit, which would tend to aerate and to percolate through the liquid slug rather than displace the slug. Rapid increase in the injection-gas casing pressure after a time-cycle controller opens will improve the gas lift valve performance and ensure a more efficient displacement of a liquid slug in a time-cycle-operated intermittent lift installation. Ample injection-gas volume must be available at the wellsite from the high-pressure injection-gas system. If the line pressure in the high-pressure system decreases immediately to the casing pressure, poor valve action is the fault of the high-pressure system and not the gas lift installation in the well.

The size and length of the flowline can significantly affect the maximum cycle frequency. A flowline should always be at least one size larger than the tubing. The maximum number of injection-gas cycles per day is controlled by the time required for the wellhead pressure to return to the separator or production header pressure after a slug surfaces. Reducing the separator pressure increases the starting slug length for the same flowing BHP but does not solve the problem of decrease in wellhead pressure. When comparing or predicting the maximum production from two high-capacity wells on intermittent gas lift, the size and length of the flowlines must be considered. If one installation requires 45 minutes and another 10 minutes for the wellhead pressure to approach the production header pressure after a slug surfaces, the difference in maximum production (assuming that both wells have the deliverability) is not the result of the gas lift installation in the well but of the surface facilities.

One definition of liquid fallback is the difference between the starting liquid slug volume, or length, and the produced slug volume, or length. The purpose of a properly designed intermittent gas lift installation is to recover as much as possible of the starting slug, thus reducing the liquid fallback. An important parameter that can be observed is the average slug velocity. The operating gas lift valve will open in less than 30 seconds after a time-cycle controller opens in most intermittent lift installations. An approximate slug velocity can be estimated by assuming the valve opens 15 seconds after the controller opens and recording the time elapsed from this instance until the slug surfaces. In most installations, the depth of the operating gas lift valve is known or can be estimated from an acoustical survey. If the average liquid slug velocity is not near or exceeding 1,000 ft/min, the liquid fallback may be excessive. A slug velocity less than 800 ft/min can result in excessive fallback.

The maximum number of injection-gas cycles per day can be estimated by assuming 2 to 3 min/1,000 ft of lift for typical flowline sizes and lengths. The actual time can be less for installations on a production platform without flowlines and much longer for intermittent installations with small ID and/or long flowlines, such as a well with 2⅞-in.-OD tubing and a 2-in. flowline that is 2 miles in length. Also, emulsions and other unique well problems can decrease the maximum number of injection cycles per day and the recoverable liquid production per cycle.

Injection Gas Requirement for Intermittent Lift

Multiphase flow correlations are not applicable for the prediction of the gas requirement to lift a well by inter-

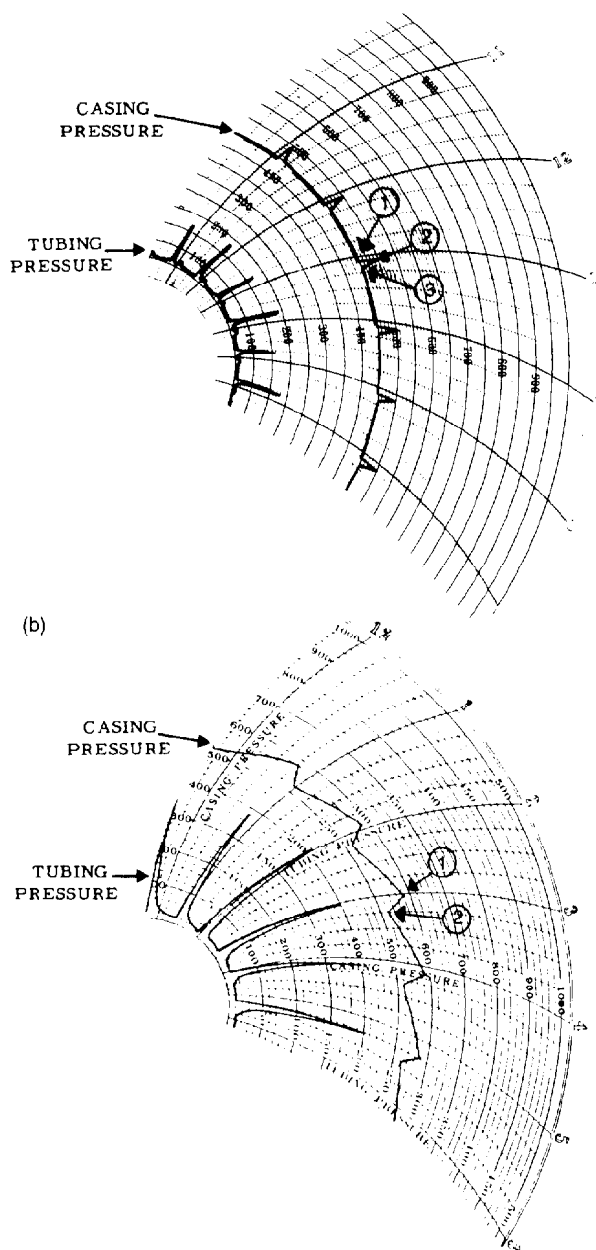


Fig. 5.27—Two-pen pressure recording charts from intermittent gas lift installations with time cycle and choke control of the injection gas. (a) Time-cycle control: (1) time-cycle controller opens, (2) time-cycle controller closes, and (3) gas lift valve closes. (b) Choke control: (1) gas lift valve opens and (2) gas lift valve closes.

mittent gas lift. Expansion and aeration of the injection and formation gas are used from the flowing production pressure at the operating gas lift valve depth to the flowing production wellhead pressure during continuous flow operations. Since intermittent gas lift is the displacement of a liquid slug by high-pressure gas, the injection-gas requirement is not based on aeration but on the volume of gas needed to fill the tubing between the bottom of the slug when it reaches the surface and the depth of the deepest gas lift valve that opens during an injection gas cycle. The injection-gas pressure following the liquid slug at the instant this slug surfaces is spent in the flowline

and does not contribute to the lift process. The energy in the formation gas does little to assist in lifting most wells.

One method for calculating the injection-gas requirement is to assume the produced slug to be a solid liquid column without any afterflow production in the tailgas. The theoretical pressure under this liquid slug at the instant the slug surfaced would be the wellhead production pressure plus the length of the produced slug times the liquid gradient. The actual average pressure in the tubing under a liquid slug is more than this pressure based on the solid slug length and a dry gas gradient because of the injection-gas penetration of the slug during the lift process and the frictional losses. An average injection-gas pressure in the tubing equal to the theoretical pressure under the produced liquid slug plus the surface closing pressure of the operating gas lift valve divided by two is a realistic assumption on the basis of numerous BHP measurements in intermittent gas lift installations. The pressure loss through the operating gas lift valve is assumed equal to the increase in gas column pressure to the depth of the valve.

The total volume of injection gas per cycle depends on the average pressure in the tubing under the slug and the physical capacity of the tubing. When the depth of lift is several thousand feet and the equivalent produced slug length is only a few hundred feet, the length of this slug may be subtracted from the tubing length above the operating gas lift valve for calculating the capacity of tubing to be filled with injection gas each cycle. This assumption implies that the rate of decrease in the pressure of the expanding injection gas volume beneath the liquid slug is less than the rate of decrease in the pressure exerted by the slug length remaining in the tubing as the upper portion of the slug enters the flowline.

Comparison of Time Cycle to Choke Control of the Injection Gas

The advantage of choke-controlled injection-gas volume for an intermittent gas lift installation is the low volumetric injection-gas rate from the high-pressure system into a well. Several conditions must be met before choke control of the injection gas can be used successfully. The gas lift valve must be suited for choke-control operation, and the casing annulus must provide adequate storage capacity for the injection-gas volume needed to displace the slug. Gas lift valves designed to operate on choke control are more complicated and expensive than an unbalanced, single-element, gas lift valve. Clean, dry gas is extremely important and very-low-capacity wells are more difficult to choke control because of the small surface injection-gas choke size required for the low daily injection gas volume needed to lift the well. A pressure-reducing regulator, to maintain a constant maximum valve opening casing pressure between valve operating cycles, may be necessary to permit the use of a larger-sized choke in the injection-gas line. Other limitations of choke control of the injection gas include the maximum liquid slug size that can be lifted each cycle and the maximum number of injection-gas cycles per day. Time-cycle control of the injection gas should be considered for high-rate intermittent-lift operations. Time-cycle and choke-control operations are illustrated by two-pen pressure recorder charts in Fig. 5.27.

Most intermittent gas lift installations use time-cycle-operated controllers on the injection-gas line because of the many advantages of time cycle over choke control of the injection gas. The rugged unbalanced, single-element, bellows-charged gas lift valves with a large port can be used, and much larger liquid slugs can be lifted because injection gas in the annulus can be supplemented with gas from the high-pressure system. The differences in time cycle and choke control of the injection gas can be explained by use of Fig. 5.28.

The curve for injection-gas requirement per cycle in Fig. 5.28 represents the injection-gas volume needed to fill the tubing beneath the liquid slug for displacing this slug to the surface. The volume of injection gas stored in the casing annulus between the initial opening and theoretical closing pressures of the operating gas lift valve is represented by the injection gas volume stored within the casing annulus curve. The slope of this curve depends on the capacity of the casing annulus and the gas lift valve spread. The maximum theoretical valve spread would occur with a production pressure at the operating gas lift valve depth equal to zero, which is not possible. However, the volume of injection gas at standard conditions stored within the casing annulus can be calculated for this condition of valve opening pressure. An operating valve will have no spread when the initial opening injection-gas pressure, production pressure, and theoretical closing pressure are the same. Again, the volume of injection gas at standard conditions in the casing at the theoretical closing pressure of the operating gas lift valve can be calculated. The volume of gas stored in the casing annulus at zero flowing production pressure is the difference between the above two volumes of injection gas at standard conditions. There is no gas available from the casing when the initial valve opening pressure is equal to its closing pressure and the spread is zero. This represents the second point for the curve. The curve defines the injection-gas volume stored in the casing annulus between a production pressure of zero and the theoretical valve closing pressure.

The size of the largest liquid slug that can be lifted by choke control with a pilot valve using the injection-gas volume stored in the casing annulus is based on the intersection of the two curves. The maximum production pressure is limited to a production pressure at this intersection where the injection-gas volume available to lift the slug is equal to injection-gas volume required to displace the slug. The well could be lifted by choke control with a production pressure less than the pressure at this intersection, but insufficient gas is available from the casing annulus for higher production pressures.

Points 1 and 2 on the dashed line represent a production pressure much higher than the pressure defined by the point of intersection. The higher production pressure represents a larger liquid slug, which requires a greater volume of injection gas than the smaller slugs. The injection gas available from the casing annulus as the result of valve spread is represented by Point 1. The greater remaining volume of injection gas required to displace the slug is furnished from the high-pressure system by setting a time-cycle controller to remain open after the gas lift valve has opened. In other words, the injection-gas volume between Points 1 and 2 is supplied from the high-pressure system by proper setting of the time-cycle controller.

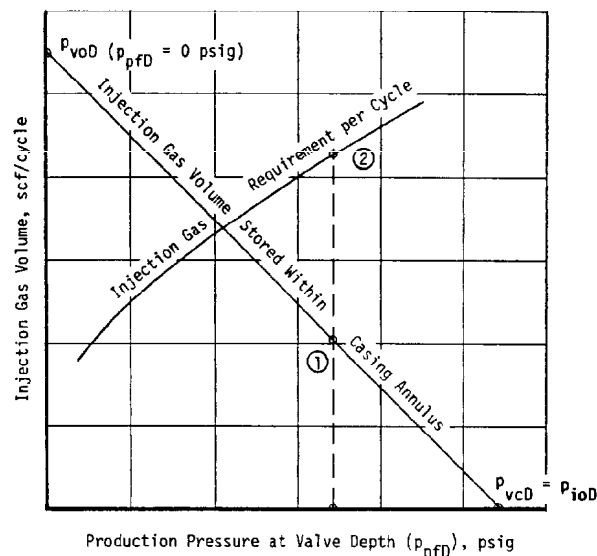


Fig. 5.28—Injection-gas volumes per cycle for intermittent gas lift operations.

The previous calculations represent several simplifying assumptions. The total available injection-gas volume per cycle should include the small volumetric gas rate through the choke while the operating gas lift valve is open for a choke-controlled installation. The advantages of being able to overrun the initial opening pressure of an operating gas lift valve with a time-cycle controller are apparent for optimizing the injection-gas volume per cycle and selecting the number of injection-gas cycles per day. Electronic timers have increased the reliability and sequence repeatability of gas injection for time-cycle-control operations.

Intermittent Gas Lift Installation Design Methods

There are many published methods and variations in these methods for designing intermittent gas lift installations. These methods can be divided into one type of design that is based on a production rate and another design that can be described as a percentage-load technique. Intermittent pressure gradient spacing factors are used for installation designs based on an assumed daily production rate. Production rate is not a consideration for a percent-load design method. The procedures for calculating a percent-load installation vary between gas lift manufacturers and between operators who have introduced slight variations in these calculations. The gas lift valve depths in most designs can be calculated or determined graphically.

Gas Lift Valves for Intermittent Lift

Most gas lift valves used for intermittent lift will be the unbalanced, single-element, bellows-charged valve with a large port. The majority of intermittent-lift designs require a gas lift valve with a large production-pressure factor. Single-element, spring-loaded gas lift valves are not recommended for intermittent lift because of the higher bellows-assembly load rate of the spring-loaded as compared to the bellows-charged gas lift valve with the same bellows and port size. The operating gas lift valve should tend to "snap" open and to provide a large port size for

injection-gas throughput so that the liquid slug can be displaced efficiently with minimal injection-gas slippage and liquid fallback. Time-cycle control of the injection gas is recommended for intermittent-lift installations with unbalanced, single-element gas lift valves. These valves may not operate on choke control of the injection gas. Most installations with unbalanced, single-element valves will not work satisfactorily on choke control.

There are gas lift valves that have been designed for choke-controlled intermittent gas lift operation. These valves will have a large port for gas passage and may be designed to operate on either time cycle or choke control of the injection gas. Several gas lift valves are designed for only choke-control operation. A properly selected pilot-operated gas lift valve will function in most wells on time cycle or choke control. There are differential-pressure opening (difference between the production and injection gas pressure for initial valve opening) and constant-injection-gas-pressure closing gas lift valves. Certain types of differential-pressure opening valves cannot be opened by an increase in injection-gas pressure and others can be opened. It is extremely important to select the proper gas lift valve if choke control for intermittent lift is mandatory.

Intermittent Pressure Gradient Spacing Factor

The intermittent pressure gradient spacing factor is similar to a flowing pressure gradient above the point of gas injection in a continuous-flow installation. This factor will increase with daily production rate and a decrease in the size of the tubing. These intermittent spacing factors ac-

count for (1) liquid fallback from injection-gas penetration of the displaced liquid slug while the slug is in the tubing, (2) fluid transfer from the casing annulus to the tubing during unloading, (3) fluid production after BHFP drawdown occurs, and (4) increase in wellhead tubing pressure with depth in deep wells with a high surface-tubing pressure.

The fluid level in the tubing immediately after an injection gas cycle is not at the operating valve depth. There is always an accumulation of liquid fallback because of gas slippage through the liquid slug during displacement. Consequently, the minimum flowing production pressure between injection-gas cycles is greater than the surface wellhead-tubing gas pressure at the operating valve depth because of liquid fallback.

The intermittent pressure gradient spacing factors (F_s) given in Fig. 5.29 were published many years before flowing pressure gradient curves were available for continuous-flow installation designs. The same unloading pressure gradients were used for intermittent-lift and continuous-flow installation design. These data were reported to have been compiled from a limited number of flowing pressure surveys from low-GLR, high-water-cut wells with 2 $\frac{3}{8}$ - and 2 $\frac{7}{8}$ -in.-OD tubing. Other tubing sizes were added at a later date. One of several important parameters missing from this correlation is depth. All these conditions accounted for by these spacing factors with the exception of fluid transfer during unloading increase with depth of lift. The only two correlating parameters in Fig. 5.29 are production rate and conduit size. Since the rate of injection-gas penetration of the slug is

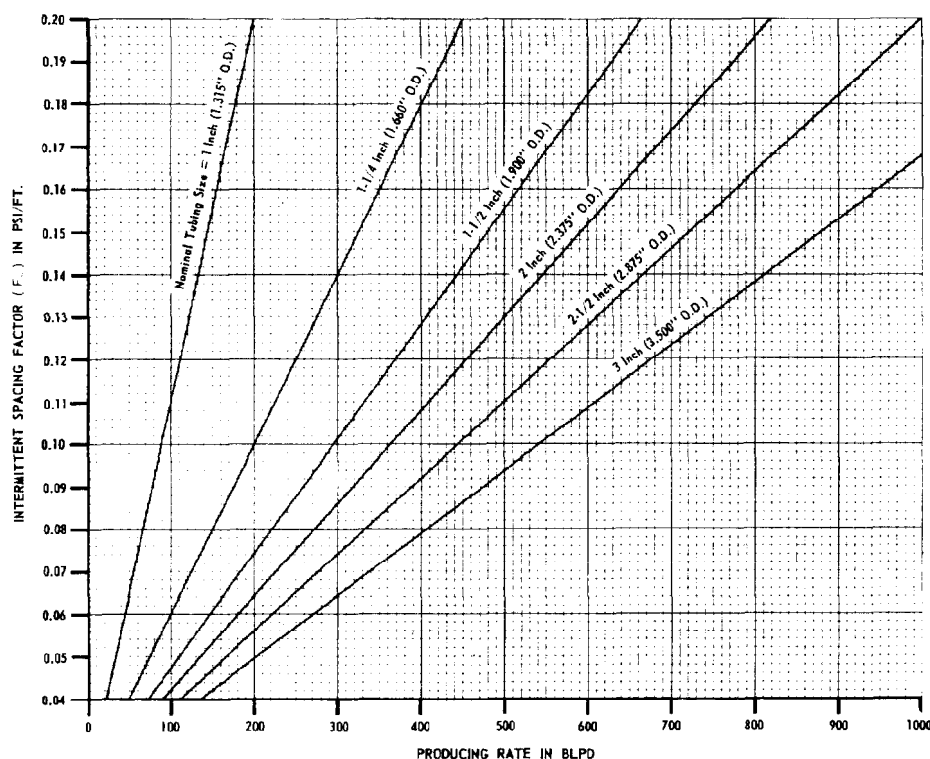


Fig. 5.29—Intermittent pressure-gradient spacing factors for varying daily production rates and different tubing sizes.

reported to be relatively constant, the liquid fallback will increase with depth because the liquid slug requires more time to reach the surface in deeper wells. These published intermittent spacing factors may be too low for very deep intermittent lift and too high for shallow lift.

Selection of Surface Closing Pressure of Gas Lift Valves

The surface closing pressure of an operating gas lift valve will be the minimum surface injection-gas pressure between gas injections if there are no leaks in the wellhead and tubing, which includes the gas lift valves. The maximum surface injection-gas pressure will occur at the instant the time-cycle controller closes or the operating gas lift valve opens on choke control of the injection gas. The available operating injection-gas-line pressure at the well-site must exceed the maximum surface casing pressure during an injection gas cycle. For this reason, an assumed gas lift valve surface closing pressure of 15% less than the available injection-gas-line pressure at the well-site is recommended for line pressures between 700 and 1,000 psig. This is the same as assuming a surface closing pressure equal to 85% of the available injection-gas-line pressure. A minimum of 100 psi difference is suggested for lower injection-gas pressures and a maximum of 200 psi for higher pressures. The maximum surface casing pressure during an injection-gas cycle for intermittent-lift operations is usually 8 to 10% higher than the surface closing pressure of the operating gas lift valve for approximate injection-gas-requirement calculations in typical tubing/casing combinations such as 2 $\frac{3}{8}$ -in.-OD tubing in 5 $\frac{1}{2}$ -in.-OD casing.

When a time-cycle controller opens, the injection-gas-line pressure upstream of the controller will decrease. To have an injection-gas volume stored in the high-pressure injection-gas lines, there must be a pressure difference in addition to the capacity of the high-pressure system. If the difference between the injection-gas-line pressure and the surface closing pressure of the operating gas lift valve is insufficient, the casing pressure will not increase at a rate necessary to ensure rapid opening of an unbalanced, single-element, gas lift valve after the controller opens. A near-instant increase in casing pressure after the controller opens improves the gas throughput performance of a single-element valve and decreases the liquid fallback. It is better to design an intermittent installation with a pressure difference between the injection-gas-line and valve closing pressures that is slightly excessive rather than insufficient to ensure fast opening of the operating gas lift valve.

Selection of Valve Port Size

Constant surface closing and percent-load intermittent gas lift installation designs require unbalanced, single-element, gas lift valves with a large port relative to the effective bellows area. The design principle is based on the production-pressure effect, which is the production pressure at the valve depth times the production-pressure factor for the valve. The valve with the highest production pressure that is less than the injection-gas pressure at valve depth will be the deepest operating gas lift valve in the installation. There is no reason to decrease the surface closing pressure for each succeeding lower unloading gas lift valve because the point of gas injection will

transfer automatically from an upper to the next lower valve after the production pressure at the lower valve depth becomes less than the injection-gas pressure at the same depth. This same design technique can be used for pilot-operated gas lift valves. The calculations for pilot valves apply to the pilot section of the valve that must have a large production-pressure factor.

There may be variations in the port size or surface closing pressure of the bottom gas lift valve. If the casing is large relative to the tubing size, such as 2 $\frac{3}{8}$ -in.-OD tubing in 7-in.-OD casing, a smaller-ported gas lift valve may be used for the bottom valve. The 1 $\frac{1}{2}$ -in.-OD unloading gas lift valves may have a $\frac{7}{16}$ - or $\frac{1}{2}$ -in. port and the bottom valve a $\frac{3}{8}$ -in. port to reduce the valve spread (that is, the difference between the initial opening and closing pressures of the bottom valve). This consideration is important for installations in wells with an anticipated low BHFP. The design surface closing pressure can be the same as the assumed closing pressure for the unloading gas lift valves with larger ports. Another variation in the installation design is to decrease the surface closing pressure of the bottom gas lift valve. The purpose of decreasing the closing pressure of the bottom valve is to provide a visible change in operating injection-gas pressure when the well is unloaded to this valve depth. This procedure is referred to as "flagging" the bottom valve, and a typical decrease in surface closing pressure would be 25 to 50 psi.

Intermittent Gas Lift Installation Design Based on Valves With a Constant Surface Closing Pressure and an Increasing Intermittent Spacing Factor Gradient With Depth

There are two advantages to a properly designed constant surface closing pressure installation design.

1. There is no decrease in operating injection-gas pressure with depth of lift. This is particularly important in deep wells with low available injection-gas pressure.
2. The depth of lift always will be the deepest valve depth where the highest production pressure in the tubing is less than the injection-gas pressure at the same depth.

Intermittent gas lift installation design based on valves with a constant surface closing pressure has been used to gas lift dual zones with a common injection-gas source in the casing annulus. The advantage of being able to predict the operating injection-gas pressure for lifting both zones with the same injection-gas pressure is apparent for duals. The higher-BHP zone may produce a slug during every injection-gas cycle and the weaker zone may operate only every other cycle. This type of operation has been observed in dual intermittent gas lift installations.

The primary disadvantage of this type installation is the difficulty of establishing the depth of the operating gas lift valve from the surface operating injection-gas pressure since the operating pressure does not decrease with each succeeding lower valve. Determining the fluid level acoustically or recording the time for a liquid slug to surface are two methods for establishing the approximate depth of lift. A slug velocity of 1,000 ft/min can be assumed for most installations. Decreasing the surface closing pressure of the bottom gas lift valve is another method used by some operators to indicate that a well has unloaded to and is operating from the deepest valve. A

decrease in the surface closing pressure of the operating gas lift should be considered if a plunger is being installed in an intermittent-lift installation. Many intermittent gas lift installations with a low productivity index will operate from the maximum possible depth of lift, which usually is limited by the packer depth.

If the daily production rate exceeds the rate for an assigned minimum intermittent spacing factor gradient, the valve depths for this design method are based on an increasing spacing factor gradient with depth. As the point of gas injection transfers to each succeeding lower gas lift valve, the drawdown in BHP and corresponding production rate will increase after the unloading BHP becomes less than the static BHP. This design method uses an increasing intermittent spacing factor gradient with an increasing production rate from a decreasing BHFP rather than a constant spacing factor for locating all valve depths on the basis of the final design production rate.

The minimum intermittent spacing factor gradient is used to locate the depth of all gas lift valves above a depth at which initial drawdown in BHP can occur on the basis of the static BHP and the load fluid gradient. A minimum intermittent spacing factor equal to 0.04 psi/ft is recommended for most installation designs. The maximum intermittent spacing factor gradient is based on the tubing size and the design daily production rate and is obtained from Fig. 5.29. The maximum spacing factor begins at a minimum depth at which the BHFP for the design daily production rate could occur. The actual depth may be deeper, and this maximum intermittent spacing factor is used below this given minimum depth when the calculated distance between the gas lift valves using the maximum spacing factor exceeds the assigned minimum distance between valves. The intermittent spacing factor gradient increases between the depth for initial BHP drawdown and the given depth for the design daily production rate. The concept of an increasing spacing factor with each succeeding lower valve is illustrated in Fig. 5.30.

Determination of the Gas Lift Valve Depths. The BHP's and BHT usually are referenced to the same depth, which is the lower end of the production conduit (D_d). The steps for establishing the gas lift valve depths on a pressure-depth worksheet are as follows.

1. Plot the static BHP (p_{wsd}) at the lower end of the production conduit (D_d) on the pressure-depth worksheet and draw the static-load fluid gradient (g_{sl}) traverse originating at p_{wsd} and extend this traverse to the static fluid level (L_{sf}) for zero wellhead pressure, where L_{sf} is calculated with Eq. 26.

$$L_{sf} = D_d - \frac{p_{wsd}}{g_{sl}} \quad (26)$$

2. Draw an unloading traverse above the point of gas injection on the basis of the minimum intermittent spacing factor $(F_s)_{\min}$ and the surface wellhead tubing pressure between the gas-injection cycles.

$$p_{pfd} = p_{wh} + (F_s)_{\min}(D_d) \quad (47)$$

Draw a straight line between the wellhead pressure, p_{wh} , at the surface and p_{pfd} for $(F_s)_{\min}$.

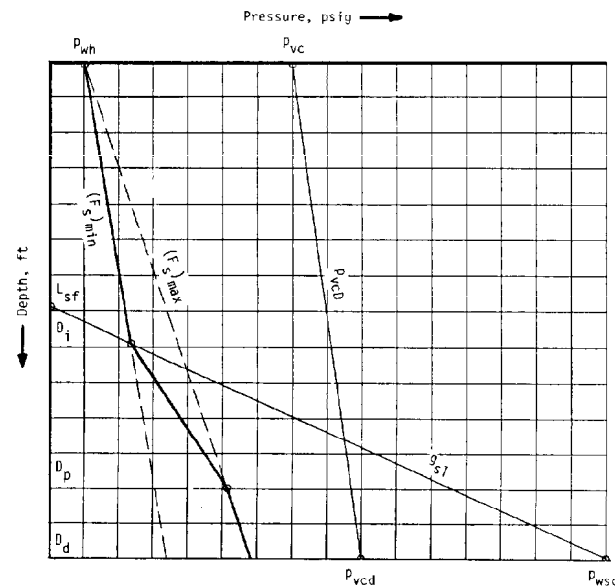


Fig. 5.30—Increasing intermittent spacing factor gradient with depth for spacing gas lift valves.

3. Determine the depth at which an initial drawdown in BHP occurs. This depth (D_i) is found at the intersection of the traverse for the $(F_s)_{\min}$ in Step 2 with the static-load fluid traverse in Step 1. The depth D_i can be calculated with the following equation:

$$D_i = \frac{g_{sl}(D_d) + p_{wh} - p_{wsd}}{g_{sl} - (F_s)_{\min}} \quad (48)$$

Record the unloading flowing production pressure at D_i between the gas-injection cycles (p_{pfdi}).

4. Determine the maximum intermittent spacing factor $(F_s)_{\max}$ from Fig. 5.29 for the given tubing size and design production rate. Draw an unloading traverse above the point of gas injection based on the $(F_s)_{\max}$.

$$p_{pfd} = p_{wh} + (F_s)_{\max}(D_d) \quad (49)$$

Draw a straight line between p_{wh} at the surface and p_{pfd} for $(F_s)_{\max}$.

5. For a given minimum depth of lift at which the design production rate may be gas lifted (D_p), record the unloading flowing production pressure between the gas-injection cycles (p_{pfdp}). This pressure occurs at the intersection of the assigned D_p depth and the traverse for the $(F_s)_{\max}$ in Step 4.

6. Draw a straight line on the pressure-depth worksheet between the pressure and depth point (p_{pfdi}) at which initial drawdown occurs in Step 3 and the pressure and depth point (p_{pfdp}) at which the design production rate may be gas lifted. This unloading intermittent spacing factor traverse above the point of gas injection represents the increase in the intermittent spacing factor with depth and daily production rate and is the minimum flowing production pressure at depth (p_{pfd}) between the gas-injection cycles.

TABLE 5.11—CALCULATION OF THE TEST-RACK-SET OPENING PRESSURES OF THE GAS LIFT VALVES ON THE BASIS OF A CONSTANT SURFACE CLOSING PRESSURE*

Valve Number	D (ft)	p_{vcD} (psig)	p_{bvD} (psig)	T_{uvD} (°F)	F_i	p_{vo} (psig)
1	1,756	707	707	106	0.910	864
2	2,992	727	727	125	0.877	856
3	4,147	745	745	142	0.850	850
4	5,018	758	758	155	0.830	844
5	5,679	768	768	165	0.816	841
6	5,950	773	773	169	0.810	840

*Valve description: 1½-in.-OD gas lift valves. Valve specifications: $A_p = 0.77$ sq in. Port ID = ½ in. $A_p/A_D = 0.255$. $(1 - A_p/A_D) = 0.745$. Surface closing pressure of gas lift valves: $p_{vc} = 680$ psig.

7. Select a surface closing pressure for the gas lift valves (p_{vc}) on the basis of approximately 85% of the available injection-gas-line pressure at the wellsite:

$$p_{vc} = 0.85(p_{io}). \quad (50)$$

Determine the valve closing pressure at the lower end of the production conduit (p_{vcd}) and draw a straight line between p_{vc} at the surface and p_{vcd} , which represents the p_{vcD} traverse.

8. Draw the unloading gas lift valve temperature at depth traverse (T_{uvD}) on the pressure-depth worksheet by assuming a straight-line traverse between the surface unloading flowing wellhead temperature (T_{whu}) and the bottomhole valve temperature (T_{vtd}).

9. Using Eq. 23, calculate the depth of the top gas lift valve (D_1) on the basis of the surface kick-off injection-gas pressure (p_{ko}), load fluid gradient (g_{sl}), and the wellhead U-tubing pressure (p_{whu}):

$$D_1 = \frac{p_{ko} - p_{whu}}{g_{sl}}.$$

The top valve may be located graphically or at the static fluid level if this depth exceeds the calculated D_1 .

10. Draw a horizontal line on the pressure-depth worksheet between the unloading intermittent spacing factor traverse and the p_{vcD} traverse at the depth D_1 and record the $(p_{pfD1})_{\min}$ at the intersection of the intermittent spacing factor traverse, the p_{vcD1} , and the T_{uvD1} on the unloading temperature traverse.

11. Draw the static-load fluid gradient (g_{sl}) traverse below the depth of the top gas lift valve on the pressure-depth worksheet with the traverse originating at $(p_{pfD1})_{\min}$ and extending to the p_{vcD} traverse.

12. Locate the depth of the second gas lift valve (D_2) on the pressure-depth worksheet at the intersection of the g_{sl} traverse and the p_{vcD} traverse.

13. Draw a horizontal line on the pressure-depth worksheet between the unloading intermittent spacing factor traverse and the p_{vcD} traverse at the depth D_2 and record the $(p_{pfD2})_{\min}$, p_{vcD2} , and T_{uvD2} .

Repeat Steps 11 through 13 until the maximum desired gas lift valve depth is attained. A minimum distance between gas lift valves can be assigned on the basis of a

percent load for locating the lower valves in deep intermittent gas lift installations.

Calculation of the Test-Rack-Set Opening Pressures of the Gas Lift Valves. A tabulation form for these calculations is illustrated in Table 5.11. The bellows-charged pressure at the valve unloading temperature (p_{bvD}) is calculated by the following equation:

$$p_{bvD} = p_{vcD}. \quad (51)$$

The flowing production pressure at valve depth is assumed equal to the injection-gas pressure at the same depth when the valve closes for this equation to be valid. This assumption is reasonable for the deeper gas lift valves with large ports. The pressure in the tubing will approach the injection-gas pressure at valve depth immediately before the valve closes. Eq. 51 will not accurately describe the closing pressure for the upper one or two valves as the point of gas injection transfers to the next lower valve.

The unloading valve temperature at the depth of the valve can be estimated from a T_{uvD} traverse on the pressure-depth worksheet or calculated using Eq. 39. The test-rack opening pressure is calculated using Eq. 38 for a tester setting temperature of 60°F and Eq. 40 for a tester setting temperature (T_{vs}) other than 60°F.

Example Problem 14. Well information for installation design calculations:

1. Tubing size = 2⅞-in. OD.
2. Tubing length = 6,000 ft.
3. Maximum valve depth = 5,950 ft.
4. Static BHP = 1,600 psig at 6,000 ft.
5. Daily production rate = 300 STB/D.
6. Minimum intermittent spacing factor = 0.04 psi/ft.
7. Minimum depth of lift for design production rate = 5,000 ft.
8. BHT = 170°F at 6,000 ft.
9. Design unloading wellhead temperature = 80°F.
10. Load fluid gradient = 0.45 psi/ft.
11. U-tubing wellhead pressure = 60 psig.
12. Flowing wellhead pressure = 100 psig (high cycle frequency).
13. Static fluid level = 0 ft (loaded).
14. Injection-gas wellhead temperature = 80°F.
15. Surface kick-off injection-gas pressure = 850 psig.
16. Surface operating injection-gas pressure = 800 psig.
17. Gas lift valve bellows area = 0.77 sq in. (1½-in. OD valve).
18. Gas lift valve with sharp-edged seat and port ID = ½ in.
19. Test-rack setting temperature = 60°F.
20. Minimum distance between gas lift valves = 350 ft.

Solution—Valve Depths. The traverse for the pressures and temperatures used for calculating the gas lift installation design are drawn on a pressure-depth worksheet in Fig. 5.31.

$$1. L_{sf} = D_1 - \frac{p_{wsd}}{g_{sl}} = 6,000 - \frac{1,600}{0.45} = 2,444 \text{ ft.}$$

Draw a straight line between 0 psig at 2,444 ft and 1,600 psig at 6,000 ft.

2. For $(F_s)_{\min} = 0.04$ psi/ft,

$$p_{pfd} = p_{wh} + (F_s)_{\min}(D_d) = 100 + 0.04(6,000) \\ = 340 \text{ psig at 6,000 ft.}$$

Draw a straight line between 100 psig at the surface and 340 psig at 6,000 ft.

3. $D_i = 2,927$ ft at intersection of $(F_s)_{\min}$ traverse in Step 2 with g_{sl} traverse in Step 1 on the pressure-depth worksheet or calculated as follows:

$$D_i = \frac{g_{sl}(D_d) + p_{wh} - p_{wsd}}{g_{sl} - (F_s)_{\min}} \\ = \frac{0.45(6,000) + 100 - 1,600}{(0.45 - 0.04)} = 2,927 \text{ ft,}$$

$$p_{pfd_i} = 217 \text{ psig at 2,927 ft.}$$

4. $(F_s)_{\max} = 0.074$ psi/ft for 300 B/D through $2\frac{7}{8}$ -in.-OD tubing from Fig. 5.29.

$$p_{pfd} = p_{wh} + (F_s)_{\max}(D_d) = 100 + 0.074(6,000) \\ = 544 \text{ psig at 6,000 ft.}$$

Draw a straight line between 100 psig at the surface and 544 psig at 6,000 ft.

5. From the pressure-depth worksheet for $D_p = 5,000$ ft,

$$p_{pfd_p} = 470 \text{ psig at 5,000 ft.}$$

6. Draw a straight line between $p_{pfd_i} = 217$ psig at 2,927 ft and $p_{pfd_p} = 470$ psig at 5,000 ft.

7. Calculate the valve surface closing pressure.

$$p_{vc} = 0.85(800) = 680 \text{ psig at surface.}$$

p_{vc} of 680 psig at surface increases to p_{vcd} of 774 psig at 6,000 ft. Draw the p_{vcd} traverse by connecting 680 psig at surface to 774 psig at 6,000 ft with a straight line.

8. Plot the unloading temperature of 80°F at the surface and 170°F at 6,000 ft and draw the T_{uvD} traverse by connecting 80°F at surface to 170°F at 6,000 ft with a straight line.

$$9. D_1 = \frac{p_{ko} - p_{whu}}{g_{sl}} = \frac{850 - 60}{0.45} = 1,756 \text{ ft.}$$

10. From the pressure-depth worksheet for $D_1 = 1,756$ ft,

$$(p_{pfd_1})_{\min} = 170 \text{ psig, } p_{vcd_1} = 707 \text{ psig, and}$$

$$T_{uvD_1} = 106^\circ\text{F.}$$

11. Draw the g_{sl} traverse (0.45 psi/ft) originating at 170 psig at 1,756 ft and extending to the p_{vcd} traverse.

12. $D_2 = 2,992$ ft at the intersection of the p_{vcd} traverse.

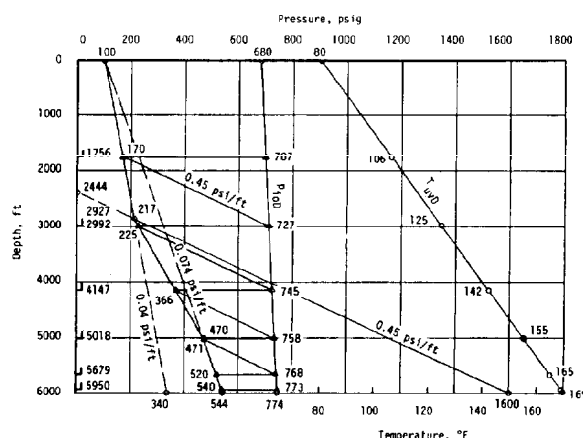


Fig. 5.31—Intermittent gas lift installation design based on a constant valve surface closing pressure and an increasing intermittent spacing factor gradient.

13. From the pressure-depth worksheet for $D_2 = 2,992$ ft [since $D_2 > D_i$, $(p_{pfd_2})_{\min}$ on intermitting spacing factor traverse between p_{pfd_i} and p_{pfd_p}],

$$(p_{pfd_2})_{\min} = 225 \text{ psig, } p_{vcd_2} = 727 \text{ psig, and}$$

$$T_{uvD_2} = 125^\circ\text{F.}$$

Repeat Steps 11 through 13 for the third gas lift valve:

11. Draw the g_{sl} traverse originating at 225 psig at 2,992 ft and extending to the p_{vcd} traverse.

12. $D_3 = 4,147$ ft.

13. $(p_{pfd_3})_{\min} = 366$ psig, $p_{vcd_3} = 745$ psig, and $T_{uvD_3} = 142^\circ\text{F.}$

Repeat Steps 11 through 13 for the fourth gas lift valve:

11. Draw the g_{sl} traverse below the third valve.

12. $D_4 = 5,018$ ft.

13. $(p_{pfd_4})_{\min} = 471$ psig, $p_{vcd_4} = 758$ psig, and $T_{uvD_4} = 155^\circ\text{F.}$

Repeat Steps 11 through 13 for the fifth gas lift valve:

11. Draw the g_{sl} traverse below the fourth valve.

12. $D_5 = 5,679$ ft.

13. $(p_{pfd_5})_{\min} = 520$ psig, $p_{vcd_5} = 768$ psig, and $T_{uvD_5} = 165^\circ\text{F.}$

Repeat Steps 11 through 13 for the sixth (bottom) gas lift valve:

11. Draw the g_{sl} traverse below the fifth valve.

12. $D_6 = 5,950$ ft (maximum valve depth).

13. $(p_{pfd_6})_{\min} = 540$ psig, $p_{vcd_6} = 773$ psig, and $T_{uvD_6} = 169^\circ\text{F.}$

Note that the minimum distance between valves of 350 ft was not used in the design of this installation. The maximum valve depth of 5,950 ft was reached before the calculated distance between valves was less than 350 ft.

The calculated test-rack opening pressure of Valve 6 (Table 5.11) is based on a $\frac{1}{2}$ -in. port. A valve with the same surface closing pressure and a $\frac{3}{8}$ -in. port can be run as the bottom valve to reduce the spread for a lower-than-predicted BHFP. The test-rack opening pressure for a valve with a $\frac{3}{8}$ -in. port would be 730 psig at 60°F on the basis of an A_p/A_h ratio of 0.143.

Percent Tubing Load Installation Designs for Intermittent Lift

Intermittent gas lift installations can be designed to require a given production pressure at valve depth for opening the gas lift valves with an available operating injection gas pressure. The production pressure is expressed as a percent load of the injection-gas pressure and can be defined as follows:

$$F_{pe} = 100 \left(\frac{p_{pfD}}{p_{ioD}} \right), \dots\dots\dots (52)$$

where F_{pe} is the production-pressure load factor, percent.

The test-rack opening pressures of the valves are based on the design injection-gas operating pressure and production load pressure at the depths of the valves. Since the transfer from an upper to the next lower gas lift valve is based on the difference in the production load pressure at each valve depth, the gas lift valves must have a large production-pressure factor, F_p . The gas lift valve with the highest production pressure at valve depth that is less than the operating injection-gas pressure at the same depth will be the operating gas lift valve.

The gas lift valve depths may be based on the percent-load production pressure or on other arbitrary percentages of the available operating injection gas pressure. Two widely used percent spacing and load design methods can be described as follows: (1) 85 to 50% spacing-load design, and (2) 40 to 70% spacing and 50% load design.

The valve depths and the test-rack opening pressures are based on the percent load for the first method. All constant percentages for spacing-load designs result in approximately the same distance between gas lift valves. The distance between the gas lift valves theoretically will increase slightly with depth because of an increase in the injection-gas pressure with depth, as can be noted from the following equation for the 85 to 50% spacing-load design:

$$L_{bv} = \frac{0.85(p_{ioD}) - 0.5(p_{ioD})}{g_{sl}},$$

Therefore,

$$L_{bv} = \frac{0.35(p_{ioD})}{g_{sl}}, \dots\dots\dots (53)$$

where L_{bv} is the distance between gas lift valves, feet.

The 40 to 70% spacing and 50% load design operate on principles similar to the other spacing-load percent design but do not result in an increasing distance between lower gas lift valves.

These installations are simple to calculate and will perform efficiently in most wells requiring intermittent lift. One disadvantage is the number of gas lift valves required for deep wells when the available injection-gas pressure is low.

Intermittent Gas Lift Installation Design Based on 40 to 70% Spacing and 50% Load

The 40 to 70% flowing production or transfer pressure line is used to locate the gas lift valve depths, and the opening pressures of the gas lift valves are based on 50% of the operating injection-gas pressure at depth. The basis

for this design method corresponds more closely to the principles of intermittent gas lift operations than the percentage spacing-load designs. As the depth of lift increases, the liquid fallback increases and the distance between gas lift valves should be less to compensate for a higher minimum flowing production pressure at valve depth between gas injections. The 40 to 70% spacing design results in the distance between gas lift valves decreasing with depth that is similar to most other types of gas lift installation designs.

The calculated theoretical closing pressure of a gas lift valve requires that the flowing production pressure be equal to the injection-gas pressure at the instant a valve closes. If the production pressure is less than the injection-gas pressure, which is usually true, the actual closing pressure will be higher than the theoretical closing pressure. For this reason, an operating injection-gas pressure for design purposes that is 50 psi less than the available injection-gas pressure at the wellsite is recommended for percent-load designs. This assumption will ensure good gas lift operation as a result of a rapid increase in the casing pressure after the time-cycle controller opens for an injection-gas cycle.

Determination of the Gas Lift Valve Depths. The BHP's and BHT usually are referenced to the same depth, which is the lower end of the production conduit (D_d). The steps for establishing the gas lift valve depths on a pressure-depth worksheet are as follows.

1. Determine the design operating injection-gas pressure at the lower end of the production conduit (p_{iod}). Generally, the design operating injection-gas pressure at the surface is assumed to be 50 psi less than the injection-gas pressure available at the wellsite to ensure a surface closing pressure that will not exceed 85% of the available injection-gas-line pressure.

2. Calculate the 40 to 70% valve spacing transfer production pressures at the surface (p_{pt}) and at the lower end of the production conduit (p_{ptd}):

$$p_{pt} = 0.4(p_{io}) \dots\dots\dots (54)$$

and

$$p_{ptd} = 0.7(p_{iod}), \dots\dots\dots (55)$$

Plot p_{pt} at the surface and p_{ptd} at the depth D_d and draw a straight line between these two pressures (p_{ptD} traverse).

3. Draw the unloading gas lift valve temperature at depth traverse (T_{wD}) by assuming a straight line between the surface unloading flowing wellhead temperature (T_{whu}) and the BHT at the lower end of the production conduit (T_{vd}). An unloading flowing wellhead temperature near the surface geothermal temperature for the area can be assumed for typical intermittent gas lift operations.

4. Calculate the depth of the top gas lift valve (D_1) on the basis of the surface kick-off injection-gas pressure (p_{ko}), the static-load fluid gradient (g_{sl}), and the wellhead U-tubing pressure (p_{whu}), or D_1 may equal the static fluid level if this depth exceeds calculated D_1 and the well will not be loaded in the future. With Eq. 23,

$$D_1 = \frac{p_{ko} - p_{whu}}{g_{sl}}.$$

TABLE 5.12—CALCULATION OF THE TEST-RACK-SET OPENING PRESSURES OF THE GAS LIFT VALVES BASED ON A 40 TO 70% SPACING AND 50% LOAD*

Valve Number	D (ft)	p_{ioD} (psig)	Load p_{pfD} (psig)	p_{bvD} (psig)	T_{uvD} (°F)	F_T	p_{vo} (psig)
1	1,699	831	416	750	105	0.912	850
2	2,681	849	425	766	120	0.886	844
3	3,608	866	433	781	134	0.863	838
4	4,485	882	441	796	147	0.842	833
5	5,314	898	448	810	160	0.823	829
6	6,097	912	456	823	171	0.807	825
7	6,838	926	463	836	183	0.791	821
8	7,538	938	469	846	193	0.778	818
9	7,970	946	473	854	200	0.769	816

*Valve description: 1½-in.-OD gas lift valves. Valve specifications: $A_b = 0.77$ sq in. Port ID = 7/16 in. $A_p/A_b = 0.195$ ($1 - A_p/A_b = 0.805$).

5. Draw a horizontal line between the p_{pfD} traverse and p_{ioD} traverse at depth D_1 . Record p_{pfD1} , p_{ioD1} , and T_{uvD1} at depth D_1 .

6. Draw the static-load fluid gradient (g_{sl}) traverse below the depth of the top gas lift valve with the traverse originating at p_{pfD1} and extending to the p_{ioD} traverse.

7. Locate the depth of the second gas lift valve (D_2) at the intersection of the static-load fluid gradient traverse with the p_{ioD} traverse. There is no pressure differential used for locating the gas lift valve depths because the p_{ioD} traverse is based on a pressure equal to 50 psi less than the minimum injection-gas pressure available at the wellsite.

8. Draw a horizontal line on the pressure-depth worksheet between the p_{pfD} traverse and p_{ioD} traverse at depth D_2 . Record p_{pfD2} , p_{ioD2} , and T_{uvD2} at depth D_2 .

9. Continue to determine the gas lift valve depths graphically by repeating Steps 6 through 8 until the maximum depth of lift is attained.

Calculation of the Test-Rack-Set Opening Pressures of the Gas Lift Valves. A tabulation form for these calculations is illustrated in Table 5.12. Since this is a 50% load intermittent gas lift installation design, the test-rack-set opening pressure of each valve is based on a load production pressure equal to 50% of the design operating injection-gas pressure at the valve depth:

$$p_{pfD} = 0.5(p_{ioD}). \quad (56)$$

The bellows-charged dome pressure at the valve unloading temperature (p_{bvD}) is calculated with the following equation:

$$p_{bvD} = p_{ioD}(1 - A_p/A_b) + p_{pfD}(A_p/A_b). \quad (57)$$

The unloading valve temperature at the depth of the valve can be estimated from a T_{uvD} traverse on the pressure-depth worksheet or calculated using Eq. 39. The test-rack opening pressure is calculated using Eq. 38 for a tester setting temperature of 60°F and Eq. 40 for a tester setting temperature (T_{ts}) other than 60°F.

Example Problem 15. Well information for installation design calculations:

1. Tubing length = 8,000 ft.
2. Maximum valve depth = 7,970 ft.
3. BHT = 200°F at 8,000 ft.
4. Load fluid gradient = 0.465 psi/ft.
5. Static fluid level = 0 ft.
6. Design unloading wellhead temperature = 80°F.
7. U-tubing wellhead pressure = 60 psig.
8. Flowing wellhead pressure = 60 psig (low gas injection frequency).
9. Surface kick-off injection-gas pressure = 850 psig.
10. Surface available injection-gas pressure = 850 psig (same as kick-off).
11. Available injection-gas pressure at depth = 1,006 psig at 8,000 ft.
12. Surface design operating injection-gas pressure = 800 psig.
13. Percentage for valve spacing line at surface = 40%.
14. Percentage for valve spacing line at 8,000 ft = 70%.
15. Percent fluid load = 50%.
16. Gas lift valve bellows area = 0.77 sq in. (1½-in.-OD valve).
17. Gas lift valve with sharp-edged seat and port ID = 7/16 in.
18. Test-rack setting temperature = 60°F.

Since this design method is not based on a daily production rate, the required data for the installation design are less than for most types of gas lift installations. The available injection-gas pressure at depth was calculated by use of Eq. 1 for the actual injection-gas gravity and temperature-at-depth gradient for the well. A gas-pressure-at-depth factor (F_g) based on the available injection-gas pressure at depth was used to calculate the injection-gas design pressure at depth. The value of F_g is 2.294 psi/100 psi/1,000 ft for this installation (refer to Eq. 3).

Solution—Valve Depths. The traverses for the pressures and temperatures used for calculating the gas lift installation design are drawn on a pressure-depth worksheet in Fig. 5.32.

1. For an available injection-gas pressure of 850 psig at the wellsite, use a surface $p_{io} = 800$ psig.

$p_{io} = 800$ psig at surface increases to $p_{iod} = 947$ psig at 8,000 ft.

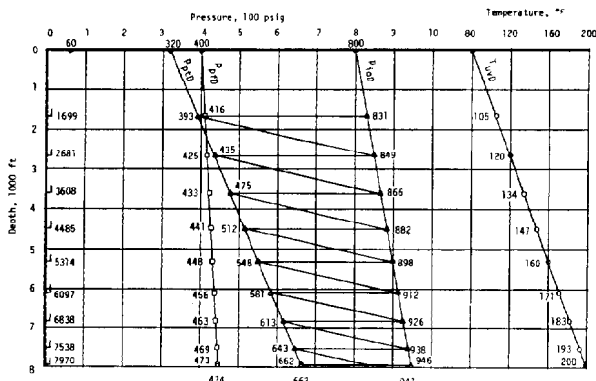


Fig. 5.32—Intermittent gas lift installation design based on a 40 to 70% spacing and 50% load.

Establish the design p_{ioD} traverse by drawing a straight line between 800 psig at the surface and 947 psig at 8,000 ft.

$$2. p_{pt} = 0.4(p_{io}) = 0.4(800) = 320 \text{ psig at surface,}$$

$$p_{ptd} = 0.7(p_{ioD}) = 0.7(947) = 663 \text{ psig at 8,000 ft.}$$

Draw a straight line between 320 psig at the surface and 663 psig at 8,000 ft to establish the p_{ptD} traverse.

3. Plot the unloading temperature of 80°F at the surface and 200°F at 8,000 ft and draw the T_{uvD} traverse.

$$4. D_1 = \frac{p_{ko} - p_{whu}}{g_{sl}} = \frac{850 - 60}{0.465} = 1,699 \text{ ft.}$$

5. From the pressure-depth worksheet for $D_1 = 1,699$ ft,

$$p_{pfD1} = 416 \text{ psig, } p_{ioD1} = 831 \text{ psig, and } T_{uvD1} = 105^\circ\text{F.}$$

6. Draw the g_{sl} traverse (0.465 psi/ft) originating at $p_{ptD} = 393$ psig at 1,699 ft and extending to the p_{ioD} traverse.

7. $D_2 = 2,681$ ft at the intersection of the p_{ioD} traverse.

8. From the pressure-depth worksheet for $D_2 = 2,681$ ft,

$$p_{pfD2} = 425 \text{ psig, } p_{ioD2} = 849 \text{ psig, and } T_{uvD2} = 120^\circ\text{F.}$$

Repeat Steps 6 through 8 for the third gas lift valve:

6. Draw the g_{sl} traverse from $p_{pfD2} = 435$ psig at 2,681 ft to the p_{ioD} traverse.

7. $D_3 = 3,608$ ft.

8. $p_{pfD3} = 433$ psig, $p_{ioD3} = 866$ psig, and $T_{uvD3} = 134^\circ\text{F.}$

This procedure is repeated until the maximum valve depth is attained (see Fig. 5.32 and Table 5.12).

The bottom gas lift valve in the test-rack opening pressure tabulation (Table 5.12) has a $\frac{7}{16}$ -in. port. If there is a possibility that this well may have a very low BHFP, a valve with a $\frac{3}{8}$ -in. port could be selected to reduce the spread in psi between the initial opening and closing pres-

ures of the bottom gas lift valve. The test-rack opening pressure for a valve with a $\frac{3}{8}$ -in. port would be 766 psig at 60°F on the basis of an A_p/A_b ratio of 0.143.

Intermittent Lift Chamber Application and Installation Design

A chamber installation is recommended for gas lifting wells with very low BHFP's and is applicable particularly for high-productivity wells with a low BHP. There are two fundamental types of chambers and many variations of each type depending on the casing size, permissible expenditure, well conditions, and the availability of special equipment for assembling a chamber installation. The more expensive chamber requires two packers. The other is an insert type that uses a bottle assembled from the largest pipe that can be run inside the casing or open hole in an openhole completion. Production accumulates in the large chamber rather than in the tubing string. Since a few feet in the chamber will represent many more feet of head in the tubing, the chamber significantly reduces the backpressure against the formation for a given volume of liquid feed-in.

The chamber must be designed properly to perform efficiently. There are accumulation chambers in wells that do not operate by the chamber principle. The chamber principle implies that the injection gas will U-tube the liquid from the chamber and into the production tubing before any injection gas enters the tubing. Other configurations in which the injection gas does not displace the liquid into the dip tube and production conduit before entering the lower end of the dip tube are not chamber installations.

A two-packer and insert chambers are illustrated in Fig. 5.33. All three chambers are designed for the injection gas to enter the chamber above the liquid and to displace the liquid into the dip tube and tubing before injection gas can enter the lower end of the dip tube. These chambers have a bleed valve near the top of the chamber to vent the gas and to allow filling with liquid production. A reliable standing valve is essential for efficient operation in most installations.

The two-packer chamber installation in Fig. 5.33a has wireline-retrievable gas lift, bleed, and standing valves. Conventional gas lift valves and nonretrievable bleed and standing valves may be used. The insert chamber installations in Figs. 5.33b and 5.33c are less expensive and are used to deplete low-capacity wells where little expenditure can be justified. The insert chamber in Fig. 5.33c is used to lower the point of gas injection in a well with a long openhole or perforated interval and low BHFP. The chamber length (L_c) is based on the capacities of the chamber annulus (V_{ca}) and the tubing above the chamber (V_t) for all installations in Fig. 5.33 and the capacity of the tubing annulus (V_{ta}) between the operating valve and the top of the chamber for the insert chamber in Fig. 5.33c.

Purposes of Intermittent Gas Lift Chamber Installations. The primary reasons for installing a chamber installation are (1) to attain the minimum possible average BHFP, (2) to lower the point of gas injection, and (3) to use an injection-gas pressure that significantly exceeds the BHFP in a well. The point of gas injection in a chamber installation is the lower end of the dip tube. The bottom

of a chamber can be located near TD in a long openhole or perforated-interval completion. Since a few feet of liquid in the chamber are converted into several feet of liquid in the tubing during unloading of a chamber, high injection-gas pressure can be used to lift a well in which the formation pressure would support only a few hundred feet of production.

Design Considerations for Chamber Installations. The unloading gas lift valve depths and the test-rack opening pressures are calculated in the same manner as the unloading gas lift valves for an intermittent gas lift installation without a chamber. An exception is the recommended maximum distance between the bottom unloading and the chamber operating gas lift valves. Several considerations are important in the design of a chamber installation to ensure operation from the chamber and the maximum liquid recovery with a minimum injection-gas requirement.

1. The chamber length should be calculated on the basis of an injection-gas pressure between 60 and 75% of the initial opening pressure at depth of the operating chamber valve to provide adequate pressure differential across the liquid slug at the instant the injection gas enters the lower end of the dip tube.

2. A bleed valve with a large port is necessary for high-rate chamber installations with a high injection-gas cycle frequency. The large bleed port is needed to vent the injection gas that is trapped in the chamber annulus between cycles.

3. Since the flowing tubing pressure at the depth of the operating chamber gas lift valve may be equal to the well-head tubing pressure plus a few psi gas column weight, the operating gas lift valve must have the proper spread to prevent excessive injection gas usage per cycle. Pilot-operated gas lift valves are used widely for this application since a large port is available with controlled spread characteristics.

4. The bottom unloading gas lift valve should be located within one to three joints of the operating chamber valve for unloading the chamber. The point of gas injection for the chamber valve is at the lower end of the dip tube and not at the depth of the chamber valve.

5. The initial opening pressure of the chamber-operating gas lift valve should be at least 50 psi less than the initial opening pressure of the bottom-unloading gas lift valve to ensure operation from the chamber.

6. The top of a chamber should not be located above the working fluid level in a well to minimize the injection-gas requirement.

7. A locking device is recommended for the standing valve in most chamber installations to prevent the standing valve from being blown out of its seating nipple by the high pressure differential across the standing valve immediately after a slug surfaces.

Chamber Length Equation. The chamber length equation is based on two assumptions. The first is that the top of the chamber is located at the working fluid level. This assumption implies that the chamber and the dip tube are full at the instant the chamber-operating gas lift valve opens. The second assumption requires that the inside diameter of the chamber and the size of the dip tube do not change for the entire length of the chamber. The chamber length equation (Eq. 58) applies to the types of cham-

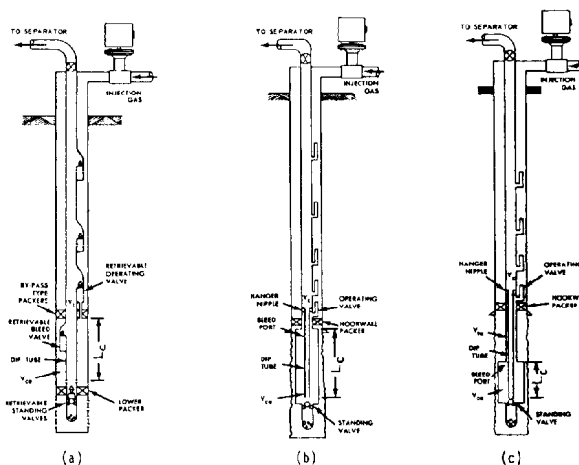


Fig. 5.33—Two-packer and insert types of chamber installations.
(a) Two-packer. (b) Insert. (c) Insert.

bers illustrated in Figs. 5.33a and 5.33b and would have to be modified slightly to account for the capacity of the tubing annulus above the chamber in Fig. 5.33c.

$$L_c = \frac{p_{iDov} - p_{tDov}}{g_l(F_{at} + 1)} \quad (58)$$

where

L_c = chamber length, ft,

p_{iDov} = injection-gas pressure at the depth of the chamber-operating valve for calculating chamber length, psig,

p_{tDov} = tubing pressure at the depth of the chamber-operating gas lift valve based on p_{wh} , psig,

g_l = pressure gradient based on liquid production, psi/ft, and

F_{at} = ratio of capacities of the chamber annulus to the tubing above the chamber (V_{ca}/V_t), consistent units.

The actual effective chamber length is the distance from the top of the chamber to the lower end of the dip tube, which is the point of gas injection. The injection-gas pressure for calculating the chamber length should be less than the initial opening pressure of the chamber-operating gas lift valve. An adequate pressure differential across the liquid slug is necessary at the instant the injection gas enters the lower end of the dip tube to attain a slug velocity that ensures maximum liquid recovery with a minimum injection-gas volume per cycle. A recommended value for p_{iDov} would be

$$p_{iDov} = 0.6 \text{ to } 0.75 (p_{oDov}), \quad (59)$$

where p_{oDov} is the initial injection-gas opening pressure of the operating-chamber pilot valve at depth, psig.

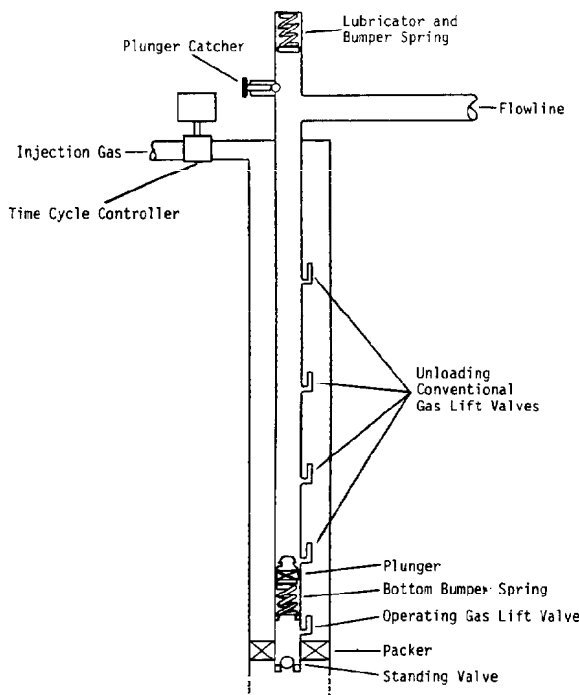


Fig. 5.34—Plunger in an intermittent gas lift installation.

Example Problem 16.

Given for chamber length calculations:

1. Two-packer chamber installation (Fig. 5.33a).
2. Casing size=7-in. OD, 26 lbf/ft.
3. Tubing and dip tube size=2 $\frac{7}{8}$ -in. OD.
4. Initial injection-gas opening pressure of operating chamber-pilot valve, p_{oDov} =800 psig at 6,000 ft.
5. Production liquid gradient, g_l =0.40 psi/ft.
6. Tubing pressure at operating chamber valve depth, p_{iDov} =100 psig at 6,000 ft for p_{wh} =85 psig at surface.

Calculate the approximate chamber length.

From the appropriate tables for the annular volumes between tubing and casing and the capacities of tubing,

$$V_{ca}=0.1697 \text{ cu ft/ft for } 2\frac{7}{8}\text{-in.-OD tubing in 7-in.-OD, 26-lbf/ft casing.}$$

$$V_t=0.0325 \text{ cu ft/ft for } 2\frac{7}{8}\text{-in.-OD, 6.5-lbf/ft EUE tubing.}$$

$$F_{at}=\frac{V_{ca}}{V_t}=\frac{0.1697}{0.0325}=5.22.$$

$$p_{iDov}=0.70(p_{oDov})=0.70(800)=560 \text{ psig at 6,000 ft.}$$

$$L_c=\frac{p_{iDov}-p_{oDov}}{g_l(F_{at}+1)}=\frac{560-100}{0.40(5.22+1)}=185 \text{ ft.}$$

Plunger Application for Intermittent Gas Lift

An important consideration related to intermittent gas lift operations is the injection-gas breakthrough and resulting

loss in the liquid production per cycle from the injection gas penetrating the liquid slug during the time required to displace this slug to the surface. The produced liquid slug can be a small fraction of the starting slug size because of injection-gas breakthrough. The losses are greater when the injection-gas pressure is low and the required depth of lift is near total depth in a deep well. For example, a 12,000-ft well with a BHFP of 300 psig and an available injection-gas pressure of only 450 psig can be gas lifted intermittently with the proper plunger. The well could not be gas lifted successfully from this depth without a plunger.

A typical plunger installation for intermittent gas lift operation is shown in Fig. 5.34. A plunger can be expected to decrease the injection-gas requirement for an intermittent gas lift installation from 30 to 70% depending on the depth of lift, injection-gas pressure, and adjustment of the injection-gas volume to the well before the plunger is installed. There will be no liquid slug recovery by intermittent gas lift from very deep wells with low injection-gas pressure unless a plunger is installed. The plunger provides a solid interface between the starting liquid slug and the displacing injection gas. The plunger will practically eliminate liquid fallback as a result of gas penetrating the liquid slug. The increase in liquid recovery and the decrease in the injection-gas requirement per cycle from installing a plunger are minimal in an intermittent gas lift installation with small liquid slugs being lifted at an exceedingly high slug velocity. Another advantage of a plunger is that it will cut paraffin in a well with a paraffin problem. Plungers are installed in some wells for the sole purpose of keeping the tubing free of paraffin deposition.

A plunger can be installed in an existing conventional gas lift installation by wireline methods. There is no need to pull the tubing. A standing valve and a bottomhole collar lock or stop with a bumper spring can be installed with wireline tools. A standing valve normally is recommended but not required in wells with a low permeability. The bottomhole bumper spring is located immediately above the operating gas lift valve and a standing valve is stationed below the valve. The remaining equipment is on the surface and includes a lubricator with a bumper spring and a plunger catcher mechanism. A plunger arrival detector to shut in the tubing is not needed for an intermittent gas lift installation since the tubing is not shut in between injection-gas cycles.

A plunger velocity of 800 to 1,000 ft/min is recommended for the most efficient lift on the basis of a study by Lea.¹⁰ A plunger may stall or tend to stop and start at plunger velocities less than 350 to 400 ft/min. Plunger velocities in excess of 1,200 to 1,500 ft/min are not recommended because of possible damage to the plunger on arrival at the surface and because of an apparent tendency to bypass a thicker than normal liquid boundary on the tubing wall. An average plunger velocity can be approximated by noting the times when a time-cycle controller opens and when the plunger arrives at the surface.

The addition of a plunger to an intermittent gas lift installation should be considered when (1) the available injection-gas pressure is low relative to the required depth of lift in a low-BHFP well, (2) the wellhead flowing pressure is excessive after a slug surfaces because of a small-ID flowline, excessive number of bends at the wellhead,

flowline choke, etc., and (3) a paraffin deposition problem exists. Actually, a plunger will increase the efficiency of most intermittent gas lift installations.

Well conditions that prohibit the use of a plunger are (1) bore opening through surface wellhead and Christmas tree valves that differ from the tubing ID; (2) excessive well deviation, which prevents a plunger from descending to its bottomhole bumper spring; (3) tight spots in the tubing; (4) wireline-retrievable, unloading, gas lift valve side-pocket mandrels—the operating gas lift valve can be retrievable; (5) appreciable sand production; and (6) high-rate intermittent gas lift operations.

The fall-time required for a plunger to descend to the bottom bumper spring can reduce the maximum production from a high-cycle-frequency intermittent gas lift installation. Manufacturers are continuing to pursue the development of a plunger that will operate successfully in wells with side-pocket mandrels. Special tandem plungers are available for wells with side-pocket mandrels. Plungers have worked in wells with a deviation near 50°, but the maximum deviation for plunger operation would depend on the construction of the plunger. The manufacturers should be able to provide the information related to their plunger operation in a deviated well.

There are numerous types of plunger sealing elements, bypass valves, plunger weights and lengths, and other features that may have been developed for unique applications. Some plungers will be particularly applicable for gas lift and other types may not. Select the proper plunger to match the well conditions and application for trouble-free service and efficient operation.

Unloading Procedures and Proper Adjustment of Injection Gas Rate

Introduction

The importance of properly unloading a gas lift installation cannot be overemphasized in terms of possible damage to gas lift valves and for attaining the optimum depth of lift. Needle valves for obtaining injection-gas operating pressure downstream of the injection-gas control device and the flowing wellhead production pressure upstream of the flowline should be in good working order before beginning the unloading operations. If a permanent meter tube is not installed in the injection-gas line to the well, provisions should be made for the installation of a portable meter tube during unloading and adjustment of the injection-gas rate to the well. Preferably, the meter tube and the orifice meter or flow computer should be located near the well's injection-gas control device so that the effect of changes in the adjustment of the injection-gas volume can be observed.

A two-pen pressure recorder should be installed before unloading all gas lift installations. The ranges of the pressure elements in the recorder should be checked before hookup. A typical recorder will have a 0- to 500- or 0- to 1,000-psi-range element for the flowing wellhead production pressure and a 0- to 1,000 or 0- to 2,000-psi-range element for the injection-gas pressure, depending on the kick-off and available operating injection-gas pressure at the wellsite. These pressure elements should be calibrated periodically with a dead-weight tester to ensure accurate recordings.

Recommended Practices Before Unloading

If the injection-gas line is new, it should be blown clean of scale, welding slag, etc., before being connected to a well. This precaution prevents damage and plugging of the surface control equipment and entry of debris with the injection gas into the casing annulus. Debris may cause serious gas lift valve operational problems.

The surface facilities for a gas lift installation should be checked before the well is unloaded. This includes all valves between the wellhead and the battery, the separator gas capacity, the stock-tank room, etc. It is important to check the pop-off safety release valve for the gas gathering facilities if this is the first gas lift installation in the system.

If a well is loaded with drilling fluid, it should be circulated clean to the perforations before gas lift valves are run. Abrasive materials in the drilling fluid can damage the gas lift valve seats and/or may result in valve malfunction during unloading operations. If the gas lift valves are run before the drilling fluid is replaced with a suitable load fluid, the well should not be reverse circulated because circulation would occur through the gas lift valves. The checks in the gas lift valves for tubing flow are designed to prevent flow from the tubing to the casing annulus; therefore, all circulation should occur around the lower end of the tubing for normal circulation.

Recommended Procedure for Unloading Gas Lift Installations

Preventing excessive pressure differentials minimizes the chance for equipment failure because of fluid and sand cutting. The following procedure avoids excessive pressure differential across the valves during the unloading operation. The permissible rate of increase in the injection-gas pressure downstream of the control device can be greater for an open installation without a packer than for an installation with a packer. Most of the load fluid from the casing annulus can U-tube through the lower end of the tubing in an open installation, whereas all the load fluid in the annulus must pass through the gas lift valves in an installation with a packer. The initial U-tubing is the most critical operation during the unloading procedure. There is no reason to hurry the U-tubing of the load fluid to uncover the top gas lift valve. Since the tubing remains full of load fluid during the U-tubing operation, there will be no drawdown in BHFP. Gas lifting does not begin until the initial U-tubing is completed and injection gas enters the tubing through the top valve. The load-fluid production rate is controlled by the rate of increase in the injection-gas pressure, which in turn depends on the injection-gas rate. Since most gas lift installations include a packer, the load fluid enters the tubing through the gas lift valves. If there are sand and debris in the load fluid and full-line injection-gas pressure is applied to the casing by opening a large valve on the injection-gas line, the gas lift valves may leak after the well is unloaded. An instantaneous pressure differential will occur across every gas lift valve that is approximately equal to the full-line injection-gas pressure because the casing and tubing are full of load fluid. The resulting high fluid velocity through the small gas lift valve ports may fluid-cut the seats—particularly if sand or debris is in the load fluid. The following procedure is recommended for monitoring and

controlling the unloading operations for all gas lift installations to prevent damage to the gas lift valves and surface facilities.

1. Install a two-pen pressure recorder that is accurate and in good working condition. The injection pressure downstream of the gas-control device and the wellhead tubing pressure should always be recorded during the entire unloading operation.

2. If the well has been shut in and the tubing pressure exceeds the separator pressure, bleed down the tubing through a $\frac{3}{4}$ - or $\frac{5}{8}$ -in. flowline choke. Do not inject lift gas before or while the tubing is being bled down.

3. Remove all wellhead and flowline restrictions including a fixed or adjustable choke if the well will not flow after all load fluid has been produced. If the gas lift installation is in a new well or a recompletion that could flow, a $\frac{2}{4}$ - to $\frac{3}{4}$ -in. flowline choke is recommended until after the well has cleaned up and obviously will not flow naturally. The selected range of the element for the flowing wellhead pressure pen in the two-pen recorder should be able to handle the maximum flowing wellhead pressure with a choke in the flowline.

4. Inject lift gas into the casing at a rate that will not allow more than a 50-psi increase in casing pressure per 10-minute interval. Continue until the casing pressure has reached at least 300 psi. Most companies will use a standard choke size in the injection-gas line for U-tubing and initial unloading operations. A typical injection-gas choke size will range from $\frac{3}{4}$ to $\frac{1}{2}$ in.

5. After the casing pressure has reached 300 to 500 psig, the injection-gas rate can be adjusted to allow a 100-psi increase per 10-minute interval until gas begins to circulate through the top gas lift valve (top valve is uncovered). After the top gas lift valve is uncovered and gas has been injected through this valve, a high pressure differential cannot occur across the lower gas lift valves. Any time the casing injection-gas pressure is increased above the opening pressure of the top valve, this valve will open and prevent a further increase in the injection-gas pressure. Gas lifting begins with the injection gas entering the top valve.

6. If the gas lift installation does not unload to the bottom valve or the design operating gas lift valve depth, adjustment of the injection-gas rate to the well will be required. An excessive or inadequate injection-gas rate can prevent unloading. This is particularly true for intermittent gas lift on time-cycle control where the maximum number of injection-gas cycles per day decreases with depth of lift. It may be necessary to decrease the number of injection-gas cycles per day and to increase the duration of gas injection as the point of gas injection transfers from an upper to a lower valve. Proper adjustment of the injection gas volume to a well is not permanent for most installations. The injection-gas requirements change with well conditions; therefore, continuous monitoring of the injection volume and the wellhead and injection-gas pressures is recommended to maintain efficient gas lift operations.

Depressing the Fluid Level, or "Rocking" a Well

If the top gas lift valve cannot be uncovered with the available injection-gas pressure, the fluid level can be depressed when there is no standing valve in the tubing. The injection-gas-line pressure is applied simultaneously

to the tubing and casing. Several hours may be required to depress the fluid level sufficiently in a "tight" low-permeability well. The tubing pressure is released rapidly and the source of the major portion of the fluid entering the tubing will be load fluid from the annulus. This procedure may be required several times to lower the fluid level in the casing annulus below the depth of the top gas lift valve.

A gas lift installation with high-production-pressure-factor valves may cease to unload after the top valve has been uncovered. This type of gas lift valve has a high degree of tubing sensitivity and requires a minimum production pressure at valve depth to open the valve with the available injection-gas pressure. This problem occurs more frequently with the top one or two gas lift valves and may be referred to as a "stymie" condition. The stymie condition can be corrected by applying an artificial increase in production pressure at valve depth by "rocking" the well. The valve cannot detect the difference between a liquid column and a pressure increase from partially equalizing the tubing and casing pressure with injection gas. If a well should stymie, the well can be rocked in the following manner:

1. With the wing valve closed, inject lift gas into the tubing until the casing and tubing pressures indicate that the gas lift valve has opened. A small copper tubing or flexible high-pressure line can be used for this purpose. When a valve opens, the casing pressure will begin to decrease and to equalize with the tubing pressure. The tubing pressure also should begin to increase at a faster rate with injection gas entering the tubing through the valve and surface connection.

2. Stop gas injection into the tubing and open the wing valve to lift the liquid slug above the valve into the flowline as rapidly as possible. A flowline choke may be required to prevent venting injection gas through the separator relief valve. Some surface facilities are overloaded easily and bleeding off the tubing must be controlled carefully.

3. The rocking process may be required several times until a lower gas lift valve has been uncovered. As the depth of lift increases, the possibility of stymie decreases because of the increase in the minimum production pressure that can be attained at the greater depths.

A stymie condition may occur in intermittent gas lift installations with very large ported gas lift valves and production-pressure-operated gas lift installations during unloading operations from the upper gas lift valves before significant BHP drawdown and reservoir fluid production are established.

Controlling the Daily Production Rate From Continuous-Flow Installations

The daily production rate from a continuous-flow gas lift installation should be controlled by the injection-gas volumetric flow rate to the well. A flowline choke should not be used for this purpose. Excessive surface flowline backpressure will increase the injection-gas requirement. Production-pressure-operated gas lift valves and injection-pressure-operated valves with a large production-pressure factor are particularly sensitive to high wellhead flowing pressure. Inefficient multipoint gas injection can result and can prevent unloading an installation to the maximum depth of lift for the available operating injection-gas pressure when the flowing wellhead backpressure is excessive.

Adjustment of a Time-Cycle-Operated Controller for Intermittent Lift Operations

When initially unloading an intermittent gas lift installation, an excessive injection-gas-cycle frequency may prevent "working down" (i.e., unloading the gas lift installation beyond a certain depth). A high injection-gas-cycle frequency can be used to transfer load fluid from the annulus for uncovering the upper unloading gas lift valves. As the depth of lift increases, the maximum possible number of injection-gas cycles per day decreases and the volume of injection gas required per cycle increases. If the number of injection cycles per day becomes excessive and there is insufficient time between gas injections for the casing pressure to decrease to the closing pressure of an upper unloading gas lift valve, the unloading process will discontinue until the number of injection-gas cycles is reduced. Many installations will require several adjustments of the time-cycle controller before the operating valve depth is reached.

The following procedure is recommended for final adjustment of a time-cycle-operated controller to minimize the injection-gas requirement when lifting from the operating gas lift valve.

1. Adjust the controller for a duration of gas injection that will ensure an excessive volume of injection gas used per cycle (approximately 500 cu ft/bbl/1,000 ft of lift). For most systems 30 sec/1,000 ft of lift will result in more gas being injected into the casing annulus than is actually needed.

2. Reduce the number of injection-gas cycles per day until the well will not lift from the required valve depth and/or the producing rate declines below the desired or maximum daily production rate.

3. Reset the controller for the number of injection-gas cycles per day immediately before the previous setting in Step 2. This establishes the proper injection-gas-cycle frequency.

4. Reduce the duration of gas injection per cycle until the producing rate decreases and then increase the duration of gas injection by 5 to 10 seconds for fluctuations in injection-gas-line pressure.

A time-cycle-operated controller on the injection-gas line can be adjusted as outlined previously, provided the line pressure remains relatively constant. If the line pressure varies significantly, the controller is adjusted to inject ample gas volume with minimum line pressure. When the line pressure is above the minimum pressure, excessive injection gas is used each cycle. One solution to this problem is a controller that opens on time and closes on a set increase in casing pressure. Several electronic timers are designed to operate in conjunction with pressure control.

Nomenclature

- A = area, sq in.
 A_b = total effective area of bellows, sq in.
 A_p = valve port area for sharp-edged seat or area of ball seat-line contact for tapered seat, sq in.
 C_d = discharge coefficient (determined experimentally), dimensionless

- C_{gT} = approximate gravity and temperature-correction factor for choke charts, dimensionless
 d_1 = orifice ID for known volumetric gas rate, in.
 d_2 = orifice ID for unknown volumetric gas rate, in.
 D = true vertical depth of gas column or valve depth, ft
 D_1 = depth of top valve, ft
 D_c = calculated depth for assumed p_{as} , ft
 D_d = reference datum depth (usually lower end of production conduit) for BHT and BHP's, ft
 D_{dl} = maximum depth for variable gradient valve spacing design line, ft
 D_i = depth at which initial BHP drawdown can be established, ft
 D_{ov} = depth of operating valve, ft
 D_p = minimum depth at which design production rate can be lifted, ft
 D_{uv} = depth of unloading valve, ft
 e = Napierian logarithm base = 2.718...
 f_o = oil cut, fraction
 F_{at} = ratio of capacities of chamber annulus/tubing above chamber, consistent units
 F_{cf} = critical flow pressure ratio

$$= \left(\frac{2}{k+1} \right)^{k/(k-1)}$$
 F_{dl} = assigned percent factor for variable gradient valve spacing design line, percent
 F_{du} = ratio of downstream pressure/upstream pressure, consistent units
 F_g = gas-pressure-at-depth factor, psi/100 psig/1,000 ft
 F_p = production-pressure factor
 F_{pe} = production-pressure load factor, percent
 F_s = intermittent pressure-gradient spacing factor, psi/ft
 $(F_s)_{\max}$ = maximum intermittent pressure-gradient spacing factor, psi/ft
 $(F_s)_{\min}$ = minimum intermittent pressure-gradient spacing factor, psi/ft
 F_{tc} = ratio of capacities of tubing/casing annulus, consistent units
 F_T = temperature correction factor for nitrogen at 60°F
 F_{T_N} = temperature correction factor for nitrogen at T_{vs}
 g = acceleration of gravity, ft/sec²
 g_{fb} = flowing pressure gradient (traverse) below point of gas injection, psi/ft
 g_{fp} = flowing pressure gradient (traverse) above point of gas injection, psi/ft
 g_g = gas gradient, psi/ft

- g_l = pressure gradient based on liquid production, psi/ft
 g_{sl} = static-load fluid gradient, psi/ft
 k = ratio of specific heats, dimensionless
 L_{bv} = distance between gas lift valves, ft
 L_c = chamber length, ft
 L_{sf} = static fluid level for zero wellhead pressure, ft
 n = number of pound-moles, lbm/mol
 p = pressure, psi
 \bar{p} = average pressure, psi
 p_1 = upstream pressure, psi
 p_2 = downstream pressure, psi
 p_{as} = assumed pressure, psi
 p_b = bellows-charged dome pressure at 60°F, psi
 p_{bvD} = bellows-charged dome pressure at T_{vD} or T_{uvD} , psi
 p_{bvx} = bellows-charged dome pressure at T_{vx} , psi
 p_{dl} = surface pressure for variable-gradient valve spacing design line, psi
 p_{dlD} = pressure for variable-gradient valve spacing design line at D_{dl} , psi
 p_{iDov} = injection-gas pressure at the depth of the chamber-operating valve for calculating chamber length, psi
 p_{io} = surface-operating injection-gas pressure, psi
 p_{iod} = operating injection-gas pressure at D_d , psi
 p_{ioD} = operating injection-gas pressure at depth, psi
 p_{ko} = surface kick-off injection-gas pressure, psi
 p_{kod} = kick-off injection-gas pressure at D_d , psi
 p_{koD} = kick-off injection-gas pressure at depth, psi
 p_o = initial valve opening pressure at surface, psi
 p_{oD} = initial valve opening pressure at valve depth, psi
 p_{oDov} = initial injection-gas opening pressure of the operating chamber valve at depth, psi
 p_{pe} = production-pressure effect, psi
 p_{pf} = flowing production pressure, psi
 p_{pfd} = unloading flowing production pressure at D_d , psi
 p_{pfd} = flowing production pressure at valve depth, psi
 p_{pfDi} = flowing production pressure at depth where initial drawdown in BHP occurs, psi
 $(p_{pfd})_{\max}$ = maximum flowing production pressure at valve depth while lifting from next lower valve, psi
 $(p_{pfd})_{\min}$ = minimum flowing production pressure at valve depth, psi
 p_{pfDp} = flowing production pressure at minimum depth where design production rate can be lifted, psi
 p_{pft} = test-rack downstream flowing production pressure, psi
 p_{pt} = surface valve-spacing transfer production pressure, psi
 p_{ptd} = valve-spacing transfer production pressure at D_d , psi
 p_{ptD} = valve-spacing transfer production pressure at valve depth, psi
 p_{sc} = standard pressure base, psi
 p_{tD} = flowing production transfer pressure at depth, psi
 p_{tDov} = tubing pressure at the depth of the chamber operating gas lift valve based on p_{wh} , psi
 p_{uvD} = minimum flowing or production transfer pressure at valve depth, psi
 p_{vc} = valve closing pressure at surface, psi
 p_{vcd} = valve closing pressure at D_d , psi
 p_{veD} = valve closing pressure at valve depth, psi
 p_{vcr} = test-rack valve closing pressure at 60°F, if, and only if, the upstream and downstream pressures across the valve port are equal at the instant the valve closes, psi
 p_{vctD} = test-rack closing pressure at valve depth, psi
 p_{vo} = test-rack valve opening pressure at 60°F, psi
 p_{voD} = valve opening pressure at T_{vD} when $p_{pfd}=0$, psi
 p_{vos} = test-rack valve opening pressure at T_{vx} , psi
 p_{wfd} = BHFP at depth D_d , psi
 p_{wh} = wellhead pressure, psi
 p_{whf} = flowing wellhead pressure, psi
 p_{whu} = wellhead U-tubing pressure, psi
 p_{wsd} = static BHP at depth D_d , psi
 Δp_a = assigned valve spacing pressure differential, psi
 Δp_{ao} = assigned design operating pressure differential across operating valve, psi
 Δp_{io} = assigned decrease in operating injection-gas pressure between valves, psi
 Δp_{oD} = difference in p_{oD} based on a change in p_{pfd} , psi
 Δp_{ov} = actual pressure differential across operating valve, psi
 Δp_{pe} = additional production-pressure effect, psi
 Δp_{pfd} = difference in p_{pfd} exerted over A_p , psi
 Δp_s = valve spread, psi
 Δp_{sD} = valve spacing pressure differential at

valve depth, psi
 q_{gsc} = gas flow rate at standard conditions
 (14.7 psia and 60°F), Mscf/D
 q_{g1} = known volumetric gas rate, Mscf/D
 q_{g2} = unknown volumetric gas rate, Mscf/D
 q_{ga} = actual volumetric gas rate, Mscf/D
 q_{gc} = chart volumetric gas rate, Mscf/D
 R = gas constant = 10.73,
 psia-cu ft/lbm-mol-°R
 R = GOR, scf/STB
 R_{glf} = formation GLR, scf/STB
 T = temperature, °F or °R
 \bar{T} = average temperature, °F or °R
 T_1 = upstream temperature, °R
 T_{gD} = temperature of injection gas at depth,
 °F or °R
 T_{sc} = standard temperature base, °F or °R
 T_{uvD} = unloading gas lift valve temperature at
 depth, °F
 T_{vd} = BHT at D_d , °F
 T_{vD} = valve temperature at depth, °F
 T_{vs} = test-rack valve or tester setting temper-
 ature (other than 60°F), °F
 T_{wh} = wellhead temperature, °F
 T_{whf} = flowing wellhead temperature, °F
 T_{whu} = assigned unloading flowing wellhead
 temperature, °F
 T_{ws} = BHT, °F
 V = volume or capacity, cu ft
 V_c = capacity of conduit, cu ft
 V_{ca} = capacity of casing or chamber annulus,
 cu ft
 V_g = volume of gas at standard conditions,
 scf
 V_{gx} = approximate gas volume, scf
 V_t = capacity of tubing, cu ft
 V_{ta} = capacity of tubing annulus, cu ft
 z = compressibility factor, dimensionless
 \bar{z} = compressibility factor for \bar{p} and \bar{T} ,
 dimensionless
 γ_g = gas specific gravity (air=1.0),
 dimensionless

Subscripts

d = reference datum depth (usually lower end
 of production conduit), ft
 D = depth (usually valve depth), ft

Key Equations in SI Metric Units

$$p_{ioD} = p_{io} e^{(\gamma_g D / 29.27 T \bar{z})}, \dots \dots \dots (1)$$

where

p_{ioD} = operating injection gas pressure at depth D ,
 kPa,
 p_{io} = operating injection gas pressure at surface,
 kPa,
 e = Napierian logarithm base = 2.718...,
 γ_g = gas specific gravity (air=1.0),
 dimensionless,
 D = true vertical depth, m,

\bar{T} = average gas temperature, K, and
 \bar{z} = compressibility factor based on average
 pressure \bar{p} and temperature T ,
 dimensionless.

$$q_{gsc} = \frac{1.347 C_d (A) p_1 \sqrt{2(g) \left(\frac{k}{k-1} \right) \left[(F_{du})^{2/k} - (F_{du})^{(k+1)/k} \right]}}{\sqrt{\gamma_g (T_1)}}, \dots \dots \dots (7)$$

where

q_{gsc} = gas flow rate at standard conditions, m³/d
 (100 kPa and 15°C),
 C_d = discharge coefficient (determined
 experimentally), dimensionless,
 A = area of opening, mm²,
 p_1 = upstream pressure, kPa,
 p_2 = downstream pressure, kPa,
 g = acceleration of gravity, m/s²,
 k = ratio of specific heats, dimensionless,
 T_1 = upstream temperature, K,
 F_{cf} = critical flow pressure
 ratio = $[2/(k+1)]^{k/(k-1)}$, and
 F_{du} = ratio of downstream pressure/upstream
 pressure, consistent units, $F_{du} = F_{cf}$ if
 $F_{du} < F_{cf}$ and $F_{du} = p_2/p_1 \geq F_{cf}$.

$$C_{gt} = 0.0730 \sqrt{\gamma_g (T_{gD})}, \dots \dots \dots (8)$$

where

C_{gt} = approximate correction factor for gas
 gravity and temperature, dimensionless,
 γ_g = gas specific gravity (air=1.0),
 dimensionless, and
 T_{gD} = gas temperature at valve depth, K.

References

1. Winkler, H.W.: "How to Design a Closed Rotative Gas Lift System—Part I: Procedure," *World Oil* (July 1960) 116-119.
2. *Gas Lift, Book 6 of Vocational Training Series*, API, Dallas, revised edition (1984) 65.
3. Winkler, H.W.: "Here's How to Improve Your Gas Lift Installations—Part I: Pressure at Depth Determinations," *World Oil* (Aug. 1959) 63-67.
4. Winkler, H.W. and Smith, S.S.: *Camco Gas Lift Manual*, Camco Inc., Houston (1962) A2-001.
5. Cook, H.L. and Dotterweich, F.H.: "Report on Calibration of Positive Flow Beans Manufactured by Thornhill-Craver Company, Inc., Houston, Texas," C. of Arts and Industries, Kingsville (Aug. 1946) 26.
6. Kirkpatrick, C.V.: "Advances in Gas-Lift Technology," *API Drill. and Prod. Prac.* (1959) 24-60.
7. Shiu, K.S. and Beggs, H.D.: "Predicting Temperatures in Flowing Oil Wells," paper presented at the 1978 ASME Energy Technology Conference, Houston, Nov. 5-9.
8. Cullender, M.H. and Smith, R.V.: "Practical Solution of Gas-Flow Equations for Wells and Pipelines with Large Temperature Gradients," *J. Pet. Tech.* (Dec. 1956) 281-87; *Trans.*, AIME, **207**.
9. *Gas Lift, Book 6 of Vocational Training Series*, API, Dallas (1965) 109.
10. Lea, J.F. and Mower, L.N.: "Defining the Characteristics and Performance of Gas Lift Plungers," *Proc.*, Southwestern Petroleum Short Course, Lubbock, TX (April 24-25, 1985) 393-420.

Chapter 6

Hydraulic Pumping

Hal Petrie, National-Oilwell*

Introduction

A well will flow if it has sufficient reservoir potential energy (pressure) to lift fluid to the surface. Artificial lift is applied to a well if the reservoir pressure is not sufficient to cause the well to flow, or when more production is desired in a flowing well. In either case, energy must be transmitted downhole and added to the produced fluid. Hydraulic pumping systems transmit power downhole by means of pressurized power fluid that flows in wellbore tubulars. Hydraulic transmission of power downhole can be accomplished with good efficiency. With 30°API oil at 2,500 psi in 2 $\frac{7}{8}$ -in. tubing, 100 surface hhp can be transmitted to a depth of 8,000 ft with a flow rate of 2,353 B/D and with a frictional pressure drop of 188 psi. This pressure loss is 7.5% of the applied power. If the transmission pressure is raised to 4,000 psi, the required flow rate drops to 1,471 B/D and the frictional pressure loss declines to only 88 psi. This is 2.2% of the applied surface power. Even higher efficiencies can be achieved with water as the hydraulic medium because of its lower viscosity.

The downhole pump acts as a transformer to convert the energy of the power fluid to potential energy or pressure in the produced fluids. The most common form of hydraulic downhole pump consists of a set of coupled reciprocating pistons, one driven by the power fluid and the other pumping the well fluids. Another form of hydraulic downhole pump that has become more popular is the jet pump, which converts the pressurized power fluid to a high-velocity jet that mixes directly with the well fluids.^{1,2} In the turbulent mixing process, momentum and energy from the power fluid are added to the produced fluids. Rotating hydraulic equipment has also been tested in oil wells.^{3,4} In this case, a hydraulic turbine driven by the power fluid rotates a shaft on which a multistage centrifugal or axial-flow pump is mounted. This type of

pump has not had widespread commercial use. The "free pump" feature, common to most designs, allows the pump to be circulated in and out of the well hydraulically without pulling tubing or using wireline services.

The operating pressures used in hydraulic pumping systems usually range from 2,000 to 4,000 psi. The most common pump used to generate this pressure on the surface is a triplex or quintiplex positive-displacement pump driven by an electric motor or a multicylinder gas or diesel engine. Multistage centrifugal pumps have also been used,⁵ and some systems have operated with the excess capacity in water-injection systems.⁶ The hydraulic fluid usually comes from the well and can be produced oil or water. A fluid reservoir at the surface provides surge capacity and is usually part of the cleaning system used to condition the well fluids for use as power fluid. Appropriate control valves and piping complete the system. A schematic of a typical hydraulic pumping system is shown in Fig. 6.1.

A wide variety of well conditions can be handled by hydraulic pumping systems. Successful applications have included setting depths ranging from 1,000 to 18,000 ft.⁷ Production rates can vary from less than 100 to more than 10,000 B/D. Surface packages are available in sizes ranging from 30 to 625 hp. The systems are flexible because the downhole pumping rate can be regulated over a wide range with fluid controls on the surface. Chemicals to control corrosion, paraffin, and emulsions can be injected downhole with the power fluid. Fresh water can also be injected to dissolve salt deposits. When pumping heavy crudes, the power fluid can serve as an effective diluent to reduce the viscosity of the produced fluids. The power fluid can also be heated for handling heavy crudes or low-pour-point crudes. Hydraulic pumping systems are suitable for wells with deviated or crooked holes that cause problems for conventional rod pumping. The surface facilities have a low profile and can be clustered into a central battery to service numerous wells. This can be

*The original chapter on this topic in the 1962 edition was written by C.J. Coberly and F. Barton Brown.

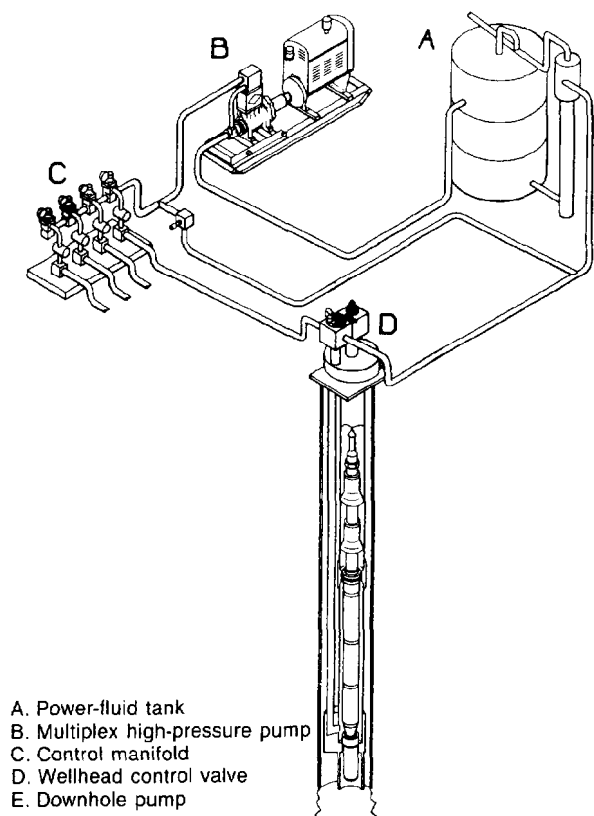


Fig. 6.1—Typical hydraulic pumping system installation.

advantageous in urban sites, offshore locations, and environmentally sensitive areas. Jet pumps can be circulated around the 5-ft-radius loop of subsea through-flowline (TFL) installations⁸ joining gas-lift valves as the only artificial lift devices suitable for these systems.

Downhole Pumps

Types of Installations

The two basic types of installations are the *fixed pump* and the *free pump* designs. In the fixed installation, the downhole pump is attached to the end of a tubing string and run into the well. Free pump installations are designed to allow downhole pump circulation into and out of the well inside the power-fluid tubing string. The downhole pump can also be installed and retrieved by wireline operations.

Fixed Pump Installations (Conventional Installations).

In the fixed insert design, the pump lands on a seating-shoe set in tubing that has a larger ID than the OD of the pump. Power fluid is directed down the inner tubing string, and the produced fluid and the return power fluid flow to the surface inside the annulus between the two tubing strings, as shown in Fig. 6.2a. This system provides a passage for venting free gas in the annular space between the outer tubing string and the inside of the well casing. To take full advantage of the gas venting passage, the pump should be set below the perforations. The power-

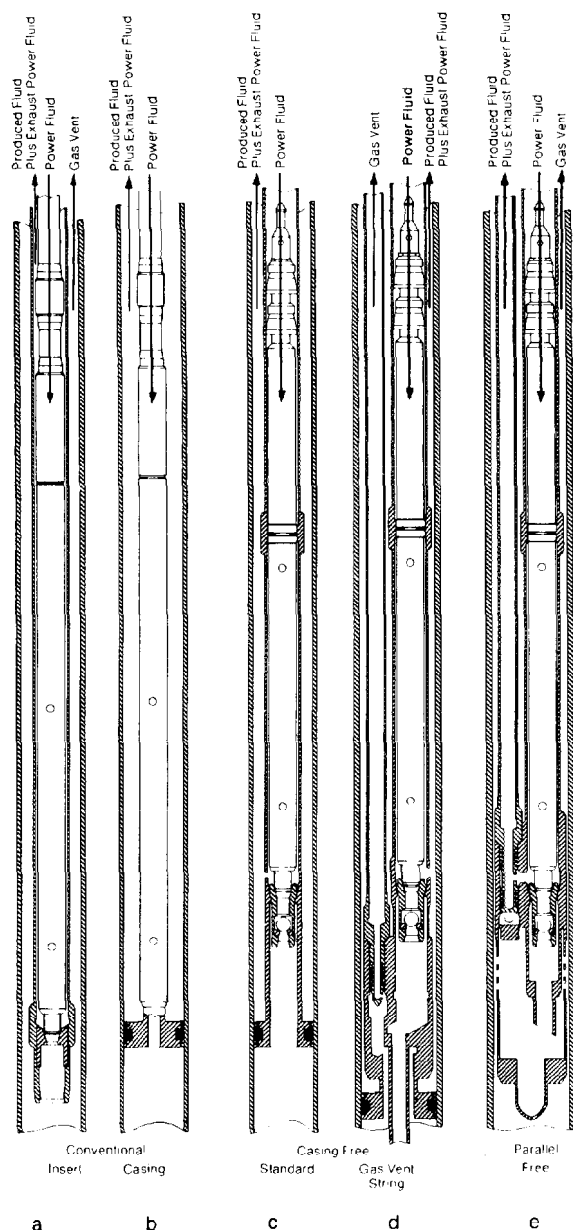


Fig. 6.2—Downhole pump installations.

fluid string is usually $\frac{3}{4}$, 1, or $1\frac{1}{4}$ in., depending on the size of the production tubing. This once-common system is now used mainly to fit a large-diameter downhole pump into restricted casing sizes and still retain the gas-vent feature. It can also be used to lift one or both zones of a dual well with parallel strings.

In the fixed casing design, the tubing, with the pump attached to its lower end, is seated on a packer, as shown in Fig. 6.2b. With this configuration, the power fluid is directed down the tubing string, and the mixed power fluid and the produced well fluids return to the surface in the tubing/casing annulus. Because the well fluids enter the pump from below the packer, all the free gas must be handled by the pump. This type of installation is normally

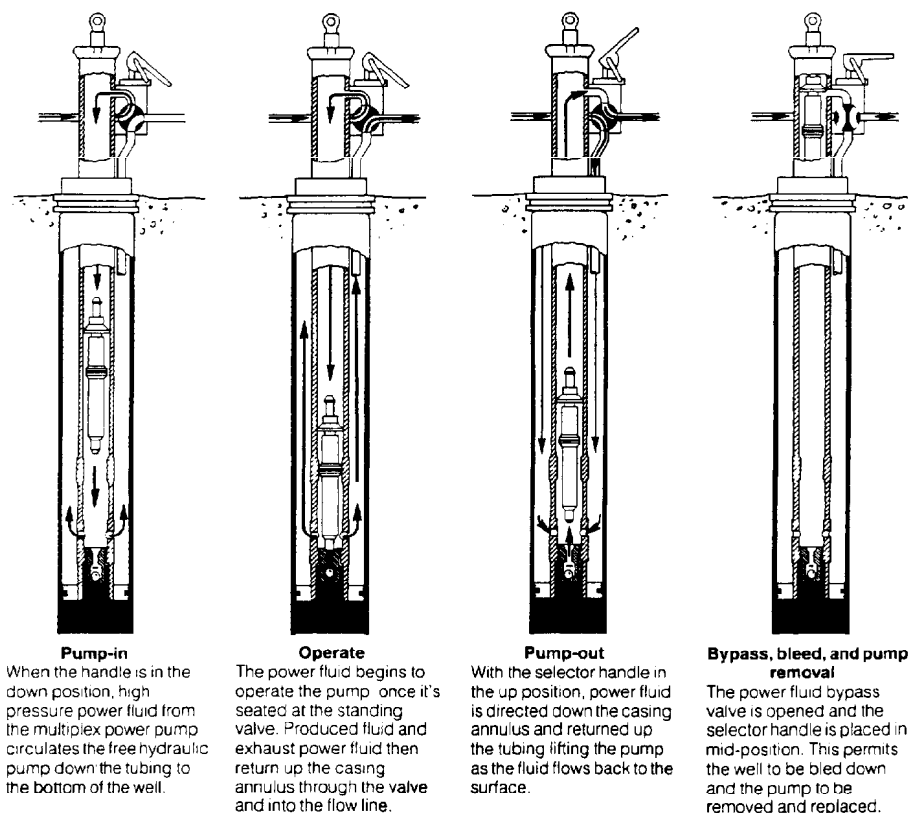


Fig. 6.3—Free-pump cycle.

used in wells without much gas and with large-diameter, high-capacity pumps. If space permits, a gas-vent string can be run from below the packer to the surface. As with the fixed insert design, this installation is no longer common, and both types have been largely supplanted by the various free pump installations. Note that in both of the fixed-type installations, the power fluid mixes with the produced fluids after passing through the pump.

Free Pump Installations. The free pump feature is one of the most significant advantages of hydraulic pumping systems. Free pump installations permit circulating the pump to bottom, producing the well, and circulating the pump back to the surface for repair or size change. Free pump installations require that a bottomhole assembly (BHA) be run in on the tubing string. The BHA consists of a seating shoe and one or more seal bores above it and serves as a receptacle for the pump itself. BHA's are of robust construction and use corrosion-resistant sealing bores to ensure a long life in the downhole environment. Once run in on the tubing string, they normally remain in place for years, even though the downhole pump may be circulated in and out numerous times for repair or resizing. As shown in Fig. 6.3, a wireline-retrievable standing valve is landed in the seating shoe below the pump. The pump is run in the hole by placing it in the power-fluid tubing string and circulating power fluid in the normal direction. When the pump reaches bottom, it enters the seal bores, begins stroking, and opens the standing valve. During normal pumping, this valve is always held

open by well fluids drawn into the pump suction. During pump-out, the normal flow of fluids is reversed at the surface with appropriate valving, and pressure is applied to the discharge flow path of the pump. This reversal of flow closes the standing valve and permits the pump to be circulated to the surface. Circulating the pump out normally takes from 30 minutes to 2 hours, depending on the well depth and the circulating flow rate.

The benefits of being able to circulate the downhole pump in and out of the well include reduced downtime and the ability to operate without a pulling unit for tubing, cable, or rod removal. Another significant advantage is that pressure and temperature recorders can be mounted on the pump to monitor downhole conditions with different pumping rates. At the conclusion of the test, circulating the pump to the surface also retrieves the recorder. Leakage of tubing pressure can be checked by substituting a dummy pump for the normal production unit. Steaming, acidizing, or other chemical treatment of the formation can be done if the pump is circulated out and the standing valve is wirelined out. A flow-through blanking tool may be run instead of the pump for such treatments if isolation of the power fluid and discharge flow paths is desired.

The casing free installation, shown in Fig. 6.2c, is attractive from an initial-cost standpoint because it uses only one string of tubing. At first glance it seems to be the same as the fixed casing design. The crucial difference is that, instead of being attached to the end of the power-fluid string, the pump fits inside it to allow circulation into and

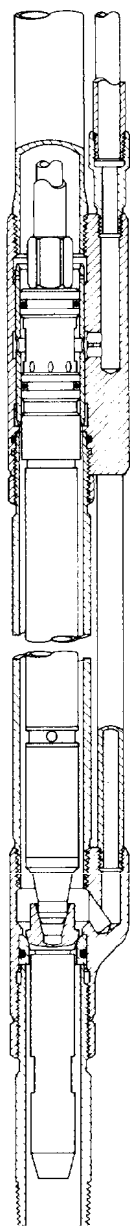


Fig. 6.4—Free-pump, parallel, closed-power BHA.

out of the well. For a given-diameter pump, this requires a larger-diameter power-fluid string, which reduces the annular flow path for the discharge fluids. In most cases, more than adequate flow area remains. Tubing as small as 1 1/2 in. can be run in systems with 2 7/8-in. tubing used as casing. In 1 1/2-in. tubing, only jet pumps can be used. In 2 3/8-in. or larger tubing, either jet or reciprocating pumps can be used. Usually, 2 3/8-in. power-fluid tubing is used in 4-in. or larger casing, 2 7/8-in. tubing in 5 1/2-in. or larger casing, and 3 1/2-in. tubing in 6 3/8-in. casing or larger. Only a very few free-pump installations have been made for 4 1/2-in. or larger tubing strings. Because the BHA sits on a packer, the pump must handle all the gas from the well in addition to the liquids. A gas-vent string can be run to below the packer if gas interference limits pump performance. Such an installation is shown in Fig. 6.2d. In both the vented and unvented systems, the power fluid mixes with the produced fluids and returns to the surface.

In wells where the produced fluids should be kept off the casing wall or where gas venting is desired, the parallel free installation should be considered. This installation, which requires two parallel tubing strings, normally does not require a packer. As shown in Fig. 6.2e, the BHA is suspended on the power-fluid tubing string, and the return string is either screwed into the BHA or is run separately with a landing spear that enters a bowl above the BHA. The tubing/casing annulus serves as a gas-vent passage, and to take full advantage of this, the unit should be set below the perforations.

If the well is not pumped off fully, well fluids will rise above the BHA until the bottomhole pressure (BHP, pump-suction pressure) increases to the point that the well inflow rate and BHP match the inflow performance relationship (IPR) curve of the well. This will expose some of the casing above the perforations to well fluids. In some cases, this may be desirable to prevent collapse of the casing, but in corrosive wells, such as those encountered in CO₂ flooding or with H₂S present, it may be undesirable. In such a case, a packer may be set above the perforations, although the gas-vent feature is then lost unless another gas-vent string is run to below the packer.

The size of the downhole pump dictates the power-fluid tubing size, and the casing size dictates how large the parallel return string can be. When the return string is limited in size, fluid friction may restrict the obtainable production or the practical setting depth.

Closed Power-Fluid Systems

All the installations discussed so far are open power-fluid types. This means that the power fluid and the produced fluid are mixed together after leaving the downhole pump and return to the surface together in a common flow passage. Jet pumps are inherently open power-fluid pumps because the energy transfer depends on mixing the power fluid and produced fluid. Reciprocating pumps, however, keep the power and produced fluids separate during the energy transfer process because there is a separate piston (or piston face) for each fluid. If the BHA has appropriate seal bores and passages to keep the two fluids separated, the power fluid can be returned to the surface in a separate tubing string. The extra tubing string for the power-fluid return classifies these installations in the

parallel free category. An example of a *closed power-fluid installation* is shown in Fig. 6.4. The principal advantage of closed power-fluid installations is that only the produced fluids need to go through the surface separating facilities, and the power fluid remains in a separate, closed loop. The resulting smaller surface facilities may be desirable in certain areas, such as townsite leases and offshore installations. In principle, the power-fluid cleanliness can be maintained better because it is not contaminated with well fluids. When water is used as the power fluid, it is generally necessary to add small amounts of corrosion inhibitors and lubricants. These would be lost in the open system, but are retained in the closed system. Offsetting the advantages of the closed system are the higher initial cost of the extra tubing string and more complex pump and BHA. Most closed power-fluid installations are found in the urban and offshore wells of California.

Reverse Flow Systems

Two considerations—the need to keep produced fluid off the casing and to minimize fluid-friction losses—have led to the use of reverse-flow installations (also known as reverse-circulation installations) in some wells. A reverse-flow casing installation is shown in Fig. 6.5. These systems are most commonly used with jet pumps, although a few installations have been made with reciprocating pumps. The casing system uses the tubing/casing annulus for power fluid, and the tubing string, which contains the pump, is used for the combined power fluid and production. This protects the casing with inhibited power fluid and is most useful when severe corrosion is anticipated. It does require the use of a heavier wall casing to avoid bursting it when power-fluid pressure is applied. The parallel system uses the smaller-size string for power fluid and the larger main string that contains the pump for the combined power fluid and production. The primary advantages of this system are reduced friction, gas venting, and protection of the casing. As discussed in the section on the parallel free design, complete casing isolation requires a packer below the BHA. Both types of reverse-flow installations may require a latch or friction hold-down to position the pump in the BHA during startup or to retain it in position during pumping, depending on the balance of forces on the downhole pump.

In reverse-flow installations, the pump is wirelined often in and out of the well, but a modified form of the free pump feature can be used. With jet pumps, the pump is run in with a pusher-type locomotive, which then circulates to the surface during pumping. To retrieve the pump, a similar blanked-off locomotive with a fishing tool attached is circulated down and latched to the pump. When flow is established in the normal pumping mode direction, the pump will surface. This sequence of operations is shown in Fig. 6.6. Fig. 6.7 shows a reverse-flow installation with a reciprocating pump. Because the engine and pump valving in these pumps does not permit flow-back to the pump suction for unseating the pump, a BHA side line must be run to the bottom of the pump. The latch assembly on top of the pump keeps it on seat during normal pumping. To retrieve the pump, a releasing tool is dropped or wirelined before the pump is circulated to the surface. Once the latch is released, the flow of fluid in the normal pumping mode will surface the pump.

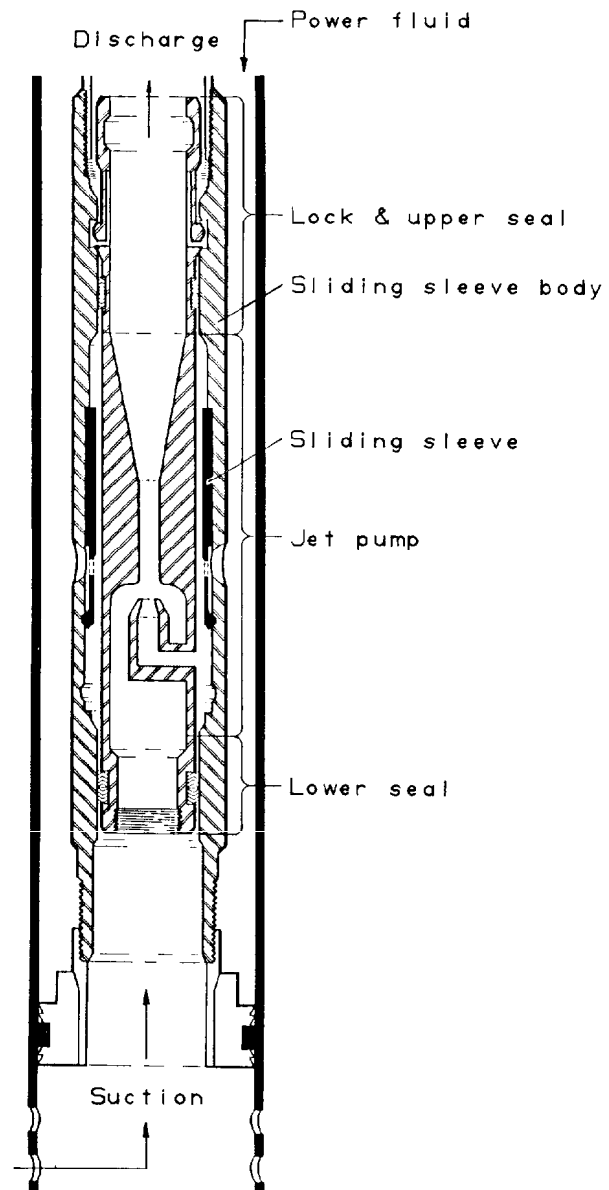


Fig. 6.5—Reverse-flow jet-pump casing type in sliding sleeve.

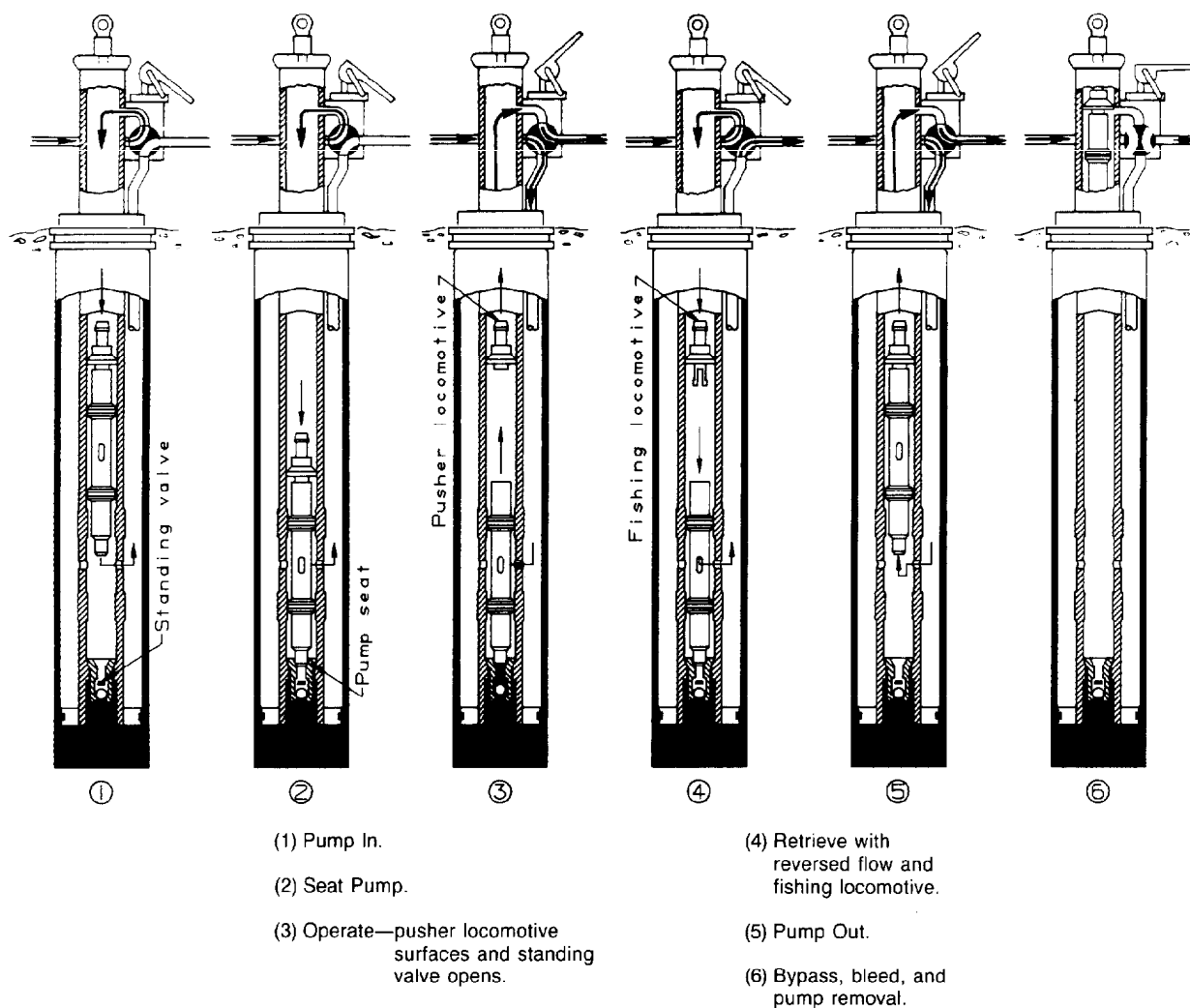


Fig. 6.6—Reverse-flow, free-pump cycle.

TFL Installations

TFL installations have been developed for offshore locations to allow circulation of various downhole tools to the bottom of remote wells from a central platform. A typical installation is shown in Fig. 6.8. Because a 5-ft-radius loop is an integral part of the subsea wellhead installation, the size of the tools that can be circulated through it is limited. Of the various artificial-lift tools, only gas-lift valves and hydraulic jet pumps are sufficiently compact to be compatible with the system. When jet pumps are used, they may be normal-flow or reverse-flow types. Fig. 6.9 is an example of the reverse-flow installation used with TFL. The normal-flow installation is the simplest because it is essentially a parallel free installation and does not require special latches or holdowns. However, the pump has more complex internal fluid passages and the discharge fluid passes through the crossover port of the downhole H-member, which serves as a BHA. Because of the potential for erosion and corrosion of the crossover

member, many operators prefer the reverse-flow installation shown in Fig. 6.9. Here, only the power fluid passes through the crossover port, and the pump flow passages are of a simpler design and can have a higher capacity. Note the compactness of the pump and the use of universal joints that allow flexibility between the pump and the lower seal section. Circulating the pump in and out, however, is more complex, and the procedures described for non-TFL reverse-flow installations must be used.

The dual-sleeve side-door choke is probably the most important item in the string other than the pump itself when TFL operations are performed. This item is run open as shown to allow bypass past the pump for circulating tools into and out of the hole because not much fluid can be circulated through the pump nozzle. Once pump operations are ready to begin, the sleeve is closed by pressuring both strings. When pulling the pump, the sleeve is reopened by pressuring the tubing string that the pump is landed in, and circulation is then re-established.

Dual Wells. Hydraulic pumps lend themselves to the complex problem of the production of two separate zones in a single wellbore. When the two zones have different reservoir pressures, it is not practical to allow communication between them because the higher-pressure zone will flow into the lower-pressure zone. To meet the artificial lift requirements of the two distinct zones, two downhole pumps are usually required. It would be highly unusual if the same power-fluid pressure and rate were required for each zone; consequently, a separate power-fluid line for each pump is usually required. A number of plumbing configurations are possible. One option is shown in Fig. 6.10. The two pumps are physically connected and are run in and retrieved as a unit. In some cases, dual zones have been produced separately by use of double pump ends with a common engine.

Tandem Pumps. When the well capacity requirements exceed what can be produced by a single pump, it is possible to install two pumps in parallel or tandem to double the displacement of the downhole equipment. Again, the pumps are physically connected to form a single unit, but each pump is free to run independently.

Historically, tandem pump installations have used reciprocating pumps. The downhole arrangement is similar to that of Fig. 6.10, but without the passages that route fluid from two separate zones. It is possible to use jet pumps in the same manner, but this is rarely done because it is usually possible to get sufficient capacity in a single jet pump. Since the introduction of jet pumps about 1970, high-volume hydraulically pumped wells have generally used jet pumps instead of tandem reciprocating pumps.

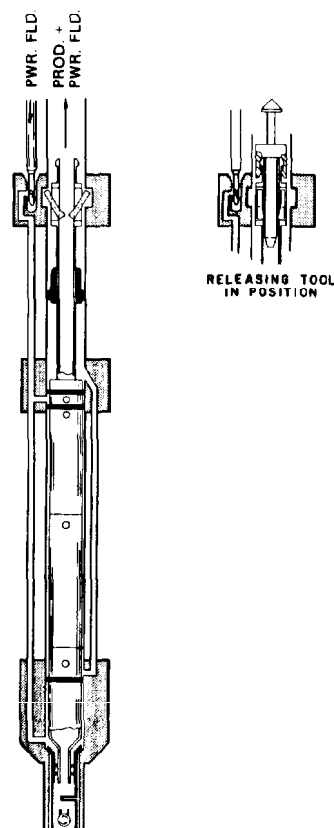


Fig. 6.7—Reverse-flow tubing arrangement (stroking pump).

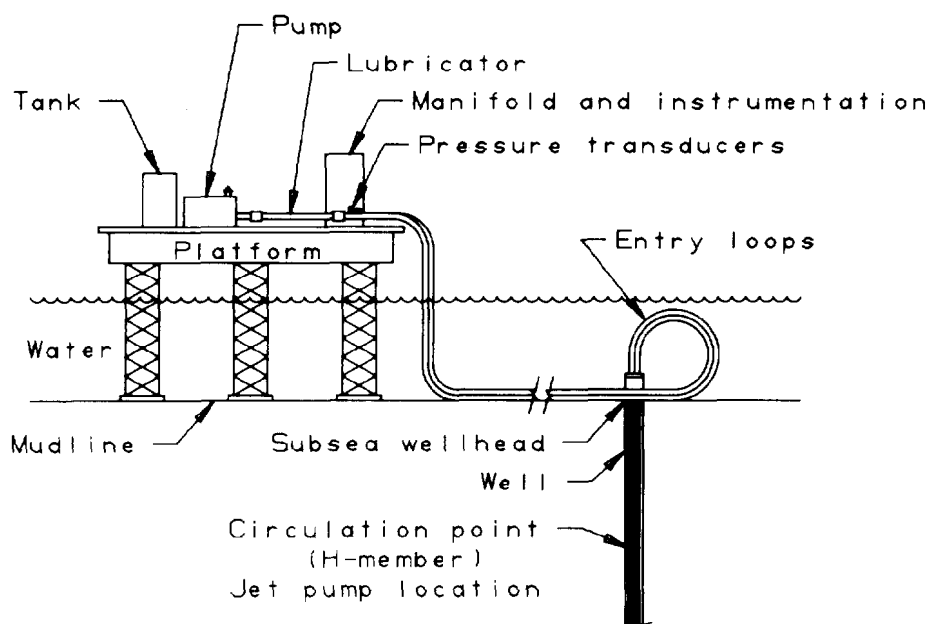


Fig. 6.8—Typical offshore TFL installation.

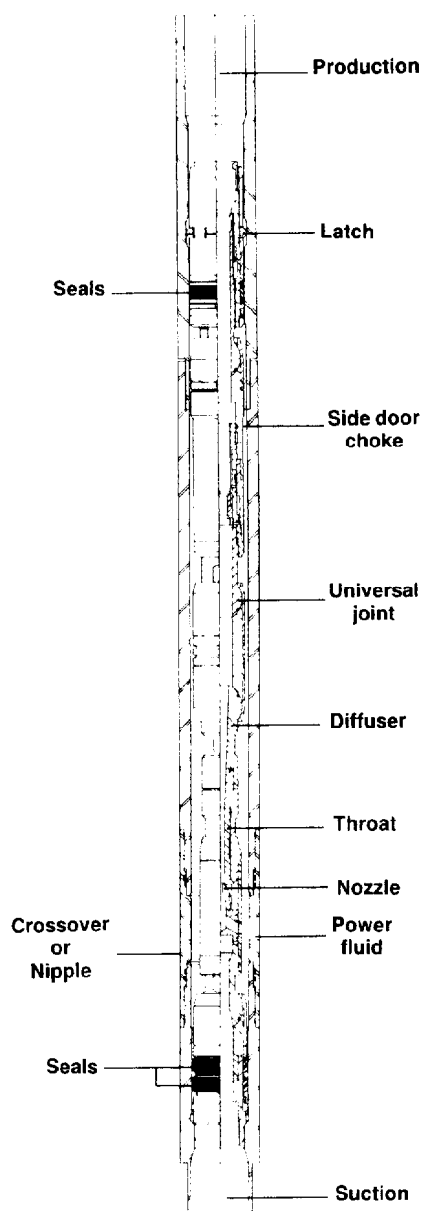


Fig. 6.9—Reverse-flow TFL jet pump.

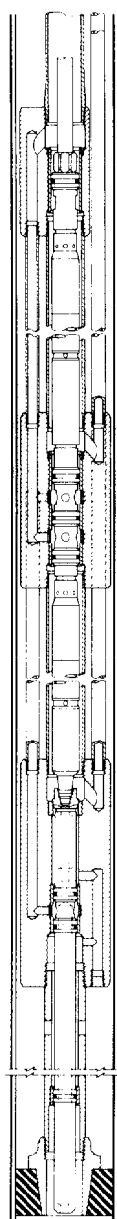


Fig. 6.10—Dual-zone installation with two free pumps operating in tandem, gas from upper zone produced through casing.

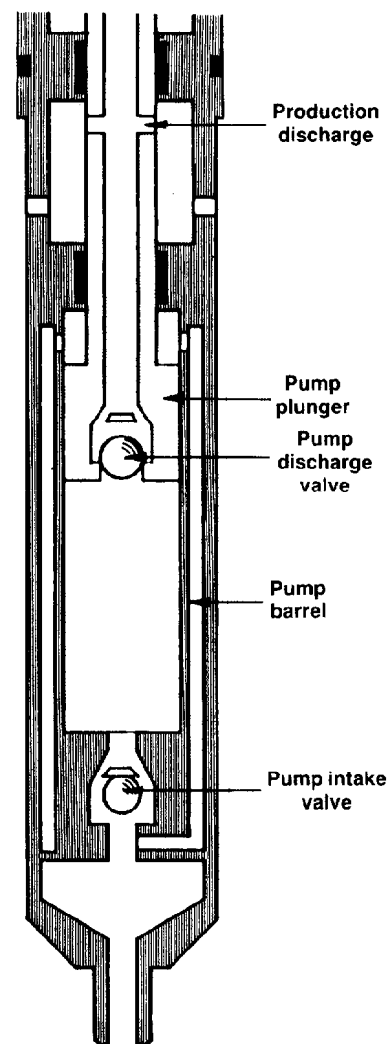


Fig. 6.11—Single-acting pump end.

Principles of Operation— Reciprocating Pumps

The pump end of a hydraulic downhole pump is similar to a sucker-rod pump because it uses a rod-actuated plunger (also called the pump piston) and two or more check valves. The pump can be either single-acting or double-acting. A single-acting pump follows rod-pump design practices closely and is called single-acting because it displaces fluid to the surface on either the upstroke or downstroke (but not on both). An example is shown schematically in Fig. 6.11. Fig. 6.12 shows a double-acting pump that has suction and discharge valves for both sides of the pump plunger, which enables it to displace fluids to the surface on both the upstroke and downstroke.

With either system, motion of the plunger away from a suction valve lowers the pressure that holds the valve closed, it opens as the pressure drops, and well fluids are allowed to enter the barrel or cylinder. At the end of the stroke, the plunger motion reverses, which forces the suction valve to close and opens the discharge valving.

In a sucker-rod installation, the rod that actuates the pump plunger extends to the surface of the well and connects to the pumping unit. In hydraulic pumps, however, the rod is quite short and extends only to the engine piston. The engine piston is constructed similarly to the pump plunger and is exposed to the power-fluid supply, which

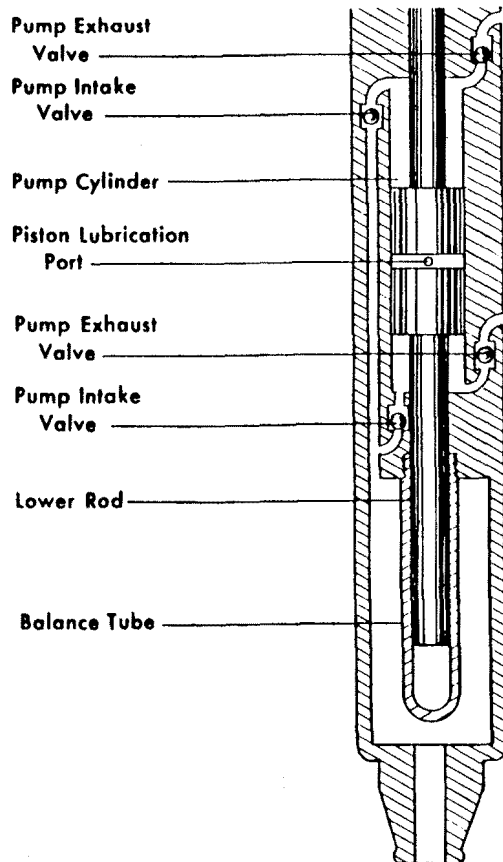


Fig. 6.12—Double-acting pump end.

is under the control of the engine valve. The engine valve reverses the flow of the power fluid on alternate half-strokes and causes the engine piston to reciprocate back and forth. Four-way engine valves are used with engines that switch from high-pressure power-fluid to low-pressure power-fluid exhaust on both sides of the engine piston in an alternating manner. These engine (or reversing) valves are used with double-acting pump ends to give equal stroking force on both upstroke and downstroke. An example of such an engine connected to a double-acting pump is illustrated in Fig. 6.13.

Three-way engine valves are used with unequal-area engine pistons that always have high-pressure power fluid on one side, and switch the power-fluid pressure from high to low pressure on the other face of the piston. This type of reversing valve is common with single-acting pumps that do not require a high force on the half-stroke that is not displacing produced fluid to the surface. An example of this type of engine attached to a single-acting pump is illustrated in Fig. 6.14.

The engine or reversing valve can be signaled by a variety of means. Commonly, ports on a rod direct pressures to control areas on the engine valve at the extremes of the upstroke and downstroke, causing the valve to shift hydraulically. The shifting of the engine valve redirects the flow of power fluid to the engine piston and causes the reversal of the rod-and-plunger system. Alternatively, the engine valve can be mechanically bumped from one position to the other by the rod and plunger system as it

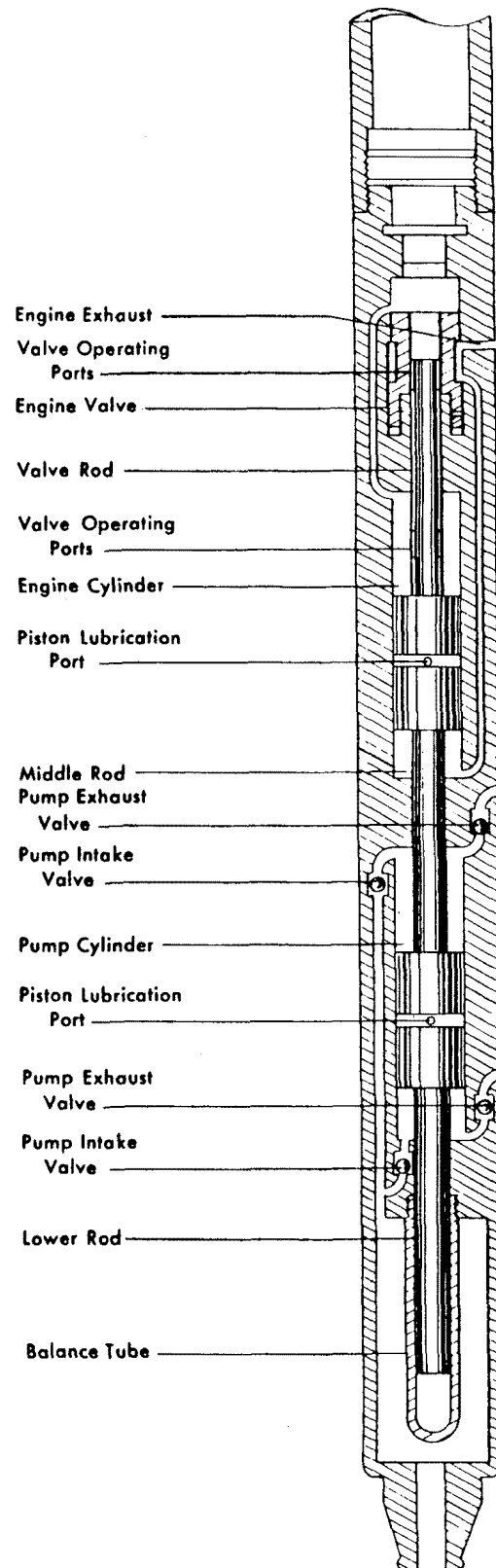


Fig. 6.13—Double-acting downhole unit.

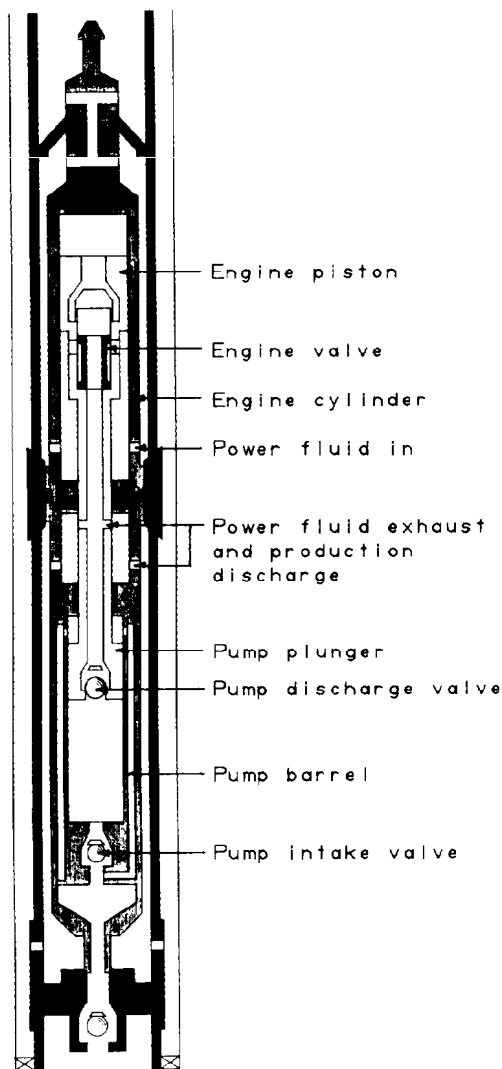


Fig. 6.14—Single-acting downhole unit.

nears the ends of the upstroke and downstroke. Combinations of mechanical and hydraulic shifting are possible. The engine valve may be located above the rod-and-plunger system, in the middle of the pump, or in the engine piston.

Note that the two designs illustrated and discussed do not exhaust the design possibilities offered by the various pump manufacturers. Examples of combinations of these and other design concepts can be seen in the cross-section schematics of the various pump types that accompany the pump specifications in Tables 6.1 through 6.4 and Figs. 6.15 through 6.18. Common to all the designs, however, is the concept of a reversing valve that causes an engine piston (or pistons) to reciprocate back and forth. This strokes the pump plunger (or plungers) that lifts fluid from the well.

Because the engine and pump are closely coupled into one unit, the stroke length can be controlled accurately. With a precise stroke length, the unswept area or clearance volume at each end of the stroke can be kept very small, leading to high compression ratios. This is very

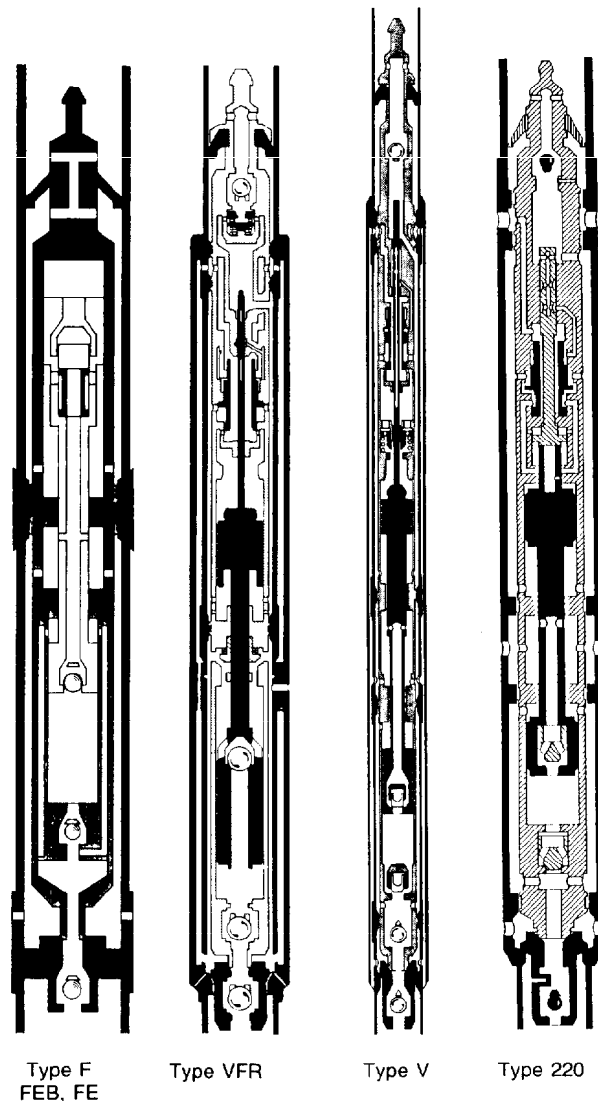


Fig. 6.15—Manufacturer "A" pump types for Table 6.1.

important in maintaining high volumetric efficiency when gas is present and generally prevents gas locking in hydraulic pumps. The engine valves and their switching mechanisms usually include controls to provide a smooth reversal and to limit the plunger speed under unloaded conditions. The unloaded plunger speed control is often called governing and minimizes fluid pound when the pump is not fully loaded with liquid. In this way, shock loads in the pump and water hammer in the tubing strings are softened, which reduces stresses and increases life.

Pressures and Forces in Reciprocating Pumps

Reciprocating hydraulic pumps are hydrostatic devices. This means that the operation of the unit depends on pressures acting against piston faces to generate forces, and that the fluid velocities are low enough that dynamic effects can be neglected. A pressurized fluid exerts a force against the walls of its container. This force is perpendicular to the walls regardless of their orientation. If the pressurized container consists of a cylinder with one end blanked off and the other end fitted with a movable plung-

TABLE 6.1—RECIPROCATING PUMP SPECIFICATIONS, MANUFACTURER “A”

Pump	Displacement					P/E	Maximum Rated Speed (strokes/min)
	B/D per strokes/min		Rated Speed (B/D)				
	Pump	Engine	Pump	Engine	Total		
Type F, Fe, FEB							
2 ³ / ₈ -in. tubing							
F201311	3.0	4.2	204	286	490	0.71	68
F201313	4.2	4.2	285	286	571	1.00	68
F201611	3.0	6.4	204	435	639	0.47	68
F201613	4.2	6.4	285	435	720	0.66	68
FEB201613	6.2	9.4	340	517	857	0.66	55
FEB201616	9.4	9.4	517	517	1,034	1.00	55
2 ⁷ / ₈ -in. tubing							
F251611	3.3	7.0	214	455	669	0.47	65
F251613	4.6	7.0	299	455	754	0.66	65
F251616	7.0	7.0	455	455	910	1.00	65
FE252011	5.0	16.5	255	842	1,097	0.30	51
FE252013	7.0	16.5	357	842	1,199	0.42	51
FE252016	10.6	16.5	540	842	1,382	0.64	51
Type VFR							
2 ³ / ₈ -in. tubing							
VFR201611	2.12	4.24	318	636	954	0.62	150
VFR201613	2.96	4.24	444	636	1,080	0.87	150
VFR201616	4.49	4.24	673	636	1,309	1.32	150
VFR20161613	2.96	6.86	444	1,029	1,473	0.54	150
VFR20161616	4.49	6.86	673	1,029	1,702	0.81	150
2 ⁷ / ₈ -in. tubing							
VFR252015	5.25	8.89	630	1,067	1,697	0.74	120
VFR252017	7.15	8.89	858	1,067	1,925	1.00	120
VFR252020	9.33	8.89	1,119	1,067	2,186	1.32	120
VFR25202015	5.25	15.16	630	1,819	2,449	0.41	120
VFR25202017	7.15	15.16	858	1,819	2,677	0.56	120
VFR25202020	9.33	15.16	1,119	1,819	2,938	0.73	120
Type V							
2 ⁷ / ₈ -in. tubing							
V-25-11-118	6.31	5.33	1,229	1,098	2,397	1.18	206
V-25-11-095	6.31	6.66	1,299	1,372	2,671	0.96	206
V-25-11-076	3.93	5.33	550	746	1,296	0.76	140
V-25-11-061	3.93	6.66	550	932	1,482	0.61	140
V-25-21-075	6.31	8.38	1,173	1,559	2,732	0.75	186
V-25-21-063	6.31	10.00	1,072	1,700	2,772	0.63	170
V-25-21-050	3.93	8.38	550	1,173	1,723	0.50	140
V-25-21-041	3.93	10.00	550	1,400	1,950	0.41	140
Type 220							
2 ³ / ₈ -in. tubing							
330-201610	4.22	8.94	422	894	1,316	0.49	100
330-201612	5.46	8.94	546	894	1,440	0.63	100
530-201615	7.86	8.94	786	894	1,680	0.89	100
2 ⁷ / ₈ -in. tubing							
348-252012	8.73	22.35	629	1,609	2,238	0.40	72
348-252015	12.57	22.35	905	1,609	2,514	0.57	72
548-252017	17.11	22.35	1,232	1,609	2,841	0.78	72
548-252019	20.17	22.35	1,452	1,609	3,061	0.93	72
536-252020	25.18	25.18	2,014	2,014	4,028	1.00	80

Note: Pump Size

F, FE, FEB, VFR Types

F

20 Nominal tubing (2 in.)

13 Engine (1.3 in.)

XX Second engine (VFR only)

11 Pump (1.1 in.)

V Types

V

25 Nominal tubing (2 $\frac{1}{2}$ in.)

11 Single engine (double = 21)

118 P/E

220 Series

3 Number of seals

48 Stroke length (in.)

25 Nominal tubing (2 $\frac{1}{2}$ in.)

20 Engine (2.000 in.)

12 Pump (1.200 in.)

Types: F, FE, FEB are single-seal, internal-porting; 220, VFR, and V are multiple-seal, external-porting.

TABLE 6.2—RECIPROCATING PUMP SPECIFICATIONS, MANUFACTURER "B"

Pump	Displacement					P/E	Maximum Rated Speed (strokes/min)
	B/D per strokes/min		Rated Speed (B/D)				
	Pump	Engine	Pump	Engine	Total		
Type A							
2³/₈-in. tubing							
2 × 1-1 ³ / ₁₆	1.15	2.15	139	260	399	0.545	121
2 × 1-1	2.10	2.15	255	260	515	1.000	121
2 × 1-1 ³ / ₁₆	3.25	2.15	393	260	653	1.546	121
2 × 1 ³ / ₁₆ -1	2.10	3.30	255	399	654	0.647	121
2 × 1 ³ / ₁₆ -1 ³ / ₁₆	3.25	3.30	393	399	792	1.000	121
2 × 1 ³ / ₁₆ -1 × 1	4.20	3.30	508	399	907	1.290	121
2 × 1 ³ / ₁₆ -1 ³ / ₁₆ × 1	5.35	3.30	647	399	1,046	1.647	121
2 × 1 ³ / ₁₆ -1 ³ / ₁₆ × 1 ³ / ₁₆	6.50	3.30	787	399	1,186	2.000	121
2⁷/₈-in. tubing							
2 ¹ / ₂ × 1 ¹ / ₄ -1	2.56	5.02	256	502	758	0.520	100
2 ¹ / ₂ × 1 ¹ / ₄ -1 ¹ / ₈	3.67	5.02	367	502	868	0.746	100
2 ¹ / ₂ × 1 ¹ / ₄ -1 ¹ / ₄	4.92	5.02	492	502	994	1.000	100
2 ¹ / ₂ × 1 ¹ / ₄ -1 ⁷ / ₁₆	7.03	5.02	703	502	1,205	1.431	100
2 ¹ / ₂ × 1 ⁷ / ₁₆ -1 ¹ / ₄	4.92	7.13	492	713	1,205	0.700	100
2 ¹ / ₂ × 1 ⁷ / ₁₆ -1 ⁷ / ₁₆	7.03	7.13	703	713	1,416	1.000	100
2 ¹ / ₂ × 1 ⁹ / ₁₆ -1 ⁷ / ₁₆	7.03	9.27	703	927	1,630	0.770	100
2 ¹ / ₂ × 1 ⁹ / ₁₆ -1 ¹ / ₂	7.45	9.27	745	927	1,672	0.820	100
2 ¹ / ₂ × 1 ⁹ / ₁₆ -1 ⁵ / ₈	9.09	9.27	909	927	1,836	1.000	100
2 ¹ / ₂ × 1 ⁷ / ₁₆ -1 ¹ / ₄ × 1 ¹ / ₄	9.84	7.13	984	713	1,697	1.400	100
2 ¹ / ₂ × 1 ⁷ / ₁₆ -1 ⁷ / ₁₆ × 1 ¹ / ₄	11.95	7.13	1,195	713	1,908	1.701	100
2 ¹ / ₂ × 1 ⁷ / ₁₆ -1 ⁷ / ₁₆ × 1 ⁷ / ₁₆	14.06	7.13	1,406	713	2,119	2.000	100
2 ¹ / ₂ × 1 ⁹ / ₁₆ -1 ⁵ / ₈ × 1 ⁵ / ₈	18.18	9.27	1,818	927	2,745	2.000	100
3¹/₂-in. tubing							
3 × 1 ¹ / ₂ -1 ¹ / ₄	5.59	9.61	486	836	1,322	0.592	87
3 × 1 ¹ / ₂ -1 ³ / ₈	7.43	9.61	646	836	1,482	0.787	87
3 × 1 ¹ / ₂ -1 ¹ / ₂	9.44	9.61	821	836	1,657	1.000	87
3 × 1 ¹ / ₂ -1 ³ / ₄	14.00	9.61	1,218	836	2,054	1.480	87
3 × 1 ³ / ₄ -1 ¹ / ₂	9.44	14.17	821	1,233	2,054	0.676	87
3 × 1 ³ / ₄ -1 ³ / ₄	14.00	14.17	1,218	1,233	2,451	1.000	87
3 × 1 ³ / ₄ -1 ¹ / ₄ × 1 ¹ / ₄	11.18	14.17	973	1,233	2,206	0.800	87
3 × 1 ³ / ₄ -1 ¹ / ₂ × 1 ¹ / ₂	18.18	14.17	1,642	1,233	2,875	1.351	87
3 × 1 ³ / ₄ -1 ³ / ₄ × 1 ¹ / ₂	23.44	14.17	2,093	1,233	3,326	1.675	87
3 × 1 ³ / ₄ -1 ³ / ₄ × 1 ³ / ₄	28.00	14.17	2,436	1,233	3,669	2.000	87
4¹/₂-in. tubing							
4 × 2-1 ³ / ₄	14.40	21.44	1,109	1,651	2,760	0.687	77
4 × 2-2	21.00	21.44	1,617	1,651	3,268	1.000	77
4 × 2-2 ³ / ₈	32.50	21.44	2,503	1,651	4,154	1.541	77
4 × 2 ³ / ₈ -2	21.00	32.94	1,617	2,536	4,153	0.649	77
4 × 2 ³ / ₈ -2 ³ / ₈	32.60	32.94	2,503	2,536	5,039	1.000	77
4 × 2 ³ / ₈ -2 × 1 ³ / ₄	35.40	32.94	2,726	2,536	5,262	1.094	77
4 × 2 ³ / ₈ -2 × 2	42.00	32.94	3,234	2,536	5,770	1.299	77
4 × 2 ³ / ₈ -2 ³ / ₈ × 2	53.50	32.94	4,120	2,536	6,656	1.650	77
4 × 2 ³ / ₈ -2 ³ / ₈ × 2 ³ / ₈	65.00	32.94	5,005	2,536	7,541	2.000	77
Type B							
2³/₈-in. tubing							
2 × 1 ³ / ₈ -1 ³ / ₁₆	3.15	4.54	381	549	930	0.700	121
2 × 1 ³ / ₈ -1 ³ / ₈	4.50	4.54	544	549	1,093	1.000	121
2 × 1 ³ / ₈ -1 ³ / ₁₆ × 1 ³ / ₁₆	6.21	4.54	751	549	1,300	1.380	121
2 × 1 ³ / ₈ -1 ³ / ₈ × 1 ³ / ₁₆	7.55	4.54	913	549	1,463	1.680	121
2 × 1 ³ / ₈ -1 ³ / ₈ × 1 ³ / ₈	8.90	4.54	1,076	549	1,625	1.980	121

Notes:

1. Pump size: nominal × engine – pump × pump (in.).
2. Illustrations for single-pump end, double available on A, B, and D.
3. Types: All double-acting.
 - A. Single seal, internal porting.
 - B. Multiple seal, external porting.
 - D. Multiple seal, external porting, double engine.
 - E. Multiple seal, external porting, opposed pistons with central engine.

TABLE 6.2—RECIPROCATING PUMP SPECIFICATIONS, MANUFACTURER "B" (continued)

Pump	Displacement					P/E	Maximum Rated Speed (strokes/min)
	B/D per strokes/min		Rated Speed (B/D)				
	Pump	Engine	Pump	Engine	Total		
Type B							
2⁷/₈-in. tubing							
2 ¹ / ₂ × 1 ³ / ₄ -1 ¹ / ₂	7.44	10.96	744	1,096	1,840	0.685	100
2 ¹ / ₂ × 1 ³ / ₄ -1 ³ / ₄	10.86	10.96	1,086	1,096	2,182	1.000	100
2 ¹ / ₂ × 1 ³ / ₄ -1 ¹ / ₂ × 1 ¹ / ₂	14.52	10.96	1,452	1,096	2,548	1.336	100
2 ¹ / ₂ × 1 ³ / ₄ -1 ³ / ₄ × 1 ¹ / ₂	17.94	10.96	1,794	1,096	2,890	1.652	100
2 ¹ / ₂ × 1 ³ / ₄ -1 ³ / ₄ × 1 ³ / ₄	21.36	10.96	2,136	1,096	3,232	1.957	100
3¹/₂-in. tubing							
3 × 2 ¹ / ₈ -1 ⁷ / ₈	15.96	21.75	1,388	1,892	3,280	0.740	87
3 × 2 ¹ / ₈ -2 ¹ / ₈	21.55	21.75	1,875	1,892	3,767	1.000	87
3 × 2 ¹ / ₈ -1 ⁷ / ₈ × 1 ⁷ / ₈	31.34	21.75	2,726	1,892	4,618	1.454	87
3 × 2 ¹ / ₈ -2 ¹ / ₈ × 1 ⁷ / ₈	36.94	21.75	3,214	1,892	5,106	1.714	87
3 × 2 ¹ / ₈ -2 ¹ / ₈ × 2 ¹ / ₈	42.53	21.75	3,700	1,892	5,592	1.974	87
Type D							
2³/₈-in. tubing							
2 × 1 ³ / ₁₆ × 1 ³ / ₈ -1 ³ / ₁₆	3.15	7.79	381	943	1,324	0.407	121
2 × 1 ³ / ₁₆ × 1 ³ / ₈ -1 ³ / ₈	4.50	7.79	544	943	1,487	0.581	121
2 × 1 ³ / ₁₆ × 1 ³ / ₈ -1 ³ / ₁₆ × 1 ³ / ₁₆	6.21	7.79	751	943	1,694	0.802	121
2 × 1 ³ / ₁₆ × 1 ³ / ₈ -1 ³ / ₈ × 1 ³ / ₁₆	7.55	7.79	914	943	1,857	0.976	121
2 × 1 ³ / ₁₆ × 1 ³ / ₈ -1 ³ / ₈ × 1 ³ / ₈	8.90	7.79	1,076	943	2,019	1.150	121
2⁷/₈-in. tubing							
2 ¹ / ₂ × 1 ⁷ / ₁₆ × 1 ³ / ₄ -1 ¹ / ₂	7.44	17.99	744	1,799	2,543	0.411	100
2 ¹ / ₂ × 1 ⁷ / ₁₆ × 1 ³ / ₄ -1 ³ / ₄	10.86	17.99	1,086	1,799	2,885	0.608	100
2 ¹ / ₂ × 1 ⁷ / ₁₆ × 1 ³ / ₄ -1 ¹ / ₂ × 1 ¹ / ₂	14.52	17.99	1,452	1,799	3,251	0.813	100
2 ¹ / ₂ × 1 ⁷ / ₁₆ × 1 ³ / ₄ -1 ³ / ₄ × 1 ¹ / ₂	17.94	17.99	1,794	1,799	3,593	0.976	100
2 ¹ / ₂ × 1 ⁷ / ₁₆ × 1 ³ / ₄ × 1 ³ / ₄	21.36	17.99	2,136	1,799	3,935	1.196	100
3¹/₂-in. tubing							
3 × 1 ³ / ₄ × 2 ¹ / ₈ -1 ⁷ / ₈	15.96	35.74	1,388	3,109	4,497	0.449	87
3 × 1 ³ / ₄ × 2 ¹ / ₈ -2 ¹ / ₈	21.55	35.74	1,874	3,109	4,983	0.606	87
3 × 1 ³ / ₄ × 2 ¹ / ₈ -1 ⁷ / ₈ × 1 ⁷ / ₈	31.34	35.74	2,726	3,109	5,835	0.882	87
3 × 1 ³ / ₄ × 2 ¹ / ₈ -2 ¹ / ₈ × 1 ⁷ / ₈	36.94	35.74	3,213	3,109	6,322	1.039	87
3 × 1 ³ / ₄ × 2 ¹ / ₈ -2 ¹ / ₈ × 2 ¹ / ₈	42.53	35.74	3,700	3,109	6,809	1.197	87
Type E							
2³/₈-in. tubing							
2 × 1 ³ / ₈	20.27	17.59	1,317	1,143	2,454	1.152	65
2⁷/₈-in. tubing							
2 ¹ / ₂ × 1 ³ / ₄	40.63	35.45	2,400	2,092	4,491	1.146	59
3¹/₂-in. tubing							
3 × 2 ¹ / ₈	71.70	62.77	4,007	3,515	7,522	1.142	56

Notes:

1. Pump size: nominal × engine – pump × pump (in.)
2. Illustrations for single-pump end, double available on A, B, and D.
3. Types: All double-acting.
 - A. Single seal, internal porting.
 - B. Multiple seal, external porting.
 - D. Multiple seal, external porting, double engine.
 - E. Multiple seal, external porting, opposed pistons with central engine.

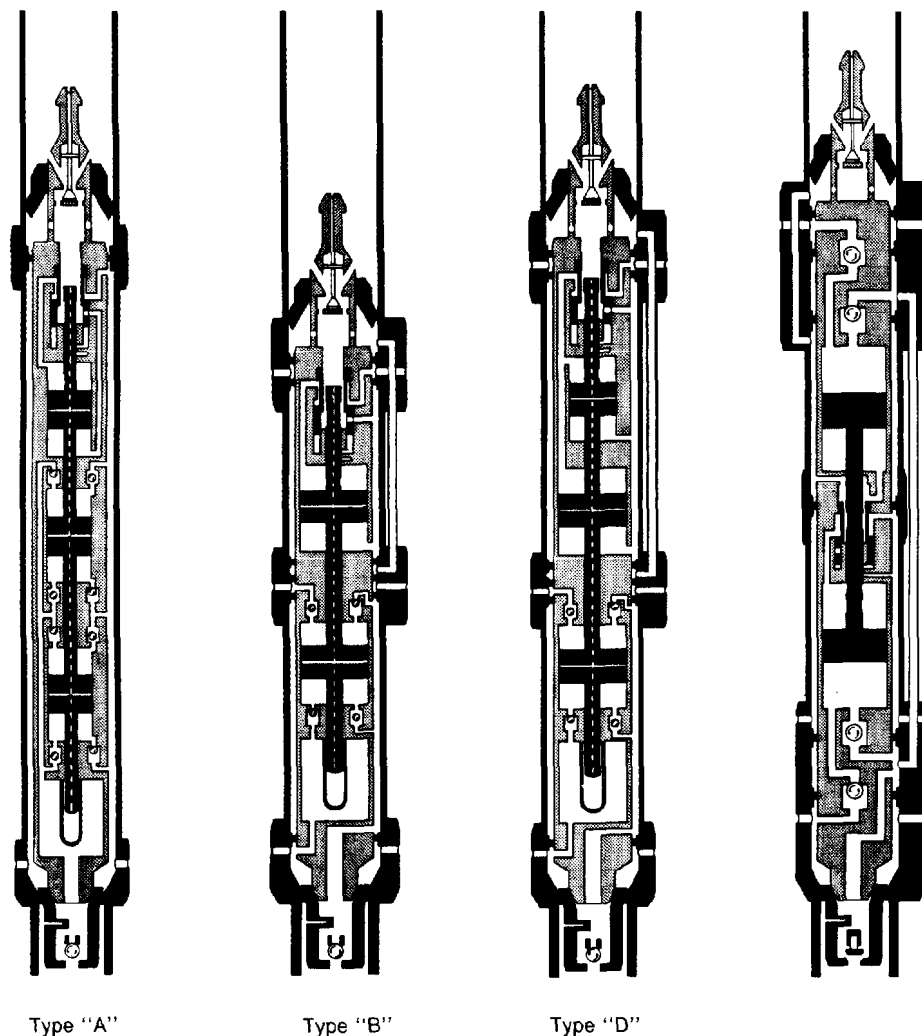


Fig. 6.16—Manufacturer "B" pump types for Table 6.2.

er, as shown in Fig. 6.19, a force will have to be applied to the plunger to resist the force exerted by the pressurized fluid. A force of 1,000 lbf will be required to restrain a plunger whose cross-sectional area is 1 sq in. if the pressure in the cylinder is 1,000 psi.

$$F = pA, \dots\dots\dots (1)$$

where

F = force, lbf,
 p = pressure, psi, and
 A = area, sq in.

This is the condition of static equilibrium for the plunger when all forces balance and no movement is taking place. Suppose next that a supply line is connected to the blanked-off end of the cylinder, as shown in Fig. 6.20, and that a pump supplies fluid at a rate of 1 cu in./sec while maintaining the pressure at 1,000 psi. This will cause the plunger to move in the cylinder at the constant speed of 1 in./sec against the 1,000-lbf restraining force. In this condition of dynamic equilibrium, work can be done by the system because work is defined as force times distance.

$$W = FL, \dots\dots\dots (2)$$

where W = work, in.-lbf, and L = distance, in.

If the plunger moves 12 in., it will do 12,000 in.-lbf of work (or 1,000 ft-lbf of work). Because the plunger is moving at 1 in./sec, it will take 12 seconds to complete its travel. Power is defined as the rate of doing work.

$$P = W/t, \dots\dots\dots (3)$$

where

P = power, ft-lbf/sec,
 t = time, seconds, and
 W = work, ft-lbf.

In this example, the power is 1,000 ft-lbf of work in 12 seconds, or 83.3 ft-lbf/sec. Horsepower is defined as 550 ft-lbf/sec (or 6,600 in.-lbf/sec), which means that the horsepower of this system can be represented as

$$P_h = \frac{P}{550}, \dots\dots\dots (4)$$

where P_h = horsepower, hp.

TABLE 6.3—RECIPROCATING PUMP SPECIFICATIONS, MANUFACTURER "C"

Pump	Displacement					P/E	Maximum Rated Speed (strokes/min)
	B/D per strokes/min		Rated Speed (B/D)				
	Pump	Engine	Pump	Engine	Total		
Powerlift I							
2³/₈-in. tubing							
2 × 1 ⁵ / ₈ × 1 ¹ / ₁₆	6.45	15.08	225	528	753	0.52	35
2 × 1 ⁵ / ₈ × 1 ¹ / ₄	8.92	15.08	312	528	840	0.72	35
2 × 1 ⁵ / ₈ × 1 ¹ / ₂	11.96	14.03	478	561	1,039	1.16	40
2 × 1 ⁵ / ₈ × 1 ³ / ₈	14.03	14.03	561	561	1,122	1.36	40
2⁷/₈-in. tubing							
2 ¹ / ₂ × 2 × 1 ¹ / ₄	12.02	30.80	264	678	942	0.44	22
2 ¹ / ₂ × 2 × 1 ¹ / ₂	17.30	30.80	467	832	1,299	0.68	27
2 ¹ / ₂ × 2 × 1 ³ / ₈	20.30	30.80	547	832	1,379	0.80	27
2 ¹ / ₂ × 2 × 1 ³ / ₄	23.60	30.80	826	1,078	1,904	1.06	35
2 ¹ / ₂ × 2 × 2	30.80	30.80	1,078	1,078	2,156	1.38	35
2 ¹ / ₂ × 1 ⁵ / ₈ × 1 ¹ / ₁₆	6.45	15.08	225	528	753	0.52	35
2 ¹ / ₂ × 1 ⁵ / ₈ × 1 ¹ / ₄	8.92	15.08	312	528	840	0.72	35
2 ¹ / ₂ × 1 ⁵ / ₈ × 1 ¹ / ₂	12.85	15.08	450	528	978	1.03	35
2 ¹ / ₂ × 1 ⁵ / ₈ × 1 ³ / ₈	15.08	15.08	528	528	1,056	1.21	35
2 ¹ / ₂ × 1 ⁵ / ₈ × 1 ¹ / ₁₆	8.69	20.30	234	548	782	0.52	27
2 ¹ / ₂ × 1 ⁵ / ₈ × 1 ¹ / ₄	12.02	20.30	325	548	873	0.72	27
2 ¹ / ₂ × 1 ⁵ / ₈ × 1 ¹ / ₂	17.03	20.30	467	548	1,015	1.03	27
2 ¹ / ₂ × 1 ⁵ / ₈ × 1 ³ / ₈	20.30	20.30	547	548	1,095	1.21	27
3¹/₂-in. tubing							
3 × 2 ¹ / ₂ × 2 ¹ / ₂	43.71	43.71	1,311	1,311	2,622	1.21	30
3 × 2 ¹ / ₂ × 2 ³ / ₄	35.41	43.71	1,062	1,311	2,373	0.98	30
3 × 2 ¹ / ₂ × 2	27.98	43.71	840	1,311	2,151	0.77	30
3 × 2 ¹ / ₂ × 1 ³ / ₄	21.42	43.71	643	1,311	1,954	0.59	30
Powerlift II							
2³/₈-in. tubing							
2 × 1 ¹ / ₁₆	5.53	12.10	597	1,307	1,904	0.524	108
2 × 1 ¹ / ₄	7.65	12.10	826	1,307	2,133	0.725	108
2 × 1 ³ / ₈	30.00	26.35	1,560	1,370	2,930	1.147	52
2⁷/₈-in. tubing							
2 ¹ / ₂ × 1 ¹ / ₂	12.59	17.69	1,322	1,857	3,179	0.725	105
2 ¹ / ₂ × 1 ¹ / ₄	8.74	17.69	918	1,857	2,775	0.503	105
2 ¹ / ₂ × 1 ³ / ₈	50.00	43.97	2,500	2,199	4,699	1.146	50

Notes:

1. Pump size: nominal × engine diameter × pump diameter.

2. Types:

Powerlift I: single seal, internal porting.

Powerlift II: Multiple seal, external porting, opposed pistons with central engine.

In our example, 83.3 ft-lbf/sec corresponds to 0.15 hp. If we were to supply the pressurized fluid at 2 cu in./sec, the plunger would move the 12 in. in 6 seconds. The work done would be the same, but because it would be done in half the time, the hp would be twice as great.

Note that we have interpreted the hp in terms of the work done through the plunger per unit time. This power is supplied by the pump pressurizing the fluid. The plunger transforms the fluid power to mechanical. This is the action of a hydraulic motor. The hydraulic equivalent of 0.15 hp is a flow rate of 1 cu in./sec at 1,000 psi. If the flow rate in cubic inches per second is multiplied by the pressure in pounds force per square inch, the product will have units of inch-pounds per second, which are the dimensions of power. Conversion of units will show that 1 cu in./sec is the same as 8.905 B/D. If 8.905 B/D at 1,000 psi is 0.15 hp, it follows that

$$P_h = q \times p \times 0.000017, \dots \dots \dots (5)$$

where q = flow rate, B/D, and p = pressure, psi.

Eq. 5 shows that the same power can be obtained with high flow rates at low pressure, or with lower flow rates at a higher pressure. This is a very useful feature of hydraulic power transmission. Only the flow rate and the pressure enter into this relationship; the density, or specific gravity, of the fluid does not.

The process described can be reversed. A force of 1,000 lbf applied to the plunger in Fig. 6.20 can force fluid out of the line at a pressure of 1,000 psi. In this case, the mechanical power of the plunger would be transformed into fluid power as it is done in pumps.

A useful consequence of the relationship expressed in Eq. 1 is demonstrated in Fig. 6.21. Two plungers of different diameters are connected together by a rod. The section of the assembly occupied by the connecting rod is vented to the atmosphere. The face area of the larger plunger is 2 sq in. and the face of the smaller plunger is 1 sq in. Fluid at 1,000-psi pressure is supplied to the cylinder that contains the larger plunger. This causes the plunger to push through the rod and against the smaller plunger with a force of 2,000 lbf. To restrain the motion of the rod-and-plunger system, an opposing force of 2,000

TABLE 6.4—RECIPROCATING PUMP SPECIFICATIONS, MANUFACTURER "D"

Pump	Displacement					P/E	Maximum Rated Speed (strokes/min)
	B/D per strokes/min		Rated Speed (B/D)				
	Pump	Engine	Pump	Engine	Total		
900 Series							
2³/₈-in. tubing							
2 × 1 ¹ / ₁₆	3.5	6.65	95	180	275	0.66	27
2 × 1 ¹ / ₈	7.0	13.30	189	359	548	0.66	27
2 × 1 ¹ / ₄	9.6	13.30	259	359	618	0.93	27
2 × 1 ¹ / ₂	13.8	13.30	372	359	731	1.33	27
2⁷/₈-in. tubing							
2 ¹ / ₂ × 1 ¹ / ₁₆	3.5	10.6	95	286	381	0.43	27
2 ¹ / ₂ × 1 ¹ / ₈	7.0	21.2	189	572	761	0.43	27
2 ¹ / ₂ × 1 ¹ / ₄	9.5	21.2	256	572	828	0.58	27
2 ¹ / ₂ × 1 ¹ / ₂	13.7	21.2	370	572	942	0.83	27
2 ¹ / ₂ × 1 ³ / ₄	18.6	21.2	502	572	1,074	1.13	27
2 ¹ / ₂ × 2	24.2	21.2	654	572	1,226	1.47	27
3¹/₂-in. tubing							
3 × 1 ¹ / ₂	15.5	36.1	419	975	1,394	0.53	27
3 × 1 ³ / ₄	21.1	36.1	570	975	1,545	0.72	27
3 × 2	27.5	36.1	743	975	1,718	0.94	27
3 × 2 ¹ / ₄	34.8	36.1	940	975	1,915	1.20	27
3 × 2 ¹ / ₂	43.0	36.1	1,160	975	2,135	1.47	27
4¹/₂-in. tubing							
4 × 2 ¹ / ₄	34.8	63.5	940	1,715	2,655	0.68	27
4 × 2 ³ / ₄	52.0	63.5	1,404	1,715	3,119	1.01	27
4 × 3 ¹ / ₄	72.6	63.5	1,960	1,715	3,675	1.41	27
924 Series							
2⁷/₈-in. tubing							
7045-92-4210	4.7	7.25	287	442	729	0.65	61
7065-92-4210	9.4	14.5	574	885	1,459	0.65	61
7100-92-4210	14.5	14.5	885	885	1,770	1.00	61

Notes: Pump Size: 900 Series—nominal × pump plunger diameter.
 Types: 900—Single-seal, single-acting, internal-porting;
 924—Single-seal, double-acting, internal-porting.

lbf must be applied to the smaller plunger. This can be accomplished with fluid in the smaller cylinder at 2,000 psi. If these pressures are maintained and fluid is supplied to the larger cylinder at a constant rate, the rod-and-plunger system will move to the right at a constant rate. Fluid will be forced out of the smaller cylinder at half the rate it is supplied to the larger cylinder, but with twice the pressure. This hydraulic transformer process is reversible, which would entail supplying 2,000-psi fluid to the smaller cylinder to make 1,000-psi fluid flow out of the larger cylinder at twice the flow rate supplied to the smaller cylinder. In either case, the input and output horsepowers are the same because no losses have been considered.

The characteristics of such a rod-and-plunger system can be used to advantage in hydraulic pumps. In shallow wells where the pressure requirements of the pump are low, a large pump plunger can be used in conjunction with a small engine piston without requiring excessively high pressures to be supplied to the engine. In deeper wells, where the discharge pressure of the pump will be high, a small pump plunger is used in conjunction with a large engine piston to reduce the power-fluid pressure requirement. The smaller pump plunger will, however, produce less fluid at the same stroking rate than the larger pump

plunger. Hydraulic pump manufacturers offer a variety of engine and pump combinations to meet the requirements of different flow rates and depth settings (see examples in Tables 6.1 through 6.4).

Pressures and Force Balance in Downhole Pumps

By looking at the pressures and forces in a downhole hydraulic pump, a generalized equation can be developed to predict the operating pressure required in a particular well. Two pumps are analyzed to show the generality of the solution. Fig. 6.22 shows a double-acting pump with the various areas identified and the pressures labeled for upstroke and downstroke conditions. In this design, both the upper and lower rods are exposed to the power-fluid pressure, p_{pf} . At the beginning and end of each half-stroke, brief periods of deceleration and acceleration occur, but the majority of the stroke is at constant velocity. For the constant-velocity condition, the sum of the forces acting downward must equal the sum of the forces acting upward. In the case of a downstroke, the downward forces are

$$F_d = p_{pf}A_{cr} + p_{pf}(A_{cp} - A_{cr}) + p_{ps}(A_{pp} - A_{pr}), \dots (6)$$

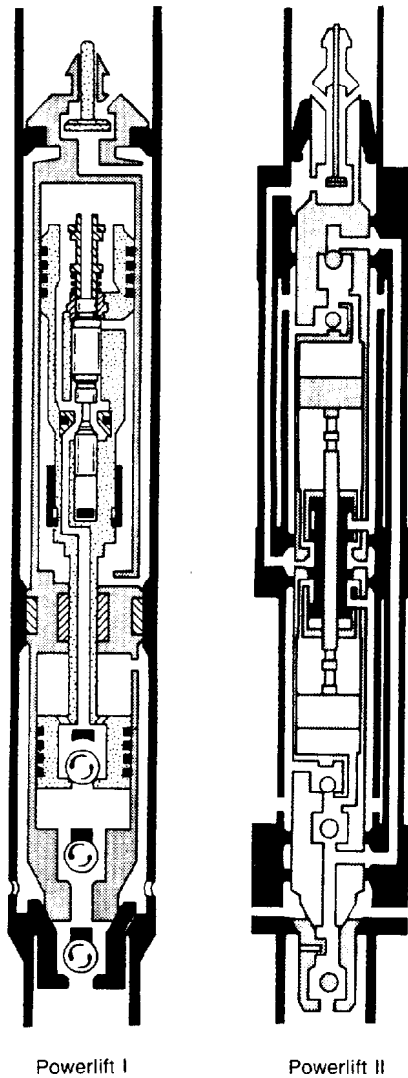


Fig. 6.17—Manufacturer "C" pump types for Table 6.3.

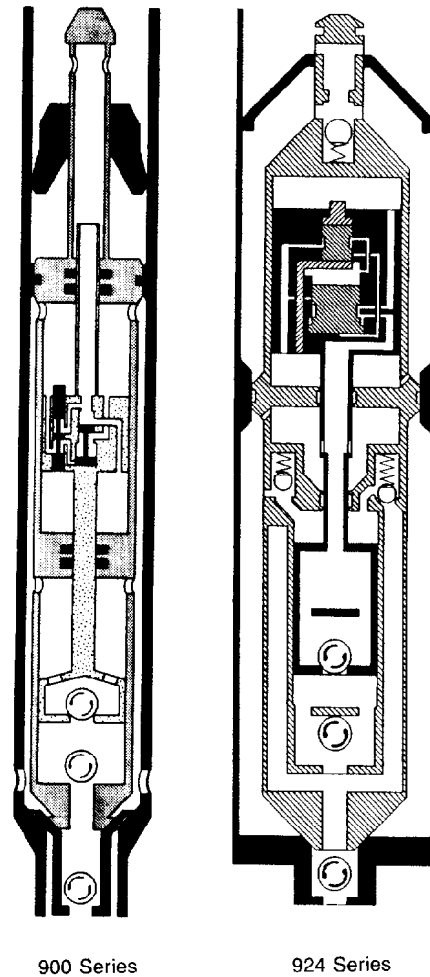


Fig. 6.18—Manufacturer "D" pump types for Table 6.4.

where

- F_d = downward force, lbf,
 p_{pf} = power-fluid pressure, psi,
 A_{er} = cross-sectional area of engine rod, sq in.,
 A_{ep} = cross-sectional area of engine piston, sq in.,
 p_{ps} = pump suction pressure, psi,
 A_{pp} = cross-sectional area of pump plunger, sq in., and
 A_{pr} = cross-sectional area of pump rod, sq in.

The upward forces are

$$F_u = p_{ed}(A_{ep} - A_{er}) + p_{pd}(A_{pp} - A_{pr}) + p_{pf}(A_{pr}), \quad (7)$$

where

- F_u = upward force, lbf,
 p_{ed} = engine discharge pressure, psi, and
 p_{pd} = pump discharge pressure, psi.

Equating the upward and downward forces and solving for the power-fluid pressure at the pump gives

$$p_{pf} = p_{ed} + p_{pd}(A_{pp} - A_{pr})/(A_{ep} - A_{er}) - p_{ps}(A_{pp} - A_{pr})/(A_{ep} - A_{er}), \quad (8)$$

If $p_{ed} = p_{pd}$, as is the case in open power-fluid systems, then

$$p_{pf} = p_{pd}[1 + (A_{pp} - A_{pr})/(A_{ep} - A_{er})] - p_{ps}(A_{pp} - A_{pr})/(A_{ep} - A_{er}), \quad (9)$$

Eq. 8 can also be written as

$$p_{pf} = p_{ed} + (p_{pd} - p_{ps})(A_{pp} - A_{pr})/(A_{ep} - A_{er}), \quad (10)$$

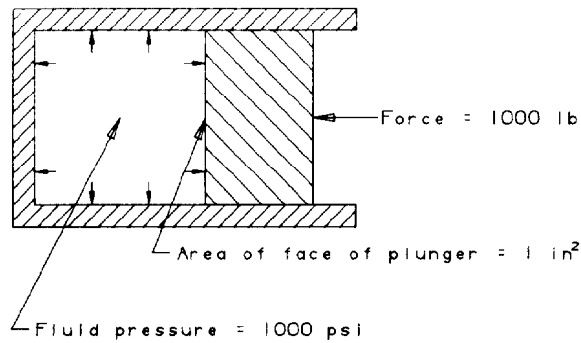


Fig. 6.19—Pressure and force in a static plunger and cylinder assembly.

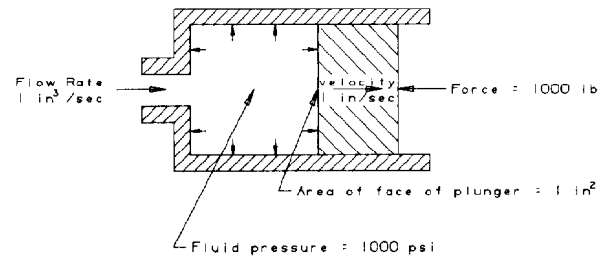


Fig. 6.20—Pressure, force, and flow in a dynamic plunger and cylinder assembly.

The same analysis for the upstroke would give the same answer because this double-acting pump is completely symmetrical.

Fig. 6.23 shows a balanced downhole unit with a single-acting pump end. First, for the downstroke, the downward forces are

$$F_d = p_{pf}(A_{ep}) + p_{ps}(A_{pp} - A_{pr}), \quad (11)$$

and the upward forces are

$$F_u = p_{pf}(A_{ep} - A_{er}) + p_{pd}(A_{er} - A_{pr}) + p_{pd}(A_{pp}). \quad (12)$$

In this pump, the areas of the engine and pump rods are half that of their respective pistons and plungers:

$$A_{er} = A_{ep}/2 \quad (13)$$

and

$$A_{pr} = A_{pp}/2. \quad (14)$$

Equating the upward and downward forces, substituting Eqs. 13 and 14, and solving for the power-fluid pressure, p_{pf} , gives

$$p_{pf} = p_{pd}(1 + A_{pp}/A_{ep}) - p_{ps}(A_{pp}/A_{ep}). \quad (15)$$

Evaluating the force balance for the upstroke gives

$$F_d = p_{ed}(A_{ep}) + p_{ps}(A_{pp} - A_{pr}) \quad (16)$$

and

$$F_u = p_{pf}(A_{ep} - A_{er}) + p_{pd}(A_{er} - A_{pr}) + p_{ps}(A_{pp}). \quad (17)$$

Eqs. 13, 14, 16, and 17 give

$$p_{pf} = 2p_{ed} - p_{pd}(1 - A_{pp}/A_{ep}) - p_{ps}(A_{pp}/A_{ep}). \quad (18)$$

Note that if $p_{ed} = p_{pd}$, which is the case in an open power-fluid installation, Eqs. 15 and 18 become the same:

$$p_{pf} = p_{pd}(1 + A_{pp}/A_{ep}) - p_{ps}(A_{pp}/A_{ep}). \quad (19)$$

Eq. 19 for the single-acting pump shown in Fig. 6.23 can be made identical to Eq. 9 for the double-acting pump shown in Fig. 6.22 by observing that, because of Eqs. 13 and 14,

$$A_{pp}/A_{ep} = (A_{pp} - A_{pr})/(A_{ep} - A_{er}). \quad (20)$$

Because it appears frequently in pressure calculations with hydraulic pumps, the term $(A_{pp} - A_{pr})/(A_{ep} - A_{er})$ is frequently simplified to P/E . This is sometimes called the “ P over E ratio” of the pump and is the ratio of the net area of the pump plunger to the net area of the engine piston. With this nomenclature, Eq. 8 for a closed power-fluid installation becomes

$$p_{pf} = p_{ed} + p_{pd}(P/E) - p_{ps}(P/E), \quad (21)$$

where $P/E = (A_{pp} - A_{pr})/(A_{ep} - A_{er})$.

Eq. 9 for an open power-fluid installation becomes

$$p_{pf} = p_{pd}[1 + (P/E)] - p_{ps}(P/E). \quad (22)$$

This approach has found widespread acceptance among the manufacturers of downhole pumps, and the ratio P/E is included in all their pump specifications (see examples in Tables 6.1 through 6.4).

P/E values greater than 1.0 indicate that a pump plunger is larger than the engine piston. This would be appropriate for shallow, low-lift wells. P/E values less than 1.0 are typical of pumps used in deeper, higher-lift wells. In some pumps, the P/E value is also the ratio of pump displacement to engine displacement, but corrections for fluid

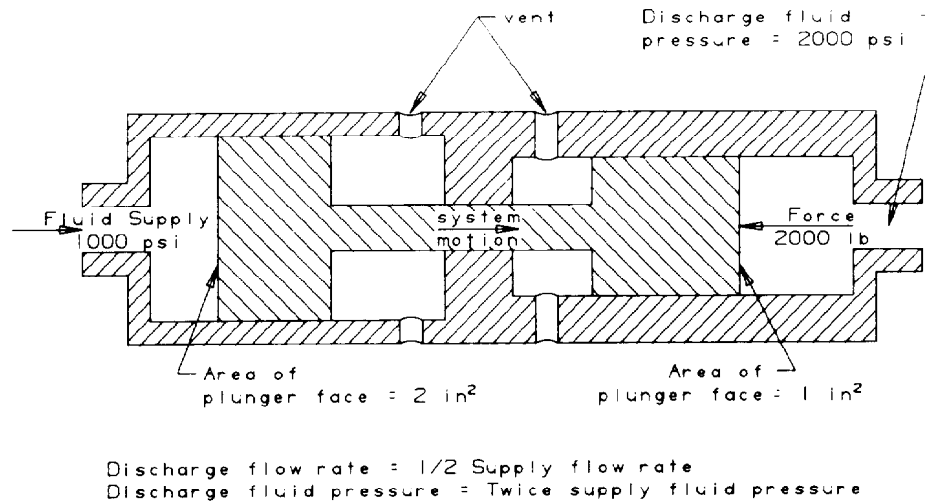


Fig. 6.21—Pressures, forces, and flows in a hydraulic transformer.

volumes to actuate engine valves and corrections for displacement volumes on the unloaded half-stroke of some single-acting pumps are necessary. Reference to specific displacement values for the engine and pump ensures proper determination of the respective flow rates.

Fluid Friction and Mechanical Losses in Hydraulic Pumps

In deriving Eqs. 9 and 19, we assume there are no fluid friction or mechanical losses. In practice, to maintain the stroking action of the pump, an additional pressure over and above the values for p_{pf} calculated with these equations is required. The largest portion of this extra pressure is a result of fluid-friction losses in the engine and pump. Because higher stroking rates require higher fluid velocities, this friction loss increases as the pump speed increases. Because of the effect of approximately constant dead times for the pump reversals, the rate of increase in pump friction with respect to increases in stroking rate tends to be higher than expected from simple pipe friction calculations based on average velocities. It has been found through testing that, for a given pump, the friction pressure can be represented by

$$p_{fr} = 50e^{K(N/N_{\max})}, \quad (23)$$

where

p_{fr} = friction pressure, psi,

K = experimentally determined constant for the particular pump,

N = pump operating rate, strokes/min., and

N_{\max} = rated maximum pump operating rate, strokes/min.

Note that the $p_{fr(\min)}$ is 50 psi, which occurs at zero strokes per minute. The value of $p_{fr(\max)}$ occurs when $N = N_{\max}$ and is

$$p_{fr(\max)} = 50e^K, \quad (24)$$

where $p_{fr(\max)}$ = maximum friction pressure, psi.

The value of $p_{fr(\max)}$ usually falls between 500 and 1,250 psi, depending on the particular pump.

If the manufacturers' reported values for $p_{fr(\max)}$ for each of their pumps are plotted vs. the maximum total flow rate of the engine and pump ends for the units, a correlation becomes apparent. For pumps designed to fit in a specific size of tubing string, the value of $p_{fr(\max)}$ increases with the maximum rated total fluid through the engine and pump ends. The form of the equation that gives a good fit is

$$p_{fr(\max)} = Ae^{Bq_{tm}}, \quad (25)$$

Here A and B are constants that depend on the tubing size for which the pump is designed, and q_{tm} is the maximum rated total flow through the engine and pump of a particular unit.

Eqs. 24 and 25 can be used to determine the value of K , which can then be substituted into Eq. 23 to give

$$p_{fr} = 50(Ae^{Bq_{tm}}/50)^{N/N_{\max}}, \quad (26)$$

The value of A in Eq. 26 is the same for all sizes of tubing—i.e., $A = 355$. Eq. 26 can therefore be written as

$$p_{fr} = 50(7.1e^{Bq_{tm}})^{N/N_{\max}}, \quad (27)$$

The values for B for different sizes of tubing are given in Table 6.5.

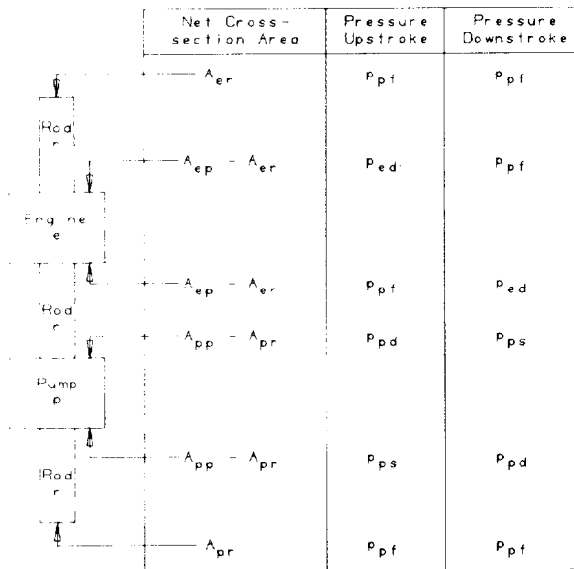


Fig. 6.22—Pressures acting on a double-acting downhole unit.

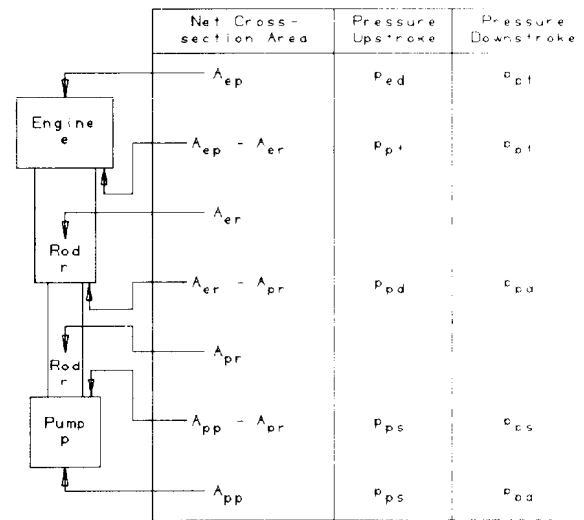


Fig. 6.23—Pressures acting on a single-acting downhole unit.

Eq. 27 is based on data accumulated from laboratory tests on water or on light test oils with viscosities less than 10 cSt and corrected to water properties. Because 75 to 80% of the losses are in the engine end of the downhole unit, specific gravity and viscosity corrections are necessary for different power fluids. To correct for density differences, the value of p_{fr} should be multiplied by the specific gravity of the power fluid, γ . A multiplying factor, F_v , which corrects for different viscosities, is given by

$$F_v = \nu_{pf}/100 + 0.99, \quad (28)$$

where ν_{pf} = power-fluid viscosity, cSt.

With both of these corrections, Eq. 27 becomes

$$p_{fr} = \gamma F_v (50) (7.1 e^{Bq_m})^{N/N_{max}}, \quad (29)$$

Curves plotted from Eq. 29 are shown in Fig. 6.24. The specific gravity of different API-gravity crudes can be determined from Table 6.6. Fig. 6.25 gives the viscosity of a variety of crudes as a function of temperature, and Fig. 6.26 gives the viscosity of water as a function of temperature with varying salt concentrations.

TABLE 6.5—TUBING SIZE VS. CONSTANT B

Tubing Size (in.)	B
2 3/8	0.000514
2 7/8	0.000278
3 1/2	0.000167
4 1/2	0.000078

Example Problem 1. Consider Manufacturer B's Type D pump—double engine, single pump end—for which the specifications are in Table 6.2. For the $2\frac{1}{2} \times 1\frac{7}{8} \times 1\frac{3}{4}$ size unit for $2\frac{1}{2}$ -in. tubing, the maximum rated engine flow rate is 1,799 B/D and the rated displacement of the pump end is 1,086 B/D for a total of 2,885 B/D. At rated speed of 100 strokes/min and using water power fluid with a specific gravity of 1.0 and a viscosity of 1 cSt, Eq. 29 gives

$$p_{fr} = (1)(1)(50) [7.1 e^{(0.000278)(2885)}]^{100/100} = 792 \text{ psi.}$$

If the pump speed is reduced to 60 strokes/min,

$$p_{fr} = 50 [7.1 e^{(0.000278)(2885)}]^{60/100} = 262 \text{ psi.}$$

These examples are shown in Fig. 6.24.

With this same unit, if the $1\frac{1}{2}$ -in. pump end is fitted, or if gas interference reduces the pump end volumetric efficiency of the $1\frac{3}{4}$ -in. pump end to 69%, the maximum rated flow through the pump end will be 744 B/D instead of 1,086 B/D, and the total flow will be reduced to 2,543 B/D. At rated speed, the friction pressure loss will then be

$$p_{fr} = 50 [7.1 e^{(0.000278)(2543)}]^{100/100} = 720 \text{ psi.}$$

If a 0.9-specific-gravity power fluid that has a viscosity of 10 cSt at bottomhole conditions was used in the last example, then

$$p_{fr} = 0.9(10/100 + 0.99)(50) [7.1 e^{(0.000278)(2543)}]^{100/100} = 706 \text{ psi.}$$

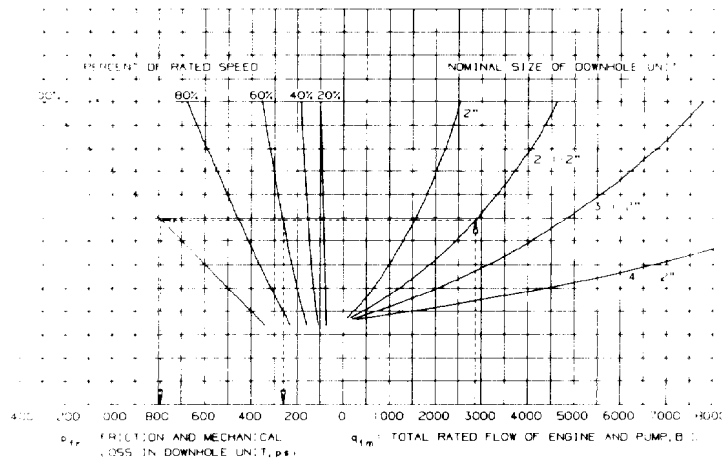


Fig. 6.24—Friction and mechanical loss in downhole pumps (specific gravity = 1.0, viscosity = 1.0 cSt).

Displacement of Downhole Pumps

Downhole pumps are normally rated by their theoretical displacement per stroke per minute on both the engine and pump ends. The theoretical displacement is the net area of the plunger times the distance traveled in a working stroke. There is also a maximum rated speed for each pump. Because of the tendency of inconsistent engine valve operation at very low stroking rates, and because of shorter pump life at very high stroking rates, downhole units are normally chosen to operate between 20 and 80% of their rated maximum speed. Choosing a pump that will meet the displacement requirements of a well at less than rated speed allows for later speed increases to offset normal pump wear. New engine efficiencies of about 95% may decline to 80% with wear. A value of 90% is often used for design purposes. New pump end efficiencies are typically high, but a worn pump end may have a volumetric efficiency as low as 70%. The specifications for downhole pumps from some major manufacturers are given in Tables 6.1 through 6.4. There are no API standards for hydraulic pumps. Consequently, there is considerable variation in designs, sizes, stroke lengths, and rated speeds, and parts are not interchangeable between brands.

At bottomhole conditions, however, the oil, water, and gas phases occupy different volumes than on the surface where flow measurements are made. Vented systems will allow significant portions of the free gas to vent to the surface, while unvented systems route all the free gas through the pump. The volume occupied by the free gas and the downhole volume of the oil with gas dissolved in it depend on several factors, including the crude gravity, gas gravity, temperature, and pressure.

The term "gas interference" has been used to describe the phenomenon of greatly reduced actual fluid displacement when gas and liquid phases are pumped at the same time. The gassy fluid is drawn into the pump suction at a low pressure and is discharged from the exhaust at a high pressure. The pump plunger, however, does not completely purge the pump barrel of fluid because of practical design and manufacturing considerations. The unswept volume is called the clearance volume. The clearance volume contains liquid and gas at pump discharge pres-

sure at the end of the discharge stroke. As the plunger reverses and moves in the suction stroke, the clearance-volume gas expands and its pressure declines. The suction valving will not open until the clearance-volume gas pressure drops below pump intake pressure. This phenomenon clearly reduces the effective stroke length of the pump, and in severe cases, the suction valves will not open for one or more pump cycles. This extreme case is referred to as "gas locking."

Hydraulic pumps usually have small clearance volumes because the engine and pump ends are very closely coupled, and control of stroke length is precise. Also, gradual leakage of power fluid or pump discharge fluid back into the pump barrel will eventually help purge clearance-volume gas. Specially designed discharge valve seats called "gas lock breakers" can be used to preclude gas lock by allowing a controlled leakage back into the pump barrel during the suction stroke. For these reasons, it is uncommon for hydraulic pumps to actually "gas lock," but the volumetric efficiency of the pump end is always reduced by the presence of gas. Even if the gas is all in solution, as when pumping above the bubblepoint of the crude, the liquid phase will occupy more volume downhole than it does in the stock tank because of dissolved gas, and this reduces the effective pump end volumetric efficiency.

Fig. 6.27, based on relationships from Standing⁹ and API Manual 14 BN,¹⁰ gives a means for determining the maximum volumetric efficiency of a pump from considerations of liquid- and gas-phase volumes. The equations used to generate Fig. 6.27 are listed in Appendix A. The gas interference effect depends on the compression ratio of the particular unit and will change with plunger size. It also depends on the ratio of intake to discharge pressure and whether the pump barrel is discharged at the top or the bottom. The magnitude of the gas interference effect is not well documented for all units. Therefore, it is common practice to assume that this effect and normal fluid leakage past fits reduces the displacement of the pump end to about 85% of the manufacturers' ratings. The pump suction rate is then

$$q_s = q_p N / N_{\max} E_{p(\max)} E_{p(\text{int})} \quad (30)$$

TABLE 6.6—SPECIFIC GRAVITIES AND UNIT PRESSURE OF FLUID COLUMNS*

Degrees API	0	0.1	0.2	0.3	0.4	0.5	0.6	0.7	0.8	0.9
10	1.0000	0.9993	0.9986	0.9979	0.9972	0.9965	0.9958	0.9951	0.9944	0.9937
	0.4331	0.4328	0.4325	0.4322	0.4319	0.4316	0.4313	0.4310	0.4307	0.4304
11	0.9930	0.9923	0.9916	0.9909	0.9902	0.9895	0.9888	0.9881	0.9874	0.9868
	0.4301	0.4298	0.4295	0.4292	0.4289	0.4286	0.4282	0.4279	0.4276	0.4274
12	0.9861	0.9854	0.9847	0.9840	0.9833	0.9826	0.9820	0.9813	0.9806	0.9799
	0.4271	0.4268	0.4265	0.4262	0.4259	0.4256	0.4253	0.4250	0.4247	0.4244
13	0.9792	0.9786	0.9779	0.9772	0.9765	0.9759	0.9752	0.9745	0.9738	0.9732
	0.4241	0.4238	0.4235	0.4232	0.4229	0.4226	0.4224	0.4221	0.4218	0.4215
14	0.9725	0.9718	0.9712	0.9705	0.9698	0.9692	0.9685	0.9679	0.9672	0.9665
	0.4212	0.4209	0.4206	0.4203	0.4200	0.4198	0.4195	0.4192	0.4189	0.4186
15	0.9659	0.9652	0.9646	0.9639	0.9632	0.9626	0.9619	0.9613	0.9606	0.9600
	0.4183	0.4180	0.4178	0.4175	0.4172	0.4169	0.4166	0.4163	0.4160	0.4158
16	0.9593	0.9587	0.9580	0.9574	0.9567	0.9561	0.9554	0.9548	0.9541	0.9535
	0.4155	0.4152	0.4149	0.4146	0.4143	0.4141	0.4138	0.4135	0.4132	0.4130
17	0.9529	0.9522	0.9516	0.9509	0.9503	0.9497	0.9490	0.9484	0.9478	0.9471
	0.4127	0.4124	0.4121	0.4118	0.4116	0.4113	0.4110	0.4108	0.4105	0.4102
18	0.9465	0.9459	0.9452	0.9446	0.9440	0.9433	0.9427	0.9421	0.9415	0.9408
	0.4099	0.4097	0.4094	0.4091	0.4088	0.4085	0.4083	0.4080	0.4078	0.4075
19	0.9402	0.9396	0.9390	0.9383	0.9377	0.9371	0.9365	0.9358	0.9352	0.9346
	0.4072	0.4069	0.4067	0.4064	0.4061	0.4059	0.4056	0.4053	0.4050	0.4048
20	0.9340	0.9334	0.9328	0.9321	0.9315	0.9309	0.9303	0.9297	0.9291	0.9285
	0.4045	0.4043	0.4040	0.4037	0.4034	0.4032	0.4029	0.4027	0.4024	0.4021
21	0.9279	0.9273	0.9267	0.9260	0.9254	0.9248	0.9242	0.9236	0.9230	0.9224
	0.4019	0.4016	0.4014	0.4011	0.4008	0.4005	0.4003	0.4000	0.3998	0.3995
22	0.9218	0.9212	0.9206	0.9200	0.9194	0.9188	0.9182	0.9176	0.9170	0.9165
	0.3992	0.3990	0.3987	0.3985	0.3982	0.3979	0.3977	0.3974	0.3972	0.3969
23	0.9159	0.9153	0.9147	0.9141	0.9135	0.9129	0.9123	0.9117	0.9111	0.9106
	0.3967	0.3964	0.3962	0.3959	0.3956	0.3954	0.3951	0.3949	0.3946	0.3944
24	0.9100	0.9094	0.9088	0.9082	0.9076	0.9071	0.9065	0.9059	0.9053	0.9047
	0.3941	0.3939	0.3936	0.3933	0.3931	0.3929	0.3926	0.3923	0.3921	0.3918
25	0.9042	0.9036	0.9030	0.9024	0.9018	0.9013	0.9007	0.9001	0.8996	0.8990
	0.3916	0.3913	0.3911	0.3908	0.3906	0.3904	0.3901	0.3898	0.3896	0.3894
26	0.8984	0.8978	0.8973	0.8967	0.8961	0.8956	0.8950	0.8944	0.8939	0.8933
	0.3891	0.3888	0.3886	0.3884	0.3881	0.3879	0.3876	0.3874	0.3871	0.3869
27	0.8927	0.8922	0.8916	0.8911	0.8905	0.8899	0.8894	0.8888	0.8883	0.8877
	0.3866	0.3864	0.3862	0.3859	0.3857	0.3854	0.3852	0.3849	0.3847	0.3845
28	0.8871	0.8866	0.8860	0.8855	0.8849	0.8844	0.8838	0.8833	0.8827	0.8822
	0.3842	0.3840	0.3837	0.3835	0.3833	0.3830	0.3828	0.3826	0.3823	0.3821
29	0.8816	0.8811	0.8805	0.8800	0.8794	0.8789	0.8783	0.8778	0.8772	0.8767
	0.3818	0.3816	0.3813	0.3811	0.3809	0.3807	0.3804	0.3802	0.3799	0.3797
30	0.8762	0.8756	0.8751	0.8745	0.8740	0.8735	0.8729	0.8724	0.8718	0.8713
	0.3795	0.3792	0.3790	0.3787	0.3785	0.3783	0.3781	0.3778	0.3776	0.3774
31	0.8708	0.8702	0.8697	0.8692	0.8686	0.8681	0.8676	0.8670	0.8665	0.8660
	0.3771	0.3769	0.3767	0.3765	0.3762	0.3760	0.3758	0.3755	0.3753	0.3751
32	0.8654	0.8649	0.8644	0.8639	0.8633	0.8628	0.8623	0.8618	0.8612	0.8607
	0.3748	0.3746	0.3744	0.3742	0.3739	0.3737	0.3735	0.3732	0.3730	0.3728
33	0.8602	0.8597	0.8591	0.8586	0.8581	0.8576	0.8571	0.8565	0.8560	0.8555
	0.3726	0.3723	0.3721	0.3719	0.3716	0.3714	0.3712	0.3710	0.3707	0.3705
34	0.8550	0.8545	0.8540	0.8534	0.8529	0.8524	0.8519	0.8514	0.8509	0.8504
	0.3703	0.3701	0.3699	0.3696	0.3694	0.3692	0.3690	0.3687	0.3685	0.3683
35	0.8498	0.8493	0.8488	0.8483	0.8478	0.8473	0.8468	0.8463	0.8458	0.8453
	0.3680	0.3678	0.3676	0.3674	0.3672	0.3670	0.3667	0.3665	0.3663	0.3661

*First line opposite each API gravity is specific gravity at 60°F, second line is column pressure in psi/ft.

TABLE 6.6—SPECIFIC GRAVITIES AND UNIT PRESSURE OF FLUID COLUMNS* (continued)

Degrees API	0	0.1	0.2	0.3	0.4	0.5	0.6	0.7	0.8	0.9
36	0.8448 0.3659	0.8443 0.3657	0.8438 0.3654	0.8433 0.3652	0.8428 0.3650	0.8423 0.3648	0.8418 0.3646	0.8413 0.3644	0.8408 0.3642	0.8403 0.3639
37	0.8398 0.3637	0.8393 0.3635	0.8388 0.3633	0.8383 0.3631	0.8378 0.3629	0.8373 0.3626	0.8368 0.3624	0.8363 0.3622	0.8358 0.3620	0.8353 0.3618
38	0.8348 0.3616	0.8343 0.3613	0.8338 0.3611	0.8333 0.3609	0.8328 0.3607	0.8324 0.3605	0.8319 0.3603	0.8314 0.3601	0.8309 0.3599	0.8304 0.3596
39	0.8299 0.3594	0.8294 0.3592	0.8289 0.3590	0.8285 0.3588	0.8280 0.3586	0.8275 0.3584	0.8270 0.3582	0.8265 0.3580	0.8260 0.3577	0.8256 0.3576
40	0.8251 0.3574	0.8246 0.3571	0.8241 0.3569	0.8236 0.3567	0.8232 0.3565	0.8227 0.3563	0.8222 0.3561	0.8217 0.3559	0.8212 0.3557	0.8208 0.3555
41	0.8203 0.3553	0.8198 0.3551	0.8193 0.3548	0.8189 0.3547	0.8184 0.3544	0.8179 0.3542	0.8174 0.3540	0.8170 0.3538	0.8165 0.3536	0.8160 0.3534
42	0.8155 0.3532	0.8151 0.3530	0.8146 0.3528	0.8142 0.3526	0.8137 0.3524	0.8132 0.3522	0.8128 0.3520	0.8123 0.3518	0.8118 0.3516	0.8114 0.3514
43	0.8109 0.3512	0.8104 0.3510	0.8100 0.3508	0.8095 0.3506	0.8090 0.3504	0.8086 0.3502	0.8081 0.3500	0.8076 0.3498	0.8072 0.3496	0.8067 0.3494
44	0.8063 0.3492	0.8058 0.3490	0.8054 0.3488	0.8049 0.3486	0.8044 0.3484	0.8040 0.3482	0.8035 0.3480	0.8031 0.3478	0.8026 0.3476	0.8022 0.3474
45	0.8017 0.3472	0.8012 0.3470	0.8008 0.3468	0.8003 0.3466	0.7999 0.3464	0.7994 0.3462	0.7990 0.3460	0.7985 0.3458	0.7981 0.3457	0.7976 0.3554
46	0.7972 0.3453	0.7967 0.3451	0.7963 0.3449	0.7958 0.3447	0.7954 0.3445	0.7949 0.3443	0.7945 0.3441	0.7941 0.3439	0.7936 0.3437	0.7932 0.3435
47	0.7927 0.3433	0.7923 0.3431	0.7918 0.3429	0.7914 0.3428	0.7909 0.3425	0.7905 0.3424	0.7901 0.3422	0.7896 0.3420	0.7892 0.3918	0.7887 0.3416
48	0.7883 0.3414	0.7879 0.3412	0.7874 0.3410	0.7870 0.3408	0.7865 0.3406	0.7861 0.3405	0.7857 0.3403	0.7852 0.3401	0.7848 0.3399	0.7844 0.3397
49	0.7839 0.3395	0.7835 0.3393	0.7831 0.3392	0.7826 0.3389	0.7822 0.3388	0.7818 0.3386	0.7813 0.3384	0.7809 0.3382	0.7805 0.3380	0.7800 0.3378
50	0.7796 0.3376	0.7792 0.3375	0.7788 0.3373	0.7783 0.3371	0.7779 0.3369	0.7775 0.3367	0.7770 0.3365	0.7766 0.3363	0.7762 0.3362	0.7758 0.3360
51	0.7753 0.3358	0.7749 0.3356	0.7745 0.3354	0.7741 0.3353	0.7736 0.3350	0.7732 0.3349	0.7728 0.3347	0.7724 0.3345	0.7720 0.3344	0.7715 0.3341
52	0.7711 0.3340	0.7707 0.3338	0.7703 0.3336	0.7699 0.3334	0.7694 0.3332	0.7690 0.3331	0.7686 0.3329	0.7682 0.3327	0.7678 0.3325	0.7674 0.3324
53	0.7669 0.3321	0.7665 0.3320	0.7661 0.3318	0.7657 0.3316	0.7653 0.3315	0.7649 0.3313	0.7645 0.3311	0.7640 0.3309	0.7636 0.3307	0.7632 0.3305
54	0.7628 0.3304	0.7624 0.3302	0.7620 0.3300	0.7616 0.3298	0.7612 0.3297	0.7608 0.3295	0.7603 0.3293	0.7599 0.3291	0.7595 0.3289	0.7591 0.3288
55	0.7587 0.3286	0.7583 0.3284	0.7579 0.3282	0.7575 0.3281	0.7571 0.3279	0.7567 0.3277	0.7563 0.3276	0.7559 0.3274	0.7555 0.3272	0.7551 0.3270
56	0.7547 0.3269	0.7543 0.3267	0.7539 0.3265	0.7535 0.3263	0.7531 0.3262	0.7527 0.3260	0.7523 0.3258	0.7519 0.3256	0.7515 0.3255	0.7511 0.3253
57	0.7507 0.3251	0.7503 0.3250	0.7499 0.3248	0.7495 0.3246	0.7491 0.3244	0.7487 0.3243	0.7483 0.3241	0.7479 0.3239	0.7475 0.3237	0.7471 0.3236
58	0.7467 0.3234	0.7463 0.3232	0.7459 0.3230	0.7455 0.3229	0.7451 0.3227	0.7447 0.3225	0.7443 0.3224	0.7440 0.3222	0.7436 0.3221	0.7432 0.3219
59	0.7428 0.3217	0.7424 0.3215	0.7420 0.3214	0.7416 0.3212	0.7412 0.3210	0.7408 0.3208	0.7405 0.3207	0.7401 0.3205	0.7397 0.3204	0.7393 0.3202
60	0.7389 0.3200	0.7385 0.3198	0.7381 0.3197	0.7377 0.3195	0.7374 0.3194	0.7370 0.3192	0.7366 0.3190	0.7362 0.3188	0.7358 0.3187	0.7354 0.3185

*First line opposite each API gravity is specific gravity at 60°F, second line is column pressure in psi/ft.

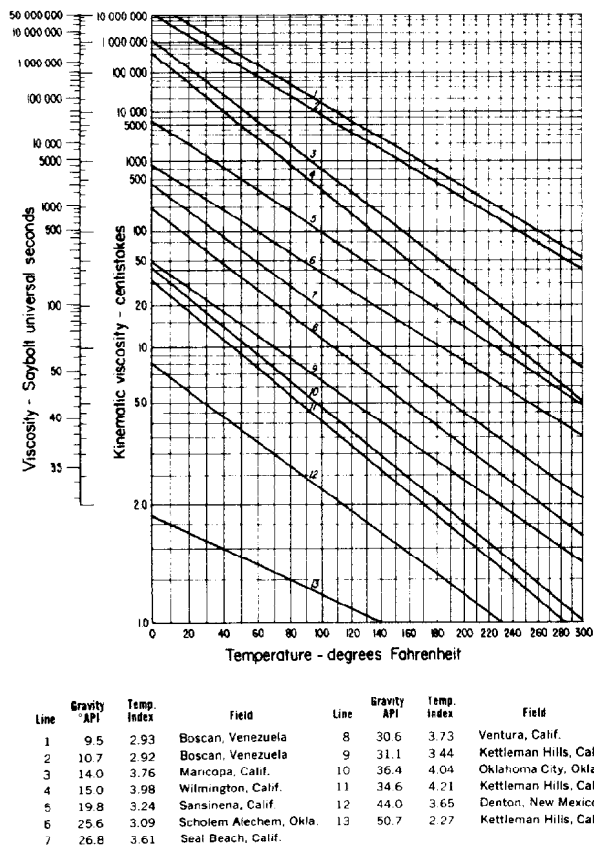


Fig. 6.25—Viscosity of oils.

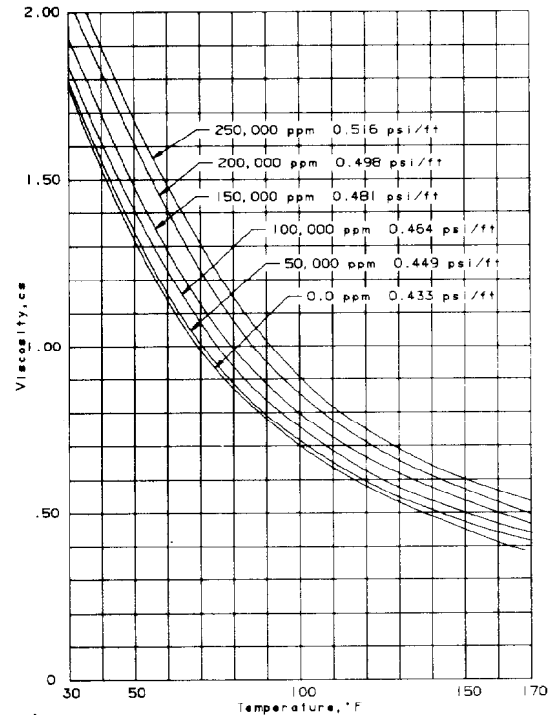


Fig. 6.26—How temperature affects viscosity of salt water (these curves indicate the effect of temperature on viscosity of salt water solutions of various concentrations).

The pump displacement required to achieve a desired pump suction rate is therefore

$$q_p = q_s / [N / N_{\max} E_{p(\max)} E_{p(\text{int})}], \quad (31)$$

where

q_s = pump suction rate, B/D,

q_p = rated pump displacement, B/D,

$E_{p(\max)}$ = maximum pump efficiency from Fig. 6.27, fraction, and

$E_{p(\text{int})}$ = pump efficiency for gas interference and pump leakage (normally = 0.85), fraction.

Example Problem 2. Consider a case where one desires to produce 250 B/D of 35°API crude at a pump intake pressure of 500 psi. The gas/oil ratio (GOR) is 500:1 and the water cut is 40%. Fig. 6.27 gives 41% theoretical volumetric efficiency. The required pump displacement at 80% of rated speed is therefore given by

$$q_p = 250 / (0.8 \times 0.41 \times 0.85) = 897 \text{ B/D.}$$

When the maximum volumetric efficiency from Fig. 6.27 is below about 50%, an installation design that in-

cludes the extra cost and complexity of a gas vent should be considered. A number of factors affect the performance of gas-vent systems. However, the saturated oil-volume line in Fig. 6.27 (the upper boundary of the downhole shaded area) can be used to account for the increased downhole volume of the oil caused by gas that remains in solution. In the previous example, saturated oil at 500 psi has a downhole volume that gives a maximum pump efficiency of 95% when calculated on surface volume where the solution gas has been liberated. The required pump displacement at 80% of rated speed is therefore given by

$$q_p = 250 / (0.8 \times 0.92 \times 0.85) = 400 \text{ B/D.}$$

System Pressures and Losses in Hydraulic Installations

The flow of fluid power in a hydraulic pumping system starts with the high-pressure pump on the surface. The power fluid passes through a wellhead control valve and down the power-fluid tubing string. The power-fluid pressure increases with depth because of the increasing hydrostatic head of fluid in the tubing. At the same time, some

of the power-fluid pressure is lost to fluid friction in the tubing string. At the pump, most of the power-fluid pressure is available for work in driving the downhole unit, with the remainder lost in the friction pressure, p_{fr} . After the downhole unit is operated, the power fluid must return to the surface. The pressure of the power fluid leaving the downhole unit depends on the hydrostatic head of fluid in the return tubing above the pump. In addition to this pressure, the fluid friction pressure lost in getting to the surface and the backpressure at the wellhead must be considered. In an open power-fluid system, the produced fluid from the well will leave the downhole unit and mix with the exhaust power fluid, thereby encountering the same pressure environment as the power fluid. In a closed power-fluid system, the production will have its own unique hydrostatic head, friction pressure loss, and wellhead or flowline backpressure. In both cases, the pump suction will be at a pump intake pressure from the well that will vary with the production rate according to the IPR of the well. Fig. 6.28 shows the system pressures and losses for an open power-fluid installation, and Fig. 6.29 shows them for a closed power-fluid installation.

The relationships shown in Figs. 6.28 and 6.29 are summarized below.

Open Power-Fluid System.

$$p_{pf} = p_{so} - p_{fpt} + g_{pf}D - p_{fr}, \dots\dots\dots (32)$$

$$p_{pd} = p_{fd} + g_d D + p_{wh}, \dots\dots\dots (33)$$

$$p_{ed} = p_{pd}, \dots\dots\dots (34)$$

and

$$p_{ps} = g_s s_p, \dots\dots\dots (35)$$

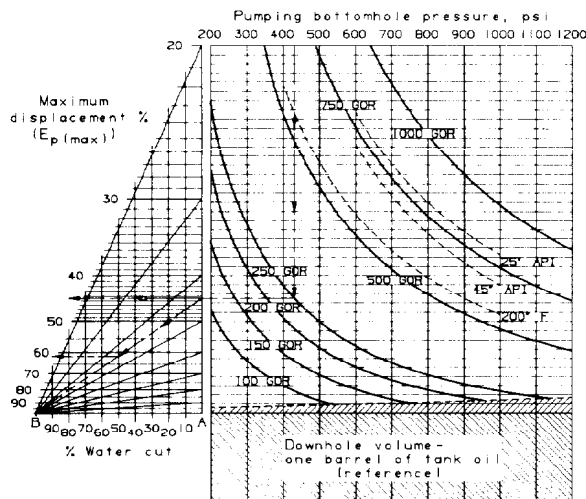


Fig. 6.27—Theoretical volumetric efficiencies of unvented downhole pumps as affected by high GOR's (volume occupied by saturated oil and free gas is based on 35° API oil at 160°F BHT). Example: To determine maximum displacement of an unvented pump with 430-psi pumping bottomhole pressure, 250 gas/oil ratio, and 50% water cut. Enter chart at 430 psi down to GOR (250). From intersection, proceed horizontally to read 44+ % oil displacement. Strike a diagonal from 44+ % on Line A to Point B, from intersection with 50% water cut, read 62% maximum displacement of water and tank oil.

Note that Eq. 32 can be solved for the surface operating pressure (triplex pressure) to give

$$p_{so} = p_{pf} + p_{fpt} - g_{pf}D + p_{fr}, \dots\dots\dots (36)$$

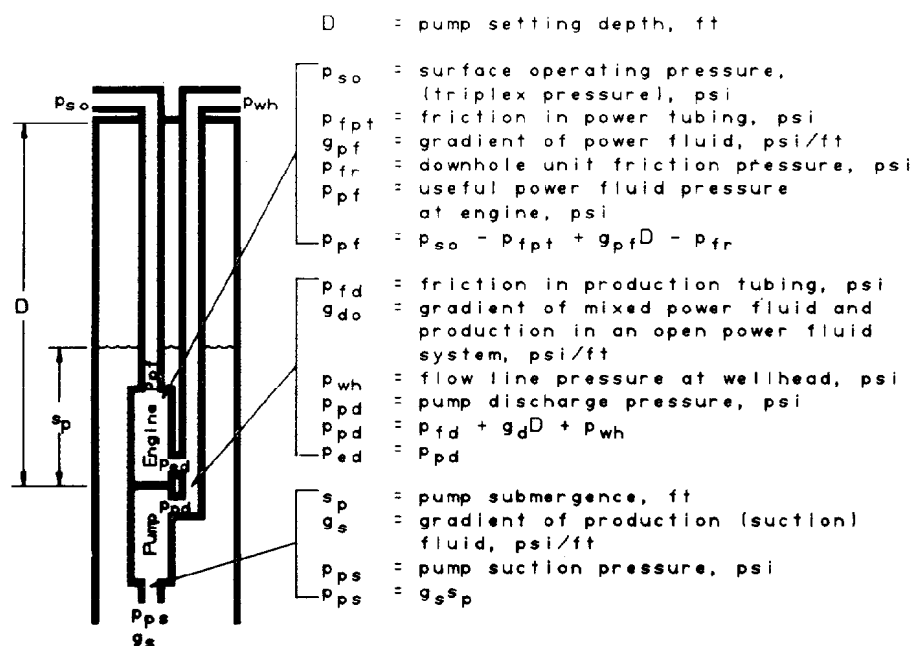


Fig. 6.28—System pressures and losses in an open power-fluid installation.

Closed Power-Fluid System.

$$p_{pf} = p_{so} - p_{fpt} + g_{pf}D - p_{fr}, \dots \dots \dots (32)$$

$$p_{ed} = p_{fet} + g_{pf}D + p_{whe}, \dots \dots \dots (37)$$

$$p_{pd} = p_{fd} + g_s D + p_{wh}, \dots \dots \dots (38)$$

and

$$p_{ps} = g_s s_p, \dots \dots \dots (35)$$

As before, solving for the surface operating pressure gives

$$p_{so} = p_{pf} + p_{fpt} - g_{pf}D + p_{fr}, \dots \dots \dots (36)$$

Calculation of Fluid Gradients. Power Fluid. Proper values for the various fluid gradients are necessary to calculate the pressures that affect the pump. The power-fluid, either oil or water, has a gradient, g_{pf} , in pounds per square inch per foot. This is also the power-fluid exhaust gradient in a closed power-fluid system. The gradient values for different-API-gravity oils are given in Table 6.6. If water is used as power fluid, its gradient may vary from the standard value of 0.433 psi/ft, depending on the amount of dissolved salt. Corrections may be made by use of the general relationship:

$$g = \gamma(0.433), \dots \dots \dots (39)$$

Produced Fluid. The gradient of the produced well fluids at the pump suction is given by

$$g_s = g_o(1 - W_c) + g_w W_c, \dots \dots \dots (40)$$

where

g_o = gradient of produced oil, psi/ft,
 g_w = gradient of produced water, psi/ft, and
 W_c = water cut (0.5 for 50% water cut),
 fraction.

This is also the value for the pump discharge gradient, g_d , in a closed power-fluid system.

Pump and Engine Discharge Gradient in an Open Power-Fluid System.

$$g_d = [(q_{pf} \times g_{pf}) + (q_s \times g_s)] / q_d, \dots \dots \dots (41)$$

where

q_{pf} = power-fluid rate, B/D,
 q_s = production (suction) fluid rate, B/D, and
 q_d = discharge fluid rate, $q_{pf} + q_s$, B/D.

Fluid Friction in Tubular and Annular Flow Passages.

Appendix B contains friction pressure-drop curves for a variety of commonly used tubing and casing sizes. Also included in Appendix B are the equations used to create the curves. Note that the pressure drops are given in pounds per square inch per 1,000 ft and that the values

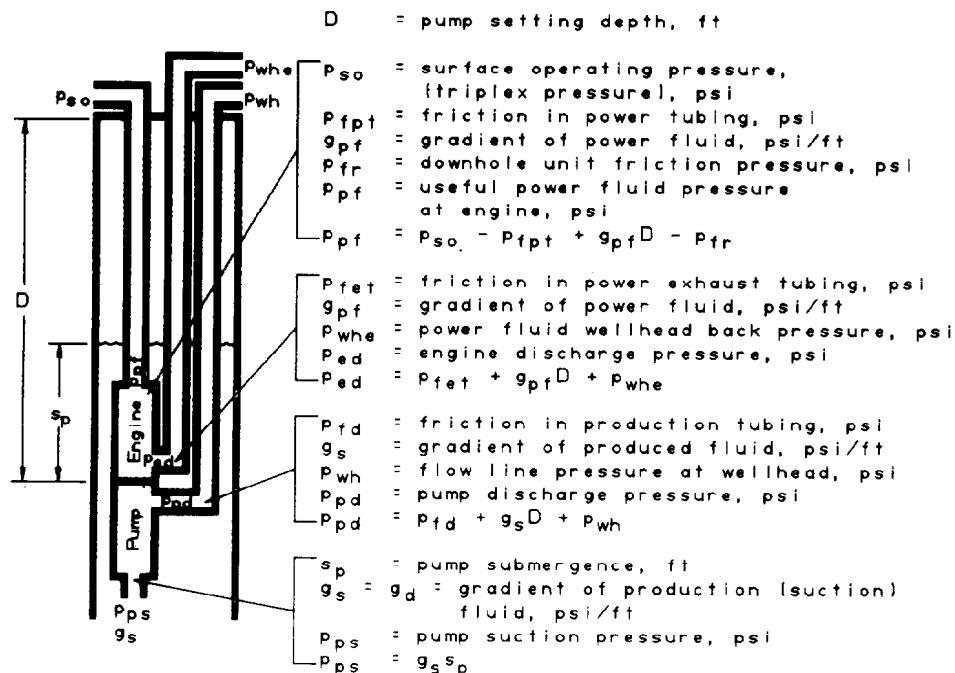


Fig. 6.29—System pressures and losses in a closed power-fluid installation.

must be multiplied by the specific gravity of the fluid. The values for the power-fluid friction pressure, p_{pft} , the power-fluid discharge pressure friction, p_{pfd} , and the production discharge friction pressure, p_{fd} , can be determined from the charts or the basic equations.

Fluid Viscosity. The viscosities of various crude oils and waters are discussed in Appendix A. The viscosity of water/oil mixtures is difficult to predict. In hydraulic pumping calculations, a weighted average is normally used. Water and oil viscosities are usually evaluated at the average temperature between surface and downhole temperatures.

$$\nu_m = (1 - W_{cd})\nu_o + W_{cd}\nu_w, \quad (42)$$

where

ν_m = mixture viscosity, cSt,

ν_o = oil viscosity, cSt,

ν_w = water viscosity, cSt, and

W_{cd} = water cut in discharge conduit to surface, fraction.

In closed power-fluid systems,

$$W_{cd} = W_c. \quad (43)$$

In open power-fluid systems using water as the power fluid,

$$W_{cd} = (q_{pf} + W_c q_s) / q_d. \quad (44)$$

For open power-fluid systems with oil as a power fluid,

$$W_{cd} = W_c q_s / q_d. \quad (45)$$

These equations do not consider the formation of any emulsions that only occasionally form in hydraulic pumping systems. Water-in-oil emulsions can cause extremely high apparent viscosities (Fig. 6.30) but the prediction of when emulsions will form is difficult. The formation of oil-in-water emulsions has been done deliberately in heavy crude wells as a means of reducing viscosity.¹¹

Multiphase Flow and Pump Discharge Pressure

Eqs. 33 and 38 for the pump discharge pressure include only the dead oil and water gradients. If the well produces significant gas, the multiphase (gas plus liquid) flow to the surface will result in pump discharge pressures lower than predicted by Eqs. 33 and 38. The magnitude of this effect on the operating pressure (and required horsepower) depends on the P/E ratio of the downhole pump. Available P/E ratios range from a low of 0.30 to a high of 2.00. By referring to Eq. 22 for open power-fluid systems, which are the most common, we can see that a change in the pump discharge pressure affects the power-fluid pressure by $(1 + P/E)$ times the change in discharge pressure. Because $(1 + P/E)$ has a range of 1.30 to 3.00, depending on the pump, a 500-psi reduction in the pump discharge pressure caused by gas effects can change the operating pressure required by 650 to 1,500 psi.

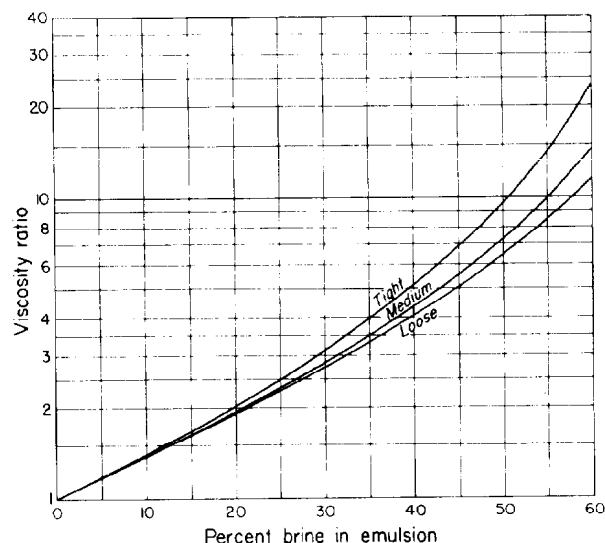


Fig. 6.30—Effect of emulsion on oil viscosity.

If the gas/liquid ratio F_{gL} is less than about 10 scf/bbl in the pump discharge flow path, the gas effects are minimal and Eqs. 33 and 38 can be used directly. For higher F_{gL} values, it is suggested that a vertical multiphase flowing gradient correlation be used to calculate the pump discharge pressure. (See Chap. 5, Gas Lift, for a detailed discussion of these calculations.) Note that in open power-fluid systems, the addition of the power fluid to the production will make the discharge F_{gl} substantially less than the formation producing GOR, R . In a closed power-fluid system,

$$F_{gL} = (1 - W_c)R. \quad (46)$$

In an open power-fluid system,

$$F_{gL} = q_s(1 - W_c)R / q_d. \quad (47)$$

The appropriate water cuts for use in vertical multiphase flowing gradient calculations are given in Eqs. 43 through 45.

Gas/Liquid Ratio in Vented Systems

Vented systems allow most of the free gas to rise to the surface without passing through the pump. The gas that is still in solution in the oil at pump intake pressure conditions, however, does pass through the pump. To determine solution GOR from Fig. 6.27, read down from the pumping BHP to the saturated oil-volume line (the upper boundary of the downhole volume shaded area). Interpolating between the intersections of the constant-GOR curves with the saturated-oil-volume line gives the solution GOR. At 500-psi pump intake pressure, the solution GOR is about 100 scf/bbl. The solution GOR should be used in Eqs. 46 and 47 when the installation includes a gas vent.

Pressure Relationships Used To Estimate Producing BHP

The pressure relationships of Eqs. 21 and 22 can be rearranged to give the pump intake pressure p_{ps} in terms of the other system pressures and the P/E ratio of the pump. For the closed power-fluid system,*

$$p_{ps} = p_{pd} - (p_{pf} - p_{ed})/(P/E). \quad (48)$$

For the open power-fluid system,

$$p_{ps} = p_{pd} - (p_{pf} - p_{pd})/(P/E). \quad (49)$$

If the appropriate relationships from Eqs. 32 through 38 are used, the equation for the closed power-fluid system becomes**

$$p_{ps} = (p_{fd} + g_s D + p_{wh}) - [(p_{so} - p_{fpt} + g_{pf} D - p_{fr}) - (p_{fet} + g_{pf} D + p_{whe})]/(P/E), \quad (50)$$

where $g_s = g_d$ in a closed power-fluid system.

For the open power-fluid system, the relationship is

$$p_{ps} = (p_{fd} + g_d D + p_{wh}) - [(p_{so} - p_{fpt} + g_{pf} D - p_{fr}) - (p_{fd} + g_d D + p_{wh})]/(P/E). \quad (51)$$

These equations can be used directly, but several problems arise. Several friction terms must be evaluated, each with a degree of uncertainty. The term p_{fr} for the losses in the pump is the least accurate number because pump wear and loading can affect it. To avoid the uncertainty in friction values, a technique called the "last-stroke method" is often used. With this method, the power-fluid supply to the well is shut off. As the pressure in the system bleeds down, the pump will continue to stroke at slower rates until it takes its last stroke before stalling out. The strokes can be observed as small kicks on the power-fluid pressure gauge at the wellhead. The power-fluid pressure at the time of the last stroke is that required to balance all the fluid pressures with zero flow and zero pump speed. At zero speed, all the friction terms are zero, except p_{fr} , which has a minimum value of 50 psi, which simplifies Eqs. 50 and 51. With the friction terms removed, the last stroke relationship for the closed power-fluid system becomes

$$p_{ps} = g_s D + p_{wh} - [(p_{so} + g_{pf} D - 50) - (g_{pf} D + p_{whe})]/(P/E). \quad (52)$$

For the open power-fluid system the relationship is

$$p_{ps} = g_d D + p_{wh} - [(p_{so} + g_{pf} D - 50) - (g_d D + p_{wh})]/(P/E). \quad (53)$$

*Eq. 48 is derived from Eq. 21 and Eq. 49 is derived from Eq. 22.

**Eq. 50 is derived from Eq. 21 and Eq. 51 is derived from Eq. 22.

These relationships have proved to be very effective in determining BHP's.¹² However, they are limited to wells that produce little or no gas for the reasons discussed in the section on Multiphase Flow and Pump Discharge Pressure. Eqs. 50 and 51 can be used in gassy wells if the hydrostatic-pressure and flowline-pressure terms are replaced by a pump discharge pressure from a vertical multiphase flowing gradient correlation. The equations for the last-stroke method, however, present a further problem because they require the gradient at a no-flow condition. The multiphase-flow correlations show a significant variation of pressure with velocity. Wilson, in Brown,⁷ suggests subtracting the friction terms from the flowing gradient for evaluating Eqs. 52 and 53 or attempting to determine p_{fr} more accurately for use in the evaluation of Eqs. 50 and 51. The method suggested here is to use a multiphase-flow correlation for determining p_{pd} at the normal operating point of the pump. With the same correlation for the same proportions of liquid and gas, determine what the p_{pd} pressure would be at a low flow rate, corresponding to the conditions when the pump is slowing down to its last stroke. By plotting the two values of p_{pd} obtained, we can extrapolate to what p_{pd} would be at zero flow. This value can be used to replace the hydrostatic-head and flowline-pressure terms.

Selecting an Appropriate P/E Ratio. As previously discussed, large values of P/E are used in shallow wells and small values in deeper wells. The larger the value of P/E , the higher the surface operating pressure to lift fluid against a given head will be. The multiplex pumps offered by the manufacturers are rated up to 5,000 psi, but few hydraulic installations use more than 4,000 psi except in very deep wells. About 80 to 90% of the installations use operating pressures between 2,200 and 3,700 psi. With the simplifying assumptions of an all-water system, no friction, 500-psi pump friction, 4,000-psi operating pressure, and a pumped-off well, Eqs. 22, 33, and 36 lead to

$$(P/E)_{\max} = 3,500/0.433L_n = 8,000/L_n, \quad (54)$$

where L_n = net lift, ft.

Eq. 54 is useful in initial selection of an appropriate P/E ratio in installation design. The actual final determination of the surface operating pressure will depend on calculation of the actual gradients and losses in the system and on the particular pump's P/E ratio.

Equipment Selection and Performance Calculations

Equipment selection involves matching the characteristics of hydraulic pumping systems to the parameters of a particular well or group of wells. A worksheet and summary of equations are given in Table 6.7.

Once a downhole unit has been selected and its power-fluid pressure and rate determined, an appropriate power supply pump must be matched to it. The section on surface equipment and pumps provides a detailed description of the types of pumps used for powering hydraulic pumping systems. Specifications for some of the pumps typically used can be found in Tables 6.1 through 6.4 (Figs. 6.15 through 6.18).

A troubleshooting guide is provided in Tables 6.8 through 6.10.

TABLE 6.7—WORKSHEET AND SUMMARY OF EQUATIONS FOR RECIPROCATING PUMPS

Well Identification Example Problem 3

Vertical setting depth, ft	9,000	Water specific gravity	1.03
Tubing length, ft	9000	Power fluid gradient, psi/ft	0.357
Tubing ID, in.	2.441	Produced oil gradient, psi/ft	0.357
Tubing OD, in.	2.875	Water gradient, psi/ft	0.446
Return ID, in.	4.892	Oil viscosity, cSt	2
Wellhead pressure, psi	100	Water viscosity, cSt	0.485
Gas specific gravity	0.75	GOR, scf/bbl	100
Oil gravity, °API	40	Water cut, %	70
Power fluid specific gravity	0.82	Surface temperature, °F	100
Produced oil specific gravity	0.82	Bottomhole temperature, °F	200

Expected net lift, ft	7,800	Vented?	Yes _____ No <input checked="" type="checkbox"/>
Desired production, B/D	250		
Pump intake pressure at above rate, psi	500		
Installation: Casing <input checked="" type="checkbox"/> Parallel _____			
OPF <input checked="" type="checkbox"/> CPF _____			

Step 1— $(P/E)_{\max} = 8,000/L_n = 1.03$ (Eq. 54)**Step 2**—Maximum pump efficiency $E_{p(\max)}$ (Fig. 6.27) _____ % (Vented)
97 % (Unvented)**Step 3**—Minimum recommended pump displacement (Eq. 31):

$$q_p = q_s / \frac{N}{N_{\max}} \times E_{p(\max)} \times E_{p(\text{int})} = 250 / (0.8 \times 0.97 \times 0.85) = 379 \text{ B/D.}$$

Step 4—Select pump from Tables 6.1 through 6.4 with P/E less than or equal to value from Step 1 and a maximum rated pump displacement equal to or greater than the value from Step 3.

Pump designation: Manufacturer B Type A 2½ × 1¼-1¼ in.

P/E	1.00
Rated displacement, B/D	492
Pump, B/D/strokes/min	4.92
Engine, B/D/strokes/min	5.02
Maximum rated speed, strokes/min	100

Step 5—Pump speed:

$$N = \frac{q_s / [(E_{p(\max)} \times E_{p(\text{int})})]}{q_p / N_{\max}} = \frac{250 / (0.97 \times 0.85)}{492 / 100} = 61.6 \text{ strokes/min.}$$

Step 6—Calculate power-fluid rate (assume 90% engine efficiency, E_e)

$$q_{pf} = N(q_e / N_{\max}) / E_e = 61.6(502 / 100) / 0.90 = 344 \text{ B/D.}$$

Step 7—Return fluid rate and properties—OPF system

- a. Total fluid rate: power fluid rate, q_{pf} = 344 B/D
+ production rate, q_s = 250 B/D
= total rate, q_d = 594 B/D

b. Water cut:

Water power fluid (Eq. 44)

$$W_{cd} = (q_{pf} + W_c q_s) / q_d = \text{_____}$$

Oil power fluid (Eq. 45)

$$W_{cd} = W_c q_s / q_d = 0.7 \times 250 / 594 = 0.29$$

c. Viscosity (Eq. 42)

$$\nu_m = (1 - W_{cd})\nu_o + W_{cd}\nu_w = (1 - 0.29)2 + 0.29 \times 0.485 = 1.56 \text{ cSt.}$$

d. Suction gradient (Eq. 40)

$$g_s = g_o(1 - W_c) + g_w W_c = 0.357(1 - 0.7) + 0.446 \times 0.7 = 0.419 \text{ psi/ft.}$$

e. Return gradient (Eq. 41)

$$g_d = [(q_{pf} \times g_{pf}) + (q_s \times g_s)] / q_d = [(344 \times 0.357) + (250 \times 0.419)] / 594 = 0.383 \text{ psi/ft.}$$

f. Gas/liquid ratio (Eq. 47)

$$F_{gL} = q_s(1 - W_c)R / q_d = 250(1 - 0.7)100 / 594 = 12.6 \text{ scf/bbl.}$$

Note: For vented installations, use solution GOR (Fig. 6.27).

TABLE 6.7—WORKSHEET AND SUMMARY OF EQUATIONS FOR RECIPROCATING PUMPS (continued)

Step 8—Return fluid rates and properties—closed power-fluid systems. Because the power fluid and produced fluid are kept separate, the power return conduit carries the flow rate from Step 6, with power-fluid gradient and viscosity. The production return conduit carries the desired production rate with production gradient, water cut, viscosity, and GOR.

- a. Power-fluid return rate _____ B/D
- b. Production return rate _____ B/D

Step 9—Return friction: If a gas lift chart or vertical multiphase flowing gradient correlation (see Chap. 5) is used for return flow calculations, it will already include friction values and the flowline backpressure. Use of gas lift charts or correlations is suggested if the gas/liquid ratio from Step 7 is greater than 10. The value from such a correlation can be used directly in Step 11c without calculating friction values. If a gas-lift chart or vertical flow correlation is not used, then with the values from Steps 7 and 8, as appropriate, determine the return conduit friction(s) from the charts or equations in Appendix B.

1. Open power-fluid friction $p_{fd} = \text{_____}$ psi.
2. Closed power-fluid friction

- a. power return $p_{fet} = \text{_____}$ psi.
- b. production return $p_{fd} = \text{_____}$ psi.

Step 10—Power-fluid friction: With the power-fluid rate from Step 6, use the appropriate charts or equations in Appendix B to determine the power-fluid friction loss.

Power fluid friction $p_{fpt} = 4.4$ psi.

Step 11—Return pressures:

- a. Open power-fluid system (Eq. 33)

$$p_{pd} = p_{fd} + g_d D + p_{wh} = \text{_____} \text{ psi.}$$

- b. Closed power-fluid system (Eqs. 37 and 38)

$$1. p_{ed} = p_{fet} + g_{pf} D + p_{whe} = \text{_____} \text{ psi.}$$

$$2. p_{pd} = p_{fd} + g_s D + p_{wh} = \text{_____} \text{ psi.}$$

- c. If a vertical multiphase flowing gradient correlation is used instead of Eqs. 33, 37, or 38, then $p_{pd} = 3,500$ psi.

Step 12—Required engine pressure p_{pf} :

- a. Open power-fluid system (Eq. 22)

$$p_{pf} = p_{pd} [1 + (P/E)] - p_{ps} (P/E) = 3,500[1 + 1] - 500(1) = 6,500 \text{ psi.}$$

- b. Closed power-fluid system (Eq. 21)

$$p_{pf} = p_{ed} + p_{pd} (P/E) - p_{ps} (P/E) = \text{_____} \text{ psi.}$$

Step 13—Calculate pump friction

- a. Rated pump displacement, $q_p = 492$ B/D
- b. Rated engine displacement, $q_e = 502$ B/D
- c. Total displacement, $q_{tm} = 994$ B/D
- d. "B" value (Table 6.5) = 0.000278
- e. $N/N_{max} = 61.6/100 = 0.616$
- f. $F_v = \nu/100 + 0.99 = 2/100 + 0.99 = 1.01$ (Eq. 28)
- g. Pump friction (Eq. 29 or Fig. 6.24)

$$p_{fr} = \gamma F_v (50) (7.1 e^{B q_{tm}^{N/N_{max}}})^{N/N_{max}}$$

$$p_{fr} = 0.82(1.01)(50)[7.1 e^{0.000278(994)}]^{0.616} = 164 \text{ psi.}$$

Step 14—Required surface operating pressure p_{so} (Eq. 36):

$$p_{so} = p_{pf} + p_{fpt} - g_{pf} D + p_{fr} = 6,500 + 4.4 - 0.357(9,000) + 164 = 3,455 \text{ psi.}$$

Step 15—Required surface horsepower, assuming 90% surface efficiency (Eq. 5):

$$P_h = q_{pf} \times p_{so} \times 0.000017/E_s = 344 \times 3,455 \times 0.000017/0.9 = 22.4 \text{ hp.}$$

Step 16—Summary:

Pump designation—Manufacturer B Type A 2½ × 1¼-1¼ in.	
Pump speed, strokes/min	61.6
Production rate, B/D	250
Power fluid rate, B/D	344
Power fluid pressure, psi	3,455
Surface horsepower	22.4

Step 17—Triplex options (from manufacturer specification sheet, Tables 6.16 through 6.18):

Type	J-30	D-323-H	
Plunger size, in.	1⅞	1⅞	
Revolutions/min	450	300	
Flow rate at revolutions/min (B/D)	400	399	
Maximum pressure rating, psi	3,590	4,000	
Horsepower	26	26	

TABLE 6.8—SUBSURFACE TROUBLESHOOTING GUIDE—RECIPROCATING PUMP

Indication	Cause	Remedy
1. Sudden increase in operating pressure—pump stroking.	(a) Lowered fluid level, which causes more net lift. (b) Paraffin buildup or obstruction in power-oil line, flow line, or valve. (c) Pumping heavy material, such as salt water or mud. (d) Pump beginning to fail.	(a) If necessary, slow pump down. (b) Run soluble plug or hot oil, or remove obstruction (c) Keep pump stroking—do not shut down. (d) Retrieve pump and repair.
2. Gradual increase in operating pressure—pump stroking.	(a) Gradually lowering fluid level. Standing valve or formation plugging up. (b) Slow buildup of paraffin. (c) Increasing water production.	(a) Surface pump and check. Retrieve standing valve. (b) Run soluble plug or hot oil. (c) Raise pump strokes/min and watch pressure.
3. Sudden increase in operating pressure—pump not stroking.	(a) Pump stuck or stalled. (b) Sudden change in well conditions requiring operating pressure in excess of triplex relief valve setting. (c) Sudden change in power-oil emulsion, etc. (d) Closed valve or obstruction in production line.	(a) Alternately increase and decrease pressure. If necessary, unseat and reseat pump. If this fails to start pump, surface and repair. (b) Raise setting on relief valve. (c) Check power-oil supply. (d) Locate and correct.
4. Sudden decrease in operating pressure—pump stroking. (Speed could be increased or reduced.)	(a) Rising fluid level—pump efficiency up. (b) Failure of pump so that part of power oil is bypassed. (c) Gas passing through pump. (d) Tubular failure—downhole or in surface power-oil line. Speed reduced. (e) Broken plunger rod. Increased speed. (f) Seal sleeve in BHA washed or failed. Speed reduced.	(a) Increase pump speed if desired. (b) Surface pump and repair. (d) Check tubulars. (e) Surface pump and repair. (f) Pull tubing and repair BHA.
5. Sudden decrease in operating pressure—pump not stroking.	(a) Pump not on seat. (b) Failure of production unit or external seal. (c) Bad leak in power-oil tubing string. (d) Bad leak in surface power-oil line. (e) Not enough power-oil supply at manifold.	(a) Circulate pump back on seat. (b) Surface pump and repair. (c) Check tubing and pull and repair if leaking. (d) Locate and repair. (e) Check volume of fluid discharged from triplex. Valve failure, plugged supply line, low power-oil supply, excess bypassing, etc., all of which could reduce available volume.
6. Drop in production—pump speed constant.	(a) Failure of pump end of production unit. (b) Leak in gas-vent tubing string. (c) Well pumped off—pump speeded up. (d) Leak in production return line. (e) Change in well conditions. (f) Pump or standing valve plugging. (g) Pump handling free gas.	(a) Surface pump and repair. (b) Check gas-vent system. (c) Decrease pump speed. (d) Locate and repair. (f) Surface pump and check. Retrieve standing valve. (g) Test to determine best operating speed.
7. Gradual or sudden increase in power oil required to maintain pump speed. Low engine efficiency.	(a) Engine wear. (b) Leak in tubulars—power-oil tubing, BHA seals, or power-oil line.	(a) Surface pump and repair. (b) Locate and repair.
8. Erratic stroking at widely varying pressures.	(a) Caused by failure or plugging of engine.	(a) Surface pump and repair.
9. Stroke "downkicking" instead of "upkicking."	(a) Well pumped off—pump speeded up. (b) Pump intake or downhole equipment plugged. (c) Pump failure (balls and seats). (d) Pump handling free gas.	(a) Decrease pump speed. Consider changing to smaller pump end. (b) Surface pump and clean up. If in downhole equipment, pull standing valve and backflush well. (c) Surface pump and repair.
10. Apparent loss of, or unable to account for, system fluid.	(a) System not full of oil when pump was started due to water in annulus U-tubing after circulating, well flowing or standing valve leaking. (b) Inaccurate meters or measurement.	(a) Continue pumping to fill up system. Pull standing valve if pump surfacing is slow and cups look good. (b) Recheck meters. Repair if necessary.

TABLE 6.9—SUBSURFACE TROUBLESHOOTING GUIDE—JET PUMPS

Indication	Cause	Remedy
1. Sudden increase in operating pressure—pump taking power fluid.	(a) Paraffin buildup or obstruction in power-oil line, flowline, or valve. (b) Partial plug in nozzle.	(a) Run soluble plug or hot oil, or remove obstruction. Unseat and reseat pump. (b) Surface pump and clear nozzle.
2. Slow increase in operating pressure—constant power-fluid rate or slow decrease in power-fluid rate, constant operating pressure.	(a) Slow buildup of paraffin. (b) Worn throat or diffuser.	(a) Run soluble plug or hot oil. (b) Retrieve pump and repair.
3. Sudden increase in operating pressure—pump not taking power fluid.	(a) Fully plugged nozzle.	(a) Retrieve pump and clear nozzle.
4. Sudden decrease in operating pressure—power-fluid rate constant or sudden increase in power-fluid rate, operating pressure constant.	(a) Tubular failure. (b) Blown pump seal or broken nozzle.	(a) Check tubing and pull and repair if leaking. (b) Retrieve pump and repair.
5. Drop in production—surface conditions normal.	(a) Worn throat or diffuser. (b) Plugging of standing valve or pump. (c) Leak or plug in gas vent. (d) Changing well conditions.	(a) Increase operating pressure. Replace throat and diffuser. (b) Surface pump and check. Retrieve standing valve. (c) Check gas-vent system. (d) Run pressure recorder and resize pump.
6. No production increase when operating pressure is increased.	(a) Cavitation in pump or high gas production. (b) Plugging of standing valve or pump.	(a) Lower operating pressure or install larger throat. (b) Surface pump and check. Retrieve standing valve.
7. Throat worn—one or more dark, pitted zones.	(a) Cavitation damage.	(a) Check pump and standing valve for plugging. Install larger throat. Reduce operating pressure.
8. Throat worn—cylindrical shape worn to barrel shape, smooth finish.	(a) Erosion wear.	(a) Replace throat. Install premium-material throat. Install larger nozzle and throat to reduce velocity.
9. New installation does not meet prediction of production.	(a) Incorrect well data. (b) Plugging of standing valve or pump. (c) Tubular leak. (d) Side string in parallel installation not landed.	(a) Run pressure recorder and resize pump. (b) Check pump and standing valve. (c) Check tubing and pull and repair if leaking. (d) Check tubing and restab if necessary.

TABLE 6.10—POWER OIL PLUNGER PUMPS TROUBLESHOOTING GUIDE

Possible Cause	Correction
<u>Knocking or Pounding in Fluid End and Piping</u>	
Suction line restricted by	
a. Trash, scale build-up, etc.	Locate and remove.
b. Partially closed valve in suction line.	Locate and correct.
c. Meters, filters, check valves, non-full-opening, cut-off valves or other restrictions.	Rework suction line to eliminate.
d. Sharp 90° bends or 90° blind tees.	Rework suction line to eliminate.
Air entering suction line through valve stem packing.	Tighten or repack valve stem packing.
Air entering suction line through loose connection or faulty pipe.	Locate and correct.
Air or vapor trapped in suction.	Locate rise or trap and correct by straightening line, providing enough slope to permit escape and prevent buildup.
Low fluid level.	Increase supply and install automatic low-level shutdown switch.
Suction dampener not operating.	Inspect and repair as required.
Worn pump valves or broken spring.	Inspect and repair as required.
Entrained gas or air in fluid.	Provide gas boot or scrubber for fluid.
Inadequate size of suction line.	Replace with individual suction line or next size larger than inlet of pump.
Leaking pressure relief valve that has been piped back into pump suction.	Repair valve and rework piping to return to supply tank—not suction line.
Bypass piped back to suction.	Rework to return bypassed fluid back to supply tank—not supply line.
Broken plunger.	Inspect when rotating pump by hand and replace as required.
Worn crosshead pin or connecting rod.	Locate and replace as required.
<u>Knock in Power End</u>	
Worn crosshead pin or connecting rod.	Locate and replace as required. Check oil quality and level.
Worn main bearings.	Replace as required. Check oil quality and level.
Loose plunger—intermediate rod—crosshead connection.	Inspect for damage—replace as required and tighten.
<u>Rapid Valve Wear or Failure</u>	
Cavitation.	Predominant cause of short valve life and is always a result of poor suction conditions. This situation can be corrected by following appropriate recommendations as listed under No. 1.
Corrosion.	Treat fluid as required.
Abrasives in fluid.	Treat to remove harmful solids.
<u>Fluid Seal Plunger Wear, Leakage, or Failure</u>	
Solids in power oil.	This is likely to cause greatest amount of wear. Power oil should be analyzed for amount and type of solids content. Proper treating to remove solids should be instigated.
Improper installation.	Follow written instructions and use proper tools. Remember, plunger and liner are matched sets. Ensure proper lubrication at startup. (Be sure air is bled out of fluid end before starting up.)
<u>Reduced Volume or Pressure</u>	
Bypassing fluid.	Locate and correct.
Air in fluid end of triplex.	Bleed off.
Inaccurate meter or pressure gauge.	Check and correct.
Pump suction cavitation due to improper hook-up, suction restriction or entrained gas.	Locate and correct.
Valves worn or broken.	Replace.
Plungers and liners worn.	Replace.
Reduced prime mover speed because of increased load, fuel or other conditions.	Determine cause and correct. (May be increased pressure caused by paraffin, temperature change, etc.)

Jet Pumps

Jet pumps are a type of downhole pump that can be used in hydraulic pumping systems instead of the reciprocating pumps previously discussed. They can be adapted to fit interchangeably into the BHA's designed for the stroking pumps. In addition, special BHA's have been designed for jet pumps to take advantage of their short length and their high-volume characteristics. Because of their unique characteristics under different pumping conditions, jet pumps should be considered as an alternative to the conventional stroking pumps.

Although technical references to jet pumps can be found as far back as 1852,¹³ it was not until 1933¹⁴ that a consistent mathematical representation was published, which included suggestions for pumping oil wells.¹⁵ Angier and Crocker¹⁶ applied for a patent on an oil well jet pump in 1864 that looked very much like those currently marketed.¹⁶ Jacuzzi¹⁷ received a patent in 1930 for jet pumps that were subsequently used in shallow water wells very successfully. McMahon¹⁸ also received the first of six patents on oilwell jet pumps in 1930. Apparently McMahon built and marketed pumps in California in the late 1930's, but they did not achieve widespread usage. Hardware improvements and the advent of computer models for correct application sizing in oil wells led to the successful marketing of jet pumps in 1970.^{1,2} Use of jet pumps has grown steadily since then. More recent publications on hydraulic pumping that describe the use of jet pumps in oil wells include those by Wilson,¹ Bell and Spisak,² Christ and Zublin,⁶ Nelson,¹⁹ Brown,²⁰ Clark,²¹ Bleakley,²² and Petrie *et al.*²³ Much of the following discussion derives from Refs. 20, 23, and 24.

An example of the simplest downhole jet free-pump completion, the single-seal style, is shown in Fig. 6.31. The most significant feature of this device is that it has no moving parts. The pumping action is achieved through energy transfer between two moving streams of fluid. The high-pressure power fluid supplied from the surface passes through the nozzle where its potential energy (pressure) is converted to kinetic energy in the form of a very-high-velocity jet of fluid. Well fluids surround the power-fluid jet at the tip of the nozzle, which is spaced back from the entrance of the mixing tube. The mixing tube, usually called the throat, is a straight, cylindrical bore about seven diameters long with a smoothed radius at the entrance. The diameter of the throat is always larger than the diameter of the nozzle exit, allowing the well fluids to flow around the power-fluid jet and be entrained by it into the throat. In the throat, the power fluid and produced fluid mix, and momentum is transferred from the power fluid to the produced fluid, causing an energy rise in it. By the end of the throat, the two fluids are intimately mixed, but they are still at a high velocity, and the mixture contains significant kinetic energy. The mixed fluid enters an expanding area diffuser that converts the remaining kinetic energy to static pressure by slowing down the fluid velocity. The pressure in the fluid is now sufficient to flow it to the surface from the downhole pump.

With no moving parts, jet pumps are rugged and tolerant of corrosive and abrasive well fluids. The nozzle and throat are usually constructed of tungsten carbide or ceramic materials for long life. Jet pumps are compact and can even be adapted to TFL completions that require the

pump to be circulated around a 5-ft-radius loop in the power-fluid tubing at the wellhead. Successful jet-pump adaptations have also been made for sliding side doors (see Fig. 6.5) in both the normal and reverse flow configurations. These are normally run in on wireline or as a fixed or conventional installation on continuous coiled tubing, and have been successful in offshore drillstem testing (DST) of heavy-crude reservoirs. Other applications include the dewatering of gas wells.²⁵

With different sizes of nozzles and throats, jet pumps can produce wells at less than 50 B/D or up to rates in excess of 10,000 B/D. As with all hydraulic pumping systems, a considerable range of production is possible from a particular downhole pump by controlling the power-fluid supply at the surface. In a given size tubing, the maximum achievable rates are usually much higher than those possible with stroking pumps. Significant free-gas volumes can be handled without the problems of pounding or excessive wear associated with positive-displacement pumps, or the inlet choking encountered in centrifugal pumps. The lack of vibration and the free-pump feature make them ideal for use with pumpdown pressure recorders to monitor BHP's at different flow rates.

Because they are high-velocity mixing devices, there is significant turbulence and friction within the pump, leading to lower horsepower efficiencies than can be achieved with positive-displacement pumps. This often leads to higher surface horsepower requirements, although some gassy wells may actually require less power. Jet pumps are prone to cavitation at the entrance of the throat at low pump intake pressures, and this must be considered in design calculations. Also, because of the nature of their performance curves, the calculations used for installation design are complex and iterative in nature and are best handled by programmable calculators or computers. Despite these limitations, their reliability and volume capability make them attractive in many wells, and their use has become widespread since commercial introduction in the early 1970's.

Performance Characteristics

Intuitively, larger-diameter nozzles and throats would seem to have higher flow capacities, and this is the case. The ratio of the nozzle area to the throat area is an important variable, however, because this determines the tradeoff between produced head and flow rate. Fig. 6.32 shows a schematic of the working section of a jet pump. If, for a given nozzle, a throat is selected such that the area of the nozzle, A_n , is 60% of the area of the throat, A_t , a relatively high-head, low-flow pump will result. There is a comparatively small area, A_s , around the jet for well fluids to enter. This leads to low production rates compared to the power-fluid rate, and because the energy of the nozzle is transferred to a small amount of production, high heads will develop. Such a pump is suited for deep wells with high lifts. Substantial production rates can be achieved if the pump is physically large, but the production rate will always be less than the power-fluid rate.

If a throat is selected such that the area of the nozzle is only 20% of the area of the throat, much more flow area around the jet is available for the production. How-

ever, because the nozzle energy is transferred to a large amount of production compared to the power-fluid rate, lower heads will be developed. Shallow wells with low lifts are candidates for such a pump.

Any number of such area combinations are possible to match different flow and lift requirements best. Attempting to produce small amounts of production compared to the power-fluid rate with a nozzle/throat-area ratio of 20% will be inefficient as a result of high turbulent mixing losses between the high-velocity jet and the slow-moving production. Conversely, attempting to produce high production rates compared to the power-fluid rate with a nozzle/throat-area ratio of 60% will be inefficient because of high friction losses as the produced fluid moves rapidly through the relatively small throat. Optimal ratio selection involves a tradeoff between these mixing and friction losses.

As a type of dynamic pump, jet pumps have characteristic performance curves similar to electric submersible pumps. An example is shown in Fig. 6.33. A family of performance curves is possible, depending on the nozzle pressure supplied to the pump from the surface. Different sizes of throats used in conjunction with a given nozzle give different performance curves. If the nozzle and throat areas of the pumps represented in Fig. 6.33 were doubled, the nozzle flow rates would double, and the production rates would double for each value of the pressure rise, Δp . The maximum Δp at zero production rate would remain the same. The curves are generally fairly flat, especially with the larger throats, which makes the jet pump sensitive to changes in intake or discharge pressure. Because variable fluid mixture densities, gas/liquid ratios, and viscosities affect the pressures encountered by the pump, the calculations to simulate performance are complex and iterative in nature, and lend themselves to a computer solution.

Cavitation in Jet Pumps

Because the production must accelerate to a fairly high velocity (200 to 300 ft/sec) to enter the throat, cavitation is a potential problem. The throat and nozzle flow areas define an annular flow passage at the entrance of the throat. The smaller this area is, the higher the velocity of a given amount of produced fluid passing through it. The static pressure of the fluid drops as the square of the

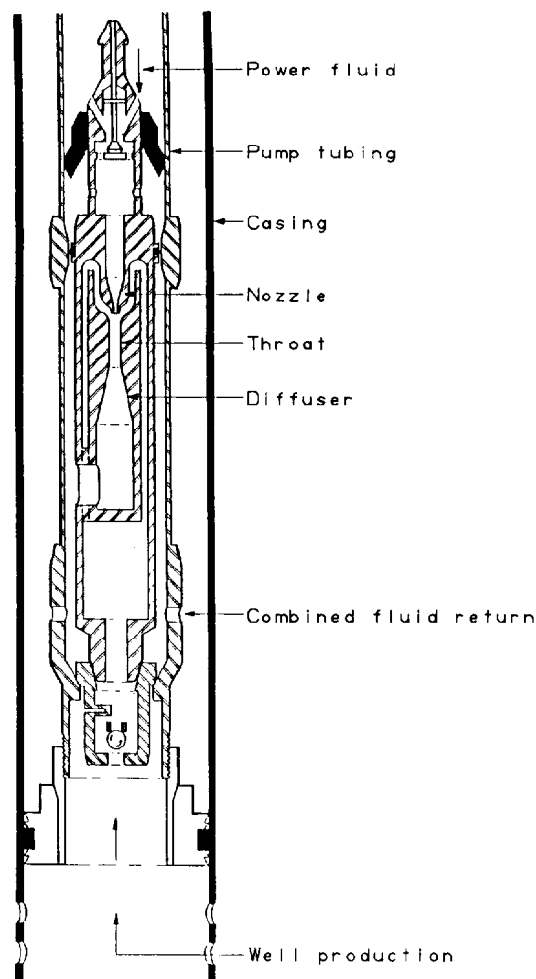


Fig. 6.31—Typical single-seal jet pump.

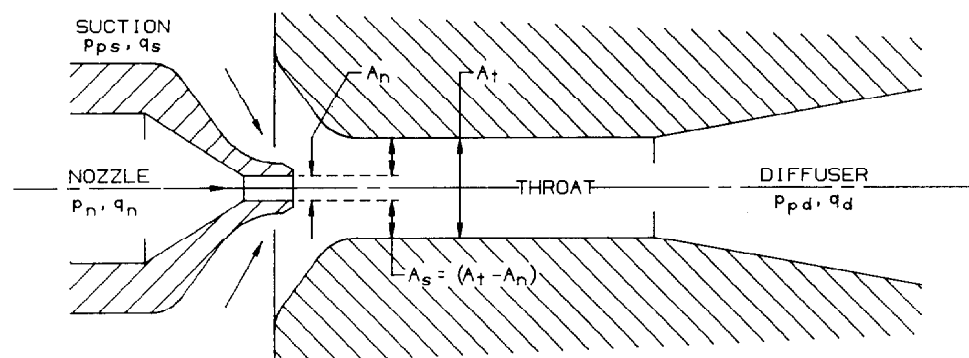


Fig. 6.32—Jet-pump nomenclature.

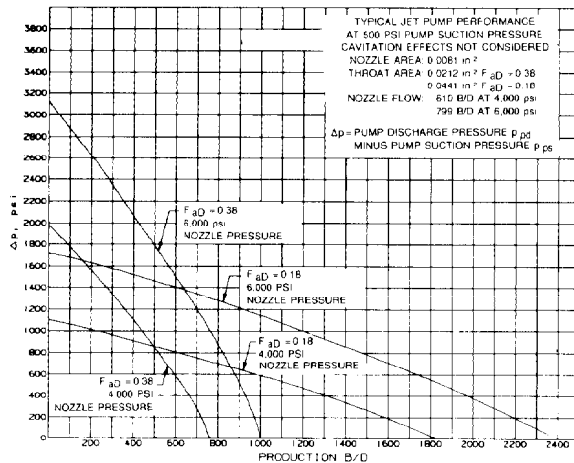


Fig. 6.33—Typical jet-pump performance.

velocity increases and will decline to the vapor pressure of the fluid at high velocities. This low pressure will cause vapor cavities to form, a process called cavitation. This results in choked flow into the throat, and production increase are not possible at that pump-intake pressure, even if the power-fluid rate and pressure are increased. Subsequent collapse of the vapor cavities as pressure is built up in the pump may cause erosion known as cavitation damage. Thus, for a given production flow rate and pump intake pressure, there will be a minimum annular flow area required to keep the velocity low enough to avoid cavitation. This phenomenon has been the subject of numerous investigations. Notable is that of Cunningham and Brown,²⁶ who used actual oilwell pump designs at the high pressures used in deep wells.

The description of the cavitation phenomenon previously discussed suggests that if the production flow rate approaches zero, the potential for cavitation will disappear because the fluid velocities are very low. Under these conditions, however, the velocity difference between the power-fluid jet and the slow-moving production is at a maximum, which creates an intense shear zone on the boundary between them. Such a shear zone constantly generates vortices, the cores of which are at a reduced pressure. Vapor cavities may form in the vortex cores, leading to erosion of the throat walls as the bubbles collapse because of vortex decay and pressure rise in the pump. Although no theoretical treatments of this phenomenon have been published, it has been the subject of experimental work. This has led to the inclusion of potential damage zones on performance prediction plots by some suppliers. This experimental correlation predicts cavitation damage at low flow rates and low pump-intake pressures before the choked flow condition occurs. Field experience has shown, however, that in most real oil wells, the erosion rate in this operating region is very low, probably because of produced gas cushioning the system by reducing the propagation velocity of the bubble-collapse shock waves. It is generally agreed that this phenomenon is of concern only in very-high-water-cut wells with virtually no gas present. Under these conditions, cavitation erosion has been observed even at very low pro-

duction rates. If a jet pump is operated near its best efficiency point, the shear vortices are a distinctly second-order effect in the cavitation process.

Mathematical Presentation

The manufacturers of oilfield jet pumps offer a large number of nozzle and throat combinations for various pumping conditions. For each nozzle size, five or more throats can be used to give different head-flow characteristics. There is no standardization of sizes, however, leading to a very large number of performance curves. Because each curve is really a family of curves that depend on the nozzle pressure, selection of the proper pump for a particular well is confusing. This problem can be greatly simplified with a unifying mathematical representation.

Cunningham^{27,28} has expanded on the original Gosline-O'Brien presentation¹⁴ in writing a set of equations describing the performance of geometrically similar pumps. If the equations are written nondimensionally, they will apply to all sizes of pumps as long as the operating Reynolds numbers are close or sufficiently high that viscosity effects are negligible. Because oilwell jet pumps necessarily require high pressures and velocities because of the large lifts involved, this latter condition is usually met.

By considering the energy and momentum equations for the nozzle, suction passage, throat (mixing tube), and diffuser, the following equations can be derived for a jet pump of the configuration shown in Fig. 6.32.

Nozzle Flow Rate (B/D).

$$q_n = 832 A_n \sqrt{(p_n - p_{ps})/g_n}, \dots \dots \dots (55)$$

where p_n = nozzle pressure, psi, and g_n = nozzle flow gradient, psi/ft.

Dimensionless Area Ratio.*

$$F_{aD} = A_n/A_1, \dots \dots \dots (56)$$

Dimensionless Mass Flow Ratio.*

$$F_{mD} = (q_s \times g_s)/(q_n \times g_n), \dots \dots \dots (57)$$

where q_s = suction flow rate, B/D, and g_s = suction gradient, psi/ft.

Dimensionless Pressure Ratio.*

$$F_{pD} = (p_{pd} - p_{ps})/(p_n - p_{pd}); \dots \dots \dots (58)$$

$$F_{pD} = \{2F_{aD} + [(1 - 2F_{aD})(F_{mD}^2 F_{aD}^2)/(1 - F_{aD})^2] - (1 + K_{td})F_{aD}^2(1 + F_{mD})^2\} / \{(1 + K_n) - \{2F_{aD} + [(1 - 2F_{aD})(F_{mD}^2 F_{aD}^2)/(1 - F_{aD})^2] - (1 + K_{td})F_{aD}^2(1 + F_{mD})^2\}\} \dots \dots \dots (59)$$

*Ref. 14 uses R_m , M , and N and Ref. 27 uses b , ϕ , and N , respectively.

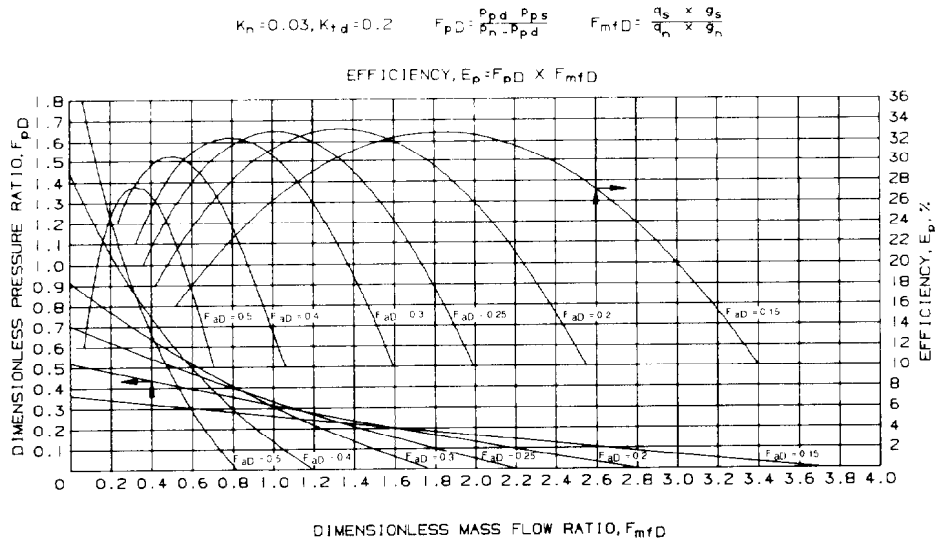


Fig. 6.34—Typical dimensionless performance curves.

Note that Eq. 59 is of the form

$$F_{pD} = \frac{\text{Numerator}}{(1 + K_n) - \text{Numerator}} \quad (60)$$

Efficiency.

$$E_p = F_{mD} \times F_{pD} = \frac{(p_{pd} - p_{ps})(q_s \times g_s)}{(p_n - p_{pd})(q_n \times g_n)} \quad (61)$$

Cavitation area, sq in.

$$A_{cm} = \frac{q_s}{691 \sqrt{\frac{p_{ps}}{g_s}}} \quad (62)$$

Eq. 55 for the nozzle flow rate can be recognized as the expression for flow through an orifice with a power fluid whose gradient is g_n psi/ft. This nozzle flow gradient is the same variable as g_{pf} used earlier for the gradient of the power fluid supplied to the engine of a stroking hydraulic pump. Eq. 56 defines F_{aD} as the dimensionless ratio of the nozzle area to that of the throat. Eq. 57 defines a dimensionless mass flow ratio equal to the production or suction flow rate divided by the nozzle flow rate times the ratio of the suction gradient divided by the nozzle fluid gradient. Eq. 58 defines a dimensionless pressure ratio. Physically, it is the ratio of the pressure rise imparted to the produced fluid to the pressure lost by the power fluid in the pump. Eq. 59 is a formulation for the dimensionless pressure of Eq. 58 in terms of the area ratio, F_{aD} , the mass flow ratio, F_{mD} , and two loss coefficients, K_{td} and K_n . These loss coefficients are experimentally

determined and are similar to orifice and pipe friction loss coefficients. Eqs. 57 and 58 can be combined to give the efficiency expressed in Eq. 61. Because hydraulic power is the product of pressure differential times flow rate, Eq. 61 is interpreted as the ratio of the power added to the produced fluid to the power lost from the power fluid. Eq. 62, derived from the orifice flow equation for the annular production flow area, A_s , at the entrance of the throat, defines the minimum flow area required to avoid cavitation if the suction flow rate is q_s and is at a pressure p_{ps} . This equation includes the assumption that the pressure at the entrance of the throat is zero at cavitation.

A slightly different formulation of these equations can be found in Brown,⁷ following the method of Gosline and O'Brien.¹⁴ The two methods give comparable results, although the formulation in Eq. 59 is more complex algebraically in the Gosline-O'Brien method. Also, the empirical loss coefficients (K_{td} and K_n) will be slightly different numerically when experimental results are correlated with the equations. The dimensionless cavitation prediction equation found in Brown will reduce to Eq. 62 if the power fluid and production have the same gradient and the dimensions from a particular size pump are used.

A representative set of dimensionless performance curves based on Eq. 59 is shown in Fig. 6.34 for typical nozzle/throat-area ratios of 0.50, 0.40, 0.30, 0.25, 0.20, and 0.15. The power fluid and produced fluid are of the same density. A nozzle loss coefficient K_n of 0.03 was used, which is typical of a well-shaped and smoothed design. A throat-diffuser loss coefficient, K_{td} , of 0.20 was used. Lower values can be obtained in laboratory tests, but this conservative value compensates for average losses in routing fluids through the rest of the pump and BHA. The peak efficiencies of about 33% shown in Fig. 6.34 can be achieved with commercially available pumps producing typical well fluids at around a 700-B/D rate.

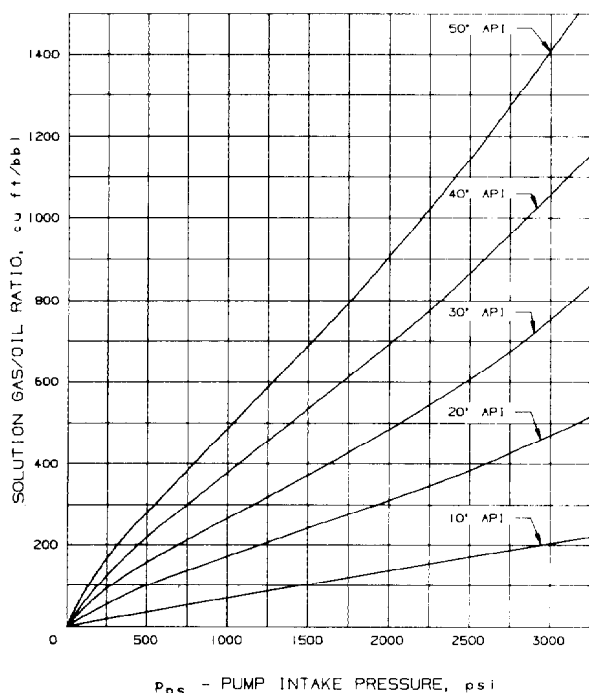


Fig. 6.35—GOR for gas-vented production.

Much larger or smaller pumps producing fluids of very low or high viscosity can result in pumps with somewhat higher or lower efficiencies, respectively. Note that each area-ratio curve has an associated efficiency curve, and that there is a most-efficient ratio for a given value of the dimensionless mass flow ratio, F_{mfD} . These curves represent the type of noncavitating performance obtainable from the jet pumps available for oilwell production. Fig. 6.34 shows that the jet pumps with area ratios, F_{aD} , of 0.30 and 0.25 have the highest peak efficiencies. Pumps with an F_{aD} value greater than 0.50 or less than 0.10 will have noticeably reduced peak efficiencies. This effect is predicted by Eq. 59. Operating under cavitating conditions will result in deviations from these curves.

By presentation of jet-pump performance in the dimensionless form of Fig. 6.34, a significant simplification has been achieved. Any jet pump, regardless of its size, will have a performance curve that corresponds to the standard one for the particular area ratio of the pump. If the pressure environment the pump encounters leads to a calculated value for F_{pD} of 0.50, the mass ratio the unit will deliver can be read from Fig. 6.34. For power and produced fluids of equal density (or gradient), the mass ratio is also the volume ratio of produced fluid to power fluid. If $F_{aD}=0.5$, then $F_{mfD}=0.47$. This means that if a nozzle size is used that supplies 100 B/D of power fluid, 47 B/D of production will be obtained. If $F_{aD}=0.4$, then $F_{mfD}=0.60$, and 60 B/D production could be obtained with 100 B/D power fluid. If $F_{aD}=0.3$, then $F_{mfD}=0.62$, and 62 B/D production would be pumped. If $F_{aD}=0.25$, then F_{mfD} drops to 0.52, and the production to only 52 B/D. This illustrates that the pump with an area ratio of $F_{aD}=0.3$ is the most efficient for this

value of F_{pD} and will produce the most fluid. If a much larger nozzle were used that supplies 1,000 B/D of power fluid, a jet pump with an area ratio of $F_{aD}=0.3$ would produce 620 B/D of production if the system pressures were such that $F_{pD}=0.50$. The many ratios available from the suppliers are not always the same as those shown in Fig. 6.34. Therefore, a calculation scheme that will consider all the possible available ratios should be based on the basic equations. This will become more apparent when the effects of gas are considered.

Approximations for Handling Gas

The equations previously presented are for liquids. The free gas present in many oil wells affects pump performance. A rigorous treatment of the pumping of multiphase and compressible fluids is outside the scope of this chapter. It has been found, however, that simple but useful approximations can be made. Cunningham²⁷ found that if the free-gas volume is added to the liquid volume as if it were liquid, pump performance follows the standard curves reasonably well. Eq. 57 then becomes

$$F_{mfD} = \frac{q_s + q_g}{q_n} \left(\frac{g_s}{g_n} \right), \dots \dots \dots (63)$$

where q_g is the flow rate of free gas in B/D at pump-intake pressure conditions.

A review of Standing's⁹ work by F.C. Christ for a variety of bottomhole conditions results in an empirical correlation for the gas-plus-liquid FVF. When this is substituted into Eq. 63, the following relationship is obtained:*

$$F_{mfD} = q_s \left\{ \left[1 + 2.8 \left(\frac{R}{p_{ps}} \right)^{1.2} \right] (1 - W_c) + W_c \right\} \times \left(\frac{g_s}{q_n \times g_n} \right), \dots \dots \dots (64)$$

where R =producing GOR, scf/bbl.

The relationship expressed in Eq. 64 is similar to that used to generate Fig. 6.27 for the stroking-pump volumetric efficiency. This simplified expression is suggested for use with jet pump calculations, however, because its simplicity is helpful if the relationships are fitted into the limited memory of hand-held programmable calculators. It was found to give very reasonable results in conjunction with the other jet pump equations in over 8 years of comparisons between predicted jet pump performance and the actual field results.

A cavitation correction for gas is also required.* If the assumption of choked flow into the throat annulus around the power fluid jet is made and the downhole fluid properties are typical, the additional area required to pass the gas is

$$A_g = \frac{q_s(1 - W_c)R}{24,650 p_{ps}}, \dots \dots \dots (65)$$

*Personal communication with F.C. Christ, Natl. Supply Co.

TABLE 6.11—NOZZLE AND THROAT SIZES

Manufacturer A				Manufacturer B				Manufacturer C			
Nozzle		Throat		Nozzle		Throat		Nozzle		Throat	
Number	Area	Number	Area	Number	Area	Number	Area	Number	Area	Number	Area
1	0.0024	1	0.0064	1	0.0024	1	0.0060	DD	0.0016	000	0.0044
2	0.0031	2	0.0081	2	0.0031	2	0.0077	CC	0.0028	00	0.0071
3	0.0039	3	0.0104	3	0.0040	3	0.0100	BB	0.0038	0	0.0104
4	0.0050	4	0.0131	4	0.0052	4	0.0129	A	0.0055	1	0.0143
5	0.0064	5	0.0167	5	0.0067	5	0.0167	B	0.0095	2	0.0189
6	0.0081	6	0.0212	6	0.0086	6	0.0215	C	0.0123	3	0.0241
7	0.0103	7	0.0271	7	0.0111	7	0.0278	D	0.0177	4	0.0314
8	0.0131	8	0.0346	8	0.0144	8	0.0359	E	0.0241	5	0.0380
9	0.0167	9	0.0441	9	0.0186	9	0.0464	F	0.0314	6	0.0452
10	0.0212	10	0.0562	10	0.0240	10	0.0599	G	0.0452	7	0.0531
11	0.0271	11	0.0715	11	0.0310	11	0.0774	H	0.0661	8	0.0661
12	0.0346	12	0.0910	12	0.0400	12	0.1000	I	0.0855	9	0.0804
13	0.0441	13	0.1159	13	0.0517	13	0.1292	J	0.1257	10	0.0962
14	0.0562	14	0.1476	14	0.0668	14	0.1668	K	0.1590	11	0.1195
15	0.0715	15	0.1879	15	0.0863	15	0.2154	L	0.1963	12	0.1452
16	0.0910	16	0.2392	16	0.1114	16	0.2783	M	0.2463	13	0.1772
17	0.1159	17	0.3046	17	0.1439	17	0.3594	N	0.3117	14	0.2165
18	0.1476	18	0.3878	18	0.1858	18	0.4642	P	0.3848	15	0.2606
19	0.1879	19	0.4938	19	0.2400	19	0.5995			16	0.3127
20	0.2392	20	0.6287	20	0.3100	20	0.7743			17	0.3750
						21	1.0000			18	0.4513
						22	1.2916			19	0.5424
						23	1.6681			20	0.6518
						24	2.1544				

Nozzle	Throat	Ratio (F_{AD})	Nozzle	Throat	Ratio (F_{AD})
N	N-1	0.483 X	N	N-1	0.517 A-
N	N	0.380 A	N	N	0.400 A
N	N+1	0.299 B	N	N+1	0.310 B
N	N+2	0.235 C	N	N+2	0.240 C
N	N+3	0.184 D	N	N+3	0.186 D
N	N+4	0.145 E	N	N+4	0.144 E

Manufacturer C ratios listed in Table 6.12.

Eq. 62 considering gas then becomes

$$A_{cm} = q_s \left[\frac{1}{691} \sqrt{\frac{g_s}{p_{ps}}} + \frac{(1 - W_c)R}{24,650 p_{ps}} \right] \dots \dots \dots (66)$$

If provisions for venting free gas are made, the solution GOR at pump suction conditions rather than the total GOR should be used in Eqs. 64 through 66. Fig. 6.35 shows the appropriate solution GOR for different values of p_{ps} and various API gravities in vented systems. Fig. 6.35 is based on Muskat's work²⁹ and shows higher GOR values at low pump-intake pressures than does Fig. 6.27, which is based on Standing's⁸ work. It has been found from field testing that the Muskat correlation gives better results in conjunction with the other approximations used in the jet-pump equations. If the total GOR is less than the value from Fig. 6.35, it indicates that all the gas is in solution (p_{ps} is above the bubblepoint) and the total GOR should be used. A vent system is not necessary in such a case. As mentioned previously, parallel installations automatically provide a gas vent unless a packer has been set or the casing outlet is shut off.

Nozzle and Throat Sizes

Each manufacturer has different sizes and combinations of nozzles and throats. Manufacturers A and B increase the areas of nozzles and throats in a geometric

progression—i.e., the flow area of any nozzle or throat is a constant multiple of the area of the next smaller size. Manufacturer B's factor is $10^{1/9} = 1.29155$ and Manufacturer A's factor is $4/\pi = 1.27324$. The system of sizes offered by Manufacturer C uses a similar geometric progression concept, but does not use the same factor over the total range. In the smaller sizes, where the change in horsepower per size is small, the rate of increase in area is more rapid than in the systems of Manufacturers A and B. In the larger, higher-horsepower sizes, the percent increase in size is less rapid than in the other systems to limit the incremental increase in horsepower. The sizes offered by Manufacturer C cover a slightly larger range than those of Manufacturers A and B. The sizes from these manufacturers are listed in Table 6.11. The maximum sizes of nozzles and throats that are practical in pumps for a given tubing size depend on the fluid passages of the particular pump, BHA, swab nose, and standing valve. Single-seal pumps cannot use nozzles as large as those practical in higher-flow, multiple-seal pumps. In general, nozzles larger than 0.035 sq in. in flow area are used only in pumps for 2½- and 3½-in. tubing.

The strict progression used by Manufacturers A and B establishes fixed area ratios between the nozzles and different throats. A given nozzle matched with the same number throat will always give the same area ratio: 0.380 in Manufacturer A's system, and 0.400 in Manufacturer B's system (Table 6.11). This is called the A ratio. Successively larger throats matched with a given nozzle give

TABLE 6.12—MANUFACTURER C RATIOS AND THROAT ANNULUS AREAS, SQ IN.

Nozzle									
DD	Throats	000	00						
	F_{aD}	0.36	0.22						
	A_s	0.0028	0.0056						
CC	Throats	000	00	0	1				
	F_{aD}	0.64	0.40	0.27	0.20				
	A_s	0.0016	0.0043	0.0076	0.0115				
BB	Throats	00	0	1	2				
	F_{aD}	0.54	0.37	0.27	0.20				
	A_s	0.0032	0.0065	0.0105	0.0150				
A	Throats	0	1	2	3				
	F_{aD}	0.53	0.39	0.29	0.23				
	A_s	0.0048	0.0088	0.0133	0.0185				
B	Throats	0	1	2	3	4	5	6	
	F_{aD}	0.92	0.66	0.50	0.40	0.30	0.25	0.21	
	A_s	0.0009	0.0048	0.0094	0.0145	0.0219	0.0285	0.0357	
C	Throats	1	2	3	4	5	6	7	
	F_{aD}	0.86	0.65	0.51	0.39	0.32	0.27	0.23	
	A_s	0.0020	0.0066	0.0118	0.0191	0.0257	0.0330	0.0408	
D	Throats	3	4	5	6	7	8	9	
	F_{aD}	0.74	0.56	0.46	0.39	0.33	0.27	0.22	
	A_s	0.0064	0.0137	0.0203	0.0276	0.0354	0.0484	0.0628	
E	Throats	4	5	6	7	8	9	10	11
	F_{aD}	0.77	0.63	0.53	0.45	0.36	0.30	0.25	0.20
	A_s	0.0074	0.0140	0.0212	0.0290	0.0420	0.0564	0.0722	0.0954
F	Throats	6	7	8	9	10	11	12	
	F_{aD}	0.69	0.59	0.48	0.39	0.33	0.26	0.22	
	A_s	0.0138	0.0217	0.0346	0.0490	0.0648	0.0880	0.1138	
G	Throats	8	9	10	11	12	13	14	
	F_{aD}	0.68	0.56	0.47	0.38	0.31	0.26	0.21	
	A_s	0.0208	0.0352	0.0510	0.0742	0.1000	0.1320	0.1712	
H	Throats	10	11	12	13	14	15	16	
	F_{aD}	0.69	0.55	0.45	0.37	0.30	0.25	0.21	
	A_s	0.0302	0.0534	0.0792	0.1112	0.1504	0.1945	0.2467	
I	Throats	11	12	13	14	15	16	17	
	F_{aD}	0.72	0.59	0.48	0.40	0.33	0.27	0.23	
	A_s	0.0339	0.0597	0.0917	0.1309	0.1750	0.2272	0.2895	
J	Throats	13	14	15	16	17	18	19	
	F_{aD}	0.71	0.58	0.48	0.40	0.34	0.28	0.23	
	A_s	0.0515	0.0908	0.1349	0.1871	0.2493	0.3256	0.4167	
K	Throats	15	16	17	18	19	20		
	F_{aD}	0.61	0.51	0.42	0.35	0.29	0.24		
	A_s	0.1015	0.1537	0.2160	0.2922	0.3833	0.4928		
L	Throats	16	17	18	19	20			
	F_{aD}	0.63	0.52	0.44	0.36	0.30			
	A_s	0.1164	0.1787	0.2549	0.3460	0.4555			
M	Throats	17	18	19	20				
	F_{aD}	0.66	0.55	0.45	0.38				
	A_s	0.1287	0.2050	0.2961	0.4055				
N	Throats	18	19	20					
	F_{aD}	0.69	0.57	0.48					
	A_s	0.1395	0.2306	0.3401					
P	Throats	19	20						
	F_{aD}	0.71	0.59						
	A_s	0.1575	0.2670						

 F_{aD} = nozzle/throat-area ratio A_s = throat annulus area.

TABLE 6.13—NOZZLE VS. THROAT ANNULUS AREA, MANUFACTURER A

Nozzle	Throat Annulus Area, A_s (sq in.)					
	X	A	B	C	D	E
1		0.0040	0.0057	0.0080	0.0108	0.0144
2	0.0033	0.0050	0.0073	0.0101	0.0137	0.0183
3	0.0042	0.0065	0.0093	0.0129	0.0175	0.0233
4	0.0054	0.0082	0.0118	0.0164	0.0222	0.0296
5	0.0068	0.0104	0.0150	0.0208	0.0282	0.0377
6	0.0087	0.0133	0.0191	0.0265	0.0360	0.0481
7	0.0111	0.0169	0.0243	0.0338	0.0459	0.0612
8	0.0141	0.0215	0.0310	0.0431	0.0584	0.0779
9	0.0179	0.0274	0.0395	0.0548	0.0743	0.0992
10	0.0229	0.0350	0.0503	0.0698	0.0947	0.1264
11	0.0291	0.0444	0.0639	0.0888	0.1205	0.1608
12	0.0369	0.0564	0.0813	0.1130	0.1533	0.2046
13	0.0469	0.0718	0.1035	0.1438	0.1951	0.2605
14	0.0597	0.0914	0.1317	0.1830	0.2484	0.3316
15	0.0761	0.1164	0.1677	0.2331	0.3163	0.4223
16	0.0969	0.1482	0.2136	0.2968	0.4028	0.5377
17	0.1234	0.1888	0.2720	0.3779	0.5128	
18	0.1571	0.2403	0.3463	0.4812		
19	0.2000	0.3060	0.4409			
20	0.2546	0.3896				

TABLE 6.14—NOZZLE VS. THROAT ANNULUS AREA, MANUFACTURER B

Nozzle	Throat Annulus Area, A_s (sq in.)					
	A -	A	B	C	D	E
1		0.0036	0.0053	0.0076	0.0105	0.0143
2	0.0029	0.0046	0.0069	0.0098	0.0136	0.0184
3	0.0037	0.0060	0.0089	0.0127	0.0175	0.0231
4	0.0048	0.0077	0.0115	0.0164	0.0227	0.0308
5	0.0062	0.0100	0.0149	0.0211	0.0293	0.0397
6	0.0080	0.0129	0.0192	0.0273	0.0378	0.0513
7	0.0104	0.0167	0.0248	0.0353	0.0488	0.0663
8	0.0134	0.0216	0.0320	0.0456	0.0631	0.0856
9	0.0174	0.0278	0.0414	0.0589	0.0814	0.1106
10	0.0224	0.0360	0.0534	0.0760	0.1051	0.1428
11	0.0289	0.0464	0.0690	0.0981	0.1358	0.1840
12	0.0374	0.0599	0.0891	0.1268	0.1749	0.2382
13	0.0483	0.0774	0.1151	0.1633	0.2265	0.3076
14	0.0624	0.1001	0.1482	0.2115	0.2926	0.3974
15	0.0806	0.1287	0.1920	0.2731	0.3780	0.5133
16	0.1036	0.1668	0.2479	0.3528	0.4881	0.6629
17	0.1344	0.2155	0.3203	0.4557	0.6304	0.8562
18	0.1735	0.2784	0.4137	0.5885	0.8142	1.1058
19	0.2242	0.3595	0.5343	0.7600	1.0516	1.4282
20	0.2896	0.4643	0.6901	0.9817	1.3583	1.8444

the B, C, D, and E ratios. In the systems of Manufacturers A and B, the size of a pump is designated by the nozzle size and ratio. Examples are 11-B, which is a No. 11 nozzle and a No. 12 throat, and 6-A, which is a No. 6 nozzle and a No. 6 throat.

Because the size progression for the nozzles and throats in Manufacturer C's system is not constant over the whole range, the nozzle/throat combinations do not yield fixed ratios. However, the ratios that result cover the same basic range as the other two systems. The actual ratios are listed in Table 6.12. In Manufacturer C's system, the nozzle and mixing tube (throat) sizes designate the size of a pump. An example is C-5, which is the size C nozzle and the No. 5 throat. This combination has an area ratio of 0.32. The annular flow areas of Manufacturer C's jet pumps used in cavitation calculations are also included in Table 6.12. The annular areas for Manufacturers A and B's jet pumps are listed in Tables 6.13 and 6.14.

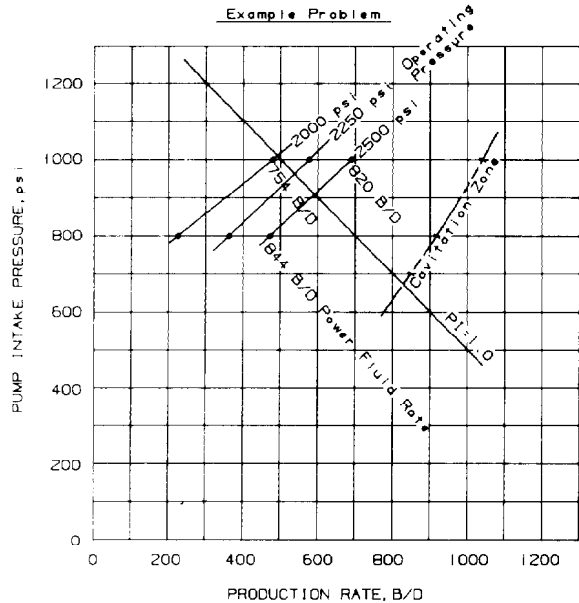
The most commonly used area ratios fall between 0.400 and 0.235. Area ratios greater than 0.400 are sometimes used in very deep wells with high lifts or when only very low surface operating pressures are available and a high head regain is necessary. Area ratios less than 0.235 are used in shallow wells or when very low BHP's require a large annular flow passage to avoid cavitation. Referring to Fig. 6.34, we see that the performance curves for the higher area ratios show higher values of the dimensionless parameter, F_{pD} , within their regions of maximum efficiency. Because F_{pD} is a measure of the pressure rise in the produced fluid, the higher area ratios are suited for high net lifts, but this is achieved only with production rates substantially less than the power-fluid rate ($F_{mD} < 1.0$). The smaller area ratios develop less head, but may produce more fluid than is used for power fluid ($F_{mD} > 1.0$). Where the curves for different area ratios cross, the ratios will have equal production and efficiency. However, different annular flow areas (A_s) may give them different cavitation characteristics.

Jet Pump Application Sizing

The current use of jet pumps can be credited to the advent of computer programs capable of making the iterative calculations necessary for application design. Jet-pump performance depends largely on the pump discharge pressure, which in turn is strongly influenced by the gas/liquid ratio, F_{gL} , in the return column to the surface. With the range of return F_{gL} seen in hydraulic pumping, higher values of F_{gL} lead to reduced pump discharge pressure. Because the jet pump is inherently an open power-fluid device, F_{gL} depends on the formation GOR and on the amount of power fluid mixed with the production. The amount of power fluid depends on the size of the nozzle and the operating pressure. As the power-fluid pressure is increased, the lift capability of the pump increases, but the additional power-fluid rate decreases F_{gL} , thereby increasing the effective lift. Finding a match between the power-fluid rate (Eq. 55), the pump performance curve (Eq. 59), and the pump discharge pressure, p_{pd} , is an iterative procedure involving successive refined guesses.

Refs. 23 and 24 provide a listing of the sequence of steps necessary in the iterative procedure and program listings for programmable calculators. This procedure has proved to be quite successful in accurately predicting the performance of oilfield jet pumps in a variety of wells. The various suppliers of jet pumps also have developed in-house computer programs for application design that are faster than the calculator routines and incorporate more correlations for fluid properties and the pump discharge pressure. The following procedure is a variation on that presented in Refs. 23 and 24 and is more suitable for hand calculations. The object of the calculation sequence will be to superimpose a jet pump performance curve on the IPR curve of the well and to note the intersections that represent the pump performance in the particular well. Therefore, a plot of the best estimate of the IPR (or PI)

DEPTH OF PUMP 5,000 ft TUBULARS 2 3/8 X 5 1/2
 OIL 42° API 0.353 psi/ft WATER 0.446 psi/ft, 30%
 GAS 150 GOR scf/bbl POWER FLUID OIL
 WELLHEAD FLOW LINE 100 psi DATE BY



NOTE—JET PUMP OPERATION MUST BE ABOVE & LEFT OF CAVITATION LINE

Fig. 6.36—Jet-pump production unit performance.

curve of the well is the starting point. An example of a completed performance plot in this format is shown in Fig. 6.36.

Calculation Sequence and Supplemental Equations

Fig. 6.37 shows a typical jet pump installation with the appropriate pressures that determine pump operation. Although a parallel installation is shown for clarity of nomenclature, the same relationships hold for the casing-type installation.

Power-Fluid Flow Through the Nozzle.

Step 1—Calculate the pump suction gradient, g_s , from Eq. 40,

$$g_s = g_o(1 - W_c) + g_w W_c.$$

Step 2—For the desired production, q_s , and pump-intake pressure, p_{ps} , calculate the minimum suction area needed to avoid cavitation (A_{cm} from Eq. 66).

Step 3—Referring to Tables 6.11 through 6.14, find a nozzle and throat combination with area ratio, F_{ad} , close to 0.4 that has an annular flow area, A_s , greater than the value of A_{cm} from Step 2. Note that this ensures that larger throats matched with this nozzle (lower values of F_{ad}) will also have annular flow areas greater than A_{cm} .

Step 4—Pick a value of the surface operating pressure, p_{so} . This is usually between 2,000 and 4,000 psi, with higher values needed in deeper wells. A good starting point is 3,000 psi.

Step 5—Determine the pressure at the nozzle, p_n . This relationship is the same as Eq. 32 without the p_{fr} term. For the first approximation, the friction term p_{fpt} can be neglected.

$$p_n = p_{so} + g_n D - p_{fpt}, \quad (67)$$

where p_{fpt} = power-fluid tubing friction pressure, psi.

Step 6—Determine the nozzle flow, q_n , from Eq. 55 for a desired pump-intake pressure, p_{ps} .

Step 7—Determine the friction in the power-fluid tubing from the charts and equations in Appendix B.

Step 8—Return to Step 5, and recalculate the pressure at the nozzle and then recalculate the nozzle flow at Step 6. This return to Steps 5 and 6 need be done only once unless the nozzle flow changed by more than 15%. Because the power-fluid rate through the nozzle depends only on the power-fluid pressure at the nozzle, p_n , and the pump-intake pressure, p_{ps} , this portion of the flow circuit has been defined and will not change with variations in the pump flow rate or pump discharge pressure so long as the pump intake pressure is held constant in the calculations.

Pump Performance and Return Flow.

Step 1—Determine the values needed to predict the pump discharge pressure, p_{pd} .

Total return flow: for a desired production rate, q_s , at a point on the IPR curve of the well,

$$q_d = q_s + q_n. \quad (68)$$

The value of q_s will be adjusted during the iteration process.

Return flow fluid gradient:

$$g_d = [(q_n \times g_n) + (q_s \times g_s)] / q_d. \quad (69)$$

Return flow water cut: for water as power fluid,

$$W_{cd} = \frac{q_n + W_c q_s}{q_d}. \quad (70)$$

For oil as power fluid,

$$W_{cd} = \frac{W_c q_s}{q_d}. \quad (45)$$

Return flow gas/liquid ratio:

$$F_{gL} = q_s(1 - W_c)R / q_d. \quad (47)$$

Return flow viscosity:

$$\nu_m = (1 - W_{cd})\nu_o + W_{cd}\nu_w. \quad (42)$$

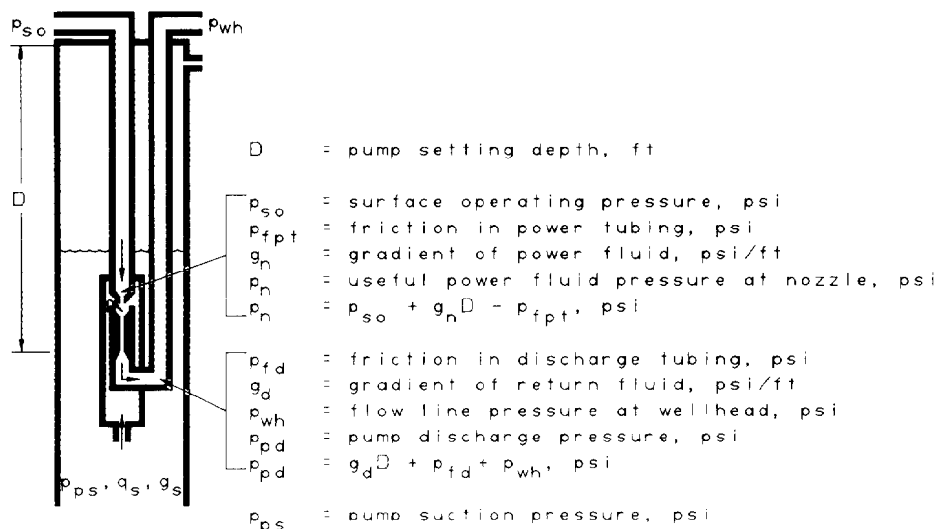


Fig. 6.37—Typical jet-pump installation.

Step 2—If F_{gL} is less than 10, it is suggested that the pump discharge pressure be calculated without considering the gas effects, particularly in casing-type installations. In such a case, the pump discharge pressure, p_{pd} , is given by

$$p_{pd} = p_{fd} + g_d D + p_{wh} \quad (33)$$

The value for the return friction can be determined from the equations or figures in Appendix B.

Step 3—If F_{gL} is greater than 10, determine the pump discharge pressure from a vertical multiphase flowing gradient correlation or from gas-lift charts.

Step 4—From the values for p_n , p_{ps} , and p_{pd} , determine the value of F_{pD} from Eq. 58.

Step 5—Calculate the value of F_{mD} from Eq. 64. Note that if the GOR is zero, F_{mD} is given by Eq. 57.

Step 6—Referring to Fig. 6.34, check whether the values of F_{mD} and F_{pD} from Steps 4 and 5 fall on one of the standard curves. Starting with the value of F_{pD} on the vertical axis, move across to the farthest curve intercepted. This will be the most-efficient-ratio curve for that value of F_{pD} . Read down to the value of F_{mD} . If this value of F_{mD} does not agree with the one from Step 5, a correction is needed in the value of q_s selected in Step 2 under Power-Fluid Flow Through the Nozzle. If the F_{mD} values do agree (within 5%), a solution has been found. The nozzle size selected in Step 3 under Power-Fluid Flow Through the Nozzle is to be used with a throat that gives a value of F_{aD} as close as possible to that found by reading across from the value of F_{pD} . The solution obtained is for the amount of production possible for the originally assumed surface operating pressure and for the originally assumed pump-intake pressure. If only one iteration was made, the value of q_s will be the originally assumed value. This solution point can be plotted on the graph of the IPR curve of the well, as shown in Fig. 6.36.

Step 7—If the values of F_{mD} did not agree closely enough, correct the value of q_s by the following method:

$$q_{s(\text{new})} = q_{s(\text{old})} \times F_{mD_6} / F_{mD_5} \quad (71)$$

where F_{mD_6} = value of F_{mD} from Step 6 and F_{mD_5} = value of F_{mD} from Eq. 64 in Step 5. By using this value of q_s , go back to Step 1 and repeat the procedure until the value of F_{mD} from Fig. 6.34 and the calculated value from Step 5 agree within about 5%.

Step 8—Determine the cavitation-limited flow rate, q_{sc} , at this particular pump intake pressure, p_{ps} .

$$q_{sc} = q_{si} (A_t - A_n) / A_{cm} \quad (72)$$

where q_{si} = initial assumed value. This value of q_{sc} can be plotted on the IPR plot for the particular value of p_{ps} under consideration.

Step 9—Because the value of q_s has been changed in the above procedure when more than one pass through the equations has been made, the combination of this value of q_s and the assumed value of p_{ps} will probably not be on the IPR curve of the well. In this case, return to Step 5 under Power-Fluid Flow Through the Nozzle with a new value of the pump-intake pressure, p_{ps} . If the solution point was below and to the left of the IPR curve, select a value of p_{ps} higher than the first one. If the solution point was above and to the right of the IPR curve, select a lower value of p_{ps} . Repeating all the remaining steps for the same area ratio, F_{aD} , will give a new solution point that can be plotted on the same graph used for the IPR curve, as shown in Fig. 6.36. The two solution points define a portion of the constant-operating-pressure curve for the particular pump. If the curve intersects the IPR curve, a match between pump performance and well performance has been found. It may be necessary to calculate a third point to extend the pump performance curve

TABLE 6.15—WORKSHEET AND SUMMARY OF EQUATIONS FOR JET PUMPS

Well Identification Example Problem 4

Vertical setting depth, ft	5,000	Water specific gravity	1.03
Tubing length, ft	6,000	Power fluid gradient, psi/ft	0.353
Tubing ID, in.	1.995	Produced oil gradient, psi/ft	0.353
Tubing OD, in.	2.375	Water gradient, psi/ft	0.446
Return ID, in.	4.892	Oil viscosity, cSt	2.5
Wellhead pressure, psi	100	Water viscosity, cSt	0.65
Gas specific gravity	0.75	GOR, scf/bbl	150
Oil gravity, °API	42	Water cut, %	30
Power fluid specific gravity	0.820	Surface temperature, °F	90
Produced oil specific gravity	0.820	Bottomhole temperature, °F	130
Desired production, B/D		500	
Pump intake pressure at above rate, psi		1,000	
Productivity index		1.0	
Installation: Casing	✓	Parallel	
Vented: Yes		No	✓

Part A—Nozzle choice and power fluid iteration**Step 1**—Pump suction gradient (Eq. 40)

$$g_s = g_o(1 - W_c) + g_w W_c \quad g_s = 0.381$$

Step 2—Minimum suction area (Eq. 66)

$$A_{cm} = q_s \left[\frac{1}{691} \sqrt{g_s / \rho_{ps}} + \frac{(1 - W_c)R}{24,650 \rho_{ps}} \right] \quad A_{cm} = 0.0163$$

Step 3—Nozzle size from Table 6.11 with $F_{aD} \approx 0.4$ such that throat annulus area (Tables 6.12, 6.13, or 6.14) is $> A_{cm}$ from Step 2.

$$\text{size} = 7 \text{ (Manufacturer A)} \\ A_n = 0.0103$$

Step 4—Operating pressure chosen.

$$p_{so} = 2,500$$

Step 5—Nozzle pressure (Eq. 67)—neglect friction on first iteration.

$$\rho_n = p_{so} + g_n D - p_{tpi} \quad \rho_n = 4,265 \quad 4,232$$

Step 6—Nozzle flow (Eq. 55)

$$q_n = 832 A_n \sqrt{(\rho_n - \rho_{ps}) / g_n} \quad q_n = 824 \quad 820$$

Step 7—Friction from Appendix B.

$$p_{tpi} = 33 \quad 33$$

Step 8—Return to Step 5 until successive values are within 15%. Then go to Part B.**Part B—Iteration on production rate****Step 1**—a. Return flow (Eq. 68)

$$q_d = q_s + q_n \quad q_d = 1,320 \quad 1,477 \quad 1,490$$

b. Return gradient (Eq. 69)

$$g_d = [(q_n \times g_n) + (q_s \times g_s)] / q_d \quad g_d = 0.364 \quad 0.365 \quad 0.366$$

c. Return water cut (Eqs. 45 and 70)

for water power fluid

$$W_{cd} = (q_n + W_c q_s) / q_d \quad W_{cd} = \quad \quad$$

for oil power fluid

$$W_{cd} = W_c q_s / q_d \quad W_{cd} = 0.113 \quad 0.133 \quad 0.139$$

d. Return gas/liquid ratio (Eq. 47)

$$F_{gL} = q_s(1 - W_c)R / q_d \quad F_{gL} = 40 \quad 47 \quad 49$$

e. Return viscosity (Eq. 42)

$$\nu_m = (1 - W_{cd})\nu_o + W_{cd}\nu_w \quad \nu_m = 2.3 \quad 2.3 \quad 2.3$$

TABLE 6.15—WORKSHEET AND SUMMARY OF EQUATIONS FOR JET PUMPS (continued)

Step 2—Discharge pressure (Eq. 31) if $F_{gL} < 10$

$$p_{fd} \text{ from Appendix B.} \quad p_{fd} = \underline{\hspace{2cm}} \quad \underline{\hspace{2cm}} \quad \underline{\hspace{2cm}}$$

$$p_{pd} = p_{fd} + g_d D + p_{wh} \quad p_{pd} = \underline{\hspace{2cm}} \quad \underline{\hspace{2cm}} \quad \underline{\hspace{2cm}}$$

Step 3—Use vertical multiphase flow correlation if $F_{gL} > 10$ to determine p_{pd}

$$p_{pd} = 1,780 \quad 1,756 \quad 1,746$$

Step 4—Calculate pressure ratio (Eq. 58)

$$F_{pD} = (p_{pd} - p_{ps}) / (p_n - p_{pd}) \quad F_{pD} = 0.318 \quad 0.305 \quad 0.300$$

Step 5—Calculate mass flow ratio (Eq. 64)

$$F_{mD} = \frac{q_s \left\{ \left[1 + 2.8 \left(\frac{R}{p_{ps}} \right)^{1.2} \right] (1 - W_c) + W_c \right\} g_s}{q_n \times g_n} \quad F_{mD_5} = 0.791 \quad 1.04 \quad 1.09$$

Step 6—Use value of F_{pD} in Fig. 6.34 to find F_{mD} from farthest curve to right at that value of F_{pD} . Note value of F_{aD} .

$$\begin{array}{ccc} F_{aD} = 0.25 & 0.25 & 0.25 \\ F_{mD_6} = 1.04 & 1.06 & 1.10 \end{array}$$

Step 7—Compare F_{mD_5} from Step 5 with F_{mD_6} from Step 6. If within 5%, go to Step 8. If not, correct q_s by Eq. 71.

$$q_{s(\text{new})} = q_{s(\text{old})} F_{mD_6} / F_{mD_5} \quad q_{s(\text{new})} = 657 \quad 670 \quad 676$$

then return to Step B.1.a.

Part C—Hardware and final calculations**Step 1**—Pick throat size closest to

$$A_t = \frac{A_n}{F_{aD}} = 0.0412 \text{ sq in.} \quad \text{Actual throat area} = 0.0441 \text{ size} = 9$$

Step 2—Cavitation limited flow (Eq. 72)

$$q_{sc} = q_{si} \times \frac{A_t - A_n}{A_{cm}} \quad q_{sc} = 1,037$$

Step 3—Hydraulic horsepower (Eq. 5)

$$P_h = q_n \times p_{so} \times 0.000017 \quad P_h = 35$$

Step 4—Triplex power at 90% efficiency = 39**Summary**

$$\begin{array}{lll} A_n = 0.0103 & p_{so} = 2,500 & q_s = 676 \\ A_t = 0.0441 & q_n = 820 & p_{ps} = 1,000 \\ F_{aD} = 0.235 & P_h = 39 & \end{array}$$

Triplex options (from manufacturer specification sheet, Tables 6.16 through 6.18)

Type	D-323-H	J-60	K-100
Plunger size, in.	1 1/2	1 1/2	1 3/4
rev/min	400	400	221
Flow rate at rev/min, B/D	945	945	945
Maximum pressure rating, psi	2,690	2,690	2,740
Horsepower	44.6	44.6	44.6

until it intersects the IPR curve. Note that in Step 8, a new value of A_{cm} will have to be calculated because p_{ps} has changed.

Step 10—Other constant-operating-pressure curves can be constructed in the same manner by assuming a different value for p_{so} in Step 4 under Power-Fluid Flow Through the Nozzle. If the intersection of a particular constant operating pressure curve with the IPR curve is at a lower-than-desired production, try a higher value of the operating pressure.

Example Problem 4. Table 6.15 can be used to aid in organizing jet pump calculations. A sample set of calculations is shown in the worksheet of Table 6.15 for one point on the 2,500-psi operating line of Fig. 6.36. Manufacturer A's jet pump sizes are used for this example. In the example calculation, the initial estimate of 500 B/D production at 2,500-psi operating pressure became 676 B/D as a result of the iterative process. This indicates that an operating pressure less than 2,500 psi is required to produce 500 B/D. Fig. 6.36 shows that the desired 500 B/D can be pumped with an operating pressure slightly more than 2,000 psi and a power-fluid rate of about 750 B/D, which is about 30 triplex hp. Higher operating pressures lead to greater production rates. For example, the 2,500-psi operating-pressure curve intersects the well PI line at about 590 B/D. The maximum production from the well with Pump 7-C is at the intersection of the cavitation line with the well's PI line at 830 B/D. The operating pressure would be about 4,000 psi.

Considering Other Sizes. In this relatively shallow well with a modest lift requirement, the selection procedure leads to a pump that is larger than necessary for 500 B/D production. This is evident from the intersection of the cavitation curve with the PI line at about 830 B/D, which is well beyond the 500-B/D production target. In a low-lift well, the value of F_{pD} will be low and area ratios less than 0.4 can be used efficiently. The No. 7 nozzle was chosen because it has sufficient annular area to avoid cavitation with an area ratio of 0.4. Ref. 24 shows that Sizes 6-B, 5-C, and 4-D are also reasonable choices in this well and that size 4-D requires the least power (23 hp), although at a higher operating pressure (2,849 psi). This suggests that when the calculation sequence leads to $F_{aD} < 0.4$, trying a smaller nozzle is warranted.

In some cases, the value of F_{aD} found by the selection procedure will be greater than 0.4. It is then necessary to check whether the throat annular area of that combination is still greater than the value of A_{cm} calculated in Step 2 under Power-Fluid Flow Through the Nozzle. If it is not, a larger nozzle size must be tried, or a higher operating pressure specified. The use of a higher operating pressure will lower the value of F_{pD} and permit the use of a throat giving a lower value of F_{aD} with a larger throat-annulus area. Larger nozzles and throats of the same area ratio will have larger throat-annulus areas.

Programming Considerations. As mentioned, Refs. 23 and 24 contain programs for hand-held programmable calculators. The method presented here can also be pro-

grammed on calculators or computers to avoid manual calculations and the use of reference charts. If Eq. 59 is solved for F_{mfd} , the following expressions emerge:

$$F_{mfd}^2(B_2 - C_2) - F_{mfd}(2C_2) + \left[(A_2 - C_2) - \frac{F_{pD}D_2}{F_{pD} + 1} \right] = 0, \quad (73)$$

where

$$A_2 = 2F_{aD}, \quad (74)$$

$$B_2 = (1 - 2F_{aD}) \frac{F_{aD}^2}{(1 - F_{aD})^2}, \quad (75)$$

$$C_2 = (1 + K_{td})F_{aD}^2, \quad (76)$$

and

$$D_2 = (1 + K_n), \quad (77)$$

Eq. 73 can then be solved by means of the familiar expression for the root of a quadratic equation:

$$F_{mfd} = \frac{2C_2 - \sqrt{(-2C_2)^2 - 4(B_2 - C_2) \left[(A_2 - C_2) - \frac{F_{pD}D_2}{F_{pD} + 1} \right]}}{2(B_2 - C_2)} \quad (78)$$

With this calculated value of F_{mfd} from Eq. 78, Eq. 71 becomes

$$q_{s(\text{new})} = q_{s(\text{old})} \frac{F_{mfd1}}{F_{mfd2}}, \quad (79)$$

where

$$F_{mfd1} = \text{dimensionless mass flow rate from Eq. 78, and}$$

$$F_{mfd2} = \text{dimensionless mass flow rate from Eq. 64.}$$

Iterating through the pump performance and return flow equations will refine the value of q_s until the desired degree of convergence is achieved. With the same value for the surface operating pressure, p_{so} , but a new value of the pump suction pressure, p_{ps} , the values for a constant operating pressure line on an IPR plot can be obtained.

Application Range

Experience in using the procedures previously described to predict jet pump performance in field applications indicates that the algorithm has a broad range of applicability. Simplifications of assumptions in the performance

equations and in correlations for liquid and gas properties, however, have been made to reduce the number of calculations during the iteration process. The IPR curve of the well is often not well known, and the gas production of an individual well may be uncertain. Jet-pump performance is strongly affected by the pump intake pressure (determined by the IPR curve) and by the pump discharge pressure (significantly determined by the GOR). For every psi error in the pump intake pressure or pump discharge pressure, the effect on surface operating pressure will be from 3 to 5 psi if the same production rate is to be obtained (see Ref. 7 for the relationships that demonstrate this effect). Higher discharge pressures or lower pump intake pressures require higher operating pressures. This multiplier effect is greater with the larger throats (low values of F_{ad}). Fluid friction losses through the passages of the particular downhole completion hardware can affect these pressures as well.

Even when accurate well data are available, the performance predictions may not always match field performance. When the volume of free gas at producing bottomhole conditions is very large, performance will probably deviate from that predicted by the equations. Current jet pump designs have been optimized for liquid production, not for pumping gas. Accuracy of prediction begins to suffer at above five parts of gas to one part liquid, and at 90% gas, the predictions are very questionable. In the case of a 42° API crude, 150 GOR, and a 30% water cut, the FVF of gas plus oil and water phases is about 1.2 RB/STB at 1,000-psi pump intake pressure, p_{ps} . If the GOR were about 2,000, the FVF would be about 5.5, which is on the boundary of the region of decreasing correlation accuracy. At higher GOR's or lower pump intake pressures or water cuts, prediction accuracy would begin to suffer. With a 500-psi pump intake pressure, a GOR of 2,000 leads to an FVF of about 11.3, which is outside the working region of the model.

If the algorithm presented here is used to evaluate wells in which the gas/liquid volume ratio is large at the downhole pumping conditions, it is suggested that the expression within the brackets in Eq. 64 be checked. This expression is the FVF for the oil, water, and gas phases in RB/STB. Up to a value of 5 or 6, the model correlates well with actual performance. Above this point, prediction accuracy diminishes, and a gas-vent system is suggested as a conservative design procedure, using the GOR value from Fig. 6.35.

Jet-pump performance with high-viscosity fluids is not modeled in these routines. Heavy crudes with viscosities above about 500 cp will cause significant deviations from predictions unless produced water is the dominant phase. Oil power fluids of less than about 22° API will also introduce losses that are not properly modeled.

A troubleshooting guide for subsurface jet pumps is given in Table 6.9.

Downhole Pump Accessories

Swab Cups. A number of accessories are available for downhole pumping systems. Free-pump systems require swab cups and a standing valve to accomplish the pump-in and pump-out operations. The swab cups are carried on a mandrel extending above the pump. The mandrel assembly may contain a check valve to limit the amount of fluid bypassing the pump as it is circulated to the surface.

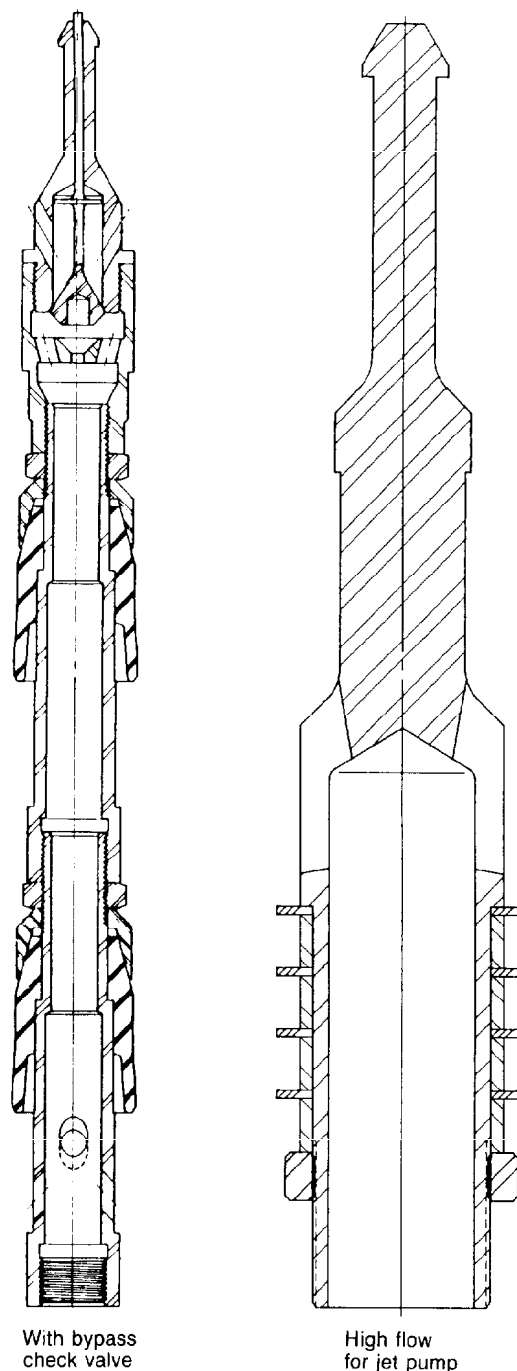


Fig. 6.38—Swab noses.

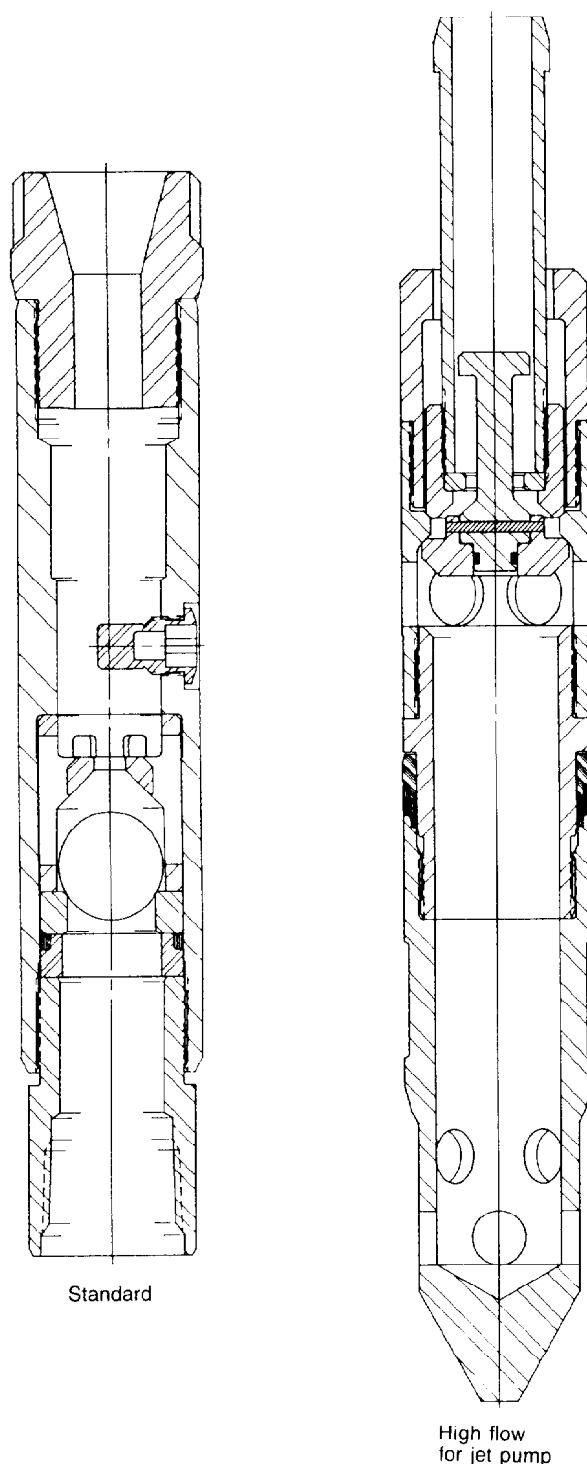


Fig. 6.39—Standing valves.

If the pump does not enter a lubricator on the wellhead, the check valve may include a check-valve bypass that is actuated when the pump enters the wellhead catcher to prevent excessive pressure buildup. Two examples of swab cup assemblies are shown in Fig. 6.38. Jet pumps usually use the simpler system.

Standing Valves. Standing valves are necessary in free-pump systems to create a "U" tube and prevent the circulating fluid from flowing back into the reservoir. During pumping operations, the standing valve is opened by flow from the formation to the pump suction, as shown in Fig. 6.3. Whenever the pump is shut down, the standing valve closes. In some cases, the standing-valve ball is held open by a small magnet to prevent it from cycling during reciprocating pump-stroking reversals. When the downhole pump is unseated, fluid attempting to flow back into the formation washes the ball off the magnet and onto the seat. The standing valve is wireline-retrievable and includes a provision for draining the tubing before attempting to pull it. In most cases, the standing valve forms the no-go and bottom seal for the pump. Some jet-pump installations, however, use high-flow designs that do not serve as a pump seat. An example of each type is shown in Fig. 6.39.

Pressure Recorders. To obtain producing BHP's at several different withdrawal rates, downhole pressure recorders are often run in conjunction with hydraulic pumps. With all hydraulic pumps, a pressure recorder can be hung below the standing valve. While this arrangement provides not only pressure drawdown but also pressure-buildup data, it has the disadvantage of requiring wireline operations to run and retrieve the recorder. Some reciprocating pumps can be run with a pressure recorder attached, which eliminates the wireline operations but does not permit observation of pressure buildup because the recorder is above the standing valve. Virtually all jet pumps can be run with recorders attached, and very smooth recordings are obtained because the jet pump is pulsation free.

Dummy Pumps. Dummy pumps are sometimes run to blank off one or more tubing strings so that they may be checked for leaks. If the dummy pump has a fluid passage in it, the terms "flow-through dummy" or "blanking tool" are often used. These tools are useful for acidizing or steaming.

Screens and Filters. To protect the downhole pump from trash in the well, various types of screens and filters are sometimes run. Because circulating pumps in and out of a well may dislodge scale and corrosion products in the tubing, a starting filter can be attached to the swab-cup assembly to filter the power fluid. Because this must be a relatively small filter, it will eventually plug up and an automatic bypass arrangement is provided. This system collects foreign material during the crucial start-up phase with a newly installed pump. For long-term operation, power-fluid and pump intake screens or strainers are used in some units. These will exclude large-diameter objects that could damage or plug the pump.

Safety Valves. In some areas, subsurface safety valves are required. When a packer is set and the BHA is above it, a wireline-retrievable safety valve can be installed be-

tween the standing valve and the packer to isolate the formation. The safety valve is normally closed unless high-pressure fluid is supplied by a small tubing line run from the main power-fluid tubing just above the pump. The pump discharge pressure provides the reference pressure to the safety valve. When the pump is on bottom and power-fluid pressure is applied to it, the safety valve opens to allow well fluid to enter the pump. Most safety valves will not hold pressure from above, so the standing valve is still necessary for circulating the pump in and out of the well. Fig. 6.40 illustrates this type of installation.

Surface Equipment

Surface Pumps

Hydraulic pumping systems have evolved toward the use of relatively high pressures and low flow rates to reduce friction losses and to increase the lift capability and efficiency of the system. Surface operating pressures are generally between 2,000 and 4,000 psi, with the higher pressures used in deeper wells. Power-fluid rates may range from a few hundred to more than 3,000 B/D. While some surface multistage centrifugal pumps are rated to this pressure range, they are generally quite inefficient at the modest flow rates associated with single-well applications. Multistage centrifugals can be used effectively when multiple wells are pumped from a central location.⁵ The surface pump for a single well or for just a few wells must be a high-head and low-specific-speed pump. Wide experience in the overall pumping industry has led to the use of positive-displacement pumps for this type of application. The vast majority of hydraulic pump installations are powered by triplex or quintiplex pumps driven by gas engines or electric motors. The multiplex pumps used for hydraulic pumping range from 30 to 625 hp. An example of a surface triplex pump is shown in Fig. 6.41. Specification sheets for multiplex pumps commonly used in hydraulic pumping systems are available from the manufacturers (Tables 6.16 through 6.18).

Multiplex pumps consist of a power end and a fluid end. The power end houses a crankshaft in a crankcase. The connecting rods are similar to those in internal combustion engines, but connect to crossheads instead of pistons. The fluid end houses individual plungers, each with intake and discharge check valves, usually spring loaded. The fluid end is attached to the power end by the spacer block, which houses the intermediate rods and provides a working space for access to the plunger system. Most units being installed in the oil field are of the horizontal configuration shown in Fig. 6.41. This minimizes contamination of the crankcase oil with leakage from the fluid end. Vertical installations are still found, however, particularly with oil as the pumped fluid or when space is at a premium, as in townsite leases.

Multiplex pumps applied to hydraulic pumping usually have stroke lengths from 2 to 7 in. and plunger diameters between 1 and 2½ in. The larger plungers provide higher flow rates, but are generally rated at lower maximum pressure because of crankshaft loading limitations. The normal maximum rating of multiplexes for continuous duty in hydraulic pumping applications is 5,000 psi, with lower ratings for the larger plungers. Actual applications above 4,000 psi are uncommon. Multiplex pumps are run at low speed to minimize vibration and wear and to avoid dynamic problems with the spring-loaded intake and dis-

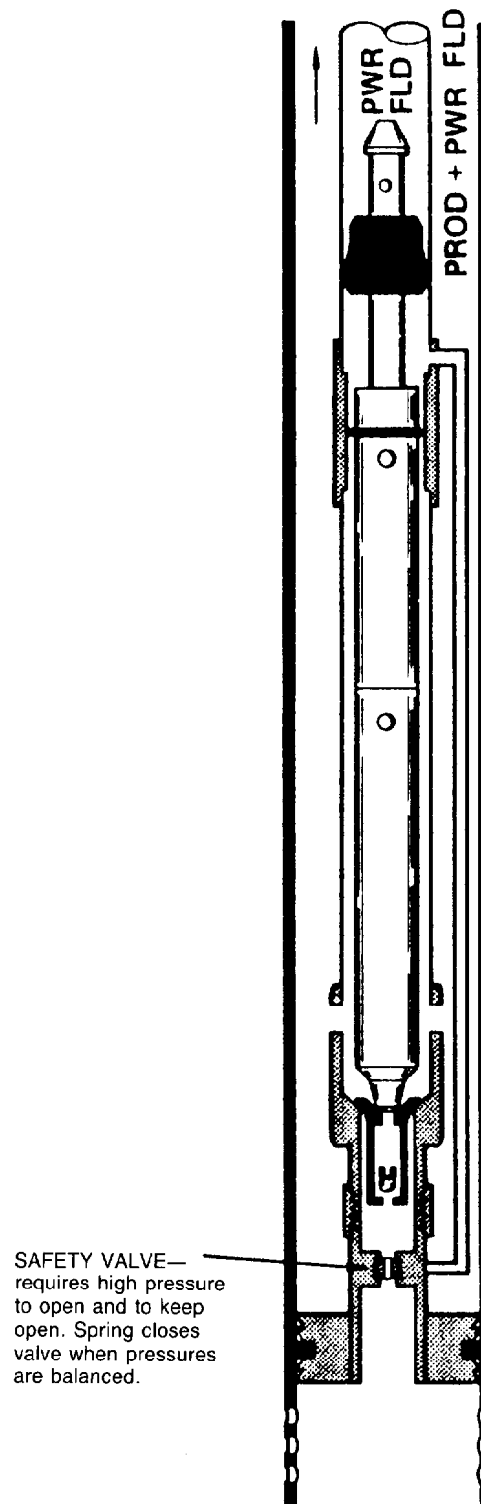


Fig. 6.40—Downhole pump with wireline-retrievable safety valve.

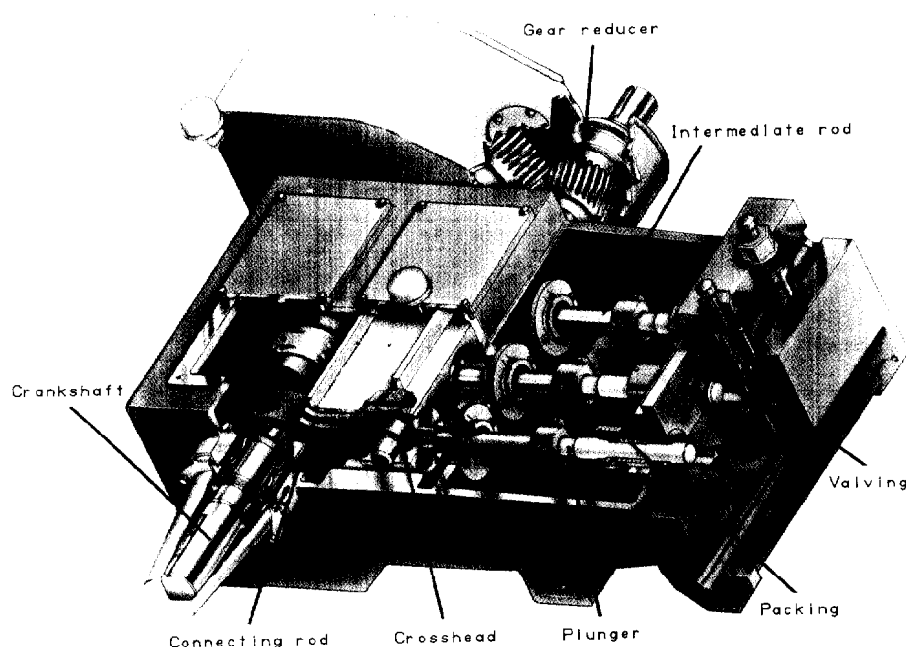


Fig. 6.41—Triplex pump.

charge valves. Most applications fall between 200 and 450 rev/min. Because this is below the speeds of gas engines or electric motors, some form of speed reduction is usually required. Belt drives are found on some units, although gear reduction is more common. Gear reduction units are integral on some multiplexes and separate on others. A variety of reduction ratios are offered for each series of pumps.

Because a positive-displacement pump has an essentially constant discharge flow rate for a given prime mover speed, bypass of excess fluid is normally used to match a particular pressure and flow demand. Another option that has been used successfully is to drive the multiplex pump through a four-speed transmission, which greatly enhances the flexibility of the system. This allows much closer tailoring of the triplex output to the demand, thereby decreasing or eliminating the bypassing of fluid and increasing efficiency. The ability to run the multiplex pump at reduced speed when needed also tends to increase the life of such components as packing and valving.

Each plunger pumps individually from a common intake manifold and into a common discharge manifold. Because discharge occurs only on the upstroke, there is some pulsation to the discharge flow. For this reason, pulsation dampeners are commonly used.

Two types of plunger systems are in common use. For oil service, a simple and effective plunger-and-liner system is used that consists of a closely fitted metallic plunger that runs inside a metallic liner. Sprayed metal coatings or other hardfacing means are often used to extend the life of the plunger and liner. When pumping water, the metal-to-metal system is not practical because the fit would have to be extremely close to keep leakage to an acceptable level. Galling and scoring are problems with close fits and the low lubricity of water. To solve this problem, spring-loaded packing systems are used that do not require adjusting. The advent of high-strength aramid

fibers for packing, in conjunction with other compounds to improve the friction characteristics, has resulted in a pronounced improvement in the ability of the pump to handle high-pressure water for extended periods of time. Water still presents a more severe challenge than oil, however, and water systems show much better life if operated at or below 3,500 psi.

Suction conditions are important to multiplex operation. Friction losses in piping, fluid end porting, and across the suction valving reduce the pressure available to fill the pumping chamber on the plunger downstroke. If these losses are sufficiently great, cavitation may result. When pumping oil with dissolved gas, the reduction in pressure will liberate free gas and cause knocking. For these reasons, it is necessary to have a positive head on the suction side to overcome the friction losses. In addition, another phenomenon known as "acceleration head" must be considered. The flow in the suction piping must accelerate and decelerate a number of times for each crankshaft revolution. For the fluid (which has inertia) to follow the acceleration, energy must be supplied, which is then returned to the fluid on deceleration. The energy supplied during acceleration comes from a reduction in the pressure in the fluid, and if this drops too low, cavitation or gas liberation will result. The standards of the Hydraulic Inst.³⁰ provide the following relationship:

$$h_a = L_s \times \bar{v}_{sl} \times N_c \times C_3 / (K_2 \times g), \dots \dots \dots (80)$$

where

- h_a = acceleration head, ft,
- L_s = actual length of suction line, ft.
- \bar{v}_{sl} = average velocity in suction line, ft/sec,
- N_c = speed of pump crankshaft, rev/min,
- C_3 = constant depending on type of pump,
- K_2 = constant depending on fluid compressibility, and
- g = gravitational constant, 32.2 ft/sec².

For a triplex, $C_3 = 0.066$, and for a quintiplex, $C_3 = 0.040$. For water, $K_2 = 1.4$, and for oil, $K_2 = 1.5$.

The minimum suction head for the multiplex pump is then the sum of the friction losses and the acceleration head. Although the pump can draw a vacuum, this will flash gas and may tend to suck air across valve or plunger packing. Manufacturers of multiplex pumps will recommend appropriate suction charging pressures for their products. It is worth noting that Eq. 80 predicts that long, small-diameter suction lines will increase the acceleration head loss. Such lines also increase the friction loss. It is therefore recommended that suction lines be short and of large diameter, with no high spots to trap air or gas. Suction stabilizers or pulsation dampeners that tend to absorb the pulsations from the pump will also reduce acceleration head.

In many cases, sufficient hydrostatic head is not available to provide the necessary suction pressure. Charge pumps are used to overcome this problem. Positive displacement pumps of the vane or crescent-gear type driven from the triplex have been used extensively. These pumps require a pressure control valve to bypass excess fluid and match the multiplex displacement. Where electric power is available, centrifugal charge pumps have given excellent service. Centrifugal pumps generally need to run at speeds considerably above the multiplex speed. Driving them from the multiplex presents problems, particularly with gas engine drive where prime mover speed variations cause significant variations in the charge-pump output pressure.

While good charging pressures are necessary to ensure proper loading and smooth operation, there are problems associated with very high charge pressures. High charge pressures add to the crankshaft loading, and for charge pressures above about 250 psi it is advisable to derate the maximum discharge pressure by one third of the charge pressure. Also, high charge pressures can adversely affect the lubrication of bearings, particularly in the cross-head wristpin. In addition, the mechanical efficiency of multiplex pumps is some 3 to 5% lower on the suction side compared to the discharge side.³¹ Consequently, the combination of a charge pump and multiplex pump will be most efficient with low charging pressures and a high boost by the multiplex pump. Charging pressures should therefore be limited to that necessary to give complete filling of the multiplex pump with a moderate safety allowance for variations in the system parameters.

In some cases, it is desirable to inject corrosion inhibitors or lubricants into the multiplex suction. Fresh water is sometimes injected to dissolve high salt concentrations. In severe pumping applications with low-lubricity fluids, a lubricating oil is sometimes injected or dripped onto the plungers in the spacer block area to improve plunger life. Injection pumps are often driven from the multiplex drive for these applications. A troubleshooting guide for multiplex pumps is given in Table 6.10.

Fluid Controls

Various types of valves are used to regulate and to distribute the power-fluid supply to one or more wellheads. Common to all free-pump systems is a four-way valve or wellhead control valve. This valve is mounted at the wellhead, as shown in Fig. 6.42. Its function is to provide for different modes of operation. To circulate the

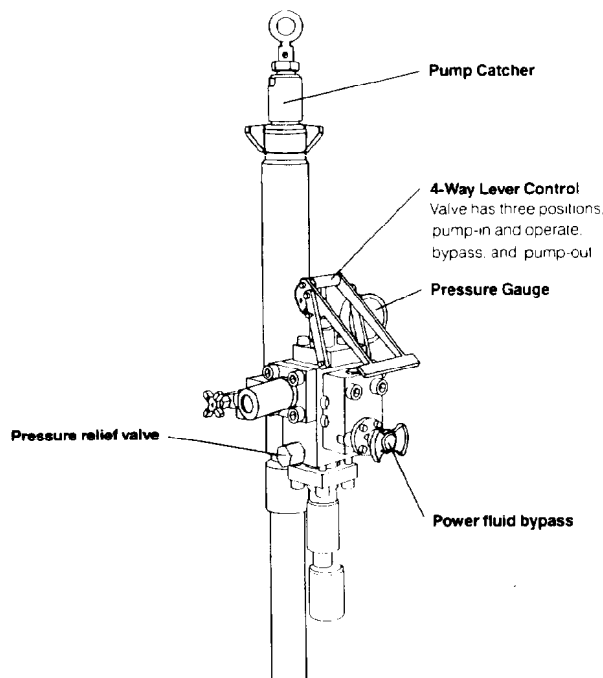


Fig. 6.42—Wellhead control valve.

pump in the hole, as shown in Fig. 6.3, power fluid is directed down the main tubing string. The power fluid begins to operate the pump once it is on bottom and seated on the standing valve. In the pump-out mode, power fluid is directed down the return tubing or casing annulus to unseat the pump and to circulate it to the surface. When the pump is on the surface, putting the valve in the bypass and bleed position permits the well to be bled down and the pump to be removed and replaced. The various functions can all be accomplished by moving the valve to different positions.

Most systems include a constant-pressure controller, as shown in Fig. 6.43. This valve maintains a discharge-pressure load on the multiplex pump by continuously bypassing the excess discharge fluid. These valves operate on the principle of an adjustable spring force on a piston-and-valve assembly that is pressure compensated. If the pressure rises on the high-pressure side, which is being controlled because of changing system loads, the pressure forces on the various areas within the valve will cause the valve to open and to bypass more fluid. This restores the high-pressure side to the preset condition. Jet pumps are frequently operated with a constant-pressure valve as the only surface control valve. The constant-pressure controller can be used to regulate the pressure on a manifold assembly serving multiple wells.

Reciprocating downhole pumps are usually regulated with a constant-flow control valve, shown in Fig. 6.44. The downhole unit can be maintained at a constant stroking rate if a constant volume of power fluid is supplied to it. The constant-flow control valve is designed to provide a preset flow rate even if the downhole operating pressure fluctuates because of changing well conditions. Because this valve does not bypass fluid, it must be used in conjunction with a constant-pressure controller on the higher-pressure or inlet side.

TABLE 6.16—MANUFACTURER A MULTIPLEX PLUNGER PUMPS

D323 Triplex; maximum rev/min 500; maximum horsepower 60.

Pump size	Plunger diameter (in.)	Maximum pressure (psi)	Displacement (B/D)	
			Per 100 rev/min	At maximum rev/min
D323-H	1 $\frac{1}{8}$	4,000	133	664
	1 $\frac{1}{4}$	3,870	164	820
	1 $\frac{3}{8}$	3,200	198	992
	1 $\frac{1}{2}$	2,690	236	1,181
D323-M	1 $\frac{5}{8}$	2,290	277	1,386
	1 $\frac{3}{4}$	1,980	321	1,607
	1 $\frac{7}{8}$	1,720	369	1,845
	2	1,510	420	2,099
	2 $\frac{1}{8}$	1,340	474	2,370
	2 $\frac{1}{4}$	1,200	531	2,657
	2 $\frac{3}{8}$	1,070	592	2,960
	2 $\frac{1}{2}$	970	656	3,280

A-324 Triplex; maximum rev/min 450; maximum horsepower 100.

A-324	1 $\frac{1}{4}$	5,000	219	984
	1 $\frac{3}{8}$	4,445	265	1,190
	1 $\frac{1}{2}$	3,735	315	1,416
	1 $\frac{5}{8}$	3,182	370	1,662
	1 $\frac{3}{4}$	2,744	429	1,928
	1 $\frac{7}{8}$	2,390	492	2,213
	2	2,101	560	2,518
	2 $\frac{1}{8}$	1,861	632	2,843
	2 $\frac{1}{4}$	1,660	708	3,187

A324-H Triplex; maximum rev/min 450; maximum horsepower 125.

A324-H	1 $\frac{1}{4}$	5,000	219	984
	1 $\frac{3}{8}$	5,000	265	1,190
	1 $\frac{1}{2}$	4,669	315	1,416
	1 $\frac{5}{8}$	3,978	370	1,662
	1 $\frac{3}{4}$	3,430	429	1,928
	1 $\frac{7}{8}$	2,988	492	2,213
	2	2,626	560	2,518
	2 $\frac{1}{8}$	2,326	632	2,843
	2 $\frac{1}{4}$	2,075	708	3,187

316-P Triplex; maximum rev/min 320; maximum horsepower 160.

316-P	1 $\frac{1}{2}$	5,650	472	1,511
	1 $\frac{9}{16}$	5,220	512	1,640
	1 $\frac{5}{8}$	4,820	554	1,774
	1 $\frac{11}{16}$	4,470	598	1,913
	1 $\frac{3}{4}$	4,160	643	2,057
	1 $\frac{13}{16}$	3,875	690	2,207
	1 $\frac{7}{8}$	3,620	738	2,362

J-30 Triplex; maximum rev/min 500; maximum horsepower 30.

J-30-H	1 $\frac{5}{16}$	5,000	61	310
	1	4,540	70	350
	1 $\frac{1}{8}$	3,590	89	445
	1 $\frac{1}{4}$	2,900	109	545
	1 $\frac{3}{8}$	2,400	132	660
	1 $\frac{1}{2}$	2,000	157	785

TABLE 6.16—MANUFACTURER A MULTIPLEX PLUNGER PUMPS (continued)

J-60 Triplex; maximum rev/min 500; maximum horsepower 60.

Pump size	Plunger diameter (in.)	Maximum pressure (psi)	Displacement (B/D)	
			Per 100 rev/min	At maximum rev/min
J-60-H	1	5,000	105	525
	1 $\frac{1}{8}$	4,780	133	665
	1 $\frac{1}{4}$	3,870	164	820
	1 $\frac{3}{8}$	3,200	198	990
J-60-M	1 $\frac{3}{8}$	3,200	198	990
	1 $\frac{1}{2}$	2,690	236	1,180
	1 $\frac{5}{8}$	2,290	277	1,385
	1 $\frac{3}{4}$	1,975	321	1,605
	2	1,500	420	2,100

J-100 Triplex; maximum rev/min 450; maximum horsepower 100.

J-100-H	1 $\frac{1}{4}$	5,000	219	980
	1 $\frac{3}{8}$	4,440	264	1,190
	1 $\frac{1}{2}$	3,730	315	1,415
	1 $\frac{5}{8}$	3,180	369	1,660
	1 $\frac{3}{4}$	2,740	428	1,925
J-100-M	1 $\frac{5}{8}$	3,180	369	1,660
	1 $\frac{3}{4}$	2,740	428	1,925
	1 $\frac{7}{8}$	2,390	492	2,210
	2	2,100	560	2,515
	2 $\frac{1}{8}$	1,860	632	2,840

J-165 Triplex; maximum rev/min 400; maximum horsepower 165.

J-165-H	1 $\frac{1}{2}$	5,000	393	1,575
	1 $\frac{5}{8}$	4,725	462	1,845
	1 $\frac{3}{4}$	4,075	536	2,140
	1 $\frac{7}{8}$	3,550	615	2,460
	2	3,120	699	2,800
J-165-M	2	3,120	699	2,800
	2 $\frac{1}{8}$	2,765	790	3,160
	2 $\frac{1}{4}$	2,465	885	3,540
	2 $\frac{3}{8}$	2,210	986	3,945
	2 $\frac{1}{2}$	2,000	1,093	4,370
	2 $\frac{5}{8}$	1,810	1,202	4,820
	2 $\frac{3}{4}$	1,650	1,322	5,290

J-275 Quintiplex; maximum rev/min 400; maximum horsepower 275.

J-275-H	1 $\frac{1}{2}$	5,000	655	2,620
	1 $\frac{5}{8}$	4,725	768	3,070
	1 $\frac{3}{4}$	4,075	891	3,565
	1 $\frac{7}{8}$	3,550	1,025	4,100
	2	3,120	1,166	4,665
J-275-M	2	3,120	1,166	4,665
	2 $\frac{1}{8}$	2,765	1,317	5,265
	2 $\frac{1}{4}$	2,465	1,474	5,895
	2 $\frac{3}{8}$	2,210	1,642	6,570
	2 $\frac{1}{2}$	2,000	1,821	7,280
	2 $\frac{5}{8}$	1,810	2,009	8,035
	2 $\frac{3}{4}$	1,650	2,205	8,820

TABLE 6.17—MANUFACTURER E MULTIPLEX PLUNGER PUMPS

B-200; maximum rev/min 400; maximum horsepower 200.

Pump size	Plunger diameter (in.)	Maximum pressure (psi)	Displacement (B/D)	
			Per 100 rev/min	At maximum rev/min
3 3/4 x 6	2 1/2	2,037	1,313	5,245
	2 3/4	1,684	1,587	6,349
	3	1,415	1,889	7,552
	3 1/4	1,205	2,215	8,859
	3 1/2	1,039	2,571	10,285
	3 3/4	905	2,952	11,807
3 x 6	2	3,183	840	3,356
	2 1/4	2,515	1,063	4,248
	2 1/2	2,037	1,313	5,245
	2 3/4	1,684	1,587	6,349
	3	1,415	1,889	7,552
	1 1/2	5,650	473	1,889
2 1/4 x 6	1 3/4	4,160	641	2,571
	2	3,183	840	3,356
	2 1/4	2,515	1,063	4,248

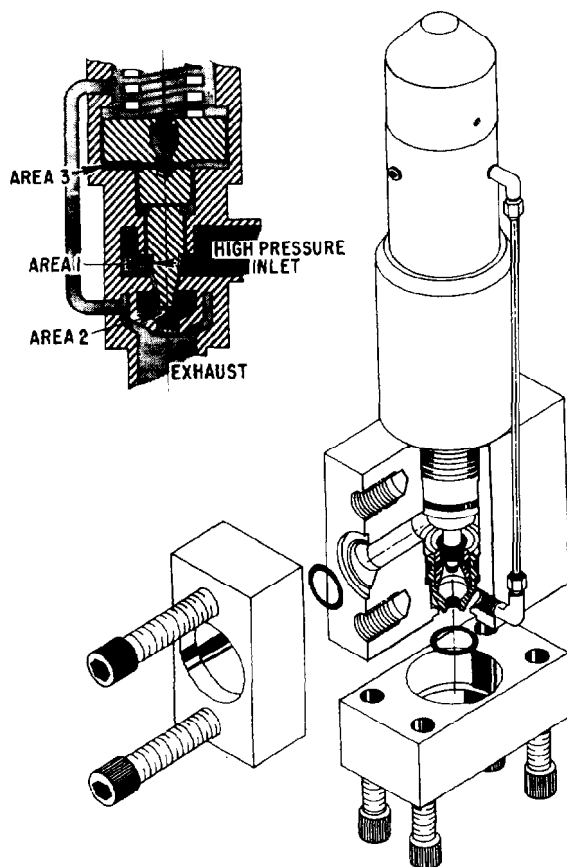


Fig. 6.43—Constant-pressure controller.

Control Manifolds

Where a number of wells are to be pumped from a central battery, a control manifold is used to direct the flows to and from the individual wells. Control manifolds are designed to be built up in a modular fashion to match the number of wells pumped and are generally rated for a 5,000-psi working pressure. Fig. 6.45 shows a power control manifold module. A constant-pressure control valve regulates the pressure on the common power-fluid side of the manifold. This pressure is generally a few hundred pounds per square inch greater than the highest pressure demanded by any well to allow proper operation of the individual well control valves. Individual constant-flow control valves regulate the amount of power fluid going to each well in the case of reciprocating pumps. Constant-pressure control valves or manual throttling valves are often used to regulate those wells on jet pumps. Meter loops or individual meters for each station can be integrated into the manifold.

Lubricator

Some wells will flow or kick back when the operator is attempting to remove or to insert a pump in the wellhead. Also, the presence of H_2S may make it inadvisable to open up the entire tubing string for pump insertion and removal. The use of a lubricator allows the master valve below the wellhead to be closed and the entire lubricator with the pump in it to be removed from the wellhead. The lubricator is essentially an extended piece of tubing with a side line to allow fluid flow when the pump is circulated up into it. A latch mechanism at the bottom prevents the pump from falling out when the lubricator is removed from the wellhead. An example of a lubricator is shown in Fig. 6.46.

Power-Fluid Systems

The function of the surface treating system is to provide a constant supply of suitable power fluid to be used to operate the subsurface production units. The successful and economical operation of any hydraulic pumping system is to a large extent dependent on the effectiveness of the treating system in supplying high-quality power fluid.

TABLE 6.18—MANUFACTURER B MULTIPLEX PLUNGER PUMPS

3K-100 Triplex; maximum rev/min 450; maximum horsepower 100.

Pump size	Plunger diameter (in.)	Maximum pressure (psi)	Displacement (B/D)	
			Per 100 rev/min	At maximum rev/min
5,000-psi fluid end	3/4	5,000	79	355
	7/8	5,000	107	481
	1	5,000	140	630
	1 1/8	5,000	177	796
	1 1/4	5,000	219	984
	1 3/8	4,446	265	1,191
	1 1/2	3,735	315	1,416
	1 5/8	3,174	369	1,666
	1 3/4	2,740	428	1,929
	1 7/8	2,395	490	2,206
3,000-psi fluid end	2	2,102	559	2,515
	2 1/8	1,863	631	2,839
	2 1/4	1,655	710	3,194
	2 3/8	1,490	789	3,549
	2 1/2	1,339	874	3,934

4K-200 Triplex; maximum rev/min 400; maximum horsepower 200.

5,000-psi fluid end	1 1/2	5,000	394	1,577
	1 5/8	5,000	463	1,851
	1 3/4	5,000	535	2,139
	1 7/8	4,309	614	2,455
	2	3,781	700	2,798
	2 1/8	3,354	789	3,154
	2 1/4	2,990	885	3,538
	2 3/8	2,678	988	3,950
	2 1/2	2,418	1,094	4,375
	2 5/8	2,197	1,203	4,814
3,000-psi fluid end	2 3/4	1,998	1,323	5,294
	2 7/8	1,828	1,447	5,787
	3	1,680	1,574	6,295
	3 1/8	1,579	1,707	6,830
	3 1/4	1,431	1,848	7,392

The presence of gas, solids, or abrasive materials in the power fluid will seriously affect the operation and wear life of the surface and downhole units. Therefore, the primary objective in treating crude oil or water for use as power fluid is to make it as free of gas and solids as possible. In addition, chemical treatment of the power fluid may be beneficial to the life of the engine end or pump end of the production unit.

On the basis of an analysis of more than 50 power-oil samples from the Permian Basin, the maximums in Table 6.19 have been established as ideal for a quality power oil in the 30 to 40°API range.³²

It has been observed, however, that acceptable performance has been achieved in many instances where these limits were exceeded moderately. Because leakage past close fits in the downhole unit is often the limiting factor, heavier power oils can perform satisfactorily with more solids because the resulting wear does not increase leakage to the same degree. The periodic analysis of power oil indicates the steps to be taken for improved operations. For example, if the power oil analysis shows that iron sulfide or sulfate compounds make up the bulk of the total solids, then a corrosion or scale problem exists that would require the use of chemical inhibitors to correct the problem.

Water is being used more frequently as a power fluid, particularly in congested locations such as townsite leases and offshore platforms where the safety and environmental advantages of water are important. Water, however, usually requires that a lubricant be added for use with

reciprocating downhole pumps, that corrosion inhibitors be added, and that all oxygen be scavenged. Because of these costly considerations, the closed power-fluid system is often used with water power fluid to minimize the amount of water treated. Filtering of water power fluid to 10 μ m is recommended, particularly with reciprocating downhole pumps.

Other considerations in the choice of water or oil as a power fluid include the following.

1. Maintenance on surface pumps is usually less with oil power fluid. The lower bulk modulus of oil also contributes to reduced pressure pulsations and vibrations, which can affect all the surface equipment.

2. Well testing for oil production is simpler with water power fluid because all the oil coming back is produced oil. With oil power fluid, the power oil rate must be metered and subtracted from the total oil returning to the surface. This can be a source of considerable error in

TABLE 6.19—QUALITY POWER OIL IN THE 30- to 40°API-RANGE MAXIMUMS

Maximum total solids,* ppm	20
Maximum salt content, lbm/1,000 bbl oil	12
Maximum particle size, μ m	15

*If the majority is not primary one kind of solid.

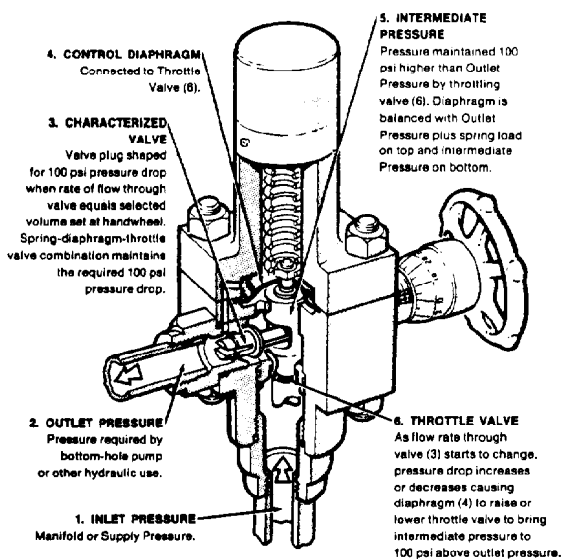


Fig. 6.44—Constant-flow control valve.

HOW IT WORKS

As illustrated at left, there are three separate pressures involved in the operation of a constant flow controller—inlet, intermediate, and outlet. The spring acts on the diaphragm with a force equivalent to 100-psi pressure; therefore the diaphragm is in equilibrium when the intermediate pressure is 100 psi greater than the outlet pressure. The outlet valve thus has a 100-psi pressure drop maintained across it at all times, which ensures a constant flow rate. The characterized outlet valve is shaped to allow, at this 100-psi pressure drop, the rate of flow selected by the handwheel.

high-water-cut wells where the power-oil rate is large compared with the net oil production. This particular objection to oil power fluid does not hold, however, with the single-well power units to be discussed later.

3. In high-friction systems, as sometimes occur with jet pumps in restricted tubulars, the lower viscosity of water can increase efficiency. With no moving parts, the jet pump is not adversely affected by the poor lubricating properties of water.

4. In deep casing-type installations, particularly with jet pumps, water power fluid can "load up" in the casing annulus return, negating any beneficial gas-lifting effects from produced gas.

The use of filters with oil power fluid has not been found to be practical unless heat and chemicals are used to eliminate waxing and emulsion plugging, and a settling process is normally used. The basic purpose of the settling process is to remove foreign particles from lease crude oil by gravity separation or settling in a continuous-flow system. All the tanking and piping specifications for an adequate power-oil system are dictated by this settling requirement. In a tank of static fluid, all the foreign particles contained in the oil would fall or settle to the bottom. Some of the particles, such as fine sand and small water droplets, will fall slowly. Heavier solids and larger water drops will fall more rapidly. This difference in rate of fall is partially because of the difference in density of the oil, water, and solids. The density, or specific gravity, of most of the solids is considerably greater than that of the oil and they will tend to settle quickly in oil. The densities of water and oil are much closer, and gravity separation will be slower. Other factors that influence the rate of separation are related to the resistance the particles encounter in dropping through oil and depend on both the size of the particles and the viscosity of the oil.

Gravity separation of small bubbles of gas, drops of water, or sand grains follows Stokes' law when the Reynolds number is less than or equal to 1.85. Stokes' law is given by

$$v_s = 4.146 \frac{d_p^2 (\gamma_{sp} - \gamma_L)}{\mu_L} \quad (81)$$

where

v_s = settling velocity, ft/hr,

d_p = diameter of particles, thousandths of an inch,

μ_L = viscosity of liquid, cp,

γ_{sp} = specific gravity of suspended particles, and

γ_L = specific gravity of liquid.

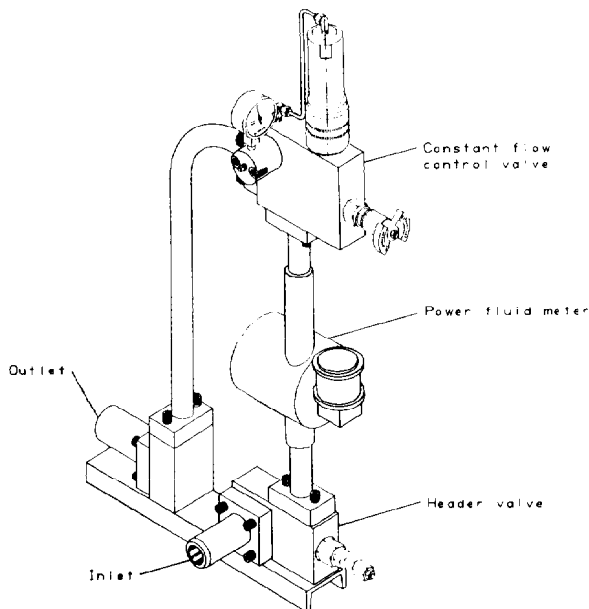


Fig. 6.45—Power control manifold module.

If the Reynolds number is greater than 1.85, a correction to Stokes' law is required and is given by

$$v_s = \frac{19.1 d_p^{1.14} (\gamma_{sp} - \gamma_L)^{0.71} F_s}{\mu_L^{0.43} \gamma_{sp}^{0.29}}, \dots\dots\dots (82)$$

where F_s = shape factor; spheres = 1.0, sand = 0.65.

Table 6.20 gives the velocity of separation of gas bubbles, water drops, and sand grains in oil having a viscosity of 10 cp and a specific gravity of 0.87.

In an actual oil system, it is neither practical nor necessary to furnish space that will provide settling under perfectly still conditions. It is necessary to provide a tank where clean crude oil can be continuously and automatically withdrawn. Proper settling under these conditions then is accomplished only if the upward flow through the settling tank is maintained at a rate that is slower than the foreign-particle fallout rate. If the upward rate of the fluid is even slightly greater than the rate at which the particles will fall, the particles will be carried upward by the fluid. Even though they may move upward very slowly, they will eventually be carried through the tank. It has been found by experience that in most cases an upward velocity of 1 ft/hr is low enough to provide sufficient gravity separation of entrained particles to clean crude oil to power-oil requirements.

Power-Oil Tank and Accessories

Open Power-Fluid System. A typical power-oil treating system that has proven adequate for most open power-fluid systems when stock-tank quality oil is supplied is shown in Fig. 6.47. This system has the general characteristic that all return fluids from the well, both production and power fluid, must pass through the surface treating facility. The power-oil settling tank in this system (shown in Fig. 6.48) is usually a 24-ft-high, three-ring, bolted steel tank. A tank of this height generally will provide adequate head for gravity flow of oil from the tank to the multiplex pump suction. If more than one multiplex pump is required for the system, individual power-oil tanks can be set for each pump, or a single large tank can be used, whichever is more economical and best meets the operating requirements. If a single large tank supplies the suction for several pumps, individual suction lines are preferred.

The gas boot is essentially a part of the power-oil tank. The purpose of the boot is to provide final gas/oil separation so that the oil will be stable at atmospheric pressure. If the gas is not sufficiently separated from the oil, entrained free gas can enter the power-oil tank and destroy the settling process by causing the fluid in the tank to roll. The following piping specifications for the gas boot are necessary to ensure undisturbed settling.

1. The gas boot inlet height should be 4 ft above the top of the power-oil tank to allow the incoming fluid to fall, and so that the agitation will encourage gas/oil separation.
2. The top section of the gas boot should be at least 3 ft in diameter and 8 ft higher than the top of the power-oil tank. These two factors will provide a reservoir that should absorb the volume of the surges.

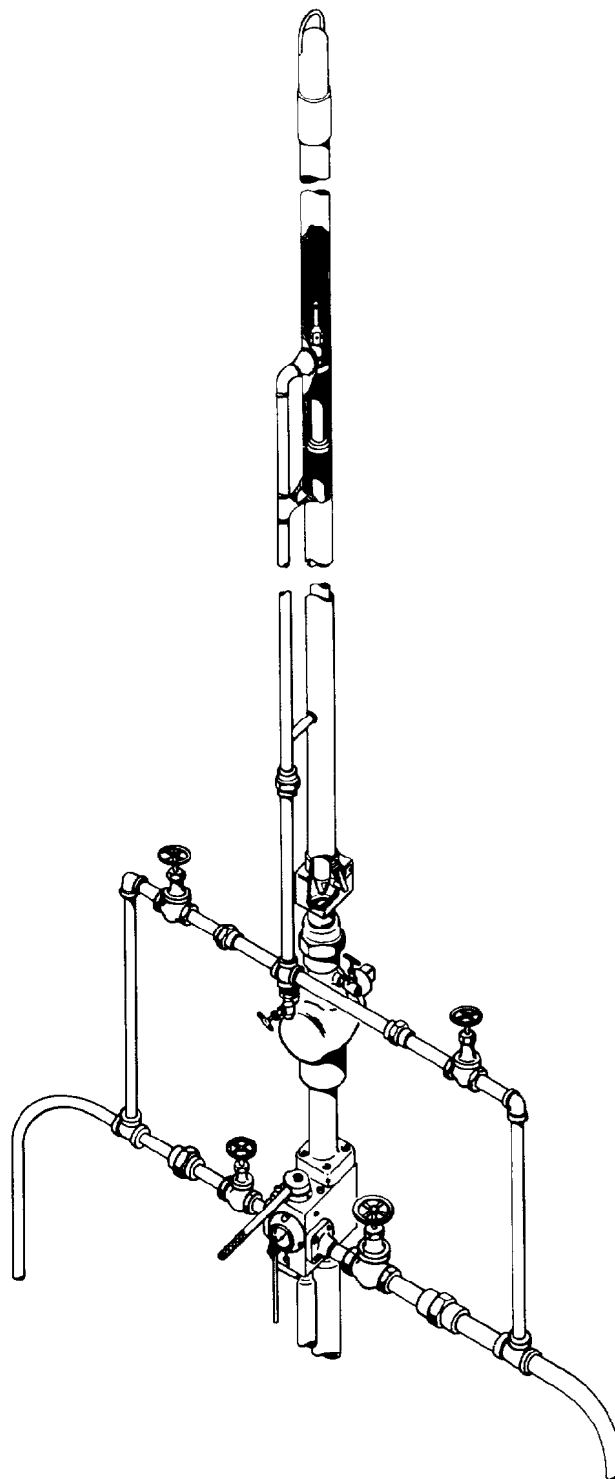


Fig. 6.46—High-pressure lubricator.

TABLE 6.20—GRAVITY SEPARATION, SETTLING VELOCITY IN OIL,
ft/hr ($\mu = 10$ cp; $\gamma = 0.87$)

Particle diameter:			100	50	10	5	1	0.5	0.1
in. $\times 10^{-3}$			2,540	1,270	254	127	25.4	12.7	2.54
μm									
Type	γ_{sp}	$\gamma_{sp} - \gamma_o$							
Gas*	0.0	-0.87	1,276	579	36.0	9.00	0.360	0.0900	0.00360
Water	1.0	0.13	331	135	5.4	1.35	0.054	0.0135	0.00054
	1.05	0.18	417	186	7.5	1.86	0.075	0.0186	0.00075
	1.10	0.23	496	224	9.5	2.38	0.095	0.0238	0.00095
	1.15	0.28	571	258	11.6	2.90	0.116	0.0290	0.00116
Solids	2.0	1.13	1,000	453	30.8	7.60	0.308	0.0760	0.00308
	2.5	1.63	1,295	587	43.9	10.98	0.439	0.1100	0.00439
	3.0	2.13	1,565	709	57.4	14.35	0.574	0.1430	0.00574
	4.0	3.13	2,060	934	84.4	21.20	0.844	0.2120	0.00844

*For this table, the density of gas is assumed to be 0.0.

3. The gas line out of the top of the boot should be tied into the power-oil tank and stock-tank vent line with a riser on the top of the power-oil tank. In the event the gas boot does become overloaded and kicks fluid over through the gas line, this arrangement will prevent the raw or unsettled fluid from being dumped in the top of the power-oil tank where it may contaminate the oil drawn off to the multiplex. A minimum diameter of 3 in. is recommended for the gas line.

4. The line connecting the gas boot to the power-oil tank should be at least 4 in. in diameter. This is necessary to minimize restrictions to flow during surge loadings of the boot.

Oil entering a large tank at the bottom and rising to be drawn off the top tends to channel from the tank inlet to the outlet. The purpose of the spreader is to reduce the velocity of the incoming fluid by distributing the incoming volume over a large area. This allows the fluid to rise

upward at a more uniform rate. The recommended spreader consists of a round, flat plate, approximately half the diameter of the tank, with a 4-in. skirt that has 60°, triangular, saw-tooth slots cut in it. The slots provide automatic opening adjustment for varying amounts of flow. It is essential that they be cut to uniform depth to obtain an even distribution of flow. This type of spreader must be installed with the tops of all the slots in a level plane to prevent fluid from dumping out under a high side. The spreader should be mounted about 2 ft above the bottom rim of the tank.

The location of the stock-tank take-off and level control is important because it establishes the effective settling interval of the power-oil tank and controls the fluid level. All fluid coming from the spreader rises to the stock take-off level where stock-tank oil is drawn off. Fluid rising above this level is only that amount required to replace the fluid withdrawn by the multiplex pump, and it is in

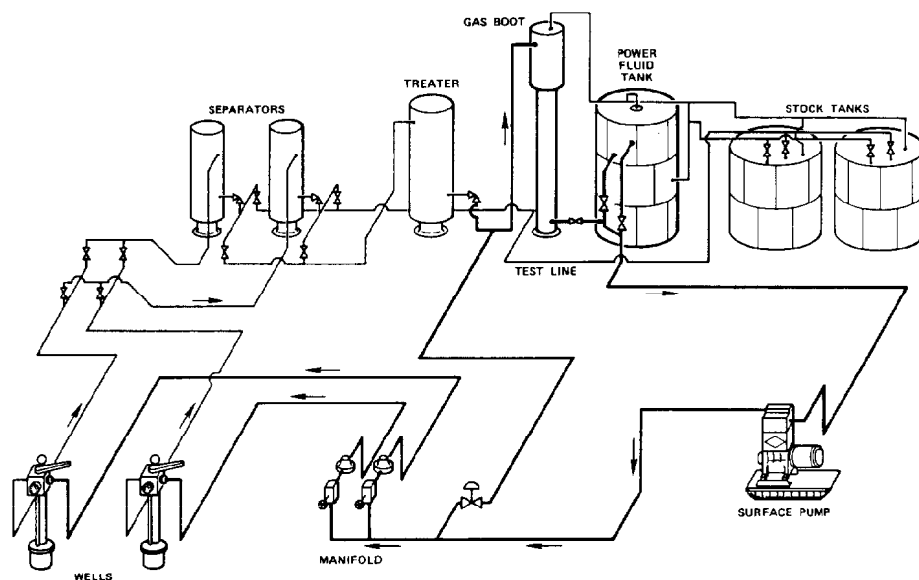


Fig. 6.47—Surface facilities for open power-fluid system.

this region that the power-oil settling process takes place. The light solids settled out are carried with the production through the stock-tank takeoff, and the heavier particles settle to the bottom where they must be periodically removed. The location of the stock take-off point should be within 6 ft of the spreader. The height to which the stock oil must rise in the piping to overflow into the stock tank determines the fluid level in the power-oil tank. For this reason, the level control should be placed a minimum of 18 in. from the top of the power-oil tank and the diameter of piping used should be sufficient to provide negligible resistance for the required volume of flow (4-in. minimum diameter recommended). The extension at the top of the level control is connected to the gas line to provide a vent that keeps oil in the power-oil tank from being siphoned down to the level of the top of the stock tank.

The power-oil outlet should be located on the opposite side of the power-oil tank from the stock take-off outlet to balance the flow distribution within the tank. Because the fluid level in the tank is maintained approximately 18 in. from the top of the tank, the upper outlet should be located 3 ft below the top of the tank to ensure an oil level above it at all times. The second, or emergency, power-oil outlet should be located below the upper outlet for use in starting up or filling tubing strings. The location of this outlet will depend on estimated emergency requirements and the capacity per foot of tank. A distance of 7 ft from the top of the tank is usually sufficient. This lower outlet line contains a shutoff valve that is to be kept closed during normal operations so that the full settling interval will be used.

Closed Power-Fluid Systems. In the closed power-fluid system, the power fluid returns to the surface in a separate conduit and need not go through the surface treating facilities. The reduction in surface treating facilities can tend to offset the additional downhole cost of the system. Virtually all closed power-fluid systems are in California because of the large number of townsite leases and offshore platforms, and water is usually the power fluid. The sur-

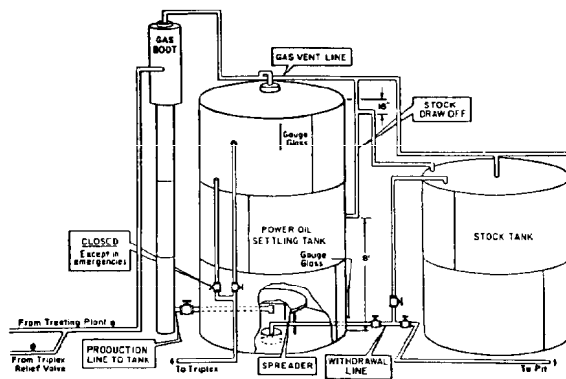


Fig. 6.48—Recommended gas-boot/settling-tank system.

face facilities for a closed power-fluid central system are shown in Fig. 6.49. Note the addition of a power-fluid tank, which is part of a closed loop including the multiplex pump and the engine end of the downhole production unit. Gravity settling separation in the power-fluid tank ensures that the power fluid remains clean despite the addition of solids from power-fluid makeup, corrosion products, and contamination during pump-in and pump-out operations. The power-fluid makeup is required to replace the small amount of fluid lost through fits and seals in the downhole pump and wellhead control valve. A certain amount of power fluid is lost during circulating operations as well. As before, if gravity separation is used, the upward velocity of the fluid in the tank should be kept below 1 ft/hr. If filtration of power water is used, the power-fluid tank size can be reduced considerably. It should be remembered that this system is not possible with the downhole jet pump because it is inherently a power-fluid and production mixing device.

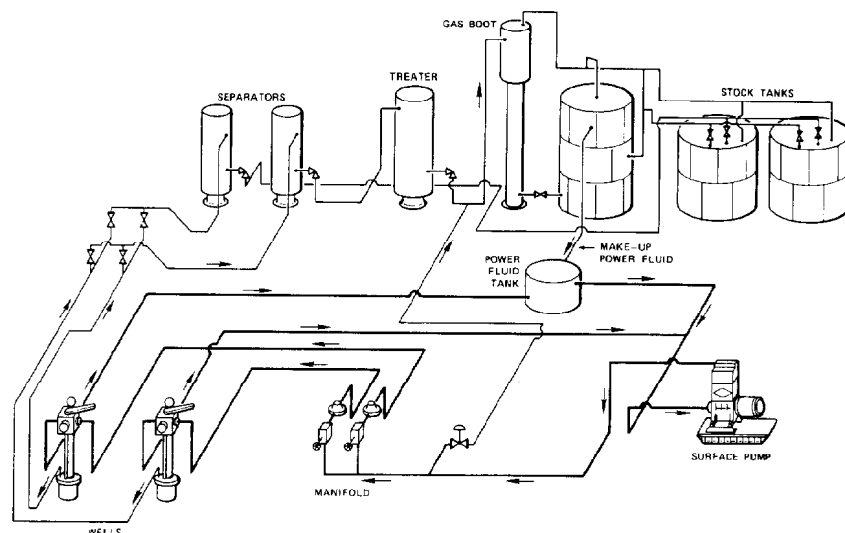


Fig. 6.49—Surface facilities for closed power-fluid system.

Single-Well Systems

The central battery systems previously discussed have been used successfully for years and provide a number of benefits. The use of lease fluid treating facilities as part of the hydraulic system ensures good, low-pressure separation of the gas, oil, water, and solid phases present in any system. Good triplex charging of clean, gas-free oil and consistently clean power fluid supplied to the down-hole pump are desirable features of this system. The lease treating facilities, however, must have sufficient capacity to process both the well production and the return power fluid. When the wells are closely spaced, the clustering of power generation, fluid treating, and control functions in one location is very efficient and allows good use of the installed horsepower. Because the system is not limited by production variations on any one well, an adequate supply of the desired power fluid is ensured by the size of the system. A further benefit associated with use of the lease separation facilities is the option of a closed power-fluid system. When well spacing is large, however, long, high-pressure power-fluid lines must be run. Also, individual well testing is complicated by the need to meter the power-fluid rate to each well, which can introduce measurement errors. As a final consideration, only a few wells in a field may be best suited to artificial lift by hydraulic pumping, and the installation of a central system is difficult to justify.

To address the limitations of the central battery system, single-well systems have been designed.^{33,34} Many of the requirements of a single-well system are the same as for a central battery. The oil, water, gas, and solid phases must be separated to provide a consistent source of power fluid. Hydraulic power to run the system must be generated. A choice of water or oil power fluid should be possible, and the fluid used as power fluid must be sufficiently clean to ensure reliable operation and be gas-free

at the multiplex suction to prevent cavitation and partial fluid end-loading. An adequate reservoir of fluid must be present to allow continuous operation and the various circulating functions associated with the free-pump procedures. Finally, a means of disposing of and measuring the well production to the lease treating and storage facilities must be provided.

To achieve these objectives, several of the manufacturers of hydraulic pumping units offer packaged single-well systems that include all the control, metering, and pumping equipment necessary. All components are skid-mounted on one or two skids to facilitate installation at the well and to make the system easily portable if the unit needs to be moved to a different well. Usually, the only plumbing required at the wellsite is for power-fluid and return-line hookup at the wellhead, and connection of the vessel outlet to the flowline.

An example of a typical single-well power unit is shown in Fig. 6.50. All units of this type share certain design concepts, with small variations depending on manufacturer preference. Two other designs are shown in Figs. 6.51 and 6.52. Either one or two pressure vessels are located at the wellsite. The size of the main reservoir vessel depends on the nature of the well and the tubular completion. The reservoir size should ensure that if the well heads and partially empties the return conduit to the flowline, adequate capacity remains to operate the down-hole unit until production returns re-enter the vessel. Even if the well does not head, extra capacity is needed. When the unit is shut down for maintenance or pump changeout, that portion of the return conduit occupied by gas will need to be filled from the vessel to unseat the pump and to circulate it to the surface. The vessel sizes normally used range from 42 × 120 to 60 × 240 in. In some wells, even the largest vessel may not be able to compensate fully for heading. In these cases, it is common to backpressure the well to stabilize heading. The vessels themselves

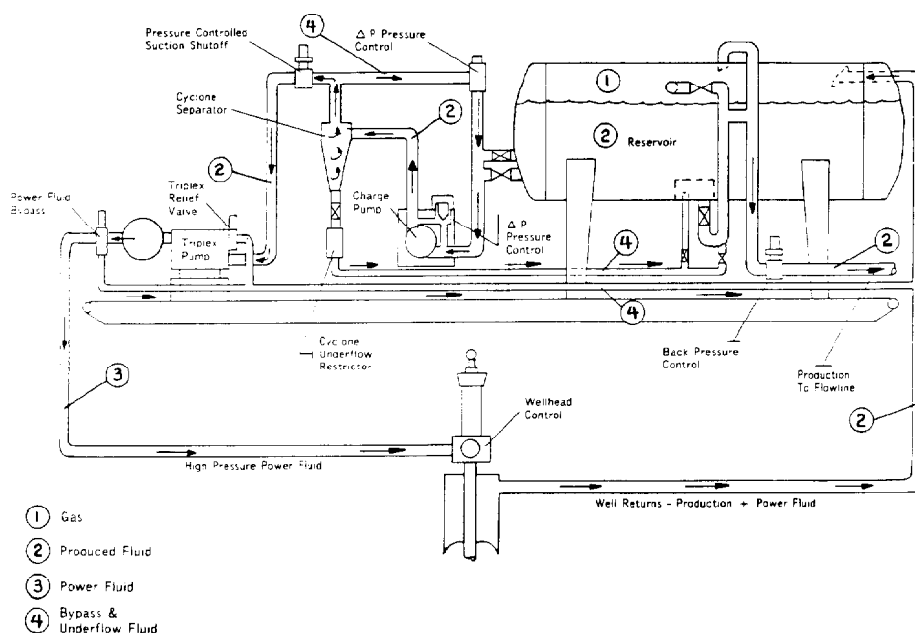


Fig. 6.50—Schematic flow diagram, single-well power unit.

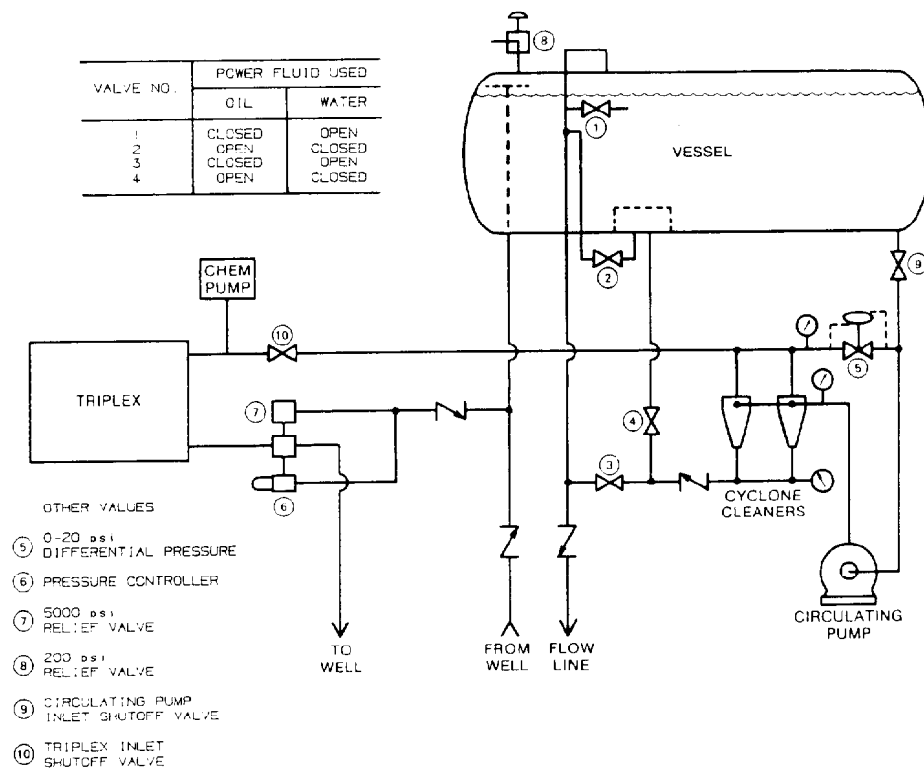


Fig. 6.51—Schematic flow diagram, single-well power unit.

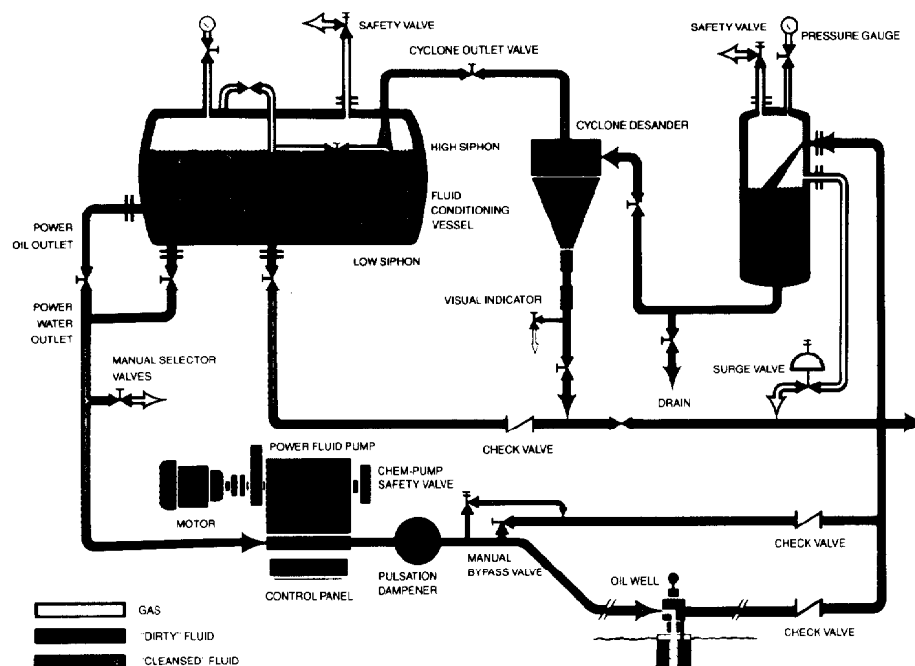


Fig. 6.52—Schematic flow diagram, dual-vessel, single-well power unit.

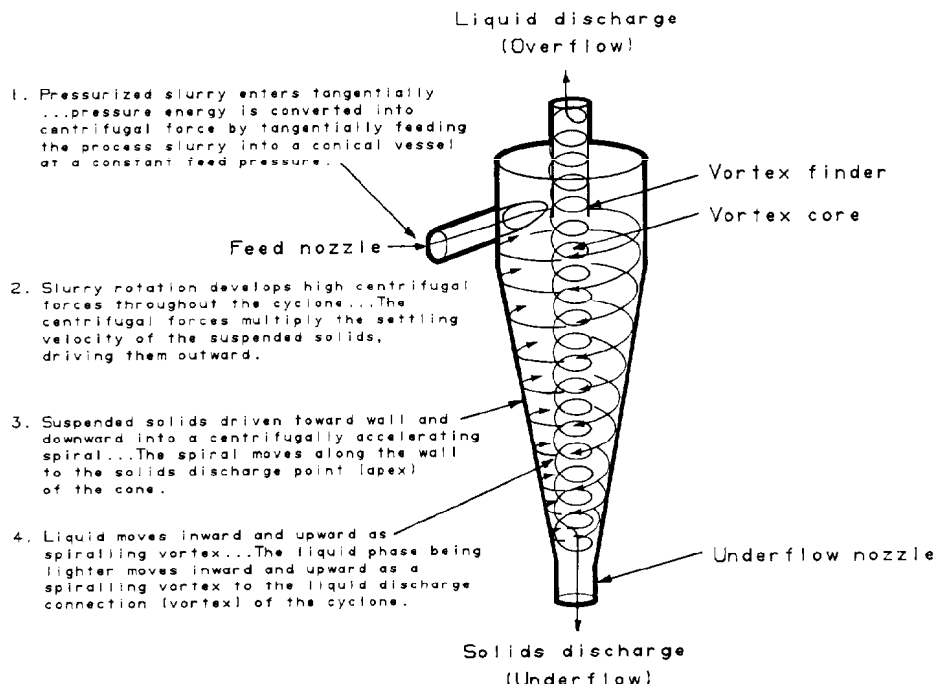


Fig. 6.53—Hydrocyclone.

are normally rated in the 150- to 175-psi range, with higher ratings available for special applications. Coal tar epoxy internal coatings are common, with special coatings available for CO_2 service.

The return power fluid and production from the well enter the vessel system where basic separation of oil, water, and gas phases take place. Free gas at vessel pressure is discharged to the flowline with a vent system that ensures a gas cap in the vessel at all times. The oil and water separate in the vessel, and the desired fluid is withdrawn for use as power fluid. The power fluid passes through one or more cyclone desanders to remove solids before entering the multiplex suction where it is pressurized for reinjection down the power-fluid tubing. Any excess multiplex output that is bypassed for downhole pump control is returned to the vessel. The underflow from the bottom of the cyclone desanders contains a high solids concentration and is discharged either into the flowline or back into the vessel system. Once the system is stabilized on the selected power fluid, the well production of oil, water, and gas is discharged into the flowline from the vessel, which is maintained at a pressure above the flowline. Because the flowline is carrying only what the well makes, additional treating and separating facilities are not needed as they are in the central battery system that encounters mixed well production and power fluid. This feature also facilitates individual well testing.

Overall fluid level in the vessel system is controlled by simple gravity dump piping that consists of a riser on the outside of the vessel. The height of the riser determines the fluid level within. To prevent siphoning of the vessel, the gas-vent line is tied into the top of the riser as a siphon breaker. The choice of oil or water power fluid is made by selection of the appropriate take-off points on the vessel so that the production goes to the flowline and

the power fluid goes to the multiplex pump. If the multiplex suction is low in the vessel and the flowline outlet is high in the vessel, water will tend to accumulate in the vessel and will be the power fluid. If the multiplex suction is high in the vessel and the flowline outlet is low, oil will tend to accumulate in the vessel and will be the power fluid. Opening and closing appropriate valves will set the system up for the chosen power fluid. The multiplex suction outlets are positioned with respect to the overall fluid level in the vessel to avoid drawing power fluid from the emulsion layer between the oil and water because this layer generally contains a significantly higher concentration of solids and is not easily cleaned in the cyclones.

The fluid cleaning is accomplished with cyclone desanders that require a pressure differential across them. In the two-vessel system, this is accomplished by a differential pressure valve between the two vessels that stages the pressure drop from the wellhead. The energy to maintain this staged pressure drop is supplied by the multiplex pump through the downhole pump. In the single-vessel system, a charge pump and a differential pressure control valve are necessary to maintain the appropriate pressures. The charge pumps are of either the positive displacement type with a pressure-relief valve, or a centrifugal pump. The centrifugal pumps are generally practical only with separate electric drive because the speed variation with gas engine drives causes excessive variations in the pump discharge pressure.

The flow path through a cyclone cleaner is shown in Fig. 6.53. Fluid enters the top of the cone tangentially through the feed nozzle and spirals downward toward the apex of the cone. Conservation of angular momentum dictates that the rotational speed of the fluid increases as the radius of curvature decreases. It is the high rotational

speed that cleans the fluid by centrifugal force. The clean fluid, called the overflow, spirals back upward through the vortex core to the vortex finder, while the dirty fluid exits downward at the apex through the underflow nozzle. The cones are usually constructed of cast iron with an elastomer interior. Different feed-nozzle and vortex-finder sizes and shapes are available to alter the performance characteristics of the cyclone. Different sizes of cyclones are available, with the smaller sizes having lower flow rates but somewhat higher cleaning efficiencies.

Maintaining the proper flows through the cyclone to ensure good cleaning depends on correctly adjusting the pressures at the feed nozzle, overflow, and underflow. At the design flow rates, a 40-to-50-psi drop normally occurs from the feed nozzle to the overflow. In a single-vessel system, the pressure is supplied by a charge pump. In a dual-vessel system, the pressure is supplied by higher backpressure on the returns from the well. Because of the centrifugal head, the cyclone overflow pressure is generally 5 to 15 psi higher than the underflow pressure. An underflow restrictor is commonly used to adjust the amount of underflow from 5 to 10% of the overflow. This ensures good cleaning without circulating excessive fluid volumes. It should be noted that the volume flow rates through a cyclone vary inversely with the specific gravity of the fluid, and that within the range of normal power fluids, increased viscosity leads to increased flow rates. This latter effect is caused by the viscosity that suppresses the internal vortex action. Therefore, proper cyclone sizing to match the charge and multiplex pump characteristics must be done carefully and with knowledge of the fluid to be processed. The manufacturers of the packaged systems will supply appropriate cyclones for the installation. Moving the portable unit to another well may require resizing of the cyclone system. A discussion of field experience and proper cyclone sizing is given by Justus.³⁵

The routing of the dirty underflow varies with different systems, and may be an adjustable option in some systems. Two basic choices are available: return of underflow to the vessel or routing of the underflow to the flowline. In a dual-vessel system, the underflow must be returned to the flowline downstream of the backpressure valve to provide sufficient pressure differential to ensure underflow. Discharging the solids to the flowline is attractive because they are disposed of immediately and are excluded from possible entry into the power fluid. Under some conditions, however, continuous operation may not be possible. If, for any length of time, the net well production is less than the underflow from the cyclone, the level of fluid in the vessel will drop. Over an extended period of time, this can result in shutdown of the system. Shutting off the cyclone underflow during these periods will stop the loss of fluid, but apex plugging may occur during the shutoff period. Returning the underflow to the vessel eliminates the problem of running the vessel dry, but does potentially reintroduce some of the solids into the power fluid. In single-vessel units, the underflow is generally plumbed back to the vessel in a baffled section adjacent to the flowline outlet. This provides for the maximum conservation of fluid, but requires a differential pressure valve between the cyclone overflow and the vessel. This valve is normally set at about 20 psi to ensure a positive pressure to the underflow fluid.

As mentioned previously, the vessel pressure is held above the flowline pressure to ensure flow into the flowline. A differential-pressure control valve is sometimes used for this purpose. This will keep the vessel pressure, which is backpressure on the well, at a minimum during flowline pressure changes that may occur during normal field operation. When water is the power fluid, ridding the flowline in this manner is acceptable. However, when oil is the power fluid, changing vessel pressures will cause flashing of gas in the power oil and will adversely affect the multiplex suction. When oil is used as power fluid, it is recommended that a pressure-control valve be used to keep the vessel at a steady pressure some 10 to 15 psi above the highest expected flowline pressure.

Although the single-well system was developed for applications involving widely spaced wells, two- or three-well installations have been successfully operated from a single-vessel system. This installation design is very attractive on offshore platforms. With a large number of highly deviated wells, offshore production is well-suited to hydraulic pumping with free pumps, but the extra fluid treating facilities required with an open power-fluid system are a drawback when severe weight and space limitations exist. The closed power-fluid system answers this problem, but the extra tubulars in deviated holes create their own set of problems and expense. Furthermore, the use of jet pumps, which are quite attractive offshore, is not possible with the closed power-fluid system. For safety and environmental reasons, water is almost always the power fluid of choice offshore. A single large vessel of the type used for single-well installations can receive the returns from all the wells and separate the power water necessary for reinjection to power downhole units. Full 100% separation of the oil from the power water is not necessary, and, in fact, some minor oil carryover will contribute to the power fluid lubricity. The platform separation facilities then have to handle only the actual production from the wells. A compact bank of cyclone cleaners completes the power fluid separation and cleaning unit.

Nomenclature

- A = pump friction constant
- A_{cm} = minimum cavitation cross-sectional area, sq in.
- A_{ep} = cross-sectional area of engine piston, sq in.
- A_{er} = cross-sectional area of engine rod, sq in.
- A_n = cross-sectional area of nozzle, sq in.
- A_{pp} = cross-sectional area of pump plunger, sq in.
- A_{pr} = cross-sectional area of pump rod, sq in.
- A_s = cross-sectional area of annulus between throat and jet, sq in.
- A_t = cross-sectional area of throat, sq in.
- A_2 = constant defined by Eq. 74
- B = pump friction constant depending on tubing-size pump designed for
- B_t = total FVF, RB/STB
- B_2 = constant defined by Eq. 75
- C_2 = constant defined by Eq. 76

- C_3 = constant depending on type of multiplex pump, Eq. 80
 d = diameter of tubing, in.
 d_p = diameter of particles, thousandths of an in.
 d_1 = ID of outer tube, in.
 d_2 = OD of inner tube, in.
 d_3 = OD of coupling, in.
 D = pump setting depth, ft
 D_2 = constant defined by Eq. 77
 e = eccentricity; also base of natural logarithm
 E_e = efficiency of engine, fraction
 E_p = efficiency of pump, fraction
 $E_{p(\text{int})}$ = pump efficiency for gas interference and pump leakage, fraction
 $E_{p(\text{max})}$ = maximum pump efficiency under downhole conditions, fraction
 E_s = efficiency of surface pump, fraction
 f = weighted average friction factor
 F_{aD} = dimensionless area ratio
 F_d = downward forces, lbf
 F_{gL} = gas/liquid ratio, scf/bbl
 F_{mFD} = dimensionless mass flow ratio
 F_{pD} = dimensionless pressure ratio
 F_s = shape factor
 F_u = upward forces, lbf
 F_v = multiplying factor correcting for viscosity
 g = gravitational constant
 g_d = gradient of discharge fluid, psi/ft
 g_n = nozzle flow gradient, psi/ft
 g_o = gradient of produced oil, psi/ft
 g_{pf} = gradient of power fluid, psi/ft
 g_s = gradient of production (suction) fluid, psi/ft
 g_w = gradient of produced water, psi/ft
 h_a = acceleration head, ft
 K = experimentally determined constant for particular pump
 K_n = nozzle loss coefficient
 K_{td} = throat-diffuser loss coefficient
 K_2 = constant depending on fluid compressibility
 L = length of annulus or tubing, ft
 L_n = net lift, ft
 L_s = actual length of suction line, ft
 N = pump rate, strokes/min
 N_c = speed of pump crankshaft, rev/min
 N_{max} = rated maximum pump rate, strokes/min
 N_{Re} = Reynolds number
 p = pressure, psi
 p_{ed} = engine discharge pressure, psi
 p_{fd} = friction pressure in discharge tubing, psi
 p_{fet} = friction pressure in power exhaust tubing, psi
 p_{fpt} = friction pressure in power tubing, psi
 p_{fr} = pump friction pressure, psi
 $p_{fr(\text{max})}$ = maximum friction pressure, psi
 p_n = pressure at the nozzle, psi
 p_{pd} = pump discharge pressure, psi
 p_{pf} = power fluid pressure, psi
 p_{ps} = pump suction pressure, psi
 p_r = reduced pressure, psi
 p_{so} = surface operating pressure, psi
 p_{wh} = flowline pressure at wellhead, psi
 p_{whe} = power-fluid exhaust wellhead backpressure, psi
 Δp = pressure rise, psi
 Δp_f = friction pressure drop, psi
 P = power, ft-lbf/sec
 P_h = horsepower, hp
 q = flow of oil, B/D
 q_d = discharge-fluid rate, B/D
 q_e = maximum rated engine displacement, B/D
 q_n = nozzle flow rate, B/D
 q_p = maximum rated pump displacement, B/D
 q_{pf} = power-fluid rate, B/D
 q_s = production (suction) fluid rate, B/D
 q_{sc} = cavitation limited flow rate, B/D
 q_{si} = initial assumed value of q_s
 q_{im} = maximum rated total flow through engine and pump, B/D
 R = producing GOR, scf/bbl
 R_s = solution GOR, scf/bbl
 R_{si} = initial solution GOR, scf/bbl
 s_p = pump submergence, ft
 T = temperature, °F
 T_r = reduced temperature, °F
 v_s = settling velocity, ft/hr
 \bar{v}_{sl} = average velocity in suction line, ft/sec
 V_s = surface volume
 V_D = downhole volume
 W_c = water cut, fraction
 W_{cd} = water cut in discharge conduit to surface
 z_g = gas compressibility factor
 γ_{sp} = specific gravity of suspended particles
 $\bar{\gamma}$ = weighted average specific gravity
 γ_{API} = API specific gravity
 γ_g = gas specific gravity
 γ_L = liquid specific gravity
 γ_o = oil specific gravity
 μ_L = viscosity of liquid, cp
 $\bar{\mu}$ = weighted average viscosity, cp
 ν_m = mixture viscosity, cSt
 ν_o = oil viscosity, cSt
 ν_{pf} = power-fluid viscosity, cSt
 ν_w = water viscosity, cSt
 $\bar{\rho}$ = weighted average density, g/cm³

Key Equations in SI Metric Units

$$F = pA, \dots\dots\dots (1)$$

where

- F = force, N,
 p = pressure, Pa, and
 A = area, m².

$$W = FL, \dots\dots\dots (2)$$

where W =work, J, and L =distance, m.

$$P = W/t, \dots\dots\dots (3)$$

where P =power, W, and t =time, seconds.

$$P_h = q \times p \times 0.000017, \dots\dots\dots (5)$$

where q =flow rate, m³/s, and p =pressure, kPa.

$$F_v = \frac{\nu}{10^{-4}} + 0.99, \dots\dots\dots (28)$$

where ν =viscosity, m²/s.

$$p_{fr} = \gamma F_v (345) (7.1 e^{Bq_{tm}})^{N/N_{max}}, \dots\dots\dots (29)$$

where

p_{fr} = friction pressure, kPa,

γ = specific gravity,

F_v = viscosity correction factor,

B = tubing size constant,

q_{tm} = maximum rated total flow through engine
and pump, m³/d,

N = strokes per minute, and

N_{max} = rated maximum strokes per minute.

Tubing Size (in.)	B
2 $\frac{3}{8}$	0.00323
2 $\frac{7}{8}$	0.00175
3 $\frac{1}{2}$	0.00105
4 $\frac{1}{2}$	0.00049

$$g = \gamma (9.79), \dots\dots\dots (39)$$

where g =fluid gradient, kPa/m.

$$(P/E)_{max} = \frac{2464}{L_n}, \dots\dots\dots (54)$$

where $(P/E)_{max}$ =maximum value of P/E , and L_n =net lift, m.

$$q_n = 0.371 A_n \sqrt{(p_n - p_{ps})/g_n}, \dots\dots\dots (55)$$

where

q_n = nozzle flow rate, m³/d,

p_n = nozzle pressure, kPa,

g_n = nozzle flow gradient, kPa/m,

A_n = nozzle area, mm², and

p_{ps} = pump suction pressure, kPa.

$$A_{cm} = \frac{q_s}{\sqrt{\frac{p_{ps}}{g_s}}} \times 3.24, \dots\dots\dots (62)$$

where

A_{cm} = cavitation area, mm²,

q_s = suction flow rate, m³/d,

p_{ps} = pump suction pressure, kPa, and

g_s = suction gradient, kPa/m.

$$F_{mfd} = q_s \left\{ \left[1 + 0.222 \left(\frac{R}{p_{ps}} \right)^{1.2} \right] (1 - W_c) + W_c \right\} \\ \times \left(\frac{g_s}{q_n \times g_n} \right), \dots\dots\dots (64)$$

where

F_{mfd} = dimensionless mass flow ratio,

R = producing GOR, std m³/m³, and

W_c = water cut fraction.

$$A_g = 6.302 \times \frac{q_s (1 - W_c) R}{p_{ps}}, \dots\dots\dots (65)$$

where A_g =area required to pass gas, mm².

$$A_{cm} = q_s \left[3.24 \sqrt{\frac{g_s}{p_{ps}}} + \frac{6.302 (1 - W_c) R}{p_{ps}} \right], \dots\dots (66)$$

where A_{cm} =minimum cavitation cross-sectional area, mm².

$$h_a = 9.54 \frac{L_s \bar{v}_{sl} N_c C_3}{K_2 g}, \dots\dots\dots (80)$$

where

h_a = acceleration head, m,

L_s = actual length of suction line, m,

\bar{v}_{sl} = average velocity in suction line, m/s,

N_c = speed of pump crankshaft, rad/s,

C_3 = constant depending on pump type,

K_2 = constant depending on fluid
compressibility, and

g = gravitational constant, 9.8 m/s².

$$v_s = 1.987 \times 10^{-6} \frac{d_p^2 (\gamma_{sp} - \gamma_L)}{\mu_L}, \dots\dots\dots (81)$$

where

v_s = settling velocity, m/h,

d_p = diameter of particles, μ m,

γ_{sp} = specific gravity of suspended particles,

γ_L = specific gravity of liquid, and

μ_L = viscosity of liquid, Pa·s.

$$v_s = \frac{0.00747 d_p^{1.14} (\gamma_{sp} - \gamma_L)^{0.71} F_s}{\mu_L^{0.43} \gamma_{sp}^{0.29}}, \dots\dots\dots (82)$$

where F_s = shape factor; spheres = 1.0 and sand = 0.65.

$$B_g = \frac{0.351z_g T}{p_a}, \dots\dots\dots (A-2)$$

$$B_t = B_o + B_g(R_{si} + R_s), \dots\dots\dots (A-3)$$

$$F = 5.55R_s \left(\frac{\gamma_g}{\gamma_o} \right)^{0.5} + 2.25T - 574.59, \dots\dots\dots (A-4)$$

and

$$R_s = \gamma_g \left[\frac{p}{515} \times \frac{10^{(1.77/\gamma_o - 1.64)}}{10^{(0.001638T - 0.418)}} \right]^{1/0.83}, \dots\dots\dots (A-5)$$

where

- B_o = oil FVF, res m³/m³,
- B_g = gas FVF, res m³/m³,
- z_g = gas compressibility factor,
- T = temperature, K,
- p = pressure, kPa,
- B_t = total (oil plus gas) FVF, res m³/m³,
- R_s = solution GOR, m³/m³,
- R_{si} = initial solution GOR, m³/m³,
- γ_g = gas specific gravity, and
- γ_o = oil specific gravity.

$$T_r = \frac{1.8T}{175 + 307\gamma_g}, \dots\dots\dots (A-12)$$

and

$$p_r = \frac{p_a}{4,830 - 324\gamma_g}, \dots\dots\dots (A-13)$$

where p_r = reduced pressure, kPa, and T_r = reduced temperature, K.

$$v = 14.73 \frac{q}{d^2}, \dots\dots\dots (B-1)$$

where

- v = fluid viscosity, m/s,
- q = quantity of oil flowing, m³/d, and
- d = diameter of tubing, mm.

$$\Delta p_f = 4.71 \times 10^5 \frac{\bar{\mu} L q}{d^4}, \dots\dots\dots (B-2)$$

and

$$\Delta p_f = 1.084 \times 10^5 \bar{\gamma} \bar{f} L \frac{q^2}{d^5}, \dots\dots\dots (B-3)$$

where

- Δp_f = friction pressure drop, kPa,
- $\bar{\mu}$ = weighted average of viscosity, Pa·s,
- $\bar{\mu}/\bar{\rho}$ = weighted average kinematic viscosity, cSt,
- $\bar{\gamma}$ = weighted average specific gravity,
- $\bar{f} = \phi(dv\bar{\rho}/\bar{\mu})$, weighted average friction factor,
- $\quad = \frac{0.0555(\bar{\mu}/\bar{\rho})^{0.21}}{(dv)^{0.21}}$, and
- L = length of tubing or annulus, m.

$$N_{Rc} = 1,000 \frac{dv}{\bar{\mu}/\bar{\rho}}, \dots\dots\dots (B-4)$$

$$v = 14.73 \frac{q}{d_1^2 - d_2^2}, \dots\dots\dots (B-5)$$

and

$$\Delta p_f = \frac{4.71 \times 10^5 \bar{\mu} L q \left(\frac{d_1}{d_1 - d_2} \right)^{0.1}}{(d_1 - d_2)^2 (d_1^2 - d_2^2) (1 + 1.5e^2)}, \dots\dots (B-6)$$

where d_1 = ID of outer tube, mm, and d_2 = OD of inner tube, mm.

$$\Delta p_f =$$

$$\frac{1.084 \times 10^5 \bar{\gamma} \bar{f} q^2 L}{(d_1 - d_2)(d_1^2 - d_2^2)^2 \left(\frac{d_1}{d_1 - d_2} \right)^{0.1} (1 + 1.5e^2)^{0.25}}, \dots\dots\dots (B-7)$$

where d_3 = OD of coupling (inner tube), mm, and e = eccentricity.

Appendix A—Fluid Properties

A detailed analysis of a hydraulic pumping system would include the properties of all the fluids under the different temperature, pressure, dissolved-gas, and emulsion conditions that can exist in different parts of the well and pumping system. Important properties that would vary include the density (or specific gravity), viscosity, and bulk modulus (or compressibility) of the various phases present. An excellent discussion of this subject as applied to hydraulic pumping is given by Brown and Coberly.³⁶

In many cases, however, the well fluid data available are not sufficiently reliable to justify detailed analysis. It has also been noted that the parameters of interest to the production engineer and foreman—notably the surface operating pressure, flow rate, and the predicted pump performance—are not sensitive to small variations in fluid properties. The deviations from expected performance can usually be compensated for readily with the inherent flexibility of the system. For these reasons, average or typical properties are often used in design calculations.

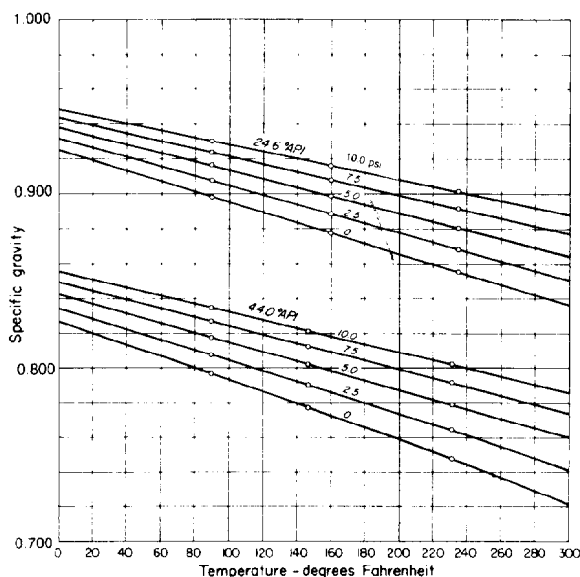


Fig. 6.54—Specific gravity of 24.6°API and 44.0°API oil at 0 to 10,000 psi.

Gravity

The values of specific gravity and gradient (pounds per square inch per foot) for different API crude gravities are given in Table 6.6. The specific gravity of oils varies with temperature and pressure, as shown in Fig. 6.54. Particularly in deep wells, variations in the specific gravity of fluids can have a significant effect on the calculated pressures. It can be seen, however, that the temperature and pressure effects are somewhat compensating. As the well gets deeper, the pressures increase, but so do the temperatures. It is usually sufficient to use reported water specific gravity and an oil specific gravity based on the API gravity from Table 6.6.

Viscosity

The viscosity of water varies with temperature as shown in Fig. 6.26. At oilfield temperatures, it is sufficiently low that variations in viscosity have a negligible effect on friction calculations unless very large volumes are being produced in restricted tubulars, as occasionally occurs with large jet pumps or turbopumps.

At normal temperature (usually 100°F for viscosity determinations), the viscosity of oils increases with specific gravity quite consistently, even though the compositions of the oils may differ. Paraffinic oils generally have somewhat higher viscosities than asphaltic crudes. Fig. 6.55 is a plot of a large number of oils (paraffinic, asphaltic, and mixed-base) from widely scattered fields, which show a good correlation with gravity. This figure has the log-log scale for kinematic viscosity as used for the ordinate of ASTM viscosity charts, and specific gravity as the abscissa. For oils on which actual viscosity determinations are not available, this figure may be used to obtain viscosities at 100°F for estimating friction losses.

Oil viscosity decreases with temperature and is represented by a straight-line relation for most oils when plot-

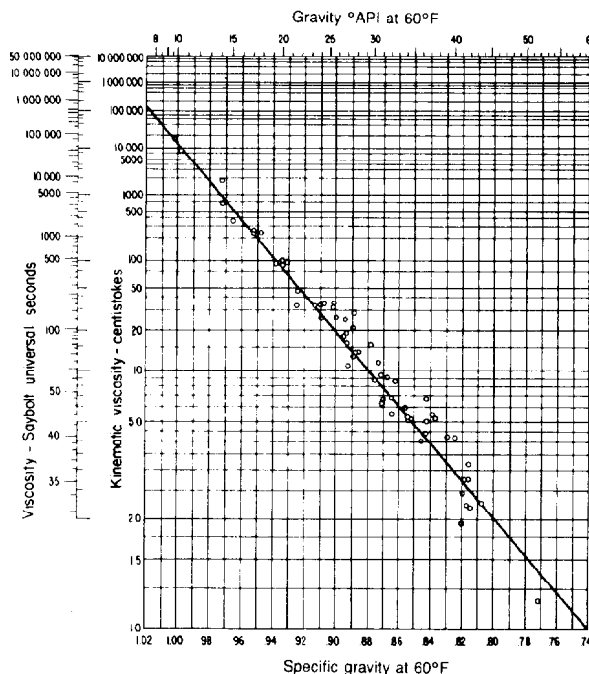


Fig. 6.55—Viscosity of oil vs. specific gravity (viscosity at 100°F).

ted on ASTM viscosity sheets having log-log of viscosity as the ordinate and log of absolute temperature as the abscissa. Fig. 6.25 is a useful plot of the variation of viscosity with temperature of 13 oils from 10 to 50° API.

Emulsion viscosity depends on several factors, most notably whether water or oil is the continuous phase. Emulsions only rarely occur in hydraulic pumping systems, and can usually be treated chemically with additives to the power fluid. Despite the vigorous turbulent mixing action of jet pumps, they have not been observed to aggravate emulsion tendencies. When water is the continuous phase, it wets the wall of the tubing, and the viscosity effects for friction calculations will be determined principally by the water properties. Fig. 6.30 shows the pronounced effect water-in-oil emulsions can have on the apparent viscosity of the fluid.

The effect of dissolved gas on oil viscosity can be significant, particularly with heavy crudes having high viscosities. The effect of dissolved gas is to decrease the viscosity of the crude. As can be seen from Fig. 6.56 (after Ref. 37), the effect is greatest with fluids of high viscosity.

Gas and Liquid FVF's

The downhole pumps must handle formation volumes of oil, water, and gas, which will change when brought to the surface. Fig. 6.27 provides a means for determining the estimated pump-end volumetric efficiency with reciprocating pumps considering these changes. The equations used for Fig. 6.27 follow.^{9,10}

The FVF equations include

$$B_o = 0.972 + 0.000147F^{1.175}, \dots \dots \dots (A-1)$$

$$B_g = 0.0283 \frac{z_g(T+460)}{p_a}, \dots \dots \dots (A-2)$$

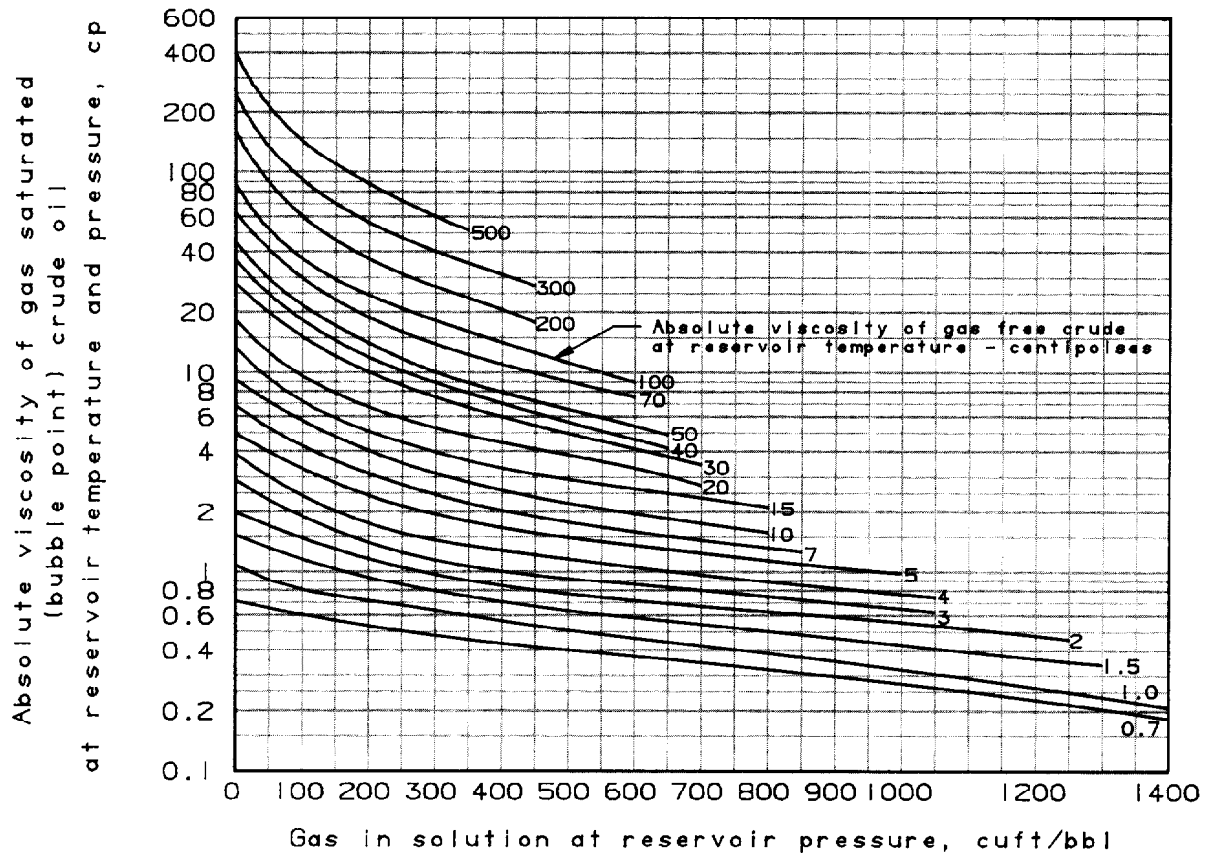


Fig. 6.56—Effect of solution gas on crude viscosity.

and

$$B_t = B_o + B_g(R_{si} + R_s) \frac{1}{5.615}, \dots \dots \dots (A-3)$$

where

$$F = R_s \left(\frac{\gamma_g}{\gamma_o} \right)^{0.5} + 1.25T, \dots \dots \dots (A-4)$$

and

$$R_s = \gamma_g \left(\frac{p_a}{18} \times \frac{10^{0.01257 \gamma_{API}}}{10^{0.000917}} \right)^{1/0.83}, \dots \dots \dots (A-5)$$

where

- B_o = oil FVF, RB/STB,
- B_g = gas FVF, RB/STB,
- z_g = gas compressibility factor,
- T = temperature, °F,
- p = pressure, psia,
- B_t = total (oil plus gas) FVF, RB/STB,
- R_s = solution GOR, scf/bbl,

R_{si} = initial solution GOR, scf/bbl,

γ_g = gas specific gravity,

γ_o = oil specific gravity, and

γ_{API} = API gravity.

The pump efficiency equations involve the ratio of the surface oil and water volume to the downhole oil, water, and gas volume.

$$E_p = \frac{V_s}{V_D} \dots \dots \dots (A-6)$$

and

$$E_p = \left[\frac{1}{W_c + (1 - W_c)B_t} \right], \dots \dots \dots (A-7)$$

where

- E_p = pump efficiency, fraction,
- V_s = surface (oil and water) volume,
- V_D = downhole (oil, water, and gas) volume,
- and
- W_c = water cut, fraction.

The compressibility of gas is a function of three variables—gas specific gravity, temperature, and pressure.

$$z_g = f(\gamma_g, T, p). \quad \text{..... (A-8)}$$

A gas compressibility equation programmed for the computer relates these variables as follows:

$$z_g = A + Bp_r + (1-A)e^{-C} - H(p_r/10)^4, \quad \text{..... (A-9)}$$

where

$$A = -0.101 - 0.36T_r + 1.3868(T_r - 0.919)^{0.5}, \quad \text{(A-10)}$$

$$B = 0.021 + 0.04275/(T_r - 0.65), \quad \text{..... (A-11)}$$

$$T_r = (T + 460)/(175 + 307\gamma_g), \quad \text{..... (A-12)}$$

$$p_r = p_a/(701 - 47\gamma_g), \quad \text{..... (A-13)}$$

$$C = p_r(D + Ep_r + Fp_r^4), \quad \text{..... (A-14)}$$

$$D = 0.6222 - 0.224T_r, \quad \text{..... (A-15)}$$

$$E = 0.0657/(T_r - 0.86) - 0.037, \quad \text{..... (A-16)}$$

$$F = 0.32e^{[-19.53(T_r - 1)]}, \quad \text{..... (A-17)}$$

and

$$H = 0.122e^{[-11.3(T_r - 1)]}, \quad \text{..... (A-18)}$$

where

p_r = reduced pressure, and
 T_r = reduced temperature.

Appendix B—Friction Relationships

Because hydraulic pumping systems require greater circulating volumes of fluid than other artificial lift systems, the proper determination of friction losses is important. This subject is thoroughly covered by F.B. Brown and C.J. Coberly³⁸ and includes the effect of viscosity gradients, laminar to turbulent transitions, proper equivalent diameters for annulus passages, and tubing eccentricity in casing/tubing annular flow passages. Their results are summarized in the following equations.

Circular Sections—Tubing

$$v = 0.01191 \frac{q}{d^2}, \quad \text{..... (B-1)}$$

where

v = velocity, ft/sec,
 q = quantity of oil flowing, B/D, and
 d = diameter of tubing, in.

$$\Delta p_f = 7.95 \times 10^{-6} \frac{\bar{\mu} L q}{d^4} \quad \text{..... (B-2)}$$

for laminar flow and

$$\Delta p_f = 11.46 \times 10^{-6} \bar{\gamma} \bar{f} L \frac{q^2}{d^5} \quad \text{..... (B-3)}$$

for turbulent flow, where

Δp_f = friction pressure drop, psi,
 $\bar{\mu}$ = weighted average viscosity, cp,
 $\bar{\mu}/\bar{\rho}$ = weighted average kinematic viscosity, cSt,
 L = length of tubing, ft,
 q = quantity of oil flowing, B/D,
 d = ID of tubing, in.,
 $\bar{\gamma}$ = weighted average specific gravity,
 \bar{f} = weighted average friction factor
 $= \phi(dv\bar{\rho}/\bar{\mu})$
 $= 0.0361 (\bar{\mu}/\bar{\rho})^{0.21} / (dv)^{0.21}.$

Transition from laminar to turbulent flow occurs when the Reynolds number (N_{Re}) is greater than 1,200.

$$N_{Re} = 7.742 \times 10^3 \frac{dv}{\bar{\mu}/\bar{\rho}}, \quad \text{..... (B-4)}$$

Annular Sections—Flow Between Tubing and Casing

Laminar flow:

$$v = 0.01191 \frac{q}{d_1^2 - d_2^2} \quad \text{..... (B-5)}$$

and

$$\Delta p_f = \frac{7.95 \times 10^{-6} \bar{\mu} L q \left(\frac{d_1}{d_1 - d_2} \right)^{0.1}}{(d_1 - d_2)^2 (d_1^2 - d_2^2) (1 + 1.5e^2)}, \quad \text{..... (B-6)}$$

where

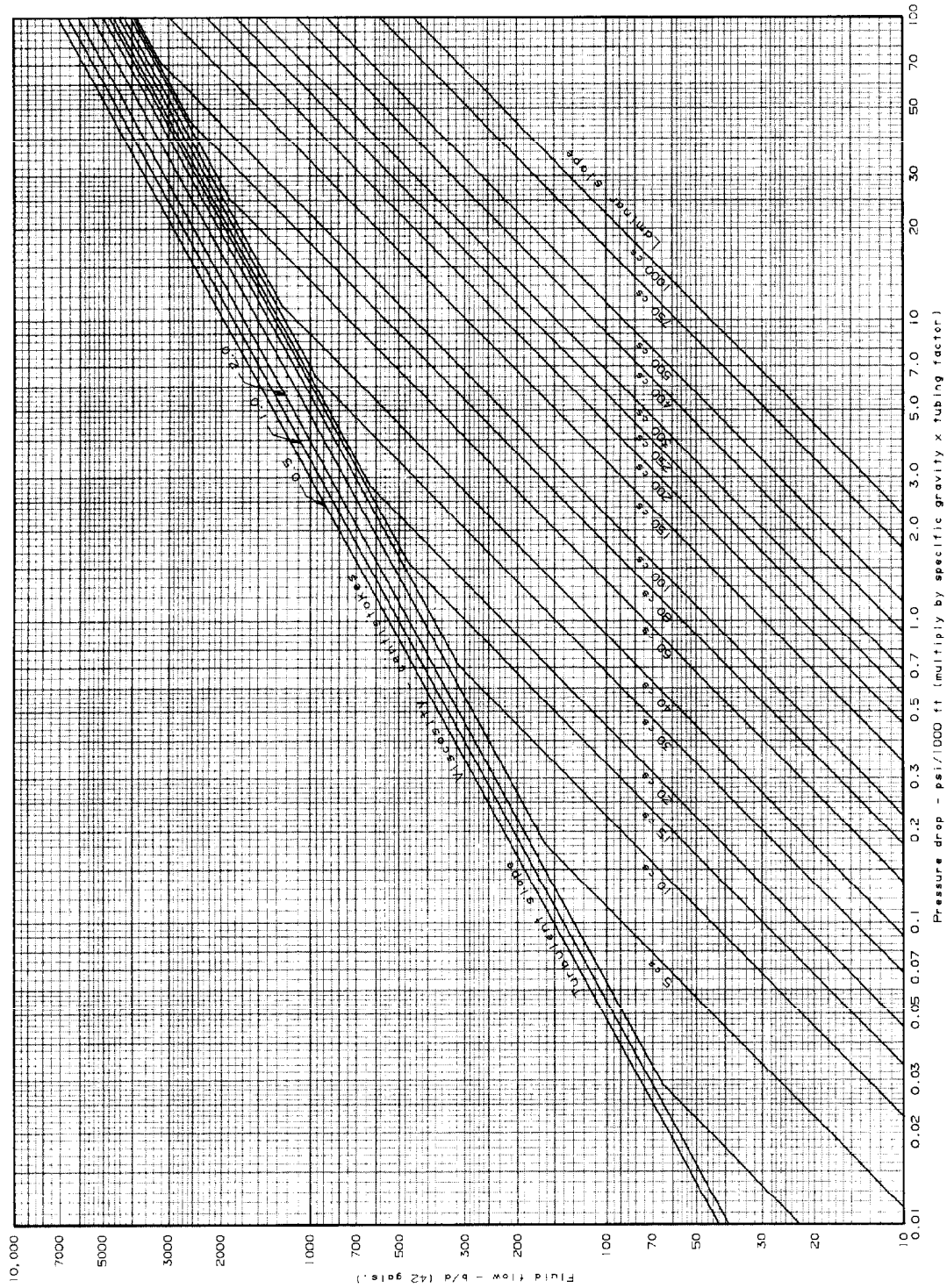
Δp_f = friction pressure drop, psi,
 $\bar{\mu}$ = weighted average viscosity, cp,
 L = length of annulus, ft,
 q = flow, B/D,
 d_1 = ID of outer tube, in.,
 d_2 = OD of inner tube, in.,
 e = eccentricity of tubes = $2d_3/(d_1 - d_2)$, and
 d_3 = distance inner tube is off center, in.

Turbulent Flow:

$$\Delta p_f = \frac{11.46 \times 10^{-6} \bar{\gamma} \bar{f} q^2 L}{(d_1 - d_2)(d_1^2 - d_2^2)^2 \left(\frac{d_1}{d_1 - d_2} \right)^{0.1} (1 + 1.5e^2)^{0.25}}, \quad \text{..... (B-7)}$$

where

Δp_f = friction pressure drop, psi,
 q = flow, B/D,
 L = length of annulus, ft,
 $\bar{\gamma}$ = weighted average specific gravity
 (water = 1.0),
 d_1 = ID of outer tube, in.,
 d_2 = OD of inner tube, in.,
 d_3 = OD of coupling (inner tube), in.,
 e = eccentricity = $(d_1 - d_3)/(d_1 - d_2)$,
 $\bar{f} = \phi(dv\bar{\rho}/\bar{\mu}) = 0.0361 (\bar{\mu}/\bar{\rho})^{0.21} / (dv)^{0.21}$, and
 $\bar{\mu}/\bar{\rho}$ = weighted average kinematic viscosity, cSt.



Tubular size multiplying factor	
	Laminar
3/4"	77.01
1"	29.32
1-1/4"	15.36
1-1/2"	9.79
2-1/16"	5.28
2-3/8"	4.91
2-7/8"	3.78
3-1/2"	2.24
4-1/2"	1.00
	0.44
	0.38
	0.10
	0.14

Fig. 6.57—Pressure drop in tubing.

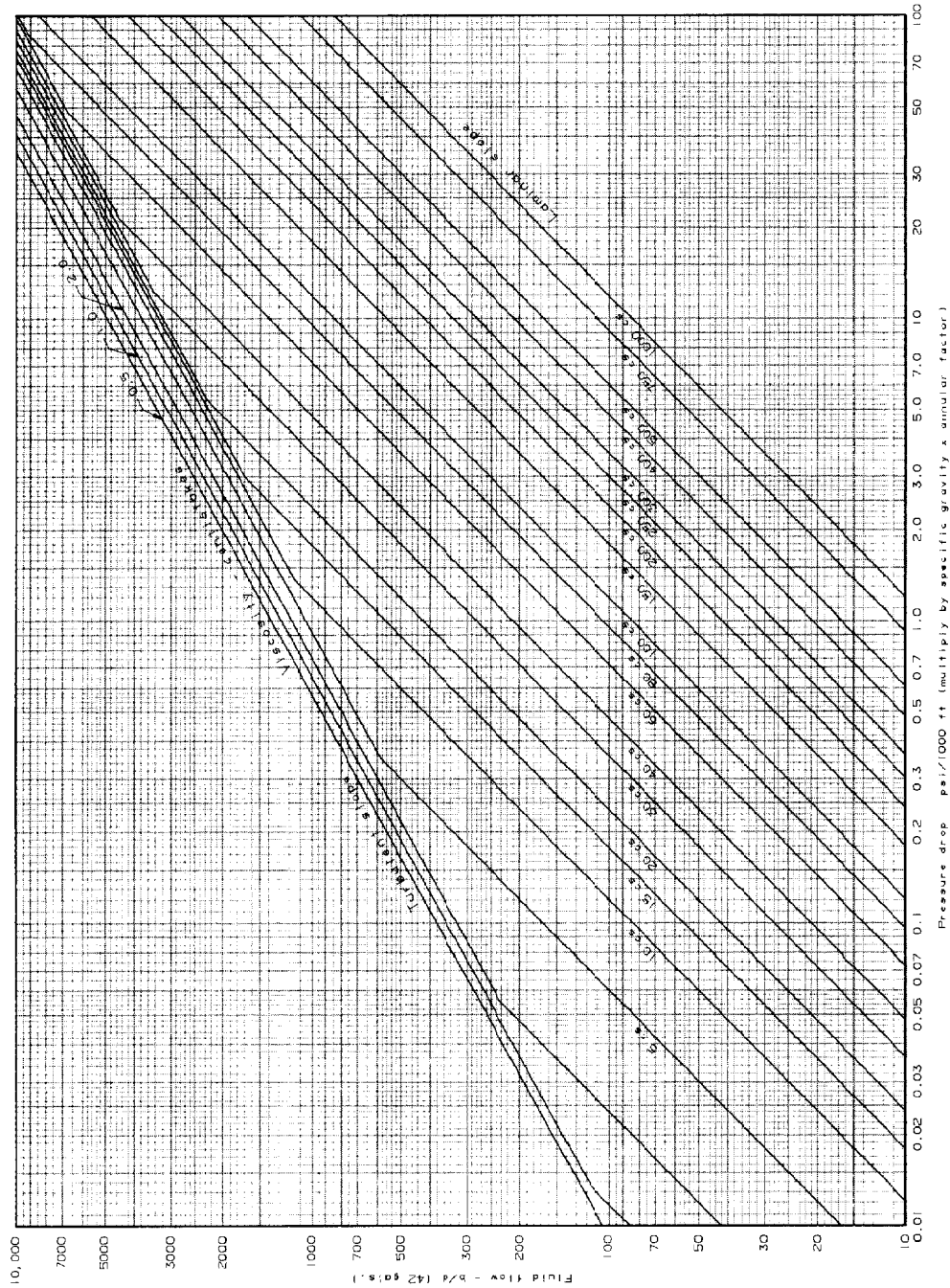


Fig. 6.58—Pressure drop in tubing, annular flow.

Annular geometry multiplying factor		Special clearance couplings required	
Tubular		Laminar	
3/4"	in 2-3/8" Tubing	23.59	23.59
1"	in 2-7/8" Tubing	21.59	21.59
1-1/4"	in 2-7/8" Tubing	55.93	36.77
1-1/2"	in 2-7/8" Tubing *	42.08	10.93
1-1/4"	in 3-1/2" Tubing	8.77	5.78
1-1/2"	in 3-1/2" Tubing	14.44	10.71
2-3/8"	in 3-1/2" Tubing *	65.04	60.93
2-3/8"	in 4-1/2" Tubing	2.98	2.59
2-7/8"	in 4-1/2" Tubing	8.00	8.48
2-3/8"	in 4-1/2" 11.6*	2.73	2.36
2-3/8"	in 5" 15*	1.25	1.08
2-3/8"	in 5-1/2" 17*	0.58	0.51
2-7/8"	in 4-1/2" 11.6*	7.07	7.46
2-7/8"	in 5" 15*	2.54	2.59
2-7/8"	in 5-1/2" 17*	1.00	1.00
2-7/8"	in 6-5/8" 24*	0.23	0.24
2-7/8"	in 7" 26*	0.16	0.16
2-7/8"	in 7-5/8" 29.7*	0.09	0.09
3-1/2"	in 6-5/8" 24*	0.41	0.48
3-1/2"	in 7" 26*	0.26	0.30
3-1/2"	in 7-5/8" 29.7*	0.13	0.15
3-1/2"	in 9-5/8" 40*	0.02	0.03
4-1/2"	in 6-5/8" 24*	1.64	2.50
4-1/2"	in 7" 26*	0.80	1.18
4-1/2"	in 7-5/8" 29.7*	0.31	0.43
4-1/2"	in 9-5/8" 40*	0.04	0.05

In calculating Reynolds numbers, N_{Re} , for annular sections, the characteristic diameter becomes $(d_1 - d_2)$ in Eq. B-4. However, the velocity, v , is calculated from the actual annular cross-sectional area between d_1 and d_2 .

These relationships have been used to construct Figs. 6.57 and 6.58. The viscosity in these figures refers to the weighted average viscosity of Eq. 42 and are for liquid flow only. Vertical or horizontal multiphase flowing gradient calculations or curves should be used when significant gas is present. Figs. 6.57 and 6.58 were constructed with values of the eccentricity, e , of one-half of its maximum value, which occurs when the tubing is against the casing.

References

1. Wilson, P.M.: "Jet Free Pump, A Progress Report on Two Years of Field Performance," Southwestern Petroleum Short Course, Texas Tech U., Lubbock (April 26-27, 1973).
2. Bell, C.A. and Spisak, C.D.: "Unique Artificial Lift System," paper SPE 4539 presented at the 1973 SPE Annual Meeting, Las Vegas, Sept. 30-Oct. 3.
3. Grant, A.A. and Sheil, A.G.: "Development, Field Experience, and Application of a New High Reliability Hydraulically Powered Downhole Pumping System," paper SPE 11694 presented at the 1983 SPE California Regional Meeting, Ventura, March 23-25.
4. Petrie, H. and Erickson, J.W.: "Field Testing the Turbo-Lift System," paper SPE 8245 presented at the 1979 SPE Annual Technical Conference and Exhibition, Las Vegas, Sept. 23-26.
5. Boone, D.M. and Eaton, J.R.: "The Use of Multistage Centrifugal Pumps in Hydraulic-Lift Power Oil Systems," paper SPE 7408 presented at the 1978 SPE Annual Technical Conference and Exhibition, Houston, Aug. 1-3.
6. Christ, F.C. and Zublin, J.A.: "The Application of High-Volume Jet Pumps in North Slope Water Source Wells," paper SPE 11748 presented at the 1983 SPE California Regional Meeting, Ventura, March 23-25.
7. Brown, K.: *The Technology of Artificial Lift Methods*, Petroleum Publishing Co., Tulsa (1980) 2b, Chaps. 5 and 6.
8. "Through Flowline (TFL) Pumpdown Systems," *API RP 66*, second edition, API, Dallas (March 1981).
9. Standing, M.B.: "A Pressure-Volume-Temperature Correlation for Mixtures of California Oil and Gases," *Drill. and Prod. Prac.*, API, Dallas (1947) 275-86.
10. *API Manual 14 BN*, API, Dallas.
11. McClafflin, G.G., Clark, C.R., and Sifferman, T.R.: "The Replacement of Hydrocarbon Diluent With Surfactant and Water for the Production of Heavy, Viscous Crude Oil," *JPT* (Oct. 1982) 2258-64.
12. Buehner, L.O. and Niebrugge, T.W.: "Determining Bottomhole Pumping Conditions in Hydraulically Pumped Wells," *JPT* (July 1976) 810-12.
13. Thomson, J.: "1852 Report British Association."
14. Gosline, J.E. and O'Brien, M.P.: "The Water Jet Pump," U. of California Publication in Eng. (1933).
15. Gosline, J.E. and O'Brien, M.P.: "Application of the Jet Pump to Oil Well Pumping," U. of California Publication in Eng. (1933).
16. Angier, J.D. and Crocker, F.: "Improvement in Ejectors for Oil Wells," U.S. Patent No. 44,587 (Oct. 11, 1864).
17. Jacuzzi, R.: "Pumping System," U.S. Patent No. 1,758,400 (May 13, 1930).
18. McMahon, W.F.: "Oil Well Pump," U.S. Patent No. 1,779,483 (Oct. 28, 1930).
19. Nelson, C.C.: "The Jet Free Pump—Proper Application Through Computer Calculated Operating Charts," Southwestern Petroleum Short Course, Texas Tech. U., Lubbock (April 17-18, 1975).
20. Brown, K.: "Overview of Artificial-Lift Systems," *JPT* (Oct. 1982) 2384-96.
21. Clark, K.M.: "Hydraulic Lift Systems for Low Pressure Wells," *Pet. Eng. Intl.* (Feb. 1980).
22. Bleakley, W.B.: "Design Considerations in Choosing a Hydraulic Pumping System Surface Equipment for Hydraulic Pumping Systems," *Pet. Eng. Intl.* (July/Aug. 1978).
23. Petrie, H., Wilson, P., and Smart, E.E.: "The Theory, Hardware, and Application of the Current Generation of Oil Well Jet Pumps," Southwestern Petroleum Short Course, Texas Tech. U., Lubbock (April 27-28, 1983).
24. Petrie, H., Wilson, P., and Smart, E.E.: "Jet Pumping Oil Wells," *World Oil* (Nov., Dec. 1983, and Jan. 1984).
25. Kempton, E.A.: "Jet Pump Dewatering, What it is and How it Works," *World Oil* (Nov. 1980).
26. Cunningham, R.G. and Brown, F.B.: "Oil Jet Pump Cavitation," paper presented at the 1970 ASME Cavitation Forum, 1970 Joint ASME Fluids Engineering, Heat Transfer, and Lubrication Conference, Detroit, May 24-27.
27. Cunningham, R.G.: "The Jet Pump as a Lubrication Oil Scavenge Pump for Aircraft Engines," Wright Air Development Center Technical Report 55-143 (July 1954).
28. Cunningham, R.G.: "Jet Pump Theory and Performance With Fluids of High Viscosity," paper ASME 56-A58 presented at the 1956 ASME Annual Meeting, New York, Nov. 25-30.
29. Muskat, M.: *Physical Principles of Oil Production*, McGraw-Hill Book Co. Inc., New York City (1949).
30. *Hydraulic Inst. Standards*, 13th edition, Hydraulic Inst., Cleveland (1975).
31. Henshaw, T.L.: "Reciprocating Pumps," *Chem. Eng.* (Sept. 1981).
32. "Hydraulic Training Manual," Natl. Production Systems, Los Nietos, CA.
33. Palmour, H.H.: "Produced Water Power Fluid Conditioning Unit," Southwestern Petroleum Short Course, Texas Tech U., Lubbock (April 15-16, 1971).
34. Feldman, H.W. and Kelley, H.L.: "A Unitized, One-Well Hydraulic Pumping System," Southwestern Petroleum Short Course, Texas Tech. U., Lubbock (April 20-21, 1972).
35. Justus, M.W.: "How to Reduce Pump Repair Costs by Resizing Cyclones on Hydraulic Pumping Units," Southwestern Petroleum Short Course, Texas Tech U., Lubbock, April 22-23, 1976.
36. Brown, F.B. and Coberly, C.J.: "The Properties of Well Fluids as Related to Hydraulic Pumping," paper SPE 1375-G presented at the 1959 California Regional Meeting, Pasadena, Oct. 22-23.
37. Chew, J.N. and Connally, C.A. Jr.: "A Viscosity Correlation for Gas-Saturated Crude Oils," *Trans., AIME* (1956) 216, 23.
38. Brown, F.B. and Coberly, C.J.: "Friction Losses in Vertical Tubing as Related to Hydraulic Pumps," paper SPE 1555-G presented at the 1960 SPE Annual Meeting, Denver, Oct. 2-5.

Chapter 7

Electric Submersible Pumps

W.J. Powers, TRW Reda Pump Div.

Introduction

The electric submersible pump (ESP), sometimes called "submergible," is perhaps the most versatile of the major oil-production artificial lift methods. This chapter provides the reader with a broad understanding of the key factors in selection, installation, and operation of electric submersible pumps. ESP topics covered include the ESP system; applications; ESP system components; selection data and methods; handling, installation, and operation; and troubleshooting.

ESP System

The ESP system comprises a downhole pump, electric power cable, and surface controls. In a typical application, the downhole pump is suspended on a tubing string hung on the wellhead and is submerged in the well fluid (see Fig. 7.1). The pump is close-coupled to a submersible electric motor that receives power through the power cable and surface controls.

The ESP has the broadest producing range of any artificial lift method. The standard 60-Hz producing range of the ESP extends from a low of 100 B/D of total fluid up to 90,000 B/D. Variable-speed drives can extend the producing range beyond these rates. Although most operators tend to associate ESP's with "high volume" lift rates, the average ESP produces less than 1,000 B/D of total fluid in continuous operation.

ESP's are used to produce a variety of fluids and the gas, chemicals, and contaminants commonly found in these fluids. Currently ESP's are operated economically in virtually every known oil field environment. The WOR is, in general, not significant in assessing an application. Relatively high gas/fluid ratios can be handled using "tapered" design pumps and a special gas separator pump intake. Aggressive fluids (those containing H_2S , CO_2 , or similar corrosives) can be produced with special materials and coatings. Sand and similar abrasive contaminants can be produced with acceptable pump life by using specially modified pumps and operation procedures.

ESP's usually do not require storage enclosures, foundation pads, or guard fences. An ESP can be operated in a deviated or directionally drilled well, although the recommended operating position is in a straight section of the well. Because the ESP can be up to 200 ft long, operation in a bend or dogleg could seriously impact unit run-life and performance by causing hot spots where the motor rests against the casing. The ESP can operate in a horizontal position. In this case, run-life will be determined by the protector's ability to isolate well fluid from the motor.

ESP's are currently operated in wells with bottomhole temperatures (BHT's) up to 350°F. Operation at elevated ambient temperatures requires special components in the motor and power cables capable of sustained operation at high ambient temperature.

ESP's have efficiently lifted fluids in wells deeper than 12,000 ft. The pumps can be operated in casing as small as 4.5 in. OD. Many studies indicate that ESP's are the most efficient lift method and the most economical on a cost per lifted barrel basis. System efficiency ranges from 18 to 68%, depending on fluid volume, net lift, and pump type.

The major disadvantage of the ESP is that it has a narrow producing rate range compared with other artificial lift forms. It does handle free gas well, but the impact of large volumes of gas can be destructive to the pump. Run life can be adversely affected by a poor quality electric power supply, but this is not limited to the ESP.

Applications

The ESP historically has been applied in lifting water or low oil-cut wells that perform similar to water wells. However, within this seemingly narrow segment there are many types of installations and equipment configurations. This section covers typical installation, booster and injection, bottom intake/discharge, cavern storage/shrouded configuration, and offshore platforms.

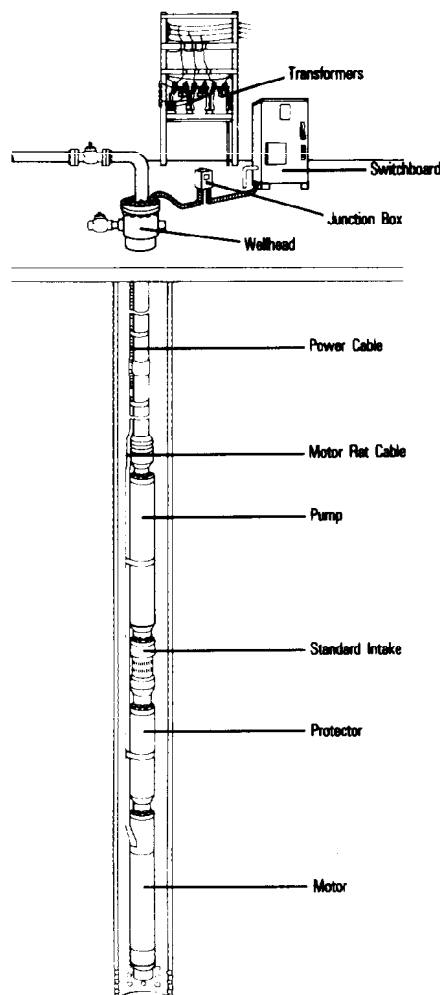


Fig. 7.1—Typical submersible pump application.

Typical Installation

A typical ESP installation is shown in Fig. 7.1. The ESP system's major surface and downhole equipment is shown. In this installation, the available surface power is transformed to the downhole power requirements by three single-phase transformers. The transformed power is supplied by a power cable to a switchboard and then through a junction box and wellhead/tubing support. The power cable is run in with the production tubing string and is banded to the tubing to prevent mechanical damage during installation and removal. The power cable is spliced to a motor flat cable, which is banded to the exterior of the pump-protector motor unit. The centrifugal pump is located at the top of the downhole unit. The pump is hung on the tubing string by the discharge head. Below the pump is a standard intake, which provides for fluid entry to the pump. The center component is the protector. The protector both equalizes external and internal pressure and isolates the motor from the well fluid. The lowest component is the motor, which drives the centrifugal pump. Note that the downhole unit is landed above the perforations. This is necessary so that fluid entering the well flows past the motor. This flow cools the motor, which is otherwise likely to overheat and fail.

These and other accessory products and system components are discussed in detail later.

Booster and Injection

Fig. 7.2 displays a booster application. In this application, a standard pump-protector motor unit is used to lift fluid from a flowline or other source and simultaneously provide injection pressure for a waterflood, pipeline, or other purpose. In a booster application, the unit is set in a short piece of casing, usually near the surface. This configuration can be used for water injection, power fluid, fluid transfer, water disposal, or as a tailgate booster.

Injection applications usually lift fluids from an aquifer at normal depths and inject the produced water into a producing zone in the same well or a second well. Injection systems can provide pressure greater than 3,000 psi. The production rate of the pump can be designed to closely match the injectivity characteristics of a reservoir during fillup.

Bottom Intake and Bottom Discharge

Fig. 7.3 displays a bottom intake configuration. In bottom intake applications, the well fluid enters the pump through a stinger landed in a permanent packer. The pump and motor sections are inverted from typical positions. The well fluid is produced up the annulus instead of the conventional tubing string. This configuration is used where casing clearance limits production volume because of tubing friction loss or pump diameter interference. Because the bottom intake pump can be suspended by small-diameter, high-tensile-strength tubing, output and efficiency are significantly improved.

Fig. 7.4 shows a bottom discharge configuration. The bottom discharge pump typically is used to inject water from a shallow aquifer into a deeper producing zone. This eliminates surface flowlines and pumping equipment completely. In this configuration, the pump and motor sections are inverted from a typical position. The pump produces the fluid through a tubing stinger landed in a permanent packer in the injection zone. Thus, the injection pressure is the sum of the interzonal hydrostatic head and the output pressure of the pump.

Shrouded Configuration/Cavern Storage

Fig. 7.5 displays a standard downhole unit that has been fitted with a shroud. Depending on the exact configuration, a shroud can serve two purposes: (1) direct fluid past the motor for cooling and (2) allow free gas to separate from the fluid before entering the pump intake. This configuration is useful in low-volume, high-gas/fluid-ratio wells where drawdown is critical. A shroud allows the pump to be set below the perforations or producing formation. Other examples are cavern or platform leg storage where a unit is suspended in the fluid on tubing and the shroud provides the necessary motor cooling-fluid flow.

Offshore Platforms

Both drilling and production platforms include ESP equipment. Typical applications are mud mixing, washdown, fire protection, sump pumps, water supply, and off-loading crude oil from storage. The major reason for the use of ESP's in these applications is its space savings when compared with conventional pump products.

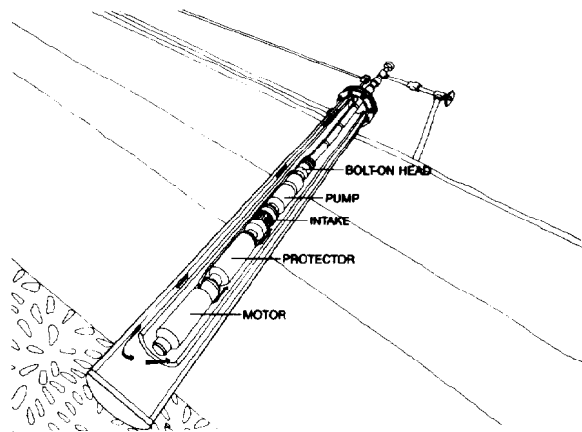


Fig. 7.2—Booster service application.

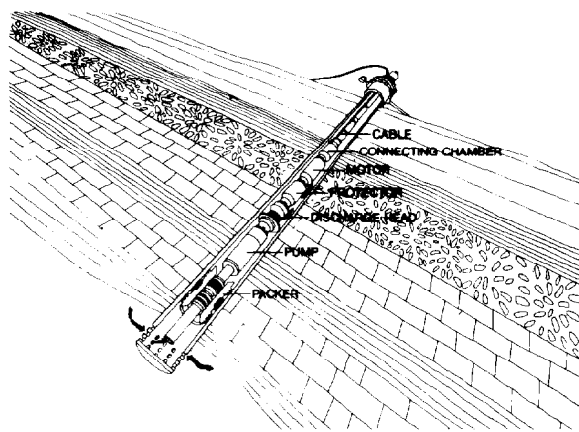


Fig. 7.3—Bottom intake application.

ESP System Components

Motor

The ESP system's prime mover is the submersible motor (see Fig. 7.6). The motor is a two-pole, three-phase, squirrel-cage induction type. Motors run at a nominal speed of 3,500 rev/min in 60-Hz operation. Motors are filled with a highly refined mineral oil that provides dielectric strength, bearing lubrication, and thermal conductivity. The standard motor thrust bearing is a fixed-pad Kingsbury type. Its purpose is to support the thrust load of the motor rotors. Other types are used in high-temperature applications above 250°F.

Heat generated by motor operation is transferred to the well fluid as it flows past the motor housing. A minimum fluid velocity of 1 ft/sec is recommended to provide adequate cooling. Because the motor relies on the flow of well fluid for cooling, a standard ESP should never be set at or below the well perforations or producing zone unless the motor is shrouded (Fig. 7.5).

Motors are manufactured in four different diameters (series) 3.75, 4.56, 5.40, and 7.38 in. Thus, motors can be used in casing as small as 4.5 in. Sixty-Hz horsepower capabilities range from a low of 7.5 hp in 3.75-in. series to a high of 1,000 hp in the 7.38-in. series. Motor construction may be a single section or

several "tandems" bolted together to reach a specific horsepower. Motors are selected on the basis of the maximum OD that can be run easily in a given casing size.

The standard motor housing material is heavy-wall, seamless, low-carbon steel tubing. The motor-shaft material is carbon steel. The rotors are supported by sleeve bearings made of Nitralloy and bronze. The squirrel cage rotor is made of one or more sections depending on motor horsepower and length. The motor stator is wound as a single unit in a fixed housing length.

Pump

The ESP is a multistage centrifugal type pump (Fig. 7.7). The type of stage used determines the design volume rate of fluid production. The number of stages determines the total design head generated and the motor horsepower required.

The materials used in manufacturing an impeller are Ni-Resist, Rytan, and bronze. Diffusers are universally manufactured of Ni-Resist. The standard shaft material is K-Monel®. Optional, high-strength shaft materials (Inconel® and Hastalloy®) are used in deep-setting applications where conventional shaft material horsepower limits are exceeded. "Bolt-on" design makes it possible to vary the capacity and total head of a pump by using

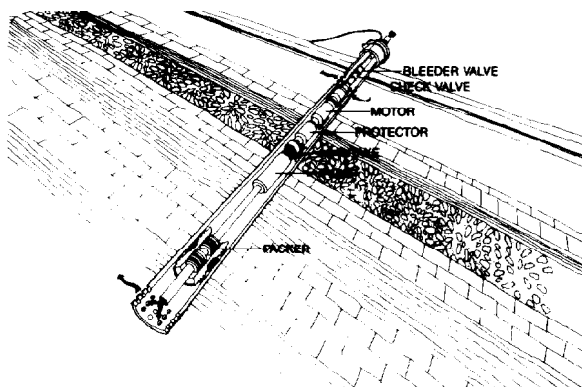


Fig. 7.4—Bottom discharge application.

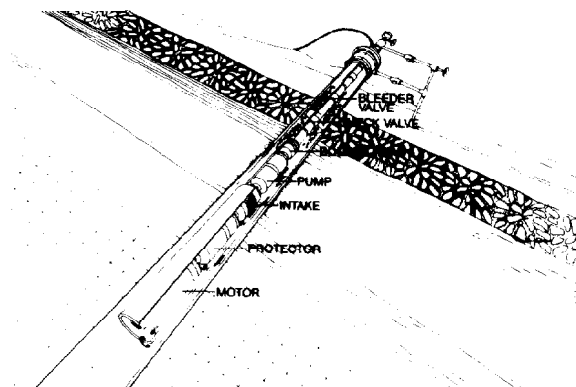


Fig. 7.5—Shrouded application.

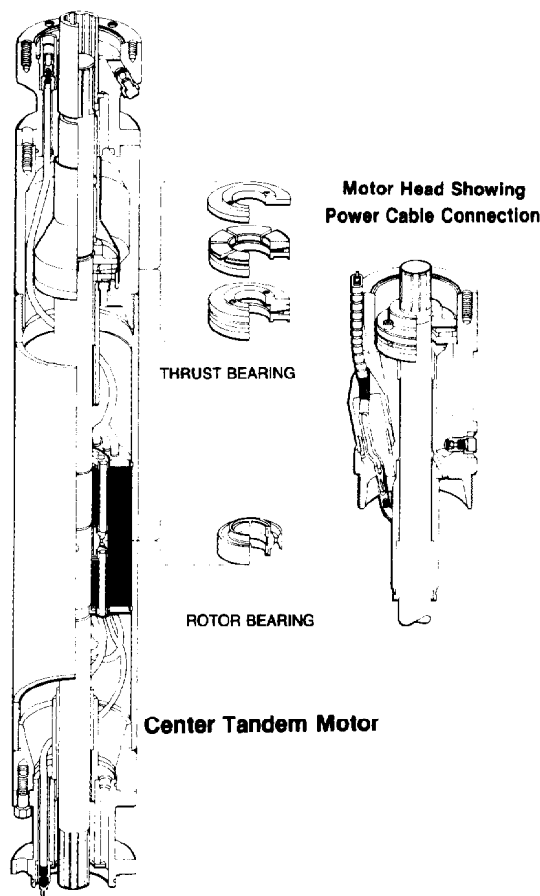


Fig. 7.6—Motor.

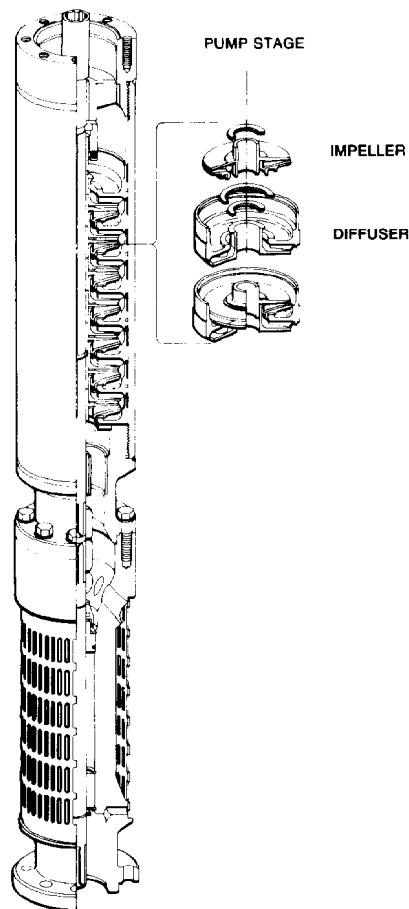


Fig. 7.7—Pump with standard intake.

more than one pump section. However, large-capacity pumps typically have integral heads and bases. The nominal OD of a pump will range from 3.38 to 11.25 in.

Protector

The protector's primary purpose is to isolate the motor oil from the well fluid while balancing bottomhole pressure (BHP) and the motor's internal pressure. There are two types of protector design—the positive seal (Fig. 7.8) and the labyrinth path (Fig. 7.9). The positive seal design relies on an elastic, fluid-barrier bag to allow for the thermal expansion of motor fluid in operation, and yet still isolate the well fluid from the motor oil. The labyrinth path design uses differential specific gravity of the well fluid and motor oil to prevent the well fluid from entering the motor. This is accomplished by allowing the well fluid and motor oil to communicate through tube paths connecting segregated chambers.

The protector performs four basic functions. The protector (1) connects the pump to the motor by connecting both the housing and drive shafts, (2) houses a thrust bearing to absorb pump shaft axial thrust, (3) isolates motor oil from well fluid while allowing wellbore-motor pressure equalization, and (4) allows thermal expansion of motor oil resulting from operating heat rise and thermal contraction of the motor oil after shutdown.

Pump Intake

Two types of intakes are used to allow fluid to enter the pump. These are the standard intake shown in Fig. 7.7 and the gas separator intake shown in Figs. 7.10 and 7.11. A gas separator intake is used when the gas/liquid ratio (GLR) is greater than can be handled by the pump. If the gas remains in solution, the pump will perform normally. However, once the GLR exceeds a value of about 0.1, the pump may produce less head than normal. As the GLR increases above 0.1 and free gas increases, the pump will eventually "gas lock," which usually drastically reduces fluid production and in extreme cases can damage the pump.

There are two types of gas separator intakes—the static type (Fig. 7.10) and the rotary type (Fig. 7.11). The static type induces gas separation by reversing the fluid flow direction. At the fluid entry ports, the reversal of fluid flow direction creates lower pressure that allows the gas to separate. The separated gas moves up the annulus and vents at the wellhead. The fluid, which still contains some gas, enters the separator and moves downward into the stand tube. The fluid is picked up by the rotating pickup impeller. The impeller creates a vortex, which forces dense, gas-free fluid to the outside and causes gas to break out and move up the shaft. This provides the first stage of the pump with a higher density of fluid than if the gas broke out in the pump.

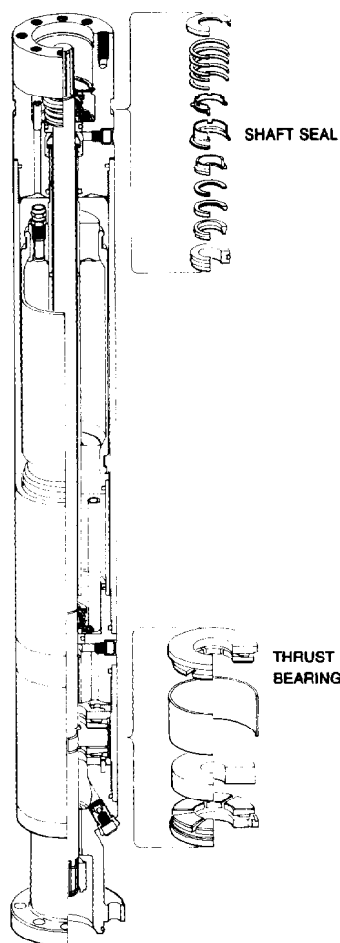


Fig. 7.8—Positive seal protector.

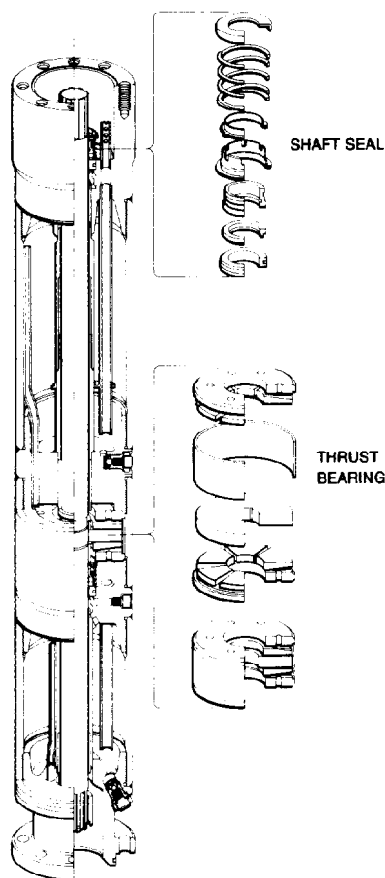


Fig. 7.9—Labyrinth path protector.

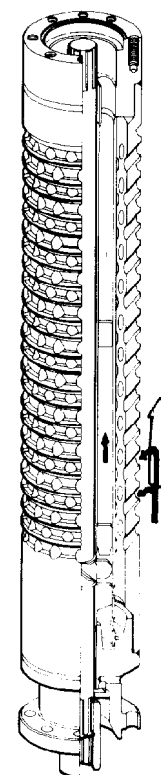


Fig. 7.10—Static type gas separator.

The rotary gas separator in Fig. 7.11 includes a rotary inducer-centrifuge to separate the gas and produced liquids. The well fluid enters the intake ports and moves into the inducer. The inducer increases the fluid pressure discharging into the centrifuge. The centrifuge forces the denser fluid to the outside. Gas rises from the center of the centrifuge through the flow divider into the crossover section where gas vents to the annulus and fluid is directed into the first stage of the pump.

Power Cable

Electric power is supplied to the downhole motor by a special submersible cable. There are two cable configurations: flat (or parallel) and round (Fig. 7.12). Round construction is used except where casing clearance requires the lower profile of flat construction. The standard range of conductor sizes is 1/0 to 6 AWG (American wire gauge). This range meets virtually all motor amperage requirements. Almost all conductors are copper.

Mechanical protection is provided by armor made from galvanized steel or, in extremely corrosive environments, Monel™. Unarmored cable is used in low-temperature (<180°F) wells with a static BHP of less than 1,500 psi.

Cable is constructed with three individual conductors—one for each power phase. Each conductor is

enclosed by insulation and sheathing material. The thickness and composition of the insulation and sheathing determines the conductor's resistance to current leakage, its maximum temperature capability, and its resistance to permeation by well fluid and gas. Electric power cable is rated to operate up to 400°F at 1,500 psi.

Round cable is also manufactured with an "I-wire." The I-wire serves as an electrical link between a downhole instrument and surface reading/processing equipment.

Motor Flat Cable

The motor flat cable is the lowest section of the power cable string. The motor flat cable has a lower profile than standard flat power cable so that it can run the length of the pump and protector in limited clearance situations (Fig. 7.1). The motor flat cable is manufactured with a special terminal called a "pothead." The function of the pothead is to allow entry of electric power into the motor while sealing the connection from well fluid entry.

Switchboard

The switchboard is basically a motor control device (Fig. 7.13). Voltage capability ranges from 600 to 4,900 V on standard switchboards. All enclosures are NEMA-3R

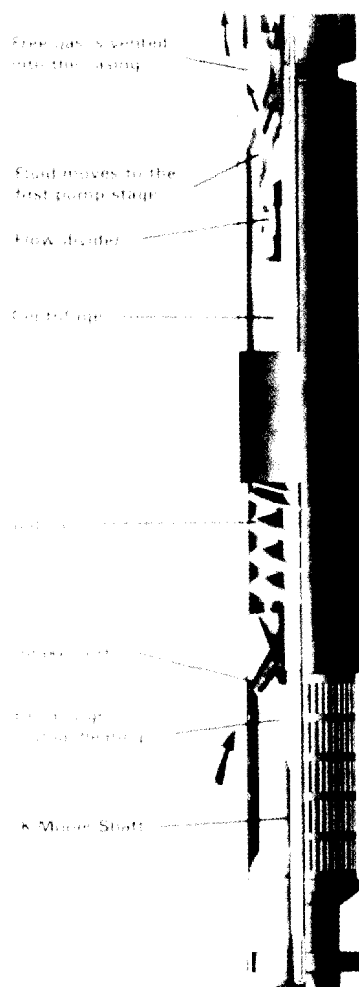


Fig. 7.11—Rotary gas separator.

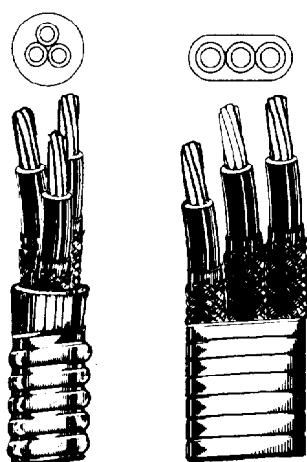


Fig. 7.12—Round and parallel power cable.

(Natl. Electrical Manufacturers Assn.), which is suitable for virtually all outdoor applications. The switchboards range in complexity from a simple motor starter/disconnect switch to an extremely sophisticated monitoring/control device.

There are two major construction types—electromechanical and solid state. Electromechanical construction switchboards provide overcurrent/overload protection through three magnetic inverse time-delay contact relays with pushbutton, manual reset. Undercurrent protection is provided by silicone-controlled rectifier (SCR) relays. These features provide protection against downhole equipment damage caused by conditions such as pumpoff, gas lock, tubing leaks, and shutoff operation.

The solid state switchboards incorporate the highly sophisticated Redalert™ motor controller. The purpose of the motor controller is to protect the downhole unit by sensing abnormal power service and shutting down the power supply if current exceeds or drops below preset limits. This is accomplished by monitoring each phase of the input power cable to the downhole motor.

The monitoring function applies to both overload and underload conditions. When a fault condition occurs, the controller shuts down the unit. It can be programmed to automatically restart the downhole motor following a user-selected time delay if the fault condition is caused by an underload. The programmed time delay can be from 1 minute up to 20 hours. Overload condition shutdown must be restarted manually, but this should be done only after the fault condition has been identified and corrected.

A valuable switchboard option is the recording ammeter. Its function is to record, on a circular strip chart, the input amperage to the downhole motor. The ammeter chart record shows whether the downhole unit is performing as designed or whether abnormal operating conditions exist. Abnormal conditions can result when a well's inflow performance is not matched correctly with pump capability or when electric power is of poor quality. Abnormal conditions that are indicated on the ammeter chart record are primary line voltage fluctuations, low amps, high amps, and erratic amps. Specific examples of typical problems encountered and the associated ammeter chart pattern are discussed later.

Transformer

The ESP system involves three different transformer configurations. These are three single-phase transformers (Fig. 7.14), one three-phase standard transformer, and one three-phase autotransformer. Transformers generally are required because primary line voltage does not meet the downhole motor voltage requirement. Oil-immersed self-cooled (OISC) transformers are used in land-based applications. Dry type transformers are sometimes used in offshore applications that exclude oil-filled transformers.

Wellhead

The ESP wellhead or tubing support is used as a limited pressure seal (Fig. 7.15). The wellhead provides a pressure tight pack-off around the tubing and power cable. High-pressure wellheads, up to 3,000 psi, use an



Fig. 7.13—Switchboard.

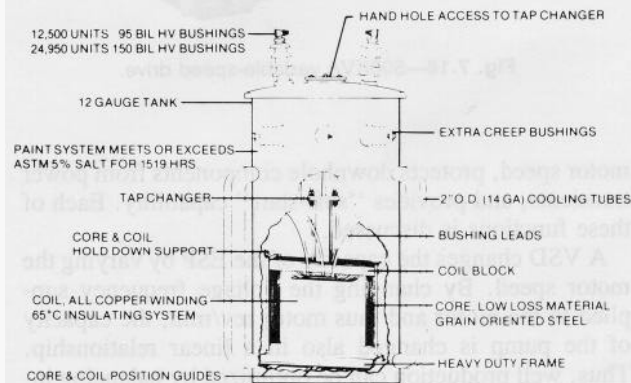


Fig. 7.14—Single-phase transformer.

electrical power feed to prevent gas migration through the cable. Wellheads are manufactured to fit standard casing sizes from 4.5 to 10% in.

Junction Box

A junction box connects the power cable from the switchboard to the well power cable (Fig. 7.16). The junction box is necessary to vent to the atmosphere any gas that may migrate up the power cable from the well. This prevents accumulation of gas in the switchboard that can result in an explosive and unsafe operating condition. *A junction box is required on all ESP installations.*

Accessory Options

The following covers two major accessory options—the pressure-sensing instrument and the variable-speed drive.

Pressure-Sensing Instrument (PSI). The PSI provides the operator with precise downhole pressure and temperature data. The PSI has two components: (1) a

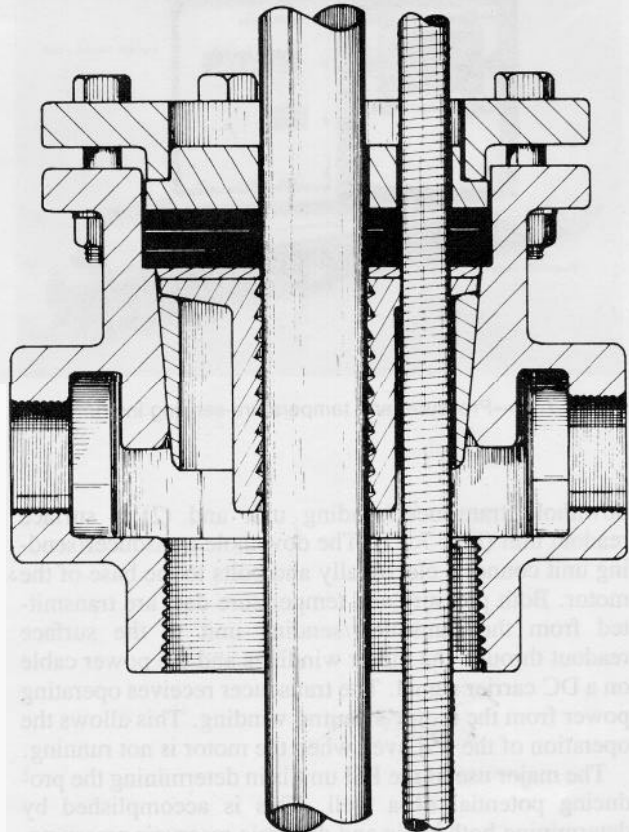


Fig. 7.15—Hercules HHS wellhead.

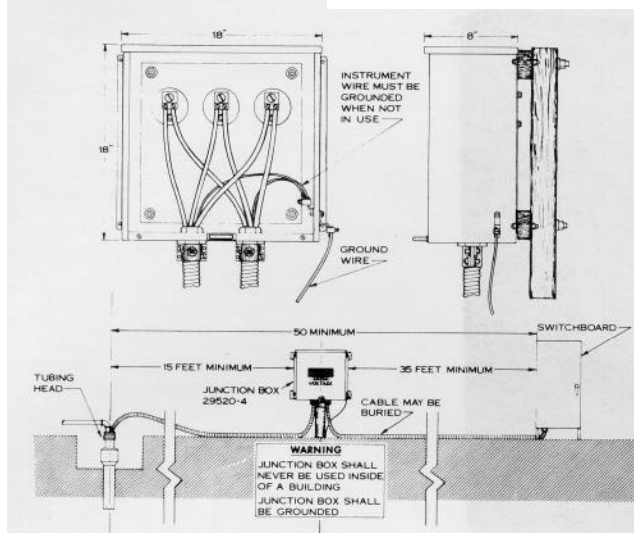


Fig. 7.16-Junction box.

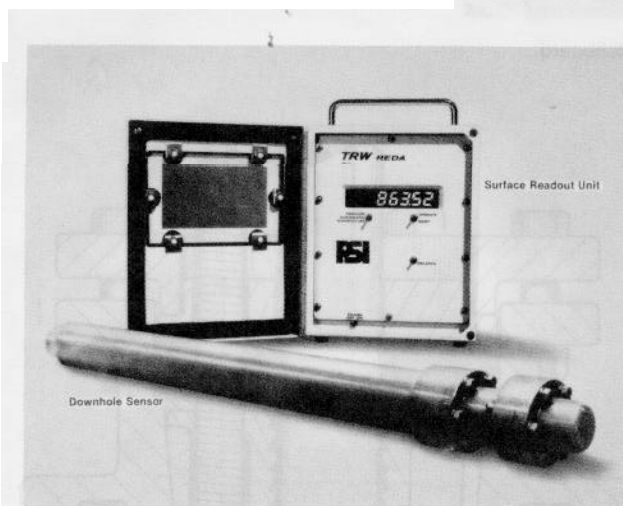


Fig. 7.17—Pressure- and temperature-sensing instrument.

downhole transducer/sending unit and (2) a surface readout unit (Fig. 7.17). The downhole transducer/sending unit connects electrically and bolts to the base of the motor. Both pressure and temperature data are transmitted from the transducer/sending unit to the surface readout through the motor windings and the power cable on a DC carrier signal. The transducer receives operating power from the motor's neutral winding. This allows the operation of the PSI even when the motor is not running.

The major use of the PSI unit is in determining the producing potential of a well. This is accomplished by determining both static and dynamic reservoir pressures. By correlating the change in pressure with a given producing rate, a well's inflow performance can be accurately quantified. This in turn will allow equipment selection, which optimizes well production.

Variable-Speed Drive. The variable-speed drive (VSD) is a highly sophisticated switchboard-motor controller (see Fig. 7.18). A VSD performs three distinct functions. It varies the capacity of the ESP by varying the



Fig. 7.18--500KVA variable-speed drive.

motor speed, protects downhole components from power transients, and provides "soft-start" capability. Each of these functions is discussed.

A VSD changes the capacity of the ESP by varying the motor speed. By changing the voltage frequency supplied to the motor and thus motor rev/min, the capacity of the pump is changed also in a linear relationship. Thus, well production can be optimized by balancing inflow performance with pump performance. This applies to both long-range reservoir changes as well as short-term transients such as those associated with high-GOR wells. This may eliminate the need to change the capacity of a pump to match changing well conditions or it may mean longer run life by preventing cycling problems. This capability is also useful in determining the productivity of new wells by documenting pressure and production values over a range of drawdown rates. The change in voltage frequency can be made manually or automatically. The VSD can operate automatically in a "closed loop" mode with a programmable controller and PSI instrument.

The VSD also protects the downhole motor from poor-quality electric power. The VSD is relatively insensitive to incoming power balance and regulation while providing closely regulated and balanced output. The VSD will not put power transients out to the downhole motor but it can be shut down or damaged by such transients. Given the choice, most operators prefer to repair surface installation equipment rather than pull and run downhole equipment. Within limits, the VSD upgrades poor-quality electric power by "rebuilding." The VSD takes a given frequency and voltage AC input, converts the AC to DC, and then rebuilds the DC to an AC

waveform. The shape of the waveform is a six-step square wave.

The soft-start capability of a VSD provides two major benefits. First, it reduces the startup drain on the power system. Second, the strain on the pump shaft is significantly reduced when compared with that of a standard start. This capability is valuable in gassy or sandy wells. In some cases, slowly ramping a pump up to operating speed may avoid pump damage.

Selection Data and Methods

This section covers the data requirements and calculation procedures required for pump selection in a typical ESP application. The single most important factor in selection of an ESP is the input data. The data used in sizing an ESP must be accurate and reliable to ensure that the unit is properly matched to the well's inflow performance.

The data requirements for selection of an ESP are categorized as mechanical data, production data, fluid data, and power supply.

Mechanical Data

The mechanical data include: (1) casing size and weight, (2) tubing size, weight, and thread, (3) well depth—both measured and true vertical, (4) perforations depth—both measured and true vertical, and (5) unusual conditions such as tight spots, doglegs, and deviation from true vertical at desired setting depth.

The casing size and weight determine the maximum diameter of the motor, pump, and protector components that will fit in the well. In general, the most efficient installation is obtained when the largest possible diameter pump, in the target flow range, is selected.

The depth of the well and the perforations determine the maximum setting depth of the ESP. If the motor is to be set below the perforations, a motor shroud must be used to provide a flow of well fluid past the motor for cooling (Fig. 7.5).

Production Data

The production data include: (1) current and desired production rate, (2) oil-production rate, (3) water-production rate, (4) GOR—free gas and solution gas or gas bubblepoint, (5) static BHP and fluid level, (6) producing BHP and stabilized fluid level, (7) BHT, and (8) system backpressure from flowlines, separator, and wellhead choke.

The inflow performance of a well establishes the maximum economical and efficient rate at which it can be produced. Liquid-level data may be used as a substitute for producing pressures and rates in water wells or in low-oil-cut wells with no gas. In these cases, a straight line PI may be used as a reasonable approximation of well capacity.

Most oil wells do not exhibit a straight-line PI because of interference caused by gas. The Vogel technique¹ yields a downward-sloping curve that corrects for gas interference. The IPR curve (Fig. 7.19) applies when wellbore pressure in the producing zone drops below the bubblepoint, which results in two-phase flow as the gas breaks out of the fluid. Again, the data obtained for this approach in sizing an ESP must be both accurate and reliable to ensure proper equipment selection.

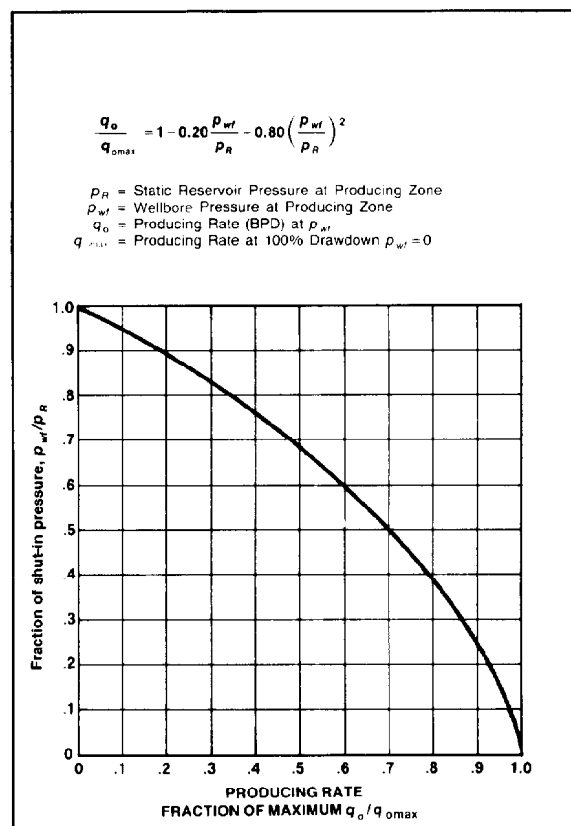


Fig. 7.19—Inflow performance relationships curve.

Fluid Data

The fluid data include: (1) oil API gravity, viscosity, pour point, paraffin content, sand, and emulsion tendency; (2) water specific gravity, chemical content, corrosion potential, and scale-forming tendency; (3) gas specific gravity, chemical content, and corrosive potential; and (4) reservoir FVF, bubblepoint pressure, and viscosity/temperature curve.

The specific gravity of the produced fluid has a direct impact on the horsepower required to turn a given size pump. Although relatively few applications encounter fluid viscosities high enough to influence pump performance, it is important to be aware that capacity, head, and horsepower correction factors may be required. In wells with a water cut of 65% or higher, the fluid will not require viscosity correction factors (except for emulsions).

The PVT data are required when gas is present. A computer program for pump selection (discussed later in this section) contains a subroutine that uses Standing's correlations² in approximating the PVT values when actual data are not available. In high-GOR applications, PVT data are very desirable because the three standard correlation estimates—Standing,² Lasater³, and Vasquez and Beggs⁴—yield large differences in calculated downhole gas volume (see Chap. 22).

Electric Power Supply

The electric power supply includes: (1) voltage available and frequency, (2) capacity of the service, and (3) quality of service (spikes, sags, etc.).

TABLE 7.1—PUMP SELECTION TABLE (60 Hz, 3,500 rpm)

Series	OD (in.)	Pump Type	Maximum BHP Rating For Pump Shaft	Capacity Range Recommended Limits	
				(B/D)	(m ³ /D)
338	3.38	A400	94	280 to 500	45 to 80
		AN550	94	425 to 700	68 to 111
		AN900	94	660 to 1100	105 to 175
		A1200	94	875 to 1575	139 to 250
		A1500	125	1100 to 1900	175 to 302
400	4.00	DN280	44	100 to 450	16 to 72
		D400	94	280 to 550	45 to 87
		DN450	94	320 to 575	51 to 91
		D550	94	375 to 650	60 to 103
		D700	94	500 to 900	80 to 143
		D950	125	600 to 1150	95 to 183
		DN1000	125	760 to 1250	121 to 199
		DN1300	125	975 to 1650	155 to 262
		D1350	125	950 to 1800	151 to 286
		DN1750	125	1200 to 2050	191 to 326
		D2000	125	1400 to 2450	223 to 390
		DN3000	256	2100 to 3700	334 to 588
		DN4000	256	3400 to 5000	540 to 795
450	4.62	EN1250	160	950 to 1600	151 to 254
		E1450	160	1050 to 1800	167 to 286
		EN3600	256	2800 to 4500	445 to 715
540	5.13	G2000	256	1500 to 2500	238 to 397
		GN2500	256	2000 to 3100	318 to 493
		G2700	256	2100 to 3400	334 to 541
		G3100	256	2200 to 3700	350 to 588
		GN4000	375		
		GN5200	375	4200 to 6600	668 to 1049
		G5600	375	4500 to 7250	715 to 1153
		GN7000	375	5500 to 8500	874 to 1351
562	5.62	HN13000	375	8000 to 12000	1272 to 1908
				9200 to 16400	1463 to 2607
650	6.62	IN7500	637	6000 to 9500	954 to 1510
		IN10000	637	8000 to 12250	1272 to 1948
675	6.75	JN16000	637	12800 to 19500	2035 to 3100
		JN21000	637	16000 to 25000	2544 to 3795
862	8.62	M520	637	12000 to 24000	1908 to 3816
		M675	637	19000 to 32500	3021 to 5167
950	9.50	N1050	1000	24000 to 47500	3816 to 7552
1000	10.00	N1500	1000	35000 to 59000	5564 to 9380
1125	11.25	P2000	1000	53600 to 95800	8521 to 15240

The power data are important because they partially determine transformer and switchboard requirements. Frequency influences pump rotation speed, capacity, and head.

Once the required data have been gathered and analyzed, the next ESP selection step is to determine the well's production capacity at a given pump-setting depth. This involves analysis of the inflow performance data as well as desired production rate. Two key factors that must be considered are the minimum pump intake pressure (net positive suction head), which the well will permit without pumpoff or gas lock, and the producing rate, which draws the fluid level down to an optimal level.

The next selection step is to determine the total dynamic head (TDH). TDH is the sum of: (1) the true vertical lift distance from the producing fluid level to the surface, (2) friction loss in the tubing string, and (3) discharge pressure head at the wellhead. The design TDH determines the number of stages required in a pump.

Selection of a specific pump involves identifying a pump of the largest possible diameter that can be run in the well. The pump should have the target capacity

within its recommended operating range and close to its peak efficiency. The initial pump capacity selection can be made from Table 7.1.

The individual pump curve should then be reviewed to determine the optimal producing range and the proximity of the design producing rate to the pump's peak efficiency (see Fig. 7.20 for a typical pump performance curve). It is very important to choose a producing rate that is in the recommended capacity range of the specific pump. When a pump operates outside this range, premature failure can result.

Once a pump is chosen, the number of stages required can be calculated using the lift-feet-per-stage data from the performance curve.

$$n_s = \frac{Z}{L_s},$$

where

n_s = number of design stages,
 Z = total dynamic head, ft, and
 L_s = lift per stage, ft.

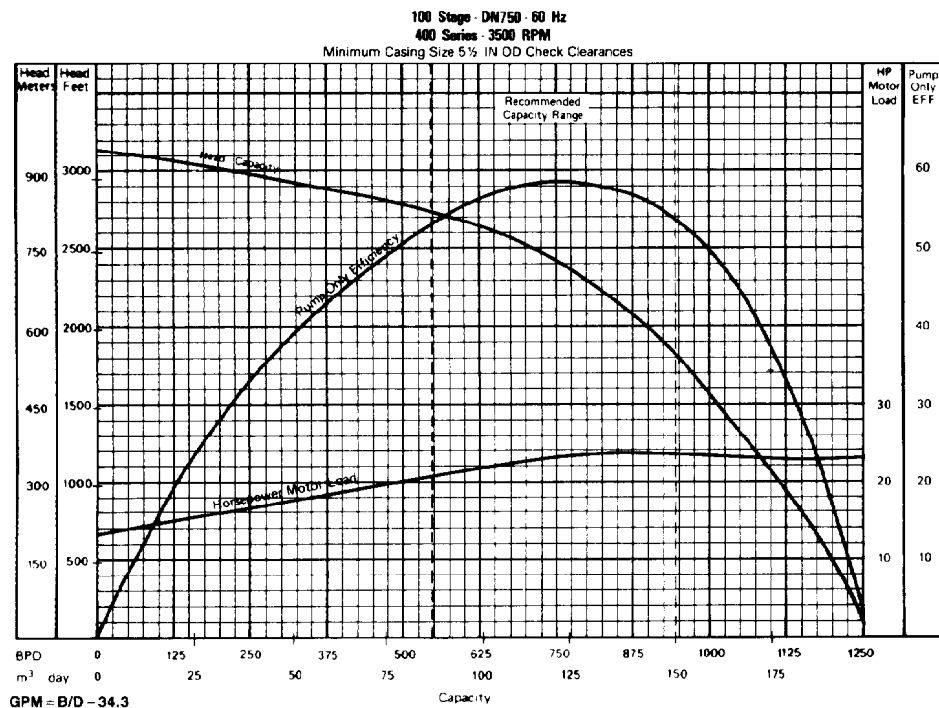


Fig. 7.20—Typical pump performance curve.

The horsepower required by the pump design then can be calculated. To accomplish this, the horsepower required per stage is read from the specific pump performance curve. The required motor horsepower is determined by multiplying the horsepower required per stage by the number of design stages. The performance curve horsepower data apply only to liquids with a specific gravity of 1.0. For other liquids (other specific gravities), the water horsepower also must be multiplied by the specific gravity of the fluid pumped. Thus we have the following equation for the motor horsepower calculation.

$$P_{hm} = P_{hs} \times n_s \times \rho_f,$$

where

$$\begin{aligned} P_{hm} &= \text{motor horsepower,} \\ P_{hs} &= \text{horsepower per stage,} \\ n_s &= \text{number of design stages, and} \\ \rho_f &= \text{specific gravity of fluid.} \end{aligned}$$

Once the design motor horsepower is determined, specific motor selection is based on setting depth, casing size, and motor voltage. Although the cost of the motor is generally unrelated to voltage, overall ESP system cost may be lowered by using higher-voltage motors in deep applications. This lower cost can sometimes occur because a higher voltage can lower the cable conductor size required. A smaller-conductor-size, lower-cost cable can more than offset the increased cost of a higher-voltage switchboard. Setting depth is a major variable in motor selection because of starting and voltage drop losses that are a function of the motor amperage and cable conductor size.

Cable selection variables are amperage, voltage drop, annulus clearance, ambient well temperature, and corrosion conditions. The standard maximum voltage drop is limited to 30V/1000 ft. If voltage drop exceeds this value, a larger conductor size should be used. Round cable normally is used unless tubing collar/annulus clearance dictates flat or parallel construction. The maximum operating temperature of a cable in relation to the specific well's ambient temperature determines the specific type of cable. Armor and lead sheathing may be recommended for wells with mechanical or clearance problems or corrosive gas such as H_2S .

The surface electrical equipment (switchboard and transformers) selection is based on the required motor horsepower, voltage, amperage, voltage loss, and cable size. The surface voltage is the sum of the downhole motor no-load voltage plus the voltage losses resulting from cable size and other component losses. Voltage losses associated with transformers range from 2.5 to 6%, depending on the manufacturer. Additional impedance is associated with VSD transformer sizing. Transformers must also be selected on the basis of the primary voltage available and the required hookup method— $\Delta\Delta$, $Y\Delta$, or YY .

The protector selection variables are motor and pump series, motor horsepower, and well temperature. Normally the protector is the same series as the pump and motor. Large horsepower motors (150 hp and larger) may require a larger oil capacity. For large horsepower motors, a positive seal double-bag model or a tandem "labyrinth path" model is used. An ambient well temperature of 250°F or higher generally requires the use of the labyrinth path protector.

ESP equipment selection in high-water-cut, low-GOR wells is relatively straightforward. Equipment selection



Fig. 7.21--Shipping boxes positioned at the wellsite.

in high GOR or viscous crude wells, however, can be very complicated. One ESP manufacturer has developed a sophisticated computer program to provide comprehensive analysis of alternative equipment selections in such situations. It can be used to select equipment or to evaluate previously selected equipment. This capability means that, over time, the engineer can evaluate the pump fit as well as changes in conditions. If well inflow performance changes significantly, the sizing of the downhole equipment may need to be checked both to optimize production and to prevent premature failure.

The computer program contains analytic models for pump performance, reservoir response, and fluid characteristics. It uses the Chew and Connally⁵ correlations for live fluid viscosity based on the quantity of gas in solution. Another option uses Orkiszewski's⁶ two-phase vertical flow model to compute pump discharge pressure and horsepower required. Standing's⁷ correlations are used to provide surrogate PVT data when actual values are not available.

Handling, Installation, and Operation

This section provides recommended practice on the handling, installation, and operation of an ESP system. Because both safety and economic run life are dependent on correct procedures, the importance of following the recommended practice cannot be overemphasized.

Handling

The downhole components—motor, pump, protector, and intake—are shipped in a metal shipping box (Fig. 7.21). The shipping boxes are painted red on the end that should be placed toward the wellhead when the equipment is delivered to the wellsite. The shipping boxes should be lifted with a spreader chain or bridled with a sling at each end. Severe equipment damage can result from dropping, dragging, or bouncing the boxes. The shipping boxes should never be lifted by the middle of the box only.

The cable reel should be lifted by using an axle and a spreader bar (Fig. 7.22). If a fork lift is used, the forks should be long enough to support both reel rims when the reel is picked up from an end. The ends of the cable should be covered or sealed to protect them from the elements.

Transformers and switchboards are provided with lifting hooks. To avoid damage, the recommended practice is to lift with a spreader bar to maintain a vertical position. Variable-speed drives are normally skid-mounted with fork lift slots and lifting eyes. Some VSD models are manufactured with pull bars.

Additional information on ESP handling and installation procedures is available in "API Recommended Practice for Electric Submersible Pump Installations."⁸

Installation

There are three segments to every ESP installation. These are well preparation, site layout, and run-in and startup of equipment. The well-preparation procedure in-

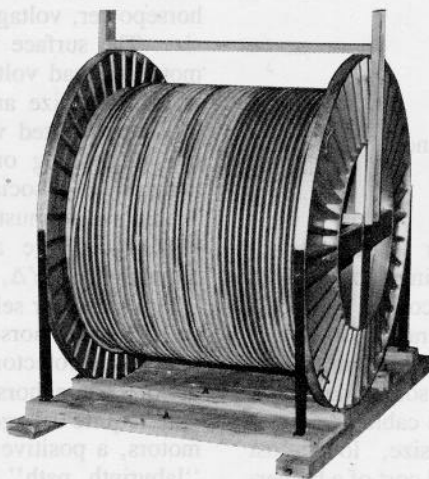


Fig. 7.22--Cable reel lifting procedures.

volves determining the **downhole** clearance conditions. Site layout prescribes equipment and rig locations as well as size and capacity. Running equipment in the well and startup procedures define the steps in equipment handling, test procedure, and responsibility of the rig crew and servicemen.

Prior to beginning installation of the ESP equipment, the well must be cleared of any tubing, rods, packers, etc., that would prevent the **downhole** equipment from reaching target setting depth. The casing flange and well head should be examined for burrs or sharp edges. This is very important in small-diameter casing because cable damage can be caused by burrs or edges catching cable bands.

A gauge ring should be run in (particularly in 4.5-in. casing) to below the setting depth of the **downhole** equipment. If gauging indicates tight spots, a scraper or reamer should be used to remove the obstruction (scale, paraffin, burrs, or partially collapsed casing). This will ensure adequate clearance for the ESP **downhole** equipment as it is run into the well.

The blowout preventer (BOP), if used, should be checked for adequate clearance as well as burrs and sharp edges. Cut-out rams are available for most tubing and cable sizes. They should be installed in the BOP for well control in the event of a kick during equipment installation.

The pulling rig should be centered over the well as closely as possible. A guide wheel/cable sheave should be secured safely to the rig mast no higher than 30 to 45 ft above the wellhead. The guide wheel should be at least 54 in. in diameter.

The cable reel or spooling truck should be positioned about 100 ft from the wellhead in direct line of sight of the rig operator. One person should be responsible for the cable operation. The responsibilities of this person are to ensure that there is minimum tension on the cable (the cable should be run at the same speed as the tubing), that the cable is kept clear of power tongs during tubing makeup or break, and that no one stands in front of the cable reel/spooler.

The cable junction box must be located at least 15 ft from the wellhead (Fig. 7.16). The switchboard must be located a minimum of 50 ft from the wellhead and 35 ft minimum from the junction box. The junction box normally is located 2 to 4 ft above ground level to ensure adequate air circulation and easy access. The junction box must **never** be located inside a building.

The ESP manufacturer's field representative checks all equipment before installation. During installation his responsibility is to supervise the pulling and/or running of the **downhole** equipment. All equipment delivered to the wellsite is checked to determine that all components necessary to complete the installation have arrived and are not damaged. The ESP manufacturer's field representative will perform the following checks and procedures.

1. Remove shipping box covers and record all component serial numbers from nameplates (Fig. 7.23).
2. Check casing, wellhead, and packoff material.
3. Check the switchboard for proper fuses, potential transformer setup, and current transformer ratios.
4. Check all couplings for shaft diameter and spline match.



Fig. 7.23—Checking nameplates.

3. Check flat cable length, size, and pothead type.
 6. Check power transformers for correct primary and secondary voltage rating.
 7. Confirm that the pump design setting depth and capacity match the well conditions.
 8. Check the power cable and flat cable with instruments and high-voltage megger.
- Once the equipment, cable, and verification procedures are completed, the assembly and run-in of **downhole** equipment can begin. The manufacturer's field representative directs the assembly and checks equipment as it is being run in. The steps of assembly and checks of equipment can be summarized as follows.
1. Assemble motor, protector, intake, and pump.
 2. Fill the motor/protector assembly with motor oil.
 3. Mechanically check free rotation of **downhole** components.
 4. Check electrical connection and test the motor, power cable, and flat cable pothead.
 5. Correct torque of connecting bolts.
 6. Band cable to tubing string.
 7. Splice cable or repair damaged cable.
 8. Connect power cable to junction box and switchboard.
 9. Pack off wellhead.
 10. Complete flowline connections and valve position.

Once the run-in procedures are completed and final electrical tests completed, the manufacturer's representative will complete the electrical connections. The switchboard underload and overload adjustments are set according to the conditions expected for each well. The pump is then started. Fluid pump-up time, load and no-load voltage, and amperage on each phase are recorded. Phase rotation should be checked carefully to ensure that the pump is rotating in the correct direction.

The quantity of production of oil, gas, and water should be monitored on startup and regularly for the time required to achieve stability. A careful study should be made on a pump installation that does not produce as designed. As much information as possible should be gathered to aid in specific identification of the problem and appropriate remedial action. This will ensure that subsequent installations will provide satisfactory run life.

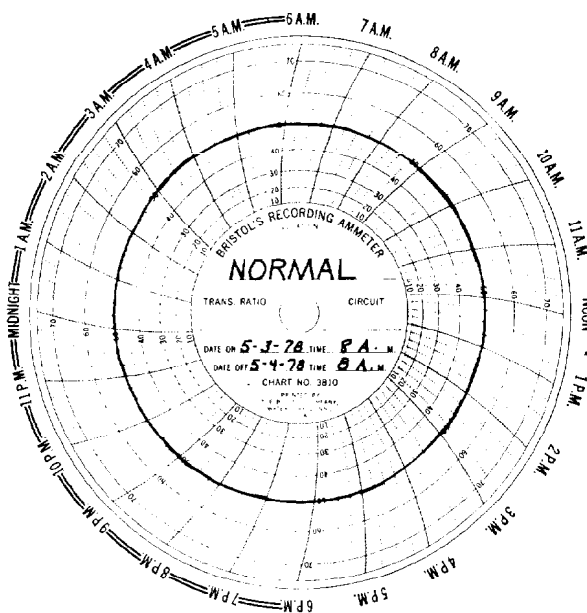


Fig. 7.24—Normal ammeter chart.

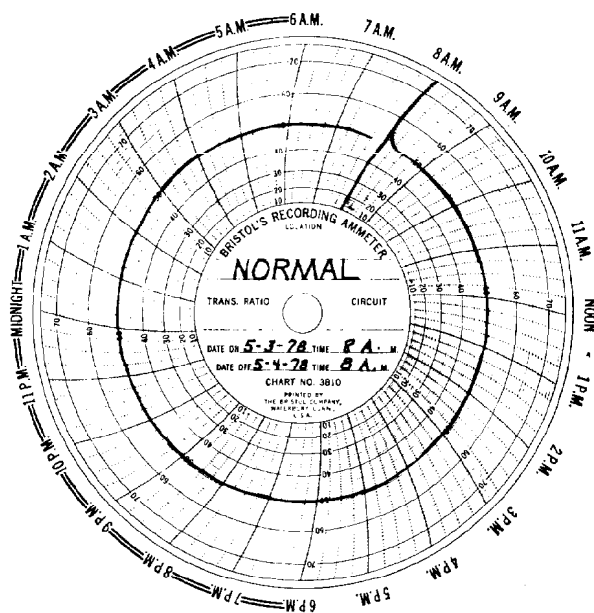


Fig. 7.25—Normal startup chart.

Pulling equipment out of a well involves essentially the reverse process of run-in. The equipment and cable should be handled with the same care as new because they are still valuable. Cable damage and missing bands should be recorded at the depth they occurred to aid in subsequent repair and evaluation. If the equipment failure is judged to be premature, the condition of cable, flat cable, pump rotation, and motor/protector fluid may be useful in determining the cause of the failure.

Troubleshooting

This section outlines a recommendation for identification and solution of typical ESP problems. The only way a failure can be analyzed and its cause determined is by data collection. When a problem occurs you simply cannot have too much information.

Information that should be routinely compiled on each ESP well includes production data (such as water, oil, and gas), run life, unit starts and stops, dynamic and static fluid level, and pump setting and perforation depth. Information also should be obtained on ammeter charts, well conditions (abrasives, corrosives, H_2S etc.), electric power quality (surges, sags, balance, negative sequence voltages, etc.), visual observations of equipment and cable condition on prior pulls, reasons for equipment pull (failure, workover, size change, etc.), and BHT.

When an ESP well is first put on production, data should be collected daily for the first week, weekly for the first month, and a minimum of monthly after the first month. Production data during the first month are very important because they will indicate whether the pump is performing as designed. If a downhole pressure instrument is installed, operating BHP is equally important.

The major source of information when troubleshooting an ESP installation is the recording ammeter. The recording ammeter is a circular strip-chart accessory

mounted in the switchboard that records the amperage drawn by the ESP motor (Fig. 7.13). A number of changes in operating conditions can be diagnosed by interpreting ammeter records. The following addresses ammeter chart "reading" and typical problem situations.

Normal Operation

A normal chart (Fig. 7.24) is smooth, with amperage at or near motor nameplate amperage draw. Actual operation may be either slightly above or below nameplate amperage. However, as long as the curve is symmetric and consistent over time, operation is considered normal.

Normal Startup

A normal startup will produce a chart similar to that shown in Fig. 7.25. The startup "spike" is caused by the inrush surge as the pump comes up to operating speed. The subsequent amperage draw is high but trending toward a normal level. This is principally a result of the fluid level being drawn down to the design TDH, resulting in a high but declining amperage draw.

Power Fluctuations

Operating ESP amperage will vary inversely with voltage. If system voltage fluctuates, the ESP amperage will fluctuate inversely to maintain a constant load (Fig. 7.26). The most common cause of this type of fluctuation is a periodic heavy load on the primary power system. This load usually occurs when starting up another ESP or other large electric motor. Simultaneous startup of several motors should be avoided to minimize the impact on the primary power system. Ammeter spikes also can occur during a thunderstorm that is accompanied by lightning strikes.

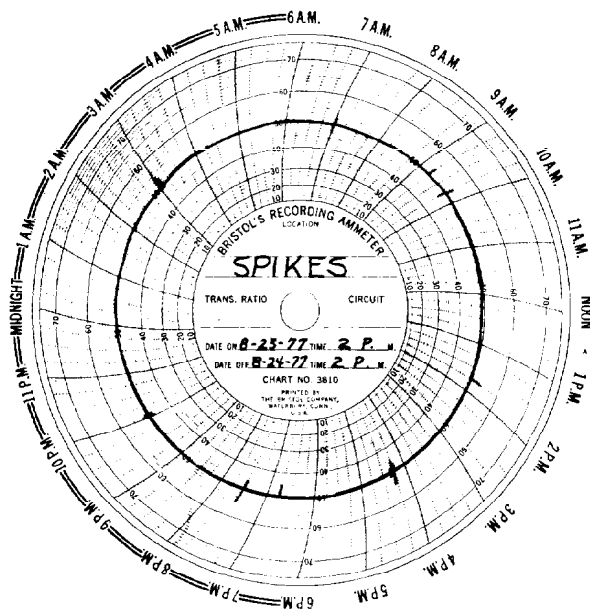


Fig. 7.26—Startup spikes chart.

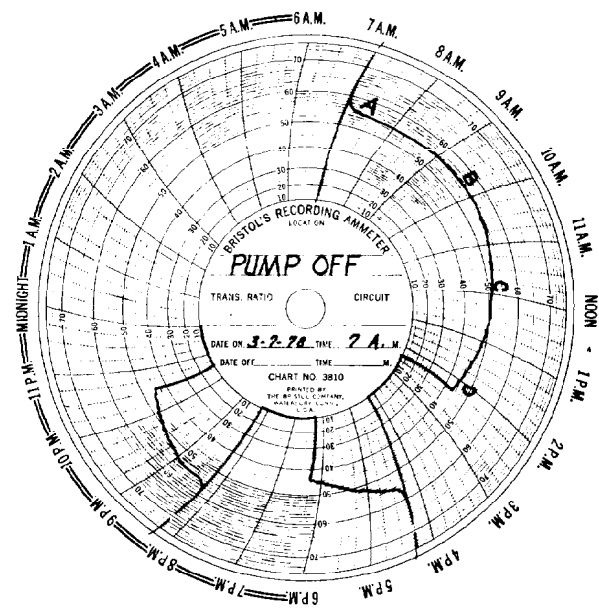


Fig. 7.28—Fluid pumpoff chart.

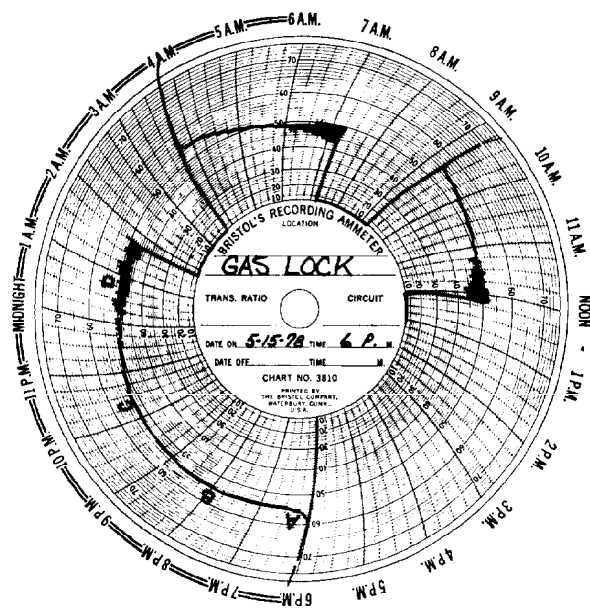


Fig. 7.27—Gas lock chart.

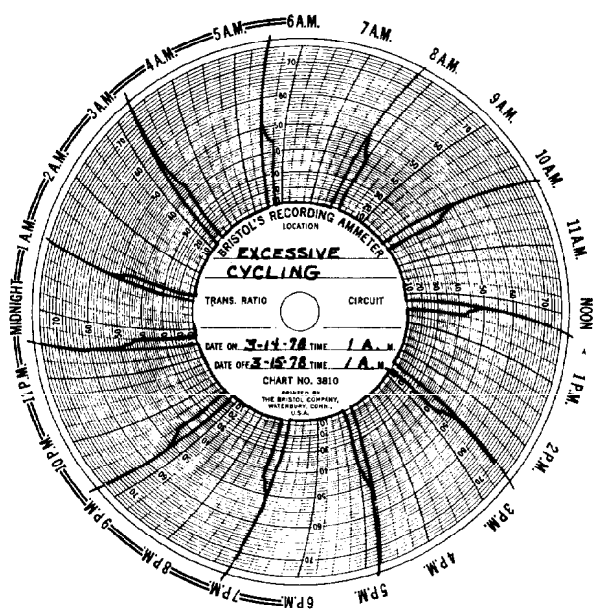


Fig. 7.29—Short duration cycling.

Gas Locking

Gas locking occurs as fluid level drawdown approaches the pump intake and intake pressure is lower than the bubblepoint. This situation is shown in Fig. 7.27. This ammeter chart shows a normal startup and amperage decline as the fluid level is drawn down. However, the chart shows erratic fluctuations as gas breaks out near the pump beginning at approximately 6:15 a.m. As the fluid level continues to draw down, cyclic loading of both free gas and fluid slugs leads to increasingly wider amperage fluctuations, ultimately resulting in shutdown at approximately 7:15 a.m. because of undercurrent loading.

There are three possible remedies for gas locking. The first is to install a gas separator intake and/or a motor shroud. The second is to lower the setting depth of the pump (but not lower than the perforations unless the motor is shrouded). The third remedy is to reduce the production rate of the pump by using a surface choke (but ensure that the production rate remains within the recommended range for that pump). It is entirely possible that none of these solutions is satisfactory. The pump should be replaced with a pump that does not draw down the fluid level or reduce intake pressure below the bubblepoint.

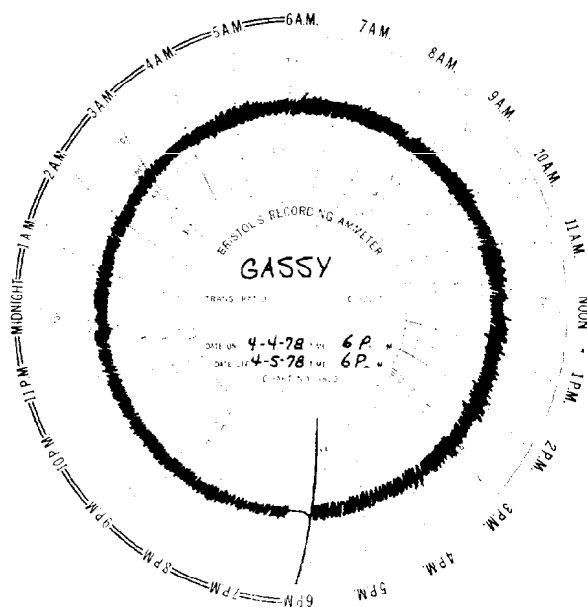


Fig. 7.30—Gassy or emulsion conditions.

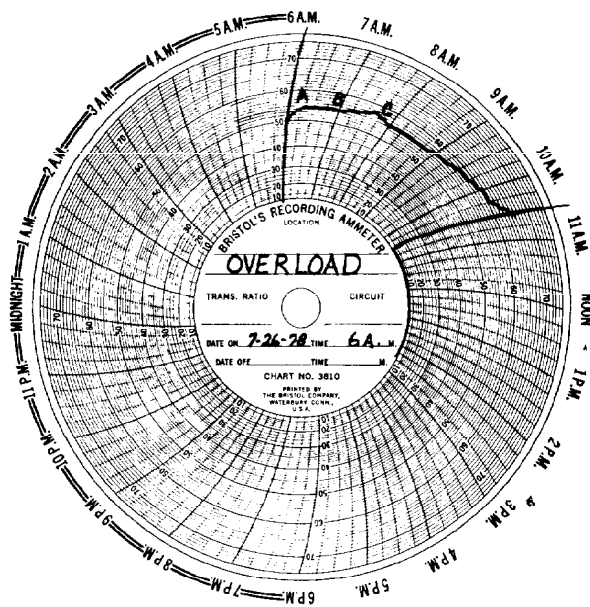


Fig. 7.32—Overload shutdown condition.

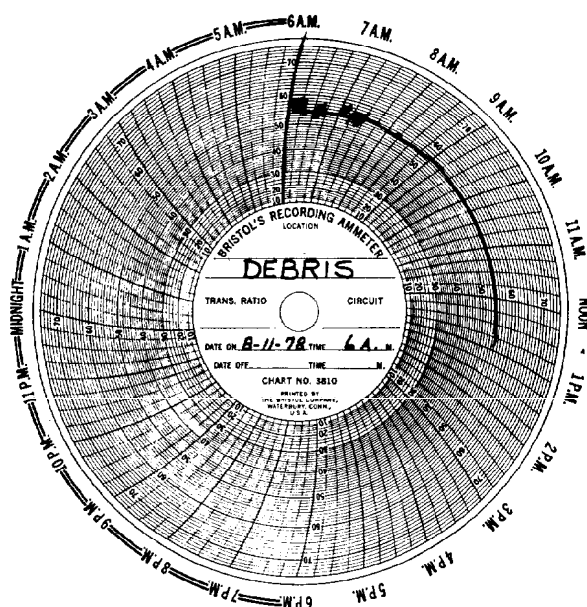


Fig. 7.31—Debris or solids in a well.

Another possible solution is to add a VSD to the existing system. The VSD controls the speed of the pump, which in turn controls the pump capacity. Thus the pump output can be fine-tuned to protect against pumpoff and gas lock while contributing to improved pump life.

Fluid Pumpoff

Fluid pumpoff occurs typically when an ESP is too large in relation to the inflow capacity of the well. This condition is illustrated in Fig. 7.28. This chart shows a normal startup at 7:00 a.m. and normal operation until approximately 10:00 a.m. Then amperage draw begins to fall

slowly until the underload setting is reached and the pump is shut down about 2:15 p.m. Subsequent automatic restarts at 4:15 p.m. and 8:15 p.m. produce similar results.

The remedial actions are much the same as those listed for gas lock and, in addition, a well stimulation treatment may increase the well's productivity closer to a match with the pump.

In general, cycling an ESP is not conducive to optimal run life. As a temporary measure, the amount of time delay before automatic restart can be increased if the switchboard is equipped with a Redalert motor controller. This may allow the fluid volume to build up to prevent a high frequency of shutdown occurrence. Nevertheless, the pump and well are not compatible and the pump size should be checked on the next changeout or the well worked over to improve productivity.

A form of frequent, short-duration cycling is shown in Fig. 7.29. This shows an extreme pumpoff condition. While the initial reaction is to suspect a badly oversized pump, there may be another cause. If a fluid level sounding, taken immediately after pump shutdown, indicates fluid over the pump, the problem may be a tubing leak or a restricted valve or discharge line. A tubing leak typically is accompanied by a somewhat low discharge pressure and low surface production rate. If shutdown is caused by a plugged valve or discharge line, tubing pressure should be abnormally high.

Gassy Conditions—Emulsion

A gassy but normal producing well is shown in Fig. 7.30. The continuous amperage fluctuations result from alternating free gas and heavy fluid pumping. Generally this condition results in a reduction of stock-tank barrels in relation to pump design rate. This figure is also typical of an emulsion. The amperage fluctuations are caused by the frequent, temporary blockage of the pump intake. If

it is an emulsion block, spikes are normally lower or below the normal amperage line.

Solids and Debris

When debris or solids are found in a well, the amperage will display fluctuations immediately after startup. This condition is shown in Fig. 7.31. Typically when solids such as sand, scale, or weighted mud are found in a well, special care must be taken on startup to avoid pump damage. It may be necessary to put backpressure on the well to prevent excess amperage until the kill fluid is removed and/or sand production begins to decline to a safe volume.

Overload Shutdown

A pump will also automatically shut down in an overload condition. This condition is shown in Fig. 7.32. However, when an overload condition shutdown occurs the unit must not be restarted until the cause of the overload has been identified and corrected. Some motor controller overload-detection circuits contain a built-in time delay, ranging from 1 to 5 seconds at 500% of the set point to 2 to 30 seconds at 200% of the set point. However, they will not automatically restart the unit on an overload condition. A restart attempt in an overload condition can destroy the downhole equipment if the cause of the overload is not identified and corrected first.

The most common causes of an overload condition are increased fluid specific gravity, sand, emulsion, scale, electric power supply problems, worn equipment, and lightning damage.

References

1. Vogel, J.V.: "Inflow Performance Relationships for Solution-Gas Drive Wells," *J. Pet. Tech.* (Jan. 1968) 83-92; *Trans.*, AIME, 243.
2. Standing, M.B.: "A Pressure-Volume-Temperature Correlation for Mixtures of California Oils and Gases," *Drill. and Prod. Prac.*, API (1975) 275.
3. Lasater, J.A.: "Bubble Point Pressure Correlation," *J. Pet. Tech.* (May 1958) 65-67; *Trans.*, AIME, 213, 379-81.
4. Vasquez, M. and Beggs, H.D.: "Correlations for Fluid Physical Property Predictions," *J. Pet. Tech.* (June 1980) 968-70.
5. Chew, J. and Connally, C.A. Jr.: "A Viscosity Correlation for Gas-Saturated Crude Oil," *J. Pet. Tech.* (Feb. 1959) 23-25; *Trans.*, AIME, 216.
6. Orkiszewski, J.: "Predicting Two-Phase Pressure Drops in Vertical Pipes," *J. Pet. Tech.* (June 1967) 829-38; *Trans.*, AIME, 240.
7. Standing, M.B.: *Volumetric and Phase Behavior of Oil Field Hydrocarbon Systems*, Reinhold Publishing Corp., New York City (1952).
8. "API Recommended Practice for Electric Submersible Pump Installation," API RP 11R (March 1980).

General References

- API Recommended Practice for the Operation, Maintenance and Trouble Shooting of Electric Submersible Pump Installations," API RP 11S, Dallas (Jan. 1982).
- Brown, K.E. et al.: *The Technology of Artificial Lift Methods*, Petroleum Publishing Co., Tulsa (1980) 2.
- Martin, J.W. and Vatalaro, F.J.: "Testing of Oil Well Power Cables Under Simulated Downhole Conditions," TRW Reda Pump Div. (1979).
- Mead, H.N.: "Oasis Submersible Lift Operations," paper SPE 5287 presented at the 1975 SPE European Spring Meeting, London, April 14-15.
- O'Neil, R.K.: "Engineered Application Submersible Pumps," paper SPE 5907 presented at the 1976 SPE Rocky Mountain Regional Meeting, Casper, May 10-11.
- Schultz, H.F.: "Extraordinary Application of Electrical Submersible Centrifugal Pump Equipment," paper SPE 4723 presented at the 1973 SPE Production Technology Symposium, Lubbock, Nov. 1-2.
- Swetnam, J.C. and Sackash, M.L.: "Performance Review of Tapered Submersible Pumps in the Three Bar Field," *J. Pet. Tech.* (Dec. 1978) 1781-87.

Chapter 8

Subsurface Sucker-Rod Pumps

James R. Hendrix, OILWELL Div. of U.S. Steel Corp.*

Introduction

The general principles of sucker-rod pumps as used in oil wells are well known. Fundamentally, they consist of the usual simple combination of a cylinder and piston or plunger with a suitable intake valve and discharge valve for displacing the well fluid into the tubing and to the surface. However, the variety of problems encountered in pumping oil wells has resulted in a great number of modifications of this fundamentally simple unit to make it more effective for the various conditions encountered. In general, the pumping of oil wells often presents the widest variety of adverse conditions possible in a single installation of any pumping application. These may include high discharge pressures; low intake pressures; severe abrasive conditions resulting from sand or other solids in suspension; severe corrosive conditions resulting from corrosive gases or salt waters; deposits of lime, salts, or other solids from the water pumped; paraffin deposits from the oil pumped; and the requirement that the pump handle liquids, permanent gases, and condensable vapors under the pressure and temperature conditions existing at the pump. Strong magnetic forces that may interfere with valve action when the valves are made of magnetic material are encountered often, and electrolytic corrosion is likely to occur as a result of using dissimilar materials.

The bores of reciprocating oilwell pumps can range from 1 to 4 $\frac{3}{4}$ in. in diameter. The 4 $\frac{3}{4}$ -in. bore pump has a displacement about 22 $\frac{1}{2}$ times that of the 1-in. pump for a given speed and stroke length. This wide range of pump capacities is necessary to permit selection of the most efficient and economical pumping equipment for all conditions encountered. In many wells it is necessary to pump large volumes of water along with the oil, so the pump must have a capacity several times that indicated by the net oil production.

Subsurface pump bores now standardized by the API

are 1 $\frac{1}{4}$, 1 $\frac{1}{2}$, 1 $\frac{3}{4}$, 2, 2 $\frac{1}{4}$, 2 $\frac{1}{2}$, and 2 $\frac{3}{4}$ in. Stroke lengths range from a few inches to more than 30 ft, and production rates with this type of pump range from a fraction of a barrel per day—with part-time operation—to approximately 3,000 B/D.

There are two broad classifications of pumps operated by sucker rods. The older type is now known as a "tubing pump." This term indicates that the pump barrel is attached directly to the tubing of a pumping well and lowered to the bottom of the well, or to any desired location for pumping, as the tubing is run into the well. The plunger, or traveling valve, of a tubing pump is run in on the lower end of the sucker rods until it contacts the lower-valve (or "standing-valve") assembly. The rods are then raised sufficiently to prevent bumping bottom at the end of the downstroke and connected to a pumping unit, or jack, at the surface.

A more recent development is the "insert" or "rod" pump in which the entire assembly of barrel, traveling valve, plunger, and standing valve is installed with the sucker rods and seated in a special seating nipple, a tubing pump barrel, or other device designed for the purpose. The rod-type pump has the obvious advantage that the entire pump may be removed from the well for repair or replacement, with only a rod-pulling job, whereas with a tubing pump it is necessary to pull both rods and tubing to remove the pump barrel. The rod pump, however, is necessarily of smaller maximum capacity for a given tubing size.

Tubing-type pumps may have a standing valve seated in a coupling or seating shoe at the lower end of the barrel, or the standing valve may be seated in a coupling at the lower end of an "extension nipple" that extends below the lower end of the barrel. The ID of the extension nipple is somewhat larger than that of the barrel to permit the pump plunger to stroke out both top and bottom to produce uniform barrel wear and prevent accumulations of solids on the barrel wall.

*Original chapter in 1962 edition written by Roy L. Chenault.

TABLE 8.1—API PUMP DESIGNATION

Type of Pump	Metal Plunger Pumps		Soft-Packed Plunger Pumps	
	Heavy-Wall Barrel	Thin-Wall Barrel	Heavy-Wall Barrel	Thin-Wall Barrel
Rod				
Stationary barrel, top anchor	RHA	RWA	—	RSA
Stationary barrel, bottom anchor	RHB	RWB	—	RSB
Traveling barrel, bottom anchor	RHT	RWT	—	RST
Tubing	TH	—	TP	—

First letter:

R = Rod or "inserted" type; run on the rods; through tubing
 T = Tubing type; noninserted, run on tubing

Second letter:

H = Heavy-wall; for metal plunger pumps
 W = Thin-wall; for metal plunger pumps
 S = Thin-wall; for soft-packed plunger pumps
 P = Heavy-wall; for soft-packed plunger pumps

Third letter:

A = Top anchor
 B = Bottom anchor
 T = Bottom anchor; with traveling barrel

Rod-type pumps may also be equipped with extension nipples above and below the barrel for similar reasons. In addition, rod pumps may be "top-seating" (pump suspended from top of barrel), "bottom-seating" (pump seated at bottom of barrel), "stationary-barrel" (traveling plunger), or "traveling-barrel."

Both tubing- and rod-type pumps are equipped with one-piece "full barrels."

The API has adopted standard designations for the combinations listed above. The classification system given in Table 8.1 is from API Standard 11AX.¹

The following definitions are provided to clarify some of the more important terms used in connection with subsurface oilwell pumps since a majority of these terms are peculiar to deep-well pumping terminology.

Barrel. The barrel of an oilwell pump is the cylinder into which the well fluid is admitted and displaced by a closely fitted piston or plunger.

Plunger. The pump plunger is a closely fitted tubular piston fitted with a check valve for displacing well fluid from the pump barrel. This may be all metal or equipped with cups, rings, or other soft packing to form a seal with the barrel.

Standing Valve. This is the intake valve of the pump and generally consists of a ball-and-seat-type check valve. The valve assembly remains stationary during the pumping cycle.

Traveling Valve. This is the discharge valve and moves with the plunger of a stationary-barrel pump and with the barrel of a traveling-barrel pump. The entire assembly of a cup-type plunger, or plunger equipped with other type of soft packing, along with the check valve, is often called a "traveling valve."

Standing Valve Puller. This is a tool designed to attach to the standing-valve cage of a tubing-type pump when the sucker rods are lowered to the bottom. The standing-valve assembly is then unseated by raising the rod string and is removed along with the pump plunger

when the rods are pulled. This avoids having to pull tubing to remove the standing valve of the tubing-type pump.

Valve Rod. Valve rods are used in rod-type stationary-barrel pumps to connect the lower end of the sucker-rod string to the pump plunger. The valve rod runs through a guide at the top of the pump. API valve-rod sizes range from $1/16$ to $1 1/16$ in. in diameter. Modified line pipe threads are standard for API valve rods (see Table 1 of Ref. 1).

Pull Tube. Pull tubes are used in rod-type traveling barrel pumps to connect the plunger with the seating assembly or "holddown." (See Ref. 1 for thread dimensions for straight threads.) Tapered threads are used on some sizes of pull tubes by some manufacturers.

Seating Assembly. A seating assembly is an anchoring device for retaining a rod pump in its working position. The seating assembly is sometimes more commonly called a "holddown." The seating assembly may be located either at the top or bottom of a stationary-barrel rod pump but can be located only at the bottom of a traveling-barrel pump. A seating assembly may be equipped with composition cups or rings that form a tight fit in a seating nipple, or coupling, to hold the pump in its working position by friction, or it may be provided with spring clips that snap into position under a shoulder and require a definite pull upward on the rods to unlatch for removal. With the cup-type seating assembly, the cups or rings also serve as a seal to prevent leakage of fluid from the tubing back to the well after it has passed through the pump. With the mechanical seating assembly, an accurately ground seating ring fitted on a tapered mandrel seats on a mating taper to form a leakproof seal.

Pump Selection

The selection of a proper subsurface pump for the application is sometimes a point of conjecture. The following recommendations generally are accepted as suitable for most applications. Fig. 8.1 shows cross sections of

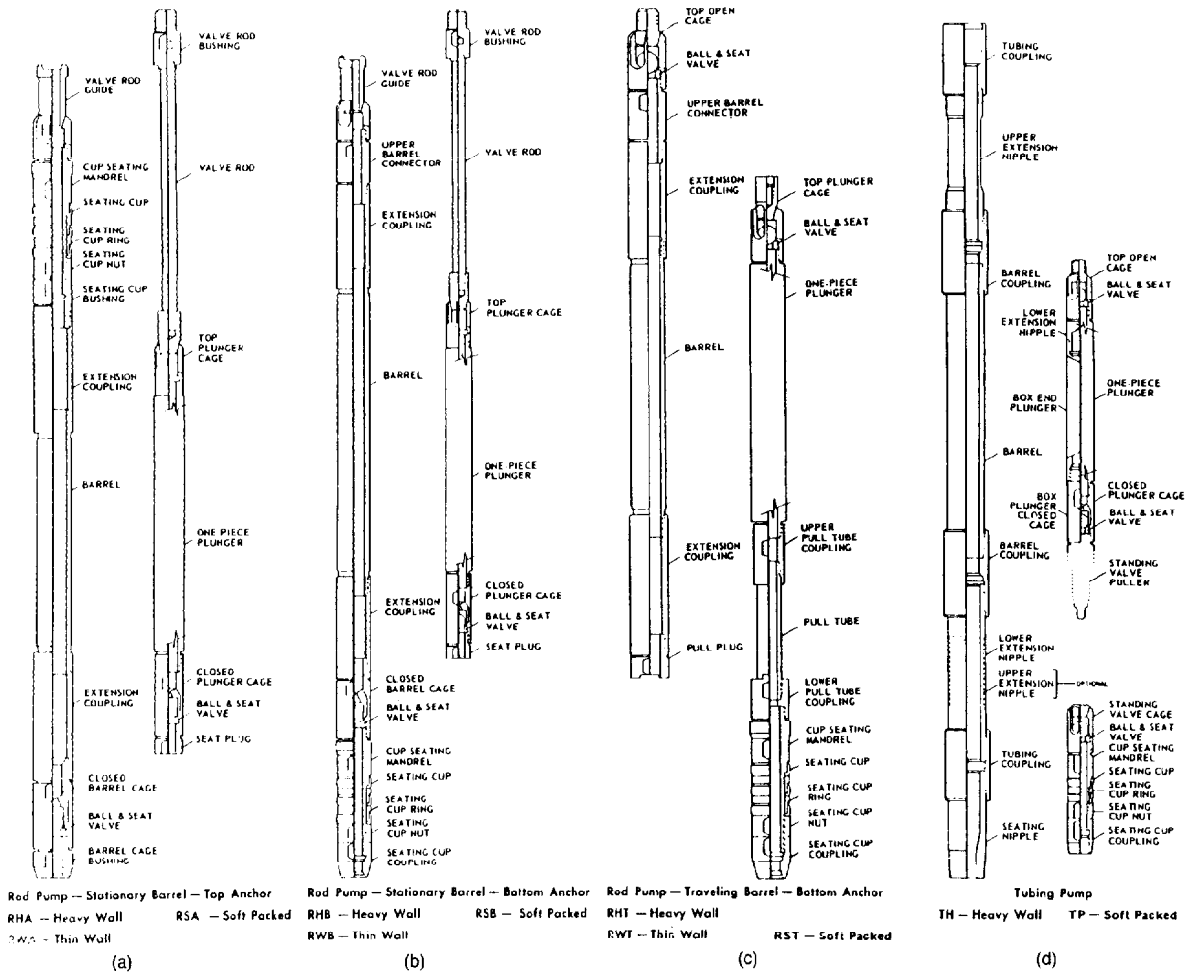


Fig. 8.1—API subsurface pump classification.

API pump classifications. There are many variations of the pumps shown, some within the specifications of API and some that are non-API that will still perform the desired function of pumping oil to the surface.

Fig. 8.1a shows a stationary-barrel rod pump with top-seating holddown. This is a pump that is run into the well with the sucker rods. In this pump the plunger is attached to, and moves up and down with, the sucker-rod string. The barrel is held stationary at its top end by the seating assembly. The barrel is on the left and the plunger assembly is on the right. This is the preferred seating for the rod pump when possible. The top seating holddown provides a seal just below the cage, where the well fluid is discharged into the tubing, so sand or other solid particles are prevented from settling between the barrel and the tubing, and the pump is not apt to become stuck in the tubing by packed sand. Since the body of the pump pivots from this top-seating arrangement, it aligns itself in crooked wells more readily than other types of pumps. Also, there is no tendency for the barrel to wear by rubbing against the tubing. This type of pump can handle low-gravity crude oil down to 400 cp quite well. In the stripper wells and in wells with low fluid levels, the top-seating design of the pump allows the standing valve to be submerged deep into the well fluid. This makes it

possible to pump the oil level lower than can be done with a bottom-seated pump. This is a particular advantage when the fluid flow from the oil reservoir is weak.

Fig. 8.1b shows a stationary-barrel rod pump with bottom-seating holddown. In this pump, the plunger is also attached to, and moves up and down with, the sucker-rod string. The barrel, on the left, is held stationary by a bottom-seating holddown, either mechanical lock or cup type, which is the type shown in the figure. This pump is more suitable for use in the deeper wells since the barrel does not elongate from the fluid column weight of the fluid in the tubing. Since the body of the pump pivots from its bottom-seating arrangement, it too can be used in crooked wells. However, there is a tendency for the valve rod to wear against the upper rod guide in this case. This pump also can handle low-gravity crude oil down to 400 cp quite well. Because of its bottom-seating arrangement, the pump can be seated easily in an old existing tubing pump barrel without pulling the tubing, where a top-seated rod pump might be too long to pass through an old tubing barrel.

The main disadvantage of this type of pump is that the pump barrel extends upward into the tubing. This makes it inadvisable to use a long pump, since it is not anchored at the top, and the action of the sucker-rod string will

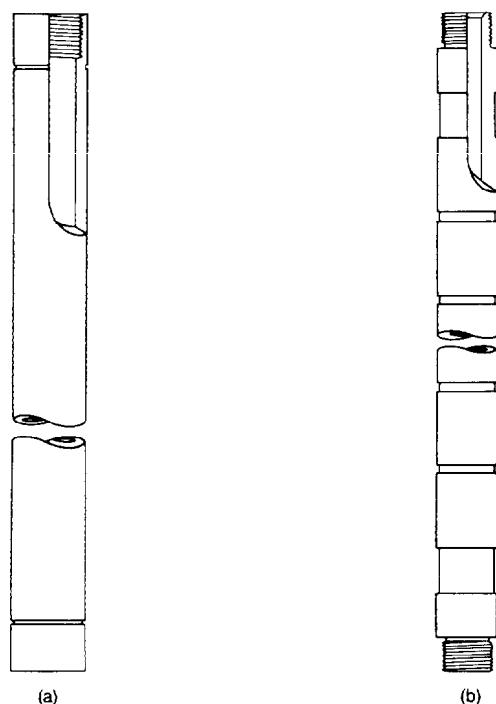


Fig. 8.2—Plain (a) and grooved (b) metal-to-metal plungers.

tend to weave it back and forth, which may cause premature failure. Also, this pump is not recommended for extremely sandy conditions, because there is no circulation of the well fluid around the outside of the barrel. For this reason, the pump may become stuck in the tubing by packed sand.

Fig. 8.1c shows a traveling-barrel rod pump. Many operators prefer this type of pump because of its simplicity and because its construction also relieves the pump barrel of a tension load resulting from the weight of the fluid column. A theoretical advantage of this type of pump is that the pressure differential across the plunger is such that the high pressure is on the bottom of the plunger on the intake stroke and the direction of leakage, or slippage, past the plunger is opposite to the direction of the force of gravity, which tends to cause sand to settle on the plunger. For this reason there is less tendency for sand to be forced into the clearance space between the plunger and barrel and accelerate wear. Although the traveling-barrel rod pump is bottom seated, it is not so likely to become sanded in the tubing as is a bottom-seated stationary-barrel rod pump since there is a continual surging of the well fluid in and out of the lower end of the barrel while in operation. Also, the construction of this pump is such that sand cannot settle into the barrel when the pump is shut down. A disadvantage of the traveling-barrel rod pump is the long and somewhat restricted inlet for oil to be admitted to the pump barrel. This may result in a relatively high pressure drop through the "pull tube" and plunger to liberate excessive quantities of free gas or to cause the formation of condensable vapors that will adversely affect the volumetric efficiency of the pump.

Some suppliers offer a combination top-seal and bottom-seating stationary-barrel rod pump. While this pump is considered "nonstandard," it combines the advantages of top-seating and bottom-seating pumps. It is particularly advantageous when a long pump is required in a deep well. This type of pump reduces the possibility of a collapsed barrel caused by external pressure and reduces sedimentation around the barrel tube. Because of additional sealing arrangements, this pump is more costly than standard API pumps.

Fig. 8.1d shows the tubing pump, so named because its barrel assembly, including barrel, extension nipples (if any), and seating nipple, is screwed onto, and becomes a part of, the tubing. Since the tubing and barrel assembly are lowered into the well together, it is easy to position a tubing pump at any desired depth for pumping. After the barrel assembly is in position, the standing-valve assembly is placed in the tubing, and it falls until it is stopped and held by the seating shoe. The plunger can be lowered into the well by attaching it to the sucker-rod string or by lowering it with the barrel assembly. In the latter case, an "off-and-on" attachment is used to connect the sucker rods to the plunger. Another device, called a "standing-valve-puller" (see Fig. 8.1d insert), can be attached to the plunger to hold the standing-valve assembly, so both can be lowered together. The standing-valve assembly is released from the standing-valve puller by turning the sucker-rod string; so the standing valve assembly remains in place, held by the seating nipple. If this action is reversed, the standing-valve assembly can be attached to the plunger and pulled out of the well with the sucker-rod string. This eliminates the necessity of pulling the complete tubing string to replace the standing-valve assembly. Another advantage of using a standing-valve puller is that the standing-valve assembly is not in danger of being damaged or becoming stuck, as is possible if it is dropped through the tubing.

Tubing pumps have larger bores and correspondingly greater displacements for a given stroke length than rod pumps that can be used with the same size tubing. Therefore, tubing pumps commonly are used where it is necessary to lift large volumes of fluid and a pump of high displacement is required. A tubing pump has fewer working parts and is often lower in cost than a rod pump of corresponding size. However, the greater volume and resulting heavier fluid load may cause a loss in this advantage by excessive sucker rod and tubing stretch. Also, the entire tubing string must be pulled to service the barrel of a tubing pump.

Plungers

Fig. 8.2 illustrates the two most common types of "metal-to-metal" plungers used for displacing well fluid in oilwell pumps. The left side shows a plain plunger with "box-end" threads. This type of plunger generally is finished somewhat undersize at each end opposite the threads. This provides for the slight expansion of the plunger when tightened, without causing binding of the plunger in the pump barrel. The right side shows a grooved "pin-end" plunger.

Most subsurface-pump manufacturers provide both plain and grooved plungers in various materials. It has never been demonstrated conclusively that either type of

**TABLE 8.2—LOSSES RESULTING FROM SLIPPAGE
OF 3-cp OIL PAST 2¼-in. PUMP PLUNGER***

Slippage Past Plunger		Slippage Loss in Pump at 15 strokes/min		
Diametral Clearance	Slippage Rate (cu in./min)	cu in./min	B/D	Percent Pump Displacement
0.003	11.43	5.72	0.85	0.2
0.006	91.5	45.8	6.8	1.6
0.010	424.0	212.0	31.5	7.4
0.020	3,390.0	1,695.0	251.8	59.2

*48 in. long with 2,000 psi differential pressure and various plunger fits. Also slippage in percent pump displacement with fifteen 48-in. strokes per minute.

construction has any particular advantage over the other. Many operators feel that grooves facilitate lubrication of closely fitted plungers by providing spaces for the well fluid to accumulate in considerable quantities. However, there is considerable slippage past any plunger operating under usual conditions where the differential pressure across the plunger is several hundred or even thousands of pounds per square inch. This slippage will provide adequate lubrication with either type of plunger if the fluid has any lubricating value. One possible advantage of a grooved plunger is that any solid particle, such as a sand grain or a steel chip that gets between the plunger and the barrel, may become lodged in a groove and minimize scoring of the barrel and plunger. With a plain plunger, particles cannot escape from the finished surfaces until they have traveled the full length of the plunger. On the other hand, a grooved plunger stroking out of a barrel increases the probability of picking up and carrying solid material into the barrel.

The high differential pressures encountered in pumping deep wells require an effective sealing or packing means on the plunger. For wells of extreme depth, a closely fitted metallic plunger is almost always used to form a satisfactory seal with the barrel. Such plungers are commonly supplied with nominal clearances of 0.001, 0.002, 0.003, or 0.005 in. in the barrel. Such plunger fits are commonly referred to as -1, -2, -3, or -5 fits. For metal-to-metal pumps the API tolerance for barrels is +0.002 in., -0.000 in., and the tolerance for plungers is +0.0000 in., -0.0005 in., making it possible for the fit of a -1 plunger, for example, to vary from 0.0010 to 0.0035 in. diametral clearance.

Slippage Past Plungers

In slippage past a closely fitted plunger, the flow between the plunger and the barrel is in the viscous range, so leakage or slippage is inversely proportional to the absolute viscosity and to the plunger length. It is directly proportional to the plunger diameter, the differential pressure between the two ends of the plunger, and the cube of the diametral clearance.

The absolute viscosity of well fluids commonly pumped will range from approximately 1 to 100 cp at temperatures existing at the pump setting. In some cases the viscosity may be as high as 1,000 cp. As a result of viscosity variations, the slippage past the plunger of a particular plunger-pump assembly with a given plunger fit, length, and diameter may vary by as much as 100 to 1 under fairly common conditions, and as much as 1,000 to 1 under extreme conditions with the same differential

pressure across the plunger. Thus it is seen that a plunger pump may operate with acceptable efficiency in a well producing a highly viscous oil, whereas the same pump operated at the same speed and stroke may fail to deliver any oil to the surface when installed at the same depth in a well producing oil of low viscosity.

The following equation can be used to determine slippage losses past a pump plunger with sufficient accuracy for most purposes.

$$q = \frac{\pi d \Delta p \Delta d_c^3}{\mu L \times 2.32 \times 10^{-7}}, \dots \dots \dots (1)$$

where

q = slippage loss, cu in./min (or 0.2371 cm³/s),

d = plunger diameter, in.,

Δp = differential pressure across plunger, psi,

Δd_c = diametral clearance, in.,

L = length of plunger, in., and

μ = absolute viscosity, cp.

A specific application of this equation will illustrate the importance of plunger fits for a pump of a particular bore and stroke, operating with various plunger fits in fluids of various viscosities.

If we assume a 2¼-in.-bore pump having a 0.003-in. diametral clearance and operating with a pressure differential of 2,000 psi between the two ends of a 48-in. plunger at a rate of fifteen 48-in. strokes per minute in oil having a viscosity of 3 cp, then Eq. 1 becomes

$$q = \frac{\pi \times 2.25 \times 2,000 \times 2.7 \times 10^{-8}}{3 \times 48 \times 2.32 \times 10^{-7}} = 11.43 \text{ cu in./min.}$$

If we assume that the volume of the barrel below the plunger is completely filled during the upstroke, this rate of leakage can occur only during the upstroke, or approximately one-half of the total time. The net slippage past the plunger is 5.72 cu in./min, or 0.85 B/D. The displacement of a 2¼-in. pump operating at fifteen 48-in. strokes per minute is 426 B/D, and the slippage in this case is only about 0.2%, which is insignificant. The results of this and other plunger clearances with 3-cp oil are shown in Table 8.2.

In the case of 0.020-in. plunger clearance, the slippage loss when water or oil with a viscosity of 1 cp is pumped would be 755 B/D, which is more than the pump displacement, and it would be impossible to pump water

to the surface, or to a level requiring 2,000-psi pressure differential across the plunger. When pumping oil with a viscosity of 100 cp, however, the slippage would be only about 7.5 B/D, or less than 1.8% of the pump displacement, and a clearance of 0.020 in. is reasonably satisfactory for these conditions.

Slippage losses result directly in power losses, since the same power is required to lift the plunger, with 90% of the fluid slipping past the plunger during the upstroke as is required with 1% or less slippage. The energy dissipated in slippage losses results in an increase in temperature of the oil within the pump and a decrease in viscosity that further increases slippage losses. Also, when water is produced with oil, excessive slippage losses increase the chances of forming emulsions.

Close plunger clearances are relatively more important with small-bore pumps than with larger bores, inasmuch as the displacement for a given stroke length and speed varies as the square of the diameter, whereas slippage varies as the first power of the diameter. Close plunger clearances are especially important in small pumps

operated at extremely low speeds, as used in stripper wells in some areas. The method outlined here should be satisfactory for evaluating maximum slippage in most cases.

Soft-Packed Plungers

Fig. 8.3 shows the cup- and ring-type plungers. The left side shows composition-formed cups used to seal the plunger against the barrel. The right side shows composition rings (generally square or rectangular in shape) used for sealing. Some operators prefer a combination of both cups and rings on a single plunger. The applications of such soft-packing arrangements generally are limited to shallow wells and to those where abrasive conditions are not excessively severe. Where this type of plunger is satisfactory, it has the advantage of being easily and less expensively reconditioned with new cups or rings, and the flexible packing will compensate for considerable wear of the barrel as long as the barrel surface remains smooth.

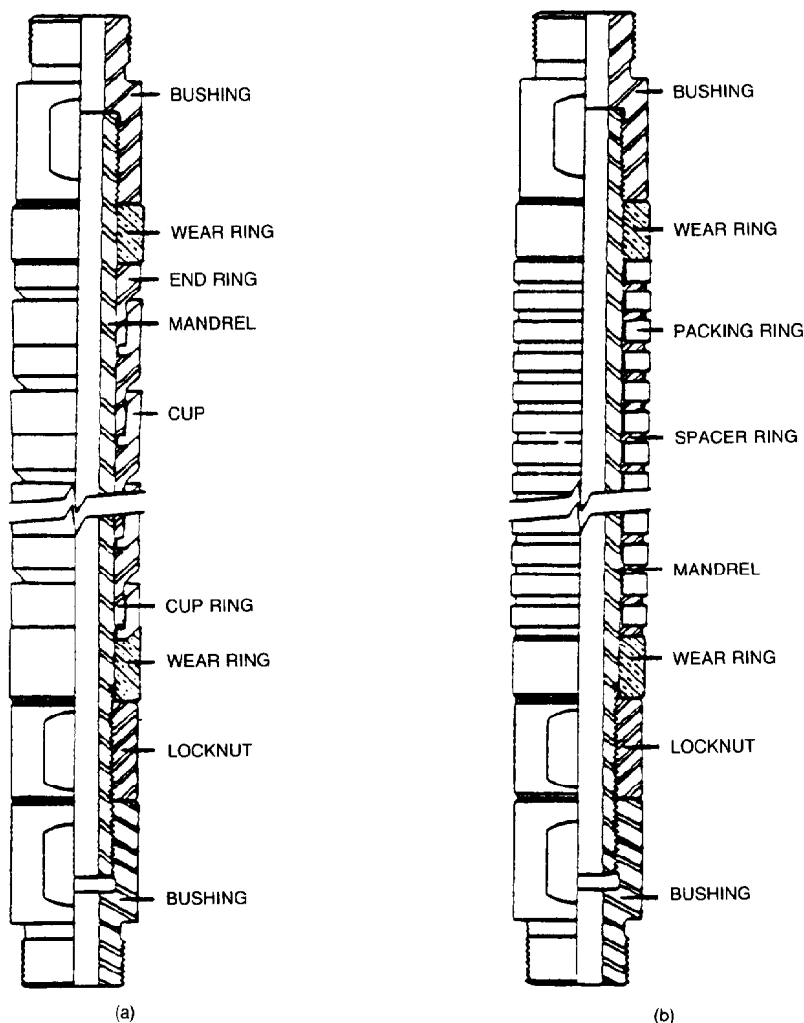


Fig. 8.3—Soft-packed plungers: (a) cup type; (b) ring type.

Balls and Seats

Fig. 8.4 illustrates the type of ball-and-seat combination commonly used for check valves in subsurface pumps. Balls and seats are made in a variety of materials to resist extremely abrasive and corrosive conditions. API Standard 11AX¹ lists the important dimensions of standard sizes along with the pump sizes with which they are commonly used.

Double Valves

Fig. 8.5 shows common arrangements of two valves in series used both as traveling valves and as standing valves. Experience has shown that two valves in series will give much longer service than a single valve if the valve life is determined by wear or fluid cutting, rather than by corrosive action. This result appears entirely logical where sand or other solid material is lifted with the oil. In such cases failure is likely to occur as a result of fluid cutting when a solid particle is caught between the ball and seat and prevents perfect seating. A pressure differential of 2,000 psi will produce a jet of fluid having a velocity of over 500 ft/sec, which can easily damage

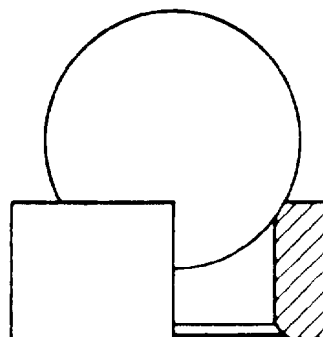


Fig. 8.4—Pump valve ball and seat.

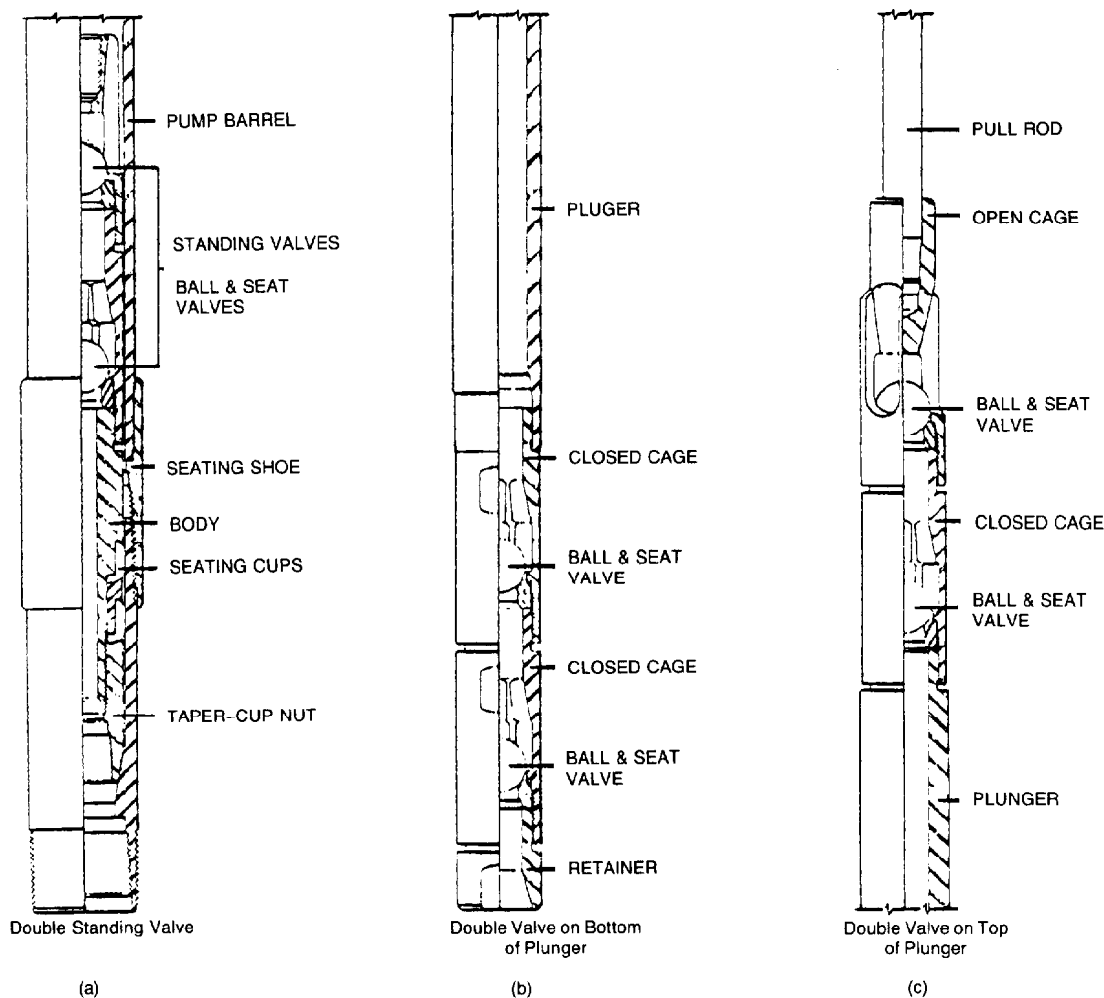


Fig. 8.5—Double-valve arrangements.

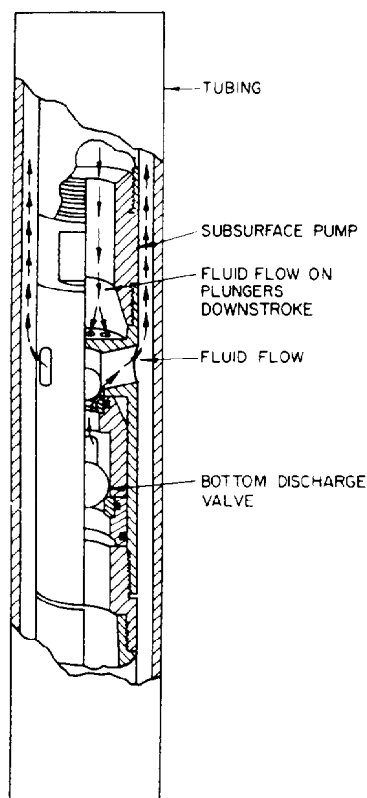


Fig. 8.6—Bottom-discharge valve for use with bottom-seating stationary-barrel rod pumps. This valve is attached to the bottom of a pump and through it part of the well fluid is diverted up the side of the pump to help dislodge sand that may have settled between the pump and the tubing.

the lapped valve-seating surface on balls and seats in a short time. The rate of damage is accelerated if the fluid jet carries solid material in suspension.

The life of a ball and seat will depend largely on the number of times it is subjected to damage by fluid jets. By use of double valves this can be greatly decreased, since a jet cannot occur until both balls are held off their seats during the same stroke. For example, if conditions are such that a single ball and seat is prevented from seating properly once out of each 100 strokes, the chances of both valves in series failing to seat properly will be reduced to 1 in 10,000 strokes. Furthermore, if the two valves fail to seat, the pressure drop will be distributed between the two valves and the cutting action will be less severe than with a single valve.

Bottom-Discharge Valve

The bottom-discharge valve shown in Fig. 8.6 is used in connection with bottom-seating stationary-barrel rod pumps and is designed to cause part of the fluid discharged from the pump to circulate up around the outside

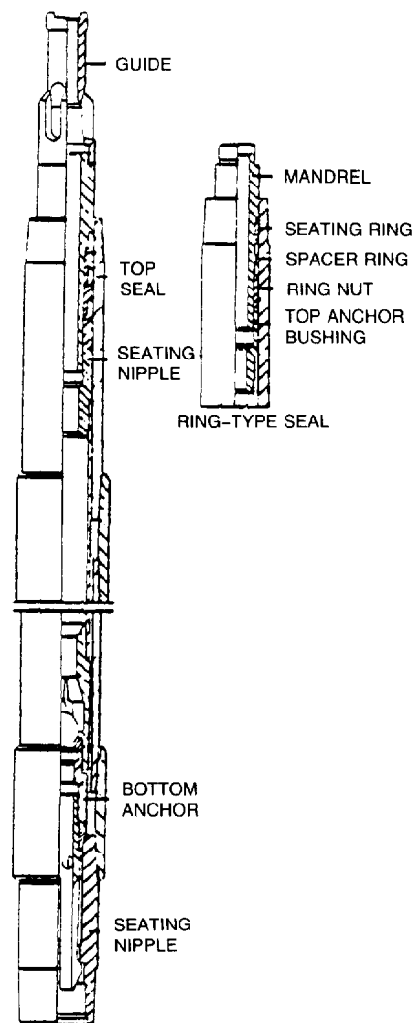


Fig. 8.7—Top seal and bottom seating for stationary-barrel rod pumps.

of the pump barrel. This is done to prevent sand from settling around the pump, which may make it impossible to pull the pump on the sucker rods. The bottom-seating arrangement for a rod-type pump is desirable in wells of extreme depth since the pump barrel is relieved of the fluid load, which places the barrel in tension. When top seating is used, the barrel is subjected to a high pressure which tends to expand the barrel.

Fig. 8.7 illustrates another means for utilizing the advantages of bottom seating with a stationary-barrel rod pump and preventing sand from settling around the outside of the pump barrel. This assembly utilizes a mechanical bottom-seating assembly, with seating cups or rings that fit into a slightly restricted seating nipple, properly spaced in the tubing to form a seal at the top of the pump barrel.

Three-Tube Pump

This type of pump is illustrated in Fig. 8.8 and gets its name from the three tubes used in its construction. The complete pump assembly is lowered into the well on the

sucker-rod string and is positioned in the well by contacting either a cup-seating assembly or a mechanical lock holddown. The middle tube of the pump is stationary, attached to the holddown. The other two tubes attached to the sucker-rod string move over the middle stationary tube, one on the outside and one on the inside. The tubes used in this pump are relatively long and have a relatively large operating clearance in comparison with the usual pump plunger. The resistance to flow between the tubes is adequate to create the seal necessary to displace the fluid past the standing valve and through the traveling valve against the tubing pressure. This pump is designed primarily to clean out wells after workover operations or formation-fracturing operations, which may make the well produce large quantities of sand for a considerable time. It is also used in wells producing from loose-sand formations that consistently produce quantities of fine floating sand.

Gas Anchors

Where conditions are such that there is considerable free gas in the well fluid at the pump intake, it is desirable to prevent as much gas as possible from entering the pump and permit the gas to rise to the surface through the casing annulus rather than through the tubing. Numerous so-called gas anchors are in use that are designed to separate the free gas and deflect it up the casing annulus. Fig. 8.9 illustrates a common type of gas-anchor arrangement in which the well fluid must enter the perforated nipple and circulate downward at a low velocity before entering the gas-anchor tube, which is attached to the pump intake. This gives the free gas an opportunity to separate and rise to the uppermost ports in the perforated nipple where it may return to the casing. A large portion of the gas will rise through the casing before passing through the perforated nipple.

Special Pumps

There are many other special types of subsurface pumps for use in special problem situations. Most of these are considered "non-API" pumps, although they may use some parts that meet API specifications in their construction. One special pump is the casing pump, which is designed to be inserted directly into the casing without a string of tubing. Such pumps are set in the casing on a packer or casing anchor that grips the casing and holds the pump in position. Such pumps are limited in size only by the casing size and can be made to have a very large capacity in relatively shallow wells. However, with this arrangement, all the gas produced with the well fluid must pass through the pump, and this may seriously limit the effective capacity in wells producing large quantities of gas.

Another special type of pump that is used to some extent is an arrangement where two displacing plungers are designed to act in series. This increases the displacement of a pump that will run in a given size of tubing and at a given stroke length. Another variation of this concept uses two valves and seats in the lower plunger and none in the upper plunger. This allows a fluid load on the lower plunger at all times and assists the sucker rods in falling on the downstroke, which is desirable for the more viscous fluids.

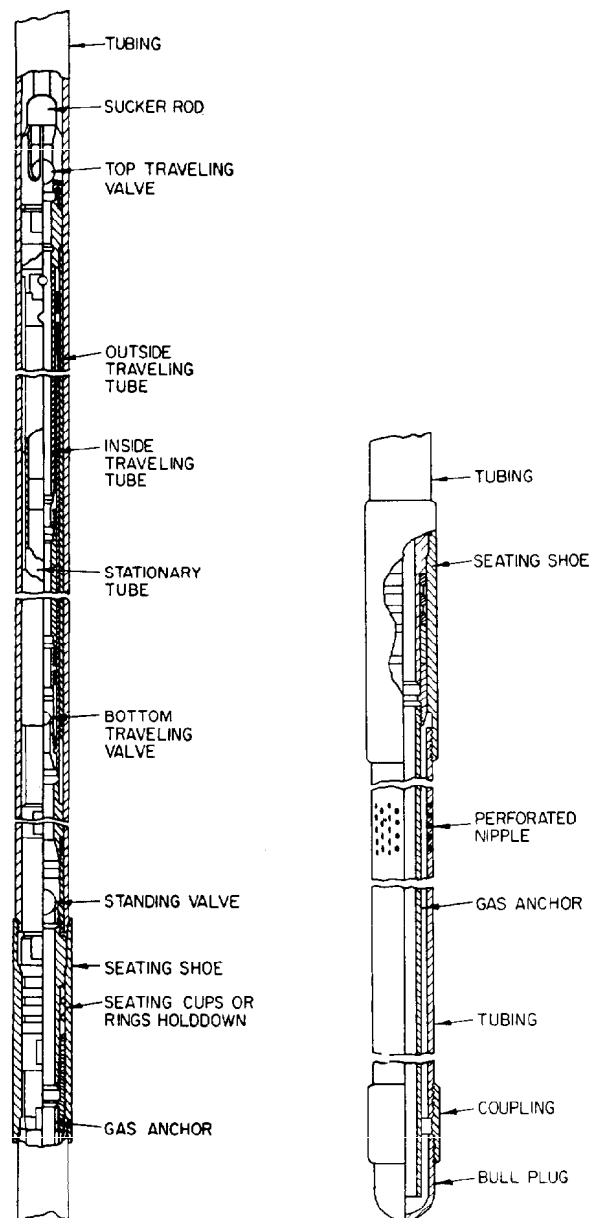


Fig. 8.8—Three-tube pump. Fig. 8.9—Gas-anchor arrangement.

Fluids with large amounts of gas can cause gas locking or at least reduced flow because of expansion of gas in the chamber between the plunger and the standing valve on the upstroke. This situation can sometimes be relieved by a special pump having two so-called compression chambers that serve to increase the compression ratio in those chambers above that normally obtainable in a standard pump.

Corrosion

In some areas resistance to corrosion of the materials used in subsurface pumps is of major importance. A wide variety of alloy irons, steels, nonferrous alloys, and elements have been used to combat corrosive conditions

in various locations. Some of the corrosive agents commonly found in various locations are hydrogen sulfide, carbon dioxide, salt waters containing sodium chloride, calcium chloride, magnesium chloride, and other salts. Chemical corrosion inhibitors are now widely used by many operators. Such inhibitors are fed either continuously or intermittently down the casing into the well. Protective films are formed on the tubing and rods, as well as on pump parts. However, since protective films cannot form on wearing surfaces, the closely fitted pump parts in rubbing contact are not protected as well as the rods and tubing by corrosion inhibitors. For this reason it is more important to use corrosion-resistant materials in the construction of subsurface pumps.

Effect of Gases and Vapors

In selecting pumping equipment for oil wells remember that in a majority of cases some of the constituents of the fluid being pumped are above or near their boiling points at the pressure and temperature conditions existing within the pump. These conditions may cause release of large volumes of dissolved gases and vapors with a slight drop in pressure of the well fluid, in addition to the free gas initially in the fluid. For this reason it is very difficult to pump some wells down. Many wells apparently will pump off with several hundred feet of fluid standing in the hole because the condensable vapors and gases occupy the entire displacement volume of the pump. Under these conditions, without a relatively high intake pressure, which decreases compression ratio, the pressure below the plunger cannot be raised to the tubing pressure. (This is necessary before the traveling valve can open and deliver oil to the tubing.) On the downstroke the vapors may condense and occupy a very small volume without an appreciable increase in pressure, and only the permanent gases are effective in increasing the pressure in accordance with the gas laws.

There are two precautions to take to minimize the adverse effects of vapors and gases.

1. The compression ratio should be made as high as possible. This is accomplished by using a closed-cage-type valve below the plunger with a stationary-barrel pump, or a valve above the plunger with a traveling-barrel-type pump. It is also important to space the pump so the traveling valve and standing valve come as near to each other as possible at the lowest position of the rods without making contact, and to use as long a stroke as possible with the equipment available.

2. Flow velocities and turbulence at the pump inlet should be kept at a minimum. This is accomplished by using the largest standing valve possible and a suitable gas anchor with the largest possible flow passages.

Conclusions

Most items covered in this section are discussed in Ref. 2, which was first issued in 1968 and is updated regularly. It is recommended that this source be referred to for state-of-the-art information about subsurface pumps.

It is well known that because of the dynamics involved in the sucker-rod string, the fluid, and the tubing during pumping cycles, the plunger stroke of the subsurface pump is seldom equal to the stroke of the pumping unit and its accompanying polished rod at the top of the well. During pump operation the fluid load, which is alternately transferred from the tubing to the sucker rods, causes the tubing to increase in length on the downstroke when the tubing is supporting the fluid load. When the rods are carrying the load on the upstroke, there is a shortening of the tubing with an increase in the length of the sucker rods. Both effects tend to shorten the plunger stroke in the well in comparison with the polished-rod stroke at the surface.

Because of the dynamic effects and the inertia and elasticity of a string of sucker rods, there will be some additional stretch in the rods during the pumping stroke. This effect is known as overtravel and results in an increase in the stroke length at the subsurface pump.

In years past, the calculation of sucker-rod and tubing stretch, as well as overtravel, was accomplished with a rather simple set of equations using tables and curves developed for this purpose. Later it was recognized that there are many factors in a pumping well that make the calculations a complex problem. In 1954 a group of users and manufacturers of sucker-rod pumping equipment formed Sucker Rod Pumping Research Inc., a non-profit organization, to study the problems of pumping wells. They in turn retained Midwest Research Inst. of Kansas City to achieve their objectives. Their study covered several hundred pumping wells and resulted in design calculation methods that more nearly match actual pumping conditions than previous methods. The results of the study were turned over to the API Production Dept. The API in turn adopted these methods.³ These design calculations are too involved and lengthy to be included in this section. It is suggested that Ref. 3 be used to determine the design values of a pumping system.

References

1. "API Specification for Subsurface Pumps and Fittings," API Spec 11AX, seventh edition, Dallas (June 1979).
2. "API Recommended Practice for Care and Use of Subsurface Pumps," API RP 11AR, second edition, Dallas (March 1983).
3. "API Recommended Practice for Design Calculations for Sucker Rod Pumping Systems (Conventional Units)," API RP 11L, third edition, Dallas (Feb. 1977).

Chapter 9

Sucker Rods

Dean E. Hermanson, LTV Energy Products Co.*

Introduction

A sucker rod is the connecting link between the surface pumping unit and the subsurface pump, which is located at or near the bottom of the oil well. The vertical motion of the surface pumping unit is transferred to the subsurface pump by the sucker rods.

Two types of sucker rods are in use today—steel rods and fiberglass-reinforced plastic sucker rods. It is estimated that slightly less than 90% of the rods sold in 1985 were steel rods, while slightly more than 10% were fiberglass rods.

Steel rods are manufactured in lengths of 25 or 30 ft. Fiberglass rods are supplied in 37½- or 30-ft lengths. Both types of rods are connected by a 4-in.-long coupling. The pin ends of the sucker rod are threaded into the internal threads of the coupling, as illustrated in Fig. 9.1. Individual rods are connected to form rod strings that can vary in length from a few hundred feet for shallow wells to more than 10,000 ft for deeper wells.

Sucker rods were originally made from long wooden poles with steel ends bolted to the wooden rod. An improvement was to use steel instead of wood and to forge the upset end on the steel rod. Forging the end generates a heat transfer zone by the upset, which is susceptible to corrosion attack. Full-length heat treating of the steel rod eliminated this problem. While the general geometry of the steel rod has remained relatively unchanged, improvements in surface finish, surface condition, end straightness, metallurgy, and quality control have been responsible for increased performance.

API Spec. 11B details information—such as workmanship and finish, material grades, dimensions, and gauging practice—on sucker rods (pony and polished rods and couplings and subcouplings).

The general dimensions for a sucker rod published by API¹ are listed in Table 9.1 and Fig. 9.2.

The general dimensions for sucker rod couplings are listed in Tables 9.2 and 9.3 and Fig. 9.3. At the present time, there is one grade of couplings, API Grade T. This coupling has a hardness designation of 16 minimum and 23 maximum on the Rockwell C scale. The hardness is controlled to provide resistance to embrittlement by H₂S and to provide a minimum strength level.

API has specified three grades of rods; their chemical and mechanical properties are listed in Table 9.4. The industry typically supplies sucker rods to the various categories, as listed in Tables 9.5 and 9.6. Other chemistries and types of rods are also available for special application.

Steel Sucker Rods

Manufacture of Sucker Rods

One-Piece Steel Sucker Rods. One-piece steel sucker rods are manufactured from hot-rolled steel finished with a special quality surface. The surface finish of the rod is very important, because rods fail prematurely as a result of discontinuities on the surface. These discontinuities can cause stress concentration that results in fatigue cracks.

The first operation in manufacturing a sucker rod is straightening the rod. In the second operation, the end of the rod is heated to about 2,250°F, and the lower bead, wrench square, pin shoulder, and pin are upset forged. The next operation is full-length heat treating. Heat treating develops the desired physical properties in the rod and provides a uniform surface structure to minimize corrosion. The type of heat treatment depends on the chemistry of the rod and the desired physical properties. Normalizing, normalizing and tempering, quenching and tempering, and surface hardening are heat treatments in use today.

*Author of the original chapter on this topic in the 1962 edition was Walter H. Ritterbusch Jr.

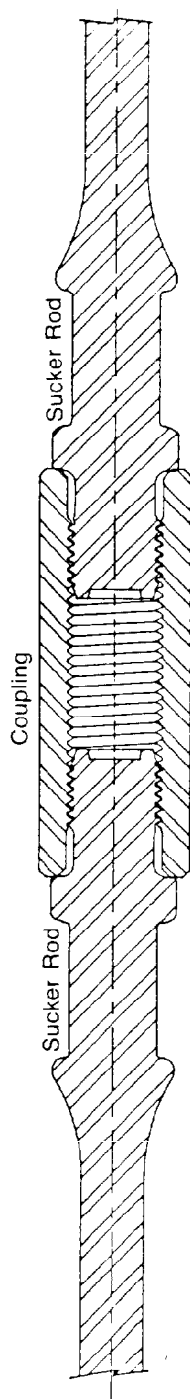


Fig. 9.1—Steel sucker rod and coupling connection.

After heat treatment, the rods are shot cleaned to remove scale. Any scale left on the rod provides the opportunity for a corrosion cell to begin. The pin ends of the rod are then machined and roll threaded. Roll threading puts the root of the pin thread in compression and hence increases the fatigue life.

The final operations are inspection, painting, and packaging. Most manufacturers protect steel sucker rods with an oil-soluble paint combined with a corrosion inhibitor.

Three-Piece Steel Sucker Rods. The three-piece sucker rod differs from a solid one-piece sucker rod in that the upset configuration is machined from a separate piece rather than integrally upset with the rod body as in a one-piece rod. The rod body of a three-piece rod is generally manufactured from cold drawn steel. The rod is threaded and screwed into the machined metal end connectors. The threads are usually joined by an adhesive. Their primary use has been in shallow wells.

Application

The selection of the size and grade of sucker rods depends on the rod stress and well conditions. The rod stress, in turn, depends on several variables—the amount of production required; the size of the tubing, which can influence the diameter of the pump, couplings, and rods; and the pumping unit, which will determine the surface stroke length. Generally, to determine rod stresses for a given well, the following information must be either known or approximated: fluid level, the net lift (in feet), pump depth (in feet), surface stroke length (in inches), pump plunger diameter (in inches), specific gravity of the fluid, nominal tubing diameter (in inches) and whether the tubing is anchored, pumping speed (in strokes per minute), sucker rod size(s) and design, and pumping-unit geometry.

With this information, the following can be calculated: plunger stroke (in inches), pump displacement (in barrels per day), peak polished rod load (in pounds force), minimum polished rod load (in pounds force), peak crank torque (in pounds force-inches), polished rod horsepower, and counterweight required (in pounds force).

Predictive Calculations

The method to perform these calculations is detailed in API RP11L.² This method was developed by simulating the sucker rod pumping system with an analog computer to resolve the many complex variables associated with a rod pumping system. API RP11L is a more reliable performance-predictive method than the previously available simplified equations. Remember that the API method, along with other methods, yields predictive performance results for typical wells.

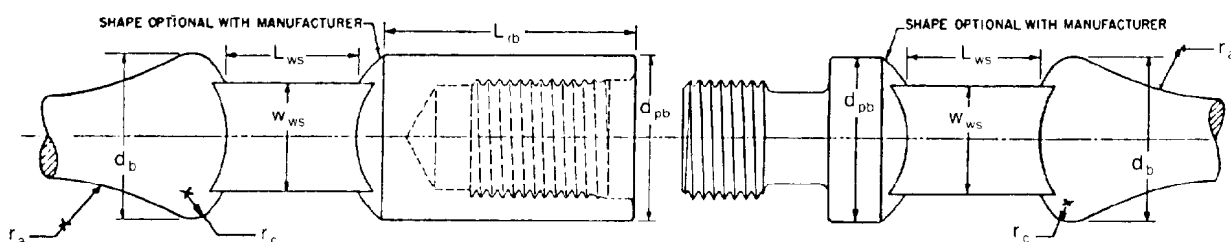


Fig. 9.2—General dimensions for sucker rod box and pin ends (see Table 9.1).

TABLE 9.1—GENERAL DIMENSIONS AND TOLERANCES FOR SUCKER RODS AND PONY RODS (see Fig. 9.2)

Rod Size (in.)	Pin Nominal Diameter (in.)	Pin Shoulder and Box OD, d_{pb} (in.)	Wrench Square Width $\pm \frac{1}{32}$ in., w_{ws} (in.)	Wrench Square Length,* L_{ws} (in.)	Minimum Rod Box Total Length, L_{rb} (in.)	Sucker Rod Length,** ± 2.0 in. (ft)	Pony Rod Length,**† ± 2.0 in. (ft)	Bead Diameter,† d_b (in.)	r_a , $\pm \frac{1}{8}$ in. (in.)	r_c , $\pm \frac{1}{16}$ in. (in.)
$\frac{1}{2}$	$\frac{3}{4}$	$1.000^{+0.005}_{-0.010}$	$\frac{5}{8}$	$\frac{3}{4}$	—	25, 30	$1\frac{1}{2}, 2, 3, 4, 6, 8, 10, 12$	$\frac{7}{8}^{+0.005}_{-\frac{1}{2}}$	$1\frac{1}{2}$	$\frac{1}{8}$
$\frac{5}{8}$	$1\frac{1}{16}$	$1.250^{+0.005}_{-0.010}$	$\frac{7}{8}$	$1\frac{1}{4}$	$2\frac{1}{8}$	25, 30	$1\frac{1}{2}, 2, 3, 4, 6, 8, 10, 12$	$1\frac{1}{8}^{+0.005}_{-\frac{1}{2}}$	$1\frac{7}{8}$	$\frac{1}{8}$
$\frac{3}{4}$	$1\frac{1}{16}$	$1.500^{+0.005}_{-0.010}$	1	$1\frac{1}{4}$	$2\frac{3}{8}$	25, 30	$1\frac{1}{2}, 2, 3, 4, 6, 8, 10, 12$	$1\frac{3}{8}^{+0.005}_{-\frac{1}{8}}$	$2\frac{1}{4}$	$\frac{1}{8}$
$\frac{7}{8}$	$1\frac{3}{16}$	$1.625^{+0.005}_{-0.010}$	1	$1\frac{1}{4}$	$2\frac{3}{8}$	25, 30	$1\frac{1}{2}, 2, 3, 4, 6, 8, 10, 12$	$1\frac{1}{2}^{+0.005}_{-\frac{1}{8}}$	$2\frac{5}{8}$	$\frac{3}{16}$
1	$1\frac{3}{8}$	$2.000^{+0.005}_{-0.010}$	$1\frac{1}{16}$	$1\frac{1}{2}$	3	25, 30	$1\frac{1}{2}, 2, 3, 4, 6, 8, 10, 12$	$1\frac{3}{4}^{+0.005}_{-\frac{1}{4}}$	3	$\frac{3}{16}$
$1\frac{1}{8}$	$1\frac{9}{16}$	$2.250^{+0.015}_{-0.010}$	$1\frac{1}{2}$	$1\frac{5}{8}$	$3\frac{1}{4}$	25, 30	$1\frac{1}{2}, 2, 3, 4, 6, 8, 10, 12$	$2^{+0.005}_{-\frac{1}{8}}$	$3\frac{3}{8}$	$\frac{3}{16}$

*Minimum length exclusive of fillet.

**The length of sucker and pony rods shall be measured from contact face of pin shoulder to contact face on the field end of the coupling.

†The length of box-and-pin rods shall be measured from contact face of pin shoulder to contact face of box.

‡Dimensions d_b , r_a , and r_c became mandatory dimensions on June 20, 1986. Before this, d_b was not to exceed d_{pb} .

Well conditions—such as slanted or crooked holes, which result in excessive well friction, and viscous fluid, which results in abnormal loads, excessive sand production, large amounts of gas production through the pump, and wells that flow off—will result in actual performance that differs from predictive performance. API RP11L was developed to predict the performance of API-designated steel-only sucker rod strings with conventional-geometry surface pumping units and medium-slip motors. Enhancements available from various manufacturers include high-slip motors, advanced pumping unit geometry, and non-API sucker rod string design.

A FORTRAN source code listing for the API design calculations can be obtained from the Dallas API office.

In addition to the API program for predicting performance, proprietary mathematical solutions using partial-differential equations are solved by numerical methods with the aid of computers. These mathematical model solutions using the wave equation are flexible and can also be used for solving fiberglass rod calculations by changing the modulus of elasticity of the input file. These programs are available for installation and use on personal computers.

API also publishes API Bull. 11L3³ for those who (1) do not have access to a computer with either the API program or a proprietary wave equation predictive program and (2) wish to avoid the tedious manual calculation of API RP11L. This design book lists a grid of conditions that have been calculated on a computer with the API RP11L method, and the results are tabulated. Pump depth varies from 2,000 to 12,000 ft in 500-ft increments. Various production rates are tabulated with different rod strings. An application can then be selected from the various pump diameters, stroke lengths, strokes per minute, peak and minimum polished rod loads, stresses, peak torques, and peak polished rod horsepower that are listed. In general, the smallest pump diameter—consistent with a reasonable cycle rate—that will achieve the desired production is the proper choice. This should result in the lightest fluid load and rod string, which, in turn, will require smaller surface equipment.

Another general rule of thumb is to use the longest stroke length and slowest cycle rate to achieve the production. The longer stroke length minimizes the effect of rod stretch, and the slower cycle rate generally minimizes the dynamic effects. A comparison of several trial calcu-

TABLE 9.2—FULL-SIZE COUPLINGS AND SUBCOUPLINGS (See Fig. 9.2)

Nominal Coupling Size* (in.)	OD, d_{oc} (in.)	Minimum Length, L_{min} (in.)	Wrench Flat Length,** L_{wf} (in.)	Distance Between Wrench Flats, l_{wf} , 0 to $\frac{1}{32}$ in. (in.)	Used With Minimum-OD Tubing Size (in.)
$\frac{5}{8}$	$1\frac{1}{2}$	4	$1\frac{1}{4}$	$1\frac{3}{8}$	$2\frac{1}{16}$
$\frac{3}{4}$	$1\frac{5}{8}$	4	$1\frac{1}{4}$	$1\frac{1}{2}$	$2\frac{3}{8}$
$\frac{7}{8}$	$1\frac{3}{4}$	4	$1\frac{1}{4}$	$1\frac{5}{8}$	$2\frac{7}{8}$
1	$2\frac{1}{8}$	4	$1\frac{1}{2}$	$1\frac{7}{8}$	$3\frac{1}{2}$
$1\frac{1}{8}$	$2\frac{3}{8}$	$4\frac{1}{2}$	$1\frac{5}{8}$	$2\frac{1}{8}$	$3\frac{1}{2}$

*Also size of rod with which coupling is to be used.

**Minimum length exclusive of fillets.

TABLE 9.3—SLIMHOLE COUPLINGS AND SUBCOUPLINGS (See Fig. 9.2)

Nominal Coupling Size* (in.)	OD, d_{oc} , ± 0.005 in. -0.010 in. (in.)	Minimum Length, L_{min} (in.)	Used With Minimum Tubing Size, OD (in.)
$\frac{1}{2}$	1	$2\frac{3}{4}$	1.660
$\frac{5}{8}$	$1\frac{1}{4}$	4	1.990
$\frac{3}{4}$	$1\frac{1}{2}$	4	$2\frac{1}{16}$
$\frac{7}{8}$	$1\frac{5}{8}$	4	$2\frac{3}{8}$
1	2	4	$2\frac{7}{8}$

*Also size of rod with which coupling is to be used.

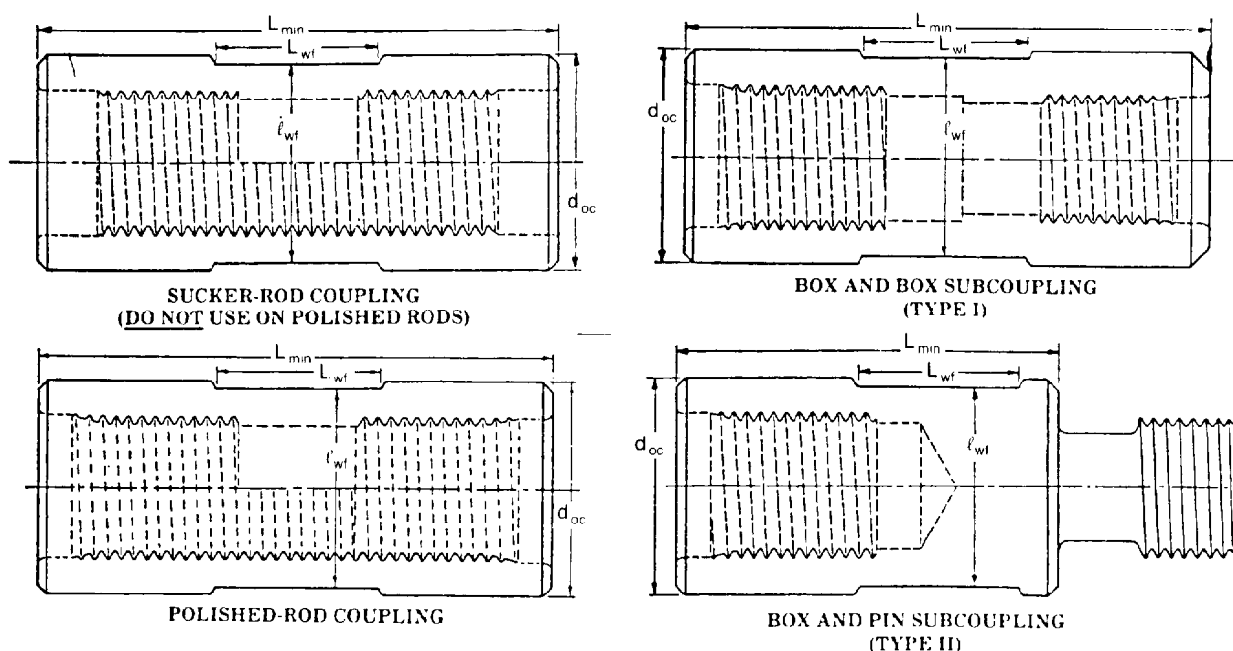


Fig. 9.3—Sucker rod couplings, polished rod couplings, and subcouplings (see Tables 9.2 and 9.3).

lations or a review of the tabulated answers in API Bull. 11L3³ will give a basis for final selection of pumping parameters. The analog computer study, which resulted in the API design calculations, did not denote any significant effects, such as increased loads, in pumping at so-called synchronous pumping speeds. The damping effects of the well system apparently nullify any theoretical loading increase.

The maximum practical pumping speed is limited by the fall of the sucker rods. It is advisable to maintain a minimum load of several hundred pounds so that the polished rod clamp does not separate from the carrier bar on the downstroke. Extraneous loads can work against free fall of the rod string. Crooked holes and viscous fluid both retard the fall of rods, thus making the minimum load less than anticipated. Fig. 9.4 can be used to approximate the maximum practical pumping speed for a given stroke length with a conventional pumping unit. The actual maximum pumping speed will depend on the well conditions and the geometry of the pumping unit. A pumping unit with a faster downstroke than upstroke will have a lower maximum permissible speed than a conventional unit.

TABLE 9.4—CHEMICAL AND MECHANICAL PROPERTIES

Grade	Chemical Composition	Tensile Strength, psi	
		Minimum	Maximum
K	AISI 46XX	85,000	115,000
C	AISI 1536*	90,000	115,000
D	Carbon or alloy**	115,000	140,000

*Generally manufactured from, but not restricted to, American Iron and Steel Inst. 1536.

**Any composition that can be effectively heat-treated to the minimum ultimate tensile strength.

The various rod string designs for given plunger diameters are listed in Table 9.7. Use of these percentages results in the stress in the top rod of each rod size being approximately equal.

Allowable Loading

The selection of a sucker rod's size and grade depends on the allowable stress and the well conditions. After the minimum and maximum stresses for the application are determined, the permissible stress is determined from the API modified Goodman diagram (see Fig. 9.5). For a given minimum stress, the maximum allowable stress can be determined from a graph of the API modified Goodman diagram for the particular rod in question or from the equivalent mathematical equation.

Example Problem 1. Assume that the minimum stress of an application is 15,000 psi [103 N/mm²]. Determine the maximum allowable stress for a Grade C rod that has a minimum tensile stress of 90,000 psi [620 N/mm²] and a service factor, F_s , of 1:

$$\begin{aligned}
 \sigma_a &= (0.25\sigma_T + 0.5625\sigma_{\min})F_s \\
 &= [0.25(90,000) + 0.5625(15,000)]1.0 \\
 &= 30,938 \text{ psi.}
 \end{aligned}$$

The application stress should be below 30,938 psi to be within the guidelines recommended by API. The diagram is not a failure diagram but is an operating diagram. The API Goodman diagram has been modified by a safety factor of 2 for the left side of the diagram and a safety factor of 1.75 for the higher portion of the diagram.

TABLE 9.5—TYPICAL SUCKER ROD CHEMISTRIES

Steel Type	C	Mn	P	S	Si	Ni	Cr	Mo	Other
API Grade K (Nickel/molybdenum)	4621	0.18 to 0.23	0.79 to 0.90	0.04	0.05	0.20 to 0.35	1.65 to 2.00	0.20 to 0.30	
API Grade C (Carbon steel)	1536	0.30 to 0.37	1.20 to 1.50	0.04	0.05	0.15 to 0.30			
API Grade D (Chrome/molybdenum)	4142	0.39 to 0.46	0.65 to 1.10	0.04	0.04	0.20 to 0.30	0.75 to 1.20	0.20 to 0.30	
API Grade D (Special alloy)	Special	0.17 to 0.22	0.80 to 1.00	0.035	0.04	0.15 to 0.30	0.90 to 1.20	0.80 to 1.05	0.20 to 0.30 0.02 to 0.03 V 0.40 to 0.60 Cu

*Maximum values.

Service Factor

The effects of corrosion and corrosion pits serve as stress raisers on the body of the rod. The effect can vary widely, and if well history does not indicate the service factor to be used, the following downward adjustments are recommended: reduce H_2S from 0.85 to 0.60, CO_2 from 0.90 to 0.70, and salt water from 0.90 to 0.80.

Some trial and error may be necessary for final selection. An effective corrosion-inhibition program should be implemented, if possible.

The limiting factor in rod string design is considered to be the rod body. The slim-hole coupling can be a limiting factor because of the reduced coupling cross-sectional area combined with the stress concentration factor of the thread. Slim-hole-coupling derating factors have been developed for use with the API modified Goodman diagram and are listed in Table 9.8. This F_d factor can be used in the same manner as the service factor—i.e., if Grade D $\frac{7}{8}$ -in. rods are used with $\frac{7}{8}$ -in. slim-hole couplings in $2\frac{3}{8}$ -in. tubing, multiply the allowable rod-body stress from the API modified Goodman diagram by the slim-hole coupling derating factor, F_d , of 0.690.

Rod Grades

The selection of which grade of rod to use should be made according to these guidelines. The lowest-cost rod is a Grade C rod, and its applicability should be checked first. The API Grade D rod (chrome moly) should be analyzed next. Other grades of rods contain various alloying elements. These alloying elements are not added in the quantity necessary to make a rod truly corrosion resistant, as the 18% chromium/8% nickel corrosion-resistant trim does on a valve. Experience has shown, however, that these relatively small alloy additions can have a positive

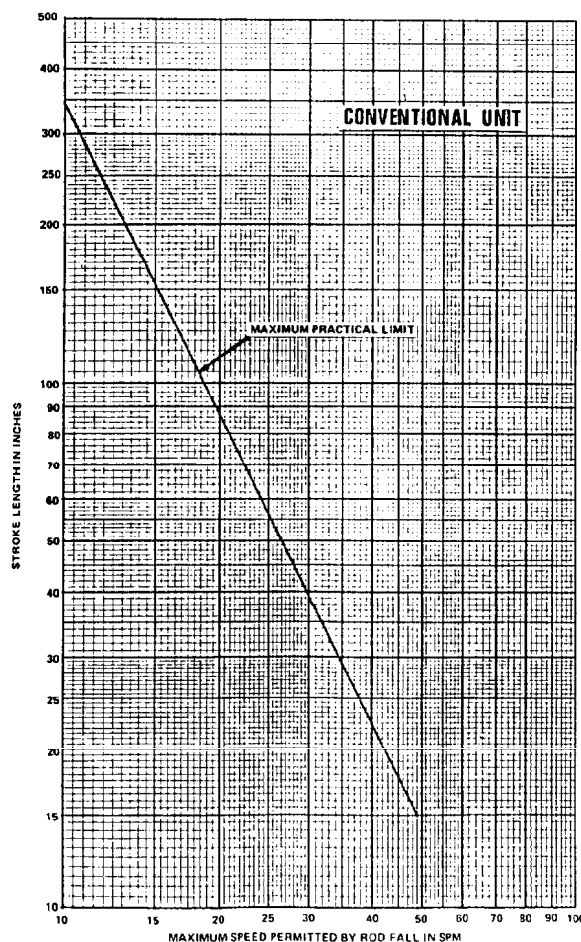


Fig. 9.4—Maximum practical pumping speed (conventional unit).

TABLE 9.6—TYPICAL SUCKER ROD MECHANICAL PROPERTIES

	Yield Strength (1,000 psi)	Tensile Strength (1,000 psi)	Elongation 8 in. (%)	Reduction of Area (%)	Brinell Hardness
API Grade K (nickel/molybdenum)	68 to 80	85 to 100	18 to 25	60 to 70	175 to 207
API Grade C (carbon steel)	60 to 75	90 to 105	18 to 25	55 to 66	187 to 217
API Grade D (chrome/molybdenum)	95 to 110	115 to 135	10 to 13	50 to 60	235 to 270
API Grade D (special alloy)	90,000	115,000	12 to 16	50 to 60	227 to 247

TABLE 9.7—ROD AND PUMP DATA

Rod*	Plunger Diameter, d_p (in.)	Rod Weight, W_r (lbm/ft)	Rod String, % of each size					
			1 1/8	1	7/8	3/4	5/8	1/2
44	All	0.726	—	—	—	—	—	100.0
54	1.06	0.892	—	—	—	—	40.5	59.5
54	1.25	0.914	—	—	—	—	45.9	54.1
54	1.50	0.948	—	—	—	—	54.5	45.5
54	1.75	0.990	—	—	—	—	64.6	35.4
54	2.00	1.037	—	—	—	—	76.2	23.8
55	All	1.135	—	—	—	—	100.0	—
64	1.06	1.116	—	—	—	28.1	33.1	38.8
64	1.25	1.168	—	—	—	31.8	37.5	30.7
64	1.50	1.250	—	—	—	37.7	44.5	17.8
64	1.75	1.347	—	—	—	44.7	52.7	2.6
65	1.06	1.291	—	—	—	31.3	68.7	—
65	1.25	1.306	—	—	—	34.4	65.6	—
65	1.50	1.330	—	—	—	39.2	60.8	—
65	1.75	1.359	—	—	—	45.0	55.0	—
65	2.00	1.392	—	—	—	51.6	48.4	—
65	2.25	1.429	—	—	—	59.0	41.0	—
65	2.50	1.471	—	—	—	67.4	32.6	—
65	2.75	1.517	—	—	—	76.6	23.4	—
66	All	1.634	—	—	—	100.0	—	—
75	1.06	1.511	—	—	22.6	26.1	51.3	—
75	1.25	1.548	—	—	24.8	28.6	46.6	—
75	1.50	1.606	—	—	28.3	32.6	39.1	—
75	1.75	1.674	—	—	32.4	37.4	30.2	—
75	2.00	1.754	—	—	37.2	42.8	20.0	—
75	2.25	1.843	—	—	42.5	49.2	8.3	—
76	1.06	1.787	—	—	25.9	74.1	—	—
76	1.25	1.798	—	—	27.8	72.2	—	—
76	1.50	1.816	—	—	30.9	69.1	—	—
76	1.75	1.836	—	—	34.3	65.7	—	—
76	2.00	1.861	—	—	38.5	61.5	—	—
76	2.25	1.888	—	—	43.1	56.9	—	—
76	2.50	1.919	—	—	48.3	51.7	—	—
76	2.75	1.953	—	—	54.1	45.9	—	—
76	3.75	2.121	—	—	82.5	17.5	—	—
77	All	2.224	—	—	100.0	—	—	—
85	1.06	1.709	—	15.9	17.7	20.1	46.3	—
85	1.25	1.780	—	17.9	19.9	22.5	39.7	—
85	1.50	1.893	—	21.0	23.4	26.5	29.1	—
85	1.75	2.027	—	24.8	27.5	31.0	16.7	—
85	2.00	2.181	—	29.0	32.3	36.3	2.4	—
86	1.06	2.008	—	19.3	21.9	58.8	—	—
86	1.25	2.035	—	20.7	23.5	55.8	—	—
86	1.50	2.079	—	23.0	26.0	51.0	—	—
86	1.75	2.130	—	25.6	29.0	45.4	—	—
86	2.00	2.190	—	28.7	32.5	38.8	—	—
86	2.25	2.257	—	32.1	36.5	31.4	—	—
86	2.50	2.334	—	35.8	41.6	22.6	—	—
86	2.75	2.415	—	40.3	45.6	14.1	—	—
87	1.06	2.375	—	22.3	77.7	—	—	—
87	1.25	2.384	—	23.5	76.5	—	—	—
87	1.50	2.397	—	25.5	74.5	—	—	—
87	1.75	2.414	—	27.9	72.1	—	—	—
87	2.00	2.432	—	30.6	69.4	—	—	—
87	2.25	2.453	—	33.7	66.3	—	—	—
87	2.50	2.477	—	37.2	62.8	—	—	—
87	2.75	2.503	—	41.0	59.0	—	—	—
87	3.75	2.632	—	60.0	40.0	—	—	—
87	4.75	2.800	—	84.7	15.3	—	—	—
88	All	2.904	—	100.0	—	—	—	—

*Rod number shown in the first column refers to the largest and smallest rod size in eighths of an inch. For example, Rod 76 is a two-way taper of 7/8 and 5/8 rods. Rod 85 is a four-way taper of 5/8, 7/8, 5/8, and 3/4 rods. Rod 109 is a two-way taper of 1 1/4 and 1 1/8 rods. Rod 77 is a straight string of 7/8 rods, etc.

TABLE 9.7—ROD AND PUMP DATA (continued)

Rod*	Plunger Diameter, d_p (in.)	Rod Weight, W_r (lbm/ft)	Rod String, % of each size					
			1 1/8	1	7/8	3/4	5/8	1/2
96	1.06	2.264	14.8	16.7	19.7	48.8	—	—
96	1.25	2.311	16.0	17.8	21.0	45.2	—	—
96	1.50	2.385	17.7	19.9	23.3	39.1	—	—
96	1.75	2.472	19.9	22.0	25.9	32.2	—	—
96	2.00	2.572	22.1	24.8	29.2	23.9	—	—
96	2.25	2.686	24.9	27.7	32.6	14.8	—	—
96	2.50	2.813	27.9	31.0	36.6	4.5	—	—
97	1.06	2.601	17.0	19.1	63.9	—	—	—
97	1.25	2.622	18.0	20.1	61.9	—	—	—
97	1.50	2.653	19.3	21.9	58.8	—	—	—
97	1.75	2.696	21.4	23.8	54.8	—	—	—
97	2.00	2.742	23.4	26.2	50.4	—	—	—
97	2.25	2.795	25.8	28.9	45.3	—	—	—
97	2.50	2.853	28.5	31.7	39.8	—	—	—
97	2.75	2.918	31.4	35.0	33.6	—	—	—
97	3.75	3.239	45.9	51.2	2.9	—	—	—
98	1.75	3.086	23.6	76.4	—	—	—	—
98	2.00	3.101	25.5	74.5	—	—	—	—
98	2.25	3.118	27.7	72.3	—	—	—	—
98	2.50	3.136	30.1	69.9	—	—	—	—
98	2.75	3.157	32.8	67.2	—	—	—	—
98	3.75	3.259	46.0	54.0	—	—	—	—
98	4.75	3.393	63.3	36.7	—	—	—	—
99	All	3.676	100.0	—	—	—	—	—
107	1.06	2.977	16.9	16.8	17.1	49.1	—	—
107	1.25	3.019	17.9	17.8	18.0	46.3	—	—
107	1.50	3.085	19.4	19.2	19.5	41.9	—	—
107	1.75	3.158	21.0	21.0	21.2	36.9	—	—
107	2.00	3.238	22.7	22.8	23.1	31.4	—	—
107	2.25	3.336	25.0	25.0	25.0	25.0	—	—
107	2.50	3.435	26.9	27.7	27.1	18.2	—	—
107	2.75	3.537	29.1	30.2	29.3	11.3	—	—
108	1.06	3.325	17.3	17.8	64.9	—	—	—
108	1.25	3.345	18.1	18.6	63.2	—	—	—
108	1.50	3.376	19.4	19.9	60.7	—	—	—
108	1.75	3.411	20.9	21.4	57.7	—	—	—
108	2.00	3.452	22.6	23.0	54.3	—	—	—
108	2.25	3.498	24.5	25.0	50.5	—	—	—
108	2.50	3.548	26.5	27.2	46.3	—	—	—
108	2.75	3.603	28.7	29.6	41.6	—	—	—
108	3.25	3.731	34.6	33.9	31.6	—	—	—
108	3.75	3.873	40.6	39.5	19.9	—	—	—
109	1.06	3.839	18.9	81.1	—	—	—	—
109	1.25	3.845	19.6	80.4	—	—	—	—
109	1.50	3.855	20.7	79.3	—	—	—	—
109	1.75	3.867	22.1	77.9	—	—	—	—
109	2.00	3.880	23.7	76.3	—	—	—	—
109	2.25	3.896	25.4	74.6	—	—	—	—
109	2.50	3.911	27.2	72.8	—	—	—	—
109	2.75	3.930	29.4	70.6	—	—	—	—
109	3.25	3.971	34.2	65.8	—	—	—	—
109	3.75	4.020	39.9	60.1	—	—	—	—
109	4.75	4.120	51.5	48.5	—	—	—	—

*Rod number shown in the first column refers to the largest and smallest rod size in eighths of an inch. For example, Rod 76 is a two-way taper of 7/8 and 5/8 rods. Rod 85 is a four-way taper of 3/4, 7/8, 5/8, and 1/2 rods. Rod 109 is a two-way taper of 1 1/4 and 1 1/8 rods. Rod 77 is a straight string of 7/8 rods, etc.

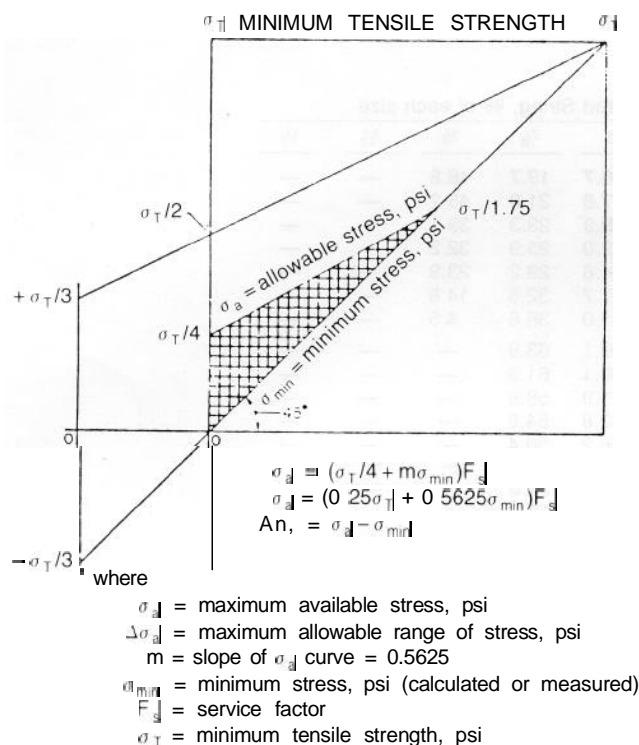


Fig. 9.5—OS-Modified Goodman diagram for allowable stress and range of stress for sucker rods in noncorrosive service.

effect on reducing the pitting of a rod. For many applications, it is the pitting of the rod that causes an increased stress concentration, which can then lead to failure.

The API Class K rod is one alloy rod specifically recognized by the API. The rod selection chart also lists special-alloy rods that meet the API Class D requirements. Because of the addition of the alloys, the initial cost of these rods is more than a Grade D chrome moly rod. This cost must be judged against possible increased life and reduced pulling costs and well expenses.

Miscellaneous and special-service rods are also available that are generally used in special situations.

Failures

The control and minimization of sucker rod failures is one of the key elements in controlling lifting costs. Proper classification of failures and the determination of the cause is the first step in corrective action. A formal failure reporting system can help provide the discipline necessary to identify the problems and causes of failures and to provide the impetus for equipment and/or operation review to remedy the situation.

TABLE 9.8—SLIM-HOLE-COUPLING
DERATING FACTOR, F_d

API Grade	Derating Factor, F_d		
	K	C	D
5/8	—	0.97	0.77
3/4	—	—	0.86
7/8	0.93	0.88	0.69
1	—	—	0.89

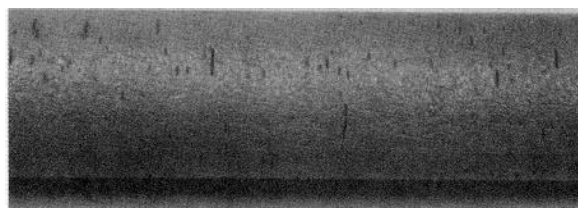


Fig. 9.6—H₂S rod part (note cracks caused by corrosion pits).

Steel sucker rod string failures can be segregated into four categories: body failures, upset failures, pin failures, and coupling failures. The most common failure is a body break. The most common cause of body breaks is corrosion caused by H₂S, CO₂, salt water, O₂, or a combination of these corrosive materials.

H₂S (sour corrosion) occurs in almost half of U.S. wells and has its own distinctive corrosion pattern. A black iron sulfide scale is deposited on the rod, and a rotten-egg odor is associated with H₂S. The corrosion pits formed are generally small and sharp and have the effect of a notch on the surface. This corrosion pit or notch creates a stress concentration effect on the surface of the rod. The stress concentration effect, along with the effect of the hydrogen in the metal, can cause rapid failure of a rod. The failure looks as though the rod were brittle. In many cases, the actual corrosion pit that initiated the failure can be seen only with the aid of magnification. Close examination of the rod may also locate adjacent corrosion pits that are the focal point for additional fatigue cracks. Fig. 9.6 illustrates this condition.

CO₂ corrosion (sweet corrosion) is caused by carbonic acid, which is formed when CO₂ combines with water. Carbonic acid combines with the iron to form iron carbonate, which is a hard, dark scale. The corrosion forms pits that appear rather smooth in nature and are usually larger than the H₂S-type pits. In addition, the pits can be connected, and the metal loss is usually much larger before breakage than the metal loss of the H₂S breaks. The stress concentration effect of CO₂ corrosion pits is generally not as severe as the H₂S pits. CO₂ corrosion is illustrated in Fig. 9.7.

The vast majority of wells contain salt water to some degree. Water is necessary for both H₂S and CO₂ corrosion. However, salt water by itself is also corrosive and causes a generalized pitting attack, but it is not as severe as other types of corrosion.

Oxygen sometimes enters the pumping system through the tubing casing annulus. In the presence of water, the corrosion, while general in nature, can occur in a comparatively short time.

An effective corrosion inhibition program abates these corrosive attacks. Such a program is required for the entire production system, including the rods. The rods are



Fig. 9.7-CO₂ corrosion

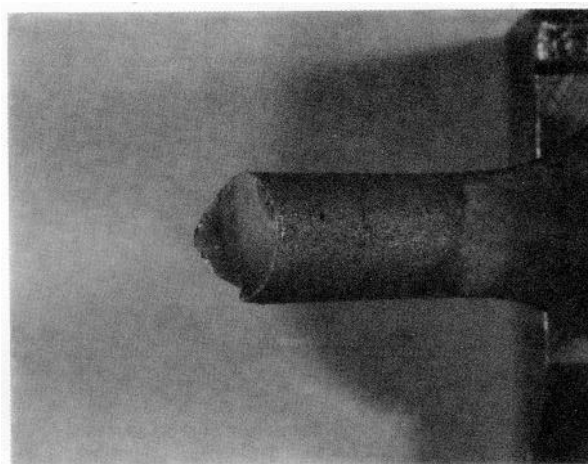


Fig. 9.8-Rod failure (cause of failure is in dark area 180° from ductile projection).

probably the most sensitive to pits because they operate in fatigue and therefore are susceptible to the effects of stress concentration.

One of the problems encountered in maintaining this effective inhibition film is wear. When the rods rub the tubing, the protective film can be destroyed. The inhibitor acts to reduce the frictional force and has deterred problems encountered with light wear. Wear on rods can be identified by a flat spot on one side of the rod.

When a rod fails, the last area to part generally fails in a ductile mode and leaves a small tip on one face. The cause for the failure usually can be found 180° opposite this tip. This condition is found in Fig. 9.8. Corrosion pits can be difficult to identify, but handling marks or marks caused by hatchets when the bundle is broken can be more easily identified.

Many body breaks occur within 2 ft or so of the upset. This can be attributed to a bend of the body in relation to the upset, which imposes a bending moment on the rod. All rods have straightness tolerances, and the maximum of the tolerance, as specified by API, will produce an added stress of about 20%. For example, if the axial stress (determined by dividing the load by the area) is 20,000 psi and the rod end has the maximum bend allowed by API, the true stress will be the summation of the axial stress and the 20% extra stress caused by the bend, or 24,000 psi.

The API modified Goodman diagram has a safety factor of about 2. The bending moment infringes on this safety factor. Because of the greater cross-sectional area of the upset, failures in this part of the rod are rare.

Sucker rod pin failures can be caused by overtightening the joint. This type of failure can be identified by the reduction in area of the undercut portion of the pin. In addition, the shoulder of the pin will generally have an indentation caused by the force exerted by the coupling face.

The load on a sucker rod pin consists of two components: the load that results from tightening the joint, or preload, and the external load resulting from the pumping cycle. As long as the face of the coupling and the face

of the pin remain in contact during the pumping cycle, the pin will see only a part of the upstroke load and a part of the downstroke load. The amount of each upstroke and downstroke load is determined by the metal cross-sectional area relationship of the pin and coupling. Because the pin experiences a varying load, it also is subject to fatigue. This fatigue failure will occur at the root of the first thread adjacent to the relief. If the joint loosens and the pin and the coupling faces separate, the failure will occur in the same place in the first engaged thread. It is extremely important that the joint be clean and the faces free from nicks so that the joint will have the best chance of retaining the preload.

API recommends the use of circumferential displacement values rather than torque to achieve the desired pin preload stress. When power tongs are used, they should be calibrated for initial use and checked each 1,000 ft.

The method of marking the joint for circumferential displacement is indicated in Fig. 9.9. The circumferential displacement values are listed in Table 9.9.

Thread galling is another joint problem that sometimes occurs. Galling is generally caused by cross threading or making up threads that were not cleaned properly.

Coupling failures typically break at the plane of the last engaged thread of the pin. This is the plane where the load is transferred totally to the coupling. If failures occur at any other location, an examination should be made to determine the origin of the failure. A likely cause is cracks created by hammer marks.

As the clearance between the coupling and tubing is minimal, the coupling can be subjected to wear. The metal spray coupling has a hard, corrosion-resistant coating with a very low friction coefficient. This coupling is popular in wells where failure as a result of corrosion or coupling wear is a problem. This coupling should not be used indiscriminately, however, because it may, in some circumstances, transfer the wear to the tubing. As with all couplings, hammer blows should not be used to loosen couplings. The metal spray coupling is especially susceptible to the formation of cracks from hammer blows because of the hard, brittle coating.

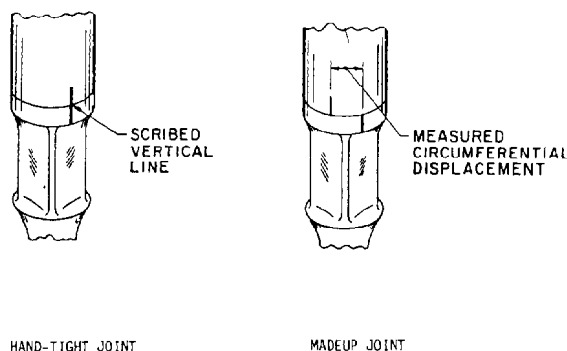


Fig. 9.9—Marking for circumferential displacement.

Care and Handling

Sucker rods are handled in the factory with equipment and facilities specially designed for protecting sucker rods from damage. The rods are shipped from the factory in packages also designed to protect the rod from damage. Care must be exercised in handling and storing the rods in the field so that the rods are run in the well in the same condition as they left the factory.

A successful sucker rod operation includes attention to detail while the rods are out of the well and a sound in-the-well program. It is particularly important to protect the surface of the rod from any handling damage, such as nicks or gouges. These discontinuities concentrate the stress in the same manner as a corrosion pit. Rods should always be properly supported so that no bends or kinks are induced. All rods with nicks, gouges, bends, or kinks should be discarded. Rods are shipped with end caps that protect not only the threads but also the pin shoulder. If any rods are without end caps, inspect the pin end, and if it is undamaged, clean and grease the end and replace the cap. Do not remove end caps until the rods are ready to be run. If it is necessary to walk across rods, provide a wooden walkway to protect the rod surface.

Unloading and Loading

Rod packages should always be lifted and laid down with handling equipment that supports the package without damaging the rods. When packages are stacked, the bottom supports should be placed directly on the top supports of the next lower package. Tie-down chains, straps,

or cables should be placed over the crosswise supports and should not be in contact with the rods.

Individual rods should be picked up and supported near each end. Locate the pickup points to minimize sag in the rod. Do not drag the rod across surfaces. Rods should never be flipped from one position to the next.

When unpackaged rods are transported, the rods should be supported with wooden or nonabrasive material so that the rod body and ends do not rest on the bed. A minimum of at least four supports is required. The rod layers should be separated by spacers positioned directly above the bottom supports. The spacers should be long enough to extend beyond the stack on each side. If the spacers are not notched, the spacers should be chocked on each side to prevent the rods from rolling off. The tie-down chains, cables, or straps should be placed over the crosswise supports and should not be in contact with the rods.

Rod Storage

Rods should be stored off the ground to minimize corrosion and grouped separately by grade and size to minimize misidentification. Inspect the rods at scheduled intervals. Replace any missing end caps and brush rusty surfaces with a wire brush until they are clean. Recoat the affected area with a suitable protective coating. Rod coatings are generally oil-soluble and contain an inhibitor. Rod manufacturers can identify a proper, compatible coating.

Good storage practices will protect the surface of the rod. The same general common-sense rules for unloading and loading also apply for storage.

Running and Pulling

At the wellsite, rods should be placed off the ground on supports. Single rods should be tailed into the mast with care, so that no contact is made with the ground or other equipment. The rods should not be raised with elevator latches during tailing. When the pin is stabbed into the coupling, the rod should be positioned directly over the well and hung straight without slack to minimize the possibility of cross threading. The couplings and pin should be brushed with a mixture of oil-soluble, film-forming corrosion inhibitor and refined oil for lubrication and corrosion protection. Use power tongs, calibrated to circumferential makeup values, for the most consistent makeup results.

The joint should never be hammered when the well is pulled or when connections are broken out. Use cheater bars, if necessary, to loosen the joint. Any overtorqued connection should be checked and thrown away if damaged. Rods should be inspected for damage—e.g., kinks, bends, and nicks—and discarded if any are found. The faces of the pins and couplings should be smooth and free of irregularities, such as scratches or nicks, that prevent proper makeup.

Fiberglass Sucker Rods

The first fiberglass rods were introduced in the 1970's. A fiberglass rod consists of long parallel strands of fiberglass embedded in a plastic matrix. Steel end fittings are then placed on the ends of the rods and held in place by wedges formed by an adhesive. The steel end fittings terminate in a standard API sucker rod pin. The rods can

TABLE 9.9—SUCKER ROD JOINT CIRCUMFERENTIAL DISPLACEMENT VALUES

Rod Size (in.)	Running New Grade D Displacement Values (in.)		Rerunning Grades C, D, and K Displacement Values (in.)	
	Minimum	Maximum	Minimum	Maximum
1/2	6/32	8/32	4/32	6/32
5/8	8/32	9/32	6/32	8/32
3/4	9/32	11/32	7/32	17/64
7/8	11/32	12/32	9/32	23/64
1	14/32	16/32	12/32	14/32
1 1/8	18/32	21/32	16/32	19/32

TABLE 9.10—GENERAL DIMENSIONS AND TOLERANCES FOR REINFORCED PLASTIC SUCKER RODS AND PONY RODS
(see Fig. 9.10)

Rod Body Nominal Size, ± 0.015 in. (in.)	Rod Pin Size (in.)	Pin Nominal Diameter (in.)	Pin Shoulder OD, d_{ps} , +0.005 in. -0.010 in. (in.)	Wrench Square Width, w_{ws} (in.)	Wrench Square Length,* L_{ws} (in.)	End Fitting Maximum Diameter, d_{ef} (in.)	End Fitting Maximum Length, L_{max} (in.)	Extension Maximum Diameter,** d_e (in.)	Pin-and-Pin Sucker Rod Length, [†] ± 0.5 in. (ft)	Pin-and-Pin Pony Rod Length, [†] ± 0.5 in. (ft)
0.625	1/2	3/4	1.000	7/8	1 1/4		Not to exceed 10 in.		25, 30, 37.5	3, 6, 9, 18
0.750	5/8	1 1/16	1.250	1	1 1/4	Not to exceed d_{ps}	exclusive of extension (if used)		25, 30, 37.5	3, 6, 9, 18
0.875	3/4	1 1/16	1.500	1 1/8	1 1/4				25, 30, 37.5	3, 6, 9, 18
1.000	7/8	1 3/16	1.625	1 5/16	1 1/4				25, 30, 37.5	3, 6, 9, 18
1.250	1	1 3/8	2.000	1 1/2	1 5/8				25, 30, 37.5	3, 6, 9, 18

*Minimum length exclusive of fillet.

**The extension is that portion of the rod body or that portion of the end fitting that is immediately adjacent to the smaller end of the elevator taper. If this section of the end fitting is longer than 0.25 in., the maximum OD shall not be more than 0.200 in. larger than the diameter of the rod body. If this section of the end fitting is 0.25 in. or less in length, the OD shall not be more than 0.25 in. larger than the diameter of the rod body.

[†]The length of pin-and-pin rods shall be measured from contact face of pin shoulder to contact face on the field end of the coupling.

be joined together with standard couplings to form rod strings. The fiberglass rods are lighter in weight than steel rods, about 0.84 lbm/ft for a 1-in. fiberglass rod compared to 2.9 lbm/ft for a 1-in. steel rod, and have a lower modulus of elasticity, about 7.0×10^6 compared to 29.5×10^6 for steel.

A typical fiberglass-reinforced plastic rod string contains about 50 to 70% fiberglass rods at the top of the rod string and 50 to 30% steel rods at the bottom. Sometimes heavy sinker bars replace the steel rods. The steel mass on the bottom of the string helps the fiberglass rods achieve overtravel and keeps the fiberglass rods in tension. Fiberglass rods are generally used in wells with relatively high fluid levels so that excessive rod stretch (also the result of high elasticity) does not destroy the efficiency of the installation.

Physical Dimensions

API has published a specification for reinforced plastic sucker rods.⁴ This document covers materials, performance, quality control, general dimensions, packaging, inspection, and recommended practice for care and handling of rods.

The general dimensions for a plastic rod published by API⁴ are listed in Table 9.10 and Fig. 9.10.

Plastic Sucker Rod Chemical and Mechanical Properties

Unlike steel, which has an infinite fatigue life when applied at stresses in a noncorrosive environment below the endurance limit, fiberglass has a finite life. If a given maximum and minimum load is cyclically applied to a plastic rod, the rod will eventually fail in fatigue. If a higher load combination is applied, the rod will fail in fewer cycles. In addition, the plastic rod is subject to loss of strength caused by increasing temperature. A stress-range diagram for plastic rods should always state the number of cycles to first expected failure and the corresponding temperature. API specifies that a basic stress-range diagram be constructed for 7.5 million cycles (1.8 years at 8 cycles/min) and 160°F. Modifiers for 5, 10, 15, and 30 million cycles to first expected failure and modifiers for other temperatures should be listed.

The end fittings for the rods are designated Grades A and B. The classifications are similar to designations for steel rods. Table 9.11 lists the end-fitting chemical and mechanical properties.

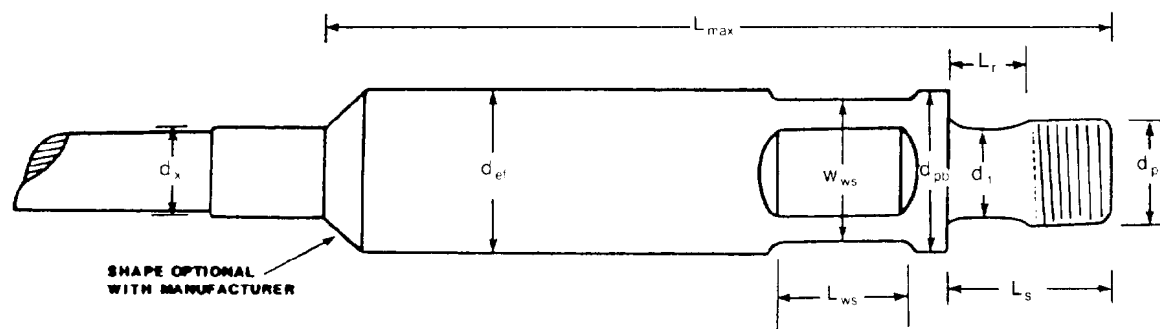


Fig. 9.10—General dimensions for reinforced plastic sucker rods (see Table 9.10).

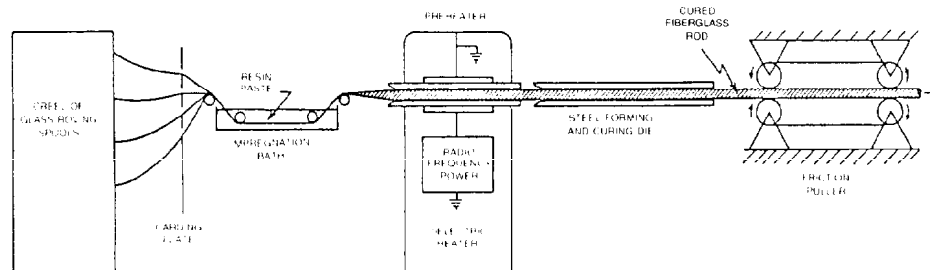


Fig. 9.11—Schematic of pultrusion process.

Manufacture of Fiberglass Sucker Rods

Fiberglass sucker rods are manufactured in three separate steps. The fiberglass rod body is produced by the pultrusion process. The metal end fittings are then assembled on the rod and locked in place with an adhesive.

The fiberglass rod body consists of high-strength fibrous glass reinforcement held in place by a resin system. A single strand of fiberglass may contain thousands of individual glass filaments. A fiberglass rod body is produced with many single-strand or multistrand glass rovings. Consequently, when a load is applied to the rod body, the load is distributed over many thousands of individual glass filaments.

The resin system protects the glass fibers and generally is the component that determines the chemical resistance and temperature performance. The resins used in fiberglass rods are thermoset resins that react during processing to form a cured material that cannot be remelted or reprocessed. Thermoset resins used in fiberglass rods, such as vinyl ester, isothalic, or epoxy, have different physical and chemical properties. This is similar to the different grades of steel, which have different physical properties and chemical resistance. The resin system also contains additives and fillers for either enhancement of properties or aids in processing.

The fiberglass rod body is manufactured by a process called pultruding. The schematic of the pultrusion process, Fig. 9.11, illustrates the manufacturing operations. Fiberglass roving spools are held on a creel and fed through a carding plate. The glass is then impregnated with the resin system paste and then preheated by a radio-frequency preheater. The final forming of the shape and curing of the rod occurs in the metal die. The power for

the system is provided by the friction pullers. The rod is cut to length by a flying saw after it leaves the friction pullers.

The metal end connectors are machined with an API pin thread on one end and an internal bore with a series of wedges on the other end. Mold release is sprayed into the ID of the steel end connector. Adhesive is then placed in the box and the rod is inserted into the cavity. The adhesive fills the machined wedges. After the adhesive has cured, the rod is then pulled on each end. Because of the mold release that was applied to the steel, the adhesive breaks loose from the steel and adheres to the fiberglass rod; thus the internal wedges are set. Fig. 9.12 shows the geometry of this unique connection.

Application

There can be several advantages to the use of fiberglass sucker rods. Because these rods cost more than steel rods, their use has to be justified. The most common and generally sought-after advantage is to increase production. The lower modulus of elasticity, about one-fourth that of steel, allows greater overtravel of the plastic rods compared to steel rods. If the fiberglass/steel rod string is operated as close to the natural frequency of the system as possible, subsurface pump stroke lengths can be achieved that are significantly longer than the surface stroke.⁵ Because the reduced modulus of elasticity is responsible for increased overtravel, it also is responsible for increased rod stretch caused by the fluid load of the pump. To decrease the effects of rod stretch, applications with fluid levels above the pump, with smaller-bore pumps, and well depths in excess of 3,000 ft are more favorable toward greater net downhole-pump-stroke length.

TABLE 9.11—END FITTING GRADES

Grade	Chemical Composition	Tensile Strength (1,000 psi)	
		Minimum	Maximum
A	*	90	115
B	**	115	140

* The material shall be such as to resist sulfide-stress corrosion cracking per NACE MR-01-75. See Ref. 6.

** Any composition that can be heat treated to give the specified tensile strength.

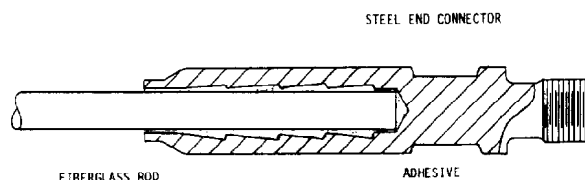


Fig. 9.12—Typical fiberglass-reinforced plastic rod-body-to-steel connector-joint design.

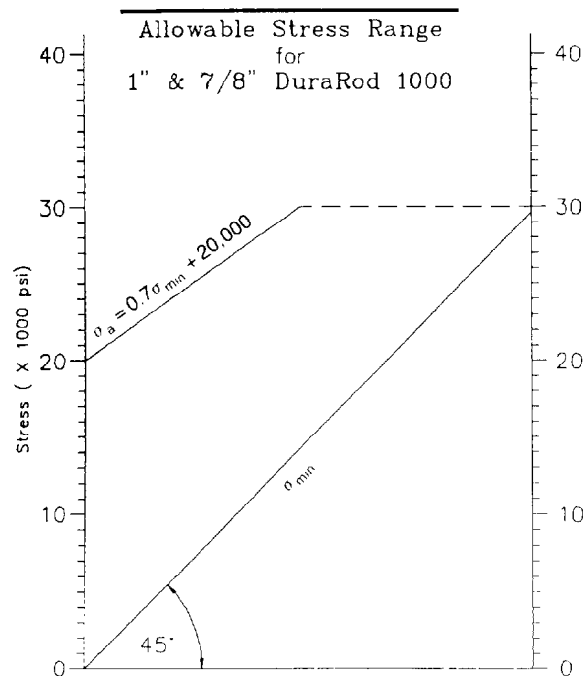


Fig. 9.13—Typical fiberglass stress-range diagram.

The lighter weight of fiberglass, about 30% that of steel, can also translate into cost savings. The total effect of the dynamics is reduced, which in turn requires less horsepower and lower power costs. In addition, the lighter weight of the total rod string means reduced pumping unit requirements, which allow smaller pumping units to be used.

Another advantage is the inherent corrosion resistance of the fiberglass. Corrosion inhibition should be used to protect the well system, casing, tubing, flowlines, and sucker rods. In many cases, however, inhibition of the rod string is ineffective. This can be a result of the physical breakdown of the film on the rod caused by rubbing against the tubing. In some instances, maintaining a film is not cost-effective. The corrosion resistance of the fiberglass rod can reduce pulling costs and well downtime. The end connectors are made from steel, and corrosion can occur on these fittings. The stresses in the connectors are relatively low, and corrosion generally has not been a factor in their performance.

Predictive well-performance calculations are made with a computer program using the wave equation discussed in the section on steel rod application. The selection of rod size is a function of stress on the rod. In practice, the most popular rod diameters by far are 1 and 1 1/4 in.

After the maximum and minimum stresses are determined, the allowable stresses are specified from a stress-range diagram. As an example, Fig. 9.13 is a stress-range diagram for 7.5 million cycles and 110°F for 7/8- and 1-in. rods. Fig. 9.14 illustrates the general relationship between stress, stress range, and expected life. A small lowering of the maximum stress can result in a significant increase in rod life. Each manufacturer publishes data and modifiers for cycles, temperature, and rod size.

Some operating and well conditions should be avoided with plastic rods. High temperatures cause a loss of

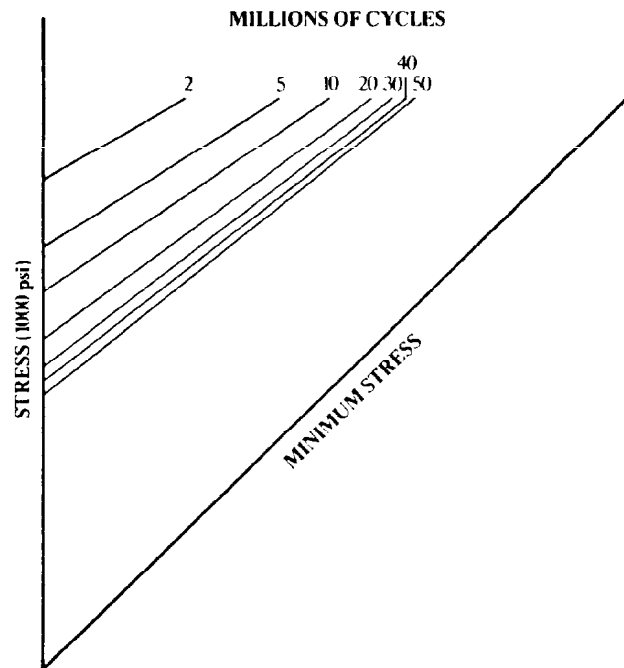


Fig. 9.14—Expected life of fiberglass rods.

strength. While bottomhole temperatures of slightly more than 200°F have been pumped with fiberglass rods, the limiting factor is the temperature that the lowest fiberglass end connector reaches. In these hot wells, more steel rods are used on the bottom of the string to reduce the operating temperature of the fiberglass rod connections. Hot oiling of wells should be done down the tubing/casing annulus.

Compression loading and wear of the rods must be avoided. These conditions can result in early failure. To prevent overstressing the fiberglass rod string when an attempt is made to pull a stuck pump, shear pin tools are usually run above the subsurface pumps.

Failures

Because fiberglass sucker rods do not have a finite endurance limit, the rods can be expected to fail eventually. The actual life of the rod can be many years and depends on the maximum and minimum stresses. The point of expected eventual failure is a breakdown of the end-connector joint, which results in the metal end connector separating from the rod. This type of failure can be fished with an overshot.

Body breaks do sometimes occur and are generally the result of mishandling, which causes nicks or damage to the surface. Occasionally, body breaks are caused by misalignment of the fiberglass rovings. Body breaks can be fished with special overshots.

Care, Handling, and Storage

The surface of the fiberglass rod is much more easily damaged than a steel rod. Therefore, it is even more important to keep the rod from contacting the ground or any object that could scratch or injure the surface.

The rods need to be protected from ultraviolet light if they are going to be exposed to the sun longer than a few months. This can be achieved by covering the rods with a dark plastic blanket.

Nomenclature

- d_b = diameter of sucker rod bead, in.
- d_{ef} = maximum diameter of end fitting, in.
- d_{oc} = outside diameter of coupling, in.
- d_p = plunger diameter, in.
- d_{pb} = outside diameter of sucker rod pin shoulder and box, in.
- d_x = maximum diameter of extension, in.
- F_d = derating factor, dimensionless
- F_s = service factor, dimensionless
- l_{wf} = distance between coupling wrench flats, in.
- L_{max} = maximum length of end fitting, ft
- L_{min} = minimum length of coupling, in.
- L_{rb} = total length of sucker rod box, in.
- L_{wf} = length of coupling wrench flat, in.
- L_{ws} = length of sucker rod wrench square, in.
- m = slope of curve
- r_a = outer radius of sucker rod bead, in.
- r_c = inner radius of sucker rod bead, in.

- w_{ws} = width of sucker rod wrench square, in.
- W_r = sucker rod weight, lbm/ft
- σ_a = maximum allowable stress, psi
- $\Delta\sigma_a$ = maximum allowable range of stress, psi
- σ_{min} = minimum stress, psi
- σ_T = minimum tensile strength, psi

References

1. *API Specification for Sucker Rods*, 21st edition, API Spec. 11B, Dallas (May 1985).
2. *API Recommended Practice for Design Calculations for Sucker Rod Pumping Systems*, third edition, API RP 11L, Dallas (Feb. 1977).
3. *API Sucker Rod Pumping System Design Book*, first edition, Bull., API 11 L3, Dallas (May 1970).
4. *API Specification for Reinforced Plastic Sucker Rods*, first edition, API Spec. 11C, Dallas (Jan. 1, 1986).
5. Tripp, H.A.: "Mechanical Performance of Fiberglass Sucker Rod Strings," paper SPE 14346 presented at the 1985 SPE Annual Technical Conference and Exhibition, Las Vegas, Sept. 23-26.
6. "Sulfide Stress Cracking Resistant Metallic Material for Oil Field Equipment," NACE MR-01-75, Natl. Assn. of Corrosion Engineers, Houston (1984).

General Reference

- API Recommended Practice for Care and Handling of Sucker Rods*, seventh edition, API RP 11BR, Dallas (May 30, 1986).

Chapter 10

Pumping Units and Prime Movers for Pumping Units: Part 1—Pumping Units

Fred D. Griffin, Lufkin Industries Inc.*

Introduction

When oil wells cease flowing, some means of artificial lift is required to produce the well. About 85% of all the artificial production of oil is accomplished by the use of sucker rods lifting the fluid. A relatively simple, reciprocating, plunger-type pump is attached to the lower end of the sucker rod string. Oil is lifted by means of a plunger and a traveling valve being moved up and down inside a polished cylinder with a valve at the bottom. The cylinder is called a "working barrel." The plunger is attached to the string of sucker rods that extends to the surface. The upper end of the rod string is attached to a polished rod, which is moved up and down by a pumping unit. Pumping units are discussed here and prime movers for pumping units in Part 2 of this chapter.

Pumping Units

A pumping unit is a mechanism which imparts reciprocating motion to a polished rod, which in turn is attached to the sucker rod string below the wellhead stuffing box. Several types of pumping units are available today. The component parts of most of the units are basically the same but the arrangement of the parts differs. Selection of the proper size and type of pumping unit for a particular application is important. Like most other machinery, pumping units must be properly installed, lubricated, and maintained. Built into the majority of pumping units is some method of counterbalance, which in most cases consists of adjustable weights on the rotating cranks or air pressure pushing up on the walking beam. The counterbalance system, whichever type is used, opposes the weight of the sucker rod string and a portion of the fluid to be lifted. The actual well load on a pumping unit should be measured and analyzed often to ensure that the counterbalance is correct and that the load and torque capacity of the unit has not been exceeded.

Types

Pumping units generally are typed according to the method of counterbalance. This is true for beam balanced units, air balanced units, conventional crank balanced units, and special geometry (or Mark II) crank balanced units.

In addition to the method of counterbalancing, the geometric arrangements of the principal components are distinguishing features. The beam balanced, the conventional crank balanced, and some special geometry units are classified as Class I lever systems because the samson post bearing (pivot point for the walking beam) is located between the well load and the actuating force of the pitman side members.

The air balanced and the Mark II crank counterbalanced units are classified as class III lever systems because the walking beam hinge point is located at the rear of the unit and the actuating force of the pitman side members is located between this pivot point and the well.

The type of pumping unit best suited for a particular pumping problem very often is a matter of personal preference. The conventional crank balanced pumping unit is the choice of many operators mainly because it has been readily accepted by field personnel for many years. Many other operators' choice is the Mark II special geometry unit with its capability of a more uniform torque pattern on the gear reducer. Usually these special geometry units will require one size smaller gear box size than other type units for a particular application. The American Petroleum Inst. (API) lists standard gear box sizes in their specification API Spec 11E.¹ Other operators specify the air balanced pumping unit, which is readily adaptable to platform or pier installations and other unstable substructures. This is because the inertia and shaking forces of air balanced units are very low. Air-balance units also are compact and light in weight compared with other types of pumping units of the same structural and gear box rat-

*Authors of the chapter on this topic in the 1962 edition were this author and L. A. Little, F. Ben Elliott Jr., J. Taylor Hood, and John H. Day Jr.

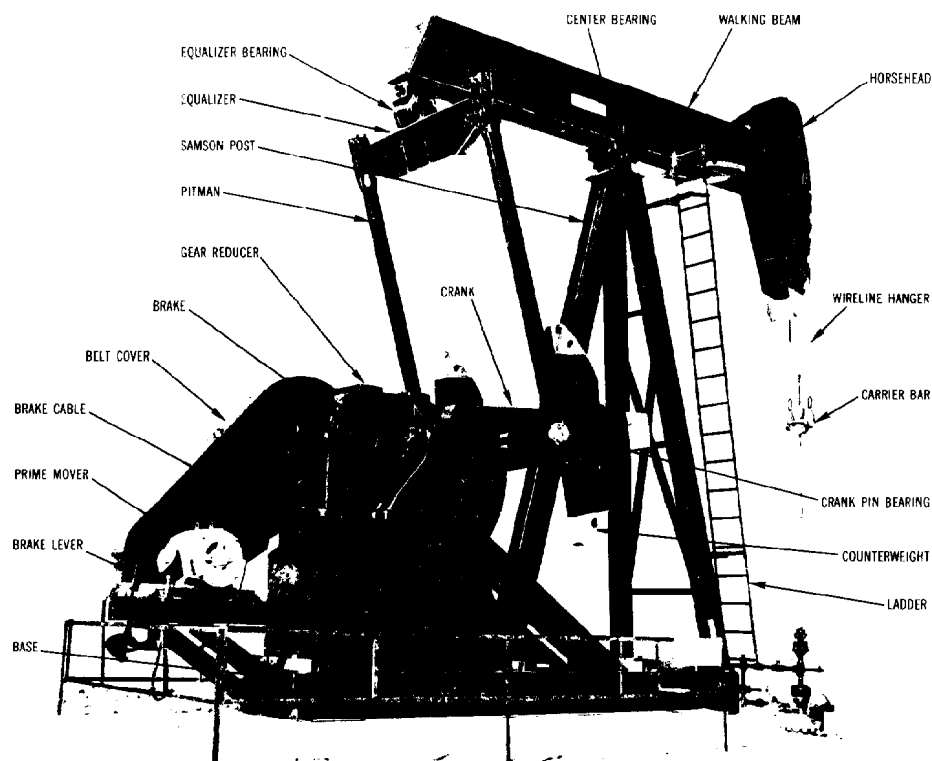


Fig. 10.1—Conventional pumping unit.

ing. The beam balanced pumping unit is manufactured only in the smaller sizes and economics is the prime factor for selecting this unit type.

Pumping Unit Geometry

Pumping units are manufactured in various geometric configurations in addition to methods of counterbalance. As mentioned before, beam balanced and conventional crank balanced units are Class I lever systems, and air balanced and Mark II units are Class III lever systems. Within these two lever systems are variations effected by moving the gear reducer on the structural base with respect to the equalizer or cross yoke.

In the case of the Mark II, the cross yoke is not located directly above the slow speed shaft of the gear reducer but shifted forward toward the horsehead. This shifting, accompanied by a specified direction of rotation of the cranks, results in a longer time interval for the upstroke and a shorter time interval for the downstroke.

Conventional Crank Balanced Units

The conventional crank balanced pumping unit is the type most commonly used today, especially in the short and medium stroke lengths. It adequately serves a wide variety of field applications. Fig. 10.1 shows a conventional crank balanced unit with the various parts labeled. The rotation of the cranks connected to the pitman side members causes the walking beam to pivot about the center bearing, thereby causing the polished rod to move up and down through its connection to the wireline and horsehead. The adjustable counterweights located on the cranks are heavy metal castings. Fig. 10.2 illustrates the mechanics of the

counterbalance system. Adjustment of the counterweights and their effect at the polished rod are discussed later in this section.

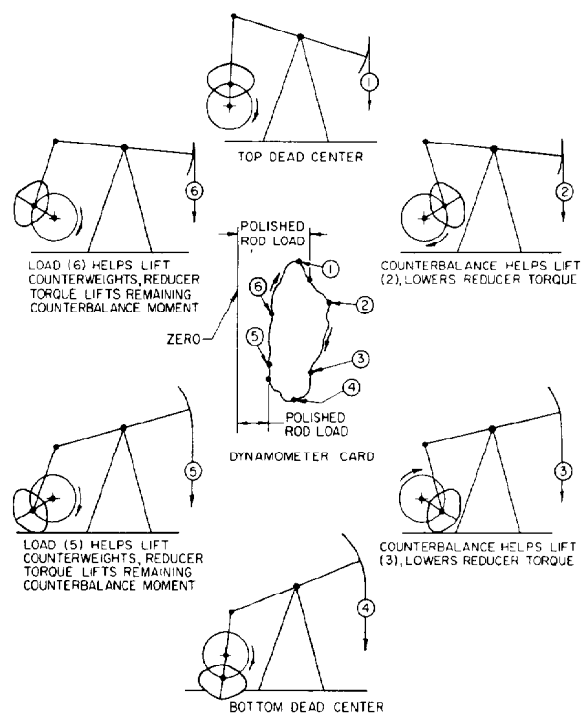


Fig. 10.2—Crank-counterbalanced diagram.

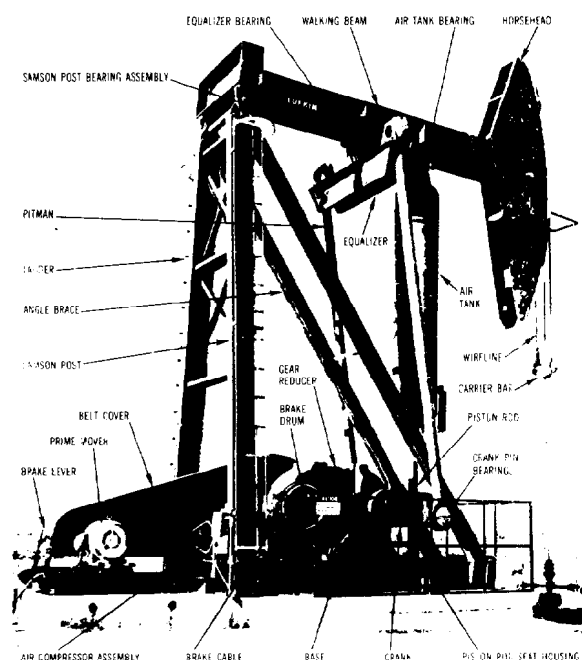


Fig. 10.3—Air-balanced pumping unit.

Air Balanced Units

The air balanced pumping unit is basically the same as the crank balanced unit in that the rotation of the cranks causes the walking beam to pivot and move the polished rod up and down. Fig. 10.3 shows a typical field installation of an air-balanced unit with the various parts labeled. The unit is compact and relatively light. The long cylindrical tank at the front of the unit houses a piston and air cylinder. Force exerted by compressing air in the cylinder is used to partially counterbalance the well load. A special sealing device is used to prevent air leaks between the piston and cylinder. One of the features of the sealing device is a pool of oil on top of the piston acting as an air seal. Fig. 10.4 shows how the counterbalance force works to partially offset the well load. An auxiliary air compressor is used to maintain the system air pressure at an optimal working level. The operation of the compressor normally is controlled automatically by a pressure switch to maintain air pressure within a manually preset range.

Beam Balanced Units

Fig. 10.5 shows a beam counterbalanced unit. This unit is very similar to the crank balanced unit except that the counterweights are mounted on an extension of the walking beam. In general, use of this type of unit has been limited to the smaller sizes. The primary reason for this is that the pumping speed is limited. High pumping speeds can result in shaking forces, which can wreck the unit unless the pumping speed is reduced.

Mark II Units

Fig. 10.6 shows the Mark II unit with the various parts labeled. This type unit has two unique features.

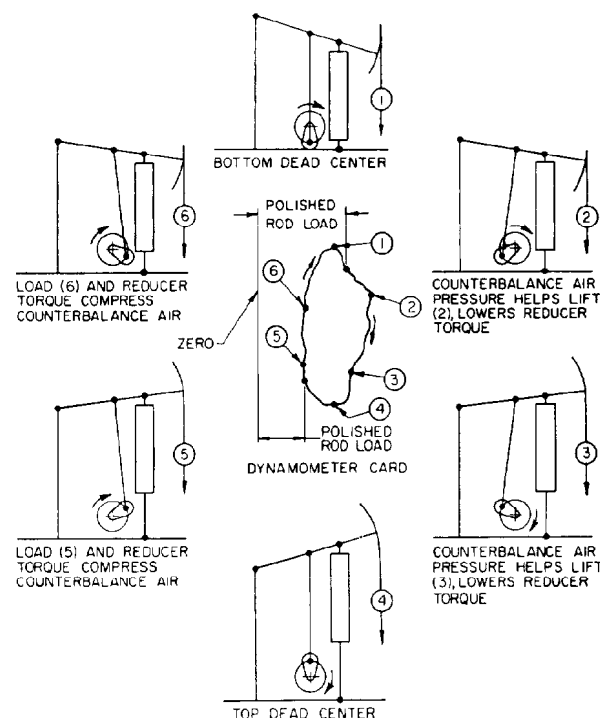


Fig. 10.4—Air-counterbalance diagram.

1. The cross yoke bearing which is actuated by the pitman side members is moved forward and is located very close to the horsehead rather than directly above the gear reducer crankshaft.

2. The cranks have a dogleg (angular offset) in them to produce an out-of-phase condition between the torque on the gear reducer exerted by the well load and the torque exerted by the counterbalance weights.

With these two unique features and with the cranks allowed to rotate in one direction only, a more uniform torque is applied to the crankshaft. The torque peaks, normally more prominent in conventional crank balanced units, are reduced in magnitude.



Fig. 10.5—Beam-balanced pumping unit.

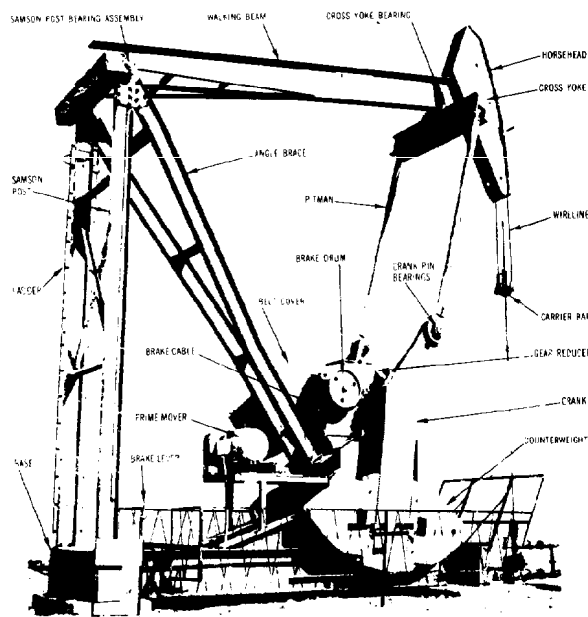


Fig. 10.6—Mark II pumping unit.

In most cases, this reduction in the torque peaks is sufficient to permit the use of one API size smaller gear reducer than would be used otherwise for a comparable conventional crank balanced unit. Fig. 10.7 illustrates how the torque on the gear reducer follows a more uniform pattern under ideal field conditions.

Crank Balanced Units (With Special Geometry)

Some crank balanced units are manufactured with the gear reducer shifted from a position directly underneath the equalizer to a position on the structural base farther away from the centerline of the well. This change from the conventional geometry causes a change in the torque factors on the upstrokes and downstrokes. This geometric change also causes a change in the time interval between the up- and downstrokes.

These type units usually have the out-of-phase system of counterbalance described previously and usually require a specific direction of rotation.

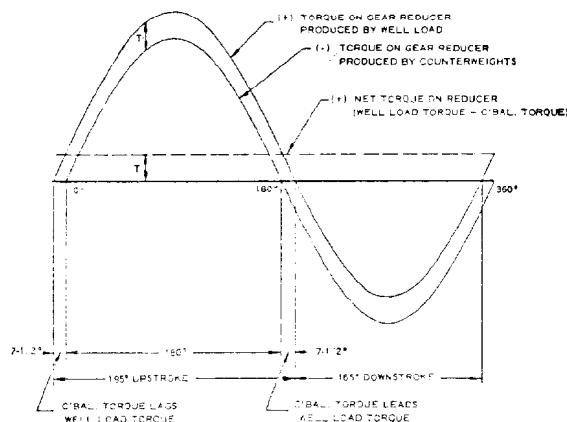


Fig. 10.7—Unitorque geometry.

Component Parts

The main parts of a pumping unit consist of structural members, bearings, speed reducer, and drive. Since the crank balanced pumping unit consists of parts typical for most units, the discussion is limited to this type.

Structure

The main structural parts of a crank balanced pumping unit are the base, samson post, walking beam, horsehead, equalizer, and pitman side members.

The structural base serves as a rigid member to which the samson post, gear reducer, and prime mover are attached for the proper alignment to effect satisfactory operation.

The samson post normally is constructed from three or four legs of rolled steel shapes. The samson post must be sufficiently rigid and strong to support at least twice the maximum polished rod load.

Centered on top of the samson post is the center bearing, which supports the large structural beam called the walking beam. The walking beam must be strong enough to resist bending caused by the well load at one end and the actuating force from the pitman side members at the other. API specifies the maximum allowable stresses and other design criteria for walking beams in API Spec 11E.¹

The horsehead is attached to the well end of the walking beam and supports the polished rod through a wireline and carrier bar assembly. The center of curvature of the horsehead is the center bearing. Thus, the polished rod moves in a straight line tangent to the arc of the horsehead.

On the other end of the walking beam are the equalizer and pitman side members. The rotary motion of the cranks attached to the speed reducer slow speed shaft is transferred to the walking beam by the equalizer and the pitman side members. The equalizer usually is mounted on the beam in such a manner that it can move and compensate for some misalignment in manufacturing and erection tolerances.

Loading on the pitman side members is tension on conventional crank balanced units, compression on Mark II units, and alternating tension and compression on air balanced units.

Structural Bearings

Trouble-free operation of a pumping unit depends on the proper functioning and design of the various structural bearings. Some characteristics to consider for proper selection of bearing design are the type and speed of the bearing as well as the direction and magnitude of load. On a conventional crank balanced pumping unit, the center bearing and equalizer bearing support an oscillating load while the crank pin shafts (and bearing inner races) rotate with respect to the load.

Various types of bearings and bearing materials have been used in these applications. High-lead bronze bearings were used for many years in all three of these bearing points. Bronze bearings operate with little damage even under marginal conditions of lubrication. In recent years, bronze structural bearings generally have been replaced by straight roller, tapered roller, or spherical roller antifriction bearings. These bearings can be grease lubricated and require less maintenance in general than do bronze bearings, which require oil lubrication.

Pumping unit bearings should be designed or selected very conservatively because they are often subjected to severe shock loads. Provision must be made for adequate lubrication and for protection from dirt and moisture.

Gear teeth proportions, hardness, and many other variables that affect the API torque rating are outlined in API Specification for Pumping Units, API Spec 11E.¹

Reducer

A speed reducer is used to convert high-speed, low-torque energy into low-speed, high-torque energy. A reduction ratio of about 30:1 commonly is used. This means that if the input speed is from 300 to 600 rev/min, the output speed or pumping speed of the pumping unit will be 10 to 20 strokes/min.

The speed reduction is accomplished by means of her-ringbone or double helical gearing in most cases. Helical gearing has been used in some instances; however, care must be taken that thrust bearings inherently required with helical gears must be adjusted properly to take the thrust from the frequently reversing loads of the pumping unit. Spur gearing and chain drives have also been used but to a much lesser extent. Pumping unit speed reducers must be sturdy and dependable. Reducer design should include provisions for adequate and proper distribution of oil.

Gear teeth proportions, hardnesses, and many other variables that affect the API torque rating are outlined in API Spec 11E.¹ This publication also outlines design parameters for chain reducers.

Drive

V-belts are the most universal driving means between the prime mover and the pumping unit gear reducer. They are dependable means of transmitting power and providing a certain amount of cushioning effect between the prime mover and gear reducer. This cushioning effect is highly desirable with slow-speed, single-cylinder engines. Sheave sizes can be changed easily to adjust pumping speeds. Provisions must be made to adjust belt tension periodically. A belt cover or guard usually is provided to protect the belts from the elements and for personnel safety (see Guarding of Pumping Units).

Pumping Unit Loading

There are many variables that affect the loading on the sucker rod string and pumping unit. Some of these variables are listed in Table 10.1.

Unfortunately, many of these variables are unknown when design calculations for sizing a pumping unit are made. See Fig. 10.8 for a visual representation of some of these loads.

Dynamometer Card Analysis

A dynamometer card is a continuous plot of polished rod load vs. polished rod displacement, or it may be a continuous plot of polished rod load vs. time. A polished rod load plot can in some instances be useful in analyzing downhole problems as well as identifying the resulting loads on the surface equipment.

A typical dynamometer card is shown in Fig. 10.8. When pumping speed is elevated above zero, the card takes on a different shape. Some of the load values are

TABLE 10.1—VARIABLES THAT AFFECT SUCKER ROD STRING AND PUMPING UNIT LOADING

Polished rod load
Pumping speed
Pump setting or depth
Physical characteristics of the rod string
Dynamic characteristics of the rod string
Plunger diameter of the pump
Specific gravity
Pump intake pressure
Polished rod acceleration pattern
Mechanical friction
Fluid friction
Pump submergence
Compressibility or gas interference
Pumping unit inertia
Pumping unit geometry
Counterbalance
Torque characteristics of prime mover
Flowline pressure

increased over the zero-pumping-speed card shown by the dotted lines and some values are decreased.

While this section is not intended as a treatise on polished rod dynamometer card interpretation, certain conclusions can be drawn from the card and knowledge of subsurface conditions.

As noted under Pumping Unit Loading (Table 10.1), there are many variables that affect loading on the polished rod. Sometimes some of these variables nullify each other, sometimes they are additive, and sometimes they are shifted time-wise because of rod string dynamics, making it virtually impossible to make a meaningful interpretation of the dynamometer card shape. This is particularly true in deep wells with a relatively elastic sucker rod string. At other times, certain type cards have a very distinctive pattern and downhole problems can be identified quite easily.

Fig. 10.9 shows a dynamometer card that is particularly detrimental to all surface and subsurface equipment. This card depicts a severe fluid pound. The condition generally is caused by attempting to produce fluid at a greater rate than the reservoir will give it up. The result is incomplete pump fillage and a fluid pound when the plunger hits the fluid on the downstroke. If the pound occurs very near the top of the pumping unit stroke, or at a low plunger speed, the effect is not so damaging; however, if the pound occurs at high plunger speeds in the pumping cycle, a progressively detrimental effect and equipment damage is

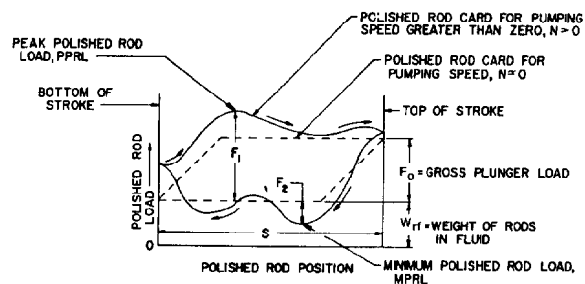


Fig. 10.8—Basic loads on polished rod.

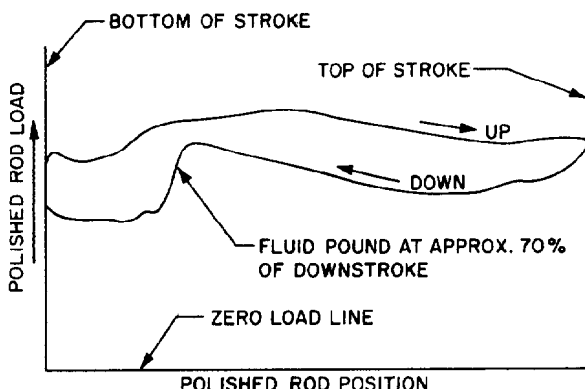


Fig. 10.9—Example of fluid pound.

generally the result. If a fluid pound does exist, the operator should make every effort to correct this costly practice by decreasing the displacement of the bottomhole pump. This can be accomplished by either reducing the pumping speed, shortening the stroke length, or installing a smaller-bore bottomhole pump. Sometimes it is necessary to try a combination of these remedies to prevent a decrease in production.

Fig. 10.10 shows a group of representative dynamometer cards illustrating the effect of pumping speed, rod stretch, and polished rod load. The abscissa, F_o/Sk_r , is a dimensionless factor representing sucker rod stretch and load. F_o is the differential fluid load on the full plunger area in pounds and Sk_r is the load in pounds necessary to stretch the sucker rod string in an amount equal to the polished rod stroke.

The ordinate, N/N_o , is a dimensionless pumping speed factor, where N is the pumping speed in cycles/min and N_o is the natural frequency of the tapered sucker rod string in cycles/min.

This family of dynamometer cards show the various effects of nondimensional pumping speeds and nondimensional sucker rod stretch on the shape of dynamometer cards. The dynamometer card on the upper left corner is a rather extreme example of an overtravel card. Overtravel cards have the distinct shape of sloping up from right to left. Undertravel cards, illustrated by the dynamometer card in the lower right-hand corners, slope up from left to right. While these two examples may be on the extreme ends of the spectrum, there are many other examples in between that reflect various combinations of pumping speeds and rod stretch.

As a general rule, most operators limit the pumping speed factor to 0.3 or 0.35 and the stretch factor to 0.5.

Very often certain card shapes favor certain types of geometry pumping units. This means that a pumping unit with a particular geometry, owing to its unique set of torque factors and perhaps phasing of counterbalance, may be able to lift the rod string with less average net torque on the gear reducer than will a pumping unit with a different geometry. In general, crank balanced units, properly balanced, will usually produce less torque on wells with undertravel cards, whereas Class III lever system units with phased counterbalance usually will show an advantage on wells with overtravel cards.

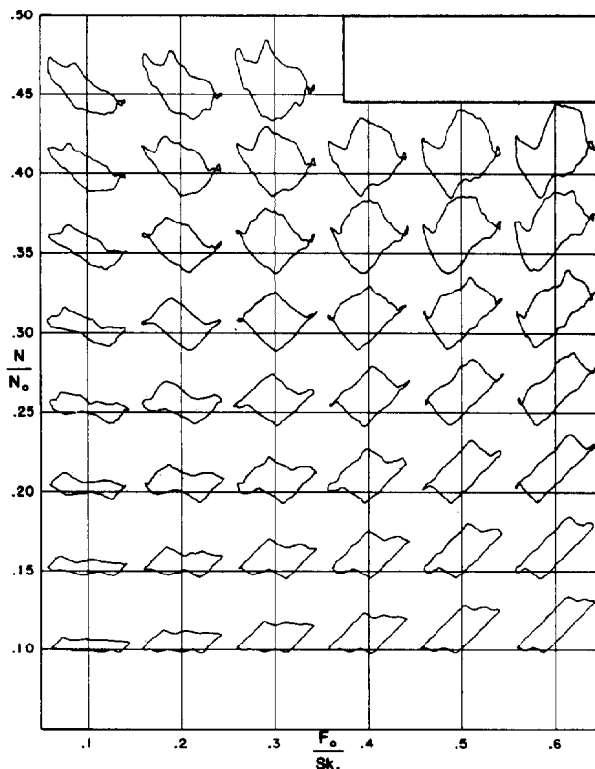


Fig. 10.10—Representative dynamometer cards.

Counterbalance

One of the most important aspects of torque loading on a gear reducer is the level of counterbalance. Improper counterbalance, either too much or too little, is probably the biggest single factor involved in overloading a pumping unit gear reducer.

In general, the counterweights are positioned on the cranks so that their effect approximately balances out the weight of the sucker rod string and a portion of the fluid to be lifted.

In some special geometry units such as the Mark II, the counterbalance torque on the gear reducer is out of phase with the torque on the gear reducer exerted by the well load. This means that when the pitman side members go over top and bottom dead center with respect to the reducer slow speed shaft, the reducer torque exerted by the counterweights is either leading or lagging the well load torque. This is accomplished by putting a dogleg in the crank so that the counterweights do not go over top and bottom dead center of the reducer slow speed shaft at the same time as do the pitman side members. The net effect of this combination of torque loading is illustrated in Fig. 10.7.

Torque Factors

For any position of the cranks there is a number, when multiplied by the polished rod load, that equals the torque on the gear reducer caused by the well load. This number is called a "torque factor." As the cranks are rotated through one complete stroke of the pumping unit, the torque factor changes for every crank position.

The pattern of torque factors around the pumping cycle is altered by the particular type geometry unit in question. This changing pattern of torque factors, in conjunction with phased counterbalance (see Counterbalance section), is used to an advantage in reducing the net torque on the gear reducer in some cases. Torque factors usually are expressed in inches.

Torque factors usually are available from the manufacturer of the pumping unit or can be calculated as illustrated in API Spec 11E¹ if the geometry dimensions of the pumping unit are known.

Polished Rod Velocities and Acceleration

Torque factors also provide a useful tool for calculating polished rod velocities and accelerations.

It can be shown that for any particular pumping speed of the pumping unit, the polished rod velocity at any Crank Position 1 is

$$v_{pr_1} = 0.00873 F_{t_1} \times N, \dots \dots \dots (1)$$

where

v_{pr_1} = polished rod velocity at Crank Position 1, ft/sec,

F_{t_1} = torque factor at Crank Position 1, in., and

N = pumping speed, strokes/min.

In Eq. 1, if v_{pr_1} is expressed in m/s, F_{t_1} in millimeters, and N in strokes/s, then the constant 0.00873 becomes 0.0121.

If the pumping speed is not constant around the pumping cycle, the equation is still true if the instantaneous pumping speed at Crank Position 1 is used in the equation.

Similarly, the average polished rod acceleration between any two Crank Positions 1 and 2 can be expressed as

$$\bar{A}_{pr_{1,2}} = 0.0524 N^2 \left(\frac{F_{t_1} - F_{t_2}}{\theta_1 - \theta_2} \right) \dots \dots \dots (2)$$

where

$\bar{A}_{pr_{1,2}}$ = average polished rod acceleration between Crank Positions 1 and 2, ft/sec²,

F_{t_1}, F_{t_2} = torque factors at Crank Positions 1 and 2, in.,

θ_1 and θ_2 = angle cranks rotate between Positions 1 and 2, degrees, and

N = pumping speed, strokes/min.

In Eq. 2, if $\bar{A}_{pr_{1,2}}$ is expressed in m/s², F_{t_1} and F_{t_2} in millimeters, θ_1 and θ_2 in rads, and N in strokes/sec, then the constant 0.0524 becomes 0.0695.

Sizing

Over the years there have been several methods of calculating the structural rating and the gear reducer rating of a pumping unit; however, it should be emphasized that the sizing of pumping unit is not an exact science. This is true because in virtually every case many of the variables previously outlined are unknown at the time the pumping unit is selected.

The most commonly used method for sizing pumping units today is outlined in API RP 11L² that was developed from test results conducted by Midwest Research Inst.

In those instances where the majority of the listed variables are known, there are more exotic computer programs available that may result in a more accurate sizing of the unit in some instances.

API RP 11L² covers the conventional pumping unit only; however, the manufacturer has modified this recommended practice to include air balanced and Mark II units.

The API, Midwest Research Inst., and the author make no guarantee as to the degree of accuracy of this sizing method when compared with measured field results and do hereby expressly disclaim any liability or responsibility for loss or damage resulting from its use.

The method of sizing conventional pumping units that is recommended by API RP 11L² and this same method as modified by the manufacturer for air balanced and Mark II units are listed on the following pages. Sample calculations for a given set of typical well conditions are filled in and circled for each type unit in Figs. 10.11 through 10.13.

Installation

An improperly installed pumping unit can result in early structural and bearing failures and overall unsatisfactory operation. An adequate foundation must be provided, and the unit must be properly erected.

Foundation

A reinforced concrete block is always the best type of foundation for a pumping unit. Concrete blocks may be cast in place although very often they are precast and moved to location for the installation of the unit. Hold-downs are provided in the concrete foundation in the form of anchor nuts or slotted pipes embedded in the concrete to receive hold-down clamp bolts.

The top of the concrete foundation should be level and smooth to support the pumping unit structural base. If the structural base members do not bear properly on the concrete, they may deflect with each stroke of the unit. This repeated deflection can result in ultimate failure of the structural steel base or the concrete foundation or both.

Other types of foundations are acceptable under certain circumstances. Foundations of heavy timbers set on alternate layers of sand and gravel have been used successfully in some areas. This board mat type of foundation must be supervised closely during its preparation to provide correct setting of the timbers. Usually, wide (portable) bases are required when board mat foundations are used.

Details for the design of the concrete foundation as well as the design of the board mat foundation is outlined in the API Recommended Practice for Lubrication of Pumping Unit Reducers, API RP 11G.³

Always use a current certified foundation print provided by the manufacturer.

Erection of the Unit

Before placing the structural base on the foundation, draw a chalk line from the center of the well along the center of the foundation. Place the base on the foundation lining

Company: _____ Well Name: _____ Date: _____
 Field: _____ County: _____ State: _____
 Req'd. Production: _____ BBL'S/Day -- Fluid Gravity 1.0 Pump Depth 8,650 Ft. -- Stroke Length 168 Inches
 Plunger Dia.: 1 3/4 Inches -- Tubing Size: _____ Inches -- Rod Size: 86 -- Pumping Speed 7.6 SPM

ALL TYPES OF UNITS

1. $F_o = \text{Depth} \times G \times \text{Fluid Load (Fig. 10.12)} = 8,650 \times 1.0 \times 1.041 = 9,005$
2. $\text{SKR} = 1000 \times \text{Stroke} + [\text{Er (Fig. 10.12)} \times \text{Depth}] = 1000 \times 168 + (.0007 \times 8,650) = 27,746$
3. $F_o/\text{SKR} = 9,005 \div 27,746 = .325$
4. $N/\text{No} = \text{SPM} \times \text{Depth} \div 245,000 = 7.6 \times 8,650 \div 245,000 = .268$
5. $N/\text{No}' = (N/\text{No}) \div F_e(\text{Fig. 10.12}) = .268 \div 1.164 = .230$
6. $\text{BPD (100\% eff.)} = \text{Pump Const. (Fig. 10.12)} \times \text{SPM} \times \text{Stroke} \times \text{SP (Fig. 10.13)} = .357 \times 7.6 \times 168 \times .771 = 351$
7. $\text{WRF} = \text{Rod Weight (Fig. 10.12)} \times \text{Depth} \times [1 - (.128 \times G)] = 2.185 \times 8,650 \times [1 - (.128 \times 1)] = 16,481$
8. $\text{WRF}/\text{SKR} = 16,481 \div 27,746 = .594$
9. $\text{TA} = 1 + [\%(\text{Fig. 10.13}) \times (\frac{\text{WRF}}{\text{SKR}} - .3) \times 10] = 1 + [(-.0075 \times (.594 - .3) \times 10)] = .978$

CONVENTIONAL UNITS

10. $\text{PPRL} = \text{WRF} + [F_1(\text{Fig. 10.13}) \times \text{SKR}] = 16,481 + (.497 \times 27,746) = 30,270$
11. $\text{MPRL} = \text{WRF} - [F_2(\text{Fig. 10.13}) \times \text{SKR}] = 16,481 - (.177 \times 27,746) = 11,570$
12. $\text{CBL} = 1.06 \times (\text{WRF} + F_o/2) = 1.06 \times (16,481 + \frac{9,005}{2}) = 22,243$
13. $\text{PT} = T(\text{Fig. 10.13}) \times \text{SKR} \times \text{Stroke}/2 \times \text{TA} = .348 \times 27,746 \times 84 \times .978 = 793,200$
14. $\text{Rod Stress} = \text{PPRL} \div \text{Area (Fig. 10.13)} = 30,270 \div .785 = 38,561$

AIR BALANCED UNITS

15. $\text{PPRL} = \text{WRF} + F_o + .85 \times [F_1(\text{Fig. 10.13}) \times \text{SKR} - F_o] = 16,481 + 9,005 + .85 \times (.497 \times 27,746 - 9,005) = 29,553$
16. $\text{MPRL} = \text{PPRL} - [F_1(\text{Fig. 10.13}) + F_2(\text{Fig. 10.13})] \times \text{SKR} = 29,553 - (.497 + .177) \times 27,746 = 10,852$
17. $\text{CBL} = 1.06 \times (\text{PPRL} + \text{MPRL}) \div 2 = 1.06 \times (29,553 + 10,852) \div 2 = 21,415$
18. $\text{PT} = T(\text{Fig. 10.13}) \times \text{SKR} \times \text{Stroke}/2 \times \text{TA} \times .96 = .348 \times 27,746 \times 84 \times .978 \times .96 = 761,500$
19. $\text{Rod Stress} = \text{PPRL} \div \text{Area (Fig. 10.13)} = 29,553 \div .785 = 37,647$

MARK II UNITS

20. $\text{PPRL} = \text{WRF} + F_o + .75 \times [F_1(\text{Fig. 10.13}) \times \text{SKR} - F_o] = 16,481 + 9,005 + .75 \times (.497 \times 27,746 - 9,005) = 29,075$
21. $\text{MPRL} = \text{PPRL} - [F_1(\text{Fig. 10.13}) + F_2(\text{Fig. 10.13})] \times \text{SKR} = 29,075 - (.497 + .177) \times 27,746 = 10,374$
22. $\text{CBL} = 1.04 \times (\text{PPRL} + 1.25 \times \text{MPRL}) \div 2 = 1.04 \times (29,075 + 1.25 \times 10,374) \div 2 = 21,862$
23. $\text{PT} = (\text{PPRL} \times .93 - \text{MPRL} \times 1.2) \times \text{Stroke} \div 4 = (29,075 \times .93 - 10,374 \times 1.2) \times 168 \div 4 = 612,800$
24. $\text{Rod Stress} = \text{PPRL} \div \text{Area (Fig. 10.13)} = 29,075 \div .785 = 37,038$
25. NOTE: Do Not Use Less Than One Size Smaller Reducer Than Required For Conventional Unit

Figure numbers in parentheses indicate where values were obtained. Abbreviations and nomenclature used here are indigenous to this form.

Fig. 10.11—Pumping unit design calculations.

BRAKE HORSEPOWER REQUIRED BASED ON 100% VOLUMETRIC EFFICIENCY:

Conventional and Air Balanced Units:

For slow speed engines & high slip electric motors

$$\text{Depth } 8,650 \text{ Ft.} \times \text{BPD } 351 = 54 \text{ BHP}$$

56,000

For multi-cylinder engines & normal slip electric motors

$$\text{Depth } 8,650 \text{ Ft.} \times \text{BPD } 351 = 68 \text{ BHP}$$

45,000

Mark II Units:

For slow speed engines & high slip electric motors

$$\text{Depth } 8,650 \text{ Ft.} \times \text{BPD } 351 \times .8 = 44 \text{ BHP}$$

56,000

For multi-cylinder engines & normal slip electric motors

$$\text{Depth } 8,650 \text{ Ft.} \times \text{BPD } 351 \times .8 = 54 \text{ BHP}$$

45,000

EXPLANATION OF SYMBOLS

Fo = Fluid Load on Full Plunger Area

SKR = Load required to stretch the rod string to an amount equal to the stroke length

Fo/SKR = Percent of the stroke length which the fluid load will stretch the rod string

N/No = Ratio of SPM to natural frequency of straight rod string

N/No' = Ratio of SPM to natural frequency of tapered rod string

BPD = Barrels per day production at 100% volumetric efficiency

WRF = Weight of rod string in fluid

TA = Torque adjustment for peak torque for values of WRF/SKR other than .3

PPRL = Peak polished rod load, pounds

MPRL = Minimum polished rod load, pounds

CBL = Counterbalance required, pounds

PT = Peak reducer torque, inch pounds

Wr = Average Weight of rods in air, pounds per foot

G = Specific Gravity of produced fluid

Plunger Dia.	Fluid Load lb. per ft.	Pump Constant
1-1/16	0.384	0.132
1-1/4	0.531	0.182
1-1/2	0.765	0.262
1-3/4	1.041	0.357
2	1.360	0.468
2-1/4	1.721	0.590
2-1/2	2.125	0.728
2-3/4	2.571	0.881
3-3/4	4.781	1.840
4-3/4	7.671	2.630

ROD AND PUMP DATA

Rod No.	Plunger Dia.	Rod Wt. lb. per ft.	Elastic Constant Er	Frequency Factor Fe	Rod String, % of Each Size				
					1	7/8	3/4	5/8	1/2
44	All	0.726	.00199	1.000	-----	-----	-----	-----	100.0
54	1.06	0.908	.00167	1.138	-----	-----	-----	44.6	55.4
54	1.25	0.929	.00163	1.140	-----	-----	-----	49.5	50.5
54	1.50	0.957	.00158	1.137	-----	-----	-----	56.4	43.6
54	1.75	0.990	.00153	1.122	-----	-----	-----	64.6	35.4
54	2.00	1.027	.00146	1.096	-----	-----	-----	73.7	26.3
55	All	1.135	.00127	1.000	-----	-----	-----	100.0	-----
64	1.06	1.164	.00138	1.229	-----	-----	33.3	33.1	33.5
64	1.25	1.211	.00132	1.215	-----	-----	37.2	35.9	26.9
64	1.50	1.275	.00123	1.184	-----	-----	42.3	40.4	17.3
64	1.75	1.341	.00114	1.145	-----	-----	47.4	45.2	7.4
65	1.06	1.307	.00114	1.098	-----	-----	34.4	65.6	-----
65	1.25	1.321	.00113	1.104	-----	-----	37.3	62.7	-----
65	1.50	1.343	.00111	1.110	-----	-----	41.8	58.2	-----
65	1.75	1.369	.00109	1.114	-----	-----	46.9	53.1	-----
65	2.00	1.394	.00107	1.114	-----	-----	52.0	48.0	-----
65	2.25	1.426	.00106	1.110	-----	-----	58.4	41.6	-----
65	2.50	1.460	.00102	1.099	-----	-----	65.2	34.8	-----
65	2.75	1.497	.00099	1.082	-----	-----	72.5	27.5	-----
66	All	1.634	.00088	1.000	-----	-----	100.0	-----	-----
75	1.06	1.566	.00100	1.191	-----	27.0	27.4	45.6	-----
75	1.25	1.604	.00097	1.193	-----	29.4	29.8	40.8	-----
75	1.50	1.664	.00094	1.189	-----	33.3	33.3	33.3	-----
75	1.75	1.732	.00089	1.174	-----	37.8	37.0	25.1	-----
75	2.00	1.803	.00085	1.151	-----	42.4	41.3	16.3	-----
75	2.25	1.875	.00080	1.121	-----	46.9	45.8	7.2	-----
76	1.06	1.802	.00082	1.072	-----	28.5	71.5	-----	-----
76	1.25	1.814	.00081	1.077	-----	30.6	69.4	-----	-----
76	1.50	1.833	.00080	1.082	-----	33.8	66.2	-----	-----
76	1.75	1.855	.00080	1.088	-----	37.5	62.5	-----	-----
76	2.00	1.880	.00079	1.093	-----	41.7	58.3	-----	-----
76	2.25	1.908	.00077	1.096	-----	46.5	53.5	-----	-----
76	2.50	1.934	.00076	1.097	-----	50.8	49.2	-----	-----
76	2.75	1.967	.00075	1.094	-----	56.5	43.5	-----	-----
76	3.25	2.039	.00072	1.078	-----	68.7	31.3	-----	-----
76	3.75	2.119	.00069	1.047	-----	82.3	17.7	-----	-----

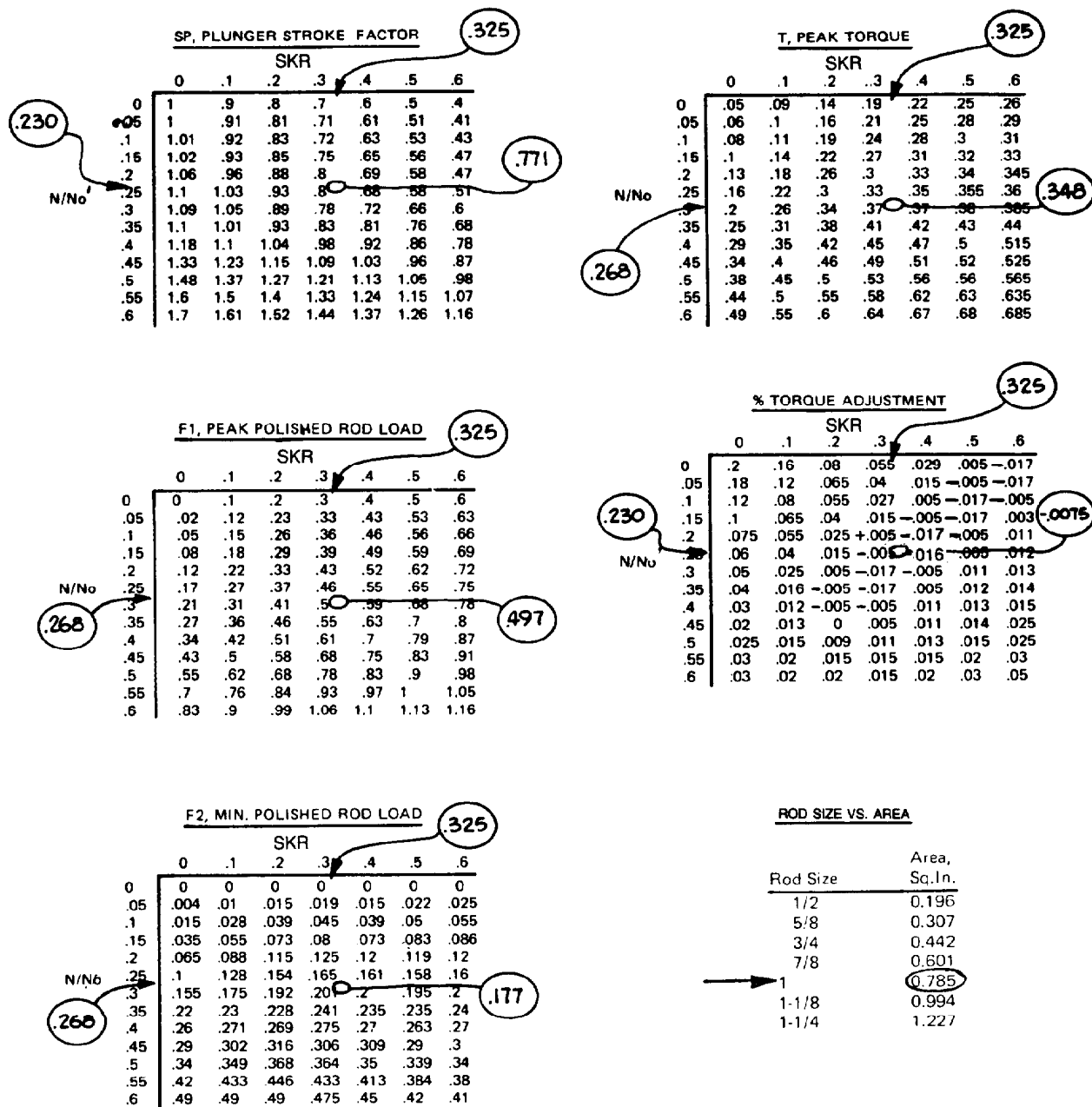
Abbreviations and nomenclature used here are indigenous to this form.

Fig. 10.12—Pumping unit design calculations.

Rod No.	Plunger Dia.	Rod Wt. lb. per ft. W_r	Elastic Constant E_r	Frequency Factor F_e	Rod String, % of Each Size					
					1-1/4	1-1/8	1	7/8	3/4	5/8
77	All	2.224	.00065	1.000	-----	-----	-----	100.0	-----	-----
85	1.06	1.883	.00087	1.261	-----	-----	22.2	22.4	22.4	33.0
85	1.25	1.943	.00084	1.263	-----	-----	23.9	24.2	24.3	27.6
85	1.50	2.039	.00079	1.232	-----	-----	26.7	27.4	26.8	19.2
85	1.75	2.138	.00074	1.201	-----	-----	29.6	30.4	29.5	10.5
86	1.06	2.058	.00074	1.151	-----	-----	22.6	23.0	54.3	-----
86	1.25	2.087	.00073	1.156	-----	-----	24.3	24.5	51.2	-----
86	1.50	2.133	.00072	1.162	-----	-----	26.8	27.0	46.3	-----
86	1.75	2.185	.00070	1.164	-----	-----	29.4	30.0	40.6	-----
86	2.00	2.247	.00068	1.161	-----	-----	32.8	33.2	33.9	-----
86	2.25	2.315	.00066	1.153	-----	-----	36.9	36.0	27.1	-----
86	2.50	2.385	.00063	1.138	-----	-----	40.6	39.7	19.7	-----
86	2.75	2.455	.00061	1.119	-----	-----	44.5	43.3	12.2	-----
87	1.50	2.413	.00061	1.062	-----	-----	27.7	72.3	-----	-----
87	1.75	2.430	.00060	1.066	-----	-----	30.3	69.7	-----	-----
87	2.00	2.450	.00060	1.071	-----	-----	33.2	66.8	-----	-----
87	2.25	2.472	.00059	1.075	-----	-----	36.4	63.6	-----	-----
87	2.50	2.496	.00059	1.079	-----	-----	39.9	60.1	-----	-----
87	2.75	2.523	.00058	1.082	-----	-----	43.9	56.1	-----	-----
87	3.75	2.641	.00056	1.078	-----	-----	61.2	38.8	-----	-----
87	4.75	2.793	.00052	1.038	-----	-----	83.6	16.4	-----	-----
88	All	2.904	.00050	1.000	-----	-----	100.0	-----	-----	-----
96	1.06	2.382	.00067	1.222	-----	19.1	19.2	19.5	42.3	-----
96	1.25	2.435	.00066	1.224	-----	20.5	20.5	20.7	38.3	-----
96	1.50	2.511	.00063	1.223	-----	22.4	22.5	22.8	32.3	-----
96	1.75	2.607	.00061	1.213	-----	24.8	25.1	25.1	25.1	-----
96	2.00	2.703	.00058	1.196	-----	27.1	27.9	27.4	17.8	-----
96	2.25	2.806	.00055	1.172	-----	29.6	30.7	29.8	9.8	-----
97	1.50	2.707	.00056	1.131	-----	22.5	23.0	54.5	-----	-----
97	1.75	2.751	.00055	1.137	-----	24.5	25.0	50.4	-----	-----
97	2.00	2.801	.00054	1.141	-----	26.8	27.4	45.7	-----	-----
97	2.25	2.856	.00053	1.143	-----	29.4	30.2	40.4	-----	-----
97	2.50	2.921	.00052	1.141	-----	32.5	33.1	34.4	-----	-----
97	2.75	2.989	.00050	1.135	-----	36.1	36.3	28.6	-----	-----
98	1.75	3.103	.00047	1.051	-----	25.7	74.3	-----	-----	-----
98	2.00	3.118	.00047	1.055	-----	27.7	72.3	-----	-----	-----
98	2.25	3.137	.00047	1.058	-----	30.1	69.9	-----	-----	-----
98	2.50	3.157	.00046	1.062	-----	32.7	67.3	-----	-----	-----
98	2.75	3.180	.00046	1.066	-----	35.6	64.4	-----	-----	-----
98	3.75	3.289	.00045	1.074	-----	49.7	50.3	-----	-----	-----
98	4.75	3.412	.00043	1.064	-----	65.7	34.3	-----	-----	-----
99	All	3.676	.00039	1.000	-----	100.0	-----	-----	-----	-----
107	1.50	3.085	.00051	1.195	19.4	19.2	19.5	41.9	-----	-----
107	1.75	3.158	.00049	1.197	21.0	21.0	21.2	36.9	-----	-----
107	2.00	3.238	.00048	1.195	22.7	22.8	23.1	31.4	-----	-----
107	2.25	3.336	.00046	1.187	25.0	25.0	25.0	25.0	-----	-----
107	2.50	3.435	.00045	1.174	26.9	27.7	27.1	18.2	-----	-----
107	2.75	3.537	.00043	1.156	29.1	30.2	29.3	11.3	-----	-----
108	1.75	3.411	.00044	1.111	20.9	21.4	57.7	-----	-----	-----
108	2.00	3.452	.00043	1.117	22.6	23.0	54.3	-----	-----	-----
108	2.25	3.498	.00043	1.121	24.5	25.0	50.5	-----	-----	-----
108	2.50	3.548	.00042	1.124	26.5	27.2	46.3	-----	-----	-----
108	2.75	3.603	.00042	1.126	28.7	29.6	41.6	-----	-----	-----
108	3.75	3.873	.00038	1.108	40.6	39.5	19.9	-----	-----	-----
109	2.50	3.911	.00037	1.048	27.2	72.8	-----	-----	-----	-----
109	2.75	3.930	.00037	1.051	29.4	70.6	-----	-----	-----	-----
109	3.75	4.020	.00036	1.063	39.9	60.1	-----	-----	-----	-----
109	4.75	4.120	.00035	1.066	51.5	48.5	-----	-----	-----	-----

Abbreviations and nomenclature used here are indigenous to this form.

Fig. 10.12—Continued.



Abbreviations and nomenclature used here are indigenous to this form.

Fig. 10.13—Pumping unit design calculations.

up the center of the base with the chalk line. The distance from the well to the front of the structural base should be given on the certified print provided by the manufacturer.

Follow the manufacturer's instructions and assemble the rest of the unit. Proper alignment of all working parts of the mechanism is essential. This may be checked by use of a level, plumb bob, or a transit. Make necessary adjustment to align the wireline hanger with the well. Tighten all bolts and nuts. Some pumping unit manufacturers specify that all structural bolts be hammer-tight.

After all other adjustments and inspection have been made and the unit is in operation, visually check alignment of moving parts. This may be done by observing the distance between the cranks and pitman side members on each side of the unit. The distances should be approximately equal. Check the wireline to see if it is tracking the horsehead properly. Objectionable noises or knocks usually indicate that some part of the unit is loose or out of alignment. All necessary adjustments should be made at this time. Misalignment may result in excessive axial motion of bearings which are designed primarily for radial load.

Guarding of Pumping Units

Guarding should be provided for all pumping units to prevent bodily injury or death from contacting moving parts of the unit by anyone inadvertently walking into the unit, falling, slipping, tripping, or any similar action. Guards should be provided around the V-belt drive as well as around the entire pumping unit.

The type of guarding around the unit depends on the location. For remote locations, usually a rail type guarding is considered satisfactory. For more populous areas, wire mesh guards several feet high are provided to ensure a greater degree of safety to personnel. Details for guarding can be found in API RP 11ER.⁴

Lubrication

Pumping units should be given periodic lubrication and maintenance checks. When they are subjected to heavy variable loads, extreme temperature conditions, or adverse moisture or dust conditions, it might be necessary to increase the frequency of the checks.

Structural Bearings

All the structural bearings (i.e., center bearings, equalizer bearings, crank pin bearings, etc.) require an adequate amount of the proper type of lubricant. A fluid lubricant

is more efficient in moving to the areas where the lubricant is most needed within the bearing housing; however, good quality grades of greases are recommended by most manufacturers for their particular bearings. In general, sleeve type bearings require oil as a lubricant and antifriction type bearings operate satisfactorily with grease lubrication.

Gear Reducers

Lubrication procedures for gear reducer drives and chain drives are recommended in accordance with API standards. Temperature and viscosity ranges for gear reducers and chain reducers are tabulated in API RP 11G³ (also see Tables 10.2 and 10.3).

It is not possible to describe adequately suitable lubricants by brief specifications or by Soc. of Automotive Engineers (SAE) or Intl. Standards Organization (ISO) viscosity numbers alone. Adequate lubrication instructions cannot be condensed sufficiently to be placed on the nameplate because of the many variables in operating conditions to which pumping units are subjected.

The proper oil for pumping unit gear reducers is best chosen with the advice of a representative of a reputable supplier of lubricants and should be based on the service conditions that are established by the design of the reducer and the service conditions of the particular installation.

The areas in contact on gear teeth and on chains and sprockets are relatively small, and, therefore, the unit pressures produced in transmitting high torque loads are correspondingly high. These gears, chains, and sprockets are designed to operate under these high unit pressures provided the lubricant used is also capable of withstanding these unit pressures during the periods of peak loads.

The temperature of the air in the vicinity of the reducer is of considerable importance in selecting oil of the proper viscosity. For high-temperature operations, an oil with a higher SAE or ISO viscosity number should be selected. For low-temperature operations, the oil should have sufficient fluidity to insure a free flow of oil through the lubricating channels.

The operating temperature of oil in pumping unit gear reducers normally would be at least 25°F above ambient temperature. The temperature increase in the oil will be

TABLE 10.2—VISCOSITY RECOMMENDATIONS FOR GEAR REDUCERS

Application* (°F)	SAE** Gear or Transmission Oil	AGMA† Oil
0 to 140	90 EP	5 EP (ISO VG 220)
-30 to 110	80 EP	4 EP (ISO VG 150)

*Operating temperature of oil in a gear reducer on a pumping unit normally will be from air temperature to 25°F above air temperature. The temperatures shown in the table are the limiting values between which satisfactory lubrication can be expected.

**Soc. of Automotive Engineers Inc., 2 Pennsylvania Plaza, New York City, NY 10001.

†American Gear Manufacturer's Assn., 1330 Massachusetts Ave., NW, Washington, DC 20005.

TABLE 10.3—VISCOSITY RECOMMENDATIONS FOR CHAIN REDUCERS

Temperature of Oil in Chain Case, °F*	SAE Viscosity Number	
	Automotive Engine Oil	Gear Oil
-50 to +50	5W	**
-20 to +80	10W	75†
0 to +100	20W	80
+10 to +125	30	80
+20 to +135	40	—
+30 to +155	50	90

*Operating temperature of oil in a chain case on a pumping unit normally will be from air temperature to 25°F above air temperature. The temperatures shown in the table are the limiting values between which satisfactory lubrication can be expected.

**SAE gear oils are not recommended for use in chain reducers for this range of temperatures.

†SAE 75 gear oil is not usually available.

negligible in slow operating, lightly loaded reducers but will reach the upper limit in heavily loaded reducers operating at the higher speeds. Because most pumping units will be stopped at times, the lowest temperature of oil in the reducer usually will be the lowest temperature reached in the locality where the pumping unit is operating. This is an important consideration when selecting the viscosity number of oil for winter operation. Most manufacturers recommend an American Gear Manufacturer's Assoc. premium grade oil with a mild extreme pressure additive and with a viscosity number suitable for the prevailing operating conditions.

The permissible range of operating oil temperature for each viscosity number of automotive-engine oil may be used provided the viscosity number of the oil is suitable for the prevailing operating conditions. In each case, the minimum temperature is based on the ability of cold oil to flow properly through the lubricating channels and the maximum temperature is based on the ability of the hot oil to maintain adequate lubrication. The temperature ranges are wide for the purpose of permitting year-long operation with one viscosity grade of oil in localities where seasonal air temperature range will allow. The operator should select the grade best meeting his temperature range. If the summer-to-winter range is too great for a single viscosity grade, the oil must be changed accordingly.

It is suggested that nameplates on pumping unit reducers carry at least a reference to API RP 11G.³

Changing the Oil

The life of a pumping unit reducer may be increased by using oil of a suitable viscosity and by keeping the oil free from foreign material, sludge, and water. Oil should be changed in the spring and fall to maintain proper viscosity if the seasonal temperature range exceeds the temperature range of the oil used in Table 10.2 or 10.3.

The method used to determine how often oil should be changed to maintain the desired condition is a matter of

policy with the individual company. Some operators periodically inspect reducers and take samples of oil for laboratory analysis to determine the percentages of water and solid material in the oil. Checks may also be made on viscosity and properties such as acidity. Oil is changed whenever the analysis shows that the limit set for any one of the various factors has been exceeded.

Other operators depend upon periodic visual inspection to determine when to change oil. An inspection includes a look inside the reducer case and an examination of a sample of oil that has been drawn off the bottom of the reducer case and allowed to settle. Oil is changed when an inspection shows (1) deposits on the surfaces inside the reducer, (2) emulsification of oil, (3) sludging of oil, or (4) contamination of oil with foreign material such as dirt, sand, or metal particles. Sludging and emulsification of the oil are usually found if there has been an excessive accumulation of water in the reducer.

A small amount of water can accumulate in the bottom of the reducer. Such water should be drawn off to prevent accumulation to the point where it will be carried with the oil and cause emulsification or sludging.

The time interval between inspections to determine the condition of the oil depends upon operating conditions. Adverse conditions that may require inspection and change of oil as often as every 3 or 4 months include (1) intermittent operation, (2) excessive dust, (3) hydrogen sulfide fumes, or (4) a combination of high humidity with high variation in daily air temperature. Under the most favorable conditions of minimum daily and seasonal temperature changes, low humidity, and freedom of atmospheric dust, a reducer may operate through one or more years before the oil becomes contaminated or deteriorates to the point that an oil change is required.

If petroleum solvent is used for flushing, all the flushing agent should be removed and the reducer immediately refilled with a suitable oil. If the reducer is not immediately returned to operation, the unit should be operated for at least 10 minutes, or longer if necessary, to ensure that all surfaces are covered with a protective film of oil.

Chapter 10

Pumping Units and Prime Movers for Pumping Units: Part 2—Prime Movers for Pumping Units

Sam Curtis, SPE, Sargent Oil Well Equipment

Ernest Showalter, SPE, Sargent Oil Well Equipment

Introduction

Pumping units are driven by either electric motors or internal-combustion engines. Each type of prime mover has characteristics that make it more appropriate, depending on field conditions and energy availability. These prime mover characteristics are covered in detail in their respective sections.

In this section, wellsite is considered the area around the well where the pumping unit and prime mover are located.

Internal-Combustion Engines

The availability and economics of the power source frequently dictate that internal-combustion engines be selected to drive pumping units. For the sake of brevity, internal-combustion engines are simply called “engines” throughout this chapter. Basically, engines used on pumping units are divided into two speed classifications: slow-speed engines and high-speed engines.

Slow-speed engines are those with one or two cylinders, which generally have a maximum crankshaft speed of 750 rev/min or less. High-speed engines are multicylinder (usually four or six cylinders) and have an average speed of more than 750 but not more than 2,000 rev/min.

Generally, high-speed engines have less torque than comparable horsepower, slow-speed engines. Therefore, high-speed engines will experience greater speed variation on the cyclic load of a pumping unit. Considerable speed variation at the prime mover has many benefits on various components of a sucker-rod-beam-type pumping unit system.^{5,6} While governors tend to limit speed var-

iation, it will not be eliminated. Speed variations of up to 35%, with resulting reductions in cyclic loads, have been measured on high-speed engine-driven pumping units.

Two-Stroke Cycle

Two-stroke cycle engines or two-cycle engines complete their work in only two strokes of the piston, which is accomplished with one revolution of the crankshaft. The two strokes are compression and power. The process of filling the cylinder with a fresh charge and exhausting the burned gases occurs almost simultaneously near the end of the power stroke. The horizontal sliding piston first uncovers exhaust ports and then uncovers intake ports, which charges the cylinder and thereby flushes out the exhaust gases. Because some of the fuel is lost at this point, two-cycle engines, above about 40 hp, are equipped with fuel injection systems that raise their fuel efficiency close to that of a four-cycle engine. Normally, a two-cycle engine, for a given displacement and speed, develops 1.6 times the power of an equivalent four-cycle engine.

The two-cycle engine normally is built as a crosshead type. This construction uses a bore in the engine base, where a crosshead is mounted to take the angular thrust of the connecting rod, and places a seal between the cylinder and crankcase. Contamination of lubricating oil is thereby reduced. Lubrication of the cylinders is accomplished by using an auxiliary oiler that injects a prescribed amount of oil into the cylinder/piston area.

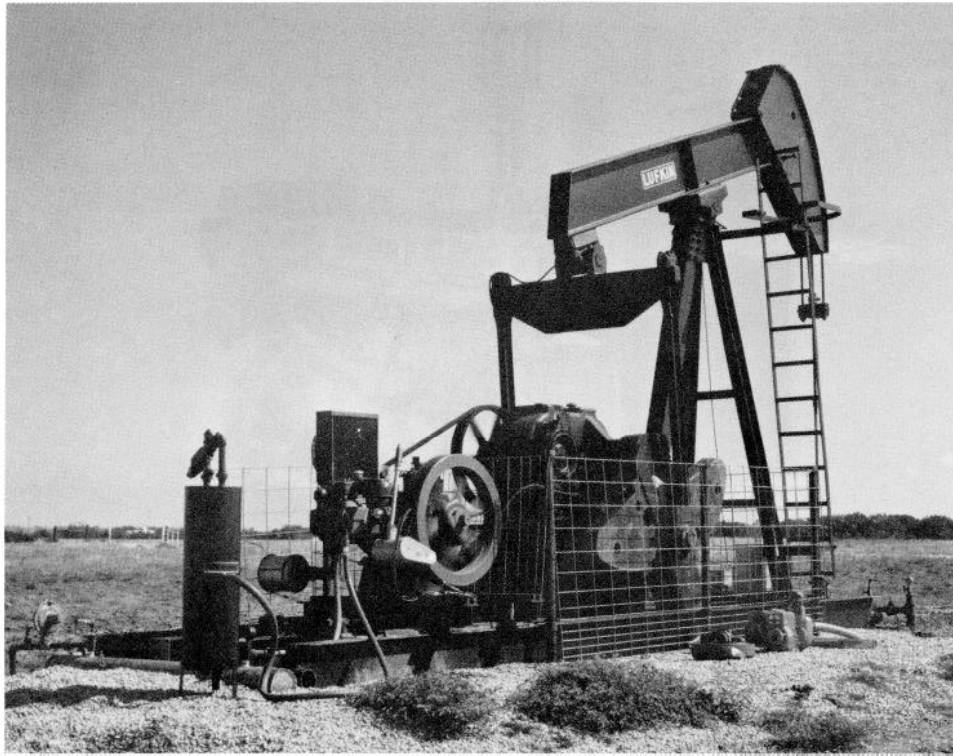


Fig. 10.14—Slow-speed, four-stroke engine on a beam-type oilwell pumping unit.

Most two-cycle engines are the slow-speed variety. These are available with a single cylinder or multiple cylinders in sizes ranging from about 15 to 325 hp. These engines have twice the power strokes of four-cycle engines and, for that reason, a smaller flywheel is required and additional speed variation is possible.

To operate most efficiently, two-cycle engines should be fairly well loaded. The proper size and length of exhaust pipe is very critical on this engine. Actually, the exhaust system completes the scavenging system. The properly sized pipe then is fitted to the correct length, as recommended by the manufacturer. This tuning of the pressure waves allows the engine to develop maximum efficiency and power. Incorrect exhaust-pipe length has a detrimental effect on the life, power, and operation of the engine.

Ideally, this type of engine operates only on natural gas or liquid petroleum (LP) gas. Some sizes may be operated on diesel fuel, but these engines must be derated.

Four-Stroke Cycle

An engine designed for four-stroke cycle or Otto cycle is called a “four-cycle engine.” The four-stroke cycle includes intake, compression, power, and exhaust. Intake and exhaust valves are mounted in the cylinder head or the block and are actuated by cams and push rods. The crankcase is connected directly to the cylinder, and contamination of the lubricating oil occurs sooner than it does in crosshead-type two-cycle engines.

The four-cycle engine is built in slow- and high-speed versions. Slow-speed engines usually have their cylinders

mounted horizontally, whereas high-speed engine cylinders are mounted vertically.

These engines use trunk pistons fastened to the crankshaft by connecting rods. Intake and exhaust valves are mounted in the cylinder head and actuated by cams and push rods.

A slow-speed, four-cycle engine as shown in Fig. 10.14 usually is built with a single horizontal cylinder. A large unenclosed flywheel is provided to store energy and deliver at a fairly constant speed to the pumping unit.

High-speed, four-cycle engines are multicylinder and can operate at speeds up to approximately 2,000 rev/min. Normally, four- and six-cylinder engines are not operated at more than 1,400 rev/min to maximize engine life.

A typical four-cycle, high-speed engine used as a prime mover on a beam-type pumping unit is shown in Fig. 10.15. This type of engine can operate on natural gas, LP gases, or gasoline.

Diesel and Oil Engines

Some slow-speed, single-cylinder engines burn diesel or fuel oil by high-pressure injections into the cylinder. The compression is much greater than gas engines. Heat, developed by compressing the air in the cylinder, ignites the fuel sprayed into the cylinder. These engines are divided into two types: full diesels, which are cold-starting, and semidiesels, which require heating to start.

The cold-starting diesel has a compression ratio of 14:1, resulting in a pressure of approximately 500 psi. The semidiesel has approximately 250 psi compression, which requires a hot tube heated by a torch or electric glow plug

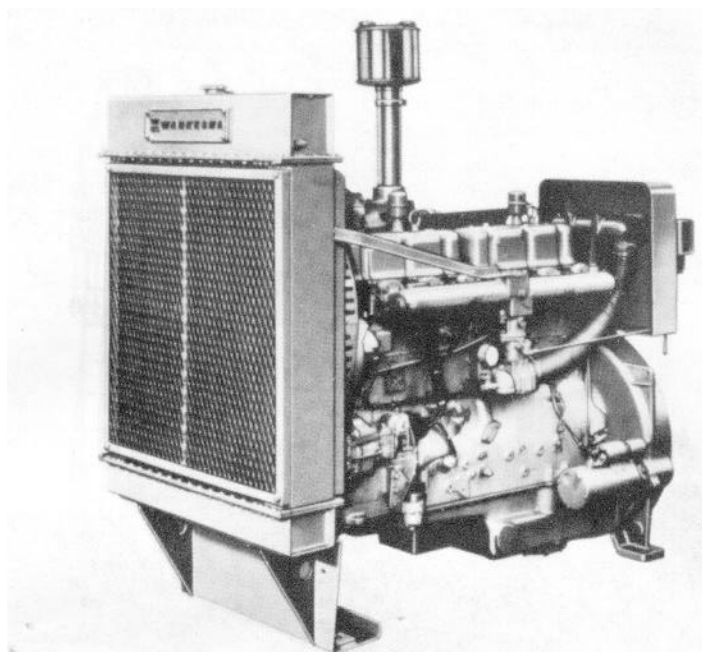


Fig. 10.15-Typical four-cycle, high-speed engine used as prime mover on a beam-type pumping unit.

to produce enough heat to ignite the charge. Once these engines are started, enough heat is produced in the cylinder to cause ignition of the fuel as it is injected into the cylinder.

High-speed, multicylinder diesel engines have been improved until they are now adaptable for oilwell pumping. These are not used commonly where gas is readily available. Diesel engines fill a need where other fuels are not readily available.

Selection of Engine

Five factors should be considered when determining which engine to purchase: fuel availability, equipment life and cost, engine safety controls, horsepower, and installation.

Fuel Availability. Natural gas is the logical choice. Taken from the wellhead casing annulus, it is called "wet gas" and is used most frequently. Where there is insufficient gas available at the wellhead, gas may be piped to the engine from the field separator. In either case, the gas must be scrubbed to remove oil and water. This is done in a double compartment volume tank where gas pressure also is reduced by a regulator. Gas from the separator will have most of the moisture and oil removed and is considered a better fuel.

Sour gas is a natural gas that contains excessive sulfur or CO_2 and is not considered a good fuel. Two percent sulfur is considered excessive. Where sour gas must be used, suitable treaters are required to improve the quality of the fuel. Sour gas causes severe etching and wear of engine parts as well as quick contamination of the lubricating oil in the four-cycle engines. Two-cycle engines fare slightly better because of their construction.

Residue gas is natural gas that has had impurities removed at a refinery and then is piped back to the field. This is sometimes called "dry gas."

LP gases, butane, and propane are excellent gases for internal-combustion engines, if economically available. Such gases must be stored under pressure in suitable pressure tanks to keep them liquefied for transportation. Vaporizers must be provided to turn the liquid into gas form for use in engines. On small engines, the vapor usually can be drawn off through a reducing regulator to provide sufficient gas; however, on larger engines, the fuel must be vaporized before entering the engine. Butane freezes to liquid at 0°C , while propane does not reach this state until -42°C . A blend of butane/propane is often used in mild climates.

Dual-fuel engines can use natural gas as long as it is available, but as soon as the pressure drops, the standby fuel is fed automatically to the engine in sufficient quantity to keep the prime mover going continuously. Such systems are designed primarily for gaseous fuels, but similar systems can switch from dry gases to gasoline or vice versa. Dual-fuel installations should not be overlooked if there is a shortage of natural gas.

Diesel fuel specifications are supplied by manufacturers of diesel engines. These fuels must be free of moisture and in clean dirt-free containers. Filters must be used to ensure that only clean fuel gets to the engine.

Some engines that are really semidiesel can burn crude oil of light gravity, but this must be cleaned satisfactorily. The type of crude must meet the standard set by the engine's manufacturer.

Equipment Life and Cost. The fact that the slow-speed engine may run at 400 rev/min and the high-speed engine may operate at 1,200 rev/min lends logic to the the-

ory that slow-speed engines generally outlast high-speed engines. Compared with high-speed engines, slow-speed engines have a longer life, are heavier, and cost more initially. A slow-speed engine requires fewer parts and is easier to repair; thus maintenance will cost more for the high-speed engine. A slow-speed engine's average life between major overhauls is somewhere between 5 and 10 years, whereas a high-speed engine's life is 2 to 5 years; albeit, there are exceptions to these averages.

Pumping unit and sucker rod life should be longer if a high-speed (lower-torque) engine is used because of greater speed variation.

Longer-interval maintenance features are available on all engines to reduce costs and extend equipment life.

1. Low-tension ignition provides better ignition with longer life to magnetos and spark plugs.

2. Extended service clutch requires lubrication only once each 6 months.

3. Automatically filling the crankcase on the engines from drums of oil ensures correct oil-level at all times.

4. Water makeup condensers provide water for the radiator automatically as required.

Engine Safety Controls. Every oilfield engine should be provided with reliable safety controls since the engines in this type of service usually are unattended. Some engine manufacturers provide safety controls as standard equipment. If not originally equipped, safety controls are available from supply companies.

Safety controls usually ground the magneto, and will shut off the fuel to stop the engine. Most desirable safety controls for engines are: (1) high water temperature, (2) low oil pressure, (3) overspeed, and (4) pumping unit vibration (to shut down the unit in case of sucker rod break).

Horsepower. API 7B-11C covers the procedure for testing and rating of engines.⁷

Maximum standard brake horsepower for engine and power unit (including accessories) is measured at various rev/min for intermittent and continuous operation. Torque and fuel consumption measuring procedures also are outlined in the API specification.

At any rotational speed, maximum brake horsepower will be the greatest horsepower corrected to standard conditions [29.4°C and 29.38 in. of mercury] as outlined under Test Procedures.

The manufacturer usually shows rating curves below the API curve, which is based on the power that the engine can produce for various conditions of service. Experience has shown that, for the cyclic load of oilwell pumping, high-speed engines must be derated more than slow-speed engines to provide a margin of safety to stand up in continuous service. Normal oilfield horsepower ratings for continuous duty, at the speed the engine will be operated, are (1) slow-speed engine (API)=maximum standard bhp×0.80, and (2) high-speed engine (API)=maximum standard bhp×0.65.

Altitude and temperature corrections (approximate) for altitude and temperature for naturally aspirated engines may be made as follows.

1. Deduct 3% of the standard brake horsepower for each 1,000-ft rise in altitude above sea level.

2. Deduct 1% of the standard brake horsepower for each 6°C rise in temperature above 29°C, or add 1% for each 6°C fall in temperature below 29°C.

Information concerning these corrections for turbo-charged engines should be secured from the manufacturer.

Calculations. Sizing prime movers to drive pumping units was discussed as part of the pumping unit load calculations in Part 1. The equation used to calculate brake horsepower, P_b , for slow-speed engines and high-slip NEMA (Nat'l. Electrical Manufacturers Assoc.) D motors* is⁸:

$$P_b = \frac{q \times D}{56,000}, \dots \dots \dots (3)$$

where

P_b = brake power, hp,

q = fluid flow rate, B/D, and

D = depth (lift), ft.

The bhp equation given for high-speed engines and normal-slip NEMA C motors** is⁷

$$P_b = \frac{q \times D}{45,000}, \dots \dots \dots (4)$$

These equations are empirical and result from modifications of the basic horsepower equations.

Hydraulic horsepower needed for actual lifting of the fluid is only a small portion of the total power required by the pumping system.

$$P_h = \frac{q \times D \times W}{33,000 \times 24 \times 60}, \dots \dots \dots (5)$$

where

P_h = hydraulic power, hp,

q = fluid flow rate, B/D,

W = weight of barrel of fluid, lbm,

D = depth (lift), ft, and

33,000 = conversion factor, ft-lbf/min.

For a fluid with 1.0 specific gravity

$$\begin{aligned} P_h &= \frac{q \times D \times 42 \times 8.3356}{33,000 \times 24 \times 60} \\ &= \frac{q \times D \times 350}{47,520,000} \\ &= \frac{q \times D}{135,735}, \dots \dots \dots (6) \end{aligned}$$

*High-slip motors are defined here as NEMA D, 5 to 8% slip. The sizing of ultrahigh-slip motors with over 13% slip is presented in the electric motor portion of this section.

**Normal-slip motors are defined as NEMA C, 3 to 5% slip.

where

42 = conversion factor, gal/bbl, and
8.3356 = conversion factor, lbm/gal.

Additional power is required to offset the frictional losses in the subsurface system.

Frictional horsepower has been defined empirically by Slonneger.⁹ (This may be low for extremely viscous crudes, such as those of 10°API gravity encountered in the Boscan field in Venezuela.)

$$P_f = \frac{\frac{1}{8}W_r \times 2S \times N}{33,000}, \dots\dots\dots (7)$$

where

P_f = power to overcome subsurface friction, hp
 W_r = weight of rods, lbm,
 S = polished-rod stroke, ft, and
 N = strokes per minute.

Frictional horsepower added to hydraulic horsepower equals polished-rod horsepower. The power required at the prime mover can be calculated by assuming a surface efficiency of 75 to 93%, depending on geometry and type of bearings in the pumping unit.

Example Problem 1. A well of 6,000-ft depth, producing 200 B/D of 1.0 specific gravity fluid using a 64-in. stroke unit, a pump with a 1½-in. bore, ¾-in. rods (1.64 lbm/ft, 14.4 strokes/min, and anchored tubing being assumed), can have its hydraulic and frictional horsepower calculated as follows:

$$\begin{aligned} P_h &= \frac{q \times D}{135,735} \\ &= \frac{200 \times 6,000}{135,735} \\ &= 8.84 \end{aligned}$$

and

$$\begin{aligned} P_f &= \frac{\frac{1}{8}W_r \times 2S \times N}{33,000} \\ &= \frac{\frac{1}{8}(1.64 \times 6,000)2(64/12) \times 14.4}{33,000} \\ &= \frac{(1,230)(10,666) \times 14.4}{33,000} \\ &= 5.72. \end{aligned}$$

The horsepower required at the polished rod, P_{pr} , is

$$\begin{aligned} P_{pr} &= P_h + P_f \dots\dots\dots (8) \\ &= 8.84 + 5.72 \\ &= 14.56. \end{aligned}$$

The horsepower required at the prime mover, P_{pm} , assuming a pumping unit with an efficiency of 85% is

$$\begin{aligned} P_{pm} &= \frac{P_{pr}}{85\%} \dots\dots\dots (9) \\ &= \frac{14.56}{0.85} \\ &= 17.13. \end{aligned}$$

Because of the cyclic nature of pumping unit loads and the fact that the preceding calculations reflect average horsepower, a factor must be applied in sizing to ensure that there is adequate horsepower available to handle peak loads.

Both high-speed engines and 3- to 5%-slip electric motors have limited torque available and should be derated 35% to handle peak loading. Generally, slow-speed engines, with higher torque capabilities, and NEMA D electric motors do not require more than 20% derating.

When using the cyclic load derating factor, F_{cl} , of 0.8 in the equation, the following prime mover horsepower will be required.

Slow-speed engine or NEMA D motor horsepower:

$$\begin{aligned} P_{pm} &= \frac{P_h + P_f}{E_{pu} \times F_{cl}} \dots\dots\dots (10) \\ &= \frac{8.84 + 5.72}{0.85 \times 0.80} \\ &= 21.41, \end{aligned}$$

where E_{pu} = pumping unit efficiency and F_{cl} = cyclic load derating factor.

High-speed engine and NEMA C horsepower:

$$\begin{aligned} P_{pm} &= \frac{8.84 + 5.72}{0.85 \times 0.65} \\ &= 26.35. \end{aligned}$$

The results of this method of horsepower calculations compare favorably with the results of the abbreviated method of Eqs. 3 and 4 as follows.

Slow-speed engine horsepower:

$$\begin{aligned} P_h &= \frac{q \times D}{56,000} \\ &= \frac{200 \times 6,000}{56,000} \\ &= 21.43. \end{aligned}$$

High-speed engine horsepower:

$$P_b = \frac{q \times D}{45,000}$$

$$= \frac{200 \times 6,000}{45,000}$$

$$= 26.66.$$

Under most conditions, the use of the illustrated method should provide adequately sized prime movers. Sizing prime movers for viscous crude may require additional frictional horsepower. In this case, experience is the best guide.

A rule commonly used in sizing high-speed engines for long life on pumping units is: 10% of engine's cubic-inch displacement as available brake horsepower. Hence, an engine with 817 cu in. of displacement can be relied on to handle an 81.7-hp pumping load.

A prime mover's minimum operating speed always should be greater than its speed at maximum torque output. This will ensure that, as the torque requirement of the pumping unit increases and the prime mover speed decreases, adequate torque capacity will be available. This is extremely important on high-speed engine drives.

Installation

The prime mover must be installed correctly to ensure good results. Most pump installations use a V-belt drive from prime mover to pumping unit. Slide rail motor mounts or some means of adjustment is necessary to provide for installation and proper tension that allows for power to be transmitted with minimal loss through belt slippage. When the prime mover is installed, the belts should be aligned and tightened properly but not over-tightened. Overtightening will overload the prime mover's shaft and bearings.

Slow-speed engines require sturdy foundations such as a steel base set on concrete or set directly on rails embedded in concrete. The slide rails should be set in line with the cylinder because of the horizontal moving forces. Cross rails, sometimes called universal rails, should be used only on small engines. Most manufacturers provide prime movers with properly designed slide rail assemblies.

Multicylinder or vertical engines, in which the forces are in a vertical plane, can be set on much lighter foundations. Cross rails on such installations are the preferred method.

Provisions must be made for exhaust and fuel lines to the engine. The manufacturer furnishes specifications for their installation. Usually, four-cycle engines come equipped with both a small silencer and a short exhaust pipe. Two-cycle engines are not equipped with such equipment unless specifically ordered by the customer.

The gas line is brought to a scrubber, then through a regulator to reduce the gas pressure to a few ounces before entering the volume tank. Normally, 1-in. pipe is the smallest size recommended from the volume tank to the engine. Larger engines may require larger lines. The purpose of the volume tank is to prevent fluctuations of gas pressure. It should have a volume of at least five times the cylinder displacement of the engine.

The gas regulator must be fitted with a properly sized orifice to maintain the proper gas flow. A regulator with too large an orifice will cause surges, whereas too small an orifice will not supply enough fuel to produce the power required.

Suitable cutoffs are required between the source line and volume tank, and the volume tank and engine. These cutoffs assist with draining the scrubber and volume tank, and also servicing of the reducing regulator.

For engine starting, many types of starters are used. Electric starters were put in automobiles, and soon were adapted to multicylinder oilfield engines. Formerly, slow-speed engines were started by manually turning the large flywheel. Some manufacturers provide electric or other built-in starters as optional equipment. Examples of starters include the following.

1. For electric starter motors requiring from 6- to 24-V direct current, power is furnished by batteries.
2. 110- to 440-V AC power and lighting circuits also are used for starter motors.
3. Air or gas motor starters in which a small vane-type air motor turns the engine through reduction gears and a Bendix-type engaging mechanism. This type of starter requires from 20 to 50 psi of gas or air pressure to operate.
4. Friction wheel starters for slow-speed engines use a small gasoline motor or an electric motor to turn a friction wheel, which engages the engine flywheel and turns the engine.
5. High-pressure air starting is sometimes applied to slow-speed engines, in which a valve admits air compressed from 125 to 200 psi into one or more cylinders to cause the engine to rotate. Usually a small engine-driven compressor is connected to a tank, which is used as a compressed air storage tank.
6. Diaphragm gas starters in which a rather large rubber diaphragm is expanded by 20- to 50-psi gas pressure cause a rack to turn a pinion attached to the engine crankshaft.
7. Gasoline-driven engine starters mounted on the engine can be used to provide power through reduction gears to start an engine.

The electric motor starter of 6 to 24 V is probably the most widely used of all starters on small engines. The battery can be located near the engine and charged by an engine-mounted generator. Portable cables from the engine can be attached easily to the batteries in trucks or automobiles. In this case, only one set of batteries would be required for starting several engines.

Large slow-speed engines are best started by using high-pressure air supplied by a small compressor and storage tank assembly. This system is simple and foolproof. The air compressor also can be used for cleaning or spray painting around the installation. Compressor units mounted on pickup trucks will accommodate starting a large number of engines and reduce the installation expense.

API RP 7C-11F is a good guide for engine operators.¹⁰ This publication should supplement the manufacturer's recommendations for installation, maintenance, and operation of internal-combustion engines.

Electric Motors for Oilwell Pumping Design Standards

Three-phase induction motors generally are classified by NEMA as being either B, C, or D. Ultrahigh-slip motors are classified by NEMA as a special purpose motor. The

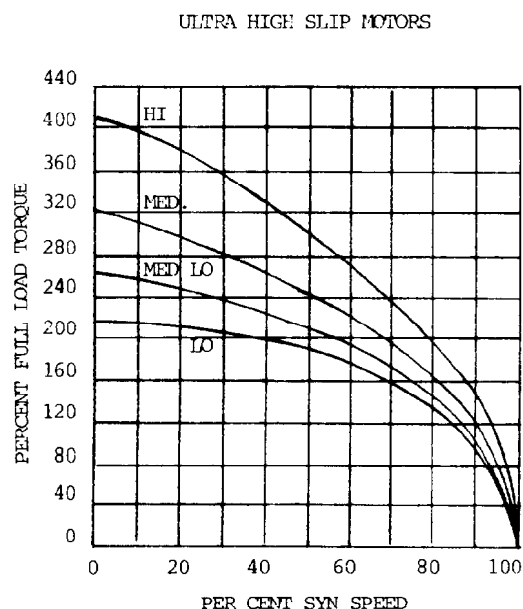
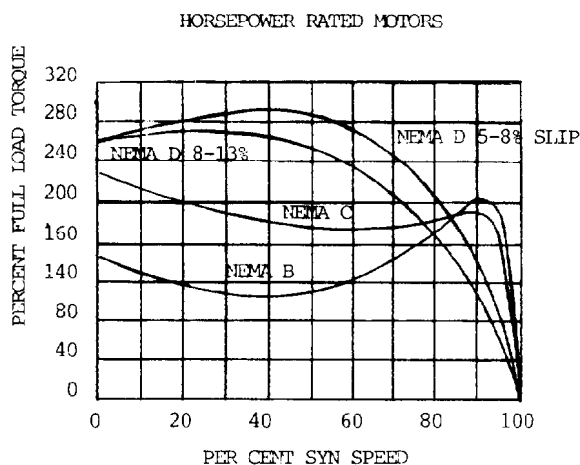


Fig. 10.16—Typical ratings for horsepower rated motors and ultrahigh-slip motors.

following is a portion of the NEMA specifications for these classified motors (Fig. 10.16).

NEMA B. Normal slip no greater than 3%, and normal starting breakaway torque 100 to 175% of full-load torque.

NEMA C. Normal slip no greater than 5%, and starting torque 200 to 250% of full-load torque.

NEMA D. High slip 5 to 8%, and starting torque 275% of full-load torque.

NEMA D Special. High slip 8 to 13%, and starting torque 275% of full-load torque.

Ultrahigh-slip motors, which have greater than 13% slip in high-torque mode, fall into an area not standardized

by NEMA. This motor, classified as a special purpose motor, is manufactured exclusively for the beam-type oil-well pumping unit. Designed with ultrahigh slip, the resulting wide speed variations produce benefits for the mechanical loading on the pumping unit. Fig. 10.16 illustrates typical ratings for one size of a multiple-rated ultrahigh-slip pumping motor.

High-Torque Mode. Maximum slip 17%, and high starting torque 410% of full-load torque.

Medium-Torque Mode. Maximum slip 21%, and starting torque 320% of full-load torque.

Medium-Low-Torque Mode. Maximum slip 27%, and starting torque 260% of full-load torque.

Low-Torque Mode. Maximum slip 32%, and starting torque 225% of full-load torque.

Horsepower Ratings of Motors

Three-phase induction motors are available in a wide range of horsepower ratings: 1, 1½, 2, 3, 4, 5, 7½, 10, 15, 20, 25, 30, 40, 50, 60, 75, 100, 125, 150, and 200. Most motors found on pumping units range from 10 to 75 hp. These motors are available in synchronous speeds of 600, 720, 900, 1,200, 1,800, and 3,600 rev/min. The majority of the three phase 460-V induction motors used on pumping units are 1,200 rev/min.

Multiple Horsepower Rated Motors

When a new well is completed, sizing is based on basic information provided by the depth of the pump and fluid, size of pump, stroke length, speed of pumping unit, and specific gravity of the fluid. There are many variables in calculations that are not always considered and may affect the required motor size. Sometimes, overlooked variables influencing loading on the motor are: actual fluid level, viscosity of fluid, deviation of hole, friction in the pump, friction in the stuffing box, excessive friction coming from the pumping unit, and quality of electric power available. Because of the many variables involved, it is sometimes difficult to size a motor accurately for new installation on the first attempt. Sometimes multiple-rated motors are considered as pumping unit drivers.

Multiple horsepower rated motors usually have three different modes available. Table 10.4 lists typical sizes available.

TABLE 10.4—TYPICAL SIZES (hp) OF MULTIPLE-HORSEPOWER-RATED MOTORS

HP	HP	HP
5	3.5	2
10	7	4
15	9	6
20	14	8
25	14	10
30	21	12
40	28	16
50	35	29
75	52	30

Multiple Size Rated Motors

An ultrahigh-slip motor is also a multiple-rated motor, usually being quadruple rated. The stator winding of this motor has been designed for multiple connections. The ultrahigh-slip capability is a result of special design characteristics incorporated in its rotor. Fig. 10.16 is two graphs that show a comparison of ultrahigh-slip motors to the horsepower rated motors. The first illustration shows the horsepower rated motors with only one torque mode available. The second shows an ultrahigh-slip motor with four-mode capability. For maximum benefits, the ultrahigh-slip motor should be used in the lowest-torque mode possible without exceeding its thermal limit.

Single-Phase Motors

Single-phase (AC) motors are also found in the oilfield in sizes up to 10 hp, although their use is limited. These single-phase motors are confined to shallow stripper wells producing in fields where three-phase power is not available.

Single-phase motors initially cost more than their three-phase counterpart with like rating. These operate less efficiently. To ensure high starting torque and low operating current, single-phase motors of the capacitor-start capacitor-run varieties should be used.

DC Motors

Direct-current (DC) motors have a very limited use on the beam-type pumping unit. DC voltage cannot be changed by transformers, which make transmission and distribution difficult without high line losses. Initial costs and maintenance for DC motors and controls are higher than for induction motors. Power available from utilities is normally 60 Hz AC, and cannot be used for DC motors.

Electric Generating Systems

Where utility-furnished power is not available, generators may be used to provide electrical power required for operation of the pumping units. This system allows the operator the benefits of electrification. When selecting equipment for the generating system, consider which type of motor will most efficiently use generator power. The ultrahigh-slip motors, which use fewer kilovoltamps (kVA) than conventional horsepower rated motors, are very popular. Distribution equipment for the generator system would be the same as for utility power if it were furnished. Generated voltage depends on the size of the electrified field. The following considerations determine the most desirable generated voltage.

1. Where the system consists of a small number of wells (one to five) with short distances from generator to well-site, the generator voltage may be the same as the motor rated voltage.

2. Where the field consists of many (5 to 50) wells, the distribution voltage should be higher than the motor rated voltage to minimize voltage drop. At each motor, a step-down transformer would be used. This system would be considered a moderately sized system with a generator having a distribution of 2,300 or 4,160 V.

3. In an exceptionally large field (50+ wells), the generator voltage would be stepped up to 7,200 or 13,800 V for distribution. At each wellsite, a transformer would be installed to drop the distribution voltage to motor rated

voltage. The generated voltage could be 2,300 or 4,160 V. The higher voltage allows smaller conductors to carry the loads and lessen line drop voltage within acceptable limits.

The procedure used in selecting primary and secondary equipment should be the same as that used by the utility companies. Protective devices and grounding procedures outlined in this chapter apply to either system.

Selecting Motor Size

Proper operation of the pumping unit depends mainly on properly sizing the components. Too often motors are oversized because the operator does not want to risk underpowering equipment. Choosing a large enough motor will ensure minimum motor failures and perhaps longevity of the motor. This does not take into consideration the effects a too-large motor has on the mechanical loading of the pumping system and the added cost in electrical power consumption.

For sizing of horsepower rated motors, refer to prime mover horsepower calculations shown in the engine section.

Proper use of the ultrahigh-slip motors requires that the motors not be oversized to obtain maximum speed variation and resulting benefits. Ultrahigh slip motor manufacturers have established methods of sizing their motors for pumping units. It is important that the sizing method used be approved by the motor manufacturer. Motors having different characteristics require different considerations for sizing. Table 10.5 shows a method used by one manufacturer.

Voltage Frequency

Induction motors may be operated from utilities or generators where frequency is other than the designed frequency. It is a common practice to operate 60-Hz motors at 50 Hz when certain conditions are met. If the V/Hz ratio is maintained as frequency is changed, the motors will operate satisfactorily but with new characteristics.

$$F_c = V/f \dots\dots\dots (11)$$

or

$$V = F_c f,$$

where

F_c = characteristics ratio, V/Hz,

V = electrical potential, V, and

f = frequency, Hz.

Example Problem 2. If a 460-V, 60-Hz motor is used where a 50-Hz frequency is available,

$$\begin{aligned} F_c &= \frac{460}{60} \\ &= 7.66 \end{aligned}$$

**TABLE 10.5—ULTRAHIGH-SLIP—OPEN DRIP-PROOF
SIZING DATA*—460 V, 60 Hz**

	Torque Modes	Full-Load Current (amp)	Maximum kVA Required	Load Capacity	Speed Variation (%)
Size 1, 215 T frame 1 $\frac{3}{8}$ -in. shaft 20-amp fuse	low	6.1	4.6	5,950	50
	medium low	7	5.3	6,300	39
	medium	9.1	6.9	8,000	32
	high	11.3	8.6	9,300	24
Size 2, 286 T frame 1 $\frac{7}{8}$ -in. shaft 30-amp fuse	low	12	9	11,500	56
	medium low	15	11	15,470	47
	medium	19	14	19,350	36
	high	22	17	22,000	30
Size 3, 326 T frame 2 $\frac{1}{8}$ -in. shaft 60-amp fuse	low	20	15	19,900	50
	medium low	23	18	23,440	40
	medium	29	22	27,970	32
	high	37	28	35,150	28
Size 4, 405 T frame 2 $\frac{7}{8}$ -in. shaft 100-amp fuse	low	38	30	39,200	53
	medium low	46	36	48,205	43
	medium	57	44	59,840	36
	high	72	55	71,590	29
Size 5, 445 T frame 3 $\frac{1}{8}$ -in. shaft 125-amp fuse	low	44	34	46,500	50
	medium low	56	43	60,500	46
	medium	71	55	77,000	39
	high	86	65	92,000	31
Size 6, 445 T frame 3 $\frac{3}{8}$ -in. shaft 175-amp fuse	low	64	48	68,000	49
	medium low	74	56	80,000	40
	medium	92	70	100,000	33
	high	122	92	130,000	29
Size 7, 509 T frame 4-in. shaft 300-amp fuse	low	118	89	127,000	52
	medium low	136	103	151,000	43
	medium	170	129	190,000	35
	high	207	157	224,000	28

*These data are applicable only to a specific manufacturer because no other motor has identical characteristics. Please call your manufacturer for assistance in sizing and applying these data.

Diameter (in.)	Constant C	Speed Factor	
		Strokes/Minute	F_s
1 $\frac{1}{16}$	0.132	20	0.277
1 $\frac{1}{4}$	0.182	19	0.268
1 $\frac{1}{2}$	0.262	18	0.259
1 $\frac{3}{4}$	0.357	17	0.250
2	0.466	16	0.239
2 $\frac{1}{4}$	0.590	15	0.228
2 $\frac{1}{2}$	0.728	14	0.217
2 $\frac{3}{4}$	0.881	13	0.205
3 $\frac{1}{4}$	1.231	12	0.193
3 $\frac{3}{4}$	1.639	11	0.180
		10	0.166
		9	0.152
		8	0.137
		7	0.122
		6	0.106
		5	0.090
		4	0.073

SIZING INSTRUCTIONS

$$\text{Load calculated} = C \times D \times S \times F_s \times \gamma,$$

where

C = a constant, the value of which is different for each size of plunger as shown above,

D = depth to fluid, ft,

S = polished rod stroke, in.,

F_s = a constant, the value of which is different for each number of strokes per minute (see above), and

γ = specific gravity of fluid being lifted.

The load capacity must be greater than load calculated.

Example: 1 $\frac{3}{4}$ -in. plunger, 120-in. polished-rod stroke, depth to fluid = 7,000 ft, 12 strokes/min., and specific gravity = 0.97.

$$\text{Load calculated} = 0.357 \times 7,000 \times 120 \times 0.193 \times 0.97 = 56,140.$$

A size 4, medium-torque mode, load capacity = 59,840.

Size 5*, medium-low-torque mode, load capacity = 59,590.

*The Size 5 MLT will have more maximum speed variation available as:

$$4 \text{ MT} = \frac{56,140}{59,840} \times 37\% = 35\% \text{ maximum SV.}$$

$$5 \text{ MLT} = \frac{56,140}{59,590} \times 45\% = 42\% \text{ maximum SV.}$$

Maximizing speed variation will maximize pumping load reductions.

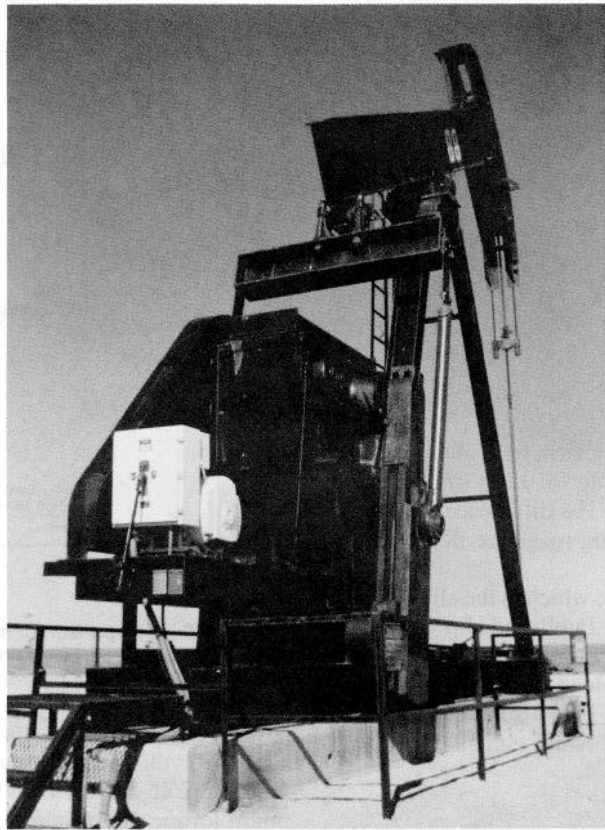


Fig. 10.17--Ultrahigh-slip motor used as prime mover on a beam-type pumping unit.

and

$$V = 7.66 \times 50$$

$$= 383.1$$

If the voltage changes to 383 V, the motor will operate satisfactorily at the new ratings. The change in performance should be obtained from the manufacturer. Approximations of changes in characteristics when using 60-Hz rated motors on 50-Hz power are: synchronous speed is $\frac{5}{6}$ of 60-Hz rating, horsepower is $\frac{5}{6}$ of 60-Hz rating, torque is approximately the same, motor amps are the same as 60-Hz rating, and applied voltage is $\frac{5}{6}$ of 60-Hz rating. A standard voltage in some countries is 415 at 50 Hz, which is 10% over the design voltage for 50 Hz. The motor will operate satisfactorily but at different characteristics. Contact the motor manufacturer for the change in ratings and performance characteristics.

On either 50- or 60-Hz operation, control components so marked have dual rating. If the voltage is changed, as shown in the example for motors, the devices would operate equally well at 50 or 60 Hz. Where control devices are not marked for dual frequency, contact the manufacturer to obtain their rating at the new frequency.

Motor Performance Factors

Electric motors have a wide variety of operating characteristics. When buying equipment for oilwell pumping

units, factors that contribute to the performance of the electric motor must be understood. This section discusses terms that describe the operating characteristics of the electric motor (see Fig. 10.17).

Motor Slip. Motor slip applies only to induction motors. Induction motors have a synchronous speed that is a function of applied voltage frequency and the number of poles in the stator winding. Table 10.6 represents a relation between the number of poles and synchronous rev/min for 50 and 60 Hz.

The majority of oilwell units use the six-pole induction motor. Three-phase voltage, when applied to the stator winding of an induction motor, causes a rotating magnetic field at the synchronous speed shown in Table 10.6. As a result of this voltage in the stator, there will be current and a magnetic field in the rotor. The interaction in

TABLE 10.6--INDUCTION MOTOR
POLES VS. SYNCHRONOUS SPEEDS
FOR 50- AND 60-HZ FREQUENCY

Number of Poles	Rev/Min at 60 Hz	Rev/Min at 50 Hz
2	3,600	3,000
4	1,800	1,500
6	1,200	1,000
8	900	750
10	720	600

TABLE 10.7—FULL-LOAD SLIP FOR NEMA RATED AND ULTRAHIGH-SLIP MOTORS

NEMA RATED	
NEMA B:	no more than 3%
NEMA C:	no more than 5%
NEMA D:	5 to 8%
NEMA D:	(special) 8 to 13%
ULTRAHIGH-SLIP	
High mode	17
Medium mode	21
Medium-low mode	27
Low mode	32

the stator between the rotor magnetic field and the rotating magnetic field is responsible for the turning action or torque of the electric motor. The difference in percent between the speed of the rotating magnetic field and the rotor is the slip of the motor.

All motors have a design slip, which is the slip the motor has when running full load. Published slip values for motors are based on full load rating.

Table 10.7 illustrates the full-load slip for NEMA rated and ultrahigh-slip motors (see Fig. 10.22).

Slip is calculated by the following equation.

$$F_s = \frac{V_s - V_{fl}}{V_s} \times 100, \dots \dots \dots (12)$$

where

F_s = motor slip factor, %,
 V_s = synchronous speed, rev/min, and
 V_{fl} = full load speed, rev/min.

Example Problem 3. If a six-pole, 1,200-rev/min synchronous induction motor has a full-load speed of 850 rev/min, the motor slip is 29.16%.

$$F_s = \frac{1,200 - 850}{1,200} \times 100$$

$$= 29.16\%.$$

The design slip of the oilwell pumping motor is a very important feature. The speed of the induction motor is reduced as more torque is required. In the case of the pumping motor, when large amounts of torque are required there will be a slowing down of the motor's rotor. As the rotor slows down, less motor torque will be required to drive the pumping unit.

There are two different torque reductions to be considered. (1) Torque resulting from polished-rod loading is reduced as a result of lower acceleration at peak torque moments.⁵ (2) Torque reduction is achieved because of inertial effects of the changing speed of the pumping unit.⁶

Fig. 10.18 shows a comparison of speed/torque curves for motors of various slip ratings. All motors on this chart have essentially equal full-load capacity on a beam-type

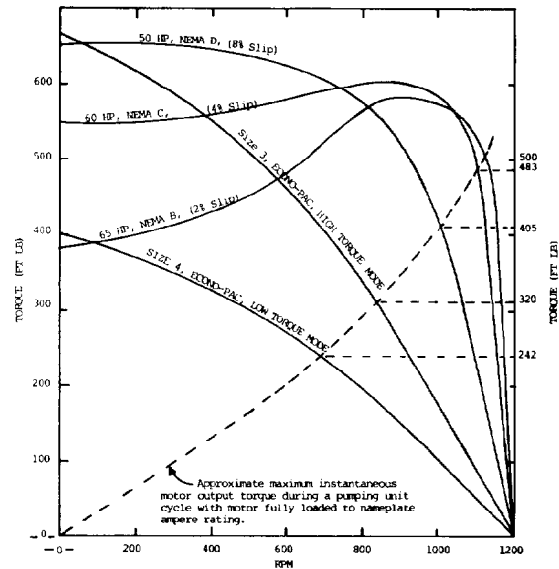


Fig. 10.18—Comparison of speed/torque curves for motors of various slip ratings.

pumping system as a result of the derating factors necessary for cyclic load operation.

The broken-line curve in Fig. 10.18 represents the maximum torque and minimum speed under which each of these motors will operate on the same pumping load. One will see that the changing speed of the higher-slip motors will have beneficial effects on the pumping equipment.

Motor Speed Variation. Motor speed variation depends on a maximum and minimum rev/min of the motor. Motor slip and motor speed variation are two different but related factors. Each is represented by a value in percent and all are calculated by very similar equations.

Speed variation:

$$F_{sv} = \frac{V_{max} - V_{min}}{V_{max}} \times 100, \dots \dots \dots (13)$$

where

F_{sv} = speed variation factor, %,
 V_{max} = maximum motor speed, rev/min, and
 V_{min} = minimum motor speed, rev/min.

Example Problem 4. An oilwell pumping motor having a maximum speed of 1,180 rev/min and a minimum speed of 690 rev/min will have a speed variation of 41.52%:

$$F_{sv} = \frac{1,180 - 690}{1,180} \times 100$$

$$= 41.52\%.$$

Speed variation on the cyclic load of the sucker rod pumping is considered beneficial. As torque demand of the system increases, motor speed decreases, thereby reducing acceleration. The force required to accomplish

work equals mass times acceleration; hence, a reduction in acceleration causes a reduction in force ($F = m \times a$).

Another benefit of increased speed variation is increased plunger overtravel, which occurs frequently. The instantaneous speed of the pumping unit is significantly greater at the top and bottom of the stroke where there is little or no torque on the pumping unit and motor. At these points, the induction motor will speed up toward its synchronous (no-load) speed, frequently increasing plunger overtravel.

Motor Power Factor. Motor power factor, being a number between zero and one, is a measure of the phase relation between the volts applied to a motor and the amps of the motor. In an induction motor, the motor current will lag the voltage by a certain amount of electrical degrees. The cosine of this angle is the power factor. In cases where the current and voltage are in phase, the angle is zero; consequently the power factor is one. The other extreme would be where the current was 90° out of phase with the voltage, which would result in a phase angle of 90° with a power factor of zero. In the case of the induction motor, which involves magnetizing devices, the current will lag the voltage. In the case of a circuit containing a large amount of capacitance, the current may lead the voltage, which results in a leading power factor.

Motors and other magnetic devices used in the electrified oilfield develop lagging power factors. Operating conditions of the oilwell pumping motor influence the power factor. Motors operating at light load or multiple rating motors operating in too high a mode have a tendency to produce low power factors. Motors allowed to regenerate as a result of the pumping unit's being unbalanced will have a momentary power factor of near zero.

High power factors reduce line losses, lower voltage drops to the motor, and reduce billing where electric utilities have power factor penalty clauses in their contract. Power factor correcting capacitors, normally connected to the motor leads, may be used to improve the power factor of the motor. Capacitors connected in this way will be in operation only when the motor is running.

There are several variables associated with the electric motor that will influence the power factor. To improve the power factor of a pumping unit motor, these factors should be considered: (1) properly balancing the pumping unit, (2) operating properly sized motors, and (3) operating in lowest-torque mode possible.

Motor Torque. Torque is a force that produces a twisting or turning effect. Torque measured in foot-pounds or inch-pounds is calculated by multiplying the distance from the center of rotation to the point where the turning force is applied by the force in pounds causing rotation. The motor adjusts its speed range in accordance with its design to develop the required torque.

Different NEMA design motors have different torque characteristics. The illustration in Fig. 10.18 shows a comparison of torque characteristics in the different classes of motors.

Motor Efficiency. The efficiency of the induction motor is a number in percent, which is the ratio of the output vs. the input.

$$E_m = \frac{P_{out}}{P_{in}} \times 100, \dots\dots\dots (14)$$

where

E_m = motor efficiency,

P_{out} = power output, and

P_{in} = power input.

During the pumping cycle when the load is light, efficiency will be low; when motor is peak loaded, efficiency will be very good. Because of the changing loads on the pumping units, a motor will travel through a varying range of speeds and its efficiency will vary accordingly. Determining or calculating the true root mean square (RMS) efficiency of the motor is extremely difficult. A very effective method of monitoring the efficiency is evaluating overall efficiency of the pumping system. This is determined on a kilowatt-per-barrel per-foot-lift basis. One should measure, over a designated period of time, kilowatts input to the motor, total production, and accurate fluid levels. If these measurements are collected under optimized conditions, they can prove beneficial in evaluating a motor's contribution to total system efficiency. Pumping motors may have a point peak efficiency of 85 to 90%. On pumping motors where loading will range from no load to 80% overload twice in one cycle, it is important that one not be overly impressed by a single-point efficiency. RMS efficiency throughout the pumping cycle and how it affects all system components is important.

Motor Cyclic Load Factor. A motor applied to the cyclic load of the oilwell pumping unit will be thermally heated more than it would be if the same average load were applied on a steady load basis. For this reason, a motor used for beam-type oilwell pumping units must incorporate the cyclic load factor in its full-load nameplate rating for proper application. Table 10.8 shows typical derating factors for two types of motors.

Motor Service Factor. Motors having single-horsepower ratings normally will include on their nameplate a service factor. The rated horsepower multiplied by this service factor represents a load that can be carried by the motor, provided that rated voltage and frequency are maintained and the temperature does not exceed the thermal limit of the motor.

The load on the motor is temperature-limited by the temperature rise of the motor or temperature limit of the insulation. Because of the cyclic load of the oilwell pumping motor, the horsepower rating or the service factor becomes meaningless. The load limit of the motor depends on the thermal amps required by the cyclic motor load.

The service factor is a rating applied to motors that are used in industries where loads are steady state. In the oilfield, the thermal amp load of the motor is compared to

TABLE 10.8—DERATING FACTORS FOR
NEMA C AND D MOTORS

Motor Type	Motor Derating Factor	Cyclic Load Factor
Design C	0.6 to 0.7	1.43 to 1.67
Design D	0.7 to 0.8	1.25 to 1.43

TABLE 10.9—MAXIMUM MOTOR TEMPERATURE AT 40°C AMBIENT TEMPERATURE (°C)

Ambient	40
Motor rise	90
Total	130
Safety factor	25
Class F insulation rating	155

TABLE 10.10—TEMPERATURE RATING OF INSULATIONS

Class	Temperature Rating	
	°C	°F
A	105	221
B	130	266
F	155	311
H	180	356

the nameplate rating of the motor. If the thermal amp load exceeds the rating of the motor, the motor is overloaded. The service factor cannot be multiplied times the full load rating of the motor to obtain a new thermal amp rating for the motor.

Motor Temperature Rise. It is important to understand how motor temperature rise and ambient temperatures influence the operating temperature of the motor. Temperature rise is the temperature that a motor, when run at full load conditions, will rise above ambient until all parts of the motor are at maximum stabilized temperature. Motor temperature rise is a design feature that normally is listed on the nameplate in degrees Celsius. If a motor starting at ambient temperature is operated at nameplate values for current, volts, and frequency until it has reached maximum operating temperature, the increase in the motor temperature above the ambient is the temperature rise of the motor. For example, if the ambient temperature is 40°C and a motor rated 90°C temperature rise is operated under full load conditions until the temperature is stabilized, the stabilized temperature of the motor would be 40°C + 90°C = 130°C. All motors have their temperature rise based on an ambient of 40°C (Table 10.9).

This same reasoning can be used to determine maximum motor temperature at other ambient temperatures. A comparison can be made between the maximum motor temperature and its insulation temperature limit. This comparison may explain why a motor fails or will not carry the desired load if ambient temperatures exceed 40°C.

In the design of the motor, the temperature rise of the motor will be limited by the class of insulation used.

Insulation for Oilwell Pumping Motors

Users responsible for oilwell pumping motors need to be aware of the type of insulation used in electric motors and how its limitations affect operation of the oilwell pumping motor. There are several classes of insulation as well as different processes of application in manufacturing. All of these influence cost and durability of the motor.

Insulation Classification. Table 10.10 shows the temperature rating (maximum hot-spot temperature) of insulations by classes.¹¹

In Table 10.9, there is a safety factor of 25°C. On days when the ambient temperature exceeds 40°C or if adverse loading causes the temperature rise to increase above 90°C, the motor will approach the maximum temperature limit of the insulation, which is 155°C. By analyzing the performance of the motor and ambient operating conditions it may be possible to determine that a motor forced to operate beyond the temperature limit of its class of insulation reduces its life by heat damaging the insulation.

Winding Insulation Materials. The winding insulation of the pumping motor has two distinct functions: (1) to provide electrical insulation of the winding and (2) to maintain a tight package, which prevents movement of motor windings that could mechanically damage the insulation on the conductors. Recognize that the torque of the motor is applied through the rotor to the shaft of the pumping unit, and this same force is applied to the winding in the motor. If the windings are not rigid, there will be moving or shifting of the windings, which will cause insulation damage. The pumping cycle of the oilwell motor may have amps as high as 180% of rating during the peak periods. These peak amps cause a high peak torque value, which may cause shifting of the windings unless they are maintained rigidly by insulating materials. Motor manufacturers should have special materials and process of application to provide a winding that has the mechanical and electrical strength required by the cyclic loading of the pumping unit motor. When motors are repaired, the manufacturer's instructions must be followed to ensure that the reconditioned motor has all the original characteristics.

Motor and Control Enclosures

Motors and their controls used on oilwell pumping units are exposed to environmental conditions. It is important to recognize the different enclosure ratings of motor and control to allow proper selection of the equipment. The ratings assigned to motor and control enclosures follow.

Motor Enclosures. The following are Natl. Electric Code (NEC) classifications of enclosures for induction motors.¹²

Drip-Proof. A drip-proof motor is an open motor in which the ventilating openings are constructed so that successful operation is not interrupted when drops of water or solid particles strike or enter the enclosures at any angle through 0 to 15° downward from the vertical.

Splash-Proof. A splash-proof motor is an open machine in which ventilating openings are constructed so that the successful operation is not interrupted when drops of liquid or solid particles strike or enter the enclosure at any angle not greater than 100° downward from the vertical.

Totally Enclosed. A totally enclosed motor is one enclosed to prevent the free exchange of air between the inside and outside of the case but not enclosed sufficiently to be determined airtight. The totally enclosed motor may be a totally enclosed fan cooled (TEFC) motor or a totally enclosed nonventilated (TENV) motor. The TEFC motor is a totally enclosed motor equipped for external cooling by a fan or fans internal with the machine but ex-

ternal with the exposed parts. The TENV motor is not equipped for cooling by means external to the enclosing parts.

Explosion-Proof. An explosion-proof motor is enclosed in a case that is capable of withstanding an explosion of a specified gas or vapor that may occur within the case. It will prevent the ignition of a specified gas or vapor surrounding the enclosure by sparks, flashes, or explosion of the gas or vapor within the case. The external temperature of the motor case will operate such that a surrounding flammable atmosphere will not be ignited.

A majority of the motors used in the oilwell pumping field are drip-proof. The TEFC motors are used in some extremely corrosive climates such as offshore or hazardous atmospheres. They are more expensive than the drip-proof motor; however, they last longer in severe environments and sometimes are justified.

Control Enclosures. The following are NEMA classifications for control enclosures.¹³

Type 1—General Purpose Indoor. This type of enclosure is intended for use indoors, primarily to prevent accidental contact of personnel with enclosed equipment in areas where unusual service conditions do not exist. In addition, they provide protection against falling dirt. Ventilation openings may be provided.

Type 3. This enclosure is intended for use outdoors to protect the enclosed equipment against windblown dust and water. They are not sleet- (-ice) tight.

Type 3R. This enclosure is intended for use outdoors to protect the enclosed equipment against rain and meet the requirements of Underwriters' Laboratories Inc., Publication No. UL 508, applying to rainproof enclosures. They are not dust-, snow-, or sleet- (ice-) proof. Ventilation openings may be provided.

Type 4. This type of enclosure is intended for use indoors or outdoors to protect the enclosed equipment against splashing water, seepage of water, falling or hose-directed water, and severe external condensation. They are sleet-resistant but not sleet- (ice-) proof.

Type 4X. This type of enclosure has the same provisions as Type 4 enclosures, and in addition, is corrosion-resistant.

Type 12. This type of enclosure is for use indoors to protect the enclosed equipment against fibers, filings, lint, dust and dirt, light splashing, seepage, dripping, and external condensation of noncorrosive liquids. There are no holes through the enclosure and no conduit knockouts or conduit openings, except that oiltight or dust-tight mechanisms may be mounted through holes in the enclosure when provided with oil-resistant gaskets. Doors are provided with oil-resistant gaskets. In addition, enclosures for combination controllers have hinged doors that swing horizontally and require a tool to open.

Although not NEMA approved for outdoor use, the Type 12 enclosure has been used successfully for many years to house disconnect switches on well locations.

Control for Oilfield Motors

Every motor used for oilwell pumping units must include a control. The components in this control have two distinct purposes. A portion of the devices serve as a means of stopping, starting, or controlling the oilwell pumping

motors. Another group of components equally important to the system are protection devices. Depending on the manufacturers, this equipment may have different appearances but the purpose is the same. Voltage ratings, size, or unique characteristics of various components may differ from one manufacturer to another. Next the major equipment used in controls is briefly described.

Equipment for Control. Hand-Off-Auto Switch. This switch normally is located on the door of the motor control and gives the operator means of selecting shutting off the motor or either automatic or manual operation. Turning this switch to the off position will not remove all power from the control but will stop the motor or prevent it from starting.

In the hand position, the motor will operate continuously, bypassing automatic functions. In the hand position, none of the protective features incorporated in the control are bypassed.

In the automatic position, the programmer or time clock is included in the function of the control devices. If there are pumpoff controls or other computerized control functions wired into the control circuit, they generally would function only when the switch is in auto position.

Local Remote Switch. This switch is a device that allows the transfer of the hand-off-auto control feature from a remote location to a site near the pumping unit. This can be very useful when the control panel is not located at the pumping unit. In some areas, electrical codes require that the starting switch be in a direct line of sight with the pumping unit.

Line Disconnect Switch. This switch serves as a means of disconnecting all electrical power from the motor control. If it is necessary to do maintenance work on the pumping unit or the motor control, it is important that all electrical power be removed from the control for safety purposes. It is not uncommon for this disconnect switch to be housed in its own separate enclosure and located near the source of utility power. When any work is performed on the pumping unit, this switch should be open. This prevents accidentally starting the pumping unit and reduces the possibility of electrical shock.

Sequence-Restart Timer. Pumping motors should be equipped to restart themselves when the electrical power is restored after a power outage. If there are a group of motors obtaining power from the same source, restarting of all motors simultaneously would create a severe drop in voltage. This voltage drop may be sufficient to prevent starting or could cause operation of safety devices at the utility substation. To prevent starting all motors simultaneously, controls should be furnished with a sequence-restart timer. This consists of a device that has an adjustable time delay period before restart of each motor is permitted. Sequence-restart timers should be set randomly at different times to prevent simultaneous starting of several motors.

Programmer. It is common for the equipment installed on a well to have the capability of lifting more fluid than the well will produce. Under these conditions, if the pumping unit operates continuously, the pump does not fill completely on the upstroke. This is commonly referred to as a "pumped-off" well. During the downstroke, fluid pounding will occur, which causes severe shock loading

of the sucker rods and pumping unit. Proper selection of these time periods allows the pumping unit to produce all of the oil that the well will give up while reducing the shock load on the system. One type of programmer is sometimes called a percentage timer, based on a total cycle of 15 minutes. If the well is capable of producing only half of the pumping system capacity, the operator should set the programmer on 12 hours. On 60-cycle current this programmer would allow the pumping unit to run $7\frac{1}{2}$ minutes and then shut down $7\frac{1}{2}$ minutes. The cycle would be repeated 96 times daily. This type of programmer does not allow the well's fluid level to build up so high that the hydrostatic head would retard inflow into the wellbore. Also, the short operating cycle can reduce electrical demand. This frequent starting and stopping has no adverse effect on equipment or power consumption. In fact, power consumption is always reduced.

Another type of programmer is a minimum 15-minute time clock that has 96 tabs. The time-clock tabs allow operators to select 15-minute operation periods. It is favored if the operator wants to operate during specific hours of the day and be off during the other hours.

Automatic pumpoff controls are also available, which shut the equipment down when pumpoff occurs detected by change of load either at the polished rod or at the motor.

Motor Starter Contactor. A magnetic-operated device applies or removes electrical power from a motor. The contactor has certain requirements that are important to maintain for its satisfactory operation and longevity. If voltage is too high, excessive current in the contactor holding coil creates heat, which reduces the life of the coil. If the voltage is low, the contactor may not pick up or maintain proper contact pressure on the main contacts that carry the motor running current. Control wires to the contactor holding coil should be kept to a minimum to reduce the effects of voltage drop. Remote stop and start switches may require auxiliary relays to limit length of wires to contactor holding coils. The contacts of this device must be of sufficient rating to handle the full load amps without deteriorating from excessive heat. For short time ratings, the contact must be of sufficient rating to handle locked rotor amps to start the motor. For continuous ratings, the contact rating should be no less than the full-load current rating for the maximum rating of the motor.

Protection Equipment. Protection equipment for oilfield motors includes the following devices.

Motor Fuses. These protective devices mounted in the disconnect switch are located between the motor control and the utility power.

Sizing fuses and the choice of fuses are very important in maintaining the protection. Fuses are not intended to prevent failure of the pumping motor. The primary purpose of the fuse is to limit damage to the system providing power to the electric motor should the motor develop electrical or mechanical difficulty. Protection of the motor should be derived from protective devices installed in the control or located in the motor winding.

Dual- and single-element fuses have similar appearances, but performance is quite different. Single-element fuses have a very high response speed to currents beyond their rating. Single-element fuses provide excellent short

circuit protection. Temporary, harmless overload or normal starting currents may cause nuisance failure of single-element fuses. The dual-element fuse is designed to be used with normal varying motor loads. The dual-element fuse has two elements in series within its housing. One of these elements functions very much like the thermal element of a standard thermal overload relay. Moderate overloads for extended periods of time will cause this fuse to operate, removing the motor from the load. The short circuit element of the fuse is sensitive only to exceptionally high current. This portion of the fuse has a very short melt time, which protects the system under electrical faults. It is always advisable to use the dual-element fuse.

Air Circuit Breaker. This protective device is used sometimes instead of fuses for distribution system protection in case electrical difficulty develops in the motor. If this happens, the air circuit breaker will operate, removing the motor from the source of power. The circuit breaker has a distinct advantage over fuses because it can be reset when the thermal element in the breaker has cooled.

Circuit breakers may be obtained with two distinct protection capabilities: thermal and magnetic. Their thermal trip capability is based on current vs. time cycle. When the rating of the breaker is exceeded, the thermal element heats up, causing operation of the breaker. The length of time it takes to trip the breaker is inversely proportional to the amount of overload. The magnetic trip capability, which is adjustable, causes instantaneous action. When the overload current exceeds the rating of the magnetic trip there is instant operation. A typical adjustment range for the magnetic circuit breaker would be 5 to 10 times the rating of the circuit breaker. The thermal portion of the circuit breaker is intended to handle continuous overload. The magnetic part of the circuit breaker is responsible for the short circuit faults in the control or the motor.

Lightning Arresters. Fuses, circuit breakers, and other protective devices cannot protect against lightning strikes. The only protection against damage caused by lightning is a properly sized and grounded lightning arrester. It must be sized according to the voltage of the system. Grounding of the lightning arrester must be through a continuous copper conductor from the lightning arrester to the ground. The wellhead at the pumping unit serves as the best ground available and should be used if at all possible. (Refer to electrical system grounding covered in electrical distribution system.)

Undervoltage Relay. Common disturbances such as overloads in the utilities distribution system may result in lower-than-normal voltages at the pumping unit. Control devices normally will operate at voltages considerably below those acceptable for the motor. Loss of voltage to the motor causes a drop in torque, which reduces the motor's rev/min and increases the amp load. Undervoltage relays are used to sense abnormal voltage and stop the motor before any permanent damage is done.

Phase Loss Relay. Electric power available to oilfields is subject to loss of one of the three phases. A phase loss relay will stop the motor if any one of the three phases is lost. In a system where there are several motors operating from the same power system, there is a degree of regeneration occurring during the loss of one phase. It is possible for motors to continue to run as well as to restart, even though there is a loss of one phase. Phase

loss relays that work well on single large-motor installations or even single small-motor installations may not operate satisfactorily on a multiple-motor electrified oil-field system. Extreme care must be exercised in selecting phase loss relays to ensure that the expected protection is provided.

Thermal Overload Relay. The standard thermal motor overload relay can play an important part in protecting motors on the oilwell pumping unit. The thermal overload relay is sensitive to the thermal amps demanded by the motor. The heaters selected should be sized to correspond to full-load amp rating for which the motor is operating. It is extremely important for motors that have multiple ratings to use heaters or settings that correspond to the full-load rating of the particular mode used. If adequate motor winding temperature sensors and controlling devices are used, thermal overload relays may not be necessary.

Motor Winding Temperature Sensor. Some of the motors manufactured for the oilwell pumping units have temperature sensors embedded in the winding to shut the pumping unit down if the temperature of the winding exceeds its limit. There are several different types of sensors including thermostats, thermistors, remote temperature devices, and thermocouples. These devices are sensitive to changes in temperature. Controlling devices attached to each of these are used to shut down the motor if conditions generate excessive winding temperature. Sensors in each phase of the motor protect against single phasing, low voltages or other abnormal loading that would cause excessively high temperatures in the motor winding.

Overtemperature Lockout Circuit. When sensors are located in the motor windings to shut down the unit because of excessive temperature, control lockout circuits should be provided to prevent automatic restart. If thermal overload has caused shut-down of the unit, it must not be restarted until the situation has been corrected. Excessive loads from loss of phase, improper counterbalance, falling fluid level, parted rods, stuck pump, or other conditions may be responsible for temperature shut-down.

Pumping Unit Vibration Switch. Pumping units are subject to severe motor overload because of breaking or parting of the sucker rods. Parting of the sucker rod causes a varying degree of unbalanced loading, depending on the location of the parted rods. Rod parts may cause an extreme overload as the motor tries to lift the counterweights. Under this condition, the motor will run until thermal protection shuts down the unit. During this period there can be serious overloading of the gear box, which may contribute to mechanical failures. Properly adjusted vibration switches mounted on the pumping unit should signal rod string failures instantly and shut down the unit.

Control Fuses. These fuses, carefully sized, are installed to protect the system should there be a failure of a component in the control package.

Electrical Distribution System

There are a variety of options concerning the type of devices and how they are used in providing electric power to pumping units. The electrical distribution system is responsible for furnishing electrical power and partial pro-

tection of the electrified oil field. It is important to the economics and longevity of the system that distribution be designed adequately before installation. This section covers topics that must be considered to ensure the most desirable benefits from the electrical system.

Primary System and Voltages. Generally, to reduce losses, electricity distributed to an oil field is brought to the field at elevated voltages, ranging between 4,000 and 15,000 V. This elevated voltage distribution system is called a primary system. Higher voltages allow smaller conductors to be used; however, the transformers are more expensive. In general, where the primary system is responsible for delivering electrical power over a long distance, a higher voltage is favored. In this situation, the cost of the smaller cable over the longer distances will offset the higher costs of the transformers and protective equipment.

An electrified oil field has a high degree of exposure to electrical storms. Electrical storms cause high static voltages, and sometimes high transient voltages, the latter being lightning. Static lines and lightning arresters are used to reduce the damage to electrical equipment by the static voltages and lightning strikes.

During electrical storms, the formation of rain clouds creates a difference in potential between the cloud and the earth. Primary electrical systems that lie in a section between the cloud and the earth may inherit a high static voltage level. This static voltage level can result in motor winding insulation damage if not reduced by properly sized and grounded lightning arresters. When the potential difference between the cloud and the earth becomes large enough, there will be an electrical discharge or lightning strike. If this lightning strikes the primary system, it will create high, transient voltages that must be arrested by the lightning arresters or failure of the insulation of the motor will occur. Other electrical equipment in the system may include transformers or reclosures and is subject to failure by the same cause. In the construction of the primary electrical system of the electrified oil field, it is extremely important to the life of the electric equipment to take measures to reduce the effects of static and transient voltages caused by electric storms.

Secondary Electrical System. The secondary portion of the electrical system of the oil field includes the transformer at the end of the primary system and all of the cables, disconnect switches, controls, and other devices, which operate at the same voltage as the motor. In general, the voltage of all the devices within the secondary system should not be greater than 600 V. A special case of the secondary system is the installation of a 796-V system. This voltage is obtained by Y-connecting three transformers whose secondary voltage is each 460 V and results in a line-to-line voltage of 796 V at the motor. This is a special case in the application of the 460-V-rated transformers. The 796-V system is used to reduce line drop to the motor. Operating at 796 V requires less current than operating at 460 V. However, this benefit is more than offset by the 796 V overstressing the insulation of motors and control components. Many operators who installed 796 V years ago have since converted to 460-V operation.

The secondary system of the electrified oil field consists of a transformer, or group of transformers, that convert the primary system voltage to the motor operating voltage. Voltage from the transformer is provided to the motors through a fused disconnect switch or a circuit breaker. The control of the motor provides for its control and protection. Where the secondary system consists of overhead cables, there is exposure of the system to electrical storms. Therefore, it is desirable to install lightning arresters at the transformer to reduce the effects of static and lightning strikes, which may damage the insulation of the electrical equipment.

All the devices selected in the secondary part of the system should be sized properly to allow full loading of the motor without any thermal damage to the equipment. Sizing of this equipment also should take into consideration the protection of the electrical devices. Fuses, circuit breakers, transformers, and wire sizes should be selected on the basis of the full-load rating of the motor.

Distribution Transformers. Distribution transformers reduce the primary high voltage to a lower voltage used by the motors. The distribution transformers are rated in kVA. They must supply reactive power (kVAR) as well as the power used for work (kW).

To obtain full-load capability of the transformers and the motors, it is desirable to use three single-phase transformers or a single three-phase transformer. One advantage of using three single-phase transformers is the convenience of replacing one, should it fail.

Open-delta or T-connected transformers will not provide the balanced, three-phase voltage even if only moderately loaded.

Distribution transformers can be connected in several different configurations to deliver three-phase power. These consist of delta-delta, wye-delta, delta-wye, wye-wye, and open-delta connections. All of these connections are used in the oil field; however, some of these have distinct advantages.

Wye-Delta. The most desirable transformer connection is the wye-delta. Do not ground the windings of the transformer or the Y point at the wellsite. If the Y point is grounded at the wellsite, as is done in many cases, danger exists. If one of the primary wires should go to ground at some point in the primary system, the groundwire at the wellsite may be at primary voltage to ground potential. This would create a personnel safety hazard. The transformer "ground" should not be connected to the grounding system at the pumping unit because the latter includes the enclosures for the electrical equipment.

The wye-delta connection has the advantage of allowing harmonic voltages existing in the system to have a self-canceling effect in the delta-connected secondary. It is not necessary for units in a three-phase bank to have equal impedances. It is important for the primary to have balanced voltage because unbalanced primary voltages can cause circulating currents in the delta secondary.

Delta-Delta. The delta-delta connection is an acceptable transformer connection; however, it is not as desirable as the wye-delta. This connection requires all units in a three-phase bank to have impedances with less than a 10% differential. Where the delta-delta connection is used, none of the endpoints or midpoints of the primary or secondary winding should be tied to the ground sys-

tem at the wellsite. If either the primary or secondary winding of the transformer is tied to the ground, be aware that if the ground is not satisfactory, the groundwire could be at a potential anywhere from zero to the line-to-ground voltage available at the transformer.

Delta-Wye. The delta-wye is an undesirable connection. It is prone to allow harmonic voltages in the distribution system to be applied to the motor and control. Harmonic voltages can cause erratic behavior of control components as well as excess motor heat. If a delta-wye system is used, neither the primary nor secondary windings of the transformer should be connected to the ground system at the motor. If grounds are attached to any part of this winding, they may be subject to the same voltage discussed under delta-delta. It is not necessary for the impedance of each unit in the three-phase transformer bank to be the same.

Wye-Wye. The wye-wye is the least desirable connection because harmonic voltages in the system are not able to circulate in the transformer winding. If they exist, they will be transmitted to the motor and control. If the wye-wye is used, no part of the transformer winding should be connected to the ground system at the wellsite. If a primary circuit has a phase-to-ground, a grounded wye will carry ground-fault current. This connection does not require transformers to have equal impedance. The delta secondary will eliminate harmonic voltage in the motor and control circuit. It is not necessary for transformers to have equal impedances.

Open-Delta. The open-delta is an incomplete delta-delta. If one transformer on the delta-delta connection is removed, the connection is an open-delta circuit. This type of connection provides unsatisfactory performance of induction motors. The open-delta connection will have unbalanced voltages, which prevent utilization of full-load rating of the transformer and motor.

At no-load, and with balanced voltages supplied to this transformer, the output will be a balanced three-phase voltage. As this two-transformer system is loaded, the impedance changes, which provides an unbalanced voltage to the motor. The use of the two-transformer open-delta transformer connection does not allow full utilization of transformer kVA (kilovoltamps) or the full output rating of the motor.

Figs. 10.19 and 10.20 show a comparison of the three-transformer delta connection with an open-delta transformer connection.

In the open-delta connection (see Figs. 10.19 and 10.20), the total kVA is only 57% of the original 100 kVA. The two 33.3-kVA transformers remaining in the circuit would have a total kVA of 66.6 kVA. With one unit removed, the remaining units with 66.6 kVA provide only 57.7 kVA, or only 86.6% of the rating. This example shows that the transformers used in open-delta connections must be derated to obtain the desired kVA rating of an open-delta connection system.

As the open-delta connected transformers are loaded, the voltage shifts from a balanced voltage at low load to a seriously unbalanced voltage at rated load. Unbalanced voltages will contain a negative sequence component of voltage. When applied to a three-phase induction motor, this causes excessive heating in the rotor as well as some lost torque in the motor. Unbalanced voltages result in unbalanced currents.

Unbalanced voltage causes a three to five times greater current unbalance. This means that for a 3% voltage unbalance, a current unbalance of 9 to 15% can be expected. These unbalanced conditions require one to derate the motor used on the pumping unit. Use the curve shown in Fig. 10.21 to determine the derating factor for percent voltage unbalance at the motor terminals.¹⁴

$$V_{ub} = \frac{\Delta V_{max}}{\bar{V}} \times 100 = \frac{\bar{V} - (V_L)_{max}}{\bar{V}} \times 100, \dots (15)$$

where

V_{ub} = voltage unbalance, %,
 ΔV_{max} = maximum voltage deviation from \bar{V} ,
 \bar{V} = average voltage, and
 $(V_L)_{max}$ = line voltage, maximum difference from average voltage.

Example Problem 5. If line voltages are 465, 460, and 435, the average voltage is 453, and the maximum deviation is $453 - 435 = 18$:

$$V_{ub} = \frac{18}{453} \times 100$$

$$= 3.97$$

and

$$F_{dr} = 0.83 \text{ (read from Fig. 10.21),}$$

where F_{dr} is the derating factor. (This curve can be used any time three-phase voltage is not balanced.)

There are many installations in the electrified oil field that use the open-delta transformer connections. The only way the open-delta transformer will operate successfully on a pumping unit is to have transformers and the motor both oversized to handle the load of the pumping unit. Only during an emergency situation where one transformer has failed is the open-delta transformer connection recommended. For this emergency condition, derating of the transformer and the motor is required.

All distribution systems have a ground of some type associated with the installation. It is extremely important that the groundwire is terminated at an adequate ground. Reference should be made to the portion of this chapter on grounding of electrical systems.

Sizing of the distribution transformer is a very important part of satisfactory operation of the oilwell pumping motor. The industrial rule of thumb for sizing transformers is 1 kVA/connected hp. Because of the cyclic nature of oilwell pumping loads, some operators use 0.9 kVA/hp. Ultrahigh-slip motors do not have horsepower ratings; therefore, a factor of 0.75 times the full-load current of the motor in the high-torque mode should be used to determine the required kVA.

Electrical System Grounding

Grounding of electrical equipment at the wellsite is a very important part of the electrical system. Grounding of electrical equipment has two distinct purposes: (1) devices are grounded for personnel safety and (2) devices must be grounded to perform satisfactorily.

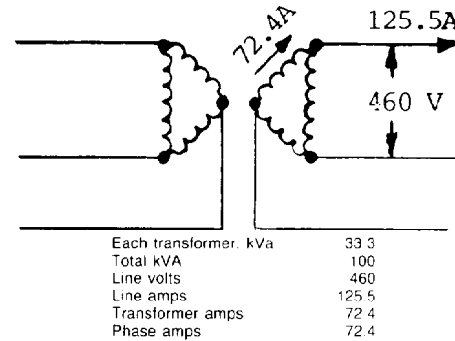


Fig. 10.19—Three transformers, delta-delta.

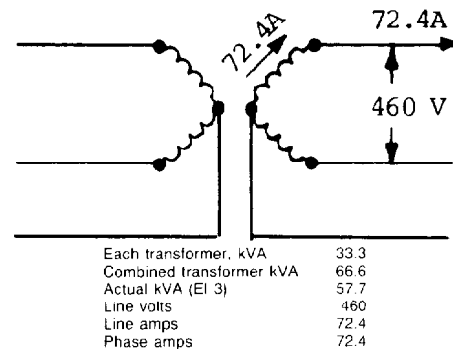


Fig. 10.20—Two transformers, open-delta.

For personnel protection at the wellsite, all enclosures that house electrical devices should be grounded. If wiring or other devices within an electrical enclosure should fail in some way and come into contact with the enclosure, it may have the same electrical potential as the broken wire. If the enclosure is grounded adequately, the stray voltage will be reduced to safe levels. If the enclosures are not grounded properly, unsafe voltages could exist, which could be fatal to the operating personnel.

The lightning arresters installed in electrical systems cannot operate satisfactorily unless they have good

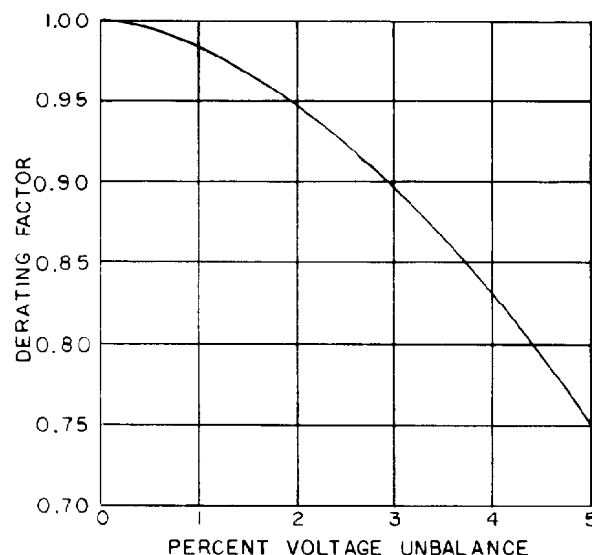


Fig. 10.21—Effects of unbalanced voltages on the performance of three-phase induction motors.

grounds. Lightning arresters under elevated static voltage or lightning strikes will short-circuit the above-normal voltages to ground. If the lightning arresters are not grounded properly, elevated voltage will enter the windings of transformers, control, or motors, causing component failures.

Obtaining a satisfactory ground at the wellsite can present some difficulties. The wellhead normally can be considered an excellent grounding source through the well casing. The ground rods used at the wellsite can vary from acceptable in moderately wet soils to very inadequate in dry soils. The wellhead should be used whenever possible for grounding of the secondary electrical system. There are some conditions that should be considered when tying equipment to the wellhead for grounding. The following directions should satisfy most conditions existing at the wellsite.

1. All the secondary electrical system devices should have their enclosures tied to the wellhead for personnel safety. This includes the transformer tank, disconnect switch enclosure, motor control, and motor frame.

2. All secondary lightning arresters should be grounded to the wellhead. Different conductors should be used to ground the secondary enclosures and lightning arresters. The wire that grounds the lightning arresters should be a continuous unbroken cable no smaller than No. 6 wire from the lightning arresters to the wellhead ground.

3. Primary lightning arresters also should be grounded at a utility primary ground and not to the secondary ground or wellhead.

4. Utility static wires or grounding of transformer connections should not be attached to the wellhead. This equipment, if connected to the wellhead, can influence the malfunction of cathodic protection of well casing and production tubing. This part of the electrical system may include many miles of line exposure and many grounds that could influence the corrosion of the production equipment. Grounds for this part of the system should be grounding rods or ground pads located at the bottom of the utility poles. Other satisfactory grounds are wells drilled or ground mats constructed for this purpose at the electrical substation.

It is desirable to install ground rods at each location for each of the separate grounding wires run to the wellhead. During the servicing of the wells, the wellhead grounds may be removed. When service work is completed, these wellhead grounds should be reconnected.

5. It is recommended not to connect the grounds of telephone systems to the grounds of oilfield pumping motors. Induction motors can generate harmonic voltages that can cause noise on telephones when they share common grounds.

Voltage Drop in Electrical Systems

The electrical system of an oil field should be designed economically, but it must be capable of delivering the required current at adequate voltage to all motors for starting and running. To satisfy these conditions, all equipment must be considered. Each device in this system will have a voltage drop based on the full load of the motor or motors. All the voltage drops should be subtracted to obtain the voltage at the motors. In most field applications, the primary system is provided by a utility company. In these cases, it is necessary to evaluate the voltage from the utility drop point to the wellsite only. It is important to obtain from the utility company the voltage and kVA available at the drop point. The voltage obtained from the utility company is that voltage available at the drop point when all the required kVA delivered to the oil field is considered. This would be the source voltage level to use to calculate voltage drops. If the utility company furnishes the distribution transformer, only the size and type of wire to the well must be determined. For short runs (1 to 200 ft), voltage drop is minimal and the selection of a cable capable of carrying 125% full-load current normally is adequate. For extended secondary cable runs, voltage drop must be calculated. This is done by use of charts, tables, or formulas designated specifically for buried cable or overhead lines. Fig. 10.22 can be used for calculating voltage drops.

To use the graphs in Fig. 10.22 draw a vertical line from wire size in the graph with or without capacitors (whichever is appropriate) to intersect with horsepower. From horsepower, draw a horizontal line to cable length. At the intersection with cable length, draw a vertical line down to percent voltage drop. For example, a 20-hp, size-2 conductor, 666 ft long, has a starting voltage drop of 8%. The running voltage drop is 1.5%.

For ultrahigh-slip motors, multiply the high-torque mode amps by 0.75 to approximate the equivalent horsepower that should be used in calculating voltage drops.

The distribution transformer's voltage drop can also be obtained from the two charts in Fig. 10.23.

Fig. 10.23 shows that the starting voltage drop of a 20-hp motor with capacitors, using a 30-kVA transformer, is 11%. The running voltage drop is 1.7%. In the example, the total drop including the transformer and motor can be determined by using Eq. 16.

$$\Delta V_m = \Delta V_t + \Delta V_l, \dots \dots \dots (16)$$

where

ΔV_m = voltage drop at motor, %,
 ΔV_t = voltage drop at transformer, %, and
 ΔV_l = line voltage drop, %.

$$\begin{aligned} \Delta V_{ms} &= 11 + 8 \\ &= 19\% \end{aligned}$$

and

$$\begin{aligned} \Delta V_{mr} &= 1.7 + 1.5 \\ &= 3.2\%, \end{aligned}$$

where

ΔV_{ms} = starting voltage drop of motor, %, and
 ΔV_{mr} = running voltage drop of motor, %.

It is desirable to limit running voltage drop to 5% and starting voltage drop to 20%.

Complete tables and charts are available for calculating voltage drops from wire and cable manufacturers. Also it is recommended that electrical codes be considered when designing systems.

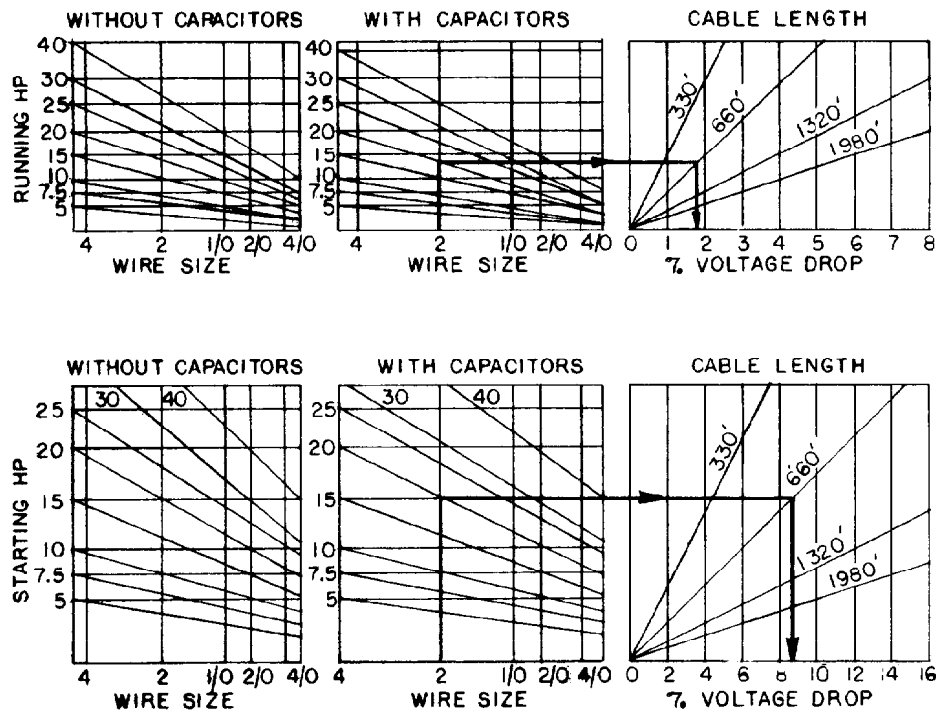


Fig. 10.22—Voltage drop for overhead and buried cable.

Power Factor and Use of Capacitors

Electric power required to drive a motor can be divided into three separate components. These are kilowatts (kW), kilovoltamp reactive (kVAR), and kilovoltamps (kVA). Kilowatts are the amount of work done by the motor and are the major quantity used for billing purposes. Kilovars are the electrical quantity needed by the motor and control for magnetizing purposes and lags kilowatts by 90°. Kilovoltamps are the amount of energy furnished by the utility company and are a resultant of kilowatts and kilovoltamps reactive (kilovars). These three components allow the creation of a motor power triangle (see Fig. 10.24).

Kilowatts are measured with a kilowatt-hour meter. Kilovoltamps can be calculated using Eq. 17.

$$EI = \frac{\sqrt{3} \times V \times I_{rms}}{1,000} \dots\dots\dots (17)$$

where

V = volts, and

I_{rms} = root mean square amps.

RMS amps are available from a thermal ammeter. The volts are the line-to-line volts to the motor. From kilovoltamps and kilowatts, the kilovoltamps reactive can be calculated as follows.

$$\text{kVAR} = \text{kVA} - \text{kW}.$$

The kilovoltamps reactive are the electrical quantity needed by the motor and control for magnetizing pur-

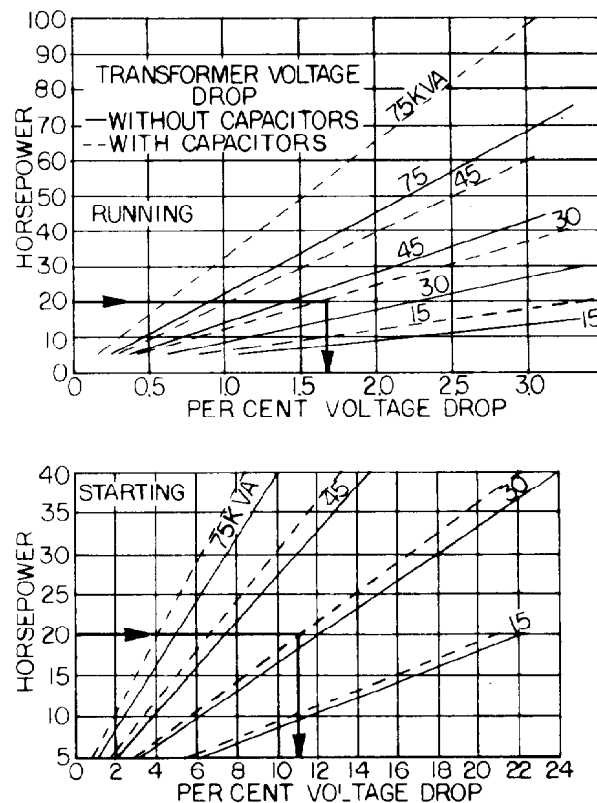


Fig. 10.23—Transformer voltage drop.

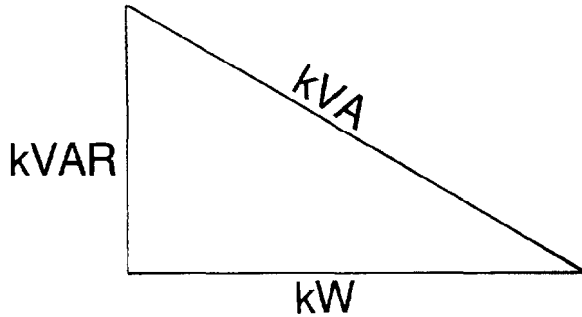


Fig. 10.24—Power triangle.

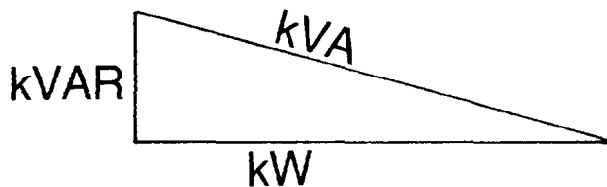


Fig. 10.25—Power triangle for heavily loaded motor.

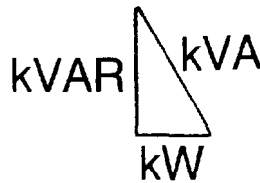


Fig. 10.26—Power triangle for lightly loaded motor.



Fig. 10.27—Power triangle for motor at synchronous revolutions per minute.

poses. The kilovoltamps reactive quantity required for a pumping motor does not follow the cyclic loading like amps and kilowatts and is approximately the same from no load to full load.

Typical power triangles drawn for a motor with different load conditions are shown in Figs. 10.25, 10.26, and 10.27.

When a motor is loaded heavily (Fig. 10.25), the kilowatts are greatest. If the motor is loaded lightly, the kilowatts decrease (Fig. 10.26). If the motor is driven at synchronous speed by the pumping unit (regeneration), the kilowatts are zero and the triangle would shift to a vertical line as in (Fig. 10.27) and consists only of kilovars. For light loads, kilovoltamps are made up predominantly of kilovars. For heavy loads, kilovoltamps are made up predominantly of kilowatts. If a utility company is furnishing the supply for the motor, they would prefer the case of maximum kilowatts as they get a better return for the kilovoltamps they are providing.

The power factor is used to show the relationship between EI (kilovoltamps) and P (kilowatts):

$$F_p = \frac{P}{EI\sqrt{3}}, \dots\dots\dots (18)$$

where

F_p = power factor,

P = power, kW,

E = electromotive force, kV,

I = current, A, and

$EI\sqrt{3}$ = voltage-current product, kVA.

Because of the cyclic nature of pumping unit motor loads, the electrical conditions illustrated in Figs. 10.25, 10.26, and 10.27 frequently occur during each stroke of a pumping cycle. This range can go from near 1.0 to 0.

If motor rev/min is at synchronous rev/min, kW is essentially zero.

$$F_p = \frac{0}{EI} = 0. \dots\dots\dots (19)$$

At light loads where kilowatts are minimal, the power factor is near zero. At heavy loads, the kilovoltamps and kilowatts approach the same magnitude. If kilowatts could be made as large as kilovoltamps, the power factor would be one. The cyclic kW load on a pumping motor can cause the power factor to range from near 1.0 to near 0 if excessive adverse pumping conditions exist. Low power factors are the result of improper counter-balance, pumped-off wells, or oversized motors. Because power factor does vary greatly throughout the pumping cycle, even under optimum conditions, one should not be misled by single-point maximum power factor rating of a motor. Overall power factor, however, is important.

A utility company furnishing electrical power must furnish both kilovars and kilowatts. In some locations, the utility company will penalize the customer if a maximum power factor is not maintained.

The magnetizing kilovars required by a motor are inductive kilovars. Capacitive reactance supplied by capac-

itors has a cancelling effect on inductive kilovars reactance required by the motors. The utility company prefers the highest possible power factors because this means they get a greater return (kW billed) for their product supplied (kVA generated). Fig. 10.28 shows by the power triangle how capacitance can improve the power factor for a motor.

Fig. 10.28 shows how capacitance kilovars are related to inductive kilovars. It also shows how an improved power factor can influence the magnitude of line amps required to operate a motor at low and high power factors.

The improved power factor does not change the current required by the motor but does change the current required from the utility company. Selection of capacitance kilovars should not be made to correct poor power factors resulting from oversized motors or unbalanced pumping units. This may cause overcorrection, which can provide a leading power factor. Lead and lag power factors will decrease from 1.0 toward 0. Lag values are assigned negative values while lead is assigned positive values. Slightly leading power factors of 1.0 to 0.96 are not harmful; however, leading power factor less than 0.96 may be detrimental to the electrical system. Excessive power factor over-correction may cause over-voltages that would cause control component failure. If the contactor to a motor with connected capacitor is opened while the pumping unit is driving the motor, voltages high enough to cause motor winding failure can occur.

Use of Phase Converters

There are areas where only single-phase power is available to drive pumping unit motors. Single-phase motors are available only in small horsepower ranges, so, if an operator chooses to electrify his well, he must use a phase converter.

A phase converter is an electrical device that creates a form of three-phase power from single-phase power. A description of three types of phase converters follows.

Capacitor-Type Converter. This is the simplest type of phase converter because the additional phases are produced by a capacitor bank in series with a part of the motor winding. Fig. 10.29 shows the general concept of this type of phase converter.

This is not a desirable phase converter for a pumping unit motor because it does not provide the full torque required for the starting and running of the cyclic loaded pumping unit motor. This requires the motor to be derated up to 40% to compensate for this condition.

Autotransformer-Type Converter. This converter uses an autotransformer-capacitor. Fig. 10.30 shows how the autotransformer is connected in the converter circuit. The autotransformer has taps for selecting the best voltage for balancing current to the three-phase induction motor.

Of the three-phase converters discussed, the autotransformer converter is, because of its cost and effectiveness, the most desirable for a single pumping unit motor installation. While the motor must be derated approximately 15%, there are adjustments available with its transformers and capacitors to obtain fairly balanced amps for the motor.

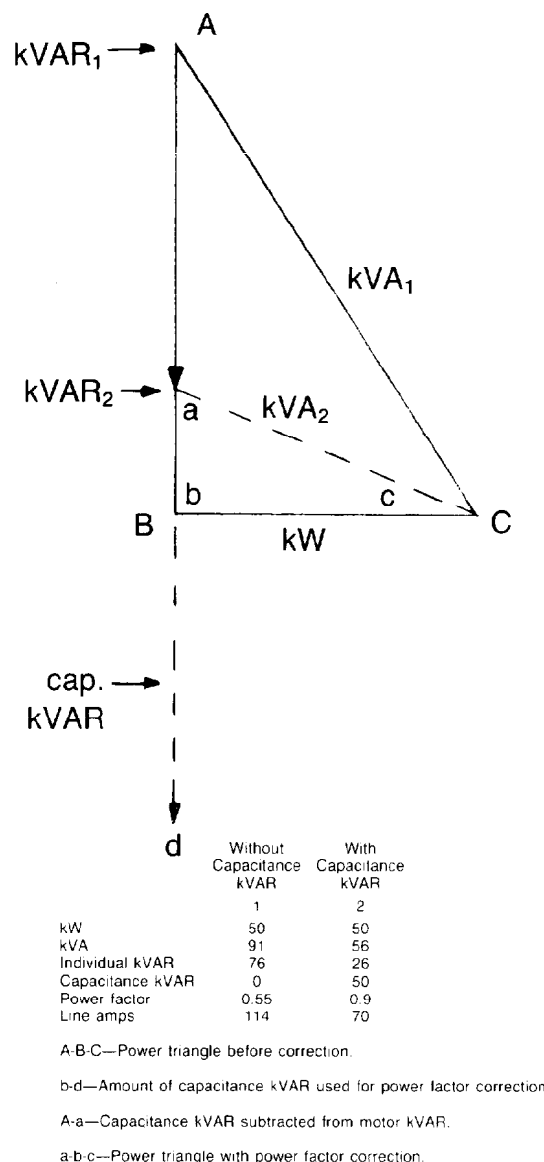


Fig. 10.28—Power triangle showing power factor correction.

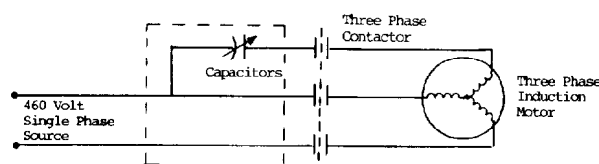


Fig. 10.29—Capacitor phase converter.

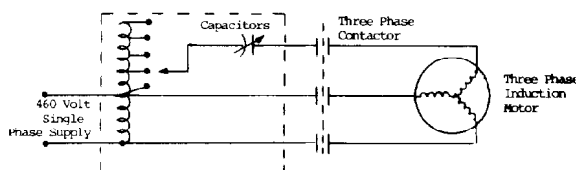


Fig. 10.30—Autotransformer capacitor.

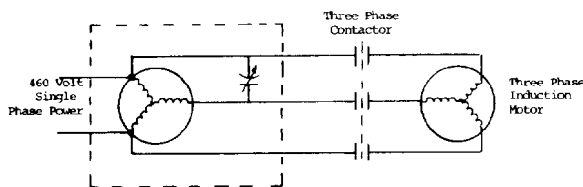


Fig. 10.31—Rotary converter.

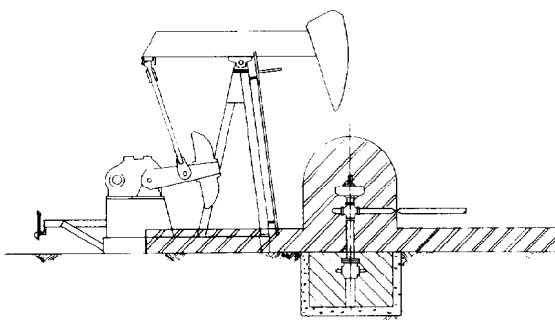


Fig. 10.32—C114D-143-64 pumping showing the classified areas.

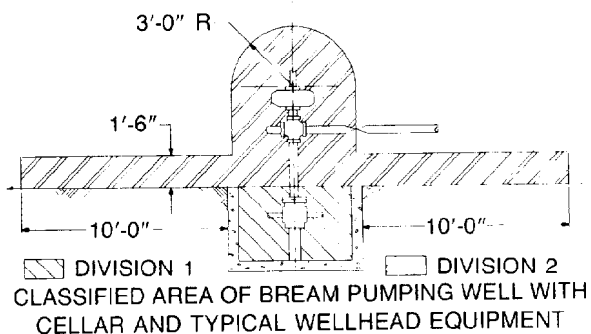


Fig. 10.33—Classified area of beam pumping well with cellar and typical wellhead equipment.

Rotary-Type Converter. The rotary converter consists of a rotating unit similar to a motor without an external shaft. Fig. 10.31 shows how the stator winding of the rotating converter is connected to the induction motor. Two of the three rotating converter terminals are connected directly to the single-phase power lines. The third rotating converting terminal is connected to one of the single-phase lines through the capacitor bank. The capacitors provide the rotating magnetic field to start and operate the converter. The generating action of the rotating converter, in combination with the phase shift of the capacitors, produces third-phase voltage to operate the motor.

The cost of rotary converters is best justified on multiple motor installations. It can provide satisfactory performance equal to the autotransformer converter. The rotary converter should be sized to be at least twice the size of the largest motor on the system and as large as the combined motor horsepower on the system, whichever is greater.

Hazardous Area Classification

NEC has classified areas surrounding production facilities both on- and offshore for safe installation of electrical equipment.¹⁵ Details of these classified areas (Figs. 10.32 and 10.33) are found later in this section. Fig. 10.33 shows classified area dimensions.

One should refer to the pumping unit dimensions to ensure that the electrical equipment is mounted in a non-classified area. All areas outside these dimensions are considered non-classified.

It is important to realize that pumping motors and controls located in non-classified areas are not required to be explosion-proof. However, other electrical equipment, such as pressure switches or other electrical devices, may require special enclosures.

Class 1 locations are those in which flammable gases or vapors are, or may be, present in the air in quantities sufficient to produce explosive or ignitable mixtures. Class 1 locations include the following.

Class 1, Div. 1.¹⁶ Locations (1) in which explosive or ignitable concentrations of flammable gases or vapors exist continuously, intermittently, or periodically under normal operating conditions; (2) in which explosive or ignitable concentrations of such gases or vapors may exist frequently because of repair or maintenance operations or because of leakages; or (3) in which breakdown or faulty operation of equipment or processes might release explosive or ignitable concentrations of flammable gases or vapors might also cause simultaneous failure of electrical equipment.

Class 1, Div. 2. Locations (1) in which volatile, flammable liquids or flammable gases are handled, processed or used, but in which the explosive or ignitable liquids, vapors, or gases will normally be confined with closed containers or closed systems from which they can escape only in case of accidental rupture or breakdown of such containers or systems, or in case of abnormal operation of equipment; (2) in which explosive or ignitable concentrations of gases or vapors are normally prevented by positive mechanical ventilation, and which might become

explosive or ignitable through failure or abnormal operation of the ventilating equipment; or (3) which are adjacent to Class 1, Division 1 locations, and to which explosive or ignitable concentrations of gases or vapors might occasionally be communicated unless such communication is prevented by adequate positive-pressure ventilation from a source of clean air, and effective safeguards against ventilation failure are provided.

Key Equations in SI Metric Units

$$v_{pr1} = 0.0121 F_{t1} \times N, \dots\dots\dots (1)$$

where

v_{pr1} = polished rod velocity at Crank Position 1, m/s,

F_{t1} = torque factor at Crank Position 1, mm, and

N = pumping speed, strokes/sec.

$$\bar{A}_{pr1,2} = 0.0695 N^2 \left(\frac{F_{t1} - F_{t2}}{\theta_1 - \theta_2} \right), \dots\dots\dots (2)$$

where

$\bar{A}_{pr1,2}$ = average polished rod acceleration between Crank Positions 1 and 2, m/s²,

F_{t1}, F_{t2} = torque factors at Crank Positions 1 and 2, mm, and

θ_1, θ_2 = angle crank rotates between Positions 1 and 2, rad.

$$P_b = \frac{q \times D}{3639}, \dots\dots\dots (3)$$

where

P_b = brake power for NEMA D motors, kW,

q = fluid flow rate, m³/d, and

D = depth (lift), m.

$$P_b = \frac{q \times D}{2924}, \dots\dots\dots (4)$$

where

P_b = brake power for NEMA C motors, kW.

$$P_h = \frac{q \times D \times W}{972.7 \times 24 \times 60}, \dots\dots\dots (5)$$

where

P_h = hydraulic power to lift the fluid, kW,

W = weight of fluid, kg,

24 = hours per day, and

60 = seconds per minute.

$$P_h = \frac{q \times D}{8821}, \dots\dots\dots (6)$$

where

P_h = hydraulic power for fluid with 1.0 specific gravity.

$$P_f = \frac{\frac{1}{8} W_r \times 2S \times N}{6118}, \dots\dots\dots (7)$$

where

P_f = power to overcome subsurface friction, kW,

W_r = weight of rods, kg,

S = polished-rod stroke, m, and

N = strokes per minute.

$$P_{pr} = P_h + P_f, \dots\dots\dots (8)$$

where

P_{pr} = polished rod power, kW.

$$P_{pm} = P_{pr} / 0.85, \dots\dots\dots (9)$$

where

P_{pm} = prime mover power, kW.

$$P_m = \frac{P_h + P_f}{E_{pu} \times F_{cl}}, \dots\dots\dots (10)$$

where

P_m = slow speed engine power or NEMA motor D, kW,

E_{pu} = pumping unit efficiency, fraction, and

F_{cl} = cyclic load derating factor, fraction.

References

1. "API Specification for Pumping Units," 12th edition, API Specification 11E, API, Dallas (Jan. 1982).
2. "Recommended Practice for Design Calculations for Sucker Rod Pumping Systems (Conventional Units)," third edition, API RP 11L, API, Dallas (Feb. 1977).
3. "Recommended Practice for Installation and Lubrication of Pumping Units," second edition, API RP 11G, API, Dallas (Feb. 1959) and Supplement (Jan. 1980).
4. "Recommended Practice for Guarding of Pumping Units," first edition, API RP 11ER, API, Dallas (March 1976).
5. Chastain, J.: "How To Pump More For Less With Extra High-Slip Motors," *Oil & Gas J.* (March 1968) 62-68.
6. Gibbs, S.G.: "Computing Gearbox Torque and Motor Loading for Beam Units With Consideration of Inertia Effects," *J. Pet. Tech.* (Sept. 1975) 1153-59.
7. "API Specifications for Internal-Combustion Reciprocating Engines for Oil Field Service," eighth edition, API 7B-11C, API, Dallas (March 1981).
8. National Electric Manufacturers Association: MG 1-1, 16 (July 1982) 16.
9. *Practical Petroleum Engineers Handbook*, fourth edition, J. Zaba and W.T. Doherty (eds.), Gulf Pub. Co., 532 (J.C. Slonneger).
10. "Recommended Practice for Installation, Maintenance, and Operating of Internal-Combustion Engines," fourth edition, API RP 7C-11F, API, Dallas (April 1981).
11. Institute of Electrical & Electronic Engineers: STD 117-1974, 23.
12. National Electric Manufacturers Association: MG 1-1.25, Part 1, 5, MG 1-1.26, Part 1, 7 (June 1978).
13. National Electric Manufacturers Association: ICS-6-1978.
14. Ward, Daniele: "Motor Voltage Unbalance Limits," *Southwest Electric Distribution Exchange* (May 9, 1979).
15. "Recommended Practice for Classification of Areas for Electrical Installations at Drilling Rigs and Production Facilities on Land and on Marine Fixed and Mobile Platforms," second edition, API RP 500B, API, Dallas (July 1973) 8.

Chapter 11

Oil Storage

William E. Roof, C-E Natco *

Types of Storage Tanks

Every facility involved in the production of petroleum and related products requires some type of storage. This chapter discusses the types of storage commonly used and also provides general guidelines to aid selection of the proper type of storage for a particular application.

References to various codes, standards, and recommended practices supplement the material provided in this chapter. Manufacturers also should be consulted for specific design information on a particular type of storage.

During the early days of oil production, the method of storing was almost exclusively white-pine wooden tanks, which were followed by cypress tanks, and then redwood tanks. However, because of the constant and steep rise in the cost of redwood lumber and the diminution of skilled erectors required, the installation of new wooden tanks is nearly nonexistent. The bolted-steel tank was developed next and virtually replaced the wooden tank.

Bolted-Steel Tanks

Bolted tanks are designed and furnished as segmental elements assembled on location to provide complete vertical, cylindrical, aboveground, closed- and open-top steel storage tanks. Standard API bolted tanks are available in nominal capacities of 100 to 10,000 bbl, and are designed for approximately atmospheric internal pressures. Bolted tanks offer the advantage of being easily transported to desired locations and erected by hand. To meet changing requirements for capacity of storage, bolted tanks can be easily dismantled and re-erected at new locations. If a tank develops a hole from corrosion or becomes damaged, a single sheet or more may be replaced. A complete tank bottom may be replaced in the field without dismantling the tank. Also, a section may be removed from the tank, a new connection installed in the sheet, and the section replaced without danger. This is not true

of any other type of steel construction. No special equipment (cranes, etc.) is required for the erection of bolted tanks. These tanks are erected by nonspecialized crews using hand tools and usually an impact wrench.

Bolted tanks are available with painted, galvanized, and special coatings, including factory-baked coatings. Painting on both sides of the sheets during fabrication gives the inside of the tank some corrosion protection. Galvanizing the sheets and all tank parts by the "hot-dip" process or applying a factory-baked coating affords high corrosion protection. The component parts of a typical bolted tank are shown in Fig. 11.1 and partial API specifications in Table 11.1.¹

Generally, bolted tanks are fabricated from 12- or 10-gauge steel and, if not galvanized or furnished with a protective coating for corrosion protection, they do not have the expected life of the welded-steel tanks, which are usually constructed of heavier steel.

Welded-Steel Tanks

Shop-fabricated welded, cylindrical-shape tanks are available in a large variety of sizes as shop-fabricated items. The API-12F specifications² for vertical shop-welded tanks (Fig. 11.2 and Table 11.2) list standard sizes for nominal capacities of 90 to 500 bbl. Shop-welded tanks fabricated to API specifications provide the oil production industry with tanks of adequate safety and reasonable economy for use in the storage of crude petroleum and other liquids commonly handled and stored by the production segment of the industry. Shop-welded tanks are usually fabricated from $\frac{3}{16}$ -in. or heavier steel and, therefore, will permit internal pressures up to 16 oz. The heavier steel also affords a corrosion allowance. Shop fabrication permits testing in the shop for leaks and also provides immediate storage. Tanks are merely up-ended from a truck on the location.

*The chapter on this topic in the 1962 edition was written by Don R. Boling

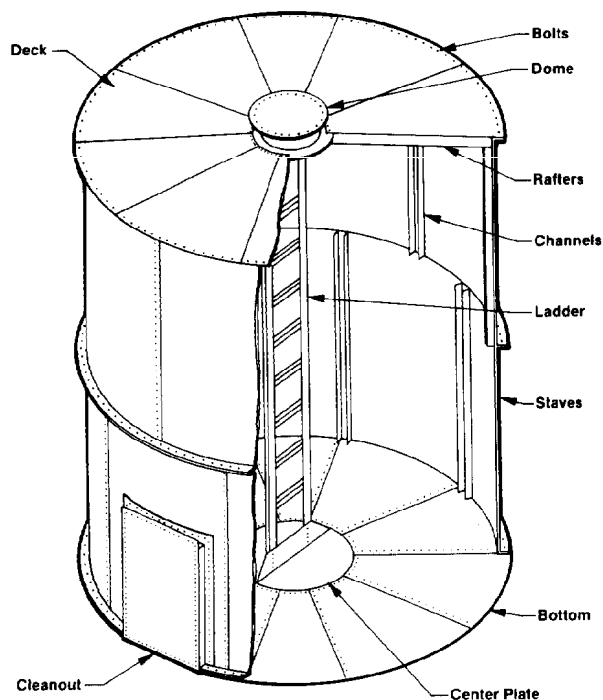


Fig. 11.1—Typical bolted tank.

Flat-Sided Tanks (Non-API)

Although cylindrical-shape tanks may be structurally best for tank construction, rectangular tanks frequently are preferred. When space is limited, such as offshore, requirements favor flat-sided tank construction because several cells of flat-sided tanks can be fabricated easily and arranged in less space than other types of tanks. Flat-sided or rectangular tanks normally are used as atmospheric-type storage.

Field-Welded Tanks

Field-welded tanks provide large storage capacities in a single unit. API Spec. 12D lists standard sizes ranging from 500- through 10,000-bbl nominal capacity. Although the sizes set forth in this specification are closely paralleled by bolted tanks, these field-welded tanks are of heavier-gauge steel with a minimum thickness of $\frac{1}{4}$ in. for the tank bottom and $\frac{3}{16}$ in. for the shell and deck.

Larger field-welded tanks providing storage capacities of 150,000 bbl or more have become quite prevalent for use in the storage of oil and petroleum products. Field-welded tanks, particularly those larger than 10,000 bbl, frequently are designed and erected in accordance with API Standard 650. This standard covers material, design, fabrication, erection, and testing requirements for welded-steel storage tanks. It also includes an alternative basis for shell design, as well as one for calculating tank-shell thickness. The API Standard 650 also may be used to govern the design and fabrication of the smaller shop-welded tanks.

Fixed Roof

Fixed roofs are permanently attached to the tank shell. Welded tanks of 500-bbl capacity and larger may be provided with a frangible roof (designed for safety release of the welded deck-to-shell joint in the event excess internal pressure occurs). In this case, the design pressure should not exceed the equivalent pressure of the dead weight of the roof including rafters, if external.

Floating Roof

Storage tanks may be furnished with floating roofs whereby the tank roof floats on the stored contents. This tank type is used primarily for storage near atmospheric pressure. Floating roofs are designed to move vertically within the tank shell to provide a constant minimum void between the surface of the stored product and the roof. Floating roofs normally are designed to provide a constant seal between the periphery of the floating roof and the tank shell. They can be fabricated in a type that is exposed to the weather or a type that is under a fixed roof. Internal floating-roof tanks, with an external fixed roof, are used in areas of heavy snowfall since accumulations of snow or water on the floating roof affect the operating buoyancy. These can be installed in existing tanks as well as new tanks. Both floating roofs and internal floating roofs are used to reduce vapor losses and to aid in conservation programs. Fig. 11.3 is a schematic of a typical internal floating-roof tank.

Cone-Bottom Tanks

The cone bottom in either the bolted or the welded tank offers a means of draining and removing water, or water-cut oil, from only the bottom of the tank, leaving the marketable oil above. The drain line from a sump-equipped cone bottom must be equipped with a vortex breaker to drain off most of the water without coning oil into the drain. With a flat-bottom tank, some of the marketable oil must be removed if all the water is removed from the tank. Corrosion on the tank bottom is kept to a minimum by keeping all water removed. A cone bottom can be kept clean without having to open the tank if 1 or 2 bbl are drained off once or twice weekly and pumped back through the treating system. If this is not done and the bottom solidifies, the tank must be opened. The cone-bottom tank can be cleaned without entering. A water hose, handled just outside the cleanout opening, can be used to flush the solids to the center of the cone and drain connection.

Pipe Storage

Pipe that is used specifically for storing and handling liquid petroleum components should be designed and constructed in accordance with applicable codes. Pipe storage consists of any number of sections of line pipe laid parallel to each other and interconnected to operate as a single unit. The size and length depend on the capacity required and economics. The exterior of buried-pipe storage should be coated and wrapped for corrosion protection. It also is recommended that any coated, wrapped, and buried carbon steel pipe be protected cathodically against the possibility of eventual holidays (imperfections) in the coating. Aboveground pipe storage should be protected against the

TABLE 11.1—PARTIAL API DIMENSIONAL SPECIFICATIONS FOR BOLTED STEEL TANKS*

Capacity		Dimensions															
Nominal Capacity (42-gal barrel)	Actual Capacity Level Full (42-gal barrel)	ID* (Nominal)				Roof and Bottom Bolt Circles (diameter)		Shell					Bottom		Cone Roof		
								Height		Staves Per Ring	USS Gauge	Rows of Bolts	Bolt Size (in.)	USS Gauge	Bolt Size (in.)	USS Gauge	Chime (in.)
		(ft)	(in.)	(ft)	(in.)	(ft)	(in.)										
100	95.80	9	2¾	9	4¼	8	½	6	12	1	½	12	½	12	½	½	
200	191.64	9	2¾	9	4¾	16	1	6	12 12	1 1	½ ½	12	½	12	½	½	
300	287.46	9	2¾	9	4¾	24	1½	6	12	1	½	12	½	12	½	½	
250	266.28	15	4⅝	15	6⅝	8	½	10	12	1	½	12	½	12	½	½	
500 high	532.56	15	4⅝	15	6⅝	16	1	10	12 12	1 1	½ ½	12	½	12	½	½	
750	798.84	15	4⅝	15	6⅝	24	1½	10	12 12 10	1 1 1	½ ½ ½	12	½	12	½	½	
500 low	522.01	21	6½	21	8½	8	½	14	12	1	½	12	½	12	½	½	
1,000 high	1,044.02	21	6½	21	8½	16	1	14	12 12	1 1	½ ½	12	½	12	½	½	
1,500**	1,566.03	21	6½	21	8½	24	1½	14	12 12 12†	1 1 2†	½ ½ ½	12 12	½ ½	12 12	½ ½	½ ½	
1,000 low	993.53	29	8⅝	29	10⅝	8	½	20	12	2	½	12	½	12	½	½	
2,000	1,987.06	29	8⅝	29	10⅝	16	1	20	12 12	2 2	½ ½	12	½	12	½	½	
3,000	2,980.59	29	8⅝	29	10⅝	24	1½	20	12 12 10	2 2 2	½ ½ ½	12	½	12	½	½	
5,000	5,037.45	38	7⅝	38	9⅝	24	1½	26	12 10 10	2 2 2	½ ½ ½	10	½	12	½	½	
10,000	10,218.49	54	11¾	55	1¾	24	2	37	10 10 3/16 in.	2 2 3	½ ½ ½	10	½	12	½	½	

*API specifications for standard bolted tanks were prepared by the API Committee on Standardization of Steel Tanks for Oil Storage. Specifications apply to new material. The specification was designed to provide the industry with a standard series of bolted tanks, comprising an adequate range and variety of sizes to meet oilfield requirements, built in accordance with modern manufacturing practice so that decks and bottom pieces and individual staves as supplied by any manufacturer will be readily interchangeable with those supplied by others. On this page are excerpts from API Std. No. 12-B. The complete specification and latest editions are available from the American Petroleum Inst., Div. of Production, Dallas.

*Nominal ID is considered as 2 in. less than bolt-circle diameter and actual capacity figured on that basis.

**Note that the first ring of staves of the 1,500-bbl tank, which is 21 ft 6½ in. ID by 24 ft 1½ in. high, will consist of 12-gauge material conforming to the usual 60-in. width and on account of the two rows of bolts required for the vertical seams of this particular ring, the net width of each of these staves will be 2 in. less than the standard, so the staves will not match up all the way round the tank, and a fill-in staff will be required.

†NOTE: A narrow fill-in staff may be used in conjunction with regular staves 60 in. wide.

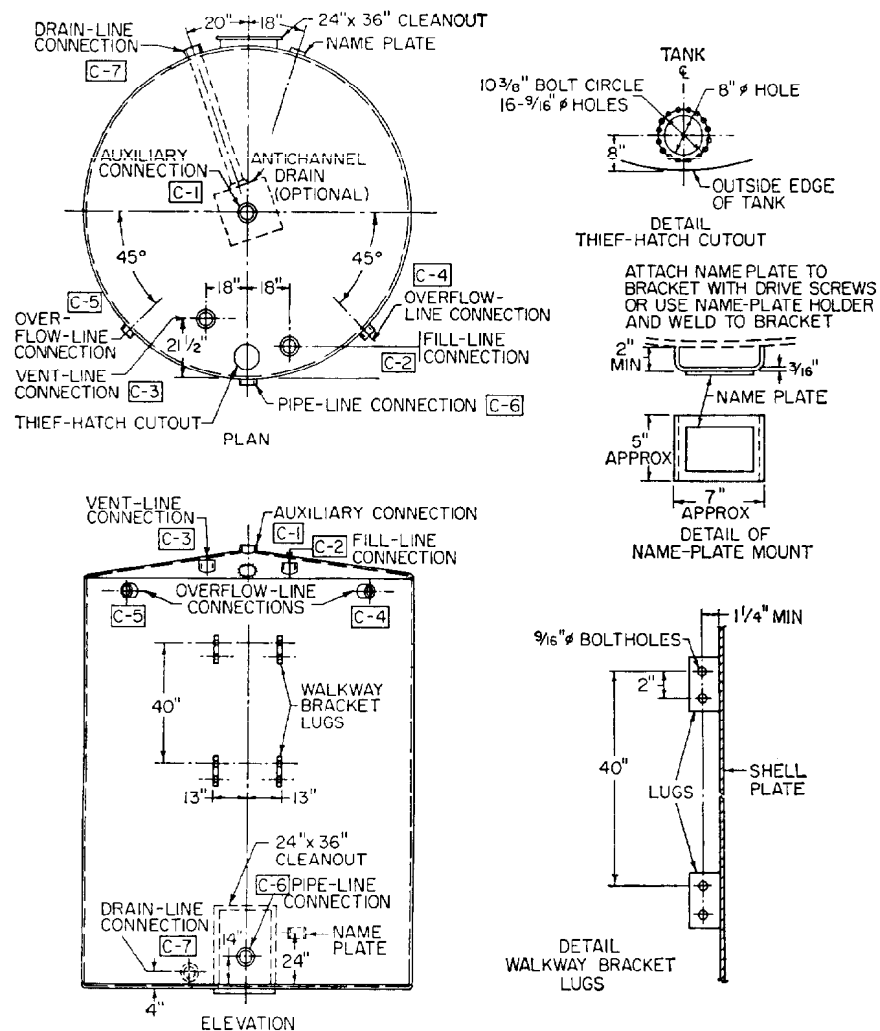


Fig. 11.2—Tank dimensions. See Table 11.2.

elements with paint or other approved coating material. In some cases, pipe storage may require insulation. The individual storage pipes are manifolded together for filling and emptying at pipeline transfer rates. The pipe storage must be protected from overpressure just like any other storage vessel.

Tank Corrosion Protection

Coating Specifications³

The primary use of internal coatings is to protect the inside surface of the tank against corrosion while also protecting the stored contents from contamination.

A coating specification should be a clearly defined list of particulars or instructions. Just as a drawing must give exact dimensions, so must a coating specification state the exact system to be used. In the preparation of such a specification, consideration must be given to such factors as (1) types of coatings available, (2) types of surfaces to be coated, (3) compatibility of coatings, and (4) number of coats required on the various types of surfaces for maximum protection. To secure high-quality coatings, consideration must be given to the following factors.

Compatibility.³ In the broadest sense, any discussion of compatibility should include a consideration of the age-old problem of heredity and environment. Environment calculates the compatibility of coatings when applied to various types of surfaces and the operating conditions to which such coatings will be subjected. Heredity concerns itself with the birth of the coating: formulation. The basic raw materials used in formulating and the art of formulation itself determine whether two paints will be "capable of existing together."

Film Thickness.⁴ Coating film thickness is now widely recognized as one of the most important factors in obtaining desired performance from a coating system. The required thickness of a coating system will vary, depending on (1) generic properties of the coating, (2) the type of substrate to which it is applied, and (3) the severity of the environment to which the coating is exposed. Film thickness for most protective paints and coatings is generally measured in mils; 1 mil is $\frac{1}{1,000}$ in.

TABLE 11.2—PARTIAL API SPECIFICATIONS FOR SHOP-WELDED TANKS—TANK DIMENSIONS

Nominal Capacity (bbl)	Design Pressure (oz/sq in.)		Approximate Working Capacity** (bbl)	OD		Height (ft)
	Pressure	Vacuum		(ft)	(in.)	
90	16	1/2	72	7	11	10
100	16	1/2	79	9	6	8
150	16	1/2	129	9	6	12
200	16	1/2	166	12	0	10
210	16	1/2	200	10	0	15
250	16	1/2	224	11	0	15
300	16	1/2	266	12	0	15
400	16	1/2	366	12	0	20
500	8	1/2	479	15	6	16
Tolerance (all sizes)				± 1/8 in.		± 3/8 in.

Height of Overflow Connection*		Height of Walkway Lugs		Location of Fill-Line Connection (in.)	Size of Connections (in.)	
(ft)	(in.)	(ft)	(in.)		C1,2,3,7	C4,5,6
9	6	7	7	14	3	3
7	6	5	7	14	3	3
11	6	9	7	14	3	3
9	6	7	7	14	3	4
14	6	12	7	14	3	4
14	6	12	7	14	4	4
14	6	12	7	14	4	4
19	6	17	7	14	4	4
15	6	13	7	14	4	4
± 1/8 in.		± 1/8 in.		± 1/8 in.		

*Viscous oil option—when so specified on the purchase order, tanks shall be furnished for viscous oil service. On such tanks, Dimension C of the overflow-line connections shall be 6 in. less than shown in Col. 6, and Dimension E of the fill-line connection shall be 6 in. ± 1/8 in.

**The approximate working capacities shown in Col. 3 apply to flat-bottom tanks.

Type A (unskirted) cone-bottom tanks have 6 in. more working height than the corresponding flat-bottom tanks. The approximate increase is 4 bbl for the 7-ft 11-in.-diameter tanks, 6 bbl for the 9-ft 6-in.-diameter tanks, 7 bbl for the 10-ft-diameter tanks, 8 bbl for the 11-ft-diameter tanks, 10 bbl for the 12-ft-diameter tanks, and 17 bbl for the 15-ft 6-in.-diameter tanks.

Type B (skirted) cone-bottom tanks have 8 in. less working height than the corresponding flat-bottom tanks. The approximate decrease in capacity is 6 bbl for the 7-ft 11-in.-diameter tanks, 8 bbl for the 9-ft 6-in.-diameter tanks, 9 bbl for the 10-ft-diameter tanks, 11 bbl for the 11-ft-diameter tanks, 13 bbl for the 12-ft-diameter tanks, and 15 bbl for the 15-ft 6-in.-diameter tanks.

Surface Preparation.⁵ The importance of surface preparation would seem so fundamental that it would not deserve mention in specifications; however, poor surface preparation is a major contributing factor of many coating failures. Detailed instructions should be given all along the line and steps taken to see that they are carried out properly. Basically, no coating can be better than the surface over which it is applied. If that surface is dirt, grease, moisture, mill scale, rust, concrete dust, or any other foreign or interference material, failure can be expected. These substances, forming a film between the surface and the coating, soon break down and fall away, taking the coating with them. Such failures cannot be called coating failures. The type of surface preparation required on various surfaces is determined by (1) the nature of the surface itself, (2) the operating conditions to which such surfaces will be subjected, and (3) the type of coating to be applied to the surfaces. As a general rule, metal surfaces that are to be submerged require more thorough surface preparation than those areas that will be

nonsubmerged. The more severe the corrosive atmospheric elements will be, the more thoroughly surface preparation must be carried out. Certain coatings have a better bonding quality than others. Once recognition is given to the unequalness of bonding qualities, it is then a relatively simple matter to be certain that the correct type of surface preparation is carried out, as required, for the various coatings.

Coatings Types. Many types of internal coatings are available for numerous protection requirements. Because of the unlimited types and applications, only a few are described here.

Coal Tar. Among the oldest and most reliable coatings, coal tar has extremely low permeability, protects the surface by the mechanical exclusion of moisture and air, is extremely water resistant, and resists weak mineral acids, alkalis, salts, brine solutions, and other aggressive chemicals well.

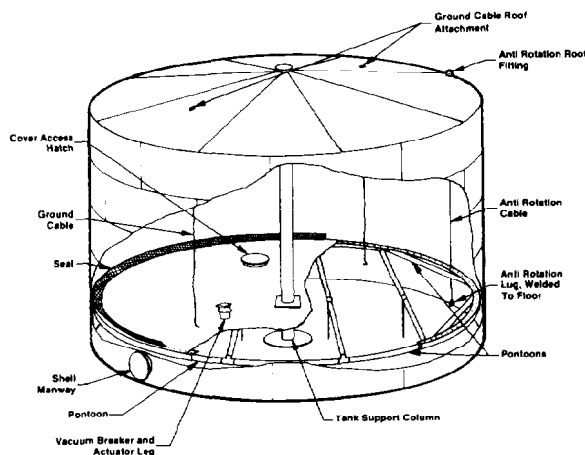


Fig. 11.3—Typical arrangement of internal floating roof.

Epoxy Resin. Epoxy resin gives excellent adhesion, toughness, abrasion resistance, flexibility, high gloss and durability, and good chemical and moisture resistance. Typical applications include linings for sour-crude tanks, floating roof tanks, solvent storage tanks, drilling mud tanks, and pipelines.

Rubber Lining. Rubber lining is used as internal lining for storage tanks that are subjected to severe service, such as elevated temperatures, or for protection from extremely corrosive contents such as concentrated chlorides, and various acids, such as chromic, sulfuric, hydrochloric, and phosphoric.

Galvanizing. Galvanizing (zinc coating) is highly resistant to most types of corrosion. Bolted steel tanks are ideally suited for galvanizing since all component parts are galvanized by the hot-dip process after fabrication but before erection. Galvanized bolted tanks are recommended where sulfur oil is produced and associated with hydrogen sulfide gas. Galvanizing is also very effective against corrosion in seacoast areas where atmospheric conditions present difficulties in maintaining tank life. Fig. 11.4 shows the expected service life of galvanized coatings in different environments for given thicknesses of galvanizing.⁶

External. The basic needs for external coatings are protection against weathering exposure and appearance. Many types of external coatings are available, ranging from basic one-coat primers to primers with one or more top coats. Environmental conditions usually dictate the extent of coating applied. Offshore and coastal installations require more extensive coatings compared with inland locations.

Cathodic Protection

Cathodic protection can be applied to control corrosion that is electrochemical in nature, whereby direct current is forced to flow onto the entire surface area of the steel structure making it cathodic and thus in a noncorroding state. Self-contained sacrificial anodes are recommended for protecting the interior of tanks and vessels. An impressed-current system is recommended for pipe storage, pipelines, casing in producing wells, etc. In this

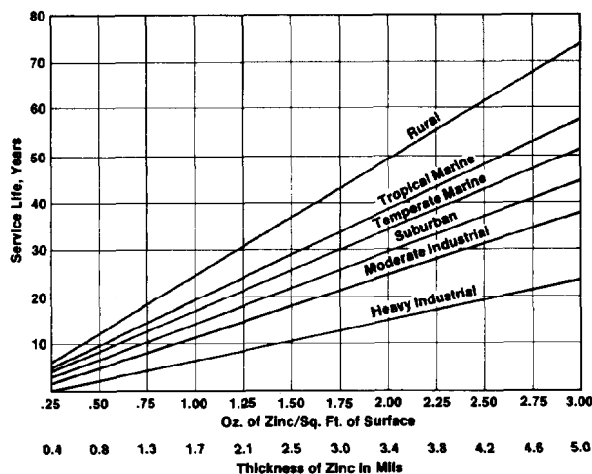


Fig. 11.4—Expected service life of galvanized coatings.

system, the current is furnished by an AC power system, then rectified to DC current and fed to the structure by the use of a semipermanent anode.

Appurtenances

Storage tanks can be provided with any number of appurtenances, depending on the appropriate design codes and user requirements. A tank may be fitted with mixers, heaters, pressure/vacuum relief devices, platforms and ladders, gauging devices, manways, and a variety of other connections. Tanks may also be equipped with sumps, inlet and outlet nozzles, temperature gauges, pressure gauges, vents, and blowdowns.

Venting Atmospheric and Low-Pressure Storage Tanks

The many abnormal variables that must be considered in connection with tank venting problems make it impracticable to set forth definite simple rules applicable to all locations and all conditions. Larger vents may be required on tanks in which oil is heated, on tanks that receive oil from wells or traps, and on tanks that are subjected to pipeline surges. Similarly, the use of flame arresters or other restrictions that may build up pressure under certain conditions may require the use of larger vents on tanks. The following recommendations for nonrefrigerated aboveground tanks are from API Standard 2000 and set forth determining factors relative to tank venting and pressure/vacuum release requirements.⁷

Nonrefrigerated Aboveground Tanks

Determination of Venting Requirements. Conditions for which venting requirements have been set forth include (1) inbreathing resulting from maximum outflow of oil from the tank, (2) inbreathing resulting from contraction of vapors caused by maximum decrease in atmospheric temperature, (3) outbreathing resulting from maximum inflow of oil into the tank and maximum evaporation caused by such inflow, (4) outbreathing resulting from expansion and evaporation that result from maximum increase in atmospheric temperature (thermal breathing), and (5) outbreathing resulting from fire exposure.

Requirements for Normal Venting Capacity. The normal venting capacity shall be obtained without exceeding the pressure or vacuum that may be applied intermittently to a tank without causing physical damage or permanent deformation to the tank.

The total normal venting capacity shall be at least the sum of the venting requirements for oil movement and thermal effect.*

Inbreathing (Vacuum Relief). The requirement for venting capacity for maximum oil movement out of a tank should be equivalent to 560 cu ft/hr of free air for each 100 bbl (4,200 gal)/hr of maximum emptying rate, including the gravity flow rate to other tanks, for oils of any flash point.

The requirement for venting capacity for thermal inbreathing for a given tank capacity for oils of any flash point should be at least that shown in Col. 2 of Table 11.3.

Outbreathing (Pressure Relief). The requirement for venting capacity for maximum oil movement into a tank and the resulting evaporation for oil with a flash point of 100°F or above should be equivalent to 600 cu ft/hr of free air for each 100 bbl (4,200 gal)/hr of maximum filling rate.**

The requirement for venting capacity for maximum oil movement into a tank and the resulting evaporation for oil with a flash point below 100°F should be equivalent to 1,200 cu ft/hr of free air for each 100 bbl (4,200 gal)/hr of maximum filling rate.³

The requirement for venting capacity for thermal outbreathing, including thermal evaporation, for a given tank capacity for oil with a flash point of 100°F or above should be at least that shown in Col. 3 of Table 11.3.

The requirement for venting capacity for thermal outbreathing, including thermal evaporation, for a given tank capacity for oil with a flash point below 100°F should be at least that shown in Col. 4 of Table 11.3.

Requirements for Emergency Venting Capacity. When storage tanks are exposed to fire, the venting rate may exceed the rate resulting from a combination of normal thermal effects and oil movement. In such cases, the construction of the tank will determine whether additional venting capacity must be provided.

Tanks With Weak Roof-To-Shell Attachment. On fixed-roof tanks with a roof-to-shell attachment (maximum $\frac{3}{16}$ -in. single-fillet weld) as described in the "Roof Design" section of API Standard 650, *Welded Steel Tanks for Oil Storage*, the roof-to-shell connection will fail preferentially to any other joint, and the excess pressure will be relieved safely if the normal venting capacity should prove inadequate. In tanks built to these specifications, consideration need not be given to any additional requirements for emergency venting.

Tanks Without Weak Roof-To-Shell Attachment. When a tank is not provided with a weak roof-to-shell attachment as previously described, the following procedure shall govern in evaluating the required venting capacity for fire exposure.

*However, the required capacity may be reduced for products whose volatility is such that vapor generation or condensation within the permissible operating range of vessel pressure will provide all or part of the venting requirements. In cases in which non-condensibles are present, this should be taken into account.

**For protection against liquid overfilling, refer to Sec. 6.05 of API Standard 620, *Recommended Rules for Design and Construction of Large, Welded, Low-Pressure Storage Tanks*.

TABLE 11.3—REQUIREMENTS FOR THERMAL VENTING CAPACITY^a

		Thermal Venting Capacity (cubic feet of free air ^b per hour)		
		Outbreathing (Pressure)		
1		2 ^c	3 ^d	4 ^e
Tank Capacity (bbl)	(gal)	Inbreathing (vacuum)	Flash Point ≥ 100°F	Flash Point < 100°F
60	2,500	60	40	60
100	4,200	100	60	100
500	21,000	500	300	500
1,000	42,000	1,000	600	1,000
2,000	84,000	2,000	1,200	2,000
3,000	126,000	3,000	1,800	3,000
4,000	168,000	4,000	2,400	4,000
5,000	210,000	5,000	3,000	5,000
10,000	420,000	10,000	6,000	10,000
15,000	630,000	15,000	9,000	15,000
20,000	840,000	20,000	12,000	20,000
25,000	1,050,000	24,000	15,000	24,000
30,000	1,260,000	28,000	17,000	28,000
35,000	1,470,000	31,000	19,000	31,000
40,000	1,680,000	34,000	21,000	34,000
45,000	1,890,000	37,000	23,000	37,000
50,000	2,100,000	40,000	24,000	40,000
60,000	2,520,000	44,000	27,000	44,000
70,000	2,940,000	48,000	29,000	48,000
80,000	3,360,000	52,000	31,000	52,000
90,000	3,780,000	56,000	34,000	56,000
100,000	4,200,000	60,000	36,000	60,000
120,000	5,040,000	68,000	41,000	68,000
140,000	5,880,000	75,000	45,000	75,000
160,000	6,720,000	82,000	50,000	82,000
180,000	7,560,000	90,000	54,000	90,000

^aInterpolate for intermediate tank sizes. Tanks with a capacity of more than 180,000 bbl require individual study.

^bAt 14.7 psia and 60°F.

^cFor tanks with a capacity of 20,000 bbl or more, the requirements for the vacuum condition are very close to the theoretically computed value of 2 cu ft of air/hr-sq ft of total shell and roof area. For tanks with a capacity of less than 20,000 bbl, the requirements for the vacuum condition have been based on 1 cu ft free air/hr-bbl of tank capacity. This is substantially equivalent to a mean rate of vapor-space-temperature change of 100°F per hour.

^dFor stocks with a flash point of 100°F or above, the outbreathing requirement has been assumed to be 60% of the inbreathing requirement. The tank roof and shell temperatures cannot rise as rapidly under any condition as they can drop, for example, during a sudden cold rain.

^eFor stocks with a flash point below 100°F, the outbreathing requirement has been assumed to be equal to the inbreathing requirement to allow for vaporization at the liquid surface and for the higher specific gravity of the tank vapors.

For tanks designed for pressures of 1 psig or below, the total rate of venting shall be determined in accordance with Table 11.4. (No increase in venting is required for tanks with more than 2,800 sq ft of wetted surface area.⁴)

For tanks and storage vessels designed for pressures of more than 1 psig, the total rate of venting shall be determined in accordance with Table 11.4. However, when the wetted surface area is more than 2,800 sq ft, the total rate of venting shall be calculated by the equation:

$$q_v = 1,107A^{0.82}, \dots\dots\dots (1)$$

where q_v = venting requirement, cu ft of free air per hour (at 14.7 psia at 60°F), and A = wetted surface area, sq ft.*

*This formula is based on $Q = 21,000A^{0.82}$ as given in API Recommended Practice 520, *Design and Installation of Pressure-Relieving Systems in Refineries, Part I—Design*. The total heat absorbed, Q , is in Btu/hr. The constant 1,107 is derived by converting the heat input value of 21,000 Btu/hr-sq ft to scf of free air by use of the latent heat of vaporization at 60°F and the molecular weight of hexane.

TABLE 11.4—TOTAL RATE OF EMERGENCY VENTING REQUIRED FOR FIRE EXPOSURE VERSUS WETTED SURFACE AREA (NONREFRIGERATED ABOVEGROUND TANKS)*

Wetted Area** (sq ft)	Venting Requirement (cu ft free air [†] /hr)	Wetted Area** (sq ft)	Venting Requirement (cu ft free air [†] /hr)
20	21,000	350	288,000
30	31,600	400	312,000
40	42,100	500	354,000
50	52,700	600	392,000
60	63,200	700	428,000
70	73,700	800	462,000
80	84,200	900	493,000
90	94,800	1000	524,000
100	105,000	1200	557,000
120	126,000	1400	587,000
140	147,000	1600	614,000
160	168,000	1800	639,000
180	190,000	2000	662,000
200	211,000	2400	704,000
250	239,000	2800	742,000
300	265,000	> 2800 [‡]	—

*Interpolate for intermediate values. The total surface area does not include the area of ground plates but does include roof areas less than 30 ft above grade.

**The wetted area of the tank or storage vessel shall be calculated as follows. For spheres and spheroids, the wetted area is equal to 55% of the total surface area or the surface area to a height of 30 ft, whichever is greater. For horizontal tanks, the wetted area is equal to 75% of the total surface area. For vertical tanks, the wetted area is equal to the total surface area of the shell within a maximum height of 30 ft above grade.

[†] At 14.7 psia and 60°F.

[‡] For wetted surfaces larger than 2,800 sq ft, see section on tanks without weak roof-to-shell attachment.

The total venting requirements, in cubic feet of free air, determined from Table 11.4 and Eq. 1 are based on the assumption that the stored liquid will have the characteristics of hexane, since this will provide results within an acceptable degree of accuracy for most liquids encountered. However, if a greater degree of accuracy is desired, the total requirement for emergency venting for any specific liquid may be determined by the following equation for cubic feet of free air per hour:

$$q_v = V \frac{1.337}{L\sqrt{M}} \sqrt{\frac{T}{520}}, \dots\dots\dots (2)$$

where

V = cubic feet of free air per hour from Table 11.4 or from Eq. 1,

L = latent heat of vaporization of the specific liquid, in Btu/lbm,

M = molecular weight of the specific liquid, and

T = temperature of the relief vapor, °R.

Full credit may be taken for the vent capacity provided for normal venting, since the normal thermal effect can be disregarded during a fire. It can also be assumed that there will be no oil movement into the tank.

If normal vents are inadequate, additional emergency vents shall be provided so that the total venting capacity is at least equivalent to that required by Table 11.4.

The vent size may be calculated on the basis of the pressure that the tank can withstand safely.

When additional protection is provided, the total rate of emergency venting determined at the beginning of this section may be multiplied by (1) a factor of 0.5 when

drainage away from the tank or vessel is provided, (2) a factor of 0.3 when a 1-in. thickness of external insulation is provided, (3) a factor of 0.15 when a 2-in. thickness of external insulation is provided, or (4) a factor of 0.075 when a 4-in. thickness of external insulation is provided.*

Water films covering the metal surfaces can, under ideal conditions, absorb substantially all of the incident radiation. However, the reliability of effective water application depends on many factors. Freezing weather, high winds, clogging of the system, unreliability of the water supply, and tank surface conditions are a few factors that may prevent adequate or uniform water coverage. Because of these uncertainties, the use of an environmental factor other than 1.0 for water spray is generally discouraged.

Means of Venting. Normal vents. Normal venting shall be accomplished by a pilot-operated relief valve, a pressure-relief valve, a pressure vacuum valve, or an open vent with or without a flame-arresting device in accordance with the following requirements.

If a pilot-operated relief valve is used, it shall be designed so that the main valve will open automatically and will protect the tank in the event of failure of the pilot valve diaphragm or another essential function device. Relief valves equipped with a weight and lever preferably should not be used.

A pressure-relief valve is applicable on tanks operating above atmospheric pressure; in cases in which a vacuum can be created within a tank, vacuum protection may be required.

Pressure vacuum valves are recommended for use on atmospheric storage tanks in which oil with a flash point

*The values for insulation are based on an arbitrary thermal conductivity of 4 Btu/hr/sq ft/(°F/in. of thickness). The insulation shall resist dislodgment by firehose streams and shall be noncombustible.

below 100°F is stored and for use on tanks containing oil that is heated above its flash point. A flame arrester is not considered necessary for use in conjunction with a pressure vacuum valve because flame speeds are less than vent velocities through pressure vacuum valves. (See API Petroleum Safety Data 2210, *Flame Arresters for Tank Vents*.)

Open vents with a flame-arresting device may be used in place of pressure vacuum valves on tanks in which oil with a flash point below 100°F is stored and on tanks containing oil that is heated above its flash point.

Open vents may be used to provide venting capacity for tanks in which oil with a flash point of 100°F or above is stored, for heated tanks in which the oil's storage temperature is below the oil's flash point, for tanks with a capacity of less than 59.5 bbl (2,500 gal) used for storing any product, and for tanks with a capacity of less than 3,000 bbl (126,000 gal) used for storing crude oil.

In the case of viscous oils, such as cutback and penetration-grade asphalts, where the danger of tank collapse resulting from sticking pallets or from plugging of flame arresters is greater than the possibility of flame transmission into the tank, open vents may be used as an exception to the previously outlined requirements for pressure vacuum valves or flame-arresting devices.

Emergency Vents. Emergency venting may be accomplished by use of (1) larger or additional open vents as limited by normal vent requirements, (2) larger or additional pressure vacuum valves or pressure relief valves, (3) a gauge hatch that permits the cover to lift under abnormal internal pressure, (4) a manhole cover that lifts when exposed to abnormal internal pressure, (5) a connection between the roof and the shell that is weaker than the weakest vertical joint in the shell or the shell-to-bottom connection,* and (6) other forms of construction demonstrably comparable for the purposes of pressure relief.

Vent Discharge. For tanks located inside a building, discharge from the vents shall be to the outside of the building. A weak roof-to-shell connection shall not be used as a means for emergency venting a tank inside a building.

Materials of Construction

Metallic

Shop- and field-welded, and bolted storage tanks are customarily fabricated from mild-quality carbon steel. Most common for welded tanks are A-36 structural steel and A-283 Grade C structural-quality carbon steel. Sheet-gauge steel for bolted tanks is of commercial quality having a minimum tensile strength of 52,000 psi. For hydrogen sulfide crude storage, aluminum bolted tanks or aluminum decks only are often used. Various API codes (listed in General References) to which the storage tank is fabricated set forth the welding procedures, inspection procedures, and testing requirements.

Nonmetallic

Nonmetallic tanks customarily are constructed from plastic materials. These have the advantage of being noncorroding, durable, low-cost, and lightweight. Plastic materials used in the construction are polyvinyl chloride,

polyethylene, polypropylene, and fiberglass-reinforced polyesters (FRP's). The FRP tanks are available in the larger sizes and are the most common.* FRP tanks are suitable for outdoor as well as indoor applications. Aboveground vertical FRP tanks can store 24,000 gal and more, depending on the shell construction.

The temperature limits of plastic tanks are approximately 40 to 150°F. Color must be added to the outer liner for protection against ultraviolet radiation. The inner liner must be selected for compatibility with the product stored. Protection from mechanical abuse such as impact loads is necessary. Good planning dictates that plastic storage should not be located next to flammable storage tanks. Special attention should be given to local codes, ordinances, and provisions for insurance relative to storing a flammable product in a flammable container. All plastic tanks used for storage service should be equipped with pressure-relief devices if designed for relatively low-pressure storage.

Production Equipment

Tank-Battery Connections

The suggested setting and connection plan for a typical tank battery is shown in Figs. 11.5 and 11.6. The pipeline connection in the tank should be located directly below the thief hatch and a minimum of 12 in. above the tank bottom. It should be equipped with a valve and sealing device immediately adjacent to the tank. Pipeline valves should be checked frequently for leaks.

Inlet connections preferably should be located in the deck of the tank and should have a valve located near the inlet capable of closing off against pressure.

Drain connections should be located immediately above the tank bottom in the side of the tank or in the tank bottom immediately adjacent to the side. They should be equipped with a valve and sealing device located next to the tank. Drains from all tanks in a battery should be connected together and piped well away from the tanks.

Equalizer or overflow connections should be installed below the deck in the tank shell. A valve and sealing device should be installed immediately adjacent to the tank if more than two tanks are in the battery and should be connected in such a manner that any two tanks can be equalized together.

Vent connections should be installed in the center of the tank deck and all tanks connected to a common line. This line should have a pressure-vacuum valve installed in the line or on the end of it. The line should be sloped to prevent accumulation of liquids in it or in the valve.

The use of gas to roll stored products is usually considered poor practice, and should be restricted to temporary or emergency use. If a roller line is used, it should enter the tank through the deck and be equipped with a valve next to the tank.

Tank-Battery Installation and Hookup

A tank battery should contain at least two tanks and usually have a capacity equal to 4 days' production. All tanks should be level with each other and have a minimum spacing of 3 ft between tanks. Local codes or specifications may require a firewall and different spacing.

*A tank with a roof-to-shell attachment (maximum 3/4-in. single-fillet weld) as described in the "Roof Design" section of API Standard 650, is recognized as having a weak-seam connection and will therefore not require emergency vents.

*An application for approval of fiberglass tanks was submitted during 1984 and the final draft is now pending approval by the API general membership.

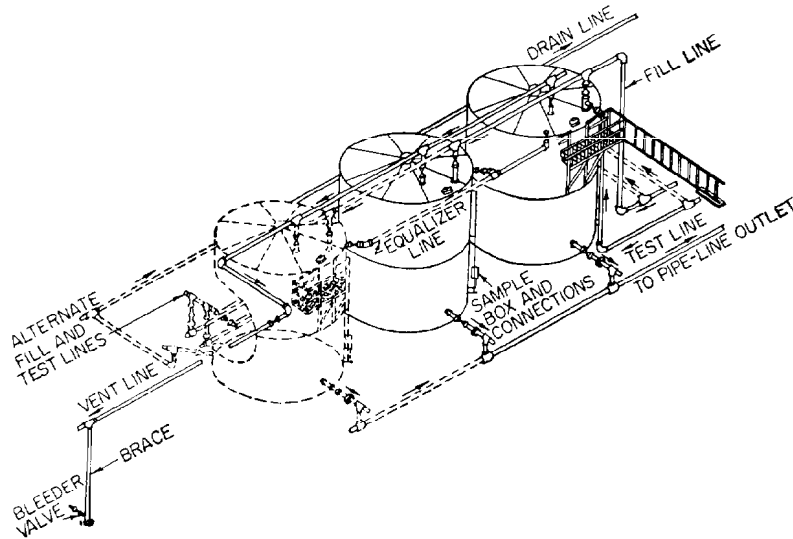


Fig. 11.5—Schematic of lease tank battery installation.

Tank Battery for Hydrogen Sulfide Crude Storage

Constant attention should be given to the hazardous condition created by iron sulfide deposits. These occur most frequently within the vapor space and particularly on the underneath exposed side of the deck. These iron sulfide deposits generate severe corrosion that can go unnoticed when deck conditions are observed from the topside only. When sour crude is stored, all openings on the tanks should be kept closed since hydrogen sulfide is poisonous. This can be accomplished by equipping the tanks with some type of ground-level gauging and thermometers located in the tank shell. Gauges and temperatures then can be read from the ground without the tank being opened. These gauging devices usually require approval by the crude purchaser. Ground-level sampling also can be accomplished by installing pipes that extend into the tank

at any desired level and to any desired distance. Valves are located at a convenient level to permit sampling on the ground without the tanks being opened. If available, a small amount of sweet gas should be fed into the top of the tank continuously to establish a "gas sweep." This will ensure positive pressure within the tank at all times and will prohibit air from entering the tank, thereby greatly reducing corrosion. It is advisable to extend the tank vent line well beyond the tank battery and to use a back-pressure valve and flash arrester in the vent line to burn the vapors.

Maintenance and Operation of Tank Batteries⁸

Steel tanks should be kept clean and free from spilled oil or other material. They should be kept painted and all water or accumulated dirt should be removed from around

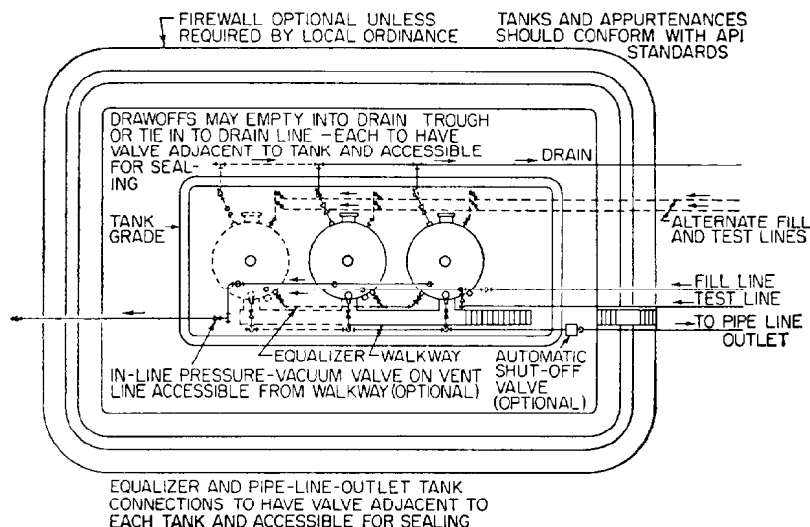


Fig. 11.6—Plan view for lease tank battery installation.

the bottom edge of the tanks. Thief hatches and vent-line valves should be kept closed and inspected periodically for proper operation and gasket condition. Should any leaks occur, they may be repaired temporarily with lead sealing plugs or toggle bolts. These leaks should be repaired permanently as soon as possible.

When a closing gauge is taken, and before the tank is filled again, the pipeline valve should be sealed closed, the drain valve checked to ensure that it is closed and the seal removed, and then the seal from the equalizer-line valve removed. Before the tank is accepted by the crude purchaser, the water should be drained from the tank if necessary and the valve sealed closed. All other valves should be sealed closed except the vapor-recovery-line valve if such a system is in use. The pipeline valve is then unsealed and opened for delivery to the purchaser.

Tank Grades

Selection. Selection of the proper location on the lease for storage tanks is of prime importance. The location should provide good drainage and be on well-packed soil—not a fill—if possible. The tank foundation or grade should be slightly elevated, level, and somewhat larger in diameter than the tank itself. For steel tanks, either bolted or welded, the best grade is one made of small gravel, crushed rock, etc., held in place by steel bands. This type of grade allows no water to stand underneath the tank and provides air circulation. If the tank is to be set directly on the ground, felt tar paper should be applied to the grade first and the tank set on this. If concrete is used for the grade, it should be slightly larger in diameter than the tank and have shallow grooves on the surface to provide air circulation. Many codes, standards, and specifications regulate the location, design, and installation of storage tanks dependent on their end use. Selecting the proper specification and providing adequate fire protection for the installation may lower insurance rates over the life of the installation.

Firewalls or Dikes. Dikes are provided to contain the volume of a certain portion of the tanks enclosed depending on the tank contents. They are used to protect surrounding property from tank spills or fires. In general, the net volume of the enclosed diked area should be the volume of the largest tank enclosed (single-failure concept). The dike walls may be earth, steel, concrete, or solid masonry designed to be watertight with a full hydrostatic head behind them. Local codes and specifications may govern construction. If more than one tank is within the diked area, curbs or preferably drainage channels should be provided to subdivide the area to protect the adjacent tanks from possible spills.

Vapor Losses

Vapors emitted from the vents and/or relief valves of a storage tank are generated in two ways: (1) they are forced out of the tank during filling operations and (2) they are generated by vaporization of the liquid stored in the tank. The total vapor produced in these two instances is the volume that would be available for recovery.

Filling Losses

Vapors that are forced out of the tank are generally called "filling losses." A storage tank generally is not pumped completely dry when emptied. The vapor above the remaining liquid in the tank will expand to fill the void space at the vapor pressure of the liquid stored in the tank at storage temperature. As the tank is filled, the vapors are compressed into a smaller void space until the set pressure on the vent/relief system is reached. There are also some filling losses that are associated with the expansion of the liquid entering the tank. Fig. 11.7 provides a graphical approach to estimating the filling losses as a percentage of the liquid being pumped into the tank.

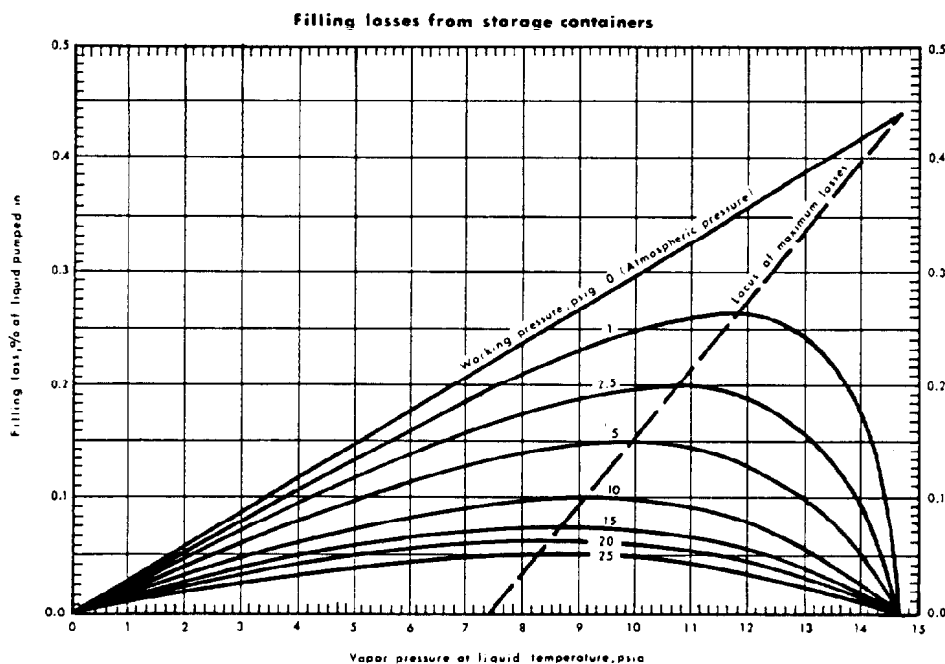


Fig. 11.7—Filling losses from storage containers.

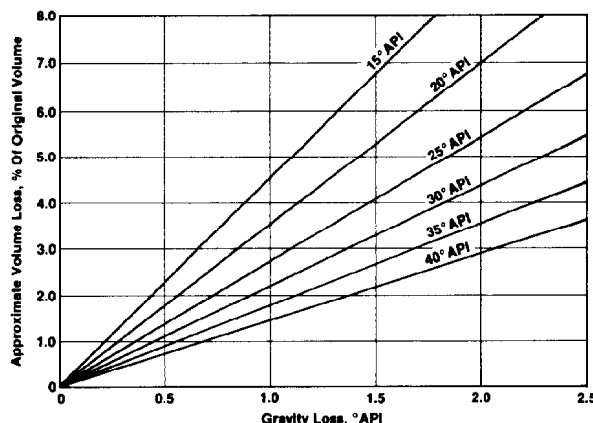


Fig. 11.8—Gravity loss in degrees API vs. percent loss by volume.

Vaporization Losses

This type of loss is characterized as the vapors generated by heat gain through the shell, bottom, and roof. The total heat input is the sum of the radiant, conductive, and convective energy forces. This type of loss is especially prevalent where light hydrocarbon liquids are stored in full-pressure or refrigerated storage. This is less prevalent but still quite common in crude oil and finished-product storage tanks. These vapors may be recovered by the use of a vapor-recovery system.

Vapor Control and Gravity Conservation With Storage Tanks⁹

Crude oils and condensates are composed of many different paraffin hydrocarbons. Propane is the lightest hydrocarbon found in any measureable amount and the hydrocarbon with the greatest tendency to evaporate or vaporize from the liquid stored. When propane and other hydrocarbons pass into the vapor phase by vaporization, the volume of the liquid stored is decreased, and because these lighter hydrocarbons are not now present in their initial amounts, the API gravity of the crude is decreased. There is a definite relationship between API gravity lost and volume lost, depending on the character of the crude (Fig. 11.8).

Factors Contributing to Vapor and Gravity Losses

Several factors affect and contribute to vapor and gravity losses in storage tanks: (1) vapor pressure of the product stored, (2) temperature of the product stored, (3) surface area of the product stored, (4) agitation of the product stored, (5) pressure on the storage tanks, (6) filling losses from the storage tanks, (7) breathing losses from the storage tanks, (8) size of the storage tanks, and (9) color of outside paint or coating.

Several, if not all, of these factors usually contribute to the total loss from any one tank or battery.

Vapor Pressure. The true vapor pressure (TVP) of a liquid is the actual pressure it exerts on the vapor space in a container at a given temperature. Water, for example, has a TVP of 1 psi at 100°F and a TVP of 14.7 psi at 212°F, yet it must be kept in a closed container to prevent evaporation. The same is true for crude oil if the TVP is below 14.7 psi. Crudes with a TVP of 10 psi and lower are usually relatively stable in closed-atmospheric storage.

Temperature. Temperature of crude is directly related to its vapor pressure. For example, a crude with a TVP of 8 psi at 50°F will have a TVP of 17 psi at 90°F. The vaporization loss is then approximately doubled at the 90°F temperature.

Surface Area. Directly related to the rate of evaporation is the surface area of the crude. Take, for example, two tanks with a capacity of 500 bbl each, one a high 500-bbl tank and the other a low 500-bbl tank. If both are filled one-half full, the high 500 bbl has 0.74 sq ft of surface area exposed per barrel stored, whereas the low 500 bbl has 1.46 sq ft of surface area exposed per barrel stored. The low 500-bbl tank then has twice the evaporation rate of the high 500-bbl tank.

Agitation. Agitation of the stored product is related directly to the vapor pressure. If two crudes under the same conditions receive equal agitation, the one with the higher vapor pressure will show the greatest evaporation loss.

Tank Pressures. The higher the pressure maintained on the storage tank, the less will be the tendency for the crude to evaporate. Pressure storage, considered to be in excess of 1 psig, is required for all stored products with a TVP in excess of 14.7 psi to prevent excessive evaporation losses. High-gravity crudes and distillates or condensates usually require a higher storage pressure than the normal 1 to 4 oz. The crude purchaser often dictates allowable storage pressure.

Filling Losses. When 475 bbl are run from a 500-bbl tank, crude-oil vapors occupy the displaced oil. When the tank is filled again, these vapors are forced from the tank into the atmosphere. These expelled vapors may be equivalent to one or more barrels, depending on the type of crude.

Breathing Losses. Temperature changes between day and night cause vapors to be expelled from the tank and air to be breathed in. These reactions are similar to, but smaller in volume than, the filling and running losses.

Storage Size. A greater vapor space and longer storage time will increase evaporation losses. As an example, consider two tanks with 100 bbl of stored crude each, one a 250-bbl tank and the other a high 500-bbl tank. The 250-bbl tank has 948 cu ft of vapor space while the high 500-bbl tank has 2,457 cu ft or two and one-half times as much. This added vapor space increases the evaporation losses from the larger tank.

Preventing Evaporation and Gravity Losses

Much can be done by the producer to prevent undue losses of crude oil by evaporation. Products should be introduced into storage as cool as possible and kept that way. Some types of heat-exchange equipment should be employed between an emulsion treater, or other heating equipment, and the tanks to cool the oil before it enters storage. If fluid heat exchangers are used, a preventive maintenance program should be employed to guard against buildup of

scale, paraffin, salt, etc., which are common to many produced fluids. Most modern tank batteries are equipped with lease automatic custody-transfer (LACT) units. The run tank should be of sufficient size to allow approximately 12 hours' settling time. Where batteries are equipped with storage for bad oil, this storage should be kept to a minimum and the battery treating capacity should be capable of treating a certain amount of bad oil. Steel tanks should be painted with a reflective or white paint. Tests show the vapor-space temperature of a tank painted with aluminum paint to average $4\frac{1}{2}^{\circ}\text{F}$ above atmospheric temperature, while a red-painted tank averaged 14°F above atmospheric temperature.

Tanks should be selected with smaller diameters, greater heights, and smaller capacities, all other considerations being equal. These factors will allow the stored product to have relatively smaller surface areas and vapor spaces as well as a shorter length of storage time before being sold.

Downcomer pipes prevent undue agitation in the tank. They are usually made by installing a line inside the tank from the inlet connection in the tank deck to 1 ft above the tank bottom. The downcomer must have a vacuum breaker hole at the top to allow gas to escape and thereby prevent agitation, splashing, and accumulation of static electricity.

All tank openings should be maintained closed and pressure on the tank should be as high as practical (at least $\frac{1}{2}$ in. of water column). Tanks in a battery all should be connected together into a common vent line to keep breathing and filling losses to a minimum. Bypass thief hatches are manufactured that will do much to prevent evaporation losses when a tank is gauged through the thief hatch. These special hatches have the tank-battery vent lines connected to them and will close off or isolate all other tanks except the one being gauged. This allows all other tanks in the battery to maintain their pressure while the tank being gauged is depressured.

The producer may install one of several types of ground-level gauging and sampling devices available that will permit gauging and sampling without opening the tank. The tank remaining closed goes far toward eliminating evaporation losses.

Vapor-Recovery System

Vapor-recovery systems are of two basic types. One type connects a vacuum line to the tank and transports the tank vapors to a processing or gasoline plant. The other type consists of a small compressor located by the tank battery, which compresses the tank vapors to a pressure suitable for lease use or sales.

Vacuum-Line System. The vacuum-line system usually is found only in large oil fields, where many tank batteries can be connected together into a relatively short gathering system. This system must employ well-maintained and properly functioning pressure/vacuum relieving devices and dependable control valves to prevent the tanks from collapsing or air from entering the gathering system.

Compression System. The compressor system is usually electrically driven and all components are skid mounted. Some of these systems use a vane-type compressor

and inject a refined oil by way of a lubrication system to seal the vanes against the compressor walls. In these systems an actual liquid recovery is accomplished by the sealing oil absorbing the condensed hydrocarbons from the compressed vapors and transporting them to storage with the returning sealing oil. Applications for this type of system are twofold: (1) compression of the rich stock-tank vapors for sale to a gasoline plant and (2) the recovery of liquids from the rich stock-tank vapors. Liquid hydrocarbons also can be recovered from the compressed vapor-recovery unit (VRU) vapor by either one or both of the following means.

1. A vapor cooling system (air-cooled or water-cooled) heat exchanger can be installed complete with a separator downstream of the hot compressed VRU vapor stream. Multiple vapor cooling systems may be used in between the stages of a multiple-staged compression system.

2. A mechanical refrigeration unit may be installed downstream of the VRU for a higher-yield liquid hydrocarbon recovery.

Underground Storage

Underground storage* is most advantageous when large volumes are to be stored. Underground storage is especially advantageous for high-vapor-pressure products. Solution-mined and conventionally mined caverns are not typically used for underground storage of refrigerated products. Underground storage allows most of the surface area (except for the entry wells) to be used for other purposes. This is especially beneficial in high-value, congested areas.

Type of Construction

Types of underground storage are (1) caverns constructed in salt by solution mining or conventional mining, (2) caverns constructed in nonporous rock by conventional mining, (3) caverns developed by conversion of depleted coal, limestone, or salt mines to storage, and (4) depleted reservoirs.

The solution-mined cavern is constructed by drilling a well or wells into the salt and circulating low-salinity water over the salt interval to dissolve the salt. Fig. 11.9 shows a typical solution-mined cavern.

Conventionally mined caverns can be constructed any place a nonporous rock is available at adequate depth to withstand product pressures. An engineer or geologist experienced in underground storage should evaluate any specific site for the feasibility of constructing underground storage. Most product caverns are constructed in shale, limestone, dolomite, or granite. This type cavern is operated "dry" (the product is recovered by pumping).

Operation

The cavern may be operated by brine displacement of product or pump-out methods (see Figs. 11.9 and 11.10).

Most solution-mined caverns are operated by the brine-displacement technique (Fig. 11.9). A suspended displacement string of casing is installed near the bottom of the cavern, and product is injected into the annulus between the product casing (casing cemented at cavern roof) and the displacement casing, forcing brine up the displace-

*Wyrick, J.: personal communication, Fenix & Scisson Inc., Tulsa (1983).

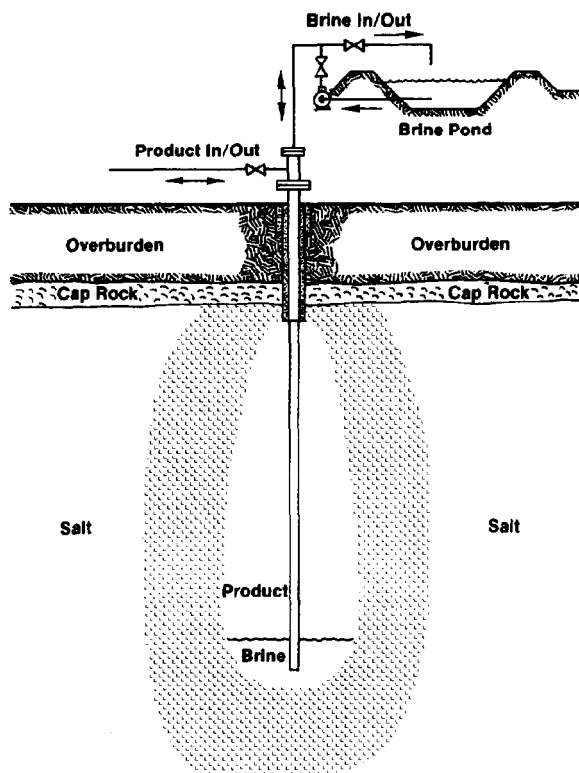


Fig. 11.9—Brine displacement cavern operation (solution-mined cavern).

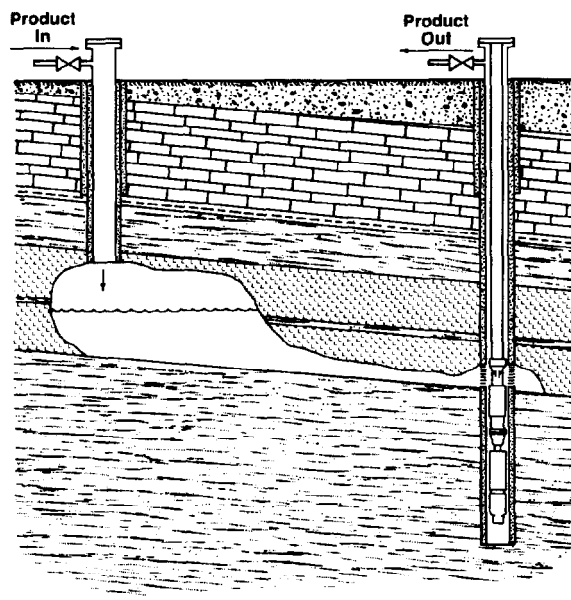


Fig. 11.10—Pump-out cavern operation (fracture-connected solution-mined cavern in bedded salt).

ment casing. The procedure is reversed for product recovery. In this type operation, a brine storage reservoir usually is provided.

Some solution-mined caverns are operated "dry" by installing a pump at cavern depth either within the cavern or in a well connected to the cavern by fracturing. Both submersible electrically driven pumps and deep-well vertical multistage pumps are used for this purpose (Fig. 11.10).

References

1. API Specification 12B: *Specifications for Bolted Production Tanks*, 12th edition, API Div. of Production, Dallas (Jan. 1977).
2. API Specification 12F: *Specifications for Shop-Welded Tanks for Storage of Production Liquids*, eighth edition, Dallas (Jan. 1982).
3. Koppers Protective Coatings, Koppers Co. Inc., Pittsburgh (Oct. 1980).
4. Koppers Protective Coatings, Koppers Co. Inc., Pittsburgh (Jan. 1980).
5. Koppers Protective Coatings, Koppers Co. Inc., Pittsburgh (March 1981).
6. *Design and Fabrication of Galvanized Products*, American Hot Dip Galvanizers Assn., and the Zinc Inst. (Nov. 1983).
7. API Standard 2000: *Venting Atmospheric and Low-Pressure Storage Tanks*, third edition, Dallas (Jan. 1982).
8. API RP 12RI: *Recommended Practice for Setting, Connecting, Maintenance and Operation of Lease Tanks*, second edition, Dallas (Feb. 1981).
9. *Vapor and Gravity Control in Crude Oil Production*, first edition, Petroleum Extension Service, U. of Texas, Div. of Extension, Austin (1956).

General References

- API Specification 12D: *Specifications for Field-Welded Tanks for Storage of Production Liquids*, ninth edition, Dallas (Jan. 1982).
- API Standard 620: *Recommended Rules for Design and Construction of Large, Welded Low-Pressure Storage Tanks*, seventh edition, Dallas (1982).
- API Standard 650: *Welded Steel Tanks for Crude Storage*, seventh edition, Dallas (Nov. 1980).
- ASTM A-123: *Zinc (Hot Galvanized) Coating on Products Fabricated From Rolled, Pressed, and Forged Steel Shapes, Plates, Bars, and Strip*, New York City (1978).
- NACE* RP-01-75: *Control of Internal Corrosion in Steel Pipelines and Piping Systems*, Washington, D.C.
- NACE RP-03-72: *Method for Lining Lease Production Tanks With Coal Tar Epoxy*, Washington, D.C.
- NACE RP-05-75: *Design, Installation, Operations, and Maintenance of Internal Cathodic Protection Systems in Oil Treating Vessels*, Washington, D.C.

*Natl. Assn. of Corrosion Engineers

Chapter 12

Oil and Gas Separators

H. Vernon Smith, Meridian Corp.

Summary

This chapter is a discussion of the design, use, functions, capacities, classifications, performance, operation, and maintenance of oil and gas separators. Vertical, horizontal, and spherical separators in both two- and three-phase arrangements are discussed. Quality of effluent fluids is approximated. Equations for calculating the sizes and capacities of separators and capacity curves and tables for sizing oil and gas separators are provided. These capacity curves and tables can be used to estimate capacities of separators as well as to determine the size of separator required to handle given volumes of fluids. Sample calculations for sizing separators are included.

Introduction

The term "oil and gas separator" in oilfield terminology designates a pressure vessel used for separating well fluids produced from oil and gas wells into gaseous and liquid components. A separating vessel may be referred to in the following ways:

1. Oil and gas separator.
2. Separator.
3. Stage separator.
4. Trap.
5. Knockout vessel, knockout drum, knockout trap, water knockout, or liquid knockout.
6. Flash chamber, flash vessel, or flash trap.
7. Expansion separator or expansion vessel.
8. Scrubber (gas scrubber), dry or wet type.
9. Filter (gas filter), dry or wet type.
10. Filter/separator.

The terms "oil and gas separator," "separator," "stage separator," and "trap" refer to a conventional oil and gas separator. These separating vessels are normally used on a producing lease or platform near the wellhead, manifold, or tank battery to separate fluids produced from oil and gas wells into oil and gas or liquid and gas. They must be capable of handling "slugs" or "heads" of well

fluids. Therefore, they are usually sized to handle the highest instantaneous rates of flow.

A knockout vessel, drum, or trap may be used to remove only water from the well fluid or to remove all liquid, oil plus water, from the gas. In the case of a water knockout for use near the wellhead, the gas and liquid petroleum are usually discharged together, and the free water is separated and discharged from the bottom of the vessel.

A liquid knockout is used to remove all liquid, oil plus water, from the gas. The water and liquid hydrocarbons are discharged together from the bottom of the vessel, and the gas is discharged from the top.

A flash chamber (trap or vessel) normally refers to a conventional oil and gas separator operated at low pressure, with the liquid from a higher-pressure separator being "flushed" into it. This flash chamber is quite often the second or third stage of separation, with the liquid being discharged from the flash chamber to storage.

An expansion vessel is the first-stage separator vessel on a low-temperature or cold-separation unit. This vessel may be equipped with a heating coil to melt hydrates, or a hydrate-preventive liquid (such as glycol) may be injected into the well fluid just before expansion into this vessel.

A gas scrubber may be similar to an oil and gas separator. Usually it handles fluid that contains less liquid than that produced from oil and gas wells. Gas scrubbers are normally used in gas gathering, sales, and distribution lines where they are not required to handle slugs or heads of liquid, as is often the case with oil and gas separators. The dry-type gas scrubber uses mist extractors and other internals similar to oil and gas separators, with preference shown to the coalescing-type mist extractor. The wet-type gas scrubber passes the stream of gas through a bath of oil or other liquid that washes dust and other impurities from the gas. The gas is flowed through a mist ex-

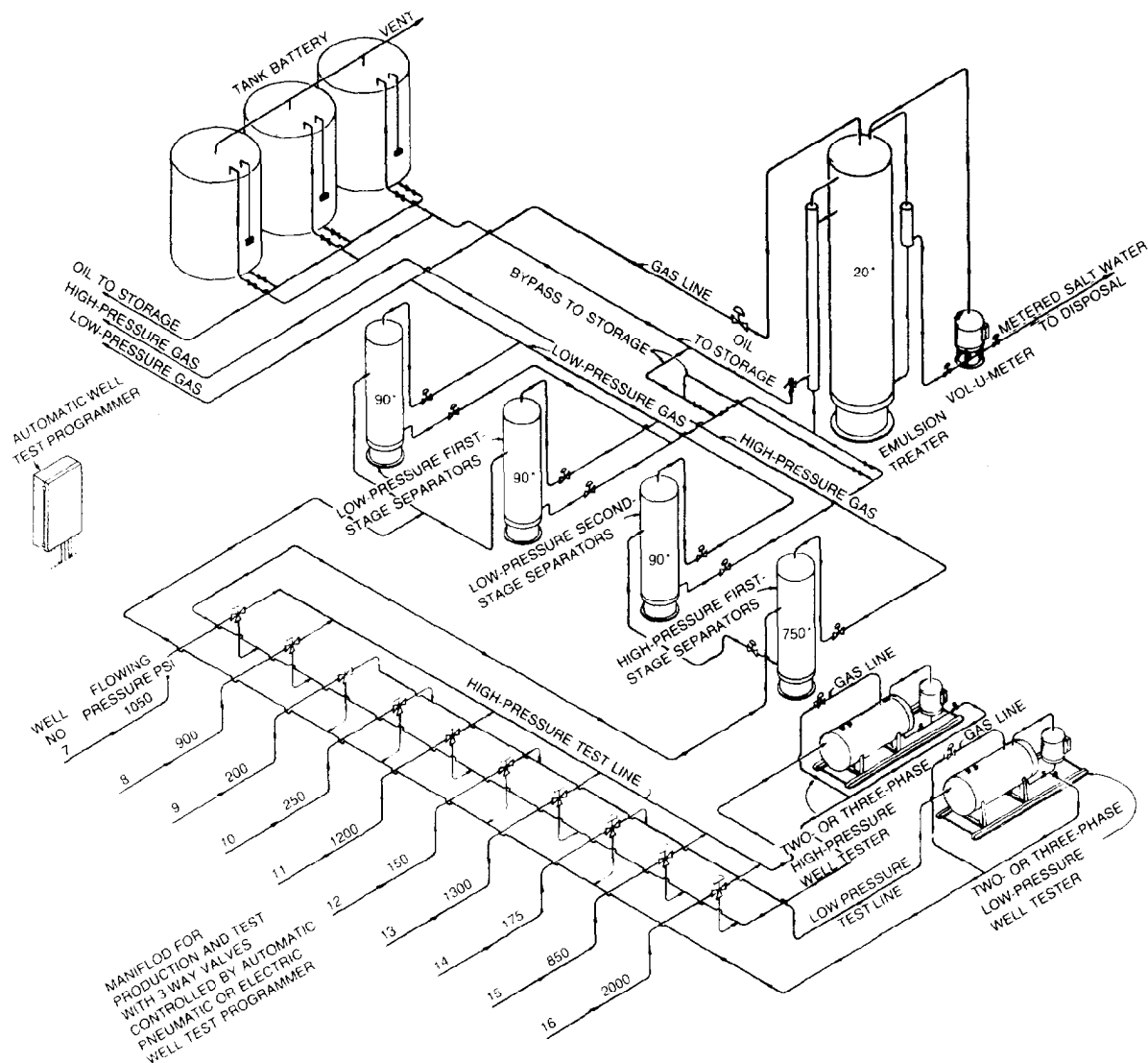


Fig. 12.1—Typical surface production equipment for handling oil and gas—oil and gas separators and other related equipment.

tractor where all removable liquid is separated from it. A “scrubber” can refer to a vessel used upstream from any gas-processing vessel or unit to protect the downstream vessel or unit from liquid hydrocarbons and/or water.

The “filter” (gas filter or filter/separator) refers to a dry-type gas scrubber, especially if the unit is being used primarily to remove dust from the gas stream. A filtering medium is used in the vessel to remove dust, line scale, rust, and other foreign material from the gas. Such units will normally remove liquid from the gas.

An oil and gas separator generally includes the following essential components and features.

1. A vessel that includes (a) primary separation device and/or section, (b) secondary “gravity” settling (separating) section, (c) mist extractor to remove small liquid particles from the gas, (d) gas outlet, (e) liquid settling (separating) section to remove gas or vapor from oil (on a three-phase unit, this section also separates water from oil), (f) oil outlet, and (g) water outlet (three-phase unit).

2. Adequate volumetric liquid capacity to handle liq-

uid surges (slugs) from the wells and/or flowlines.

3. Adequate vessel diameter and height or length to allow most of the liquid to separate from the gas so that the mist extractor will not be flooded.

4. A means of controlling an oil level in the separator, which usually includes a liquid-level controller and a diaphragm motor valve on the oil outlet. For three-phase operation, the separator must include an oil/water interface liquid-level controller and a water-discharge control valve.

5. A backpressure valve on the gas outlet to maintain a steady pressure in the vessel.

6. Pressure relief devices.

In most oil and gas surface production equipment systems, the oil and gas separator is the first vessel the well fluid flows through after it leaves the producing well. However, other equipment—such as heaters and water knockouts—may be installed upstream of the separator. Fig. 12.1 shows a typical surface production equipment system for handling crude oil using an oil and gas separator along with related equipment.

Well Fluids and Their Characteristics

Some of the physical characteristics of well fluids handled by oil and gas separators are briefly outlined in this section.

Crude Oil. Crude oil is a complex mixture of hydrocarbons produced in liquid form. The API gravity of crude oil can range from 6 to 50°API and viscosity from 5.0 to 90,000 cp at average operating conditions. Color varies through shades of green, yellow, brown, and black. Detailed characteristics of crude oils are given in Chap. 21.

Condensate. This is a hydrocarbon that may exist in the producing formation either as a liquid or as a condensible vapor. Liquefaction of gaseous components of the condensate usually occurs with reduction of well-fluid temperature to surface operating conditions. Gravities of the condensed liquids may range from 50 to 120°API and viscosities from 2.0 to 6.0 cp at standard conditions. Color may be water-white, light yellow, or light blue.

Natural Gas. A gas may be defined as a substance that has no shape or volume of its own. It will completely fill any container in which it is placed and will take the shape of the container. Hydrocarbon gas associated with crude oil is referred to as natural gas and may be found as “free” gas or as “solution” gas. Specific gravity of natural gas may vary from 0.55 to 0.90 and viscosity from 0.011 to 0.024 cp at standard conditions.

Free Gas. Free gas is a hydrocarbon that exists in the gaseous phase at operating pressure and temperature. Free gas may refer to any gas at any pressure that is not in solution or mechanically held in the liquid hydrocarbon.

Solution Gas. Solution gas is homogeneously contained in oil at a given pressure and temperature. A reduction in pressure and/or an increase in temperature may cause the gas to be emitted from the oil, whereupon it assumes the characteristics of free gas.

Condensible Vapors. These hydrocarbons exist as vapor at certain pressures and temperatures and as liquid at other pressures and temperatures. In the vapor phase, they assume the general characteristics of a gas. In the liquid phase, condensible vapors vary in specific gravity from 0.55 to 4.91 (air=1.0), and in viscosity from 0.006 to 0.011 cp at standard conditions.

Water. Water produced with crude oil and natural gas may be in the form of vapor or liquid. The liquid water may be free or emulsified. Free water reaches the surface separated from the liquid hydrocarbon. Emulsified water is dispersed as droplets in the liquid hydrocarbon.

Impurities and Extraneous Materials. Produced well fluids may contain such gaseous impurities as nitrogen, carbon dioxide, hydrogen sulfide, and other gases that are not hydrocarbon in nature or origin. Well fluids may contain liquid or semiliquid impurities, such as water and paraffin. They may also contain solid impurities, such as drilling mud, sand, silt, and salt.

Primary Functions of Oil and Gas Separators

Separation of oil from gas may begin as the fluid flows through the producing formation into the wellbore and may progressively increase through the tubing, flowlines, and surface handling equipment. Under certain conditions, the fluid may be completely separated into liquid and gas before it reaches the oil and gas separator. In such cases, the separator vessel affords only an “enlargement” to permit gas to ascend to one outlet and liquid to descend to another.

Removal of Oil From Gas

Difference in density of the liquid and gaseous hydrocarbons may accomplish acceptable separation in an oil and gas separator. However, in some instances, it is necessary to use mechanical devices commonly referred to as “mist extractors” to remove liquid mist from the gas before it is discharged from the separator. Also, it may be desirable or necessary to use some means to remove non-solution gas from the oil before the oil is discharged from the separator.

Removal of Gas From Oil

The physical and chemical characteristics of the oil and its conditions of pressure and temperature determine the amount of gas it will contain in solution. The rate at which the gas is liberated from a given oil is a function of change in pressure and temperature. The volume of gas that an oil and gas separator will remove from crude oil is dependent on (1) physical and chemical characteristics of the crude, (2) operating pressure, (3) operating temperature, (4) rate of throughput, (5) size and configuration of the separator, and (6) other factors.

Rate of throughput and liquid depth in the separator determine the “retention” or “settling” time of the oil. Retention time of 1 to 3 minutes is generally adequate to obtain satisfactory separation of crude oil and gas unless foaming oil is being handled. When foaming oil is separated, retention time should be increased to 5 to 20 minutes, dependent on the stability of the foam and on the design of the separator. Advancements in field processing systems and production procedures—such as automatic custody transfer—emphasize the need for complete removal of nonsolution gas from the oil. Agitation, heat, special baffling, coalescing packs, and filtering materials can assist in the removal of nonsolution gas that otherwise may be retained in the oil because of the viscosity and surface tension of the oil.

Separation of Water From Oil

In some instances it is preferable to separate and to remove water from the well fluid before it flows through pressure reductions, such as those caused by chokes and valves. Such water removal may prevent difficulties that could be caused downstream by the water—such as corrosion, hydrate formation, and the formation of tight emulsion that may be difficult to resolve into oil and water.

The water can be separated from the oil in a three-phase separator by use of chemicals and gravity separation. If the three-phase separator is not large enough to separate the water adequately, it can be separated in a free-water

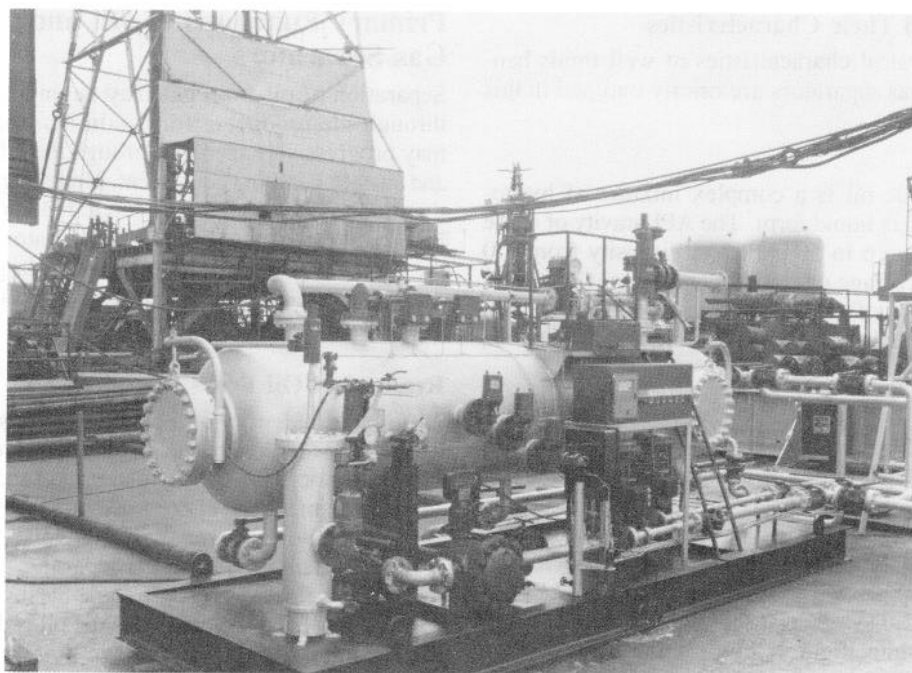


Fig. 12.2—Horizontal skid-mounted three-phase well tester on offshore drilling platform off coast of Brazil.

knockout vessel installed upstream or downstream of the separators. If the water is emulsified, it may be necessary to use an emulsion treater to remove it. Figs. 12.2 through 12.5 are illustrations of three-phase separators.

Secondary Functions of Oil and Gas Separators

Maintain Optimum Pressure on Separator

For an oil and gas separator to accomplish its primary functions, pressure must be maintained in the separator so that the liquid and gas can be discharged into their respective processing or gathering systems. Pressure is

maintained on the separator by use of a gas backpressure valve on each separator or with one master backpressure valve that controls the pressure on a battery of two or more separators. Fig. 12.6 shows a typical low-pressure gas backpressure valve, and Fig. 12.7 shows a typical high-pressure gas backpressure valve used to maintain the desired pressure in separators.

The optimum pressure to maintain on a separator is the pressure that will result in the highest economic yield from the sale of the liquid and gaseous hydrocarbons. This optimum pressure can be calculated theoretically or determined by field tests.

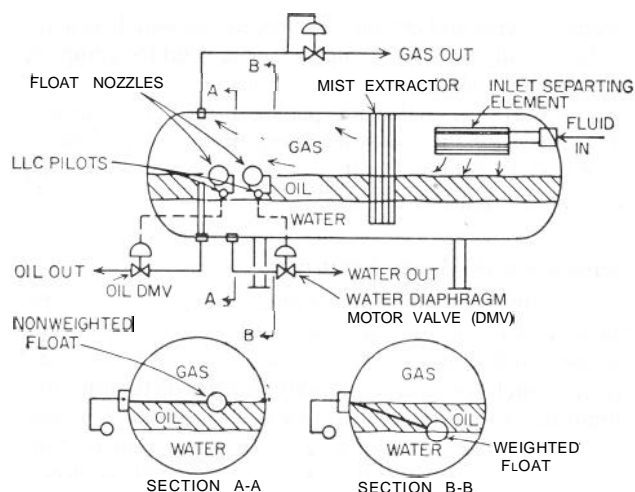


Fig. 12.3—Schematic of typical horizontal three-phase oil/gas/water separator.

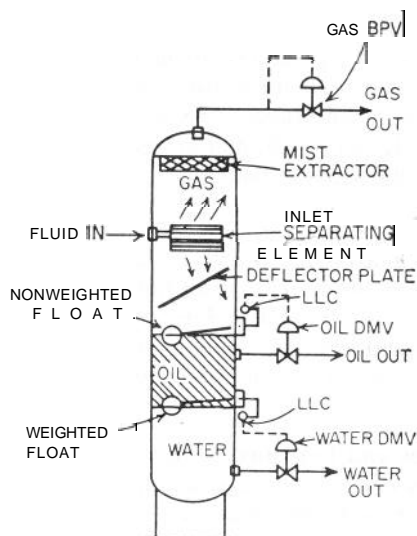


Fig. 12.4—Schematic of a typical vertical three-phase oil/gas/water separator.

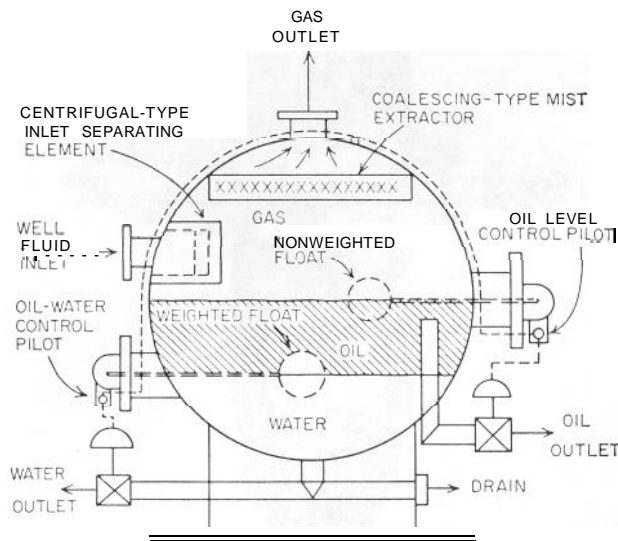


Fig. 12.5—Schematic of a typical spherical three-phase oil/gas/water separator.

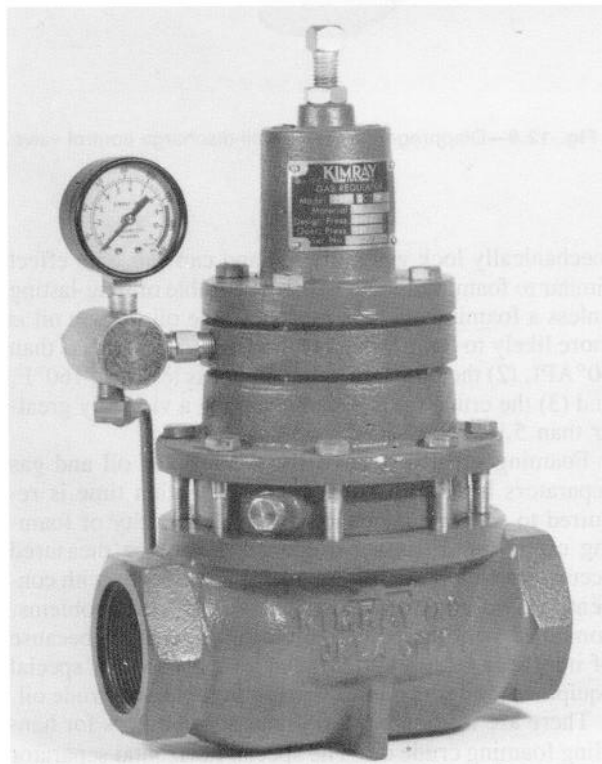


Fig. 12.6—Low-pressure-gas backpressure valve.

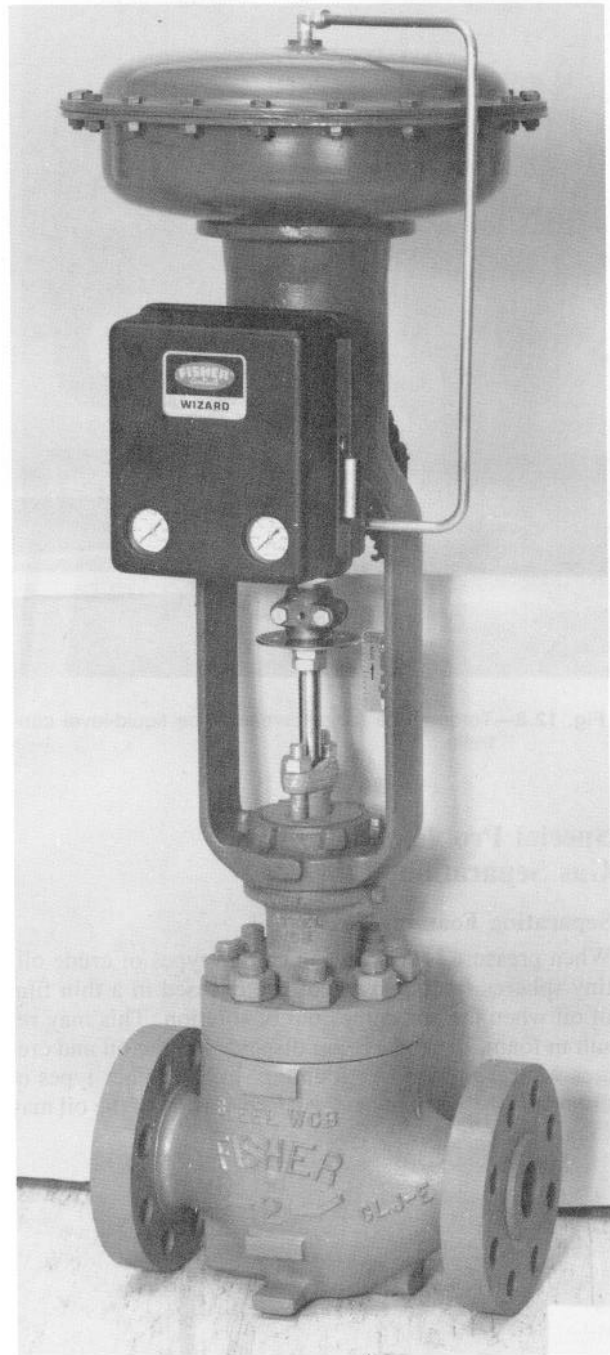


Fig. 12.7—High-pressure-gas backpressure valve.

Maintain Liquid Seal in Separator

To maintain pressure on a separator, a liquid seal must be effected in the lower portion of the vessel. This liquid seal prevents loss of gas with the oil and requires the use of a liquid-level controller and a valve similar to those shown in Figs. 12.8 and 12.9. A lever-operated valve similar to the one shown in Fig. 12.10 can be used to

maintain the liquid seal in a separator when the valve is operated by a float that is actuated by the oil level in the separator. The oil discharge control valve shown in Fig. 12.9 can be actuated by a float-operated pilot (not illustrated), by a floatless liquid-level controller similar to the one shown in Fig. 12.11, or by a torque tube-type (displacement) liquid-level controller similar to the one shown in Fig. 12.8.

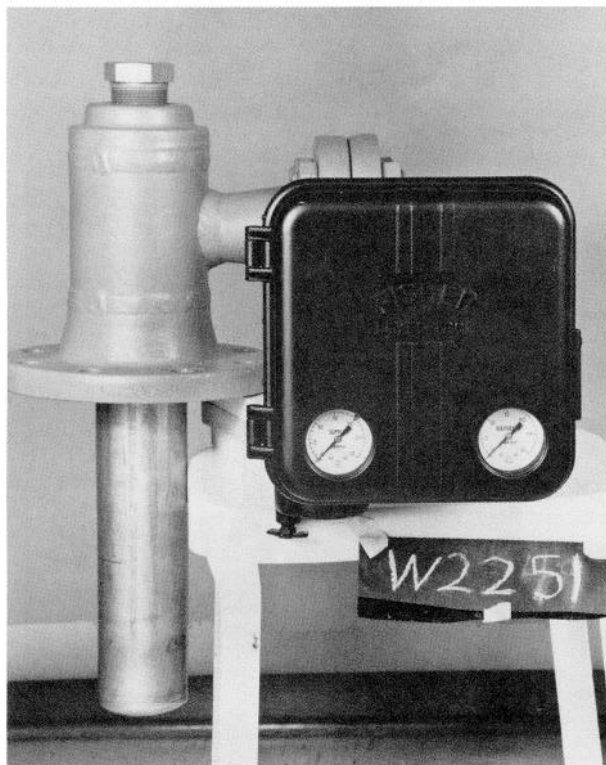


Fig. 12.8—Torque-tube (displacement)-type liquid-level controller.

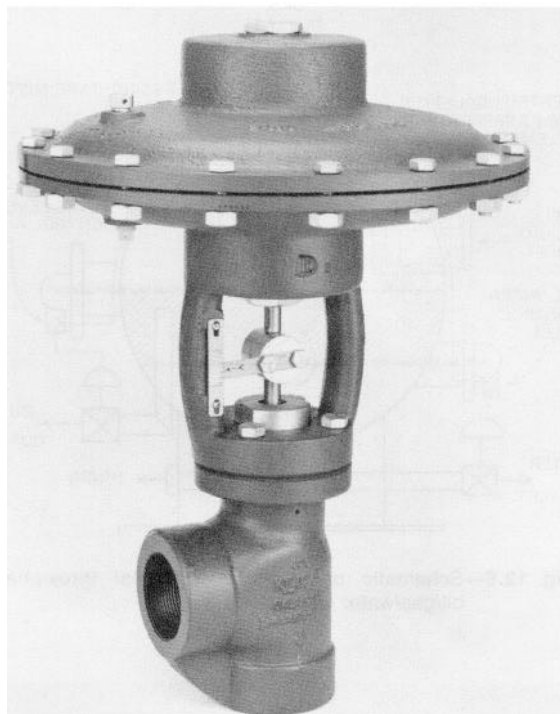


Fig. 12.9—Diaphragm-motor-type oil-discharge control valve.

Special Problems in Oil and Gas Separation

Separating Foaming Crude Oil

When pressure is reduced on certain types of crude oil, tiny spheres (bubbles) of gas are encased in a thin film of oil when the gas comes out of solution. This may result in foam, or froth, being dispersed in the oil and creates what is known as “foaming” oil. In other types of crude oil, the viscosity and surface tension of the oil may

mechanically lock gas in the oil and can cause an effect similar to foam. Oil foam will not be stable or long-lasting unless a foaming agent is present in the oil. Crude oil is more likely to foam when (1) the API gravity is less than 40° API, (2) the operating temperature is less than 160°F, and (3) the crude oil is viscous, having a viscosity greater than 5,000 SSU (about 53 cp).

Foaming greatly reduces the capacity of oil and gas separators because a much longer retention time is required to separate adequately a given quantity of foaming crude oil. Foaming crude oil cannot be measured accurately with positive-displacement meters or with conventional volumetric metering vessels. These problems, combined with the potential loss of oil and gas because of improper separation, emphasize the need for special equipment and procedures in handling foaming crude oil.

There are many special designs of separators for handling foaming crude oil. The special horizontal separator for handling foaming oil shown in Fig. 12.12 is one of the simpler, more effective units available for this service. The special degassing element used on the inlet of this separator shown in Section CC of Fig. 12.12 gently agitates the well fluid and assists in removing gas from the oil and in breaking foam bubbles as they flow through the inlet element.

The defoaming plates, which extend from near the inlet end to near the outlet end of the separator, are spaced 4 in. apart and are shaped with an apex at the vertical center of the separator. The plates that are immersed in oil assist in removing nonsolution gas from the oil and in breaking foam in the oil. The plates that are above the oil/gas interface in the gas section of the separator remove

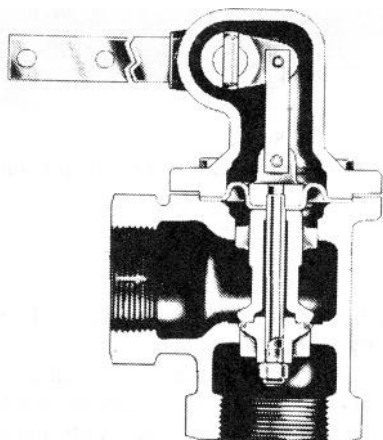


Fig. 12.10—Lever-type valve for controlling oil discharge from oil and gas separators. Valve is float operated.

oil mist from the gas and assist in breaking foam that may exist in the gas section of the vessel.

The 6-in.-thick knitted-wire-mesh mist extractor (located below the gas outlet) removes the remainder of the liquid mist from the gas and breaks or removes the remaining foam bubbles from the gas.

The vertical separator shown in Fig. 12.13 can be used to handle foaming crude oil. As the oil cascades down the plates in this unit, the foam bubbles will be distorted and broken. This design can increase the capacity of the separator to handle foaming oil by 10 to 50%.

The main factors that assist in "breaking" foaming oil are settling, agitation (baffling), heat, chemicals, and centrifugal force. These factors or methods of "reducing" or "breaking" foaming oil are also used to remove entrained gas from oil. They are discussed on Pages 12-13 through 12-15. Many different designs of separators for handling foaming crude oil have evolved. They are available from various manufacturers—some as standard foam-handling units and some designed especially for a specific application.

Paraffin

Paraffin deposition in oil and gas separators reduces their efficiency and may render them inoperable by partially filling the vessel and/or blocking the mist extractor and fluid passages. Paraffin can be effectively removed from separators by use of steam or solvents. However, the best

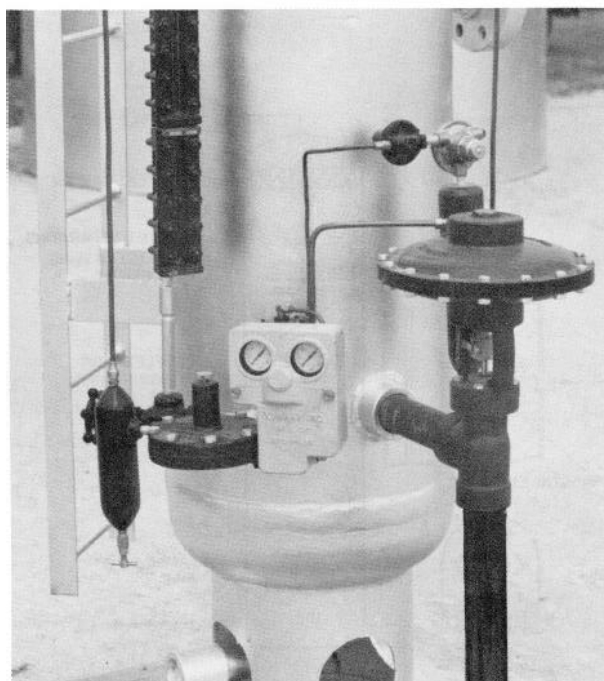


Fig. 12.11—Floatless liquid-level controller and diaphragm-motor oil-control valve on high-pressure oil and gas separator.

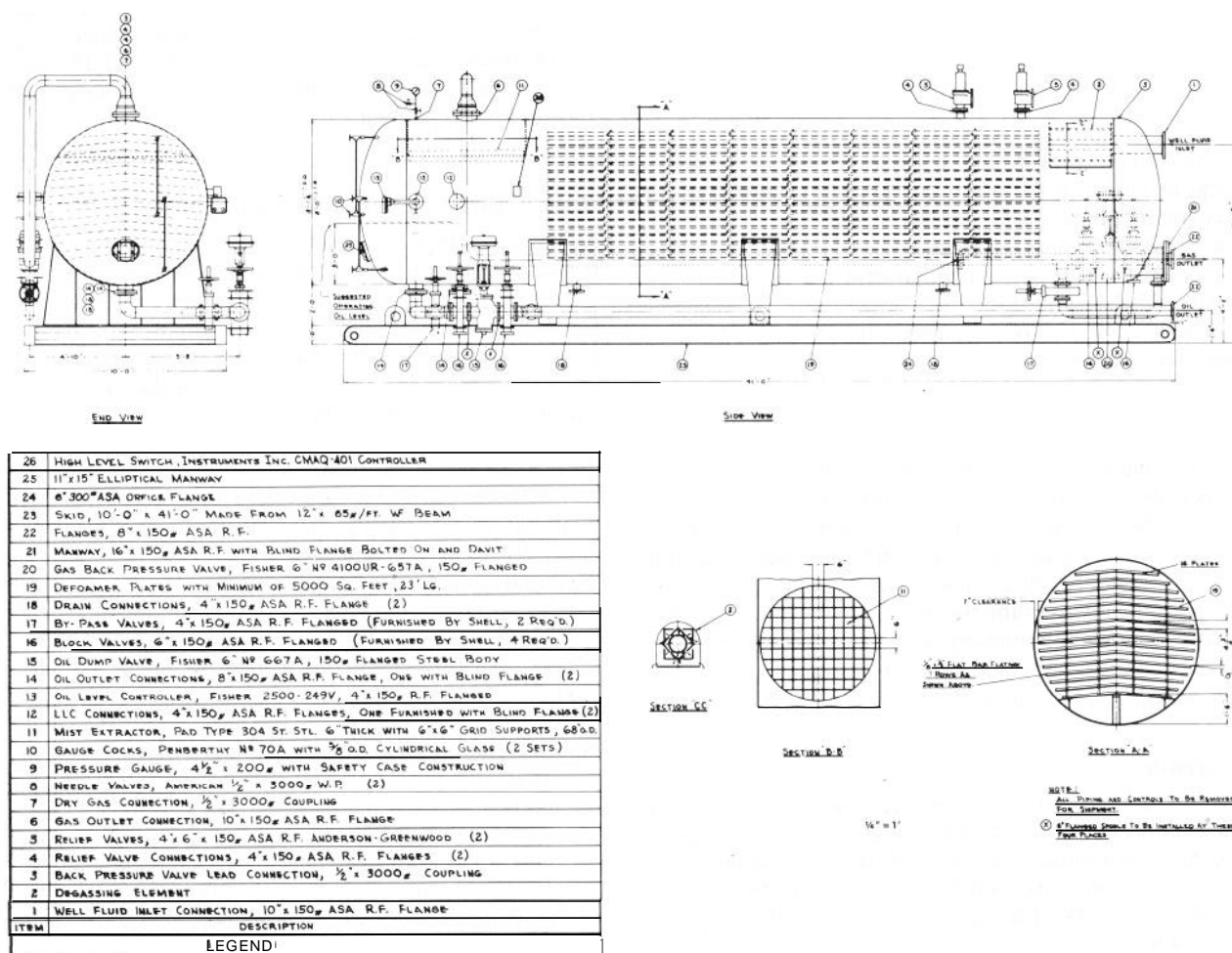


Fig. 12.12—Horizontal oil and gas separator with special internals for separating foaming crude oil.

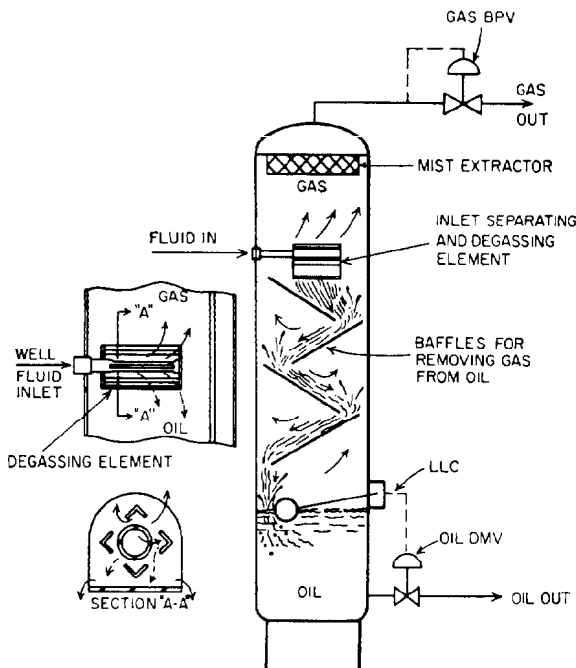


Fig. 12.13—Vertical oil and gas separator with special baffling to remove gas from oil, especially beneficial in handling foaming oil. Upper left view and Section A-A show inlet separating element that assists in removing gas from oil.

solution is to prevent initial deposition in the vessel by heat or chemical treatment of the fluid upstream of the separator. Another deterrent, successful in most instances, involves the coating of all internal surfaces of the separator with a plastic for which paraffin has little or no affinity. The weight of the paraffin will cause it to slough off of the plastic-coated surface before it builds up to harmful thickness.

Sand, Silt, Mud, Salt, Etc.

If sand and other solids are continuously produced in appreciable quantities with well fluids, they should be removed before the fluids enter the pipelines. Medium-grained sand in small quantities can be removed by settling in an oversized vertical vessel with a conical bottom and by periodically draining the residue from the vessel. Salt may be removed by mixing water with the oil, and after the salt is dissolved, the water can be separated from the oil and drained from the system.

Corrosion

Produced well fluids can be very corrosive and cause early failure of equipment. The two most corrosive elements are hydrogen sulfide and carbon dioxide. These two gases may be present in the well fluids in quantities from a trace up to 40 to 50% of the gas by volume. A discussion of the problems caused by these two corrosive gases is included in Chaps. 14 and 44.

Methods Used To Remove Oil From Gas in Separators

Liquid mist can be effectively removed from the gas stream in an oil and gas separator by a well-designed mist extractor. Condensable vapors in the gas cannot be removed by mist extractors. Condensation of these vapors, caused by reduction of temperature, may occur after the gas has been discharged from the separator. Thus, existence of liquid in the effluent gas from an oil and gas separator in many instances may not necessarily reflect the efficiency of the separator. Because condensable vapors may have the characteristics of natural gas at separator temperature and pressure, condensation of these vapors may occur immediately after being discharged from the separator.

Density difference of liquid and gas may accomplish separation of liquid droplets from a gas stream where the velocity of the stream is slow enough and sufficient time is allowed to accomplish separation. Limiting the gas velocity in a separator may obtain satisfactory separation without a mist extractor. However, mist extractors are generally installed in conventional oil and gas separators to assist in separation and to minimize the amount of liquid (mist) carried out with the gas.

The methods used to remove oil from gas in oil and gas separators are density difference (gravity separation), impingement, change of flow direction, change of flow velocity, centrifugal force, coalescence, and filtering. Mist extractors used in oil and gas separators can be of many different designs using one or more of these methods. Fig. 12.14 shows a vane-type mist extractor, Fig. 12.15 a centrifugal one, and Fig. 12.16 shows a knitted-wire-mesh (coalescing)-type mist extractor.

Density Difference (Gravity Separation)

Natural gas is lighter than liquid hydrocarbon. Minute particles of liquid hydrocarbon that are temporarily suspended in a stream of natural gas will, by density difference or force of gravity, settle out of the stream of gas if the velocity of the gas is sufficiently slow. The larger droplets of hydrocarbon will quickly settle out of the gas, but the smaller ones will take longer.

At standard conditions of pressure and temperature, the droplets of liquid hydrocarbon may have a density 400 to 1,600 times that of natural gas. However, as the operating pressure and temperature increase, the difference in density decreases. At an operating pressure of 800 psig, the liquid hydrocarbon may be only 6 to 10 times as dense as the gas. Thus, operating pressure materially affects the size of the separator and the size and type of mist extractor required to separate adequately the liquid and gas.

The fact that the liquid droplets may have a density 6 to 10 times that of the gas may indicate that droplets of liquid would quickly settle out of and separate from the gas. However, this may not occur because the particles of liquid may be so small that they tend to "float" in the gas and may not settle out of the gas stream in the short period of time the gas is in the oil and gas separator.

Particles of liquid hydrocarbon with diameters of 100 μm and larger will generally settle out of the gas in most average-sized separators. However, mist extractors usually are needed to remove smaller particles from the gas.

As the operating pressure on a separator increases, the density difference between the liquid and gas decreases. For this reason, it is desirable to operate oil and gas separators at as low a pressure as is consistent with other process variables, conditions, and requirements.

Impingement

If a flowing stream of gas containing liquid mist is impinged against a surface, the liquid mist may adhere to and coalesce on the surface. After the mist coalesces into larger droplets, the droplets will gravitate to the liquid section of the vessel. If the liquid content of the gas is high, or if the mist particles are extremely fine, several successive impingement surfaces may be required to effect satisfactory removal of the mist. A mist extractor that provides repeated impingement to remove fine oil mist from the gas is shown in Fig. 12.14a.

Change of Flow Direction

When the direction of flow of a gas stream containing liquid mist is changed abruptly, inertia causes the liquid to continue in the original direction of flow. Separation of liquid mist from the gas thus can be effected because the gas will more readily assume the change of flow direction and will flow away from the liquid mist particles. The liquid thus removed may coalesce on a surface or fall to the liquid section below. The mist extractor shown in Fig. 12.14a uses this method of mist extraction.

Change of Flow Velocity

Separation of liquid and gas can be effected with either a sudden increase or decrease in gas velocity. Both conditions use the difference in inertia of gas and liquid. With a decrease in velocity, the higher inertia of the liquid mist carries it forward and away from the gas. The liquid may then coalesce on some surface and gravitate to the liquid section of the separator. With an increase in gas velocity, the higher inertia of the liquid causes the gas to move away from the liquid, and the liquid may fall to the liquid section of the vessel. Fig. 12.14a shows one version of a vane-type mist extractor that uses change of flow velocity. This mist extractor is used in the typical vertical oil and gas separator shown in Fig. 12.14b.

Centrifugal Force

If a gas stream carrying liquid mist flows in a circular motion at sufficiently high velocity, centrifugal force throws the liquid mist outward against the walls of the container. Here the liquid coalesces into progressively larger droplets and finally gravitates to the liquid section below. Centrifugal force is one of the most effective methods of separating liquid mist from gas. Efficiency of this type of mist extractor increases as the velocity of the gas stream increases. Thus for a given rate of throughput, a smaller centrifugal separator will suffice.

Fig. 12.15 illustrates a horizontal, dual-tube, two-phase oil and gas separator that uses two stages of centrifugal mist extraction to remove liquid mist from the gas. The inlet impingement element is a cone with outwardly spiraling vanes that impart a swirling motion to the well fluid as it enters the separator. The larger droplets of liquid are thrown outward against the shell of the separator and gravitate down to the liquid section of the vessel. The gas

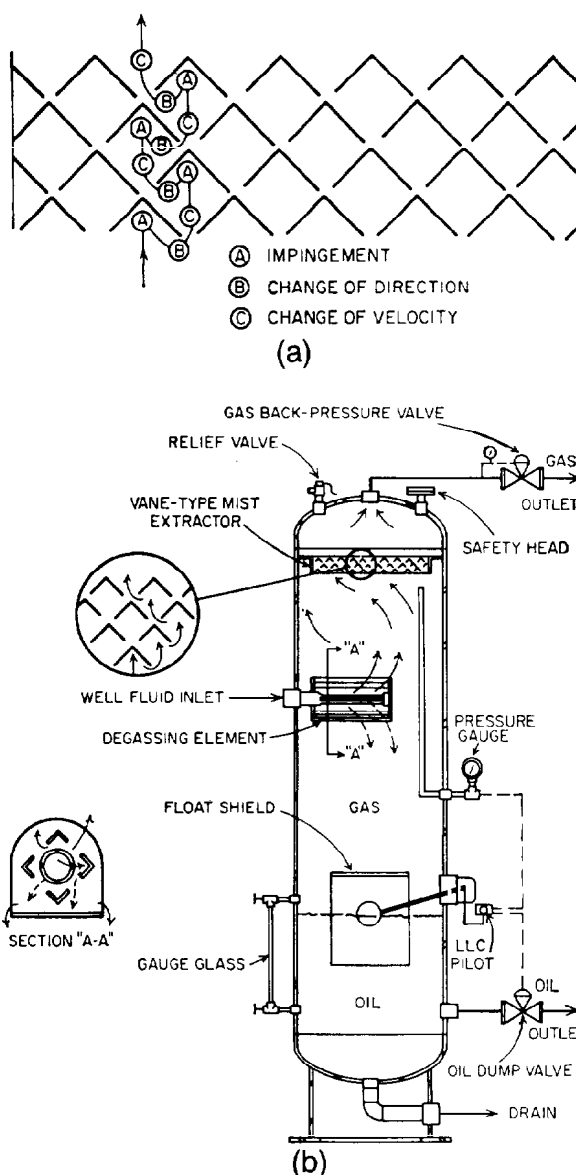


Fig. 12.14—Vertical two-phase oil and gas separator. (a) Illustration of impingement, change of flow direction, and change of flow velocity methods of mist extraction. (b) Separating and degassing element on inlet of vessel shown in detail in Section A-A.

flows to the secondary element, which consists of inward-spiraling vanes that accelerate the gas to around 80 ft/sec at normal capacity. This high velocity forces the particles of the liquid mist to the center of the element where they coalesce and separate from the gas when the velocity reduces to 2 to 8 ft/sec downstream of the secondary element. Oil separated by the primary centrifugal element flows from the upper shell cylinder to the lower one through the downcomer at the left. Oil removed from the gas by the secondary centrifugal element flows from the upper shell cylinder to the lower shell cylinder through the downcomer at the right. The lower cylinder of the separator is divided into two compartments with crude oil being discharged from each by use of two liquid-level controllers and two oil-discharge control valves.

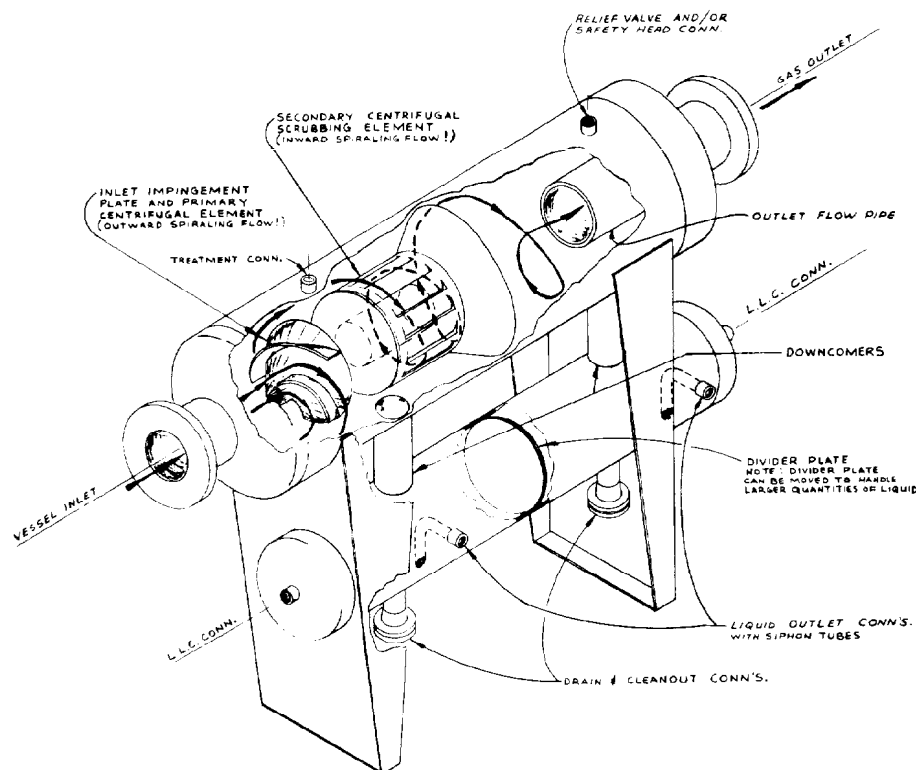


Fig. 12.15—Dual-tube horizontal two-phase oil and gas separator with centrifugal primary and secondary separating elements.

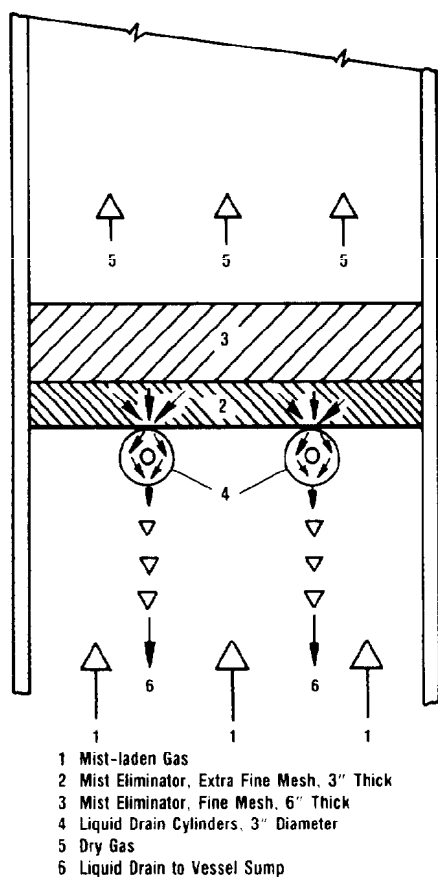


Fig. 12.16—Coalescing-type mist-eliminator pad with drain cylinders.

Separators and scrubbers using centrifugal force for the removal of liquid mist from the gas can handle large volumes of gas. One such unit installed near Princess, Alta., Canada, handles 3.5×10^9 scf/D at 1,000 psig.¹ This type of gas-cleaning unit is generally used in gas gathering, transmission, and distribution systems.

Small-diameter oil and gas separators (below 3 or 4 ft in diameter) using centrifugal force are generally not used as the primary separator on producing leases. This is because of the possibility that the small vessels may be inundated with a "slug" or "head" of liquid that may allow excessive liquid to exit with the gas and excessive gas to exit with the liquid. Therefore, primary separators on oil and gas streams are usually "conventional" units (other than centrifugal) to prevent the possibility of "overloading" the separators with liquid.

Coalescence

Coalescing packs afford an effective means of separating and removing liquid mist from a stream of natural gas. One of their most appropriate uses is the removal of liquid mist from gas in transmission and distribution systems where the amount of liquid in the gas is low.

Coalescing packs can be made of Berl saddles, Raschig rings, knitted wire mesh, and other such tower-packing materials. The packs use a combination of impingement, change of direction, change of velocity, and coalescence to separate and to remove liquid mist from gas. These packs provide a large surface area for collection and coalescence of the liquid mist. Fig. 12.17 is a schematic of a knitted wire mesh coalescing pack-type mist extractor used in some oil and gas separators and gas scrubbers.

A word of caution is appropriate concerning the use of coalescing packs in oil and gas separators for general field use. Coalescing packs may be made of frangible material that can be damaged during transit or installation if they are installed in the separator in the manufacturing shop before shipment to point of use. Knitted wire mesh may foul or plug from paraffin deposition and other foreign material and thus make a separator inoperative after a short period of service. Also, excessive pressure drop across the pack may force the pack out of place and allow channelling around or through the pack.

Even though coalescing packs are very effective in the removal of liquid mist from gas, it is usually preferred to use vane-type mist extractors for most oil and gas separators because they may be used under widely varying field conditions. Because of the "fouling" tendency of coalescing-type mist extractors, their use may appropriately be restricted to gas scrubbers used in gas gathering, transmission, and distribution systems.

Filtering

Porous filters are effective in the removal of liquid mist from gas in certain applications. In effect, the porous material strains or filters the liquid mist from the gas. The porous material may use the principles of impingement, change of flow direction, and change of velocity to assist in separation of liquid mist from gas.

Pressure drop through mist extractors used in separators should be as low as practical while maximum separating efficiency is still maintained. Generally, filter-type mist extractors will have the highest pressure drop per unit volume of capacity and the coalescing type will have the lowest. Pressure drop through the other types of mist extractors will usually range between these two extremes.

Mist Extractors Used in Oil and Gas Separators

Vane-Type Mist Extractors

Vane-type mist extractors are widely used in oil and gas separators to remove the liquid mist from the gas. These mist extractors can be of many designs. One design is shown in Fig. 12.14B. An enlargement of the mist extractor is shown in Fig. 12.14A. This is a simple but effective mist extractor, consisting of four layers of steel angles placed parallel to each other with the apex of the angle pointing upward. The angles are spaced $\frac{1}{2}$ in. apart horizontally; that is, they have a $\frac{1}{2}$ -in. gap between the legs of the angles in the horizontal plane. There is also a $\frac{1}{2}$ -in. space between the apex of the angle and the leg of the angles in the row above.

Gas flowing through the mist extractor follows the path illustrated in Fig. 12.14A. This flow pattern takes advantage of impingement, change of flow direction, change of flow velocity, and coalescence to separate liquid mist from the gas. Literally thousands of these mist extractors have been used, with all of them giving good performance. They are inexpensive to manufacture and usually will not plug or foul with foreign material and paraffin.

Another design of a vane-type mist extractor is shown in Fig. 12.18. As the gas enters the mist extractor, it is divided into many vertical ribbons (A). Each ribbon of gas is subjected to multiple changes of direction of flow

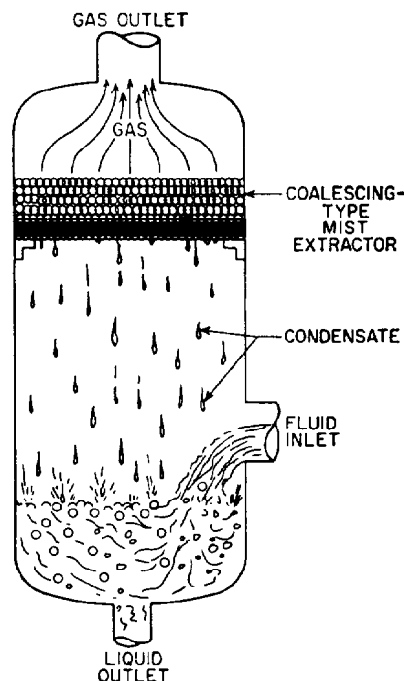
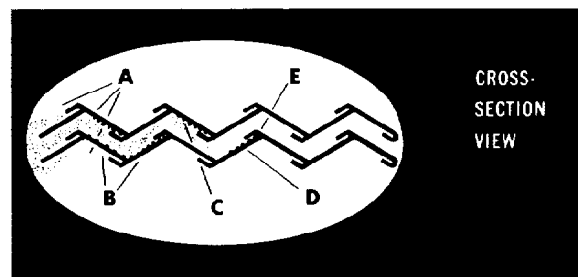


Fig. 12.17—Coalescing-type mist extractor with knitted wire mesh. Used in gas scrubbers and oil and gas separators.

(B) as it flows through the mist extractor. This causes mild turbulence and causes the gas to roll against the vanes, as at (C). The entrained droplets of liquid impinge against the vanes, where they adhere and coalesce (D). The liquid droplets move into the vane pockets (E). The liquid flows downward in these channels to the bottom of the mist extractor and then through the drain to the liquid reservoir in the bottom of the vessel where it can be drained from the separator.² The liquid drainage from this mist extractor occurs with the liquid out of the gas stream and with the movement of the liquid flow at a right angle to the direction of flow of the gas.

The separating efficiency of this mist extractor depends on the (1) number of vanes in the element, (2) distance between the vanes, (3) number of drainage channels, (4)



PRINCIPLE OF OPERATION

Fig. 12.18—Vane-type mist extractor with liquid channels.

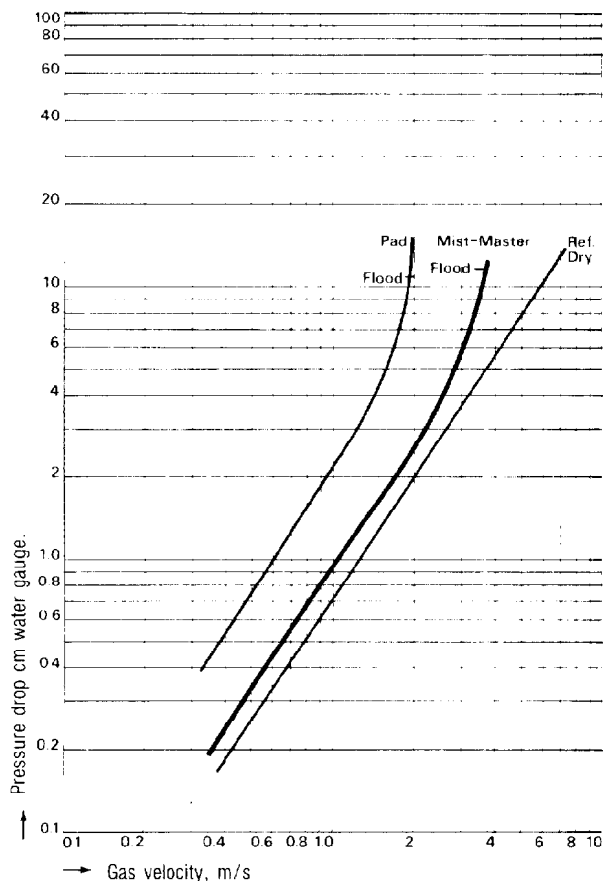


Fig. 12.19—Pressure drop and flooding velocity for 6-in.-thick mist-eliminator pad with and without drain cylinders.

width and depth of drainage channels, (5) distance between drainage channels, and (6) size of liquid particles to be removed from the gas.

It is claimed that this mist extractor will remove all entrained liquid droplets that are 8 to 10 μm and larger. If liquid particles smaller than 8 μm in diameter are present in the gas, an agglomerator should be installed upstream of the separator to coalesce the liquid into particles that are large enough for the vane-type mist extractor to remove. Some agglomerators are capable of achieving removal of 99.5% of all particles 1.0 μm and larger. Pressure drop across this vane mist extractor is very low, varying from 2 to 3 in. of water up to 6 to 8 in. of water.²

Fibrous-Type Mist Extractors

Fibrous packing has been used to remove liquid mist from natural gas since the early 1950s. Most of these fibrous packs have been knitted wire mesh. The main use of such mist eliminators has been to remove fine droplets, 10 to 100 μm in diameter, from a stream of gas. Standard mist-eliminator pads made of knitted wire mesh have low pressure drop, high separating efficiency, relatively low initial cost, and low maintenance cost.

In the late 1960's and early 1970's, considerable developmental work was done to improve the separating efficiency of knitted-wire-mesh mist-eliminator pads. It was

found that through use of a combination of filaments of different materials and diameters, the separating capacity of the pads could be greatly increased. It was found that a pad 9 in. thick with one 3-in.-thick pad of cknitted 0.0008-in.-diameter fiberglass filaments and 0.011-in.-diameter stainless steel filaments used as the bottom portion and one 6-in.-thick pad of 0.011-in.-diameter stainless-steel wire mesh as the top portion of the pad would give the highest separating efficiency at the lowest initial cost. In Fig. 12.16, No. 2 is the multifilament bottom portion of the pad, and No. 3 is the coarser monofilament top portion of the pad.

The extra-fine fiberglass filaments (0.0008 in. in diameter) cknitted with the 0.011-in. stainless-steel wire used in the bottom portion of the pad will agglomerate mist particles of 1 to 10 μm into larger particles so that the larger-diameter wire fibers (0.011 in. in diameter) used in the upper 6 in. of the mist eliminator can remove these agglomerated particles from the gas. Even though these combination multifilament pads appreciably increased the separating efficiency, they could not be used widely because they would flood at velocities 50% below those of regular (0.011-in. diameter) wire pads.

U.S. Patent No. 4,022,593³ issued May 10, 1977, solved this flooding problem for fine-wire pads. This patent discloses that the use of liquid drain cylinders installed underneath the mist eliminator pad, No. 4 of Fig. 12.16, will cause liquid to drain from the mist eliminator pad as quickly as it collects so that the mist pads remain free of liquid. This reduces the pressure drop through the pads and increases their separating capacity and efficiency.

These drain cylinders are made of the same material as the bottom portion of the mist eliminator pad, are about 3 in. in diameter, and are spaced underneath the pad on 12-in. centers. The drain cylinders provide a preferential "escape" route from the pad for the liquid. The preferential drain route results from the added gravity head provided by the drain cylinders.⁴ The drain cylinders are generally made of the same material and mesh as the bottom portion of the mist-eliminator pad. The liquid draining from the drain cylinders is shielded from the drag friction of the upflowing gas. Small rivulets or streams of liquid flow down through and across the mist pads down through the drain cylinders. The liquid flows from the drain cylinders in large drops or small streams. Re-entrainment is minimized or eliminated by use of the drain cylinders at the same time the separating efficiency of the pad is increased. Any free liquid anywhere in the pad tends to flow into the drain cylinder and be removed from the pad.

Fig. 12.19 shows the comparative pressure drop and flooding characteristics of a 6-in.-thick knitted-mesh mist-eliminator pad made of high-density polypropylene with and without drain cylinders. The fluids used in this test were air and water. The left curve is for the 6-in.-thick pad without drain cylinders. The middle curve is with the same pad but with drain cylinders installed. The straight line marked "Ref. Dry" represents the pressure drop through the same pad with no water in the pad, i.e., with the pad dry. The two points marked "Flood" indicate the air velocity that caused the pad to flood with water. The flood velocity for the pad without drain cylinders was almost 7 ft/sec. For the pad with drain cylinders, the flood velocity was 11.8 ft/sec.

Methods Used To Remove Gas From Oil In Separators

Because of higher prices for natural gas, the widespread reliance on metering of liquid hydrocarbons, and other reasons, it is important to remove all nonsolution gas from crude oil during field processing.

Methods used to remove gas from crude oil in oil and gas separators are settling, agitation, baffling, heat, chemicals, and centrifugal force.

Settling

Gas contained in crude oil that is not in solution in the oil will usually separate from the oil if allowed to settle a sufficient length of time. An increase in retention time for a given liquid throughput requires an increase in the size of the vessel and/or an increase in the liquid depth in the separator. Increasing the depth of oil in the separator may not result in increased emission of nonsolution gas from the oil because "stacking up" of the oil may prevent the gas from emerging. Optimum removal of gas from the oil is usually obtained when the body of oil in the separator is thin—i.e., when the ratio of surface area to retained oil volume is high.

Agitation

Moderate, controlled agitation is helpful in removing nonsolution gas that may be mechanically locked in the oil by surface tension and oil viscosity. Agitation usually will cause the gas bubbles to coalesce and to separate from the oil in less time than would be required if agitation were not used. Agitation can be obtained by properly designed and placed baffling.

Baffling

An inlet degassing element similar to that shown in Fig. 12.13 can be installed on the inlet of the separator to assist in introducing the well fluid into the separator with minimum turbulence and in removing gas from the oil. This element disperses the oil in such a manner that gas can more readily escape from the oil. This type of element eliminates high-velocity impingement of fluid against the opposite wall of the separator. The baffles placed in the separator (Fig. 12.13) between the inlet and the oil level spread the oil into thin layers as it flows downward from the inlet to the oil section. The oil is rolled over and over as it cascades down the baffles, and the combination of spreading and rolling is effective in releasing entrained gas bubbles. This type of baffling is effective in handling foaming oil.

Special perforated baffles or tower packing can be used to remove nonsolution gas from crude oil. Such baffling or packing provides slight agitation, which allows the gas bubbles to break out of the oil as it flows through the baffles or packing.

Heat

Heat reduces surface tension and viscosity of the oil and thus assists in releasing gas that is hydraulically retained in the oil. The most effective method of heating crude oil is to pass it through a heated-water bath. A spreader plate that disperses the oil into small streams or rivulets increases the effectiveness of the heated-water bath. Upward flow of the oil through the water bath affords slight

agitation, which is helpful in coalescing and separating entrained gas from the oil. A heated-water bath is probably the most effective method of removing foam bubbles from foaming crude oil. A heated-water bath is not practical in most oil and gas separators, but heat can be added to the oil by direct or indirect fired heaters and/or heat exchangers, or heated free-water knockouts or emulsion treaters can be used to obtain a heated-water bath.

Chemicals

Chemicals that reduce the surface tension of crude oil will assist in freeing nonsolution gas from the oil. Such chemicals will appreciably reduce the foaming tendency of the oil and thereby increase the capacity of a separator when foaming oil is handled. In one particular case, the capacity of an oil and gas separator was increased from 3,800 to 9,600 B/D when silicone was injected into and mixed with the oil upstream of the separator with no other change made in the system. Silicone is effective in reducing the foaming tendency of crude oil when it is mixed with the oil in such small quantities as parts per million or parts per billion.

Centrifugal Force

Centrifugal force is effective in separating gas from oil. The heavier oil is thrown outward against the wall of the vortex retainer while the gas occupies the inner portion of the vortex. A properly shaped and sized vortex will allow the gas to ascend while the liquid flows downward to the bottom of the unit. The separators and scrubbers shown in Figs. 12.15 and 12.20 through 12.22 use centrifugal force for separation. Oil from such units will usually contain less nonsolution gas than that from units that do not use centrifugal force.

Estimated Quality of Separated Fluids

Crude Oil

The free (nonsolution) gas content of separated crude oil will vary widely depending on many factors, such as size and configuration of the separator, design and arrangement of the separator internals, operating pressure and temperature, rate of flow, GOR, depth of liquid in the separator, viscosity, and surface tension of the oil. Table 12.1 indicates the estimated free gas and water content of separated crude oil discharged from average oil and gas separators operating under average field conditions. The values shown in this table are only approximate and are intended as an indication of the general range of results that may be expected; they are not intended to be exact and limiting. Table 12.1 indicates that appreciable quantities of free gas and water may be left in the separated crude oil; such undesirable performance may be obtained unless particular attention is given to the controlling factors indicated previously.

The water content of separated crude oil probably will be within the wide range indicated in Table 12.1. The factors listed previously, in addition to the agitation resulting from pressure reduction and flow, well-fluid water content, impurities, and degree of emulsification of the oil and water will determine the water content of the separated crude oil.

The approximate values given in Table 12.1 assume that special chemicals, equipment, procedures, and techniques

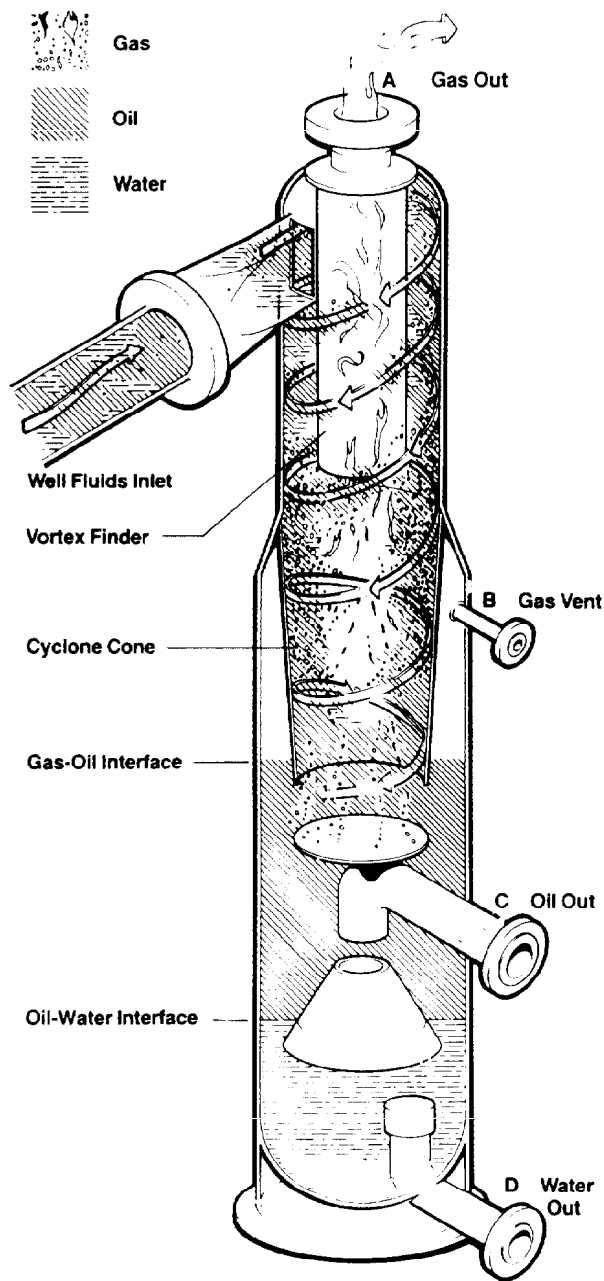


Fig. 12.20—Vertical three-phase separator with centrifugal force to obtain primary separation.

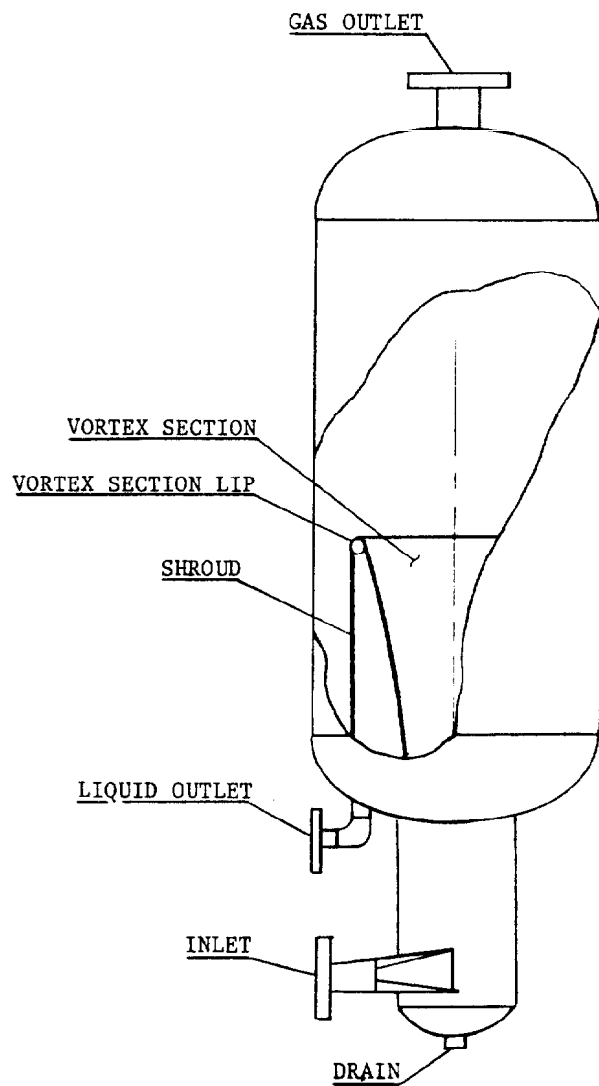


Fig. 12.21—Diverging vortex separator.

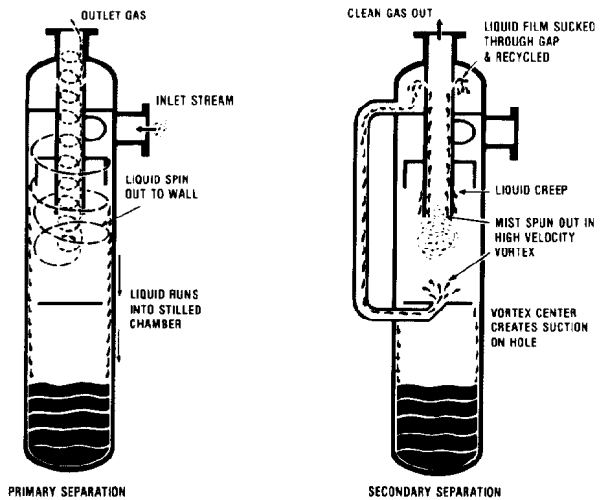


Fig. 12.22—Schematic of vertical recycling separator with centrifugal force to obtain primary and secondary separation of oil and gas.

TABLE 12.1—ESTIMATED QUALITY OF SEPARATED CRUDE OIL

Approximate Oil Retention Time (minutes)	Estimated Free (Nonsolution) Gas Content of Effluent Oil (%)*		Estimated Range of Water Content of Effluent Oil			
	Minimum	Maximum	Minimum		Maximum	
			(ppm)	(%)* **	(ppm)	(%)* **
1 to 2	5.0	20.0	16,000	1.60	80,000	8.00
2 to 3	4.0	16.0	8,000	0.80	40,000	4.00
3 to 4	3.0	12.0	4,000	0.40	20,000	2.00
4 to 5	2.5	10.0	2,000	0.20	10,000	1.00
5 to 6	2.0	8.0	1,000	0.10	5,000	0.50
6 +	1.5	6.0	500	0.05	2,500	0.25

*Expressed as a percent of the total oil volume with the gas measured at standard pressure and temperature.

**Volume basis.

have not been used or applied to improve the quality of the separated crude oil. When these are applied, appreciably improved results may be obtained.

Separated Water

It is probable that the effluent water from a three-phase separator will contain oil somewhere within the range indicated in Table 12.2. The quality of the separated water discharged from a three-phase separator depends on the same factors as previously listed for controlling the water content of the effluent oil. It is assumed that special chemicals and separating methods have not been used to improve the estimated quality of the effluent water shown in Table 12.2.

If the difference in the specific gravities of the oil and water at separator operating conditions is less than 0.20, special attention is required because the small difference in the densities of the oil and water will result in limited and incomplete separation. Lower qualities of effluent oil and water may result in such cases.

Gas

The oil (liquid hydrocarbon) content of the gas discharged from an oil and gas separator probably will be in the range shown in Table 12.3. Currently, it is difficult to measure the amount of oil in the separated gas under field operating conditions. With experience and patience, it can be done with a laser liquid particle spectrometer. The range of oil content in the separated gas shown in Table 12.3 has been accepted in recent years as an approximation of the performance of standard commercially available oil and gas separators under normal or average conditions equipped with suitably designed mist extractors.

TABLE 12.2—ESTIMATED QUALITY OF SEPARATED WATER

Water Retention Time (minutes)	Estimated Range of Oil Content of Effluent Water			
	Minimum		Maximum	
	(ppm)	(%)*	(ppm)	(%)*
1 to 2	4,000	0.40	20,000	2.00
2 to 3	2,000	0.20	10,000	1.00
3 to 4	1,000	0.10	5,000	0.50
4 to 5	500	0.05	2,500	0.25
5 to 6	200	0.02	1,000	0.10
6 +	40	0.004	200	0.02

*Volume basis.

Gas Quality From Scrubbers

The liquid content of gas discharged from gas scrubbers is usually less than the liquid content of gas discharged from oil and gas separators. Gas scrubbers are normally installed downstream of oil and gas separators or other separating equipment. If there is a separator upstream of the scrubber, the liquid hydrocarbon content of the scrubbed gas should be less than 0.10 gal/MMscf (less than 0.01335 ppm on a volume basis).

Measuring Quality of Separated Fluids

The quality of separated fluids discharged from oil and gas separators and similar equipment can be measured by state-of-the-art instruments currently available from various manufacturers. The measurements of the quality of effluent fluids and the instruments used to make these measurements are presented in Table 12.4

The instruments indicated are delicate. Each must be carefully selected, calibrated, applied, and operated, and

TABLE 12.3—ESTIMATED QUALITY OF SEPARATED GAS

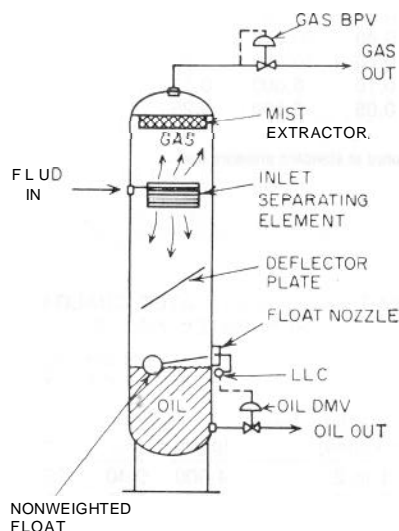
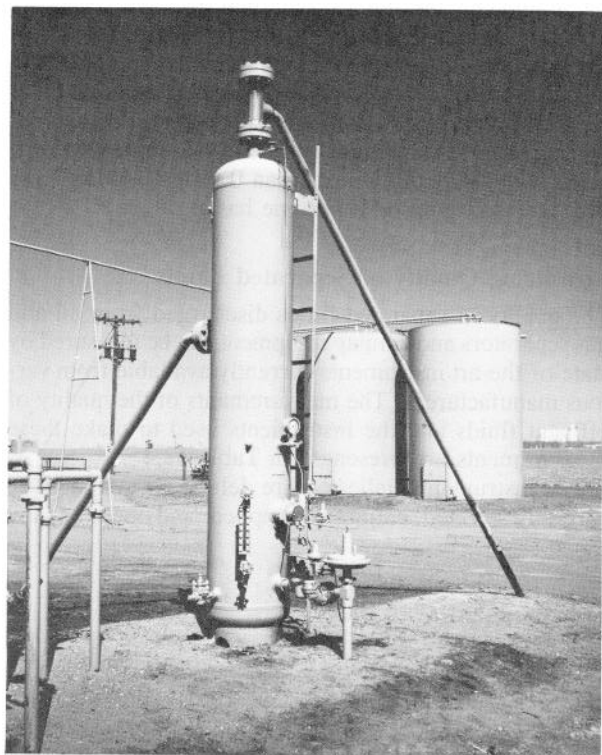
Operating Pressure (psig)	Operating Temperature (°F)	Estimated Oil Content of Effluent Gas			
		Minimum		Maximum	
		(ppm)	(gal/MMscf)	(ppm)	(gal/MMscf)
0 to 3,000	60 to 130	0.01335	0.10*	0.1335	1.00**

*Equivalent to 14.129 L/NM³ × 10⁶.

**Equivalent to 141.29 L/NM³ × 10⁶.

TABLE 12.4-MEASUREMENTS OF EFFLUENT FLUIDS QUALITY

Measurement	Instrument
Oil in effluent gas	Laser liquid particle spectrometer
Gas in effluent-oil	Nucleonic Densitometer
Water in effluent oil	BS&W monitor (capacitance measurement unit)
Oil in effluent water	Ultraviolet absorption unit
Oil in effluent water	Solvent extraction/infrared absorbance

**Fig. 12.23-Schematic of typical vertical two-phase oil and gas separator.****Fig. 12.24-Typical field installation of a vertical two-phase oil and gas separator.**

the results must be expertly analyzed and interpreted to obtain reliable and reproducible results.

Classification of Oil and Gas Separators

Classification by Configuration

Oil and gas separators can have three general configurations: vertical, horizontal, and spherical. Vertical separators can vary in size from 10 or 12 in. in diameter and 4 to 5 ft seam to seam (S to S) up to 10 or 12 ft in diameter and 15 to 25 ft S to S. Vertical separators are shown in Figs. 12.4, 12.13, 12.14, and 12.20 through 12.24.

Horizontal oil and gas separators are manufactured with monotube and dual-tube shells. Monotube units have one cylindrical shell, and dual-tube units have two cylindrical parallel shells with one above the other. Both types of units can be used for two-phase and three-phase service. A monotube horizontal oil and gas separator is usually preferred over a dual-tube unit. The monotube unit has a greater area for gas flow as well as a greater oil/gas interface area than is usually available in a dual-tube separator of comparable price. The monotube separator will usually afford a longer retention time because the larger single-tube vessel retains a larger volume of oil than the dual-tube separator. It is also easier to clean than the dual-tube unit.

In cold climates, freezing will likely cause less trouble in the monotube unit because the liquid is usually in close contact with the warm stream of gas flowing through the separator. The monotube design normally has a lower silhouette than the dual-tube unit, and it is easier to stack them for multiple-stage separation on offshore platforms where space is limited.

Horizontal separators may vary in size from 10 or 12 in. in diameter and 4 to 5 ft S to S up to 15 to 16 ft in diameter and 60 to 70 ft S to S. Horizontal separators are shown in Figs. 12.2, 12.3, 12.12, 12.15, and 12.25 through 12.27.

Spherical separators are usually available in 24 or 30 in. up to 66 to 72 in. in diameter. Spherical separators are shown in Figs. 12.5 and 12.28.

Classification by Function

The three configurations of separators are available for two- and three-phase operation. In the two-phase units, gas is separated from the liquid with the gas and liquid being discharged separately. In three-phase separators, well fluid is separated into gas, oil, and water with the three fluids being discharged separately.

Classification by Operating Pressure

Oil and gas separators can operate at pressures ranging from a high vacuum to 4,000 to 5,000 psi. Most oil and gas separators operate in the pressure range of 20 to 1,500 psi.

Separators may be referred to as low pressure, medium pressure, or high pressure. Low-pressure separators usually operate at pressures ranging from 10 to 20 up to 180 to 225 psi. Medium-pressure separators usually operate at pressures ranging from 230 to 250 up to 600 to 700 psi. High-pressure separators generally operate in the wide pressure range from 750 to 1,500 psi.

Classification by Application

Oil and gas separators may be classified according to application as test separator, production separator, low-temperature separator, metering separator, elevated separator, and stage separators (first stage, second stage, etc.).

Test Separator. A test separator is used to separate and to meter the well fluids. The test separator can be referred to as a well tester or well checker. Test separators can be vertical, horizontal, or spherical. They can be two-phase or three-phase. They can be permanently installed or portable (skid or trailer mounted). Test separators can be equipped with various types of meters for measuring the oil, gas, and/or water for potential tests, periodic production tests, marginal well tests, etc.

Production Separator. A production separator is used to separate the produced well fluid from a well, group of wells, or a lease on a daily or continuous basis. Production separators can be vertical, horizontal, or spherical. They can be two phase or three phase. Production separators range in size from 12 in. to 15 ft in diameter, with most units ranging from 30 in. to 10 ft in diameter. They range in length from 6 to 70 ft, with most from 10 to 40 ft long.

Low-Temperature Separator. A low-temperature separator is a special one in which high-pressure well fluid is jetted into the vessel through a choke or pressure-

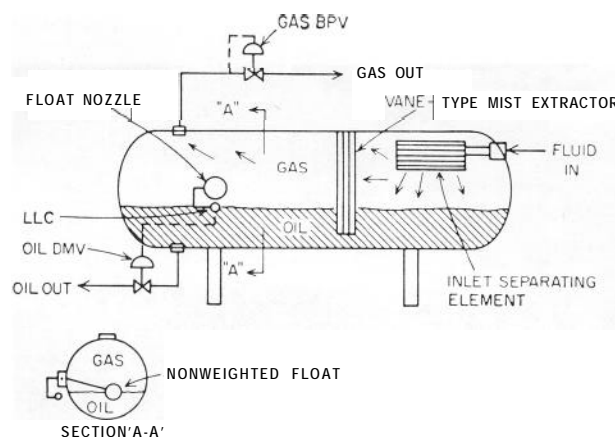


Fig. 12.25--Schematic of typical horizontal two-phase oil and gas separator.

reducing valve so that the separator temperature is reduced appreciably below the well-fluid temperature. The temperature reduction is obtained by the Joule-Thompson effect of expanding well fluid as it flows through the pressure-reducing choke or valve into the separator. The lower operating temperature in the separator causes condensation of vapors that otherwise would exit the separator in the vapor state. Liquids thus recovered require stabilization to prevent excessive evaporation in the storage tanks.

Metering Separator. The function of separating well fluids into oil, gas, and water and metering the liquids can be accomplished in one vessel. These vessels are commonly referred to as metering separators and are available for two- and three-phase operation. These units are available in special models that make them suitable for accurately metering foaming and heavy viscous oil.

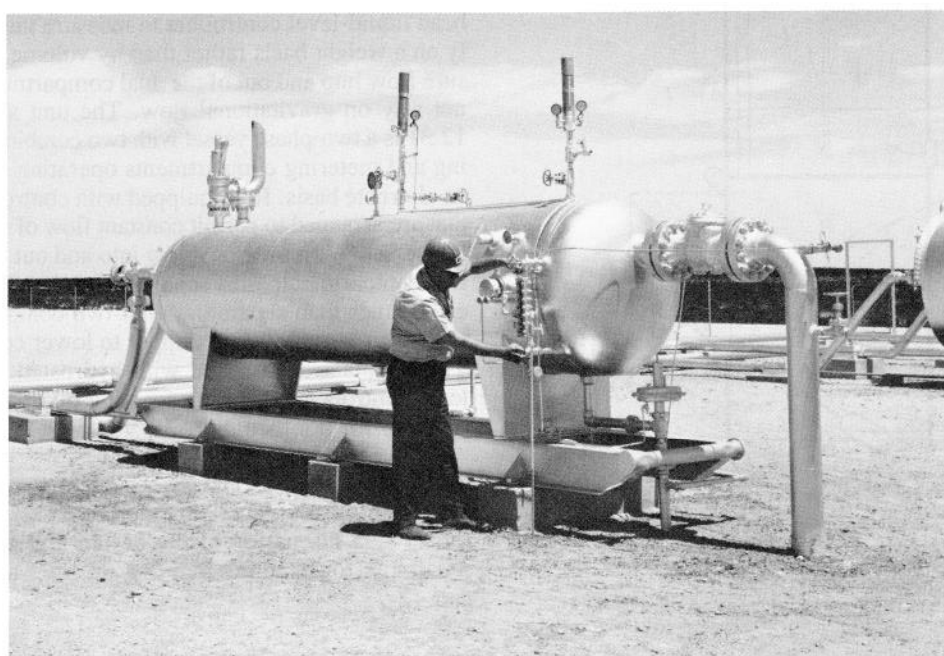


Fig. 12.26--Horizontal monotube two-phase oil and gas separator. Unit is skid mounted with accessories. Operator is checking liquid level in separator.

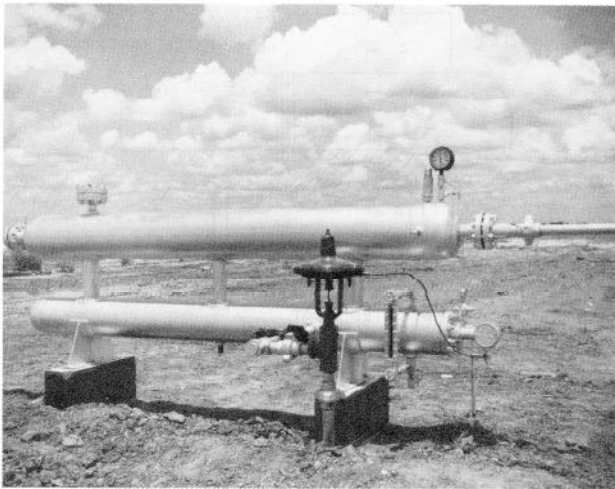


Fig. 12.27—Typical horizontal dual-tube two-phase oil and gas separator.

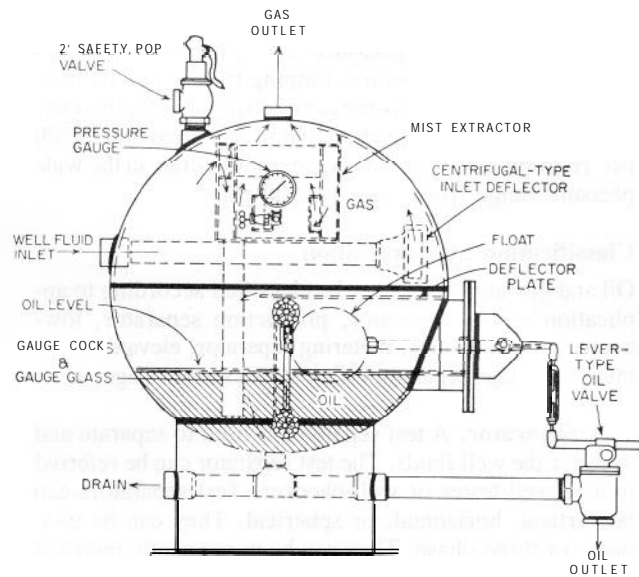


Fig. 12.28—Schematic of a typical spherical two-phase oil and gas separator with float-operated lever-type oil control valve.

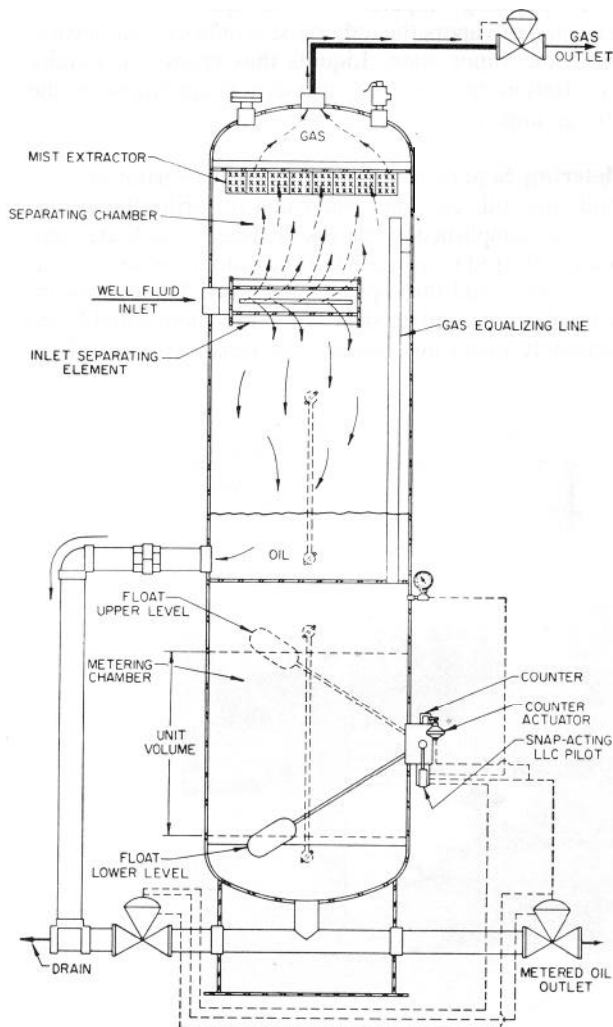


Fig. 12.29—Schematic of a vertical two-phase metering separator. Liquid is metered in integral metering compartment in lower portion of vessel.

A two-phase metering separator separates well fluids into liquid and gas and measures the liquid in the lower portion of the vessel. A typical two-phase metering separator is shown in Fig. 12.29. A three-phase metering separator separates the oil, water, and gas and measures only the oil or both the oil and water. Metering of the liquid is normally accomplished by accumulation, isolation, and discharge of given volumes in a metering compartment in the lower portion of the vessel.

Fig. 12.30 illustrates a three-phase metering separator in which the free water is measured with a positive-displacement meter. The metering separator shown in Fig. 12.31 is designed especially for separating large volumes of foaming and/or viscous oil. This unit uses hydrostatic-head liquid-level controllers to measure the oil accurately on a weight basis rather than by volume. It uses pressure flow into and out of the dual compartments and does not rely on gravitational flow. The unit shown in Fig. 12.31 is a two-phase vessel with two combination separating and metering compartments operating in parallel on an alternate basis. It is equipped with controls and valves that are arranged to permit constant flow of well fluid into the vessel. With pressure flow into and out of each of the two compartments, this separator can handle much larger volumes than separators with two compartments that rely on gravity flow from upper to lower compartments. These units are furnished with hydrostatic-head liquid-level controls for metering foaming oil or float-operated controls for nonfoaming oil.

Foam Separator. Oil and gas separators that handle foaming crude oil are generally referred to as foam separators. For a discussion of the design and application of separators for handling foaming oil refer to Pages 12-6 and 12-7.

Elevated Separators. Separators can be installed on platforms at or near tank batteries or on offshore platforms so that the liquid can flow from the separator to storage

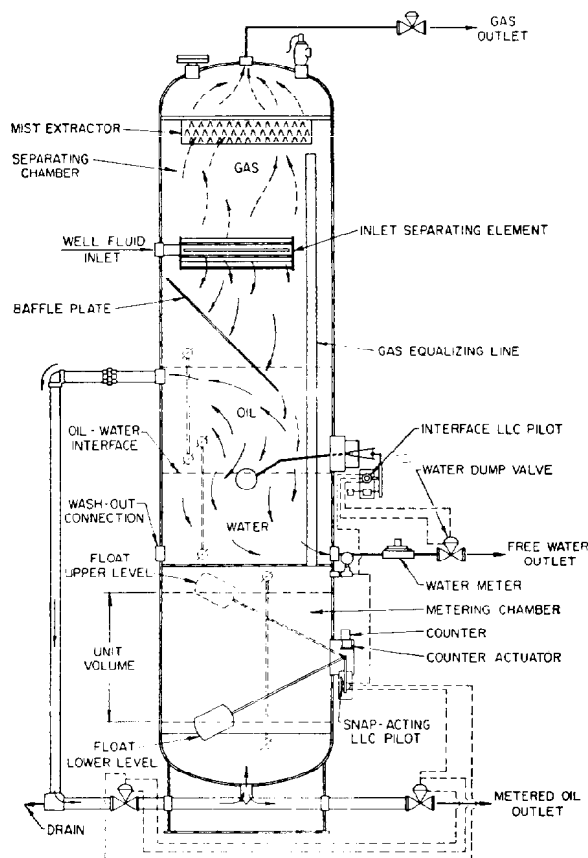


Fig. 12.30—Schematic of a vertical three-phase metering separator with free water metered with a positive displacement meter.

or to downstream vessels by gravity. This permits the separator to be operated at the lowest possible pressure to capture the maximum amount of liquid and to minimize the loss of gas and vapor to the atmosphere or to the low-pressure gas system.

Stage Separators. When produced well fluid is flowed through more than one separator with the separators in series, the separators are referred to as stage separators. The first separator is referred to as the first-stage separator, the second separator is called the second-stage separator, etc. For a more detailed discussion on stage separation refer to Page 12-32.

Classification by Principle Used for Primary Separation

Separators may be classified according to the method used to accomplish primary separation in the separator. Such a classification is density difference (gravity separation), coalescence and/or impingement, and centrifugal force.

Density Difference (Gravity Separation). This classification includes all units that have no inlet element, deflector, impingement plate, or pack on the inlet to the vessel.

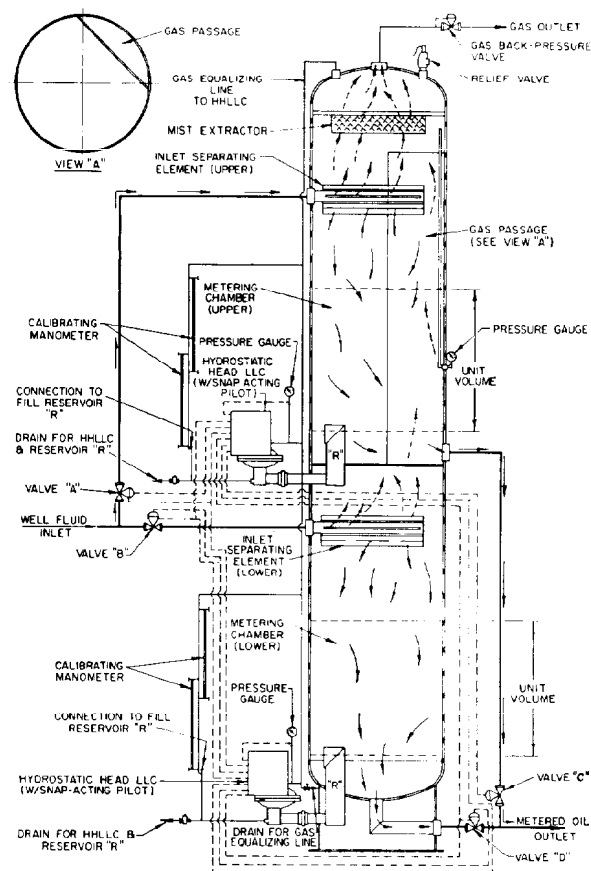


Fig. 12.31—Schematic of vertical two-phase metering separator for separating and metering viscous and/or foaming oil on a weight basis. Pressure flow into and out of the dual separating and metering compartments increases fluid-handling capacity.

Primary separation is obtained solely by the difference in density of the oil and gas or vapor. These units are few in number and most separators will have a mist extractor near the gas outlet to remove oil mist from the gas.

Impingement and/or Coalescence. This type of separator includes all units that use an impingement plate or device or a pack of tower packing on the inlet of the separator to accomplish initial separation of the oil and gas. An infinite number of design arrangements can be used on the inlet of a separator, but one of the simplest and most effective arrangements is illustrated in Fig. 12.14.

Centrifugal Force. Centrifugal force can be used for both primary and secondary separation of oil and gas in a separator. The centrifugal force can be obtained with either a properly sized tangential inlet in the separator (see Figs. 12.20 through 12.22) or a properly sized internal spiral or involute element with the top and bottom of the element open or partially open. These centrifugal elements cause cyclonic flow of the incoming fluid at velocities high enough to separate the fluid into an outer layer or cylinder of liquid and an inner cone or cylinder of gas or vapor. The velocity required for centrifugal separation will vary

from about 40 to about 300 ft/sec. The most common operating velocity range is between about 80 and 120 ft/sec.

Most centrifugal separators are vertical. However, a centrifugal separating element can be used on the inlet of horizontal separators to accomplish the initial separation of oil and gas. A second centrifugal element can be installed in the vessel to remove liquid mist from the exiting gas.

Centrifugal Oil and Gas Separators and Gas Scrubbers

Increased use of oil and gas separators on offshore platforms for handling larger volumes of well fluid has increased efforts to develop more compact separators to reduce space and weight on offshore platforms. Positive results have been achieved from these efforts, resulting in some separators that use centrifugal force to accomplish both initial and final separation of the oil and gas. Three centrifugal-force separators are illustrated in Figs. 12.20 through 12.22.

Centrifugal Separators

The vertical centrifugal oil and gas separator shown in Fig. 12.20 operates as described here.⁵ Well fluid enters the separator through the adjustable tangential slot at high velocity, inducing a cyclone within the vessel. The cyclone, stabilized by the vortex finder, moves down the cyclone cone. High cyclonic velocity ensures that a stable, thin film of liquid is maintained. The cyclone cone provides a long path for well fluid, enabling free gas to break out, a factor that is very effective with foaming oil. Residence time is not critical in gas/liquid separation. When the gas/oil interface is reached, the gas cyclone is reversed with the gas flowing upward and exiting from Nozzle A. The cyclone cone provides a smooth transition for the liquid to flow to the sump, preventing re-entrainment and assisting oil/water separation.

Oil/water separation is accomplished by gravity with the required residence time dependent on the well-fluid properties. Oil and water are drawn off from Nozzles C and D, respectively. Gas Vent B is provided to equalize the pressure and remove any gas that separates in the sump. Gas Vent B is normally connected to Gas Outlet A.

Diverging Vortex Separator

Fig. 12.21 shows a centrifugal gas/liquid separator that has been designed and patented recently.^{6,7} This unit uses centrifugal force to separate the gas and liquids. If the liquid is separated into oil and water, the separation is done by gravity.

The diverging vortex separator (DVS) is a bottom-entry, high-performance cyclone separator. Performance ranges from 99% to 99.99+ % over a flow rate range of 10 to 1. Mist particles are typically removed to below 5 μm and, depending on design specifications, additional condensate can be obtained because of the centrifugal force field. There are no moving parts and no change in gas flow direction. Pressure losses are minimal, ranging from inches of water to a few psi.

The oil-laden gas tangentially enters the bottom of the DVS vortex section, Fig. 12.21. Both the separated oil and gas corotationally spiral outward and up in a constant

vortex flow field. At the top of the vortex section, the oil circumferentially flows over the vortex section lip (Coanda effect), around and down the shroud to the vessel bottom, and out the liquid outlet. The gas continues an upward spiral to the gas outlet. This flow regime minimizes the oil-to-gas relative velocity, thereby minimizing re-entrainment and maximizing vortex-section surface area for coalescing and gathering oil. This surface is flow-wise continuous, allowing the oil to form a nearly uniform film. This film is stable, and the oil movement is consistent with inlet velocity and centrifugal force. Separation performance is independent of inlet liquid loadings up to 10 lbm of liquid per pound of gas.

The shroud extends below the oil level in the annular liquid section. The large annular liquid volume allows the separator to accommodate flow surges and liquid slugs. Performance is not affected by oil level within control range.

The oil and gas equilibrium is affected by centrifugal force in the vortex section. The equilibrium shift favors condensate formation, thereby effecting a dewpoint depression in the outlet gas. This dewpoint depression correlates directly with vortex section centrifugal force and is thus a function of inlet velocity. In-situ condensate formation is greatest at the vortex section inlet. This aids in the coalescing of entrained oil in the inlet stream, which improves separator performance. The outlet gas dewpoint depression means both a drier gas and a slightly higher liquid vapor pressure. If the inlet gas contains water vapor, moisture recovery will be consistent with the dewpoint-depression characteristic. This moisture will collect with the oil and condensate, allowing their final separation in the annulus formed by the vortex wall and the shell of the separator vessel.

Centrifugal Gas Scrubbers

Several different designs of centrifugal gas scrubbers are available from several suppliers. One of the most popular and effective centrifugal gas scrubbers is illustrated in Fig. 12.22. Operation of this unit is as follows.⁸ The centripetal-flow-type recycling separator has two effective stages of separation. The term centripetal flow denotes gas flow converging toward the center of the vessel, as in a whirlpool. In the first stage, all the free liquid and most of the entrained liquid are spun out of the gas by centrifugal force. In the second stage, the small amount of entrained liquid remaining in the gas is spun out under the influence of greatly increased centrifugal force and is collected by a recycling circuit as indicated in Fig. 12.22.

The well fluid enters the separator through the tangential inlet nozzle, which causes the stream to whirl around the inlet chamber. The spinning stream then moves downward between the smoothing sleeve and the separator shell into the vortex chamber. Liquid in the spinning stream is thrown outward by centrifugal force to the wall of the vortex chamber and runs down past the baffle plate into the liquid chamber, from which it is discharged. The gas, still spinning, converges toward the center of the vortex chamber, increasing in velocity, and enters the vortex finder tube. In the vortex finder tube, entrained liquid remaining in the rapidly spinning gas collects on the vortex finder wall and is swept upward by the gas toward the gas outlet. This liquid, together with a sidestream of about

5% of the total gas, is then sucked through a gap in the tube wall, down the recycling line, and through the central hole of the baffle plate into the vortex chamber. The low-pressure area along the axis of the vortex provides the necessary suction. Recycled liquid and sidestream gas thus entering the vortex chamber through the hole in the baffle plate mix with the rapidly spinning gas in the core of the vortex, and the liquid is thrown out to the wall and runs down with the rest of the liquid into the liquid chamber. The mainstream gas, now clean, continues up the vortex finder past the gap to the gas outlet.

The liquid chamber in these separators contains baffles for liquid stilling or for isolation of the level-control float as needed. The liquid chamber may be made oversized to handle very large liquid flows and may be constructed for gravity separation of the oil and water.

Illustrations of Oil and Gas Separators

Typical oil and gas separators are illustrated in Figs. 12.2 through 12.5 and 12.23 through 12.28. Fig. 12.25 is a schematic of a typical horizontal two-phase oil and gas separator. Fig. 12.26 is a photograph of a horizontal monotube two-phase oil and gas separator. Fig. 12.2 shows a horizontal skid-mounted three-phase oil/gas/water well tester on an offshore drilling platform off the coast of Brazil. The well tester is a separator with oil, gas, and water meters piped on it so that the well fluid can be separated into oil, gas, and water and each of the fluids metered before they are recombined or discharged separately.

Fig. 12.23 is a schematic of a typical vertical two-phase oil and gas separator. Fig. 12.24 is a photograph of a typical field installation of a vertical two-phase oil and gas separator. Fig. 12.28 depicts a typical two-phase spherical oil and gas separator with float-operated lever-type oil-control valve.

Fig. 12.3 is a schematic of a typical horizontal three-phase oil/gas/water separator. Fig. 12.4 shows a typical vertical three-phase oil/gas/water separator, and Fig. 12.5 illustrates a typical spherical three-phase oil/gas/water separator. Fig. 12.27 is a photograph of a horizontal dual-tube two-phase oil and gas separator.

Comparison of Oil and Gas Separators

Table 12.5 compares the advantages and disadvantages of two- and three-phase horizontal, vertical, and spherical oil and gas separators. This table is not intended as an "absolute" guide but affords a relative comparison of the various characteristics or features of the different separators over the range of types, sizes, and working pressures. The comparison of oil and gas separators in Table 12.5 assumes that the horizontal oil and gas separators are monotube vessels.

Estimating the Sizes and Capacities of Oil and Gas Separators

The oil and gas capacities of oil and gas separators will vary as the following factors vary.

1. Size (diameter and length) of separator.
2. Design and arrangement of separator internals.
3. Number of stages of separation.
4. Operating pressure and temperature of separator.
5. Physical and chemical characteristics of well fluid (gravity, viscosity, phase equilibrium, etc.)
6. Varying gas/liquid ratio.
7. Size and distribution of liquid particles in gas in the separator upstream of mist extractor.
8. Liquid level maintained in separator.
9. Well-fluid pattern, whether steady or surging.
10. Foreign-material content of well fluid.
11. Foaming tendency of oil.
12. Physical condition of separator and its components.
13. Other factors.

Items 5 and 7 are generally not known with sufficient detail and accuracy to permit accurate calculation of the size or performance of a separator. However, such calculations can be based on empirical data and assumptions for comparative and budgetary purposes. When separators are being sized for maximum performance and when the performance must be guaranteed, Items 5 and 7 become very important and must be available to the designer.

In a vertical separator, the liquid particles to be removed from the gas must settle downward against the upflowing column of gas. Conversely, in a horizontal separator, the

TABLE 12.5—COMPARISON OF ADVANTAGES AND DISADVANTAGES OF HORIZONTAL, VERTICAL, AND SPHERICAL OIL AND GAS SEPARATORS, TWO- AND THREE-PHASE

Considerations	Horizontal (Monotube)*	Vertical (Monotube)*	Spherical (One Compartment)*
Efficiency of separation	1	2	3
Stabilization of separated fluids	1	2	3
Adaptability to varying conditions	1	2	3
Flexibility of operation	2	1	3
Capacity (same diameter)	1	2	3
Cost per unit capacity	1	2	3
Ability to handle foreign material	3	1	2
Ability to handle foaming oil	1	2	3
Adaptability to portable use	1	3	2
Space required for installation			
Vertical plane	1	3	2
Horizontal plane	3	1	2
Ease of installation	2	3	1
Ease of inspection and maintenance	1	3	2

*Ratings: (1) most favorable; (2) intermediate; (3) least favorable.

path of a liquid particle to be separated from the gas as it flows through the vessel resembles the trajectory of a bullet fired from a gun. This difference in the flow pattern of the separated liquid particles indicates that a horizontal separator of a given diameter and length will separate a larger volume of well fluid than a vertical vessel of the same size. This is generally true, but the liquid level that must be carried in a monotube horizontal separator subtracts from this advantage and may cancel it out completely if a high liquid level is maintained in the horizontal separator.

The maximum gas velocity in an oil and gas separator that will allow separation of liquid mist from the gas can be calculated with the following form of Stokes' law:

$$v_g = F_{co} \left(\frac{\rho_L - \rho_g}{\rho_g} \right)^{1/2}, \quad (1)$$

where

- v_g = maximum allowable gas velocity, ft/sec,
- F_{co} = configuration and operating factor
(empirical) (see Fig. 12.32 for values),
- ρ_L = density of liquid at operating conditions,
lbm/cu ft, and
- ρ_g = density of gas at operating conditions,
lbm/cu ft.

The value of F_{co} in Eq. 1 is an empirical independent variable; it includes all factors that affect separation of liquid from gas in an oil and gas separator except (1) the compressibility factor of the gas, (2) base and operating pressure, (3) base and operating temperature, and (4) density of the fluids to be separated. F_{co} does include and varies with the length/diameter (L/D) ratio of the separator, the configuration of the separator vessel, the design of the internals of the separator, the liquid depth in the separator, foaming tendency of the oil, steady or pulsating flow of gas, heading or steady flow of liquid, gas/liquid ratio, presence of foreign materials and impurities,

and the degree of separation required. F_{co} varies in direct proportion to the L/D ratio. Of the variables listed above on which F_{co} is dependent, the L/D ratio of the separator vessel is the most dominant. The use of straightening vanes or cylinders, baffling, and special inlet degassing elements can increase the value of F_{co} and the separating capacity of a separator.

The original values of F_{co} used in Eq. 1 were determined by the assignment of values to F_{co} that would result in a velocity in the separator, expressed in feet per second and calculated by Eq. 1, that would provide the desired degree of separation. Thus the original values of F_{co} were for the customary system of units. To change the velocity calculated by Eq. 1 from customary to SI units, a multiplier of 30.48 must be used. That is, the velocity in feet per second must be multiplied by 30.48 to change it to centimeters per second.

The maximum allowable gas velocity v_g of Eq. 1 is the maximum velocity at which the gas can flow in the separator and still obtain the desired quality of gas/liquid separation. Only the open area of the separator available for gas flow is considered in calculating its capacity. The gas separating capacity of an oil and gas separator can be stated as

$$q_g = A_g v_g, \quad (2)$$

where

- q_g = volume of gas flowing through separator,
cu ft/sec,
- A_g = cross-sectional area of separator for gas
flow, sq ft, and
- v_g = gas velocity, ft/sec, from Eq. 1.

The ρ_g of Eq. 1 is calculated from Eq. 3 as follows:

$$\rho_g = \frac{pM_g}{z_g RT}, \quad (3)$$

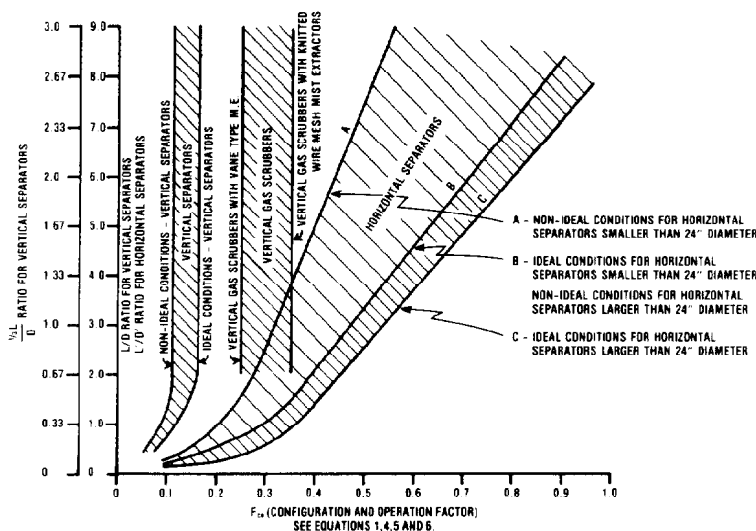


Fig. 12.32—Configuration and operation factor F_{co} for oil and gas separators and gas scrubbers (see Eqs. 1 and 4 through 6).

where

- p = separator operating pressure, psia,
 M_g = molecular weight of gas,
 z_g = compressibility factor of gas,
 R = gas constant, 10.732, and
 T = operating temperature, °R.

Substituting in Eq. 2 for v_g and simplifying yields

$$q_g = A_g F_{co} \left(\frac{\rho_L - \rho_g}{\rho_g} \right)^{1/2} \quad (4)$$

Equation for Gas Capacity of Oil and Gas Separator

When Eq. 4 is corrected for compressibility, pressure, and temperature and when units are changed to cubic feet per day, the equation becomes

$$q_g = 86,400 A_g F_{co} \left(\frac{1}{z_g} \right) \left(\frac{p}{p_b} \right) \left(\frac{T_b}{T} \right) \left(\frac{\rho_L - \rho_g}{\rho_g} \right)^{1/2} \quad (5)$$

where

- p_b = base pressure, psia, and
 T_b = base temperature, °R.

Equation for Sizing an Oil and Gas Separator for Gas Capacity

Eq. 5 can be rewritten to solve for A_g .

$$A_g = \frac{q_g}{86,400 F_{co} \left(\frac{1}{z_g} \right) \left(\frac{p}{p_b} \right) \left(\frac{T_b}{T} \right) \left(\frac{\rho_L - \rho_g}{\rho_g} \right)^{1/2}} \quad (6)$$

Eq. 5 can be used to calculate the volume of gas a separator of a given size will handle under given operating conditions. Eq. 6 can be used to calculate the size of separator required to handle a given volume of gas under certain operating conditions.

When Eqs. 5 and 6 are used for horizontal separators, A_g is the area for gas flow. The area occupied by liquid must be excluded. In a vertical separator, A_g is usually the entire internal cross-sectional area of the vessel.

The range of values of F_{co} normally used in Eqs. 5 and 6 is as follows. For vertical separators, the range is 0.10 to 0.167, and for horizontal separators, the range is 0.35 to 0.707. Values of F_{co} can be obtained from Fig. 12.32. The values of F_{co} shown in Fig. 12.32 are in customary units. Multiply these values by 30.48 for SI Units. For the L/D ratio of any given separator, any value of F_{co} indicated in Fig. 12.32 can be used. Experience aids in the selection of the optimum value of F_{co} . The nonideal (conservative) values of F_{co} will result in lower gas velocities, i.e., larger vessels. Use of F_{co} values for ideal (liberal) conditions will result in higher gas velocities, i.e., smaller vessels. Where the oil and gas tend to separate clean and dry and ideal operating conditions prevail, the ideal (liberal) values of F_{co} can be used. Where condi-

tions are less than ideal—such as slugging flow, high operating pressure and temperature, and excessive platform vibration or movement—the nonideal (conservative) values of F_{co} should be used. For estimating purposes for unknown operating conditions, the nonideal (conservative) values of F_{co} should be used. As experience is gained in a particular oil field or producing zone or area, it may be possible and practical to use higher values of F_{co} until the optimum balance between cost and performance is reached.

The values of F_{co} for horizontal separators are higher than for vertical separators. A typical value of F_{co} for vertical separators is 0.167; for horizontal separators a typical value of F_{co} is 0.500.

If the proper F_{co} value is used in Eq. 5, all liquid particles larger than 100 μm should be removed by gravity separation upstream of the mist extractor. If a properly designed and sized mist extractor is used, all liquid particles larger than 10 μm should be removed by the mist extractor.

The value of F_{co} in Eqs. 1 and 4 through 6 varies as the L/D ratio of the separator vessel varies. With a given diameter separator, as the length of the separator increases, the value of F_{co} increases. With a given length separator, as the diameter of the separator increases, the value of F_{co} decreases. This relationship is more pronounced in horizontal separators than it is in vertical separators; in vertical separators, if the L/D is greater than about 2.0, the value of F_{co} will change little, if at all, regardless of how much the L/D is increased. Refer to Fig. 12.32 for an indication of the relationship between L/D and F_{co} for both vertical and horizontal separators.

There is a range of length-to-diameter (L/D) ratios for oil and gas separators that will adequately meet each separator capacity requirement. This range of L/D ratios is minimum at about 1.0 to 2.0 and maximum at about 8.0 to 9.0. There is not just one diameter and length of separator that will satisfy a given capacity requirement; rather, there is a series of sizes (L/D ratios) that can be used for each application.

In a vertical separator, the well-fluid inlet is located about one-third of the length of the shell below the top head-shell weld seam, and the gas flows from the inlet up through the vessel to the gas outlet at the top of the vessel. The oil (liquid) flows downward from the inlet to the bottom of the vessel. Thus either the gas volume (above the inlet) or the liquid oil volume (below the inlet) can determine the required separator diameter.

For vertical separators, if the gas volume determines the size of the vessel, the L/D ratio of the vessel should be from about 2.0 to 3.0; if the liquid volume determines the separator size, the L/D ratio should be from about 2.0 to 6.0.

For horizontal separators, the L/D ratio of the vessel should be from about 2.0 to 6.0. The gas and liquid added together determine the size of a horizontal separator because the two fluids flow concurrently through the vessel from inlet end to outlet end.

For vertical separators similar to the configuration shown in Fig. 12.33, L/D or $1/3 L/D$ can be used to determine the value of F_{co} from Fig. 12.32. From the standpoint of determining the gas separating capacity of a vertical separator, the only pertinent part of the separator is that from the well-fluid inlet to the gas outlet. This

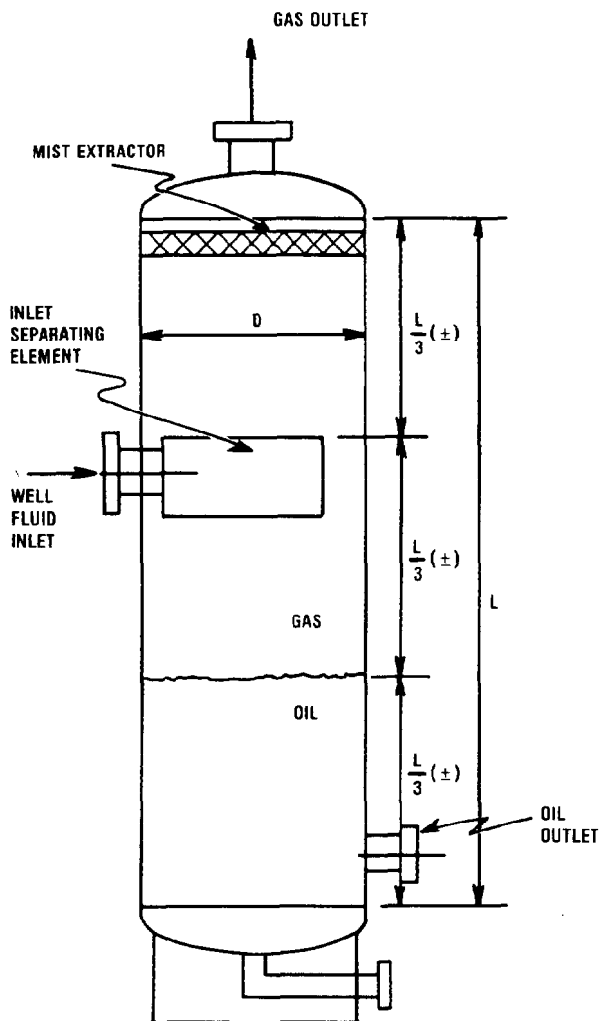


Fig. 12.33—One-third L/D vs. L/D for vertical oil and gas separators.

TABLE 12.6—VALUES FOR EXAMPLE PROBLEM 1

$L/D = 10/2 = 5.0$	$L'/D' = 7.0/1.33 = 5.26$	Difference in Values of F_{co} (%)
$F_{co} = 0.725$ (ideal conditions)	$F_{co} = 0.747$ (ideal conditions)	+ 3.03
$F_{co} = 0.636$ (nonideal conditions)	$F_{co} = 0.655$ (nonideal conditions)	+ 2.99

can include the mist extractor because the mist extractor should be as effective as density-difference separation would be in the space that it occupies. Fig. 12.32 shows both L/D and $\frac{1}{3}L/D$ for vertical separators.

Above an L/D ratio of 2.0 and a $\frac{1}{3}L/D$ ratio of 0.67, additional shell length does not increase the gas capacity of vertical separators. Additional shell length can increase the liquid capacity of the separator when the additional shell length is located between the inlet and the oil outlet.

For configurations of horizontal separators similar to the one shown in Fig. 12.34, L'/D' instead of L/D should be used to determine the value of F_{co} . This usually will result in a smaller separator for a given volume of gas, as indicated in the following three examples.

Example Problem 1. Assume a 24-in.-diameter \times 10-ft (S to S) horizontal separator operating with a liquid depth of 8 in. and with dimensions $A=1.5$ ft and $B=1.5$ ft (Fig. 12.34). The values of F_{co} are from Fig. 12.32. Refer to Table 12.6 for further data.

Example Problem 2. Assume a 48-in.-diameter \times 16 ft S to S horizontal separator operating with a liquid depth of 24 in. and with dimensions $A=2$ ft and $B=2$ ft (Fig. 12.34). Refer to Table 12.7 for more data.

Example Problem 3. Assume a 96-in.-diameter \times 30 ft S to S horizontal separator operating with a liquid depth of 32 in. and with dimensions $A=3$ ft and $B=4$ ft (Fig. 12.34). Refer to Table 12.8 for more data.

For a given horizontal separator, the value of F_{co} obtained by use of L'/D' will vary directly with the liquid depth.

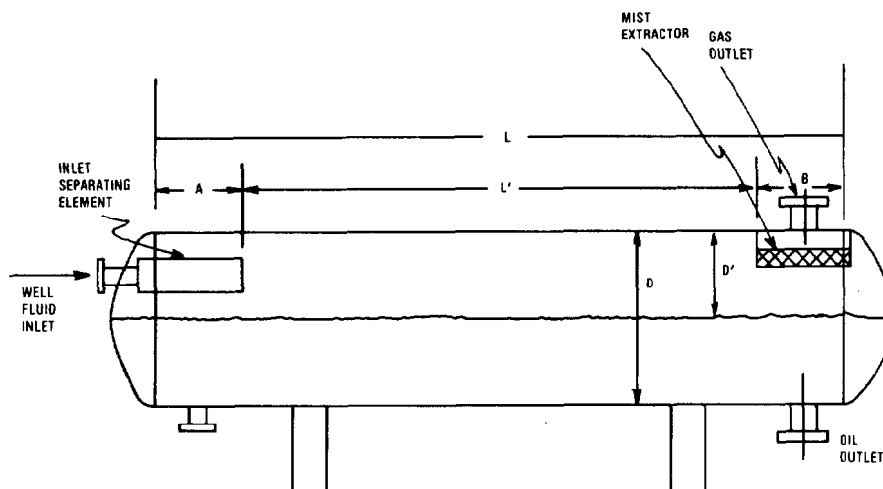


Fig. 12.34— L'/D' vs. L/D for horizontal oil and gas separators.

TABLE 12.7—VALUES FOR EXAMPLE PROBLEM 2

$L/D = 16/4 = 4.00$	$L'/D' = 12/2 = 6.00$	Difference in Values of F_{co} (%)
$F_{co} = 0.640$ (ideal conditions)	$F_{co} = 0.808$ (ideal conditions)	+ 26.25
$F_{co} = 0.560$ (nonideal conditions)	$F_{co} = 0.716$ (nonideal conditions)	+ 15.60

TABLE 12.8—VALUES FOR EXAMPLE PROBLEM 3

$L/D = 30/8 = 3.75$	$L'/D' = 23/5.33 = 4.32$	Difference in Values of F_{co} (%)
$F_{co} = 0.618$ (ideal conditions)	$F_{co} = 0.670$ (ideal conditions)	+ 8.41
$F_{co} = 0.541$ (nonideal conditions)	$F_{co} = 0.582$ (nonideal conditions)	+ 4.10

The use of straightening tubes, cylinders, plates, vanes, and Dixon plates will generally increase the value of F_{co} and increase the capacity of a given separator. The increase in capacity to be obtained by such devices and other design features can be estimated from empirical data that must be verified by field tests.

Computer Sizing of Oil and Gas Separators

Tables 12.9 and 12.10 are printouts of a computer program⁹ for sizing vertical and horizontal separators. The format of the computer printout has been modified.

The L/D for the vertical separator was indicated by the computer to vary from 2.0 to 2.8. The L/D for the horizontal separator was indicated by the computer to vary from 2.0 to 6.0. Fig. 12.32 shows the relation between L/D and the values of F_{co} . The values of F_{co} to be used in Eqs. 5 and 6 can be obtained from Fig. 12.32. Table 12.9 is an example of computer sizing of a vertical oil and gas separator. Table 12.10 is an example of computer sizing of a horizontal separator.

The liquid separating capacity of most oil and gas separators is controlled by retention or residence time, the time liquid is retained in the separator. This time usually var-

TABLE 12.9—COMPUTER DESIGN OF TWO-PHASE
VERTICAL OIL AND GAS SEPARATOR

Input Data			Output Data	
Gas rate, MMscf/D	50		GOR, scf/bbl	1,666.7
Oil rate, B/D	30,000		Density of gas, lbm/cu ft	0.68
Specific gravity of gas (air = 1)	0.70		Density of oil, lbm/cu ft	58.30
Specific gravity of oil (water = 1)	0.934		Compressibility factor	0.970
Operating temperature, °F	115		Inlet nozzle size, in.	14
Operating pressure, psig	185		Gas outlet size, in.	14
Maximum design pressure, psig	250		Oil outlet size, in.	6
Oil retention time, minutes	2		Relief valve	
			Inlet body size, in.	6
			Orifice area, * sq in.	8.067

Output Data

Number	Length to Diameter Ratio	ID (ft)	Height of Water Level (ft)	Height of Oil Level (ft)	Total Liquid Height (ft)	Distribution inlet Connection From Bottom Seam (ft)	Inside Cross-Sectional Area (sq ft)	Mist-Extractor Cross-Sectional Area (sq ft)
1	2.8	6.15	0.00	7.94	7.94	9.92	29.67	14.16
2	2.7	6.25	0.00	7.68	7.68	9.68	30.68	14.16
3	2.6	6.50	0.00	7.10	7.10	9.15	33.18	14.16
4	2.4	6.75	0.00	6.58	6.58	8.69	35.78	14.16
5	2.3	7.00	0.00	6.12	6.12	8.28	38.48	14.16
6	2.2	7.25	0.00	5.71	5.71	7.92	41.28	14.16
7	2.1	7.50	0.00	5.33	5.33	7.60	44.18	14.16
8	2.1	7.75	0.00	4.99	4.99	7.32	47.17	14.16
9	2.0	8.00	0.00	4.69	4.69	7.07	50.27	14.16

Output Data

Minimum Shell Height (ft)	Length of Shell Plus Heads (ft)	Minimum Shell Thickness (in.)	Minimum Head Thickness (in.)	Approximate Weight of Head Plus Shell (lbm)	Approximate Vessel Weight (lbm)	Actual Velocity of Gas (ft/sec)
17.06	20.56	0.53	0.53	9,299	10,693	1.54
16.93	20.48	0.54	0.54	9,591	11,029	1.49
16.65	20.33	0.56	0.56	10,331	11,881	1.38
16.44	20.25	0.58	0.58	11,127	12,797	1.28
16.28	20.22	0.61	0.60	11,982	13,780	1.19
16.17	20.24	0.63	0.62	12,897	14,832	1.11
16.10	20.29	0.65	0.64	13,875	15,956	1.04
16.07	20.39	0.67	0.67	14,917	17,154	0.97
16.07	20.52	0.69	0.69	16,025	18,429	0.91

*Based on gas volume only with maximum backpressure of 10%.
Any one of the nine separators indicated will satisfy the design capacity requirements.

**TABLE 12.10—COMPUTER DESIGN OF TWO-PHASE
HORIZONTAL OIL AND GAS SEPARATOR**

Input Data		Output Data	
Gas rate, MMscf/D	100	GOR, scf/bbl	2,000.00
Oil rate, B/D	50,000	Compressibility factor of gas	0.834
Specific gravity of gas (air = 1)	0.80	Density of gas, lbm/cu ft	3.70
Specific gravity of oil (water = 1)	0.85	Density of oil, lbm/cu ft	53.06
Operating temperature, °F	110	Inlet nozzle size, in.	14
Operating pressure, psig	800	Gas outlet size, in.	10
Maximum design pressure, psig	1,000	Oil outlet size, in.	8
Oil retention time, minutes	1.5	Relief valve	
L/D	2.0, 3.0, 4.0, 5.0, 6.0	Inlet body size, in.	4
		Orifice area,* sq in.	4.480

*Based on gas volume only with maximum backpressure of 10%.

Output Data

Number	L/D	Minimum ID (ft)	Minimum Shell Length (ft)	Minimum Shell Thickness (in.)	Minimum Head Thickness (in.)	Mist-Extractor Area (sq ft)	Vessel Area (sq ft)
1	2.0	6.97	13.93	2.47	2.40	14.95	38.12
2	3.0	6.24	18.72	2.22	2.15	14.95	30.60
3	4.0	5.67	22.68	2.01	1.96	14.95	25.26
4	5.0	5.26	26.32	1.87	1.82	14.95	21.77
5	6.0	4.99	29.92	1.77	1.72	14.95	19.53

Output Data

Area Assigned to						Actual Velocity of Gas (ft/sec)
Oil		Dead Space		Gas		
(sq ft)	(%)	(sq ft)	(%)	(sq ft)	(%)	
20.97	55.0	4.63	12.1	12.52	32.8	1.53
15.60	51.0	4.19	13.7	10.80	35.3	1.77
12.88	51.0	3.88	15.3	8.50	33.7	2.25
11.10	51.0	2.77	12.7	7.89	36.3	2.42
9.77	50.0	2.36	12.1	7.40	37.9	2.58

Output Data

Height of Oil Level		Height of Dead Space	
Vessel Diameter (%)	Feet	Vessel Diameter (%)	Feet
53.94	3.76	9.71	0.68
50.79	3.17	10.86	0.68
50.79	2.88	12.20	0.69
50.79	2.67	10.10	0.53
50.00	2.49	9.57	0.48

Output Data

Height of Gas		Approximate Weight of Shell and Heads (lbm)	Approximate Weight of Separator (lbm)
Vessel diameter (%)	ft		
36.36	2.53	44,292.8	50,936.7
38.36	2.39	43,324.0	49,822.6
37.01	2.10	41,100.9	47,266.0
39.12	2.06	39,760.2	45,724.2
40.43	2.02	39,636.4	45,581.9

Any one of the five separators indicated will satisfy the design capacity requirements.

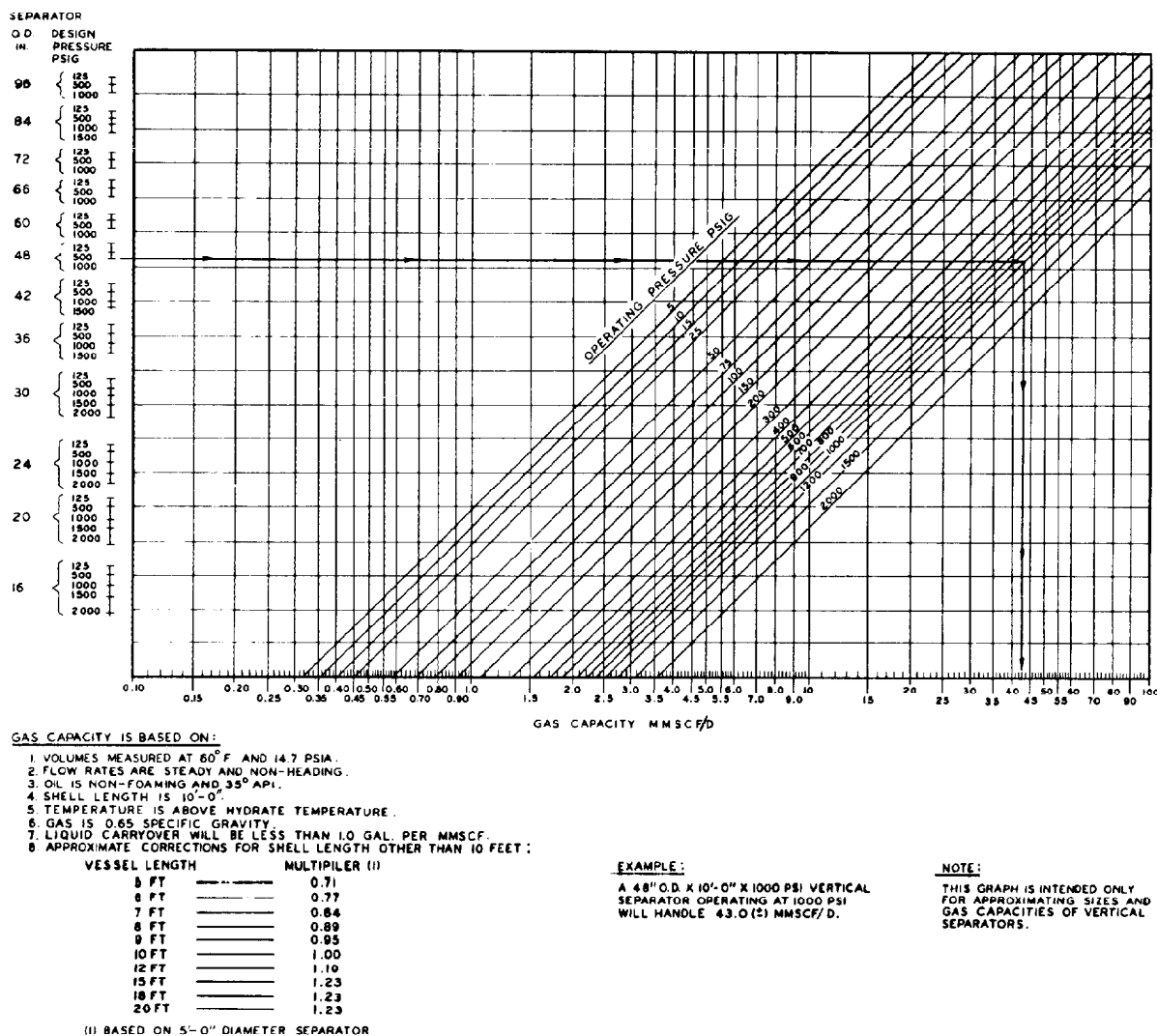


Fig. 12.35—Gas capacity of vertical oil and gas separators.

ies from 20 seconds to 1 to 2 hours, depending on many factors. For retention time to result in separation of water from oil, the liquid must be relatively quiet and free from agitation. Typical retention time for two-phase separation is 30 seconds to 2 minutes. Typical retention time for three-phase separation is from 2 to 10 minutes, with 2 to 4 minutes the most common.

Separators can be sized for liquid capacity in two ways. One way is to base the sizing on test data on the well fluid to be separated. The other way is to base the sizing on experience in separating fluid from that producing zone or area from neighboring wells or leases. If it is known that a certain retention time will be required to accomplish separation, sizing the separator for liquid becomes a simple volume calculation.

Capacity Curves for Vertical and Horizontal Oil and Gas Separators

The gas and liquid capacities of vertical and horizontal oil and gas separators can be estimated from the curves shown in Figs. 12.35 through 12.38. These capacity curves are based on calculations made with a computer

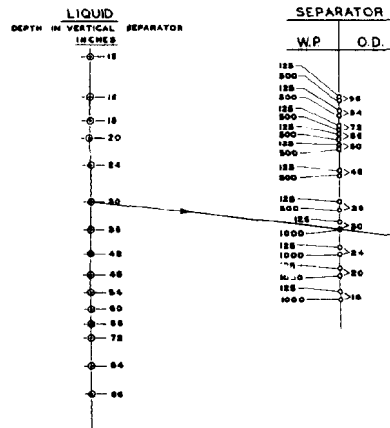
program developed by George O. Ellis⁹ and the author. Sample printouts of this computer program for vertical and horizontal separators listing the input and output data for each is shown in Tables 12.9 and 12.10.

The oil and gas capacity curves in Figs. 12.35 through 12.38 can be used reversibly to determine (1) the size separator required to separate a given volume of fluid under given operating conditions and (2) the volume of fluid a given separator will handle under given operating conditions.

The gas capacity of vertical separators is shown in Fig. 12.35. The capacities shown are based on the assumptions listed at the lower left side of Fig. 12.35. Conditions other than these will result in different capacities. These capacities are suitable for preliminary sizing and estimating purposes. If accurate sizing or performance data are required, calculations should be made with pertinent data. The gas capacity of a vertical separator does not vary directly with a change in shell length. If a standard length of 10 ft is assumed, an increase in shell length of 100%, to 20 ft, will result in an increase in gas capacity of about 23%.

LIQUID CAPACITIES ARE BASED ON:

1. RETENTION TIME INDICATED.
2. STEADY NON-HEADING FLOW.
3. NON-FOAMING OIL.
4. TEMPERATURE OF OIL MUST BE ABOVE POUR POINT.
5. OIL GRAVITY OF 35° API OR HIGHER.
6. VISCOSITY OF 50 SSU OR LESS.
7. LIQUID DEPTH IN SEPARATOR SHOULD NOT EXCEED APPROX. ONE TO THREE TIMES DIAMETER OF SEPARATOR DEPENDING ON EXACT DESIGN OF SEPARATOR.



EXAMPLE
A 30" X 10' X 1000 PSI SEPARATOR WITH A 30" LIQUID DEPTH WILL HANDLE 2700 BBL/DAY WITH ONE MINUTE RETENTION TIME.

MINIMUM RECOMMENDED RETENTION TIME	
0 — 600 PSI	= 1 MINUTE
600 — 1000 PSI	= 45 SECONDS
OVER 1000 PSI	= 30 SECONDS

NOTE: IF OIL FOAMS, RETENTION TIME MAY NEED TO BE INCREASED TO 5 MINUTES OR MORE.

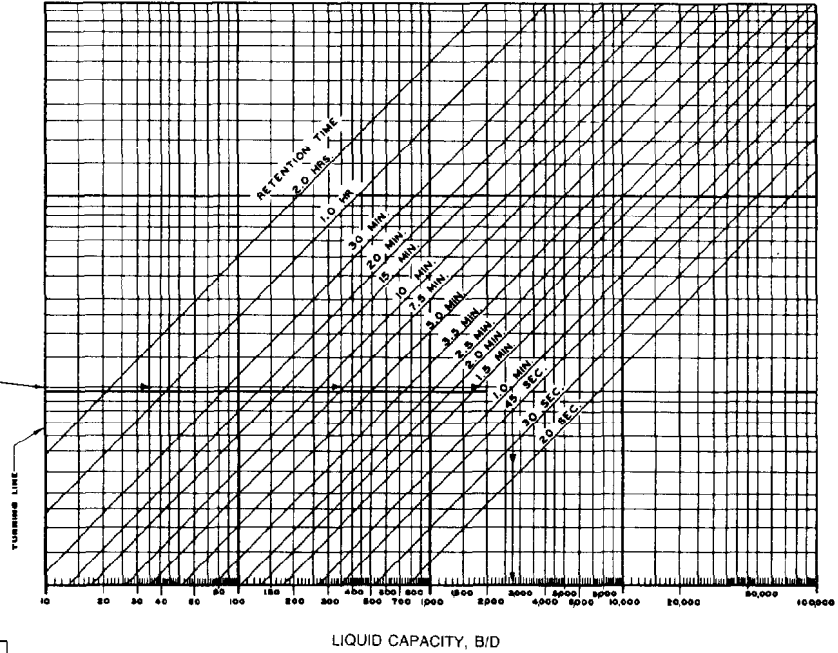
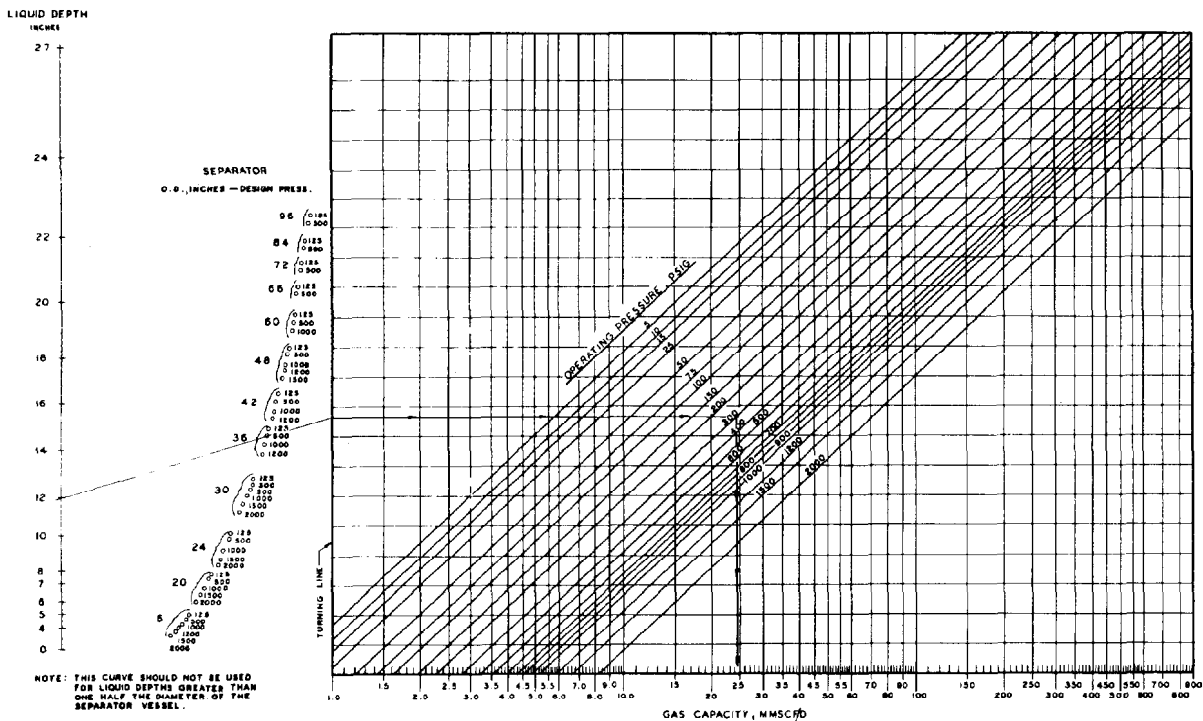


Fig. 12.36—Liquid capacity of vertical oil and gas separators.



NOTE: THIS CURVE SHOULD NOT BE USED FOR LIQUID DEPTHS GREATER THAN ONE HALF THE DIAMETER OF THE SEPARATOR VESSEL.

GAS CAPACITY IS BASED ON:

1. VOLUME MEASURED AT 60°F AND 14.7 PSIA.
2. FLOW RATES ARE STEADY AND NON-HEADING.
3. OIL IS NON-FOAMING AND 35° API.
4. SHELL LENGTH IS 10 FT.
5. OPERATING TEMPERATURE IS 100°F.
6. GAS IS 0.65 SPECIFIC GRAVITY.
7. LIQUID CARRYOVER WILL BE LESS THAN 1.0 OAL. MMSCF.
8. APPROXIMATE CORRECTIONS FOR SHELL LENGTH OTHER THAN 10 FT.

VESEL LENGTH	MULTIPLIER (1)
5 FT	0.78
8 FT	0.82
7 FT	0.87
4 FT	0.91
9 FT	0.95
10 FT	1.00
12 FT	1.05
15 FT	1.24
18 FT	1.37
20 FT	1.46

(1) BASED ON 48" DIAMETER SEPARATOR

EXAMPLE:

A 30" BY 10' BY 800 PSI HORIZONTAL OIL AND GAS SEPARATOR WITH A LIQUID DEPTH OF 30" IS OPERATING AT 300 PSI WILL HANDLE 24.2 MMSCF/D.

NOTE:

THIS GRAPH IS INTENDED ONLY FOR APPROPRIATE SIZES AND GAS CAPACITIES OF HORIZONTAL SEPARATORS.

Fig. 12.37—Gas capacity of horizontal oil and gas separators.

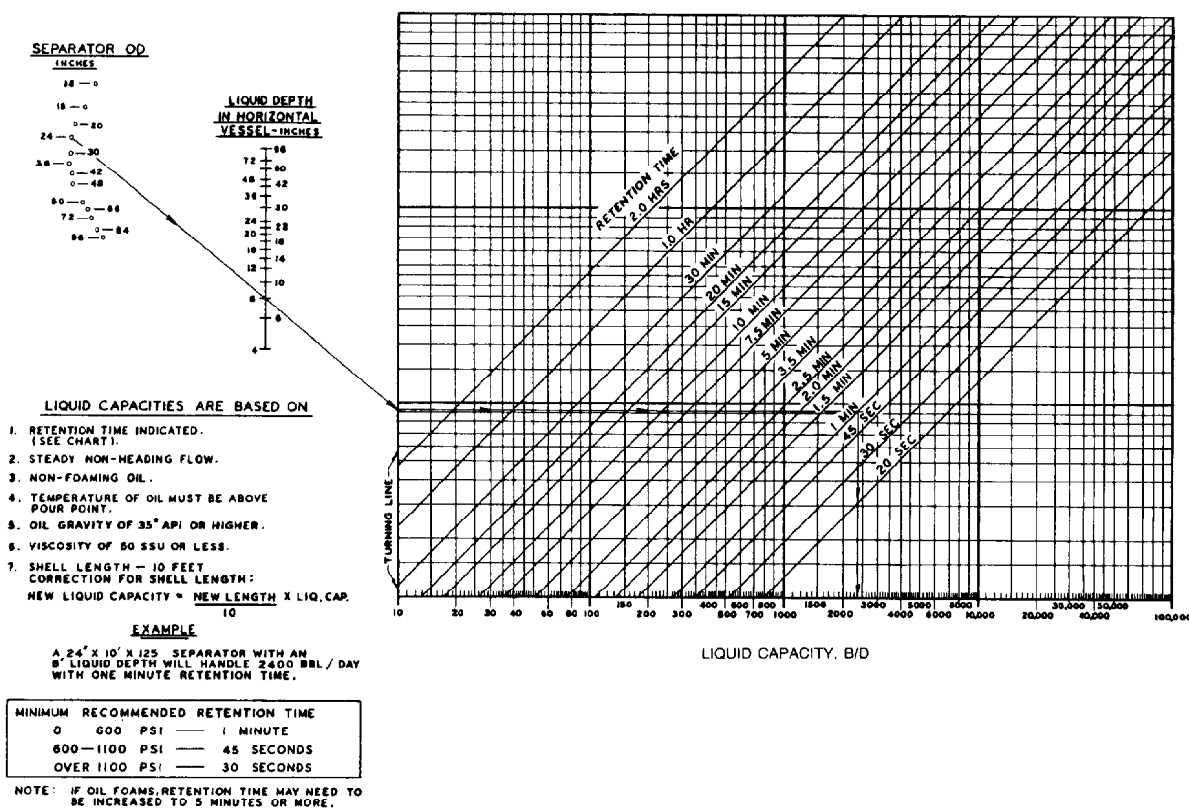


Fig. 12.38—Liquid capacity of horizontal oil and gas separators.

The liquid (oil) capacity of vertical separators is shown in Fig. 12.36. The liquid capacity of a vertical separator is controlled primarily by the volume of liquid retained in the accumulation (settling) section of the separator. Normal practice is to maintain a liquid depth above the oil outlet connection of from one to three diameters of the vessel. The optimum liquid depth depends on the design of the separator, the rate of throughput, and the characteristics of the fluid being separated.

The gas capacity of horizontal separators is shown in Fig. 12.37. The gas capacity of a horizontal separator is directly proportional to the cross-sectional area of the vessel available for gas flow. Thus, the diameter of a horizontal separator and the depth of liquid maintained in the vessel determine its gas capacity under given conditions. The gas separating capacity of a horizontal separator is proportional to the length but not directly proportional. For instance, if the length of the separator is increased from 10 to 20 ft, the gas separating capacity will increase 46%. Refer to the lower left corner of Fig. 12.37 for the relationship between shell length and gas capacity of a horizontal separator. The indicated multipliers assume that no special internals are used in the separators.

The liquid (oil) capacity of horizontal separators is shown in Fig. 12.38. The liquid capacity of a horizontal separator depends on the volumetric liquid-settling capacity of the accumulation (retention) section of the separator. This volumetric capacity is determined by inside shell diameter, shell length, and liquid depth.

The liquid depth in a horizontal separator for two-phase operation is normally assumed to be one-third of the diameter of the vessel. However, it can vary from 3 to 4 inches up to 60 to 70% of the cross-sectional area of the

separator. The liquid depth in a horizontal separator for three-phase operation is normally assumed to be at the horizontal centerline of the vessel (one-half full of liquid). However, it can vary from 8 to 10 inches up to 80 to 90% of the cross-sectional area of the vessel.

The gas capacities shown in the graphs in Figs. 12.35 and 12.37 are only approximate. These graphs should be used only for approximating the sizes and performance of separators. Calculations are recommended for more precise sizing and performance requirements especially where performance must be guaranteed.

Vertical Separator Sizing

Example Problem 4. See Table 12.11 for the given data. From Fig. 12.32, $F_{co}=0.167$; $M_g=M_{air}\gamma_g=28.97\times 0.7=20.28$.

Gas Sizing. Substituting in Eq. 3 yields

$$\rho_g = \frac{(199.7)(20.28)}{(0.97)(10.73)(575)} = 0.68 \text{ lbm/cu ft.}$$

TABLE 12.11—GIVEN DATA FOR SIZING
VERTICAL SEPARATORS—EXAMPLE PROBLEM 4

Maximum gas flow rate, MMscf/D	50.0
Specific gravity of gas	0.70
Maximum oil rate, B/D	30,000
Specific gravity of oil	0.934
Operating temperature, °F	115
Operating pressure, psig	185
Design pressure, psig	250
Oil retention time, minutes	2.0
Gas compressibility factor	0.97
Two-phase operation	No water

TABLE 12.12—GIVEN DATA FOR SIZING HORIZONTAL SEPARATORS—EXAMPLE PROBLEM 5

Maximum gas flow rate, MMscf/D	100.0
Specific gravity of gas	0.80
Maximum oil rate, B/D	50,000
Specific gravity of oil	0.85
Operating temperature, °F	110
Operating pressure, psig	800
Design pressure, psig	1,000
Oil retention time, minutes	1.5
Gas compressibility factor	0.834
Two-phase operation	No water

Substituting in Eq. 6 gives

$$A_g = \frac{50,000,000}{(86,400)(0.167) \left(\frac{1}{0.97} \right) \left(\frac{199.7}{14.7} \right) \left(\frac{520}{575} \right) \left(\frac{58.28 - 0.68}{0.68} \right)^{1/2}}$$

$$A_g = 29.76 \text{ sq ft for gas flow, and}$$

$$D = (29.76/0.7854)^{1/2} = 6.15 \text{ ft ID.}$$

A 72-in.-ID vessel can be used if the volume of 50.0 MMscf/D includes a small safety margin. If the separator must handle 50.0 MMscf/D with a written guarantee for performance, then a 78-in.-OD or -ID vessel can be used.

Oil Sizing for the Same Separator. Volume required in the separator for oil, V_o , is

$$V_o = \frac{30,000}{1440/2} = 41.67 \text{ bbl} = 233.98 \text{ cu ft.}$$

The height of oil, h_o , in the vertical separator is

$$h_o = \frac{233.98}{28.27} = 8.28 \text{ ft in a 72-in.-ID vessel,}$$

where the cross-sectional area of the 72-in.-ID vessel is 28.27 sq ft. If the separator has a 78-in. ID, the h_o will be

$$h_o = \frac{233.98}{33.18} = 7.05 \text{ ft,}$$

where the cross-sectional area of the 78-in.-ID vessel is 33.18 sq ft.

The length required for this separator shell will be about 16 to 18 ft.

Horizontal Separator Sizing

Example Problem 5. See Table 12.12 for the given data. From Fig. 12.32, $F_{co} = 0.707$; $M_g = M_{air} \gamma_g = 28.97 \times 0.80 = 23.18$.

Gas Sizing. Substituting in Eq. 3 yields

$$\rho_g = \frac{(814.7)(23.18)}{(0.834)(10.73)(570)} = 3.70 \text{ lbm/cu ft.}$$

Substituting in Eq. 6 gives

$$A_g = \frac{100,000,000}{(86,400)(0.707) \left(\frac{1}{0.834} \right) \left(\frac{814.7}{14.7} \right) \left(\frac{520}{570} \right) \left(\frac{53.04 - 3.70}{3.70} \right)^{1/2}}$$

$$A_g = 7.40 \text{ sq ft for gas.}$$

Oil Sizing for the Same Separator. The oil volume required in the vessel is

$$V_o = \frac{50,000 \times 5.615}{24 \times 60} \times 1.5 = 292.4 \text{ cu ft.}$$

Select a vessel length of 30 ft.

The cross-sectional area of oil is

$$A_o = \frac{292.4}{30} = 9.74 \text{ sq ft.}$$

For vessel sizing,

Area for gas = 7.40 sq ft

Area for oil = 9.74 sq ft

Dead space = 2.00 sq ft (about 25% of area for gas)

Total area = 19.14 sq ft

Note that dead space is considered to be "reserve" space between oil and gas and is usually assumed to be about 10 to 30% of the gas space for reserve capacity.

The vessel will be $9.74/19.14 = 51\%$ full of liquid. The area of the vessel's ID = 19.14 sq ft.

$$D = \left(\frac{19.14}{0.7854} \right)^{1/2} = 4.94 \text{ ft} = 59.2 \text{ in.}$$

Use a 60-in.-ID or 66-in.-OD \times 30-ft S to S separator, depending on reserve capacity desired.

The volume of the two heads on horizontal separators is normally not considered in separator-sizing calculations. This volume will compensate for the internals and for other variables.

Capacities of Spherical Separators

Spherical oil and gas separators use the same principles of separation used in horizontal and vertical separators. A spherical separator can be considered as a truncated vertical separator. When the fluid-handling capacity of spherical separators is considered, allowance must be made for the reduced height available for separation above the fluid inlet. The same consideration must be applied to spherical separators that is applied to the trays in a frac-

tionating column: the smaller the tray spacing, the lower the allowable capacity. Fig. 12.28 is a schematic of a typical two-phase spherical oil and gas separator. A typical three-phase spherical separator is shown in Fig. 12.5.

The chief advantage of spherical separators is their relatively low silhouette, which allows all component parts to be readily accessible to operating personnel. However, the horizontal separator offers this same advantage. The spherical separator may be easier and less expensive to install; on smaller units a gin-pole truck or crane may not be required to unload and place it on location.

The oil capacities of spherical oil and gas separators are shown in Table 12.13. The gas capacities of spherical oil and gas separators are shown in Fig. 12.39. The table and curves were originated by Vondy.¹⁰ The gas capacities shown in Fig. 12.39 for spherical separators are conservative and assume that the spherical vessels contain no internals. If a properly designed separating element is used on the inlet of the spherical separators, and if an effective mist extractor is used, the gas capacities shown in Fig. 12.39 can be increased by a multiplier that ranges from 1.0 to 3.0, as shown in Table 12.14.

The amount of increase in spherical separator capacity that can be obtained by vessel design is dependent on several factors: (1) location of inlet connection in the vessel with respect to the liquid level in the separator; (2) size, configuration, and location of the inlet separating and spreading element; (3) vertical distance between the inlet separating and spreading element and the mist extractor; (4) size, design, and location of the mist extractor; (5) physical and chemical characteristics of the well fluid being separated; (6) operating pressure and temperature of the separator; (7) flow pattern into the separator (heading or steady); and (8) other factors.

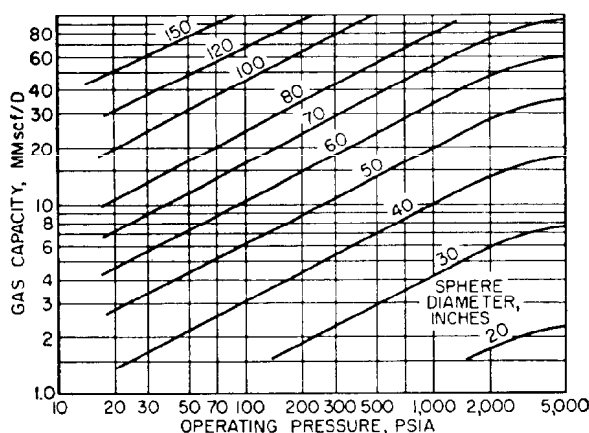


Fig. 12.39—Gas capacity of spherical oil and gas separators.

The oil (liquid hydrocarbon) capacity of spherical oil and gas separators is shown in Table 12.13. The liquid capacity for each size unit is shown for two different liquid depths in the vessel—with the liquid depth equal to one-third and one-half the ID of the sphere. The first condition is appropriate for two-phase (oil/gas) separation; the second condition is appropriate for three-phase (oil/gas/water) separation.¹⁰

Spherical separators are more appropriately used for two-phase separation than for three-phase separation. This is especially true of sizes smaller than 36 in. in diameter. Field tests should be made on spherical separators to determine and/or to confirm their capacity because, of the three shapes of separator vessels available, they are the most difficult to rate properly for oil and gas capacities.

TABLE 12.13—LIQUID CAPACITIES OF SPHERICAL OIL AND GAS SEPARATORS

ID of Sphere (in.)	Assumed Liquid Depth in Sphere (in.)	Liquid Capacity, B/D, 42 gal/bbl, Steady Flow									
		Liquid-Retention Time									
		20 seconds	30 seconds	60 seconds	2.5 minutes	5.0 minutes	10 minutes	20 minutes	30 minutes		
16 (1)*	5.33	248	165	83	33	17	8	4	3		
(2)**	8.00	447	318	159	64	32	16	8	5		
20 (3)	6.66	483	322	161	64	32	16	8	5		
(4)	10.00	932	622	311	124	62	31	16	10		
24 (5)	8.00	836	557	278	111	56	28	14	9		
(6)	12.00	1,611	1,074	537	215	107	54	27	19		
30 (7)	10.00	1,632	1,088	544	218	109	54	27	18		
(8)	15.00	3,147	2,098	1,049	420	210	105	52	35		
36 (9)	12.00	2,820	1,880	940	376	188	94	47	31		
(10)	18.00	5,438	3,625	1,813	725	363	181	91	60		
42 (11)	14.00	4,478	2,985	1,493	597	299	149	75	50		
(12)	21.00	8,636	5,757	2,879	1,151	576	288	144	96		
48 (13)	16.00	6,684	4,456	2,228	891	446	223	111	74		
(14)	24.00	12,890	8,594	4,297	1,719	859	430	215	143		
60 (15)	20.00	13,056	8,704	4,352	1,741	870	435	216	145		
(16)	30.00	25,177	16,785	8,392	3,357	1,678	839	420	280		
72 (17)	24.00	22,560	15,040	7,520	3,008	1,502	752	375	250		
(18)	36.00	43,505	29,004	14,502	5,801	2,900	1,450	725	483		
84 (19)	28.00	35,825	23,880	11,942	4,777	2,388	1,194	597	398		
(20)	42.00	69,085	46,057	23,028	9,211	4,606	2,303	1,151	768		
96 (21)	32.00	53,477	35,652	17,826	7,130	3,565	1,783	891	594		
(22)	48.00	103,125	68,750	34,375	13,750	6,875	3,437	1,719	1,146		
100 (23)	33.33	60,444	40,296	20,148	8,059	4,030	2,015	1,007	672		
(24)	50.00	116,560	77,707	38,853	15,541	7,771	3,885	1,943	1,295		

*Odd-numbered conditions recommended for two-phase operation.

**Even-numbered conditions recommended for three-phase operation.

TABLE 12.14—MULTIPLIERS FOR GAS CAPACITIES SHOWN IN FIG. 12.39

Type of Separator Service	Design of Vessel Internals	Multipliers for Gas Capacities Shown in Fig. 12.39
Foaming crude oil	Average	0.25 to 0.75
Nonfoaming crude oil	Average	1.0 to 1.5
Nonfoaming crude oil	Superior	1.5 to 2.0
Distillate or condensate	Average	2.0 to 2.5
Distillate or condensate	Superior	2.5 to 3.0

Practical Considerations in Sizing Oil and Gas Separators

To ensure acceptable separation at all times, an oil and gas separator should be sized so that it will never operate above its maximum rated capacity. A separator must be sized for the maximum instantaneous flow rate to which it will be subjected rather than for the total daily production rate. Many wells produce by "heads" or "slugs" as a result of natural causes or intermittent gas lift. Such a well may produce a total of only 200 bbl of liquid in 24 hours. However, if that well "heads" or "intermits" only once each hour, it may produce $\frac{1}{4}$ of its total daily production in a matter of 2 or 3 minutes, which would result in an instantaneous flow rate of about 4,000 to 6,000 B/D. The separator should be sized to handle the maximum instantaneous rate of fluid produced during these short intervals, or it must be of sufficient size to store a portion of these slugs while it separates and discharges the balance.

In addition to serving as a means for separating the well fluid into gas and liquids, the separator vessel, in some instances, must also serve as an accumulation or storage vessel, particularly when the wells flow by "heads," when intermittent gas lift is used, when the tubing string and/or flowlines may unload liquid into the separator at high instantaneous flow rates and when the liquid is transferred from the separator by pump and the separator must serve as the accumulator/reservoir vessel for the pumping operation. In these instances the separator vessel must be large enough to store the extra volume of liquid in addition to performing the function of separating. This consideration of storage may often dictate larger vessels than otherwise would be required if the flow of fluid into and out of the separator were steady and continuous.

It is extravagant to install grossly oversized separators where their excess capacities will never be used. Most pumping wells, continuous-flow gas-lift wells, and some naturally flowing wells always produce at uniform rates. For such wells, separator sizes may be selected on the basis of maximum total daily production.

Field tests should be made on oil and gas separators to determine their oil- and gas-handling capacities under

actual conditions. Manufacturers' rated capacities for separators are intended for "general" or "average" conditions. The only way to determine the exact capacity of a particular separator under a given set of conditions is to actually test the separator under those conditions.

Stage Separation of Oil and Gas

Theoretical Considerations of Stage Separation

Stage separation of oil and gas is accomplished with a series of separators operating at sequentially reduced pressures. Liquid is discharged from a higher-pressure separator into the next-lower-pressure separator. The purpose of stage separation is to obtain maximum recovery of liquid hydrocarbons from the well fluid and to provide maximum stabilization of both the liquid and gas effluent.

Two processes liberate gas (vapor) from liquid hydrocarbon under pressure. They are flash separation (vaporization) and differential separation (vaporization). Flash separation is accomplished when pressure is reduced on the system with the liquid and gas (vapor) remaining in contact; i.e., the gas (vapor) is not removed from contact with the liquid as reduction in pressure allows the gas to come out of solution. This process yields the most gas (vapor) and the least liquid. Differential separation is accomplished when the gas (vapor) is removed from contact with the liquid as reduction in pressure allows the gas (vapor) to come out of solution. This process yields the most liquid and least gas (vapor).

In a multiple-stage-separator installation, both processes of gas liberation are obtained. When the well fluid flows through the formation, tubing, chokes, reducing regulators, and surface lines, pressure reduction occurs with the gas in contact with the liquid. This is flash separation. When the fluid passes through a separator, pressure is reduced; also, the oil and gas are separated and discharged separately. This is differential separation. The more nearly the separation system approaches true differential separation from producing formation to storage, the higher the yield of liquid will be.

An ideal oil and gas separator, from the standpoint of maximum liquid recovery, is one constructed so that it reduces the pressure of the well fluid from the wellhead at the entrance of the separator vessel to, or near, atmospheric pressure at the discharge from the separator. The gas and/or vapor is removed from the separator continuously as soon as it is separated from the liquid. This special application of differential vaporization or separation is not practical and is never used.

Some of the benefits of an ideal separator may be obtained by use of multiple-stage separation. The number of stages does not have to be large to obtain an appreciable benefit, as can be seen from Table 12.15.¹¹ Economics usually limits the number of stages of separation to

TABLE 12.15—NUMBER OF STAGES VS. DIFFERENTIAL SEPARATION

Number of Stages of Separation	Approximate Percent Approach to Differential Vaporization
2	0
3	75
4	90
5	96
6	98½

three or four, but five or six will pay out under favorable conditions. Seven stages have been used on large volumes of oil, but such installations are rare.

Ratios of operating pressures between stages in multiple-stage separation can be approximated from the following equations¹¹:

$$F = \sqrt[n]{\frac{p_1}{p_s}}, \dots\dots\dots (7)$$

$$p_2 = \frac{p_1}{F} = p_s F^{n_i-1}, \dots\dots\dots (8)$$

and

$$p_3 = \frac{p_2}{F} = p_s F^{n_i-2}, \dots\dots\dots (9)$$

where

F = stage pressure ratio $p_1/p_2 = p_2/p_3$

$= \dots p_n/p_s$,

n_i = number of interstages (number of stages - 1),

p_1 = first-stage separator pressure, psia,

p_2 = second-stage separator pressure, psia,

p_3 = third-stage separator pressure, psia, and

p_s = storage-tank pressure, psia.

Equilibrium flash calculations should be made for several assumed conditions of pressures and temperatures to determine the conditions that will yield the most stock-tank liquid. However, the above equations will give a practical approximation that can be used when no other information is available. Fig. 12.40 schematically shows typical two-, three-, and four-stage separation systems.

Two-stage separation is normally considered to be obtained when one oil and gas separator is used in conjunction with a storage tank. Three-stage separation is obtained when two separators are used in a series at different pressures in conjunction with a storage tank. The storage tank is considered a separation stage because of the gas contained in solution in the oil at a pressure below the operating pressure of the low-pressure separator. Some of this gas will not separate from oil immediately upon entry into the tank but will "weather" from the oil for a period of a few minutes up to a few days. Such gas or vapors can be captured with a vapor recovery system (see Chap. 14).

Flash Calculations for Oil and Gas Separators

Flash (equilibrium) calculations can be made to determine accurately the gas and liquid analysis and yield from oil and gas separators if the composition of the well fluid is known. As an example, fluid produced from seven wells is gathered and separated in three stages in such a system as that depicted in Fig. 12.41.

In Fig. 12.41, F1 represents the first-stage separator, F2 represents the second-stage separator, and F3 represents the third stage, the storage tank. The fluid streams are represented by numbers as follows:

- (1) well fluid inlet to first-stage separator,
- (2) gas and vapors from first-stage separator,
- (3) liquid from first-stage separator,

- (4) gas and vapors from second-stage separator,
- (5) liquid from second-stage separator,
- (6) gas and vapors from storage tank (third stage), and
- (7) liquid in storage tank (stock-tank oil) (third stage).

The first-stage separator operates at 850 psia and 90°F; the second-stage separator operates at 250 psia and 76°F; the third stage (storage tank) is maintained at atmospheric pressure (14.7 psia) and is assumed to be at 100°F (summer conditions).

Flash calculations were made on this system with a computer program available from Simulation Sciences, Inc.¹² The results are shown in Table 12.16.

Economic Considerations of Stage Separation

The extent of application of stage separation will depend on two principal considerations: the terms of the gas sales contract and the price structure for the gaseous and liquid hydrocarbons.

If gas is sold on volume only, it will usually be desirable to remove most condensible vapors from it. If, on the other hand, gas is sold on liquid content, it may be desirable to permit condensible vapors to remain in the gas, depending on conditions, facilities, and location.

If the liquid hydrocarbon is sold on the basis of volume and API gravity, it may be desirable to remove the condensible vapors from the gas and add them to the liquid to increase its sales price. If, on the other hand, the liquid is sold on the basis of volume only, it may be desirable to leave the condensible vapors in the gas.

Other considerations in the application of stage separation are (1) physical and chemical characteristics of the well fluid, (2) flowing wellhead pressure and temperature, (3) operating pressures of available gas-gathering systems, (4) conservation features of liquid-storage facilities, and (5) facilities for transporting liquids.

The point of diminishing returns in stage separation is reached when the cost of additional stages of separation is not justified by increased economic gains. The optimum number of stages of separation can be determined by field testing and/or by equilibrium calculations based on laboratory tests of the well fluid. Flash calculations can be made for various numbers of stages of separation to determine the optimum number of stages of separation for each installation.

Stabilization of Separated Liquid Hydrocarbons

If an oil and gas separator is operated under a vacuum and/or at a temperature higher than well-stream temperature, the liquid hydrocarbons flowing through the separator will have more gas and/or vapors removed than otherwise would be removed. This tends to stabilize the liquid and results in loss of less gas and condensible vapors from the storage tanks. By the use of a stabilization unit similar to that shown in Fig. 12.42, the yield of stock-tank liquid has been increased by 10 to 15% over that obtainable with standard two-stage separation.

When a stabilizer of this type is used, a separator installed upstream of the stabilizer removes gas from the liquid, and the liquid is discharged to the stabilizer. The liquid discharged from the stabilizer to the tanks is completely stabilized and has a Reid vapor pressure of 11 to 13 psi, which is less than atmospheric pressure. Therefore, there will be no loss of gas or vapor from the storage

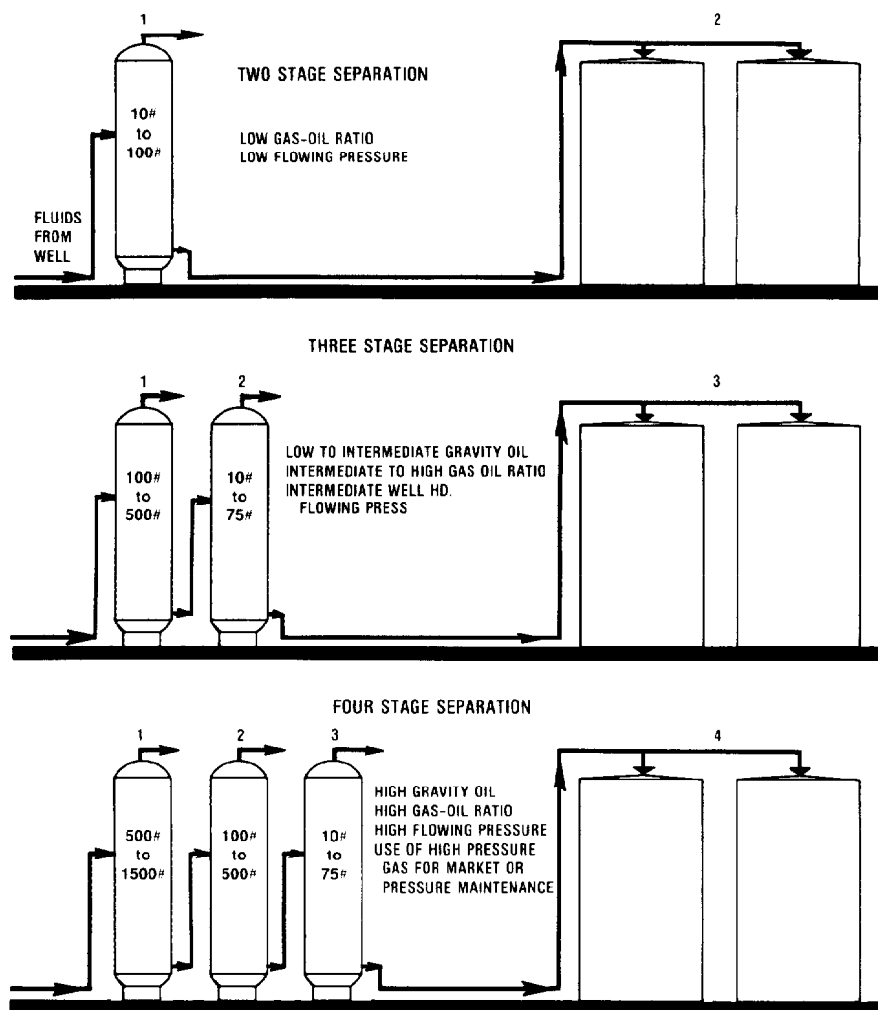


Fig. 12.40—Flow diagrams for two-, three-, and four-stage separation.

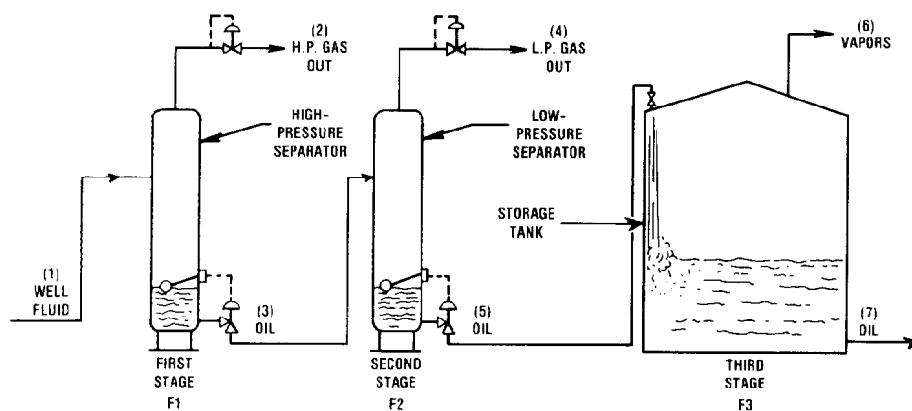


Fig. 12.41—Three-stage separator installation with two separators and storage tank(s). Refer to equilibrium flash calculations on Page 12-33 and Table 12.16.

tanks. In some installations the initial cost of a stabilizer may be less than the initial cost of multiple-stage oil and gas separators. Use of a stabilization unit has resulted in liquid recovery comparable to that from four to six stages of separation. Each new installation should be studied to determine whether a stabilizer should be used. If a highly volatile liquid is being handled, the use of stabilizers may result in increased profit.

Selection and Application of Separators and Scrubbers

Oil and gas separators are manufactured in three basic configurations: vertical, horizontal, and spherical. Gas scrubbers are manufactured in two basic shapes: vertical and horizontal. Each of these units has specific advantages and uses. Selection of the particular unit to use for each application is usually based on which will obtain the desired results at the lowest equipment, installation, and maintenance costs. Table 12.5 gives a comparison of the advantages and disadvantages of vertical, horizontal, and spherical separators.

The following summary indicates the general recommended uses of vertical, horizontal, and spherical oil and gas separators and gas scrubbers.

Vertical Oil and Gas Separators

Applications for vertical oil and gas separators include the following.

1. Well fluids having a high liquid/gas ratio.
2. Well fluids containing appreciable quantities of sand, mud, and similar finely divided solids.
3. Installations with horizontal space limitations but with little or no vertical height limitations, such as crowded tank batteries and/or offshore production platforms.
4. Well fluids where liquid volume may vary widely and instantaneously, such as slugging wells and/or intermittent gas lift wells.
5. Downstream of other production equipment that allows or causes liquid condensation or coalescence.
6. Upstream of other field process equipment that will not perform properly with entrained liquid in the gas.
7. Where economics favors the vertical separator.

Horizontal Oil and Gas Separators

Applications for horizontal oil and gas separators include these situations.

1. Liquid/liquid separation in three-phase separator installations to obtain more efficient oil/water separation.
2. Separating foaming crude oil where the larger liquid/gas contact area of the horizontal vessel will allow and/or cause faster foam breakdown and more efficient gas/liquid separation.
3. Installations where vertical height limitations indicate the use of a horizontal vessel because of its lower silhouette.
4. Well fluids with a high GOR.
5. Well with relatively constant flow rate and with little or no liquid heading or surging.
6. Installations where the operator and/or conditions require or indicate internal water-weir and oil-bucket construction to eliminate the use of oil/water interface liquid level controller.
7. Where portable units (either skid or trailer mounted) are required for either test or production use.

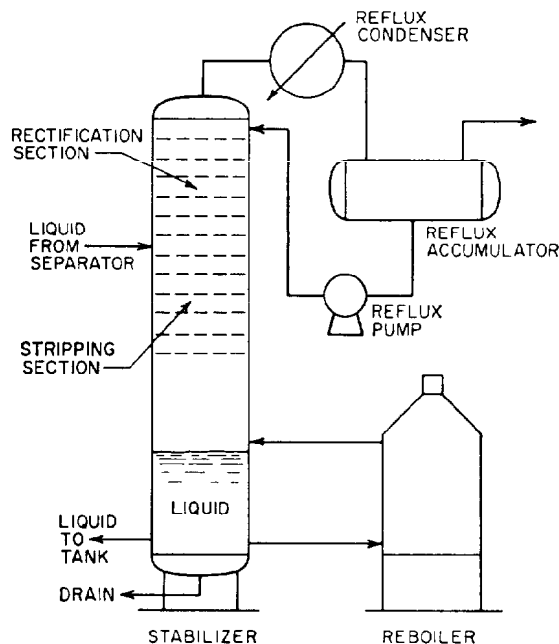


Fig. 12.42—Schematic of typical stabilization unit used for stabilizing and increasing the yield of liquid hydrocarbons at field separation stations.

8. Where multiple units can be stacked to conserve floor space.

9. Upstream of other field process equipment that will not perform satisfactorily with entrained liquid in the gas.

10. Downstream of other production equipment that allows or causes liquid condensation or coalescence.

11. Where economics favors the horizontal separator.

Spherical Oil and Gas Separators

The following is a list of applications for spherical oil and gas separators.

1. Well fluids with high GOR's, constant flow rates, and no liquid slugging or heading.
2. Installations where both vertical and horizontal space and height limitations exist.
3. Downstream of process units—such as glycol dehydrators and gas sweeteners—to scrub and to salvage the expensive process fluids, such as amine and glycol.
4. Installations where economics favors the spherical separator.
5. Installations requiring a small separator where one man can transport the spherical separator to location and install it.
6. Scrubber for fuel and process gas for field and/or plant use.

Gas Scrubbers

Most vertical and horizontal gas scrubbers are used where the gas previously has been separated, cleaned, transported and/or processed with other equipment. That is, most of the impurities—such as entrained liquids, silt, line scale, and dust—have been removed from the gas by other equipment, and the gas scrubber is being used to “polish” the gas. Gas scrubbers generally are used to ensure that the gas contains no materials that will be detrimental to the equipment that the scrubber is installed to protect—such as compressors, dehydrators, sweeteners, meters, and regulators.

TABLE 12.16—SEPARATOR FLASH CALCULATIONS

Unit Identification	F1	F2	F3
Type	Flash	Flash	Flash
Feeds	(1)	(3)	(5)
Products	(2) (V)	(4) (V)	(6) (V)
	(3) (L)	(5) (L)	(7) (L)
Temperature, °F	90.00	75.82	100.00
Pressure, psia	850.00	250.00	14.70
Fraction liquid	0.062	0.748	0.597
Duty, MMBtu/D	0.000	0.000	5.694

Stream Component Flow Rates, lbm mol/D				
Stream Identification	(1)	(2)	(3)	(4)
Phase	Well Fluid	Vapor	Liquid	Vapor
1 C1	26,081.7315	25,585.5952	496.1363	385.1366
2 C2	1,783.4190	1,663.0260	120.3930	48.3420
3 C3	1,098.4380	925.2687	173.1693	29.1554
4 IC4	296.2080	217.4148	78.7932	6.3136
5 NC4	398.0295	268.3454	129.6841	7.4733
6 IC5	185.1300	94.2998	90.8302	2.2505
7 NC5	129.5910	59.1854	70.4056	1.3462
8 NC6	249.9255	65.1978	184.7277	1.1809
9 NC7	316.2638	40.4824	275.7814	0.5803
10 NC8	316.2638	18.6834	297.5804	0.2113
Totals	30,855.0000	28,937.4988	1,917.5012	481.9902

Temperature, °F	90.0000	90.0000	90.0000	75.8247
Pressure, psia	850.0000	850.0000	850.0000	250.0000
Mole fraction liquid	0.0621	0.0000	1.0000	0.0000

Stream Identification	(5)	(6)	(7)
Phase	Liquid	Vapor	Liquid
C1	110.9998	110.1207	0.8791
2 C2	72.0510	69.2178	2.8332
3 C3	144.0139	126.8146	17.1993
4 IC4	72.4796	55.0069	17.4727
5 NC4	122.2108	84.3322	37.8786
6 IC5	88.5797	42.4336	46.1461
7 NC5	69.0594	28.6450	40.4144
8 NC6	183.5467	34.6597	148.8870
9 NC7	275.2010	19.5618	255.6392
10 NC8	297.3691	7.4581	289.9110
Totals	1,435.5110	578.2504	857.2606

Temperature, °F	75.8247	100.0000	100.0000
Pressure, psia	250.0000	14.7000	14.7000
Mole fraction liquid	1.0000	0.0000	1.0000

Stream Molal Compositions				
Stream Identification	(1)	(2)	(3)	(4)
Phase	Well Fluid	Vapor	Liquid	Vapor
1 C1	8.4530×10^{-1}	8.8417×10^{-1}	2.5874×10^{-1}	7.9905×10^{-1}
2 C2	5.7800×10^{-2}	5.7470×10^{-2}	6.2786×10^{-2}	1.0030×10^{-1}
3 C3	3.5600×10^{-2}	3.1975×10^{-2}	9.0310×10^{-2}	6.0490×10^{-2}
4 IC4	9.6000×10^{-3}	7.5133×10^{-3}	4.1092×10^{-2}	1.2099×10^{-2}
5 NC4	1.2900×10^{-2}	9.2733×10^{-3}	6.7632×10^{-2}	1.5505×10^{-2}
6 IC5	6.0000×10^{-3}	3.2587×10^{-3}	4.7369×10^{-2}	4.6692×10^{-3}
7 NC5	4.2000×10^{-3}	2.0453×10^{-3}	3.6717×10^{-2}	2.7930×10^{-3}
8 NC6	8.1000×10^{-3}	2.2531×10^{-3}	9.6338×10^{-2}	2.4501×10^{-3}
9 NC7	1.0250×10^{-2}	1.3990×10^{-3}	1.4382×10^{-1}	1.2040×10^{-3}
10 NC8	1.0250×10^{-2}	6.4565×10^{-4}	1.5519×10^{-1}	4.3836×10^{-4}
Totals	30,855.0000	28,937.4988	1,917.5012	481.9902

Temperature, °F	90.0000	90.0000	90.0000	75.8247
Pressure, psia	850.0000	850.0000	850.0000	250.0000
Mole fraction liquid	0.0621	0.0000	1.0000	0.0000

TABLE 12.16—SEPARATOR FLASH CALCULATIONS (continued)

Stream Identification Phase	(5) Liquid	(6) Vapor	(7) Liquid
1 C1	7.7324×10^{-2}	1.9044×10^{-1}	1.0254×10^{-3}
2 C2	5.0192×10^{-2}	1.1970×10^{-1}	3.3050×10^{-3}
3 C3	1.0032×10^{-1}	2.1931×10^{-1}	2.0063×10^{-2}
4 IC4	5.0490×10^{-2}	9.5126×10^{-2}	2.0382×10^{-2}
5 NC4	8.5134×10^{-2}	1.4584×10^{-1}	4.4186×10^{-2}
6 IC5	6.1706×10^{-2}	7.3383×10^{-2}	5.3830×10^{-2}
7 NC5	4.8108×10^{-2}	4.9537×10^{-2}	4.7144×10^{-2}
8 NC6	1.2786×10^{-1}	5.9939×10^{-2}	1.7368×10^{-2}
9 NC7	1.9171×10^{-1}	3.3829×10^{-2}	2.9820×10^{-1}
10 NC8	2.0715×10^{-1}	1.2898×10^{-2}	3.3818×10^{-1}
Totals	1,435.5110	578.2504	857.2606
Temperature, °F	75.8247	100.0000	100.0000
Pressure, psia	250.0000	14.7000	14.7000
Mole fraction liquid	1.0000	0.0000	1.0000

Stream Summary				
Stream Identification Phase	(1) Well Fluid	(2) Vapor	(3) Liquid	(4) Vapor
lbm mol/D	30,855.000	28,937.499	1,917.501	481.990
Temperature, °F	90.000	90.000	90.000	75.825
Pressure, psia	850.000	850.000	850.000	250.000
H, Btu/lbm	38.422	41.548	24.098	76.102
Mole fraction liquid	0.06214	0.00000	1.00000	0.00000
M lbm/D	672.911	552.396	120.515	10.163
Molecular weight	21.809	19.089	62.850	21.085
Specific gravity	0.3586	0.3302	0.5919	0.3470
Vapor				
M lbm/D	552.396	552.396	0.000	10.163
Standard M cu ft/D	10,981.491	10,981.491	0.000	182.910
Actual M cu ft/D	174.741	174.741	0.000	10.455
z	0.87018	0.87018	0.00000	0.94366
Liquid				
M lbm/D	120.515	0.000	120.515	0.000
Standard liquid cu ft/D	3,268.282	0.000	3,268.282	0.000
Actual gallons per minute	19.3504	0.0000	19.3504	0.0000
cu ft/D	3,724.960	0.000	3,724.960	0.000

Stream Summary			
Stream Identification Phase	(5) Liquid	(6) Vapor	(7) Liquid
lbm mol/D	1,435.511	578.250	857.261
Temperature, °F	75.825	100.000	100.000
Pressure, psia	250.000	14.700	14.700
H, Btu/lbm	19.306	179.133	33.287
Mole fraction liquid	1.00000	0.00000	1.00000
M lbm/D	110.352	28.467	81.885
Molecular weight	76.873	49.229	95.520
Specific Gravity	0.6330	0.5315	0.6781
Vapor			
M lbm/D	0.000	28.467	0.000
Standard M cu ft/D	0.000	219.440	0.000
Actual M cu ft/D	0.000	232.310	0.000
z	0.00000	0.98332	0.00000
Liquid			
M lbm/D	110.352	0.000	81.885
Standard liquid cu ft/D	2,798.155	0.000	1,938.415
Actual gallons per minute	16.3754	0.0000	11.7773
cu ft/D	3,152.270	0.000	2,267.129

Some of the uses for gas scrubbers are to clean gas (1) for fuel for heaters, boilers, steam generators, and engines; (2) for control gas for processing plants and equipment; (3) upstream of compressors; (4) upstream of dehydrators and sweeteners; (5) downstream of dehydrators and sweeteners to conserve processing fluids; (6) upstream of gas distribution systems; (7) upstream of and in gas transmission lines to remove liquid, dust, rust, and scale; (8) upstream and/or downstream of pressure regulation stations; and (9) downstream of gas-transmission-line compressor stations to remove lubricating oil from the line.

Both vertical and horizontal scrubbers can be effective and efficient in the applications listed above. The selection of a vertical or horizontal scrubber may be a matter of personal preference, space limitations, cost consideration, and/or availability.

Gas scrubbers normally are limited to applications where there is little or no liquid to be removed and where liquid slugging seldom or never occurs. A large number of different types, designs, and sizes are available from many manufacturers.

Construction Codes for Oil and Gas Separators

ASME Code for Unfired Pressure Vessels

Most oil and gas separators furnished for field use are designed, constructed, pressure tested, and labelled in accordance with the ASME Code for Unfired Pressure Vessels.¹³ Outside the U.S., other similar codes may be used (Table 12.17). Sec. VIII, Div. I of the ASME code is used for most unfired pressure vessels. Div. II of Sec. VIII may be used for offshore installations because of weight reduction obtained by its use. Div. I design equations are based on a safety factor of 4.0, while Div. II equations are based on a safety factor of 3.0. Quality control is more stringent under Div. II than Div. I.

Use of the ASME or some equivalent code for construction of pressure vessels ensures the purchaser of receiving vessels that are designed, constructed, and pressure-tested in accordance with established standards, inspected by a disinterested party, and certified safe for use at specified design pressures and temperatures. All vessels labeled with ASME code stamp must be constructed in accordance with the ASME code requirements, and written reports verifying this information must be furnished to the purchaser if requested.

The ASME Code for Unfired Pressure Vessels, Sec. VIII, Div. I, is generally preferred in the U.S. Information about and copies of the ASME Code may be obtained from Ref. 13. Information on other codes for construction of pressure vessels can be obtained from the government authorities shown in Table 12.17.¹⁴

Design equations for shell and head thicknesses and working pressures according to ASME Code for Unfired Pressure Vessels, Sec. VIII, Div. I¹³ are as follows.

Cylindrical shells.

$$h_{cs} = \frac{p_{cs} r_i}{\sigma E - 0.6 p_{cs}}$$

and

$$p_{cs} = \frac{\sigma E h_{cs}}{r_i + 0.6 h_{cs}}$$

Spherical shells.

$$h_{ss} = \frac{p_{ss} r_i}{2\sigma E - 0.2 p_{ss}}$$

and

$$p_{ss} = \frac{2\sigma E h_{ss}}{r_i + 0.2 h_{ss}}$$

Ellipsoidal heads.

$$h_{eh} = \frac{p_{eh} d_i}{2\sigma E - 0.2 p_{eh}}$$

and

$$p_{eh} = \frac{2\sigma E h_{eh}}{d_i + 0.2 h_{eh}}$$

Torispherical heads.

$$h_{th} = \frac{0.885 p_{th} r_c}{\sigma E - 0.1 p_{th}}$$

and

$$p_{th} = \frac{\sigma E h_{th}}{0.885 r_c + 0.1 h_{th}}$$

Hemispherical heads.

$$h_{hh} = \frac{p_{hh} r_c}{2\sigma E - 0.2 p_{hh}}$$

and

$$p_{hh} = \frac{2\sigma E h_{hh}}{r_c + 0.2 h_{hh}}$$

where

h = minimum required thickness (exclusive of corrosion allowance), in.,

p = design pressure, psi,

r_i = inside radius of shell course under consideration before corrosion allowance is added, in.,

σ = maximum allowable stress value, psi (use one-quarter of tensile strength listed in Table 12.19 for a safety factor of 4.0),

E = joint efficiency for appropriate joint in cylindrical shells and any joint in spherical shells or the efficiency of ligaments between openings, whichever is less (see Table 12.18),

d_i = inside diameter, in., and

r_c = inside spherical or crown radius, in.

Joint efficiency, E , for the above ASME design equations is shown in Table 12.18.

Materials of Construction for Separator

The most common steels used in the shells, heads, nozzles, and flanges in pressure vessels built under the ASME

TABLE 12.17—CODE AUTHORITIES FOR VARIOUS COUNTRIES

Country	Government Authority and Address*	Country	Government Authority and Address*
Australia	SAA, Standards Assn. of Australia 8-86 Arthur Street North Sydney, NSW 2060, Australia	The Netherlands	NNI, Nederlands Normalisatie Instituut Kalfjeslaan 2 P.O. Box 5059 2600 GB Delft, The Netherlands
Austria	ONORM, Oesterreichisches Normungsinstitut Leopoldgasse 4A-1021 Wein 2, Austria	Norway	SSF, Norges Standardiseringsforbund Haakon VII's Gate 2 Oslo 1, Norway
Canada	CSA, Canadian Standards Assn. 178 Rexdale Blvd. Rexdale 603, Ont., Canada	Saudi Arabia	SASO, Saudi Arabian Standards Organization P.O. Box 3437 Riyadh, Saudi Arabia
People's Republic of China	China Assn. for Standardization P.O. Box 820 Beijing, China	Singapore	SIRU, Singapore Institute of Standards and Industrial Research Maxwell Road P.O. Box 2611 Singapore, Singapore
France	AFNOR, Association Française de Normalization Tour Europe, Cedex 7, 92080 Paris, La Defense, France	Sweden	SIS, Standardiseringskommissionen Tegnergatan 11 P.O. Box 3295 S-103-66 Stockholm, Sweden
West Germany	DNA, DIN, Deutsches Normenausschuß 4-7 Burggrafenstraße Postfach 1107 Berlin 30, West Germany	Switzerland	SNV, Association Suisse de Normalisation Kirchenweg 4 Zurich, Switzerland
Indonesia	Badan Kerjasama Standardisasi Lipi-Ydni Jln. Teuku Chik Ditiro 43 P.O. Box 250 Jakarta, Indonesia	United Kingdom	BSI, British Standards Institute 2 Park Street London W1A-2BS, England
Italy	UNI, Ente Nazionale Italiano de Unificazione Piazza Armando Diaz 2, 120123 Milano, Italy	USSR	USSR State Committee for Standards Leninsky Prospekt 9 Moskva 117049, USSR
Japan	JISC, Japanese Industrial Standards Committee Agency of Industrial Science and Technology Ministry of International Trade and Industry 1-3-1 Kasumigaseki Chiyoda-Ku Tokyo 100, Japan	Venezuela	COVENIN, Comision Venezolana de Normas Industriales Avenida Andres Bello Edificio Torre Fondo Comun Piso 11 Caracas 1050, Venezuela
Mexico	DGN, Direccion General de Normas Calle Puente de Tecamachalco No. 6 Lomas de Tecamachalco Seccion Fuentes Naucalpan de Juarez 53-950 Mexico DF, Mexico		

*The names and addresses of the government agencies for other countries can be obtained from Ref. 14.

Code for Unfired Pressure Vessels, Sec. VIII, Div. I, are listed in Table 12.19, along with the most important information concerning these materials. For more detailed information on these steels refer to the corresponding ASTM specifications indicated in Table 12.19.

Controls, Valves, Accessories, and Safety Features for Oil and Gas Separators

Controls

The controls required for oil and gas separators are liquid-level controllers for oil and oil/water interface (three-phase operation) and gas back-pressure control valve with pressure controller.

Valves

The valves required for oil and gas separators are oil-discharge control valve, water-discharge control valve (three-phase operation), drain valves, block valves, pressure relief valve, and valves for sight glasses.

Accessories

The accessories required for oil and gas separators are pressure gauges, thermometers, pressure-reducing regulators (for control gas), level sight glasses, safety head with rupture disk, piping, and tubing.

Safety Features for Oil and Gas Separators

Oil and gas separators should be installed at a safe distance from other lease equipment. Where they are installed on offshore platforms or in close proximity to other equipment, precautions should be taken to prevent injury to personnel and damage to surrounding equipment in case the separator or its controls or accessories fail.

The following safety features are recommended for most oil and gas separators.

High- and Low-Liquid-Level Controls. High- and low-liquid-level controls normally are float-operated pilots that actuate a valve on the inlet to the separator, open a bypass around the separator, sound a warning alarm, or perform some other pertinent function to prevent damage that might result from high or low liquid levels in the separator.

High- and Low-Pressure Controls. High- and low-pressure controls are installed on separators to prevent excessively high or low pressures from interfering with normal operations. These high- and low-pressure controls can be mechanical, pneumatic, or electric and can sound a warning, actuate a shut-in valve, open a bypass, or perform other pertinent functions to protect personnel, the separator, and surrounding equipment.

TABLE 12.18—JOINT EFFICIENCY, ASME SEC. VIII, DIV. I

Single-welded Butt Joints (back-up strip left in place)		Double-Welded Butt Joints
(%)	(% Radiograph)	(%)
90	100	100
80	Spot	85
65	None	70

High- and Low-Temperature Controls. Temperature controls may be installed on separators to shut in the unit, to open or to close a bypass to a heater, or to sound a warning should the temperature in the separator become too high or too low. Such temperature controls are not normally used on separators, but they may be appropriate in special cases.

Safety Relief Valves. A spring-loaded safety relief valve is usually installed on all oil and gas separators. These valves normally are set at the design pressure of the vessel. Safety relief valves serve primarily as a warning, and in most instances are too small to handle the full rated fluid capacity of the separator. Full-capacity safety relief valves can be used and are particularly recommended when no safety head (rupture disk) is used on the separator.

Safety Heads or Rupture Disks. A safety head or rupture disk is a device containing a thin metal membrane that is designed to rupture when the pressure in the separator exceeds a predetermined value. This is usually from $1\frac{1}{4}$ to $1\frac{1}{2}$ times the design pressure of the separator vessel. The safety head disk is usually selected so that it will not rupture until the safety relief valve has opened and is incapable of preventing excessive pressure buildup in the separator.

Operation and Maintenance Considerations for Oil and Gas Separators

Periodic Inspection

In refineries and processing plants, it is normal practice to inspect all pressure vessels and piping periodically for corrosion and erosion. In the oil fields, this practice is not generally followed, and equipment is replaced only after actual failure. This policy may create hazardous conditions for operating personnel and surrounding equipment. It is recommended that periodic inspection schedules for all pressure equipment be established and followed to protect against undue failures.

Installation of Safety Devices

All safety relief devices should be installed as close to the vessel as possible and in such manner that the reaction force from exhausting fluids will not break off, unscrew, or otherwise dislodge the safety device. The discharge from safety devices should not endanger personnel or other equipment.

Safety Heads (Rupture Disks)

The discharge from a safety head should be open and without restriction. The discharge line from a safety device should be parallel to a vertical separator and perpendicular to a horizontal one; otherwise the separator may be blown over by the reaction force from exhaust-

ing fluids. A valve should not be used between the safety head and the separator because it may inadvertently be closed. Water should not be allowed to accumulate on top of the rupture disk because ice could form and alter the rupture characteristics of the disk. Operation of an oil and gas separator without a properly sized and installed safety head (rupture disk) is not recommended.

Pressure relief valves may corrode and leak or may "freeze" in the closed position. They should be checked periodically and replaced if not in good working condition. Discharge lines, especially those on full-capacity relief valves, should be such that reaction force from discharge will not move the separator. Safety relief valves with "try" handles are recommended for general use. Some operators use pilot-operated relief valves where frequent testing of the relief valves is required.

Mist Extractors

Some mist extractors in oil and gas separators require a drain or liquid downcomer to conduct liquid from the mist extractor to the liquid section of the separator. This drain will be a source of trouble when pressure drop through the mist extractor becomes excessive. If the pressure drop across the mist extractor, measured in inches of oil, exceeds the distance from the oil level in the separator to the mist extractor, the oil will flow from the bottom of the separator up through the mist-extractor drain and out with the gas. This condition may be aggravated by partial plugging of the mist extractor with paraffin or other foreign material. This explains why some separators have definite fixed capacities that cannot be exceeded without liquid carryover through the gas outlet, and it also explains why the capacities of some separators may be lowered with use. In recent years, separators of advanced design have used mist extractors that do not require drains or downcomers. These designs eliminate this source of trouble (see Fig. 12.14).

Low Temperatures

Separators should be operated above hydrate-formation temperatures. Otherwise hydrates may form in the vessel and partially or completely plug it, thereby reducing the capacity of the separator and, in some instances when the liquid or gas outlet is plugged or restricted, causing the safety valve to open or the safety head to rupture. Steam coils can be installed in the liquid section of oil and gas separators to melt hydrates that may form there. This is especially appropriate on low-temperature separators.

Corrosive Fluids

A separator handling corrosive fluid should be checked periodically to determine whether remedial work is required. Extreme cases of corrosion may require a reduction in the rated working pressure of the vessel. Periodic hydrostatic testing is recommended, especially if the fluids being handled are corrosive. Expendable anodes can be used in separators to protect them against electrolytic corrosion. Some operators determine separator shell and head thickness with ultrasonic thickness indicators and calculate the maximum allowable working pressure from the remaining metal thickness. This should be done yearly offshore and every two to four years onshore.

TABLE 12.19—PROPERTIES OF MATERIALS OF CONSTRUCTION FOR PRESSURE VESSELS

Properties of Materials Carbon and Low Alloy Steel*										
Form	Nominal Composition	Specification		Application	Specification		P Number	Tensile Strength (1,000 psi)	Yield Point (1,000 psi)	Notes
		Number	Grade		Number	Grade				
Plate	C	SA-283	C	Structural quality. For pressure vessel may be used with limitations. See Note 1.	SA-283	C	1	55.0	30.0	1
	C	SA-285	C	Boilers for stationary service and other pressure vessels	SA-285	C	1	55.0	30.0	2,6
	C-Si	SA-515	55	Primarily for intermediate- and high-temperature service	SA-515	55	1	55.0	30.0	3
	C-Si	SA-515	60	Primarily for intermediate- and high-temperature service	SA-515	60	1	60.0	32.0	3
	C-Si	SA-515	65	Primarily for intermediate- and high-temperature service	SA-515	65	1	65.0	35.0	3
	C-Si	SA-515	70	Primarily for intermediate- and high-temperature service	SA-515	70	1	70.0	38.0	3
	C-Si	SA-516	55	For moderate- and lower-temperature service	SA-516	55	1	55.0	30.0	3,8
	C-Si	SA-516	60	For moderate- and lower-temperature service	SA-516	60	1	60.0	32.0	3,8
	C-Mn-Si	SA-516	65	For moderate- and lower-temperature service	SA-516	65	1	65.0	35.0	3,8
	C-Mn-Si	SA-516	70	For moderate- and lower-temperature service**	SA-516	70	1	70.0	38.0	3,8,10
Flange and Fitting	C-Mn-Si	SA-105		For high-temperature service	SA-105	—	1	70.0	36.0	2,3
	C-Si	SA-181	I	For general service	SA-181	I	1	60.0	30.0	2,3
	C-Mn	SA-350	LF1	For low-temperature service	SA-350	LF1	1	60.0	30.0	—
	C-Mn-Si		LF2		SA-350	LF2	1	70.0	36.0	—
Pipe	C-Mn	SA-53	B	For general service	SA-53	B	1	60.0	35.0	2,3,4,7
	C-Mn	SA-106	B	For high-temperature service	SA-106	B	1	60.0	35.0	3
	C-Mn	SA-333	6	Low-temperature and sour-gas service	SA-333	6	1	60.0	35.0	9
Bolting	1Cr-1/5 Mo.	SA-193	B7	For high-temperature service 2½-in. diameter or less	SA-193	B7	—	125.0	105.0 < 2½-in. diameter	—
		SA-194	2H	For high-temperature service nut	SA-194	2H	—	55.0	—	—
		SA-307	B	Machine bolt for general use	SA-307	B	—	55.0	5	—

*Data of the most frequently used materials from ASME Code Sec. II and VIII.

**With charpy tests, this steel is used for low-temperature and sour-gas service.

- SA-283 C plate may be used for pressure parts in pressure vessels provided all of the following requirements are met.
 - The vessels are not used to contain lethal substances, either liquid or gaseous;
 - The material is not used in the construction of unfired steam boilers;
 - The design temperature at which the material is used is between -20°F and 650°F;
 - For shells, heads, and nozzles only, the thickness of plates on which strength welding is applied does not exceed ½ in.; and
 - The steel is manufactured by the electric furnace, open-hearth process, or the basic oxygen process.
- For service temperatures above 850°F, it is recommended that killed steels containing not less than 0.10% residual silicon be used. Killed steels that have been deoxidized with large amounts of aluminum and rimmed steels may have creep and stress-rupture properties in the temperature range above 850°F, which are somewhat less than those on which the values in the table are based.
- Upon prolonged exposure to temperatures above about 800°F, the carbide phase of carbon steel may be converted to graphite.
- Only killed steel shall be used above 850°F.
- Not permitted above 450°F; allowable stress value 7,000 psi.
- The material shall not be used in thicknesses above 2 in.
- For welded pipe the maximum allowable stress values are 15% less. No increase in these stress values shall be allowed for the performance of radiography.
- The stress values to be used for temperatures below -20°F when steels are made to conform with Supplement (5) SA-20 shall be those that are given in the column for -20 to 650°F.
- SA-333 pipe is SA-106-B pipe with charpy tests made at the mill by the manufacturer of the pipe.
- For low-temperature and sour-gas service, charpy tests must be made on this steel before fabrication of the vessel.
- Most of the information for this table was taken from Ref. 14.

Paraffin

A separator handling paraffin-based oil may need to be steamed periodically to prevent plugging and a resultant decrease in capacity. This reduction in capacity often results in liquid carryover in the gas or discharge of excessive gas with the liquid.

High-Capacity Operation

Where separators are operating near or at their maximum rated capacity, they should be checked carefully and periodically to determine whether acceptable separation is being accomplished.

Pressure Shock Loads

Wells should be switched in and out of the separator slowly. Fast opening and closing of valves causes damaging shock loads on the vessel, its components, and piping.

Throttling Discharge of Liquid

Throttling discharge of small volumes of liquid from separators normally should be avoided. Throttling may cause erosion or wire drawing of the inner valves and seats of the liquid-dump valves and may erode the dump-valve bodies to the extent that they may burst at or below rated working pressures.

However, throttling discharge may be necessary because processing units, such as lower-pressure separators or stabilization units, downstream of the separator may require relatively steady flow. Liquid-discharge control valves on separators should be sized for the volume of liquid the separator must handle. Such valves usually should be smaller than the lines in which they are installed. Reduced inner valves can be used to size the valve properly to minimize wire drawing during throttling service.

Pressure Gauges

Pressure gauges and other mechanical devices on separators should be tested for accuracy at regular intervals. Isolating valves should be used so that pressure gauges can be easily removed for testing, cleaning, repairs, or replacement.

Gauge Cocks and Glasses

Gauge cocks and gauge glasses should be kept clean so that the liquid level observed in the sight glass indicates at all times the true liquid level in the separator. Periodic flushing of the gauge glass or cleaning with special solvents and swabs is recommended.

Cleaning of Vessels

It is recommended that all separator vessels be equipped with manways, cleanout openings, and/or washout connections so that the vessels can be cleaned periodically. Larger vessels can be equipped with manways to facilitate their cleaning. Smaller vessels can be equipped with handholes and/or washout connections so that they can be easily cleaned or washed out periodically.

SI Metric Unit Conversions

Most conversions from customary units to SI metric units in Chap. 12 can be made directly by using the conversion factors presented in the tables in the publication entitled "The SI Metric System of Units and SPE Metric Standard." The exceptions are listed below.

The values of F_{co} in Fig. 12.32 should be multiplied by 30.48 to change them for use in the SI metric units. F_{co} is used in Eqs. 1, 4, 5, and 6.

In Eq. 3, the gas constant R in customary units has the value 10.732. In SI metric units, the value of R is 0.083145 where the gas volume is in cubic meters, pressure in bars, temperature in degrees Kelvin, and n in kmol.¹⁶

Nomenclature

- A_g = cross-sectional area of separator for gas flow, sq ft
- A_o = cross-sectional area of separator for oil flow, sq ft
- d_i = ID, in.
- D = diameter of separator, in. (see Fig. 12.34 for D')
- E = joint efficiency for appropriate joint in cylindrical shells and any joint in spherical shells or the efficiency of ligaments between openings, whichever is less (Table 12.18)
- F = stage pressure ratio $p_1/p_2 = p_2/p_3 = \dots p_n/p_s$
- F_{co} = configuration and operation factor (empirical) (see Fig. 12.32 for values)
- h = thickness (exclusive of corrosion allowance), in.
- h_o = height (or depth) of oil in separator, ft
- L = length of separator, ft (see Fig. 12.34 for L')
- M_g = molecular weight of gas
- n_i = number of interstages (number of stages - 1)
- p = design pressure or separator operating pressure, psia
- p_b = base pressure, psi
- p_s = storage-tank pressure, psia
- p_1 = first-stage separator pressure, psia
- p_2 = second-stage separator pressure, psia
- p_3 = third-stage separator pressure, psia
- q_g = volume of gas flowing through separator, cu ft/sec
- r_c = inside spherical or crown radius, in.
- r_i = inside radius of shell course under consideration before corrosion allowance is added, in.
- R = gas constant
- T = operating temperature, °R
- T_b = base temperature, °R
- v_g = gas velocity, ft/sec
- V_o = volume required in separator for oil, cu ft
- z_g = gas compressibility factor
- γ_g = specific gravity of gas
- ρ_g = density of gas at operating conditions, lbm/cu ft
- ρ_L = density of liquid at operating conditions, lbm/cu ft

σ = maximum allowable stress value, psi (use
 1/4 of tensile strength listed in Table
 12.19 for a safety factor of 4.0)

Acknowledgments

Appreciation is expressed to George O. Ellis of Ellis Engineering Co., Houston, for allowing the usage of the Comsign Computer Program to calculate the oil and gas capacities for vertical and horizontal separators shown in Figs. 12.35 through 12.38 and for the sample calculations in Tables 12.9 and 12.10.

References

1. *Sales Bulletin*, Porta-Test Systems Ltd, Edmonton, Alta. (1982) 4.
2. "Peerless Vane-Type Line Separators," *Bull.* 11000, Peerless Manufacturing Co., Dallas (1965).
3. Lerner, B.J.: "Mist Elimination," U.S. Patent No. 4,022,593 (1977).
4. "Mist Eliminator Allows 100% Greater Throughput in Vessels," *Chemical Engineering*, ACS Industries Inc. (Aug. 20, 1984) 53, 54.
5. *Sales Bulletin*, Plenty Metrol Ltd., Newbury, Berkshire, England (1980).
6. Schilling, J.R.: "Diverging Vortex Separator," U.S. Patent No. 4,394,138 (1982).
7. "Gas-Liquid Separation Systems," Vortec Inc., Woodside, CA (1984).
8. "People, Products, Porta-Test," Porta-Test Systems Ltd., Edmonton, Alta. (1979).
9. Comsign Computer Program, Ellis Engineering Inc., Houston.
10. Vondy, D.: "Spherical Process Vessels," *Oil and Gas J.* (Oct. 15, 1956) 148; (Nov. 12, 1956) 213; (Dec. 3, 1956) 135; (Jan. 7, 1957) 130; (Feb. 4, 1957) 136; (Feb. 11, 1957) 130; (March 11, 1957) 189; (April 8, 1957) 121-122.
11. Kimmell, G.O.: "Stage Separation," paper 48-PET-15 presented at the ASME Annual Meeting, Oklahoma City, Oct. 1949.
12. "Separator Flash Calculations, Process Version 0882," Simulation Sciences Inc., Houston.
13. *ASME Boiler and Pressure Vessel Code*, Sec. VIII, Div. I (1986).
14. *KWIC Index of International Standards*, Intl. Organization for Standardization, Geneva.
15. Megyesy, E.F.: *Pressure Vessel Handbook*, Pressure Vessel Handbook Publishing Inc., Tulsa.
16. *Engineering Data Book*, Gas Processors Assoc., Tulsa (1981) 14-4.
- Cooper, F.E. *et al.*: "Field Separation of Liquids," *Oil and Gas J.* (Feb. 9, 1959) 91-99.
- Davies, E.E. and Watson, P.: "Miniaturized Separators Provide High Performance," *World Oil* (April 1980).
- Dixon, P.C.: "Method of and Means for Separating Liquid and Gas or Gaseous Fluid," U.S. Patent No. 2,349,944 (1944).
- Dotterweich, F.H.: "Mechanical Removal of Entrained Materials From Natural Gas," *Pet. Eng.* (May 1949) 546-49.
- Field Handling of Natural Gas*, third ed., Petroleum Extension Service, U. of Texas, Austin (1974).
- Fekete, L.A.: "Vortex Tube Separator May Solve Weight/Space Limitations," *World Oil* (July 1986) 40-44.
- Gaskell, T.F. and Wood, P.M.: "Production Improved in New Domains," *Oil and Gas Intl.* (June 1963) 102-04.
- Gravis, C.K.: "The Oil and Gas Separator," *World Oil* (Jan. 1960) 84-92.
- Guerrero, E.T.: "How To Make Stage-Separation Calculations," *Oil and Gas J.* (Oct. 3, 1966).
- "Gulf of Mexico Region Production Safety Systems," OCS Order No. 5, U.S. Dept. of the Interior, Metairie, LA (1980).
- Hydrogen Sulphide Corrosion in Oil and Gas Production: A Compilation of Classic Papers*, Natl. Assn. of Corrosion Engineers, Houston (1981).
- Katz, D.L.: "Overview of Phase Behavior in Oil and Gas Production," *J. Pet. Tech.* (June 1983) 1205-14.
- Mapes, G.J.: "The Low Temperature Separation Unit," *World Oil* (Jan. 1960) 93-99.
- Morris, J.K. and Smith, R.S.: "Crude Stabilizer Can Save Money Offshore," *Oil and Gas J.* (May 7, 1984) 112-16.
- Penick, D.P. and Thrasher, W.B.: "Challenges Associated With the Design of Oil-Gas Separation Systems for North Sea Platforms," *Proc.*, Ninth Annual Offshore Technology Conference, May 2-5, 1977.
- Penick, D.P. and Thrasher, W.B.: "Mobil's Design Considerations for North Sea Oil/Gas Separation Facilities," *Pet. Eng.* (Oct. 1977) 22, 24, 26.
- Peters, B.A.: "Get Better Separation With Proper Water-Weir Heights," *Oil and Gas J.* (Nov. 19, 1973) 73, 74, 77.
- Pollak, A. and Work, L.T.: "The Separation of Liquid From Vapor Using Cyclones," *Trans.*, ASME (Jan. 1942) 31-41.
- "Pressure Vessel Inspection Code—Maintenance, Inspection, Rating, Repair, and Alteration," *API Std. 510*, third ed. (1983).
- "Recommended Practice for Analysis Design, Installation, and Testing of Basic Surface Safety Systems on Offshore Production Platforms," *API RP 14-C*, third ed. (April 1984).
- "Recommended Practice for Design and Installation of Offshore Production Platform Piping Systems," *API RP 14-E*, fourth ed. (April 1984).
- Robinson, J.: "Fundamentals of Oil and Gas Separation," *Proc.*, 1979 Gas Cond. Conference, March 5-7.
- "Separator Loses Weight, Bulk—But Boosts Production," *Offshore Services and Technology*, Newbury, England (May 1980).
- "Separators-Technique," *Oil and Gas Separation Theory, Application and Design*, AIME (1977) 5.
- Aliev, S.N. *et al.*: "Uliyanie Fizicheskikh Svoystv Zhidkosti Na Rabotu Gazovykh Separatorov," *Neft Khoz* (Jan. 1982) 40-43.
- Barrett, R.: "Unique High Efficiency Cyclone Separator," *Europe and Oil* (1970).
- Barry, A.F. and Parks, A.S.: "Low Temperature Separation Increases Recovery of Condensate from Natural Gas," *World Oil*, 7, 203.
- Broussard, W.F. and Gravix, C.K.: "Three-Phase Separators," *World Oil* (April 1960) 127-32.
- Campbell, J.M.: *Gas Conditioning and Processing*, Campbell Petroleum Series, Norman, OK (1979) 1, 119-14.
- Carbon Dioxide Corrosion in Oil and Gas Production: Selected Papers, Abstracts and References*, Natl. Assn. of Corrosion Engineers, Houston (1984).
- Chepkasov, V.M., Ovchinnikov, A.A., and Nikolaev, N.A.: "Raschet Gidravlicheskogo Soprotivleniya Vikhrevykh Separatorov S Aksialnymi Zavikhrityami," *Izv Vyssh Uchebn Zaved Neft Gaz* (May 1981) 43-48.

- Sinaiskii, E.G.: "O Razdelenii Gazozhidkostnykh Smesei V Separatorakh," *Izv Vyssh Uchebn Zaved Neft Gaz* (March 1980) 44-54.
- "Specification for Oil and Gas Separators," *API Spec. 12-J*, fifth ed. (Jan. 1982).
- "Standard for Welding Pipelines and Related Facilities," *API Std. 1104*, 16th ed. (1983).
- Warner, B.J. and Scauzillo, F.: "The Design of Fibrous Filters for Mist Elimination," paper presented at the 1963 Gas Technology Conference, Norman, OK.
- Whinery, K.F. and Campbell, J.M.: "A Method for Determining Optimum Second Stage Pressure in Three Stage Separation," *J. Pet. Tech.* (April 1958) 53-54.
- Worley, S.M. and Lawrence, L.L.: "Oil and Gas Separation is a Science," *J. Pet. Tech.* (April 1957) 11-16.

Chapter 13

Gas Measurement and Regulation

John M. Campbell Sr., The Campbell Companies*

Introduction

Measurement and regulation are an integral part of the production of gas. As the value of gas has increased, the need for more accurate measurement has become apparent. Proper regulation is necessary to prevent unnecessary flaring or production curtailment.

Today the engineer has a choice from among many instruments and controls, some of which are rather sophisticated. The advent of electronic and digital equipment offers many alternatives. Remote metering and control now are more commonly employed to minimize personnel overhead. The net result is a more complex production system than the traditional one.

Many seemingly superior instruments and controls are not suitable for some production systems. They may not be packaged to withstand exposure to the weather and elements in the environment—rain, salt spray, sand, wind, lightning, etc. Some devices are so sensitive that mere vibration may be a problem. Calibration and other like necessities may be inconvenient (or maybe impractical) in remote locations. Also, properly trained personnel may not be available for maintenance.

If transfer of custody is involved, contractual obligation may limit the choice of system. Other factors like spare parts availability and vendor service all influence the proper selection of equipment and vendor.

Gas Measurement

The choice of meter depends on the absolute volume involved and the *rangeability*—the ratio of maximum to minimum flow rate that a given size meter can accommodate. Reliability also is a factor. Both accuracy and precision must be considered. Accuracy is the difference between true and measured rate. Precision is the repeatability of a measurement, however wrong it may be.

*This author also wrote the chapter on this topic in the 1962 edition.

There are a series of volumetric meters that measure volume directly by use of bellows, reciprocating pistons, rotating vanes and cams, etc.¹ These are used primarily for measuring small volumes of low-pressure gas and have little application in production operations.

Velocity Meters

A velocity meter is any device that measures flow by impact kinetic energy or by using the change in pressure that accompanies a controlled change in velocity. However this change is induced, meter performance is governed by an energy balance.

The Energy Balance. Fig. 13.1 illustrates a general flow system on which a general flow equation may be based. Points 1 and 2 represent any two points in a flow system between which an energy balance may be written.

The fluid entering at Point 1 has an internal energy, U_1 , which is the result of previous energy obtained. In addition, a certain amount of pV work must be done to get the fluid past Point 1—i.e., the energy necessary for it to flow. This fluid also possesses potential energy, X_1 , above the datum plane, and kinetic energy $v_1^2/2g$. The fluid leaving at Point 2 possesses the same forms of energy but the amount depends on the work W or heat Q gained or lost by the system between the two points. The general equation may then be written

$$\begin{aligned}
 U_1 + p_1 V_1 + Z_1 + \frac{v_1^2}{2g} + Q - W \\
 = U_2 + p_2 V_2 + Z_2 + \frac{v_2^2}{2g}, \dots\dots\dots (1)
 \end{aligned}$$

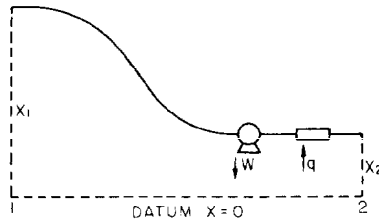


Fig. 13.1—General flow system.

where

- U = internal energy, which includes all energy such as heat, electrical, chemical, and surface,
- p = pressure,
- V = volume or specific volume,
- Z = height above an arbitrary datum plane,
- v = velocity in conduit,
- Q = heat gained or lost by system (plus if gained, minus if lost), and
- W = work done by system (plus if done by system, minus if done on system).

The many ramifications of Eq. 1 are developed in any standard text on thermodynamics.

Eq. 1 may be applied to any of the systems shown in Fig. 13.2. When writing it between Points 1 and 2 of any of the three systems shown, it may be reduced to

$$p_1 V_1 - p_2 V_2 = \frac{v_2^2}{2g} - \frac{v_1^2}{2g} \quad \dots \dots \dots (2)$$

Eq. 2 develops on the normally correct premise that Q , W , and ΔU are substantially zero between the two points. These two points are, furthermore, so close together that any change in potential energy is negligible in comparison with the other changes involved. Eq. 2 is the basic equation governing velocity or head meters and expresses the general fact that changes in velocity in such a system must be accompanied by a corresponding change in static pressure.

Forms of Meter. Fig. 13.2 shows several common ways in which a velocity change may be imposed on the system. In each instance, a constriction is supplied for increasing the velocity (decreasing static pressure), following which the velocity returns to normal. The amount of *permanent* pressure loss across the device is small and depends largely on the amount of turbulence and friction loss involved.

The Venturi tube shown in Part a is designed so that a high-pressure differential can be induced and still minimize the permanent pressure loss due to turbulence and eddy currents. In general, it will restore at least 90% of the pressure drop at the throat. The sections involved, though, are expensive to manufacture and bulky to handle, especially at elevated pressures. Consequently, their

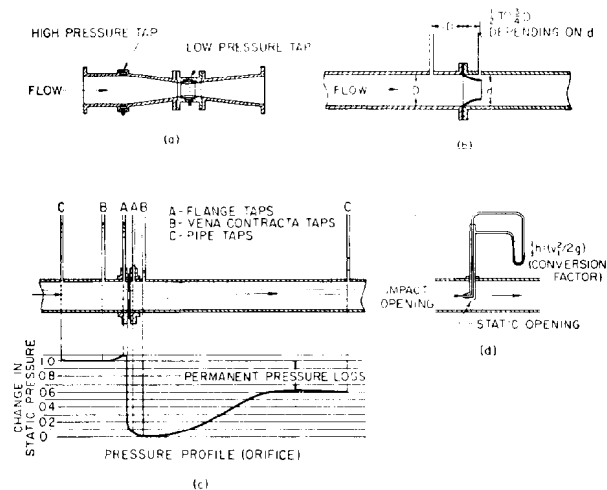


Fig. 13.2—Diagrammatic representation of fluid flow through a flat-plate orifice showing relative positions of the pressure taps in common use and the change in static pressures (flow is from left to right). (a) Venturi tube, cross section; (b) flow nozzle, cross section; (c) location of taps; (d) schematic view of pitot tube.

use is usually limited to low-pressure applications where high-pressure recovery is essential. The flow nozzle is essentially a cross between the three devices shown and represents an attempt to incorporate the best features of each. General usage is limited.

The flat-plate orifice is used in the majority of all gas-production and transportation facilities. It is simple, inexpensive, handy to change and stock, and gives reproducible results. Although the pressure recovery is seldom higher than 65%, this is not a critical fault, for most systems are designed to operate with a low differential pressure.

Derivation of an Orifice Equation. Eq. 2 may be simplified by assuming that $V_1 = V_2 = V$, an assumption that is approximately true and is later corrected by a term called the expansion factor. Then

$$v_1^2 - v_2^2 = 2gV(p_2 - p_1) = 2gh \quad \dots \dots \dots (3)$$

The term h is the differential head loss between Points 1 and 2 expressed as "feet of fluid" (that fluid flowing in the system).

The velocities may be expressed in terms of volume rate of flow q_g and diameters d_i and d_o (internal diameter of pipe and orifice opening, respectively). This substitution yields an intermediate equation

$$q_g = A_2 \frac{1}{\sqrt{1 - F_d^4}} \sqrt{2gh} \quad \dots \dots \dots (4)$$

where A_2 = area of orifice plate opening, and $F_d = d_o/d_i$. The second term on the right side of Eq. 4 is often referred to as the approach factor.

Further modification of our theoretical equation is necessary. Part c of Fig. 13.2 shows that the diameter of the flowing stream becomes smaller than that of the orifice opening. This point, known as the *vena contracta*, is really the limiting diameter, and some correction must be made when using the orifice-opening diameter in the equation. There is also an energy loss due to turbulence and friction not yet accounted for. Both of these considerations are easily handled by use of an efficiency factor, K_o , that must be determined experimentally.

For convenience we furthermore like to express h in terms of inches of water, h_w . If all these corrections and conversions are superimposed on Eq. 4 the equation reads

$$q_g = 218.44 K_o d_o^2 \frac{p_f}{p_{sc}} \frac{T_{sc}}{T_f} \sqrt{\frac{h_w T_f}{p_f \gamma_g}}, \dots \dots \dots (5)$$

where

- q_g = gas-flow rate, std cu ft/hr measured at p_b and T_b ,
- d_i = internal diameter, in.,
- d_o = orifice-opening diameter, in.,
- p_f = flowing pressure, psia,
- p_{sc} = base pressure, psia,
- T_f = flowing temperature, °R,
- T_{sc} = base temperature, °R,
- h_w = differential across orifice, in. H₂O,
- γ_g = specific gravity of gas (air=1.0), and
- K_o = efficiency factor, which includes the approach factor.

Eq. 5 may be modified to a more standard form by (1) combining terms, (2) writing it for a gas whose specific gravity=1.0, and (3) assuming that $p_{sc}=14.73$ psia and $T_{sc}=T_f=520^\circ\text{R}$.

This yields the two basic orifice equations

$$q_g = C' \sqrt{h_w p_f} \dots \dots \dots (6)$$

and

$$C' = F_b F_{pb} F_{tb} F_g F_{tf} F_r Y F_{pv} F_m F_v F_a \dots \dots \dots (7)$$

The value C' is known as the orifice constant. It is determined primarily from F_b , the basic orifice flow factor, which is equal to $338.17 K_o d_o^2$. The other multipliers shown in Eq. 7 are correction factors to correct for the basic assumptions necessary to arrive at Eq. 6. Only the first five are usually used in routine lease operations, in measuring gas for proration records and the like. The last six correction factors are relatively small and are used to obtain accurate records in the sale or purchase of gas. The last two apply only to meters with mercury manometers.

Table 13.1 summarizes these constants except for F_{pv} , which is calculated from compressibility factor, and F_a , calculated from the expansibility of metals used for orifice construction.^{2,3}

The comparable metric standard for the orifice equations and constants is ANSI/API 2530.² At the time this material was being prepared, the conversion effort to SI units had not been completed. Until it is, calculations may be made in English units and converted.

$$q_g (\text{m}^3) = (0.02833) (\text{cu ft}),$$

where $q_g = \text{m}^3$ measured at 101.315 kPa and 15°C and cu ft=volume measured at 14.73 psia and 60°F.

Orifice Constants

The value of the constants in Eq. 7 depends in many cases on the points between which the differential head loss, h_w , is measured. Two standards are provided in gas measurement—flange taps and pipe taps. With the former, the flange or orifice holder is so tapped that the center of the upstream and downstream taps is 1 in. from the respective orifice-plate surfaces. For standard pipe taps, the upstream tap is located two and one-half pipe diameters upstream and eight pipe diameters downstream. The location of Sec. 1 (Tables 13.1a, g, i, and l) of the orifice tables is for *flange taps* and Sec. 3 (Tables 13.1b, h, j, and m) is for *pipe taps*. Sec. 2 (the remaining parts of Table 13.1) shows the fluid-condition factors common to both types.

Basic Orifice Factor F_b . This factor, as noted above, is based on those assumptions necessary to go from Eq. 5 to 6. These are $T_{sc}=520^\circ\text{R}$, $\gamma_g=1.00$, and $T_f=520^\circ\text{R}$. It is a function of the experimental constant K_o , which means that it depends on the location of the differential pressure taps and the internal pipe diameter, in addition to the orifice diameter.

The value of F_b may be found from tables of F_b shown in Table 13.1a for flange taps and Table 13.1b for pipe taps if the meter run is of standard internal diameter. For gas-measurement work involving sale and purchase by a gas-transmission or distribution company, corrections are provided for values of F_b not fitting the standard tables. These are not shown here, for they are not normally used in production operations.

Pressure-Base Factor F_{pb} . Values of this factor are shown in Sec. 2 (Table 13.1c) of the charts. It corrects the value of F_b for the case where the pressure base used is not 14.73 psia. It may be determined by the equation $F_{pb}=14.73 p_{sc}$.

Temperature-Base Factor F_{tb} . This is shown in Table 13.1d and corrects for any contract wherein the base temperature is not 520°R (60°F). This factor may be computed by the equation $F_{tb}=T_{sc}/520$.

Specific-Gravity Factor F_g . This factor, shown in Table 13.1e, is to correct the basic orifice equation for those cases where the specific gravity of the gas is other than 1.00. The equation is $F_g=(1/\gamma_g)^{0.5}$.

Flowing-Temperature Factor F_{tf} . This factor corrects for those cases where the flowing temperature of the gas is other than 60°F. The equation is $F_{tf}=(520/T_f)^{0.5}$. Values are given in Table 13.1f.

(continued on Page 8)

TABLE 13.1a—FLANGE TAPS: BASIC ORIFICE FACTORS, F_b

Orifice Diameter, d_o , (in.)	Internal Diameter of Pipe, d_i , in.						
	2			3			
	1.689	1.939	2.067	2.300	2.626	2.900	3.068
0.250	12.695	12.707	12.711	12.714	12.712	12.708	12.705
0.375	28.474	28.439	28.428	28.411	28.393	28.382	28.376
0.500	50.777	50.587	50.521	50.435	50.356	50.313	50.292
0.625	80.090	79.509	79.311	79.052	78.818	78.686	78.625
0.750	117.09	115.62	115.14	114.52	113.99	113.70	113.56
0.875	162.95	159.56	158.47	157.12	156.00	155.41	155.14
1.000	219.77	212.47	210.22	207.44	205.18	204.04	203.54
1.125	290.99	276.20	271.70	266.35	262.06	259.95	259.04
1.250	385.78	353.58	345.13	335.12	327.39	323.63	322.03
1.375	—	448.57	433.50	415.75	402.18	395.80	393.09
1.500	—	—	542.26	510.86	487.98	477.36	472.96
1.625	—	—	—	623.91	586.82	569.65	562.58
1.750	—	—	—	—	701.27	674.44	663.42
1.875	—	—	—	—	834.88	793.88	777.18
2.000	—	—	—	—	—	930.65	906.01
2.125	—	—	—	—	—	1091.2	1052.5
2.250	—	—	—	—	—	—	1223.2
2.375	—	—	—	—	—	—	—
2.500	—	—	—	—	—	—	—
2.625	—	—	—	—	—	—	—
2.750	—	—	—	—	—	—	—
2.875	—	—	—	—	—	—	—
3.000	—	—	—	—	—	—	—
3.125	—	—	—	—	—	—	—
3.250	—	—	—	—	—	—	—
3.375	—	—	—	—	—	—	—
3.500	—	—	—	—	—	—	—
3.625	—	—	—	—	—	—	—
3.750	—	—	—	—	—	—	—
3.875	—	—	—	—	—	—	—
4.000	—	—	—	—	—	—	—
4.250	—	—	—	—	—	—	—
4.500	—	—	—	—	—	—	—
4.750	—	—	—	—	—	—	—
5.000	—	—	—	—	—	—	—
5.250	—	—	—	—	—	—	—
5.500	—	—	—	—	—	—	—
5.750	—	—	—	—	—	—	—
6.000	—	—	—	—	—	—	—
6.250	—	—	—	—	—	—	—
6.500	—	—	—	—	—	—	—
6.750	—	—	—	—	—	—	—
7.000	—	—	—	—	—	—	—
7.250	—	—	—	—	—	—	—
7.500	—	—	—	—	—	—	—
7.750	—	—	—	—	—	—	—
8.000	—	—	—	—	—	—	—
8.250	—	—	—	—	—	—	—
8.500	—	—	—	—	—	—	—
8.750	—	—	—	—	—	—	—
9.000	—	—	—	—	—	—	—
9.250	—	—	—	—	—	—	—
9.500	—	—	—	—	—	—	—
9.750	—	—	—	—	—	—	—
10.000	—	—	—	—	—	—	—
10.250	—	—	—	—	—	—	—
10.500	—	—	—	—	—	—	—
10.750	—	—	—	—	—	—	—
11.000	—	—	—	—	—	—	—
11.250	—	—	—	—	—	—	—

TABLE 13.1a—FLANGE TAPS: BASIC ORIFICE FACTORS, F_b (continued)

Orifice Diameter, d_o , (in.)	Internal Diameter of Pipe, d_i , in.							
	4				6			
	3.152	3.438	3.826	4.026	4.897	5.189	5.761	6.065
0.250	12.703	12.697	12.687	12.683	—	—	—	—
0.375	28.373	28.364	28.353	28.348	—	—	—	—
0.500	50.284	50.258	50.234	50.224	50.197	50.191	50.182	50.178
0.625	78.598	78.523	78.450	78.421	78.338	78.321	78.296	78.287
0.750	113.50	113.33	113.15	113.08	112.87	112.82	112.75	112.72
0.875	155.03	154.71	154.40	154.27	153.88	153.78	153.63	153.56
1.000	203.33	202.75	202.20	201.99	201.34	201.19	200.96	200.85
1.125	258.65	257.63	256.69	256.33	255.31	255.08	254.72	254.56
1.250	321.37	319.61	318.03	317.45	315.83	315.48	314.95	314.72
1.375	391.97	389.03	386.45	385.51	382.99	382.47	381.70	381.37
1.500	471.14	466.39	462.27	460.79	456.93	456.16	455.03	454.57
1.625	559.72	552.31	545.89	543.61	537.77	536.64	535.03	534.38
1.750	658.96	647.54	637.84	634.39	625.73	624.09	621.79	620.88
1.875	770.44	753.17	738.75	733.68	721.03	718.69	715.44	714.19
2.000	896.06	870.59	849.41	842.12	823.99	820.68	816.13	814.41
2.125	1038.1	1001.4	970.95	960.48	934.97	930.35	924.07	921.71
2.250	1499.9	1147.7	1104.7	1089.9	1054.4	1048.1	1039.5	1036.3
2.375	—	1311.7	1252.1	1231.7	1182.9	1174.2	1162.6	1158.3
2.500	—	1498.4	1415.0	1387.2	1320.9	1309.3	1293.8	1288.2
2.625	—	—	1595.6	1558.2	1469.2	1453.9	1433.5	1426.0
2.750	—	—	1797.1	1746.7	1628.9	1608.7	1582.1	1572.3
2.875	—	—	—	1955.5	1801.0	1774.5	1740.0	1727.5
3.000	—	—	—	2194.9	1986.6	1952.4	1907.8	1891.9
3.125	—	—	—	—	2187.2	2143.4	2086.4	2066.1
3.250	—	—	—	—	2404.2	2348.8	2276.5	2250.8
3.375	—	—	—	—	2639.5	2569.8	2479.1	2446.8
3.500	—	—	—	—	2895.5	2808.1	2695.1	2654.9
3.625	—	—	—	—	3180.8	3065.3	2925.7	2876.0
3.750	—	—	—	—	—	3345.5	3172.1	3111.2
3.875	—	—	—	—	—	3657.7	3435.7	3361.5
4.000	—	—	—	—	—	—	3718.2	3628.2
4.250	—	—	—	—	—	—	4354.8	4216.6
4.500	—	—	—	—	—	—	—	4900.9
4.750	—	—	—	—	—	—	—	—
5.000	—	—	—	—	—	—	—	—
5.250	—	—	—	—	—	—	—	—
5.500	—	—	—	—	—	—	—	—
5.750	—	—	—	—	—	—	—	—
6.000	—	—	—	—	—	—	—	—
6.250	—	—	—	—	—	—	—	—
6.500	—	—	—	—	—	—	—	—
6.750	—	—	—	—	—	—	—	—
7.000	—	—	—	—	—	—	—	—
7.250	—	—	—	—	—	—	—	—
7.500	—	—	—	—	—	—	—	—
7.750	—	—	—	—	—	—	—	—
8.000	—	—	—	—	—	—	—	—
8.250	—	—	—	—	—	—	—	—
8.500	—	—	—	—	—	—	—	—
8.750	—	—	—	—	—	—	—	—
9.000	—	—	—	—	—	—	—	—
9.250	—	—	—	—	—	—	—	—
9.500	—	—	—	—	—	—	—	—
9.750	—	—	—	—	—	—	—	—
10.000	—	—	—	—	—	—	—	—
10.250	—	—	—	—	—	—	—	—
10.500	—	—	—	—	—	—	—	—
10.750	—	—	—	—	—	—	—	—
11.000	—	—	—	—	—	—	—	—
11.250	—	—	—	—	—	—	—	—

TABLE 13.1a—FLANGE TAPS: BASIC ORIFICE FACTORS, F_o (continued)

Orifice Diameter, d_o , (in.)	Internal Diameter of Pipe, d_i , in.					
	8			10		
	7.625	7.981	8.071	9.564	10.020	10.136
0.250	—	—	—	—	—	—
0.375	—	—	—	—	—	—
0.500	—	—	—	—	—	—
0.625	—	—	—	—	—	—
0.750	—	—	—	—	—	—
0.875	153.34	153.31	153.31	—	—	—
1.000	200.46	200.39	200.38	200.20	—	—
1.125	253.99	253.89	253.87	253.55	253.48	253.47
1.250	313.91	313.78	313.74	313.31	313.20	313.18
1.375	380.25	380.06	380.02	379.44	379.29	379.26
1.500	453.02	452.78	452.72	451.95	451.76	451.72
1.625	532.27	531.95	531.87	530.87	530.63	530.57
1.750	618.02	617.60	617.50	616.21	615.90	615.83
1.875	710.32	709.77	709.64	707.99	707.61	707.51
2.000	809.22	808.50	808.34	805.23	805.76	805.65
2.125	914.79	913.86	913.64	910.97	910.38	910.24
2.250	1027.1	1025.9	1025.6	1022.2	1021.5	1021.3
2.375	1146.2	1144.7	1144.3	1140.1	1139.2	1139.0
2.500	1272.3	1270.3	1269.8	1264.5	1263.4	1263.1
2.625	1405.4	1402.9	1402.3	1395.6	1394.2	1393.9
2.750	1545.7	1542.5	1541.8	1533.4	1531.7	1531.3
2.875	1693.4	1689.3	1688.4	1678.0	1675.9	1675.4
3.000	1848.6	1843.5	1842.3	1829.4	1826.9	1826.3
3.125	2011.6	2005.2	2003.8	1987.8	1984.7	1984.0
3.250	2182.6	2174.6	2172.9	2153.2	2149.5	2148.6
3.375	2361.8	2352.0	2349.9	2325.7	2321.2	2320.2
3.500	2549.7	2537.7	2535.0	2505.6	2500.1	2498.9
3.625	2746.5	2731.8	2728.6	2692.8	2686.2	2684.7
3.750	2952.6	2934.8	2930.8	2887.6	2879.7	2877.9
3.875	3168.3	3146.9	3142.1	3090.1	3080.7	3078.5
4.000	3394.3	3368.5	3362.9	3300.6	3289.3	3286.8
4.250	3879.4	3842.3	3834.2	3746.1	3730.2	3726.7
4.500	4412.8	4360.5	4349.0	4226.0	4204.1	4199.2
4.750	5000.7	4928.1	4912.2	4742.7	4712.8	4706.2
5.000	5650.0	5551.1	5529.5	5298.6	5258.5	5249.6
5.250	6369.3	6236.4	6207.3	5897.4	5843.6	5831.8
5.500	7170.9	6992.0	6953.6	6543.1	6471.9	6456.3
5.750	—	7830.0	7777.8	7240.0	7146.9	7126.5
6.000	—	—	8706.9	7993.3	7873.0	7846.6
6.250	—	—	—	8808.9	8654.8	8621.1
6.500	—	—	—	9693.3	9498.1	9455.3
6.750	—	—	—	10654	10409	10355
7.000	—	—	—	11711	11394	11327
7.250	—	—	—	—	12467	12381
7.500	—	—	—	—	13656	13541
7.750	—	—	—	—	—	—
8.000	—	—	—	—	—	—
8.250	—	—	—	—	—	—
8.500	—	—	—	—	—	—
8.750	—	—	—	—	—	—
9.000	—	—	—	—	—	—
9.250	—	—	—	—	—	—
9.500	—	—	—	—	—	—
9.750	—	—	—	—	—	—
10.000	—	—	—	—	—	—
10.250	—	—	—	—	—	—
10.500	—	—	—	—	—	—
10.750	—	—	—	—	—	—
11.000	—	—	—	—	—	—
11.250	—	—	—	—	—	—

TABLE 13.1a—FLANGE TAPS: BASIC ORIFICE FACTORS, F_b (continued)

Orifice Diameter, d_o , (in.)	Internal Diameter of Pipe, d_i , in.					
	12			16		
	11.376	11.938	12.090	14.688	15.000	15.250
0.250	—	—	—	—	—	—
0.375	—	—	—	—	—	—
0.500	—	—	—	—	—	—
0.625	—	—	—	—	—	—
0.750	—	—	—	—	—	—
0.875	—	—	—	—	—	—
1.000	—	—	—	—	—	—
1.125	—	—	—	—	—	—
1.250	312.94	312.85	312.83	—	—	—
1.375	378.94	378.82	378.79	—	—	—
1.500	451.30	451.14	451.10	450.53	450.48	—
1.625	530.04	529.83	529.78	529.06	528.99	528.94
1.750	615.16	614.90	614.84	613.94	613.85	613.78
1.875	706.68	706.36	706.28	705.18	705.07	704.99
2.000	804.61	804.23	804.13	802.78	802.65	802.55
2.125	908.98	908.51	908.39	906.77	906.61	906.49
2.250	1019.8	1019.2	1019.1	1017.1	1017.0	1016.8
2.375	1137.1	1136.4	1136.2	1133.9	1133.7	1133.5
2.500	1260.8	1260.0	1259.8	1257.1	1256.8	1256.6
2.625	1391.1	1390.1	1389.9	1386.7	1386.4	1386.1
2.750	1528.0	1526.8	1526.5	1522.7	1522.4	1522.1
2.875	1671.4	1670.0	1669.6	1665.2	1664.8	1664.5
3.000	1821.4	1819.7	1819.3	1814.1	1813.7	1813.3
3.125	1978.1	1976.1	1975.6	1969.6	1969.0	1968.6
3.250	2141.5	2139.2	2138.6	2131.5	2130.9	2130.4
3.375	2311.7	2308.9	2308.2	2299.9	2299.2	2298.7
3.500	2488.7	2485.4	2484.6	2474.9	2474.1	2473.5
3.625	2672.6	2668.7	2667.7	2656.4	2655.5	2654.8
3.750	2863.5	2858.8	2857.7	2844.6	2843.5	2842.7
3.875	3061.4	3055.9	3054.6	3039.4	3038.1	3037.2
4.000	3266.4	3260.0	3258.5	3240.8	3239.4	3238.3
4.250	3698.4	3689.6	3687.5	3663.8	3661.9	3660.5
4.500	4160.4	4148.4	4145.5	4113.9	4111.5	4109.7
4.750	4653.4	4637.2	4633.4	4591.5	4588.4	4586.0
5.000	5179.0	5157.4	5152.3	5097.2	5093.1	5090.1
5.250	5738.5	5710.0	5703.3	5631.4	5626.1	5622.3
5.500	6333.8	6296.6	6287.9	6194.8	6188.1	6183.1
5.750	6966.9	6919.0	6907.8	6788.1	6779.6	6773.3
6.000	7640.4	7579.0	7564.7	7412.3	7401.5	7393.6
6.250	8357.3	8278.9	8260.7	8068.4	8054.8	8044.8
6.500	9121.0	9021.7	8998.7	8757.3	8740.3	8727.9
6.750	9935.2	9810.5	9781.6	9480.4	9459.4	9444.0
7.000	10804	10649	10613	10239	10213	10194
7.250	11732	11540	11496	11035	11003	10980
7.500	12725	12489	12434	11869	11831	11803
7.750	13787	13500	13433	12745	12698	12664
8.000	14927	14578	14498	13664	13607	13566
8.250	16158	15730	15633	14628	14560	14511
8.500	17505	16962	16845	15642	15560	15501
8.750	—	18296	18148	16706	16609	16539
9.000	—	—	19565	17826	17711	17628
9.250	—	—	—	19004	18868	18770
9.500	—	—	—	20245	20085	19969
9.750	—	—	—	21552	21365	21230
10.000	—	—	—	22930	22712	22555
10.250	—	—	—	24385	24132	23948
10.500	—	—	—	25924	25628	25416
10.750	—	—	—	27567	27210	26962
11.000	—	—	—	29331	28899	28600
11.250	—	—	—	—	30710	30348

TABLE 13.1b—PIPE TAPS—BASIC ORIFICE FACTORS, F_b

Orifice Diameter, d_o , (in.)	Internal Diameter of Pipe, d_i , in.								
	2			3				4	
	1.689	1.939	2.067	2.300	2.626	2.900	3.068	3.152	3.438
0.250	12.850	12.813	12.800	12.782	12.765	12.753	12.748	12.745	12.737
0.375	29.359	29.097	29.005	28.882	28.771	28.710	28.682	28.669	28.634
0.500	53.703	52.816	52.481	52.019	51.591	51.353	51.243	51.196	51.064
0.625	87.212	84.919	84.083	82.922	81.795	81.142	80.835	80.703	80.332
0.750	132.23	126.86	124.99	122.45	120.06	118.67	118.00	117.70	116.86
0.875	192.74	181.02	177.08	171.92	167.23	164.58	163.31	162.76	161.17
1.000	275.45	251.10	243.27	233.30	224.56	219.76	217.52	216.55	213.79
1.125	391.93	342.98	327.98	309.43	293.79	285.48	281.66	280.02	275.42
1.250	—	465.99	437.99	404.52	377.36	363.41	357.12	354.45	347.03
1.375	—	—	583.96	524.68	478.68	455.82	445.74	441.48	429.83
1.500	—	—	—	679.10	602.45	565.79	549.94	543.31	525.40
1.625	—	—	—	—	755.34	697.43	672.95	662.81	635.76
1.750	—	—	—	—	946.99	856.37	819.05	803.77	763.51
1.875	—	—	—	—	—	1050.4	993.98	971.19	911.98
2.000	—	—	—	—	—	1290.7	1205.6	1171.8	1085.5
2.125	—	—	—	—	—	—	1465.1	1415.0	1289.7
2.250	—	—	—	—	—	—	—	—	1532.0
2.375	—	—	—	—	—	—	—	—	1822.8

Reynolds-Number Factor F_r . This takes into account the variation of the discharge coefficient with Reynolds number. In gas measurement, the variation is slight and is often ignored in production operations. Values are shown in Tables 13.1g and 13.1h. It has been assumed in preparation of these tables that gas viscosity is substantially constant. The constant b shown in the tables is then primarily a function of pipe diameter, orifice diameter, and the location of the differential-pressure taps.

Expansion Factor Y . This factor accounts for the change in gas density as the pressure changes across the orifice. Inasmuch as the differential involved is usually small, this correction is small and often ignored. The value used depends on which one of the differential-pressure taps is used to measure static pressure and the location of the tap. The additional primary variables involved are (1) F_d , (2) ratio of differential pressure to absolute pressure, and (3) the specific-heat ratio C_p/C_v . In the standard table the last variable is taken as constant and equal to 1.3. This factor is shown in Tables 13.1i through 13.1m.

Supercompressibility Factor F_{pv} . The variation from the ideal-gas laws by an actual gas is the function of this factor. The factor may be measured experimentally or determined by detailed methods outlined in AGA Committee Report 3.² The correction is usually small and is often ignored. It may be estimated from the equation $F_{pv} = (1/z)^{0.5}$, where z is equal to the compressibility factor obtained from standard correlations.

Manometer Factor F_m . This is used only with mercury-type meters to correct for the slight error in measurement caused by having different heads of gas above the two legs of the manometer. For all practical purposes it is insignificant. Table 13.1n lists this factor vs. gas specific gravity.

Gauge Location Factor, F_ℓ . This corrects the manometer factor, F_m , for elevation and latitudes other than sea level and 45° latitude (see Table 13.1o).

Thermal Expansion Factor, F_a . This corrects for expansion or contraction of the orifice opening when operating at temperatures substantially different from that at which the orifice was made. Normally, it is applied only at temperatures above 120°F or below 0°F.

Example Problem 1. A 0.7-specific-gravity natural gas is measured in an orifice meter having flange taps. Determine the flow rate in scf/hr at 14.4 psia and 60°F if the following data apply:

$$\begin{aligned}\bar{h}_w &= 40 \text{ in. H}_2\text{O}, \\ \bar{p}_f &= 143 \text{ psig (measured} \\ &\quad \text{downstream),}\end{aligned}$$

$$\text{avg flowing temp} = 84^\circ\text{F},$$

$$\text{line size} = 4.026 \text{ in., and}$$

$$\text{orifice-plate opening} = 1.50 \text{ in.}$$

Solution.

The respective factors are

$$F_b = 460.79,$$

$$F_{pb} = 1.0229,$$

$$F_{tb} = 1.0000,$$

$$F_g = 1.1952,$$

$$F_{ff} = 0.9777,$$

$$F_r = 1.0004,$$

$$Y = 1.0016, \text{ and}$$

$$C' = 551.89 \text{ (the product of the above numbers).}$$

Then, $q_g = 551.89 [(40)(143 + 14.73)]^{0.5} = 43,810$ scf/hr.

As a practical matter, the accuracy of the meter device itself does not justify the number of significant figures shown in the charts. Consequently, in most production operations and engineering calculations the values of the coefficients may be rounded off and sometimes ignored with no practical loss of accuracy.

(continued on Page 36)

TABLE 13.1b—PIPE TAPS—BASIC ORIFICE FACTORS, F_b (continued)

Orifice Diameter, d_o , (in.)	Internal Diameter of Pipe, d_i , in.								
	20			24			30		
	18.814	19.000	19.250	22.626	23.000	23.250	28.628	29.000	29.250
2.000	806.71	806.57	806.40	—	—	—	—	—	—
2.125	911.51	911.35	911.13	—	—	—	—	—	—
2.250	1022.9	1022.7	1022.4	—	—	—	—	—	—
2.375	1141.0	1140.7	1140.4	1136.8	1136.5	1136.3	—	—	—
2.500	1265.7	1265.4	1265.0	1260.6	1260.2	1259.9	—	—	—
2.625	1397.2	1396.8	1396.3	1390.9	1390.5	1390.2	—	—	—
2.750	1535.5	1535.0	1534.4	1527.9	1527.3	1527.0	—	—	—
2.875	1680.7	1680.1	1679.3	1671.5	1670.9	1670.4	1663.8	—	—
3.000	1832.7	1832.1	1831.2	1821.9	1821.1	1820.6	1812.7	1812.3	1812.0
3.125	1991.8	1991.0	1990.0	1978.9	1978.0	1977.4	1968.1	1967.7	1967.4
3.250	2158.0	2157.0	2155.8	2142.8	2141.7	2141.0	2130.2	2129.6	2129.3
3.375	2331.3	2330.2	2328.7	2313.5	2312.3	2311.5	2298.8	2298.2	2297.7
3.500	2511.9	2510.6	2508.8	2491.2	2489.7	2488.8	2474.1	2473.3	2472.9
3.625	2699.7	2698.2	2696.2	2675.8	2674.0	2673.0	2656.0	2655.2	2654.6
3.750	2895.0	2893.2	2890.9	2867.4	2865.4	2864.1	2844.6	2843.7	2843.0
3.875	3097.7	3095.7	3093.0	3066.0	3063.8	3062.3	3040.0	3038.9	3038.2
4.000	3308.0	3305.7	3302.7	3271.8	3269.2	3267.6	3242.2	3240.9	3240.1
4.250	3751.6	3748.7	3744.8	3705.0	3701.7	3699.6	3669.6	3665.3	3664.3
4.500	4226.8	4223.0	4218.1	4167.6	4163.4	4160.7	4119.3	4117.3	4116.0
4.750	4734.1	4729.4	4723.3	4660.0	4654.8	4651.4	4599.6	4597.1	4595.4
5.000	5274.6	5268.7	5261.1	5183.0	5176.4	5172.3	5108.2	5105.0	5103.0
5.250	5849.0	5841.9	5832.6	5737.1	5729.1	5723.9	5645.4	5641.6	5639.1
5.500	6458.6	6449.9	6438.7	6322.9	6313.2	6307.0	6211.8	6207.2	6204.2
5.750	7104.4	7094.0	7080.4	6941.3	6929.7	6922.2	6807.7	6802.1	6798.5
6.000	7787.9	7775.4	7759.1	7592.8	7579.0	7570.1	7433.6	7426.9	7422.6
6.250	8510.4	8495.4	8476.0	8278.3	8262.0	8251.5	8089.9	8082.0	8076.9
6.500	9273.4	9255.6	9232.5	8998.8	8979.5	8967.1	8777.2	8768.0	8761.9
6.750	10079	10058	10030	9755.0	9732.4	9717.9	9496.0	9485.2	9478.1
7.000	10928	10903	10871	10548	10522	10505	10247	10234	10226
7.250	11823	11794	11756	11379	11348	11329	11030	11016	11006
7.500	12767	12733	12689	12249	12214	12191	11847	11830	11819
7.750	13762	13722	13670	13160	13119	13093	12697	12678	12665
8.000	14810	14763	14703	14113	14065	14035	13582	13560	13546
8.250	15914	15860	15791	15109	15054	15020	14501	14477	14461
8.500	17073	17015	16935	16150	16087	16048	15457	15429	15411
8.750	18305	18232	18139	17237	17166	17121	16450	16418	16397
9.000	19598	19515	19408	18373	18292	18241	17480	17444	17421
9.250	20963	20866	20743	19560	19468	19409	18548	18508	18482
9.500	22402	22292	22151	20800	20695	20628	19656	19611	19582
9.750	23923	23796	23634	22094	21976	21900	20805	20754	20721
10.000	25529	25384	25198	23447	23312	23227	21995	21938	21901
10.250	27227	27061	26849	24859	24708	24612	23228	23165	23124
10.500	29023	28834	28592	26335	26164	26056	24505	24434	24388
10.750	30925	30709	30434	27878	27685	27563	25827	25749	25698
11.000	32940	32694	32381	29490	29273	29136	27196	27109	27052
11.250	35078	34798	34443	31175	30932	30779	28613	28516	28453
11.500	37348	37030	36626	32938	32666	32494	30080	29972	29903
11.750	39761	39400	38941	34783	34478	34285	31598	31479	31402
12.000	42330	41920	41399	36714	36373	36158	33169	33038	32953
12.500	47991	47461	46790	40855	40429	40161	36478	36318	36215
13.000	54463	53778	52914	45406	44877	44544	40024	39829	39704
13.500	—	—	—	50420	49763	49352	43823	43589	43437
14.000	—	—	—	55959	55147	54638	47898	47615	47433
14.500	—	—	—	62099	61094	60468	52271	51932	51714
15.000	—	—	—	68929	67687	66915	56967	56562	56301
15.500	—	—	—	76562	75025	74074	62017	61583	61223
16.000	—	—	—	—	83231	82055	67453	66878	66509
16.500	—	—	—	—	—	—	73314	72630	72193
17.000	—	—	—	—	—	—	79641	78831	78313
17.500	—	—	—	—	—	—	86485	85525	84913
18.000	—	—	—	—	—	—	93900	92765	92042
18.500	—	—	—	—	—	—	101950	100610	99758
19.000	—	—	—	—	—	—	110720	109130	108130
19.500	—	—	—	—	—	—	120300	118420	117230
20.000	—	—	—	—	—	—	130780	128560	127150

TABLE 13.1c—PRESSURE-BASE FACTORS, F_{pb}

$$F_{pb} = 14.73 \div \text{base pressure, psia}$$

Pressure base, psia	Factor F_{pb}	Pressure base, psia	Factor F_{pb}
14.4	1.0229	15.2 (8 oz. above 14.7)	0.9691
14.65 (4 oz. above 14.4)	1.0055	15.325 (10 oz. above 14.7)	0.9612
14.73	1.0000	15.4 (1 psi above 14.4)	0.9565
14.9 (8 oz. above 14.4)	0.9886	15.7 (1 psi above 14.7)	0.9382
14.95 (4 oz. above 14.7)	0.9853	16.4 (2 psi above 14.4)	0.8982
15.025 (10 oz. above 14.4)	0.9804	16.7 (2 psi above 14.7)	0.8820

TABLE 13.1d—TEMPERATURE-BASE FACTORS, F_{tb}

$$F_{tb} = \frac{460 + \text{temperature base } ^\circ\text{F}}{520}$$

Temperature base, $^\circ\text{F}$	Factor F_{tb}	Temperature base, $^\circ\text{F}$	Factor F_{tb}	Temperature base, $^\circ\text{F}$	Factor F_{tb}
45	0.9712	65	1.0096	85	1.0481
50	0.9808	70	1.0192	90	1.0577
55	0.9904	75	1.0288	95	1.0673
60	1.0000	80	1.0385	100	1.0769

TABLE 13.1e—SPECIFIC-GRAVITY FACTORS, F_g

$$F_g = \sqrt{\frac{1.0000}{\gamma_g}}$$

Specific gravity γ_g	Factor F_g	Specific gravity γ_g	Factor F_g	Specific gravity γ_g	Factor F_g	Specific gravity γ_g	Factor F_g
0.500	1.4142	0.675	1.2172	0.850	1.0847	1.05	0.9759
0.505	1.4072	0.680	1.2127	0.855	1.0815	1.06	0.9713
0.510	1.4003	0.685	1.2082	0.860	1.0783	1.07	0.9667
0.515	1.3935	0.690	1.2039	0.865	1.0752	1.08	0.9623
0.520	1.3868	0.695	1.1995	0.870	1.0721	1.09	0.9578
0.525	1.3801	0.700	1.1952	0.875	1.0690	1.10	0.9535
0.530	1.3736	0.705	1.1910	0.880	1.0660	1.11	0.9492
0.535	1.3672	0.710	1.1868	0.885	1.0630	1.12	0.9449
0.540	1.3608	0.715	1.1826	0.890	1.0600	1.13	0.9407
0.545	1.3546	0.720	1.1785	0.895	1.0570	1.14	0.9366
0.550	1.3484	0.725	1.1744	0.900	1.0541	1.15	0.9325
0.555	1.3423	0.730	1.1704	0.905	1.0512	1.16	0.9285
0.560	1.3363	0.735	1.1664	0.910	1.0483	1.17	0.9245
0.565	1.3304	0.740	1.1625	0.915	1.0454	1.18	0.9206
0.570	1.3245	0.745	1.1586	0.920	1.0426	1.19	0.9167
0.575	1.3188	0.750	1.1547	0.925	1.0398	1.20	0.9129
0.580	1.3131	0.755	1.1509	0.930	1.0370	1.21	0.9091
0.585	1.3074	0.760	1.1471	0.935	1.0342	1.22	0.9054
0.590	1.3019	0.765	1.1433	0.940	1.0314	1.23	0.9017
0.595	1.2964	0.770	1.1396	0.945	1.0287	1.24	0.8980
0.600	1.2910	0.775	1.1359	0.950	1.0260	1.25	0.8944
0.605	1.2856	0.780	1.1323	0.955	1.0233	1.26	0.8909
0.610	1.2804	0.785	1.1287	0.960	1.0206	1.27	0.8874
0.615	1.2752	0.790	1.1251	0.965	1.0180	1.28	0.8839
0.620	1.2700	0.795	1.1215	0.970	1.0153	1.29	0.8805
0.625	1.2649	0.800	1.1180	0.975	1.0127	1.30	0.8771
0.630	1.2599	0.805	1.1146	0.980	1.0102	1.31	0.8737
0.635	1.2549	0.810	1.1111	0.985	1.0076	1.32	0.8704
0.640	1.2500	0.815	1.1077	0.990	1.0050	1.33	0.8671
0.645	1.2451	0.820	1.1043	0.995	1.0025	1.34	0.8639
0.650	1.2403	0.825	1.1010	1.00	1.0000	1.35	0.8607
0.655	1.2356	0.830	1.0976	1.01	0.9950	1.36	0.8575
0.660	1.2309	0.835	1.0944	1.02	0.9901	1.37	0.8544
0.665	1.2263	0.840	1.0911	1.03	0.9853	1.38	0.8513
0.670	1.2217	0.845	1.0879	1.04	0.9806	1.39	0.8482

TABLE 13.1f—FLOWING-TEMPERATURE FACTORS, F_H

$$F_H = \sqrt{\frac{520}{460 + \text{actual flowing temperature}}}$$

°F	Factor	°F	Factor	°F	Factor	°F	Factor	°F	Factor	°F	Factor
1	1.0621	21	1.0398	41	1.0188	61	0.9990	81	0.9804	110	0.9551
2	1.0609	22	1.0387	42	1.0178	62	0.9981	82	0.9795	120	0.9469
3	1.0598	23	1.0376	43	1.0168	63	0.9971	83	0.9786	130	0.9388
4	1.0586	24	1.0365	44	1.0157	64	0.9962	84	0.9777	140	0.9309
5	1.0575	25	1.0355	45	1.0147	65	0.9952	85	0.9768	150	0.9233
6	1.0564	26	1.0344	46	1.0137	66	0.9943	86	0.9759	160	0.9158
7	1.0552	27	1.0333	47	1.0127	67	0.9933	87	0.9750	170	0.9085
8	1.0541	28	1.0323	48	1.0117	68	0.9924	88	0.9741	180	0.9014
9	1.0530	29	1.0312	49	1.0107	69	0.9915	89	0.9732	190	0.8944
10	1.0518	30	1.0302	50	1.0098	70	0.9905	90	0.9723	200	0.8876
11	1.0507	31	1.0291	51	1.0088	71	0.9896	91	0.9715	210	0.8810
12	1.0496	32	1.0281	52	1.0078	72	0.9887	92	0.9706	220	0.8745
13	1.0485	33	1.0270	53	1.0068	73	0.9877	93	0.9697	230	0.8681
14	1.0474	34	1.0260	54	1.0058	74	0.9868	94	0.9688	240	0.8619
15	1.0463	35	1.0249	55	1.0048	75	0.9859	95	0.9680	250	0.8558
16	1.0452	36	1.0239	56	1.0039	76	0.9850	96	0.9671	260	0.8498
17	1.0441	37	1.0229	57	1.0029	77	0.9840	97	0.9662	270	0.8440
18	1.0430	38	1.0219	58	1.0019	78	0.9831	98	0.9653	280	0.8383
19	1.0419	39	1.0208	59	1.0010	79	0.9822	99	0.9645	290	0.8327
20	1.0408	40	1.0198	60	1.0000	80	0.9813	100	0.9636	300	0.8272

TABLE 13.1g—*b* VALUES FOR REYNOLDS NUMBER FACTOR, F_r , FLANGE TAPS (continued)
$$F_r = 1 + \frac{b}{\sqrt{h_w \rho_f}}$$

Orifice Diameter, d_o , (in.)	Internal Diameter of Pipe, d_i , in.					
	12			16		
	11.376	11.938	12.090	14.688	15.000	15.250
0.250	—	—	—	—	—	—
0.375	—	—	—	—	—	—
0.500	—	—	—	—	—	—
0.625	—	—	—	—	—	—
0.750	—	—	—	—	—	—
0.875	—	—	—	—	—	—
1.000	—	—	—	—	—	—
1.125	—	—	—	—	—	—
1.250	0.0698	0.0714	0.0718	—	—	—
1.375	0.0654	0.0671	0.0676	—	—	—
1.500	0.0612	0.0631	0.0635	0.0706	0.0713	—
1.625	0.0573	0.0592	0.0597	0.0670	0.0678	0.0684
1.750	0.0536	0.0555	0.0560	0.0636	0.0644	0.0650
1.875	0.0501	0.0521	0.0526	0.0604	0.0612	0.0618
2.000	0.0469	0.0488	0.0492	0.0572	0.0581	0.0587
2.125	0.0438	0.0458	0.0463	0.0542	0.0551	0.0558
2.250	0.0410	0.0429	0.0434	0.0514	0.0523	0.0529
2.375	0.0383	0.0402	0.0407	0.0487	0.0496	0.0502
2.500	0.0359	0.0377	0.0382	0.0461	0.0470	0.0476
2.625	0.0336	0.0354	0.0358	0.0436	0.0445	0.0452
2.750	0.0316	0.0332	0.0336	0.0413	0.0422	0.0428
2.875	0.0297	0.0312	0.0317	0.0391	0.0399	0.0406
3.000	0.0278	0.0294	0.0298	0.0370	0.0378	0.0385
3.125	0.0264	0.0278	0.0282	0.0350	0.0358	0.0365
3.250	0.0251	0.0263	0.0266	0.0331	0.0339	0.0346
3.375	0.0239	0.0250	0.0253	0.0314	0.0321	0.0328
3.500	0.0229	0.0238	0.0241	0.0298	0.0305	0.0311
3.625	0.0221	0.0228	0.0230	0.0282	0.0290	0.0295
3.750	0.0214	0.0219	0.0221	0.0268	0.0275	0.0281
3.875	0.0208	0.0212	0.0213	0.0255	0.0262	0.0267
4.000	0.0204	0.0206	0.0207	0.0243	0.0249	0.0254
4.250	0.0200	0.0198	0.0198	0.0223	0.0228	0.0232
4.500	0.0201	0.0195	0.0194	0.0206	0.0210	0.0213
4.750	0.0207	0.0196	0.0194	0.0193	0.0196	0.0198
5.000	0.0217	0.0202	0.0199	0.0184	0.0185	0.0187
5.250	0.0231	0.0212	0.0208	0.0178	0.0178	0.0179
5.500	0.0249	0.0226	0.0221	0.0176	0.0174	0.0174
5.750	0.0270	0.0243	0.0237	0.0176	0.0174	0.0172
6.000	0.0294	0.0263	0.0255	0.0180	0.0176	0.0173
6.250	0.0320	0.0285	0.0277	0.0186	0.0180	0.0177
6.500	0.0347	0.0309	0.0300	0.0195	0.0188	0.0183
6.750	0.0376	0.0335	0.0325	0.0206	0.0198	0.0192
7.000	0.0406	0.0362	0.0351	0.0220	0.0210	0.0202
7.250	0.0435	0.0390	0.0379	0.0235	0.0224	0.0216
7.500	0.0463	0.0418	0.0407	0.0252	0.0240	0.0230
7.750	0.0491	0.0446	0.0434	0.0271	0.0257	0.0246
8.000	0.0517	0.0473	0.0461	0.0291	0.0276	0.0264
8.250	0.0540	0.0498	0.0487	0.0312	0.0296	0.0283
8.500	0.0560	0.0522	0.0511	0.0334	0.0317	0.0303
8.750	—	0.0543	0.0534	0.0357	0.0338	0.0324
9.000	—	—	0.0553	0.0380	0.0361	0.0346
9.250	—	—	—	0.0402	0.0383	0.0368
9.500	—	—	—	0.0425	0.0406	0.0390
9.750	—	—	—	0.0447	0.0428	0.0412
10.000	—	—	—	0.0469	0.0449	0.0434
10.250	—	—	—	0.0489	0.0470	0.0455
10.500	—	—	—	0.0508	0.0490	0.0475
10.750	—	—	—	0.0526	0.0509	0.0495
11.000	—	—	—	0.0541	0.0526	0.0513
11.250	—	—	—	—	0.0541	0.0528

$$F_r = 1 + \frac{b}{\sqrt{h_w p_f}}$$

Orifice Diameter, d_o (in.)	Internal Diameter of Pipe, d_i , in.								
	20			24			30		
	18.814	19.000	19.250	22.626	23.000	23.250	28.628	29.000	29.250
0.250	—	—	—	—	—	—	—	—	—
0.375	—	—	—	—	—	—	—	—	—
0.500	—	—	—	—	—	—	—	—	—
0.625	—	—	—	—	—	—	—	—	—
0.750	—	—	—	—	—	—	—	—	—
0.875	—	—	—	—	—	—	—	—	—
1.000	—	—	—	—	—	—	—	—	—
1.125	—	—	—	—	—	—	—	—	—
1.250	—	—	—	—	—	—	—	—	—
1.375	—	—	—	—	—	—	—	—	—
1.500	—	—	—	—	—	—	—	—	—
1.625	—	—	—	—	—	—	—	—	—
1.750	—	—	—	—	—	—	—	—	—
1.875	—	—	—	—	—	—	—	—	—
2.000	0.0667	0.0671	0.0676	—	—	—	—	—	—
2.125	0.0640	0.0644	0.0649	—	—	—	—	—	—
2.250	0.0614	0.0618	0.0622	—	—	—	—	—	—
2.375	0.0588	0.0592	0.0597	0.0659	0.0665	0.0669	—	—	—
2.500	0.0563	0.0568	0.0573	0.0636	0.0642	0.0646	—	—	—
2.625	0.0540	0.0544	0.0549	0.0614	0.0620	0.0624	—	—	—
2.750	0.0517	0.0521	0.0526	0.0592	0.0599	0.0603	—	—	—
2.875	0.0494	0.0499	0.0504	0.0571	0.0578	0.0582	0.0662	—	—
3.000	0.0473	0.0477	0.0483	0.0551	0.0557	0.0562	0.0644	0.0649	0.0652
3.125	0.0452	0.0457	0.0462	0.0531	0.0538	0.0542	0.0626	0.0631	0.0634
3.250	0.0433	0.0437	0.0442	0.0511	0.0520	0.0523	0.0608	0.0613	0.0616
3.375	0.0414	0.0418	0.0423	0.0493	0.0500	0.0504	0.0590	0.0596	0.0599
3.500	0.0395	0.0399	0.0405	0.0474	0.0481	0.0486	0.0574	0.0579	0.0582
3.625	0.0378	0.0382	0.0387	0.0457	0.0464	0.0468	0.0557	0.0562	0.0566
3.750	0.0361	0.0365	0.0370	0.0440	0.0447	0.0451	0.0541	0.0546	0.0550
3.875	0.0345	0.0349	0.0354	0.0423	0.0430	0.0435	0.0525	0.0530	0.0534
4.000	0.0329	0.0333	0.0339	0.0407	0.0414	0.0419	0.0509	0.0515	0.0518
4.250	0.0301	0.0304	0.0310	0.0376	0.0384	0.0388	0.0479	0.0485	0.0488
4.500	0.0275	0.0279	0.0283	0.0348	0.0355	0.0360	0.0450	0.0456	0.0460
4.750	0.0252	0.0256	0.0260	0.0322	0.0328	0.0333	0.0423	0.0429	0.0433
5.000	0.0232	0.0235	0.0239	0.0297	0.0304	0.0308	0.0397	0.0403	0.0407
5.250	0.0214	0.0217	0.0220	0.0275	0.0281	0.0285	0.0373	0.0378	0.0382
5.500	0.0199	0.0201	0.0204	0.0254	0.0260	0.0264	0.0349	0.0355	0.0359
5.750	0.0186	0.0188	0.0191	0.0236	0.0241	0.0245	0.0327	0.0333	0.0337
6.000	0.0176	0.0177	0.0179	0.0219	0.0224	0.0228	0.0306	0.0312	0.0316
6.250	0.0167	0.0168	0.0170	0.0204	0.0208	0.0212	0.0287	0.0292	0.0296
6.500	0.0161	0.0162	0.0163	0.0191	0.0195	0.0198	0.0269	0.0274	0.0277
6.750	0.0157	0.0157	0.0157	0.0179	0.0183	0.0185	0.0252	0.0257	0.0260
7.000	0.0155	0.0155	0.0154	0.0169	0.0172	0.0174	0.0236	0.0240	0.0244
7.250	0.0155	0.0154	0.0153	0.0161	0.0163	0.0165	0.0221	0.0226	0.0229
7.500	0.0157	0.0155	0.0154	0.0154	0.0156	0.0157	0.0208	0.0212	0.0215
7.750	0.0160	0.0158	0.0156	0.0148	0.0150	0.0151	0.0195	0.0199	0.0202
8.000	0.0166	0.0163	0.0160	0.0144	0.0145	0.0146	0.0184	0.0187	0.0190
8.250	0.0172	0.0169	0.0165	0.0142	0.0142	0.0142	0.0174	0.0177	0.0179
8.500	0.0180	0.0177	0.0172	0.0141	0.0140	0.0140	0.0164	0.0168	0.0170
8.750	0.0190	0.0186	0.0180	0.0141	0.0140	0.0139	0.0156	0.0159	0.0161
9.000	0.0201	0.0196	0.0190	0.0143	0.0141	0.0140	0.0149	0.0152	0.0153
9.250	0.0213	0.0208	0.0201	0.0146	0.0143	0.0141	0.0143	0.0145	0.0146
9.500	0.0226	0.0220	0.0213	0.0150	0.0146	0.0144	0.0138	0.0139	0.0141
9.750	0.0240	0.0234	0.0226	0.0155	0.0150	0.0147	0.0133	0.0135	0.0136
10.000	0.0256	0.0249	0.0240	0.0161	0.0155	0.0152	0.0130	0.0131	0.0132
10.250	0.0271	0.0264	0.0255	0.0168	0.0162	0.0158	0.0128	0.0128	0.0128
10.500	0.0288	0.0280	0.0270	0.0176	0.0169	0.0164	0.0126	0.0126	0.0126
10.750	0.0305	0.0297	0.0286	0.0185	0.0176	0.0172	0.0125	0.0125	0.0125
11.000	0.0322	0.0314	0.0303	0.0194	0.0186	0.0181	0.0125	0.0124	0.0124
11.250	0.0340	0.0332	0.0320	0.0205	0.0196	0.0190	0.0126	0.0125	0.0124
11.500	0.0358	0.0349	0.0338	0.0216	0.0207	0.0200	0.0128	0.0126	0.0125
11.750	0.0376	0.0367	0.0355	0.0228	0.0218	0.0211	0.0130	0.0128	0.0127
12.000	0.0394	0.0385	0.0373	0.0241	0.0230	0.0223	0.0134	0.0131	0.0129
12.500	0.0429	0.0420	0.0408	0.0267	0.0255	0.0248	0.0142	0.0138	0.0136
13.000	0.0463	0.0454	0.0442	0.0296	0.0282	0.0274	0.0153	0.0148	0.0145
13.500	0.0494	0.0485	0.0474	0.0326	0.0311	0.0302	0.0166	0.0160	0.0157
14.000	0.0520	0.0512	0.0502	0.0356	0.0341	0.0331	0.0182	0.0175	0.0171
14.500	—	—	—	0.0386	0.0370	0.0360	0.0199	0.0192	0.0187
15.000	—	—	—	0.0415	0.0400	0.0390	0.0218	0.0209	0.0204
15.500	—	—	—	0.0443	0.0428	0.0418	0.0239	0.0230	0.0224
16.000	—	—	—	0.0470	0.0455	0.0446	0.0260	0.0250	0.0244
16.500	—	—	—	0.0494	0.0480	0.0471	0.0283	0.0273	0.0266
17.000	—	—	—	—	0.0503	0.0494	0.0307	0.0296	0.0288
17.500	—	—	—	—	—	—	0.0331	0.0319	0.0312
18.000	—	—	—	—	—	—	0.0355	0.0343	0.0335
18.500	—	—	—	—	—	—	0.0379	0.0366	0.0358
19.000	—	—	—	—	—	—	0.0402	0.0390	0.0382
19.500	—	—	—	—	—	—	0.0424	0.0412	0.0404
20.000	—	—	—	—	—	—	0.0446	0.0434	0.0426
20.500	—	—	—	—	—	—	0.0466	0.0455	0.0448
21.000	—	—	—	—	—	—	0.0485	0.0475	0.0467
21.500	—	—	—	—	—	—	—	0.0492	0.0485

TABLE 13.1g—*b* VALUES FOR REYNOLDS NUMBER FACTOR, F_r , FLANGE TAPS (continued)
$$F_r = 1 + \frac{b}{\sqrt{h_w p_f}}$$

Internal Diameter of Pipe, d_i , in.

F_d	2			3				4			
	1.689	1.939	2.067	2.300	2.626	2.900	3.068	3.152	3.438	3.826	4.026
0.10	0.1062	0.1027	0.1012	0.0987	0.0958	0.0928	0.0927	0.0921	0.0905	0.0886	0.0877
0.11	0.1020	0.0985	0.0970	0.0945	0.0916	0.0896	0.0885	0.0880	0.0863	0.0844	0.0835
0.12	0.0981	0.0945	0.0930	0.0905	0.0876	0.0856	0.0845	0.0840	0.0823	0.0804	0.0795
0.13	0.0943	0.0907	0.0892	0.0867	0.0838	0.0818	0.0807	0.0802	0.0785	0.0766	0.0757
0.14	0.0906	0.0871	0.0856	0.0831	0.0802	0.0782	0.0771	0.0765	0.0749	0.0730	0.0721
0.15	0.0872	0.0837	0.0822	0.0797	0.0768	0.0748	0.0736	0.0731	0.0715	0.0696	0.0687
0.16	0.0840	0.0805	0.0789	0.0764	0.0736	0.0715	0.0704	0.0699	0.0682	0.0663	0.0654
0.17	0.0809	0.0774	0.0759	0.0734	0.0705	0.0685	0.0673	0.0668	0.0652	0.0633	0.0624
0.18	0.0780	0.0745	0.0730	0.0705	0.0676	0.0656	0.0645	0.0639	0.0623	0.0604	0.0595
0.19	0.0753	0.0718	0.0703	0.0678	0.0649	0.0629	0.0617	0.0612	0.0596	0.0577	0.0568
0.20	0.0728	0.0693	0.0677	0.0653	0.0624	0.0603	0.0592	0.0587	0.0570	0.0551	0.0542
0.21	0.0703	0.0668	0.0652	0.0628	0.0599	0.0579	0.0567	0.0562	0.0546	0.0527	0.0518
0.22	0.0681	0.0646	0.0630	0.0606	0.0577	0.0556	0.0545	0.0540	0.0524	0.0505	0.0496
0.23	0.0660	0.0625	0.0610	0.0585	0.0556	0.0536	0.0525	0.0520	0.0503	0.0484	0.0475
0.24	0.0642	0.0606	0.0591	0.0566	0.0538	0.0517	0.0506	0.0501	0.0484	0.0465	0.0457
0.25	0.0624	0.0589	0.0574	0.0549	0.0520	0.0500	0.0489	0.0483	0.0467	0.0448	0.0439
0.26	0.0607	0.0572	0.0557	0.0532	0.0504	0.0483	0.0472	0.0467	0.0451	0.0431	0.0423
0.27	0.0593	0.0558	0.0543	0.0518	0.0489	0.0469	0.0458	0.0452	0.0436	0.0417	0.0408
0.28	0.0580	0.0545	0.0530	0.0505	0.0476	0.0456	0.0445	0.0440	0.0423	0.0404	0.0395
0.29	0.0569	0.0534	0.0518	0.0494	0.0465	0.0444	0.0433	0.0428	0.0412	0.0393	0.0384
0.30	0.0559	0.0524	0.0508	0.0484	0.0455	0.0434	0.0423	0.0418	0.0402	0.0383	0.0374
0.31	0.0549	0.0514	0.0499	0.0474	0.0445	0.0425	0.0414	0.0409	0.0392	0.0373	0.0364
0.32	0.0541	0.0506	0.0491	0.0467	0.0438	0.0417	0.0406	0.0401	0.0385	0.0366	0.0357
0.33	0.0534	0.0499	0.0484	0.0460	0.0431	0.0411	0.0399	0.0394	0.0378	0.0359	0.0350
0.34	0.0529	0.0495	0.0479	0.0455	0.0426	0.0406	0.0395	0.0389	0.0373	0.0354	0.0345
0.35	0.0525	0.0490	0.0475	0.0450	0.0422	0.0401	0.0390	0.0385	0.0369	0.0350	0.0341
0.36	0.0521	0.0487	0.0471	0.0447	0.0418	0.0398	0.0387	0.0382	0.0366	0.0347	0.0338
0.37	0.0520	0.0485	0.0470	0.0446	0.0417	0.0397	0.0386	0.0380	0.0364	0.0345	0.0337
0.38	0.0519	0.0484	0.0469	0.0445	0.0416	0.0396	0.0385	0.0380	0.0363	0.0344	0.0336
0.39	0.0520	0.0485	0.0470	0.0445	0.0417	0.0397	0.0386	0.0380	0.0364	0.0345	0.0337
0.40	0.0521	0.0486	0.0471	0.0446	0.0418	0.0398	0.0387	0.0382	0.0365	0.0346	0.0338
0.41	0.0523	0.0488	0.0473	0.0449	0.0420	0.0400	0.0389	0.0384	0.0368	0.0349	0.0340
0.42	0.0526	0.0491	0.0476	0.0452	0.0423	0.0403	0.0392	0.0387	0.0371	0.0352	0.0343
0.43	0.0530	0.0495	0.0480	0.0456	0.0427	0.0407	0.0396	0.0391	0.0375	0.0356	0.0348
0.44	0.0534	0.0500	0.0485	0.0461	0.0432	0.0412	0.0401	0.0396	0.0380	0.0361	0.0353
0.45	0.0540	0.0506	0.0490	0.0466	0.0438	0.0418	0.0407	0.0402	0.0386	0.0367	0.0359
0.46	0.0546	0.0512	0.0497	0.0473	0.0445	0.0425	0.0414	0.0409	0.0393	0.0374	0.0365
0.47	0.0553	0.0519	0.0504	0.0479	0.0451	0.0431	0.0421	0.0415	0.0400	0.0381	0.0372
0.48	0.0561	0.0527	0.0512	0.0488	0.0459	0.0440	0.0429	0.0424	0.0408	0.0389	0.0380
0.49	0.0569	0.0535	0.0520	0.0496	0.0468	0.0448	0.0437	0.0432	0.0416	0.0397	0.0389
0.50	0.0578	0.0544	0.0529	0.0505	0.0477	0.0457	0.0446	0.0441	0.0426	0.0407	0.0398
0.51	0.0587	0.0553	0.0538	0.0514	0.0486	0.0467	0.0456	0.0451	0.0435	0.0417	0.0408
0.52	0.0598	0.0564	0.0549	0.0525	0.0497	0.0478	0.0467	0.0462	0.0446	0.0427	0.0419
0.53	0.0608	0.0574	0.0559	0.0535	0.0508	0.0488	0.0477	0.0472	0.0457	0.0438	0.0430
0.54	0.0617	0.0584	0.0569	0.0546	0.0518	0.0498	0.0488	0.0483	0.0467	0.0449	0.0440
0.55	0.0629	0.0595	0.0580	0.0557	0.0529	0.0510	0.0499	0.0494	0.0479	0.0460	0.0452
0.56	0.0639	0.0606	0.0591	0.0568	0.0540	0.0521	0.0511	0.0506	0.0490	0.0472	0.0464
0.57	0.0651	0.0618	0.0603	0.0580	0.0553	0.0534	0.0523	0.0518	0.0503	0.0484	0.0476
0.58	0.0663	0.0630	0.0615	0.0592	0.0565	0.0545	0.0535	0.0530	0.0515	0.0496	0.0488
0.59	0.0675	0.0642	0.0628	0.0605	0.0578	0.0558	0.0548	0.0543	0.0528	0.0510	0.0501
0.60	0.0687	0.0654	0.0640	0.0617	0.0590	0.0571	0.0560	0.0556	0.0540	0.0522	0.0514
0.61	0.0698	0.0666	0.0651	0.0628	0.0602	0.0583	0.0572	0.0567	0.0552	0.0534	0.0526
0.62	0.0711	0.0678	0.0664	0.0641	0.0614	0.0595	0.0585	0.0580	0.0565	0.0548	0.0539
0.63	0.0722	0.0690	0.0676	0.0653	0.0626	0.0608	0.0597	0.0593	0.0578	0.0560	0.0552
0.64	0.0733	0.0701	0.0687	0.0665	0.0638	0.0620	0.0610	0.0605	0.0590	0.0572	0.0564
0.65	0.0745	0.0713	0.0699	0.0677	0.0651	0.0632	0.0622	0.0617	0.0602	0.0585	0.0577
0.66	0.0756	0.0724	0.0710	0.0688	0.0662	0.0643	0.0633	0.0629	0.0614	0.0597	0.0589
0.67	0.0766	0.0735	0.0721	0.0699	0.0673	0.0655	0.0645	0.0640	0.0626	0.0608	0.0601
0.68	0.0777	0.0745	0.0732	0.0710	0.0684	0.0666	0.0656	0.0652	0.0637	0.0620	0.0612
0.69	0.0786	0.0755	0.0741	0.0720	0.0694	0.0676	0.0667	0.0662	0.0648	0.0631	0.0623
0.70	0.0795	0.0765	0.0751	0.0730	0.0704	0.0687	0.0677	0.0672	0.0658	0.0641	0.0634
0.71	0.0803	0.0773	0.0759	0.0738	0.0713	0.0695	0.0686	0.0681	0.0667	0.0651	0.0643
0.72	0.0811	0.0781	0.0768	0.0747	0.0722	0.0704	0.0695	0.0690	0.0676	0.0660	0.0652
0.73	0.0818	0.0789	0.0776	0.0755	0.0730	0.0713	0.0704	0.0699	0.0685	0.0669	0.0662
0.74	0.0825	0.0795	0.0782	0.0762	0.0738	0.0721	0.0711	0.0707	0.0693	0.0677	0.0670
0.75	0.0829	0.0800	0.0788	0.0767	0.0743	0.0726	0.0718	0.0713	0.0699	0.0683	0.0677

$$F_r = 1 + \frac{b}{\sqrt{h_w p_f}}$$

	6				8				10				12		
F_d	4.897	5.189	5.761	6.065	7.625	7.981	8.071	9.564	10.020	10.136	11.376	11.938	12.090		
0.10	0.0859	0.0846	0.0825	0.0815	0.0777	0.0771	0.0769	0.0747	0.0742	0.0741	0.0729	0.0724	0.0725		
0.11	0.0818	0.0805	0.0783	0.0773	0.0736	0.0729	0.0727	0.0706	0.0700	0.0699	0.0687	0.0682	0.0681		
0.12	0.0777	0.0764	0.0742	0.0732	0.0695	0.0688	0.0687	0.0665	0.0660	0.0658	0.0646	0.0642	0.0640		
0.13	0.0738	0.0725	0.0703	0.0694	0.0656	0.0649	0.0648	0.0626	0.0621	0.0619	0.0607	0.0603	0.0602		
0.14	0.0701	0.0688	0.0666	0.0657	0.0619	0.0612	0.0611	0.0589	0.0584	0.0583	0.0571	0.0566	0.0565		
0.15	0.0666	0.0653	0.0631	0.0622	0.0584	0.0578	0.0576	0.0554	0.0549	0.0548	0.0536	0.0531	0.0530		
0.16	0.0633	0.0620	0.0598	0.0589	0.0551	0.0545	0.0543	0.0522	0.0516	0.0515	0.0503	0.0498	0.0497		
0.17	0.0601	0.0589	0.0567	0.0558	0.0520	0.0514	0.0512	0.0491	0.0485	0.0484	0.0472	0.0467	0.0466		
0.18	0.0571	0.0558	0.0537	0.0527	0.0490	0.0484	0.0482	0.0461	0.0455	0.0454	0.0442	0.0438	0.0436		
0.19	0.0544	0.0531	0.0510	0.0500	0.0463	0.0456	0.0455	0.0433	0.0428	0.0427	0.0415	0.0410	0.0409		
0.20	0.0517	0.0504	0.0483	0.0474	0.0436	0.0430	0.0428	0.0407	0.0402	0.0401	0.0389	0.0384	0.0383		
0.21	0.0492	0.0480	0.0459	0.0449	0.0412	0.0405	0.0404	0.0383	0.0377	0.0376	0.0364	0.0360	0.0359		
0.22	0.0469	0.0457	0.0436	0.0426	0.0389	0.0383	0.0381	0.0360	0.0355	0.0353	0.0342	0.0337	0.0336		
0.23	0.0448	0.0435	0.0414	0.0405	0.0368	0.0362	0.0360	0.0339	0.0334	0.0333	0.0321	0.0316	0.0315		
0.24	0.0428	0.0416	0.0395	0.0385	0.0349	0.0342	0.0341	0.0320	0.0314	0.0313	0.0302	0.0297	0.0296		
0.25	0.0410	0.0398	0.0377	0.0367	0.0331	0.0324	0.0323	0.0302	0.0297	0.0296	0.0284	0.0279	0.0278		
0.26	0.0393	0.0381	0.0360	0.0350	0.0314	0.0308	0.0306	0.0285	0.0280	0.0279	0.0267	0.0263	0.0262		
0.27	0.0378	0.0366	0.0345	0.0336	0.0299	0.0293	0.0292	0.0271	0.0266	0.0264	0.0253	0.0248	0.0247		
0.28	0.0365	0.0352	0.0332	0.0322	0.0286	0.0280	0.0278	0.0258	0.0252	0.0251	0.0240	0.0235	0.0234		
0.29	0.0352	0.0340	0.0319	0.0310	0.0274	0.0268	0.0266	0.0245	0.0240	0.0239	0.0228	0.0223	0.0222		
0.30	0.0341	0.0328	0.0308	0.0299	0.0263	0.0257	0.0255	0.0235	0.0230	0.0228	0.0217	0.0213	0.0211		
0.31	0.0331	0.0319	0.0298	0.0289	0.0254	0.0247	0.0246	0.0225	0.0220	0.0219	0.0208	0.0203	0.0202		
0.32	0.0322	0.0310	0.0290	0.0280	0.0245	0.0239	0.0237	0.0217	0.0212	0.0211	0.0199	0.0195	0.0194		
0.33	0.0314	0.0302	0.0282	0.0273	0.0238	0.0232	0.0230	0.0210	0.0205	0.0204	0.0192	0.0188	0.0187		
0.34	0.0308	0.0296	0.02												

$$F_r = 1 + \frac{b}{\sqrt{h_w p_t}}$$

Orifice Diameter, d_o , (in.)	Internal Diameter of Pipe, d_i , in.								
	10			12			16		
	9.564	10.020	10.136	11.376	11.938	12.090	14.688	15.000	15.250
1.000	0.0728	—	—	—	—	—	—	—	—
1.125	0.0674	0.0690	0.0694	—	—	—	—	—	—
1.250	0.0624	0.0641	0.0646	0.0687	0.0704	0.0708	—	—	—
1.375	0.0576	0.0594	0.0599	0.0643	0.0661	0.0666	—	—	—
1.500	0.0532	0.0550	0.0555	0.0601	0.0620	0.0625	0.0697	0.0705	—
1.625	0.0490	0.0509	0.0514	0.0561	0.0580	0.0585	0.0662	0.0670	0.0676
1.750	0.0452	0.0471	0.0476	0.0523	0.0543	0.0548	0.0628	0.0636	0.0642
1.875	0.0417	0.0436	0.0440	0.0488	0.0508	0.0513	0.0594	0.0603	0.0610
2.000	0.0385	0.0403	0.0407	0.0454	0.0475	0.0480	0.0563	0.0572	0.0578
2.125	0.0355	0.0372	0.0377	0.0423	0.0443	0.0449	0.0532	0.0541	0.0548
2.250	0.0329	0.0345	0.0349	0.0394	0.0414	0.0419	0.0503	0.0512	0.0519
2.375	0.0305	0.0320	0.0324	0.0367	0.0387	0.0392	0.0475	0.0484	0.0492
2.500	0.0283	0.0298	0.0301	0.0342	0.0361	0.0366	0.0449	0.0458	0.0466
2.625	0.0265	0.0277	0.0281	0.0319	0.0337	0.0342	0.0424	0.0433	0.0440
2.750	0.0248	0.0260	0.0262	0.0298	0.0316	0.0320	0.0400	0.0409	0.0417
2.875	0.0234	0.0244	0.0246	0.0279	0.0295	0.0300	0.0378	0.0387	0.0394
3.000	0.0222	0.0230	0.0232	0.0262	0.0277	0.0281	0.0356	0.0365	0.0372
3.125	0.0212	0.0218	0.0220	0.0244	0.0260	0.0264	0.0336	0.0345	0.0352
3.250	0.0204	0.0209	0.0210	0.0232	0.0245	0.0249	0.0317	0.0326	0.0332
3.375	0.0199	0.0201	0.0202	0.0220	0.0232	0.0235	0.0300	0.0308	0.0314
3.500	0.0195	0.0195	0.0196	0.0210	0.0220	0.0222	0.0283	0.0291	0.0297
3.625	0.0193	0.0191	0.0191	0.0200	0.0209	0.0212	0.0268	0.0275	0.0281
3.750	0.0192	0.0188	0.0188	0.0193	0.0200	0.0202	0.0254	0.0261	0.0267
3.875	0.0193	0.0187	0.0186	0.0187	0.0192	0.0194	0.0240	0.0247	0.0253
4.000	0.0195	0.0187	0.0186	0.0182	0.0185	0.0187	0.0228	0.0235	0.0240
4.250	0.0203	0.0192	0.0189	0.0176	0.0176	0.0177	0.0207	0.0213	0.0217
4.500	0.0215	0.0200	0.0197	0.0175	0.0172	0.0171	0.0190	0.0194	0.0198
4.750	0.0230	0.0212	0.0208	0.0178	0.0171	0.0170	0.0176	0.0180	0.0182
5.000	0.0248	0.0228	0.0223	0.0185	0.0174	0.0173	0.0166	0.0168	0.0170
5.250	0.0267	0.0244	0.0239	0.0195	0.0181	0.0178	0.0160	0.0161	0.0162
5.500	0.0287	0.0263	0.0257	0.0207	0.0190	0.0186	0.0156	0.0156	0.0156
5.750	0.0307	0.0282	0.0276	0.0221	0.0202	0.0197	0.0155	0.0154	0.0153
6.000	0.0326	0.0302	0.0295	0.0231	0.0215	0.0210	0.0157	0.0154	0.0153
6.250	0.0343	0.0320	0.0316	0.0253	0.0230	0.0224	0.0161	0.0157	0.0154
6.500	0.0358	0.0336	0.0331	0.0270	0.0246	0.0239	0.0167	0.0162	0.0159
6.750	—	0.0351	0.0346	0.0288	0.0262	0.0256	0.0174	0.0169	0.0164
7.000	—	0.0363	0.0359	0.0304	0.0279	0.0272	0.0184	0.0177	0.0172
7.250	—	—	—	0.0320	0.0295	0.0288	0.0195	0.0187	0.0181
7.500	—	—	—	0.0334	0.0310	0.0304	0.0206	0.0198	0.0191
7.750	—	—	—	0.0347	0.0325	0.0318	0.0219	0.0209	0.0202
8.000	—	—	—	—	0.0338	0.0332	0.0232	0.0222	0.0214
8.250	—	—	—	—	0.0349	0.0344	0.0246	0.0235	0.0227
8.500	—	—	—	—	—	—	0.0259	0.0248	0.0240
8.750	—	—	—	—	—	—	0.0273	0.0262	0.0253
9.000	—	—	—	—	—	—	0.0286	0.0276	0.0267
9.250	—	—	—	—	—	—	0.0299	0.0288	0.0280
9.500	—	—	—	—	—	—	0.0311	0.0300	0.0292
9.750	—	—	—	—	—	—	0.0322	0.0312	0.0304
10.000	—	—	—	—	—	—	0.0332	0.0323	0.0315
10.250	—	—	—	—	—	—	0.0341	0.0333	0.0326
10.500	—	—	—	—	—	—	—	0.0341	0.0333

TABLE 13.1h—*b* VALUES FOR REYNOLDS NUMBER FACTOR, F_r , PIPE TAPS (continued)
$$F_r = 1 + \frac{b}{\sqrt{h_w p_t}}$$

Orifice Diameter, d_o , (in.)	Internal Diameter of Pipe, d_i , in.								
	20			24			30		
	18.814	19.000	19.250	22.626	23.000	23.250	28.628	29.000	29.250
2.000	0.0663	0.0667	0.0672	—	—	—	—	—	—
2.125	0.0635	0.0639	0.0644	—	—	—	—	—	—
2.250	0.0609	0.0613	0.0618	—	—	—	—	—	—
2.375	0.0583	0.0588	0.0593	0.0658	0.0665	0.0669	—	—	—
2.500	0.0558	0.0562	0.0568	0.0635	0.0642	0.0646	—	—	—
2.625	0.0534	0.0539	0.0544	0.0613	0.0620	0.0624	—	—	—
2.750	0.0510	0.0515	0.0520	0.0591	0.0598	0.0603	—	—	—
2.875	0.0488	0.0492	0.0498	0.0570	0.0577	0.0582	0.0667	—	—
3.000	0.0466	0.0470	0.0476	0.0549	0.0556	0.0561	0.0649	0.0654	0.0657
3.125	0.0445	0.0449	0.0455	0.0529	0.0536	0.0541	0.0630	0.0636	0.0639
3.250	0.0425	0.0429	0.0435	0.0509	0.0516	0.0521	0.0613	0.0616	0.0622
3.375	0.0406	0.0410	0.0416	0.0490	0.0497	0.0502	0.0595	0.0601	0.0604
3.500	0.0387	0.0391	0.0397	0.0471	0.0479	0.0484	0.0578	0.0584	0.0587
3.625	0.0369	0.0373	0.0379	0.0454	0.0461	0.0466	0.0561	0.0567	0.0571
3.750	0.0352	0.0356	0.0362	0.0436	0.0444	0.0449	0.0545	0.0550	0.0554
3.875	0.0336	0.0340	0.0346	0.0419	0.0427	0.0432	0.0528	0.0534	0.0538
4.000	0.0320	0.0324	0.0330	0.0403	0.0411	0.0416	0.0513	0.0518	0.0522
4.250	0.0291	0.0295	0.0301	0.0372	0.0380	0.0385	0.0482	0.0488	0.0492
4.500	0.0265	0.0269	0.0274	0.0343	0.0351	0.0356	0.0453	0.0459	0.0463
4.750	0.0242	0.0246	0.0250	0.0316	0.0324	0.0328	0.0425	0.0431	0.0435
5.000	0.0221	0.0225	0.0229	0.0292	0.0299	0.0303	0.0399	0.0405	0.0409
5.250	0.0203	0.0206	0.0210	0.0269	0.0276	0.0280	0.0374	0.0380	0.0384
5.500	0.0188	0.0190	0.0194	0.0248	0.0255	0.0259	0.0350	0.0356	0.0360
5.750	0.0175	0.0177	0.0180	0.0230	0.0236	0.0240	0.0328	0.0334	0.0338
6.000	0.0164	0.0165	0.0168	0.0212	0.0218	0.0222	0.0307	0.0313	0.0317
6.250	0.0155	0.0156	0.0158	0.0197	0.0202	0.0206	0.0287	0.0293	0.0297
6.500	0.0148	0.0149	0.0150	0.0184	0.0189	0.0192	0.0269	0.0274	0.0278
6.750	0.0143	0.0144	0.0145	0.0172	0.0176	0.0179	0.0252	0.0257	0.0260
7.000	0.0141	0.0141	0.0141	0.0162	0.0166	0.0168	0.0236	0.0241	0.0244
7.250	0.0140	0.0140	0.0139	0.0153	0.0156	0.0158	0.0221	0.0226	0.0229
7.500	0.0140	0.0140	0.0139	0.0146	0.0148	0.0150	0.0207	0.0212	0.0215
7.750	0.0142	0.0141	0.0140	0.0140	0.0142	0.0144	0.0195	0.0199	0.0202
8.000	0.0146	0.0144	0.0142	0.0136	0.0138	0.0138	0.0183	0.0187	0.0190
8.250	0.0151	0.0148	0.0146	0.0133	0.0134	0.0132	0.0173	0.0177	0.0179
8.500	0.0156	0.0154	0.0151	0.0132	0.0132	0.0130	0.0164	0.0167	0.0169
8.750	0.0163	0.0160	0.0157	0.0131	0.0130	0.0130	0.0155	0.0158	0.0161
9.000	0.0171	0.0168	0.0163	0.0131	0.0130	0.0130	0.0148	0.0151	0.0153
9.250	0.0180	0.0176	0.0171	0.0133	0.0131	0.0130	0.0142	0.0144	0.0146
9.500	0.0189	0.0185	0.0180	0.0136	0.0133	0.0132	0.0136	0.0138	0.0140
9.750	0.0198	0.0194	0.0189	0.0139	0.0136	0.0134	0.0132	0.0133	0.0134
10.000	0.0209	0.0204	0.0198	0.0143	0.0140	0.0138	0.0128	0.0129	0.0130
10.250	0.0219	0.0214	0.0208	0.0148	0.0144	0.0142	0.0125	0.0126	0.0127
10.500	0.0230	0.0225	0.0219	0.0154	0.0150	0.0147	0.0123	0.0124	0.0124
10.750	0.0241	0.0236	0.0229	0.0160	0.0155	0.0152	0.0122	0.0122	0.0122
11.000	0.0252	0.0247	0.0240	0.0168	0.0162	0.0158	0.0121	0.0121	0.0121
11.250	0.0263	0.0261	0.0251	0.0175	0.0169	0.0165	0.0122	0.0121	0.0121
11.500	0.0273	0.0268	0.0262	0.0183	0.0176	0.0172	0.0122	0.0121	0.0122
11.750	0.0284	0.0278	0.0272	0.0191	0.0184	0.0180	0.0124	0.0123	0.0122
12.000	0.0293	0.0288	0.0282	0.0200	0.0192	0.0190	0.0126	0.0124	0.0123
12.500	0.0312	0.0307	0.0301	0.0218	0.0210	0.0204	0.0132	0.0130	0.0128
13.000	0.0327	0.0323	0.0318	0.0236	0.0228	0.0222	0.0140	0.0137	0.0135
13.500	—	—	—	0.0254	0.0246	0.0240	0.0150	0.0146	0.0143
14.000	—	—	—	0.0272	0.0264	0.0258	0.0161	0.0156	0.0153
14.500	—	—	—	0.0289	0.0280	0.0275	0.0173	0.0168	0.0165
15.000	—	—	—	0.0304	0.0296	0.0291	0.0186	0.0181	0.0177
15.500	—	—	—	0.0318	0.0311	0.0306	0.0200	0.0194	0.0190
16.000	—	—	—	—	0.0323	0.0318	0.0215	0.0209	0.0204
16.500	—	—	—	—	—	—	0.0230	0.0223	0.0219
17.000	—	—	—	—	—	—	0.0244	0.0238	0.0233
17.500	—	—	—	—	—	—	0.0259	0.0252	0.0248
18.000	—	—	—	—	—	—	0.0272	0.0266	0.0261
18.500	—	—	—	—	—	—	0.0286	0.0279	0.0275
19.000	—	—	—	—	—	—	0.0298	0.0292	0.0288
19.500	—	—	—	—	—	—	0.0309	0.0303	0.0299
20.000	—	—	—	—	—	—	0.0318	0.0313	0.0310

TABLE 13.1h—b VALUES FOR REYNOLDS NUMBER FACTOR, F_r , PIPE TAPS (continued)
$$F_r = 1 + \frac{b}{\sqrt{h_w \rho_i}}$$

Internal Diameter of Pipe, d_i , in.

F_d	2			3				4			
	1.689	1.939	2.067	2.300	2.626	2.900	3.068	3.152	3.438	3.826	4.026
0.10	0.1295	0.1209	0.1173	0.1118	0.1058	0.1017	0.0996	0.0986	0.0957	0.0924	0.0909
0.11	0.1253	0.1167	0.1132	0.1077	0.1016	0.0976	0.0954	0.0945	0.0915	0.0882	0.0867
0.12	0.1212	0.1126	0.1090	0.1035	0.0975	0.0934	0.0913	0.0903	0.0874	0.0841	0.0826
0.13	0.1172	0.1086	0.1051	0.0996	0.0935	0.0895	0.0874	0.0864	0.0835	0.0802	0.0787
0.14	0.1134	0.1049	0.1013	0.0958	0.0898	0.0858	0.0837	0.0827	0.0797	0.0765	0.0750
0.15	0.1098	0.1013	0.0978	0.0923	0.0863	0.0823	0.0801	0.0792	0.0762	0.0729	0.0715
0.16	0.1065	0.0980	0.0944	0.0889	0.0829	0.0789	0.0768	0.0758	0.0729	0.0696	0.0682
0.17	0.1033	0.0948	0.0912	0.0856	0.0798	0.0758	0.0737	0.0727	0.0698	0.0665	0.0650
0.18	0.1001	0.0916	0.0881	0.0827	0.0767	0.0727	0.0706	0.0696	0.0667	0.0634	0.0620
0.19	0.0973	0.0888	0.0853	0.0799	0.0739	0.0699	0.0678	0.0669	0.0639	0.0607	0.0592
0.20	0.0945	0.0861	0.0825	0.0771	0.0712	0.0672	0.0651	0.0642	0.0613	0.0580	0.0566
0.21	0.0919	0.0835	0.0800	0.0746	0.0687	0.0647	0.0626	0.0617	0.0588	0.0555	0.0541
0.22	0.0894	0.0811	0.0776	0.0722	0.0663	0.0623	0.0603	0.0593	0.0564	0.0532	0.0518
0.23	0.0872	0.0788	0.0753	0.0700	0.0641	0.0602	0.0581	0.0571	0.0543	0.0510	0.0496
0.24	0.0851	0.0767	0.0733	0.0679	0.0621	0.0581	0.0561	0.0551	0.0523	0.0490	0.0476
0.25	0.0831	0.0748	0.0714	0.0660	0.0602	0.0563	0.0542	0.0533	0.0504	0.0472	0.0458
0.26	0.0812	0.0730	0.0695	0.0642	0.0584	0.0545	0.0524	0.0515	0.0487	0.0455	0.0441
0.27	0.0796	0.0713	0.0679	0.0626	0.0568	0.0530	0.0509	0.0500	0.0471	0.0440	0.0426
0.28	0.0781	0.0699	0.0665	0.0612	0.0554	0.0516	0.0495	0.0486	0.0458	0.0426	0.0412
0.29	0.0766	0.0685	0.0651	0.0598	0.0541	0.0502	0.0482	0.0473	0.0445	0.0413	0.0399
0.30	0.0753	0.0672	0.0638	0.0586	0.0529	0.0490	0.0470	0.0461	0.0433	0.0401	0.0388
0.31	0.0741	0.0661	0.0627	0.0575	0.0518	0.0480	0.0460	0.0451	0.0423	0.0391	0.0378
0.32	0.0730	0.0650	0.0616	0.0564	0.0508	0.0470	0.0450	0.0441	0.0413	0.0382	0.0368
0.33	0.0720	0.0640	0.0606	0.0555	0.0499	0.0461	0.0441	0.0432	0.0405	0.0374	0.0360
0.34	0.0712	0.0632	0.0599	0.0548	0.0492	0.0455	0.0435	0.0426	0.0398	0.0368	0.0354
0.35	0.0705	0.0626	0.0593	0.0542	0.0486	0.0449	0.0429	0.0420	0.0393	0.0362	0.0349
0.36	0.0699	0.0620	0.0587	0.0537	0.0481	0.0444	0.0424	0.0416	0.0388	0.0358	0.0345
0.37	0.0693	0.0615	0.0582	0.0532	0.0477	0.0440	0.0421	0.0412	0.0385	0.0355	0.0341
0.38	0.0689	0.0611	0.0578	0.0529	0.0474	0.0437	0.0418	0.0409	0.0382	0.0352	0.0339
0.39	0.0684	0.0607	0.0575	0.0525	0.0471	0.0435	0.0415	0.0407	0.0380	0.0350	0.0337
0.40	0.0681	0.0604	0.0572	0.0523	0.0469	0.0433	0.0414	0.0405	0.0379	0.0349	0.0336
0.41	0.0678	0.0603	0.0571	0.0522	0.0468	0.0432	0.0414	0.0405	0.0379	0.0349	0.0336
0.42	0.0677	0.0602	0.0570	0.0521	0.0468	0.0433	0.0414	0.0405	0.0379	0.0350	0.0337
0.43	0.0676	0.0601	0.0570	0.0522	0.0469	0.0434	0.0415	0.0402	0.0381	0.0352	0.0339
0.44	0.0675	0.0601	0.0570	0.0522	0.0470	0.0435	0.0417	0.0408	0.0382	0.0354	0.0341
0.45	0.0675	0.0602	0.0571	0.0524	0.0472	0.0437	0.0419	0.0410	0.0385	0.0357	0.0344
0.46	0.0676	0.0603	0.0572	0.0526	0.0474	0.0440	0.0422	0.0413	0.0388	0.0360	0.0347
0.47	0.0676	0.0604	0.0574	0.0528	0.0476	0.0442	0.0424	0.0416	0.0391	0.0363	0.0351
0.48	0.0677	0.0606	0.0576	0.0530	0.0479	0.0446	0.0428	0.0420	0.0395	0.0367	0.0355
0.49	0.0678	0.0608	0.0578	0.0532	0.0482	0.0449	0.0431	0.0423	0.0399	0.0372	0.0359
0.50	0.0680	0.0611	0.0581	0.0536	0.0486	0.0453	0.0436	0.0428	0.0404	0.0377	0.0365
0.51	0.0682	0.0613	0.0584	0.0539	0.0490	0.0458	0.0440	0.0433	0.0409	0.0382	0.0370
0.52	0.0684	0.0615	0.0587	0.0543	0.0494	0.0462	0.0445	0.0437	0.0413	0.0387	0.0375
0.53	0.0687	0.0619	0.0590	0.0547	0.0499	0.0467	0.0450	0.0442	0.0419	0.0393	0.0381
0.54	0.0689	0.0622	0.0594	0.0551	0.0503	0.0472	0.0455	0.0448	0.0424	0.0398	0.0387
0.55	0.0692	0.0625	0.0598	0.0555	0.0508	0.0477	0.0460	0.0453	0.0430	0.0404	0.0393
0.56	0.0694	0.0628	0.0601	0.0559	0.0513	0.0482	0.0466	0.0458	0.0435	0.0410	0.0399
0.57	0.0696	0.0632	0.0605	0.0563	0.0517	0.0487	0.0471	0.0464	0.0441	0.0416	0.0405
0.58	0.0699	0.0635	0.0608	0.0567	0.0522	0.0492	0.0476	0.0469	0.0447	0.0422	0.0412
0.59	0.0701	0.0638	0.0612	0.0571	0.0527	0.0497	0.0482	0.0474	0.0453	0.0428	0.0418
0.60	0.0704	0.0641	0.0615	0.0575	0.0532	0.0502	0.0487	0.0480	0.0458	0.0434	0.0424
0.61	0.0705	0.0643	0.0618	0.0578	0.0535	0.0506	0.0491	0.0484	0.0463	0.0439	0.0429
0.62	0.0706	0.0645	0.0620	0.0581	0.0539	0.0510	0.0495	0.0489	0.0468	0.0444	0.0434
0.63	0.0707	0.0648	0.0623	0.0585	0.0543	0.0515	0.0500	0.0493	0.0473	0.0450	0.0440
0.64	0.0708	0.0649	0.0625	0.0587	0.0546	0.0518	0.0504	0.0497	0.0477	0.0454	0.0444
0.65	0.0709	0.0651	0.0627	0.0590	0.0549	0.0522	0.0508	0.0501	0.0481	0.0459	0.0449
0.66	0.0708	0.0651	0.0628	0.0591	0.0551	0.0525	0.0511	0.0504	0.0485	0.0463	0.0453
0.67	0.0708	0.0653	0.0629	0.0594	0.0554	0.0528	0.0514	0.0508	0.0489	0.0467	0.0458
0.68	0.0708	0.0653	0.0630	0.0595	0.0556	0.0531	0.0517	0.0511	0.0492	0.0471	0.0462
0.69	0.0705	0.0652	0.0629	0.0595	0.0557	0.0532	0.0518	0.0512	0.0494	0.0473	0.0464
0.70	0.0704	0.0651	0.0629	0.0595	0.0558	0.0533	0.0520	0.0514	0.0496	0.0476	0.0467

TABLE 13.1h—*b* VALUES FOR REYNOLDS NUMBER FACTOR, F_r , PIPE TAPS (continued)
$$F_r = 1 + \frac{b}{\sqrt{h_w d_i}}$$

Internal Diameter of Pipe, d_i , in.

	6				8			10			12		
F_d	4.897	5.189	5.761	6.065	7.625	7.981	8.071	9.564	10.020	10.136	11.376	11.938	12.090
0.10	0.0845	0.0836	0.0821	0.0814	0.0784	0.0778	0.0777	0.0757	0.0752	0.0751	0.0739	0.0734	0.0733
0.11	0.0803	0.0795	0.0779	0.0772	0.0742	0.0736	0.0735	0.0716	0.0710	0.0709	0.0697	0.0692	0.0691
0.12	0.0763	0.0755	0.0739	0.0732	0.0702	0.0696	0.0695	0.0676	0.0670	0.0669	0.0657	0.0652	0.0651
0.13	0.0725	0.0717	0.0701	0.0694	0.0664	0.0658	0.0657	0.0638	0.0632	0.0631	0.0619	0.0614	0.0613
0.14	0.0689	0.0680	0.0665	0.0658	0.0628	0.0622	0.0621	0.0601	0.0596	0.0595	0.0583	0.0578	0.0577
0.15	0.0655	0.0646	0.0631	0.0624	0.0594	0.0588	0.0587	0.0567	0.0562	0.0561	0.0549	0.0544	0.0543
0.16	0.0623	0.0614	0.0599	0.0591	0.0561	0.0556	0.0554	0.0535	0.0530	0.0528	0.0516	0.0512	0.0510
0.17	0.0592	0.0583	0.0568	0.0561	0.0531	0.0525	0.0524	0.0504	0.0499	0.0498	0.0486	0.0481	0.0480
0.18	0.0563	0.0554	0.0539	0.0532	0.0502	0.0496	0.0495	0.0475	0.0470	0.0469	0.0457	0.0452	0.0451
0.19	0.0536	0.0527	0.0512	0.0505	0.0475	0.0469	0.0468	0.0448	0.0443	0.0442	0.0430	0.0425	0.0424
0.20	0.0511	0.0502	0.0487	0.0479	0.0449	0.0444	0.0442	0.0423	0.0418	0.0416	0.0404	0.0400	0.0398
0.21	0.0486	0.0477	0.0462	0.0455	0.0425	0.0419	0.0418	0.0398	0.0393	0.0392	0.0380	0.0375	0.0374
0.22	0.0464	0.0455	0.0440	0.0433	0.0403	0.0397	0.0396	0.0376	0.0371	0.0370	0.0358	0.0353	0.0352
0.23	0.0444	0.0435	0.0420	0.0412	0.0382	0.0377	0.0375	0.0356	0.0351	0.0350	0.0338	0.0333	0.0332
0.24	0.0425	0.0416	0.0401	0.0393	0.0364	0.0358	0.0357	0.0337	0.0332	0.0331	0.0319	0.0314	0.0313
0.25	0.0407	0.0399	0.0383	0.0376	0.0346	0.0341	0.0339	0.0320	0.0315	0.0313	0.0301	0.0297	0.0295
0.26	0.0391	0.0382	0.0367	0.0360	0.0330	0.0324	0.0323	0.0303	0.0298	0.0297	0.0285	0.0280	0.0279
0.27	0.0377	0.0368	0.0353	0.0345	0.0315	0.0310	0.0309	0.0289	0.0284	0.0283	0.0271	0.0266	0.0265
0.28	0.0364	0.0355	0.0340	0.0332	0.0303	0.0297	0.0296	0.0276	0.0271	0.0270	0.0258	0.0253	0.0252
0.29	0.0352	0.0343	0.0328	0.0321	0.0291	0.0286	0.0284	0.0265	0.0260	0.0258	0.0246	0.0242	0.0240
0.30	0.0342	0.0333	0.0318	0.0311	0.0281	0.0275	0.0274	0.0255	0.0249	0.0248	0.0236	0.0231	0.0230
0.31	0.0333	0.0324	0.0309	0.0302	0.0272	0.0266	0.0265	0.0245	0.0240	0.0239	0.0227	0.0222	0.0221
0.32	0.0325	0.0317	0.0301	0.0294	0.0264	0.0259	0.0257	0.0238	0.0233	0.0232	0.0220	0.0215	0.0214
0.33	0.0319	0.0310	0.0295	0.0288	0.0258	0.0252	0.0251	0.0231	0.0226	0.0225	0.0213	0.0208	0.0207
0.34	0.0314	0.0305	0.0290	0.0283	0.0253	0.0247	0.0246	0.0226	0.0221	0.0220	0.0208	0.0203	0.0202
0.35	0.0310	0.0301	0.0286	0.0278	0.0249	0.0243	0.0242	0.0222	0.0217	0.0216	0.0204	0.0199	0.0198
0.36	0.0306	0.0298	0.0283	0.0275	0.0246	0.0240	0.0239	0.0219	0.0214	0.0213	0.0201	0.0196	0.0195
0.37	0.0305	0.0296	0.0281	0.0274	0.0244	0.0239	0.0237	0.0218	0.0213	0.0212	0.0200	0.0195	0.0194
0.38	0.0304	0.0285	0.0280	0.0273	0.0244	0.0238	0.0237	0.0217	0.0212	0.0211	0.0199	0.0195	0.0193
0.39	0.0305	0.0296	0.0281	0.0274	0.0244	0.0239	0.0238	0.0218	0.0213	0.0212	0.0200	0.0195	0.0194
0.40	0.0306	0.0296	0.0283	0.0276	0.0246	0.0240	0.0239	0.0220	0.0215	0.0213	0.0202	0.0197	0.0196
0.41	0.0309	0.0300	0.0285	0.0278	0.0248	0.0243	0.0241	0.0222	0.0217	0.0216	0.0204	0.0199	0.0198
0.42	0.0312	0.0303	0.0288	0.0281	0.0252	0.0246	0.0245	0.0226	0.0221	0.0219	0.0208	0.0203	0.0202
0.43	0.0316	0.0308	0.0293	0.0286	0.0256	0.0251	0.0249	0.0230	0.0225	0.0224	0.0212	0.0207	0.0206
0.44	0.0321	0.0313	0.0298	0.0291	0.0261	0.0256	0.0254	0.0235	0.0230	0.0229	0.0217	0.0213	0.0211
0.45	0.0327	0.0319	0.0304	0.0297	0.0267	0.0262	0.0261	0.0241	0.0236	0.0235	0.0223	0.0219	0.0217
0.46	0.0334	0.0326	0.0311	0.0304	0.0274	0.0269	0.0267	0.0248	0.0243	0.0242	0.0230	0.0226	0.0224
0.47	0.0341	0.0333	0.0318	0.0311	0.0282	0.0276	0.0275	0.0256	0.0251	0.0249	0.0238	0.0233	0.0232
0.48	0.0350	0.0341	0.0326	0.0319	0.0290	0.0284	0.0283	0.0264	0.0259	0.0258	0.0246	0.0242	0.0240
0.49	0.0358	0.0349	0.0335	0.0328	0.0299	0.0293	0.0292	0.0273	0.0268	0.0267	0.0255	0.0250	0.0249
0.50	0.0368	0.0359	0.0344	0.0337	0.0308	0.0303	0.0302	0.0283	0.0278	0.0276	0.0265	0.0260	0.0259
0.51	0.0378	0.0369	0.0354	0.0347	0.0318	0.0313	0.0312	0.0293	0.0288	0.0287	0.0275	0.0270	0.0269
0.52	0.0388	0.0380	0.0365	0.0358	0.0329	0.0324	0.0323	0.0304	0.0299	0.0298	0.0286	0.0281	0.0280
0.53	0.0399	0.0391	0.0376	0.0369	0.0340	0.0335	0.0334	0.0315	0.0310	0.0309	0.0297	0.0293	0.0291
0.54	0.0410	0.0402	0.0387	0.0380	0.0351	0.0346	0.0345	0.0326	0.0321	0.0320	0.0308	0.0304	0.0303
0.55	0.0422	0.0413	0.0399	0.0392	0.0363	0.0358	0.0357	0.0338	0.0333	0.0332	0.0321	0.0316	0.0315
0.56	0.0433	0.0425	0.0411	0.0404	0.0375	0.0370	0.0369	0.0350	0.0345	0.0344	0.0333	0.0328	0.0327
0.57	0.0446	0.0438	0.0423	0.0416	0.0388	0.0383	0.0381	0.0363	0.0358	0.0357	0.0346	0.0341	0.0340
0.58	0.0458	0.0450	0.0436	0.0429	0.0401	0.0395	0.0394	0.0376	0.0371	0.0370	0.0358	0.0354	0.0353
0.59	0.0472	0.0463	0.0449	0.0442	0.0414	0.0409	0.0408	0.0389	0.0384	0.0383	0.0372	0.0367	0.0366
0.60	0.0484	0.0476	0.0462	0.0455	0.0427	0.0422	0.0421	0.0402	0.0398	0.0397	0.0385	0.0381	0.0380
0.61	0.0497	0.0489	0.0474	0.0468	0.0440	0.0435	0.0433	0.0415	0.0411	0.0409	0.0398	0.0394	0.0393
0.62	0.0510	0.0502	0.0488	0.0481	0.0452	0.0448	0.0447	0.0429	0.0424	0.0423	0.0412	0.0407	0.0406
0.63	0.0523	0.0515	0.0501	0.0494	0.0466	0.0461	0.0460	0.0442	0.0437	0.0436	0.0425	0.0421	0.0420
0.64	0.0535	0.0527	0.0513	0.0507	0.0479	0.0474	0.0473	0.0455	0.0451	0.0449	0.0438	0.0434	0.0433
0.65	0.0548	0.0540	0.0526	0.0520	0.0492	0.0487	0.0486	0.0468	0.0464	0.0463	0.0452	0.0447	0.0446
0.66	0.0560	0.0552	0.0538	0.0532	0.0505	0.0500	0.0499	0.0481	0.0476	0.0475	0.0465	0.0460	0.0459
0.67	0.0572	0.0564	0.0551	0.0544	0.0517	0.0512	0.0511	0.0494	0.0489	0.0488	0.0477	0.0473	0.0472
0.68	0.0584	0.0576	0.0563	0.0556	0.0530	0.0525	0.0523	0.0506	0.0502	0.0500	0.0490	0.0486	0.0484
0.69	0.0595	0.0587	0.0574	0.0567	0.0541	0.0536	0.0535	0.0518	0.0513	0.0512	0.0502	0.0497	0.0496
0.70	0.0606	0.0598	0.0585	0.0579	0.0552	0.0548	0.0546	0.0529	0.0525	0.0524	0.0513	0.0509	0.0508
0.71	0.0616	0.0608	0.0595	0.0589	0.0563	0.0558	0.0557	0.0540	0.0535	0.0534	0.0524	0.0520	0.0519
0.72	0.0625	0.0618	0.0605	0.0599	0.0573	0.0568	0.0567	0.0550	0.0546	0.0545	0.0535	0.0530	0.0529
0.73	0.0635	0.0627	0.0614	0.0608	0.0583	0.0578	0.0577	0.0560	0.0556	0.0555	0.0545	0.0541	0.0540
0.74	0.0643	0.0636	0.0623	0.0617	0.0592	0.0587	0.0586	0.0570	0.0565	0.0564	0.0554	0.0550	0.0549
0.75	0.0650	0.0643	0.0630	0.0624	0.0599	0.0594	0.0594	0.0577	0.0573	0.0572	0.0562	0.0558	0.0557

TABLE 13.1h—*b* VALUES FOR REYNOLDS NUMBER FACTOR, F_r , PIPE TAPS (continued)

$$F_r = 1 + \frac{b}{\sqrt{h_w \rho_f}}$$

Internal Diameter of Pipe, d_i , in.

F_d	16			20			24			30		
	14.688	15.000	15.250	18.814	19.000	19.250	22.626	23.000	23.250	28.628	29.000	29.250
0.10	0.0706	0.0705	0.0704	0.0690	0.0689	0.0688	0.0680	0.0679	0.0678	0.0669	0.0669	0.0668
0.11	0.0665	0.0663	0.0662	0.0648	0.0647	0.0647	0.0638	0.0637	0.0637	0.0628	0.0627	0.0627
0.12	0.0624	0.0622	0.0621	0.0607	0.0607	0.0606	0.0597	0.0596	0.0596	0.0587	0.0586	0.0586
0.13	0.0585	0.0584	0.0582	0.0569	0.0568	0.0567	0.0558	0.0558	0.0557	0.0548	0.0548	0.0547
0.14	0.0549	0.0548	0.0546	0.0532	0.0531	0.0530	0.0522	0.0521	0.0520	0.0511	0.0511	0.0511
0.15	0.0514	0.0512	0.0511	0.0497	0.0497	0.0496	0.0487	0.0486	0.0486	0.0477	0.0476	0.0476
0.16	0.0481	0.0479	0.0478	0.0464	0.0464	0.0463	0.0454	0.0453	0.0453	0.0444	0.0443	0.0443
0.17	0.0450	0.0448	0.0447	0.0433	0.0433	0.0432	0.0423	0.0423	0.0422	0.0413	0.0413	0.0412
0.18	0.0420	0.0419	0.0417	0.0404	0.0403	0.0402	0.0394	0.0393	0.0392	0.0383	0.0383	0.0383
0.19	0.0393	0.0391	0.0390	0.0376	0.0376	0.0375	0.0366	0.0366	0.0365	0.0356	0.0356	0.0355
0.20	0.0367	0.0365	0.0364	0.0350	0.0350	0.0349	0.0340	0.0340	0.0339	0.0330	0.0330	0.0329
0.21	0.0343	0.0341	0.0340	0.0326	0.0326	0.0325	0.0316	0.0316	0.0315	0.0306	0.0306	0.0305
0.22	0.0320	0.0318	0.0317	0.0304	0.0303	0.0302	0.0294	0.0293	0.0293	0.0284	0.0283	0.0283
0.23	0.0299	0.0298	0.0296	0.0283	0.0282	0.0281	0.0273	0.0272	0.0272	0.0263	0.0262	0.0262
0.24	0.0280	0.0278	0.0277	0.0264	0.0263	0.0262	0.0254	0.0253	0.0253	0.0244	0.0243	0.0243
0.25	0.0262	0.0261	0.0260	0.0246	0.0246	0.0245	0.0236	0.0236	0.0235	0.0226	0.0226	0.0226
0.26	0.0246	0.0244	0.0243	0.0230	0.0229	0.0228	0.0220	0.0219	0.0219	0.0210	0.0210	0.0209
0.27	0.0231	0.0230	0.0229	0.0215	0.0215	0.0214	0.0206	0.0205	0.0204	0.0196	0.0195	0.0195
0.28	0.0218	0.0217	0.0216	0.0202	0.0202	0.0201	0.0193	0.0192	0.0191	0.0183	0.0182	0.0182
0.29	0.0206	0.0205	0.0204	0.0191	0.0190	0.0189	0.0181	0.0180	0.0180	0.0171	0.0171	0.0170
0.30	0.0196	0.0194	0.0193	0.0180	0.0179	0.0179	0.0170	0.0170	0.0169	0.0161	0.0160	0.0160
0.31	0.0187	0.0185	0.0184	0.0171	0.0170	0.0170	0.0161	0.0161	0.0160	0.0152	0.0151	0.0151
0.32	0.0179	0.0177	0.0176	0.0163	0.0162	0.0162	0.0153	0.0153	0.0152	0.0144	0.0143	0.0143
0.33	0.0172	0.0170	0.0169	0.0156	0.0156	0.0155	0.0147	0.0146	0.0146	0.0137	0.0137	0.0136
0.34	0.0166	0.0165	0.0164	0.0151	0.0150	0.0150	0.0142	0.0141	0.0140	0.0132	0.0131	0.0131
0.35	0.0162	0.0161	0.0160	0.0147	0.0146	0.0145	0.0137	0.0137	0.0136	0.0128	0.0127	0.0127
0.36	0.0159	0.0157	0.0156	0.0144	0.0143	0.0142	0.0134	0.0134	0.0133	0.0125	0.0124	0.0124
0.37	0.0157	0.0155	0.0154	0.0141	0.0141	0.0140	0.0132	0.0132	0.0131	0.0123	0.0122	0.0122
0.38	0.0155	0.0154	0.0153	0.0140	0.0140	0.0139	0.0131	0.0130	0.0130	0.0122	0.0121	0.0121
0.39	0.0155	0.0154	0.0153	0.0140	0.0139	0.0139	0.0131	0.0130	0.0130	0.0122	0.0121	0.0121
0.40	0.0156	0.0154	0.0153	0.0141	0.0140	0.0139	0.0132	0.0131	0.0130	0.0122	0.0122	0.0122
0.41	0.0157	0.0155	0.0154	0.0142	0.0142	0.0141	0.0133	0.0132	0.0132	0.0124	0.0124	0.0123
0.42	0.0159	0.0158	0.0157	0.0144	0.0144	0.0143	0.0136	0.0135	0.0134	0.0126	0.0126	0.0126
0.43	0.0162	0.0161	0.0160	0.0148	0.0147	0.0146	0.0139	0.0138	0.0138	0.0130	0.0129	0.0129
0.44	0.0166	0.0164	0.0163	0.0151	0.0151	0.0150	0.0143	0.0142	0.0141	0.0134	0.0133	0.0133
0.45	0.0170	0.0169	0.0168	0.0156	0.0155	0.0155	0.0147	0.0146	0.0146	0.0138	0.0138	0.0137
0.46	0.0175	0.0174	0.0173	0.0161	0.0160	0.0160	0.0152	0.0151	0.0151	0.0143	0.0143	0.0143
0.47	0.0180	0.0179	0.0178	0.0166	0.0166	0.0165	0.0158	0.0157	0.0157	0.0149	0.0149	0.0148
0.48	0.0186	0.0185	0.0184	0.0172	0.0172	0.0171	0.0164	0.0163	0.0163	0.0155	0.0155	0.0154
0.49	0.0192	0.0191	0.0190	0.0178	0.0178	0.0177	0.0170	0.0169	0.0169	0.0162	0.0161	0.0161
0.50	0.0199	0.0198	0.0197	0.0185	0.0185	0.0184	0.0177	0.0176	0.0176	0.0169	0.0168	0.0168
0.51	0.0206	0.0205	0.0204	0.0193	0.0192	0.0191	0.0184	0.0184	0.0183	0.0176	0.0176	0.0175
0.52	0.0213	0.0212	0.0211	0.0200	0.0199	0.0199	0.0192	0.0191	0.0191	0.0183	0.0183	0.0183
0.53	0.0221	0.0220	0.0219	0.0208	0.0207	0.0207	0.0200	0.0199	0.0199	0.0191	0.0191	0.0191
0.54	0.0229	0.0227	0.0226	0.0215	0.0215	0.0214	0.0208	0.0207	0.0207	0.0199	0.0199	0.0199
0.55	0.0237	0.0235	0.0234	0.0224	0.0223	0.0223	0.0216	0.0215	0.0215	0.0208	0.0207	0.0207
0.56	0.0244	0.0243	0.0242	0.0232	0.0231	0.0231	0.0224	0.0223	0.0223	0.0216	0.0216	0.0215
0.57	0.0253	0.0251	0.0250	0.0240	0.0239	0.0239	0.0232	0.0232	0.0231	0.0224	0.0224	0.0224
0.58	0.0261	0.0260	0.0259	0.0248	0.0248	0.0247	0.0241	0.0240	0.0240	0.0233	0.0233	0.0232
0.59	0.0269	0.0268	0.0267	0.0256	0.0256	0.0255	0.0249	0.0248	0.0248	0.0241	0.0241	0.0241
0.60	0.0277	0.0276	0.0275	0.0265	0.0264	0.0264	0.0257	0.0257	0.0256	0.0250	0.0249	0.0249
0.61	0.0284	0.0283	0.0282	0.0272	0.0272	0.0271	0.0265	0.0265	0.0264	0.0258	0.0257	0.0257
0.62	0.0292	0.0291	0.0290	0.0280	0.0280	0.0279	0.0273	0.0272	0.0272	0.0266	0.0265	0.0265
0.63	0.0299	0.0298	0.0297	0.0288	0.0287	0.0287	0.0281	0.0280	0.0280	0.0273	0.0273	0.0273
0.64	0.0306	0.0305	0.0304	0.0295	0.0295	0.0294	0.0288	0.0288	0.0287	0.0281	0.0281	0.0280
0.65	0.0313	0.0312	0.0312	0.0302	0.0302	0.0301	0.0295	0.0295	0.0294	0.0288	0.0288	0.0288
0.66	0.0320	0.0319	0.0318	0.0309	0.0308	0.0308	0.0302	0.0301	0.0301	0.0295	0.0295	0.0295
0.67	0.0326	0.0325	0.0324	0.0315	0.0315	0.0314	0.0309	0.0308	0.0308	0.0302	0.0302	0.0302
0.68	0.0332	0.0331	0.0330	0.0322	0.0321	0.0321	0.0315	0.0315	0.0314	0.0308	0.0308	0.0308
0.69	0.0337	0.0336	0.0335	0.0327	0.0326	0.0326	0.0320	0.0320	0.0320	0.0314	0.0314	0.0313
0.70	0.0342	0.0341	0.0340	0.0332	0.0332	0.0331	0.0326	0.0325	0.0325	0.0319	0.0319	0.0319

TABLE 13.1i—EXPANSION FACTORS: FLANGE TAPS, Y_1 ; STATIC PRESSURE TAKEN FROM UPSTREAM TAPS

$$F_d = \frac{d_o}{d_i}$$

$\frac{h_w}{P_{f1}}$ Ratio	0.1	0.2	0.3	0.4	0.45	0.50	0.52	0.54	0.56	0.58	0.60	0.61	0.62
0.0	1.0000	1.0000	1.0000	1.0000	1.0000	1.0000	1.0000	1.0000	1.0000	1.0000	1.0000	1.0000	1.0000
0.1	0.9989	0.9989	0.9989	0.9988	0.9988	0.9988	0.9988	0.9988	0.9988	0.9988	0.9987	0.9987	0.9987
0.2	0.9977	0.9977	0.9977	0.9977	0.9976	0.9976	0.9976	0.9976	0.9975	0.9975	0.9975	0.9975	0.9974
0.3	0.9966	0.9966	0.9966	0.9965	0.9965	0.9964	0.9964	0.9963	0.9963	0.9963	0.9962	0.9962	0.9962
0.4	0.9954	0.9954	0.9954	0.9953	0.9953	0.9952	0.9952	0.9951	0.9951	0.9950	0.9949	0.9949	0.9949
0.5	0.9943	0.9943	0.9943	0.9942	0.9941	0.9940	0.9940	0.9939	0.9938	0.9938	0.9937	0.9936	0.9936
0.6	0.9932	0.9932	0.9931	0.9930	0.9929	0.9928	0.9927	0.9927	0.9926	0.9925	0.9924	0.9924	0.9923
0.7	0.9920	0.9920	0.9920	0.9919	0.9918	0.9916	0.9915	0.9915	0.9914	0.9913	0.9912	0.9911	0.9910
0.8	0.9909	0.9909	0.9908	0.9907	0.9906	0.9904	0.9903	0.9902	0.9901	0.9900	0.9899	0.9898	0.9897
0.9	0.9898	0.9897	0.9897	0.9895	0.9894	0.9892	0.9891	0.9890	0.9889	0.9888	0.9886	0.9885	0.9885
1.0	0.9886	0.9886	0.9885	0.9884	0.9882	0.9880	0.9879	0.9878	0.9877	0.9875	0.9874	0.9873	0.9872
1.1	0.9875	0.9875	0.9874	0.9872	0.9870	0.9868	0.9867	0.9866	0.9864	0.9863	0.9861	0.9860	0.9859
1.2	0.9863	0.9863	0.9862	0.9860	0.9859	0.9856	0.9855	0.9853	0.9852	0.9850	0.9848	0.9847	0.9846
1.3	0.9852	0.9852	0.9851	0.9849	0.9847	0.9844	0.9843	0.9841	0.9840	0.9838	0.9836	0.9835	0.9833
1.4	0.9841	0.9840	0.9840	0.9837	0.9835	0.9832	0.9831	0.9829	0.9827	0.9825	0.9823	0.9822	0.9821
1.5	0.9829	0.9829	0.9828	0.9826	0.9823	0.9820	0.9819	0.9817	0.9815	0.9813	0.9810	0.9809	0.9808
1.6	0.9818	0.9818	0.9817	0.9814	0.9811	0.9808	0.9806	0.9805	0.9803	0.9800	0.9798	0.9796	0.9795
1.7	0.9806	0.9806	0.9805	0.9802	0.9800	0.9796	0.9794	0.9792	0.9790	0.9788	0.9785	0.9784	0.9782
1.8	0.9795	0.9795	0.9794	0.9791	0.9788	0.9784	0.9782	0.9780	0.9778	0.9775	0.9772	0.9771	0.9769
1.9	0.9784	0.9783	0.9782	0.9779	0.9776	0.9772	0.9770	0.9768	0.9766	0.9763	0.9760	0.9758	0.9756
2.0	0.9772	0.9772	0.9771	0.9767	0.9764	0.9760	0.9758	0.9756	0.9753	0.9750	0.9747	0.9745	0.9744
2.1	0.9761	0.9761	0.9759	0.9756	0.9753	0.9748	0.9746	0.9744	0.9741	0.9738	0.9734	0.9733	0.9731
2.2	0.9750	0.9749	0.9748	0.9744	0.9741	0.9736	0.9734	0.9731	0.9729	0.9725	0.9722	0.9720	0.9718
2.3	0.9738	0.9738	0.9736	0.9732	0.9729	0.9724	0.9722	0.9719	0.9716	0.9713	0.9709	0.9707	0.9705
2.4	0.9727	0.9726	0.9725	0.9721	0.9717	0.9712	0.9710	0.9707	0.9704	0.9700	0.9697	0.9694	0.9692
2.5	0.9715	0.9715	0.9713	0.9709	0.9705	0.9700	0.9698	0.9695	0.9692	0.9688	0.9684	0.9682	0.9680
2.6	0.9704	0.9704	0.9702	0.9698	0.9694	0.9688	0.9686	0.9683	0.9679	0.9675	0.9671	0.9669	0.9667
2.7	0.9693	0.9692	0.9691	0.9686	0.9682	0.9676	0.9673	0.9670	0.9667	0.9663	0.9659	0.9656	0.9654
2.8	0.9681	0.9681	0.9679	0.9674	0.9670	0.9664	0.9661	0.9658	0.9654	0.9650	0.9646	0.9644	0.9641
2.9	0.9670	0.9669	0.9668	0.9663	0.9658	0.9652	0.9649	0.9646	0.9642	0.9638	0.9633	0.9631	0.9628
3.0	0.9658	0.9658	0.9656	0.9651	0.9647	0.9640	0.9637	0.9634	0.9630	0.9626	0.9621	0.9618	0.9615
3.1	0.9647	0.9647	0.9645	0.9639	0.9635	0.9628	0.9625	0.9622	0.9617	0.9613	0.9608	0.9605	0.9603
3.2	0.9635	0.9635	0.9633	0.9628	0.9623	0.9616	0.9613	0.9609	0.9605	0.9601	0.9595	0.9593	0.9590
3.3	0.9624	0.9624	0.9622	0.9616	0.9611	0.9604	0.9601	0.9597	0.9593	0.9588	0.9583	0.9580	0.9577
3.4	0.9613	0.9612	0.9610	0.9604	0.9599	0.9592	0.9589	0.9585	0.9580	0.9576	0.9570	0.9567	0.9564
3.5	0.9602	0.9601	0.9599	0.9593	0.9588	0.9580	0.9577	0.9573	0.9568	0.9563	0.9558	0.9554	0.9551
3.6	0.9590	0.9590	0.9587	0.9581	0.9576	0.9568	0.9565	0.9560	0.9556	0.9551	0.9545	0.9542	0.9538
3.7	0.9579	0.9578	0.9576	0.9570	0.9564	0.9556	0.9553	0.9548	0.9543	0.9538	0.9532	0.9529	0.9526
3.8	0.9567	0.9567	0.9564	0.9558	0.9552	0.9544	0.9540	0.9536	0.9531	0.9526	0.9520	0.9516	0.9513
3.9	0.9556	0.9555	0.9553	0.9546	0.9540	0.9532	0.9528	0.9524	0.9519	0.9513	0.9507	0.9504	0.9500
4.0	0.9545	0.9544	0.9542	0.9535	0.9529	0.9520	0.9516	0.9512	0.9506	0.9501	0.9494	0.9491	0.9487

TABLE 13.1i—EXPANSION FACTORS: FLANGE TAPS, Y_1 ; STATIC PRESSURE TAKEN FROM UPSTREAM TAPS (continued)
$$F_d = \frac{d_o}{d_i}$$

$\frac{h_w}{p_1}$ Ratio	0.63	0.64	0.65	0.66	0.67	0.68	0.69	0.70	0.71	0.72	0.73	0.74	0.75
0.0	1.0000	1.0000	1.0000	1.0000	1.0000	1.0000	1.0000	1.0000	1.0000	1.0000	1.0000	1.0000	1.0000
0.1	0.9987	0.9987	0.9987	0.9987	0.9987	0.9987	0.9986	0.9986	0.9986	0.9986	0.9986	0.9986	0.9986
0.2	0.9974	0.9974	0.9974	0.9974	0.9973	0.9973	0.9973	0.9973	0.9972	0.9972	0.9972	0.9971	0.9971
0.3	0.9961	0.9961	0.9961	0.9960	0.9960	0.9960	0.9959	0.9959	0.9958	0.9958	0.9958	0.9957	0.9957
0.4	0.9948	0.9948	0.9948	0.9947	0.9947	0.9946	0.9946	0.9945	0.9945	0.9944	0.9943	0.9943	0.9942
0.5	0.9935	0.9935	0.9934	0.9934	0.9933	0.9933	0.9932	0.9931	0.9931	0.9930	0.9929	0.9929	0.9928
0.6	0.9923	0.9922	0.9921	0.9921	0.9920	0.9919	0.9918	0.9918	0.9917	0.9916	0.9915	0.9914	0.9913
0.7	0.9910	0.9909	0.9908	0.9907	0.9907	0.9906	0.9905	0.9904	0.9903	0.9902	0.9901	0.9900	0.9899
0.8	0.9897	0.9896	0.9895	0.9894	0.9893	0.9892	0.9891	0.9890	0.9889	0.9888	0.9887	0.9886	0.9884
0.9	0.9884	0.9883	0.9882	0.9881	0.9880	0.9879	0.9878	0.9877	0.9875	0.9874	0.9873	0.9871	0.9870
1.0	0.9871	0.9870	0.9869	0.9868	0.9867	0.9865	0.9864	0.9863	0.9861	0.9860	0.9859	0.9857	0.9855
1.1	0.9858	0.9857	0.9856	0.9854	0.9853	0.9852	0.9851	0.9849	0.9848	0.9846	0.9844	0.9843	0.9841
1.2	0.9845	0.9844	0.9843	0.9841	0.9840	0.9838	0.9837	0.9835	0.9834	0.9832	0.9830	0.9828	0.9826
1.3	0.9832	0.9831	0.9829	0.9828	0.9827	0.9825	0.9823	0.9822	0.9820	0.9818	0.9816	0.9814	0.9812
1.4	0.9819	0.9818	0.9816	0.9815	0.9813	0.9812	0.9810	0.9808	0.9806	0.9804	0.9802	0.9800	0.9798
1.5	0.9806	0.9805	0.9803	0.9802	0.9800	0.9798	0.9796	0.9794	0.9792	0.9790	0.9788	0.9786	0.9783
1.6	0.9793	0.9792	0.9790	0.9788	0.9787	0.9785	0.9783	0.9781	0.9778	0.9776	0.9774	0.9771	0.9769
1.7	0.9780	0.9779	0.9777	0.9775	0.9773	0.9771	0.9769	0.9767	0.9764	0.9762	0.9760	0.9757	0.9754
1.8	0.9768	0.9766	0.9764	0.9762	0.9760	0.9758	0.9755	0.9753	0.9751	0.9748	0.9745	0.9743	0.9740
1.9	0.9755	0.9753	0.9751	0.9749	0.9747	0.9744	0.9742	0.9739	0.9737	0.9734	0.9731	0.9728	0.9725
2.0	0.9742	0.9740	0.9738	0.9735	0.9733	0.9731	0.9728	0.9726	0.9723	0.9720	0.9717	0.9714	0.9711
2.1	0.9729	0.9727	0.9725	0.9722	0.9720	0.9717	0.9715	0.9712	0.9709	0.9706	0.9703	0.9700	0.9696
2.2	0.9716	0.9714	0.9711	0.9709	0.9706	0.9704	0.9701	0.9698	0.9695	0.9692	0.9689	0.9685	0.9682
2.3	0.9703	0.9701	0.9698	0.9696	0.9693	0.9690	0.9688	0.9685	0.9681	0.9678	0.9675	0.9671	0.9667
2.4	0.9690	0.9688	0.9685	0.9683	0.9680	0.9677	0.9674	0.9671	0.9668	0.9664	0.9661	0.9657	0.9653
2.5	0.9677	0.9675	0.9672	0.9669	0.9666	0.9663	0.9660	0.9657	0.9654	0.9650	0.9646	0.9643	0.9639
2.6	0.9664	0.9662	0.9659	0.9656	0.9653	0.9650	0.9647	0.9643	0.9640	0.9636	0.9632	0.9628	0.9624
2.7	0.9651	0.9649	0.9646	0.9643	0.9640	0.9637	0.9633	0.9630	0.9626	0.9622	0.9618	0.9614	0.9610
2.8	0.9638	0.9636	0.9633	0.9630	0.9626	0.9623	0.9620	0.9616	0.9612	0.9608	0.9604	0.9600	0.9595
2.9	0.9625	0.9623	0.9620	0.9616	0.9613	0.9610	0.9606	0.9602	0.9598	0.9594	0.9590	0.9585	0.9581
3.0	0.9613	0.9610	0.9606	0.9603	0.9600	0.9596	0.9592	0.9588	0.9584	0.9580	0.9576	0.9571	0.9566
3.1	0.9600	0.9597	0.9593	0.9590	0.9586	0.9583	0.9579	0.9575	0.9571	0.9566	0.9562	0.9557	0.9552
3.2	0.9587	0.9584	0.9580	0.9577	0.9573	0.9569	0.9565	0.9561	0.9557	0.9552	0.9547	0.9542	0.9537
3.3	0.9574	0.9571	0.9567	0.9564	0.9560	0.9556	0.9552	0.9547	0.9543	0.9538	0.9533	0.9528	0.9523
3.4	0.9561	0.9558	0.9554	0.9550	0.9546	0.9542	0.9538	0.9534	0.9529	0.9524	0.9519	0.9514	0.9508
3.5	0.9548	0.9545	0.9541	0.9537	0.9533	0.9529	0.9524	0.9520	0.9515	0.9510	0.9505	0.9500	0.9494
3.6	0.9535	0.9532	0.9528	0.9524	0.9520	0.9515	0.9511	0.9506	0.9501	0.9496	0.9491	0.9485	0.9480
3.7	0.9522	0.9518	0.9515	0.9511	0.9506	0.9502	0.9497	0.9492	0.9487	0.9482	0.9477	0.9471	0.9465
3.8	0.9509	0.9505	0.9502	0.9497	0.9493	0.9488	0.9484	0.9479	0.9474	0.9468	0.9463	0.9457	0.9451
3.9	0.9496	0.9492	0.9488	0.9484	0.9480	0.9475	0.9470	0.9465	0.9460	0.9454	0.9448	0.9442	0.9436
4.0	0.9483	0.9479	0.9475	0.9471	0.9466	0.9462	0.9457	0.9451	0.9446	0.9440	0.9434	0.9428	0.9422

TABLE 13.1j—EXPANSION FACTORS: PIPE TAPS, Y_1 ; STATIC PRESSURE TAKEN FROM UPSTREAM TAPS

$$F_d = \frac{d_o}{d_i}$$

$\frac{h_w}{P_{t1}}$ Ratio	0.1	0.2	0.3	0.4	0.45	0.50	0.52	0.54	0.56	0.58	0.60
0.0	1.0000	1.0000	1.0000	1.0000	1.0000	1.0000	1.0000	1.0000	1.0000	1.0000	1.0000
0.1	0.9990	0.9989	0.9988	0.9985	0.9984	0.9982	0.9981	0.9980	0.9979	0.9978	0.9977
0.2	0.9981	0.9979	0.9976	0.9971	0.9968	0.9964	0.9962	0.9961	0.9959	0.9957	0.9954
0.3	0.9971	0.9968	0.9964	0.9956	0.9952	0.9946	0.9944	0.9941	0.9938	0.9935	0.9931
0.4	0.9962	0.9958	0.9951	0.9942	0.9936	0.9928	0.9925	0.9921	0.9917	0.9913	0.9908
0.5	0.9952	0.9947	0.9939	0.9927	0.9919	0.9910	0.9906	0.9902	0.9897	0.9891	0.9885
0.6	0.9943	0.9937	0.9927	0.9913	0.9903	0.9892	0.9887	0.9882	0.9876	0.9870	0.9862
0.7	0.9933	0.9926	0.9915	0.9898	0.9887	0.9874	0.9869	0.9862	0.9856	0.9848	0.9840
0.8	0.9923	0.9916	0.9903	0.9883	0.9871	0.9857	0.9850	0.9843	0.9835	0.9826	0.9817
0.9	0.9914	0.9905	0.9891	0.9869	0.9855	0.9839	0.9831	0.9823	0.9814	0.9805	0.9794
1.0	0.9904	0.9895	0.9878	0.9854	0.9839	0.9821	0.9812	0.9803	0.9794	0.9783	0.9771
1.1	0.9895	0.9884	0.9866	0.9840	0.9823	0.9803	0.9794	0.9784	0.9773	0.9761	0.9748
1.2	0.9885	0.9874	0.9854	0.9825	0.9807	0.9785	0.9775	0.9764	0.9752	0.9739	0.9725
1.3	0.9876	0.9863	0.9842	0.9811	0.9791	0.9767	0.9756	0.9744	0.9732	0.9718	0.9702
1.4	0.9866	0.9853	0.9830	0.9796	0.9775	0.9749	0.9737	0.9725	0.9711	0.9696	0.9679
1.5	0.9857	0.9842	0.9818	0.9782	0.9758	0.9731	0.9719	0.9705	0.9690	0.9674	0.9656
1.6	0.9847	0.9832	0.9805	0.9767	0.9742	0.9713	0.9700	0.9685	0.9670	0.9652	0.9633
1.7	0.9837	0.9821	0.9793	0.9752	0.9726	0.9695	0.9681	0.9666	0.9649	0.9631	0.9610
1.8	0.9828	0.9811	0.9781	0.9738	0.9710	0.9677	0.9662	0.9646	0.9628	0.9609	0.9587
1.9	0.9818	0.9800	0.9769	0.9723	0.9694	0.9659	0.9643	0.9626	0.9608	0.9587	0.9565
2.0	0.9809	0.9790	0.9757	0.9709	0.9678	0.9641	0.9625	0.9607	0.9587	0.9566	0.9542
2.1	0.9799	0.9779	0.9745	0.9694	0.9662	0.9623	0.9606	0.9587	0.9566	0.9544	0.9519
2.2	0.9790	0.9768	0.9732	0.9680	0.9646	0.9605	0.9587	0.9567	0.9546	0.9522	0.9496
2.3	0.9780	0.9758	0.9720	0.9665	0.9630	0.9587	0.9568	0.9548	0.9525	0.9500	0.9473
2.4	0.9770	0.9747	0.9708	0.9650	0.9613	0.9570	0.9550	0.9528	0.9505	0.9479	0.9450
2.5	0.9761	0.9737	0.9696	0.9636	0.9597	0.9552	0.9531	0.9508	0.9484	0.9457	0.9427
2.6	0.9751	0.9726	0.9684	0.9621	0.9581	0.9534	0.9512	0.9489	0.9463	0.9435	0.9404
2.7	0.9742	0.9716	0.9672	0.9607	0.9565	0.9516	0.9493	0.9469	0.9443	0.9414	0.9381
2.8	0.9732	0.9705	0.9659	0.9592	0.9549	0.9498	0.9475	0.9449	0.9422	0.9392	0.9358
2.9	0.9723	0.9695	0.9647	0.9578	0.9533	0.9480	0.9456	0.9430	0.9401	0.9370	0.9335
3.0	0.9713	0.9684	0.9635	0.9563	0.9517	0.9462	0.9437	0.9410	0.9381	0.9348	0.9312
3.1	0.9704	0.9674	0.9623	0.9549	0.9501	0.9444	0.9418	0.9390	0.9360	0.9327	0.9290
3.2	0.9694	0.9663	0.9611	0.9534	0.9485	0.9426	0.9400	0.9371	0.9339	0.9305	0.9267
3.3	0.9684	0.9653	0.9599	0.9519	0.9469	0.9408	0.9381	0.9351	0.9319	0.9283	0.9244
3.4	0.9675	0.9642	0.9587	0.9505	0.9452	0.9390	0.9362	0.9331	0.9298	0.9261	0.9221
3.5	0.9665	0.9632	0.9574	0.9490	0.9436	0.9372	0.9343	0.9312	0.9277	0.9240	0.9198
3.6	0.9656	0.9621	0.9562	0.9476	0.9420	0.9354	0.9324	0.9292	0.9257	0.9218	0.9175
3.7	0.9646	0.9611	0.9550	0.9461	0.9404	0.9336	0.9306	0.9272	0.9236	0.9196	0.9152
3.8	0.9637	0.9600	0.9538	0.9447	0.9388	0.9318	0.9287	0.9253	0.9216	0.9175	0.9129
3.9	0.9627	0.9590	0.9526	0.9432	0.9372	0.9301	0.9268	0.9233	0.9195	0.9153	0.9106
4.0	0.9617	0.9579	0.9514	0.9417	0.9356	0.9283	0.9249	0.9213	0.9174	0.9131	0.9083

TABLE 13.1j—EXPANSION FACTORS: PIPE TAPS, Y_1 ; STATIC PRESSURE TAKEN FROM UPSTREAM TAPS
(continued)

$$F_d = \frac{d_o}{d_i}$$

$\frac{h_w}{p_{t1}}$ Ratio	0.61	0.62	0.63	0.64	0.65	0.66	0.67	0.68	0.69	0.70
0.0	1.0000	1.0000	1.0000	1.0000	1.0000	1.0000	1.0000	1.0000	1.0000	1.0000
0.1	0.9976	0.9976	0.9975	0.9974	0.9973	0.9972	0.9971	0.9970	0.9969	0.9968
0.2	0.9953	0.9951	0.9950	0.9948	0.9947	0.9945	0.9943	0.9941	0.9938	0.9935
0.3	0.9929	0.9927	0.9925	0.9923	0.9920	0.9917	0.9914	0.9911	0.9907	0.9903
0.4	0.9906	0.9903	0.9900	0.9897	0.9893	0.9890	0.9886	0.9881	0.9876	0.9871
0.5	0.9882	0.9879	0.9875	0.9871	0.9867	0.9862	0.9857	0.9851	0.9845	0.9839
0.6	0.9859	0.9854	0.9850	0.9845	0.9840	0.9834	0.9828	0.9822	0.9814	0.9806
0.7	0.9835	0.9830	0.9825	0.9819	0.9813	0.9807	0.9800	0.9792	0.9784	0.9774
0.8	0.9811	0.9806	0.9800	0.9794	0.9787	0.9779	0.9771	0.9762	0.9753	0.9742
0.9	0.9788	0.9782	0.9775	0.9768	0.9760	0.9752	0.9742	0.9733	0.9722	0.9710
1.0	0.9764	0.9757	0.9750	0.9742	0.9733	0.9724	0.9714	0.9703	0.9691	0.9677
1.1	0.9741	0.9733	0.9725	0.9716	0.9707	0.9696	0.9685	0.9673	0.9660	0.9645
1.2	0.9717	0.9709	0.9700	0.9690	0.9680	0.9669	0.9657	0.9643	0.9629	0.9613
1.3	0.9694	0.9685	0.9675	0.9664	0.9653	0.9641	0.9628	0.9614	0.9598	0.9581
1.4	0.9670	0.9660	0.9650	0.9639	0.9627	0.9614	0.9599	0.9584	0.9567	0.9548
1.5	0.9646	0.9636	0.9625	0.9613	0.9600	0.9586	0.9571	0.9554	0.9536	0.9516
1.6	0.9623	0.9612	0.9600	0.9587	0.9573	0.9558	0.9542	0.9525	0.9505	0.9484
1.7	0.9599	0.9587	0.9575	0.9561	0.9547	0.9531	0.9514	0.9495	0.9474	0.9452
1.8	0.9576	0.9563	0.9550	0.9535	0.9520	0.9503	0.9485	0.9465	0.9443	0.9419
1.9	0.9552	0.9539	0.9525	0.9510	0.9493	0.9476	0.9456	0.9435	0.9412	0.9387
2.0	0.9529	0.9515	0.9500	0.9484	0.9467	0.9448	0.9428	0.9406	0.9381	0.9355
2.1	0.9505	0.9490	0.9475	0.9458	0.9440	0.9420	0.9399	0.9376	0.9351	0.9323
2.2	0.9481	0.9466	0.9450	0.9432	0.9413	0.9393	0.9371	0.9346	0.9320	0.9290
2.3	0.9458	0.9442	0.9425	0.9406	0.9387	0.9365	0.9342	0.9317	0.9289	0.9258
2.4	0.9434	0.9418	0.9400	0.9381	0.9360	0.9338	0.9313	0.9287	0.9258	0.9226
2.5	0.9411	0.9393	0.9375	0.9355	0.9333	0.9310	0.9285	0.9257	0.9227	0.9194
2.6	0.9387	0.9369	0.9350	0.9329	0.9307	0.9282	0.9256	0.9227	0.9196	0.9161
2.7	0.9364	0.9345	0.9325	0.9303	0.9280	0.9255	0.9227	0.9198	0.9165	0.9129
2.8	0.9340	0.9321	0.9300	0.9277	0.9253	0.9227	0.9199	0.9168	0.9134	0.9097
2.9	0.9316	0.9296	0.9275	0.9252	0.9227	0.9200	0.9170	0.9138	0.9103	0.9064
3.0	0.9293	0.9272	0.9250	0.9226	0.9200	0.9172	0.9142	0.9108	0.9072	0.9032
3.1	0.9269	0.9248	0.9225	0.9200	0.9173	0.9144	0.9113	0.9079	0.9041	0.9000
3.2	0.9246	0.9223	0.9200	0.9174	0.9147	0.9117	0.9084	0.9049	0.9010	0.8968
3.3	0.9222	0.9199	0.9175	0.9148	0.9120	0.9089	0.9056	0.9019	0.8979	0.8935
3.4	0.9199	0.9175	0.9150	0.9122	0.9093	0.9062	0.9027	0.8990	0.8948	0.8903
3.5	0.9175	0.9151	0.9125	0.9097	0.9067	0.9034	0.8999	0.8960	0.8918	0.8871
3.6	0.9151	0.9126	0.9100	0.9071	0.9040	0.9006	0.8970	0.8930	0.8887	0.8839
3.7	0.9128	0.9102	0.9075	0.9045	0.9013	0.8979	0.8941	0.8900	0.8856	0.8806
3.8	0.9104	0.9078	0.9050	0.9019	0.8987	0.8951	0.8913	0.8871	0.8825	0.8774
3.9	0.9081	0.9054	0.9025	0.8993	0.8960	0.8924	0.8884	0.8841	0.8794	0.8742
4.0	0.9057	0.9029	0.9000	0.8968	0.8933	0.8896	0.8856	0.8811	0.8763	0.8710

TABLE 13.1k—EXPANSION FACTORS: FLANGE TAPS, γ_2 ; STATIC PRESSURE TAKEN FROM DOWNSTREAM TAPS

$$F_d = \frac{d_o}{d_i}$$

$\frac{h_w}{P_{f2}}$ Ratio	0.1	0.2	0.3	0.4	0.45	0.50	0.52	0.54	0.56	0.58	0.60	0.61	0.62
0.0	1.0000	1.0000	1.0000	1.0000	1.0000	1.0000	1.0000	1.0000	1.0000	1.0000	1.0000	1.0000	1.0000
0.1	1.0007	1.0007	1.0007	1.0006	1.0006	1.0006	1.0006	1.0006	1.0006	1.0006	1.0005	1.0005	1.0005
0.2	1.0013	1.0013	1.0013	1.0013	1.0013	1.0012	1.0012	1.0012	1.0012	1.0011	1.0011	1.0011	1.0011
0.3	1.0020	1.0020	1.0020	1.0020	1.0019	1.0018	1.0018	1.0018	1.0017	1.0017	1.0016	1.0016	1.0016
0.4	1.0027	1.0027	1.0027	1.0026	1.0026	1.0025	1.0024	1.0024	1.0023	1.0023	1.0022	1.0022	1.0021
0.5	1.0033	1.0033	1.0033	1.0032	1.0031	1.0030	1.0029	1.0029	1.0028	1.0028	1.0027	1.0027	1.0027
0.6	1.0040	1.0040	1.0040	1.0039	1.0038	1.0036	1.0036	1.0035	1.0034	1.0033	1.0032	1.0032	1.0031
0.7	1.0047	1.0047	1.0047	1.0045	1.0044	1.0043	1.0042	1.0041	1.0040	1.0039	1.0038	1.0038	1.0037
0.8	1.0053	1.0053	1.0053	1.0051	1.0050	1.0049	1.0048	1.0047	1.0046	1.0045	1.0044	1.0043	1.0043
0.9	1.0060	1.0060	1.0060	1.0058	1.0057	1.0055	1.0054	1.0053	1.0052	1.0050	1.0049	1.0048	1.0048
1.0	1.0067	1.0066	1.0066	1.0064	1.0063	1.0061	1.0060	1.0059	1.0058	1.0056	1.0055	1.0054	1.0053
1.1	1.0074	1.0073	1.0073	1.0071	1.0069	1.0067	1.0066	1.0065	1.0063	1.0061	1.0060	1.0059	1.0058
1.2	1.0080	1.0080	1.0079	1.0077	1.0075	1.0073	1.0072	1.0071	1.0069	1.0067	1.0066	1.0065	1.0064
1.3	1.0087	1.0087	1.0086	1.0084	1.0082	1.0080	1.0078	1.0077	1.0075	1.0073	1.0071	1.0070	1.0069
1.4	1.0094	1.0093	1.0093	1.0090	1.0088	1.0086	1.0084	1.0083	1.0081	1.0079	1.0077	1.0076	1.0074
1.5	1.0100	1.0100	1.0099	1.0097	1.0094	1.0091	1.0090	1.0088	1.0086	1.0084	1.0082	1.0081	1.0080
1.6	1.0108	1.0107	1.0106	1.0104	1.0101	1.0097	1.0097	1.0095	1.0093	1.0090	1.0088	1.0086	1.0085
1.7	1.0114	1.0114	1.0113	1.0110	1.0108	1.0104	1.0103	1.0101	1.0099	1.0096	1.0094	1.0092	1.0091
1.8	1.0121	1.0120	1.0120	1.0117	1.0114	1.0110	1.0108	1.0106	1.0104	1.0102	1.0100	1.0097	1.0096
1.9	1.0128	1.0127	1.0126	1.0123	1.0120	1.0116	1.0115	1.0112	1.0110	1.0107	1.0104	1.0103	1.0101
2.0	1.0134	1.0133	1.0132	1.0129	1.0126	1.0122	1.0121	1.0118	1.0116	1.0113	1.0110	1.0108	1.0106
2.1	1.0140	1.0140	1.0139	1.0136	1.0133	1.0129	1.0127	1.0124	1.0122	1.0119	1.0115	1.0114	1.0111
2.2	1.0147	1.0147	1.0146	1.0142	1.0139	1.0135	1.0133	1.0130	1.0128	1.0125	1.0121	1.0120	1.0118
2.3	1.0154	1.0154	1.0153	1.0149	1.0146	1.0141	1.0139	1.0136	1.0133	1.0130	1.0127	1.0125	1.0123
2.4	1.0160	1.0160	1.0159	1.0154	1.0151	1.0146	1.0144	1.0141	1.0138	1.0135	1.0133	1.0130	1.0128
2.5	1.0167	1.0167	1.0166	1.0162	1.0158	1.0153	1.0150	1.0148	1.0145	1.0141	1.0137	1.0135	1.0133
2.6	1.0174	1.0173	1.0172	1.0168	1.0164	1.0159	1.0156	1.0154	1.0151	1.0147	1.0143	1.0141	1.0139
2.7	1.0183	1.0182	1.0181	1.0176	1.0172	1.0167	1.0164	1.0161	1.0158	1.0154	1.0150	1.0148	1.0146
2.8	1.0187	1.0186	1.0185	1.0180	1.0176	1.0171	1.0168	1.0165	1.0162	1.0158	1.0154	1.0152	1.0149
2.9	1.0194	1.0194	1.0192	1.0187	1.0183	1.0177	1.0175	1.0172	1.0168	1.0164	1.0160	1.0157	1.0155
3.0	1.0200	1.0200	1.0198	1.0193	1.0189	1.0183	1.0180	1.0177	1.0173	1.0169	1.0165	1.0162	1.0160
3.1	1.0207	1.0206	1.0205	1.0200	1.0195	1.0189	1.0186	1.0183	1.0179	1.0175	1.0171	1.0168	1.0166
3.2	1.0213	1.0213	1.0211	1.0206	1.0201	1.0195	1.0192	1.0189	1.0185	1.0180	1.0176	1.0173	1.0171
3.3	1.0220	1.0220	1.0218	1.0213	1.0208	1.0202	1.0199	1.0195	1.0191	1.0186	1.0181	1.0178	1.0176
3.4	1.0227	1.0227	1.0225	1.0219	1.0214	1.0208	1.0205	1.0201	1.0197	1.0192	1.0187	1.0184	1.0182
3.5	1.0233	1.0233	1.0231	1.0225	1.0220	1.0214	1.0210	1.0207	1.0202	1.0198	1.0192	1.0190	1.0187
3.6	1.0240	1.0239	1.0237	1.0232	1.0227	1.0220	1.0216	1.0212	1.0208	1.0203	1.0198	1.0195	1.0192
3.7	1.0246	1.0246	1.0244	1.0238	1.0232	1.0225	1.0221	1.0217	1.0213	1.0208	1.0203	1.0200	1.0197
3.8	1.0252	1.0252	1.0250	1.0244	1.0238	1.0231	1.0227	1.0223	1.0219	1.0214	1.0209	1.0206	1.0203
3.9	1.0259	1.0259	1.0257	1.0250	1.0245	1.0237	1.0234	1.0229	1.0225	1.0220	1.0214	1.0211	1.0208
4.0	1.0265	1.0265	1.0263	1.0256	1.0251	1.0243	1.0240	1.0235	1.0231	1.0225	1.0220	1.0217	1.0213

TABLE 13.1k—EXPANSION FACTORS: FLANGE TAPS, Y_2 ; STATIC PRESSURE TAKEN FROM DOWNSTREAM TAPS
(continued)

$$F_d = \frac{d_o}{d_i}$$

$\frac{h_w}{p_{t2}}$ Ratio	0.63	0.64	0.65	0.66	0.67	0.68	0.69	0.70	0.71	0.72	0.73	0.74	0.75
0.0	1.0000	1.0000	1.0000	1.0000	1.0000	1.0000	1.0000	1.0000	1.0000	1.0000	1.0000	1.0000	1.0000
0.1	1.0005	1.0005	1.0005	1.0005	1.0005	1.0005	1.0004	1.0004	1.0004	1.0004	1.0004	1.0004	1.0004
0.2	1.0010	1.0010	1.0010	1.0010	1.0010	1.0009	1.0009	1.0009	1.0008	1.0008	1.0008	1.0008	1.0007
0.3	1.0016	1.0015	1.0015	1.0015	1.0014	1.0014	1.0014	1.0013	1.0013	1.0012	1.0012	1.0011	1.0011
0.4	1.0021	1.0021	1.0020	1.0020	1.0019	1.0019	1.0018	1.0018	1.0017	1.0017	1.0016	1.0015	1.0015
0.5	1.0026	1.0026	1.0025	1.0025	1.0024	1.0024	1.0023	1.0022	1.0022	1.0021	1.0020	1.0019	1.0019
0.6	1.0031	1.0030	1.0030	1.0029	1.0028	1.0027	1.0027	1.0026	1.0025	1.0024	1.0023	1.0022	1.0022
0.7	1.0036	1.0036	1.0035	1.0034	1.0033	1.0032	1.0031	1.0031	1.0030	1.0029	1.0028	1.0026	1.0025
0.8	1.0042	1.0041	1.0040	1.0039	1.0038	1.0037	1.0036	1.0035	1.0034	1.0033	1.0032	1.0031	1.0029
0.9	1.0047	1.0046	1.0045	1.0043	1.0042	1.0041	1.0040	1.0039	1.0039	1.0037	1.0036	1.0035	1.0033
1.0	1.0052	1.0051	1.0050	1.0049	1.0048	1.0046	1.0045	1.0044	1.0043	1.0041	1.0040	1.0039	1.0037
1.1	1.0057	1.0056	1.0055	1.0054	1.0053	1.0051	1.0050	1.0049	1.0047	1.0046	1.0044	1.0042	1.0040
1.2	1.0062	1.0061	1.0060	1.0059	1.0057	1.0056	1.0054	1.0053	1.0051	1.0050	1.0048	1.0046	1.0044
1.3	1.0067	1.0066	1.0065	1.0064	1.0062	1.0061	1.0059	1.0058	1.0056	1.0054	1.0052	1.0050	1.0048
1.4	1.0073	1.0072	1.0070	1.0069	1.0067	1.0065	1.0063	1.0062	1.0060	1.0058	1.0056	1.0054	1.0052
1.5	1.0078	1.0077	1.0075	1.0074	1.0072	1.0070	1.0068	1.0067	1.0065	1.0063	1.0060	1.0058	1.0056
1.6	1.0083	1.0081	1.0080	1.0078	1.0076	1.0075	1.0073	1.0071	1.0069	1.0066	1.0064	1.0062	1.0059
1.7	1.0089	1.0087	1.0086	1.0084	1.0082	1.0080	1.0078	1.0076	1.0074	1.0071	1.0069	1.0066	1.0064
1.8	1.0094	1.0092	1.0091	1.0089	1.0087	1.0084	1.0082	1.0080	1.0078	1.0075	1.0073	1.0070	1.0067
1.9	1.0099	1.0097	1.0095	1.0093	1.0091	1.0089	1.0087	1.0084	1.0082	1.0079	1.0077	1.0074	1.0071
2.0	1.0104	1.0102	1.0100	1.0098	1.0096	1.0094	1.0092	1.0089	1.0087	1.0084	1.0081	1.0078	1.0075
2.1	1.0110	1.0108	1.0105	1.0103	1.0101	1.0099	1.0096	1.0094	1.0091	1.0088	1.0085	1.0082	1.0079
2.2	1.0116	1.0114	1.0111	1.0109	1.0107	1.0104	1.0101	1.0098	1.0095	1.0094	1.0089	1.0086	1.0083
2.3	1.0121	1.0119	1.0116	1.0114	1.0111	1.0109	1.0106	1.0103	1.0100	1.0097	1.0093	1.0090	1.0086
2.4	1.0126	1.0124	1.0121	1.0119	1.0116	1.0114	1.0111	1.0108	1.0105	1.0102	1.0098	1.0095	1.0091
2.5	1.0131	1.0128	1.0126	1.0123	1.0120	1.0118	1.0115	1.0112	1.0109	1.0106	1.0102	1.0098	1.0094
2.6	1.0136	1.0134	1.0131	1.0128	1.0125	1.0123	1.0120	1.0116	1.0113	1.0110	1.0106	1.0102	1.0099
2.7	1.0143	1.0141	1.0138	1.0135	1.0132	1.0129	1.0126	1.0123	1.0119	1.0115	1.0111	1.0107	1.0103
2.8	1.0147	1.0144	1.0141	1.0139	1.0136	1.0132	1.0129	1.0126	1.0122	1.0118	1.0114	1.0110	1.0106
2.9	1.0152	1.0150	1.0147	1.0144	1.0141	1.0137	1.0134	1.0130	1.0127	1.0123	1.0119	1.0114	1.0110
3.0	1.0157	1.0155	1.0152	1.0149	1.0146	1.0142	1.0139	1.0135	1.0131	1.0127	1.0123	1.0119	1.0114
3.1	1.0163	1.0160	1.0157	1.0153	1.0150	1.0147	1.0143	1.0139	1.0135	1.0131	1.0127	1.0123	1.0118
3.2	1.0168	1.0165	1.0162	1.0158	1.0155	1.0152	1.0148	1.0144	1.0140	1.0136	1.0131	1.0127	1.0122
3.3	1.0173	1.0170	1.0166	1.0163	1.0159	1.0156	1.0152	1.0148	1.0144	1.0139	1.0135	1.0130	1.0125
3.4	1.0179	1.0175	1.0172	1.0169	1.0165	1.0161	1.0157	1.0153	1.0149	1.0144	1.0139	1.0135	1.0129
3.5	1.0183	1.0180	1.0177	1.0173	1.0169	1.0165	1.0161	1.0157	1.0153	1.0148	1.0143	1.0139	1.0133
3.6	1.0188	1.0185	1.0182	1.0178	1.0174	1.0170	1.0166	1.0162	1.0158	1.0153	1.0148	1.0143	1.0138
3.7	1.0193	1.0190	1.0187	1.0183	1.0179	1.0175	1.0171	1.0166	1.0162	1.0157	1.0152	1.0146	1.0141
3.8	1.0199	1.0196	1.0192	1.0189	1.0185	1.0180	1.0176	1.0171	1.0167	1.0162	1.0156	1.0151	1.0145
3.9	1.0205	1.0201	1.0197	1.0193	1.0189	1.0185	1.0180	1.0176	1.0171	1.0166	1.0160	1.0155	1.0149
4.0	1.0210	1.0206	1.0202	1.0198	1.0194	1.0190	1.0185	1.0180	1.0175	1.0170	1.0164	1.0159	1.0153

TABLE 13.1I—EXPANSION FACTORS: PIPE TAPS, Y_2 ; STATIC PRESSURE TAKEN FROM DOWNSTREAM TAPS

$$F_d = \frac{d_o}{d_i}$$

$\frac{h_w}{P_{t2}}$ Ratio	0.1	0.2	0.3	0.4	0.45	0.50	0.52	0.54	0.56	0.58	0.60
0.0	1.0000	1.0000	1.0000	1.0000	1.0000	1.0000	1.0000	1.0000	1.0000	1.0000	1.0000
0.1	1.0008	1.0007	1.0006	1.0003	1.0002	1.0000	0.9999	0.9998	1.9997	0.9996	0.9995
0.2	1.0017	1.0015	1.0012	1.0007	1.0004	1.0000	0.9998	0.9997	0.9995	0.9993	0.9990
0.3	1.0025	1.0023	1.0018	1.0010	1.0006	1.0000	0.9998	0.9995	0.9992	0.9989	0.9985
0.4	1.0033	1.0031	1.0024	1.0014	1.0008	1.0000	0.9997	0.9994	0.9989	0.9985	0.9980
0.5	1.0042	1.0037	1.0029	1.0018	1.0010	1.0001	0.9997	0.9993	0.9987	0.9982	0.9975
0.6	1.0051	1.0045	1.0035	1.0021	1.0012	1.0001	0.9996	0.9991	0.9985	0.9979	0.9972
0.7	1.0059	1.0053	1.0042	1.0024	1.0014	1.0001	0.9996	0.9989	0.9983	0.9976	0.9968
0.8	1.0068	1.0060	1.0048	1.0028	1.0016	1.0002	0.9995	0.9988	0.9981	0.9972	0.9963
0.9	1.0076	1.0068	1.0053	1.0032	1.0018	1.0003	0.9995	0.9987	0.9978	0.9969	0.9958
1.0	1.0084	1.0075	1.0059	1.0036	1.0021	1.0003	0.9994	0.9986	0.9976	0.9965	0.9954
1.1	1.0093	1.0082	1.0065	1.0039	1.0023	1.0004	0.9994	0.9984	0.9974	0.9962	0.9949
1.2	1.0101	1.0090	1.0071	1.0043	1.0025	1.0004	0.9994	0.9984	0.9972	0.9959	0.9945
1.3	1.0110	1.0098	1.0077	1.0047	1.0027	1.0004	0.9994	0.9982	0.9969	0.9956	0.9941
1.4	1.0119	1.0106	1.0083	1.0050	1.0030	1.0005	0.9993	0.9981	0.9967	0.9953	0.9937
1.5	1.0127	1.0113	1.0089	1.0054	1.0032	1.0005	0.9993	0.9980	0.9965	0.9950	0.9932
1.6	1.0136	1.0121	1.0095	1.0058	1.0034	1.0006	0.9993	0.9979	0.9964	0.9947	0.9928
1.7	1.0143	1.0128	1.0101	1.0062	1.0036	1.0006	0.9993	0.9978	0.9962	0.9944	0.9924
1.8	1.0152	1.0136	1.0107	1.0065	1.0038	1.0007	0.9992	0.9977	0.9960	0.9942	0.9920
1.9	1.0161	1.0143	1.0113	1.0069	1.0041	1.0008	0.9992	0.9976	0.9958	0.9938	0.9916
2.0	1.0169	1.0150	1.0119	1.0073	1.0044	1.0008	0.9992	0.9975	0.9956	0.9935	0.9912
2.1	1.0177	1.0158	1.0125	1.0077	1.0046	1.0008	0.9992	0.9974	0.9954	0.9933	0.9908
2.2	1.0185	1.0165	1.0131	1.0081	1.0048	1.0009	0.9992	0.9973	0.9953	0.9930	0.9905
2.3	1.0194	1.0173	1.0137	1.0084	1.0050	1.0010	0.9992	0.9972	0.9951	0.9928	0.9902
2.4	1.0202	1.0180	1.0142	1.0089	1.0053	1.0011	0.9992	0.9971	0.9949	0.9924	0.9897
2.5	1.0210	1.0188	1.0148	1.0092	1.0056	1.0012	0.9992	0.9971	0.9948	0.9922	0.9894
2.6	1.0219	1.0195	1.0154	1.0096	1.0058	1.0013	0.9992	0.9970	0.9946	0.9919	0.9890
2.7	1.0230	1.0205	1.0162	1.0101	1.0061	1.0014	0.9992	0.9969	0.9944	0.9916	0.9885
2.8	1.0236	1.0210	1.0166	1.0104	1.0063	1.0014	0.9992	0.9969	0.9943	0.9914	0.9882
2.9	1.0244	1.0217	1.0173	1.0107	1.0065	1.0015	0.9992	0.9968	0.9941	0.9912	0.9879
3.0	1.0251	1.0224	1.0179	1.0111	1.0067	1.0017	0.9992	0.9967	0.9939	0.9910	0.9875
3.1	1.0259	1.0232	1.0185	1.0115	1.0070	1.0018	0.9993	0.9966	0.9938	0.9907	0.9872
3.2	1.0267	1.0239	1.0190	1.0119	1.0072	1.0018	0.9993	0.9966	0.9936	0.9905	0.9869
3.3	1.0276	1.0247	1.0196	1.0122	1.0075	1.0019	0.9993	0.9966	0.9935	0.9903	0.9866
3.4	1.0284	1.0253	1.0202	1.0126	1.0077	1.0020	0.9994	0.9965	0.9934	0.9901	0.9863
3.5	1.0291	1.0261	1.0208	1.0130	1.0080	1.0021	0.9994	0.9964	0.9933	0.9898	0.9860
3.6	1.0301	1.0268	1.0214	1.0134	1.0083	1.0022	0.9994	0.9964	0.9931	0.9896	0.9857
3.7	1.0309	1.0276	1.0219	1.0137	1.0085	1.0023	0.9995	0.9964	0.9930	0.9894	0.9854
3.8	1.0316	1.0287	1.0225	1.0141	1.0088	1.0024	0.9995	0.9963	0.9929	0.9892	0.9850
3.9	1.0324	1.0290	1.0231	1.0145	1.0091	1.0025	0.9995	0.9963	0.9928	0.9889	0.9847
4.0	1.0332	1.0297	1.0237	1.0149	1.0093	1.0025	0.9995	0.9963	0.9927	0.9887	0.9844

TABLE 13.1m—EXPANSION FACTORS: FLANGE TAPS, Y_m ; STATIC PRESSURE, MEAN OF UPSTREAM AND DOWNSTREAM
$$F_d = \frac{d_o}{d_i}$$

$\frac{h_{sc}}{\bar{p}_{lm}}$ Ratio	0.1	0.2	0.3	0.4	0.45	0.50	0.52	0.54	0.56	0.58	0.60	0.61	0.62
0.0	1.0000	1.0000	1.0000	1.0000	1.0000	1.0000	1.0000	1.0000	1.0000	1.0000	1.0000	1.0000	1.0000
0.1	0.9998	0.9998	0.9998	0.9997	0.9997	0.9997	0.9997	0.9997	0.9997	0.9997	0.9996	0.9996	0.9996
0.2	0.9995	0.9995	0.9995	0.9995	0.9994	0.9994	0.9994	0.9994	0.9993	0.9993	0.9993	0.9993	0.9992
0.3	0.9993	0.9993	0.9993	0.9992	0.9992	0.9991	0.9991	0.9990	0.9990	0.9990	0.9989	0.9989	0.9989
0.4	0.9991	0.9991	0.9990	0.9990	0.9989	0.9988	0.9988	0.9987	0.9987	0.9986	0.9986	0.9985	0.9985
0.5	0.9988	0.9988	0.9988	0.9987	0.9986	0.9985	0.9985	0.9984	0.9983	0.9983	0.9982	0.9981	0.9981
0.6	0.9986	0.9986	0.9985	0.9984	0.9984	0.9982	0.9982	0.9981	0.9980	0.9979	0.9978	0.9978	0.9977
0.7	0.9984	0.9984	0.9983	0.9982	0.9981	0.9979	0.9979	0.9978	0.9977	0.9976	0.9975	0.9974	0.9973
0.8	0.9981	0.9981	0.9981	0.9979	0.9978	0.9976	0.9976	0.9975	0.9974	0.9972	0.9971	0.9970	0.9970
0.9	0.9979	0.9979	0.9978	0.9977	0.9975	0.9973	0.9973	0.9972	0.9971	0.9969	0.9968	0.9967	0.9967
1.0	0.9977	0.9977	0.9976	0.9975	0.9973	0.9971	0.9970	0.9969	0.9968	0.9967	0.9965	0.9964	0.9963
1.1	0.9975	0.9974	0.9974	0.9972	0.9971	0.9968	0.9967	0.9966	0.9965	0.9963	0.9961	0.9960	0.9959
1.2	0.9973	0.9973	0.9972	0.9970	0.9968	0.9966	0.9964	0.9963	0.9961	0.9960	0.9958	0.9957	0.9955
1.3	0.9971	0.9970	0.9970	0.9967	0.9965	0.9963	0.9961	0.9960	0.9958	0.9956	0.9954	0.9953	0.9952
1.4	0.9968	0.9968	0.9967	0.9965	0.9963	0.9960	0.9958	0.9957	0.9955	0.9953	0.9951	0.9949	0.9948
1.5	0.9966	0.9966	0.9965	0.9962	0.9960	0.9957	0.9955	0.9954	0.9952	0.9950	0.9948	0.9946	0.9945
1.6	0.9964	0.9964	0.9962	0.9960	0.9957	0.9954	0.9952	0.9950	0.9948	0.9946	0.9944	0.9943	0.9941
1.7	0.9962	0.9962	0.9960	0.9958	0.9955	0.9952	0.9950	0.9948	0.9946	0.9943	0.9941	0.9939	0.9938
1.8	0.9959	0.9959	0.9958	0.9955	0.9953	0.9949	0.9947	0.9945	0.9943	0.9940	0.9937	0.9936	0.9934
1.9	0.9957	0.9957	0.9956	0.9953	0.9950	0.9948	0.9944	0.9942	0.9940	0.9937	0.9934	0.9933	0.9931
2.0	0.9955	0.9954	0.9953	0.9950	0.9946	0.9942	0.9940	0.9938	0.9935	0.9932	0.9929	0.9927	0.9925
2.1	0.9953	0.9953	0.9952	0.9948	0.9945	0.9940	0.9938	0.9936	0.9933	0.9930	0.9927	0.9925	0.9923
2.2	0.9951	0.9951	0.9950	0.9947	0.9943	0.9938	0.9936	0.9934	0.9931	0.9927	0.9924	0.9922	0.9920
2.3	0.9949	0.9949	0.9947	0.9944	0.9940	0.9936	0.9933	0.9931	0.9928	0.9924	0.9921	0.9919	0.9917
2.4	0.9947	0.9947	0.9945	0.9941	0.9938	0.9933	0.9930	0.9927	0.9924	0.9921	0.9917	0.9915	0.9913
2.5	0.9945	0.9944	0.9943	0.9938	0.9935	0.9930	0.9927	0.9924	0.9921	0.9918	0.9914	0.9912	0.9909
2.6	0.9943	0.9942	0.9941	0.9936	0.9933	0.9928	0.9925	0.9922	0.9919	0.9915	0.9911	0.9909	0.9907
2.7	0.9941	0.9941	0.9939	0.9934	0.9930	0.9925	0.9922	0.9919	0.9916	0.9912	0.9907	0.9905	0.9903
2.8	0.9939	0.9938	0.9937	0.9932	0.9928	0.9922	0.9919	0.9916	0.9913	0.9909	0.9904	0.9902	0.9900
2.9	0.9937	0.9936	0.9934	0.9929	0.9925	0.9919	0.9916	0.9913	0.9909	0.9905	0.9901	0.9899	0.9896
3.0	0.9935	0.9934	0.9932	0.9927	0.9923	0.9917	0.9914	0.9911	0.9907	0.9903	0.9898	0.9895	0.9892
3.1	0.9932	0.9932	0.9930	0.9925	0.9920	0.9914	0.9911	0.9908	0.9904	0.9900	0.9895	0.9892	0.9890
3.2	0.9931	0.9931	0.9929	0.9923	0.9919	0.9912	0.9909	0.9905	0.9901	0.9897	0.9892	0.9889	0.9886
3.3	0.9929	0.9928	0.9926	0.9921	0.9916	0.9909	0.9906	0.9902	0.9898	0.9894	0.9889	0.9886	0.9883
3.4	0.9927	0.9926	0.9924	0.9918	0.9913	0.9907	0.9903	0.9899	0.9895	0.9890	0.9885	0.9882	0.9879
3.5	0.9925	0.9924	0.9922	0.9916	0.9911	0.9905	0.9901	0.9897	0.9893	0.9888	0.9883	0.9880	0.9877
3.6	0.9923	0.9923	0.9920	0.9914	0.9909	0.9902	0.9898	0.9894	0.9890	0.9885	0.9878	0.9876	0.9873
3.7	0.9921	0.9920	0.9918	0.9912	0.9907	0.9899	0.9895	0.9891	0.9887	0.9882	0.9876	0.9873	0.9870
3.8	0.9919	0.9918	0.9916	0.9910	0.9905	0.9897	0.9893	0.9889	0.9884	0.9879	0.9873	0.9870	0.9866
3.9	0.9918	0.9917	0.9915	0.9908	0.9902	0.9894	0.9890	0.9886	0.9881	0.9876	0.9870	0.9867	0.9863
4.0	0.9916	0.9915	0.9913	0.9906	0.9900	0.9892	0.9888	0.9884	0.9879	0.9873	0.9867	0.9864	0.9861

TABLE 13.1m—EXPANSION FACTORS: FLANGE TAPS, Y_m , STATIC PRESSURE, MEAN OF UPSTREAM AND DOWNSTREAM (continued)

$$F_d = \frac{d_o}{d_i}$$

$\frac{h_w}{\rho_{lm}}$ Ratio	0.63	0.64	0.65	0.66	0.67	0.68	0.69	0.70	0.71	0.72	0.73	0.74	0.75
0.0	1.0000	1.0000	1.0000	1.0000	1.0000	1.0000	1.0000	1.0000	1.0000	1.0000	1.0000	1.0000	1.0000
0.1	0.9996	0.9996	0.9996	0.9996	0.9996	0.9996	0.9995	0.9995	0.9995	0.9995	0.9995	0.9995	0.9995
0.2	0.9992	0.9992	0.9992	0.9992	0.9991	0.9991	0.9991	0.9991	0.9990	0.9990	0.9990	0.9989	0.9989
0.3	0.9988	0.9988	0.9988	0.9987	0.9987	0.9987	0.9986	0.9986	0.9986	0.9985	0.9985	0.9984	0.9984
0.4	0.9984	0.9984	0.9984	0.9983	0.9983	0.9982	0.9982	0.9981	0.9981	0.9980	0.9980	0.9979	0.9978
0.5	0.9981	0.9980	0.9980	0.9979	0.9978	0.9978	0.9977	0.9977	0.9976	0.9975	0.9974	0.9974	0.9973
0.6	0.9977	0.9976	0.9975	0.9975	0.9974	0.9973	0.9973	0.9972	0.9971	0.9970	0.9969	0.9968	0.9967
0.7	0.9973	0.9972	0.9971	0.9971	0.9970	0.9969	0.9968	0.9967	0.9966	0.9965	0.9964	0.9963	0.9962
0.8	0.9969	0.9968	0.9967	0.9967	0.9965	0.9965	0.9964	0.9963	0.9962	0.9961	0.9960	0.9959	0.9957
0.9	0.9966	0.9965	0.9964	0.9963	0.9962	0.9961	0.9960	0.9959	0.9957	0.9956	0.9955	0.9953	0.9952
1.0	0.9962	0.9961	0.9960	0.9959	0.9958	0.9957	0.9955	0.9954	0.9953	0.9951	0.9950	0.9948	0.9947
1.1	0.9958	0.9957	0.9956	0.9955	0.9953	0.9952	0.9951	0.9949	0.9948	0.9946	0.9945	0.9943	0.9941
1.2	0.9954	0.9953	0.9952	0.9951	0.9949	0.9948	0.9946	0.9945	0.9943	0.9941	0.9940	0.9938	0.9936
1.3	0.9951	0.9949	0.9948	0.9946	0.9945	0.9943	0.9942	0.9940	0.9938	0.9936	0.9934	0.9933	0.9931
1.4	0.9947	0.9945	0.9944	0.9942	0.9941	0.9939	0.9938	0.9936	0.9934	0.9932	0.9930	0.9928	0.9926
1.5	0.9944	0.9942	0.9941	0.9939	0.9937	0.9935	0.9933	0.9932	0.9929	0.9927	0.9925	0.9923	0.9920
1.6	0.9940	0.9938	0.9937	0.9935	0.9933	0.9931	0.9929	0.9927	0.9925	0.9922	0.9920	0.9918	0.9915
1.7	0.9936	0.9934	0.9933	0.9931	0.9929	0.9927	0.9925	0.9923	0.9921	0.9918	0.9916	0.9913	0.9910
1.8	0.9932	0.9930	0.9928	0.9927	0.9925	0.9923	0.9920	0.9918	0.9916	0.9913	0.9911	0.9908	0.9905
1.9	0.9929	0.9927	0.9925	0.9923	0.9921	0.9919	0.9916	0.9914	0.9911	0.9908	0.9906	0.9903	0.9900
2.0	0.9923	0.9921	0.9919	0.9917	0.9915	0.9912	0.9910	0.9907	0.9904	0.9901	0.9899	0.9896	0.9892
2.1	0.9921	0.9919	0.9917	0.9915	0.9913	0.9910	0.9908	0.9905	0.9902	0.9899	0.9896	0.9893	0.9890
2.2	0.9918	0.9916	0.9913	0.9911	0.9908	0.9906	0.9903	0.9900	0.9897	0.9894	0.9892	0.9888	0.9884
2.3	0.9915	0.9913	0.9910	0.9908	0.9905	0.9902	0.9900	0.9897	0.9894	0.9891	0.9887	0.9884	0.9880
2.4	0.9911	0.9909	0.9906	0.9904	0.9901	0.9898	0.9895	0.9892	0.9889	0.9886	0.9882	0.9878	0.9875
2.5	0.9907	0.9905	0.9902	0.9900	0.9897	0.9894	0.9891	0.9888	0.9885	0.9881	0.9878	0.9874	0.9870
2.6	0.9904	0.9902	0.9899	0.9896	0.9893	0.9890	0.9887	0.9884	0.9880	0.9876	0.9873	0.9869	0.9865
2.7	0.9900	0.9898	0.9895	0.9892	0.9889	0.9886	0.9883	0.9880	0.9876	0.9872	0.9869	0.9864	0.9860
2.8	0.9897	0.9895	0.9892	0.9889	0.9886	0.9882	0.9879	0.9875	0.9871	0.9867	0.9864	0.9859	0.9855
2.9	0.9893	0.9891	0.9888	0.9885	0.9882	0.9878	0.9874	0.9871	0.9867	0.9863	0.9859	0.9855	0.9850
3.0	0.9890	0.9887	0.9884	0.9881	0.9877	0.9874	0.9870	0.9867	0.9863	0.9859	0.9854	0.9850	0.9845
3.1	0.9887	0.9884	0.9881	0.9877	0.9874	0.9870	0.9867	0.9863	0.9859	0.9854	0.9850	0.9845	0.9840
3.2	0.9883	0.9880	0.9877	0.9873	0.9870	0.9866	0.9862	0.9858	0.9854	0.9850	0.9845	0.9840	0.9835
3.3	0.9880	0.9877	0.9873	0.9870	0.9866	0.9863	0.9859	0.9854	0.9850	0.9845	0.9841	0.9836	0.9831
3.4	0.9876	0.9873	0.9869	0.9866	0.9862	0.9858	0.9854	0.9850	0.9845	0.9841	0.9836	0.9831	0.9825
3.5	0.9873	0.9870	0.9866	0.9863	0.9859	0.9855	0.9850	0.9846	0.9841	0.9837	0.9832	0.9826	0.9821
3.6	0.9869	0.9866	0.9862	0.9859	0.9855	0.9851	0.9846	0.9842	0.9837	0.9833	0.9827	0.9822	0.9816
3.7	0.9866	0.9863	0.9859	0.9855	0.9851	0.9847	0.9842	0.9838	0.9833	0.9828	0.9822	0.9817	0.9811
3.8	0.9863	0.9859	0.9855	0.9851	0.9847	0.9843	0.9838	0.9834	0.9829	0.9824	0.9818	0.9813	0.9807
3.9	0.9860	0.9856	0.9852	0.9848	0.9844	0.9839	0.9835	0.9830	0.9825	0.9820	0.9814	0.9808	0.9802
4.0	0.9857	0.9853	0.9849	0.9845	0.9840	0.9836	0.9831	0.9826	0.9820	0.9815	0.9809	0.9803	0.9797

TABLE 13.1n—MANOMETER FACTORS (MERCURY METERS), F_m

Specific Gravity, γ_g	Flowing pressure, psig						
	0	500	1000	1500	2000	2500	3000
Ambient Temperature = 0°F							
0.55	1.0000	0.9989	0.9976	0.9960	0.9943	0.9930	0.9921
0.60	1.0000	0.9988	0.9972	0.9952	0.9932	0.9919	0.9910
0.65	1.0000	0.9987	0.9967	0.9941	0.9920	0.9908	0.9900
0.70	1.0000	0.9985	0.9961	0.9927	0.9907	0.9896	0.9890
0.75	1.0000	—	—	—	—	—	—
Ambient Temperature = 40°F							
0.55	1.0000	0.9990	0.9979	0.9967	0.9954	0.9942	0.9932
0.60	1.0000	0.9989	0.9976	0.9962	0.9946	0.9933	0.9923
0.65	1.0000	0.9988	0.9973	0.9955	0.9937	0.9923	0.9913
0.70	1.0000	0.9987	0.9970	0.9947	0.9926	0.9912	0.9903
0.75	1.0000	0.9986	0.9965	0.9937	0.9915	0.9902	0.9893
Ambient Temperature = 80°F							
0.55	1.0000	0.9991	0.9981	0.9971	0.9960	0.9950	0.9941
0.60	1.0000	0.9990	0.9979	0.9967	0.9955	0.9943	0.9933
0.65	1.0000	0.9989	0.9977	0.9963	0.9948	0.9935	0.9925
0.70	1.0000	0.9988	0.9974	0.9958	0.9940	0.9926	0.9915
0.75	1.0000	0.9987	0.9971	0.9951	0.9931	0.9916	0.9906
Ambient Temperature = 120°F							
0.55	1.0000	0.9992	0.9983	0.9974	0.9965	0.9956	0.9948
0.60	1.0000	0.9991	0.9981	0.9971	0.9960	0.9950	0.9941
0.65	1.0000	0.9990	0.9979	0.9967	0.9955	0.9944	0.9934
0.70	1.0000	0.9989	0.9977	0.9963	0.9950	0.9937	0.9926
0.75	1.0000	0.9988	0.9975	0.9959	0.9943	0.9929	0.9918

TABLE 13.1o—GAUGE LOCATION FACTOR— F_ℓ

Degrees Latitude	Gauge Elevation Above Sea Level, ft					
	Sea Level	2,000	4,000	6,000	8,000	10,000
0 (Equator)	0.9967	0.9986	0.9985	0.9984	0.9983	0.9982
5	0.9987	0.9986	0.9985	0.9984	0.9983	0.9982
10	0.9968	0.9987	0.9986	0.9985	0.9984	0.9983
15	0.9989	0.9988	0.9987	0.9986	0.9985	0.9984
20	0.9990	0.9989	0.9988	0.9987	0.9986	0.9985
25	0.9991	0.9990	0.9989	0.9988	0.9987	0.9986
30	0.9993	0.9992	0.9991	0.9990	0.9989	0.9988
35	0.9995	0.9994	0.9993	0.9992	0.9991	0.9990
40	0.9996	0.9997	0.9996	0.9996	0.9994	0.9993
45	1.0000	0.9999	0.9998	0.9997	0.9996	0.9996
50	1.0002	1.0001	1.0000	0.9999	0.9998	0.9997
55	1.0004	1.0003	1.0002	1.0001	1.0000	0.9999
60	1.0007	1.0006	1.0005	1.0004	1.0003	1.0002
65	1.0008	1.0007	1.0006	1.0005	1.0004	1.0003
70	1.0010	1.0009	1.0008	1.0007	1.0006	1.0005
75	1.0011	1.0010	1.0009	1.0008	1.0007	1.0006
80	1.0012	1.0011	1.0010	1.0009	1.0008	1.0007
85	1.0013	1.0012	1.0011	1.0010	1.0009	1.0008
90 (Pole)	1.0013	1.0012	1.0011	1.0010	1.0009	1.0008

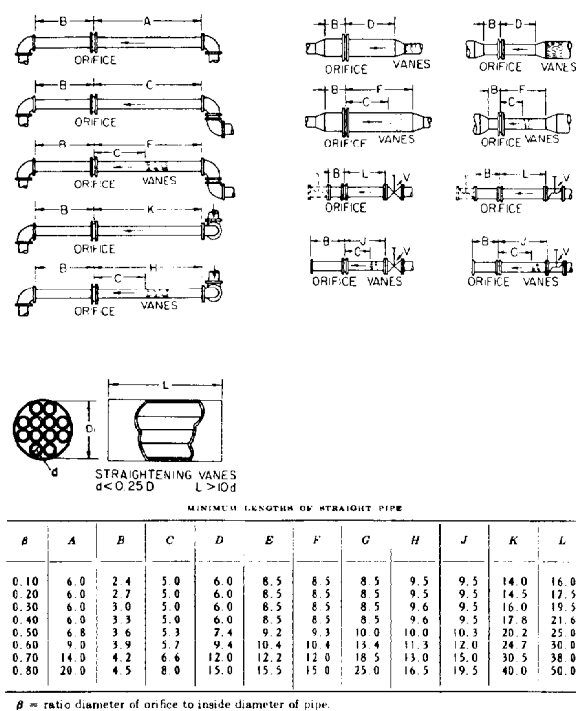


Fig. 13.3—Proper installation of a meter run for an orifice meter.

Physical Setup of System

Inasmuch as standard tables are used, careful attention must be paid to the physical setup of the metering system. Otherwise the results would vary with the installation.

Straightening Vanes. The purpose of these vanes is to minimize the effect of swirls, eddy currents, or irregular velocity distribution on meter accuracy. These vanes are built into a nipple and consist of a bundle of small pipe or tubing as shown in Fig. 13.3. The dimension of each tube d should not exceed one-fourth of the inside pipe diameter d_i . The length should be at least $10d$.

Unless necessary, vanes should not be used because they are susceptible to erosion, introduce additional pressure loss, and clog easily.

Orifice Location. Fig. 13.3 shows the minimum distance the orifice should be from valves and fittings in order that proper metering might result.

Size of Orifice and Meter Run. The meter run should be sized so that the anticipated maximum and minimum flow rates may be handled within the satisfactory ratio of orifice to pipe diameter. In doing this, it should be kept in mind that (1) the differential h_w should not exceed the static pressure p_s (based on numerical values only, not units); (2) the meter run ID should be at least one-third larger than the orifice opening; and (3) both the differential- and static-pressure pens should preferably operate within the middle 60% of the recording-chart range.

As a practical matter, the meter run ID should not be less than 3 in. in nominal diameter regardless of the small quantity of gas flowing. As a first approximation, Eq. 6 should be solved for C' at the flow rate h_w and p_f desired. Then

$$d_o = \left(\frac{C'}{250} \right)^{0.5} \quad (8)$$

If the maximum anticipated flow rate is used to find C' , multiplying the orifice size found in Eq. 8 by 1.5 gives the approximate minimum pipe diameter needed. Once this has been established, it is a relatively simple matter to change orifice plates as the flow varies to keep the values of h_w , and p_f in the desired range. If flow is small and fairly constant (e.g. fuel meter) and/or a 1/4-in. orifice is used, a 2-in. run should be used to avoid low F_d (below 0.10).

Standard sharp-edged orifice plates should be used, the thickness of which is at least 1/16 in. For pipes larger than 4 in., thickness is at least 1/8 in. The thickness should not exceed one-eighth the orifice opening.

Recorder. The normal orifice meter is equipped with a two-pen recorder for measuring both static and differential pressure. The differential pen is normally actuated through a mechanical system using either a mercury manometer or a bellows. Both types are shown in Fig. 13.4.

With the former, a slight change in flow rate changes the level in the mercury manometer. A large float resting on the mercury changes level correspondingly and transmits this movement to the chart pen through a system of levers.

The bellows-type or mercuryless meter consists of two bellows filled with fluid such as glycol. As the pressure differential changes, this fluid moves between the bellows through a damping device, causing the bellows to expand or contract. The pen is actuated by a center rod, which is connected to the free ends of the bellows. The small liquid-filled bellows located on the high-pressure side serves as an expansion device to correct for changes in ambient temperature.

Both types of instruments are equipped with check valves to protect them from differential pressures that exceed the range of the instrument. This is more of a problem with the mercury meter, for excessive differential pressure can blow mercury out of the meter, which destroys its calibration. In the bellows meter, soft-seated check valves prevent the flow of fluid between the bellows. The bellows are then not likely to rupture for they are supported internally by the fluid contained within them.

The bellows meter has gained increasing popularity, particularly in field operations. Even though the initial cost is higher, many operators feel that this is compensated for by decreased maintenance. It also offers the advantage of operating either properly or not at all, with little range in between. Eliminated are the problems of mercury loss, worrying about the change in calibration with the amount of mercury, and the like. Until it fails, experience has shown that this meter needs little routine calibration.

With both types, the static pressure is read from a pen actuated by a bourdon tube. The lead for this may come off either the upstream or downstream tap. In most installations, it is good practice to order a bourdon tube having about twice the maximum pressure anticipated. This minimizes the problem of distortion, which destroys the original calibration of the tube. These tubes are available in many materials, the type depending on the service and the pressure rating desired.

Most meters are hooked up using a standard five-valve manifold of the type shown just above the bellows meter in Fig. 13.4. One valve is placed on each of the leads to the pressure taps, two valves on the bypass, plus a vent valve. When the meter is placed in operation the bypass valves would be open, as would the two main valves, with the vent valve closed. The meter is then placed in service by slowly closing the bypass valves, followed by opening of the vent valve. This procedure prevents momentary pressure surges that might damage the meter or upset the calibration. The reverse procedure would be used in taking the meter out of service. When the leads are bypassed, the vent valve is an excellent place to obtain a gas sample. A slightly more complex manifold is shown above the mercury meter, with drip pots for removing any liquid in the gas.

Standard calibration procedure on the differential pen calls for connecting one side of a water manometer into the high-pressure side of the meter. The low-pressure side of the meter is then opened to the atmosphere. This gives two manometers in parallel. By superimposing pressure on the high-pressure cell with a hand pump or similar device, one may compare the meter reading with that of the manometer. If they are different, the meter must be adjusted accordingly.

The bourdon tube may be calibrated simply by placing a dead-weight tester (preferred) or a calibrated pressure gauge in the lead line to the bourdon tube. By proper manipulation of the valves, the vent valve may be used to make this connection.

The circular charts used usually cover a time period of 24 hours or 7 days. Many meters have clocks that may be easily adjusted for either time period. In most production operations, 7-day periods are preferred, because this minimizes the cost of changing charts and the number of charts to be handled.

Other Forms of Metering Systems

For well-test purposes, other forms of velocity meters are used—orifice well testers, critical-flow provers, pitot tubes, and side-static methods. These methods are not so accurate as the meters discussed previously but are convenient and often yield results accurate enough for the purpose.

Orifice Well Tester. This consists of a 2-in. nipple with provision for attaching different sharp-edged orifice plates on the end. The static pressure just upstream from this plate may then be measured. Tables 13.2a and b show various applicable charts for measuring flow.⁴

The accuracy of this device is limited but it is suitable for measuring the amount of gas being produced where the pressures are relatively low and the production is to the atmosphere.

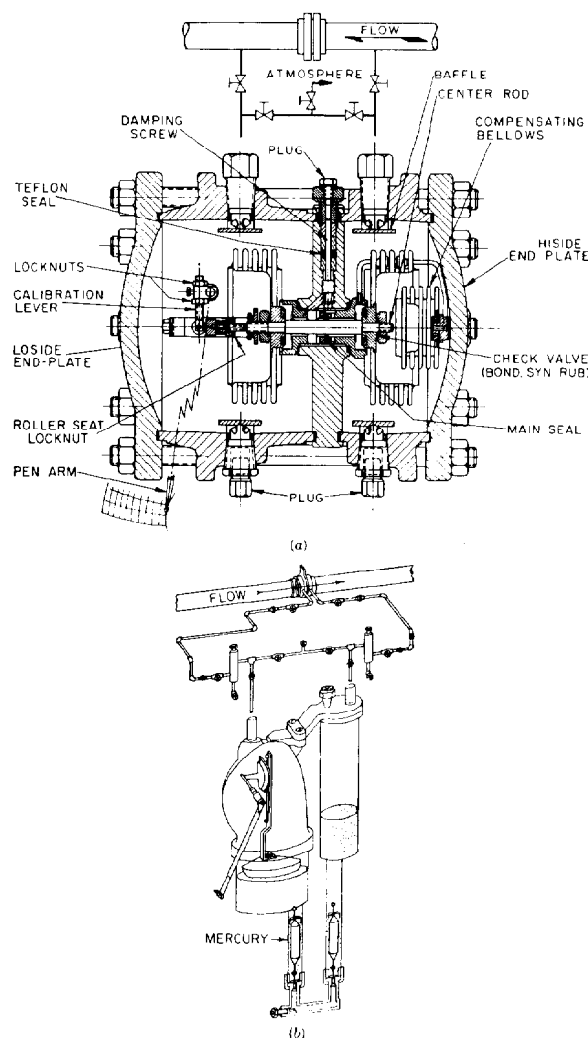


Fig. 13.4—Views showing construction of meters.

Critical-Flow Prover. The critical-flow prover is a similar device that exhausts the gas to the atmosphere. It is also a special pipe nipple with a flange for holding special plates to the end. It is based on the principle that the velocity of sound represents the maximum speed at which a pressure effect may be propagated through a gas—i.e., once this velocity is reached, further increase in the pressure differential will not increase the pressure at the throat. This means that the mass rate of flow would not increase as the pressure differential p_2/p_1 was decreased below this critical value. With ideal gases, the critical ratio is 0.49 for monatomic gases and 0.53 for diatomic gases, with slightly higher values for complex gases. Saturated steam, for example, shows a critical pressure ratio of 0.55. The range of these values is the source of the common rule of thumb that, once the pressure reduction is twofold, critical-flow phenomena limit the mass rate of flow.

When metering gas under such conditions, the volume rate of flow will be a function of upstream pressure, gas gravity, and gas temperature, since it is a compressible fluid.

(continued on Page 45)

TABLE 13.2a—CAPACITIES OF ORIFICE WELL TESTERS*

Pressure, in. of water	Specific gravity								
	0.60	0.70	0.80	0.90	1.00	1.10	1.20	1.30	1.50
1/8-in. Orifice in 1/8-in. Plate									
1.0	528	489	458	432	409	390	374	359	334
1.2	578	536	501	473	448	427	409	393	366
1.4	625	579	541	511	484	462	442	425	395
1.6	669	619	579	546	518	494	473	454	423
1.8	709	657	614	579	549	524	502	482	449
2.0	747	692	647	610	579	552	528	508	473
2.2	784	726	679	640	607	579	554	532	496
2.4	818	758	709	669	634	605	579	556	518
2.6	852	789	738	696	660	629	603	579	539
2.8	884	819	766	722	685	653	625	601	559
3.0	915	848	793	747	709	676	647	622	579
3.2	945	875	819	772	732	698	669	642	598
3.4	975	902	844	796	755	720	689	662	616
3.6	1000	928	868	819	777	740	709	681	634
3.8	1030	954	892	841	798	761	728	700	651
4.0	1060	979	915	863	819	781	747	718	669
4.5	1120	1040	971	915	868	823	793	762	709
5.0	1180	1090	1020	965	915	873	836	803	747
5.5	1240	1150	1070	1010	960	915	876	842	784
6.0	1290	1200	1120	1060	1000	956	915	879	819
6.5	1340	1250	1170	1100	1040	995	953	916	852
7.0	1390	1290	1210	1140	1080	1030	989	950	885
8.0	1500	1380	1290	1220	1160	1100	1060	1020	945
9.0	1590	1470	1370	1290	1230	1170	1120	1080	1000
10.0	1670	1550	1450	1360	1290	1230	1180	1140	1060
11.0	1750	1620	1520	1430	1360	1300	1240	1190	1110
12.0	1830	1700	1590	1500	1420	1350	1300	1250	1160
13.0	1910	1770	1650	1560	1480	1410	1350	1300	1200
14.0	1980	1830	1720	1620	1540	1460	1400	1350	1250
15.0	2050	1900	1780	1680	1590	1520	1450	1390	1300
1/4-in. Orifice in 1/8-in. Plate									
1.0	1680	1560	1460	1370	1300	1240	1190	1140	1060
1.2	1850	1710	1600	1510	1430	1360	1300	1250	1170
1.4	1990	1840	1730	1630	1540	1470	1410	1350	1260
1.6	2130	1970	1840	1740	1650	1570	1510	1450	1350
1.8	2260	2090	1960	1840	1750	1670	1600	1530	1430
2.0	2370	2200	2060	1940	1840	1760	1680	1620	1510
2.2	2490	2310	2160	2040	1930	1840	1770	1700	1580
2.4	2610	2410	2260	2130	2020	1930	1840	1770	1650
2.6	2710	2510	2350	2220	2100	2000	1920	1840	1720
2.8	2810	2610	2440	2300	2180	2080	1990	1910	1780
3.0	2920	2700	2530	2380	2260	2150	2060	1980	1840
3.2	3010	2790	2610	2460	2330	2220	2130	2050	1900
3.4	3110	2870	2690	2540	2410	2290	2200	2110	1960
3.6	3190	2960	2770	2610	2470	2360	2260	2170	2020
3.8	3280	3040	2840	2680	2540	2420	2320	2230	2070
4.0	3370	3120	2920	2750	2610	2490	2380	2290	2130
4.5	3580	3310	3090	2920	2770	2640	2530	2430	2260
5.0	3710	3490	3260	3070	2920	2780	2660	2560	2380
5.5	3950	3650	3420	3220	3060	2920	2790	2680	2500
6.0	4120	3820	3570	3370	3190	3040	2910	2800	2610
6.5	4300	3970	3720	3500	3330	3170	3040	2920	2710
7.0	4450	4120	3860	3640	3450	3290	3150	3030	2820
8.0	4760	4410	4120	3890	3690	3520	3370	3230	3010
9.0	5050	4680	4370	4120	3910	3730	3570	3430	3190
10.0	5320	4930	4610	4350	4120	3930	3760	3620	3370
11.0	5600	5180	4850	4570	4340	4140	3960	3810	3540
12.0	5860	5420	5070	4780	4540	4325	4150	3980	3700
13.0	6100	5650	5280	4980	4730	4510	4320	4140	3860
14.0	6330	5860	5480	5170	4900	4670	4480	4300	4000
15.0	6550	6070	5670	5350	5080	4840	4640	4450	4140

TABLE 13.2a—CAPACITIES OF ORIFICE WELL TESTERS* (continued)

Pressure, in. of water	Specific gravity								
	0.60	0.70	0.80	0.90	1.00	1.10	1.20	1.30	1.50
3⁄8-in. Orifice in 1⁄8-in. Plate									
1.0	3560	3300	3090	2910	2760	2640	2520	2430	2260
1.2	3910	3620	3390	3190	3030	2890	2760	2660	2470
1.4	4220	3910	3660	3450	3270	3120	2990	2870	2670
1.6	4520	4180	3910	3690	3500	3340	3190	3070	2860
1.8	4790	4440	4150	3910	3710	3540	3390	3250	3030
2.0	5050	4670	4370	4120	3910	3780	3570	3430	3190
2.2	5290	4900	4580	4320	4100	3910	3740	3600	3350
2.4	5520	5120	4790	4510	4280	4080	3910	3760	3500
2.6	5760	5330	4980	4700	4460	4250	4070	3910	3640
2.8	5980	5530	5170	4880	4630	4410	4220	4060	3780
3.0	6180	5720	5350	5050	4790	4570	4370	4200	3910
3.2	6390	5910	5530	5210	4950	4720	4520	4340	4040
3.4	6580	6090	5700	5370	5100	4860	4650	4470	4160
3.6	6780	6270	5860	5530	5250	5000	4790	4600	4280
3.8	6960	6440	6020	5680	5390	5140	4920	4730	4400
4.0	7140	6610	6180	5830	5530	5270	5050	4850	4520
4.5	7580	7010	6560	6180	5870	5590	5350	5140	4790
5.0	7980	7390	6910	6520	6180	5890	5640	5420	5050
5.5	8370	7750	7250	6830	6480	6180	5920	5690	5290
6.0	8740	8090	7570	7140	6770	6460	6180	5940	5530
6.5	9100	8430	7880	7430	7050	6720	6440	6180	5760
7.0	8450	8740	8180	7710	7320	6980	6680	6420	5970
8.0	10100	9350	8740	8240	7820	7460	7140	6860	6380
9.0	10700	9910	9270	8740	8300	7910	7570	7280	6770
10.0	11300	10400	9770	9200	8740	8340	7980	7670	7140
11.0	11900	11000	10300	9700	9200	8780	8410	8070	7510
12.0	12400	11500	10800	10100	9620	9180	8790	8440	7860
13.0	12900	12000	11200	10600	10000	9560	9160	8790	8190
14.0	12400	12400	11600	11000	10400	9920	9510	9120	8490
15.0	13900	12900	12000	11300	10800	10300	9840	9440	8790
1⁄2-in. Orifice in 1⁄8-in. Plate									
1.0	6270	5810	5430	5120	4860	4630	4440	4260	3970
1.2	6870	6360	5950	5610	5320	5070	4860	4670	4350
1.4	7420	6870	6430	6060	5750	5480	5250	5040	4690
1.6	7940	7350	6870	6480	6150	5860	5610	5390	5020
1.8	8430	7880	7290	6870	6520	6220	5950	5720	5330
2.0	8870	8210	7680	7240	6870	6550	6270	6030	5610
2.2	9310	8610	8060	7600	7210	6870	6580	6320	5880
2.4	9720	9000	8420	7940	7530	7180	6870	6600	6150
2.6	10100	9360	8760	8260	7830	7470	7150	6870	6400
2.8	10500	9720	9090	8570	8130	7750	7420	7130	6640
3.0	10900	10100	9410	8870	8420	8030	7680	7380	6870
3.2	11200	10400	9720	9170	8700	8290	7940	7630	7100
3.4	11600	10700	10000	9450	8960	8550	8180	7860	7320
3.6	11900	11000	10300	9720	9220	8790	8420	8090	7530
3.8	12200	11300	10600	9980	9470	9030	8650	8310	7730
4.0	12500	11600	10900	10200	9720	9270	8870	8530	7940
4.5	13300	12300	11500	10900	10300	9830	9410	9040	8420
5.0	14100	13000	12100	11500	10900	10400	9920	9530	8870
5.5	14700	13600	12700	12000	11400	10900	10400	10000	9310
6.0	15400	14200	13300	12500	11900	11300	10900	10400	9720
6.5	16000	14800	13900	13100	12400	11800	11300	10900	10100
7.0	16700	15400	14400	13600	12900	12300	11700	11300	10500
8.0	17200	16400	15400	14500	13700	13100	12500	12100	11200
9.0	18800	17400	16300	15400	14600	13900	13300	12800	11900
10.0	19900	18400	17200	16200	15400	14700	14000	13500	12500
11.0	20900	19400	18100	17100	16200	15500	14800	14200	13200
12.0	21900	20300	19000	17900	17000	16200	15500	14900	13800
13.0	22800	21100	19700	18600	17700	16800	16100	15500	14400
14.0	23700	21900	20500	19300	18300	17500	16700	16100	15000
15.0	24500	22700	21200	20000	19000	18100	17300	16600	15500

TABLE 13.2a—CAPACITIES OF ORIFICE WELL TESTERS* (continued)

Pressure, in. of water	Specific gravity								
	0.60	0.70	0.80	0.90	1.00	1.10	1.20	1.30	1.50
¾-in. Orifice in ½-in. Plate									
1.0	14200	13100	12300	11600	11000	10500	10000	9260	8960
1.2	15500	14400	13400	12700	12000	11500	11000	10500	9810
1.4	16800	15500	14500	13700	13000	12400	11800	11400	10600
1.6	17900	16600	15500	14600	13900	13200	12700	12200	11300
1.8	19000	17600	16500	15500	14700	14000	13400	12900	12000
2.0	20000	18500	17300	16400	15500	14800	14200	13600	12700
2.2	21000	19400	18200	17100	16300	15500	14900	14300	13300
2.4	21900	20300	19000	17900	17000	16200	15500	14900	13900
2.6	22900	21100	19800	18600	17700	16800	16100	15500	14400
2.8	23800	21900	20500	19300	18400	17500	16800	16100	15000
3.0	24500	22700	21200	20000	19000	18100	17300	16700	15500
3.2	25300	23500	21900	20700	19600	18700	17900	17200	16000
3.4	26100	24200	22600	21300	20200	19300	18500	17700	16500
3.6	26900	24900	23300	21900	20800	19800	19000	18300	17000
3.8	27600	25600	23900	22500	21400	20400	19500	18800	17500
4.0	28300	26200	24500	23100	21900	20900	20000	19200	17900
4.5	30100	27800	26000	24500	23300	22200	21200	20400	19000
5.0	31600	29300	27400	25900	24500	23400	22400	21500	20000
5.5	33200	30700	28800	27100	25700	24500	23500	22600	21000
6.0	34700	32100	30000	28300	26900	25600	24500	23600	21900
6.5	36100	33400	31300	29500	28000	26700	25500	24500	22800
7.0	37400	34700	32500	30600	29000	27700	26500	25500	23700
8.0	40000	37100	34700	32700	31000	29600	28300	27200	25300
9.0	42500	39300	36800	34700	32900	31400	30000	28900	26900
10.0	44800	41500	38800	36600	34700	33100	31700	30400	28300
11.0	47200	43700	40900	38500	36500	34800	33400	32000	29800
12.0	49300	45700	42700	40300	38200	36400	34900	33500	31200
13.0	51400	47600	44500	42000	39800	38000	36400	34900	32500
14.0	53300	49300	46200	43500	41300	39400	37700	36200	33700
15.0	55200	51100	47800	45100	42800	40800	39100	37500	34900
1-in. Orifice in ½-in. Plate									
1.0	25800	23900	22400	21100	20000	19100	18300	17500	16300
1.2	28300	26200	24500	23100	21900	20900	20000	19200	17900
1.4	30600	28300	26500	24900	23700	22600	21600	20800	19300
1.6	32700	30200	28300	26700	25300	24100	23100	22200	20700
1.8	34600	32100	30000	28300	26800	25600	24500	23500	21900
2.0	36500	33800	31600	29800	28300	27000	25800	24800	23100
2.2	38300	35400	33200	31300	29700	28300	27100	26000	24200
2.4	40000	37000	34600	32700	31000	29500	28300	27200	25300
2.6	41600	38500	36000	34000	32200	30700	29400	28300	26300
2.8	43200	40000	37400	35300	33500	31900	30500	29300	27300
3.0	44700	41400	38700	36500	34600	33000	31600	30400	28300
3.2	46200	42800	40000	37700	35800	34100	32700	31400	29200
3.4	47600	44100	41200	38900	36900	35200	33700	32300	30100
3.6	48900	45300	42400	40000	37900	36200	34600	33300	31000
3.8	50300	46600	43600	41100	39000	37200	35600	34200	31800
4.0	51600	47800	44700	42200	40000	38100	36500	35100	32700
4.5	54700	50700	47400	44700	42400	40400	38700	37200	34600
5.0	57700	53400	50000	47100	44700	42600	40800	39200	36500
5.5	60500	56100	52400	49400	46900	44700	42800	41100	38300
6.0	63300	58500	54800	51600	49000	46700	44700	43000	40000
6.5	65800	61000	57000	53800	51000	48600	46600	44700	41600
7.0	68300	63200	59200	55800	52900	50500	48300	46400	43200
8.0	73100	67600	63200	59600	56600	53900	51600	49600	46200
9.0	77500	71700	67100	63200	60000	57200	54800	52600	49000
10.0	81600	75600	70700	66700	63200	60300	57700	55500	51600
11.0	85900	79500	74400	70100	66500	63500	60800	58400	54300
12.0	89800	83200	77800	73300	69600	66400	63600	61000	56800
13.0	93600	86600	81000	76400	72500	69100	66200	63600	59200
14.0	97300	89900	84100	79300	75200	71700	68700	66000	61400
15.0	101000	93000	87100	82100	77900	74200	71200	68300	63600

TABLE 13.2a—CAPACITIES OF ORIFICE WELL TESTERS* (continued)

Pressure, in. of water	Specific gravity								
	0.60	0.70	0.80	0.90	1.00	1.10	1.20	1.30	1.50
1¼-in. Orifice in ⅛-in. Plate									
1.0	43900	40600	38000	35800	34000	32400	31000	29800	27700
1.2	48000	44500	41600	39200	37200	35500	34000	32600	30400
1.4	51900	48000	44900	42400	40200	38300	36700	35300	32800
1.6	55500	51400	48100	45300	43000	41000	39200	37700	35100
1.8	58900	54500	51000	48100	45600	43500	41600	40000	37200
2.0	62000	57400	53700	50600	48000	45800	43900	42100	39200
2.2	65100	60200	56300	53100	50400	48000	46000	44200	41100
2.4	67900	62900	58800	55500	52600	50200	48100	46200	43000
2.6	70700	65500	61200	57700	54800	52200	50000	48000	44700
2.8	73300	67900	63600	59900	56800	54200	51900	49900	46400
3.0	76000	70300	65800	62000	58900	56100	53700	51600	48100
3.2	78500	72700	68000	64100	60800	58000	55500	53300	49600
3.4	80900	74900	70100	66000	62700	59700	57200	55000	51200
3.6	83300	77000	72100	67900	64500	61500	58800	56500	52600
3.8	85500	79200	74000	69800	66200	63100	60500	58100	54100
4.0	87800	81200	76000	71600	68000	64800	62000	59600	55500
4.5	93100	86100	80600	76000	72100	68700	65800	63200	58800
5.0	98100	90800	84900	80100	76000	72400	69400	66600	62000
5.5	103000	95200	89100	84000	79700	76000	72700	69900	65100
6.0	107000	99500	93000	87700	83200	79300	76000	73000	67900
6.5	112000	104000	96900	91300	86600	82600	79100	76000	70700
7.0	116000	107000	101000	98400	89900	85700	82100	78900	73400
8.0	124000	115000	107000	101000	96100	91600	87700	84300	78500
9.0	132000	122000	114000	107000	102000	92700	93100	89400	83200
10.0	138000	128000	120000	113000	107000	102000	98100	94200	87700
11.0	145000	135000	126000	119000	113000	107000	103000	98800	92000
12.0	152000	141000	132000	124000	118000	112000	108000	103000	96200
13.0	158000	147000	137000	129000	123000	117000	112000	108000	100000
14.0	164000	152000	142000	134000	127000	121000	116000	112000	104000
15.0	170000	158000	147000	139000	132000	126000	120000	116000	108000

* Values are cu ft in 24 hours at a base pressure of 14.65 psia; base and flowing temperature, 60°F. The volumes obtained from these tables apply only to Orifice Well Testers manufactured by American Meter Company. For other testers, use the tables recommended by the manufacturer. The rates given in the tables for water are based on the following equation:

$$q = C\sqrt{p}$$

where

q = rate in cubic feet in 24 hours,
 C = rate for 1 in. given in the tables, and
 p = pressure in inches of water.

The rates given in the tables for mercury are based on the following equation which was determined from a series of 100 tests covering the limits of the tables:

$$q = C\sqrt{p_m(29.32 + 0.3p_m)} + \gamma_g$$

where

q = rate in thousands of cubic feet in 24 hours,
 C = 7.464 for ¾-in. orifice,
 = 13.61 for 1-in. orifice,
 = 23.10 for 1¼-in. orifice,
 p_m = pressure in inches of mercury,
 29.32 = assumed atmospheric pressure in inches of mercury
 = 14.4 psi,
 0.3 = factor determined by tests, and
 γ_g = specific gravity of gas.

TABLE 13.2b—CAPACITIES OF ORIFICE WELL TESTERS*

Pressure, in. of mercury	Specific gravity								
	0.60	0.70	0.80	0.90	1.00	1.10	1.20	1.30	1.50
	¾-in. Orifice in ⅛-in. Plate								
1.0	52	49	45	43	41	39	37	36	33
1.1	55	51	48	45	43	41	39	37	35
1.2	58	53	50	47	45	43	41	39	36
1.3	60	55	52	49	46	44	42	41	38
1.4	62	58	54	51	48	46	44	42	39
1.5	64	60	56	53	50	48	45	44	41
1.6	67	62	58	54	52	49	47	45	42
1.7	69	64	59	56	53	51	48	47	43
1.8	71	65	61	58	55	52	50	48	45
1.9	73	67	63	59	56	54	51	49	46
2.0	75	69	65	61	58	55	53	51	47
2.2	78	72	68	64	61	58	55	53	49
2.4	82	76	71	67	63	60	58	56	52
2.6	85	79	74	70	66	63	60	58	54
2.8	89	82	77	72	69	65	63	60	56
3.0	92	85	79	75	71	68	65	62	58
3.2	95	88	82	77	73	70	67	64	60
3.4	98	91	85	80	76	72	69	67	62
3.6	101	93	87	82	78	74	71	69	64
3.8	104	96	90	85	80	77	73	70	66
4.0	107	99	92	87	82	79	75	72	67
4.5	113	105	98	92	88	84	80	77	72
5.0	120	111	103	98	93	88	85	81	76
5.5	126	116	109	103	97	93	89	85	79
6.0	132	122	114	108	102	97	93	89	83
6.5	137	127	119	112	106	102	97	93	87
7.0	143	132	124	117	111	106	101	97	90
8.0	154	142	133	125	119	113	108	104	97
9.0	164	151	142	134	127	121	116	111	103
10.0	173	160	150	142	134	128	122	118	109
11.0	183	169	158	149	141	135	129	124	115
12.0	192	177	166	156	148	142	135	130	121
13.0	200	185	173	164	155	148	142	136	127
14.0	209	193	181	170	162	154	148	142	132
15.0	217	201	188	177	168	160	153	148	137
16.0	225	208	195	184	174	166	159	153	142
17.0	233	216	202	190	180	172	165	158	147
18.0	241	223	209	197	187	178	170	164	152
19.0	249	230	215	203	192	184	176	169	157
20.0	256	237	222	209	198	189	181	174	162
21.0	264	244	228	215	204	195	186	179	167
22.0	271	251	234	221	210	200	191	184	171
23.0	278	257	241	227	215	205	197	189	176
24.0	285	264	247	233	221	211	202	194	180
25.0	292	271	253	239	226	216	207	199	185
26.0	300	277	259	245	232	221	212	204	189
27.0	306	284	265	250	237	226	216	208	194
28.0	313	290	271	256	242	231	221	213	198
29.0	320	296	277	261	248	236	226	218	202
30.0	327	302	283	267	253	241	231	222	207
31.0	334	309	289	272	258	246	236	227	211
32.0	340	315	294	278	263	251	240	231	215
33.0	347	321	300	283	268	256	245	236	219
34.0	353	327	306	289	273	261	250	240	223
35.0	360	333	311	294	278	266	254	245	227
36.0	366	339	317	299	283	271	259	249	231
37.0	373	345	323	304	288	275	263	253	236
38.0	379	351	328	310	293	280	268	258	240
39.0	386	357	334	315	298	285	272	262	244
40.0	392	363	339	320	303	289	277	266	248

TABLE 13.2b—CAPACITIES OF ORIFICE WELL TESTERS* (continued)

Pressure, in. of mercury	Specific gravity							
	0.60	0.70	0.80	0.90	1.00	1.10	1.20	1.30
	1-in. Orifice in 1/8-in. Plate							
1.0	96	89	83	78	74	71	68	65
1.1	100	93	87	82	78	74	71	68
1.2	105	97	91	86	81	77	74	71
1.3	109	101	95	89	85	81	77	74
1.4	113	105	98	93	88	84	80	77
1.5	117	109	102	96	91	87	83	80
1.6	121	112	105	99	94	90	86	83
1.7	125	116	108	102	97	92	88	85
1.8	129	119	112	105	100	95	91	88
1.9	132	123	115	108	103	98	94	90
2.0	136	126	118	111	105	100	96	92
2.2	143	132	124	117	111	105	101	97
2.4	149	138	129	122	116	110	105	101
2.6	155	144	135	127	120	115	110	106
2.8	161	150	140	132	125	119	114	110
3.0	167	155	145	137	130	124	118	114
3.2	173	160	150	141	134	128	122	117
3.4	179	165	155	146	138	132	126	121
3.6	184	170	159	150	142	136	130	125
3.8	189	175	164	154	146	140	134	128
4.0	194	180	168	159	150	143	137	132
4.5	206	191	179	169	160	153	146	140
5.0	218	202	189	178	169	161	154	148
5.5	229	212	199	187	178	169	162	156
6.0	240	222	208	196	186	177	170	163
6.5	251	232	217	205	194	185	177	170
7.0	261	241	226	213	202	192	184	177
8.0	280	259	242	229	217	207	198	190
9.0	298	278	258	244	231	220	211	203
10.0	316	293	274	258	245	233	223	215
11.0	333	308	288	272	258	246	235	226
12.0	349	323	303	285	271	258	247	237
13.0	365	338	316	298	283	270	258	248
14.0	381	352	330	311	295	281	269	259
15.0	396	366	343	323	306	292	280	269
16.0	411	380	356	335	318	303	290	279
17.0	425	394	368	347	329	314	300	289
18.0	439	407	381	359	340	325	311	299
19.0	453	420	393	370	351	335	320	308
20.0	467	432	405	381	362	345	330	317
21.0	481	445	416	392	372	355	340	327
22.0	494	457	428	403	383	365	349	336
23.0	507	470	439	414	393	375	358	345
24.0	520	482	451	425	403	384	368	354
25.0	533	494	462	435	413	394	377	362
26.0	546	506	473	446	423	403	386	371
27.0	559	517	484	456	433	413	395	380
28.0	571	529	495	466	442	422	404	388
29.0	583	540	505	477	452	431	412	397
30.0	596	552	516	487	462	440	421	405
31.0	608	563	527	496	471	449	430	413
32.0	620	574	539	506	480	458	438	421
33.0	632	585	548	516	490	467	447	430
34.0	644	596	558	526	499	476	455	438
35.0	656	607	568	536	508	485	464	446
36.0	668	618	578	545	517	493	472	454
37.0	679	629	589	555	526	502	480	462
38.0	691	640	599	565	535	511	489	470
39.0	703	651	609	574	544	519	497	478
40.0	714	661	619	583	553	528	505	485

TABLE 13.2b—CAPACITIES OF ORIFICE WELL TESTERS* (continued)

Pressure, in. of mercury	Specific gravity								
	0.60	0.70	0.80	0.90	1.00	1.10	1.20	1.30	1.50
	1¼-in. Orifice in ⅛-in. Plate								
1.0	162	150	141	132	126	120	115	110	103
1.1	170	158	147	139	132	126	120	116	108
1.2	178	165	154	145	138	132	126	121	113
1.3	185	171	160	151	143	137	131	126	117
1.4	192	178	167	157	149	142	136	131	122
1.5	199	184	173	163	154	147	141	135	126
1.6	206	191	178	168	160	152	146	140	130
1.7	212	197	184	173	164	157	150	144	134
1.8	219	202	189	178	169	161	155	149	138
1.9	225	208	195	184	174	166	159	153	142
2.0	231	214	200	188	179	171	163	157	146
2.2	242	224	210	198	188	179	171	165	153
2.4	253	234	219	206	196	187	179	172	160
2.6	264	244	229	215	204	195	187	179	167
2.8	274	254	237	224	212	202	194	186	173
3.0	284	263	246	232	220	210	201	193	180
3.2	293	272	254	240	227	217	208	199	186
3.4	303	281	262	247	235	224	214	206	192
3.6	312	289	270	255	242	230	221	212	197
3.8	321	297	278	262	249	237	227	218	203
4.0	330	305	285	269	255	243	233	224	208
4.5	350	324	304	286	271	259	248	238	222
5.0	370	343	321	302	287	273	262	251	234
5.5	389	360	337	318	301	287	275	264	246
6.0	407	377	353	333	316	301	288	277	258
6.5	425	394	368	347	329	314	301	289	269
7.0	442	409	383	361	343	327	313	300	280
8.0	475	440	411	388	368	351	336	323	300
9.0	506	469	439	413	392	374	358	344	320
10.0	536	496	464	438	415	396	379	364	339
11.0	565	523	489	461	438	417	399	384	357
12.0	593	549	514	484	459	438	419	403	375
13.0	620	574	537	506	480	458	438	421	392
14.0	646	598	559	527	500	477	457	439	409
15.0	672	622	582	548	520	496	475	456	425
16.0	697	645	604	569	540	515	493	473	441
17.0	721	668	625	589	559	533	510	490	456
18.0	746	690	646	609	578	551	527	507	472
19.0	769	712	666	628	596	568	544	523	487
20.0	793	734	687	647	614	586	561	539	501
21.0	816	755	706	666	632	603	577	554	516
22.0	838	776	726	684	649	619	593	570	530
23.0	861	797	745	703	667	636	609	585	544
24.0	883	818	765	721	684	652	624	600	558
25.0	905	838	784	739	701	668	640	615	572
26.0	927	858	803	757	718	684	655	629	586
27.0	948	878	821	774	734	700	670	644	600
28.0	969	897	839	789	751	716	685	658	613
29.0	990	917	858	809	761	732	700	673	626
30.0	1011	936	876	826	783	747	715	687	640
31.0	1032	955	894	843	799	762	730	701	653
32.0	1052	974	912	859	815	777	744	715	666
33.0	1073	993	929	876	831	793	759	729	679
34.0	1093	1012	947	893	847	808	773	743	691
35.0	1113	1031	964	909	862	822	787	756	704
36.0	1133	1049	982	925	878	837	801	770	717
37.0	1153	1068	999	942	893	852	816	783	729
38.0	1173	1086	1016	958	909	867	830	797	742
39.0	1193	1104	1033	974	924	881	844	810	754
40.0	1212	1122	1050	990	939	896	857	824	767

*Values are thousands of cu ft in 24 hours at a base pressure of 14.65 psia; base and flowing temperature, 60°F.

The orifice used differs from that in the orifice meter. This one is thicker and has a rounded edge. This edge is placed toward the flow, for experience has shown that a sharp-edged orifice does not give reproducible results under critical-flow conditions. In fact, sharp-edged orifices do not conform to existing theories and correlations.

The general equation for a critical-flow prover is

$$q_g = \frac{Cp}{(\gamma_g T)^{0.5}}, \quad \dots \dots \dots (9)$$

where

p = pressure on prover, psia,

C = orifice coefficient for prover,

q_g = rate of flow, thousands of standard cu ft/24 hr, measured at 14.4 psia and 60°F,

γ_g = specific gravity of gas (air=1.00), and

T = absolute temperature, °R.

The critical-flow prover is one of the basic devices used for determining the gas-flow rate in the open-flow testing of gas wells. Values of the coefficient C may be found in Table 13.3.*

Pitot Tube. The pitot tube is another measuring device used extensively for testing flow rates during tests. It works by measuring the difference between the impact pressure at the tip and the static pressure in the flowing stream. This impact pressure results from conversion of the kinetic energy of the flowing gas to pressure. If the conversion efficiency is relatively constant, a conversion between pressure and flow rate is possible. The pitot tube is normally made of 1/8-in.-ID pipe and is inserted in the center of a nipple at least eight diameters long.

Table 13.4 gives the flow rate in thousands of cubic feet per day for a pitot tube inserted in different-diameter nipples.

A pitot tube is used largely for temporary flow measurement since it is small and easy to handle. Very few permanent installations are made, for it produces low-pressure differentials, is difficult to calibrate, and often clogs.

A pitot tube measures a point velocity, i.e., the velocity at only one point across the cross section of the pipe. Inasmuch as the velocity varies throughout this cross section, the problem of proper location presents itself. In the absence of unknown disturbing elements such as pipe burrs or undue roughness, the velocity at the center is theoretically 20% greater than the mean velocity. For approximate measurement, the standard tables use this factor to convert readings taken at the center of the pipe to a volume flow rate. For exact work, the mean velocity would be found by taking a series of experimental velocity measurements across the pipe diameter.

A similar method is used for large gas-flow rates and/or where debris produced with the gas makes other methods unfeasible. This consists simply of measuring

TABLE 13.3—ORIFICE COEFFICIENTS
FOR CRITICAL-FLOW PROVERS

Size of orifice (in.)	Orifice Coefficient	
	2-in. Prover	4-in. Prover
1/16	1.524	—
3/32	3.355	—
1/8	6.301	—
5/16	14.47	—
7/32	19.97	—
1/4	25.86	24.92
5/16	39.77	—
3/8	56.68	56.01
7/16	81.09	100.2
1/2	101.8	156.1
5/8	154.0	223.7
3/4	224.9	304.2
7/8	309.3	396.3
1	406.7	499.2
1 1/8	520.8	616.4
1 1/4	657.5	742.1
1 3/8	807.8	884.3
1 1/2	1,002.0	1,208.0
1 3/4	—	1,596.0
2	—	2,566.0
2 1/2	—	3,904.0
3	—	—

the static pressure through a side opening four diameters from the end of a nipple at least eight diameters long. Values for this system are also shown in Table 13.4. This is the least desirable of the methods discussed because of the potential error involved.

Further data on the use of these four devices for the measurement of gas flow may be found in U.S. Bureau of Mines Monograph 7.

Other Meters That Use Velocity. *Rotameter.* This is a variable-orifice meter useful for the indication of flow rates in operations (Fig. 13.5). It is economical in sizes up to 10 cm [4 in.], at moderate pressures. It can transmit electrical or pneumatic signals. Its rangeability is about 10:1.

Eccentric Orifices. These are used for many two-phase streams including those containing solids (Fig. 13.6). Substantial straight-line pipe sections are required both upstream and downstream.

Segmental Orifices. These possess the same basic applicability as the eccentric orifices with an additional advantage that they do not dam solids on the upstream side of the plate (Fig. 13.7). These are used primarily for large line sizes and low fluid viscosities.

Centrifugal (Elbow) Meters. This is used for large pipe sizes primarily. It is based on the centrifugal force induced as the fluid changes direction (Fig. 13.8). This centrifugal force is a function of velocity, R and D , as well as fluid properties. A common pipe elbow is generally used. If very accurate results are desired, calibration is necessary. Its rangeability is about 3:1.

Turbine Meters. The turbine meter has a wide range of applicability except for high-viscosity fluids. Rangeability is about 20:1. Turbine meters come in various configurations, but they all transmit a signal based on rotation speed, which in turn is a function of flow rate and fluid properties (Fig. 13.9). It is difficult to generalize about this type of meter because some have

*A set of constants in SI metric units has not been officially adopted at this time. Therefore the constants in customary units are used (Table 13.3) and final results are converted to SI metric units. The readers are advised, however, to refer to the official standards in their area for the appropriate tables and equations presented in this chapter.

TABLE 13.4—PITOT-TUBE VALUES

Impact pressure			Open flow, Mcf/D								
in. of water	in. of mercury	psi	1 in.	2 in.	3 in.	4 in.	5 in.	6 in.	8 in.	10 in.	12 in.
0.1	—	—	10.97	44	99	176	274	395	702	1,100	1,580
0.2	—	—	15.52	62	140	248	388	559	944	1,550	2,240
0.3	—	—	19.00	76	171	304	475	684	1,220	1,900	2,740
0.4	—	—	21.95	88	198	351	549	790	1,410	2,200	3,160
0.5	—	—	24.53	98	221	392	613	882	1,570	2,450	3,530
0.6	—	—	26.89	108	242	430	672	968	1,720	2,690	3,870
0.7	—	—	29.03	116	261	464	726	1,050	1,860	2,900	4,180
0.8	—	—	31.02	124	279	497	776	1,120	1,990	3,100	4,470
0.9	—	—	32.92	132	296	526	823	1,180	2,110	3,290	4,740
1.0	—	—	34.69	139	312	555	867	1,250	2,200	3,470	5,000
1.25	—	—	38.78	155	349	620	969	1,400	2,480	3,880	5,580
1.36	0.10	—	40.45	162	364	648	1,010	1,460	2,590	4,050	5,820
1.6	0.12	—	43.89	175	395	702	1,100	1,580	2,810	4,390	6,320
1.8	0.13	—	46.56	186	419	744	1,160	1,680	2,980	4,660	6,700
2.0	0.15	—	49.00	196	441	784	1,230	1,760	3,140	4,900	7,060
2.2	0.16	—	51.45	206	463	823	1,290	1,850	3,290	5,150	7,410
2.4	0.18	—	53.74	214	483	860	1,340	1,930	3,440	5,370	7,740
2.7	0.20	—	57.20	228	515	915	1,430	2,060	3,660	5,720	8,230
3.0	0.22	—	60.02	240	540	961	1,500	2,160	3,840	6,000	8,640
3.5	0.26	—	64.91	260	584	1,040	1,620	2,340	4,160	6,490	9,340
4.1	0.30	—	70.01	280	630	1,120	1,750	2,520	4,480	7,000	10,100
4.5	0.33	—	73.60	295	662	1,180	1,840	2,650	4,710	7,360	10,600
5.0	0.37	—	77.57	310	698	1,240	1,940	2,790	4,960	7,760	11,200
5.4	0.40	—	80.90	324	728	1,300	2,020	2,910	5,180	8,090	11,700
6.0	0.44	—	84.91	340	764	1,360	2,120	3,060	5,430	8,490	12,200
6.8	0.50	—	90.48	362	814	1,450	2,260	3,260	5,790	9,500	13,000
8.2	0.60	—	99.20	396	892	1,590	2,480	3,570	6,350	10,000	14,300
9.0	0.66	—	104.0	416	936	1,670	2,600	3,750	6,660	10,400	15,000
9.5	0.70	—	107.0	428	962	1,710	2,680	3,850	6,850	10,700	15,400
10.0	0.74	—	109.7	439	987	1,760	2,740	3,950	7,020	11,000	15,800
10.9	0.80	—	114.5	458	1,030	1,830	2,860	4,120	7,330	11,500	16,500
12.0	0.88	—	120.1	481	1,080	1,920	3,000	4,300	7,690	12,000	17,300
12.2	0.90	—	121.4	486	1,090	1,940	3,040	4,370	7,770	12,100	17,500
13.9	1.02	0.5	129.2	517	1,160	2,070	3,230	4,650	8,270	12,900	18,600
15.0	1.1	—	134.2	537	1,210	2,150	3,360	4,830	8,590	13,400	19,300
16.3	1.2	—	140.1	560	1,260	2,240	3,500	5,040	8,960	14,000	20,200
17.7	1.3	—	145.8	584	1,310	2,330	3,650	5,250	9,330	14,600	21,000
19.0	1.4	—	151.4	606	1,360	2,420	3,790	5,450	9,680	15,100	21,900
20.4	1.5	—	156.7	627	1,410	2,510	3,920	5,640	10,000	15,700	22,600
21.8	1.6	—	161.8	648	1,460	2,590	4,050	5,820	10,400	16,200	23,300
24.5	1.8	—	171.7	686	1,550	2,750	4,290	6,180	11,100	17,200	24,700
27.2	2.0	1.0	180.9	734	1,630	2,890	4,520	6,510	11,600	18,100	26,000
29.9	2.2	—	189.7	768	1,710	3,040	4,740	6,830	12,100	19,000	27,300
32.6	2.4	—	198.0	802	1,780	3,170	4,950	7,130	12,700	19,800	28,500
—	2.6	—	206.1	824	1,860	3,300	5,150	7,420	13,200	20,600	29,700
—	2.8	—	214.0	857	1,930	3,420	5,350	7,700	13,700	21,400	30,800
—	3.0	1.5	221.6	887	2,000	3,500	5,540	7,980	14,200	22,600	31,900
—	3.2	—	228.9	917	2,060	3,660	5,720	8,240	14,600	22,900	32,000
—	3.4	—	235.8	943	2,120	3,770	5,900	8,480	15,100	23,600	34,000
—	3.6	—	242.8	971	2,180	3,880	6,070	8,740	15,500	24,300	35,000

TABLE 13.4—PITOT-TUBE VALUES (continued)

Impact pressure		Open flow, Mcf/D								
in. of mercury	psi	1 in.	2 in.	3 in.	4 in.	5 in.	6 in.	8 in.	10 in.	12 in.
3.8	—	249.4	998	2,240	3,990	6,230	8,980	16,000	24,900	35,900
4.0	2.0	255.9	1,020	2,300	4,090	6,400	9,210	16,400	25,600	36,800
4.2	—	262.0	1,050	2,360	4,190	6,550	9,430	16,800	26,200	37,700
4.4	—	268.4	1,070	2,410	4,290	6,710	9,650	17,200	26,800	38,600
4.6	—	274.5	1,100	2,470	4,390	6,860	9,880	17,600	27,500	39,500
4.8	—	280.3	1,120	2,520	4,490	7,010	10,100	18,000	28,000	40,400
5.0	2.5	286.1	1,140	2,570	4,580	7,150	10,300	18,300	28,600	41,200
5.2	—	291.8	1,170	2,630	4,670	7,300	10,500	18,700	29,200	42,000
5.4	—	297.4	1,190	2,680	4,760	7,440	10,700	19,000	29,700	42,800
5.6	—	302.7	1,210	2,720	4,840	7,560	10,900	19,400	30,300	43,600
5.8	—	308.1	1,230	2,770	4,920	7,700	11,100	19,700	30,800	44,300
6.0	3.0	313.4	1,250	2,820	5,010	7,830	11,300	20,000	31,300	45,100
6.5	—	326.0	1,300	2,930	5,220	8,150	11,700	20,900	32,600	47,000
7.0	3.5	338.6	1,350	3,050	5,420	8,460	12,200	21,700	33,900	48,800
7.5	—	350.0	1,400	3,150	5,600	8,760	12,600	22,400	35,000	50,400
8.0	4.0	361.5	1,450	3,250	5,780	9,040	13,000	23,100	36,200	52,100
8.5	—	373.9	1,500	3,370	5,980	9,340	13,400	23,900	37,400	53,700
9.0	4.5	383.9	1,540	3,460	6,140	9,600	13,800	24,600	38,400	55,300
9.5	—	394.2	1,580	3,550	6,310	9,860	14,200	25,200	39,400	56,800
10.0	—	404.6	1,620	3,640	6,470	10,100	14,600	25,900	40,500	58,200
10.2	5.0	408.1	1,630	3,689	6,540	10,200	14,700	26,100	40,800	58,800
11.2	5.5	428.0	1,710	3,850	6,850	10,700	15,400	27,400	42,800	61,600
12.2	6.0	447.0	1,790	4,030	7,150	11,200	16,100	28,600	44,700	64,400
13.2	6.5	465.5	1,860	4,190	7,450	11,600	16,800	29,800	46,600	67,000
14.3	7.0	483.0	1,930	4,350	7,730	12,100	17,400	30,900	48,600	69,600
15.3	7.5	500.0	2,000	4,500	8,000	12,500	18,000	32,000	50,000	72,000
16.3	8.0	516.0	2,060	4,650	8,260	12,900	18,600	33,000	51,600	74,300
17.3	8.5	532.1	2,130	4,790	8,520	13,300	19,200	34,100	53,200	76,600
18.3	9.0	548.0	2,190	4,930	8,770	13,700	19,700	35,100	54,800	78,900
19.3	10.0	563.0	2,250	5,070	9,000	14,100	20,300	36,000	56,300	81,100
20.4	10.0	577.6	2,310	5,200	9,240	14,400	20,800	37,000	57,800	83,200
22.4	11.0	605.6	2,420	5,450	9,680	15,100	21,800	38,800	60,600	87,200
24.4	12.0	632.5	2,530	5,700	10,100	15,800	22,800	40,500	63,300	91,200
26.5	13.0	658.0	2,630	5,920	10,500	16,500	23,700	42,100	65,800	94,800
28.5	14.0	683.8	2,740	6,150	10,900	17,100	24,600	43,800	68,400	98,600
	15.0	707	2,830	6,360	11,300	17,700	25,500	45,200	70,700	102,000
	16.0	731	2,930	6,580	11,700	18,300	26,300	46,800	73,100	105,000
	17.0	755	3,020	6,800	12,100	18,900	27,200	48,300	75,500	109,000
	18.0	779	3,120	7,010	12,500	19,500	28,000	49,900	77,900	112,000
	19.0	802	3,210	7,220	12,800	20,100	28,900	51,300	80,200	115,000
	20.0	826	3,310	7,440	13,200	20,700	29,700	52,900	82,600	119,000
	21.0	850	3,400	7,650	13,600	21,300	30,600	54,400	85,000	122,000
	22.0	874	3,500	7,870	14,000	21,900	31,500	55,900	87,400	126,000
	23.0	898	3,590	8,080	14,400	22,500	32,300	57,500	89,800	129,000
	24.0	922	3,690	8,300	14,800	23,100	33,200	59,000	92,200	133,000
	25.0	946	3,780	8,520	15,100	23,700	34,100	60,500	94,600	136,000
	26.0	969	3,880	8,720	15,500	24,200	34,900	62,000	96,900	140,000
	27.0	993	3,970	8,940	15,900	24,800	35,700	63,500	98,300	143,000
	28.0	1,017	4,070	9,150	16,300	25,400	36,600	65,100	102,000	146,000
	29.0	1,040	4,160	9,360	16,600	26,200	37,400	66,600	104,000	150,000

TABLE 13.4—PITOT-TUBE VALUES (continued)

Impact pressure	Open flow, Mcf/D									
	psi	1 in.	2 in.	3 in.	4 in.	5 in.	6 in.	8 in.	10 in.	12 in.
30.0	1,064	4,260	9,580	17,000	26,600	38,300	68,100	106,000	153,000	
32.0	1,112	4,450	10,000	17,800	27,800	40,100	71,200	111,000	160,000	
34.0	1,159	4,640	10,400	18,600	29,000	41,700	74,200	116,000	167,000	
36.0	1,207	4,830	10,900	19,300	30,200	43,500	77,300	121,000	174,000	
38.0	1,255	5,020	11,300	20,100	31,400	45,200	80,300	126,000	181,000	
40.0	1,302	5,210	11,700	20,800	32,600	46,900	83,400	130,000	188,000	
45.0	1,421	5,690	12,800	22,800	35,500	51,200	91,000	142,000	205,000	
50.0	1,540	6,160	13,900	24,700	38,500	55,400	98,600	154,000	222,000	
55.0	1,660	6,640	15,000	26,600	41,500	59,800	106,000	166,000	239,000	
60.0	1,778	7,120	16,000	28,500	44,500	64,000	114,000	178,000	256,000	
65.0	1,898	7,600	17,100	30,400	47,500	68,400	122,000	190,000	273,000	
70.0	2,017	8,060	18,200	32,300	50,400	72,600	129,000	202,000	290,000	
75.0	2,136	8,840	19,200	34,200	53,400	76,800	137,000	214,000	308,000	
80.0	2,252	9,010	20,300	36,000	56,400	81,100	144,000	225,000	324,000	
90.0	2,492	9,980	22,400	39,900	62,400	89,800	160,000	249,000	359,000	
100.0	2,732	10,900	24,600	43,700	68,400	98,400	175,000	273,000	394,000	
110.0	2,970	11,900	26,700	47,500	74,200	107,000	190,000	297,000	428,000	
120.0	3,208	12,800	28,900	51,300	80,200	116,000	205,000	321,000	462,000	
130.0	3,445	13,800	31,000	55,100	86,200	124,000	221,000	345,000	496,000	
140.0	3,681	14,700	33,100	58,900	92,000	133,000	236,000	368,000	530,000	
150.0	3,921	15,700	35,300	62,800	98,000	141,000	251,000	392,000	565,000	
160.0	4,160	16,700	37,500	66,600	104,000	150,000	266,000	416,000	599,000	
170.0	4,399	17,600	39,600	70,400	110,000	158,000	282,000	440,000	634,000	
180.0	4,635	18,600	41,700	74,200	116,000	167,000	297,000	464,000	668,000	
190.0	4,870	19,500	43,900	78,000	122,000	175,000	312,000	487,000	702,000	
200.0	5,108	20,500	46,000	81,800	128,000	185,000	327,000	511,000	736,000	

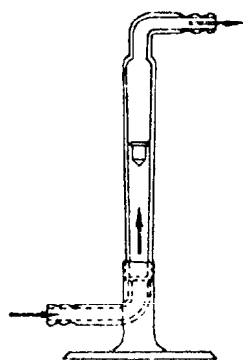


Fig. 13.5—A typical rotameter.



Fig. 13.6—An eccentric orifice.

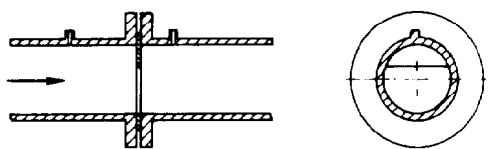


Fig. 13.7—A segmental orifice.

proven very good and some very bad in a given application. For this reason, the choice should be based on experience with a given model in a given service.

Bearings can be troublesome. Ball bearings may be susceptible to damage by abrasive solids; sleeve bearings tend to be more trouble-free but rangeability may be reduced.

When properly selected, turbine meters are very acceptable. Their acceptability for custody transfer has been slow in some areas because of lack of proven experience compared with the orifice meter. Liquid turbine meters have been accepted more readily than those for gas service because they could be tested more readily.

Repeatability is often $\pm 0.05\%$ on test and accuracy is within $\pm 1\%$. Like all meters, these values are a function of meter condition.

The axial flow turbine meter has proved useful for high gas-flow rates. Its rangeability is up to 100:1 and it has a linear response to flow rate. A summary of performance of these meters is found in Refs. 5 and 6.

Vortex Shedding Meter. This is a newer meter for measuring all fluids that do not have too high a viscosity (Fig. 13.10). It has no moving parts, wide rangeability, and is linear over wide ranges of flow.

Fig. 13.11 shows the principle involved when a fluid flows around a blunt object. The flow is unable to follow the surface of the object and sheds from it at some point to form a continuous series of eddy currents. The frequency of shedding is proportional to flow velocity and inversely proportional to the diameter of the object. This shedding may be sensed by thermistors or by what is called a "shuttle ball" contained in the fixed flow element. Movement of this ball is detected by a magnetic sensor. This ball-type is suitable for low-density, clean liquids.

Sonic Meters. Sonic meters offer many potential advantages if they can be made so that they remain stable electronically and overcome drift tendencies. They possess no moving parts and have linearity.

They contain three components: a transducer assembly, transmitter, and a receiver. The transducer assembly shown in Fig. 13.12 contains two transducers that alternately transmit sonic pulses diagonally across the pipe. The difference in transit times is proportional to flow velocity.

Regulation

Principles of Control

The regulation of pressure and temperature flow or level is an integral part of the regulation of gas and liquid streams. A means is necessary to sense the value of the controlled variables and then cause the movement of a valve to maintain the value desired. The communication link between sensing element and valve may use gas (pneumatic), liquid (hydraulic), electricity, and electronics. More than one may be used in a given system by employing a *transducer*, a device for converting signals.

Historically, most of the systems used pneumatic controls, so they will be used to illustrate the principles involved. However, the use of electrical and electronic controls is increasing rapidly. When a control system is chosen, these also should receive serious consideration.

Many of the routine problems encountered with lease equipment stem from failure or misapplication of controls. This has become even more pronounced in recent years as this equipment has become more complex.

Oilfield instrumentation is less complex than that in plants and refineries but imposes severe service conditions. In such service, the instruments often have only wet supply gas and rare adjustment by expert servicemen and are exposed to the elements, yet must give continuous and trouble-free service. Even with these severe conditions, it must be concluded that many troubles stem from improper application rather than inadequacy of the controls themselves, although many types are not suitable for oil-field use.

Definitions

To choose controls properly, it is necessary to know not only the requirements of the process but also the corresponding characteristics of the controls available. No understanding of controls may be complete without a familiarity with applicable definitions.

Pneumatic controls are those actuated by air or gas (the most common type used in the field).

Diaphragm motor valve is the term applied to a complete valve that uses pressure to open and close it.

Topworks (motor) is that portion of the motor valve that contains the mechanism to open and close the valve.

Inner-valve assembly (trim) includes the stem and seat within the valve body that actually controls the flow of fluid.

Fluid is any liquid or gas being controlled.

Proportional control describes the system whereby the valve opening is proportional to the degree of change in the controlled variable.

Snap action is a mode of control whereby the valve is either wide open or closed (on/off control).

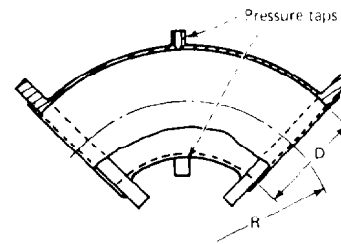


Fig. 13.8—A centrifugal (elbow) meter.

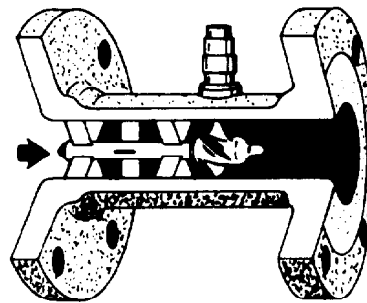


Fig. 13.9—A turbine meter.

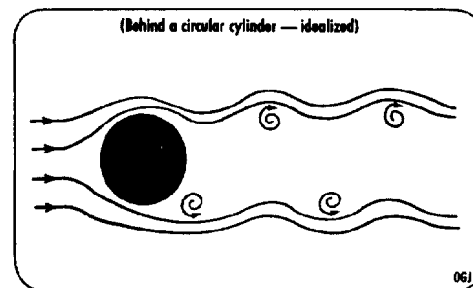


Fig. 13.10—Karman vortex trail.

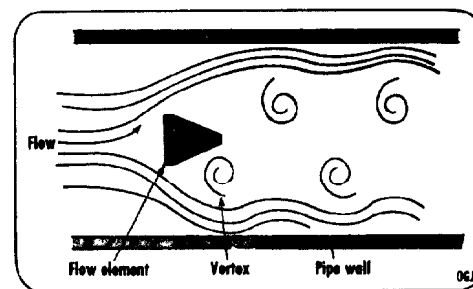


Fig. 13.11—Vortex flow pattern.

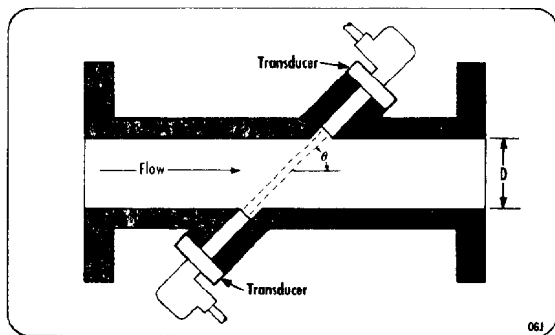


Fig. 13.12—A sonic flowmeter.

Reset is an addition to a proportional-control system to enable the instrument to hold itself at the control point as the process load varies.

Derivative response is a further addition that provides corrective action based on the time rate of change of the deviation from the control point.

Self-operated controller is a valve that is actuated directly by the controlled variable.

Pilot is a relay that transforms the controlled variable into an equivalent signal to the control valve, such signal controlling the action of that valve.

Supply gas is that gas necessary in a pneumatic pilot to operate it.

Controlled variable is the pressure, liquid level, temperature, or flow rate being controlled.

Measuring means is the means used to detect any change in the controlled variable.

Sensitivity is the ability to detect small deviations in the controlled variable.

Reproducibility is the ability of an instrument to repeat and measure consistently the values of a static condition over a period of time.

Static error is the difference between the absolute value of the controlled variable and the measured value.

Lag is the period of time by which the measured value follows the change in the absolute value of the controlled variable.

Static conditions occur when all changes in the controlled variable are instantaneous.

Dynamic conditions occur when the controlled variable is continually changing.

Normally closed valve is a valve that is held closed by a spring or some similar device and is opened by the action of pilot and/or the controlled variable.

Normally open valve is the reverse of the above; one that is closed by the action of the pilot and/or the controlled variable.

Drift includes reproducibility and the inability to repeat a measurement because of changes in the measured variable.

Process Characteristics

Because the purpose of an automatic controller is to regulate a process, it is fundamental that the properties and characteristics of a process be understood. A process is defined as the collective functions performed in and by equipment in which a variable is controlled. As an example, a field heater that heats well effluent by circulating hot water is a unit of equipment in which the process of heating the wellstream is accomplished. The process consists of a controlled variable (the temperature) and a controlled medium (the wellstream). Other controlled variables could be rate of flow, liquid level, or pressure. A control agent (circulating water) is the medium for effecting the temperature change, and thus regulation of the control agent regulates the controlled variable. The total requirements of the process for the control agent at any one time are defined as the process load. If the rate of flow of the wellstream increases, then more or hotter water is required to maintain the same temperature, and a change in process load has taken place. By the same token, a drop in inlet temperature at the original rate of flow would also constitute a process-load change.

The properties of an entire process include its potential, capacitance, resistance, and dead time. Capacitance, not to be confused with capacity, is the change in the quantity of energy or material per unit change in some variable, usually the controlled variable.

Resistance, or opposition to the flow of energy or material, is another process characteristic. The most familiar concept of resistance is in electricity when it is expressed as the ohm.

Potential is most generally recognized in the concept of electricity where it is expressed as a volt. Table 13.5 summarizes the characteristics of a process.

Dead time is the time lag that occurs when energy is being transferred at a constant rate of flow through a given distance. It is equal to the time it takes the energy to move the distance. The dead time is a characteristic of the process, and it is not to be confused with the time lag inherent in the automatic controller itself.

The purpose of the automatic controller is to prevent deviation of a process from a desired standard. This may be accomplished by various modes of control action, each of which incorporates a distinct limit, range, and speed of correction.

TABLE 13.5—PROCESS CHARACTERISTICS

Process Characteristic	Thermal	Pressure	Liquid Level	Electrical
Capacity	Btu	cu ft	cu ft	Coulomb
Potential	degree	psi	ft	volt
Capacitance	Btu/degree	cu ft/psi	cu ft/ft	Farad
Resistance	degree	psi	ft	ohm
	Btu/sec	cu ft/sec	cu ft/sec	

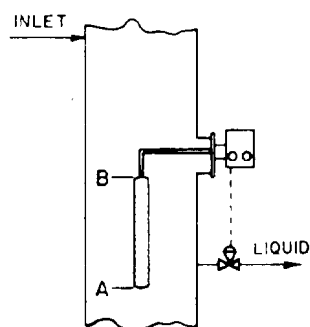


Fig. 13.13—Liquid-level control using displacement-type float.

Proportional Control. The modes used depend on the frequency and magnitude of the process load changes, the degree of control needed, and the dynamic lag inherent in the process and controls used.

Proportional control is the basic action that is employed in all controllers not using snap (on/off) action. Because it is defined as control action in which a continuous linear relation exists between the value of the controlled variable and the position of the valve, the following equation may be written.

$$\frac{dp}{dr} = S \frac{dy}{dr}, \dots\dots\dots (10)$$

where

dy/dr = rate of change of the controlled variable with time (level, pressure, etc.),

dp/dr = rate of change of pilot output pressure or current signal with time, and

S = characteristic constant of the pilot relating output to input.

This characteristic is represented by the sensitivity usually expressed as a percentage. The proportional band or range, expressed as a percentage, relates the percentage of the full range of the measuring means that the controlled variable has to traverse to stroke the valve fully. This is illustrated in Fig. 13.13.

This figure represents a typical level-control application using a displacement-type controller—i.e., one that does not float on top of the liquid but depends on the varying buoyancy of the liquid as the level changes. Consequently, the control range is represented by the distance between Points A and B, because below A or above B a change in level has no effect on the buoyancy of the float.

Therefore, at 100% proportional control the level would have to move from A to B or vice versa, to stroke the valve fully from full open to closed. At 25%, a level change of $0.25 \times \text{distance AB}$ would fully stroke the valve, etc. The same principles apply with all other modes of control, including gas regulation.

Example Problem 2. A backpressure controller with a range of 0 to 100 psig is set at 50% proportional control,

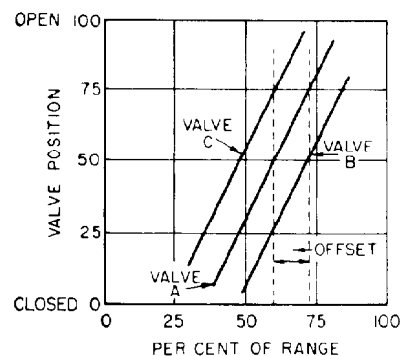


Fig. 13.14—Characteristics of proportional control.

using a normally open valve. If the valve is open at 100 psig, (a) at what pressure will it be fully closed? (b) what is the opening at 75 psig?

Solution. The control range is 100 psig, which at 50% proportional control means that a $0.50 \times 100 = 50$ psig change will fully stroke the valve; therefore it is fully closed at 50 psig. At 75 psig it would be half open.

The amount of fluid that a valve will pass at a given position depends on the size and characteristic of the inner-valve assembly. Ideally, the amount of fluid passed under given conditions, with a given valve, should be directly proportional to the valve opening. Often it is not, however; so that the type of inner valve has a definite effect on the proper proportional setting. Also ideally, the diameter of the inner valve should be such that the range of anticipated process loads may be handled when the valve is between 25 and 75% open. In the final analysis, the choice of the proportional band to use in a given installation must be governed by experience and adjustment on the job.

This is illustrated in Fig. 13.14. The slope of the lines depends on the proportional band used, each line representing a valve of given size. Under these conditions, each valve may operate only along a single line, in accordance with Eq. 1.

If the instrument was set to control at 60% of the range, Valve A would be 50% open; Valve B, 25% open; and Valve C, 75% open.

Suppose, however, that an instrument set to operate along Line A is in gas-regulation service and the flow rate increases such that a valve opening of 75% is needed to maintain the pressure. According to Line A, the only way the proportional controller can provide this opening is for the pressure to be at 70% of the range, or 10% above the set point. This 10% is called offset.

Consequently, with proportional control alone a change in process load brings a change in the valve position and some change in the liquid level. The proper proportional setting is therefore one which makes the lines in Fig. 13.14 as perpendicular as possible.

Zero per cent proportional control represents a special case. It is the upper limit of a range where the pressure is controlled by the valve alternately opening and closing. This is normally called snap action or on-off control. At a given snap setting, the valve will stay closed until the liquid level reaches a certain point between A and B and

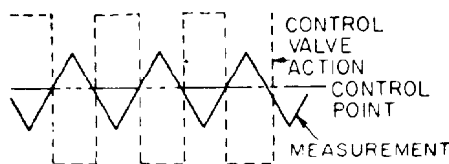


Fig. 13.15—On/off action of a controller.

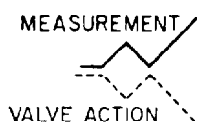


Fig. 13.16—Proportional action of a controller.

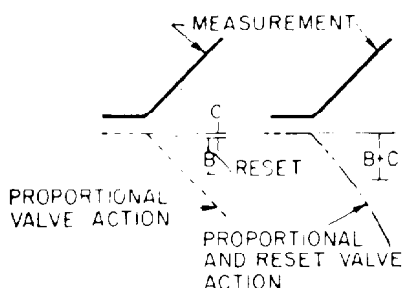


Fig. 13.17—Valve action for reset and proportional controllers (at left); valve action for combined proportional/reset controller (at right).

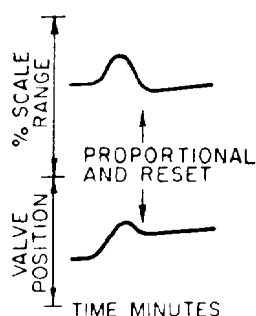


Fig. 13.18—Typical control curves when using a proportional/reset controller.

then remain full open until the liquid level drops to the control point. Where rapid process load changes are encountered, such as surging flow through separators, snap action is normally recommended.

Reset. The "offset" obtained with proportional control is sometimes too great to be tolerated and it is necessary to add other modes of control. One such addition is known as *reset*.

Figs. 13.15 and 13.16 show on/off action and proportional action, respectively. In the latter, it is seen that the amount of valve movement is proportional to the deviation of the measured variable. By contrast, the amount of correction applied with reset action depends on both the magnitude and duration of the deviation away from the control point. The prime purpose of reset is therefore to prevent "offset" and keep the controlled variable at the control point even as the process load changes.

The differential equation of a controller with proportional plus reset action is

$$\frac{dp}{dt} = S \frac{dy}{dt} + SR(y - y_o), \dots\dots\dots (11)$$

where dp/dt , S , and dy/dt have been previously defined, R = controller reset constant, and $y - y_o$ = duration of the controlled variable from the control point.

In this type of controller, the two corrections occur simultaneously as shown in Fig. 13.17 (this figure also shows whether the actions took place separately).

Fig. 13.18 shows typical curves in a process being controlled by this combination action. When a change in process load takes place the valve returns the measurement to the control point with a minimum of cycling. The original motion of the valve corresponding to the measurement change is caused by proportional action, but the change of the valve to its new position is due entirely to reset. In other words, the valve has moved to a new position to maintain the controlled condition. With only proportional control both the valve and controller would have changed.

Derivative Response. Proportional control plus reset does not provide correction that is rapid enough for certain processes. Derivative response may therefore be added to anticipate a change in process load and transmit a corrective signal to minimize the lag. This action corrects on the basis of the rate of change of the deviation from the desired standard. This term stems from the fact that the first derivative of the change from the desired standard is incorporated into the control mechanism. The equation for an instrument with proportional plus reset plus derivative response is therefore

$$\frac{dp}{dt} = SR(y - y_o) + S \frac{dy}{dt} + SF_{ia} \frac{d^2y}{dt^2}, \dots\dots\dots (12)$$

where F_{ia} is an instrument-adjustment factor. The action of a controller with this response is shown in Fig. 13.19.

The general applications of the various combinations of control action may be summarized as follows:

Proportional. Where process time lag is small in comparison with the apparatus capacity such as tank heating or large surge vessels, or where "offset" may be tolerated.

Proportional Plus Reset. Where it is necessary to use a narrow band to prevent "hunting" or overcontrol, and as the frequency and magnitude of the process load changes become greater.

Proportional Plus Derivative Response. In processes involving long time lags and large capacities when small and frequent load changes occur. Does not provide compensation for process load changes.

Proportional Plus Reset Plus Derivative Response. Where long time lags and large capacities are combined with large and sudden load changes.

Because the addition of reset and derivative response increases the investment cost, they should not be used unless their action is needed for proper control.

Liquid-Level Control

The control of liquid level is an integral part of gas processing. It furthermore affords a means of illustrating the general problem of instrumentation and gas regulation. In view of the widespread applications and the variety of conditions encountered, it is not surprising that a number of mechanisms are used. These may be conveniently subdivided as: (1) mechanically operated valve actuated by a float; (2) pilot-operated valve actuated by a float; (3) diaphragm motor valve actuated by (a) displacement-type controller and (b) "floatless" level controller; and (4) external devices, including inverted bucket traps, float traps, etc.

Either snap action or proportional control is normally employed on most lease equipment. Most applications do not justify the cost of reset and/or derivative response since small changes in level with flow rate and time lag are usually not critical problems.

Separator controls, in fact, are usually set on snap action because this enables the controller to handle a surging condition better. The degree of snap action will depend on the conditions encountered. However, it should be set so that not over 25% of the vessel's liquid capacity is filled, above the control point, before the valve opens. The inner-valve size should be determined on the basis of 110% of the maximum flow to be encountered. This means that during a surging condition the valve can handle the volume and prevent the separator from filling up.

Some uncertainty always exists, of course, when one tries to estimate future flow rates. On low-pressure separators, sizing is not a serious problem because of the low-pressure drop across the valve. On high-pressure gas-condensate separators, however, where the liquid flow rate is low, too large an inner valve on snap action can blow all the liquid out of the separator and allow gas to enter the stock tank before the valve can close. The author observed one such installation when 1,000-psig gas hit a 100-bbl tank, knocked the cover off the vent valve, sprayed oil over the countryside, and lifted the tank off the ground.

The manufacturers of control valves furnish sizing curves, and these should be consulted. In using these, it should be remembered that critical-flow conditions occur when the upstream pressure is approximately twice the valves' downstream pressure. Consequently, only twice the downstream absolute pressure should be used with these sizing curves if the actual pressure ratio exceeds 2.

When handling very small volumes of liquid, the use of such curves often indicates the use of so-called "metering trim." Its use is not recommended in field applications, for the small quantities of solid materials often present may clog the valve. For this reason, nothing smaller than $\frac{3}{16}$ -in. needle trim is usually recommended in field service.

Float-operated mechanical oil valves are satisfactory at pressures up to 125 psig. Such valves are directly actuated by movement of the float on top of the liquid,

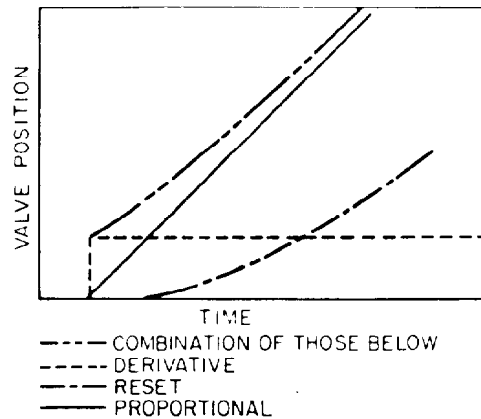


Fig. 13.19—Typical control curves for proportional, reset and derivative-action controllers.

through an adjustable linkage. At higher pressure, the leverage supplied by the float is insufficient to provide satisfactory valve action because of the pressure acting on the valve seat. On separators with greater than 125-psig working pressure, the use of a pilot-operated valve is advisable. Whenever applicable this type of control is very dependable and simple to adjust and repair.

Float-actuated pilot-operated valves are particularly applicable at pressure to 1,000 psig on vertical vessels. Such control has been "standard" on separators for years because the pilot is rugged and simple and will operate satisfactorily with the "wet" supply gas from the separator overhead.

This overhead gas contains entrained liquid so that a drip pot ahead of the pilot is advisable. With high-pressure separators, the expansion of gas from separator to instrument pressure may cause sufficient temperature drop to condense some water. This in turn presents hydrate or freezing problems, particularly in cold weather. A variety of solutions have been used, including tracing with warm separator gas, use of dehydrator pots, running such gas through a heater or treater if available, and insulation of the lines.

Displacement-type liquid-level controls use the buoyant effect of liquid on the float. The average float movement does not exceed $\frac{3}{16}$ in. As the level varies on the float, the weight changes correspondingly and this change in torque is transmitted to the pilot, which, in turn, controls the valve movement. This type of control is applicable in all pressure ranges but is used primarily at high pressures and/or in horizontal vessels. Because of the small movement and small float diameter, the vessel opening may be decreased. This advantage becomes pronounced at high pressure or on small-diameter horizontal vessels.

The pilots on such controls are more sensitive than those discussed above, which allows one to control the level more closely. Most such pilots also allow the valve action to be changed from snap to varying degrees of proportional control by a simple adjustment.

They are necessarily more complex and expensive. Consequently, their use must be justified by process requirements. The instrument gas requirements are also more critical, because as little as one drop of water may plug the small orifice in some pilots.

Floatless level controls are a relatively new development. With these, the pilot is actuated by the varying liquid head in the vessel. As the liquid rises in the separator, it overcomes the pilot spring and forces the pilot assembly upward, closing the upper seat and opening the lower separator seat, which vents the diaphragm pressure to atmosphere. The separator fluid pressure then opens the valve. When the valve is throttling, the nonbleed three-way valve action of the pilot plug against its seat adjusts the motor-valve diaphragm pressure. This type of control has the obvious advantage of eliminating large vessel openings and offering application on very small vessels.

External devices such as float cages and traps find application particularly on vessels with small and/or infrequent liquid loads. Some types of float cages offer no particular economic advantage at high pressure. They are most commonly used on low-pressure plant suction and instrument systems. Inverted bucket traps have been successfully used on small glycol absorbers for economic reasons but regular level controls certainly offer advantages.

At high pressures, a choke nipple downstream from the control valve is advisable, for it (1) provides a factor of safety if the valve "cuts out" or fails to close for any reason; (2) reduces the pressure differential across the valve, which improves the valve action and enables it to shut off tighter; and (3) prevents damage to low-pressure equipment downstream if the instrument supply gas fails on a normally open valve.

The control range with a float-operated controller is limited by the flange diameter and the float-arm length. With a displacement element, control is possible only throughout the float length, for a change in level above or below the float does not affect the buoyancy. Therefore, the desired change in level should not exceed the float length.

The choice of a liquid-level control is somewhat arbitrary, but it is good policy to choose the simplest control that will meet process requirements. Average lease-operating conditions impose severe service on the control, and the ability to make repairs with field personnel will generally reduce downtime.

Types of Regulators

The regulation of backpressure and pressure reduction in a system may be conveniently divided into three categories when considering the type of system needed. The low-pressure range is usually 0 to 125 psig; the intermediate pressure 125 to 500 psig; and the high pressure greater than 500 psig. The use of these ranges is primarily for convenience since some types of valves can operate satisfactorily in all of them.

All pressure regulators are similar in principle, the specification of type being dependent on the process requirements, pressure drop, variation in flow rate, limitations of the loading device, and the maximum pressure. In either of these services, pressure is regulated by the control of flow rate.

This flow is controlled through movement of the regulator inner valve, which is held either open or closed by some means of preloading. The amount of preloading and the size of the diaphragm used, if any, are such that the inner valve will move to the opposite extreme of

travel shortly after the diaphragm pressure passes the desired working pressure. The control pressure, therefore, is varied by changing the amount of preload, thus upsetting the equilibrium between it and the diaphragm pressure. With most valves, increasing preload increases pressure.

The preloading may be accomplished through the use of spring compression, dead weight, or fluid pressure. Valves a and b in Fig. 13.20 are examples of weight-loaded and spring-loaded valves, respectively. Valve c is a spring-loaded valve incorporating a pilot.

In backpressure service, the preloading normally closes the valve, while in pressure reduction the valve is normally open. With the former, the upstream pressure is introduced under the diaphragm and works against the loading device to position the valve properly. In pressure-reduction service, the downstream pressure is introduced under the diaphragm and tends to close the valve until the inner valve is properly positioned. Many valves may be changed from one service to the other by simply reversing the valve body and the stem, while still others have provision for reversing the diaphragm action.

Some applications require that a certain differential pressure be maintained across the valve regardless of how much the upstream or downstream pressures vary. The chief application of this is with positive-displacement pumps where the maximum pressure ratio is controlled by a valve located on a bypass.

In this service, the valve is normally closed with the downstream (higher) pressure under the diaphragm and the upstream (lower) pressure on top of the diaphragm. The desired differential is then established with the loading device.

Each of the types of preloading has its distinct applications and limitations. The weight-loaded regulator is very sensitive within its pressure range if the flow rate does not vary widely. This is true primarily because the inner valve may move through a greater change of position than with a spring-loaded valve. The greater sensitivity is particularly pronounced when the diaphragm is in direct communication with the valve body, which eliminates friction in the stuffing box.

Very few weight-loaded regulators are recommended above 50 psig because at greater pressures heavy weights are necessary. As a result, a small change in controlled pressure is only a small portion of the loading weight, and there is less subsequent movement of the inner valve, which in turn renders control more difficult.

A spring-loaded regulator is generally slightly less sensitive than a comparable weight-loaded regulator under constant-flow conditions. In low-pressure service, (particularly between 0 and 20 psig) it is an ideal type of loading, for the springs used tend to compress in direct proportion to the load, with constant load increase being required for each increment of compression. Consequently, spring loading is excellent in low-pressure systems and where the diaphragm is loaded with a pilot. Because each compression increment is a valve-travel increment, the valve travel is always in proportion to the relationship of the controlled pressure to the preloading. At high pressure, this characteristic does not exist because of the heavy springs required. Therefore, non-pilot-operated spring-loaded regulators are not normally

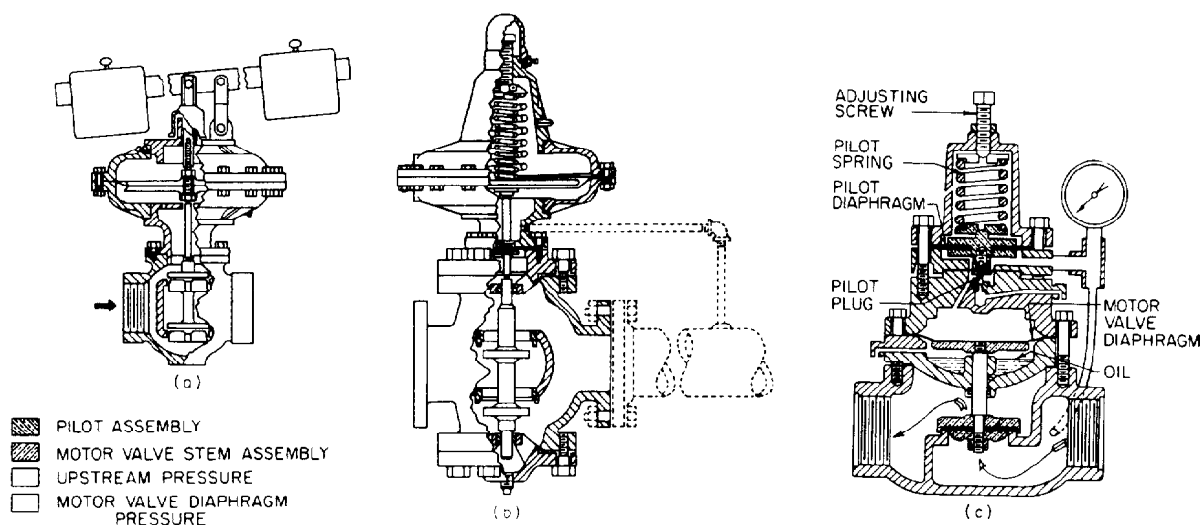


Fig. 13.20—(a) Weight-loaded backpressure regulator. (b) Pressure-reducing valve. (c) Backpressure valve with self-contained pilot.

recommended above 125 psig because of this loss in sensitivity and their closer approach to the price of pilot-loaded regulators.

With either a direct-acting weight or spring-loaded regulator, a change in the uncontrolled pressure will cause a corresponding change in the controlled pressure if the pressure drop is low. This is true especially if the pressure drop is less than 25% of the inlet pressure. Therefore, when accurate control is necessary under these circumstances, pressure-loaded or pilot-operated valves are recommended.

Both the regulation of flow and tight shut-off should not normally be attempted with the same valve unless absolutely necessary. If this is required by operating conditions, a single-seated valve should be used. Double-seated valves are seldom operated under the actual conditions at which they were manufactured and tested.

Consequently, as temperature changes the distance between the two seats, only one of the two will seal off tight.

Single-ported valves will seal off tight but the unbalancing force on the inner valve increases with the square of diameter. Because the diaphragm/spring combination must overcome this force and still control travel, it is logical that the inner-valve size is limited by practical diaphragm size. As a general rule of thumb, direct-acting spring- and weight-loaded regulators up to 2-in. diameter may be used with single-port construction.

Pilot-loaded valves, either pressure-balanced or spring-loaded, offer particular advantage at higher pressure since the pilot presents a means of increasing the control-valve travel with a given change in controlled pressure. This enables one to use a more accurately sized valve. The resultant smaller valve gives better shutoff and closer control because the full range of travel may be utilized.

Low-Pressure Service. It is in this pressure range that weight- and spring-loaded regulators find particular application on the lease. One of the most common applica-

tions is in back-pressure service on low-pressure separators operating at less than 40 psig. All the valves shown in Fig. 13.20 are applicable. One modification of a diaphragm-type weight-loaded valve is used where the weight simply acts to counteract the unbalanced force acting under the inner valve. The choice of this valve is predicated primarily from cost considerations since it is the cheapest of the valves. No diaphragm is used.

The simple weight-loaded valve has the advantage of being cheap and simple. Its primary disadvantage stems not from its operation but from the circumstances surrounding its use. The weights become loose and shift, are lost, or are hindered in movement by outside obstructions. It is not too uncommon to see rocks and other miscellaneous objects used as substitutes for, or additions to, the proper weights. Consequently, these regulators serve as a proper but not necessarily completely satisfactory backpressure control.

Not too many spring-loaded regulators are used on separators because of their higher price, although they are generally satisfactory below 40 psig. The best regulator in this range is Valve c, Fig. 13.20. It gives fine control throughout the range with widely fluctuating flow rates and uncontrolled pressures. Where fine control is necessary, particularly above 40 psig, the extra investment is normally justifiable.

Because of the almost infinite number of different field conditions that arise, the above considerations can at best serve only as a general guide. Unfortunately, the actual choice of type must often stem largely from past experience.

High-Pressure Service. At pressures above 125 psig, it is usually difficult to justify anything other than a pilot-operated diaphragm motor valve for pressure control. Non-pilot-loaded valves are sometimes applicable but usually only in those circumstances where pronounced load changes are not encountered. At these higher pressures, the cost differential also becomes less, which further encourages the use of pilot-operated controls.

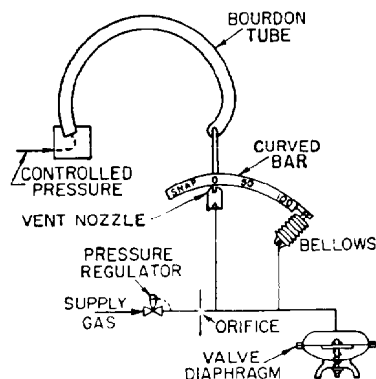


Fig. 13.21—Proportional pilot for pneumatic service.

Most pilots now in use in the oil field are pneumatic in nature and use natural gas as the actuating fluid. Any natural gas that is free of fluids and at a pressure greater than 15 psig is suitable in this service.

Fig. 13.21 is a schematic view of a pressure pilot that will give both proportional and on/off control. As the controlled pressure varies, the bourdon tube will change shape and, in turn, raise or lower the curved bar.

The supply pressure is held constant between 15 and 20 psig by the pressure regulator. The vent nozzle is so sized that when wide open (curved bar away from it) it will pass more gas than the orifice. Consequently, the pressure on the valve diaphragm and the valve position depends on the opening of the vent, which in turn depends on the position of the curved bar, as fixed by the bourdon tube. If the vent is wide open, the pressure on the diaphragm is zero, while if it is fully closed, the diaphragm pressure equals the controlled supply pressure.

It is necessary that both the vent and orifice be very small to minimize the amount of gas vented. If the curved bar had a fixed pivot rather than a bellows, only on/off (snap) action would be possible because of these small openings. From a purely mechanical standpoint, any small movement of the curved bar would in effect make the vent wide open.

The bellows is used to impart a rotating motion to the curved bar around the end of the vent. When the bar begins to rise off the vent, the bellows contracts, which tends to keep part of the vent opening covered. As a result, more vertical movement of the bar is necessary to open (or close) the valve fully. All points in between then represent some degree of proportional control.

The vertical distance that the bourdon tube has to lift the bar to stroke the valve completely increases as the lever arm decreases. This then allows for adjustment of the proportional band.

If the vent is close to the left end of the curved bar, the movement of the bellows imparts little rotation to the bar and on-off action results.

Most pressure pilots have the bar marked to show various percentages of proportional control. The percentage shown indicates that the controlled variable must vary through that percentage of the instrument's range to open or close the valve fully.

Example Problem 3. If a pressure pilot has a bourdon tube with a range of 0 to 200 psig and it is set on 50% proportional control, how much must the pressure vary to make the valve be fully stroked?

Solution. It must vary $(0.50)(200 - 0) = 100$ psig to stroke the valve fully.

From the discussion above it therefore follows that the closer the vent is to the bellows, the higher the percentage of proportional control obtained.

Most pressure pilots are slightly more complex than the schematic presentation in Fig. 13.21, to improve the mechanical action and the sensitivity. However, the basic mechanism and principle of operation shown is common to all pneumatic pilots.

In most applications, the valve is spring-loaded, but there are some applications where a large quantity of high-pressure gas must be controlled with a low-pressure drop. Such an application is encountered with the switching valves of a dry-desiccant dehydrator. A large inner-valve assembly is required, which increases the unbalanced forces on the diaphragm, which in turn necessitates a heavy spring. In such cases, the use of a pressure-loaded balanced diaphragm valve is indicated. With this type, greater valve travel may be obtained, with less change of controlled pressure than with any other type. With a constant loading pressure, on a larger balanced diaphragm, the available force to travel the valve with incremental change of control pressure is greater than with a spring-loaded valve because of spring characteristics. However, spring loading is simpler wherever applicable.

The greater the pressure drop across a valve, the greater the unbalanced force that exists. Where this pressure drop is greater than several hundred psi, it is good practice to install a choke nipple downstream from the valve. This choke nipple should preferably be about 10 to 25% larger than the inner valve so that the latter is the controlling element. The nipple serves two purposes:

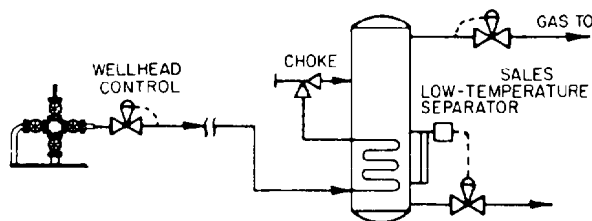


Fig. 13.22—Typical pressure control for a high-pressure well.

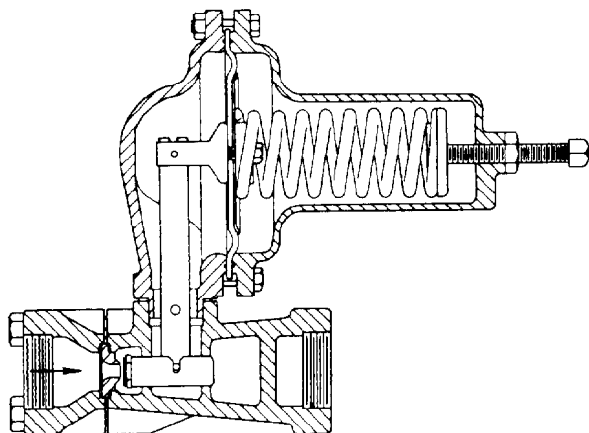


Fig. 13.23—Small high-pressure spring-loaded pressure regulator.

(1) it reduces the pressure drop across the valve and increases sensitivity; and (2) it acts as a secondary control in the event the valve fails to close or cuts out.

The pilot shown in Fig. 13.21 may be modified to give what is known as high-low shut-off. A pilot so modified will cause the valve to close if the controlled pressure becomes higher (or lower) than the preset condition. This modification has particular application in high-pressure wells to (1) shut in the well in the event a line break is encountered; and (2) prevent overpressuring of a separator or other piece of equipment downstream from a choke or valve.

In some instances, it is desirable to use an automatic rather than a manual adjustable positive choke. A regular diaphragm-motor-valve topworks may then be combined with the choke body to give a control valve and choke combined. Although it costs more, there is some advantage to using the positive choke as a rough control with a separate valve at the wellhead for safety. Fig. 13.22 illustrates such a scheme where several wells are being flowed to a central low-temperature separation unit, the pressure drop being taken at the unit. The valve at the well protects against line break while the back-pressure valve at the separator holds the separation pressure constant regardless of how the sales line pressure varies. The two control valves fix the pressure drop across the choke, with the flow rate being determined by the choke setting.

Where very high formation pressures are encountered, one or more "storm chokes" in the well proper make a desirable installation.

Fig. 13.23 shows a spring-loaded valve for pressure-reduction service. This is a popular valve for pressure regulation in services where the rate of flow is not large. The pivot point on the arm is so located that it ratios the force on the inner valve down to where the spring can control properly.

Fig. 13.24 shows a double-port diaphragm motor valve that would be controlled by a separate pilot, such as that shown in Fig. 13.21. Fig. 13.25 shows several of the different types of inner valves that might be used in the double-port valve shown. The shape used depends on the service and the type of control desired. The same

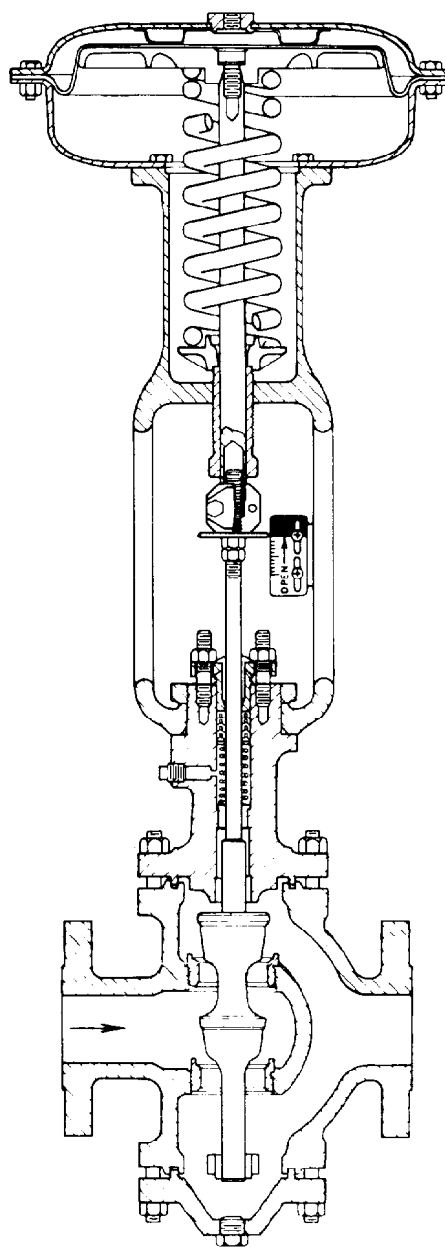


Fig. 13.24—Typical spring-loaded motor valve.

general shapes of inner valves are also available in single-port valves.

Control of Field Compressors

Most of the controls on a field booster compressor are designed to protect the equipment and facilitate operation with minimum attention; it is theoretically possible to operate the system with little more than manual control. The exact scheme used will of course vary with the application, but that shown in Fig. 13.26 is typical of small-lease operations where low-pressure gas is compressed in one stage.

No control and cooling system is shown for the engine since this will depend on the engine manufacturer. On most small portable units, the engine is self-contained

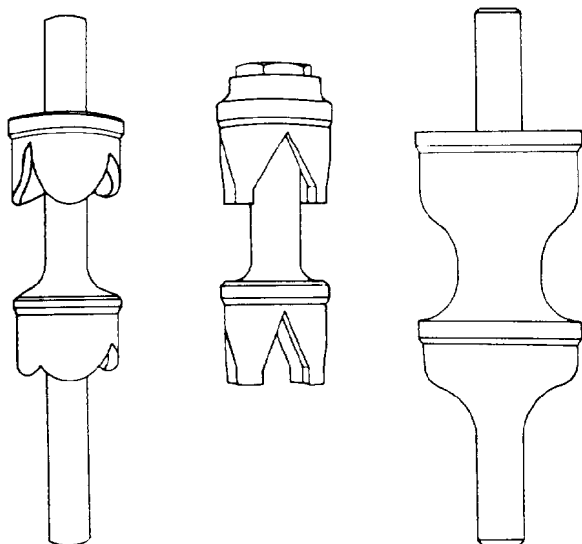


Fig. 13.25—Several types of inner valves used in double-port valves.

with its own radiator and pump. If two-, or more, stage compression is used, the controls shown for the inlet scrubber would be duplicated for each interstage scrubber. A provision would also have to be made for interstage gas cooling.

The backpressure controller shown on the vent is to prevent overpressuring of the separator in case the compressor plant is down. The other backpressure valve on the suction line is to prevent the plant from lowering the separator pressure by drawing off gas faster than it is produced. It should be set several pounds lower than the valve on the vent line.

The meter run is shown at the plant, although it could be conveniently located at the separator. A check valve (Location 12) is included to prevent the backflow that may result when multiple units feed the same compressor.

A butterfly valve (Location 14) is an optional but desirable item to control the compressor suction pressure. All compressors are rated using a given suction and discharge pressure, and this valve simply prevents the former from getting too low and overloading the unit. This valve is particularly desirable if the deliverability of gas to the plant is widely variant.

The inlet scrubber is primarily a protective device to keep liquid out of the cylinders and should not be used as a primary oil and gas separator. This vessel serves simply as a liquid sump and a convenient device on which to hang certain necessary controls. As a convenient rule of thumb, this vessel should have a cross-sectional area of at least 100 sq in./MMcf/D of gas processed. The minimum size is normally 12 in. A float-operated trap (Location 6) is very satisfactory for controlling the liquid level.

Switches (Locations 1, 2, 7, and 8), constitute the basic safety shutdown system. These switches are normally open, but if the condition at any one goes beyond set limits, it closes, grounding out the engine magneto, which in turn stops the engine. All are simple and inexpensive and afford positive protection. A horn and/or remote indicator may be incorporated that is actuated at any time the compressor stops.

Switches at Locations 1 and 8 are high- and low-pressure shutdown, respectively. They serve to keep these pressures within the limits set up for the compressor. The switch at Location 2 is a high-temperature shutdown that is actuated by the hot water leaving the cylinder jacket. It shuts down the unit when any failure occurs in the cooling system.

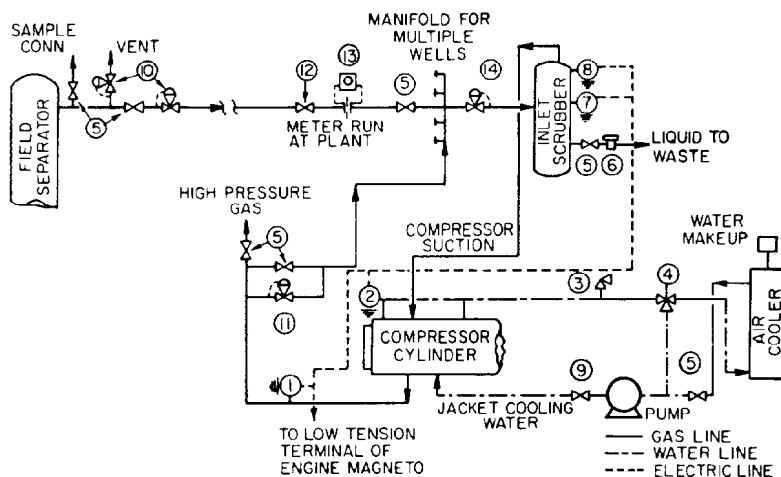


Fig. 13.26—Typical control system for field compression of natural gas. (1) High-pressure shutdown switch. (2) Water-temperature safety switch. (3) Low-pressure liquid-relief valve. (4) Water-temperature bypass control. (5) Plug valve. (6) Trap-type level control. (7) High-level shutdown. (8) Low-pressure shutdown switch. (9) Globe valve. (10) Low-pressure backpressure controllers. (11) Relief valve. (12) Check valve. (13) Orifice meter. (14) Low-pressure pilot-controlled butterfly valve.

The switch at Location 8 is a high-level shutdown that operates when the liquid level becomes too high in the scrubber because of either failure of the valve at Location 6 or an excess quantity of liquid entering the plant.

The bypass valve at Location 5 is desirable because it provides a means of taking the load off the compressor, particularly during start-up. During normal start-up, this valve would be open and gradually closed once the compressor and engine reached running speed.

The bypass relief valve (Location 11) is an optional and, to a certain extent, a luxury item because it duplicates the protection offered by the switch at Location 1. It provides relief in the event the outlet or bypass plug valves are inadvertently closed, without shutting down the compressor. If used, it would normally be set to open 5 to 10 psig before the high-pressure switch closes.

The water-temperature bypass control (Location 4) serves to control the jacket water temperature by governing the amount of water to the cooler. In its simplest and cheapest form, it consists of an automobile-radiator-type thermostat in a three-way cast-iron valve body. It is substantially the same device used on most oil-field engines. A conventional temperature control would of course be satisfactory but its cost cannot be justified unless it is a large installation or is used where the complexity of the system does not lend itself to this type of control. In some cases where several services are handled by the same cooler, it is often more satisfactory to control the temperature by varying the speed or pitch of the fan.

Although no scale trap is shown, it is normally a good policy to have one to prevent accumulation and possible system damage. Some provision for water make-up is necessary; so a small surge tank on top of the cooler should be provided for this purpose. Drains should be provided so that the system may be completely drained.

The pop-off valve (Location 3) is primarily to prevent overpressure of the system, particularly the radiator. A simple brass valve 1/2 in. in size is normally sufficient.

On large systems, a standpipe may be used ahead of the pump suction to handle surges and serve as a water reservoir.

Nomenclature

- A_2 = area of orifice plate opening
- b = values for Reynolds number factor, Tables 13.1g and 13.1h
- C = orifice coefficient for prover
- C' = orifice constant
- d_i = internal diameter of pipe
- d_o = orifice-opening diameter
- F_a = thermal expansion factor
- F_b = basic orifice factor
- F_d = ratio of orifice opening diameter to internal pipe diameter
- F_g = specific-gravity factor
- F_{ia} = instrument-adjustment factor

- F_L = gauge location factor
- F_m = manometer factor
- F_{pb} = pressure-base factor
- F_{pc} = supercompressibility factor
- F_r = Reynolds-number factor
- F_{tb} = temperature-base factor
- F_{tf} = flowing-temperature factor
- g = force-mass conversion factor
- h_w = differential water head across orifice
- K_o = efficiency factor, which includes approach factor
- p = pressure
- p_{fm} = flowing mean pressure
- p_m = pressure in inches of mercury
- q_g = gas-flow rate
- Q = heat gained or lost by system
- R = controller reset constant
- S = characteristic constant of the pilot relating output to input
- t = time
- T = absolute temperature
- U = internal energy, which includes all energy such as heat, electrical, chemical, and surface
- v = velocity in conduit
- V = volume
- W = work done by system
- X = 0, datum defined in Fig. 13.1
- X_1, X_2 = potential energy above the datum plane defined in Fig. 13.1
- Y = expansion factor
- Z = height above an arbitrary datum plane
- γ_g = specific gravity of gas (air=1.0)

Subscripts

- f = flowing conditions
- g = gas
- o = orifice
- s_c = base or standard conditions

References

1. Campbell, J.M.: "Gas Conditioning and Processing," Campbell Petroleum Series, Norman, OK (1984).
2. *Orifice Constant Tables*, American Gas Assn., Report No. 3, revised (1969). Also, ANSI/API 2530.
3. *Handbook E-2, Orifice Constant Tables*, American Meter Co., revised (1973).
4. *Engineering Data Book*, GPSA, Tulsa, OK (1972).
5. November, M.H.: "How to Use High-Capacity Axial-Flow Turbine Meters for Gas Measured," *Oil and Gas J.* (April 3, 1972) 69.
6. Evans, H.J.: "Turbine Meters Gain in Gas Measurement," *Oil and Gas J.* (Aug. 20, 1973) 67.

General References

- Supercompressibility Tables NX-19*, American Gas Assn.
- Supercompressibility Tables IS-561, IS-461*, Pacific Energy Association.

Chapter 14

Lease-Operated Hydrocarbon Recovery Systems

Robert N. Maddox, Oklahoma State U.*

Introduction

In lease production of natural gas, the marketing specifications as prescribed by the gas sales contract must be considered when selecting the system for processing wellhead gas for liquid recovery. Natural gas at the wellhead can contain liquefied hydrocarbons, free water, water vapor, acid gases, and other undesirable components. To make wellhead gas merchantable, these components must be reduced to a composition that will satisfy the marketing specifications. The first part of this chapter is devoted to the removal of liquefiable hydrocarbons from natural gas. The latter part of the chapter describes techniques for removal of some of the other components.

The removal of liquefiable hydrocarbons, which are called "condensate," is necessary for efficient transmission of natural gas in pipelines. If hydrocarbons condense in the pipeline, additional horsepower is required to overcome the increased pressure drop. Where the heating value of the natural gas is specified by the gas sales contract, there must be control of the condensate removal to satisfy this limitation. A final consideration for removal of condensate is that additional revenue is derived over that from sale of natural gas. In many instances this additional revenue will readily pay out the cost of process equipment required to produce gas of merchantable quality.

Low-Temperature Separation (LTS) Systems

Theoretical Considerations

Before various methods for removing condensate from natural gas are discussed, some of the physical phenomena involved in the formation of condensate are examined.

Retrograde Condensation. Retrograde condensation is a phenomenon that occurs at the high temperatures and

pressures frequently encountered in condensate hydrocarbon reservoirs. In the retrograde condensation region, as shown in Fig. 14.1, condensate forms at constant temperature with a reduction in pressure or at constant pressure with an increase in temperature, both of which are contrary to the normal expectations for condensation. If fluid in the reservoir existed at Point A, condensation would occur as the pressure in the reservoir declined from A to B. Less frequently encountered is the case shown by Line C-D. Here the fluid is in the single-phase region at Point C. As the temperature is increased at constant pressure from C to D, condensation occurs.

Retrograde condensation also can occur at lower temperatures and pressures than those encountered in the reservoir. This phenomenon¹ can occur at normal processing conditions for lease-operated equipment. Gas removed from a separator at typical high-pressure separator conditions (100°F and 1,000 psia) will undergo an increase in dewpoint temperature as the pressure is lowered. In many cases this "bulge" in the dewpoint line at lower pressures can amount to as much as 20°F or more, enough to cause troublesome condensation in lines thought to be at constant temperature as relatively small pressure drops occur.

Fig. 14.2 shows the calculated dewpoint curve for the off-gas from a separator operating at 120°F and 1,000 psia. The maximum dewpoint temperature is 136°F and occurs at about 500 psia. Also shown in Fig. 14.2 are constant mol% liquid lines. Over nominal line pressure drops very little liquid will form but that formed will be primarily the heaviest components in the gas stream.

Cooling. A second phenomenon to consider in condensate removal from natural gas is the cooling that can occur when the pressure on the gas is decreased. This temperature decrease can have one of two causes. When natural gas expands from a high pressure to a lower pressure without heat transfer or work being done (a constant-

*The author of the chapter on this topic in the 1962 edition was Edwin C. Young.

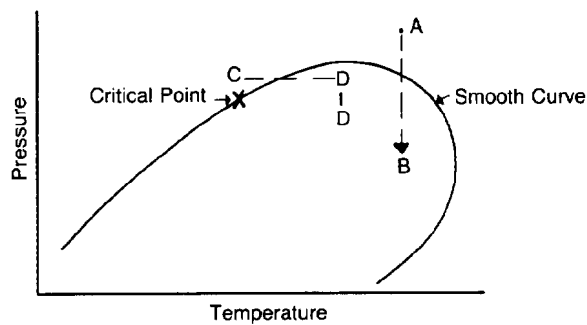


Fig. 14.1—Pressure-temperature diagram for typical natural gas and showing retrograde behavior.

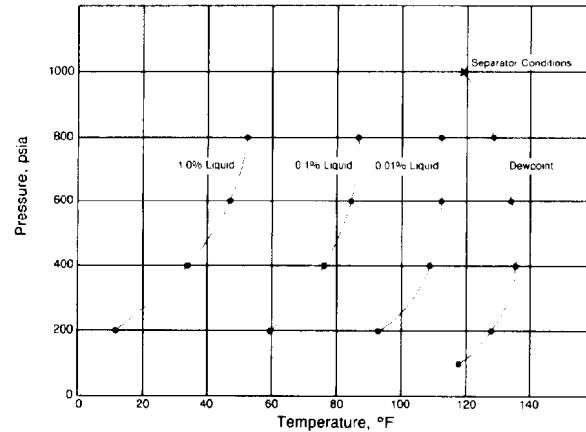


Fig. 14.2—Retrograde condensation of separator off-gas.

enthalpy expansion), there is an accompanying temperature drop or refrigeration effect normally referred to as the Joule-Thomson effect. If, however, the expansion occurs through a turbine then work is removed from the gas during the expansion and cooling occurs also. Advantage can be taken of the available pressure drop to lower the separation temperature of the hydrocarbon mixture and cause more liquid to form from the natural gas. Cooling from turbine expansion must be modeled along the lines of compression calculations and is not easily correlated. Cooling available from constant-enthalpy expansion can be estimated by charts such as Fig. 14.3. One must be cautious in using charts like Fig. 14.3 because they are composition-dependent and cooling depends on gas composition and amount of liquid formed as well as the initial and final pressures.

Hydrate Formation. A third phenomenon that must be considered is the possible formation of hydrates when

water is present in the natural gas stream. Hydrates are materials that have fixed chemical compositions but exist without chemical bonds and are called "clathrates." They form a solid similar to snow at temperatures above 32°F (the freezing point of water) when the gas is under pressure. They appear to be hydrates of a mixture of the component gases and not a mixture of the hydrates of the individual gases. The hydrates form at a temperature that is characteristic of a given gas mixture rather than at the hydrate temperature for the individual components in the mixture. The hydrates normally include several water molecules for each hydrocarbon molecule so that the presence of liquid water is generally considered necessary for the formation of hydrates in sufficient quantity to cause plugging of a line, valve, etc. Turbulence accelerates the formation of hydrates and for this reason they frequently occur downstream from valves, regulators, chokes, orifice plates, sharp bends, etc. Fig. 14.4 can be used to estimate hydrate-forming conditions for different natural

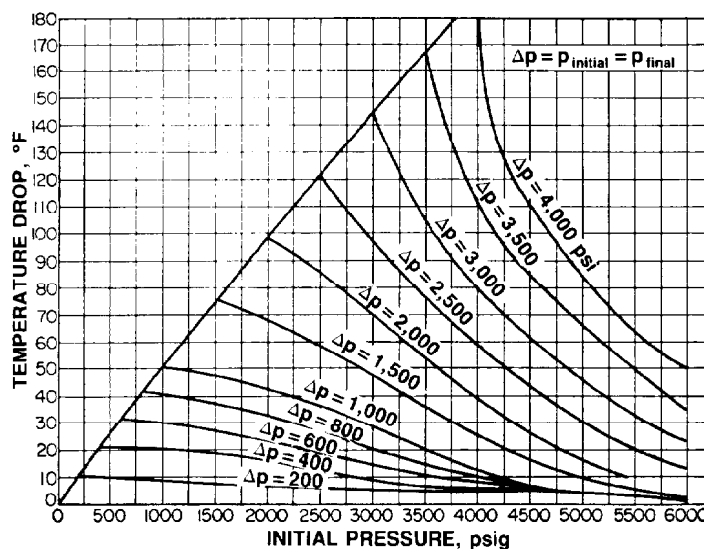


Fig. 14.3—Temperature drop associated with a given pressure drop.

gases. Caution also must be used in Fig. 14.4 because, as shown by the different hydrate-forming lines for 0.6-gravity gases, there can be considerable difference in the hydrate temperature of gases of the same gravity.

If the composition of the gas is known, a composition-dependent calculation of the hydrate temperature, either by hand³ or by computer,¹ will give a much better estimate of the hydrate temperature than will Fig. 14.4.

A necessary condition for hydrate formation is the presence of liquid water. Prediction of the temperature where free water will occur will help identify the first point at which hydrates might form. The chart shown in Fig. 14.5 gives the water vapor content of sweet [no hydrogen sulfide (H_2S) or CO_2] natural gas as a function of temperature and pressure. As the temperature decreases at a given pressure the water content required for saturation also decreases. This will result in condensation of liquid water for a saturated gas stream as it is cooled. As an example, suppose a well is flowing 1 MMscf/D of natural gas at 1,000 psia saturated with water vapor but containing no liquid water at 110°F. The gas is cooled to 60°F because of ground and atmospheric cooling. At 1,000 psia and 110°F, the gas contains 80 lbm water vapor/MMscf and at 60°F it contains only 18 lbm/MMscf. One day of gas production will result in the formation of 62 lbm of free water because of the cooling. Referring to Fig. 14.4, if the gas flowing has a specific gravity greater than 0.6, hydrates are likely to form in the flow line at some point of turbulence.

Constant-Enthalpy Expansion Systems

The constant-enthalpy expansion systems use the refrigeration effect that results from a pressure drop taken on a high-pressure wellstream. This expansion occurs across a choke and the resulting refrigeration effect is dependent on the temperature on the upstream side of the choke, the pressure differential across the choke, and the amount of liquid formed. For obtaining the maximum removal of liquefiable hydrocarbons from the gas stream for a given pressure differential and sales-gas pressure, the lowest possible temperature within reasonable limits should be attained in the separator. This in turn means the lowest possible temperature upstream of the choke. Two basic methods commonly used to accomplish condensate removal are low-temperature separation with or without hydrate inhibitors. Each method is discussed in the following sections.

Low-Temperature Separation Without Hydrate Inhibitor.

The basic unit for low-temperature separation without hydrate inhibitor includes essentially a choke, separator, and heat-exchange coils. Assuming that the inlet wellstream contains a minimum amount of free water and is of sufficient temperature to prevent formation of hydrates upstream of the choke, the operation is as follows. The wellstream enters the unit shown in Fig. 14.6 through the heat-exchange coil, where it is cooled through heat exchange with the liquid external to the coil. The wellstream then passes through an adjustable choke used to control the flow rate through the system and establish a means for introducing the necessary pressure drop. The turbulence and temperature drop created by the expansion across the choke cause the formation of hydrates and the

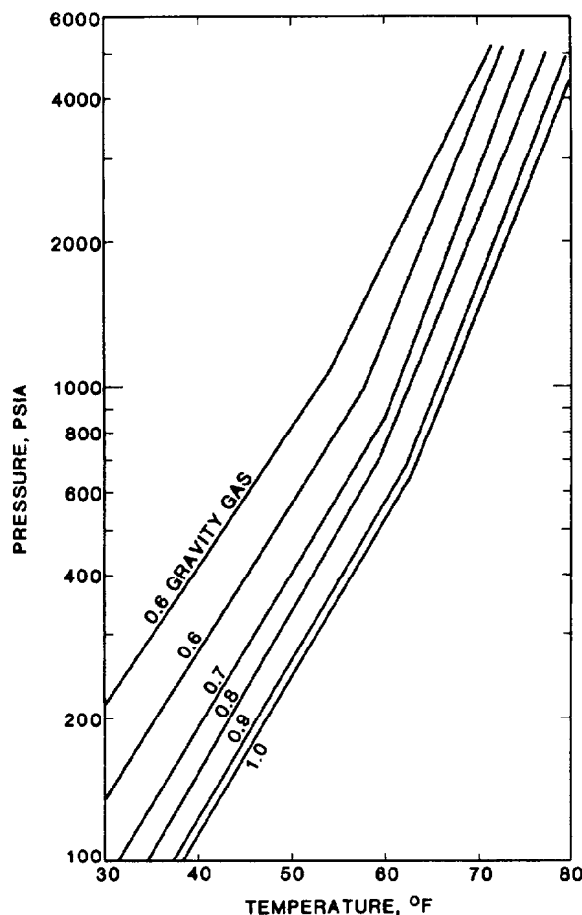


Fig. 14.4—Approximate hydrate-forming conditions for natural gas mixtures.

condensation of the liquefiable hydrocarbons. The hydrates and condensate are separated from the gas by means of centrifugal force, normally generated by locating the choke tangential to the shell of the separator, and by gravity. The hydrates and condensate collect in the bottom of the separator where they absorb heat from the inlet coil, causing the hydrates to be melted. The liquid level is maintained by a level controller such that the coils are always submerged in the liquid.

Two possible operating problems might occur in this simple system. Either the wellstream could be near the hydrate temperature on entering the coil and further cooling would create hydrates upstream of the choke, or there is an insufficient amount of the liquid bottoms causing hydrates to build up inside the separator. In either case the system will malfunction. To use low-temperature separation successfully, the pressure of the gas upstream of the choke must be approximately twice the pressure in the low-temperature separator. Certainly, the higher the pressure upstream of the choke the lower the temperature that can be achieved in the low-temperature separator.

The common solution to this problem is to install an indirect heater upstream of the low-temperature separator. The indirect heater temperature would be maintained at a level to ensure wellstream gas temperatures above the hydrate temperature. Heat transfer is accomplished

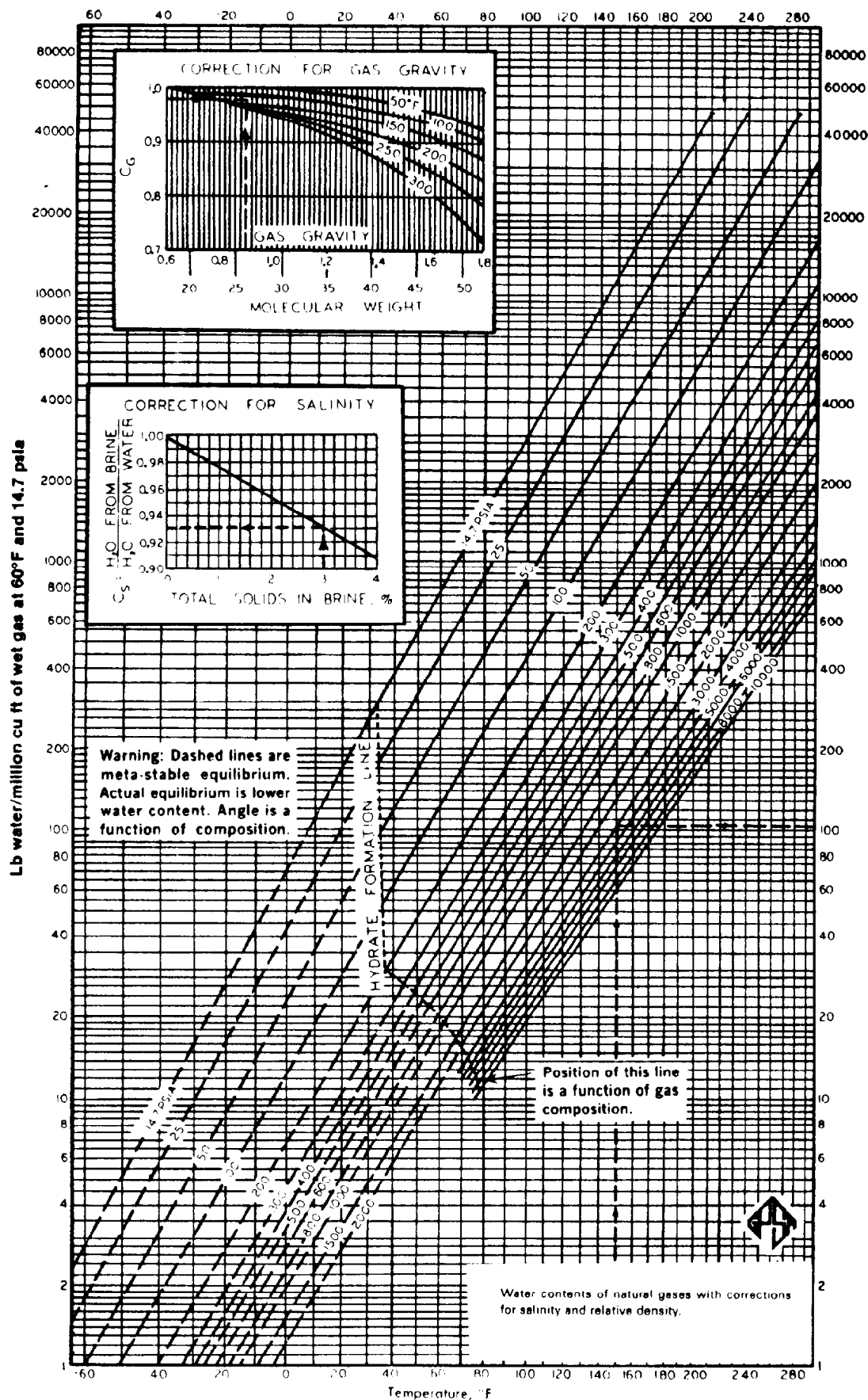


Fig. 14.5—Water dewpoint of natural gas.

by flowing the wellstream through the coils in the indirect heater. The gas temperature is controlled by a thermostat located in the outlet end of the coil. A second thermostat can be located in the liquid section of the low-temperature separator to override the heater controls in the event the liquid temperature is too low.

For the simple system outlined here, the prime concern was to keep the temperature high enough upstream of the choke to ensure continuous operation. One of the necessary elements for hydrate formation, as pointed out previously, is the presence of free liquid water. In cases where free water and liquid hydrocarbons are present in the wellstream, and where these liquids are formed because of the chilling effect in the coil, a high-pressure separator can be placed between the coil and the choke. The liquids separated in this vessel are dumped at a relatively warm temperature into the bottom of the low-temperature separator and combined with the liquids in the separator. This reduces the amount of free water and liquid hydrocarbons passing through the choke and allows more net cooling to occur. Since the sensible heat transfer to these liquids can be used for cooling the gas and condensing additional hydrocarbon vapor, it also reduces the amount of hydrates formed by minimizing the amount of free water passing through the choke.

A further refinement to this system is possible for increasing the condensate removed from the wellstream. This includes the addition of a heat exchanger located between the inlet high-pressure liquid separator and the choke. The high-pressure wellstream flows through the tube side of this heat exchanger, and cold sales gas off the top of the low-temperature separator flows through the shell side. The amount of sales gas flowing on the shell side is controlled by a three-way bypass valve actuated by a temperature controller upstream of the choke. In this manner the upstream temperature at the choke can be maintained at a minimum value but still above hydrate

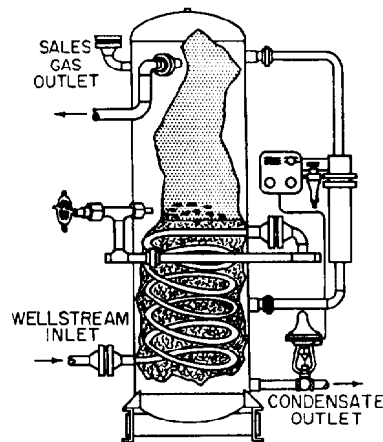


Fig. 14.6—Typical low-temperature separator.

temperature. From the analysis given, the lower this inlet temperature, the lower will be the temperature in the separator and the greater will be the amount of condensate removed.

The complete system is shown in Fig. 14.7. The wellstream flows through the coil in the low-temperature separator where it is slightly chilled, then to the inlet high-pressure liquid separator where free liquids are separated from the gas. The gas then flows through the gas-to-gas heat exchanger, through the choke, and into the low-temperature separator. The cold gas flows from the separator, through the gas-to-gas heat exchanger, and into the sales-gas line. The liquids from the bottom of the low-temperature separator are dumped to some form of stabilization before going into storage.

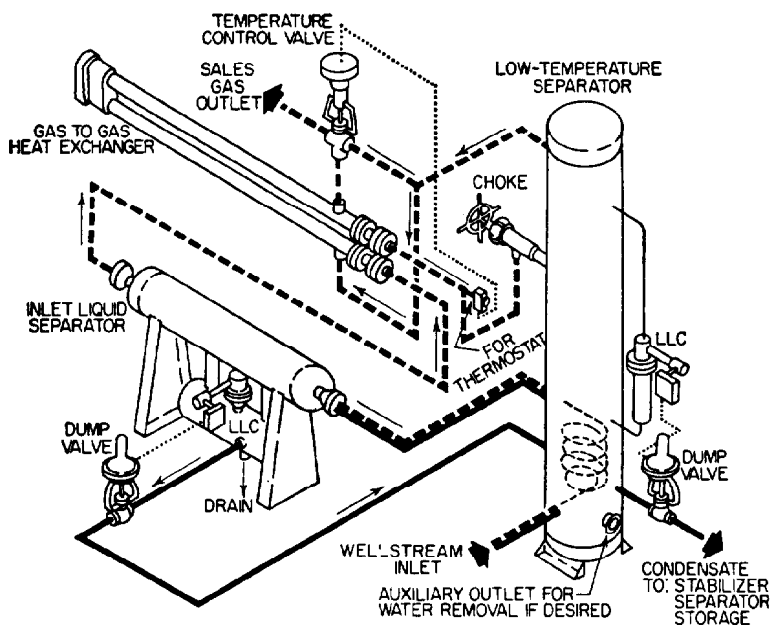


Fig. 14.7—Typical LTS system with inlet separator and intermediate heat exchanger.

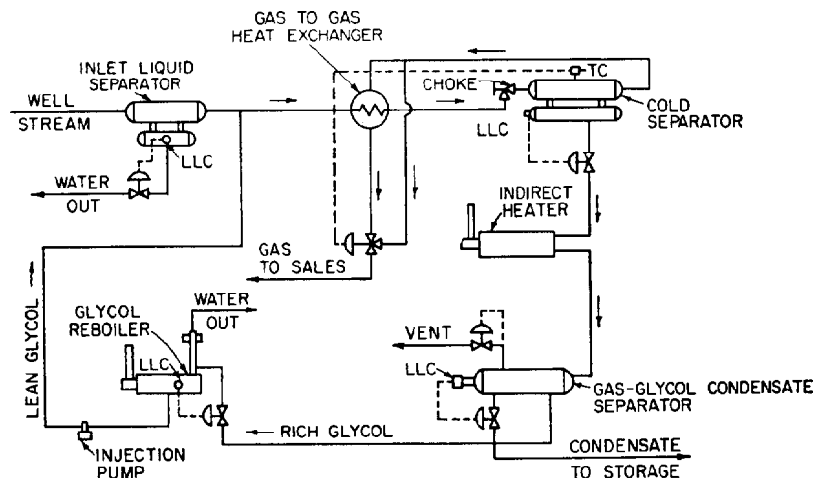


Fig. 14.8—Schematic flow diagram of a glycol injection LTS system.

In summary, the following considerations are necessary for operation of low-temperature separation systems without hydrate inhibitors. The controlled temperature of the high-pressure stream must be kept slightly above the hydrate temperature to prevent freezing upstream of the choke. The hydrate temperature can be determined by reference to the hydrate curve for natural gas (Fig. 14.4). The temperature of the low-temperature separator can be estimated from pressure-temperature drop curves for natural gas in Fig. 14.3. Allowances must be made for the liquid content, which will slightly reduce the temperature drop if the liquid hydrocarbons are not separated in a high-pressure separator upstream of the choke.

On wellstreams with low flowing temperatures a heater may have to be installed upstream of the low-temperature unit. In such cases the temperature is controlled with the heater and the gas-to-gas heat exchanger may not be required. If a well makes little free water and/or no waxy distillates or free condensate, the inlet high-pressure liquid separator can be eliminated.

This type of system is economically feasible from a liquid-recovery standpoint for gas streams with liquid content of a few barrels up to about 100 bbl/MMscf gas. The optimal recovery pressure will vary with different wellstreams but may be as low as 350 psig.

A rough rule of thumb is that 0.05 bbl additional liquid can be recovered per MMscf of gas for each degree lowering of the temperature. Below 20°F the increase in recovery becomes lower, and in some cases only slight additional recovery of net stock-tank liquid can be realized by lower temperatures.

Low-Temperature Separation With Hydrate Inhibitor.

The formation of hydrates can be prevented by changing the character of the water in such a way that it will not hydrate with the natural gas. This is accomplished through the use of a substance known as a "hydrate inhibitor." The most commonly used hydrate inhibitors are glycols and alcohols. Either will function satisfactorily. The system with a hydrate inhibitor is similar to the one in Fig. 14.7 except that the inhibitor is injected between the inlet high-pressure separator and the regenerative heat ex-

changer. The inhibitor mixes with free water formed on cooling and prevents hydrate formation. The advantages and disadvantages of alcohols and glycols as inhibitors are discussed by Campbell,² as is the required amount of either material necessary for preventing hydrate formation. Further discussion here centers on the use of glycol as a hydrate inhibitor. A typical system using glycol is shown in Fig. 14.8.

The presence of the inlet high-pressure liquid separator is very important in this system. The produced water must be removed in this inlet separator to prevent contamination of the glycol and to keep the regeneration equipment from having to handle this extra vaporization load. The contamination occurs as (1) excessive dilution of the glycol, which reduces its inhibiting qualities; (2) as salt water, which is detrimental to the regeneration system; and (3) as solids, which can cause foaming and other problems in the separation and regeneration systems. If the wellstream contains waxy heavy ends these must be removed and kept out of the low-temperature separator where they could build up and cause the system to malfunction.

Glycol, which has been processed through the regeneration system to remove the water picked up in the system, is pumped from a storage tank to an injection point downstream of the inlet separator. The glycol rate is controlled by setting the speed of the pump. The rate is established by calculating the amount of water to be inhibited while going from the saturated condition downstream of the inlet separator to a saturated condition in the low-temperature separator. The glycol concentration, resulting from dilution with this water to be picked up, must be maintained sufficiently above the freezing point of the solution to prevent freeze-up in the low-temperature separator or the regenerative heat exchanger. There are published curves³ that can be used to calculate the necessary quantity of glycol.

The inhibited wellstream passes through the regenerative heat exchanger, to the choke, and into the low-temperature separator. The cold sales gas off the separator passes through the shell side of the heat exchanger. A three-way valve is used to control the amount of heat

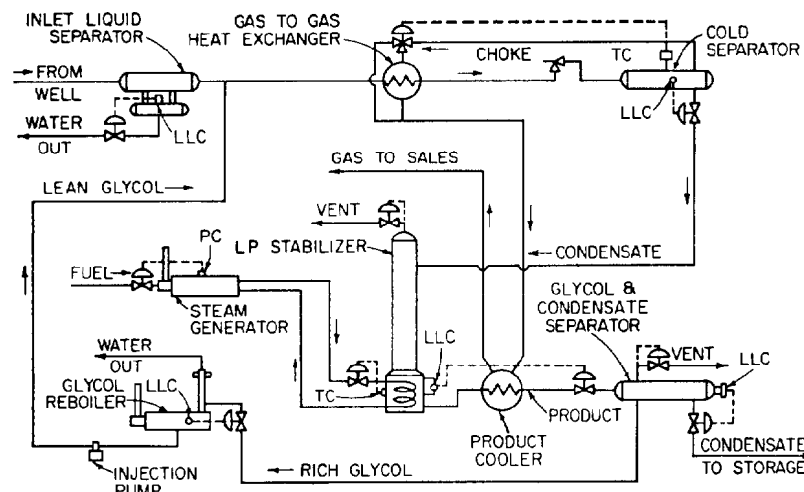


Fig. 14.9—Schematic flow diagram of a glycol injection LTS system with low-temperature stabilization.

transferred from the wellstream to the sales gas to maintain a specified temperature in the low-temperature separator. This valve is actuated by a temperature controller located in the low-temperature separator. Since the inhibited wellstream can be cooled below hydrate temperature ahead of the choke, lower temperatures are possible in this system than with the uninhibited system. This allows more liquefiable hydrocarbons to be condensed out of the wellstream and separated along with the rich glycol.

The liquids from the low-temperature separator contain condensate and rich glycol. The step of separating these liquids is difficult because of the low temperature and high viscosity. One method of handling this separation is to pass the liquids through a heater, as shown in Fig. 14.8, to bring the temperature to a level where separation can be achieved. However, this decreases the potential liquids recovery because of the warming up of the liquid hydrocarbons. Since condensates from glycol injection systems are commonly stabilized to give better stock tank recovery, in some cases the glycol hydrocarbon mixture passes through the stabilizer before separation. A flowsheet for this process is shown in Fig. 14.9.

If the gas being processed contains aromatic hydrocarbons, these will dissolve preferentially in the glycol. They may then cause degradation and decomposition problems in the glycol regeneration system.

The glycol from the injection system is rich in water and must be reconcentrated before it can be recirculated. This is accomplished in the glycol reboiler as shown in Figs. 14.8 and 14.9. The rich glycol is fed into a still column where it contacts the steam rising from the reboiler. This serves to preheat the glycol, strip out any dissolved gases, and condense any glycol that may be entrained in the steam vapors. With diethylene glycol the reboiler is operated at around 240 to 250°F to provide outlet glycol concentrations of about 80 to 85 wt%. The glycol-condensate separator is usually designed to act as a surge to take up the slack in the event that glycol might be temporarily accumulated elsewhere in the system.

Glycols are expensive, so the system must be designed and operated to keep losses at a minimum. Losses occur because of the slight solubility of glycols in condensate

and the vaporization of glycols in the regeneration system. Proper equipment design and sizing for separation in the low-temperature separator and the glycol-condensate separator can keep mechanical losses to a minimum. In considering the type of glycol best suited for an injection system, both the solubility and the vaporization characteristics must be considered. Ethylene glycol has the least solubility in condensates but the highest vaporization losses. The vaporization can be reduced through a more elaborate regeneration system but at a higher initial equipment cost. Triethylene glycol has the least vaporization loss but is the most soluble. Diethylene glycol is usually considered a good compromise. In a typical condensate, 70 to 80 wt% diethylene glycol solution is about 0.4 wt% soluble. More concentrated solutions are more soluble but these are seldom encountered in glycol injection systems. Aromatic hydrocarbons tend to increase the solubility of the glycol in the condensate and higher losses can be expected when they are present. In installations where extreme care is exercised to eliminate glycol losses of a mechanical nature, such as leakage past the pump packing and unnecessary spillage, glycol losses have been found to be approximately 0.2 gal/MMscf of gas processed.

Hydrocarbons separated in the inlet high-pressure liquid separator can be recombined in the low-temperature separator provided they are not of a waxy base. The solution gas flashed in discharging from the high-pressure separator can be recombined with the sales gas and the liquids recombined with the condensate prior to stabilization. Waxy-based hydrocarbon liquids are best discharged directly to the stabilizer, where the temperatures are higher and they are more easily handled.

The low-temperature separation system with hydrate inhibitor eliminates the formation of hydrates and allows the gas to be cooled below the hydrate temperature before expansion. This results in an increase in the amount of condensate removed from the wellstream. The operating costs are higher than for the system using expansion without inhibitor, but the increased recovery will normally more than offset this. Glycol injection can be used more effectively on wellstreams where the pressure drop is low-

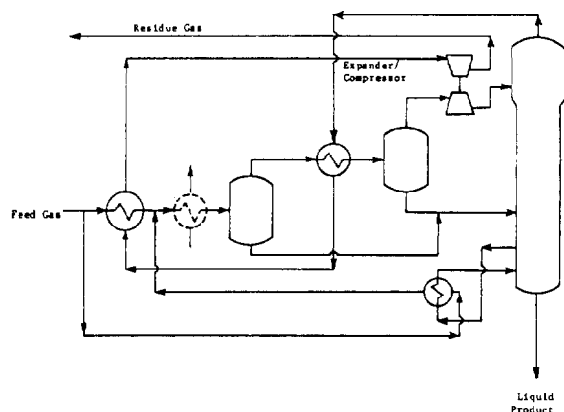


Fig. 14.10—Process flow for expansion process.

er than can the straight expansion system. Approximately 1,000 psi of pressure drop should be available for operation of an LTS system while a glycol injection system can function well with pressure drops as low as 500 psi.

Turbine Expansion Systems

The turbine expansion low-temperature liquid recovery system differs from the choke or valve expansion in that the turbine turns a shaft from which work is extracted. A typical turbo-expander process is shown in Fig. 14.10. The gas enters through an inlet separator with any liquid separated at this point being introduced to a low point in the stabilizer tower. The gas then goes through heat exchange with the cold gas leaving the stabilizer. Another separator is installed if sufficient liquid is formed in the gas-to-gas exchanger with the liquid being introduced at an intermediate point in the stabilizer. The cold gas then flows to the expander where the pressure is reduced and low temperature achieved. The gas and liquid mixture

leaves the expander and flows to the separator that normally is on top of the stabilizer column. Sales gas flows back through the exchanger and may be compressed in the direct-connected centrifugal compressor before being put into the sales gas line. Since extremely low temperatures are reached in a typical turbo-expander plant, dehydration normally is a first step though some plants do use alcohol injection. The gas frequently is expanded below sales gas pressure and then recompressed to make use of the work that must be extracted from the shaft of the turbine. The stabilizer is either a demethanizer or deethanizer with the mixed hydrocarbon product being sold.

A fairly recent development in gas processing, the turbo-expander process is one of great simplicity and ease of operation. The favorable operating characteristics allow the plant to run unattended through long periods and its simplicity and relatively low investment cost make it an attractive option.

Mechanical Refrigeration Systems

Because mechanical refrigeration systems frequently chill to as low as 0°F, they involve essentially the same problems encountered in the low-temperature systems where the temperature is obtained by pressure expansion. The systems really are quite similar. The only essential difference is that the choke in the low-temperature separator systems is replaced by a chiller in the mechanical refrigeration systems.

Although glycol-injection systems are used extensively, there are many installations where inlet dehydration is used to lower the water dewpoint of the gas below the operating temperature in the chiller. There is merit to this system since the glycol does not come in contact with the condensate and glycol losses are, therefore, much smaller. Some of the other operating problems such as separation of glycol and condensate also are eliminated. The dehydrator, if it exists in the flowsheet, would ordinarily be placed between the inlet liquid separator and the chiller. The dehydrator could either be a liquid or granular desiccant type.

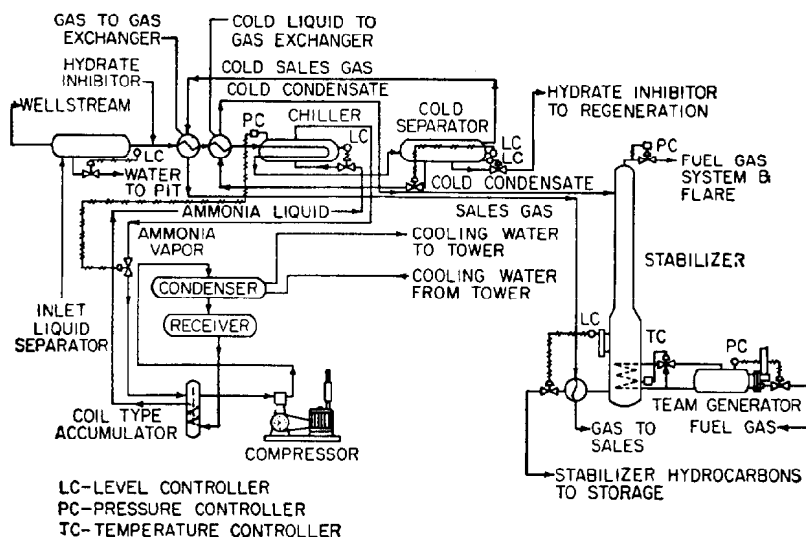


Fig. 14.11—Hydrocarbon-liquid recovery system with mechanical refrigeration and stabilization.

TABLE 14.1—COMPARISON OF COMMON REFRIGERANTS*

		Evaporator Temperature (°F)														
		-80	-70	-60	-50	-40	-30	-20	-10	0	10	20	30	40	50	60
Evaporator Pressure (psia)																
Ammonia				5.55	7.67	10.4	13.9	18.3	23.7	30.4	38.5	48.0	59.7	73.0	89.2	107.5
Propylene	7.20	9.50	12.50	16.1	20.7	26.0	32.1	39.0	48.0	58.0	70.0	82.5	96.0	113.0	131.0	
Propane	5.55	7.45	9.78	12.6	16.2	20.5	25.5	31.3	38.1	46.4	56.0	67.3	80.0	94.1	110.0	
Freon 12	2.88	3.97	5.36	7.12	9.3	12.0	15.3	19.2	23.8	29.3	35.7	43.1	51.7	61.4	72.4	

Condensed liquid temperature 95°F. Condenser pressure in psia: ammonia 197; propylene 212; propane 177; Freon 12 123.

Pounds of Refrigerant per Minute per Ton of Refrigeration																
Ammonia			0.454	0.450	0.446	0.442	0.438	0.435	0.432	0.429	0.426	0.424	0.422	0.420	0.418	
Propylene	2.07	2.01	1.96	1.92	1.87	1.83	1.79	1.76	1.72	1.69	1.66	1.63	1.60	1.57	1.54	
Propane	2.18	2.11	2.04	1.98	1.93	1.88	1.83	1.78	1.74	1.71	1.67	1.63	1.59	1.56	1.53	
Freon 12	5.18	5.03	4.89	4.77	4.65	4.53	4.42	4.32	4.22	4.13	4.05	3.95	3.88	3.81	3.74	

CFM of Refrigerant per Minute per Ton of Refrigeration																
Ammonia			20.4	14.9	11.1	8.40	6.45	5.00	3.96	3.13	2.52	2.04	1.69	1.38	1.14	
Propylene	27.1	20.2	15.7	12.0	9.18	7.30	5.85	4.74	3.84	3.11	2.53	2.12	1.80	1.51	1.28	
Propane	37.4	27.4	20.0	15.5	12.0	9.37	7.29	5.79	4.77	3.87	3.12	2.59	2.13	1.77	1.50	
Freon 12	59.9	43.2	31.7	23.7	18.0	13.9	10.8	8.52	6.79	5.47	4.44	3.63	3.00	2.50	2.09	

Brake Horsepower per Ton of Refrigeration																
Ammonia			4.31	3.74	3.23	2.80	2.41	2.08	1.78	1.50	1.26	1.03	0.835	0.648	0.483	
Propylene	5.00	4.47	3.96	3.51	3.10	2.69	2.35	2.06	1.74	1.46	1.20	1.00	0.830	0.647	0.485	
Propane	4.98	4.39	3.87	3.43	3.03	2.67	2.32	2.03	1.75	1.49	1.24	1.01	0.800	0.622	0.458	
Freon 12	5.70	4.98	4.33	3.79	3.31	2.86	2.47	2.14	1.83	1.55	1.30	1.06	0.848	0.668	0.490	

Condensed liquid temperature 125°F. Condenser pressure in psia: ammonia 303; propylene 314; propane 260; Freon 12 184.

Pounds of Refrigerant per Minute per Ton of Refrigeration																
Ammonia			0.492	0.487	0.483	0.478	0.474	0.469	0.466	0.463	0.460	0.457	0.454	0.452	0.450	
Propylene	2.67	2.58	2.50	2.42	2.35	2.28	2.22	2.16	2.11	2.06	2.01	1.97	1.93	1.89	1.86	
Propane	2.86	2.74	2.63	2.53	2.44	2.36	2.29	2.22	2.16	2.10	2.04	1.99	1.94	1.89	1.84	
Freon 12	6.42	6.19	5.98	5.80	5.61	5.45	5.28	5.14	5.00	4.87	4.75	4.64	4.53	4.43	4.33	

CFM of Refrigerant per Minute per Ton of Refrigeration																
Ammonia			22.0	16.1	12.0	9.09	6.97	5.40	4.26	3.38	2.72	2.19	1.82	1.49	1.23	
Propylene	35.2	26.0	20.0	15.4	11.5	9.40	7.32	5.85	4.72	3.81	3.08	2.60	2.18	1.84	1.56	
Propane	50.0	35.6	25.8	19.7	15.4	11.8	9.16	7.20	5.94	4.79	3.79	3.14	2.63	2.19	1.80	
Freon 12	74.0	53.0	38.8	28.8	21.7	16.6	12.9	10.1	8.05	6.45	5.21	4.25	3.50	2.90	2.42	

Brake Horsepower per Ton of Refrigeration																
Ammonia			5.68	4.96	4.38	3.81	3.33	2.92	2.54	2.19	1.90	1.63	1.38	1.16	0.952	
Propylene	7.49	6.72	5.96	5.32	4.71	4.14	3.66	3.23	2.79	2.41	2.03	1.78	1.55	1.31	1.10	
Propane	7.47	6.60	5.85	5.18	4.60	4.06	3.59	3.18	2.81	2.43	2.07	1.77	1.50	1.25	1.03	
Freon 12	8.09	7.11	6.25	5.46	4.78	4.18	3.67	3.20	2.78	2.41	2.07	1.77	1.49	1.24	1.02	

*Notes

1. Gases considered saturated at compressor inlet. Heat of liquid assumed condenser pressure and temperature shown.
2. Horsepowers are average values, based on centrifugal compressor efficiencies, without economizing.
3. Properties of ammonia from U.S. Bureau of Standards; propylene and propane from Elliot Co. Bull. (1951) P-11; and Freon 12 from "Thermodynamic Properties of Freon 12," DuPont Co. (1955).
4. All cases shown can be handled by one compressor body except ammonia at 0°F and colder (95°F condensing) and 20°F and colder (125°F condensing).
5. One ton of refrigeration = 12,000 Btu-hr.

In a refrigeration process, low temperature is achieved by cooling the gas using a refrigerant at low pressure. The heat in the incoming stream vaporizes the refrigerant at low pressure. The refrigerant must then have its pressure increased so that it can be liquefied. The pressure may be raised in two ways—compression or by absorbing the refrigerant in a liquid, which is then pumped to high pressure with the refrigerant being stripped and subsequently condensed. Compression refrigeration systems are more common, but either should work satisfactorily.

Compression Refrigeration Systems

A typical compression refrigeration system is shown in

Fig. 14.11. The inlet gas stream flowing through the chiller causes the refrigerant to boil. The cold refrigerant vapors flow out of the chiller and to the compressor. Only one chiller is shown in Fig. 14.11. However, frequently in larger systems two or even three chillers may be used with each operating at a different pressure. The chiller pressures are fixed at interstage compression pressures for the compressor.

After compression, the refrigerant vapors are liquefied by cooling with either water or air. The liquid refrigerant is stored in the receiver until required in the chiller. A number of different materials may be used as refrigerants. Tables 14.1 and 14.2³ compare properties of a number of commonly used refrigerants.

TABLE 14.2—PROPERTIES OF SIX REFRIGERANTS

Refrigerant Number (ARI Designation)	Trichloromono- fluoromethane 11	Dichlorodi- fluoromethane 12	Monochlorodi- fluoromethane 22	Trichlorotri- fluoroethane 113	Dichlorotetra- fluoroethane 114	Azeotrope of Dichlorodi- fluoromethane and Difluoroethane 500
	CCl_3F	CCl_2F_2	CHClF_2	$\text{CCl}_3\text{F}-\text{CClF}_3$	$\text{C}_2\text{Cl}_2\text{F}_4$	73.8% CCl_2F_2 26.2% CH_3CHF_2
Molecular weight	137.38	120.93	86.48	187.39	170.93	99.29
Gas constant, R (ft-lbf/lbm-°R)	11.25	12.78	17.87	8.25	9.04	15.57
Boiling point at 1 atm, °F	74.7	-21.62	-41.4	117.6	38.4	-28.0
Freezing point at 1 atm, °F	-168	-252	-256	-31	-137	-254
Critical temperature, °F	388.0	233.6	204.8	417.4	294.3	221.1
Critical pressure, psia	635.0	597.0	716.0	495.0	474.0	631.0
Specific heat of liquid, 86°F	0.220	0.235	0.335	0.218	0.238	
Specific heat of vapor, C_p , 60°F at 1 atm	*	0.146	0.149	*	0.156	0.171
Specific heat of vapor, C_v , 60°F at 1 atm	*	0.130	0.127	*	0.145	0.151
Ratio of $C_p/C_v = K$ (86°F at 1 atm)	1.11	1.14	1.18	1.12	1.09	1.13
Ratio of specific heats, liquid (105°F)/vapor, C_p (40°F), saturation pressure	2.04	1.55	2.14	1.47	1.59	1.77
Liquid head (1 psi at 105°F), ft	1.61	1.84	2.04	1.51	1.65	2.10
Saturation pressure at, psi						
-50°F	0.52	7.12	11.74	*	1.35	*
0°F	2.55	23.85	38.79	0.84	5.96	27.96
40°F	7.03	51.67	83.72	2.66	15.22	60.94
105°F	25.7	141.25	227.65	11.58	50.29	167.85
Net refrigeration effect (40 to 105°F; no subcooling), Btu-lbm	67.56	49.13	66.44	54.54	43.46	59.82
Cycle efficiency (40 to 105°F) % Carnot cycle	90.5	83.2	81.8	87.5	84.9	82.0
Solubility of water in refrigerant	negligible	negligible	negligible	negligible	negligible	negligible
Miscibility with oil	miscible	miscible	limited	miscible	miscible	miscible
Toxic concentration, vol%	above 10%	above 20%	*	*	above 20%	above 20%

The refrigeration load on the chiller for a given gas flow rate is a function of the wellstream analysis, pressure, and the inlet temperature to the chiller. The two factors involved in this cooling load are the sensible heat required to reduce the wellstream from flowing temperature to chiller temperature and the latent heat required to condense the liquefiable hydrocarbons. Obviously, the richer the wellstream the greater the refrigeration load required. The chiller and refrigeration system must be designed to meet the requirements of each individual installation. These requirements are based on the wellstream analysis, pressure, and temperature.

For economical operation the system must be designed to use as much of the cooling as possible. This is done by taking advantage of heat exchange between cold and hot streams wherever possible.

Selective Adsorption Systems

On lean wellstreams where economic justification and payout of the equipment necessary for hydrocarbon removal by refrigeration are not possible, a selective adsorption system should be considered. This type of system frequently will be competitive in hydrocarbon recovery with mechanical refrigeration for lean gas streams.

The selective adsorption system consists basically of two or more adsorption towers filled with a solid material capable of adsorbing hydrocarbons. The towers are controlled on a time cycle to be adsorbing, regenerating, and/or cooling. Alternatively, the bed is used to adsorb the desired quantity of hydrocarbon from the gas stream. When the bed becomes saturated with hydrocarbons, the gas stream is switched to another bed. The saturated bed then is regenerated by passing hot gas through the bed. The hot gas vaporizes and drives off the adsorbed hydrocarbons. During the regeneration cycle, the bed and some of the parts of the adsorber become heated and must be cooled before the bed can again be used on an adsorbing cycle.

The approach used in hydrocarbon adsorption is the same as is widely used in dry-desiccant dehydrators. The basic difference is in the time allowed for the adsorption cycle. Dehydrators normally operate on a 6-hour or longer cycle. Hydrocarbon recovery units operate on a much shorter time cycle and for this reason are frequently called "short-" or "quick-cycle" units.

When a multicomponent mixture like natural gas is adsorbed, the lighter components saturate the bed first. They then are displaced gradually by the heavier hydrocarbons and, eventually, the hydrocarbons would be displaced by

TABLE 14.2—PROPERTIES OF SIX REFRIGERANTS (continued)

Refrigerant Number (ARI Designation)	Trichloromono- fluoromethane 11	Dichlorodi- fluoromethane 12	Monochlorodi- fluoromethane 22	Trichlorotri- fluoroethane 113	Dichlorotetra- fluoroethane 114	Azeotrope of Dichlorodi- fluoromethane and Difluoroethane 500
	CCl ₃ F	CCl ₂ F ₂	CHClF ₂	CCl ₂ F-CClF ₂	C ₂ Cl ₃ F ₄	73.8% CCl ₂ F ₂ 26.2% CH ₃ CHF ₂
Odor	Ethereal, odorless when mixed with air	same as R 11	same as R 11	same as R 11	same as R 11	same as R 11
Warning Properties	none	none	none	none	none	none
Explosive range, vol%	none	none	none	none	none	none
Safety group, U.L.	5	6	5A	4 to 5	6	5A
Safety Group, ASA 89.1	1	1	1	1	1	1
Toxic decomposition products	yes	yes	yes	yes	yes	yes
Viscosity, cp						
saturated liquid	95°F	0.3893	0.2463	0.2253	0.5845	0.2150
105°F	0.3723	0.2395	0.2207	0.5472	0.3272	0.2100
vapor at 1 atm	30°F	0.0101	0.0118	0.0120	0.0097	0.0108
40°F	0.0103	0.0119	0.0122	0.0098	0.0109	0.0111
50°F	0.0105	0.0121	0.0124	0.0100	0.0111	0.0111
Thermal conductivity, k						
saturated liquid	95°F	0.0596	0.0481	0.0573	0.0512	0.0435
105°F	0.0581	0.0469	0.0553	0.0500	0.0421	0.0350
vapor at 1 atm	30°F	0.0045	0.0047	0.0060	0.0037	0.0056
40°F	0.0046	0.0049	0.0061	0.0039	0.0057	0.0057
50°F	0.0046	0.0051	0.0063	0.0040	0.0059	0.0059
Liquid circulated, lbm/min/ton (40 to 105°F)	2.96	4.07	3.02	3.66	4.62	3.35
Theoretical displacement, cu ft/min/ton (40 to 105°F)	16.1	3.14	1.98	39.5	9.16	2.69
Theoretical hp/ton (40 to 105°F)	0.676	0.736	0.75	0.70	0.722	0.747
Performance coefficient, 4.71/(hp/ton) (40 to 105°F)	6.95	6.39	6.29	6.74	6.52	6.31
Cost compared with R 11	1.00	1.57	2.77	2.15	2.97	2.00

*Data not available or not applicable.

water present in the gas. The secret to operating a hydrocarbon recovery unit is determining the point where the largest percentage of desired liquefiable hydrocarbons has been adsorbed. The cycle time normally has to be a compromise since it is done on a time basis.

Fig. 14.12 shows a typical installation for a selective adsorption system. The wellstream flows into an inlet-liquid separator to remove any free liquids and thus cut down on possible adsorbent contamination. The gas then flows through a pressure-reducing valve, used to control the flow of gas through the regeneration and cooling cycles, and into a manifold for switching to the tower on stream by the time-cycle controller. As the gas passes through the bed, the heavier hydrocarbons and water vapor are adsorbed. Stripped dry gas leaves the tower and flows through the gas-to-gas heat exchanger into the sales-gas line.

The tower being regenerated has been saturated through previous contact with the main gas stream. Gas for regeneration is taken off the main gas line upstream of the pressure-reducing valve, and the flow rate through the regeneration system is controlled by the pressure drop across this valve. The regeneration gas flows through the heater where it is heated and then to the tower being

regenerated. The heavier hydrocarbons and water vapor that were adsorbed are driven off by the hot gases. The gas and vaporized fluids pass through an air-cooled heat exchanger where the temperature is lowered, condensing some of the liquid. Additional cooling is obtained in the main gas-to-gas heat exchanger with further condensation. The regeneration gas and condensates are passed through the regeneration-system separator where the condensates are removed from the gas. The gas off the separator flows back into the main gas stream downstream of the pressure-reducing valve. The condensates are separated, the water is dumped, and the hydrocarbon liquid typically flows to a stabilizer.

The system just described is commonly called an "open regeneration system." This means that the regeneration gas flows continuously out and into the main gas stream on either side of the pressure-reducing valve. This requires that a pressure drop be taken in the main gas stream. In applications where pressure drops cannot be tolerated, a closed regeneration system can be used. Such a system can be seen in Fig. 14.13.

A blower is used to recirculate the regeneration gas through the regeneration heating and cooling cycles. The blower picks up gas downstream from the regeneration-

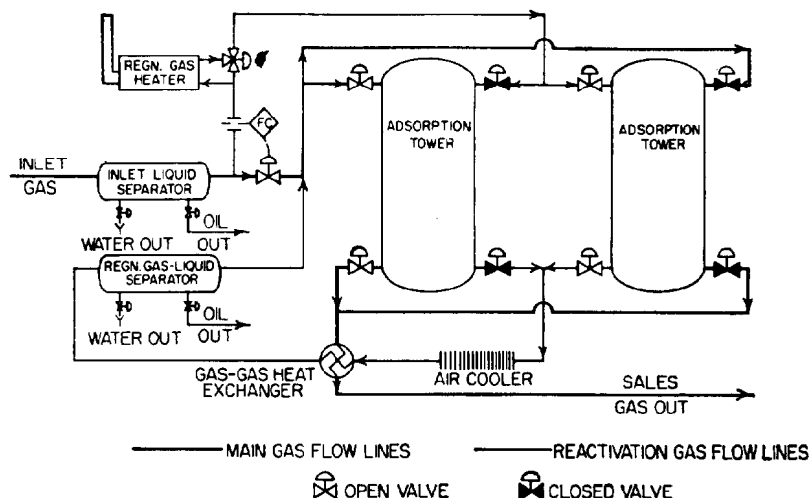


Fig. 14.12—Typical two-tower open-cycle selective hydrocarbon-adsorption system.

liquid separator and boosts the pressure sufficiently to produce the required circulation rate of the regeneration gas. Although the system shown in Fig. 14.13 is for a three-tower system, the blower will work equally well on the two-tower system shown in Fig. 14.12. The blower discharge would connect into the meter run going to the regeneration gas heater. The pressure-reducing valve and extra piping shown in Fig. 14.13 are included to ensure continuous operation while the blower is shut in for maintenance. Under these circumstances the unit operates as an open-cycle system. To compensate for varying pressures in the reactivation-gas system caused by temperature changes, equalizer lines are connected into the system with check valves. In the event that gas is required in the system, dry gas is taken from the sales-gas end of the system. If the reverse is the case, then gas within the regeneration system is discharged ahead of the adsorber so that

wet gas can be processed before entering the sales-gas line.

One advantage of the closed system is that the regeneration gas never becomes a factor in the drying cycle. Essentially the same gas is used over and over again. This results in slightly higher recoveries with an additional operating expense that requires an economic study for justification. The inclusion of the blower in the system adds considerably to the maintenance expense and operating problems encountered over the open system. The main advantage of the closed system is that the pressure drop on the main gas stream can be held to a minimum.

The size of the adsorption beds is a function of the amount of liquid to be removed. This quantity of liquid may be obtained from a small volume of rich gas or a large volume of lean gas. The diameter of the tower is established from the allowable velocity of the gas through

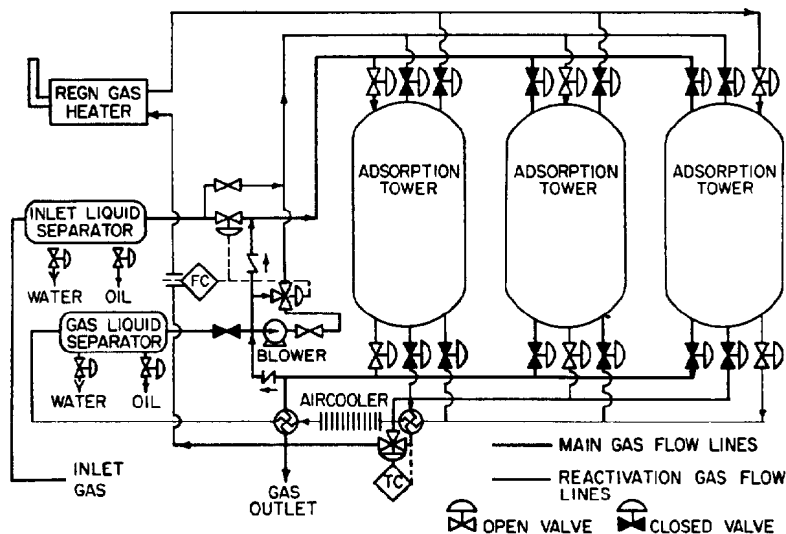


Fig. 14.13—Typical three-tower closed-cycle selective hydrocarbon-adsorption system.

the bed. At low pressures this diameter can become quite large if a given capacity must be satisfied. The depth of the bed is determined by the amount of adsorbent required, the allowable pressure drop, or the minimum bed depth. The length of the time cycle affects the size of the bed for a given amount of liquid removed. The amount of adsorbent decreases with decreasing time, but the heating and cooling requirements increase as the cycle is shortened. The heat required is a function only of the pounds of liquids to be removed and the materials to be heated such as the adsorbent and portions of the towers. The heating and cooling rates are thus inversely proportional to the time of the cycle.

For a given wellstream, the design of the equipment and the operation and control are most important in effecting liquid removal. The time cycle is important and is good only for a range of variation in the wellstream analysis. If the wellstream becomes richer, the cycle may be too long and all liquids are not removed. If the wellstream becomes leaner, the cycle is too short and the adsorbent is not used to the maximum capacity.

The quality of process cooling can also affect the process efficiency. If sufficient cooling is not accomplished, condensation of the liquefiable hydrocarbons will not be complete. In the open cycle this means that the regeneration gas will carry these vapors back into the bed to be adsorbed again. This could result in a considerable amount of recycling of hydrocarbon vapors.

The nonhydrocarbons present in the natural gas will have some effect on the process. This is especially true of the water vapors that eventually replace the hydrocarbons adsorbed in the bed and allow them to be expelled. The short-cycle unit is an excellent dehydrator as well as a hydrocarbon-removal unit. Presence of H_2S has little effect on the process unless oxygen is present. In this event, the oxygen causes free sulfur to form which will tend to foul the desiccant. CO_2 , nitrogen, and other gases occasionally found in natural gas do not affect the process significantly.

When selecting a short-cycle unit, the following can be used as a guide. When the butanes and heavier hydrocarbons to be adsorbed amount to 10 bbl/MMscf of gas or less, then the application of this type of system is normally feasible. Between 10 and 15 bbl/MMscf the choice must be made between the quick-cycle and the refrigeration system. Only through an economic analysis of both these systems can the proper choice be made. On wellstreams in excess of 15 bbl/MMscf the refrigeration system is more feasible. The normal application for the quick-cycle unit is downstream of low-temperature separation systems in which the reservoir pressure has decreased to the extent that the refrigeration from expansion cannot effectively remove the liquefiable hydrocarbons.

Hydrocarbon Stabilization

The previous discussion covers the processes by which a maximum removal of liquefiable hydrocarbons from the gaseous phase of the well stream is accomplished to satisfy gas pipeline specifications and derive additional revenue from the liquid hydrocarbons. Unless the liquid hydrocarbons are handled properly after separation from the main gas stream, the maximum revenue will not be derived. The maximum is obtained by retaining the maximum volume of separated hydrocarbon liquids in atmospheric

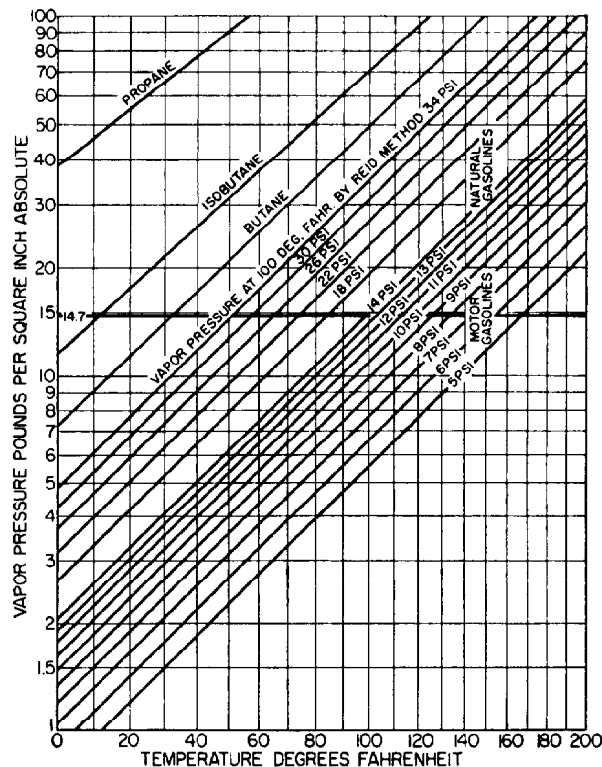


Fig. 14.14—Vapor pressure-temperature curves for motor and natural gasolines.

storage and salvaging or recovering the maximum amount of light vapors that flash from the separated liquids.

If a liquid is to be stored at atmospheric pressure without vaporization losses, it must have a vapor pressure no greater than the existing atmospheric pressure at the maximum temperature it will reach in the storage tank. The vapor pressure exerted by the liquid is called its "true vapor pressure." Measuring the true vapor pressure of a liquid is difficult. For this reason a standard vapor pressure, called the "Reid vapor pressure" (RVP) is much more frequently determined for the liquid. The RVP is determined by using a standard ASTM technique in a 100°F controlled-temperature bath. By sampling the liquid hydrocarbon product, the actual RVP of the liquid being produced can be determined.

Fig. 14.14 shows a correlation for approximating the true vapor pressure of a liquid for which the RVP has been determined. Because vapor pressure is composition-dependent, Fig. 14.14 should be considered an approximation only. If the maximum storage temperature were expected to be 60°F, Fig. 14.14 shows that approximately a 29-psi RVP product could be stored. If the maximum storage temperature were 100°F, the maximum RVP for the product would be approximately 14 psi.

When the hydrocarbon liquids are dumped from the high-pressure separator, the liquids are at their boiling point for the pressures involved. Each reduction in pressure causes some vapors to be boiled off. If the liquids were dumped directly to a storage tank, violent boiling would take place, resulting in a loss of not only the lighter vapors but also some of the heavier ends. By taking

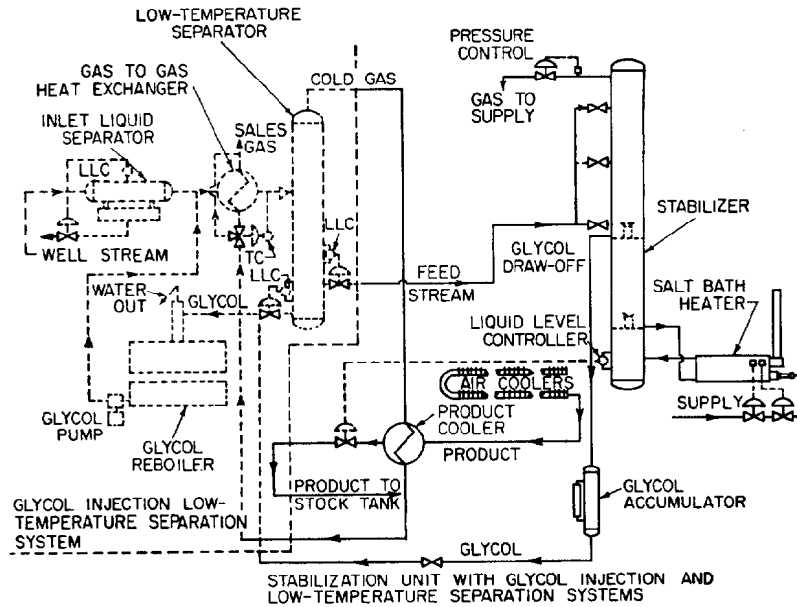


Fig. 14.16—Stabilization unit with glycol-injection LTS system.

the column to reflux itself. This eliminates the relatively expensive reflux system required on stabilizers where the feed is at higher temperatures. The elimination of reflux condenser, reflux control, and reflux pump greatly simplifies the operation of a stabilizer on an oilfield lease where operational supervision is limited. In most cases sufficient refrigeration is available in the system to chill the liquid from the heated-liquid-type low-temperature separation system. The simplified stabilizer can then be used with the heated-liquid system as well as with the glycol-injection low-temperature system.

By this method, the separator liquid is separated into its heavier components, which will remain liquid at atmospheric pressure and temperatures, and its lighter components, which will become a gas at atmospheric conditions. A minimum of liquid components is lost with the lighter components in this method of separation.

For selective adsorption units the liquefied hydrocarbons are recovered on a batch basis. This means that the liquids build up fast over a short period of time and no more are produced until the cycle switches. This means that an accumulator must be used between the separator and the stabilizer so that a more continuous flow of liquids can be provided to effect efficient stabilizer operation.

In stage separation all the increased volume of normally liquid hydrocarbons is not reflected in the stock tanks because a larger amount of it is carried out as a vapor during the separation of the lighter components. By the use of stabilization, almost all the increased volume of normally liquid components in the low-temperature separator is retained in the stock tanks under stable conditions. In addition to producing a larger stock-tank volume of liquid from a given volume of low-temperature separator liquid, the stabilizer produces all the lighter normally gaseous components overhead at one point in the system at relatively high pressure. Gas at this pressure can be compressed back to gas-transmission line pressure at a much reduced compression cost as compared with the low-

pressure vapors from the same system using stage separation. The vapors from the stabilizer are also lean in heavy hydrocarbon components and therefore more desirable in a gas-transmission line than the hydrocarbon-liquid-laden vapors from stage separation.

When the overhead vapors from a stabilizer are compressed into the sales-gas line and the stabilized liquid is stored in a vapor-tight tank, every pound of the produced well fluid, with the exception of that used for fuel gas in lease heaters (if any) and the stabilizer reboiler, can be marketed.

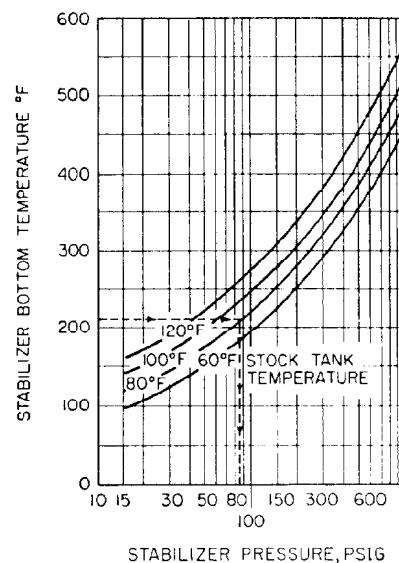


Fig. 14.17—Stabilizer operating conditions. Initial settings for determining the point of maximum recovery.

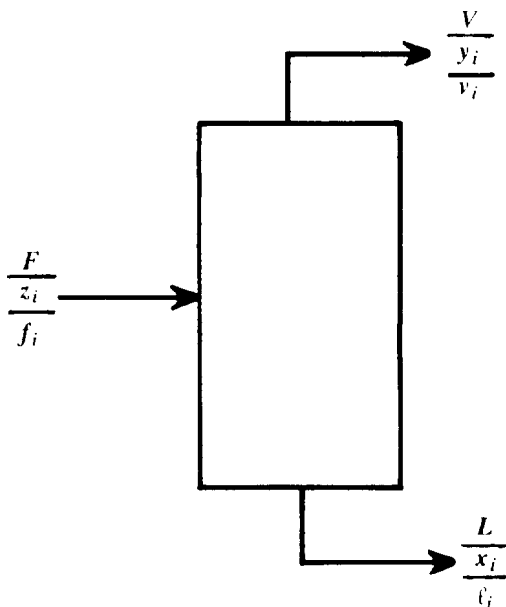


Fig. 14.18—Equilibrium flash separation.

To evaluate the requirements of the lease from an equipment standpoint, the operator must understand the principles of material balance and equilibrium as they apply to multicomponent light hydrocarbon mixtures. Before undertaking such an evaluation, the complete properties of the wellstream must be known. This includes a component-by-component analysis, the temperature, pressure, and the quantities of gas and liquid that can be marketed. These quantities are essential if a payout for the equipment is to be estimated. If sufficient information is available, liquid recoveries can be calculated by using the procedure outlined next.

In making hydrocarbon liquid recovery calculations, compositions and flow rate normally must be expressed in terms of the number of molecular weight equivalent of the material present (moles). The feed to the recovery unit, F , is the sum of the liquid, L , and the vapor or gas, V , as given by

$$F = L + V. \quad (1)$$

Individual component compositions are expressed in mole fractions. The mole fraction of any component in a stream is the moles of that component divided by the total number of moles for all components in the stream. The mole fraction of any component in a liquid stream is denoted x_i ; in the vapor phase y_i ; and in the feed or wellstream z_i . A material balance for any component on the same basis as Eq. 1 can be written

$$z_i F = x_i L + y_i V \quad (2)$$

or

$$f_i = l_i + v_i. \quad (3)$$

By definition the vapor/liquid equilibrium (VLE) constant, K_i , for a given component is the ratio of the mole

fraction of that component in the vapor, y_i , to the mole fraction in the liquid, x_i , that would be in equilibrium with that vapor at the temperature and pressure as given by

$$K_i = \frac{y_i}{x_i} = \frac{v_i/V}{l_i/L} \quad (4)$$

The value of K_i for a given component in a stream is a function of the temperature, pressure, and composition of the stream. In light hydrocarbon systems containing essentially only the paraffin hydrocarbons, the composition dependency of the VLE constant is slight. For this reason many calculations only approximate the composition dependency of K_i .

By definition the summation of the mole fractions in any stream is equal to unity and shown by $\Sigma x_i = 1$, $\Sigma y_i = 1$, and $\Sigma z_i = 1$.

The operating equations used for equilibrium flash calculations are derived by assuming that the separator operates with the vapor and liquid leaving the separator in equilibrium as shown in Fig. 14.18.

Combining Eqs. 3 and 4 and eliminating v_i leads to

$$l_i = \frac{f_i}{1 + \frac{K_i V}{L}} \quad (5)$$

If l_i had been eliminated we would get

$$v_i = \frac{K_i f_i}{K_i + L/V} \quad (6)$$

In either case $L = \Sigma l_i$, $V = \Sigma v_i$.

Eqs. 5 and 6 apply at any point in the process step where the liquid and vapor are in equilibrium. In normal lease processing, there will be many instances where the vapor and liquid are separated. Eqs. 5 and 6 can be used to predict the amount and composition of vapor and liquid present. Solution of either Eq. 5 or 6 is by trial and error because both equations involve V and L , the total vapor and liquid rates leaving the separator. To use the equations, the recommended procedure is to solve for the stream that is expected to be present in smallest amount. A value for that stream is assumed and the appropriate equation used to solve for the moles of the individual components in that stream. These are summed to give the total-stream flow rate. If the value calculated differs from the value assumed, the next assumption should be even further in the direction of the difference.

Keep in mind that the terms involved in Eqs. 5 and 6 are molar flows and not the normal units used to describe liquid and vapor flow rates.

If a digital computer program is available it can readily be used for solution of Eqs. 5 and/or 6. In most instances the computer program will incorporate an appropriate equation of state (EOS) to evaluate equilibrium constants. The user of such a program should be aware that the results will differ for different EOS's. Also, two programs written by different people using the same EOS may give significantly different quantities of liquid and vapor for the same separator at the same temperature and pressure

conditions. In addition, the manner in which the undefined components (C_6+ or C_7+ fractions) are characterized also will have an impact on the calculated liquid present.¹

To determine the volume of gas at any point in the process, the number of moles of gas present may be multiplied by 379.5 to determine the number of standard cubic feet. If the actual volume of the gas under the temperature and pressure are required the procedure followed in determining the gas volume in Chap. 20 must be used. To estimate the liquid production, the number of gallons per mole for each component should be determined from a standard reference such as the GPSA's *Engineering Data Book*.³ These densities in gallons per mole should be multiplied by the number of moles of each component and the results summed to give the total volume of liquid formed.

For the case of hydrocarbon recoveries from a stabilizer or from short-cycle adsorption units, no attempt is made to present the methods of calculations here. They are beyond the scope of this treatment but should be checked carefully for reasonableness and apparent accuracy.

Gas-Treating Systems for Removal of Water Vapor, CO_2 , and H_2S

Natural gas can contain any number of nonhydrocarbon impurities in the formation or at wellhead conditions. Some of these are detrimental to efficient pipeline operation, whereas others have no effect on operation but do affect the heat content or Btu rating of the natural gas.

In almost every case natural gas contains water vapor to some extent. The characteristics of the rock in the formation will determine largely the extent to which water occurs. In some cases the gas is supersaturated, which means that free water will be present. In other cases the gas is saturated at reservoir conditions, which would mean that at producing conditions it will be supersaturated. Finally, the water content can be much lower than saturation but higher than specifications to be satisfied for pipeline acceptance. The formation of free water with pressure and/or temperature reduction can result in the formation of hydrates if the temperature falls below the hydrate-forming temperature. This phenomenon is discussed more fully in the preceding section. In addition to the problems of hydrates, the formation of free water because of condensation can add to the horsepower requirements for pipelines because of increased pressure drops caused when water collects in low spots in the line and reduces the flow area of the gas. This condition is also conducive to corrosion in the pipe. Water vapors must be removed from the gas, and various methods used for this removal are discussed in the following.

Sour gas is the name commonly given to natural gas containing H_2S . This H_2S is found in concentrations varying from a trace on up to 30 mol%. The presence of H_2S causes severe corrosion to occur when free water is present in natural-gas pipelines. When burned it forms sulfur dioxide, which is very toxic and can be a serious problem on the marketing end of the pipeline. Various methods for removal of H_2S are discussed in the following.

A companion to H_2S is CO_2 . It occurs quite frequently in natural gas but is not nearly so serious a detriment as H_2S . The main difficulty encountered is the corrosive

characteristics of CO_2 in the presence of water. Since it is not combustible, it lowers the heat content of the natural gas, and this becomes a factor especially where large volumes of CO_2 are present. The same systems that are used to remove the H_2S also can remove the CO_2 . The presence of both these acid gases in the same wellstream will require larger recirculation and regeneration equipment than if only one were present.

Other impurities can be found in natural gas but their occurrence is not so frequent. Mercaptans, compounds similar to alcohols but with sulfur replacing the oxygen (RSH instead of ROH), are found occasionally. Because mercaptans contain sulfur, they will form sulfur dioxide on combustion and this could present a problem. In addition, mercaptans may present a problem because they are foul smelling. Interestingly, even if mercaptans have to be removed from the gas to make it salable, a small amount of mercaptan will normally be added to the gas intentionally before it is sold. This is done so that natural gas leaks can be detected by smell. Nitrogen is frequently found in natural gas. It has no detrimental effects other than lowering the heat content of the gas. Oxygen is sometimes encountered but the quantities are usually so low as to be negligible. Another impurity that is only rarely encountered is helium. Because manufacture of helium is all but impossible, and because of its importance in many industrial applications, the U.S. government has established helium-recovery facilities. Production of helium is a specialized low-temperature process that will not be discussed further.

Removal of Water Vapor

In the preceding sections the removal of liquefiable hydrocarbons is discussed. The basic processes used for this removal of hydrocarbons invariably result in the removal of water vapors. Experience has shown that the water-vapor dewpoint of the gas leaving the low-temperature separator in these processes is from 10 to 12°F below LTS temperature for systems not using hydrate inhibitors and from 20 to 40°F below LTS temperature for systems using hydrate inhibitors. Dewpoint depressions for selective adsorption systems will be discussed further, and the use of liquid desiccants will be covered for the field of gas dehydration in this section.

To understand water-vapor dewpoint and dewpoint depression better, refer to Fig. 14.5. As was explained, this curve shows the saturation conditions for water vapor in natural gas. The water dewpoint temperature is the same as the saturation temperature for a given pressure. Assume that gas is flowing into a dehydration unit at 1,000 psia and 100°F and that it must be dehydrated to 7 lbm water/MMscf gas to meet contract specifications. At 1,000 psia and 100°F the gas contains 62 lbm of water. The inlet water-vapor dewpoint temperature is 100°F. From the chart for 1,000 psia and 7 lbm water/MMscf the outlet water-vapor dewpoint temperature is 33°F. The dehydrator must be capable of producing a 67°F dewpoint depression and removing 55 lbm water/MMscf gas.

Dehydration With Organic Liquid Desiccants. Since 1949 the removal of water from natural gas with organic liquid desiccants has become one of the most widely accepted methods of dehydration. Though a large number of organic materials can be used as liquid desiccants, by

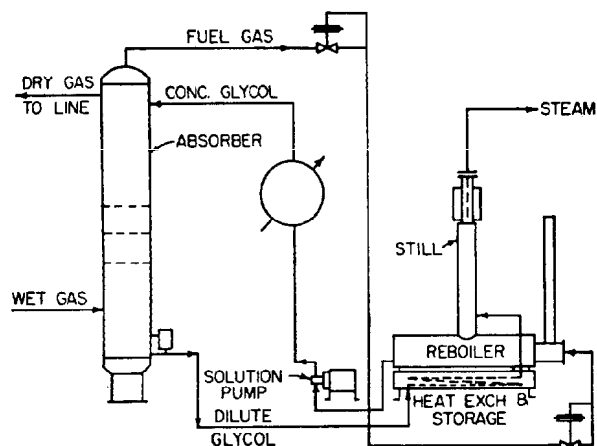


Fig. 14.19—Glycol-absorption gas dehydrator.

far the most generally used are the ethylene glycols. Ethylene glycol (EG), diethylene glycol (DEG), triethylene glycol (TEG), and tetraethylene glycol (TRG) all can be satisfactorily used for dehydration of natural gas. However, by far the most widely used and generally accepted is TEG. Figure 14.19 shows a schematic flowsheet for absorption dehydration of natural gas using an ethylene glycol. The flowsheet will vary little from one glycol to the next. Wet gas enters the absorber and flows up through a series of plates coming into contact with the concentrated glycol solution. The glycol removes from 75 to 95% of the incoming water vapor in the gas, depending on the efficiency of the overall system. This lowers the dewpoint of the gas and the dehydrated gas leaves the absorber top and flows to the sales gas line.

The dilute glycol solution leaves the bottom of the absorber and flows through a heat exchanger and is heated prior to discharging into the still column. The heated glycol flashes off solution gases and enters the still column and comes into countercurrent contact with vapor rising from the reboiler. These vapors are essentially steam but do contain some hydrocarbon vapor and a small amount of glycol. The cooler glycol feed tends to condense the glycol vapors but does not affect appreciably the flow rate of the steam or hydrocarbon vapors which are discharged from the top of the still column. The dilute glycol then dumps into the reboiler where it is heated to the temperature required for producing glycol of high enough concentration to allow the outlet gas to be sufficiently dehydrated. The regenerated glycol overflows the weir in the reboiler and flows into the storage tank. Glycol from the storage tank is pumped to the top tray of the absorber where it comes in contact again with the gas being dehydrated. The glycol flows through the absorber by gravity, removing water vapors from the gas. Since the gas contains more water with each subsequent lower stage, the water picked up on the lower trays is greater than that on the upper trays. The dilute glycol is dumped from the absorber by a liquid level controller (LLC). Some glycol dehydrators use spent glycol and some high pressure gas as the driving force for the diaphragm pump for circulating lean glycol. If this is done, the contactor will not have an LLC.

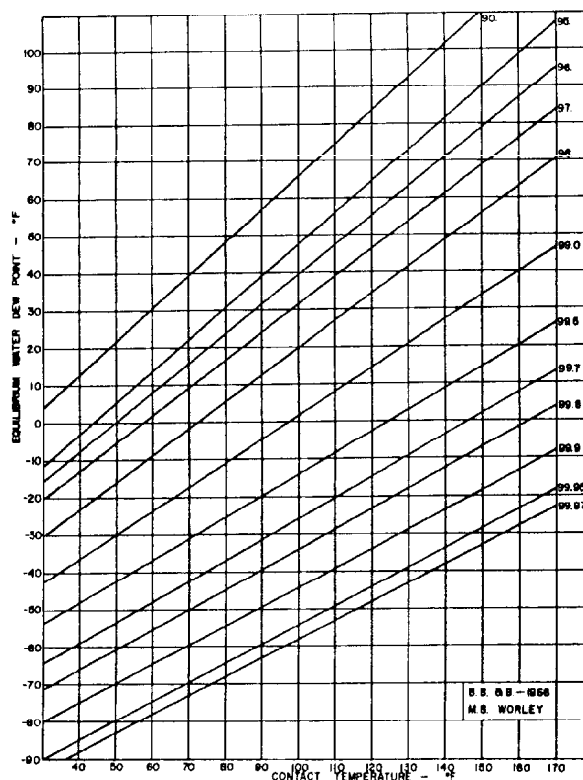


Fig. 14.20—Equilibrium (minimum) water dewpoint obtainable for a given lean TEG concentration and effective contactor temperature.

Glycol dehydration units have been designed for capacities ranging from a few Mcf/D to those designed for millions of scf/D. Where the dehydration required is within the range of the TEG unit, it generally will be the most economical method of natural gas dehydration.

TEG has gained its position of prominence in gas dehydration because of several advantages. The first is that TEG will give a greater dewpoint depression with less loss of glycol than with any of the others. For equal concentrations, DEG can theoretically produce greater dewpoint depressions than is possible with TEG. However, the temperature to which the glycol/water solution can be heated without decomposing the glycol is only about 330°F for DEG, whereas TEG begins to decompose at temperatures above about 400°F. This allows for greater concentrations of TEG in the glycol solution with consequently higher dewpoint depressions.

The concentrations of the glycol solution are normally given in weight percent. This is somewhat misleading as the absorption of water takes place on a mole-composition rather than a weight-composition basis; 98 wt% TEG contains almost 15 mol% water. Thus the weight concentrations can be somewhat misleading because of the great difference in molecular weight for TEG and water.

Fig. 14.20 shows the equilibrium dewpoint for natural gas streams in equilibrium with TEG solutions of a given concentration. You will note that the higher the contactor temperature, the higher the equilibrium dewpoint. The effective contactor temperature for a glycol absorber will

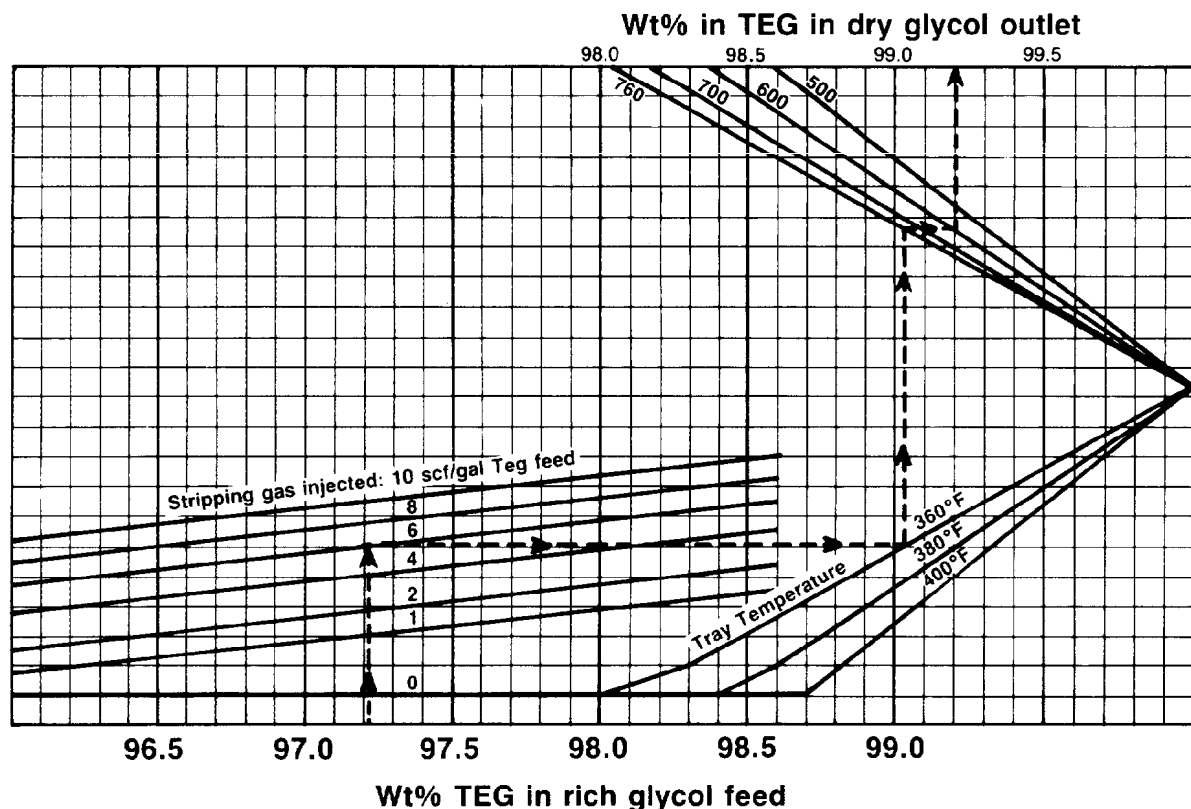


Fig. 14.21—Effect of stripping gas and vacuum on TEG regeneration.

be at the temperature of the wet gas coming to the absorber. Some heat is released when the water is absorbed but the masses of water and glycol involved are so small in comparison with the mass of the gas flowing that, in general, the contactor will operate at the gas temperature.

The dashed line on Fig. 14.20 shows the approximate concentration of TEG solution that can be obtained by a reboiler operating at 400°F and atmospheric pressure. This concentration is in the range of 98.5 to 98.7 wt% glycol. If a higher concentration of glycol is required to obtain the desired outlet dewpoint, some additional means of regeneration must be employed. This can either be stripping gas, whose effect on glycol concentration can be estimated by the use of Fig. 14.21, or there are a number of patented closed regeneration recycle processes that also give higher TEG concentrations. In addition, a vacuum pump can be used to lower the pressure in the reboiler and still column as indicated in Fig. 14.21.

One important variable in selecting the glycol to be used for dehydration is the loss of solution that can be expected. These losses result from vaporization, mechanical entrainment, and vaporization with the still overhead. TEG is more favorable from a loss or replacement standpoint because the consumption resulting from vapor losses is much less than for DEG or EG for the same operating conditions. The vaporization losses are directly proportional to the vapor pressure of the liquid and the vapor pressure of TEG is considerably less than for the other glycols. Glycol consumption can be kept to losses in the range of 0.1 gal/MMscf gas under normal operating conditions with contactor temperatures of 100°F or lower and

pressures above about 200 psi. Glycol contactors should always contain a well-designed mist pad to remove entrained glycol from the dehydrated gas.

There are practical limitations to using TEG for dehydration from both a dehydration-efficiency and an operating-cost standpoint. The lower the temperature in the contactor, the greater the viscosity of the glycol solution. As the viscosity of the solution increases, the efficiency of the contactor decreases, which results in less water-vapor removal per stage or plate. At temperatures below 50°F, a pronounced reduction in efficiency has been observed. At temperatures approaching the freezing point of water, the TEG solution becomes so viscous that the liquid is all but impossible to move through the system. As the contact temperature increases, the vapor pressure of the solution increases, which results in higher vaporization losses of glycol and higher outlet water content of the gas. If the contactor temperature is increased to 120°F the vapor pressure of a 99-wt% glycol TEG solution will be almost twice what it is at 100°F with consequently larger vapor losses of the circulating solution.

There is no reasonable pressure limitation on the use of TEG for dehydration. However, the maximum dewpoint depression appears to increase with pressure up to about 500 psi and then remains essentially constant for higher pressures. Dehydration units have been designed and operated satisfactorily at pressures as high as 2,000 psi.

The higher the ratio of glycol circulated to the water vapor removed from the gas, the less will be the dilution on the individual trays and the dewpoint depression will,

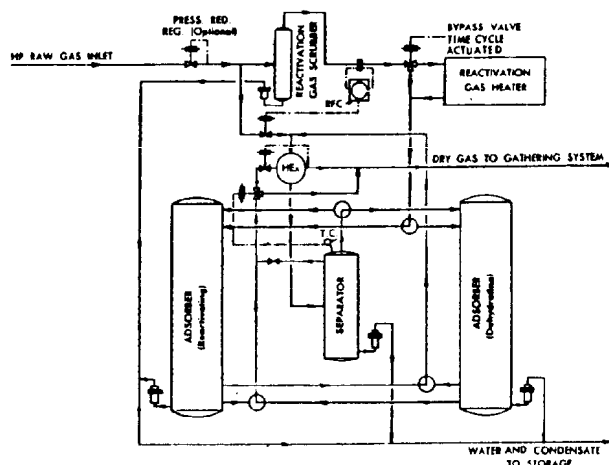


Fig. 14.22—Typical flow sheet for a dry-desiccant plant.

theoretically, be increased. However, since the dilution on the top tray is relatively small the overall effect of increasing the circulation rate is not appreciable. The overall effect could be obtained by increasing the number of plates or trays in the contactor. From an economic standpoint a circulation rate of 3 to 5 gal/lbm water absorbed appears best for most applications.

The number of trays in the contactor varies with the dewpoint depression desired. For normal pipeline-quality gas on a typical wellhead installation, four actual plates should be sufficient in the contactor. When higher dewpoint depressions are required, higher TEG concentrations are used and more trays are in the contactor. For high dewpoint depression operations as many as 10 to 12 or more plates may be installed in the contactor.

Various contaminants that enter the absorber under operating conditions can prove troublesome. A small amount of liquid water entering the absorber will have no serious effects on the system. If the water contains salt, however, the salt will be deposited in the reboiler and potentially can cause reduced efficiency of heat transfer and even the formation of hotspots and tube failures. Large quantities of water will overload the regeneration equipment causing inefficient regeneration of the glycol and perhaps other operational problems.

Liquid hydrocarbons are potentially a source of trouble for the system. An inlet separator capable of separating all liquid water and hydrocarbons before introducing the gas to the absorber is a must. Presence of liquid hydrocarbons will tend to clog the filter and flood the still column and reboiler. This may result in a serious fire hazard if the overhead from the still column is not piped away from the unit. Liquid hydrocarbons also can cause glycol foaming in the absorber and seriously reduce the capacity of the unit and increase glycol losses. Heavier hydrocarbon liquids will accumulate in the glycol and not be separated. Hydrocarbons may also decompose and deposit out on the firetube along with the decomposed glycol. This will cause the glycol to become discolored and also to lose its effectiveness for dehydration.

Ordinarily, there should not be serious corrosion in a TEG dehydrator unless CO_2 and/or H_2S is present. These acid gases do cause serious corrosion and other

operating problems in the dehydrator. Oxygen also causes glycol degradation. For this reason, storage tank and surge drums should be gas blanketed.

Dehydration by Adsorption. Water vapor also can be removed from natural gas by use of a solid desiccant as an adsorption medium. The adsorption process is a very complex phenomenon involving transfer of the component adsorbed from the gas phase to contact with the solid. For this reason the most effective adsorbents have extremely large surface areas per unit of mass. This means that their surface is honeycombed with capillaries that serve to provide the necessary surface area.

A flowsheet of a typical dry desiccant dehydration unit is shown in Fig. 14.22. There must be at least two desiccant beds for continuous operation because adsorption is a batch process. The main gas stream flows through an inlet separator where all free liquids are removed. Any liquids can be harmful to the dehydration process. Free water will reduce the capacity of the unit if not removed. Hydrocarbons can poison the bed if not properly regenerated. The main gas stream then flows through a pressure-reducing valve that controls the flow of the regeneration gas by inducing a pressure drop in the main gas stream. The gas then flows through one of the two adsorption towers where it contacts the desiccant and the water vapors are removed. The main gas stream flows to the sales gas line through a gas-to-gas heat exchanger where heat is removed from the regeneration gas.

The second adsorption tower is regenerated while the other tower adsorbs water vapor from the main gas stream. Regeneration gas (approximately 10 to 15% of the total gas flow) is taken from the main gas stream upstream of the pressure reducing valve and passed through a heater where the temperature is raised to approximately 450°F . The hot gas then passes through the desiccant bed. The water adsorbed through the bed is vaporized and swept out of the bed by the regeneration gas. The hot, wet regeneration gas passes through the gas-to-gas exchanger where it is cooled by the main gas stream. The water condensed from the gas is separated in the regeneration gas scrubber. The regeneration gas flows into the main gas stream downstream of the pressure-reducing valve. Because of the regeneration gas flow, the pressure drop through a solid desiccant dehydration unit will be higher than for a TEG unit and will be approximately 25 psi for the system.

An adsorption dehydration unit is controlled automatically on a time-cycle basis. The most frequently used cycle is 8 hours for the adsorption and regeneration. This requires that the towers be sized to handle 8 hours of flow from a water-vapor-capacity standpoint and that the heating and cooling requirements must be satisfied on the same basis. The time-cycle controller switches the three-way valves to place one tower on stream and the other on regeneration. The three-way valve on the heater system is controlled so that, when the heating cycle is completed, the valve switches to allow cool gas to flow through the system to cool the desiccant and tower prior to placing it on adsorption.

Some of the significant factors that must be considered in the design of these units are gas pressure and temperature, gas velocity, design outlet water content, adsorption capacity of the desiccant, and free liquids to be removed from the main gas stream. For good operation,

low spots in the flowlines and equipment where water might collect during the regeneration cycle must be avoided. Proper sequencing of the valve switching must be accomplished so that no unusual pressure or velocity surges will occur and no wet gas will be allowed to pass from the unit to the sales-gas line. Precautions should be taken to ensure that no high temperatures occur in the main gas stream.

There are a number of materials that can be used satisfactorily for desiccants. Activated aluminas, silica gel beads, and molecular sieves have all been used satisfactorily. Several grades or types of each desiccant are available and the final choice of the one to be used depends on the outlet water dewpoint required and an economic balance.

The capacities of the desiccants to adsorb water vary. However, in all cases, the initial desiccant capacity will indicate that the desiccant is capable of picking up far more water than can be designed for on a long-term basis. The capacities tend to drop off fairly rapidly initially and then gradually taper off until the desiccant becomes ineffective and must be replaced. The capacity and life of the desiccant are strongly dependent on the nature of the application. Under ideal operating conditions, a life of several years can be expected. Under severe fouling conditions the life of the desiccant may be reduced to one year or less. The design capacity to be used for the individual desiccant must be determined through an economic balance between the first cost of the unit and the additional operating cost for occasional desiccant replacement.

The heating required in the regeneration cycle is the sum of the heat of vaporization of the water adsorbed; the sensible heat to raise the desiccant, water, and water vapor to the regeneration temperature; and the heat required to heat the piping, vessels, etc. to regeneration temperature. Fuel requirements are directly proportional to the heat requirement. Cooling requirements are also directly proportional to the heat requirements. Proper design of the unit to minimize heat requirements can have a substantial effect on the size of heating and cooling equipment required.

The desiccant beds must be protected from slugs of liquid water and liquid hydrocarbons. Slugs of water will serve at least to decrease the adsorptive capacity of the unit and at worst can result in loss of the desiccant. Slugs of liquid hydrocarbons can cause fouling and reduce capacity for adsorbing water. The higher-molecular-weight hydrocarbons can plug the pores in the desiccant pellets and seriously affect the adsorptive capacity for water.

Protection of the beds is sufficiently important that an inlet separator must be included as an integral part of the unit. In addition, a guard or protective bed of desiccant placed ahead of the main adsorption vessel or as a top layer of desiccant in the adsorber can serve to protect the main desiccant bed from such items as compressor oil. The heavy oil when adsorbed on the desiccant can seriously affect the adsorptive capacity.

Corrosion usually is not considered a serious problem in dry desiccant dehydration. However, where there are large quantities of CO_2 and/or H_2S , corrosion may occur in the regeneration gas heat exchanger. At this point free water is condensing from the system and the water in combination with CO_2 and/or H_2S can create serious corrosion problems.

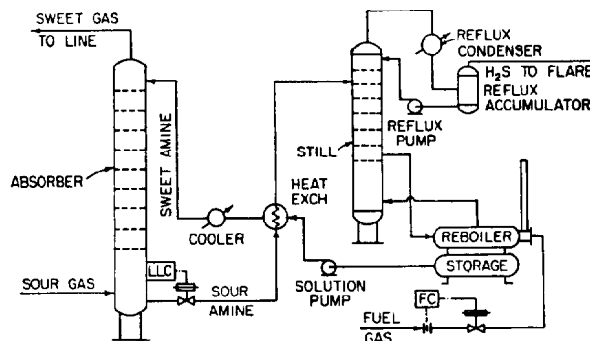


Fig. 14.23—Amine gas desulfurizer.

Removal of Acid Gases

The presence of acid gases, H_2S and/or CO_2 , in natural gas is undesirable from many standpoints. Perhaps the principal objection is the corrosion that results when free water is present. For this reason the H_2S and CO_2 normally are removed at the wellhead or relatively close to it. There are a number of systems that can be used for removal of acid gases.

Sweetening by Ethanolamines. Perhaps the most widely used type of acid-gas-removal system involves the use of an ethanolamine. A simplified flow diagram of a typical ethanolamine-type desulfurization unit is shown in Fig. 14.23.

In this process a solution of water and ethanolamine that may vary from about 15 to 60 wt% ethanolamine is used for removing H_2S and CO_2 from the incoming gas stream. The process is based on the principle that the acid gases, H_2S and CO_2 , will react with the ethanolamine at ordinary temperatures. The reaction can be reversed by reducing the pressure and heating the solution. The sour gas passes up through the contactor and the lean ethanolamine solution passes downward. The foul solution is discharged from the bottom of the contactor and flows through a heat exchanger before it discharges into the top of the still or regenerator column. The ethanolamine solution is boiled by application of heat in the reboiler. This boiling action supplies vapors, primarily steam, that pass up through the still column sweeping the H_2S and CO_2 from the ethanolamine solution.

The regenerated ethanolamine leaves the reboiler and passes through the amine-to-amine heat exchanger into a storage tank from which it is recirculated to the contactor with the amine pump. The H_2S and CO_2 leaving the top of the still column have a large volume of steam with them. To keep down the quantity of makeup water required and to minimize ethanolamine losses the overhead product usually is cooled. The water condensed in this cooling is returned to the regenerator as reflux.

A number of different types of ethanolamine can be used in the process. Monoethanolamine (MEA), diethanolamine (DEA), diglycolamine (DGA), and methyldiethanolamine (MDEA) are among those that are the most popular. There are a number of things that can affect the choice of ethanolamine to be used in a given system. MEA is a stronger base and has a lower molecular weight than

the others. This means that lower concentrations should be possible and that the removal of H_2S and CO_2 should be greater. DGA is also a primary amine with good removal properties but has the same molecular weight as DEA. DEA is a secondary ethanolamine and slightly less basic and therefore will not make specification sweet gas at as low a pressure as MEA and/or DGA. MDEA is said to offer selectivity when only H_2S removal is desired. Other sulfur compounds such as carbonyl sulfide (COS) also can affect the choice. COS reacts irreversibly with MEA and this requires the installation of a reclaimer to control MEA losses.

In many ethanolamine sweetening units, corrosion is the greatest operating problem. Corrosion can occur in the reboiler, storage tank, still column, heat exchangers, and the contactor. Most of the corrosion problems can be minimized by correct design. Limiting the heat flux in the reboiler and condenser can serve to minimize corrosion there. Maintaining pressure on the sour amine solution until it is passed through the heat exchanger and to the point of introduction to the still column can help minimize corrosion in the heat exchanger and piping. Limiting the amount of acid gas pickup per unit of circulating solution will also help. Limiting the temperature on the stream introduced to the top of the still column will help. The lowest possible pressure should be maintained on the still column because this lowers the boiling temperature of the ethanolamine solution.

Another severe problem that can occur in ethanolamine-type desulfurizers is foaming. This foaming most frequently occurs in the contactor and can result in excessive amine losses. Foaming has many causes but the presence of liquid hydrocarbons in the contactor is a frequent one. In addition, particulate matter can stabilize foam. A good filter should be used to remove any iron sulfide or other solid materials from the circulating solution. If oxygen enters the system it will cause problems. It can cause the

formation of thiosulfates and also cause direct degradation of the amine solution.

Iron Sponge Sweetening. Hydrated iron oxide can also be used for removing H_2S from natural gas. This process is "selective" and removes only the H_2S from the gas. It is suitable for removing small quantities (a few grains per 100 scf) of H_2S from natural gas streams. The flow sheet is similar for that of a solid desiccant dehydration unit except for the fact that there is no regeneration gas stream. The iron oxide or sponge is generally suspended on wood chips to disperse it and limit the heat release caused by the reaction of H_2S with the iron oxide. The iron oxide must be kept in a basic environment ($pH \geq 8$) so that soda ash or caustic soda solution is normally injected into the bed with the natural gas. The gas leaving the bed has essentially all the H_2S removed.

Since the iron sponge is consumed in the process and must be replaced frequently, the vessels must be constructed in such a way that the bed can be replaced easily. Iron sulfide will self-ignite when exposed to air, so extreme caution must be used when replacing the iron sponge bed. In addition, disposal of the spent sponge can present a problem because, when it burns, sulfur dioxide is formed.

In all desulfurization units, disposal of the H_2S gas presents a problem. Increasingly, government agencies forbid exhausting the H_2S to the atmosphere either as H_2S or, after incineration or flaring, as SO_2 . For this reason disposal of the removed H_2S must be an integral part of the planning for any desulfurization unit.

References

1. Maddox, R.N. and Erbar, J.H.: "Advanced Techniques and Applications," *Gas Conditioning and Processing*, Campbell Petroleum Series, Norman, OK (1981) 3.
2. Campbell, J.M.: *Gas Conditioning and Processing*, Campbell Petroleum Series, Norman, OK (1982) 2.
3. *GPSA Engineering Data Book*, ninth edition, fifth revision, Gas Processors Suppliers Assoc., Tulsa (1981).

Chapter 15

Surface Facilities for Waterflooding and Saltwater Disposal

K.E. Arnold, Paragon Engineering Services*

Introduction

In producing operations it is often necessary to handle brine that is produced with the crude oil. This brine must be separated from the crude oil and disposed of in a manner that does not violate environmental criteria. In offshore areas the governing regulatory body specifies a maximum hydrocarbon content in water that it will allow to be discharged overboard. Currently this ranges from 7 to 72 mg/L depending on the specific location. In most onshore locations the water cannot be disposed of on the surface because of possible salt contamination and it must be injected into an acceptable disposal formation or disposed of by evaporation. On the other hand, it is often desirable to inject water into the producing formation to maintain reservoir pressure or increase recovery through waterflooding. Produced water that is properly treated to remove hydrocarbons and solids can be used for this purpose. In addition, supplemental sources of water from other formations or from surface sources could be used for waterflooding.

The purpose of this chapter is to discuss the equipment and design criteria that are employed in common systems for either waterflooding or for saltwater disposal. In both cases the design engineer may be concerned with designing piping systems, selecting pumps, separating solids from water, treating hydrocarbons from water, removing dissolved gases and solids from water, treating hydrocarbons from solids, and overall project management.

Piping System Design

In any waterflood or disposal system, it is necessary to gather the water from one or more sources for treatment and then to distribute it to one or more points for injection or disposal. This section discusses criteria for selecting pipe diameter, pipe materials, and wall thickness, as well as general design considerations for cross-country piping systems.

Pipe Diameter

The choice of pipe diameter depends on the pressure drop available, or on a range of acceptable velocities for fluid flow in the pipe.

Pressure at a Point. The pressure at any point in a system can be determined from Bernoulli's theorem, if the pressure at any other point is known. This theorem, which is derived from conservation of energy, is given by

$$Z_1 + \frac{p_1}{\rho_1} + \frac{(v_1)^2}{2g} = Z_2 + \frac{p_2}{\rho_2} + \frac{(v_2)^2}{2g} + Z_{fl}, \dots (1)$$

where

Z = elevation above a datum,

p = pressure,

ρ = density,

v = velocity,

g = gravitational constant, and

Z_{fl} = head loss due to friction between Points 1 and 2.

Darcy demonstrated that head loss was given by

$$Z_{fl} = \frac{fLv^2}{2gd_i}, \dots (2)$$

where

f = friction factor,

L = length, and

d_i = pipe ID.

The friction factor is, in turn, a function of the non-dimensional Reynold's number, given by

$$N_{Re} = \frac{\rho dv}{\mu} \dots (3)$$

* Authors of the original chapter on this topic in the 1962 edition were W.F. Ellison and R.H. Lasater.

where N_{Re} is the Reynold's number and μ is the viscosity. The relationship between Reynold's number and the friction factor is given in the classical Moody diagram (Fig. 15.1).

Pressure Drop in Liquid Lines. The pressure drop for liquid lines can be derived from Eq. 1 as

$$\Delta p = \frac{0.000115 f (q_L)^2 \gamma_L L}{(d_i)^5}, \dots\dots\dots (4)$$

where

Δp = pressure drop, psi,
 q_L = liquid flow rate, B/D,
 γ_L = specific gravity of liquid relative to water,
 L = length of line, ft, and
 d_i = pipe ID, in.

This relationship is shown graphically in Fig. 15.2.

For liquid flow in pipelines, a friction factor of 0.02 is sometimes used for preliminary calculations. In determining the actual friction factor from Fig. 15.1, it is sometimes convenient to use either of the following equations.

$$N_{Re} = 7,734 \frac{\gamma_L d_i v}{\mu} \dots\dots\dots (5)$$

or

$$N_{Re} = 92.1 \frac{\gamma_L q_L}{\mu d_i} \dots\dots\dots (6)$$

where v is velocity, ft/s, and μ is viscosity, cp.

The roughness, ϵ , to use in determining which relative-roughness, ϵ/d , curve governs in Fig. 15.1 depends on the age of the pipe and the material that lines its inside surface. Cast-iron pipe could be expected to be rougher than bare-steel pipe and bare-steel pipe rougher than plastic-lined steel pipe. Roughness factors for new pipe are given in Table 15.1. These should be increased by a factor of two to four to account for corrosion or incrustation effects that could occur with age.

In the past, the empirical Hazen-Williams¹ equation has been used by some engineers for flow of water through pipelines. With the advent of computers and programmable calculators, these empirical equations are no longer recommended. However, for completeness, the Hazen-Williams equation is given as

$$Z_f = 0.015 \frac{(q_L)^{1.85} L}{(d_i)^{4.87} (C_{HW})^{1.85}}, \dots\dots\dots (7)$$

where

Z_f = friction head loss, ft of liquid,
 q_L = liquid flow rate, B/D,
 L = length of line, ft,
 d_i = pipe ID, in., and
 C_{HW} = constant with a value of 80 to 140,
 depending on the inside pipe material
 and its age.

In determining the length to be used in either Eq. 4 or 7, it is necessary to include an allowance for valves, ells, tees, reducers, and entrance and exit losses from vessels. The most common way of accounting for these pressure losses is to include a certain additional length of pipe to the actual length of pipe in the value used for L . Table 15.2 shows the length of pipe that should be added for various valves and fittings.

Velocity in Liquid Lines. Although it is necessary that a selected pipe diameter ensures that the pressure drop is not excessive, in many cases the velocity in the line, and not the pressure drop, will determine the pipe diameter. In most of the short liquid lines within the plant, there will be more than sufficient pressure available to transport the liquid from one piece of equipment to another. However, if the entire pressure drop were taken in the piping, and only a marginal pressure drop were taken across a liquid-control valve, the velocities in the pipe would be high enough to cause noise, erosion of products of corrosion, or water-hammer problems. For this reason a maximum liquid flow velocity of 15 ft/s usually is recommended.

Consideration should also be given to a minimum velocity necessary to prevent solids buildup in the bottom of the pipe. Experiments have shown that when the liquid velocity falls below a certain value, any solids present will settle in a horizontal bed until an equilibrium velocity is reached over the bed. At this velocity, erosion of the solid particles on the surface of the bed is exactly balanced by the deposition of additional particles. It can be shown that, for situations likely to be encountered in oilfield pipelines, a velocity of between 2 and 4 ft/s is required to keep from building up such a bed. For this reason a minimum velocity of 3 ft/s is usually preferred for any liquid piping likely to contain solids.

The following equation has proved useful in calculating velocities.

$$v = 0.012 \frac{q_L}{(d_i)^2} \dots\dots\dots (8)$$

This equation is shown graphically in Fig. 15.3.

Choosing Pipe Diameters in Liquid Lines. The choice of a pipe diameter for a liquid line thus becomes one of choosing a diameter large enough for the pressure available while attempting to keep the velocity between 3 and 15 ft/s. On short lines within a plant, it is usually quicker to choose a diameter based on velocity considerations and then check for pressure drop. On longer lines, or on lines within a plant that flow between atmospheric tanks (low available pressure), it is usually desirable to choose a diameter based on pressure-drop considerations first and then to check velocity.

On lines that experience large variations in elevation, it is desirable to employ Bernoulli's theorem (Eq. 1) at all high points to ensure that there is sufficient positive pressure so that a vacuum is not created. Although it is possible to operate a line with a high-point vacuum, relying on a syphon effect may make it difficult to restart a line if the syphon ever loses its liquid seal. In addition, at any point where a vacuum exists, there is a very real feasibility of drawing oxygen into the system with resultant corrosion and bacteria problems.

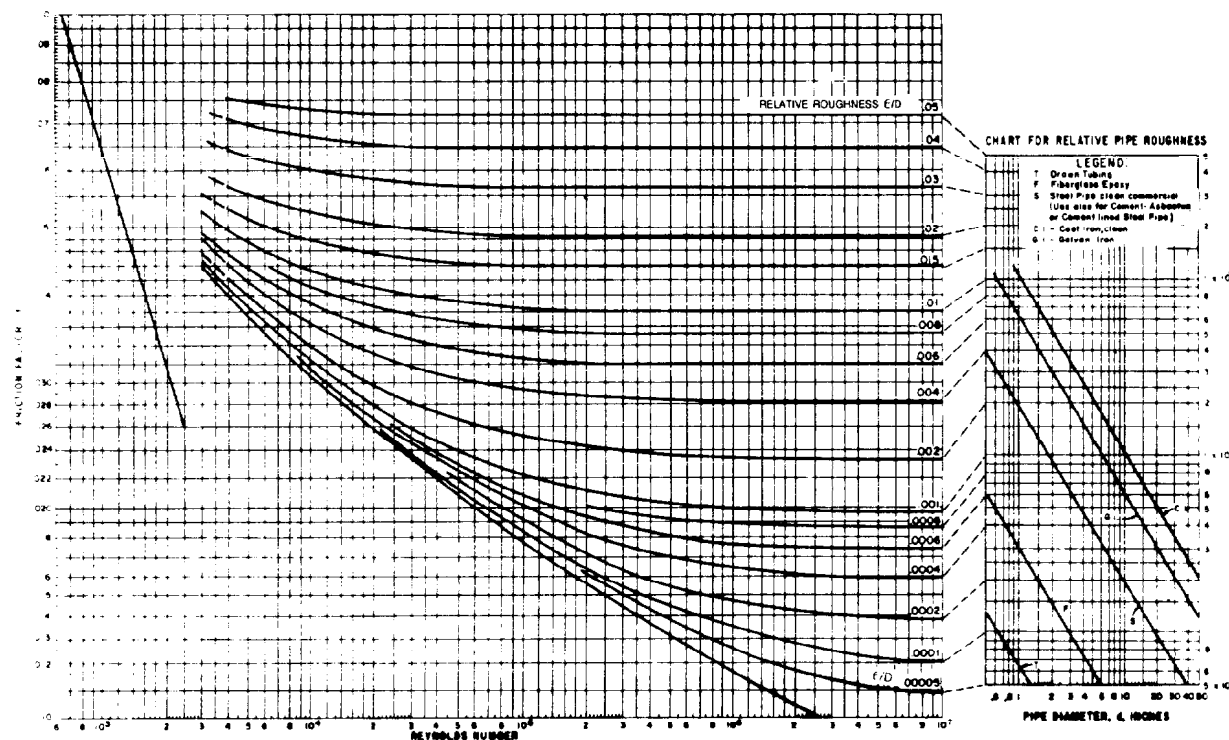


Fig. 15.1—Friction factor chart.

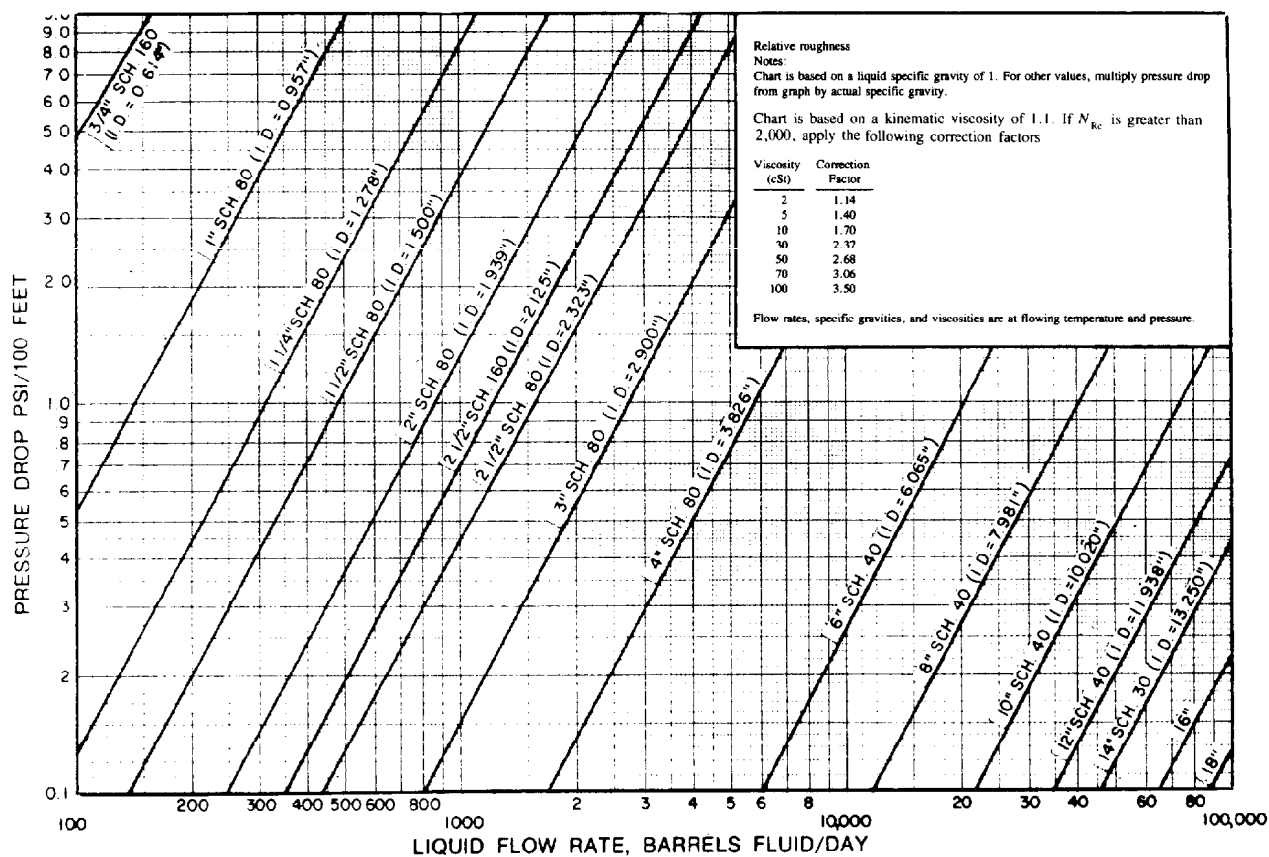


Fig. 15.2—Pressure drop in liquid lines.

**TABLE 15.1—ABSOLUTE PIPE ROUGHNESS (IN.),
NEW PIPE**

Unlined concrete	0.01 to 0.1
Cast iron	0.01
Galvanized iron	0.006
Carbon steel	0.0018
Fiberglass epoxy	0.0003
Drawn tubing	0.0001

TABLE 15.2—EQUIVALENT LENGTH OF 100% OPENING VALVES AND FITTINGS (FT)

Nominal Pipe Size (in.)	Globe Valve or Ball Check Valve	Angle Valve	Swing Check Valve	Plug Cock	Gate or Ball Valve	Weld Thread				
						45° Ell	Short	Long	Hard T	Soft T
							Radius Ell	Radius Ell		
1½	55	26	13	7	1	1-2	3-5	2-3	8-9	2-3
2	70	33	17	14	2	2-3	4-5	3-4	10-11	3-4
2½	80	40	20	11	2	2	5	3	12	3
3	100	50	25	17	2	2	6	4	14	4
4	130	65	32	30	3	3	7	5	19	5
6	200	100	48	70	4	4	11	8	28	8
8	260	125	64	120	6	6	15	9	37	9
10	330	160	80	170	7	7	18	12	47	12
12	400	190	95	170	9	9	22	14	55	14
14	450	210	105	80	10	10	26	16	62	16
16	500	240	120	145	11	11	29	18	72	18
18	550	280	140	160	12	12	33	20	82	20
20	650	300	155	210	14	14	36	23	90	23
22	688	335	170	225	15	15	40	25	100	25
24	750	370	185	254	16	16	44	27	110	27
30	—	—	—	312	21	21	55	40	140	40
36	—	—	—	—	25	25	66	47	170	47
42	—	—	—	—	30	30	77	55	200	55
48	—	—	—	—	35	35	88	65	220	65
54	—	—	—	—	40	40	99	70	250	70
60	—	—	—	—	45	45	110	80	260	80

			Enlargement				Contraction					
			Sudden			Standard Reducer		Sudden			Standard Reducer	
90° Miter Bends			Equivalent L in Terms of Small d*									
Two-miter	Three-miter	Four-miter	d/D = ¼	d/D = ½	d/D = ¾	d/D = ½	d/D = ¾	d/D = ¼	d/D = ½	d/D = ¾	d/D = ½	d/D = ¾
—	—	—	5	3	1	4	1	3	2	1	1	—
—	—	—	7	4	1	5	1	3	3	1	1	—
—	—	—	8	5	2	6	2	4	3	2	2	—
—	—	—	10	6	2	8	2	5	4	2	2	—
—	—	—	12	8	3	10	3	6	5	3	3	—
—	—	—	18	12	4	14	4	9	7	4	4	1
—	—	—	25	16	5	19	5	12	9	5	5	2
—	—	—	31	20	7	24	7	15	12	6	6	2
28	21	20	37	24	8	28	8	18	14	7	7	2
32	24	22	42	26	9	—	—	20	16	8	—	—
38	27	24	47	30	10	—	—	24	18	9	—	—
42	30	28	53	35	11	—	—	26	20	10	—	—
46	33	32	60	38	13	—	—	30	23	11	—	—
52	36	34	65	42	14	—	—	32	25	12	—	—
56	39	36	70	46	15	—	—	35	27	13	—	—
70	51	44	—	—	—	—	—	—	—	—	—	—
84	60	52	—	—	—	—	—	—	—	—	—	—
98	69	64	—	—	—	—	—	—	—	—	—	—
112	81	72	—	—	—	—	—	—	—	—	—	—
126	90	80	—	—	—	—	—	—	—	—	—	—
190	99	92	—	—	—	—	—	—	—	—	—	—

*d is ID of smaller outlet and D is ID of larger outlet.

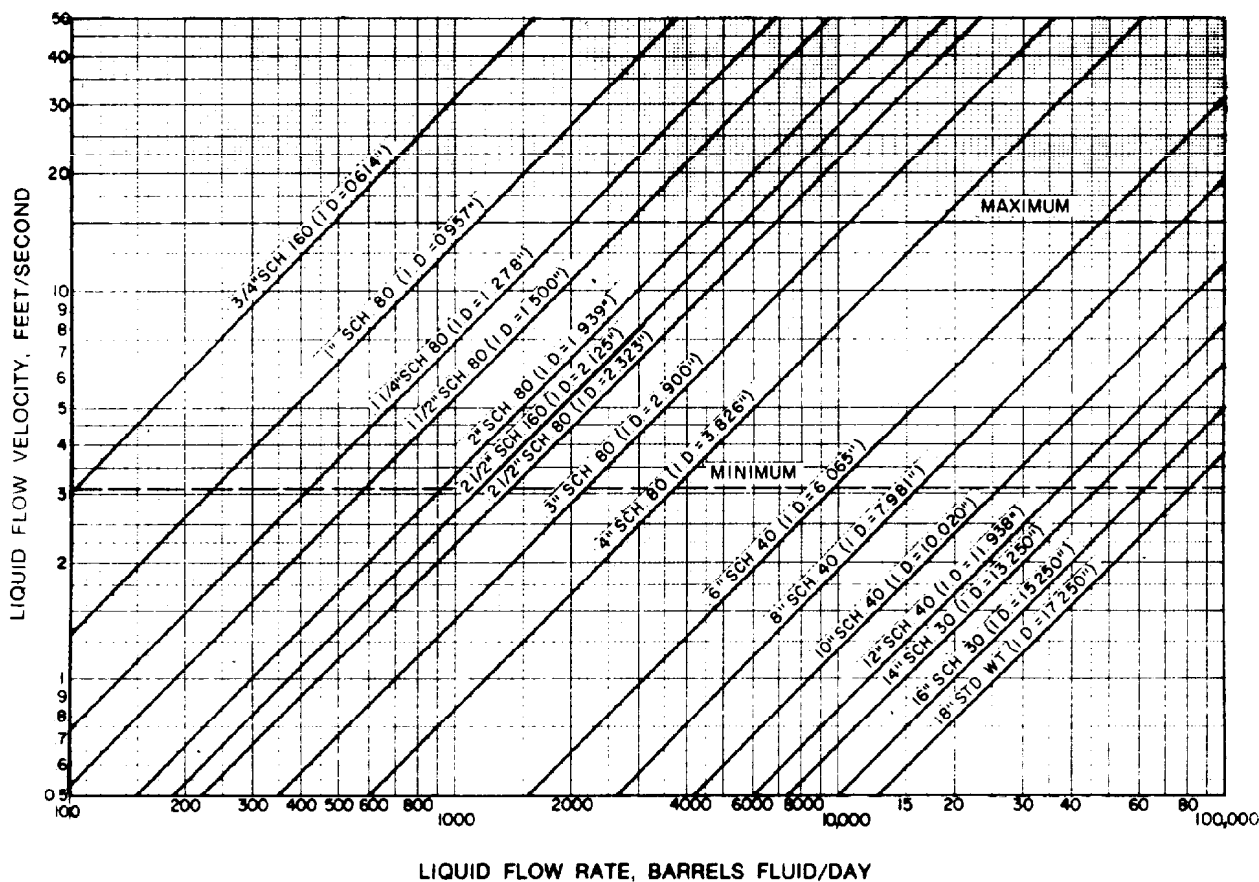


Fig. 15.3—Velocity in liquid lines.

Sometimes, it is not feasible to satisfy minimum velocity criteria during the early stages of a project, where flow velocities are low, without violating pressure drop or maximum velocity criteria at peak flow rates. In such cases, engineering judgment is needed to choose between alternatives such as (1) installing a smaller line initially and either looping the line or installing more pumps at a later date, (2) allowing an equilibrium-solids bed to be deposited initially and relying on it being eroded as flow velocities increase, or (3) allowing a velocity greater than 15 ft/s at peak flow rates.

Pressure Drop in Gas Lines. Although this chapter deals primarily with liquid flow, it may be necessary to size gas lines as part of the project. Source water may come from gas-lifted wells, which would require a gas-lift gas-distribution system, produced water may have flash gas associated with its separation and treating equipment, flotation units and gas strippers require gas lines to operate, and fuel, instrument and utility gas undoubtedly will be required.

Flow in gas lines is considered isothermal. That is, there is sufficient heat transfer to and from the surrounding air, water, or soil to keep the temperature of the gas in the line from changing as the pressure changes because of friction losses. If we assume steady-state gas flow, an ideal gas ($z = 1.0$), and a constant friction factor over the length of the line, the following equation can be derived.

$$(p_1)^2 - (p_2)^2 = 25.2 \frac{\gamma_g (q_g)^2 T f L}{(d_i)^5}, \quad \dots \dots \dots (9)$$

where

- p_1 = pressure at pipe inlet, psia,
- p_2 = pressure at pipe outlet, psia,
- q_g = flow rate of gas at standard conditions, MMscf/D,
- γ_g = specific gravity of the gas at standard conditions relative to air, and
- T = temperature, °R.

When the Reynold's number is calculated to determine the friction factor from Fig. 15.1, it is often convenient to use either

$$N_{Re} = 20,102 \frac{q_g \gamma_g}{d_i \mu_{gf}} \quad \dots \dots \dots (10)$$

or

$$N_{Re} = 335 \frac{v_{gf} p_1 d_i \gamma_g}{T \mu_{gf}}, \quad \dots \dots \dots (11)$$

where v_{gf} is the velocity of gas at specific flow conditions, ft/s, and μ_{gf} is the viscosity of gas at specific flow conditions, cp.

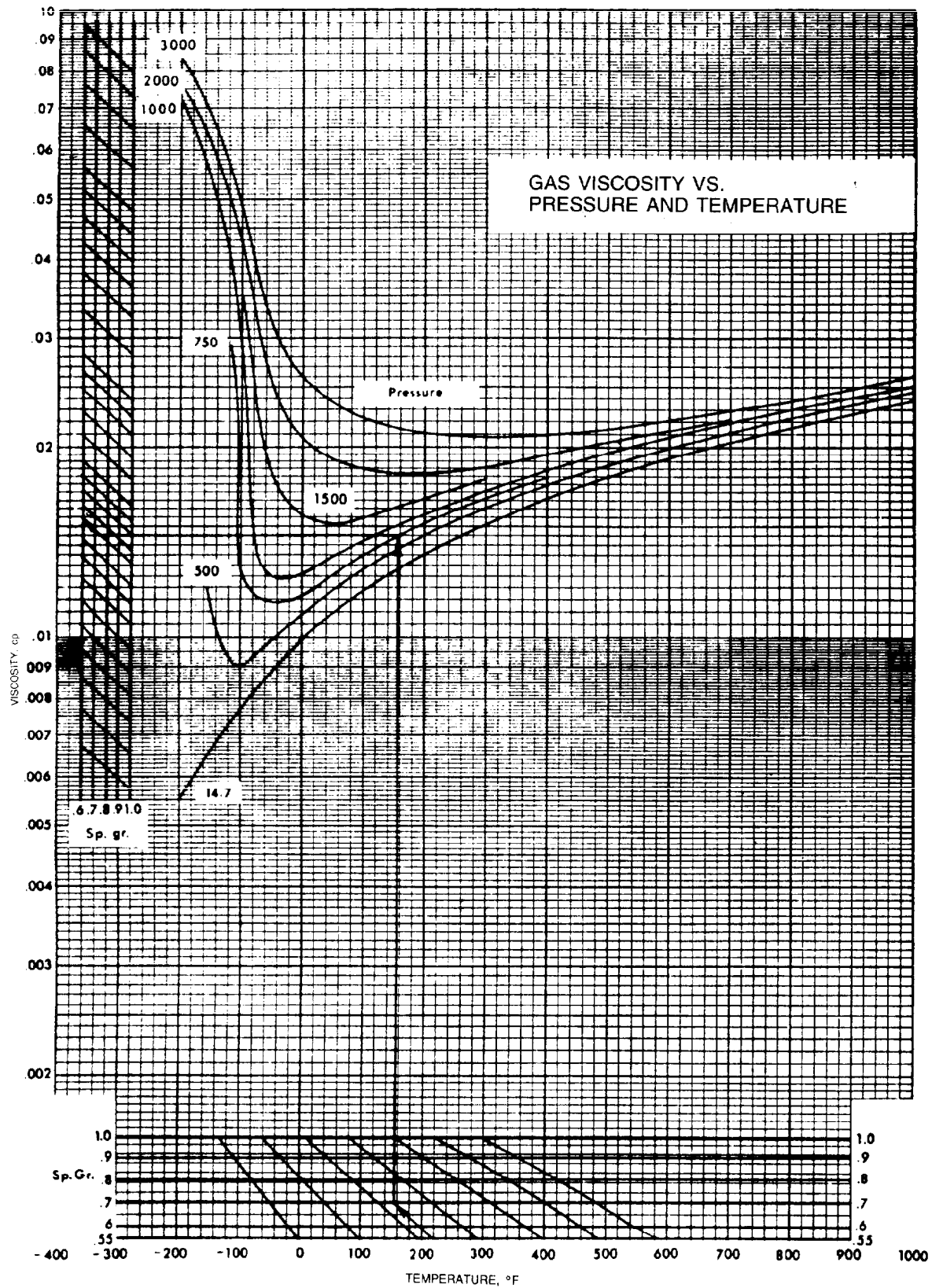


Fig. 15.4—Hydrocarbon gas viscosity.

The viscosity of the gas at flow conditions can be derived from Fig. 15.4. Where

$$\frac{p_1 - p_2}{p_1} < 0.1,$$

Eq. 9 reduces to

$$\Delta p = 12.6 \frac{\gamma_g T f L (q_g)^2}{p_1 (d_i)^5} \quad \dots \dots \dots (12)$$

It is recommended that either Eq. 9 or 12 be used. However, in the past, two empirical equations were developed that have been used extensively. The Weymouth equation² is used for lines with high Reynold's numbers. It assumes that the friction factor is merely a function of pipe diameter. That is, flow is occurring in the flat part of the relative roughness curves on the Moody diagram. The Weymouth equation can be written as

$$(p_1)^2 - (p_2)^2 = 0.81 \frac{\gamma_g (q_g)^2 T L}{(d_i)^{5.33}} \quad \dots \dots \dots (13)$$

This equation would normally apply to short lines within the plant where gas velocities, and thus Reynold's numbers, would probably be high. Figs. 15.5 and 15.6 can be used to solve this equation.

For long gas lines, where velocities are likely to be less and the friction factor will depend on both the line size and the flow rate, the Panhandle equation² has been developed:

$$(p_1)^2 - (p_2)^2 = 0.2 \frac{\gamma_g^{0.96} q_g^{1.96} T L}{E d_i^{4.96}} \quad \dots \dots \dots (14)$$

where E is flow efficiency (1.00 for new pipe, 0.92 for average conditions, and 0.85 for unfavorable conditions).

Velocity in Gas Lines. As in liquid lines, there is a velocity consideration in picking a pipe diameter for a gas line. At high velocities, there could be problems with both noise and erosion of the layer of corrosion products on the inside of the pipe. The greater the rate of erosion of these products, the greater the rate of corrosion the line would experience.

From a noise consideration, the velocity in the pipe should be limited to 60 to 80 ft/s at actual flow condition of pressure and temperature. Experiments have shown that there is a correlation between velocity and erosion of the products of corrosion, which is given by

$$v_{gf} = \frac{C_E}{\sqrt{\rho_g}} \quad \dots \dots \dots (15)$$

where ρ_g is the density of the gas at actual conditions, lbm/cu ft, and C_E is a constant for erosional flow. Eq. 15 can be rewritten as

$$v_{gf} = 0.6 C_E \sqrt{\frac{T}{(\gamma_g) p}} \quad \dots \dots \dots (16)$$

API Recommended Practice 14E³ for offshore piping systems proposes using a value of 125 for intermittent service and 100 for continuous service for the constant C_E . Recent experimental data indicate a C_E as high as 300 may be appropriate for an allowable corrosion rate of 10 mil/yr.

The choice of a value to use between 100 and 300 depends on the judgment of the design engineers as to the corrosivity of the gas and the cost of being overly conservative. Where pressures are below 1,000 to 1,500 psi, the noise criteria will govern and the erosional criteria can be neglected.

If the gas is saturated to the extent that liquids are likely to condense from the vapor phase because of ambient cooling, it is recommended that a minimum velocity of 10 ft/s be maintained. This will sweep the liquid out of the line. At lower velocities, liquid may accumulate at low spots, accelerating corrosion and potentially leading to liquid slugging in the line.

Choosing a Pipe Diameter in Gas Lines. As in liquid lines, the choice of pipe diameter will depend on satisfying both the pressure-drop and velocity criteria. For almost all lines within the plant, the velocity criteria will govern, and the pressure drop will probably not even have to be checked. For long gathering or distribution lines the pressure drop available may govern, or a study of pipe diameter and cost vs. compressor horsepower and cost may be necessary.

Materials

Selection of materials for pipe, valves, and fittings for any piping system must take into account the pressure rating of the application, the corrosivity of the fluid, and the location of the line. There is some economic cost over life for each selection and this must be taken into account in determining the types of material to use for a given application.

Asbestos-Cement Pipe. Because of its resistance to corrosion and low cost, asbestos-cement pipe is recommended for use in large-diameter lines on gravity or low-pressure water systems (200-psi maximum working pressure). The joint connection consists of asbestos-cement couplings with rubber rings. The pipe itself is not flexible, but a deflection of 6° can be obtained at the coupling. This proves advantageous in eliminating abrupt bends when it is necessary to lay pipe on horizontal or vertical curves. Care must be exercised in the actual laying of the pipe by providing a conditioned ditch for the pipe. Installation guides have been published by the manufacturers of asbestos-cement pipe and are available to the design engineer on request.

Asbestos-cement pipe can be coated internally with plastic or fiberglass to lower the friction factor and to protect against seepage of any crude oil that may be in the water stream. Asbestos-cement has the disadvantage of being more brittle than steel pipe, which could make it susceptible to damage from external loads. In addition, proper bedding and backfill compaction is required to prevent future pipe movement resulting from external loads, which could cause joint leakage.

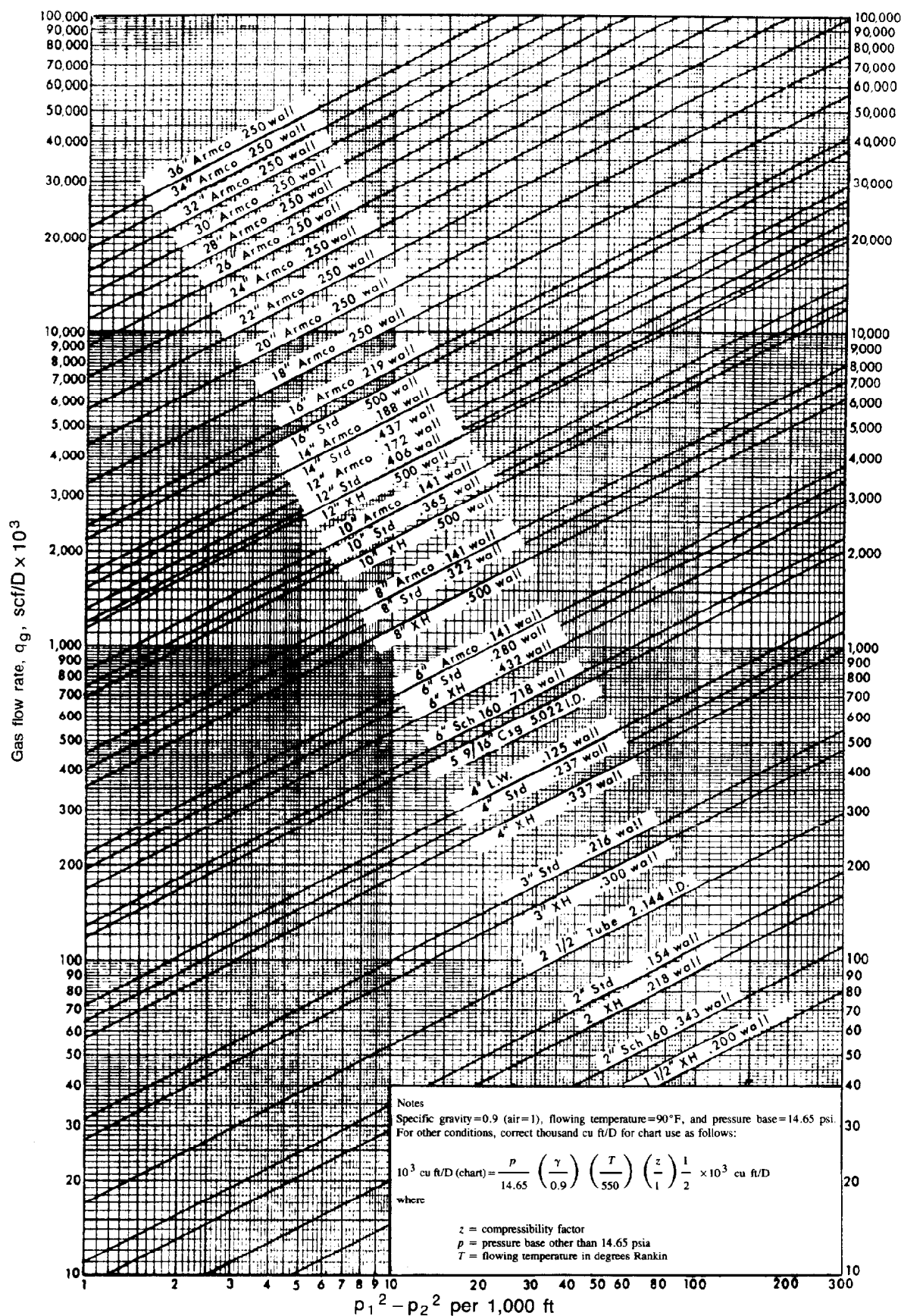


Fig. 15.5—Gas flow based on Weymouth formula.

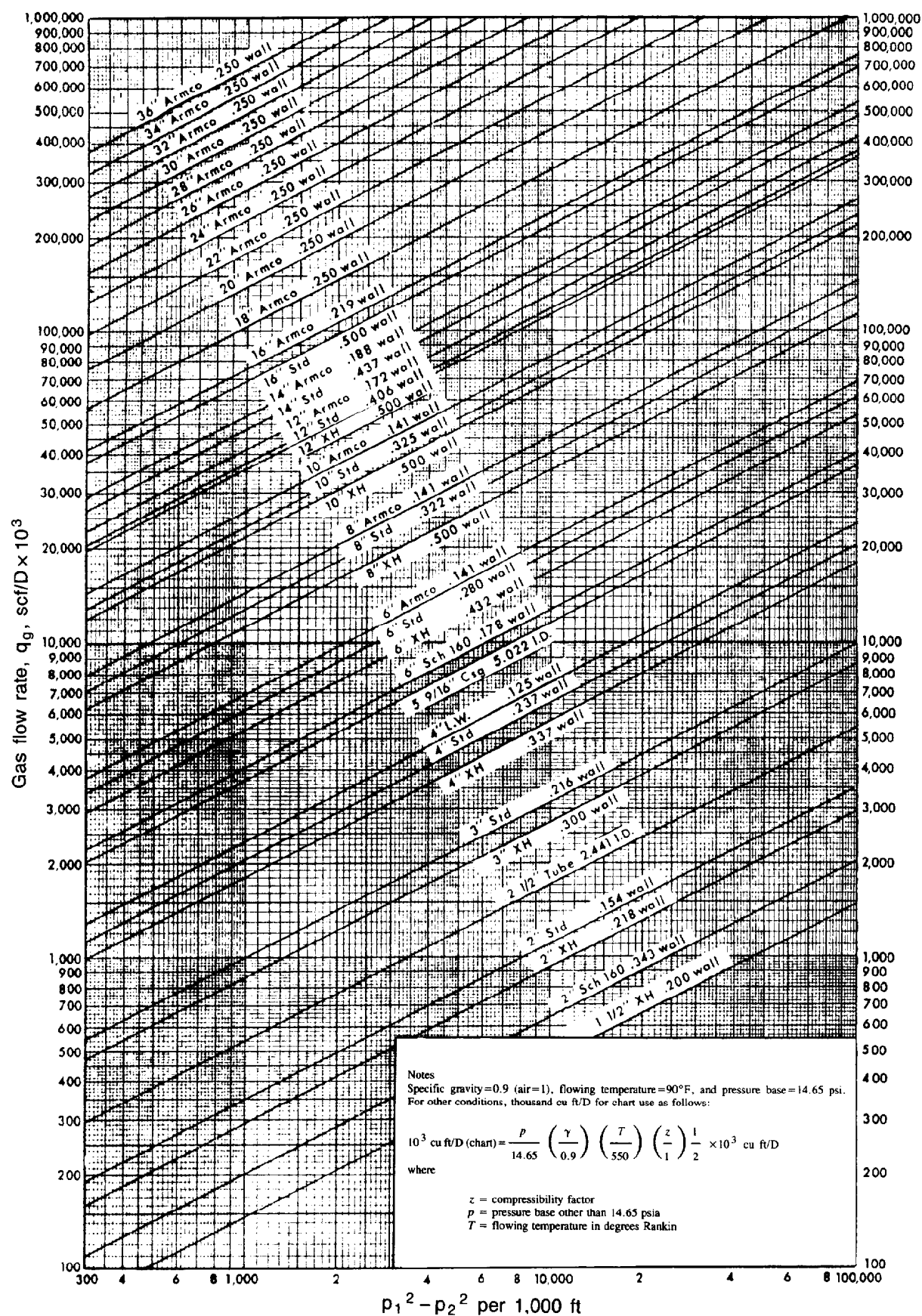


Fig. 15.6—Gas flow based on Weymouth formula.

Plastic Pipe. In recent years, there has been a continuing increase in the use of the various types of plastic pipe especially in moderately low-pressure (300 psi), small-diameter (6 in. and lower) water service. Plastic pipe is not susceptible to either internal or external corrosion, it has a low friction factor, and its light weight makes it easy to install. This is a rapidly developing field and there are numerous proprietary brands. However, in general, plastic pipe can be purchased in accordance with the following API specifications: Spec. 5LE for polyethylene line pipe (PE),⁴ Spec. 5LP for thermoplastic line pipe (PVC and CPVC),⁵ and Spec. 5LR for reinforced thermosetting resin line pipe (RTRP).⁶

The latter category, which includes fiber-reinforced plastic (FRP) pipe, is the strongest, with PVC next, and PE last. All plastic pipe is sensitive to temperature and must be derated as temperature increases. PE pipe is limited to 100°F, PVC pipe to 140°F, and RTRP pipe is limited to 150°F unless specific tests are run by the manufacturer.

The pressure rating of plastic pipe also depends on the fluid being handled. PE pipe handling crude oil has 50% of the pressure rating of the same pipe handling water. PVC pipe must be derated to 40% of its water strength if handling crude oils because of the long-term effect of hydrocarbons on the material. The deration of RTRP pipe is specified by the manufacturer.

Because of the superior strength and greater resistance to heat and hydrocarbons, the use of FRP pipe is increasing. Pipe is available in diameters to 12 in. and pressure ratings that exceed those in 5LR by a factor of two. However, plastic pipe has the disadvantage of being extremely brittle. This can lead to damage in installation. More important, if the ditch is not prepared correctly in rocky soil, over time as the line settles, rocks can come in contact with the underside of the line and cause a stress concentration and eventual failure. It also has the disadvantage of becoming brittle with time when exposed to direct sunlight.

Cast-Iron Pipe. Satisfactory installations of cast-iron pipe have been made on systems where pressures are more than 200 psi but less than 250 psi. Cast-iron pipe has a high corrosion-resistant quality. This pipe has a higher initial cost than either asbestos-cement or plastic pipe. While it is less susceptible to impact and temperature effects than plastic pipe, it is more brittle than steel pipe. For this reason, it must have flat-faced flanges and care must be exercised to ensure that it is not connected to a valve fitting with a more standard, raised-face flange.

If cast-iron pipe is subjected to a fire and then hit by a stream of cold water, it is susceptible to cracking. For this reason, it is not generally acceptable for services containing hydrocarbons.

Carbon Steel Pipe. The most commonly used material for piping systems is Grade B line pipe (35,000-psi yield) manufactured in accordance with API Spec. 5L for line pipe.⁷ Because of its strength, this material can withstand high pressures and is available in diameters to 64 in.

Steel pipe has excellent impact resistance and flexural strength. Unfortunately, it is much more susceptible to both internal and external corrosion, and its installation is more expensive than the lighter plastic pipes.

Where oxygen is excluded from the system, internal corrosion may not be a problem. External corrosion can be reduced by burying and protecting the pipe with a cathodic-protection system. The system could consist of sacrificial zinc or aluminum anodes, which are attached electrically to the pipe at specified intervals. For long pipelines, an impressed-current system may be considered, which would enable the use of fewer anodes.

External corrosion could also be combatted with a coating system. For pipe that is exposed to salt air, a three-coat epoxy-paint system is often specified. Less-elaborate systems are employed in less-severe atmospheres. Underground or underwater pipe may be protected by a thin-film-epoxy, coal-tar-epoxy, or extruded-plastic system. Thin-film-epoxy systems seem to be more popular lately, because of their greater toughness to potential handling and installation damage.

Most long pipelines are protected both with a coating system and cathodically. The coating system decreases the current demand, while the cathodic-protection system provides protection for any breaks, gaps, or scratches that develop in the coating.

Where internal corrosion is anticipated, carbon steel can be protected in four ways.

1. **Cement lining.** Individual joints have a $\frac{3}{8}$ -in. cement-mortar mix applied by a centrifugal spinning procedure. The field joints are protected by an asbestos welding gasket compressed between the joints. Cement-lined pipe is available in sizes from 3 to 24 in. API RP 10E⁸ specifies cement thickness vs. pipe size. The accepted tolerance is $\pm 1/32$ in.

2. **Coal-tar-epoxy lining.** Typically this is a $\frac{3}{32}$ -in. lining that is centrifugally spun into the pipe section after a field joint is made. This technique is limited to large-diameter lines.

3. **Plastic lining.** Various types of epoxies have been installed in steel lines. These can be installed in a small section at a time, or by use of cylindrical devices (pigs), which are run into the line in sections up to 1 mile long. Some success has been reported with plastic lining used to protect pipe against further deterioration, but the necessity of cleaning the pipe wall before applying the plastic coating makes this very difficult. At the present time, manufacturers claim the smallest pipe that can be internally plastic coated is 1 $\frac{1}{4}$ in. nominal.

4. **Use of liners.** There have been several successful installations of FRP and other liners in steel pipe. The steel provides the strength to resist high pressures and the liner provides corrosion resistance. Other than the high cost of installation, this system has the further drawback in that because of long-term permeability through the liner, the pressure in the annulus between the liner and steel can reach an equilibrium with the line pressure. When the line is depressured for maintenance, this may cause collapse of the liner if the system is not carefully designed. Liners have been installed in pipe from 2- to 30-in. diameter and for distances as long as 0.5 mile in a single pull.

TABLE 15.3—DESIGN PROPERTIES AND ALLOWABLE WORKING PRESSURES FOR PIPING*

Nominal Pipe Size (in.)	Schedule Number	Weight of Pipe (lbm/ft)	OD (in.)	Wall Thickness (in.)	ID d_i (in.)	d_o^5	Flow Area (sq ft)	Allowable Working Pressures for Temperatures (°F) Not To Exceed						
								- 20 to 100	200	300	400	500	600	700
½	S40	0.851	0.840	0.109	0.622	0.0931	0.00211	2,258	2,258	2,258	2,258	2,134	1,953	1,863
¾	S40	1.131	1.050	0.113	0.824	0.3799	0.00371	1,933	1,933	1,933	1,933	1,827	1,672	1,595
1	X80	1.474		0.154	0.742	0.2249	0.00300	3,451	3,451	3,451	3,451	3,261	2,985	2,847
	S40	1.679	1.315	0.133	1.049	1.2700	0.00600	2,103	2,103	2,103	2,103	1,998	1,819	1,735
	X80	2.172		0.179	0.957	0.8027	0.00499	3,468	3,468	3,468	3,468	3,277	3,000	2,861
	160	2.844		0.250	0.815	0.3596	0.00362	5,720	5,720	5,720	5,720	5,405	4,948	4,719
	XX	3.659		0.358	0.599	0.0771	0.00196	9,534	9,534	9,534	9,534	9,010	8,247	7,866
1½	S40	2.718	1.900	0.145	1.610	10.820	0.01414	1,672	1,672	1,672	1,672	1,580	1,446	1,379
	X80	3.632		0.200	1.500	7.594	0.01225	2,777	2,777	2,777	2,777	2,624	2,402	2,291
	160	4.866		0.281	1.338	4.288	0.00976	4,494	4,494	4,494	4,494	4,247	3,887	3,707
	XX	6.409		0.400	1.100	1.611	0.00680	7,228	7,228	7,228	7,228	6,831	6,253	5,963
	S40	3.653	2.375	0.154	2.067	37.72	0.02330	1,469	1,469	1,469	1,469	1,388	1,270	1,212
2	X80	5.022		0.218	1.939	27.41	0.02050	2,488	2,488	2,488	2,488	2,351	2,152	2,053
	160	7.445		0.343	1.687	13.74	0.01556	4,617	4,617	4,617	4,617	4,363	3,994	3,809
	XX	9.030		0.436	1.503	7.67	0.01232	6,284	6,284	6,284	6,284	5,939	5,436	5,185
	S40	7.58	3.500	0.216	3.068	271.80	0.05130	1,640	1,640	1,640	1,640	1,550	1,419	1,353
	X80	10.25		0.300	2.900	205.10	0.04587	2,552	2,552	2,552	2,552	2,412	2,207	2,105
4	160	14.33		0.438	2.624	124.40	0.03755	4,122	4,122	4,122	4,122	3,895	3,566	3,401
	XX	18.58		0.600	2.300	64.36	0.02885	6,089	6,089	6,089	6,089	5,754	5,267	5,024
	S40	10.79	4.500	0.237	4.026	1,058.0	0.08840	1,439	1,439	1,439	1,439	1,359	1,244	1,187
	X80	14.99		0.337	3.826	819.8	0.07986	2,275	2,275	2,275	2,275	2,150	1,968	1,877
	160	22.51		0.531	3.438	480.3	0.06447	3,978	3,978	3,978	3,978	3,760	3,441	3,282
6	XX	27.54		0.674	3.152	311.1	0.05419	5,307	5,307	5,307	5,307	5,015	4,590	4,378
	S40	18.98	6.625	0.280	6.065	8,206	0.2006	1,205	1,205	1,205	1,205	1,139	1,042	994
	X80	28.58		0.432	5.761	6,346	0.1810	2,062	2,062	2,062	2,062	1,948	1,783	1,701
	160	45.30		0.718	5.187	3,762	0.1469	3,759	3,759	3,759	3,759	3,552	3,251	3,101
	XX	53.17		0.864	4.897	2,816	0.1308	4,659	4,659	4,659	4,659	4,403	4,030	3,844
8	S40	28.56	8.625	0.322	7.981	32,380	0.3474	1,098	1,098	1,098	1,098	1,037	950	906
	X80	43.4		0.500	7.625	25,775	0.3171	1,864	1,864	1,864	1,864	1,761	1,612	1,537
	XX	72.4		0.875	6.875	15,360	0.2578	3,554	3,554	3,554	3,554	3,359	3,074	2,932
	160	74.7		0.906	6.813	14,679	0.2532	3,699	3,699	3,699	3,699	3,496	3,200	3,052
	S40	40.5	10.750	0.365	10.020	101,000	0.5475	1,022	1,022	1,022	1,022	966	884	843
10	X80	54.7		0.500	9.750	88,110	0.5185	1,484	1,484	1,484	1,484	1,403	1,284	1,224
	160	115.7		1.125	8.500	44,371	0.3941	3,736	3,736	3,736	3,736	3,531	3,232	3,082
	S	49.6	12.750	0.375	12.000	248,800	0.7854	976	976	976	976	922	844	805
	X	65.4		0.500	11.750	223,970	0.7528	1,245	1,245	1,245	1,245	1,177	1,077	1,027
	160	160.3		1.312	10.126	106,461	0.5592	3,113	3,113	3,113	3,113	2,942	2,693	2,569
14	10	36.7	14.000	0.250	13.500	448,400	0.9940	486	486	486	486	460	421	401
	S30	54.6		0.375	13.250	408,394	0.9575	807	807	807	807	763	698	666
	X	72.1		0.500	13.000	371,290	0.9211	1,132	1,132	1,132	1,132	1,069	979	934
	16	42.1	16.000	0.250	15.500	894,660	1.310	425	425	425	425	402	368	351
	S30	62.6		0.375	15.250	824,801	1.268	705	705	705	705	666	609	581
18	S40	82.8		0.500	15.000	759,375	1.227	987	987	987	987	933	854	815
	10	47.4	18.000	0.250	17.500	1,641,309	1.670	377	377	377	377	357	326	311
	S	70.6		0.375	17.250	1,527,400	1.622	625	625	625	625	591	541	516
	X	93.5		0.500	17.000	1,419,900	1.575	876	876	876	876	823	757	722
	20	52.7	20.000	0.250	19.500	2,819,500	2.074	339	339	339	339	321	293	280
20	S20	78.6		0.375	19.250	2,643,352	2.021	562	562	562	562	531	486	464
	X30	104.1		0.500	19.000	2,476,099	1.969	787	787	787	787	743	680	649
	24	63.4	24.000	0.250	23.500	7,167,030	3.012	282	282	282	282	267	244	233
	S20	94.8		0.375	23.250	6,793,832	2.948	468	467	467	467	442	404	386
	X	125.5		0.500	23.000	6,436,300	2.883	660	654	654	654	618	565	539

*ASTM A106, grade B seamless pipe—petroleum refinery piping code for pressure piping ANSI B31.3-1976—corrosion allowance = 0.05.

Exotic Metals. In some highly corrosive environments, especially those associated with CO₂ floods, stainless-steel pipe has been employed. This is extremely expensive. However, it may be the only acceptable long-term solution.

Pressure Ratings for Steel Pipe

Pipe-Wall Thickness. Water-injection lines may have to withstand extremely high pressures. In addition, some of the piping in the plant may include high-pressure gas, oil, or water piping. Thus, steel pipe-wall thicknesses other than "standard" weight may be needed.

The thickness for any pipe depends on the pressure rating, temperature, diameter, and piping code applicable to that pipe. Piping codes generally used are: (1) ANSI B31.1—power piping,⁹ (2) ANSI B31.3—chemical plant and petroleum refinery piping,¹⁰ (3) ANSI B31.4—liquid petroleum transportation piping systems,¹¹ and (4) ANSI B31.8—gas transmission and distribution piping systems.¹²

Generally, B31.1 and B31.3 have the same equation for determining pipe thickness. This tends to be more conservative than that contained in the other two codes. Wall thicknesses determined from this equation are shown in Table 15.3. These are primarily used for steam piping at all locations, for all piping on offshore platforms, and in large onshore plants that represent a large capital investment.

B31.4 and B31.8 have the same equation for pipe-wall thickness. The allowable pressure in a given pipe is dependent on the "construction factor," which is a measure of the potential cost of failure at a given location. The greater the hazard to the public because of failure, the smaller the construction factor. Allowable pressures for various grades of steel and construction factors are given in Table 15.4 and 15.5.

Generally, oil or water lines can be specified with a construction factor of 0.72. The factor for lines containing gas depends on the location of the line. Table 15.5 indicates, in general, the factors to be used. However, care should be taken, since there are specific definitions

TABLE 15.4—GAS TRANSMISSION AND DISTRIBUTING PIPING SPECIFICATIONS FOR CARBON STEEL AND HIGH YIELD STRENGTH PIPE*

Nominal Pipe Size	O.D. (in.)	Wall Thickness (in.)	Allowable Working Pressures up to 250°F																					
			Construction Type Design Factors																					
			Type A, $F = 0.72^{**}$					Type B, $F = 0.60$					Type C, $F = 0.50$					Type D, $F = 0.40$						
			35,000	42,000	46,000	52,000	60,000	35,000	42,000	46,000	52,000	60,000	35,000	42,000	46,000	52,000	60,000	35,000	42,000	46,000	52,000	60,000		
2	2.375	0.154	3,268					2,723					2,270					1,816						
		0.218	4,626					3,855					3,213					2,570						
3	3.500	0.125	1,800					1,500					1,250					1,000						
		0.156	2,246					1,872					1,560					1,248						
		0.188	2,707					2,256					1,880					1,504						
		0.216	3,110					2,592					2,160					1,728						
		0.250	3,600					3,000					2,500					2,000						
		0.281	4,046					3,372					2,810					2,248						
		0.300	4,320					3,600					3,000					2,400						
4	4.500	0.125	1,400	1,680	1,840			1,167	1,400	1,533			973	1,167	1,278			778	933	1,022				
		0.156	1,747	2,097	2,296			1,456	1,747	1,913			1,214	1,456	1,595			971	1,165	1,276				
		0.188	2,105	2,526	2,767			1,754	2,105	2,306			1,462	1,755	1,922			1,170	1,404	1,537				
		0.219	2,453	2,943	3,223			2,044	2,453	2,686			1,704	2,044	2,239			1,363	1,635	1,791				
		0.237	2,654	3,185	3,488			2,212	2,654	2,907			1,844	2,212	2,423			1,475	1,770	1,938				
		0.250	2,800	3,360	3,680			2,333	2,800	3,067			1,945	2,333	2,556			1,556	1,869	2,044				
		0.281	3,147	3,775	4,136			2,623	3,147	3,447			2,186	2,622	2,873			1,748	2,098	2,298				
		0.312	3,494	4,193	4,593			2,912	3,494	3,827			2,427	2,912	3,190			1,941	2,330	2,552				
		0.337	3,774	4,530	4,981			3,145	3,775	4,134			2,621	3,146	3,445			2,097	2,516	2,756				
6	6.625	0.156	1,187	1,424	1,580	1,763		989	1,187	1,300	1,469		824	989	1,083	1,224		659	791	866	980			
		0.188	1,429	1,718	1,880	2,124		1,192	1,430	1,567	1,770		993	1,192	1,306	1,475		794	954	1,044	1,180			
		0.219	1,666	2,000	2,190	2,475		1,388	1,666	1,825	2,063		1,157	1,389	1,521	1,719		926	1,111	1,216	1,375			
		0.250	1,902	2,282	2,500	2,826		1,585	1,902	2,063	2,355		1,321	1,585	1,736	1,963		1,057	1,288	1,389	1,570			
		0.280	2,130	2,556	2,799	3,164		1,775	2,130	2,355	2,637		1,479	1,775	1,944	2,198		1,183	1,420	1,555	1,758			
		0.312	2,373	2,848	3,120	3,527		1,978	2,374	2,600	2,933		1,649	1,978	2,167	2,449		1,319	1,582	1,733	1,959			
		0.375	2,853	3,424	3,750	4,237		2,377	2,853	3,125	3,531		1,981	2,378	2,604	2,943		1,585	1,902	2,083	2,354			
		0.432	3,287	3,943	4,319	4,863		2,739	3,286	3,596	4,069		2,283	2,738	3,000	3,391		1,826	2,191	2,400	2,713			
8	8.625	0.156	912	1,094	1,198	1,354		760	912	998	1,128		633	760	832	940		506	608	666	752			
		0.188	1,098	1,318	1,444	1,632		915	1,098	1,203	1,360		763	915	1,003	1,133		610	732	802	907			
		0.203	1,186	1,424	1,559	1,762		989	1,186	1,299	1,469		824	989	1,083	1,224		659	791	866	979			
		0.219	1,280	1,535	1,681	1,901		1,067	1,280	1,401	1,584		869	1,067	1,168	1,320		711	853	934	1,056			
		0.250	1,461	1,753	1,920	2,170		1,217	1,461	1,600	1,809		1,014	1,217	1,333	1,507		812	974	1,067	1,206			
		0.277	1,618	1,942	2,128	2,405		1,349	1,618	1,773	2,004		1,124	1,349	1,478	1,670		899	1,079	1,182	1,336			
		0.312	1,823	2,189	2,396	2,709		1,520	1,823	1,997	2,258		1,266	1,520	1,664	1,881		1,013	1,216	1,331	1,505			
		0.322	1,882	2,258	2,473	2,796		1,568	1,882	2,061	2,329		1,307	1,568	1,717	1,941		1,045	1,254	1,374	1,553			
		0.344	2,011	2,412	2,642	2,988		1,676	2,011	2,202	2,490		1,396	1,676	1,835	2,075		1,117	1,340	1,468	1,660			
		0.375	2,191	2,628	2,880	3,256		1,826	2,191	2,399	2,713		1,521	1,826	1,999	2,261		1,217	1,460	1,599	1,808			
		0.438	2,560	3,071	3,364	3,803		2,133	2,560	2,804	3,170		1,778	2,133	2,336	2,641		1,422	1,705	1,869	2,113			
		0.500	2,922	3,506	3,840	4,341		2,435	2,922	3,200	3,617		2,029	2,435	2,667	3,014		1,623	1,948	2,133	2,412			
10	10.750	0.188	881	1,058	1,158	1,310		733	881	965	1,091		612	735	804	909		490	588	644	728			
		0.203	952	1,143	1,251	1,415		794	952	1,043	1,179		661	794	869	983		529	635	695	788			
		0.219	1,026	1,231	1,348	1,525		855	1,026	1,124	1,271		713	855	936	1,059		570	684	749	847			
		0.250	1,172	1,407	1,540	1,741		977	1,172	1,284	1,451		814	977	1,070	1,209		651	781	856	967			
		0.279	1,309	1,570	1,719	1,944		1,091	1,309	1,433	1,620		909	1,091	1,194	1,350		727	872	955	1,080			
		0.307	1,440	1,728	1,892	2,138		1,200	1,440	1,577	1,782		1,000	1,200	1,314	1,486		800	960	1,051	1,189			
		0.344	1,613	1,936	2,120	2,396		1,344	1,613	1,767	1,997		1,120	1,344	1,473	1,664		896	1,075	1,178	1,331			
		0.365	1,711	2,054	2,249	2,542		1,426	1,711	1,874	2,119		1,188	1,426	1,562	1,766		951	1,141	1,249	1,412			
		0.438	2,054	2,464	2,700	3,051		1,712	2,054	2,250	2,543		1,426	1,712	1,875	2,119		1,141	1,369	1,500	1,695			
12	12.750	0.500	2,344	2,813	3,081	3,483		1,953	2,344	2,567	2,902		1,628	1,953	2,140	2,419		1,302	1,563	1,712	1,935			
		0.188	743	892	977	1,104		619	743	814	920		516	619	678	767		413	495	543	613			
		0.203	803	963	1,055	1,193		669	803	879	995		558	669	733	829		446	535	586	663			
		0.219	866	1,039	1,138	1,287		722	866	948	1,073		601	722	790	894		481	577	632	711			
		0.250	988	1,186	1,299	1,468		824	988	1,082	1,224		686	824	902	1,020		549	659	722	816			
		0.281	1,111	1,332	1,460	1,651		926	1,111	1,217	1,378		771	926	1,014	1,146		617	740	811	917			
		0.312	1,233	1,480	1,620	1,832		1,028	1,233	1,350	1,527		856	1,028	1,123	1,273		685	822	900	1,016			
		0.330	1,305	1,566	1,715	1,939		1,088	1,305	1,430	1,616		906	1,088	1,191	1,346		725	870	953	1,077			
		0.344	1,359	1,631	1,796	2,020		1,133	1,359	1,488	1,663		944	1,133	1,240	1,403		755	906	992	1,122			
		0.375	1,482	1,779	1,948	2,202		1,235	1,482	1,624	1,835		1,029	1,235	1,353	1,529		824	988	1,082	1,224			
		0.406	1,606	1,926	2,110	2,385		1,338	1,606	1,758	1,988		1,115	1,338	1,465	1,656		892	1,070	1,172	1,325			
		0.438	1,732	2,077	2,275	2,572		1,443	1,732	1,896	2,144		1,203	1,443	1,580	1,786		962	1,148	1,254	1,428			
		0.500	1,976	2,372	2,598	2,936		1,647	1,976	2,165	2,447		1,373	1,647	1,804	2,039		1,098	1,318	1,443	1,631			
16	16.000	0.219	669	828	905	1,024	1,183		575	669	755	854	986		479	575	629	711	822	383	460	503	569	657
		0.250	788	945	1,035	1,170	1,350		656	788	883	975	1,125	547	656	719	813	938	438	525	575	650	750	
		0.281	886	1,063	1,164	1,316	1,																	

TABLE 15.7—ANSI PRESSURE RATINGS FOR MATERIAL GROUP 1.1.

Class	Allowable Pressure (psig)	
	– 20 to 100°F	101 to 200°F
150	285	260
300	740	675
400	990	900
600	1,480	1,350
900	2,220	2,025
1,500	3,705	3,375
2,500	6,170	5,625

Looped Networks. In large gathering and distribution systems, the potential savings associated with looping the system (i.e., installing pipelines parallel to existing lines to increase the system's capacity) or installing pumps at different locations must be investigated. Although simple loops may be calculated by hand, the ready availability of many fine looped-network computer models make this a fairly easy choice. In most instances, some simple calculations and assumptions can be made that narrow the choices to a few practical alternatives. An experienced engineer can use these techniques to greatly reduce computer time and costs.

Gravity Systems. In gravity-systems design, careful consideration must be given to pressure drops in the pipe. Valves and fittings must be considered in these calculations since there is normally little room for error. It is absolutely necessary that accurate elevations of all tanks and equipment and an accurate profile be determined along the line of the pipe. The hydraulic gradient must be plotted along this profile for worst-case conditions of working levels in the tanks or operating pressure in vessels. The hydraulic gradient should be higher than the pipe at each point to ensure that a syphon is not developed. Fig. 15.7 shows an example profile.

High-point vents should be installed in the line to keep gas from accumulating and potentially blocking the flow. Gas eliminators such as those used in lease automatic custody transfer (LACT) units can be installed for this purpose.

Pigging. On long lines where paraffin, scale, or solids may be deposited, periodic pigging of the line may be required. A pig is a sphere or cylinder, often containing scrapers, which is injected into the line at the beginning in a "pig launcher" and collected in a "pig trap" at the end.

Launchers and traps must be installed wherever the pipeline changes size and at all junction points. Where pigging is expected, care must be exercised in selecting valves and radius of curvature of the pipe to allow the pig to move through the line. Fig. 15.8 shows a typical pig trap which can be used to remove a pig from a line without having to shut in flow.

Selecting Pumps and Drivers

Pumps are used in all water gathering, treating, and disposal systems. Indeed, the most costly single piece of equipment in a water-injection system is often the injection pump and driver. The factors to consider in the selection of pumps include capacity, head, suction lift,

TABLE 15.8—API PRESSURE RATINGS

Class	Allowable Pressure at 100°F (psi)	ANSI Dimensional Equivalent	
		Class	Rating at 100°F (psi)
2,000	2,000	600	1,480
3,000	3,000	900	2,220
5,000	5,000	1,500	3,705
10,000	10,000	—	—
15,000	15,000	—	—
20,000	20,000	—	—
30,000	30,000	—	—

space, efficiency, flexibility to varying throughput and pressure conditions, and type of prime mover. It is beyond the scope of this chapter to discuss any of these in detail. Instead, a broad description of commonly used pump types and their characteristics, types of drivers and their characteristics, and some comments as to pump piping and installation are presented.

Pump Types

There are many types of pumps in use. However, most of the common ones can be classified as either positive displacement or centrifugal by the action they employ to move the liquid to a higher pressure level.

Positive-Displacement Pumps. Positive-displacement pumps employ a moving piston, plunger, diaphragm, or rotor to move a fixed volume of liquid per revolution of the pump. The amount of liquid pumped per revolution is independent of the speed of the pump or the discharge pressure.

Reciprocating pumps are positive-displacement pumps that operate as a result of the movement of a piston or plunger inside a cylinder. Piston pumps can be double-acting in that the fluid could be forced out of the cylinder into the discharge piping ahead of the piston and liquid drawn into the cylinder behind the piston regardless of the direction of the piston travel. If liquid is pumped during a piston movement in one direction only, the pump is classified as single-acting. Pumps with two cylinders are called "duplex," three cylinders "triplex," etc.

Advantages of reciprocating pumps are (1) for a given speed, the rate of discharge is practically constant, regardless of head, and the pump is limited only by the power of the prime mover and the strength of the pump parts; (2) efficiency is high regardless of the head and speed; (3) owing to low operating speed and the low velocities of fluids, they are well adapted to handling viscous fluids; (4) they are usually self-priming.

Disadvantages of reciprocating pumps include (1) heavy weight and large physical size; (2) valve trouble can occur, especially when pumping liquid containing solids; (3) pulsating flow in both suction and discharge lines; (4) high net positive suction head requirements; (5) not generally suitable for handling liquids containing solids, abrasives, or dirt.

Rotary pumps are positive-displacement pumps that operate by having a rotating member turn inside a housing in such a way that it creates one or more cavities that move from suction to discharge forcing the trapped liquid through the pump.

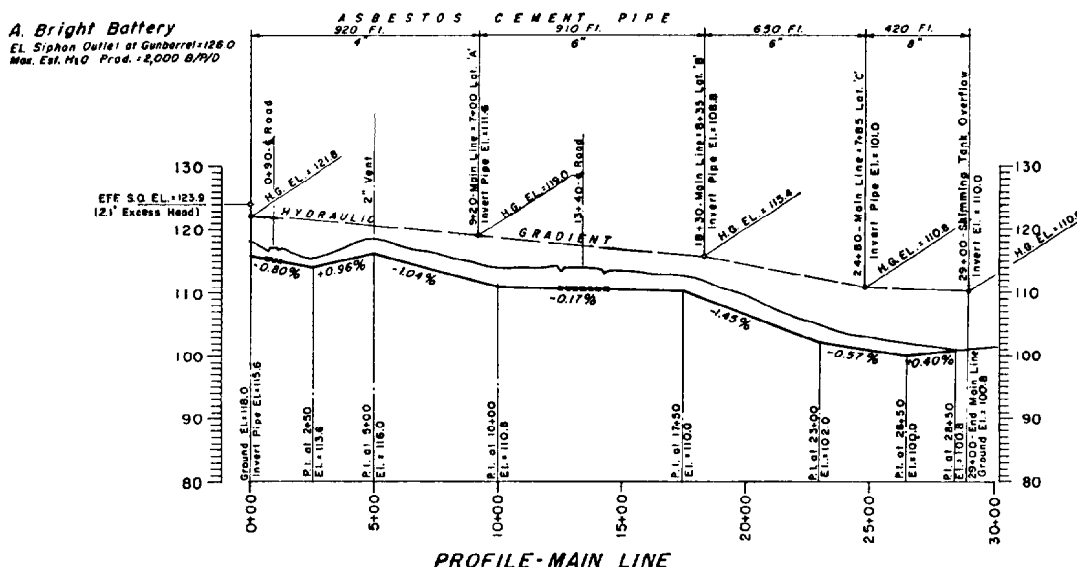


Fig. 15.7—Profile of the main line in a gravity system.

Advantages of rotary pumps are (1) in general, these are the same as for reciprocating pumps; (2) rotary pumps are relatively inexpensive and require small space; (3) they will operate over wide ranges of capacity, head, and viscosity; (4) rotaries are self-priming and are good vapor-handlers; (5) they deliver relatively pulsation-free flow.

Disadvantages of rotary pumps are (1) close clearances and/or rubbing contacts restrict the choice of materials for construction; (2) close clearances require that liquids to be pumped have lubricating value and be noncorrosive—therefore, they are suitable for oil but not suited for water; (3) rotaries have low volumetric efficiency at low speeds because the slip approaches the displacement. This effect increases directly with the pressure/viscosity ratio.

The **diaphragm pump** is a type of reciprocating positive-displacement pump that operates by the action of a diaphragm moving back and forth within a fixed chamber. Raising the diaphragm creates a vacuum, drawing liquid (or air) into the pump through the suction check valve. Lowering the diaphragm forces the liquid (or air) out through the discharge check valve. This type of pump will handle clear water or water containing large quantities of mud, sand, sludge, and trash. Its popularity for low-volume applications stems from its ability to operate where the quantity of water varies considerably so that much of the time air is being pumped. The suction effect of the diaphragm motion makes the pump self-priming. For high discharge pressure requirements, diaphragm pumps are limited to very low fluid rates. Although they tend to be easy to repair in the field, the frequency of maintenance required is higher than with other pump types.

Centrifugal Pumps. A centrifugal pump contains a central rotating wheel, called an impeller, which imparts high velocity to the liquid by centrifugal force and then

converts most of this velocity to pressure. The liquid flows from the pump even against considerable discharge pipe pressure. By its very nature, the centrifugal pump operates at relatively high rotative speeds. It is the most common type of pump used today.

Centrifugal pumps can be of radial-flow construction, axial-flow construction, or some combination of the two. In radial-flow pumps, flow enters the center of the wheel and is propelled radial to the outside. Radial construction provides maximum head per stage.

Axial flow pumps develop their head by the propelling or lifting force developed in the fluid by the impeller vanes, which, in cross section, are shaped like airfoils. The flow is parallel to the pump shaft axis. The diameter of the impeller is the same at the suction and discharge sides. Velocity energy is converted to pressure by stationary diffuser vanes.

Advantages of centrifugal pumps are (1) simple construction, quiet operation; (2) inexpensive; (3) small space requirement in relation to capacities; (4) no close clearances, therefore, it can handle liquids containing dirt, abrasives, large solids, etc.; (5) low maintenance, dependable; (6) low net positive suction head requirements; (7) capacity adjusts automatically to changes in head. Thus, capacity may be controlled over a wide range at constant speed.

Disadvantages of centrifugal pumps are (1) cannot achieve high pressures like reciprocating pumps; (2) viscosity effects on head, capacity, and efficiency are appreciable at 200 Saybolt Universal Seconds (S.S.U.) and serious at 500 S.S.U.; (3) low efficiencies when compared to reciprocating pumps; (4) efficiency is a function of flow rate. At throughput rates and pressures less than design, considerable additional horsepower may be required.

Pump Drivers

Depending on the location, type of pump, availability, and cost of natural gas for fuel, pump drivers will be gas

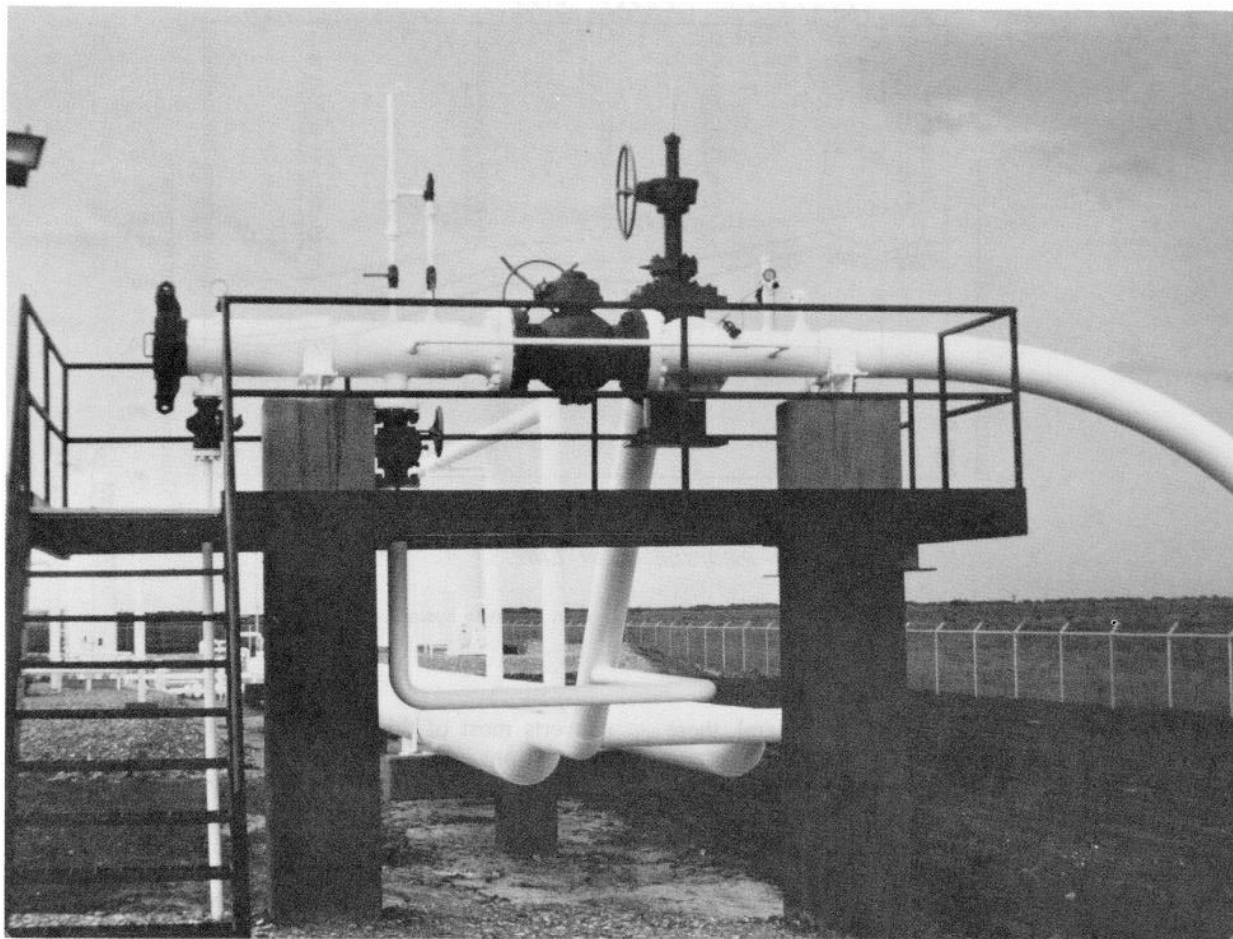


Fig. 15.8—Pig trap.

engines, gas turbines, or electric motors. The amount of horsepower required for a given installation can be calculated from

$$P_{bh} = \frac{q_L \Delta p}{1714 E_p} = \frac{q_L Z \gamma_L}{3960 E_p}, \quad \dots \dots \dots (17)$$

where

- P_{bh} = brake horsepower,
- q_L = flow of liquid, gal/min,
- Δp = differential pressure, psi,
- E_p = pump efficiency at flow conditions, %
- Z = head of liquid, ft, and
- γ_L = specific gravity of liquid relative to water.

Bump efficiencies of between 80 and 90% for reciprocating pumps and 55 and 65% for centrifugal pumps are common.

Natural Gas Engines. The reciprocating internal-combustion natural-gas engine is the leading prime mover in the oil field because of its high efficiency, availability, and ease of maintenance. Both two- and four-cycle engines are in use.

In general, for a given engine, the horsepower output depends on engine speed in rev/min and whether an exhaust-gas turbocharger is installed to increase the flow

of air to the power cylinders. At higher operating speed, the engine is capable of producing greater horsepower. A turbocharged engine will be able to develop more horsepower than a naturally aspirated engine. Unfortunately, maintenance costs and downtime increase as an engine is accelerated above a certain limit and when turbochargers are added. A turbocharged engine has the added disadvantage of being able to load itself to mechanical destruction.

Most engine drivers are built to operate in the 900- to 1,400-rev/min range. For sustained operations, most mechanics do not like to operate their engines above 1,000 to 1,200 rpm. Turbocharged engines can be expected to use 7,000 to 8,000 Btu/bhp-hr of fuel while naturally aspirated units will use 8,000 to 10,000 Btu/bhp-hr. Fuel efficiency is fairly constant over large ranges in bhp.

Care must be exercised with nitric and nitrous oxide (NO_x) emissions on large installations (over 2,000 hp) or in nonattainment areas. Catalytic converters are available for most engines if this becomes a problem.

Gas Turbines. Gas turbine engines have three basic sections—an air-generation section, a combustion section, and a power-turbine section. In the compressor, or air-generator section, ambient air is drawn into the turbine

and compressed with a combination of radial and axial flow elements for delivery to the combustion section. Fuel is mixed with the air in the combustion section and the combustion products are mixed with additional air to provide a specific temperature at the power turbine inlet. The hot gas expands across the power turbine providing power to drive the air generator and the load.

Advantages of turbines over gas engines include the following.

1. Gas turbines can be made very light and compact in relation to horsepower ($\frac{1}{4}$ to $\frac{1}{2}$ lbm/hp) in jet aircraft. The weight/horsepower ratio varies from 1 to 12 lbm/hp for industrial turbines. High-speed turbocharged gas engines weigh from 15 to 40 lbm/hp.

2. Turbine maintenance cost is normally lower and its availability higher. This is true, however, only for turbines in continuous service. Starting and stopping units has a severe effect on maintenance costs.

3. Turbines reject large quantities of high-temperature heat in their exhaust, which can be used to provide process heat.

4. Turbines are available in larger sizes (100,000 hp and higher).

5. Turbines are clean burning from an air pollution standpoint and do not require catalytic converters.

Disadvantages of turbines are (1) high fuel consumption if waste heat is not needed (9,000 to 11,000 Btu/hp-hr at peak efficiency) and (2) large falloff in fuel efficiency when operating at less than peak load.

Electric Motors. In areas where electricity is available from either commercial sources or onsite generators, electric-motor drives are the least expensive in initial capital and maintenance costs. Their use is recommended where the additional cost of purchasing or generating electricity is not too great.

Pump Piping and Installation Details

Suction Piping. It is essential that a flooded suction be furnished for reciprocating pumps. A pump should never be allowed to run "dry" or "starved." The net positive suction head (NPSH) recommended by the manufacturer is shown on the performance curves for the pump and must be provided. To furnish this head and ensure a flooded suction at all times, it is necessary that (1) the storage tank or basin supplying the pump be set at a sufficient elevation above the fluid end of the pump and (2) that the suction piping be of sufficient size to minimize friction losses in the pipe between the storage tank or basin and the pump. In cases where it is possible to secure sufficient elevation head between the storage tank and pump, a centrifugal pump, commonly called a "booster pump," is employed. Normally the booster pump is tied into the storage tank and delivers the water in sufficient quantity to the suction header of the reciprocating pumps to furnish the flooded suction and provide the required NPSH.

The recommended NPSH curve, supplied by manufacturers of reciprocating and centrifugal pumps, is the NPSH that results in a 3% drop in capacity. Cavitation usually starts at a higher NPSH. In cases where no cavitation damage can be tolerated, the NPSH required for no loss in capacity should be used for designing suction and charge systems.

The following features relative to suction-piping installations should be provided.

1. Suction pipe should be as large as or, preferably, larger than the pump suction-inlet size. Table 15.9 indicates acceptable flow velocities in suction lines.

2. Long-radius elbows are recommended to eliminate sharp turns.

3. Suction lines should be laid to a constant grade from the storage tank to pump to eliminate high points where vapor may accumulate.

4. For reciprocating pumps, a pulsation dampener should be installed. These can be elastomer diaphragm or acoustic in design. One common alternative is to install an air- or gas-volume chamber. The chamber allows the pump to fill properly by relieving excessive acceleration and deceleration of the fluid with each stroke of the pump. The required size of an air-volume chamber and its air space depends on the type of pump, displacement per revolution, and speed of the pump. The air-volume chamber may vary from two to eight times the piston displacement of a single stroke. A sight glass is also installed for gauging the liquid level in the chamber so that gas or air can be added periodically to replace what is absorbed by the liquid being pumped.

5. The suction piping should be flushed out and cleaned prior to starting the pump to remove slag, mill scale, rust, welding splatter, etc.

Discharge Piping. As in the suction piping, the discharge piping should be well planned with a minimum of turns, fittings, restrictions, etc. The discharge piping should be of sufficient size to minimize friction losses in the pipe to furnish the required pressure of the pump discharge. Other factors to be considered in discharge piping include the following.

1. A pressure-relief valve must be employed on positive-displacement pumps in the discharge line ahead of any other valve or restriction.

2. A pulsation damper, or desurger, should be installed in the discharge line near a reciprocating pump to relieve shock or vibratory forces. These forces are the result of pressure variations, or surges, prevalent in positive-displacement pump operation. They also result from water hammer because of valve closures and restrictions in the line.

The design and theory of pulsation dampers, or desurgers, are based on the concept that a constant pressure can be maintained if the liquid can be accumulated as the pressure increases and discharged as the pressure decreases. Several types of dampers, or

TABLE 15.9—TYPICAL FLOW VELOCITIES (ft/sec)

	Suction velocity	Discharge velocity
Reciprocating pumps		
Speeds up to 250 rev/min	2	6
Speeds 251 to 330 rev/min	1½	4½
Speeds above 330 rev/min	1	3
Centrifugal pumps	2 to 3	6 to 9

desurgers, are available. Operational features should be investigated and a damper, or desurger, selected to fit each condition.

3. On installations where the fluid is pumped to a level higher than the pump outlet, a gate valve or check valve should be placed downstream of the pressure-relief valve near the pump in the discharge line. This permits shutoff of fluid backing through the pump while pump valves or plungers are being serviced.

The general practice is to connect pumps in parallel through a common suction and discharge header on systems where two or more pumps are installed. A better but somewhat more costly practice is to use separate suction lines for each pump. Headers should be sized to ensure sufficient capacity for satisfactory operation. Each reciprocating pump should have its own separate pressure-relief valve to ensure protection regardless of which pump may be shut down or out of service.

Foundations. For adequate support to maintain alignment and to reduce vibration, a foundation of sufficient size and strength should be provided. Steel-reinforced-concrete foundations are ordinarily used for rotating equipment and are recommended for onshore locations. The pump and prime mover must be set level to ensure good operation. To accomplish this, the pump and mover are mounted on a skid base; the skid base is set on the concrete foundation, leveled, and approximately 1 in. of grout is used to set the equipment.

The required dimensions of the foundation will vary relative to the size and shape of the equipment. The depth to which the foundation must be carried depends on the soil conditions where the foundation is to be set.

The foundation should have sufficient bearing area, which is calculated by using the allowable soil-bearing capacity. Where unbalanced forces are unknown, a rule of thumb that the weight of the concrete-mass foundation should be from 1.5 to 2 times the weight of the reciprocating equipment is sometimes used. Under certain combinations of poor soil and large unbalanced forces, the foundation weight may have to be as much as four times the weight of the equipment.

The size and shape of the skid base will determine the plan dimensions of the foundation and, with acceptable soil conditions, the depth of the foundation is carried to a point that will furnish the required mass. Temperature stresses in normal concrete foundations for pumps and engines govern the amount of steel reinforcing used. The amount of such steel can be estimated by: area of steel (sq in./sq ft of slab area) = $0.002 \times$ cross-sectional area (sq in. of concrete slab). Maximum spacing between bars should not exceed 18 in. Where unbalanced forces and couples are known and for large offshore installations where weight is important, a more detailed dynamic calculation should be made.

Separating Suspended Solids From Heater

The water that is being treated may have suspended solids such as produced sand, rust, and scales. These can be separated from the water stream by gravity settling, cyclone desanders, centrifuges, filters, or flotation.

Gravity Settling

Solid particles, because of their heavier density than water and net negative buoyant force, will settle to the bottom with a terminal velocity that can be derived from Stoke's law as

$$v = \frac{\Delta\rho(d_p)^2}{18\mu_L}, \dots\dots\dots (18)$$

where

$\Delta\rho$ = difference in density of the particle and the liquid,

d_p = solid particle diameter, and

μ_L = viscosity of the liquid.

This equation can also be expressed as

$$v = \frac{1.78 \times 10^{-6} \Delta\gamma(d_p)^2}{\mu_w}, \dots\dots\dots (19)$$

where

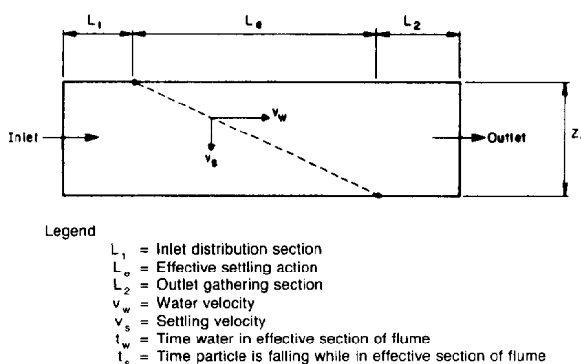
d_p = particle diameter, microns,

$\Delta\gamma$ = difference in specific gravity relative to water,

μ_w = viscosity of water, cp, and

v = velocity, ft/sec.

This equation can be used to size a tank, vertical pressure vessel, horizontal pressure vessel, rectangular sedimentation chamber, or a device of any other configuration to allow a particle of a certain diameter and specific gravity to settle to the bottom.



$$t_s = \frac{Z_f}{v_s} \quad t_w = \frac{L_e}{v_w}$$

$$t_w = t_s$$

$$v_w = \frac{L_e v_s}{Z_f}$$

Fig. 15.9—Model for calculation of sedimentation flume capacity.

Most sedimentation basins are rectangular flumes with length-to-width ratios of 4:1 or greater to limit crossflow. The width of the flow channel can be determined by setting the time required for a particle to settle from the top of the flume to the bottom equal to the time required for the water to traverse from the inlet of the flume to the outlet as shown in Fig. 15.9. This can be expressed as

$$b = \frac{36q_w \mu_w}{\Delta\gamma(d_p)^2 L_e}, \dots\dots\dots (20)$$

where

b = width (breadth) of flow channel, ft,

q_w = water flow rate, B/D, and

L_e = effective length, ft.

Note that the width and length of the settling chamber are independent of its depth. The API Manual on Disposal of Refinery Wastes¹⁵ recommends a turbulence and short-circuiting factor of between 1.3 and 1.8, depending on the ratio of water velocity to solids settling velocity. Using a factor of 1.8, Eq. 20 can be rewritten as

$$b = \frac{65q_w \mu_w}{\Delta\gamma(d_p)^2 L_e}, \dots\dots\dots (21)$$

API also recommends that water velocity be limited to 15 times the settling velocity, or 3 ft/min, whichever is less. The settling velocity can be calculated from Eq. 19 and the water velocity can be calculated from

$$v_w = 6.5 \times 10^{-5} \frac{q_w}{h_f b}, \dots\dots\dots (22)$$

where v_w is the velocity of water, ft/sec, and h_f is the height of flume, ft. For practical considerations, b should be between 6 and 20 ft and ratio of h_f to b should be between 0.3 and 0.5.

The flume can be concrete lined or constructed as a soil pit. Solids that settle in the bottom of the flume can be cleaned out with a bucket. A mechanical sludge scraper run on a chain could be installed to concentrate the solids in one location for easy removal.

Cyclone Desanders

Cyclone desanders are conical-shaped devices that make use of centrifugal force to separate the heavier particles from the liquid. Fig. 15.10 shows the basic operation of a cyclone desander. Pressurized fluid enters a common inlet manifold, which distributes the stream to individual cyclones. Flow proceeds through a tangential feed inlet, which directs the fluid against the wall of a cylindrical section above a truncated cone. The fluid and solid particles move downward in a spiral pattern forcing the heavy particles to move toward the outer perimeter of the cone. Gravity forces these particles to slide downward and to be rejected at the cone apex and carried away in the "underflow" slurry. The water moves toward the vacuum created at the center of the cone, and is drawn off as the "overflow."

The size particle that is separated depends on the pressure drop through the cone. The pressure drop, in turn, depends on the flow rate. Thus, there is a minimum flow and a pressure drop that must be provided for each cone to settle a certain size particle. With pressure drops in the range of 25 to 50 psi, cyclones can be used to remove 99% of the 30- to 100-micron particles.

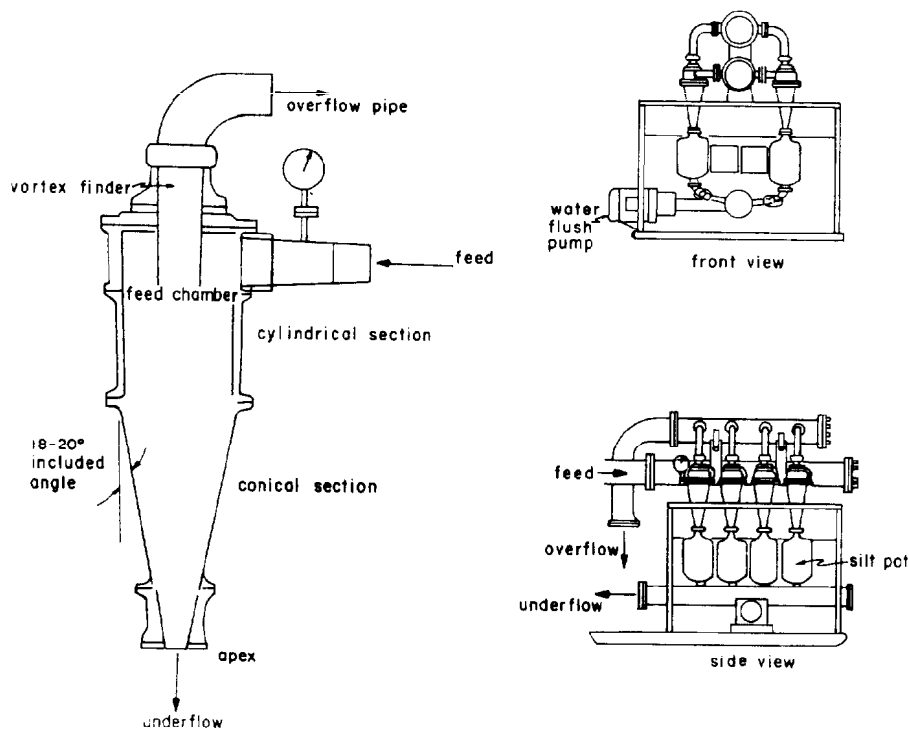


Fig. 15.10—Hydrocyclone operation.

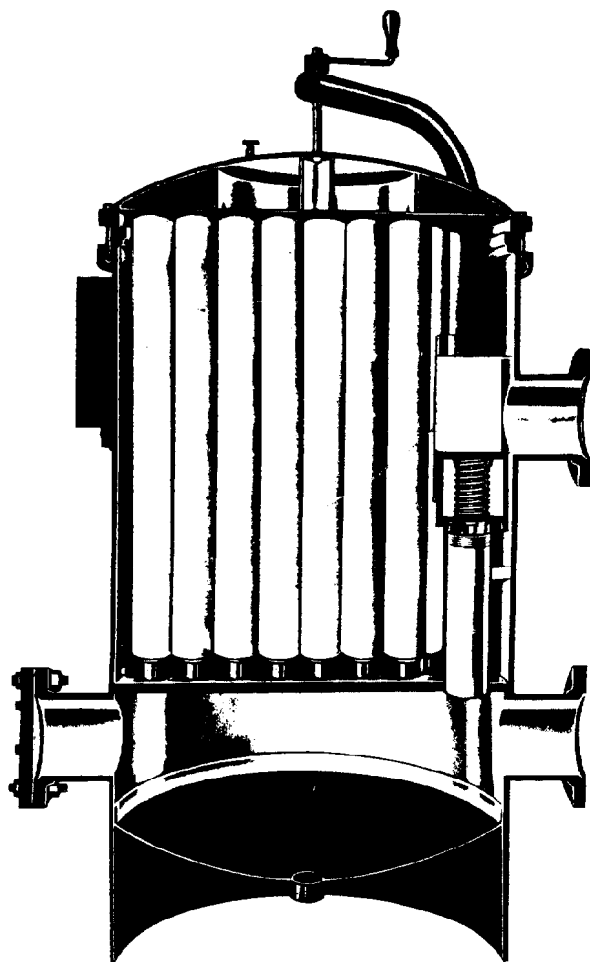


Fig. 15.11—Cartridge filter.

Centrifuges

Centrifuges are used on drilling rigs to separate low-gravity drill solids and reclaim high percentages of the heavy solids. They have not found wide use in producing operations because of the high maintenance associated with their use. Normally, if it is desirable to separate particles of diameter less than that resulting from sedimentation or cyclones, filters are used.

TABLE 15.10—CARTRIDGE DESIGN CONDITIONS
FOR BRINE

Cartridge Type	Particle Size (microns)	Flow Rate for 3-in. OD x 36-in. Element (gal/min)
Pleated wire screen	80	12
Pleated cellulose paper	5 to 10	4
Rolled laminated cotton and acrylic excelsior filler	5 to 10	2 to 3
Molded fiberglass	2	6

Filtration

To avoid plugging the injection formation it may be necessary to separate small-diameter suspended particles by filtration. Filters cannot handle the volume of solids that can be handled by sedimentation and cyclones. By proper choice of filter element, filters can remove fine solids in the 0.5- to 50-micron range and are used as a form of secondary treatment.

Cartridge Filters. Cartridge filters are the simplest to install, require no backwash, and are capable of removing solid particles of 2-micron or larger diameter. Their drawback is that they can take only very low solid loadings. The filter vessel must be taken out of service, depressured, and the cartridges replaced whenever the volume of solids trapped causes the differential pressure to exceed a predetermined maximum (usually 25 psi). Some modern cartridge filters can be backwashed.

Fig. 15.11 shows a typical cartridge filter. The cylindrical filters are encased in a pressure vessel. Flow enters the vessel and flows from the outside of the cartridges to the center, where it enters a perforated pipe that is open on the bottom. A bypass mechanism is included that will automatically allow flow to pass from the inlet to the outlet chambers if the differential pressure exceeds the capacity of the cartridges.

Table 15.10 indicates the particle size that can be separated and the recommended flow rate through various standard-size cartridges. The molded fiberglass has the least solid storage area and the pleated wire screen and pleated paper the most.

Sand Filters. Sand filters have beds of graded sand, gravel, anthracite, or graphite. The beds may be of a single medium or may be graded from coarse to fine media to allow for greater solids loading.

The media are arranged in a pressure vessel for either downflow filtration and upflow backwash as shown in Fig. 15.12 or for upflow filtration and upflow backwash. Conventional downflow filters are limited to flow rates of 2 to 5 gal/(min-sq ft) and total solids loads (before backwashing) of ½ to 1½ lbm/sq ft. With appropriately designed distribution systems, high-rate filters can be operated at 7 to 15 gal/(min-sq ft). This higher loading forces the solids farther into the bed allowing for solid loadings of between 1 and 4 lbm/sq ft.

Upflow filters have a greater capacity for solids loading. Flow tends to loosen the bed allowing for greater penetration of the solids. This allows up to 6 lbm/sq ft of solid loading. However, because of the danger of losing the bed, upflow filters are limited to flow rates of 6 to 8 gal/(min-sq ft). They also require longer backwashing time and more backwash fluid.

Walnut hulls are used as filter media in some new filters. There is a system that removes, cleans, and returns this medium to the filter automatically.

Sand filters are good for separating 25-micron particles. Some manufacturers claim their filters are good for 5- to 10-micron separation.

Diatomaceous Earth (DE) Filters. For filtration of 0.5- to 1.0-micron particles, DE filters are used. Typically, these have low solids-loading capabilities [½ to 1 gal/(min-sq ft)]. A typical DE filter is shown in Fig. 15.13.

The individual leaves, which are spaced at approximately 3-in. intervals, are made up of a wire screen of corrosion-resistant materials such as stainless steel, Monel®, or Inconel®. A precoat slurry of DE is mixed and flowed through the filter to provide an approximately $\frac{1}{16}$ -in.-thick coating to the leaves. Flow then is turned into the filter with a "body feed" of "filter aid" (DE and cellulose fiber or perlite) equal on a weight basis to the amount of solids to be filtered. The body feed helps to build an even, permeable filter cake on the leaves.

When a pressure differential of 25 to 35 psi is reached, the unit must be taken out of service and the filter cake removed. This can be done by backwashing alone, backwashing and vibrating, or backwashing and water sluicing the cake. Water with good filtering characteristics may build up a large permeable filter cake that requires backwashing before a large pressure differential is developed.

Flotation

It is possible to remove small particles by use of dispersed or dissolved-gas flotation devices. These units are used primarily for treating hydrocarbons from water and are discussed in that section. Normally gas is dispersed into the water or released from solution in the water and forms bubbles approximately 30 to 120 microns in diameter. The bubbles form on the surfaces of the suspended particles and create a particle whose average density is less than that of water. These rise to the surface and are mechanically skimmed. Because of the difficulty of predicting particle removal efficiencies with the method, it is normally not used in oil field land operations. However, it is being used increasingly in off-shore operations and in some underground disposal systems.

Treating Hydrocarbons From Water

Produced water, which may have to be treated, will enter the water treating plant from a three-phase separator, free water knockout, gun barrel, heater treater, or other lease equipment, which are discussed in previous chapters. This water will contain small amounts (100 to 2,000 mg/L) of suspended hydrocarbons in oil droplets. Since the water flows out of these pieces of equipment through dump valves or pumps, the oil particle diameters will be very small.

Theory

Treating equipment to handle this problem relies on one or more of the following principles: gravity separation of the lighter oil droplets from the water, coalescence of the smaller oil droplets, or gas flotation of the oil droplets. In applying these concepts, one must keep in mind the dispersion of large oil droplets to smaller droplets, which will take place if energy is added to the system.

Gravity Separation. As in the case of settling of sand from water, Stoke's Law, Eqs. 18 and 19, holds true for the buoyant rise velocity of an oil droplet in a water-continuous phase. Several immediate conclusions can be drawn from this equation.

1. The larger the size of an oil droplet, the greater its vertical velocity. That is, the bigger the droplet size, the

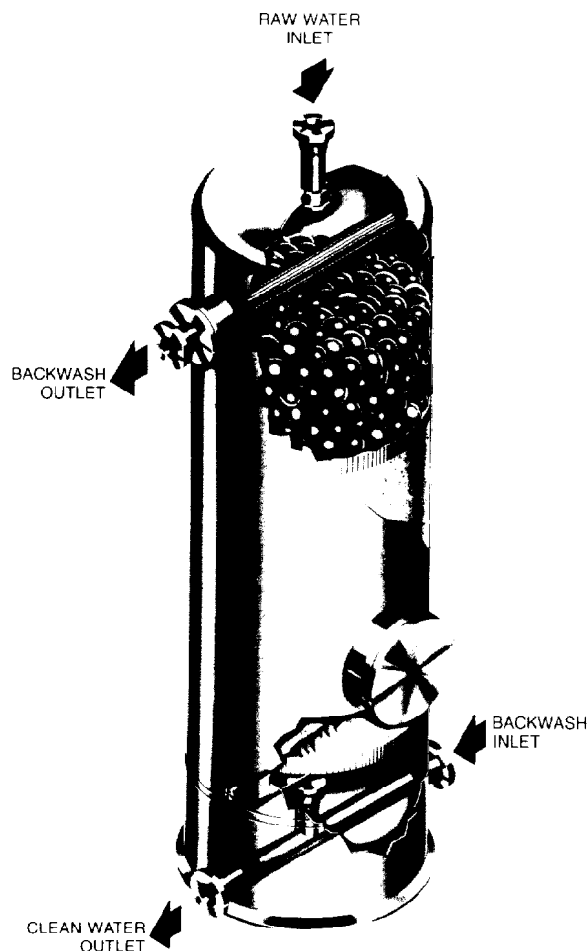


Fig. 15.12—Sand filter.

less time it takes for the droplet to rise to a collection surface and thus the easier it is to treat the water.

2. The greater the difference in density between the oil droplet and the water phase, the greater the vertical velocity. That is, the lighter the crude, the easier it is to treat the water.

3. The higher the temperature, the lower the viscosity of the water, and thus, the greater the vertical velocity. That is, it is easier to treat the water at high temperatures than at low temperatures.

The last conclusion requires some further elaboration. Heat is the primary mechanism used in treating small water droplets from oil in oil-treating equipment because of the effect heat has on the oil viscosity, which prompts more rapid settling, and because of the effect heat has on the emulsifier stabilizing the water-in-oil emulsion. Heat is not commonly used in water treating because (1) the percentage change in viscosity per degree of temperature change is much greater in oil than in water, (2) water-in-oil emulsions tend to have a higher percent of the dispersed phase than oil-in-water emulsions, and the dispersed phase tends to have larger-diameter droplets stabilized by heat-sensitive emulsifiers, and (3) it takes twice as much heat input to raise a barrel of water as it takes to raise a barrel of oil to the same temperature.

The time it takes to “grow” a large droplet from a relatively small droplet, in a “quiet” gravity settler, is approximated by

$$t = \frac{(d_d)^4}{2f_v K_s}, \quad (24)$$

where

d_d = droplet diameter,
 f_v = volume fraction of the dispersed phase, and
 K_s = empirical settling constant.

While it is impossible to determine K_s for an actual installation, the following qualitative conclusions can be drawn.

1. A doubling of residence time will cause an increase in droplet size of only 19%.

2. The more dilute the dispersed phase, the greater the residence time needed to grow a given particle size. That is, coalescence occurs more rapidly in concentrated dispersions.

Gravity Separation Devices

Most water-treating equipment makes use of gravity separation of the oil droplets. Included in this category are skim tanks, API separators, plate coalescers, and skim piles. Unfortunately, it is necessary to know both the oil concentration in the effluent water and the particle size distribution to design a gravity separator to meet a certain effluent quality.

This information can be determined from experience-derived relationships such as those shown in Fig. 15.14. Further work is needed to define these relationships. For the present, the design engineer must rely on a judgment factor or on laboratory tests for the particular crude oil and water.

Skim Tanks and Vessels. The simplest form of treatment equipment is a skim tank or pressure vessel. These are normally designed to provide large residence times during which coalescence and gravity separation can occur. They can be either pressure vessels or atmospheric tanks.

Skim tanks can be either vertical or horizontal in configuration. They may be set up for vertical downward flow of the water with or without inlet spreaders or outlet collectors. They may also be designed as horizontal vessels where the water enters on one side and flows over a weir on the far end.

In vertical vessels the oil droplets must flow upward against the downward velocity of the water. For this reason, horizontal vessels are more efficient in gravity separation of the two liquid phases. In spite of this, vertical vessels and tanks are sometimes used for two reasons.

1. Sand and other solid particles can be more easily handled in vertical vessels with either the water outlet or a sand drain off the bottom. Experience with elaborately designed sand drains in the large horizontal vessels has not been very satisfactory.

2. Vertical vessels are less susceptible to high-level shut-downs because of liquid surges. Internal waves resulting from surging in horizontal vessels can trigger a level float even though the volume of liquid between the

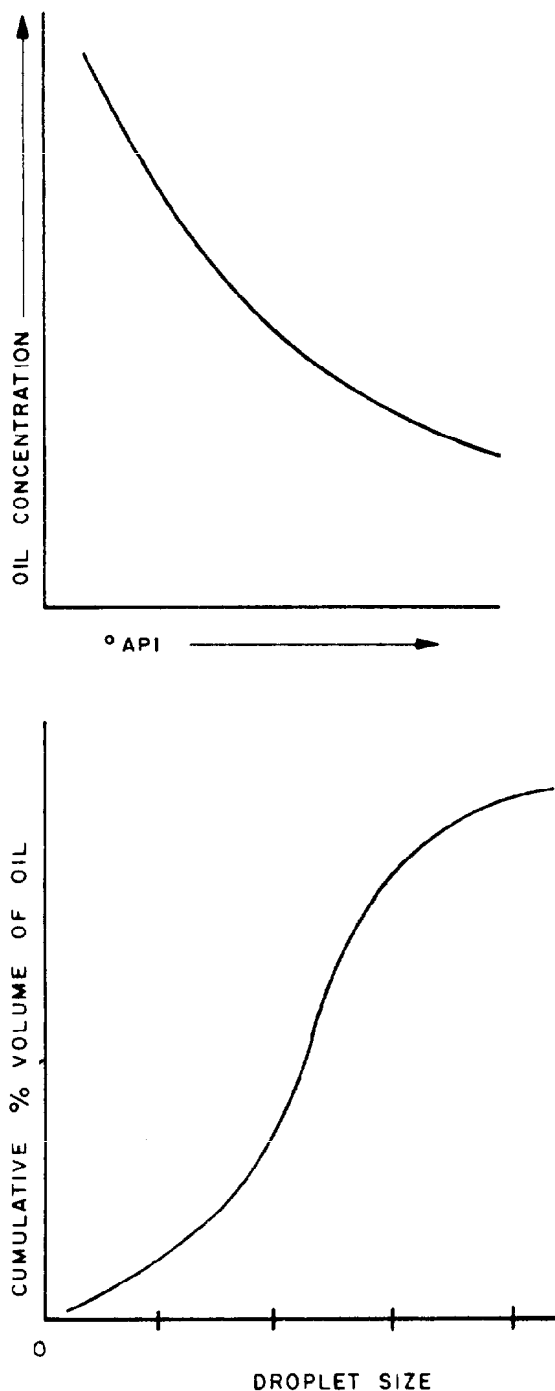


Fig. 15.14—Form of empirical curves for oil concentration and droplet size distribution.

normal operating level and the high-level shut-down is equal to or larger than that in a vertical vessel.

Tracer studies have shown that large skim tanks, even those with carefully designed spreaders and baffles, exhibit poor flow behavior and short circuiting. This is probably because of density and temperature differences, deposition of solids, corrosion of spreaders, etc. In one case, a tank with a design mean residence time of 33 hours had a breakthrough of the tracer with a peak within minutes of tracer injection.

As seen previously, the provision of residence time to allow for coalescence does not appear to be cost efficient. However, a minimum residence time of 10 minutes to one hour should be provided to ensure that surges do not upset the system and to provide for some coalescence.

Horizontal Pressure Vessel Sizing. The required diameter and length of a horizontal cylinder operating one-half full of water can be determined by use of a model similar to that used for settling solids. The following equation can be derived from the model.

$$d_i L_e = \frac{1000 q_w \mu_w}{\Delta \gamma_{ow} (d_d)^2} \quad (25)$$

where

- d_i = vessel ID, in.,
- q_w = water flow rate, BWPD,
- μ_w = water viscosity, cp,
- d_d = oil droplet diameter, micron,
- L_e = effective length in which separation occurs, ft (for design use 75% of the seam-to-seam length), and
- $\Delta \gamma_{ow}$ = difference in specific gravity between oil and water.

While Eq. 25 will govern the design, it is also necessary to check for adequate retention time.

$$t_r = 0.7 \frac{(d_i)^2 L_e}{q_w} \quad (26)$$

where t_r is the retention time in minutes.

Vertical Cylindrical Vessel. The required diameter of a vertical cylindrical pressure vessel or tank can be determined from

$$(d_i)^2 = 7,000 F \frac{q_w \mu_w}{\Delta \gamma_{ow} (d_d)^2}, \quad (27)$$

where F is a factor to account for turbulence and short circuiting. For small-diameter vessels (48 in. or less), $F=1.0$. For larger diameters, F depends on the type of inlet and outlet spreaders, collectors, and baffles that are provided. Large tanks (10 ft or more in diameter) should be considered to have an $F > 2.0$, depending on the inlet and outlet conditions. Tanks greater than 10 ft in diameter should be discouraged because of short circuiting.

The height of the water column can be determined from retention time requirements:

$$Z_w = 0.7 \frac{t_r q_w}{(d_i)^2}, \quad (28)$$

where Z_w is the height of the water column in feet.

API Separators. An API separator is the name given to a horizontal, rectangular cross-section, atmospheric oil skimmer that follows the sizing equations and guidelines included in the *API Manual on Disposal of Refinery Wastes*.¹⁵ Fig. 15.15 shows a typical API separator. The equations for sizing and their derivations have been discussed previously in the solids settling section.

Plate Coalescers. The use of flow-through parallel plates to help the gravity separation in skim tanks was pioneered in 1959¹⁶ as a method of converting existing API separators to treatment of droplets less than 150 microns in diameter.

Various configurations of plate coalescers have been devised. These are commonly called parallel plate interceptors (PPI), corrugated plate interceptors (CPI), or crossflow separators. All of these depend on gravity separation to allow the oil droplets to rise to a plate surface where coalescence and capture occur. Flow is split between a number of parallel plates spaced a short distance apart. To facilitate capture of the oil particles, the plates are inclined to the horizontal.

As shown in Fig. 15.16, an oil droplet entering the space between the plates will rise in accordance with Eq. 19. At the same time, it will have a forward velocity equal to the bulk water velocity. By solving for the vertical velocity needed by a particle entering at the base of the flow to reach the coalescing plate at the top of the flow, the resulting diameter can be determined. A restriction is placed on the Reynold's number for the water to ensure that turbulence in this flow does not affect the oil sheet on the coalescing plate.

General Sizing Equation. For a plate coalescer with flow either parallel to or perpendicular to the direction of flow the general sizing equation for the droplet size removal is:

$$(d_d)^2 = \frac{4.7 q_w L_p \mu_w}{\cos \theta Z_p b_p L \Delta \gamma_{ow}}, \quad (29)$$

where

- d_d = design oil droplet diameter, micron,
- q_w = bulk water flow rate, BWPD,
- L_p = perpendicular distance between plates, in.
- μ_w = viscosity of the water, cp,
- θ = angle of the plate with the horizontal,
- Z_p = height of the plate section perpendicular to the axis of water flow, ft,
- b_p = width of the plate section perpendicular to the axis of water flow, ft,
- L = length of plate section parallel to the axis of water flow, ft, and
- $\Delta \gamma_{ow}$ = difference in specific gravity between oil and water.

Experiments have indicated that Reynold's number for the flow regime cannot exceed 400, on the basis of the hydraulic radius as the characteristic dimension. Thus the maximum flow rate is given by

$$(q_w)_{\max} = \frac{1562 Z_p b_p}{L_p} \quad (30)$$

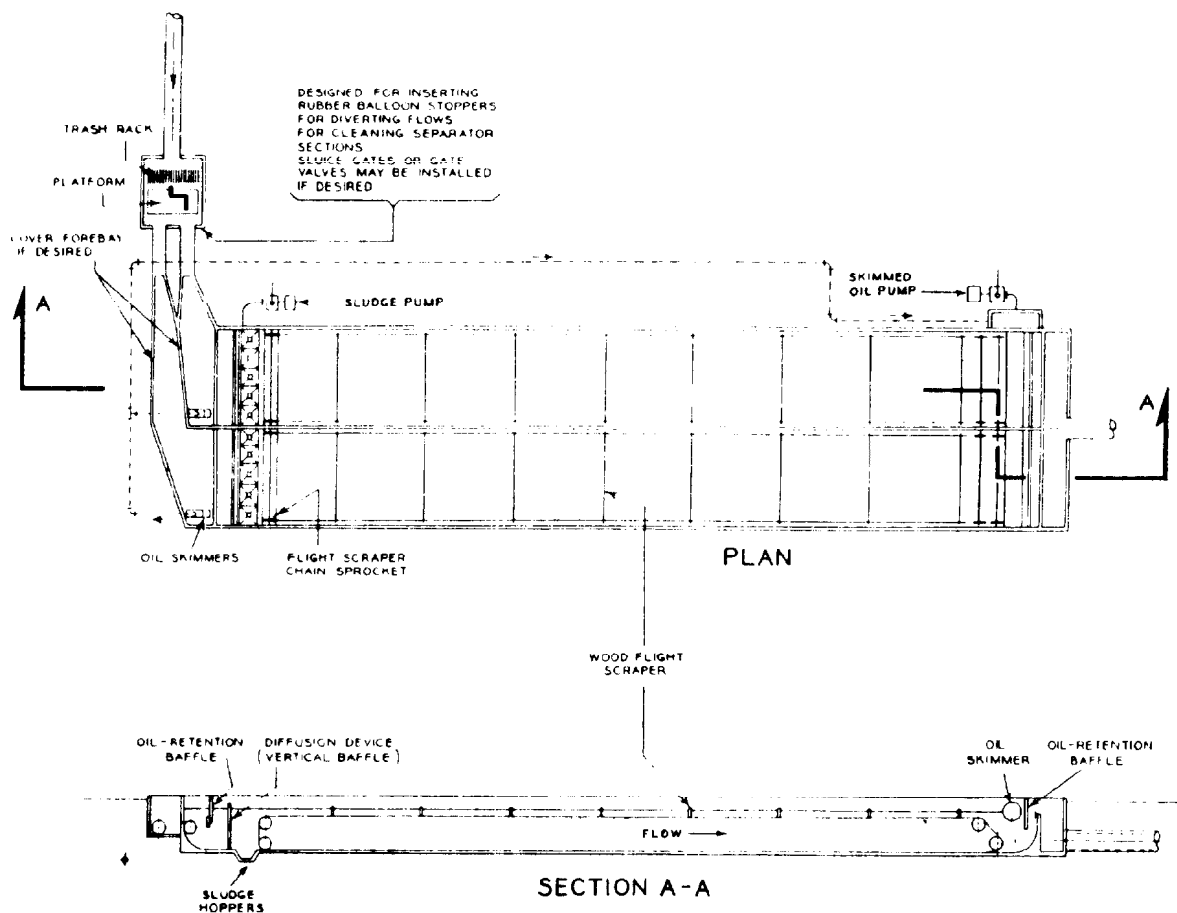


Fig. 15.15—API oil-water separator.

Parallel Plate Interceptor (PPI). The first form of plate coalescer was the PPI. This involved installing a series of plates parallel to the longitudinal axis of an API separator (a horizontal, rectangular cross-sectioned skimmer). The plates form a "V" when viewed perpendicular to the axis of flow so that the oil sheet migrates up the underside of the coalescing plate and to the sides. Sediments migrate toward the middle and down to the bottom of the separator, where they are removed.

Corrugated Plate Interceptor (CPI). The most common form of parallel plate interceptor used offshore is the CPI. This is a refinement of the PPI in that it takes up less platform space (length) for the same particle size removal, and has the added benefit of making sediment handling easier. Fig. 15.17 is a typical design using a corrugated plate.

In CPI's, the parallel plates are corrugated (like roofing material) with the axis of the corrugations inclined to an angle of 45° . The bulk water flow is forced downward. The oil sheet rises upward counter to the water flow and is concentrated in the top of each corrugation. When the oil reaches the end of the plate pack it is collected in a vertical channel and brought to the oil/water interface. CPI's require frequent cleaning of the plate packs where large amounts of sediments are handled.

Crossflow Devices. Recently manufacturers have

modified the CPI configuration for horizontal water flow perpendicular to the axis of the corrugations in the plates. This allows the plates to be put on a steeper angle to facilitate sediment removal and to enable the plate pack to be more conveniently packaged in a pressure vessel. The latter benefit may be required if gas blowby through an upstream dump valve could cause relief problems with an atmospheric tank.

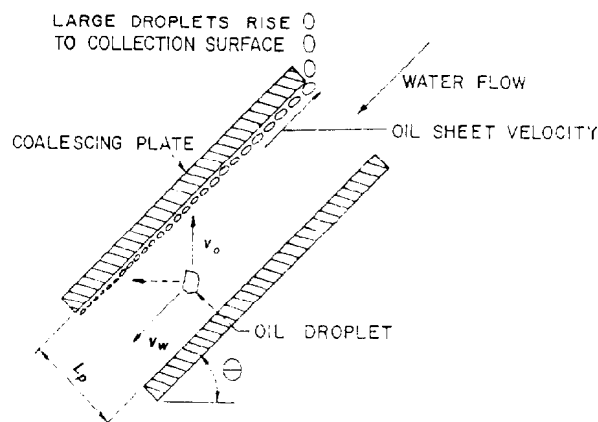


Fig. 15.16—Plate coalescers.

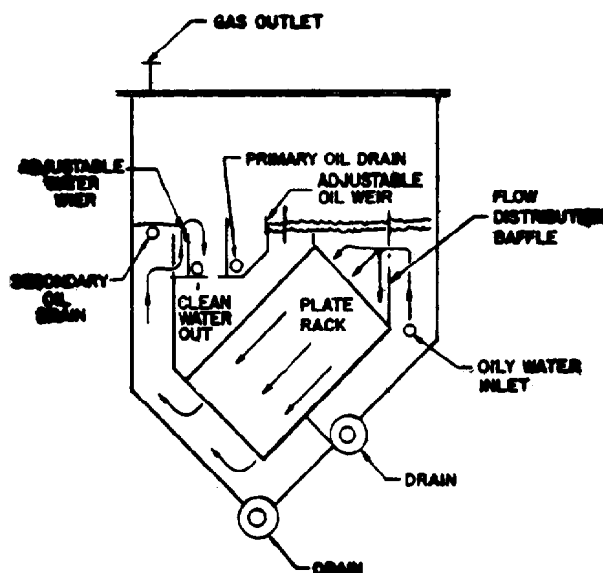


Fig. 15.17—CPI separator flow pattern.

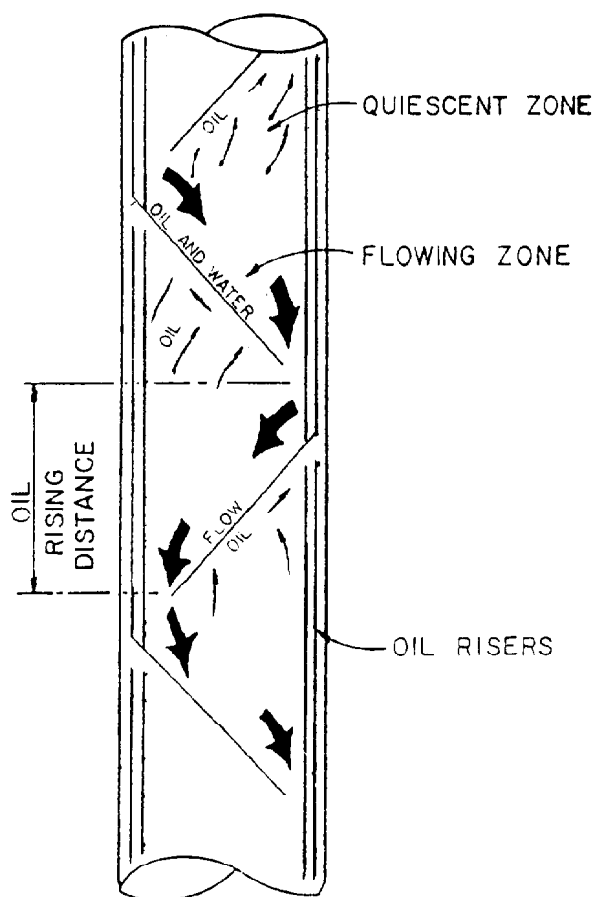


Fig. 15.18—Skim pile flow pattern.

Crossflow devices can be constructed in either horizontal or vertical pressure vessels. The horizontal vessels require less internal baffling as the ends of nearly every plate conduct the oil directly to the oil/water interface and the sediments to the sediment area below the water flow area. The vertical units, although requiring collection channels on one end to enable the oil to rise to the oil/water interface and on the other end to allow the sand to settle to the bottom, can be designed for more efficient sand removal. Crossflow separators are used where sand is considered a problem and it is not removed in the process upstream of the CPI.

Practical Limitations. Stoke's law theory should apply to oil droplets as small in diameter as 1 to 10 microns. However, field experience indicates that 30 microns sets a reasonable lower limit on the droplet sizes that can be removed. Below this size small pressure fluctuations, platform vibration, etc., tend to impede the rise of the droplets to the coalescing surface. Thus, the practical limit for sizing plate coalescers is 30-micron removal.

Skim Pile. Skim piles are gravity water-treating devices that are used offshore. As shown in Fig. 15.18, flow through the multiple series of baffle plates creates quiescent zones that reduce the distance a given oil droplet must rise to be separated from the main flow.

Once in the quiescent zone, there is plenty of time for coalescence and gravity separation. The larger droplets then migrate up the underside of the baffle to an oil collection system. Skim piles are used extensively to treat deck drainage of washdown or rainwater that has been contaminated with oil. They have the added benefit of providing for some degree of sand cleaning. Sand traversing the length of a skim pile will abrade on the baffles and be water washed. This removes the free oil, which is then captured in a quiescent zone.

Skim Pile Sizing—Deck Drainage. Field experience has indicated that acceptable effluent is obtained with 20 minutes of retention time in the baffled section of the pile. Using this,

$$(d_i)^2 L_{bs} = 14.3 (q_w + 0.356 A_d q_r), \dots (31)$$

where

L_{bs} = length of baffle section, ft,

A_d = area of deck, sq ft, and

q_r = rainfall rate, in./hr.

Intermittent Flow. During periods of no flow, oil droplets rise to the area of the quiescent zone and become trapped and protected from being swept back into the flow stream when flow is resumed. The net effect of the baffles is to reduce this rise distance. Each time flow is stopped as the water traverses the baffled section more oil particles are trapped in the quiescent zone.

This phenomenon can be used when it is desired to use a skim pile downstream of a skim tank or CPI for further treating. By use of a snap acting water dump on the influent, intermittent flow is established in the pile.

If t is the time in seconds for the dump cycle,

$$N_c = \frac{41.7 (d_i)^2 L_{bs}}{q_w t} \dots (32)$$

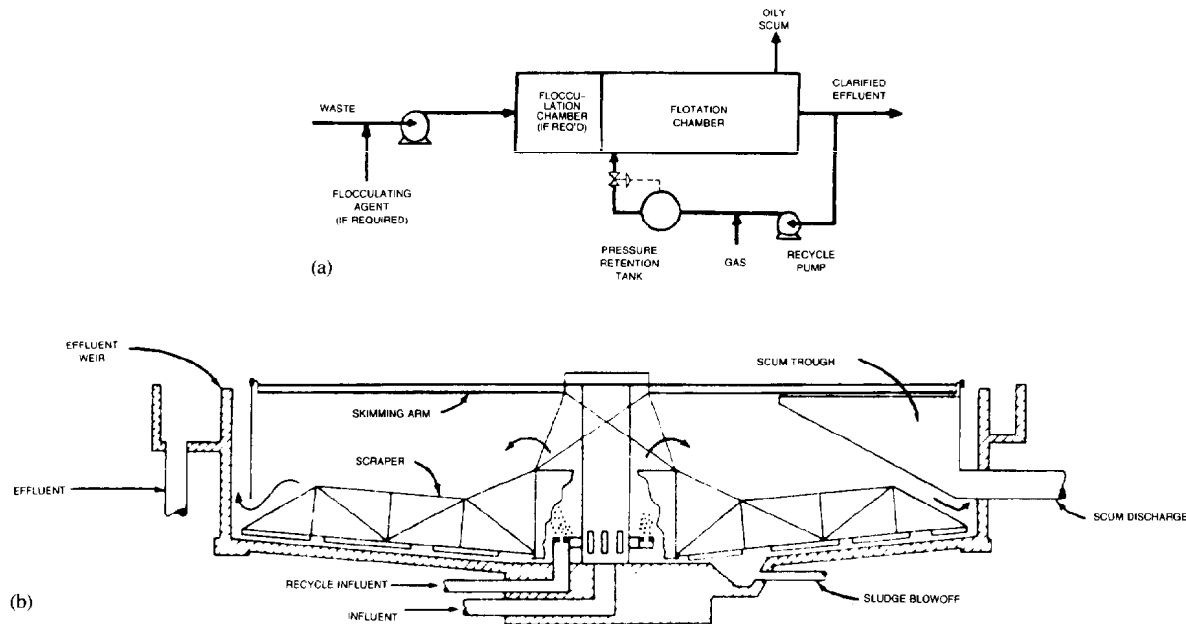


Fig. 15.19—(a) air flotation process; (b) circular flotation chamber details.

where N_c is the number of cycles of no flow a particle sees as it traverses the baffle section.

If t_c is the time the valve is closed, the removal efficiency on any cycle of a particular drop size is

$$E_{rc} = \frac{4.3 \times 10^{-5} (\Delta \gamma_{ow}) (d_p)^2 t_c}{\mu_w d_i} \quad (33)$$

The overall removal efficiency of that particle size can then be determined by

$$E_{ro} = 1 - [1 - E_{rc}]^{N_c} \quad (34)$$

Gas Flotation Units

Flotation units are the only commonly used water-treatment equipment that does not rely on gravity separation of the oil droplets. In fact, the action of these units is independent of the oil droplet size. In gas flotation units, large quantities of small-diameter gas bubbles are injected into the water stream. The bubbles attach to the oil droplets suspended in the stream and cause them to rise to the water surface as a froth. Experimental results have shown that very small-diameter oil droplets in dilute suspension can be removed easily by flotation. High percentages of oil removal are achieved.

Two distinct types of flotation units have been used, which are distinguished by the method employed in producing the small gas bubbles needed to contact the water. These are dissolved-gas units and dispersed-gas units.

Dissolved-Gas Units. Dissolved-gas designs take a portion of the treated water effluent and saturate the water with natural gas or air in a contactor. The higher the pressure, the more gas can be dissolved in the water.

However, most units are designed for a contact pressure of 20 to 40 psig. Normally, 20 to 50% of the treated water is recirculated for contact with the gas.

The gas-saturated water is then injected into the flotation chamber as shown in Fig. 15.19. The dissolved gas breaks out of solution in small-diameter bubbles when the flow enters the chamber, which is operated at near-atmospheric pressure.

Design parameters are recommended by the individual manufacturers but normally range from 0.2 to 0.5 scf/bbl of water to be treated and flow rates of treated plus recycled water of between 2 and 4 gal/(min-sq ft). Retention times of 10 to 40 minutes and depths of between 6 and 9 ft are specified.

Dissolved-gas units have been used successfully in refinery operations where air can be used as the gas and where large areas are available. In treating produced water for injection, it is desirable to use natural gas to exclude oxygen. This requires the venting of the gas or installation of a vapor recovery unit. Field experience with dissolved-natural-gas units have not been as successful as experience with dispersed-gas units.

Dispersed-Gas Units. In dispersed-gas units, gas bubbles are dispersed in the total stream either by use of an inductor device or by a vortex set up by mechanical rotors. Fig. 15.20 shows a schematic cross section of such a unit.

Most dispersed-gas units contain three or four cells. Bulk water flow moves in series from one cell to the other by underflow baffles. Field tests have indicated that the high intensity of mixing in each cell creates the effect of plug flow of the bulk water from one cell to the next. That is, there is virtually no short circuiting or breakthrough of a part of the inlet flow to the outlet weir box.

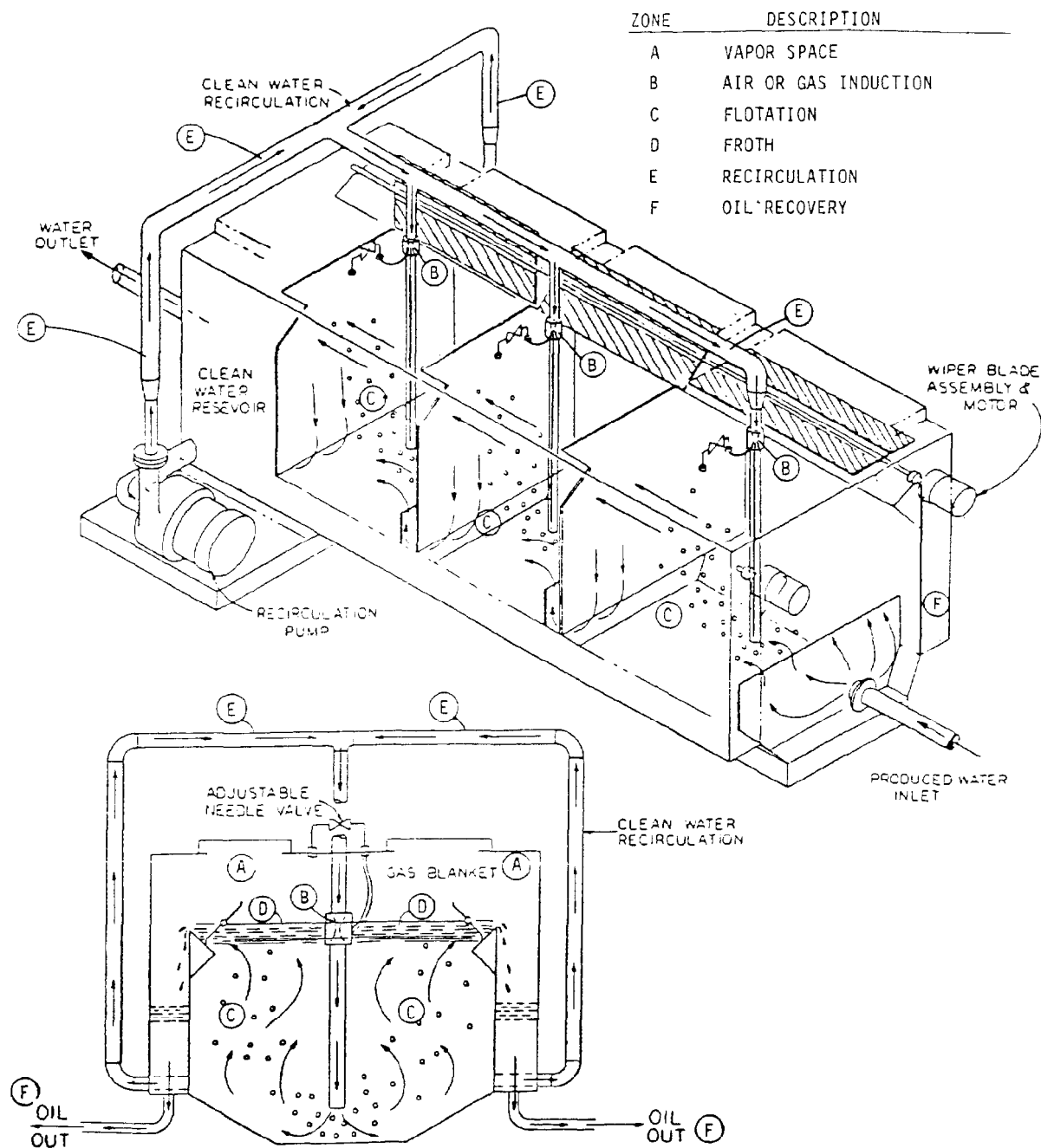


Fig. 15.20—Dispersed-gas unit with inductor device.

Field tests and theory both indicate that these units operate on a constant percent removal basis. Within normal ranges, their oil removal efficiency is independent of inlet concentration or oil droplet diameter. The design of the induction nozzle or rotor and internal baffles is critical for determining overall efficiency.

Field experiments indicate that most designs can be expected to have efficiencies of about 90%. Because the gas is recycled by the unit, a natural gas blanket can easily be maintained with little or no venting. The low required retention times makes this an ideal choice for offshore facilities where space and weight are at a premium.

Dissolved Gas Removal

Often, produced or surface waters will contain dissolved gases, which must be removed by the water-treating plant. Oxygen in concentrations of 0.05 ppm in hydrogen-sulfide-free water and 0.01 ppm in water containing hydrogen sulfide is generally considered to be sufficient to cause corrosion problems in the facilities and bacteria plugging problems in an injection reservoir. For this reason, attempts are made to exclude oxygen from produced-water systems by maintaining gas blankets on all tanks. However, sometimes these

systems must be designed to handle rainwater, which may introduce dissolved oxygen in sufficient quantities to require removal. The location of surface water intakes can be arranged to minimize the oxygen content in the surface water but, in almost all cases, oxygen may have to be removed.

Some waters may contain ammonia, H_2S , or CO_2 , which must be removed. Dissolved gases are commonly removed by either chemical scavenging, gas stripping, or liquid extraction. It is beyond the scope of this book to deal with the design of the complex processes and equipment that can be employed in removing all dissolved gases. Since oxygen is the most common contaminant, we will briefly describe the treatment processes commonly in use to remove dissolved oxygen.

Oxygen Scavengers

Chemical scavengers are used quite often to remove dissolved oxygen from water streams of less than 10,000 B/D. Sulfite is the most common scavenging agent for water treating. The most common forms are sodium sulfite, sodium bisulfite, ammonium bisulfite, and sulfur dioxide. To speed the reaction rate, a catalyst such as cobalt is required.

Gas Stripping

The basic principle employed in gas stripping is that the quantity of oxygen dissolved in the water is directly proportional to the partial pressure of the gas that is in contact with the water (Henry's law). Since partial pressure of the gas is a function of the mole fraction of that gas, the addition of other gases to the solution will decrease the partial pressure of oxygen and thus the concentration of oxygen in the water.

In a typical gas stripping column, natural gas or steam, if available, is introduced in the base of a packed or trayed column (similar to the familiar glycol contactor used in gas dehydration) and flows upward countercurrent to the water, which is introduced in the top of the column and flows downward.

If natural gas is used, the oxygen-contaminated gas from the top of the tower can be used for fuel, compressed for inclusion in the sales gas stream, or vented, depending on the process design and gas sales contract. Stripping gas usage of between 2 and 5 scf/bbl is common.

It is also feasible to strip oxygen from water by use of a concurrent flow. This is common in cases where lift gas is used as the artificial-lift mechanism for obtaining the water from a reservoir or subsea source. Sometimes, the gas is injected into the water with a static mixer in concurrent flow in a pipe. While this may require more stripping gas, it may be more economical from the standpoint of equipment cost, space, and weight when the value of the stripping gas is low. Stripping gas usage in concurrent flow can be in excess of 10 scf/bbl.

Vacuum Deaeration

Since the partial pressure of oxygen in the gas is a function of the total pressure of the system, the partial pressure of oxygen can also be reduced by applying a vacuum to the water-gas system. Vacuum deaerators can be combined with either counterconcurrent or concurrent

stripping gas to provide very low oxygen concentrations in the water. Stripping gas usages of a fraction of a cubic foot per barrel are common. Vacuum stripping towers are used where no stripping gas is available, the available stripping gas contains contaminants such as CO_2 and H_2S , and stripping gas has a high value.

Dissolved Solids Removal

The removal of dissolved solids is of major importance if the water is to be used in steam generation or for some EOR projects. In particular, magnesium and calcium ions in the water may cause boiler scale, react adversely with an EOR chemical, or precipitate in the reservoir as a plugging solid.

Various processes have been used to create chemical reactions to cause the dissolved solids to form precipitates, which can then be settled or filtered out of the water. Aeration has been used to oxidize soluble ferrous compounds to insoluble ferric compounds, and soluble bicarbonates to insoluble carbonates. However, this process introduces dissolved oxygen, which must then be stripped out of the solution.

The addition of chemicals, such as lime and soda ash, under correct conditions of temperatures and pH can form insoluble carbonates. Alum or other coagulants are then added to help in the settling or filtering of the precipitate. The equilibrium constants for these reactions are usually such that the low total dissolved solids (TDS) required cannot be easily met. For this reason, ion exchange has become the most common process for control of dissolved solids.

Ion exchange can be defined as a reversible exchange of ions between a solid and a liquid in which there is no significant change in the structure of the solid. Ion-exchange solids of various types can be used. The usual ion-exchange material takes the form of granules, or beads, ranging in size from approximately 0.3 to 1.0 mm in diameter.

As a very broad generalization, the synthetic ion-exchange resins can be categorized into four groups.

1. **Strong acid resins.** These are polystyrene resins that are strongly acid, have a high exchange capacity, and are not damaged by strongly alkaline hot water.

2. **Strong base resins.** Typical resins in this category incorporate a quaternary ammonium type of structure. The hydrocarbon groups may include methyl groups, polymeric benzyl groups, ethanol groups, and the like.

3. **Weak acid resins.** These resins usually contain carboxylic groups as the active, or functional, ion sites. They have a limited use in water treatment, but can be used to remove basic materials from solution.

4. **Weak base resins.** Typical resins in this category are of the polyamine type. They usually contain a mixture of primary, secondary, and tertiary amine groups and their chemical properties are analogous to amine or ammonium hydroxide solutions. They can be used to remove free acids from solution.

Table 15.11 presents general guidelines for the use of different combinations of resins.

In ion-exchange units the influent water flows through the bed of ion-exchange material. Ions from the bed are exchanged for the undesirable ionic species in the water. When a bed is close to breakthrough, it is regenerated

TABLE 15.11—GUIDELINES FOR CATALYST SELECTION

Feed		Resin	Process
TDS	Hardness		
<2,000	<700	strong acid	single bed
700 to 5,000	<2,000	strong acid	series bed
5,000 to 10,000	<500	weak acid	single bed
5,000 to 10,000	500 to 2,000	strong to weak acid	series operation
10,000 to 25,000	<2,000	weak acid	series bed
>25,000	<500	chelating	single bed

with a strong solution of the ionic species originally contained in the ion-exchange material. The exit solution from the regeneration stage is thus a concentrated solution of the contaminants removed from the water.

Removing Hydrocarbons From Solids

Fortunately, most solids that must be handled in a water treating plant are water-wet. Reservoir sand in its in-situ condition is almost always water-wet. As it flows up the tubing and through the process system, it may become coated with an oil layer but, since this layer is on top of a water-wet solid, it is easily removed. The two most common solids cleaning processes are abrasion and water washing.

In separating solids with a hydrocyclone, the solids rub against the inside wall of the cone and against each other. The high centrifugal velocities involved abrade the oil layer, cleaning the solid. In most applications, one pass through a hydrocyclone is sufficient to clean the solids sufficiently for disposal. Some installations include two or three cyclones, in series, to ensure adequate cleaning. In some installations, an air flotation step is used between cyclones to separate any oil that may exit through the cyclone underflush.

Another cleaning method involves the routing of the underflush to a batch cleaning vessel. Water is induced in the vessel to agitate and wash the solids. The solid bed is then allowed to settle while the oil is skimmed from the top. The procedure is repeated several times until the solids are clean enough to be educted from the bottom of the vessel and disposed of as a slurry.

On offshore platforms, skim piles have been used effectively to water wash and abrade solids. The solids move down the pile and are abraded as they bounce along the baffle surfaces. These are water-washed in the mixture around the end of each baffle. Oil removal occurs in the normal manner within each baffle section.

Process Selection and Project Management

The process selection for a specific project must provide an overall cost-effective system using the individual techniques described previously. In some cases, the process selection and design of the system may be obvious and easily handled by hooking up some standard pieces of equipment in the field with no further engineering design. However, in most cases, several alternative schemes may have to be analyzed, and the process will be complex enough to require the system to be engineered to work as designed. Cost may be significant

enough to necessitate competitive bids for equipment and installation.

Every project, no matter how small, must proceed through the following steps. On small projects, the engineer alone may handle some of these steps in a matter of minutes. On larger projects, these may take months of analysis and work by teams of individuals.

Conceptual Studies

The first step of any project, the conceptual study, investigates one or more means of accomplishing the objective. An economic and technical assessment and comparison of the various methods or schemes is made. Block diagrams may be used to develop a selected process or alternative into specific descriptions and recommendations for equipment. Equipment type and arrangement are studied and a design philosophy established. An analysis of cost and economic benefit of each alternative is performed and a recommendation made.

Project Definition

The next phase is to define the project for the scheme selected in the conceptual study. Tools used are process flow sheets, layout drawings, preliminary cost estimate, and project execution plan.

The block diagram is converted into a process flow sheet to better define the project. The flow sheet shows all major equipment, main piping, and operating pressures and temperatures. Instrumentation that controls the main process flow is shown and every major line is assigned a stream number. A table is included listing pertinent operating data for these streams.

Layout drawings locate the equipment on the process flow sheets. A well-planned layout is the key to good operation, economical construction, and efficient maintenance. The layout drawing must be integrated with the development of the process flow sheet and must be settled before detailed piping, structural, and electrical design can begin.

A plan of execution for a project begins when the first information is received. This plan must consider the alternatives for breaking the job down into individual work items for bid solicitation. It must balance time and ease of management against cost for such decisions as (1) the scope of work to be included in individual work, (2) degree of engineering to perform prior to bid, (3) potential suppliers' work load, capability, and competitive situations, and (4) operator sole source preferences.

The preliminary cost estimate is an important tool in the generation of the initial authority for expenditure (AFE). For effective cost control, the preliminary estimate must be made accurately and upgraded when information is received that affects it. Revisions may be necessary because of a change in scope or a realization that the amount of work was over- or underestimated.

Design Engineering

Once the need and extent of engineering assistance is determined, design engineering must begin to translate the process flow sheets into specific objectives and to determine activities required to attain these objectives. The basic item on which all other activities depend and which must be completed early in an engineering design project is the mechanical flow sheet.

Mechanical flow sheets are established from the process flow sheets and show every piece of equipment for the entire facility, including process, utilities, fire-water system, safety systems, spare equipment, etc. Every instrument, valve, and specialty item is shown schematically. Piping should be shown with flow arrows and line numbers indicating size, pressure rating, heat tracing, and insulation.

Vessel and equipment specifications are established for long-delivery items to expedite both the design and purchasing effort. Every facility is designed for a specific function, and thus the criteria by which the equipment is selected are applicable to that facility only. Therefore, this equipment is not normally produced off-the-shelf items. However, an experienced engineer will maximize the use of standard items to minimize cost and delivery time.

Detail Engineering

Once design engineering is completed and major equipment items have been specified and sent out for bid, the next step is to perform the detail engineering. This consists of piping drawings, structural drawings, electrical one-line drawings, instrument data sheets, and control schematics.

Piping drawings translate to the fabrication contractor the piping arrangement, as defined in the mechanical flow sheets. In many cases, a good set of piping drawings is the key to any easy to build and operate facility. In all cases, a good set of drawings is required to speed installation and keep the cost for extras to a minimum.

Structural drawings for an onshore facility detail the foundation site development and road work required, as well as detailing any pipe supports or skids for the production equipment. For an offshore facility, these drawings can include platform drawings as well as those for production skids themselves. The skids could be installed on wooden or concrete piles, steel or concrete barges, or steel jackets with steel decks.

Procurement

A large part of the *engineering* effort is involved in bidding, evaluating, expediting, and coordinating vendors and vendor information. This is true whether the work is performed by the operator, the engineering consultant, or a turnkey contractor.

Special, long-delivery equipment, vessels, and instrumentation usually are ordered as soon as the

specification can be written, checked, bids obtained and evaluated, and the purchase order issued.

All bids should be opened at one time to minimize any possibility of a bidder receiving an unfair advantage. While it is possible to play one bidder against another by "bid shopping," any experienced project engineer knows that in the long run this will be counterproductive. If vendors expect the work to be given to the low bidder, they will put their best effort into the price. If an auction is expected, the bid price will reflect this.

Inspection and Expediting

An important phase of the project is inspection. It is the inspector's responsibility to ensure that the finished equipment or material is of acceptable quality and complies with all requirements of the purchase order.

The inspector witnesses tests on mechanical equipment such as pumps and compressors, observes and approves fabrication methods of vessels, pipe, and structural steel, and generally ensures that the best workmanship is being performed on the purchased equipment.

The purchaser's expeditor can do much to ensure that the estimated delivery dates will be met by working with both the manufacturer and his own organization. The expeditor should seek and study all information that might affect delivery, anticipate delays or bottlenecks, and resolves these with the vendor. He should assist the vendor in obtaining priorities and solving procurement problems by communicating with subsuppliers. If delivery schedules must change, he should advise his employer as early as possible. On small projects, these functions are performed by the inspectors.

Startup

The conscientious preparation of a startup and operations procedure is the best possible check of the practicability, operability, and safety of a system. The procedure may contain only a few pages or may take the form of a book. In any case, it describes (1) overall purpose and design of the installation, (2) operation of the process, (3) details and operating descriptions of all systems, including overall instrumentation (pneumatic and/or electronic) electrical, data transmission, utility and fire-water, etc., (4) instructions for equipment installation, (5) purge and preparation for operation, and (6) procedure for starting.

Project Execution Format

Every project goes through the steps of project management described above. This is true no matter whether the tasks are performed by the operator's staff, the engineering consultant, or contractors. The project must progress from one step to the next; engineering, procurement, and inspection must be accomplished; and the cost of performing these functions must be borne by the project.

There are several different project execution formats that must be considered. The choice of a specific format will determine which of these functions will be performed by a particular organization.

Although there are almost as many formats as there are projects, most can be separated into the following four basic types which we shall call turnkey, negotiated turnkey, modified turnkey, and cost plus.

Turnkey. The turnkey format is used when the work is not completely designed. The conceptual study and project definition are normally complete. In this case, the scope of the contractor's work would include the design engineering, detail engineering, procurement, inspection and expediting, and possibly, startup.

Five advantages are claimed by proponents of this format: (1) the project cost is established before work starts, (2) a single point of responsibility is established, (3) the contractor can design to take advantage of construction efficiencies, (4) the contractor can speed up equipment delivery by performing engineering in such a manner as to get long lead time equipment on order sooner, and (5) the contractor assumes risk.

Several problems have been experienced with this format.

1. Owner loses design control or can exercise it only at high cost in extra work.

2. Competition is limited to select firms with total design and construction capability.

3. Most large firms have different engineering and construction profit centers. Many large contractors bid the work to outside engineering firms. In either case, the contractor's engineers may be no more or less aware of construction efficiencies than a third party.

4. Because of the design risks assumed by the contractor, a contingency factor will be added to the price.

5. By necessity, there will be a large number of subcontractors furnishing individual items of equipment to the turnkey contractor. Other than initial approval, the owner has no control over subcontractors.

6. The contractor's and owner's interests are not identical. The contractor has an incentive to provide the least costly quality for the fixed price and does not profit or lose nearly as much as the owner with timely delivery. Therefore, the owner must provide inspection and expediting. It is very difficult to do this for subcontractors where no direct commercial relationship exists.

Negotiated Turnkey. The negotiated turnkey format recognizes that, before the detail engineering is complete, it is difficult for a contractor to provide a fixed price for the work while maintaining adequate owner control. In this format, the design and detail engineering are performed (normally for a fixed fee), so that long-delivery items can be placed on order prior to completion of detail engineering. Once the scope of work is defined, a turnkey price is negotiated.

The advantages claimed for this format are the same as those for the turnkey format with the added advantages of maintaining owner control and reducing contractor's design risk. The disadvantages are identical with the added disadvantage of eliminating much of the owner's leverage when it comes to negotiating the final contract.

Modified Turnkey. In the modified turnkey format, each work item is separated and bid turnkey as the scope of that work item is defined. In the previous two formats, the prime contractor does this in bidding out items of equipment to subcontractors. The difference in this format is that the owner, or engineering consultant, do the bidding, awarding, and expediting. In addition, those items which are "sole sourced" to the contractors construction arm in the two previous formats must be bid

and evaluated. The main advantages claimed for this format are (1) control of the project is maintained, (2) competition is maximized as individual work items can be bid to firms specializing in such work, (3) owner's inspectors and expeditors have a direct commercial relationship to all suppliers, and (4) contractor's risk and contingency is controlled to the extent desired by owner. For example, scope of work contingency can be eliminated while weather contingencies are included.

The disadvantages with this format are (1) increased coordination of the contracts is required by either the owner or the engineering consultant, (2) the owner, or consultant, must develop and monitor the plan of execution rather than this being a function of the turnkey contractor, and (3) engineering and project management costs are explicitly determined and not hidden in contract cost.

Cost Plus. The cost-plus format requires the contractor to be reimbursed for all direct costs plus a percentage of costs for overhead and profit. Typically, this format is used where risk is high, or when there is insufficient time to solicit firm bids. Such a case would occur if construction were required within an operating plant, it were necessary to repair storm damage, or a simple field routing job were envisioned. The major disadvantage of this format is that the owner bears the risk of inefficient labor and job organization.

Comparison of Formats. The type of project format to employ depends on the nature of the project, the type of contractors available and their competitive position, and the priorities of the owner. There is no one answer as each project is different and competition and priorities change from time to time.

The author had the opportunity to be involved in two similar projects for the same owner, which occurred almost simultaneously. One was set up as a turnkey format and the other in a modified turnkey format to test the validity of the claimed advantages and disadvantages. The cost of the modified turnkey approach was 15% less, and it took 10% less time to complete because of greater owner control of the schedule. On another recent project, the design was done by the owner and each work item bid out separately. In addition, two turnkey bids were solicited from companies who expressed a desire to construct the complete installation. The additional cost for awarding the low turnkey bid would have been 40% more than the cost of awarding 10 individual bids.

Project Control

No matter what the project execution format, it is necessary to implement procedures for controlling both project cost and timing. The most important part of project control begins at the outset of the project with controlling the engineering effort. Priorities set and decisions made at this point will affect project timing and cost throughout the job.

An activities schedule will help in project scheduling. This is a detailed plan of execution for the project's engineering phase and is similar to, but more detailed than, the overall project plan of execution described previously. When preparing the activities list, an effort should be made to separate activities into logical cost categories.

The main tool for project cost control is the preliminary cost estimate developed during project definition, which lists budget costs for each item in the plan of execution. Budgets should be established for scheduled work packages. It is important for cost control purposes that activities have definite starting and ending points.

Costs are periodically updated as the project becomes better defined. Differences can then be explained and total project cost revised—even before the first item is purchased. As bids are awarded and commitments are made, the total project amount can be adjusted accordingly.

Accounting for costs can be routine, but controlling costs is another matter. Once a project is committed, a large part of final cost is beyond control of the project engineer. It is not unusual for bid items to vary significantly from time to time because of contractor work load, weather conditions, and availability of equipment. Also, difference in price between low bidder and next low bidder can vary 10 to 20%. If the low bidder had not been included in the bid list, item cost would be that much higher. On a recent project, the sum of second low bidders' prices was 5% higher than that of low bidders.

Early in the project, timing is controlled through the engineering effort to ensure that bids are sent out, evaluated, and awarded in accordance with the project plan of execution. Once bids are awarded, the inspector and/or expeditor are responsible for determining if work is progressing on schedule. A schedule thus must be worked out with the successful bidder, preferably before bid award. When delays are spotted, meetings with the contractor are required to return the job to schedule. On occasion, it may be necessary to appeal to higher levels of management in both companies. The sooner a problem is spotted, the better the chance that corrective action can be agreed on. On large complex projects, the use of computer-based network analysis of activities is sometimes beneficial.

Nomenclature

A_d = area of deck, sq ft
 b = width (breadth), ft
 b_p = width (breadth) of the plate section perpendicular to the axis of water flow, ft
 C_d = dispersion constant
 C_E = constant for erosional flow
 C_{HW} = constant with a value of 80 to 140, depending on the inside pipe material and its age
 d_d = oil droplet diameter, micrometers
 $(d_d)_{\max}$ = maximum oil droplet diameter, micrometers
 d_i = pipe inside diameter, in.
 d_p = particle diameter, microns
 E = flow efficiency, fraction
 E_p = pump efficiency at flow conditions
 E_{rc} = removal efficiency on any cycle of a particular drop size
 E_{ro} = overall particle removal efficiency

f = friction factor
 f_V = volume fraction of the dispersed phase
 F = factor to account for turbulence and short circuiting
 h_f = height of flume, ft
 K_s = empirical settling constant
 L = length of line or length of plate section parallel to the axis of water flow, ft
 L_1 = inlet distribution section
 L_2 = outlet gathering section
 L_{bs} = length of baffle section, ft
 L_e = effective settling section
 L_p = perpendicular distance between plates, in.
 N_c = number of cycles of no flow a particle sees as it traverses the baffle section
 N_{Re} = Reynolds number
 p_{bh} = brake horsepower
 p_1 = pressure at pipe inlet, psia
 p_2 = pressure at pipe outlet, psia
 q_g = flow rate of gas at standard conditions, MMscf/D
 q_L = liquid flow rate, B/D
 q_r = rainfall rate, in./hr
 q_w = bulk water flow rate, BWPD
 t = time for the dump cycle, seconds
 t_c = time valve is closed, seconds
 t_r = retention time, minutes
 t_s = time particle is falling while in effective section of flume
 t_w = time water is in effective section of flume
 v_{gf} = velocity of gas at specific flow conditions, ft/sec
 v_s = settling velocity, ft/sec
 Z_{fl} = friction head loss, ft of liquid
 Z_p = height of the coalescer plate section perpendicular to the axis of water flow, ft
 Z_w = height of water column, ft
 γ_g = specific gravity of the gas at standard conditions relative to air
 γ_L = specific gravity of liquid relative to water
 $\Delta\gamma$ = difference in specific gravity relative to water
 $\Delta\gamma_{ow}$ = difference in specific gravity between oil and water
 θ = angle of the plate with the horizontal
 μ_{gf} = viscosity of gas at specific flow conditions, cp

References

1. Daugherty, R.L. and Ingersoll, A.C.: *Fluid Mechanics with Engineering Applications*, McGraw-Hill Book Co. Inc., New York City (1954) 205.
2. "Flow of Fluids Through Valves, Fittings and Pipe," Crane Co., Houston (1969) Technical Paper 410, 1-8.
3. *Design and Installation of Offshore Production Platform Piping Systems*, third edition, API RP14E, API, Dallas (1981) 22.
4. *API Specification for Polyethylene Line Pipe (PE)*, third edition, API Spec. 5LE, API, Dallas (Nov. 1981).
5. *API Specification for Thermoplastic Line Pipe (PVC and CPVC)*, fifth edition, API Spec. 5LP, API, Dallas (Nov. 1981).

6. *API Specification for Reinforced Thermosetting Resin Line Pipe (RTRP)*, fourth edition, API Spec. 5LR, API, Dallas (March 1976).
7. *API Specification for Line Pipe*, 33rd edition, API Spec. 5L, API, Dallas (March 1983).
8. *Recommended Practice for Application of Cement Lining to Steel Tubular Goods, Handling Installation and Joining (Tentative)*, first edition, API RP 10E, API, Dallas (March 1978).
9. *American National Code for Pressure Piping, Power Piping*, ANSI B31.1, American Soc. of Mechanical Engineers, New York City (1977).
10. *ASME Code for Pressure Piping, B31, Chemical Plant and Petroleum Refinery Piping*, ANSI/ASME B31.3, American Soc. of Mechanical Engineers, New York City (1980).
11. *American National Standard Code for Pressure Piping, Liquid Petroleum Transportation Piping System*, ANSI/ASME B31.4, American Soc. of Mechanical Engineers, New York City (1979).
12. *American National Standard Code for Pressure Piping, Gas Transmission and Distribution Piping Systems*, ANSI B31.8, American Soc. of Mechanical Engineers, New York City (1975).
13. *American National Standard, Pipe Flanges and Flanged Fittings*, ANSI B16.5, American Soc. of Mechanical Engineers, New York City (1981).
14. *API Specifications for Wellhead Equipment*, 14th edition, API Spec. 6A, API, Dallas (March 1983).
15. "Oil-Water Separator Process Design," *Manual on Disposal of Refinery Wastes, Volume on Liquid Wastes*, API, Dallas (1975) Chapter 5.
16. Brunsmann, J.J., Cornelissen, J., and Eilers, H.: "Improved Oil Separation in Gravity Separators," paper presented to the 1959 API Committee on Disposal of Refinery Wastes, Denver, Oct. 14-16.

Chapter 16

Automation of Lease Equipment

G.R. Burrell, Exxon Co. U.S.A.*

Introduction

Automation in the oil and gas producing industry covers a broad spectrum of supported functions. In a simple application, automation may be defined as linking together instruments and controls to perform lease-operating procedures automatically in a predetermined manner. Automation in a more complex environment will have digital computers in some form of a supervisory control and data acquisition (SCADA) system. Automation in the industry has tended to evolve as new tools become available and are accepted by industry and regulatory agencies. Generally, automation has advanced by a more complex linkage of instruments and control devices. Some of the more important tools and/or techniques that have enhanced lease automation are (1) solid-state electronics, (2) lease automatic custody transfer (LACT), (3) tank battery consolidation, and (4) SCADA.

Solid-State Electronics

The development of solid-state electronics first as discrete components and then as integrated circuits has been a key factor in advancing lease automation. Electronics have provided the base for improvements in instrumentation, control elements, communication, and digital computers that form the primary components of enhanced automation facilities. Pneumatic and electromagnetic (relay) logic have been, and will continue to be, used in various forms of automation, but the extent of logic implementation is limited substantially compared with that available for electronics. Pneumatic and/or electromagnetic functions are effective as complementary features to electronic forms of automation and as stand-alone automation for less complex applications.

Microprocessors and their extension to microcomputers are having an impact on automation that may well

exceed that of integrated circuits in the initial form of "hard-wired" logic. Microcomputers combine the advantages of electronic components and program instructions into a flexible, capable, and reliable form that has substantial advantages for automation. These functional advantages have been complemented by a reduction in cost compared to implementation with integrated circuits. Microcomputers are being used in almost every component of automation related equipment from individual instruments through digital computers.

Lease Automatic Custody Transfer (LACT)

LACT is the process of transferring (running) lease-produced oil into a connected pipeline on an unattended basis. LACT includes the capability to determine automatically the quantity and quality of oil being transferred and the control functions to prevent transfer of unacceptable quality and/or volumes. Before LACT, lease oil was produced into a tank, quantity and quality (opening gauge and thieving, etc.) were determined, and a valve was opened to the pipeline to initiate transfer. When the transfer was complete, the pipeline valve was closed and a final (closing) gauge was made as basis for determining net volume transferred. All these steps were manual activities with some related duplication of effort between the lease operator and the pipeline gauger. In addition to being labor intensive, the process was inherently inefficient in use of related treating and storage facilities. LACT is an important tool in the evolution of lease automation. LACT is a significant automation element and has been widely accepted and implemented by industry. In addition, it has become an important building block for other forms of automation in lease operations.

Tank Battery Consolidation

Many oil and gas fields have multiple operators or working interest owners. In addition, most fields consist of a number of separate leases (common royalty ownership,

* Author of the original chapter on this topic in the 1962 edition was Don R. Patterson.

etc.) that require individual oil and gas processing (separation, treating, storage and transfer, etc.) facilities to account for production to each owner.

LACT initially was applied to these separate lease operations. The automatic transfer of produced oil and recycling of unacceptable quality oil [high basic sediment and water (BS&W) content] to treating facilities increased the effectiveness of treating and storage equipment. In addition, the incremental cost of larger meters, pumps, and related equipment of LACT's was low compared to the increased oil volume transfer capability. Thus, a technical basis was available to process and transfer much higher produced-oil volumes than present on the average lease.

Historically, individual lease oil-production volumes had been treated to pipeline quality (2% BS&W or less) before custody transfer from the lease. In the 1960's, regulatory agencies began to approve operator requests to commingle wet-oil (not pipeline quality) production from multiple leases into a common or central oil processing and custody transfer facility. Oil production from each lease was determined by measuring the wet-oil volume (separator positive-volume or positive-displacement meters, etc.) and correcting for water content with automatic samplers and later with capacitance probes and related net-oil computers. Final sales volume to each separate lease was determined by allocating the custody transferred (sales) volume back to each lease on the basis of its proportion of total wet-oil lease measurements. In other cases, tank battery consolidation was implemented when a field was unitized under a single operator for initiation of secondary recovery activities.

Tank battery consolidation eliminated oil treating and storage facilities on the individual lease. In some fields, the pipeline trunk lines used to gather individual lease oil volumes were converted to wet-oil gathering lines for the consolidated tank battery operation. Tank battery consolidation converts a field's operation from a number of stand-alone lease functions to a central process with multiple inputs. Oil treating and storage, water treating and disposal, vapor recovery facility, etc., became more efficient and controllable in the consolidated environment.

Supervisory Control and Data Acquisition (SCADA)

SCADA is a common name applied to computer-driven automation systems used in oil and gas production operations. Basic functions generally include status/alarm reporting, production volume accumulation/reporting, well testing, and control. These systems vary from small units that are applied to only a few leases in a single field to large units that serve multiple fields containing several thousand total wells.

SCADA systems are tied directly to the instrumentation and control devices on the process equipment used in oil and gas production. This provides timely and continuous access to the operational information being sensed by the instrumentation. Some SCADA systems emphasize data gathering and reporting to operating personnel for "open-loop" control while others use program logic to analyze input information and initiate control actions directly ("close-loop" control). SCADA

systems may be oriented primarily to operating personnel needs, or they may be multipurpose by providing functions for operating, accounting, engineering, and management groups.

SCADA is a logical extension of automation in the sequence from manual lease operation, to use of LACT, and then to centralized treating, storage, and automatic custody transfer (ACT) with tank battery consolidation. This sequence moved from essentially independent individual lease operations to a single overall process that has a number of closely related functions. SCADA provides the ability to obtain timely operational information for optimization of the interrelated process functions. For example, if a compressor outage reduces the gas processing capacity below a field's gas-producing rate, well-test information from SCADA allows shutting-in of wells with high GOR's and thus minimizes reduction of the related oil producing rate. In general, timely and accurate operational information can be used to obtain maximum utility of existing process equipment and minimize need for stand-by capacity.

Some form of automation is used on every lease that produces oil and gas. The extent of practical automation depends primarily on economics. Some of the benefits of automation that may be used in the economic justification are as follows:

1. Capital investment in lease production equipment is reduced.
2. Operating expenses are reduced through savings in labor costs, maintenance expenses, travel expenses, and power and fuel costs.
3. Ability to initiate and document actions required for regulatory compliance is improved.
4. Surveillance capability of management and supporting staff groups is improved.
5. The quantity and quality of operational information available for making business decisions is increased, which results in revenue increases and operating cost decreases.

Automation in oil and gas production activities will continue to evolve as additional tools are developed and applied. Most advances (including improved communications and "smart" end devices) will take the form of (1) improvements in existing devices, (2) new devices with improved capability/reliability to replace older equipment, and, less frequently, (3) new devices with new features/functions that are applicable to the production process. Much of the basic instrumentation and control equipment (primarily pneumatic-based) that has been used for years with oil and gas processing facilities will continue to be applicable. Implementation of some form of enhanced automation (as described earlier) will be a primary force to increase use of electronic and electronic/pneumatic equipment. On this basis, it appears reasonable to elucidate the topic of automation first by discussing some of the commonly used equipment and then by depicting equipment application in automation systems.

Automatic Production-Control Equipment

Automatically Controlled Valves and Accessories

Automatic control valves can be classified in a number of ways, but classification by the energy medium that actuates the valve operator is most pertinent to automation.

By using this method of classification, automatic control valves can be grouped into three major categories: fluid-controlled valves, electrically controlled valves, and fluid-electric-controlled valves. In the latter category a fluid energy generally is used to operate the valve and electric energy is used to control the fluid-energy source.

Fluid-Controlled Valves. The most common types of automatic fluid-controlled valve operators are diaphragm operators and fluid cylinders. Both of these valve operators can be used on any style of valve body whose inner valve can be positioned by longitudinal displacement of the valve stem. The fluid cylinder operator normally is used with valve-body styles requiring 90° rotation for operation. Diaphragm operators most commonly are applied to valves that have globe, angle, butterfly, and Saunders-type valve bodies. Fluid-cylinder operators are more commonly used with plug valves.

In oilfield applications, the most common fluid used to actuate both valve operators is natural gas, generally taken directly off a separator or heater-treater on the lease. If natural gas is not available, or if for some reason the available natural gas supply is not suitable, a bottled gas (nitrogen, etc.), compressed air, or hydraulic fluid could be used. Diaphragm operators normally require only 15- to 30-psi fluid pressure to actuate the valve. Pressures up to 100 psi and over often are desired for the fluid cylinders because, the higher the fluid pressure available to operate the cylinder, the smaller size the cylinder may be, and consequently the lower the cost. Valves using these types of operators, as a class, are frequently called "pneumatic control valves" even though the control fluid may be something other than air.

Some fluid-controlled valves can be controlled with the fluid flowing in the line in which the valve is located. These types of valves generally use the differential pressure principle for control purposes. A reference control pressure is established by spring-loading or pressure-loading the valve operator. The control valve is actuated when the line pressure upstream and/or downstream sensed by the valve operator algebraically exceeds the reference control pressure—i.e., the valve can be actuated by pressures either excessively high or excessively low, or both. This feature makes this type of valve particularly suited for use as safety shut-in valves on wellheads.

Electrically Controlled Valves. Automatic electrically controlled valve operators are of two general types, electric-solenoid (or magnetic) and electric motor. Magnetic operators are used for valves requiring longitudinal motion to position the inner valve. The use of magnetic operators generally is limited to valves 2 in. and smaller in size and of relatively low working pressures. Electric-motor operators can be used with any type of valve but in all cases must include accessories that provide a torque-limiting means and a limit switch to prevent damaging the motor when either extreme valve position is reached. On valves requiring longitudinal motion to seat the inner valve electric-motor, operators also must include a gear rack and pinion to convert the motor's rotary motion to longitudinal displacement. Because of the relative expense of electric-motor

operators, they normally are used only on large-sized valves and/or valves having high working pressures.

Fluid-Electric Controlled Valves. Self-contained valve operators in the third category are generally hydroelectric-type operators. Operators of this type essentially consist of a self-contained reservoir of hydraulic fluid, a small electric motor, a pump, and a fluid-cylinder device—all within a single housing. The fluid-cylinder principle limits this type of operator to valves requiring longitudinal motion or 90° rotation to seat the inner valve. Valve operators of this type are available for a wide variety of valve sizes and working-pressure ranges.

In addition to the hydroelectric-type operators, any of the fluid-controlled operators mentioned can be made combination-type operators. By the addition of electric-solenoid valves in the fluid-control lines, an electric signal can be used to control the release of fluid energy to the valve operator. Combination-type operators of this kind are commonly called "electropneumatic operators."

Valve Switches. It is frequently essential that an automatic control system be able to sense the position of certain valves whether automatically or manually operated. This is accomplished by means of a "valve switch" coupled directly to the stem of the valve in question. In electrical control systems, the valve switch may be a mercury switch, a microswitch, or a position-sensing switch. In pneumatic control systems, the "valve switch" is a three-way pilot valve. The switches may be adjusted to open or close a circuit as the valve opens and closes. One of the most common applications of valve switches is on tank-run valves, in which case they are generally called "pipeline valve switches." Another common use of valve switches is to indicate remotely the operational position (open, closed, etc.) of automatic control valves on wellheads, well manifolds, metering-tank inlets and outlets. In these general applications, valve switches normally will be referred to as "limit switches." When interlocked with an automatic control system, valve switches perform the very important function of preventing subsequent steps in an automatic operation from proceeding unless certain valves are in the proper position. Other type devices can be used to sense "control" valve positions at intermediate points (or continuously) between the open and closed positions.

Automatic Production Programmers

Time-Cycle Controller. Automatic production programmers are scheduling devices that control the particular times and lengths of time that operating functions are performed. The simplest form of automatic production programmer is a time-cycle controller. A time-cycle controller basically consists of a clock with a timing wheel or wheels, containing a number of programming points at regular intervals around its circumference. The clock may be electrically driven, gas driven, or mechanically driven by a spring. It may have a 1-, 2-, 4-, 6-, 8-, 12-, or 24-hour rotation period, the rotation period being the time required for the timing wheel(s) to

make one complete revolution. Programming is accomplished by positioning the contacts on the timing wheel(s) such that the rotation of the wheel(s) generates the proper control signal to open or close valves controlled by the time-cycle controller at the proper times.

As commonly applied, a time-cycle controller in conjunction with a diaphragm control valve compose a "stopcock controller" and/or an "intermitter controller." The primary difference in a stopcock controller and an intermitter controller is in the application. A stopcock controller generally is installed in a well's flowline at the Christmas tree. It controls the times that the well is opened for production, normally for short intervals several times a day. An "intermitter controller" is installed in high-pressure-gas supply line at the wellhead of a well being gas lifted intermittently. It controls the times that gas is admitted to the well to actuate the gas-lift valves and lift the fluid to the surface. A time-cycle controller in conjunction with any type of automatic control valve may be used to produce a naturally flowing well where it is desired to produce the well less than 24 hours per day and/or 7 days a week.

A time-cycle or percentage-time controller plus a motor starter basically compose an automatic production programmer for an electrically driven rod-pumping unit. The rod-pumping unit controls also generally contain several safety devices: undervoltage relay, which drops out on power failure, overload relays to prevent burning up the motor, lightning arrester, circuit-breaking devices, etc.

The electronic (solid state) timer frequently is used in new installations that require timer functions. Mechanical and electro-mechanical timers will continue to be used in many existing installations.

Any time that these automatic production-programming devices are actuated electrically, the control point for individual wells may be centralized at the well manifolds, a central point on the lease, or even a point remote from the field. The time-cycle controllers, automatic control valves, motor starters, etc. still may remain located at the wellheads while control is exercised remotely. This is not true for similar devices that are actuated pneumatically unless the pilot gas for these devices is controlled electrically. Too much dampening and distortion occurs in pneumatic control signals for effective control when transmitted distances of more than about 150 ft.

Other Programmers

The programmers discussed previously have been used in oil and gas production facilities for many years. Currently, the more complex sequential control will be electronic- and combined electronic/pneumatic-based in many applications. This trend is expected to increase as general-purpose programmable controllers, developed initially in the plant applications, find more use in oil and gas production. The functions of the programmable controller and the remote terminal unit (RTU) may well be combined into a more capable unit for oil and gas production monitoring and control applications.

Production Safety Controls

In some respects, virtually all automatic control equipment is also safety-control equipment: automatic control

equipment nearly always is made to be "fail safe"—i.e., upon loss of power from the controlling energy medium, the controls return to the position that will result in the safest condition. Some automation controls, however, primarily perform safety functions rather than normal operational functions. These include high-/low-pressure safety shut-in valves, excess-flow valves, pressure and temperature switches, and pump-off controls.

Safety Shut-In Valves

High-/low-pressure safety shut-in valves and excess-flow valves are both fluid-controlled valves of the type that is actuated by line fluid. This valve type was discussed briefly in the section on automatic control valves. The use of an excess-flow valve or low-pressure control with a safety shut-in valve primarily safeguards against a flowline break and the resultant loss of oil and surface property damage. High-pressure control with a safety shut-in valve guards against pressures in excess of the allowable limit building up in the flowline. Either of these two kinds of valves normally would be installed at the wellhead.

Pressure Switches

Another means of protecting against excessive flowline pressures and/or flowline breaks is the use of a pressure switch and an automatic control valve. Pressure switches are available that produce either an electric or pneumatic signal, as required, to actuate the automatic control valve. On rod-pumped wells, the control signal from the pressure switch also must shut down the pumping unit—i.e., turn off the switch on an electric motor or ground the magneto on an internal-combustion engine. On rod-pumped wells that have no tendency to "head" or flow when the pumping unit is shut down, the automatic control valve may be omitted.

A "pressure switch" in the sense it is used here consists primarily of a pressure-sensing element, limit pressure contact(s), and an electrical, mechanical, or pneumatic means to transmit the control signal to the object(s) controlled by the pressure switch. The pressure-sensing element is commonly a bourdon tube, though some requirements could necessitate the use of a helical-, spiral-, diaphragm-, piston-, or bellows-type pressure-sensing element. In electrical control systems, the displacement of the pressure-sensing element is made to "make" or "break" an electrical switch, normally a mercury or microswitch, when the line pressure reaches the preset pressure limit(s). In pneumatic control systems, reaching the preset pressure limit(s) may actuate a pneumatic transmitter, relay, or slide valve.

Liquid-Level Controls

Another automatic safety-control device, which also frequently performs an operational-control function, is a liquid-level controller. These devices commonly are used to control liquid levels in separators, heater-treaters, storage tanks, surge tanks, accumulator vessels, metering vessels, etc. They may be used (1) to control high liquid levels to prevent running over a vessel, (2) to control low liquid levels to maintain pump submergence, (3) to control intermediate operational levels to open and close dump valves, to start and stop pumps, etc., or (4) to maintain the interface of two liquids at a given level.

There are many types of liquid level controls. Some of the more common types of level control devices used in production equipment are float operated, pressure operated, ground-level tank gauges, electric and/or electronic, sonic, and vibration. A float-operated level switch generally consists of a spherical or cylindrical float attached to one end of a mechanical lever with either an electrical switch or a pneumatic relay on the other end. The switch or relay is located in a separate portion of the device housing and is isolated from the float area with a pressure seal. The float is displaced by the rise and/or fall of the liquid level being controlled and the motion is transmitted through the pressure seal to activate the switch/relay. A pressure level control switch may control liquid level on the basis of either differential or static pressure. The differential type devices commonly are used as a form of "pilot operated" dump valves on pressure vessels. The static pressure devices frequently are used for well shut-down service and level control in tanks.

Ground level tank gauges consist of tape, tape drum, and a tank gauge float that are linked to cause the tape to be spooled on and off the tape drum as the liquid level rises and falls within the tank. By extending the tape drum shaft and using appropriate cams, gears, etc., electrical or pneumatic control systems may be activated to control liquid levels in the tank. One type of sonic level control consists of a sound transmitter and receiver that are suitably arranged for separation by the liquid being controlled. The transmitter and receiver are driven with an electronic circuit that can measure the intensity of the sound reaching the receiver. The change in the received sound intensity between air/gas and the liquid as the separation material can be used to sense and control a liquid level. Ultrasonic level devices sense the reflection of a sound wave from the gas/liquid interface and use the delay time between transmitting and receiving to determine distance from sensor to liquid level.

Some liquid level devices induce vibration into a detecting element. The degree of vibration dampening caused by the medium surrounding the element can be sensed to differentiate between gas and liquid materials. Electric and/or electronic level controls depend on the different electrical properties (capacitance, conductance, etc.) of the liquid to be controlled and that of the related medium (air, gas, and/or other liquid). An electronic circuit is used to sense the change in electrical property as the liquid level changes and thus controls the level as required.

Other types of level controls are available for specific installation needs. Level controllers should be selected to provide the required function in the least complex and most reliable form. It is advantageous to select equipment that has demonstrated satisfactory application experience within the operating environment that is to be controlled.

Automatic Quantitative Measurement

Gross volumes frequently must be adjusted by quantitative measurements such as water content, temperature, pressure, and density before net volumes at standard conditions can be determined. Several of these quantitative parameters are necessary for automation of lease operations.

Liquid Measurement

There are three types of quantitative (volume) devices commonly used for automatic liquid measurement on the lease: positive-volume meters, positive-displacement meters, and inferential meters. Positive-volume meters are essentially extensions of tank measurement with automatic "filling" and "running" functions. Positive-displacement meters "trap" a fixed volume of liquid within moving elements of the meter. Inferential meters measure liquid by detecting some property of the moving stream that is a basis for determining volume indirectly.¹

Positive-Volume Meters. Positive-volume meters operate on a "fill" and "dump" cycle rather than being a continuous operation. This type meter is essentially the automatic gauging of a tank by using level controls to move a fixed volume through the tank on each complete cycle. The volume that is "dumped" or measured is related to the displacement volume in the meter between the high "fill" point and the low "dump" point in the meter. Various types of level controls are used to control the fluid levels in the meter. Each complete "fill" and "dump" cycle is registered on a counter as a basis for total volume determination. Since the positive-volume meter is cyclic with a separate "fill" and "dump" period, allowance for handling produced volumes while the meter is in the "dump" cycle must be made. Continuous operation is possible by having a pair of meters that are sequenced to have alternating cycles. This essentially requires duplication of facilities and some increased complexity in the controls. A more common arrangement is to provide surge volume capacity upstream of a single meter.

Volume-type dump tanks or meters have been built in a variety of shapes and volumes. Capacities per dump have ranged from less than ¼ bbl to several hundred barrels. The metering chamber may be in a stand-alone vessel or it may be an integral portion of a vessel such as a separator or heater treater. The positive-volume meter is not as compatible with qualitative measurement as the positive-displacement and inferential meters since the volume measurement cannot be separated easily into smaller increments to drive sampling and other qualitative measurement devices.

Positive-Displacement Meters. A positive-displacement meter, regardless of specific type, consists of two primary elements: a stationary case and a mobile element, which acts to isolate within the case fixed volume of fluid each cycle of operation. The mobile element may be a rotor with sliding vanes, rotatable vanes, or rotatable buckets. It may be two rotors that mesh somewhat similarly to two helical or cycloidal gears as they rotate. The mobile element may be a disk that nutates about a camlike follower in three-dimensional motion or a cylinder that oscillates about a cam follower in two-dimensional motion. Or, finally, the mobile element could be a conventional piston such as that found in a power pump. Most positive-displacement meters are, in fact, closely akin to positive-displacement pumps.

Positive-displacement meters rapidly became the standard for ACT use. The positive-displacement meter provided a less costly and less complex facility than the

positive-volume meter. In addition, the positive-displacement meter provides a means to drive samplers and/or net oil computers with signals on a small increment of volume that is more compatible with automatic qualitative measurement requirements.

Care must be exercised in the installation design for a positive-displacement meter. All free gas must be removed upstream to avoid spinning the meter, which would cause erroneous readings and, possibly, damage to the meter. For greatest accuracy, a constant flow rate should be maintained through the meter and at a rate at least 15% or greater of the rated capacity of the meter. Standards for calibration frequency, methods, etc., are set forth in API Std. 1101.¹

Inferential Meters. The turbine meter and the orifice meter are commonly used inferential meters for liquid measurement. These meters indirectly determine volume by sensing some property of the moving stream that can be related to volume. For example, the rotation of the turbine blades in the turbine meter and the differential pressure developed across the orifice plate in an orifice meter can be used as basis of volume determination.

Turbine meters became important in volume measurement when electronics were accepted as an element of a measuring device. The rotation of the turbine blades can be sensed electronically without need for any mechanical connection to the turbine rotor. This provides a simple arrangement that is inherently reliable and particularly suitable for high-pressure service. Thus, turbine meters initially were applied to measure injection water volumes. However, high-viscosity fluids drastically reduce the range of turbine meters.

Turbine meters are being used for well testing and wet-oil lease production measurements when combined with net-oil computers. These meters tend to be more tolerant of short over-range periods and sandy fluid than are positive volume meters. Turbine meters also are being used for ACT, particularly for high-volume and/or high-pressure service.

Orifice meters are used more commonly for gas measurement but they have some applications in liquid measurement. Compressible liquids that require pressure correction for volume determination frequently are measured with orifice meters.

Gas Measurement

The primary device for lease gas volume measurement has been and continues to be the orifice meter, which initially measured gas volume by using a mercury manometer before development of the bellows-type chart recorder. Orifice meters have these advantages: (1) no moving parts in the gas stream, (2) the ability to handle wide range of flow rates (long term) by means of plate size changes, (3) reliable and nonexternal powered recorder, and (4) a reliable sensor (bellows). The chart recorder is not compatible with automatic data acquisition; other types of gas measurement devices are used with SCADA. These gas measurement devices include positive-displacement meters, gas-flow computers, turbine meters, and vortex meters.¹

Positive-Displacement Meters

The installation of SCADA systems with automatic well

testing generated a need for gas measurement over a wide flow range with direct readout capability. The "rotary" positive-displacement gas meter is similar to the liquid "lobed-impeller" or gear-type meter. The rotary gas meter has the capability to measure gas accurately over a range of about 15 to 1 compared with about 4 to 1 for an orifice meter with a fixed orifice plate size. The rotary meter can be equipped with mechanical compensation on indicated volume for static pressure and flowing temperature corrections. The rotary meter needs to be protected from over-range and liquid accumulation within the measuring elements. These meters are usually applied to low-pressure gas measurement service.

Gas-Flow Computers

Gas-flow computers were developed to use existing orifice-meter runs and to provide a direct readout of gas volume that was compatible with SCADA. These devices use static and differential pressure electrical transducers on a standard orifice meter as a basis for gas measurement. The computer integrates the signals from the transducers and combines with fixed data on meter run size, plate size, etc. to develop a gas volume. The volume readout will be in the form of a switch closure that will register on an internal counter and provide input to electronic counter in an RTU.

Some gas-flow computers can accept a temperature transducer input to measure temperature of flowing gas stream for improved accuracy of volume measurement. Computers also may have capability to use two differential pressure transducers (e.g., 0 to 20 and 0 to 200 in.) and to select input from the unit providing most accurate instantaneous reading for integration. Early gas-flow computers were analog devices. Many current designs are digital units based on a microcomputer. The flow computer integration function also is being done by the microcomputer-based RTU. All designs have integration accuracy compatible with the basic measurement capability of the orifice meter.

Gas Turbine Meters

Gas turbine meters also are used to obtain direct readout on gas volume measurement that is compatible with SCADA. Turbine meters can measure gas volumes accurately over a range of about 20 to 1 at medium pressures. Rangeability tends to increase with increasing static pressure. These meters are usually somewhat less subject to over-range damage than the positive-displacement meter if over-range period is of short duration. Meter proving and checking may require installation of prover loop for a master meter. Gas turbine meters can be equipped with temperature and static pressure volume compensation capability. Many gas (or liquid) turbine meters are destroyed when they are over-ranged while pressuring up the system.

Vortex Meter

Vortex meters have a "bluff body" that spans the flow area through the meter and causes vortices to form in the flowing medium. These vortices are shed off the bluff body at a frequency that is proportional to the volumetric flow rate through the meter. The vortices can be

“counted” with suitable pressure or other flow pattern sensors, which are connected to an electronic component for flow accumulation. Vortex meters have rangeability characteristics similar to positive displacement and turbine meters without the moving parts of these devices.

Temperature Measurement

Types of temperature-sensing devices commonly used in oil and gas production include filled-thermal, resistance thermal detection, thermocouple, thermister, and solid-state. The filled-thermal device operates on the basis of the principle that a fluid expands or contracts with changes in temperature. The device consists of a temperature-sensitive bulb connected by capillary tubing to an expansible element that is sensitive to pressure change. The bulb may be filled with a liquid, a liquid and its vapors, or a gas. The expansible element may be a diaphragm, a bellows, or a bourdon tube.

The *filled-thermal* device has sufficient output force to be used directly for temperature compensation on positive-displacement meters used for LACT. The bellows assembly is connected to an infinitely variable transmission, which corrects the meter's volume output to a base temperature of 60°F.

A *resistance thermal detector* (RTD) works on the principle that a change in resistance of a wire is related directly to a change in temperature of the wire. The device consists of a resistance element (sensing element) and a related electrical circuit, which uses the changing resistance of the element to control an output signal. The output signal can drive recorders and controllers.

A *thermocouple* works on the principle that heat applied to one end of two strips of metal of different composition, which are bonded at either end, develops an electromotive force (EMF) that is proportional to the temperature. Thermocouples may be of the wire type, in which both elements are in wire form, or of the Pyrod type, in which one element is a closed tube and the other a wire welded to the inside bottom of the tube. The thermocouple is connected to an electrical circuit, which senses the generated EMF and develops an output signal that can drive recorders and controllers. Thermocouple devices are used in applications where temperatures may exceed 1,000°F.

Thermister and *solid-state* devices exhibit a resistance change with temperature change. Both these devices respond rapidly to a temperature change because of the small mass of the sensing element. Electrical circuits are required to convert the “sensed” resistance change into an output signal that is proportional to temperature.

Automatic Sampler

An automatic sampler is a device that removes a representative volume of fluid from a moving stream and retains it in a container for later processing and analysis. Factors that improve probability of obtaining a representative sample include the following: (1) sampling probe should be located in a vertical downrun of pipe at the center of the pipe and with probe opening facing upstream; (2) the total flowstream should be in turbulent flow; (3) sample size and sampling interval should be such that the sample is proportional to the total stream flow; (4) sample metering chamber should be closely coupled to sampler probe and located below the center

line of sample probe; and (5) samples should be collected and stored at pressures exceeding the vapor pressure of the sample liquid to prevent evaporation and deterioration during storage.

Samplers also are used with positive-volume and positive-displacement meters in well testing and wet-oil (not pipeline quality) lease volume measurements. Representative sampling becomes more difficult with increasing water content in the oil stream. For improved accuracy, fluid mixtures that may have both free water and oil emulsion (oil-external phase) components should be processed through a three-phase separator before the remaining oil emulsion stream is sampled.

The capacitance probe and net-oil computer have not replaced the automatic sampler on most LACT installations because (1) crude oil value frequently is based on gravity (determined on sample volume), (2) the gross-oil volume available directly from LACT counters is satisfactory for daily operating needs, and (3) the potential operating cost reduction by eliminating sampler use is not significant. Most major purchasers will have a recommended (or required) design for automatic sampler installation.

BS&W Monitor

Pipelines specify the maximum BS&W content that a crude oil may contain to be acceptable for transfer. The development of LACT equipment required a means to monitor the quality of crude oil as it was being measured and transferred automatically to a pipeline. The commonly accepted device for this function is a capacitance probe BS&W monitor. The dielectric constants of crude oil and water are about 2 and 80, respectively. The BS&W monitor uses a concentric probe, which senses the apparent dielectric constant of a fluid stream by measuring its capacitance between the probe electrodes.

The capacitance probe generally is installed in a vertical riser on the premise that a more uniform mixing of stream components will result and thus, that a more accurate sensing of water content is ensured. Temperature compensation is required since dielectric constants of oil and water vary with temperature. The BS&W monitors used with LACT generally have a 0 to 3% BS&W range. The monitors have a variable set-point that is used to divert the oil stream back through the treating facilities when the selected BS&W content is reached and/or exceeded. In this application, a BS&W monitor controls the crude oil stream being transferred to the pipeline, but it does not determine the BS&W content as basis for gross volume adjustment.

Net-Oil Computer

The application of SCADA systems to production operations increased the need to read directly the net-oil content of an emulsion stream for well testing and lease oil production measurements. The basic principle of the capacitance probe used in BS&W monitors was extended to oil emulsions of higher water content by probe redesign.

The capacitance probe, with modification to give a linear output, provides a technique to obtain instantaneous value of water content in an oil emulsion stream. By combining the probe output with volume output from a positive-displacement or turbine meter, the net-oil and

water volumes in an emulsion stream can be determined. The device that combines the capacitance probe and meter volume information to obtain net-oil and water volumes is designated as a net-oil computer.

The net-oil computer can determine the oil/water content of an emulsion stream with reasonable accuracy (1 to 2% in oil measurement to about 35% water). The capacitance probe will continue to indicate water content above this value (if in an emulsion form), but the decreasing oil percentage of the total stream causes increased error in the measured oil fraction. A limitation of the capacitance probe is that any "free" water moving across a probe with oil emulsion will distort the indicated water content and cause substantial errors. Applications with water cuts above 35% can be measured by using three-phase separators (for well testing and/or lease oil production). Treating chemicals can be used with three-phase separators, if necessary, to keep water content in the emulsion to 35% or less. With these procedures, well testing and lease oil production can be processed with total water production of more than 99%.

Supervisory Control and Data Acquisition (SCADA) Systems

SCADA systems applied to oil and gas producing operations vary in function and overall capability. Some systems are oriented primarily to local operating personnel needs and may only monitor/control a few wells in a single field. Other systems are applied to multiple fields that have several thousand total wells. Even with the wide variations, SCADA systems consist of the following basic elements: (1) supervisory control/data acquisition equipment, (2) field instrumentation and cabling systems, (3) communication facilities, and (4) digital computer systems.

SCADA Equipment

This equipment functions to interconnect digital computer systems and instrumentation and control devices that are related to the oil and gas producing process. The equipment consists of a communication adapter and RTU's. A communication adapter is attached directly to the digital computer by a high-speed data link and attached indirectly to RTU's by communication circuits. The communication adapter serves as a data concentrator for the digital computer, which can drive several communication circuits simultaneously. A number of RTU's generally share a common communication circuit.

The communication adapter and the RTU's are designed to use a specific message protocol or structure for the transmission of information. This message structure generally will contain the RTU address, function being requested, function modifiers, and supplemental information used for checking validity of message transfer. A primary feature shared by the communication adapter and the RTU's is the checking for valid message transmission between the devices. Manufacturers use different techniques to ensure receipt of valid messages and most of these have a high probability of detecting invalid transmissions. Earlier communication adapters were designed with "hard-wire" logic and were separate devices. Many of the current designs are microcomputer-based units that may be an integral part of the digital computer rather than a separate unit. These units fre-

quently can handle multimessage protocols to allow more flexibility in attached devices.

RTU's are electronic devices that connect the SCADA system directly to the oil and gas production facilities that are being automated. An RTU has the capability to store information from several input points and to transmit this information in a serial mode over a single communication circuit to a digital computer on demand. The RTU also may receive control information from the computer that it routes to a selected control point. The RTU generally is located within a few thousand feet of its connected instrumentation and control equipment but may be up to several hundred miles from the computer location.

RTU's commonly sense input information related to status/alarm (on-off, etc.), volume accumulation (oil and gas meter counts), and instantaneous analog values (temperature, pressure, flow rate, etc.). The RTU can provide control output in the form of relay activate (on-off, start-stop) and a set-point value. The set-point is commonly a 4 to 20 mA or 10 to 50 mA signal that is compatible with control devices. Although these basic RTU capabilities may appear limited, most data input and control output functions related to oil and gas production can be implemented directly. Some specific functions may require supplemental logic in local control panels for implementation.

The basic RTU functions described previously are common to units designed with "hard-wired" logic. Many of the current and most future RTU designs will be microcomputer-based. The microcomputer allows substantial increases in RTU functions with relatively small incremental hardware expansion and cost. For example, RTU's are being used to replace stand-alone gas-flow computers simply by adding to the microcomputer program logic that integrates static pressure, differential pressure, and temperature transducer data from an orifice meter. The microcomputer in the RTU can handle all basic RTU functions and process gas-volume accumulation for 30 to 50 m runs without timing constraints. With continuing developments in electronic technology and improving program support, the outlook is for significant expansion in RTU capability.

Initial RTU designs that incorporated microcomputers tended simply to implement "hard-wired" logic in the microcomputer. In addition, microcomputers used with RTU's generally did not have any internal error checking such as parity on memory, data bus, and address bus transfers. These conditions resulted in microcomputer-based RTU's that were difficult to trouble-shoot when malfunctions were experienced. Self-diagnostic capabilities should be the first functional extension of microcomputer-based RTU's. Good diagnostic features usually will require a combination of extended hardware and software. Diagnostic checks should be run at startup and at frequent intervals during the regular operation of the RTU. RTU's should have a "watch-dog" timer that will attempt to restart the microcomputer if it stalls as a result of hardware and/or software malfunction. The restart feature also should provide a means to document its use.

The RTU as an electronic device has two primary environmental factors that adversely affect operational reliability. These factors are heat and electrical tran-

sients. All solid-state electronic components suffer decreased life with increasing operating temperatures. Many users of RTU's routinely have placed these units in air-conditioned buildings to decrease the mean time between failures. More recent introduction of low-power electronic components such as complementary metal-oxide silicon (CMOS) may minimize the need to provide cooling below normal ambient temperatures.

Solid-state electronic components are subject to damage by extremely short-duration (microseconds) higher voltage electrical transients (e.g., noise, spikes). These transients may enter an RTU by means of primary power or by the many signal loops connecting the RTU to the instruments and control devices associated with the production process. RTU's frequently are provided battery backup power to allow for continued operation with primary power outages. Common procedure is to operate the RTU continuously on battery power with primary power driving a battery charger. This arrangement provides relatively good isolation for the RTU from power line transients.

All RTU input/output connections to the field cable system also must be protected from voltage transients. Status/alarm and accumulator input points frequently use optical isolation between field cables and internal circuitry. Each field signal loop also should use a gas tube (or similar device) to route induced voltage transients to earth ground. Lightning can induce sufficient energy to literally evaporate protective components in extreme cases but many of the otherwise damaging transients can be suppressed with proper protection equipment. Electrical noise also may be caused by inductive devices such as relay and solenoid valve coils. Inductive components should have suppression diodes placed across the input terminals to minimize electrical transient generation.

Field Instrumentation and Cabling Systems

Field instrumentation and control devices are selected primarily to meet needs of the oil and gas producing facilities. If these devices are also to interface with the RTU of a SCADA system, some additional features may be required. RTU status/alarm and accumulator inputs require an electrical switch closure to convey information to the RTU. For example, a separator high-level float control may have a pneumatic switch for control valve activation. An electrical pressure switch may be added to the pneumatic control line to allow the RTU to sense the position of the high-level control. In general, reliability of interface increases when the primary instrumentation has a direct electrical connection compared to the example that required a pneumatic to electrical conversion.

Meters for liquid and gas measurement also need to have an electrical switch activation to indicate some increment of volume accumulation. Liquid meters, for example, frequently will have an electrical switch closure at nominal 1-bbl volume increments. The switch closure must be maintained for some minimum time increment (about 50 milliseconds) to ensure that electrical transients will not cause invalid volume counts. The RTU will have a separate signal loop (wire pair) and internal electronic counter associated with each meter being monitored.

Pressure, temperature, flow rate, position, and similar

operational parameters are sensed by the RTU as an analog input value from electrical transducers. Nominal electrical transducer output ranges of 1 to 5, 4 to 20, and 10 to 50 mA usually can be processed by the RTU. A current output transducer is preferred since the signal is less susceptible to electrical transient distortion than a voltage output.

Multiconductor cables are used to connect the RTU to the instrumentation and control devices associated with the production process. The signal cables consist of individually insulated copper wires generally of 19 or 22 gauge that commonly are used for commercial telephone service. The cables usually are buried to minimize probability of mechanical damage and electrical noise intrusion. Cables can be damaged when buried and repairs should be made immediately to prevent further deterioration. Cable lengths are controlled by cost relationships between installing more RTU's at separate locations and the amount of cable required for interconnection. Most cable systems will be limited by economics to a few thousand feet.

Radio communication links between RTU's and a central location within a field can reduce overall cabling costs substantially. This technique can use a master radio station in a "polling" mode to communicate with the individual RTU's. Separate transmit and receive frequencies enhance the radio communication procedure. In this arrangement, the master radio transmits an outbound message to all RTU's and the RTU's will decode the address portion of the message. The addressed RTU then will decode the function portion of the message and reply to the master radio by bringing up its transmit radio link for the period required by the return message. The master radio is linked to a regular four-wire communication circuit for communication outside the field area.

The low-energy signals used in the cable system require careful connection of wiring to instrumentation. Any damage to wiring insulation or collection of moisture at connection points may result in sufficient signal leakage to cause invalid sensing of operational information. Some installations are made with the signal loop power supply "floating" or not connected to earth ground. Maintenance checks then can be made to determine current leakage to the positive and negative terminals of the power supply from earth ground as a measure of signal leakage. With selective isolation of the signal loops, leakage problems usually can be identified. Common practice is to design alarm-signal loops to be in normal condition when the sensing device has a closed electrical switch. This feature makes the alarm signal more fail-safe in that any failure of the signal path will cause indication of an alarm condition also. Less critical "status" loops frequently are open in the normal state to minimize total power needs.

Communication Facilities

SCADA systems require capable and reliable communication facilities to connect the communication adapters on the digital computer system with the RTU's that are located in fields being automated. Most SCADA systems use dedicated or nonswitched communication circuits that have a four-wire configuration. The four-wire designation provides two independent communication paths that will support simultaneous data transfer in

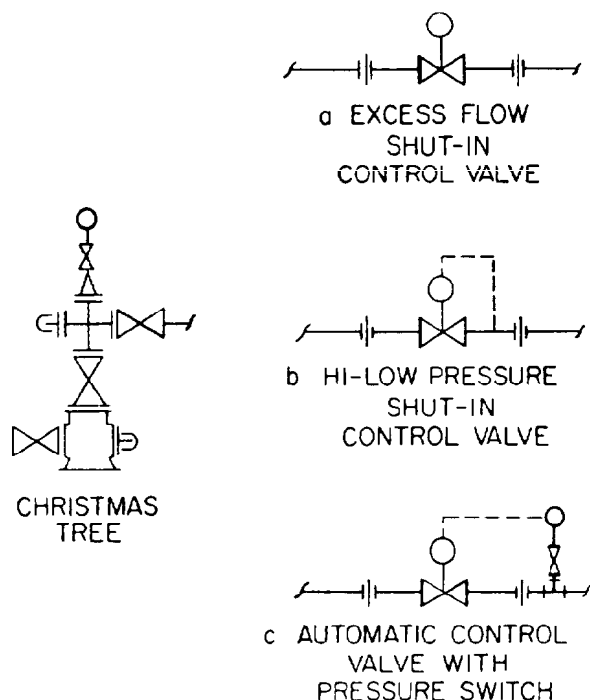


Fig. 16.1—Automatic wellhead safety controls.

two directions (full duplex). Data transmission in SCADA generally is operated in one direction at a time (half duplex) with transmit over one path and receive over the other path but at different time periods. Data are transmitted over the communication circuits with the aid of modems. Modems are electronic devices that convert voltage or current level from the communication adapter into analog signals that can be transmitted over the communication circuit. A similar modem at the RTU receives the analog signals and converts them into voltage or current levels that are compatible with the electronic circuitry in the RTU. A data transmission from an RTU to the communication adapter operates in the reverse cycle.

SCADA can use commercially available voice-grade (telephone) communication circuits. Communication speeds of 1,200 bits/sec can be used with long term reliability over these circuits by using conventional modem equipment. Higher communication rates can be obtained by using more complex modems and higher quality communication circuits if the application being monitored requires more critical timing responses. Increased communication rates tend to require more maintenance time or fine tuning of communication equipment to achieve a constant reliability of performance.

SCADA communication circuits may require multiple ownership and maintenance responsibility links to reach particular locations. Circuits with divided maintenance responsibility tend to have more reliability problems. In these cases, adequate test facilities at the computer site can aid in defining the particular link causing problems. The four-wire circuit is compatible with testing since it can be turned around to receive a transmitted test signal from the computer site. If remotely operated turn-around

devices are located at each link interconnection, the circuit can be tested and problems isolated to the responsible maintenance group.

Digital Computer Systems

SCADA became possible with the development of process-control-type computer systems in the late 1950's. The process control computer was a special hardware implementation that provided for direct connection to plant instrumentation and control equipment. This same hardware also provided a means to interconnect with the communication adapter of a SCADA system. The SCADA equipment then allowed the process control computer to be connected indirectly to oil and gas facility instrumentation at remote locations.

Process control computers had software operating systems with program execution control that was compatible with SCADA needs. The operating systems were designed to recover automatically from minor program malfunctions to minimize computer operator needs in the continuously operating SCADA applications. Early process control computers had limited memory size that tended to require assembler language routines for some functions. Frequently, bulk storage (disk or drum) devices also were limited in capacity. Most earlier SCADA systems were based on a central computer system concept.

Currently, SCADA systems have extremely capable computer systems available for system implementation. Process-control-type computers are available with few practical limitations on memory size, speed of execution, and random access storage capacity. In addition, many of the general-purpose-type computers (business and scientific applications) now have extensive communication capabilities and operating system features that are compatible with most SCADA requirements. Distributed computing, which uses multiple computers at remote sites, became practical in the mid- to late 1970's as manufacturers developed capable network software. The network software provided capability to develop application programs at central locations and download through communication links into computer systems at field locations. Increased use of distributed computers in SCADA is anticipated.

Basic application software is generally available from manufacturers of the SCADA systems. The rapidly changing technology, however, has made it difficult for suppliers to develop general purpose application software that is transportable to new computer systems. Most larger SCADA systems have tended to be specialized software applications that have continuing program development to meet the changing operational needs. Application software for both small and large SCADA systems should have flexibility to allow changes/additions to the implemented functions.

Typical Automatic-Control Installations

Automatic Well Control

Automatic Wellhead Controls. Wells may be controlled at the wellhead or at the well manifold. Frequently, it is necessary or desirable to control them at both places. Fig. 16.1 depicts three different types of

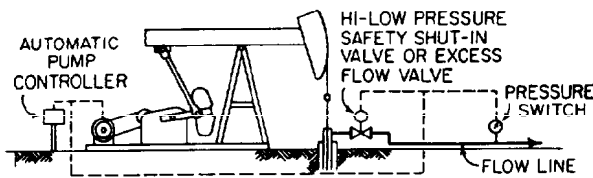


Fig. 16.2—Automatic controls for rod-pumped wells.

places. Fig. 16.1 depicts three different types of automatic control valves that could be installed at the wellhead immediately adjacent to the tubing wing valve. Although Fig. 16.1 pictures a naturally flowing well, the same types of automatic controls would be applicable for artificially lifted wells of all types, if required. The excess-flow valve shown in Fig. 16.1a generally is used only to protect against flowline breaks when the wells are choked and controlled at the well manifold. The high/low pressure shut-in valve in Fig. 16.1b may be used whether the well is choked at the wellhead or at the well manifold. It is protection against both flowline breaks and chokes cutting out or plugging. The control valve and separate pressure-sensing element shown in Fig. 16.1c perform exactly the same functions as the high/low pressure shut-in valve.

Rod-Pumped-Well Control. The typical automatic-control system for a rod-pumped well is shown in Fig. 16.2. The high-low pressure safety shut-in valve is necessary only when the well has a tendency to flow naturally when the pumping unit is shut down. The excess-flow valve, again, is protection against flow-line breaks. Some operators use them; others do not. They are not always effective unless line pressures are high enough, and the size of the break large enough, to create a substantial pressure drop. The pressure switch is the most common automatic safety control used with rod-pumped wells, particularly where the wells are remotely controlled. Regardless of which of these three types of controls are used, when the control pressure is reached, that automatic control must furnish a signal to shut down the pumping unit. This is accomplished by grounding the magneto of a gas engine or shutting off an electric motor. A pump-off control, if used, would be installed in the flow line immediately adjacent to the pumping tee.

Gas-Lift-Well Control. Fig. 16.3 shows a typical arrangement of controls on the gas-supply line to a well that is produced by an intermitter-type gas-lift installation. The "time-cycle controller" shown on the right is an automatic production programmer. It automatically opens and closes the diaphragm control valve, to which it is connected by instrument lines, according to the schedule manually created in the programmer. The "flow-control valve" is a manually actuated valve used to control the rate at which gas is admitted to a well. Automatic-control valves on the flow line, if required, would be one of the types shown in Fig. 16.1.

Hydraulic-Pumped-Well Control. Fig. 16.4 depicts the typical automatic controls for a hydraulic pumping

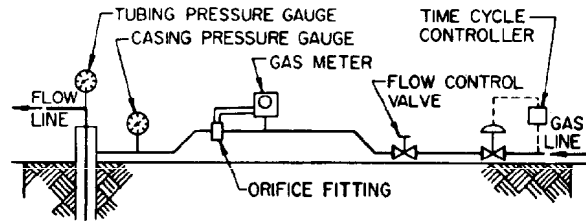


Fig. 16.3—Typical automatic control of gas-lift well.

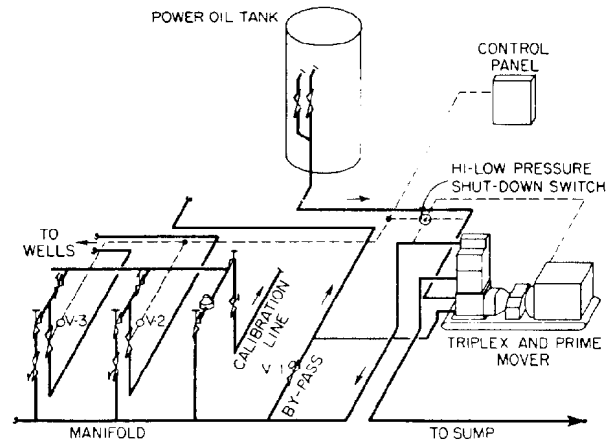


Fig. 16.4—Typical hydraulic-pumping-system control.

system. A high/low pressure switch protects the triplex pump and its prime mover against overloading from abnormally low suction pressures and/or high discharge pressures. In either case, the pressure switch would shut down the prime mover. Automatic Control Valve V-1 in the manifold bypass is generally a diaphragm-type regulator valve which is normally closed. It would open at a pressure slightly under the setting of the high/low pressure shutdown switch and divert sufficient power oil back to the power-oil tank to maintain system pressure at a safe level. Automatic Control Valves V-2 and V-3 are in the power-oil lines to individual wells. They would be closed automatically in the event the pressure switch shut down the triplex and prime mover. With an appropriate programmer, they could also be used to produce individual wells selectively on an intermittent schedule.

Automatic Well Manifolds. In Figs. 16.5 and 16.6 are shown two typical automatic well manifolds designed for controlling the wells at the well manifold rather than at the wellhead. The single-wing well manifold shown in Fig. 16.5 has a maximum of flexibility to meet any system of stage separation and/or treating that might arise. It has another advantage in that it could be installed initially on new leases as they are developed without the automatic-control valve and still add the valve later with a minimum of expense. The dual-wing well manifold shown in Fig. 16.6 is limited to situations where all production in a well manifold is processed through a single vessel or a common sequence of vessels. Both these manifold designs would require flow lines capable of withstanding full wellhead pressure and

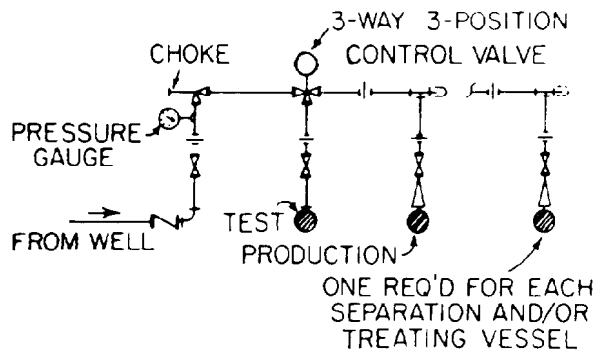


Fig. 16.5—Typical single-wing automatic well manifold.

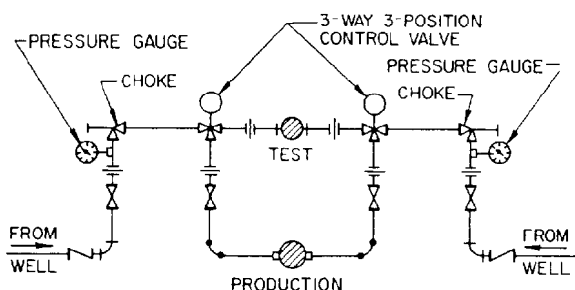


Fig. 16.6—Typical dual-wing automatic well manifold.

would choke and control the wells at the manifold. All manifold designs should provide for monitoring valve leakage.

Some operators prefer to use three-way, two-position control valves in the well manifold and to control the wells at the wellhead. Automatic-control valves of the types shown in Fig. 16.1 then would be installed at the wellhead in addition to the control valves in the well manifold. Other operators would prefer to use a two-way control valve in each riser to each pressure vessel served by the well manifold.

Automatic Well Testing

A typical automatic well-testing system is illustrated in Fig. 16.7. The sequence control logic for conducting the test and for calculating test results may be self-contained in the control panel or it may originate in a SCADA system that is remote from the site. In either case, a three-way control valve in the test/production manifold is activated to divert the selected well to the test vessel when the related signals are received from the control panel. The test vessel may be either a separator or a heater treater. The liquid-metering elements commonly will be either positive-displacement or turbine meters. The oil meter will be combined with a capacitance probe and net-oil computer to provide measurement of net-oil and emulsion-water volumes. The free water volume will be measured by a separate water meter. Well-test control logic will combine the emulsion-water and free water measurements to obtain total test water volume.

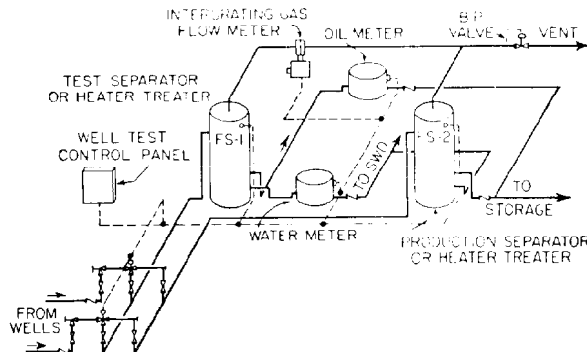


Fig. 16.7—Typical automatic well-testing system.

The test-gas volume can be determined with a positive-displacement meter, turbine meter, or gas-flow computer. The three-way control valves should be equipped with position switches that can be used to confirm that only the selected well is in the test vessel. The test vessel normally will have a high-level float switch that will automatically divert the on-test well back to production status when a high liquid level is detected. The same switch can be used to notify the SCADA system of the test vessel malfunction.

Some operators have extended the use of measurement equipment, as described for well testing, to total lease production. For example, with more logic in the control panel and manifold of dump lines from test and production vessels, the oil-measurement equipment can be time-shared to measure both test and production oil volumes. The control panel determines (one at a time) which vessel dumps through the oil-measurement equipment and routes the volume counts to the related counter. Separate gas-measurement facilities are required for test and production volume determination.

The time-sharing concept has been extended further in certain instances. For example, a number of separate leases, each having only a few wells, were arranged to have all production separators located at a common site. The oil production from each separate lease production separator was determined by time-sharing a single oil-measurement facility. In addition, a single test separator was used to test all wells at the site. The site control panel routed test volume counts to the test counters and to the appropriate lease counters related to the well on test.

LACT

The first efforts to design an acceptable LACT installation tried to incorporate the existing equipment on the lease and familiar operating principles insofar as possible. Thus, understandably, the first officially accepted LACT system was a weir-tank system installed by Gulf Oil Corp. on its Ames Lease in the Bloomer field, KS, in 1955. Shell Oil Co. also pioneered in the development of the weir-tank-type LACT system on its leases in the Antelope and Wasson fields in Texas, beginning unofficial experiments as early as 1948. The next significant development in LACT system design was the meter-tank-type system.

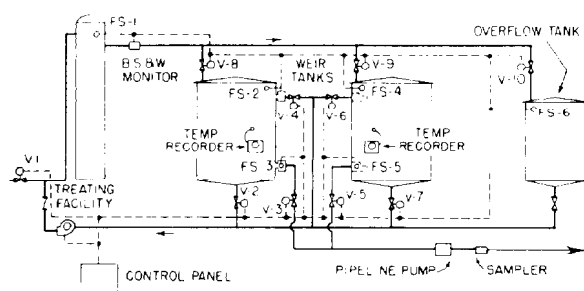


Fig. 16.8—Typical weir-tank-type automatic-custody-transfer system.

The meter-tank-type system is closely akin to the weir-tank system in many respects, but perhaps it deserves consideration as a separate category because these vessels were designed solely as measuring vessels. The great similarity between measurement with the larger-sized positive-volume dump meters and conventional lease tanks assured their early acceptance. Officially accepted LACT installations of this type of the Phillips Petroleum Co. and Amoco in Oklahoma and Texas followed closely on the heels of the Gulf weir-tank-type system in Kansas. The third type of LACT design which has gained wide acceptance to date is the positive-displacement-meter-type system. Exxon Co. U.S.A. was perhaps the strongest early proponent of this type of system, and they performed much development work on their leases in south Texas.

The positive-displacement-meter-type equipment rapidly became the LACT standard primarily because of substantial cost and operating reliability advantages over the other two units. The positive-displacement-meter LACT assembly was skid-mounted for relatively simple installation within existing production facilities. Figs. 16.8 and 16.9 are included for reference to the historical development of LACT as an important element of lease automation.

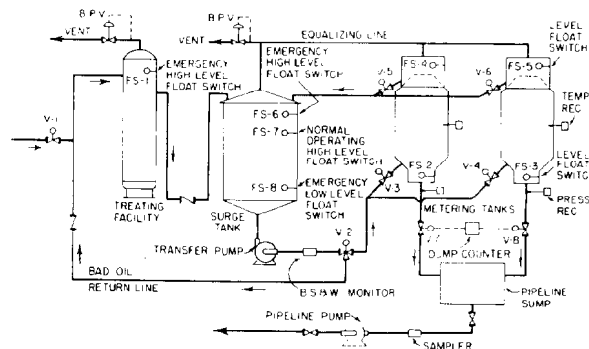


Fig. 16.9—Typical automatic-custody-transfer system using metering dump tanks.

Positive-Displacement-Meter LACT System. Fig. 16.10 shows a positive-displacement-meter LACT installation. Option B indicates a two-meter arrangement that was recommended strongly in earlier installations for improved measurement reliability. Operational experience found the single meter arrangement (Option A) to have satisfactory reliability and most LACT's were installed with the single meter. Some LACT's have two meters but most of these operate the second meter in a stand-by mode rather than simultaneous measurement through both meters. Most major purchasers have recommended (or required) certain designs for LACT installations.

The routine operation of crude-oil transfer is controlled by the normal operating high-level float switch with an override to shut down on emergency with the low-level float switch. The BS&W monitor will divert fluid stream to the treating facility on detection of high BS&W content. The strainer is used to protect the meter from particles that could damage the meter. The meter is temperature-compensated to indicate oil volume at 60°F standard condition. Daily and monthly volume limit switches prevent overrun of lease on either daily or monthly allowable volumes. A calibration loop is located downstream of the meters to allow convenient

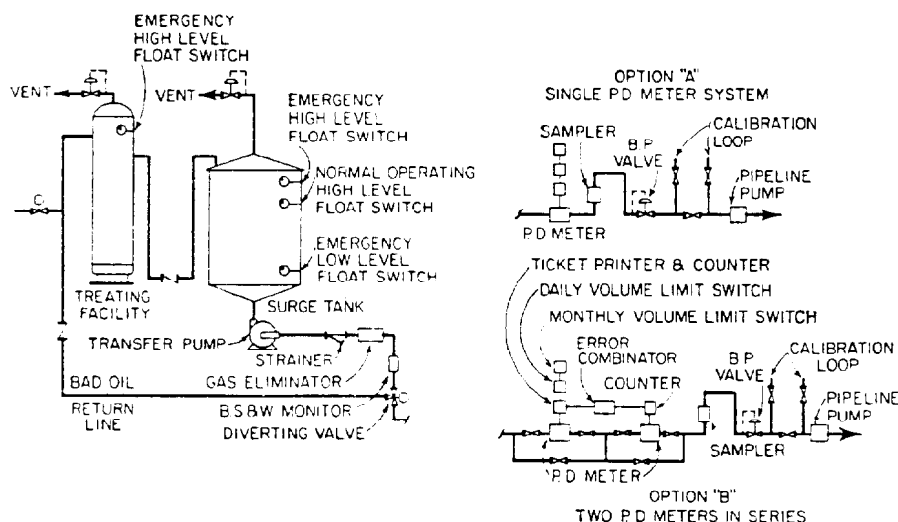


Fig. 16.10—Typical automatic-custody-transfer systems using positive-displacement meters.

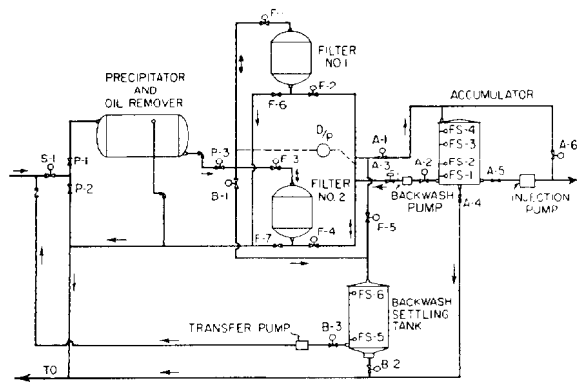


Fig. 16.11—Automatic backwash of rapid sand filters in water-treatment plant.

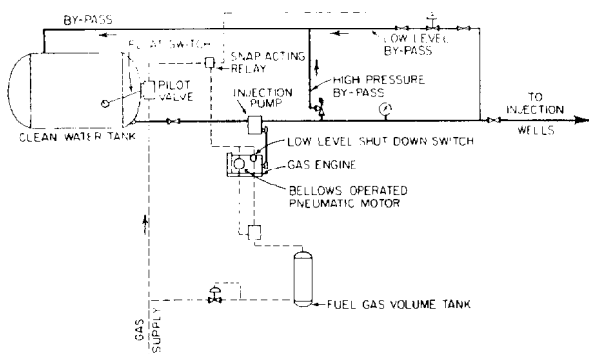


Fig. 16.12—Typical method of controlling injection-pumping rate.

meter-proving or calibration with a master meter. A sampler is used to collect sample volumes for basis of BS&W correction and oil gravity determination. The back-pressure valve is used to minimize gas break-out or "flashing" in the crude stream prior to being metered. A check valve (not shown) should be located downstream from the back-pressure valve (or combined with it). API Standards 1101, 2502, 2531, 2542, 2544, and 2546, and supplements thereto provide recognized industry codes for liquid petroleum measurement.²

Automatic Lease Process Control

There are many normal lease-operating processes that may be automated or that already are automated completely and not recognized as such by the average individual. Space limitations will permit only a brief look at a few of these control systems to show what can be and is being done.

Automatic Water-Treating Plant. Fig. 16.11 depicts a rather elaborate automatic backwash system for rapid sand filters in water-treating plants. Normal flow is from the precipitator and oil remover through the sand filters into the accumulator. When the differential pressure across the bank of filters reaches a predetermined value, the backwash cycle is initiated automatically. Valves

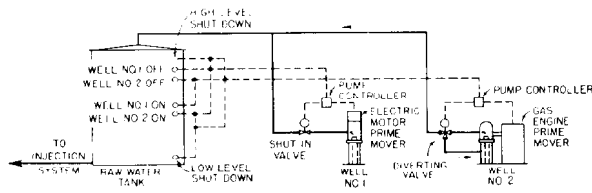


Fig. 16.13—Automatic control of water-supply wells.

P-3, F-1, F-3, F-4, and A-1 are closed; Valve A-2 is opened; and the backwash pump is started. After a slight delay, Valves F-1 and B-1 are opened and Filter 1 is backwashed into the backwash-settling tank for a predetermined, but adjustable, time. At the end of this time, Valves B-1 and A-2 are closed and Valves P-3 and F-5 are opened. Normal flow is permitted through Filter 1 into the backwash-settling tank for a short interval to settle the filter bed. At the end of this interval, Valves P-3 and F-5 are closed, Valves A-2 and F-4 are opened, and the backwash pump is started. After a slight delay, Valve F-3 opens and the same cycle is completed for Filter 2.

Four float switches are required in the accumulator. Float Switch FS-1 is an emergency low-level float switch, which maintains a flooded pump suction and prevents gas from locking the pump since the accumulator normally will be gas-blanketed. The volume between Float Switches FS-1 and FS-2 is large enough to backwash the filters. Normally the fluid level is not permitted to fall below FS-2. If it should, the injection pump is shut down if it has an electric prime mover, or Valve A-6 is opened and the injection-pump output is bypassed back into the accumulator if the injection pump has a gas-engine prime mover. When the fluid level reaches Float Switch FS-3, the normal injection process is resumed. Float Switch FS-4 is an emergency high-level control that would cause Valve S-1 to close to prevent running over the accumulator.

Valve A-3 is shown as a backpressure valve that is intended to keep a constant head on the backwash pump. The backwash pump probably will be a centrifugal pump because of the high rate normally recommended for proper backwashing. If the injection process ceases for the backwash cycle, then gas pressure applied to the top of the accumulator can be used in place of the backwash pump.

After all the filters have been backwashed and settled into the backwash-settling tank, the solids in the water are permitted to settle out in the bottom of the tank. Then Valve B-2 is opened automatically to permit the solids to be washed out to the pit. Then Valve B-2 closes, Valve B-3 opens, and the transfer pump returns the clear water back through the system. Float switch FS-5 is for the purpose of maintaining a flooded suction on the transfer pump, and Float Switch FS-6 is to prevent running over the vessel.

The system just described represents a composite situation. All automatic water-treating plants would not have to be this elaborate. For example, a backwash-settling tank would be desirable only where it was necessary to keep the water going into the pit at a minimum. On the other hand, by a few small changes,

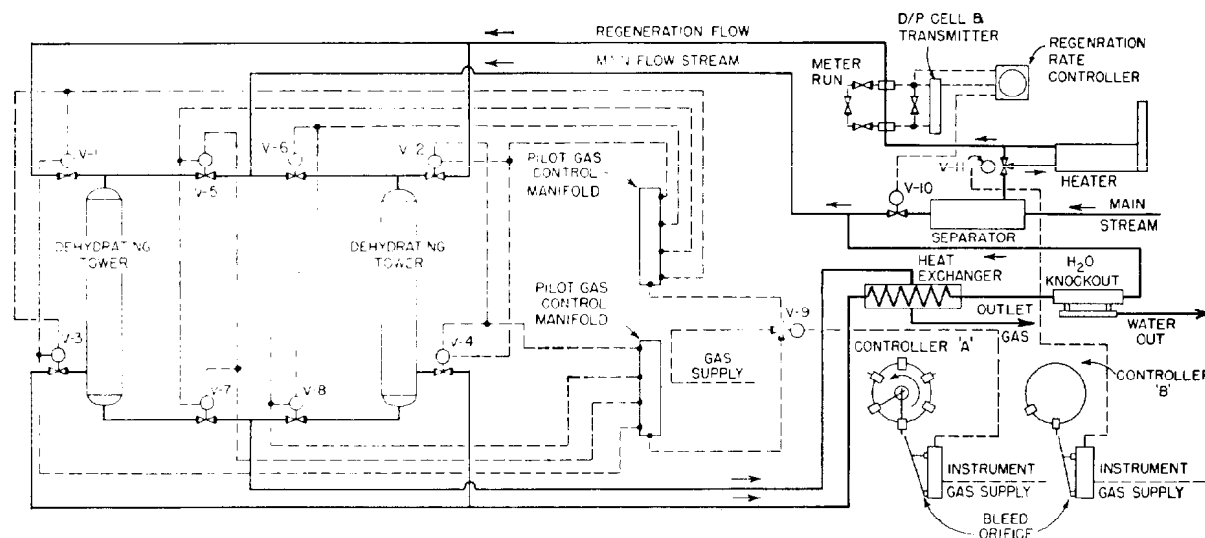


Fig. 16.14—Automatic cycling of desiccant beds in dry-desiccant-type gas dehydrators.

the systems shown in Fig. 16.11 could also be altered to provide for continuous through-put and injection while one of the filters was being backwashed.

Automatic Control of Injection-Pumping Rate. Fig. 16.12 shows a typical method of controlling the injection-pumping rate of a gas-engine-driven injection pump. A float switch and pilot valve, acting through a snap-active pneumatic relay, controls the position of (1) a low-level bypass regulator, and (2) a bellows-operated pneumatic motor that adjusts the engine throttle linkage relative to the position of the float switch in the clean-water tank. In the event the fluid level drops too low in the clean-water tank, the pilot valve sends a signal to a low-level shutdown switch, which grounds the magneto on the engine and shuts it down.

Automatic Control of Water-Supply Wells. Fig. 16.13 shows a method of using float switches to control the operation of several water-supply wells to maintain an adequate supply of water in the raw-water tank. As always, high- and low-level emergency float switches are provided. Additional float switches are included to program the addition and subtraction of supply wells feeding the system to assure an adequate volume of water is always in the raw-water tank. The well-on float switches would be actuated by a dropping fluid level, and the well-off float switches by a rising fluid level.

At the water-supply wells, there are several ways to control the pumping equipment. If the pump is driven electrically, it might be necessary to start up and shut down the pump motor only as called for. If the water-supply well were artesian or had a tendency to flow naturally, it would be necessary, of course, to furnish a shut-in valve. If the pump is driven by a gas engine, it would be necessary either to provide the engine with an electric ignition system (battery or electric motor) and a startup sequence programmer or to install a diverting valve and leave the engine running while diverting production back into a casing annulus.

Automatic Control of Dry-Desiccant-Type Gas Dehydrators. As a final example, let us consider a lease

process that has been fully automatic since its inception, but one which is rarely thought of in terms of automation: the automatic cycling of desiccant beds in dry-desiccant-type gas dehydrators. Fig. 16.14 is a schematic of a typical dry-desiccant-type dehydrator. The wet gas stream enters the horizontal separator and is divided, with a part of the gas going to the regeneration stream and the remainder continuing in the main gas stream through the dehydrating tower. The proportioning of the flow between the two streams is controlled by the regeneration-rate controller. The rate of flow in the regeneration gas line is measured by a differential-pressure cell and transmitted to the regeneration-rate controller. The regeneration-rate controller, in turn, acts to position Automatic-Control Valve V-10 to maintain the predetermined rate of flow of gas through the regeneration system.

Automatic-Control Valve V-11 in the regeneration gas line is controlled by Controller B. Each time the controller rotates until the pin on the next trip clamp unlatches the pilot arm, Valve V-11 reverses its position. In the one position, it diverts gas through the heater to provide hot gas for expelling moisture from the desiccant bed of the tower being regenerated. In the other position, it bypasses the heater and provides unheated gas to cool the desiccant bed in the same tower before placing it back into service. By the time the controller rotates one more position, the regeneration valves on the towers will have switched so that the hot gas goes to the other tower.

Automatic-Control Valves V-1, V-2, V-3, and V-4 control the flow of regeneration gas to dehydrating towers, and Valves V-5, V-6, V-7, and V-8 control the flow of the main gas stream. Valves V-1, V-3, V-6 and V-8 are always in the opposite position from Valves V-2, V-4, V-5, and V-7. The main-stream valves and the regeneration-stream valves are manifolded in such a manner that only one tower at a time receives the main-stream gas and that tower is blocked off from the regeneration gas. The other tower receives the regeneration gas and is blocked off from the main-stream gas. The position of all these valves is controlled by Controller A acting through relay Valve V-9 and the pilot-

gas-control manifolds. Each time the controller rotates until the pin on the next trip clamp unlatches the pilot arm, instrument gas will flow through the bleed orifice instead of flowing to the Relay Valve V-9. Relay Valve V-9 then will reposition itself and allow instrument gas to flow to the other pilot-gas-control manifold and vent the gas from the pilot-gas-control manifold supplied in its original position. This, in turn, will cause each of these control valves to reverse their positions, and thus the flows of main and regeneration gas streams will also reverse. The length of each cycle is controlled by the spacing of the trip clamps on the controller.

References

1. *API Manual of Petroleum Measurement Standards*, first edition, API, Dallas (1981) Chaps. 1, 5, and 6.
2. "Specifications for Lease Automotive Custody Transfer (LACT) Equipment," second edition, API Spec. 11N, API, Dallas (March 1979).

General References

- Anderson, G.L. and Reed, G.A.: "Automation in the South Swan Hills Unit," *J. Can. Pet. Tech.* (Oct.-Dec. 1981) 20, 105.
- Atkinson, M.H., and Newberg, A.H.: "Crude-oil Measurement Is Going Automatic," *Oil and Gas J.* (June 4, 1956) 102.
- "Automatic Custody Transfer," *Oil and Gas J.* (July 11, 1956) 110.
- "Automatic Sale Slated," *Oil and Gas J.* (Feb. 13, 1956) 90.
- "Automation," *Pet. Week* (Nov. 16, 1956) 71.
- Barrett, M.L. Jr.: "Meter Proving," *Oil and Gas J.* (Feb. 24, 1958) 153 (March 10, 1958) 201 (March 24, 1958) 213 (April 21, 1958) 179 (May 5, 1958) 133.
- Bayless, C.R., and Mikeska, F.J.: "Automatic Control of Production," *Oil and Gas J.* (June 4, 1956) 78 (June 11, 1956) 129 (June 25, 1956) 110.
- Beach, F.W.: "Fail-safe LACT Unit; Here's How It Works," *World Oil* (Nov. 1957) 133.
- Brainerd, H.A. and Piros, J.J.: "New Controller Recorder Gravimeter," *Oil and Gas J.* (Dec. 2, 1957) 78.
- Case, R.C. and Fritsch, D.R.: "Automation for the Ekofisk Offshore Operation," paper presented at the 1976 Automation in Offshore Oil Field Operations Symposium, Bergen, Norway, June 14-17.
- DeVerter, P.L. and Scovill, W.E.: "Part I: Continuous Automatic Sampling," *Oil and Gas J.* (April 2, 1956) 125. Warren, F.H.: "Part II: Continuous Automatic Sampling," *Oil and Gas J.* (April 9, 1956) 124. Johnson, R.P.: "Part III: Continuous Automatic Sampling," *Oil and Gas J.* (April 23, 1956) 119. Berglund, J.H.: "Part IV: Continuous Automatic Sampling," *Oil and Gas J.* (April 30, 1956) 210.
- Doble, P.A.C.: "Computer-Assisted Operations in a Northern North Sea Operation," *J. Pet. Tech.* (April 1983) 701-08.
- Dunham, C.L.: "A Distributed Computer Network for Oilfield Computer Production Control," *J. Pet. Tech.* (Nov. 1977) 1417-26.
- EnDean, H.J.: "Oil Field Watchman Checks BS&W Content," *World Oil* (Nov. 1957) 151.
- "First LACT System for Low Gravity, Viscous Crudes," *Oil and Gas J.* (Dec. 2, 1957) 82.
- Foster, K.W.: "Centralia Water Flood: Pre-planned Automation Pays Off," *Pet. Engr.* (March 1958) B-116.
- Hebard, G.G.: "Automatic Lease Custody Transfer," *Oil and Gas J.* (Nov. 5, 1956) 86.
- Hill, R.W.: "Factory-built LACT Unit Is Gas Operated," *Oil and Gas J.* (May 6, 1957) 98.
- Hubby, L.M.: "Automatic Production Controls," Paper API 926-1-C presented at the 1956 Southern District Spring Meeting, Division of Production, San Antonio, Mar. 9.
- "LACT: A Youngster Now, Soon a Giant," *Oil and Gas J.* (Sept. 22, 1958) 74.
- "LACT Is for Stripper Leases, Too," *Oil and Gas J.* (Dec. 15, 1958) 70.
- "Lease Automatic Custody Transfer," *Bull.* 2509A, API, Dallas (Aug. 1956)
- "Lease Is Fully Automatic," *Pet. Week* (Feb. 15, 1957) 11.
- LeVelle, J.A.: "New Production Programming System," *Pet. Engr.* (April 1956) B-30.
- Matheny, S.L. Jr.: "Computer Production Control Expands," *Oil and Gas J.* (March 23, 1981).
- McGhee, E.: "Automatic Switching, 9-mile Radio Link," *Oil and Gas J.* (Sept. 10, 1956) 114.
- McGhee, E.: "How Cities Service Is Using P.D. Meters for LACT," *Oil and Gas J.* (Jan. 13, 1958) 74.
- McGhee, E.: "How Shell's Antelope LACT Works," *Oil and Gas J.* (June 3, 1957) 90.
- McGhee, E.: "It's Automatic—Even to Sample Taking," *Oil and Gas J.* (Feb. 13, 1956) 104.
- McGhee, E.: "LACT—And Why We Like It," *Oil and Gas J.* (Jan. 20, 1958) 131.
- McGhee, E.: "When a Field Outgrows Its Facilities," *Oil and Gas J.* (Apr. 15, 1957) 108.
- McKinley, D.C.: "P.D. Meters Get the Job Done," *Oil and Gas J.* (Oct. 1, 1956) 87.
- Meyers, D.C.: "How Shell Designs an Automatic Lease," *Oil and Gas J.* (Oct. 17, 1955) 111.
- Northern, T.P.: "Automatic Lease Operations—Weeks Island Field," *J. Pet. Tech.* (Jan. 1954) 21-24.
- Packard, H.C., Kelley, H.S., and Newburg, A.H.: "Automatic Custody Transfer of Crude Oil. Part I: General Considerations. Part II: From the Producer's Viewpoint. Part III: From the Pipeliner's Viewpoint," paper presented at the 1956 API Annual Meeting, Chicago, Nov. 13.
- Patterson, D.R.: "Production Automation," *Pet. Engr.* (Jan. 1959) B-31.
- Pope, S.H. and Stutz, R.M.: "Lease Automatic Custody Transfer Becomes a Reality," *Oil and Gas J.* (April 23, 1956) 96.
- "Pneumatic LACT System," *Pet. Engr.* (Jan. 1957) B-104.
- "Principles of Lease Automation," *Pet. Equipment* (1957) 21.
- "Production Automation Forges Ahead," *Pet. Week* (July 26, 1957) 21.
- Reese, C.P.: "Automatic Control of the Wattenberg Gas Field—Colorado," paper SPE 11111 presented at the 1982 SPE Annual Technical Conference and Exhibition, New Orleans, Sept. 26-29.

- Resen, L.: "Humble Tries LACT, Gives A Stamp of Approval," *Oil and Gas J.* (March 4, 1957) 94.
- Saye, H.A.: "Automatic Well Testing," *Oil and Gas J.* (Jan. 6, 1958) 102.
- Scott, J.O.: "Automation Pays Off in Big Mineral Producing Operations," *Oil and Gas J.* (Sept. 19, 1955) 114.
- Scott, V.B.: "Automatic Lease Operation," paper presented at West Texas Oil Lifting Short Course, Texas Technological C., Lubbock, April 11-12, 1957.
- Shatto, H.L.: "Comments on the Status and Future of ACT from the Production Viewpoint," paper presented at the 1958 ASME Mechanical Engineering Conference, Denver, Sept. 21-24.
- Shatto, H.L. and Hall, A.H.: "Greater Rewards from LACT," *Oil and Gas J.* (April 7, 1958) 133.
- Stormont, D.H.: "Tank Bottoms Are Recycled," *Oil and Gas J.* (Nov. 12, 1956) 173.
- Taylor, D.M.: "New Auto-pneumatic Lease Programming System," *Pet. Engr.* (Dec. 1956) B-28.
- Todd, M.: "Automation Applied to Flooding at Naval Reserve Pool," *Oil and Gas J.* (March 4, 1957) 84.
- Travis, R.H.: "Complete Automation in Water Injection," *Pet. Engr.* (Feb. 1957) B-76.
- Warren, F.H.: "Automatic Gaging, Sampling, and Testing," *Oil and Gas J.* (Nov. 8, 1951) 271.
- Wasicek, J.J., Kleppinger, K.B., and Grovenburg, W.W.: "An Integrated Design of Lease Programming and Custody Transfer Facilities, paper 1125-G presented at the 33rd Annual Fall Meeting of the Society of Petroleum Engineers, AIME, in Houston, Tex., Oct. 3-8, 1958.
- Water-flood Project Is Fully Automatic," *Oil and Gas J.* (July 7, 1958) 135.
- Weaver, E.G. and Hildebrand, S.M.: "Unique Automation System Monitors South Florida Production Operations," *J. Pet. Tech.* (June 1982) 1307-12.
- "Weight Measures Flow in New Unit," *Oil and Gas J.* (Sept. 8, 1958) 66.
- "What's Ahead for Oil in Automation," *Oil and Gas J.* (June 27, 1955) 62.
- Wrightsmann, L.S.: "Experience with P.D. Meters and Fixed-volume Tank-measurement Procedures in LACT," paper presented at the 1958 ASME Mechanical Engineering Conference, Denver, Sept. 21-24.

Chapter 17

Measuring, Sampling, and Testing Crude Oil

Don G. Chancey, ARCO Oil & Gas Co.*

Introduction

In the early days of the petroleum industry, crude oil was sold by the producer in various-size containers called "the barrel." It was not until 1866 that the Pennsylvania Oil Producers had a meeting and established the size of a standard oil barrel to be 42 U.S. gal at 60°F. As the value of the oil increased and as the size and number of sales grew, it became necessary to establish a set of codes or standards by which the oil could be measured accurately and a net volume determined.

The American Petroleum Inst. (API) first established its Code 25 in April 1929, under the tentative title "API Code on Measuring Field Production and Field Tanks." This code was superseded by API Standard 2500, "Measuring, Sampling, and Testing Crude Oil" in 1955. API now publishes a two-volume, comprehensive *Manual of Petroleum Measurement Standards*, which represents all branches of the industry and is the recognized standard. It serves as the unified method and practice in measuring, sampling, and testing crude oil. As the manual is revised and as new chapters are completed, the standard designations will be replaced by chapter designations. The manual is being updated continually and care should be taken that the current standard or chapter is used.

Procedure for Typical Measuring, Sampling, and Testing

The procedure given here is the API method currently in effect for running a field tank of crude oil. Since there are many variables that would alter this method, this procedure is applicable *only* under specific conditions.

1. The tank is vertical, nonpressurized, fixed roof with side outlets, and it is to be gauged by the innage method.

2. The oil is less than 100 seconds at 100°F (Saybolt universal viscosity) and is a liquid at atmospheric temperature and pressure.

3. A cup case thermometer is used to read temperature of the oil in the tank.

4. A thief is used to obtain fluid samples from the tank.

5. The API gravity scale hydrometer test method is used to determine the API gravity of the oil; the temperature of the oil has to be near 60°F ($\pm 5^\circ\text{F}$).

6. The water and sediment in the oil is to be determined by the centrifuge method with a 203-mm [8-in.] cone-shaped tube.

The following outline gives the sequence of steps to be taken and the key points to be noted at each step.

1. Isolate the tank to be checked.

2. Use face mask and fresh air bottles if H₂S hazard exists.

3. Ground your body to stair railing or tank shell before reaching the top. This prevents static electrical discharge in a hazardous area.

4. Stand to the side of the hatch when opening to permit wind to blow gas away from face.

5. Measure temperature. Suspend thermometer in oil tank. Thermometer should be 12 in. or more from tank shell and must be immersed in oil for 5 minutes.

Use an ASTM-approved, wood-back or corrosion-resistant metal cup case. If atmospheric temperature differs by more than 20°F from that of the liquid in the tank, the cup case should be given at least two preliminary immersions. Empty the cup case after each immersion.

Rapidly withdraw the thermometer and read and record the temperature to the nearest 1°F.

Note: The number of temperature measurements varies with the depth of the liquid.¹

*The original chapter on this topic in the 1962 edition was taken from API Standard 2500.

In a tank containing more than 15 ft of liquid, three measurements should be taken: (1) 3 ft below the top surface of the liquid; (2) middle of the liquid; and (3) 3 ft above bottom of the liquid.

In a tank containing 10 to 15 ft of liquid, two measurements should be taken: (1) 3 ft below the top surface of liquid; and (2) 3 ft above the bottom surface of liquid.

In a tank containing less than 10 ft of liquid, one measurement should be taken in the middle of the liquid.

For tanks over 10 ft high with a capacity of less than 5,000 bbl, one measurement in the middle of the liquid should be taken.

6. With a thief, take sample(s) for basic sediment and water (BS&W) centrifuge test.

Note: The number of samples to be taken for BS&W determination varies.²

In tanks larger than 1,000-bbl capacity that contain more than 15 ft of liquid, equal-volume samples should be taken (1) 6 in. below the top of the liquid, (2) at the middle of the liquid, and (3) at the outlet connection of the merchantable oil, in the order named. This method also may be used in tanks up to and including a capacity of 1,000 bbl.

In a tank larger than 1,000-bbl capacity that contains more than 10 ft and up to 15 ft of liquid, equal-volume samples should be taken (1) 6 in. below the top surface of the liquid and (2) at the outlet connection of the merchantable oil, in the order named. This method may be used on tanks up to and including a capacity of 1,000 bbl.

In a tank larger than 1,000-bbl capacity that contains 10 ft or less liquid, one sample may be taken in the middle of the column of liquid.

7. Place BS&W composite sample in sample container. Sample should be a blend of the upper, middle, and lower (if three samples were required) containing equal parts from the samples taken.

8. Seal sample container. In the lower 48 states, with the exception of California, the sample is ready to be tested for BS&W as described below in Step 17. In California, the container should be labeled and delivered to the laboratory for BS&W determination.

9. With a thief, take sample for gravity determination.³ The sample should be taken midway between oil surface and pipeline connection. Hang the thief in the hatch. Remove bubbles. Place hydrometer in oil sample.

10. Determine and record sample temperature to nearest 0.5°F. Hydrometer must float away from wall of cylinder; temperature of surrounding media should not change more than 5°F.

Depress hydrometer two scale divisions and release.

Read hydrometer to nearest 0.05°API on scale at which surface of liquid cuts scale.

11. Read and record sample temperature to nearest 0.5°F. Repeat gravity reading if temperature of sample before and after reading of gravity has changed more than 1°F. Apply any relevant correction to observed hydrometer reading (correction scale on bulb) to nearest 0.1°API. Record the mean temperature reading observed before and after final hydrometer reading to nearest 1°F.

Note: Hydrometer scale readings at temperatures other than calibration temperatures (60°F) should not be considered more than scale readings since the hydrometer bulb changes with temperature.

12. Convert relevant corrected value to standard temperatures. Use Table 5A* for crude oils.

13. Take bottom thief sample for BS&W height. Lower the clean, dry thief slowly into the oil to the desired depth, trip thief and raise slowly to avoid agitation. When sample is taken, the top of the thief must be two inches above the bottom of the pipeline connections.

14. Determine and record BS&W height in the tank. Pour remaining thief sample over a test glass until contamination appears. Measure and record (as the BS&W height) the distance from the bottom of the thief to the top of the contamination in the thief. If BS&W height is less than 4 in. from the bottom of the pipeline connection, do not run the tank.

15. Gauge the tank.⁴ Do not gauge a boiling or foaming tank. Use steel innage tape with innage plumb bob. Always make contact between gauge line and hatch while running tape into tank.

Gauge the tank only at the reference point on the gauging hatch. On tanks of 1,000-bbl capacity or less, read to the nearest ¼ in. On tanks of 1,000 bbl or more, read to the nearest ⅛ in.

Record the reading immediately. Repeat the above until two identical gauges are obtained.

16. Saturate solvent with water.⁵ Toluene is approved solvent. It is flammable and toxic. Care should be taken when using toluene.

Fill a 1-qt or 1-L glass bottle with a screw top with 700 to 800 mL toluene. Add 25 mL of either distilled or tap water. Screw cap on. Shake vigorously for 30 seconds. Loosen cap.

Place bottle in bath for 30 minutes. Maintain bath at a constant temperature of 140°F ± 5°F.

Remove, tighten cap and shake vigorously for 30 seconds. Repeat three times.

Allow bottle of water/toluene mixture to sit in bath for 48 hr before using. Be sure no free water is left in bottle.

17. Shake sample container until sample is well mixed.

Fill each of two 203-mm [8-in.] cone-shaped centrifuge tubes with 50 mL of sample.

Use pipette to add 50 mL of toluene. Toluene should be water saturated at 140°F. Read top of meniscus at both the 50 and 100 mL marks.

Add 0.2 mL demulsifier if necessary for clean break in oil/water contact.

Stopper the tube tightly. Invert tube 10 times to ensure that oil and solvent are uniformly mixed.

18. Loosen stopper slightly. Immerse tube to the 100 mL mark in bath for 15 minutes. Bath must maintain 140°F ± 5°F; by contract agreement the bath temperature may be 120°F ± 5°F.

Remove tube from bath and tighten stopper. Invert tube 10 times to ensure that oil and solvent are uniformly mixed.

19. Place tubes in trunnion cups on opposite sides of centrifuge. Spin for 10 minutes while maintaining minimum relative centrifuge force of 600.

Following spinning, read and record the combined volume of water and sediment at the bottom of each tube. Read to the nearest 0.05 mL for oil from 0.1 to 1

* See API Manual, Chap. 11.1, Vol. 1 (1980) listed on Page 17-5.

mL graduation. Read to nearest 0.1 mL above 1 mL graduation. Estimate to nearest 0.025 mL below 0.1-mL graduation.

Return tube to centrifuge without agitation. Spin for 10 minutes at same rate. Repeat this operation until the combined volume of water and sediment remains constant on two consecutive readings.

20. Record final volume of water and sediment in each tube. The sum of the two admissible readings is the percentage by volume of water and sediment in the sample.

After the tank has been run, the following closing data should be obtained.

21. Closing oil temperature: no closing temperature is necessary on tanks of 5,000 bbl or less; on tanks 5,000 bbl or more, always read to the nearest 1°F.

22. Obtain closing gauge reading at the same point and in the same manner as the opening gauge reading.

23. Obtain bottom thief. If BS&W level is lower than the opening gauge, report to supervisor.

Abstract of API Manual

Publications and Distribution Section, American Petroleum Inst., 2101 L St. NW, Washington, DC 20037.

Since the *API Manual of Petroleum Measurement Standards* is the industry's standard on this subject and since the manual is quite long, this chapter is a reference to the API manual.

The following table of contents of the API manual lists the chapter titles, the API stock number, and a short abstract of the content of each chapter. These chapters can be ordered from the API.

API Chap. 1—Vocabulary

First edition (April 1977).

The words and terms used throughout the entire *Manual of Petroleum Measurement Standards* are defined and described in this vocabulary.

API Chap. 2—Tank Calibration

Measurement and Calibration of Upright Cylindrical Tanks. *API Publication 852-25500, API Standard 2550, first edition (Oct. 1965).* This standard describes the procedures for calibrating upright cylindrical tanks larger than a barrel or drum. It is presented in two parts. Part I (Secs. 8 through 41) outlines procedures for making necessary measurements to determine total and incremental tank volumes; Part II (Secs. 42 through 58) presents the recommended procedure for computing volumes.

Measurement and Calibration of Horizontal Tanks. *API Publication 852-25510, API Standard 2551, first edition (Oct. 1965).* This standard describes external measurement procedures for calibrating horizontal aboveground stationary tanks larger than a barrel or drum. It is presented in two parts.

Part I (Secs. 7 through 21) includes procedures for the measurement of horizontal, and tilted, cylindrical aboveground tanks with various types of heads; descriptions of tank-measuring equipment and procedures for the calibration of that equipment for which calibration is required; and suggestions for the orderly and complete recording of field measurement data, including tank measurement record forms.

Part II (Secs. 22 through 44) includes procedures for calculating the incremental tank capacities from the field data, suitable for the preparation of incremental capacity gauge tables. Typical examples of calculations are included in Appendix I, as are convenient tables of shape factors for determining contained liquid volume in horizontal cylinders and in formed heads at any liquid depth.

Measurement and Calibration of Spheres and Spheroids. *API Publication 852-25520, API Standard 2552, first edition (Oct. 1965).* This standard describes the procedures for calibrating spheres and spheroids that are used as liquid containers. It is presented in two parts. Part I (Secs. 2 through 10) outlines the procedures for the measurement and calibration of spherical tanks; Part II (Secs. 11 through 20) outlines the procedures for the measurement and calibration of spheroidal tanks.

Measurement and Calibration of Barges. *API Publication 852-25530, API Standard 2553, first edition (Oct. 1966).* This standard describes procedures for calibrating barge tanks. It is presented in two parts.

Part I (Secs. 7 through 9) includes procedures for determining the required field measurement data, description of tank measurement equipment, and suggestions for the orderly and complete recording of field data.

Part II (Secs. 10 through 13) includes procedures for calculating the total and incremental tank capacities from the field data, suitable for preparation of the capacity gauge table. Typical examples of calculations are included in Appendix II.

Measurement and Calibration of Tank Cars. *API Publication 852-25540, API Standard 2554, first edition (Oct. 1965).* This standard describes the procedures for calibrating tank cars. It is presented in two parts: Part I (Secs. 2 through 21) outlines procedures for nonpressure-type tank cars; Part II (Secs. 22 through 31) outlines procedures for pressure type tank cars.

Method for Liquid Calibration of Tanks. *API Publication 852-25550, API Standard 2555 (Sept. 1966).* This standard describes the procedure for calibrating tanks, or portions of tanks, larger than a barrel or drum by introducing or withdrawing measured quantities of liquid.

Correcting Gauge Tables for Incrustation. *API Publication 852-25560, API RP 2556, first edition (Aug. 1968); supersedes supplement No. 1 to API Standard 2500.* This recommended practice defines incrustation, describes the materials involved and recommends methods to correct the observed volume gauged.

API Chap. 3—Tank Gauging

Method of Gauging Petroleum and Petroleum Products. *API Publication 852-25450, API Standard 2545 (Oct. 1965).* This standard describes the procedures for gauging crude petroleum and its liquid products in various types of tanks, containers, and carriers. Secs. 3 through 58 are applicable for measuring quantities of liquids having Reid vapor pressure (Rvp) under 40 psig;

Secs. 59 through 64 are applicable for measuring liquefied petroleum gases and other products having Rvp of 40 psig or more. The determination of temperature, API gravity, and sediment and water are not within the scope of this standard; however, brief descriptions of portable equipment used for this purpose are included in Secs. 8 and 9.

API Chap. 4—Proving Systems *API Publication 852-2315, first edition (May 1978).*

This publication serves as a guide for the design, installation, calibration and operation of meter proving systems. All types of proving systems commonly used by the petroleum industry are covered, including field standards, pipe provers, tank provers, master meter provers, meter proving, and analysis of sphere position repeatability.

Proving systems covered in former API Standards 1101, 2531, 2533, and 2534 (*Measurement of Petroleum Liquid Hydrocarbons by Positive Displacement Meter; Mechanical Displacement Meter Provers; Metering Viscous Hydrocarbons; and Measurement of Liquid Hydrocarbons by Turbine Meter Systems*) are combined in this publication, which supersedes the former standards.

This publication is intended primarily for use in the U.S. and, therefore, is related to the standards, specifications, and procedures of the (U.S.) Natl. Bureau of Standards (NBS). When it is desired to use the publication in other countries, the appropriate national standards organizations and their specifications and procedures apply.

API Chap. 5—Metering

Sec. 1—Foreword, General Considerations, and Scope of Chap. 5—Metering. *API Publication 852-30101, first edition (Nov. 1976).* This is an overall introduction to Chap. 5, Metering.

Sec. 2—Measurement of Liquid Hydrocarbons by Displacement Meter Systems. *API Publication 852-30102, first edition (Jan. 1977).* This section specifies the characteristics of displacement meters and gives rules for systematically applying appropriate consideration to the nature of the liquids to be measured, to the installation of a metering system, and to the selection, performance, operation, and maintenance of the same. It does not apply to two-phase fluids. Special precautions should be taken when used in mass measurement systems.

Sec. 3—Turbine Meters. *API Publication 852-30103, first edition (July 1976).* This section specifies the characteristics of turbine meters and gives rules for applying appropriate considerations to the nature of the liquids to be measured, to the installation of a metering system using a turbine meter, and to the performance, operation, and maintenance of the same in liquid hydrocarbon service.

Sec. 4—Instrumentation or Accessory Equipment for Liquid Hydrocarbon Metering Systems. *API Publication 852-30104, first edition (July 1976).* This publication serves as a guide for the instrumentation of liquid

hydrocarbon meters to obtain optimal accuracy and service life of metering systems. Selection of any piece of accessory equipment described herein depends on the function, design, purpose, and manner in which a measurement installation is to be used.

The application of this publication is limited to instrumentation by accessory equipment made essentially to enhance the usage of liquid hydrocarbon meters. Thus, all valves, manifolding, vents, etc. are not included. Thermometers, hydrometers, and pressure gauges are discussed but only so far as certain minimum requirements must be met.

Sec. 5—Fidelity and Security of Flow Measurement Pulsed-Data Transmission Systems. *API Publication 852-30105, first edition (June 1982).* This chapter provides a guide to the selection, operation, and maintenance of pulsed-data, cabled transmission systems for fluid metering systems to provide the desired level of fidelity and security of transmitted data.

API Chap. 6—Metering Assemblies

Sec. 1—LACT Systems. *API Publication 852-30121, first edition (Feb. 1981).* This chapter serves as a guide for the design, installation, calibration, and operation of lease automatic custody transfer (LACT) systems.

Sec. 5—Metering Systems for Loading and Unloading Marine Bulk Carriers. *API Publication 852-30125, first edition (July 1980).* This section deals with the operation and special arrangements of meters, provers, manifolding, instrumentation, and accessory equipment used for measurement in loading and unloading marine bulk carriers.

The information provided in this section is applicable to shore-to-carrier and carrier-to-shore measurement of crude oils and refined products. These procedures are not intended to apply to hydrocarbons and other materials such as liquefied petroleum gas (LPG) or liquefied natural gas (LNG), which require specialized measurement and handling equipment.

Sec. 6—Pipeline Metering Systems. *API Publication 852-30126, first edition (Aug. 1981).* This section provides guidelines for the selection of the type and size of meter(s) to be used to measure pipeline oil movements. Types of accessories and instruments that may be desirable are specified, and the relative advantages and disadvantages of three methods of proving meters (by tank prover, by pipe prover, and by master meter) are discussed. This section also includes discussions on obtaining the best operating results from a pipeline meter station.

Sec. 7—Metering Viscous Hydrocarbons. *API Publication 852-30127, first edition (Jan. 1981).* This section serves as a guide for the design, installation, operation, and proving of meters and their auxiliary equipment used to meter viscous hydrocarbons.

Measurement of Petroleum Liquid Hydrocarbons by Positive Displacement Meter. *API Publication 852-11010, API Standard 1101, first edition (Aug. 1960).* This section covers the installation of positive

displacement meters, their auxiliary proving equipment, and other accessories. All types of meter installations must meet certain fundamental requirements. These include accurate proving facilities; adequate protective devices, such as strainers, relief valves, and air or vapor eliminators; and dependable pressure and flow controls. A further fundamental installation requirement is that physical conditions during operations and proving should be identical.

API Chap. 7—Temperature Determination

This chapter is in preparation. It will cover the sampling, reading, averaging, and rounding of the temperature of liquid hydrocarbons in both the static and dynamic modes of measurement for volumetric purposes.

The following API standard now covers the subject of temperature determination.

Method of Measuring the Temperature of Petroleum and Petroleum Products. *API Publication 852-25430, API Standard 2543 (Oct. 1965).* This standard describes the thermometer assemblies and temperature levels used in various tanks and carriers of petroleum.

API Chap. 8—Sampling

Sec. 1—Manual Sampling of Petroleum and Petroleum Products. *API Publication 852-30161 (ASTM D 4057), first edition (Oct. 1981).* This section covers the procedures for obtaining representative samples of stocks or shipments of uniform petroleum products, except electrical insulating oils and fluid power hydraulic fluids. Sampling crude petroleum and nonuniform petroleum stocks and shipments also are covered, although the representative nature of these sampling methods is in doubt.

API Chap. 9—Density Determination

Sec. 1—Hydrometer Test Method for Density, Relative Density (Specific Gravity), or API Gravity of Crude Petroleum and Liquid Petroleum Products.

API Publication 852-30181 (ASTM D 1298), first edition (June 1981). This section describes the methods and practices relating to the determination of the density, relative density, or API gravity of crude petroleum and liquid petroleum products by using the hydrometer method (laboratory determination).

Sec. 2—Pressure Hydrometer Test Method for Density or Relative Density. *API Publication 852-30182, first edition (April 1982).* This section provides a guide for determining the density, relative density (specific gravity), or API gravity of light hydrocarbons, including liquefied petroleum products, using a pressure hydrometer.

API Chap. 10—Sediment and Water

Sec. 1—Determination of Sediment in Crude Oils and Fuel Oils by the Extraction Method. *API Publication 852-30201, first edition (April 1981).* This section specifies a method for the determination of sediment in crude oils and fuel oils by extraction with toluene.

Sec. 2—Determination of Water in Crude Oil by the Distillation Method. *API Publication 852-30202, first*

edition (April 1981). This publication specifies a method for the determination of water in crude oil.

Sec. 3—Determination of Water and Sediment in Crude Oil by the Centrifuge Method (Laboratory Procedure). *API Publication 852-30203, first edition (April 1981).* This method describes the laboratory determination of water and sediment in crude oil by means of the centrifuge procedure. This centrifuge method is not entirely satisfactory. The amount of water detected is almost always lower than the actual water content. When a highly accurate value is required, the revised procedures for water by distillation (API Chap. 10.2) and sediment by extraction (API Chap. 10.1) must be used.

API Chap. 11—Physical Properties Data

Chap. 11 includes the physical data that have direct application to volumetric measurement of liquid hydrocarbons. It is presented in table form, in equations relating volume to temperature and pressure, computer subroutines, magnetic tape, and microfilm.

Chap. 11.1, "Volume Correction Factors, 1980," (ASTM D 1250) (IP 200) is available on magnetic tape and includes a paper edition of Vol. X. [*API Publication 852-27150, first edition (Aug. 1980).*] The tape is nine-track, 1,600 bites/in., EBCDIC, unlabeled, fixed block and requires a 32-bit or higher machine. Chap. 11.1 is also available as a FORTRAN card deck (includes paper edition of Vol. X) [*API Publication 852-27151, first edition (Aug. 1980).*] and on microfiche (includes paper edition of Vol. X) [*API Publication 852-27152, first edition (Aug. 1980).*]

The following is a list of tables and computer subroutines to found in Chap. 11.1 through 11.3.

Chap. 11.1, Vol. I, 1980. *ASTM publication (ASTM D 1250).* (*ASTM publications can be ordered from ASTM, 1916 Race St., Philadelphia, PA 19103.*) Table 5A—Generalized Crude Oils, Correction of Observed API Gravity to API Gravity at 60°F.

Table 6A—Generalized Crude Oils, Correction of Volume to 60°F Against API Gravity at 60°F.

Chap. 11.1, Vol. II, 1980. *API Publication 852-27015, first edition (Aug. 1980).* Table 5B—Generalized Products, Correction of Observed API Gravity to API Gravity at 60°F.

Table 6B—Generalized Products, Correction of Volume to 60°F Against API Gravity at 60°F.

Chap. 11.1, Vol. III, 1980. *ASTM publication (ASTM D 1250).* Table 6C—Volume Correction Factors for Individual and Special Applications, Volume Correction to 60°F Against Thermal Expansion Coefficients at 60°F.

Chap. 11.1, Volume IV, 1980. *API Publication 852-27045, first edition (Aug. 1980).* Table 23A—Generalized Crude Oils, Correction of Observed Relative Density to Relative Density at 60/60°F.

Table 24A—Generalized Crude Oils, Correction of Volume to 60°F Against Relative Density 60/60°F.

Chap. 11.1, Vol. V, 1980. *API Publication 852-27060, first edition (Aug. 1980).* Table 23B—Generalized Pro-

ducts, Correction of Observed Relative Density to Relative Density at 60/60°F.

Table 24B—Generalized Products, Correction of Volume to 60°F Against Relative Density 60/60°F.

Chap. 11.1, Vol. VI, 1980. *API Publication 852-27085, first edition (Aug. 1980).* Table 24C—Volume Correction Factors for Individual and Special Applications, Volume Correction to 60°F Against Thermal Expansion Coefficients at 60°F.

Chap. 11.1, Vol. VII, 1980. *API Publication 852-27100, first edition (Aug. 1980).* Table 53A—Generalized Crude Oils, Correction of Observed Density to Density at 15°C.

Table 54A—Generalized Crude Oils, Correction of Volume to 15°C Against Density of 15°C.

Chap. 11.1, Vol. VIII, 1980. *API Publication 852-27115, first edition (Aug. 1980).* Table 53B—Generalized Products, Correction of Observed Density to Density at 15°C.

Table 54B—Generalized Products, Correction of Volume to 15°C Against Density at 15°C.

Chap. 11.1, Vol. IX, 1980. *API Publication 852-27130, first edition (Aug. 1980).* Table 54C—Volume Correction Factors for Individual and Special Applications, Volume Corrections to 15°C Against Thermal Expansion Coefficients at 15°C.

Chap. 11.1, Vol. X, 1980. *API Publication 852-27145, first edition (Aug. 1980).* This volume gives the background, development, and computer documentation for all tables listed in Chap. 11.1 Vol. I through Vol. IX.

Chap. 11.1, Vol. XI, 1982, "Petroleum Measurement Subsidiary." *ASTM Publication (ASTM D 1250).*

Table 1—Interrelation of Units of Measurement.

Table 2—Temperature Conversions.

Table 3—API Gravity at 60°F to Relative Density 60/60°F and to Density at 15°C.

Table 4—U.S. Gallons at 60°F and Barrels at 60°F to Liters at 15°C Against API Gravity at 60°F.

Table 8—Pounds per U.S. Gallon at 60°F and U.S. Gallons at 60°F per Pound against API Gravity at 60°F.

Table 9—Short Tons per 1000 U.S. Gallons at 60°F and per Barrel at 60°F Against API Gravity at 60°F.

Table 10—U.S. Gallons at 60°F and Barrels at 60°F per Short Ton Against API Gravity at 60°F.

Table 11—Long Tons per 1000 U.S. Gallons at 60°F and per Barrel at 60°F Against API Gravity at 60°F.

Table 12—U.S. Gallons at 60°F and Barrels at 60°F per Long Ton Against API Gravity at 60°F.

Table 13—Metric Tons (Tonnes) per 1000 U.S. Gallons at 60°F and per Barrel at 60°F Against API Gravity at 60°F.

Table 14—Cubic Meters at 15°C per Short Ton and per Long Ton Against API Gravity at 60°F.

Chap. 11.1, Vol. XII, 1982, "Petroleum Measurement Subsidiary." *ASTM Publication (ASTM D 1250).* Table 21—Relative Density 60/60°F to API Gravity at 60°F and to Density at 15°C.

Table 22—U.S. Gallons at 60°F to Liters at 15°C and Barrels at 60°F to Cubic Meters at 15°C.

Table 26—Pounds per U.S. Gallon at 60°F and U.S. Gallons at 60°F per Pound Against Relative Density 60/60°F.

Table 27—Short Tons per 1000 U.S. Gallons at 60°F and per Barrel at 60°F Against Relative Density 60/60°F.

Table 28—U.S. Gallons at 60°F and Barrels at 60°F per Short Ton Against Relative Density 60/60°F.

Table 29—Long Tons per 1000 U.S. Gallons at 60°F and per Barrel at 60°F Against Relative Density 60/60°F.

Table 30—U.S. Gallons at 60°F and Barrels at 60°F per Long Ton Against Relative Density 60/60°F.

Table 31—Cubic Meters at 15°C per Short Ton and per Long Ton Against Relative Density 60/60°F.

Table 33—Specific Gravity Reduction to 60°F for Liquefied Petroleum Gases and Natural Gasoline.

Table 34—Reduction of Volume to 60°F Against Specific Gravity 60/60°F for Liquefied Petroleum Gases.

Table 51—Density at 15°C to Relative Density 60/60°F and to API Gravity at 60°F.

Table 52—Barrels at 60°F to Cubic Meters at 15°C and Cubic Meters at 15°C to Barrels at 60°F.

Table 56—Kilograms per Liter at 15°C and Liters at 15°C per Metric Ton Against Density at 15°C.

Table 57—Short Tons and Long Tons per 1000 Liters at 15°C Against Density at 15°C.

Table 58—U.S. Gallons and Barrels per Metric Ton Against Density at 15°C.

Chap. 11.1, Vol. XIII, 1982. *API Publication 852-27185, first edition (Jan. 1982).* Table 5D—Generalized Lubricating Oils, Correction of Observed API Gravity to API Gravity at 60°F.

Table 6D—Generalized Lubricating Oils, Correction of Volume to 60°F Against API Gravity at 60°F.

Chap. 11.1, Vol. XIV, 1982. *API Publication 852-27200, first edition (Jan. 1982).* Table 53D—Generalized Lubricating Oils, Correction of Observed Density to Density at 15°C.

Table 54D—Generalized Lubricating Oils, Correction of Volume to 15°C Against Density at 15°C.

Chap. 11.1.77, Extrapolation of Table 6A to -50°F, Volume Reduction Factors, 1976. *API Publication 852-25393.* This chapter is a computer printout of Subroutine Table 6 in extrapolated form.

Standard Tables for Positive Displacement Meter Prover Tanks, 1966. *API Publication 852-25410, API Standard.* These tables provide multipliers for converting to 60°F the volumes of petroleum and petroleum products measured at temperatures between 0 and 125°F in insulated, mild steel prover tanks for positive displacement meters.

Chap. 11.3.2.1, Ethylene Density. *API Publication 852-25650, first edition (1974).* This chapter is a computer subroutine and includes subordinate subroutines "rubin" and "taint" on one FORTRAN IV card deck. It

will produce either a density (lbm/cu ft) or a compressibility factor for vapor-phase ethylene over the temperature range of 65 to 167°F and the pressure range of 200 to 2,100 psia.

Chap. 11.3.3.1, Propane Compressibility Table. *API Publication 852-25654, first edition (1974).* This FORTRAN IV subroutine is applicable to liquid-phase propane in the following ranges: relative density, 0.500 to 0.510; temperature, -20 to 120°F; saturation pressure to 1,500 psia. The subroutine computes the following two values: average compressibility per psi (this factor would be applied in the same manner as compressibilities in the current API Standard 1101) and the ratio of volume at flowing temperature and pressure to volume at flowing temperature and saturation pressure.

Chap. 11.3.3.2, Propylene Compressibility Table. *API Publication 852-25656, first edition (1974).* This FORTRAN IV subroutine is applicable to liquid-phase propylene in the following ranges: temperature, 30 to 165°F; and saturation pressure to 1,600 psia. The subroutine computes the following two values: density in lbm/cu ft at flowing temperature and pressure, and the ratio of density at flowing conditions to density at 60°F and saturation pressure.

API Chap. 12—Calculation of Petroleum Quantities

Sec. 2—Calculation of Liquid Petroleum Quantities Measured by Turbine or Displacement Meters. *API Publication 852-30302, first edition (Sept. 1981).* This publication defines the various terms (words or symbols) employed in the calculation of metered petroleum quantities. Where two or more terms customarily are employed in the oil industry for the same thing, this publication selects what should become the new standard term—for example, “run tickets,” “receipt and delivery tickets,” and the like are herein simply “measurement tickets.”

The publication also specifies the equations that allow the values of correction factors to be computed. Rules for sequence, rounding, and significant figures to be employed in a calculation are given. In addition, some tables, convenient for manual as well as computer calculations, are provided.

Field Manual, Sec. 2—Instructions for Calculating Liquid Petroleum Quantities Measured by Turbine or Displacement Meters. *API Publication 852-30303, first edition (Sept. 1981).* This document is the user's field manual. It is addressed to those who need instructions without explanations as to why a particular course of action is necessary to achieve the same answer from the same data, regardless of who or what does the computing.

The user's field manual is an instruction document. Those who wish or need to know more about the background to a set of instructions should obtain Chap. 12, Sec. 2, which is an instruction and explanation document.

API Interim Chap. 13—Measurement Control

Charts and Statistical Methods for Petroleum Metering Systems. *API Publication 852-25342, API Standard*

2534, Appendix B, first edition (March 1970). The more accurate petroleum measurement becomes, the more its practitioners stand in need of statistical methods to express residual uncertainties. This chapter covers the application of statistical methods to petroleum measurement and sampling. Chap. 13 is in preparation.

API Chap. 14—Natural Gas Fluids Measurement

Sec. 1—Measuring, Sampling, Testing, and Base Conditions for Natural Gas Fluids. *API Publication 852-30341, third edition (March 1975).* This chapter presents recommended practices that cover the production, transportation, and custody transfer of natural gas and the products recovered excluding LNG.

Sec. 3—Orifice Metering of Natural Gas. *API Publication 852-30343, first edition (Sept. 1981).* This standard provides guidance on the measurement of natural gas flow. It provides the standards for construction and installation of orifice plates and associated fittings and instructions for computing the flow of natural gas through orifice meters. Also included are the necessary tables providing the basic factors to apply to adjust for expansion, Reynolds number, temperature, pressure, specific gravity, and supercompressibility.

Sec. 5—Calculation of Gross Heating Value, Specific Gravity, and Compressibility of Natural Gas Mixtures From Compositional Analysis. *API Publication 852-30345, first edition (Jan. 1981).* This publication outlines a procedure for calculating from compositional analysis the following properties of natural gas mixtures: heating value, specific gravity, and compressibility factor.

Sec. 6—Installing and Proving Density Meters Used To Measure Hydrocarbon Liquid with Densities Between 0.3 and 0.7 g/cm³ at 15.56°C [60°F] and Saturation Vapor Pressure. *API Publication 852-30346, first edition (Sept. 1979).* This publication provides a method for installation and accurately proving density meters that measure light hydrocarbons used in static or dynamic conditions.

API Chap. 15—Guidelines for the Use of the Intl. System of Units (SI) in the Petroleum and Allied Industries. *API Publication 852-25640, second edition (Dec. 1980).*

This publication specifies the API preferred units for quantities involved in petroleum industry measurements and indicates factors for conversion of quantities expressed in customary units to the API-preferred metric units. The quantities that comprise the tables are grouped into convenient categories related to their use. They were chosen to meet the needs of the many and varied aspects of the petroleum industry but also should be useful in other, similar process industries. Chap. 58 of this edition of *Petroleum Engineering Handbook* is the *SPE Metric Standard*.

API Chap. 16—Measurement of Petroleum by Weight (in preparation)

The purpose of this chapter is to provide references to model regulations promulgated by the National Con-

ference of Weights and Measures regarding commercial weighing, tolerances, and other technical requirements, and to describe the recognized practices of the petroleum industry when products are handled on a weight basis.

API Chap. 17—Marine Measurement

This chapter provides guidelines that suggest the actions to be taken in measuring and reporting quantities of crude oil or petroleum product marine transfers by shore terminal operators, vessel personnel, and other parties involved in cargo transfer measurement and accountability operations.

Sec. 1—Guidelines for Marine Cargo Inspection. *API Publication 852-30401, first edition (April 1982).* This chapter provides guidelines to encourage uniform marine cargo inspection practices and to simplify the making of contracts that can be interpreted clearly and executed between parties.

References

1. *Method of Measuring the Temperature of Petroleum and Petroleum Products*, API Standard 2543, API, Washington, DC (Oct. 1965).
2. API Chap. 8, *Manual of Petroleum Measurement Standards, Sampling; Sec. 1—Manual Sampling of Petroleum and Petroleum Products*, API, Washington, DC (Oct. 1981).
3. API Chap. 9, *Manual of Petroleum Measurement Standards, Density Determination; Sec. 1—Hydrometer Test Method for Density, Relative Density (Specific Gravity), or API Gravity of Crude Petroleum and Liquid Petroleum Products*, API, Washington, DC (June 1981).
4. *Method of Gauging Petroleum and Petroleum Products*, API Standard 2545, API, Washington, DC (Oct. 1965).
5. API Chap. 10, *Manual of Petroleum Measurement Standards, Sediment and Water; Sec. 3—Determination of Water and Sediment in Crude Oil by the Centrifuge Method (Laboratory Procedure)*, API, Washington, DC (April 1981) Appendix A.

Chapter 18

Offshore Operations

William H. Silcox, Chevron Corp.

James A. Bodine, Chevron Corp.

Gerald E. Burns, Chevron Corp.

Carter B. Reeds,* Chevron Corp.

Donald L. Wilson, Chevron Corp.

Edward R. Sauve, Chevron Corp.

Introduction

Offshore petroleum operations emerged in the 20th century and brought new dimensions of challenge and excitement to oil exploration and production. When a structure taller than a 100-story building is launched from a barge, or when a small city is built and placed offshore in 2 years, those involved deserve their feelings of pride and accomplishment.

In nearly every corner of the globe, thousands of offshore installations with payloads from 5 to 50,000 tons are producing gas and oil today in water depths from 10 to 1,000 ft. Although subjected to winds and waves up to hurricane intensity, earthquakes, sheet ice, severe tides and currents, or shifting foundations, surprisingly few structures have succumbed to the environment despite the difficulty in predicting environmental forces, equipment failure, or reservoir behavior.

This chapter can only scratch the surface of offshore operations; detailed procedures for design and construction of structures, equipment, and facilities would require volumes. Furthermore, such volumes would be obsolete before they were published. Because there is no concise reference or set of references, this chapter describes the fundamentals of standard practice in several disciplines and offers guidance for the selection of appropriate offshore codes of practice and technical references.

Historical Review

In 1859, Col. Edwin Drake drilled and completed the first known oil well near a small town in Pennsylvania. This well, which was drilled with cable tools, started the modern petroleum industry. Drilling methods and tools remained in their infancy for more than 40 years, until hydraulic rotary drilling techniques were first used to drill

the Spindletop well in 1901. By then, the petroleum industry was already moving offshore.

In 1897, near Summerland, CA, H.L. Williams extended an onshore oil field into the Santa Barbara Channel by drilling a submarine well from a pier. This first offshore well was drilled just 38 years after Col. Drake's well. Five years later, more than 150 offshore wells were producing oil. Production from the California piers continues even today.

From this start, offshore drilling actually turned inland with activity in the Great Lakes, Caddo Lake in Louisiana, and Lake Maracaibo in Venezuela. Initially, wells were drilled from shore-connected piers and later from wooden single-well platforms. During this period of inland offshore drilling, platform technology remained basic. The one step forward was the change from wooden platforms to concrete structures in Lake Maracaibo.

In the late 1920's, steel production piers that extended a quarter of a mile into the ocean at Rincon and Elwood, CA, were built and new high-producing wells stimulated exploration activity. In 1932, a small company called Indian Petroleum Corp. determined that there was a likely prospect about ½ mile from shore. Instead of building a monumentally long pier, they decided to build a portion of a pier with steel piles and crossmembers. Adding a deck and barging in a derrick completed the installation. By Sept. 1932, the 60×90-ft "steel island" was completed in 38 ft of water with a 25-ft air gap. This first open-seas offshore platform supported a standard 122-ft steel derrick and associated rotary drilling equipment. Successful drilling with largely unsuccessful results was carried on intermittently on the "steel island" until 1939, when the third well was completed on the pump at 40 B/D.

In Jan. 1940, a Pacific storm destroyed the steel island. During the subsequent cleanup, divers were used for the first time to remove well casing and to set abandonment plugs.¹

*Deceased

Meanwhile, the first offshore field was discovered in the Gulf of Mexico in 1938. A well was drilled to 9,000 ft off the coast of Texas in 1941. With the start of World War II, however, offshore activities came to a halt. Activity did not resume until 1945 when the State of Louisiana held its first offshore lease sale.

At the end of the war, surplus Navy ships and barges became available to the oil industry. At first, Navy landing craft (LST's) were converted into tenders to support drilling operations on offshore platforms. By installing mud systems and electrical generation equipment, and by storing consumables on the tender, engineers reduced drilling platform payloads by a factor of 10.

The development of tender-supported platform rigs pointed the way toward mobile exploratory rigs that could move on and off location, thereby eliminating the cost of fixed drilling platforms. During the late 1940's and early 1950's, a number of mobile rigs were developed in rapid succession.

First was the posted barge, which consisted of a submersible barge with the drilling rig mounted on steel columns. The barge was sunk on location with the drilling rig clear of the water. Next came the submersible, with large vertical columns that provided enough buoyancy to transport the drilling rig while floating. These rigs were sunk on location with the drilling rig and deck remaining above water. Finally came the jackup rig. This rig consisted of a barge hull fitted with vertical legs that could be jacked down until they contacted the ocean floor, thus raising the barge, which supported the drilling rig, clear of the water. While the bottom-supported drilling rigs were being developed for the shallow waters of the Gulf of Mexico, floating drilling vessels and techniques were being developed for offshore California. There, water depths in excess of 500 ft were found inside the 3-mile limit.

Civil and structural engineers were largely responsible for the development of submersible and jackup rigs, but naval architects and marine engineers were called on to convert military ships for the drilling industry. Mechanical engineers from the oil fields designed the specialized subsea and shipboard drilling equipment.

The first floating drilling vessels were converted mine sweepers with A-frames over the side for handling pipe and jet bits. The pipe was jetted into the ocean floor, and core barrels were dropped through the pipe to get cores from the bottom of the hole. Next, Navy patrol boats were converted into drillships with "over-the-side" masts and rotary tables. The first rotary floating drilling vessel went into service in 1953 and was capable of drilling in 400 ft of water to depths of 3,000 ft.

The adverse motion characteristics of these ship-shaped vessels, combined with the "over the side" rotary table, encouraged offshore drillers and engineers to find ways to reduce vessel motions. In 1955, innovative drilling engineers moved the drilling rig from over the side to the center of the ship to reduce the effects of vessel motion. A center well, or moon pool, was installed vertically through the hull, and the drilling rig was mounted over it. This breakthrough led the way to modern-day drilling vessels. Technological advances in subsea systems, vessel station-keeping systems, moored and dynamic positioning, motion compensators, control systems, and navigation systems have all contributed to the success of

drillships during the past 30 years. They will be discussed in more detail later in this chapter.

While ship-shaped vessels were being developed for California waters, a different approach to improving vessel stability was taken in Gulf of Mexico waters. The semi-submersible, or column-stabilized drilling vessel, was developed by addition of buoyant hulls to a submersible so that it could drill while floating instead of sitting on the seafloor. These rigs exhibited superior motion characteristics and now are used extensively in such rough-water areas as the North Sea and off the east coast of Canada.

While mobile drilling rigs were being developed into today's sophisticated drilling systems, platform technology was keeping pace. In 1947, the first platform "out of sight of land" was built off the coast of Louisiana in 20 ft of water. From then until the 1970's, the gulf coast dominated offshore petroleum activity with the installation of more than 5,000 offshore drilling or drilling/producing structures. During the 1970's, the North Sea captured most of the offshore attention with the advent of huge payload requirements, and concrete gravity structures competed with the steel "template." Eighteen concrete structures have been installed in water depths from 240 to 540 ft with payloads up to 40,000 tons.

Meanwhile, steel-structure technology competed successfully for smaller payloads in the North Sea and regained favor as deeper U.S. waters were explored. In 1976, "Hondo," a pile-supported two-piece jacket, was installed in 850 ft of water off the coast of California. In 1978, "Cognac" was installed in three pieces in 1,025 ft of water in the Gulf of Mexico. Single-piece structures became viable for deeper water as launch barges and transportation technology developed. "Garden Banks" was installed in one piece in 680 ft of water in the Gulf of Mexico in 1976. "Cerveza," in 935 ft, and "Liguera," in 915 ft, were installed in the gulf in 1981 and 1982. Designs for steel jackets for up to 1,200 ft of water are in the final design stages for placement in the Santa Barbara Channel and the Gulf of Mexico.

Many other specialty structures have been installed. In 1966, a steel gravity-oil-storage structure was placed in service in the Gulf of Mexico. Three 500,000-bbl steel storage domes that resemble inverted champagne glasses were installed in the Arabian Gulf in 1969, 1971, and 1972. Buoyant articulated columns were installed in the North Sea in the 1970's to serve as tanker mooring devices for loading out crude oil. Tankers and drilling vessels have been moored by various means to support gas/water/oil separation facilities and to provide temporary oil storage. Breast mooring and single-point mooring systems have been installed in water depths exceeding 100 ft to accommodate a supertanker's draft. A steel gravity structure with storage capacity of 1 million bbl of oil and a deck payload of 30,000 tons has been installed in the North Sea as an alternative to the concrete structures. A guyed tower was installed in 1,000 ft of water in the Gulf of Mexico in 1983. A tension-leg platform, the commonly favored concept for water depths of more than 1,200 ft, was installed in 485 ft of water in the North Sea in 1984. Each of these special-purpose structures represents an advance in ocean engineering technology and forward-thinking business management to support untried ideas.

Progress is not always the result of new ideas or concepts but often a step-by-step improvement in existing technology. For example, the skirt pile that is currently part of most steel deepwater structures was first implemented in 1955, but the idea had been patented in the 19th century. The North Sea gravity structure had a precedent in a gravity platform constructed offshore in California more than 30 years ago. The guyed tower was patented before the turn of the century. The tension-leg platform was invented during World War II as a seadrome or floating airport. Current improvements in computerized design, transportation, and installation equipment, coupled with an ever-increasing need for new oil supplies, is the driving force for technological advance.

During the evolution of offshore platforms, the new ocean engineering discipline also evolved. Ocean engineers are versed in structural engineering, soil mechanics, the hydrodynamic effects of waves and currents, structural dynamics, statistical analysis methods, and reliability analysis techniques.

The equipment, methods, and techniques for completing, producing, and maintaining wells on the ocean floor have also undergone tremendous advancements since the first subsea wells were completed in the late 1950's. Early subsea Christmas trees were made up of the same conventional valves and flanges as trees for land wells. The one concession to underwater operations was fail-safe hydraulic actuators on remote-control valves. These early trees were usually diver-installed and connected by Bowlines to shore. One company developed a swimming hydraulic wrench that was fitted with television cameras and maneuvering thrusters. This system, integrated into the wellhead system, was successful to a degree. It was the first attempt to eliminate divers from subsea operations. Over the past 25 years, there has been a continuous effort to reduce dependency on divers, but divers are still a very important part of the offshore oil industry.

Complex multiwell systems have been installed on the ocean floor. Single-well completions have been made in 1,300 ft of water. Control systems that involve hydraulic, electronic multiplex, and acoustic signal transmission systems are now common. Unmanned, remotely operated vehicles now are being developed that will become an integral part of the subsea completion system. Much has been accomplished in the past 25 years, but with exploratory drilling being done in 6,500 ft of water, even more remains to be done in this area of subsea completions.

The search for offshore oil and gas reserves has directed the petroleum industry to the ice-covered waters of the Arctic. In 1963, the first commercial oil field was discovered in the upper Cook Inlet of Alaska. For the first time, ice driven by extreme tidal currents produced loads on the production facilities *far* in excess of other environmental forces. By the end of 1968, 14 platforms were producing oil and gas from the inlet.

The onshore oilfield discoveries of Prudhoe Bay in 1968 and Kuparuk in 1969 established the Alaska North Slope as an oil province. In 1977, construction of the Trans-Alaska Pipeline System was completed, and oil began flowing directly to the ice-free port of Valdez. This development has inspired extensive exploration activity in the Arctic offshore continental shelves of the U.S. and Canada.

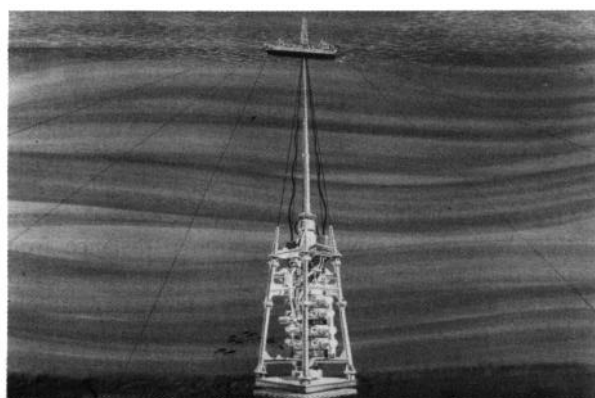


Fig. 18.1— Typical floating drilling arrangement.

The industry has constructed 26 sand and gravel islands for exploratory drilling in water depths to 100 ft since 1972. Several caisson-retaining systems have been implemented to speed construction and to reduce the fill requirements for the islands. Beyond 100 ft, drillships have been used, but they operate only during the ice-free summer season. In 1983, a floating conical drilling unit was deployed in the Canadian Beaufort Sea. The unit is capable of resisting early winter ice loads, hence extending the drilling season to 6 months a year.

At the current time, at least four major Arctic marine projects are in the planning phases: the Arctic Pilot Project in the Canadian Arctic Islands, the Arctic Marine Hydrocarbon Production Project in the Canadian Beaufort Sea, the Endicott Development nearshore U.S. Beaufort Sea, and the Hibernia Development off the east coast of Canada. Permanent production platforms, subsea pipelines, icebreaking tankers, supply vessels, and evacuation systems are a few of the facilities being developed.

In summary, though the offshore industry has come a long way since the wooden pier days of Summerland, the technological requirements have barely been addressed.

Offshore Drilling

The Introduction brought us quickly from the very early days of the oil industry to today's jackup drilling units, semisubmersibles, and drillships. This section will discuss the planning, preparation, and equipment necessary to conduct a typical floating drilling operation (see Fig. 18.1). Focus will be primarily on floating drilling because operations from jackups, submersibles, and platforms generally follow land drilling practices. The last portion of the section will be devoted to special considerations, such as deepwater and high-current drilling and considerations for cold and hostile environmental conditions. For a general discussion of the technology of offshore drilling, completion, and production, see Ref. 2.

Planning and Preparations

Site Conditions and Considerations. The culmination of the sometimes arduous and complex task of geologic evaluation of a potential offshore play is for the exploration geologist to put a finger on the map and say "drill

here." This decision sets in motion a series of actions that will eventually lead to the drilling of an offshore well.

The first major step is to select a rig to drill the well. Because all rigs have specific operating criteria and limits, however, certain data must be known about the drillsite and surrounding area. Basic rig selection criteria consist of water depth, expected environmental conditions during the forecasted drilling period (wind, waves, current profile, and climatological conditions), distance from nearest dock facility, and availability of consumable supplies (such as drilling mud, cement, pipe, rental tools, and spare parts).

Water Depth. A rough idea of the water depth is an important criterion for rig selection. If the water depth does not exceed approximately 350 ft, any of the three major rig types can be considered. Jackups can handle a water depth range from their shallow draft limit of 20 to 30 ft to a maximum depth of 350 ft. The maximum depth limitation is a function of other environmental constraints, such as wind, wave, and current conditions at the site. Severe conditions tend to lower the jackup rig's maximum water-depth capacity.

Drillship water depths range from approximately 100 to 8,000 ft with today's technology. The shallow side is limited by clearance between the bottom of the hull and the subsea blowout preventer (BOP) equipment. Maximum water-depth limits occur because of riser-system limitations and other constraints that will be discussed later.

Semisubmersible water depths range from approximately 150 to 8,000 ft. The semisubmersible must stay in slightly deeper water than a ship because of the clearance between the submerged hull (60 to 90 ft below the water surface during normal drilling operations) and the subsea BOP equipment. Until 1978, semisubmersible maximum water depth was limited by the practical depth of conventional mooring systems—approximately 2,200 ft. One dynamically positioned semisubmersible that required no conventional mooring system, thus extending the design working depth to 8,000 ft, was commissioned in 1978. Today, several dynamically positioned semisubmersibles are under construction or in service.

The industry water-depth record currently stands at 6,848 ft for a well drilled off the U.S. east coast during the summer 1983.

Expected Environmental Conditions. Wind, waves, and current are all important site-specific data to help in rig selection and in determination of vessel heading, mooring pattern, mooring line tensions, riser tensions, subsea equipment selection, and equipment operational limits.

Wind, wave, current, and climatological data are generally the responsibility of an oceanographic consulting firm or your own company's oceanographer. Many sources of environmental data are available—the marine climatic atlas, ship observations, U.S. Navy publications, privately funded oceanographic studies, and university-sponsored research. Converting these data into useful site-specific wind, wave, and current information is the scientific specialty of oceanography.

The oceanographer must have specified coordinates of the location and the time of the year (with some cushion on both ends) in which operations are expected. With that, he can develop the expected wind, wave, and current conditions for the location. For an exploratory location, the oceanographer may provide environmental data for oper-

ational weather, seasonal one-year storm, and seasonal 10-year storm. With that information, the drilling engineer and technical support staff can accomplish several tasks necessary in planning the well.

1. A preliminary rig selection can be made based on water depth, wind, wave, and current information.

2. A preliminary estimate of vessel heading can be determined. Before a final heading is specified, however, local knowledge of the area should be considered. Local conditions—such as swell, tide-generated currents, and rapidly changing wind directions—frequently can affect the optimum vessel heading significantly. The primary objective of optimum vessel heading is to minimize vessel motion (primarily pitch, roll, and heave) while keeping the vessel's mooring line forces within acceptable limits and providing a lee side (calm-water side) for supply and crew boats to tie up.

3. To assist in vessel selection, a vessel motion or downtime analysis can be run. Computer programs that compare a particular vessel's motion characteristics with the predicted wind and waves are available. The result indicates vessel motion. The resulting motion can be compared with a previously established set of acceptable operating limits (by computer analysis or manually) to determine an approximate downtime to be expected. This analytical tool is most useful in comparing two rigs for a particular location.

4. After the vessel is selected, mooring and riser analyses can be run to determine whether the vessel is adequately equipped for the location. In addition, both mooring and riser operating tensions can be determined. Both are necessary after the rig arrives on location. Typically, the mooring system is analyzed with a one-year seasonal storm to determine what operating tensions should be pulled on the anchor lines. A 10-year storm can be analyzed to determine the level of proof test to pull on each mooring line. With reasonable risk considered, if each line can withstand a 10-year storm proof test, normal operations should be safe without the fear of slipping an anchor or breaking a mooring line. Drilling riser top tensions are developed to minimize ball-joint angles and riser sag while keeping riser-pipe stresses within acceptable limits.

For jackup rig evaluation, comparing water depth, current, wind, and tides with the maximum recommended criteria established by the rig designer is extremely important. In water depths nearing the rig's maximum capability, strong current or other environmental factors may reduce the acceptable water depth.

Soil or foundation competency at the site must be known for jackup operations also. At an exploratory location with unknown soil consistency, soil borings generally will be required before the rig's arrival on location. They are useful in determining depth of leg penetration and to ensure that the soil can adequately support the rig.

Logistics Considerations. Logistics must also be considered in rig selection. Remote locations require substantially more planning and preparation than do locations adjacent to established bases and supplies. Consideration must be given to (1) frequency of consumables supply; (2) distance from supply base (length of boat run); (3) number of people the rig can accommodate; (4) availability of spare parts; and (5) shipment delays caused by customs regulations.

Floating rigs' (ships and semisubmersibles) variable deck-load capacity must be considered and compared with frequency of consumable supplies required. Ships, as an example, have much greater variable deck-load capacity than semisubmersible drilling rigs (15,000 vs. 3,000 tons). If the location is in an extremely rough environment, however, the semisubmersible is more stable in rough seas than the ship. Trade-offs and compromises are necessary ingredients in rig selection.

Availability of pipe, mud, fuel, water, and other consumables must be carefully determined during the planning effort. Helicopters to transport personnel and light equipment in routine and emergency situations are a necessary part of most floating drilling operations. Those located within a few minutes of the coastline and support bases are sometimes exceptions.

Climatological conditions have a major effect on helicopter operations. Fog and impaired visibility conditions will ground flight operations and, depending on their extent, can have a major effect on the resupply of consumables, transportation of crews to and from support bases, and overall rig operations. Floating ice, low temperature, and high currents offer special considerations that are discussed at the end of the Offshore Drilling section of this chapter.

Seismic and Other Location Studies. Preparation to drill an exploratory location will include running and evaluating a suite of location surveys. Site surveys generally are run by seismic companies specializing in prespud site studies. These companies will conduct the surveys, evaluate the data, and prepare formal reports that present the data that will be useful in selecting the exact location, in preparing the mooring plan, and in determining how the top hole will be drilled.

For exploratory drilling in federal offshore waters, the U.S. Mineral Management Service issued a set of guidelines that require certain surveys to be performed and analyzed before it will issue a permit to drill. These guidelines cover studies on shallow geological hazards, culture and archaeology, and biology.

The operator or lease holder must cover a minimum prescribed grid of traverse lines in carrying out these studies. In addition, certain minimum instrumentation is required to be run during the surveys. These include sparker, uniboom, sub-bottom profiler, side-scan sonar, and fathometer for surveys of shallow geological hazards. If the drilling equipment is to be on board a floating vessel, no bottom sampling is required. If a bottom-setting jack-up barge is to be used, then a bottom sample or core must be obtained. Side-scan-sonar, magnetometer, and fathometer are required for cultural and archaeological surveys. For biological surveys, box-core samples of hard-bottom areas and ocean-floor photography or TV view of hard-bottom areas are required.

The shallow-hazard surveys are required for all sites. The grid must be at least 8,000 ft on a side, centered on the proposed location, and surveyed on 1,000-R grid lines. The cultural surveys need to be run only in waters of less than 400-ft depth. The biological surveys must be run in areas where endangered species exist or hard-bottom sediments might be disturbed. Navigation and location of the survey grid during the water-borne surveys must be accurate to within $50 \pm$ ft.



Fig. 18.2— Jackup rig.

Rig-Selection Considerations

Rig-selection criteria and rig types were discussed briefly earlier. In this section, we will discuss the differences in four rigs that are used for offshore drilling: jackups, submersibles, semisubmersibles, and ships. We will also consider drilling equipment, mooring systems, and procedure manuals.

Rig types. Jackup rigs (see Fig. 18.2) consist of barge-shaped hulls with three or four (sometimes more) structural or tubular legs. Jackups must be towed to location or loaded on specially built ships for major moves. Ship transportation of jackups is becoming more frequent as new special transport vessels become available. Ship transport is considerably faster for long moves (6 to 8 vs. 2 to 3 knots) and much less risky. Loading and offloading the jackup requires a calm-water site at both ends of the move. Once the jackup is in its "jacked-up" position, drilling proceeds in a way similar to land or platform operations. However, several subtle differences should be mentioned.

First, water conditions must be relatively calm—generally less than 6- to 7-ft waves—before the rig can jack its hull out of the water. Major concerns are impact and lateral loading on the legs just as it comes in contact with the ocean floor. If the rig is rolling and pitching beyond specified limits, the jacking operation must be suspended until calmer conditions prevail. The same logic applies when the rig is jacking down.

Second, once the rig is jacked up to working position with a safe air gap between the ocean surface and the underside of the hull, primary concerns are lateral loading on the legs and scouring around the leg mats caused by current. Excessive current can cause troublesome vibration, and scouring can lead to foundation failure. Both conditions are monitored closely, and corrective actions are taken when necessary.



Fig. 18.3— Submersible rig

Third, the drilling operation is similar to a land operation after the outer casing is driven or drilled and cemented in place. Surface BOP and conventional drilling equipment are used.

Fourth, the casing extending from the ocean floor to the rig is a structural member and should be analyzed before installation. Wall thickness and strength of the pipe should be specified (and will vary if a mudline suspension system is used) to ensure that it will withstand the lateral loads of the current and the axial loads of the surface BOP and successive casing strings.

Submersible rigs (see Fig. 18.3) are limited to shallow-water drilling. Once the rig is on location and ballasted to sit on the ocean floor, drilling operations proceed as on a land site. Foundation considerations are as important here as in jackup operations. Logistics and supply considerations are common to all offshore operations, so jackups and submersibles can be just as severely hampered by fog and bad weather as floating drilling rigs.

Semisubmersible rigs (see Fig. 18.4) evolved from submersibles. Some semisubmersibles can operate when resting on the ocean floor or in their normal semisubmerged



Fig. 18.4— Semisubmersible rig

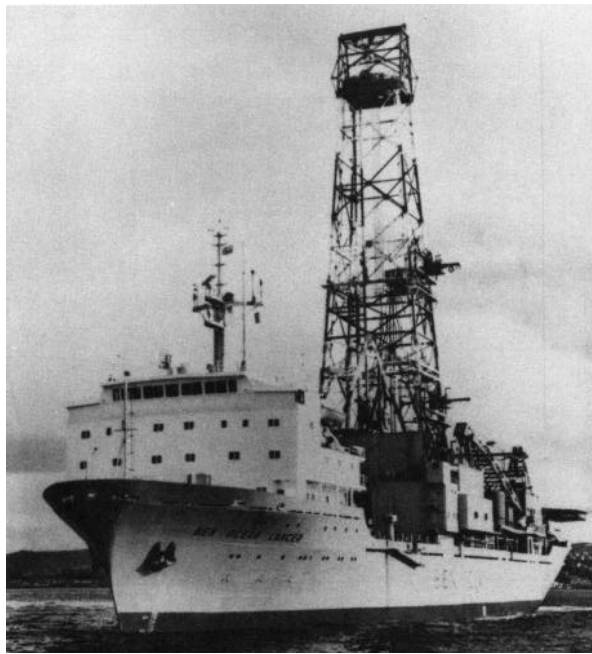


Fig. 18.5— Drillships.

position. The major advantage of a semisubmersible is that it provides a stable floating drilling platform. Roll, pitch, and heave are minimized because minimum structure is exposed to the water plane. The rig's main disadvantage is that variable deck-load capacity is limited by its reserve buoyancy or the amount of watertight volume above the water line. A semisubmersible with four 50-ft-diameter columns breaking the water plane displaces about 62 tons of seawater for each foot of displacement of the column. An equivalent 400-ft-long by 60-ft-wide ship displaces 756 tons for each foot of hull displacement. Because semisubmersibles are sensitive to variations in deck load, they are outfitted with extensive ballasting systems that are capable of shifting ballast rapidly to maintain proper trim and of deballasting or ballasting as cargo is loaded or offloaded. The semisubmersible is highly regarded as the year-round drilling vessel for the open-sea environment because it is very stable in pitch, roll, and heave.³

Drillships (see Fig. 18.5) are noted for their mobility and high storage capacity. Drillships have a definite advantage over semisubmersibles because of their size and speed. Most drillships are designed to pass through the major canals of the world, thereby substantially reducing the distance between oceans. The distance from the Gulf of Mexico to the U.S. west coast by the way of the Panama Canal is 4,500 miles. The distance around South America to the U.S. west coast (the route a semisubmersible must travel because it is too large to pass through the Panama Canal) is 15,000 miles. The cost of moving the ship to the west coast is generally much less than that of moving a semisubmersible because of time savings (less day rate) and distance savings (less fuel). Ships generally can travel at a higher speed than a semisubmersible (12 to 13 vs. 8 to 9 knots) for even more time savings. As pointed out in the semisubmersible discussion, the drillship can carry a much larger variable deck load, which offers the advantage of less frequent resupply.

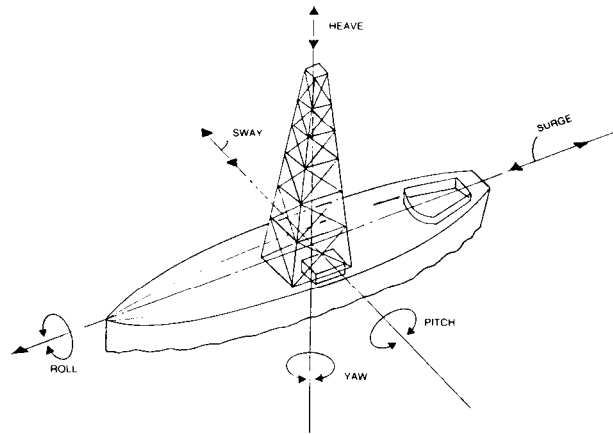


Fig. 18.6— Vessel-motion terminology.

The very nature of drillships (long, narrow hulls with large water planes), however, dictates their sensitivity to sea conditions in pitch, roll, and heave. Operations can be carried out with minimum weather downtime, however, by working drillships in protected waters at seasons when conditions are best for open-sea drilling. Clearly, the biggest disadvantage of a drillship working in severe environments is its motion characteristics, especially in pitch, roll, and heave.³

Motion Characteristics. To compare the advantage of one drilling vessel over another, their relative motion characteristics must be considered carefully. Vessel motions for ships and semisubmersibles can be analyzed by determining the rig's response in the six degrees of freedom (pitch, roll, heave, yaw, surge, and sway) relative to the uniform waves (see Fig. 18.6). All vessels should have a set of motion-response curves. The curves generally are obtained for each rig configuration in a model basin. Each hull shape has a unique set of curves. Roll and heave generally control the limiting operation. With curves like those shown in Figs. 18.7 and 18.8, vessel motion in roll and heave can be determined for a particular set of wave data representing the drilling period. Ocean waves represent a spectrum of wave heights and wave periods. Computer programs are available to calculate vessel motion by entering wave data and the rig's motion curves. The result will be a motion history of that particular rig for a specific drilling period.

Performance Evaluation. The next step is to compare the performance of the two rigs. One performance yardstick is the weather-related downtime the rigs will suffer under the same environmental conditions. Downtime analysis can be particularly useful when comparing available drilling vessels for a one-well project or a complete drilling program. While one vessel may appear to be more

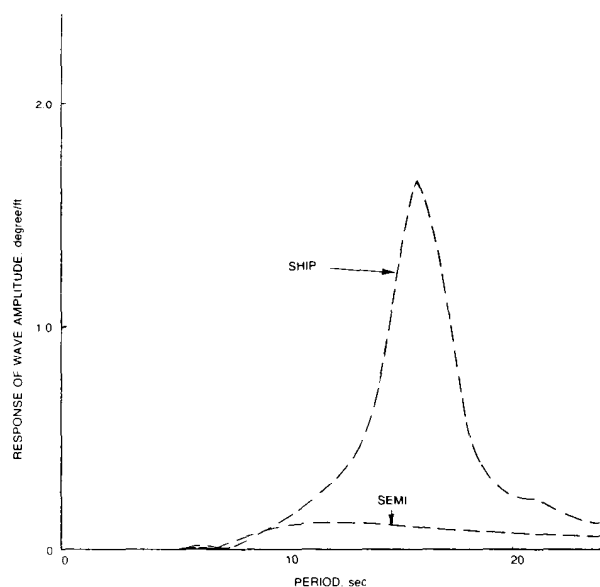


Fig. 18.7—Vessel response—roll.

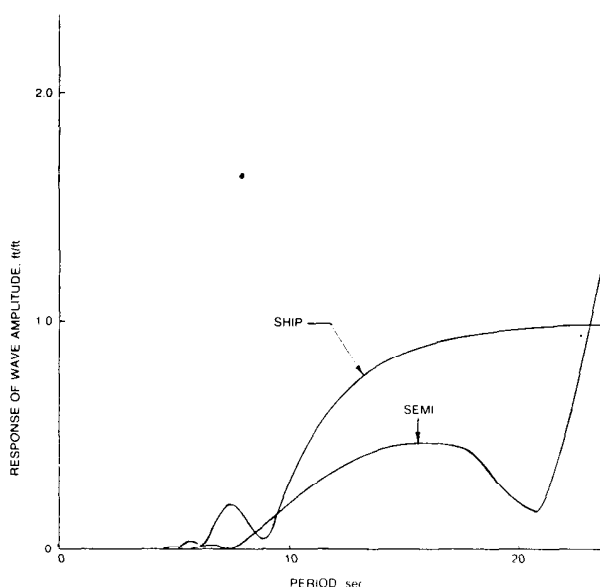


Fig. 18.8—Vessel response—heave.

economical because it has a lower day rate, it may cost more to complete the job because of weather-related downtime.

The key to weather-related downtime is identifying the maximum limit in degrees of roll, feet of heave, degrees of pitch, etc., that can be tolerated during each discrete operation of floating drilling. The maximum level may be based on equipment operating limits, safety considerations, work efficiency, potential for damage, or other factors. Although such a limit is seldom concise, it can be a fair comparison to evaluate relative rig performance. Implementing an operating limit by shutting down an operation on the rig is completely a judgment call with many variables to be considered on the spot. Each rig should have its own set of operating limits established from experience with the rig or from experience of the rig operating personnel. Table 18.1 is an example of limiting vessel motions for most floating drilling operations.

With the appropriate operating limits, the percent of the time each applies, and the rig's motion history, weather-related downtime can be calculated. A number of papers have been published on downtime analysis. Various techniques (both manual and computer-aided analyses) can be applied to calculate weather-related downtime.⁴

TABLE 18.1—DRILLING VESSEL OPERATING LIMITS

Operation	Heave Limit		Roll Limit (deg.)	Time Criterion Applied Per Well (%)
	ft	m		
Anchoring, running riser, landing BOP	6	1.8	3	10
Running casing, coring, well testing	10	3.0	3	40
Drilling, tripping, logging	12	3.6	6	30
Circulate and condition mud	20	6.1	10	20

An additional item normally not included in the motion-related operating limits is wind. High winds frequently result in shutdown because the rig crane cannot safely handle casing or riser. This is a valid input to the rig's overall performance and should be included in the final downtime comparison. Occurrences other than severe weather also cause operating downtime. Equipment breakdown and repair downtime (sometimes the result of severe weather, but not always) must be determined from experience and operating history with a particular rig or company. This increment of downtime is unpredictable and difficult to estimate.

Mooring Systems (Stationkeeping). Once the engineers are satisfied that a particular rig or group of rigs is capable of handling the environment of a specified offshore location, other equipment systems must be evaluated and compared.

Mooring equipment provided to keep the rig on location is of major significance. Major questions to be answered regarding mooring equipment include the following: (1) is the mooring line (chain, wire, or a combination of chain and wire) strong enough to withstand the loads during the strongest anticipated storm; (2) does the rig have sufficient wire or chain on board or available for the water depth at the specified location; (3) do the anchor handling or supply boats that are being considered have adequate pennant-wire-handling equipment on board (lengths must be greater than the water depth and sufficiently strong to handle the 30- to 40-ton anchors and can approach 2.5 to 3 in. diameter); (4) does the vessel have adequate instrumentation to monitor mooring-line loads; and (5) does the rig have adequate chain-locker capacity to hold the desired amount of chain, or must part or all of the chain be stored on supply boats? (Vessels that don't carry their own chain have greater in-transit deck-load capability but normally will require longer to moor up because of the additional chain-handling requirements.)

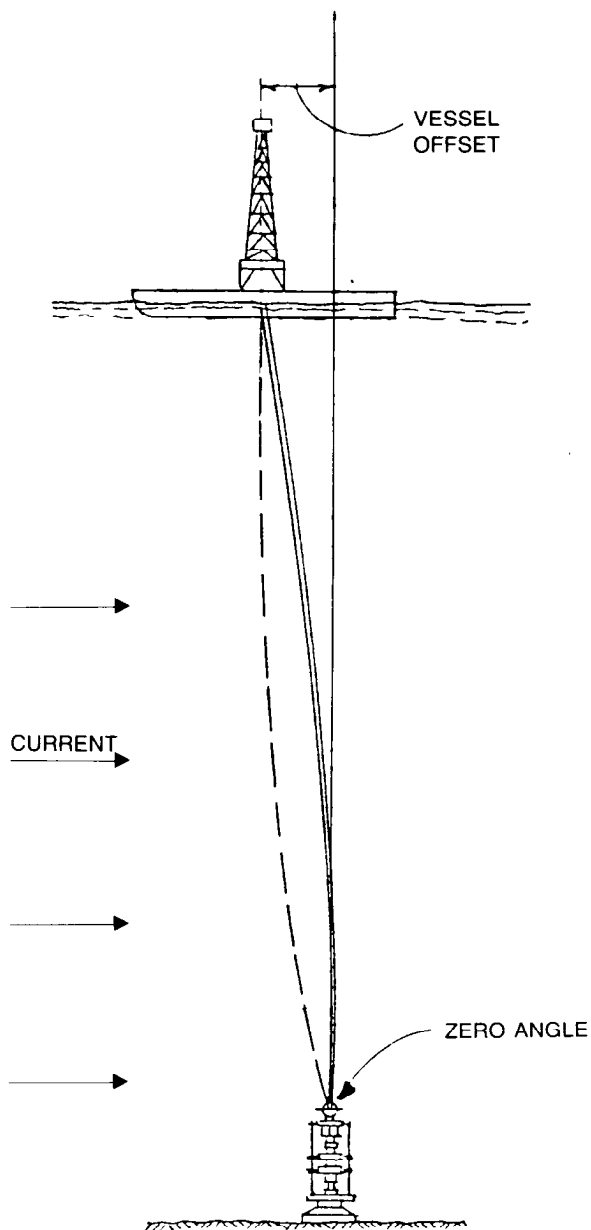


Fig. 18.9—Optimum vessel position.

These questions must be answered to specify an adequate mooring system properly. Mooring analysis, which is necessary to answer several of the questions, will be discussed later in this section.

Adequate stationkeeping (keeping the vessel within acceptable limits on the location) is a result of a properly designed and operated mooring system. Why is stationkeeping important? Ideally, the vessel should be located directly over the well. However, wind and current forces can cause the vessel to take an offset downstream from the wellhead location. Waves cause the vessel to oscillate around that offset position.

It is important to keep the vessel reasonably close to the wellhead position for several reasons: (1) the subsea drilling equipment can accommodate angular offsets of up to 10° , but beyond that the equipment mechanically locks up; (2) drillpipe that is rotating in the ball joint at

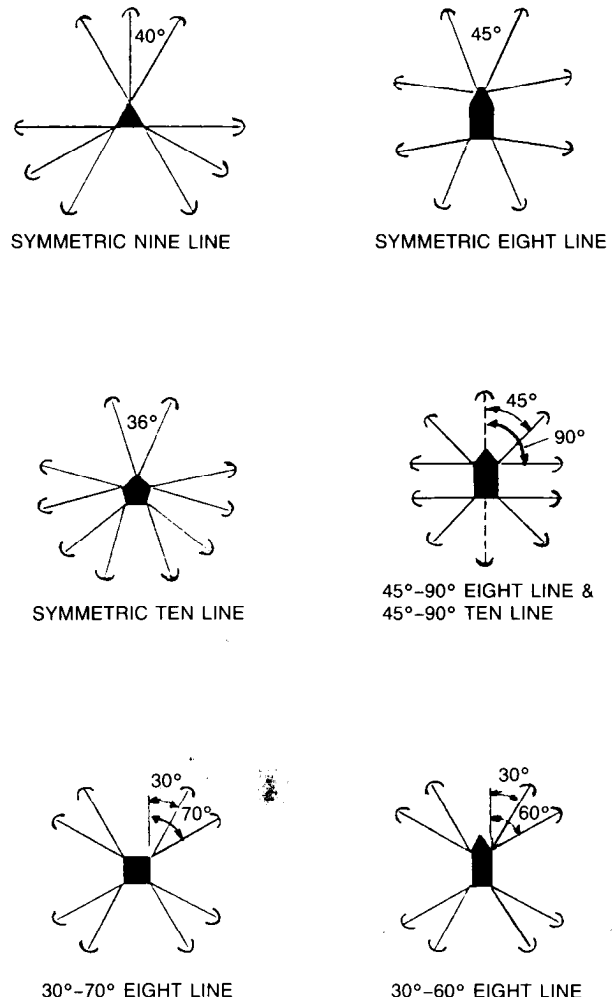


Fig. 18.10—Typical spread mooring patterns.

the top of the BOP can cause rapid and excessive wear if the angular offset exceeds 1 to 2° for an extended length of time; (3) excessive vessel offset can cause increased riser sag, compounding both the ball-joint offset and the wear problems. Proper monitoring of the ball-joint angle and adjustment of the mooring system will result in a vessel offset upstream of the current and wind that will minimize the lower ball-joint angle. Optimum vessel offset would yield a zero ball-joint angle (see Fig. 18.9).

There are many variations in mooring patterns. Differently shaped vessels will require different mooring patterns (see Fig. 18.10).

One criterion in mooring-system design is that the restoring forces should be able to withstand nearly the same storm conditions from any direction.⁵ The mooring pattern is designed to fit the vessel and particular environmental conditions anticipated at the site.

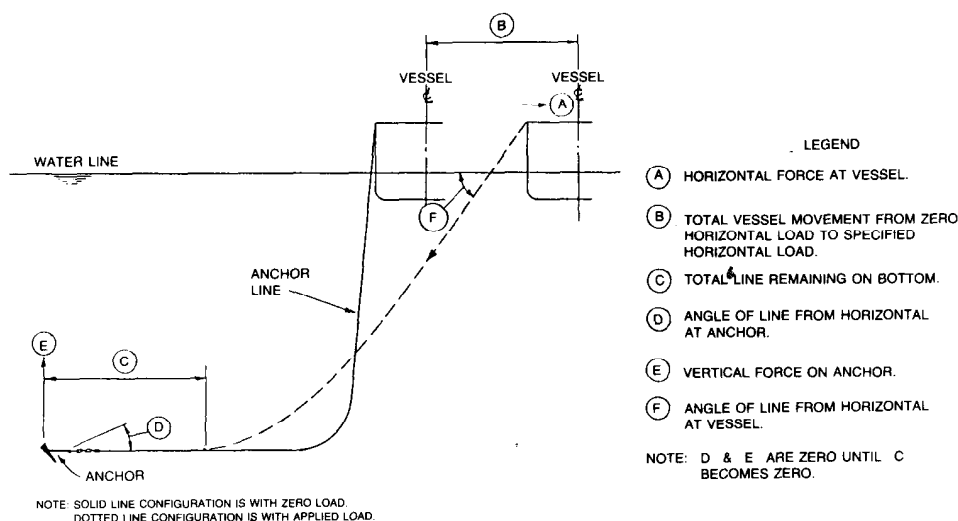


Fig. 18.11—Typical catenary configuration.

The restoring forces are generated by the mooring line. Environmental loads acting on a vessel displace it horizontally until an equal and opposite horizontal force (restoring force) is developed by the anchor and mooring lines. As the vessel is displaced, tension in the anchor line increases because of additional line being lifted off the ocean floor and because the vertical component of anchor line tension, which increases as line is lifted off-bottom, is affected by the angle in the anchor line at the vessel (see Fig. 18.11).

Vertical or uplifting forces on the anchor are zero as long as line remains on bottom. A properly designed and operated mooring system should always have line remaining on bottom during maximum storm conditions. If all the line comes off-bottom, the chances of dislodging an anchor are high.

With a spread mooring system, vessel excursion in moderate weather conditions can be restricted to 2 to 3% of water depth by pulling initial operating tensions in each line. Fig. 18.12 shows the nonlinear behavior of horizontal force (horizontal component of line tension) and vessel displacement for a typical spread mooring. If the vessel

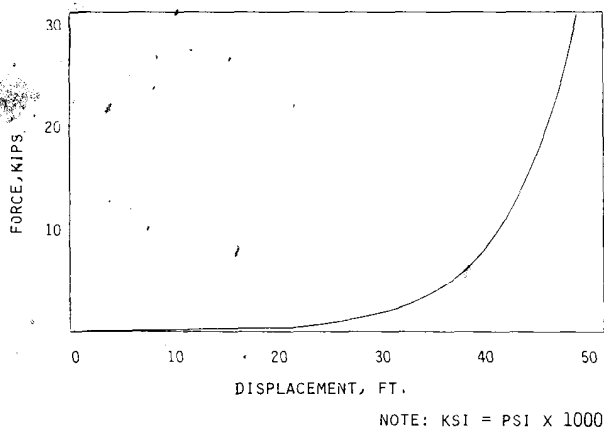


Fig. 18.12—Single-line catenary horizontal force vs. horizontal displacement.

had two opposing mooring lines and could pull tension on each line initially, vessel displacement could be greatly reduced for the same environmental loads because the line would operate in a much "stiffer" region of its horizontal force vs. displacement curve.

Initial operating tension, however, does affect the maximum line tension that will be required in maximum storm weather. The same environmental loads on the vessel are produced during maximum storm weather regardless of the value of initial operating tension. This force must be balanced by one or more mooring lines. This restoring force is in addition to most of the horizontal components of the initial tension in the line. The vessel will probably not be displaced enough to reduce the initial tension in the leeward lines completely. In actual operations, leeward lines can be slacked off during maximum storm weather to reduce maximum line tension and vessel offset. In general, the higher the initial tension, the higher the maximum line tension during maximum storm conditions. Too little initial tension, however, will result in unacceptable vessel offset during operating weather conditions. Table 18.2 identifies desirable stationkeeping criteria.

Dynamic positioning is another method of stationkeeping where no mooring lines are used. These systems require acoustic positioning beacons, multiple thrusters on the vessel, and an on-board computer system and are primarily for deepwater drilling. Dynamic positioning will be discussed briefly in the last section, Special Considerations.

Drilling-Equipment Considerations. Rig-selection considerations should include a review of the vessel's drilling equipment. Much of the drilling equipment found on board floating drilling vessels is identical or similar to equipment on land drilling rigs. This discussion will be limited to equipment unique to floating drilling.

Fig. 18.13 identifies the major components of the subsea drilling system and related shipboard systems. The figure shows some of the components of the drilling system that have been developed to accommodate vessel motion and water depth. The components to be explained

TABLE 18.2—DESIRABLE CRITERIA OF STATIONKEEPING

Operational:	Drilling operations can be carried out
Minimal weather	That which results in $\leq 3^\circ$ lower ball-joint angle, generally
Maximum vessel excursion	2 to 3% of water depth
Nonoperational, But Riser-Connected:	Seasonal 1-year storm
Maximum weather condition	$\frac{1}{3}$ breaking strength
Maximum line tension	500 ft
Minimum line remaining on bottom	That which results in $\leq 5^\circ$ lower ball-joint angle, generally
Maximum vessel excursion	5 to 6% of water depth
Riser-Disconnected:	Seasonal 10-year storm
Weather conditions	$\frac{1}{2}$ breaking strength
Maximum line tension	100 ft
Minimum line remaining on bottom	

are the BOP, the flex joint, riser, riser slip joint, riser and guideline tensioners, drillstring motion compensator, guidelines, and control system.

BOP. The subsea BOP stack is a major change from land or platform drilling operations. Drilling riser, extended kill and choke lines, remote hydraulic and electrohydraulic control systems, and subsea wellhead equipment are all product modifications needed because the BOP was relocated on the ocean floor. The well's major pressure-containing components were put on the ocean floor because of the need to compensate for vessel motion.

A BOP stack, whether located on the surface or subsea, is considered a last resort for preventing a well kick from becoming a blowout. Several steps are taken to control unusual well conditions before use of the well shut-in device (BOP). If the previous steps have failed and it becomes necessary to shut the well in, the shut-in equipment must be highly reliable. BOP equipment is designed with reliability as its ultimate criterion. Because of its relative inaccessibility, the subsea BOP requires additional redundancy and reliability.

The BOP stack is a combination of individual BOP's designed to shut in a well under pressure so that formation fluids that have moved into the wellbore can be circulated out while continuous control of the well is maintained.

A description of the BOP stack components is included below (see Fig. 18.14).

Ram Preventers. The massive steel rams have rubber seals, and are hydraulically actuated to seal off the wellbore. Pipe rams seal the annulus around the drillpipe and are designed so that an entire string of drillpipe and collars can be suspended from a pipe joint landed on a ram. The ram seals must be the correct size to seal; 3-in. seals cannot be used for 5-in. drillpipe. Conventionally, three pipe rams are used. A fourth ram, a blind-shear ram, is used to seal over the open hole and to shear drillpipe when necessary. Shearing pipe is, of course, one of the last resorts in an emergency situation.⁵ Variable-bore rams are an option that is offered for tapered drillstrings.

Annular Preventers. Annular preventers are comprised of specially designed, reinforced rubber elements that can seal around any tubular or near-tubular objects that will go through the BOP's. They will also seal over the open hole and can pass drillpipe tool joints without severely

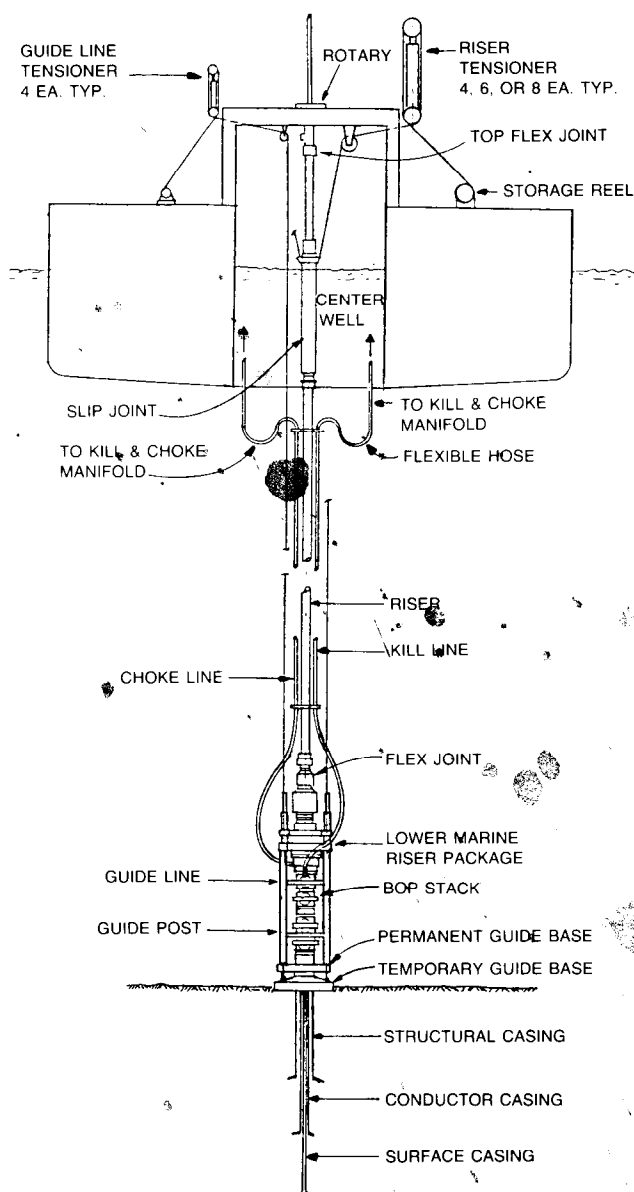


Fig. 18.13—Floating drilling system.

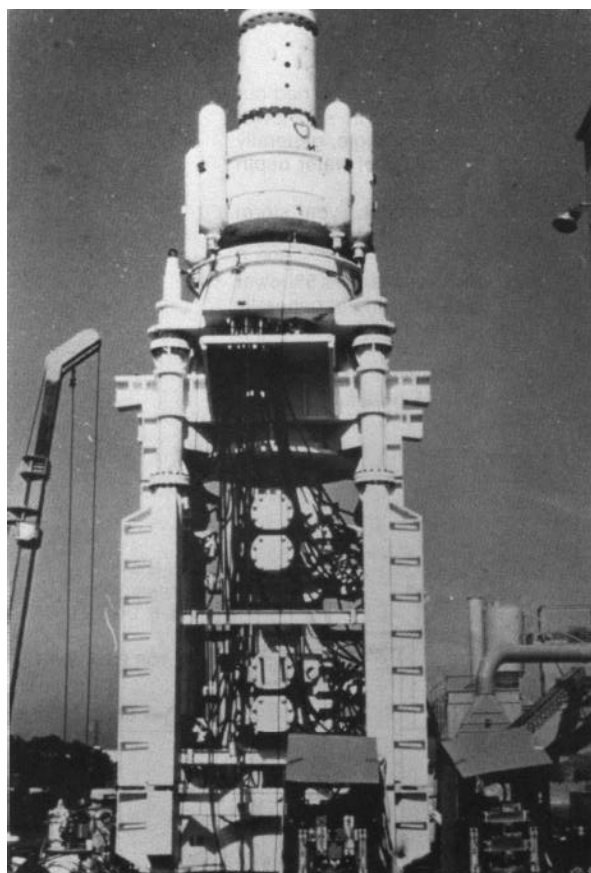


Fig. 18.14— BOP stack

damaging the sealing element. Annular preventers are actuated by an annular piston that squeezes the seal into the bore. The piston area is large relative to the other functions on the stack and, except for initial closure, should be operated at pressures lower than the other stack functions. This decreases the possibility of extruding the rubber seal out of the preventer.⁵ Frequently, two annular preventers are used. One normally will be located above the upper hydraulic connector so that it can be retrieved with the riser.

Hydraulic Connectors.³ Hydraulic connectors provide the main pressure seal between the wellhead housing and the BOP and between the top of the BOP and the lower marine riser package (LMRP—usually contains the top annular preventer, flex joint, control system, and crossover to the bottom riser joint). The high-pressure wellhead housing is the male portion of the connector. It will be a mandrel or a hub type. The connector is the female portion and consists of a series of hydraulic cylinders that actuate locking dogs into grooves machined into the wellhead housing or collet fingers that clamp over the wellhead housing hub. Both types of connectors use metal-ring seals. This provides continuous metal-to-metal sealing up through the BOP.

Kill-and-Choke Valves. These valves are the subsea shutoff of the high-pressure kill and choke (K&C) lines that run from the BOP's to the choke manifold on the rig. K&C valves are hydraulically controlled from the surface and are designed to close by spring action when opening pressure is released. Some valves close hydraulically

in addition to the spring or fail-safe close feature. Two valves in each line should always be used for redundancy. They should be located as close to the stack as possible for mechanical protection.⁵

Unitized BOP Stack. The unitized BOP stack that consists of two hydraulic connectors, three or four ram preventers, one or two annular preventers, four K&C valves, one flex joint, and a control system is generally handled in one or two pieces on board the rig. The complete assembly can weigh from 200,000 to 400,000 lbm and stand 25 to 30 ft high.³

Handling and moving the BOP stack from its storage position to the moonpool and back presents unique problems. Generally, either special overhead cranes or hydraulically actuated carts are used to move the stacks.

BOP maintenance is extremely important. The only time available for routine maintenance is between locations. On short field moves, this can present problems. Land BOP systems are frequently broken down and sent to the shop for maintenance between wells, but that is virtually impossible to do without causing major delays on a floating drilling rig. A few rigs are equipped with backup BOP stacks to minimize the chance of major delay.

BOP testing is done in two steps. The stack must be completely function-tested (each of the 30 to 40 hydraulic functions actuated to verify that each works) before running. It must also be completely pressure-tested before it leaves the deck. Each pressure-containing component (rams, annulars, and K&C valves) must be tested to a pressure specified by the operator. API RP 53 on BOP's⁶ identifies testing procedures as a minimum safe guideline. After the BOP has been run and latched on to the subsea wellhead, it must again be pressure-tested. Following procedures defined by regulatory agencies, periodic function and pressure-testing must be done on the BOP equipment during the course of a well. A complete deck and subsea BOP testing checklist simplifies frequent testing requirements.

Flex Joints.³ A flex joint is installed between the lower end of the riser and the BOP stack. This joint essentially acts as a pinned connection to minimize bending stresses in the riser as the drilling vessel is moved by wind, wave, and current action.

The first flex joints were made from bag-type annular BOP's fitted over a mandrel flanged to the top of the BOP stack. The rubber element in the preventer was inflated against the mandrel to a pressure high enough to keep drilling fluid in the riser from leaking past it. This type of flex joint, which was not positively locked to the BOP, worked fine in shallow waters (200 ft or less) where tension was not pulled on the riser.

The next flex joints were the pressure-balanced ball joints. These joints came into existence when operations moved into deeper waters and it became necessary to pull tension in the riser through the ball joint into the BOP itself. With this positive pull upward on the ball joint, it was necessary to provide a pressurized oil pad between the male and female halves of the ball joint to minimize wear. Pressurized oil was provided through a line from the surface and was contained between upper and lower O-ring seals within the ball joint. The balancing pressure on the ball joint was determined by dividing the tension pulled through the ball joint by the projected horizontal area between the ball-joint seals.

Steel-laminated elastomers now are replacing ball joints as riser flex joints. These joints are longer-lived and require less maintenance than the pressurized ball joints. They also eliminate the need for the pressure source and hydraulic lines.

Some operators also require the installation of a flex joint between the upper end of the riser and the slip joint. Pressurized ball joints and elastomeric joints have been used successfully in this application. Most flex joints are designed for an angular travel of $\pm 10^\circ$ for a total included angle of 20° .

Slip Joints.³ All floating drilling vessels, ship-shaped or semisubmersible, heave up and down as swells go by. A slip joint is the link between the riser fastened to the bottom of the ocean and the heaving drilling vessel. The slip joint, similar in action to a trombone, consists of an inner and an outer barrel. The outer barrel is connected to the riser and the inner barrel to the ship. As the ship heaves up and down, the inner barrel strokes in and out of the outer barrel. A pair of inflatable rubber elements mounted on the upper end of the outer barrel serve as the seal between the barrels to prevent loss of drilling fluid. The second seal is for redundancy.

Riser Tensioner. For a drilling riser to survive, two things must happen.³ First, the drilling vessel must be kept within prescribed limits as it moves about in surge and sway. Second, the riser must be tensioned properly so that it will not sag and ultimately be overstressed in bending.

The controlling criterion is not vessel position relative to the well on the ocean floor, but the angle between the axis of the lower end of the riser and the vertical axis of the BOP stack. This angle is called the lower riser angle. During drilling, this angle should be kept at less than 3° . A greater angle will cause the rotating drillpipe to cut into the flex joint and BOP stack. In extreme cases, lost circulation has resulted from a worn-through flex joint. In normal drilling, the riser angle is kept to less than 1° . If it exceeds 3° , drilling is stopped until the vessel can be repositioned.

To keep the lower riser angle as near 0° as possible in areas where ocean current is a factor, the drilling vessel may have to be located up-current from the well.

If the drilling vessel is located up-current, as shown in Fig. 18.9, but inadequate tension is pulled on the riser, the riser could sag, as denoted by the dotted line. If the drilling vessel is moving about and there is heavy drilling fluid in the riser, the angle at the flex joint could exceed 10° and put bending stresses in the riser. If this situation is not corrected, the riser ultimately will fail.

Hydropneumatic tensioning units were developed to keep constant tension pulled on the riser. Determination of the tension required is a complex problem in which water depth, riser size, mud weight, ocean current, vessel motion, and sea conditions must be considered. A number of computer programs, both time and frequency domain, have been developed to determine the tension needed. Many oil companies that operate offshore have their own riser programs or have access to them. These programs give the riser tension required and the desired vessel offset.

The tensioner system works on the principle that displacement of a relatively small amount of hydraulic fluid against a large pressurized volume of air results in a very

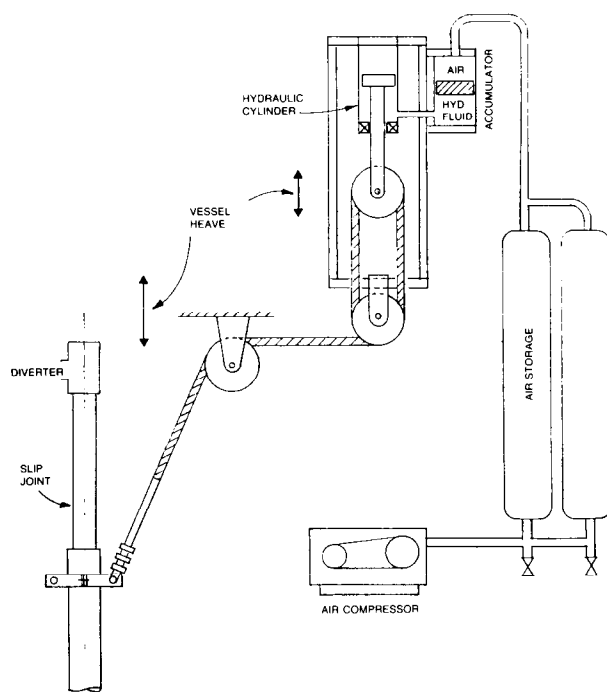


Fig. 18.15—Riser tensioner unit.

small change in the hydraulic pressure. Variation in tension on the riser can be kept to less than 5% by proper design.

The tensioning unit (see Fig. 18.15) consists of a series of large air storage tanks that are connected to the air or gas side of an accumulator that serves as the interface between the air and hydraulic systems. The tensioner is a cylinder/piston arrangement that has wire-rope sheaves mounted on the lower end of the cylinder and on the upper end of the piston rod that extends out of the cylinder. A wire rope that is dead-ended on a storage reel is reeved through the sheaves over alignment sheaves and is attached to the outer barrel of the slip joint. As the drilling vessel heaves up, it pulls on the line, which pulls the piston into the cylinder, displacing fluid into the accumulator against the large volume of air. The air is precharged to give the desired tension. Similarly, when the vessel moves down, the gas pressure displaces hydraulic fluid against the piston, extending the piston rod and maintaining a constant pull on the riser.

Guideline tensioning systems, developed to keep constant tension in the guidelines, operate in much the same manner as the riser tensioners. The only difference is that they are smaller because less tension is required on the guidelines.

Drillstring Motion Compensators. Without drillstring motion compensation,³ the drill bit would be constantly lifting off and banging down into the bottom of the hole as the drilling vessel heaves up and down. Weight control on the bit under these conditions without some type of motion compensation is next to impossible. Bumper subs (trombone-type slip joints) in the drillstring above the drill collars were used initially to provide some relief from vessel motion. However, with bumper subs, once the drillstring was in the hole, the weight on the bit (WOB) (weight of the drill collars) was fixed and could be changed

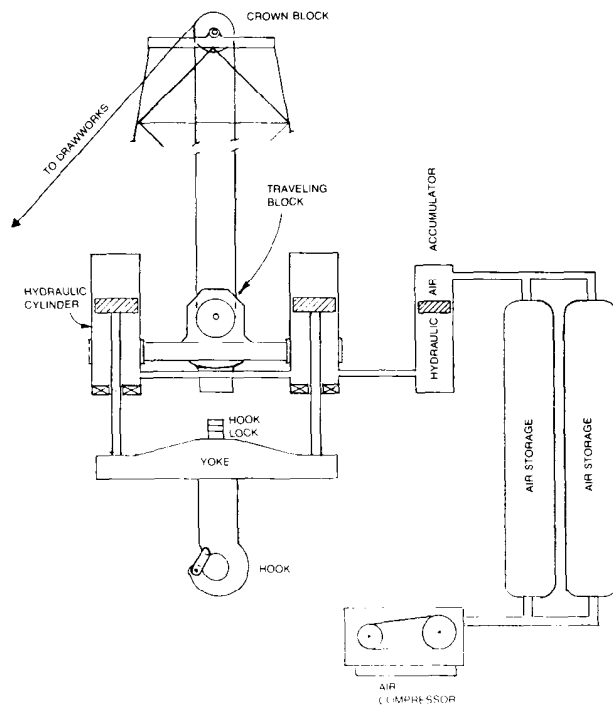


Fig. 18.16—Drillstring motion compensator.

only by pulling the drilling assembly and changing the number of drill collars. Another disadvantage was that the early bumper subs were not hydraulically balanced. Mud pressure in the drillstring that was higher than the external pressure in the drillpipe/hole annulus, as when jet bits are used, caused the bumper subs to “pump” open and to become as stiff as the drillpipe, making them ineffective.

Balanced bumper subs that have the internal pressure routed to both sides of the stroking member were invented to solve this problem. These solved one problem and created another. When working in sandy drilling fluids, the balanced bumper subs’ seals wore out after relatively short runs, making it necessary to come out of the hole with “green” bits to replace the worn-out, leaking subs. Because of their short lives, the worn-out bumper subs were repaired on board, which required an inventory of spare parts and personnel trained in their repair.

These considerations led to development of drillstring motion compensators (see Fig. 18.16). These hydropneumatic units are installed either between the traveling blocks and the hook or in the crown block at the top of the derrick. These units have been successful for both drilling-bit weight control and running and landing heavy subsea equipment (such as 400,000-lbm BOP stacks). They are common on most drilling vessels today.

Drillstring motion compensators are similar to riser tensioners in the way they function—i.e., a small volume of hydraulic fluid is displaced against a large volume of pressurized gas. The weight of the drillstring is supported on a vertical piston inside a cylinder that is connected to the rig blocks. The piston is supported by pressurized hydraulic fluid between the piston and cylinder. As the vessel heaves up, the piston is pulled down into the cylinder, displacing hydraulic fluid into a gas-charged accumula-

tor. When the vessel heaves down, the piston is forced up by the pressurized hydraulic fluid from the accumulator. The gas side of the accumulator is connected to large-volume gas bottles. The small volume of fluid displaced by the piston against the large volume of gas gives a low compression ratio. This means that there is very little change in the gas pressure and the hydraulic pressure, resulting in an almost constant WOB.

At the start of drilling, the gas pressure is adjusted so that it will barely support the weight of the drillstring. WOB is increased simply by reducing the gas pressure. This transfers weight from the drillstring motion compensator to the bit. As a hole is made, the blocks are lowered to keep the compensator at midstroke of the piston. To reduce the WOB, the gas pressure is increased. Large air bottles are kept charged with high-pressure air for this purpose.

Re-Entry Systems. Re-entering a 3-ft-diameter hole in the ocean floor in shallow waters without too much current, say less than half a knot, isn’t too difficult.³ If that same hole is put under half a mile of water in an area with 1- to 2-knot currents, the problem obviously is more difficult.

Almost from the beginning of floating drilling, wire-rope guidelines have been used to guide drillstrings, casing, BOP stacks, and riser pipe into or onto subsea wells. In most instances, the guidelines are anchored to the ocean floor by the temporary guidebase. In some cases, when the hole for the structural pile is spudded without a temporary guidebase, the mud pumps were run at full capacity as the bit entered the ocean bottom. This washed a large conical hole in the ocean floor that, with luck, could be re-entered without guidelines. However, under these conditions, when the structural casing and the permanent guidebase are run, the guidelines are attached to the permanent guidebase for subsequent re-entry operations.

With the advent of dynamically positioned drillships, guidelineless re-entry systems were developed. These systems still had temporary and permanent guidebases; however, instead of using guidelines and guideposts, they were fitted with guidecones that provided a large target for the tools or casing being run. TV cameras were run through the drillpipe, casing, riser, or BOP stack (depending on what was being run) to provide guidance into the hole or back onto the BOP stack. Combinations of TV and sonar also have been used for re-entry guidance. With the dynamic-positioning system, the driller can take control of the drilling vessel from his station and position it as required for re-entry. Re-entry by means of these systems has been made in waters as deep as 6,800 ft.

Marine Risers. The first floating-drilling systems did not use marine risers for mud returns.³ Hoses that were connected below a rotating packer mounted on top of the BOP stack brought mud returns back to the drilling vessel. The rotating packers, which sealed around the drillpipe, were very short-lived and allowed drilling fluid to leak into the ocean when they failed. It was the failure of rotating packers that led to development of today’s marine risers.

As may be seen in Fig. 8.14, the marine riser extends from the BOP stack on the ocean floor up to the drilling vessel. The marine riser, in the parlance of land drilling, is just a very long pitcher nipple. In addition to serving

as a pitcher nipple or mud-return conduit, the marine riser serves another useful purpose: it guides the drillstring through the BOP's and into the hole being drilled in the ocean floor.

The riser joints can be ordered in any length desired, but the length normally is determined by the geometry of the drillship. Normal riser joints are 50 ft long, and at least one riser made of 75-ft joints is in service.

In the beginning, riser couplings were simply threaded collars. Cross threading of couplings being made up on a moving vessel led to the development of clamp-type couplings, piloted union-type couplings, and finally the radially driven dog-and-groove couplings. Riser couplings now being developed for waters in excess of 7,000 ft are of a piloted-bolted type.

As drilling entered deeper waters and drilling vessels ran out of space to install more and more riser tensioners, it became necessary to reduce the weight of the riser by adding buoyancy material. Syntactic foam was used first. Later, air cans were installed around the riser joints to make them air buoyant. Both types of buoyancy are now in everyday use. The cost of the dense syntactic foam that is required for deeper waters is offset by the cost of high-pressure air compressors for air-buoyancy risers. Air-buoyant risers do have one advantage over the foam riser package: the air in the buoyancy cans can be dumped so that the riser will plumb bob vertically below the drilling vessel and not tend to drift off with the current.

For ultradeep waters (deeper than about 10,000 ft), free-standing risers are visualized. Work done in conjunction with the Natl. Science Foundation's proposed Advanced Ocean Drilling Program indicates that to provide the means for rapid disconnect of the drilling vessel from the well, it will be necessary to establish a disconnect point in the riser at about 1,000 ft below the ocean surface. To support the riser vertically below the disconnect point after a disconnect, 10-ft-diameter buoyancy cans will be fitted to an appropriate number of riser joints. The disconnect point will include shear rams to cut the drillpipe if an emergency disconnect becomes necessary. This intermediate disconnect point is essential because it is estimated that pulling 10,000 ft of riser could take from 7 to 10 days, well outside our weather-forecasting capability.

K&C Systems. On land rigs, the K&C outlets³ on the BOP stack are plugged directly into the K&C manifolds on the rig floor. In floating drilling, where the BOP's may be from several hundred to several thousand feet below the rig floor, K&C lines must be provided to bridge the water depth.

In the early days in relatively shallow waters, high-pressure hoses were connected to the BOP stack and, as the stack was lowered, were paid off hose reels. When the stack was landed on the wellhead, the hoses were connected to the K&C manifolds. As water depths became greater, the hose reels became too large for convenient use, and another way to bridge the water depth had to be found. This was done first by installing guide funnels at about 15-ft intervals along the length of the riser as it was run. These funnels were lined up with receptacles immediately above the K&C valves on the BOP stack. With the riser in place, screwed-pipe K&C lines were run down through the guide funnels and stabbed into the receptacles on the stack. Their upper ends were connected into the K&C manifolds.

This system, while functionally satisfactory, was time-consuming to run and test, so another method was developed. This method was to make the K&C lines integral with the riser. The tops of the K&C joints were fitted with a female seal pocket filled with chevron packing, and the lower end fitted with a male seal nipple. When the riser was run, the seal nipples dropped vertically into the female seal assembly. No rotation or screwing was required. The joints were held together by the riser couplings.

Some manufacturers of flexible high-pressure pipe now are proposing to provide long K&C lines that would be stored on reels and paid out with the BOP stack when it is run down to the ocean floor. On the larger vessels now in service, there is space for the large hose reels required.

Control Systems. The simplest way to operate an actuator in a hydraulic control system is to connect hydraulic lines from a pressure source through control valves directly to the actuator.³ Some actuators require two lines to complete the control cycle; others, such as spring-return fail-safe actuators, require only one line.

Subsea BOP's were controlled this way during the start of floating drilling. An early stack consisting of a hydraulically actuated connector top and bottom, K&C valves, four ram preventers, an annular preventer, and a pressure-balanced ball joint would require as many as 17 control hoses. These hoses, bundled together, were stored on a large hose reel. All hoses first were connected directly to their function on the stack, then pressure- and function-tested before the stack was run. Improperly tagged hoses led to many hours of troubleshooting to get the stack to work properly. This time-consuming job had to be done each time the stack was run.

Eventually, male and female multifunction stab plates were developed that reduced some of the hookup time, but the same problem of larger hose reels in deeper waters resulted. In addition, as BOP's became more complex, as many as 30 to 40 hoses were included in the hose bundles, doubling and tripling their size. To solve the problem of large hose reels, multihose bundles, and their slower actuator response times in deeper waters, two new types of control systems were developed: the piloted all-hydraulic control system and the direct-wired electrohydraulic control system.

Backup Control Systems. In spite of the best-laid plans and even with two control pods providing 100% redundancy, problems or failures still occur in the most modern control systems. It is desirable to have reliable backup systems if the primary controls fail. This has led to development of two types of backup control systems: the acoustic control system and the last-chance hydraulic stab system.³

The acoustic backup system uses acoustic signals through the water as the control link between the drilling vessel and the BOP stack on the ocean floor. Energy to power the acoustic signal receiver and to position control valves is provided by dry-cell batteries. Hydraulic energy to power selected functions on the BOP stack comes from accumulators mounted on the BOP stack. These accumulators are kept charged because they are part of the normal control system. Typical functions are to close shear rams, to close pipe rams, and to disconnect the riser at the lower marine-riser package.

An acoustic transmitter located on a surface vessel, drilling vessel, work boat, or other vessel is used to send

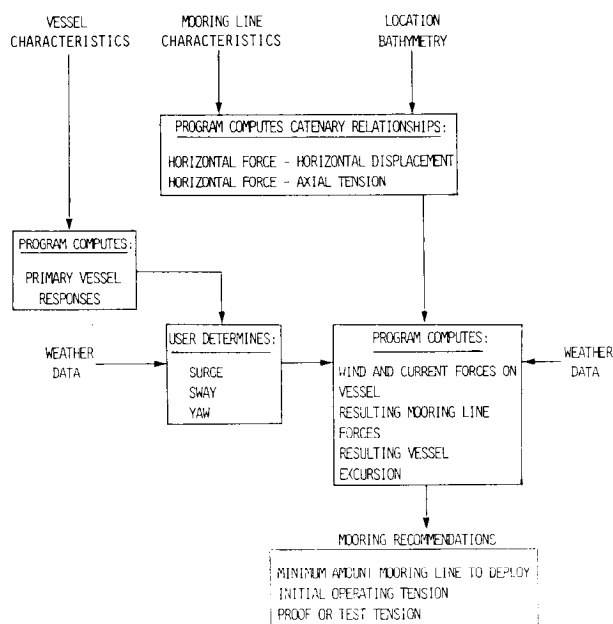


Fig. 18.17—Mooring analysis method.

a signal that is coded for the desired function, down to the receiver on the BOP stack. This signal is interpreted and the proper control valve is actuated, directing hydraulic fluid from the accumulators to the desired function. Acoustic backup systems now are installed on most deep-water drillships. Solid-propellant gas generators also have been tested successfully as backup subsea energy sources.

The last-chance hydraulic stab system provides the means for actuating several selected functions when all else has failed. A hydraulic stab that is ported to accommodate the desired functions is run down to the BOP stack on drillpipe. It may be guided down guidelines or directed by sonar or TV. Hydraulic hoses are connected to the stab and are run in with the drillpipe as the stab is lowered down to the receptacle on the stack. Once the stab is in place, control is accomplished by pressuring up the appropriate hydraulic line. The stab also can retrieve the lower-marine-riser package or the complete BOP stack in the event of a failed riser. The stab receptacle is connected with shear bolts to a mounting plate on the lower-marine-riser package. The receptacle also is attached to the lower-marine-riser package with a heavy wire-rope bridle. The stab contains a connector that, when lowered into the receptacle, latches the stab to the receptacle. To retrieve the lower-marine-riser package, for example, the stab is run in on drillpipe and is stabbed and latched into the receptacle. After the lower-marine-riser-package disconnect is actuated, the drillpipe is picked up, the shear bolts sheared, and the load transferred to the wire-rope bridle. The piece then is recovered by pulling the drillpipe.

Extended-Water-Depth Capability. Occasionally, a drilling vessel is considered that has a maximum-water-depth capability just short of the wellsite water depth (1,300-ft water depth with a 1,000-ft capacity rig as an example). To ensure that the rig is adequate for the location, consider additional riser availability and storage space; additional riser tension (or added buoyancy); lengthened control hoses and TV cable; additional guideline length; mooring system adequacy (mooring lines and

pennant wire); size of control hose reels (large enough to hold additional hose; ease of installing larger ones); size of guideline winch drums (large enough to handle additional line); and substructure strength (enough to support the added tension requirement).

Generally, the added water depth can be accommodated, but each rig and each site should be considered separately.

Operating Manuals and Emergency Procedures

Rig selection considerations should include a review of each drilling vessel's operations manual and emergency procedures plan. The operations manual will include drilling operations and equipment-handling procedures. Normal operating limits for discrete drilling operations will be specified. The emergency procedures plan should cover detailed responses and courses of action to be followed during marine emergencies, well emergencies, and bad weather situations. Disconnect and hang-off procedures must be identified, and special equipment should be on board to accomplish the suspension under adverse conditions. An agreement on well-control procedures should be reached between the drilling contractor and the oil company personnel. The drilling contractor personnel will implement the procedure, so if it is different from their previous procedures, additional training should be conducted.

Mooring and Riser Analyses

Mooring Analysis. Mooring systems and the objectives of station-keeping have been discussed briefly. The concept of the catenary and horizontal restoring force were mentioned. Combining these forces with the wellsite water depth, physical description of the rig's mooring equipment, and environmental data is the task of a mooring analysis. Several commercial computer programs are available to perform mooring analysis. Some companies have developed their own programs. Mooring-analysis methods are documented in numerous articles and papers. Two are referenced at the end of the Floating Drilling section. In addition, API RP 2P discusses mooring analyses.⁷

Fig. 18.17 describes the basic procedure followed in mooring analysis. Combining vessel characteristics and mooring-equipment specifics with bathymetry and weather data yields the length of mooring line to deploy, the initial operating tension, and the proof or test tension. The results can be obtained for a number of mooring configurations to determine which is optimum or simply to verify a recommended configuration.

Riser Analysis. Marine or drilling risers were described earlier. Accurate performance of drilling risers can be determined only by analysis. In floating drilling operations, the riser behaves as a string. It gains all of its structural integrity from tension. The single most important parameter in operation of the system, therefore, is riser top tension. Insufficient top tension can result in operational problems associated with large ball-joint angles and, if low enough, buckling of the riser pipe body. Overtensioning, however, produces high stresses in the riser that can result in a shortening of its life because of fatigue cracking. For each combination of environmental conditions, mud weight, riser weight, and vessel offset, there is an optimum range of riser top tension.

Commercial programs are available to do riser analysis. As with mooring analysis, some companies have developed their own programs. API RP 2Q addresses riser design⁸ and API RP 2K discusses riser use and maintenance.⁹ Papers written on riser-analysis procedures are referenced at the end of the Floating Drilling section. The following discussion covers riser-analysis criteria and operational considerations, but not details of the complex analysis.

The items considered in riser analysis are riser stress, ball-joint angle, top tension, riser top angle, tensioner line angle, sheave friction, and riser pipe collapse.

Riser Pipe Stress. Static and dynamic stresses in riser pipe are calculated by the riser-analysis program. Static loads are caused by the riser weight, mud weight, current-induced hydrodynamic forces, the applied top tension, and deflection of the top of the riser. Deflection of the top of the riser is caused by vessel offset. Dynamic loads result from wave-induced water-particle motion and vessel surge/sway motion. Wave-induced surge/sway motion produces dynamic riser deflections and hydrodynamic forces because of the relative motion of the riser and the water.

The criteria for acceptable static and dynamic stress levels is shown in Fig. 18.18. For purely static loads (no dynamic load applied), stresses up to 50% of the pipe-material yield strength are allowed for normal operations and stresses up to 67% of yield strength for limited or emergency operations. These allowable stresses have factors of safety of 2.0 and 1.5, respectively. For purely dynamic stresses, the allowables have been reduced to 25% of the pipe-material yield strength and 25% of the pipe-material ultimate strength because of fatigue considerations. Combined static and dynamic stress states must fall within the recommended range indicated on the graph. High stresses occur in the pipe-to-connector weld and at the base of the groove in the connector pin. These two areas should be inspected frequently.

Ball Joint Angle. To minimize wear by the drillpipe, the angle of approach of the riser to the BOP stack should be kept as small as possible. Problems are minimized if this angle is maintained to less than 1°—a goal readily attainable in a mild environment. With moderate to severe environments, establishing an allowable ball-joint angle of 3° is a compromise between wear problems and the application of criteria too restrictive to permit economical drilling operations.

The lower ball-joint angle is affected by many variables. Of these, rig personnel can readily adjust only riser top tension and vessel position. The rig's riser-angle indicator should be monitored continuously and the vessel position and/or riser tension adjusted accordingly. Changing the vessel location relative to the wellhead is the best method of minimizing ball-joint angle. The lower ball-joint (flex-joint) angle is the most important operating criterion to maintain.

Top Tension. For long-term operations, it is not desirable to work riser-tensioner systems at more than about 75% of their rated capacity. To do so will result in premature failure, generally in the tensioner lines. Tension requirements can be reduced by the use of buoyancy.

Sufficient tension/buoyancy should be specified to prevent drastic consequences should one tensioner fail. After ball-joint angle, this criterion is the most restrictive

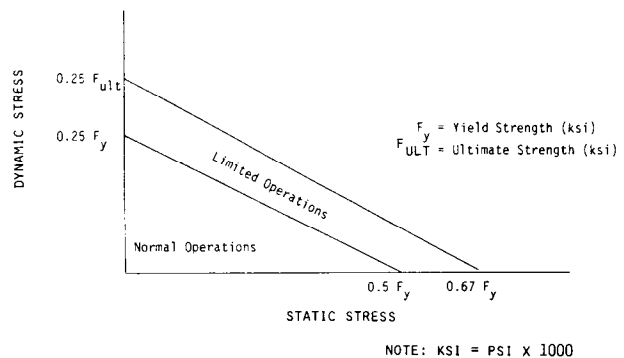


Fig. 18.18—Recommended stress ranges.

on tension requirements. When operating at the recommended tension, failure of one tensioner should not cause increases in ball-joint angle past 3°, and stress should remain in the recommended range for normal operations (see Fig. 18.18).

Minimum operating tension should always be sufficient for emergency disconnect. An overpull at the lower-marine-riser package connector of about 50,000 lbf is recommended to ensure that the lower-marine-riser package and riser will retract sufficiently to clear the top of the BOP.

Increasing riser top tension within the specified range can reduce bottom ball-joint angle. Increased tension beyond the maximum recommended, however, will significantly increase pipe stresses and have very little effect on decreasing ball-joint angle. At that point, the vessel must be moved to correct excessive ball-joint angle.

Riser Top Angle. Although the lower ball-joint angle is the most critical, the top angle must also be controlled. Tensions selected for drilling operations include a top angle of less than 4°.

Tensioner Line Angle and Sheave Friction. Variation in tensioner line angle generally has very little effect on riser tension. Sheave friction, however, may be substantial in some systems. If so, its effect should be compensated for in the tensioner control system so that the desired tension is maintained on the top of the riser.

Riser Pipe Collapse. Riser-pipe material strength and wall thickness should be sufficient to prevent collapse owing to seawater hydrostatic pressure when the riser is completely void. Reduction in collapse strength because of axial loading and bending stress should be included. In general, collapse considerations become important in water depths greater than 800 ft.

The objective of riser analysis is to specify recommended top tensions that keep the system within safe working limits under all anticipated conditions, as described in Table 18.3.

Field Operations

With the major planning and preparation completed, we will now discuss the sequential steps of drilling a well from a floating vessel. The sequence of events in this description is not necessarily followed for every well drilled from a floating vessel, but it is a method that has worked in the past and will work in the future.

TABLE 18.3—RECOMMENDED OPERATING LIMIT

Ball-Joint Angle Range	Comments
0 to 1°	Maintain ball-joint angle within these limits, if at all possible.
1 to 3°	Maximum limit for normal operations. Preferably should be in this range only temporarily.
3° and increasing	Start drillpipe hang-off procedure.
5° and increasing	Drillpipe hung off. Start riser disconnect procedure.

Establishing Location

The location has been plotted on the map, the seismic work reviewed, and the drilling program written. Materials have been delivered (especially subsea wellhead equipment, 30- and 20-in. pipe), and it is time to survey the location. Surveys must be accurate for several reasons. Locations near lease boundaries must be accurately placed from a legal or ownership viewpoint. Well location relative to seismic mapping is critical. If the rig has moved off location, getting back on location requires good survey data.

Today's techniques can provide accuracy within 10 ft. In well-established areas—such as around the perimeters of the U.S., Canada, and in the North Sea—radio triangulation systems are used. In remote areas, satellite navigation (SAT NAV) systems, with receivers located on the floating vessels, are used. SAT NAV systems are accurate to within 3 ft. Depending on the well location relative to available satellites, however, it will take multiple satellite passes and approximately 24 hours to achieve that accuracy. The site may be marked with a buoy or the rig may be surveyed indirectly. Once on location with the mooring system set and tested, drilling is ready to begin. See Fig. 18.19 for the sequence of operations.

Spudding The Well

Step 1 in drilling from a floating vessel is to lower the temporary guidebase to the ocean floor.³ The temporary guidebase is generally 12 by 12 ft and is outfitted with a bull's-eye that is observed by TV for levelness determination. This base is run on drillpipe connected to it with a J-tool or hydraulic connector. Four wire-rope guidelines are attached to the subbase before it is lowered. The base may be loaded with weighted rotary mud so that necessary tension can be pulled in the guidelines when drilling equipment is lowered to the ocean floor. With the base on bottom, the drillpipe running string is marked at the kelly bushing, averaging out the vessel heave, so that the water depth may be determined by measuring the pipe when it is pulled. This measurement, corrected for tide, is the water depth from the kelly bushing to the ocean floor that is used in all subsequent drilling, logging, casing, and testing operations.

Step 2 consists of running the drilling assembly—the bit, drill collars, bumper subs, and drillpipe—down the guidelines, through the temporary guidebase, and into the ocean floor to drill the hole for the structural casing. This hole must be drilled carefully to ensure that it is kept within 1° of vertical because it later will control how vertical the BOP stack will be when it is landed on the wellhead.

Several single shots should be taken while this hole is drilled. When drilling is completed, heavy mud is spotted in the hole to prevent sloughing or caving in. This hole generally has a 36-in. diameter and is 100 to 200 ft deep. The structural casing probably will be 30 in. in diameter with a ¾- or 1-in.-thick wall. It is called structural casing because it serves as a foundation to provide lateral support for the BOP's during subsequent drilling operations. In addition to drilling a hole for the structural casing, it may be driven or jetted in. In these instances, some drillers elect not to use the temporary guidebase.

Running 30-in. Casing

In Step 3, the structural casing (with the permanent guidebase attached and the guidelines threaded through the guideposts) is run down the guidelines into the hole.³ Care must be taken while the 30-in. casing is run to ensure that it is filled with water. Should this be overlooked, it is possible to collapse the 30-in. casing. It is run on, and cemented through, the drillpipe lowering string. Cement returns are taken on the ocean floor and may be observed on TV. To ensure a good cement job for this critical casing string, the cement may be overdisplaced by as much as 100%.

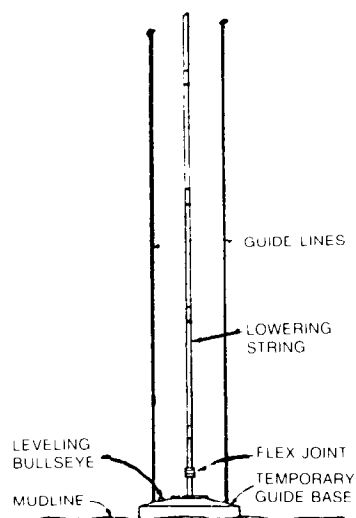
In Step 4, hole is drilled for the conductor casing. If the soil the structural casing was set in is competent, a riser is run and latched into the permanent guidebase, and drilling returns are taken on the drilling vessel. Riser top tension should be sufficient only to minimize lower ball-joint angle. Too much top tension could result in pulling the 30-in. casing out of the ground. If the soil is not competent, the riser is not run and returns are taken on the ocean floor. If the riser were used with incompetent soil, the hydrostatic head of the drilling fluid could break down the soil at the shoe of structural casing, resulting in lost circulation. The conductor hole may range in depth from 298 to 499 ft. The size of conductor casing commonly used has a 20-in. OD. If the riser has been used, it is pulled before the conductor is run.

Running 20-in. Casing

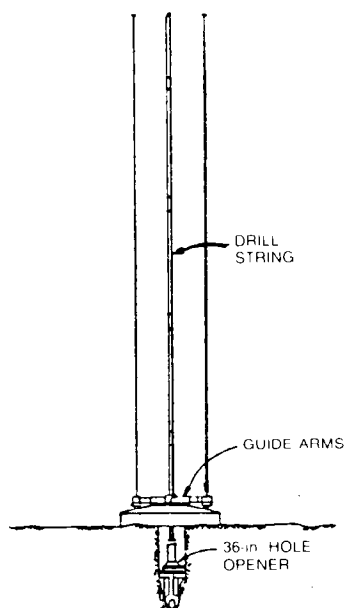
In Step 5, the 20-in. conductor is run down the guidelines on drillpipe, landed in the housing on the structural casing, and cemented back to the ocean floor.³ The top of the 20-in. conductor is fitted with a 16¾- or 18½-in. high-pressure wellhead housing prepared internally to receive subsequent casing strings. The size of the casing head is determined by the size of the BOP's on the drilling vessel. The external profile on the upper end of the casing head is prepared to match the type of wellhead connector installed on the BOP stack. A metal-on-metal seal ring provides the pressure seal between the connector and wellhead.

Running the BOP

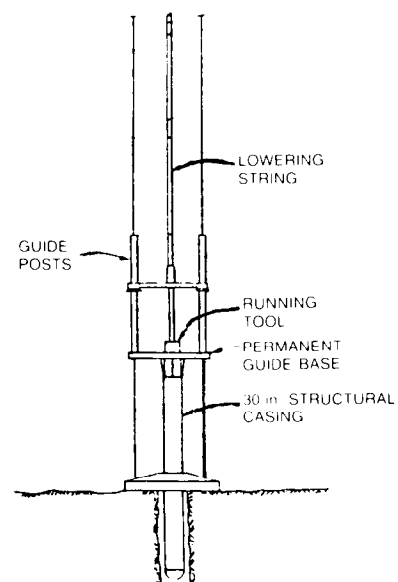
Step 6 consists of function- and pressure-testing the BOP stack on the deck, then running it down the guidelines and latching it to the casing head.³ The BOP's, which can weigh as much as 400,000 lbm and range in height from 30 to 40 ft, normally are run on the drilling riser. Depending on water depth, running the BOP stack can be a short or long procedure (from a few hours to several days). Each riser joint must be carefully inspected as it



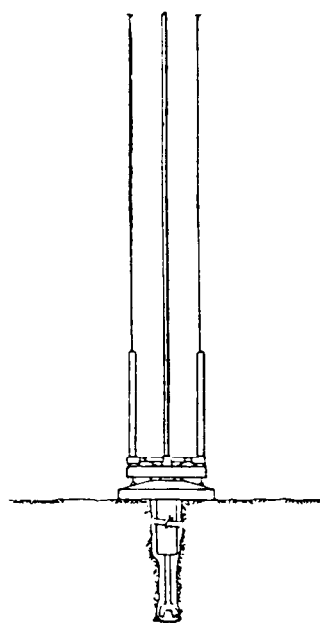
STEP 1 LANDING TEMPORARY GUIDE BASE



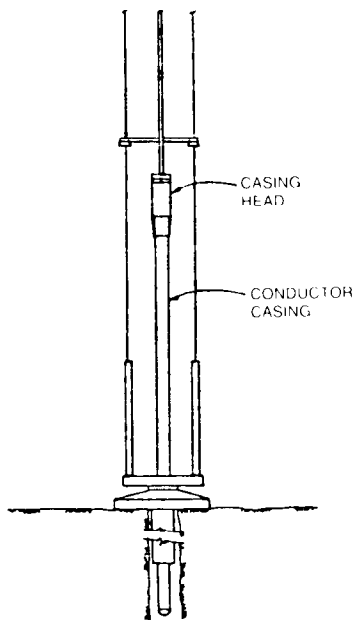
STEP 2 DRILLING STRUCTURAL CASING HOLE



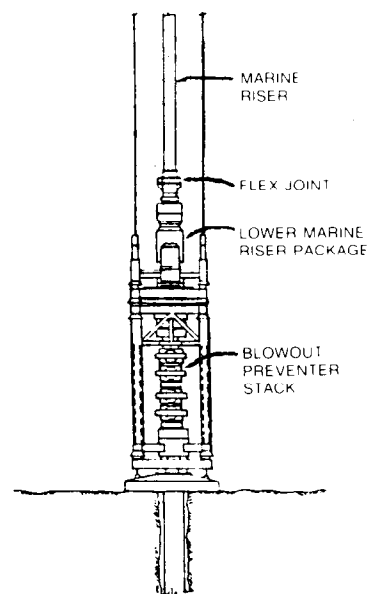
STEP 3 RUNNING PERMANENT GUIDE BASE AND STRUCTURAL CASING



STEP 4 DRILLING HOLE FOR CONDUCTOR



STEP 5 RUNNING CONDUCTOR WITH CASING HEAD



STEP 6 BOP'S INSTALLED READY TO DRILL TO T.D.

Fig. 18.19—Floating drilling—subsea systems.

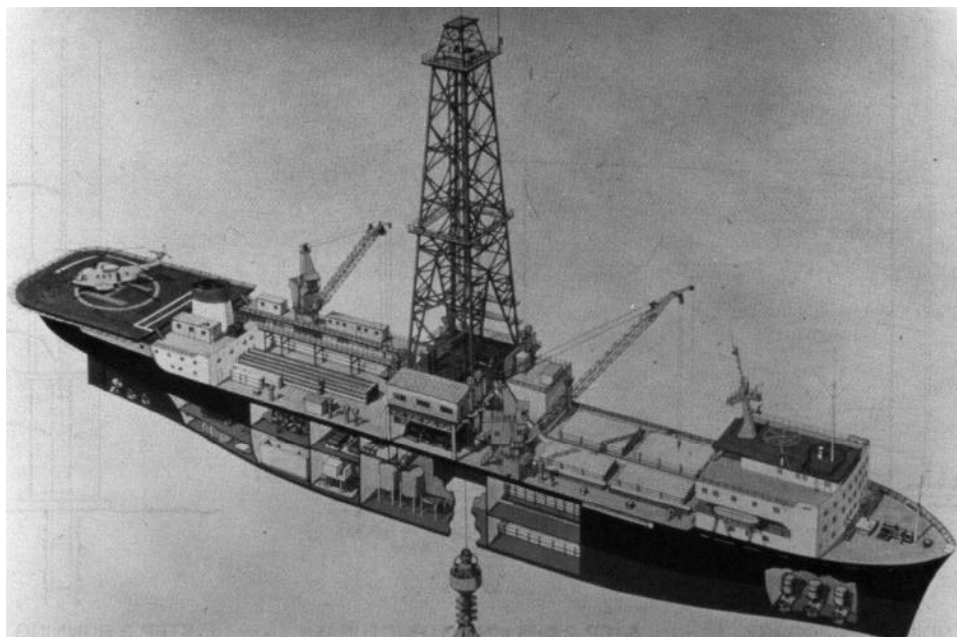


Fig. 18.20— Dynamically positioned drillship.

is run. Each riser connection must be checked for correct makeup. The total weight of the BOP is supported by each connection. Integral K&C lines (and hydraulic supply line if it is hard-piped) should be pressure-tested every second or third joint to avoid an unnecessary pulling of the BOP for leak repair. In addition to careful riser inspection, riser handling tools and the riser spider should be inspected for cracks or damage. The riser handling tool supports the total weight of the BOP and riser each time another joint is added to the string. The top of the riser is fitted with a slip joint to accommodate vessel heave and offset. The slip joint lands in a diverter housing immediately under the rotary table. Riser tensioning lines are connected to the slip-joint barrel so that tension can be applied to the riser when the stack is landed on the wellhead. Once in place, the stack is function- and pressure-tested, and all is ready to begin drilling to total depth (TD). As hole is drilled, additional casing strings may be run through the riser and BOP's. Periodic BOP testing after the first casing string is landed in the wellhead housing must be done carefully. A leaking casing-hanger-seal assembly could collapse the casing if test pressure exceeds casing-collapse pressure. API RP 53⁶ includes testing guidelines. If the well is to be put on production, the tubing string also is run through the BOP's and hung off in the casing head.

Drillstem Testing

Drillstem testing (DST) requires specific equipment not normally installed on floating vessels. An inside-the-BOP production tree includes redundant master valves and a surface-actuated hydraulic latch for emergency disconnect, high-pressure piping and valves from the choke manifold to production-equipment area, test trap with metering equipment, storage tanks with transfer pumps, and a flare boom. This equipment requires considerable space. Storage-tank location may require beefing up the local deck structure. Flare booms require special foun-

dations. Installation and operation of production well-test equipment requires planning and significant rig-up time.

The BOP production tree space-out is critical. The tree lands in the subsea wellhead housing, and BOP pipe rams seal the casing tubing annulus. The tree height, including the emergency disconnect mandrel, must not extend above the bottom of the blind shear ram. In case of emergency disconnect, the blind-shear-ram area must be clear for shut-in.

DST is a critical operation. It must be conducted under carefully controlled conditions. If H_2S is possible in the production, special precautions are necessary. Local regulations and API RP 49 cover H_2S requirements.¹⁰

Plug and Abandonment

If the decision is made to abandon the well, it must be plugged first. Local regulations dictate plugging details. Abandonment plugging generally consists of laying cement plugs in the wellbore at specified intervals to just below the ocean floor. The plugs are pressure tested as they are installed.

Next, the subsea wellhead and bases must be recovered. This is accomplished by cutting the casing strings approximately 15 ft below the mudline. Cutting can be done with mechanical cutters (tools are available that can cut 13 $\frac{3}{8}$ -in., 20-in., and 30-in. strings in one step) or with explosives. If explosives are used, the rig may have to be moved several hundred feet away from the wellhead, depending on water depth, so that the explosion shock wave won't damage the vessel's hull. Retrieved wellhead equipment and bases can be reconditioned and reused.

Special Considerations

Deepwater Drilling

Maximum water depths continue to extend. During 1983, a well was drilled in approximately 6,800 ft of water off the U.S. east coast. Locations in water depths greater than

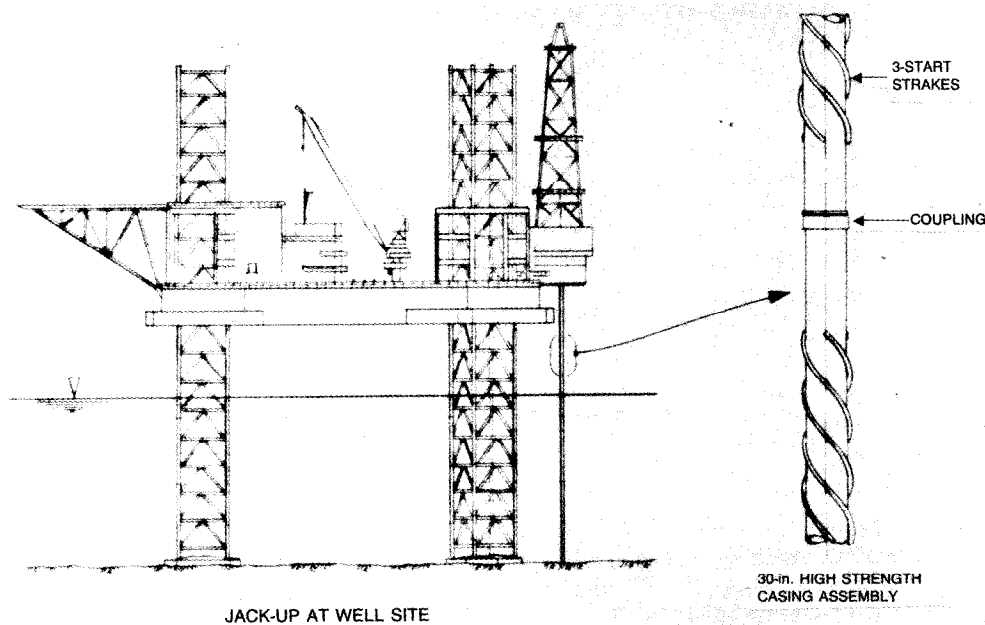


Fig. 18.21—Thirty-inch casing with helical strakes.

2,000 ft should be considered deep water. Mooring becomes more difficult, subsea equipment is heavier, collapse under hydrostatic conditions becomes critical, equipment performance under emergency disconnect conditions, and well-control procedures require additional considerations.

The major differences in shallow vs. deepwater floating drilling equipment are station-keeping (moored vs. dynamic positioning), riser design (material strength vs. buoyancy needed), BOP control systems (hydraulic vs. multiplex), and backup systems (diver vs. unmanned).

Deepwater operations require longer calm-weather periods and improved weather forecasting to accomplish specific tasks. Running and retrieving BOP's can take just a few hours in shallow water. In deep water, 2 or even 3 days may not be unreasonable. Relatively calm sea conditions are required during that time.

Dynamic-positioning (DP) systems have extended station-keeping capabilities to depths of more than 10,000 ft. DP systems consist of acoustic beacons located on the ocean floor, hydrophones mounted on the vessel's hull, thruster units fore and aft, and an on-board computer system for control. Dynamically positioned drilling vessels are equipped with from 12,000 to 20,000 hp for station-keeping. Increased fuel consumption while operating in the DP mode is a major cost increment in a rig's day rate (see Fig. 18.20).

Cold Environment

A few special cold-weather drilling vessels are available today. However, most rigs operating in cold environments today were not designed with low-temperature steel requirements. Highly loaded or highly stressed components—such as the derrick substructure, lifting subs, riser running tools, riser connectors, and elevators—must be fabricated from steels with low-temperature resistance (Charpy impact values comparable to the temperatures encountered) if they are to function safely. Material specifica-

tions of highly loaded components should be checked and verified before an unknown rig is taken into a low-temperature work situation.

Other cold-weather equipment considerations include quarters, insulation and heating, work-area heating, control-fluid freeze protection, water-system freeze protection, water-tank heating, and superstructure de-icing capability.

The American Bureau of Shipping specifies requirements for ice-class rigs.¹¹ Those specifications include hull strength in the ice zone, thruster or propeller protection from ice chunks, and other specific requirements that must be met before a rig (ship or semisubmersible) can be certified to work in ice areas.

High-Current Drilling

The first concern in drilling high-current locations is station-keeping. Does the mooring system have adequate strength, or the dynamic-positioning system adequate horsepower, to keep the drilling vessel on the location? With the mooring analysis previously discussed or with more sophisticated techniques to evaluate dynamic-positioning station-keeping, we can determine the adequacy of the proposed rig's station-keeping system.

The next concern is possible fatigue failure of 30- and 20-in. casing strings (generally in a connector) owing to vibration. High currents can cause vibrations that induce failure in hours under the right conditions. Any surface current of more than 3 knots should be considered high current. Casing strings of 30 and 20 in. have been fabricated with helical strakes to break up the vortices that cause the severe vibrations (see Fig. 18.21).

Vortex shedding, which causes high-amplitude vibration at 90° to the direction of the current, can create severe problems in drilling risers also. Riser fairings have been developed and used on several occasions to eliminate the troublesome vortex-shedding vibrations successfully (see Fig. 18.22). Special equipment, in addition to

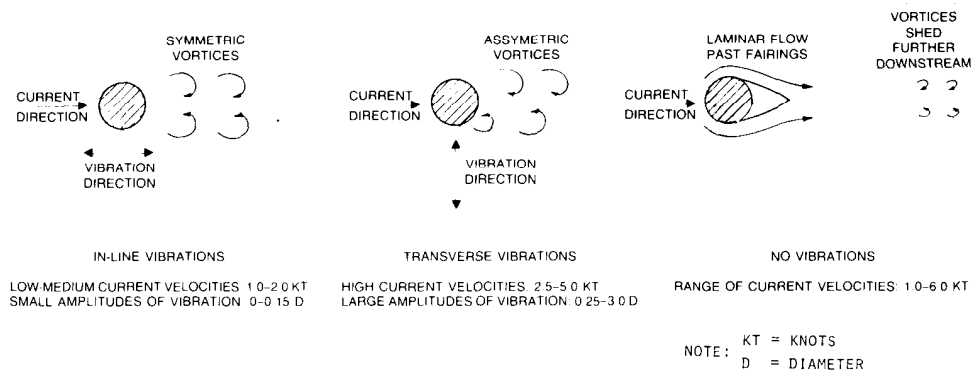


Fig. 18.22—Riser vortex shedding.

strakes and fairing, can be installed on the drilling vessel to allow successful drilling operations in high-current areas. A floating rotary table and a moonpool riser-centralizing system have been developed to accommodate the high loads and high angles imparted on pipes and risers during high-current periods. If current direction is fairly consistent, installing early-warning current-meter strings 2 to 3 miles upstream from the rig can greatly assist in coping with the oncoming current conditions.

Structures

Background and Philosophy

As exploration and production encroaches into deeper water and harsher environments, the challenges of structural design increase. Environmental load predictions, transportation analyses, and installation procedures are as important to understand as the more obvious structural-frame analysis. Seldom is a designer afforded the luxury of optimizing a structure on the basis of in-place stress analysis. More often, the transportation and installation (lasting a few weeks out of perhaps a 20-year structure life) will dictate the major framing patterns. Equally disconcerting to the structural designer is that most of his accomplishment is seen by only a handful of people, especially once it is in place. For the structure's lifetime, it is expected to support drilling and/or production operations, and the operator cares little beyond that.

So the structural engineer's job can be simply defined as getting it designed, built, and in place as quickly and economically as possible, while ensuring functionality and providing for minimal maintenance.

Structure Classification

As indicated in the Historical Review, many types of offshore structures are in service. Some are better suited to certain environmental and operational criteria; some are limited by availability of construction sites; and some are chosen simply by subjective preference of an owner/operator. Selecting a structure type is the first major structural design task after environmental and operational criteria have been defined and might require preliminary design of several concepts before a choice is made.

Template/Jacket. "Template" was derived from the function of the first offshore structures: to serve as a guide for the piles. The piles, after being driven, are cut off

above the template, and the deck is placed on top of the piles. The template is prevented from settling by being welded to the pile tops with a series of rings and gussets. Hence, the template carries no load from the deck but merely hangs from the top of the piles and provides lateral support to them.

Some companies prefer to place packers in the bottom of each template leg and to grout the annular space between the leg and pile from bottom to top. The structure and piles share the axial load from the deck and the compressive and tensile loads from the overturning moment produced by lateral wave loads. The grouted pile also provides additional strength to the tubular joints where horizontal and diagonal bracing are welded to the legs. Drawbacks to this system are the difficulty in ensuring that the grout is adequately placed and of sufficient strength to be counted in the analysis and the additional difficulty in platform removal.

Although both top-hung and grouted structures are loosely called templates, some prefer to call the latter a jacket to distinguish the difference in load path. This path is substantially different for the overturning moment as well as axial loads. The top-hung template requires that moment from lateral wave loads be transmitted up the structure to be resolved into axial pile loads. The grouted jacket has a direct downward load path for shear and moments. The novice designer would do well to learn this distinction early in his career.

When steel structures are designed for deeper water (in excess of 250 ft), pile-leg grouting is prevalent. Deep-water jacket designs are heavily influenced by lateral wave loads that produce high base shear and overturning. Piles placed through the legs of the jacket are not always sufficient to transfer these loads to the soil, so "skirt piles" are added, normally in clusters around the corner legs. This adds a new dimension to the installation procedure. Pile guides are required up to water level, and a removable "follower" must be used during pile-driving operations. Grouting procedures for the skirt sleeve-to-pile must recognize that grout placement and inspection will be done remotely.

Template/Jacket Construction. A typical construction sequence for a template or jacket calls for yard constructing the unit on a pair of skid rails, skidding the structure onto a barge with matching skid rails, towing the barge to location, and launching. After the structure comes to

rest, usually floating horizontally, it is upended by ballasting members at the lower end. Once upright, it is moved onto the final site and lowered to the seabed by continued ballasting.

To date, the maximum water depth feasible for a single-piece jacket appears to be about 1,000 ft. The constraint is a result of construction equipment and facility limitations, although contractors are quick to point out that capability can be extended quickly if the business climate warrants. Meanwhile, an alternative for deeper water is the multipiece structure. These structures are built in either two or three pieces that are launched from separate barges. The pieces can be mated while floating horizontally, like the Hondo¹² platform, or stacked vertically and grouted together with pin piles, like the Cognac¹³ platform. Mating of large structural sections has proved to be expensive and involves added risk over single-piece structures, so plans are under way to extend single-piece construction to water depths beyond 1,000 ft.

Yard facilities are tailored to build structures in the horizontal position. Lifting equipment is huge in both capacity and reach because a deepwater structure might have a base width of more than 200 ft, which would require lifts to be placed to the height of a 20-story building! A structure for 1,200 to 1,500 ft of water could have a base width of more than 300 ft, which is beyond the reach of today's equipment.

Since 1975, several large transportation barges have been built with lengths of more than 600 ft and capacities of 40,000 tons. Such a barge was used to place the single-piece Cerveza¹⁴ platform in 935 ft of water. Several installation contractors now have plans for "super barges" with lengths of 900 to 1,000 ft and the capability of transporting jackets more than 1,500 ft long.

The increased pile loads on deepwater structures have necessitated advancements in pile-placing technology. In 1960, driving a 48-in. pile to 300 ft penetration for an axial capacity of 2,500 tons was a major feat. In 1984, a designer can plan for an 84-in. pile driven to about 400 ft to develop an axial capacity of 15,000 tons. Most of the advancement has come in the area of pile hammers. Hammers can be built to energy levels of 1.2 million ft-lbf, nearly 10 times that of the hammers used in 1960. Also, underwater hammers are becoming more dependable, which has the advantage of eliminating pile guides and followers for skirt piles and saving the energy normally lost through the follower.

Concrete Gravity Structures. As the name implies, these structures have large mat foundations instead of piles and are heavy enough to resist overturning and base shear from lateral wave and wind loads. Whereas steel template/jacket technology was largely a product of the U.S., the concrete gravity structures were European designs. Three reasons are offered for the emergence of these designs: (1) the European countries with offshore oilfields demanded a high percentage of national content—i.e., design and construction money had to be spent within their borders; (2) European design expertise, construction facilities, and construction skills leaned heavily toward concrete and away from steel; and (3) template/jacket technology was not prepared for the huge payloads and severe environment of the North Sea. The first major steel structure met with severe design changes and inadequate

fabrication and transportation facilities and was finally placed with high cost overruns. The high cost overruns of the first steel structures opened the door to concrete structures. Although these structures also ran into severe cost overruns, they had the advantage of not being payload-sensitive.

The concrete structures were necessarily massive to resist overturning. Furthermore, the concrete members were often controlled more from pressure than from axial forces of the deck load. Hence, changes in the payload requirement that occurred during construction and even for years after placement could be accommodated with relative ease. This proved valuable as the prolific North Sea fields were developed and facilities were continually added to existing structures.

Most concrete gravity structures were designed to store crude oil until it could be loaded on a transport tanker. This was required in the early stages of development because building an adequate pipeline network for the North Sea took many years. Only a few of the structures still are used for oil storage, and tanker-loading systems are active only in Norwegian fields where a deep coastal trench has delayed pipelines from coming ashore.

Concrete structures have two basic shapes. The French design generally consists of a large, vertical, cylindrical structure surrounded by a perforated wall. The internal structure is capable of storing oil and supports the center of the deck structure. Typically, the perforated wall has 6.6-ft-diameter holes at 13-ft spacing that allow seawater to flow through as the wave passes, thereby reducing the wave force. The wall ends about 33 ft above the water level, and bracing extends up to support the edges of the deck.

Gravity Platform Construction. Concrete structures are nearly always built vertically. The lower portion of the base is built in a graving dock. The dock is flooded to sea level, thereby floating the base. The gate or dike is removed and the structure is towed to a protected deepwater site in a fjord or firth. The remainder of the structure is built by use of slipform methods and increases in draft as construction continues. If the platform has been designed for 450 ft of water, the draft of the completed substructure might be 300 ft.

Meanwhile, the deck is built, outfitted, and skidded onto one or two barges, depending on the configuration. Substructure and barge-mounted deck are towed to a mating site where water depth exceeds the design depth. The substructure is ballasted until only a few feet are above water. The barge-mounted deck is towed carefully over the substructure, and the substructure is deballasted until it picks the deck off the barges.

After the mating is complete, the platform is deballasted to minimum draft for towing to location. Minimum draft is still deep—perhaps 350 ft—and is limited by platform stability; further deballasting would raise the platform until it became top-heavy and toppled over.

The tow to site is nearly as critical as the mating operation. The tow route must be carefully surveyed, charted, and marked. Deviation from this route could result in stranding the structure on a sand bar or hitting a submerged canyon wall. A fleet of the world's largest tugboats is required to tow the platform safely. Power, steerage, and standby tugs must all respond to the direction of the tow master.

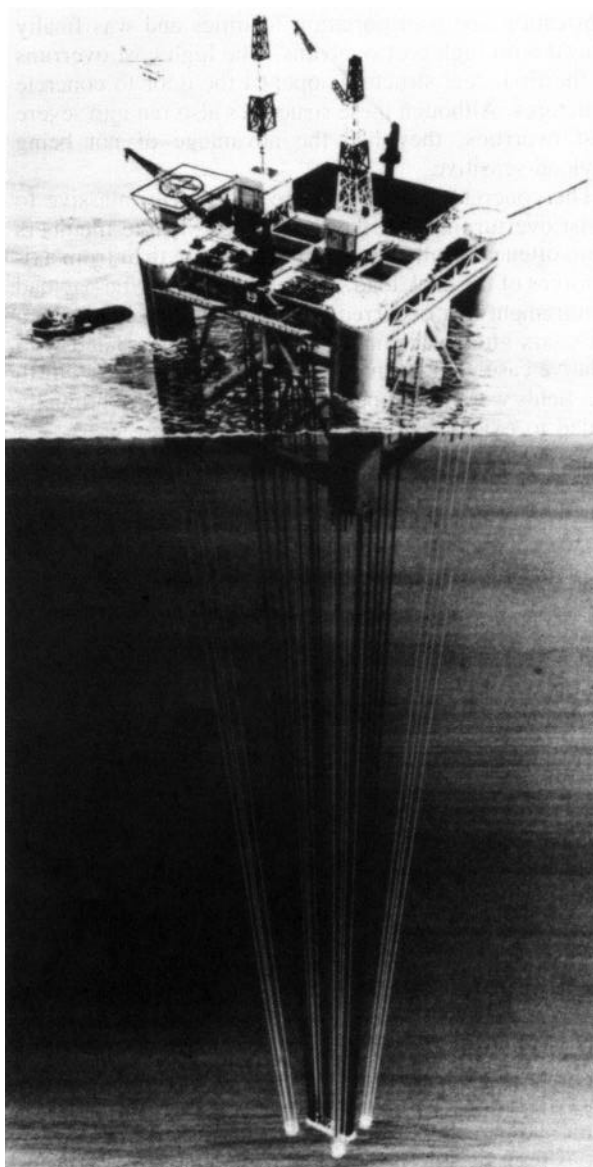


Fig. 18.23— Tension leg platform

Once on site, ballasting will set the structure on bottom, and grouting fills any voids under the base. Offshore construction and hook-up time can be held to a minimum because onshore deck construction should have included commissioning most of the systems.

Guyed Towers

The guyed tower is intended for use in deep water—perhaps 1,000 to 2,000 ft. It applies the principle of “compliance” to wave forces. Wave forces are cyclic in nature, pushing a structure first in the wave direction and then against it. By pinning the structure to the seafloor instead of making it a fixed cantilever, the guylines allow the structure to sway back and forth with the wave force, transmitting only small loads to the foundation. The guyline system holds the tower upright and resists the steady forces from wind and current. Depending on the size and configuration of the guyline system, the tilt an-

gle of the tower can be restrained to 2 or 3°. The Lena platform in the Gulf of Mexico is the only guyed tower built and in service to date. Twenty-four guylines support the structure; their diameter varies between 5 and 5½ in.

The vertical support system resembles the template in that the tower is welded to the top of the piles and hangs in tension. The piles carry the deck load directly and, in addition, the vertical component of the guyline tension.

An additional, undesirable, axial load is caused by the tilting of the tower. The piles on one side compress as the tower tilts, and on the opposite side they stretch. The resulting stress cannot be eliminated, only controlled. The piles are clustered near the center of the tower to reduce the stretching and compressing. The system can be designed successfully by limiting the tilt angle and providing sufficient pile length to absorb the compression.

As the tower tilts, the piles must bend through the tilt angle in a relatively short distance near the mudline. The stress can be controlled in this case by locating the guides properly and determining the stiffness of the soil. The influence of the tilt angle on the pile stresses must be evaluated before the guyline system is sized.

Guyed Tower Construction. The guyed tower is lighter and more slender than a jacket would be for the same depth. Therefore, yard and transportation equipment can handle a guyed tower for depths greater than that for a template. Installation procedures, however, are more complex because of the heavy guyline system and the large piles.

After the tower is upended and set on the seafloor, buoyancy must hold the structure upright until the guylines are installed. A derrick barge is needed for driving piles, placing the deck, and setting equipment modules. This barge normally relies on its own mooring system for station keeping, but in this case, some modification will probably be required to prevent the tangling of mooring lines with guylines. The entire installation sequence must be planned carefully to ensure safety of the structure, guyline system, and floating equipment.

Tension Leg Platform

The tension leg platform (TLP) is another structural system based on the “compliance” principle. The platform is composed of a deck structure and a buoyant hull that is made up of a series of vertical cylindrical columns, horizontal submerged pontoons, and tubular member bracing. The platform is tied to the seabed by a number of tendons that are kept taut by excess buoyancy in the hull. Fig. 18.23 shows a TLP designed for 1,600 ft of water. Four vertical 52-ft-diameter columns are tied together with 28-ft-diameter pontoons, and four tendons at each corner column (16 total) tie the platform to the seafloor foundation template.

To date, the Hutton platform in the North Sea is the only TLP in service. It was placed in only 485 ft of water, although the TLP is considered by many as the most promising structure for water depths from 1,000 to 4,000 ft.

Because the TLP is lightly restrained horizontally, steady forces from wind and current will cause large excursions of about 5 to 10% of water depth. Second-order wave forces, insignificant on fixed platforms or guyed

towers, can cause substantial steady offset and "slow-drift oscillation" at the natural surge period of 60 to 120 seconds.

The tendon system and well system on the TLP are the most structurally critical and set the limits on horizontal excursion. Often containing flex joints or tapered cantilevered pipe sections, these systems require careful analysis both for maximum stress and for fatigue life.

The foundation system is subjected to cyclic loads superimposed on a high tension. This system also requires careful analysis based on the best possible geotechnical data for the site.

TLP Construction. The TLP is structurally similar to the common semisubmersible drilling structure, and most efforts to design it differently or to different standards result in extreme cost and schedule overruns. The size of the TLP is related directly to the payload required and the environment it will withstand. This normally means that the displacement (buoyancy) will be between two and five times that of a semisubmersible. Therefore, many shipyard facilities used for semisubmersible construction will be too small for a TLP.

Two distinctly different construction methods are available. The first is separate construction of the deck and hull, requiring a mating sequence similar to that described for a concrete gravity platform. The second method is single-piece construction where the deck is built onto the hull and equipment placed on the completed platform. The first method offers reduced construction time; the second allows for intermediate structural bracing to support the deck because clearance is not required for a barge. The choice between these two construction methods must be made early in the planning stage to take advantage of the benefits afforded by either concept.

The most difficult and uncertain part of TLP construction is the placement of the seafloor template or templates and the piling. Again, several options are open—a single template for the foundation and well system or separate templates. Tendons may be attached to the template or directly to the piles. Again, each system has advantages and disadvantages, and all aspects of allowable tolerances, seabed levelness, potential for settlement, and preference for separate structural systems should be considered.

Special-Service Structures

Many structures have been built for a specific location or specific purpose and are essentially one of a kind or perhaps one of a select few. Self-floating jackets, steel gravity platforms, tanker-mooring articulated towers, mooring dolphins, and single-well caissons are some special-service structures. Each of these concepts and the innovative effort that went into them deserves a chapter in a book, but unfortunately there is not room here. The author recognizes the effort needed to learn the special hydrodynamics, structural dynamics, stress analysis, and construction methods needed for a unique design. Many unheralded innovative engineers have gone virtually unnoticed because their structure, though successful in the purpose for which it was intended, simply was not needed anywhere else.

Structure Selection

From the preceding discussion, it should be obvious that the chosen structure is not always the one that theoreti-

cally has the least concrete or steel. Construction facilities and skills in the area are important, and often the operator's preference will prevail. Here are some guidelines, though, on the four concepts discussed.

Template/Jackets. Around the U.S., these structures are the norm for water depths from 10 to 1,000 ft. Most U.S. offshore structures have a payload based on less than 50,000 B/D production. These small payloads are conducive to templates and jackets. Future technology might push these structures to 1,500 ft of water; limitations will be based on the structure's natural period and cost.

Concrete Gravity Structures. These structures require deepwater construction sites in protected water. Norway and England have such sites; the U.S. does not. These structures can readily carry the equipment for up to 200,000-B/D production. The North Sea will probably need more structures with these production rates; we hope the U.S. will also. Depth limitation is probably around 700 ft, unless new construction methods are developed.

Guyed Towers. These structures should be good for deep water and heavy payloads. Because deckloads are carried directly by the piles and only indirectly affect the tower and guyline system, heavy payloads should not cause a substantial increase in structure costs.

TLP. These structural systems should be relatively economical for deep water and light payloads. Increased payload directly affects buoyancy requirements, which in turn directly increases waveloads and tendon and foundation requirements. Conversely, deeper water requires only longer tendons. With a design based on realistic understanding, this concept could be extended to a 4,000-ft water depth.

It will be interesting to see how the future will bring about changes.

Structural Design Process

As previously indicated, there are many types of offshore structures, but the following example will be confined to a barge-launched jacket. The considerations and procedures, however, have a parallel in the design and construction of any structure.

Methods for determining environmental loads and for analyzing structures are outlined in API RP 2A, "API Recommended Practice for Planning, Designing, and Constructing Fixed Offshore Platforms." This document is one of a series of recommended practices that are reviewed frequently and reflect the state of the art.

Fig. 18.24 shows a rather large offshore jacket for about 500 ft of water. Drilling and production facilities are assumed to be in modules for placement on top of the module support frame.

The structure must be designed for a variety of conditions, including fabrication, transportation on a barge, launching, upending, placement, and operation. Each condition controls the size of some members. The members controlled by in-service conditions may require several separate analysis procedures to size them adequately.

Field Development Plan. To put the design process in a time frame, Fig. 18.25 shows that portion of a possible field-development program that relates to the jacket,

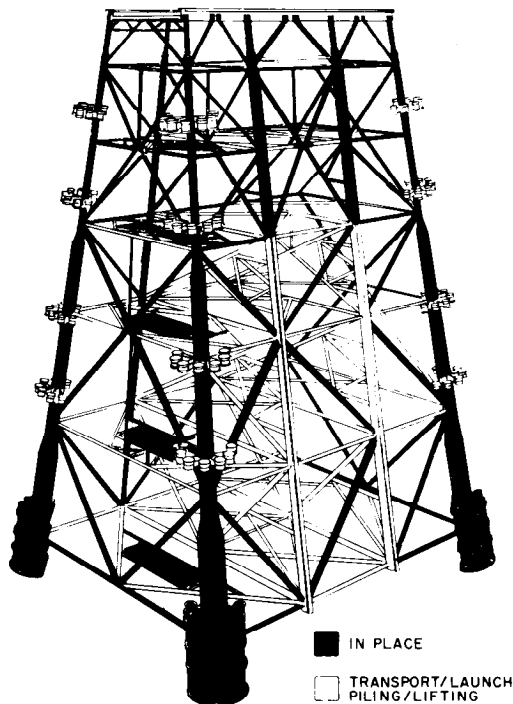


Fig. 18.24—Jacket members as sized by design conditions.

recognizing that facilities design and construction are parallel. The economic studies are to determine the viability of the program and must include a preliminary design of the jacket to determine a cost estimate. Analysis will probably be limited to a single topside load and the maximum storm wave, using a first guess at water depth, wind speed, wave height, and current velocity.

Environmental Criteria. As the design progresses through two or three of the cycles shown in Fig. 18.25, more exact environmental data will be needed, and the oceanographers probably will be working to firm the data up in parallel with the design. Close coordination between the designer and the oceanographer is critical. The information must be available on time, sufficiently detailed, and in a format compatible with the design procedures.

Storm directionality might determine the orientation of the platform. Because of transportation requirements, a jacket is rarely symmetrical, so it will resist lateral wave loading better along one axis than the other. The pattern of well conductors is often dictated by the reservoir characteristics, however, so aligning the strong axis with the most severe storm direction is not always possible.

In addition to maximum storm criteria, statistical wave data and scatter diagrams are needed for fatigue, transportation, and launch analysis, and for determining weather windows for derrick barges that will be used for pile-driving and lifting modules. This information might point out a substantial seasonal variation in weather statistics that will dictate the time of year for installation. The designer should anticipate the required magnitude and format of environmental data and pass this requirement to the oceanographer early in the project.

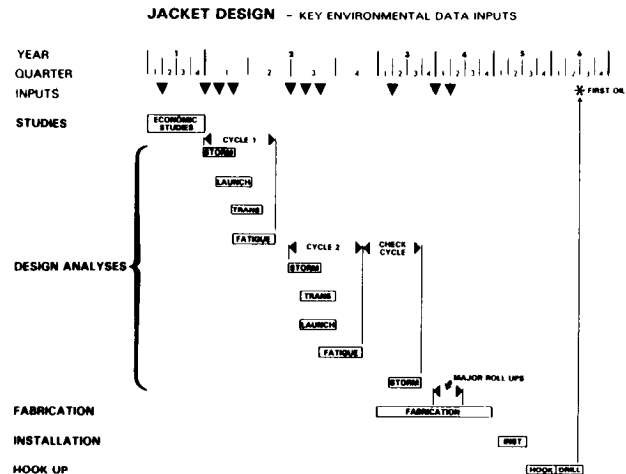


Fig. 18.25—Jacket design—key environmental data inputs.

In-Situ Analyses. The in-situ static procedure in Fig. 18.26 shows the loading systems applied to the jacket. The stiffness analysis assumes these loads to be static, and the results must be combined with the wave data and the natural periods of the structure to derive a dynamic amplification factor. The “combination processor” must combine static and dynamic loads to determine member and joint forces, moments, and displacements. These are then converted to stresses and compared with those permitted by the design codes. If the design is not acceptable, members and joints must be resized and the process repeated.

The linear stiffness analysis usually is adequate for the steel framework, but must be adjusted for the pile/soil interaction that is commonly nonlinear when extreme-event loads are applied. Various linearization techniques or iteration procedures are used to arrive at the correct pile displacement and rotation. This is probably the most difficult and critical area in the analysis because improper stiffness assumptions, either too high or too low, can result in a nonconservative structure.

Transportation and Launch. The approximate location where the structure is to be fabricated must be known to estimate the tow route and duration. Also, the season must be established so that sea-state predictions are appropriate. For Gulf of Mexico structures, tow routes normally are short, and weather forecasts often can cover the entire duration of tow and launch. For the west coast, fabrication might be in the orient, with a tow duration of 6 to 10 weeks. Thus, early construction planning is required for adequate design and analysis.

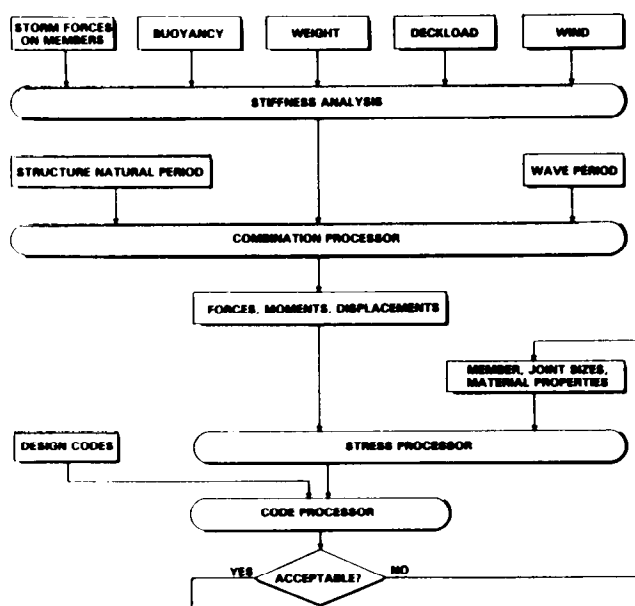


Fig. 18.26—In-situ "static" analysis.

The analysis procedure for both tow and launch is shown in Fig. 18.27. A wave-scatter diagram is used to define significant wave height and period combinations for the various sea states to be encountered. Barge motions can be determined either by analysis or model tests. Member accelerations, dead weight, and tiedown reactions can then be fed into the jacket stiffness analysis to determine stress levels for checking against design-code allowables.

The launch analysis requires a step-by-step simulation of the jacket tipping off the barge on the rocker arms until it is floating freely. Loads and reactions, including hydrodynamic loads on submerged members, must be retained for a stiffness analysis.

Fatigue Analysis. There are two distinct methods of fatigue analysis that are used in industry. The first and most easily understood is the deterministic analysis (shown in Fig. 18.28). This procedure will be described in some depth. The second method is spectral analysis, which involves a statistical prediction of stress magnitude and cycle distribution in each sea state and over the life of the structure. This method is gaining favor in industry but is too complicated to treat adequately in the context of this chapter.

The basic principle of fatigue damage is straightforward, although its accuracy is often debated. It states that for a given stress level, the fatigue damage, F_d , is equal to the number of applied cycles, n , divided by the number of cycles required for failure, N , or $F_d = n/N$. For example, if a steel can withstand 2.5×10^7 cycles at 10 ksi before failure occurs and 6.1×10^6 cycles are applied, then the damage is $F_d = (6.1 \times 10^6) / (2.5 \times 10^7) = 0.244$. This indicates that the member is 24.4% damaged. The common procedure for checking total damage is Miner's rule, which requires that the summation of all damage be less than 1.0. The recommended fatigue curves and al-

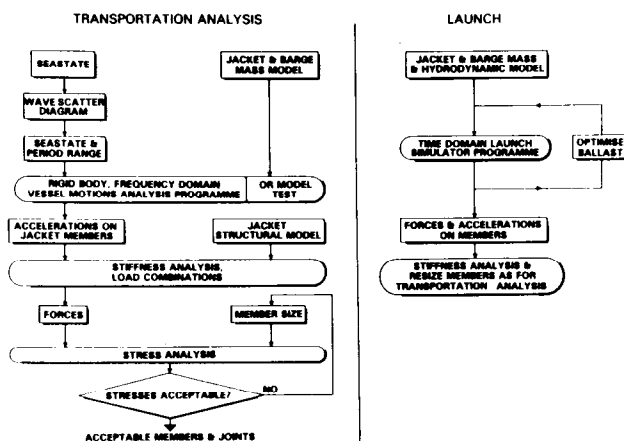


Fig. 18.27—Analysis procedure for tow and launch.

lowable cumulative damage can be found in API RP 2A. The fatigue curves show stress, S , plotted against the number of cycles to failure, N , and are often called $S-N$ curves.

If the natural period of the structure exceeds 3 seconds, API RP 2A recommends that a dynamic amplification factor (DAF) be included in the analysis. The DAF accounts for increased stress because of structural vibration. A complete dynamic analysis may be performed in lieu of using DAF's, but this can become extremely expensive.

Fig. 18.29 shows a spectral fatigue analysis that can be compared to the deterministic analysis in Fig. 18.28. Ref. 13 outlines this procedure.

The previous discussion covers most of the major analyses required for a platform, but don't be misled by the brevity. Between 75 and 100 complete stress analyses usually are required to determine stresses for in-place fatigue. Transportation fatigue might require twice that many. If seismic analyses are included, the total bill for computer time might exceed \$1 million for a thorough final analysis.

Other structures will have unique design and analysis problems. Generally, the same types of analyses are required, but they differ in areas of dynamic response or hydrodynamic loading. Ultimately, the extent and choice of the analysis procedure falls back to engineering judgment, and there is absolutely no substitute for experience.

Offshore Production Operations

Offshore production installations can be either very similar to or radically different from land installations. The purpose of this section is to provide a general overview that will acquaint inexperienced persons with typical designs and requirements for completing and producing wells offshore and describe alternative installations that are currently available to engineers and operators for meeting production objectives under varying conditions.

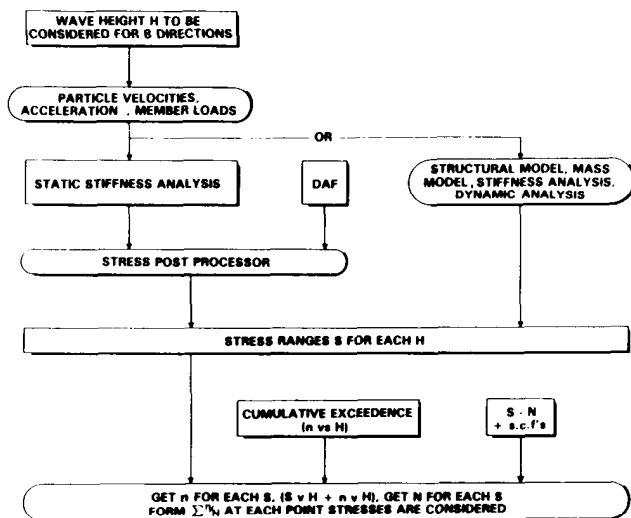


Fig. 18.28—Deterministic procedure analysis.

Platform Production

Well systems and crude-oil and gas process facilities installed on platforms account for more than 99% of current offshore production capacity. A small number of wells are completed on manmade islands. From a design and operating standpoint, these island wells are handled the same as platform wells. Wells that are completed sub-sea number fewer than 300 worldwide and will be discussed separately.

Well Completions. Except for a few innovative installations, wellheads and Christmas trees on platforms are basically the same as for land wells (Fig. 18.30). Control valves, safety valves, and piping outlets are configured the same and use the same or similar components. Some of the valves probably will have pneumatic or hydraulic actuators to facilitate remote and rapid closure in an emergency. Also, some Christmas trees may have composite block valves instead of individual valves flanged together.

The major difference, however, between land and platform well completions is the economic incentive on platforms to reduce equipment weight wherever possible and to minimize space requirements. Simply put, lighter, smaller equipment and more compact installations result in less-expensive platforms. A good example is the use of composite block valves to reduce Christmas-tree size and weight. Another example is the spacing of wellheads as close together as drilling operations will permit, with just enough room for safe and efficient operation of tree valves, control valves, and well-workover equipment. Typically, this means centerline distances of 6 to 10 ft between wellheads.

Where only one drilling rig is on a platform, all the wellheads usually are located in one bay. Larger platforms that are designed to accommodate two drilling rigs may have two well bays (one for each rig) with two or more rows of wells in each bay.

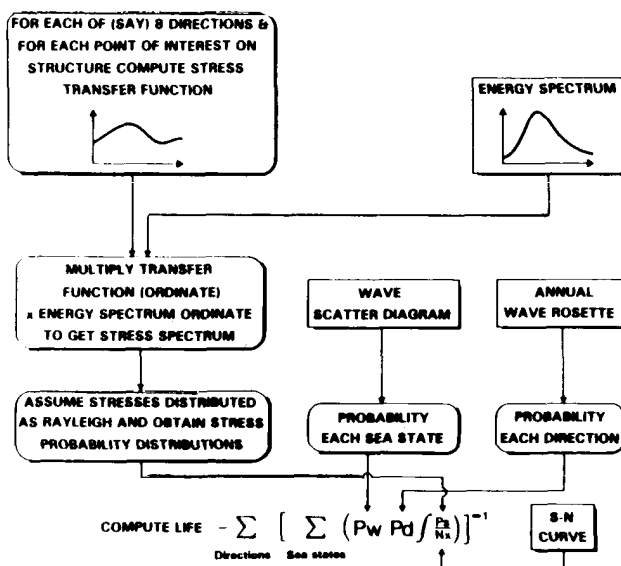


Fig. 18.29—Spectral fatigue analysis procedure.

Process Equipment. The primary function of process equipment, whether on a platform or on land, is to stabilize produced fluids and to prepare them for shipping or disposal. Well production is separated into components of oil, gas, and water (and sometimes condensate). The separated fluids are measured and then either shipped, injected back into the reservoir, or flared.

Differences between the process equipment (oil and gas separators, free-water knockouts, gas scrubbers, pumps, compressors, etc.) installed on a platform and those installed on land are minor (Fig. 18.31). Where possible, consideration is given to using vessels and machinery that are compact and lightweight—e.g., electric motors are commonly used instead of gas engines for driving pumps and compressors. Vertical clearance between decks may impose height limitations and dictate, for example, the use of horizontal instead of vertical separators.

There is a major difference, however, in the way equipment is packaged. If it is to be installed offshore after placement of the platform jacket and decks, process equipment usually is built in modules at a land site. The module assemblies then are barged offshore, lifted onto the platform, and hooked up. This significantly reduces expensive offshore installation and hookup time. In any event, the equipment and its piping, wiring, and controls are installed as compactly as possible. The extra engineering and fabrication costs needed to reduce deck area to an absolute minimum are more than offset by savings in platform structure cost.

Well Servicing and Well Workovers. On relatively small platforms with no more than 5 to 10 wells, it is common practice in some areas to drill all the wells before any of them is placed on production. The drilling rig is removed after the last well is drilled, and future well workovers are performed with a portable workover rig or well-pulling unit. Downhole work that does not require pulling tubing (e.g., replacing safety valves, gas lift valves, or standing valves) normally is accomplished with a wire-line unit.

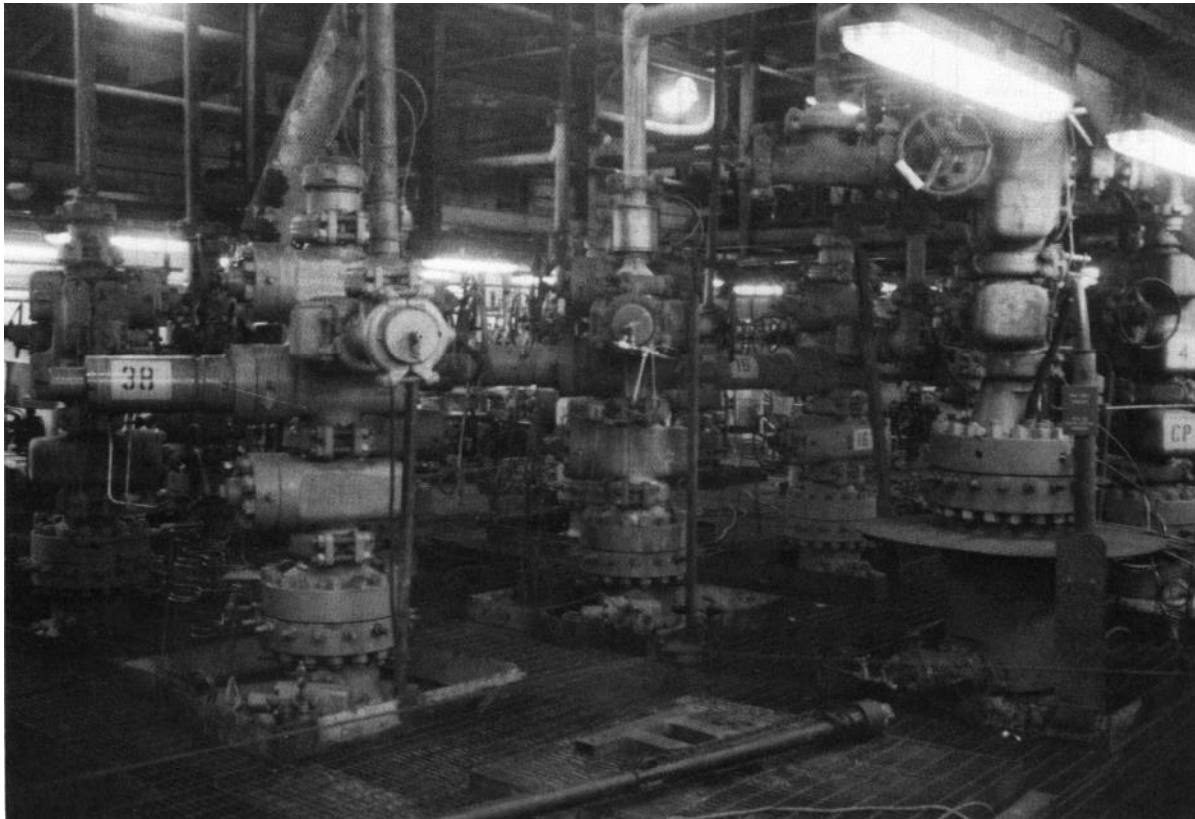


Fig. 18.30– Platform well bay

On larger platforms with more wells, drilling and production operations generally are carried on concurrently. In this case, well workovers are performed by the drilling rig if it is still on the platform. Depending on the urgency of the workover and on economic considerations, the work typically is scheduled to follow completion of the well that is currently being drilled. Wireline repairs can be performed without interfering with drilling operations unless the two wells involved are too close together for safety considerations.

Even on the largest platforms, drilling rigs normally are removed after all scheduled wells have been drilled. Depending on the number of wells and the amount of downhole work anticipated, a special workover rig may be installed permanently on the platform. An economic comparison between using a portable rig and using a permanently installed rig should be the basis for selection.

Crude-Oil Disposal. In the great majority of cases, crude-oil production is “shipped” from platforms by subsea pipelines. Because most offshore producing areas involve multiple platforms and more than one operating company, the pipelines are generally common carriers.

In the simplest of installations, where a pipeline transports only one type of crude oil from a single platform, an optimum pipeline design and installation can be involved and expensive. Numerous factors must be evaluated, such as seawater temperature, seafloor profile and geologic features, water currents between surface and

seafloor, hazards from commercial fishing equipment and boat anchors, the possible need for a weight coating such as concrete to ensure negative buoyancy, cathodic protection, corrosion-prevention coatings, water depth, the possible need for burial beneath the seafloor, the type of beach crossing that will best protect the pipe and also be environmentally acceptable, the best riser to use at the platform to afford protection from corrosion and physical damage from boats and waves, total length of pipeline, pumping rates and pressures, the need for periodic pigging and inspection, safety shutdowns to prevent or to minimize pollution in the event of failure or accident, and the crude-oil properties and rheology. When crude oil is shipped from more than one platform, a more detailed study of rates and pressures will be required, and if crudes from different reservoirs are being pumped through the same pipeline, a much more detailed study of oil properties and rheology will be necessary.

Depending on pipe diameter, length, need for burial, need for coatings and cathodic protection, water depth, and various construction considerations, an offshore pipeline can be the single most expensive element of an offshore installation, sometimes far exceeding the cost of one or more platforms. In the great majority of cases, however, piping is still the safest, most economical way to transport crude-oil production to a land site.

Occasionally, an offshore oil field is too remote, production rates are too low, or the field is too short-lived to justify a pipeline economically. The alternative is to

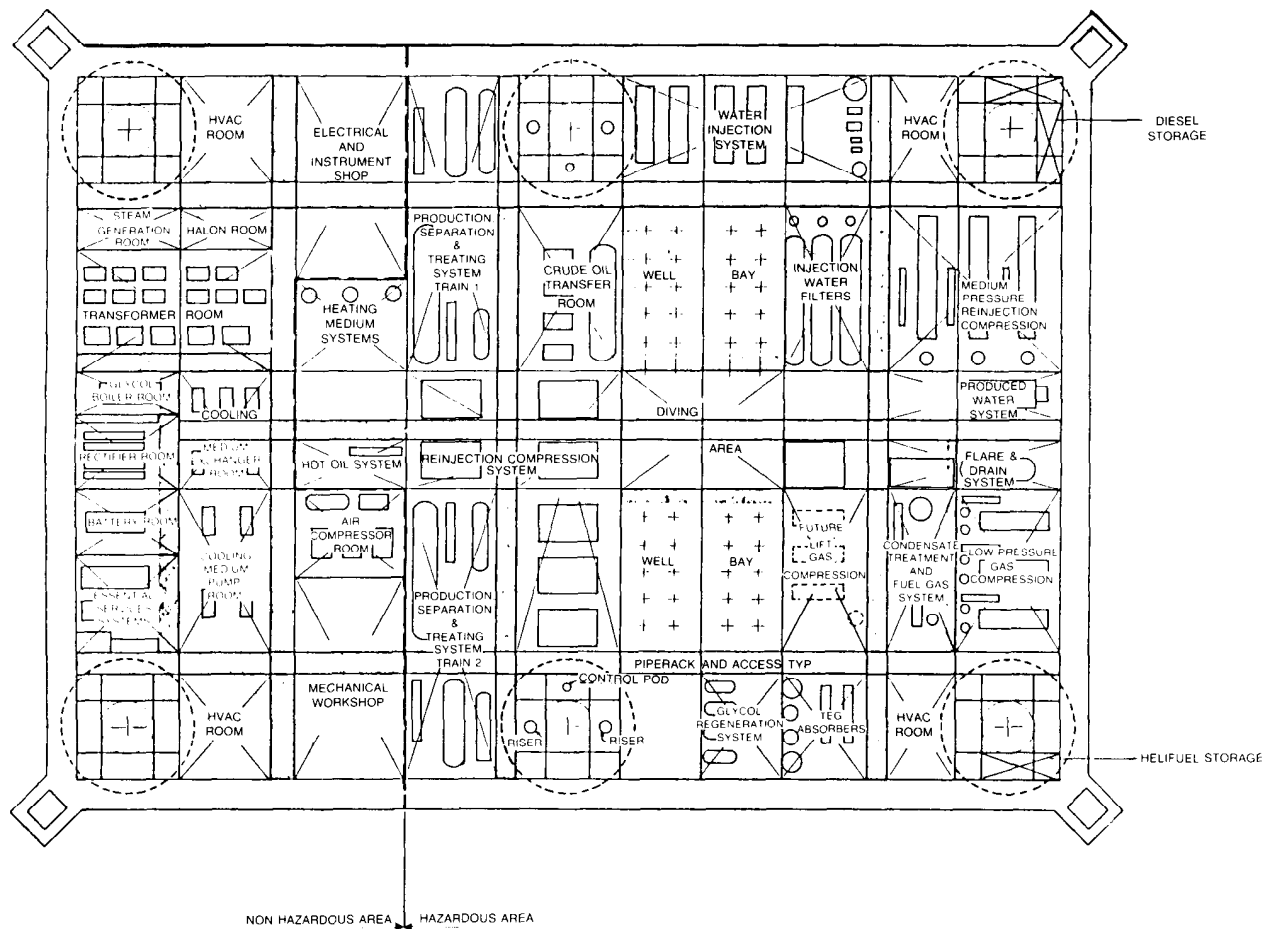


Fig. 18.31—Platform deck layout for process facilities.

ship the oil by tankers. This usually requires some type of loading system installed 1 to 2 miles from the platform, such as a moored buoy or articulated loading tower. A seafloor pipeline connects the loading facility to the platform, and a tanker is moored to the loading facility during the transfer of oil.

The two most important drawbacks of a tanker-loading operation are sensitivity to weather and the need for separate oil storage. Tanker loading is best suited to mild-weather areas to minimize downtime from storms. Oil storage requirements will depend on total field producing rates and reservoir characteristics (can the wells be shut in for short periods without loss in productivity) as well as tanker downtime. This has led to the development of permanently moored storage tankers.

Gas Disposal. Disposition of gas from an offshore production site will depend on a combination of reservoir and economic factors. If well production is primarily oil, the gas may be handled as a byproduct and be disposed of in the most economical way. Piping the gas to a land site for sale and use as fuel is generally preferred if it can be done economically. Injection back into the producing formation is a common alternative. This helps to maintain reservoir pressure and conserves the gas for possible fu-

ture sale. In some areas, gas flaring is still acceptable, but many countries now forbid it except for short test periods and for the disposal of small amounts of residual waste gas.

Water Disposal. Produced water is normally cleaned so that it may be either discharged offshore in accordance with governmental regulations or reinjected. In either case, a combination of mechanical and chemical means may be used to condition the produced water before disposal. Tankage and filtration are used to remove oil and other contaminants from the water. Chemical treatment is common to control bacteria and corrosion in injection wells.

Subsea Completions

Seafloor well completions occupy a very small niche in the offshore petroleum industry, but they attract a lot of attention. Their primary use has been as single satellite wells producing to a nearby platform. They are a means of producing field extremities that cannot be reached by directional drilling from an existing platform and where the economics do not justify the installation of one or more additional platforms. Some multiwell templates and piping manifolds have been installed that go beyond the satellite well concept.

The main benefit of subsea completion efforts is that the petroleum industry and political governments now recognize and accept them as a technically viable means for producing offshore oil and gas wells. This, in turn, means that future installations can be evaluated on the basis of actual field experience and realistic economic considerations. Subsea completions probably will increase in popularity in coming years, especially if significant discoveries are made in deep water where conventional platforms are either extremely expensive or impractical.

Wet vs. Dry. Seafloor installations are made either with the equipment protected by a dry, one-atmosphere pressure chamber (Fig. 18.32) or with the equipment exposed to the sea environment (Figs. 18.33 and 18.34). The dry chambers are large enough for workmen to install and to repair valves, flanges, and control systems in a shirt-sleeve environment. Access is by way of a diving bell lowered from a work boat. Successful installations have been made in water depths greater than 500 ft.

Most subsea completions are of the wet type and require varying amounts of diver intervention during installation and removal of the seafloor equipment. Minor repairs and trouble-shooting can sometimes be accomplished in place, but major equipment or control-system repairs are made above water after the faulty equipment is removed. Running tools operated from a floating drilling or workover rig are used for installation and removal of well completion equipment in much the same way that drilling operations are conducted when running and retrieving a BOP stack for a subsea well. Wet well completions have been made in water depths greater than 1,300 ft, and a satellite system has been constructed in 2,500 ft of water. The latter is designed to use tethered, remotely operated vehicles with manipulators instead of divers for trouble-shooting installation problems and for assisting with repairs.

Single Satellite Wells. Functionally, seafloor well completions are no different than wells on platforms or land. Completions in shallow water where divers are used extensively for installing the equipment may even look like land wells.

In deeper water, however, where diving requires expensive saturation systems for the divers, more reliance is placed on equipment that can be installed and removed with special tools that are run and operated from a floating drilling rig. Hydraulically actuated wellhead connectors are used instead of flanged or clamped connectors. Tubing hangers that can be locked in place and tested remotely are used. Precise equipment systems that can be remotely connected and disconnected and that permit personnel on the drilling rig to test and to function all of the wellhead equipment are required. Hydraulic controls are generally used for this work. The result is a Christmas tree that may be 20 to 40 ft tall when combined with its drilling bases and that may cost several times more than a land tree.

One very important requirement for subsea-well-completion equipment is that it be totally compatible with the drilling equipment that is used in drilling the well (Fig. 18.35). This requires extensive pre-engineering and preplanning between persons responsible for the drilling, completion, and producing operations.

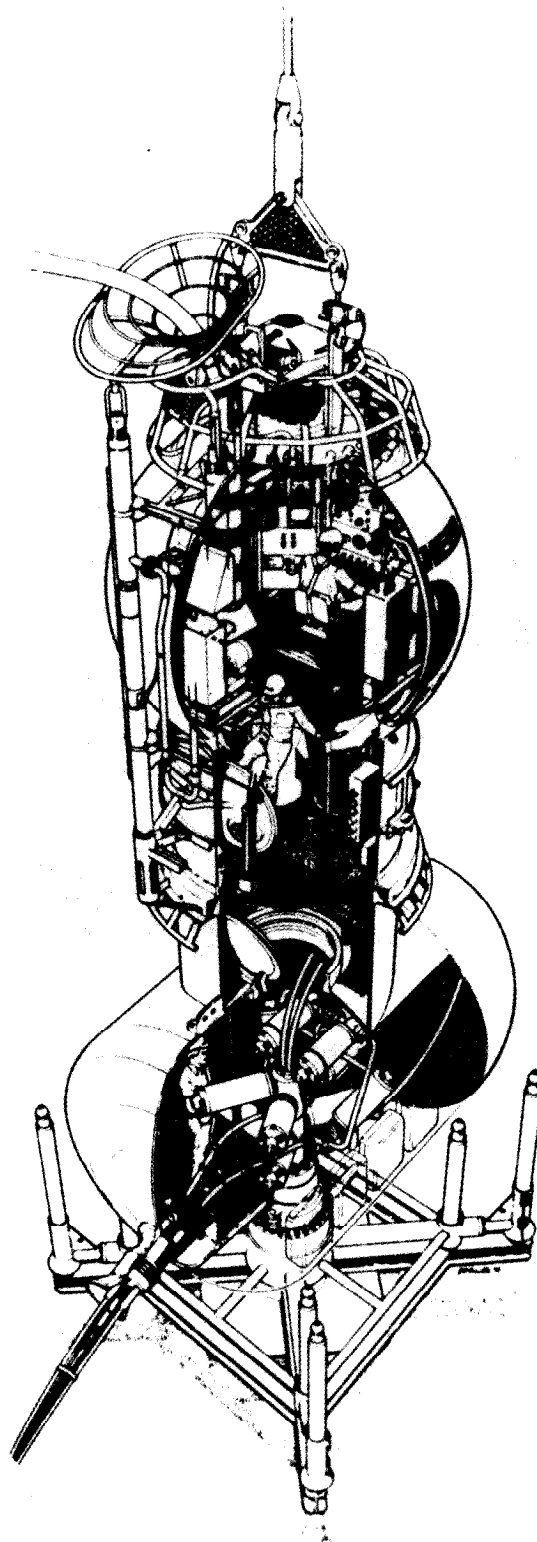


Fig. 18.32—Subsea tree—dry type with diving bell in place.

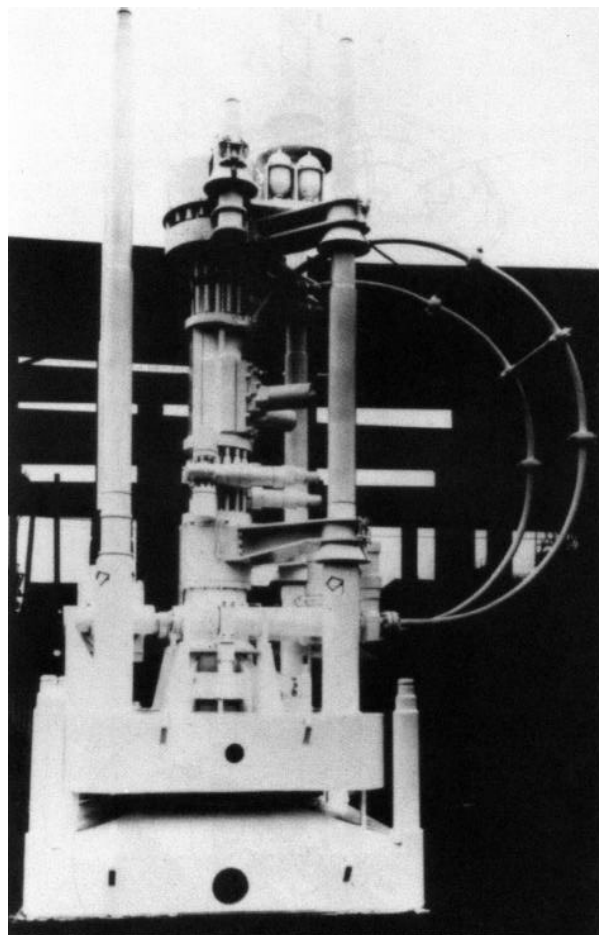


Fig. 18.33— Subsea tree-wet type.

Multiwell Templates. A seafloor template with guide posts and wellhead receptacles for more than one well is suitable for drilling a number of satellite wells in close proximity to one another. Minor cost savings are realized during drilling operations because the drilling vessel does not have to be moved and reanchored between wells. Any slight adjustment in position can be accomplished by taking in or letting out opposing anchor lines. A major savings in flowlines may be possible by commingling well production at the template and transferring it through one large pipeline instead of individual flowlines. Well testing can still be accomplished by installing one separate flowline with a valve manifold for switching wells. Multiwell templates offer additional opportunities for reduced costs for control systems, gas-lift piping, and water-injection piping. Obviously, potential cost savings will be the greatest with a large number of wells. Multiwell template designs should consider poten-

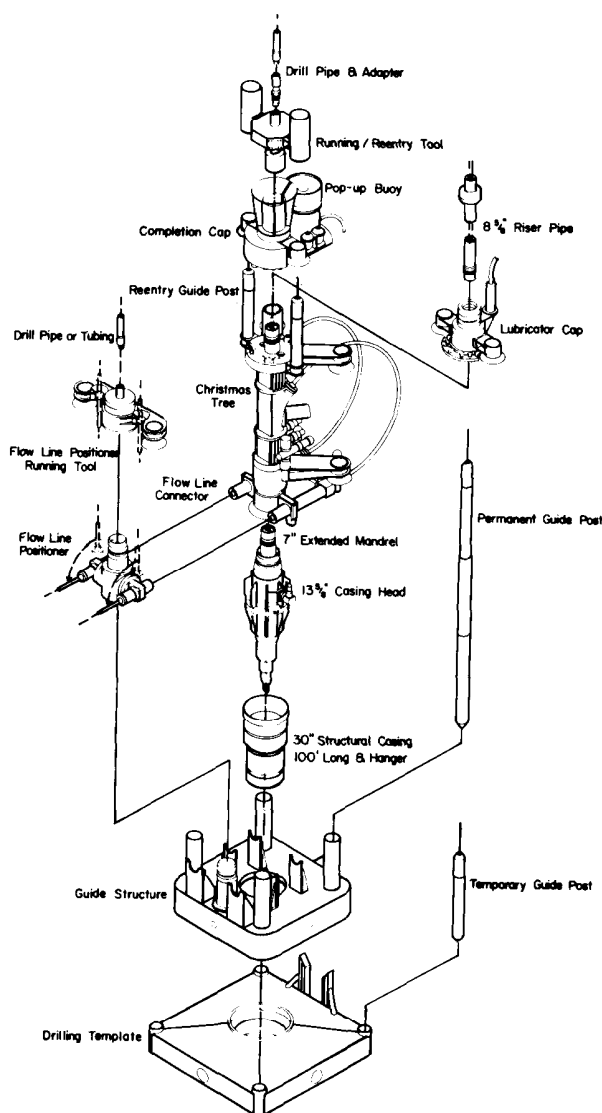


Fig. 18.34— Exploded view of diverless subsea tree and running tools.

tial hazards from accidentally dropped tool joints or other heavy equipment during drilling operations. This may be a deterrent to producing completed wells until all wells in the template have been drilled. For a large template with many wells, this would have a significant effect on cash flow. A detailed economic analysis of all relevant factors is essential to determine the optimum size and configuration of a multiwell template.

Manifolds. One technique for combining some of the advantages of single satellite wells with the piping savings for multiwell templates is to produce moderately spaced satellite wells to a central, seafloor manifold installation (Fig. 18.36). The manifold would include valves and controls to commingle or test each well selectively and would reduce overall piping- and control-system costs if platform process facilities are located several miles away. Both dry and wet manifolds have been successfully installed and operated.

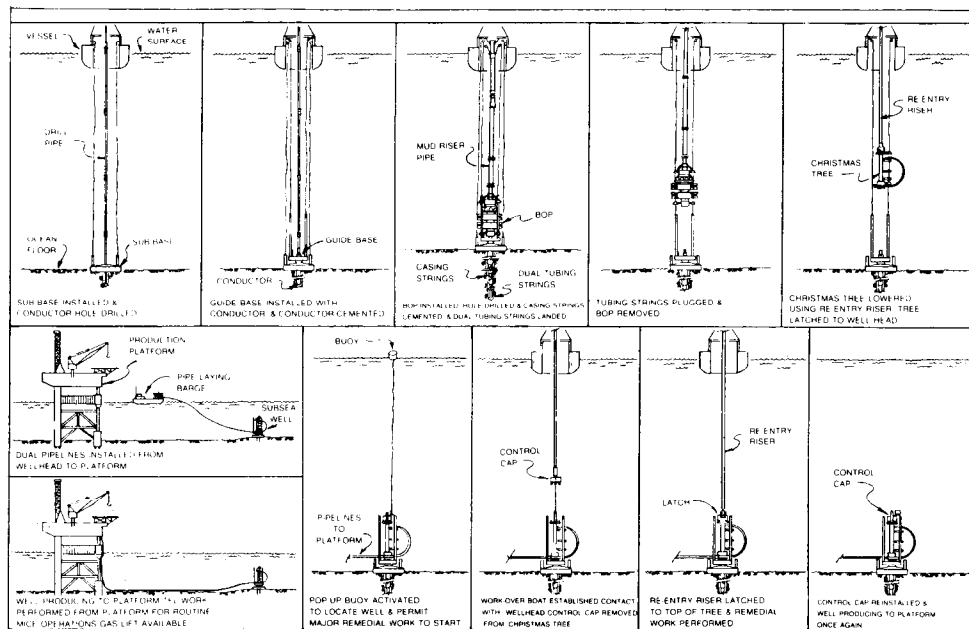


Fig. 18.35—Sequence drawings for drilling and completing a subsea well and for well re-entry workover.

Flowlines and Control Lines. Subsea satellite wells may be installed with either one or two flowlines, depending on well conditions and operating requirements. The production flowline is usually 2 to 6 in. in diameter. Size is dictated primarily by flow rate, flowline length, and wellhead pressure. A second flowline frequently is installed for communicating with the tubing/casing annulus. This line is effective for monitoring annulus pressure and for circulating kill fluid if needed. It can be hooked up to pump pigs, paraffin scrapers, or through flowline tools. It can also be used as a second production line.

In some cases, a decision to bury flowlines below the

seafloor can be made because of local regulations or obvious hazards. Generally, however, the pros and cons for burial and the overall costs and economics should be evaluated carefully before a decision is made to bury flowlines. If the answer is not clear-cut, leaving the lines unburied is probably best. Unburied lines cost less to install, are less expensive to repair, and are easier to inspect for leaks and damage.

Conventional welded steel pipe is used for most flowlines. It can be protected against external corrosion by either anodes, a corrosion coating, or a combination of both. Cathodic-protection methods should be compat-

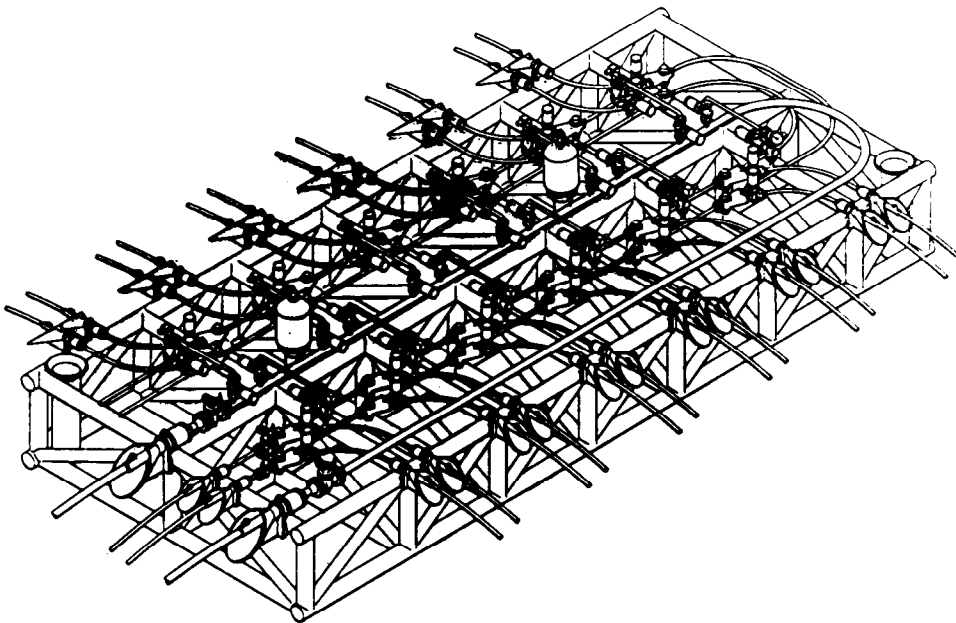


Fig. 18.36—Seafloor manifold for satellite subsea wells.

ible with corrosion-prevention designs for equipment at both ends of the flowline (wellhead equipment and usually a platform jacket), as well as other nearby or crossing pipelines.

In recent years, flexible pipe made of laminations of steel wires and other materials has become popular for flowline service. Although the material cost for flexible pipe is usually very high in comparison with conventional pipe, this may be more than offset by savings in the installation cost. Work boats or special-purpose vessels equipped with large-diameter reels can lay long lengths of flexible pipe in short periods of time. Flexible pipe normally does not require a separate coating on the outside, but it may require cathodic protection of the end connections.

All flowlines should be protected from abrasion and physical damage from other crossing pipelines, and expansion loops may be necessary if the installed configuration does not allow for expansion and contraction from temperature changes. Other considerations include possible scour damage or vibration fatigue where bottom currents exist and high stresses where the line bridges low spots on uneven seafloor. Installation methods for flowlines are generally the same as for other subsea pipelines. These are discussed in the Offshore Pipelines section.

Control lines, both hydraulic and electrical, for subsea well completions are discussed in the Electrical, Instrumentation and Control Systems section.

Well Servicing—Wireline vs. Through Flowline. There are two common techniques for performing downhole work on subsea wells when the work tasks do not require removing the Christmas tree and tubing. The most common procedure is to install a workover riser between the surface vessel (drilling or workover rig) and the top of the Christmas tree above the swab valves and to install a wireline lubricator on top of the riser. Conventional wireline tools and equipment can be used to remove and to install safety valves and gas-lift valves, to shift sliding sleeves, or to make temperature and pressure surveys. Vessel heave must be compensated for, but otherwise the procedure is the same as for land and platform wells.

To overcome the delays and high cost associated with wireline work on subsea wells (vessel availability, high daily rates, and weather delays), a procedure for servicing wells remotely from the process platform has been developed. It is called "through flowline" (TFL). It is basically a set of tools that are inserted into the flowline at the platform and hydraulically pumped through the flowline, through 5-ft-radius flowline loops (bends) at the subsea Christmas tree, and down the tubing. A complete hydraulic loop is required between the platform and the well to pump the tools down and back. This means that a second flowline is necessary for work to be performed at or immediately below the wellhead and a second tubing string is required, with controllable communication between the tubing strings downhole to perform work downhole. TFL tools are available to fit common tubing sizes and to perform virtually all the same tasks as wireline tools. Numerous technical papers have been written on TFL tools and techniques.

Gas wells generally are not suitable candidates for TFL servicing because a gas-free hydraulic loop is required

for circulating the tools. A decision favoring either wireline- or TFL-servicing procedures for an oil well should be based on a full evaluation of operating conditions, anticipated downhole service requirements, the availability of trained personnel, and an economic comparison of installed costs and servicing costs.

Well Workovers. Work on subsea wells that requires the tubing to be pulled or is otherwise beyond the scope of wireline or TFL tools is a major undertaking and requires extensive planning and preparation. Unless a special-purpose vessel is available that is suitable for workovers, a semisubmersible or ship-shaped drilling rig must be scheduled and mobilized with a workover riser and running tools specially designed for the Christmas tree and tubing hanger. This equipment is needed in addition to a regular drilling riser and BOP stack, which must have a hydraulic connector that is compatible with the wellhead. Space limitations on some drilling vessels may preclude their use, which further complicates the workover.

Floating Production Facilities

For many years, floating drilling rigs (semisubmersibles, ships, and barges) have conducted drillstem tests and short-term production tests of newly drilled wells. These wells were nearly always drilled for exploratory or delineation purposes. Common practice was to abandon the wells temporarily or permanently after testing. Following the installation of a platform, development wells were then drilled and produced. Because brief production tests frequently provided insufficient reservoir data, and because delaying well production until platforms could be fabricated and installed resulted in poor cash flow, the concept of floating production facilities (FPF's) was developed. This concept requires some type of floating vessel (ship, barge, or semisubmersible) that is equipped for processing crude-oil production instead of for drilling. The vessel is either moored in place with multiple anchors, or is connected to some type of single-point mooring (SPM) or articulated tower. Crude-oil production from one or more seafloor wells is produced to the FPF either directly through individual pipe risers or through a seafloor manifold center and multiple-bore riser assembly (Figs. 18.37 through 18.39).

Applications. Two applications for FPF's were mentioned above: long-term production tests and accelerated (early) production. The use for long-term testing nearly always involves only one well and may be for a duration of anywhere from 2 to 3 months to a year or longer. Some reservoirs, particularly limestone as opposed to sandstone, cannot be evaluated from a short-term test, and full field development may be unacceptably risky without extended test data. The simplest FPF installation for production tests is a vessel moored with multiple anchors directly over a seafloor well connected by drillpipe or tubing to a subsea test tree installed in a BOP on the wellhead. A similar installation generally preferred for longer-term testing would use a flexible pipe riser instead of drillpipe or tubing and a conventional subsea Christmas tree instead of a BOP with test tree.

The same installations described above can also be used for early production if only one or two wells are involved. For more wells (up to 5 or 10), a seafloor manifold center

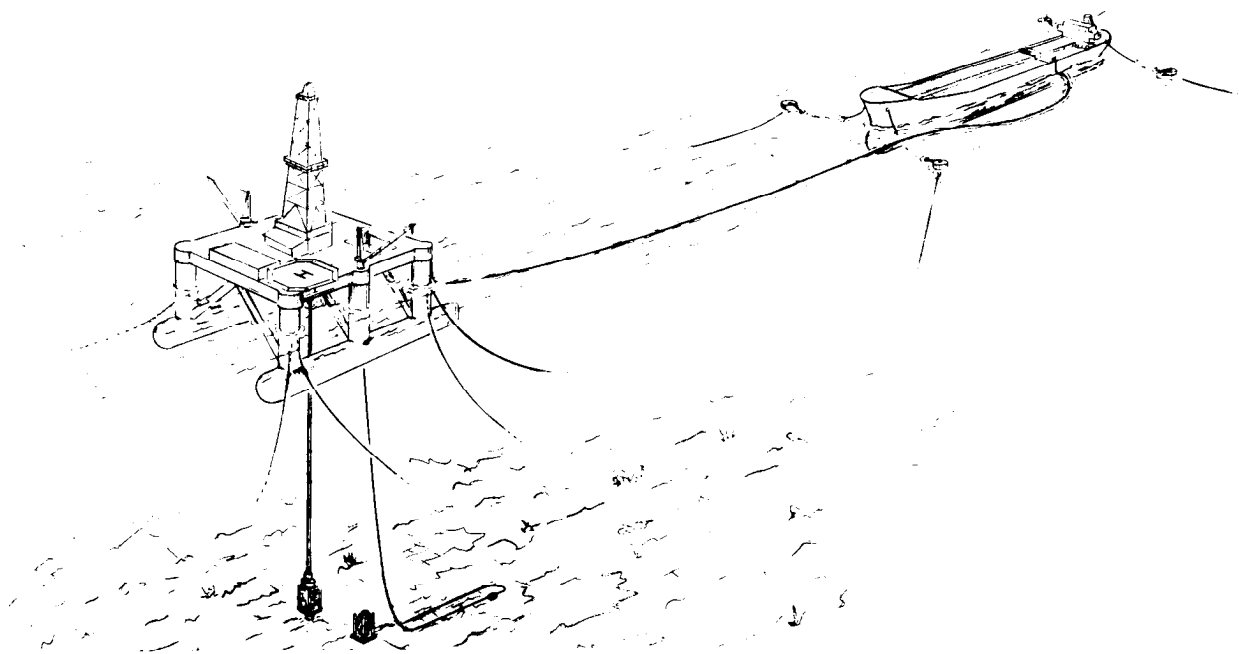


Fig. 18.37—FPF with flexible pipe risers and floating loading hose for two subsea wells.

may be used with a multiple-bore riser and some type of SPM or articulated tower. An SPM or tower has the added advantage of permitting the process vessel to weather-vane into the wind and seas and thus to mitigate the effect of bad weather on process equipment.

A third application for FPF's is permanent process facilities for a small or short-lived oil field where a conventional platform is either uneconomical or marginally

economical. Particularly where reuse of the facility may be a factor, the ease of moving an FPF to a different location or field may have a significant impact on overall economics.

Semisubmersibles vs. Tankers. Most FPF installations have been converted semisubmersible drilling rigs or converted oil tankers. Semisubmersibles are characteristically

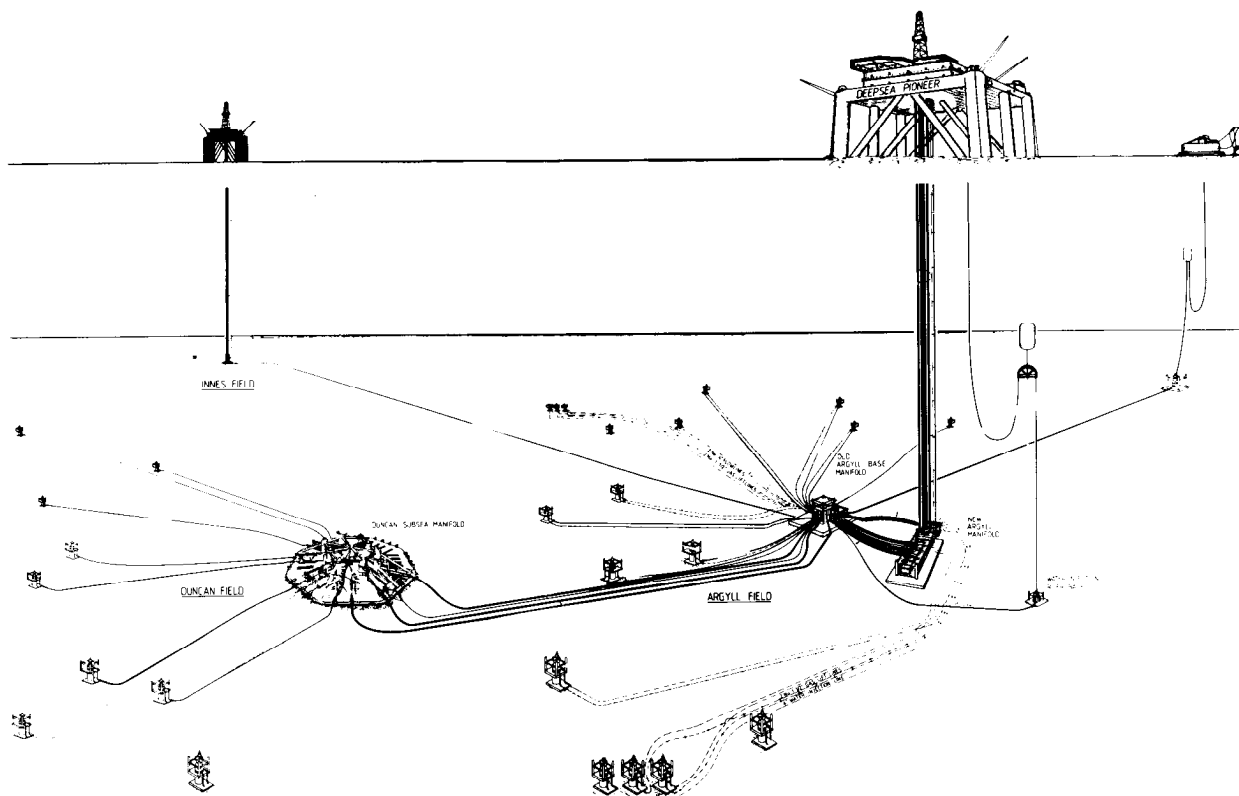


Fig. 18.38—FPF with seafloor manifold, composite riser, and seafloor pipeline to loading buoy and tanker.

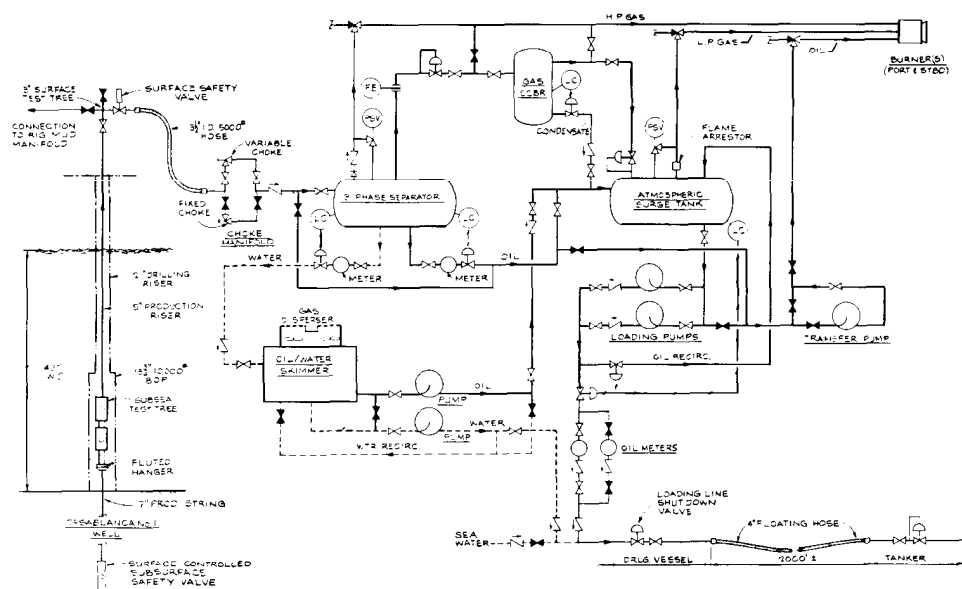


Fig. 18.39—Flow diagram for FPF process equipment for one-well, long-term test.

better suited to severe weather areas such as the North Sea, because of their superior stability. Their main drawback from an operating standpoint is the lack of sufficient oil storage capacity to prevent shutdowns when tanker-loading operations are disrupted. Loading disruptions are not uncommon and can result from either equipment failure or bad weather.

In relatively mild weather areas, converted tankers perform satisfactorily as FPF's, especially when moored to SPM's or loading towers that permit the tanker to weather-vane. Large oil-storage capacity, inherent to tankers, greatly facilitates the scheduling of shuttle tankers to transport the crude oil to refineries or terminals.

The choice between semisubmersibles and tankers for FPF service is heavily influenced by the availability of surplus vessels, the operating conditions, and the geographic area. A careful investigation of the used-vessel market is essential to an economic decision. At the time of this writing, new special-purpose vessels designed specifically for FPF service are being promoted. These include semisubmersibles with some storage capacity to offset that drawback and ship-shaped vessels with anti-roll devices to improve stability. A wide selection of FPF designs and vessels probably will make their use more economically and operationally attractive in coming years.

Disposal of Oil, Gas, and Water. Technically, there is no reason why oil cannot be shipped from an FPF by pipeline. Most installations to date, however, have transported oil with shuttle tankers. Loading operations can be accomplished by a floating hose directly between the FPF and the shuttle tanker. This inexpensive approach is practical in mild weather areas, especially with low production rates. For higher production and transfer rates and for adverse weather conditions, a seafloor pipeline or hose between the FPF and a dedicated loading buoy is safer and generally will result in less downtime.

Water produced with crude oil can be treated and disposed of the same as on a platform. It can be cleaned and

treated for reinjection into the reservoir, or, where local regulations permit, it can be cleaned and discharged into the ocean. Depending on downstream terminal or refinery conditions, shipment of small amounts of water production with the crude oil may be possible.

Small amounts of gas production have to be flared in a typical FPF installation. If flaring is not permitted, or if economics favors reinjection, compressors can be installed for this purpose. Use of FPF's in fields producing large amounts of gas may require additional facilities for gas treating, processing, and disposal.

Offshore Pipelines

The design and installation of subsea pipelines bear only slight resemblance to their counterpart activities on land. Preliminary sizing of lines can be based on general-purpose pressure-drop curves as long as the effects of the ocean environment on fluid rheology are understood. Also, preliminary cost estimates can be made on the basis of either estimating manuals prepared for this purpose or historical data for similar installations. Final pipeline designs, detailed plans, and cost estimates for fabrication and installation, however, are best handled by pipeline contractors or consultants who specialize in this activity.

Flowlines. Flowlines for subsea wells range in size from 2 to 6 in. As indicated previously in the Subsea Completions section, conventional steel pipe is used for most installations. It is readily available and does a good job when protected against corrosion and physical hazards. Flexible pipe made of laminations of steel wires and other materials is now available from several sources and has been used in a number of instances. It is made in a range of pressure ratings and a variety of materials that are suitable for most applications.

Welded flowlines sometimes are made up on the beach and then towed to the point of placement. Towing can be at or near the surface of the water with the pipe supported by buoys or other buoyant material, or it can be just off-bottom by a combination of buoys and chains for

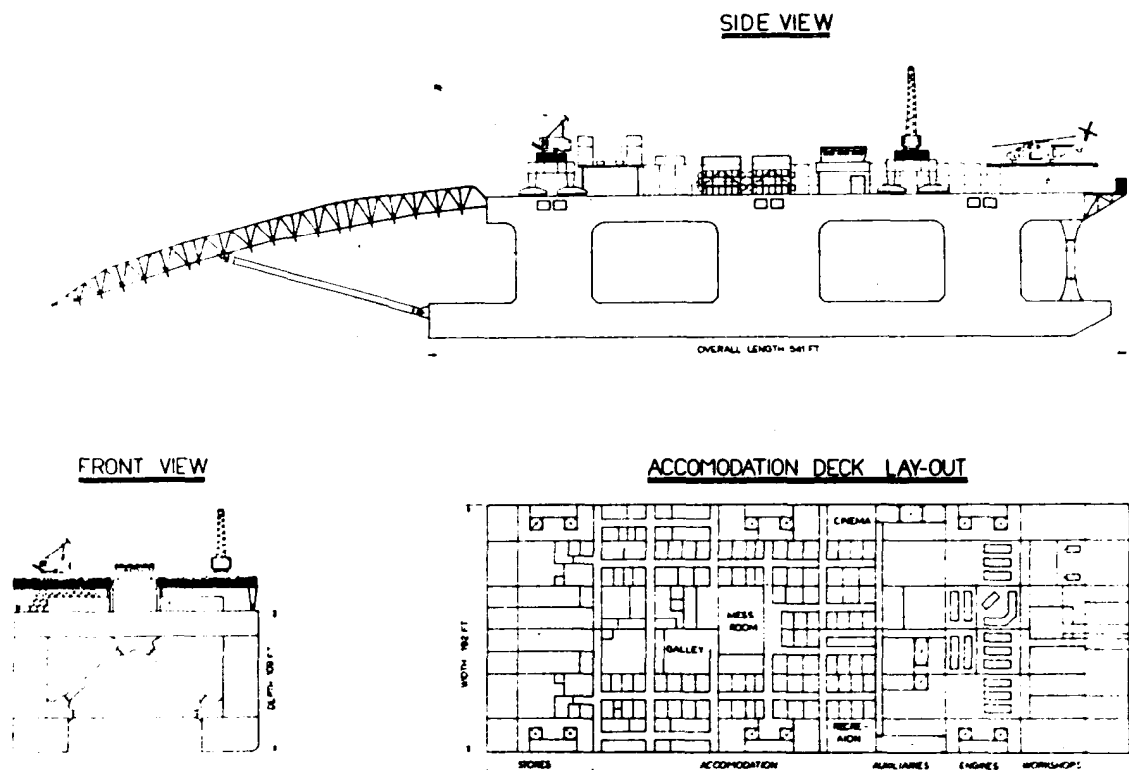


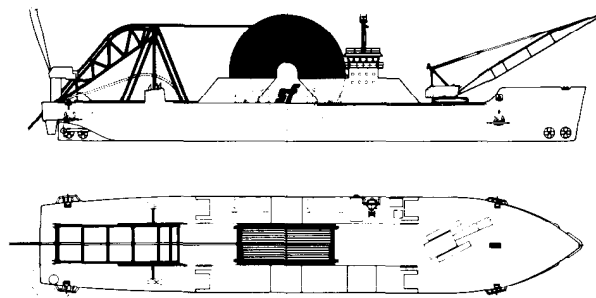
Fig. 18.40—Conventional pipe-lay barge.

buoyancy control. More common methods of installation, however, are either by conventional lay barges (Fig. 18.40) or by reel barges (Fig. 18.41). The former make up straight lengths of pipe on the barge and feed it into the water by way of a curved stinger as the barge is winched along the flowline route. The purpose of the stinger is to control radius of curvature as the pipe is lowered into the water and thus to prevent buckling. Buckling and overtensioning of the pipe as it contacts the seafloor are prevented by maintaining a predetermined amount of tension on the pipe as it leaves the barge and by controlling the forward movement of the barge.

Probably the most popular method of installing flowlines, both conventional steel pipe and flexible pipe, is with special-purpose reel ships or reels mounted on large work boats. Depending on pipe diameter, several miles of pipe can be reeled onto one or more large reels at a shore-mobilization site and then rapidly reeled off at the placement site. The main advantage of this technique is the speed of installation. Fast installation reduces not only the number of offshore construction days but also costly interruptions caused by bad weather. A job that might require a week of offshore construction time with a conventional lay barge is much more susceptible to weather downtime than a job that can be completed in 1 or 2 days with a reel ship.

Flowline connections at platforms generally are made by pulling the line up through a curved conductor pipe called a J tube and then securing the line at the platform deck opening with a flange or clamp. Several procedures are used for connections to subsea wells, depending on Christmas tree configuration and whether the flowline in-

stallation starts at the tree (a first-end connection) or ends at the tree (a second-end connection). Most tree connections have been a pull-in type, where the flowline is first laid on the seafloor and then pulled into a receptacle on the tree base with a wire rope. One advantage of this is that it can be performed either on a first-end or second-end connection. A pull-in procedure can also be used as the flowline is being lowered to the seafloor, making a connection at the tree base before laying the flowline on



Reel Capacity

Nominal Pipe Size (Inches)	Approximate Capacity (Feet)	
4	267,000	50.5
6	160,000	30.3
8	104,000	19.7
10	73,000	13.8
12	54,000	10.2
14	45,000	8.5
16	30,000	5.7

Fig. 18.41—Work boat with pipe-laying reels.

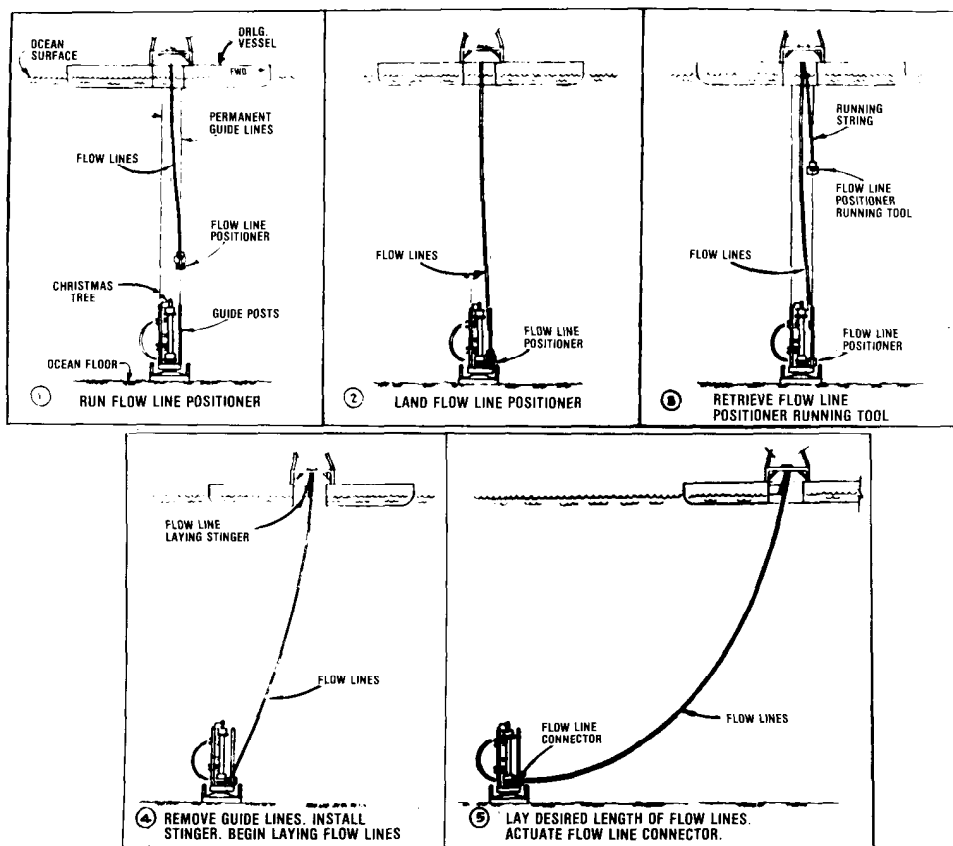


Fig. 18.42—J-lay method for installing flowlines away from subsea well (first-end connection).

the seafloor. A procedure particularly applicable to subsea wells in very deep water is the J-lay first-end connection (Fig. 18.42), where the flowline is run vertically to the tree base from the drilling rig, stabbed into a receptacle, and then laid down into a horizontal position as the drilling rig or pipe-lay vessel moves away from the well-site toward the platform. A trunnion-type assembly on the end of the flowline permits the line to be laid down without bending. The mating of the flowline to the Christmas tree is made after the line is fully horizontal.

Many different devices and procedures have been developed for making the actual connection between the Christmas tree and the flowline. In shallow water, divers can install a piping spool with flanges or couplings on each end. Diverless connections usually have some type of hydraulically actuated device that is operated remotely from the drilling rig.

Larger Pipelines. Pipeline diameters from 8 to 36 in. or more are used extensively for the transfer of crude oil and gas from offshore fields to land sites. Installations typically have been made with conventional pipe-lay barges as described previously, but reel barges also are used extensively for the smaller sizes. Both bottom tows and surface tows are used in limited applications where logistics favor them. As discussed previously, a pipeline can be the single most expensive element of an offshore installation, sometimes exceeding the cost of one or more platforms. Numerous factors must be considered when

designing a line and planning its construction to minimize installation difficulties and to ensure satisfactory operation throughout the expected life of the line. Many technical papers and magazine articles have been written about this subject and are excellent sources of further information—e.g., proceedings from the annual Offshore Technology Conference.

Arctic

Production operations in the offshore Arctic regions are within the reach of existing technology. Procedures used onshore and offshore in less hostile regions, however, must be modified to meet the challenges of the harsh climatic conditions in these remote locations.¹⁵

In the last decade, the major areas of industry interest have been the offshore regions of Alaska¹⁶ and Canada. The environmental conditions vary significantly in each of these regions. Major factors that affect normal offshore operations are extremely cold temperatures, fog, gusty winds, short open-water seasons, permafrost, and the persistence of ice. The specific production system that is selected must be tailored to each unique combination of these factors to ensure safe oilfield development.

Environmental Conditions

Ice Characteristics. Sea ice is the principal environmental factor in all of the offshore Arctic areas.¹⁷ The most abundant type of sea ice that is encountered offshore is less than 1 year old. This first-year ice begins to form

during fall and grows to a thickness of 4 to 8 ft during the winter. Sheets of ice close to shore become landfast and remain locked in place throughout the winter. Beyond the landfast zone, the ice is kept in constant motion by wind, currents, and, in some areas, the influence of the Arctic polar pack. This dynamic movement causes shearing and impacting between ice features that produce ridges of ice several miles in length. Ice ridges formed in this manner are called pressure ridges. Localized ridging around a grounded ice feature, the shoreline, or a structure is considered a rubble pile. In areas of extremely cold winter temperatures, the ice blocks within a ridge or rubble pile begin to refreeze into a contiguous feature. Depending on the conditions, the refrozen consolidated thickness could become several times larger than the first-year ice thickness.

Sea ice that survives one or more melt seasons is considered multiyear ice. The predominant source of multiyear ice features is the polar pack. The pack consists primarily of floes 25 to 50 ft thick with embedded ridges 50 to 100 ft deep. During the summer, northerly winds break off portions of the pack and push them toward shore. These multiyear floes are commonly 1,000 to 2,000 ft in diameter.

The other major type of ice is not formed from seawater but is freshwater ice from the glaciers of Northern Canada. In the Arctic Ocean, the glacial fragments are called ice islands. These tabular-shaped features are several thousand feet in diameter and more than 200 ft deep. Because of the enormous size and slow movement rates of these features, they can be tracked for several months before encroachment upon a given area. Most of the areas of interest for oilfield development in the Arctic Ocean are also in relatively shallow water. This shallow bathymetry causes these freshwater ice features to run aground before they are a threat. In the North Atlantic, similar glacial features are called icebergs. Icebergs that weigh more than 50 million tons have been observed in water depths beyond 1,600 ft. Again, the local bathymetry dictates the maximum size iceberg that could encroach upon a given area.

Ice Loading. Ice exerts the predominant forces on Arctic offshore structures. Extensive laboratory and field tests have been conducted on small- and large-scale specimens to determine in-situ strength characteristics for design. From the results of these tests, the mechanical properties of ice are predicted that consider its salinity, temperature, crystallographic structure, and loading rate.

Newly formed sea ice is relatively warm—only a few degrees above seawater temperature—and high in salinity. As the ice sheet grows, the temperature at the surface reduces to the ambient air temperature, while the bottom remains near the seawater temperature. The salt in the crystal structure of the sheet begins to consolidate into brine droplets. These droplets migrate down through the thickness of the sheet, creating drainage channels and lowering the overall salinity. Fresh water, from precipitation or melting snow cover, fills these channels and refreezes, thereby further reducing the salinity. The result is an ice feature with varying strength, strongest at the surface and reducing through the thickness with increasing salinity and warmer temperature. For multiyear ice, this process ap-

proaches equilibrium. The multiyear ice floe is near zero salinity and has a relatively cold temperature through its thickness. This results in an ice strength several times greater than a first-year ice sheet.

Another parameter that influences the strength of sea ice is the loading rate. When ice is loaded at a very slow strain rate, it exhibits a plastic behavior. Loaded rapidly, it behaves as a brittle material. Empirical equations have been developed that relate the ice movement rate and shape of the structure or indenter to the strain in the ice feature.

The shape of the structure is also a primary factor in producing a crushing, buckling, or flexural failure of the ice feature. For narrow structures relative to the ice thickness, crushing is the predominant failure mode. As the width increases, a combination of crushing and buckling of the ice field around the platform results in the development of a rubble pile. This rubble pile will then shield the structure from direct impact of subsequent ice floes and ensure failure of the ice mantle away from the production facility. And finally, sloping-sided structures normally force a flexural ice failure. Because ice flexural strength is 20 to 40% of the crushing strength, an appreciable reduction in ice forces can be achieved when a bending failure is induced.

Waves. The wave conditions in the Arctic are similar to other offshore areas, and the design of structures or islands against wave loading is well established. Nearshore sea states can be defined by determination of the open-water area along the storm route or fetch and the water depth. In the Arctic Ocean, the presence of sea ice and the polar pack limits the open-water fetch for storms to generate and consequently reduces the design wave height. Breaking wave conditions exist in most shallow-water-depth locations and around gravel islands. This diffraction, shoaling, and refraction of the waves produces highly irregular sea states. Because the interaction of the waves and structure is dependent on structural geometry, the forces the design wave exerts on the structure should be determined by model testing or approximated by linear diffraction analysis.

Scour of the foundation around the structure caused by waves must also be considered and appropriate protection methods implemented. The scour protection could consist of rock, sand bags, or precast concrete elements placed around the structure after installation. For artificial islands, this becomes slope protection and can be used to reduce wave and ice run-up by providing an artificially rough surface.

Permafrost. Permafrost is soil at a temperature below 32°F with partially or completely frozen pore water. Drilling and producing operations in areas with permafrost have been well defined from the experience of the Prudhoe Bay field. In most nearshore areas of the Arctic, permafrost has been found at or near the mudline. These soils are very stiff and can make excavation for pipelines or driving of piling nearly impossible. Permafrost normally is soil bonded by ice and is very susceptible to changes in temperature. This can result in significant changes in the soil characteristics and must be considered in the design.

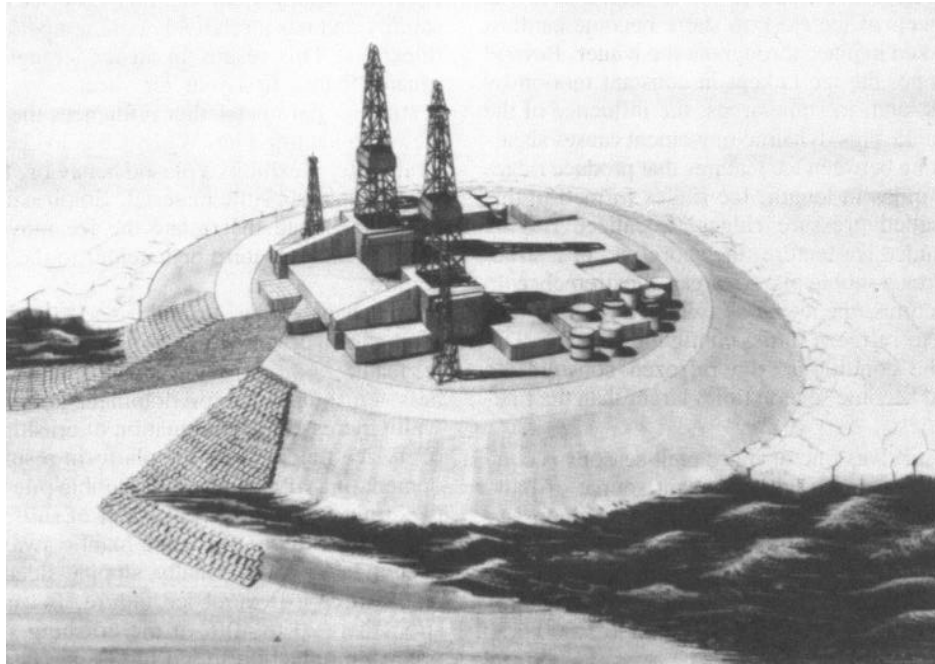


Fig. 18.43A— Protected-slope production island.

Production Structures ¹⁶

Artificial Islands. Artificial islands already are used in many shallow-water areas throughout the world for permanent drilling and producing facilities. The islands that are currently being used for drilling in the Arctic consist of either unretained or retained beach slope systems, as shown in Figs. 18.43A and 18.43B. Because of the short summer construction season and, in some areas, the lack

of island fill material, the quantity of fill required for the island should be minimized. The minimum island working surface is determined by the area required for drilling and production operations. To reduce the quantity of island fill, the steepest side slopes that the mode of construction and fill material will allow should be provided. The minimum side slopes of unretained islands depend on whether the island is constructed by summer dredg-

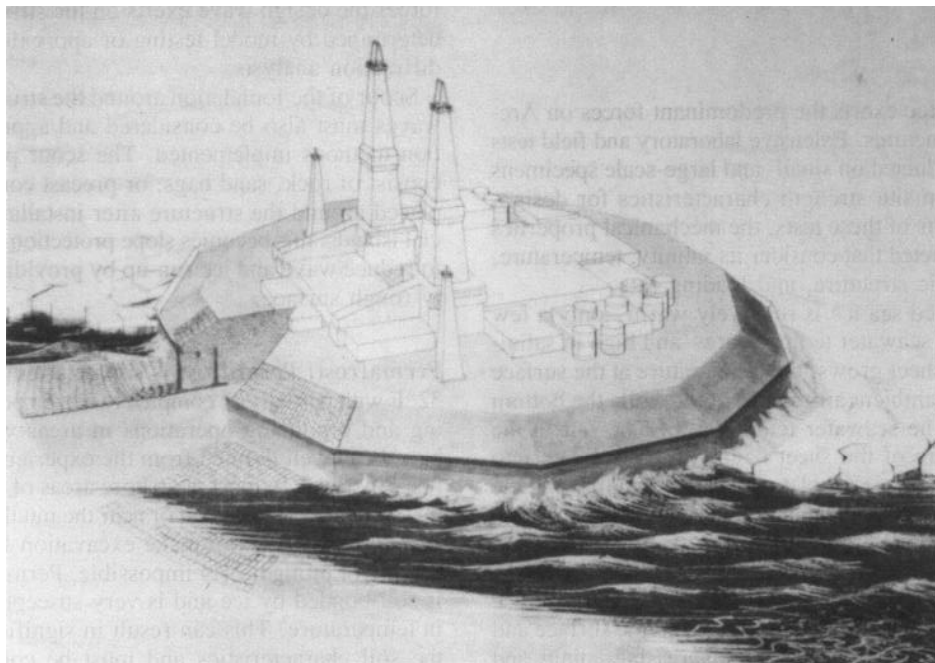


Fig. 18.43B— Caisson-retained production island

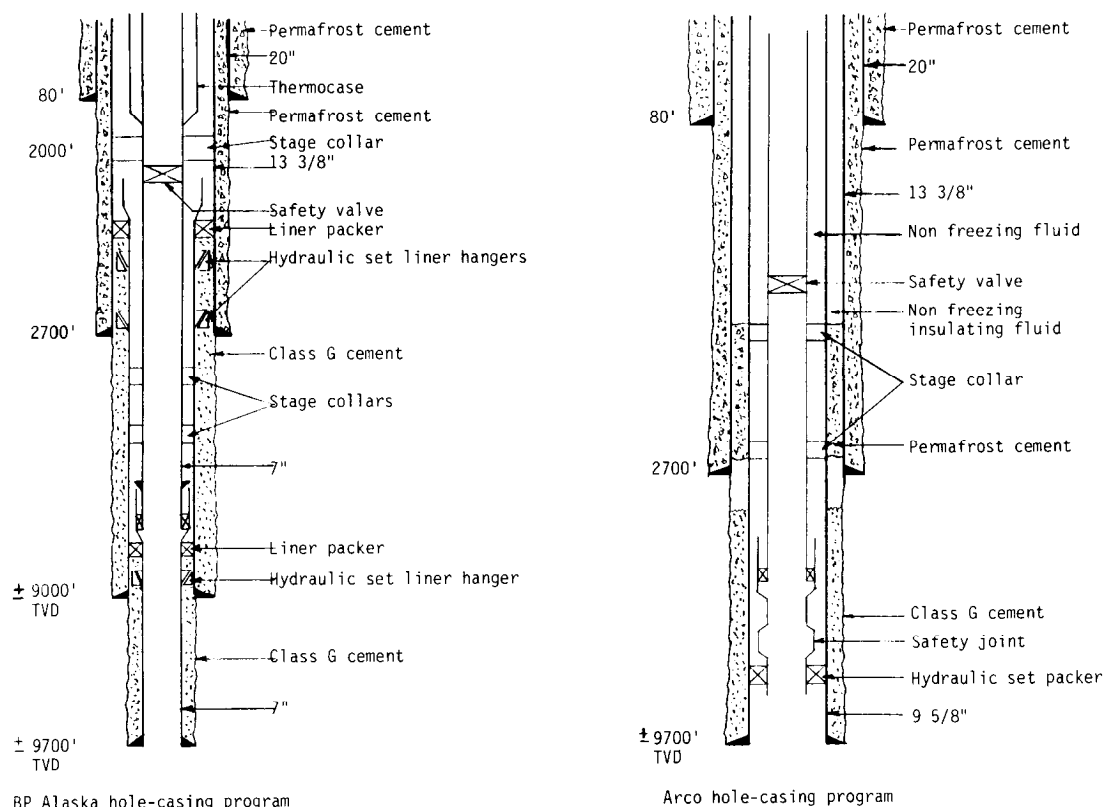


Fig. 18.44—Hole casing programs, Alaska.

ing or winter transport of onshore borrow material over the ice to the desired location. The side slopes for summer dredging are approximately 1:20 (vertical to horizontal), and for winter construction are 1:3. On completion, sandbags or concrete mats are placed on the exposed slopes of the island to prevent ice and wave erosion. Sandbags, stiffer soils for embankments, or caisson units are used on retained islands during construction to reduce the required volume of fill. The caisson units typically consist of vertical walled concrete or steel units. The caissons also provide easy access to the island as a dock for resupply and could be used for storage of consumables or oil.

Artificial islands must be designed to withstand the horizontal forces exerted by ice. The potential failure modes of the island consist of slope instability, bearing failure, or horizontal shearing of the island near the waterline. Each of these failure modes can be predicted by classic geotechnical analysis. The only variable in the analysis is the properties of the island fill material. During winter construction, the fill is delivered to the site at the cold ambient temperature and dumped into the sea. Ice forms on the granular material and inhibits consolidations. As the island surface thaws, considerable settlement may take place. To minimize the effects of thaw settlements, thermal analysis of the freezing and thawing interface should be conducted to determine the proper gradations of fill material.

The design of production facilities placed on an island is similar to that on land. Equipment foundations must be designed and insulated to reduce the potential for frost heaving, pile jacking, and thaw settlements from seasonal thawing and freezing of the island surface and, in some

areas, subsea permafrost. To prevent thaw settlement, an artificial refrigeration system for the fill material could be installed. Placement of equipment and accommodation modules should account for predominant wind, ice movement, and wave directions to ensure safe year-round operations.

The well systems should be vertically drilled through the frost-susceptible island surface and permafrost and then directionally drilled to true vertical depth (TVD). Wells should be spaced close together to minimize the overall size of the island surface and to reduce the effects of thaw subsidence. The casing program should be designed to withstand freeze-back loading during periods of well inactivity and to accommodate differential movement in the tubing string owing to the thermal effects of the drilling fluids. Two casing programs in the Prudhoe Bay field are shown in Fig. 18.44,¹⁸ which shows that both systems incorporate the use of a permafrost cement and provide a safety valve in the production tubing string below the permafrost for emergency shut-in.

Gravity Structures. Various types of gravity structures are being proposed for use in the Arctic. Many of the conventional gravity structures that are used in the North Sea are being adapted for the deepwater and moderate-ice-concentration areas. In the more hostile areas of the high Arctic, vertical- and sloping-sided gravity structures are being proposed. These structures provide the large deck load and space requirements, protection of the wells within tower shafts, and storage of oil. Because of the extreme winter ice conditions in many areas, the production facilities will have to operate 9 months without major resupply.

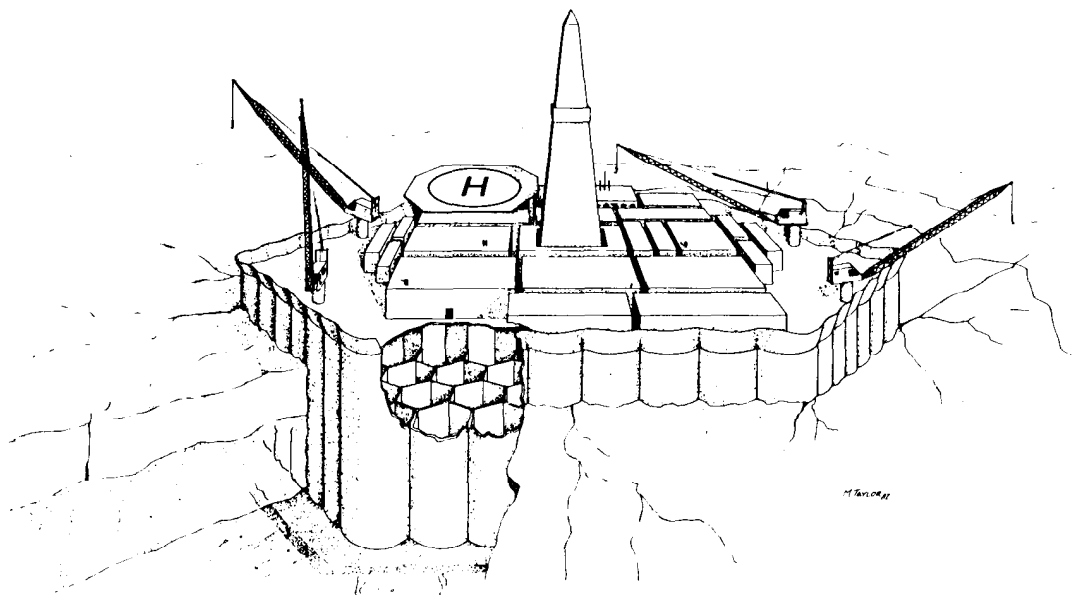


Fig. 18.45—Vertical-sided structure.

The vertical-sided structures (Fig. 18.45) are proposed for the shallow, nearshore areas in the Arctic. These structures typically are rectangular or hexagonal and are capable of being installed directly on the seabed or subsea berm. Production equipment can be placed directly on the working surface of the top slab or integrated into the hull of the structure. Wells are drilled and produced directly from the deck of the structure. Because of the large width of this concept, the structural integrity of the system is

not sensitive to local discontinuities in the seabed from ice gouges or settlements in the foundation from local degradation of permafrost.

Conical, sloping-sided structures (Fig. 18.46) are being proposed for the deeper-water, dynamic-ice-movement areas. This geometry induces flexural failure of the ice features and is relatively transparent to pack-ice movements. The deck is fully outfitted with processing equipment before it is mated with the structure. Wells are confined to a central moon-pool area in the cylindrical throat. Consumables and oil can be stored in the base.

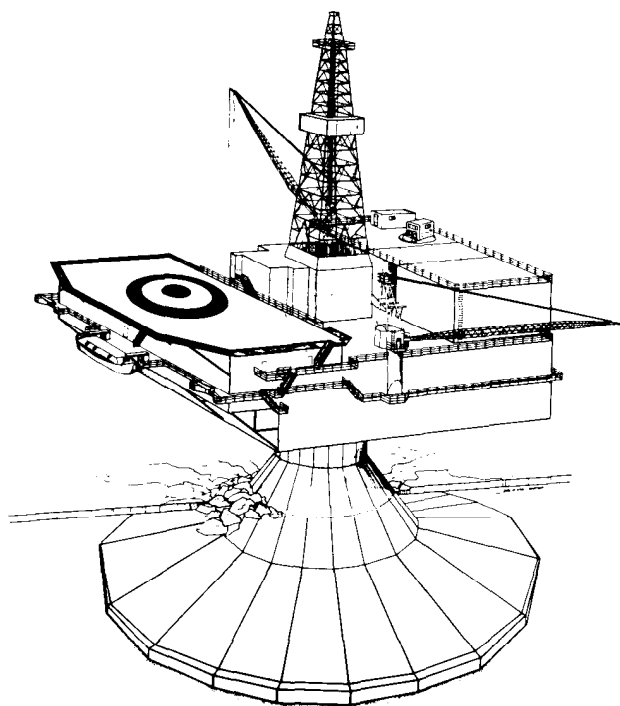


Fig. 18.46—Arctic mobile drilling structure: sloping-sided structure.

Piled Structures. Piled steel structures have been developed primarily for the Bering Sea area of offshore Alaska. These structures are similar to conventional template or jacket concepts but must be modified to resist annual sheet-ice loading. A typical geometry is shown in Fig. 18.47. The platform concept consists of four or eight main pile legs with intermediate bracing of the legs omitted in the ice-loading zone near the waterline. Well conductors and oil-transport lines are positioned within the legs of the platform for protection from ice loading. This requires close spacing of the wells and, in some cases, completion of the wells at different levels of the deck. Diver-access tubes may also be located in the legs to facilitate the repair and inspection of subsea components of the platform during complete ice coverage.

In most other Arctic areas, pile structures are not practical. Subsea permafrost makes pile installation nearly impossible. The short construction season also does not accommodate the installation, pile driving, and placement of the topside modules in one season. Also, the hookup and commissioning of the production equipment modules would be very expensive in these remote areas.

Transportation Systems

Pipelines. Offshore pipelining is the predominant mode of crude-oil transport proposed for Arctic regions. The pipelines will interconnect platform facilities, mooring

structures, and land-based facilities in much the same manner as in conventional offshore locations. The principal factors affecting the construction and operations of Arctic pipelines are the short open-water seasons, subsea permafrost, scour, and ice gouging of the seafloor.

Pipelines can be placed directly on the seabed in deep water, in trenches in areas susceptible to ice gouging or scour, and on causeways or elevated bridges at shore crossings. In areas of extreme ice gouging, redundant lines may be used to lower the risk of interrupted production.

In deepwater, moderate-ice areas of the Bering Sea, the lines will be laid directly on the seabed by conventional lay-barge methods. The 6- to 9-month open-water season, extreme summer wave conditions, and logistics of operating several hundred miles offshore reduce the efficiency of the construction process. The distance from shore or an offshore loading terminal may also require pump stations along the pipelining route.

Marine pipelines in the Arctic Ocean are considered feasible but will require the greatest challenge to existing technology. The open-water season lasts approximately 1 to 3 months a year. In shallow-water locations, the keels of ice features may gouge the seafloor for several miles in a single ice-movement event. Pipelines must be buried in trenches that are deep enough to ensure no damage. Offshore permafrost may also cause difficulty in obtaining the desired trench depth and may require the use of cutter-suction dredges to remove the ice-rich soil. Once the pipeline is installed, refrigeration of the trench may be required to ensure no subsequent thawing of the permafrost. Nearshore pipelines may also have to be designed for wave-induced erosion or strudel scour. Strudel scour, which is common at the mouth of rivers, is the process in which river-water outwash flows over the nearshore sheet ice and floods down through holes and cracks in the ice. This jet of water could create large, eroded pockets in the seabed and produce long, unsupported spans of pipe.

Marine Terminals and Tankers. Transportation of crude-oil products from many of the remote Arctic oil fields also can be accomplished by offshore terminal and tanker systems. The systems could consist of an interfield pipeline-gathering network with processed crude shipped directly to shore. Once onshore, the crude could be stored until it is loaded onto tankers and shipped to market. Another form of marine terminal system is direct shipment of processed crude from offshore platforms to tankers through single-point mooring systems.

The design, construction, and operation of these systems have been proved in many sub-Arctic areas. However, some of the components must be modified for the cold temperatures and persistence of ice. Loading arms must be designed to ensure that hoses remain elevated above the ice mantle and can accommodate loading of tankers from any location around the terminal. Tanker-mooring systems must be designed for both wave- and ice-loading conditions. Extreme ice areas may require offshore loading directly from fixed platforms or from subsea facilities, making maneuvering and stationkeeping very difficult. Icebreaker assistance vessels may also be required to ensure safe access and departure from the terminal by tankers.

To travel through the offshore Arctic regions, purpose-built icebreaking tankers may be required. The amount

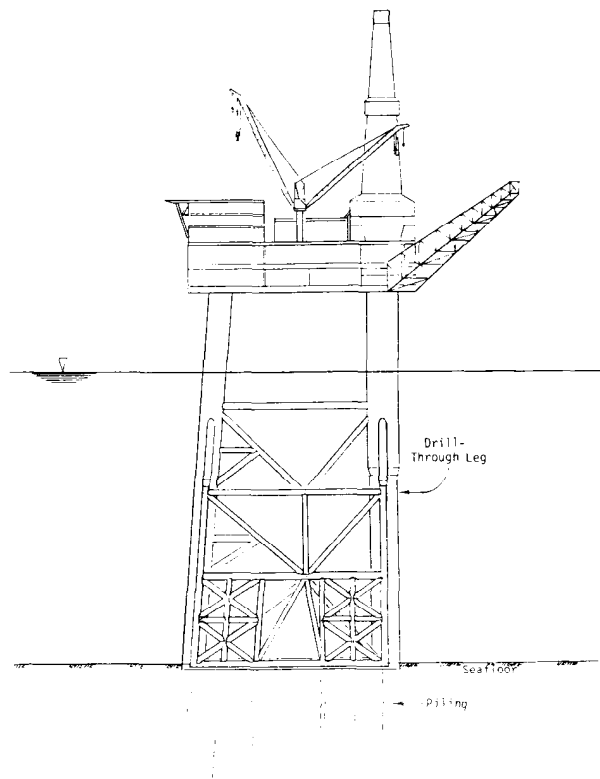


Fig. 18.47—Piled structure.

of hull stiffening will be dictated by the ice conditions for its area of operation. The modifications could range from simply thickening the hull plate to the requirement of an icebreaking bow and turbine-powered propulsion system. Internal bulkhead arrangements should also be arranged to ensure that oil storage tanks are adequately stiffened and not susceptible to direct ice impact.

Special Considerations

Ice Management. A critical support system, unique to the Arctic, is the ice-management system. The key component of this system is instrumentation of the structure, foundation, and ice field around the structure to monitor both local and global ice loading. Other elements of ice management include icebreaker support vessels for tankers or supply boats, tractor-mounted ditch diggers for slotting the ice to reduce loads, and water-pumping units to flood areas around a platform to stabilize ice movement.

Electrical, Instrumentation and Control Systems

Offshore production facilities have the same basic requirements for electric power and control systems as onshore facilities. These are a power source with a reliable distribution system, instrumentation to control and to monitor production operations, and a safety shutdown system tailored for the installation.

Although offshore and onshore installations have similar needs in these areas, the two operations are significantly different in other respects. As pointed out earlier, deck size and payload significantly affect offshore structure costs. Consequently, offshore electrical facilities must

be designed for minimum weight and space while still offering a high degree of flexibility, reliability, access, and maintainability. Because of deck space and layout limitations, hazardous area considerations are more complex and often are governed by different regulatory codes depending on the type of structure, its location, and the responsible governmental agency. Additionally, environmental considerations are much more demanding because of the generally salt-laden atmosphere and the possibility of saltwater washdowns and sea spray.

Several wiring methods are approved for offshore installations, but the method used frequently depends on local practices and personal preferences. There is no single correct method for wiring an offshore installation as long as the appropriate codes are satisfied and the craftsmanship is of average quality or better.

Offshore-production instrumentation and control systems also tend to differ from their onshore counterparts. Offshore oilfield operations are confined to a relatively small spot on the ocean rather than being spread over several acres. Consequently, controls tend to be much more centralized. This trend toward centralization has become more pronounced with increased use of computer-based production-monitoring and control systems.

Safety shutdown systems onshore and offshore are roughly equivalent. However, offshore requirements regarding functionality and reliability are somewhat more stringent because of the greater potential for spills and resultant pollution. Increased concern for personal safety and environmental protection creates a more stringent atmosphere for approval, testing, and inspection by outside agencies, as well as thorough documentation of the entire process and facility by the operator.

Alternative methods of addressing and satisfying these and other considerations peculiar to offshore operations will be discussed. The intent is to lay out the problems, to highlight areas of concern, and to discuss possible solutions, rather than to present specific, detailed engineering methods for design and installation of electrical and/or control systems.

Codes and Regulatory Authorities

Offshore electrical installations are governed by one or more codes and regulations, depending on the type of offshore structure involved and its location. In U.S. waters, electrical designs are governed by local or state electrical codes and in most cases the Natl. Electrical Code.¹⁹ Generally, the installation should be in accord with the more stringent requirements of the applicable codes. The guidelines given in API RP 14F²⁰ provide direction for accepted good practice in accordance with most applicable codes. If the facility falls under U.S. Coast Guard jurisdiction (e.g., TLP's, mobile offshore drilling units and FPF's), all or portions of the electrical system also must be designed, installed, and operated in accordance with the applicable portions of U.S. Coast Guard Regulations 46 CFR Chapter I, Subchapter IA, Mobile Offshore Drilling Units, Part 108 and Subchapter J—Electrical Engineering, Parts 110–113.²¹ Overseas installations frequently fall within the jurisdiction of local/national codes or regulatory agencies. This situation occurs in the North Sea where Lloyds of London or Det norske Veritas frequently are named as certifying authority, and their requirements must be met. If there is no lo-

cal certifying authority, it generally is good practice to design all systems to meet normal U.S. requirements for that type of facility.

Platform Loads

With the exception of the hotel loads that serve accommodations and personnel needs, normal platform loads are not greatly different from the normal assortment of onshore loads. Processes are likely to be concentrated in a single location offshore, and the loads are appropriately higher. Loads usually consist of a mix of transfer pumps, compressors, fans, and heaters as well as utilities (air compressors, sump pumps, fire water pumps, water makers, sewage facilities, etc.). Other typical loads include pumps and gas compressors associated with shipping, artificial lift, secondary recovery, and pressure-maintenance operations. Depending on platform type and production facilities and rates, the loads on any given platform in a field can range from less than 25 kVA to more than 40 MVA.

Layout of Facilities

Considerations that govern layout of offshore electrical facilities are similar to those for land installations, but the options are more restricted because of the space limitations. The primary requisite is to separate to the maximum extent possible the sources of ignition from the process facilities. Electrical equipment should be kept out of hazardous areas when economically feasible. Primary electrical switch gear is frequently grouped in a pressurized, central electrical-equipment room. Remote motor-control centers (MCC's) sometimes are used to reduce the amount of platform wiring. Installing MCC's near load concentrations and supplying the MCC's with high-voltage feeders shortens branch circuits that feed individual loads. Remote MCC's frequently must be purged or pressurized because of their location. The design approach appropriate in each individual case must be based on practicality and economics.

Detailed load analyses must be made early in the design stage. Each analysis must consider both initial and anticipated future load. Results of the analysis should control design of primary power facilities, layouts of conduit or cable ways, switchgear space, and distribution-equipment layouts. Designs must allow for expansion in each of these areas. The designer must carefully consider possible future system expansion and pay particular attention to possible future artificial-lift and water-injection requirements. Hydraulic pumping and electric submersibles can add significantly to the ultimate electrical load. It is important to consider the potential for future changes in facilities as reservoir conditions change and possible increased demand on the electric power system.

Primary Electric Power

Typically, offshore facilities either generate power locally or they are fed by submarine cables. Generated power ranges from 480 to 4,160 V. The higher voltage levels are more prevalent where there are high horsepower loads or where platform drilling rigs are not set up to generate their own power. Very large platforms are sometimes designed with primary power system voltages of up to 13.8 kV.

The primary source of generated power usually consists of one or more brushless synchronous generators with either diesel-engine or turbine prime movers. Turbines may be gas- or diesel-fueled or they may be dual fueled. Dual-fueled turbines generally are set up to run on diesel initially and then to cut over to produced gas as production builds to a stable supply. Turbines offer the advantages of lighter weight and the opportunity for the use of waste heat in oil production processing. Turbine-generator packages, however, are very costly, require more maintenance, and in some cases, may require more deck space than internal-combustion-engine-driven generators of the same capacity. In addition, primarily because of the somewhat limited selection of turbine sizes available, it can be more difficult to match turbine generator packages to the electrical system loads.

The second source of offshore power, submarine cable, offers an efficient means of electrification if adequate sources are located nearby. Depending on the loads and the distances involved, cable-system voltages can range between 480 and 35,000 V. Submarine-power-cable technology is well established. Power cables generally include one or more pairs of small-gauge wires dedicated to telecommunications or telemetry and also are protected with torque-balanced double layers of galvanized armor wires that may be plastic-coated for additional protection. Power cables may be buried, depending on local conditions or regulations. Tubular risers are required at each platform served by submarine cables to protect the cables as they rise from the seabed to the platform deck. The riser generally should be filled with a corrosion-inhibiting fluid to preserve the long-term integrity of the armor wires. When the submarine cables originate on land, they must be buried and suitably protected through the surf zone. Mechanical protection is frequently provided by additional armor or by the installation of heavy-wall pipe through this area.

Secondary/Back-up Power

Essential loads on offshore facilities must remain energized even when the main power source fails. These loads usually fall in the category of navigation lights (ship and aircraft), foghorns, communications, emergency lighting, and possibly some selected hotel loads. In some instances where marine regulatory bodies have jurisdiction, the emergency system may have to be expanded to serve other loads related to the safety of personnel on board.

High-volume oil and gas facilities are frequently designed to shut in completely in the event of power failure, in which case process or shipping loads do not have to be considered in determining backup power loads. Some smaller facilities, such as wellhead platforms, are designed to continue production operations without any electrification other than lighting, navigation lights, and foghorns.

Emergency power generally is derived from onboard generators, storage batteries, or both. The generators usually are small (less than 500 kW) and diesel-engine driven. Diesel engines that are used in emergency service normally are equipped with automatic starters. These engines also are equipped with cooling water and lube-oil heaters to ensure that they will start reliably and instantaneously (within 10 seconds) on loss of primary power.

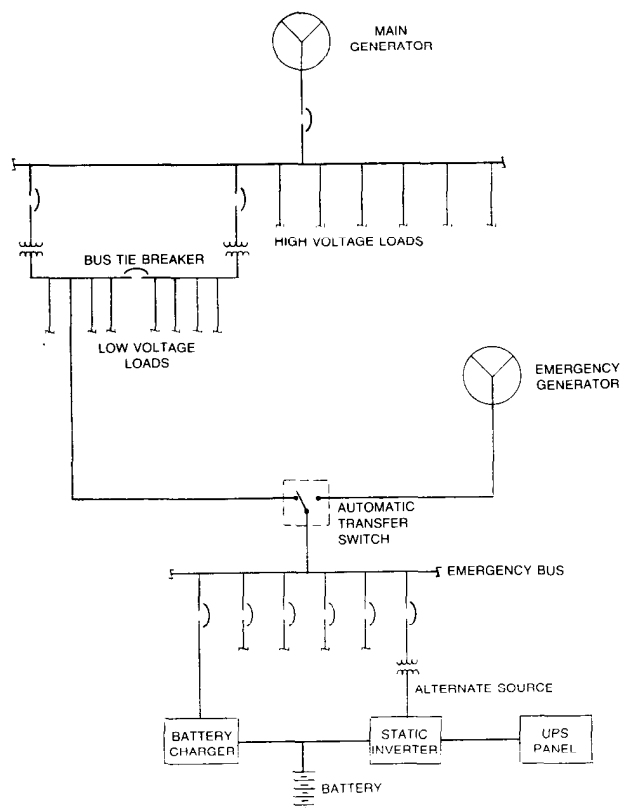


Fig. 18.48—Typical electrical one-line diagram with ups and emergency generator.

Offshore facilities with electronic instrumentation or computer-based monitoring or telemetry systems generally need uninterruptable power supplies (UPS's) to provide reliable, clean power for these loads. A UPS is essential on platforms where some loads are supplied from onboard, solid-state, silicon-controlled rectifiers (SCR's) because of the high level of electrical noise injected into the power system by the SCR's.

The emergency bus typically is tied into the normal power bus through an automatic transfer switch. The emergency bus receives power during normal operation from the main bus. On failure of the primary power, the transfer switch opens the tie between the two buses to isolate the emergency bus and its loads from the remainder of the platform loads. Additional controls automatically start the emergency generator to energize the emergency bus. Normally, no provisions are made for operating the emergency generator in parallel with the main power supply. Interlock circuits should be provided, however, to permit testing the emergency generator offline without energizing the emergency bus.

Typical one-line diagrams for a UPS and an emergency generator bus tie are shown in Fig. 18.48.

Distribution System

Offshore power-distribution systems and associated equipment do not differ substantially from land-based operations. Depending on load sizes, distribution voltages will normally range from 120 to 2,400 V. Distribution systems with 4,160 V and higher are rare except on very

large platforms with high horsepower loads. As with land-based systems, accepted good practice and system capacity determine the maximum allowable horsepower for individual loads and the appropriate supply voltages.

Motor-control centers and switchgear usually are installed inside pressurized or purged enclosures or modules. The pressurizing or purging frequently is required to ensure a nonhazardous operating environment for the electrical equipment so that air-break switching equipment can be used safely. Code requirements for purging are prescribed in the Natl. Electrical Code¹⁹ and Natl. Fire Protection Assn. Bull. NFPA 496.²³ As indicated in the references, interlocks usually are provided either to sound an alarm or to shut down all supplies when a loss of pressurization or purge occurs. Depending on the particular operations involved, a simple alarm may be permissible if shutdown of the process could create a greater hazard than continuing operation during a short-term loss of pressurization or purge protection. Each installation is site-specific and must be considered on its own merits.

System transformers may be installed either indoors or outdoors. Both single- and double-ended line-ups are used offshore, depending on the nature of the operation. Double-ended 100%-capacity supplies with bus tie breakers are frequently used for increased reliability and continuity of service in the event of equipment failures.

Hazardous Areas

The possibility of fire or explosion because of the ignition of leaking gas or liquids is a concern in all producing facilities. The concern is even greater offshore because of the concentration of personnel and facilities in a relatively confined area where fire can be difficult to extinguish and platform evacuation can be a complex problem. The requirements for classifying areas according to their degree of hazard and for selecting equipment for the various areas are covered in API RP 500B²²; Section 500 of the Natl. Electrical Code¹⁹; and USCG Regulations 46 CFR, Chapter I, Subchapter I-A, Part 108 and Subchapter J, "Electrical Engineering," Parts 110-113.²¹ Certifying agencies outside the U.S. have some different rules and categories, but in general, they are no more strict than the U.S. rules for the same situation.

Wiring Methods and Equipment Enclosures

Several wiring methods are applicable to offshore installations, and opinions differ as to whether conduit-and-wire or cable-and-cable-tray systems are best. Each has advantages and disadvantages. If the installation complies with the appropriate procedures as outlined in the Natl. Electrical Code¹⁹ and API RP 14F,²⁰ each method is safe and reliable. Rigid steel conduit and wire systems provide the maximum mechanical integrity, but the conduit and fittings should be coated with plastic (PVC) to eliminate corrosion effectively. PVC-coated fittings and accessories are readily available in most locations. Copper-free aluminum conduit systems have been used successfully in lieu of galvanized steel. Aluminum systems require special wrapping of the conduit wherever steel support clamps are used to prevent setting up corrosion cells where dissimilar metals would come in contact. Overall, conduit systems provide excellent protection for wiring systems, but they have the disadvantage of being bulky and relatively expensive to install, maintain, and modify.

Type MC (metal-clad) cable, which has a corrugated aluminum sheath and an overall PVC jacket, is another preferred system that is frequently used offshore. Armored shipboard cable and type TC tray cable are viable alternatives to MC cable in many instances and are suitable as long as the installation complies with the Natl. Electrical Code.¹⁹ Cable systems are more flexible, quicker to install, and less subject to corrosion than conduit offshore, but they are more subject to mechanical damage.

As with onshore facilities, all electrical equipment installed in locations classified as Class I, Div. 1 must be explosion-proof. Requirements for equipment in Class I, Div. 2 areas are slightly less stringent as long as no arcing contacts are exposed. Electrical equipment in nonhazardous areas generally is chosen for its applicability to the situation. Switches, for instance, generally are provided with explosion-proof enclosures for mechanical protection and durability even if the contacts are enclosed. General-purpose enclosures are normally used in protected areas. Fiberglass enclosures are seldom used in open areas because of their susceptibility to mechanical impact damage.

Explosion-proof motors are required in Div. 1 areas. Fractional horsepower motors in Divs. 1 or 2 areas must be explosion-proof. Otherwise, both Div. 2 and unclassified areas permit the use of totally enclosed fan-cooled (TEFC), totally enclosed nonventilated (TENV), or encapsulated, open drip-proof motors. Choice of enclosure must be based on exposure and service. Motors operating at 2,400 V or higher should be equipped with integral heaters or low-voltage winding heating systems if they are in exposed locations to ensure that the integrity of the insulation resistance is maintained during periods of nonuse. As warm windings cool in the relatively high-humidity offshore atmosphere, moisture is pulled into the windings, giving rise to a high chance of an internal short circuit. Motors of 500 hp or more that have been shut down for an extended period should always be checked with an insulation tester before they are restarted, regardless of whether they have been heated in the interim.

General Instrumentation

The primary guide for the instrumentation of offshore installations is API RP 14C.²⁴ In conjunction with the applicable U.S. OCS Orders,^{25,26} the API guide provides an excellent reference for guidelines in the design of monitoring and control systems for offshore-production facilities. Most offshore installations have local control panels for packaged equipment, such as gas compressors, low-temperature gas separation (LTS) units, and electrical generators. Beyond this, the choice of individual local display/controllers or centralized control rooms with field transmitters and local displays depends on the nature of the facility, the complexity of the operation, economics, and preference of the operator. Most large, modern offshore facilities are planned with centralized controls. The one design principle that must be followed regardless of the overall design philosophy is that all systems should be designed to be fail-safe so that loss of a signal represents an alarm or shutdown condition.

Even when a centralized control room has been provided, continuous remote, closed-loop (analog) control is seldom used. Remote, closed-loop controls usually are

considered only when the process includes complex separation processes, sulfur removal and handling, or gas processing. Most oil/gas handling processes are sufficiently simple and straightforward that local control loops are satisfactory.

Centralized controls can be based on conventional instrument and relay control panels, but advances in electronics have increased the use of programmable controllers and microprocessor-based instrument systems. These advanced system designs have multiplexed monitoring and control systems that frequently offer significant savings in wiring costs and space for a complex installation. They are more compact and much more flexible than conventional control panels.

Offshore instrumentation is very similar to onshore instrumentation. Process controls frequently include a combination of pneumatic, hydraulic, electric, and electronic instrumentation. Process variables that must be monitored and/or controlled include level, pressure, temperature, flow, oil/water interface, and gas/oil interface. In most offshore installations, the considerations in designing instrument systems to accommodate these variables are identical to those for their land-based equivalent. Foam, gas cutting, sand, wax, and H_2S are typical considerations. Radios are used extensively for offshore communications, and radio interference can present some unique problems. Some electronic-based sensors are sensitive to radio-frequency interference and may give false alarms or shutdown signals when high-powered radios are keyed nearby.

Most operators prefer to separate emergency shutdown circuits from alarm and control circuits. Typical examples are high- and low-level shutdowns on tanks or separators, high/low pilots on manifolds, and gas and fire detectors.

Regardless of the level of complexity of an instrument and control system, a conscientious, well-disciplined, and well-documented program of regular testing and maintenance is essential. Offshore instrument systems are not overly complicated, and given adequate maintenance and correct initial installation, every instrument should perform its intended function reliably over the life of the facility.

Safety Systems

Separation of process-related shutdowns from instrument-control loops was mentioned earlier. Process shutdowns generally involve process-related variables that have exceeded preset limits. Other key safety-related systems should be kept separate. These systems are covered in various U.S. Coast Guard Regulations and OCS Orders.²⁶ Examples of these systems are combustible-gas detectors, poisonous-gas sensors, fire detectors, surface-controlled subsurface safety valves (SCSSV's), surface safety valves (SSV's), and emergency shutdowns (ESD's). Proper design and installation of these systems is perhaps the single most critical aspect of offshore instrumentation and control systems. (Safety shut-in systems are covered in more detail in Chap. 3).

Combustible-gas detection systems are required in most offshore operations. They are intended as early warning devices to alert operators to potentially hazardous conditions where none normally exist. Modern systems have catalytic sensing heads whose electrical characteristics depend on the concentration of hydrocarbon gases surround-

ing the sensor. Units are calibrated and have known variations in their electrical output that are based on the gas concentration in the area of the sensor. Gas sensors normally are connected to a central monitoring panel equipped with individual sensor readouts calibrated in percent of lower explosive limit (LEL). Each readout has at least two alarm outputs. Normally, one alarm is set for about 20% LEL and the other for 60% LEL. Some operations/regulations require automatic shut-in at the higher level. Although gas detection technology has improved over the years, malfunctioning caused by poisoning of the sensing heads by contaminants in the air and loss of circulation caused by dirt accumulations on the sensors continues to be a problem.

H_2S gas detectors are essential where sour crude and sour gas is handled or produced because of the extreme toxicity of H_2S . Sensors continue to improve, but reliability and maintenance are continuing problems.

Because of their vulnerability, gas detectors must be installed where they are protected from water spray, drilling mud, and other contaminants; yet they must be in areas where they can adequately monitor the environment. They generally are installed in areas where leaks or accumulations might be expected under abnormal conditions—above gas compressors, in a wellhead or manifold area, over drilling mud pits, or in dead-air spaces—or in areas where a gas build-up could be catastrophic, such as in ventilation system inlets.

Fire-detection systems generally are based on the use of ultraviolet (UV) sensors or fusible plugs. The operating principle of UV sensors is that their sensitivity to the UV radiations from flame provides an alarm output in the presence of UV radiations from open flames. Unfortunately, they also are somewhat sensitive to direct and reflected UV radiation from welding arcs. Because of their extreme sensitivity, most UV fire systems include a brief time delay to minimize false triggering of a fire alarm. The layout of UV sensors at a site is important. Considerable care must be taken in laying out a coverage that considers viewing angles, range, and sensitivity.

Infrared (IR) fire sensors were tried on early offshore platforms, but they had many operating problems. IR sensors are seldom used today, primarily because of difficulties with their calibration and reliability.

Fusible plug fields that consist of pressurized stainless steel or plastic tubing, heat-sensitive solder plugs, and pneumatically held pilot shutdown valves are popular and reliable systems for fire detection. With this system, tubing is run through and around various critical areas of an offshore facility. The tubing runs are segregated by process area or some other criterion. Multiple solder plugs are included within each field. If a fire occurs in that field, the solder plug melts, depressurizing the field and tripping a shutdown valve. The major problem with plug fields is maintenance and accidental shutdown because of leaks.

Overall, a judicious combination of strategically placed UV sensors and fusible plugs forms the optimum fire detection and automatic shut-in system. With such a system, it is possible to shut in production facilities, to blow down pressurized vessels, and to activate the appropriate fire suppression system simultaneously and immediately, thus minimizing fire danger.

SCSSV's should form an integral part of every offshore production system. These valves are installed in the production tubing below the mudline. They are hydraulically actuated and held open during normal operation by pressurized hydraulic fluid in their individual control lines. They are designed to be fail-safe in that they close when a loss of hydraulic pressure occurs. On modern platforms, the SCSSV hydraulic system is generally a separate, centralized, hydraulic power unit dedicated solely to their control. Surface power units and their associated alarms and controls are available as specialty packaged units. Their design and component selections have been developed over the years to the point where it is not cost-effective to try to design alternative units.

Platform wells also are equipped with surface safety valves (SSV's) between the wellhead and the production manifold. The actuators on these valves are designed to be fail-safe closed and can be actuated either hydraulically or pneumatically by the automatic safety shutdown system and/or the manual emergency shutdown.

SCSSV's normally are actuated only in extreme emergency to preserve their integrity. Repairs are expensive. SSV's, on the other hand, usually are activated in almost all platform or process shut-ins. They are simpler devices that are less expensive to repair, more rugged, and more accessible.

Nearly all platforms are equipped with automatically controlled riser shutoff valves on pipelines and flowlines feeding or leaving the platform. The intent of these valves is to allow isolation of the platform from any outside source of flammable fuel in the event of a platform accident. In the case of subsea wells, it frequently is desirable to shut in the wells by simply blocking the flowline rather than operating the subsea valves unnecessarily. The flowline riser valves commonly are operated first in the event of a subsea well shut-in and last on startup to avoid cutting out seafloor valves by closing or opening them unnecessarily against a flowing stream. Riser valves are far more accessible and maintainable than the subsea tree valves.

The final element in any safety system should be the manual ESD. These controls can be either electrically operated solenoids or pneumatically or hydraulically held pilot valves that control various shutdown control circuits around the facility. ESD stations usually are located on boat landings, on helidecks, in process areas, and in control rooms.

Control of Subsea Production Facilities

The mechanics of subsea production systems, such as wells and manifold centers, were covered under Production Facilities. This section presents various operating philosophies and discusses methods of providing remote control of subsea equipment.

Subsea controls should be as simple and straightforward as possible and still meet requirements for operational considerations and the physical layout of the field. System reliability, maintainability, control response times, and the need for feedback of tubing or annulus pressure and valve position to the operator are some of the most important factors that must be considered. Physical aspects of the oilfield—water depth, lateral offset of the subsea equipment from its associated platform, anticipated sea or ice conditions, and the potential for well damage caused

by shut-ins—and the complexity of the subsea facility determine the optimal design of the control system.

Subsea facilities require two separate sets of controls. Production controls provide day-to-day operational control of the subsea equipment. Initial completion and subsequent workover of subsea wells require controls designed specifically for installation/maintenance functions. Completion/workover systems generally provide control over more functions than the associated production system. Production controls normally exclude control over hydraulic connectors, test ports, and vertical access valves.

Reliability/Maintainability

Reliability of a control system can be considered to be the probability that the control will not malfunction in such a manner as to preclude performing an intended function. Reliability usually is quoted over some specified period, such as the intended operating life of a particular project or the planned time between scheduled maintenance. For any system, the probability that the system will fail to perform its intended functions over a given time period is a function of the design, quality of the system components, built-in redundancy, and the quality of manufacture. Regardless of how well a system is designed and built and how short an operating period is considered, there will be a finite probability that it may malfunction during that period.

The likelihood of a failure can be minimized, but it can never be completely eliminated. Consequently, rather than going to great lengths and expense to design a system that "can't fail," it may be more cost-effective to set realistic reliability goals and to concentrate on designing the equipment for maximum maintainability. This approach is aimed at minimizing the effect of a problem instead of trying to avoid the inevitable and generally results in a sound design that maximizes ease of retrieval and reinstallation. How best to implement increased reliability and maintainability should be determined by the incremental cost involved and the benefits to be derived.

Redundancy

A system fault generally results in a well shut-in, and recovery of the control equipment for repair and reinstallation is then required before the well can be returned to production. The ultimate cost of the repairs is reflected in the expense of mobilization for repair, the repair, and subsequent demobilization.

One of the most economic and effective means of increasing system reliability is to include active backup for weaker elements within the basic subsea control module or, in the extreme, to provide a completely redundant module.

This approach may be cost-effective in situations where field conditions could impose severe economic penalties or pose a safety hazard in the event of a control system malfunction. The value of deferred/lost production and the possibility of premature well work necessitated by the shut-in also must be taken into account in evaluating the economics of providing redundancy.

Redundancy does not eliminate the ultimate need for repairs, but it may permit postponing them to take advantage of favorable weather windows, contracting rate trends, or vessel availabilities, all of which can work to

substantially reduce repair costs. In addition, built-in redundancy allows operations personnel to schedule the work on the basis of convenience without incurring unnecessary production losses or potential well damage.

Although potentially economical, redundancy is not free. The decision on the extent to which it should be included in a design must be based on a careful examination of the cost impact on the project and the potential benefits.

Operational Considerations

Many operational factors and operating philosophies must be weighed when the control system for a specific installation is selected. Among the items that should be considered are response-time requirements; potential need for diver or remote-operated vehicle intervention; requirements for feedback regarding subsea valve operation, wellhead pressures, and temperatures; single-well or multiwell completions; use of subsea manifolds, commingling, and application of subsea chokes; type of control fluid; and the type of control-system design.

Response time for opening a tree valve usually is not critical if it is not unreasonably long, particularly with low flow velocities and clean production. Closing times are of considerable concern, however, and closing response may determine the type of control system to be employed. Excessively long closing times are neither desirable nor necessary. From the standpoint of pollution potential in the event of a flowline rupture, closing response times are less critical for water-injection wells than clean-gas wells, which, in turn, are less critical than oil wells.

All other factors being equal, a system that provides discrete control over each subsea valve and allows the operator to verify or to infer valve operations would always be recommended over one that does not. Some type of feedback on valve position is almost mandatory for safe operation of subsea facilities. If there is any concern about wellhead temperature or pressure because of flowline materials or other considerations, the ability to sense this information and to transmit it to the surface can be an overriding consideration in the selection of a control system.

Control Fluids

High-pressure control fluid is the means of converting a control command into subsea valve operation in both all-hydraulic and electrohydraulic control systems. Military-grade, low-viscosity, conventional oil-based hydraulic oil and highly water-based fluids are the two types of fluids in subsea control systems. Oil-based fluids provide the best system performance from the standpoints of lubricity, component wear, internal leakage, corrosion protection, and ultimately, system reliability. Oil can be used only in closed systems, however, because it cannot be discharged into the ocean when a control loop is vented to deactivate a control. Closed systems imply higher costs and, over long distances, slower response times. Oil-based systems can be particularly troublesome in cold climates. Water-based fluids, on the other hand, are inexpensive, are biodegradable (so they can be discharged into the environment), exhibit very low viscosity, and provide the fastest response times.

Unfortunately, water-based fluids also have certain inherent deficiencies. They exhibit lower lubricity, en-

courage higher leak rates, display lower corrosion inhibition, and are subject to biofouling from bacterial growth. All of these shortcomings can be overcome with proper component selection, design, and operating practices. Water-based fluids are used in most subsea and drilling control systems.

The single most important factor with any hydraulic control system, regardless of the type of fluid, is fluid cleanliness. Failure to keep the hydraulic system clean virtually guarantees an early malfunction.

Umbilicals

Platform control of subsea facilities requires a control umbilical between the platform and the subsea facility. The umbilical may consist of multiple hydraulic lines in a common jacket, a composite of hydraulic hoses, power wires, and communication pairs in a common jacket, or separate hydraulic and electrical bundles. The makeup of the umbilical depends entirely on the nature of the control system and the field conditions.

Hydraulic bundles can be fabricated with either stainless steel tubes or elastomeric hoses. Because of the importance of quick response and because hose expansion is a major determining factor in response time, manufacturers have upgraded hoses to the point that their expansion characteristics approach that of steel tubing. Hose and tubing display different installation and operational characteristics, however, and the decision on umbilical design must consider the unique aspects of the materials and specific project requirements.

Protection of control lines laid on the ocean floor is always a concern. One of the principal means of protecting control lines that are not buried is to armor them with galvanized wires applied in two separate, contrahelically wound layers. Because of the cost of armoring the large diameters encountered in most hose bundles, however, they are seldom armored. As armoring costs are reduced with improved technology, armoring of hose bundles may become more common. Hose bundles that are armored usually have a polyethylene bedding jacket under the armor and may have a thin covering over the armor. Some unarmored designs include a small-diameter wire rope molded integrally with the jacket to provide tensile strength and additional weighting. An alternative hose-bundle design makes use of a thick outer urethane jacket in lieu of armor. The high density of urethane provides the necessary negative buoyancy, and it provides excellent abrasion resistance.

A viable alternative to hose bundles uses stainless steel tubes laid side-by-side in a flat configuration. Relatively large-diameter wirelines (ropes) normally are placed on the outside of a flat bundle to provide mechanical protection and resistance to kinking.

The generally accepted practice is to armor subsea electric control cable for mechanical protection, weighting, and tensile strength. Even though it means a substantial reduction in cost, few, if any, unarmored cables have been installed subsea.

Alternative Subsea Control System

There are currently two primary approaches to the control of subsea equipment—all hydraulic and a hybrid of electric and hydraulic (electrohydraulic). Each offers a number of variations with unique advantages, disadvantages, and associated costs that must be considered and

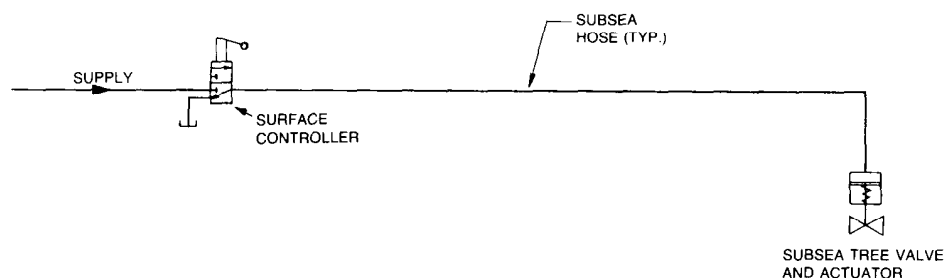


Fig. 18.49—Direct hydraulic subsea control.

evaluated before a system design is finalized. Usually, one design will prove superior to the others for a given situation. Applicability of a given design depends on factors such as water depth, operating environment, offset distances, equipment to be controlled, operating requirements, operating philosophies, reservoir characteristics, and field economics.

The following sections include brief discussions of several basic system designs and their primary advantages and disadvantages. When the final selection is made, trade-offs must be made between simplicity, response time, operability, and costs on a site/project-specific basis.

Direct Hydraulic Control

Direct hydraulic control (Fig. 18.49) is the most straightforward design approach. It uses a single three-way surface control valve—a single, relatively large-diameter, dedicated high-pressure control line between the surface control valve and the subsea tree hydraulic-valve actuator and the valve actuator. When the surface control valve is operated, high-pressure fluid is introduced into the control hose, causing the subsea valve actuator to open the tree valve. When the surface valve is deactivated, the fluid that opened the subsea valve is returned to the surface fluid reservoir. The advantages of this system are simplicity, discrete remote control over each subsea function,

inherent feedback on subsea operations, and minimum cost of the basic control hardware. The disadvantages are slowest response time for a given control-line size, highest control-line costs, and potential problems with corrosion and biofouling of the subsea actuator when a water-based control fluid is used because the fluid is never renewed. System costs are directly proportional to the number of functions controlled and the distance between the control point and the subsea device. This type of system is seldom used with producing wells at offset distances of more than 10,000 ft, or with injection wells at more than 15,000 ft, because of the cost and response-time considerations.

Response time of the direct hydraulic controls for the valve-closing (shut-in) operation over a given distance with a given line size can be improved significantly by installing a subsea dump valve on each tree-valve actuator. This approach also permits the introduction of new control fluid into the control lines because the fluid in the actuators is vented to the ocean whenever a valve is closed. This provides a gradual renewal of control fluid with each valve operation.

The disadvantage of dump valves is that they introduce additional flow-rate/direction-sensitive hydraulic-control elements that require very clean control fluid. This increases subsea hardware cost and markedly reduces the overall system reliability.

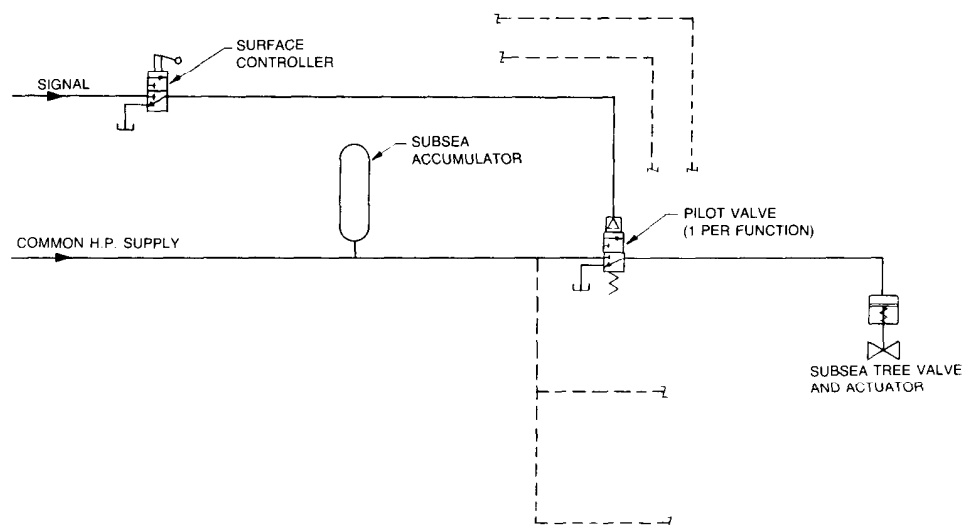


Fig. 18.50—Discrete-piloted hydraulic subsea control.

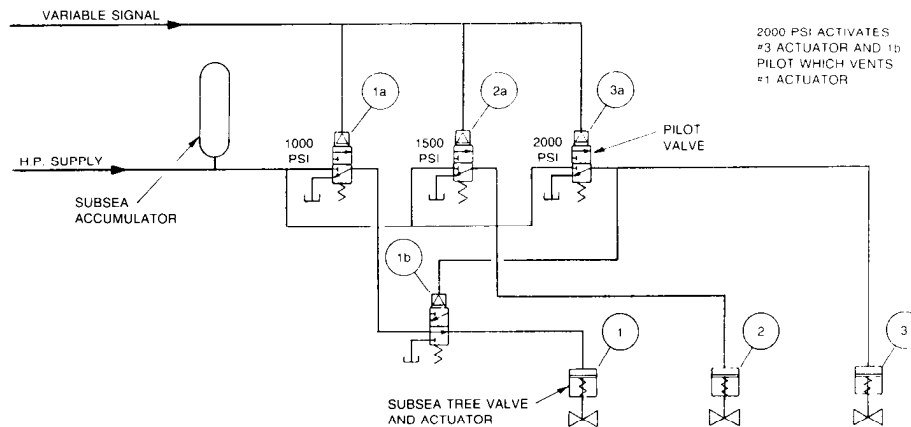


Fig. 18.51—Sequential-piloted hydraulic subsea control.

Discrete-Piloted Hydraulic

Discrete-piloted control (Fig. 18.50) has a single three-way control valve at the surface for each subsea function, a corresponding subsea pilot control valve, and single small-diameter dedicated signal line between the two control valves. A single common high-pressure line provides hydraulic supply from the surface to the tree. When the subsea pilot valve is actuated, it switches high-pressure fluid from the supply line to the subsea valve actuator. When the pilot valve is deactuated, it vents the actuator fluid subsea rather than returning it to the surface.

The advantages of this design are its relative simplicity, discrete remote control over each subsea function, inherent inferred feedback on subsea operations, relatively low-cost hardware, and relatively fast response compared to the direct hydraulic design. The disadvantages are that cost and response time are both proportional to distance just as they are with direct hydraulics, but the effects are significantly less. The pilot lines are dead-ended, but cor-

rosion is not a problem because pilot valves usually are made of stainless alloys. Biofouling, however, can still be a problem.

Sequential-Piloted Hydraulic

Sequential control is similar to discrete-piloted control in that it also has subsea pilot valves that direct high-pressure hydraulic fluid to tree-valve actuators (Fig. 18.51). However, subsea pressure-sensitive pilot valves that are manifolded to a common signal line are used in this design. Rather than discrete control over each individual pilot valve, they are switched in groups according to the signal pressure and the pilot-valve set points. The valves are interconnected so that supply pressure is applied to the subsea tree actuators in a predetermined sequence in response to changes in signal pressure. Up to six combinations of valve operations can be implemented reliably with a single control line and a single supply line. The advantage of this system is its relatively lower cost for

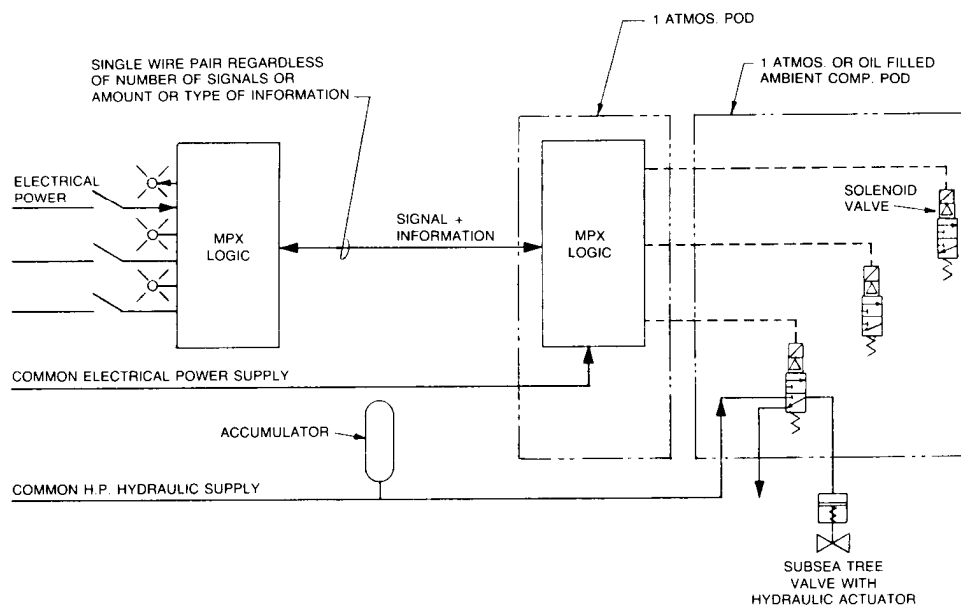


Fig. 18.52—Multiplexed control with hydraulic valve actuators.

hardware and control lines. It has a somewhat slower response than a discrete-piloted hydraulic system, and it is less reliable because it is more complex. The really significant disadvantages, however, are that independent valve control is impossible, there is no ready means of confirming valve operations, and operating sequences must be predetermined before manufacture and installation. Further, the sequence approach offers no means for independent valve control for performing operational tests, troubleshooting or diagnosis, or for changing flow paths through a subsea system in the event of a malfunction.

Multiplexed Electrohydraulic Control

This design (Fig. 18.52) has a single high-pressure hydraulic supply line and an electric cable that, in its simplest form, consists of one pair of signalling wires and one pair of power wires. The limited number of electrical conductors permits the use of inductive couplers rather than the more conventional pin-and-socket connectors. Pin connectors historically have been troublesome in subsea production applications, while inductive couplers have proved to be relatively foolproof. Inductive couplers are easily and reliably remotely mated and unmated subsea, which provides maximum flexibility in hardware layout. Encoding and decoding multiplex logic are provided at the surface and subsea to enable transmission of coded valve-open and valve-close commands and associated status feedback over one pair of single wires. The multiplexed valve commands trigger electric solenoid pilot valves that activate hydraulic-switching valves to direct high-pressure fluid to the tree-valve actuators. The advantages of this system are (1) fastest possible response independent of distance, (2) simplicity of control lines, and (3) total flexibility. With some designs, a totally hydraulic backup system can be included with the multiplexed system at little increase in cost to provide some measure of temporary operability in the event of an electrical failure. The obvious disadvantages of this design are its increased complexity and higher costs.

With a multiplexed electrohydraulic system, a recirculating (closed) subsea hydraulic power unit is also feasible in the control housing. This approach offers the possibility of eliminating the hydraulic supply line if system leakage can be controlled to a very low level. If this design approach is used, some provision still must be made for fluid makeup to account for long-term leakage. The primary advantage is that it allows the use of conventional oil-based hydraulic fluids, thus ensuring maximum life and reliability. The obvious disadvantages are the substantial increase in system complexity and consequent overall lower system reliability.

References

1. Rintoul, B.: "Drilling From The Steel Island," *Pacific Oil World/Annual*, Petroleum Publishers, Brea, CA (Jan. 1980) 73, 18-28.
2. *The Technology of Offshore Drilling, Completion and Production*, ETA Offshore Seminars, Inc., The Petroleum Publishing Co., Tulsa (1976).
3. Silcox, W.H.: "Floating Drilling: The First 30 Years—Part I and Part 2," *J. Pet. Tech.* (Jan. and Feb. 1983).
4. Burke, B.G.: "Downtime Evaluation for Operations from Floating Vessels in Waves," *Proc.*, 1977 Society of Naval Architects and Marine Engineers Second Ship Tech. and Research Symposium, New York City, 279-301.
5. Sheffield, R.: "Floating Drilling: Equipment and Its Use," *Practical Drilling Technology*, Gulf Publishing Co., Houston (1980) 2.
6. "Recommended Practice for Blowout Prevention Equipment Systems," second edition, API RP 53, API, Dallas (Jan. 1984).
7. "The Analysis of Spread Mooring Systems for Floating Drilling Units," latest edition, API RP 2P, API, Dallas.
8. "Design and Operation of Marine Drilling Riser Systems," latest edition, API RP 2Q, API, Dallas.
9. "Recommended Practice for Care and Use of Marine Drilling Risers," latest edition, API RP 2K, API, Dallas.
10. "Recommended Practices for Safe Drilling of Wells Containing Hydrogen Sulfide," latest edition, API RP 49, API, Dallas.
11. "Strengthening for Navigation in Ice," *Rules for Building and Classing Steel Vessels*, latest edition, American Bureau of Shipping, New York City.
12. Bardgett, J.J. and Irick, J.T.: "Construction of the Hondo Platform in 850 Feet of Water," paper OTC 2959 presented at the 1977 Offshore Technology Conference, Houston, May 2-5.
13. Kinra, R.K. and Marshall, P.W.: "Fatigue Analysis of the Cognac Platform," paper OTC 3378 presented at the 1979 Offshore Technology Conference, Houston, April 30-May 3.
14. Tannahill, C.A., Isenhower, W.M., and Engle, D.D.: "Cerveza—A Project Overview of a Deep-Water Platform," paper OTC 4185 presented at the 1982 Offshore Technology Conference, Houston, May 3-6.
15. Goodman, M.A.: *Handbook of Arctic Well Completions*, Gulf Publishing Co., Houston (1978).
16. "U.S. Arctic Oil and Gas," Natl. Petroleum Council, Washington, DC (Dec. 1981).
17. "API Bulletin on Planning, Designing, and Constructing Fixed Offshore Structures in Ice Environments," latest edition, *Bull.* 2N, API, Dallas.
18. Willits, K.L. and Lindsey, W.C.: "Well Completions in the Prudhoe Bay Field," *Pet. Eng. Intl.* (Feb. 1976) 48-56.
19. *Natl. Electrical Code*, latest edition, Natl. Fire Protection Assn., Quincy, MA.
20. "Recommended Practice for Design and Installation of Electrical Systems for Offshore Production Platforms," latest edition, API RP 14F, API, Dallas.
21. USCG Regulation 46 CFR Shipping, Chap. I, Subchapter I-A, "Mobile Offshore Drilling Units," Subchapter J, "Electrical Engineering," U.S. Government Printing Office, Washington, DC, Parts 108 and 110-13.
22. "Recommended Practice for Classification of Areas for Electrical Installations at Drilling Rigs and Production Facilities on Land and on Marine Fixed and Mobile Platforms," latest edition, API RP 500B, API, Dallas.
23. "Standards for Purged and Pressurized Enclosures for Electrical Equipment in Hazardous (Classified) Locations," *Bull.* 496, Natl. Fire Protection Assn., Quincy, MA.
24. "Recommended Practice for Analysis, Design, Installation and Testing of Basic Surface Safety Systems on Offshore Production Platforms," latest edition, API RP 14C, API, Dallas.
25. USCG Regulation 33 CFR, Chap. I, Subchapter N, "Outer Continental Shelf Activities," U.S. Government Printing Office, Washington, DC, Parts 140 through 147.
26. USCG Regulation 30 CFR, Part 250, "Oil and Gas and Sulfur Operations in the Outer Continental Shelf," Minerals Management Service, U.S. Dept. of Interior, Washington, D.C.

Chapter 19

Crude Oil Emulsions

H. Vernon Smith, Meridian Corp.

Kenneth E. Arnold, Paragon Engineering Services Inc.

Introduction

Much of the oil produced worldwide is accompanied by water in an emulsion that requires treating. Even in those fields where there is essentially no initial water production, water cuts may increase in time to the point where it is necessary to treat the emulsion. Water content of the untreated oil may vary from a fraction of 1% to over 90%.

To prevent increased transportation costs, water treatment and disposal costs, and deterioration of equipment, purchasers of crude oil limit the basic sediment and water (BS&W) content of the oil they purchase. Limits vary depending on local conditions, practices, and contractual agreements and typically range from 0.2 to 3.0%. BS&W is usually predominantly water but may contain solids. The solids contained in the BS&W come from the producing formation and consist of sand, silt, mud, scale, and precipitates of dissolved solids. These troublesome solids vary widely from producing field to field, zone to zone, and well to well.

Purchasers may also limit the salt content of the oil. Removing water from the stream decreases the salt content. Salt content along with BS&W are the two important crude purchasing requirements.

When water forms a stable emulsion with crude oil and cannot be removed in conventional storage tanks, emulsion-treating methods must be used. The methods, procedures, equipment, and systems generally used in treating crude oil emulsions are considered in this chapter. Space limitation does not permit the rigorous treatment of crude oil emulsions. Many topics and sub-topics exist on which entire chapters can be written. This chapter contains an abbreviated discussion of only a few of the most important and pertinent considerations of crude oil emulsions. More detailed and diversified discussions on crude oil emulsions can be found in the General References at the end of the chapter.

Theories of Emulsions

Definition of an Emulsion

An emulsion is a heterogeneous liquid system consisting of two immiscible liquids with one of the liquids intimately dispersed in the form of droplets in the second liquid. An emulsion is distinguished from a simple dispersion of one liquid in another by the fact that, in an emulsion, the probability of coalescence of droplets on contact with one another is greatly reduced because of the presence of an emulsifier, which inhibits coalescence. Such inhibition is not present in a dispersion.

The stability of the emulsion is controlled by the type and amount of surface-active agents and/or finely divided solids, which commonly act as emulsifying agents or emulsifiers. As shown in Fig. 19.1, these emulsifying agents form interfacial films around the droplets of the dispersed phase and create a barrier that slows down or prevents coalescence of the droplets.

The matrix of an emulsion is called the external or continuous phase. The portion of the emulsion that is in the form of small droplets is called the internal, dispersed, or discontinuous phase. The emulsions considered in this chapter consist of crude oil and water or brine produced with it.

In most emulsions of crude oil and water, the water is finely dispersed in the oil. The spherical form of the water globules is a result of interfacial tension (IFT), which compels them to present the smallest possible surface area to the oil. This is a water-in-oil emulsion and is referred to as a "normal" emulsion. The oil can be dispersed in the water to form an oil-in-water emulsion, which is referred to as an "inverse" or "reverse" emulsion. A typical reverse emulsion is shown in Fig. 19.2.

Emulsions are sometimes interrelated in a more complex form. The emulsion may be either water-in-oil or oil-in-water to begin with, but additional agitation may



Fig. 19.1—Photomicrograph of water-in-oil emulsion. Observe the rigid-appearing film or skin that retards coalescence.

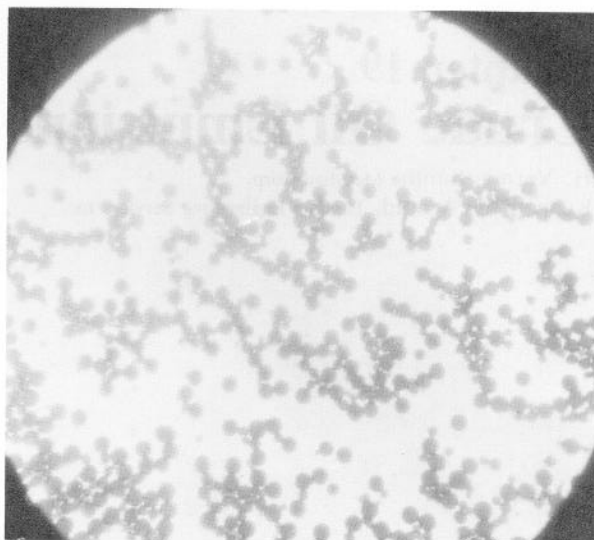


Fig. 19.2—Photomicrograph of reverse emulsion. Uniformly sized oil particles are about 10 μm in diameter and are dispersed in the continuous water phase.

cause it to become multistage. If it is a water-in-oil emulsion initially, a water-in-oil-in-water emulsion can be formed if a small volume of the original water-in-oil emulsion is enveloped in a film of water. It is also possible to form multistage emulsions in an oil continuous phase as shown in Figs. 19.3 and 19.4. This alternating external-phase/internal-phase/external-phase arrangement has been known to exist in eight stages. Multistage emulsions usually add appreciably to the problem of separating the emulsion into oil and water. The more violent the agitation, the more likely multistage emulsions are to form.

How Crude Oil Emulsions Form

The three conditions necessary for the formation of an emulsion are (1) the two liquids forming the emulsion must be immiscible, (2) there must be sufficient agitation to disperse one liquid as droplets in the other, and (3) there must be an emulsifying agent present. Crude oil and water are immiscible. If gently poured into the same container, they will quickly separate. If the oil and water are violently agitated, small drops of water will be dispersed in the continuous oil phase and small drops of oil will be dispersed in the continuous water phase. If left undisturbed, the oil and water will quickly separate into layers of oil and water. If any emulsion is formed, it will be between the oil above and the water below.

When considering crude oil emulsions, we are usually concerned with water-in-oil emulsions because most emulsions are this type. Oil-in-water emulsions are encountered in some heavy oil production, however, such as that

found in areas of Canada, California, Venezuela, and other areas. Oil-in-water emulsions are generally resolved in the same way as water-in-oil emulsions, except electrostatic treaters cannot be used on oil-in-water emulsions.

The agitation necessary to form an emulsion may result from any one or a combination of several sources: (1) the bottomhole pump, (2) flow through the tubing, wellhead, manifold, or flowlines, (3) the surface transfer pump, or (4) pressure drop through chokes, valves, or other surface equipment. The greater the amount of agitation, the smaller the droplets of water dispersed in the oil. Figs. 19.5 through 19.9 show common crude oil emulsions that demonstrate the range of droplet sizes normally encountered. Studies of water-in-oil emulsions have shown that water droplets are of widely varying sizes, ranging from less than 1 to about 1,000 μm . Emulsions that have smaller droplets of water are usually more stable and difficult to treat than those that have larger droplets.

Crude oils vary widely in their emulsifying tendencies. Some may form very stable emulsions that are difficult to separate, while others may not emulsify or may form a loose emulsion that will separate quickly. The presence, amount, and nature of an emulsifying agent determines whether an emulsion will be formed and the stability of that emulsion. If the crude oil and water contain no emulsifying agent, the oil and water may form a dispersion that will separate quickly because of rapid coalescence of the dispersed droplets. On the other hand, if an emulsifying agent is present in the crude oil, a very stable emulsion can be formed.

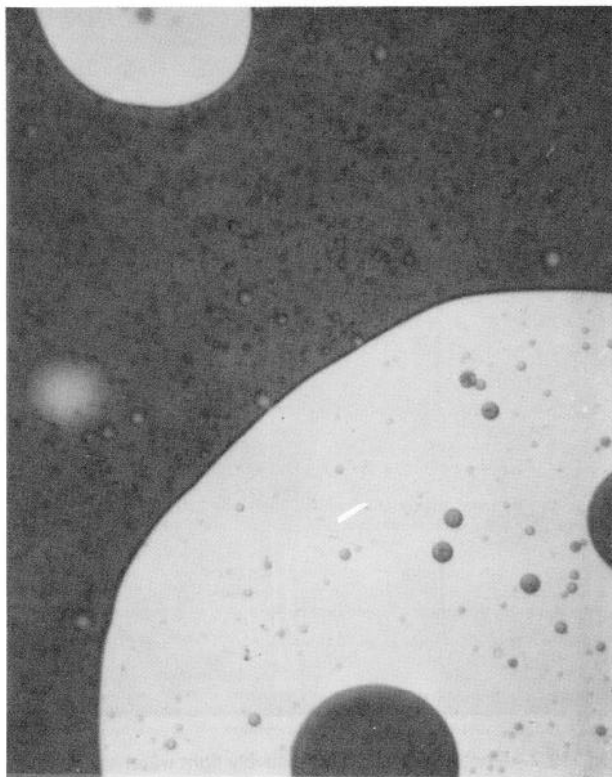


Fig. 19.3—Photomicrograph of oil-in-water-in-oil emulsion. Oil droplets are shown dispersed in water droplets that are dispersed in the continuous oil phase.

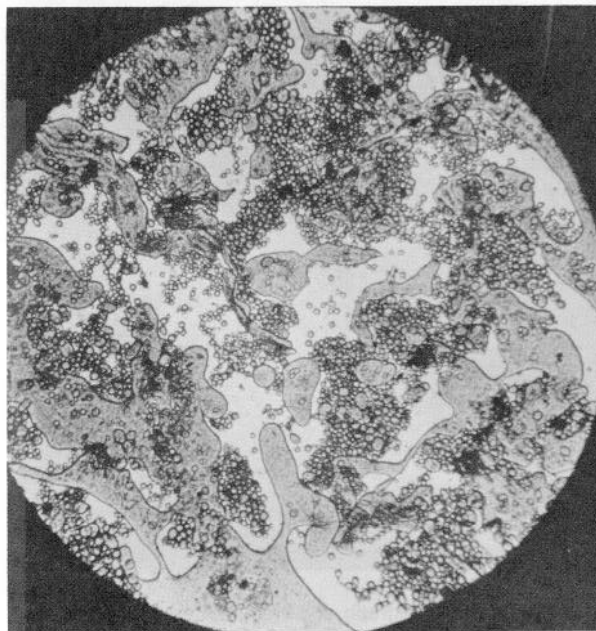


Fig. 19.4—Photomicrograph of multiple-stage emulsion from Rocky Mountain field. The dispersed water phase contains small oil particles.

If an emulsion is not treated, a certain amount of water will separate from the oil by natural coalescence and settling because of the difference in density of oil and water. Unless some form of treatment is used to accomplish complete separation, however, there probably will be a small percentage of water left in the oil even after extended settling. The water that remains in the oil will be in minute droplets that have extremely slow settling velocities. They will be widely dispersed so that there will be little chance for them to collide, coalesce into larger droplets, and settle.

The amount of water that emulsifies with crude oil in most production systems may vary from less than 1 to more than 60% in rare cases. The most common range of emulsified water in light crude oil—i.e., oil above 20° API—is from 5 to 20 vol%. The most common range of emulsified water in crude oil heavier than 20° API is from 10 to 35%.

Emulsifying Agents

Emulsifying agents are surface-active compounds that attach to the water-drop surface and lower the oil/water IFT. When energy is added to the mixture by agitation, the dispersed-phase droplets are broken into smaller droplets. The lower the IFT, the smaller the energy input required for emulsification—i.e., with a given amount of agitation, smaller droplets will form.

There are many theories on the nature of emulsifying agents in crude oil emulsions. Some emulsifiers are thought to be asphaltic in nature. They are barely soluble

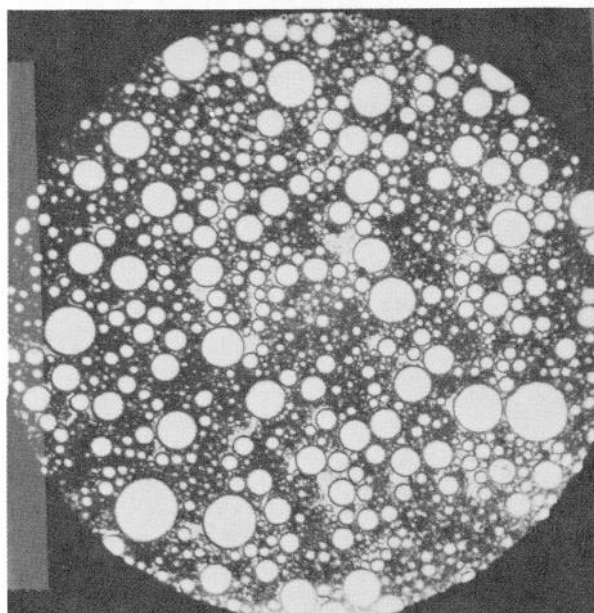


Fig. 19.5—Photomicrograph of loose emulsion from western Kansas containing about 30% emulsified water in the form of droplets ranging in diameter from about 60 μm downward.

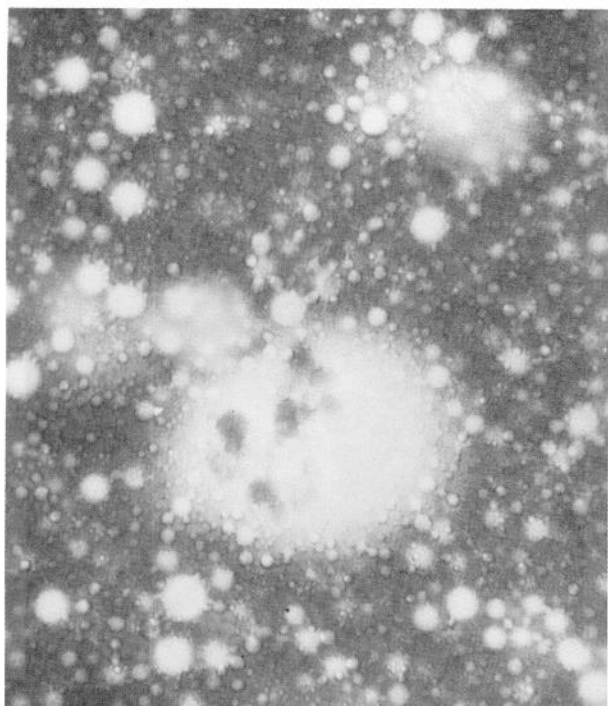


Fig. 19.6—Photomicrograph of water-in-oil emulsion with dispersed particles of water ranging in size from about 250 to about 1 μm .

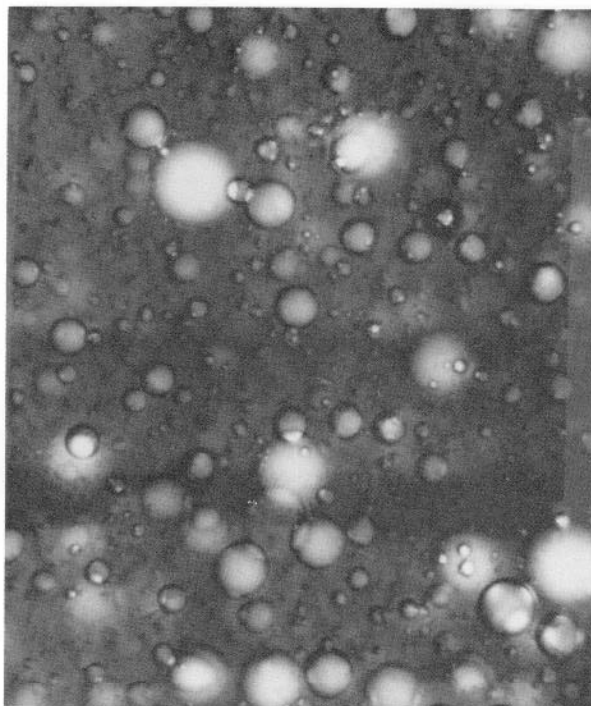


Fig. 19.7—Photomicrograph of relatively tight water-in-oil emulsion. Largest water droplets are about 60 μm , medium droplets are about 40 μm , and the smallest ones are about 1 to 20 μm .

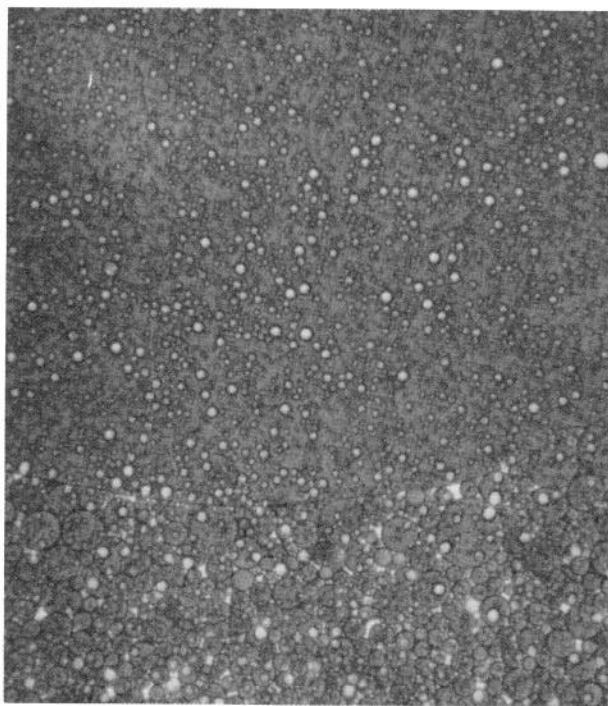


Fig. 19.8—Photomicrograph of tight emulsion with the dispersed water particles varying in size from 1 to 20 μm .

in oil and are strongly attracted to the water. They come out of solution and attach themselves to the droplets of water as these droplets are dispersed in the oil. They form thick films that surround the water droplets and prevent the surfaces of the water droplets from contacting, thus preventing coalescence when the droplets collide.

Oil-wet solids—such as sand, silt, shale particles, crystallized paraffin, iron, zinc, aluminum sulfate, calcium carbonate, iron sulfide, and similar materials—that collect at the oil/water interface can act as emulsifiers. Fig. 19.10 shows some of these solids removed from a crude oil emulsion. These substances usually originate in the oil formation but can be formed as the result of an ineffective corrosion-inhibition program.

Many emulsions are prepared for commercial use. An emulsion of kerosene and water is used for spraying fruit trees; soap is used as the emulsifying agent. Eggs supply the emulsifying agent used in the preparation of mayonnaise from vegetable oil and vinegar. These are very stable emulsions.

Most but not all crude oil emulsions are dynamic and transitory. The interfacial energy per unit of area in petroleum emulsions is rather high compared with familiar industrial emulsions. They are therefore thermodynamically unstable in the sense that if the dispersed water coalesced and separated, the total free energy would decrease. Only the presence of an emulsifier film introduces an energy barrier that prevents the “breaking” or separation process from proceeding.

The characteristics of an emulsion change continually from the time of formation to the instant of complete resolution. This occurs because there are numerous types of

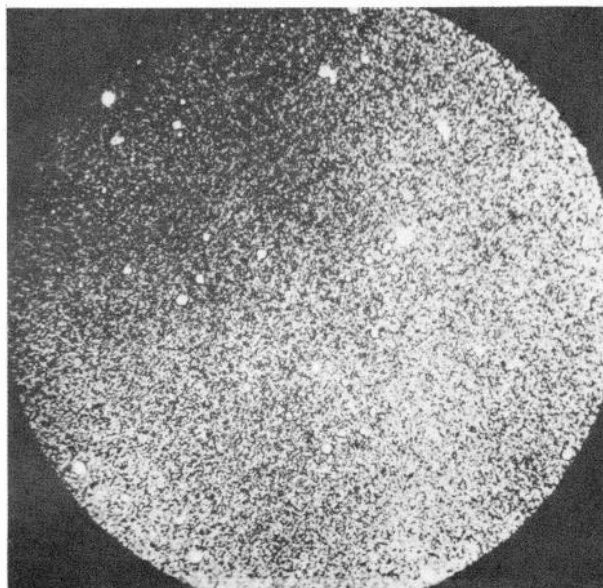


Fig. 19.9—Photomicrograph of tight emulsion from Huntington Beach, CA; water content 20%, with the average water droplet diameter less than 5 μm .

adsorbable materials in a given oil. Also, the adsorption rate of the emulsion and permanence of location at the interface may vary as the fluid flows through the process. Furthermore, the emulsion characteristics are changed as the liquid is subjected to changes in temperature, pressure, and degree of agitation.

Prevention of Emulsions

If all water can be excluded from the oil as it is produced and/or if all agitation of well fluids can be prevented, no emulsion will form. Exclusion of water in some wells is difficult or impossible, and the prevention of agitation is almost impossible. Therefore, production of emulsion from many wells must be expected. In some instances, however, emulsification is increased by poor operating practices.

Operating practices that include the production of excess water as a result of poor cementing or reservoir management can increase emulsion-treating problems. In addition, a process design that subjects the oil/water mixture to excess turbulence can result in greater treating problems. Unnecessary turbulence can be caused by over-pumping and poor maintenance of plunger and valves in rod-pumped wells, use of more gas-lift gas than is needed, and pumping the fluid where gravity flow could be used. Some operators use progressive cavity pumps as opposed to reciprocating, gear, or centrifugal pumps to minimize turbulence. Others have found that some centrifugal pumps can actually cause coalescence if they are installed



Fig. 19.10—Photomicrograph showing a collection of inorganic solids removed from an emulsion by filtering and washing. These solids include calcite, silica, iron compounds, obsidian, and black carbonaceous materials.

in the process without a downstream throttling valve. Wherever possible, pressure drop through chokes and control valves should be minimized before oil/water separation.

Color of Emulsions

The color of a crude oil emulsion can vary widely, depending on the oil and water content of the emulsion and the characteristics of the oil and water. The most common color of emulsions is a dark reddish brown. However, any color from light green or yellow to grey or black may be found. "Brightness" is an indicator of the presence of an emulsion. Oil-free water and water-free oil are clear and bright. Emulsions are murky and opaque because of reflection and scattering of light at the oil/water interfaces of the dispersed phase. The greater the total interfacial area between the oil and water, the lighter the color of the emulsion. That is, an emulsion containing many small droplets of water will tend to be lighter than one containing an equal volume of water in larger droplets because the latter has less total interfacial surface area.

Stability of Emulsions

Generally, crude oils with low API gravity (high density) will form a more stable and higher-percentage volume of emulsion than will oils of high API gravity (low density). Asphaltic-based oils have a tendency to emulsify more readily than paraffin-based oils. High-viscosity crude oil

will usually form a more stable emulsion than low-viscosity oil. Emulsions of high-viscosity crude oil usually are very stable and difficult to treat because the viscosity of the oil hinders or prevents movement of the dispersed water droplets and thus retards their coalescence. In addition, high-viscosity/high-density oils usually contain more emulsifiers than lighter oils.

Effect of Emulsion on Viscosity of Fluids

Emulsions are always more viscous than the clean oil contained in the emulsion. The ratio of the viscosity of an emulsion to the viscosity of the clean crude oil in oilfield emulsions depends on the shear rate to which it has been subjected. The authors have found that for many emulsions and the shear rates normally encountered in piping systems, this shear rate can be approximated by the following equation if no other data are available.

$$\mu_e/\mu_o = 1 + 2.5f + 14.1f^2, \dots\dots\dots (1)$$

where

- μ_e = viscosity of emulsion,
- μ_o = viscosity of clean oil, and
- f = fraction of the dispersed phase.

Sampling and Analyzing Crude Oil Emulsions

Purchasers of crude oil have established certain specifications that must be met before they will accept oil from a producer. These specifications limit the amount of BS&W in the oil. The limitations are usually strict, and if the amount of BS&W in the oil exceeds the specified limit, the oil may not be accepted by the purchaser. The seller and buyer must agree on the procedure for sampling and analyzing the oil to provide consistent and mutually acceptable data.

The performance of emulsion-treating units or systems can be observed and studied by the practice of regularly and periodically withdrawing and analyzing samples of the contents at multiple levels in the vessels or multiple points in the systems. This is particularly beneficial in treating emulsions involving viscous oils. Samples of emulsions should be representative of the liquid from which they are taken. Emulsification should not occur when the sample is extracted. Samples obtained at the wellhead, manifold, or oil and gas separator may show a high percentage of emulsion, but the oil and water in the system may actually not be emulsified. This indicates that emulsification occurred because of the turbulence created as the sample was removed from the pressure zone to the sample container.

It is possible to take a sample from a pressure zone without further emulsification of the liquids if the velocity of the discharging liquid is controlled. One method is to use a piece of small-diameter tubing approximately 10 to 15 ft long. One end of the tubing is connected to a bleeder valve on the line or vessel from which the sample is to be extracted, and the other end is connected to the sample container. The bleeder valve should be opened fully and the sample allowed to flow through the small-diameter tubing into the container. The pressure drop from

the line to the container is absorbed by flow through the tubing. Flow through the tubing, however, can cause either coalescence or additional emulsification.

Another method of withdrawing a representative sample of emulsion is to use a sample container initially filled with water. The sample container is equipped with valves at the top and bottom with the top valve connected to the point from which the sample is to be extracted. The top valve of the container is opened first and the container pressured from the line. The valve at the bottom of the container is then opened and the water discharged into the atmosphere as the sample enters the container. There will be no emulsification in the container because there is no pressure drop between the source and sample container to cause turbulence. Once the sample is taken, pressure can be bled off through a third valve with little effect on the sample.

Small centrifuges are used to determine BS&W content of crude oil. The centrifuges may be driven by hand or electric motor. A small measured volume of sample is diluted with solvent and placed in graduated glass containers. These are then inserted into the centrifuge and rotated at high speed for a few minutes. Separation of the oil, water, and solids is accomplished by centrifugal force. The percentages of each constituent can be read directly from the graduated containers in which the sample is centrifuged. The speed used in these small centrifuges varies from 2,000 to 4,000 rev/min.

Methods of taking and analyzing samples of crude oil for custody transfer are included in the *API Manual of Petroleum Measurement Standards*. Also see Chap. 17.

Methods Used in Treating Crude Oil Emulsions

Three basic steps usually are required to separate a crude-oil/water emulsion into bulk phases of oil and water.

Step 1—Destabilization. An emulsion is destabilized by counteracting the stabilizing effect of the emulsifier. The tough skin or film surrounding the dispersed water droplets must be weakened and broken. This is usually accomplished by adding heat and/or a properly selected, interfacially active chemical compound to the emulsion.

Step 2—Coalescence. After the films encasing the dispersed droplets are broken, the dispersed droplets must coalesce into drops large enough to settle out of the continuous phase of oil. Fig. 19.11 shows a small droplet of water breaking through a destabilized emulsion film to coalesce with the bigger drop. This usually is accomplished by imposing a period of moderate agitation or by subjecting the destabilized emulsion to an alternating electric field. This will increase the dispersed droplets contacting rate. Thus coalescence will increase, resulting in larger droplets.

Step 3—Gravity Separation. A quiet period of settling must be provided to allow the coalesced drops to settle out of the oil because of the difference in density between the water and oil. This is accomplished by providing a sufficient residence time and a favorable flow pattern in a tank or vessel that will allow the coalesced drops of water to separate from the oil.

Another way of stating the general emulsion-treating procedure is that to resolve a crude-oil/water emulsion into bulk oil and water three things must be done:

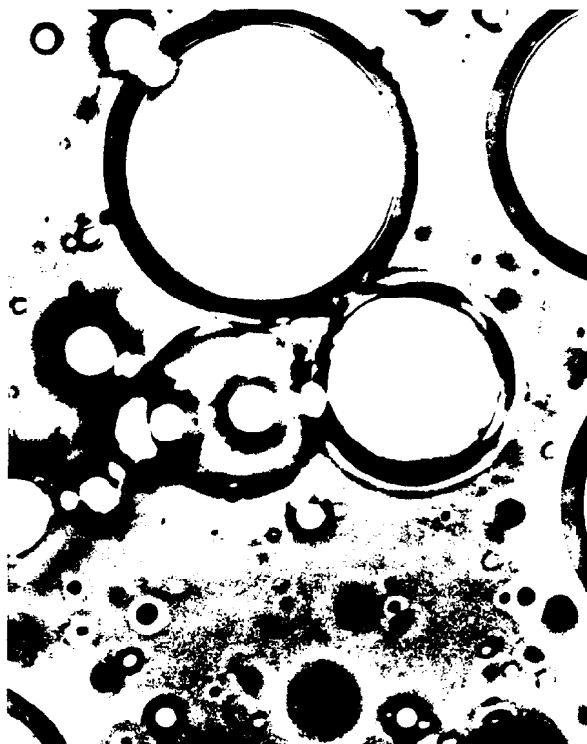


Fig. 19.11—A water-in-oil emulsion with the film or skin surrounding the water droplet in the process of rupturing.

(1) increase the probability of coalescence of dispersed water droplets on contact, (2) make the rate of contact of dispersed water droplets high without creating high shear forces, and then (3) allow the liquids to settle quietly so that they can separate into bulk phases of oil and water. All the incidental variables, such as selection of proper chemical, rate of chemical injection, treating temperature and pressure, oil and emulsion viscosity, flow rate, vessel design, vessel size, and fluid levels, are controlled to execute these three steps in the quickest and most economical manner.

An emulsion-treating unit or system will use one or more of the methods in Table 19.1 to aid in destabilizing, coalescence, and/or settling. Each of these treating methods that can be used to resolve an emulsion is discussed separately.

Heating

The use of heat in treating crude oil emulsions has four basic benefits.

1. Heat reduces the viscosity of the oil, resulting in a greater force during collision of the water droplets. Also, the reduced oil viscosity allows the water droplets to settle more rapidly through the less viscous oil. Fig. 19.12 can be used to estimate crude oil viscosity/temperature relationships. Viscosities vary widely from one crude to another. The curves should be used only in the absence of specific data. If the viscosity of the crude is known at two temperatures, the viscosity at other temperatures can be approximated by a straight line. If the viscosity is known at one temperature, it can be approximated at

TABLE 19.1—METHODS TO AID DESTABILIZATION, COALESCENCE, AND/OR SETTLING

Destabilization
Chemical
Heating
Coalescence
Agitation
Coalescing plates
Electric field
Water washing
Filtering
Fibrous packing
Heating
Retention time
Centrifugation
Gravity Separation
Gravity settling
Heating
Centrifugation

other temperatures by drawing a straight line parallel to the others. If the viscosity is unknown at any temperature, the lines on the chart may be used. API Spec. 12L recommends that crude be heated so that its viscosity is below 150 SSV (about 50 cSt) for treating.

2. Heat increases the droplets' molecular movement. This aids in coalescence through increased collision frequency of the dispersed-phase droplets.

3. Heat may deactivate the emulsifier (e.g., dissolving paraffin crystals) or it can enhance the action of treating chemicals, causing the chemical to work faster and more thoroughly to break the film surrounding the droplets of the dispersed phase of the emulsion.

4. Heat may also increase the difference in density between the oil and the water, thus accelerating settling. In general, at temperatures below 180°F, the addition of heat will increase the difference in density. Most light oils are treated below 180°F; thus the effect of heat on gravity is beneficial. For heavy crudes (below 20° API), which normally are treated above 180°F, heat may have a negative effect on difference in density. In special cases, increased heat may cause the density of water to be less than that of oil. This effect is shown in Fig. 19.13.

Heating well fluids is expensive. Adding heat can cause a significant loss of the lower-boiling-point hydrocarbons (light ends). This results in "shrinkage" of the oil, or loss of volume. Because the light ends are boiled off, the remaining liquid has a lower API gravity and thus may have a lower value. Figs. 19.14 and 19.15 illustrate typical gravity and volume losses for 33° API crude vs. temperature. The molecules leaving the oil phase may be vented or compressed and sold with the gas. Even if they are sold with the gas, there probably will be a net loss in income.

The gas liberated when crude oil is treated may also create a problem in the treating equipment if the equipment is not properly designed. In vertical emulsion treaters and gun barrels, some gas may rise through the coalescing section. The liberated gas can create enough turbulence and disturbance to inhibit coalescence. Perhaps more important, the small gas bubbles have an attraction for surface-active material and hence for the water droplets; thus they have a tendency to keep the water droplets from settling and even may cause them to be discharged with the oil.

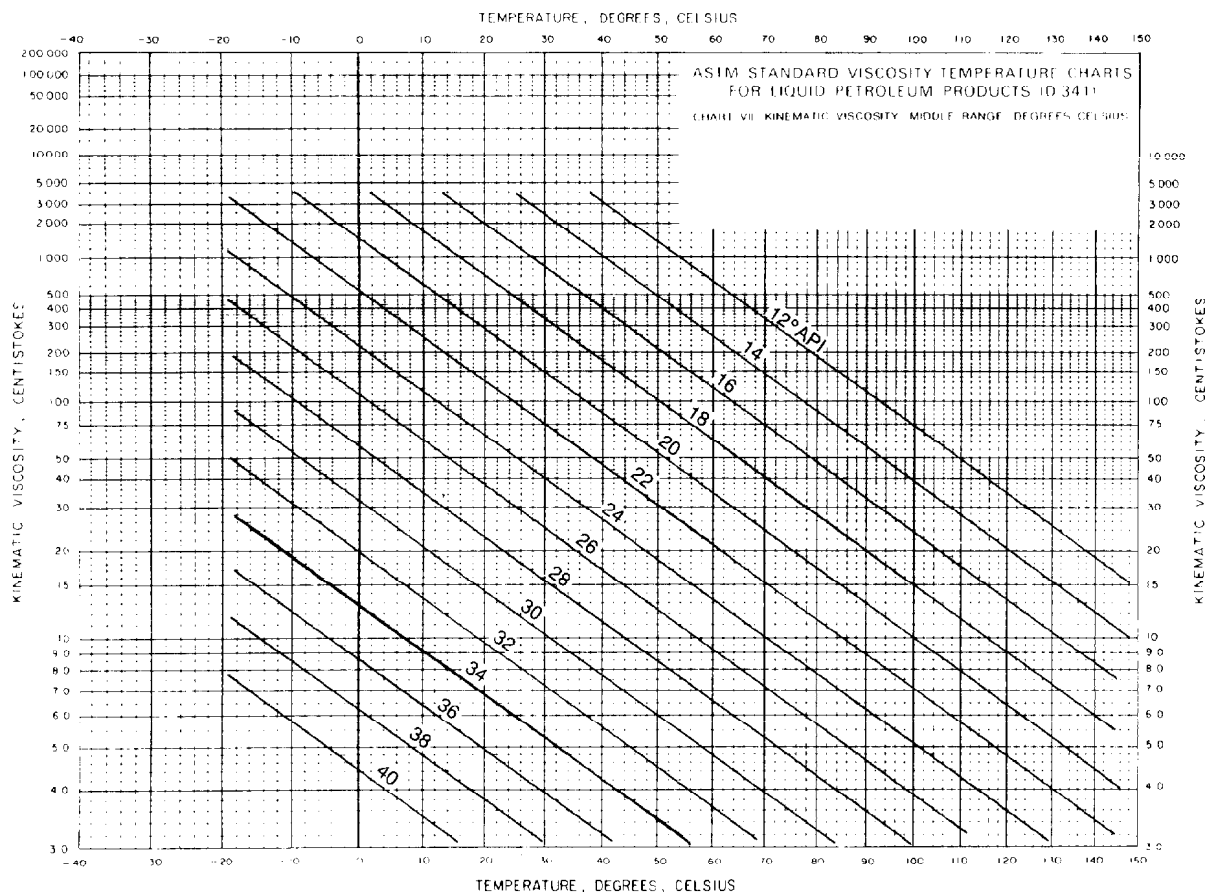


Fig. 19.12—Approximate viscosity/temperature relationships for crude oil.

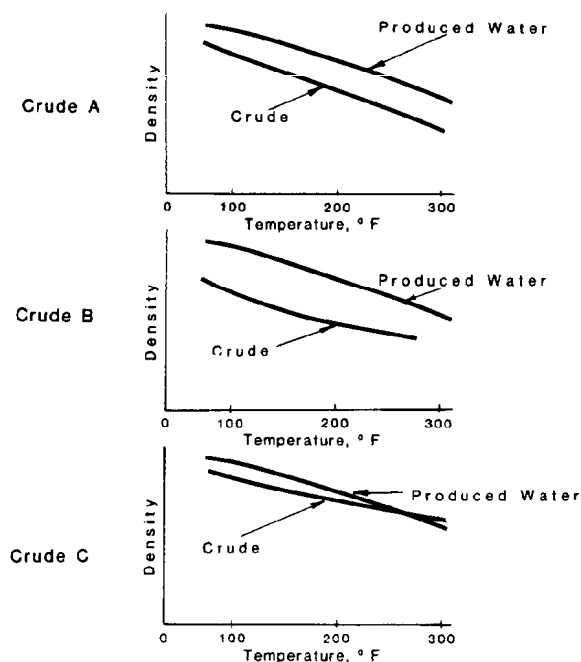


Fig. 19.13—Relationship of specific gravity with temperature for three crude oils.

Fuel is required to provide heat, and the cost of fuel must be considered. If the oil is much above ambient temperature when discharged from the treating unit, it can be flowed through a heat exchanger with the incoming well fluid to transfer the heat to the cooler incoming well fluid. This will minimize evaporation losses and reduce fuel cost. It will also increase the vapor pressure of the crude, however, which may be limited by contract.

If properly applied, heating an emulsion can have great beneficial effect on water separation. The most economical emulsion treating may be obtained by use of less heat and a little more chemical, agitation, and/or settling space.

In some geographic areas, emulsion heating requirements vary in accordance with daily and/or seasonal atmospheric temperatures. Emulsions are usually more difficult to treat when it is cool—at night, during a rain, or in winter months when the atmospheric temperatures are lowest. Treatment, especially heating, may not be required in warmer summer months. Where the treating problem is seasonal, some emulsions can be resolved successfully by addition of more chemical demulsifiers during winter months. Study is required to determine the proper economic balance of heat and chemicals.

Crude oil emulsions with similar viscosity ranges do not always require the same type of treating equipment or the same treating temperature. Emulsions produced

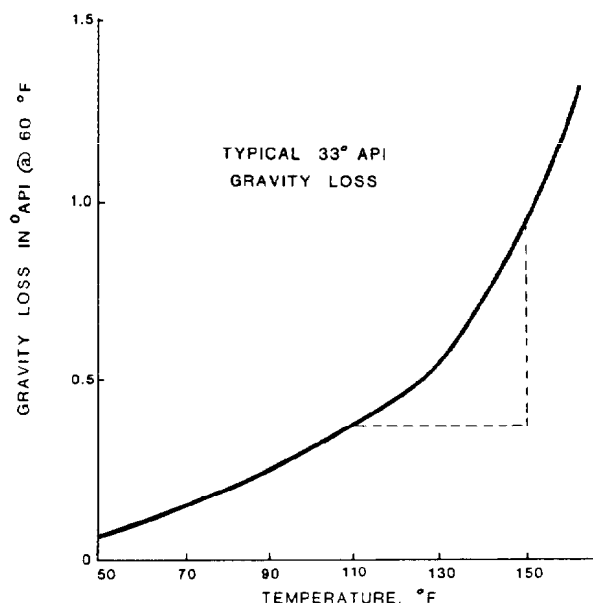


Fig. 19.14—API gravity loss vs. temperature for crude oil.

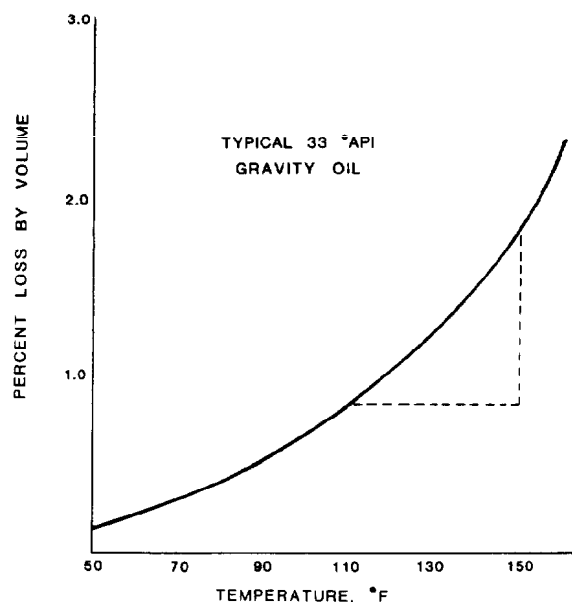


Fig. 19.15—Percent loss by volume vs. temperature for crude oil.

from different wells on the same lease or from the same formation in the same field may require different treating temperatures. For this reason, it is recommended that low treating temperatures be tested so that the lowest practical treating temperature for each emulsion and treating unit or system can be determined by trial.

The heat input and thus the fuel required for treating depends on the temperature rise, amount of water in the oil, and the flow rate. It requires about twice as much energy to heat a given volume of water as it does to heat the same volume of oil. For this reason, it is beneficial to separate free water from the emulsion to be treated. Often this is accomplished in a separate free-water knock-out vessel upstream of the point where heat is added. Sometimes it is accomplished in a separate section of the same vessel.

The required heat input for an insulated vessel (heat loss is assumed to be 10% of heat input) can be approximated from

$$Q = 16\Delta T(0.5q_o\gamma_o + q_w\gamma_w), \quad (2)$$

where

- Q = heat input, Btu/hr,
- ΔT = increase in temperature, °F,
- q_o = oil flow rate, B/D,
- q_w = water flow rate, B/D,
- γ_o = specific gravity of oil, and
- γ_w = specific gravity of water.

Chemical Demulsifiers

Certain chemical compounds are widely used to destabilize and to assist in coalescence of crude oil emulsions. These are referred to as dehydration chemicals or demulsifiers. This treatment method is popular because the

chemicals are easily applied to the emulsion, usually are reasonable in cost, and usually minimize the amount of heat and settling time required.

The chemical counteracts the emulsifying agent, allowing the dispersed droplets of the emulsion to coalesce into larger drops and settle out of the matrix. For demulsifiers to work, they must (1) be injected into the emulsion, (2) intimately mix with the emulsion and migrate to all of the protective films surrounding all of the dispersed droplets, and (3) displace or nullify the effect of the emulsifying agent at the interface. A period of continued moderate agitation of the treated emulsion to produce contact between and coalescence of the dispersed droplets and a quiet settling period must exist to allow separation of the oil and water.

Four actions are required of a chemical demulsifier.

Strong attraction to the oil/water interface. The demulsifier must have ability to migrate rapidly through the oil phase to reach the droplet interface where it must counteract the emulsifying agent.

Flocculation. The demulsifier must have an attraction for water droplets with a similar charge and bring them together. In this way, large clusters of water droplets gather, which look like bunches of fish eggs under a microscope.

Coalescence. After flocculation, the emulsifier film is still continuous. If the emulsifier is weak, the flocculation force may be enough to cause coalescence. This is not true in most cases, and the demulsifier must therefore neutralize the emulsifier and promote rupture of the droplet interface film. This allows coalescence to occur. With the emulsion in a flocculated condition, the film rupture results in growth of water drop size.

Solids Wetting. Iron sulfides, clays, and drilling muds can be made water-wet, causing them to leave the interface and be diffused into the water droplets. Paraffins and

asphaltenes can be dissolved or altered by the demulsifier to make their films less viscous, or they can be made oil-wet so that they will be dispersed in the oil.

The demulsifier selection should be made with all functions of the treating system in mind. If the process is a settling tank, a relatively slow-acting demulsifier can be applied with good results. On the other hand, if the system is an electrostatic process, where some of the flocculation and coalescing action is accomplished by the electric field, there is need for a quick-acting demulsifier. Time for demulsifier action in a vertical emulsion treater normally will be somewhere between that of a settling tank and that of an electrostatic treater.

As field conditions change and/or the treating process is modified, the chemical requirements may change. Seasonal changes may cause paraffin-induced emulsion problems. Well workovers may change solids content, which may alter emulsion stability. So no matter how satisfactory a demulsifier is, it cannot be assumed that it will always be satisfactory over the life of the field.

While the first commercial emulsion-treating chemical was a solution of soap, present-day chemicals are based on highly sophisticated materials. Chemical emulsion breakers are complex organic compounds with surface-active characteristics. The active properties may be derived from any one or a combination of nonionic, cationic, and anionic materials. Within each of these types, compositions are used that will confer various degrees of hydrophobe/hydrophile balance to the chemical as desired. The active components are highly viscous and sometimes even solids. It is necessary to use a carrier that will make handling easier; this carrier is almost without exception an organic solvent. Solvent systems are designed to make emulsion breakers compatible with the crude oil system in which they are used. It is also necessary to omit materials that will interfere with refining processes, such as those that will poison catalysts. Therefore, no organic chlorides, bromides, iodides, fluorides, or compounds of arsenic or lead are used in the manufacture of most emulsion-treating chemicals.

There is no simple designation of specific chemicals to treat specific emulsions. There are, however, certain common demulsifier types that tend to produce a consistent reaction in many water-in-oil emulsions. Some of the demulsifier types are as follows.

Polyglycol esters are characterized by quick brightening of emulsions, but frequently tend toward slow water drop and sludging; they are subject to overtreating problems.

Low-molecular-weight resin derivatives tend toward rapid water drop and fair to good overall demulsification properties; they show some tendency toward overtreatment in high-API-gravity emulsions.

High-molecular-weight resin derivatives generally have a strong wetting tendency and fair brightening and water-drop characteristics; they are always used in combination with other materials.

Sulfonates exhibit fair to good wetting and water-drop performance, some ability to brighten oil, and very little tendency to overtreat, particularly in high-gravity emulsions.

Polymerized oils and esters produce specific characteristics on particular emulsions; they are generally poor for widespread application and are always used in combination with other materials.

Alkanolamine condensates promote water drop in some emulsions and may produce some brightening; they are blended with other materials for overall good performance.

Oxyalkylated phenols are predominantly wetting agents with fair to poor demulsification properties; they are used in blending to improve demulsifier performance.

Polyamine derivatives produce good brightening characteristics and are good blending agents; they are relatively poor in other respects.

There are many specific variations within each of these broad categories. Most demulsifiers used in breaking crude oil emulsions are blends of the above and other compounds. The components selected for a given demulsifier are chosen to provide the necessary actions to achieve complete emulsion treatment. The number of different surface-active materials that can act as emulsifiers in crude oil is large. The possible combinations of these emulsifying agents is almost infinite. Therefore, the number of demulsifiers and their combinations must likewise be numerous to treat the emulsions. The type and composition of the crude oil in the emulsion being treated has more influence on how a certain chemical demulsifier will perform than does the specific category of components included in the treating chemical. For example, a low-molecular-weight resin used in treating an emulsion of 35°API oil may exhibit rapid water drop, but that same chemical, when used in treating an emulsion of 15°API oil, may not cause rapid water drop. This illustrates that demulsifying chemicals must be compounded for each particular emulsion.

Each treating system must be tested and checked to ensure that the chemicals used for treating the water for disposal do not conflict with chemicals used for treating the oil emulsion. One chemical must not react with the other to cause problems, such as stabilizing the oil in the water. Compatibility of the two chemicals must be tested by bottle tests and then by field tests in the actual treating system. Also, compatibility tests should be performed for any other chemicals added to the produced fluids.

Selection of the optimum chemical to use usually starts with bottle tests. A representative sample of fluid is taken and transferred into several test bottles. Several demulsifying chemicals are added to the test bottles in various amounts to determine which chemical will best break the emulsion. Additional tests are made to determine the optimum ratio of chemical to fluid. Several series of tests may be necessary at various ratios and temperatures before a selection can be made. Many factors—such as the color and appearance of the oil, clarity of the water, interface quality, required operating temperature, settling time, and BS&W content—are observed during these bottle tests.

Bottle tests can be made with the samples of emulsion taken at the wellhead, anywhere in the flowline, at the manifold, or at the entrance to the treating system or tank. Well-equipped mobile laboratories are available, so this type of work can be done in the field. These mobile units should be operated by trained technicians who can minimize testing and optimize selection of chemical demulsifiers.

After the bottle tests are made and the best two or three chemicals have been selected, they should be field tested in the treating system to verify that the best chemicals have been selected. Tests should be made in the treating sys-

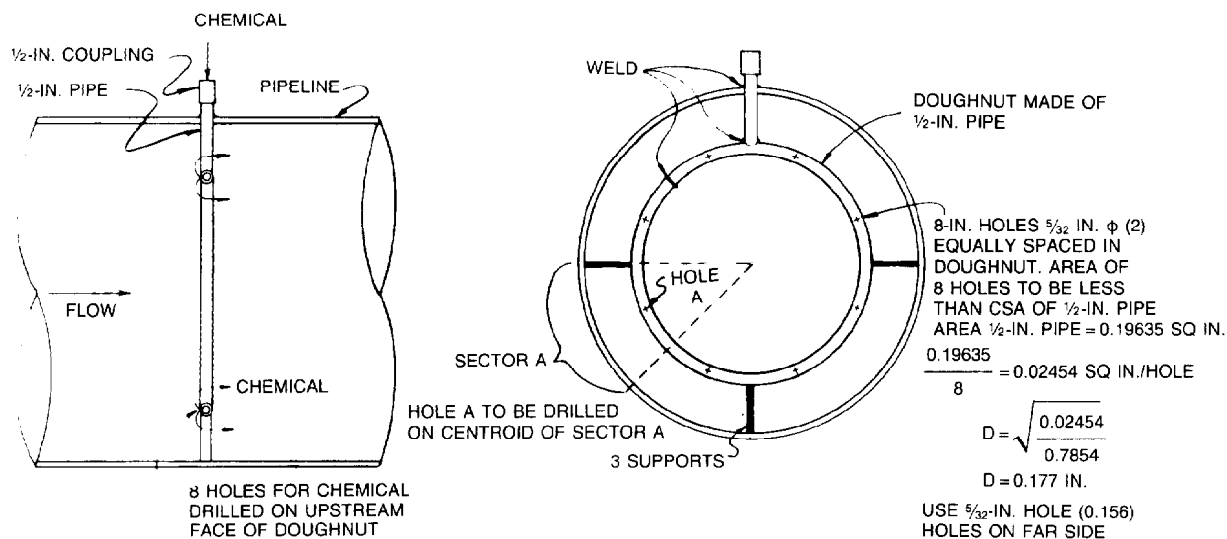


Fig. 19.16—Chemical distributor for flowlines 10 in. and larger.

tem at various concentrations, operating temperatures, settling times, degrees of mixing, etc., before the final selection is made on the basis of performance and cost. The optimum chemical is one that will provide the clearest, cleanest separation of water from oil at the lowest temperature in the shortest time at the lowest cost per barrel treated and that will not interfere with subsequent deoiling of the water.

The required concentration of demulsifying chemical may be as high as 8 gal/1,000 bbl (about 200 ppm) or as low as 1 gal/5,000 bbl (about 5.0 ppm). This is a range of 40 to 1. The most common range of chemical injection is between 10 and 60 ppm.

Application of heat to an emulsion after a demulsifier has been mixed with it increases effectiveness of the chemical by reducing the viscosity of the emulsion and facilitating more intimate mixing of chemical with emulsion. Chemical reaction at the oil/water interface takes place at a more rapid rate at higher temperatures.

The point of injection of demulsifier chemical into the emulsion is important. The chemical should be injected into the emulsion and mixed with it so that it is evenly and intimately distributed throughout the emulsion when it is heated, coalesced, and settled in the treating system. The demulsifying chemical should be injected in a continuous stream, with the chemical volume directly proportional to the emulsion volume. Certain demulsifiers should not be present in the emulsion during excessively prolonged agitation because the beneficial effect of the demulsifier may be spent or counteracted by the agitation and re-emulsification may occur.

Turbulence accelerates the diffusion of the demulsifier throughout the emulsion and increases the number and intensity of impacts between water droplets. Turbulence must be prolonged for a sufficient time to permit the chemical to reach the interface between the oil and all the dispersed water droplets, but the intensity and duration of the turbulence must be controlled so that it will not cause further emulsification. Turbulence is the dynamic factor that disperses the water in the oil and is a prerequisite

to emulsion formation. A moderate level of controlled turbulence, however, causes the dispersed droplets to collide and coalesce. Usually, this turbulence is provided by normal flow in surface lines, manifolds, and separators and by flow through the emulsion-treating unit or system.

One way of assisting in dispersing the chemical throughout the entire volume of emulsion is to mix a small volume of chemical with a diluent and then to inject and mix the diluted chemical with the emulsion. The larger volume of the mixture may make it possible for the chemical to be more uniformly and intimately mixed with the emulsion.

When flow rates are low (less than 3 ft/sec) or when laminar flow is encountered, the injection of chemical into a coupling welded in the side of the pipe is not recommended. In such cases, an injection quill (which injects the chemical in the stream at a location removed from the wall), a chemical distributor (Fig. 19.16), and/or a kinetic mixer (Fig. 19.17) is recommended. The kinetic mixer consists of a series of staggered, helically convoluted vanes that use the velocity of the fluid to accomplish mixing.

When a tank of wet oil (oil containing more than the permissible amount of water) accumulates, the tank contents can be treated by adding a small proportion of demulsifier, agitating or circulating the tank contents, and then allowing time for the water to settle in the tank. Trailer-mounted units that include a heater, circulating pump, and chemical injector are sometimes used for this method of tank treating. This batch-treatment method normally is used as an emergency measure.

Excessive amounts of treating chemical can result in increased stability of the water-in-oil emulsion or of the oil-in-water emulsion in the produced water, increase the stability or the volume of the interfacial emulsion and/or sludge, or waste money equal to the cost of the excessive volume of chemical over the optimum volume. Also, the cost of handling and injecting the excessive amount of chemical must be considered along with the purchase cost of the chemical. Insufficient treating chemical can fail to

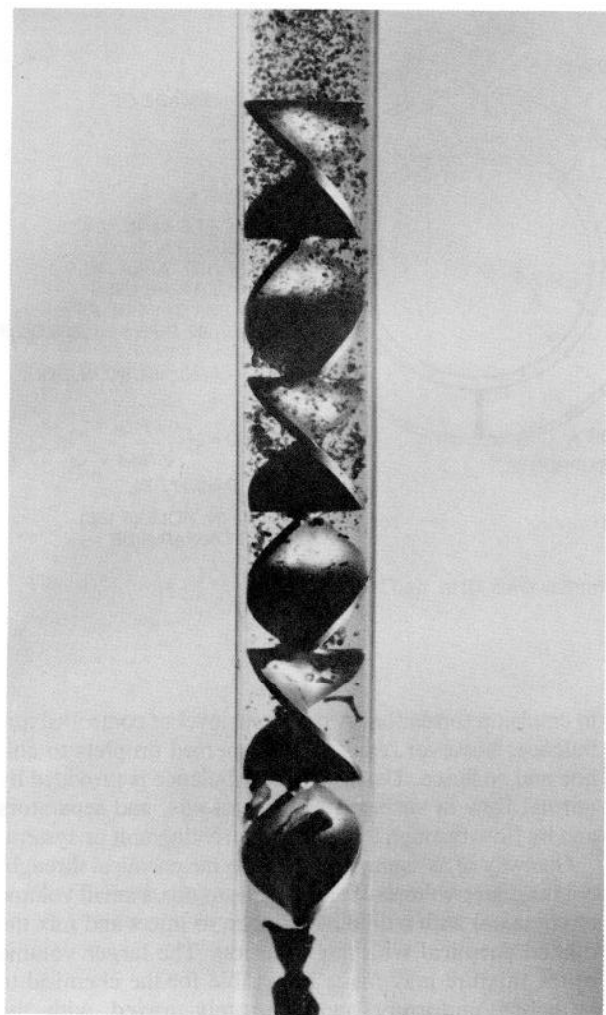


Fig. 19.17—Kinetic (static) mixer for mixing chemical demulsifier with emulsion.

break the emulsion; allow a quick buildup of excessive amounts of emulsion and/or sludge; and result in a need for excessive heat to break the emulsion, a need for excessive settling time to resolve the emulsion, reduced capacity of the treating equipment, excessive water remaining in the crude oil causing accumulation of unsalable oil and the resultant cost of retreating the crude, or more difficulty in removing oil from the produced water.

Agitation

Agitation or turbulence is necessary to form a crude oil emulsion. When turbulence is controlled, however, it can assist in resolving the emulsion. Agitation causes increased collisions of dispersed particles of water and increases the probability that they will coalesce and settle from the emulsion. Caution should be exercised to prevent excessive agitation that will result in further emulsification instead of resolving the emulsion. If the turbulence is kept to moderate Reynolds numbers of 50,000 to 100,000, good coalescing conditions usually should be achieved.

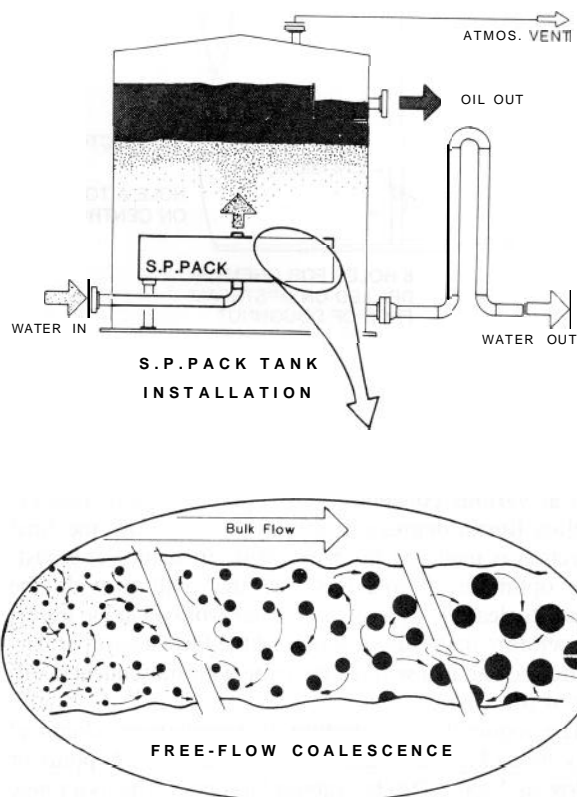


Fig. 19.18—The S. P. Pack™ grows a larger drop size on the inlet separator of a gravity settler.

The flow of emulsions at moderate Reynolds numbers through long pipelines has been shown to cause coalescence and develop droplets that exceed 1,000 μm in diameter. The length of the pipeline required to obtain coalescence can be dramatically decreased by using a defined flow path as in the special flow coalescing device shown in Fig. 19.18.

The demulsification process may be assisted by the use of baffle plates placed inside the treating vessel. Properly designed and located baffle plates can evenly distribute emulsion in a vessel and cause gentle agitation that may bring about collisions of dispersed water particles to aid in coalescing the droplets. Excessive baffling should be avoided because it can cause excessive turbulence, which may result in increased emulsification and impede water-droplet settling. Special baffling in the form of perforated plates properly placed inside treating vessels affords surfaces upon which water droplets in the emulsion may coalesce. As the emulsion flows through the perforations, slight agitation in the form of eddy currents is created, causing coalescence. If the perforations are too small, however, shearing of the water droplets can occur, resulting in a tighter emulsion.

Other designs of baffle plates provide coalescing surfaces for the water droplets, as shown in Fig. 19.19. Flow through the plates is laminar, but directional changes enable the water droplets to contact the plates and coalesce. Such a device may plug easily and become inoperable quickly.

Electrostatic Coalescing

The small water drops dispersed in the crude oil can be coalesced by subjecting the water-in-oil emulsion to a high-voltage electrical field. When a nonconductive liquid (oil) containing a dispersed conductive liquid (water) is subjected to an electrostatic field, the conductive particles or droplets are caused to combine by one of three physical phenomena.

1. The water droplets become polarized and tend to align themselves with the lines of electric force. In so doing, the positive and negative poles of the droplets are brought adjacent to each other. Electrical attraction brings the droplets together and causes them to coalesce.

2. The water droplets are attracted to an electrode because of an induced electric charge. In an AC field, because of inertia, small droplets vibrate a greater distance than larger droplets, promoting coalescence. In a DC field, the droplets tend to collect on the electrodes, forming larger and larger droplets until eventually they settle by gravity.

3. The electric field tends to distort and thus to weaken the film of emulsifier surrounding the water droplets. Water droplets dispersed in oil subjected to a sinusoidal alternating-current field will be elongated along the lines of force as voltage rises during the first half-cycle. As they are relaxed during the low-voltage portion, the surface tension pulls the droplets back toward spherical shape. The same effect is obtained in the next half of the alternating cycle. The weakened film is thus more easily broken when droplets collide.

Whatever the actual mechanism, the electrical field causes the droplets to move about rapidly in random directions, which increases the chances of collision with other droplets. When droplets collide with the proper velocity, coalescence occurs. The greater the voltage gradient, the greater the forces causing coalescence. Experimental data show, however, that at some voltage gradient, the water droplet can be pulled apart and a tighter emulsion can result. For this reason, electrostatic treaters normally are equipped with a mechanism for adjusting the voltage gradient in the field.

If the quantity of water in the oil is large there is a tendency for the formation of a chain of charged water particles, which may form links between the two electrodes, causing short-circuiting. This is referred to as "chaining" and has been observed in emulsions containing 4% or less water. The short-circuit releases a burst of electrical energy that immediately causes this chain of water particles to become steam. The resulting explosions sound like popping popcorn. If chaining occurs, the voltage gradient is too large (i.e., the electrical grids of the electrostatic treater are too close together or the voltage is too high) for the amount of water being handled. Small amounts of gas breaking out of solution may also create sufficient turbulence and impede the coalescing process.

Water-Washing

In some emulsion-treating vessels, separation of liquids

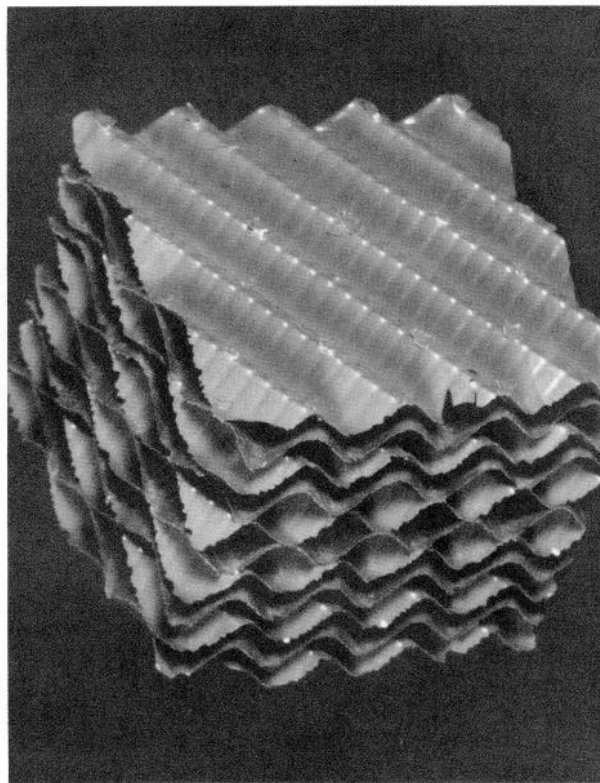


Fig. 19.19—Performax™ plate pack, a special coalescing medium for crude oil emulsions.

and vapors takes place in the inlet diverter, flume, or gas boot located at the top of the vessel. The liquid flows by gravity to the bottom of the vessel through a large conductor pipe or conduit. A spreader plate on the lower end of the conduit spreads the emulsion into many small streams or rivulets that move upward through the water, accomplishing a water-wash. After the emulsion has passed through the water-wash, it flows to the upper portion of the vessel, where the coalesced water droplets settle out of the oil by gravity separation.

If an emulsion is flowed through an excess of the internal phase of the emulsion, the droplets of the internal phase will tend to coalesce with the excess of the internal phase and thus be removed from the continuous phase. This is the principle on which a water-wash operates. The water-wash is more beneficial if the emulsion has been destabilized by addition of a demulsifier and if the water is heated. The effectiveness of a water-wash greatly depends on the ability of the spreader plate or distributor to divide the emulsion into small streams or rivulets and to cause the emulsion to be in maximum intimate contact with the water bath so that the small drops of water can coalesce with the water.

If an emulsion-treating system or unit uses a water-wash, it can be charged with water to facilitate initial operation. Water from the emulsion to be treated should be used if available. If it is not available, extraneous water may be used.

Filtering

A filtering material with the proper size of pore spaces and the proper ratio of pore spaces to total area can be used to filter out the dispersed water droplets of a crude oil emulsion by preferentially wetting the filtering material with oil and keeping it submerged in oil. When used in this manner, the pack is correctly called a "filter" because it filters out the liquid that it prevents from passing through.

When excelsior is used as a filter in an emulsion treating, it is immersed in oil above the oil/water interface level. Excelsior is preferentially wetted by water because of the high affinity the cellulose fibers have for water. If the excelsior is initially wetted by oil, however, the dispersed water droplets in the oil will not normally take possession of the excelsior fibers because the fibers are saturated with oil. If the water droplets do take possession of the excelsior fibers, possession will occur at a slow rate and penetration of the pack by the water will be only partially complete.

Excelsior is wood that is cut into small shreds or fibers. Observed under a microscope, the surfaces of each strand of excelsior bristle with tiny sharp barbs. When emulsion flows through an excelsior pack, these rough surfaces cause distortion of the film surrounding the water droplets, thereby encouraging adherence of the droplets to the strands of excelsior. This results in coalescence of the water droplets into drops large enough to settle out of the oil. Excelsior should be made from pitch-free woods, such as aspen, cottonwood, or poplar. Pine excelsior is not recommended for crude oil emulsion-treating purposes. Excelsior should be used at less than 180°F treating temperature. Higher temperature will delignify and deteriorate the excelsior. It will also make it difficult to remove from the vessel.

Glass wool and other porous materials have been used as filtering material. Glass wool, when the fibers are properly sized and compacted, can serve as a filtering material for filtering water droplets out of a crude oil emulsion. If the glass wool is coated with silicone, its filtering effect will be enhanced because the silicone-coated fibers will be more wettable by oil than untreated glass wool fibers. Glass wool is not widely used for filtering because of its initial expense and its fouling problems.

Porous materials, both plastics and metals, are available that will filter dispersed water droplets from a crude oil emulsion. These porous materials are not widely used because of the difficulty of obtaining and maintaining the proper size pores and because they easily foul and become inoperable.

Treating crude oil emulsions by filtering is not widely used because of the difficulty in obtaining and maintaining the desired filtering effect and because the filtering material is easily plugged by foreign material.

Fibrous Packing

Fibrous coalescing packs are not commonly used in oil treating. They are mentioned for completeness and to differentiate between filtering and coalescence. A coalescing pack is a section or compartment in an emulsion-treating tank or vessel that is packed with a material that is wetted by the water, causing the water to coalesce into larger drops. Separation of two emulsified liquids by use

of a coalescing pack operates on the principle that two immiscible liquids with different surface tensions cannot simultaneously take possession of a given surface. The coalescing pack is wetted with or submerged in water. When the dispersed droplets of water come in contact with the water-wet coalescing material, the water droplets coalesce and adhere to the coalescing surfaces. Oil will pass through the pore spaces of the coalescing material. Separation of the two liquids in a coalescing pack is not caused by filtering but by the greater affinity of the water-wet coalescing material for the water droplets.

The film of oil containing the emulsifying agent surrounding the dispersed water particles must be broken before these droplets will adhere to a coalescing medium. The film is broken with the aid of demulsifying chemicals and/or heat and by repeated contact between the water particles and the surface of the coalescing materials as the emulsion flows through the pack. When this film has been broken, the water particles adhere to the surface of the coalescing material until they combine into drops large enough to settle out of the oil.

Glass wool can be used as coalescing material in emulsion-treating vessels. It will not deteriorate like wood excelsior and will prolong the service life of the coalescing pack. Glass wool fouls rather easily and may cause channeling. Woven wire mesh can also be used but tends to be more expensive than glass wool.

Gravity Settling

Gravity settling is the oldest, simplest, and most widely used method of treating crude oil emulsions. The difference in density of the oil and water causes the water to settle through and out of the oil. Because the water droplets are heavier than the volume of oil they displace, they have a downward gravitational force exerted on them. This force is resisted by a drag force caused by their downward movement through the oil. When the two forces are equal, a constant velocity is reached that can be computed from Stokes' law as

$$v = \frac{1.78 \times 10^{-6} (\Delta\gamma_{ow}) d^2}{\mu_o}, \dots\dots\dots (3)$$

where

v = downward velocity of the water droplet relative to the oil, ft/sec,

d = diameter of the water droplet, μm ,

$\Delta\gamma_{ow}$ = difference in specific gravity between the oil and water, and

μ_o = dynamic viscosity of the oil, cp.

Several conclusions can be drawn from this equation.

1. The larger the size of a water droplet, the greater its downward velocity—i.e., the bigger the droplet size, the less time it takes for the droplet to settle to the bottom of the vessel, and thus the easier it is to treat the oil.

2. The greater the difference in density between the water droplet and the oil, the greater the downward velocity—i.e., the lighter the oil, the easier it is to treat the oil. If the oil gravity were 10°API and the water fresh, the settling velocity would be zero because there is no gravity difference.

3. The higher the temperature, the lower the viscosity of the oil, and thus the greater the downward velocity of the water droplets—i.e., it is easier to treat the oil at high temperatures than at low temperatures (assuming a small effect on gravity difference because of increased temperature).

Gravity settling alone can be used to treat only loose, unstable emulsions. When other treating methods destabilize the emulsion and create coalescence, which increases water droplet size, however, gravity settling provides separation of water from oil.

Retention Time

In a gravity settler, such as an oil-treating tank or the coalescing section of an oil-treating vessel, coalescence will occur. Because of the small forces at work, however, the rate of contact between water droplets is small and coalescence seldom occurs immediately when two droplets collide. Thus the process of coalescence, although it will occur with time, follows a steep exponential curve where successive doubling of retention time results in small incremental increases in droplet size.

The addition of retention time alone, after some small amount necessary for initial coalescence, may not significantly affect the size of the water droplet that must be separated by gravity to meet the desired oil quality. A taller tank will increase the retention time but will not decrease the upward velocity of the oil or may not significantly increase the size of the water drop that must be separated from the oil. Thus the additional retention time gained by the taller tank may not materially affect the water content of the outlet oil.

A larger-diameter tank will increase the retention time. More important, it will slow the upward velocity of the oil and thus allow smaller droplets of water to settle out by gravity. In this case, it may not have been the increase in retention time that improved the oil quality but rather the reduction in flow velocity, which decreased the size of the water droplets that can be separated from the oil by gravity.

Centrifugation

Because of the difference in density between oil and water, centrifugal force can be used to break an emulsion and separate it into oil and water. Small centrifuges are used to determine the BS&W content of crude oil emulsion samples. A few centrifuges have been installed in the oil field to process emulsions. They have not been widely used for treating emulsions, however, because of high initial cost, high operating cost, low capacity, and a tendency to foul.

Distillation

Distillation can be used to remove water from crude oil emulsions. The water, along with lighter oil fractions, can be distilled by heating and then separated by appropriate means. The lighter oil fractions are usually returned to the crude oil.

The only current use of distillation is in the "flash system" used in 15°API and lower oil. These systems use the excess heat in the oil received from the treater or treating system and convert this sensible heat to latent heat at or near atmospheric pressure. The flashed steam is condensed in a surface condenser in the incoming cooler

stream of raw crude, thus scavenging the excess heat that would ordinarily be wasted. Fig. 19.20 shows a typical flash distillation system for dehydrating emulsions of heavy viscous crude oils.

The disadvantage of distillation is that it is expensive and that all the dissolved and suspended solids contained in the water are left in the oil when the water is removed by evaporation.

Emulsion-Treating Equipment and Systems

The design of equipment or a system for treating crude oil emulsions and the sizing of each piece of equipment for a specific application requires experience and engineering judgment. It would be ideal if a procedure existed that would permit the engineer to infer from measured properties of the emulsion the most economical treating process, taking into account treating temperature, chemical usage, and physical size of treating equipment. Unfortunately, such a procedure is not available and the engineer must rely on experience and empirical data from other wells or fields in the area and on laboratory experiments.

For example, the economic balance between the amount of chemical and heat to use to destabilize the emulsion and aid in coalescence is difficult to predict. Almost all emulsion-treating systems use demulsifying chemicals. In most instances, the lower the treating temperature, the greater the amount of chemical required to treat the emulsion. In many areas of west Texas and the Gulf of Mexico, some operators do not add heat to treat the relatively light crudes that are produced. Other operators under the same conditions add heat when treating similar crudes to minimize chemical cost and the size of the emulsion-treating equipment.

Another example is the economic balance that must be considered between those factors that promote coalescence (chemicals, water wash, heat, coalescing plates, etc.) and the size of the treating vessels. The larger the size of the treating vessel, the smaller the size of water droplets that can be separated from the emulsion. Thus the use of coalescing aids may reduce the size of the equipment by increasing the size of the water droplet that must be separated from the oil to meet the required quality. The savings in vessel costs must be balanced against the increased capital and operating cost (e.g., fuel and increased maintenance because of plugging) of the coalescing aids.

Bottle tests in the laboratory provide a means for estimating ranges of treating temperature and retention time for design purposes. Unfortunately, these tests are static in nature and do not model closely the dynamic effects of water droplet dispersion and coalescence that occur in the actual equipment because of flow through control valves, pipes, inlet diverters, baffles, and water-wash sections. Bottle tests, however, can be useful in estimating treating parameters such as temperature, demulsifier volume, settling time, etc.

When evaluating empirical data from similar wells or fields, the designer should recognize that the temperature at which an emulsion is treated may not be as critical as the viscosity of the crude at that temperature. The design of an oil-treating system can be assisted by observing an existing system, knowing the viscosity of the crude at treating temperature, and calculating from the flow geometry and Stokes' law the minimum size water droplet

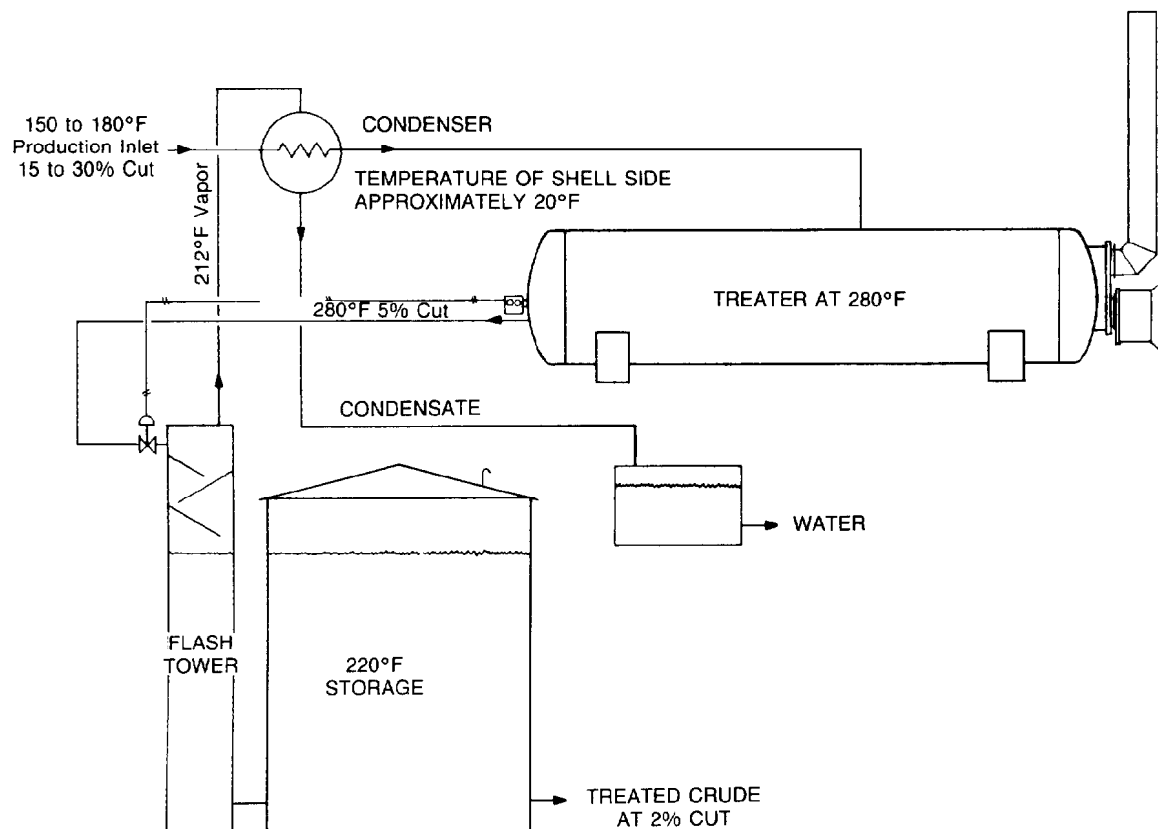


Fig. 19.20—Typical flash distillation system for dehydrating emulsions of heavy viscous crude oils.

that can be settled from the crude. A treating system can then be designed that will heat the emulsion to the temperature required to obtain the same viscosity that exists in the sample field, and then any one of the pieces of equipment or combinations thereof described in the next section can be selected and sized so that all water droplets larger than the calculated minimum diameter can be separated from the oil.

Because of the uncertainties in attempting to scale up from laboratory data or to infer designs from empirical data from similar wells or fields, a new treating system should be designed with either larger equipment or more heat input capacity than the engineer calculates to be necessary. The amount of "overdesign" to be built into the treating system depends on an assessment of the cost of the extra capacity balanced against the risk of not being able to treat the design throughput.

Description of Equipment Used in Treating Crude Oil Emulsions

The characteristics of the emulsion to be treated should be understood before a treating system is selected. Several different types of equipment or systems may satisfactorily resolve an emulsion, but one particular type of equipment or system may be superior to others because of basic considerations in design, operation, initial cost, maintenance

cost, operating cost, and performance. Effort should be made to select the minimum number of pieces of equipment or the simplest design for each treating system to optimize initial and operating costs.

The combination of the various emulsion-treating methods that will provide the lowest use of chemical, lowest treating temperature, lowest loss of light hydrocarbons, lowest overall treating cost, and the best performance should be used. Experience and empirical data may guide the buyer to the optimum combination of treating methods, but field testing will be required to confirm the selection.

The following discussion describes various emulsion-treating equipment and systems. Each piece of treating equipment and each treating system affords a wide selection of the type, configuration, size, component selection, component design, and usage. Additional treating equipment can usually be added to each unit or system until the desired treating results are obtained. The design and selection of all the components of the treating system should be made at the time of initial purchase and installation. Because of the modular design of most systems, however, if the selected equipment does not perform as desired or if operating conditions change, additional features can usually be added or operating procedures altered to obtain the desired results.

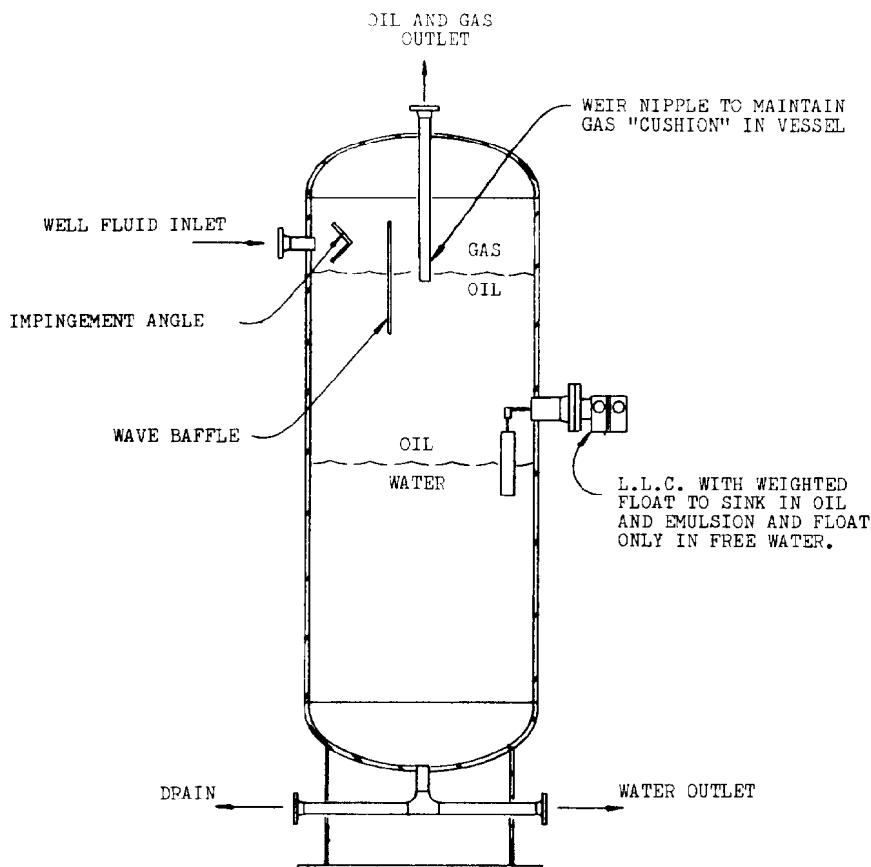


Fig. 19.21—Typical vertical FWKO.

Free Water Knockouts

Where large quantities of water are produced, it usually is desirable to separate the free water before attempting to treat the emulsion. When oil and water are agitated with moderate intensity and then allowed to settle for a period of time, three distinct phases normally will form: a layer of essentially clean oil at the top with a small amount of water dispersed in the oil in very small droplets, relatively clean water (free water) at the bottom with a small amount of dispersed oil in very small droplets, and an emulsion phase in between. With time, the amount of emulsion will approach zero as coalescence occurs.

The free water is the water that separates in 3 to 10 minutes. It may contain small droplets of dispersed oil that may require treatment before disposal. Equipment to do this is discussed in Chap. 15.

Free-water knockouts (FWKO's) are designed as either horizontal or vertical pressure vessels. Fig. 19.21 is a schematic of a vertical FWKO, and Fig. 19.22 shows a horizontal FWKO. The fluid enters the vessel and flows against an inlet diverter. This sudden change in momentum causes an initial separation of liquid and gas, which will prevent the gas from disturbing the settling section of the vessel. In some designs, the separating section contains a downcomer that directs the liquid flow below the oil/water interface to aid in water-washing the emulsion.

The liquid-collecting section of the vessel provides sufficient time for the oil and emulsion to form a layer of oil at the top, while the free water settles to the bottom. When there is appreciable gas in the inlet stream, a three-phase separator can be used as an FWKO. See Chap. 12 for a description of both vertical and horizontal three-phase separators.

Sometimes a cone-bottom vertical three phase separator is used. This design is used if sand production is anticipated to be a major problem. The cone is normally at an angle to the horizontal of between 45 and 60°. If a cone is used, it can be the bottom head of the vessel, or for structural reasons, it can be installed internally in the vessel. In such a case, a gas-equalizing line must be installed to ensure that the vapor behind the cone is always in pressure equilibrium with the interior of the vessel. Water jets can be used to dislodge and flush the sand from the vessel.

Oil and water are usually separated more quickly and completely in an FWKO when the liquid travels through the vessel in a horizontal rather than a vertical direction. Horizontal flow permits a less restricted downward movement of the water droplets. If the emulsion flows vertically upward, the water must move downward through an upward-moving stream; therefore, the downward movement of water is retarded by upward movement of the oil and emulsion.

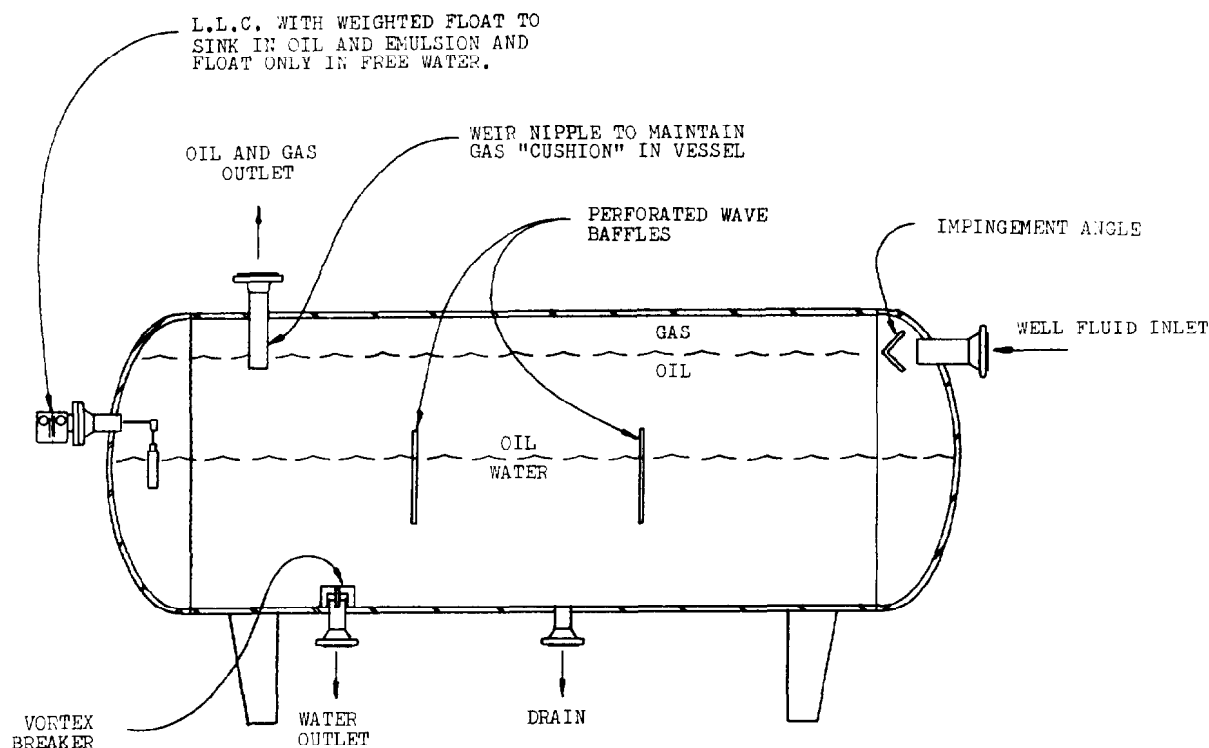


Fig. 19.22—Typical horizontal FWKO.

It is possible to add a heating tube to an FWKO, as shown in Fig. 19.23, or to add heat upstream of the FWKO. In such cases, even though the vessel may be called an FWKO, it is performing the function of an emulsion treater.

Many configurations are possible for providing baffles and maintaining levels in an FWKO. A good design will provide the functions described previously, i.e., degassing, water-washing, and providing sufficient retention time and correct flow pattern so that free water will be removed from the emulsion.

When the free water is removed, it may or may not be necessary to treat the oil further. In many fields producing light oil, a well-designed FWKO with ample settling time and with a reasonable chemical-treating program can provide pipeline-quality oil. Most often, however, further emulsion treating is required downstream of the FWKO.

Storage Tanks

Oil generally should be water-free before it is flowed into lease storage tanks. If there is only a small percentage of water in the oil and/or if the water and oil are loosely emulsified, however, it may be practical to allow the water to settle to the bottom of the oil storage tank and to draw off the water before oil shipment. This practice is not generally recommended or followed, but for small volumes of free or loosely emulsified water on small leases or for low-volume marginal wells, it may be a practical and economical procedure.

When a storage tank is used for dehydration, the oil is flowed into the tank and allowed to settle. When the tank is full of liquid, flow into the tank is stopped or

switched to another tank and the tank is allowed to remain idle while water settles out of the oil. After the water has been separated from the oil by settling, water is drained from the bottom of the tank and the oil is gauged, sampled, and pumped or drained to a truck or pipeline. No water-wash is used in conjunction with the standard storage tank. If there is a water-wash, its shallowness and the absence of a proper spreader causes it to be of little or no benefit.

Settling Tanks

Various names are given to settling tanks used to treat oil. Some of the most common are gunbarrels, wash tanks, and dehydration tanks. The design of these tanks differs in detail from field to field and company to company. All contain all or most of the basic elements shown in Fig. 19.24.

The emulsion enters a gas separation chamber or gas boot where a momentum change causes separation of gas. Gas boots can be as simple as the piece of pipe shown in Fig. 19.24, or they can contain more elaborate nozzles, packing, or baffles to help separate the gas. If there is much gas in the well stream, it is usually preferable to use a two- or three-phase separator upstream of the settling tank. In this case, the gas boot must separate only the gas that is liberated as the pressure decreases during flow from the separator to the settling tank.

A downcomer directs the emulsion below the oil/water interface to the water-wash section. On most large tanks, a spreader is used to distribute the flow over the entire cross section of the tank. This minimizes short-circuiting. The more the upward-flowing emulsion spreads out and

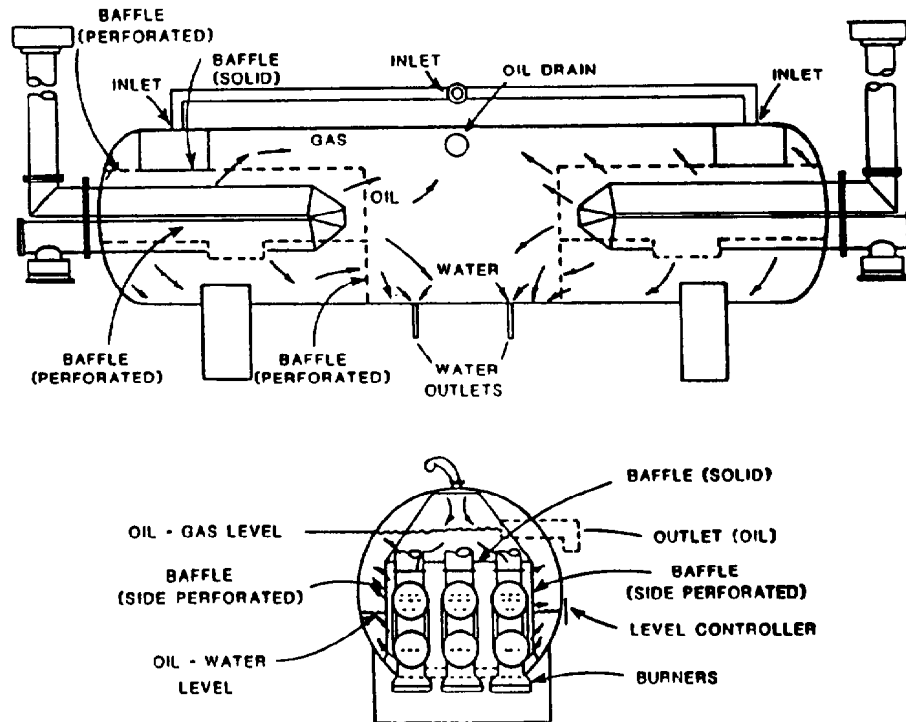


Fig. 19.23—Schematic view of FWKO with heating element in each end.

approaches plug (or uniform) flow, the slower its average upward velocity and the smaller the water droplets that will settle out of the emulsion.

There are many types of spreader designs. Spreaders can be made by cutting slots in plate, use of angle iron, or holes in pipe. By causing the emulsion stream to separate into many small streams, the spreader causes a more intimate contact with the water to help promote coalescence in the water-wash section. This is shown in Figs. 19.25 and 19.26. Most spreaders contain small holes or slots to divide the oil and emulsion into small streams. Large holes (3 to 4 in. in diameter) will not be nearly as effective in dividing the stream as small holes ($\frac{3}{8}$ to 1 in. in diameter). In designing a spreader, however, it is important that the fluid is not agitated to the point where shearing of the water droplets in the emulsion takes place, causing the emulsion to become harder to separate. In addition, small holes can be more easily plugged with solids and are difficult to clean. Free-flow coalescing devices, such as S.P. PacksTM (Fig. 19.18), can be installed on the downcomer/spreader to promote coalescence and to minimize shearing of the water droplets by the spreader.

As the emulsion rises above the oil/water interface, water droplets settle from the oil countercurrent to the flow of the oil by gravity. Because there may be very little coalescence above the oil/water interface, increasing the height of the oil-settling section above some minimum to aid in spreading out the flow may not materially affect the oil outlet quality.

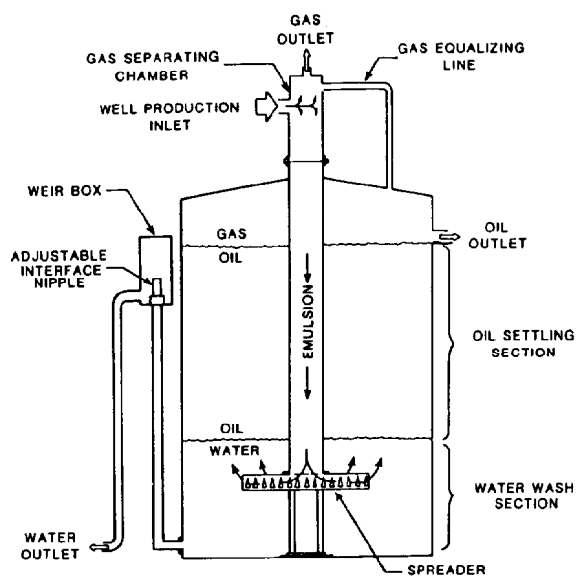


Fig. 19.24—Typical settling tank with internal downcomer and emulsion spreader.

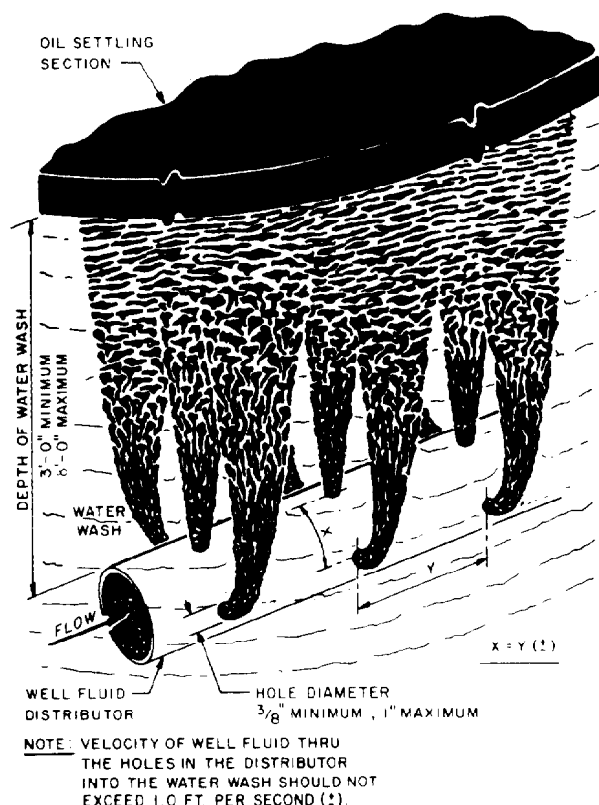


Fig. 19.25—Proper design of well fluid inlet distributor for wash or gunbarrel tank showing use of small holes in distributor.

Sometimes oil collectors similar in design to oil spreaders are used to aid in establishing plug flow. The oil collector must not allow vortexing and should collect oil from the top of the tank in such a way that horizontal movement of the oil will be minimized.

Some tanks discharge the water through a water collector designed to cause the flow of water to approach plug flow conditions more nearly. The water outlet collector must prevent vortexing of the water and must minimize horizontal movement of the water. The water outlet collector should be located near the tank bottom. There must be enough vertical distance between it and the inlet spreader to allow sufficient clarification of the water, and it should be at least 6 to 12 in. above the tank bottom to allow for accumulation of sand.

Some tanks have elaborate sand-jetting and drain systems that may or may not be part of the water-collector system. It may be difficult to make these drains operate satisfactorily because the water flow to each drain must be on the order of 3 ft/sec to suspend the sand. Sand drains may lengthen the amount of time between tank cleanings, but the additional cost of sand drains in tanks may not be warranted.

In Fig. 19.24, the oil/water interface is established by an external adjustable weir sometimes called a water leg. The height of the interface is determined by the difference in height of oil outlet and weir and the fluid properties. It may be calculated from

$$h_{wd} = (h_{oo} - h_{ww}) \frac{\gamma_o}{\gamma_w} + h_{ww} \quad (4)$$

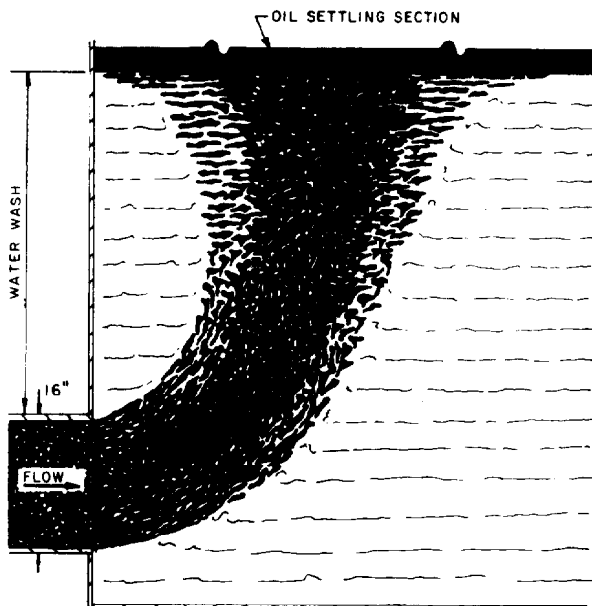


Fig. 19.26—Improper design of well fluid inlet for wash or gunbarrel tank.

where

h_{wd} = height of water-draw-off overflow nipple in weir box above tank bottom, ft,

h_{oo} = height of clean oil outlet above tank bottom, ft,

h_{ww} = desired height of water-wash in tank above tank bottom, ft,

γ_o = specific gravity of oil, and

γ_w = specific gravity of water.

Water legs are used successfully for emulsions where the gravity is above 20°API and there is sufficient difference in gravity between the oil and water. Marginal performance is obtained on oil between 15 and 20°API. Below 15°API, water legs normally are not used.

It is also common to control the oil/water interface with internal weirs or with an interface liquid-level controller and a water-dump valve. In heavy oils, electronic probes are most often used to sense the interface and operate a water-dump valve. In lighter oils, floats that sink in the oil and float in the water are more common.

Not all settling tanks contain all the sections and design details described previously. The choice depends on the overall process selected for the facility, emulsion properties, flow rates, and desired effluent qualities. While Fig. 19.24 is representative of the majority of settling tanks currently in use, other tanks have a different flow pattern. A series of parallel vertical baffles from the bottom of the vertical tank to above the oil level, as shown in Fig. 19.27, cause the flow of the emulsion to be

horizontal rather than vertical. With this type of flow path, the water droplets fall at right angles to the oil flow, rather than countercurrent to the oil flow. Some settling tank designs employ a vortex or swirling motion at the inlet of the tank to aid in coalescence and settling and to minimize short-circuiting. Many settling tanks employ heat to aid in the treatment process. Heat can be added to the liquid by an indirect heater, a direct heater, or any type of heat exchanger.

A direct fired heater, sometimes referred to as a "jug" heater, is one in which the fluid to be heated comes in direct contact with the immersion-type heating tube or element of the heater. Direct fired heaters are generally used to heat low-pressure noncorrosive liquids. These units normally are constructed so that the heating tube can be removed for cleaning, repair, or replacement.

An indirect fired heater is one in which the fluid passes through pipe coils or tubes immersed in a bath of water, oil, salt, or other heat-transfer medium that, in turn, is heated by an immersion-type heating tube similar to the one used in the direct fired heater. The contents of the bath of an indirect fired heater are caused to circulate by thermosiphonic currents. The immersion-type heating tube heats the bath, which heats the fluid flowing through coils immersed in the bath. When water is used as the bath, water free of impurities will prolong the life of the heater and prevent fouling of the surface of the heating tube and coils.

Indirect fired heaters are less likely to catch on fire than direct fired heaters and generally are used to heat corrosive or high-pressure fluids. They usually are constructed so that the heating tube and pipe coil are individually removable for cleaning and replacement. They tend to be more expensive than direct fired heaters.

Heat exchangers normally are used where waste heat is recovered from an engine, turbine, or other process stream or where fired heaters are prohibited. In complex facilities, especially offshore, a central heat-transfer system recovering waste heat and supplying it through heat exchangers to all process heat demands is sometimes more economical and may be the only way to meet established safety regulations.

Advantages of heating the entire stream of emulsion before it enters the settling tank are as follows.

1. After the fluid is heated, it flows through piping and into the flume pipe or gas boot of the gunbarrel tank. This moderate agitation of the heated fluid can assist in coalescence of water droplets.

2. The emulsion is heated before it reaches the gunbarrel, which aids in removing gas from the oil in the gas boot. This helps maintain quiescence in the settling portion of the gunbarrel.

3. The heater and gunbarrel can be sized independently, which allows flexibility in sizing the system.

4. Water-wash volume in the gunbarrel can be adjusted over a wide range, providing additional flexibility.

5. Continuous flow of fresh fluids through the heater tends to prevent coking and scaling and helps keep the heating surface clean, which will prolong the heater life.

Heat can also be supplied to the system by circulating the water in the water-wash section to a heater and back to the tank. The hot-water-wash section warms the incoming emulsion. A thermosiphon caused by density differences of the hot and the cold water can be used as the

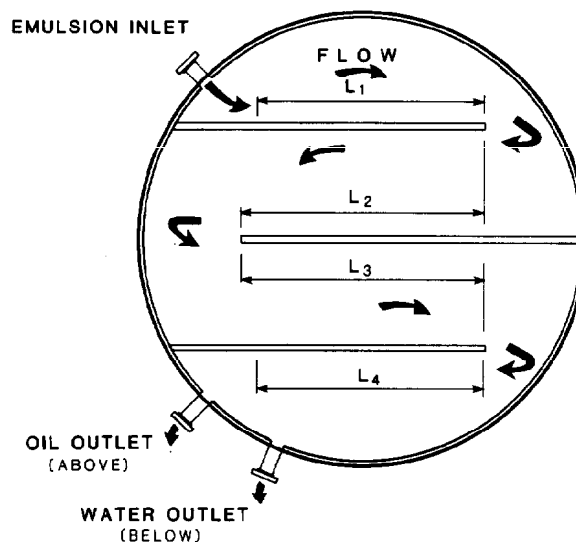


Fig. 19.27—Plan view of vertical tank with horizontal flow settling pattern.

driving force for the circulation if the heat source is not far from the tank. The water also may be pumped to the heater and circulated back through the flume, as shown in Fig. 19.28. In this system, the settling space in the gunbarrel may be disturbed by gas released from the oil when it comes in contact with the hot water. It has two advantages. First, oil will not be overheated because it never comes in contact with the heating element in the heater but is heated by the water bath in the gunbarrel. This minimizes vapor losses from the oil and tends to maintain maximum oil gravity. It also minimizes coking and scaling. Second, this system is as safe from fire hazards as a system involving a fired vessel can be because only water flows through the heater. There is no oil or gas in the fired vessel.

Settling or gunbarrel tanks can also be heated directly with a fire tube, as shown in Fig. 19.29, or with internal heat exchangers, using steam or other heat media. Heat exchangers can be either pipe coils or plate-type heating elements.

Plate-type heating elements are usually 18 to 32 in. by about 5 to 8 ft. These usually are preferred over pipe coils because the heat-transfer coefficient is 10 to 20% higher for the plate-type heating elements when immersed in oil than for a corresponding area of pipe. Further, the gentle agitation brought about by the convection flow of the oil up the surface of the plate-type element assists in coalescence. Plate-type heating elements are available with a wide range of pressure ratings. They can be purchased for steam service or hot-water service, but the same unit should not be used for both because the construction of the cells is different for the two types of heating media.

Pipe coils are popular because of the local availability of materials. The cost is normally slightly higher than for plate-type exchangers, however, especially in larger installations.

When settling tanks are heated directly, they operate in much the same manner as vertical or horizontal emulsion treaters.

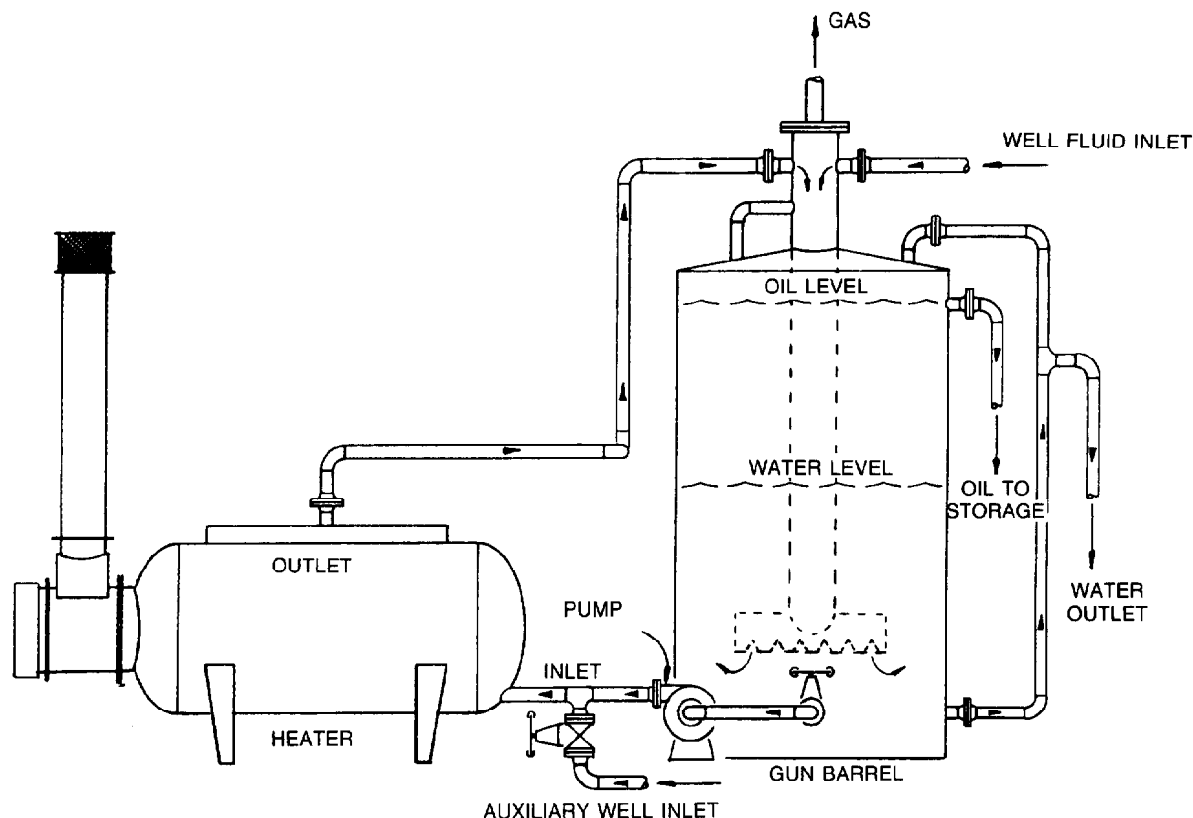


Fig. 19.28—Heater and gunbarrel in forced circulation method of heating.

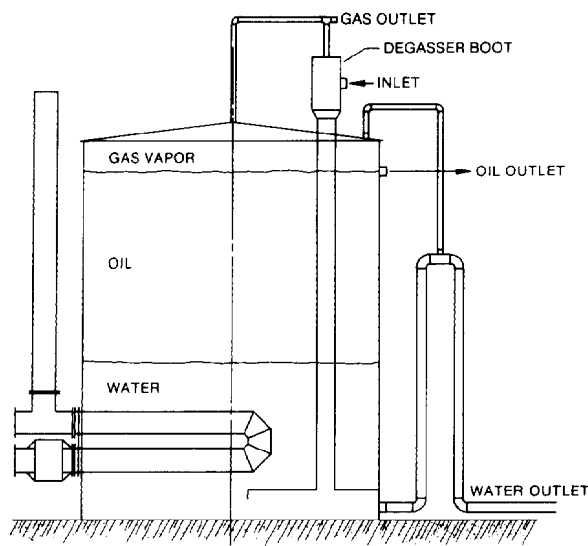


Fig. 19.29—Heated gunbarrel emulsion treater.

Vertical Emulsion Treaters

The most commonly used one-well lease emulsion treater is the vertical unit. A typical design is shown in Fig. 19.30. Flow enters near the top of the treater into a gas separation section. This section must have adequate dimensions to separate the gas from the liquid. If the treater is located downstream of a separator, this section can be very small. The gas separation section should have an inlet diverter and a mist extractor.

The liquid flows through a downcomer to the bottom portion of the treater, which serves as an FWKO and water-wash section. If the treater is located downstream of an FWKO, the bottom section can be very small. If the total wellstream is to be treated, this section should be sized for sufficient retention time to allow the free water to settle out. This will minimize the amount of fuel gas needed to heat the liquid rising through the heating section.

The oil and emulsion flows upward around the fire tubes to a coalescing section, where sufficient retention time is provided to allow the small water droplets to coalesce and to settle to the water section. Treated oil flows out the oil outlet. Any gas flashed from the oil because of heating flows through the equalizing line to the gas space above. The oil level is maintained by pneumatic or lever-operated dump valves. The oil/water interface level is controlled by an interface controller or an adjustable external water leg.

It is necessary to prevent steam from being formed on the fire tubes. This can be done by employing the "40° rule"—i.e., the operating pressure is kept equal to the

pressure of saturated steam at a temperature equal to the operating temperature plus 40°F. This is desirable because the normal full-load temperature difference between the fire tube wall and the surrounding oil is approximately 30°F in most treaters. Allowing 10°F for safety, the 40° rule will prevent flashing of steam on the wall of the heating tube.

Baffles and spreader plates may be placed in the coalescing section of the treater above the fire tubes. Many treaters were originally equipped with excelsior or "hay" packs. In most applications these may not be needed, but a manway may be provided in case one may need to be added in the field.

Although Fig. 19.30 shows a treater with a fire tube, it is also possible to use an internal heat exchanger to provide the required heat or to heat the emulsion before it enters the treater. For safety reasons, some offshore operators prefer a heat-transfer fluid and a pipe or plate heat exchanger inside the treater rather than a fire tube.

Horizontal Emulsion Treaters

For most multiwell leases, horizontal treaters normally are preferred. Fig. 19.31 shows a typical design of a horizontal treater. Flow enters the front section of the treater where gas is flashed. The liquid flows downward to near the oil/water interface where the liquid is water-washed and the free water is separated. Oil and emulsion rises past the fire tubes and flows into an oil surge chamber. The oil/water interface in the inlet section of the vessel is controlled by an interface-level controller, which operates a dump valve for the free water.

The oil and emulsion flows through a spreader into the back or coalescing section of the vessel, which is fluid-packed. The spreader distributes the flow evenly throughout the length of this section. Treated oil is collected at the top through a collection device used to maintain uniform vertical flow of the oil. Coalescing water droplets fall countercurrent to the rising oil. The oil/water interface level is maintained by a level controller and dump valve for this section of the vessel.

A level control in the oil surge chamber operates a dump valve on the oil outlet line regulating the flow of oil out the top of the vessel and maintaining a liquid-packed condition in the coalescing section. Gas pressure on the oil in the surge section allows the coalescing section to be liquid-packed.

The inlet section must be sized to handle separation of the free water and heating of the oil. The coalescing section must be sized to provide adequate retention time for coalescence to take place and to allow the coalescing water droplets to settle downward countercurrent to the upward flow of the oil.

Fig. 19.32 shows another design of a horizontal emulsion treater with a different flow pattern that minimizes vertical flow of the emulsion. Oil, water, and gas enter the top of the treater at the left side (facing the burners) and travel toward the front and downward. Gas remains at the top, and oil and water are heated as required. Some heat is applied to the water in this section, but because this section has its own temperature controller, it can be regulated up or down for optimum performance.

The cross section in Fig. 19.32 shows that the emulsion flows under a longitudinal baffle and through a large slot in the partition plate near the front of the treater at

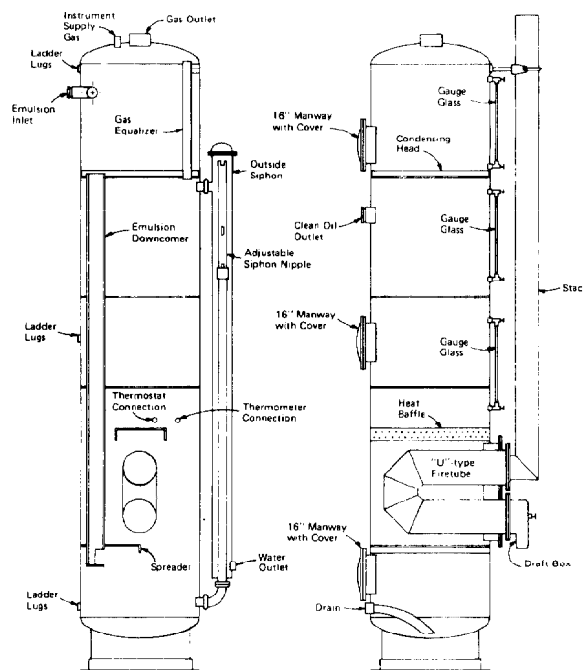


Fig. 19.30—Schematic view of typical vertical emulsion treater.

the bottom of the fire tube where it is water-washed. In the right compartment of Section AA, the oil and emulsion flow longitudinally up across the fire tube at about a 10 to 15° incline from horizontal.

The heating and settling section separation baffle blocks the passage of foam at the top and blocks emulsion at the bottom. Heated oil travels through a slot in a partition that is about at the centerline of the top fire tube. Free water is allowed to travel under the baffle. As emulsion accumulates at the interface, it rises to touch the fire tube, which is only 6 in. above the interface. The fire tube then tends to heat and eliminate the emulsion pad to maintain a uniform emulsion-pad thickness.

Channeling, skimming, and stratifying are all reduced by the application of louvered baffles, which are made of a stainless steel sheet punched with a louvered pattern that ranges from 15 to 60% open area. The baffles are solid at the top to prevent foaming or skimming and extend down near but do not touch the water. All the emulsion goes through the louvered openings, which provide a slight impedance to flow to develop even flow distribution and aid in coalescence.

Oil level in the treater is maintained by a weir and an oil box. Water level in the treater is critical; thus a weir is placed approximately 5 ft from the rear head seam, and the oil/water interface level upstream of this weir is maintained by the weir. Adjustment of the water-level controller, which is located downstream of this weir, has no effect on the water level in the main treater body upstream of the weir.

Because the emulsion flow path in this design is essentially horizontal, the water particles are not opposed by the velocity of upflowing oil as in a treater with a vertical flow pattern. This is especially important in heavy crudes where the differential specific gravity between oil and water is small and the settling velocity is low.

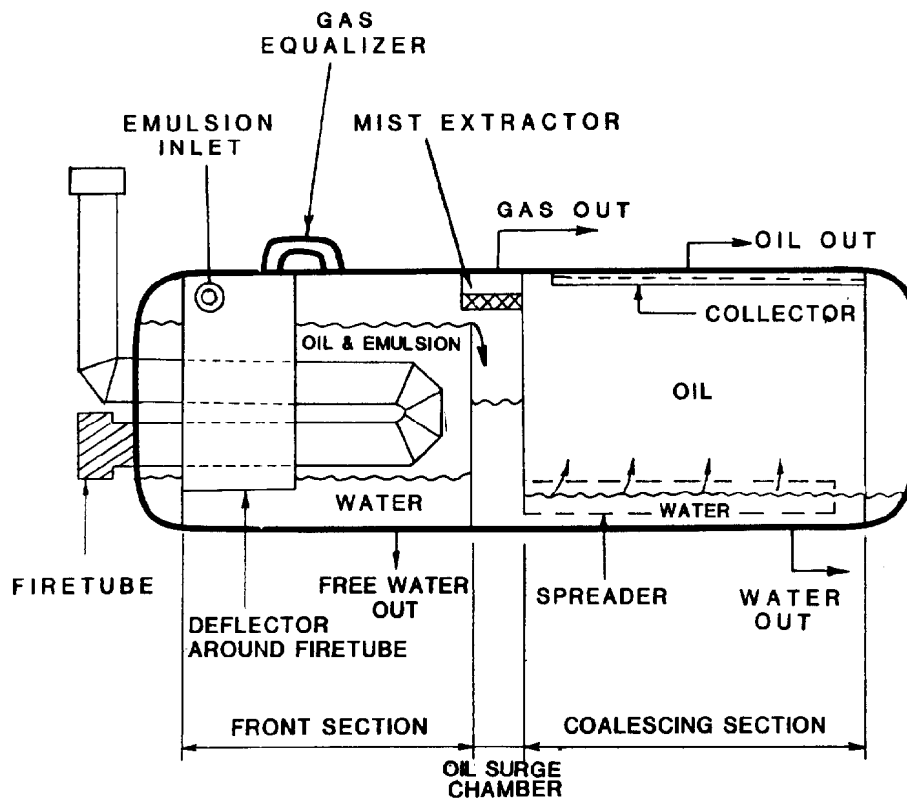


Fig. 19.31—Typical horizontal emulsion treater with vertical flow.

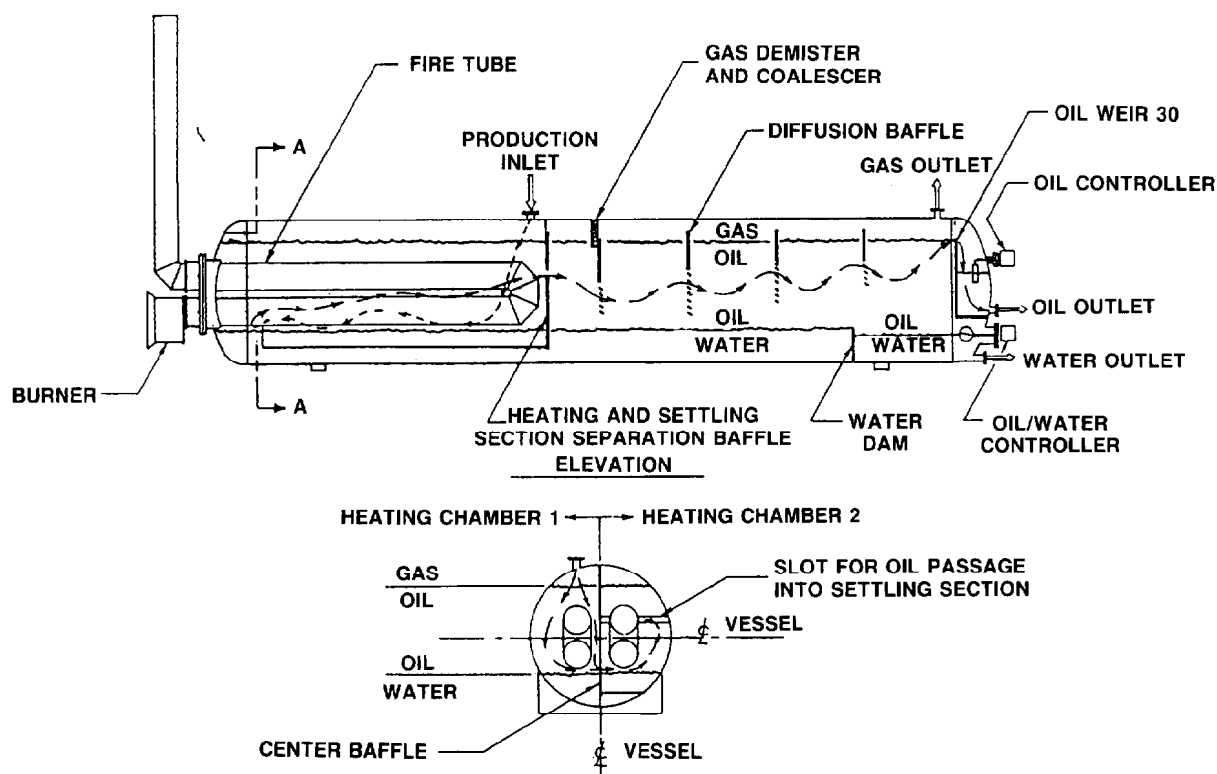


Fig. 19.32—Horizontal emulsion treater with horizontal flow.

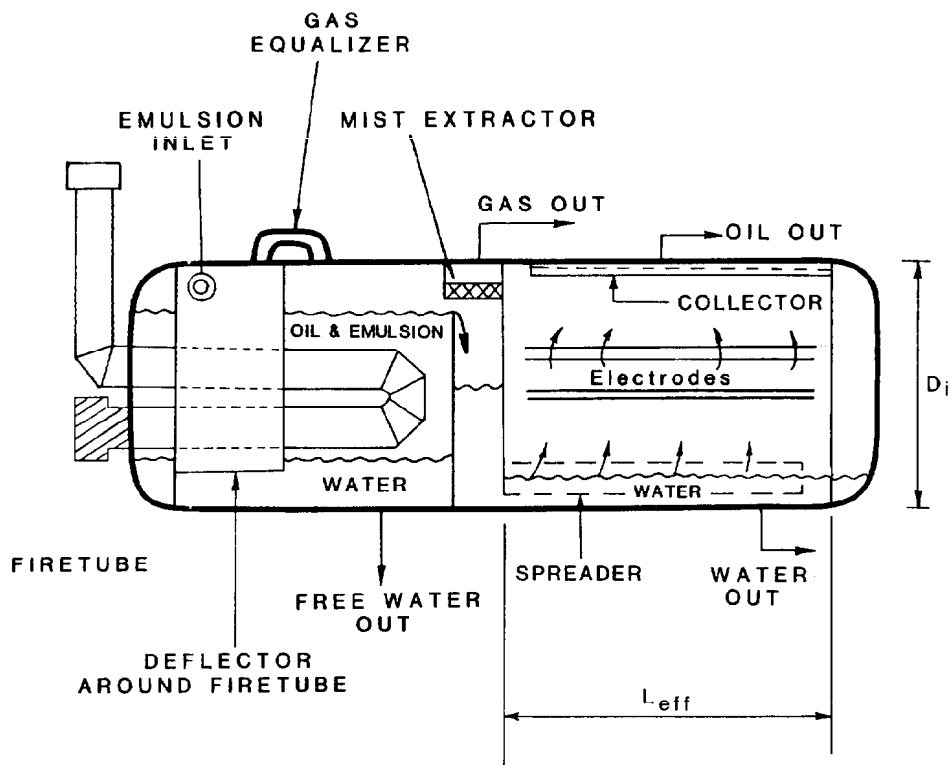


Fig. 19.33—Typical horizontal electrostatic emulsion treater with vertical flow.

Other flow patterns are available if different baffle designs are used in horizontal treaters. The two described previously are examples to show the concepts that are most generally applied. Other methods of heating the emulsion can be used if it is desirable to eliminate the fire tubes.

Electrostatic Coalescing Treaters

Electrostatic treating can be used in either vertical or horizontal emulsion treaters by including electrical grids in the settling or coalescing sections. Figs. 19.33 and 19.34 show how grids can be installed in the horizontal treaters shown in Figs. 19.31 and 19.32.

Two grids of electrodes typically are installed in electrostatic emulsion treaters. One is wired to a source of electric current and the other is grounded. The emulsion flows between these electrodes, which are charged with a very high voltage. The electrodes are installed in the vessel to provide a final stage of coalescence to the emulsion after it has already been treated to near pipeline quality. In the design of Fig. 19.33, the upflowing oil passes the "hot" electric grid, which is usually steel or stainless steel rods or bars spaced 4 to 6 in. apart. This grid is stationary and hangs from multiple electric insulators. AC current is wired to this grid from an external single-phase transformer. The "cold" electric grid is mounted directly above the hot grid and is adjustable from 2.5 to 12 in. from the hot grid. The normal operating spacing between the two grids is usually 4 to 6 in.

Coalescing takes place between the oil/water interface and the hot grid, as well as between and above the grids. The oil continues vertically to the outlet collector pipe with

small calibrated holes in the top of the pipe to ensure uniform distribution. The electric section has no oil/gas interface. All gas must be removed in the heating section.

The electric coalescing function in the treater shown in Fig. 19.34 is similar to the horizontal grid unit of Fig. 19.33 except that the vertical grids provide the advantage of the horizontal flow pattern for the emulsion and improve the performance of this unit.

In addition to the safety controls normally found on emulsion treaters with fireboxes, there are also low-liquid-level safety switches on the electric treater to avoid the possibility of the electric power being applied when the high-voltage grid is surrounded with gas instead of liquid.

The greater the voltage gradient, the greater the forces causing coalescence. Experimental data show, however, that at some voltage gradient the water droplets can be pulled apart and a tighter emulsion can result. For this reason, electrostatic treaters are normally equipped with a mechanism for adjusting the voltage gradient in the field so that the optimum can be obtained.

The voltage gradient can be changed (1) by selecting optional transformer voltage taps. (2) by adjusting the voltage gradient by raising or lowering the oil/water interface in units using horizontal grids—the water level is, in effect, a grounded electrode against which most of the coalescing takes place; or (3) by adjusting the hot or cold grid location to change the voltage gradient.

The transformer is normally an 18,000- to 20,000-V secondary, single-phase, oil-filled, 100%-reactance-type transformer. It is mounted on the top, side, or end of the treater with a short, high-voltage conduit connected to an

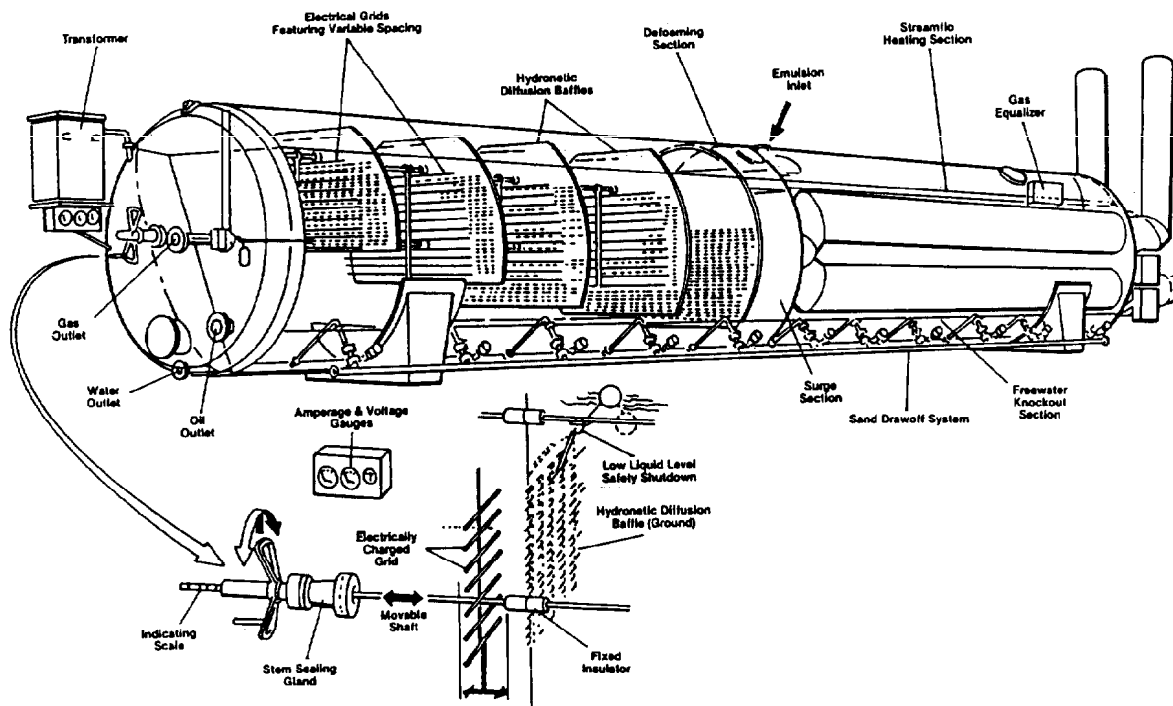


Fig. 19.34—Typical horizontal electrostatic emulsion treater with vertical electric grids for horizontal flow of fluids.

appropriate entrance probe assembly. The high-voltage line is entirely submerged in transformer oil, which is normally a highly refined hydrocarbon that has been vacuum dried and contains no moisture.

The application of electrostatic treaters should be limited to "polishing" of oil to avoid chaining and short-circuiting of the grids. They are particularly effective in reducing the water content of oil to very low levels (less than 0.5 to 1.0%). Electrostatic coalescence may also aid in reducing heat and/or chemicals required to treat crude oil to a specific quality.

Desalting Crude Oil

Most produced water contains salts, which may cause problems in production and refining processes when the solids precipitate to form scale on heaters, plug exchangers, etc. This can cause accelerated corrosion in piping and equipment.

In almost all cases, the salt content of crude oil consists of salt dissolved in small droplets of water that are dispersed in the crude. In some instances, the produced oil can contain crystalline salt, which forms because of changes in pressure and temperature as the fluid flows up the wellbore and through the production equipment. Crystalline salt will flow out with the water and is not of importance in desalting operations.

The salinity of produced brine varies widely, but most produced water falls in the range of 15,000 to 130,000 ppm of equivalent NaCl. Crude oil containing only 1.0% water with a 15,000 ppm salt content will have 55 lbm salt/1,000 bbl of water-free crude. The chemical composition of these salts varies, but the major portion is nearly always NaCl with lesser amounts of calcium and

magnesium chloride. Because of the operational problems associated with salts, most refineries buy crude at a salt content of 10 to 20 lbm/1,000 bbl, then desalt the oil to 1 to 5 lbm/1,000 bbl before charging to crude stills.

The purpose of a desalting system is to reduce the salt content of the treated oil to acceptable levels. In cases where the salinity of the produced brine is not too great, salt content can be reduced by merely ensuring a low fraction of water in the oil. In this case, the terms desalting and emulsion treating are identical, and the concepts and equipment described previously can be used.

The required maximum concentration of water in oil to meet a known salt specification can be derived from

$$C_{so} = 0.35 C_{sw} \gamma_w f_w, \quad (5)$$

where

C_{so} = salt content of the oil, lbm/1,000 bbl,

C_{sw} = concentration of salt in produced water, ppm,

γ_w = specific gravity of produced water, and

f_w = volume fraction of water in crude oil.

If the produced brine has a high salt concentration, it may not be possible to treat the oil to a low enough water content (less than 0.2 to 0.25% is difficult to guarantee). In such a case, desalting implies the mixing of low-salt-content water with the emulsion before treating, as shown in Fig. 19.35. This lowers the effective value of C_{sw} in Eq. 5. If a single-stage desalting system will require too much dilution water, then a two-stage system, such as that shown in Fig. 19.36, is used.

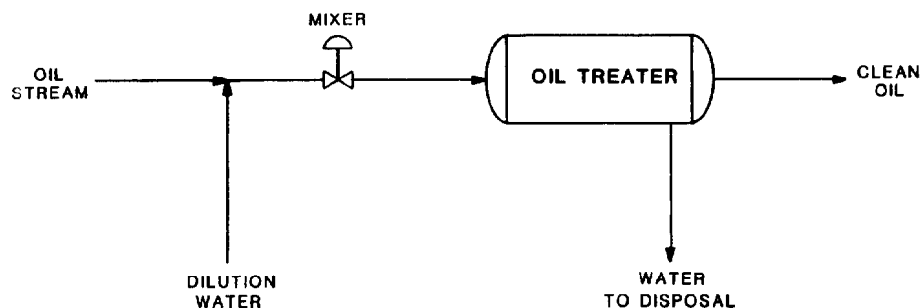


Fig. 19.35—Single-stage desalting with dilution water injection.

Although it is possible to desalt with most of the emulsion-treating equipment discussed previously, most desalting systems use electrostatic treaters to obtain the lowest possible water content in the oil and thus minimize the amount of dilution water needed.

One of the most important parts of desalting systems is the method and efficiency of the method of mixing the wash water with the crude. The smaller the diameter of the wash-water drops dispersed in the oil, the greater the possibility of their coming in contact and coalescing with entrained saltwater droplets.

Excessive agitation when mixing the wash water with the crude oil can result in emulsions that are too tight (stable) to resolve easily. Therefore, the amount of mixing provided should be adjustable to zero. This requirement tends to make pumps and level-control valves poor choices for mixing. The most commonly used mixing system consists of some type of special mixing tee or static mixer followed by a globe-type mixing valve.

Mixing efficiency in a desalting system refers to the fraction of wash water that actually mixes with the produced water. The remainder of the water, in effect, bypasses the desalting stage and is disposed of as free water. A mixing efficiency of 70 to 85% can be considered a reasonable range of attainment. Part of the energy for mixing is obtained from the pressure of the wash water, which should enter the mixer at approximately 25 psi above the pressure in the vessel.

Reverse Emulsions

Most emulsions are the water-in-oil type; they occur much more frequently than the oil-in-water type. Oil-in-water (reverse) emulsions are most likely to be produced where the WOR is high, the dissolved solids content of the water is low, the water is slightly alkaline, and the oil has a naphthenic base. The oil content of these emulsions may vary from as low as a few ppm to 40%. They may vary in consistency from watery thin to a moderately heavy cream.

The produced water from some leases and ballast water from some oil tankers contain sufficient oil to be or have the characteristics of an oil-in-water emulsion. Such water is usually treated with chemicals formulated for water treating and with equipment described in Chap. 15.

Reverse emulsions may not require much, if any, heat. Because the external phase is water, the viscosity is quite low at ambient temperature. The chemicals used to treat reverse emulsions are usually some type of surface-active compounds that will neutralize the charges on the oil particles and allow them to coalesce during the gentle agitation that should follow introduction and mixing of the chemical with the emulsion. Overtreatment of this type of emulsion with chemical can result in stabilization rather than breaking of the emulsion.

Empirical data and experience are required to design equipment and/or systems for resolving reverse emulsions.

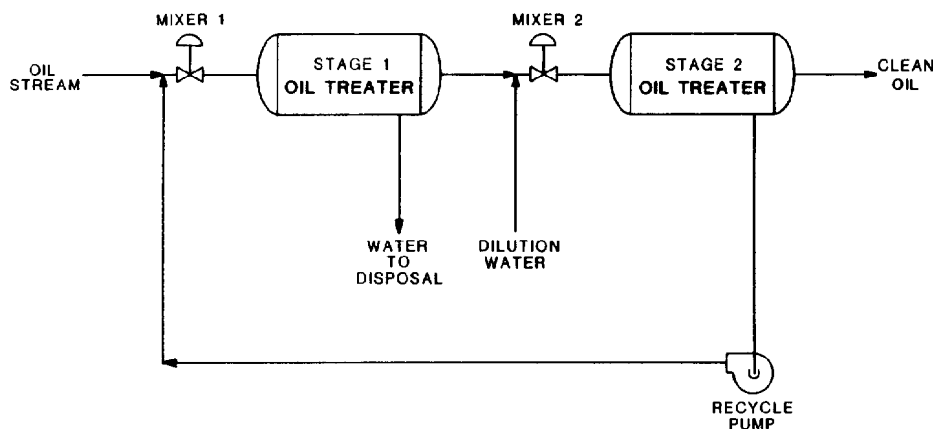


Fig. 19.36—Two-stage desalting using second-stage recycle.

Treating Emulsions Produced From EOR Projects

Standard emulsion-treating procedures, equipment, and systems used during primary and secondary oil production may not be adequate to treat the emulsions encountered in EOR projects. EOR methods of oil production—such as in-situ combustion and steam, CO_2 , caustic, polymer, and micellar (surfactant/polymer) floods—may result in the production of emulsions that may not respond to treatment normally used in primary and secondary oil production operations.

The treatment of the emulsions from EOR projects is usually handled independent of the primary and secondary emulsions from the same fields. Emulsion-treating procedures, equipment, and systems have been and are continuing to be developed for use in these EOR projects.

Clarification of Water Produced with Emulsions

Even though a normal (water-in-oil) emulsion exists in the oil production system, when produced water is separated from crude oil, the water usually contains small quantities of oil. The oil has been divided into small particles and dispersed in the water by agitation and turbulence caused by flow in the formation; into the wellbore; through the bottomhole pump, standing valve, traveling valve, and tubing; reciprocation of sucker rods; flow through the wellhead choke, flowline, manifold, oil and gas separator, and treating system; and by surface transfer pumps.

These small particles of oil will be suspended in the water and held there by mechanical, chemical, and electrical forces. The amount of oil contained in the untreated produced water in most systems will vary from an average low of about 5.0 ppm to an average high of about 2,000 ppm. In some water systems, oil contents as high as 20,000 ppm (2.0%) have been observed.

The oil particles in the untreated produced water will usually vary in size from 1 to about 1,000 μm , with most of the oil particles ranging between 5 and 50 μm in diameter.

Nine methods can be used to remove oil from the produced water: chemical, heat, gravity settling (skim tanks, API separators, etc.), coalescence (plate, pipe/free flow), tilted plate (corrugated) interceptors, flotation, flocculation, filtering, and combinations of the above. Refer to Chap. 15 for a discussion of the details of deoiling the produced water.

Operational Considerations for Emulsion-Treating Equipment

Burners and Fire Tubes

The design of burners and fire tubes is of importance because of the high cost of fuel and the operating problems that can occur when they malfunction. The burner should be designed to provide a flame that does not impinge on the walls of the fire tube, but that is almost as long as and concentric with the fire tube. If the flame touches the fire-tube wall, hot spots can develop, which can lead to premature failure.

Burners should not be allowed to cycle off and on frequently because thermal stresses caused by temperature reversals can damage the firebox. The combustion con-

trols should be accessible and designed so that the operator can easily adjust the air and gas to achieve optimum flame pattern and peak combustion efficiency.

A reliable pilot burner is required. Many operators and some regulatory agencies require burner safety shutdown valves that will shut off fuel to the burner in case of pilot failure. Unless specifically requested by the purchaser, most small emulsion treaters normally will not include this feature.

API RP 14C, "Analysis, Design, Installation and Testing of Basic Surface Safety Systems for Offshore Production Platforms," contains a basic description of recommended safety devices needed for fired- and exhaust-heated units. Consideration should be given to installing these devices on onshore, as well as offshore, fired treaters. They include process high-temperature shutdown, burner exhaust high-temperature shutdown, low-flow devices and check valves for heat exchangers, high- and low-pressure shutdown sensors, pressure-relief valves, flame arresters, fan motor starter interlocks on forced draft burners, etc.

Every gas-fired crude oil heating unit should be provided with fuel gas from which liquids have been "scrubbed." In large facilities, this can be accomplished with a central fuel-gas scrubber or filter providing fuel gas to all fired units. Many small facilities are equipped with individual fuel-gas scrubber vessels for each fired unit. These fuel-gas scrubbers are typically 8 to 12 in. in diameter and 2 to 4 ft tall, and contain a float-operated shutoff valve. If liquid enters the fuel-gas scrubber, the float will close a valve and stop gas flow to the burners of the heating unit. This will prevent oil from entering the combustion chamber and possibly prevent a fire.

Most fire tubes that transfer heat to crude oil or emulsion are sized to transfer 7,500 Btu/hr-sq ft, although some manufacturers use heat-transfer rates as high as 10,000 Btu/hr-sq ft. Fire tubes that transfer heat to the water-wash section of a treater, as in a vertical treater, are sized for 10,000 Btu/hr-sq ft, although some manufacturers use heat-transfer rates as high as 15,000 Btu/hr-sq ft. These higher rates are not recommended because they can be overly optimistic and thus may undersize the required fire tube area.

The temperature controller, fuel control valve, pilot burner, main burner, combustion safety controls, and fuel-gas scrubber for controlling and cleaning the fuel gas for fired treating vessels should be inspected and cleaned periodically as required. A schedule of preventive maintenance is recommended for this equipment.

Deposits of soot, carbon, sulfur, and other solids, if any, should be removed from the combustion space periodically to prevent reduction in heating capacity and loss of combustion efficiency. On oil-fired units, the following items should be inspected and maintained periodically: combustion controls, burner nozzles, combustion refractory, air/fuel control linkages, oil pump, oil preheater, pressure and temperature gauges, and O_2 and/or CO_2 analyzers.

Cleaning Vessels

Crude oil emulsions may contain mud, silt, sand, salts, asphalt, paraffin, and other impurities produced in conjunction with crude oil and accompanying water. In most

instances, these impurities are present in small quantities and add little to the treating problem. However, the treating problem may be made difficult and expensive because of the presence of one or more of these impurities in appreciable quantity. Special equipment and techniques may be required to handle these materials.

It is good practice to equip all treating vessels with cleanout openings and/or washout connections so that the vessels can be drained and cleaned periodically. Larger vessels should be equipped with manways to facilitate cleaning them. Steam cleaning may be required periodically. Acidizing may be required to remove calcium carbonate or similar deposits that cannot be removed by hot water or by steam cleaning.

One of the most likely causes of difficulty in operating fired emulsion-treating vessels is the deposition of solids on heating tubes and nearby surfaces. It is desirable to prevent such deposits, but if they cannot be prevented, these surfaces should be cleaned periodically. The deposits insulate the heating tube, reducing heating capacity and efficiency. Also, these materials may cause accelerated corrosion.

Of the salts commonly found in oilfield waters, the chlorides, sulfates, and bicarbonates of sodium, calcium, and magnesium are predominant. The most prevalent of the chlorides is NaCl. Calcium and magnesium chloride are next in quantity. These salts can be found in practically all water associated with crude oil. Salts are seldom found in the crude oil, but if they are present, they are mechanically suspended and not dissolved in it.

Emulsion-heating equipment is particularly susceptible to scaling and coking. These processes of deposition are not distinctly separate but may occur simultaneously. Also, one may hasten the other.

Calcium and magnesium carbonates and calcium and strontium sulfates are readily precipitated on heating surfaces in emulsion-treating equipment by decomposition of their bicarbonates and the resultant reduced solubility in the water carrying them. These materials will be deposited in pipes, tubes, fittings, and the inside surface of treating vessels. Maximum deposition will occur at the hottest surfaces, such as on heating coils and fire tubes.

Scale deposition also may occur when pressure on the fluid is reduced. This is the result of release of CO₂ from the bicarbonates in salt water to form insoluble salts that tend to adhere to surfaces of equipment containing the fluid.

Coke is not generally a primary fouling material. When deposits of salt, scale or any other fouling material build up, however, coking begins as soon as the insulating effect of the fouling material causes the skin temperature of the heating surface (heating tube or element) to reach 600 to 650°F. At this temperature, coke begins to form, which further aggravates fouling and reduces heat transfer. Once coking starts, a burnout of the firebox may follow quickly.

In areas where fluids cause considerable scaling or coking, the amount of such deposits can be reduced to a minimum by decreasing the treating temperature or by use of chemical inhibitors, properly designed spreader plates, and favorable fluid velocities through the equipment. Arranging the internals of the equipment so that all surfaces are as smooth and continuous as possible will also reduce such deposits. The operator should periodically inspect the equipment internally and clean the surfaces as required

if trouble-free operation is to be obtained over a long period of time. It is impossible to eliminate the deposition of solids entirely in emulsion-treating equipment, but it can be minimized.

Removing Sand and Other Settled Solids

Sand and silt may be produced with many crude oils. They may settle out in the vessel and be difficult to remove. It is common to shut down and drain the vessel periodically for cleaning. Sand can be removed from the unit with rakes and shovels or with a vacuum truck. The use of "sand pans," automated water jets, and drain systems can eliminate or minimize the problem of sand and silt in emulsion-treating vessels, but it is very difficult to eliminate sand buildup in large-diameter tanks.

Sand pan is the name given to a special perforated or slotted box or enclosure located in the bottom portion of a vessel or tank. Sand pans are designed to cover the area of the vessel that the flow of discharging water will clean. Often they are designed to work in conjunction with a set of water jets. The sand pans for horizontal vessels usually consist of elongated, inverted V-shaped troughs that are located parallel with and on the bottom of the vessels and that straddle the vertical centerline of the vessel. In the design in Fig. 19.37, the sand pans have sides that make an angle of 60° with the horizontal. The bottom edges of the sloping sides are serrated with 2-in. V-shaped slots and are welded to the interior of the shell of the treater. Most sand pans used in horizontal vessels are 5 ft long; a 60-ft-long horizontal vessel will typically have 11 sand pans and 11 sand-dump valves.

Sand pans, without a water jet system, have satisfactorily removed sand from most horizontal vessels up to 6 or 8 ft in diameter. Horizontal vessels larger than 4 ft in diameter should be equipped with a water jet system in addition to sand pans to keep sand cleaned from the vessel. Typical sand pans with a water jet system are illustrated in Fig. 19.37.

In vertical vessels, the sand pan may be a flanged and dished head approximately one-third the diameter of the vessel in which it is concentrically located. The sand pan is usually serrated around the periphery where it is welded to the bottom head of the vertical vessel concentric with the water outlet.

Water jets usually are designed to flow approximately 3.0 gal/min of water through each jet with a differential pressure of 30 psi. Standard jets are available for this service that have a 60° flat fan jet pattern. The jets are usually spaced on 12- or 16-in. centers. The water jet header is U-shaped so that the vessel is cleaned on both sides of the sand pan simultaneously. The water jets can be programmed for all the jets to flow at the same time, or they can be controlled by operation of the water jets and the sand dump valves in sequential cycles.

One problem in removing sand from vessels is that very few, if any, water-discharge control valves can withstand the abuse of sand-cutting during the water-discharge period for the long term. The partial answer to this problem is to arrange the instrumentation to open and close the water-discharge control valve on clean sand-free water and to use special slurry-type valves.

The most sophisticated sand-removal systems use programmable logic controllers. This solves the problem of selection of the proper time intervals between dumps

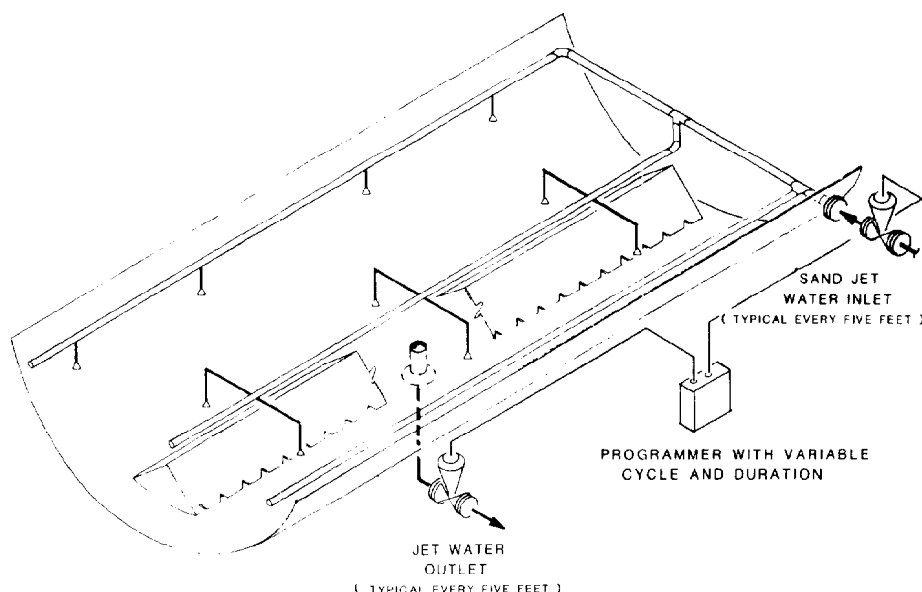


Fig. 19.37—Sand pans and water jet system in a horizontal vessel.

and automatically controls the length of the water/sand discharge. The timing must be coordinated with the water jet system and the normal water-dump controller. A properly designed sand-removal system with proper water-jetting and water/sand dumping can operate for many years without the need for a shutdown to clean out the sand or to repair or replace the dump valve.

Most emulsion-treating systems that handle large volumes of sand should not rely on hand or non-programmed operation for removal of the sand. If the operator fails to activate the dump valve often enough, the sand will cover the sand pans and plug or partially plug the water outlet, and the drains will become inoperative. With sand pans in the treater but without a programmer, large volumes of sand will usually cause trouble by plugging or partially plugging the water outlets and/or by cutting or wearing the drain valve.

Because both the amount and type of sand vary greatly, the length and frequency of the water-jetting and dumping cycles must vary to suit local conditions. Most of the coarser sand will settle out in the inlet end of the treater; the fine sand will settle out near the outlet end of the treater. It may be necessary to cycle the water jets and drain valves near the inlet end of the treater three to four times more frequently than those near the outlet end of the unit. Many timers are set for 30 minutes between jetting and dumping cycles and for 20- to 60-second jetting and dumping periods.

Interfacial Buildup

Interfacial buildup, sometimes referred to as sludge, is material that may collect at or near the oil/water interface of emulsion-treating tanks and vessels. Interfacial

buildup may contain paraffin, asphaltenes, bitumen, water, sand, silt, salt, carbonates, oxides, sulfides, and other impurities mixed with the emulsion. It can be removed from the vessel through a drain installed at the interface. The most common procedure, however, is to close the water dump valve and float it out to a bad-oil tank for further processing or disposal. Interfacial buildup can also be discharged with the water by opening the water-drain valve.

Corrosion

Emulsion-treating equipment that handles corrosive fluids should periodically be inspected internally to determine whether remedial work is required. Extreme cases of corrosion may require a reduction in the working pressure of the vessel or repair or replacement of vessel and piping. Periodic ultrasonic tests can measure the wall thickness of vessels and piping to detect the existence and extent of corrosion.

Corrosion of emulsion-treating equipment is usually mitigated or controlled by a combination of the following.

Exclusion of Oxygen. Corrosion rates in most oilfield applications can be kept low if O_2 is excluded from the system. Care must be taken in the process design to install and maintain gas blankets on all tanks in the process and to exclude rainwater from the system. Recycled water from sump systems and storage tanks is a prime source for O_2 entry into the process.

Corrosion Inhibitors. An inhibitor is a material that, when added in small amounts to an environment potentially corrosive to a metal or alloy, effectively reduces

the corrosion rate by diminishing the tendency of the metal or alloy to react with the solution. Inhibitors, in the form of liquid solutions or compounds, can be injected into the flow stream in the flowline, manifold, or production system to inhibit corrosion that would occur otherwise.

Cathodic Protection. Sacrificial galvanic anodes are commonly used for cathodic protection. They are made of a metal that will provide sacrificial protection to the steel vessel because of its relative position in the galvanic series. Most galvanic anodes used in emulsion treaters are about 3 to 6 in. in diameter and about 3 to 4 ft long. Multiple anodes usually are installed in each vessel. The anodes usually are sized to last from 10 to 20 years. They are considered expendable and are always installed in the vessel through a flange or quick coupling so that they can be easily replaced when expended.

The galvanic anodes must be installed so that they are immersed in the water, which serves as an electrolyte. They will not protect the treater if they are immersed in the oil. The anodes must "see" all metal surfaces that are to be protected—i.e., there must be no obstructions between the anodes and the surface they are to protect. Each anode should be located as near the center of the compartment or area they are to protect as practical.

An impressed electric-current cathodic protection system can also be used to inhibit corrosion. It is a direct electric current supplied by a device using a power source external to the electrode system. The DC current can be obtained by rectifying AC current. When resistivity of the electrolyte ranges from 25 to 300 $\Omega \cdot \text{cm}$ and above, consideration should be given to the use of an impressed current system. Impressed current systems are difficult and costly to maintain, however, and usually require skilled technicians.

Electrical current density requirements for cathodic protection of emulsion-treating vessels usually range from 5 to 40 mA/sq ft of bare water-immersed steel.

Internal Coating. Emulsion-treating vessels can be coated internally for protection from corrosion. It is important that the internal surfaces and the welds of the vessels be properly prepared to receive the coating. A coating system must be selected that will withstand the physical and chemical environment to which it will be exposed. Coating specifications, application techniques, and final inspection are very important considerations. Most coating systems will contain some holidays (breaks in the coating) or may be damaged in shipping or installation. Therefore, coating alone should not be relied on to prevent corrosion.

Steel tanks can be galvanized or lined in the field with fiberglass or other coatings. Some operators use fiberglass tanks in their emulsion-treating process, while others feel that this represents an unnecessary fire hazard.

Special Metallurgy. In particularly severe environments, such as where large quantities of CO_2 are expected and where O_2 cannot be practically eliminated from the system, it is possible to minimize corrosion by using stainless steel vessels or an internal stainless cladding in carbon steel vessels. In most low-pressure applications, stainless vessels are less expensive than clad vessels. It may also be cheaper to use a stainless vessel than one that is internally coated because of the labor required to prepare and to coat the internal surfaces of the vessel.

Level Controllers and Gauges

A wide selection of liquid-level controllers is available for liquid/gas control and for oil/water interface control in light crude oil (above 20°API) systems. For interfacial controllers in light crude oils, floats that sink in the oil but float in the water normally are used.

For heavy crude oils, electronic interface controllers have been very successful. These operate on the principle of the differences between oil and water electrical conductivity, electrical capacitance, or radio frequency. The most common type is called "capacitance probes"; they use the dielectric strength of the fluid in which they are immersed.

Standard gauge glasses (reflex or transparent) are used on 20°API crude oil and higher. Reflex gauges normally are used on liquid/gas levels and transparent gauges for oil/water levels. Armored gauge glasses normally are used on pressure vessels and tubular gauge glasses on tanks. Some operators use the tubular gauge glasses on low-pressure treating equipment. Tubular gauge glasses normally are furnished on standard low-pressure vessels unless armored gauges are specified.

For API gravities below 20°API, gauge glasses are not recommended, particularly for interfacial service, because they are difficult or impossible to read. In lieu of gauge glasses, a system of sample valves is used with the sample lines all piped to a single point just above a sample box. Generally, the lines are insulated to keep them warm. A nameplate is clamped on each sample valve to designate the elevation it represents in the treater. The sample box is fitted with a drain line piped to the sump.

Water-in-Oil Detectors (BS&W Monitors)

Several companies manufacture devices for detecting and measuring the water content of crude oil. They are commonly called BS&W monitors. BS&W monitors are typically analog instruments that measure dielectric strength and are specifically designed for determination of the water content of crude oil containing a low percent of water. They do not operate satisfactorily on streams containing free water. The unit provides a water reading corresponding to the water content of the oil. It can be made to alarm, record, and control if the detected percentage exceeds the field-selectable preset limit of BS&W content.

Special Safety Features for Electrostatic Treaters

Because of the high voltage and the associated potential hazard to personnel that can result from entering a drained vessel with the grids activated, electrostatic treaters require a positive shutdown switch for the high-voltage transformer. This disconnects the transformer if the fluid level falls below a predetermined level in the treating vessel. Some manufacturers install an internal grounding device inside the treater that grounds the hot grid if fluid is not present.

Changing Excelsior Packs

Excelsior used in treating emulsions may have a serviceable life ranging from just a few days to several years. The best grade excelsior should be used because cost of the excelsior is small compared to the expense of removing and replacing it. In some fields, the excelsior must be chopped into blocks with an ax and removed in chunks.

Serviceable life of the excelsior may be extended by periodically washing it with hot water. The water level can be allowed to build up above the top of the excelsior pack and the water heated to about 210°F. The temperature should be kept this high for about 1 hour. The water should be drained quickly from the vessel while it is hot. The hot water may carry most of the foreign material with it. If the application of heat only partially cleans the excelsior, a second heating may clean it further. Care should be taken to use water that will not deposit solids in the treater while it is being heated.

Economics of Treating Crude Oil Emulsions

The object of operating oil-producing properties is to deliver consistently the maximum volume of highest-API-gravity oil to the pipeline at the lowest possible cost. Emulsions should be prevented wherever feasible and treated at the lowest cost where they cannot be prevented.

Implementation of the following directives can minimize the occurrence of emulsions and the costs of treating.

1. Eliminate production of water with oil where possible and practical.

2. Minimize the investment in emulsion-treating equipment by studying the treating problem and the selection and use of appropriate treating methods, equipment, and procedures. The emulsion treating system should be as small as possible, yet capable of adequately handling treating requirements on the lease. Treating systems may be initially oversized to allow for future development, lease expansion, or increased water production. Such anticipation of future needs should be considered when treating equipment is purchased; however, needlessly oversized systems involve unnecessary expense and accomplish nothing that properly sized systems will not accomplish.

3. Minimize the loss of oil with water and salvage oil from interfacial sludge and tank bottoms where feasible. Oil may be discharged with the water as it flows from FWKO's, emulsion treaters, gunbarrels, or other treating vessels. The fraction of oil is low and the oil is usually dispersed in small droplets. Sometimes this oil is pumped along with the water to disposal wells or delivered to operators of water disposal companies without recovery or without credit being received by the lease. This oil loss can be minimized by maintaining proper operating variables with adequately sized and maintained vessels and controls and by properly designed water treating systems.

4. Minimize chemical treating costs by use of the most appropriate chemical demulsifier compound(s), the optimum quantity of chemical, the proper location and method of injection of chemical, the proper means of intimately mixing chemical with emulsion, and the proper use of heat. Treating chemicals are not recoverable and constitute a continuing expense. Some crude oil can be adequately treated by chemical injection used in conjunction with coalescing and/or settling without heat. However, some emulsions require an increased temperature during the coalescing and settling period. A proper balance of chemical and heat aids in providing the most economical and efficient treating system. The chemicals must be intimately mixed with emulsion so that a minimum amount of chemical will provide maximum benefit. Chemicals may be wasted by being injected into the oil in large slugs and not intimately mixed with the emulsions.

5. Ensure that chemicals added to the produced fluids are compatible. Some corrosion inhibitors can cause emulsions or affect the action of oil-treating chemicals. Chemicals used in produced-water-treating systems may be recycled to the oil-treating system with the skimmed oil and cause emulsion-treating problems.

6. Conserve gravity and volume of oil by using optimum treating temperature, cooling oil before discharging to storage, discharging vent gases from treating vessels through cooler oil in stock tanks, maintaining slight gas pressure on treating system and storage tanks, and using vapor recovery equipment on vessels and tanks. Crude oil emulsions should be resolved at the lowest effective temperature. Excessive heat drives condensable vapors from the oil, and they are discharged with the gas. Loss of these light ends lowers the API gravity of the oil and simultaneously reduces the oil volume. A further disadvantage of overheating is the increased maintenance required on treating systems caused by hot spots, salt deposition, scaling, and increased rate of corrosion, especially of the fireboxes.

7. Use all treating equipment to the best advantage. By careful observations, supervision, and record keeping, emulsion-treating equipment can be used to maximum efficiency. Transfer of equipment and alterations or additions to the treating system may be made to use existing equipment better. Constant testing and vigilance are required to obtain maximum results.

8. Practice preventive maintenance to minimize irretrievable loss of oil production because of downtime for equipment repairs. The more complex the treating system, the greater will be the possibility of mechanical failure. Oversized and overly complex systems have a greater failure frequency than more appropriately designed, simpler, and more compact systems.

9. Exchange information on treating methods and results among company personnel, with other operators, engineering firms, vendors, and chemical-treating companies. Experience can be gained and shared by personnel responsible for handling treating problems, which will result in lower treating costs.

Cost records are important in oil emulsion-treating operations. To achieve optimum operation of emulsion-treating equipment at minimum cost, proper records must be kept of operating temperatures, pressures, fuel and/or power consumption, chemical usage, performance, etc. Such records should be kept on a daily, weekly, or monthly basis, reviewed regularly, and kept available for supervisory personnel.

Cost records make it possible to predict whether an existing system should be modified or replaced. Justification for modifying or replacing an existing system will depend on the efficiency of the system, and this can be determined best from accurate and reliable cost and performance records. Cost records on existing methods or systems will assist in determining the type, kind, and size of treating systems for new leases. Treating cost records should make it possible to determine current operating costs, probable installation costs for new systems, and probable future operating costs of similar systems.

Each operator should determine what is to be charged to emulsion-treating costs. Listed in Table 19.2 is an outline of items that may be considered part of the data base for a cost-accounting system. Some of these items will

not be applicable to all treating systems, and some operators may elect to group some of the categories. A comprehensive general listing is presented for those who wish to consider all items of cost. Special systems and conditions may require additional cost items.

It is necessary to consider all factors listed in Table 19.2 if complete and accurate treating cost records are to be compiled. This information should be obtained and recorded on a continuous daily, weekly, or monthly basis, and it must be accurate and concise if cost records are to be of maximum value.

Investment costs must include the initial cost of all equipment used, including the cost of transporting it to the location, of erecting and installing the equipment, and of readying the system for operation. Such items as pipe and pipe fittings, valves, grade work, foundations, and fencing should be included.

The labor cost should include supervisory personnel, cost of company gang and contract gang, and other labor required to obtain, install, and put the treating system into operation. Operating cost should be kept separate from maintenance cost and should include such items as supervisory labor, operating labor, chemicals, fuel, and miscellaneous supplies. Maintenance cost should include cost of maintaining and repairing all treating equipment. This should include such items as cleaning, repairing, painting, and other similar items.

The Overall System Performance section should include an accurate record of the volume of oil treated and the volume of water separated, treated, and handled. This part of the record should also include reference to troubles experienced with the system and a commentary on day-to-day performance of the unit or system.

Key Equations in Metric Units

$$Q = 53.09 \Delta T (0.5 q_o \gamma_o + q_w \gamma_w), \quad (2)$$

where

Q is in watts,
 ΔT is in Kelvin,
 q_o is in m^3/d ,
 γ_o is dimensionless,
 q_w is in m^3/d , and
 γ_w is dimensionless.

$$v = \frac{5.43 \times 10^{-10} (\Delta \gamma_{ow}) d^2}{\mu_o}, \quad (3)$$

where

v is in m/s ,
 $\Delta \gamma_{ow}$ is dimensionless,
 d is in μm , and
 μ_o is in $\text{Pa}\cdot\text{s}$.

General References

Arnold, K. and Stewart, M.: *Surface Production Operations, Volume 1: Design of Oil-Handling Systems and Facilities*, Gulf Publishing Co., Houston (1986).

Bansback, P.L. and Bessler, D.U.: "Cold Treating of Oilfield Emulsions," presented at the Southwestern Petroleum Short Course, Dept. of Petroleum Engineering, Texas Tech U., Lubbock, April 1975.

TABLE 19.2—COSTS OF EMULSION TREATING

Equipment Investment Costs

Material

Treating equipment and facilities
 Auxiliary equipment, controls, and accessories

Labor to install equipment

Company labor
 Contract labor

Other expenses

Surface rights
 Special services
 Other

Operating Costs

Material

Chemicals
 Chemical injection equipment
 Diluents and solvents
 Testing apparatus
 Depreciation allowances
 Other

Labor

Supervisory
 Operator or pumper
 Steaming or cleaning crew
 Gang
 Contract
 Other

Other expenses

Equipment rental
 Fuel (gas or liquid)
 Electric current
 Transportation
 Laboratory expenses
 Other

Maintenance Costs

Material

Maintenance
 Replacements and additions
 Repairs

Labor

Supervisory
 Pumper or operator
 Mechanic
 Painting
 Gang
 Contract
 Other

Other Expenses

Equipment rental
 Transportation
 Other

Overall System Performance

Volume of oil treated
 Water content of treated oil
 Volume of water produced
 Volume of water treated
 Volume of oil salvaged from water treatment
 Remarks or observations

- Becher, P.: *Principles of Emulsion Technology*, Reinhold Publishing Corp., New York City (1955).
- Bessler, D.U.: "Demulsification of Enhanced Oil Recovery Produced Fluids," Tretolite Div.-Petrolite Corp., St. Louis, MO (March 23, 1983).
- Blair, C.M.: "Handling the Emulsion Problem in the Oil Fields," Magna Corp., Santa Fe Springs, CA (Dec. 6, 1971).
- Blair, C.M.: "Interfacial Films Affecting the Stability of Petroleum Emulsions," *Chemistry and Industry* (1960) 538-44.
- Breaking Emulsions by Chemical Technology—Theories of Emulsion Breaking*, Technology Series CTS-V3, Nalco Chemical Co., Sugarland, TX (1983).
- Coppel, C.P.: "Factors Causing Emulsion Upsets in Surface Facilities Following Acid Stimulation," *JPT* (Sept. 1975) 1060-66.
- "Corrosion Control," *Corrosion*, L.L. Shreir (ed.), John Wiley and Sons Inc., New York City (1963) 2, 18.12.
- Corrosion Control in Petroleum Production*, NACE TPC-5, Item 51103, Natl. Assn. of Corrosion Engineers, Houston (1979).
- Corrosion Inhibitors*, Item 51073, Natl. Assn. of Corrosion Engineers, Houston (1973).
- CO₂ Corrosion in Oil and Gas Production: Selected Papers, Abstracts, and References*, Item 51120, Natl. Assn. of Corrosion Engineers, Houston (1984).
- "Demulsification," Tretolite Div.-Petrolite Corp., St. Louis, MO (1975).
- "Design, Installation, Operation, and Maintenance of Internal Cathodic Protection Systems in Oil Treating Vessels," NACE Standard RP-05-75, Natl. Assn. of Corrosion Engineers, Houston (Oct. 1975).
- Fontaine, E.T.: "Oilfield Brine Vessels—Cathodic Protection for Brine Handling Equipment," *Materials Protection* (March 1967) 6, No. 3, 41-44.
- H₂S Corrosion in Oil and Gas Production: A Compilation of Classic Papers*, Item 51113, Natl. Assn. of Corrosion Engineers, Houston (1981).
- Impurities in Petroleum: Occurrence, Analysis, and Significance to Refiners*, Petrolite Corp., St. Louis, MO (1958).
- Introduction to Oilfield Water Technology*, Item 52140, Natl. Assn. of Corrosion Engineers, Houston (1979).
- Jones, T.J., Neustadter, E.L., and Whittingham, K.P.: "Water-in-Crude Oil Emulsion Stability and Emulsion Destabilization by Chemical Demulsifiers," *J. Cdn. Pet. Tech.* (April-June 1979) 17, No. 2, 100-08.
- Mansurov, R.I. *et al.*: "Sravnitel'nye Ispytaniya Elektrodegidratorov Trekh Konstruktsii (Comparative Tests of Three Differently Designed Electrodehydrators)," *Neft Khoz* (Dec. 1976) No. 12, 50-53.
- Manual of Petroleum Measurement Standards*, API Manual, Item No. 852-25235, API, Dallas.
- McClafflin, G. *et al.*: "The Replacement of Hydrocarbon Diluent With Surfactant and Water for the Production of Heavy, Viscous Crude Oil," *JPT* (Oct. 1982) 2258-64.
- McGhee, E.: "Una Sola Planta Deshidratara 150,000 BPD," *Petróleo Interamericano* (Aug. 1965) 42-46.
- Mennon, V.B. and Wassan, D.T.: "Demulsifications," *Encyclopedia of Emulsion Technology*, P. Becher (ed.), Marcel Dekker, New York City (1984) 2.
- Moilliet, J.L., Collie, B., and Black, W.: *Surface Activity, the Physical Chemistry, Technical Applications, and Chemical Constitution of Synthetic Surface-Active Agents*, D. Van Nostrand Co. Inc., Princeton, NJ (1960).
- "Nalco Announces New Emulsion Breaker High Temperature/Pressure Heater Treater Simulator," *Vispatch* (Sept. 1984) 3, No. 2.
- "New Mechanical Coalescing Medium is Used in Treaters," *Oil and Gas J.* (Jan. 23, 1984) 82-83.
- Petrov, A.A. and Shtof, I.K.: "Investigation of Structure of Crude Oil Emulsion Stabilizers by Means of Infrared Spectroscopy," *Chemical Technology Fuels Oils* (July-Aug. 1974) 10, No. 7-8, 654-57.
- "Practices and Methods of Preventing and Treating Crude Oil Emulsions," *Bull.* 417, U.S. Bureau of Mines, Superintendent of Documents, Washington, D.C. (1939).
- "Recommended Practice for Analysis, Design, Installation, and Testing of Basic Surface Safety Systems on Offshore Production Platforms," latest edition, API RP 14C, API, Dallas.
- "Recommended Practice for Analysis of Oil-Field Waters," latest edition, API RP 45, API, Dallas.
- "Recommended Practice for Design and Installation of Offshore Production Platform Piping Systems," latest edition, API RP 14E, API, Dallas.
- "Specification for Indirect-Type Oil Field Heaters," latest edition, API Spec. 12K, API, Dallas.
- "Specification for Vertical and Horizontal Emulsion Treaters," latest edition, API Spec. 12L, API, Dallas.
- "Standard for Welding Pipelines and Related Facilities," latest edition, API Std. 1104, API, Dallas.
- Stockwell, A., Graham, D.E., and Cairns, R.J.: "Crude Oil Emulsion Dehydration Studies," paper presented at the 1980 Oceanology Intl., Brighton, England, March 2-7, available from BPS Exhibitions Ltd., London, England.
- Treating Oil Field Emulsions*, third edition, Petroleum Extension Service, U. of Texas, Austin (1974).
- "Tretolite Chemical Demulsifiers for Petroleum Producers," *Bull.*, Tretolite Div.-Petrolite Corp., St. Louis, MO (Sept. 1978).
- Wassan, D.T. *et al.*: "Observations on the Coalescence Behavior of Oil Droplets and Emulsion Stability in Enhanced Oil Recovery," *SPEJ* (Dec. 1978) 409-17.
- Zanker, K.J.: "Radio-Wave Interface Detector Measures Low Concentrations of Oil in Water, Controls Dumping," *Oil and Gas J.* (Jan. 30, 1984) 150-52.

Chapter 20

Gas Properties and Correlations

Robert S. Metcalfe, Amoco Production Co.*

Molecular Weight

Molecules of a particular chemical species are composed of groups of atoms that always combine according to a specific formula. The chemical formula and the international atomic weight table provide us with a scale for determining the weight ratios of all atoms combined in any molecule. The molecular weight, M , of a molecule is simply the sum of all the atomic weights of its constituent atoms. It follows, then, that the number of molecules in a given mass of material is inversely proportional to its molecular weight. Therefore, when masses of different materials have the same ratio as their molecular weights, the number of molecules present is equal. For instance, 2 lbm hydrogen contains the same number of molecules as 16 lbm methane. For this reason, it is convenient to define the term "lbm mol" as a weight of the material in pounds equal to its molecular weight. (Similarly, a "g mol" is its weight in grams.) One lbm mol of any compound, therefore, represents a fixed number of molecules.

Ideal Gas

The kinetic theory of gases postulates that a gas is composed of a large number of very small discrete particles. These particles can be shown to be identified with molecules. For an ideal gas, the volume of these particles is assumed to be so small that it is negligible compared with the total volume occupied by the gas. It is assumed also that these particles or molecules have neither attractive nor repulsive forces between them. The average energy of the particles or molecules can be shown to be a function of temperature only. Thus, the kinetic energy, E_k , is independent of molecule type or size. Since kinetic energy is related to mass and velocity by

$$E_k = \frac{1}{2}mv^2,$$

it follows that small molecules (less mass) must travel faster than large molecules (more mass) when both are

at the same temperature. Molecules are considered to be moving about in all directions in a random manner as a result of frequent collisions with one another and with the walls of the containing vessel. The collisions with the walls create the pressure exerted by the gas. Thus, as the volume occupied by the gas is decreased, the collisions of the particles with the walls are more frequent, and an increase in pressure results. It is a statement of Boyle's law that this increase in pressure is inversely proportional to the change in volume at constant temperature.

$$\frac{V_1}{V_2} = \frac{p_2}{p_1},$$

where p is the absolute pressure and V is the volume.

Further, if the temperature is increased, the velocity of the molecules and, therefore, the energy with which they strike the walls of the containing vessel will be increased, resulting in a rise in pressure. To maintain the pressure constant while heating a gas, the volume must be increased in proportion to the change in absolute temperature. This is a statement of Charles's law,

$$\frac{V_1}{V_2} = \frac{T_1}{T_2},$$

where T is the absolute temperature and p is constant.

From a historical viewpoint, it is interesting to note that the observations of Boyle and Charles in no small degree led to the establishment of the kinetic theory of gases, rather than vice versa.

It follows from this discussion that, at zero degrees absolute, the kinetic energy of an ideal gas, as well as its volume and pressure, would be zero. This agrees with the definition of absolute zero, which is the temperature at which all the molecules present have zero kinetic energy.

*Author of the original chapter on this topic in the 1962 edition was Charles F. Weinaug.

TABLE 20.1—VALUES OF THE GAS CONSTANT, R , IN $pV = RT$ FOR 1 MOLE OF IDEAL GAS

Temperature Units	Pressure Units	Volume Units	Energy Units	$R/g \text{ mol}$
K	—	—	calories	1.9872
K	—	—	absolute joules	8.3144
K	—	—	international joules	8.3130
K	atm	cm ³	—	82.057
K	atm	L	—	0.082054
K	mm Hg	L	—	62.361
K	bar	L	—	0.08314
K	kg/cm ²	L	—	0.08478
				$R/lbm \text{ mol}$
R	—	—	Btu (IT)	1.986
R	—	—	hp-hr	0.0007805
R	—	—	kw-hr	0.0005819
R	atm	cu ft	—	0.7302
R	in. Hg	cu ft	—	21.85
R	mm Hg	cu ft	—	555.0
R	lbm/sq in., abs.	cu ft	—	10.73
R	lbm/sq ft, abs.	cu ft	ft-lbm	1545.0
K	atm	cu ft	—	1.314
K	mm Hg	cu ft	—	998.9
K	—	—	—	1.986

Because the kinetic energy of a molecule is dependent only on temperature, and not on size or type of molecule, equal molecular quantities of different gases at the same pressure and temperature would occupy equal volumes. The volume occupied by an ideal gas, therefore, depends on three things: temperature, pressure, and number of molecules (moles) present. It does not depend on the type of molecule present. The ideal-gas law, which is actually a combination of Boyle's and Charles's laws, is a statement of this fact:

$$pV = nRT, \dots\dots\dots (1)$$

where

p = pressure,

V = volume,

n = number of moles,

R = gas-law constant, and

T = absolute temperature.

The gas-law constant, R , is a proportionality constant dependent only on the units of p , V , n , and T . Table 20.1 presents different values of R for the various units of these parameters.

Critical Temperature and Pressure

Typical PVT relationships for a pure fluid are illustrated in Fig. 20.1. The curve segment B-C-D defines the limits of vapor/liquid coexistence, B-C being the bubblepoint curve of the liquid and C-D, the dewpoint curve of the vapor. Any combination of temperature, pressure, and volume above that line segment indicates that the fluid exists in a single phase. At low temperatures and pressures, the properties of equilibrium vapors and liquids are extremely different—e.g., the density of a gas is low while that of a liquid is relatively high. As the pressure and temperature are increased along the coexistence curves, liquid density, viscosity, etc. generally decrease while vapor density, viscosity, etc. generally increase. Thus, the difference in physical properties of the coexisting phases decreases. These changes continue as the temperature and pressure are raised until a point is reached where the properties of the equilibrium vapor and liquid become equal. The temperature, pressure, and volume at this point are called the "critical" values for that species. Location C on Fig. 20.1 is the critical point. The critical temperature and pressure are unique values for each species and are useful in correlating physical properties. Critical constants for some of the commonly occurring hydrocarbons and other components of natural gas can be found in Table 20.2.

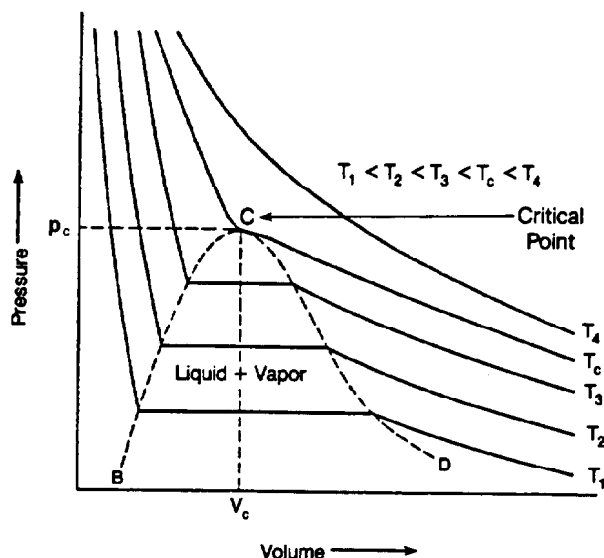


Fig. 20.1—Typical pressure volume diagram for pure component.

TABLE 20.2—SOME PHYSICAL CONSTANTS OF HYDROCARBONS

Number	Compound	Formula	Molecular Weight	Vapor Pressure (100°F, psia)	Critical Constants			Gas Density (60°F, 14.696 psia) Calculated as Ideal Gas*
					Pressure (psia)	Temperature (°F)	Volume (cu ft/lbm)	
1	methane	CH ₄	16.043	(5000)	667.8	-116.68	0.0988	59.1*
2	ethane	C ₂ H ₆	30.070	(800)	707.8	90.1	0.0788	37.48**
3	propane	C ₃ H ₈	44.097	188.0	616.3	206.01	0.0737	36.49**
4	n-butane	C ₄ H ₁₀	58.124	51.54	550.7	305.62	0.0703	31.80**
5	isobutane	C ₄ H ₁₀	58.124	72.39	529.1	274.96	0.0724	30.65**
6	n-pentane	C ₅ H ₁₂	72.151	15.575	488.6	385.6	0.0674	27.67
7	isopentane	C ₅ H ₁₂	72.151	20.4444	490.4	369.03	0.0679	27.38
8	neopentane	C ₅ H ₁₂	72.151	36.66	464.0	321.08	0.0673	26.16**
9	n-hexane	C ₆ H ₁₄	86.178	4.960	436.9	453.6	0.06887	24.38
10	2-methylpentane	C ₆ H ₁₄	86.178	6.767	436.6	435.74	0.0682	24.16
11	3-methylpentane	C ₆ H ₁₄	86.178	6.103	453.1	448.2	0.0682	24.56
12	neohexane	C ₆ H ₁₄	86.178	9.859	446.9	420.04	0.0668	24.02
13	2,3-dimethylbutane	C ₆ H ₁₄	86.178	7.406	453.5	440.0	0.0665	24.47
14	n-heptane	C ₇ H ₁₆	100.205	1.620	396.8	512.7	0.0690	21.73
15	2-methylhexane	C ₇ H ₁₆	100.205	2.2719	396.5	494.89	0.0673	21.56
16	3-methylhexane	C ₇ H ₁₆	100.205	2.131	408.1	503.67	0.0646	21.84
17	3-ethylpentane	C ₇ H ₁₆	100.205	2.013	419.3	513.36	0.0665	22.19
18	2,2-dimethylpentane	C ₇ H ₁₆	100.205	3.494	402.2	477.12	0.0665	21.41
19	2,4-dimethylpentane	C ₇ H ₁₆	100.205	3.293	397.0	475.84	0.0668	21.39
20	3,3-dimethylpentane	C ₇ H ₁₆	100.205	2.774	427.1	505.74	0.0662	22.03
21	triptane	C ₇ H ₁₆	100.205	3.375	428.4	496.33	0.0636	21.93
22	n-octane	C ₈ H ₁₈	114.232	0.537	360.6	564.10	0.0690	19.58
23	diisobutyl	C ₈ H ₁₈	114.232	1.1017	360.6	530.31	0.0676	19.33
24	isooctane	C ₈ H ₁₈	114.232	1.709	372.5	519.33	0.0657	19.28
25	n-nonane	C ₉ H ₂₀	128.259	0.1796	331.8	610.54	0.0684	17.81
26	n-decane	C ₁₀ H ₂₂	142.286	0.0609	304.4	651.6	0.0679	16.32
27	cyclopentane	C ₅ H ₁₀	70.135	9.914	653.0	461.6	0.0594	33.85
28	methylcyclopentane	C ₆ H ₁₂	84.162	4.503	549.0	499.24	0.0607	28.33
29	cyclohexane	C ₆ H ₁₂	84.162	3.266	590.9	536.6	0.0589	29.45
30	methylcyclohexane	C ₇ H ₁₄	98.189	1.6093	503.6	570.15	0.0601	24.92
31	ethylene	C ₂ H ₄	28.054	—	731.1	48.56	0.0748	—
32	propene	C ₃ H ₆	42.081	227.6	667.2	197.06	0.0689	39.25**
33	1-butene	C ₄ H ₈	56.108	62.10	583.5	295.48	0.0686	33.91**
34	cis-2-butene	C ₄ H ₈	56.108	45.95	612.1	324.37	0.0668	35.36**
35	trans-2-butene	C ₄ H ₈	56.108	49.94	587.1	311.86	0.0679	34.40**
36	isobutene	C ₄ H ₈	56.108	63.64	580.0	292.55	0.0682	33.86**
37	1-pentene	C ₅ H ₁₀	70.135	19.117	591.8	376.93	0.0676	29.13**
38	1,2-butadiene	C ₄ H ₆	54.092	36.5	(653.0)	(340.0)	(0.0649)	38.4**
39	1,3-butadiene	C ₄ H ₆	54.092	59.4	628.0	305.0	0.0655	36.69**
40	isoprene	C ₅ H ₈	68.119	16.68	(558.4)	(412.0)	(0.0650)	31.87
41	acetylene	C ₂ H ₂	26.038	—	890.4	95.32	0.0695	—
42	benzene	C ₆ H ₆	78.114	3.225	710.4	552.22	0.0525	35.82
43	toluene	C ₇ H ₈	92.141	1.033	595.5	605.57	0.0549	29.94
44	ethylbenzene	C ₈ H ₁₀	106.168	0.376	523.4	651.29	0.0565	25.97
45	o-xylene	C ₈ H ₁₀	106.168	0.263	541.6	674.92	0.0557	26.36
46	m-xylene	C ₈ H ₁₀	106.168	0.325	512.9	651.02	0.0567	25.88
47	p-xylene	C ₈ H ₁₀	106.168	0.3424	509.2	649.54	0.0570	25.80
48	styrene	C ₈ H ₈	104.152	0.238	580.0	706.0	0.0541	27.68
49	isopropylbenzene	C ₉ H ₁₂	120.195	0.188	465.4	676.3	0.0572	22.80
50	methyl alcohol	CH ₄ O	32.042	4.63	1,174.4	463.08	0.0589	78.61
51	ethyl alcohol	C ₂ H ₆ O	46.069	2.125	925.3	465.39	0.0580	54.36
52	carbon monoxide	CO	28.010	—	507.5	-220.4	0.0532	—
53	carbon dioxide	CO ₂	44.010	—	1,071.0	87.87	0.0342	59.78**
54	hydrogen sulfide	H ₂ S	34.076	387.1	1,306.0	212.6	0.046	73.07
55	sulfur dioxide	SO ₂	64.059	85.46	1,145.0	315.8	0.0306	69.01
56	ammonia	NH ₃	17.031	211.9	1,636.0	270.4	0.0681	114.71
57	air	N ₂ O ₂	28.964	—	546.9	-221.4	0.0517	—
58	hydrogen	H ₂	2.016	—	188.1	-399.9	0.5164	—
59	oxygen	O ₂	31.999	—	736.9	-181.2	0.0367	—
60	nitrogen	N ₂	28.013	—	493.0	-232.7	0.0516	—
61	chlorine	Cl ₂	70.906	154.9	1,118.4	291.0	0.0280	63.53
62	water	H ₂ O	18.015	0.9495	3,207.9	705.5	0.0509	175.6
63	helium	He	4.003	—	32.99	-450.308	0.230	—
64	hydrogen chloride	HCl	36.461	906.3	205.1	124.8	0.0356	74.88

* Apparent value at 60°F.

** Saturation pressure at 60°F.

Specific Gravity (Relative Density)

The specific gravity of a gas, γ , is the ratio of the density of the gas at a given pressure and temperature to the density of air at the same pressure and temperature. The ideal-gas laws can be used to show that the specific gravity (ratio of densities)* is also equal to the ratio of the molecular weights. When the ideal-gas assumptions are not valid (high pressures or most real gases), this will not always be true. By convention, specific gravities of all gases at all pressures are defined as the ratio of the molecular weight of the gas to that of air (28.966).

Mole Fraction and Apparent Molecular Weight of Gas Mixtures

The analysis of a gas mixture can be expressed in terms of a mole fraction, y_i , of each component, which is the ratio of the number of moles of a given component to the total number of moles present. Analyses also can be expressed in terms of the volume, weight, or pressure fraction of each component present. Under limited sets of conditions, where gaseous mixtures conform reasonably well with the ideal-gas laws, the mole fraction can be shown to be equal to the volume fraction but not to the weight fraction. The apparent molecular weight of a gas mixture is equal to the sum of the mole fraction times the molecular weight of each component.

Specific Gravity of Gas Mixtures

The specific gravity (γ_g) of a gas mixture is the ratio of the density of the gas mixture to that of air. It is measured easily at the wellhead in the field and, therefore, is used as an indication of the composition of the gas. As mentioned earlier, the specific gravity of gas is proportional to its molecular weight (M_g) if it is measured at low pressures where gas behavior approaches ideality. Once again, by convention, the specific gravity is defined as the mole weight of the gas mixture divided by 28.966. Specific gravity also has been used to correlate other physical properties of natural gases. To do this, it is necessary to assume that the analyses of gases vary regularly with their gravities. Since this assumption is only an approximation and is known to do poorly for gases with an appreciable nonhydrocarbon content, it should be used only in the absence of a complete analysis or of correlations based on a complete analysis of the gas.

Dalton's Law

The partial pressure of a gas in a mixture of gases is defined as the pressure that the gas would exert if it alone were present at the same temperature and volume as the mixture. Dalton's law states that the sum of the partial pressures of the gases in a mixture is equal to the total pressure of the mixture. This law can be shown to be true if the ideal-gas laws apply.

Amagat's Law

The partial volume of a gas in a mixture of gases is defined as that volume which the gas would occupy if it alone were present at the same temperature and pressure as the

mixture of the gases. If the ideal-gas laws hold, then Amagat's law, that the sum of the partial volumes is equal to the total volume, also must be true.

Real Gases

At low pressures and relatively high temperatures, the volume of most gases is so large that the volume of the molecules themselves may be neglected. Also, the distance between molecules is so great that the presence of even fairly strong attractive or repulsive forces is not sufficient to affect the behavior in the gas state. However, as the pressure is increased, the total volume occupied by the gas becomes small enough that the volume of the molecules themselves is appreciable and must be considered. Also, under these conditions, the distance between the molecules is decreased to the point where the attractive or repulsive forces between the molecules become important. This behavior negates the assumptions required for ideal-gas behavior, and serious errors are observed when comparing experimental volumes to those calculated using the ideal-gas law. Consequently, a real-gas law was formulated (in terms of a correction to the ideal-gas law) by use of a proportionality term called the compressibility factor, z . The real-gas law is thus

$$pV = znRT. \quad \dots \dots \dots (2)$$

Tables of compressibility factors are available for most pure gases as functions of temperature and pressure. Compressibility factors for mixtures (or unknown pure compounds) are measured easily in a Burnett¹ apparatus or a variable-volume PVT equilibrium cell. Excellent correlations are also available for the calculation of compressibility factors as discussed in the section on equations of state (EOS's). For this reason, compressibility factors are no longer routinely measured on dry gas mixtures or most of the leaner wet gases. Rich gas condensate systems require other equilibrium studies, and compressibility factors can be obtained routinely from these data. A knowledge of the compressibility factor means that the density, ρ , is also known from the relationship

$$\rho = \frac{pM}{zRT},$$

because $V = (nM)/\rho$, where M is the molecular weight.

Many times it is more convenient to report compressibilities than densities because the range in z is usually small—e.g., between 0.3 and 2.0.

Principle of Corresponding States

The principle of corresponding states has been useful in correlating the properties of gases. This principle was developed because observers noticed that the behavior of pure gases was qualitatively similar when compared (on p - V plots, for instance) even though the quantitative values of p and V were very dissimilar. The idea was advanced that the properties of substances could be correlated if they were all compared at "corresponding" values of T and p , which could be referenced easily. In the application

*Although specific gravity is used throughout this chapter, this traditional term will not be used under the SI system. It will be replaced by "relative density." Also, API gravity eventually will disappear as a measure of relative density.

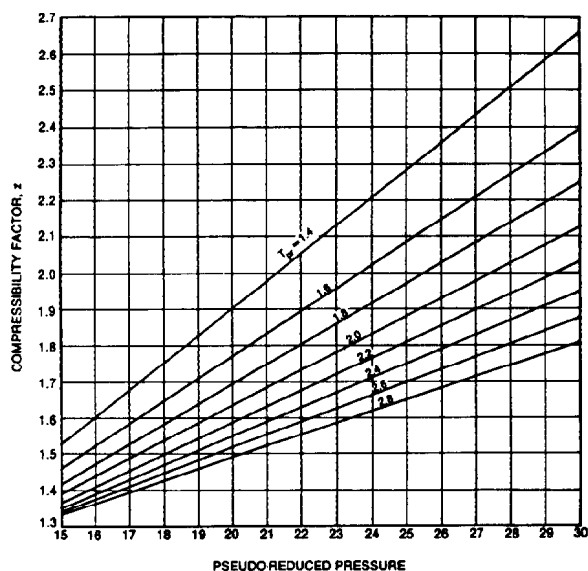


Fig. 20.2A—Compressibility factor for natural gases at pressures of 10,000 to 20,000 psia (from Ref. 2).

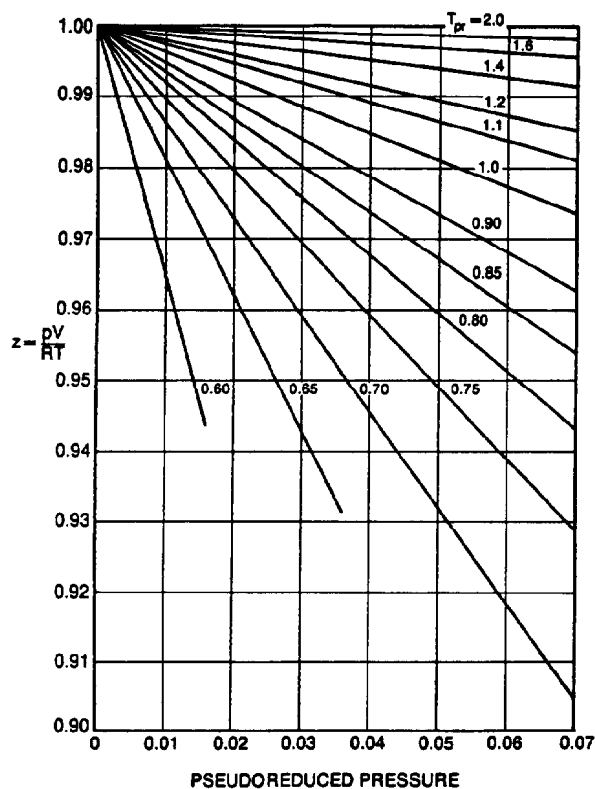


Fig. 20.2B—Compressibility factors for natural gases near atmospheric pressures.

and

$$p'_{pc} = \frac{p_{pc} T'_{pc}}{T_{pc} + y_{H_2S}(1 - y_{H_2S})\epsilon},$$

where

$$\epsilon = 120[(y_{CO_2} + y_{H_2S})^{0.9} - (y_{CO_2} + y_{H_2S})^{1.6}]$$

$$+ 15(y_{H_2S}^{0.5} - y_{H_2S}^{4.0}), \dots \dots \dots (4)$$

T'_{pc} = corrected pseudocritical temperature,
 p'_{pc} = corrected pseudocritical pressure,
 y_{CO_2} = mole fraction of CO_2 in mixture, and
 y_{H_2S} = mole fraction of H_2S in mixture.

The correction factor, ϵ , has been plotted against hydrogen sulfide and carbon dioxide concentrations in Fig. 20.4 for convenience. This correction is reported to reproduce compressibility factors with less than 1% error.

Equations of State

An EOS seeks to describe specific PVT relationships of fluids mathematically. There are hundreds of these equations ranging from those for a specific pure compound to generalized forms that claim to relate the properties of multicomponent mixtures. Naturally, there is a large range of complexity from the simple ideal-gas law to

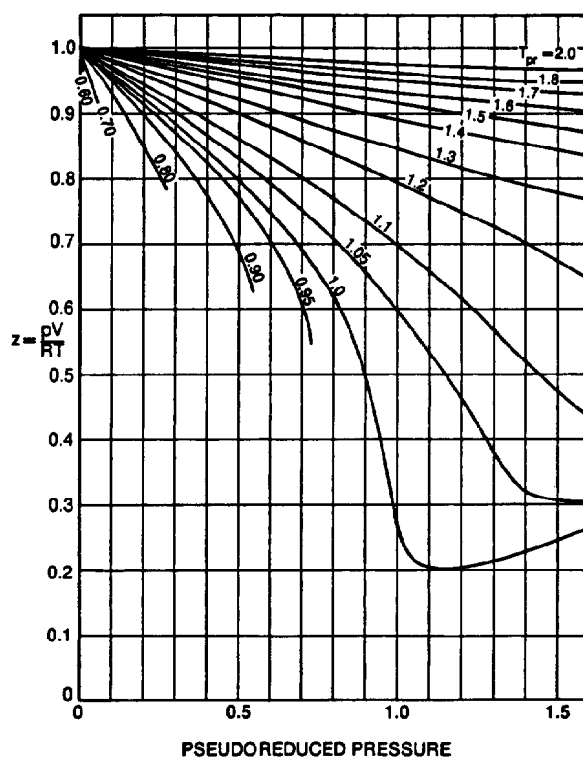


Fig. 20.2C—Compressibility factors for natural gases at low reduced pressures.

modern equations with 15 or more universal constants plus adjustable parameters. Historically, use of these equations has been limited to applications by researchers having large computing facilities. Recently, however, operating engineers have been provided with the same computing tools previously reserved only for researchers and special projects. The use of EOS's, therefore, has become relatively common. Some applications, such as calculation of compressibility factors, are possible on hand-held programmable calculators. The modern engineer should not forget the use of EOS's when the need arises for calculation or estimation of fluid properties.

Van der Waals' Equation

Van der Waals⁶ added terms to the ideal-gas law in an attempt to take into account forces between molecules as well as volume of the molecules themselves. His equation becomes

$$\left(p + \frac{a}{V_M^2}\right)(V_M - b) = RT, \quad \dots\dots\dots (5)$$

where V_M is the molar volume and a and b are constants characteristic of the gas.

The term b is a constant to correct for the volume occupied by the molecules themselves. The term a/V_M^2 is a correction factor to account for the attraction between molecules as a function of the average distance between them (which is related to the molar volume). When an EOS such as the van der Waals equation is applied to mixtures, either special constants for a and b must be developed for each mixture or constants for each gas in the mixture must be included in the equation along with adjustments for the interaction between unlike gases. The latter is the more common approach.

Van der Waals' law extends the range of pressures and temperatures for describing gas behavior beyond that of the ideal-gas law. However, it has two disadvantages in actual application. The correction factors are inadequate at very high pressures and it is not always easy to obtain the mixture coefficients and interaction constants. In addition, this two-parameter formulation does not really treat the attractive and repulsive forces correctly. Despite these criticisms, modifications of the van der Waals equation have been used successfully in industry for many years.

Redlich and Kwong⁷ developed the first major extension of the two-parameter EOS when they proposed their own form and showed how they related the a and b terms to R , p_c , and T_c . Other researchers since have modified the original Redlich and Kwong equation to improve its accuracy and generality further. Most notable of the modifications are those of Soave,⁸ Zudkevitch and Joffe,⁹ and Peng and Robinson.¹⁰ Some companies have their own versions, such as the one published by Yarbrough.¹¹

The most common equations of state in use today and the computer programs available are the following.

1. The Starling-Hon¹² extension of the Benedict-Webb-Rubin¹³ EOS:

$$\begin{aligned} p = RT\rho_M + & \left(B_o RT - A_o - \frac{C}{T^2} + \frac{D_o}{T^3} - \frac{E_o}{T^4}\right)\rho_M^2 \\ & + \left(bRT - a - \frac{d}{T}\right)\rho_M^3 + \alpha(a+d)\rho_M^6 \\ & + \left(\frac{c\rho_M^2}{T^2}\right)(1 + \gamma\rho_M^2) \exp(-\gamma\rho_M^2), \quad \dots\dots\dots (6) \end{aligned}$$

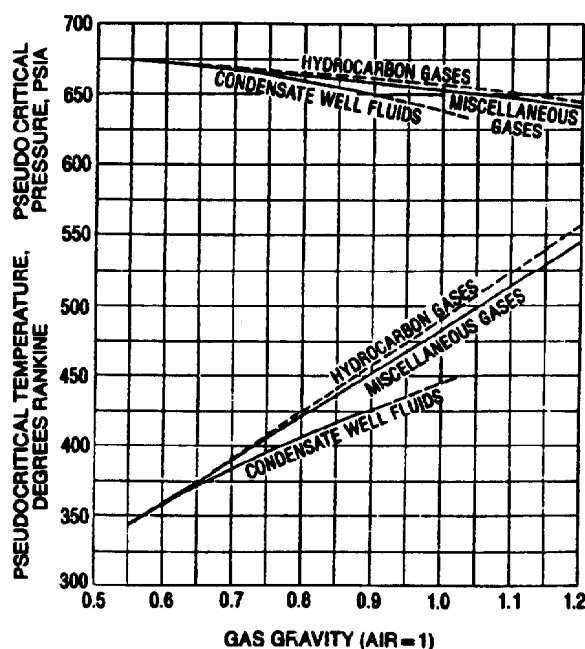


Fig. 20.3—Pseudocritical properties of natural gases.

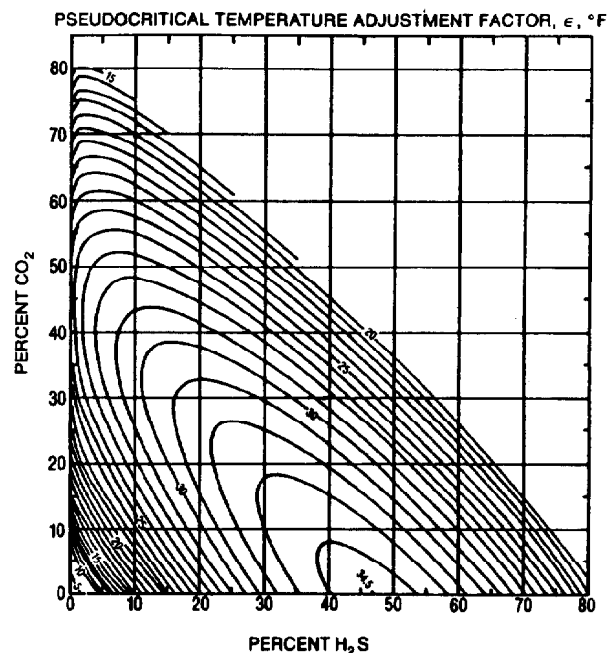


Fig. 20.4—Pseudocritical temperature adjustment factor, ϵ , °F.

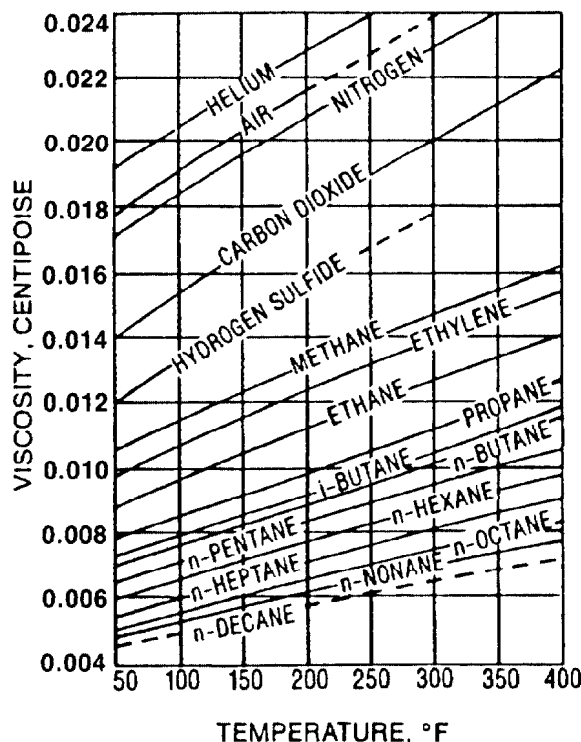


Fig. 20.5—Viscosity of pure compounds at 14.7 psia.

where A_o , B_o , C , D_o , E_o , a , b , c , d , α , and γ are empirical constants, and ρ_M equals n/V_M (subscript M refers to molar values). This equation usually is called the "BWRS" and is available from Exxon Corp.

2. The Peng-Robinson¹⁰ EOS (EquiphaseTM):

$$p = \frac{RT}{V_M - b} - \frac{a(T)}{V_M(V_M + b) + b(V_M - b)}, \quad (7)$$

where a and b are constants characteristic of the fluid, $a(T)$ is a functional relationship, and V_M is the molar volume. It is available from the Gas Processors Suppliers Assn. (GPSA).

3. The Soave⁸ modification of the Redlich-Kwong⁷ EOS:

$$p = \frac{RT}{V_M - b} - \frac{a(T)}{V_M(V_M + b)}, \quad (8)$$

where $a(T)$ is a functional relationship. It, too, is available from the GPA.

The first equation, BWRS, is an empirical form using 11 constants. The values of these constants have been determined from properties measured on many different fluids. It is extremely accurate in the prediction of most thermodynamic properties. Eqs. 7 and 8 are variations of the original equation proposed by van der Waals and as such are not as accurate as the BWRS for calculation of pure component properties or properties of mixtures of light hydrocarbons. Both the Peng-Robinson and the

Soave RK EOS's are more reliable for phase equilibrium calculations or for calculation of properties of gas condensate systems. One cannot assess their accuracy directly because it is dependent on how well the constants represent the specific components.

The Redlich-Kwong EOS and its extension are cubic in compressibility factor. J.J. Martin¹⁴ proposed a generalized cubic equation that, through suitable adjustment of parameters, can be used to obtain any other cubic including those that have been proposed after his work was published. All cubic equations have limitations in their ability to represent behavior at near-critical conditions. They are incorrect in the prediction of the critical compressibility factor and/or the shape of the critical isotherm. They can be manipulated by additional terms to circumvent this problem but errors then appear in some other region of pressure-temperature-composition space. In general, however, EOS's can be used routinely to calculate gas properties for both hydrocarbon and nonhydrocarbon systems and their mixtures.

One particularly useful application of EOS's in gas property estimations is the direct calculation of the compressibility factor, z . As noted previously, the principle of corresponding states can be used to obtain compressibilities with reasonable accuracy. However, one can solve an EOS directly for z quite readily. The most reliable methods for typical natural gases are those of Robinson and Jacoby¹⁵ and Hall and Yarborough.¹⁶ Robinson and Jacoby proposed the following equations.

$$p = \frac{RT}{V_M - b} - \frac{a}{\sqrt{T}V_M(V_M + b)}, \quad (9)$$

$$a_i = \alpha_i + \beta_i T, \quad (10)$$

and

$$b_i = \gamma_i + \delta_i T, \quad (11)$$

where α , β , γ , and δ are constants for Substance i , and for mixtures

$$a_{ij} = \frac{1}{2}[K_{ij}a_i + (1 - K_{ij})a_j],$$

$$a_m = \sum_i \sum_j y_i y_j a_{ij},$$

and

$$b_m = \sum_i y_i b_i,$$

where K_{ij} is a constant for each binary pair when used for mixtures.

Their equations are another modification of the Redlich-Kwong equation designed specifically for the region of temperatures from 70 to 250°F and pressures below 1,500 psia. It is untested for gas mixtures containing large amounts of C₄₊ material. Within these stated limits, it should be expected to calculate compressibility factors with less than 2% error.

The Hall-Yarborough equation is

$$z = \frac{(1 + x + x^2 - x^3) - Ax + Bx^C}{(1 - x)^3}, \quad (12)$$

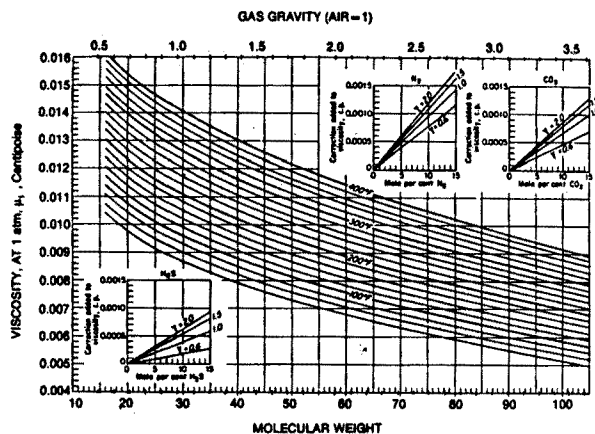


Fig. 20.6—Viscosity of gases at 14.7 psia.

where

$$\begin{aligned} z &= \text{compressibility factor,} \\ A &= (14.76t - 9.76t^2 + 4.58t^3), \\ B &= (90.7t - 242.2t^2 + 42.4t^3), \\ C &= 1.18 + 2.82t, \\ x_i &= b\rho_M/4, \\ b &= 0.245(RT_c/p_c) \exp[-1.2(1-t)^2], \text{ and} \\ t &= T_c/T. \end{aligned}$$

It is designed specifically to fit the Standing-Katz charts and provides excellent results for multicomponent systems. Hall and Yarborough also include the correction factors proposed by Wichert and Aziz for systems with high concentrations of nonhydrocarbons. The method has been programmed for hand calculators by Ajitsaria.¹⁷ Note that the equations contain both z and ρ_M , making the solution trial and error and not well suited for use without a computer or calculator algorithm.

Viscosity

Viscosity is an important property in determining resistance to flow during production and marketing of gas. Generally, the viscosity of a gas increases with increasing pressure, except at very low pressures where it becomes more or less independent of the pressure. At low pressures, the viscosity of a gas, unlike that for liquids, increases as the temperature is raised. This is caused by the increasing activity of the molecules as temperature increases. Viscosity of a fluid is obtained by determining the force per unit area necessary to shear two parallel planes with a standard spacing and velocity difference. The standard unit of viscosity is the poise, which is defined as 1 dyne·s/cm² [6.9 lbf·sec/sq in.]. However, the common unit is the centipoise (0.01 poise). Carr *et al.*¹⁸ used the data of many researchers to produce Fig. 20.5, which presents viscosities as a function of temperature at atmospheric pressure for a number of pure compounds.

Viscosity Correlations

Viscosities can be estimated both by the principle of corresponding states and by a residual viscosity function based on reduced density. Carr *et al.*,¹⁸ using the the-

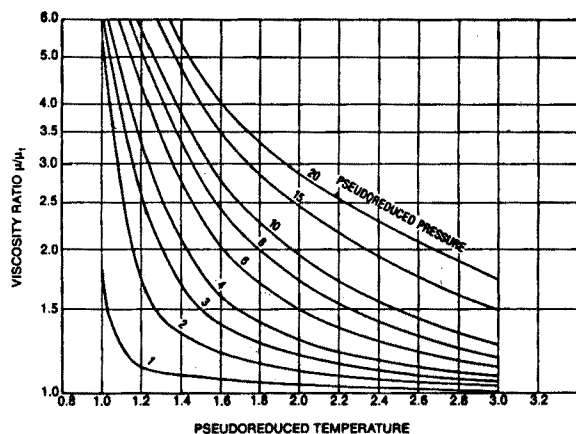


Fig. 20.7—Viscosity ratio vs. pseudoreduced temperature.

ories of transport processes, correlated viscosities of pure gases and gas mixtures against molecular weight and temperature. Fig. 20.6 presents their correlation for viscosities at atmospheric pressure. Fig. 20.7 permits estimation of a pressure correction for gas viscosities by corresponding-states techniques. The ratio of the viscosity at some elevated pressure to the viscosity from Fig. 20.6 is plotted against pseudoreduced temperature and pressure. Viscosities calculated from this correlation should be expected to have less than 2% error.

The residual viscosity function ($\mu - \mu^*$) also has been used to correlate gas viscosities with even better success than the corresponding-states technique described previously. (μ^* is a correlating parameter obtained from Fig. 20.8.) Thodos *et al.*^{19,20} have shown that the residual viscosity function can be well correlated against density, thereby making it a useful tool for both gas and liquid viscosities. The Thodos method requires two steps, as does the technique of Carr *et al.* First μ^* must be estimated, then the effect of pressure can be calculated from another correlation. The correlation for μ^* is shown in Fig. 20.8, and the effects of pressure can be estimated

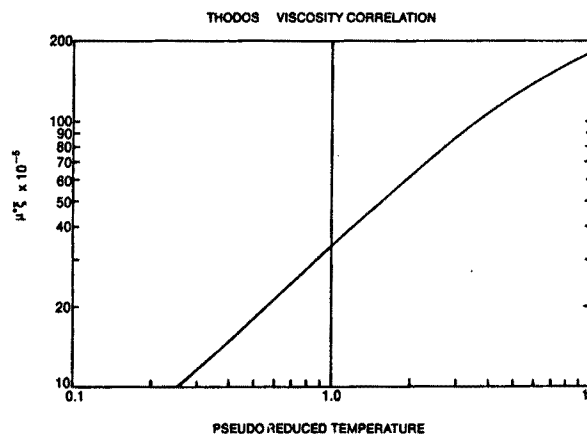


Fig. 20.8—Thodos viscosity correlation.

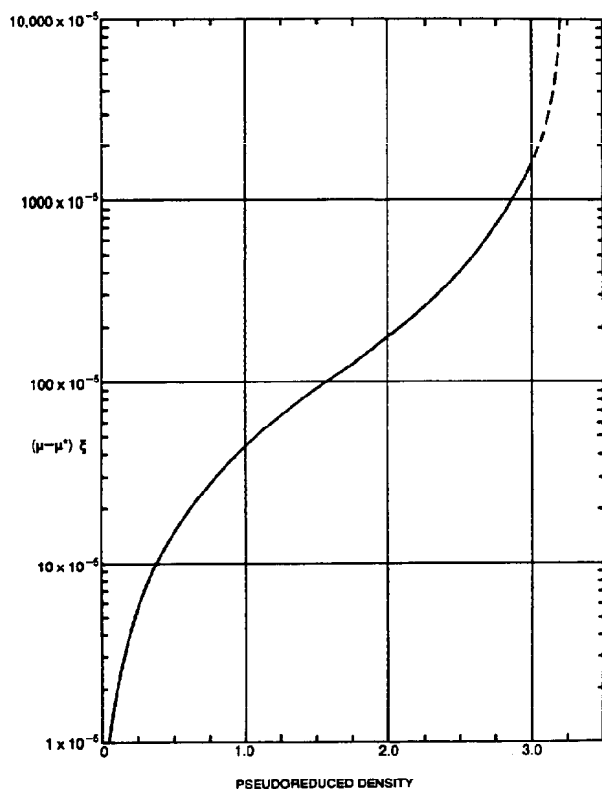


Fig. 20.9—Thodos viscosity correlation—pressure correction.

from Fig. 20.9. Viscosities calculated using the correlations of Thodos *et al.* can be expected to have an accuracy on the order of 3%.

To use Figs. 20.8 and 20.9, one must first calculate the average mole weight of the mixture, $\bar{M}_g = \sum y_i M_i$, and the pseudocritical temperature, pressure, and volume by Kay's rules (T_c in units of Kelvin and V_c in $\text{cm}^3/\text{g mol}$) or Fig. 20.3 if the C_{7+} concentration is small. Alternatively, the correlation of Matthews *et al.*²¹ (Fig. 20.10) may be used to get T_c and p_c for C_{7+} fractions. The following may be used for V_c of the C_{7+} fraction.

$$(V_c)_{C_{7+}} = 1.561(M_{C_{7+}}/\rho_R)^{1.15},$$

where $M_{C_{7+}}$ is the molecular weight of the C_{7+} fraction, and ρ_R is the relative density of the C_{7+} fraction.

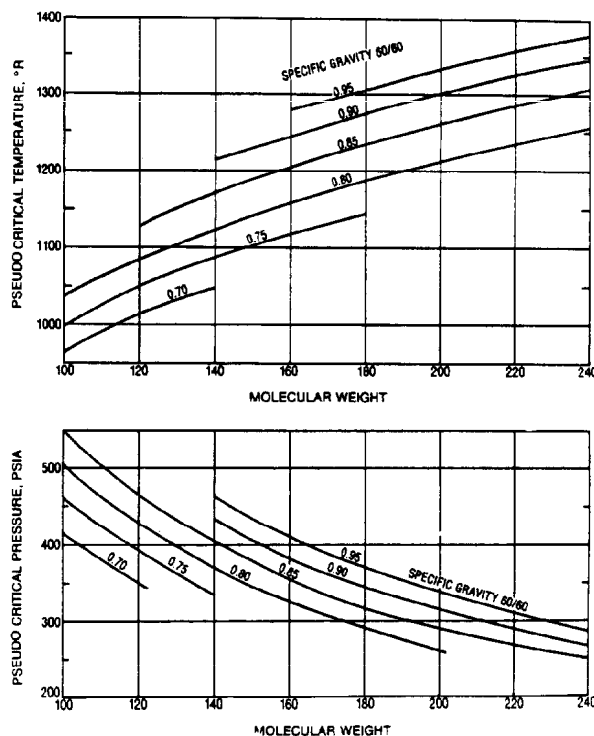
Calculation of the pseudocritical density, ρ_{pc} , and the viscosity parameter, ξ , are as follows.

$$\rho_{pc} = \bar{M}_g/V_{pc} \quad \dots \dots \dots (13)$$

and

$$\xi = \frac{(T_{pc})^{1/2}}{(\bar{M}_g)^{1/2}(p_{pc})^{1/2}}, \quad \dots \dots \dots (14)$$

where T_{pc} is the pseudocritical temperature, K, and p_{pc} is the pseudocritical pressure, atm. Caution: This is a correlation and the terms should not be converted to a consistent set of units.

Fig. 20.10—Pseudocritical properties of C_{7+} fractions.

For very quick estimations, Katz² provides graphs of viscosity vs. temperature ($^{\circ}\text{F}$) and pressure (psia) for gas gravities ranging from 0.6 to 1.0. Errors can be expected to be on the order of 4 to 5%.

If gas density is not known it can be obtained from the compressibility factor through $\rho_g = M_g p / (z_g RT)$. Compressibility factors can be obtained by using the methods discussed above. Reduced conditions then can be calculated making sure ρ and ρ_{pc} are in the same units. It is possible to use Fig. 20.8 to obtain μ^* and then obtain ξ from $\mu^* = (\mu^* \xi) / \xi$. The final step is to obtain $(\mu - \mu^*)\xi$ from Fig. 20.9 and solve for μ with $\mu = \mu^* + [(\mu - \mu^*)\xi] / \xi$.

Within the limitations of each correlation, that of Carr *et al.* may have a slight advantage. That of Thodos *et al.* is a more general relationship and can be used for both gases and liquids, making it the preferred method for phase equilibrium calculations or for the near-critical region.

Natural Gasoline Content of Gas

In the handling and evaluating of gas, determination of natural gasoline or liquefiable content is important. This can be accomplished because the liquid volumes of the heavier components in natural gasoline are essentially additive. The required number of cubic feet of gas to form, by condensation, 1 gal of various materials is shown in Table 20.2 under the heading "cu ft gas/gal liquid." Mole fraction, or cubic feet of any component per cubic foot of mixture, divided by the cubic feet of gas per gallon of liquid gives the total gallons of liquid that each component could contribute to the natural gasoline per cubic

foot of gas mixture. If only a part of the component under consideration is to be recovered as liquid, a suitable correction must be made. Using the principle of additive volumes, the sum of contributions of each component can be assumed to give the recoverable gasoline content per cubic foot. Use of this procedure can lead to errors of about 10% if relatively large amounts of aromatic and/or naphthenic compounds are present.

Formation Volume Factor

The gas FVF, B_g , is defined as barrels of reservoir gas contained in 1 scf. It is sometimes erroneously reported as the reciprocal of this definition. In either case, it is a way of relating reservoir PV to produced surface volumes. The definition of B_g assumes that no liquids will condense as the reservoir gas is brought to standard conditions (60°F and 1 atm [288 K and 100 kPa]). This may be an invalid assumption for gas condensates but is probably acceptable for most wet gases.

The real-gas law, $pV = znRT$, can be used to convert measurements at standard conditions to reservoir conditions. If the above assumption holds, then

$$\frac{p_{rc} V_{rc}}{z_{rc} T_{rc}} = \frac{p_{sc} V_{sc}}{z_{sc} T_{sc}}, \quad \dots \dots \dots (15)$$

where the subscript rc refers to reservoir conditions and sc to standard conditions. Since, by definition,

$$B_g = \frac{V_{rc}}{V_{sc}},$$

it follows that

$$B_g = 0.005035 \frac{T_{rc} z_{rc}}{p_{rc} z_{sc}} \quad \dots \dots \dots (16)$$

when T is in °R and p in psia, or

$$B_g = 0.34722 \frac{T_{rc} z_{rc}}{p_{rc} z_{sc}}$$

when T is in K and p in kPa.

Many times it is assumed that $z_{sc} = 1.0$, but this is not necessarily true. If greater precision is desired, Fig. 20.2B or 20.2C can be used to determine z for the gas at standard conditions. For rough engineering calculations, this extra precision may not be required.

Coefficient of Isothermal Compressibility

Reservoir engineering equations that deal with system compressibility require a gas compressibility term. This is not the gas compressibility factor, z , but the coefficient of isothermal compressibility, c_g . It is defined as the rate of change of volume with respect to pressure at constant

temperature divided by the actual volume. It can be written in differential form as

$$c_g = -\frac{1}{V} \left(\frac{\partial V}{\partial P} \right)_T.$$

If a gas is ideal it can easily be shown that $c_g = 1/p$. As we have already discussed, however, reservoir gases and most surface gases do not follow the ideal-gas law. Consequently, this result should only be considered as an order-of-magnitude approximation.

When the real-gas law, $pV = znRT$, is differentiated to calculate c_g , the result is

$$c_g = \frac{1}{p} - \frac{1}{z} \left(\frac{\partial z}{\partial p} \right)_T. \quad \dots \dots \dots (17)$$

If z 's are known as function of pressure, it can be evaluated over a small range as

$$c_g = \frac{1}{p} - \frac{1}{z} \left(\frac{\Delta z}{\Delta p} \right).$$

However, Trube²² has correlated a term called pseudoreduced compressibility against pseudoreduced pressure to eliminate the need for these evaluations. His definition of pseudoreduced compressibility is

$$c_{pr} = c_g \times p_{pc}, \quad \dots \dots \dots (18)$$

and is nondimensional. The correlating work of Trube is presented in Figs. 20.11 and 20.12. A knowledge of pseudoreduced temperature and pseudoreduced pressure is required to obtain the pseudoreduced compressibility. The coefficient of isothermal compressibility then can be calculated directly from this relationship. Trube does not give any estimates of the accuracy of his correlation, but a method based on pseudoreduced properties should be at least as accurate as the z -factor correlations on which it is based because the coefficient of compressibility is a slope rather than an absolute number.

Vapor Pressure

At a given temperature, the vapor pressure of a pure compound is the pressure at which vapor and liquid coexist at equilibrium. The term "vapor pressure" should be used only in conjunction with pure compounds and is usually considered as a liquid (rather than gas) property. For a pure compound, there is only one vapor pressure at any temperature. A plot of these pressures for various temperatures is shown in Fig. 20.13 for n-butane. The temperature at which the vapor pressure is equal to 1 atm (14.696 psia or 101.32 kPa) is known as the normal boiling point.

The Clapeyron equation gives a rigorous quantitative relationship between vapor pressure and temperature:

$$\frac{dp_v}{dT} = \frac{L_v}{T \Delta V}, \quad \dots \dots \dots (19)$$

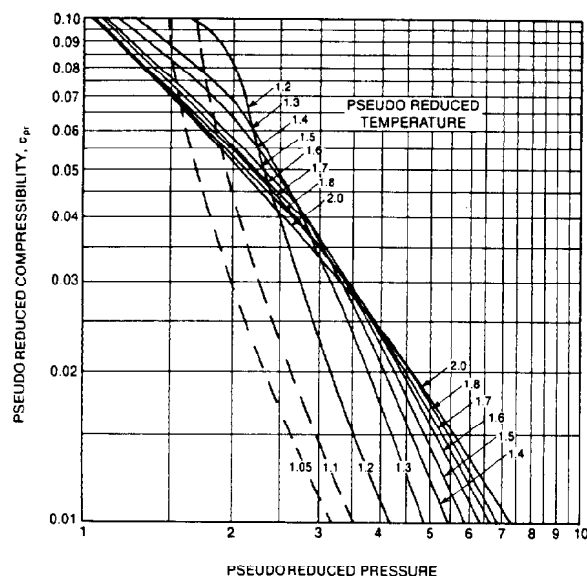


Fig. 20.11—Reduced compressibility coefficients for low pseudoreduced pressures and fixed pseudoreduced temperatures.

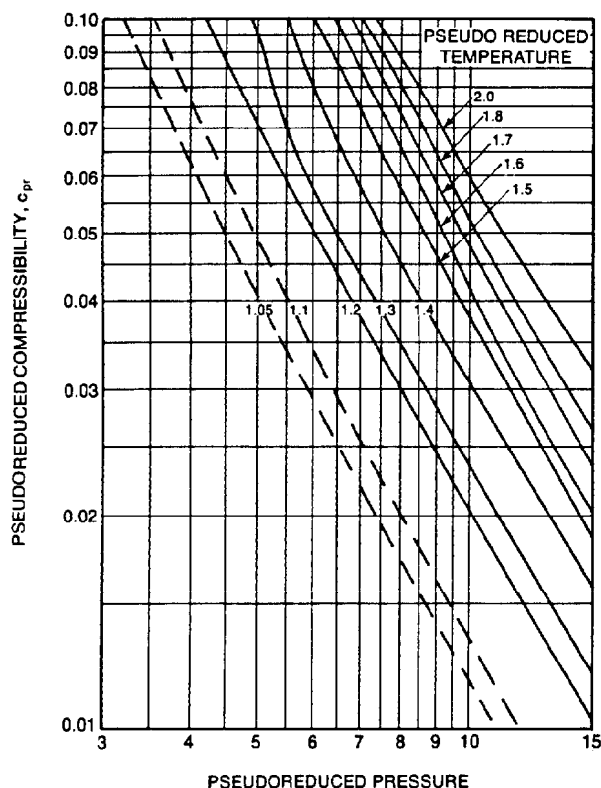


Fig. 20.12—Reduced compressibility coefficients for moderate pseudoreduced pressures and fixed pseudoreduced temperatures.

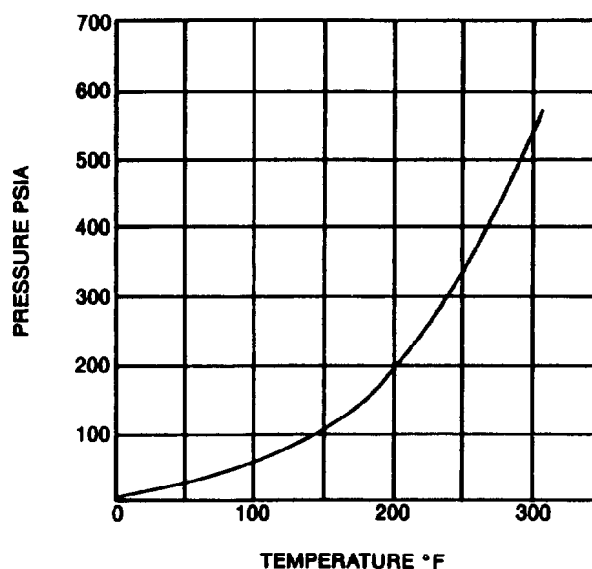


Fig. 20.13—Vapor pressure of n-butane.

where

p_v = vapor pressure,

T = absolute temperature,

ΔV = increase in volume while vaporizing 1 mole, and

L_v = molal latent heat of vaporization.

Assuming ideal-gas behavior of the vapor and neglecting the liquid volume, the Clapeyron equation can be simplified over a small temperature range to give the approximation

$$\frac{d \ln p_v}{dT} = \frac{L_v}{RT^2},$$

which is known as the Clausius-Clapeyron equation.

This equation suggests that a plot of logarithm of vapor pressure against the reciprocal of the absolute temperature would approximate a straight line. Such a plot is useful in interpolating and extrapolating data over short ranges. However, the shape of this relationship for real substances is not a straight line but rather S-shaped. Therefore, the use of the Clausius-Clapeyron equation is not recommended when other methods are available.

Cox Chart

Cox²³ further improved the method of estimating vapor pressure by plotting the logarithm of vapor pressure against an arbitrary temperature scale. The vapor-pressure/temperature plot forms a straight line, at least for the reference compound, and usually for most of the materials related to the reference compound. This is especially true for petroleum hydrocarbons. A Cox chart using water as a reference material is shown in Fig. 20.14. In addition to forming nearly straight lines, compounds of the same family appear to converge on a single point.

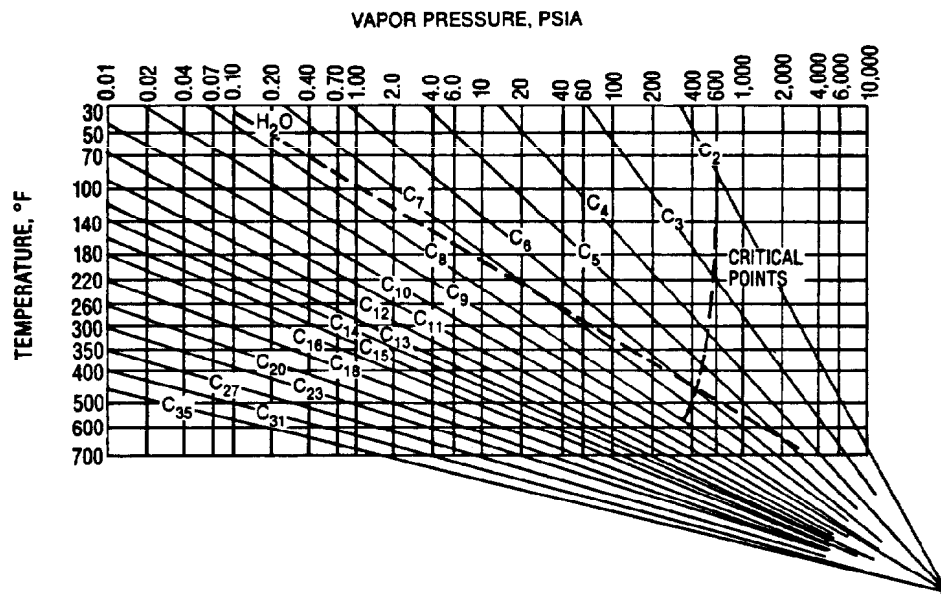


Fig. 20.14—Cox chart for normal paraffin hydrocarbons.

Thus, it is necessary to know only vapor pressure at one temperature to estimate the position of the vapor-pressure line. This approach is very handy and can be much better than the previous method. Its accuracy is dependent to a large degree on the readability of the chart.

Calingeart and Davis Equation

The Cox chart was fit with a three-parameter function by Calingeart and Davis.²⁴ Their equation is

$$\ln p_v = A - \frac{B}{T - C}, \quad (20)$$

where A and B are empirical constants, and, for compounds boiling between 32 and 212°F, C is a constant with a value of 43 when T is in K, and C is a constant with a value of 77.4 when T is in °R.

This equation generally is known as the Antoine²⁵ equation because he proposed one of very similar nature that used 13 K for the constant C . Knowledge of the vapor pressure at two temperatures will fix A and B and permit approximations of vapor pressures at other temperatures. Generally, the Antoine approach can be expected to have less than 2% error and is the preferred approach if the vapor pressure is expected to be less than 1,500 mm Hg [200 kPa] and if the constants are available.

Lee-Kesler

Vapor pressures also can be calculated by corresponding-states principles. The most common expansions of the Clapeyron equation lead to a two-parameter expression. Pitzer extended the expansion to contain three parameters:

$$\ln p_{vr} = f^0(T_r) + \omega f^1(T_r), \quad (21)$$

where p_{vr} is the reduced vapor pressure (vapor pressure/critical pressure), f^0 and f^1 are functions of reduced temperature, and ω is the acentric factor.

Lee and Kesler²⁶ have expressed f^0 and f^1 in analytical forms:

$$f^0 = 5.92714 - (6.09648/T_r) - 1.28862 \ln T_r + 0.169347(T_r)^6 \quad (22)$$

and

$$f^1 = 15.2518 - (15.6875/T_r) - 13.4721 \ln T_r + 0.43577(T_r)^6, \quad (23)$$

which can be solved easily by high-speed computer or a hand-held calculator. Lee-Kesler is the preferred method of calculation but should be used only for nonpolar liquids.

The advent of computers and calculators makes use of approximations and charts much less advantageous than they were in the 1960's. Values of acentric factors can be found in Ref. 27, which also presents many other available vapor-pressure correlations and calculation techniques with comments about their advantages and limitations.

Example Problems

Example Problem 1. Calculate relative density (specific gravity) of the following natural gas. All compositions are in mole percent.

C ₁	83.19
C ₂	8.48
C ₃	4.37
iC ₄	0.76
nC ₄	1.68
iC ₅	0.57
nC ₅	0.32
C ₆	0.63
Total	100.00

TABLE 20.3—DATA FOR EXAMPLE PROBLEM 1

i	y_i	M_i^*	$y_i M_i$
C ₁	0.8319	16.04	13.344
C ₂	0.0848	30.07	2.550
C ₃	0.0437	44.10	1.927
iC ₄	0.0076	58.12	0.442
nC ₄	0.0168	58.12	0.976
iC ₅	0.0057	72.15	0.411
nC ₅	0.0032	72.15	0.231
C ₆	0.0063	86.18	0.543
Total	1.0000		20.424

*From Table 20.2.

TABLE 20.4—DATA FOR EXAMPLE PROBLEM 2

	Mole Fraction	T_c (°R*)	p_c (psia*)	M_i^*
Methane	0.8319	343	668	16.04
Ethane	0.0848	550	708	30.07
Propane	0.0437	666	616	44.09
i-butane	0.0076	735	529	58.12
n-butane	0.0168	766	551	58.12
i-pentane	0.0057	829	490	72.15
n-pentane	0.0032	846	489	72.15
Hexanes	0.0063	914	437	86.17
	1.0000			

*From Table 20.2.

Solution. First calculate the apparent mole weight from information in Table 20.3.

$$\bar{M}_g = \sum y_i M_i = 20.424.$$

Then

$$\begin{aligned}\gamma_g &= \bar{M}_g / M_a = \sum y_i M_i / 28.966 \\ &= 20.424 / 28.966 \\ &= 0.705,\end{aligned}$$

where M_a is the molecular weight of air = 28.966.

Example Problem 2. Calculate actual density of the same mixture at 1,525 psia and 75°F.

Solution.

$$\rho_g = \frac{p \bar{M}_g}{z_g R T},$$

$$p = 1,525 \text{ psia},$$

$$\bar{M}_g = 20.424,$$

$$R = 10.73 \frac{\text{psia} \times \text{cu ft}}{^\circ\text{R} \times \text{lbm mol}} \quad (\text{from Table 20.1}),$$

$$T = 75^\circ\text{F} + 460 = 535^\circ\text{R}, \text{ and}$$

$$z_g \text{ must be obtained from Fig. 20.2.}$$

Calculate z_g from known composition or gas gravity in Table 20.4. From the known gas composition we obtain

$$T_{pc} = \sum y_i T_{ci} = 393.8^\circ\text{R},$$

$$T_{pr} = \frac{535}{393.8} = 1.36,$$

$$p_{pc} = \sum y_i p_{ci} = 662.6 \text{ psia},$$

$$p_{pr} = \frac{1,525}{662.6} = 2.30, \text{ and}$$

$$z_g = 0.712.$$

From gas gravity we obtain

$$\bar{M}_g = \sum y_i M_i = 20.424$$

and

$$\gamma_g = \frac{\bar{M}_g}{M_a} = \frac{20.424}{28.966} = 0.705.$$

From Fig. 20.3 we obtain

$$T_{pc} = 392^\circ\text{R},$$

$$T_{pr} = \frac{535}{392} = 1.36,$$

$$p_{pc} = 663 \text{ psia},$$

$$p_{pr} = \frac{1,525}{663} = 2.30,$$

and

$$z_g = 0.712.$$

Conclusion. Composition and gas gravity methods yield identical results for this hydrocarbon gas at surface processing conditions. Then,

$$\rho_g = \frac{1,525 \times 20.424}{0.712 \times 10.73 \times 535}$$

$$= 7.62 \text{ lbm/cu ft} = 0.122 \text{ g/cm}^3.$$

Example Problem 3. Calculate the z factor for the reservoir fluid in Table 20.5 at 307°F and 6,098 psia. For the C₇₊ fraction:

$$\gamma = 0.825 (40^\circ\text{API}),$$

$$\bar{M}_g = 119, \text{ and}$$

the experimental $z_g = 0.998$.

Solution. From the known gas composition we obtain (Fig. 20.2)

$$T_{pc} = \sum y_i T_{ci} = 487^\circ\text{R},$$

$$T_{pr} = \frac{767}{487} = 1.58,$$

$$p_{pc} = \sum y_i p_{ci} = 822 \text{ psia},$$

$$p_{pr} = \frac{6,098}{824} = 7.42, \text{ and}$$

$$z_g = 0.962 \text{ } (-4\% \text{ error}).$$

TABLE 20.5—DATA FOR EXAMPLE PROBLEM 3

	Mole Fraction	T_c (°R)	p_c (psia)	M_g
Nitrogen	0.1186	228	493	28.02
Methane	0.3836	343	668	16.04
Carbon Dioxide	0.0849	548	1071	44.01
Ethane	0.0629	550	708	30.07
Hydrogen sulfide	0.2419	673	1306	34.08
Propane	0.0261	666	616	44.09
i-butane	0.0123	735	529	58.12
n-butane	0.0154	766	551	58.12
i-pentane	0.0051	829	490	72.15
n-pentane	0.0052	846	489	72.15
Hexanes	0.0067	914	437	86.17
Heptanes plus	0.0373	1,116*	453*	119.00
Total	1.0000			

* Obtained from Fig. 20.10.

From gas gravity we obtain

$$\bar{M}_g = \sum y_i M_i = 31.87, \text{ and}$$

$$\gamma_g = \bar{M}_g / M_a = \frac{31.87}{28.966} = 1.100.$$

$$T_{pc} = 524^\circ \text{R},$$

$$T_{pr} = \frac{767}{524} = 1.464,$$

$$p_{pc} = 652 \text{ psia},$$

$$p_{pr} = \frac{6,098}{652} = 9.35, \text{ and}$$

$$z_g = 1.087 \text{ (9\% error)}.$$

By including corrections to calculated criticals with Wichert and Aziz's chart we obtain

$$\epsilon = 31.2 \text{ (Fig. 20.4),}$$

$$T'_{pc} = 487 - 31 = 456^\circ \text{R},$$

$$p'_{pc} = (822)(456) / [487 + (0.2419)(1 - 0.2419)(31.2)],$$

$$= 762 \text{ psia}.$$

$$T_{pr} = \frac{767}{456} = 1.68,$$

$$p_{pr} = \frac{6,098}{762} = 8.00, \text{ and}$$

$$z_g = 1.010 \text{ (1\% error)}.$$

Example Problem 4. Calculate the viscosity at 150°F and 2,012 psia for the gas of the composition shown in Table 20.6.

TABLE 20.6—DATA FOR EXAMPLE PROBLEM 4

	Mole Fraction	M_i Molecular Weight	T_c (°R)	p_c (psia)
Nitrogen	0.158	28.02	228	492
Methane	0.739	16.04	343	668
Ethane	0.061	30.07	550	708
Propane	0.034	44.09	666	616
i-butane	0.002	58.12	735	529
n-butane	0.006	58.12	765	551
Total	1.000			

Solution by the Carr-Kobayashi-Burrows Method.

$$T_{pc} = \sum y_i T_{ci} = 350^\circ \text{R},$$

$$T_{pr} = \frac{460 + 150}{350} = 1.74,$$

$$p_{pc} = \sum y_i p_{ci} = 639 \text{ psia},$$

$$p_{pr} = \frac{2,012}{639} = 3.15,$$

$$\bar{M}_g = \sum y_i M_i = 19.98, \text{ and}$$

$$\gamma_g = \frac{19.98}{28.966} = 0.690.$$

$$\text{Viscosity at } 150^\circ \text{F, } 1 \text{ atm (Fig. 20.6)} = 0.0116 \text{ cp}$$

$$\text{Correction for N}_2 \text{ (Fig. 20.6)} = +0.0013 \text{ cp}$$

$$\text{Viscosity, } \mu_1 = 0.0129 \text{ cp}$$

$$\text{Viscosity ratio, } \mu/\mu_1 \text{ (Fig. 20.7)} = 1.32$$

$$\text{Viscosity, } \mu = (1.32)(0.0129) = 0.0170 \text{ cp}$$

Solution by the Thodos Method.

$$v_{pc} = \sum y_i v_{ci} = 104.5 \text{ cm}^3/\text{g mol}.$$

Viscosity parameter,

$$\xi = \frac{(T_{pc})^{1/6}}{(\bar{M}_g)^{1/2} (p_{pc})^{1/3}}$$

$$= \frac{(350/1.8)^{1/6}}{(19.98)^{1/2} (639/14.7)^{1/3}} = 0.0435.$$

Pseudocritical density,

$$\rho_{pc} = \frac{\bar{M}_g}{v_{pc}} = \frac{19.98}{104.5} = 0.1912 \text{ g/cm}^3.$$

$$\text{Viscosity factor, } \mu^* \xi \text{ (Fig. 20.8)} = 55 \times 10^{-5},$$

$$\mu^* = 55 \times 10^{-5} / 0.0435 = 0.0126 \text{ cp}.$$

Density,

$$z_g = 0.876 \text{ (Fig. 20.2),}$$

$$\rho_g = \frac{\bar{M}_g p}{z_g R T} = \frac{(19.98)(2,012)}{(0.876)(10.73)(610)} = 7.017 \text{ lbm/cu ft}$$

$$= 0.112 \text{ g/cm}^3, \text{ and}$$

$$\rho_{pr} = 0.112/0.1912 = 0.58.$$

Viscosity factor, $(\mu - \mu^*)\xi = 18.9 \times 10^{-5}$ (from Fig. 20.9).

Viscosity, $\mu = \mu^* + (\mu - \mu^*)\xi/\xi$

$$= 0.0126 + 18.9 \times 10^{-5}/0.0435$$

$$= 0.0169 \text{ cp.}$$

Results. Carr *et al.* = 0.0170 cp, Thodos *et al.* = 0.0169 cp, and experimental = 0.0172 cp.

Conclusion. Excellent results are obtained from either correlation for viscosity of a natural gas.

Example Problem 5. A new discovery in the Lower Tuscaloosa formation produces a gas consisting of 96% C₁ and 4% C₂. There is no liquid production at the surface. Reservoir conditions are 6,000 psia and 245°F. Calculate the gas formation volume factor and the coefficient of isothermal compressibility.

Solution. The pseudocritical pressure and temperature of the mixture are

$$\begin{aligned} T_{pc} &= 0.96 \times 343 = 329.3 \\ &+ 0.04 \times 550 = \underline{22.0} \\ &= 351.3^\circ\text{R.} \end{aligned}$$

and

$$\begin{aligned} p_{pc} &= 0.96 \times 668 = 641.3 \\ &+ 0.04 \times 708 = \underline{28.3} \\ &= 669.6 \text{ psia.} \end{aligned}$$

The reduced quantities at reservoir (subscript *rc*) and surface (subscript *sc*) conditions are

$$(T_{pr})_{rc} = \frac{245 + 459.6}{351.3} = \frac{704.6}{352.24} = 2.00,$$

$$(T_{pr})_{sc} = \frac{60 + 459.6}{351.3} = 1.48,$$

$$(p_{pr})_{rc} = \frac{6,000}{669.6} = 8.96,$$

and

$$(p_{pr})_{sc} = \frac{14.7}{669.6} = 0.022.$$

From Fig. 20.2, $z_{rc} = 1.095$, $z_{sc} = 0.998$ (probably could have assumed 1.0), and

$$B_g = 0.005035 \frac{T_{rc} z_{rc}}{p_{rc} z_{sc}} = \frac{0.005035 \times 704.6 \times 1.095}{6,000 \times 0.998}$$

$$= 0.00065 \text{ RB/scf.}$$

From Fig. 20.11, by using $T_{pr} = 2.00$ and $p_{pr} = 8.96$, we obtain:

$$c_{pr} = 0.074,$$

$$c_{pr} = c_g \times p_{pc},$$

and

$$c_g = \frac{c_{pr}}{p_{pc}} = \frac{0.074}{669.6} = 0.0001105$$

$$= 110.5 \times 10^{-6} \text{ psi}^{-1}.$$

By using a computer to calculate the numerical derivative of z with respect to pressure, we get $c_g = 107.4 \times 10^{-6} \text{ psi}^{-1}$, which indicates Trube's correlation to be in error by about 3%.

Example Problem 6. The vapor pressure of pure hexane as a function of temperature is 54.04 kPa at 50°C and 188.76 kPa at 90°C. Estimate the vapor pressure of hexane at 100°C, using all the methods outlined in the text.

Solution. Clausius-Clapeyron. The Clausius-Clapeyron equation can be solved graphically by plotting log of vapor pressure vs. reciprocal absolute temperature and extrapolating. It also can be solved by slopes.

$$T_1 = 50^\circ\text{C} [581.67^\circ\text{R}],$$

$$1/T_1 = 0.001719,$$

$$T_2 = 90^\circ\text{C} [617.67^\circ\text{R}],$$

$$1/T_2 = 0.001619,$$

$$p_v \text{ at } T_1 = 54.04 \text{ kPa} = 7.8374 \text{ psia,}$$

$$\log p_v = 0.89417,$$

$$p_v \text{ at } T_2 = 105.37 \text{ kPa} = 15.2826 \text{ psia,}$$

$$\log p_v = 1.18420,$$

$$\Delta \log p_v = -0.29003,$$

$$1/T_1 - 1/T_2 = 0.0001, \text{ and}$$

$$\text{slope} = \Delta \log p_v / \left(\frac{1}{T_1} - \frac{1}{T_2} \right) = \frac{-0.29003}{0.0001}$$

$$= -2900.3.$$

Solving $\log p_v = -2900.3(1/T) + b$ for b yields

$$b = 5.87977,$$

$$T_3 = 100^\circ\text{C} = 671.67^\circ\text{R, and}$$

$$1/T_3 = 0.001489.$$

Solving for p_v at 100°C:

$$\log p_v = -2900.3(0.001489) + 5.87977$$

$$= 1.56122, \text{ and}$$

$$p_v = 36.4102 \text{ psia [251.04 kPa]}.$$

However, if you know that the vapor pressure at 70°C is 105.37 kPa, you can use the 70 to 90°C temperature differential to calculate the slopes and ultimately will calculate $p_v = 35.81 \text{ psia} = 246.7 \text{ kPa}$.

Cox Chart.²⁸ From Fig. 20.14, the vapor pressure at 100°C can be approximated between 35 and 36 psia. A larger chart is required for more precise readings.

The Calingart and Davis or Antoine Equation. This can be used by obtaining the Antoine constants from Reid *et al.*²⁷ For n-hexane, with temperature in K, these constants are $A = 15.8366$, $B = 2697.55$, and $C = -48.78$. Then,

$$\ln p_v = A - \frac{B}{T + C}$$

$$= 15.8366 - \frac{2697.55}{373 - 48.78} = 3.60223, \text{ and}$$

$$p_v = 36.68 \text{ psia [252.73 kPa]}.$$

Lee-Kesler. The use of the Lee-Kesler equation requires p_c , T_c , and ω for n-hexane. These can be obtained from Table 20.2.

$$p_c = 436.9 \text{ psia [29.7 atm]}$$

$$T_c = 453.7^\circ\text{F or } 913.3^\circ\text{R or } 507.4 \text{ K, and}$$

$$\omega = 0.3007.$$

For 100°C,

$$T_r = 0.7351,$$

$$(T_r)^6 = 0.15782,$$

$$\ln T_r = -0.30775,$$

$$f^0 = 5.92714 - (6.09648/0.7351) + 1.28862(0.30775)$$

$$+ 0.169347(0.15782),$$

and

$$f^1 = 15.2518 - (15.6875/0.7351) + 13.4721(0.30775)$$

$$+ 0.43577(0.15782).$$

Therefore,

$$f^0 = 5.92714 - 8.29340 + 0.39657 + 0.02673$$

$$= -1.94296,$$

$$f^1 = 15.2518 - 21.34063 + 4.14604 + 0.06877$$

$$= -1.87402,$$

$$\ln p_{vr} = -1.94296 + 0.3007(-1.87402)$$

$$= -2.50648,$$

$$p_{vr} = \frac{p_v}{p_c} = 0.0816,$$

and

$$p_v = 0.0816 \times 29.7 = 2.4235 \text{ atm} = 35.62 \text{ psia}$$

$$= 245.59 \text{ kPa}.$$

Experimental Value. 35.69 psia = 245.90 kPa.

Conclusions. Lee-Kesler gives the best answer, but the Clausius-Clapeyron method can be even more accurate if the extrapolation is short.

Nomenclature

- a = constant characteristic of the fluid
- a_i = constant for Substance i
- a_{ij} = mixture parameter
- a_m = Parameter a characteristic
- $a(T)$ = functional relationship
- A = empirical constant
- A_o = empirical constant
- b = constant characteristic of the fluid
- b_i = constant characteristic for Substance i
- b_m = Parameter b for mixture
- B = empirical constant
- B_g = gas FVF
- B_o = empirical constant
- c = empirical constant
- c_g = coefficient of isothermal compressibility
- C = constant with value of 43 when temperature is in K, and a value of 77.4 when temperature is in °R
- d = empirical constant
- D_o = empirical constant
- E_k = kinetic energy
- E_o = empirical constant
- f^0, f^1 = functions of reduced temperature
- K_{ij} = constant for each binary pair when used for mixtures
- L_v = molar latent heat of vaporization
- m = mass
- M = molecular weight
- M_a = molecular weight of air
- $M_{C_{7+}}$ = molecular weight of C_{7+} fraction
- M_g = average mole weight of gas mixture
- p = absolute pressure
- p_c = critical pressure

p_{ci} = critical pressure of Component i in gas mixture
 p_{pc} = pseudocritical pressure of gas mixture
 p'_{pc} = corrected pseudocritical pressure
 p_r = reduced pressure
 p_{rc} = pressure at reservoir conditions
 p_{sc} = pressure at standard conditions
 p_v = vapor pressure
 p_{vr} = reduced vapor pressure (vapor pressure/critical pressure)
 R = absolute temperature
 t = ratio of critical to absolute temperature
 T_c = critical temperature
 T_{ci} = critical temperature of Component i in gas mixture
 T_{pc} = corrected pseudocritical temperature
 T_r = reduced temperature
 T_{rc} = temperature at reservoir conditions
 T_{sc} = temperature at standard conditions
 v = velocity
 V = volume
 V_c = critical volume
 $(V_c)_{C_7+}$ = critical volume of C_7+ fraction
 V_M = molar volume
 V_r = reduced volume
 V_{rc} = volume at reservoir conditions
 V_{sc} = volume at standard conditions
 ΔV = increase in volume while vaporizing 1 mole
 x_i = mole fraction of Component i in liquid
 y_{CO_2} = mole fraction of CO_2 in mixture
 y_{H_2S} = mole fraction of H_2S in mixture
 y_i = mole fraction of Component i in gas mixture
 z = compressibility factor
 z_{rc} = compressibility factor at reservoir conditions
 z_{sc} = compressibility factor at standard conditions
 α_i = empirical constant for Substance i
 β_i = empirical constant for Substance i
 γ_g = specific gravity for gas
 γ_i = empirical constant for Substance i
 δ_i = empirical constant for Substance i
 ϵ = correction factor
 μ = viscosity
 μ^* = correlating parameter
 ξ = viscosity parameter
 ρ_M = molar density
 ρ_{pc} = pseudocritical density
 ρ_R = relative density of C_7+ fraction
 ω = acentric factor

References

1. Burnett, E.S.: "Compressibility Determinations Without Volume Measurements," *J. Applied Mechanics* (1936) **3**, A136-40.
2. Katz, D.L. *et al.*: *Handbook of Natural Gas Engineering*, McGraw-Hill Book Co. Inc., New York City (1959).
3. Standing, M.B. and Katz, D.L.: "Density of Natural Gases," *Trans., AIME* (1942) **146**, 140-44.
4. Brown, G.G. *et al.*: "Natural Gasoline and the Volatile Hydrocarbons," Natural Gas Assn. of America, Tulsa (1948).
5. Wichert, E. and Aziz, K.: "Compressibility Factor for Sour Natural Gases," *Cdn. J. Chem. Eng.* (1972) **49**, 269-75.
6. van der Waals, J.D.: *Proc., Acad. Sci. Amsterdam* (1901) **3**, 515.
7. Redlich, O. and Kwong, J.N.S.: "On the Thermodynamics of Solutions. V—An Equation of State. Fugacities of Gaseous Solutions," *Chem. Reviews* (1949) **44**, 233-44.
8. Soave, G.: "Equilibrium Constants from a Modified Redlich-Kwong Equation of State," *Chem. Eng. Sci.* (1972) **27**, 1197-1203.
9. Zudkevitch, D. and Joffe, J.: "Correlations and Predictions of Vapor-Liquid Equilibrium with the Redlich-Kwong Equation of State," *AIChE J.* (1970) **16**, 112-19.
10. Peng, O.Y. and Robinson, D.B.: "A New Two-Constant Equation of State," *Ind. and Eng. Chem. Fundamentals* (1976) **15**, No. 1, 59-64.
11. Yarborough, L.: "Application of a Generalized Equation of State to Petroleum Reservoir Fluids," *Equations of State in Engineering and Research*, K.C. Chao and R.L. Robinson (eds.), Advances in Chemistry Series No. 182, ACS, Washington, DC (1979) 385-439.
12. Starling, K.E. and Hon, M.S.: "Thermo Data Refined for LPG," *Hydrocarbon Processing* (May 1972) 129-33.
13. Benedict, M., Webb, G.B., and Rubin, L.C.: "An Empirical Equation for Thermodynamic Properties of Light Hydrocarbons and Their Mixtures," *Chem. Eng. Prog.* (1951) **47**, 419; and *J. Chem. Phys.* (1940) **8**, 334; (1942) **10**, 747.
14. Martin, J.J.: "Cubic Equations of State—Which?" *Ind. Eng. Chem. Fundamentals* (May 1979), **18**, No. 2, 81-97.
15. Robinson, R.L. Jr. and Jacoby, R.H.: "Better Compressibility Factors," *Hydrocarbon Processing* (April 1965) 141-45.
16. Hall, K.R. and Yarborough, L.: "A New Equation of State for Z-Factor Calculations," *Oil and Gas J.* (June 18, 1971) **71**, 82-91.
17. Ajitsaria, N.K.: "Hand Held Calculator Programs Determine Natural Gas Physical Properties," *Oil and Gas J.* (June 6, 1983) **81**, 69-72.
18. Carr, N.L., Kobayashi, R., and Burrows, D.B.: "Viscosity of Hydrocarbon Gases Under Pressure," *Trans., AIME* (1954) **201**, 264-78.
19. Stiel, L.I. and Thodos, G.: "The Viscosity of Non-Polar Gases at Normal Pressures," *AIChE J.* (1961) **7**, 611-20.
20. Jossi, J.A., Stiel, L.I., and Thodos, G.: "The Viscosity of Pure Substances in the Dense Gaseous and Liquid Phases," *AIChE J.* (1962) **8**, 59-70.
21. Matthews, T.A., Roland, C.H., and Katz, D.L.: "High Pressure Gas Measurement," *Proc., Natural Gas Assn. of America* (1942) 41-51.
22. Trube, A.S.: "Compressibility of Natural Gases," *Trans., AIME* (1957) **210**, 355-57.
23. Cox, E.R.: "Pressure Temperature Chart for Hydrocarbon Vapors," *Ind. Eng. Chem.* (1923) **15**, 592-98.
24. Calingart, G. and Davis, D.S.: "Pressure Temperature Charts Extended Ranges," *Ind. Eng. Chem.* (1925) **17**, 1287-1300.
25. Antoine, C.: *Chem. Reviews* (1888) **107**, 836-50.
26. Lee, B.I. and Kesler, M.G.: "A Generalized Thermodynamic Correlation Based on Three-Parameter Corresponding States," *AIChE J.* (May 1975) **21**, 510-27.
27. Reid, R.C., Prausnitz, J.M., and Sherwood, T.K.: *The Properties of Gases and Liquids*, 3rd ed., McGraw-Hill Book Co. Inc., New York City (1977).
28. Perry, J.H. and Chilton, C.H.: *Chemical Engineer's Handbook*, fifth edition, McGraw-Hill Book Co. Inc., New York City (1975).
29. *GPSA Engineering Databook*, ninth edition, fifth revision, Gas Processors Suppliers Assn., Tulsa (1981).

Chapter 21

Crude Oil Properties and Condensate Properties and Correlations

Paul Buthod, U. of Tulsa*

Introduction

All crude oils are composed primarily of hydrocarbons, which are made by the combination of the elements carbon and hydrogen. In addition, most crudes contain sulfur compounds and trace quantities of oxygen, nitrogen, and heavy metals. The difference in crude oils is caused by the amount of sulfur compounds and by the types and molecular weights of the hydrocarbons making up the oil.

The hydrocarbons found in crude oil range in size from the smallest molecule, methane, which contains 1 atom of carbon, to the largest ones, which contain nearly 100 atoms of carbon. The types of hydrocarbon compounds are paraffin, naphthene, and aromatic, found in raw crude, and olefin and diolefin, which are sometimes found in refined products after thermal treatment. Since any crude oil will have several thousand different compounds in it, it has been impossible so far to develop exact analyses of the actual compounds present. Three methods of reporting analyses are available—ultimate analysis, chemical analysis, and evaluation analysis.

Ultimate analysis lists the composition in percentages of the elements carbon, hydrogen, nitrogen, oxygen, and sulfur. This tells very little about the type of compounds present or the physical characteristics of the oil. It is useful, however, in determining the amount of sulfur that must be removed. Table 21.1 shows the ultimate analysis of several crude oils.

Chemical analysis gives composition in percentage of paraffin, naphthene, and aromatic-type compounds present in the crude. This type of analysis can be determined with fair accuracy by means of chemical reaction and solvency tests. An analysis of this sort gives an idea of the usefulness of refined products but does not give any

means of predicting the amount of various refined products. Table 21.2 gives the chemical analysis of several fractions of four crude oils.

The crude-oil evaluation consists primarily of a fractional distillation of the oil followed by physical-property tests (for parameters such as gravity, viscosity, and pour point) on the distillation products. Since the primary means of separating products in the refinery is fractionation, this analysis makes it possible to predict yields of refined products and physical properties studied in the evaluation. The evaluation curves shown in Fig. 21.1 make it possible to predict the physical properties of the refined products. As an example of the use of evaluation curves, Table 21.3 shows product yields and properties when a refinery is operated for maximum gasoline yield, and Table 21.4 shows product yields and properties when the objective is to produce lubricating oils and diesel fuel.

Since the early 1970's, much research has been performed on the use of the gas chromatograph to generate simulated distillations. This has the advantage of producing crude-oil evaluation curves with very small samples of crude and in a period of about an hour, compared with about a gallon of crude for a fractional distillation column and about 2 days for the analysis. The simulated distillation is called ASTM Test Method D2887.¹

Base of Crude Oil

Since the beginning of the oil industry in the U.S., it has been convenient to separate crude oils into three broad classifications or bases. These three, paraffin, intermediate, and naphthene, are useful as general classifications but lead to ambiguity in many instances. Because a crude may exhibit one set of characteristics for

*This author also wrote the original chapter on this topic in the 1962 edition.

TABLE 21.1—ULTIMATE CHEMICAL ANALYSES OF PETROLEUM

Petroleum	Specific Gravity γ	Temperature (°C)	Component (%)					
			C	H	N	O	S	Base
Pennsylvania pipeline	0.862	15	85.5	14.2				paraffin
Mecook, WV	0.897	0	83.6	12.9		3.6		paraffin
Humbolt, KS	0.912		85.6	12.4			0.37	mixed
Healdton, OK			85.0	12.9			0.76	mixed
Coalinga, CA	0.951	15	86.4	11.7	1.14		0.60	naphthene
Beaumont, TX	0.91		85.7	11.0	2.61*		0.70	naphthene
Mexico	0.97	15	83.0	11.0	1.7*		4.30	naphthene
Baku, USSR	0.897		86.5	12.0		1.5		
Colombia, South America	0.948	20	85.62	11.91	0.54			

*Combined nitrogen and oxygen.

TABLE 21.2—CHEMICAL ANALYSES OF PETROLEUM, %

Fraction (°F)	Grozny ("High Paraffin") 45.3% at 572°F			Grozny ("Paraffin-Free Upper Level"), 40.9% at 572°F			Oklahoma (Davenport), 64% at 572°F			California (Huntington Beach), 34.2% at 572°F		
	Aromatic	Naphthene	Paraffin	Aromatic	Naphthene	Paraffin	Aromatic	Naphthene	Paraffin	Aromatic	Naphthene	Paraffin
140 to 203	3	25	72	4	31	65	5	21	73	4	31	65
203 to 252	5	30	65	8	40	52	7	28	65	6	48	46
252 to 302	9	35	56	13	52	35	12	33	55	11	64	25
302 to 392	14	29	57	21	55	24	16	29	55	17	61	22
392 to 482	18	23	59	26	63	11	17	31	52	25	45	30
482 to 572	17	22	61	35	57	8	17	32	51	29	40	31

TABLE 21.3—EVALUATION WHEN OPERATING PRIMARILY FOR GASOLINE*

Material	Basis	Percent Distilled			Gravity (°API)	Other Properties
		Range	Midpoint	Yield		
Gas loss		0 to 1.3		1.3		
Straight-run gasoline (untreated)	54.5 octane number	1.3 to 32	16.6	30.7	56**	390°F ASTM endpoint†
Catalytic charge	900°F cut	32 to 80.5	56.2	48.5	28.8	165°F aniline point or 47.5 diesel index
Vis-breaker charge or asphalt	remainder	80.5 to 100		19.5	6.4‡	110 penetration
Crude oil				100.0	32.0	11.65 characterization factor

*Topping followed by vacuum flashing to produce a gas oil for catalytic cracking. The cycle stock from catalytic cracking is thermally cracked along with the asphalt or vis-breaker charges stock.

**Average gravity from instantaneous curve of API gravity.

†At about 400°F endpoint the true-boiling-point cut point is about 22°F higher than the ASTM end point.

‡By a material balance.

TABLE 21.4—EVALUATION WHEN OPERATING PRIMARILY FOR LUBRICATING-OIL STOCK^a

Material	Basis	Percent Distilled			API Gravity	Viscosity, SU's	Other Properties
		Range	Midpoint	Yield			
Gas loss		0 to 1.3		1.3			
Light gasoline (untreated)	300 EP ^b	1.3 to 21.0	10.5	19.7	61.2 ^c		63.8 octane number ^d
Re-forming naphtha	445 EP ^b	21.0 to 38.5	29.7	17.5	41.3 ^e		0.16% sulfur
Diesel fuel	156 aniline point	38.5 to 56.5	47.5	18.0	32.1	41 (estimated)	50 diesel index; 0.82% sulfur
Light lube or cracking stock	remainder	56.5 to 74.9	65.7	18.4	25.9	145 at 100°F	1.49% sulfur ^f
Lube stock (untreated)	100 SU's viscosity at 210°F	74.9 to 80.9	77.9	6.0	19.1	100 at 210°F	
Asphalt	100 penetration	80.9 to 100.0		19.1			100 penetration at 77°F ^g
Crude oil				100.0	32.0		

^aTopping followed by vacuum distillation. The light lube stock can be thermally or catalytically cracked if desired.^bIn the range of 300°F endpoint, the true-boiling-point cut point is about the same as the ASTM endpoint. At 445 EP, the difference in temperature is about 20°F.^cAn average of the gravity from 1.3 to 21%.^dRead at 19.7 on the octane-number-yield curve.^eRead at the mid-point on the instantaneous-gravity curve.^fPlotted curves are never accurate enough to read viscosity index from them.^gRead at 19.1 (80.9% distilled) in the penetration-yield curve.

TABLE 21.5—BASES OF CRUDE OILS*

Low-Boiling Part	High-Boiling Part	API Gravity at 60°F		Approximate UOP** Characterization Factor	
		Key Fraction 1	Key Fraction 2	Low-Boiling	High-Boiling
paraffin	paraffin	40 +	30 +	12.2 +	12.2 +
paraffin	intermediate	40 +	20 to 30	12.2 +	11.4 to 12.0
paraffin	naphthene	40 +	20 -	12.2 +	11.4 -
intermediate	paraffin	33 to 40	30 +	11.5 to 12.0	12.2 +
intermediate	intermediate	33 to 40	20 to 30	11.4 to 12.1	11.4 to 12.1
intermediate	naphthene	33 to 40	20 -	11.4 to 12.1	11.4 -
naphthene	intermediate	33 -	20 to 30	11.5 -	11.4 to 12.1
naphthene	paraffin	33 -	30 +	11.5 -	12.2 +
naphthene	naphthene	33 -	20 -	11.4 -	11.4 -

*USBM, Report 3279 (Sept. 1935).

**Universal Oil Products Co., Chicago.

its light materials and another set for the heavy-lube fractions, the USBM has developed a more useful method of classifying oils.

Two fractions (called "key fractions") are obtained in the standard Hempel distillation procedure. Key Fraction 1 is the material that boils between 482 and 527°F at atmospheric pressure. Key Fraction 2 is the material that boils between 527 and 572°F at 40 mm absolute pressure. Both fractions are tested for API gravity, and Key Fraction 2 is tested for cloud point. In naming the type of oil, the base of light material (Key Fraction 1) is named first, and the base of the heavy material (Key Fraction 2) is named second. If the cloud point of Key Fraction 2 is above 5°F, the term "wax-bearing" is added. If the pour point is below 5°F, it is termed "wax-free."

Thus, "paraffin-intermediate-wax-free" would mean a crude that has paraffinic characteristics in the gasoline portion and intermediate characteristics in the lube portion and has very little wax. Table 21.5 shows the criteria used in establishing bases of oil by the USBM method.

Several attempts have been made to establish an index to give a numerical correlation for the base of a crude oil. The most useful of these is the characterization factor K developed in Ref. 2,

$$K = \frac{\sqrt[3]{\bar{T}_B}}{\gamma}$$

in which \bar{T}_B is the molal average boiling point (degrees Rankine) and γ is the specific gravity at 60°F. This has been used successfully in correlating not only crude oils, but refinery products both cracked and straight-run. Typical numerical values for characterization factors are listed in Table 21.6.

In addition to the relationship between the characterization factor and the specific gravity and boiling point defined above, a number of other physical properties have been shown to be related to the characterization factor. Among these properties are viscosity, molecular weight, critical temperature and pressure, specific heats, and percent hydrogen.

Table 21.7 shows characterization factors for a

TABLE 21.6—TYPICAL CHARACTERIZATION FACTOR VALUES

Product	Characterization Factor
Pennsylvania stocks (paraffin base)	12.1 to 12.5
Mid-Continent stocks (intermediate)	11.8 to 12.0
Gulf Coast stocks (naphthene base)	11.0 to 11.8
Cracked gasoline	11.5 to 11.8
Cracking-plant combined feeds	10.5 to 11.5
Recycle stocks	10.0 to 11.0
Cracked residuum	9.8 to 11.0

number of worldwide crudes and products and typical hydrocarbon compounds that have the same characterization factor as the oil in question.

Physical Properties

Fig. 21.2 shows the relationship of carbon-to-hydrogen ratio, average molecular weight, and mean average boiling point as a function of API gravity and characterization factor. The *API Technical Data Book*³ has published a number of correlations for physical properties of petroleum. For the most accurate data, this reference should be consulted.

When oil is heated or cooled in a processing operation, the amount of heat required is best obtained by the use of the specific heat. Fig. 21.3 shows the specific heat of liquid petroleum oils as a function of API gravity and temperature. This chart is based on a characterization factor of 11.8, and if the oil being studied is other than that, there is a correction shown at the lower right side of the chart. The number obtained for the specific heat should be multiplied by this correction factor. Certain paraffin hydrocarbons are also shown on the chart. No correction need be applied to these.

If vaporization or condensation occurs in a processing operation, the heat requirements are most easily handled by the use of total heats. Fig. 21.4 gives total heats of petroleum liquid and vapor, with liquid at 0°F as a reference or zero point. This eliminates the necessity of selecting a latent heat, specific heats of both vapor and liquid, and deciding at what temperature to apply the latent heat. Certain corrections must be applied for characterization factor and for pressure.

TABLE 21.7—CHARACTERIZATION FACTORS OF A FEW HYDROCARBONS, PETROLEUMS, AND TYPICAL STOCKS

Characterization Factor	Hydrocarbons	Typical Crude Oils	Miscellaneous Products
14.7	propane		
14.2	propylene		
13.85	isobutane		
13.5 to 13.6	butane		94.5 API adsorption gasoline
13.0 to 13.2	butane-1 and isopentane		Four Venezuelan paraffin waxes
12.8	hexane and tetradecene-7		paraffin wax*: M.C. 82.2 API natural gasoline
12.7	2-methylheptane and tetradecane		CA 81.9 API natural gasoline
12.6	pentene-1, hexene-1, and cetene		
12.55	2,2,4-trimethylpentane	Cotton Valley (LA) lubes	debutanized E. TX natural gasoline
12.5	hexene-2 and 1,3-butadiene		San Joaquin (Venezuela) wax distillate
12.1 to 12.5	2,2,3,3-tetramethyl butane	Pennsylvania-Rodessa (LA)	Panhandle (TX) lubes
12.2 to 12.44	2,11-dimethyl dodecadiene	Big Lake (TX)	Six Venezuelan wax distillates
12.0 to 12.2		Lance Creek (WY)	paraffin-base gasolines
11.9 to 12.2		Mid-Continent (M.C.)	Middle East light products
		Oklahoma City (OK)	cracked gasoline from paraffinic feeds
			E. TX gas oil and lubes
11.9	hexylcyclohexane		light cycloversion gasoline from M.C. feeds
11.8 to 12.1		Fullerton (W. TX)	Middle East gas oil and lubes
11.85		Illinois; Midway (AR)	cracked gasoline from intermediate feeds
11.7 to 12		W. TX; Jusepin (Venezuela)	E. TX and LA white products
11.75		Cowden (W. TX)	cracked gas oil from paraffinic feeds
11.7	butylcyclohexane	Santa Fe Springs (CA)	catalytic cycle stocks from paraffinic feeds
11.6	octyl or diamyl benzene	Slaughter (W. TX); Hobbs (NM)	cracked gasoline from naphthene feeds
11.5 to 11.8		Colombian	Tia Juana (Venezuela) gas oil and lubes
11.5		Hendrick and Yates (W. TX)	naphthenic gasoline; catalytic (cracked) gasoline
			catalytic cycle stocks from M.C. feeds
11.45	ethylcyclohexane and 9-hexyl-11-methylheptadiene	Elk Basin, heavy (WY)	cracked gasoline from highly naphthenic feeds
11.4	methylcyclohexane	Kettleman Hills (CA)	high-conversion catalytic cycle stocks from paraffinic feeds
		Smackover (AR)	typical catalytic cycle stocks
11.3 to 11.6		Lagunillas (Venezuela)	light-oil coil thermal feeds
11.3	cyclobutane and 2,6,10,14-tetramethyl hexadiene	Gulf Coast light distillates	catalytic cycle stocks from 11.7-characterization-factor feeds
			gasoline from catalytic re-forming

*12.88 (range 12.1 to 13.65) calculated from factors of raw and dewaxed lube stocks.

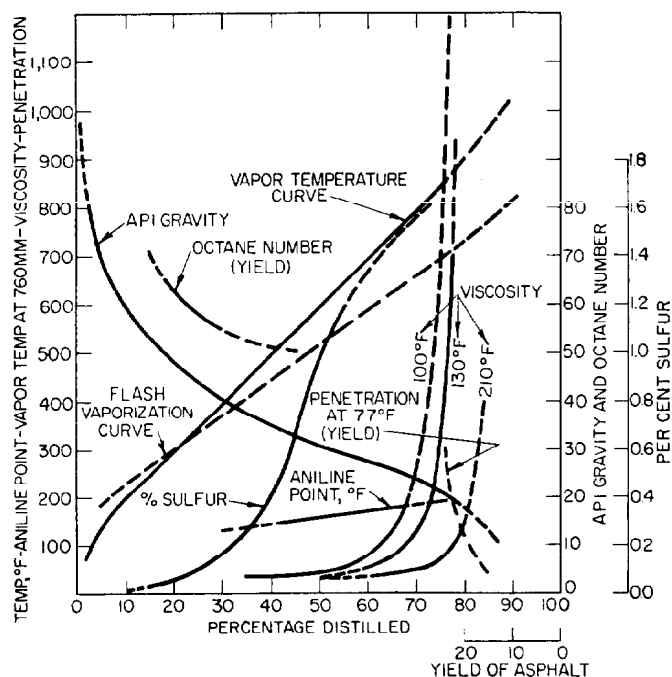


Fig. 21.1—Evaluation curves of a 32.0°API intermediate-base crude oil of characterization factor 11.65.

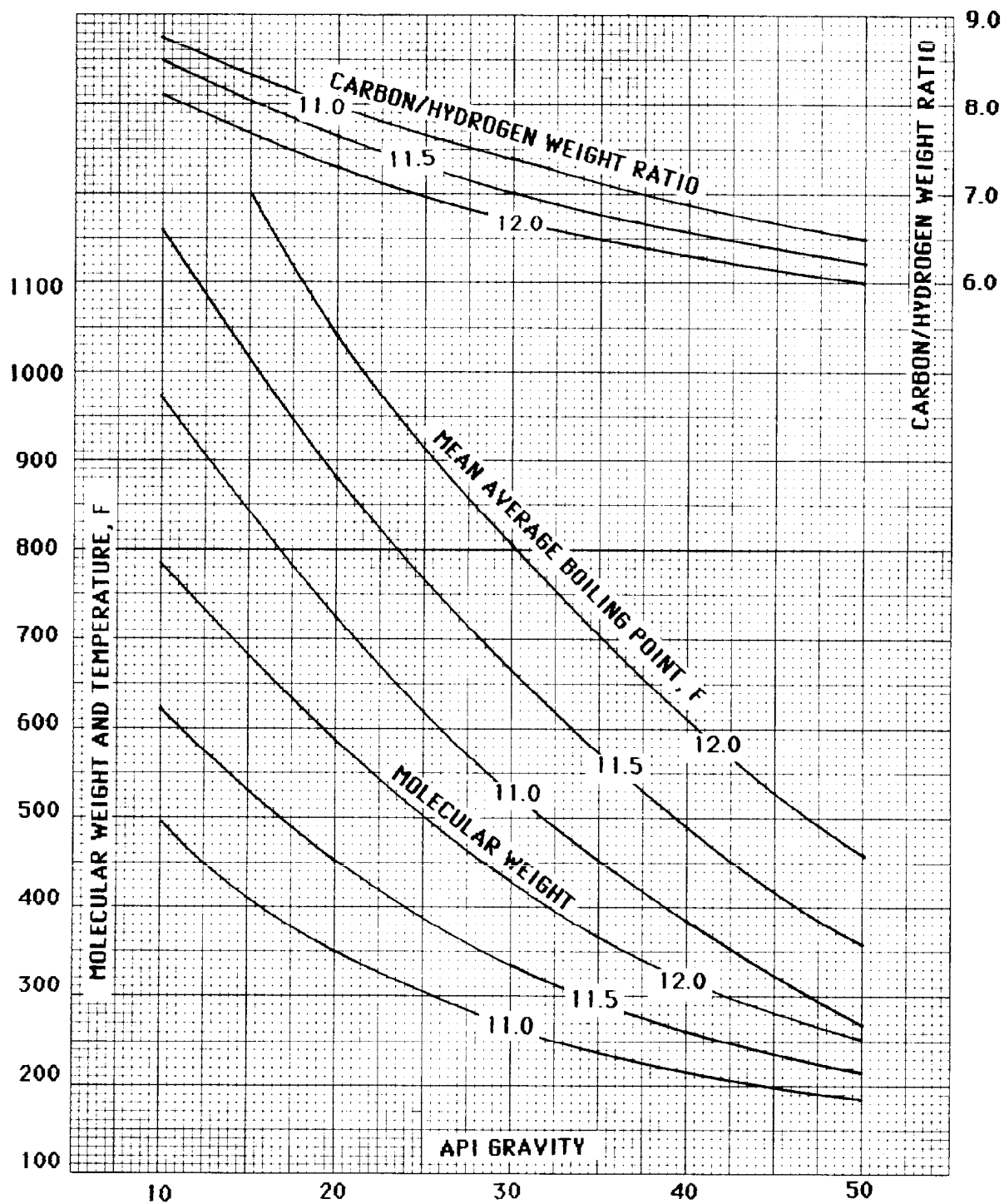


Fig. 21.2—Petroleum properties as a function of API gravity and characterization factor. Note: the parameters in the curves refer to the characterization factor.

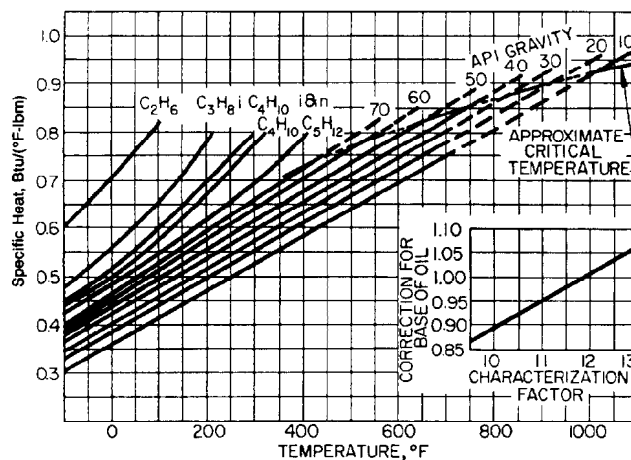


Fig. 21.3—Specific heats of Mid-Continent liquid oils with a correction factor for other bases of oils.

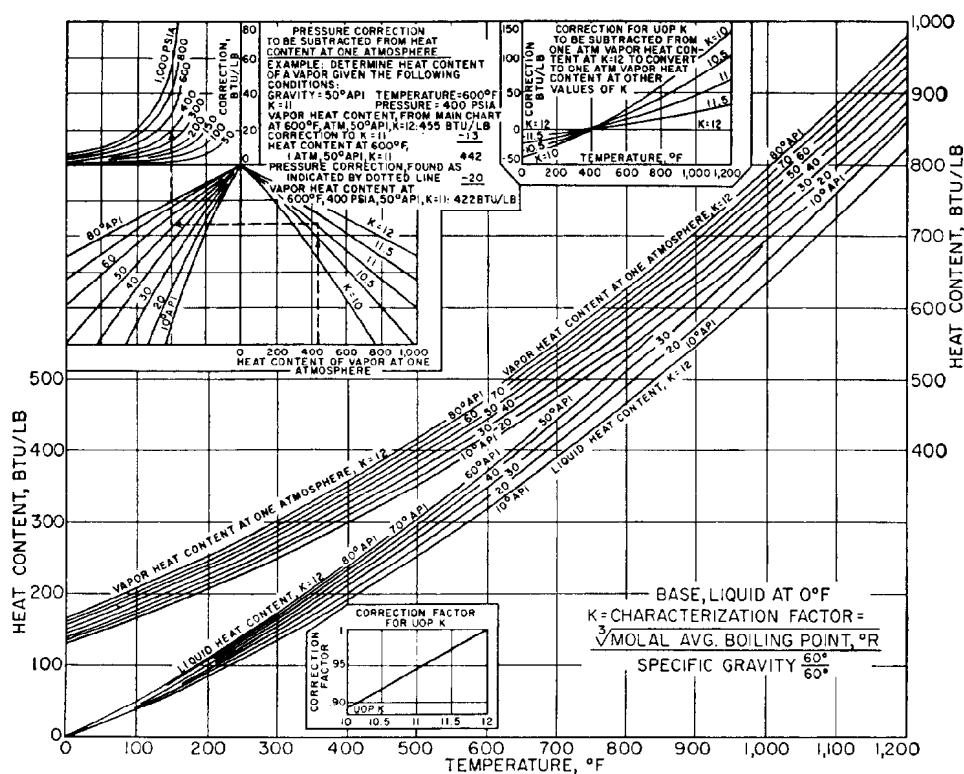


Fig. 21.4—Heat content of petroleum fractions including the effect of pressure.

TABLE 21.8—TRUE-BOILING-POINT CRUDE OIL ANALYSES

	Location					
	Smackover, AR	Atlanta, AR (limestone)	Kern River, CA	Santa Maria, CA	Coalinga (East), CA	Coalinga, CA
Gravity, API	20.5	44.5	10.7	15.4	20.7	31.1
Sulfur, %	2.30	0.48 ^c	1.23	4.63	0.51	0.31
Viscosity, SUS at 100°F	270	35	6,000 +	368	178	48
Date	4/3/39			8/2/54		
Characterization factor						
At 250°F	11.62	11.82		11.90		11.5
At 450°F	11.48	12.05	11.13	11.42	11.28	11.53
At 550°F	11.47	12.08	11.15	11.29	11.20	11.59
At 750°F	11.55	12.25	11.15	11.11	11.23	11.72
Average	11.53	12.05		11.48		11.58
Base	I	IP	N	IN	N	I
Loss, %	0	1.5	0	0	3.0	1.1
Gasoline						
% at 300°F	6.0	25.2 ^d	0	7.0	1.2 ^d	21.6 ^d
Octane number, clear	73.2 ^a					72.0 ^b
Octane number, 3 cc TEL	89.0 ^a					
% to 400°F	11.0	39.2 ^d	1.2 ^d	13.2	9.6 ^d	31.6 ^d
Octane number, clear	66.0 ^b	48.5 ^b		59.8 ^e	67.0 ^b	66.7 ^b
Octane number, 3 cc TEL				70.3 ^e		
% to 450°F	14.4	45.3 ^d	2.2 ^d	17.0	15.6 ^d	35.6 ^d
Quality	good ^b				good ^b	excellent ^b
Jet stock						
% to 550°F	24.1	56.3 ^d	6.1 ^d	25.0	29.3 ^d	46.2 ^d
API gravity	41.9	57.4	29.5 ^b	43.0	36.9	46.0 ^d
Quality	good			good		good
Kerosene distillate						
%, 375 to 500°F	9.5	15.0 ^d	2.7 ^d	8.5	16.0 ^d	11.0 ^d
API gravity	38.0	46.0	32.5 ^d	34.5	34.0 ^d	37.8
Smoke point	16.0 ^b	27.0 ^b	13.0 ^b		14.5 ^b	17.0 ^b
Sulfur, %	0.29 ^b	0.06 ^b	0.38 ^b	1.8 ^d	0.14 ^b	0.06 ^b
Quality		excellent				
Distillate or diesel fuel						
%, 400 to 700°F	29.2	35.0 ^d	19.7 ^d	23.8	38.4 ^d	28.0 ^d
Diesel index	43.0 ^b	76.0 ^d	30.0 ^b	33.0	33.0 ^b	48.5 ^b
Pour point	0 ^b	high	−30.0 ^b	−3.0	−25.0 ^b	20.0 ^b
Sulfur, %	0.82 ^b	0.15 ^b	0.8 ^b	2.5 ^d	0.35 ^b	0.27 ^b
Quality						
Cracking stock (distilled)						
%, 400 to 900°F	48.2	51.4 ^d	41.8 ^d	39.8	59.4 ^d	45.6 ^d
Octane number (thermal)	71.4 ^b	64.5 ^b	75.6 ^b	75.6 ^d		70.4 ^b
API gravity	25.7	35.5	20.0	22.8	22.3	28.0
Quality			good		excellent	good
Cracking stock (residual)						
% above 550°F	75.9	42.2 ^d	93.9 ^d	75.0	67.7 ^d	52.7 ^d
API gravity	14.7	27.1	9.1	8.0	11.0	18.2
API cracked fuel	4.8	9.6		8.0	4.2	5.0
% gasoline (on stock)	35.5	54.9		15.0	27.5	42.2
% gasoline (on crude oil)	27.0	23.2		11.0	18.6	22.2
Lube distillate (undewaxed)						
%, 700 to 900°F ^c	19.0	16.4 ^d	22.2 ^d	16.0	13.0 ^d	17.6 ^d
Pour point						
Viscosity index	37.0 ^b	113.0 ^b				58.0 ^b
Sulfur, %	2.45 ^b	0.8 ^b	1.5 ^b		0.67 ^b	0.43 ^b
Quality		excellent				
Residue, % over 900°F	40.8	7.9 ^d	57.0 ^d	47.0	28.0 ^d	21.7 ^d
Asphalt quality	good		excellent	excellent	excellent	good

^a Simply aviation gasoline, not always 300°F cut point.^b Estimated from general correlations.^c Sour oils (i.e., oils containing more than 0.5 cu ft hydrogen sulfide per 100 gal before stabilization.)^d Approximated from data on other fractions of same oil.^e Research method octane number.

TABLE 21.9—ANALYSIS OF CONDENSATE LIQUID AND GAS FROM SELECTED TEXAS ZONES

	Chapel Hill Palusy Zone	Carthage Upper Pettite Zone	Carthage Lower Pettite Zone	Old Ocean Chenault Zone	Old Ocean Larson Zone	Seeligson 21 D Zone	Seeligson 21 A Zone	Saxet
Sampling pressure	645	607	632	752	702	810	410	1087
Sampling temperature	82	70	67	85	85	80	85	88
Total fluid mol wt	25.03	19.62	20.19	20.76	20.51	20.64	20.63	21.34
Liquid/gas ratio, bbl per million scf	88.74	16.23	29.28	29.33	28.71	29.88	24.48	41.33
Gas mol wt	20.16	18.25	18.25	18.70	18.17	18.42	18.69	18.89
Gas analysis, mol%								
Carbon dioxide	0.794	0.695	0.646	0.448	0.468	0.130	0.200	0.299
Nitrogen	1.375	1.480	1.967	0.370	0.414	0.075	0.253	0.281
Methane	76.432	89.045	88.799	87.584	90.162	89.498	88.731	86.733
Ethane	7.923	4.691	3.363	5.312	4.067	4.555	5.224	4.816
Propane	4.301	1.393	1.536	2.302	1.616	1.909	1.795	2.673
i-butane	1.198	0.401	0.335	0.584	0.464	0.465	0.486	0.836
n-Butane	1.862	0.394	0.583	0.630	0.390	0.493	0.452	0.788
i-pentane	0.937	0.283	0.302	0.416	0.274	0.266	0.172	0.583
n-Pentane	0.781	0.191	0.254	0.207	0.123	0.209	0.241	0.256
Hexanes	1.415	0.379	0.574	0.505	0.418	0.385	0.414	0.633
Heptane plus	2.992	1.098	1.641	1.642	1.604	2.015	2.032	2.102
Total	100.00	100.00	100.00	100.00	100.00	100.00	100.00	100.00
Liquid gravity, °API	71.8	61.0	64.8	54.0	47.6	52.7	52.1	60.0
Liquid mol wt	68.64	91.51	81.55	85.93	110.07	94.49	103.22	68.73
Liquid analysis	Vol %	°API	Vol %	°API	Vol %	°API	Vol %	°API
Light gasoline	55.1	82.9	29.1	74.8	40.7	76.6	21.2	71.2
Naphtha	37.2	60.5	48.4	59.2	47.0	59.3	55.3	52.9
Kerosene distillate	21.1	50.6	18.2	48.1	7.9	47.6	15.0	42.6
Gas oil							17.4	42.1
Nonviscous lube							15.9	43.6
Residuum and loss	5.6	4.3	4.4	4.7	2.3	6.5	6.5	4.3

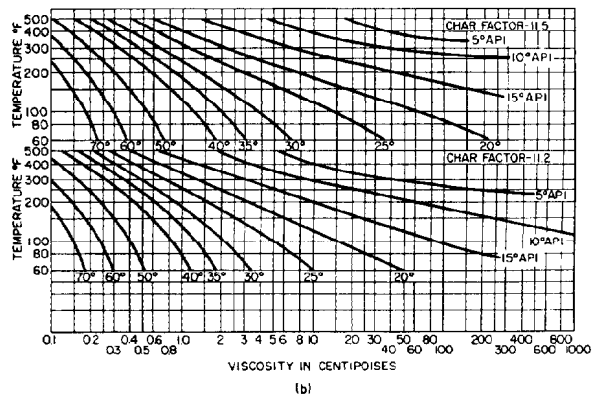
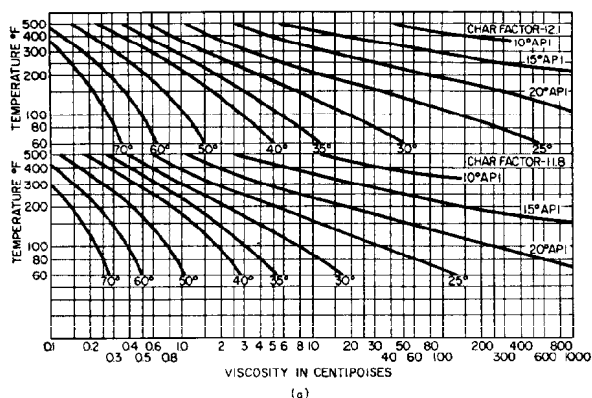


Fig. 21.5—Approximate relation between viscosity, temperature, and characterization factor.

An important physical property of petroleum necessary in studying flow characteristics is viscosity. Viscosity of petroleum is often reported in Saybolt Universal Seconds (SUS), derived from one of the common routine tests for oils. For engineering calculation, however, the viscosity should be obtained in centipoise. The relation between these two systems, according to the U.S. Bureau of Standards, is

$$\frac{\mu_o}{\gamma_o} = 0.219 t_{SU} - \frac{149.7}{t_{SU}},$$

where

μ_o = viscosity, cp

γ_o = specific gravity of oil at measured temperature, and

t_{SU} = Universal Saybolt viscosity, seconds.

An accurate correlation for viscosity is difficult, especially for viscous oils, but an estimate of viscosity may be obtained from Fig. 21.5. Four characterization factors are given, and interpolation must be made for other factors.

True-Boiling-Point Crude-Oil Analyses

A number of true-boiling-point crude-oil analyses are included in Table 21.8. In addition to the gravity, viscosity, sulfur content, and characterization factor, there is a breakdown of typical products made from each crude. This table may be used either to estimate the value of the products listed or to plot and evaluate any set of products obtained (see Fig. 21.1). The table is separated first according to state, and within each group according to gravity.

When the quality of a product is indicated as good or excellent, it means not only that the quality is good but that it is present in normal amounts and that a salable product can be made without excessive treatment.

Table 21.9 shows the analysis of the gas and liquid phases after a stage separation of several condensates.

Nelson⁴ gives a compilation of 164 crudes and lists the gravity, characterization factor, sulfur content, and viscosity of each. Those tables include yields of typical refined products, along with their physical properties and an indication of their quality. A true-boiling-point curve can be generated by plotting the end points of these products against the cumulative volume percent yield. If the characterization factor is plotted on the same graph, the characterization factor at any instantaneous boiling point can be calculated. When instantaneous temperatures and characterization factors at different percents are known, specific gravity, API gravity, and viscosity curves may be estimated. Thus, evaluation curves such as those in Fig. 21.1 may be produced for any of the 164 crudes listed. A typical page of these data is shown in Table 21.8.

More recently, a series on evaluations of non-U.S. crude oils was published.⁵ The format is similar to those in Nelson's compilation,⁴ but the physical properties are usually more complete. An example of an analysis from this series is shown in Table 21.10.

The USBM in Bartlesville, OK, began making distillation analyses before 1920. This laboratory [U.S. DOE Bartlesville Energy Technology Center (BETC)] has continued to evaluate crude oil up to the present time and has two publications^{6,7} that show the distillation data along with gravity and viscosity of the distilled fractions. They also show the percentage composition of the fractions in terms of paraffins, naphthenes, and aromatics. This set of tables uses the correlation index rather than characterization factor as a correlating number. In general, low correlation index (I_c) numbers indicate highly paraffinic (pure paraffin hydrocarbons, $I_c=0$). High numbers indicate a high degree of aromaticity (benzene, $I_c=100$). The correlation index is defined as follows.

$$I_c = 473.7 \gamma - 456.8 + 87552/\bar{T}_B,$$

where γ is the specific gravity of the fraction at 60°F and \bar{T}_B is the average normal boiling point in degrees Rankine.

All U.S. DOE analysis data have been built into the BETC Crude Oil Analysis Data Bank.⁸ The data retrieval system, Crude Oil Analysis System (COASYS), is available by telephone hookup, and customers may search, sort, and retrieve analyses from the file. More than 30 keywords are available for searching; for example, YEAR, APIG, LOC, GEOL and SULF, allow a search on year analyzed, API gravity, location by state and country, geological formation, and percent sulfur in the oil, respectively. Table 21.11 shows the type of information obtained in a typical analysis retrieved from a computer search by COASYS.

Bubblepoint Pressure Correlations*

In the study of reservoir flow properties, it is important to know whether the fluid in the reservoir is in the liquid,

TABLE 21.10—TYPICAL CRUDE OIL EVALUATION, EKOFISK, NORWAY

Crude	
Gravity, °API	36.3
Basic sediment and water, vol%	1.0
Sulfur, wt%	0.21
Pour test, °C	+20
Viscosity, SUS at 100°F	42.48
Reid vapor pressure, psi at 100°F	5.1
Salt, lbm/1,000 bbl	14.5
Nitrogen compounds and lighter, vol%	1.0
Gasoline	
Range, °F	60 to 200
Yield, vol%	10.7
Gravity, °API	77.2
Sulfur, wt%	0.003
Research octane number, clear	74.4
Research octane number, -3 mL tetraethyl lead per gallon	90.0
Gasoline	
Range, °F	60 to 400
Yield, vol%	31.0
Gravity, °API	60.1
Paraffins, vol%	56.52
Naphthenes, vol%	29.52
Aromatics, vol% (O + A)	13.96
Sulfur, wt%	0.0024
Research octane number, clear	52.0
Research octane number, +3 mL tetraethyl lead per gallon	76.0
Kerosene	
Range, °F	400 to 500
Yield, vol%	13.5
Gravity, °API	40.2
Viscosity, SUS at 100°F	32.33
Freezing point, °F	-38
Aromatics, vol% (O + A)	13.1
Sulfur, wt%	<0.05
Aniline point, °F	146.2
Smoke point, mm	21
Light Gas Oil	
Range, °F	500 to 650
Yield, vol%	15.7
Gravity, °API	33.7
Viscosity, SUS at 100°F	43.83
Pour point, °F	-25
Sulfur, wt%	0.11
Aniline point, °F	164.3
Carbon residue, Ramsbottom, wt%	0.08
Cetane index	56.5
Topped Crude	
Range, °F	650 +
Yield, vol%	38.8
Gravity, °API	21.5
Viscosity, SUS at 122°F	80.25
Pour point, °F	-85
Sulfur, wt%	0.39
Carbon residue, Ramsbottom, wt%	4.0
Nickel, vanadium, ppm	5.04, 1.95

*The remainder of this chapter was written by M.B. Standing in the 1962 edition.

TABLE 21.11—ADAPTATION OF BETC COMPUTER SEARCH PRINTOUT

Crude Petroleum Analysis: BETC Sample—B75008

Identification

Webb W Field, Grant County, OK

Red Fork, Des Moines, Middle Pennsylvanian—4,464 to 4,482 ft

General CharacteristicsGravity, specific [$^{\circ}$ API] 0.820 [41.1]

Sulfur, wt% 0.24

Viscosity, SUS

at 77°F 42

at 100°F 39

Pour point, °F < 5

Nitrogen, wt% 0.054

Color brownish-black

Distillation, USBM Method (First drop at 79°F)Stage 1—Distillation at Atmospheric Pressure 746 mm Hg

Fraction Number	Cut (°F)	Vol%	Cumulative Vol%	Gravity at 60°F		Correlation Index	Refraction Index at 20°C	Specific Dispersion	Viscosity at 100°F (SUS)	Cloud point (°F)	wt%	
				Specific	API						Residuum	Crude
1	122	1.5	1.5	0.639	89.9							
2	167	2.2	3.7	0.670	79.7	7	1.38560	126.3				
3	212	5.5	9.2	0.712	67.2	17	1.39755	131.1				
4	257	7.4	16.6	0.738	60.2	21	1.41082	133.0				
5	302	5.8	22.4	0.757	55.4	22	1.42186	134.0				
6	347	6.7	29.1	0.773	51.6	23	1.43039	134.7				
7	392	6.0	35.1	0.785	48.8	22	1.43770	135.2				
8	437	5.9	41.0	0.798	45.8	23	1.44415	135.5				
9	482	6.8	47.8	0.812	42.8	24	1.45102	137.6				
10	527	5.1	52.9	0.823	40.4	25	1.45771	138.0				

Stage 2—Distillation continued at 40 mm Hg

11	392	7.2	60.1	0.842	36.6	30	1.46481	141.2	40	14		
12	437	6.2	66.3	0.851	34.8	30	1.47017	145.6	47	34		
13	482	5.8	72.1	0.863	32.5	33	1.47736	148.4	61	60		
14	527	4.8	76.9	0.874	30.4	35			96	76		
15	572	5.1	82.0	0.887	28.0	38			179	98		
Residuum		17.0	99.0	0.934	20.0						7.1	1.4
Carbon											0.67	
Sulfur											0.235	
Nitrogen												

Approximate Summary

Light gas	9.2		0.690	73.6								
Gas + Naph	35.1		0.743	58.9								
Kerosene	17.8		0.311	43.1								
Gas oil	11.6		0.845	35.9								
Non viscous lub	10.3		0.854 to 0.875	34.3 to 30.3					50 to 100			
Med viscous lub	6.0		0.875 to 0.890	30.3 to 27.4					100 to 200			
Viscous lub	1.3		0.890 to 0.894	27.4 to 26.8					>200			
Residue	17.0		0.934	20.0								
Loss	1.0											

vapor, or two-phase state. With crude oils, the fluid may be subcooled liquid, but with some dissolved gas. Upon reduction in reservoir pressure, a point where the gas starts to come out of solution, called "bubblepoint pressure," is reached. At this point the flow characteristics change. Some of the earliest work in this field was done by Lacey, Sage, and Kircher.⁹

Several empirical correlations have been developed to predict the bubblepoint pressure, and some of these are presented later.

Dewpoint-Pressure Correlations

The dewpoint, like the bubblepoint, is characterized by a substantial amount of one phase in equilibrium with an infinitesimal amount of the other phase. At the dew-

point, the liquid phase is at its minimum. In general, petroleum-reservoir systems that involve dewpoint behavior at reservoir conditions are characterized by (1) surface gas/oil ratios (GOR's) greater than 6,000 cu ft/bbl in most instances; (2) lightly colored tank oils, usually straw-colored to light orange for reservoir systems at 3,000 to 5,000 psi but grading to brown for systems at 7,000 psi and greater; (3) tank oil gravity usually greater than 45°API; and (4) methane content usually greater than 65 mol%.

Few dewpoint-pressure correlations of reservoir systems have been published. Sage and Olds¹⁰ published a very general correlation of the behavior of several San Joaquin Valley, CA, systems. A correlation developed by Organick and Golding¹¹ is discussed in

TABLE 21.11—ADAPTATION OF BETC COMPUTER SEARCH PRINTOUT (continued)

Hydrocarbon-type Analysis for Crude Petroleum Analysis B75008

Fraction Number	Vol% of Crude	Specific Gravity	Correlation Index	Aromatics (vol% of Fraction)	P-N* (vol% of Fraction)	Correlation Index of P-N	Specific Gravity of P-N
1	1.5	0.639	—	0.0	100.0	—	0.639
2	2.2	0.670	7	2.4	97.6	5	0.665
3	5.5	0.712	17	5.9	94.1	13	0.702
4	7.4	0.738	21	7.5	92.5	16	0.727
5	5.8	0.757	22	9.1	90.9	17	0.746
6	6.7	0.773	23	10.2	89.8	17	0.761
7	6.0	0.785	22	10.6	89.4	16	0.772
8	5.9	0.798	23	10.7	89.3	16	0.784
9	6.8	0.812	24	11.5	88.5	17	0.796
10	5.1	0.823	25	10.4	89.6	18	0.809
11	7.2	0.842	30	13.0	87.0	22	0.825
12	6.2	0.851	30	16.2	83.8	21	0.831

Analysis of Naptha Fractions

Fraction Number	Vol% of P-N		Vol% of Fraction		Fraction Number	Number of Total	Aromatic Rings	Naphthenes per mol
	Naptha	Paraffin	Naptha	Paraffin				
2	7.1	92.9	6.9	90.7	12	1.4	0.3	1.1
3	23.7	76.3	22.3	71.8	14	1.7	0.6	1.1
4	38.6	61.4	35.7	56.8				
5	44.0	56.0	40.0	50.9				
6	43.6	56.4	39.2	50.7				
7	43.6	56.4	39.0	50.4				

Summary Data for Blends

	Naptha Blend (Fractions 1 through 7)	Gas/oil Blend (Fractions 8 through 12)
Vol% of Crude in Blend	35.1	31.2
Aromatic, vol% of Blend	7.9	12.5
Paraffin-Naphtene, vol% of Blend	92.1	87.5
Naphtene, vol% of Blend	32.6	
Paraffin, vol% of Blend	59.5	
Naphtene, vol% of P-N in Blend	35.3	
Paraffin, vol% of P-N in Blend	64.7	
Naphtene Ring, wt% of P-N in Blend	20.0	28.3
Paraffin + Side Chains, wt% of P-N in Blend	80.0	71.7

*Paraffin-Naptha.

detail. Calculation of the dewpoint pressure by means of the composition and equilibrium ratios is discussed in Chap. 23.

Sage and Olds' Correlation

Laboratory studies on five San Joaquin Valley systems resulted in the correlation shown in Table 21.12. The basis for the 160°F data presented in this table is shown in Fig. 21.6. Although the five systems correlate within themselves, it is not known how representative the correlation is of systems from other fields. The data are reproduced here more as a guide to dewpoint-pressure behavior than as a means of estimating precise values of dewpoints.

Organick and Golding's Correlation

This correlation relates saturation pressure of a system directly to its chemical composition by means of two generalized composition characteristics \bar{T}_B , the molal average boiling point, and \bar{W}_m , a modified weight average equivalent molecular weight. The saturation pressure may be either bubble-point pressure, dewpoint pressure, or the very special case of critical pressure. The 15 working charts (Figs. 21.7 through 21.21) cover

primarily conditions that pertain to dewpoints, and it is in this capacity that they will be discussed. The reader should be aware, however, that the charts also may be used to estimate critical pressure and temperature of the more volatile systems. The correlation has limited usefulness as a bubblepoint-pressure correlation because it covers primarily high-volatility systems. system. The short-cut method suffices for most calculations.

Calculation of \bar{T}_B . The molal average boiling point of the system is defined as

$$\bar{T}_B = \sum y \times \bar{T}_a, \dots \dots \dots (1)$$

where y is the mole fraction and \bar{T}_a the atmospheric boiling point.

Boiling points of the pure compounds (methane, ethane, nitrogen, carbon dioxide, etc.) are listed in Chap. 20. The boiling point of the C_7^+ fraction is taken as the Smith and Watson¹² mean average boiling point (MABP). The MABP can be calculated from the ASTM distillation curve, the procedure being first to calculate the ASTM volumetric average boiling point (VABP, °F) and then to apply a correction factor to obtain the

TABLE 21.12—RELATION OF DEWPOINT PRESSURE OF CALIFORNIA CONDENSATE SYSTEMS

Tank-Oil Gravity (°API)	GOR (cu ft/bbl)					
	15,000	20,000	25,000	30,000	35,000	40,000
160°F						
52	4,440	4,140	3,880	3,680	3,530	3,420
54	4,190	3,920	3,710	3,540	3,410	3,310
56	3,970	3,730	3,540	3,390	3,280	3,180
58	3,720	3,540	3,380	3,250	3,140	3,060
60	3,460	3,340	3,220	3,100	3,010	2,930
62	3,290	3,190	3,070	2,970	2,880	2,800
64	3,080	3,010	2,920	2,840	2,770	2,700
160°F						
52	4,760	4,530	4,270	4,060	3,890	3,650
54	4,400	4,170	3,950	3,760	3,610	3,490
56	4,090	3,890	3,690	3,520	3,380	3,270
58	3,840	3,650	3,470	3,320	3,200	3,110
60	3,610	3,430	3,280	3,150	3,040	2,960
62	3,390	3,240	3,100	2,990	2,890	2,810
64	3,190	3,060	2,930	2,820	2,740	2,670
220°F						
54	4,410	4,230	4,050	3,890	3,750	3,620
56	3,990	3,780	3,600	3,440	3,300	3,180
58	3,700	3,480	3,280	3,110	2,970	2,850
60	3,430	3,210	3,030	2,880	2,760	2,660
62	3,150	2,970	2,800	2,670	2,570	2,480
64	2,900	2,740	2,590	2,470	2,380	2,300

TABLE 21.14—VALUES OF EQUIVALENT MOLECULAR WEIGHTS FOR NATURAL-GAS CONSTITUENTS

Methane	16.0
Ethane	30.1
Propane	44.1
i-butane	54.5
n-Butane	58.1
i-pentane	69.0
n-Pentane	72.2
Hexanes	85
Ethylene	26.2
Nitrogen	28.0
Carbon dioxide	44.0
Hydrogen sulfide	34.1

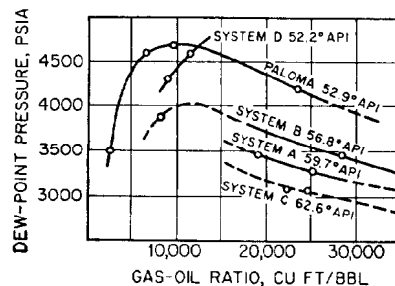
MABP. The VABP is the average of the temperatures at which the distillate plus loss equals 10, 30, 50, 70, and 90% by volume of the ASTM charge, that is,

$$\bar{T}_V = \frac{T_{10\%} + T_{30\%} + T_{50\%} + T_{70\%} + T_{90\%}}{5}, \dots\dots(2)$$

where \bar{T}_V is the ASTM volumetric average boiling point.

The correction to add to \bar{T}_V to obtain the mean average boiling point is given in Table 21.13 as a function of \bar{T}_V and the slope of the ASTM curve between the 10 and 90% distilled points. In the correlation, \bar{T}_V is in degrees Rankine (i.e., °F+460).

Calculation of \bar{W}_m . The modified weight average equivalent molecular weight, \bar{W}_m , is a more complex function to evaluate. It is defined as the equivalent molecular weight multiplied by the summation of the weight fractions. The equivalent molecular weight of a paraffin hydrocarbon compound is its true molecular

**Fig. 21.6—Influence of gas/oil ratio and tank-oil gravity on retrograde dewpoint pressure at 160°F.****TABLE 21.13—CORRECTION TO ADD TO ASTM VOLUMETRIC AVERAGE BOILING POINT TO OBTAIN MEAN AVERAGE BOILING POINT**

Slope of ASTM Curve (°F/%) 10 to 90% points	ASTM VABP (°F)			
	200	300	400	500
2.0	-13	-11.5	-10.5	-9.5
2.5	-17	-15.5	-14	-13
3.0	-22	-20	-18.5	-17
3.5	-27	-25	-23	-21.5
4.0	-33	-30.5	-28.5	-26.5
4.5	—	—	-34.5	-32.5

TABLE 21.15—CORRECTION TO ADD TO ASTM VOLUMETRIC AVERAGE BOILING POINT TO OBTAIN CUBIC AVERAGE BOILING POINT

Slope of ASTM Curve (°F/%) 10 to 90% points	ASTM VABP (°F)		
	200	400	600
2.0	-5.0	-4.0	-3.5
2.5	-6.5	-5.5	-4.5
3.0	-8.0	-7.0	-5.5
3.5	-10.0	-8.5	-7.0
4.0	-12.5	-10.0	-8.5
4.5	-15.0	-12.5	-10.0

weight. For other than straight-chain paraffin compounds (isoparaffins and olefins), the equivalent molecular weight is defined as the molecular weight that an n-paraffin would have if it boiled at the same temperature as the isoparaffin or olefin in question. Values of the equivalent molecular weights for natural-gas constituents are given in Table 21.14.

The equivalent molecular weight of the C₇+ fraction is determined by calculating the Watson characterization factor, K_W , and using Fig. 21.7. Use of the characterization factor permits some account to be taken of the paraffinicity of the heavy-end material.

$$K_W = \frac{\sqrt[3]{\bar{T}_C}}{\gamma_g}, \dots\dots\dots(3)$$

where \bar{T}_C is the cubic average boiling point, °R. The cubic average boiling point (\bar{T}_C) is obtained by adding the corrections in Table 21.15 to the ASTM \bar{T}_V , °F.

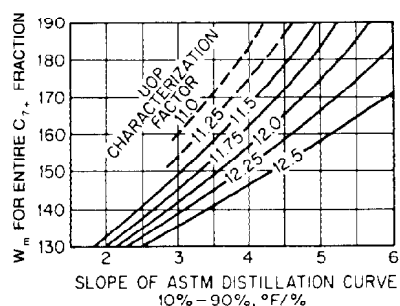


Fig. 21.7—Equivalent molecular weight of C_7+ fraction. Organick and Golding dewpoint/pressure correlation.

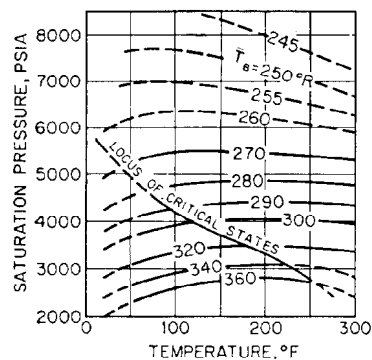


Fig. 21.10—Saturation pressure vs. temperature at $W_m = 80$. Parameter T_b .

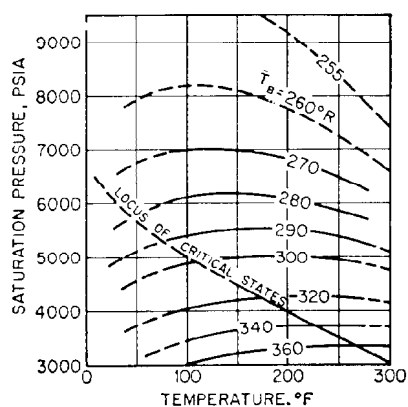


Fig. 21.8—Saturation pressure vs. temperature at $W_m = 100$. Parameter T_b .

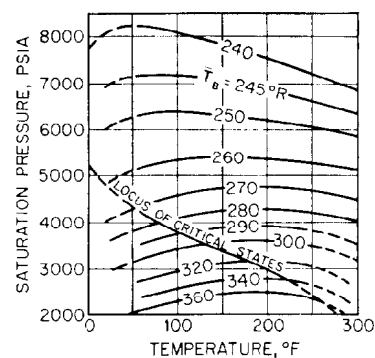


Fig. 21.11—Saturation pressure vs. temperature at $W_m = 70$. Parameter T_b .

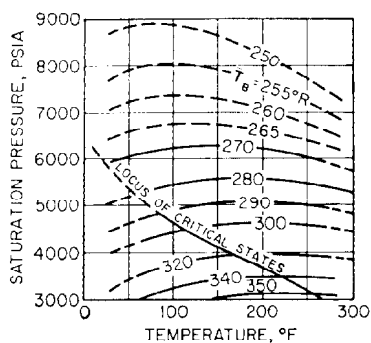


Fig. 21.9—Saturation pressure vs. temperature at $W_m = 90$. Parameter T_b .

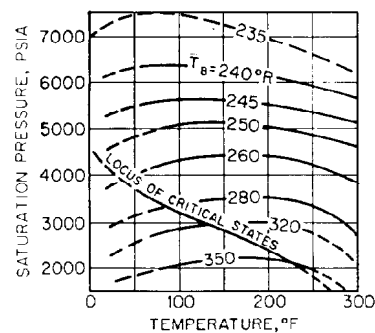


Fig. 21.12—Saturation pressure vs. temperature at $W_m = 60$. Parameter T_b .

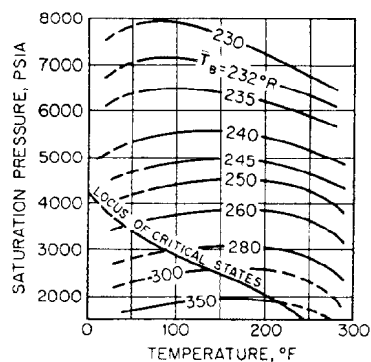


Fig. 21.13—Saturation pressure vs. temperature at $\bar{W}_m = 55$. Parameter T_B .

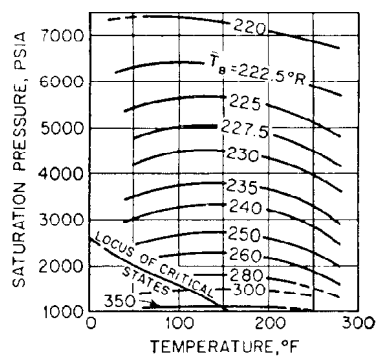


Fig. 21.16—Saturation pressure vs. temperature at $W_m = 40$. Parameter T_B .

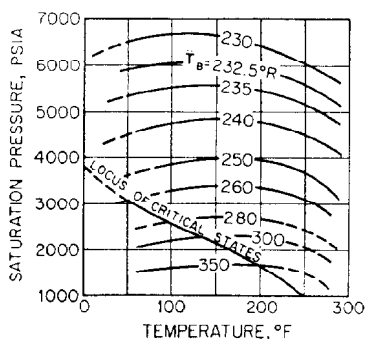


Fig. 21.14—Saturation pressure vs. temperature at $W_m = 50$. Parameter T_B .

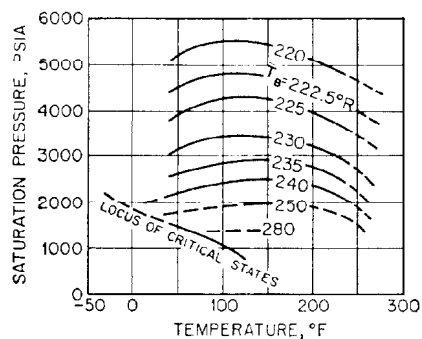


Fig. 21.17—Saturation pressure vs. temperature at $W_m = 35$. Parameter T_B .

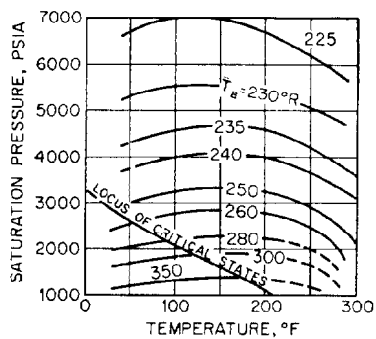


Fig. 21.15—Saturation pressure vs. temperature at $\bar{W}_m = 45$. Parameter T_B .

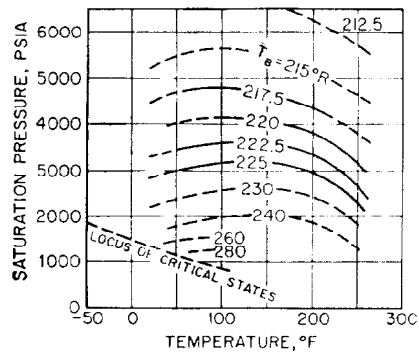


Fig. 21.18—Saturation pressure vs. temperature at $W_m = 32.5$. Parameter T_B .

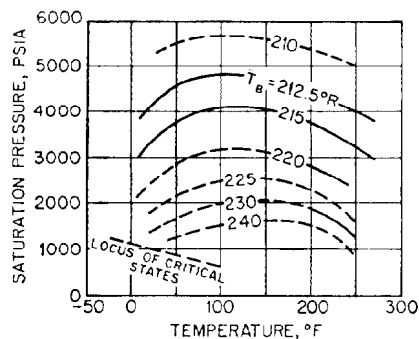


Fig. 21.19—Saturation pressure vs. temperature at $W_m = 30$. Parameter T_B .

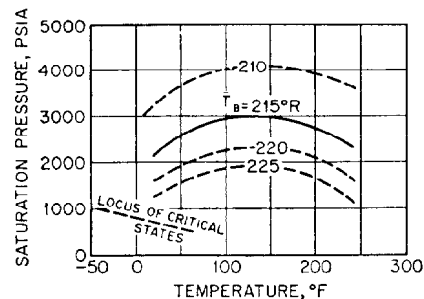


Fig. 21.20—Saturation pressure vs. temperature at $W_m = 27.5$. Parameter T_B .

Example Problem 1. The dewpoint pressure at 200°F for a well effluent having the composition shown in Table 21.16 is predicted as follows.

1. Calculating first the properties of the separator liquid C_7^+ , we have

$$\bar{T}_V = \frac{232 + 260 + 313 + 383 + 497}{5} = 337^\circ\text{F}$$

and

$$10-90\% \text{ slope} = \frac{497 - 232}{80} = 3.31.$$

From Table 21.13, MABP is $337 - 22.5 = 315^\circ\text{F}$ or 775°R . From Table 21.15, CABP is $337 - 8.3 = 329^\circ\text{F}$ or 789°R , giving

$$K_w = \frac{\sqrt[3]{789}}{0.7535} = 12.3.$$

From Fig. 21.7 the \bar{W}_m for the C_7^+ material from the separator liquid is estimated to be 142.

Properties of the C_7^+ material from the separator gas are assumed to be equal to those of n-octane (i.e., $T_B = 718^\circ\text{R}$, $W_m = 114$).

2. Calculating values of \bar{T}_B and \bar{W}_m for the well effluent, we obtain the results shown in Table 21.17.

3. Having calculated \bar{T}_B and \bar{W}_m for the well effluent, we can now determine the desired dewpoint pressure at 200°F by interpolation between Figs. 21.14 and 21.15. At $\bar{T}_B = 240^\circ\text{F}$, the dewpoint pressure is

$$\frac{\bar{W}_m = 50}{4,850} = \frac{\bar{W}_m = 45}{4,000},$$

and the calculated dew point (at $\bar{W}_m = 49$) is 4,680 psia.

It will be noticed that at 4,680 psia and 200°F the material is about 200°F and 900 psi above the critical temperature and pressure of the system. (From Figs. 21.14 and 21.15, the locus of critical states line gives $T_c = 0^\circ\text{F}$ and $p_c = 3,800$ psia.)

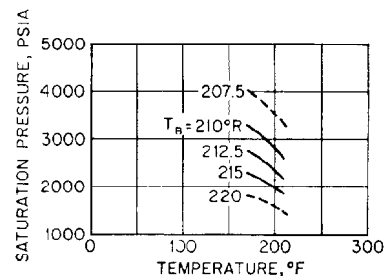


Fig. 21.21—Saturation pressure vs. temperature at $W_m = 25$. Parameter T_B .

Accuracy of Organick-Golding Correlation. About 50% of the 214 points that form the basis for the correlation were in error less than 5% and 82% were in error less than 10%. Standard deviation of all points is about 7.0%.

Total Formation Volume Correlations

The total formation volume factor (FVF) defines the total volume of a system regardless of the number of phases present. Vink *et al.*¹³ have shown that it is possible to have more than two hydrocarbon phases in equilibrium when the system contains an excessively large amount of one component. Naturally occurring systems usually exist in either one or two phases. For this reason, the term “two-phase formation volume” has become synonymous with total formation volume.

The relationship of specific volume and density to the total formation volume is the same as indicated in the preceding section for the oil-formation volume.

Total Formation Volume Factors of Gas-Condensate Systems

Total formation volume factors, specific volumes, and densities of gas-condensate systems may be calculated by use of the ideal gas-law equation with the proper compressibility factor applied provided that the liquid phase present does not amount to an appreciable fraction of the

TABLE 21.16—WELL EFFLUENT COMPOSITION

Component	Mole Fraction		
	Separator Gas	Separator Liquid	Well Effluent**
CO ₂	0.0060	—	0.0056
N ₂	0.0217	—	0.0204
C ₁	0.8986	0.0988	0.8498
C ₂	0.0461	0.0350	0.0454
C ₃	0.0131	0.0381	0.0146
i-C ₄	0.0043	0.0201	0.0053
n-C ₄	0.0043	0.0382	0.0064
i-C ₅	0.0019	0.0495	0.0048
n-C ₅	0.0017	0.0313	0.0035
C ₆	0.0019	0.1284	0.0096
C ₇₊ *	0.0004	—	0.0004
C ₇₊ **	—	0.5606	0.0342
	1.0000	1.0000	1.0000

Properties of C₇₊**Separator gas C₇₊ molecular weight = 114**Separator liquid C₇₊

Molecular weight = 139

Density = 0.7535 g/cc = 56.3°API

ASTM distillation

IBP (%)	216°F
10	232
20	245
30	260
40	289
50	313
60	349
70	383
80	416
90	497
95	

Endpoint

†Effluent composition calculated on the basis of separator liquid/gas ratio 3.0 gal/10³ cu ft.

system volume. Usually, at reservoir pressures and temperatures and for systems whose composition can be expressed as having a surface GOR greater than 10,000 cu ft/bbl, the presence of 10 vol% liquid phase will not cause errors greater than 2 or 3% when the two-phase mixture density is calculated as though the mixture existed in only a single phase. This comes about because the partial volumes of components in the liquid phase are substantially the same as the partial volumes of the same components in the vapor phase.

Calculations from Composition of the Condensate System. As outlined previously, the formation volume (total or single phase) can be calculated from the relation

$$B = \frac{M_{ro} v_{ro}}{L M_{st} v_{st}}, \quad \dots \dots \dots (4)$$

where

- M_{ro} = molecular weight of reservoir system,
- v_{ro} = specific volume of reservoir system,
- M_{st} = molecular weight of stock-tank oil,
- v_{st} = specific volume of stock-tank oil, and
- L = moles of stock-tank oil per 1 mole of reservoir system.

L can be calculated by use of equilibrium ratios and the methods outlined in Chap. 23.

To use the pseudoreduced-temperature/pseudoreduced-pressure/compressibility chart in the calculation of v_{ro} , it is necessary to determine suitable pseudocritical temperature and pressure values for the heptanes and

heavier components. These values can be obtained by the chart shown in Fig. 21.22. The following example illustrates the calculation of M_{ro} and v_{ro} .

Example Problem 2. The specific volume of a gas-condensate system at reservoir conditions given the system molal analysis shown in Table 21.18 is calculated as follows, assuming 1 pound mole of system.

$$T_{pr} = \frac{460 + 199}{370.7} = 1.78,$$

$$p_{pr} = \frac{2,500}{666.0} = 3.75,$$

$$z = 0.885 \text{ (from Fig. 20.2)}$$

and at 2,500 psia and 199°F

$$v_{ro} = \frac{zRT}{Mp} = \frac{0.885 \times 10.73 \times 659}{19.39 \times 2,500} = 0.129,$$

where T_{pr} is the pseudoreduced temperature, p_{pr} the pseudoreduced pressure, z the compressibility factor, and v_{ro} the specific volume (cu ft/lbm) at reservoir conditions.

In the above solution, two phases are present at 2,500 psia, as the dewpoint pressure calculated by the method of Organick and Golding is 2,690 psia at 199°F. Probably no correlation will indicate directly the amount of liquid present at pressures less than the dewpoint pressure, although it can be calculated by use of suitable equilibrium-ratio and density data.

Calculations from GOR and Produced Fluid Properties. A second method of calculating specific volume or formation volume on the basis of the gas-law equation was developed by Standing.¹⁴ This method uses a correlation (Fig. 21.23) to obtain the gravity of the well effluent (or reservoir system) from the condensate liquid/gas ratio, gas gravity, and the stock-tank-oil gravity of the surface products. The effluent gravity is then used to obtain values of pseudocritical temperatures and pressures and, by means of these, to evaluate compressibility factors for the entire effluent. The condensate curve of Fig. 21.24 should be used when employing this method.

Example Problem 3. The total formation volume of a gas-condensate system at reservoir conditions given the parameters in Table 21.19 is calculated as follows, assuming 1 bbl of stock-tank condensate.

$$\gamma_g = \frac{3,700 \times 0.65 + 170 \times 1.20}{3,700 + 170} = 0.675$$

and 1 bbl condensate per million cubic feet is

$$\frac{325}{3.70 + 0.17} = 84,$$

where γ_g is the gravity of total surface gas.

TABLE 21.17—CALCULATED VALUES OF \bar{T}_B and \bar{W}_m

Component	Mole Fraction	Boiling Point (°R)	Mole Fraction Times Boiling Point (°R)	Weight Fraction	Equivalent Molecular Weight	Weight Fraction Times Equivalent Molecular Weight
CO ₂	0.0056	350	2.0	0.0107	44	0.47
N ₂	0.0204	139	2.8	0.0244	28	0.68
C ₁	0.8498	201	170.8	0.5831	16.0	9.33
C ₂	0.0454	332	15.1	0.0586	30.1	1.76
C ₃	0.0146	416	6.1	0.0274	44.1	1.21
i-C ₄	0.0053	471	2.5	0.0133	54.5	0.72
n-C ₄	0.0064	491	3.1	0.0158	58.1	0.92
i-C ₅	0.0048	542	2.6	0.0150	69.0	1.03
n-C ₅	0.0035	557	1.9	0.0107	72.2	0.77
C ₆	0.0096	600	5.8	0.0356	85	3.03
C ₇₊ separator gas	0.0004	718	0.3	0.0019	114	0.22
C ₇₊ separator liquid	0.0342	788	26.9	0.2035	142	28.90
	1.0000		$\bar{T}_B = 239.9$	1.0000		$\bar{W}_m = 49.04$

TABLE 21.18—CALCULATION OF SPECIFIC VOLUME OF GAS-CONDENSATE SYSTEM*

Component	Mole Fraction, y	Molecular Weight, M	Weight, yM (lbm)	Critical Temperature of Components, T _c (°R)	yT _c (°R)	Critical Pressure of Components, p _c (psia)	yp _c
CO ₂	0.0059	44.0	0.26	548	3.2	1,072	6.3
N ₂	0.0218	28.0	0.61	227	4.9	492	10.7
C ₁	0.8860	16.0	14.18	344	304.8	673	596.3
C ₂	0.0460	30.1	1.39	550	25.3	709	32.6
C ₃	0.0134	44.1	0.59	666	8.9	618	8.3
i-C ₄	0.0045	58.1	0.26	733	3.3	530	2.4
n-C ₄	0.0048	58.1	0.28	766	3.7	551	2.6
i-C ₅	0.0026	72.1	0.19	830	2.2	482	1.3
n-C ₅	0.0021	72.1	0.15	847	1.8	485	1.0
C ₆	0.0037	86.2	0.32	915	3.4	434	1.6
C ₇₊	0.0084	138	1.16	1,090**	9.2	343**	2.9
	1.0000		19.39		370.7		666.0

*Reservoir pressure = 2,500 psia.
 Reservoir temperature = 199°F.
 Molecular weight of C₇₊ = 138.
 Specific gravity of C₇₊ = 0.7535.
 **Pseudocritical values from Fig. 21.22.

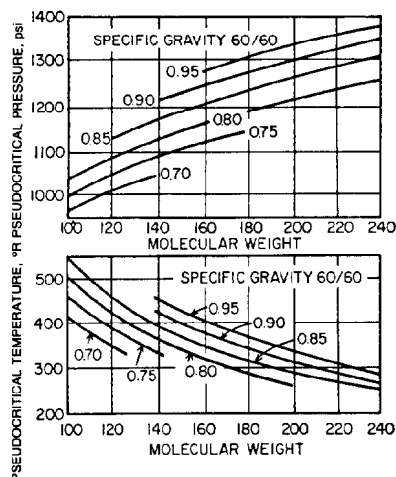


Fig. 21.22—Pseudocritical temperatures and pressures for heptanes and heavier.

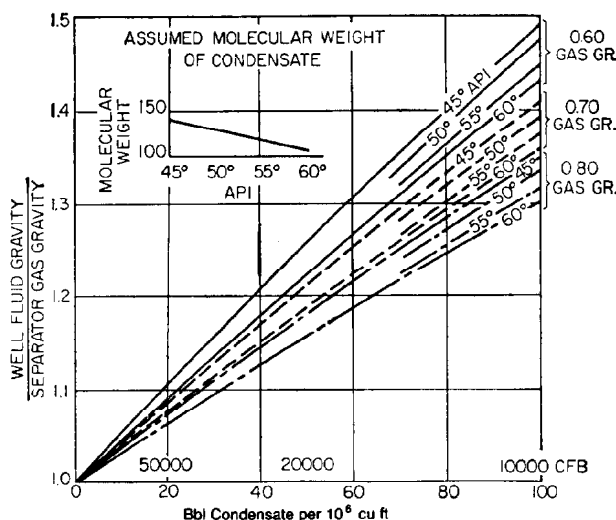


Fig. 21.23—Effect of condensate volume on the ratio of surface-gas gravity to well-fluid gravity.

TABLE 21.19—DATA FOR CALCULATING TOTAL FORMATION VOLUME OF A GAS-CONDENSATE SYSTEM*

Reservoir pressure, psia	3,000
Reservoir temperature, °F	250
Stock-tank-condensate production, B/D	325
Stock-tank condensate gravity, °API	45
Tank vapor rate, 10 ³ cu ft/D	170
Tank vapor gravity (air = 1)	1.20
Trap gas rate, 10 ³ cu ft/D	3,700
Trap gas gravity, (air = 1.0)	0.65

*Basis: 1 bbl of stock-tank condensate.

TABLE 21.20—DATA FOR CORRELATION FOR OBTAINING TOTAL FORMATION VOLUME FACTORS OF DISSOLVED GAS AND GAS-CONDENSATE SYSTEMS SHOWN IN FIG. 21.25

Pressure, psia	400 to 5,000
GOR, cu ft/bbl	75 to 37,000
Temperature, °F	100 to 258
Gas gravity	0.59 to 0.95
Tank-oil gravity, °API	16.5 to 63.8

From Fig. 21.23, at 45°API

$$\gamma_{lw}/\gamma_{gt} = 1.367$$

and

$$\gamma_{lwr} = 1.367 \times 0.675 = 0.923,$$

where

γ_{lw} = well fluid gravity,

γ_{gt} = trap gas gravity,

and

γ_{lwr} = well fluid reservoir gravity.

From Fig. 21.24,

$$T_{pc} = 432$$

and

$$p_{pc} = 647.$$

At reservoir conditions of 3,000 psia and 250°F,

$$T_{pr} = \frac{460 + 250}{432} = 1.64,$$

$$p_{pr} = \frac{3,000}{647} = 4.64,$$

and from Fig. 20.2

$$z = 0.845.$$

By using 350 lbm/bbl for water, the weight of stock-tank condensate per barrel is

$$\frac{350 \times 141.5}{131.5 + ^\circ\text{API}} = 281.$$

TABLE 21.21—DATA FOR CALCULATING TOTAL FORMATION VOLUME OF THE GAS-CONDENSATE SYSTEM DESCRIBED IN EXAMPLE PROBLEM 4

Reservoir pressure, psia	3,000
Reservoir temperature, °F	250
GOR (condensate total), cu ft/bbl	11,900
Gas gravity (total)	0.675
Tank-oil gravity, °API	45

TABLE 21.22—DATA USED TO CALCULATE TOTAL FORMATION VOLUME FACTOR IN EXAMPLE PROBLEM 5

Reservoir pressure, psia	1,329
Reservoir temperature, °F	145
GOR, cu ft/bbl	
Separator	566
Tank	37
Total	603
Gas gravity	0.674
Tank-oil gravity, °API	36.4

From Fig. 21.23 the molecular weight of stock-tank condensate, M_c , is 140, moles of stock-tank condensate per barrel is $281/140 = 2.00$, moles of surface gas per barrel of stock-tank condensate is $1/325 \times (3,870 \times 10^3) \times 1/379 = 31.4$, and total moles per barrel of stock-tank condensate is $2.00 + 31.4 = 33.4$.

From gas law,

$$V = \frac{nzRT}{p} = \frac{33.4 \times 0.845 \times 10.73 \times 710}{3,000} = 71.7$$

and

$$V = \frac{71.7}{5.615} = 12.8,$$

where the first value of V is in cubic feet and the second in barrels, giving a formation volume B_i of 12.8 bbl/bbl of stock-tank condensate.

Total Formation Volume Factors of Dissolved Gas Systems

A suitable correlation for obtaining total formation volume factors of both dissolved gas and gas-condensate systems was developed by Standing.¹⁵ This correlation is shown in Fig. 21.25, and the graphical chart for simplified use of the correlation is given by Fig. 21.26. The correlation contains 387 experimental points, 92% of which are within 5% of the correlation. Range of the data comprising the correlation is given in Table 21.20.

Example Problem 4. The total formation volume of the gas-condensate system described in Example Problem 3 is calculated as follows, given the data in Table 21.21.

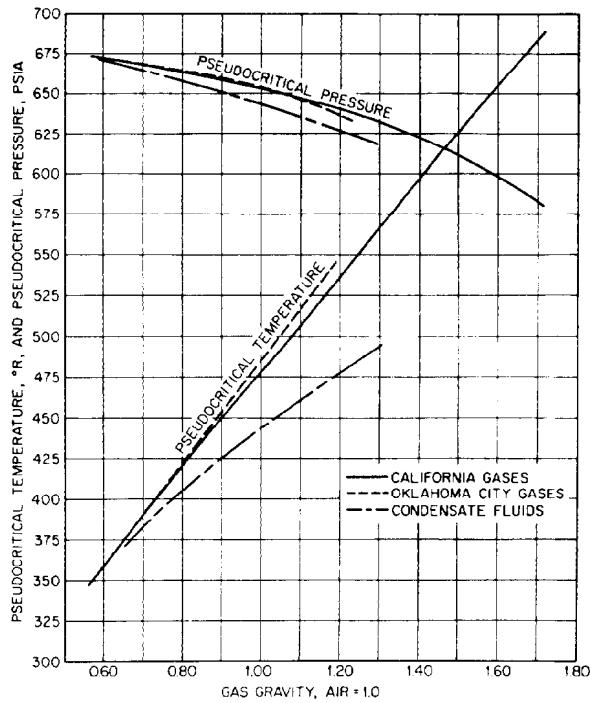


Fig. 21.24—Pseudocritical properties of gases and condensate well fluids.

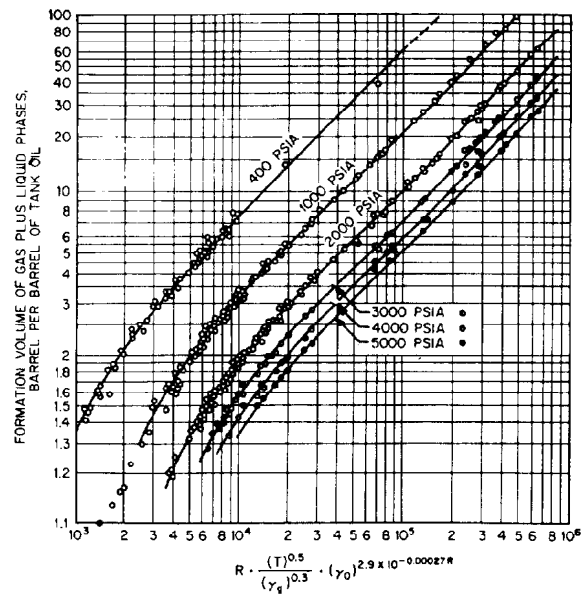


Fig. 21.25—Formation volume of gas plus liquid phases from GOR, total gas gravity, tank-oil gravity, temperature, and pressure.

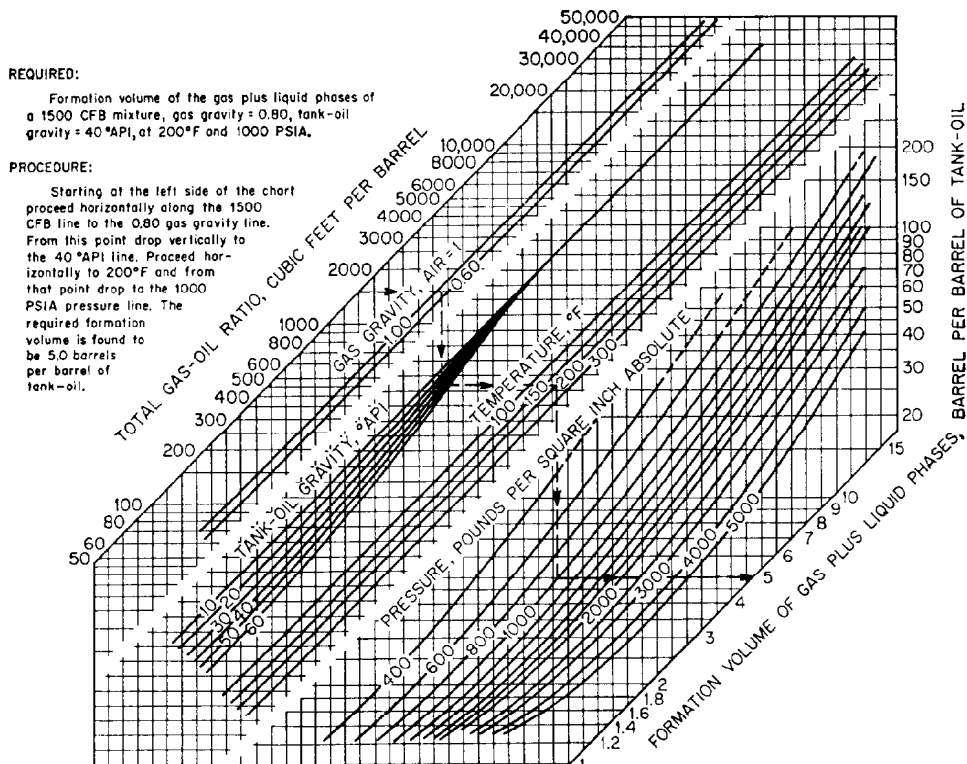


Fig. 21.26—Chart for calculating total formation volume by Standing's correlation.

$$\gamma_o = \frac{141.5}{131.5 + 45} = 0.802$$

and

$$\begin{aligned} & \frac{R(T)^{0.5}}{(\gamma_g)^{0.3}} \times (\gamma_o)^{2.9 \times 10^{-0.00027R}} \\ &= 11,900 \frac{(250)^{0.5}}{(0.675)^{0.3}} \times (0.802)^{2.9 \times 10^{-0.00027 \times 11,900}} \\ &= 11,900 \frac{15.8}{0.877} \times (0.802)^{1.0} \\ &= 1.72 \times 10^5 \end{aligned}$$

where γ_o is the tank-oil specific gravity.

From Fig. 21.25, $B_t = 13 + \text{bbl/bbl of tank oil}$.

From Fig. 21.26, $B_t = 13.7 \text{ bbl/bbl of tank oil}$.

Example Problem 5. The total formation volume of well production at reservoir conditions given the data in Table 21.22 is calculated as follows.

From Fig. 21.26, $B_t = 1.72 \text{ bbl/bbl of tank oil}$. Experimental value calculated from PVT test results is 1.745 bbl/bbl of tank oil.

Nomenclature

B = formation volume, m^3 (bbl)
 I_c = correlation index
 K = characterization factor
 L_c = moles of stock-tank condensate per barrel
 L_o = moles of stock-tank oil per 1 mole of reservoir system, kmol/m^3 (lbm mol/gal)
 M = molecular weight
 M_{ro} = molecular weight of reservoir system
 M_{st} = molecular weight of stock-tank oil
 n = total moles
 p_c = critical pressure, psia (lbf/sq in.)
 p_{pr} = pseudoreduced pressure
 R = universal gas constant
 t_{SU} = Universal Saybolt viscosity, seconds
 T = temperature, $^{\circ}\text{F}$
 T_c = critical temperature, $^{\circ}\text{C}$ ($^{\circ}\text{F}$)
 T_{pr} = pseudoreduced temperature
 \bar{T}_a = atmospheric boiling point, K ($^{\circ}\text{R}$)
 \bar{T}_B = molal average boiling point, K ($^{\circ}\text{R}$)

\bar{T}_C = cubic average boiling point, K ($^{\circ}\text{R}$)
 \bar{T}_m = mean average boiling point, K ($^{\circ}\text{R}$)
 \bar{T}_m = mean average boiling point, K ($^{\circ}\text{R}$)
 \bar{T}_V = volumetric average boiling point, $^{\circ}\text{F}$
 v_{ro} = specific volume of reservoir system
 v_{st} = specific volume of stock-tank oil
 \bar{W}_m = modified weight average equivalent molecular weight
 y = mole fraction
 z = compressibility factor
 γ_g = gas specific gravity
 γ_{gt} = trap gas gravity
 γ_{lw} = well fluid gravity
 γ_{lwr} = well fluid reservoir gravity
 γ_o = tank-oil specific gravity
 μ = viscosity, $\text{Pa} \cdot \text{s}$ (cp)

References

1. *ASTM Standards on Petroleum Products and Lubricants*, Part 24, ASTM, Philadelphia (1975) 796.
2. Watson, K.M., Nelson, E.F., and Murphy, G.B.: "Characterization of Petroleum Fractions," *Ind. and Eng. Chem.* (Dec. 1935) 1460-64.
3. *Technical Data Book—Petroleum Refining*, API, Washington, D.C. (1970) 2-11.
4. Nelson, W.L.: *Petroleum Refinery Engineering*, fourth edition, McGraw-Hill Book Co. Inc., New York City (1958), 910-37.
5. "A Guide to World Export Crudes," *Oil and Gas J.* (1976).
6. Ferrero, E.P. and Nichols, D.T.: "Analyses of 169 Crude Oils from 122 Foreign Oil Fields," U.S. Dept. of the Interior, Bureau of Mines, Bartlesville, OK (1972).
7. Coleman, H.J. et al.: "Analyses of 800 Crude Oils from United States Oil Fields," U.S. DOE, Bartlesville, OK (1978).
8. Woodward, P.J.: *Crude Oil Analysis Data Bank*, Bartlesville Energy Technology Center, U.S. DOE, Bartlesville, OK (Oct. 1980) 1-29.
9. Lacey, W.N., Sage, B.H., and Kircher, C.E. Jr.: "Phase Equilibria in Hydrocarbon Systems III, Solubility of a Dry Natural Gas in Crude Oil," *Ind. and Eng. Chem.* (June 1934) 652-54.
10. Sage, B.H. and Olds, R.H.: "Volumetric Behavior of Oil and Gas from Several San Joaquin Valley Fields," *Trans., AIME* (1947) 170, 156-62.
11. Organick, E.I. and Golding, B.H.: "Prediction of Saturation Pressures for Condensate-gas and Volatile-oil Mixtures," *Trans., AIME* (1952), 195, 135-48.
12. Smith, R.L. and Watson, K.M.: "Boiling Points and Critical Properties of Hydrocarbon Mixtures," *Ind. and Eng. Chem.* (1937) 1408.
13. Vink, D.J. et al.: "Multiple-phase Hydrocarbon Systems," *Oil and Gas J.* (Nov. 1940) 34-38.
14. Standing, M.B.: *Volumetric and Phase Behavior of Oil Field Hydrocarbon Systems*, Reinhold Publishing Corp., New York City (1952).
15. Standing, M.B.: "A Pressure-Volume-Temperature Correlation for Mixtures of California Oils and Gases," *Drill. and Prod. Prac.*, API (1947), 275.

Chapter 22

Oil System Correlations

H. Dale Beggs, Petroleum Consultant*

Introduction

Knowledge of petroleum fluids' physical properties is required by petroleum engineers for both reservoir and production system calculations. These properties must be evaluated at reservoir temperature and various pressures for reservoir performance studies, and at conditions of both changing pressure and temperature for wellbore hydraulics calculations.

If reservoir fluid samples are available, the fluid properties of interest can be measured with a pressure-volume-temperature (PVT) analysis. However, these analyses usually are conducted at reservoir temperature only and the variation of the properties with temperature is not available for production system calculations. Also, in many cases a PVT analysis may not be available early in the life of the reservoir or may never be available because of economic reasons. To overcome these obstacles, empirical correlations have been developed for predicting various fluid physical properties from limited data. The development and application of several of these empirical correlations are presented in this chapter. Methods for estimating physical properties for both saturated and undersaturated oils as functions of pressure, temperature, stock-tank oil gravity, and separator gas gravity are given.

Fluid properties are calculated here only for oil systems with and without fluid composition known. Methods for calculating physical properties of gas-condensate systems are presented in Chaps. 21, 23, and 30. Therefore, no correlations for dewpoint pressure are presented, as the dewpoint pressure can be calculated with the procedures outlined in Chap. 21 if the composition of the fluid is known.

Many of the older correlations were presented in graphical form only and are therefore not suitable for use in computers or programmable calculators. These graphs are converted to equation form where possible.

The generally accepted definitions of the fluid properties correlated in this chapter are as follows.*

Oil density, ρ_o , is the ratio of the mass of the oil plus its dissolved or solution gas per unit volume, which varies with temperature and pressure.

Bubblepoint pressure, p_b , is the pressure at which the first bubble of gas evolves as the pressure on the oil is decreased. It also is frequently called "saturation pressure," as the oil will absorb no more gas below that pressure. The bubblepoint pressure varies with temperature for a particular oil system.

Solution gas/oil ratio (GOR), R_s , is the amount of gas that will evolve from the oil as the pressure is reduced to atmospheric from some higher pressure. It is usually expressed in units of scf/STB. The gas is frequently referred to as "dissolved gas."

Oil formation volume factor (FVF), B_o , is the volume occupied by 1 STB oil plus its solution gas at some elevated pressure and temperature. It is usually expressed as bbl/STB. It is a measure of the shrinkage of the oil as it is brought to stock-tank conditions.

Total FVF, B_t , means the volume occupied at some elevated pressure and temperature by 1 STB oil, its remaining solution gas, and the free gas ($R_{sf} - R_s$) that has evolved from the oil. It is also expressed as bbl/STB.

Oil viscosity, μ_o , measures the oil's resistance to flow, defined as the ratio of the shearing stress to the rate of shear induced in the oil by the stress. It is usually measured in centipoise and is required for both reservoir and piping system calculations.

Interfacial tension (IFT), σ_o , is the force per unit length existing at the interface between two immiscible fluids. This property is not required in most reservoir calculations but is a parameter in some correlations for piping system calculations. It is usually expressed in units of dyne/cm.

*The original chapter on this topic in the 1962 edition was written by Marshall B. Standing.

*General terms are defined in the Glossary at the end of this chapter.

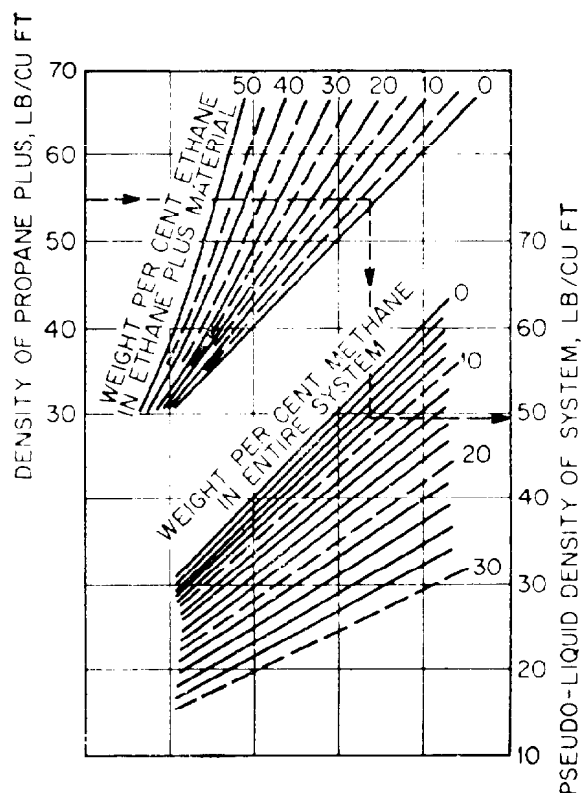


Fig. 22.1—Pseudoliquid density of systems containing methane and ethane.

Oil Density Determination

Oil density is required at various pressures and at reservoir temperature for reservoir engineering calculations. The variation with temperature must be calculated for production system design calculations. An equation for oil density is

$$\rho_o = \frac{350\gamma_o + 0.0764\gamma_g R_s}{5.615B_o}, \quad (1)$$

where

- ρ_o = oil density, lbm/cu ft,
- γ_o = oil specific gravity,
- γ_g = gas specific gravity,
- R_s = solution or dissolved gas, scf/STB,
- B_o = oil FVF, bbl/STB,
- 350 = density of water at standard conditions, lbm/STB,
- 0.0764 = density of air at standard conditions, lbm/scf, and
- 5.615 = conversion factor, cu ft/bbl.

If the pressure and temperature conditions are such that all of the available gas is in solution—i.e., the pressure is above the bubblepoint at the temperature of interest—

increased pressure will merely compress the liquid and increase its density. For the case of $p > p_b$, the oil density is calculated from

$$\rho_o = \rho_{ob} \exp[c_o(p - p_b)], \quad (2)$$

where

- ρ_o = oil density at p , T ,
- ρ_{ob} = oil density at p_b , T ,
- p = pressure, psia,
- p_b = bubblepoint pressure at T , psia, and
- c_o = oil isothermal compressibility at T , psi^{-1} .

Correlations for calculating R_s , B_o , c_o and p_b at various conditions are presented later.

In the petroleum industry, it is common to express gravity in terms of the API gravity of the oil, or:

$$\gamma_o = \frac{141.5}{131.5 + \gamma_{\text{API}}}, \quad (3)$$

where γ_o is oil specific gravity, and γ_{API} is oil gravity, °API.

Density From Ideal Solution Principles—Composition Known

The principle of ideal solutions states that the volume of the total solution is the sum of the individual component volumes. The principle applies at atmospheric pressure for fluids in which the components are closely related chemically, such as petroleum. If the composition of the fluid is known, the density at standard conditions (14.7 psia and 60°F) may be calculated from

$$\rho_{sc} = \frac{\sum_{i=1}^C m_i}{\sum_{i=1}^C V_i} = \frac{\sum m_i}{\sum m_i / \rho_i}, \quad (4)$$

where

- m_i = mass of the i th component,
- V_i = volume of the i th component,
- ρ_i = density of the i th component at standard conditions, and
- C = number of components.

Once the density at standard conditions is calculated, it must be corrected for compressibility and thermal expansion if the density at other conditions is required. This can be accomplished by use of charts presented by Standing.¹

When the ideal solution principle is applied to reservoir oils that contain large amounts of dissolved gas, it is obvious that the fluid cannot be brought to standard or stock-tank conditions and still remain in the liquid phase. This limitation is overcome by calculating a pseudoliquid density, the value of which depends on the mass or weight fractions of methane and ethane in the fluid. The pseudoliquid density correlation was presented by Standing¹ and is illustrated in Fig. 22.1.

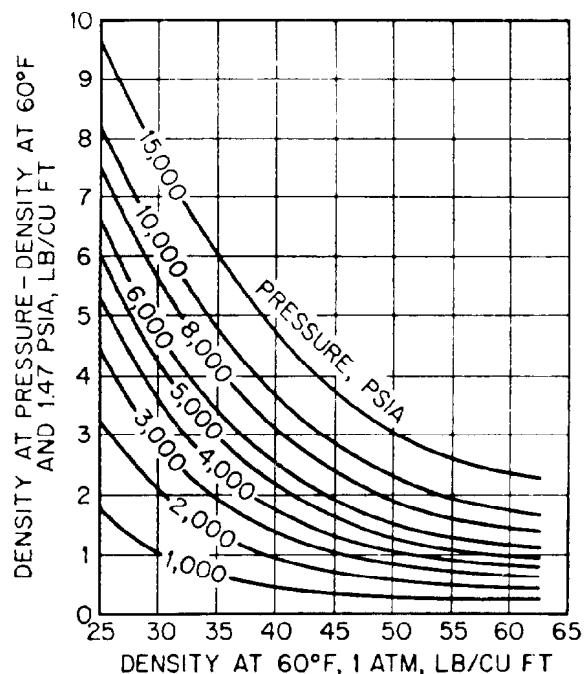


Fig. 22.2—Density correction for compressibility of hydrocarbon liquids.

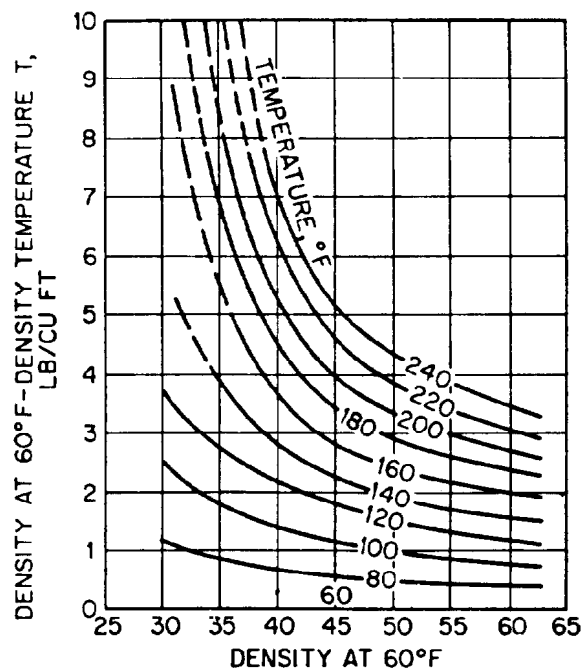


Fig. 22.3—Density correction for thermal expansion of hydrocarbon liquids.

The procedure for calculating oil density at any pressure and temperature when the composition is known is as follows.

1. Calculate the mass or weight of the ethane and heavier components in the mixture.
2. Calculate the density of the propane and heavier components with Eq. 4.
3. Calculate the weight or mass percent of ethane in the ethane and heavier mixture.
4. Calculate the weight percent methane in the total mixture.
5. Determine the pseudoliquid density from Fig. 22.1.
6. Correct for compressibility with Fig. 22.2
7. Correct for thermal expansion with Fig. 22.3.

Example Problem 1. Using the known composition of a reservoir fluid as given in Table 22.1, calculate the den-

sity at the bubblepoint pressure of 3,280 psi and temperature of 218°F.

Solution.

1. Weight of ethane plus = $130.69 - 7.046 = 123.46$ lbm.

2. Density of propane plus equals (weight of propane plus) divided by (volume of propane plus):

$$\frac{130.69 - 7.046 - 1.296}{2.227} = 54.94 \text{ lbm/cu ft.}$$

3. Weight percent ethane in ethane plus:

$$\frac{1.296(100)}{123.46} = 1.05.$$

TABLE 22.1— EXAMPLE PROBLEM 1 SOLUTION

Component	Mole Fraction, y_i	Mole Weight of Components, M_i	Weight of Components $m_i = y_i M_i$ (lbm)	Liquid Density of Components,* ρ_i	Liquid Volume of Components,* $V_i = m_i / \rho_i$ (cu ft)
C ₁	0.4404	16.0	7.046		
C ₂	0.0432	30.1	1.296		
C ₃	0.0405	44.1	1.786	31.66	0.0564
C ₄	0.0284	58.1	1.650	35.77**	0.0461
C ₅	0.0174	72.2	1.256	39.16**	0.0321
C ₆	0.0290	86.2	2.500	41.43	0.0603
C ₇₊	0.4011	287	115.1	56.6	2.032
Total	1.0000		130.69		2.227

* at 60°F and 14.7 psia.

** Arithmetic average of iso and normal values.

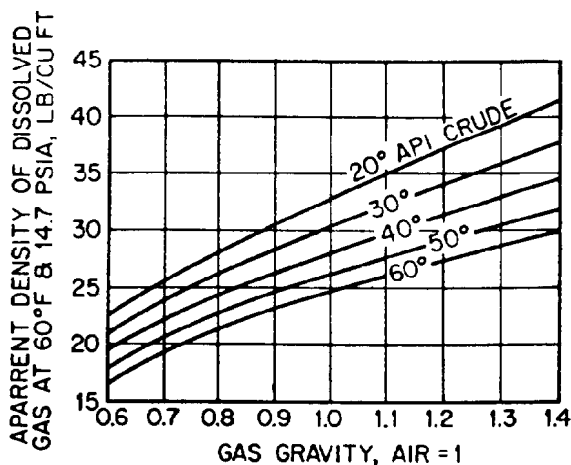


Fig. 22.4—Apparent liquid density of natural gases.

4. Weight percent methane in methane plus:

$$\frac{7.046(100)}{130.69} = 5.39.$$

5. From Fig. 22.1, $\rho_{sc} = 50.8$ lbm/cu ft at 60°F and 14.7 psia.

6. From Fig. 22.2, the correction for pressure is 0.89 lbm/cu ft.

Therefore, the density at 3,280 psia and 60°F is $50.8 + 0.89 = 51.7$ lbm/cu ft.

7. From Fig. 22.3, the correction for temperature is -3.57 lbm/cu ft. Therefore, the density at 3,280 psia and 218°F is

$$51.7 - 3.57 = 48.1 \text{ lbm/cu ft.}$$

Density From Ideal Solution Principles—Composition Unknown

The procedure for estimating oil density outlined in the preceding section used charts for determining the apparent gas density, which required knowledge of the total fluid composition. Katz² extended the apparent density concept to apply to natural gases in general. This results in a method that can be used when solution GOR stock-tank-oil gravity, and gas gravity are known. The fluid composition is not required. The correlation for the apparent density of the dissolved gas as a function of oil and gas gravity is shown in Fig. 22.4. The gravity of the produced gas is calculated as a volume-weighted average of the gas evolved at the separator and the stock tank.

Application of Fig. 22.4 in estimating the oil density from limited data is illustrated in Example Problem 2. In this example, the fluid passed through two separators between the wellhead and the stock tank.

Example Problem 2. Calculate the density and specific volume of the oil system at the bubblepoint conditions of $p_b = 3,280$ psia at $T = 218^\circ\text{F}$. The stock-tank oil gravity

is 27.4°API and the quantities and gravities of the produced gas are given in Table 22.2.

Solution.

1. Average gas gravity, $\bar{\gamma}_g = \Sigma R_i \gamma_{gi} / \Sigma R_i$,

$$\bar{\gamma}_g = \frac{(414)(0.640) + 90(0.897) + 25(1.540)}{414 + 90 + 25} = 0.726,$$

and

$$\gamma_o = \frac{141.5}{131.5 + 27.4} = 0.89.$$

2. Molecular weight of produced gas, $M_g = \gamma_g (M_{\text{air}})$;

$$M_g = 0.726(28.97) = 21.03 \text{ lbm/mol.}$$

3. Mass of dissolved gas, m_g , is given by

$$\frac{529 \text{ scf/STB}}{379.5 \text{ scf/mol}} (21.03 \text{ lbm/mol}) = 29.32 \text{ lbm/STB.}$$

4. Mass of stock-tank oil, m_o , is given by

$$350 \text{ lbm/STB}(0.89) = 311.50 \text{ lbm/STB.}$$

Fig. 22.4 shows that the apparent liquid density of the dissolved gas is about 24.9 lbm/cu ft at 60°F and 14.7 psia. This is used to calculate the volume of the dissolved gas.

5. Volume of dissolved gas, V_g , is given by

$$\frac{m_g}{\rho_g} = \frac{29.32 \text{ lbm/STB}}{24.9 \text{ lbm/cu ft}} = 1.178 \text{ cu ft/STB.}$$

6. Volume of stock-tank oil, V_o , is given by

$$5.615 \text{ cu ft/STB.}$$

7. Pseudoliquid density, ρ_{sL}

$$\begin{aligned} &= \frac{m_o + m_g}{V_o + V_g} \\ &= \frac{311.50 \text{ lbm/STB} + 29.32 \text{ lbm/STB}}{5.615 \text{ cu ft/STB} + 1.178 \text{ cu ft/STB}} \\ &= 50.17 \text{ lbm/cu ft.} \end{aligned}$$

TABLE 22.2—PRODUCED GAS CHARACTERISTICS

	R (scf/STB)	γ_g
First-stage separator	414	0.640
Second-stage separator	90	0.897
Stock tank	25	1.540
Total	529	

Correction of the density for compression and thermal expansion is accomplished with Figs. 22.2 and 22.3.

Fig. 22.2 shows that the pressure correction to 3,280 psia is 0.90 lbm/cu ft. Therefore,

$$\rho_{3280, 60} = 50.17 + 0.90 = 51.07 \text{ lbm/cu ft.}$$

Fig. 22.3 shows that the temperature correction to 218°F is -3.63 lbm/cu ft. Therefore,

$$\rho_{3280, 218} = 51.07 - 3.63 = 47.44 \text{ lbm/cu ft.}$$

The specific volume of the oil is defined as the reciprocal of the density. Therefore,

$$V_o = \frac{1}{\rho_o} = \frac{1}{47.44} = 0.021 \text{ cu ft/lbm.}$$

Bubblepoint-Pressure Correlations

Reservoir performance calculations require that the reservoir bubblepoint pressure be known. This is determined from a PVT analysis of a reservoir fluid sample or calculated by flash calculation procedures if the composition of the reservoir fluid is known. However, since this information is frequently unavailable, empirical correlations for estimating p_b from limited data were developed. These correlations may be used to estimate bubblepoint or saturation pressure as a function of reservoir temperature, stock-tank oil gravity, dissolved-gas gravity, and solution GOR at initial reservoir pressure. That is,

$$p_b = f(T_R, \gamma_{API}, \gamma_g, R_{sb}).$$

A value for $R_{sb} = R_{si}$ can be obtained from the initial solution GOR (produced) if the reservoir pressure is above p_b , where R_{sb} is the solution GOR at bubblepoint pressure and R_{si} is the solution GOR at initial reservoir pressure.

Three methods for estimating bubblepoint pressure are presented. The correlations were developed by use of experimentally measured bubblepoint pressures obtained from PVT analyses on reservoir fluid samples. Other correlations were developed for application in specific reservoirs, but the methods presented here gave good results over a wide range of oil systems.

Standing Correlations

Standing³ presented an equation and nomograph to estimate bubblepoint pressures greater than 1,000 psia. The correlation was based on 105 experimentally determined bubblepoint pressures of California oil systems. The average error of the correlation when applied to the data used to develop the method was 4.8% and 106 psi. The ranges of data used to develop the method are given in Table 22.3.

The gases evolved from the systems used to develop the correlation contained essentially no nitrogen or hydrogen sulfide. Some of the gases contained CO₂, but in quantities less than 1 mol%. No attempt was made to

characterize the tank oils other than by the API gravity. The value for gas gravity to be used is apparently the volume-weighted average of the gas from all stages of separation. The correlation should apply to other oil systems as long as the compositional makeup of the gases and crudes is similar to those used in developing the method.

The equation for estimating bubblepoint pressure is

$$p_b = 18 \left(\frac{R_{sb}}{\gamma_g} \right)^{0.83} \times 10^{\gamma_g}, \dots \dots \dots (5)$$

where

- y_g = mole fraction gas,
- = $0.00091(T_R) - 0.0125\gamma_{API}$,
- p_b = bubblepoint pressure, psia,
- R_{sb} = solution GOR at $p \geq p_b$, scf/STB,
- γ_g = gas gravity (air=1.0),
- T_R = reservoir temperature, °F, and
- γ_{API} = stock-tank oil gravity, °API.

A nomograph developed from Eq. 5 is shown in Fig. 22.5. The example bubblepoint determination shown in the nomograph is calculated with Eq. 5 in the following example.

Example Problem 3. Estimate p_b where $R_{sb} = 350$ scf/STB, $T_R = 200^\circ\text{F}$, $\gamma_g = 0.75$, and $\gamma_{API} = 30^\circ\text{API}$.

Solution.

$$y_g = 0.00091(200) - 0.0125(30) = -0.193.$$

$$p_b = 18 \left(\frac{350}{0.75} \right)^{0.83} \times 10^{-0.193}.$$

$$p_b = 1,895 \text{ psia.}$$

Lasater Correlation

A correlation by Lasater⁴ was developed in 1958 from 158 experimental data points, which included the ranges of variables shown in Table 22.4.

The correlation was presented graphically in the form of two charts. Equations were fitted to these graphical correlations to enhance the use of this method with computers or calculators. The graphical correlations are shown in Figs. 22.6 and 22.7.

The following procedure is used to estimate p_b using Figs. 22.6 and 22.7.

TABLE 22.3—DATA PARAMETERS AND RANGES

p_b , psia	130 to 7,000
T_R , °F	100 to 258
R_{sb} , scf/STB	20 to 1,425
γ_{API} , °API	16.5 to 63.8
γ_g (air = 1.0)	0.59 to 0.95

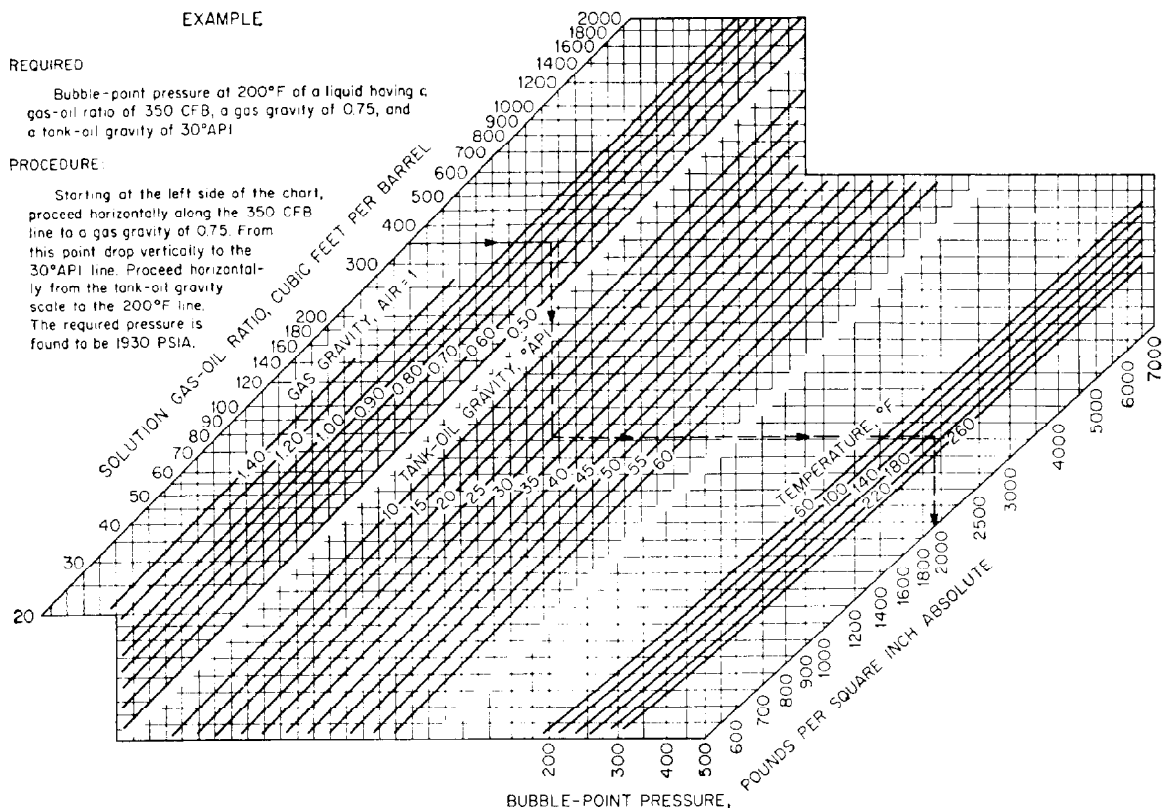


Fig. 22.5—Chart for calculating bubblepoint pressure by Standing's correlation.

1. Find the effective molecular weight of the stock-tank oil from the API gravity using Fig. 22.6.

2. Calculate the mol fraction of gas in the system from

$$y_g = \frac{R_{sb}/379.3}{R_{sb}/379.3 + 350\gamma_o/M_o} \quad (6)$$

3. Find the bubblepoint pressure factor, $p_b\gamma_g/T_R$, from Fig. 22.7

4. Calculate the bubblepoint pressure $p_b = [(p_b\gamma_g)/T] \cdot T_R/\gamma_g$ where T_R is in °R.

The following equations can be used to replace Figs. 22.6 and 22.7.

Equations for Fig. 22.6

For $\text{API} \leq 40$:

$$M_o = 630 - 10\gamma_{\text{API}} \quad (7)$$

For $\text{API} > 40$:

$$M_o = 73,110 (\gamma_{\text{API}})^{-1.562} \quad (8)$$

Equations for Fig. 22.7

For $y_g \leq 0.60$:

$$\frac{p_b\gamma_g}{T_R} = 0.679 \exp(2.786y_g) - 0.323 \quad (9)$$

TABLE 22.4—VARIABLE RANGES

p_b , psia	48 to 5,780
T_R , °F	82 to 272
γ_{API} , °API	17.9 to 51.1
γ_g	0.574 to 1.223
R_{sb} , scf/STB	3 to 2,905

For $y_g > 0.60$:

$$\frac{p_b\gamma_g}{T_R} = 8.26y_g^{3.56} + 1.95 \quad (10)$$

A nomograph that combines Figs. 22.6 and 22.7 is presented in Fig. 22.8. The example given in Fig. 22.8 is worked with the equations in the following example.

Example Problem 4. Given the following data, use the Lasater method to estimate p_b .

$R_{sb} = 500$ scf/STB, $T_R = 200^\circ\text{F} = 660^\circ\text{R}$, $\gamma_g = 0.80$, $\gamma_{\text{API}} = 30$, and $\gamma_o = 0.876$.

Solution.

$$M_o = 630 - 10(30) = 330.$$

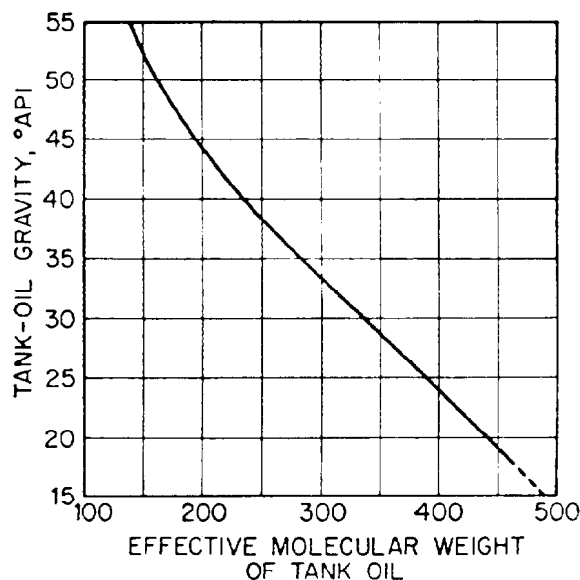


Fig. 22.6—Effective molecular weight related to tank-oil gravity.

$$y_g = \frac{500/379.3}{500/379.3 + 350(0.876)/330} = 0.587.$$

$$\frac{p_b \gamma_g}{T_R} = 0.679 \exp[2.786(0.587)] - 0.323;$$

$$\frac{p_b \gamma_g}{T_R} = 3.161.$$

$$p_b = \frac{3.161(660)}{0.80} = 2,608 \text{ psia.}$$

Vasquez and Beggs Correlation

Vasquez and Beggs⁵ used results from more than 600 oil systems to develop empirical correlations for several oil properties including bubblepoint pressure. The data encompassed very wide ranges of pressure, temperature, oil gravity, and gas gravity and included approximately 6,000 measured data points for R_s , B_o and μ_o at various pressures and temperatures. The ranges of the pertinent parameters are given in Table 22.5.

It was found that the gas gravity was a strong correlating parameter and, unfortunately, usually is one of the variables of most questionable accuracy. The gravity of the evolved gas depends on the pressure and temperature of the separators, which may not be known in many cases. The gas gravity used to develop all the correlations reported by Vasquez and Beggs was that which would result from a two-stage separation. The first-stage pressure was chosen as 100 psig and the second stage was the stock tank. If the known gas gravity resulted from a first-stage separation at a pressure other than 100 psig, the corrected gas gravity to be used in the correlations can be obtained from Eq. 11. If separator conditions are unknown,

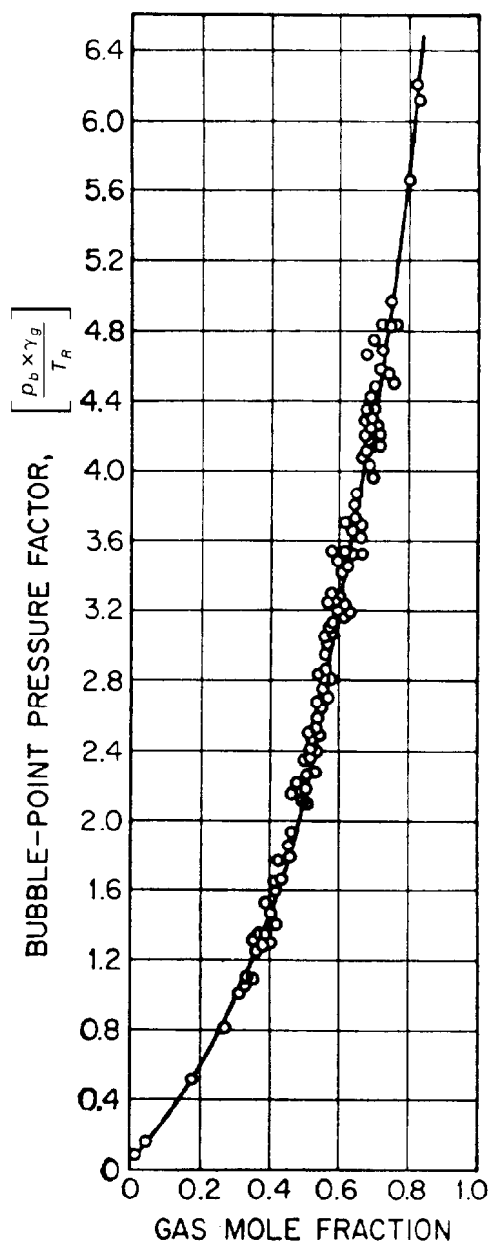


Fig. 22.7—Lasater's correlation of bubblepoint-pressure factor with gas-mole fraction.

the uncorrected gas gravity may be used in the correlations for p_b , R_s , B_o , and c_o .

$$\gamma_{gc} = \gamma_g [1.0 + 5.912 \times 10^{-5} \gamma_{API} T_s \log(p_s/114.7)], \quad (11)$$

where

γ_{gc} = corrected gas gravity,

γ_g = gas gravity resulting from a separation at p_s , T_s

T_s = separator temperature, °F,

p_s = separator pressure, psia, and

γ_{API} = oil gravity, °API.

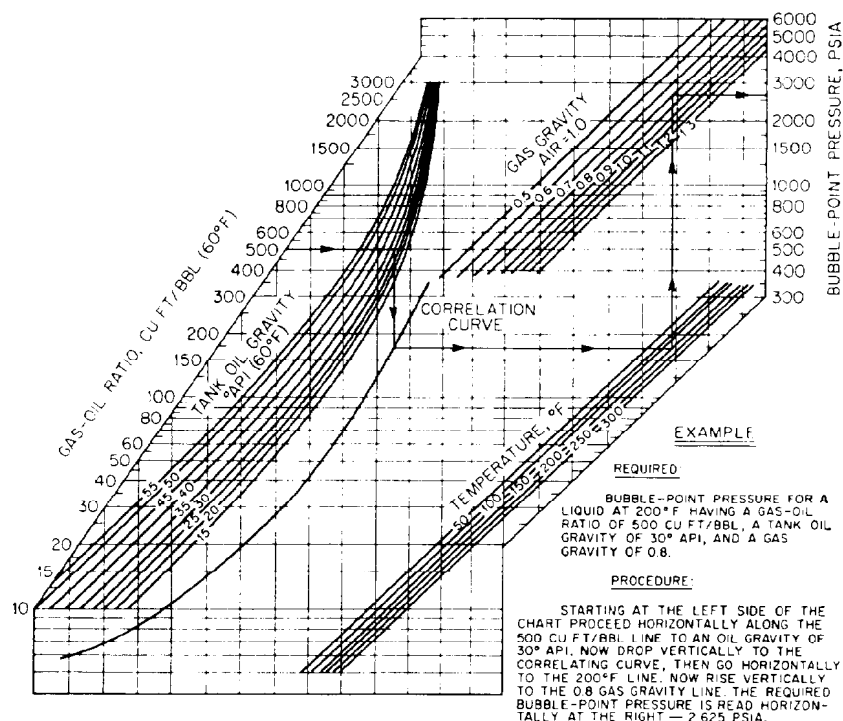


Fig. 22.8—Chart for calculating bubblepoint pressure by Lasater's correlation.

The correlations are presented in equation form only. The bubblepoint pressure is calculated from

$$p_b = \left\{ \frac{R_{sb}}{C_1 \gamma_g \exp[C_3 \gamma_{API}/(T_R + 460)]} \right\}^{1/C_2}, \quad (12)$$

where

- p_b = bubblepoint pressure, psia,
- R_{sb} = solution GOR at p_b , scf/STB,
- γ_g = gas gravity,
- γ_{API} = oil gravity, °API, and
- T_R = temperature, °F.

The accuracy of the correlation was greater if the samples were divided into ranges of oil API gravity. A dividing point of 30°API was chosen. The values of the constants in Eq. 12 depend on API gravity of the stock-tank oil and are given in Table 22.6.

TABLE 22.5—VARIABLE RANGES

p_b , psia	50 to 5,250
T_R , °F	70 to 295
R_{sb} , scf/STB	20 to 2,070
γ_{API} , °API	16 to 58
γ_g	0.56 to 1.18

Example Problem 5. Calculate the bubblepoint pressure for the oil system given in Example Problem 4 using the Vasquez and Beggs correlation and the following data. Use the uncorrected gas gravity. R_{sb} = 500 scf/STB, T_R = 220°F, γ_g = 0.80, and γ_{API} = 30°API.

Solution.

Eq. 12 and the correct C values from Table 22.1 give:

$$p_b = \left[\frac{500}{0.0362(0.80) \exp[25.724(30)/680]} \right]^{1/1.0937};$$

$$p_b = 2,562 \text{ psia.}$$

This compares well with the value of 2,608 obtained in Example Problem 4 with Lasater's correlation. With Standing's Eq. 5, a value of 2,415 psia is obtained.

Accuracy of Bubblepoint Correlations

Comparison of the accuracy with which the measured bubblepoint pressures used in each correlation agreed with

TABLE 22.6—CONSTANTS FOR BUBBLEPOINT EQUATION

	°API ≤ 30	°API > 30
C_1	0.0362	0.0178
C_2	1.0937	1.1870
C_3	25.7240	23.9310

TABLE 22.7—COMPARISON OF ACCURACY OF BUBBLEPOINT-PRESSURE CORRELATIONS

	Standing	Lasater	Vasquez-Beggs
Number of points in correlations	105	158	5,008
Data points within 10% of correlation, %	87	87	85
Data points more than 200 psi in error, %	27		
Mean error, %	4.8	3.8	-0.7

values determined from the final correlation shows that the Vasquez and Beggs correlation is the most accurate, followed by Lasater's and then by Standing's. This is shown in Table 22.7.

Solution GOR for Saturated Oils

Both reservoir engineering and production engineering calculations require estimates of the amount of dissolved gas remaining in solution at oil system pressures below bubblepoint pressure. The amount of free gas—that is, the gas that has evolved from 1 STB oil as the pressure is reduced below p_b —is $R_{sb} - R_s$, where R_s is the gas remaining in solution at the pressure of interest. In effect, any pressure below the original bubblepoint pressure is also a bubblepoint pressure, since the oil is saturated with gas at this pressure. Therefore, the correlations presented in the previous section can be solved for solution GOR and a value of R_s can be obtained at any pressure less than the reservoir p_b . That is, $R_s = f(p, T, \gamma_{API}, \gamma_g)$.

The nomographs presented in Figs. 22.5 and 22.8 can be used to determine R_s by entering the bubblepoint axis at the pressure of interest and proceeding "backward" through the graph to determine R_s .

Standing Correlation

$$R_s = \gamma_g \left(\frac{p}{18 \times 10^{\gamma_g}} \right)^{1.204}, \quad (13)$$

where

$$\begin{aligned} \gamma_g &= 0.00091(T) - 0.0125(\gamma_{API}), \\ R_s &= \text{solution GOR, scf/STB,} \\ p &= \text{pressure, psia,} \\ \gamma_g &= \text{gas gravity,} \\ \gamma_{API} &= \text{oil gravity, } ^\circ\text{API, and} \\ T &= \text{temperature of interest, } ^\circ\text{F.} \end{aligned}$$

Lasater Correlation

$$R_s = \frac{132755 \gamma_o \gamma_g}{M_o (1 - \gamma_g)}, \quad (14)$$

where M_o is obtained from Eq. 7 or 8 and γ_g is calculated by either Eq. 9 or 10, depending on whether the value of the pressure factor is less than or greater than 3.29.

$$\text{For } \frac{p\gamma_g}{T} < 3.29:$$

$$\gamma_g = 0.359 \ln \left(\frac{1.473 p \gamma_g}{T} + 0.476 \right), \quad (15)$$

$$\text{For } \frac{p\gamma_g}{T} \geq 3.29:$$

$$\gamma_g = \left(\frac{0.121 p \gamma_g}{T} - 0.236 \right)^{0.281}, \quad (16)$$

where T is in $^\circ\text{R}$.

Vasquez and Beggs Correlation

$$R_s = C_1 \gamma_g p^{C_2} \exp \left(\frac{C_3 \gamma_{API}}{T + 460} \right), \quad (17)$$

where

$$\begin{aligned} R_s &= \text{gas in solution at } p \text{ and } T, \text{ scf/STB,} \\ \gamma_g &= \text{gas gravity,} \\ p &= \text{pressure of interest, psia,} \\ \gamma_{API} &= \text{stock-tank oil gravity, } ^\circ\text{API} \\ T &= \text{temperature of interest, } ^\circ\text{F, and} \\ C_1, C_2, C_3 &= \text{are obtained from Table 22.6.} \end{aligned}$$

Example Problem 6. Estimate the solution GOR of the following oil system using the correlations of Standing, Lasater, and Vasquez and Beggs and the data: $p = 765$ psia, $T = 137^\circ\text{F}$, $\gamma_{API} = 22^\circ\text{API}$, and $\gamma_g = 0.65$.

Standing

$$\gamma_g = 0.00091(137) - 0.0125(22) = -0.15.$$

$$R_s = 0.65 \left[\frac{765}{18 \times 10^{-0.15}} \right]^{1.204} = 90 \text{ scf/STB.}$$

Lasater

$$\frac{p\gamma_g}{T} = \frac{765(0.65)}{137 + 460} = 0.833.$$

$$\gamma_g = 0.359 \ln[1.473(0.833) + 0.476] = 0.191 \text{ (Eq. 15).}$$

$$M_o = 630 - 10(22) = 410 \text{ (Eq. 7).}$$

$$\gamma_o = \frac{141.5}{131.5 + 22} = 0.922.$$

$$R_s = \frac{132755(0.922)(0.191)}{410(1 - 0.191)} = 70 \text{ scf/STB (Eq. 14).}$$

If γ_g is read from Fig. 22.7 rather than calculated from Eq. 15, a value of approximately 0.25 is obtained. This gives a value of $R_s = 100$ scf/STB. In this example, the graphical value is closer to those calculated from the other two correlations. The accuracy of the Lasater equation is much better at higher R_s values.

Vasquez and Beggs

$$R_s = 0.0362(0.65)(765)^{1.0937} \exp \left[\frac{25.724(22)}{137 + 460} \right];$$

$$R_s = 87 \text{ scf/STB.}$$

Oil FVF Correlations

The oil FVF is required for both reservoir and production system calculations. The reservoir engineer must be able to relate stock-tank volumes to reservoir volumes at various pressures and a constant reservoir temperature. Production engineering involves converting surface-measured volumetric flow rates to in-situ flow rates at various pressures and changing temperatures as the fluid is produced to the surface.

As defined previously, the oil FVF is the volume that would be occupied at some pressure and temperature by 1 STB oil plus any gas dissolved in the oil at these pressure and temperature conditions. It is a function of the composition of the system and the conditions under which the gas and liquid are separated.

Values of oil FVF at reservoir temperature and various pressures can be obtained from a standard PVT analysis of a reservoir fluid sample. However, this type of analysis is often unavailable and the engineer must then resort to empirical correlations that require only limited data. Two empirical correlations for saturated oil systems will be presented in this section. Both require values for solution GOR, R_s , which can be obtained by the methods presented in the previous section.

At pressures above the bubblepoint, the oil is undersaturated and the liquid expands as pressure is reduced. Calculation of oil FVF thus requires a value for oil compressibility. Two correlations for estimating the compressibility of an undersaturated oil system will be presented.

Saturated Systems

If an oil system is saturated with gas at given conditions of pressure and temperature, a reduction in pressure will allow solution gas to evolve, thus causing the oil to shrink. The liquid volume is also affected by temperature. Solution gas increases as temperature is decreased, but the liquid volume decreases as the oil is cooled. The correlations presented in this section can be expressed as

$$B_o = f(R_s, \gamma_{API}, \gamma_g, T).$$

Standing Correlation. Standing⁴ used the same oil systems described in the bubblepoint correlation section to develop a correlation for B_o at pressures less than p_b . The method was presented in both equation and nomograph form. In equation form,

$$B_o = 0.972 + 0.000147F^{1.175}, \dots \dots \dots (18)$$

where F is a correlating function and is determined from the equation

$$F = R_s(\gamma_g/\gamma_o)^{0.5} + 1.25T,$$

B_o = oil FVF, bbl/STB,
 R_s = solution GOR, scf/STB,
 γ_g = gas gravity,
 γ_o = oil specific gravity = $141.5/(131.5 + \gamma_{API})$,
 and
 T = temperature of interest, °F.

A nomograph that solves Eq. 18 graphically is presented in Fig. 22.9.

Example Problem 7. Use both Standing's equation and nomograph to estimate the oil FVF for the oil system described by the data $T = 200^\circ\text{F}$, $R_s = 350$ scf/STB, $\gamma_g = 0.75$, and $\gamma_{API} = 30^\circ\text{API}$.

Solution.

$$\begin{aligned} \gamma_o &= 141.5/(131.5 + 30) = 0.876. \\ F &= 350(0.75/0.876)^{0.5} + 1.25(200) = 574. \\ B_o &= 0.972 + 0.000147(574)^{1.175}; \\ B_o &= 1.228 \text{ bbl/STB.} \end{aligned}$$

A value of 1.22 bbl/STB is obtained from the nomograph, Fig. 22.9.

Vasquez and Beggs Correlation. In conjunction with development of the bubblepoint and solution GOR correlations, Vasquez and Beggs⁵ also presented an equation for oil FVF for saturated oils. To improve the accuracy of the correlation, the 600 oil systems were divided into two groups, those having API gravities ≤ 30 and those having gravities > 30 . The gas gravity used in the equation should be the corrected gravity calculated by Eq. 11 if the separator pressure is known. If separator conditions are unknown, the uncorrected gas gravity may be used. The equation is

$$B_o = 1 + C_1 R_s + C_2 (T - 60)(\gamma_{API}/\gamma_{gc}) + C_3 R_s (T - 60)(\gamma_{API}/\gamma_{gc}), \dots \dots \dots (19)$$

where

$$\begin{aligned} B_o &= \text{oil FVF at } p \text{ and } T, \text{ bbl/STB} \\ R_s &= \text{solution GOR at } p, T, \text{ scf/STB} \\ T &= \text{temperature of interest, } ^\circ\text{F} \\ p &= \text{pressure of interest, psia} \\ \gamma_{API} &= \text{stock-tank oil gravity, } ^\circ\text{API, and} \\ \gamma_{gc} &= \text{gas gravity, corrected, air} = 1. \end{aligned}$$

The constants are determined from Table 22.8.

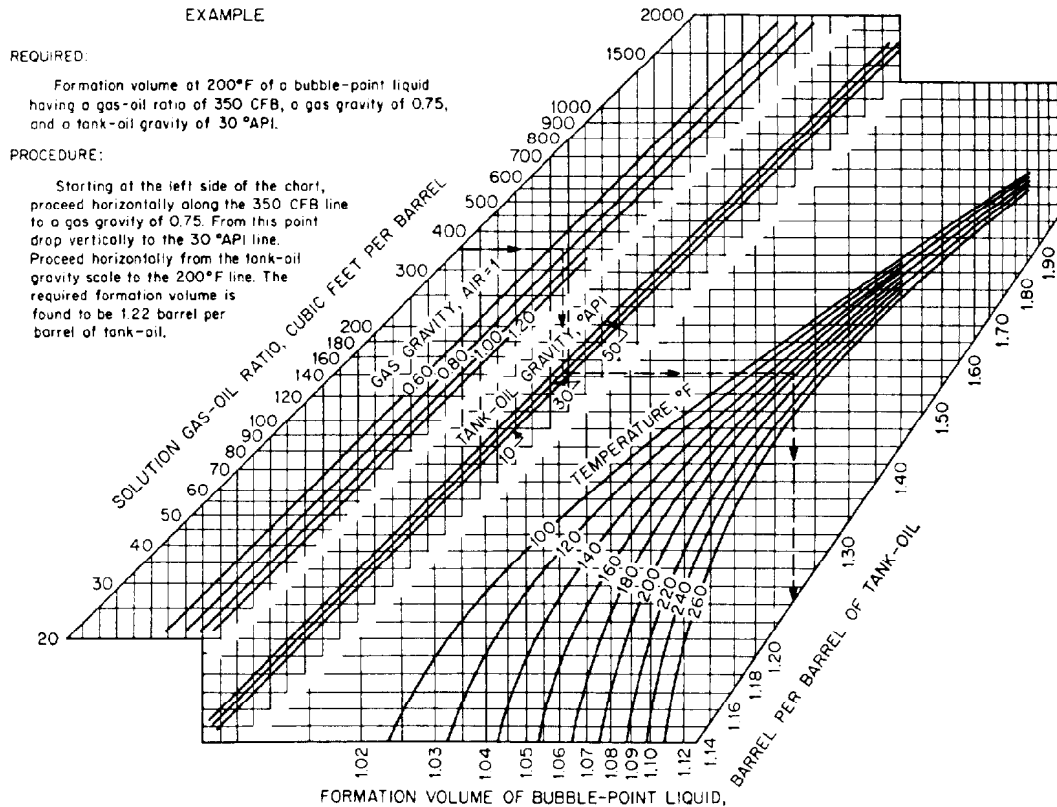


Fig. 22.9—Chart for calculating oil-formation volume by Standing's correlation.

Example Problem 8. Use the Vasquez and Beggs equation to determine the oil FVF at bubblepoint pressure for the oil system described by $p_b = 2,652$ psia, $R_{sb} = 500$ scf/STB, $\gamma_{gc} = 0.80$, $\gamma_{API} = 30^\circ$ API, and $T = 220^\circ$ F.

Solution.

$$B_{ob} = 1 + 4.677 \times 10^{-4} (500) + 1.751 \times 10^{-5} (160) \cdot (30/0.80) - 1.811 \times 10^{-8} (500)(160) \cdot (30/0.80).$$

$$B_{ob} = 1.285 \text{ bbl/STB.}$$

Undersaturated Systems

The oil FVF decreases with pressure increase at pressures above the bubblepoint. In this case, B_o is calculated from

$$B_o = B_{ob} \exp[c_o(p_b - p)], \quad (20)$$

where

- B_{ob} = oil FVF at p_b ,
- p_b = bubblepoint pressure, psia,
- p = pressure of interest, psia, and
- c_o = oil isothermal compressibility, psi^{-1} .

Values for B_{ob} can be calculated with the Standing or Vasquez and Beggs correlation. The oil compressibility can be determined from a PVT analysis or estimated from empirical correlations. Two correlations for c_o will be presented.

TABLE 22.8—CONSTANTS FOR OIL FVF

	$^\circ\text{API} \leq 30$	$^\circ\text{API} > 30$
C_1	4.677×10^{-4}	4.670×10^{-4}
C_2	1.751×10^{-5}	1.100×10^{-5}
C_3	-1.811×10^{-8}	1.337×10^{-9}

Oil Isothermal Compressibility—Trube Method. The Trube method⁶ makes use of the following relationships.

$$c_{pr} = c_o p_{pc},$$

$$p_{pr} = \frac{p}{p_{pc}},$$

and

$$T_{pr} = \frac{T}{T_{pc}},$$

where

- c_{pr} = pseudoreduced compressibility,
- c_o = oil isothermal compressibility,
- p_{pc} = pseudocritical pressure,
- T_{pc} = pseudocritical temperature.

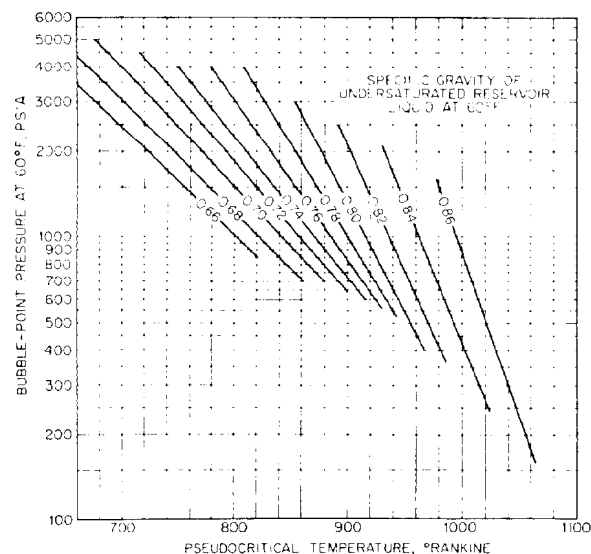


Fig. 22.10—Variation of pseudocritical temperature of reservoir oils with 60°F bubblepoint pressure; Trube's correlation.

p_{pr} = pseudoreduced pressure,
 T_{pr} = pseudoreduced temperature,
 p = pressure of interest, and
 T = temperature of interest.

The pseudoreduced compressibility is a function of p_{pr} and T_{pr} . Once c_{pr} is obtained, c_o is calculated from

$$c_o = c_{pr}/p_{pc} \quad (21)$$

Three graphs are required to obtain the necessary parameters to calculate c_o . The pseudocritical temperature T_{pc} is obtained from Fig. 22.10 as a function of the specific gravity of the undersaturated liquid at the bubblepoint pressure and 60°F. It also depends on the bubblepoint pressure of the oil at 60°F. Values for these parameters may be estimated using the correlations for density and bubblepoint pressure presented previously.

A value for p_{pc} is obtained from Fig. 22.11 using the liquid specific gravity at 60°F and the value of T_{pc} obtained from Fig. 22.10. Once p_{pc} and T_{pc} are known, p_{pr} and T_{pr} at the pressure and temperature of interest can be calculated. A value of c_{pr} is obtained from Fig. 22.12 using p_{pr} and T_{pr} . Then c_o is calculated by Eq. 21.

Application of the Trube method using a computer or calculator would require digitization of Figs. 22.10, 22.11, and 22.12.

Because of its complexity, no example will be given illustrating the application of this method. An example problem may be found in Ref. 6.

Oil Isothermal Compressibility—Vasquez and Beggs Method. Vasquez and Beggs⁵ used approximately 2,000 experimentally measured values of c_o from more than 600 oil systems to develop a correlation for c_o as a function of R_{sb} , T , γ_g , γ_{API} , and p . This method is much simpler to use than the Trube method and is more accurate

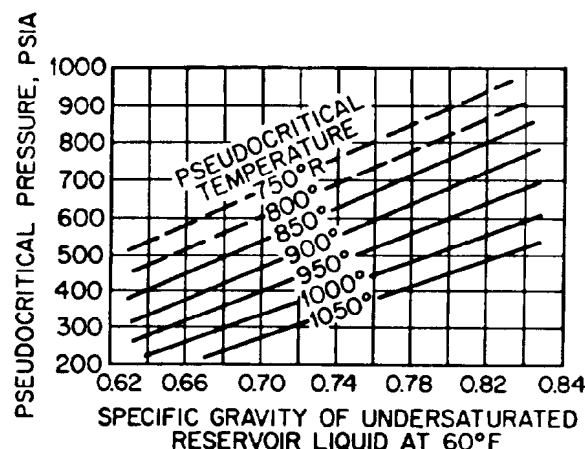


Fig. 22.11—Pseudocritical pressure variation with pseudocritical temperature and 60°F specific gravity of reservoir oil; Trube's correlation.

when used to predict the 2,000 measured values of c_o from which the correlation was developed. No comparison of the two methods is available using independent data. The equation for c_o is

$$c_o = \frac{5R_{sb} + 17.2T - 1,180\gamma_g + 12.61\gamma_{API} - 1,433}{p \times 10^5} \quad (22)$$

where

c_o = oil isothermal compressibility, psi^{-1}
 R_{sb} = solution GOR, scf/STB
 T = temperature of interest, °F
 p = pressure of interest, psia
 γ_g = gas gravity, and
 γ_{API} = stock-tank oil gravity, °API.

Example Problem 9. Calculate the oil FVF for the oil system described in Example Problem 8 at a pressure of 3,000 psia. Use Eq. 22 to determine a value for c_o where $p_b = 2,652$ psia, $R_{sb} = 500$ scf/STB, $\gamma_g = 0.80$, $\gamma_{API} = 30^\circ\text{API}$, $T = 220^\circ\text{F}$, and $B_{ob} = 1.285$ bbl/STB.

Solution.

$c_o =$

$$\frac{5(500) + 17.2(220) - 1,180(0.80) + 12.61(30) - 1,433}{3,000 \times 10^5};$$

$$c_o = 1.43 \times 10^{-5} \text{ psi}^{-1}.$$

With Eq. 20,

$$B_o = 1.285 \exp[1.43 \times 10^{-5}(2,652 - 3,000)];$$

$$B_o = 1.285(0.995) = 1.279 \text{ bbl/STB.}$$

Total FVF's

When material-balance calculations are made for reservoir engineering, it is often convenient to calculate the volume at reservoir conditions that is occupied by all the material associated with a stock-tank barrel of oil—i.e., the volume of the saturated oil and the volume of the evolved or liberated gas. This can be expressed as a total FVF, B_t .

The total FVF can be calculated if B_o and the amount of liberated gas is known. That is, B_t equals volume of oil plus dissolved gas/STB plus volume of liberated gas/STB.

In equation form,

$$B_t = B_o + B_g(R_{sb} - R_s), \dots\dots\dots(23)$$

where

B_t = total FVF, bbl/STB,

B_o = oil FVF, bbl/STB,

R_{sb} = solution GOR at p_b , scf/STB,

R_s = solution GOR at pressure of interest, scf/STB, and

B_g = gas FVF at pressure and temperature of interest, bbl/scf.

The gas FVF requires a value for the gas compressibility or z_g factor that may be obtained from Chap. 17.

$$B_g = \frac{0.00504 z_g T}{p}, \dots\dots\dots(24)$$

where

B_g = gas FVF, bbl/scf,

z_g = gas compressibility factor at p , T ,

p = pressure of interest, psia, and

T = temperature of interest, °R.

A nomograph for estimating total FVF was presented by Standing.³ The correlation was developed from 387 experimental data points that included the ranges given in Table 22.9.

The nomograph, on which an example calculation is worked, is shown in Fig. 22.13.

Oil Viscosity Correlations

The absolute viscosity of a fluid is a measure of the fluid's resistance to flow. The resistance to flow is caused by internal friction generated when the fluid molecules are sheared. The viscosity can be quantified as the ratio of the shearing stress required to induce a particular rate of shear in the fluid at specific conditions of pressure and temperature. The absolute viscosity of a Newtonian fluid is independent of the rate of shear. Only Newtonian fluids are considered in this section.

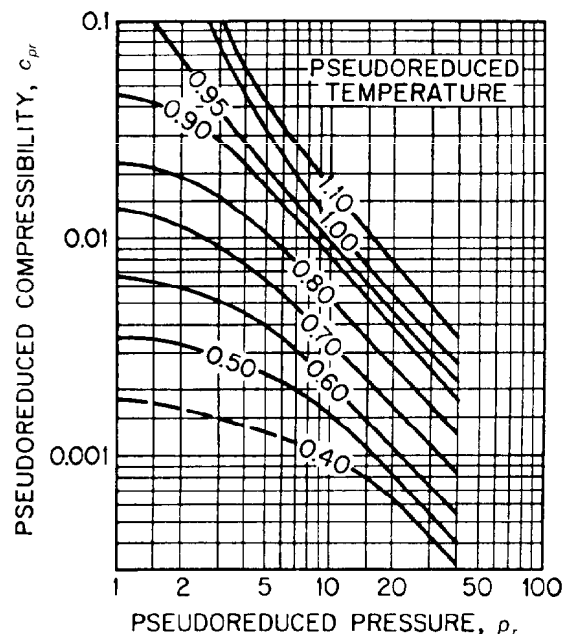


Fig. 22.12—Variation of pseudoreduced compressibility with pseudoreduced pressure and temperature.

Values of oil viscosity are required at various pressures and temperatures for both reservoir and production engineering calculations. If a PVT analysis is available, measured values of oil viscosity will be reported at reservoir temperature and at various pressures. However, as the fluid flows through the production system, the temperature also changes. This necessitates correcting the viscosity for temperature changes, which is usually accomplished by empirical correlations.

The absolute viscosity, which is usually referred to merely as the viscosity, can be expressed in various units. The so-called "oilfield unit" is the centipoise or poise. A relationship among various systems of units is given as 1 cp = 0.01 poise = 0.001 Pa·s = 6.72×10^{-4} lbm/(ft·sec).

The kinematic viscosity of a fluid is the absolute viscosity divided by the density, or

$$\nu = \frac{\mu}{\rho}$$

The most commonly used unit of kinematic viscosity is the centistoke (cSt), where the conversion to SI units is 1 cSt = 10^{-6} m²/s.

In addition to absolute and kinematic viscosity units, the units of Saybolt seconds universal (SSU) and Saybolt

TABLE 22.9—DATA RANGES FOR STANDING CORRELATION

Pressure, psia	400 to 5,000
GOR, scf/STB	75 to 37,000
Temperature, °F	100 to 258
Gas gravity	0.59 to 0.95
Oil gravity, °API	16.5 to 63.8

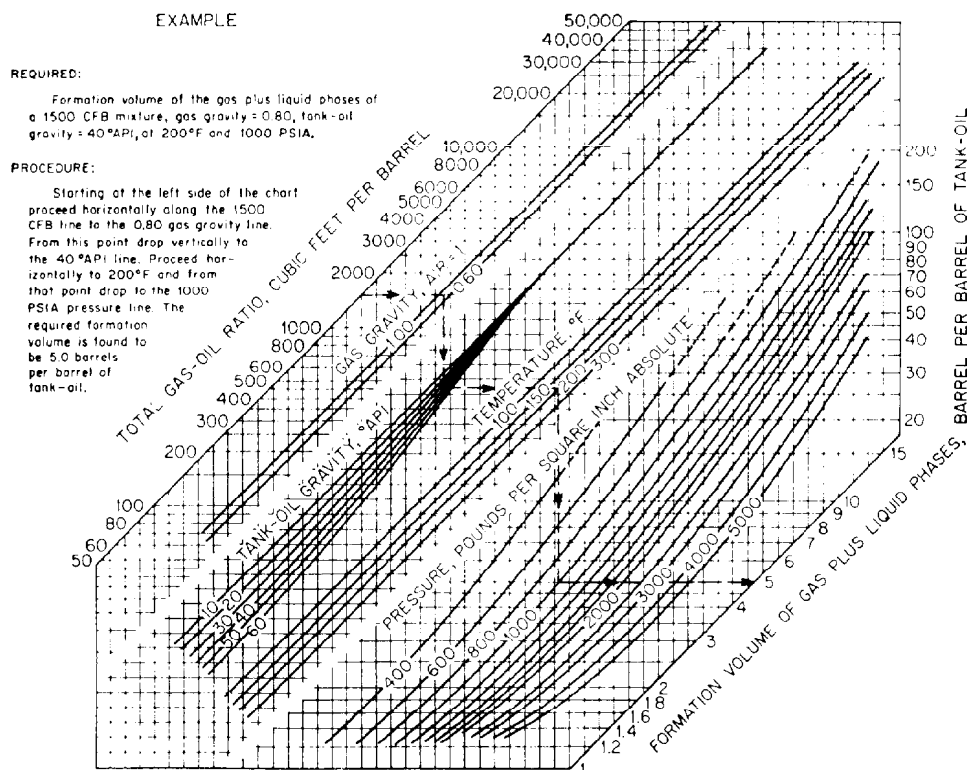


Fig. 22.13—Chart for calculating total formation volume by Standing's correlation.

seconds furol (SSF) are commonly used. An approximate conversion between centistokes and the time units can be made with the following equations.

$$\nu = 0.220t_{SU} - 180/t_{SU},$$

and

$$\nu = 2.12t_{SF} - 139/t_{SF}, \quad (25)$$

where

- ν = kinematic viscosity in cSt,
- t_{SU} = Saybolt seconds universal, and
- t_{SF} = Saybolt seconds furol.

Factors Affecting Oil Viscosity

The principal factors of interest to the petroleum engineer that affect viscosity are composition, temperature, dissolved gas, and pressure. Oil viscosity increases with a decrease in API gravity and also increases with a decrease in temperature.

The effect of dissolved gas is to lighten the oil and thus decrease its viscosity, while an increase in pressure on an undersaturated oil compresses the oil and causes the viscosity to increase.

Oil Viscosity Correlations—Saturated Systems

The most common method for obtaining the viscosity of a crude oil that contains dissolved gas is first to estimate the viscosity of the gas-free or dead oil and then to cor-

rect this value for dissolved gas. The dead-oil viscosity depends on API gravity of the stock-tank oil and the temperature of interest.

The dead-oil viscosity can be obtained from empirical correlations or, if measured values are available at two temperatures, the viscosity at any other temperature can be calculated from the equation

$$\log[\log(\nu + 0.8)] = A + B \log T, \quad (26)$$

where

- ν = kinematic viscosity at T ,
- T = temperature of interest, and
- A, B = constants for a particular oil that can be determined if two measured values of ν and T are available.

Beal's Correlation for Dead Oils. Beal⁷ presented a graphical correlation showing the effects of both oil gravity and temperature on dead-oil viscosity. The correlation was developed from measurements made on 655 oil samples. The relationship among viscosity, API gravity, and temperature is shown in Fig. 22.14.

Effect of Dissolved Gas—Chew and Connally Method.

The decrease in the dead-oil viscosity as gas goes into solution can be estimated with Fig. 22.15, which was published by Chew and Connally⁸ in 1959. The procedure for using the chart and an example problem are shown

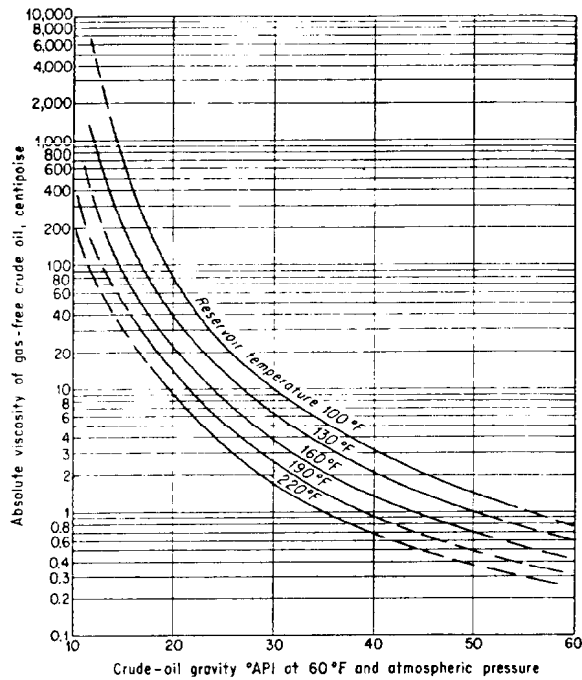


Fig. 22.14—Gas-free crude viscosity as a function of reservoir temperature and stock-tank crude gravity.

in the figure. They also proposed an equation for correcting for the dissolved gas:

$$\mu_{os} = a\mu_{od}^b \quad (27)$$

where

μ_o = saturated oil viscosity,
 μ_{od} = gas-free or dead-oil viscosity, and
 a, b = functions of R_s , shown in Fig. 22.16.

Beggs and Robinson Correlation. A method for calculating both dead-oil and saturated-oil viscosity was presented by Beggs and Robinson⁹ in 1975. The correlation was developed from more than 2,000 measured data points using 600 oil systems. The range of variables of the data is given in Table 22.10.

The equation developed reproduced the measured data with an average error of -1.83% and a standard deviation of 27% .

The equation for dead-oil viscosity is

$$\mu_{od} = 10^x - 1.0, \quad (28)$$

where

$x = T^{-1.163} \exp(6.9824 - 0.04658\gamma_{API})$,
 μ_{od} = dead-oil viscosity, cp,
 T = temperature of interest, °F, and
 γ_{API} = stock-tank oil gravity, °API.

To correct for the effect of dissolved gas, an equation similar to Eq. 27 was developed.

$$\mu_{os} = A\mu_{od}^B, \quad (29)$$

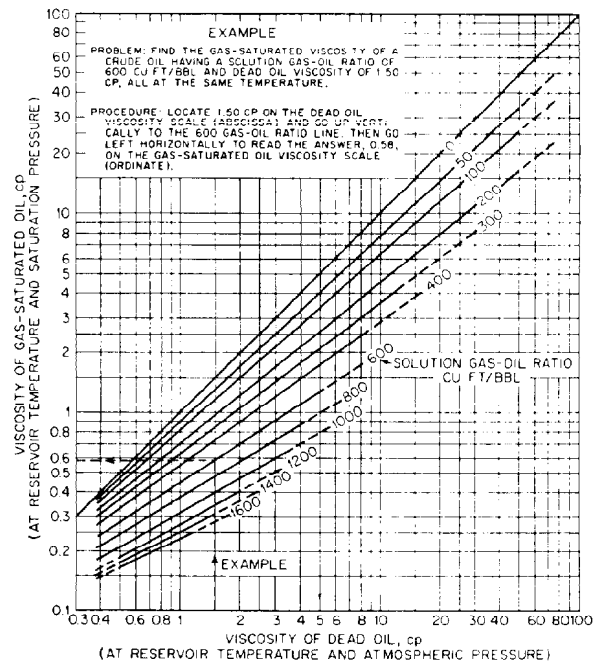


Fig. 22.15—Viscosity and gas-saturated crude oils at reservoir temperature and pressure; Chew and Connally's correlation.

where

μ_{os} = saturated-oil viscosity

μ_{od} = dead-oil viscosity,

A, B = functions of R_s ,

$$A = 10.715(R_s + 100)^{-0.515}, \quad (30)$$

and

$$B = 5.44(R_s + 150)^{-0.338}, \quad (31)$$

where R_s is the solution GOR in scf/STB. No graphs are required to apply this method.

Example Problem 10. Calculate the viscosity of the saturated oil system described next using the Beal and Chew and Connally correlations and the Beggs and Robinson correlation where $T = 137^\circ\text{F}$, $\gamma_{API} = 22^\circ\text{API}$, and $R_s = 90$ scf/STB.

Solution—Beal with Chew and Connally. From Fig. 22.14, $\mu_{od} = 20$ cp. From Fig. 22.16, $a = 0.82$ and $b = 0.9$. $\mu_{os} = 0.82(20)^{0.9} = 12.15$ cp.

Interpolation was necessary on both Figs. 22.14 and 22.16 to obtain values for μ_{od} , a , and b . Use of Fig. 22.15 to correct for R_s gives a value of approximately 12 cp for μ_o .

Solution—Beggs and Robinson.

$$x = (137)^{-1.163} \exp[6.9824 - 0.04658(22)];$$

$$x = 1.2658.$$

$$\mu_{od} = 10^{1.2658} - 1.0 = 17.44 \text{ cp.}$$

$$A = 10.715(90 + 100)^{-0.515} = 0.719.$$

$$B = 5.44(90 + 150)^{-0.338} = 0.853.$$

$$\mu_{os} = 0.719(17.44)^{0.853} = 8.24 \text{ cp.}$$

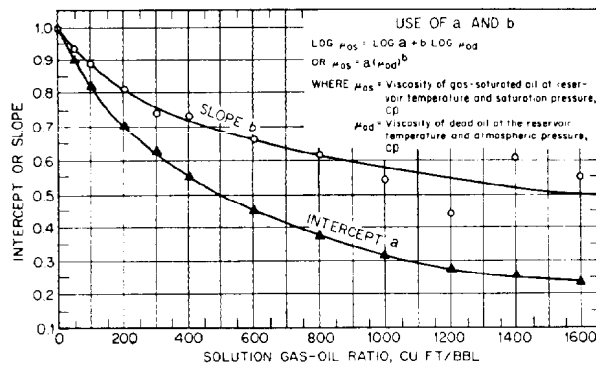


Fig. 22.16—*a* and *b* factors for use in Chew and Connally's viscosity correlation.

TABLE 22.10—BEGGS AND ROBINSON CORRELATION DATA

R_s , scf/STB	20 to 2,070
γ_{API} , °API	16 to 58
p , psig	0 to 5,250
T , °F	70 to 295

Oil Viscosity Correlations—Undersaturated Systems

The effect of increasing the pressure on an oil system above the bubblepoint is to compress the liquid and to increase the viscosity. This effect was measured by Beal and presented graphically in Fig. 22.17. The graph gives the viscosity increase in cp/1,000-psi increase in pressure above p_b as a function of the saturated or bubblepoint viscosity, μ_{ob} .

Vasquez and Beggs⁵ extended the Beggs and Robinson correlation for undersaturated oils with the equation

$$\mu_o = \mu_{ob}(p/p_b)^m, \quad (32)$$

where

- μ_o = viscosity at $p > p_b$,
- μ_{ob} = viscosity at p_b ,
- p = pressure of interest, and
- p_b = bubblepoint pressure.

The exponent m is pressure dependent and is calculated from

$$m = C_1 p^{C_2} \exp(C_3 + C_4 p), \quad (33)$$

where

- p = pressure of interest, psia,
- $C_1 = 2.6$,
- $C_2 = 1.187$,
- $C_3 = -11.513$, and
- $C_4 = -8.98 \times 10^{-5}$.

Example Problem 11. Calculate the viscosity of the oil system described at a pressure of 4,750 psia, with $T=240^\circ\text{F}$, $\gamma_{API}=31^\circ\text{API}$, $\gamma_g=0.745$, and $R_{sb}=532$ scf/STB.

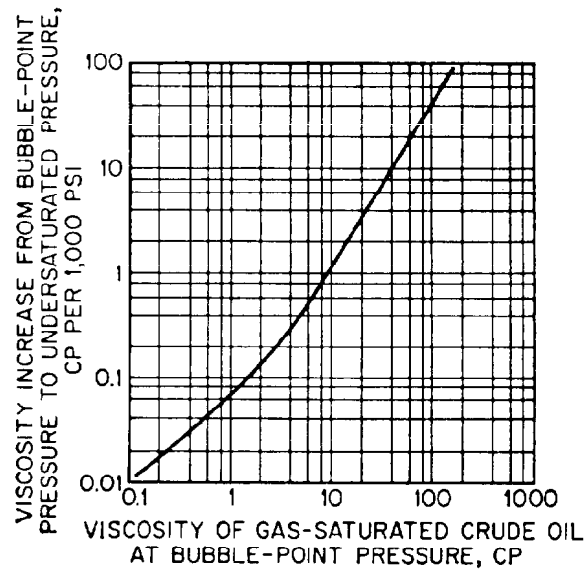


Fig. 22.17—Effect of pressure on viscosity of gas-saturated crude oils; Beal's correlation.

Solution.

From Eq. 12:

$$p_b =$$

$$\left[\frac{532}{0.0178(0.745) \exp 23.931(31)/(240+460)} \right]^{1/1.187};$$

$$p_b = 3,093 \text{ psia.}$$

From Eq. 28:

$$x = (240)^{-1.163} \exp[6.9824 - 0.04658(31)];$$

$$x = 0.4336,$$

$$\mu_{ob} = 10^{0.4336} - 1.0 = 1.71 \text{ cp.}$$

From Eqs. 29, 30, and 31:

$$A = 10.715(532+100)^{-0.515} = 0.387,$$

$$B = 5.44(532+150)^{-0.338} = 0.599,$$

and

$$\mu_{ob} = 0.387(1.71)^{0.599} = 0.53 \text{ cp.}$$

From Eqs. 32 and 33:

$$m = 2.6(4,750)^{1.187} \exp[-11.513 - 4,750(8.98 \times 10^{-5})];$$

$$m = 0.393, \text{ and}$$

$$\mu_o = 0.53(4,750/3,093)^{0.393} = 0.63 \text{ cp.}$$

Gas/Oil IFT

The interfacial or surface tension existing between a liquid and gas is required for estimating capillary-pressure

forces in reservoir engineering and is a parameter in some correlations used in wellbore hydraulics calculations. The surface tension between natural gas and crude oil ranges from zero to about 35 dyne/cm. It is a function of pressure, temperature, and compositions of the phases.

The surface tension of a hydrocarbon mixture can be calculated if the composition of the mixture at the pressure and temperature of interest is known. The parachor of each component must also be known. The parachor is the molecular weight of a liquid times the fourth root of its surface tension, divided by the difference between the density of the liquid and the density of the vapor in equilibrium with it. It is essentially constant over wide ranges of temperature. An equation for estimating surface tension is

$$\sigma^{0.25} = \sum_{i=1}^C P_{\text{chi}} \left(\frac{x_i \rho_L}{M_L} + \frac{y_i \rho_v}{M_v} \right), \quad \dots \dots \dots (34)$$

where

- σ = surface tension, dyne/cm,
- P_{chi} = parachor of i th component,
- x_i = mole fraction of i th component in the liquid phase,
- y_i = mole fraction of i th component in the vapor phase,
- ρ_L = density of the liquid phase, g/cm³,
- ρ_v = density of the vapor phase, g/cm³,
- M_L = molecular weight of liquid phase,
- M_v = molecular weight of vapor phase, and
- C = number of components.

Parachors for some hydrocarbons, nitrogen, and carbon dioxide are given in Table 22.11. A correlation of the parachor with molecular weight was presented by Katz¹⁰ and is shown in Fig. 22.18.

Empirical correlations in the form of graphs were presented by Baker and Swerdloff¹¹ where surface tension is correlated with temperature, API gravity, and pressure. The correlations are shown in Figs. 22.19 and 22.20. Equations that approximate Figs. 22.19 and 22.20 are:

$$\sigma_{68} = 39 - 0.2571 \gamma_{\text{API}}, \quad \dots \dots \dots (35)$$

and

$$\sigma_{100} = 37.5 - 0.2571 \gamma_{\text{API}}, \quad \dots \dots \dots (36)$$

where

- σ_{68} = IFT at 68°F, dyne/cm,
- σ_{100} = IFT at 100°F, dyne/cm, and
- γ_{API} = gravity of stock-tank oil, °API.

It has been suggested that if the temperature is greater than 100°F, the value at 100°F should be used. Also, if $T < 68^\circ\text{F}$, use the value calculated at $T = 68^\circ\text{F}$. For intermediate temperatures, use linear interpolation between the values obtained at 68 and 100°F. That is:

$$\sigma_T = \sigma_{68} - \frac{(T - 68^\circ\text{F})(\sigma_{68} - \sigma_{100})}{32}, \quad \dots \dots \dots (37)$$

where σ_T = IFT at $68^\circ\text{F} < T < 100^\circ\text{F}$.

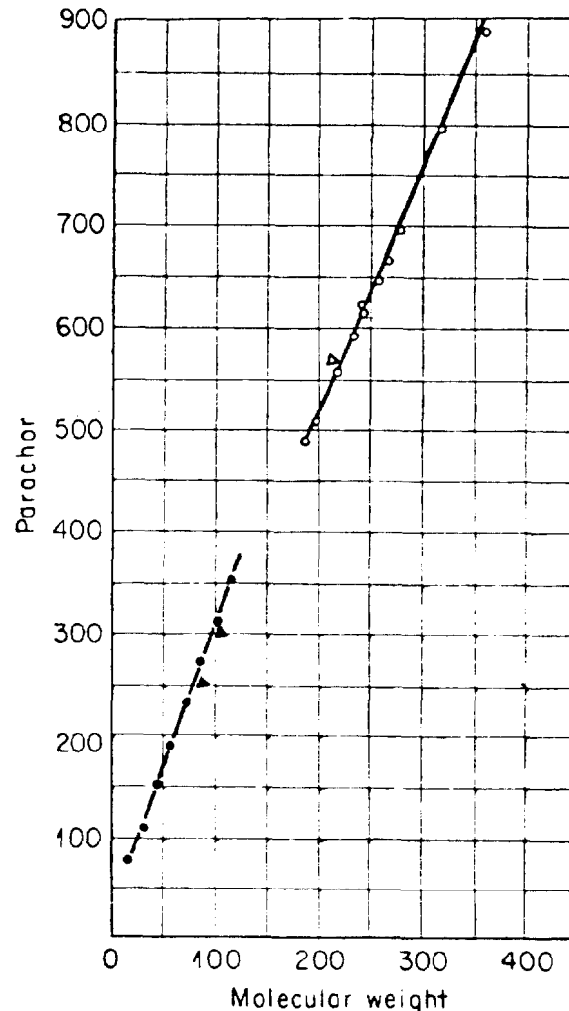


Fig. 22.18—Parachors for hydrocarbons. ●, n-paraffins; ○, heptanes plus; ▲, gasolines; Δ, crude oil.

TABLE 22.11—PARACHORS FOR PURE SUBSTANCES

Methane	77.0
Ethane	108.0
Propane	150.3
Isobutane	181.5
n-Butane	190.0
Isopentane	225
n-Pentane	232
n-Hexane	271
n-Heptane	311
n-Octane	352
Nitrogen (in n-heptane)	41.0
Carbon dioxide	78.0

The effect of gas going into solution as pressure is increased on the gas/oil mixture is to reduce the IFT. The dead-end oil IFT can be corrected by multiplying it by the following correction factor.

$$F_c = 1.0 - 0.024p^{0.45}, \quad \dots \dots \dots (38)$$

where p is in psia.

The IFT at any pressure is then obtained from

$$\sigma_o = F_c \sigma_T \quad (39)$$

The IFT becomes zero at miscibility pressure, and for most systems, this will be at any pressure greater than about 5,000 psia.

Most of the correlations presented in this chapter are included in a calculator program for the HP-41C. The program is available from Hewlett-Packard.¹²

Nomenclature

- a = function of R_s in Eq. 27
- A = constant in Eq. 26
- b = function of R_s in Eq. 27
- B = constant in Eq. 26
- B_g = gas formation volume factor
- B_o = oil formation volume factor
- c_o = oil isothermal compressibility
- c_{pr} = pseudo-reduced compressibility
- C = number of components
- C_1, C_2, C_3, C_4 = various constants
- F = correlating function in Eq. 18
- F_c = correcting factor for dead oil interfacial tension, Eq. 38
- m = pressure-dependent exponent in Eq. 32
- m_i = mass of i th component
- M_o = molecular weight of stock-tank oil
- p = pressure of interest
- p_b = bubblepoint pressure
- p_{pc} = pseudo-critical pressure
- p_{pr} = pseudo-reduced pressure
- P_{chi} = parachor of i th component
- R_F = free gas/oil ratio
- R_s = solution gas/oil ratio
- R_{sb} = solution gas/oil ratio at the bubblepoint pressure
- t_{SU} = Saybolt seconds universal
- t_{SF} = Saybolt seconds furol
- T = temperature of interest
- T_{pc} = pseudo-critical temperature
- T_{pr} = pseudo-reduced temperature
- T_R = reservoir temperature
- v = specific volume
- V_i = volume of i th component
- x = symbol for various groups of terms, Eq. 28
- y_g = symbol for various groups of terms, Eqs. 5, 6, 9, 10, and 13-16
- z_g = gas compressibility factor
- γ = fluid specific gravity
- γ_{API} = oil API gravity
- γ_{gc} = corrected gas gravity
- γ_o = oil specific gravity
- μ = fluid viscosity
- μ_{ob} = oil viscosity at bubblepoint pressure

- μ_{od} = dead oil viscosity
- μ_{os} = saturated oil viscosity
- ν = kinematic viscosity
- ρ = fluid density
- σ = surface tension, interfacial

Key Equations in SI Metric Units

$$\rho_o = \frac{1000\gamma_o + 1.224\gamma_g R_s}{B_o} \quad (1)$$

$$p_b = 519.7 \left(\frac{R_{sb}}{\gamma_g} \right)^{0.83} \times 10^{y_g} \quad (5)$$

where y_g = mole fraction gas,

$$= 1.225 + 0.00164T_R - 1.769/\gamma_o.$$

$$y_g = \frac{0.0148R_{sb}}{0.0148R_{sb} + 350\gamma_o/M_o} \quad (6)$$

For $\gamma_o \leq 0.825$:

$$M_o = 1945 - 1415/\gamma_o \quad (7)$$

For $\gamma_o > 0.825$:

$$M_o = \left(\frac{0.109}{\gamma_o} - 0.101 \right)^{-1.562} \quad (8)$$

For $y_g \leq 0.60$:

$$\frac{p_b \gamma_g}{T_R} = 8.427 \exp(2.78y_g) - 4.01 \quad (9)$$

For $y_g > 0.60$:

$$\frac{p_b \gamma_g}{T_R} = 102.51y_g^{3.56} + 24.20 \quad (10)$$

$$\gamma_{gc} = \gamma_g \left[1.0 + \left(\frac{0.0151T_s}{\gamma_o} - \frac{3.848}{\gamma_o} - 0.014T_{st} 3.576 \right) \log \left(\frac{p_s}{790} \right) \right] \quad (11)$$

$$p_b = \left[\frac{R_{sb}}{C_1 \gamma_g \exp \left(\frac{C_3}{\gamma_o T} - \frac{C_4}{T} \right)} \right]^{C_2} \quad (12)$$

where the following constants apply.

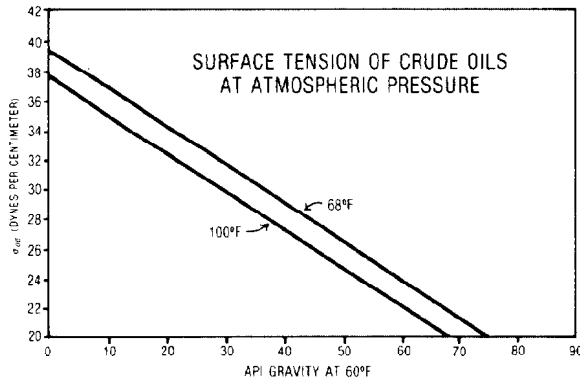


Fig. 22.19—Surface tension of crude oils at atmospheric pressure.

	$\gamma_o < 0.876$	$\gamma_o \geq 0.876$
C_1	3.204×10^{-4}	7.803×10^{-4}
C_2	0.8425	0.9143
C_3	1881.24	2022.19
C_4	1748.29	1879.28

$$R_s = \gamma_g \left(\frac{p}{519.7 \times 10^{y_s}} \right)^{1.204}, \quad (13)$$

where

$$y_g = 1.225 + 0.00164T - 1.769/\gamma_o.$$

$$R_s = \frac{23\,643\gamma_o y_g}{M_o(1-y_g)}, \quad (14)$$

For $\frac{p\gamma_g}{T} < 40.7$:

$$y_g = 0.359 \ln \left(\frac{0.1187p\gamma_g}{T} + 0.476 \right), \quad (15)$$

For $\frac{p\gamma_g}{T} \geq 40.7$:

$$y_g = \left(\frac{0.0098p\gamma_g}{T} - 0.236 \right)^{0.281}, \quad (16)$$

$$R_s = C_1 \gamma_g^{C_2} \exp \left(\frac{C_3}{\gamma_o T} - \frac{C_4}{T} \right), \quad (17)$$

where the following constants apply.

	$\gamma_o < 0.876$	$\gamma_o \geq 0.876$
C_1	3.204×10^{-4}	7.803×10^{-4}
C_2	1.1870	1.0937
C_3	1881.24	2022.19
C_4	1748.29	1879.28

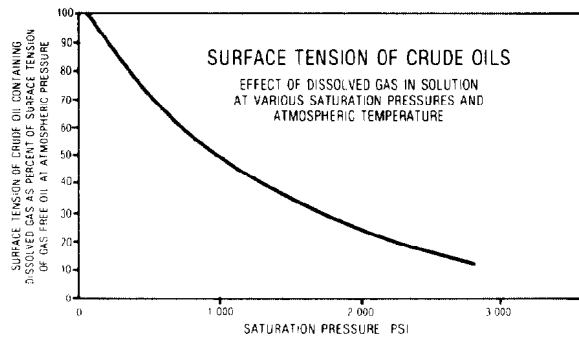


Fig. 22.20—Effect of solution gas on surface tension of crude oils.

$$B_o = 0.972 - 0.000147F^{1.175}, \quad (18)$$

where

$$F = 5.615R_s \left(\frac{\gamma_g}{\gamma_o} \right)^{0.5} + 2.25T - 5.75.$$

$$B_o = 1 + C_1 R_s + F(C_2 + C_3 R_s), \quad (19)$$

where

$$F = \frac{254.7T}{\gamma_o} - 236.7T - \frac{73\,580}{\gamma_o} + 68\,380$$

and the following constants apply.

	$\gamma_o < 0.876$	$\gamma_o \geq 0.876$
C_1	2.622×10^{-3}	2.626×10^{-3}
C_2	1.100×10^{-5}	1.751×10^{-5}
C_3	1.337×10^{-9}	-1.811×10^{-8}

$$C_o = \frac{28.1R_s + 30.6T - 1180\gamma_g + \frac{1784}{\gamma_o} - 10\,910}{p \times 10^5}, \quad (22)$$

$$\mu_o = 10^{(x-3)} - 0.001, \quad (28)$$

where

$$x = (1.8T - 460)^{-1.163} \exp(13.108 - 6.591/\gamma_o).$$

$$A = 10.715(5.615R_s + 100)^{-0.515}, \quad (30)$$

$$B = 5.44(5.615R_s + 150)^{-0.338}, \quad (31)$$

$$m = 0.263p^{1.187} \exp(-11.513 - 1.302 \times 10^{-5}p), \quad (33)$$

where

B_o is in m^3/m^3 ,

C_o is in kPa^{-1} ,

M_o is in $\text{kg}/\text{kg-mole}$,

p is in kPa ,

R_s is in m^3/m^3 ,

T is in K ,

ρ_o is in kg/m^3 , and

μ_o is in $\text{Pa}\cdot\text{s}$.

Glossary

These are generally accepted definitions, peculiar to reservoir engineering phase-behavior work.

Apparent liquid density is the ratio of mass to volume of a gas when dissolved in a liquid. It normally is calculated for conditions of 14.7 psia and 60°F by correcting the observed density of the system to that state and subtracting the mass and volume of the liquid component of the system.

Bubblepoint of a system is the state characterized by the coexistence of a substantial amount of liquid phase and an infinitesimal amount of gas phase in equilibrium.

Compressibility factor (gas-deviation factor, supercompressibility factor) is a multiplying factor introduced into the ideal-gas law to account for the departure of true gases from ideal behavior ($pV = nzRT$; z is the compressibility factor).

Condensate (distillate) liquids are liquids formed by condensation of a vapor or gas. The term usually identifies a light-colored liquid, usually of 50°API gravity or higher, obtained from systems that exist in the gaseous phase in the reservoir.

Critical state is the term used to identify the unique condition of pressure, temperature, and composition wherein all properties of coexisting vapor and liquid become identical.

Critical temperature T_c and/or pressure p_c is the temperature or pressure at the critical state.

Dewpoint of a system is analogous to the bubblepoint in that a large volume of gas and an infinitesimal amount of liquid coexist in equilibrium.

Dewpoint pressure p_d is the gas pressure in a system at its dewpoint.

Differential-gas liberation indicates removal of a gas phase from the system as the gas forms at bubblepoint conditions. It is generally believed that the differential-gas-liberation process is the one that predominates in solution-gas-drive reservoirs during the greater part of their producing life.

Differential process is a term used primarily in PVT work to indicate that, as a system is caused to move through a bubblepoint or dewpoint and as a result forms two phases, the minor phase is removed from further contact with the major phase. Thus, during a differential process, the "system" is continuously changing in quantity and composition.

Dissolved gas (solution gas) identifies material ordinarily gaseous at atmospheric conditions but which is part of a liquid phase at elevated pressure and temperature.

Dissolved-gas drive (solution-gas drive) is a primary recovery process whereby liquid (oil) is displaced from the reservoir rock by energy of expansion of gas components originally dissolved in the liquid.

Flash gas liberation means that a gas forms from a liquid (usually on reduction of pressure) under conditions wherein the total composition of the system remains the same in time. An example of flash gas liberation occurs during the steady-state flow of oil and gas through a gas-oil separator.

Flash process is one in which the composition of the system remains constant but the proportion of gas and liquid phases that comprise the system changes as pressure or some other independent variable is changed. For example, the determination of the PV relations of a reservoir fluid sample involves a flash process.

Formation volume factor (FVF) is a means of expressing a volumetric relation of a system. The volume of fluid, at formation pressure and temperature, that results in 1 bbl stock-tank oil is, by definition, the formation volume B . If the system is in a single condensed state in the formation, the term oil-FVF B_o is used. If two phases exist, the term used is total-FVF B_t or two-phase formation volume. Oil-formation volumes normally are between 1.1 and 2.0. Total formation volumes may be as great as 200, depending on the system composition and the pressure involved. Gas-formation volume B_g refers to the volume in the reservoir (usually expressed as barrels) per 1,000 std surface cu ft of the gas. Water-formation volume B_w designates the volume in the formation occupied by 1 surface bbl water and its attendant gases. Water-formation volumes are usually in the range of 0.99 to 1.07. In all instances, the reference state is standard surface conditions of 14.7 psia and 60°F unless specified otherwise.

Gas gravity is a simple means of expressing the molecular weight of a gas. The unit of gas gravity is dry air of molecular weight 28.97. Thus, methane (molecular weight = 16.04) has a gas gravity of $16.04/28.97 = 0.55$.

Gas-oil ratio (GOR) is a loose expression of system composition. Normally, the units involved are cubic feet of gas per 1 bbl liquid, both measured at 14.7 psia and 60°F. However, in some instances, local usage calls for measuring the gas at some pressure other than 14.7 psia. Further, the barrel of liquid may refer to some pressure other than the usual stock-tank oil. The units of reservoir oil and residual oil are encountered quite often in PVT work. Lastly, several kinds of GOR are used in reser-

voir engineering, such as solution (gas solubility in oil) R_s , producing R , and cumulative R_p . Pressure and temperature of separation and the number of stages used affect the GOR number obtained for a given system.

Mole is one molecular weight unit of any substance. For example, 16.04 lbm methane is a lbm-mol. Likewise, 16.04 g methane constitute a gmol. The lbm-mole is used for petroleum engineering work. A lbm-mol of gas (perfect) occupies 379.4 cu ft at 14.7 psia and 60°F.

Phase is a portion of a system that differs in its intensive properties from adjacent portions of the system. An interface exists between phases because of this difference in properties. Systems involved in petroleum production normally occur in not more than two phases, gas and liquid. On occasion and for hydrocarbon systems of unusual composition, two liquid phases or a solid phase may occur.

Properties, Extensive and Intensive. Properties directly proportional to the amount of material making up the system are termed extensive properties. Examples are area, mass, inertia, and volume. An intensive property is one that is independent of the amount of material. Density, pressure, temperature, viscosity, and surface tension are intensive properties. Energy is the product of an intensive property and an extensive property; for example, pressure times volume is mechanical energy.

Pseudocritical and Pseudoreduced Properties (Temperature, Pressure). Properties of pure hydrocarbons are often the same when expressed in terms of their reduced properties. The same reduced-state relationships often apply to multicomponent systems if "pseudo" critical temperatures and pressures are used rather than the true criticals of the systems. Calculation of the pseudocritical values from the composition of the system varies depending on the correlation being used. The ratio of the property to the pseudocritical property is called the pseudoreduced property, e.g., pseudoreduced pressure $p_{pr} = p/p_{pc}$.

Reduced properties (temperature, pressure, volume) are the ratio of the property to the critical property; for example, the reduced pressure $p_r = p/p_c$.

Relative oil volume is analogous to formation volume except that the reference state is other than at standard surface conditions and the oil is other than stock-tank oil. For example, the term is used often on the basis of 1 bbl bubblepoint oil, or saturated oil, as the reference volume. Relative oil volumes must specify pressure, temperature, and some composition parameter, e.g., relative oil volume = 0.7 (2,520 psia, 185°F, bubblepoint oil = 1.0).

Residual oil is a term common in PVT work to identify the liquid remaining in a PVT cell at the completion of a differential process carried out at or near the reservoir temperature. By analogy, it refers also to the liquid that remains in an oil reservoir at depletion. General usage is that residual oil volumes and gravities are reported in PVT work at 60°F and 14.7 psia. Residual oil is to a dif-

ferential gas-removal process as stock-tank oil is to a flash-gas process—the end liquid product.

Saturated liquid is a liquid in equilibrium with vapor at the saturation pressure. Likewise, saturated vapor denotes equilibrium with liquid. These terms are often used synonymously with the term "bubblepoint liquid" (dewpoint vapor) at the bubblepoint (dewpoint) pressure. Note that the terms "bubblepoint" and "dewpoint" identify the special case where the minor phase is present only in an infinitesimal amount, whereas the term "saturated liquid" does not involve the relative amounts of phases present.

Shrinkage refers to the decrease in volume of a liquid phase caused by release of solution gas and/or by the thermal contraction of the liquid. Shrinkage may be expressed (1) as a percentage of the final resulting stock-tank oil or (2) as a percentage of the original volume of the liquid. Shrinkage factor is the reciprocal of FVF expressed as barrels of stock-tank oil per barrel of reservoir oil. A reservoir oil that resulted in 0.75 bbl of stock-tank oil per 1 bbl of reservoir oil would have a shrinkage of $0.25/0.75 = 33\%$ under Definition 1, a shrinkage of $0.25/1.00 = 25\%$ under Definition 2, a shrinkage factor of 0.75, and an FVF of $1.00/0.75 = 1.33$.

Solution gas-oil ratio, R_s , expresses the amount of gas in solution, or dissolved, in a liquid. The reference oil may be stock-tank oil or residual oil. On occasion, reservoir saturated oil is used as the reference.

Standard conditions (surface) are 14.7 psia and 60°F. Gas volumes may be specified on occasion at pressures slightly removed from 14.7 psia.

Stock-tank oil is the liquid that results from production of reservoir material through surface equipment that separates normally gaseous components. Stock-tank oil may be caused to vary in composition and properties by varying the conditions of gas/liquid separation. Stock-tank oil is normally reported at 60°F and 14.7 psia but may be measured under other conditions and corrected to the standard condition.

System refers to a body or to a composition of matter that represents the material under consideration. The term "system" may be defined further as a **homogeneous system** or a **heterogeneous system**. In a homogeneous system, the intensive properties vary only in a continuous manner with respect to the extent of the system. A heterogeneous system is made up of a number of homogeneous parts, and abrupt changes in the intensive properties occur at the interface between the homogeneous parts.

Undersaturated fluid (liquid or vapor) is material capable of holding additional gaseous or liquid components in solution at the specified state.

References

1. Standing, M.B.: *Volumetric and Phase Behavior of Oil Field Hydrocarbon Systems*, Reinhold Publishing Corp., New York City (1952).
2. Katz, D.L.: "Prediction of the Shrinkage of Crude Oils," *Drill. and Prod. Prac.*, API (1942).

3. Standing, M.B.: "A Pressure-Volume-Temperature Correlation for Mixtures of California Oils and Gases," *Drill. and Prod. Prac.*, API (1947).
4. Lasater, J.A.: "Bubble Point Pressure Correlation," *Trans.*, AIME (1958) **213**, 379-81.
5. Vasquez, M. and Beggs, H.D.: "Correlations for Fluid Physical Property Prediction," *J. Pet. Tech.* (June 1980) 968-70.
6. Trube, A.S.: "Compressibility of Undersaturated Hydrocarbon Reservoir Fluids," *Trans.*, AIME (1957) **210**, 355-57.
7. Beal, C.: "The Viscosity of Air, Water, Natural Gas, Crude Oil and Its Associated Gases at Oil Field Temperatures and Pressures," *Trans.*, AIME (1946) **165**, 94-115.
8. Chew, J. and Connally, C.A.: "A Viscosity Correlation for Gas-Saturated Crude Oils," *Trans.*, AIME (1959) **216**, 23-25.
9. Beggs, H.D. and Robinson, J.R.: "Estimating the Viscosity of Crude Oil Systems," *J. Pet. Tech.* (Sept. 1975) 1140-41.
10. Katz, D.L., Monroe, R.R., and Trainer, R.R.: "Surface Tension of Crude Oils Containing Dissolved Gases," *Pet. Tech.* (Sept. 1943) 1-10.
11. Baker, O. and Swerdloff, W.: "Finding Surface Tension of Hydrocarbon Liquids," *Oil and Gas J.* (Jan. 2, 1956).
12. HP-41C Petroleum Fluids Pac, Hewlett-Packard, 1000 N.E. Circle Blvd., Corvallis, OR 97330.
- Herschel, W.H.: "The Change in Viscosity of Oils with Temperature," *Ind. and Engr. Chem.* (1922) **14**, 715.
- Lacey, W.N., Sage, B.H., and Kircher, C.E. Jr.: "Phase Equilibria in Hydrocarbon Systems: III — Solubility of a Dry Natural Gas in Crude Oil," *Ind. and Engr. Chem.* (1934) **26**, 652.
- Lewis, W.K. and Squires, L.: "Mechanism of Oil Viscosity," *Oil and Gas J.* (1934) **33**, No. 26, 92.
- Nelson, W.L.: "How to Handle Viscous Crude Oil," *Oil and Gas J.* (1954) **53**, No. 28, 269.
- Norton, A.E.: *Lubrication*, McGraw-Hill Book Co. Inc., New York City (1942).
- Perry, J.H.: *Chemical Engineer's Handbook*, McGraw-Hill Book Co. Inc., New York City (1950).
- Schilthuis, R.I.: "Active Oil and Reservoir Energy," *Trans.*, AIME (1936) **118**, 33-52.
- Standing, M.B. and Katz, D.L.: "Density of Crude Oils Saturated With Natural Gas," *Trans.*, AIME (1942) **146**, 159-65.
- van Wijk, W.R., deVries, D.A., and Thijssen, H.A.C.: "Study of PVT Relations of Reservoir Fluids," *Proc.*, Fourth World Petroleum Congress, **II**, 313.
- Vink, D.J. *et al.*: "Multiple-Phase Hydrocarbon Systems," *Oil and Gas J.* (1940) **39**, No. 28, 34.
- Wiggins, W.R.: "Viscosity-Temperature Characteristics of Petroleum Products," *Science of Petroleum*, **2**, 1071.

General References

- Borden, G. Jr. and Rzasa, M.J.: "Correlation of Bottom Hole Sample Data," *Trans.*, AIME (1950) **189**, 345-48.
- Dodson, C.R., Goodwill, D., and Mayer, E.H.: "Application of Laboratory PVT Data to Reservoir Engineering Problems," *Trans.*, AIME (1953) **198**, 287-98.
- Gosline, J.E. and Dodson, C.R.: "Solubility Relations and Volumetric Behavior of Three Gravities of Crudes and Associated Gases," *Drill. and Prod. Prac.*, API (1942) **137**.

Chapter 23

Phase Diagrams

F.M. Orr Jr., New Mexico Inst. of Mining and Technology
J.J. Taber, New Mexico Inst. of Mining and Technology*

Introduction

Petroleum reservoir fluids are complex mixtures containing many hydrocarbon components that range in size from light gases such as methane, ethane, and so on to very large hydrocarbon molecules containing 40 or more carbon atoms. Nonhydrocarbon components such as nitrogen, hydrogen sulfide (H_2S), or CO_2 also may be present. Water, of course, is usually present in large quantities in all reservoirs. At a given temperature and pressure, the components distribute between whatever *solid*, *liquid*, and *vapor* phases are present. A *phase* may be defined as that portion of a system that is homogeneous, bounded by a surface, and physically separable from other phases present. *Equilibrium phase diagrams* offer convenient representations of the ranges of temperature, pressure, and composition within which various combinations of phases coexist. Phase behavior plays an important role in a variety of reservoir engineering applications ranging from pressure maintenance to separator design to enhanced oil recovery (EOR) processes. This chapter reviews the fundamentals of phase diagrams used in such applications.

Single-Component Phase Diagrams

Fig. 23.1 summarizes the phase behavior of a single component. The saturation curves shown in Fig. 23.1 indicate the temperatures and pressures at which phase changes occur. At temperatures below the *triple point*, the component forms a vapor if the pressure is below that indicated by the *sublimation curve*, and forms a solid at pressures above the curve. At pressures and temperatures lying on the sublimation curve, solid and vapor can coexist, and on the *melting curve*, solid and liquid are in equilibrium. At higher temperatures, liquid and vapor can coexist along the vaporization or *vapor-pressure curve*. If the pressure is greater than the vapor pressure, a liquid forms, if lower, a vapor. The vapor-pressure curve

terminates at the *critical point*. At temperatures above the *critical temperature*, T_c , a single phase forms over the entire range of pressures. Thus, for a single component, the critical temperature is the maximum temperature at which two phases can exist. Critical temperatures of hydrocarbons vary widely. Small hydrocarbon molecules have low critical temperatures, while those of large ones are much higher. Critical pressures generally decline as the molecular size increases. For instance, the critical temperature and pressure of methane are -117°F and 668 psia. For decane, the values are 652°F and 304 psia. (Fig. 23.9 shows additional vapor pressure curves and critical points for several other light hydrocarbon molecules.)

For many reservoir engineering applications liquid/vapor equilibrium is of greatest interest, though liquid/liquid equilibria are important in some EOR processes. Solid/liquid phase changes, such as asphaltene or paraffin precipitation, occasionally occur in petroleum production operations. Fig. 23.2 shows typical volumetric behavior of a single component in the range of temperatures and pressures near the vapor-pressure curve in Fig. 23.1. If the substance under consideration is placed in a pressure cell at constant temperature T_1 below T_c and at a low pressure (Point A, for instance), it forms a vapor phase of high volume (low density). If the volume of the sample is decreased with the temperature held constant, the pressure rises. When the pressure reaches $p_v(T_1)$, the sample begins to condense. The pressure remains constant at the vapor pressure until the sample volume is reduced from the saturated vapor volume (V_v) to that of the saturated liquid (V_L). With further reductions in volume, the pressure rises again as the liquid phase is compressed. Note that small decreases in volume give rise to large pressure increases in the liquid phase because of the low compressibility of liquids. At a temperature T_2 above the critical temperature, no phase change is observed. Instead, the sample can be

*The chapter on this topic in 1962 edition was written by Murray F. Hawkins.

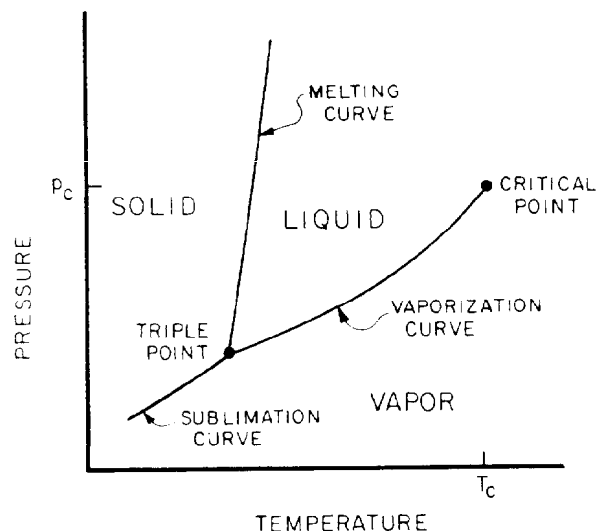


Fig. 23.1—Phase behavior of a pure component.

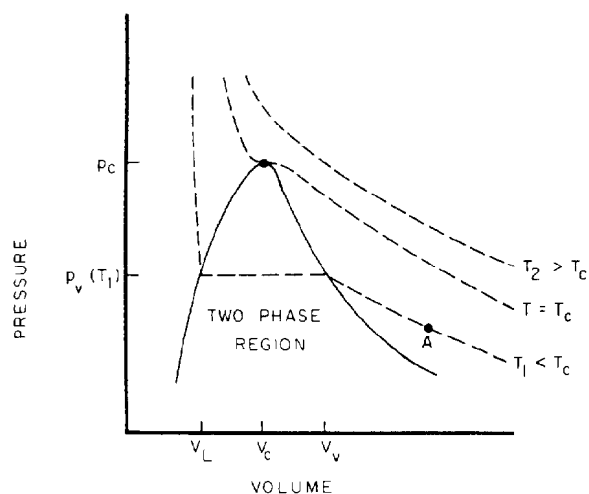


Fig. 23.2—Volumetric behavior of a pure component in the liquid/vapor region.

compressed from high volume (low density) and low pressure to low volume (high density) and high pressure with only one phase present.

Phase Rule

The maximum number of phases that can coexist at fixed temperature and pressure is determined by the number of components present. The phase rule states that

$$F = 2 + C - P - n_C, \quad (1)$$

where F is the number of degrees of freedom, C is the number of components, P is the number of phases, and n_C is the number of constraints. For a single-component system, the maximum number of phases occurs when there are no constraints ($n_C = 0$) and there are no degrees

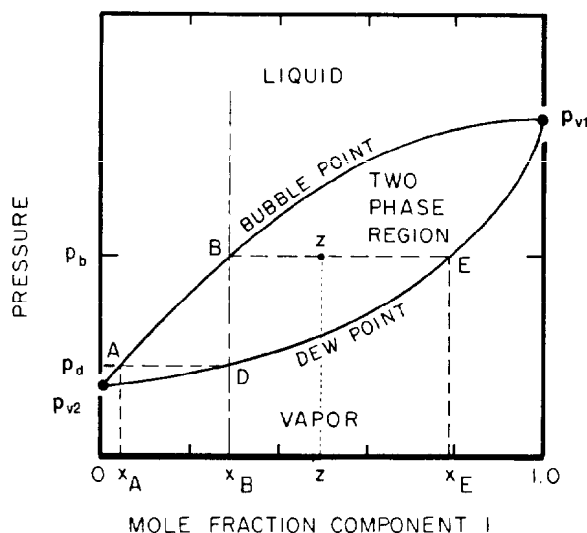


Fig. 23.3—Pressure-composition phase diagram for a binary mixture at a temperature below the critical temperature of both components.

of freedom ($F=0$). Thus, the maximum number of phases possible is three. Therefore, if three phases coexist in equilibrium (possible only at the triple point), the pressure and temperature are fixed. If only two phases are present for a pure component, then either the temperature or the pressure can be chosen. Once one is chosen, the other is determined. If the two phases are vapor and liquid, for example, choice of the temperature determines the pressure to be the vapor pressure at that temperature. These permitted pressure-temperature values lie on the vapor pressure curve of Fig. 23.1.

In a binary system, two phases can exist over a range of temperatures and pressures. The number of degrees of freedom is

$$F = 2 - n_C, \quad (2)$$

and hence both the temperature and pressure can be chosen, though there is no guarantee that two phases will occur at a specific choice of T and p . For multicomponent systems, the phase rule provides little guidance, since the number of phases is always far less than the maximum number that can occur. Hence, as the number of components increases, more component concentrations must be known to determine the system.

Types of Diagrams

Binary Phase Diagrams

Fig. 23.3 shows typical vapor/liquid phase behavior for a binary system at a fixed temperature below the critical temperature of both components. Such a diagram is known as a pressure-composition phase diagram. At pressures below the vapor pressure of Component 2, p_{v2} , any mixture of the two components forms a single vapor phase. At pressures between p_{v1} and p_{v2} , two phases can coexist for some compositions. For instance, at pressure p_b two phases will occur if the mole fraction of Component 1 lies between x_B and x_E . If the mixture

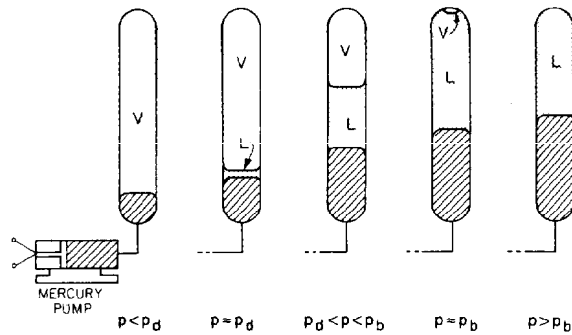


Fig. 23.4—Volumetric behavior of a binary mixture at constant temperature.

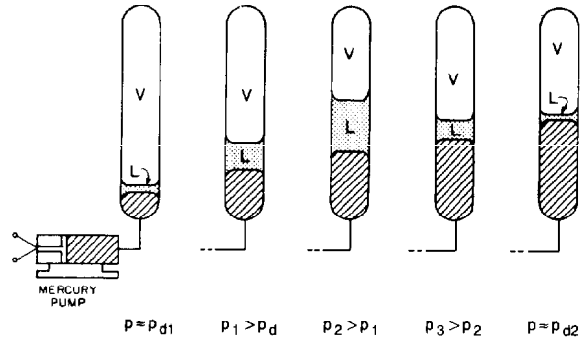


Fig. 23.6—Volumetric behavior of a binary mixture at a constant temperature showing retrograde vaporization.

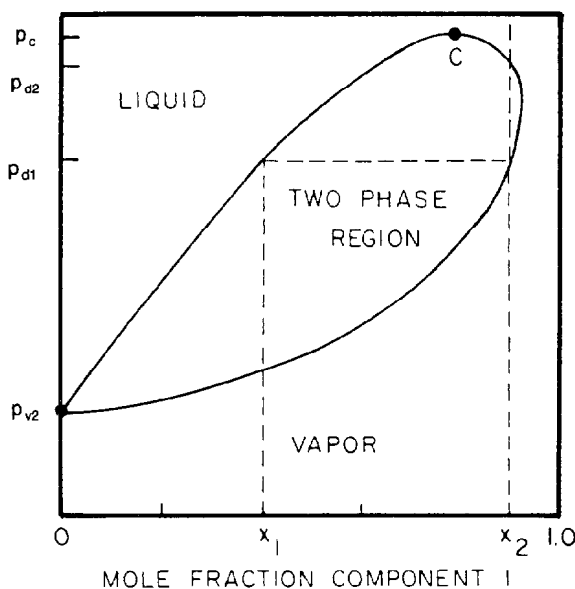


Fig. 23.5—Pressure-composition phase diagram for a binary mixture at a temperature above the critical temperature of Component 1.

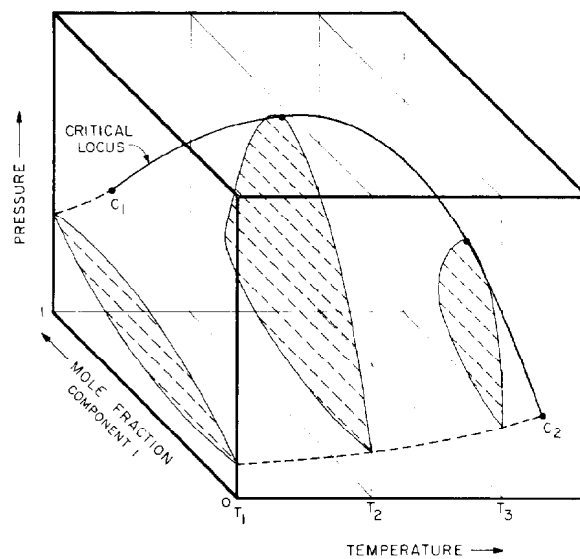


Fig. 23.7—Regions of temperature, pressure, and composition for which two phases occur in a binary liquid/vapor system.

composition is x_B , it will be all liquid, if it is x_E , all vapor. For 1 mol of mixture of overall composition, z , between x_B and x_E , the number of moles of liquid phase is

$$L = \frac{x_E - z}{x_E - x_B} \quad (3)$$

Eq. 3 is known as an inverse lever rule because it is equivalent to a statement concerning the distances along a tie line from the overall composition to the liquid and vapor compositions; $L = ZE/BE$, where ZE and BE are lengths on the tie line shown in Fig. 23.3. Thus, the amount of liquid is proportional to the distance from the overall composition to the vapor composition divided by the length of the tie line. The line connecting the compositions of phases in equilibrium is known as a tie line. In binary phase diagrams such as Fig. 23.3, the tie lines are always horizontal.

Phase diagrams such as Fig. 23.3 can be determined experimentally by placing a mixture of fixed overall composition in a high-pressure cell and measuring the pressures at which phases appear and disappear. For example, a mixture of composition x_B would show the behavior indicated qualitatively in Fig. 23.4. At a pressure less than p_d (Fig. 23.3), the mixture is a vapor. If the mixture is compressed by injecting mercury into the cell, the first liquid, which has composition x_A , appears at the dewpoint pressure, p_d . As the pressure is further increased, the volume of liquid grows as more and more of the vapor phase condenses. The last vapor, of composition x_E , disappears at the bubblepoint pressure, p_b .

If the system temperature is above the critical temperature of one of the components, the phase diagram is similar to that shown in Fig. 23.5. (See Fig. 23.13 for additional examples of this type of phase diagram.) At the higher temperature, the two-phase region no longer extends to the pure Component 1 side of

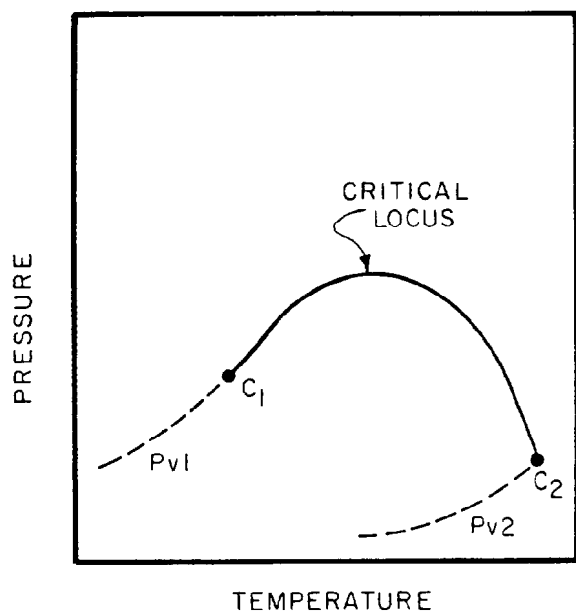


Fig. 23.8—Projection of the vapor pressure (p_{v1} and p_{v2}) curves and locus of critical points for binary mixtures. Points C_1 and C_2 are the critical points of the pure components.

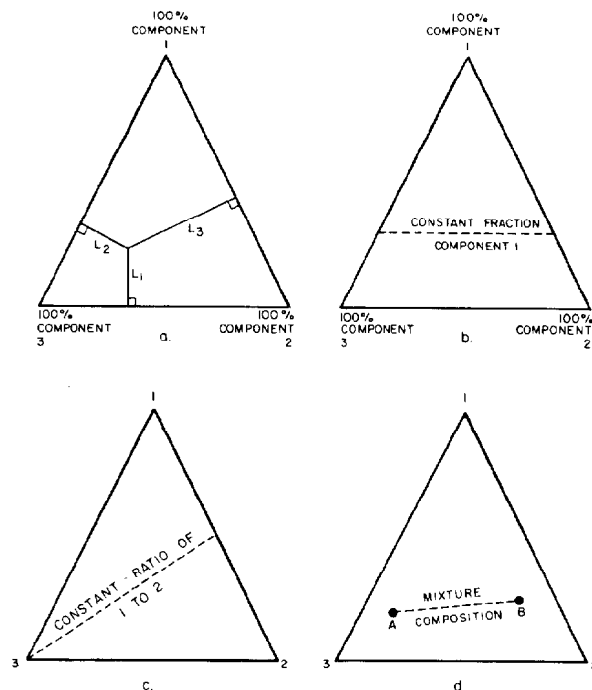


Fig. 23.10—Properties of ternary diagrams.

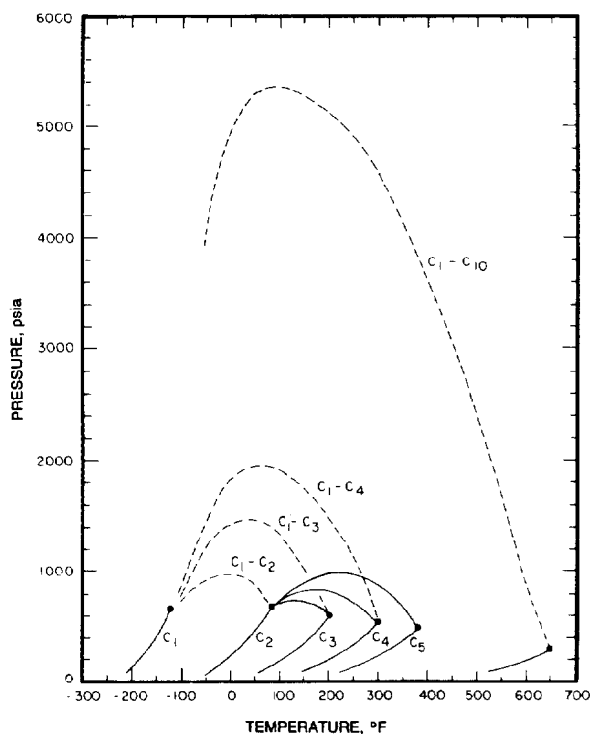


Fig. 23.9—Vapor pressure curves for light hydrocarbons and critical loci for selected hydrocarbon pairs.

the diagram. Instead, there is a critical point, C , at which liquid and vapor phases are identical. The critical point occurs at the maximum pressure of the two-phase region. The volumetric behavior of mixtures containing less Component 1 than the critical mixture is like that shown in Fig. 23.4. Fig. 23.6 shows the volumetric behavior of mixtures containing more Component 1. Compression of mixture of composition x_2 (in Fig. 23.5) leads to the appearance of liquid phase of composition x_1 when pressure p_{D1} is reached. The volume of liquid first grows and then declines with increasing pressure. The liquid phase disappears again when pressure p_{D2} is reached. Such behavior is called "retrograde vaporization" (or "retrograde condensation" if the pressure is decreasing).

If the system temperature is exactly equal to the critical temperature of Component 1, the critical point on the binary pressure-composition phase diagram is located at a Component 1 mole fraction of 1.0. Fig. 23.7 shows the behavior of the two-phase regions as the temperature rises. As the temperature increases, the critical point moves to lower concentrations of Component 1. As the critical temperature of Component 2 is approached, the two-phase region shrinks, disappearing altogether when the critical temperature is reached. A typical locus of critical temperatures and pressures for a pair of hydrocarbons is shown in Fig. 23.8. The critical locus shown in Fig. 23.8 is the projection of the critical curve in Fig. 23.7 onto the p - T plane. Thus, each point on the critical locus represents a critical mixture of different composition, though composition information is not shown on this diagram. For temperatures between the critical temperature of Component 1 and Component 2, the critical pressure of the mixtures can be much

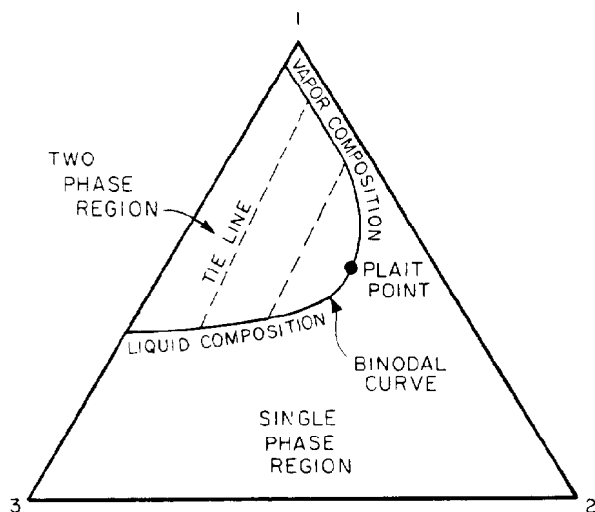


Fig. 23.11—Ternary phase diagram at a constant temperature and pressure for a system that forms a liquid and a vapor.

higher than the critical pressure of either component. Thus, two phases can coexist at pressures much greater than the critical pressure of either component. If the difference in molecular weight of the two components is large, the critical locus may reach very high pressures. Fig. 23.9 gives critical loci for some hydrocarbon pairs.¹

The binary phase diagrams reviewed here are those most commonly encountered. More complex phase diagrams involving liquid/liquid and liquid/liquid/vapor equilibria do occur, however, in hydrocarbon systems at very low temperatures (well outside the range of conditions encountered in reservoirs or surface separators) and in CO₂/crude oil systems at temperatures below about 50°C. For reviews of such phase behavior see Refs. 2 and 3.

Ternary Phase Diagrams

Phase behavior of mixtures containing three components is conveniently represented on a triangular diagram such as that shown in Fig. 23.10a. Such diagrams are based on the property of equilateral triangles that the sum of the perpendicular distances from any point to each side of the diagram is a constant equal to length of any of the sides. Thus, the composition of a point in the interior of the triangle is

$$x_1 = \frac{L_1}{L_T}, x_2 = \frac{L_2}{L_T}, x_3 = \frac{L_3}{L_T},$$

where

$$L_T = L_1 + L_2 + L_3. \quad (4)$$

Several other useful properties of triangular diagrams are also a consequence of this fact. For mixtures along any line parallel to a side of the diagram, the fraction of the component of the corner opposite to that side is constant

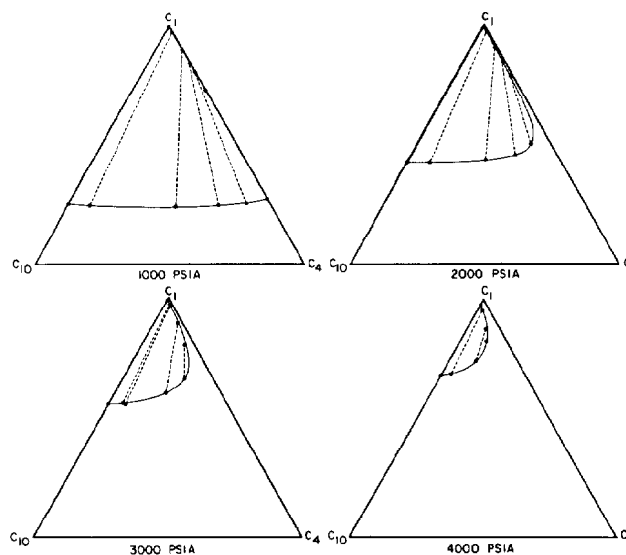


Fig. 23.12—Ternary phase diagram for the methane/butane/decane system at 160°F [71°C].

(Fig. 23.10b). In addition, mixtures lying on any line connecting a corner with the opposite side contain a constant ratio of the components at the ends of the side (Fig. 23.10c). Finally, mixtures of any two compositions, such as A and B in Fig. 23.10d, lie on a straight line connecting the two points on the ternary diagram. Compositions represented on a ternary diagram can be expressed in volume, mass, or mole fractions. For vapor/liquid equilibrium diagrams, mole fractions are most commonly used.

Typical features of a ternary phase diagram for a system that forms a liquid and a vapor at fixed temperature and pressure are shown in Fig. 23.11. Mixtures with overall compositions that lie inside the binodal curve will split into liquid and vapor. Tie lines connect compositions of liquid and vapor phases in equilibrium. Any mixture on one tie line gives the same liquid and vapor compositions. Only the amounts of liquid and vapor change as the overall composition changes from the liquid side of the binodal curve to the vapor side. If the mole fractions of component i in the liquid, vapor, and overall mixture are x_i , y_i , and z_i , the fraction of the total moles in the mixture in the liquid phase is given by

$$L = \frac{y_i - z_i}{y_i - x_i}. \quad (5)$$

Eq. 5 is another lever rule similar to that described for binary diagrams. The liquid and vapor portions of the binodal curve meet at the plait point, a critical point where the liquid and vapor phases are identical. Thus, the plait point mixture has a critical temperature and pressure equal to the conditions for which the diagram is plotted. Depending on the pressure and temperature and components, a plait point may or may not be present.

Any one ternary diagram is given for fixed temperature and pressure. As either the temperature or pressure is varied, the location of the binodal curve and

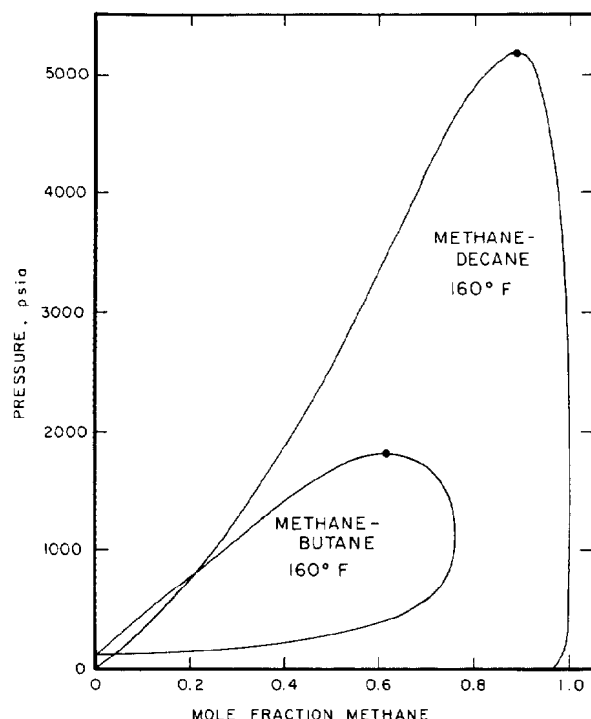


Fig. 23.13—Pressure-composition phase diagrams for methane/butane and methane/decane binary systems at 160°F [71°C].

slopes of the tie lines may change. Fig. 23.12 shows the effect of increasing pressure on ternary phase diagrams for mixtures of methane (C_1), butane (C_4), and decane (C_{10}) at 160°F.^{4,5} The sides of the ternary diagram represent a binary system, so the ternary diagram includes whatever binary tie lines exist at the temperature and pressure of the diagram. Fig. 23.13 shows the corresponding binary phase diagrams for the C_1 - C_4 and C_1 - C_{10} pairs. The C_4 - C_{10} pair is not shown because it forms two phases only below the vapor pressure of C_4 , about 120 psia at 160°F (see Fig. 23.9).

As shown in Fig. 23.12, at 1,000 psia the two-phase region is a band that stretches from the C_1 - C_{10} side of the diagram to the tie line on the C_1 - C_4 side. If the pressure is increased above 1,000 psia, the liquid composition line shifts to higher methane concentrations; methane is more soluble in both C_4 and C_{10} at the higher pressure (see Fig. 23.13). The two-phase region detaches from the C_1 - C_4 side of the diagram at the critical pressure of the C_1 - C_4 pair (about 1,800 psia). As the pressure increases above that critical pressure, the plait point moves into the interior of the diagram (Fig. 23.12, lower diagrams). With further increases in pressure, the two-phase region continues to shrink. It would disappear completely from the diagram if the pressure reached the critical pressure of the C_1 - C_{10} system at 160°F (nearly 5,200 psia).

Reservoir Fluid Systems

Real reservoir fluids contain many more than the two or three components, so phase composition data can no longer be represented with two or three coordinates. In-

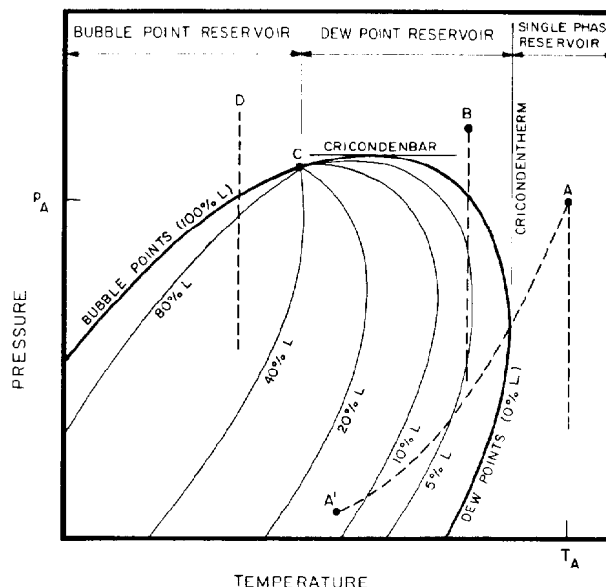


Fig. 23.14—Pressure-temperature phase diagram for a mixture of fixed composition.

stead, phase diagrams, which give more limited information, are used. Fig. 23.14 shows one such diagram for a multicomponent mixture. Fig. 23.14 gives the region of temperatures and pressures at which the mixture forms two phases. The analog of Fig. 23.14 for a binary system can be obtained by taking a slice at constant mole fraction of Component 1 through the diagram in Fig. 23.7. Also given are contours of liquid volume fractions, which indicate the fraction of total sample volume occupied by the liquid phase. Fig. 23.14 does not give any compositional information, however. In general, the compositions of coexisting liquid and vapor will be different at each temperature and pressure.

At temperatures below the critical temperature (Point C), a sample of the mixture described in Fig. 23.14 splits into two phases at the bubblepoint pressure (Fig. 23.4) when the pressure is reduced from a high level. At temperatures above the critical temperature, dewpoints are observed (Fig. 23.6). In this multicomponent system, the critical temperature is no longer the maximum temperature at which two phases can exist. Instead, the critical point is the temperature and pressure at which the phase compositions and all phase properties are identical.

The bubblepoint, dewpoint, and single-phase regions shown in Fig. 23.14 are sometimes used to classify reservoirs. At temperatures above the *cricondentherm*, the maximum temperature for the formation of two phases, only one phase occurs at any pressure. For instance, if the hydrocarbon mixture of Fig. 23.14 were to occur in a reservoir at temperature T_A and pressure p_A (Point A), a decline in pressure at approximately constant temperature caused by removal of fluid from the reservoir would not cause the formation of a second phase. While the fluid in the reservoir remains a single phase, the produced gas splits into two phases as it cools and expands to surface temperature and pressure at Point A'. Thus, some condensate would be collected at the

surface even though only one phase is present in the formation. The amount of condensate collected depends on the operating conditions of the separator (or separators). The lower the temperature at a given pressure, the larger the volume of condensate collected (Fig. 23.14).

Dewpoint reservoirs are those for which the reservoir temperature lies between the critical temperature and the cricondentherm for the reservoir fluid. Production of fluid from a reservoir starting at Point B in Fig. 23.14 causes liquid to appear in the reservoir when the dewpoint pressure is reached, and as the pressure declines further, the saturation of liquid increases because of retrograde condensation. Because the saturation of liquid is low, only the vapor phase flows to producing wells. Thus, the overall composition of the fluid remaining in the reservoir changes continuously. However, the phase diagram shown in Fig. 23.14 is for the original composition only. The preferential removal of light hydrocarbon components in the vapor phase generates new hydrocarbon mixtures which have a greater fraction of the heavier hydrocarbons. Differential liberation experiments, in which a sample of the reservoir fluid initially at high pressure is expanded through a sequence of pressures, can be used to investigate the magnitude of the effect of pressure reduction on the vapor composition. At each pressure, a portion of the vapor is removed and analyzed. Such an experiment simulates what happens when condensate is left behind in the reservoir as the pressure declines. As the reservoir fluid becomes heavier, the boundary of the two-phase region in a diagram like Fig. 23.14 shifts to higher temperatures. Thus, the composition change also acts to drive the system toward higher liquid condensation. Such reservoirs are candidates for pressure maintenance by lean gas injection to limit the retrograde loss of condensate or for gas cycling to vaporize and recover some of the liquid hydrocarbons.

Bubblepoint reservoirs are those in which the temperature is less than the critical temperature of the reservoir fluid (Point D in Fig. 23.14). These reservoirs are sometimes called "undersaturated" because there is insufficient gas for a gas phase at that temperature and pressure. Isothermal pressure reduction causes the appearance of a vapor phase at the bubblepoint pressure. Because the compressibility of the liquid phase is much lower than that of a vapor, the pressure in the reservoir declines rapidly during production in the single-phase region. The appearance of the much more compressible vapor phase reduces the rate of pressure decline. The volume of vapor present in the reservoir grows rapidly with reduction of reservoir pressure below the bubblepoint. Because the vapor viscosity is much lower than the liquid viscosity, and the gas relative permeability goes up markedly with increasing gas saturation, the vapor phase flows more easily. Hence, the produced GOR climbs rapidly. Again, pressure maintenance by water drive, water injection, or gas injection can substantially improve oil recovery over the 10 to 20% recovery typical of pressure depletion in these solution-gas-drive reservoirs. As in dewpoint reservoirs, the composition of the reservoir fluid changes continuously once the two-phase region is reached.

There is, of course, no reason why initial reservoir temperatures and pressures cannot lie within the two-phase region. Oil reservoirs with gas caps and gas reser-

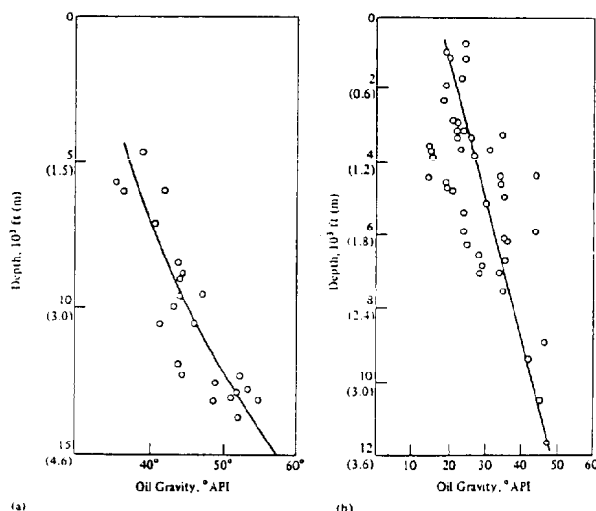


Fig. 23.15—Increase in °API gravity with depth: (a) Ordovician Ellenberger reservoirs in Delaware Val Verde basin; (b) Pennsylvanian Tensleep reservoirs in Wyoming.

voirs with some liquids present are common. There also can be considerable variation in the initial composition of the reservoir fluid. The discussion of single-phase, dewpoint, and bubblepoint reservoirs was based on a phase diagram for one fluid composition. Even for one fluid, all the types of behavior occur over a range of temperatures. In actual reservoir settings, the composition of the reservoir fluid correlates with depth and temperature. Deeper reservoirs usually contain lighter oils.⁶ Fig. 23.15 shows the relationships between oil gravity and depth for two basins. The higher temperatures of deeper reservoirs alter the original hydrocarbon mixtures to produce lighter hydrocarbons over geologic time.⁶ Low oil gravity, low temperature, and relatively small amounts of dissolved gas all combine to produce bubblepoint reservoirs. High oil gravity, high temperatures, and high GOR's produce dewpoint or condensate systems.

Phase Diagrams for EOR Processes

Phase behavior plays an important role in a variety of EOR processes. Such processes are designed to overcome, in one way or another, the capillary forces that act to trap oil during waterflooding. In surfactant/polymer processes, the effects of capillary forces are reduced by injection of surfactant solutions that contain molecules with oil- and water-soluble portions. Such molecules migrate to the oil/water interface and reduce the interfacial tension, thereby reducing the magnitude of the capillary forces that resist movement of trapped oil. Miscible displacement processes are designed to eliminate interfaces between the oil and the displacing phase, thereby removing the effects of capillary forces between the injected fluid and the oil. Unfortunately, fluids that are strictly miscible with oil are too expensive for general use. Instead, fluids such as methane or methane enriched with intermediate hydrocarbons, CO₂, or nitrogen are injected, and the required miscible displacing fluid is generated by mixing of the injected fluid with oil in the reservoir.

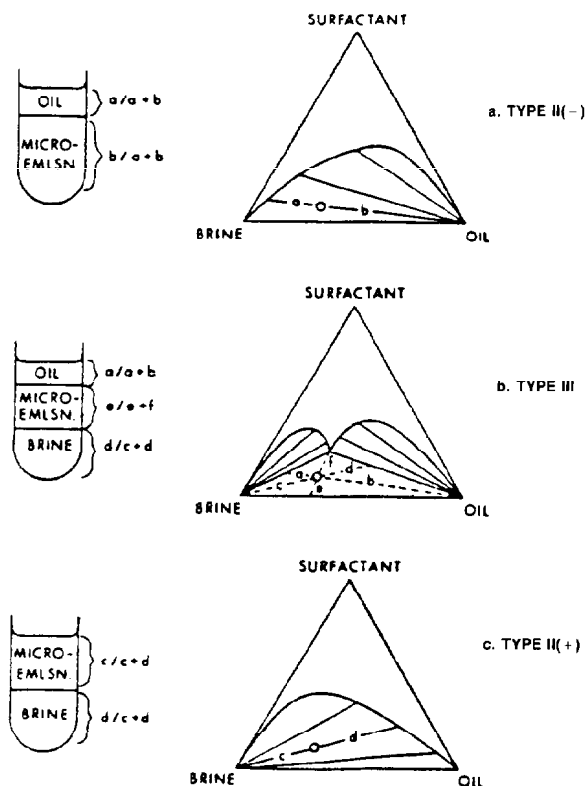


Fig. 23.16—Ternary representation of phase diagrams.

Phase diagrams typical of those used to explain the behavior of surfactant systems are shown in Fig. 23.16.⁷ In those ternary diagrams, the components shown are no longer true thermodynamic components since they are mixtures. A crude oil contains hundreds of components, and the brine and surfactant pseudocomponents may also be complex mixtures. The simplified representation, however, has obvious advantages for describing phase behavior, and it is reasonably accurate as long as each pseudocomponent has approximately the same composition in each phase. In Fig. 23.16a for instance, the “oil” pseudocomponent can appear in an oil-rich phase or in a phase containing mostly surfactant and brine. If the oil solubilized into the surfactant/brine phase is nearly the same mixture of hydrocarbons as the original “oil,” then the representation in terms of pseudocomponents is reasonable. The compositions shown in Fig. 23.16 are in volume fractions. An inverse lever rule similar to Eqs. 3 or 5 gives the relationship between the volumes of the two phases for a given overall composition, as illustrated in Fig. 23.16.

Fig. 23.16a is a phase diagram for the liquid/liquid equilibrium behavior typical of mixtures of brines of low salinity with oil. If there is no surfactant present, the oil and brine are immiscible; mixture compositions on the base of the diagram split into essentially “pure” brine in equilibrium with “pure” oil. Addition of surfactant causes some oil to be solubilized into a microemulsion rich in brine. That phase is in equilibrium with a phase containing nearly pure oil. Thus in the low-salinity brine, the surfactant partitions into the brine phase,

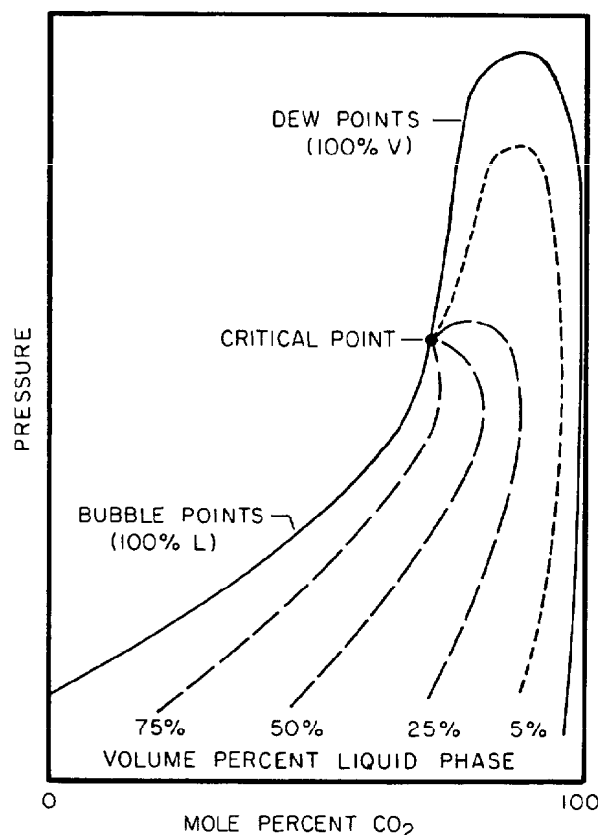


Fig. 23.17—Typical pressure-composition phase diagram for a binary mixture of CO_2 with a crude oil at temperatures above 120°F [49°C].

solubilizing some oil. The plait point in Fig. 23.16a lies close to the oil corner of the diagram. Because only two phases occur and the tie lines all have negative slope, such phase is often called “Type II(-).”

Phase diagrams for high-salinity brines are often similar to Fig. 23.16c. In the high-salinity systems the surfactant partitions into the oil phase and solubilizes water into an oil-external microemulsion. In this case the plait point is close to the brine apex on the ternary diagram. For intermediate salinities, the phase behavior can be more complex, as shown in Fig. 23.16b. According to the phase rule, if the temperature and pressure are set, then up to three phases can coexist for a three component system. If three phases do occur, then the compositions of the phases are fixed at a given temperature and pressure. The three-phase region on a ternary diagram is represented as a triangle (Fig. 23.16b). Any overall composition lying within the three-phase region splits into the same three phases. Only the amounts of each phase change as the overall composition varies in the three-phase region. The edges of the three-phase region are tie lines for the associated two-phase regions. Thus, there is a two-phase region adjacent to each of the sides of the three-phase triangle. In Fig. 23.16b, the two-phase region at low surfactant concentrations is too small to show on the diagram. It must be present, however, since oil and brine form only two phases in the absence of surfactant.

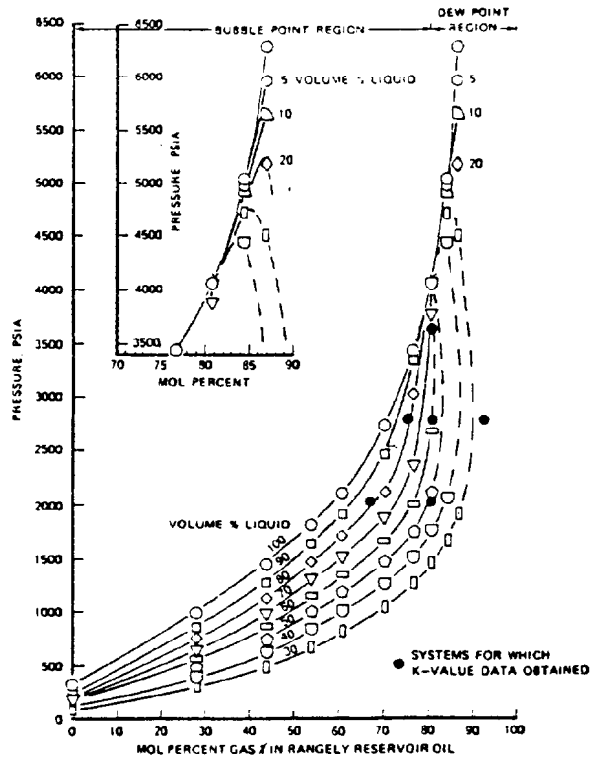


Fig. 23.18—Pressure composition diagram—Gas 1 system for Rangely oil: 95% CO_2 and 5% methane gas system at 160°F [71°C].

Phase behavior of CO_2 /crude oil systems is often summarized in pressure-composition (p - x) diagrams such as those shown in Fig. 23.17. Fig. 23.18 is an example of a p - x diagram for mixtures of CO_2 (containing a small amount of methane contamination) with crude oil from the Rangely field.⁸ In such diagrams, the behavior of binary mixtures of CO_2 with a particular oil is reported for a fixed temperature. Thus, the oil is represented as a single pseudocomponent on such a diagram. Such diagrams indicate bubble- and dewpoint pressures, the regions of pressure and composition for which two or more phases exist, and information about the volume fractions of the phases. However, they provide no information about the compositions of the phases in equilibrium. The reason for the absence of composition data is illustrated in Fig. 23.19,³ which gives data reported by Metcalfe and Yarborough⁹ for a ternary system of CO_2 , C_4 , and C_{10} . Binary phase data for the CO_2 - C_4 (Ref. 10) and CO_2 - C_{10} (Ref. 11) systems also are included. Fig. 23.19 shows a triangular solid within which all possible compositions (mole fractions) of CO_2 - C_4 - C_{10} mixtures for pressures between 400 and 2,000 psia are contained. The two-phase region is bounded by a surface that connects the binary phase envelope for the CO_2 - C_{10} binary pair to that on the CO_2 - C_4 side of the diagram. That surface is divided into two parts—liquid compositions and vapor compositions. Tie lines (heavy dashed lines in Fig. 23.19) connect the compositions of liquid and vapor phases in equilibrium at a fixed pressure. Thus, the ternary phase diagram for CO_2 - C_4 - C_{10} mixtures at any pressure is just a constant

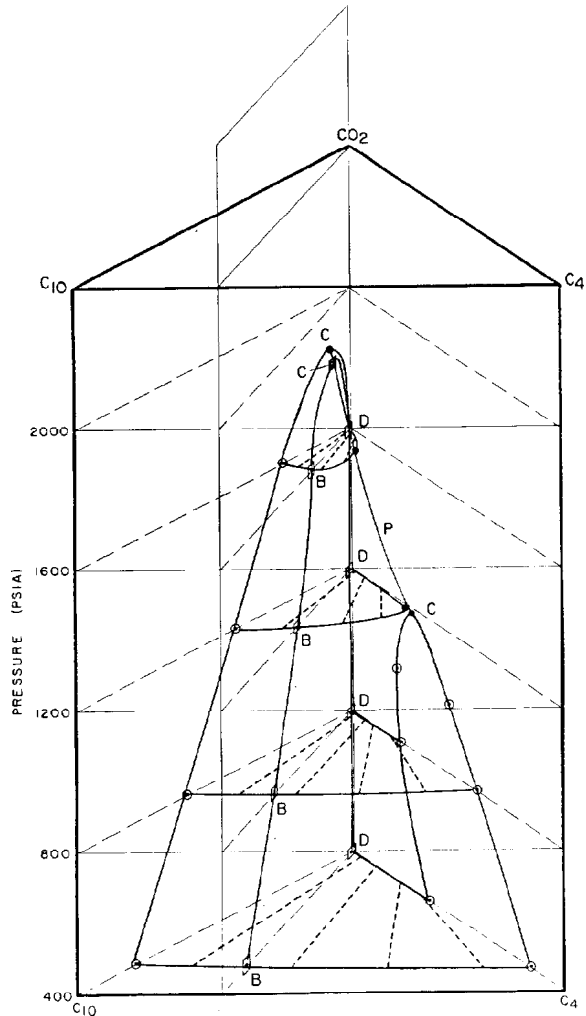


Fig. 23.19—Phase behavior of CO_2 - C_4 - C_{10} mixtures at 160°F [71°C].

pressure (horizontal) slice through the triangular prism. Several such slices at different pressures are shown in Fig. 23.19. At pressures below the critical pressure of CO_2 - C_4 mixtures (1,184 psia), both CO_2 - C_{10} mixtures and CO_2 - C_4 mixtures form two phases for some range of CO_2 concentrations. At 400 and 800 psia, the two-phase region is a band across the diagram. Above the critical pressure of CO_2 - C_4 mixtures, CO_2 is miscible with C_4 , and ternary slices at higher pressures show a continuous binodal curve on which the locus of liquid compositions meets that of vapor compositions at a plait point. The locus of plait points (labeled "P" in Fig. 23.19) connects the critical points of the two binary pairs.

To see the effect of representing the phase behavior of a ternary system on a pseudobinary diagram, consider a p - x diagram for an "oil" composed of 70 mol% C_{10} and 30 mol% C_4 . At any fixed pressure, the mixtures of CO_2 and oil which would be investigated in an experiment to determine a p - x diagram lie on a straight line (the dilution line), which connects the original oil composition with the CO_2 apex. Thus, a p - x diagram for this

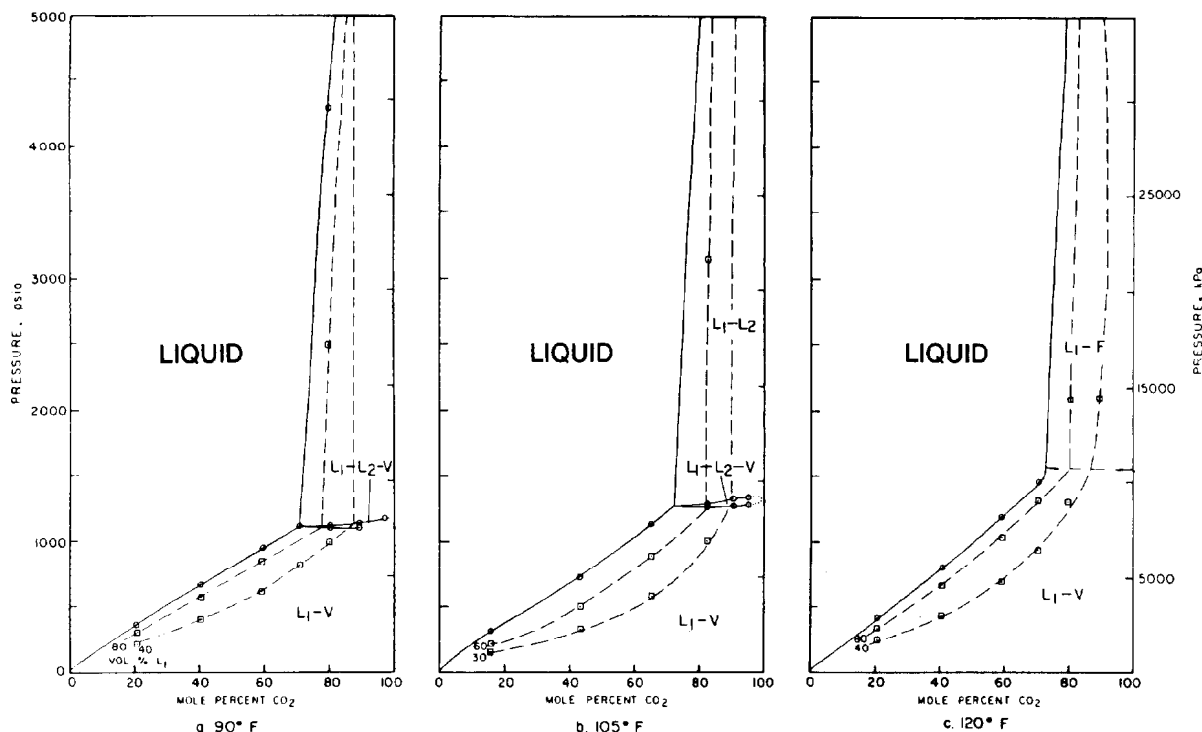


Fig. 23.20— p - x diagrams for mixtures of CO₂ with Wasson oil, where L₁ is Liquid Phase 1 (oil-rich phase), L₂ is Liquid Phase 2 (CO₂-rich phase), and V is the vapor phase. Dashed lines indicate constant volume fraction of L₁ phase.

system is a vertical slice through the triangular prism shown in Fig. 23.19. The saturation pressures on a p - x diagram are those at which the dilution plane intersects the surface which bounds the two-phase region. Bubble-point pressures (B) occur where the dilution plane intersects the liquid composition side of the two-phase surface, while dewpoint pressures (D) occur at the intersection with vapor compositions. Comparison of the phase envelope on the resulting p - x diagram with binary phase diagrams yields the following observations.

1. Tie lines do not, in general, lie in the dilution plane. Instead, they pierce that plane. This means that the composition of vapor in equilibrium with a bubblepoint mixture on the p - x diagram is not the same as that of the dewpoint mixture at the same pressure.

2. The critical point on the p - x diagram occurs where the locus of plait points pierces the dilution plane. It is not, in general, at the maximum saturation pressure on the p - x diagram. The maximum pressure occurs where the binodal curve is tangent to the dilution plane. The critical point on the p - x diagram can lie on either side of the maximum pressure, depending on the position of locus of plait points on the two-phase surface.

It is apparent from Fig. 23.19 that the composition of the original oil has a strong influence on the shape of the saturation pressure curve, and on the location of the critical point on the p - x diagram. If the oil had been richer in C₄, the critical pressure and maximum pressure both would have been lower. Thus, it should be anticipated that the appearance of p - x diagrams for CO₂/crude oil systems should depend on the composition of the oil.

Figs. 23.18 and 23.20 illustrate the complexity of

phase behavior observed for CO₂/crude oil systems. Fig. 23.18 gives the behavior of mixtures of CO₂ (with about 5% methane as a contaminant) with Rangely crude oil at 160°F. The oil itself has a bubblepoint pressure of about 350 psia. Mixtures containing up to about 80 mol% CO₂ (+C₁) show bubblepoints, while those containing more CO₂ show dewpoints. At the relatively high temperature of the Rangely field, only two phases, a liquid and a vapor, form. At lower temperatures, more complex phase behavior can occur. Figs. 23.20a, b and c show the behavior of mixtures of a dead oil from the Wasson field³ with CO₂. At 90°F and 105°F, the mixtures form a liquid and a vapor at low pressures and two liquid phases at high pressures and high CO₂ concentrations. They form three phases, two liquids and a vapor, for a small range of pressures at high CO₂ concentrations. The liquid/liquid and liquid/liquid/vapor behavior disappears if the temperature is high enough. At 120°F (Fig. 23.20c), the three-phase region had disappeared. For the systems studied to date, 120°F appears to be a reasonable estimate of the maximum temperature for liquid/liquid/vapor separations. For detailed discussions of such phase behavior, see Refs. 2 and 3.

Calculation of Phase Compositions

Calculations of the compositions of phases that occur for multicomponent mixtures are important for the design of surface separators and for the design of EOR processes such as high-pressure and condensing-gas drives and CO₂ floods. There are two widely used methods for such calculations— K -value correlations and equations of state (EOS's).

The use of K -values, also called "equilibrium ratios" or "equilibrium constants," is based on the behavior of mixtures of gases at relatively low pressures and temperatures. According to Raoult's law, the partial vapor pressure p'_{vi} of component i in a liquid mixture is equal to the product of the mole fraction of component i in the liquid and its pure component vapor pressure

$$p'_{vi} = x_i p_{vi} \quad (6)$$

In addition, Dalton's law states that the partial pressure of component i in the vapor is

$$p'_{vi} = y_i p_t \quad (7)$$

where y_i is the mole fraction of component i in the vapor and p_t is the total pressure. Rearrangement of Eqs. 6 and 7 gives the definition of K -value for an ideal (low pressure) system:

$$K_i = \frac{y_i}{x_i} = \frac{p_{vi}}{p_t} \quad (8)$$

Thus, for a multicomponent mixture at low pressure, the equilibrium value can be estimated from the vapor pressure, which is a function of temperature only, and the total pressure. The assumption of an ideal gas in Raoult's and Dalton's laws is reasonable only if the pressure is below about 50 to 100 psia.¹² At higher pressures, equilibrium ratios are functions of pressure, temperature, and composition. Fig. 23.21 shows a typical set of equilibrium ratios for a hydrocarbon system containing some CO₂ at 220°F.¹³ Also shown (as dashed lines) are the ideal equilibrium ratios. At high pressures, the K -values for ethane and heavier hydrocarbons pass through a minimum and appear to converge to a value of one, in this case at 4,200 psia. This observation is the basis for a widely used empirical correlation for K -values. K -value charts for a variety of convergence pressures and a recommended technique for estimating the convergence pressure are given in GPSA's *Engineering Data Book*.¹

If K -values are known or can be estimated, then amounts of liquid and vapor and phase compositions can be calculated easily. Consider 1 mol of a mixture in which the overall mole fraction of the i th component is z_i . If the mole fractions of component i in the liquid and vapor are x_i and y_i , and the fraction of the mole of mixture that is liquid is L , then a material balance gives

$$z_i = x_i L + y_i (1 - L) \quad (9)$$

Substitution of the definition of $K_i = y_i/x_i$ into Eq. 9 and rearrangement gives

$$x_i = \frac{z_i}{K_i + (1 - K_i)L} \quad (10)$$

Similarly, Eq. 9 can be solved for y_i , giving

$$y_i = \frac{K_i z_i}{K_i + (1 - K_i)L} \quad (11)$$

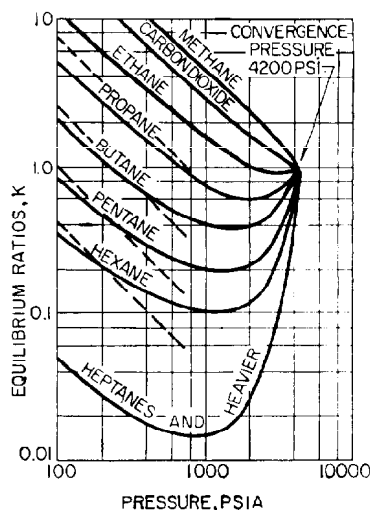


Fig. 23.21—Typical equilibrium ratios at 220°F [104°C] (dashed lines are the ideal ratios).

By definition, $\sum x_i = \sum y_i = 1$, so $\sum x_i - \sum y_i = 0$ which gives the nonlinear function $f(L)$:

$$f(L) = \sum_i \frac{z_i (K_i - 1)}{K_i + (1 - K_i)L} = 0 \quad (12)$$

Eq. 12 can be solved for L by application of a Newton-Raphson iteration. If L_k is the k th estimate of the solution, an improved estimate is given by

$$L_{k+1} = L_k - \frac{f(L_k)}{\left. \frac{df}{dL} \right|_{L_k}} \quad (13)$$

where

$$\frac{df}{dL} = \sum_i \frac{z_i (1 - K_i)^2}{[K_i + (1 - K_i)L]^2} \quad (14)$$

The iterative calculation is complete when $f(L)$ as given by Eq. 12 and $\Delta L = L_{k+1} - L_k$ are both smaller than some preset tolerances. Once the liquid mole fraction has been determined, the x_i and y_i are obtained from Eqs. 10 and 11.

If the mixture is at its bubblepoint pressure, then $L = 1$ and $\sum z_i = 1$, and Eq. 12 reduces to

$$\sum (z_i K_i) = 1 \quad (15)$$

Thus, if K_i 's are known as a function of pressure, then the bubblepoint pressure can be obtained as the pressure at which Eq. 15 is satisfied. Bubblepoint pressures are generally most sensitive to the K -values of the lightest components, which are the largest. If the mixture is at its dewpoint pressure, then $L = 0$, $\sum z_i = 1$, and

$$\sum \left(\frac{z_i}{K_i} \right) = 1 \quad (16)$$

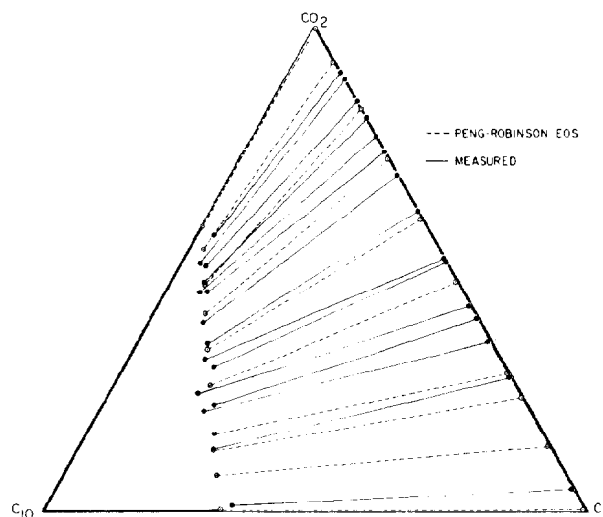


Fig. 23.22—Comparison of calculated and measured phase compositions for ternary mixtures of CO₂, methane (C₁), and decane (C₁₀), at 160°F [71°C] and 1,250 psia.

Dewpoint pressures are most sensitive to the smallest K -values, those of the heavy components, which often are least accurately known. Thus, there is often more uncertainty in calculated values of dewpoint pressure. The sums of Eqs. 15 and 16 also are useful for determining whether the mixture forms one or two phases. If $\Sigma(K_i z_i) < 1$, the mixture is all liquid. If $\Sigma(z_i/K_i) < 1$, the mixture is all vapor. If both $\Sigma(K_i z_i) > 1$ and $\Sigma(z_i/K_i) > 1$, the mixture forms two phases.

In recent years, EOS's also have been used extensively for phase equilibrium calculations. Most of the widely used EOS's are refinements of the equation proposed by van der Waals:

$$p = \frac{RT}{V-b} - \frac{a}{V^2}, \quad (17)$$

where p is the pressure, R the gas constant, T the temperature, and V the molar volume. The constants a and b can be determined for a particular component from thermodynamic constraints at the critical point, which requires that

$$(\partial p / \partial V)_{T_c} = (\partial^2 p / \partial V^2)_{T_c} = 0,$$

which gives

$$a = \frac{27}{64} \frac{R^2 T_c^2}{p_c}$$

and

$$b = \frac{RT_c}{8p_c}, \quad (18)$$

where T_c is the critical temperature and p_c is the critical pressure.

van der Waals' equation reduces to the ideal gas law if the molar volume is large (low pressure). If the molar

volume is small enough to be close to the constant b , then the pressure increases rapidly as the volume is reduced. Thus, the EOS is qualitatively consistent with liquid behavior when the pressure is high.

The calculation of phase compositions is based on the fact that, at thermodynamic equilibrium, the fugacity of each component must be the same in each phase. The fugacity of a component in a phase can be calculated if the volumetric behavior of the phase is known. It can be shown¹⁴ that the fugacity of component i , f_i , in a phase is given by

$$RT \ln f_i = \int_{V_i}^{\infty} \left[\left(\frac{\partial p}{\partial n_i} \right)_{T, V_i, n_j} - \frac{RT}{V_i} \right] dV_i - RT \ln \frac{V_i}{n_i RT}, \quad (19)$$

where T is the temperature, p the pressure, V_i the total volume, n_i the number of moles of component i , and R the gas constant. If the relationship between pressure, composition, and total volume is known from an EOS, then $(\partial p / \partial n_i)_{T, V_i, n_j}$ can be obtained and the integral evaluated. A variety of EOS's have been suggested for hydrocarbon mixtures. For example, the original Redlich-Kwong equation has the form

$$p = \frac{n_i RT}{V_i - n_i b_m} - \frac{n_i^2 a_m}{T^{1/2} V_i (V_i + n b_m)}, \quad (20)$$

where $n_i = \Sigma n_i$ is the total number of moles and a_m and b_m depend on the mixture composition and the critical properties of the components as follows.

$$a_m = \frac{(\Sigma y_i A_i^{1/2})^2 R^2 T^{5/2}}{p}, \quad (21)$$

where

$$A_i = \frac{\Omega_a (p/p_{ci})}{(T/T_{ci})^{5/2}}, \quad (22)$$

and

$$\Omega_a = \frac{1}{9(2^{1/2} - 1)} \cong 0.4275. \quad (23)$$

$$b_m = \frac{(\Sigma y_i B_i) RT}{p}, \quad (24)$$

where

$$B_i = \frac{\Omega_b (p/p_{ci})}{(T/T_{ci})}, \quad (25)$$

and

$$\Omega_b = \frac{2^{1/2} - 1}{3} \cong 0.08664. \quad (26)$$

In Eqs. 21 through 26, y_i is the mole fraction of component i in the mixture, and p_{ci} and T_{ci} are the critical pressure and temperature of component i . The constants Ω_a and Ω_b arise from the thermodynamic constraints, $(\partial p/\partial V)_{T_c} = (\partial^2 p/\partial V^2)_{T_c} = 0$, at the critical point. From Eqs. 19 through 26, an expression for the fugacity of each component in a phase can be obtained. To calculate phase compositions, the following procedure is used.

1. Estimate compositions of liquid and vapor.
2. Calculate fugacities of each component in each phase.
3. If $f_{iv} = f_{iL}$ stop. Otherwise, obtain improved phase compositions and return to Step 2.

Similar calculations can be performed for liquid/liquid and even liquid/liquid/vapor systems. Because the equations for fugacities are complex and nonlinear, computer implementation of this iterative scheme to find phase compositions is required.

The Redlich-Kwong EOS given as an example here is by no means the only equation available. Many modifications to the Redlich-Kwong equation have been proposed to improve the accuracy of the predictions of phase compositions, and equations with different analytical forms are also in use. The Soave modification of the Redlich-Kwong equation and the Peng-Robinson equation are among the most widely used. Ref. 14 gives details of a variety of EOS's, and Ref. 15 is a useful collection of papers relevant to phase equilibrium calculations for hydrocarbon systems. Computer programs for such calculations are available.*

EOS's currently in use are quite accurate for mixtures of light hydrocarbons for which critical properties are known and extensive phase behavior data are available. For instance, Fig. 23.22 shows a comparison of phase compositions calculated with the Peng-Robinson EOS with measured values for mixtures of CO₂, C₁, and C₁₀ at 1,250 psia and 160°F. For this well-characterized system, the calculated values agreed well with the measured compositions. For crude oil systems, phase behavior predictions are less reliable because the characterization of heavy components is less certain. For such systems some experimental data are required to tune the EOS to represent the particular hydrocarbon system. Improvement of the predictive power of EOS's for complex hydrocarbon systems is an area of active current research.

Nomenclature

- a_m = defined by Eq. 21
- A_i = defined by Eq. 22
- b_m = defined by Eq. 24
- B_i = defined by Eq. 25
- C = critical point when liquid and vapor phases are identical
- f_{iL} = liquid fugacity of Component i
- f_{iv} = vapor fugacity of Component i
- K_i = K-value of Component i
- L = total moles of liquid-phase in mixture
- L_k = k th estimate of L by Newton-Raphson iteration
- n_C = number of constraints

- p = pressure
- p_b = bubblepoint pressure
- p_d = dewpoint pressure
- p_t = total pressure
- p_v = vapor pressure
- p_{vi} = vapor pressure of Component i in liquid mixture
- p'_{vi} = partial vapor pressure of Component i in liquid mixture
- p_{vz} = any mixture of two components which form a single vapor phase
- p_{v1} = pressure below vapor pressure of Component z which may form a single vapor phase
- p_{v2} = pressure above vapor pressure of Component z which may form a single vapor phase
- T_c = critical temperature
- T_1 = constant temperature below T_c
- T_2 = constant temperature above T_c
- V_L = saturated liquid volume
- V_v = saturated vapor volume
- z_i = overall mole fraction of the i th component
- Ω_a = defined in Eq. 23
- Ω_b = defined in Eq. 26

Subscripts

- C = number of components
- F = number of degrees of freedom
- P = number of phases

References

1. *Engineering Data Book*, Gas Processors Suppliers Assn., ninth edition, Tulsa (1972).
2. Stalkup, F.I. Jr.: *Miscible Displacement*, Monograph Series, SPE, Dallas (1983) 8.
3. Orr, F.M. Jr. and Jensen, C.M.: "Interpretation of Pressure-Composition Phase Diagrams for CO₂-Crude Oil Systems," *Soc. Pet. Eng. J.* (Oct. 1984) 485-97.
4. Reamer, H.H., Fiskin, J.M., and Sage, B.H.: "Phase Equilibria in Hydrocarbon Systems," *Ind. Eng. Chem.* **41** (Dec. 1949) 2871.
5. Sage, B.H. and Lacey, W.N.: *Thermodynamic Properties of the Lighter Paraffin Hydrocarbons and Nitrogen*, Monograph on API Research Project 37, American Petroleum Inst., New York City (1950).
6. Hunt, J.M.: *Petroleum Geochemistry and Geology*, W.H. Freeman and Co., San Francisco (1979).
7. Nelson, R.C. and Pope, G.A.: "Phase Relationships in Chemical Flooding," *Soc. Pet. Eng. J.* (Oct. 1978) 325-38.
8. Graue, D.J. and Zana, E.T.: "Study of a Possible CO₂ Flood in the Rangely Field, Colorado," *J. Pet. Tech.* (July 1981) 1312-18.
9. Metcalfe, R.S. and Yarbrough, L.: "The Effect of Phase Equilibria on the CO₂ Displacement Mechanism," *Soc. Pet. Eng. J.* (Aug. 1979) 242-52; *Trans.*, AIME, **267**.
10. Olds, R.H. et al.: "Phase Equilibria in Hydrocarbon Systems," *Ind. Eng. Chem.* **41** (March 1949) 475-82.
11. Reamer, H.H. and Sage, B.H.: "Phase Equilibria in Hydrocarbon Systems. Volumetric and Phase Behavior of the n-Decane-CO₂ System," *J. Chem. Eng. Data* **8**, No. 4 (1963) 508-13.
12. Standing, M.B.: *Volumetric and Phase Behavior of Oil Field Hydrocarbon Systems*, SPE, Dallas (1977).
13. Allen, F.H. and Roe, R.P.: "Performance Characteristics of a Volumetric Condensate Reservoir," *Trans.*, AIME (1950) **189**, 83-90.
14. Reid, R.C., Prausnitz, J.M., and Sherwood, T.K.: *The Properties of Gases and Liquids*, third edition, McGraw-Hill Book Co. Inc., New York City (1977).
15. *Phase Behavior*, Reprint Series, SPE, Dallas (1981) **15**.

*Gas Processors Suppliers Assn., Tulsa, OK

Chapter 24

Properties of Produced Waters

A. Gene Collins,* U.S. DOE Bartlesville Energy Technology Center**

Introduction and History

Early U.S. settlements commonly were located close to salt licks that supplied salt to the population. Often these salt springs were contaminated with petroleum, and many of the early efforts to acquire salt by digging wells were rewarded by finding unwanted increased amounts of oil and gas associated with the saline waters. In the Appalachian Mts., many saline water springs occurred along the crests of anticlines.¹

In 1855 it was found that distillation of petroleum produced a light oil that was similar to coal oil and better than whale oil as an illuminant.² This knowledge spurred the search for saline waters that contained oil. Using the methods of the salt producers, Col. Edward Drake drilled a well on Oil Creek, near Titusville, PA, in 1859. He struck oil at a depth of 70 ft, and this first oil well produced about 35 B/D.³

The early oil producers did not realize the significance of the oil and saline waters occurring together. In fact, it was not until 1938 that the existence of interstitial water in oil reservoirs was generally recognized.⁴ Torrey⁵ was convinced as early as 1928 that dispersed interstitial water existed in oil reservoirs, but his belief was rejected by his colleagues because most of the producing wells did not produce any water upon completion. Occurrences of mixtures of oil and gas with water were recognized by Griswold and Munn,⁶ but they believed that there was a definite separation of the oil and water, and that oil, gas, and water mixtures did not occur in the sand before a well tapped the reservoir.

It was not until 1928 that the first commercial laboratory for the analysis of rock cores was established, and the first core tested was from the Bradford third sand (from the Bradford field, McKean County, PA). The

percent saturation and percent porosity of this core were plotted vs. depth to construct a graphic representation of the oil and water saturation. The soluble mineral salts that were extracted from the core led Torrey to suspect that water was indigenous to the oil-productive sand. Shortly thereafter a test well was drilled near Custer City, PA, that encountered higher than average oil saturation in the lower part of the Bradford sand. This high oil saturation resulted from the action of an unsuspected flood, the existence of which was not known when the location for the test well had been selected. The upper part of the sand was not cored. Toward the end of the cutting of the first core with a cable tool core barrel, oil began to come into the hole so fast that it was not necessary to add water for the cutting of the second section of the sand. Therefore, the lower 3 ft of the Bradford sand was cut with oil in a hole free from water. Two samples from this section were preserved in sealed containers for saturation tests, and both of them, when analyzed, had a water content of about 20%PV. This well made about 10 BOPD and no water after being shot with nitroglycerine. Thus, the evidence developed by the core analysis and the productivity test after completion provided a satisfactory indication of the existence of immobile water, indigenous to the Bradford sand oil reservoir, which was held in its pore system and could not be produced by conventional pumping methods.⁵

Fettke⁷ was the first to report the presence of water in an oil-producing sand. However, he thought that it might have been introduced by the drilling process.

Munn⁸ recognized that moving underground water might be the primary cause of migration and accumulation of oil and gas. However, this theory had little experimental data to back it until Mills⁹ conducted several laboratory experiments on the effect of moving water and gas on water/oil/gas/sand and water/oil/sand systems. Mills concluded that "the up-dip migration of

*Now with the Natl. Inst. of Petroleum and Energy Research, Bartlesville, OK.

**The author of the original chapter on this topic in the 1962 edition was J. Wade Watkins.

oil and gas under the propulsive force of their buoyancy in water, as well as the migration of oil, either up or down dip, caused by hydraulic currents, are among the primary factors influencing both the accumulation and the recovery of oil and gas." This theory was seriously questioned and completely rejected by many of his contemporaries.

Rich¹⁰ assumed that "hydraulic currents, rather than buoyancy, are effective in causing accumulation of oil or its retention." He did not believe that the hydraulic accumulation and flushing of oil required a rapid movement of water but rather that the oil was an integral constituent of the rock fluids and that it could be carried along with them whether the movement was very slow or relatively rapid.

The effect of water displacing oil during production was not recognized in the early days of the petroleum industry in Pennsylvania. Laws were passed, however, to prevent operators from injecting water into the oil reservoir sands through unplugged wells. In spite of these laws, some operators at Bradford secretly opened the well casing opposite shallow groundwater sands to start a waterflood in the oil sands. Effect of artificial waterfloods were noted in the Bradford field in 1907, and became evident about 5 years later in the nearby oil fields of New York.¹¹ Volumetric calculations of the oil-reservoir volume that were made for engineering studies of these waterflood operations proved that interstitial water was generally present in the oil sands. Garrison¹² and Schilthuis⁴ gave detailed information concerning the distribution of water and oil in porous rocks, and of the origin and occurrence of "connate" water with information concerning the relationship of water saturation to formation permeability.

The word "connate" was first used by Lane and Gordon¹³ to mean interstitial water that was deposited with the sediments. The processes of rock compaction and mineral diagenesis result in the expulsion of large amounts of water from sediments and movement out of the deposit through the more permeable rocks. It is therefore highly unlikely that the water now in any pore is the same as that which was there when the particles that surround it were deposited. White¹⁴ redefined connate water as "fossil" water because it has been out of contact with the atmosphere for an appreciable part of a geologic time period. Thus, connate water is distinguished from "meteoric" water, which has entered the rocks in geologically recent times, and from "juvenile" water, which has come from deep in the earth's crust and has never been in contact with the atmosphere.

Meanwhile, petroleum engineers and geologists had learned that waters associated with petroleum could be identified with regard to the reservoir in which they occurred by a knowledge of their chemical characteristics. Commonly, the waters from different strata differ considerably in their dissolved chemical constituents, making the identification of a water from a particular stratum easy. However, in some areas the concentrations of dissolved constituents in waters from different strata do not differ significantly, and the identification of such waters is difficult or impossible.

The amount of water produced with the oil often increases as the amount of oil produced decreases. If this is edge water, nothing can be done about it. If it is bottom-

water, the well can be plugged back. However, it often is intrusive water from a shallow sand gaining access to the well from a leaky casing or faulty completion and this can be repaired.

Enormous quantities of water are produced with the oil in some fields, and it is necessary to separate the oil from the water. Most of the oil can be removed by settling. Often, however, an oil-in-water emulsion forms, which is very difficult to break. In such cases, the oil is heated and various surface-active chemicals are added to induce separation.

In the early days, the water was dumped on the ground, where it seeped below the land surface. Until about 1930, the oilfield waters were disposed into local drainage, frequently killing fish and even surface vegetation. After 1930, it became common practice to evaporate the water in earthen pits or inject it into the producing sand or another deep aquifer. The primary concern in such disposal practice is to remove all oil and basic sediment from the waters before pumping them into injection wells to prevent clogging of the pore spaces in the formation receiving the waste water. Chemical compatibility of waste water and host aquifer water also must be ensured.

Waters produced with petroleum are growing in importance. In years past, these waters were considered waste and had to be disposed of in some manner. Injection of these waters into the petroleum reservoir rock serves three purposes: it produces additional petroleum (secondary recovery), it utilizes a potential pollutant, and in some areas it controls land subsidence.

The volume of water produced with petroleum in the U.S. is large. In 1981 domestic oil production was about 8.6×10^6 B/D and the amount of water produced with the oil ranges from 4 to 5 times the oil production. Therefore, the water production, assuming a factor of 4.5, would be about 38.7×10^6 B/D.

Secondary and tertiary oil recovery processes that use water injection usually result in the production of even more water along with the oil. To inject these waters into reservoir rocks, suspended solids and oil must be removed from the waters to prevent plugging of the porous formations. Water injection systems require separators, filters, and, in some areas, deoxygenating and bacteria control equipment with chemical and physical methods to minimize corrosion and plugging in the injection system.

In waterflooding most petroleum reservoirs, the volume of produced water is not sufficient to recover the additional petroleum efficiently. Therefore, supplemental water must be added to the petroleum reservoir. The use of waters from the other sources requires that the blending of produced water with supplemental water must yield a chemically stable mixture so that plugging solids will not be formed. For example, a produced water containing considerable calcium should not be mixed with a water containing considerable carbonate because calcium carbonate may precipitate and prevent injection of the floodwater. The design and successful operation of a secondary or tertiary recovery operation requires a thorough knowledge of the composition of the waters used.

Chemical analyses of waters produced with oil are useful in oil production problems, such as identifying the

source of intrusive water, planning waterflood and saltwater disposal projects, and treating to prevent corrosion problems in primary, secondary, and tertiary recovery. Electrical well-log interpretation requires a knowledge of the dissolved solids concentration and composition of the interstitial water. Such information also is useful in correlation of stratigraphic units and of the aquifers within these units, and in studies of the movement of subsurface waters. It is impossible to understand the processes that accumulate petroleum or other minerals without insight into the nature of these waters.

Sampling

The composition of subsurface water commonly changes with depth and also laterally in the same aquifer. Changes may be brought about by the intrusion of other waters, and by discharge from and recharge to the aquifer. It is thus difficult to obtain a representative sample of a given subsurface body of water. Any one sample is a very small part of the total mass, which may vary widely in composition. Therefore, it is generally necessary to obtain and analyze many samples. Also, the samples may change with time as gases come out of solution and supersaturated solutions approach saturation.

The sampling sites should be selected, if possible, to fit into a comprehensive network to cover an oil-productive geologic basin.

There is a tendency for some oilfield waters to become more diluted as the oil reservoir is produced. Such dilution may result from the movement of dilute water from adjacent compacting clay beds into the petroleum reservoir as pressure declines with the continued removal of oil and brine.¹⁵

The composition of oilfield water varies with the position within the geologic structure from which it is obtained. In some cases the salinity will increase upstructure to a maximum at the point of oil/water contact.

Few of the samples collected by drillstem test (DST) are truly representative formation-water samples. During drilling, the pressure in the wellbore is intentionally maintained higher than that in the formations. Filtrate from the drilling mud seeps into the permeable strata, and this filtrate is the first liquid to enter the test tool.

The most truly representative formation-water sample usually is obtained after the oil well has produced for a period of time and all extraneous fluids adjacent to the wellbore have been flushed out. Samples taken immediately after the well is completed may be contaminated with drilling fluids and/or with well completion fluids, such as filtrate from cement, tracing fluids, and acids, which contain many different chemicals.

Sampling methods are discussed in publications of the American Petroleum Inst. (API),¹⁶ American Soc. for Testing and Materials (ASTM),¹⁷ and the Natl. Assn. of Corrosion Engineers (NACE).¹⁸

Drillstem Test

The DST, if properly made, can provide a reliable formation water sample. It is best to sample the water after each stand of pipe is removed. Normally, the total dissolved solids (TDS) content will increase downward and become constant when pure formation water is ob-

tained. A test that flows water will give even higher assurance of an uncontaminated sample. If only one DST water sample is taken for analysis, it should be taken just above the tool, since this is the last water to enter the tool and is least likely to show contamination.

Analyses of water obtained from a DST of Smackover limestone water in Rains County, TX, show how errors can be caused by improper sampling of DST water. Analyses of top, middle, and bottom samples taken from a 50-ft fluid recovery show an increase in salinity with depth in the drillpipe, indicating that the first water was contaminated by mud filtrate.¹⁹ Thus, the bottom sample was the most representative of Smackover water.

Sample Procedure

No single procedure is universally applicable for obtaining a sample of oilfield water. For example, information may be desired concerning the dissolved gas or hydrocarbons in the water or the reduced species present, such as ferrous or manganous compounds. Sampling procedures applicable to the desired information must be used.

Some of the special information and sample location cases, with appropriate procedures or references cited for proper sampling, follow.

Sample Containing Dissolved Gas. Knowledge of certain dissolved hydrocarbon gases is used in exploration.^{20,21}

Sampling at the Flowline. Another method of obtaining a sample for analysis of dissolved gases is to place a sampling device in a flowline. Fig. 24.1 illustrates such a device. The device is connected to the flowline, and water is allowed to flow into and through the container, which is held above the flowline, until 10 or more volumes of water have flowed through. The lower valve on the sample container is closed and the container removed. If any bubbles are present in the sample, the sample is discarded and a new one is obtained.

Sampling at the Wellhead. It is common practice in the oil industry to obtain a sample of formation water from a sampling valve at the wellhead. A plastic or rubber tube can be used to transfer the sample from the sample valve into the container (usually plastic). The source and sample container should be flushed to remove any foreign material before a sample is taken. After flushing the system, the end of the tube is placed in the bottom of the container, and several volumes of fluid are displaced before the tube is removed slowly from the container and the container is sealed. Fig. 24.2 illustrates a method of obtaining a sample at the wellhead. An extension of this method is to place the sample container in a larger container, insert the tube to the bottom of the sample container, allow the brine to overflow both containers, and withdraw the tube and cap the sample under the fluid.

At pumping wellheads the brine will surge out in heads and be mixed with oil. In such situations a larger container equipped with a valve at the bottom can be used as a surge tank or an oil-water separator or both. To use this device, place the sample tube in the bottom of the large container, open the wellhead valve, rinse the large container with the well fluid, allow the large container to

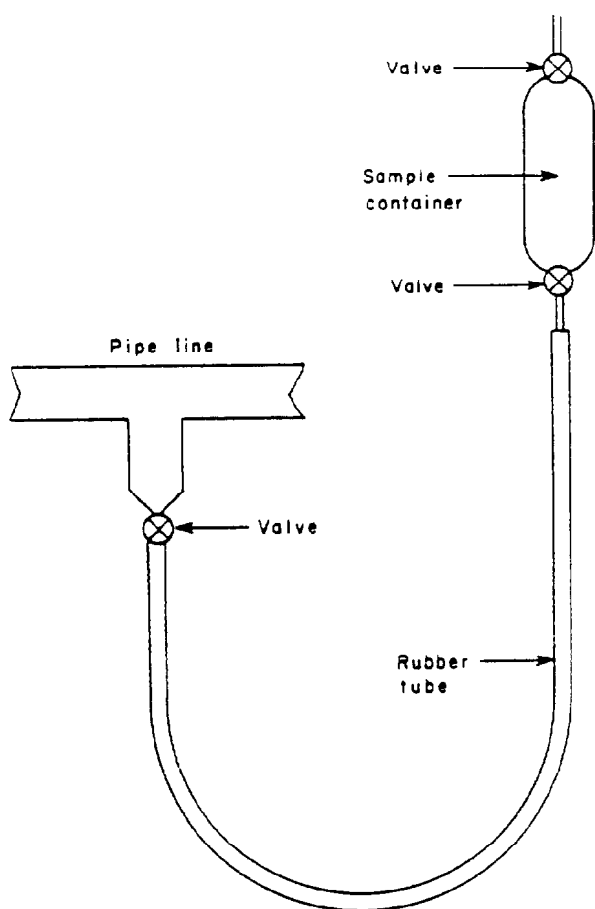


Fig. 24.1—Flowline sampler.

fill, and withdraw a sample through the valve at the bottom of the large container. This method will serve to obtain samples that are relatively oil-free.

Field Filtered Sample. In some studies it is necessary to obtain a field filtered sample. The filtering system shown in Fig. 24.3 was designed and has proved successful for various applications.

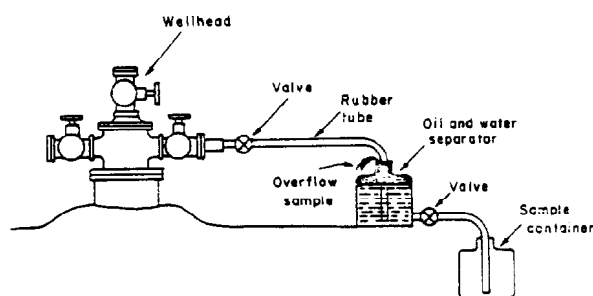


Fig. 24.2—Example of the method used for obtaining a sample at the wellhead.

This filtering system is simple and economical. It consists of a 50-mL disposable syringe, two check valves, and an inline-disk-filter holder. The filter holder takes size 47-mm diameter, 0.45- μ m pore size filters, with the option of a prefilter and depth prefilter.

After the oilfield brine is separated from the oil, the brine is drawn from the separator into the syringe. With the syringe, it is forced through the filter into the collection bottle. The check valves allow the syringe to be used as a pump for filling the collection bottle. If the filter becomes clogged, it can be replaced in a few minutes. About 2 minutes are required to collect 250 mL of sample. Usually two samples are taken, with the one being acidified to pH 3 or less with concentrated HCl or HNO₃. The system can be cleaned easily or flushed with brine to prevent contamination.

Sample for Stable-Isotope Analysis. Stable isotopes have been used in several research studies to determine the origin of oilfield brines.²²⁻²⁴

Sample for Determining Unstable Properties or Species. A mobile analyzer was designed to measure pH, Eh (redox potential), O₂, resistivity, S⁼, HCO₃⁻, CO₃⁼, and CO₂ in oilfield water at the wellhead. When oilfield brine samples are collected in the field and transported to the laboratory for analysis, many of the unstable constituents change in concentration. The amount of change depends on the sampling method, sample storage, ambient conditions, and the amounts of the constituents in the original sample. Therefore an analysis of the brine at the wellhead is necessary to obtain reliable data.²⁵

Sample Containers. Containers that are used include polyethylene, other plastics, hard rubber, metal cans, and borosilicate glass. Glass will adsorb various ions such as iron and manganese, and may contribute boron or silica to the aqueous sample. Plastic and hard rubber containers are not suitable if the sample is to be analyzed to determine its organic content. A metal container is used by some laboratories if the sample is to be analyzed for dissolved hydrocarbons such as benzene.

The type of container selected depends on the planned use of the analytical data. Probably the more satisfactory container, if the sample is to be stored for some time

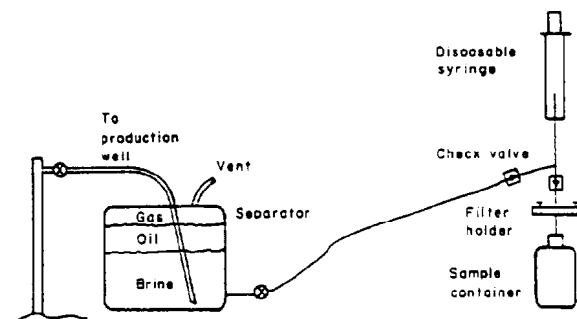


Fig. 24.3—Example of field filtering equipment.

TABLE 24.1—DESCRIPTION NEEDED FOR EACH OILFIELD WATER SAMPLE

Sample Number _____	Field _____
Farm or lease _____	Well No. _____ in the _____
of Section _____	Township _____ Range _____
County _____	State _____ Operator _____
Operator's address (main office) _____	
Sample obtained by _____	Date _____
Address _____	Representing _____
Sample obtained from (lead line, separatory flow tank, etc.) _____	
Completion date of well _____	
Name of productive zone from which sample is produced _____	
Sand _____	Shale _____ Lime _____ Other _____
Name of productive formation _____	Names of formations well passes through _____
Depths: Top of formation _____	Bottom of formation _____
Top of producing zone _____	Bottom of producing zone _____
Top of depth drilled _____	Present depth _____
Bottomhole pressure and date of pressure _____	
Bottomhole temperature _____	
Date of last workover _____	Are any chemicals added to treat well _____ If yes, what? _____
Well production _____	Initial _____ Present _____ Casing service record: _____
Oil, B/D _____	_____
Water, B/D _____	_____
Gas, cu ft/D _____	_____
Method of production (primary, secondary, or tertiary) _____	

Remarks: (such as casing leaks, communication or other pay in same well, lease or field)

before analysis. is the polyethylene bottle. Not all polyethylenes are satisfactory because some contain relatively high amounts of metal contributed by catalysts in their manufacture. The approximate metal content of the plastic can be determined by a qualitative emission spectrographic technique. If the sample is transported during freezing temperatures, the plastic container is less likely to break than is glass.

Tabulation of Sample Description. Information such as that in Table 24.1 should be obtained for each sample of oilfield water.

Analysis Methods for Oilfield Waters

Analytical methods for analyzing oilfield waters are improving with respect to precision, accuracy, and speed. There have been at least two groups trying to standardize methods of oilfield water analysis during the past 20 years. They are the API and ASTM. The API published Recommended Practice 45 for Analysis of Oilfield Waters.¹⁶

The ASTM's Committee D-19 standardizes methods of analyzing oilfield brines. Methods standardized by rigorous round-robin testing by several laboratories and subsequent ASTM committee balloting procedures are found in Ref. 17.

Table 24.2 illustrates the analyses for various properties or constituents of oilfield water. Methods to determine most of these properties or constituents can be found in Refs. 16, 17, and 25 through 30.

Chemical Properties of Oilfield Waters

Oilfield waters are analyzed for various chemical and physical properties. Most oilfield waters contain a variety of dissolved inorganic and organic compounds.

TABLE 24.2—GEOCHEMICAL WATER ANALYSES*

	Produced Water	Injection Water	Steam Generation Water	Disposal Water
pH	X	X	X	X
Eh	O	X		O
Specific resistivity	X			
Specific gravity	X	X	X	X
Bacteria	O	X		O
Barium	X	X		X
Bicarbonate	X	X	X	X
Boron	O			
Bromide	O			
Calcium	X	X	X	X
Carbonate	X	X	X	X
Carbon dioxide	O	X	X	O
Chloride	X	X	X	X
Hydrogen sulfide	O	X		O
Iodine	O			
Iron	X	X	X	O
Magnesium	X	X	X	X
Manganese	O	O	O	O
Oxygen	O	X	O	O
Potassium	O			
Residual hydrocarbons		X		O
Sodium	X	O	O	O
Silica	O	X	X	O
Strontium	O	X	O	O
Sulfate	X	X	X	X
Suspended solids		X		X
Total dissolved solids	X	X	X	X

*X = usually requested.
O = sometimes requested

TABLE 24.3—CHARACTERISTICS OF SOME WATERS PRODUCED FROM APPALACHIAN FIELDS

Number of Analyses*	System	Formation	Subsurface Depth (ft)	Constituents (mg/L)			
				Ca	Mg	Na	K
Kentucky ^{23,24}							
4	Devonian-Silurian	Corniferous	400 to 1,506	1,520	670	9,520	120
8	Mississippian	McClosky	1,390 to 2,618	12,160	3,350	44,740	1,290
				1,700	990	15,700	ND**
5	—	Jett	939 to 1,534	3,400	2,180	33,600	ND
				370	130	1,860	ND
				830	320	15,500	ND
Ohio ^{35,36}							
8	Mississippian	Blue Lick	1,843 to 3,263	1,390	650	10,500	150
7	Ordovician	Sub Trenton	3,820 to 5,815	9,230	2,900	33,600	1,510
				11,000	2,700	39,500	0
8	Mississippian	Second Water Big Lime	2,175 to 3,270	44,000	6,600	58,600	2,890
				32,300	5,180	36,000	1,950
10	Upper Devonian	First Water Big Lime	5,175 to 5,300	51,200	10,200	60,700	2,330
				25,900	4,100	21,600	270
12	Mississippian	Berea	401 to 1,592	29,600	10,000	86,400	2,370
				4,600	1,500	25,000	120
				11,900	3,000	43,900	220
Pennsylvania ^{37,38}							
10	Devonian	Bradford	—	40	30	1,600	—
7	Devono-Mississippian	Venango	—	32,400	1,940	39,500	—
				7,000	70	3,600	—
12	Devonian	Bradford III	—	82,000	2,020	16,000	—
				420	40	300	—
				16,900	2,530	39,200	—
West Virginia ³⁹							
29	Mississippian	Big Injun	1,390 to 3,215	30	300	50	10
6	Mississippian	Squaw	1,908 to 2,019	1,730	3,910	52,200	750
				630	200	6,300	290
21	Mississippian	Maxton	1,287 to 3,259	8,920	2,250	38,100	340
				100	40	3,800	30
44	Pennsylvanian	Salt Sand	450 to 1,960	15,300	2,740	35,100	660
				400	340	2,500	60
43	Devonian	Oriskany	3,036 to 8,089	20,600	2,650	50,900	3,680
				2,500	480	34,000	200
				33,600	3,800	98,300	6,900

*Upper figure in each column is minimum value and lower figure is maximum value for number of analyses indicated.

**Not determined

However, oil producers usually are interested in only a few of the macro properties. This is understandable because oil producers wish to spend the least amount of money possible. Therefore, they will look at only the properties that are necessary to evaluate any treatment for reinjection to recover more oil or to dispose of the oilfield waters.

Composition of Oilfield Waters

The composition of oilfield waters varies from relatively dilute waters to heavy brines. Several thousand oilfield water analyses are available on computerized files.³¹ Tables 24.3 through 24.14 show characteristics of produced waters, and much of the text was taken from the 1962 edition of this book.³²

The tabulated data on water analyses following are listed alphabetically in order of general oil-productive areas of the U.S., Canada, and Venezuela, rather than by the smaller subdivisions of basins, geologic provinces, or geosynclines. An exception to this is the Illinois

basin, a large area not generally otherwise identifiable. This division has been made arbitrarily for convenience and because of the lack of a uniform system and is not intended as a precedent for any system of classification. The states or provinces from which reliable analyses were available are listed alphabetically in the tables under each area.

The reader is referred to the original indicated sources of analytical data for more complete information.

Appalachian Area. The Appalachian area was the first in the U.S. in which petroleum was produced commercially and is one of the best known and studied geologic features of North America. Table 24.3 gives the characteristics of some waters produced from Appalachian fields.³³⁻³⁹

Petroleum and associated water are produced from more than 50 strata in systems from the Cambrian to the Permian. Most of the productive strata are sandstones, although some limestones are productive. Many of the

TABLE 24.3—CHARACTERISTICS OF SOME WATERS PRODUCED FROM APPALACHIAN FIELDS (continued)

Constituents (mg/L)							Specific Gravity 60°/60°	TDS (mg/L)
Ba	Sr	HCO ₃	SO ₄	Cl	I	Br		
—	0	20	10	19,600	Trace	120	1.022	31,600
—	630	680	690	93,900	10	820	1.120	158,330
—	ND	60	910	31,700	ND	ND	1.036	51,060
—	ND	230	3,320	61,000	ND	ND	1.070	103,730
—	ND	120	50	14,000	ND	ND	1.020	16,530
—	ND	250	3,200	26,000	ND	ND	1.039	46,100
—	Trace	110	30	18,200	0	0	1.025	31,030
—	315	380	380	77,600	10	570	1.089	125,180
—	0	20	150	113,500	10	150	1.150	167,030
—	900	510	490	189,400	30	600	1.224	304,020
—	0	60	30	113,000	ND	580	1.151	189,100
—	1,240	140	100	216,300	ND	1,900	1.240	344,110
—	Trace	30	210	114,200	ND	1,230	1.125	167,540
—	Trace	230	550	193,100	ND	2,100	1.211	324,350
—	0	20	0	52,700	ND	320	1.063	84,260
—	1,800	20	60	93,400	ND	520	1.115	154,820
—	—	30	30	1,100	—	—	—	2,790
—	—	560	1,080	83,200	—	—	—	158,680
—	—	0	260	30,900	—	—	—	41,830
—	—	0	1,270	75,300	—	—	—	176,590
—	—	0	0	490	—	—	—	1,260
—	—	40	1,080	97,600	—	—	—	157,350
Trace	10	10	5	70	Trace	Trace	1.001	475
300	830	70	320	121,000	20	1,750	1.149	191,580
0	0	0	0	11,330	2	80	1.010	18,832
540	70	40	10	81,130	10	700	1.101	132,110
10	5	10	20	5,830	Trace	Trace	1.007	9,825
1,500	220	1,680	530	89,900	10	500	1.115	148,090
10	30	10	5	2,500	Trace	5	1.004	5,810
870	210	1,330	400	125,000	10	780	1.159	206,430
20	Trace	Trace	10	44,300	2	40	1.059	51,552
760	1,570	270	900	170,000	30	2,500	1.219	318,630

sandstones are nonuniform and discontinuous, although the Big Injun and Berea sands have been traced across wide areas. The oil-producing states included in the Appalachian area from which analyses were available are Kentucky, Ohio, Pennsylvania, and West Virginia. The concentrations of dissolved salts in waters produced with petroleum range from a few hundred to more than 300,000 mg/L.

California. In different fields of California, oil is produced from many reservoirs, ranging in age from Cretaceous to Pleistocene. Sandstones and sands are the principal productive rocks. Many of the formations are of massive thickness, and much folding and faulting are evident. In general, mineralized water produced with petroleum from California reservoirs is by no means as concentrated as that from reservoirs in many other areas, especially the midcontinent. Table 24.4 gives the characteristics of some water produced from California fields.^{40,41}

U.S. Gulf Coast. For many years since the Spindletop dome was discovered in 1901, copious quantities of oil have been produced from Tertiary and Quaternary formations on the flanks, in the caprock, and in structures above the caprock of massive salt domes, usually considered intrusive in nature. During recent years, offshore drilling has focused attention on drilling off the coasts of Louisiana and Texas. Some waters produced from gulf coast fields are quite fresh; others have concentrations of dissolved salts as high as 170,000 mg/L (Table 24.5).⁴²⁻⁴⁴

Illinois Basin. The Illinois basin, divided roughly into halves by the LaSalle anticline, comprises much of Illinois and southwestern Indiana. Oil is produced here from many fields, principally from Pennsylvanian and Mississippian sandstones and, to a smaller extent, from limestones. TDS in the produced waters range from about 1,000 to more than 160,000 mg/L (Table 24.6).⁴⁵

TABLE 24.4—CHARACTERISTICS OF SOME WATERS PRODUCED FROM CALIFORNIA FIELDS

Number of Analyses*	System	Formation	Subsurface Depth (ft)	Constituents (mg/L)							TDS (mg/L)
				Ca	Mg	Na	CO ₃	HCO ₃	SO ₄	Cl	
17	Tertiary	Coalinga	1,104 to 1,916	20	10	40	50	180	190	90	580
10	Tertiary	Midway	1,495 to 3,250	390	340	3,290	480	360	7,260	2,520	14,640
				20	10	910	0	180	10	1,010	2,140
5	Tertiary	Sunset	2,270 to 3,550	2,890	690	13,250	360	360	1,380	23,550	42,120
				60	20	3,650	0	50	5	4,360	8,145
4	Tertiary	Kern River	400 to 3,000	1,280	570	11,650	90	4,270	40	21,420	39,320
				10	10	50	0	0	0	10	80
2	Tertiary	Lost Hills	—	20	20	1,550	390	70	20	60	2,130
				200	140	4,770	150	0	20	7,740	13,020
26	Tertiary	Maricopa	—	220	230	7,640	460	0	630	11,950	21,120
				200	10	1,300	0	4	2	1,170	2,686
18	Tertiary	Zone A	—	2,900	1,300	15,015	510	1,020	110	27,100	47,995
				10	3	2,050	0	1,700	1	1,300	5,064
				80	140	7,090	340	3,900	90	9,560	21,200

*Upper figure in each column is minimum value and lower figure is maximum value for number of analyses indicated. ^{40,41}

Midcontinent Area. The midcontinent oil productive area is the largest geographically of all oil-productive areas in the U.S. For purposes of this section, it is considered to include Arkansas, Kansas, northern Louisiana, Missouri, Nebraska, Oklahoma, and all of Texas except the gulf coast fields.

Oil and associated brines are produced from many sandstones and limestones, as well as from other types of formations, in geologic systems ranging from the Cambrian through the Upper Cretaceous. Waters produced with petroleum from midcontinent fields have a wide range of concentration of dissolved salts, from little more than 1,000 to more than 350,000 mg/L. Tables 24.7 through 24.9 present the characteristics of some produced waters from the midcontinent fields of Kansas, Oklahoma, and Texas. ⁴⁶⁻⁵⁴

Rocky Mt. Area. Petroleum is produced in Colorado, Montana, New Mexico, Utah, and Wyoming from many fields in the Rocky Mt. area. The principal production is from rocks of the Cretaceous system, although oil and

associated waters also are produced from Jurassic, Permian, Pennsylvanian, and Mississippian rocks. Produced waters from Rocky Mt. fields have comparatively low concentrations of dissolved salts and often are characterized by comparatively high concentrations of bicarbonate. Tables 24.10 and 24.11 give the characteristics of some waters produced from Rocky Mt. fields of Colorado, Montana, and Wyoming. ⁵⁵⁻⁵⁹

Canada. The principal oil-productive areas in Canada are the lower Ontario Peninsula, where oil is produced from rocks ranging from Ordovician to Devonian age, and the western provinces, principally Alberta, Saskatchewan, and the Northwest Territories. Reservoir rocks in western Canada range in age from Devonian to Cretaceous. Although many of the waters produced with petroleum have quite low concentrations of dissolved salts, others are quite concentrated. Tables 24.12 and 24.13 present the characteristics of some waters from Canadian fields in Alberta, Manitoba, and Saskatchewan. ⁶⁰⁻⁶⁵

TABLE 24.5—CHARACTERISTICS OF SOME WATERS PRODUCED FROM GULF COAST FIELDS (TEXAS)

Number of Analyses*	System	Formation or field	Subsurface Depth (ft)	Constituents (mg/L)						TDS (mg/L)
				Ca	Mg	Na	HCO ₃	SO ₄	Cl	
42	Tertiary	Frio	2,579 to 11,400	200	50	2,240	30	0	3,180	5,700
5	—	Norm Coastal	406 to 1,100	5,100	1,000	40,600	990	110	69,100	116,900
				30	10	60	230	3	20	353
6	Oligocene	Goose Creek	1,305 to 3,296	80	30	1,330	770	160	2,130	4,500
				450	120	3,800	70	120	6,300	10,860
6	Upper Eocene	Humble	775 to 3,200	1,430	540	18,200	400	210	33,700	54,480
				380	100	3,600	290	Trace	6,100	10,470
5	Oligocene	Damon Mound	250 to 3,470	2,200	750	61,000	600	1,750	105,000	171,300
				530	70	6,700	70	270	11,300	18,900
4	Pliocene-Miocene	Barber Hill Dome	—	2,100	400	40,800	280	3,010	63,400	109,990
				40	10	340	70	16	110	570
6	—	Powell-Mexia	—	200	90	30	550	230	610	1,710
				90	200	4,460	30	10	6,700	11,490
				920	700	12,730	240	210	21,600	36,400

*Upper figure in each column is minimum value and lower figure is maximum value for number of analyses indicated. ⁴²⁻⁴⁴

TABLE 24.6—CHARACTERISTICS OF SOME WATERS PRODUCED FROM ILLINOIS FIELDS

Number of Analyses*	System	Formation or field	Subsurface Depth (ft)	Constituents (mg/L)						TDS (mg/L)
				Ca	Mg	Na	HCO ₃	SO ₄	Cl	
12	Mississippian	Waltersburg	1.994	1,200	640	22,660	30	0	38,300	62,830
			2,437	2,970	1,020	32,220	390	1,620	56,700	93,920
18	Mississippian	Tar Springs	1,125	960	10	240	20	0	700	62,930
			2,596	6,020	1,730	42,810	1,050	980	76,000	128,590
57	Mississippian	Cypress	1,045	840	510	3,970	10	10	25,800	31,140
			2,960	6,600	1,680	47,900	1,660	3,840	83,200	143,940
17	Ordovician	Trenton	672 to 4,000	50	40	340	20	30	200	680
				7,500	1,830	41,830	960	1,350	82,400	135,870
134	Mississippian	St. Genevieve	1,104 to 3,519	1,900	910	8,740	20	30	14,000	25,600
				18,430	3,460	47,660	1,470	2,990	95,400	167,940

*Upper figure in each column is minimum value and lower figure is maximum value for number of analyses indicated.⁴⁵

Venezuela. The principal productive formations in Venezuela are Tertiary sandstones and Cretaceous limestones. In general, the various waters produced with petroleum have low concentrations of dissolved salts (Table 24.14).⁶⁶⁻⁶⁹

Inorganic Constituents

Petroleum companies often analyze oilfield waters to determine their major dissolved inorganic constituents. The major constituents usually are sodium, calcium, magnesium, chloride, bicarbonate, and sulfate. The analytical data are used in studies such as water identification, log evaluation, water treatment, environmental impact, geochemical exploration, and recovery of valuable minerals.²⁶

Cations

The presence of various cations and anions in oilfield waters can cause solubility, acidity, and redox (Eh) potential changes as well as the precipitation and adsorption of some constituents. The major cations in most

oilfield waters are sodium, calcium, and magnesium. The concentrations of these ions can range from less than 10,000 mg/L for sodium, and from less than 1,000 mg/L to more than 30,000 mg/L for calcium and/or magnesium.

Other cations that often are present in oilfield waters in concentrations greater than 10 mg/L are potassium, strontium, lithium, and barium. Some oilfield waters contain concentrations in excess of 10 mg/L of aluminum, ammonium, iron, lead, manganese, silicon, and zinc.^{26,70,71}

Anions

The major anion in most oilfield waters is chloride. The chloride concentration can range from less than 10,000 to more than 200,000 mg/L. There are exceptions to this—e.g., some Venezuelan oilfield waters contain more bicarbonate than chloride.⁷²

Most oilfield waters contain bromide and iodide. The concentrations of these anions range from less than 50 to more than 6,000 mg/L for bromide and from less than 10

TABLE 24.7—CHARACTERISTICS OF SOME WATERS PRODUCED FROM MID-CONTINENT FIELDS (KANSAS)

Number of Analyses*	System	Formation	Subsurface Depth (ft)	Constituents (mg/L)										Specific Gravity (60°/60°)	TDS (mg/L)
				Ca	Mg	Na	Ba	HCO ₃	SO ₄	Cl	I	Br			
87	Pennsylvanian	Kansas City Lansing	1,228 to 3,409	2,040	840	16,940	4	5	0	34,100	2	30	1,040	53,959	
				16,000	3,950	77,000	70	450	2,160	156,800	15	400	1,159	256,830	
8	Ordovician	Wilcox	3,500 to 3,600	790	5,560	10,800	0	20	80	10,870	Trace	80	1,015	28,120	
				14,400	68,500	142,500	0	530	300	142,600	3	350	1,140	369,180	
123	Ordovician	Arbuckle	2,750 to 3,770	700	240	6,820	0	50	0	12,300	0	Trace	1,014	20,180	
				19,800	10,900	34,450	0	640	2,700	79,200	Trace	60	1,091	145,060	
76	Ordovician	Viola	2,091 to 4,141	620	230	5,240	0	10	20	330	0	5	1,012	6,455	
				11,000	3,110	52,000	0	650	1,180	112,700	10	90	1,116	180,740	
27	Pennsylvanian	Bartlesville	625 to 3,200	420	180	7,550	0	10	1	12,600	2	20	1,016	20,782	
				12,100	3,480	69,600	10	520	750	141,200	10	200	1,141	224,870	
20	Mississippian	Mississippian	1,010 to 4,679	560	220	9,150	0	30	0	14,400	1	2	1,017	24,363	
				12,900	2,660	59,300	20	670	3,540	122,000	60	3	1,140	201,153	
8	Basal Pennsylvanian	Conglomerate	3,320 to 3,469	1,000	360	11,600	0	0	0	20,700	0	200	1,023	33,850	
				8,480	2,000	47,000	0	180	700	58,300	Trace	400	1,105	116,660	
24	Pennsylvanian	Chat	2,697 to 3,365	3,120	640	24,400	0	30	0	42,700	2	10	1,068	70,902	
				13,480	1,950	66,500	0	130	2,200	137,700	3	420	1,143	222,383	
12	Silurian	Hunton	2,390 to 2,893	230	90	3,610	0	70	100	5,300	0	10	1,007	9,410	
				5,220	1,460	36,600	3	480	1,230	68,400	2	70	1,075	113,460	
10	Basal Pennsylvanian	Gorham	3,300 to 3,854	920	280	6,560	0	160	40	11,300	0	5	1,019	19,265	
				3,960	1,030	17,100	10	840	3,010	36,000	0	10	1,045	58,940	
9	Pennsylvanian	Prue	1,032 to 2,400	2,310	720	14,300	0	20	0	28,000	0	0	1,033	45,350	
				11,300	2,610	68,700	10	330	50	138,900	0	0	1,139	221,900	
12	Cambrian	Reagan	3,175 to 3,609	1,390	310	9,300	0	80	30	14,700	ND	ND	1,021	26,810	
				5,250	1,370	43,000	0	410	2,570	76,900	ND	ND	1,088	126,930	

*Upper figure in each column is minimum value and lower figure is maximum value for number of analyses indicated.^{46,47}

TABLE 24.8—CHARACTERISTICS OF SOME WATERS PRODUCED FROM MID-CONTINENT FIELDS (OKLAHOMA)

Number of Analyses*	System	Formation	Subsurface Depth (ft)	Constituents (mg/L)							Specific Gravity (60°/60°)	TDS (mg/L)
				Ca	Mg	Na	Ba	HCO ₃	SO ₄	Cl		
75	Pennsylvanian	Bartlesville	4,489 to 5,524	1,900	910	12,100	0	0	0	24,100	1.031	39,010
94	Ordovician	Wilcox	3,436 to 7,233	19,000	2,740	83,800	730	300	890	144,000	1.175	251,460
				6,800	1,400	48,300	0	20	0	91,300	1.103	147,820
25	Pennsylvanian	Layton	1,240 to 4,800	18,500	3,300	80,200	130	160	720	163,000	1.178	266,010
				5,300	1,800	31,300	0	10	0	34,900	1.075	73,310
28	Ordovician	Arbuckle	542 to 6,094	18,900	4,300	79,000	380	80	510	160,000	1.179	263,170
				2,200	900	14,000	0	0	0	33,000	1.034	50,100
19	Pennsylvanian	Cromwell	1,480 to 5,430	18,800	2,700	63,800	110	850	1,880	127,000	1.147	214,140
				4,600	1,400	34,600	1	0	0	65,000	1.073	105,701
12	Pennsylvanian	Burgess	1,800 to 2,490	11,900	4,300	51,500	20	310	1,130	113,500	1.130	182,660
				5,900	2,000	42,500	1	15	0	81,600	1.091	132,016
22	Mississippian	Mississippi	1,837 to 4,872	13,300	2,600	57,700	200	120	200	115,000	1.129	189,120
				6,400	2,000	43,600	2	10	24	84,200	1.095	136,212
18	Mississippian	Misener	3,927 to 5,977	22,400	2,500	72,000	30	80	430	157,000	1.173	254,440
				4,600	1,100	29,500	0	30	60	55,400	1.066	90,690
17	Pennsylvanian	Pennsylvanian	1,258 to 6,025	18,400	3,200	76,000	10	110	1,920	156,000	1.173	250,640
				1,700	600	17,600	10	20	0	29,800	1.039	49,730
10	Ordovician	Simpson	1,213 to 6,495	15,800	3,100	61,300	280	90	2,750	121,000	1.134	204,320
				5,600	1,200	24,400	0	0	0	50,900	1.059	82,100
22	Pennsylvanian	Skinner	1,030 to 4,567	17,600	3,000	71,900	2	110	440	140,000	1.159	233,042
				6,200	1,500	31,700	0	10	30	64,100	1.075	103,540
22	Pennsylvanian	Booch	1,876 to 2,300	18,700	3,200	67,400	10	130	450	139,000	1.157	228,890
				6,600	1,500	42,500	0	5	0	90,000	1.103	141,050
22	Siluro-Devonian	Hunton	3,197 to 5,021	12,700	2,500	56,500	240	140	680	117,000	1.131	189,760
				300	80	4,000	0	15	0	8,200	1.012	11,995
27	Pennsylvanian	Red Fork	2,403 to 4,650	28,900	4,300	75,900	170	660	7,010	142,000	1.155	258,948
				9,700	1,700	42,800	5	3	0	101,000	1.115	155,208
12	Ordovician	Viola	3,458 to 5,004	19,600	2,600	71,700	220	170	370	149,000	1.164	243,660
				200	60	2,900	0	40	0	4,400	1.005	7,600
20	Pennsylvanian	Prue	2,267 to 3,587	16,000	2,400	62,000	10	940	980	122,000	1.137	204,330
				8,500	1,300	43,400	5	50	30	86,300	1.110	139,885
13	Pennsylvanian	Healdton	982 to 3,163	11,700	3,100	72,900	20	120	480	142,000	1.158	230,320
				740	230	10,800	0	20	2	18,600	1.022	30,392
15	Pennsylvanian	Tonkawa	2,417 to 3,254	7,300	2,900	27,900	50	380	40	63,600	1.076	102,170
				14,000	2,200	23,800	0	0	130	132,800	1.160	172,930
24	Pennsylvanian	Burbank	790 to 5,000	17,400	3,100	76,400	5	50	370	156,200	1.171	253,525
				10,900	1,800	43,200	2	20	15	99,300	1.109	155,235
15	Pennsylvanian	Dutcher	1,882 to 3,218	20,000	3,500	69,000	40	130	260	149,000	1.163	241,930
				5,500	900	32,000	0	50	40	45,500	1.073	86,900
14	Ordovician	Bromide	2,173 to 7,569	13,900	2,000	54,700	10	130	760	108,000	1.122	179,500
				700	400	11,500	10	0	0	19,500	1.024	32,110
				22,400	3,500	80,500	450	500	920	167,000	1.183	275,270

*Upper figure in each column is minimum value and lower figure is maximum value for number of analyses indicated. ^{48,49}**TABLE 24.9—CHARACTERISTICS OF SOME WATERS PRODUCED FROM MID-CONTINENT FIELDS (TEXAS)**

Number of Analyses*	System	Formation	Subsurface Depth (ft)	Constituents (mg/L)						Specific Gravity (60°/60°)	TDS (mg/L)
				Ca	Mg	Na	HCO ₃	SO ₄	Cl		
North-Central Texas ⁵⁰⁻⁵²											
33	Upper Pennsylvanian	Gose	—	20	5	530	1	1	460	ND**	1,017
8	Upper Pennsylvanian	Dyson	1,884 to 2,081	10,700	2,450	48,200	610	690	97,900	ND	160,550
				14,400	2,440	58,300	0	300	122,200	ND	197,640
7	Upper Pennsylvanian	Landreth	2,540 to 2,668	16,700	2,860	66,800	0	520	139,800	ND	226,680
				10,200	2,030	52,500	0	630	106,000	ND	171,360
13	Upper Cretaceous	Woodbine	3,844 to 4,446	13,800	2,440	61,000	10	740	119,000	ND	196,990
				3,100	370	32,100	130	250	57,500	ND	93,450
				7,900	600	62,900	410	370	112,500	ND	184,680
North and West Texas ^{53,54}											
21	Pennsylvanian	Cisco	700 to 1,950	500	160	6,030	0	10	10,000	1.015	16,700
35	Pennsylvanian	Canyon	2,200 to 7,000	23,100	3,000	60,400	180	400	134,000	1.157	221,080
				2,200	640	15,700	10	40	31,400	1.044	50,010
47	Cambro-Ordovician	Ellenberger	3,800 to 8,370	14,000	2,300	57,100	650	4,840	109,500	1.145	188,390
				1,700	350	12,000	4	20	25,300	1.035	39,374
56	Pennsylvanian	Strawn	1,700 to 6,900	22,300	2,850	55,700	1,840	2,140	130,500	1.173	214,330
				3,200	810	25,500	2	2	82,900	1.105	112,414
50	Permian	San Andres	—	21,300	3,500	74,300	710	710	161,800	1.212	262,320
				740	310	4,400	210	350	19,000	1.033	25,010
42	Permian	Big Lime	—	19,800	7,900	67,000	1,840	4,900	140,500	1.154	241,940
				250	200	210	0	160	890	ND	1,710
				9,800	3,700	122,500	0	8,600	212,000	ND	356,600

*Upper figure in each column is minimum value and lower figure is maximum value for number of analyses indicated.

**Not determined.

TABLE 24.10—CHARACTERISTICS OF SOME WATERS PRODUCED FROM ROCKY MOUNTAIN FIELDS (COLORADO AND MONTANA)

Number of Analyses*	System	Formation	Subsurface Depth (ft)	Constituents (mg/L)							TDS (mg/L)
				Ca	Mg	Na	CO ₃	HCO ₃	SO ₄	Cl	
Colorado ⁵⁵⁻⁵⁶											
7	Cretaceous	Dakota	2,819 to 5,830	0	0	310	0	210	40	40	560
6	Cretaceous	Frontier	1,230 to 3,464	1,180	290	13,000	160	3,600	890	22,100	41,220
				0	0	820	0	340	0	820	1,980
6	Eocene	Wasatch	2,230 to 5,283	190	70	8,200	240	4,900	90	12,800	26,490
				30	40	1,800	0	120	20	2,000	3,990
4	Jurassic	Morrison	3,020 to 4,395	900	410	10,600	150	2,000	870	18,900	33,830
				0	0	1,400	0	540	160	260	2,360
3	Jurassic	Sundance	4,564 to 6,263	80	30	3,600	120	3,350	980	5,000	13,160
				0	0	1,070	0	200	0	260	1,530
				380	80	5,250	0	3,030	1,040	8,060	17,840
Montana ⁵⁵⁻⁵⁷											
9	Jurassic	Montana	—	0	0	3,900	0	140	0	10	4,050
10	Upper Cretaceous	Colorado	—	100	70	220	0	2,000	1,850	5,530	9,770
				0	0	710	0	260	0	280	1,250
11	Lower Cretaceous	Kootenai	—	130	120	6,200	0	1,400	250	8,800	16,900
				0	0	280	0	500	0	10	790
55	Upper Jurassic	Ellis	—	90	60	4,670	0	4,900	290	6,000	16,010
				trace	0	1,110	0	1,670	0	370	3,150
22	Pennsylvanian	Quadrant	—	90	80	3,140	0	4,040	820	2,890	11,060
				60	trace	30	0	150	1,310	10	1,560
25	Upper Mississippian	Tensleep	—	680	700	1,390	0	400	5,540	440	8,470
				0	0	20	0	220	trace	10	250
	Lower Mississippian	Madison		500	430	2,330	0	4,830	2,110	2,790	12,990

*Upper figure in each column is minimum value and lower figure is maximum value for number of analyses indicated.

TABLE 24.11—CHARACTERISTICS OF SOME WATERS PRODUCED FROM ROCKY MT. FIELDS (WYOMING)

Number of Analyses*	System	Formation	Subsurface Depth (A)	Constituents (mg/L)							TDS (mg/L)
				Ca	Mg	Na	CO ₃	HCO ₃	SO ₄	Cl	
24	Cretaceous	Shannon	900 to 1,300	10	10	410	trace	280	0	20	730
35	Cretaceous	Frontier	1,000 to 3,080	250	330	5,560	230	1,900	3,710	7,670	19,650
				trace	trace	550	trace	1,270	trace	70	1,890
45	Cretaceous	First Wall Creek	—	220	130	20,000	1,050	7,800	240	27,900	57,340
				trace	trace	200	trace	1,000	trace	220	1,420
50	Cretaceous	Second Wall Creek	—	30	100	5,320	320	5,460	60	5,940	17,230
				trace	trace	1,740	trace	890	trace	1,170	3,800
14	Jurassic	Cloverly	1,400 to 1,500	40	10	7,000	590	6,950	880	6,600	22,070
				trace	trace	1,040	trace	110	0	150	1,300
22	Jurassic	Dakota	4,050 to 4,505	110	20	6,210	300	2,290	110	7,590	16,630
				trace	trace	180	trace	230	20	20	450
24	Jurassic	Dakota	4,353 to 8,500	230	160	13,000	280	6,900	980	19,200	40,750
				trace	trace	630	trace	1,000	trace	110	1,740
5	Jurassic	Greybull	—	60	60	5,560	380	3,680	60	1,930	11,730
				trace	trace	180	0	480	60	40	760
60	Jurassic	Sundance	—	40	trace	430	60	980	820	90	2,420
				0	0	520	0	410	40	140	1,110
20	Permian	Embar	—	400	60	6,800	330	6,850	5,880	7,700	28,020
				140	30	140	0	210	190	10	620
50	Pennsylvanian	Tensleep	—	630	220	5,170	0	1,690	5,790	3,930	17,430
				40	10	5	0	30	10	3	98
19	Mississippian	Madison	—	720	250	790	10	1,000	2,500	1,080	6,350
				20	trace	20	trace	20	50	4	114
20	Triassic	Minnelusa	—	870	180	580	20	1,080	1,940	1,070	5,740
				250	50	630	0	190	1,930	250	3,300
				450	60	1,670	0	550	3,870	610	7,210

*Upper figure in each column is minimum value and lower figure is maximum value for number of analyses indicated. ^{55,56,58,59}

TABLE 24.12—CHARACTERISTICS OF SOME WATERS PRODUCED FROM CANADIAN FIELDS

Number of Analyses*	System	Formation	Subsurface Depth (ft)	Constituents (mg/L)								Specific Gravity (60°/60°)	TDS (mg/L)	
				Ca	Mg	Na	CO ₃	HCO ₃	SO ₄	Cl	I			Br
Province of Alberta ⁶⁰⁻⁶³														
4	—	Milk River	215 to 1,890	10	10	660	0	320	5	200	ND	ND	ND	1,205
				50	10	3,000	80	790	600	4,500	ND	ND	ND	9,030
3	Cretaceous	Viking	1,670 to 2,072	70	20	6,400	0	580	20	6,400	10	10	1,010	13,510
				620	230	19,000	60	840	40	29,200	40	620	1,060	64,160
4	Mississippian	Banff	2,708 to 2,744	5	60	1,030	0	180	0	870	ND	ND	1,006	2,145
				1,250	190	9,100	410	1,250	2,500	11,000	ND	ND	1,032	25,700
6	Cretaceous	Basal Quartz	—	—	—	—	—	—	—	—	0	10	—	—
				—	—	—	—	—	—	—	20	460	—	—
6	Jurassic	Rundle	—	—	—	—	—	—	—	—	2	20	—	—
				—	—	—	—	—	—	—	20	220	—	—
6	Devonian	Wabamun	—	—	—	—	—	—	—	—	3	90	—	—
				—	—	—	—	—	—	—	10	110	—	—
6	Devonian	Leduc	—	—	—	—	—	—	—	—	2	200	—	—
				—	—	—	—	—	—	—	20	1,500	—	—
Province of Manitoba ⁶⁴														
86	Mississippian	Lodgepole	1,570 to 3,323	160	980	850	0	100	1,000	850	—	—	1,010	3,940
				3,260	67,340	44,900	40	2,140	4,800	94,900	—	—	1,089	150,380
35	Devonian	Nisku	2,200 to 2,942	1,000	240	4,900	0	110	900	7,000	—	—	1,016	14,150
				10,700	2,000	81,400	30	360	4,900	149,600	—	—	1,157	248,990
47	Jurassic	Mission Canyon	3,000 to 3,422	2,200	550	21,300	0	80	3,900	34,900	—	—	1,031	62,930
				3,900	1,400	72,800	80	780	4,300	120,700	—	—	1,136	203,880
22	—	Ashville	870 to 2,060	280	30	1,900	0	0	200	740	—	—	1,004	3,150
				1,200	570	19,300	30	380	4,000	31,200	—	—	1,033	25,680
21	Jurassic	Swan River	1,322 to 2,553	10	0	850	40	210	200	530	—	—	1,002	1,840
				850	330	11,700	870	1,100	3,000	8,800	—	—	1,025	25,780
11	—	Souris River	2,516 to 4,604	1,040	150	5,300	0	80	1,750	7,800	—	—	1,025	16,120
				5,500	1,300	104,600	0	470	4,700	173,500	—	—	1,180	290,070
14	Devonian	Duperow	1,698 to 3,717	1,100	470	7,800	0	90	3,100	14,300	—	—	1,026	26,760
				10,500	2,400	89,900	0	600	6,100	154,900	—	—	1,178	264,300

*Upper figure in each column is minimum value and lower figure is maximum value for number of analyses indicated.

**Not determined

to more than 1,400 mg/L for iodide.²⁶ Bromide concentration is important in determining the origin of an oilfield brine and is an important geochemical marker constituent.⁷³ Bicarbonate and sulfate are present in many oilfield waters. Their concentrations can range from none to several thousand milligrams per liter.

Other anions found in oilfield waters include arsenate, borate, carbonate, fluoride, hydroxide, organic acid salts, and phosphates. Boron concentrations in excess of 100 mg/L can affect electric log deflections.²⁶

Physical Properties of Oilfield Waters*

Compressibility

The compressibility of formation water at pressures above the bubblepoint is defined as the change in water volume per unit water volume per psi change in pressure. This is expressed mathematically as

$$c_w = -\frac{1}{V} \left(\frac{\partial V}{\partial p} \right) T, \dots \dots \dots (1a)$$

*This section, except for the pH and Eh, was written by Howard B. Bradley.

TABLE 24.13—CHARACTERISTICS OF SOME WATERS PRODUCED FROM CANADIAN FIELDS, PROVINCE OF SASKATCHEWAN

Number of Analyses*	System	Formation	Subsurface Depth (ft)	Constituents (mg/L)								Specific Gravity (60°/60°)	TDS (mg/L)
				Ca	Mg	Na	CO ₃	HCO ₃	SO ₄	Cl	I		
27	Cretaceous	Blairmore	998 to 3,713	trace	trace	2,200	—	190	—	2,800	—	1.000	6,190
				2,300	870	20,300	80	1,300	3,500	38,900	—	1.048	67,250
5	—	Shaunavon	3,205 to 3,413	170	100	8,800	—	190	2,100	890	—	1.007	12,250
				1,850	230	12,400	—	300	3,100	13,800	—	1.014	31,580
5	—	Gravelbourg	3,290 to 4,175	470	220	11,700	—	140	270	14,500	—	1.022	27,300
				620	370	12,900	—	350	2,100	20,100	—	1.026	36,440
25	—	Mission Canyon	3,700 to 5,785	100	130	760	—	60	—	280	—	1.001	1,330
				7,100	3,100	73,700	—	440	3,200	155,000	—	1.093	242,540
12	Devonian	Nisku	4,682 to 6,927	740	190	1,000	—	200	Trace	640	—	1.002	2,770
				14,100	7,150	73,000	—	2,350	2,500	142,800	—	1.186	242,600
9	Devonian	Duperow	2,253 to 4,024	680	170	940	—	100	2,200	700	—	1.002	4,790
				9,000	900	17,700	—	860	5,000	31,100	—	1.040	64,560
11	Mississippian	Mississippian	4,487 to 5,665	trace	trace	4,300	—	120	340	5,700	—	1.004	10,460
				5,600	1,600	71,000	110	850	3,900	123,800	—	1.150	206,860
4	Mississippian	Lodgepole	2,305 to 4,470	730	90	1,400	—	480	3,400	580	—	1.004	6,680
				2,800	610	27,000	—	600	3,900	45,700	—	1.061	80,610
11	Lower Cretaceous	Viking	2,395 to 3,026	trace	trace	1,100	—	70	0	2,100	—	1.002	3,270
				190	100	9,300	—	2,600	790	12,700	—	1.014	25,680
8	Devonian	Devonian	3,356 to 6,605	0	0	0	—	40	190	4,800	—	1.012	5,030
				1,100	1,200	69,100	—	1,580	2,400	111,000	—	1.160	185,380
8	Jurassic	Jurassic shale	3,105 to 4,325	trace	trace	4,300	—	290	0	2,800	—	1.002	7,390
				8,100	160	10,900	—	1,320	3,600	15,400	—	1.029	39,480

*Upper figure in each column is minimum value and lower figure is maximum value for number of analyses indicated.⁶⁵

TABLE 24.14—CHARACTERISTICS OF SOME WATERS PRODUCED FROM VENEZUELAN FIELDS

Number of Analyses	System	Formation or Field	Constituents (mg/L)							TDS (mg/L)
			Ca	Mg	Na	CO ₃	HCO ₃	SO ₄	Cl	
5	Tertiary	Zeta (Quiriquire)	170	100	1,750	0	3,050	4	1,910	7,190
7	Tertiary	Eta (Quiriquire)	330	270	5,150	0	5,400	10	5,420	18,260
			70	50	2,040	0	3,050	5	710	6,900
6	Tertiary	Cabimas field, La Rosa formation	400	300	12,360	0	7,410	30	11,170	36,500
			60	60	1,740	0	2,010	0	1,780	5,643
7	Cretaceous	Lagunillas field, Iceota formation	10	60	2,000	120	5,260	0	90	5,260
8	Tertiary	Bachaquero field, Pueblo Viejo main sandstone	40	60	4,610	0	6,250	5	3,700	14,657
8	Tertiary	Mene Grande field, Pauji and Mason-Trujillo range	30	20	1,800	100	3,570	0	690	6,210
7	Tertiary	La Concepcion field, Punta Gorda sands and deeper sands	50	20	4,700	1,900	30	0	6,250	12,955
8	Cretaceous	La Paz field, Guasare formation	30	20	6,000	80	1,230	0	8,550	15,911
			30	50	2,660	0	1,130	0	3,450	7,320
10	Cretaceous	S. El Mene field, El Salto formation	30	40	3,000	0	1,130	0	1,260	5,460
			150	50	9,000	0	2,440	0	9,000	20,640
11	Tertiary	Oficina and W. Guará fields								
		OF ₇ sand	50	20	1,260	0	2,330	140	640	4,424
		AB ₃ sand	40	30	1,360	0	2,780	60	560	4,830
		D ₄ sand	40	30	3,080	0	1,100	130	4,230	8,520
		Du and Eu sands	40	60	4,000	0	1,430	0	5,500	11,030
		F ₇ sand	140	70	7,900	0	3,500	150	10,500	22,260
		H sand	70	70	8,400	0	2,050	10	12,090	22,690
		L ₁ sand	160	100	7,300	0	4,420	trace	9,260	21,240
		M sand	110	30	7,700	0	2,100	20	10,900	20,860
		P sand	140	80	7,800	0	970	0	11,600	20,590
		S sand	330	80	8,600	0	1,700	100	13,050	23,860
		U sand	940	180	11,800	0	1,100	0	19,800	33,820

*Upper figure in each column is minimum value and lower figure is maximum value for number of analyses indicated. 66-69

or

$$\bar{c}_w = \frac{1}{\bar{V}} \left(\frac{V_2 - V_1}{p_1 - p_2} \right), \dots \dots \dots (1b)$$

or

$$\bar{c}_w = \frac{B_{w2} - B_{w1}}{\bar{B}_w(p_1 - p_2)}, \dots \dots \dots (1c)$$

where

c_w = water compressibility at the given pressure and temperature, bbl/bbl-psi,

\bar{c}_w = average water compressibility within the given pressure and temperature interval, bbl/bbl-psi,

V = water volume at the given pressure and temperature, bbl,

\bar{V} = average water volume within p and T intervals, bbl,

p_1 and

p_2 = pressure at conditions 1 and 2 with $p_1 > p_2$, psi,

B_{w1} and

B_{w2} = water FVF p_1 and p_2 , bbl/bbl, and

\bar{B}_w = average water FVF corresponding to \bar{V} , bbl/bbl.

In an oil reservoir, water compressibility also depends on the salinity. In contrast to the literature, laboratory measurements by Osif⁷⁴ show that the effect of gas in

solution on compressibility of water with NaCl concentrations up to 200 g/cm³ is essentially negligible. Osif's results show no effect at gas/water ratios (GWR's) of 13 scf/bbl, at GWR's of 35 scf/bbl probably no effect, but certainly no more than a 5% increase in the compressibility of brine.

Laboratory measurements⁷⁴ of water compressibility resulted in linear plots of the reciprocal of compressibility vs. pressure. The plots of $1/c_w$ vs. p have a slope of m_1 , and intercepts linear in salinity and temperature. Data points for the systems tested containing no gas in solution resulted in Eq. 2.

$$1/c_w = m_1 p + m_2 C + m_3 T + m_4, \dots \dots \dots (2)$$

where

c_w = water compressibility, psi⁻¹,

p = pressure, psi,

C = salinity, g/L of solution,

T = temperature, °F,

$m_1 = 7.033$,

$m_2 = 541.5$,

$m_3 = -537$, and

$m_4 = 403.3 \times 10^3$.

Eq. 2 was fit for pressures between 1,000 and 20,000 psi, salinities of 0 to 200 g NaCl/L, and temperatures from 200 to 270°F. Compressibilities were independent of dissolved gas.

Where conditions overlap, the agreement with the results reported by both Dorsey⁷⁵ and Dotson and Standing⁷⁶ is very good. Results from the Rowe and Chou⁷⁷

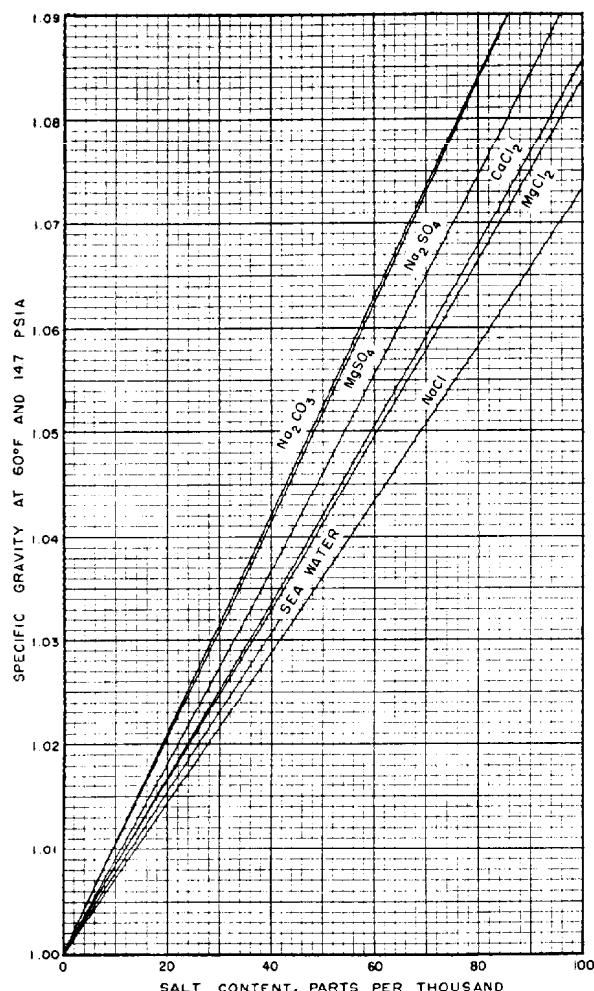


Fig. 24.4—Specific gravity of salt solutions at 60°F and 14.7 psia.

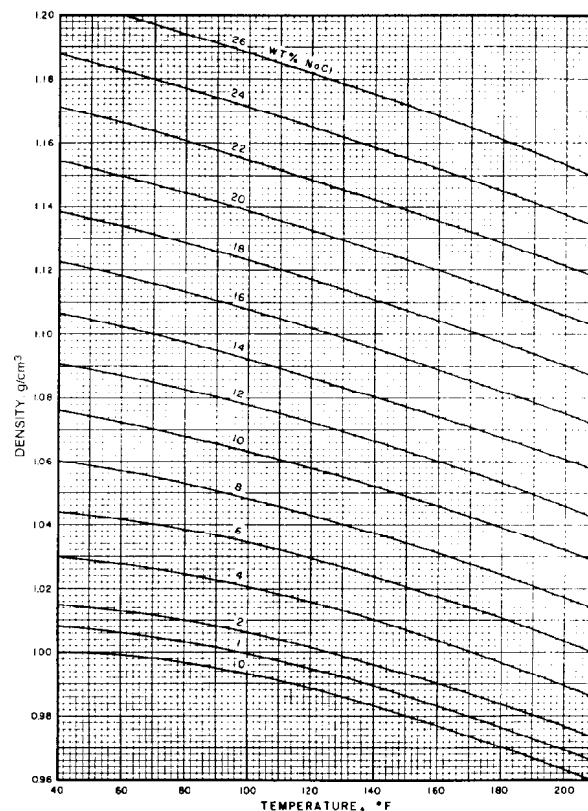


Fig. 24.5—Density of NaCl solutions at 14.7 psia vs. temperature.

equation agree well up to 5,000 psi (their upper pressure limit) but result in larger deviations with increasing pressure. In almost all cases, the Rowe and Chou compressibilities are less than that of Eq. 2.

Density

The density of formation water is a function of pressure, temperature, and dissolved constituents. It is determined most accurately in the laboratory on a representative sample of formation water.¹⁷ The formation water density is defined as the mass of the formation water per unit volume of the formation water. For engineering purposes, density in metric units (g/cm^3) is considered equal to specific gravity. Therefore, for most engineering calculations density and specific gravity are interchangeable.¹⁶

When laboratory data are not available, the density of formation water at reservoir conditions can be estimated (usually to within $\pm 10\%$) from correlations (Figs. 24.4 through 24.6). The only field data necessary are the density at standard conditions, which can be obtained from the salt content by use of Fig. 24.4. The salt content can

be estimated from the formation resistivity (obtained from electric log measurements) by use of Fig. 49.3 (see Chap. 49). The density of formation water at reservoir conditions can be calculated in four steps.

1. Using the temperature and density at atmospheric pressure, obtain the equivalent weight percent NaCl from Fig. 24.5.

2. Assuming the equivalent weight percent NaCl remains constant, extrapolate the weight percent to reservoir temperature and read the new density.

3. Knowing the density at atmospheric pressure and reservoir temperature, use Fig. 24.6 to find the increase in specific gravity (density) when compressed to reservoir pressure. Note that for oil reservoirs below the bubblepoint, the "saturated-with-gas" curves should be used; for water considered to have no solution gas, the "no-gas-in-solution" curves should be used. These curves were computed from data given by Ashby and Hawkins.⁷⁸

4. The density of formation water (g/cm^3) at reservoir conditions is the sum of the values read from Figs. 24.5 and 24.6. They can be added directly since the metric

units are referred to the common density base of water (1 g/cm³). The metric units can be changed to customary units (lbm/cu ft) by multiplying by 62.37.

Also the specific gravity of formation water can be estimated if the dissolved solids are known. The equation is

$$\gamma_w = 1 + C_{sd} \times 0.695 \times 10^{-6}, \dots \dots \dots (3)$$

where C_{sd} is the concentration of dissolved solids (mg/L).

For precise but very detailed calculations, the reader is referred to a recent paper by Rogers and Pitzer.⁷⁹ They tabulated a large number of values of compressibility, expansivity and specific volume vs. molality, temperature, and pressure. A semiempirical equation of the same type found to be effective in describing thermal properties of NaCl (0.1 to 5 molality) was used to reproduce the volumetric data from 0 to 300°C and 1 to 1,000 bars.

Formation Volume Factor (FVF)

The water FVF, B_w , is defined as the volume at reservoir conditions occupied by 1 STB of formation water plus its dissolved gas. It represents the change in volume of the formation water as it moves from reservoir conditions to surface conditions. Three effects are involved: the liberation of gas from water as pressure is reduced, the expansion of water as pressure is reduced, and the shrinkage of water as temperature is reduced.

The water FVF also depends on pressure. Fig. 24.7 is a typical plot of water FVF as a function of pressure. As the pressure is decreased to the bubblepoint, p_b , the FVF increases as the liquid expands. At pressures below the bubblepoint, gas is liberated, but in most cases the FVF still will increase because the shrinkage of the water resulting from gas liberation is insufficient to counterbalance the expansion of the liquid. This is the effect of the small solubility of natural gas in water.

The most accurate method of obtaining the FVF is from laboratory data. It also can be calculated from density correlations if the effects of solution gas have been accounted for properly. The following equation is used to estimate B_w if solution gas is included in the laboratory measurement or correlation of ρ_{rc} :

$$B_w = \frac{V_{rc}}{V_{sc}} \times \frac{\rho_{sc}}{\rho_{rc}}, \dots \dots \dots (4)$$

where

V_{rc} = volume occupied by a unit mass of water at reservoir conditions (weight of gas dissolved in water at reservoir or standard conditions is negligible), cu ft,

V_{sc} = volume occupied by a unit mass of water at standard conditions, cu ft,

ρ_{sc} = density of water at standard conditions, lbm/cu ft, and

ρ_{rc} = density of water at reservoir conditions, lbm/cu ft.

The density correlations and the methods of estimating ρ_{sc} and ρ_{rc} were described previously.

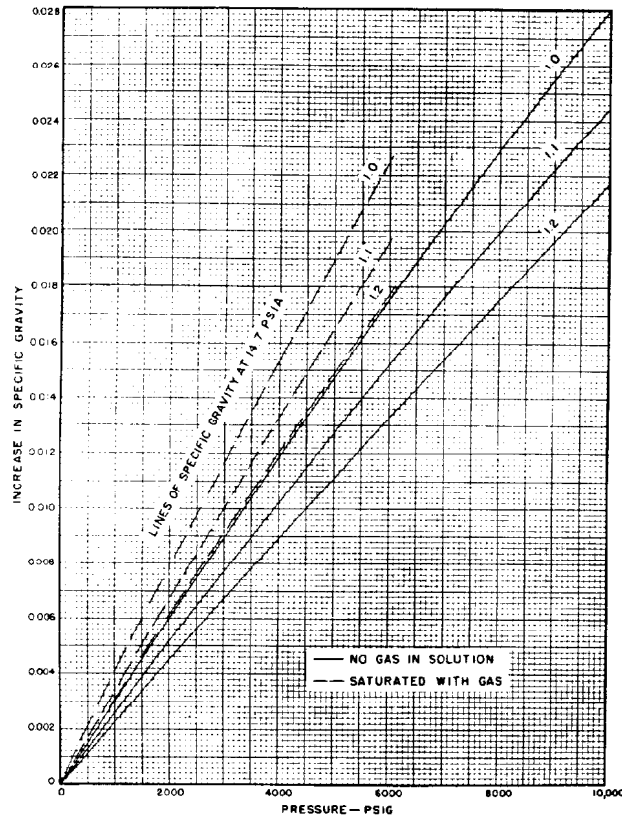


Fig. 24.6—Specific gravity increase with pressure—salt water.

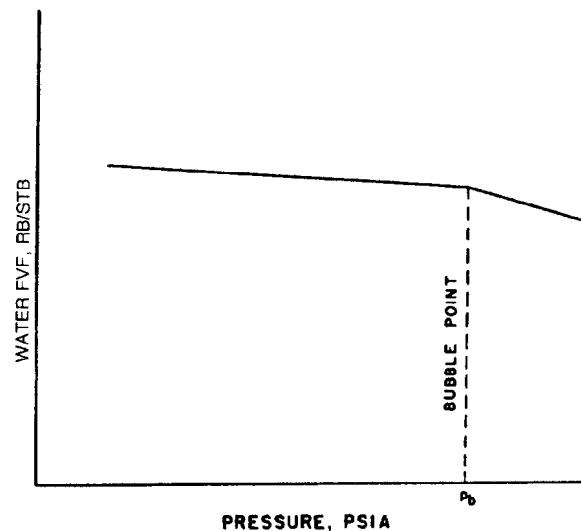


Fig. 24.7—Typical plot of water FVF vs. pressure.

The FVF of water can be less than one if the increase in volume resulting from dissolved gas is not great enough to overcome the decrease in volume caused by increased pressure. The value of FVF is seldom higher than 1.06.

Resistivity

The resistivity of formation water is a measure of the resistance offered by the water to an electrical current. It can be measured directly or calculated.¹⁶ The direct-measurement method is essentially the electrical resistance through a 1-m² cross-sectional area of 1 m³ of formation water. The formation water resistivity, R_{wg} , is expressed in units of $\Omega\cdot m$. The resistivity of formation water is used in electric log interpretation and for such use the value is adjusted to formation temperature.⁸⁰ (See Chap. 49 for more information).

Surface (Interfacial) Tension (IFT)

Surface tension is a measure of the attractive force acting at a boundary between two phases. If the phase boundary separates a liquid and a gas or a liquid and a solid, the attractive force at the boundary usually is called "surface tension"; however, the attractive force at the interface between two liquids is called "IFT." IFT is an important factor in enhanced recovery processes (see Chap. 47, Chemical Flooding, describing "Low-IFT Processes" and "Phase Behavior and IFT" in the Micellar/Polymer Flooding section).

Surface tension is measured in the laboratory by a tensiometer, by the drop method, or by other methods. Descriptions of these methods are found in most physical chemistry texts.

Viscosity

The viscosity of formation water, μ_w , is a function of pressure, temperature, and dissolved solids. In general, brine viscosity increases with increasing pressure, increasing salinity, and decreasing temperature.⁸¹ Dissolved gas in the formation water at reservoir conditions generally results in a negligible effect on water viscosity. There is little information on the actual numerical effect of dissolved gas on water viscosity.

Gas in solution behaves entirely differently from gas in hydrocarbons.* In water the presence of the gas actually causes the water molecules to interact with each other more strongly, thus increasing the rigidity and viscosity of the water. However, this effect is very small and has not been measured to date. In the physical chemistry literature there is an enormous amount of indirect evidence to support this concept.

For the best estimation of the viscosity of water, the reader is referred to a paper by Kestin *et al.*⁸² Their correlating equations involve 32 parameters for calculating the numerical effect of pressure, temperature, and concentration of aqueous NaCl solutions on the dynamic and kinematic viscosity of water. Twenty-eight tables generated from the correlating equations cover a temperature range from 20 to 150°C, a pressure range from 0.1 to 35 mPa, and a concentration range from 0 to 6 molal.

Figs. 24.8 through 24.10 may be used to approximate water viscosity for engineering purposes. These figures show the effects of pressure, temperature, and NaCl content on the viscosity of water. They may be used when the primary contaminant is sodium chloride.

Some engineers assume that reservoir brine viscosity is equal to that of distilled water at atmospheric pressure and reservoir temperature. In this case it is assumed that the viscosity of brine is essentially independent of pressure (a valid premise for the pressure ranges usually encountered).

The pH

The pH of oilfield waters usually is controlled by the CO₂/bicarbonate system. Because the solubility of CO₂ is directly proportional to temperature and pressure, the pH measurement should be made in the field if a close-to-natural-conditions value is desired. The pH of the water is not used for water identification or correlation purposes, but it does indicate possible scale-forming or corrosion tendencies of a water. The pH also may indicate the presence of drilling-mud filtrate or well-treatment chemicals.

The pH of concentrated brines usually is less than 7.0, and the pH will rise during laboratory storage, indicating that the pH of the water in the reservoir probably is appreciably lower than many published values. Addition of the carbonate ion to sodium chloride solutions will raise the pH. If calcium is present, calcium carbonate precipitates. The reason the pH of most oilfield waters rises during storage in the laboratory is because of the formation of carbonate ions as a result of bicarbonate decomposition.

The Redox Potential (Eh)

The redox potential often is abbreviated "Eh," and also may be referred to as oxidation potential, oxidation-reduction potential, or pE. It is expressed in volts, and at equilibrium it is related to the proportions of oxidized and reduced species present. Standard equations of chemical thermodynamics express the relationships.

Knowledge of the redox potential is useful in studies of how compounds such as uranium, iron, sulfur, and other minerals are transported in aqueous systems. The solubility of some elements and compounds depends on the redox potential and the pH of their environment.

Some water associated with petroleum is interstitial ("connate") water, and has a negative Eh; this has been proved in various field studies. Knowledge of the Eh is useful in determining how to treat a water before it is reinjected into a subsurface formation. For example, the Eh of the water will be oxidizing if the water is open to the atmosphere, but if it is kept in a closed system in an oil-production operation the Eh should not change appreciably as it is brought to the surface and then reinjected. In such a situation, the Eh value is useful in determining how much iron will stay in solution and not deposit in the wellbore.

Organisms that consume oxygen cause a lowering of the Eh. In buried sediments, it is the aerobic bacteria that attract organic constituents, which remove the free oxygen from the interstitial water. Sediments laid down in a shoreline environment will differ in degree of oxidation

* Personal communication: Melrose, J.C., Mobil R&D Corp., Dallas (Sept. 25, 1985).

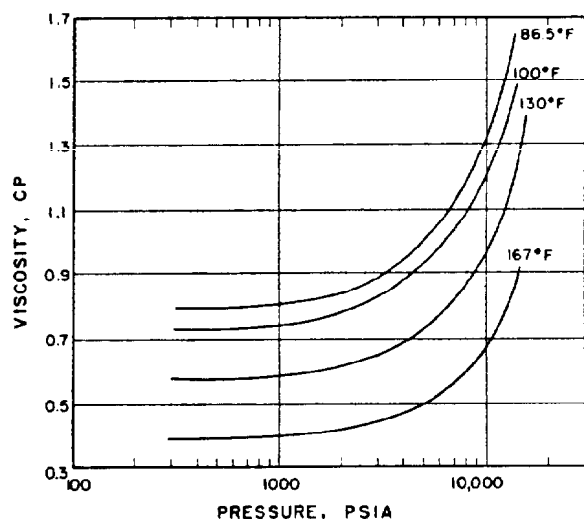


Fig. 24.8—Effect of pressure on the viscosity of water.

compared with those laid down in a deepwater environment. For example, the Eh of the shoreline sediments may range from -50 to 0 mV, but the Eh of deepwater sediments may range from -150 to -100 mV.

The aerobic bacteria die when the free oxygen is totally consumed; the anaerobic bacteria attack the sulfate ion, which is the second most important anion in the seawater. During this attack, the sulfate reduces to sulfite and then to sulfide; the Eh drops to -600 mV, H_2S is liberated, and $CaCO_3$ precipitates as the pH rises above 8.5.

Dissolved Gases

Large quantities of dissolved gases are contained in oilfield brines. Most of these gases are hydrocarbons; however, other gases such as CO_2 , N_2 , and H_2S often are present. The solubility of the gases generally decreases with increased water salinity, and increases with pressure.

Hundreds of drillstem samples of brine from water-bearing subsurface formations in the U.S. gulf coast area were analyzed to determine their amounts and kinds of hydrocarbons.²⁰ The chief constituent of the dissolved gases usually was methane, with measurable amounts of ethane, propane, and butane. The concentration of the dissolved hydrocarbons generally increased with depth in a given formation and also increased basinward with regional and local variations. In close proximity to some oilfields, the waters were enriched in dissolved hydrocarbons, and up to 14 scf dissolved gas/bbl water was observed in some locations. A more detailed discussion of this topic is given in Chap. 22.

Organic Constituents

In addition to the simple hydrocarbons, a large number of organic constituents in colloidal, ionic, and molecular form occur in oilfield brines. In recent years, some of these organic constituents have been measured quantitatively. However, many organic constituents are present that have not been determined in some oilfield

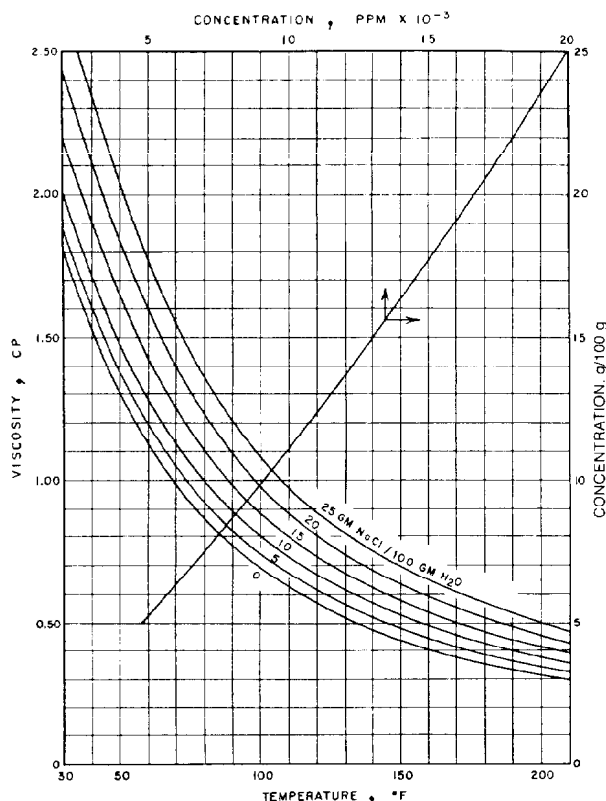


Fig. 24.9—Viscosity of sodium chloride solutions as a function of temperature and concentration at 14.7 psia.

brines primarily because the analytical problems are difficult and very time-consuming.

Knowledge of the dissolved organic constituents is important because these constituents are related to the origin and/or migration of an oil accumulation, as well as to the disintegration or degradation of an accumulation. The concentrations of organic constituents in oilfield brines vary widely. In general, the more alkaline the water, the more likely that it will contain higher concentrations of organic constituents. The bulk of the organic matter consists of anions and salts of organic acids; however, other compounds also are present.

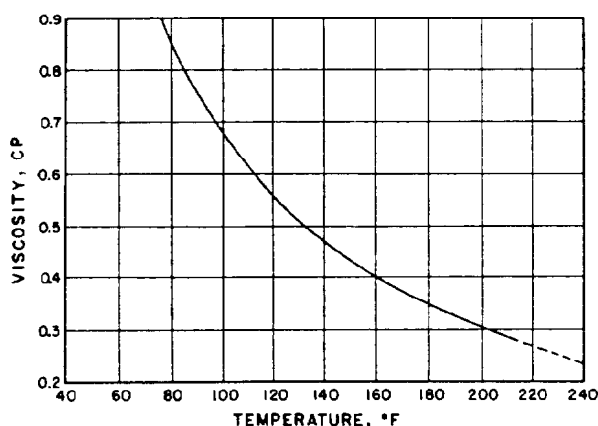


Fig. 24.10—Effect of temperature on viscosity of water.

Knowledge of the concentrations of benzene, toluene, and other components in oilfield brines is used in exploration. The solubilities of some of these compounds in water at ambient conditions and in saline waters at elevated temperatures and pressures have been determined.^{83,84}

However, the actual concentrations of these and other organic constituents in subsurface oilfield brines is another matter. It has been shown experimentally that the solubilities of some organic compounds found in crude oil increase with temperature and pressure if pressure is maintained on the system. The increased solubilities become significant above 150°C. The solubilities decrease with increasing water salinity. Waters associated with paraffinic oils are likely to contain fatty acids, while those associated with asphaltic oils more likely contain naphthenic acids.

Quantitative recovery of organic constituents from oilfield brines is difficult. Temperature and pressure changes, bacterial actions, adsorption, and the high inorganic/organic-constituents ratio in most oilfield brines are some reasons why quantitative recovery is difficult.

Interpretation of Chemical Analyses

Oilfield waters include all waters or brines found in oilfields. Such waters have certain distinct chemical characteristics.

About 70% of the world petroleum reserves are associated with waters containing more than 100 g/L dissolved solids. A water containing dissolved solids in excess of 100 g/L can be classified as a brine. Waters associated with the other 30% of petroleum reserves contain less than 100 g/L dissolved solids. Some of these waters are almost fresh. However, the presence of fresher waters usually is attributed to invasion after the petroleum accumulated in the reservoir trap.

Examples of some of the low-salinity waters can be found in the Rocky Mt. areas in Wyoming fields such as Enos Creek, South Sunshine, and Cottonwood Creek. The Douleb oil field in Tunisia is another example.

The composition of dissolved solids found in oilfield waters depends on several factors. Some of these factors are the composition of the water in the depositional environment of the sedimentary rock, subsequent changes by rock/water interaction during sediment compaction, changes by rock/water interaction during water migration (if migration occurs), and changes by mixing with other waters, including infiltrating younger waters such as meteoric waters. The following are definitions of some types of water.

Types of Water

Meteoric Water. This is water that recently was involved in atmospheric circulation; furthermore, "the age of meteoric groundwater is slight when compared with the age of the enclosing rocks and is not more than a small part of a geologic period."¹⁴

Seawater. The composition of seawater varies somewhat, but in general will have a composition relative to the following (in mg/L): chloride—19,375, bromide—67, sulfate—2,712, potassium—387, sodium—10,760, magnesium—1,294, calcium—413, and strontium—8.

Interstitial Water. Interstitial water is the water contained in the small pores or spaces between the minute grains or units of rock. Interstitial waters are *syngenetic* (formed at the same time as the enclosing rocks) or *epigenetic* (originated by subsequent infiltration into rocks).

Connate Water. The term "connate" implies born, produced, or originated together—connascent. Therefore, connate water probably should be considered an interstitial water of syngenetic origin. Connate water of this definition is fossil water that has been out of contact with the atmosphere for at least a large part of a geologic period. The implication that connate waters are only those "born with" the enclosing rocks is an undesirable restriction.¹⁴

Diagenetic Water. Diagenetic waters are those that have changed chemically and physically, before, during, and after sediment consolidation. Some of the reactions that occur in or to diagenetic waters include bacterial, ion exchange, replacement (dolomitization), infiltration by permeation, and membrane filtration.

Formation Water. Formation water, as defined here, is water that occurs naturally in the rocks and is present in them immediately before drilling.

Juvenile Water. Water that is in primary magma or derived from primary magma is juvenile water.¹⁴

Condensate Water. Water associated with gas sometimes is carried as vapor to the surface of the well where it condenses and precipitates because of temperature and pressure changes. More of this water occurs in the winter and in colder climates and only in gas-producing wells. This water is easy to recognize because it contains a relatively small amount of dissolved solids, mostly derived from reactions with chemicals in or on the well casing or tubing.

Water analyses may be used to identify the water source. In the oil field one of the prime uses of these analyses is to determine the source of extraneous water in an oil well so that casing can be set and cemented to prevent such water from flooding the oil or gas horizons. In some wells a leak may develop in the casing or cement, and water analyses are used to identify the water-bearing horizon so that the leaking area can be repaired. With the current emphasis on water pollution prevention, it is very important to locate the source of a polluting brine so that remedial action can be taken.

Comparisons of water-analysis data are tedious and time-consuming; therefore, graphical methods are commonly used for positive, rapid identification. A number of systems have been developed, all of which have some merit.

Graphic Plots

Graphic plots of the reacting values can be made to illustrate the relative amount of each radical present. The graphical presentation is an aid to rapid identification of a water and classification as to its type. Several methods have been developed.

Tickell Diagram. The Tickell diagram was developed using a six-axis system or star diagram.⁸⁵ Percentage reaction values of the ions are plotted on the axes. The percentage values are calculated by summing the equivalent proton masses (EPM's) of all the ions, dividing the EPM of a given ion by the sum of the total EPM's, and multiplying by 100.

The plots of total reaction values, rather than of percentage reaction values, are often more useful in water identification because the percentage values do not take into account the actual ion concentrations. Water differing only in concentrations of dissolved constituents cannot be distinguished.

Reistle Diagram. Reistle devised a method of plotting water analyses by using the ion concentrations.⁸⁶ The data are plotted on a vertical diagram, with the cations plotted above the central zero line and the anions below. This type of diagram often is useful in making regional correlations or studying lateral variations in the water of a single formation because several analyses can be plotted on a large sheet of paper.

Stiff Diagram. Stiff plotted the reaction values of the ions on a system of rectangular coordinates.⁸⁷ The cations are plotted to the left and the anions to the right of a vertical zero line. The endpoints then are connected by straight lines to form a closed diagram, sometimes called a "butterfly" diagram. To emphasize a constituent that may be a key to interpretation, the scales may be varied by changing the denominator of the ion fraction, usually in multiples of 10. However, when a group of waters is being considered, all must be plotted on the same scale.

Many investigators believe that this is the best method of comparing oilfield water analyses. The method is simple, and nontechnical personnel can be easily trained to construct the diagrams.

Other Methods. Several other water identification diagrams have been developed, primarily for use with fresh waters, and they are not discussed here. The Stiff and Piper diagrams,^{87,88} were adapted to automatic data processing by Morgan *et al.*⁸⁹ and Morgan and McNellis.⁹⁰ The Piper diagram uses a multiple trilinear plot to depict the water analysis, and this quaternary diagram shows the chemical composition of the water in terms of cations and anions.⁸⁸ Angino and Morgan applied the automated Stiff and Piper diagrams to some oilfield brines and obtained good results.⁹¹

Occurrence, Origin, and Evolution of Oilfield Waters

The sedimentary rocks that now consist of stratified deposits originally were laid down as sediments in oceans, seas, lakes, and streams. Naturally, these sediments were filled with water. This water is still present in the stratified sediments and millions of years later would be considered truly connate water.

Many large sedimentary strata originally were associated with oceans and seas. The original associated water, therefore, was marine in such sediments. Sediments laid down by lakes and streams would not contain a marine water during their initial deposition.

However, with time and tectonic events plus transgression and regression of oceans and seas, even these sediments probably were subjected to marine waters by infiltration.

In any event, the petroleum, which formed from organic matter deposited with the sediments, migrated from what usually is called the "source rock" into more porous and permeable sedimentary rock. Petroleum (i.e., oil and gas) is less dense than water; therefore, it tends to float to the top of a water body regardless of whether the water is on the surface or in the subsurface.

Therefore, water associated with petroleum in a subsurface reservoir is called an "oilfield water." By this definition, any water associated with a petroleum deposit is an oilfield water.

The question of the origin of oilfield brines is difficult to answer in a general manner. The water involved and the constituents dissolved in the water to form the brine can involve divergent histories. Subsurface water is there either because it originally was there or because it infiltrated to the subsurface from the surface. If it was there originally, it would be endogenetic, whereas if it infiltrated from the surface and/or penetrated with sediment accumulations, it would be exogenetic.

Obviously these two types of waters could meet and mix in the subsurface and thus the mixture would contain water of two separate origins. The problem could multiply if more than one exogenetic water were involved.

The chemical composition of an oilfield brine is an end product of several variables. These variables include (1) dissolved ions, salts, gases, and organic matter, (2) reactions between these dissolved constituents, and (3) interaction of the brine with the surrounding rocks, petroleum, etc. There are a number of pertinent reactions that could cause the composition of a subsurface oilfield brine to change in composition, including leaching of the rocks, ion exchange between water and rock, redox, mineral hydration, mineral formation and/or dissolution, ion diffusion, gravitational segregation of ions, and membrane filtration, or other osmotic effects.

It is rather difficult to rank the factors that might be more important for general consideration. However, two of the more important factors probably are the original composition of the water and interaction of that water with the rocks. If one assumes that the original water was a marine water and that the associated sediments (subsequently sedimentary rocks) were marine, then the original composition of the marine water could be an important factor.

However, even the salinity in the various oceans and seas is not constant. For example, the salinity of the waters in the major oceans ranges from 33,000 to 38,000 mg/L, about 40,000 mg/L in the Mediterranean Sea, up to 70,000 mg/L in the Red Sea, about 18,000 to 22,000 mg/L in the Black Sea, and only about 1,000 mg/L in the Baltic Sea. Some land-locked waters, such as the Dead Sea, Great Salt Lake, etc., contain waters that are nearly saturated with dissolved solids.

Studies of formation waters in the western Canada sedimentary basin indicate that 85% of the strata were deposited under marine conditions, while 15% were deposited under brackish-water and possibly under freshwater conditions.⁹² These investigators estimated that 80% of all the sedimentary strata in Alberta were

deposited under marine conditions. This led to the conclusion that one could assume with negligible error that all sedimentary strata originally contained seawater.

Further, the study indicated that evaporites form an important volumetric part of several of the stratigraphic units. Some of the stratigraphic units possibly contain bitterns subsequent to halite precipitation but preceding precipitation of potassium salts. They calculated an average formation water salinity of about 46,000 mg/L TDS, which indicated a net gain of dissolved salts. Of the major and some minor components, all showed a net gain with the exception of Mg and SO_4 .

Factor analysis was used in interpretation of the analyses, and the following factors were considered to be major controls: composition of the original seawater, dilution by freshwater recharge, membrane filtration, solution of halite, dolomitization, bacterial reduction of sulfate, formation of chlorite, cation exchange on clays, contribution from organic matter, and solubility relationships.

It was concluded that (1) the formation waters of western Canada are ancient seawaters in which the deuterium concentration was changed because of mixing with infiltrating fresh water, (2) oxygen-18 was exchanged with carbonates in the rocks, and (3) dissolved salts are in equilibrium with the rock matrix subsequent to their redistribution by membrane filtration and/or dilution by freshwater recharge. Equilibrium was attained by such processes as dissolution of evaporates, new mineral formation, cation exchange on clays, desorption of ions from clays and organic matter, and mineral solubilities.

The majority of the published research studies seem to agree that all these controls and/or reactions are involved in establishing the composition of oilfield brines. Further, most investigators agree with the assumption that marine water usually is a part of the original material from which formation waters evolve. Opinions, however, are not unanimous with respect to how they evolved. The major disagreements are related to the membrane filtration theory and to other modes of concentrating the dissolved solids such as seawater evaporation.

It is possible to reconstruct the evolution of some oilfield brines in sedimentary basins if one reasons that they are genetically related to evaporites. For example, geochemical and geological studies of some very concentrated brines indicate that in deep quiescent bodies of water, strong bitterns can persist for long periods of time under a layer of near-normal seawater. As a result, carbonates can precipitate from the less saline water and fall through the bittern at the bottom, and, as compaction proceeds, the pore spaces remain filled with bitterns. Some fossil brines once trapped have not moved very far or very fast.

A geochemical model can be built to represent the origin and evolution of this type of brine by using the relatively simple operations and processes of (1) evaporation, (2) precipitation, (3) sulfate reduction, (4) mineral formation and diagenesis, (5) ion exchange, (6) leaching, and (7) expulsion of interstitial fluids from evaporites during compaction.

Experimental work indicated that about 14% of the bromide in seawater precipitates with the halite as seawater evaporates. The average concentration of

bromide in the Smackover brines is 3,100 mg/L. Therefore, the average degree of concentration of these brines compared to seawater is $3,100 \div 65 = 48$. Assuming that seawater is concentrated 50-fold, the approximate composition of a brine can be calculated.²⁶

Shale Compaction and Membrane Filtration

Some investigators believe that the salinity variations found in oilfield waters are the result of filtration of water through shale.⁹³ The membrane filtration theory first was suggested by De Sitter.⁹⁴ Laboratory experiments indicated that natural shales can act as semipermeable membranes.^{95,96} This system working in nature should cause a water to be more saline on one side of the shale membrane and almost fresh or less saline on the other side. This follows because the shale membrane should filter out the dissolved ions on the upflow side, causing the water on the downflow side to contain few or no dissolved ions.

Quantities of Produced Water

An analysis was made of the approximate amount of water produced with crude oil in 14 states. The states and their percent of total U.S. crude oil production in 1981 are: Alabama, 0.3%; Alaska, 19.9%; California, 11.7%; Colorado, 1.0%; Florida, 1.4%; Louisiana, 13.4%; Montana, 1.0%; Mississippi, 1.2%; Nebraska, 0.2%; New Mexico, 2.3%; North Dakota, 1.4%; Texas, 31.2%; Utah, 0.8%; and Wyoming, 4.2%.

Fig. 24.11 indicates the crude oil and water production from wells in the 14 states. The figure indicates production of about 4.3 bbl water/bbl oil. Fig. 24.12 is a similar graph for 13 states excluding Alaska. This figure indicates production of about 5.2 bbl water/bbl oil. Further, it can be shown that oil wells produce more water as cumulative oil production increases. In other words, the older the well, the higher the WOR.

Recovery of Minerals From Brines

Extraction of minerals from oilfield brines should be considered in production planning (1) to recoup exploration and development costs, (2) to prevent environmental damage from brine, (3) to produce potable water, and (4) to conserve all valuable minerals and energy.

Precipitation is the most common separation process used in separating minerals from any type of brine. Minerals recovered from brines in the U.S. include compounds of iodine, bromine, chlorine, sodium, lithium, potassium, magnesium, and calcium.

Evaporation of a saline water or brine will cause the precipitation of calcium carbonate, calcium sulfate, sodium chloride, magnesium sulfate, potassium chloride, and finally magnesium chloride. These are the major chemicals in most brines, and this is the sequence order in which these compounds will precipitate. Mere precipitation will not produce a very pure chemical from a brine; therefore, other chemical or physical processes are used.

For example, iodine, which is in the form of iodide in a brine, is recovered by these steps: (1) the iodide is oxidized to iodine, (2) the iodine is stripped from the brine, (3) the iodine then is reduced back to iodide, (4) the iodide is oxidized again to iodine, (5) the iodine is

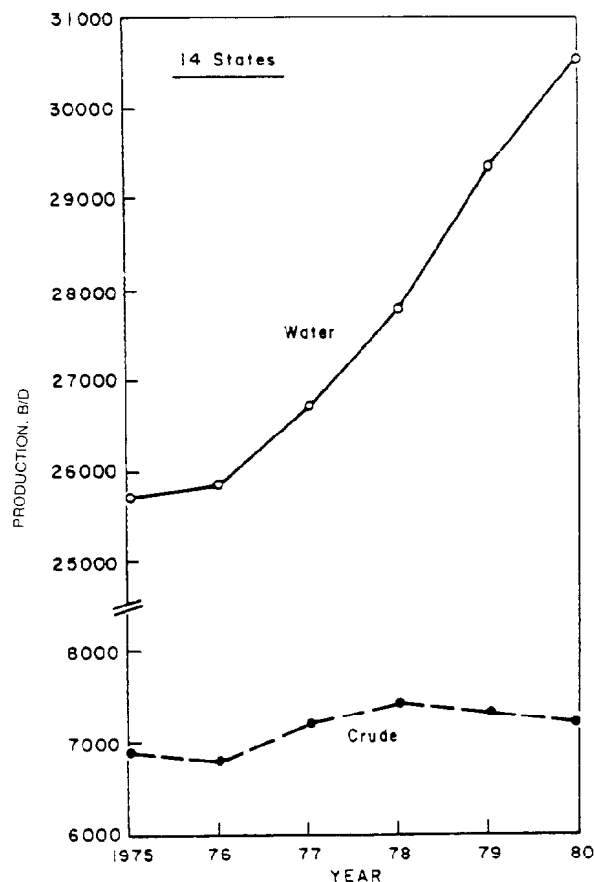


Fig. 24.11—Crude oil and water produced ($\times 1,000$ B/D) from wells in 14 states including Alaska.

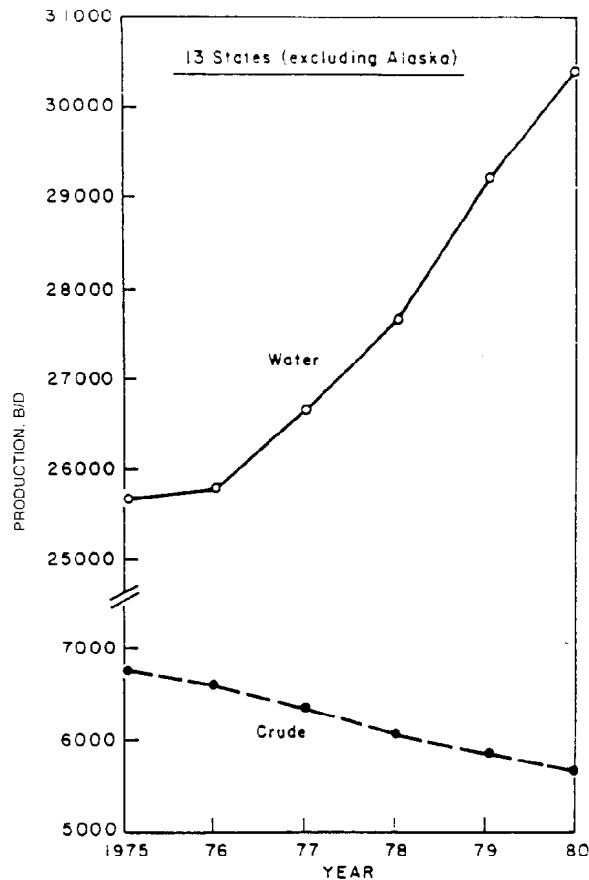


Fig. 24.12—Crude oil and water produced ($\times 1,000$ B/D) from wells in 13 states excluding Alaska.

crystallized and filtered, and (6) the iodine crystals are purified further.

Bromine is recovered by a similar though, of course, different process. It is present in a brine as bromide. The *U.S. Bureau of Mines Yearbook*⁹⁷ contains information on general recovery technology, domestic production, consumption and uses, prices, stocks, etc., of minerals recovered from brines as well as minerals recovered from other sources.

The first plant in the U.S. in more than 40 years built solely to produce iodine from brine went on stream in 1977 near Woodward, OK. It has a design capacity of 2 million lbm iodine/yr or about 30% of the annual U.S. demand. Some smaller-scale operations to recover iodine started in 1982 near Kingfisher, OK.

Several plants recover bromine and other constituents from brine near El Dorado, AR. The brine is produced from the Smackover formation.

Magnesium and other chemicals are recovered from lake brines, well brines, and seawater in plants located near Ogden, UT; Ludington, MI; Freeport, TX; and Port St. Joe, FL. Lithium is recovered from brine near Clayton Valley, NV.⁹⁸

Economic Evaluation

It is true that market demand fluctuates with supply; therefore, any company considering an enterprise to

recover minerals from brines should make an in-depth study of the current and potential economics. Some of the factors that must be determined are (1) concentrations of valuable minerals in a brine, (2) amount of brine available, (3) costs of gathering the brine, (4) costs of recovering the minerals from the brine, (5) present and potential market demand for the recovered minerals, and (6) costs of delivering the minerals to the market.²⁶

References

1. Rogers, W.B. and Rogers, H.D.: "On the Connection of Thermal Springs in Virginias with Anticlinal Axes and Faults," *Am. Geol. Rep.* (1843) 323-47.
2. Howell, J.V.: "Historical Development of the Structural Theory of Accumulation of Oil and Gas," W.E. Wrather and F.H. Lahee (eds.), AAPG, Tulsa (1934) 1-23.
3. Dickey, P.A.: "The First Oil Well," *J. Pet. Tech.* (Jan. 1959) 14-26.
4. Schilthuis, R.J.: "Connate Water in Oil and Gas Sands," *Trans., AIME* (1938) 127, 199-214.
5. Torrey, P.D.: "The Discovery of Interstitial Water," *Prod. Monthly* (1966) 30, 8-12.
6. Griswold, W.T. and Munn, M.J.: "Geology of Oil and Gas Fields in Steubenville, Burgettstown and Claysville Quadrangles, Ohio, West Virginia and Pennsylvania," *Bull., USGS* (1907) No. 318, 196.
7. Fetteke, C.R.: "Bradford Oil Field, Pennsylvania, and New York," *Bull., Pennsylvania Geologic Survey, Fourth Ser.* (1938) M21, 1-454.
8. Munn, M.J.: "The Anticlinal and Hydraulic Theories of Oil and Gas Accumulation," *Econ. Geol.* (1920) 4, 509-29.

9. Mills, F. van A.: "Experimental Studies of Subsurface Relationships in Oil and Gas Fields," *Econ. Geol.* (1920) **15**, 398-421.
10. Rich, J.L.: "Further Notes on the Hydraulic Theory of Oil Migration and Accumulation," *Bull.*, AAPG (1923) **7**, 213-25.
11. Torrey, P.D.: "A Review of Secondary Recovery of Oil in the United States," *Secondary Recovery of Oil in the United States*, API, New York City (1950) 3-29.
12. Garrison, A.D.: "Selective Wetting of Reservoir Rock and Its Relation to Oil Production," *Drill. and Prod. Prac.*, New York City (1935) 130-40.
13. Lane, A.C. and Gordon, W.C.: "Mine Waters and Their Field Assay," *Bull.*, Geologic Soc. of America (1908) **19**, 501-12.
14. White, D.E.: "Magmatic, Connate, and Metamorphic Water," *Bull.*, Geologic Soc. of America (1957) **68**, 1659-82.
15. Wallace, W.E.: "Water Production from Abnormally Pressured Gas Reservoirs in South Louisiana," *J. Pet. Tech.* (Aug. 1969) 969-82.
16. *Recommended Practice for Analysis of Oilfield Waters*, API RP-45, API, Dallas (1968).
17. "Saline and Brackish Waters, Sea Waters and Brines," American Society for Testing and Materials, *Annual Book of ASTM Standards*, Part 31—Water, Section VII, Philadelphia (1982).
18. Ostroff, A.G.: "Introduction to Oilfield Water Technology," NACE, Houston (1979) 394.
19. Noad, D.F.: "Water Analysis Data, Interpretation and Application," *J. Cdn. Pet. Tech.* (1962) **1**, 82-89.
20. Buckley, S.E., Hocott, C.R. and Taggart, M.S. Jr.: "Distribution of Dissolved Hydrocarbons in Subsurface Waters," *Habitat of Oil*, L.C. Weeks (ed.), AAPG, Tulsa (1958) 850-82.
21. Zarrella, W.M. et al.: "Analysis and Significance of Hydrocarbons in Subsurface Brines," *Geochim. Cosmochim. Acta.* (1967) **31**, 1155-66.
22. Bailey, N.J.L. et al.: "Alteration of Crude Oils by Water and Bacteria—Evidence from Geochemical and Isotope Studies," *Bull.*, AAPG (1973) **57**, No. 7, 1276-90.
23. Carothers, W.W.: "Aliphatic Acid Anions and Stable Carbon Isotopes of Oil Field Waters in the San Joaquin Valley, California," Master's thesis, San Jose (CA) State U. (1976).
24. Sunwall, M.T. and Pushkar, P.: "The Isotopic Composition of Strontium in Brines from Petroleum Fields of Southeastern Ohio," *Chem. Geol.* (1979) **24**, 189-97.
25. Hoke, S.H. and Collins, A.G.: "Mobile Wellhead Analyzer for the Determination of Unstable Constituents in Oil-Field Waters," ASTM STP 735 (1981) 34-48.
26. Collins, A.G.: *Geochemistry of Oilfield Waters*, Elsevier Scientific Publishing Co., New York City (1975) 496.
27. Beestecher, E.: *Petroleum Microbiology—an Introduction to Microbiological Engineering*, Elsevier Scientific Publishing Co., New York City (1954) 375.
28. Davis, J.B.: *Petroleum Microbiology*, Elsevier Scientific Publishing Co., New York City (1967) 604.
29. Patton, C.C.: *Oilfield Water Systems*, Campbell Petroleum Series, Norman, OK (1974) 65.
30. Postgate, J.R.: *The Sulfate Reducing Bacteria*, Cambridge U. Press, New York City (1979) 151.
31. Bright, J.: "Oilfield Water Analysis Data Bank," DOE/EC/10116-2, U.S. DOE (1983).
32. Watkins, J.W.: "Properties of Produced Water," *Petroleum Production Handbook*, T.C. Frick and R.W. Taylor (eds.), SPE, Richardson, TX (1962) **II**, 21.1-21.20.
33. McGrain, P. and Thomas, G.R.: "Preliminary Report on the Natural Brines of Eastern Kentucky," *Kentucky Geol. Survey Report* (1951) **3**.
34. McGrain, P.: "Miscellaneous Analyses of Kentucky Brines," *Kentucky Geol. Survey Report* (1953) **7**.
35. Lamborn, R.E.: "Additional Analyses on Brines from Ohio," *Ohio Geol. Survey Report* (1952) **11**.
36. Stout, W., Lamborn, R.E., and Schnaf, D.: "Brines of Ohio," *Bull.*, Ohio Geol. Survey, 4th Series (1932) **37**.
37. Barb, C.F.: "Oil-field Waters of Pennsylvania," *Penn. State. Coll. Bull.* (1931) **8**.
38. Torrey, P.D.: "Composition of Oil-Field Waters of the Appalachian Region," *Sidney Powers Memorial Volume*, AAPG (1934) 841-53.
39. Price, P. et al.: "Salt Brines of West Virginia," *West Virginia Geol. Survey* (1937) **8**.
40. Rogers, G.S.: "Chemical Relation of the Oil-Field Waters in San Joaquin Valley, Calif.," *Bull.*, U.S. Geol. Survey (1917) **653**, 5.
41. Jensen, J.: "California Oil-field Waters," *Sidney Powers Memorial Volume*, AAPG (1934) 953-85.
42. Jessen, F.W. and Rolshausen, F.W.: "Waters from the Frio Formation, Texas Gulf Coast," *Trans.*, AIME (1944) **155**, 23-38.
43. Rogers, G.S.: "Some Oil-field Waters of the Gulf Coast," *Bull.*, AAPG (1919) **3**, 310-31.
44. Minor, H.E.: "Oil-field Waters of the Gulf Coast Plain," *Sidney Powers Memorial Volume*, AAPG (1934) 891-905.
45. Meents, W.F. et al.: "Illinois Oil-field Brines," *Illinois Geol. Survey Div., Ill. Pet.* (1952) **66**.
46. Schoewe, W.H.: "Kansas Oil-field Brines and Their Magnesium Content," *Bull.*, U. of Kansas Publ. (1943) **47**, pt. 2.
47. Rall, C. and Wright, J.: "Analyses of Formation Brines in Kansas," RI 4974, USBM (1953).
48. "Survey of Oklahoma Formation Waters," Mid-Continent District Study Comm. and the U. of Tulsa (1957).
49. Wright, J. et al.: "Analyses of Brines from Oil-productive Formations in Oklahoma," RI 5326, USBM (1957).
50. Plummer, F.B. and Sargent, E.C.: "Underground Waters and Subsurface Temperatures of the Woodbine Sand in Northeast Texas," *Bull.*, U. of Texas Publications (1931) **3138**.
51. Plummer, F.B.: "Texas Water Resources," *Bull.*, U. of Texas Publications (1943) **4301**, 301-12.
52. Barnes, V.E.: "Earth Temperatures and Oil-field Waters of North-Central Texas," *Bull.*, U. of Texas Publications (1943) **4301**, 313-57.
53. Berger, W.R. and Fash, R.H.: "Relation of Water Analyses to Structure and Porosity in the West Texas Permian Basin," *Sidney Powers Memorial Volume*, AAPG (1934) 869-89.
54. Beeler, H.S., McKinney, O.B., and White, V.C.: "The Chemical Analyses of Brines from Some Fields in North and West Texas," Petroleum Branch, AIME (1953).
55. Coffin, C.R. and DeFord, R.K.: "Waters of the Oil and Gas Bearing Formations of the Rocky Mountains," *Sidney Powers Memorial Volume*, AAPG (1934) 927-52.
56. Crawford, J.G.: "Waters of Producing Fields in the Rocky Mountain Region," *Trans.*, AIME (1948) **179**, 264-86.
57. Crawford, J.G.: "Oil-field Waters of Montana Plains," *Bull.*, AAPG (1942) **26**, pt. 2, 1317-74.
58. Ross, J.S. and Swedenborg, E.A.: "Analyses of Waters of the Salt Creek Field Applied to Underground Problems," *Trans.*, AIME (1929) **82**, 207-20.
59. Crawford, J.G.: "Oil-field Waters of Wyoming and Their Relation to Geological Formations," *Bull.*, AAPG (1940) **24**, pt. 2, 1214-1329.
60. Campbell, W.P.: "Oil-field Waters of Alberta and Saskatchewan," *Trans.*, Cdn. Inst. Mining Met. (1929) **32**, 316-32.
61. Elworthy, R.T.: "A Field Method and Apparatus for the Determination by Means of Electrical Conductivity Measurements of the Character of Waters Leaking into Oil and Gas Wells," Cdn. Dept. Mines Summary Rept. No. 605 (1922) 58-70.
62. Hitchon, B.: "Formation Fluids," *Geological History of Western Canada*, R.G. McCrossan and R.P. Glaister (eds.), Alberta Soc. of Petroleum Geologists, Calgary, Alta. (1964) 201-17.
63. Harris, W.E. et al.: "Viking Formation Waters of Alberta," *Alta. Soc. Pet. Geol.* (July 1957).
64. "Analyses of Formation Water Samples," Dept. Mining Resources, Mines Branch, Province of Manitoba, Canada.
65. "Analyses of Formation Water Samples," Dept. Mining Resources, Mines Branch, Province of Saskatchewan, Canada.
66. Borger, H.D.: "Case History of Quiriquire Field, Venezuela," *Bull.*, AAPG, **31**, 2291-2330.
67. "Oil Fields of Royal Dutch-Shell Group in Western Venezuela," *Bull.*, AAPG (1948) **31**, 517-623.
68. Suter, H.H.: "El Mene De Acosta Field, Falcon, Venezuela," *Bull.*, AAPG, **31**, 2193-2206.
69. Hedberg, H.D., Sass, L.C., and Funkhouser, H.J.: "Oil Fields of Greater Oficina Area, Central Anaoategui, Venezuela," *Bull.*, AAPG (1947) **31**, No. 12, 2089-2169.
70. Rittenhouse, G. et al.: "Minor Elements in Oilfield Waters," *Chem. Geol.* (1969) **4**, 189-209.
71. Krejci-Graf, K.: "Data on the Geochemistry of Oilfield Waters," *Geologisches Jahrbuch Reihe D* (1978) **3**, No. 174, 21-25.
72. Bockmeulen, H., Barker, C., and Dickey, P.A.: "Geology and Geochemistry of Crude Oils, Bolivar Coastal Fields, Venezuela," *Bull.*, AAPG (1983) 242-70.
73. Collins, A.G.: "Geochemistry of Some Tertiary and Cretaceous Age Oil-Bearing Formation Waters," *Environmental Science and Technology* (1967) **1**, 725-30.

74. Osif, T.L.: "The Effects of Salt, Gas, Temperature, and Pressure on the Compressibility of Water," paper SPE 13174 presented at the 1984 SPE Annual Technical Conference and Exhibition, Houston, Sept. 16-19.
75. Dorsey, N.E.: *Properties of Ordinary Water Substances*, Monograph Series, American Chemical Soc. (1940) **208**, No. 81, 246.
76. Dotson, C.R. and Standing, M.B.: "Pressure, Volume, Temperature and Solubility Relations for Natural Gas-Water Mixtures," *Drill. and Prod. Prac.*, API (1944) 173-79.
77. Rowe, A.M. Jr. and Chou, J.C.S.: "Pressure-Volume-Temperature-Concentration Relations of Aqueous NaCl Solutions," *J. Chem. Data* (1970) **15**, 61-66.
78. Ashby, W.H. Jr. and Hawkins, M.F.: "The Solubility of Natural Gas in Oil-Field Brines," paper presented at the 1948 SPE Annual Meeting, Dallas, Oct. 4-6.
79. Rogers, P.S.Z. and Pitzer, K.S.: "Volumetric Properties of Aqueous Sodium Chloride Solutions," *J. Phys. Chem. Ref. Data* (1982) **11**, No. 1, 15-81.
80. Wyllie, M.R.J.: *The Fundamentals of Well Log Interpretation*, second edition, Academic Press Inc., New York City (1954) rev. 1957.
81. Amyx, J.W., Bass, C.M. Jr., and Whiting, R.L.: *Petroleum Reservoir Engineering*, McGraw-Hill Book Co. Inc., New York City (1960).
82. Kestin, J., Khalifa, H.E., and Correia, R.J.: "Tables of the Dynamic and Kinematic Viscosity of Aqueous NaCl Solutions in the Temperature Range 20-150°C and the Pressure Range 0.1-35 MPa," *J. Phys. Chem. Ref. Data* (1981) **10**, No. 1, 71-87.
83. McAuliffe, C.D.: "Solubility in Water of Paraffin, Cycloparaffin, Olefin, Acetylene, Cyclo-olefin and Aromatic Hydrocarbons," *J. Phys. Chem.* (1966) **70**, 1267-75.
84. Prince, L.C.: "Aqueous Solubility of Petroleum as Applied to Its Origin and Primary Migration," *Bull.*, AAPG (1976) 213-44.
85. Tickell, F.G.: "A Method for Graphical Interpretation of Water Analysis," *Calif. State Oil Gas Superv.* (1921) **6**, 5-11.
86. Reistle, C.E.: "Identification of Oilfield Waters by Chemical Analysis," U.S. Bur. Min. Technical Paper, 404 (1927).
87. Stiff, H.A. Jr.: "The Interpretation of Chemical Water Analysis by Means of Patterns," *J. Pet. Tech.* (1951) **192**, 15-17.
88. Piper, A.M.: "A Graphic Procedure in the Geochemical Interpretation of Water Analysis," U.S. Geol. Surv. Ground Water Note 12, (1953).
89. Morgan, C.O., Dingman, R.J., and McNellis, J.M.: "Digital Computer Methods for Water-quality Data," *Ground Water* (1966) **4**, 35-42.
90. Morgan, C.O. and McNellis, J.M.: "Stiff Diagrams of Water-quality Data Programmed for the Digital Computer," Kansas State Geol. Surv. Spec. Distrib. Publ. 43 (1969).
91. Angino, E.E. and Morgan, C.O.: "Application of Pattern Analysis to the Classification of Oilfield Brines," Kansas State Geol. Surv. Comput. Contrib. 7 (1966) 53-56.
92. Hitchon, B., Billings, G.K., and Klován, J.E.: "Geochemistry and Origin of Formation Waters in the Western Canada Sedimentary Basin—III. Factors Controlling Chemical Composition," *Geochim. Cosmochim. Acta* (1971) **35**, 567-98.
93. Clayton, R.N. *et al.*: "The Origin of Saline Formation Waters. I. Isotopic Composition," *J. Geophys. Res.* (1966) **71**, 3869-82.
94. De Sitter, L.U.: "Diagenesis of Oil-field Brines," *Bull.*, AAPG (1947) 2030-40.
95. Kharaka, Y.K. and Berry, F.A.F.: "Simultaneous Flow of Water and Solutes Through Geological Membranes I. Experimental Investigations," *Geochim. Cosmochim. Acta.* (1973) **37**, 2577-2603.
96. McKelvey, J.G. and Milne, J.H.: "The Flow of Salt Solution Through Compacted Clay, in Clays and Clay Minerals," 9th Natl. Conf. Clays and Clay Minerals (1962) 248-59.
97. *U.S. Bureau of Mines Minerals Yearbook, Metals, Minerals, and Fuels*, U.S. Bureau of Mines, Washington, D.C. (Yearly).
98. Vine, J.D.: "Lithium Resources and Requirements by the Year 2000," U.S. Geological Survey Professional Paper 1005, U.S. Government Printing Office, Washington D.C. (1976).

Chapter 25

Phase Behavior of Water/Hydrocarbon Systems

Riki Kobayashi, Rice U. *

Kyoo Y. Song, Rice U.

E. Dendy Sloan, Colorado School of Mines

Introduction

The occurrence of water with hydrocarbons both in the reservoir and in the produced states represents the norm. Even though streams saturated with water enter the producing tubing, subsequent cooling generally produces separate phases of low mutual solubilities. Nevertheless, the mutual solubility of water and hydrocarbons is extremely significant in the processing of produced fluids. In the reservoir, their mutual solubilities increase as the temperature increases, either as a result of reservoir depth or external heating, as in the case of a steamflooding operation. Thus, the definition of the saturated water content in the equilibrium phases is the subject of this chapter. The coexisting phases may be gas, G , hydrocarbon-rich liquid, L_{HC} , water-rich liquid, L_w , or hydrate, H , although the coexisting phases are seldom pure. The advent of EOR processes that use CO_2 gives rise to the occurrence of a CO_2 -rich liquid phase, which we designate L_{CO_2} .

General Hydrocarbon/Water Phase Diagrams and Equilibrium Data Sources

For a given mixture of oil, water, and gas, the definition of the phases in equilibrium at any given pressure and temperature is of importance to the reservoir engineer. The prediction of the extent, composition, and other equilibrium properties of the phases in equilibrium is the objective of thermodynamic calculations. Given the number of components in the mixture and the number of coexisting phases, the number of independent variables that must be specified to describe the system (thermodynamically) is given by the phase rule of Gibbs,¹

which states that the “degrees of freedom” or number of independent variables required to define the system, F , equals the number of components, C , minus the number of phases, $P+2$, or $F=C-P+2$. A few examples given this important relationship are summarized in Table 25.1.

The phase rule is essentially a “rule of algebra” applied to equations of equilibrium and as such does not specify which phases are in equilibrium or their equilibrium concentrations. Nevertheless, its value in the organization of knowledge regarding phases in equilibrium and their relationship is important and always should be respected and used.

The pressure-temperature projection of the univariant coexistence lines of binary hydrocarbon/water systems represents a unique way of summarizing the phase behavior of the system. The methane/water system is one in which the critical point of the gas falls far below the ice point. With high pressures, even at moderate temperatures, solid hydrates are formed. The pressure-temperature projection of the system is given by Fig. 25.1.² Of particular interest to petroleum production engineers is the precise location of the L_w - H - G line or the initial hydrate formation condition. Since natural gases vary in composition, the L_w - H - G line is usually compositionally dependent.

Fig. 25.2 shows a constant-pressure trace of the saturation conditions of the methane/water binary system at a constant pressure exceeding the critical pressure of methane. Among the important features of this diagram are the dissolved gas concentration of the water-rich liquid phase (e.g., at Point 4), the equilibrium dewpoint locus, the initial hydrate formation temperature along the horizontal line 7-2-5-6, and the equilibrium and

*Authors of the original chapter on this topic in the 1962 edition were John J. McKetta and Albert H. Wehe.

TABLE 25.1—SUMMARY AND MEANING OF DEGREES OF FREEDOM

Number of Components	Equilibrium Phases	Number of Independent Variables Required To Represent each Locus of States
1	1	2
1	2	1
1	3	0
2	2	2
2	3	1
2	4	0
3	3	2
3	4	1

metastable dewpoint locus (Line 7-8) below the initial hydrate formation temperature and below the stable dewpoint line. The definition of the equilibrium dewpoint water content for methane has been determined by Olds *et al.*³ and the initial hydrate formation condition by Villard,⁴ Deaton and Frost,⁵ Kobayashi and Katz,² and Marshall *et al.*⁶

The definition of the gas-hydrate equilibrium locus, as distinguished from the metastable equilibrium locus erroneously reported in most dewpoint charts, has been reported by Sloan *et al.*⁷ The measurement of the gas hydrate compositions or hydrate numbers for methane was conducted successfully by Galloway *et al.*⁸ and found in essential agreement with the statistical

mechanical theory of van der Waals and Platteeuw,⁹ as applied by Saito *et al.*²⁰⁰ as well as Parrish and Prausnitz,¹⁰ and other subsequent workers.

The second type of pressure-temperature projection presented is for the propane-water system in which the critical temperature of the hydrocarbon exceeds the ice point. Since the aqueous and hydrocarbon-rich phases exhibit low mutual solubilities, a three-phase $H-L_w-G$ condition occurs in the neighborhood of the vapor pressure of condensable hydrocarbons such as propane.

Fig. 25.4 presents a constant-pressure trace of Fig. 25.3 at a pressure less than the critical pressure of propane (Kobayashi¹¹). The principal qualitative difference between Figs. 25.2 and 25.4 is the existence of the $L_{HC}-G$ region in the latter that is absent in the former, at least at moderate temperatures. Note that in the $L_{HC}-G$ region of Fig. 25.4, the water concentration of the gas phase is larger than in the equilibrium liquid phase at the same temperature. On the contrary, in the $G-L_w$ region, the water concentration in the saturated gas is rather less than in the equilibrium water-rich liquid phase.

Owing to the differences in the molecular sizes of methane and propane, the hydrate structures of methane hydrate (Structure I) and of propane hydrate (Structure II) are quite different.

By using phase diagrams such as Figs. 25.2 and 25.4, it is possible to trace the phase transitions one would expect to encounter for various composition mixtures as the temperature of the system is lowered. It is important to note that hydrates can form directly from the fluid hydrocarbon phase (i.e., in the absence of free liquid

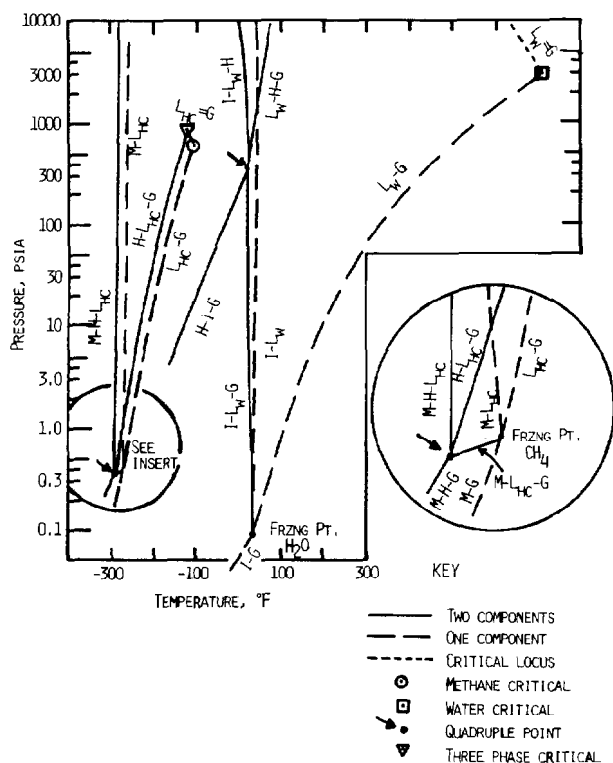


Fig. 25.1—Pressure-temperature projection of univariant heterogeneous equilibrium in the methane-water system.

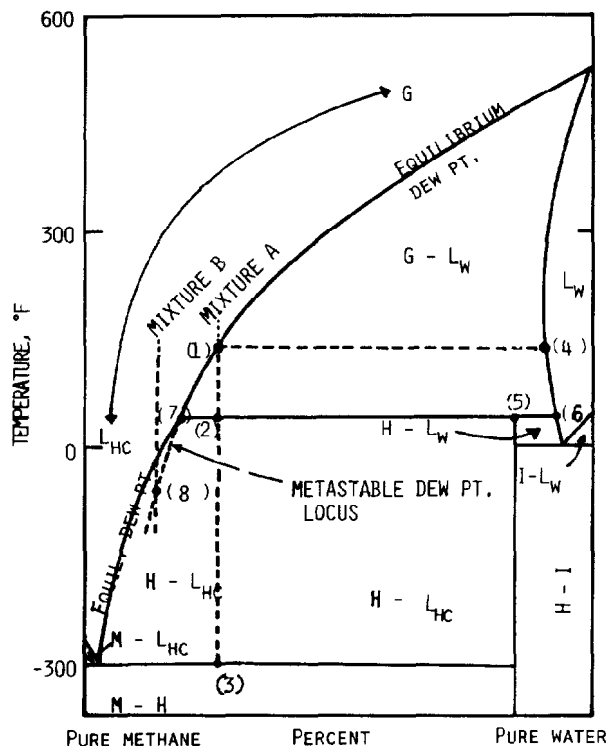


Fig. 25.2—Constant-pressure trace of the methane/water system at a pressure greater than the methane critical pressure.

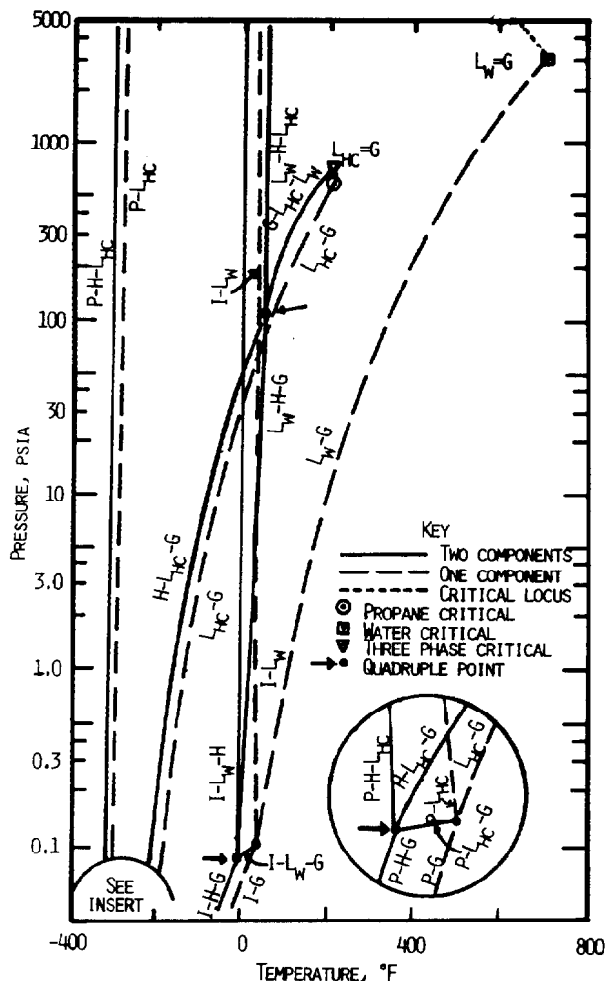


Fig. 25.3—Pressure-temperature projection of univariant heterogeneous equilibrium in the propane-water system.

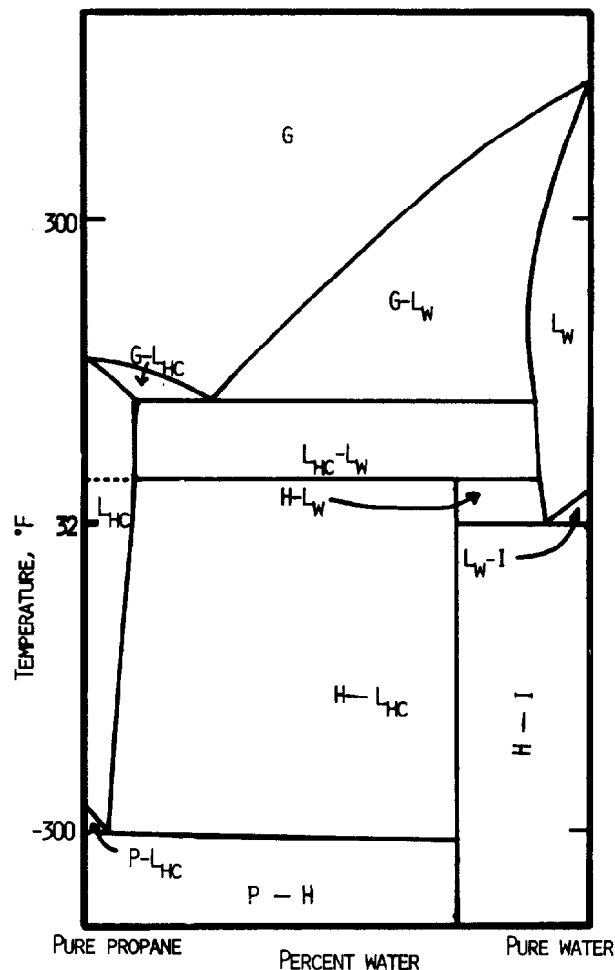


Fig. 25.4—Constant-pressure trace of the propane/water system at a pressure less than the propane critical pressure.

water at low water compositions) provided that the temperature is sufficiently low and turbulence is present or the equilibration times are large, as shown by Cady.¹² The metastable dewpoint line shown in Fig. 25.2 (Line 7-8) rather than the true equilibrium state may be attained under certain situations to give a false or metastable indication of equilibrium (Kobayashi and Katz¹³).

References for aqueous/volatile-gas systems related to petroleum production are listed in the references at the end of the chapter. These are for methane/water system (Refs. 3 and 14 through 44), natural-gas/water (Refs. 13 and 45 through 52), CO₂/water (Refs. 31, 44, and 53 through 96), and for nitrogen/water (Refs. 24, 31, 33 through 36, 62, and 97 through 120). References for other binary and ternary hydrocarbon/water systems are listed in the general references.

References for hydrate/volatile-gas systems are for methane/water (Refs. 2, 4, 6 through 8, and 121 through 129), natural-gas/water (Refs. 126 and 130 through 135), CO₂/water (Refs. 5 and 136 through 139), and nitrogen/water (Refs. 6, 140, and 201). References for other binary and ternary hydrocarbon/hydrate systems are listed in the general references.

As shown in Figs. 25.1 through 25.4 for the methane/water and propane/water systems, the phase behavior of such systems is complicated by the existence of multiphase equilibria, including solid phases such as hydrate or ice. The former phase is particularly troublesome in petroleum production since solid hydrates can form at temperature above the ice point wherein the concentration of water in the system is quite low. Fig. 25.5 presents the univariant three-phase loci for various binary hydrocarbon/water systems and shows their critical hydrate formation loci (solid lines).

The variability of the water content of hydrocarbon-rich phases for a condensable system perhaps is illustrated best by Fig. 25.6, which shows the concentration of water in the propane-rich phases in the propane/water system. In the low-pressure gaseous region the water content is determined primarily by the vapor pressure of water, whereas in the condensed propane region the solubility of water in the propane-rich liquid phase is determined by the strong repulsion of water by the hydrocarbon owing to the thorough hydrogen-bond-breaking ability of the condensed hydrocarbon phase. This phenomenon can be illustrated further by Fig. 25.7, a composite plot of the activity coefficient of water at

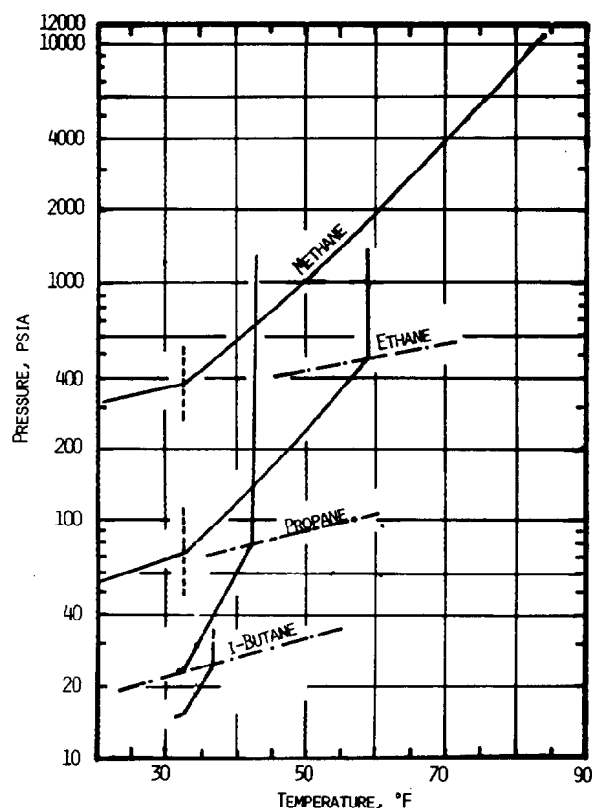


Fig. 25.5—Hydrate-forming conditions for paraffin hydrocarbons.

moderate pressures from hydrocarbon molecules vs. temperature for molecules ranging from propane to liquids as heavy as naphtha and SAE 20 lubricating oil.¹⁴¹ Fig. 25.7 also shows that at higher temperatures water becomes increasingly miscible with hydrocarbons, with total miscibility conditions having been reported for intermediate-range hydrocarbons. This phenomenon, which is relevant to high-pressure steamfloods, also is illustrated by Fig. 25.8, which gives their three-phase miscibility conditions.¹⁴²

In addition to fluid condensed phases, as the pressure is increased and the temperature decreased, nonpolar molecules and weakly ionizing molecules of appropriate molecular sizes form solid gas hydrates. Davidson¹⁴³ presents the approximate molecular diameters and structure type of the hydrate formers and their theoretical hydrate chemical formulas.

Hydrate Stability Conditions

Table 25.2 presents the physical data of the two known hydrate lattices, the diamond type or structure II hydrate, and the body-centered type or Structure I hydrate. Owing to their critical sizes, some molecules, such as cyclopropane, stabilize both hydrate Structures I and II at higher temperatures but only Structure II at lower temperatures with a phase transition temperature in between (see Sloan¹⁴⁴).

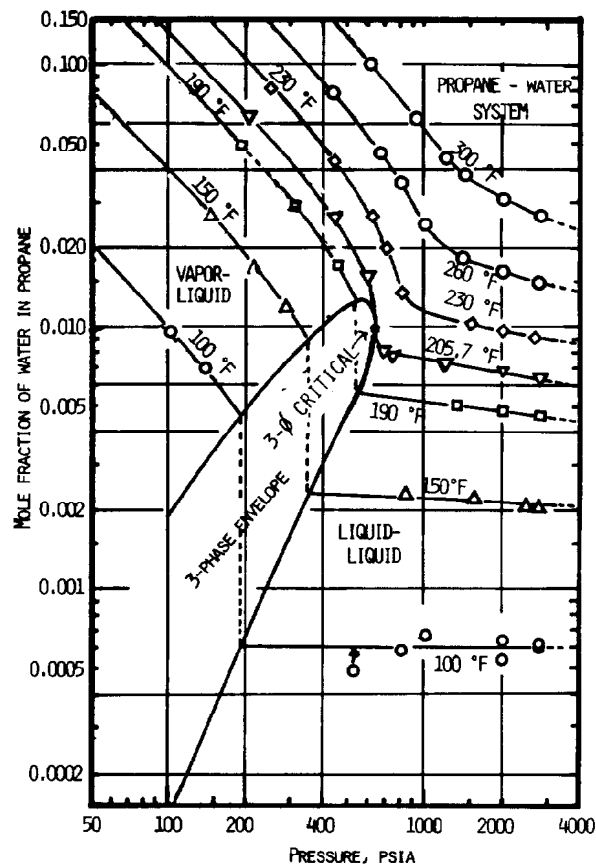


Fig. 25.6—Concentration of water in propane-rich fluid phases in the two- and three-phase regions.

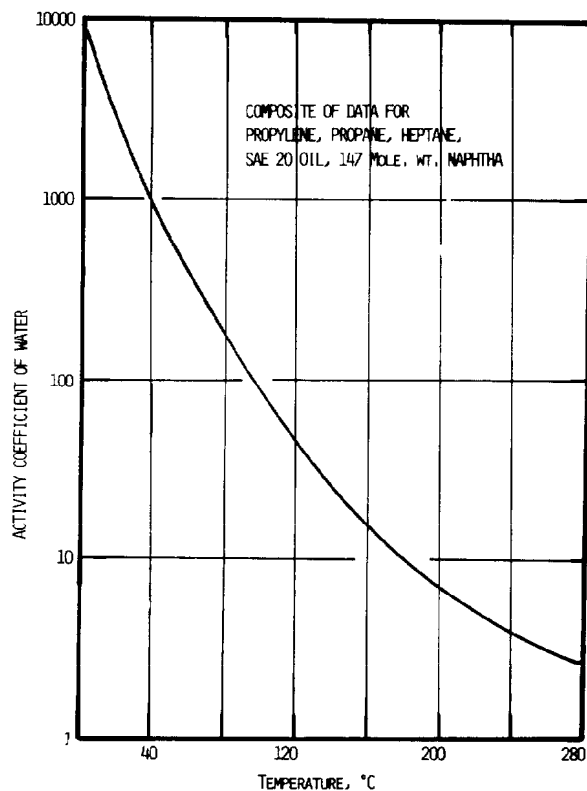


Fig. 25.7—Composite activity coefficient plot for water in hydrocarbon systems.

Estimating Initial Hydrate Formation

The estimation for the stability conditions of the hydrates when liquid water is present, the L_w - H - G equilibrium locus, can be estimated by various means.

Sweet Natural Gas Systems Method. The initial hydrate formation condition can be estimated for sweet natural gas systems by using pressure, temperature, and gas gravity as parameters (see Katz^{145,146}) as shown in Figs. 25.9 and 25.10. These figures should be confined for usage when the natural gas mixtures are similar to those used in developing them, with data taken from Deaton and Frost,⁵ Wilcox *et al.*,¹³⁵ Kobayashi and Katz,² and Katz.¹⁴⁵ Typical compositions of natural gases corresponding to gas gravities of Fig. 25.9 are given in Table 25.3. It should be noted that no H_2S or CO_2 content is tolerated by the correlations.

Vapor/Solid Equilibrium Ratios Method. The second approach involves the development and application of vapor/solid equilibrium ratios for gas/liquid/hydrate equilibrium (Carson and Katz,¹⁴⁷ Unruh and Katz,¹³⁹ Noaker and Katz,¹⁴⁸ Robinson,¹⁴⁹ and Robinson and Ng¹⁵⁰), as shown in Figs. 25.11 through 25.16. The development of the vapor/solid K -values involved experimental hydrate formation conditions for mixtures of methane with other gas(es) and the hypothesis that hydrates could be treated as solid solutions, in hindsight a brilliant hypothesis. The vapor/solid $K_{i(v-s)}$ values are used to calculate the hydrate "frost point" in direct analogy with dewpoint calculations:

$$K_{i(v-s)} \equiv \frac{y_i}{x_i}$$

where $K_{i(v-s)}$ is the vapor/solid equilibrium values of component i , y_i is the mole fraction of component i in the vapor phase, and x_i is the mole fraction of component i in the solid phase, so that

$$\sum_{i=1}^n y_i / K_{i(v-s)} = 1.0. \quad (1)$$

An example calculation for a complex mixture is presented in Table 25.4.¹⁴⁴ As suggested, the K -value of n -butane is taken numerically as that for ethane.

Statistical Mechanics for Adsorption Approach. A third method of estimating initial hydration formation involves the application of statistical mechanics (van der Waals and Platteeuw¹⁵¹) in well-defined hydrate cages as determined by X-ray crystallography by von Stackelberg and Müller^{152,153} and others. The theory of van der Waals and Platteeuw was applied to predict the initial hydrate formation of pure gases at temperature above the ice point by Marshall *et al.*⁶ and later to binary mixtures by Saito and Kobayashi.¹⁵⁴ Nagata and Kobayashi¹⁵⁵ used the Kihara potential to calculate the dissociation pressures of hydrates, following the earlier work of McKoy and Sinanoglu.¹⁵⁶ A more convenient estimation method for hydrate decomposition conditions

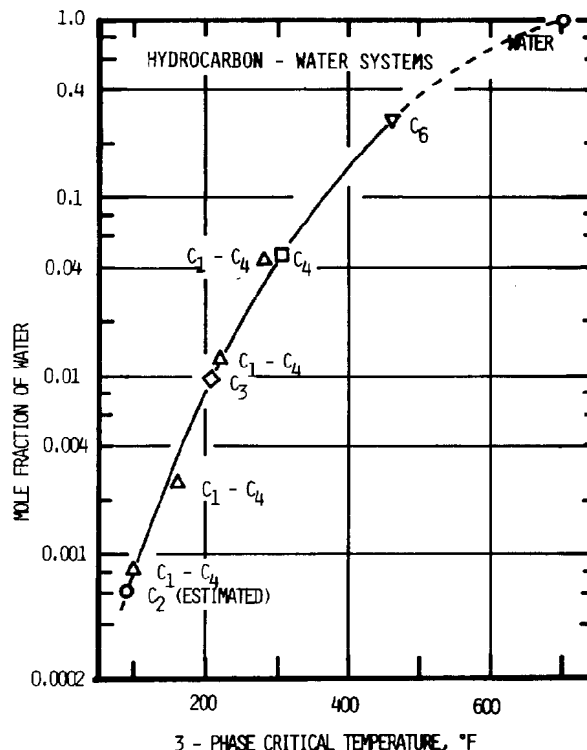


Fig. 25.8—Composition of hydrocarbon-rich phase at three-phase critical conditions.

was developed by Parrish and Prausnitz,¹⁰ using the Kihara potential and the method of van der Waals and Platteeuw.⁹

Computer Method For Hydrate Dissociation Predictions. Parrish and Prausnitz Development.¹⁰ The method of van der Waals and Platteeuw as developed by Parrish and Prausnitz is slightly more complex than the previous method, but it has two considerable advantages: (1) the equations are related to the microscopic hydrate structure, and (2) the theoretical nature of the model allows it to be extended beyond the G - L_w - H region.

TABLE 25.2—PHYSICAL DATA OF TWO KNOWN HYDRATE LATTICES

	Structure I	Structure II
Water molecules per unit cell	46	136
Cavities per unit cell		
Small	2	16
Large	6	8
Cavity radius, r_c		
Small	3.97	3.91
Large	4.30	4.73
Typical gases that form in each cavity of this structure	methane* ethane**	propane** i-butane** n-butane** neo-pentane**

*Small.
**Large.

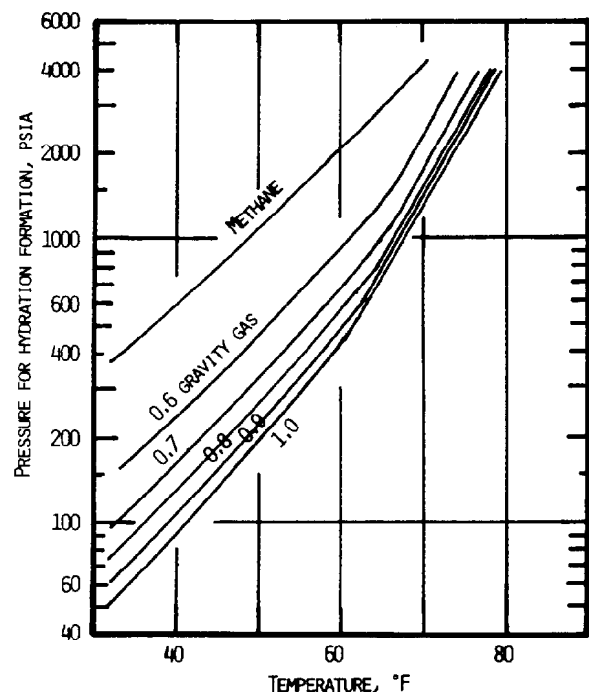


Fig. 25.9—Initial hydrate-formation conditions for natural gases with varying gas gravities.

In the late 1940's and early 1950's the molecular structures of hydrates, shown in Table 25.2, were studied through the use of X-ray diffraction.^{152,153} The structural determination enabled van der Waals and Platteeuw⁹ to develop a model for the prediction of hydrate dissociation pressure at any temperature. Their basic equation looks complex until one considers it as being very similar to the basic equation for the chemical potential of Component 1 in a mixture of Components 1 and 2. This equation, which relates the chemical potential of

TABLE 25.3—TYPICAL COMPOSITIONS AND CORRESPONDING GAS GRAVITIES OF NATURAL GASES OF FIG. 25.9

	Mole Fraction				
CH ₄	0.9267	0.8605	0.7350	0.6198	0.5471
C ₂ H ₆	0.0529	0.0606	0.1340	0.1777	0.1745
C ₃ H ₈	0.0138	0.0339	0.0690	0.1118	0.1330
i-C ₄ H ₁₀	0.00182	0.0084	0.0080	0.0150	0.0210
n-C ₄ H ₁₀	0.00338	0.0136	0.0240	0.0414	0.0640
C ₅ H ₁₂ + Gravity calculation	0.0014	0.0230	0.0300	0.0343	0.0604
	0.603	0.704	0.803	0.906	1.023

component i , μ_i , to the activity of a component is

$$\mu_i = \mu_i^0 + RT \ln a_i, \dots \dots \dots (2)$$

where

μ_i^0 = chemical potential of pure component i ,

R = universal gas constant,

T = absolute temperature, and

a_i = activity of component i in mixture.

Van der Waals and Platteeuw used theory to derive a similar equation for the chemical potential of water in the hydrate structure as follows.

$$\mu_{wH} = \mu_{wMT} + RT \sum_i n_{ci} \ln \left(1 - \sum_j y_{ji} \right), \dots \dots (3)$$

where

μ_{wH} = chemical potential of water in filled hydrate,

μ_{wMT} = chemical potential of water in empty hydrate,

n_{ci} = number of cavities of type i per water molecule in basic lattice, and

y_{ji} = fractional occupancy of type i cavity by type j molecule.

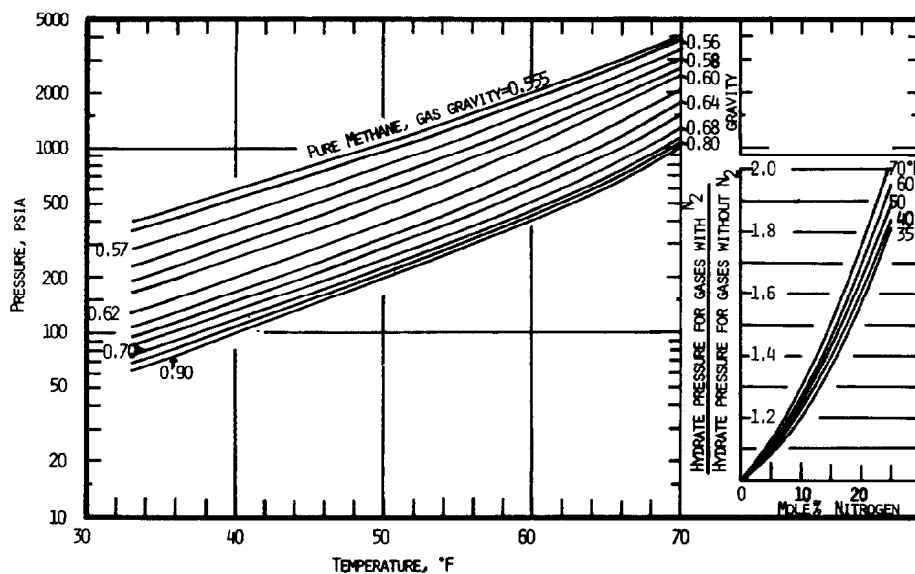


Fig. 25.10—Initial hydrate-formation condition.

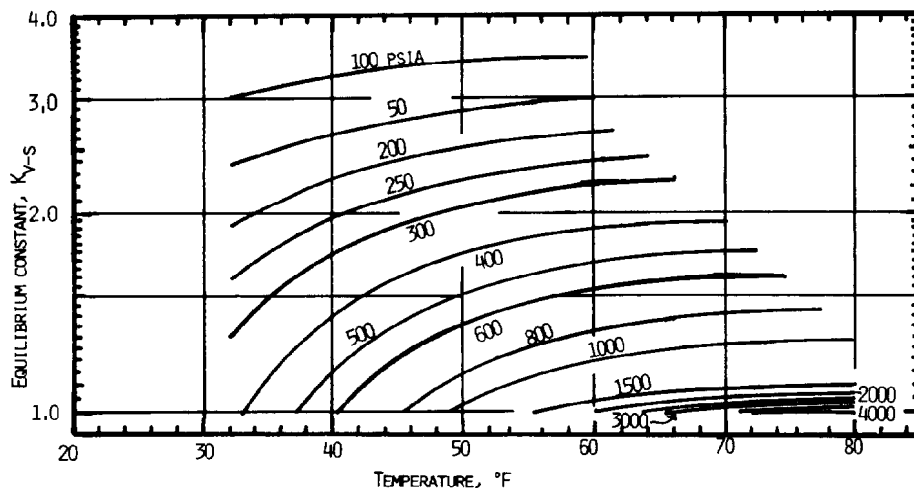


Fig. 25.11—Vapor/solid equilibrium constant for methane.

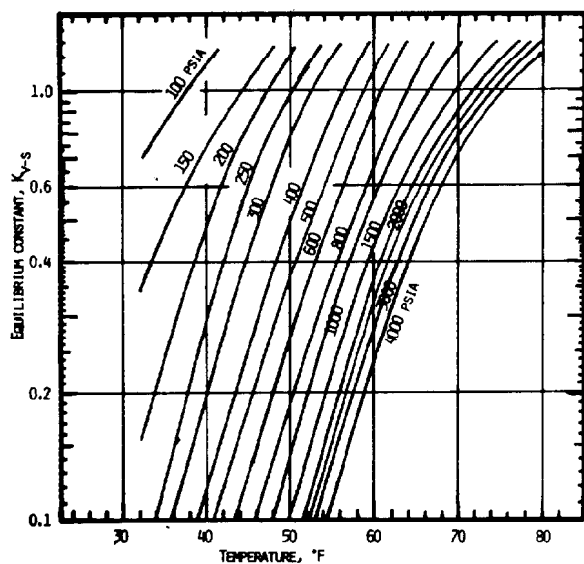


Fig. 25.12—Vapor/solid equilibrium constant for ethane.

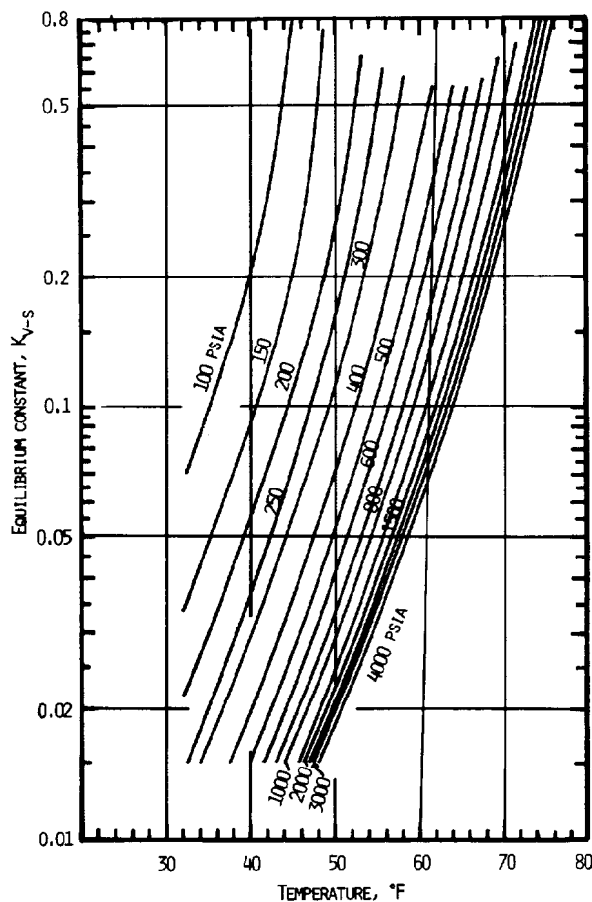


Fig. 25.13—Vapor/solid equilibrium constant for propane.

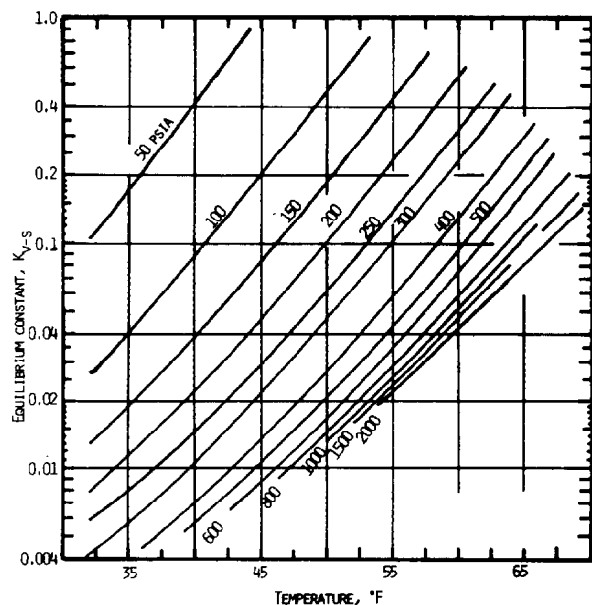
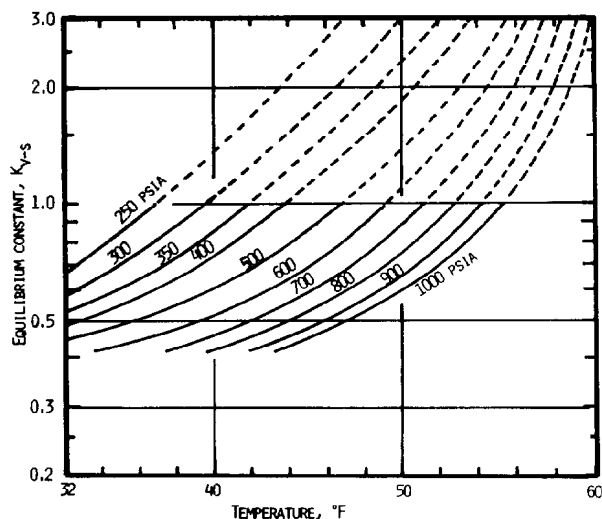


Fig. 25.14—Vapor/solid equilibrium constant for isobutane.

Fig. 25.15—Vapor/solid equilibrium constants for CO₂.TABLE 25.4—CALCULATION OF PRESSURE FOR
HYDRATE FORMATION OF A COMPLEX MIXTURE
AT 50°F*

	Mole Fraction in Gas	At 300 psia		At 350 psia	
		K	y/K	K	y/K
CH ₄	0.784	2.04	0.3841	1.90	0.4126
C ₂ H ₆	0.060	0.79	0.0759	0.63	0.0952
C ₃ H ₈	0.036	0.113	0.3186	0.085	0.4234
i-C ₄ H ₁₀	0.005	0.046	0.1087	0.034	0.1471
n-C ₄ H ₁₀	0.019	0.79	0.024	0.63	0.030
N ₂	0.094	∞	0	∞	0
CO ₂	0.002	3.0	0.0007	2.3	0.0008
Total	1.000		0.912		1.10

*The linearly interpolated answer is 322 psia and the experimentally observed hydrate formation pressure at 50°F was 325 psia.

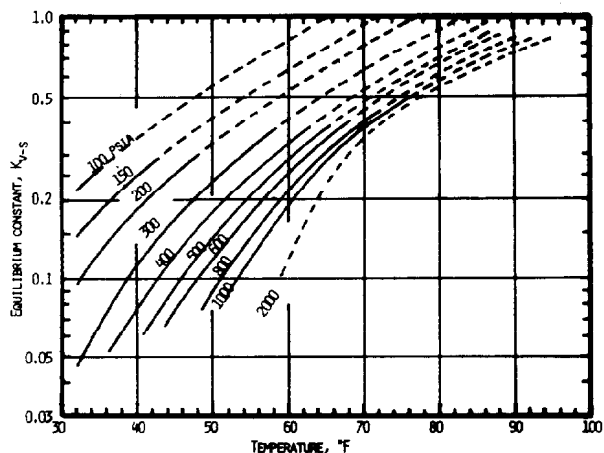


Fig. 25.16—Vapor/solid equilibrium constants for hydrogen sulfide.

The second term on the right accounts for hydrocarbon filling of the lattice. The term y_{ji} is given by

$$y_{ji} = \frac{C_{ji}f_j}{1 + \sum_k C_{ki}f_k}, \quad \dots \dots \dots (4)$$

where C_{ji} is a unique function of temperature for each guest molecule in each size cavity, f_j and f_k are the fugacities of j and k in the gas phase, and k is ordered from one to the number of components.

The fugacity term is determined by an equation of state (EOS), such as Peng-Robinson (PREOS).¹⁵⁷ The C_{ji} functions may be calculated using the Lennard-Jones-Devonshire spherical cell model. The interaction between the guest molecule and a uniform spherical surface representing the cage commonly is described by a Kihara potential function. The method is described by Parrish and Prausnitz.¹⁰ The Kihara parameters are determined from single or binary gas dissociation conditions and then may be used to predict dissociation conditions for multicomponent gases. A fit of C_{ji} for common gases is given in Table 25.5.

To predict hydrate formation conditions from liquid water and gas, the following conditions must be satisfied.

$$\mu_{wL} = \mu_{wH} = \mu_{wg}, \quad \dots \dots \dots (5a)$$

$$T_L = T_H = T_g, \quad \dots \dots \dots (5b)$$

and

$$p_L = p_H = p_g, \quad \dots \dots \dots (5c)$$

where p is the absolute pressure and subscripts L , H , and g are liquid water, hydrate, and gas, respectively.

TABLE 25.5—PARAMETERS FOR THE HYDRATE DISSOCIATION MODEL

	Structure I*	Structure II**
$\Delta\mu_w(T_o, p_o)$, J/mol	1297	874
$\Delta h_w(T_o)$, J/mol	1389	1624.6
Δv_w , cm ³ /mol	3.0	3.4

Parameters for Calculating Langmuir Constant Between 260 K and 300 K

$$C_{ji} = A/T \exp(B/T) \text{ atm}^{-1}$$

	Small Cavities of Structure I		Large Cavities of Structure I		Small Cavities of Structure II		Large Cavities of Structure II	
	$A \times 10^3$	B	$A \times 10^2$	B	$A \times 10^2$	B	$A \times 10^2$	B
CH ₄	2.7711	2752.8047	1.4865	2878.0682	2.1778	2713.4259	6.6777	2310.0682
C ₂ H ₆	0.0	0.0	0.4071	3820.7119	0.0	0.0	2.9157	3277.9254
C ₃ H ₈	0.0	0.0	0.0	0.0	0.0	0.0	1.3212	4506.9810
n-C ₄ H ₁₀	0.0	0.0	0.0	0.0	0.0	0.0	0.0404	2687.9744
i-C ₄ H ₁₀	0.0	0.0	0.0	0.0	0.0	0.0	0.0788	3083.9044
N ₂	17.7986	1931.5130	5.7883	1669.2292	14.8724	2002.6644	15.6182	1319.4734
CO ₂	1.5227	2943.9948	1.0242	3172.6655	1.1620	2837.3018	5.3986	2478.0545
H ₂ S	2.3458	3701.3170	1.3532	3739.3355	1.8306	3671.9126	6.4567	2976.4243

*Dharmawardhana.¹⁵⁶**Weiler.¹⁵⁹

Eq. 5a may be combined with Eqs. 3 and 2 to obtain

$$\Delta\mu_w = \mu_{wMT} - \mu_{wL} = -RT \sum_i n_{ci} \ln \left(1 - \sum_j y_{ji} \right) + RT \ln a_i, \dots\dots\dots(6)$$

where $\Delta\mu_w$ is the difference in chemical potential of pure water and a_i accounts for the normally small solubility of the guest gas in the aqueous phase. Now given T , p , and f_j , one may calculate $\Delta\mu_w$ in Eq. 6 by using Eq. 3 and the Kihara potential. However, the $\Delta\mu_w$ obtained are useless until they are matched to the $\Delta\mu_w$ from the following equation.

$$\frac{\Delta\mu_w(T, p)}{RT} = \frac{\Delta\mu_w(T_o, p_o)}{RT} - \int_{T_o}^T \frac{\Delta h_w}{RT^2} dT + \int_{p_o}^p \frac{\Delta v_w}{RT} dp, \dots\dots\dots(7)$$

where

- T_o = reference temperature,
- p_o = reference pressure,
- Δh_w = specific enthalpy difference, and
- Δv_w = specific volume difference.

Eq. 7 corrects a chemical potential difference at a standard T_o (0°C) and p_o (0 atm), $\Delta\mu_w(T_o, p_o)$ for the change in temperature and pressure of the hydrate of interest. The constants $\Delta\mu_w(T_o, p_o)$ and $\Delta h_w(T_o)$, measured recently by Dharmawardhana¹⁵⁸ and Weiler,¹⁵⁹ and parameters for Langmuir constants are given in Table 25.5.

Procedure for Determining Hydrate Formation Pressure. The procedure for determining hydrate formation pressures for a given gas at a given temperature is as follows.

1. Estimate a pressure, p .
2. At the estimated pressure, for the given temperature and gas mole fraction of component j , determine the fugacity of j from an EOS, such as PREOS.¹⁵⁷
3. By using C_{ji} values from the Kihara potential and y_{ji} values from Eq. 4, determine $\Delta\mu_w$ from Eq. 3.
4. By using constants from Table 25.5, calculate $\Delta\mu_w$ from Eq. 7 at the temperature and estimated pressure.
5. If the $\Delta\mu_w$ values for Eqs. 6 and 7 are equal, then the p value is correct for hydrate formation. If not, estimate a new value of p and return to Step 2.

A computer program that performs the above procedure has been written by Ng and Robinson and is available commercially through the Gas Processors Assn. (GPA). A second hydrate program generated by Erickson and Sloan¹⁶⁰ at the Colorado School of Mines is also available through GPA.

That the model predicts the three-phase data accurately is demonstrated in Fig. 25.17 for the methane/propane system. The dramatic decrease of dissociation pressure for a 1% addition of propane is evidence that the hydrate has changed structure (from I to II) as mentioned earlier. In other words, as small amounts of propane are added, a greater temperature at constant pressure is tolerated for hydrate formation.

Fig. 25.18 also demonstrates the accuracy of the model while indicating that hydrates denude the gas of propane. At 5 atm, while the gas phase has about 8% propane, the solid phase has 50% propane. From Figs. 25.17 and 25.18 and typical earth temperature gradients, Davidson¹⁶¹ proposed the following in-situ, onshore hydrate conditions.

Going toward the center of the earth, one may encounter Structure II hydrate at relatively shallow depths until the point at which the hydrate denudes the gas of propane. No more hydrate is encountered until the range of Structure I stability conditions is obtained. Continuing downward from the Structure I region no hydrates are encountered. Finally, a Structure II region is realized for gases rich in propane.

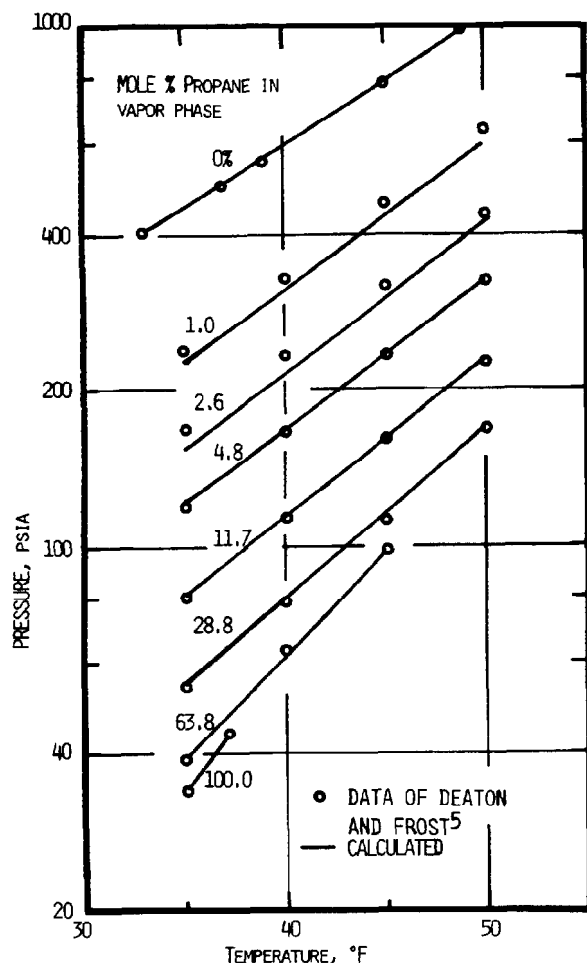


Fig. 25.17—Hydrate formation conditions for the methane/propane/water system.

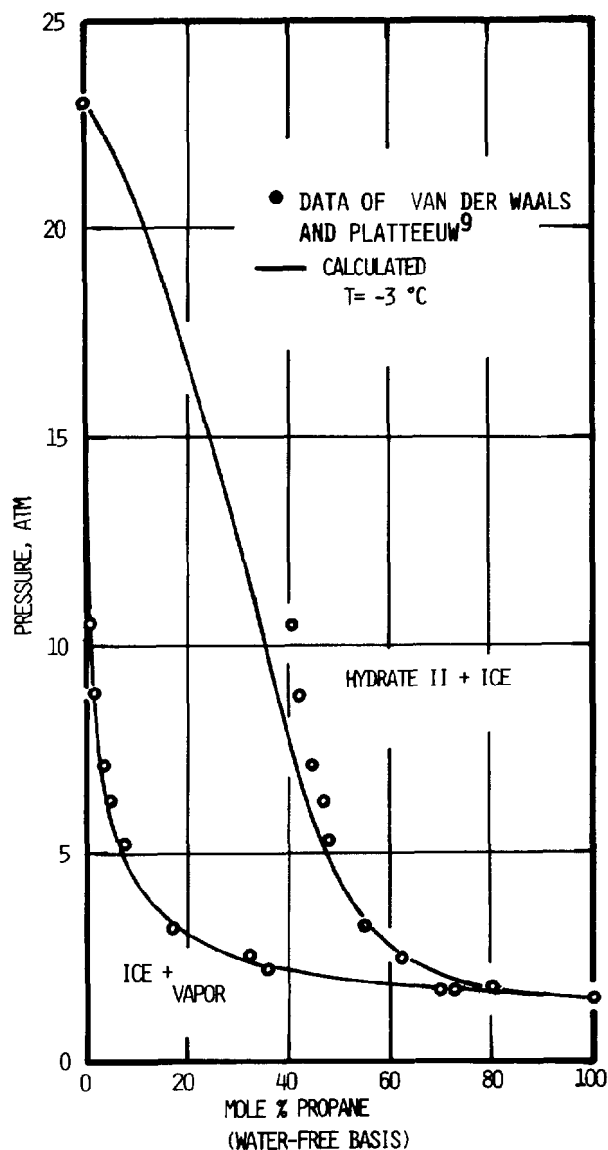


Fig. 25.18—Pressure-composition diagram for the methane/propane/water system.

Determining the Water Content of Gas (or Hydrocarbon-Rich Liquid) in Equilibrium with Hydrates

The position of lines $G-H$ and $L_{HC}-H$ in Figs. 25.2 and 25.4 determines the extent to which the hydrocarbon must be dried to prevent the formation of hydrate from the gas phase. The water content in this region is relatively small and difficult to measure. Until recently, straight lines (log water content vs. $1/T$ from the gas/liq-uid region were extrapolated into the gas/hydrate region with only limited experimental justification. However, as indicated by Kobayashi and Katz,¹³ thermodynamics tells us that such concentration extrapolations across phase boundaries yield severe errors. This observation, that straight-line extrapolation into the gas hydrate region represents gas in equilibrium with metastable liq-uid water, explains the field data anomalies observed by

Records and Seely.¹⁶² Laboratory confirmation that the water content of gas in equilibrium with hydrate should be much different from the extrapolated values has been verified by Sloan *et al.*⁷ for methane hydrates, and Song and Kobayashi¹⁶³ for methane/propane hydrates.

When one predicts the water content of a single fluid phase, such as a fluid, in equilibrium with hydrates, the basic equation is as follows.

$$f_{wf} = f_{wH}, \quad (8)$$

where f_{wf} is the fugacity of water in the fluid phase and f_{wH} is the fugacity of water in the hydrate phase.

In this equation the fugacity of water in the fluid phase is determined from

$$f_{wf} = y_w K_{wf} p, \quad (9)$$

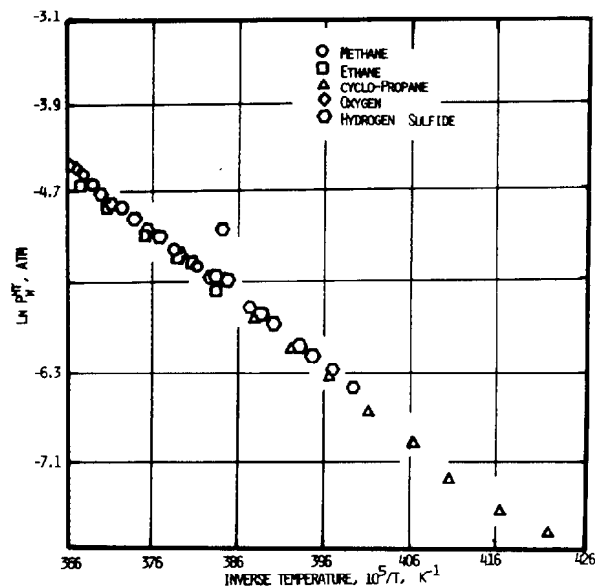


Fig. 25.19—Structure I empty hydrate vapor pressure as a function of reciprocal temperature.

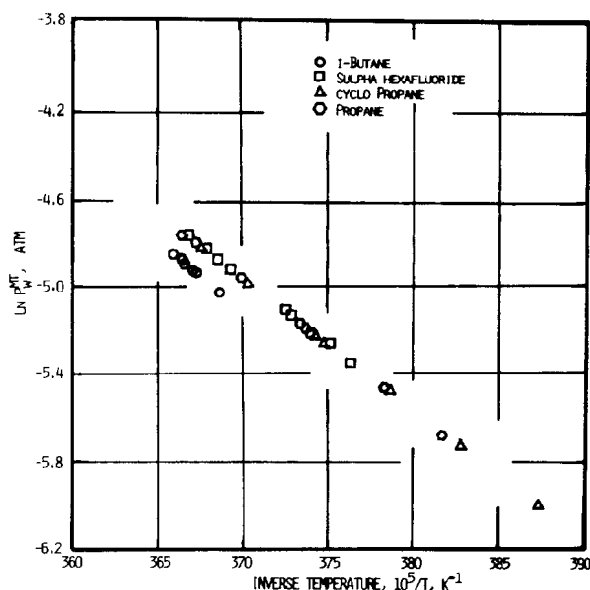


Fig. 25.20—Structure II empty hydrate vapor pressure as a function of reciprocal temperature.

where K_{wf} is the fugacity coefficient* of water (determined by an EOS) and y_w is the mole fraction of water in the hydrocarbon.

The value y_w is the solution to this problem, stated as: given a flowing hydrocarbon at T and p , determine how much the fluid should be dried to prevent hydrate formation.

The quantity f_{wH} in Eq. 8 is determined by

$$f_{wH} = f_{wMT} \exp(-\Delta\mu_w/RT), \quad \dots\dots\dots (10)$$

where f_{wHT} is the fugacity of water in empty hydrate.

Ng and Robinson¹⁶⁴ give an expression for f_{wMT} in both structures, obtained by fitting the vapor/hydrate data of Kobayashi *et al.*^{7,121,165} Therefore, their method may be considered a correlation of existing two-phase (vapor/hydrate) data.

By equating the fugacity of hydrate to ice in three-phase data, Dharmawardhana¹⁵⁸ showed that f_{wMT} of Eq. 10 can be expressed as an empty hydrate vapor pressure as follows:

$$p_{vI} K_{fI} \exp \frac{V_I(p - p_I)}{RT} = p_{vMT} K_{fMT} \exp(\Delta\mu/RT), \quad \dots\dots\dots (11)$$

where

- p_{vI} = vapor pressure of ice,
- K_{fI} = fugacity coefficient of ice,
- V_I = volume of ice,
- p_I = vapor pressure of ice,
- p_{vMT} = vapor pressure of empty hydrate, and
- K_{fMT} = fugacity coefficient of empty hydrate.

*In some prior publications, ϕ was used as the symbol for fugacity coefficient.

In this equation, all of the ice properties are well known, the $\Delta\mu$ is obtained from three-phase data fit to Eqs. 3 and 4; the only unknown is p_{vMT} , which was fit to a number of hydrates' three-phase data below 273 K and found to be a single function of temperature; Figs. 25.19 and 25.20 show these values for empty hydrate vapor pressure as determined from a number of hydrates. Recent work at the Colorado School of Mines has shown the method represented by Eqs. 9 and 10 and Figs. 25.19 and 25.20 to represent the water-in-liquid hydrocarbon/hydrate equilibria accurately.

Hydrate Formation on Expansion of Gases

The simultaneous solution of the isenthalpic (throttling) expansion of natural gases with initial hydrate formation conditions, Fig. 25.9 yields a first approximation of the prediction of permissible expansions. Katz¹⁴⁵ presented a useful chart for various gas gravities of natural gases.

Definition of the Saturated Water Content of Natural Gases in Equilibrium With Aqueous Phases

The saturated water content of natural gases in equilibrium with aqueous phases generally is presented in the familiar dewpoint chart. Fig. 25.21 presents a dewpoint chart for methane-rich gases synthesized from several sources of data. The upper limit of the dewpoint chart given in Fig. 25.21 is defined by the properties of steam. Fig. 25.22 presents a correction to Fig. 25.21 caused by the hydrate formation of methane gas, and a mixture of methane and propane gas. The water content at temperatures above the hydrate stability conditions up to 10,000 psia are based primarily on the data of Olds *et al.*³ At temperatures below the initial hydrate formation

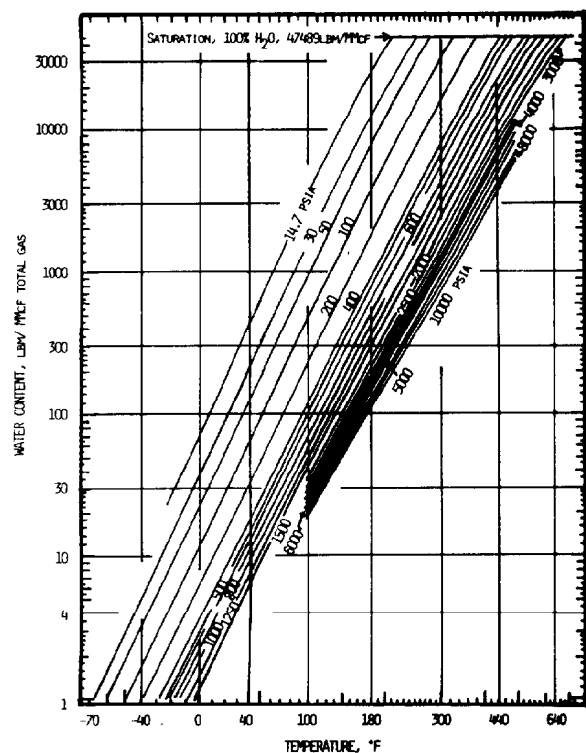


Fig. 25.21—Dewpoint water content chart for methane-rich gas.

conditions, the data are primarily those measured by Skinner.¹⁶⁶ However, below the initial hydrate formation conditions, as initially observed (in the gas fields) by Records and Seely,¹⁶² Fig. 25.21 presents metastable values. Using the hydrate theory discussed previously, and recent measurements on the water content of two gases (a methane/5.31-mol% propane and a pure methane in the gaseous state in equilibrium with hydrates), a corrective correlation to Fig. 25.21 in the gas/hydrate region was developed.

A typical replacement chart is shown in Fig. 25.22.¹⁶³ In this figure the high-temperature vapor/liquid-water region is separated from the low-temperature vapor/hydrate region by a line representing the three-phase (vapor/liquid-water/hydrate) boundary. The isobaric data in the vapor/hydrate region follow semilogarithmic straight lines when plotted against reciprocal temperature, but these lines have slopes different from the straight lines in the vapor/liquid-water region. In addition, the three-phase lines are indicated to be a function of gas composition, so that the change in the slope of an isobar from the vapor/liquid region occurs at different temperatures. With the above complexities, a comprehensive water content chart (or series of charts) for gases of differing compositions would be cumbersome. Instead, a mathematical method for determining the water content of gases in the vapor/hydrate region is used.

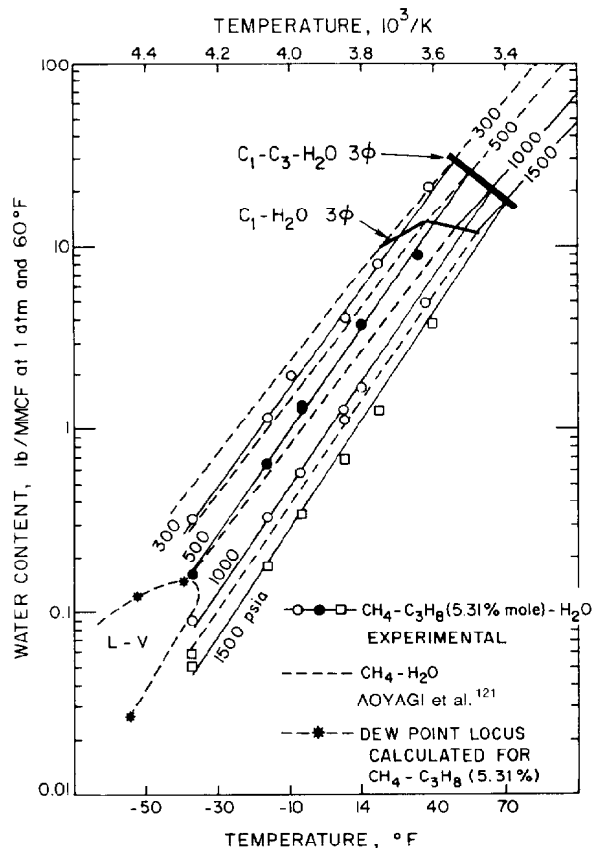


Fig. 25.22—Depression of metastable dewpoint below initial hydrate temperature.

Steps in Determining the Water Content of Vapor in Equilibrium with Hydrates

The method for determining the water content of vapor in equilibrium with hydrates, at a given temperature and pressure, is composed of six steps.

1. Calculate the metastable water content at the temperature and pressure of interest by using Eq. 12.
2. Calculate the three-phase temperature at the pressure and gas gravity of interest by using Eq. 13. Obtain the temperature difference (ΔT) by subtracting the temperature of interest from the calculated three-phase temperature.
3. Calculate the displacement from the metastable water content (ΔW) at the above ΔT and pressure of interest using both Eq. 14a for methane and Eq. 14b for a 94.69-mol% methane/5.31-mol% propane mixture.
4. Calculate the ΔW for the gas composition of interest by a linear interpolation between the ΔW for methane (gravity=0.552) and the ΔW for the mixture containing 5.31% propane (gravity=0.603), using gravity as an interpolation parameter.
5. Calculate the equilibrium water content by subtracting the ΔW value obtained in Step 4 from the metastable water value obtained in Step 1.
6. Consider the range of data used to fit Eqs. 12, 13, 14a, and 14b, as discussed later, to determine whether the answer obtained in Step 5 is within the bounds of the correlation.

TABLE 25.6—COEFFICIENTS FOR EQUATIONS

	Eq. 12	Eq. 13	Eq. 14a	Eq. 14b
C ₁	2.8910758E + 1	2.7707715E - 3	-1.605505E + 3	2.59097E + 3
C ₂	-9.6681464E + 3	-2.782238E - 3	8.181485E + 2	-1.51351E + 3
C ₃	-1.6633582E + 0	-5.649288E - 4	9.289352E + 2	-1.16506E + 2
C ₄	-1.3082354E + 5	-1.298593E - 3	-1.578381E + 2	3.26066E + 2
C ₅	2.0353234E + 2	1.407119E - 3	-3.899544E + 2	6.65280E + 1
C ₆	3.8508508E - 2	1.785744E - 4	-2.009926E + 1	-1.17697E + 1
C ₇		1.130284E - 3	1.368723E + 1	-3.05990E + 1
C ₈		5.9728235E - 4	5.500387E + 1	-1.20352E + 1
C ₉		-2.3279181E - 4	4.088990E + 0	2.94244E + 0
C ₁₀		-2.6840758E - 5	1.517650E + 0	7.83747E - 1
C ₁₁		4.6610555E - 3	-4.524342E - 1	1.04913E + 0
C ₁₂		5.5542412E - 4	-2.590273E + 0	7.23943E - 1
C ₁₃		-1.4727765E - 5	-2.46599E - 1	-2.94560E - 1
C ₁₄		1.3938082E - 5	-7.543630E - 2	7.08799E - 2
C ₁₅		1.4885010E - 6	1.034443E - 1	-1.24938E - 1

Equations for Determining the Water Content of Vapor in Equilibrium with Hydrates

In the following equations, the pressure is expressed in psia, the temperature in degrees Rankine, and the water content is expressed in pounds of water per million cubic feet of gas at 1 atm and 60°F. A listing of the coefficients in each equation is found in Table 25.6.

Fit of Methane-Rich Gas (Fig. 25.21). The following equation, which is a fit of Fig. 25.21, is in the pressure range of 200 to 2,000 psia, and in the temperature range of -40 to 120°F, for metastable water content, W_{ms} , as a function of temperature, T , and pressure, p :

$$W_{ms} = \exp[C_1 + C_2/T + C_3(\ln p) + C_4/T^2 + C_5(\ln p)/T + C_6(\ln p)^2], \dots (12)$$

where $C_1 \dots C_6$ are obtained from Table 25.6.

Fit of Three-Phase (Vapor/Liquid/Hydrate) Formation Conditions. The three-phase condition was fit in the temperature range of 34 to 62°F, the pressure range of 65 to 1,500 psia, and the gas gravity, γ , range from 0.552 to 0.9. Only hydrocarbons were used in the fit, and gases containing CO₂ and hydrogen sulfide were excluded specifically.

$$T = 1/[C_1 + C_2(\ln p) + C_3(\ln \gamma) + C_4(\ln p)^2 + C_5(\ln p)(\ln \gamma) + C_6(\ln \gamma)^2 + C_7(\ln p)^3 + C_8(\ln p)^2(\ln \gamma) + C_9(\ln p)(\ln \gamma)^2 + C_{10}(\ln \gamma)^3 + C_{11}(\ln p)^4 + C_{12}(\ln p)^3(\ln \gamma) + C_{13}(\ln p)^2(\ln \gamma)^2 + C_{14}(\ln p)(\ln \gamma)^3 + C_{15}(\ln \gamma)^4], \dots (13)$$

where $C_1 \dots C_{15}$ are obtained from Table 25.6.

Fit of Water Content Suppression. The suppression of the water content from the metastable region, ΔW , was

fit as a function of pressure and of the temperature difference from the three-phase condition, ΔT , for both methane and a mixture containing 5.31 mol% propane. The fit for methane was in the pressure range of 500 to 1,500 psia and in the temperature range of -28 to 26°F; coefficients for methane in the following equation are labelled Eq. 14a in Table 25.6. The fit for the mixture was in the pressure range of 500 to 1,500 psia, and in the temperature range of -38 to 40°F; coefficients for the mixture are labelled Eq. 14b in Table 25.6. The general regression equation for both gases is:

$$\begin{aligned} \Delta W = & \exp[C_1 + C_2(\ln p) + C_3(\ln \Delta T) + C_4(\ln p)^2 \\ & + C_5(\ln p)(\ln \Delta T) \\ & + C_6(\ln \Delta T)^2 + C_7(\ln p)^3 \\ & + C_8(\ln p)^2(\ln \Delta T) \\ & + C_9(\ln p)(\ln \Delta T)^2 + C_{10}(\ln \Delta T)^3 + C_{11}(\ln p)^4 \\ & + C_{12}(\ln p)^3(\ln \Delta T) + C_{13}(\ln p)^2(\ln \Delta T)^2 \\ & + C_{14}(\ln p)(\ln \Delta T)^3 + C_{15}(\ln \Delta T)^4], \dots (14) \end{aligned}$$

Example Calculation of Water Content of a Vapor in Vapor/Hydrate Region. Determine the water content of a gas whose gravity is 0.575 in equilibrium with hydrate at 1,000 psia and 8.4°F.

1. The metastable water content of the gas is calculated from Eq. 12 at 1,000 psia and 8.4°F as 2.745 lbm/10⁶ scf.

2. The three-phase temperature at 1,000 psia is calculated to be 60.35°F from Eq. 13. The ΔT value is 51.95°F.

3. The displacement from the metastable condition is calculated for methane to be 0.653 lbm/10⁶ scf from Eq. 14a. The displacement from the metastable condition is calculated for the mixture containing 5.31 mol% propane as 1.55 lbm/10⁶ scf from Eq. 14b.

4. An interpolation between the values obtained in Step 3 (based on gas gravity) is done to determine the displacement for a gas with a gravity of 0.575. The resulting displacement is 1.0575 lbm/10⁶ scf.

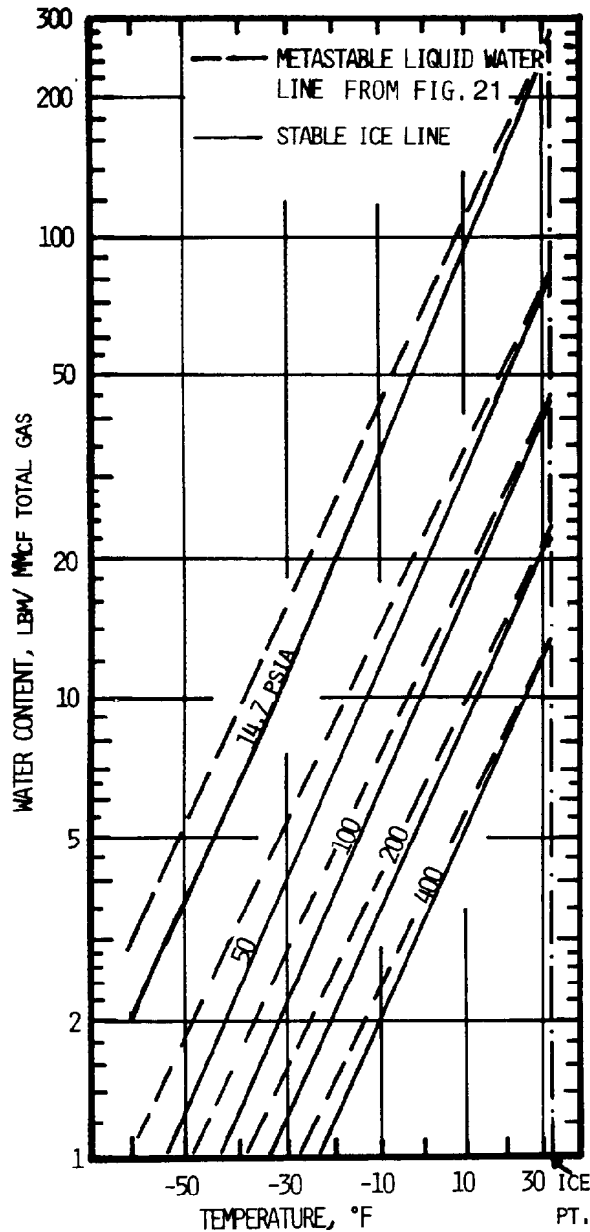


Fig. 25.23—Depression of metastable dewpoint below ice temperature.

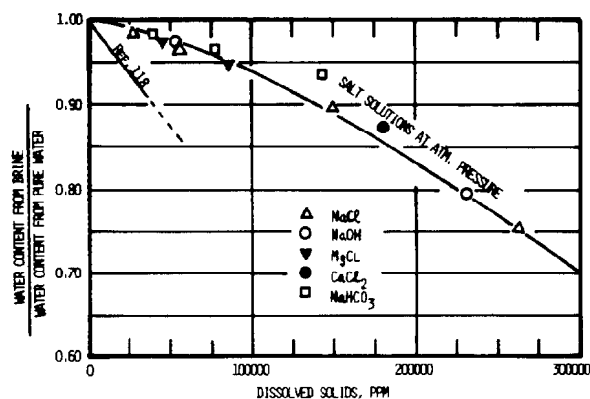


Fig. 25.24—Correction to water content for natural gas in equilibrium with brines.

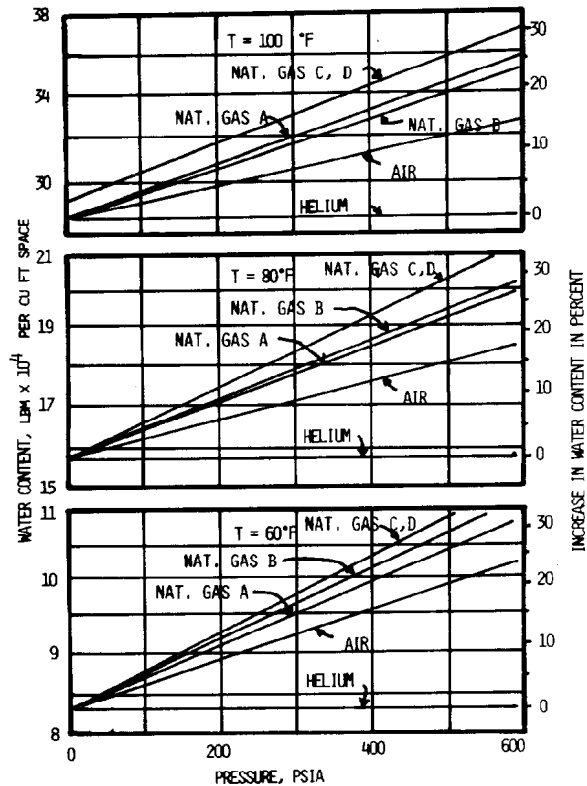


Fig. 25.25—Water content per cubic feet of volume occupied by various gases at system pressure and temperature.

5. The displacement in Step 4 is subtracted from the metastable value in Step 1 to obtain a water concentration of $1.687 \text{ lbm}/10^6 \text{ scf}$. The 0.575-gravity gas must be dried to less than $1.687 \text{ lbm}/10^6 \text{ scf}$ to prevent hydrate formation at 1,000 psia and 8.4°F .

6. A check of the conditions of regression of Eqs. 12 through 14 indicates that the correlation should apply for the conditions of the example.

Fig. 25.23 presents the corrective correlation below the ice/gas region. Fig. 25.24 gives corrections to Fig. 25.21 from the salinity of the aqueous phase. The work of Deaton and Frost⁵ indicated that the water content of gases in equilibrium with liquid water fall in the order

$$y_{\text{He}} < y_{\text{Air}} < y_{\text{CH}_4} < y_{\text{NG}} < y_{\text{CO}_2}$$

where y is the mole fraction of water in each subscripted gas at the same pressure and temperature as shown in Fig. 25.25. The water content of nitrogen up to moderate pressures has been reported by Rigby and Prausnitz.³⁴ No data exist, however, on the water content of nitrogen in equilibrium with hydrates.

The water content of liquid and gaseous CO_2 in equilibrium with hydrates has become increasingly more important in the development of EOR technology.

Fig. 25.26 presents a pressure-temperature projection of the univariant loci for the CO_2 /water system. It defines both the univariant and two-phase regions presently being studied and the regions over which the various combinations of binary equilibrium exist. Like

**TABLE 25.7—VAPOR PRESSURE OF WATER
USED TO CALCULATE ENHANCEMENT
OF THE WATER CONTENT OF
THE CO₂-RICH FLUID PHASES**

T (°F)	p_w (psia)
0	0.02215*
15	0.04352**
30	0.08162**
45	0.1487†
65	0.3089†
77	0.4641†
87.8	0.6518‡
122	1.789‡

*Extrapolated to lower temperature from high temperatures of **.

**Data from Perry, R.H. and Chilton, C.H.: *Chemical Engineer's Handbook*, fifth edition, McGraw-Hill Book Co. Inc., New York City (1973), Table 3-4.

†Data from "Tables of Thermal Properties of Gases," U.S. Dept. of Commerce, Washington D.C. (1955) Circular 564, Table 9-9/a.

‡Data from "Tables of Thermal Properties of Gases," U.S. Dept. of Commerce, Washington D.C. (1955) Circular 564, Table 3-5.

propane, the location of the critical point of CO₂ relative to the $H-L_w-G$ line results in an invariant quadruple point in which $H-L_w-L_{CO_2}-G$ coexist, the hub from the other four univariant three-phase lines emanate.

A second quadruple point involving $H-I-L_w-G$ exists at lower pressure in the neighborhood of the ice point.

The pioneering work of Wiebe and Gaddy provides extensive data on the solubility of CO₂ in water^{90,91} and the vapor-phase composition of CO₂/water mixtures.⁹² The measurements were confined to temperatures exceeding the initial hydrate formation condition. Measurement of the water concentration of gas and liquid in equilibrium with hydrates currently is being pursued by Song and Kobayashi.^{137,138} By using the vapor pressure of water or metastable liquid water given in Table 25.7, the experimental data from several sources have been presented as enhancement of the vapor pressure resulting from the CO₂ pressure on the system (Fig. 25.27). In Fig. 25.27, p is the total pressure, p_w^0 is the saturation pressure of water, and y_w is the mole fraction of water. The water content of coexisting CO₂-rich liquid and gas along the three-phase region is shown as a loop terminating at its three-phase critical point in the neighborhood of the critical temperature of CO₂. Fig. 25.27 shows that the enhancement of the water vapor pressure is favored by lower temperatures and high pressure, variables that also favor a substantial increase in the density of fluid CO₂. It is noted that the solubility of water in liquid CO₂ is greater than in gaseous CO₂ at the same pressure and temperature, precisely the reverse of the solubility sequence for liquid and gaseous hydrocarbons. This phenomenon is related to the excessive collection of water in the middle of a distillation column separating a CO₂-rich feed from its associated LPG constituents.

Fig. 25.28 presents the water content of CO₂ vs. inverse absolute temperature along isobars demonstrating the complexity of the system. The curves show a break downward at the initial hydrate formation conditions as methane and natural gases.

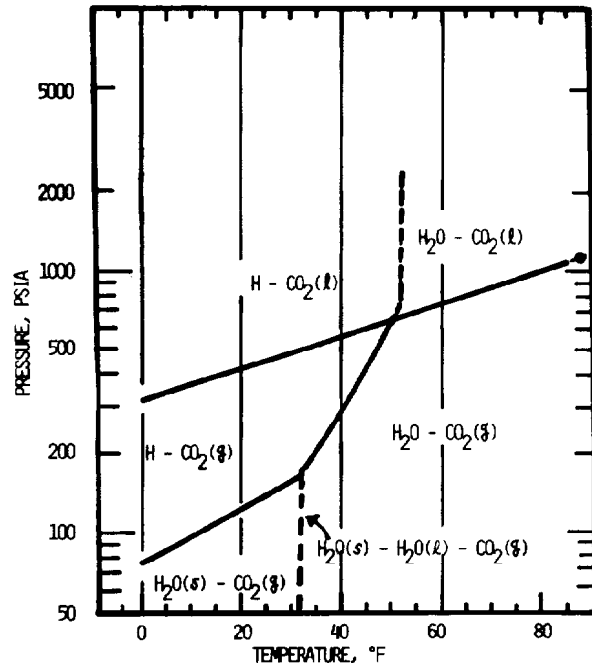


Fig. 25.26—Pressure temperature projection of univariant loci for CO₂/water system.

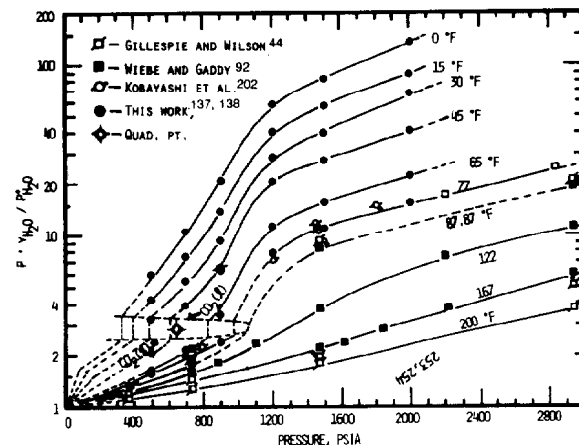


Fig. 25.27—Enhancement of the vapor pressure of water caused by CO₂ total pressure at various temperatures.

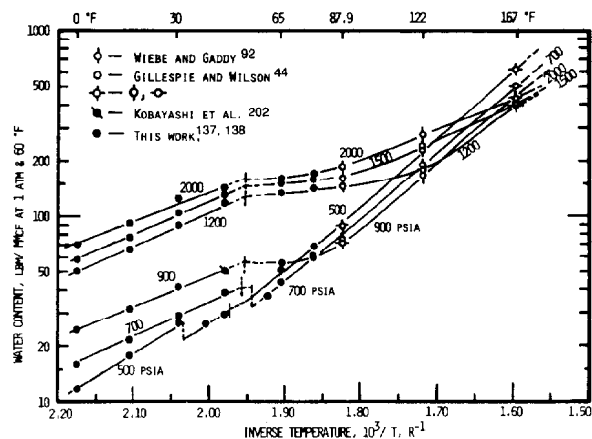


Fig. 25.28—Water content of CO₂ vs. inverse absolute temperature along isobars.

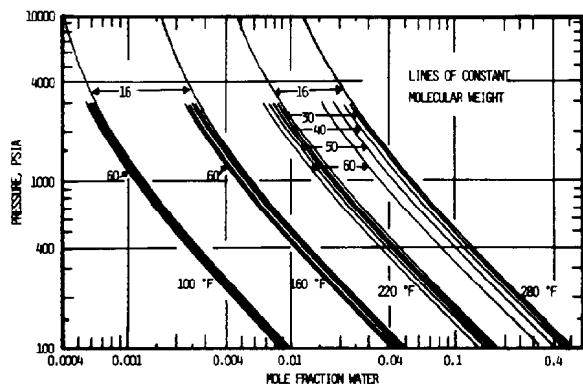


Fig. 25.29—The effect of molecular weight on the water content in the vapor phase (from Ref. 167).

Quantitative Prediction of Water Content in Light Hydrocarbon Systems

A systematic study of the effect of molecular weight on the water content of the vapor phase made by McKetta and Katz^{52,167} is given in Fig. 25.29. The effect of molecular weight is seen to be most pronounced at the highest temperature of the study, 280°F.

The solubility of water in various liquid hydrocarbons at their vapor pressures is presented in Fig. 25.30.

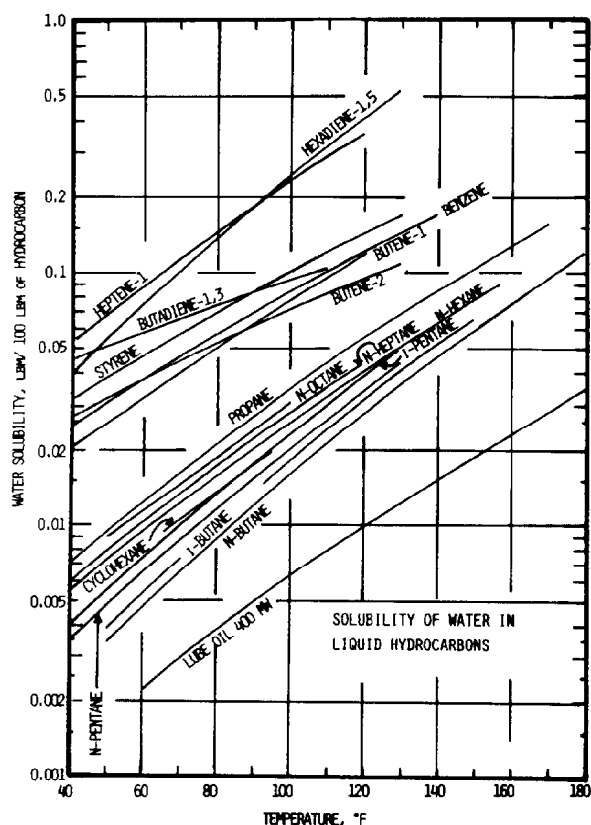


Fig. 25.30—The solubility of water in various liquid hydrocarbons at their vapor pressures.

In recent years estimations of water in both the non-aqueous and aqueous phases in both the two- and three-phase regions have been carried out successfully by Peng and Robinson,¹⁶⁸ Baumgaertner *et al.*,¹⁶⁹ and Moshfeghian *et al.*¹⁷⁰ In these exercises various EOS's were used—the PREOS (Peng-Robinson equation of state),¹⁵⁷ the Schmidt-Wenzel EOS,¹⁶⁹ and the PFGC-MES (Parameter from Group Contribution—Moshfeghian, Erbar, Shariot) EOS.¹⁷⁰ Collectively, these correlation procedures are able to describe vapor/liquid equilibria in systems as diverse as $\text{CH}_4/\text{H}_2\text{O}$, $\text{C}_2\text{H}_6/\text{H}_2\text{O}$ through $\text{n-C}_8\text{H}_{18}/\text{H}_2\text{O}$, $\text{N}_2/\text{H}_2\text{O}$, $\text{CO}_2/\text{H}_2\text{O}$, $\text{CO}/\text{H}_2\text{O}$, $\text{O}_2/\text{H}_2\text{O}$, $\text{H}_2/\text{H}_2\text{O}$, $\text{C}_6\text{H}_6/\text{H}_2\text{O}$, air/ H_2O , $\text{H}_2\text{S}/\text{H}_2\text{O}$, and $\text{NH}_3/\text{H}_2\text{O}$. Both the PREOS and PFGC-MES EOS require temperature-dependent interaction parameters, while the method of Baumgaertner *et al.*¹⁶⁹ describes the water structure in terms of its degree of polymerization in the liquid as a function of the temperature. Examples of the successful application of the calculational method to multicomponent systems by Moshfeghian *et al.*¹⁷⁰ are reported.

Quantitative Predictions of Solute Concentrations in the Aqueous Phase

General references are presented for the solubility of various gases in water, along with other types of data on aqueous systems. The low-pressure references are included because of their contributions to calculational methods for sour water systems.

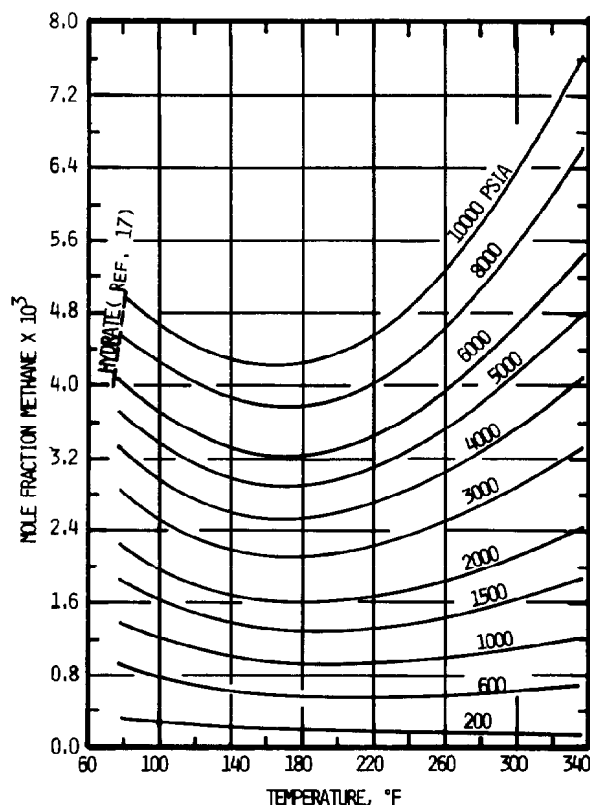


Fig. 25.31—The solubility of methane in water.

Fig. 25.31 presents the volumetric solubility of methane in water to 10,000 psia as measured by Culbertson and McKetta.¹⁷ The solubility of methane increases monotonically with pressure but shows a relative minimum with respect to temperature as do the Henry's law constants.¹⁴² Dodson and Standing,⁴⁵ on the other hand, presented the solubility of a typical natural gas in water and gave corrections for the solubility due to brine salinity, Fig. 25.32. The relative solubility of gas in brine relative to its solubility in pure water is given in Fig. 25.32.

The analytical prediction of the solubility of nonpolar or low-polarity solutes in water can be used by the application of the relationships introduced by Krichevskii and Kasarnovskii¹⁷¹ and Wiebe and Gaddy,⁹⁰ which were later applied by Kobayashi and Katz¹⁴² and Leland *et al.*¹⁷² to condensing light-hydrocarbon systems.

The expression is given as follows.

$$\ln \left(\frac{\hat{f}_1}{x_1} \right) - \ln K_H = \frac{\hat{V}_{M1}}{RT} p_t p_{vs}, \dots (15)$$

where

\hat{f}_1 = partial fugacity of the solute in water at T and p_t ,

K_H = an empirical constant that is a function of temperature only but is equal numerically to Henry's law constant for noncondensable gases and a hypothetical Henry's law constant for condensable gases,

x_1 = mole fraction of the dissolved solute,

R = gas constant per mole,

\hat{V}_{M1} = partial molal volume of components in the solution,

T = absolute temperature,

p_t = total pressure, and

p_{vs} = vapor pressure of the solvent for a noncondensable gas, but equal to some constant pressure slightly above the three-phase pressure determined from experimental data.

The usual absence of values for the partial volume of the solute \hat{V}_m precludes the application of Eq. 15. However, given a good set of experimental data to moderate pressures, Eq. 15 provides a good method of extending the solubility data to higher pressures, particularly if the solute remains essentially pure at the higher pressures. Fig. 25.33 gives an application of Eq. 15 to the aqueous phase of the propane/water system.¹⁴²

Examples of the agreement in the experimental and predicted water compositions are given for the methane/water^{38,40} and ethane/water^{173,174} and propane/water¹⁴² systems in Figs. 25.34 through 25.36 by Peng and Robinson.¹⁶⁸

Both the Peng-Robinson¹⁶⁸ and the Baumgaertner *et al.*¹⁶⁹ methods present successful predictions of the aqueous-phase concentrations as well as in the nonaqueous phase.

Sour Water Stripper Correlations

With the development of a collective environmental consciousness, waste disposal has become an integral part of

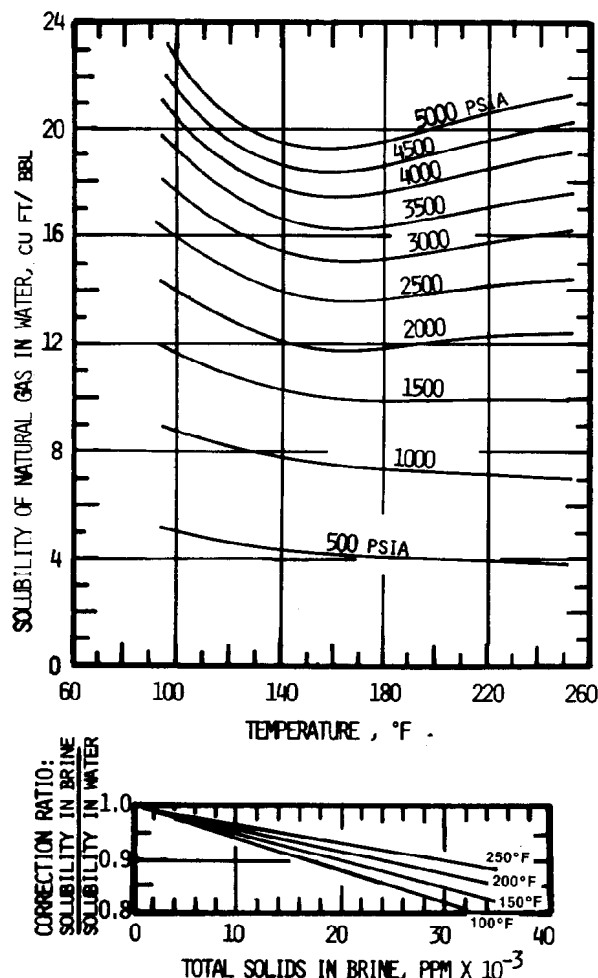


Fig. 25.32—Solubility of natural gas in water with correction for brine salinity.

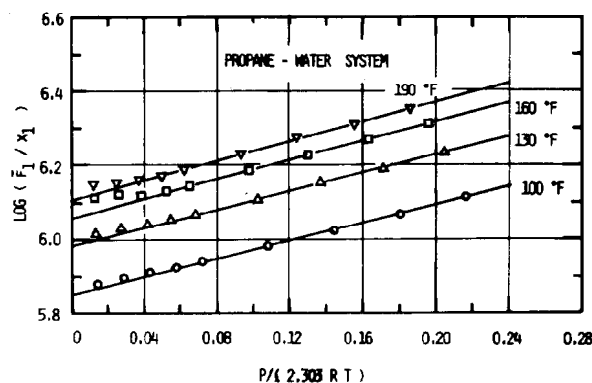


Fig. 25.33—Solubility of propane in water to determine partial molar volume and Henry's law constant.

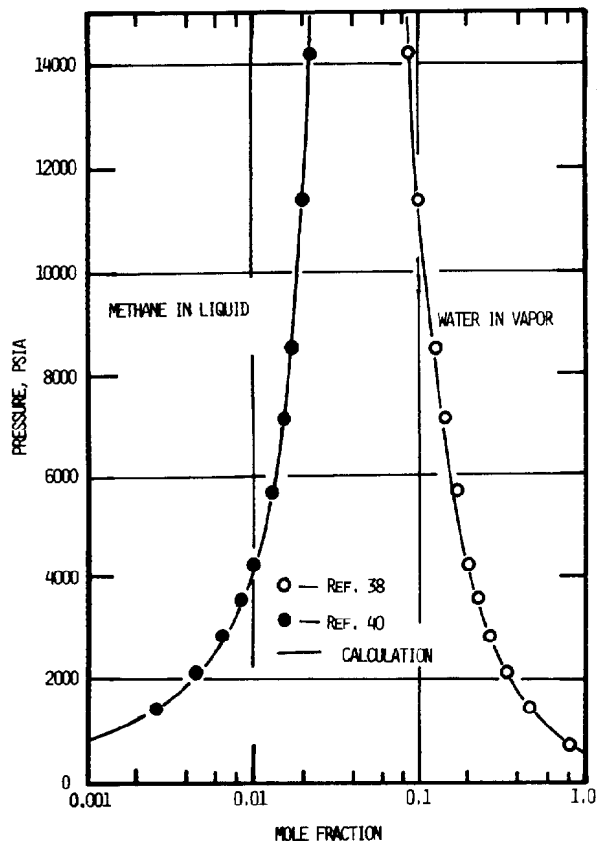


Fig. 25.34—Experimental and predicted vapor and liquid phase compositions for methane/water system at 250°C.

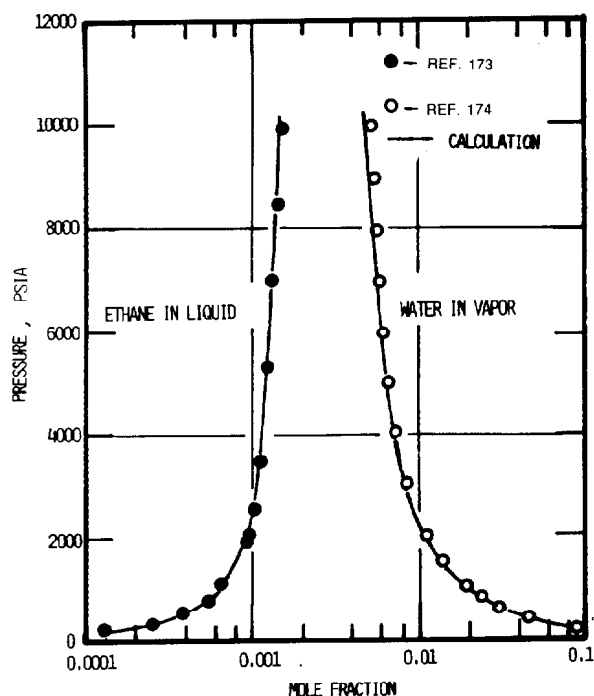


Fig. 25.35—Experimental and predicted vapor and liquid phase compositions for the ethane/water system at 220°F.

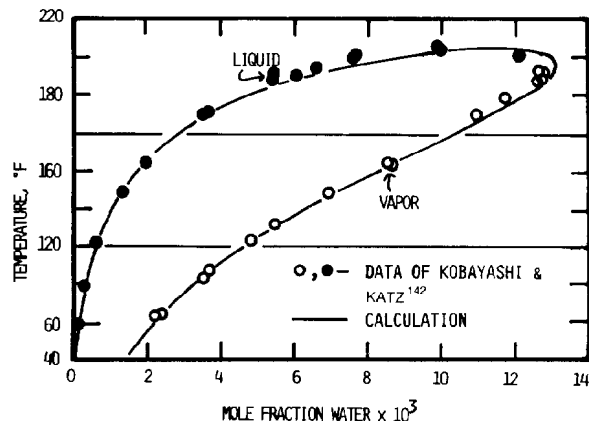


Fig. 25.36—Experimental and predicted water content of propane liquid and vapor phases along three-phase locus.

petroleum production and processing. From an experimental standpoint the developments have been spurred by the accumulation of experimental data typically encountered in sour water processes.¹⁷⁵⁻¹⁷⁸ Meanwhile, basic theoretical work had been laid for the interpretation of such data.¹⁷⁹⁻¹⁸² Interpretations of these and other theories are reviewed by Friedman and Krishnan,¹⁷⁹ Newman,¹⁸³ and Knapp and Sandler.¹⁸⁴

Thus, predictive methods have been developed to estimate vapor/liquid equilibria in complex mixtures containing such components as $\text{NH}_3/\text{CO}_2/\text{H}_2\text{S}$ (Wilson¹⁷⁵), $\text{N}_2/\text{CO}_2/\text{H}_2\text{S}/\text{CH}_4\text{OH}$ (Moshfeghian *et al.*¹⁷⁰), $\text{NH}_3/\text{H}_2\text{S}/\text{H}_2\text{O}$, $\text{NH}_3/\text{SO}_2/\text{H}_2\text{O}$, and $\text{NH}_3/\text{CO}_2/\text{H}_2\text{O}$ (Renon¹⁸⁵), $\text{NH}_3/\text{CO}_2/\text{H}_2\text{S}/\text{H}_2\text{O}$ (Mauerer¹⁸⁶), $\text{CO}_2/\text{NaCl}/\text{KCl}/\text{H}_2\text{O}$ (Chen *et al.*¹⁸⁷), and many others.¹⁸³ The calculations now enable the estimation of physical and chemical equilibria from purely aqueous to strong electrolyte solutions.

Oil and Gas Reservoirs That Exist in the Gas Hydrate Region

In recent years an increasing number of oil and gas reservoirs in the hydrated state have been discovered by Katz,¹⁸⁸ Stoll *et al.*,¹⁸⁹ Makogon *et al.*,¹⁹⁰ Bily and Dick,¹⁹¹ Verma *et al.*,¹⁹² Holder *et al.*,¹⁹³ and Trofimuk *et al.*¹⁹⁴ In fact, hydrate cores have been recovered from below the ocean floor in the Mid-American Trench off Central America.¹⁹⁵ A review of geologic occurrences of hydrates is presented by Kvenvolden and McMenamin.¹⁹⁶

In Feb. 1982 a hydrate core was recovered by the Deep Sea Drilling Project from the Mid-American Trench off Guatemala in 1718 m of water. All evidence to date indicates that these hydrates are of biogenic origin, since they are composed mainly of products from anaerobic digestion. These hydrates are of the Structure I form.

In May 1983 a second hydrate core was recovered by a Getty drilling operation from the Gulf of Mexico in 530 m of water. These hydrates are thermogenic in origin with probable prior biogenesis and have substantial amounts of ethane, propane, and isobutane. These hydrates are of the Structure II form.

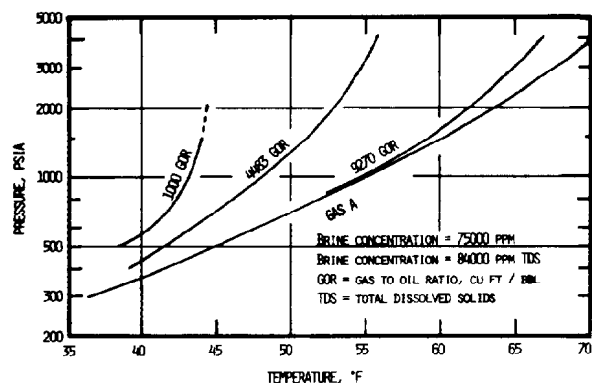


Fig. 25.37—Effect of GOR on hydrate formation conditions for a 46.8°API oil in the presence of excess fluid brine.

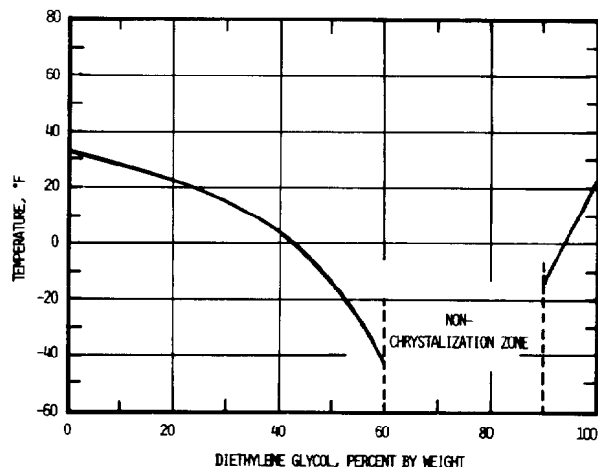


Fig. 25.39—Crystallization temperatures of aqueous diethylene glycol solutions.

These natural hydrates bring many implications to mind; however, only a few will be outlined.

1. The simultaneous solution of hydrate formation for the occurrence of hydrates and earth temperature gradients yields possible environments for the occurrence of hydrates.

2. The potential reserve of natural gas existing in nature as solid hydrates is probably very enormous.

3. Petroleum reservoirs existing in the hydrate region may be denuded of a substantial amount of the lighter constituents and, thus, will be energy deficient for production by a gas-drive mechanism.

4. Waterflooding of dissolved gas reservoirs with near-freezing water may cause hydrate formation in the reservoir.

5. A tremendous amount of technological development will be necessary to unleash hydrocarbons from hydrated reservoirs.

Hydrate Inhibition

While crude oils may not inhibit hydrate formation per se, their oils with dissolved gases affect the initial hydrate formation significantly, as shown in Fig. 25.37.¹⁹⁷

Under some circumstances it may be advantageous to inhibit hydrate formation rather than dehydrate oil and/or gas streams. While many ionic and hydrogen-bonding substances inhibit hydrate formation, the two compounds that are used most frequently for hydrate inhibition are methanol and ethylene glycol. Natural brines cause only a few degrees of hydrate depression.¹³⁴ Figs. 25.38 through 25.40 present the freezing points of aqueous glycol solutions showing their eutectics in the absence of gas.¹⁹⁸ Fig. 25.41 presents the freezing point depression of diethylene/glycol/water solutions.¹⁹⁷

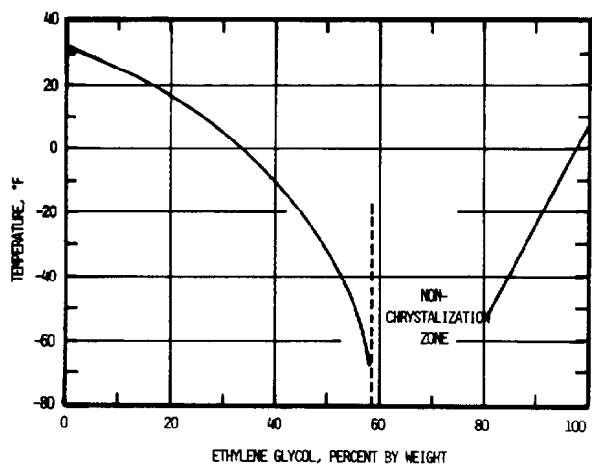


Fig. 25.38—Crystallization temperatures of aqueous ethylene glycol solutions.

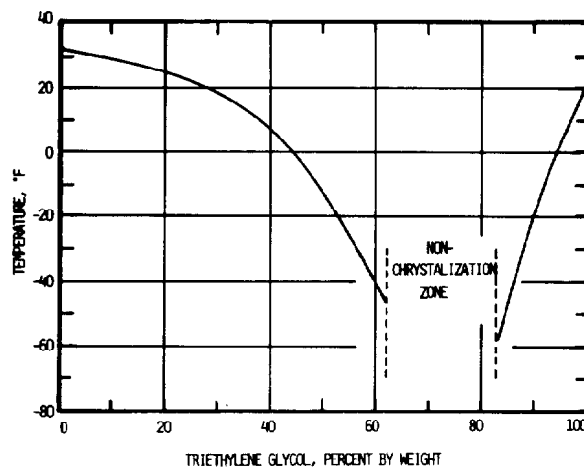


Fig. 25.40—Crystallization temperatures of aqueous triethylene glycol solutions.

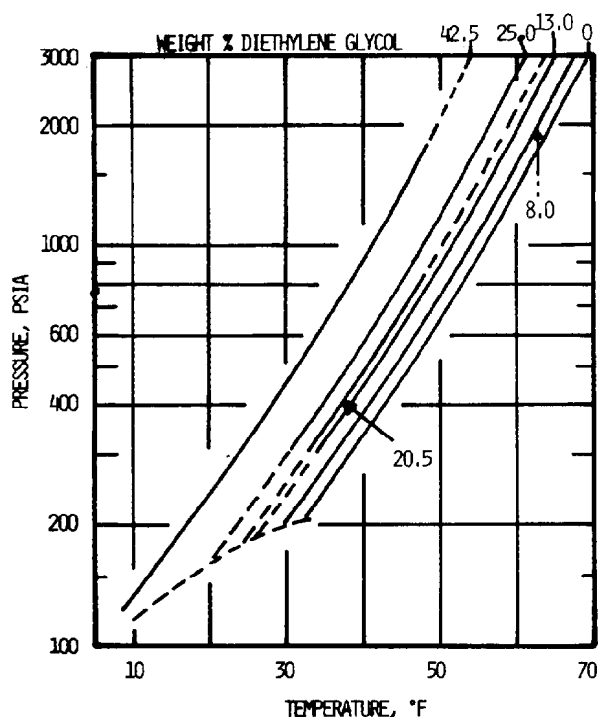


Fig. 25.41—Effect of diethylene glycol on conditions for hydrate formations.

The inhibition effect of methanol and ethylene glycol on the hydrate formation condition of a methane/12-mol% propane mixture is currently under study at Rice U.

Recently, Ng and Robinson¹⁹⁹ have presented the hydrate formation conditions of methane, ethane, propane, CO₂, hydrogen sulfide, methane/10.49-mol% ethane, 90.09-mol% methane/9.91-mol% CO₂, 95.01-mol% methane/4.99-mol% propane, a synthetic natural mixture, and a synthetic natural gas mixture containing CO₂, each in the presence of methanol solutions of 10 to 20 wt% methanol in water. With the increasing amount of oil and gas transmission along ocean floors prior to dehydration, such data are of increasing usefulness.

Nomenclature

- a_i = activity of component i in mixture
 C_{ji} = a unique function of temperature for each guest molecule in each size cavity
 f_j = fugacity of j in the gas phase
 \hat{f}_1 = partial fugacity of the solute in water at T and p_t
 f_{wf} = fugacity of water in the fluid phase
 Δh_w = enthalpy difference
 K_1 = an empirical constant that is a function of temperature only but is equal numerically to Henry's law constant for noncondensable gases and a hypothetical Henry's law constant for condensable gases
 K_{fl} = fugacity coefficient of ice

- K_{fMT} = fugacity coefficient of empty hydrate
 $K_{i(v-s)}$ = vapor/solid equilibrium values of Component i
 K_{wf} = fugacity coefficient of water
 n_{ci} = number of cavities of type i per water molecule in basic lattice
 p_o = reference pressure
 p_{vl} = vapor pressure of ice
 p_{vMT} = vapor pressure of empty hydrate
 p_{vs} = vapor pressure of the solvent for a noncondensable gas, but equal to some constant pressure slightly above the three-phase pressure determined from experimental data
 T_o = reference temperature
 Δv_w = specific volume difference
 \hat{V}_{M1} = partial molal volume of components in the solution
 W_{ms} = metastable water content
 x_1 = mole fraction of the dissolved solute
 y_{ji} = fractional occupancy of type i cavity by type j molecule
 μ_i = chemical potential of Component i
 μ_i^o = chemical potential of pure Component i
 $\Delta \mu_w$ = difference in chemical potential of water
 μ_{wH} = chemical potential of water in filled hydrate
 μ_{wMT} = chemical potential of water in empty hydrate

Subscripts

- L = liquid water
 H = hydrate
 g = gas

References

- Gibbs, J.W.: *The Collected Works of J. Willard Gibbs, Volume I, Thermodynamics*, Yale U. Press, New Haven, CN (1948).
- Kobayashi, R. and Katz, D.L.: "Methane Hydrate at High Pressure," *Trans., AIME* (1949) **186**, 66–70.
- Olds, R.H., Sage, B.H., and Lacey, W.N.: "Composition of Dew Point Gas Methane-Water System," *Ind. Eng. Chem.* (1942) **34**, 1223–27.
- Villard, P.: "On Some Hydrates," *Compt. Rend.* (1888) **106**, 1602–03; (1888) **107**, 395–97.
- Deaton, W.M. and Frost, E.M.: *Gas Hydrates and Their Relation to the Operation of Natural Gas Pipe Lines*, Monograph 8, USBM, Washington D.C. (1946).
- Marshall, D.R., Saito, S., and Kobayashi, R.: "Hydrates at High Pressures: Part I. Methane-Water, Argon-Water, and Nitrogen-Water Systems," *AIChE J.* (1964) **10**, No. 2, 202–05.
- Sloan, E.D., Khoury, F., and Kobayashi, R.: "Water Content of Methane Gas in Equilibrium with Hydrates," *Ind. Eng. Chem. Fund.* (1976) **15**, No. 4, 318–22.
- Galloway, T.J. et al.: "Experimental Measurement of Hydrate Numbers for Methane and Ethane and Comparison with Theoretical Values," *Ind. Eng. Chem. Fund.* (1970) **9**, No. 2, 237–43.
- van der Waals, J.H. and Platteeuw, J.C.: "Clathrate Solutions," *Adv. in Chemical Physics*, Vol. II, I. Prigogine (ed.), Interscience Publishers Inc., New York City (1959) 1–58.
- Parrish, W.R. and Prausnitz, J.M.: "Dissociation Pressures of Gas Hydrates," *Ind. Eng. Chem. Proc. Des. Dev.* (1972) **11**, No. 1, 26–35.
- Kobayashi, R.: "Vapor-Liquid Equilibria in Binary Hydrocarbon-Water Systems," PhD dissertation, U. of Michigan, Ann Arbor (1951).

12. Cady, G.H.: "Compositions of Clathrate Gas Hydrates of CHClF_2 , CCl_3F , Cl_2 , ClO_3F , H_2S , and SF_6 ," *J. Phys. Chem.* (1981) **85**, No. 22, 3225-30.
13. Kobayashi, R. and Katz, D.L.: "Metastable Equilibrium in the Dew Point Determination of Natural Gases in the Hydrate Region," *Trans., AIME* (1955) **204**, 262-63.
14. Ben-Naim, A., Wilf, J., and Yaacobi, M.: "Hydrophobic Interaction in Light and Heavy Water," *J. Phys. Chem.* (1973) **77**, No. 1, 95-102.
15. Claussen, W.F. and Polglase, M.F.: "Solubilities and Structures in Aqueous Aliphatic Hydrocarbon Solutions," *J. Am. Chem. Soc.* (1952) **74**, 4817-19.
16. Culberson, O.L. and McKetta, J.J.: "Phase Equilibria in Hydrocarbon-Water Systems, IV. Vapor-Liquid Equilibrium Constants in the Methane-Water and Ethane-Water Systems," *Trans., AIME* (1951) **192**, 297-300.
17. Culberson, O.L. and McKetta, J.J.: "Phase Equilibria in Hydrocarbon-Water Systems, III. Solubility of Methane in Water at Pressures up to 10,000 psia," *Trans., AIME* (1951) **192**, 223-26.
18. Culberson, O.L., Horn, A.B., and McKetta, J.J.: "Phase Equilibria in Hydrocarbon-Water Systems, The Solubility of Ethane in Water at Pressures to 1,200 psi," *Trans., AIME* (1950) **189**, 1-6.
19. Davis, J.E. and McKetta, J.J.: "Solubility of Methane in Water," *Pet. Refiner* (1960) **39**, No. 3, 205-6.
20. Duffy, J.R., Smith, N.A., and Nagy, B.: "Solubility of Natural Gases in Aqueous Salt Solutions. I. Liquid Surfaces in the System $\text{CH}_4\text{-H}_2\text{O-NaCl-CaCl}_2$ at Room Temperatures and Pressures below 1000 Lb./Sq.in. abs.," *Geochim. Cosmochim. Acta* (1961) **24**, 23-31.
21. Eucken, A. and Hertzberg, G.: "Salting Out Effects and Ion Hydration," *Z. Physik Chem.* (1950) **195**, 1-23.
22. Feillolay, A. and Lucas, M.: "The Solubility of Helium and Methane in Aqueous Tetrabutyl Ammonium Bromide Solutions at 25 and 35°," *J. Phys. Chem.* (1972) **76**, 3068-72.
23. Fischer, F. and Zerbe, C.: "The Solubility of Methane in Water and Organic Solvents under Pressure," *Brennstoff-Chem.* (1923) **4**, 17-19.
24. Frolich, P.K. et al.: "Solubilities of Gases in Liquids at High Pressure," *Ind. Eng. Chem.* (1931) **23**, 548-50.
25. Greco, G., Casale, C., and Negri, G.: "Liquid-Vapor Equilibrium at Elevated Pressures of One Component in the Presence of Noncondensable Components," *Industria Chim. Belge* (1955) **20**, Spec. No. 251-57.
26. Harder, A.H. and Holden, W.R.: "Measurement of [Methane] Gas in Ground Water," *Water Resources Research* (1965) **1**, No. 1, 75-82.
27. Lannung, A. and Gjaldraek, J.C.: "The Solubility of Methane in Hydrocarbons, Alcohols, Water and Other Solvents," *Acta Chem. Scand.* (1960) **14**, 1124-28.
28. McAuliffe, C.: "Solubility in Water of $\text{C}_1\text{-C}_9$ Hydrocarbons," *Nature* (1963) **200**, 1092-93.
29. Michels, A., Grever, J., and Bijl, A.: "The Influence of Pressure on the Solubilities of Gases," *Physica* (1936) **3**, 797-808.
30. Moore, J.C. et al.: "Partial Molar Volumes of 'Gas' at Infinite Dilution in Water at 298.15 K," *J. Chem. Eng. Data* (1982) **27**, 22-24.
31. Morrison, T.J. and Billett, F.: "The Salting Out of Non-electrolytes. Part II. The Effect of Variation in Non electrolyte," *J. Chem. Soc.* (1952) 3819-22.
32. Navone, R. and Fenninger, W.D.: "Determination of CH_4 in Water by Gas Chromatography," *J. Am. Water Works Assoc.* (1967) **59**, No. 6, 757-59.
33. O'Sullivan, T.D. and Smith, N.O.: "Solubility and Partial Molar Volume of Nitrogen and Methane in Water in Aqueous Sodium Chloride from 50 to 125 deg and 100 to 600 atm," *J. Phys. Chem.* (1970) **74**, No. 7, 1460-66.
34. Rigby, M. and Prausnitz, J.M.: "Solubility of Water in Compressed Nitrogen, Argon, and Methane," *J. Phys. Chem.* (1968) **72**, No. 1, 330-34.
35. Schroeder, W.: "Gas Solubility in Water," *Naturwissenschaften* (1968) **55**, No. 11, 542.
36. Schroeder, W.: "Observations on Solutions of Gases in Liquids," *Z. Naturforschung* (1969) **B24**, 500-08.
37. Shoor, S.K., Walker, R.D., and Gubbins, K.E.: "Salting Out of Nonpolar Gases in Aqueous Potassium Hydroxide Solutions," *J. Phys. Chem.* (1969) **73**, 312-17.
38. Sultanov, R.G., Skripka, V.G., and Namiot, A.Y.: "Moisture Content of Methane at High Temperatures and Pressures," *Gazov. Prom.* (1971) **16**, No. 4, 6-8.
39. Sultanov, R.G., Skripka, V.G., and Namiot, A. Y.: "Phase Equilibriums and Critical Phenomena in the Water-Methane System at Increased Temperatures and Pressures," *Zh. Fiz. Khim.* (1972) **46**, No. 8, 2160.
40. Sultanov, R.G., Skripka, V.G., and Namiot, A.Y.: "Solubility of Methane in Water at High Temperatures and Pressures," *Gazov. Prom.* (1972) **17**, No. 5, 6-7.
41. Wen, W.-Y. and Hung, J.H.: "Thermodynamics of Hydrocarbon Gases in Aqueous Tetraalkylammonium Salt Solutions," *J. Phys. Chem.* (1970) **74**, 170.
42. Winkler, L.W.: "The Solubility of Gases in Water," *Ber. Deut. Chem. Ges.* (1901) **34**, 1408-22.
43. Yamamoto, S., Alcauskas, J.B., and Crozier, T.E.: "Solubility of Methane in Distilled Water and Sea Water," *J. Chem. Eng. Data* (1976) **21**, No. 1, 78-80.
44. Gillespie, P.C. and Wilson, G.M.: "Vapor-Liquid and Liquid-Liquid Equilibria," Research Report RR-48, GPA, Tulsa (April 1982).
45. Dodson, C.R. and Standing, M.B.: "Pressure-Volume-Temperature and Solubility Relations for Natural Gas-Water Mixtures," *Drill. and Prod. Prac.*, API, Dallas (1944) 173-79.
46. Hall, K.R., Eubank, P.T., and Holste, J.C.: "Experimental Densities and Enthalpies for Water-Natural Gas Systems," *Proc., Gas Processors Assoc. Annual Conv.*, Denver (1979) **58**, 1-2.
47. Lauhere, B.M. and Briscoe, C.F.: "The Partial Dehydration of High-Pressure Natural Gas," *Gas* (1939) **15**, No. 9, 21-24.
48. McCarty, E.L., Boyd, W.S., and Reid, L.S.: "Water-Vapor Content of Essentially Nitrogen-free Natural Gas Saturated with Water at Various Conditions of Temperature and Pressure," *Oil and Gas J.* (1950) **48**, No. 35, 59.
49. McKetta, J.J. and Wehe, A.H.: "How to Determine the Water Content of Natural Gases," *World Oil* (1958) **147**, No. 1, 122.
50. Russell, G.B. et al.: "Experimental Determination of Water Vapor Content of a Natural Gas up to 2000 Pounds Pressure," *Trans., AIME* (1945) **160**, 150-56.
51. Tsaturyants, A.B., Rachinskii, M.A., and Izabakarov, M.: "Solubility of Water in Natural Gas," *Gazov. Delo* (1967) 6-10.
52. McKetta, J.J. and Katz, D.L.: "Methane-n-Butane-Water System in Two and Three-Phase Regions," *Ind. Eng. Chem.* (1948) **40**, 853-63.
53. Coan, C.R.: "Solubility of Water in Compressed Carbon Dioxide, Nitrous Oxide, and Ethane. Evidence for Hydration of Carbon Dioxide and Nitrous Oxide in the Gas Phase," PhD dissertation, U. of Georgia, Athens (1971).
54. Coan, C.R. and King, A.D. Jr.: "Solubility of Water in Compressed Carbon Dioxide, Nitrous Oxide, and Ethane. Evidence for Hydration of Carbon Dioxide and Nitrous Oxide in the Gas Phase," *J. Am. Chem. Soc.* (1971) **93**, No. 8, 1857-62.
55. Bartholome, E. and Friz, H.: "Solubility of Carbon Dioxide in Water at High Pressures," *Chem. Ing. Tech.* (1956) **28**, 706-08.
56. Barton, J.R. and Hsu, C.C.: "Solubility of Cyclobutane in Alkyl Carboxylic Acids," *J. Chem. Eng. Data* (1971) **16**, No. 1, 93-95.
57. Bohr, C.: "Method of Determination of Solubility Coefficients for Gases in Liquids: Carbon Dioxide in Water and Sodium Chloride Solutions," *Ann. Physik. Chem.* (1899) **68**, 500-25.
58. DeKiss, A.V., Lajtai, I., and Thury, G.: "Solubility of Gases in Nonelectrolyte Water Mixtures," *Z. Anorg. Allg. Chem.* (1937) **233**, 346-52.
59. Dodds, W.S., Stutzman, L.F., and Sollami, B.J.: "Carbon Dioxide Solubility in Water," *Ind. Eng. Chem.* (1956) **1**, 92-95.
60. Ellis, A.J.: "The Solubility of Carbon Dioxide in Water at High Temperatures," *Am. J. Sci.* (1959) **257**, 217-34.
61. Ellis, A.J. and Golding, R.M.: "The Solubility of Carbon Dioxide above 100°C in Water and in Sodium Chloride Solutions," *Am. J. Sci.* (1963) **261**, 47-60.
62. Enns, T., Scholander, P.F., and Bradstreet, E.B.: "Effect of Hydrostatic Pressure on Gases Dissolved in Water," *J. Phys. Chem.* (1965) **69**, 389-91.
63. Franck, E.U. and Todheide, K.: "Thermal Properties of Supercritical Mixtures of Carbon Dioxide and Water up to 750° and 2000 atms," *Z. Physik. Chem.* (1959) **22**, 232-45.
64. Haehnel, O.: "The Strength of Carbonic Acid at Higher Pressures," *Centr. Min. Geol.* (1920) 25-32.

65. Hayduk, W. and Malik, V.K.: "Density, Viscosity, and Carbon Dioxide Solubility and Diffusivity in Aqueous Ethylene Glycol Solutions," *J. Chem. Eng. Data* (1971) **16**, No. 2, 143-46.
66. Houghton, G., McLean, A.M., and Ritchie, P.D.: "Compressibility, Fugacity, and Water Solubility of Carbon Dioxide in the Region 0-36 atm., 0-100°," *Chem. Eng. Sci.* (1957) **6**, 132-37.
67. Khitarov, N.I. and Malinin, S.D.: "Experimental Characteristics of a Part of the System H_2O-CO_2 ," *Geokhimiya* (1956) **3**, 18-27.
68. Khitarov, N.I. and Malinin, S.D.: "Phase Equilibrium Relation in the System H_2O-CO_2 ," *Geokhimiya* (1958) **7**, 678-79.
69. Krichevskii, J.I., Zhavoronkov, N.M., and Aepelbaum, V.A.: "Measured Solubilities of Gases in Liquids under Pressure. I. Solutions of Carbon Dioxide in Water and Mixtures with Hydrogen at 20, and 30°C and Pressures to 30 Kg/cm²," *Z. Phys. Chem.* (1936) **A175**, 232-38.
70. Kuerth, W.: "Solubility of CO_2 and H_2O in Certain Solvents," *Phys. Rev.* (1922) **19**, 512-24.
71. Loprest, F.J.: "A Method for the Rapid Determination of the Solubility of Gases in Liquids at Various Temperatures," *J. Phys. Chem.* (1957) **61**, 1128-30.
72. Maas, O. and Mennie, J.H.: "Aberrations from the Ideal Gas Laws in Systems of One and Two Components," *Proc. Roy. Soc., London* (1926) **A110**, 198-232.
73. Malinin, S.D. and Savel'eva, N.I.: "Carbon Dioxide Solubility in Sodium Chloride and Calcium Chloride Solutions at Temperatures of 25, 50, and 75 deg. and Elevated Carbon Dioxide Pressure," *Geokhimiya* (1972) **6**, 643-53.
74. Malinin, S.D.: "The System Water-Carbon Dioxide at High Temperatures and Pressures," *Geokhimiya* (1959) **3**, 235-45.
75. Malinin, S.D.: "Solubility of Carbon Dioxide in Water at Low Partial Pressures at High Temperatures," *Trans., Soveshch. Eksp. Tekh. Mineral. Petrogr.* (1971) **8**, 229-34.
76. Markham, A.E. and Kobe, K.A.: "Solubility of Carbon Dioxide and Nitrous Oxide in Aqueous Salt Solutions," *J. Am. Chem. Soc.* (1941) **63**, 449-54.
77. Marous, J. et al.: "Solubility of Carbon Dioxide in Water at Pressures up to 40 atm.," *Collect. Czech. Chem. Commun.* (1969) **34**, No. 12, 3982-85.
78. McCay, R.C., Seely, D.H. Jr., and Gardner, F.H.: "Distribution of Gaseous Solutes between Aqueous and Liquid-Hydrocarbon Phases. Carbon Dioxide," *Ind. Eng. Chem.* (1949) **41**, 1377-80.
79. Murray, C.N. and Riley, J.P.: "Solubility of Gases in Distilled Water and Sea Water. IV. Carbon Dioxide," *Deep-Sea Res. Oceanogr. Abstr.* (1971) **18**, No. 5, 533-41.
80. Nezdoininoga, N.A.: "Solubility of Carbon Dioxide in Water," *Izv. Akad. Nauk Arm. SSSR, Ser. Tekh. Nauk* (1968) **21**, No. 3, 11-17.
81. Pollitzer, F. and Strebel, E.: "The Influence of an Indifferent Gas on the Saturation Vapor Concentration of a Liquid," *Z. Physik. Chem.* (1924) **110**, 768-85.
82. Sander, W.: "The Solubility of CO_2 in Water and Other Solutions at Higher Pressures," *Z. Physik. Chem.* (1912) **78**, 513-49.
83. Stewart, P.B. and Munjal, P.K.: "Solubility of Carbon Dioxide in Distilled Water, Synthetic Sea Water, and Synthetic Sea-Water Concentrates," *U. of Calif., Sea Water Convers.* (1969) **69**, No. 2, 44.
84. Stewart, P.B. and Munjal, P.K.: "Solubility of Carbon Dioxide in Pure Water, Synthetic Sea Water Concentrates at -5 deg. to 25 deg. and 10- to 45-atm. Pressure," *J. Chem. Eng. Data* (1970) **15**, No. 1, 67-71.
85. Takenouchi, S. and Kennedy, G.C.: "The Binary System H_2O-CO_2 at High Temperatures and Pressures," *Am. J. Sci.* (1964) **262**, 1055-74.
86. Todheide, K. and Franck, E.U.: "Two Phase Range and the Critical Curve in the System Carbon Dioxide-Water up to 3500 bar," *Z. Physik. Chem.* (1963) **NF37**, 387-401.
87. Vanderzee, C.E. and Haas, N.C.: "Second Virial Coefficients B_{12} for the Gas Mixture (Carbon Dioxide+Water) from 300 to 1000 K," *J. Chem. Thermodynamics* (1981) **13**, No. 3, 203-11.
88. Vilcu, R. and Gainar, I.: "Solubility of Gases in Liquid Under Pressure. I. Carbon Dioxide-Water System," *Rev. Roum. Chim.* (1967) **12**, No. 2, 1819.
89. Weiss, R.F.: "Carbon Dioxide in Water and Sea Water," *Marine Chem.* (1974) **2**, No. 3, 203-15.
90. Wiebe, R. and Gaddy, V.L.: "The Solubility in Water of Carbon Dioxide at 50, 75 and 100° at Pressures to 700 Atmospheres," *J. Am. Chem. Soc.* (1939) **61**, 315-18.
91. Wiebe, R. and Gaddy, V.L.: "The Solubility of Carbon Dioxide in Water at Various Temperatures from 12 to 40° and at Pressures to 500 Atmospheres. Critical Phenomena," *J. Am. Chem. Soc.* (1940) **62**, 815-17.
92. Wiebe, R. and Gaddy, V.L.: "Vapor Phase Composition of Carbon Dioxide-Water Mixtures at Various Temperatures and at Pressures to 700 Atmospheres," *J. Amer. Chem. Soc.* (1941) **63**, 475-77.
93. Wroblewski, S.: "Investigation of the Absorption of Gases in Liquids at High Pressure. I. Carbon Dioxide in Water," *Ann. Physik. Chem.* (1882) **17**, 103-28.
94. Yeh, S.-Y. and Peterson, R.E.: "Solubility of Carbon Dioxide, Krypton, and Xenon in Aqueous Solution," *J. Pharm. Sci.* (1964) **53**, No. 7, 822-24.
95. Zawisza, A. and Malesinska, B.: "Solubility of Carbon Dioxide in Liquid Water and of Water in Gaseous Carbon Dioxide in the Range of 0.2 to 5 MPa and at Temperature up to 473 K," *J. Chem. Eng. Data* (1981) **26**, No. 4, 388-91.
96. Zel'evskii, Y.D.: "The Solubility of Carbon Dioxide under Pressure," *J. Chem. Ind. (USSR)* (1937) **14**, 1250-57.
97. Paratella, A.A., and Sagradora, G.: "Solubilities of Liquids in Gases," *Ricerca Sci.* (1959) **29**, 2605-13.
98. Adeney, W.E. and Becker, H.G.: "The Determination of the Rate of Solution of Atmospheric Nitrogen and Oxygen in Water," *Sci. Proc. Roy. Dublin Soc.* (1919) **15**, 609-28.
99. Bartlett, E.P.: "The Concentration of Water Vapor in Compressed Hydrogen, Nitrogen and a Mixture of These Gases in the Presence of Condensed Water," *J. Am. Chem. Soc.* (1927) **49**, 65-78.
100. Basset, J. and Dode, M.: "Solubility of Nitrogen in Water at High Pressures to 4500 Kg/cm²," *Compt. Rend.* (1936) **203**, 775-77.
101. Benson, B.B. and Krause, D.J.: "Empirical Laws for Dilute Aqueous Solutions of Nonpolar Gases," *J. Chem. Phys.* (1976) **64**, 689-709.
102. Benson, B.B. and Parker, P.D.M.: "Relations among the Solubilities of Nitrogen, Argon, and Oxygen in Distilled Water and Sea Water," *J. Phys. Chem.* (1961) **65**, 1489-96.
103. Douglas, E.: "Solubilities of Oxygen, Argon and Nitrogen in Distilled Water," *J. Phys. Chem.* (1964) **68**, 169-74.
104. Farhi, L.E., Edwards, A.T.W., and Homma, T.: "Determination of Dissolved N_2 in Blood by Gas Chromatography and (a-A) N_2 Difference," *J. Appl. Physiol.* (1963) **18**, 97-106.
105. Fox, C.J.J.: "On the Coefficients of Absorption of Nitrogen and Oxygen in Distilled Water and Sea-Water, and of Atmospheric Carbonic Acid in Sea-Water," *Trans., Faraday Soc.* (1909) **5**, 68-87.
106. Goodman, J.B. and Krase, N.W.: "Solubility of Nitrogen in Water at High Pressures and Temperatures," *Ind. Eng. Chem.* (1931) **23**, 401-4.
107. Klotz, C.E. and Benson, B.B.: "Solubilities of Nitrogen, Oxygen, and Argon in Distilled Water," *J. Marine Res.* (1963) **21**, 48-57.
108. Maslennikova, V.Y.: "Solubility of Nitrogen in Water," *Tr. Gas. Nauch.-Issled. Proekt. Inst. Azotn. Prom. Prod. Org. Sin.* (1971) **12**, 82-87.
109. Maslennikova, V.Y., Vdovina, N.A., and Tsiklis, D.S.: "Solubility of Water in Compressed Nitrogen," *Zh. Fiz. Khim.* (1971) **45**, No. 9, 2384.
110. Murray, C.N. and Riley, J.P.: "Solubility of Gases in Distilled Water and Sea Water. II. Oxygen," *Deep-Sea Res. Oceanography Abstr.* (1969) **3**, 311-20.
111. Pray, H.A., Schweickent, C.E., and Minnich, B.H.: "Solubility of Hydrogen, Oxygen, Nitrogen, and Helium in Water," *Ind. Eng. Chem.* (1952) **44**, 1146-51.
112. Saddington, A.W. and Krase, N.W.: "Vapor-Liquid Equilibria in the System Nitrogen-Water," *J. Am. Chem. Soc.* (1934) **56**, 353-61.
113. Smith, N.O., Keleman, S., and Nagy, B.: "Solubility of Natural Gases in Aqueous Salt Solutions. II. Nitrogen in Aqueous NaCl, $CaCl_2$, Na_2SO_4 and $MgSO_4$ at Room Temperatures and at Pressures below 1000 lb/sq. in. abs.," *Geochim. Cosmochim. Acta* (1962) **26**, 921-26.
114. Suci, S.N. and Sibbitt, W.L.: "Study of the Nitrogen and Water and Hydrogen and Water Systems at Elevated Temperatures and Pressures," U.S. Atomic Energy Commission, Washington, ANL (1951) **2**, 4603.

115. Tsiklis, D.S. and Maslennikova, V.Y.: "Limited Mutual Solubility of Gases in the Water-Nitrogen System," *Dokl. Akad. Nauk SSSR* (1965) **161**, 645-47.
116. Wiebe, R., Gaddy, V.L., and Heins, C.: "Solubility of Nitrogen in Water at 25°C from 25 to 1000 Atmospheres," *Ind. Eng. Chem.* (1932) **24**, 927.
117. Wiebe, R., Gaddy, V.L., and Heins, C.: "The Solubility of Nitrogen in Water at 50, 75 and 100° from 25 to 1000 Atmospheres," *J. Am. Chem. Soc.* (1933) **55**, 947-55.
118. Wilcock, R.J. and Battino, R.: "Solubility of Oxygen-Nitrogen Mixture in Water," *Nature*, London (1974) **252**, No. 5484, 614-15.
119. Winkler, L.W.: "The Solubility of Gases in Water," *Ber. Deut. Chem. Ges.* (1891) **24**, 3602-10; 89-101.
120. Winkler, L.W.: "Measurements of the Absorption of Gases in Liquids," *Z. Physik. Chem.* (1892) **9**, 171-75.
121. Aoyagi, K., et al.: "Improved Measurements and Correlation of the Water Content of Methane Gas in Equilibrium with Hydrate," paper presented at the 1979 GPA Annual Conference, Denver.
122. Byk, S.S., and Fomina, V.I.: "Water Content of Hydrates of Gases at Different Temperature," *Zh. Fiz. Khim.* (1978) **52**, No. 5, 1306-08.
123. Falabella, B.J. and Vanpee, M.: "Experimental Determination of Gas Hydrate Equilibrium below the Ice Point," *Ind. Eng. Chem. Fund.* (1974) **13**, No. 3, 228-31.
124. Frost, E.M. and Deaton, W.M.: "Gas Hydrate Composition and Equilibrium Data," *Oil and Gas J.* (1946) **45**, No. 12, 170-78.
125. Glew, D.N.: "Aqueous Solubility and the Gas Hydrates. The Methane-Water System," *J. Phys. Chem.* (1962) **66**, 605-09.
126. Hammerschmidt, E.G.: "Formation of Gas Hydrates in Natural Gas Transmission Lines," *Ind. Eng. Chem.* (1934) **26**, No. 8, 851-55.
127. McLeod, H.D. Jr. and Campbell, J.M.: "Natural Gas Hydrates at Pressures to 10,000 psia," *J. Pet. Tech.* (1961) **13**, 590-94.
128. Roberts, O.L., Brownscombe, E.R., and Howe, L.S.: "Constitution Diagrams and Composition of Methane and Ethane Hydrates," *Oil and Gas J.* (1940) **39**, No. 30, 37-40.
129. Snell, L.E., Otto, F.D., and Robinson, D.G.: "Hydrates in Systems Containing Methane, Ethylene, Propylene, and Water," *AIChE J.* (1961) **7**, No. 3, 482-85.
130. Ballard, D.: "How to Operate a Glycol Plant," *Hydrocarbon Process. Pet. Refiner* (1966) **45**, No. 6, 171-80.
131. Deaton, W.M. and Frost, E.M.: "Gas Hydrates in Natural Gas Pipe Lines," *Oil and Gas J.* (1937) **36**, No. 1, 75-81.
132. Hammerschmidt, E.G.: "Preventing and Removing Hydrates in Natural Gas Pipe Lines," *Gas* (1939) **15**, No. 5, 30-40.
133. Trebin, F.A. and Makogan, Y.I.: "Process of Hydrate Formation in Natural Gas. Conditions of Formation and Decomposition of Hydrates," *Tr. Mosk. Inst. Neftekhim. i Gaz. Prom.* (1963) **42**, 196-208.
134. Kobayashi, R., et al.: "Gas Hydrate Formation with Brine and Ethanol Solutions," *Proc., Nat. Gas Assoc. Am.* (1951) 27-31.
135. Wilcox, W.I., Carson, D.B., and Katz, D.L.: "Natural Gas Hydrates," *Ind. Eng. Chem.* (1941) **33**, 662-65.
136. Larson, S.: "Phase Studies of the Two-Component Carbon Dioxide-Water System Involving the Carbon Dioxide Hydrate," PhD thesis, U. of Illinois, Urbana (1955).
137. Song, K.Y. and Kobayashi, R.: "The Water Content of CO₂-Rich Fluids in Equilibrium with Liquid Water and/or Hydrate," Research Report, GPA, Tulsa (Sept. 1983).
138. Takahashi, S., Song, K.Y., and Kobayashi, R.: "Availability and Deficiencies in Thermodynamic Data Needed for the Design of Glycol Dehydrators for CO₂-Rich Fluids," paper 67e presented at the 1983 AIChE Summer National Meeting, Denver, Aug. 28-31.
139. Unruh, C.H. and Katz, D.L.: "Gas Hydrates of Carbon Dioxide-Methane Mixtures," *Trans., AIME* (1949) **186**, 83-86.
140. van Cleeff, A., et al.: "Studies of the Ternary System Ethylene-Ethanol-Water. II. Formation of Ethylene Hydrate," *Brennstoff-Chem.* (1960) **41**, 55-57.
141. Alder, S.B. and Spencer, C.F.: "Case Studies of Industrial Problems. Phase Equilibria and Fluid Properties in the Chemical Industry," *Proc., Equilibrium Fluid Properties in the Chemical Industry* (1980) 465-95.
142. Kobayashi, R. and Katz, D.L.: "Vapor-Liquid Equilibria for Binary Hydrocarbon-Water Systems," *Ind. Eng. Chem.* (1953) **45**, 440-51.
143. Davidson, D.W.: "Cathrate Hydrates," *Water—A Comprehensive Treatise*, Vol. 2, *Water in Crystalline Hydrates—Aqueous Solutions of Simple Nonelectrolytes*, F. Franks (ed.), Plenum Press, New York City (1973) 115-234.
144. Sloan, E.D.: "Phase Equilibria of Natural Gas Hydrates," paper 67f presented at the 1983 AIChE Summer Natl. Meeting, Denver, Aug. 28-31.
145. Katz, D.L.: "Prediction of Conditions for Hydrate Formation in Natural Gases," *Trans., AIME* (1945) **160**, 140-49.
146. Katz, D.L. et al.: "Water-Hydrocarbon Systems," *Handbook of Natural Gas Engineering*, McGraw-Hill Book Co. Inc., New York City (1959) 189-221.
147. Carson, D.B. and Katz, D.L.: "Natural Gas Hydrates," *Trans., AIME* (1942) **146**, 150-59.
148. Noaker, L.J. and Katz, D.L.: "Gas Hydrates of Hydrogen Sulphide-Methane Mixtures," *Trans., AIME* (1954) **201**, 237-39.
149. Wu, B.-J., Robinson, D.B., and Ng, H.-J.: "Three- and Four-Phase Hydrate Forming Conditions in Methane-Isobutane-Water," *J. Chem. Thermodynamics* (1976) **8**, 461-69.
150. Robinson, D.B. and Ng, H.-J.: "Improve Hydrate Predictions," *Hydrocarbon Proc.* (Dec. 1975) **54**, No. 12, 95-98.
151. Platteau, J.C. and van der Waals, J.H.: "Thermodynamic Properties of Gas Hydrates. II. Phase Equilibrium in the System," *Rec. Trav. Chim.* (1959) **78**, 126-33.
152. von Stackelberg, M.: "Solid Gas Hydrates," *Naturwissenschaften* (1949) **36**, 327-33, 359-62.
153. von Stackelberg, M. and Muller, H.G.: "On the Structure of Gas Hydrates," *J. Chem. Phys.* (1951) **19**, 1319-20.
154. Saito, S. and Kobayashi, R.: "Hydrates at High Pressures: Part III. Methane-Argon-Water, Argon-Nitrogen-Water Systems," *AIChE J.* (1965) **11**, No. 1, 96-99.
155. Nagata, I. and Kobayashi, R.: "Calculation of Dissociation Pressures of Gas Hydrates Using the Kihara Model," *Ind. Eng. Chem. Fund.* (1966) **5**, 344-48.
156. McKoy, V. and Sinanoglu, O.: "Theory of Dissociation Pressures of Some Gas Hydrates," *J. Chem. Phys.* (1963) **38**, No. 12, 2946-56.
157. Peng, D.-Y. and Robinson, D.B.: "A New Two-Constant Equation of State," *Ind. Eng. Chem.* (1976) **15**, 59-64.
158. Dharmawardhana, P.B.: "The Measurement of the Thermodynamic Parameters of the Hydrate Structure and Application of Them in the Prediction of Natural Gas Hydrates," PhD dissertation, Colorado School of Mines, Golden (1980).
159. Weiler, B.E.: "Experimental Determination of the Thermodynamic Parameters of Structure II Hydrate Using Propane," MS thesis, Colorado School of Mines, Golden (1982).
160. Erickson, D.D.: "Development of a Natural Gas Hydrate Prediction Computer Program," MS thesis, Colorado School of Mines, Golden (1982).
161. Davidson, D.W.: "Thermodynamic Aspects of Natural Gas Hydrates," paper presented at the CIC Conference, Ottawa (June 1980).
162. Records, J.R. and Seely, D.H. Jr.: "Low Temperature Dehydration of Natural Gas," *Trans. AIME* (1951) **192**, 61-68.
163. Song, K.Y. and Kobayashi, R.: "Measurement and Interpretation of the Water Content of a Methane-Propane Mixture in the Gaseous State in Equilibrium with Hydrate," *Ind. Eng. Chem. Fund.* (1982) **21**, No. 4, 391-95.
164. Ng, H.-J. and Robinson, D.B.: "A Method for Predicting the Equilibrium Gas Phase Water Content in Gas-Hydrate Equilibrium," *Ind. Eng. Chem. Fund.* (1980) **19**, No. 1, 33-36.
165. Aoyagi, K. and Kobayashi, R.: "Report on the Water Content Measurement of High Carbon Dioxide Content Simulated Prudhoe Bay Gas in Equilibrium with Hydrates," *Proc., 50th Annual GPA Convention*, New Orleans (1978).
166. Skinner, W. Jr.: "The Water Content of Natural Gas at Low Temperatures," MS thesis, U. of Oklahoma, Norman (1948).
167. McKetta, J.J. and Katz, D.L.: "Phase Relationships of Hydrocarbon-Water Systems," *Trans., AIME* (1947) **170**, 34-43.
168. Peng, D.-Y. and Robinson, D.B.: "Two- and Three-Phase Equilibrium Calculations for Coal Gasification and Related Process," *Thermodynamics of Aqueous Systems with Industrial Applications*, S.A. Newman (ed.) Symposium Series 133, ACS (1980) 393-414.
169. Baumgaertner, M., Moorwood, R.A.S., and Wenzel, H.: "Phase Equilibrium Calculations by Equation of State for

- Aqueous Systems with Low Mutual Solubility," *Thermodynamics of Aqueous Systems with Industrial Applications*, S.A. Newman (ed.), Symposium Series 133, ACS (1980) 415-34.
170. Moshfeghian, M., Shariot, A., and Erbar, J.H.: "Application of the PFGC-MES Equation of State to Synthetic and Natural Gas Systems," *Thermodynamics of Aqueous Systems with Industrial Applications*, S.A. Newman (ed.), Symposium Series 133, ACS (1980) 333-59.
 171. Krichevskii, I.R. and Kasarnovskii, J.S.: "Thermodynamical Calculations of Solubilities of Nitrogen and Hydrogen in Water at High Pressures," *J. Am. Chem. Soc.* (1935) **57**, 2168-71.
 172. Leland, T.W. Jr., McKetta, J.J., and Kobe, K.A.: "Phase Equilibrium in 1-Butene-Water System and Correlation of Hydrocarbon-Water Solubility," *Ind. Eng. Chem.* (1955) **47**, 1265-71.
 173. Culberson, O.L. and McKetta, J.J.: "Phase Equilibria in Hydrocarbon-Water Systems. II. The Solubility of Ethane in Water at Pressures to 10,000 psi," *Trans., AIME* (1950) **189**, 319-22.
 174. Reamer, H.H. *et al.*: "Composition of Dew-Point Gas in Ethane-Water System," *Ind. Eng. Chem.* (1943) **35**, 790-93.
 175. Wilson, G.M.: "A New Correlation of NH_3 , CO_2 and H_2S Volatility Data from Aqueous Sour Water Systems," *API Data Book*, API, Dallas (Feb. 1978).
 176. Otsuka, E.: "Measure Vapor Liquid Equilibria of NH_3 - CO_2 - H_2 ," *Kogyo Kagaku Zasshi* (1960) **63**, 1214.
 177. Yasunishi, A. and Yashida, F.: "Solubility of Carbon Dioxide in Aqueous Electrolyte Solution," *J. Chem. Eng. Data* (1979) **24**, 11-14.
 178. Malinin, S.D. and Kurovskaya, N.A.: "Solubility of CO_2 in NaCl - H_2O Solutions at Elevated Temperatures and Pressures," *Geo. Chem. Anal. Chem.* (1975) **4**, 547-50.
 179. Friedman, R.L. and Krishnan, C.V.: *Water—A Comprehensive Treatise*, Vol. 3, F. Franks (ed.) Plenum Press, New York City (1973) 55-59.
 180. Pitzer, K.S.: "Thermodynamics of Electrolytes I. Theoretical Basis and General Equations," *J. Phys. Chem.* (1973) **77**, 268-77.
 181. Pitzer, K.S. and Mayorga, G.: "Thermodynamics of Electrolytes. II. Activity and Osmotic Coefficients for Strong Electrolytes with One or Both Ions Univalent," *J. Phys. Chem.* (1973) **77**, No. 19, 2300-08.
 182. Pitzer, K.S. and Kim, J.J.: "Thermodynamics of Electrolytes. IV. Activity and Osmotic Coefficients for Mixed Electrolytes," *J. Am. Chem. Soc.* (1974) **96**, 5701-07.
 183. *Thermodynamics of Aqueous Systems with Industrial Applications*, S.A. Newman (ed.), Symposium Series 133, ACS (1980).
 184. Knapp, H. and Sandler, S.: "Phase Equilibria and Fluid Properties in the Chemical Industry," paper presented at the 1980 Second Intl. EFCE Conf., West Berlin, March 17-21.
 185. Renon, H.: "Representation of NH_3 - H_2S - H_2O , NH_3 - SO_2 - H_2O , and NH_3 - CO_2 - H_2O Vapor-Liquid Equilibrium," *Thermodynamics of Aqueous Systems with Industrial Applications*, S.A. Newman (ed.), Symposium Series 133, ACS (1980) 173-86.
 186. Mauerer, O.: "Einrichtung zur Messung des Wasserdampfanteils in Gasen," Auslegeschrift DE 2713617 B2, Deutsches Patentamt (1981).
 187. Chen, C.-C., Britt, H.I., Boston, J.F., and Evans, L.B.: "The New Activity Coefficient Models for the Vapor-Liquid Equilibrium of Electrolyte Systems," *Thermodynamics of Aqueous Systems with Industrial Applications*, S.A. Newman (ed.) Symposium Series 133, ACS (1980) 61-89.
 188. Katz, D.L.: "Depths to Which Frozen Gas Fields (Gas Hydrates) May be Expected," *J. Pet. Tech.* (1971) **23**, 419-23.
 189. Stoll, R.D., Ewing, J., and Bryan, G.M.: "Anomalous Wave Velocities in Sediments Containing Gas Hydrates," *J. Geophys. Res.* (1971) **76**, 2090-94.
 190. Makogon, Y.F. *et al.*: "Detection of a Pool of Natural Gas in a Solid (Hydrated Gas) State," (in Russian) *Dokl. Akad. Nauk SSSR* (1971) **196**, 203.
 191. Bily, C. and Dick, J.W.L.: "Naturally Occurring Gas Hydrates in the Mackenzie Delta, N.W.T.," *Bull., Cdn. Pet. Geol.* (1974) **22**, No. 4, 340-52.
 192. Verma, V.K. *et al.*: "Denuding Hydrocarbon Liquids of Natural Gas Constituents by Hydrate Formation," *J. Pet. Tech.* (Feb. 1975) 223-26.
 193. Holder, G.D., Katz, D.L., and Hand, J.H.: "Hydrate Formation in Subsurface Environments," *Bull., AAPG* (1976) **60**, No. 6, 981-88.
 194. Trofimuk, A.A., Cherskii, N.V., and Tsarev, V.P.: "Gas Hydrates—New Sources of Hydrocarbons," *Priroda*, Moscow (1979) **1**, 18-27.
 195. *Geotimes* (1979) **24**, No. 12, 18-19.
 196. Kvenvolden, K.A. and McMenamin, M.A.: "Hydrates of Natural Gas: A Review of Their Geologic Occurrence," *Geol. Surv. Circ.* (1980) **825**, 14.
 197. Scauzillo, F.R.: "Inhibiting Hydrate Formations in Hydrocarbon Gases," *Chem. Eng. Progr.* (1956) **52**, No. 8, 324-28.
 198. Gas Conditioning Fact Book, Dow Chemical Co., Midland, MI (1962) 69-71.
 199. Ng, H.-J. and Robinson, D.B.: "Equilibrium Phase Compositions and Hydrating Conditions in Systems Containing Methanol, Light Hydrocarbons, CO_2 and H_2S ," Research Report, GPA, Tulsa (Feb. 1983).
 200. Saito, S., Marshall, D.R., and Kobayashi, R.: "Hydrates at High Pressures: Part II. Application of Statistical Mechanics to the Study of the Hydrates of Methane, Argon, and Nitrogen," *AIChE J.* (1964) **10**, No. 5, 734-40.
 201. van Cleeff, A. and Diepen, G.A.M.: "Gas Hydrates of Nitrogen and Oxygen," *Rec. Trav. Chim.* (1960) **79**, 582-86.
 202. Kobayashi, R. *et al.*: "Final Revised Report on the Water Content of Carbon Dioxide Gas and Liquid Equilibrium with Liquid Water and with Gas Hydrates," Report to ARCO Oil and Gas Co., Dallas (June 1979).

General References

Water/Volatile Gas Systems

Acetylene/Water

Billitzer, J.: "The Acid Nature of the Acetylenes," *Z. Phys. Chem.* (1902) **40**, 535-44.

Flid, R.M. and Golynets, Y.F.: "Solubility of Acetylene in Aqueous Solutions of Electrolytes in Relation to the Temperature and Concentration of Salt," *Izv. Vyssh. Uchebn. Zaved. Khim. Technol.* (1959) **2**, 173.

Hiraoka, H.: "The Solubilities of Compressed Acetylene Gas in Liquids. I. Water," *Rev. Phys. Chem. Jpn.* (1954) **24**, 13.

See also Ref. 30.

Ethylene/Water

Bradbury, E.J. *et al.*: "Solubility of Ethylene in Water—Effect of Temperature and Pressure," *Ind. Eng. Chem.* (1952) **44**, 211-12.

Davis, J.E. and McKetta, J.J.: "Solubility of Ethylene in Water," *J. Chem. Eng. Data* (1960) **5**, 374-75.

Sanchez, M. and Lentz, H.: "Phase Equilibrium of Water-Propene and Water-Ethene Systems at High Temperatures and Pressures," *High Temp.-High Pressures* (1973) **5**, 6, 689-99.

See also Refs. 30, 31, and 97.

Ethane/Water

Abou El-Nour, F., Harting, P., and Schuetze, H.: "Thermodynamic Carbon Isotope Effect for Solubility of Ethane in Water," *Isotopenpraxis* (1977) **13**, No. 8, 296-98.

Ben-Naim, A. and Yaacobi, M.: "Effects of Solutes on the Strength of Hydrophobic Interaction and its Temperature," *J. Phys. Chem.* (1974) **78**, 170-78.

Danniel, A., Todheide, K., and Franck, E.V.: "Vaporization Equilibria and Critical Curves in the Systems Ethane/Water and n-Butane/Water at High Pressures," *Chem. Ing. Tech.* (1967) **39**, 816-22.

Diepen, G.A.M. and Scheffler, F.E.C.: "The Solubility of Water in Supercritical Ethane," *Rec. Trav. Chim.* (1950) **69**, 604-09.

Gjaldbaek, J.C. and Niemann, H.: "The Solubility of Nitrogen, Argon and Ethane in Alcohols and Water." *Acta Chem. Scand.* (1958) **12**, 1015-23.

Murzin, V.I. and Afanas'eva, N.L.: "Solubility of Water in Liquefied Ethane near its Critical Point." *Zh. Fiz. Khim.* (1968) **42**, No. 8, 1942-45.

See also Refs. 14, 15, 16, 18, 21, 28, 30, 31, 41, 42, 53, 54, 173, and 174.

Propylene/Water

Azamoosh, A. and McKetta, J.J.: "Solubility of Propylene in Water." *J. Chem. Eng. Data* (1959) **4**, 211-12.

Kazaryan, T.S. and Ryabtsev, N.I.: "Solubility of Saturated Propylene, Isobutylene, Isobutane, and n-Butane in Water and Aqueous Solutions." *Nefi. Khoz.* (1969) **47**, No. 10, 54-56.

Klausutis, N.A.: "Phase Equilibrium in the Propane-Propylene-Water System in the Three-Phase Region." PhD dissertation, U. of Texas, Austin (1968).

Li, C.C. and McKetta, J.J.: "Vapor-Liquid Equilibria in the Propylene-Water Systems." *J. Chem. Eng. Data* (1963) **8**, 271-75.

McBain, J.W. and O'Connor, J.J.: "The Effect of Potassium Oleate Upon the Solubility of Hydrocarbon Vapors in Water." *J. Am. Chem. Soc.* (1941) **63**, 875-77.

McBain, J.W. and Soldate, A.M.: "The Solubility of Propylene Vapor in Water as Affected by Typical Detergents." *J. Am. Chem. Soc.* (1942) **64**, 1556-57.

Oleinikova, A.L. and Bogdanov, M.I.: "Solubility of Propylene in Water and Aqueous Sulfuric Acid Solutions." *Uch. Zap., Yaroslav. Tekhnol. Inst.* (1971) **27**, 28-31.

Petrov, A.N., Pankov, A.G., and Bogdanov, M.I.: "Liquid-Gas Chromatographic Determination of the Solubility of Hydrocarbon Gases in Water." *Uch. Zap., Yaroslav. Tekhnol. Inst.* (1970) **13**, 186-90.

Sleinikova, A.L., Petrov, A.N., and Bogdanov, M.I.: "Thermodynamics of Dissolution of Unsaturated C₃-C₅ Hydrocarbons in Water." *Uch. Zap., Yaroslav. Tekhnol. Inst.* (1971) **26**, 35-41.

See Ethylene/Water: Sanchez and Lentz.

See also Ref. 30.

Propyne/Water

Inga, R.F. and McKetta, J.J.: "Solubility of Propyne in Water." *J. Chem. Eng. Data* (1961) **6**, 337-38.

Simpson, L.B. and Lovell, F.P.: "Solubility of Ethyl, and Vinyl Acetylene in Several Solvents." *J. Chem. Eng. Data* (1962) **7**, 498-500.

Cyclopropane/Water

Hafemann, D.R. and Miller, S.L.: "The Clathrate Hydrates of Cyclopropane." *J. Phys. Chem.* (1969) **73**, No. 5, 1392-97.

Imai, S.: "Biophysicochemical Studies on Cyclopropane. I. Solubility Coefficient of Cyclopropane for Various Solutions." *Nara. Igaku Zasshi.* (1961) **12**, 973-79.

Thomson, E.S. and Gjaldbaek, J.C.: "Solubility of Cyclopropane in Perfluoro-Heptane, n-Hexane, Benzene, Dioxane, and Water." *Dan. Tidsskr. Farm.* (1963) **37**, 9-17.

See also Ref. 30.

Cyclopropane/KCl/Water

Zerpa, C. et al.: "Solubility of Cyclopropane in Aqueous Solutions of Potassium Chloride." *J. Chem. Eng. Data* (1979) **24**, No. 1, 26-28.

Propane/Water

Chaddock, R.E.: "Liquid-Vapor Equilibrium in Hydrocarbon Water Systems [Propane-Water]." PhD dissertation, U. of Michigan, Ann Arbor (1942).

DeLoos, T.W., Wijen, A.J.M., and Diepen, G.A.M.: "Phase Equilibria and Critical Phenomena in Fluid (Propane+Water) at High Pressures and Temperatures." *J. Chem. Thermodynamics* (1980) **12**, 193-204.

Goldup, A. and Westaway, M.T.: "Determination of Trace Quantities of Water in Hydrocarbons. Application of the Calcium Carbide-Gas Chromatographic Method to Streams Containing Methanol." *Anal. Chem.* (1966) **38**, No. 12, 1657-61.

Hachmuth, K.H.: "Dehydrating Commercial Propane." *Western Gas* (1931) **8**, No. 1, 55-56, 62, 64.

Perry, C.W.: "Determining Dissolved Water in Liquefied Gases." *Ind. Eng. Chem. Anal. Ed.* (1938) **10**, 513-14.

Krescheck, G.C., Schneider, H., and Scheraga, H.A.: "The Effect of D₂O on the Thermal Stability of Proteins. Thermodynamic Parameter for the Transfer of Model Compounds from H₂O to D₂O." *J. Phys. Chem.* (1965) **69**, 3132.

Poettmann, F.H. and Dean, M.R.: "Water Content of Propane." *Pet. Refiner* (1946) **25**, No. 12, 125-28.

Sanchez, M. and Coll, R.: "Propane-Water System at High Pressures and Temperatures. I. Two-Phase Region." *Ann. Quim.* (1978) **74**, No. 11, 1329-35.

Wehe, A.H. and McKetta, J.J.: "Method for Determining Total Hydrocarbons Dissolved in Water." *Ann. Chem.* (1961) **33**, No. 20, 291-93.

Wetlaufer, D.B. et al.: "Nonpolar Group Participation in the Desaturation of Proteins by Urea and Guanidinium Salts Model Compound Studies." *J. Am. Chem. Soc.* (1964) **86**, 508-14.

See Propene/Water: Azamoosh and McKetta.

See also Refs. 15, 28, 30, 31, 41, and 142.

1,3-Butadiene/Water

See Ref. 30.

1-Butene/Water

Brooks, W.B. and McKetta, J.J.: "The Solubility of 1-Butene in Water at Pressures to 1000 psia." *Pet. Refiner* (1955) **34**, No. 2, 143-44.

Brooks, W.B. and McKetta, J.J.: "The Solubility of Water in 1-Butene." *Pet. Refiner* (1955) **34**, No. 4, 138.

Brooks, W.B., Haughn, J.E., and McKetta, J.J.: "The 1-Butene-Water System in the Vapor and Three-Phase Regions." *Pet. Refiner* (1955) **34**, No. 8, 129-30.

See also Ref. 172.

Isobutane/Water

Razaryan, T.S. and Ryabtsev, N.I.: "Solubility of Saturated Propylene, Isobutylene, Isobutane, and n-Butane in Water and Aqueous Solutions." *Nefi. Khoz.* (1969) **47**, No. 10, 54-56.

Black, C., Joris, G.G., and Taylor, H.S.: "The Solubility of Water in Hydrocarbons." *J. Chem. Phys.* (1948) **16**, No. 5, 537-43.

Nosov, E.F. and Barlyaev, E.V.: "Solubility of Hexafluoropropylene and Isobutane in Water." *Zh. Obshch. Khim.* (1968) **38**, No. 2, 211-12.

Reed, C.D. and McKetta, J.J.: "The Solubility of Isobutane in Water," *Pet. Refiner* (1959) **38**, No. 4, 159-60.

See also Ref. 28.

Isobutane-Furfural/Water

Jordan, D. *et al.*: "Vapor-Liquid Equilibrium of C₄ Hydrocarbon-Furfural-Water Mixtures. Experimental and Theoretical Methods for Three- and Four-Component Systems," *Chem. Eng. Progr.* (1950) **46**, 601-13.

n-Butane/Water

Brooks, W.B., Gibbs, G.B., and McKetta, J.J.: "Mutual Solubility of Light Hydrocarbon-Water Systems," *Pet. Refiner* (1951) **30**, No. 10, 118-20.

LeBreton, J.G. and McKetta, J.J.: "Low Pressure Solubility of n-Butene in Water," *Hydrocarbon Proc. Petro. Ref.* (1964) **43**, No. 6, 136-38.

Reamer, H.H. *et al.*: "Composition of Co-Existing Phases of n-Butane-Water System in the Three-Phase Region," *Ind. Eng. Chem.* (1944) **36**, 381-83.

Reamer, H.H. *et al.*: "n-Butane-Water System in the Two-Phase Region," *Ind. Eng. Chem.* (1952) **44**, 609-15.

Rice, P.A., Gale, R.P., and Barduhn, A.J.: "Solubility of Butane in Water and Soft Solutions at Low Temperatures," *J. Chem. Eng. Data* (1976) **21**, 204-06.

Tsiklis, D.S. and Maslennikova, V.Y.: "Limited Mutual Solubility of Gases in the Water-Butane System," *Pokl. Akad. Nauk SSSR* (1964) **157**, 426-29.

See Ethane/Water: Dannel *et al.*

See Propane/Water: Goldup and Westaway; Krescheck *et al.*; and Wetlaufer *et al.*

See Isobutane/Water: Black *et al.* and Kazaryan and Ryabtsev.

See also Refs. 14, 15, 28, 30, 31, 41, and 55.

2,2-Dimethylbutane/Water and Cyclopentane/Water

See Ref. 28.

n-Pentane/Water

Connolly, J.F.: "Solubility of Hydrocarbons in Water Near the Critical Solution Temperature," *J. Chem. Eng. Data* (1966) **11**, 13-16.

Fuhner, H.: "Water Solubility in Homologous Series," *Ber. Deut. Chem. Ges.* (1924) **5713**, 510-15.

Liabastre, A.A.: "Experimental Determination of the Solubility of Small Organic Molecules in Water and Dideuterium Oxide and the Application of the Scaled Particle Theory to Aqueous and Non-aqueous Solutions," PhD dissertation, Georgia Inst. of Tech., Atlanta (1974).

Namiot, A.Y. and Beider, S.Y.: "The Water Solubility of n-Pentane and n-Hexane," *Khim. Tekhnol. Topliv. Masel* (1960) **5**, 52-55.

See Isobutane/Water: Black *et al.*

See also Refs. 28 and 44.

Methylcyclopentane/Water; 2,4-Dimethylpentane/Water; and 2,2,4-Trimethylpentane/Water

See Ref. 28.

2-Methylpentane/Water and n-Heptane/Water

See n-Pentane/Water: Connolly, J.F.

See also Ref. 28.

Isopentane/Water

Pavlova, S.P. *et al.*: "Mutual Solubility of C₅ Hydrocarbons and Water," *Prom. Sin. Kauch.* (1966) **3**, 18-20.

See Isobutane/Water: Black *et al.*

See also Ref. 28.

Neopentane/Water

See Refs. 30 and 37.

Cyclohexane/Water

Farkas, E.J.: "New Method for Determination of Hydrocarbon-in-Water Solubilities," *Anal. Chem.* (1965) **37**, No. 9, 1173-75.

Roddy, J.W. and Coleman, C.F.: "Solubility of Water in Hydrocarbons as a Function of Water Activity," *Talanta* (1968) **15**, No. 11, 1281-86.

Sultanov, R.G. and Skripka, V.G.: "Solubility of Water in n-Hexane, Cyclohexane, and Benzene at Elevated Temperatures and Pressures," *Zh. Fiz. Khim.* (1973) **47**, No. 4, 1035.

See also Ref. 28.

n-Hexane/Water

Gester, G.C.: "Design and Operation of a Light Hydrocarbon Distillation Drier," *Chem. Eng. Progr.* (1947) **43**, 117-22.

See Cyclohexane/Water: Roddy and Coleman, and Sultanov and Skripka.

See also Ref. 28.

Methylcycloheptane/Water and n-Octane/Water

See Ref. 28.

n-Decane/Water

Lotter, Y.G., Asmyan, K.D., and Skripka, V.G.: "The Volume Properties of the Coexisting Phases of the n-Decane-Water System at 275°C," *Zh. Fiz. Khim.* (1976) **50**, 2171.

Methane/Ethane/Water

Amirjafari, B. and Campbell, J.M.: "Solubility of Gaseous Hydrocarbon Mixtures in Water," *Soc. Pet. Eng. J.* (Feb. 1972) **12**, No. 1, 21-27.

Villareal, J.F., Bissey, L.T., and Nielson, R.F.: "Dew Point Water Contents of Methane-Ethane Mixtures at a Series of Pressures and Temperatures," *Prod. Monthly* (1954) **18**, No. 7, 15-17.

Methane/Propane/Water; Ethane/Propane/Water; and

Methane/Ethane/Propane/Water

See Methane/Ethane/Water: Amirjafari and Campbell.

Methane/n-Butane/Water

Anthony, R.G. and McKetta, J.J.: "How to Estimate H₂O in Hydrocarbons," *Hydrocarbon Process.* (1968) **47**, No. 6, 131-34.

See also Refs. 52 and 167.

Methane/n-Pentane/Water

See Ref. 44.

Ethylene/Ethane/Water

Anthony, R.G. and McKetta, J.J.: "Phase Equilibrium in the Ethylene-Ethane-Water System," *J. Chem. Eng. Data* (1967) **12**, No. 1, 21-28.

Aromatic-Hydrocarbon/Water

Eganhouse, R.P. and Calder, J.A.: "The Solubility of Medium Molecular Weight Aromatic Hydrocarbon(s) and the Effects of Hydrocarbon Co-Solutes and Salinity," *Geochim. Cosmochim. Acta*. (1976) **40**, No. 5, 555-61.

Kerosine/Water and Oil/Water

Griswold, J. and Kasch, J.E.: "Hydrocarbon-Water Solubilities at Elevated Temperatures and Pressures," *Ind. Eng. Chem.* (1942) **34**, 804-06.

Groschuff, E.: "Solubility of Water in Benzene, Petroleum and Paraffin Oil," *Elektrochem.* (1911) **17**, 348.

Naphtha/Water

Amero, R.C., Moore, J.W., and Capell, R.G.: "Design and Use of Adsorptive Drying Units," *Chem. Eng. Progr.* (1947) **43**, 349-70.

See Kerosine-Water: Griswold and Kasch.

Natural-Gas/Glycol/Water

Russell, G.F., Reid, L.S., and Huntington, R.L.: "Experimental Determinations of the Vapor-Liquid Equilibria Between Natural Gas and 95% Diethylene Glycol up to a Pressure of 2000 psi," *Trans., AIChE* (1945) **41**, 315-25.

Gasoline/Water

Derr, R.B. and Willmore, C.B.: "Dehydration of Organic Liquids with Activated Alumina," *Ind. Eng. Chem.* (1939) **31**, 866-68.

Wachter, A. and Smith, S.S.: "Preventing Internal Corrosion of the Pipe Lines—Sodium Nitrite Treatment for Gasoline Lines," *Ind. Eng. Chem.* (1943) **35**, 358-67.

Argon/Methane/Water and Helium/Methane/Water

Namiot, A.Y. and Bondareva, M.M.: "Solubility of Helium-Methane Mixture in Water at High Pressures," *Nauch. Tekhn. SB. PO Dobyshchenefti Vses. Neftgaz Nauch. Issled. Inst.* (1962) **18**, 82-91.

Nitrogen/Methane/Water

Maharajh, D.M. and Walkley, J.: "Thermodynamic Solubility of Gas Mixtures. I. Two Component Gas Mixtures in Water at 25 deg.," *J. Chem. Soc. Far. Trans.* (1973) **69**, No. 5, 842-48.

Oxygen/Methane/Water

Maharajh, D.M. and Walkley, J.: "Lowering of the Separation Solubility of Oxygen by Presence of Another Gas," *Nature*, London (1972) **236**, No. 5343, 165.

See Nitrogen/Methane/Water: Maharajh and Walkley.

Hydrogen-Sulfide/Carbon-Dioxide/Methane/Water

Froning, H.R., Jacoby, R.H., and Richards, W.L.: "Vapor-Liquid Equilibria of the Methane, Carbon Dioxide, Hydrogen Sulfide, Water System and Application to the Design of a Water Wash System for Removing Acid Gases," *Proc., Annual Convention of the Natural Gas Assoc. Am.* (1963) **42**, 32-39.

Hydrogen-Sulfide/Water

Selleck, F.T., Carmichael, L.T., and Sage, B.H.: "Phase Behavior in the Hydrogen Sulfide-Water System," *Ind. Eng. Chem.* (1952) **44**, 2219-26.

Hydrate/Volatile Gas SystemsMethane/Brine (NaCl)/Water and Methane/EtOH/Water

See Ref. 134.

Ethylene/Water

van Cleef, A. and Diepen, G.A.M.: "Ethylene Hydrate at High Pressures," *Rec. Trav. Chim.* (1962) **81**, 425-29.

Diepen, G.A.M. and Scheffer, F.E.C.: "The Ethylene-Water System," *Rec. Trav. Chim.* (1950) **69**, 593-603.

See also Ref. 122.

Ethylene/EtOH/Water

Reamer, H.H., Selleck, F.T., and Sage, B.H.: "Some Properties of Mixed Paraffinic and Olefinic Hydrates," *Trans., AIME* (1952) **195**, 197-201.

See also Ref. 129 and 140.

Ethane/Water

See Ethylene/EtOH/Water: Reamer *et al.*

See also Refs. 4, 8, 123, 124, 126, and 128.

Cyclopropane/Water

Callahan, J.E. and Sloan, E.D.: "Heat Capacity Measurements on Structure I and II Pure Hydrates at Low Pressures and Below Room Temperature," Research Report, Gas Research Inst. (Sept. 1982) Contract No. 5081-360-0487.

Dharmawardhana, P.B., Parrish, W.R. and Sloan, E.D.: "Experimental Thermodynamic Parameters for the Prediction of Natural Gas Hydrate Dissociation Conditions," *Ind. Eng. Chem. Fund.* (1980) **19**, 410-14.

Hafemann, D.R. and Miller, S.L.: "The Clathrate Hydrates of Cyclopropane," *J. Phys. Chem.* (1969) **73**, No. 5, 1392-97.

Cyclopropane/KCl/Water and Cyclopropane/CaCl₂/Water

Menten, P.D., Parrish, W.R. and Sloan, E.D.: "Effect of Inhibitors on Hydrate Formation," *Ind. Eng. Chem. Processes Des. Dev.* (1981) **20**, No. 2, 399-401.

Cyclopropane/Methanol/Water

Giussani, A.: "Inhibition of Natural Gas Hydrates," MS thesis, Colorado School of Mines, Golden (1981).

See Cyclopropane/KCl/Water: Menten *et al.*

Propane/Water

Miller, B. and Strong, E.R. Jr.: "Possibilities of Strong Natural Gas in the Form of a Solid Hydrate; a Method for Determining the Ratio of Hydrocarbon to Water in a Solid Hydrate of a Normally Gaseous Hydrocarbon, and its Application to Propane Hydrate," *Proc. Am. Gas Assoc.* (1945) **27**, No. 2, 80-94.

See Ethylene/EtOH/Water: Reamer *et al.*

See also Refs. 5, 122, 126, 134, and 135.

Isobutane/Water

Rouher, O.S. and Barduhn, A.J.: "Hydrates of Iso- and Normal Butane and Their Mixtures," *Desalination* (1969) **6**, 57-73.

See also Refs. 126 and 149.

1,4-Dioxane/Water and 1,3-Dioxane/Water

Davidson, D.W. and Ripmeester, J.A.: "Clathrate Ices—Recent Results," *J. Glaciol.* (1978) **21**, No. 85, 33-49.

Methane/Ethylene/Water and Methane/Ethylene/Propylene/Water

See Ref. 129.

Methane/Ethane/Water

Holder, G.D. and Grigoriou, G.C.: "Hydrate Dissociation Pressures of (Methane-Ethane-Water). Existence of a Locus of Minimum Pressures," *J. Chem. Thermodynamics* (1980), 1093-1104.

See also Refs. 5, 127, and 128.

Methane/Propylene/Water

Otto, F.D. and Robinson, D.B.: "A Study of Hydrates in the Methane-Propylene-Water System," *AIChE J.* (1960) **6**, No. 4, 602-05.

Methane/Propane/Water

Carson, D.B. and Katz, D.L.: "Natural Gas Hydrates," *Trans., AIME* (1941) **146**, 150-53.

Verma, V.K., Hand, J.H., and Katz, D.L.: "Gas Hydrates from Liquid Hydrocarbons (Methane-Propane-Water Systems)," paper presented at the GVC/AIChE Joint Meeting, Munich, Germany, Sept. 17-21.

See also Refs. 5, 127, and 163.

Methane/Isobutane/Water

Ng, H.-J. and Robinson, D.B.: "The Measurement and Prediction of Hydrate Formation in Liquid Hydrocarbon-Water Systems," *Ind. Eng. Chem. Fund.* (1976) **15**, No. 4, 293-98.

See also Refs. 5, 127, and 149.

Methane/n-Butane/Water

John, V.T. and Holder, G.D.: "Improved Predictions of Hydrate Equilibria," paper presented at the 1981 AIChE Annual Meeting, New Orleans.

Ng, H.-J. and Robinson, D.B.: "The Prediction of Hydrate Formation in Condensed Systems," *AIChE J.* (1977) **23**, No. 4, 477-82.

See also Ref. 127.

Methane/Pentane/Water and Methane/Hexane/Water

See Methane-Propane-Water: Carson and Katz.

Ethylene/Ethane/Water

Koshelev, V.S. *et al.*: "Study of Hydrate-Gas Phase Equilibrium in the Ethane-Ethylene System," *Zh. Prikl. Khim.*, Leningrad (1971) **44**, 2573-74.

Ethylene/Propane/Water

Fomina, V.I. and Byk, S.S.: "Study of Hydrate-Gas Phase Equilibrium in the Ethylene-Propane System," *Zh. Prikl. Khim.*, Leningrad (1969) **42**, 2855-58.

Ethane/Propane/Water and Methane/Ethane/Propane/Water

Holder, G.D. and Hand, J.H.: "Multiple-Phase Equilibria in Hydrates from Methane, Ethane, Propane and Water Mixtures," *AIChE J.* (1982) **28**, No. 3, 440-47.

Propane/Propylene/Water

Fomina, V.I. and Byk, S.S.: "Hydrate-Gas Phase Equilibrium in the Propane-Propylene-Water System," *Gaz. Prom.* (1967) **12**, No. 3, 50-56.

See Ethylene/EtOH/Water: Reamer *et al.*

Methane/Ethane/Propane/CO₂/Water

See Refs. 164 and 165.

Methane/Ethane/Propane/Isobutane/n-Butane/Water

See Ref. 127.

Methane/Propane/Condensate/Water andMethane/Propane/Crude-Oil/Water

See Ref. 192.

Methane/Propane/Hydrogen-Sulfide/Water

Schroeter, J.P., Kobayashi, R., and Hildebrand, M.A.: "Hydrate Decomposition Conditions in the System H₂S-Methane-Propane," *Ind. Eng. Chem. Fund.* (1983) **22**, No. 4, 361-64.

Isobutylene/Propane/Isobutane/Water andIsobutylene/Propane/Isoheptane/Propylene/Water

See Propane/Propylene/Water: Fomina and Byk.

Cracked-Gas/Water

Byk, S.S.: "Experiments on the Conditions for the Formation of Hydrates of Cracked Gases," *Gaz. Prom.* (1957) **4**, 33-35.

Oil/Water

See Ref. 193.

Methane/Argon/Water

See Ref. 154.

Methane/Nitrogen/Water

Jhaveri, I. and Robinson, D.B.: "Hydrates in the Methane-Nitrogen System," *Cdn. J. Chem. Eng.* (1965) **43**, No. 2, 75-78.

Propane/Nitrogen/Water

Ng, H.-J., Petrunia, J.P., and Robinson, D.B.: "Experimental Measurement and Prediction of Hydrate Forming Conditions in the N₂-Propane-H₂O System," *Fluid Phase Equil.* (1978) **1**, 283-91.

Methane/Carbon-Dioxide/Water

See Ref. 139.

Propane/Carbon-Dioxide/Water

Robinson, D.B. and Mehta, B.R.: "Hydrates in the Propane-CO₂-H₂O System," *J. Cdn. Pet. Tech.* (1971) **10**, 33-35.

Propane/Hydrogen-Sulfide/Water

See Ref. 151.

Methane/Hydrogen-Sulfide/Carbon-Dioxide/Water

Robinson, D.B. and Hutton, J.M.: "Hydrate Formation in Systems Containing Methane, Hydrogen Sulfide and Carbon Dioxide," *J. Cdn. Pet. Tech.* (1967) **6**, No. 1, 6-9.

Natural-Gas/Glycol/Water

See Ref. 197.

Natural-Gas/Ammonium/Water

Russell, J.T.: "Anhydrous Ammonia to Inhibit Gas Hydrate Formation," *Gas* (1937) **13**, No. 6, 38-40.

Natural-Gas/NaCl/Water

See Ref. 134.

Natural-Gas/CaCl₂/Water

See Ref. 5.

Chapter 26

Properties of Reservoir Rocks

Daniel M. Bass Jr., Colorado School of Mines*

Introduction

This chapter deals with the fundamental properties of reservoir rocks. The properties discussed are (1) *porosity*—a measure of the void space in a rock; (2) *permeability*—a measure of the fluid transmissivity of a rock; (3) *fluid saturation*—a measure of the gross void space occupied by a fluid; (4) *capillary-pressure relations*—a measure of the surface forces existing between the rock and the contained fluids; and (5) *electrical conductivity of fluid-saturated rocks*—a measure of the conductivity of the rock and its contained fluids to electric current. These properties constitute a set of fundamental parameters by which the rock may be described quantitatively.

Typical core-analysis data are presented to illustrate the description of porous media by these fundamental properties.

Porosity

Porosity is defined as the ratio of the void space in a rock to the bulk volume (BV) of that rock, multiplied by 100 to express in percent. Porosity may be classified according to the mode of origin as primary and secondary. An original porosity is developed during the deposition of the material, and later compaction and cementation reduce it to the primary porosity. Secondary porosity is that developed by some geologic process subsequent to deposition of the rock. Primary porosity is typified by the intergranular porosity of sandstones and the intercrystalline and oolitic porosity of some limestones. Secondary porosity is typified by fracture development as found in some shales and limestones and the vugs or solution cavities commonly found in limestones. Rocks having primary porosity are more uniform in their

characteristics than rocks in which a large part of the porosity is induced. For direct quantitative measurement of porosity, reliance must be placed on formation samples obtained by coring.

Unit cells of two systematic packings of uniform spheres are shown in Fig. 26.1. The porosity for cubical packing (the least compact arrangement) is 47.6% and for rhombohedral packing (the most compact arrangement) is 25.96%.¹ Considering cubical packing, the porosity may be calculated as follows. The unit cell is a cube with sides equal to $2r$ where r is the radius of the sphere. Therefore, $V_b = (2r)^3 = 8r^3$, where V_b is the bulk volume. Since there are $8\frac{1}{8}$ spheres in the unit cell, the sand-grain volume, V_s , is given by

$$V_s = \frac{4\pi r^3}{3}$$

The porosity, ϕ , is given by

$$\phi = \frac{V_p}{V_b} \times 100 = \frac{V_b - V_s}{V_b} \times 100,$$

where V_p is PV. Therefore,

$$\begin{aligned} \phi &= \frac{8r^3 - 4/3\pi r^3}{8r^3} \times 100 = \left(1 - \frac{\pi}{2 \times 3}\right) \times 100 \\ &= 47.6\%. \end{aligned}$$

Of particular interest is the fact that the radii cancel and the porosity of uniform spheres is a function of packing only.

*This author also wrote the original chapter on this topic in the 1962 edition with coauthor James W. Amyx (deceased). D.M. Bass Jr. is currently a petroleum consultant.

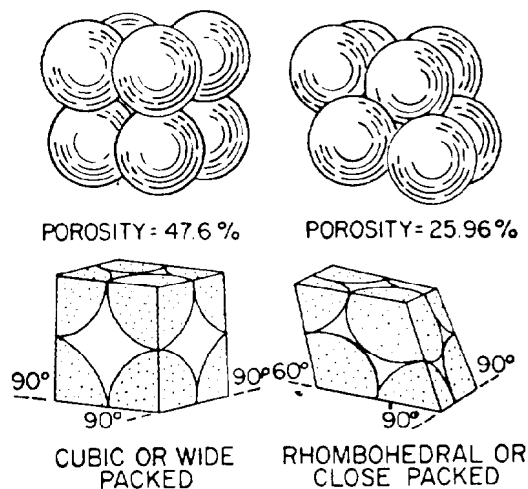


Fig. 26.1—Unit cells and groups of uniform spheres for cubic and rhombohedral packing.

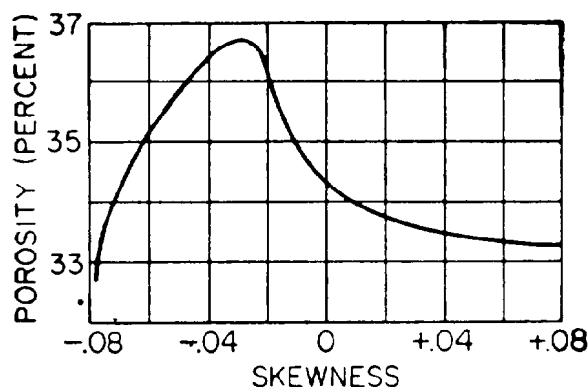


Fig. 26.2—Variation of porosity with skewness of grain-size distribution.

Tickell *et al.*² has presented experimental data indicating that, for packings of Ottawa sand, porosity was a function of skewness of the grain-size distribution (see Fig. 26.2). Skewness is a statistical measure of the uniformity of distribution of a group of measurements. Other investigators have measured the effects of distribution, grain size, and grain shape. In general, greater angularity tends to increase the porosity, while an increase in range of particle size tends to decrease porosity.

In dealing with reservoir rocks (usually consolidated sediments), it is necessary to define total porosity and effective porosity because cementing materials may seal off a part of the PV. *Total porosity is the ratio of the total void space in the rock to the BV of the rock, while effective porosity is the ratio of the interconnected void space in the rock to the BV of the rock, each expressed in percent.* From the reservoir-engineering standpoint, effective porosity is the desired quantitative value because it represents the space that is occupied by mobile fluids. For intergranular materials, poorly to moderately well cemented, the total porosity is approximately equal to the effective porosity. For more highly cemented materials and for limestones, significant differences in total-porosity and effective-porosity values may occur.

Photographs of oilwell cores are presented in Fig. 26.3.³ The pore configuration of the sandstones shown is complex, but the pores are distributed relatively uniformly. Complex pore configurations arise from the interaction of many factors in the geologic environment of the deposit. These factors include the packing and particle-size distribution of the framework fraction, the type of interstitial material, and the type and degree of cementation. The influence of these various factors may be evaluated as statistical trends.

Material having induced porosity, such as the carbonate rocks shown in Fig. 26.3, have even more complex pore configurations. In fact, two or more systems of pore openings may occur in such rocks. The basic rock material is usually finely crystalline and is called the "matrix." The matrix contains uniformly small pore openings that comprise one system of pores. One or more systems of larger openings usually occur in carbonate rocks as a result of leaching, fracturing, or dolomitization of the primary rock material. Vugular pore openings are frequently as large as an ordinary lead pencil and usually are attributed to leaching of the rock subsequent to deposition. Fractures also may be quite large and contribute substantially to the volume of pore openings in the rock.

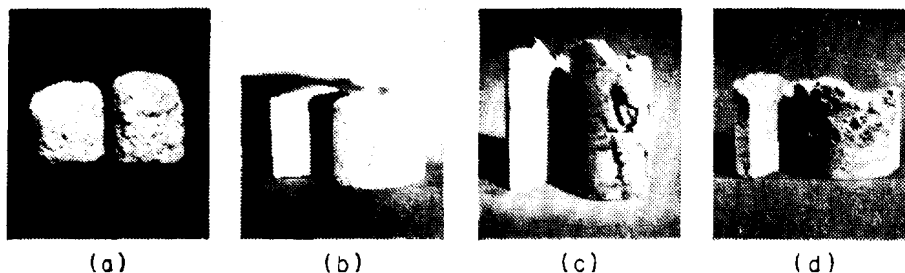


Fig. 26.3—Oilwell cores. Consolidated sandstone: (a) wireline core, Lower Frio; (b) whole core, Seven Rivers. Vugular, solution cavities, and crystalline limestone and dolomite: (c) whole core, Devonian; (d) whole core, Hermosa.

Laboratory Measurement of Porosity

Numerous methods have been developed for the determination of the porosity of consolidated rocks having intergranular porosity. Most of the methods developed have been designed for small samples, roughly the size of a walnut. Since the pores of intergranular material are quite small, determining the porosity of such a sample involves measuring the volume of literally thousands of pores. The porosity of larger portions of the rock is represented statistically from the results obtained on numerous small samples.

In the laboratory measurement of porosity, it is necessary to determine only two of the three basic parameters (BV, PV, and grain volume). In general, all methods of BV determination are applicable to determining both total and effective porosity.

BV. Usual procedures use observation of the volume of fluid displaced by the sample. This procedure is particularly desirable because the BV of specially shaped samples may be determined as rapidly as that of shaped samples.

The fluid displaced by a sample may be observed either volumetrically or gravimetrically. In either procedure, it is necessary to prevent fluid penetration into the pore space of the rock. This may be accomplished by (1) coating the rock with paraffin or a similar substance, (2) saturating the rock with the fluid into which it is to be immersed, or (3) using mercury, which by virtue of its surface tension and wetting characteristics does not tend to enter the small pore spaces of most intergranular materials.

Gravimetric determinations of BV may be accomplished by observing the sample's weight loss when immersed in a fluid or the difference in weight of a pycnometer when filled with a fluid and when filled with fluid and the core sample. The details of gravimetric determinations of BV are best summarized by Example Problems 1 through 3.

Example Problem 1—Coated Sample Immersed in Water.

Given that the weight of dry sample in air, $A=20.0$ g, weight of dry sample coated with paraffin, $B=20.9$ g (density of paraffin $=0.9$ g/cm³), and weight of coated sample immersed in water at 40°F, $C=10.0$ g (density of water $=1.00$ g/cm³),

we can then calculate that

$$\text{weight of paraffin} = B - A = 20.9 - 20.0 = 0.9 \text{ g,}$$

$$\text{volume of paraffin} = \frac{0.9}{0.9} = 1 \text{ cm}^3,$$

$$\text{weight of water displaced} = B - C = 20.9 - 10.0 = 10.9 \text{ g,}$$

$$\text{volume of water displaced} = \frac{10.9}{1.0} = 10.9 \text{ cm}^3,$$

$$\begin{aligned} \text{volume of water displaced} - \text{volume of paraffin} \\ = 10.9 - 1.0 = 9.9 \text{ cm}^3, \text{ and} \\ \text{BV of rock, } V_b, = 9.9 \text{ cm}^3. \end{aligned}$$

Example Problem 2—Water-Saturated Sample Immersed in Water.

Given that weight of saturated sample in air, $D=22.5$ g, and weight of saturated sample in water at 40°F, $E=12.6$ g,

we can calculate that

$$\begin{aligned} \text{weight of water displaced} &= D - E = 22.5 - 12.6 \\ &= 9.9 \text{ g, and} \end{aligned}$$

$$\text{volume of water displaced} = \frac{9.9}{1.0} = 9.9 \text{ cm}^3.$$

Therefore,

$$\text{BV rock, } V_b, = 9.9 \text{ cm}^3.$$

Example Problem 3—Dry Sample Immersed in Mercury Pycnometer.

Given A from Example Problem 1 and the following values,

weight of pycnometer filled with mercury at 20°C, $F=350.0$ g and

weight of pycnometer filled with mercury and sample at 20°C, $G=235.9$ g (density of mercury $=13.546$ g/cm³),

we can calculate that

$$\text{weight of sample + weight of pycnometer filled with mercury} = A + F = 20 + 350 = 370 \text{ g,}$$

$$\text{weight of mercury displaced} = A + F - G = 370 - 235.9 = 134.1 \text{ g, and}$$

$$\text{volume of mercury displaced} = \frac{134.1}{13.546} = 9.9 \text{ cm}^3.$$

Therefore,

$$\text{BV of rock} = 9.9 \text{ cm}^3.$$

Determinations of BV volumetrically use a variety of specially constructed pycnometers or volumeters. An electric pycnometer from which the BV may be read directly is shown in Fig. 26.4. The sample is immersed in the core chamber, causing a resulting rise in the level of the connecting U tube. The change in mercury level is measured by a micrometer screw connected to a low-voltage circuit. The electric circuit is closed as long as the measuring point is in contact with the mercury. The travel of the measuring point is calibrated in volume units such that the difference in the open-circuit readings with and without the sample in the core chamber represents the BV of the sample. Either dry or saturated samples may be used in the device.

Sand-Grain Volume (GV). The various porosity methods usually are distinguished by the means used to determine the GV or PV. Several of the oldest methods of porosity measurement are based on the determination of GV.

The GV may be determined from the dry weight of the sample and the sand-grain density. For many purposes, results of sufficient accuracy may be obtained by using the density of quartz (2.65 g/cm³) as the sand-grain density.

For more rigorous determinations either the A.F. Melcher-Nutting⁴ or Russell⁵ method may be employed. The BV of a sample is determined; then this sample, or an adjacent sample, is reduced to grain size and the GV is determined. In the Melcher-Nutting technique, all the measurements are determined

TABLE 26.1—METHODS OF DETERMINING POROSITY

	Effective Porosity Methods			
	Washburn-Bunting Porosimeter	Stevens Porosimeter	Kobe Porosimeter	Boyle's Law Porosimeter
Type of sampling	One to several pieces per increment (usually one).	One to several pieces per increment (usually one).	One to several pieces per increment (usually one).	One to several pieces per increment (usually one).
Preparation	Solvent extraction and oven drying. Occasionally use retort samples.	Solvent extraction and oven drying. Occasionally use retort samples.	Solvent extraction and oven drying. Occasionally use retort samples.	Solvent extraction and oven drying. Occasionally use retort samples.
Functions measured	PV and BV.	Sand grain volume and unconnected PV and BV.	Sand grain volume and unconnected PV and BV.	Sand grain volume and unconnected PV and BV.
Manner of measurement	Reduction of pressure on a confined sample and measurement of air evolved. BV from mercury pycnometer.	Difference in volume of air evolved from a constant-volume chamber when empty and when occupied by sample. BV by Russell tube.	Difference in volume of air evolved from a constant-volume chamber when empty and when occupied by sample. BV by Russell tube.	Difference in volume of air evolved from a constant-volume chamber when empty and when occupied by sample. BV by Russell tube.
Errors	Air from dirty mercury; possible leaks in system; incomplete evacuation caused by rapid operation or tight sample.	Mercury does not become dirty. Possible leaks in system; incomplete evacuation caused by rapid operation or tight sample.	Mercury does not become dirty. Possible leaks in system; incomplete evacuation caused by rapid operation or tight sample.	Mercury does not become dirty. Possible leaks in system; incomplete evacuation caused by rapid operation or tight sample.

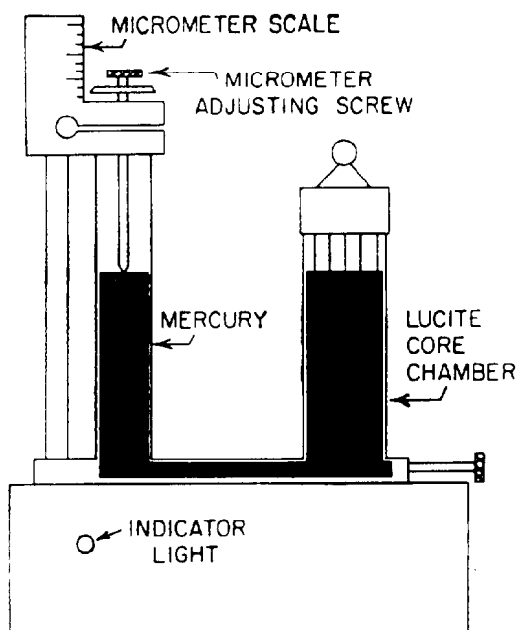


Fig. 26.4—Electric pycnometer.

gravimetrically, using the principle of buoyancy (Example Problem 2). The Russell method uses a specially designed volumeter, and the BV and GV are determined volumetrically. The porosity determined is total porosity, ϕ_t . Thus,

$$\phi_t = \frac{V_b - V_s}{V_b} \times 100.$$

From the data of Example Problem 2 and using a sand-grain density of 2.65 g/cm^3 ,

$$V_b = 9.9 \text{ cm}^3,$$

$$V_g = \frac{20}{2.65} = 7.55 \text{ cm}^3,$$

and

$$\phi_t = \frac{9.9 - 7.55}{9.9} \times 100 = 23.8\%.$$

The Stevens⁶ porosimeter is a means of determining the "effective" GV. The porosimeter (Fig. 26.5) consists of a core chamber that may be sealed from atmospheric pressure and closed from the remaining parts of the porosimeter by a needle valve. The accurate volume of the core chamber is known. In operation, a core is placed in the core chamber; a vacuum is established in the

TABLE 26.1—METHODS OF DETERMINING POROSITY (continued)

Saturation*	Effective Porosity Methods		Total Porosity Method
	Core Laboratories, Wet Sample	Core Laboratories, Dry Sample	Sand Density
One to several pieces per increment (usually one).	Several pieces for retort; one for mercury pump.	One to several pieces per increment (usually one).	Several pieces per increment.
Solvent extraction and oven drying. Occasionally use retort samples.	None.	Solvent extraction and oven drying. Occasionally use retort samples.	Solvent extraction; then, in second step, crush sample to grain size.
PV and BV.	Volumes of gas space, oil, and water. BV.	Sand-grain volume and unconnected PV, and BV.	BV of sample and volume of sand grains.
Weight of dry sample; weight of saturated sample in air; weight of saturated sample immersed in saturated fluid.	Weight of retort sample; volume of oil and water from retort sample; gas volume and BV of mercury-pump sample.	Difference in volume of air evolved from a constant-volume chamber when empty and when occupied by sample.	Weight of dry sample; weight of saturated sample immersed; weight and volume of sand grains.
Possible incomplete saturation.	Obtain excess water from shales. Loss of vapors through condensers.	Possible leaks in system; incomplete evacuation caused by rapid operation or tight sample.	Possible loss of sand grains in crushing. Can be reproduced most accurately.

*Best method

system by manipulating the mercury reservoir; the air in the core chamber is expanded repeatedly into the evacuated system and measured at atmospheric pressure in the graduated tube. The Stevens method is an adaptation of the Washburn-Bunting⁷ procedure, which will be discussed with the measurement of PV.

Example Problem 4—Determination of Grain Volume by Gas Expansion (Stevens Porosimeter).

Given that

volume of core chamber, $H = 15 \text{ cm}^3$

and

total reading, $I = 7.00 \text{ cm}^3$

where

volume of air (first reading) = 6.970,

volume of air (second reading) = 0.03, and

volume of air (third reading) = 0,

we can calculate

effective grain volume = $H - I = 8 \text{ cm}^3$,

bulk volume of sample (from pycnometer) = 10 cm^3 ,

and effective porosity, $\phi_e = [(10 - 8)/10] \times 100 = 20\%$.

PV. All methods of measuring PV yield "effective" porosity. The methods are based on either the extraction of a fluid from the rock or the introduction of a fluid into the pore space of the rock.

The Washburn-Bunting⁷ porosimeter measured the volume of air extracted from the pore space by creating a partial vacuum in the porosimeter by manipulation of the attached mercury reservoir. In the process, the core is exposed to contamination by mercury and, therefore, is

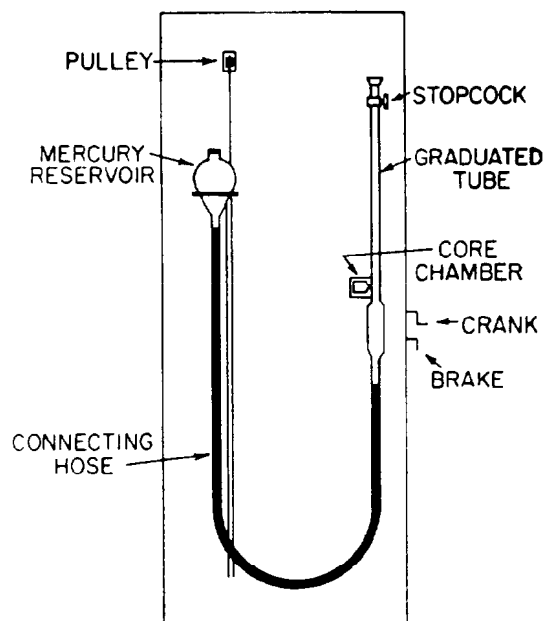


Fig. 26.5—Stevens porosimeter.

TABLE 26.2—CHARACTERISTICS OF SAMPLES USED IN POROSITY-MEASUREMENT COMPARISONS

Sample Number	Type of Material	Approximate Gas Permeability (md)	Porosity (%)				
			Average	Average From Gas Methods	Average From Saturation Methods	Value From High Observation*	Value From Low Observation**
1	Limestone	1	17.47	17.81	16.96	18.50	16.72
2	Fritted glass	2	28.40	28.68	27.97	29.30	27.56
3	Sandstone	20	14.00	14.21	13.70	15.15	13.50
4	Sandstone	1,000	30.29	31.06	29.13	31.8	26.8
BZE	Semiquartzitic sandstone	0.2	3.95	4.15	3.66	4.60	3.50
BZG	Semiquartzitic sandstone	0.8	3.94	4.10	3.71	4.55	3.48
61-A	Alundum	1,000	28.47	28.78	28.00	29.4	27.8
722	Alundum	3	16.47	16.73	16.08	17.80	16.00
1123	Chalk	1.6	32.67	33.10	32.03	33.8	31.7
1141-A	Sandstone	45	19.46	19.68	19.12	20.2	18.8

*Highest reported porosity value for the sample.

**Lowest reported porosity value for the sample.

not suitable for additional tests. The previously described Stevens method is a modification of the Washburn-Bunting procedure especially designed to prevent mercury contamination of the samples.

A number of other devices have been designed for measuring PV; these include the Kobe⁸ porosimeter, the Oilwell Research porosimeter, and the mercury-pump porosimeter. Kobe and Oilwell Research porosimeters are Boyle's-law-type porosimeters designed for use with nitrogen or helium with negligible adsorption on rock surfaces at room temperature. The mercury-pump porosimeter is designed so that the BV may be obtained as well as the PV.

The saturation method of determining porosity consists of saturating a clean dry sample with a fluid of known density and determining the PV from the gain in weight of the sample. The sample usually is evacuated in a vacuum flask to which the saturation fluid may be admitted by means of a separatory funnel. If care is exercised to achieve complete saturation, this procedure is believed to be one of the best available techniques for intergranular materials. Example Problem 5 illustrates the saturation technique of measuring PV.

Example Problem 5—Effective Porosity by the Saturation Method. From the data of Example Problems 1 and 2, we can calculate

$$\begin{aligned}\text{weight of water in pore space} &= D - A = 22.5 - 20 \\ &= 2.5 \text{ g,}\end{aligned}$$

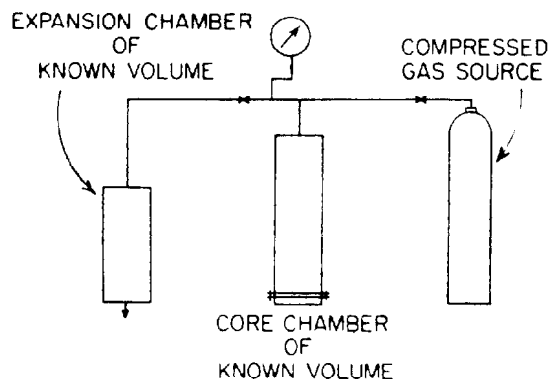


Fig. 26.6—Gas-expansion porosimeter for large cores.

$$\text{volume of water in pore space} = \frac{2.5 \text{ g}}{1 \text{ g/cm}^3} = 2.5 \text{ cm}^3,$$

$$\text{effective PV} = 2.5 \text{ cm}^3, \text{ and}$$

$$\text{BV (Example Problem 2)} = 9.9 \text{ cm}^3.$$

Therefore,

$$\phi_e = \frac{2.5}{9.9} \times 100 = 25.3\%.$$

Several methods of determining effective porosity are compared in Table 26.1.

Precision of Porosity Measurements. A group⁹ of major company laboratories conducted a series of tests to determine the precision of porosity measurements. The method used was either gas expansion or a saturation technique. Table 26.2 summarizes the results of these tests. Note that the gas-expansion method is consistently higher than the saturation method. This undoubtedly results from the fact that the errors inherent to each tend to be in opposite directions. In the case of the gas-expansion method, errors caused by gas adsorption would cause high values to be obtained while, for the saturation techniques, incomplete saturation of the sample would result in low values. The difference in the average values obtained by the two methods is about 0.8% porosity, which is approximately a 5% error for a 16% porosity sample. However, it is felt that all the methods commonly used to determine effective porosity yield results with the desired degree of accuracy if carefully performed.

Carbonate Rocks. Small samples, such as used in the routine techniques already discussed, yield values of porosity that do not include the effect of vugs, solution cavities, etc. The saturation methods of determining PV and BV are unsatisfactory because drainage will occur from the larger pore spaces. Therefore, it is necessary to use larger core samples and to determine the BV by measurement of the core dimensions or after coating the sample. The effective grain volume is obtained by using a large gas-expansion porosimeter of the type shown in Fig. 26.6. This porosimeter is based on Boyle's law in

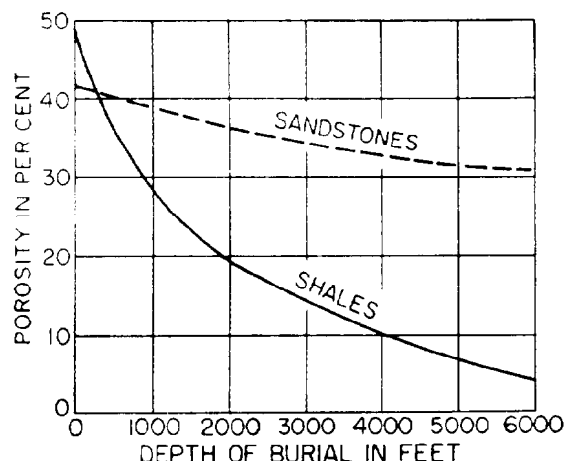


Fig. 26.7—Effect of natural compaction on porosity.

which high-pressure gas is equalized between two chambers. The porosity may be calculated from the measured pressures, the volume of either chamber, and the bulk-sample volume by the use of Boyle's law.

Kelton¹⁰ reported results of whole-core analysis, a method utilizing large sections of the full-diameter core. The following table of matrix vs. whole-core data summarizes a part of Kelton's work.¹⁰

	Group			
	1	2	3	4
Matrix porosity, % bulk	1.98	1.58	2.56	7.92
Total porosity, % bulk	2.21	2.62	3.17	8.40

Matrix porosity is that determined from small samples; total porosity is that determined from the whole core. Whole-core analysis satisfactorily evaluates most carbonate rocks. However, no satisfactory technique is available for the analysis of extensively fractured materials because the samples cannot be put together in their natural state.

Compaction and Compressibility of Porous Rocks

The porosity of sedimentary rocks has been shown by Krumbein and Sloss¹¹ to be a function of the degree of compaction of the rock. The compacting forces are a function of the maximum depth of burial of the rock. The effect of natural compaction on porosity is shown in Fig. 26.7. This effect is caused principally by the resulting packing arrangement after compaction; thus, sediments that have been buried deeply, even if subsequently uplifted, exhibit lower porosity values than sediments that have not been buried at great depth.

Geertsma¹² states that three kinds of compressibility must be distinguished in rocks: (1) rock-matrix compressibility, (2) rock-bulk compressibility, and (3) pore compressibility. Rock-bulk compressibility is a combination of pore and rock matrix compressibility.

Rock-matrix compressibility is the fractional change in volume of the solid rock material (grains) with a unit change in pressure. Pore compressibility is the fractional change in PV of the rock with a unit change in pressure.

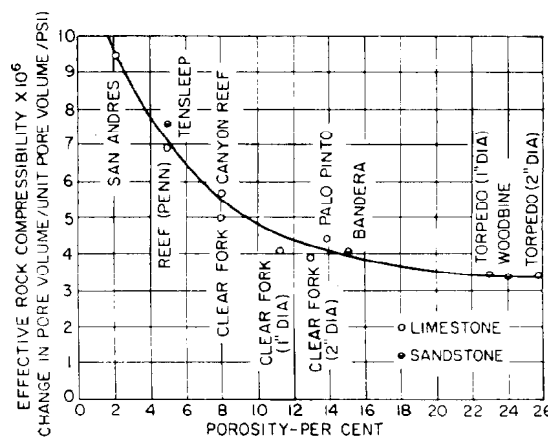


Fig. 26.8—Effective reservoir-rock compressibilities.

The depletion of fluids from the pore space of a reservoir rock results in a change in the internal stress in the rock, thus causing the rock to be subjected to a different resultant stress. This change in stress results in changes in the GV, PV, and BV of the rock. Of principal interest to the reservoir engineer is the change in the PV of the rock. The change in rock-bulk compressibility may be of importance in areas where surface subsidence could cause appreciable property damage.

Hall¹³ reported PV compressibility as a function of porosity. These data are summarized in Fig. 26.8. The effective rock compressibility in Fig. 26.8 results from the change in porosity caused by grain expansion and decrease in pore space because of compaction of the matrix.

Fatt¹⁴ indicates that the pore compressibility is a function of pressure. Within the range of his data, he was unable to find a correlation with porosity.

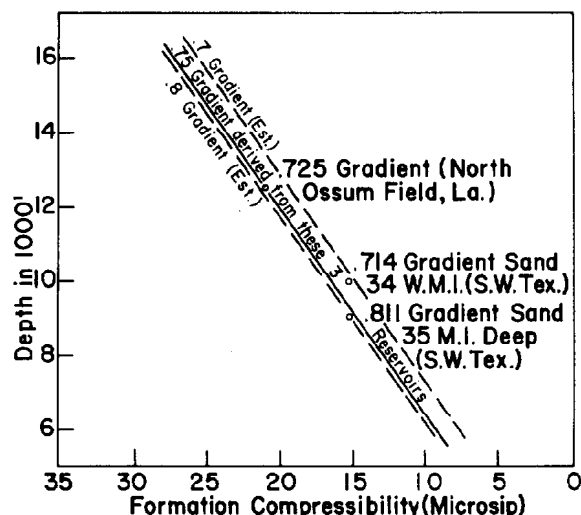


Fig. 26.9—Depth vs. formation compressibility in abnormally pressured segment of an abnormally pressured reservoir.

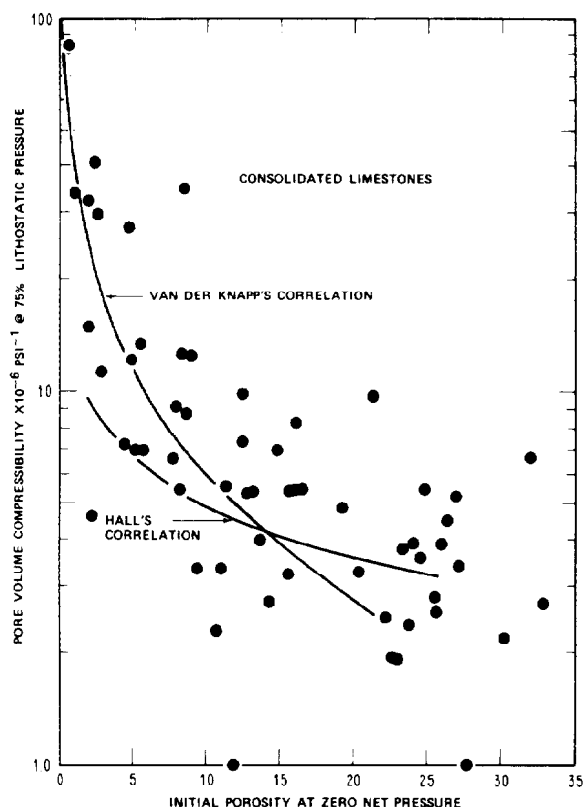


Fig. 26.10—PV compressibility at 75% lithostatic pressure vs. initial sample porosity for limestones.

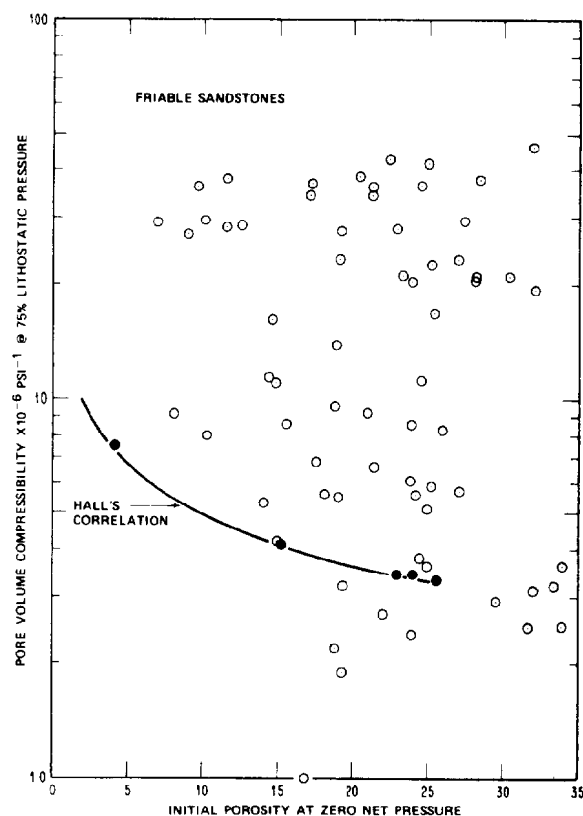


Fig. 26.12—PV compressibility at 75% lithostatic pressure vs. initial sample porosity for friable sandstones.

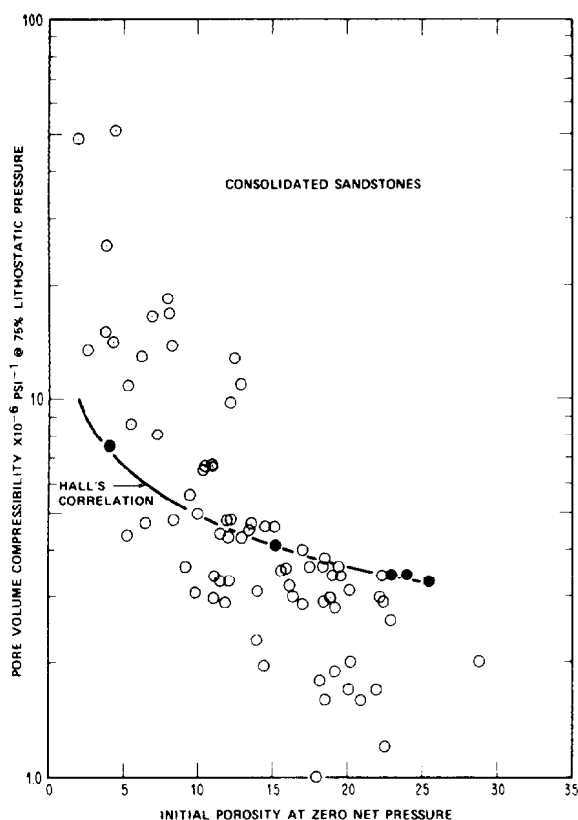


Fig. 26.11—PV compressibility at 75% lithostatic pressure vs. initial sample porosity for consolidated sandstones.

The additional significance of changes in porosity with the discovery of oil at deeper depths and new geological areas resulted in the need for a better understanding of the changes in porosity with the depletion of reservoir fluid pressure.

Hammerlindl¹⁵ developed a correlation from measured field data that indicates the change in porosity compressibility with depth of burial of an unconsolidated sand (Fig. 26.9). Similar correlations have also been presented by others in the technical literature.

Considerable laboratory work has been performed recently in an attempt to understand better the effect of formation compaction on porosity. Newman¹⁶ performed measurements on samples of limestone and consolidated, friable, and unconsolidated sandstones. He compared his results with those of Hall¹³ and van der Knaap,¹⁷ as illustrated in Figs. 26.10 through 26.13. As noted in his data, an approximate correlation may exist between PV compressibility and porosity for limestones and consolidated sandstones. Little or no correlation exists between PV compressibility and porosity for friable and unconsolidated sandstones. By averaging the PV compressibility in 5% ranges of porosity, Newman attempted to correlate all four types of porous media. The results of this averaging technique are presented in Fig. 26.14.

The methods used to measure PV compressibility have come under discussion. PV compressibility can be measured in the laboratory by the hydrostatic (same pressure in all three directions) or the triaxial (different pressure in the z direction than in the x and y directions) techniques. The test samples also can be stress cycled

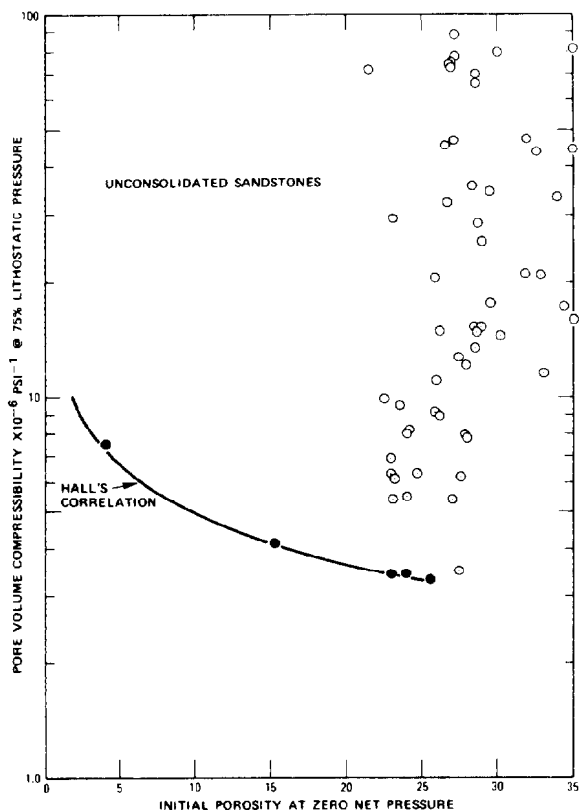


Fig. 26.13—PV compressibility at 75% lithostatic pressure vs. initial sample porosity for unconsolidated sandstones.

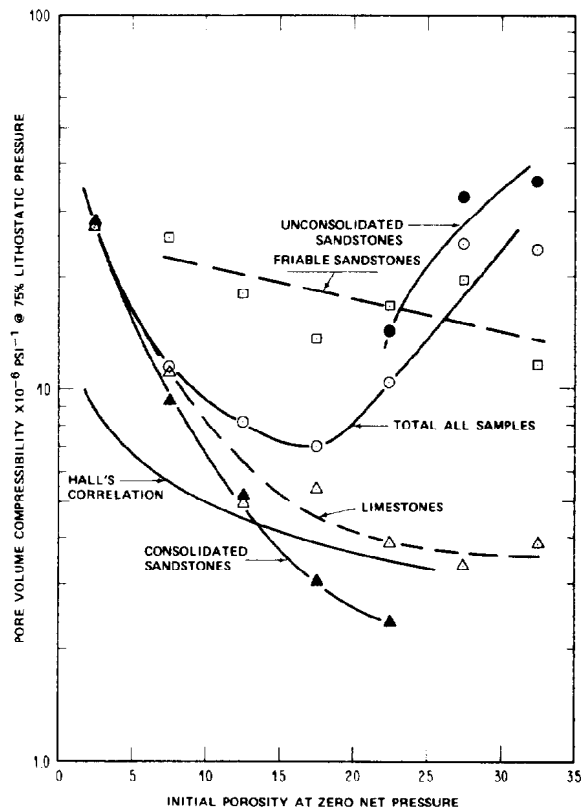


Fig. 26.14—Class averages of PV compressibility vs. initial sample porosity.

until the strain resulting from a supplied stress is constant, or the sample can be placed under stress and the strain measured for purposes of calculating PV compressibility.

Krug¹⁸ and Graves¹⁹ demonstrated that when a formation sample was stress cycled to a stable strain condition, the sample gave repeatable values of PV compressibility even when the sample was left in an unstressed condition for 30 days or more. The data reported by Newman were for samples that were not stress cycled.

Lachance²⁰ compared PV compressibilities obtained by the hydraulic and triaxial methods. The reported results (Fig. 26.15) indicate a large difference in the magnitude of PV compressibilities obtained by the two methods. The triaxial data indicate that PV compressibility is essentially independent of the sample porosity. Newman's¹⁶ data were obtained by the hydrostatic method, whereas Krug's¹⁸ and Graves'¹⁹ data were obtained by the triaxial method.

In summary, rock compressibility is an important factor in reservoir evaluation. Oil reservoirs with high initial pressures and low fluid bubblepoint pressures are sensitive to the true value of PV compressibility. Gas reservoirs with initial reservoir pressures in excess of 6,000 psi are also sensitive to the value of PV compressibility. Newman,¹⁶ Krug,¹⁸ and Graves¹⁹ all recommend that PV compressibility be measured on

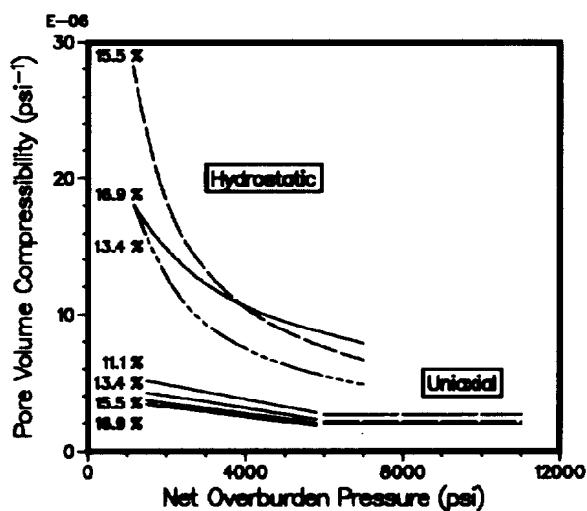


Fig. 26.15—Calculated PV compressibility (porosity $\geq 8\%$).

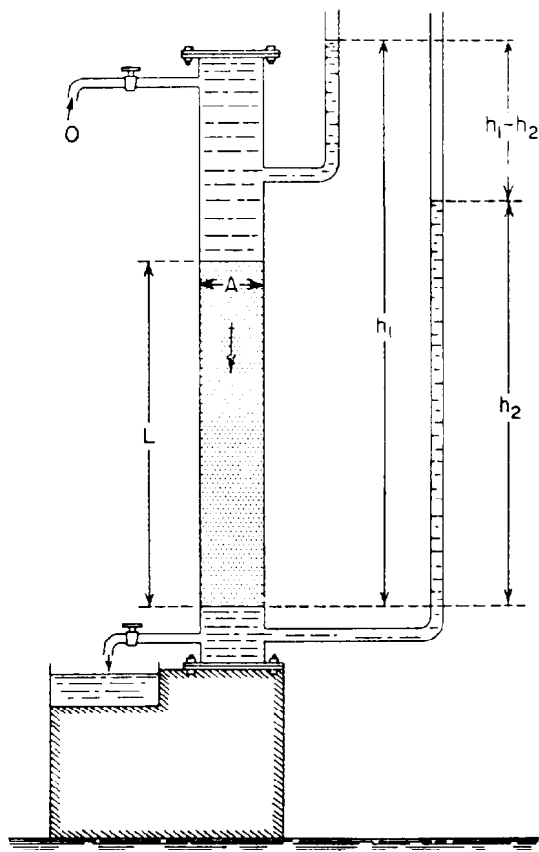


Fig. 26.16—Schematic of Henry Darcy's experiment on flow of water through sand.

samples from the reservoir in question when the PV compressibility may be significant in reservoir evaluation.

Permeability

Introductory Theory

It is the purpose of this section to discuss the ability of the formation to conduct fluids. In the introduction to API Code 27,²¹ it is stated that permeability is a property of the porous medium and a measure of the medium's capacity to transmit fluids. The measurement of permeability, then, is a measure of the fluid conductivity of the particular material. By analogy with electrical conductors, the permeability represents the reciprocal of the resistance that the porous medium offers to fluid flow.

The following equations for flow of fluids in circular conduits are well known.

Poiseuille's equation for viscous flow:

$$v = \frac{d^2 \Delta p}{32 \mu L}, \quad (1)$$

Fanning's equation for viscous and turbulent flow:

$$v^2 = \frac{2 d \Delta p}{f \rho L}, \quad (2)$$

where

- v = fluid velocity, cm/s,
- d = diameter of conductor, cm,
- Δp = pressure loss over length L , dynes/cm²,
- L = length over which pressure loss is measured, cm,
- μ = fluid viscosity, Pa·s,
- ρ = fluid density, g/cm³, and
- f = friction factor, dimensionless.

A more convenient form of Poiseuille's equation is

$$q = \frac{\pi r^4 \Delta p}{8 \mu L}, \quad (3)$$

where r is the radius of the conduit, cm, q is the volume rate of flow, cm³/s, and the other terms are as previously defined.

If a porous medium is conceived to be a bundle of capillary tubes, the flow rate q_t through the medium is the sum of the flow rates through the individual tubes. Thus,

$$q_t = \frac{\pi \Delta p}{8 \mu L} \sum_{j=1}^k n_j r_j^4, \quad (4)$$

where n_j is the number of tubes of radius r_j . If

$$(\pi/8) \sum_{j=1}^k n_j r_j^4$$

is treated as a flow coefficient for the particular grouping of tubes the equation reduces to

$$q_t = C \frac{\Delta p}{\mu L}, \quad (5)$$

where

$$C = \frac{\pi}{8} \sum_{j=1}^k n_j r_j^4. \quad (6)$$

The pore structure of rocks does not permit simple classification of the flow channels. Therefore, empirical data are required in most cases.

In 1856, Darcy investigated the flow of water through sand filters for water purification. His experimental apparatus is shown schematically in Fig. 26.16.²² Darcy interpreted his observations to yield results essentially as given in Eq. 7.

$$q = KA \frac{h_1 - h_2}{L}. \quad (7)$$

q represents the volume rate of flow of water downward through the cylindrical sandpack of cross-sectional area A and length L . h_1 and h_2 are the heights above the standard datum of the water in manometers located at the input and output faces and represent the hydraulic head at

Points 1 and 2. K , a constant of proportionality, was found to be characteristic of the sandpack. Darcy's investigations were confined to flow of water through sandpacks that were 100% saturated with water.

Later investigators found that Darcy's law could be extended to fluids other than water and that the constant of proportionality K could be written as k/μ , where μ is the viscosity of the fluid and k is a proportionality constant for the rock. The generalized form of Darcy's law as presented in API Code 27 is presented in Eq. 8.

$$u_s = -\frac{k}{\mu} \left(\frac{dp}{ds} - g\rho \frac{dz}{ds} \right), \quad (8)$$

where

s = distance in direction of flow, always positive,

u_s = volume flux across a unit area of the porous medium in unit time along flow path s ,

z = vertical coordinate, considered positive downward, cm,

ρ = density of the fluid,

g = acceleration of gravity,

$\frac{dp}{ds}$ = pressure gradient along s at the point to which u refers,

μ = viscosity of the fluid,

k = permeability of the medium, and

$\frac{dz}{ds} = \sin \theta$, where θ is the angle between s and the horizontal.

u_s may further be defined as q/A where q is the volume rate of flow and A is the average cross-sectional area perpendicular to the lines of flow.

The portion of Eq. 8 in parentheses may be interpreted as the total pressure gradient minus the gradient caused by a head of fluid. Thus, if the system is in hydrostatic equilibrium, there is no flow and the quantity inside the parentheses will be zero. Eq. 8 may be rewritten as

$$u_s = -\frac{k}{\mu} \frac{d}{ds} (\rho g z - p). \quad (9)$$

The quantity $d(\rho g z - p)/ds$ may be considered to be the negative gradient of a potential function Φ , where

$$\Phi = p - \rho g z. \quad (10)$$

The potential function is defined such that flow will be from higher to lower values.

The dimensions of permeability may be established from an analysis of Eq. 8 as $k = L^2$. In the cgs system of units, the unit of permeability would be cm^2 , a large unit for common usage; therefore, the petroleum industry adopted the darcy as the standard unit of permeability, which is defined as follows.

A porous medium has a permeability of one darcy when a single phase fluid of one centipoise viscosity that completely fills the voids of the medium, will flow through it under conditions of viscous flow at a rate of one cubic centimeter per second per square centimeter cross sectional area under a pressure or equivalent hydraulic gradient of one atmosphere per centimeter.²¹

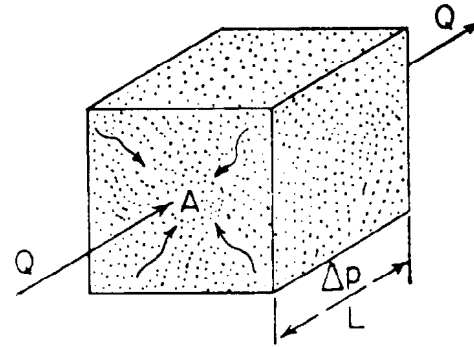


Fig. 26.17—Sand model for rectilinear flow of fluids.

Conditions of viscous flow mean that the rate of flow will be sufficiently low to be directly proportional to the potential gradient.

Darcy's law holds only for conditions of viscous flow as defined. Further, for the permeability k to be a proportionality constant of the porous medium, the medium must be 100% saturated with the flowing fluid when the determination of permeability is made. In addition, the fluid and the porous medium must not react—i.e., by chemical reaction, adsorption, or absorption. If a reactive fluid flows through a porous medium, it alters the porous medium and, therefore, changes the permeability of the medium as flow continues.

Flow Systems of Simple Geometry

Horizontal Flow. Horizontal rectilinear steady-state flow is common to virtually all measurements of permeability. If a rock is 100% saturated with an incompressible fluid and is horizontal (Fig. 26.17), then $dz/ds = 0$, $dp/ds = dp/dx$, and Eq. 8 reduces to

$$u_x = \frac{q}{A} = -\frac{k}{\mu} \frac{dp}{dx},$$

which on integration becomes

$$q = \frac{kA(p_1 - p_2)}{\mu L}, \quad (11)$$

where k is the specific permeability.

If a compressible fluid flows through a porous medium, Darcy's law, as expressed in Eq. 8, is still valid. However, for steady flow, the mass rate of flow rather than the volume rate of flow is constant through the system. Therefore, the integrated form of the equation differs. Considering steady rectilinear flow of compressible fluids, Eq. 8 becomes

$$\rho u_x = -\frac{k\rho}{\mu} \frac{dp}{dx}, \quad (12)$$

or, for steady-state flow,

$$\rho u_x = \rho \frac{q}{A} = \text{constant}.$$

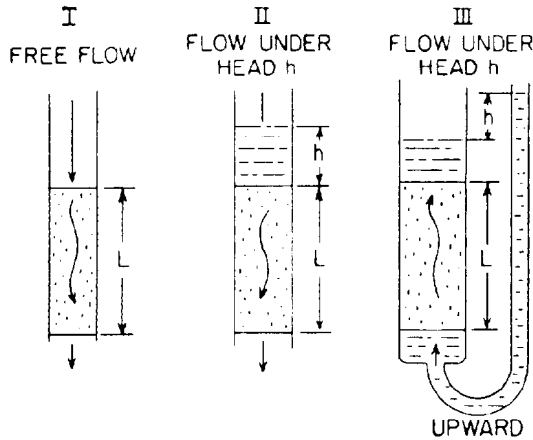


Fig. 26.18—Sand model for vertical flow.

The density-pressure relationship for isothermal conditions of a slightly compressible fluid may be expressed as

$$\rho = \rho_o e^{cp}$$

and

$$\frac{\partial \rho}{\partial p} = \frac{\rho}{cp}, \quad (13)$$

where c is the fluid compressibility. Thus,

$$\frac{\rho_o q_o}{A} = \frac{-k\rho}{\mu} \frac{dp}{dx} = \frac{-k}{\mu c} \frac{d\rho}{dx},$$

where q_o is the volume rate of flow of a fluid of density ρ_o .

On integration,

$$\rho_o q_o = \frac{kA(\rho_1 - \rho_2)}{\mu c L}, \quad (14)$$

If terms of cp of second and higher order are neglected, the density can be expressed as

$$\rho = \rho_o(1 + cp),$$

such that Eq. 14 reduces to

$$q_o = \frac{kA(p_1 - p_2)}{\mu L}.$$

The density-pressure relationship for isothermal conditions of an ideal gas may be expressed as

$$\frac{p}{p_b} = \frac{\rho}{\rho_b} \text{ or } \rho = \frac{p\rho_b}{p_b}, \quad (15)$$

Thus,

$$\frac{\rho_b q_b}{A} = -\frac{k\rho}{\mu} \frac{dp}{dx},$$

where ρ_b and q_b are the density and volume rate of flow, respectively, at the base pressure, p_b .

Substituting for ρ

$$\frac{p_b q_b}{A} = -\frac{k}{\mu} p \frac{dp}{dx}, \quad (16)$$

which on integration yields

$$q_b = \frac{kA}{2\mu L} \frac{p_1^2 - p_2^2}{p_b}, \quad (17)$$

Define \bar{p} as $(p_1 + p_2)/2$, and q_p as the volume rate of flow at \bar{p} such that $p q_p = p_b q_b$; then

$$q_p = \frac{kA(p_1 - p_2)}{\mu L}. \quad (18)$$

Therefore, flow rates of ideal gases may be computed from the equations for incompressible liquids so long as the volume rate of flow is defined at the algebraic mean pressure.

Vertical Flow. Fig. 26.18 shows three sandpacks in which linear flow occurs in the vertical direction.

First consider Case 1 (Fig. 26.18)—when the pressure at the inlet and outlet are equal (free flow), such that only the gravitational forces are driving the fluids. Given

$$s = z, \quad \frac{dz}{ds} = 1, \text{ and } \frac{dp}{ds} = 0,$$

the flow is then defined by

$$q = \frac{kA}{\mu} \rho g. \quad (19)$$

Next consider Case 2—the case of downward flow when the driving head (difference in hydraulic head of inlet and outlet) is h (Fig. 26.18). We know that

$$\frac{dz}{ds} = 1 \text{ and } \frac{dp}{ds} = \frac{-\rho g h}{L}.$$

Therefore, from Eq. 8,

$$q = \frac{kA}{\mu} \rho g \left(\frac{h}{L} + 1 \right). \quad (20)$$

When the flow is upward and the driving head is h , Case 3 (Fig. 26.18), and z is defined as positive downward,

$$\frac{dz}{ds} = -1, \quad \frac{dp}{ds} = -\frac{dp}{dz} = \left(-\frac{\rho gh}{L} - \rho g \right),$$

and

$$u = +\frac{k}{\mu} \left(+\frac{\rho gh}{L} + \rho g - \rho g \right),$$

then

$$q = \frac{kA\rho gh}{\mu L} \quad (21)$$

Radial Flow. A radial-flow system, analogous to flow into a wellbore, is idealized in Fig. 26.19. If flow is considered to occur only in the horizontal plane under steady-state conditions, an equation of flow may be derived from Darcy's law to be

$$q = \frac{2\pi kh(p_e - p_w)}{\mu \ln r_e/r_w} \quad (22)$$

where r_e is the radius at the external boundary at which p_e (pressure at the external boundary) is measured, and r_w is the radius of the wellbore at which p_w (pressure at the wellbore) is measured. All other terms are as defined for linear flow.

Eq. 22 may be modified appropriately for the flow of compressible fluids. The details of modifying this equation are omitted because they are essentially the same as the ones used in the horizontal rectilinear flow systems.

After modification for variations in flowing volumes with changing pressures, Eq. 22 becomes for slightly compressible fluids

$$w = \frac{2\pi kh(\rho_e - \rho_w)}{c\mu \ln r_e/r_w} \quad (23)$$

where w is the mass rate of flow, g/s, or

$$q_o = \frac{2\pi kh(p_e - p_w)}{\pi \rho_o \ln r_e/r_w},$$

where q_o is defined at the pressure p_o where the density is ρ_o .

For ideal gases, Eq. 22 becomes

$$q_b = \frac{\pi kh(p_e^2 - p_w^2)}{\mu p_b \ln r_e/r_w} \quad (24)$$

or

$$q_p = \frac{2\pi kh(p_e - p_w)}{\mu \ln r_e/r_w} \quad (25)$$

where q_p is the volume rate of flow at the algebraic mean pressure $(p_e + p_w)/2$.

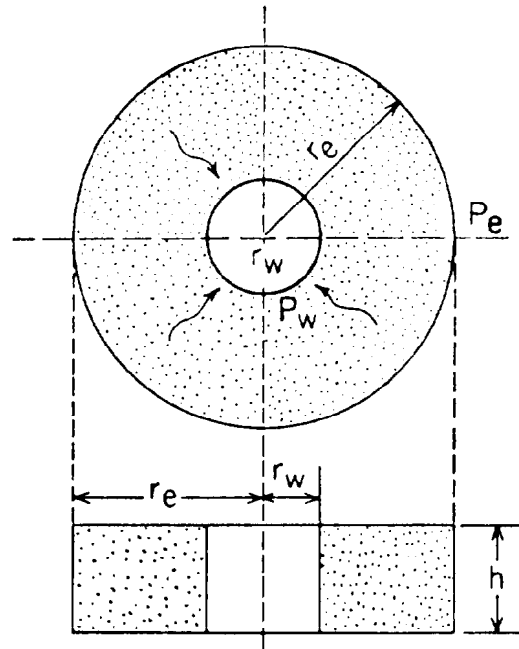


Fig. 26.19—Sand model for radial flow of fluids to central wellbore.

Conversion of Units in Darcy's Law

It is convenient in many applications of Darcy's law to introduce commonly used oilfield units. The following is a summary of the more common equations with the conversion factors to convert to oilfield terminology.

Linear-Flow Liquids (or Gases with Volume at Mean Pressure). Rate, B/D, is given by

$$q = 1.1271 \frac{kA(p_1 - p_2)}{\mu L} \quad (26)$$

Rate, cu ft/D, is given by

$$q = 6.3230 \frac{kA(p_1 - p_2)}{\mu L} \quad (27)$$

Radial-Flow Liquids (or Gases with Volume at Mean Pressure). Rate, liters per day, is given by

$$q = 92.349 \times 10^3 \frac{kh(p_e - p_w)}{\mu \ln r_e/r_w} \quad (28)$$

Rate, cu ft/D, is

$$q = 92.349 \times 10^3 \frac{kh(p_e - p_w)}{\mu \ln r_e/r_w} \quad (29)$$

Gases at Base Pressure, p_b , and Average Flowing Temperature, \bar{T}_f . Linear flow rate, cu ft/D, is given by

$$q_b = \frac{3.1615 T_b k A (p_1^2 - p_2^2)}{\bar{T}_f \mu_g L p_b} \quad (30)$$

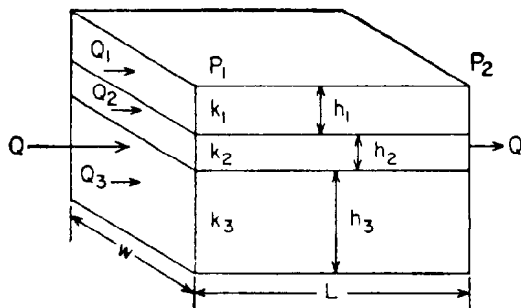


Fig. 26.20—Linear flow—parallel combination of beds.

and radial flow rate, cu ft/D, is given by*

$$q_b = \frac{19.88 T_b k h (p_e^2 - p_w^2)}{\bar{T}_f \bar{z} \mu_g p_b \ln r_e / r_w}, \quad (31)$$

where k is in darcies; A is in sq ft; h is in ft; p_1 , p_2 , p_e , p_w , and p_b are in psia; μ is in cp; L is in ft; and r_e and r_w are in consistent units.

Since the previous equations describe the flow in the medium, appropriate volume factors must be introduced to account for changes in the fluids caused by any decrease in pressure and temperature from that of the medium to standard or stock-tank conditions.

Permeability Conversion Factors. Following is a list of various unit conversions from darcy units to other systems of units.

$$k = \frac{q\mu}{A(p/L)}$$

1 darcy (d) = 1,000 millidarcies (md)

$$\begin{aligned} &= \frac{(\text{cm}^3/\text{s})\text{cp}}{\text{cm}^2(\text{atm}/\text{cm})} \\ &= 9.869 \times 10^{-7} \frac{(\text{cm}^3/\text{s})\text{cp}}{\text{cm}^2 \left(\frac{\text{dyne}/\text{cm}^2}{\text{cm}} \right)} \\ &= 9.869 \times 10^{-9} \text{ cm}^2 \\ &= 1.062 \times 10^{-11} \text{ sq ft} \\ &= 7.324 \times 10^{-5} \frac{(\text{cu ft}/\text{sec})\text{cp}}{\text{sq ft}(\text{psi}/\text{ft})} \\ &= 9.697 \times 10^{-4} \frac{(\text{cu ft}/\text{sec})\text{cp}}{\text{cm}^2(\text{cm water}/\text{cm})} \\ &= 1.127 \frac{(\text{B}/\text{D})\text{cp}}{\text{sq ft}(\text{psi}/\text{ft})} \\ &= 1.424 \times 10^{-2} \frac{(\text{gal}/\text{min})\text{cp}}{\text{sq ft}(\text{ft water}/\text{ft})} \end{aligned}$$

*Because pseudosteady rather than steady state normally exists in the reservoir, average reservoir pressure is used instead of external boundary pressure. Therefore, the $\ln(r_e/r_w)$ term becomes $\ln(r_e/r_w) - 0.75$. See Chaps. 32 and 35 for further discussion. Also, if there is a large temperature difference between the base temperature and flowing temperature, then the z at both conditions should be used.

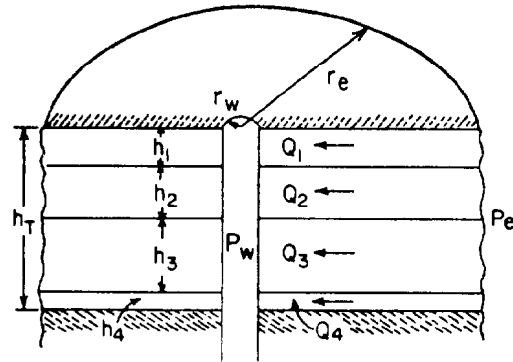


Fig. 26.21—Radial flow—parallel combination of beds.

Flow Systems of Combinations of Beds

Consider the case where the flow system comprises layers of porous rock separated from each other by infinitely thin, impermeable barriers as shown in Fig. 26.20. The average permeability \bar{k} may be evaluated by Eq. 32.

$$\bar{k} = \frac{\sum_{j=1}^n k_j h_j}{\sum_{j=1}^n h_j} \quad (32)$$

Fig. 26.21 shows that the same terms appear in the radial flow network as in the linear system. The only difference in the two systems is the manner of expressing the length over which the pressure drop occurs. Because all these terms are the same in each of the parallel layers, an evaluation of the parallel radial system yields the same solution as obtained in the linear case.

Example Problem 6—Average Permeability of Beds in Parallel. What is the equivalent linear permeability of four parallel beds having equal widths and lengths under the following conditions?

Bed	Pay Thickness (ft)	Horizontal Permeability (md)
1	20	100
2	15	200
3	10	300
4	5	400

$$\begin{aligned} \bar{k} &= \frac{\sum_{j=1}^n k_j h_j}{\sum_{j=1}^n h_j} ; \\ k &= \frac{(100 \times 20) + (200 \times 15) + (300 \times 10) + (400 \times 5)}{20 + 15 + 10 + 5} \end{aligned}$$

$$= \frac{10,000}{50} = 200 \text{ md.}$$

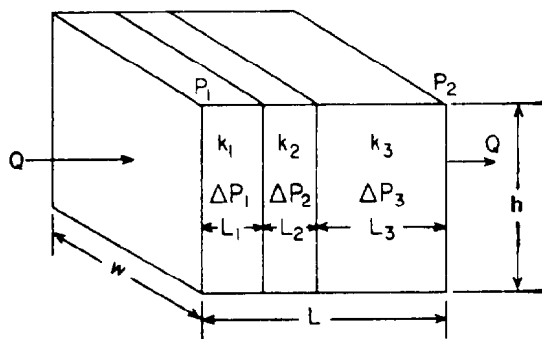


Fig. 26.22—Linear flow—series combination of beds.

Another possible combination for flow systems is to have the beds of different permeabilities to be arranged in series as shown in Fig. 26.22. In the case of linear flow, the average series permeability may be evaluated by Eq. 33.

$$\bar{k} = \frac{L}{\sum_{j=1}^n L_j/k_j} \quad \dots \dots \dots (33)$$

The same reasoning can be used in the evaluation of the average permeability for the radial system (Fig. 26.23) so as to yield

$$\begin{aligned} \bar{k} &= \frac{\ln r_e/r_w}{\sum_{j=1}^n \frac{\ln r_j/r_{j-1}}{k_j}} \\ &= \frac{\log r_e/r_w}{\sum_{j=1}^n \frac{\log r_j/r_{j-1}}{k_j}} \quad \dots \dots \dots (34) \end{aligned}$$

Example Problem 7—Average Permeability of Beds in Series. What is the equivalent permeability of four beds in series, having equal formation thicknesses under the following conditions?

Assume Bed 1 adjacent to the wellbore (1) for a linear system and (2) for a radial system if the radius of the penetrating wellbore is 6 in., and the radius of effective drainage is 2,000 ft.

Bed	Length of Bed (ft)	Horizontal Permeability (md)
1	250	25
2	250	50
3	500	100
4	1,000	200

For a linear system,

$$\bar{k} = \frac{L}{\sum_{j=1}^n L_j/k_j}$$

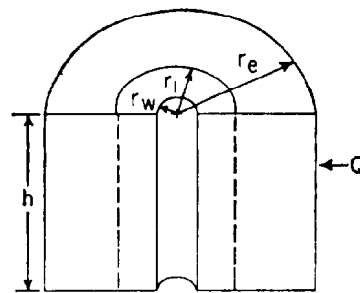


Fig. 26.23—Radial flow—series combination of beds.

Therefore,

$$\begin{aligned} \bar{k} &= \frac{250 + 250 + 500 + 1,000}{\frac{250}{25} + \frac{250}{50} + \frac{500}{100} + \frac{1,000}{200}} \\ &= \frac{2,000}{10 + 5 + 5 + 5} = 80 \text{ md.} \end{aligned}$$

For a radial system,

$$\begin{aligned} k &= \frac{\log 2,000/0.5}{\frac{\log 250/0.5}{25} + \frac{\log 500/250}{50} + \frac{\log 1,000/500}{100} + \frac{\log 2,000/1,000}{200}} \\ &= 30.4 \text{ md.} \end{aligned}$$

Permeability of Channels and Fractures

Only the matrix permeability has been discussed in the analysis to this point. In some sand and carbonate reservoirs, the formation frequently contains solution channels and natural or artificial fractures. These channels and fractures do not change the permeability of the matrix but do change the effective permeability of the flow network.

Circular Channel. Equating Darcy's and Poiseuille's equations for fluid flow in a tube, the permeability may be expressed as a function of the tube radius.

$$k = \frac{r^2}{8} \quad \dots \dots \dots (35)$$

where k and r are in consistent units.

If r is in centimeters, then k in darcies is given by

$$k = \frac{r^2}{8(9.869 \times 10^{-9})} \approx 12.50 \times 10^6 r^2,$$

where 9.869×10^{-9} is a conversion factor from the previous list. Then, if r is in inches,

$$\begin{aligned} k &= 12.50 \times 10^6 (2.54)^2 r^2 \\ &= 80 \times 10^6 r^2 = 20 \times 10^6 d^2, \end{aligned}$$

where d is the diameter of the opening in inches.

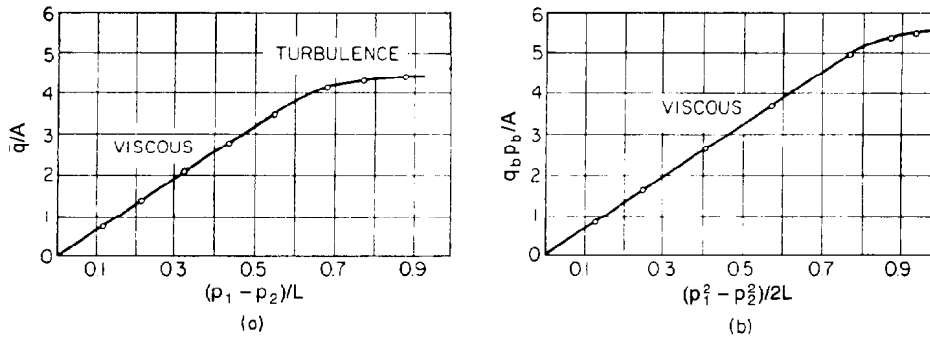


Fig. 26.24—Plot of experimental results for calculation of permeability—(a) from $k/\mu = qL/[A(p_1 - p_2)]$; (b) from $k/\mu = 2qBp_B L/[A(p_1^2 - p_2^2)]$.

Therefore, the permeability of a circular opening 0.005 in. in radius is 2,000,000 md.

Fracture. For flow through slots of fine clearances and unit width, Buckingham²⁵ reports that

$$\Delta p = \frac{12\mu vL}{h^2},$$

such that the permeability of the slot is given by

$$k = \frac{h^2}{12} \dots \dots \dots (36)$$

When h is in centimeters and k in darcies, the permeability of the slot is given by

$$k = \frac{h^2}{12(9.869 \times 10^{-9})} = 84.4 \times 10^5 h^2,$$

and when h is in inches and k is in darcies, permeability is given by

$$k = 54.4 \times 10^6 h^2,$$

so that the permeability of a fracture 0.01 in. in thickness would be 5,440 darcies or 5,440,000 md.

Physical Analogies to Darcy's Law

Ohm's law as commonly written is

$$I = \frac{E}{r},$$

where

- I = current, A,
- E = voltage drop, V, and
- r = resistance of the circuit, Ω ,

but

$$r = \rho \frac{L}{A} \text{ or } r = \frac{L}{\sigma A},$$

where

- ρ = resistivity, $\Omega\text{-cm}$,
- $\sigma = 1/\rho$ = conductivity,
- L = length of flow path, cm, and
- A = cross-sectional area of conductor, cm^2 .

Therefore,

$$I = \frac{AE}{\rho L}.$$

Comparing with Darcy's law for a linear system,

$$q = -\frac{k}{\mu} A \frac{\Delta p}{L}.$$

Note that

$$\begin{aligned} q &\approx I, \\ \frac{k}{\mu} &\approx \frac{1}{\rho}, \text{ and} \\ \frac{\Delta p}{L} &\approx \frac{E}{L}. \end{aligned}$$

The Fourier heat equation may be written as

$$\dot{Q} = k_h A \frac{\Delta T}{L},$$

where

- \dot{Q} = rate of heat flow, Btu/hr,
- A = cross-sectional area, sq ft,
- ΔT = temperature drop, $^{\circ}\text{F}$,
- L = length of the conductor, ft, and
- k_h = thermal conductivity, Btu/(ft-hr- $^{\circ}\text{F}$).

A comparison with Darcy's law indicates that

$$\begin{aligned} q &\approx \dot{Q}, \\ \frac{k}{\mu} &\approx k_h, \text{ and} \\ \frac{\Delta p}{L} &\approx \frac{\Delta T}{L}. \end{aligned}$$

Electrical and heat models (based on these analogies) of rock and well systems frequently are used to solve fluid-flow problems involving complex geometry.

Measurement of Permeability

The permeability of a porous medium may be determined from samples extracted from the formation or by in-place testing. The procedures discussed in this section pertain to the permeability determinations on small samples of extracted media.

Two methods are used to evaluate the permeability of cores. The method most used on clean, fairly uniform formations uses small cylindrical samples called perm plugs that are approximately $\frac{3}{4}$ in. in diameter and 1 in. in length. The second method uses full-diameter core samples in lengths of 1 to $1\frac{1}{2}$ ft. The fluids used with either method may be gas or any nonreactive liquid.

Perm-Plug Method. As core samples ordinarily contain residual oil, water, and gas, it is necessary that the sample be subjected to preparation before the determination of the permeability. The residual fluids normally are extracted by retorting or solvent extraction. The core is dried before permeability measurements are taken. Air commonly is used as the fluid in permeability measurements. The requirement that the permeability be determined for conditions of viscous flow is best satisfied by obtaining data at several flow rates and plotting results, as shown in Fig. 26.24, based on either Eq. 17 or 18. For conditions of viscous flow, the data should plot a straight line, passing through the origin. Turbulence is indicated by curvature of the plotted points. The slope of the straight-line portion of the curve is equal to k/μ , from which the permeability may be computed. To obtain k in darcies, q must be in cm^3/s , A in cm^2 , p_1 and p_2 in atm, L in cm, and μ in cp.

A permeameter designed for the determination of the permeability of rocks with either gas or liquid is illustrated in Fig. 26.25. Data ordinarily are taken from this device at only one flow rate. To assure conditions of viscous flow, the lowest possible rate that can be measured accurately is used.

Example Problem 8—Permeability Measurement. The following data were obtained during a routine permeability test. Compute the permeability of this core.

1. Flow rate = $1,000 \text{ cm}^3$ of air at 1 atm absolute and 70°F in 500 seconds.
2. Pressure, downstream side of core = 1 atm absolute; flowing temperature, 70°F .
3. Viscosity of air at test temperature = 0.02 cp .
4. Cross-sectional area of core = 2.0 cm^2 .
5. Length of core = 2 cm.
6. Pressure, upstream side of core = 1.45 atm absolute.

$$p_1 V_1 + p_2 V_2 = \bar{p} \bar{V}$$

where 1 is upstream conditions and 2 is downstream conditions, and

$$\bar{p} = \frac{p_1 + p_2}{2} = \frac{1.45 + 1}{2} = 1.225,$$

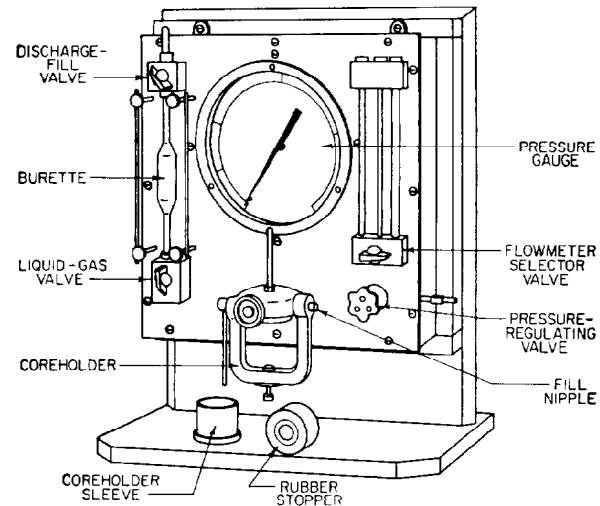


Fig. 26.25—Ruska universal permeameter.

and

$$1 \times 1,000 = 1.225 \bar{V}.$$

$$\bar{V} = 816 \text{ cm}^3,$$

$$\bar{q} = \frac{\bar{V}}{t} = \frac{816}{500} = 1.63,$$

$$k = \frac{\bar{q} L}{A \Delta p} \mu \times 1,000$$

$$= \frac{1.63 \times 2 \times 0.02}{2 \times 0.45} \times 1,000$$

$$= 72.5 \text{ md.}$$

Assuming that the data indicated were obtained, but water was used as the flowing medium, compute the permeability of the core. The viscosity of water at test temperature was 1.0 cp .

$$\bar{q} = \frac{\bar{V}}{t} = \frac{1,000}{500} = 2.0$$

and

$$k = \frac{\bar{q} \mu L}{A \Delta p} \times 1,000 = \frac{2 \times 1 \times 2}{2 \times 0.45} \times 1,000 = 4,444 \text{ md.}$$

Whole-Core Measurement. The core must be prepared in the same manner as perm plugs. The core is then mounted in special holding devices as shown in Fig. 26.26. The measurements required are the same as the perm plugs but the calculations are slightly different.

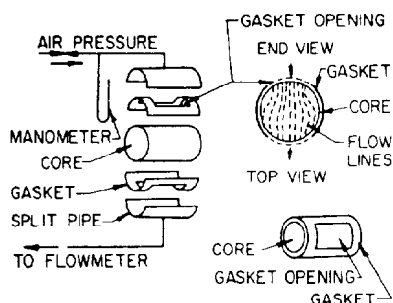


Fig. 26.26—Clamp-type permeameter for large cores.

In the case of the clamp-type permeameter, the geometry of the flow paths is complex, and an appropriate shape factor must be applied to the data to compute the permeability of the sample. The shape factor is a function of the core diameter and the size of the gasket opening. The shape factor affects the quantity L/A in the previous equations.

Factors Affecting Permeability Measurements

In the techniques of permeability measurement previously discussed, certain precautions must be exercised to obtain accurate results. When gas is being used as the measuring fluid, corrections must be made for gas slippage. When liquid is the testing fluid, care must be taken that it does not react with the solids in the core sample. Also, corrections may be applied for the change in permeability because of the reduction in confining pressure on the sample.

Effect of Gas Slippage on Permeability Measurements

Klinkenberg²⁴ has reported variations in permeability determined by using gases as the flowing fluid from that determined by using nonreactive liquids. These variations were ascribed to slippage, a phenomenon well known with respect to gas flow in capillary tubes. The phenomenon of gas slippage occurs when the diameter of the capillary openings approaches the mean free path of the gas.

Fig. 26.27 is a plot of the permeability of a porous medium as determined at various mean pressures using hydrogen, nitrogen, and carbon dioxide as the flowing fluids. Note that for each gas a straight line is obtained for the observed permeability as a function of the reciprocal of the mean pressure of the test. The data obtained with the lowest-molecular-weight gas yield the straight line with the greatest slope, indicative of a greater slippage effect. All the lines when extrapolated to infinite mean pressure ($1/\bar{p}=0$) intercept the permeability axis at a common point. This point is designated as the equivalent liquid permeability, k_L . Klinkenberg and

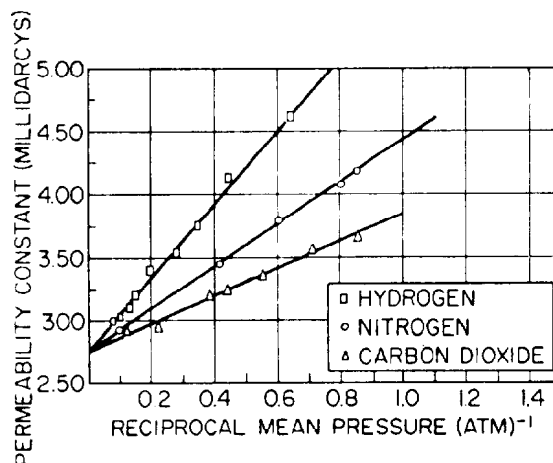


Fig. 26.27—Permeability constant of core sample L to hydrogen, nitrogen, and CO_2 at different pressures (permeability constant to iso-octane, 2.55 md).

others established that the permeability of a porous medium to a nonreactive homogeneous single-phase liquid was equal to the equivalent liquid permeability.

The linear relationship between the observed permeability and the reciprocal of mean pressure may be expressed as follows.

$$k_L = \frac{k_g}{1 + b/\bar{p}} = k_g - m \frac{1}{\bar{p}}, \quad \dots \dots \dots (37)$$

where

k_L = permeability of the medium to a single liquid phase completely filling the pores of the medium,

k_g = permeability of the medium to a gas completely filling the pores of the medium,

\bar{p} = mean flowing pressure of the gas at which k_g was observed,

b = constant for a given gas in a given medium, and

m = slope of the curve.

Reactive Fluids. While water commonly is considered to be nonreactive in the ordinary sense, the occurrence of swelling clays in many reservoir rock materials results in water's being the most frequently occurring reactive liquid in connection with permeability determinations. Reactive liquids alter the internal geometry of the porous medium. This phenomenon does not vitiate Darcy's law but rather results in a new porous medium, the permeability of which is determined by the new internal geometry.

While fresh water may cause the cementation material in a core to swell because of hydration, it is a reversible process. A highly saline water may be flowed through the core and return the permeability to its original value. The effect of water salinity on permeability is shown in Table 26.3.²⁵

TABLE 26.3—EFFECT OF WATER SALINITY ON PERMEABILITY OF NATURAL CORES (Grains/gal Chloride ion*)

Field	Zone	k_a	$k_{1,000}$	k_{500}	k_{300}	k_{200}	k_{100}	k_w
S	34	4,080	1,445	1,380	1,290	1,190	885	17.2
S	34	24,800	11,800	10,600	10,000	9,000	7,400	147
S	34	40,100	23,000	18,600	15,300	13,800	8,200	270
S	34	39,700	20,400	17,600	17,300	17,100	14,300	1,680
S	34	12,000	5,450	4,550	4,600	4,510	3,280	167
S	34	4,850	1,910	1,430	925	736	326	5.0
S	34	22,800	13,600	6,150	4,010	3,490	1,970	19.5
S	34	34,800	23,600	7,800	5,460	5,220	3,860	9.9
S	34	27,000	21,000	15,400	13,100	12,900	10,900	1,030
S	34	12,500	4,750	2,800	1,680	973	157	2.4
S	34	13,600	5,160	4,640	4,200	4,150	2,790	197
S	34	7,640	1,788	1,840	2,010	2,540	2,020	119
S	34	11,100	4,250	2,520	1,500	866	180	6.2
S	34	6,500	2,380	2,080	1,585	1,230	794	4.1
T	36	2,630	2,180	2,140	2,080	2,150	2,010	1,960
T	36	3,340	2,820	2,730	2,700	2,690	2,490	2,460
T	36	2,640	2,040	1,920	1,860	1,860	1,860	1,550
T	36	3,360	2,500	2,400	2,340	2,340	2,280	2,060
T	36	4,020	3,180	2,900	2,860	2,820	2,650	2,460
T	36	3,090	2,080	1,900	1,750	1,630	1,490	1,040

*For example, k_a means permeability to air, k_{500} means permeability to 500-grain/gal chloride solution, and k_w means permeability to fresh water.

Care must be taken that laboratory permeability values are corrected to liquid values obtained with water whose salinity corresponds to formation water.

Overburden Pressure. When the core is removed from the formation, all the confining forces are removed. The rock matrix is permitted to expand in all directions, partially changing the shapes of the fluid-flow paths inside the core.

Compaction of the core caused by overburden pressure may cause as much as a 25% reduction in the permeability of various formations, as observed in Fig. 26.28.²⁶ Note that some formations are much more compressible than others; thus, more data are required to develop empirical correlations that will permit the correction of surface permeability for overburden pressures.

Factors in Evaluation of Permeability From Other Parameters

Permeability, like porosity, is a variable that can be measured for each rock sample. To aid in understanding fluid flow in rocks and possibly to reduce the number of measurements required on rocks, correlations among porosity, permeability, surface area, pore size, and other variables have been made. The reasoning behind some of the correlations among porosity, permeability, and surface area is presented here to enable the reader to gain some understanding of the interrelation of the physical properties of rocks. Although these relations are not quantitative, they are indicative of the interdependence of rock characteristics.

Use of Capillary Tubes for Flow Network. The permeability of a tube derived from Darcy's and Poiseuille's equation is

$$k = \frac{r^2}{8}$$

If a porous system is conceived to be a bundle of capillary tubes, then it can be shown that the permeability of the medium depends on the pore-size distribution and porosity. A flow network of tubes would be similar to layers of different permeability in parallel, such that the average permeability could be calculated by adapting Eq. 32 to read

$$\bar{k} = \frac{\sum_{j=1}^m k_j A_j}{\sum_{j=1}^m A_j}, \dots \dots \dots (38)$$

where k_j is the permeability of one capillary tube and A_j is the area of flow represented by a bundle of tubes of permeability k_j .

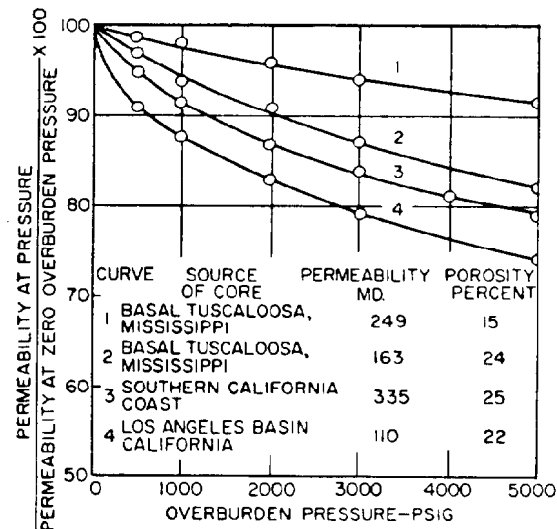


Fig. 26.28—Change in permeability with overburden pressure.

The quantities k_j and A_j can be defined in terms of the radius of capillary tubes.

$$A_j = \pi n_j r_j^2$$

and

$$k_j = \frac{r_j^2}{8},$$

where n_j is the number of tubes of radius r_j .

$$\sum_{j=1}^m A_j = \phi A_t,$$

where ϕ is the porosity of the flow network and A_t is the total cross-sectional area of the flow network. By substitution, Eq. 38 reduced to

$$\bar{k} = \frac{\phi}{8} \frac{\sum_{j=1}^m n_j r_j^4}{\sum_{j=1}^m n_j r_j^2}, \quad (39)$$

where \bar{k} is the average permeability of the tube bundle.

Note that the permeability of a bundle of tubes is a function not only of the pore size but of the arrangement or porosity of the system.

Consider a system that comprises a bundle of capillary tubes of the same radii and length; k , the permeability, may be written from Eq. 39 as

$$k = \frac{\phi r^2}{8}. \quad (40)$$

The internal surface area per unit PV, A_s , may be defined in terms of the tube radius by

$$A_s = \frac{2}{r}. \quad (41)$$

Combining Eqs. 40 and 41 gives the permeability as a function of porosity and internal surface area. This function is

$$k = \frac{4\phi}{8A_s^2} = \frac{\phi}{2A_s^2}.$$

If $1/K_z$ is substituted for the constant $1/2$, the resulting expression is Kozeny's equation wherein K_z is defined as the Kozeny's constant.

$$k = \frac{\phi}{K_z A_s^2}. \quad (42)$$

Wyllie²⁷ derived the Kozeny equation from Poiseuille's law by using a specified flow network. The resulting permeability for this flow network is given by Eq. 43.

$$k = \frac{\phi}{F_s A_s^2} \left(\frac{L}{L_a} \right)^2, \quad (43)$$

where

k = permeability of the porous medium,

F_s = shape factor,

L = length of the sample, and

L_a = actual length of the flow path.

If

$$\left(\frac{L_a}{L} \right)^2 = \tau = \text{tortuosity of the porous medium}$$

and $K_z = F_s \tau$ = Kozeny constant, then Wyllie's equation will reduce to the same form as Eq. 42.

Fluid Saturations

In the previous sections of this chapter, the storage and the conduction capacity of a porous rock were discussed. To the engineer there is yet another important factor to be determined—i.e., the fluid content of the rock. In most oil-bearing formations, it is believed that the rock was completely saturated with water before the invasion of the rock by petroleum. The oil will not displace all the water from the pore space. Therefore, to determine the quantity of hydrocarbons accumulated in a porous rock formation, it is necessary to determine the fluid saturation (oil, water, and gas) of the rock.

There are two approaches to the problem of determining the fluid saturations within a reservoir rock. The direct approach is to measure, in the laboratory, the saturations of selected rock samples recovered from the parent formation. The indirect approach is to determine the fluid saturation by measuring some related physical property of the rock.

Factors Affecting Fluid Saturations of Cores

The core samples delivered to the laboratory for fluid-saturation determinations are obtained from the ground by either rotary, sidewall, or cable-tool coring. In all cases, the fluid content of these samples has been altered by two processes. First, in the case of rotary drilling, the mud column exerts a greater pressure at the formation wellbore surface than the fluid in the formation. The differential pressure between the mud column and the formation fluids causes mud and mud filtrate to invade the formation, thus flushing the formation with mud and its filtrate. The filtrate displaces some of the original fluids. This displacement process changes the original fluid contents of the in-place rock. Second, as the sample is brought to the surface, the confining pressure of the fluid column is constantly decreasing. The reduction of pressure permits the expansion of the entrapped water, oil, and gas. Gas, having the greater coefficient of expansion, expels oil and water from the core. Thus, the content of the core at the surface has been changed from that which existed in the formation. Because the invasion

of the filtrate precedes the core bit, it is not possible to use pressurized core barrels to obtain undisturbed samples.

Drill cuttings, chips, or cores from cable-tool drilling also have undergone definite physical changes. If little or no fluid is maintained in the wellbore, the formation adjacent to the well surface is depleted because of pressure reduction. As chips are formed in the well, they may or may not be invaded, depending on the fluids in the wellbore and the physical properties of the rock. In all probability, fluid will permeate this depleted sample, resulting in flushing. Thus, even cable-tool cores undergo the same two processes as was noted in the case of rotary coring, although in reverse order.

Sidewall cores from either rotary- or cable-tool-drilled holes are subjected to these same processes.

In an attempt to understand better the overall effect of the physical changes that occur in the core because of flushing and fluid expansion, Kennedy *et al.*²⁸ undertook a study to simulate rotary-coring techniques. The effects of both invasion and expansion because of pressure reduction were measured.

Schematics of the changes in saturation resulting from these two processes for oil- and water-based muds are shown in Fig. 26.29. For the water-based mud, the original displacing action of the water filtrate reduced the oil saturation by approximately 14%. The expansion to surface pressure displaced water and additional oil. The final water saturation was greater than the water saturation before coring. With oil-based mud, wherein the filtrate is oil, the displacing action did not alter the initial water saturations but did result in replacement of approximately 20% of the initial oil. On pressure depletion, a small fraction of the water was expelled, reducing the water saturation from 49.1 to 47.7%. The oil saturation was reduced by both processes from 50.9 to 26.7%. Thus, even when high water saturations are involved, up to approximately 50%, the water-saturation values obtained with oil-based muds may be considered to be representative of the initial water saturations in the reservoir. Hence, it is possible to obtain fairly representative values of in-place water saturations by using oil-based muds.

Attempts have been made to use tracers in the drilling fluid to determine the amount of water in the core that is caused by mud-filtrate invasion. The theory was that mud filtrate displaced only oil. Thus, upon recovering the core to the surface, the salt concentration of the core water could be determined. Thus, if the salt concentration in the reservoir water and the tracer concentration in the drilling fluid were known, the volume of filtrate and reservoir water in the core could be calculated. Because a large fraction of the initial reservoir water may have been displaced by the invading filtrate, the tracer method results in incorrect values for reservoir-water saturation.

To obtain realistic values of fluid saturation, it is necessary to choose the proper drilling fluid or to use indirect methods of saturation determination.

Determination of Fluid Saturations from Rock Samples

One of the most popular means of measuring fluid saturations of cores is the retort method. This method takes a small rock sample and heats the sample to

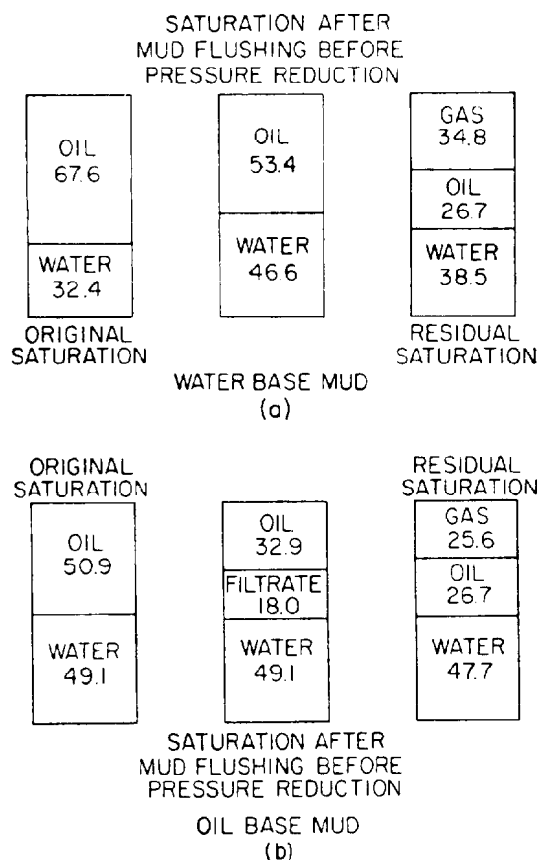


Fig. 26.29—Typical changes in saturations of cores flushed with water-based and oil-based muds.

vaporize the water and the oil, which is condensed and collected in a small receiving vessel. The retort method has several disadvantages as far as commercial work is concerned. The water of crystallization within the rock is driven off, causing the water-recovery values to be too high. The second error that occurs from retorting samples is that the oil, when heated to high temperatures, has a tendency to crack and coke. This change of hydrocarbon molecules tends to decrease the liquid volume. The fluid wetting characteristics of the sample surface may be altered during the retorting process as a result of the two previous factors. Before retorts can be used, calibration curves must be prepared for water and oils of various gravities to correct for losses and other errors. These curves can be obtained by running "blank" runs (retorting known volumes of fluids of known properties). The retort is a rapid method for determining fluid saturations and, if the corrections are used, yields satisfactory results. It gives both water and oil volumes such that the oil and water saturations can be calculated from the following equations.

$$S_w = \frac{V_w}{V_p},$$

$$S_o = \frac{V_o}{V_p},$$

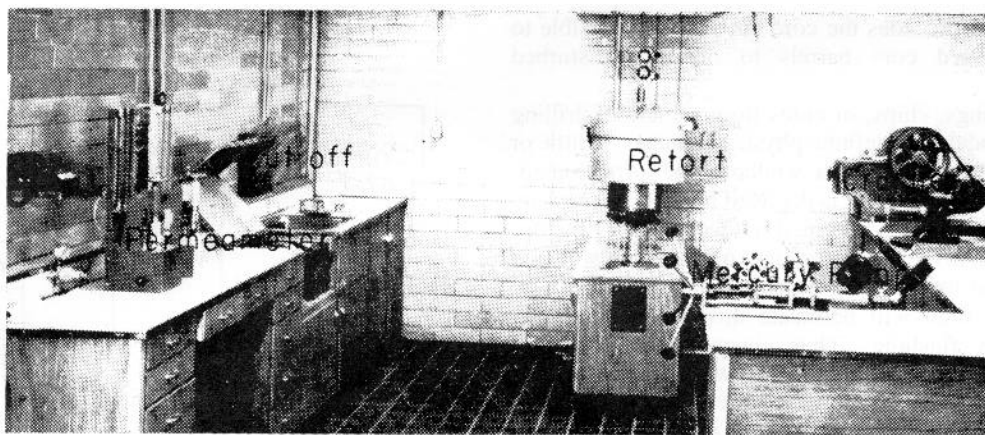


Fig. 26.30—Laboratory layout for performing routine core analysis

and

$$S_g = 1 - S_w - S_o$$

{ live

- S_w water saturation,
- S_o oil saturation,
- S_g gas saturation,
- V_w water volume, cm^3 ,
- V_p pore volume, cm^3 , and
- V_o oil volume, cm^3 .

The other method of determining fluid saturation is by extraction with a solvent. Extraction may be accomplished by a modified ASTM distillation method or a centrifuge method. In the standard distillation test, the core is placed such that a vapor of either toluene, pentane, octane, or naphtha rises through the core. This process leaches out the oil and water in the core. The water and extracting fluid are condensed and collected in a graduated receiving tube. The water settles to the bottom of the receiving tube because of its greater density, and the extracting fluid refluxes over the core and into the main heating vessel. The process is continued until no more water is collected in the receiving tube. The water saturation may be determined directly by

$$S_w = \frac{V_w}{V_p}$$

The oil saturation is an indirect determination. The oil saturation as a fraction of PV is given by

$$S_o = \frac{W_{cw} - W_{cd} - W_w}{V_p - \rho_o},$$

where

- W_{cw} = weight of wet core, g,
- W_{cd} = weight of dry core, g,
- W_w = weight of water, g,
- V_p = PV, cm^3 , and
- ρ_o = density of oil, g/cm^3 .

The gas saturation is obtained in the same manner as the retort.

Another method of determining water saturation is to use a centrifuge. A solvent is injected into the centrifuge just off center. Because of centrifugal force, it is thrown to the outer radii and forced to pass through the core sample. The outflow fluid is trapped and the quantity of water in the core is determined. The use of the centrifuge provides a very rapid method because of the high forces that can be applied. In both extraction methods, at the same time that the water content is determined, the core is cleaned in preparation for the other measurements such as porosity and permeability.

There is another procedure for saturation determination that is used in conjunction with either of the extraction methods. The core as received from the well is placed in a modified mercury porosimeter in which the BV and gas volume are measured. The volume of water is determined by one of the extraction methods. The fluid saturations can be calculated from these data.

In connection with all procedures for determination of fluid content, a value of PV must be established in order that fluid saturations may be expressed as percent of PV. Any of the porosity procedures previously described may be used. Also, the BV and gas volume determined from the mercury porosimeter may be combined with the oil and water volumes obtained from the retort to calculate PV, porosity, and fluid saturations.

Porosity, permeability, and fluid-saturation determinations are the measurements commonly reported in routine core analysis. A laboratory equipped for such determinations is shown in Fig. 26.30.

Interstitial Water Saturations

Essentially, three methods are available to the reservoir engineer for the determination of interstitial water saturations. These methods are (1) determination from cores cut with oil-based muds, (2) determination from capillary-pressure data, and (3) calculation from electric-log analysis (see Chap. 49).

Oil-Based Mud. The obtaining of water saturations by using oil-based muds has been discussed. A correlation between water saturation and air permeability for cores obtained with oil-based muds is shown in Fig. 26.31.²⁹

A general trend of increasing water saturation with decreasing permeability is indicated. It is accepted from field and experimental evidence that the water content determined from cores cut with oil-based mud reflects closely the water saturation as it exists in a reservoir, except in transition zones where some of the interstitial water is replaced by filtrate or displaced by gas expansion.

Fig. 26.32 shows permeability/interstitial-water relationships reported in the literature for a number of fields and areas. There is no general correlation applicable to all fields; however, an approximately linear correlation between interstitial water and the logarithm of permeability exists for each individual field. The general trend of the correlation is decreasing interstitial water with increasing permeability.

Capillary Pressure. Capillary pressure may be thought of as a force per unit area resulting from the interaction of surface forces and the geometry of the medium in which they exist. Capillary pressure for a capillary tube is defined in terms of the interfacial tension between the fluids, σ , the angle of contact of the interface of these two fluids and the tube, θ_c , and the radius of the tube, r_t .

This relationship is expressed in Eq. 44.

$$P_c = \frac{2\sigma \cos \theta_c}{r_t} \quad (44)$$

where the angle θ_c is measured through the more dense fluid.

In a packing of spheres, the capillary pressure is expressed in terms of any two perpendicular radii of cur-

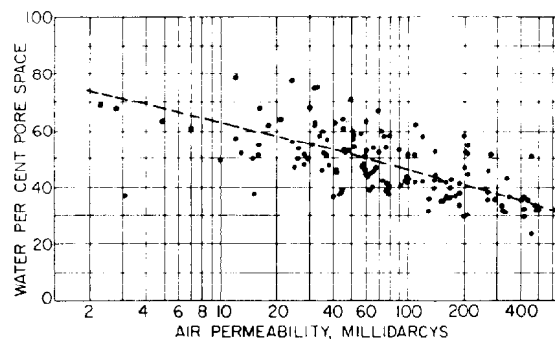


Fig. 26.31—Relation of air permeability to the water content of the South Coles Levee cores.

vature (these radii touch at only one point), r_1 and r_2 , and the interfacial tension of the fluids. This relationship is given in Eq. 45.

$$P_c = \sigma \left(\frac{1}{r_1} + \frac{1}{r_2} \right) \quad (45)$$

Comparing Eq. 45 with the equation for capillary pressure as determined by the capillary-tube method, it is found that the mean radius \bar{r} is defined by

$$\frac{1}{\bar{r}} = \frac{1}{r_1} + \frac{1}{r_2} = \frac{2 \cos \theta_c}{r_t};$$

$$\bar{r} = \frac{r_1 r_2}{r_1 + r_2} = \frac{r_t}{2 \cos \theta_c} \quad (46)$$

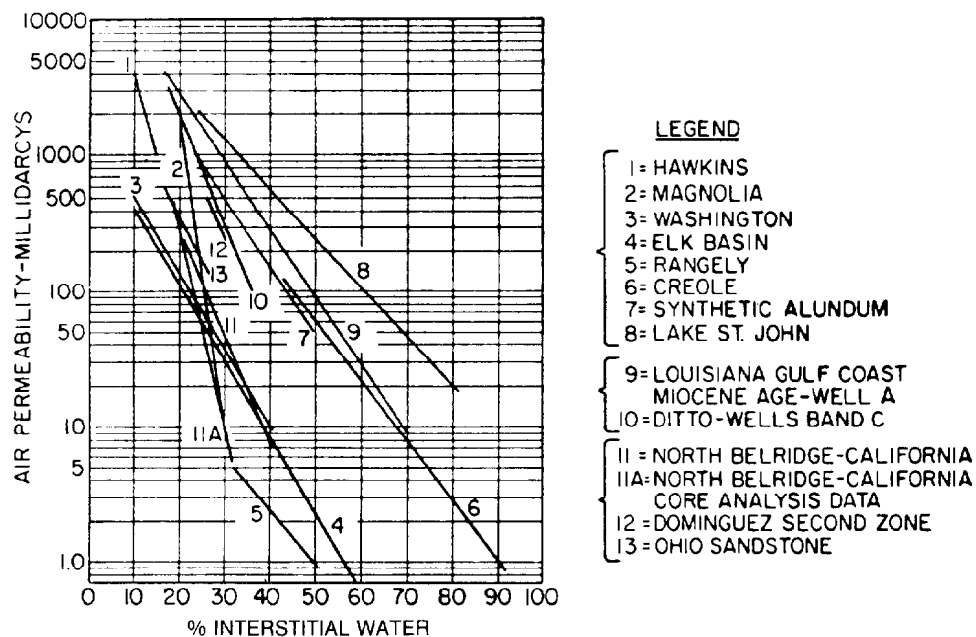


Fig. 26.32—Interstitial water vs. permeability relationships.

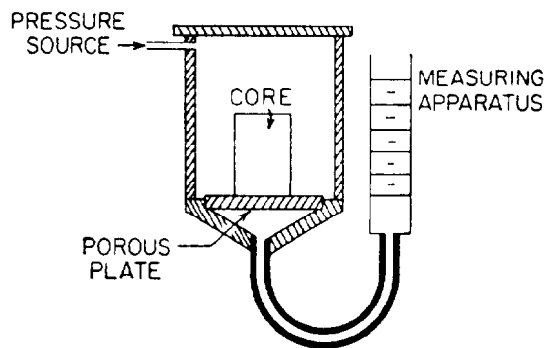


Fig. 26.33—Schematic of porous-diaphragm method of capillary pressure.

It is practically impossible to measure the values of r_1 and r_2 ; hence, they generally are referred to by the mean radius of curvature and empirically determined from other measurements on a porous medium.

The distribution of the liquid in a porous system depends on the wetting characteristics. It is necessary to determine which is the wetting fluid so as to ascertain which fluid occupies the small pore spaces. From packings of spheres, the wetting-phase distribution within a porous system has been described as either funicular or pendular in nature. In funicular distribution, the wetting phase is continuous, completely covering the surface of the solid. The pendular ring is a state of saturation in which the wetting phase is not continuous and the nonwetting phase is in contact with some of the solid surface. The wetting phase occupies the smaller interstices. As the wetting-phase saturation progresses from the funicular to the pendular-ring distribution, the volume of the wetting phase decreases and the mean radius of curvature or the values of r_1 and r_2 tend to decrease in magnitude. Referring to Eq. 46, we see that if r_1 and r_2 decrease in size, the magnitude of the capillary pressure would have to increase in value. Since r_1 and r_2 can be related to the wetting-phase saturation, it is possible to express the capillary pressure as a function of fluid saturation when two immiscible phases are within the porous matrix.

Laboratory Measurements of Capillary Pressure

Essentially, five methods of measuring capillary pressure on small core samples are used. These methods are (1) the desaturation or displacement process, through a porous diaphragm or membrane (restored-state method of Welge³⁰), (2) the mercury-injection method, (3) the centrifuge or centrifugal method, (4) the dynamic-capillary-pressure method, and (5) the evaporation method.*

Porous Diaphragm. The first of these, illustrated in Fig. 26.33, is the displacement or diaphragm method. The essential requirement of the diaphragm method is a

permeable membrane of uniform pore-size distribution containing pores of such size that the selected displacing fluid will not penetrate the diaphragm when the pressures applied to the displacing phase are below some selected maximum pressure of investigation. Various materials including fritted glass, porcelain, and cellophane have been used successfully as diaphragms. Pressure applied to the assembly is increased by small increments. The core is allowed to approach a state of static equilibrium at each pressure level. The saturation of the core is calculated at each point defining the capillary-pressure curve. Any combination of fluids may be used: gas, oil, and/or water. Although most determinations of capillary pressure by the diaphragm method are drainage tests, by suitable modifications imbibition curves similar to Leverett's may be obtained.

Mercury Injection. The mercury-capillary-pressure apparatus was developed to accelerate the determination of the capillary-pressure/saturation relationship. Mercury is normally a nonwetting fluid. The core sample is inserted in the mercury chamber and evacuated. Mercury is forced into the core under pressure. The volume of mercury injected at each pressure determines the nonwetting-phase saturation. This procedure is continued until the core sample is filled with mercury or the injection pressure reaches some predetermined value. Two important advantages are gained by this method: (1) the time for determination is reduced to a few minutes, and (2) the range of pressure investigation is increased because the limitation of the diaphragm's properties is removed. Disadvantages are the difference in wetting properties and permanent loss of the core sample.

Centrifuge Method. A third method for determining capillary properties of reservoir rocks is the centrifuge method.³¹ The high accelerations in the centrifuge increase the field of force on the fluids, in effect subjecting the core to an increased gravitational force. By rotating the sample at various constant speeds, a complete capillary-pressure curve may be obtained. The speed of rotation is converted into force units in the center of the core sample, and the fluid saturation is read visually by the operator. The advantage of the method is the increased speed of obtaining the data. A complete curve may be established in a few hours, while the diaphragm method requires days.

Dynamic Method. Brown³² reported the results of determining capillary-pressure/saturation curves by a dynamic method. Simultaneous steady-state flow of two fluids is established in the core. By the use of special wetted disks that permitted hydraulic pressure transmission of only the selected fluid phase, the difference in the resulting measured pressures of the two fluids in the core is the capillary pressure. The saturation is varied by regulating the quantity of each fluid entering the core. Thus, it is possible to obtain a complete capillary-pressure curve.

Comparison of Methods of Measurement

Intuitively, it appears that the diaphragm method (restored state) is superior in that oil and water are used; therefore, actual wetting conditions are more nearly ap-

*Since this method is seldom used today, it will not be discussed. The procedure consists of continuously monitoring the decrease in weight caused by evaporation of a core sample initially 100% saturated with a wetting fluid. See Messner, E.S.: "Interstitial Water Determination By An Evaporation Method," *Trans., AIME* (1951) 192, 269-74.

proached. Hence, the diaphragm method is used as the standard to which all other methods are compared. The mercury-injection test data must be corrected for wetting conditions before they can be compared with results from the restored-state method. If it is assumed that the mean curvature of an interface in rock is a unique function of fluid saturation, then the ratio of mercury to water capillary-pressure data is given by

$$\frac{P_{cm}}{P_{cw}} = \frac{\sigma_m}{\sigma_w} = \frac{480}{70} = 6.57, \quad (47)$$

where σ_m is the surface tension of mercury and σ_w is the surface tension of water. Experimentation has shown the ratio to vary between 5.8 (for limestones) and 7.5 (for sandstones). Thus, no conversion factor can be defined that will apply to all rocks.

Good agreement of centrifuge data with those from the diaphragm method was reported by Slobod.³¹ Unlike the mercury-injection method, there is no need of conversion factors to correct for wetting properties. The same fluids are used in the centrifugal and diaphragm methods.

Excellent correlation was obtained by Brown³² between the diaphragm and dynamic methods. The dynamic data were obtained by simultaneous steady flow of oil and gas through the porous sample at a predetermined level of pressure difference between the fluids. Care was taken to maintain uniform saturations throughout the core as well as to conduct the test such that a close correspondence to drainage conditions existed.

If capillary-pressure data are to be used for determining fluid saturations, the values obtained should be comparable with those of other methods. Water distributions, as determined from electric logs, and capillary-pressure data are normally in good agreement. A comparison of these methods is shown in Fig. 26.34.³³ Shown also is the approximate position of the gas/oil contact as determined from other test data. In the gas-bearing portion of the formation there is no significant variation in water saturation with depth or method of determination. However, in a thin oil zone, such as that shown in Fig. 26.34, there is a significant variation in the water saturation with depth. Variations in water saturations with depth within an oil zone must be taken into account to determine accurately average reservoir interstitial-water saturations.

Water Saturation from Capillary-Pressure Data. In oilfield terms, the capillary pressure may be stated as

$$P_c = \frac{h}{144} (\rho_1 - \rho_2), \quad (48)$$

where h is in feet and ρ_1 and ρ_2 are the densities of Fluids 1 and 2, respectively, in lbm/cu ft at the conditions of the capillary pressure.

Converting Laboratory Data. To use laboratory capillary-pressure data, it is necessary to convert them to reservoir conditions. Laboratory data are obtained with a

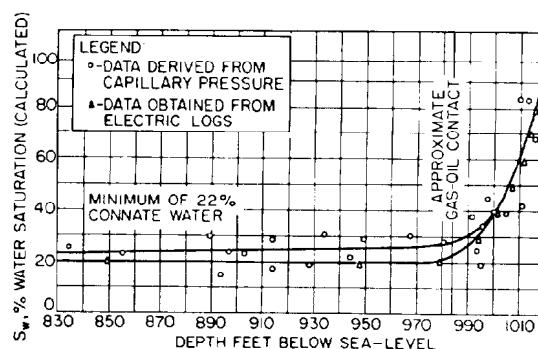


Fig. 26.34—Comparison of water saturation from capillary pressure and electric log.

gas/water or an oil/water system that normally does not have the same physical properties as the reservoir water, oil, and gas.

Essentially two techniques, differing only in the initial assumptions, are available for correcting laboratory capillary-pressure data to reservoir conditions.

$$P_{c,R} = \frac{\sigma_{wo} \cos \theta_{cwo}}{\sigma_{wg} \cos \theta_{cwg}} P_{c,L}$$

or

$$P_{c,R} = \frac{\sigma_R}{\sigma_L} P_{c,L}, \quad (49)$$

where

- σ_{wo} = interfacial tension water/oil,
- σ_{wg} = interfacial tension water/gas,
- θ_{cwo} = water/oil contact angle,
- θ_{cwg} = water/gas contact angle,
- subscript
- R = reservoir conditions, and
- subscript
- L = laboratory conditions.

Since the interfacial tensions enter as a ratio, pressure in any consistent units may be used together with the interfacial tension in dynes/cm.

Averaging Capillary-Pressure Data. Two methods have been proposed for correlating capillary-pressure data of similar geologic formations. The first correlating procedure is a dimensionless grouping of the physical properties of the rock and the saturating fluids. This function is called a J function³⁴ and is expressed as

$$J(S_w) = \frac{P_c}{\sigma} \left(\frac{k}{\phi} \right)^{1/2}, \quad (50)$$

where

- S_w = water saturation, fraction of PV,
- P_c = capillary pressure, dyne/cm²,
- σ = interfacial tension, dyne/cm,
- k = permeability, cm², and
- ϕ = fractional porosity.

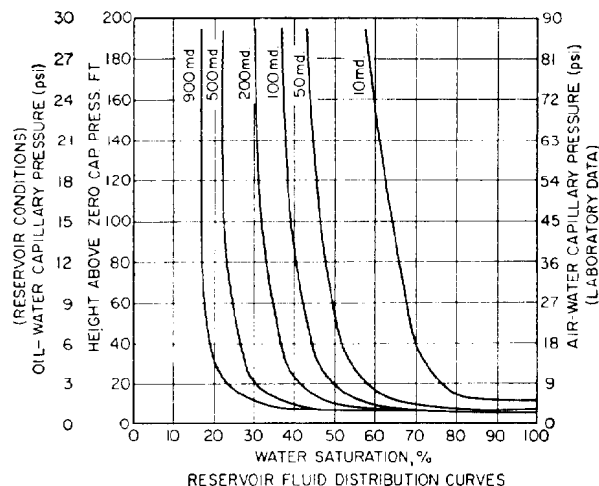


Fig. 26.35—Series of capillary-pressure curves as a function of permeability.

Some authors alter the above expression by including the $\cos \theta_c$ (where θ_c is the contact angle) as follows.

$$J(S_w) = \frac{P_c}{\sigma \cos \theta_c} \left(\frac{k}{\phi} \right)^{1/2}$$

The J function originally was proposed as a means of converting all capillary-pressure data to a universal curve. There exist significant differences in correlation of the J function with water saturation from formation to formation such that no universal curve may be obtained, but the J function may be used to correlate the data from one formation.

The second method of evaluating capillary-pressure data is to analyze a number of representative samples and treat the data statistically to derive correlations that, together with the porosity and permeability distribution data, may be used to compute the interstitial-water saturations for a field. A first approximation for the correlation of capillary-pressure data is to plot water saturation against the logarithm of permeability for constant values of capillary pressure. A straight line may be fitted to the data for each value of capillary pressure, and average-capillary-pressure curves may be computed from permeability-distribution data for the field. The resulting straight-line equation takes the general form of

$$S_w = m \log k + b \quad (51)$$

Fluid-distribution curves are reported for several values of permeability, ranging from 10 to 900 md in Fig. 26.35.³⁵ These data also may be considered to be capillary-pressure curves. The ordinate on the right reflects values of capillary pressure determined by displacing water with air in the laboratory. The ordinates on the left include the corresponding oil/water capillary pressure that would exist at reservoir conditions and the fluid distribution with height above the free-water surface.

The results of the statistical correlation previously discussed applied to the capillary-pressure data presented in Fig. 26.35 are shown in Fig. 26.36. The reader should note the linearity of the curves for each value of capillary pressure and the tendency of all capillary-pressure curves to converge at high permeability values. This behavior is what normally would be expected because of the larger capillaries associated with high permeabilities.

To convert capillary-pressure saturation data to height saturation, it is necessary only to rearrange the terms in Eq. 48 so as to solve for the height instead of the capillary pressure—i.e.,

$$h_{fw} = \frac{P_c \times 144}{\rho_w - \rho_o} \quad (52)$$

where

h_{fw} = height above the free-water surface, ft,

ρ_w = density of water at reservoir conditions, lbm/cu ft,

ρ_o = density of oil at reservoir conditions, lbm/cu ft, and

P_c = capillary pressure at some particular saturation for reservoir conditions (it must be converted from laboratory data first, psi).

Example Problem 9—Calculation of Saturation Plane From Laboratory Capillary-Pressure Data. If

$P_{c,L} = 18$ psi for $S_w = 0.35$,

$\sigma_{wo} = 24$ dynes,

$\rho_w = 68$ lbm/cu ft,

$\sigma_{wg} = 72$ dynes, and

$\rho_o = 53$ lbm/cu ft,

then, from Eq. 49,

$$P_{c,R} = 18(24/72) = 18/3 = 6 \text{ psi,}$$

and

$$h = \frac{P_{c,R} \times 144}{\rho_w - \rho_o} = \frac{6 \times 144}{68 - 53} = 58 \text{ ft.}$$

Thus, a water saturation of 35% exists at a height of 58 ft above the free-water surface.

To calculate the fluid saturation in the gas zone, it is necessary to consider all three phases: oil, water, and gas. If all three phases are continuous, it can be shown that

$$P_{c,wg} = P_{c,wo} + P_{c,og},$$

where

$P_{c,wg}$ = capillary pressure at a given height above the free-water surface determined by using water and gas,

$P_{c,wo}$ = capillary pressure at a given height above the free-water surface, using water and oil, and

$P_{c,og}$ = capillary pressure at a given height above the free-oil surface, using oil and gas.

If the wetting phase becomes discontinuous, then the wetting-phase saturation takes on a minimum value, and, at all heights above the point of discontinuity, the wetting-phase saturation cannot be less than this minimum value. It is then possible to calculate the fluid saturations above the free-oil surface by the following relations.

1. S_w at h is calculated using oil and water as the continuous phases.

2. S_L at h is calculated using oil and gas as the continuous phases and height denoted by the free-oil surface.

3. $S_g = 1 - S_L$ and $S_o = S_L - S_w$, where S_L is the total liquid saturation, oil plus water, fraction.

Example Problem 10—Calculation of Water and Oil Saturation in Gas Zone From Capillary-Pressure Data. Let oil-zone thickness, h_o , equal 70 ft and

$$\begin{aligned}\sigma_{wg} &= 72 \text{ dynes,} \\ \sigma_{og} &= 50 \text{ dynes,} \\ \sigma_{wo} &= 25 \text{ dynes,} \\ \rho_w &= 68 \text{ lbm/cu ft} \\ \rho_g &= 7 \text{ lbm/cu ft, and} \\ \rho_o &= 53 \text{ lbm/cu ft.}\end{aligned}$$

From Fig. 26.28 for a 900-md sample, let

$P_{c,L} = 54$ psi by the method illustrated in

Example Problem 9,

$P_{c,R} = 18$ psi,

$h_{fw} =$ height above free-water level = 120 ft, and

$S_w = 16\%$ at a height of 70 ft or greater (read from curve).

Since the oil zone is only 70 ft thick, the height of 120 ft above the free-water surface must be at least 50 ft into the gas-saturated zone. The first step is to calculate the total fluid saturation, S_L , using gas and oil as the continuous phases.

$$h_{fo} = h_{fw} - h_o = 120 - 70 = 50 \text{ ft;}$$

$$P_{c,R} = \frac{h_{fo}}{144} (\rho_o - \rho_g),$$

where h_{fo} is the height above free-oil level, ft.

$$P_{c,R} = 50/144 \times (53 - 7) = 50/144 \times 46,$$

$$P_{c,R} = 15.97,$$

and

$$P_{c,L} = P_{c,R} \frac{\sigma_{wg}}{\sigma_{og}} = 15.97 \times 72/50 = 23 \text{ psi.}$$

From Fig. 26.35, for a laboratory capillary pressure of 23 psi and a permeability of 900 md, the total wetting saturation, S_L , equals 18%. Therefore,

$$S_o = S_L - S_w = 18 - 16 = 2\%$$

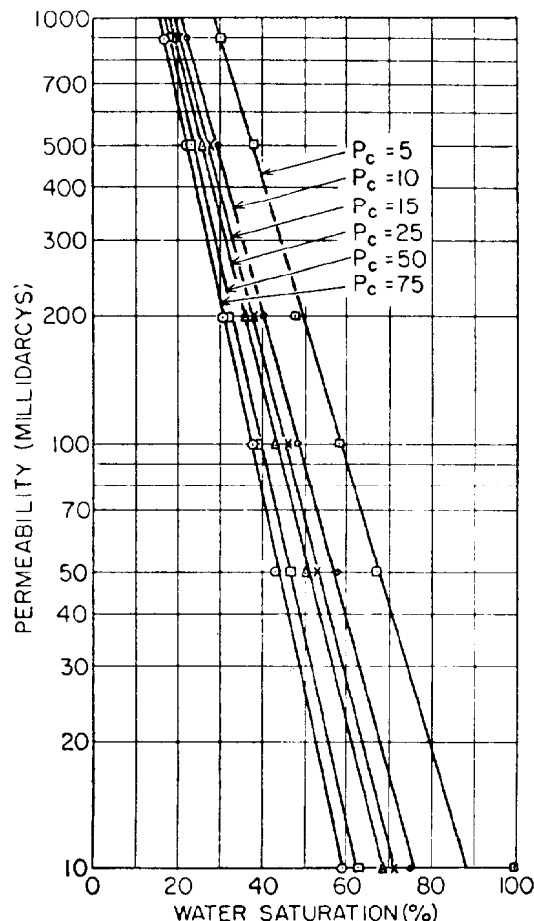


Fig. 26.36—Correlation of water saturation with permeability for various capillary pressures.

and

$$S_g = (100 - S_L) = 100 - 18 = 82\%.$$

It must be understood that the relationships used in Example Problem 10 for calculating the fluid saturations in the gas zone were based on continuity of all three phases. Since this is not normally the case, it might be expected that saturations somewhat different from the calculated values exist. Because the capillary pressure for a discontinuous phase could vary from pore to pore, it is impossible to ascertain the exact relationships that should exist. Hence, the preceding method of calculating fluid distributions is not exact but is usually as accurate as the data available for making the computation.

Electrical Conductivity of Fluid-Saturated Rocks

Porous rocks comprise an aggregate of minerals, rock fragments, and void space. The solids, with the exception of certain clay minerals, are nonconductors of electricity. The electrical properties of a rock depend on the geometry of the voids and the fluids that fill the voids. The fluids of interest in petroleum reservoirs are oil, gas, and water. Oil and gas are nonconductors. Water is a

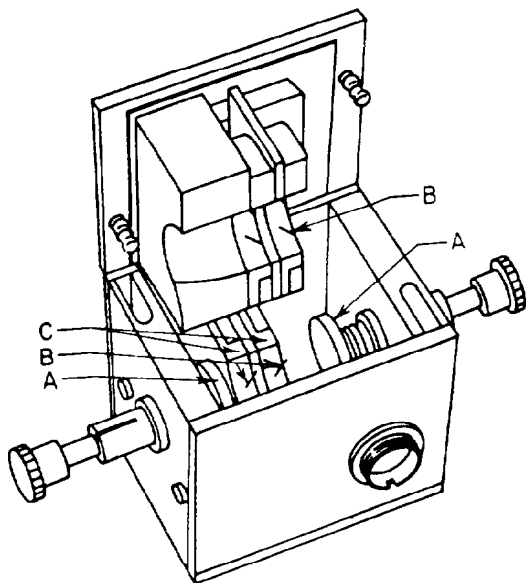


Fig. 26.37—Core-sample resistivity cell.

conductor when it contains dissolved salts. Current is conducted in water by movement of ions and therefore may be termed electrolytic conduction. The resistivity of a material is the reciprocal of conductivity and commonly is used to define the ability of a material to conduct current. The resistivity of a material is defined by the following equation.

$$\rho = \frac{rA}{L}, \quad (53)$$

where

- ρ = resistivity,
- r = resistance,
- A = cross-sectional area of the conductor, and
- L = length of the conductor.

For electrolytes, ρ is commonly reported in Ω -cm, and r is expressed in ohms, A in cm^2 , and L in cm. In the study of the resistivity of soils and rocks, it has been found that the resistivity may be expressed more conveniently in Ω -m. To convert to Ω -m from Ω -cm, divide the resistivity in Ω -cm by 100. In oilfield practice, the resistivity in Ω -m commonly is represented by the symbol R with an appropriate subscript to define the condition to which R applies.

Fundamental Concepts

The definition of electrical formation resistivity factor is perhaps the most fundamental concept in considering electrical properties of rocks. The formation resistivity factor as defined by Archie²⁷ is

$$F_R = \frac{R_0}{R_w}, \quad (54)$$

where R_0 is the resistivity of the rock when saturated with water having a resistivity of R_w .

The second fundamental notion of electrical properties of porous rock is the resistivity index, I_R , which is defined as

$$I_R = \frac{R_t}{R_0}, \quad (55)$$

where R_t is the true resistivity of the rock system at some particular value of water saturation and R_0 is as previously defined.

Three idealized representations have been introduced in the literature from which the formation resistivity factor, F_R , and the resistivity index, I_R , have been related to the porosity, ϕ , and the rock tortuosity, τ .

From Wyllie's²⁷ analysis the relations are

$$F_R = \tau \frac{1}{\phi}$$

and

$$I_R = \tau_e \frac{1}{S_w},$$

where τ_e is the effective rock tortuosity at some water saturation.

Cornell and Katz³⁶ presented an analysis of a slightly different model. The relationships developed are as follows.

$$F_R = \sqrt{\tau} \frac{1}{\phi}$$

and

$$I_R = \sqrt{\tau_e} \frac{1}{S_w}.$$

Wyllie and Gardner³⁷ later presented an analysis based on a probability theory from which the following relationships were obtained.

$$F_R = \frac{1}{\phi^2}$$

and

$$I_R = \frac{1}{S_w^2}.$$

From the analysis of the electrical properties of the foregoing idealized pore models, general relationships between electrical properties and other physical properties of the rock may be deduced. The formation resistivity factor has been shown to be some function of the porosity and the internal geometry of the rock system. In particular, the formation resistivity factor may be expressed in the following form.

$$F_R = K\phi^{-m}, \quad (56)$$

where K is some function of the tortuosity and m is a function of the number of reductions in pore-opening sizes or closed channels. It is suggested that K should be 1 or greater. The value of m has been shown from theory to range from 1 to 2.

Both the formation resistivity factor, F_R , and the resistivity index, I_R , depend on ratios of path length or tortuosities. Therefore, to compute the formation resistivity factor or resistivity index from the relations derived from models, it is necessary to determine the electrical tortuosity. Since direct measurement of the path length is impossible, reliance has been placed primarily on empirical correlations based on laboratory measurements. Winsauer *et al.*³⁸ devised a method of determining tortuosity by transit time of ions flowing through a rock under a potential difference. The data obtained were correlated with the product $F_R\phi$. The resulting correlation of formation resistivity factor, porosity, and tortuosity is given in Eq. 57.

$$\left(\frac{L_a}{L}\right)^{1.67} = F_R\phi,$$

where L_a is the actual length of flow path, and L is the length of the sample, or

$$\tau^{1.67/2} = F_R\phi. \quad (57)$$

The deviation from the theory is believed to be an indication of the greater complexity of the actual pore system than that of the models on which the theory was based.

Archie suggested that the formation resistivity factor could be correlated with porosity and have the form

$$F_R = \phi^{-m}, \quad (58)$$

where ϕ is the fractional porosity and m is the cementation factor. Archie further reported that the cementation factor probably ranged from 1.8 to 2.0 for consolidated sandstones and, for clean unconsolidated sands, was about 1.3.

Measurement of Electrical Resistivity of Rocks

Laboratory measurements of electrical properties of rocks have been made with a variety of devices. The measurements require a knowledge of the dimensions of the rock, the fluid saturation of the rock, the resistivity of the water contained in the rock, and a suitable resistivity cell in which to test the samples. A simple cell is shown in Fig. 26.37.³⁹ A sample cut to suitable size is placed in the cell and clamped between electrodes A. Current is then passed through the sample and the potential drop observed. The resistance of the sample is computed from Ohm's law,

$$r = \frac{E}{I},$$

and R (the resistivity) is computed from

$$R = \frac{rA}{L},$$

where A is the cross-sectional area of the sample and L is the length of the sample. The saturation conditions of the test may be established at known values before measurement or determined by an extraction procedure after measurement.

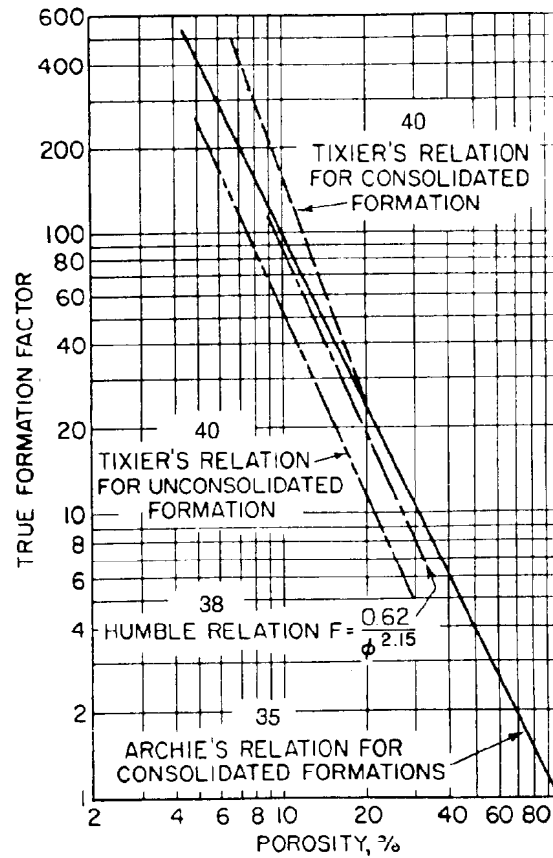


Fig. 26.38—Comparison of various formation resistivity factor correlations.

Empirical Correlation of Electrical Properties

Archie, as previously mentioned, reported the results of correlating laboratory measurements of formation factor with porosity. He expressed his results in the form $F_R = \phi^{-m}$.

Winsauer *et al.*³⁸ reported a similar relationship based on correlations of data from a large number of sandstone cores. This equation, commonly referred to as the Humble relation, is

$$F_R = 0.62\phi^{-2.15}. \quad (59)$$

In discussing the theory of the formation resistivity factor, it was stated that K should be greater than 1 and that m should be 2 or less. At this time, the discrepancy between theory and experiment must be attributed to the possible effect of conducting solids.

Improved correlations should result from considering other parameters, such as permeability, as variables in the relations.

A comparison of suggested relationships between porosity and the formation resistivity factor is shown in Fig. 26.38.

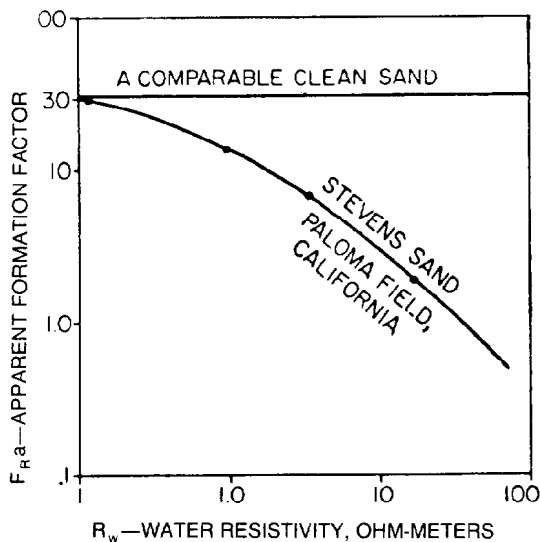


Fig. 26.39—Effect of interstitial clay on formation resistivity factors.

Effect of Conductive Solids

Investigations by Wyllie⁴¹ indicate that clays contribute substantially to the conductivity of a rock when the rock is saturated with a low-conductivity water. The effect of water resistivity on the formation resistivity factor for sands containing clay minerals is shown in Fig. 26.39. The formation resistivity factor for a comparable clean (clay-free) sand is a constant. The formation resistivity factor for the clayey sand increases with decreasing water resistivity and approaches a constant value at a

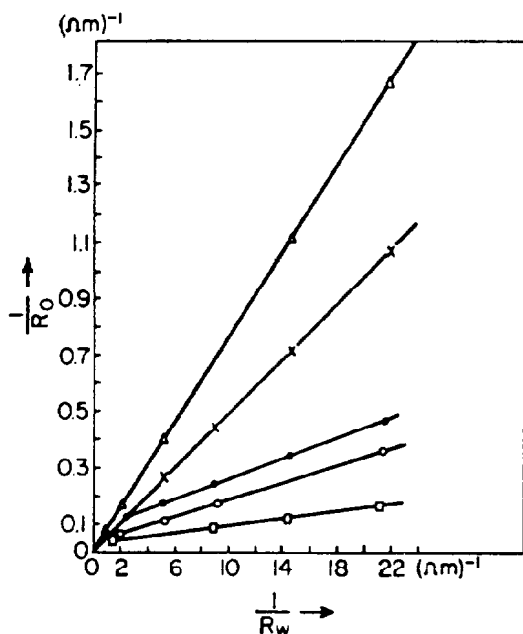


Fig. 26.40—Water-saturated rock conductivity plotted against water conductivity yields these measurements: (Δ) Suite 1 No. 40; (X) Suite 1 No. 21; (●) Suite 1 No. 4; (○) Suite 2 No. 13; (□) Suite 6 No. 2.

water resistivity of about 0.1 Ω-m. Wyllie proposed that the observed effect of clay minerals was similar to having two electric circuits in parallel—the conducting clay minerals and the water-filled pores. Thus,

$$F_{Ra} = \frac{R_{0sh}}{R_w} \text{ and } \frac{1}{R_{0sh}} = \frac{1}{R_{cl}} + \frac{1}{F_R R_w}, \dots \dots (60)$$

where

F_{Ra} = apparent formation resistivity factor,

R_{0sh} = resistivity of a shaly sand when 100% saturated with water of resistivity R_w ,

R_{cl} = resistivity caused by the clay minerals,

R_w = resistivity caused by the distributed water, and

F_R = true formation resistivity factor of the rock (i.e., the constant value of formation factor approached when the rock contains low-resistivity water).

The data presented in Fig. 26.40 represent graphically the confirmation of the relationship expressed in Eq. 60. The graphs were plotted by deWitte⁴² from data presented by Hill and Milburn.⁴³ The plots are linear and are of the general form

$$\frac{1}{R_{0sh}} = m \frac{1}{R_w} + b, \dots \dots \dots (61)$$

where m is the slope of the line and b is the intercept. Comparing Eq. 60 with Eq. 61, note that $m = 1/F_R$ and $b = 1/R_{cl}$. The curve labeled Suite 1 No. 40 indicates a clean sand because the line passed through the origin, thus having a zero intercept $b = 1/R_{cl} = 0$. Then $1/R_{0sh} = m(1/R_w) = (1/F_R R_w)$, or $R_0 = F_R R_w$. The remaining samples are from shaly sands, which have a finite conductivity of the clay minerals, as indicated by the intercepts of the lines. The linearity of the plots indicates that $1/R_{cl}$ is a constant independent of R_w . This phenomenon may be explained in terms of the ions absorbed on the clay. When the clay is hydrated, the absorbed ions form an ionic conducting path, which is closely bound to the clay. The number of absorbed ions is apparently little changed by the salt concentration of the interstitial water.

Eq. 60 may be rearranged to express the apparent formation resistivity factor in terms of R_{cl} and $F_R R_w$.

$$R_{0sh} = \frac{R_{cl} R_w}{R_w + R_{cl}/F_R}$$

and

$$F_{Ra} = \frac{R_{cl}}{R_w + (R_{cl}/F_R)}$$

As $R_w \rightarrow 0$,

$$\lim F_{Ra} = \frac{R_{cl}}{R_{cl}/F_R} = F_R.$$

Therefore, F_{Ra} approaches F_R as a limit as R_w becomes small. This behavior was observed in Fig. 26.39.

Hill and Milburn⁴³ evaluated 450 samples from both sandstone and limestone formations. The formation resistivity factor was determined at a water resistivity of 0.01 Ω -m, a value at which the apparent formation resistivity factor, F_{Ra} , approaches the formation resistivity factor, F_R . They designated the formation resistivity factor as $F_{R,0.01}$. The data were fitted by the method of least squares to yield

$$F_{R,0.01} = 1.4\phi^{-1.78} \quad (62)$$

This equation conforms to the theory previously discussed. They also fitted the data with K in Eq. 56 restricted to a value of 1. This yielded $F_{R,0.01} = \phi^{-1.93}$, which corresponds closely to Archie's original expression $F = \phi^{-2}$.

In summary, Eqs. 58 (with $m=2.0$) and 59 have been used widely to represent the relation between formation resistivity factor and porosity. Both equations yield results satisfactory for most engineering purposes. However, we propose that Eq. 62 be considered as more valid because the data were taken to minimize the effect of clays. The selection of a particular relation should be based on independent observations on the formations or formations of interest in a given geologic province.

Resistivity of Partially Water-Saturated Rocks

A rock containing both water and hydrocarbon has a higher resistivity than when fully saturated with water. The resistivity of partially water-saturated rocks has been shown to be a function of the water saturation, S_w . From theoretical developments, the following generalization may be drawn.

$$I_R = K' S_w^{-n}, \quad (63)$$

where $I_R = R_t/R_0$, the resistivity index; K' is some function of tortuosity; and n is the saturation exponent.

Archie compiled and correlated experimental data from various sources from which he suggested that the data could be represented by

$$I_R = S_w^{-2}. \quad (64)$$

Wyllie confirmed the suggested relationship for clean sands but found that the presence of clays (conductive solids) altered the relationship. A comparison of Archie's relationship and that for a core containing conductive solids is shown in Fig. 26.41. The change in the relationship depends on both the amount of clays and the water resistivity. Therefore, a general correlation for sands containing conductive solids is not available, although deWitte⁴² has proposed a method of using Eq. 64 for evaluation of shaly sands.

Use of Electrical Parameters in Characterizing Porous Media

In the section on permeability, the Kozeny equation was developed as follows.

$$k = \frac{\phi}{F_s A_s^2 \tau}, \quad (65)$$

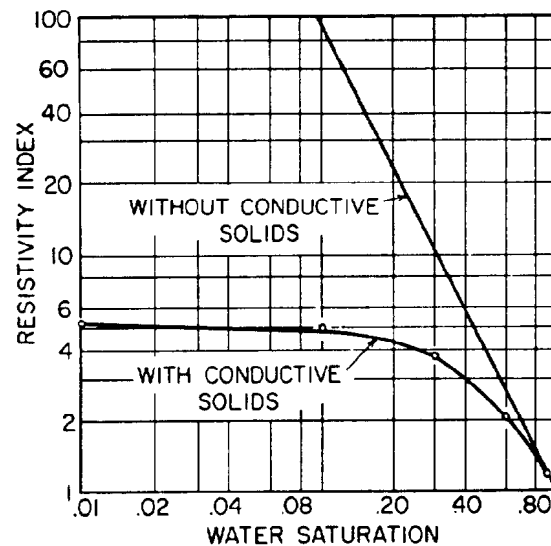


Fig. 26.41—Effect of conductive solids on the resistivity-index-vs.-saturation relationship in Stevens sandstone core.

where

- k = permeability,
- ϕ = porosity, fraction,
- F_s = shape factor,
- A_s = internal surface area/unit PV, and
- τ = Kozeny tortuosity.

τ has been shown to be a function of $F_R \phi$ —i.e., $\tau = (F_R \phi)^x$, where x ranges between 1 and 2. If the internal surface area is expressed in terms of the mean hydraulic radius, \bar{r}_H , by

$$A_s = \frac{1}{\bar{r}_H}, \quad (66)$$

the general form of the relationship may be stated as

$$k = \frac{\phi(\bar{r}_H)^2}{F_s (F_R \phi)^x}$$

or

$$\frac{(\bar{r}_H)^2}{k} = F_s \frac{(F_R)^x}{\phi}. \quad (67)$$

Eq. 67 perhaps provides an improved basis for the correlation of characteristic physical data of porous media with the electrical formation resistivity factor.

The electrical properties of porous rocks, as discussed in the foregoing sections, form the basis of quantitative evaluation of electrical-logging records. In particular, the Humble relation (Eq. 59) has been used widely by service companies in estimating porosity from measurements made with "contact" resistivity devices such as the Microlog.TM Eq. 64 forms the basis of interpretation of water saturations from deeper-penetration

resistivity devices such as the conventional resistivity curves of the standard electrical log or from the various "focused" electrical-resistivity devices.

Improvements in the statistical correlations of electrical properties of rocks will improve the results of such analyses.

Nomenclature

- A = cross-sectional area
 A_j = area of flow represented by a bundle of tubes of permeability k_j
 A_s = internal surface area/unit PV
 b = constant for a given gas in a given medium
 c = fluid compressibility
 C = flow coefficient
 d = diameter
 E = voltage drop
 f = friction factor
 F_s = shape factor
 F_R = formation resistivity factor
 F_{Ra} = apparent formation resistivity factor
 g = acceleration of gravity
 h = driving head
 h_{fo} = height above free-oil level
 h_{fw} = height above free-water level
 h_j = thickness of j th layer
 I = current
 I_R = resistivity index
 J = J function, Eq. 48
 k = permeability of the medium
 k_a = permeability to air
 k_g = permeability of the medium to a gas completely filling the pores of the medium
 k_h = thermal conductivity
 k_j = permeability of one capillary tube
 k_L = permeability of the medium to a single liquid phase completely filling the pores of the medium
 k_w = permeability to fresh water
 k_{500} = permeability to 500-grain/gal chloride solution
 K = constant of proportionality, Eq. 7
 K' = some function of the tortuosity, Eq. 63
 K_z = Kozeny's constant
 L = length of flow path or length of the sample
 L_a = actual length of the flow path
 L_j = length of j th layer
 m = slope of the curve or cementation factor
 n_j = number of tubes of radius r_j
 \bar{p} = mean flowing pressure
 Δp = pressure loss over length L
 p_b = base pressure
 p_e = pressure at the external boundary
 p_w = pressure at the wellbore
 P_c = capillary pressure
 $P_{c,L}$ = capillary pressure, laboratory conditions
 P_{cm} = capillary pressure of mercury
 $P_{c,og}$ = capillary pressure at height above free-oil surface, using oil and gas
 $P_{c,R}$ = capillary pressure, reservoir conditions
 P_{cw} = capillary pressure of water
 $P_{c,wg}$ = capillary pressure at a given height above the free-water surface determined by using water and gas
 $P_{c,wo}$ = capillary pressure at a given height above the free-water surface, using water and oil
 q_b = volume rate of flow at the base pressure
 q_o = volume rate of flow of oil
 q_p = volume rate of flow at the algebraic mean pressure $(p_e + p_w)/2$
 q_t = total flow rate
 \dot{Q} = rate of heat flow
 r = radius or resistance
 \bar{r} = mean radius
 r_e = radius at the external boundary
 r_H = hydraulic radius
 r_w = radius of the wellbore
 R_{cl} = resistivity caused by the clay minerals
 R_0 = resistivity of the rock when saturated with water having a resistivity of R_w
 R_{0sh} = resistivity of a shaly sand when 100% saturated with water of resistivity R_w
 s = distance in direction of flow, always positive
 S_g = gas saturation
 S_L = total wetting saturation
 S_o = oil saturation
 S_w = water saturation
 \bar{T}_f = average flowing temperature
 ΔT = temperature drop
 u_s = volume flux across a unit area of the porous medium in unit time along flow path s
 u_x = volume flux across a unit area of the porous medium in unit time along flow path x
 v = fluid velocity
 V_b = BV
 V_o = oil volume
 V_p = PV
 V_s = sand-grain volume
 V_w = water volume
 w = mass rate of flow
 W_{cd} = weight of dry core
 W_{cw} = weight of wet core
 W_w = weight of water
 z = vertical coordinate, considered positive downward
 θ = angle between s and the horizontal
 θ_c = angle of contact of the interface of two fluids and the capillary tube
 θ_{cwg} = water/gas contact angle
 θ_{cwo} = water/oil contact angle
 μ = fluid viscosity
 ρ = fluid density or resistivity
 ρ_b = fluid density at base pressure
 ρ_o = oil density
 σ = IFT or conductivity
 σ_m = surface tension of mercury

- σ_w = surface tension of water
 σ_{wg} = water/gas IFT
 σ_{wo} = water/oil IFT
 τ = Kozeny tortuosity
 τ_e = effective rock tortuosity
 ϕ = fractional porosity
 ϕ_e = effective porosity
 Φ = potential function

Key Equations in SI Metric Units

$$q = 14.696 \times 10^3 \frac{kA(p_1 - p_2)}{\mu L}, \dots \dots \dots (26)$$

$$q = 92.349 \times 10^3 \frac{kh(p_e - p_w)}{\mu \ln r_e/r_w}, \dots \dots \dots (28)$$

$$q_b = 23.1454 \times 10^4 \frac{T_b kA(p_1^2 - p_2^2)}{\bar{T}_f \mu_g L p_b}, \dots \dots \dots (30)$$

$$q_b = 1.4554 \times 10^6 \frac{T_b kh(p_e^2 - p_w^2)}{\bar{T}_f \mu_g p_b \ln r_e/r_w}, \dots \dots \dots (31)$$

where

- q is in m^3/d ,
 k is in μm^2 ,
 A is in m^2 ,
 p is in kPa ,
 μ is in $\text{Pa}\cdot\text{s}$,
 L is in m ,
 h is in m ,
 r is in m , and
 T is in $^\circ\text{C}$.

References

- Fraser, H.J. and Gratton, L.C.: "Systematic Packing of Spheres—With Particular Relation to Porosity and Permeability," *J. Geol.* (Nov.-Dec. 1935) 785-909.
- Tickell, F.G., Mechem, O.E. and McCurdy, R.C.: "Some Studies on the Porosity and Permeability of Rocks," *Trans., AIME* (1933) **103**, 250-60.
- Core Laboratories Inc., Dallas, TX.
- Nutting, P.G.: "Physical Analysis of Oil Sands," *Bull., AAPG*, (1930) **14**, 1337-49.
- Russell, W.L.: "A Quick Method for Determining Porosity," *Bull., AAPG* (1926) **10**, 931-38.
- Stevens, A.B.: *A Laboratory Manual for Petroleum Engineering 308*, Texas A&M U., College Station, TX (1954).
- Washburn, E.W. and Bunting, E.N.: "Determination of Porosity by the Method of Gas Expansion," *J. Am. Ceram. Soc.*, **5**, 48.
- Beeson, C.M.: "The Kobe Porosimeter and Oilwell Research Porosimeter," *Trans., AIME* (1950) **189**, 313-18.
- Dotson, B.J. et al.: "Porosity Measurement Comparison by Five Laboratories," *Trans., AIME* (1951) **192**, 341-46.
- Kelton, F.C.: "Analysis of Fractured Limestone Cores," *Trans., AIME* (1950) **189**, 225-34.
- Krumbein, W.C. and Sloss, L.L.: *Stratigraphy and Sedimentation*, Appleton-Century-Crofts Inc., New York City (1951) 218.
- Geertsma, J.: "Effect of Fluid Pressure Decline on Volumetric Changes of Porous Rocks," *Trans., AIME* (1957) **210**, 331 and 339.
- Hall, H.N.: "Compressibility of Reservoir Rocks," *Trans., AIME* (1953) **198**, 309.
- Fatt, I.: "Pore Volume Compressibilities of Sandstone Reservoir Rocks," *Trans., AIME* (1958) **213**, 362-64.
- Hammerlindl, D.J.: "Predicting Gas Reservoirs in Abnormally Pressured Reservoirs," paper SPE 3479 presented at the 1971 SPE Annual Meeting, New Orleans, Oct. 3-6.
- Newman, G.H.: "Pore-Volume Compressibility of Consolidated, Friable, and Unconsolidated Reservoir Rocks Under Hydrostatic Loading," *J. Pet. Tech.* (Feb. 1973) 129-34.
- Van der Knaap, W.: "Nonlinear Behavior of Elastic Porous Media," *Trans., AIME* (1959) **216**, 179-87.
- Krug, J.A.: "The Effect of Stress on the Petrophysical Properties of Some Sandstones," PhD dissertation (T-1964), Colorado School of Mines, Golden, CO (1977).
- Graves, R.M.: "Biaxial Acoustic and Static Measurement of Rock Elastic Properties," PhD dissertation (T-2596), Colorado School of Mines, Golden, CO (1982).
- Lachance, D.P. and Anderson, M.A.: "Comparison of Uniaxial Strain and Hydrostatic Stress Pore-Volume Compressibilities in the Nugget Sandstone," paper SPE 11971 presented at the 1983 SPE Annual Technical Conference and Exhibition, San Francisco, Oct. 5-8.
- API Code 27—*Recommended Practice for Determining Permeability of Porous Media*, Div. of Production, API, Dallas (Sept. 1952).
- Hubbert, M.K.: "Entrapment of Petroleum Under Hydrodynamic Conditions," *Bull., AAPG* (Aug. 1953) 1954-2026.
- Croft, H.O.: *Thermodynamics, Fluid Flow and Heat Transmission*, McGraw-Hill Book Company Inc., New York City (1938) 129.
- Klinkenberg, L.J.: "The Permeability of Porous Media to Liquids and Gases," *Drill. and Prod. Prac.*, API, Dallas (1941) 200-13.
- Johnston, N. and Beeson, C.M.: "Water Permeability of Reservoir Sands," *Trans., AIME* (1945) **160**, 43-55.
- Fatt, I. and Davis, D.H.: "Reduction in Permeability with Overburden Pressure," *Trans., AIME* (1952) **195**, 329.
- Wyllie, M.R.J. and Spangler, M.B.: "Application of Electrical Resistivity Measurements to Problem of Fluid Flow in Porous Media," *Bull., AAPG* (Feb. 1952) 359-403.
- Kennedy, H.T., VanMeter, O.E., and Jones, R.G.: "Saturation Determination of Rotary Cores," *Pet. Engr.* (Jan. 1954) B.52-B.64.
- Gates, G.L., Morris, F.C., and Caraway, W.H.: *Effect of Oil-Base Drilling Fluid Filtrate on Analysis of Cores from South Coles Levee, California and Rangely, Colorado Field*, technical report, Contract No. RI 4716, USBM (Aug. 1950).
- Welge, H.J. and Bruce, W.A.: "The Restored-state Method for Determination of Oil in Place and Connate Water," *Drill. and Prod. Prac.*, API, Dallas (1947) 166-74.
- Slobod, R.L., Chambers, A., and Prehn, W.L. Jr.: "Use of Centrifuge for Determining Connate Water, Residual Oil, and Capillary Pressure Curves of Small Core Samples," *Trans., AIME* (1951) **192**, 127-34.
- Brown, H.W.: "Capillary Pressure Investigations," *Trans., AIME* (1951) **192**, 67-74.
- Owen, J.D.: "Well Logging Study—Quinduno Field, Roberts County, Texas," paper 593-G presented at the 1955 AIME Formation Evaluation Symposium, Houston, Oct. 27-28.
- Leverett, M.C.: "Capillary Behavior in Porous Solids," *Trans., AIME* (1941) **142**, 152-68.
- Wright, H.T. Jr. and Wooddy, L.D. Jr.: "Formation Evaluation of the Borregas and Seeligson Fields, Brooks and Jim Wells Counties, Texas," paper 591-G presented at the 1955 AIME Formation Evaluation Symposium, Houston, Oct. 27-28.
- Cornell, D. and Katz, D.L.: "Flow of Gases Through Consolidated Porous Media," *Ind. and Engr. Chem.* (Oct. 1953) **45**.
- Wyllie, M.R.J. and Gardner, G.H.F.: "The Generalized Kozeny Carman Equation," *World Oil* (March and April 1958).
- Winsauer, W.O. et al.: "Resistivity of Brine-Saturated Sands in Relation to Pore Geometry," *Bull., AAPG* (Feb. 1952) 253-77.
- Rust, C.F.: "Electrical Resistivity Measurements on Reservoir Rock Samples by the Two-Electrode and Four-Electrode Methods," *Trans., AIME* (1952) **195**, 217-24.
- Tixier, M.P.: "Porosity Index in Limestone from Electrical Logs—Part 1," *Oil and Gas J.* (Nov. 15, 1951) 140.
- Wyllie, M.R.J. and Gregory, A.R.: "Formation Factors of Unconsolidated Porous Media: Influence of Particle Shape and Effect of Cementation," *Trans., AIME* (1953) **198**, 103-09.
- de Witte, A.J.: "Saturation and Porosity from Electrical Logs in Shaly Sands—Part 1," *Oil and Gas J.* (March 4, 1957) 89.
- Hill, H.J. and Milburn, J.D.: "Effect of Clay and Water Salinity on Electrochemical Behavior of Reservoir Rocks," *Trans., AIME* (1956) **207**, 65-72.

Chapter 27

Typical Core Analysis of Different Formations

R.E. Jenkins. Core Laboratories Inc.*

Introduction

The early-day analysis of cores was largely an art, a qualitative matter of odors and tastes, sucking on the rock, and visual examination. The science of core analysis has evolved from such early beginnings, using developments in instrumental methods of chemical and physical analyses as they became available. Electron microscopy, mass spectrometry, gas chromatography, high-frequency phase analysis, acoustic wave train analysis, and nuclear magnetic relaxation analysis are among the tools being used in the more sophisticated core testing today.

Many other techniques are available now to assist the geologist and petroleum engineer in the completion of wells and the evaluation and operation of oil and gas reservoirs, but core analysis still remains the basic tool for obtaining reliable information on the rock material penetrated. Study of representative core samples of an oil- or gas-bearing formation provides the only means for direct measurement of many important properties of the formation.

The minimum basic measurements made on cores generally comprise determination of porosity at no confining pressure, permeability at low confining pressure, and residual fluid saturations. Various supplementary routine tests such as chloride, oil gravity, directional permeability, grain density, and grain size frequently are made as an aid in interpretation and evaluation. These data are the subject of this chapter.

Porosity

Porosity is a measure of the void space or storage capacity of a reservoir material. Normally it is expressed as a percentage of bulk volume (%BV). Porosity may be determined by measurement of any two of the three quantities—grain volume, void volume, and bulk volume. Various generally acceptable methods and techniques for determining porosity are used by different laboratories. The void volume may be determined on a previously cleaned and dried sample by extraction or gas or air con-

tent, by saturation with a liquid, or by calculation from Boyle's law upon compression or expansion of gas in the pore spaces of the sample. The other widely used method involves the separate determination of the gas, oil, and water contents of the sample, and the summation of these three values to obtain PV.

Most of the porosity data reported in the tables here were determined by the *summation-of-fluids* method. Comparison of porosity values obtained on samples from several thousand feet of core where measurements were made by both the *summation-of-fluids* method and by a *Boyle's law* method showed agreements, in general, of 0.1 to 0.5% porosity. Extensive checks of porosity values by resaturation with brine have shown values slightly lower than by the other procedures, indicating approximately 98 to 99% resaturation.

Permeability

The permeability of a formation sample is a measure of its ability to transmit fluid. The permeability determination involves measurement of the rate of flow of a fluid of known viscosity through a shaped sample under a measured pressure differential. Air is the fluid normally used because of its convenience, availability, and relative inertness toward the core material. For many years, air-permeability measurements were corrected to an "equivalent" liquid permeability by use of the well-known Klinkenberg corrections. The permeability values reported in Tables 27.1 through 27.11 have been corrected to the "equivalent" liquid-permeability values, except as noted in the next paragraph.

In the whole-core or *full-diameter* core analysis procedures, permeability is frequently measured in two horizontal directions. One measurement is made in the direction of the major fracture planes and is reported as *k*. This value indicates the effectiveness of the fractures as flow channels. The core sample is then rotated 90° and the second measurement is made in a direction of flow perpendicular to the direction of the first measurement. This

(continued on page 9)

* Author of the original chapter on this topic was E.H. Koepf.

TABLE 27.1—ARKANSAS

Formation	Fluid Production	Range of Production Depth (ft)	Average Production Depth (ft)	Range of Production Thickness (ft)	Average Production Thickness (ft)	Range of Permeability (md)
Blossom	C/O*	2,190 to 2,655	2,422	3 to 28	15	1.6 to 8,900
Cotton Valley	C/O	5,530 to 8,020	6,774	4 to 79	20	0.6 to 4,820
Glen Rose	O	2,470 to 3,835	3,052	5 to 15	10	1.6 to 5,550
Graves	C/O	2,400 to 2,725	2,564	2 to 26	11	1.2 to 4,645
Hogg	O	3,145 to 3,245	3,195	12 to 33	17	6.5 to 5,730
Meakin	G/C/O*	2,270 to 2,605	2,485	2 to 20	11	3.0 to 6,525
Nacatoch	C/O	1,610 to 2,392	2,000	6 to 45	20	0.7 to 6,930
Paluxy	O	2,850 to 4,890	3,868	6 to 17	12	5 to 13,700
Pettit	O	4,010 to 5,855	4,933	4 to 19	11	0.1 to 698
Rodessa [†]	O	5,990 to 6,120	6,050	8 to 52	16	0.1 to 980
Smackover [‡]	G/C/O	6,340 to 9,330	8,260	2 to 74	18	0.1 to 12,600
Tokio	C/O	2,324 to 2,955	2,640	2 to 19	13	0.5 to 11,500
Travis Peak	C/O	2,695 to 5,185	3,275	3 to 25	10	0.4 to 6,040
Tuscaloosa	C/O	3,020 to 3,140	3,080	4 to 25	15	0.4 to 3,760

*Indicates fluid produced: G = gas; C = condensate; O = oil.

**Specific zone not identified locally.

†Includes data from Mitchell and Gloyd zones.

‡Includes data from Smackover Lime and Reynolds zones.

TABLE 27.2—EAST TEXAS AREA

Formation	Fluid Production	Range of Production Depth (ft)	Average Production Depth (ft)	Range of Production Thickness (ft)	Average Production Thickness (ft)	Range of Permeability (md)
Bacon	C/O	6,685 to 7,961	7,138	3 to 24	11	0.1 to 2,040
Cotton Valley	C	8,448 to 8,647	8,458	7 to 59	33	0.1 to 352
Fredericksburg	O	2,330 to 2,374	2,356	5 to 8	7	0.1 to 4.6
Gloyd	C/O	4,812 to 6,971	5,897	3 to 35	19	0.1 to 560
Henderson	G/C/O	5,976 to 6,082	6,020	3 to 52	12	0.1 to 490
Hill	C/O	4,799 to 7,668	5,928	3 to 16	9	0.1 to 467
Mitchell	O	5,941 to 6,095	6,010	3 to 43	21	0.1 to 487
Mooringsport	O	3,742 to 3,859	3,801	4 to 12	8	0.4 to 55
Nacatoch*	O	479 to 1,091	743	2 to 21	12	1.9 to 4,270
Paluxy	O	4,159 to 7,867	5,413	7 to 46	27	0.1 to 9,600
Pecan Gap	O	1,233 to 1,636	1,434	5 to 20	13	0.5 to 55
Pettit**	G/C/O	5,967 to 8,379	7,173	2 to 23	11	0.1 to 3,670
Rodessa	C/O	4,790 to 8,756	6,765	4 to 42	17	0.1 to 1,180
Sub-Clarksville [†]	O	3,940 to 5,844	4,892	3 to 25	12	0.1 to 9,460
Travis Peak [‡]	C/O	5,909 to 8,292	6,551	2 to 30	11	0.1 to 180
Wolfe City	O	981 to 2,054	1,517	6 to 22	13	0.3 to 470
Woodbine	C/O	2,753 to 5,993	4,373	2 to 45	14	0.1 to 13,840
Young	C	5,446 to 7,075	6,261	4 to 33	17	0.1 to 610

*Small amount of Navarro data combined with Nacatoch.

**Data for Pittsburg, Potter, and upper Pettit combined with Pettit.

†Small amount of Eagleford data combined with sub-Clarksville.

‡Data for Page combined with Travis Peak.

TABLE 27.1—ARKANSAS (continued)

Average Permeability (md)	Range of Porosity (%)	Average Porosity (%)	Range of Oil Saturation (%)	Average Oil Saturation (%)	Range of Calculated Interstitial-Water Saturation (%)	Average Calculated Interstitial-Water Saturation (%)
1,685	15.3 to 40	32.4	1.2 to 36	20.1	24 to 55	32
333	11.3 to 34	20.3	0.9 to 37	13.1	21 to 43	35
732	17.3 to 38	23.4	4.0 to 52	21.0	28 to 50	38
1,380	9.8 to 40	34.9	0.3 to 29	16.8	19 to 34	30
1,975	14.4 to 41	30.9	2.6 to 56	19.9	26 to 34	27
1,150	17.1 to 40	31.8	0.6 to 43	12.9	24 to 63	43
142	9.9 to 41	30.5	0.2 to 52	4.9	41 to 70	54
1,213	15.1 to 32	26.9	7.5 to 49	21.2	28 to 43	35
61	6.2 to 28	15.4	9.1 to 29	12.7	25 to 44	30
135	5.1 to 28	16.5	0.7 to 26	14.8	25 to 38	31
850	1.1 to 34	14.2	0.7 to 41	12.8	21 to 50	31
2,100	13.6 to 42	32.1	0.9 to 57	25.6	17 to 43	27
460	9.4 to 36	24.3	0.5 to 36	14.3	16 to 48	36
506	15.6 to 39	27.3	0.3 to 53	14.0	31 to 63	45

TABLE 27.2—EAST TEXAS AREA (continued)

Average Permeability (md)	Range of Porosity (%)	Average Porosity (%)	Range of Oil Saturation (%)	Average Oil Saturation (%)	Range of Calculated Interstitial-Water Saturation (%)	Average Calculated Interstitial-Water Saturation (%)
113	1.5 to 24.3	15.2	2.7 to 20.6	8.6	9 to 22	16
39	6.9 to 17.7	11.7	1.1 to 11.6	2.5	13 to 32	25
1.2	11.9 to 32.8	23.1	3.3 to 39.0	20.8	35 to 43	41
21	8.0 to 24.0	14.9	trace to 24.3	8.2	16 to 45	31
19	7.0 to 26.2	15.2	0.8 to 23.3	10.6	21 to 44	27
70	6.4 to 32.2	15.6	0.9 to 26.7	12.2	23 to 47	33
33	7.2 to 29.0	15.5	1.8 to 25.9	12.5	15 to 47	29
5	5.3 to 19.6	14.6	2.8 to 26.6	13.8	29 to 48	40
467	13.4 to 40.9	27.1	0.6 to 37.4	14.5	24 to 55	41
732	6.3 to 31.1	21.6	2.2 to 48.7	24.1	22 to 47	30
6	16.3 to 38.1	26.6	3.5 to 49.8	12.9	30 to 56	46
65	4.5 to 25.8	14.7	0.9 to 31.6	9.8	10 to 35	23
51	2.3 to 29.0	14.5	trace to 25.3	5.3	6 to 42	23
599	8.2 to 38.0	24.8	1.4 to 34.6	17.9	12 to 60	33
42	5.6 to 25.8	15.0	0.1 to 42.8	12.5	17 to 38	28
32	17.1 to 38.4	27.9	1.5 to 37.4	15.6	23 to 68	46
1,185	9.7 to 38.2	25.5	0.7 to 35.7	14.5	14 to 65	35
112	4.4 to 29.8	19.7	trace to 4.5	0.8	13 to 27	21

TABLE 27.3—NORTH LOUISIANA AREA

Formation	Fluid Production	Range of Production Depth (ft)	Average Production Depth (ft)	Range of Production Thickness (ft)	Average Production Thickness (ft)	Range of Permeability (md)
Annona Chalk	O	1,362 to 1,594	1,480	15 to 69	42	0.1 to 2.5
Buckrange	C/O	1,908 to 2,877	2,393	2 to 24	13	0.1 to 2,430
Cotton Valley ^a	G/C/O	3,650 to 9,450	7,450	4 to 37	20	0.1 to 7,350
Eagleford ^b	C	8,376 to 8,417	8,397	9 to 11	10	3.5 to 3,040
Fredericksburg	G/C	6,610 to 9,880	8,220	6 to 8	7	1.6 to 163
Haynesville	C	10,380 to 10,530	10,420	22 to 59	40	0.1 to 235
Hosston	C/O	5,420 to 7,565	6,480	5 to 15	12	0.4 to 1,500
Nacatoch	O	1,223 to 2,176	1,700	6 to 12	8	27 to 5,900
Paluxy	C/O	2,195 to 3,240	2,717	2 to 28	16	0.2 to 3,060
Pettit ^c	C/O	3,995 to 7,070	5,690	3 to 30	14	0.1 to 587
Pine Island ^d	O	4,960 to 5,060	5,010	5 to 13	9	0.2 to 1,100
Rodessa ^e	G/C/O	3,625 to 5,650	4,860	6 to 52	18	0.1 to 2,190
Schuler ^f	G/C/O	5,500 to 9,190	8,450	4 to 51	19	0.1 to 3,180
Sligo ^g	C/O	2,685 to 5,400	4,500	3 to 21	7	0.1 to 1,810
Smackover	C/O	9,960 to 10,790	10,360	6 to 55	24	0.1 to 6,190
Travis Peak ^h	C/O	5,890 to 7,900	6,895	7 to 35	18	0.1 to 2,920
Tuscaloosa	G/C/O	2,645 to 9,680	5,164	4 to 44	24	0.1 to 5,750

^a Data reported where member formation of Cotton Valley group not readily identifiable.^b Data reported as Eutaw in some areas.^c Includes data reported as Pettit, Upper Pettit, and Mid-Pettit, sometimes considered the same as Sligo.^d Sometimes referred to as Woodruff.^e Includes data reported locally for Jeter, Hill, Kilpatrick, and Fowler zones.^f Includes data reported locally for Bodcaw, Vaughn, Doris, McFerrin, and Justiss zones.^g Includes data reported as Birdsong-Owens.^h Frequently considered the same as Hosston.

TABLE 27.4—CALIFORNIA

Formation	Area	Fluid Production	Range of Production Depth (ft)	Average Production Depth (ft)	Range of Production Thickness (ft)	Average Production Thickness (ft)	Range of Permeability (md)	Average Permeability (md)
Eocene, lower	San Joaquin Valley ^a	O	6,820 to 8,263	7,940	—	—	35 to 2,000	518
Miocene	Los Angeles Basin and Coastal ^b	O	2,870 to 9,530	5,300	60 to 450	165	10 to 4,000	300
Miocene, upper	San Joaquin Valley ^c		1,940 to 7,340	4,210	10 to 1,200	245	4 to 7,500	1,000
	Los Angeles Basin and Coastal ^d	O	2,520 to 6,860	4,100	5 to 1,040	130	86 to 5,000	1,110
Miocene, lower	San Joaquin Valley ^e	O	2,770 to 7,590	5,300	30 to 154	76	15 to 4,000	700
	Los Angeles Basin and Coastal ^f	O	3,604 to 5,610	4,430	20 to 380	134	256 to 1,460	842
Oligocene	San Joaquin Valley ^g	O	4,589 to 4,717	4,639	—	—	10 to 2,000	528
	Coastal ^h	O	5,836 to 6,170	6,090	—	—	20 to 400	107
Pliocene	San Joaquin Valley ⁱ	O	2,456 to 3,372	2,730	5 to 80	33	279 to 9,400	1,250
	Los Angeles Basin and Coastal ^j	O	2,050 to 3,450	2,680	—	100	25 to 4,500	1,410

^a Mainly data from Gatchell zone.^b Includes Upper and Lower Terminal, Union Pacific, Ford, 237, and Seson zones.^c Includes Kernco, Republic, and 26R zones.^d Includes Jones and Main zones.^e Includes JV, Olcese, and Phacoides zones.^f Mainly data from Vaqueros zone.^g Mainly data from Oceanic zone.^h Mainly data from Sespe zone.ⁱ Includes Sub Mulina and Sub Salez No. 1 and No. 2 zones.^j Includes Ranger and Tar zones.^k Oil-based data show high oil saturation (average 61%) and low water (3 to 54%, average 15%).^l Oil-based data show range 27.6 to 52.4 and average of 42.3% not included in above oil saturation values.

TABLE 27.3—NORTH LOUISIANA AREA (continued)

Average Permeability (md)	Range of Porosity (%)	Average Porosity (%)	Range of Oil Saturation (%)	Average Oil Saturation (%)	Range of Calculated Interstitial-Water Saturation (%)	Average Calculated Interstitial-Water Saturation (%)
0.7	14.3 to 36.4	26.8	6.0 to 40	22.0	24 to 40	37
305	13.4 to 41	31.4	0.7 to 51	22.6	29 to 47	35
135	3.5 to 34	13.1	0.0 to 14	3.1	11 to 40	24
595	12.8 to 28	22.9	1.6 to 28	4.3	—	36
90	12.8 to 23.1	19.9	1.7 to 4.3	2.7	35 to 49	41
32	5.5 to 23.1	13.4	1.1 to 14.5	5.1	31 to 41	38
140	8.8 to 29	18.6	0.0 to 35	8.8	18 to 37	28
447	25.8 to 40	31.4	2.5 to 33	19.5	45 to 54	47
490	9.6 to 39	27.2	0.1 to 48	11.8	23 to 55	35
26	4.5 to 27	14.3	0.1 to 59	15.6	10 to 43	29
285	8.5 to 27	20.6	13.3 to 37	24.1	16 to 30	22
265	5.1 to 34	19.1	0.0 to 31	2.9	21 to 38	30
104	3.6 to 27.4	15.0	0.0 to 24	4.8	8 to 51	25
158	7.3 to 35	21.1	0.6 to 27	9.8	12 to 47	31
220	3.4 to 23	12.9	1.1 to 22	7.2	9 to 47	25
357	7.0 to 27	19.4	0.1 to 35	8.6	26 to 38	31
706	10.7 to 36	27.6	0.0 to 37	8.5	31 to 61	43

TABLE 27.4—CALIFORNIA (continued)

Range of Porosity (%)	Average Porosity (%)	Range of Oil Saturation (%)	Average Oil Saturation (%)	Range of Total Water Saturation (%)	Average Total Water Saturation (%)	Range of Calculated Interstitial-Water Saturation (%)	Average Calculated Interstitial-Water Saturation (%)	Range of Gravity (°API)	Average Gravity (°API)
14 to 26	20.7	8 to 23	14.1	16 to 51	35	15 to 49	35	28 to 34	31
15 to 40	28.5	6 to 65	18.8	25 to 77	50	15 to 72	36	15 to 32	26
17 to 40	28.2	9 to 72	32 ^k	20 to 68 ^k	50 ^k	12 to 62	30	13 to 34	23
19.5 to 39	30.8	10 to 55	25	22 to 72	44	12 to 61	30	11 to 33	21
20 to 38	28.4	4 to 40	19	25 to 80	51	14 to 67	36	15 to 40	34
21 to 29	24.3	13 to 20	15.8	32 to 67	53	27 to 60	37	34 to 36	35
19 to 34	26.3	12 to 40	22	2 to 60	43	3 to 45	30	37 to 38	38
15 to 22	19.5	6 to 17	11.8	19 to 56	46	15 to 52	42	—	25
30 to 38	34.8	7 to 43 ^l	24.1 ^l	33 to 84	54	10 to 61	34	18 to 44	24
24 to 41	35.6	15 to 80	45	19 to 54	38	10 to 40	21	12 to 23	15

TABLE 27.5—TEXAS GULF COAST—CORPUS CHRISTI AREA*

Formation	Fluid Production	Range of Production Depth (ft)	Average Production Depth (ft)	Range of Production Thickness (ft)	Average Production Thickness (ft)	Range of Permeability (md)	Average Permeability (md)
Catahoula	O	3,600 to 4,800	3,900	1 to 18	8	45 to 2,500	670
Frito	C/O	1,400 to 9,000	6,100	3 to 57	13	5 to 9,000	460
Jackson	O	600 to 5,000	3,100	2 to 23	9	5 to 2,900	350
Marginulina	C	6,500 to 7,300	7,000	5 to 10	7	7 to 300	75
Oakville	O	2,400 to 3,100	2,750	5 to 35	22	25 to 1,800	700
Vicksburg	C/O	3,000 to 9,000	6,200	4 to 38	12	4 to 2,900	220
Wilcox	C	6,000 to 8,000	7,200	30 to 120	60	1 to 380	50
Yegua	O	1,800 to 4,000	3,000	3 to 21	7	6 to 1,900	390

*Includes counties in Texas Railroad Commission Dist. 4: Jim Wells, San Patricio, Webb, Brooks, Nueces, Jim Hogg, Hidalgo, Willacy, Starr, Aransas, and Duval.

TABLE 27.6—TEXAS GULF COAST—HOUSTON AREA

Formation	Fluid Production	Range of Production Depth (ft)	Average Production Depth (ft)	Range of Production Thickness (ft)	Average Production Thickness (ft)	Range of Permeability (md)	Average Permeability (md)
Frio	C	4,000 to 11,500	8,400	2 to 50	12.3	18 to 9,200	810
	O	4,600 to 11,200	7,800	2 to 34	10.4	33 to 9,900	1,100
Marginulina	C	7,100 to 8,300	7,800	4 to 28	17.5	308 to 3,870	2,340
	O	4,700 to 6,000	5,400	4 to 10	5.7	355 to 1,210	490
Miocene	C	2,900 to 6,000	4,000	3 to 8	5.5	124 to 13,100	2,970
	O	2,400 to 8,500	3,700	2 to 18	7.2	71 to 7,660	2,140
Vicksburg	C	7,400 to 8,500	8,100	1 to 6	2.0	50 to 105	86
	O	6,900 to 8,200	7,400	3 to 18	9.3	190 to 1,510	626
Wilcox	C	5,800 to 11,500	9,100	5 to 94	19.1	3.0 to 1,880	96
	O	2,300 to 10,200	7,900	3 to 29	10.0	9.0 to 2,460	195
Woodbine	O	4,100 to 4,400	4,300	6 to 13	8.2	14 to 680	368
Yegua	G/C	4,400 to 8,700	6,800	3 to 63	11.0	24 to 5,040	750
	O	3,700 to 9,700	6,600	2 to 59	8.5	23 to 4,890	903

TABLE 27.7—LOUISIANA GULF COAST

Formation	Fluid Production	Range of Production Depth (ft)	Average Production Depth (ft)	Range of Production Thickness (ft)	Average Production Thickness (ft)	Range of Permeability (md)	Average Permeability (md)
Miocene	C	5,200 to 14,900	11,200	3 to 98	20.2	36 to 6,180	1,010
	O	2,700 to 12,700	9,000	3 to 32	11.0	45 to 9,470	1,630
Oligocene	C	7,300 to 14,600	9,800	2 to 80	14.6	18 to 5,730	920
	O	6,700 to 12,000	9,400	2 to 39	8.3	64 to 5,410	1,410
Tuscaloosa	G/C	17,533 to 18,906	17,742	15 to 94	61	1 to 2,000	139

*Water saturations from logs.

TABLE 27.5—TEXAS GULF COAST—CORPUS CHRISTI AREA (continued)

Range of Porosity (%)	Average Porosity (%)	Range of Oil Saturation (%)	Average Oil Saturation (%)	Range of Calculated Interstitial-Water Saturation (%)	Average Calculated Interstitial-Water Saturation (%)	Range of Gravity (°API)	Average Gravity (°API)
17 to 36	30	1 to 30	14	30 to 44	36	23 to 30	29
11 to 37	27	2 to 38	13	20 to 59	34	23 to 48	41
16 to 38	27	3 to 32	15	21 to 70	45	22 to 48	37
14 to 30	24	1 to 4	2	20 to 48	34	55 to 68	60
21 to 35	28	9 to 30	18	32 to 48	44	23 to 26	25
14 to 32	24	1 to 17	7	26 to 54	38	37 to 65	48
15 to 25	19	0 to 10	1	22 to 65	37	53 to 63	58
22 to 38	29	4 to 40	17	14 to 48	36	20 to 40	32

TABLE 27.6—TEXAS GULF COAST—HOUSTON AREA (continued)

Range of Porosity (%)	Average Porosity (%)	Range of Oil Saturation (%)	Average Oil Saturation (%)	Range of Total Water Saturation (%)	Average Total Water Saturation (%)	Range of Calculated Interstitial-Water Saturation (%)	Average Calculated Interstitial-Water Saturation (%)	Range of Gravity (°API)	Average Gravity (°API)
18.3 to 38.4	28.6	0.1 to 6.0	1.0	34 to 72	54	20 to 63	34		
21.8 to 37.1	29.8	4.6 to 41.2	13.5	24 to 79	52	12 to 61	33	25 to 42	36
35.0 to 37.0	35.9	0.2 to 0.8	0.5	33 to 61	46	14 to 31	21		
28.5 to 37.3	32.6	8.1 to 21.8	15.3	48 to 68	59	25 to 47	36	25 to 30	28
28.6 to 37.6	33.2	0.2 to 1.5	0.5	55 to 73	66	23 to 53	38		
23.5 to 38.1	35.2	11.0 to 29.0	16.6	45 to 69	58	21 to 55	34	21 to 34	25
26.5 to 31.0	27.1	0.0 to 1.5	0.2	66 to 78	74	53 to 61	56		
29.5 to 31.8	30.4	14.4 to 20.3	15.3	45 to 55	53	26 to 36	35	22 to 37	35
14.5 to 27.4	19.6	0.2 to 10.0	1.5	27 to 62	46	20 to 54	38		
16.2 to 34.0	21.9	4.6 to 20.5	9.7	32 to 72	47	20 to 50	37	19 to 42	34
23.5 to 28.7	25.5	10.7 to 27.4	20.1	34.4 to 72.7	46	24 to 59	36	26 to 28	27
23.4 to 37.8	30.7	0.1 to 15.5	1.2	26 to 74	57	17 to 59	33		
22.9 to 38.5	31.6	3.5 to 21.8	11.4	31 to 73	57	17 to 53	34	30 to 46	37

TABLE 27.7—LOUISIANA GULF COAST (continued)

Range of Porosity (%)	Average Porosity (%)	Range of Oil Saturation (%)	Average Oil Saturation (%)	Range of Total Water Saturation (%)	Average Total Water Saturation (%)	Range of Calculated Interstitial-Water Saturation (%)	Average Calculated Interstitial-Water Saturation (%)	Range of Gravity (°API)	Average Gravity (°API)
15.7 to 37.6	27.3	0.1 to 4.7	1.5	37 to 79	53	20 to 74	35	—	—
18.3 to 39.0	30.0	6.5 to 26.9	14.3	30 to 72	51	18 to 50	32	25 to 42	36
16.7 to 37.6	27.7	0.5 to 8.9	2.3	33 to 71	51	19 to 57	32	—	—
22.1 to 36.2	29.0	5.2 to 20.0	11.1	34 to 70	54	23 to 60	35	29 to 44	38
5 to 29	18	26* to 44*	—	38 to 60	40*	55	—	40 to 53	47

TABLE 27.8—COMPARATIVE DATA—SIDEWALL (S.W.) VS. CONVENTIONAL (CONV.) ANALYSIS, TEXAS AND LOUISIANA GULF COAST AREAS

Formation	Area	Fluid Production	Type Analysis	Average Depth (ft)	Average Permeability (md)	Average Porosity (%)	Average Oil Saturation (% pore space)	Average Total Water Saturation (% pore space)
Frio	Houston	C	S.W.	8,945	62	27.5	0.7	64
			Conv.	9,037	813	26.7	0.7	49
		O	S.W.	7,174	317	30.8	14.6	56
	Corpus Christi	C	Conv.	8,622	1,895	27.7	14.6	47
			S.W.	4,902	238	27.2	0.8	64
		O	Conv.	6,789	1,496	28.5	1.1	53
Yegua (includes Cockfield)	Louisiana	C	S.W.	5,456	681	29.5	19.5	53
			Conv.	6,399	641	28.5	16.3	51
			S.W.	8,148	75	27.3	4.2	69
		O	Conv.	8,826	235	26.8	1.9	60
			S.W.	8,276	176	27.1	10.0	63
			Conv.	8,415	791	28.7	7.9	56
	Houston	C	S.W.	7,240	147	27.9	0.2	62
			Conv.	7,693	277	29.7	0.7	55
		O	S.W.	7,369	302	29.9	10.5	59
	Corpus Christi	C	Conv.	7,099	603	31.6	11.7	58
			S.W.	3,861	119	26.8	3.2	68
		O	Conv.	4,194	558	31.8	1.7	65
Miocene (includes Catahoula)	Louisiana	C	S.W.	2,824	634	33.3	20.9	53
			Conv.	3,625	576	31.8	19.9	57
			S.W.	10,664	312	28.2	2.5	63
		O	Conv.	11,500	748	27.4	2.1	52
			S.W.	8,996	327	28.2	10.1	62
			Conv.	10,171	1,300	26.6	14.8	49
	Corpus Christi	C	S.W.	4,286	180	28.5	0.5	69
			Conv.	4,040	578	29.0	0.7	61
		O	S.W.	4,504	346	30.4	17.7	60
			Conv.	4,383	867	29.8	20.0	53

second value is normally reported as k_{90} , and it is usually representative of the matrix permeability. Values for k_{90} are reported in the following tables for formations that are normally subjected to the whole-core or full-diameter core analysis procedures. These values are not corrected to "equivalent" liquid-permeability values.

Liquid Saturations

In the coring process, the core is exposed to the drilling fluid at a pressure greater than formation pressure. If the core contains oil or gas, some portion of this is flushed out and replaced by the drilling-fluid filtrate. As the core is brought to the surface and the external pressure is reduced, the expansion of free gas or dissolved gas expels both oil and water from the core. As a result, the pore spaces of the cores recovered at the surface contain free gas, water, and oil if oil is present in situ. The oil and water contents normally are called "*residual liquids*."

The residual oil and water contents of core samples normally are determined by retorting, vacuum distillation, or solvent extraction and distillation. The oil and water contents are converted to oil and water saturations as percentages of PV. The oil and water saturation values reported in these tables represent data obtained by the retorting or the vacuum distillation procedures.

The water content of the core as recovered is generally called "*total water*," and it may include some drilling-fluid filtrate or invasion water. The water saturation actually existing at a given interval in a reservoir may be spoken of as the *connate water* or *interstitial water*. This interstitial-water saturation value, as reported in the ta-

bles, was determined in some cases by an empirical correlation factor applied to the total water value and in some cases by the use of capillary-pressure data for the specific reservoirs.

The API oil gravity values reported normally were measured on the oil recovered in the retorting or vacuum-distillation procedures. Comparison of gravity values obtained in oil recovered from cores with values obtained on produced or drillstem test (DST) oil indicates general agreement to within $\pm 2^\circ$ API.

The liquid saturation data presented in the tables are from formations interpreted to be hydrocarbon-productive to some degree. In some cases, it was feasible to make a distinction between gas-, condensate-, and oil-productive zone characteristics. Table 27.9 shows core analysis data for zones identified as "transition" zones. These represent intervals or zones where an appreciable water cut is encountered during the life of a field. Such transition zones are present in many other areas and fields, but the available data did not permit a similar breakdown. It should be pointed out that the relative average depths reported for the gas-condensate, oil, and transition zones do not contradict the basic premises that gas overlies oil and that oil overlies water. The condensate-producing zones in the major formations in the U.S. gulf coast area, as presented in Tables 27.6 and 27.7, frequently are found at greater depths than are the oil-producing zones of the same formations. In a similar manner, the gas, oil, and transition zones shown in Table 27.9 for the extensive geologic groups and formations in the Oklahoma-Kansas area are found at different subsurface depths in different parts of the area.

Percussion Sidewall Core Data

Percussion sidewall sampling is used extensively in the U.S. gulf coast area, and in other areas where productive intervals are encountered in relatively soft formations and where this type of coring has been found satisfactory. The limited size of the individual samples has made it necessary to develop special procedures for handling and measuring the properties and fluid contents of these samples. Also, the percussion-sampling technique and the limitation of sampling to a small distance from the walls of the wellbore frequently result in questions of the degree to which sidewall core analysis data compare with data obtained on conventional wireline or diamond cores. Table 27.8 summarizes a study of core analysis results from more than 5,300 samples where approximately half were obtained by percussion-type sidewall sampling and the other half were obtained by conventional coring procedures.

Data From U.S. Areas

Data from areas in the U.S. including Alaska, are presented in Tables 27.1 through 27.12. The formation and zone

names were selected in an effort to represent generally recognized nomenclature over large areas rather than local terminology. Some important producing formations are not included because of the lack of sufficient data at this time or because of their proprietary nature.

Data From Non-U.S. Areas

The data from non-U.S. areas generally are lacking in pore liquid saturation values because of the formation evaluation practices in general use. The small quantity of data reported is a result of the problems of data being released. Data from Australia are presented in Table 27.13. Most of the Canadian data (Table 27.14) were provided by the Energy Resources Conservation Board of Alberta. The Middle East data are presented in Table 27.15. The North Sea data (Table 27.16) were published in the *European Continental Shelf Guide*.¹ Venezuela data presented in Table 27.17 were provided by Petroleum de Venezuela S.A.

Reference

1. *European Continental Shelf Guide*, Oilfield Publications Ltd., Ledbury, Herefordshire, England (1982).

TABLE 27.9—OKLAHOMA-KANSAS AREA^a

Formation	Fluid Production	Range of Production Depth (ft)	Average Production Depth (ft)	Range of Production Thickness (ft)	Average Production Thickness (ft)	Range of Permeability (md)	Average Permeability (md)	Range of Permeability, k_{90} (md)
Arbuckle	G	2,700 to 5,900	4,500	5.0 to 37	18.3	3.2 to 544	131	—
	O	500 to 6,900	3,500	1.0 to 65.5	11.8	0.2 to 1,530	140	0.1 to 1,270
	T ^b	800 to 11,600	3,600	2.0 to 33	14.3	0.1 to 354	57	0.1 to 135
Atoka ^c	G	3,700 to 3,800	3,700	1.0 to 9.0	4.0	1.3 to 609	174	—
	O	500 to 4,500	2,600	3.0 to 16	7.8	0.3 to 920	144	0.6 to 2.8
	T	300 to 3,700	2,100	2.0 to 10	6.5	9 to 166	67.3	—
Bartlesville	G	700 to 7,400	2,600	1.5 to 42	11.4	0.2 to 36	10.4	5.5
	O	200 to 5,700	1,500	1.0 to 72	14.0	0.2 to 537	32.7	1.5
	T	500 to 2,600	1,200	4 to 40	14.5	0.1 to 83	18.2	0.07
Bois D'Arc	G	4,800 to 5,100	5,000	4 to 48	19.0	0.1 to 43	24.4	—
	O	3,700 to 7,800	6,500	2.3 to 50	12.5	0.3 to 664	36.0	0.1 to 2.2
Booch	G	2,600 to 3,200	2,900	5 to 8	6.5	1.4 to 6.6	4.0	—
	O	1,000 to 3,800	2,600	2 to 26.5	8.8	0.3 to 160	19.3	—
	T	2,700 to 3,300	3,000	4 to 5	4.5	3.1 to 13	8.0	—
Burgess	G	—	1,600	—	20	—	142	—
	O	300 to 2,800	1,800	2.5 to 9	5.8	0.2 to 104	19	22
First Bromide ^d	G	6,800 to 7,600	7,200	3.0 to 19.5	11.3	0.6 to 62	31.3	0.4
	O	3,700 to 13,800	8,600	2.0 to 82	18.7	0.1 to 2,280	175	0.2 to 7.4
	T	6,000 to 13,200	11,500	15 to 161.3	65.1	0.9 to 40	18.3	1.40
Second Bromide ^e	G	6,900 to 16,200	12,800	20 to 53.6	37.9	3.4 to 72	21.4	0.3 to 0.9
	O	4,500 to 11,200	9,000	3.0 to 69	16.2	2.0 to 585	118	—
	T	4,400 to 13,300	9,700	5 to 44.5	18.4	0.8 to 42	12.9	—
Burbank	O	1,300 to 4,500	2,800	3 to 48	17.3	0.1 to 226	8.64	—
	T	2,800 to 3,700	3,000	3 to 19	9.1	0.1 to 4.8	1.53	0.9 to 3.5
	G	4,200 to 6,700	5,700	2 to 45	10.9	0.1 to 269	33.0	0 to 0.5
Chester	O	4,700 to 6,700	5,700	2 to 23	8.6	0.1 to 61	9.11	0.1 to 5.0
	T	4,800 to 6,100	5,700	4 to 20.5	10.0	0.1 to 13	2.38	—
	G	2,200 to 5,700	3,500	2 to 17	9.0	2.5 to 338	50.6	1.4 to 2.3
Cleveland ^f	O	300 to 6,400	3,200	1 to 70	13.4	0.1 to 135	15.4	—
	T	1,900 to 3,900	3,100	3 to 22	7.7	0.1 to 112	12.9	0.80
	G	4,300 to 11,800	6,500	5 to 55	19.3	7.8 to 232	94.1	1.10
Deese ^g	O	600 to 10,000	5,200	2 to 60.3	11.7	0.4 to 694	62.8	—
	G	2,200 to 6,800	4,000	4 to 49	16.6	1.9 to 200	61.8	—
	O	1,800 to 2,100	2,000	3 to 37	11.9	1.3 to 974	288	—
Hoover	T	1,900 to 2,000	2,000	2 to 17	8.4	55 to 766	372	—
	G	3,800 to 8,800	6,300	9 to 11	10.0	6.4 to 61	33.7	—
	O	1,000 to 10,300	4,200	2 to 63	14.4	0.1 to 1,620	277	—
Hoxbar	T	2,900 to 3,000	3,000	3 to 13	9.3	0.5 to 31	14.4	0 to 77.0
	O	1,800 to 9,600	4,600	2 to 77.3	14.0	0.1 to 678	34.5	0.1 to 7.9
	T	2,500 to 8,700	4,900	2 to 73	14.7	0.1 to 48	5.3	0.3 to 162
Lansing	O	1,900 to 5,800	3,800	3 to 16.2	6.5	0.3 to 390	101	—
	T	—	3,300	—	22.0	—	14	—
Layton	G	700 to 6,100	3,900	4 to 18	9.3	0.2 to 210	26.3	0.5 to 162
	O	500 to 6,300	2,900	1 to 57	10.3	0.3 to 280	54.1	—
	T	1,800 to 5,700	3,200	3 to 15.5	7.4	1.1 to 143	23.8	0.20
Marmaton	O	4,300 to 4,600	4,400	1.5 to 7.5	4.7	24 to 105	46.4	—
	G	8,100	8,100	3 to 14	8.5	37 to 171	104	0 to 2.1
Misner	O	2,600 to 6,500	4,300	2 to 56.5	10.6	0.1 to 803	89.7	—
	T	4,900 to 6,200	6,000	8 to 21	15.8	0.1 to 120	41.8	0.2 to 74
	G	1,800 to 5,100	4,000	2 to 34.4	16.1	0.4 to 516	33.5	0 to 216
Mississippi Chat	O	800 to 5,200	3,100	2 to 48.1	12.2	0.1 to 361	21.9	0 to 163
	T	1,200 to 5,200	3,900	1 to 43	10.9	0.2 to 229	21.3	0.1 to 89
Mississippi Lime	G	900 to 8,800	4,600	3 to 27.1	13.3	0.1 to 129	22.2	0.1 to 185
	O	600 to 6,600	4,100	1.5 to 95.3	12.0	0.1 to 1,210	43.5	0.1 to 36
	T	400 to 7,200	4,000	4 to 70.1	17.4	0.1 to 135	7.5	—
McLish	G	3,600 to 17,000	10,100	14 to 58	35.3	12 to 98	48.0	—
	O	1,600 to 11,200	8,100	3 to 42	12.2	0.7 to 157	39.0	6.2 to 8.8

TABLE 27.9—OKLAHOMA-KANSAS AREA (continued)

Average Permeability, k_{90} (md)	Range of Porosity (%)	Average Porosity (%)	Range of Oil Saturation (%)	Average Oil Saturation (%)	Range of Total Water Saturation (%)	Average Total Water Saturation (%)	Range of Calculated Interstitial-Water Saturation (%)	Average Calculated Interstitial-Water Saturation (%)	Range of Gravity (°API)	Average Gravity (°API)
—	9.0 to 20.9	14.4	0.7 to 9.4	3.7	34.5 to 62.7	43.1	28 to 62	40	—	—
67.8	2.1 to 24.3	12.0	5.2 to 42.3	17.1	20.6 to 79.3	52.4	20 to 79	47	29 to 44	37
21.8	3.7 to 23.1	9.2	0 to 23.8	7.1	37.2 to 91.9	69.2	37 to 91	52	42	42
—	8.5 to 17.3	12.9	0 to 8.1	2.0	36.4 to 65.2	47.2	32 to 65	45	—	—
1.7	5.9 to 28.6	14.5	5.1 to 35.1	20.7	16.4 to 61.5	38.7	19 to 61	37	31 to 42	38
—	11.9 to 18.6	14.9	5.8 to 21.1	12.1	42.7 to 55.4	47.0	40	40	—	—
5.5	8.4 to 21.1	15.6	0 to 11.1	4.7	23.4 to 70.0	54.1	23 to 68	48	—	—
1.5	8.5 to 25.8	17.8	3.3 to 60.6	18.2	17.4 to 85.2	44.4	17 to 72	40	28 to 42	34
0.07	8.5 to 20.1	14.6	0.9 to 35.7	12.2	43.9 to 88.0	63.5	43 to 67	54	35	35
—	3.8 to 19.8	12.2	0 to 8.7	4.3	32.9 to 62.4	42.8	26 to 62	40	—	—
0.45	1.2 to 19.3	7.2	3.3 to 25.8	15.0	14.6 to 58.5	32.4	15 to 59	32	32 to 42	40
—	11.9 to 14.8	13.4	4.6 to 8.8	6.7	50.0 to 51.3	50.7	50	50	—	—
—	8.3 to 21.4	15.6	4.8 to 49.7	21.5	15.3 to 60.0	40.0	15 to 59	37	29 to 42	35
—	16.9 to 18.1	17.5	7.4 to 7.8	7.6	47.3 to 55.2	51.3	44	44	—	—
—	—	14.2	—	6.3	—	37.3	—	35	—	—
22	8.1 to 22.8	13.2	16.2 to 33	21.5	19.3 to 65.4	42.2	19 to 58	40	31 to 38	36
0.40	1.5 to 6.5	4.0	0 to 7.6	3.8	35.7 to 71.8	53.8	36 to 72	54	—	—
2.23	1.4 to 15.7	9.8	3.1 to 24	11	12.8 to 67.2	35.4	12 to 67	34	31 to 42	40
1.40	1.5 to 10.9	6.5	0.4 to 6.8	2.2	29.5 to 78.8	48.3	—	—	—	—
0.60	3.5 to 14.5	6.8	0 to 6.9	4.0	28.2 to 45.7	37.9	28 to 45	32	42	42
—	5.6 to 11.7	9.3	2.4 to 24.2	11.5	8.9 to 44.9	25.1	8 to 44	25	37 to 42	41
—	5.8 to 11.4	7.4	0 to 13.6	4.8	21.1 to 57.6	43.5	40	—	—	—
—	8.4 to 21.6	15.7	9.3 to 26.6	15.3	31.5 to 73.4	47.2	31 to 73	43	35 to 41	39
—	7.1 to 17.0	13.7	2.0 to 15.7	11.2	45.7 to 80.7	57.8	45 to 81	51	—	—
1.87	2.6 to 20.7	12.2	0 to 7.5	1.1	20.9 to 80.7	46.8	19 to 81	43	—	—
0.21	2.3 to 16.0	10.1	7.2 to 35.9	19.1	17.7 to 80.8	42.1	17 to 81	33	38 to 42	40
1.18	3.2 to 17.8	7.7	0 to 11.1	1.2	40.9 to 89.2	61.7	40 to 89	61	—	—
—	9.8 to 23.5	16.9	0 to 7.1	4.1	40.0 to 64.4	48.9	30 to 64	42	—	—
1.85	7.4 to 24.6	15.2	5.8 to 35.5	13.1	10.2 to 74.0	46.7	10 to 74	44	27 to 56	42
—	11.0 to 20.4	15.6	0 to 21.1	7.8	32.9 to 77.2	55.3	32 to 77	49	—	—
0.80	9.8 to 22.6	16.7	2.2 to 6.3	3.8	19.1 to 54.9	42.1	19 to 49	37	—	—
1.10	4.7 to 26.4	17.4	5.9 to 46.4	20.4	14.0 to 56.6	37.8	13 to 57	33	17 to 42	32
—	11.7 to 23.4	18.3	0 to 7.0	0.8	41.1 to 77.1	53.8	19 to 76	45	—	—
—	12.7 to 24.1	19.7	12.6 to 23.1	16.0	14.6 to 48.5	40.2	14 to 47	35	36 to 42	42
—	16.7 to 22.5	20.5	6.6 to 17.1	14.5	34.8 to 50.7	42.9	31 to 42	35	42	42
—	13.9 to 18.2	16.1	0.7 to 4.4	2.6	40.1 to 40.6	40.4	34 to 39	37	—	—
—	3.1 to 29.7	18.5	3.2 to 48.7	21.4	13.8 to 68.5	45.1	13 to 68	39	29 to 42	34
—	14.3 to 22.7	18.5	3.3 to 11.4	6.6	50.5 to 69.8	57.9	—	—	—	—
5.24	1.6 to 33.8	10.9	1.6 to 34.5	15.3	16.7 to 93.4	48.6	17 to 93	46	24 to 42	38
2.04	1.1 to 19.5	7.3	0 to 61.1	10.6	16.0 to 88.7	54.5	16 to 89	48	—	—
52.3	8.4 to 16.0	12.2	6.5 to 28.9	18.1	37.4 to 68.6	51.9	28 to 69	49	31 to 39	37
6.7	—	7.2	—	12.8	—	75.5	—	—	—	—
—	5.1 to 25.9	14.5	0 to 7.8	2.4	38.2 to 83.7	54.1	34 to 83	47	—	—
23.3	4.6 to 27.2	17.8	1.6 to 37.3	15.3	28.0 to 76.3	45.5	23 to 76	41	30 to 42	37
—	14.2 to 21.3	17.1	0 to 14.3	6.9	33.2 to 69.4	45.9	31 to 69	43	—	—
0.20	1.8 to 21.4	14.0	6.4 to 16.1	11.7	42.8 to 66.4	55.5	42 to 66	53	36 to 42	40
—	11.0 to 12.1	11.6	2.1 to 2.3	2.2	19.8 to 22.9	21.4	18 to 22	20	—	—
0.62	2.1 to 20.9	11.9	4.1 to 41.6	14.8	16.9 to 86.7	41.5	14 to 87	38	36 to 48	42
—	1.9 to 11.3	8.1	0 to 8.2	4.7	21.4 to 51.7	33.0	20 to 51	32	—	—
13.9	6.5 to 37.8	21.0	0 to 6.8	2.4	60.3 to 93.4	76.7	60 to 93	77	—	—
13.7	5.7 to 39.3	22.3	1.4 to 30.0	12.9	27.1 to 94.8	64.0	27 to 95	58	22 to 42	35
14.2	1.5 to 38.0	18.7	1.1 to 18.3	7.6	47.4 to 84.9	71.5	43 to 85	63	—	—
13.2	1.5 to 23.6	10.3	0 to 9.3	2.8	22.6 to 93.5	63.2	22 to 93	53	—	—
9.44	1.3 to 34.1	13.4	2.1 to 56.5	15.0	16.9 to 85.3	50.7	16 to 85	46	22 to 45	39
4.23	1.1 to 26.1	9.3	0 to 41.2	6.9	32.9 to 94.0	67.6	32 to 94	61	—	—
—	2.8 to 9.6	6.7	4.0 to 14.7	7.8	19.3 to 76.5	43.9	19 to 77	44	—	—
—	5.5 to 16.5	11.0	5.1 to 27.7	13.2	14.8 to 52.2	32.1	14 to 52	31	35 to 48	38

TABLE 27.9—OKLAHOMA-KANSAS AREA (continued)

Formation	Fluid Production	Range of Production Depth (ft)	Average Production Depth (ft)	Range of Production Thickness (ft)	Average Production Thickness (ft)	Range of Permeability (md)	Average Permeability (md)	Range of Permeability, k_{90} (md)
Morrow	G	4,300 to 9,700	6,100	2 to 64	11.0	0.1 to 1,450	115	0.3 to 55
	O	4,100 to 7,500	5,700	2 to 37	9.8	0.2 to 1,840	117	0.1 to 48
	T	5,500 to 6,900	6,100	3 to 30	9.5	0.1 to 410	34.4	—
Oil Creek	G	7,100 to 14,000	10,900	14 to 149	46.3	0.1 to 132	32.0	0.2 to 230
	O	5,100 to 11,700	8,300	3 to 71	12.6	0.1 to 615	131	—
	T	8,400 to 13,700	12,300	8 to 27	15.0	0.1 to 87	22.1	—
Oswego	G	4,500 to 4,600	4,600	8 to 9	8.5	2.4 to 151	76.7	0.1 to 66
	O	300 to 6,300	3,800	3.6 to 34.1	12.3	0.2 to 296	27.3	0 to 41
	T	1,200 to 5,800	3,300	2 to 21	10.6	0.1 to 117	27.0	—
Peru	G	1,200 to 5,300	3,100	4 to 17	9.8	3.1 to 42	15.0	—
	O	200 to 3,200	1,200	2 to 42	12.4	0.2 to 284	20.8	—
	T	700 to 2,500	1,500	4 to 21	10.3	1.7 to 804	205	—
Prue	G	3,000 to 6,600	4,000	5 to 22	13.8	0.7 to 42	18.3	—
	O	600 to 6,700	3,100	2 to 81	14.6	0.1 to 254	22.6	—
	T	3,000 to 5,400	3,700	3 to 18	11.7	0.5 to 133	42.8	—
Purdy	O	4,200 to 7,400	4,500	3 to 30	14.8	7.4 to 500	182	51 to 266
	T	—	4,200	—	4.8	—	195	—
Reagan	G	3,500 to 3,600	3,600	2 to 13	7.4	1.1 to 173	39.3	—
	O	2,100 to 3,700	3,600	1 to 32	11.0	0.2 to 2,740	255	—
	T	3,600	3,600	5 to 7	6.0	19.0 to 37	38.0	—
Redfork	G	2,300 to 7,400	4,300	4 to 19	7.9	0.1 to 160	23.4	—
	O	300 to 7,600	3,100	1 to 63	10.5	0.1 to 668	14.2	—
	T	1,200 to 3,800	3,100	2 to 9	5.3	0 to 23	6.3	—
Skinner	G	1,000 to 5,300	3,700	4 to 29	11.8	0.1 to 127	27.7	—
	O	1,000 to 5,800	3,200	1 to 42.5	9.2	0.1 to 255	20.6	2 to 6.6
	T	2,400 to 4,600	3,400	6 to 35.9	11.5	0.3 to 16	6.0	2.40
Strawn	G	—	1,100	—	12.0	—	71.0	—
	O	1,000 to 7,400	3,500	2 to 40.5	12.4	0.1 to 599	58.1	—
	O	2,600 to 6,700	4,600	2 to 84	26.4	0.1 to 3.1	0.67	0 to 1.3
Tonkawa	G	5,000 to 7,100	5,600	2 to 27.5	9.8	0.3 to 283	46.7	—
	O	2,400 to 5,700	4,800	2 to 28.5	8.7	1.4 to 278	98.6	8 to 22
	T	2,300 to 3,100	2,700	4 to 9	7.0	1.3 to 406	106	—
Tucker	O	1,300 to 2,900	2,200	2 to 14	7.6	2.1 to 123	36	—
	T	2,700 to 2,900	2,800	8.9 to 16	12.5	4.3 to 252	128	53
Tulip Creek	G	7,200 to 16,700	13,400	21 to 268.4	78.1	0.9 to 24	7.63	0.5 to 1.0
	O	700 to 16,800	8,000	2 to 136	15.3	0.1 to 1,470	154.0	0.2 to 1.8
	T	1,400 to 12,900	8,600	3 to 86.5	20.0	2.0 to 143	44.6	0.40
Viola	G	4,300 to 7,300	5,400	3 to 73	39.1	3.6 to 23	10.8	3.40
	O	2,100 to 11,100	4,900	2 to 111.7	17.2	0.1 to 1,150	52.3	0.2 to 186
	T	2,600 to 10,300	4,600	2 to 117	19.6	0.1 to 997	45.1	0.03 to 49
Wayside	O	300 to 2,800	800	3.1 to 34	10.8	0.2 to 133	22.2	—
	G	2,800 to 5,400	4,300	2 to 35	11.3	0.7 to 145	72.1	—
	O	2,800 to 7,400	4,900	2 to 28	10.0	0.2 to 445	91.3	—
First Wilcox	T	3,200 to 6,100	3,900	1.9 to 29	7.7	0.3 to 418	84.1	0.80
	G	5,000 to 10,000	6,700	5 to 28	13.4	0.2 to 154	76.2	—
	O	3,700 to 8,400	6,500	1.3 to 32	11.3	0.4 to 2,960	214.0	—
Second Wilcox	T	4,700 to 7,500	6,000	1.5 to 5	4.4	0.4 to 756	246.0	—
	O	4,100 to 5,000	4,600	2.6 to 30.4	16.2	1.4 to 250	87.1	2.4 to 156

TABLE 27.9—OKLAHOMA-KANSAS AREA (continued)

Average Permeability, k_{90} (md)	Range of Porosity (%)	Average Porosity (%)	Range of Oil Saturation (%)	Average Oil Saturation (%)	Range of Total Water Saturation (%)	Average Total Water Saturation (%)	Range of Calculated Interstitial-Water Saturation (%)	Average Calculated Interstitial-Water Saturation (%)	Range of Gravity (°API)	Average Gravity (°API)
7.5	4.2 to 24.4	14.8	0 to 33.0	4.3	29.0 to 77.0	46.5	16 to 77	36	—	—
23.1	5.7 to 23.2	14.6	0.7 to 44.5	15.1	23.9 to 75.5	42.1	16 to 54	35	33 to 43	40
28.0	5.5 to 16.2	11.3	0 to 15.2	5.0	31.1 to 90.1	57.2	31 to 90	38	—	—
—	6.1 to 13.5	9.0	0 to 6.5	1.6	12.5 to 40.6	25.2	12 to 40	24	—	—
75.6	1.8 to 23.9	13.1	1.3 to 29.5	13.0	14.2 to 76.4	39.1	14 to 76	34	29 to 42	36
—	5.2 to 16.1	10.9	0 to 5.8	2.6	21.7 to 74.9	46.6	21 to 74	—	—	—
—	12.0 to 17.3	14.7	5.1 to 6.4	5.8	39.8 to 55.5	47.7	34 to 55	45	—	—
9.24	2.6 to 21.6	10.1	0 to 27.1	15.0	16.2 to 73.4	41.5	15 to 73	37	35 to 48	44
11.5	4.7 to 20.9	8.7	0 to 14.5	5.8	41.7 to 89.7	63.4	42 to 89	57	—	—
—	12.3 to 17.5	15.6	0.1 to 7.9	4.1	44.3 to 59.4	52.5	44 to 56	51	—	—
—	12.7 to 33.8	18.7	6.7 to 36.8	14.7	34.4 to 73.1	50.6	28 to 73	44	25 to 43	36
—	13.6 to 24.4	19.2	2.8 to 25.5	12.0	38.0 to 60.4	50.7	36 to 56	51	—	—
—	13.8 to 22.4	17.8	2.3 to 9.1	5.5	31.4 to 53.4	42.2	25 to 49	37	—	—
—	7.6 to 23.8	17.0	4.7 to 34.1	16.9	24.4 to 73.1	41.6	20 to 72	38	34 to 46	42
—	9.8 to 23.4	17.5	3.7 to 34.3	19.0	40.7 to 60.9	47.1	32 to 60	36	—	—
179	12.3 to 18.8	16.7	10.1 to 27.2	20.0	31.4 to 58.1	41.5	16 to 50	29	39 to 44	41
166	—	17.8	—	13.6	—	56.2	—	—	—	—
—	9.3 to 12.7	10.8	1.1 to 7.9	4.2	28.4 to 68.4	44.4	28 to 68	40	41	41
—	6.9 to 21.5	13.3	3.0 to 42.0	14.2	17.5 to 72.9	32.9	12 to 72	31	24 to 43	38
—	10.6 to 12.8	11.7	1.8 to 10.5	6.2	33.3 to 46.7	40.0	29 to 45	29	—	—
—	3.8 to 21.2	14.5	0 to 21.7	4.7	16.2 to 63.6	45.8	16 to 63	39	—	—
—	6.6 to 26.1	16.2	5.4 to 30.8	16.9	29.5 to 57.7	43.7	27 to 55	41	32 to 48	37
—	10.1 to 18.6	15.3	0.3 to 36.3	9.9	41.4 to 69.7	52.6	41 to 69	49	—	—
—	13.3 to 19.8	15.7	0 to 9.9	4.2	30.6 to 48	40.8	26 to 47	38	—	—
3.30	7.4 to 21.7	15.3	2.5 to 39.7	20.1	14.3 to 78.7	40.3	14 to 78	38	30 to 46	36
2.40	11.7 to 19.0	15.5	4.9 to 18.2	8.5	39.9 to 71.1	52.4	39 to 71	39	—	—
—	—	21.3	—	9.9	—	61.8	—	38	—	—
—	8.2 to 23.5	16.8	5.7 to 31.1	15.1	28.5 to 61.5	45.6	22 to 56	41	31 to 44	40
0.50	7.2 to 18.4	13.3	9.2 to 33.5	21.1	36.0 to 61.6	45.5	32 to 62	43	33 to 36	35
—	11.7 to 21.4	16.4	0 to 8.1	2.0	31.6 to 56.3	44.5	27 to 56	41	—	—
15.0	13.2 to 22.9	18.4	7.5 to 16.5	12.5	36.1 to 78.0	45.0	31 to 78	38	40 to 45	43
—	15.4 to 18.9	17.1	6.9 to 17.3	11.4	45.1 to 52.6	49.0	44 to 52	45	—	—
—	12.4 to 20.3	15.6	7.3 to 29.8	16.0	35.6 to 50.1	40.7	33 to 43	38	29 to 40	36
53	11.8 to 19.5	15.7	7.1 to 10.9	9.0	58.0 to 64.3	61.2	52 to 62	52	—	—
0.40	2.0 to 11.9	6.1	0 to 6.6	4.1	23.7 to 54.8	33.2	23 to 55	34	49.5	49.5
0.80	2.5 to 25.0	11.6	3.0 to 44.5	12.2	10.0 to 63.0	34.9	9 to 63	33	32 to 50	40
0.40	0.7 to 26.0	11.0	0.7 to 7.7	2.6	15.9 to 82.8	45.7	15 to 82	46	—	—
3.40	8.1 to 10.1	9.3	1.7 to 9.4	5.0	19.7 to 37.2	30.7	19 to 37	30	—	—
18.3	1.0 to 16.1	8.4	3.2 to 41.0	15.5	24.1 to 85.5	54.4	24 to 86	51	28 to 48	37
4.38	0.6 to 18.8	7.1	0 to 33.7	8.6	39.0 to 90.8	65.7	39 to 90	58	—	—
—	13.2 to 24.9	18.6	8.1 to 33.8	18.6	29.4 to 68.0	51.3	28 to 67	47	29 to 42	35
—	5.2 to 15.6	10.8	0.7 to 8.3	3.6	29.7 to 60.5	43.9	29 to 60	44	—	—
—	5.4 to 20.5	12.0	3.6 to 40.5	11.7	15.0 to 58.2	32.0	14 to 58	31	33 to 50	42
0.80	6.8 to 17.7	10.9	0 to 16.9	7.9	24.8 to 63.6	41.7	—	—	—	—
—	5.0 to 15.1	11.2	0 to 3.8	1.5	17.7 to 45.8	30.9	17 to 43	29	—	—
—	4.2 to 20.6	12.4	2.9 to 19.2	10.2	19.0 to 56.3	36.9	18 to 56	34	34 to 42	40
—	1.9 to 20.4	12.9	0 to 8.4	6.1	41.4 to 60.5	42.5	40 to 60	43	—	—
79.2	1.9 to 6.6	4.4	8.3 to 16.7	11.8	43.0 to 87.9	60.1	43 to 87	60	41	41

^a General geologic sections taken at different points in Oklahoma-Kansas areas indicate some variations in the properties and an appreciable variation in the occurrence and relative depths of many of the more important oil- and/or gas-producing zones, formations, geologic groups, and their members. The general identification of core samples from these producing intervals reflects local conditions or activities significantly. In the development of average data values, an attempt has been made to combine data originally reported for locally named zones into more generally recognized formations or geologic groups. In some instances (i.e., Deese, Cherokee) data are reported for a major geologic group as well as for some of its individual members. The values designated by the major group name represent areas where the general characteristics permit identification as to the geologic group but not as to group member. In other areas the group members or zones are readily identifiable. The combinations of data and the use of local rather than regional geologic names in some instances are explained in the footnotes.

^b T represents transition zone or production of both water and either gas or oil.

^c Includes data reported as Dornick Hills and Dutcher.

^d Includes Bromide first and second as reported on McClain County area.

^e Data reported locally as Bromide third, Bromide upper third, and Bromide lower have been considered as part of the Tulip Creek.

^f Includes data reported as Cleveland sand, Cleveland lower, and Cleveland upper.

^g Includes the numerous zones (Deese first, second, third, fourth, fifth, Zone A, Zone B, Zone C, and Zone 1) reported locally for the Anadarko, Ardmore, and Marietta Basin areas. In northwest Oklahoma, these different zones are normally referred to as Cherokee. In other areas the zones are frequently identifiable and properties are reported as for Redfork, Bartlesville, etc.

TABLE 27.10—ROCKY MOUNTAIN AREA

Formation	Fluid Production	Range of Production Depth (ft)	Average Production Depth (ft)	Range of Production Thickness (ft)	Average Production Thickness (ft)	Range of Permeability (md)	Average Permeability (md)	Range of Permeability, k_{90} (md)
Aneth	O	5,100 to 5,300	5,200	3.8 to 23.1	14.0	0.7 to 34	9.35	0.2 to 23
Boundary Butte	G	5,500 to 5,600	5,600	8 to 27	17.5	0.1 to 2.0	1.05	—
	O	5,400 to 5,900	5,600	2 to 68	16.2	0.1 to 114	13.3	0.2 to 23
Cliffhouse	G	3,600 to 5,800	4,800	2 to 56	13.7	0.1 to 3.7	0.94	—
D Sand	O	4,350 to 5,050	5,800	7 to 33	15.0	0 to 900	192	—
Dakota	G	500 to 7,100	5,700	2 to 75	32.0	0.1 to 915	106	—
	O	653 to 7,293	5,600	13 to 75	32.0	0.1 to 915	106	—
Desert	O	5,400 to 5,500		11.6 to 18.3	14.9	1.0 to 11	4.4	0.4 to 2.4
Entrada	G	3,600 to 3,700	3,640	4 to 10	6.0	5 to 300	100	—
Frontier Sands	O	265 to 8,295	2,950	8 to 100	46.0	0 to 534	105	—
Gallop	G	1,500 to 6,900	5,000	5 to 25	11.6	0.1 to 324	26.5	0.3 to 20
	O	500 to 6,400	4,600	2 to 43	12.4	0.1 to 2,470	48.2	0.1 to 3.2
Hermosa	G	4,900 to 7,700	5,600	5 to 30	14.1	0.1 to 91	18.6	45.0
	O	5,300 to 6,000	5,600	3 to 38.2	15.1	0.1 to 37	7.32	0 to 26
Hospa	G	4,800 to 7,100	5,500	3 to 17	10.5	0.1 to 70	18.2	—
	O	4,600 to 5,100	4,800	6 to 18	13.3	0.7 to 25	8.63	—
Ismay	O	5,544 to 5,887	5,707	10 to 90	36.4	0.1 to 142	10.4	—
J Sand	O	4,470 to 5,460	4,900	15 to 62	25.0	0 to 1,795	330	—
	G	6,970 to 8,040	7,500	20 to 76	45.0	0.01 to 0.50	0.20	—
Leadville	G	9,950 to 10,100	9,950		15.0	0 to 21	3.0	—
McCracken	O	8,264 to 9,466	8,820	2 to 142	56.4	0.01 to 272	5.8	—
Madison*	O	3,400 to 6,200	4,900	41 to 450	186.0	0 to 1,460	13	—
Menefee	G	5,200 to 5,700	5,400	7 to 25	12.7	0.1 to 20	5.04	—
Mesaverde	O	1,500 to 6,100	4,700	2 to 22	10.0	0.1 to 17	3.57	—
	O	—	300	—	4.0	—	60	—
Morrison	O	1,600 to 6,900	4,500	24 to 54	40.0	0 to 1,250	43	—
Muddy	O	930 to 8,747	1,845	7 to 75	20.0	0 to 2,150	173	—
Nugget	G	9,900 to 10,300	10,100	60 to 700	385.0	0.8 to 65	40	—
	O	9,500 to 10,800	10,375	250 to 700	475.0	0.5 to 85	20	—
Paradox	G	5,100 to 9,500	6,900	4 to 44.2	12.2	0.2 to 42	11.6	0.1 to 28
	O	5,300 to 6,100	5,700	2 to 66	14.8	0.1 to 119	10.4	0 to 57
Phosphoria (formerly Embar)	O	700 to 10,500	4,600	5 to 100	64.0	0 to 126	3.7	—
Pictured Cliffs	G	1,200 to 5,800	3,400	3.0 to 72.0	17.0	0.01 to 135	7.7	—
	O	—	2,900		23.0		0.5	—
Point Lookout	G	4,300 to 6,500	5,500	2 to 101	22.9	0.1 to 16	1.74	—
	O	—	4,700	—	7.0	—	2.90	—
Shannon	O	4,700 to 5,500	4,900	10 to 20	15.0	0.05 to 5.0	0.8	—
Sundance	O	1,100 to 6,860	3,100	5 to 100	44.0	0 to 1,250	100	—
Sussex	O	4,300 to 5,100	4,500	10 to 30	20.0	0.05 to 20	1.0	—
Tensleep	O	600 to 11,800	4,700	10 to 200	118.0	0 to 2,950	120	—
Tocito	G	—	7,900	—	7.0	—	230	—
	O	1,400 to 5,100	4,600	4 to 58	17.3	0 to 31	3.36	—

TABLE 27.10—ROCKY MOUNTAIN AREA (continued)

Average Permeability, K_{90} (md)	Range of Porosity (%)	Average Porosity (%)	Range of Oil Saturation (%)	Average Oil Saturation (%)	Range of Total Water Saturation (%)	Average Total Water Saturation (%)	Range of Calculated Interstitial-Water Saturation (%)	Average Calculated Interstitial-Water Saturation (%)	Range of Gravity (°API)	Average Gravity (°API)
6.10	4.4 to 10.5	8.1	14.5 to 35.9	25.0	12.5 to 30.5	23.6	13 to 31	24	41	41
—	4.3 to 6.5	4.7	4.7	4.7	23.8 to 35.0	29.4	23 to 35	29	—	—
12.5	5.4 to 21.6	11.0	4.8 to 26.7	12.5	9.3 to 48.8	28.3	7 to 45	27	40 to 41	41.1
—	7.0 to 16.2	11.3	0 to 19.8	4.5	10.2 to 60.3	36.9	10 to 59	36	—	—
—	8.6 to 29.5	21.6	8.4 to 39.5	13.2	—	—	9 to 48	23	36 to 42	38
—	4.5 to 21.6	14.8	0.0 to 7.8	3.5	14.8 to 55.3	40.6	—	—	—	—
—	5.0 to 23.3	11.2	13.8 to 54.5	24.4	11.6 to 44.3	31.0	—	—	38 to 43	40
1.13	11.9 to 13.8	12.7	13.4 to 16.8	15.2	14.8 to 24.7	19.2	14 to 22	18	—	41
—	12.0 to 27.0	25.0	trace to 6.0	3.0	—	—	—	—	—	—
—	6.3 to 29.8	20.0	7.6 to 37.6	14.9	—	—	28 to 45	33	31 to 50	41
10.2	8.5 to 20.8	13.3	0 to 25.6	5.7	20.7 to 59.2	40.0	20 to 54	37	39	39
0.7	6.9 to 23.1	12.5	8.5 to 43.7	25.3	17.2 to 76.9	35.7	14 to 77	34	36 to 42	39
45.0	5.5 to 16.5	10.2	0 to 6.5	3.0	14.2 to 45.3	32.7	12 to 45	32	—	—
4.26	2.7 to 17.9	8.3	3.9 to 29.1	10.8	11.6 to 60.0	35.6	12 to 60	35	41 to 42	40
—	7.4 to 11.9	10.5	0.5 to 23.8	7.5	8.7 to 49.7	38.1	8 to 49	37	—	—
—	6.6 to 14.8	11.3	20.4 to 29.8	25.0	32.3 to 44.8	36.0	31 to 45	35	40	40
—	0.5 to 22.2	7.6	1.6 to 26.4	8.4	—	—	—	—	—	39
—	8.9 to 32.7	19.6	8.8 to 46.5	13.9	—	—	6 to 42	20	36 to 42	38
—	3.0 to 20.0	10.0	0.0 to 22.2	2.0	10.0 to 65.0	35.0	—	—	—	—
—	2.0 to 16.0	3.0	trace to 6.0	7.5	—	—	—	—	—	—
—	0.5 to 15.1	6.5	0.0 to 50.1	14.4	—	—	—	—	45 to 46	45.5
—	1.8 to 26.4	11.9	6.0 to 43.5	17.4	—	—	22 to 33	27	21.6 to 30	26
—	8.7 to 13.5	11.2	0.3 to 5.3	1.6	14.5 to 45.1	27.5	15 to 43	27	—	—
—	10.0 to 19.8	14.6	0 to 6.8	3.3	14.5 to 68.4	42.0	15 to 64	40	—	—
—	—	26.2	—	8.3	—	61.0	—	44	—	—
—	9.9 to 25.5	17.5	5.0 to 26.0	13.1	—	—	15 to 41	35	29 to 56	42
—	2.3 to 32.9	22.3	7.6 to 48.5	30.8	—	—	5 to 47	19	26 to 42	38
—	10.0 to 18.0	13.7	0.0 to 5.0	3.6	20.0 to 60.0	28.0	20 to 56	26	—	—
—	10.0 to 18.0	13.4	5.0 to 10.0	6.4	20.0 to 50.0	32.5	18 to 40	26	—	48
4.43	1.4 to 19.4	7.4	0 to 10.1	3.1	9.9 to 57.9	34.7	10 to 58	34	—	—
4.57	3.3 to 21.8	10.5	3.6 to 38.7	12.4	10.8 to 60.5	33.6	10 to 61	33	40 to 43	41
—	2.0 to 25.0	8.9	3.0 to 40.0	22.5	—	—	5 to 30	21	15 to 42.3	25.4
*	3.1 to 31.0	17.5	0.0 to 21.1	2.6	16.0 to 88.0	47.0	—	—	*	55
—	—	11.4	—	23.2	—	40.9	—	—	—	39
—	5.6 to 21.6	10.9	0 to 9.1	2.9	11.9 to 55.6	36.7	12 to 55	36	—	—
2.40	—	13.3	—	23.8	40	40.9	—	41	—	39
—	6.0 to 15.0	12.0	3.0 to 22.0	16.0	30.0 to 60.0	45.0	—	—	—	44
—	15.0 to 25.0	19.0	8.0 to 25.0	17.0	—	—	20 to 49	35	22 to 63	39
—	8.0 to 20.0	13.0	5.0 to 20.0	11.0	35.0 to 60.0	45.0	—	—	40 to 43	42
—	5.0 to 27.0	13.6	6.0 to 30.0	23.3	7.0 to 59	25.7	5 to 50	19	17 to 58.5	26.2
—	—	20.2	—	4.0	—	51.8	—	43	—	—
—	12.8 to 17.8	14.7	11.9 to 26.6	21.3	40.8 to 55	46.3	40 to 55	46	36 to 40	36

* Not enough wells to justify range of variations.

** Data limited to Bighorn Basin.

TABLE 27.11—WEST TEXAS—SOUTHEASTERN NEW MEXICO AREAS

Formation	Group ^a	Area ^b	Fluid Production	Range of Production Depth (ft)	Average Production Depth (ft)	Range of Production Thickness (ft)	Average Production Thickness (ft)	Range of Permeability (md)	Average Permeability (md)
Bend Conglomerate	1	1,2,4 5,6,8	O	6,000 to 6,100	6,000	3 to 22	13.2	4 to 311	150
Blinberry	2	3	O	10,300 to 10,500	10,400	10 to 28	20.0	1.6 to 11	5.7
	—	8	G	5,383 to 5,575	5,480	23 to 50	36	1.6 to 3.8	2.4
	—	—	O	5,262 to 5,950	5,610	4 to 95	43	0.1 to 5.3	1.8
Cambrian	—	3	O	5,500 to 6,300	5,900	2.0 to 95	30.3	0.8 to 1,130	173
Canyon reef	—	2,3,4 5,6,7	O	4,200 to 10,400	7,100	4.0 to 222	36.8	0.6 to 746	42
Canyon sand	—	2,3,4,7	G	—	5,000	—	8.0	—	1.7
	—	—	O	3,000 to 10,000	5,500	3.0 to 57	16.9	0.1 to 477	38
Clearfork	1	3,4,7	G	—	2,400	—	95	—	11
	—	2(part)	O	1,500 to 6,800	4,400	4.0 to 180	41	0.1 to 43	4.6
	2	5,6	O	5,400 to 8,300	6,600	3.0 to 259	3.3	< 0.1 to 136	5.8
Dean	—	2,4,7	O	7,700 to 9,100	8,200	6.0 to 68	26.2	< 0.1 to 0.3	0.12
	—	1 ^c	G	4,700 to 5,000	4,800	5.2 to 39	18.6	1.1 to 33	12.9
Delaware	—	—	O	3,500 to 5,100	4,200	3.0 to 52	14.5	0.6 to 84	24.5
	—	—	O	—	—	—	—	—	—
Devonian	1	2,5 ^d	G	11,200 to 11,600	11,400	14 to 117	54	0.5 to 36	10.5
	—	—	O	11,300 to 12,300	11,800	8 to 299	99	0.2 to 23	4.0
	2	2,5 ^e	G	—	9,200	—	17	—	0.4
Ellenburger	—	—	O	5,500 to 9,900	7,700	8 to 113	34	2.5 to 50	14.9
	—	—	C	11,000 to 11,200	11,100	19 to 34	27	< 0.1 to 2.2	1.1
	—	6,7,8 ^f	O	7,800 to 12,800	11,200	6.5 to 954	69	1.0 to 2,840	177
Fuselman	—	All	C	4,100 to 10,600	7,400	11 to 18	14.3	203 to 246	225
	—	—	O	5,500 to 16,600	10,100	3.0 to 347	55	0.1 to 2,250	75
Glorietta	—	All	C	8,700 to 12,700	10,300	18 to 51	34	1.2 to 26	8.4
	—	—	O	9,500 to 12,500	12,000	8 to 49	32	0.5 to 25	10.3
(Paddock) ^g	—	All	G	2,200 to 2,600	2,400	3 to 44	16.3	4.6 to 12	5.6
	—	—	O	2,300 to 6,000	4,300	3 to 103	22.3	0.4 to 223	11.5
Granite wash	—	3,4,6,7	G	3,000 to 8,600	4,700	4 to 8	5.1	11 to 2,890	477
	—	—	O	2,300 to 3,400	3,000	2 to 81	15.6	5 to 3,290	609
Grayburg	1	8	G	3,600 to 4,200	3,800	3.0 to 5.0	4.2	1.6 to 9.3	6.5
	—	—	O	2,400 to 4,500	4,100	3.0 to 123	27.4	0.5 to 159	13.7
	2	4,5,6,7	G	4,400	4,400	12 to 26	20.8	0.6 to 3.7	2.5
Pennsylvania sand (Morrow) ^h	—	—	O	3,000 to 4,800	4,400	6 to 259	45	0.2 to 118	5.5
	3	1,2,3	O	1,300 to 3,900	2,700	4.5 to 182	50	0.3 to 1,430	37.7
	—	2,3,4	O	4,100 to 11,400	9,100	1.7 to 77	22.3	0.3 to 462	34.9
Queen (Penrose) ^g	—	All	G	3,000 to 3,200	3,100	4.0 to 29	9.9	10 to 318	64
	—	—	O	800 to 4,900	3,500	1.5 to 38	10.2	0.2 to 4,190	123
San Andres	1	8	O	3,900 to 4,700	4,500	6 to 39	18.6	0.3 to 461	61
	2	5,6	O	4,100 to 5,300	4,500	4.7 to 124	40.1	0.3 to 295	6.9
	3	1,2,3 4,7	O	1,500 to 5,100	3,300	3.0 to 197	30.2	0.2 to 593	9.7
Seven Rivers	—	1,2,5,8	G	3,600 to 4,100	3,900	3.0 to 8.0	5.6	0.6 to 23	12.2
	—	—	O	800 to 4,000	2,600	4.0 to 136	18.5	0.4 to 428	51.4
Sprayberry	1	4,7	O	4,800 to 8,500	7,100	2.0 to 59	21.7	0.2 to 71	6.3
	2	2	O	5,000 to 9,200	6,900	2.0 to 120	18.5	0.1 to 124	4.8
Strawn lime	—	All	G	—	5,600	11 to 57	34.4	4.5 to 310	179
	—	—	O	5,200 to 6,700	5,900	2.0 to 101	36.7	1.9 to 196	43
Strawn sand	—	2,3,4,7	G	3,800 to 10,500	7,800	3.0 to 39	16.8	0.3 to 42	11.4
	—	—	O	1,100 to 11,300	5,200	2.0 to 76	15.1	0.2 to 718	47
	—	Others ^h	O	915 to 7,366	3,938	6 to 21	14	1.0 to 400	45
Tubb	—	1,2,5,8	O	6,100 to 7,300	6,500	15 to 43	33.5	0.2 to 135	27.6
Wolfcamp (Abo) ^g	1	2	O	—	9,800	—	10.6	—	2.3
	2	4,5,6,7	O	8,400 to 9,200	8,800	13 to 129	41.7	2.3 to 9,410	419
	3	3(part)	G	2,500 to 4,100	3,600	4.0 to 119	22.5	0.1 to 1,380	57
	—	—	O	2,400 to 4,100	3,500	2.0 to 114	28.0	1.0 to 1,270	60
Yates	—	8	O	9,000 to 10,600	9,700	4.5 to 204	59	0.2 to 147	20.4
	—	1,2,5,8	G	1,400 to 3,500	2,800	3.0 to 53	10.8	0.2 to 145	19.3
—	—	—	O	1,400 to 4,000	2,300	3.0 to 66	16.6	1.0 to 4,000	42.7

^a More than one group indicates distinct differences in formation as found in different areas.^b Area numbers refer to map of Fig. 27.1.^c Plus Ward, Pecos, and Southwestern Lea County.^d Midland and Ector counties only.^e Crane, Ward, Winkler, and Pecos counties only.^f Except counties in 4 and 5 above.^g Names in parentheses are those commonly used in New Mexico. Area 8.^h Archer, Baylor, Clay, Jack, Montague, Wichita, Wise, and Young counties.

TABLE 27.11—WEST TEXAS-SOUTHEASTERN NEW MEXICO AREA (continued)

Range of Permeability, k_{90} (md)	Average Permeability, k_{90} (md)	Range of Porosity (%)	Average Porosity (%)	Range of Oil Saturation (%)	Average Oil Saturation (%)	Range of Total Water Saturation (%)	Average Total Water Saturation (%)	Range of Calculated Interstitial-Water Saturation (%)	Average Calculated Interstitial-Water Saturation (%)	Range of Gravity (°API)	Average Gravity (°API)
—	—	13.8 to 16.9	15.0	8.1 to 8.6	8.3	43 to 64	52	42 to 62	50	40 to 42	14
0.9 to 5.1	2.2	4.0 to 15.7	10.9	9.5 to 16.1	11.5	21 to 41	33	21 to 39	32	41 to 45	43
—	—	10.7 to 14.8	12.7	2.1 to 9.1	4.9	34 to 40	36	31 to 33	33	—	—
0.2 to 4.2	1.4	3.1 to 12.5	7.8	9.6 to 19.3	12.8	29 to 57	40	27 to 56	39	39 to 42	40
—	—	4.1 to 16.8	12.0	6.9 to 21.2	11.8	22 to 71	39	22 to 71	38	44 to 51	48
0.3 to 249	17	3.0 to 21.5	8.9	3.6 to 39.2	11.6	18.3 to 73	44	18 to 73	43	30 to 47	42
—	—	—	15.1	—	5.8	—	46	—	44	—	—
—	—	5.5 to 22.1	14.3	4.8 to 27.7	13.7	21 to 72	43	21 to 72	41	37 to 43	40
—	7.8	—	13.5	—	5.7	—	50	—	50	—	—
<0.1 to 24	2.5	4.1 to 20.6	9.2	7.5 to 31.4	15.6	18 to 84	54	18 to 84	53	23 to 42	28
<0.1 to 109	3.1	1.9 to 19.4	5.8	5.6 to 27.1	16.5	22 to 69	47	21 to 69	47	28 to 40	32
—	—	7.5 to 12.7	10.3	22 to 44	33.7	20 to 52	34	19 to 51	33	37 to 40	39
—	—	13.8 to 21.8	17.9	2.0 to 10.3	6.0	45 to 66	53	36 to 63	49	—	—
—	—	15.2 to 25.4	21.0	3.9 to 15.6	11.2	33 to 65	49	31 to 64	42	35 to 42	40
0.1 to 1.3	0.5	1.7 to 5.3	3.3	2.1 to 6.6	3.7	37 to 68	53	37 to 68	53	—	—
0.1 to 5.8	0.8	1.3 to 6.8	4.3	3.3 to 16.7	9.2	19 to 53	33	19 to 53	33	48 to 52	49
—	—	—	6.7	—	5.7	—	62	—	61	—	—
0.2 to 18	7.0	5.5 to 27.7	15.2	6.8 to 22.9	11.0	41 to 76	51	41 to 76	51	35 to 46	42
<0.1 to 0.9	0.5	2.2 to 7.7	5.0	3.1 to 4.8	4.0	45 to 69	57	45 to 69	57	—	—
0.3 to 1,020	37	1.8 to 25.2	6.0	5.3 to 24.6	12.9	22 to 65	46	22 to 65	46	36 to 49	42
1.4 to 54	27.7	3.7 to 4.6	4.2	0.8 to 7.6	4.2	47 to 67	57	47 to 67	57	—	—
<0.1 to 396	22.9	1.3 to 13.8	3.8	1.0 to 19.2	8.4	40 to 84	61	40 to 84	60	37 to 52	47
0.3 to 1.3	0.9	2.6 to 3.7	3.3	0.2 to 3.9	1.7	32 to 47	40	32 to 47	40	—	—
0.2 to 17	3.9	1.4 to 10.7	3.3	5.2 to 16	10.4	25 to 65	42	24 to 64	38	47 to 50	48
—	9.3	14 to 18.2	15.0	3.9 to 4.4	3.7	39 to 60	51	37 to 60	50	—	—
0.2 to 126	8.1	5.2 to 20.9	13.6	3.1 to 22.1	15.4	24 to 72	48	24 to 71	47	28 to 40	33
—	53	12.1 to 20.4	14.4	2.9 to 8.7	5.2	39 to 66	55	39 to 66	53	—	—
—	30	3.5 to 26.1	17.7	4.8 to 22.5	14.7	42 to 71	54	35 to 66	49	40 to 45	42
—	—	11.1 to 14.3	12.4	7.1 to 42	18.6	22 to 53	39	22 to 52	38	—	—
0.2 to 48	5.2	7.0 to 20.0	11.3	6.2 to 37.9	17.6	26 to 56	36	25 to 55	35	31 to 41	36
0.3 to 2.1	1.3	6.3 to 6.6	6.4	2.4 to 7.1	4.7	55 to 68	60	55 to 68	60	—	—
0.1 to 110	2.7	2.7 to 16.2	7.9	4.8 to 22.1	13.9	32 to 84	55	32 to 84	55	23 to 40	32
0.1 to 228	14.3	5.3 to 24.3	11.9	8.3 to 34	18.2	31 to 78	58	31 to 78	56	28 to 35	31
0.1 to 168	14.7	2.7 to 13.9	7.7	4.7 to 18.8	9.7	28 to 58	42	28 to 58	41	38 to 47	41
—	—	10.7 to 22.2	16.6	2.6 to 7.6	7.4	36 to 62	48	35 to 58	45	—	—
—	1.0	5.7 to 27.0	17.2	4.2 to 34.7	15.6	32 to 68	49	30 to 66	45	30 to 42	33
0.1 to 482	53	3.2 to 14.0	8.5	8.9 to 33.9	18.7	21 to 49	36	19 to 49	36	34 to 38	37
0.1 to 208	3.8	3.1 to 12.8	7.1	4.9 to 30.6	14.7	26 to 69	52	25 to 69	51	30 to 37	33
0.2 to 510	8.4	3.3 to 25.1	15.5	3.5 to 24.2	13.2	39 to 74	58	37 to 74	56	26 to 37	32
—	0.3	15.5 to 16.6	16.0	3.4 to 9.5	6.4	51 to 66	56	46 to 65	54	—	—
—	8.0	5.9 to 28.9	16.5	4.2 to 41.7	16.2	38 to 70	54	38 to 61	50	28 to 38	32
—	4.0	10.1 to 23.3	15.8	7.0 to 24.5	15.3	32 to 68	45	30 to 67	43	36 to 42	39
—	—	4.4 to 20.6	11.7	7.0 to 30	15.5	25 to 72	43	25 to 72	42	36 to 43	38
27 to 189	108	10.9 to 14.8	12.9	5.5 to 6.3	5.9	38 to 39	39	38 to 39	38	—	—
0.6 to 148	19.1	3.1 to 12.6	7.2	4.9 to 26.3	11.2	15 to 66	44	15 to 66	43	39 to 47	41
0.1 to 0.4	0.2	2.1 to 14.2	6.9	1.7 to 5.2	3.0	48 to 60	52	48 to 60	52	—	—
0.1 to 138	11.7	1.0 to 20.3	12.6	2.7 to 27.9	12.2	23 to 77	43	23 to 77	41	29 to 48	42
—	—	6.0 to 27	16.2	5.0 to 27	14.1	25 to 60	43	23 to 59	41	—	—
0.1 to 1.1	0.5	2.5 to 7.1	4.9	8.5 to 25.3	12.9	37 to 64	54	37 to 64	54	38	38
—	0.4	—	4.3	—	19.6	—	25	—	25	42	42
1.5 to 6,210	274	4.9 to 18.5	9.9	6.6 to 16.8	9.7	32 to 56	44	31 to 56	44	36 to 45	40
—	3.4	7.2 to 24.5	15.3	0.5 to 16.1	4.6	30 to 64	48	26 to 64	45	—	—
—	4.3	5.4 to 26.3	15.5	1.6 to 26.8	14.3	32 to 65	46	29 to 64	44	40 to 50	48
0.2 to 36	5.4	2.6 to 12.8	8.1	5.3 to 23.6	14.4	28 to 56	39	28 to 56	39	40 to 44	42
—	—	12.1 to 27.4	17.9	1.3 to 17.0	5.6	43 to 79	59	36 to 78	53	—	—
—	27.8	2.4 to 27.0	18.8	3.7 to 37.3	16.0	31 to 75	53	31 to 75	47	27 to 41	32

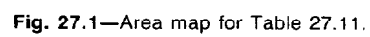


TABLE 27.12—ALASKA

Formation	Fluid Production	Range of Production Depth (ft)	Average Production Depth (ft)	Range of Production Thickness (ft)	Average Production Thickness (ft)	Range of Permeability (md)	Average Permeability (md)
Beluga	G	4,500 to 8,100	5,640	40 to 106	82	100 to 300	125
Hemlock	O	6,100 to 10,800	8,600	20 to 1,300	420	1 to 35	10
Kuparek*	O	6,200 to 6,700	6,200	30 to 80	—	3 to 200	—
Sadlerochit*	O	8,300 to 8,800	8,600	350 to 630	—	—	265
Sterling	G	2,850 to 7,500	6,230	22 to 130	82	20 to 4,400	480
Tyonek	G	6,950 to 7,800	7,200	36 to 92	60	3.5 to 1,600	—
Tyonek	O	4,400 to 14,800	6,150	90 to 1,000	265	10 to 350	43

*Data from report.

TABLE 27.12—ALASKA (continued)

Formation	Range of Porosity (%)	Average Porosity (%)	Range of Oil Saturation (%)	Average Oil Saturation (%)	Range of Calculated Interstitial-Water Saturation (%)	Average Calculated Interstitial-Water Saturation (%)	Range of Gravity (°API)	Average Gravity (°API)
Beluga	19.8 to 28.0	23.0	0.0 to 0.1	0.1	35 to 50	40	30 to 38	37
Hemlock	11.2 to 18.0	14.6	—	10.0	35 to 46	39	—	23
Kuparek*	—	23.0	—	—	—	—	—	28
Sadlerochit*	—	22.0	—	—	—	—	—	—
Sterling	28.0 to 34.0	30.0	—	—	—	—	—	—
Tyonek	11.0 to 21.0	16.0	—	—	—	—	—	—
Tyonek	14.0 to 26.0	16.0	10 to 18	15.0	—	—	35 to 44	40

*Data from report

TABLE 27.13—AUSTRALIA (GIPPSLAND BASIN)

Formation (Reservoir)	Production Unit	Fluid Production	Range of Production Depth (m)	Average Production Thickness (m)	Range of Permeability (md)	Average Permeability (md)	Average Porosity (%)	Average Oil Saturation (%)	Average Calculated Interstitial-Water Saturation (%)
L-1	Mackerel	O	2,299 to 2,396	88.4	600 to 3000	—	22	—	21
L-1	Tuna	O	1,650 to 1,950	6.0	800 to 3000	—	21	—	25
M-1	Marlin	G	1,521 to 1,556	7.5	—	2,000	25	0	25
M-1	Tuna	G	1,299 to 1,377	58.1	—	3,000	21	0	10
M-1	Barracuda	O	1,018 to 1,151	37.2	—	5,000	27	—	26
M-1	Cobia	O	2,352 to 2,396	40.0	500 to 5000	—	22	—	24
N-1	Snapper	G	1,186 to 1,383	99.0	—	1,000	27	0	16
N-4	Barracuda	O	1,330 to 1,339	2.7	—	1,000	25	—	40

TABLE 27.14—ALBERTA, CANADA

Formation	Pool	Fluid Production	Average Production Depth (ft)	Average Permeability (md)	Average Porosity (%)	Average Oil Saturation	Average Calculated Interstitial-Water Saturation
Cardium A	Barrington	O	6,634	3.7	10.1	37.9	22.9
Cardium A	Willesden Green	O	6,225	7.4	15.1	30.3	23.3
Beaver Hill Lake A&B	Swan Hills	O	8,345	32.2	7.9	13.3	21.9
Falher (conglomerate)	Elmworth	G	6,500	1.0	10.0	0	23.0
Falher (sandstone)	Elmworth	G	6,500	40.1	9.0	0	35.0
Gilwood	Nipisi	O	5,651	208.0	12.9	9.3	42.5
Keg River	Rainbow	G	6,082	95.0	4.4	0	14.0
Keg River	Rainbow	O	6,381	187.0	10.0	16.1	19.9
Leduc 03	Red Water	O	3,208	302.0	6.3	19.4	25.6
Leduc 03A	Bonnie Glen	O	6,000	682.0	9.4	4.7	24.2
Taber	Taber	O	3,500	1,000.0	26.0	20.0	25.0
Viking	Viking Kimsella	G	2,400	14.0	18.0	0	35.0
Viking A	Gilbey	O	6,401	238.0	10.6	13.0	35.6

TABLE 27.15—MIDDLE EAST

Formation	Location	Fluid Production	Range of Production Depth (ft)	Range of Permeability (md)	Average Permeability (md)	Range of Porosity (%)	Average Porosity (%)	Range of Reservoir Water Saturation (%)	Average Reservoir Water Saturation (%)
Arab IV	Quatar	0	7,400 to 7,980	0.3 to 6,000	300	5 to 34	21	9 to 100	25
Shubaliba/Wasai	Oman	0	4,125 to 4,422	2.0 to 10	8	27 to 37	33	8 to 16	10
Buhasa	Abu Dhabi	0	10,000 to 12,000	0.5 to 1,000	20	15 to 22	18	15 to 40	25
Umm Shaiff	Abu Dhabi	0	10,000 to 12,000	0.2 to 500	8	10 to 20	15	25 to 45	35
Asab	Abu Dhabi	0	10,000 to 12,000	0.5 to 1,500	25	15 to 30	20	15 to 35	20

TABLE 27.16—NORTH SEA *

Formation	Field	Fluid Production	Depth (ft)	Production Thickness (ft)	Range of Permeability (md)	Average Permeability (md)	Range of Porosity (%)	Average Porosity (%)	Average Reservoir Water Saturation (%)
(Paleocene)	Forties	O	7,200	509	400 to 3,900	—	25 to 30	27	23
Brent	Brent	G&O	—	740	10 to 8,000	—	7 to 37	—	—
Brent	Statfjord	O	7,700	778	—	3,000	—	28	—
Statfjord	Brent	G&O	—	900	100 to 5,500	—	10 to 26	—	—
Statfjord	Statfjord	O	8,900	800	10 to 2,000	—	—	23	—
(Upper Cretaceous) to Danian	Ekofisk	O	10,400	700	—	12	—	30	20

TABLE 27.17—VENEZUELA

Formation	Fluid Production	Range of Production Depth (ft)	Average Production Depth (ft)	Range of Production Thickness (ft)	Average Production Thickness (ft)	Range of Permeability (md)	Average Permeability (md)	Range of Porosity (%)	Average Porosity (%)
Upper Laguna	O	7,200 to 10,900	9,500	20 to 170	88	100 to 470	270	18 to 35	30.3
Upper Lagunillas inferior	O	8,100 to 11,400	10,000	20 to 220	142	200 to 3,000	1,500	20 to 32	28.7
Bachaquero inferior	O	9,000 to 11,000	10,000	20 to 150	83	100 to 700	450	17 to 28	21.8

Chapter 28

Relative Permeability

Walter Rose, Consultant *

Introduction

This chapter was written as an overview of relative permeability: the basic ideas are given and their evolution is traced. Also presented are some laboratory measurement details and comments on the use of relative permeability information in problem solving. Many unresolved issues still exist, regardless of the fact that the literature is quite rich with the descriptions of what previous workers have thought about this complex subject.

Fluid flow is the major transport process that is involved in the recovery of oil, gas, and associated formation waters from subsurface petroleum reservoirs. As a consequence, process descriptions are needed to understand, to forecast, to manage, and to control production operations. Relative permeability is the concept that is often used as a framework for describing two- and three-phase flow of immiscible fluids through porous sedimentary rocks.

The term *permeability* historically has been adopted as a measure of the porous rocks' ability to conduct fluid. If only one fluid is present in the interstices, this transport coefficient is called the *specific* permeability, but otherwise one must make reference to the *effective* permeability of each of the immiscible fluids in the connected pore space. *Relative* permeability by convention is the ratio of the effective to the specific permeability.

In transport theory one deals with *fluxes*, *forces*, and the coefficients by which these variables are interconnected. As soon as the force-flux relationships are established for particular cases, they can be written in such a way that the various permeability functions will appear explicitly. In other words, just as specific

permeability has the sense of a transport coefficient that appears in Darcy's equation for single-phase flow, effective and corresponding relative permeability functions also can be thought of analogously as important transport coefficients by which multiphase flow processes are best described.

Central to the relative permeability idea is that we are dealing with material response types of parameters that cannot be derived from theory alone. On the contrary, laboratory measurements generally also will have to be made. All measurements are to be made in accordance with how the experimental variables properly are defined and used later.

To simplify the discussion, assume that we are dealing with the steady flow of an incompressible fluid that is moving macroscopically in a horizontal direction. Then,

$$q = \frac{kA\Delta p}{\mu L}, \dots\dots\dots (1)$$

where Δp is the pressure drop that can be measured across a specimen sample of length L and cross-sectional area A , and q is the volumetric rate of discharge of the flowing fluid whose viscosity is μ . Eq. 1 serves to prescribe an experimental measurement methodology by which values for k can be determined unambiguously.

In particular, it is seen that a plot of q vs. Δp should be a straight line whose slope is proportional to the specific permeability, k , as long as certain limiting conditions prevail. These are that (1) the fluid is homogeneous; (2) the temperature is constant; (3) the transport process is free of electrokinetic effects (as occur when certain dilute electrolytes are being moved through electrically nonconducting media), and of film surface flow (as oc-

* Author of the chapter on this topic in the 1962 edition was M.R.J. Wyllie.

curs when a gas is moving at such low mean pressure that the frequency of molecular collisions at the interstitial surface boundaries becomes important); and (4) the porous rock is sufficiently rigid and inert to preclude rapid changes in the pore geometry.

Accordingly, in what follows, we adopt the idea that if Darcy's law adequately describes single-phase flow, analogs of it can be postulated just as well as useful descriptions of multiphase flow phenomena.

Historical Background

In the 1930's and 1940's, serious ideas about the meaning and measurement of relative permeability phenomena first appeared. Principal authors were Muskat, Botset, Hassler, Leverett, and perhaps a dozen more whose names punctuate the milestones described in the standard references.^{1,2} These people were connected predominantly in one way or another with the U.S. petroleum industry at a time when quantitative study of recovery of hydrocarbon fluids from subsurface sedimentary environments was in its infancy. In focusing on how reservoir fields of fluid flow would be influenced by the nature and number of the coexistent interstitial fluids, the early workers took advantage of the fact that the existing and well-developed understandings about single-phase flow in porous rocks, when generalized, seemed to provide credible descriptions of multiphase flow situations. When L.A. Richards³ published his classic 1931 paper on the flow of capillary-bound moisture in so-called unsaturated soils, Darcy's pioneering work already had stood the test of three-quarters of a century of scrutiny, use, and amplification by diverse groups of technologists that included groundwater specialists as well as petroleum, chemical, and civil engineers.

Framework Ideas

By analogy to Eq. 1, a set of separate equations can be written to describe multiphase flow phenomena under the restricted conditions that no gravity forces are affecting the steady flow of each of the incompressible immiscible fluids, or

$$q_j = (k_j A)(\Delta p_j)/(\mu_j L) = (kk_{rj} A)(\Delta p_j)/(\mu_j L), \dots (2)$$

where the subscript j refers to the j th fluid phase (oil, gas, water). Following the usual terminology, k_j is called the effective permeability, k_{rj} is called the relative permeability, and p_j denotes values of pressure locally measured in the various fluid phases that are separated by interfaces of contact.

In particular, k_j and k_{rj} are to be considered measures of the flow conductivity afforded by the porous rock when saturated with the immiscible fluid phases in some particular way. As will be seen, reference must be made to fluid saturation configurations and distributions as well as to fluid saturation levels. For example, and in analogy to the porosity concept where ϕ is given by the local ratio of pore to bulk volume, the saturation of the j th fluid, S_j , is defined as

$$S_j = \frac{V_{fj}}{V_{pt}}, \dots (3)$$

where V_{fj} is the volume of fluid j and V_{pt} is the total pore volume. In other words, the product ϕS_j can be thought of as an effective porosity of that portion of the partitioned pore space occupied by the j th fluid phase.

It follows that locally (i.e., in any representative volume element of the reservoir rock system of interest) $\Sigma S_j = 1$, even when saturation is changing with time and position. In any case, it would appear that the relative permeability, k_{rj} , has a first-order dependency on the saturation level, S_j . But this is only one of the dependencies, because usually many interstitial fluid phase distributions are possible for each level of saturation. Also, the reduced pore space occupied by each of the several pore fluid saturants is not necessarily everywhere bounded by interstitial (solid pore wall) surfaces; hence, it is possible that the influence of prevalent fluid/fluid interfacial boundaries also may have to be considered. Thus, the statement

$$0 < k_{rj} < 1 \text{ for } 0 < S_j < 1, \dots (4)$$

while always true, ignores the fact that k_{rj} may equal zero even when S_j is finite, and may be greater than unity even for values for S_j less than unity.^{4,5} Moreover, Eq. 4 is too crude to indicate explicitly that k_{rj} can have more than one value for each value of S_j (e.g., because of hysteresis).

Hysteresis

From the thermodynamic point of view, the fluid flow processes under consideration are irreversible (i.e., nonequilibrium); therefore, they are inherently path-dependent. One consequence is that the equilibrium states approached in one direction can be different from those approached in another. This phenomenon is called hysteresis, and explanations for it are not hard to find. For example, while specific permeability depends mostly on the interstitial pore geometry, effective (hence, relative) permeability depends on the fluid saturation geometry as well. Usually there will be more than one way a given fraction of the pore space can be occupied by each fluid phase of interest. The result is that relative permeability data give values that are functions of the history and sequence of the prior saturation changes as well as being merely functions of the fluid saturation levels.

As will be seen later in this chapter, little laboratory work has been published to prove that Eq. 2 truly describes multiphase flow phenomena. Nor can much reassurance be taken from the fact that the validity of Eq. 1 as a description of the characteristics of single phase flow has been confirmed experimentally for a large number of cases. This is because the unsteady states are of the greatest interest when dealing with petroleum recovery problems, but this aspect is ignored by the Darcian modeling.

In other words, Eq. 2 by itself does not make it possible to account for and to predict the saturation changes that occur as flood fronts move through reservoir space during production. And in the real processes to be modeled, the various phases may be flowing in separate directions rather than colinearly. The greatest limitation of Eq. 2, however, is that it gives no explicit prescription

of how to avoid end effects (the buildup of wetting fluid saturation levels at surfaces of capillary discontinuity such as core end-faces) in laboratory work.

Immiscible Wetting and Nonwetting Pore Fluids

Whenever wetting and nonwetting immiscible fluids compete to occupy the same pore space, it is clear that at inflow and outflow surfaces of so-called capillary discontinuity, there will tend to be a buildup of wetting fluid saturation levels during the course of multiphase flow processes. This has been understood from the earliest days.^{3,6} The central idea is that immiscible fluids that are co-existent in contiguous capillary pore space generally will be separated by curved interfaces of contact instead of by stress-free flat interfaces at contacts that occur exterior to the flow system.

In fact, the interfacial curved boundaries are a reflection of the balance between capillary and gravity forces in the static (stationary) cases, and of the viscous forces as well in the dynamic cases. This means that locally there usually will be a pressure difference between the immiscible fluids. This pressure difference, commonly called the capillary pressure, P_c , by convention is defined as the local difference between p_n and p_w (where the subscripts n and w refer to the nonwetting and the wetting fluids, respectively).

In systems at equilibrium, immiscible fluids tend to be distributed such that the free surface energy of the system is at a minimum, subject to the constraints imposed by the S_j levels and by the hysteretic path of saturation change being followed as successive equilibrium states are being established. This usually means that the wetting fluid will be found in the smaller pore spaces, and that the interfaces of contact will be concave toward the nonwetting fluid (hence, P_c will have positive values). In fact, capillary pressure, like k_j and k_{rj} , frequently is assumed to be primarily saturation-dependent, but it depends substantially on the fluid/fluid interstitial configurations at each saturation level.

The Buckley-Leverett equation⁶ takes the following special form in describing two-phase displacement processes involving one-dimensional (horizontal) flow of incompressible fluids. With density $\rho_j = \text{constant}$ and $\partial q_j / \partial x = 0$, we have

$$\begin{aligned} & \phi(\partial S_w / \partial t) + \partial \{ [(q_w + q_n) M_w] / [(M_w + M_n) A_f] \} / \partial L_h \\ & + \partial [(M_n M_w)(dP_c / dS_w)(\partial S_w / \partial L_h) / (M_w + M_n)] / \partial L_h \\ & = 0. \end{aligned} \quad (5)$$

where ϕ is the local porosity independent of time, A_f is the cross-sectional area of flow path, P_c is the capillary pressure, L_h is the horizontal distance parameter, and t is the time (both independent variables); and M_n and M_w are the mobilities of the nonwetting and wetting fluids, respectively (i.e., $M_j = k_j / \mu_j$). As can be seen from the derivations of Eq. 5 given in Refs. 1, 2, and 6, the saturation levels vary with position and time in a way that depends on the variation of P_c with S_w , on the saturation gradient, on the relative permeabilities, and on the initial and boundary conditions of the problem [as well as on certain controllable and disposable variables

such as porosity, fluid viscosities, the specific permeability, and the total flow rate given by $(q_w + q_n)$].

Indeed, the importance of having relative permeability information is to make it possible to solve reservoir engineering problems modeled by process descriptions such as given by Eq. 5. The more elaborate modeling technique involving equations with the transport and interaction coefficients described by Rose⁷ require considering more than simple relative permeability information, however. Even so, the experiments prescribed by the Buckley-Leverett⁶ and Rose⁷ equations will not be easy to perform. The laboratory difficulties obviously multiply if unsteady states are to be considered (where S_j changes with time and spatial position). This is why only state-of-the-art methodologies will be described here. Nonetheless, it is clear that future workers will continue to be challenged by the need to develop and to perfect measurement methods that are based on modeling that goes beyond the simplistic Darcian reasoning embedded in Eq. 2.

Measurement Methodologies

A number of measurement methodologies have been described in the literature; these are classified and explained to some extent as follows, along with some of the data that have been reported. Two controversial questions are (1) do the various methods yield equivalent data, and (2) if not, which are the most trustworthy ones?

Laboratory measurement techniques for relative permeability determination are of two sorts. In the so-called steady-state methods, the effective permeability as a function of saturation is calculated from the flow data that are obtained on the assumption that Eq. 2 is correct in form. The trick is to make direct measurements prescribed by the theory, of parameters such as volumetric flow rates, pressure drops, and fluid saturation levels. In one variant of the method, known as the Hassler technique,⁸ provision also is made to control and to measure the local values of capillary pressure to avoid the troublesome end effects.

The so-called unsteady-state methods are based on using integrals of Eq. 5 as the process model. The idea is to observe the consequences (i.e., the outcomes in terms of cumulative production) of controlled multiphase displacement experiments, and then to back-calculate the relative permeability values that are consistent with, and serve to explain, those outcomes. The cumulative production data also are processed to provide a basis for calculating average saturation levels to be associated with the relative permeability values.

As will be seen, the steady-state methods are more time-consuming than the unsteady-state methods; still, the data obtained by them are at least as believable as the plausible model on which they are based (Eq. 2), especially if convincing measures are taken to minimize the capillary end effects mentioned previously. On the other hand, the unsteady-state methods, comparatively speaking, supply the wanted data quickly and cheaply. This latter advantage, it may be argued, is only a partial compensation for the uncertainties in data interpretation inherent in the indirect nature of such measurements. To expose the rationale for selecting one type of procedure over another, the ideas of recent authors are reviewed below.

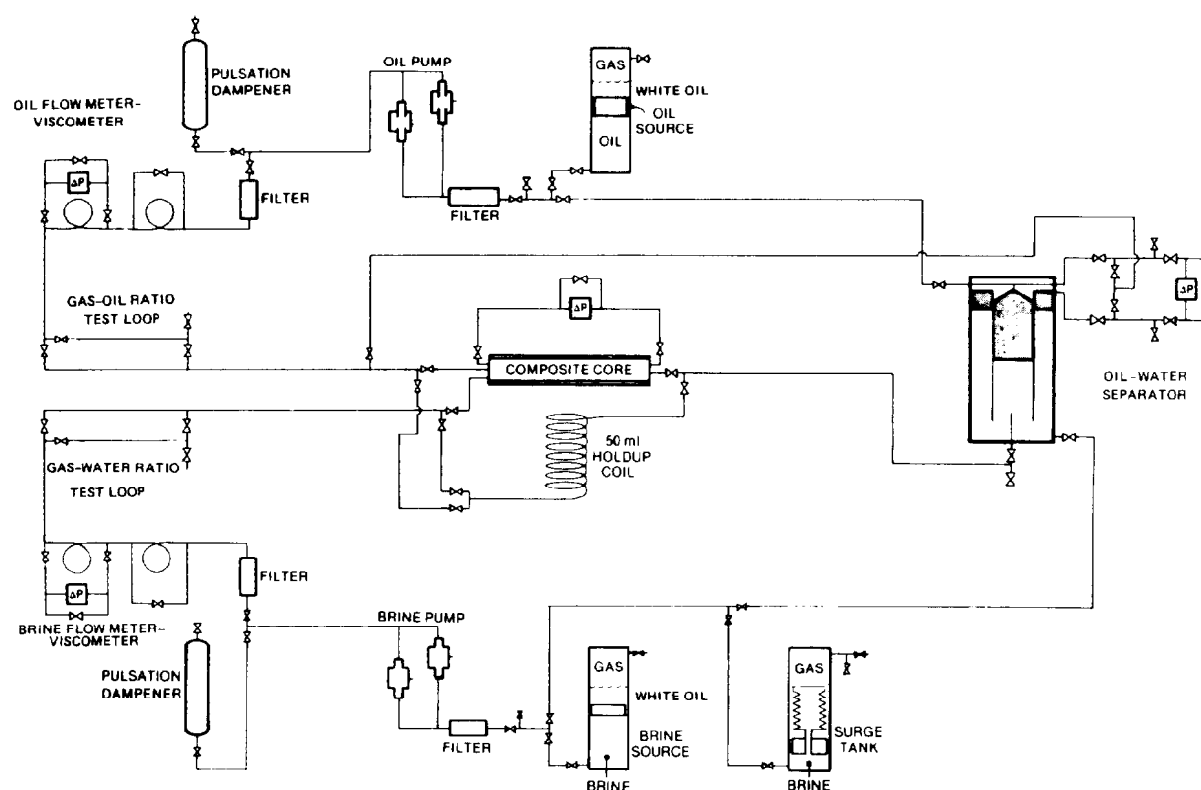


Fig. 28.1—Details of steady-state relative permeability apparatus.

Steady-State k_r Methods

Experimental Procedure. Blackwell and Braun⁹ provide a comprehensive statement of how some people think the steady-state relative permeability method should be practiced when given the understandings and instrumentation opportunities available at the start of the 1980's. Fig. 28.1 is a schematic of the laboratory system that can be used. Positive displacement or other types of constant-rate pumps, one for each fluid, discharge a fixed-ratio mixture into the core sample. Regardless of the initial saturation conditions within the core sample, the effluent fluid mixture eventually will be identical in composition to that being delivered by the pumps upstream. At this steady-state condition, effective permeabilities for the immiscible fluids can be calculated because the separate pump rates (q_o and q_w) will be known, and because an approximation of the pressure drop across the core sample can be used as the indicated driving force for each fluid.

For example, suppose that the reservoir process under consideration involves edgewater encroachment into a uniform sand that has a certain level of interstitial water saturation, with the rest of the pore space filled with an unsaturated oil. A core sample representative of the formation could be selected and, after cleaning, an appropriate initial condition with respect to water and oil saturation could be established by the so-called restored-state capillary pressure technique. Alternatively (and perhaps ideally), a "fresh" core sample could be brought into the laboratory as recovered by a pressure core barrel so that the wanted initial saturation conditions already would prevail. Or, as still another preparation

procedure, an "as-received" core could be processed so that the mud filtrate was replaced by simulated formation water that, thereafter, was displaced down to interstitial levels by flooding the sample with "live" oil. That is, in one way or another, the imbibition water/oil relative permeability data could be obtained where the experiment is started from a proper initial condition in fluid saturations and saturation distributions. And, if reservoir conditions of wettability were to be somehow preserved or restored as preparations for the experimental work are made, and if the ensuing displacement process were to be undertaken under conditions where reservoir-like overburden stress, pore fluid pressure, and/or temperature were simulated, then so much the better. However, the final saturation levels at steady state still would have to be measured. Several methods are available from which this information can be obtained.

Saturation Measurements. What the Braun and Blackwell method⁹ does is have a downstream water/oil separator where (as shown in Fig. 28.1) the bulk of each effluent phase is directed back to the inflow sides of the respective pumps, but where the differential amount between inflow and outflow of each phase is collected in a column and gravimetrically or volumetrically measured. In other schemes, X-ray absorbers or radioactive tracers can be added to one or more of the flowing fluids so that external instrument scans of the core will give the information that can be converted back to saturation levels. Even more simply, the core sample can be removed from the core holder after each steady-state condition is

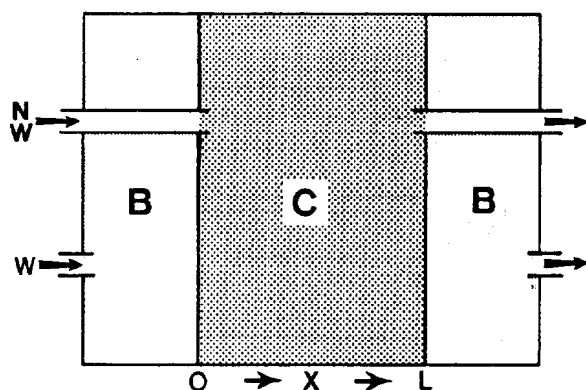


Fig. 28.2—The Hassler "sandwich." C denotes the core sample of length L and B denotes the inflow and outflow capillary end barriers. NW and W designate the ports through which the nonwetting and wetting fluids are directed collinearly as shown by the arrows.

reached, and then weighed so that saturation values can be calculated from independent knowledge of fluid densities and core sample PV.

More details about the steady-state procedure under discussion are available in the references. Suffice it to say that entire curves of relative permeability vs. saturation are to be obtained, following well-defined imbibition or drainage paths, by proceeding stepwise from one steady-state condition to the next. For example, in the water influx experiment under discussion, the q_w/q_o ratio delivered by the pumps could be set at successively higher values while going from one steady state to the next until finally the high produced WOR's would confirm that a condition of residual oil saturation had been achieved.

The previous discussion provides a brief description of the sense of the steady-state relative permeability measurement scheme as used when no special effort is made to control end effects (e.g., the buildup of wetting fluid saturation levels at surfaces of capillary discontinuity such as core end-faces). Early data obtained by equivalent steady-state procedures are reported in Muskat's classic work.¹⁰ Remarkably, there does not appear to be much learned from more recently obtained data than was at least qualitatively apparent in the beginning.

For example, one conclusion that can be drawn consistently from laboratory observations is that the inequalities given previously as Eq. 4 can be written more exactly as

$$0 < k_{rj} < 1 \text{ for } S_{ij} < S_j < 1, \dots \dots \dots (6)$$

where S_{ij} is the minimum (irreducible) value of S_j when the j th fluid of interest no longer has phase continuity over sensible distances within the pore space. On the other hand, the idea that relative permeability can be greater than unity for saturations less than unity has been reported^{4,5} and explained as a reflection of the "lubrication" provided as one fluid slides by an adjacent immiscible one.

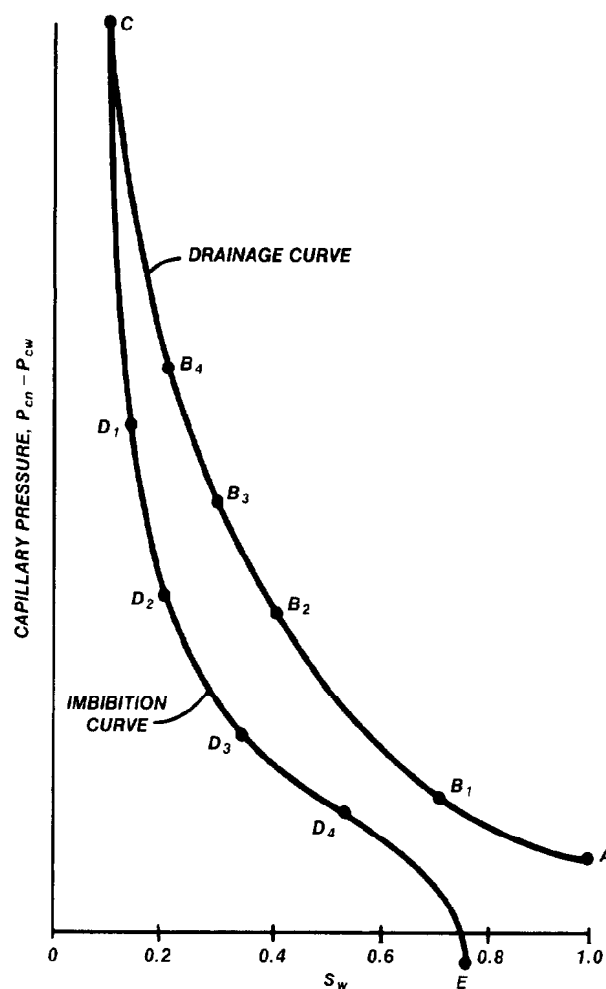


Fig. 28.3—Schematic capillary pressure curves.

On the other hand, when attention needs to be given to end effects, some workers have proposed that long cores be used so that measurements could be confined to an inner portion.¹¹ Even in such a so-called Penn State arrangement, however, the pressure-drop terms of Eq. 2 still are not measured separately for each of the immiscible fluids, and that is why it makes sense to refer back to Hassler's almost-forgotten work.

The *Hassler method* for relative permeability determination has had a curious history. The patent was granted in 1944⁸ and although cited occasionally, it has been ignored by most workers intent on developing simple state-of-the-art procedures. Scheidegger² referred to the method as superior, but difficult and time-consuming to apply, and at one point Rose¹² gave an analysis of why operational difficulties were to be expected in some applications. More recently, however, a patent has appeared that teaches how Hassler's ideas indeed might be reduced to a practical operating scheme.¹³ Whether or not these claims eventually are substantiated by the facts, it is nonetheless of interest to examine in some detail the principle of the Hassler method for relative permeability determination. Thereby, a reference frame can be established to which other steady-state relative permeability procedures can be compared.

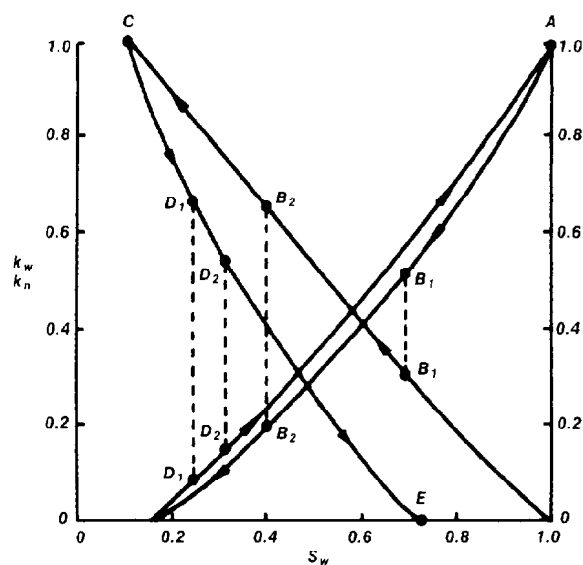


Fig. 28.4—Schematic relative permeability curves.

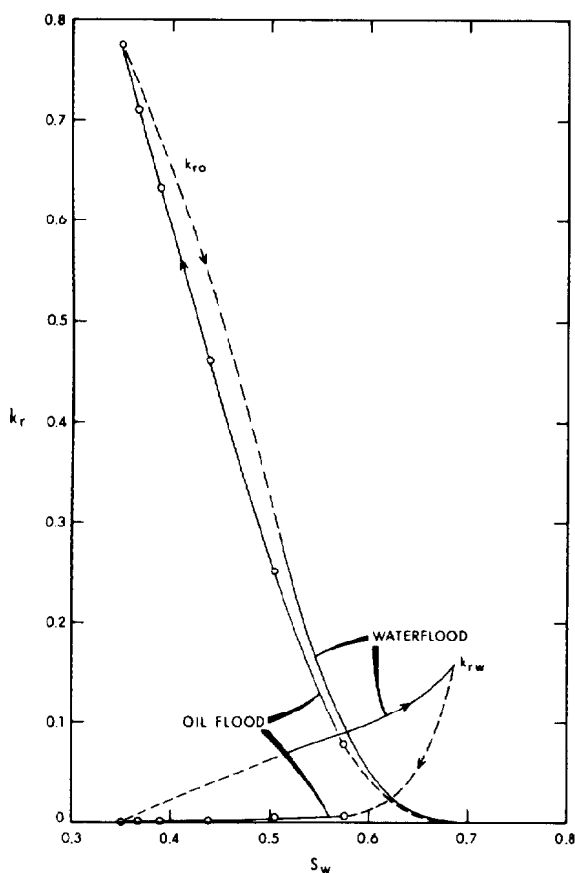


Fig. 28.5—Hysteresis in waterflood vs. oilflood relative permeability curves.

Fig. 28.2 is a schematic that shows the sandwich arrangement where the wetting fluid (denoted by W) passes in series through an inflow capillary barrier as it enters the core sample, and then exits through a similar downstream barrier. The nonwetting fluid (denoted by NW) flows in parallel with the wetting fluid in the core sample but does not enter the pore space of the barriers. This exclusion is achieved by never letting the pressure in the nonwetting phase locally be so great that the barrier threshold pressure is exceeded; hence, the endflow barriers will always remain 100% saturated with the wetting fluid during the course of the test.

Fig. 28.3 is a schematic of a representative capillary pressure drainage and imbibition curve for the reservoir rock sample of interest where the relative permeability relationships are wanted. Suppose that, as an initial condition, the core (as well as the end barriers in series with it) is 100% saturated with water (say with a simulated oilfield brine). Let the threshold pressure for the core sample be P_{CA} and that for the barrier material be greater than P_{CC} . * Threshold pressure is being defined here as the lowest capillary pressure ($P_{cn} - P_{cw}$), where the nonwetting fluid will enter a wetting-fluid-saturated porous medium. Since the capillary end barriers are made of material considerably less permeable than the core sample material, $P_{CC} \gg P_{CA}$.

Hassler's way of performing the relative permeability experiment is to measure the effective permeability to each phase by using Eq. 2 at various successive capillary pressure conditions, such as $P_A, P_{B1}, P_{B2} \dots P_C, P_{D1}, P_{D2} \dots P_E$. The result is a succession of saturation states such as $S_{A1}, S_{B1}, S_{B2} \dots S_{C1}, S_{D1}, S_{D2} \dots S_E$ in the sense that from A to C a drainage curve is being traced since the wetting-phase saturation is always decreasing, while from C to E an imbibition curve is being traced since the wetting-phase saturation is always increasing. Note that at A the wetting-phase saturation, S_A , is 1.0, at C the wetting-phase saturation is close to the interstitial water level, S_{iw} , while at E the wetting-phase saturation is $(1 - S_{rn})$, where S_{rn} designates the residual (nonproducing) nonwetting fluid saturation level.

Corresponding to the saturation points where capillary pressure values have been measured and shown in Fig. 28.3 during drainage and imbibition, the associated relative permeability data to be obtained by the Hassler method are shown in Fig. 28.4 in schematic format. It is instructive to draw some comparisons between these presentations. Capillary pressure as well as relative permeability functions are saturation-dependent. They both appear as parameters in the Buckley-Leverett description of multiphase flow and displacement processes (Eq. 5). Both functions are a direct reflection of the network structure of the pore space (size, shape, orientation, mode of branching, tortuosity, etc.). It is for these reasons that early workers were quick to search for the direct dependency between capillary pressure and relative permeability phenomena¹⁴ and that Hassler, with such great insight, was provoked to emphasize the interconnections that still earlier had been recognized by Leverett¹⁵ and Richards.³

* P_{CC} is the highest value of capillary pressure to be used in the experiment to obtain the lowest value of S_w .

The process under discussion is complicated and not easy to describe without many details. Since these are fully covered in the original references,^{1,2,7} it is enough to end the discussion here with the observation that there are at least two ways, in principle, to practice the Hassler method. One is to impose fixed boundary conditions in pressure upstream as well as downstream, and then to observe flow rates needed for the calculations of permeability data.⁸ The other¹³ is to have constant flow rate as the upstream boundary condition while keeping constant pressure as the downstream boundary condition. What is gained thereby is circumvention of the practical difficulties of avoiding end effects encountered when the boundary conditions are set in terms of upstream and downstream pressure only.

Unsteady-State k_r Method

Compared to the unsteady-state methods to be described now, the steady-state methods are quite straightforward and involve few uncertainties. The following analyses will reveal why this is so.

Experimental Procedure. In so-called unsteady-state procedures, effluent production from a core sample during the course of an imposed displacement process is recorded, and relative permeability functions are generated on the basis of a mathematical modeling of the process that is supposed to be consistent with what is being observed. In practice, the mathematical model usually selected is a simplified form of an integral of the Buckley-Leverett Eq. 5. By linearizing the equation by dropping the capillary pressure (end effect) terms, back-calculating the relative permeability functions appears to be possible.

Since the aim is to get more resolution for calculation of intermediate values of relative permeability and for calculation of the associated saturation values, one needs to spread out the effluent production data. The whole enterprise is compromised, however, when a very *unfavorable mobility ratio* is chosen as the way to prolong the transient period before total breakthrough of the displacing phase. The reader is referred to one analysis of this situation⁷ for further information.

Methods of Calculation

Institut Français du Pétrole Method. The reader also is referred to the definitive paper by authors at the Institut Français du Pétrole¹⁶ for full details about how to practice the unsteady-state method for relative permeability determination. Constant-flow-rate and constant-pressure schemes are described, precautions are enumerated, and calculation schemes are given. Fig. 28.5 is taken from another paper¹⁷ that shows how representative data and the associated relative permeability curves might look in a representative case.

Automated Centrifuge Technique. To finish with the discussion of the variants of the unsteady-state methodologies, it will be useful to cite the work of O'Meara and Lease,¹⁸ who gave three-phase data obtained with an automated centrifuge technique. By spinning core samples in a centrifugal field of known strength and observing effluent volumes as a function of

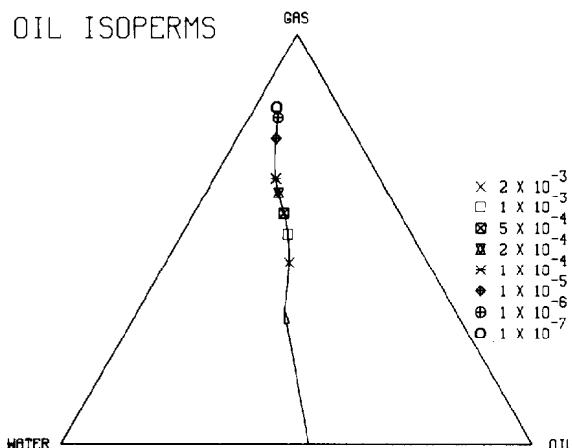


Fig. 28.6—Three-phase saturation trajectory and oil isoperms ranging from 1×10^{-7} to 2×10^{-3} .

time, a back-calculation of relative permeability can be made (which, again, will be at most of qualitative value because of the limiting assumptions that have been used in the mathematical modeling).

Claims made for the centrifuge technique are (1) it does not suffer from viscous fingering distortions, as in the case of the conventional unsteady-state procedures, and (2) it is faster than the competing steady-state procedures. However, the capillary end-effect problem still has to be faced. Another disadvantage is that in any given run, the information obtained applies only to the relative permeability of the invading phase. Since the conventional unsteady-state procedures give relative permeabilities for the displaced (as well as the displacing) fluids, and since larger samples can be processed than is possible in the centrifuge, the conventional approaches are the ones that are considered to be state-of-the-art. In fact, the appeal that the centrifuge technique holds for experimenters is related to its suitability for automation, and to the fact that it is already generating three-phase data. Fig. 28.6, for example, is a display of some of the data that have been reported.

Critique of Methods

To summarize what has been published about relative permeability measurement methodologies, the critique originally given by Scheidegger,² and more recently affirmed,¹⁸ is accepted enthusiastically here. The consensus seems to be that the steady-state methods, Hassler's in particular, give the most believable results since they are based on a plausible (however naive) definition of relative permeability (i.e., as embedded in Eq. 2). Unsteady-state methods, while quicker and easier to apply from the laboratory operational point of view, nonetheless are beset with enormous interpretation difficulties. This is mostly because they involve drawing inferences (by way of back-calculations) from a rough-integral form of the Buckley-Leverett Eq. 5. As noted previously, Eq. 5 is at most an imperfect model of the flow process under study.⁷

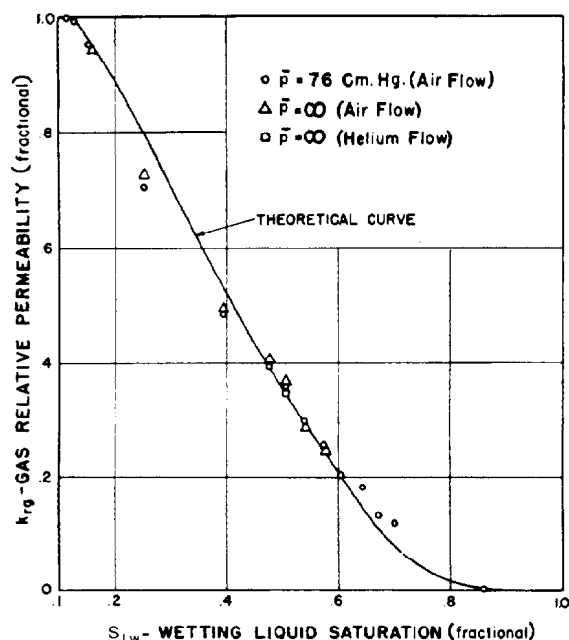


Fig. 28.7—Gas relative permeability vs. total wetting-liquid saturation.

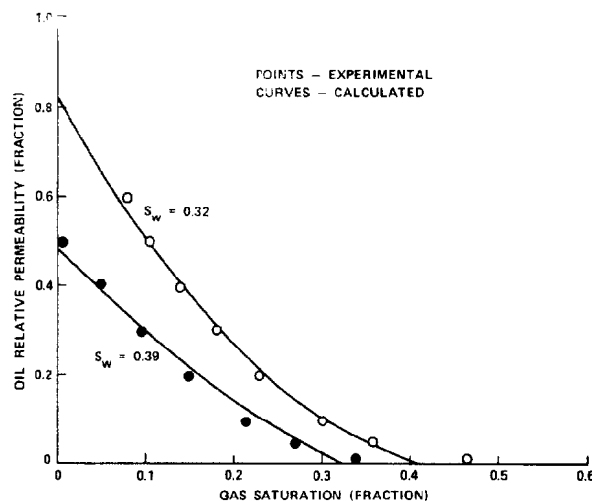


Fig. 28.8—Matching Corey *et al.* Berea sandstone data.

Other k_r Methods

Still other methods to arrive at relative permeability information remain to be cited for completeness. For example, there are the so-called stationary fluid methods¹⁹ and the calculation methods based on capillary pressure and endpoint displacement data associated with Corey *et al.*²⁰ and Stone.²¹ Figs. 28.7 and 28.8 display some of the results given by these investigators.

In the stationary fluid methods, the effective permeability of one phase is measured by flowing that fluid at such a low pressure gradient that the contiguous immiscible fluid is left (it is hoped) unaffected. Clearly, the method can be trusted most when the stationary fluid has a saturation level close to its minimum (irreducible) value (i.e., $S_j \rightarrow S_{ij}$ for the stationary fluid). Otherwise, it may be concluded that the data generated by applying the method will be distorted by the ever-present end effects. On the other hand, the method is easy to apply operationally, and the data generated giving k_o at S_{iw} (irreducible water saturation) and k_w at S_{io} (irreducible oil saturation) are needed along with other parameters when calculated values of relative permeability are to be made by the popular Corey *et al.* and Stone methodologies. In any case, values for k_o at S_{iw} give an indication of the initial productivity of oil wells from horizons where there is only initial oil plus interstitial water saturation. Similarly, values for k_w at S_{io} can be used to indicate the level of the effective water/brine permeabilities when residual oil saturation conditions are reached at the end of a waterflood recovery process.

To understand better the rationale for using relative permeability calculation schemes, reference can be made to the early papers where they were first advocated.^{14,22} All along, the idea underlying them has been that petrophysical properties (e.g., relative permeability and capillary pressure relationships, specific surface area,

electrical resistivity parameters, etc.) depend in one way or another on the nature of the pore structure, and on how it will be partitioned in representative cases between the intertwining filaments of the adjacent immiscible fluid phases. Of the pore textural properties enumerated previously, relative permeability turns out to be the most difficult one to measure in the laboratory. This has been the origin of the thought (and hope) that an economy could be expected if relative permeability information somehow could be extracted (by way of calculations) from the more easily obtainable data. Wyllie,²³ a foremost advocate of these ways of thinking, is the authority to be consulted when more information is needed.

Eqs. 7a and 7b are the ones given by Corey *et al.*²⁰ for calculating k_{ro} under three-phase saturation conditions, and Eq. 8 is the one proposed by Stone.²¹ For $S_L > S_{Lr}$,

$$k_{ro} = (1 - S_g - S_w)^3 (1 - S_g + S_w - 2S_{Lr}) / (1 - S_{Lr})^4, \quad \dots \dots \dots (7a)$$

and for $S_L \leq S_{Lr}$

$$k_{ro} = (1 - S_g - S_w) / (1 - S_{Lr})^4. \quad \dots \dots \dots (7b)$$

Also,

$$k_{ro} = (k_{row} + k_{rw})(k_{rog} + k_{rg}) - (k_{rw} + k_{rg}), \quad \dots \dots \dots (8)$$

where

S_L = total liquid saturation, fraction,

S_{Lr} = residual liquid saturation left in pore space, fraction,

k_{row} = relative permeability to oil in a gas-free system, and

k_{rog} = relative permeability to oil in a water-free system.

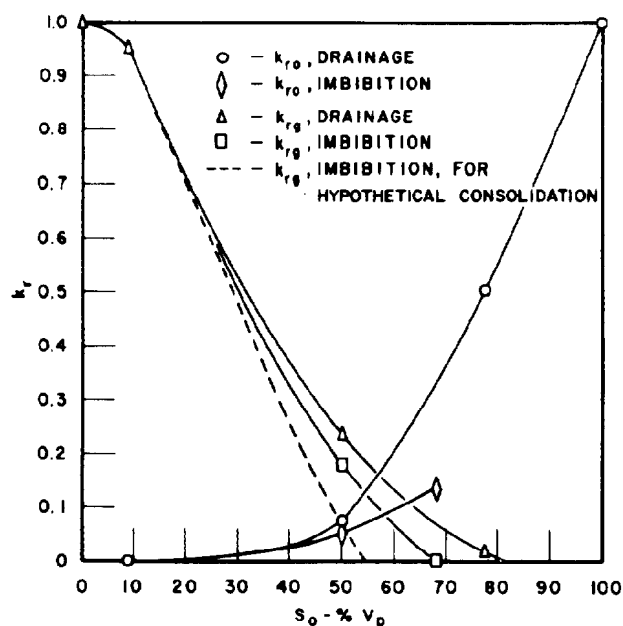


Fig. 28.9—Gas/oil relative permeability in poorly consolidated sandstone.

The recommendation for using Eqs. 7 and 8 to obtain calculated values for the difficult-to-measure k_{ro} under three-phase saturation conditions is that one only needs to enter more easily obtained two-phase data. Inspection will show that while such equations give plausible results (e.g., compatible with the indications of Eq. 6), the results are no more trustworthy than the modeling assumptions when measured relative permeability values are needed but are otherwise unavailable.

Comments. A conclusion to be drawn from this analysis is that if there is any merit to taking short-cuts, it is only when the benefits outweigh the risks. While many (perhaps most) of the readers of this chapter will never have to go to the laboratory to make relative permeability measurements, it is important for them to realize that someone, some day, has to make such measurements before any of the calculation schemes can be used with confidence. In other words, computer guesswork in general will be no substitute for laboratory work. This is because direct observations always will be needed before reliable predictions can be made for processes that inherently depend on material response parameters such as relative permeability.

Recent Literature

More than 30 years have elapsed between an early and a later time when the author of this chapter was provoked to write papers on the then-current problems of relative permeability measurement.^{24,25} It is as though some of the problems have continued to be unsolved and/or unsolvable, while other vexing ones have emerged to take the place of any of the earlier ones that somehow were resolved. In the meantime, work continues on many fronts such as those critiqued in this paper. Note that all the papers now to be referenced have appeared after

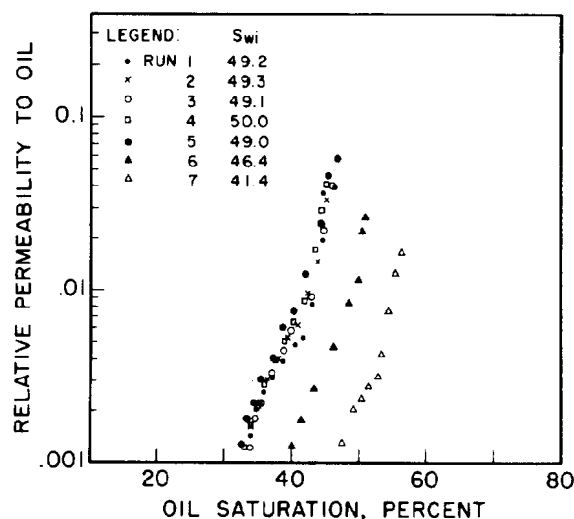


Fig. 28.10—Unsteady-state, three-phase relative mobility (relative permeability to oil, Berea sandstone).

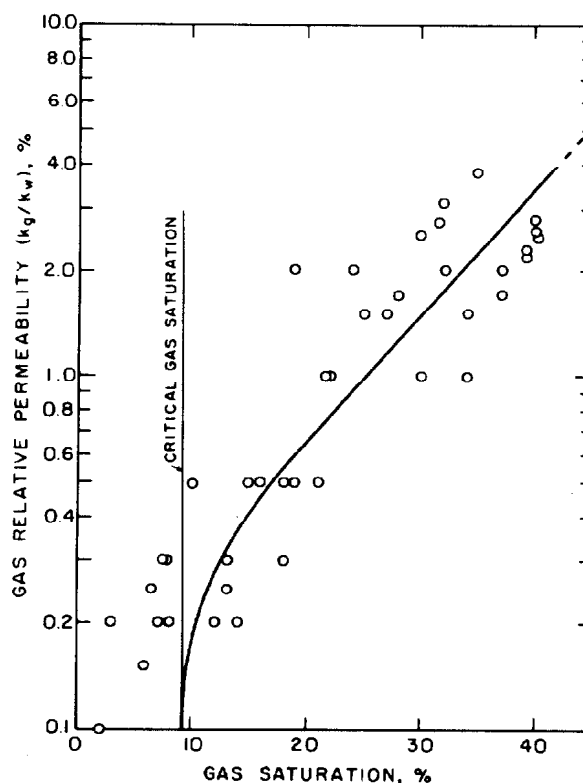


Fig. 28.11—Relative permeability to gas in three-phase flow as a function of gas saturation.

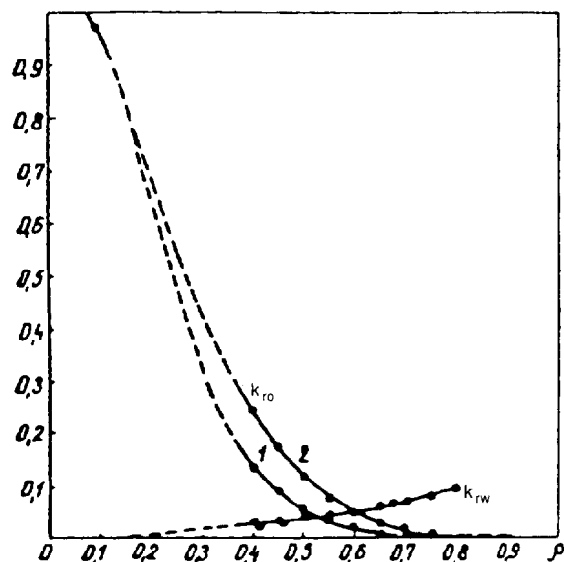


Fig. 28.12—Relative permeability to oil and water showing the effect of displacement (Curve 1) vs. carbonated water displacement (Curve 2).

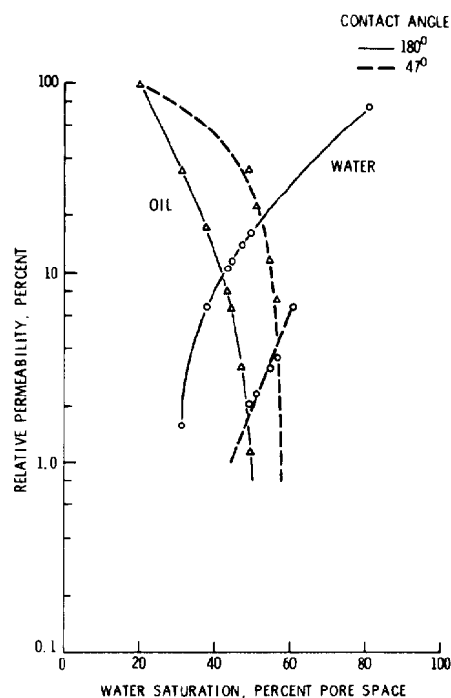


Fig. 28.14—Imbibition relative permeabilities for two wetting conditions, Torpedo sandstone.

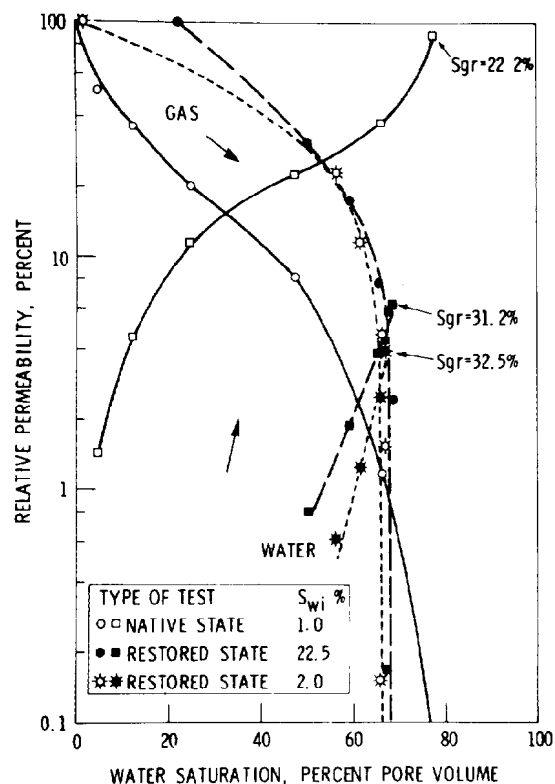


Fig. 28.13—A comparison of restored-state and native-state water/gas relative permeability data.

Wyllie wrote the original chapter on "Relative Permeability" in the first edition of this handbook (in 1962) referencing the literature through the 1950's.²³

Critique of Recent Work

Loomis and Crowell²⁶ present an early but extensive comparison of data obtained by various methods, and as calculated by various mathematical modeling schemes. The high degree of conformity reported makes suspect the objectivity of the work. On the other hand, the authors were quick to point out that wettability was an uncontrolled laboratory variable in their work. This disquieting contention was matched by the surprising result reported without explanation by other workers at the same time, namely that hysteresis effects were different for unconsolidated vs. consolidated core samples.²⁷ Fig. 28.9 shows the trends observed.

The paper of Sarem²⁸ was one of several describing three-phase measurements by an unsteady-state method. One observation (see Fig. 28.10) of this work had to do with the important role played by the initial saturation conditions. At about the same time, Saref and Fatt²⁹ reported success in the development of a nuclear magnetic resonance technique for measurements of fluid saturation levels. These workers, moreover, confirmed the long-held view that relative permeability to gas in three-phase systems depended mostly on the total liquid saturation. This calculation is supported by the data shown in Fig. 28.11.

Two papers appeared in the early 1970's^{30,31} indicating that relative permeability to oil is greatly increased if CO₂ is present (see Fig. 28.12). At this same point in time, Lefebvre du Prey³² was dealing with the question of interfacial tension effects on relative

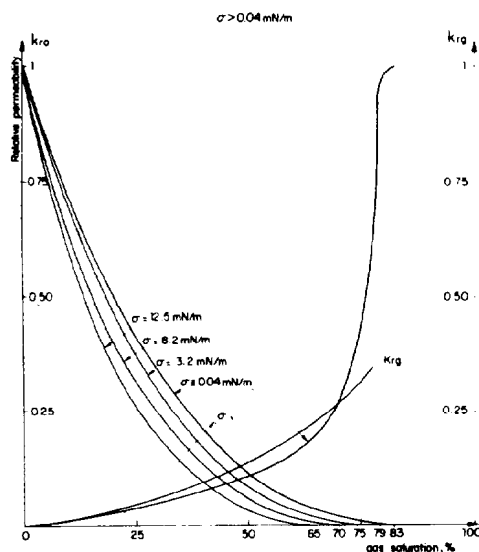


Fig. 28.15—Gas/oil relative permeability calculated from production data from experiments.

permeability while Schneider and Owens³³ and Owens and Archer³⁴ were concluding that because of wettability effects, experimenters were advised to make use of so-called native-state cores. The work of Bardon and Longeron³⁵ also dealt with this subject. And somewhat later Sigmund and MacCaffery³⁶ were trying to sort out the influence of reservoir rock heterogeneity on relative permeability characteristics. Some of the data presented by these authors are shown in Figs. 28.13, 28.14, and 28.15.

In the 1980's, numerous relative permeability papers continue to appear as though a renaissance interest in the old subject is developing. A noteworthy one was by Hagoort,³⁷ who used a centrifuge technique to show the high efficiency of the gravity drainage recovery process in water-wet cores. Bogdanov and Markhasin³⁸ introduced the less familiar subject that speculated that viscosity changes (because of molecular-surface interactions with the rock matrix) could distort relative permeability data. At the same time, Ashford,³⁹ in a very comprehensive paper, was reopening the dubious issue of how relative permeability and capillary pressure data can be linked directly. (As implied above, it is nice to have a conceptual theory available to explain relative permeability effects, but to expect that calculations avoid the need for careful experimental work is a kind of wishful thinking that can be justified only when there is a great urgency to have qualitative inputs for reservoir process simulations). Fig. 28.16 is representative of the fits reported by Ashford between calculated and measured values.

Delshad *et al.*⁴⁰ currently have addressed the interesting question of whether the transport of low-tension micellar fluids will significantly change classical relative permeability trends. They show that the residual (end-point) saturations decrease and relative permeabilities increase as interfacial tension decreases. The predicted nearly 45° relative permeability curves are shown for one case in Fig. 28.17. Yokoyama⁴¹ has been dealing

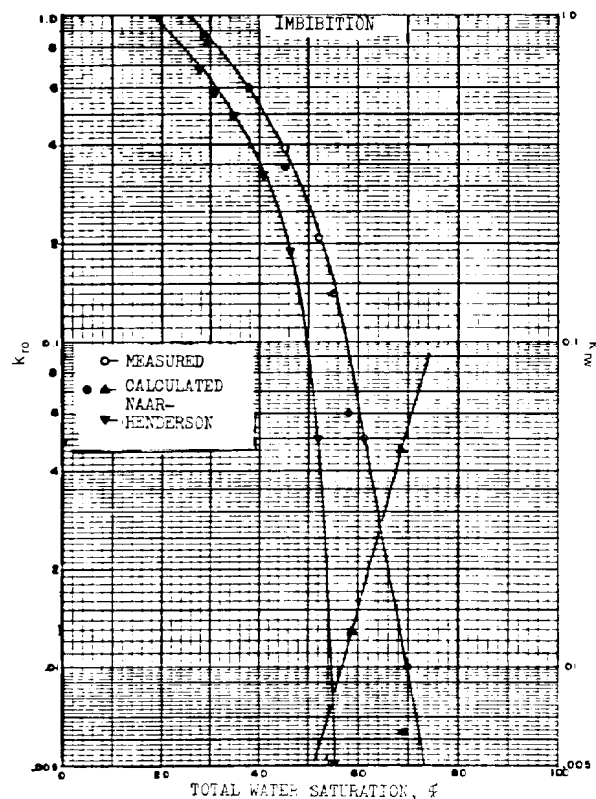


Fig. 28.16—Relative permeability relations for imbibition and drainage experiments, with values calculated by Naar *et al.* method.

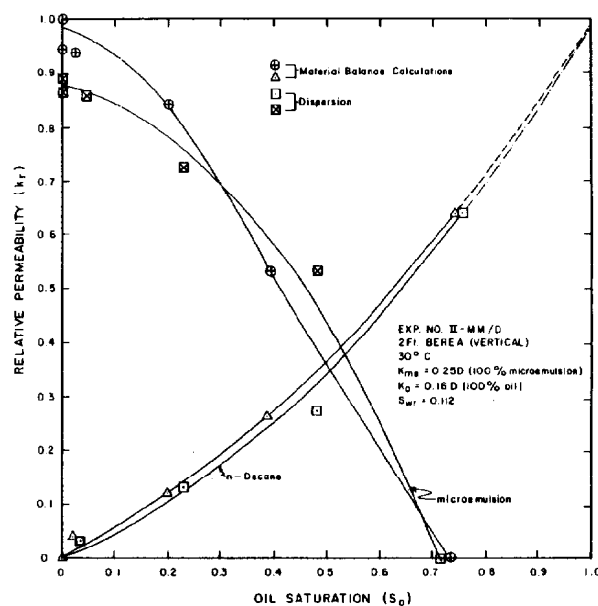


Fig. 28.17—Imbibition relative permeability curves for microemulsion and decane vs. oil saturation in Berea sandstone.

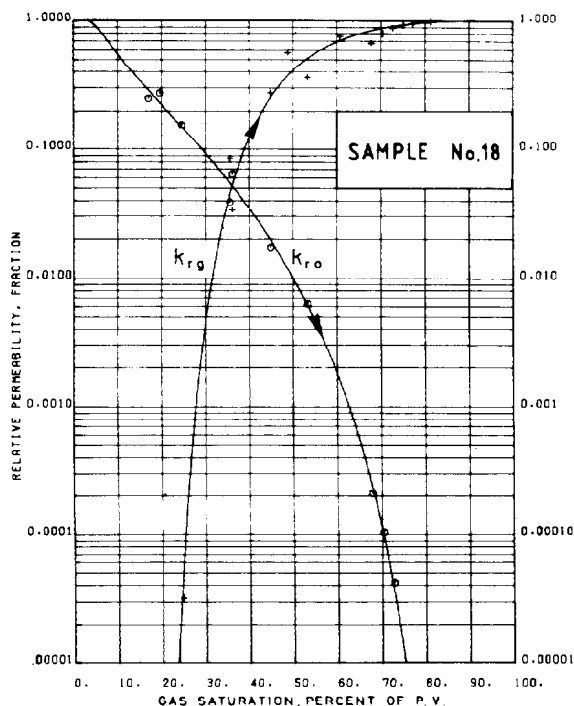


Fig. 28.18—Drainage k_{ro} and k_{rg} curves.

with the equally complex problem of accounting for transverse and longitudinal capillary imbibition during displacements in stratified media.

In another direction, Carlson⁴² extends Land's⁴³ earlier prescriptions for calculating flow from independent measurements of rock properties. Chierici⁴⁴ does the same thing, on the basis of the "bundle of capillary tubes" model described earlier by Brooks and Corey.⁴⁵ Some of these data are shown in Fig. 28.18.

Finally, Lin and Slattery⁴⁶ and Mohanty and Salter⁴⁷ carry pore structure (network) modeling as a basis for arriving at calculated relative permeabilities to still higher plateaus of sophistication. Extensive bibliographies are provided by these latter authors. Some of their results are given in Figs. 28.19 and 28.20.

For example, Fig. 28.20 indicates that (1) relative permeabilities to the nonwetting phase k_{rn} during secondary imbibition (SI) and imbibition (IM) are essentially the same but lower than the values that refer to the primary drainage (PD) conditions, and (2) relative permeabilities to the wetting phase k_{rw} during primary drainage is lower than that in either secondary drainage or imbibition. In other words, those authors⁴⁷ conclude that "the ratio of conductivity or nooks and crannies to that of a full throat feature influences the wetting fluid permeabilities only at low saturation."

Other recent papers are those of Salter and Mohanty,⁴⁸ who made observations to justify a modeling of multiphase flow that postulates flowing, dendritic, and isolated configurations for each phase, and of Maini and Batycky,⁴⁹ who claim (see Fig. 28.21) that temperature influences both the endpoint saturation and the shape of the relative permeability curves. A different view about the importance of temperature effects had been expressed earlier by Sufi *et al.*⁵⁰

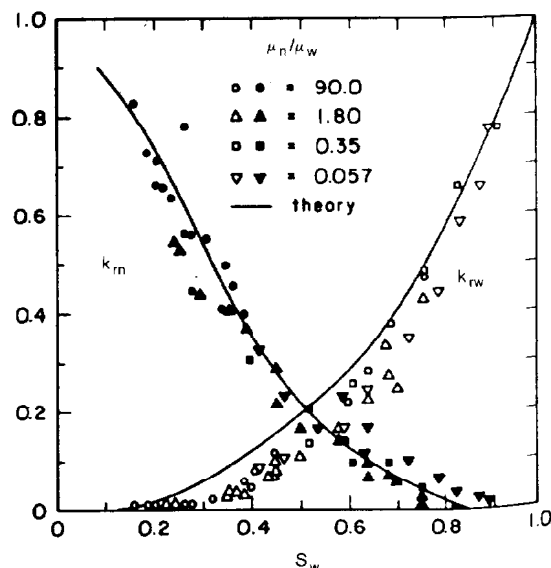


Fig. 28.19—Comparison of drainage relative permeabilities from randomized network model with experimental data for 100 to 200 mesh sand.

The paper of O'Meara and Lease¹⁸ has been cited previously in connection with the unsteady-state determination of three-phase relative permeabilities using the centrifuge technique. It, along with the Maini and Batycky paper,⁴⁹ are just two of nine other papers on relative permeability presented at the 1983 Society of Petroleum Engineers Annual Technical Conference and Exhibition in San Francisco, Oct. 5-8. Listing them by topic is one way to expose the depth and breadth of current interests in the subject. Thus, Kortekass⁵¹ describes displacement in cross-bedded reservoirs. Meads and Bassiouni⁵² speak of combining production history and petrophysical correlations to enhance the representativeness of relative permeability data. Miller and Ramey⁵³ deal further with temperature effects for oil/water systems. Mohanty and Salter⁵⁴ extend their work on oil mobilization, transverse dispersion, and wettability effects. Fulcher *et al.*⁵⁵ and Harbert⁵⁶ deal further with low interfacial systems. Heiba *et al.*⁵⁷ address the wettability questions. And in companion papers, Heaviside *et al.*⁵⁸ cover the experimental and theoretical aspects of relative permeability phenomena. Such are the extensive details currently being discussed.

Ramifications Needing Attention

In summary, the reader who has studied the representative papers cited here, and the even larger number that are scattered in the literature at large, will conclude that this chapter is not the final one to be written on what amounts to be a very complex subject. Some of the ramifications that appear to need further attention include studies of the following effects: (1) phase changes such as gas evolution during multiphase flow, (2) non-collinear flow in a gravity force field between immisci-

ble fluids of differing densities, and counterflow imbibition, (3) reservoir rock anisotropy and heterogeneity by which sample size and sampling frequency requirements are to be determined, (4) "fines" movements, (5) overburden stress simulation and related stress-relaxation and creep compaction phenomena, (6) viscous drag at interstitial interfaces between contiguous immiscible fluids, (7) chemical precipitation and dissolution phenomena, (8) chemical reactions, (9) high Reynolds-number conditions (nonlinear laminar and turbulent flow regimes) (10) Klinkenberg gas-slippage effects, (11) concentration and/or thermal gradients being superimposed on fields of flow primarily caused by mechanical energy gradients, (12) non-Newtonian rheology, (13) systems characterized by more than one local pore space type, (14) fluid/solid interactions, for example, as related to the mineralogy of interstitial clays, (15) viscous fingering, and (16) hysteresis related to wettability changes.

While theoretical considerations may permit a qualitative prediction of the nature of some of these effects, in the final analysis, any truly quantitative assessments should be based on directly undertaken experimental work, if possible. This is not to say that in every case the laboratory data obtained on small hand specimens will reveal everything that needs to be known about large composite petroleum reservoirs, but rather that observations generally are more trustworthy indicators than are blind guesses.

Conclusions

Several questions come to mind whenever the subject of relative permeability is raised: how is it to be defined? where can the information be obtained? why is it needed and by whom? What are the proper (fruitful) ways to use it? Only partial answers to some of these questions have been given in this chapter. This is because the subject is too vast to be dealt with fully in limited space and because the details not covered are probably too specialized for the average reader, whose concern is only with the ordinary applications.

Here we have asserted that definitions of permeability (specific, effective, relative) are embedded in the differential equations that describe the transport equations governing fluid flow in petroleum reservoirs. Eqs. 1 and 5 are examples that apply to special situations (steady single-phase flow and unsteady multiphase flow of immiscible fluids, respectively). Obviously, the differential equations of transport will have other forms for more general cases of fluid flow, such as those observed when there is coupling with chemical diffusion and/or heat transfer processes. This is to say that there may be different kinds of relative permeability to deal with according to the nature of the process under consideration. In all cases, however, one must start by constructing the defining equations to be compatible with the underlying principles of nonequilibrium thermodynamics.

Relative permeability information can be obtained in two major ways. The preferred method is to have an experiment performed on a representative sample of the reservoir rock according to the procedure prescribed by the appropriate integral form of the defining differential equation. Eqs. 1 and 2 are examples of integrals that involve measurable terms (such as volumetric flow rates

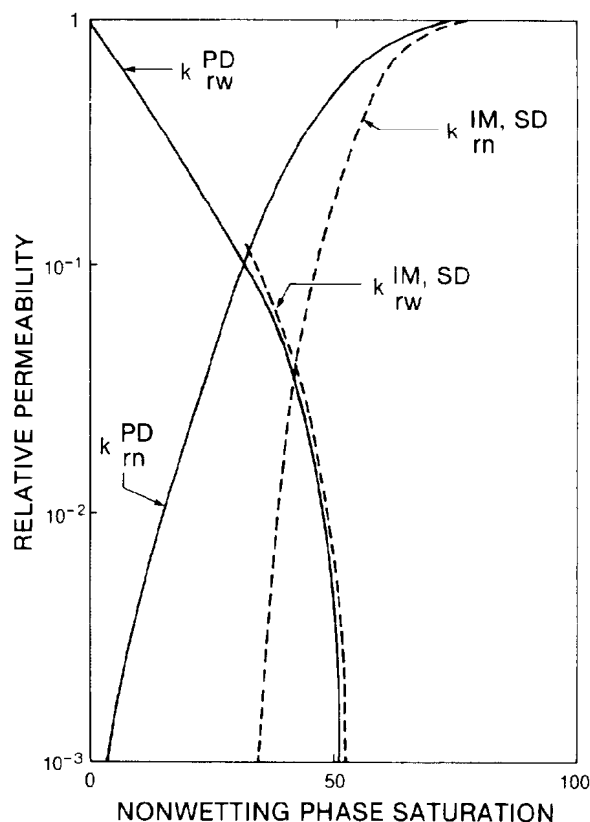


Fig. 28.20—Relative permeability curves.

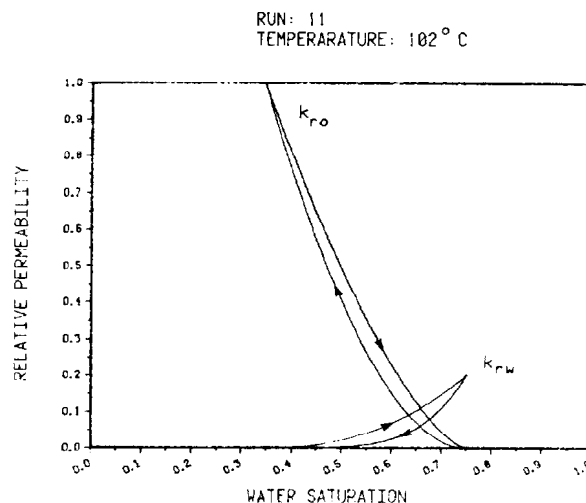


Fig. 28.21—High-temperature relative permeability curves for oil and water.

and pressures, p_i , at bounding sample surfaces). Since the parent differential equations themselves have terms that cannot be directly measured in the laboratory (such as velocity and mechanical energy gradients), integral forms that apply to the particular initial and boundary conditions of the problem must be derived and used for each specific case.

In these connections, it will be revealing (and disturbing) to mention that the degree of equivalence of relative permeability functions obtained by different methods (e.g., the steady- vs. the unsteady-state schemes mentioned previously) so far has not been established fully. Eq. 2 prescribes how the steady-state results are to be obtained, while integrals of Eq. 5 prescribe how the unsteady-state results are to be obtained. Until the definitive laboratory work is done and the comparisons are reported in the literature, users of relative permeability information today will continue to be left in the dark as to which procedure can be used with the most confidence when applications are being made.

As for ordinary applications, relative permeability information is used by petroleum reservoir engineers when interpretations and assessments are being made about the outcomes of observed and probable petroleum recovery processes. These applications are referenced in other chapters in this handbook (e.g., on reservoir simulation, well testing analysis, etc.), and will not be discussed further here. Suffice it to say that the same governing transport equations and their integrals by which relative permeability is defined, necessarily are used again in the ensuing analyses of reservoir performance; hence, relative permeability will be needed as input data whenever analytical studies are undertaken. Among other things, this means that using drainage relative permeability data to describe an imbibition process (such as waterflooding) should be avoided.

A second way to obtain relative permeability information is to develop suitable models of the processes under consideration for use as calculation algorithms. Eqs. 7 and 8 are examples that in use require laboratory data more easily obtained than the relative permeability functions themselves. For example, to calculate three-phase oil relative permeability as a function of oil saturation (where $S_o = 1 - S_w - S_g$) by Eq. 7, all that is needed is prior knowledge of the interstitial water saturation. Naturally, such calculation schemes cannot be used blindly except for cases where it has been independently validated that calculated and experimental values are equivalent. In other words, even the most carefully constructed calculation scheme does not circumvent the need to have experimental measurement methods also developed and available.

However, calculation schemes usually involve analytical functions that can be entered directly into the computer software used for such things as qualitative economic forecasting. Similarly, the related way to obtain relative permeability information, namely by inferring it from the values that force history matches of observed field data, also has a utility when qualitative assessments are being made using reservoir simulators.

The points being made here are both subtle and self-evident. The aim has been simply to convey a certain set of useful ideas to users of relative permeability information such as (1) that relative permeability methodologies

are still in the developmental state even after more than a half century of well-intentioned labor by hundreds of workers and (2) that users of relative permeability information must put the burden of proof on those that supply it, to demonstrate that credible schemes have been used.

Acknowledgment

Any author who has been writing narrowly on a specialized subject like relative permeability for more than a third of a century (specifically from 1948¹⁹ to 1984²⁵) has to be deeply indebted to all those inspiring workers who have managed to keep the issues alive and in focus over such a long period. A few of them, but not all, are named in the abbreviated references that appear here. Likewise, any teacher for a similarly long period must be deeply indebted to the generations of inquisitive students who were willing to ask the provocative questions before they graduated and left to disappear into oblivion. What a lucky thing it was to have had so many companions on what otherwise would have been a dreary Orwellian journey.

Nomenclature

A	= cross-sectional area
A_f	= cross-sectional area of flow path
k	= specific permeability
k_j	= effective permeability, Fluid j (gas, oil, or water)
k_{rj}	= relative permeability, Fluid j (gas, oil, or water)
k_{rog}	= relative permeability to oil in water-free system
k_{row}	= relative permeability to oil in gas-free system
k_{rw}	= relative permeability of wetting fluid
K_{me}	= microemulsion dispersion coefficient
L	= length
L_h	= horizontal distance
M_n	= mobility of nonwetting phase
M_w	= mobility of wetting phase
p_j	= pressure, Fluid j
Δp	= pressure drop
P_c	= capillary pressure
q	= volumetric flow rate
S_{gr}	= residual gas saturation
S_{ij}	= irreducible (minimum) value of S_j
S_{iw}	= irreducible (interstitial) water saturation
S_j	= fractional saturation of j th fluid
S_L	= total liquid saturation
S_{Lr}	= residual liquid saturation
S_{Lw}	= wetting liquid saturation
S_{rn}	= residual (nonproduced) nonwetting fluid saturation
S_w	= water saturation
S_{wr}	= residual water saturation
t	= time
V_{fj}	= volume of Fluid j
V_{pt}	= total PV
Δp	= pressure drop
μ	= fluid viscosity

σ = interfacial tension

ϕ = porosity

Subscripts

g = gas

j = j th fluid (gas, oil, or water)

n = nonwetting

o = oil

w = water or wetting

References

1. Bear, J.: *Dynamics of Fluids in Porous Media*, Elsevier Scientific Publishing Co. Inc., New York City (1972).
2. Scheidegger, A.E.: *Physics of Flow Through Porous Media*, third edition, U. of Toronto Press, Toronto, Canada (1974).
3. Richards, L.A.: "Capillary Conduction of Liquids Through Porous Mediums," *Physics* (1931) 1, 318-33.
4. Odeh, A.S.: "Effect of Viscosity Ratio on Relative Permeability," *Trans., AIME* (1959) 216, 346-52.
5. Yuster, S.T.: "Theoretical Consideration of Multiphase Flow in Idealized Capillary Systems," *Proc., Third World Pet. Cong., The Hague* (1951) 436-45.
6. Buckley, S.E. and Leverett, M.C.: "Mechanism of Fluid Displacement in Sands," *Trans., AIME* (1942) 146, 107-16.
7. Rose, W.: "Some Problems Connected With the Use of Classical Descriptions of Fluid/Fluid Displacement Processes," *Fundamentals of Transport Processes in Porous Media*, Elsevier Scientific Publishing Co. Inc., Amsterdam (1972) 229-40.
8. Hassler, G.L.: U.S. Patent No. 2,345,935 (1944).
9. Braun, E.M. and Blackwell, R.J.: "A Steady-State Technique for Measuring Oil-Water Relative Permeability Curves at Reservoir Conditions," paper SPE 10155 presented at the 1981 Annual Technical Conference and Exhibition, San Antonio, Oct. 4-7.
10. Muskat, M.: *Physical Principles of Oil Production*, McGraw-Hill Book Co. Inc., New York City (1949).
11. Osoba, J.S. et al.: "Laboratory Measurements of Relative Permeability," *Trans., AIME* (1951) 192, 47-56.
12. Rose, W.: "Some Problems in Applying the Hassler Relative Permeability Method," *J. Pet. Tech.* (July 1980) 1161-63.
13. Rose, W.: U.S. Patent No. 4,506,542 (1985).
14. Rose, W. and Bruce, W.A.: "Evaluation of Capillary Character in Reservoir Rock," *Trans., AIME* (1949) 186, 127-42.
15. Leverett, M.C.: "Capillary Behavior in Porous Solids," *Trans., AIME* (1940) 142, 152-69.
16. "Measurement of Relative Permeabilities by the Welge Method (Investigation)," *Revue de l'Institut Français du Pétrole* (1973) 28, No. 5, 695-714.
17. Jones, S.C. and Roszelle, W.O.: "Graphical Techniques for Determining Relative Permeability From Displacement Experiments," *J. Pet. Tech.* (May 1978) 807-17; *Trans., AIME*, 265.
18. O'Meara, D.J. Jr. and Lease, W.O.: "Multiphase Relative Permeability Measurements Using an Automated Centrifuge," paper SPE 12128 presented at the 1983 SPE Annual Technical Conference and Exhibition, San Francisco, Oct. 5-8.
19. Rose, W.: "Permeability and Gas Slippage Phenomena," *Drill. and Prod. Prac.*, API, Dallas (1948) 127-35.
20. Corey, A.T. et al.: "Three-Phase Relative Permeability," *J. Pet. Tech.* (Nov. 1956) 63-65; *Trans., AIME*, 207.
21. Stone, H.L.: "Probability Model for Estimating Three-Phase Relative Permeability," *J. Can. Pet. Tech.* (Oct. 1973) 53-59.
22. Rose, W.: "Theoretical Generalizations Leading to the Evaluation of Relative Permeability," *Trans., AIME* (1949) 186, 111-26.
23. Wylie, M.R.J.: "Relative Permeability," *Petroleum Production Handbook*, SPE, Richardson, TX (1962) 2, 1-14.
24. Rose, W.: "Some Problems of Relative Permeability Measurement," *Proc., Third World Pet. Cong.* (1951) Sec. 2, 446-59.
25. Rose, W.: "Formation Evaluation by Reservoir Rock and Fluid Sample Analyses," paper SPE 11858 presented at the 1983 SPE Rocky Mountain Regional Meeting, Salt Lake City, May 22-25.
26. Loomis, A.G. and Crowell, D.C.: "Report of Investigations," *Bull.* 599, U.S. Bureau of Mines (1962).
27. Naar, J. et al.: "Imbibition Relative Permeability in Unconsolidated Porous Media," *Soc. Pet. Eng. J.* (March 1962) 13-17; *Trans., AIME*, 225.
28. Sarem, A.M.: "Three-Phase Relative Permeability Measurements by Unsteady-State Method," *Soc. Pet. Eng. J.* (Sept. 1966) 199-205; *Trans., AIME*, 237.
29. Saraf, D.N. and Fatt, I.: "Three-Phase Relative Permeability Measurement Using a Nuclear Magnetic Resonance Technique for Estimating Fluid Saturation," *Soc. Pet. Eng. J.* (Sept. 1967) 235-42; *Trans., AIME*, 240.
30. Bálint, V. et al.: "Relative Permeability Curves for Oil Displacement by Carbon Dioxide," *Koolag és Földgáz* (1971) 4, 140-44.
31. Panteleev, V.G. et al.: "Influence of Carbon Dioxide on Three Phase Permeability by Oil and Water," *Neftepromyslovoe delo* (1973) No. 6, 11-13.
32. Lefebvre du Prey, E.J.: "Factors Affecting Liquid-Liquid Relative Permeabilities of a Consolidated Porous Medium," *Soc. Pet. Eng. J.* (Feb. 1973) 39-47.
33. Schneider, F.N. and Owens, W.W.: "Relative Permeability Studies of Gas-Water Flow Following Solvent Injection in Carbonate Rocks," *Soc. Pet. Eng. J.* (Feb. 1976) 23-30; *Trans., AIME*, 261.
34. Owens, W.W. and Archer, D.L.: "The Effect of Rock Wettability on Oil-Water Relative Permeability Relationships," *J. Pet. Tech.* (July 1971) 873-78; *Trans., AIME*, 251.
35. Bardon, C. and Longeron, D.G.: "Influence of Very Low Interfacial Tensions on Relative Permeability," *Soc. Pet. Eng. J.* (Oct. 1980) 391-401.
36. Sigmund, P.M. and McCaffery, F.G.: "An Improved Unsteady-State Procedure for Determining Relative-Permeability Characteristics of Heterogeneous Porous Media," *Soc. Pet. Eng. J.* (Feb. 1979) 15-28.
37. Hagoort, J.: "Oil Recovery by Gravity Drainage," *Soc. Pet. Eng. J.* (June 1980) 139-50.
38. Bogdanov, V.S. and Markhasin, I.L.: "Determination of Relative Permeability to Oil With Allowance for the Change in its Viscosity Due to Molecular Surface Interaction with Rock," *Izv. Vyssh. Ucheb. Zaved. Neft' i Gaz* (Oct. 1980) No. 10, 57-60.
39. Ashford, F.E.: "Determination of Two Phase and Multiphase Relative Permeability for Drainage and Imbibition Cycles Based on Capillary Pressure Measurement," *Revista Tecnica Intevep* (1981) 1, 77-94.
40. Delshad, M. et al.: "Multiphase Dispersion and Relative Permeability Experiments," *Soc. Pet. Eng. J.* (Aug. 1985) 524-34.
41. Yokoyama, Y. and Lake, L.W.: "The Effects of Capillary Pressure on Immiscible Displacements in Stratified Porous Media," paper SPE 10109 presented at the 1981 SPE Annual Technical Conference and Exhibition, San Antonio, Oct. 4-7.
42. Carlson, F.M.: "Simulation of Relative Permeability Hysteresis to the Nonwetting Phase," paper SPE 10157 presented at the 1981 SPE Annual Technical Conference and Exhibition, San Antonio, Sept. 4-7.
43. Land, C.S.: "Calculation of Imbibition Relative Permeability for Two- and Three-Phase Flow from Rock Properties," *Soc. Pet. Eng. J.* (June 1968) 149-56; *Trans., AIME*, 243.
44. Chierici, G.L.: "Novel Relations for Drainage and Imbibition Relative Permeabilities," *Soc. Pet. Eng. J.* (June 1984) 275-76.
45. Brooks, R.H. and Corey, A.T.: *Hydraulic Paper No. 3*, Colorado State U. (1964).
46. Lin, C. and Slattery, J.C.: "Three-Dimensional, Randomized, Network Model for Two-Phase Flow Through Porous Media," *AIChE J.*, 28 (1982) No. 2, 311-24.
47. Mohanty, K.K. and Salter, S.J.: "Multiphase Flow in Porous Media: II. Pore-Level Modeling," paper SPE 11018 presented at the 1982 SPE Annual Technical Conference and Exhibition, New Orleans, Sept. 26-29.
48. Salter, S.J. and Mohanty, K.K.: "Multiphase Flow in Porous Media: I. Macroscopic Observations and Modeling," paper SPE 11017 presented at the 1982 SPE Annual Technical Conference and Exhibition, New Orleans, Sept. 26-29.
49. Maini, B.B. and Batycky, J.P.: "Effect of Temperature on Heavy-Oil/Water Relative Permeabilities in Horizontally and Vertically Drilled Core Plugs," *J. Pet. Tech.* (Aug. 1985) 1500-10.
50. Sufi, A.H. et al.: "Temperature Effects on Relative Permeabilities of Oil-Water Systems," paper SPE 11071 presented at the 1982 SPE Annual Technical Conference and Exhibition, New Orleans, Sept. 26-29.
51. Kortekaas, T.F.M.: "Water/Oil Displacement Characteristics in Crossbedded Reservoir Zones," *Soc. Pet. Eng. J.* (Dec. 1985) 917-26.

52. Meads, R. and Bassiouni, Z.: "Combining Production History and Petrophysical Correlations to Obtain More Representative Relative Permeability Data," paper SPE 12113 presented at the 1983 SPE Annual Technical Conference and Exhibition, San Francisco, Oct. 5-8.
53. Miller, M.A. and Ramey, H.J. Jr.: "Effect of Temperature on Heavy-Oil/Water Relative Permeabilities of Unconsolidated and Consolidated Sands," *Soc. Pet. Eng. J.* (Dec. 1985) 945-54.
54. Mohanty, K.K. and Salter, S.J.: "Multiphase Flow in Porous Media: Part 3—Oil Mobilization, Transverse Dispersion, and Wettability," paper SPE 12127 presented at the 1983 SPE Annual Technical Conference and Exhibition, San Francisco, Oct. 5-8.
55. Fulcher, R.A. *et al.*: "Effect of Capillary Number and Its Constituents on Two-Phase Relative Permeability Curves," *J. Pet. Tech.* (Feb. 1985) 249-60.
56. Harbert, L.W.: "Low-Interfacial-Tension Relative Permeability," paper SPE 12171 presented at the 1983 SPE Annual Technical Conference and Exhibition, San Francisco, Oct. 5-8.
57. Heiba, A.A. *et al.*: "Effect of Wettability on Two-Phase Relative Permeabilities and Capillary Pressures," paper SPE 12172 presented at the 1983 SPE Annual Technical Conference and Exhibition, San Francisco, Oct. 5-8.
58. Heaviside, J., Black, C.J.J., and Berry, J.F.: "Fundamentals of Relative Permeability: Experimental and Theoretical Considerations," paper SPE 12173 presented at the 1983 SPE Annual Technical Conference and Exhibition, San Francisco, Oct. 5-8.

General References

- Honarpour, M.: *Relative Permeability of Petroleum Reservoirs*, CRC Press Inc., Boca Raton, FL (1986).
- Whitaker, S.: "Flow in Porous Media II: The Governing Equations for Immiscible, Two-Phase Flow," *Transport in Porous Media* (1986) **1**, 105-25.

Chapter 29

Petroleum Reservoir Traps

Raymond T. Skirvin, J.R. Butler and Co
Brian E. Ausburn, J.R. Butler and Co.*

Introduction

A reservoir trap is a combination of physical conditions that will cause hydrocarbon liquids and/or gases and water to accumulate in porous and permeable rock and prevent them from escaping either laterally or vertically because of differences in specific gravity, pressure, fluid/gas characteristics, and/or lithology. It has the capability of collecting, holding, and yielding hydrocarbon fluids and water.

The portion of the trap that contains oil and/or gas accumulations is the petroleum reservoir. It generally occupies a limited portion of the trap capacity, the remainder being occupied by formation waters that underlie and are interspersed within the petroleum accumulation.

Traps are formed by an infinite variety of structural and stratigraphic conditions of rock formations combined with pressure differentials among the various fluids within the reservoir rock. A trap consists of an impervious cover or roof rock overlying a porous and permeable rock. Reservoir pressure gradients and fluid flow within the reservoir rock can create traps that do not have structural closure. The boundary between oil and water or between gas and water need not be flat or level when these pressure gradients are present. Generally, however, traps do have structural closure, and as viewed from below, the impervious cover is concave, preventing the oil and gas, if present, from escaping vertically or laterally. The water underlying the oil and gas exerts a buoyant force on the oil/water boundary or contact, lifting and holding the oil and gas to the crest of the structure or area of minimum hydrostatic pressure.

Trap Classification

Classification of traps logically falls into three broad general groups: (1) structural, (2) stratigraphic, and (3) combination. More detailed classifications have been

made by geologists attempting to include all factors and conditions that account for petroleum reservoirs. Many reservoirs have unique features that cause the oil to accumulate at a given location. The purpose of this chapter is to illustrate the more common geological conditions that cause traps and to point out a few of the infinite variety of minor variations that help create and hold petroleum accumulations in place.

Structural Traps

Structure implies some form of rock deformation, commonly expressed as a positive uplift, which may result in four-way dip closure. With the proper stratigraphy, structural traps may be present. Domes, anticlines, and folds are common structures. Fault-related features also may be classified as structural traps if closure is present. Structural traps are the easiest to locate by surface and subsurface geological and geophysical studies. They are the most numerous among traps and have received a greater amount of attention in the search for oil than all other types of traps. In new areas of exploration the prime search is for potential reservoir rock, source beds for hydrocarbons, and structural deformation. This structural deformation provides opportunities for several types of structural traps.

Domes, Anticlines, and Folds. Domes, anticlines, and folds in general must have structural closure to become effective traps. The reservoir rock must dip away in all directions from the crest of the structure. If there is not dip in all directions away from the crest but hydrocarbons are present, there are other contributing physical factors that helped complete the trap.

Domes, anticlines, and folds caused by structural deformation of sedimentary rocks generally create many potential traps because the deformation extends vertically through potential reservoirs. Thus a single well can reveal many possible pay zones when drilled on the crest of a domal structure.

*Fred L. Oliver wrote the original chapter on this topic in the 1962 edition.

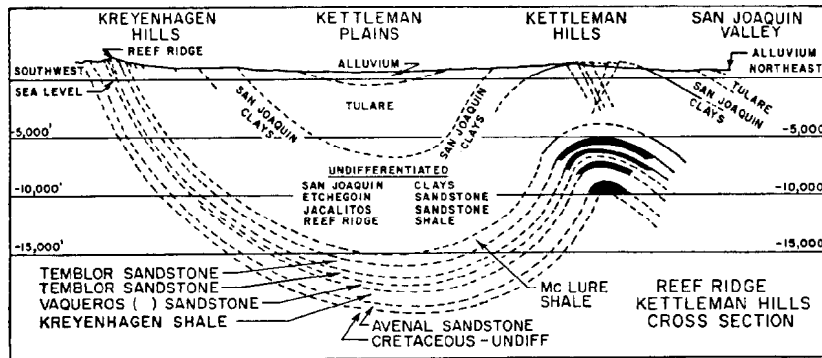


Fig. 29.1—Example of anticlinal folds creating structural traps; Kettleman Hills field.

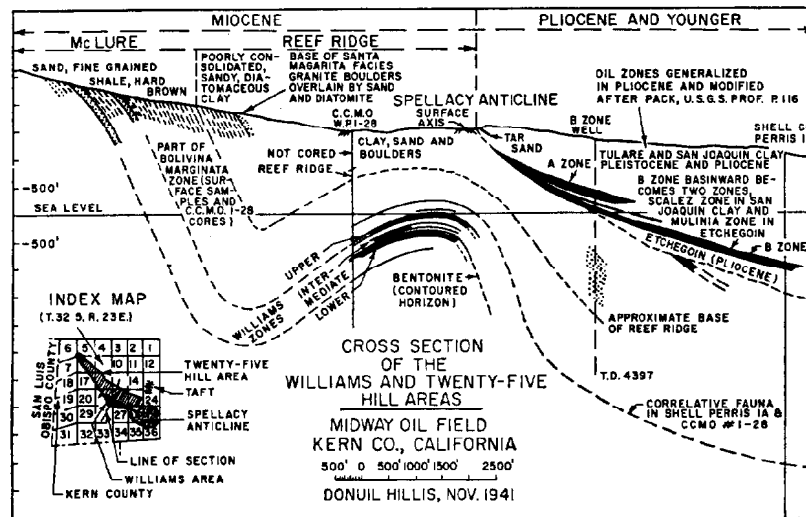


Fig. 29.2—Example of anticlinal folds creating structural and stratigraphic traps; Midway oilfield.

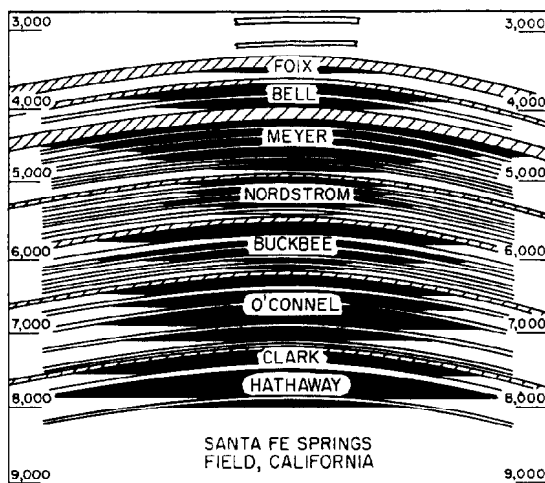


Fig. 29.3—Example of anticlinal folds creating many separate reservoirs; Santa Fe Springs field.

Figs. 29.1, 29.2, and 29.3 are cross sections of Kettleman Hills, Midway, and Santa Fe Springs fields, CA.¹ These are examples of single folds creating many separate accumulations. The separation between the various reservoirs is demonstrated in each case by different oil/water and gas/oil contacts in most reservoirs. The Midway field also illustrates stratigraphic traps formed on the flanks of the anticlinal fold.

Folds, anticlines, and domes are the easiest to interpret in subsurface studies. They vary in size from a few acres to several thousand acres. Folds and anticlines were created by compressional or tensional forces in the earth's crust or by differential compaction of the sediments. Asymmetrical anticlines, overturned anticlines, thrust faulting, and fracturing generally indicate areas of compression. Symmetrical folds and anticlines, low-angle normal faulting, monoclines, homoclines, and low-relief domal structures generally indicate areas of tensional forces or compaction.

Mountainous areas usually result from compressional forces. Torsion and shearing help cause local complex structures but are generally forces resulting from the more regional compressional forces of the earth's crust.

Stable areas or areas of subsidence are the counterpart to mountain-building compressional areas. They are areas where structures are caused by differential

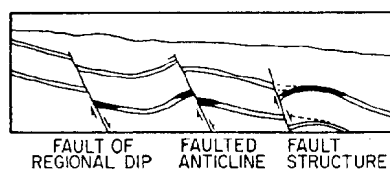


Fig. 29.4—Examples of fault traps: normal or gravity faults.

downwarping, as in the midcontinent area of the U.S. and areas where structures are created by the lengthening of the earth's crust, such as the gulf coast of Texas and Louisiana. This lengthening causes regional horizontal tensional forces that create simple and more predictable local structures. The many prolific structural and stratigraphic oil trends that parallel the U.S. gulf coast today are the result of regional downwarping and tensional forces.

Fault Traps. Fault traps are classified as structural traps where closure is effected in one or more directions by faulting or where faulting has caused definite changes in the reservoir configuration (such as along strike-slip faults). Many structures are faulted without being limited by the faults or without changing the reservoir configuration. Fault traps can occur in both the up- and downthrown blocks. Closure against the fault can result from faults striking across regional dip or across anticlines or domes. Horsts and grabens and other closed fault blocks can result in traps with relatively no structural closure.

Normal or gravity faults (Fig. 29.4) occur as a result of tensional or gravitational forces. The angle of the fault plane with the horizontal generally ranges between 25 and 60°. Normal faults involve horizontal lengthening of the earth's crust and are recognized in the subsurface by loss of stratigraphic section in wells drilled through the fault plane. Geophysically, they are recognized by interruptions in the continuity of reflective interfaces.

Two common types of normal fault-related traps are: (1) fault closures and (2) rollover fault closures. Any structural nose cut at right angles by a fault results in a fault closure. The direction of throw on the fault is not important but the closure created by the fault is. For example, a south-plunging structural nose cut at right angles by a fault will result in a potential trap. The fault throw may be in either direction. A trap will result if the fault acts as a seal or if the potential reservoir is thrown against a shale or other impermeable member on the opposite side of the fault.

Gravity-type faulting commonly occurs in areas of tension and over the crests of domes and anticlines because of the stresses involved. Fault traps are common in such an environment, and hydrocarbon accumulations may occur on either the up- or downthrown blocks, in horsts, and/or in grabens.

Rollover fault closures are common in sedimentary basins receiving great quantities of sediments. Closure is created on the downthrown block by contemporaneous sedimentation and fault movement. Through this interaction, more deposition takes place next to the active fault plane, resulting in a "downbending" of the deposits into

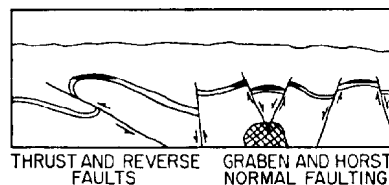


Fig. 29.5—Examples of fault traps: reverse or thrust faults.

the fault. This "downbending" creates a reversal in dip and this results in closure. This type of trap is extremely common in the Cenozoic formations of the U.S. gulf coast.

Reverse or thrust faults (Fig. 29.5) result from compressional forces and involve horizontal shortening of the earth's crust. The angle of the fault plane with a horizontal plane can vary from a few degrees to 90° and can be recognized in the subsurface by repetition of stratigraphic section in wells drilled through the fault plane. Structural traps of this nature are common on both the east and west coasts of North America. The occurrence of a trap against a fault depends on the fault plane sealing the porous reservoir rock and preventing migration across or along the fault plane.

Fractured formations usually are caused by local deformation, faulting and folding, reduction in overburden permitting expansion of the underlying rock, and differential compaction. Brittle rocks are more commonly affected because of their inelasticity. In many cases minor joints, fractures, and fissures are modified by solution and combine with primary and secondary porosity to give a greater effective reservoir porosity and permeability. Fractures in reservoirs increase the wellbore radius and permit extremely tight and impermeable areas to bleed into the fractures over a wide area and thus be connected with channels leading to the wellbore.

Production is sometimes obtained from igneous and metamorphosed rock as a result of fracturing. The fractures provide the reservoir space as well as the permeability to permit oil and gas migration, accumulation, and production from the reservoir.

For a trap to occur in a fractured formation, it must be overlain by a more pliable or less brittle rock that has not been fractured by the deformation. Otherwise, migration would occur up through the fractures and there would be no trap.

Where faulting caused the fracturing, production is limited to a narrow band along the fault. When folding or other deformation has caused the fracturing, the reservoir can become very complex in shape and unpredictable in production performance. Generally, the areas of greatest deformation have the greater number of fractures, which results in better well performance and recovery of more oil or gas.

Stratigraphic Traps

Traps created by changes in stratigraphy have the same physical requirements as structural traps. There is an up-dip limitation or termination of the reservoir rock, creating an area of minimum hydrodynamic potential or concave closure. In case of structural limitations, this is

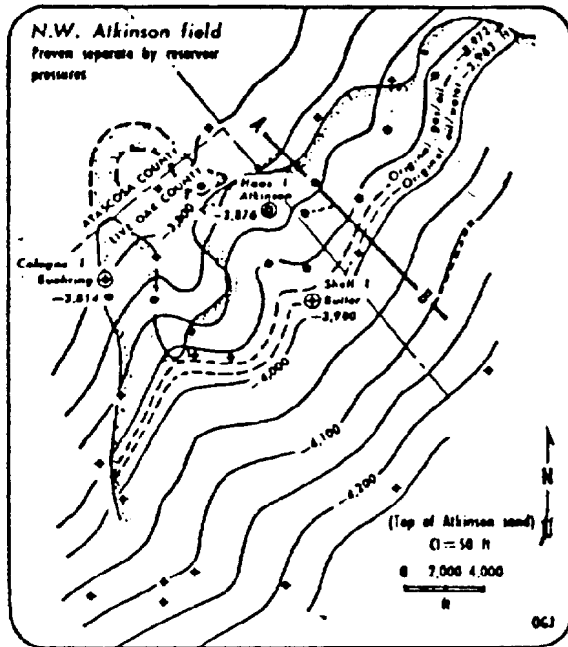


Fig. 29.6—Structural/stratigraphic interpretation; Northwest Atkinson field, TX.

obtained by faulting or a turnover of the reservoir rock. In stratigraphic traps, this limitation is accomplished by changes in porosity and permeability, which result from nondeposition, erosion and overlap, facies, and lithological changes caused by depositional variations, truncation, and differential compaction.

Stratigraphic traps can be classified as primary or secondary. Primary traps are those formed during sedimentary deposition: lenses, facies changes, shoestring sands, offshore sandbars, reefs, and detrital limestone or dolomite reservoirs can be classified as primary. Secondary traps are those resulting from later causes such as solution, cementation, erosion, fracturing, and chemical alteration or replacement.

Primary Stratigraphic Traps. These traps result from deposition of clastic or chemical materials. Shoestring sands, lenses, sand patches, bars, channel fillings, facies changes, strand-line (shoreline) deposits, coquinas, and weathered or reworked igneous materials are classified as clastic sedimentary deposits and can result in stratigraphic traps. Fig. 29.6 is a structural/stratigraphic interpretation of the northwest Atkinson field in Live Oak County, TX.² An ancient sand-filled stream channel meander has cut into older south-dipping shales and created a perfect stratigraphic trap. Fig. 29.7 is a cross section³ across the Yoakum Channel in Lavaca County, TX. This is an example of a channel filled with shale. The shale plug served as the seal for reservoirs within a west-plunging structural nose. Hydrocarbons are trapped in the truncated updip portions of the reservoirs.

Organic reefs or bioherms and biostromes are the primary chemical stratigraphic traps; they are built by organisms and are foreign bodies to the surrounding deposits. A cross section of Scurry field in Scurry County, TX (Fig. 29.8) gives an example of a primary chemical stratigraphic trap.⁴ The Strawn and Cisco-Canyon series are limestone reefs that have had younger sediments deposited on the flanks and eventually over the crest of the reef deposits. The shale serves as the seal. Differential compaction of the thicker shales on the

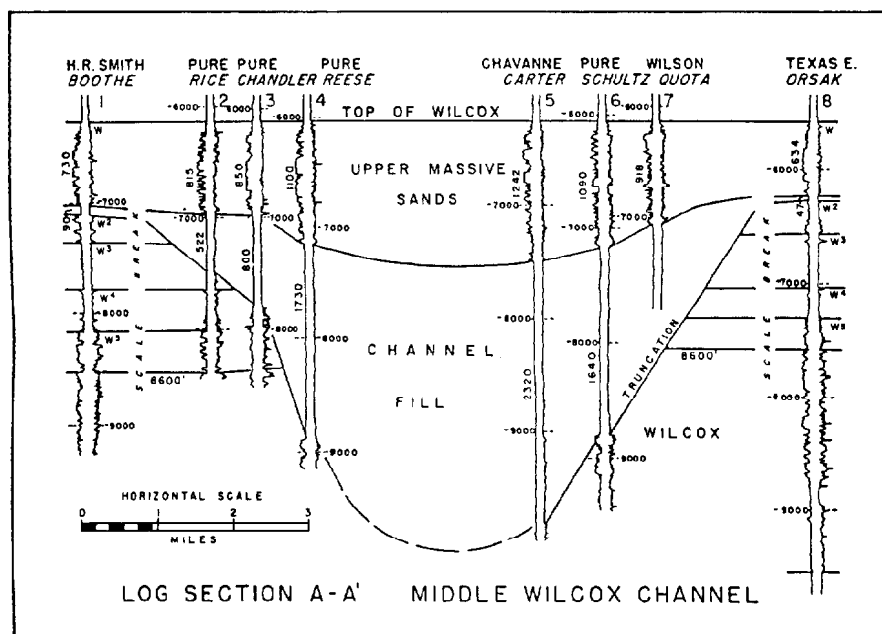


Fig. 29.7—Cross section showing stratigraphic position of upper Wilcox Yoakum channel.

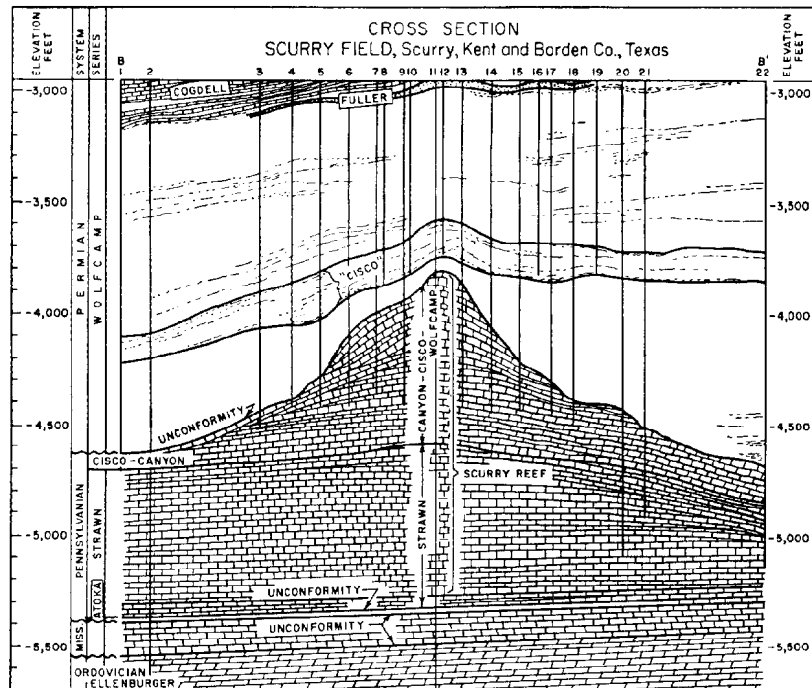


Fig. 29.8—Example of a stratigraphic reef field; structure and cross section of Scurry field.

flanks of the reef as compared with the thinner shale at the crest has created structural closure in younger overlying formations. Hydrocarbon accumulations have occurred in the Cisco and Fuller formations as a result of this differential compaction. Additional traps in other reservoirs are the result of updip permeability and porosity barriers and are either primary or secondary stratigraphic traps.

Secondary Stratigraphic Traps. Traps of this type were formed after the deposition of the reservoir rock by erosion and/or alteration of a portion of the reservoir rock through solution or chemical replacement.

Secondary stratigraphic traps actually should fall into the combination-trap classification because most are associated with or are the result of structural relief during some stage of development of porosity and permeability or limitation of the reservoir rock. However, many of the so-called typical "stratigraphic traps" fall into this category, and it is felt that it would be impossible to change the historical usage of this term. Therefore, secondary stratigraphic traps are defined for this discussion as those traps created after deposition and having limitations caused by lithology changes.

Erosion creates a major part of these through truncation of the reservoir rock. On-lap deposition (when the water is encroaching landward), off-lap deposition (when the water is regressing), and the chemical alteration of limestone result in many secondary stratigraphic traps.

The East Texas field (Figs. 29.9 and 29.10) is perhaps the most famous field in this classification. It is a truncation of the Woodbine formation as it approaches the regional Sabine uplift.⁵ A certain amount of leaching of the cementing material by waters over the unconformity

has resulted in increased porosity and permeability in the field as compared with similar Woodbine sands in the deeper portions of the East Texas basin.

Combination Traps

Combination traps are structural closures or deformations in which the reservoir rock covers only part of the structure. Both structural and stratigraphic changes are essential to the creation of this type of trap. Traps of this nature are dependent on stratigraphic changes to limit permeability and structure to create closure and complete the trap. Updip shale-outs, strand-lines, and facies changes on anticlines, domes, or other structural features causing dip of the reservoir rock create many combination traps. Unconformities, overlap of porous rocks, and truncation are equally important in forming combination traps. Faulting is also a controlling factor in many of these traps. Asphalt seals and other secondary plugging agents may assist in creating traps.

Salt Domes. These structures are of enough importance to justify a separate classification. However, sometimes they are difficult to identify, and many of the traps result from both stratigraphic variations and structural deformation.

Intrusion of rocks into overlying sediments may result in many different types of traps. Salt intrusions are more commonly associated with petroleum traps, although some igneous intrusions have also resulted in the formation of petroleum traps.

Salt domes are classified as piercement, intermediate, and deep-seated domes. Salt plugs or masses have moved up from greater depths through overlying sediments, forming traps in the sediments that have not been penetrated by the salt. Most salt intrusions took

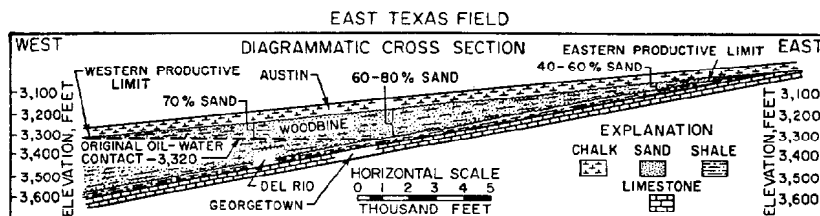


Fig. 29.9—Example of a secondary stratigraphic trap: structure and cross section of East Texas field.

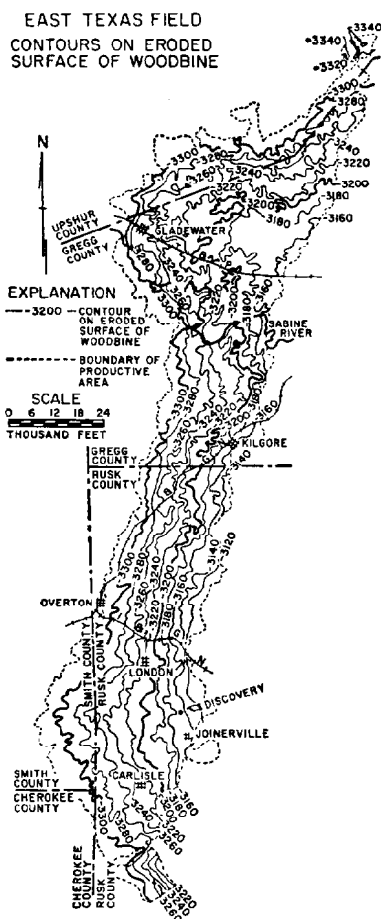


Fig. 29.10—Example of a secondary stratigraphic trap: structure and cross section of East Texas field.

considerable geologic time to reach their current position in the crust of the earth. Some are still growing, and apparently all have grown intermittently, allowing sands to be deposited over the crest of the structure at certain times and limiting deposition to the flanks of the structure at other times. The movement of the salt mass up through the surrounding rock creates many complex structures and sedimentary variations. Radial and peripheral faulting provide the avenue for the salt pushing up through overlying sediments. At times, the overlying formations were competent enough to stop or delay the growth of the salt plug. At other times, the salt

apparently grew steadily and contemporaneously with the deposition. Many times the salt masses of some domes must have reached the surface or near surface, where groundwaters could act on the intrusive salt mass. Some of the domes are very near the surface of the ground. Some have reached the surface and are currently extruding salt. In areas of very low rainfall, such as southwest Iran, salt has reached a height of 5,000 ft above the surrounding terrain.

Deep-seated salt domes are normally those at considerable depths where the salt may not have been penetrated by drilling. These can be identified by the overlying characteristic structure or by geophysical data, which help prove salt is present at depths of 12,000 ft or more and can be assumed to have caused the overlying complex structure. Intermediate domes can be defined arbitrarily as those where the salt is deeper than 2,500 ft but has been penetrated by drilling at depths less than 12,000 ft.

Traps occur on the flanks of salt domes where sands have been faulted and deformed or terminate against the salt mass and where facies changes have resulted because of the associated uplift. These conditions are illustrated in Fig. 29.11.⁶ Traps occur in the caprock, which consists of calcite, anhydrite, and limestone. Caprock is the insoluble residue on top of the plug that results from the dissolution of the salt from the crest of the plug. Porosity and permeability in the caprock result from fracturing, solution, chemical alteration, or any combination of these and are generally restricted to the calcite or limestone portions of the caprock.

Traps also overlie the salt mass and may result entirely from structural closure, faulting, differential compaction, or stratigraphic variations combined with the deformation, as indicated in Fig. 29.12.⁷

Characteristics of Reservoir Rocks

Classification of reservoirs* can be made on the basis of the texture, composition, and origin of the containing rock or the geometric configuration of the reservoir trap. Classification of reservoirs on the basis of rock texture and composition can assist in the prediction of reservoir performance. Variations in the mineralogy of reservoir rocks can be as important in reservoir performance as structural configuration or areal extent of the reservoir rock.

Sedimentary reservoir rocks can be divided into two groups: chemical and detrital. Sedimentary rocks are created by the weathering, disintegration, erosion, reworking, and deposition of material from older rocks.

*For more detailed coverage of this subject, refer to Refs. 8 and 9.

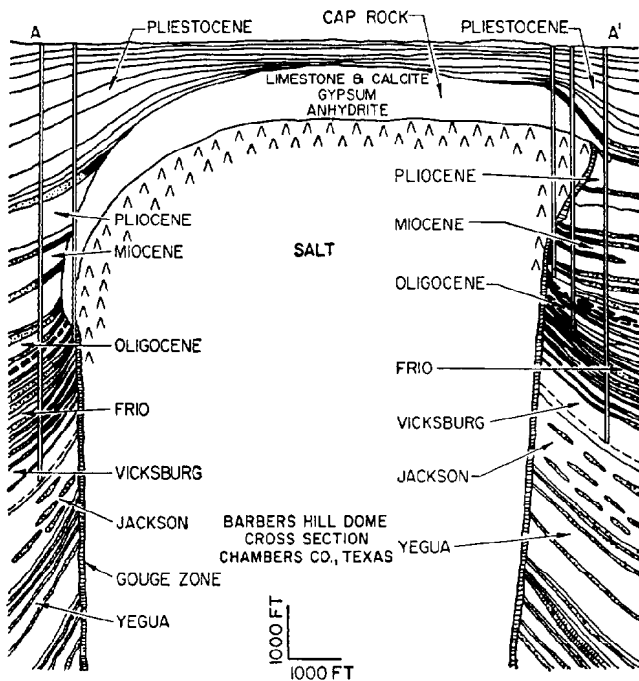


Fig. 29.11—Example of piercement-type dome showing termination of sands on the flanks of the salt plug and the resultant reservoir traps.

Clastic or detrital rocks are created from fragments transported by wind or water and allowed to settle out of suspension when the weight of the fragments is sufficient to exceed the carrying capacity of the transporting agent (wind or water). Chemical rocks are the result of precipitation of materials out of aqueous solution by organic growth and deposition or evaporation of seawater in closed basins, which precipitates salt and other evaporites. A list of reservoir rocks is given in Table 29.1.

Detrital Reservoirs

Clastic or Detrital Granular Reservoirs. These reservoirs can be classified according to rock types, depend-

ing on variations in source rock, transport distance, and depositional environment.

Quartzose-Type. Quartzose-type sediments occur in periods of geologic quiescence, with relatively flat coastal plains bordered by shallow seas. Weathering and chemical decay are at a maximum and erosion is at a minimum. Only stable minerals remain, and these are well sorted and generally uniform in texture and composition. Blanket sands and shales over extensive areas are general factors and the sandstones demonstrate high vertical as well as horizontal permeability. Waterdrive reservoir mechanisms can be expected and high recoveries by primary methods of production are the general rule because of the homogeneity of the reservoir rock. The coastal plains, embayments, and continental shelf along the Gulf of Mexico from Texas to Florida are typical of the physical requirements for this type of deposition.

Graywacke Sediments. These sediments occur in periods of moderate geologic disturbances. The coastal region is moderately uplifted and the depositional basins are somewhat deeper with a shorter continental shelf. More rapid erosion and shorter distances of transportation prevent the complete weathering and chemical decay of the sediments, and some of the more unstable minerals are able to remain. The land and adjacent basin areas are unstable, and minor isostatic adjustments occur from time to time, causing abrupt changes in the sediments being deposited. This causes poor sorting, lenticularity, irregular porosity and permeability variations, and heterogeneous deposition. Vertical permeability is poor, limiting water drive and gravity drainage. Production is normally gas-depletion drive, and the opportunities for secondary recovery operations are excellent. The New England coast is typical of the environment necessary for these types of deposits.

Arkose Sediments. Arkose sediments result from deposition during periods of intense orogenic movements. Certain land areas are sharply elevated above other land areas and/or the shoreline. Faulting and major isostatic adjustments occur frequently. The con-

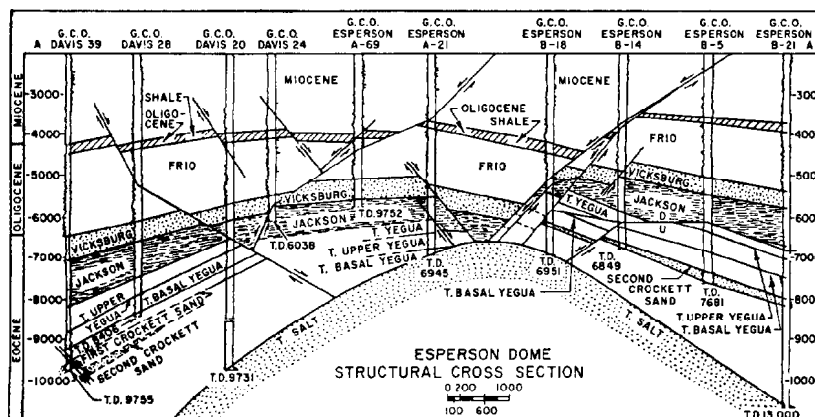


Fig. 29.12—Example of traps caused by a combination of structural and stratigraphic variations and of the complex faulting occurring above an intrusive salt mass.

TABLE 29.1—RESERVOIR ROCKS

Clastic and Detrital Porosity

1. Sand, conglomeratic sand, and gravel (clean, argillaceous, silty, lignitic, etc.)
2. Porous calcareous sandstone and siliceous sandstone (incomplete cementation)
3. Arkosic (feldspathic) sand, arkose, arkosic conglomerate (granite wash)
4. Detrital limestone and dolomite, oolitic and pisolitic limestone, coquina, and shell breccia

Fractured Porosity

1. Fractured sandstone and conglomerate
2. Fractured limestone, shale, and chert

Crystalline Porosity

1. Crystalline limestone and dolomite
2. Sugary dolomite "saccharoidal" porosity

Solution Porosity

1. Crystalline limestone and dolomite
2. Cavernous limestone and dolomite
3. Porous caprock
4. Honeycombed anhydrite
5. Oolitic limestone

tinental shelf is extremely narrow or nonexistent. Maximum erosion and the short distance of transportation virtually eliminate chemical decay and weathering. Sediments are deposited and covered over by younger sediments before any appreciable sorting and weathering can take place. Unstable minerals are present in the thick heterogeneous deposits. Highly porous stratigraphic traps are developed by lensing, pinchouts, and unconformities. Depletion-drive reservoirs are the general rule and recoveries are usually low. Much of the California coast is typical of the depositional environment for the deposition of arkosic sediments.

Chemical Reservoirs

Limestones and Dolomites. Limestones and dolomites also are deposited in quiescent geologic environments. Deposition of limy deposits is occurring along the west coast of Florida and some of the Bahama Islands while clastic sediments are being deposited in other nearby local areas.

Carbonate Reservoirs. Carbonate reservoirs include reefs, clastic limestones, chemical limestones, and dolomite. Porosity may be intercrystalline, intergranular, oolitic or oolitic, vuggy fractured, fossiliferous, cavernous, or saccharoidal. Production characteristics are highly variable in carbonate reservoirs, depending almost entirely on the type of porosity and fracturing developed and the resultant permeability.

Other types of reservoirs are given in Table 29.2.

Glossary of Terms

Bioherm: A moundlike, domelike, lenslike, or reeflike mass of rock built by sedentary organisms (such as corals, algae, foraminifers, mollusks, and gastropods), composed almost exclusively of their calcareous remains and enclosed or surrounded by rock of different lithology.

Biotrom: A distinctly bedded and widely extensive or broadly lenticular, blanketlike mass of rock built by and composed mainly of the remains of sedentary organisms and not swelling into a

TABLE 29.2—TYPES OF RESERVOIRS

Shale Reservoirs

Sometimes present in brittle, siliceous fractured shales

Anhydrite Evaporites

Develop porosity from leaching by circulating waters

Igneous or Metamorphic Rock

1. Very uncommon
2. Sometimes contain oil when secondary porosity is developed by fracturing or weathering
3. Best-known igneous reservoirs are the serpentine plugs of Bastrop and Caldwell counties, Texas

moundlike or lenslike form. As an organic layer, such as a bed of shells, crinoids, or corals or a modern reef in the course of formation.

Breccia: A coarse-grained clastic rock composed of angular broken fragments held together by a mineral cement or in a fine-grained matrix.

Closure: In a subsurface fold, dome, or other structural trap, the vertical distance between the structure's highest point and its lowest closed structure contour. Four-way dip is determined by in-line and cross-line right angle control demonstrating dip in four directions away from the crest of the closure.

Coquina: A detrital limestone composed wholly or chiefly of mechanically sorted fossil debris that experienced abrasion and transport before reaching the deposition site, and weakly to moderately cemented but not completely endurated.

Detrital: Pertaining to or formed from detritus of rocks, minerals, and sediments. The term may indicate a source outside or inside the depositional basin.

Facies: The aspect, appearance, and characteristics of a rock unit, usually reflecting the conditions of its origin; especially as differentiating the unit from adjacent or associated units.

Graben: An elongate, relatively depressed crustal unit or block that is bounded by faults on its long sides.

Horst: An elongate, relatively uplifted crustal unit or block that is bounded by faults on its long sides.

Minimum hydrodynamic potential: As used here, a geologic position or condition due to impermeability in the reservoir rock where the dynamic action of fluid movement is abated.

Minor isostatic adjustment: The minor adjustment of the lithosphere of the earth to maintain equilibrium among units of varying mass and density; excess mass above is balanced by a deficit of density below and vice versa.

Normal fault: A fault in which the hanging wall appears to have moved downward relative to the foot wall. The angle of the fault is usually 45° to 90°. A low-angle normal fault is a normal fault with the angle of the fault less than 45°.

Off-lap deposition: The progressive offshore regression of the updip terminations of the sedimentary units within a conformable sequence of rocks in which each successively younger unit leaves exposed a portion of the older unit on which it lies. The successive contraction in the lateral extent of strata (as seen in an upward sequence) resulting from their being deposited in a shrinking sea or on the margin of a rising land mass.

On-lap deposition: The regular and progressive pinching out toward the margins or shores of a depositional basin of the sedimentary units within a conformable sequence of rocks in which the boundary of each unit is transgressed by the next overlying unit and each unit, in turn, terminates farther from the point of reference.

Oolicast: One of the small, subspherical openings found in an oolitic rock, produced by the selective solution of ooliths without destruction of the matrix.

Oolicastic porosity: The porosity produced in an oolitic rock by removal of the ooids and formation of oolcasts.

Oolith: One of the small round or oval accretionary bodies in a sedimentary rock resembling the roe of fish, usually formed of calcium carbonate and having a diameter of 0.25 to 2 mm.

Pisolith: One of the small, round or ellipsoidal accretionary bodies in a sedimentary rock, resembling a pea in size and shape, and constituting one of the grains that make up a pisolite. It is often formed of calcium carbonate and some are thought to have been produced by a biochemical algae-encrustation process. A pisolith is larger and less regular in form than an oolith.

Pisolitic: Pertaining to pisolite or to the texture of a rock made up of pisoliths or pealike grains.

Pisolitic limestone: A limestone with pisolitic texture.

Saccharoidal: Said of a granular or crystalline texture resembling sugar.

Shell breccia: A breccia composed of angular broken shell fragments.

Shoestring sands: A shoestring of sand or sandstone usually buried in the midst of mud or shale as in a buried sandbar or channel fill.

Strand line: The ephemeral line or level at which a body of standing water meets the land; the shoreline, especially a former shoreline now elevated above the present water level.

Strike-slip fault: A fault on which the movement is parallel to the fault's strike.

Torsion: The state of stress produced by two force couples of opposite movement acting in different but parallel planes about a common axis. Torsion faults are wrench faults or lateral faults in which the fault surface is more or less vertical.

Truncation: An act or instance of cutting or breaking off the top or end of a geologic structure or land form, as by erosion.

Unconformity: A substantial break or gap in the geologic record where a rock unit is overlain by another that is not next in stratigraphic succession, such as interruption in the continuity of a depositional sequence of sedimentary rocks or a break between eroded igneous rocks and younger sedimentary strata. It results from a change that caused deposition to cease for a considerable span of time, and it normally implies uplift and erosion with loss of the previously formed record.

References

- Galloway, T.J.: Bull. 118, California Division of Mines, Sacramento (Aug. 1957).
- Sams, H.: "Atkinson Field; Good Example of 'Subtle Stratigraphic Trap,'" *Oil and Gas J.* (Aug. 12, 1974), 145-63.
- Hoyt, W.V.: "Erosional Channel in the Middle Wilcox Near Yoakum, Lavaca County, Texas," *Trans., Gulf Coast Assn. of Geological Societies* (Nov. 1959) 9, 41-50.
- "Occurrence of Oil and Gas in West Texas," F.A. Herald (ed.) Bureau of Economic Geology and West Texas Geological Soc. (Aug. 1957).
- "Occurrence of Oil and Gas in Northeast Texas," F.A. Herald (ed.) Bureau of Economic Geology and East Texas Geological Soc. (April 1951).
- An Introduction to Gulf Coast Oil Fields*, Houston Geological Soc. (1941).
- A Guide Book*, Houston Geological Soc. (1953).
- Pirson, S.J.: *Oil Reservoir Engineering*, second edition, McGraw-Hill Book Co. Inc., New York City (1958).

- Krynine, P.D.: "The Megascopic Study and Field Classification of Sedimentary Rocks," *J. Geol.*, 56, No. 2.

General References

- Aguilera R.: *Natural Fractured Reservoirs*, Petroleum Publishing Co., Tulsa (1980).
- Bates, R.L. and Jackson, J.A.: *Glossary of Geology*, second edition, American Geological Inst. (1980).
- Beebe, Warren B.: "Natural Gases of North America, Vols. 1 and 2," Memoir 9, AAPG (1968).
- Bouma, H., Moore, G.T., and Coleman, J.M.: "Framework, Facies and Oil Trapping Characteristics of the Upper Continental Margin," AAPG (1978) Studies No. 7.
- Braunstein, J.: "North American Oil and Gas Fields," AAPG (1976) Memoir 24.
- Busch, D.A.: "Stratigraphic Traps in Sandstone," AAPG (1974) Memoir 21.
- "Geologic Formation and Economic Development of Oil and Gas Fields of California," California Department of Natural Resources, Sacramento (1943).
- Halbouty, M.T.: "Giant Oil and Gas Fields of the Decade 1968-1978," AAPG (1980) Memoir 30.
- Halbouty, M.T.: "Salt Domes, Gulf Region, United States and Mexico," second edition, Gulf Publishing Co., Houston (1979).
- Halbouty, M.T.: "The Deliberate Search for the Subtle Trap," AAPG (1982) Memoir 32.
- Hanna, M.A.: "Gulf Coast Salt Domes," *Problems in Petroleum Geology*, AAPG (1934).
- Hubbert, M.K.: "Entrapment of Petroleum under Hydrodynamic Conditions," *Bull.*, AAPG (Aug. 1953) 37, 1954-2026.
- King, R.E.: "Stratigraphic Oil and Gas Fields: Classification, Exploration Methods and Case Histories," AAPG (1972) Memoir 16, S.E.G. Special Publication No. 10.
- Levorsen, A.I.: *Geology of Petroleum*, W.H. Freeman and Co., San Francisco (1954).
- Mazzullo, S.J.: "Stratigraphic Traps in Carbonate Rocks," AAPG (1980) Reprint 23.
- Payton, E.: "Seismic Stratigraphy—Applications to Hydrocarbon Exploration," AAPG (1977) Memoir 26.
- Russel, W.L.: *Structural Geology for Petroleum Geologists*, McGraw-Hill Book Co. Inc., New York City (1955).
- Scholle, P.A., Bebout, D.G., and Moore, C.H.: "Carbonate Depositional Environments," AAPG (1983).
- "Structure of Typical American Oil Fields," *Bull.*, AAPG (1929).
- Weeks, L.G.: "Habitat of Oil," AAPG (1958).
- Wilhelm, O.: "Classification of Petroleum Reservoirs," *Bull.*, AAPG (Nov. 1945) 29, 1537-79.
- Woodland, A.W.: *Petroleum and the Continental Shelf of Northwest Europe, Vol. 1, Geology*, John Wiley Sons Inc., New York City (1975).
- Young, A. and Galley, J.E.: "Fluids in Subsurface Environments," AAPG (1965) Memoir 4.

Chapter 30

Bottomhole Pressures

G.J. Plisga, Sohio Alaska Petroleum Co.*

Introduction

The practice of using bottomhole pressure (BHP) to improve oil production and to solve petroleum engineering problems started in about 1930. Pressures in oil wells were first calculated from fluid levels and later by injecting gas into the tubing until the pressure became constant. The earliest BHP measurements were made with pressure bombs and with maximum-indicating or maximum-recording pressure gauges that did not have the accuracy, reliability, or durability now demanded. These early pressure measurements were occasional, or spot tests rather than systematic diagnostic engineering measurements.

BHP Instruments

The development of precision recording pressure gauges small enough in diameter to be run through tubing made it feasible to make BHP measurements in sufficient number to develop the science that now makes them indispensable to petroleum engineering. BHP now is determined with continuously recording pressure gauges, which are either self-contained or surface-recording.

Self-Contained Gauges

Mechanical self-contained pressure gauges are used universally. The pressure element and recording section are encased and sealed against external pressure except for an opening to communicate the pressure to the element. The entire instrument is run to the depth at which the pressure is to be measured, allowed to stabilize thermally, and then returned to the surface and the pressure determined from the chart. Modern pressure measurement systems incorporate force summing devices that convert energy into physical displacement or deformation. These force summing devices can take many forms, three of which are shown in Fig. 30.1. Although there

are numerous mechanical self-contained pressure devices available (Table 30.1) only the most commonly used continuously recording BHP gauges are discussed fully. Regardless of the type of force summing device incorporated into the BHP gauge, whether physical displacement (piston elements) or deformation (bellows/bourdon tubes), the generated force is coupled to a recording device.

The Amerada pressure gauge has a helical bourdon tube as a pressure element that is of sufficient length to rotate the stylus the full inside circumference of the cylindrical chart holder without multiplication of movement. A clock moves the chart longitudinally. The gauge is made in both 1 1/4- and 1-in. diameters with a length of approximately 74 in. A vapor-pressure-type recording thermometer can be run in combination with this to obtain continuously recorded temperatures and allow correction of pressure measurements. This will also ensure that thermal stabilization has occurred.

The Humble gauge pressure element has a piston, which moves through a stuffing box against a helical spring in tension. Attached to the inner end of the piston is a stylus that records longitudinally on a chart in a cylindrical holder, which is rotated by a clock. The instrument is made in two sizes, with 1 1/4- and 15/16-in. OD's, and is approximately 60 in. long. Thermometer elements are available for both sizes.

Other recording gauges have been described in the literature, two of which were continuously recording, but they are no longer available on the market. The Gulf BHP gauge has a pressure element consisting of a long metallic bellows restrained by a double helical spring in tension. The recording mechanism is a cylindrical chart holder rotated by a clock. The USBM BHP gauge pressure element is a multiple-bellows type with a movement of about 0.6 in., which is multiplied through a rack and gears to about 5 1/2 in. of stylus movement. The stylus records longitudinally on a cylindrical chart that is

*The original chapter on this topic in the 1962 edition was written by C.V. Millikan.

TABLE 30.1—MECHANICAL RECORDING BHP GAUGES

	Amerada			Kuster				Johnston
	RPG-3	RPG-4	RPG-5	KPG	AK-1	K-2	K-3	Leutert
OD, in.	1.25	1	1.5	1.25	2.25	1	1.25	1.42
Length, in.	77	76	20	73	36	41	43	139
Type pressure element*	B	B	B	B	B	B	B	RP
Maximum pressure, psi**	25,000	25,000	20,000	30,000	30,000	20,000	20,000	10,000
Accuracy, %FS†	± 0.2	± 0.2	± 0.25	± 0.2	± 0.25	± 0.25	± 0.25	± 0.025
Resolution, %FS†	± 0.05	± 0.056	± 0.05	± 0.05	± 0.025	± 0.05	± 0.04	± 0.005
Maximum service temperature, °F	500	500	450	700	350	700	700	300
Maximum clock running time, hours	360	144	120	360	120	120	120	360
								192

*B = bourdon tube, RP = Rotating piston, P = Piston.

**Normally, elements are available in several ranges.

†FS = Full scale, NS = Not stated.

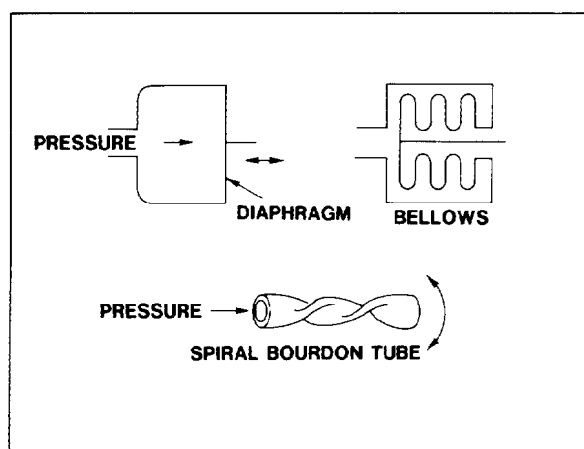


Fig. 30.1—Force summing devices.

rotated by a helical spring but controlled by a watch movement.

BHP gauges, although rugged and capable of service in severe conditions, must be considered precision instruments. Proper attention to adjustment, calibration, and operation is required to obtain consistently reliable and accurate pressure measurements. A comparison of the commonly used mechanical continuously recording BHP gauges is shown in Table 30.1.

Charts

Charts used in a BHP gauge are paper or metal. Paper charts have an abrasive coating and are marked by a brass or gold stylus. Metal charts, which are made of brass, copper, or aluminum, are generally preferred because they are not affected by humidity. Plain metal charts require a sharp pointed stylus. Coated metal charts are generally preferred because they produce less stylus friction. Black-coated charts are marked with a steel or jewel stylus, which burnishes the coated surface. White-coated charts are used with a brass or gold stylus. A finer line can be made on the black chart, but it is more difficult to read. A brass or gold stylus used with white-coated charts, paper, or metal, must be sharpened very frequently.

A small magnifying lens and steel scale with 0.01-in. divisions are most frequently used for reading charts with static pressure—i.e., where only one or two

pressures readings are made on a chart. When a number of readings are to be made from a chart, it is advantageous to use one of the several available chart scanners. Some engineers have used microscopic comparators to read pressure deflection to 0.0001 in., but the inherent errors of a pressure element even under most careful handling are usually greater than the added accuracy of such precise measurement of the chart. New electronic chart scanners have improved the readability and accuracy of mechanical BHP gauges.

Calibration

Self-contained pressure gauges, like all pressure gauges used for precision work, must be calibrated on a dead-weight tester at regular intervals. To obtain maximum accuracy, the pressure gauge is calibrated before a survey at the anticipated bottomhole temperature, (BHT), the survey conducted, and then the chart read using the presurvey calibration lines. New pressure elements should be calibrated frequently until they have become seasoned in service and their ability to retain calibration has been established. Before calibration, pressure equal to the maximum range of the element should be applied and released several times. The number of calibration points should be more on a new element, and two or more curves should be run as a check. The element should also be calibrated at the reservoir temperature at which the pressures are to be determined, or a temperature-correction factor should be determined to correct pressures measured at other than calibration temperature (Fig. 30.2). During calibration, the gauge should be tapped lightly to relieve residual friction in the moving parts of the element. Under normal operating conditions, pressure determination in a well should have an accuracy within a range of 0.2% of the maximum range of the element. The pressure element range should be selected to operate in the upper two-thirds range when at bottomhole conditions. Greater accuracy can be obtained by greater attention to details of calibration and the use of instruments that are well-seasoned by service. Pressure increase inside the gauge caused by an increase in temperature is considered only when extra effort is made to obtain precision pressures.

Temperature Effect

Temperature effect is an inherent property of metals and is present in all gauges, although for some alloys it is very small. Except for such alloys, temperature change

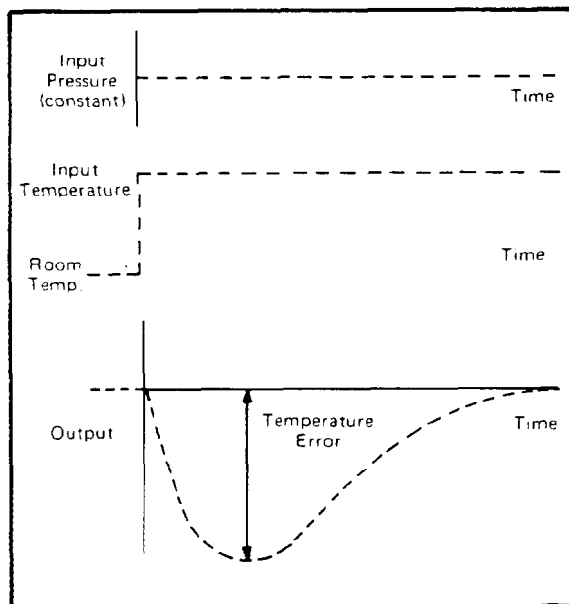


Fig. 30.2—Temperature effect on pressure gauges.

must be considered in pressure measurements. The preferred method is to calibrate the pressure element at the temperature of the reservoir in which pressures are to be measured. The calibration curve for most pressure elements is practically a straight line; therefore, a temperature-correction coefficient may be determined for a given pressure element and used to correct for temperatures other than the calibration temperature as follows. For a given pressure, preferably about three-fourths of the maximum for the element, determine the pressure deflection and the temperature. For the same pressure, determine the deflection at a higher temperature, preferably 100°F higher.

Then¹

$$C_T = \frac{d_2 - d_1}{d_1(T_2 - T_1)}, \dots\dots\dots (1)$$

where

- C_T = temperature coefficient,
- T_1 = lower temperature,
- T_2 = higher temperature,
- d_1 = deflection at T_1 for given pressure, and
- d_2 = deflection at T_2 for same pressure.

The corrected deflection can be calculated as

$$d_c = \frac{d_o}{1 + C_T(T_o - T_c)}, \dots\dots\dots (2)$$

where

- d_c = deflection at calibration temperature,
- d_o = observed deflection,
- T_c = calibration temperature, and
- T_o = observed temperature.

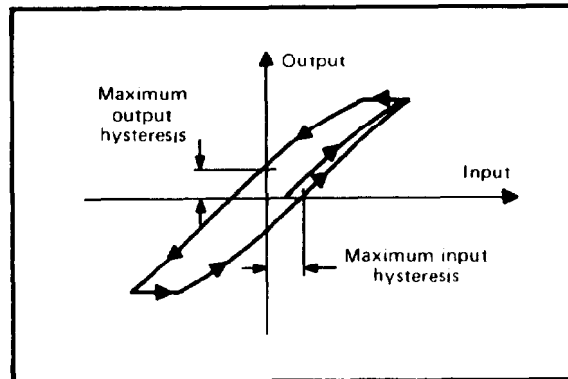


Fig. 30.3—Hysteresis.

If it is more convenient, pressure readings may be substituted for deflections in Eq. 2. Gauges with a steel pressure element usually have a temperature coefficient of about 0.0002 in./°F.

When the pressure gauge is run to the depth of the pressure determination, it should remain long enough to stabilize thermally, usually 15 to 20 minutes. If the instrument cannot remain long enough to reach temperature equilibrium, a maximum-indicating thermometer run in a closed container as part of the gauge will give a satisfactory reading for temperature correction.

Many BHP gauge elements are made of an alloy with a very low temperature coefficient such as Ni-Span C®, and a temperature correction may be neglected up to 200°F except where extra precautions are taken to obtain very precise pressure measurements. For temperatures above 200°F, most elements require a varying correction that can be determined only by actual calibration.

Hysteresis

Hysteresis is a characteristic of metals under strain that must be recognized in pressure gauges. Because of hysteresis, the calibration of a gauge made with increasing pressures will differ slightly from a calibration made with decreasing pressures (Fig. 30.3). If only static pressures are to be determined, a calibration at increasing pressure is satisfactory. When a flowing pressure starting from a static condition is to be determined, hysteresis may be of sufficient magnitude to take into account. To determine the hysteresis effect, the pressure element should be pressurized somewhat higher than the highest anticipated well pressure and released several times before running the calibration, first with increasing pressures, then with decreasing pressures. Flexing the element several times will substantially reduce the hysteretic effect and should be done each time just before the gauge is run into a well.²

Operating Equipment

The BHP gauge, a self-contained instrument, is run on a wireline and depth is measured by the line running in contact with a calibrated measuring wheel, which operates a counter. The most frequently used calibration of the measuring wheel is 2 ft/rev. When the contact of the line is tangent to the measuring wheel, the wheel

TABLE 30.2—WIRELINE TENSILE STRENGTHS AND WEIGHTS

	Tensile Strength (psi)	Nominal Tensile Strength (lbf)			
		Diameter Line (in.)			
		0.066	0.072	0.082	0.092
Plow steel	232,000	794	945	1,225	1,542
Stainless steel	170,000	582	692	898	1,130
Monel	150,000	513	611	792	997
Nominal Weight per 1,000 ft of Line (lbm)					
Plow steel		11.4	14.0	18.0	22.6
Stainless steel		11.8	14.1	18.3	23.0
Monel		13.1	15.6	20.2	25.4

diameter in inches is $24/\pi$. When the contact is an arc of the wheel, the wheel diameter is $D=(24/\pi)-d$, where d is the diameter of the wireline. This applies if the greatest distance of the chord of the contact arc from the periphery of the wheel is greater than the diameter of the wireline. The measuring wheel diameter should be checked at reasonable intervals to maintain accuracy of depth measurements. A decrease in the diameter of the wireline caused by wear or by permanent stretch resulting from a hard pull will also cause errors in depth measurements.

The most common wirelines have diameters of 0.066, 0.072, 0.082, or 0.092 in. In areas having noncorrosive well fluids, plow steel lines are most satisfactory, but for corrosive conditions, stainless steel and Monel® lines are used. Both plow steel and stainless steel are subject to hydrogen embrittlement, but are satisfactory for short runs such as static-pressure tests, except under severe conditions. For an operation that requires the line to be in the hole under corrosive conditions for several hours, a Monel line should be used. Nominal tensile strengths of wire lines and their weights are given in Table 30.2.

Equipment for operating a wireline varies greatly. The most frequently used unit is a trailer-mounted reel driven by a 2- to 4-hp air-cooled gasoline engine. Power is transmitted to the reel by V-belt, through a disk clutch, or by hydraulic drive. On smaller equipment, an idler pulley permits the V-belt to serve as a clutch also. Braking may be by friction disk, brakeband, or hydraulic

pump. When the equipment is used for a continuous program it may be mounted in a pickup truck, with housing to protect against the weather.

Pressure Bombs

Pressure bombs were used to some extent before recording pressure gauges small enough in diameter for oilwell use became available. They were usually made from tubing approximately 1½ in. in diameter with a small needle valve in the top and a ball and seat in the bottom to hold maximum pressure in the well. When the bomb was recovered, the pressure was determined by attaching a pressure gauge to the valve. The bomb had to be long enough to leave a volume of gas (or air) in the top to reduce the error of filling the bourdon tube of the pressure gauge. There was also substantial correction for temperature unless the bomb was raised to BHT before the pressure was read. An ordinary commercial maximum-indicating pressure gauge enclosed in a pressure-tight container was used occasionally, and in some cases a recording mechanism and clock were added. Such instruments were 3 in. or larger in diameter, which limited their use to wells without tubing.

Surface Recording Gauges

Surface recording pressure gauges can be used either permanently installed or wireline retrievable. All surface recording pressure gauges must be run on a single-

TABLE 30.3—SURFACE RECORDING BHP GAUGES

Pressure Measurement System	Amerada EMR-502 with EPG-512 Pressure/Temperature Gauge	Lynes DMH-312 PTS-SK	Lynes DMH-314 PTS-SK	Sperry Sun	Johnston-Macco/Schlumberger SDR-1 Solid State Downhole Recorder	Johnston-Macco/Schlumberger J-300 Acoustic Pressure Recorder	Amerada EPG-512 Pressure/Temperature Gauge	Lynes Conductor Wire Line Probe	Hewlett Packard 2813B Quartz Pressure Gauge	Johnston-Macco/Flopetrol Schlumberger DPTT
Dimensions and Weight										
OD, in.	1.25	1.25	1.65	1.7	1.7	3	1.25	1.65	1.44	1.5
Length, in.	85	50.5	60.75	108	150	76	13	28.5	39.38	44
Weight, lbm	3	8.5	10	NS	46.75 (with battery)	117 (with battery)	3	9.5	11	12
Pressure Channel										
Transducer type	capacitance	strain gauge	quartz crystal	bourdon tube	sputtered thin film strain gauge	sputtered thin film strain gauge	capacitance	quartz crystal	quartz crystal	sputtered thin film strain gauge
Calibrated range, psi	0 to 2,500 0 to 5,000 0 to 10,000	0 to 5,000 0 to 10,000 2 × FS	0 to 5,000 0 to 10,000 1.1 × FS	0 to 15,000 0 to 10,000 NS	0 to 10,000 0 to 10,000 1.5 × FS	0 to 10,000 0 to 10,000 NS	0 to 2,500 0 to 5,000 0 to 10,000	0 to 5,000 0 to 10,000 NS	200 to 11,000 1.1 × FS NS	0 to 10,000 1.5 × FS NS
Operating range, psi	NS**	NS**	NS	NS	NS	NS	NS	NS	NS	NS
Accuracy, %FS*	±0.09	±0.25	±0.05	±0.05	±0.04	±0.04	±0.09	±0.05	±0.0039	±0.0002
Resolution, %FS*	±0.0004	±0.025	±0.006	±0.005	±0.0002	±0.0002	±0.0004	±0.001	±0.0004	±0.0002
Repeatability							±0.09% FS	NS	±0.4 psi	NS
Temperature Channel										
Range, °F	0 to 302	32 to 257	32 to 257	no temperature channel	32 to 302	32 to 302	0 to 302	32 to 257	no temperature channel	32 to 302
Accuracy	±0.1°F	±0.33% of reading	±0.33% of reading	no temperature channel	±0.5°F	±0.5°F	±0.1°F	±0.33% of reading	no temperature channel	±0.5°F
Resolution, °F	±0.01	±0.06	±0.26	no temperature channel	±0.10	±0.05	±0.01	±0.26	no temperature channel	±0.02
Power Supply and Signal Processor							GSC-501 gauge signal converter	DSR-300 digital surface recorder	Hewlett Packard 2816A pressure signal processor	SPRO test system
Environment										
Vibration	NS	NS	NS	NS	NS	±10G 10 to 60 Hz				
Shock	NS	NS	NS	NS	NS	200 G for 11 milliseconds (half-sine wave)				

*FS = Full scale.

**NS = Not stated by manufacturer or available to author.

†Accuracy of HP 2813B if operating temperature is known: within 1.8°F: ±0.5 psi or ±0.025% of reading, whichever is greater; within 18°F: ±1.0 psi or ±0.1% of reading, whichever is greater; and within 36°F: ±5 psi or ±0.25% of reading, whichever is greater.

TABLE 30.4—SUMMARY OF TRANSDUCER CRITERIA

Sensor	Excitation	Output Level	Accuracy (%)	Pressure Range (psi)	Frequency Response (Hz)	Temperature Range and Effects (°F)	Shock and Vibration Sensitivity	Stability* (%/yr)	Life or Calibration Shift with Use*
Capacitive	AC-DC special	high level (5V) frequency/bridge	0.02	0.01 to 5,000	0 to >100	0 to +165	poor to good	0.05	> 10 ⁷ cycles with <0.05% calibration shift
Differential transformer	AC special	high level (5V) phase demod/bridge	0.5	30 to 10,000	> 100	0 to +165	poor	0.5	> 10 ⁶ cycles life
Force balance	AC line power	high level (5V) with servo	0.01	1 to 5,000	0 to <5	40 to +165 (0.01%/°F)	poor	0.05%/month	> 10 ⁷ cycles with <0.5% calibration shift
Piezoelectric	DC amp and self-generating AC	medium level with amp	1	0.1 to 40,000	1 to >100,000	-450 to +400 (0.01%/°F)	excellent	1	unmeasurable use effects
Potentiometer	AC-DC regulated	high level	1	5 to 10,000	0 to >50	-65 to +300 (0.01%/°F)	poor	0.5	< 10 ⁶ cycles life
Strain gauge	AC-DC regulated								
Unbonded	10V AC-DC	low level 4 mV/V	0.25	0.5 to 40,000	0 to >2,000	-320 to +600 (0.005%/°F over limited compensated range)	good	0.5	< 0.5% calibration shift after 10 ⁶ cycles
Bonded foil	10V AC-DC	low level 3 mV/V	0.5	5 to 10,000	0 to >1,000	-65 to +250 (0.01%/°F over limited compensated range)	very good	0.5	> 10 ⁶ cycles
Thin film	10V AC-DC	3 mV/V	0.25	15 to 10,000	0 to >1,000	-320 to +525 (0.005%/°F over limited compensated range)	very good	0.05	> 10 ⁶ cycles with <0.25% calibration shift
Diffused semiconductor	10 to 28 V DC	medium level 3 mV/V to 20 mV/V	0.25	15 to 5,000	0 to >1,000	-85 to 250 (0.005%/°F over limited compensated range)	very good	0.05	< 0.25% calibration shift after 10 ⁶ cycles
Bonded bar semiconductor	10V AC-DC	medium level 3 mV/V to 20 mV/V	0.25	5 to 10,000	0 to >1,000	-65 to +250 (0.01%/°F over limited compensated range)	very good	0.5	< 0.5% calibration shift after 10 ⁶ cycles
Variable reluctance	AC special	40 mV/V	0.5	0.04 to 10,000	0 to >1,000	-320 to +600 (0.02%/°F over limited compensated range)	very good	0.5	> 10 ⁶ cycles life
Vibrating wire and tube	AC special	high level and frequency	0.02	1 to 100	0 to >100	-65 to +200 requires temperature control	poor	0.01	> 10 ⁶ cycles life
Vibrating quartz	AC special	high level and frequency	0.01	1 to 10,000	0 to >100	0 to +302	good	0.005	> 10 ⁶ cycles life

*Stability and calibration shift should be considered together.

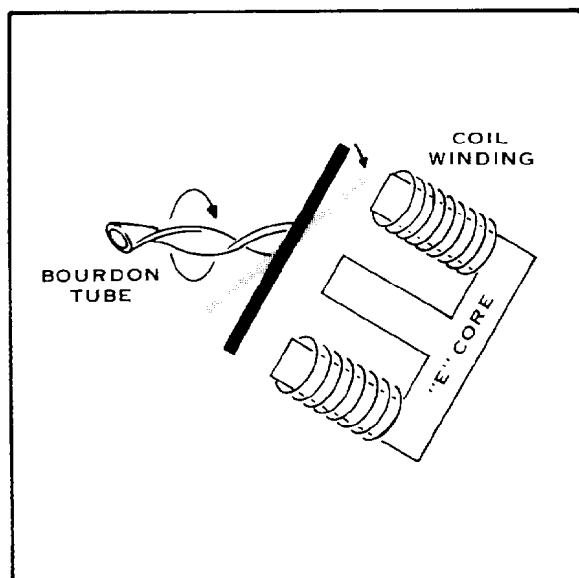


Fig. 30.4—E-Core transformer

conductor armored cable that carries a direct current from the surface to the transducer in the bottomhole instrument. Oscillating current returns through the same circuit from the transducer to surface instruments that determine and record its frequency. A transducer is any device that converts energy from one form to another. There is a large variety of transducers that allow nonelectrical variations to be converted into changes in resistance, current, voltage, capacitance, etc. Some examples are the strain gauge, thermistor, and the microphone. Readings are made at selected intervals of 1 second to 30 minutes or more. The frequency recorded in cycles per second is translated to pounds per square inch from a calibration curve. Table 30.3 shows a comparison of commonly used surface recording pressure gauges.

A permanently installed surface recording pressure gauge requires a gauge carrier or receiver and either a single conductor line or small diameter tubing (0.092 in.) strapped to the production tubing. The pressure gauge can be run with the tubing or by wireline retrievable, which sits in a gas lift mandrel or some other device to complete the circuit. The surface instruments may be connected permanently, or one set can be used to monitor BHP in several wells.

Modern precision pressure-measuring systems incorporate force summing devices that convert gas or liquid entry into physical displacement or deformation. The following sections discuss various concepts of pressure transducer technology shown in Table 30.4.³

Pressure Transducer Technology

Capacitive Transducer

In a capacitive transducer, a diaphragm is spaced evenly between capacitor plates. BHP causes displacement of the diaphragm and a change in capacitance. The advantages of a capacitive transducer are excellent frequency response, low hysteresis, good linearity, and excellent stability and repeatability. Disadvantages are high sensitivity to temperature variations and vibration.

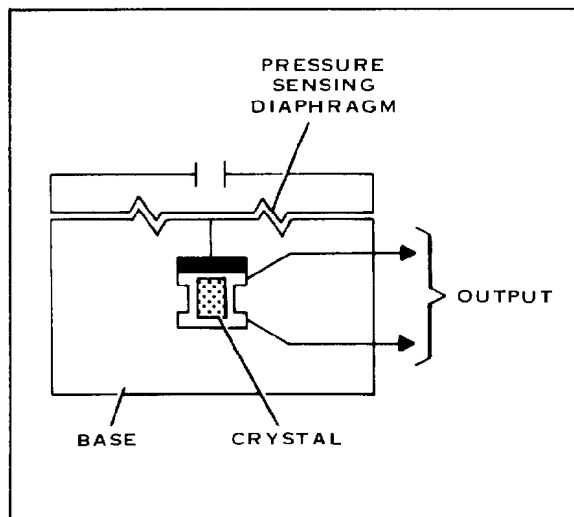


Fig. 30.5—Piezoelectric transducer.

Variable Inductance Transducer

In the variable inductance transducer, a flux linkage bar is mechanically linked to a spiral bourdon tube, diaphragm, or bellows (Fig. 30.1). The flux linkage bar is in the magnetic path of an E-core transformer (Fig. 30.4). Displacement of the flux linkage bar by pressure changes the E-core flux density resulting in a transformer output proportional to the pressure applied. The advantages are medium-level output and rugged construction. Disadvantages are a requirement for AC excitation, poor linearity, and susceptibility to stray magnetic fields.

Piezoelectric Transducer

The piezoelectric effect is the property exhibited by certain crystals of generating voltage when subjected to pressure (Fig. 30.5). When a strain is applied to an asymmetrical crystalline material such as barium, titanite, quartz, or rochell salt, an electrical charge is generated. When a piezoelectric crystal is connected to a diaphragm, bellows, or bourdon tube, the generated charge can be made proportional to the applied pressure. Advantages are very high frequency response (250 kHz), small size, rugged construction, and ability to accept large overpressures without damage. Disadvantages are temperature sensitivity, inability to make static measurements, and special electronics required.

Potentiometric Transducer

This transducer is constructed by coupling the wiper of a multiturn potentiometer to an amplifying mechanical linkage to a diaphragm, bellows, or bourdon tube. Advantages are low-cost, high-level output and simple electronic circuits. Disadvantages are limited life, poor resolution, large hysteresis, and low frequency response.

Vibrating Wire Transducer

A thin wire is connected in tension to a diaphragm, bellows, or bourdon tube and is caused to vibrate under the influence of a magnetic field (Fig. 30.6). The wire's frequency of vibration is directly related to its tension.

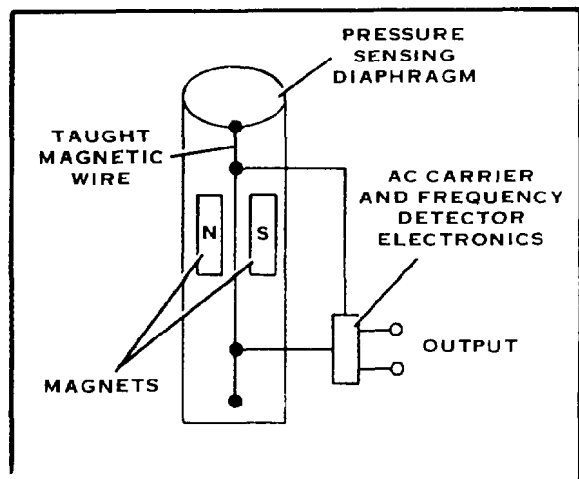


Fig. 30.6—Vibrating wire transducer.

Advantages are very high accuracy, low hysteresis, and excellent long-term stability. Disadvantages are sensitivity to shock and vibration, temperature sensitivity, and additional electronics.

Strain Gauge Transducers

A strain gauge transducer is a strain-sensitive resistor mounted to a diaphragm, bellows, or bourdon tube. When pressure is applied, the resistor changes its physical length thereby causing change in resistance. This effect is expressed by

$$F_g = \frac{\Delta r/r}{\Delta L/L}, \dots \dots \dots (3)$$

where

- F_g = gauge factor,
- Δr = change in resistance,
- r = unstrained resistance,
- ΔL = change in length, and
- L = unstrained length.

There are four basic types of strain gauge transducers; unbonded wire, bonded foil, thin film, and semiconductor. A rule that applies to strain gauge transducers is the larger the gauge factor, the higher the output of the device. For unbonded wire, the gauge factor is four. Bonded foil and thin film (Fig. 30.7) have factors of two. For semiconductor transducers, the factor ranges from 80 to 150.

Vibrating Crystal Transducer

In vibrating crystal transducers, a crystal is forced by external electronic circuits to oscillate at its resonate frequency when external stress is applied to the crystal by mechanical linkage to the diaphragm, bellows, or bourdon tube. The resonate frequency of the crystal shifts in proportion to the stress. In at least one transducer of this type, the pressure is applied directly to the crystal itself. The vibrating crystal is usually manufactured out of quartz because of its excellent elastic properties, long-

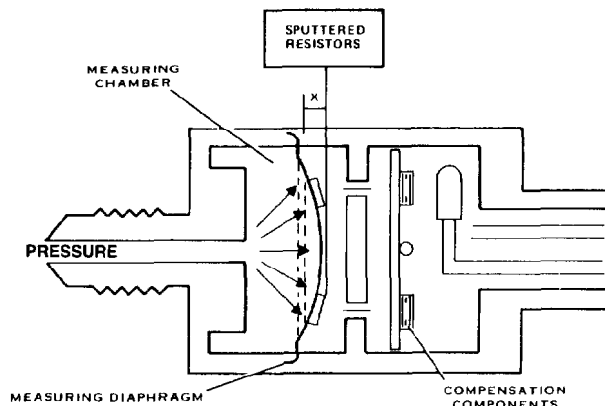


Fig. 30.7—Thin film strain gauge transducer.

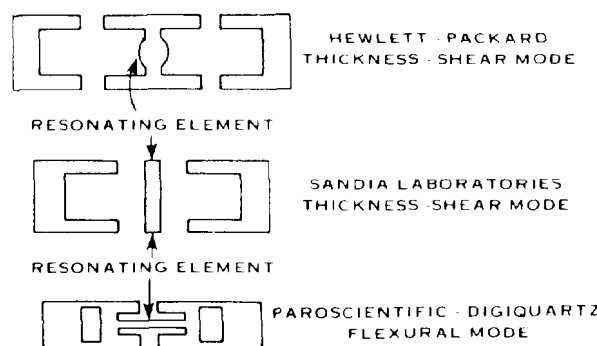


Fig. 30.8—Cross-sections showing different modes of motion of quartz crystals.

term stability characteristics, and ease of vibrational excitement. Fig. 30.8 shows various modes of motion of quartz crystal. Advantages are excellent accuracy, resolution, and long-term stability. Disadvantages are sensitivity to temperature and extremely high costs.

New technology is constantly evolving a new generation of surface recording pressure gauges that are more and more advantageous to the petroleum engineer and petroleum engineering problems.

Calculated BHP

BHP calculated from surface pressure and fluid level, although less accurate than measured pressure, is sufficient for many practical uses. In an open hole or open tubing, the fluid level can be determined by a float run on a measuring line.

In pumping wells, the fluid level can be determined by sound reflection. There are four types of commercial instruments available. These are the depthograph, echometer, sonoloy, and acoustical well sounder. Each of these instruments records sound reflection initiated by firing a blank shotgun shell or pistol cartridge or venting pressure into a chamber attached to the casing head. A sound reflection is received and recorded from each tubing collar. By counting the collar reflections and knowing the tubing tally, the depth to the fluid can be calculated. In deep wells, attenuation of the collar reflection makes accurate counting difficult. In some oil wells,

usually those having considerable gas, a foaming condition makes the fluid level difficult to identify or may indicate a fluid level much higher than actual. A foaming condition is usually indicated when the fluid level changes several feet on tests made at short intervals of time. Fluid level can also be calculated from the time interval for the reflection to be received from the fluid level, but the variation in the speed of sound through gases of different compositions and the effect of temperature make the procedures more laborious and usually less accurate than the simpler method of counting collar reflections.

In calculating the pressure caused by the column of fluid, allowances should be made for gas in solution in the oil, which will reduce its specific gravity below that measured in the stock tank. This can reduce the gradient 5 psi/100 ft or more where much gas is in solution under high pressure. For wells producing water, it is customary to calculate the fluid head on a basis of a column of oil and water in the same ratio as normal production for the well, but this calculation is less reliable for low-capacity wells with high casinghead pressure and for pumping wells in which the pump is several hundred feet above the producing formation. If the surface pressure is low, the pressure caused by the weight of a column of gas may be too small to warrant consideration, but under high pressure it should be calculated and added to the hydrostatic head by the same equation used for calculating BHP in a gas well, where D is the depth of the fluid level.

Producing BHP of a pumping well that is sufficiently accurate for practical use may be calculated by shutting in the casing head until the gas pressure depresses the fluid level to the inlet of the pump, at which time fluid delivery is stopped. The casinghead pressure at that time, plus the head of the column of gas from the casing head to the pump inlet, plus the head of the column of liquid from the pump inlet to the producing formation is the producing BHP. A check of the determination should be made by releasing and controlling the pressure a few pounds less than the maximum pressure read and determining the rate of production under such conditions.

The BHP in a gas well can be calculated with an equation developed by Pierce and Rawlins⁴:

$$p_{ws} = (p_{wh})^{e^{0.0000347\gamma_g D}}, \quad \dots \dots \dots (4)$$

where

- p_{ws} = static BHP, psia,
- p_{wh} = wellhead pressure, psia,
- e = base, natural logarithms,
- γ_g = specific gravity of gas (air=1), and
- D = depth of well, ft.

This equation is based on an average temperature of the column of gas of 60°F. While the temperature gradient in a producing well is rarely a straight line, the average temperature at a depth below seasonal effect (20 to 30 ft) and at a depth of the pressure is sufficiently accurate for practical purposes. The equation can then be written⁵:

$$p_{ws} = (p_{wh})^{e^{\gamma_g D/(53.34T)}}$$

or

$$\log p_{ws} = \log p_{wh} + \frac{\gamma_g D}{122.82 \bar{T}}, \quad \dots \dots \dots (5)$$

where \bar{T} is the average temperature in the borehole, °F+460.

Deviation of a gas from Boyle's law will affect the calculated BHP enough to be considered only in high pressure deep wells. USBM Monograph 7 presents the following equation.⁵

$$\frac{p_{ws}}{1 + p_{ws}z} = \left(\frac{p_{wh}}{1 + p_{wh}z} \right)^{e^{\gamma_g D/(53.34T)}} \quad \dots \dots \dots (6)$$

where z is the deviation coefficient, deviation per psi expressed as a decimal.

Application of BHP

The importance of pressure analysis in projecting and enhancing the performance of producing oil and gas wells emphasizes the need for precision pressure measurement systems. Today's petroleum engineer must have sufficient information about the reservoir to adequately analyze current performance and predict and optimize future performance. More specifically, such pressures are a basic part of reservoir calculations, rate of equalization of pressures, interference tests for well spacing or rate of development, formation damage during completion, rework or workover operations, and indication of deposition of salts, sediments, or other restrictions at the wellbore. Other applications are design of downhole equipment for artificial lifting, efficiency of operation of such equipment, and evaluation of drillstem test (DST) information.

Static Pressure

Static pressure is the most frequent BHP measurement. Most such measurements are made as a pressure survey of a pool where the pressures in all wells are determined in a short period of time either by cooperation of the operators or by order of a conservation commission, usually as a result of a recommendation by the operators. Pressures are taken under reasonably uniform conditions after the wells have been shut in a specified length of time such as 24 or 48 hours, or longer, if the pressure buildup is at a slow rate. The pressures should be measured at or adjusted to a common data plane. In many pools, the pressures will not reach equilibrium in the specified shut-in time. However, if the pressures are determined for several surveys under the same conditions, the indicated rate of decline of the reservoir pressure should be reasonably accurate. Tests in representative wells which have been shut in long enough to reach pressure equilibrium will show the relation of the measured pressure to the actual reservoir pressure. Pressures in inactive wells may be used to confirm the actual pressure and the rate of decline.

Average Reservoir Pressure

The average reservoir pressure for a pool may be determined by arithmetically averaging the pressures of all

wells. For some pools it is preferable to determine a weighted average by weighting each pressure by the productive thickness of the reservoir at that point. When for any reason the pressure cannot be determined in substantially all wells or where wells are irregularly spaced, a better average reservoir pressure is determined by recording the pressures, either actual or weighted, on a map of the area and drawing isobars from which the average pressure weighted for an area is determined by planimeter, grid system, or other means.

Static Pressure from Partial Buildup

Many low-permeability reservoirs require excessive shut-in time to reach static or equilibrium pressure. Several methods have been proposed for calculating the reservoir pressure from partial buildup of pressure. Muskat⁶ proposed plotting $\log(p_{ws} - p_t)$ vs. time, where p_{ws} is an estimated static BHP and p_t is the measured pressure at different times, p_{t_1} , p_{t_2} , p_{t_3} , etc. When plotted on semilog cross-sectional paper with pressure on the log scale, the selected p_{ws} is the static pressure when the plot is a straight line.

Arps and Smith⁷ proposed plotting increments of pressure increase for uniform time periods against measured pressure on rectangular cross-sectional paper, and extrapolating the curve to intersect the zero line of the incremental-pressure scale, which gives the static pressure. Both the Arps and Smith and the Muskat methods are more commonly used in cases of rapid pressure buildup.

Miller *et al.*⁸ presented an equation to calculate the static pressure from a partial buildup curve:

$$p_{ws} = p^* + \frac{(p_{sd} - \Delta\bar{p})q\mu B}{0.00708 kh}, \quad \dots \quad (7)$$

where

- p_{ws} = static BHP, psi
- p^* = last pressure on buildup curve, psi
- $p_{sd} = \log_e(r_d/r_w)$ for constant pressure at radius of drainage, or
 $= \log_e(r_d/r_w) - 0.75$ when no influx across external boundary,
- q = production rate at shut-in, B/D,
- μ = reservoir fluid viscosity, cp,
- B = formation volume factor for total fluid produced, RB/STB
- k = permeability of reservoir, md,
- h = effective thickness of reservoir, ft,
- $\Delta\bar{p}$ = dimensionless pressure variable from curves (see Fig. 30.9),
- $\Delta p = p_{wf} - p_{ws}$,
- p_{wf} = BHP during buildup, psi,
- p_{ws} = BHP at time of shut-in, psi, and
- t = time after well was shut in, hours.

The value of p^* is determined by plotting the buildup pressure vs. the time on semilog paper, with time on the log scale. When afterflow is completed following shut-in, the points should fall on a straight line and p^* is the

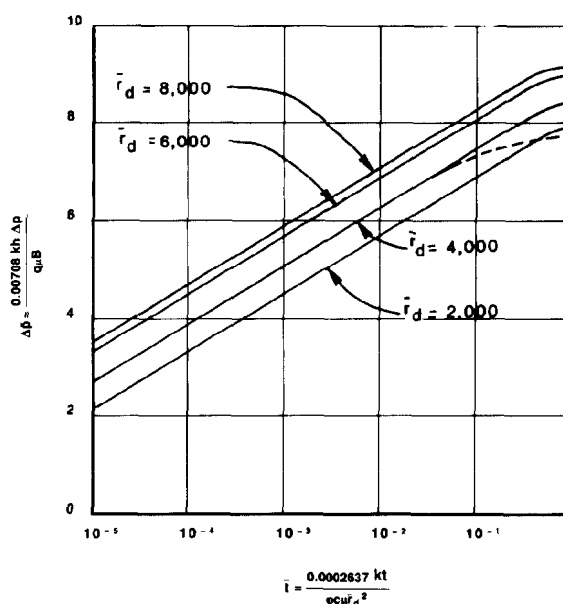


Fig. 30.9—Curves from which $\Delta\bar{p}$ is determined in the Miller *et al.* equation for calculating static pressure from buildup pressure curve. Solid lines assume influx at r_d and dotted line indicates direction of curves when no influx at r_d .

highest measured pressure lying on the straight line. This is the same straight line by which the slope, m , is determined in the equation for permeability from buildup pressures by the same authors and is discussed further under that topic.

The straight line by which the slope m is determined comes from the middle time region of a Horner plot. Afterflow causes lack of development of the middle time region (with long periods of afterflow), early onset of boundary effects, and development of several false straight lines that could be mistaken for the middle time region. This makes the middle time region difficult for the buildup test analyst to recognize. Recognition of the middle time region is essential for successful buildup curve analysis based on Horner plot method. The line must be identified to estimate reservoir permeability, to calculate skin factor, and to estimate static drainage area pressure.

A log-log graph of the pressure change, $p_{ws} - p_{wf}$ (Δp), in a buildup test vs. shut-in time t presents a good estimation of where the straight line portion, or middle time region, begins (Fig. 30.10).⁹ A log-log graph of pressure change $p_{ws} - p_{wf}$ vs. Δt ¹⁶ is an even more diagnostic indicator of the end of afterflow distortion. Fig. 30.11 shows a semilog plot of theoretical buildup test data. The use of type curves has greatly improved identification of the straight line portion of the buildup curve after wellbore storage effects have ended.

Horner¹⁰ plotted buildup pressure vs. $(t + \Delta t)/\Delta t$ on semilog paper with $(t + \Delta t)/\Delta t$ on the log scale where t = total producing time since well completion, hours, and Δt = time since the well was closed in, hours. Extrapolation of the curve to a value of $(t + \Delta t)/\Delta t = 1$ is the approximate static pressure.

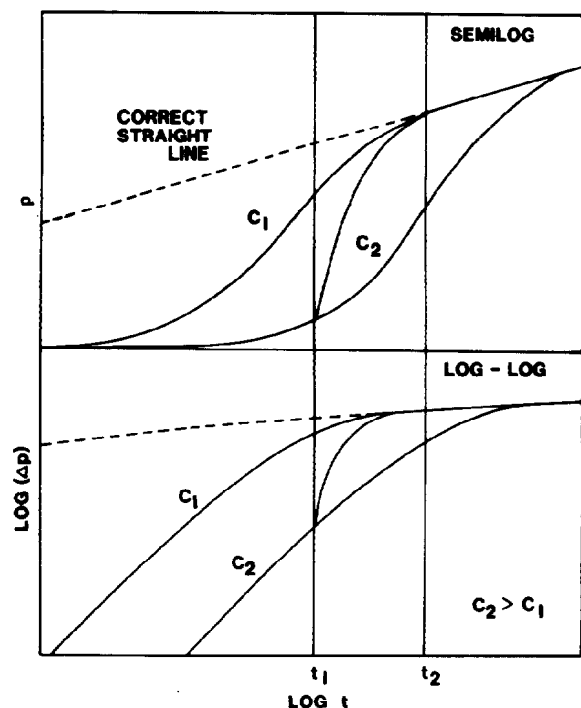


Fig. 30.10—Log-log vs. semilog plots.

The value of t is determined by dividing the cumulative production of the well by the rate of production per hour at the time the well is shut in. The uncertainty of the value of t increases with the age of the well. Experience indicates that using the time of the flow period before the well is shut in for the buildup test is often more reliable than using the total time since completion provided fully stabilized conditions exist both when the well is opened and when it is shut in.

Thomas,¹¹ with Horner's basic equation, preferred using the reciprocal of $(t + \Delta t)/\Delta t$ and therefore plotted pressure vs. $\Delta t/(t + \Delta t)$ on semilog paper with $\Delta t/(t + \Delta t)$ on the log scale, and extrapolated the curve to a value of $\Delta t/(t + \Delta t) = 1$, which gives the approximate reservoir pressure.

Hurst¹² plotted the buildup pressure vs. the shut-in time in minutes on semilog paper with time on the log scale. A straight line is drawn through the points and extrapolated to an intercept time value of 1. The slope is the value of pressure change in one log cycle. Expressing his equation in English units, the static pressure is calculated:

$$p_{ws} = b + m \log 625 m, \quad (8)$$

where

p_{ws} = static BHP, psi,

m = slope of buildup curve, and

b = intercept of curve with time value of 1 minute.

Correct identification of the straight-line portion of the buildup curve is necessary for the interpretation of pressure buildup data. The straight-line portion of the

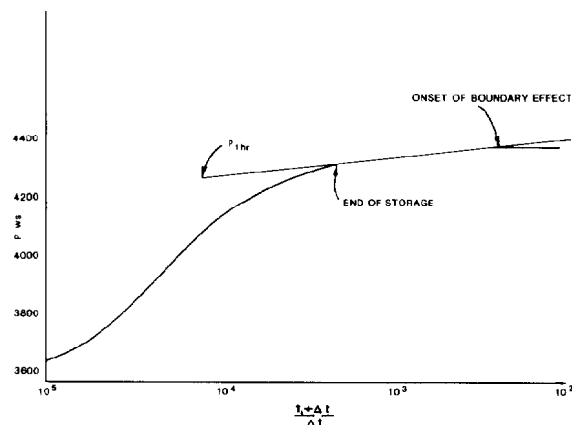


Fig. 30.11—Plot of typical buildup with afterflow.

curve is frequently masked by one or more factors, such as skin effect, afterflow, and the early onset of boundary effects. Chap. 35, "Well Performance Equations," addresses these problems.

The capacity of a well to produce can be estimated from the BHP drawdown on a flow test. For gas wells, the open-flow capacity is calculated by the procedure proposed in Ref. 5 except that both the static pressure and the flowing pressure are measured with a BHP gauge. Open-flow capacity of oil wells having large capacity and high pressure is rarely of value, and little work has been reported on such determinations. Theoretically, so long as single-phase flow maintains, the rate of flow should increase in proportion to the drawdown pressure. But, because of gas coming out of solution below the bubblepoint, turbulence in the flow, and borehole restrictions, the flow conditions change and the proportionality does not hold. Engineers who have investigated the problem usually consider that little increase will be obtained after the drawdown pressure is one-half the static pressure. For low-pressure wells, the rate of production will usually continue to increase until the flowing pressure is equal to or close to atmospheric pressure.

Productivity Index

PI is defined as the barrels of oil produced per day per pound decline in BHP. To determine the PI, a well is shut in until static or reservoir pressure is reached. The well then is opened and produced until the BHP and rate of production are stabilized. Since a stabilized pressure at surface does not necessarily indicate a stabilized BHP, the BHP should be recorded continuously from the time the well is opened. The PI is then

$$J = \frac{q_o}{p_{ws} - p_{wf}}, \quad (9)$$

where

J = PI, B/D-psi,

q_o = rate of oil production, B/D,

p_{ws} = static BHP, psi, and

p_{wf} = flowing BHP, psi.

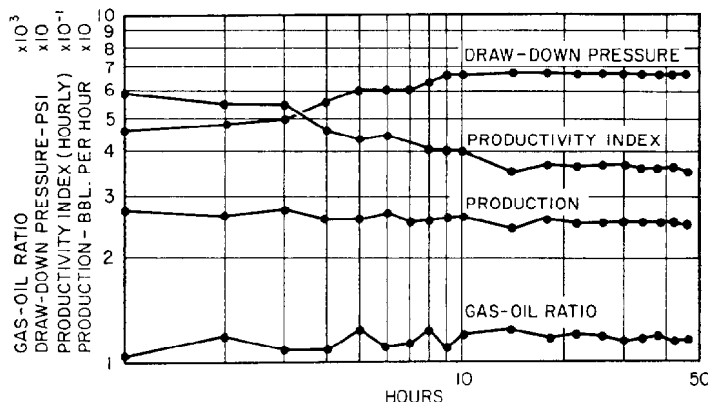


Fig. 30.12—Flow-test data on a well having a negligible transient or stabilization period.

Specific PI is defined as barrels of oil produced per day per pound decline in BHP per foot of effective reservoir thickness, and is expressed as

$$J_s = \frac{q_o}{(p_{ws} - p_{wf})h}, \quad (10)$$

where J_s is the specific PI and h is the effective reservoir thickness, ft.

On a flow test the time required for a well to reach a stabilized BHP and rate of production, that is, the transient period, may require several hours or even days and occasionally several weeks. The duration of the transient period and the rate of the pressure decline and the PI decline during the transient period will indicate the quality of the reservoir. A short transient period indicates a high-quality reservoir, and a long transient indicates a low-quality reservoir which will have a comparatively low recovery of the amount of oil calculated to be in place. Reservoir quality is not related to the numerical value of the PI. The nature of the transient period is most conveniently expressed by plotting the productivity index by hours on log-log paper.

Typical well test data are presented in Figs. 30.12 through 30.15. The negligible transient period of the test shown in Fig. 30.12 indicates a high-quality reservoir from which relatively high recovery may be expected. The short transient period in the flow test in Fig. 30.13 indicates a comparatively high recovery of the original oil in place. In Fig. 30.14, the transient period is quite long but the continuous flattening of the slope of the PI curve indicates eventual stabilization. Fig. 30.15 is the flow test of a well in which the continuous decline in pressure, production, and PI shows that the flow will not stabilize and therefore the ultimate recovery will be lower than that reasonably expected from a consideration of the producing formation and its apparent productivity.

Flow tests and PI tests are conducted by other procedures. Some prefer to run the test at two or more different rates of flow. There is usually some difference in the PI at different rates, sometimes more than can be accounted for by inherent limitation of accuracy of pressure measurement and production gauging. Changing GOR or WOR will affect the relative permeability

and therefore the PI. Calculating a PI based on total fluid mass instead of liquid production has given more consistent results in some pools.

Permeability

Permeability of the reservoir rock can be calculated from the PI. Wycoff *et al.*¹³ used

$$k = \frac{q\mu B \log(r_d/r_w)}{0.003076 h(p_{ws} - p_{wf})} \\ = 325 J_s \mu B \log \frac{r_d}{r_w}, \quad (11)$$

where

- k = permeability, md,
- r_d = radius of drainage area, ft,
- r_w = wellbore radius, ft,
- q = production rate, B/D,
- μ = viscosity of produced fluid, cp,
- B = formation volume factor, RB/STB,
- h = effective reservoir thickness, ft,
- p_{ws} = static BHP,
- p_{wf} = flowing BHP, and
- J_s = specific PI.

Permeability can be calculated from the buildup curve obtained when a producing well is shut in following a flow test. Muskat discussed this in 1937 and presented an equation in 1949.¹⁴ The equation in commonly used units is

$$k = \frac{40.37 md^2 \mu B \log(r_d/r_w)}{h\gamma}, \quad (12)$$

where m = slope of $\log(p_{ws} - p_{wf})$ vs. t , d = diameter of flow pipe, in., t = time, hours, since well was closed in, and other parameters are as previously defined.

The equation has limitations, but it may be helpful in cases of severe reservoir damage such as interpretation of DST buildup curves where recovery is low.

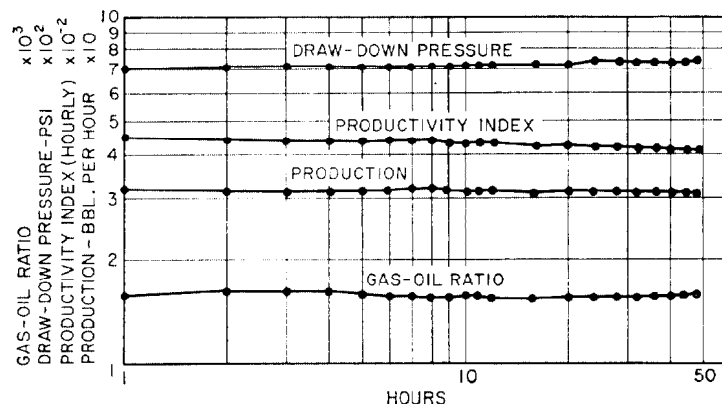


Fig. 30.13—Flow-test data on a well having a short transient period.

Miller *et al.*⁸ calculated permeability from a BHP buildup curve with the equation

$$k_o = \frac{162.5 q_o \mu_o B_o}{hm}, \quad (13)$$

where

- k_o = effective oil permeability, md,
- k = permeability, md,
- q_o = oil production rate, B/D,
- μ_o = viscosity of reservoir oil, cp,
- B_o = formation volume factor of oil, RB/STB,
- h = effective reservoir thickness, ft, and
- m = slope of buildup curve.

The slope m can be determined most conveniently by plotting BHP against time in hours on semilog paper, with time on the log scale. The initial part of the curve is affected by the afterflow into the wellbore, and the last part of the buildup curve may be too flat and therefore unreliable because of interference of drainage areas or limited reservoir. The calculation is simplified by extrapolating the buildup curve to encompass one complete cycle of the log scale. The slope is then the difference in the pressure reading at the beginning and at the end of the cycle.

The part of the curve representing the slope of the buildup curve is usually evident, but occasionally interferences and irregularities in the reservoir make the slope uncertain. We consider that if the value

$$m = \frac{0.0002637kt}{\phi c_L r_d^2 \mu}, \quad (14)$$

where

- k = permeability, md,
- t = time, hours, from closed in to end of straight-line portion,
- ϕ = porosity, fractional,
- c_L = liquid compressibility, psi⁻¹,
- μ = viscosity, cp,
- r_d = drainage radius, ft,

falls to the range 10^{-1} to 10^{-2} , the slope m is proper and the calculated value of k is valid. This tacitly assumes that the values of the other factors are known and that the conditions exist for which the equation was derived. A valid calculation of permeability from buildup curves requires stabilized conditions of pressure and rate of production at the time the well is closed in.

These equations for calculating permeability are based on liquid single-phase flow. When a small amount of free gas is produced with the liquid, adjustment by the relative permeability will give an acceptable answer. When gas only is produced from the reservoir, the equations for permeability are as follows.

Radial flow equation:

$$k = \frac{q_g \mu_g T_R z \log(r_d/r_w)}{0.00306h(p_{ws}^2 - p_{wf}^2)}, \quad (15)$$

Pressure buildup¹⁵:

$$k = \frac{1,637 q_g \mu_g T_R z}{hm_g}, \quad (16)$$

where

- k = permeability, md,
- q_g = rate of production, Mcf/D at 14.7 psi and 60°F,
- μ_g = viscosity of reservoir gas, cp,
- T_R = reservoir temperature, °F + 460,
- z = gas deviation factor, reservoir conditions,
- h = effective reservoir thickness, ft,
- p_{ws} = static BHP, psia,
- p_{wf} = flowing BHP, psia,
- r_d = drainage radius,
- r_w = wellbore radius, and,
- m_g = slope of pressure buildup curve, p_w^2 vs. $\log t$, where t = time after shut-in, hours,
- p_w = BHP at t .

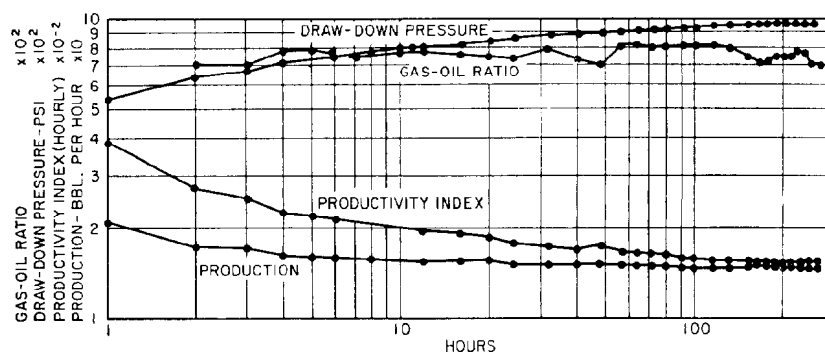


Fig. 30.14—Flow-test data on a well having a long but finite transient period.

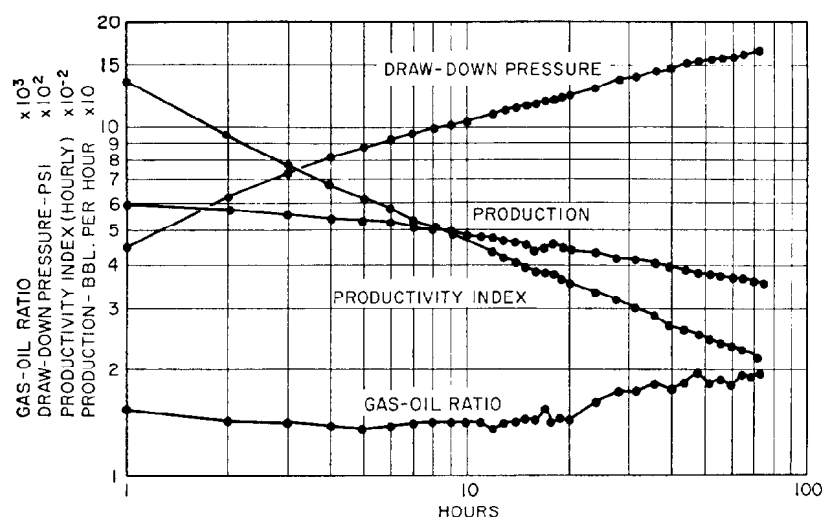


Fig. 30.15—Flow-test data on a well having a very long transient period.

Permeability Damage

The permeability of the reservoir adjacent to the borehole is frequently reduced by the invasion of drilling mud, water blocking by invasion of filtrate water from drilling fluid or other source, swelling of clay particles, or deposition of salts or wax. Blinding or partial clogging of screens or perforations will give a similar effect. A substantial restriction of flow can be observed on the BHP chart by the straight-line buildup until near the maximum pressure instead of the normal exponential shaped curve. On the other hand, permeability adjacent to the borehole may be increased as a result of acidizing, fracturing, or shooting.

The amount of damage or improvement to the permeability adjacent to the borehole is determined by comparing the permeability calculated from flow test with the permeability calculated from the buildup and is expressed as the productivity ratio:

$$F_P = \frac{k_j}{k_b} \quad \dots \dots \dots (17)$$

where

- F_P = productivity ratio,
- k_j = permeability calculated from productivity index, and
- k_b = permeability calculated from buildup pressure.

Substituting the equated expressions of k_j and k_b and simplifying:

$$F_P = \frac{2m \log(r_d/r_w)}{p_{ws} - p_{wf}} \quad \dots \dots \dots (18)$$

A fractional F_P indicates restricted flow at the borehole and an F_P greater than unity indicates better permeability at the borehole, usually the result of stimulation.

Dolan *et al.*¹⁶ presented an empirical equation to determine "damage factor" that does not involve the use of the amount of production. It is of particular value for interpretation of drillstem test charts that have an acceptable buildup but negligible fluid recovery. His equation expressed as productivity ratio is

$$F_P = \frac{\Delta p}{0.183(p_{ws} - p_{wf})} \quad \dots \dots \dots (19)$$

where

F_P = productivity ratio,
 p_{ws} = static BHP,
 p_{wf} = flowing BHP, and
 Δp = slope of plot of p vs. $\log(t + \Delta t / \Delta t)$,

where

t = time well was open, minutes,
 Δt = time after well was shut in, minutes, and
 p = pressure at $t + \Delta t$.

Hurst¹² has developed equations for calculating restrictions to flow through the reservoir adjacent to the borehole, which they have called "skin effect." Expressed in oilfield units, these equations are

for oil:

$$p_s = m \left[\frac{(p_t - p_{wf})}{m} - \log \left(\frac{q_o B_o}{10.4 m h \phi c_o r_w^2} \right) \right] \dots \dots \dots (20)$$

and for gas:

$$p_s = m_g \left[\frac{(p_t - p_{wf})}{m_g} - \log \left(\frac{q_g z T_R}{2.063 \phi h m_g c_g \bar{p} r_w^2} \right) \right], \dots \dots \dots (21)$$

where

p_s = pressure loss due to skin effect, psi,
 p_{ws} = static BHP, psi,
 p_{wf} = flowing BHP, psi,
 p_t = well pressure 1 hour after shut-in, psi,
 q_o = production rate for oil, B/D,
 q_g = production rates for gas, Mcf/D at 14.7 psia and 60°F,
 B_o = formation volume factor of oil, RB/STB,
 z = compressibility factor (gas deviation factor),
 h = effective reservoir thickness, ft,
 T_R = reservoir temperature, °F + 460,
 ϕ = porosity reservoir rock, fraction,
 c_o = compressibility of reservoir oil, psi⁻¹,
 r_w = borehole radius, ft,
 m = slope, p_t vs. $\log t$, and
 m_g = slope p_t^2 vs. $\log t$, where p_t is the well pressure at time t and t is time after well shut-in, hours.

Positive values of p_s indicate damage and negative values of p_s indicate improvement of permeability adjacent to the wellbore in terms of pressure loss due to skin effect.

It is usually difficult to delineate specific heterogeneities from well test results only because different heterogeneities may cause the same or similar well test response. A higher degree of confidence is achieved when the interpretation of test results is confirmed by geological and geophysical evidence of heterogeneities.

Linear discontinuities, faults, and barriers affect a pressure buildup behavior and are manifested by a second straight line, the slope of which is double the initial straight line. For a well near a linear fault, drawdown testing can be used to estimate reservoir permeability and skin factor in the usual fashion, as long as wellbore storage effects do not mask the initial straight-line section. If the well is very close to the fault, the initial straight-line section may end so quickly that it will be masked by wellbore storage.

As the drawdown proceeds and the pressure at the producing well falls below the initial semilog straight line, the following equation indicates that p_{wf} vs. $\log t$ plot will have a second straight line portion with a slope double that of the initial straight line.

$$p_{wf} = 2(m \log t + p_{thr}) + p_i + m \left[0.86859s + \log \left(\frac{4L^2}{r_w^2} \right) \right], \dots \dots \dots (22)$$

where

$$m = \frac{-162.5 q_o \mu_o B_o}{kh},$$

p_{thr} = pressure on straight-line portion of semilog plot one hour after beginning a transient test, psi,

p_i = initial reservoir pressure, psi,

s = skin effect, and

L = distance to a linear discontinuity, ft.

However, the simple occurrence of a doubling slope in a transient test does not guarantee the existence of a linear boundary near the well.

To estimate the distance to a linear discontinuity, we use the intersection time, t_x , of the two straight line segments of the drawdown curve. The following equation applies for drawdown testing.¹⁷

$$L = 0.01217 \sqrt{\frac{k_o t_x}{\phi c_t \mu_o}}, \dots \dots \dots (23)$$

where c_t is compressibility of the total system, psi⁻¹. The effects of reservoir heterogeneities and method of determining them are discussed in Chap. 26.

Lifting Equipment

BHP measurements are valuable to the engineer for determining the size and type of artificial lift to install and to monitor the efficiency of such equipment.

The efficiency of a gas lift depends, among other factors, on the pressure at the depth of gas injection. From

the flowing pressure or PI, the pressure can be calculated for a given rate of production and after a gas lift is in operation. Knowing the PI, the producing efficiency can be calculated from the rate of production. The change in pressure gradient in a well being gas lifted will determine the point at which gas is entering the flow string, which is of interest where multiple flow or unloading valves are installed.

The PI is used to determine the amount of fluid available to be pumped from a well and therefore the size of the pump that should be run and the depth at which it should be set. After a well has been on the pump for some time and declined in production, the question frequently arises as to whether the productivity of the well has declined or the pumping equipment has decreased in efficiency. The correct condition can be determined by measuring the static and producing pressures, either with a bottomhole gauge or from fluid-level calculation by sound reflections as described previously. If fluid-level determinations are known to be unreliable for a given pool or are proved uncertain in a given well because of fluctuating fluid-level by several determinations, a BHP gauge should be run. Many operators have successfully run a pressure gauge in the annulus between the tubing and casing. During such runs the wireline will sometimes wrap around the tubing or the gauge will wedge between the tubing and casing. It can usually be released by starting the pumping equipment, but sometimes it is necessary to move in a pulling unit to lift the tubing to free the gauge. Many operators use an eccentric tubing head to position the tubing against one side of the casing instead of its normal central position and thus minimize chances of the gauge's becoming hung up in the annulus. The BHP gauge can be run on the rods in most wells by attaching it, preferably rigidly, to the standing valve. A pressure gauge under these conditions is subject to severe vibrations resulting from both the vibration of the pumping equipment and a "water-hammer" effect from the liquid at the pump level.

Drillstem Tests

The most common use of BHP gauges in a drilling well is in evaluating DST's. Pressure gauges were first used to determine that the valve functioned properly and was open during the test. Subsequently the pressure information has become important. The detailed pressure information obtained on a DST can be used to determine the productivity of the formation by calculating the PI from the amount of fluid recovered during the test and the static and drawdown pressures. A more recent use has been to confirm indicated productivity from the buildup after the valve is closed. It is not unusual to have a very poor recovery of fluid and obtain a good buildup curve such as can be obtained only when the producing capacity is much better than indicated by the quantity of fluid recovered. The permeability can be calculated from the buildup curve. While subject to a high probable error because of the short time of the test and usually high reservoir damage adjacent to the borehole, it is sufficient to indicate whether further testing may be warranted.

Mud Weight

The pressure at the depth of a DST, before seating the packer and also after the test is completed and the packer

unseated, permits calculating the average weight of mud in the hole and is used to verify mud weight as measured by routine tests.

Nomenclature

- b = intercept of curve with time value of 1 minute
- B = formation volume factor for total fluid produced
- B_o = formation volume factor of oil
- c_L = liquid compressibility
- c_o = compressibility of reservoir oil
- c_t = compressibility of the total system
- C_g = gas compressibility
- C_T = temperature coefficient
- d = diameter of flow pipe
- d_c = deflection of calibration temperature
- d_o = observed deflection
- d_1 = deflection at T_1 for given pressure
- d_2 = deflection at T_2 for same pressure
- D = depth of well
- e = base, natural logarithms
- F_g = gauge factor
- F_p = productivity ratio
- h = effective reservoir thickness
- J = PI
- J_s = specific PI
- k = permeability of reservoir
- k_b = permeability calculated from buildup pressure
- k_j = permeability calculated from productivity index
- k_o = effective permeability of oil
- L = distance to a linear discontinuity and unstrained length
- ΔL = change in length
- m = slope of buildup curve, p_t vs. $\log t$ or slope of $\log(p_{ws} - p_{wf})$ vs. t
- m_g = slope of pressure buildup curve, p_w^2 vs. $\log t$
- p = pressure at $t + \Delta t$
- Δp = slope of plot of p vs. $\log t + \Delta t / \Delta t$ or $\Delta p = p_{wf} - p_{ws}$
- $\tilde{\Delta p}$ = dimensionless factor from curves (see Fig. 30.9)
- p^* = last pressure on buildup curve
- p_i = initial reservoir pressure
- p_s = pressure loss due to skin effect
- $p_{sd} = \log e \, r_d / r_w$ for constant pressure at radius of drainage or $\log e \, (r_d / r_w) - 0.75$ when no influx across external boundary
- p_t = well pressure 1 hour after shut-in
- p_w = BHP at t
- p_{wf} = flowing BHP
- p_{wh} = wellhead pressure
- p_{ws} = static BHP
- p_{1hr} = pressure on straight-line portion of semilog plot one hour after beginning a transient test

q = production rate at shut-in
 q_g = rate of production
 q_o = rate of oil production
 r = unstrained resistance
 Δr = change in resistance
 r_d = drainage radius
 r_w = wellbore radius
 s = skin effect
 t = time
 t = time from closed in to end of straight-line portion of buildup curve
 Δt = time after well was shut in
 t_x = intersection time of the two straight line segments of the drawdown curve
 \bar{T} = average temperature in the borehole
 T_c = calibration temperature
 T_o = observed temperature
 T_R = reservoir temperature
 T_1 = lower temperature
 T_2 = higher temperature
 z = compressibility factor (gas deviation factor)
 γ_g = specific gravity of gas (air=1)
 μ = viscosity of produced fluid
 μ_g = viscosity of reservoir gas
 μ_o = viscosity of reservoir oil
 ϕ = porosity reservoir rock

$$m = \frac{kt}{\phi c_L r_d^2 \mu} \quad (14)$$

$$k = \frac{254.359 q_g \mu_g T_R z \log \left(\frac{r_d}{r_w} \right)}{h(p_{ws}^2 - p_{wf}^2)} \quad (15)$$

$$k = \frac{127.2 q_g \mu_g T_R z}{hm_g} \quad (16)$$

$$p_s = m \left[\frac{p_t - p_{wf}}{m} - \log \left(\frac{0.412 q_o B_o}{\phi m h c_o r_w^2} \right) \right] \quad (20)$$

$$p_s = m_g \left[\frac{p_t - p_{wf}}{m_g} - \log \left(\frac{142.817 q_g z T_R}{\phi h m_g c_g r_w^2 \bar{p}} \right) \right] \quad (21)$$

$$L = \sqrt{\frac{kt_x}{1.781 \phi c_L \mu_o}} \quad (23)$$

Key Equations in SI Metric Units

$$p_{ws} = p_{wh} \exp(1.139 \times 10^{-4} \gamma_g D) \quad (4)$$

$$\log p_{ws} = \log p_{wh} + \frac{\gamma_g D}{67.37 T} \quad (5)$$

$$\frac{p_{ws}}{1 + p_{ws} z} = \frac{p_{wh}}{1 + p_{wh} z} \exp \left(\frac{\gamma_g D}{29.26 T} \right) \quad (6)$$

$$p_{ws} = p^* + \frac{(p_{sd} - \Delta \bar{p}) q \mu B}{2 \pi h k} \quad (7)$$

$$k = \frac{q \mu B \log \left(\frac{r_d}{r_w} \right)}{2 \pi h (p_{ws} - p_{wf})} = \frac{J_s \mu B \log \left(\frac{r_d}{r_w} \right)}{2 \pi} \quad (11)$$

$$k = \frac{44,330 \text{ m}^2 \mu B \log \left(\frac{r_d}{r_w} \right)}{h \gamma} \quad (12)$$

$$k_o = \frac{q_o \mu_o B_o}{5.4575 h m} \quad (13)$$

where

p 's are in Pa,
 D is in m,
 γ_g is in kg/m³,
 T is in K,
 μ is in Pa·s,
 h is in m,
 k is in m²,
 q is in m³/s,
 r 's are in m,
 t is in s, and
 c 's are in m³/m³.

References

1. Millikan, C.V.: "Bottom-Hole Pressures," *Petroleum Production Handbook* (1962) **2**, 27-1-27-14.
2. Brownscombe, E.R. and Conlon, D.R.: "Precision in Bottom-Hole Pressure Measurement," *Trans., AIME* (1946) **165**, 159-74.
3. Bergman, J.C., Guimard, A., and Hageman, P.S.: "High Performance Pressure Measurement Systems," *Johnston-Macco* (1980) 10.
4. Pierce, H.R. and Rawlins, E.L.: "The Study of Fundamental Basis for Controlling and Gauging Natural Gas Wells, Part 1," R1 2929, USBM (1929).
5. *Back-Pressure Data on Natural Gas Wells and Their Application to Production Practices*, USBM Monograph 7 (1935) 168.
6. Muskat, M.: "Use of Data in the Build-Up of Bottomhole Pressures," *Trans., AIME* (1937) **123**, 44-48.
7. Arps, J.J. and Smith, A.E.: "Practical Use of Bottom-Hole Pressure Build-Up Curves," *Drill. and Prod. Prac.*, API (1949) 155.

8. Miller, C.C., Dyes, A.B., and Hutchinson, C.A. Jr.: "Estimation of Permeability and Reservoir Pressure from Bottomhole Pressure Build-Up Characteristics," *Trans., AIME* (1950) **189**, 91-104.
9. Earlougher, R.C. Jr., Kersch, K.M., and Ramey, H.J. Jr.: "Wellbore Effects in Injection Well Testing," *J. Pet. Tech.* (Nov. 1973) 1244-50.
10. Horner, D.R.: "Pressure Build-Up in Wells," *Proc., Third World Pet. Cong.* (1951).
11. Thomas, G.B.: "Analysis of Pressure Build-Up Data," *J. Pet. Tech.* (April 1953) 125-28; *Trans., AIME*, **198**.
12. Hurst, W.: "Establishment of the Skin Effect and Its Impediment to Fluid Flow into a Wellbore," *Pet. Eng.* (1953) **25**, No. 11, B-6.
13. Wycoff, R.D. *et al.*: "Measurement of Permeability of Porous Media," *Bull., AAPG* (1934) **18**, 161.
14. Muskat, M.: *Physical Properties of Oil Production*, McGraw-Hill Book Co. Inc., New York City (1949).
15. Tracy, G.W.: "Why Gas Wells Have Low Productivity," *Oil and Gas J.* (Aug. 6, 1955) **54**, No. 66, 84.
16. Dolan, J.P., Einarsen, C.A., and Hill, G.A.: "Special Applications of Drill Stem Test Pressure Data," *J. Pet. Tech.* (Nov. 1957) 318-24; *Trans., AIME*, **210**.
17. Gray, K.E.: "Approximating Well-to-Fault Distance from Pressure Build-Up Tests," *J. Pet. Tech.* (July 1965) 761-67.

Chapter 31

Temperature in Wells

G.J. Plisga, Sohio Alaska Petroleum Co.*

Introduction

Frequently, when working with a wildcat or deepening old production into zones that are relatively unknown, it becomes necessary to know the underground temperatures expected at a predetermined depth. In the 1920's, API Research Project 25 investigated the relationship between geothermal gradients and the geologic structures of oil fields.¹ Initially, interest in subsurface temperatures in oil fields focused on high temperature in deep wells, which caused cement to take initial set before it was placed behind the casing. More recently, cements with low hydration heat have been developed to protect permafrost intervals in northern frontier areas. Temperature surveys in wells were used to determine the top of the column of cement behind the casing.² With continual development of temperature devices, the reliability, accuracy, and speed of response have opened new horizons to temperature logging. Temperature logs are used currently to identify fluid entry into the wellbore, fluid migration behind the casing, tubing/casing leaks, and the extent of hydraulic fracturing and to monitor injectivity profiles.

Thermometers

Self-Contained Recording Thermometers

Self-contained recording thermometers, as used in the oil fields, use the same mechanism to record as the bottomhole pressure (BHP) gauge, with a thermometer element substituted for a pressure element. Temperature elements are made for some of the commercially available BHP gauges.

Humble Gauge Temperature Element. The temperature element for the Humble gauge is a container filled with mercury. With an increase in temperature, the mercury expands into a small-diameter cylinder at the end of

a piston, which extends through a packing gland against a tense helical spring. A stylus arm attached to the end of the piston extends into the cylindrical chart holder of the recording mechanism. The temperature range may be changed by varying the diameter of the cylinder and piston. To prevent the well pressure from affecting the temperature element, the mercury container is enclosed within an outer tube, which is filled with mercury to reduce thermal lag. With reasonable care in calibration and operation, temperature readings are accurate to 2°F and differential temperatures of 0.5°F can be read.

Amerada Gauge Temperature Element. The temperature element for an Amerada gauge is a pressure element with a bulb attached to the pressure end of the helical Bourdon tube, but thermally insulated from the gauge to reduce thermal lag. The bulb contains a liquid that has a substantial vapor pressure in the temperature range of interest. For various temperature ranges, different liquids and different ranges of helical Bourdon tubes are selected, preferably in such a combination that the maximum temperature range is near the critical temperature of the liquid, which gives maximum deflection per degree change in temperature. Ranges of approximately 120 and 200°F are used most frequently, with the minimum or maximum temperature as requested on the order. For maximum chart readability, the span between the minimum and maximum should be no greater than 200°F. Thermometers with a range of 120 to 200°F, as ordinarily calibrated, have a sensitivity of about 0.5°F and temperature changes of 0.1°F can be detected. The absolute accuracy of the Amerada temperature gauges is $\pm 2^\circ\text{F}$. The time required for thermal equilibrium is 20 minutes, but some 70% of the change in temperature will be recorded in 30 to 45 seconds when the instrument is immersed in liquid. A faster-responding gauge design, which increases the

*Author of the original chapter on this topic in the 1962 edition was C.V. Millikan.

temperature sensing area and reduces the heated mass, reaches thermal equilibrium in 8 to 10 minutes. The response of a liquid-vapor element is not a straight line, and therefore the accuracy and sensitivity of the element depend on the temperature to be measured.

Time Response. The time response of a thermometer to a change in temperature is directly related to the rate of movement through fluid, or flow of fluid past the thermometer. When a long section of hole is to be surveyed for a possible anomaly, the thermometer can be run at 50 to 100 ft/min followed by a second run at 2 to 5 ft/min through intervals of interest indicated on the first run.

Thermometers in Gas. The thermal conductivity of a gas is much lower than that of liquid. Therefore, a thermometer in gas has greater thermal lag for a given change in temperature. However, in most wells in which a thermometer is run through gas, any anomaly present is caused by expansion of gas, and the change in temperature is much greater than normally found when the anomaly is caused by migration of liquids. Because of the greater change in temperature, the presence of an anomaly is recorded as quickly in gas as in liquid. If a wellbore contains gas through the interval of interest and no gas expansion is present, such as a survey to determine migration of fluid behind the pipe, it is preferable to fill the well with liquid. If this is not feasible, then the thermometer must be run much slower (one-fifth to one-tenth) than the normal rate in liquid.

Electrical Surface-Recording Thermometers

Electrical surface-recording thermometers have a thermocouple, resistance wire, or thermistor as a temperature element. As normally calibrated for oil well use, electrical surface-recording thermometers have a sensitivity of 0.5°F and a thermal lag of only a few seconds. They are run on armored, insulated cables and the measuring wheel is geared to drive a chart recorder, camera, or computer to record temperature against depth.

Differential thermometers have been developed that record very small changes in temperature, 0.1°F or less, and are useful for identifying an anomaly in a long section when surveying at logging speeds of 100 to 150 ft/min. Once an anomaly is recorded, the thermometer can be run at slower speeds to completely define the anomaly. The differential thermometer is usually run in conjunction with an electrical thermometer to allow the absolute temperature to be measured in conjunction with the differential temperature.

By using electrical surface-recording thermometers, any temperature change noted can be checked by a rerun without returning the instrument to the surface. Very small anomalies under static conditions may be disturbed by the movement of the instrument, and therefore when a check of such condition is run, it should be delayed long enough to reestablish temperature equilibrium in the hole.

Advantages and Disadvantages

Self-contained thermometers and electrical surface-recording thermometers each have advantages and disad-

vantages. Self-contained thermometers have the advantages of portability and low investment. Disadvantages are much greater thermal lag and the necessity of returning the instrument to surface and reading the charts before the results are known. Electrical surface-recording thermometers have the advantage of quick response to temperature change, which permits running faster, plotting temperature against depth as the survey progresses, and checking any temperature anomaly without having to recover the instrument from the well. Disadvantages include a much greater investment, larger and heavier equipment, and delicate instrumentation.

Thermometry

Introduction

Two types of temperature surveys are used in the oil fields. One determines the true temperature at the depth of interest, and the second determines the depth or interval of a change in temperature. Usually, true temperature is measured with a maximum-recording thermometer. However, the use of electrical surface-recording thermometers is becoming more widespread for measuring true temperatures. Determination of a change in temperature requires a continuous record some distance above and below (as well as through) the interval of interest. In this case, the use of a differential thermometer will show the existence of a change in temperature rather than the true temperature or the actual magnitude of the change.

Actual Temperature

The geothermal gradient is very different in the various sedimentary basins, but within a given basin the change is gradual from one part to another.^{3,4} In most oil-producing areas, the gradient is usually within the range of 1 to 2°F increase for each 100 ft of depth. Temperatures just below the seasonal effect, ordinarily 30 ft below the surface, are about 1.5°F higher than the isotherms of the average annual temperature, as shown by climatological data of the U.S. Weather Bureau (Fig. 31.1). An exception to this is in northern latitudes where continuous permafrost exists. A geothermal gradient determined from such surface temperatures and the temperature of the producing formation is sufficiently accurate for most practical uses (Fig. 31.2). The rate of temperature increase in some areas is greater with depth, especially below 10,000 ft, and marked increases have been reported below 18,000 ft. When a precise geothermal gradient is to be determined, the hole selected must not have been disturbed for several months. In any event, the survey must be conducted while the well is in operation, since the passage of the thermometer will alter the static gradient.

The thermal conductivity of geological strata varies. The average heat conductivity of common sediments is given approximately by the figures in Table 31.1.⁴

When fluid movement continues in a borehole for periods of time, such as in drilling operations or a producing well, the temperature effect will be different on each formation. Any effect on a given formation will depend on its thermal conductivity, the difference in temperature between the moving fluid and the formation, and the length of time such movement continues. When fluid movement is stopped, temperature equalization

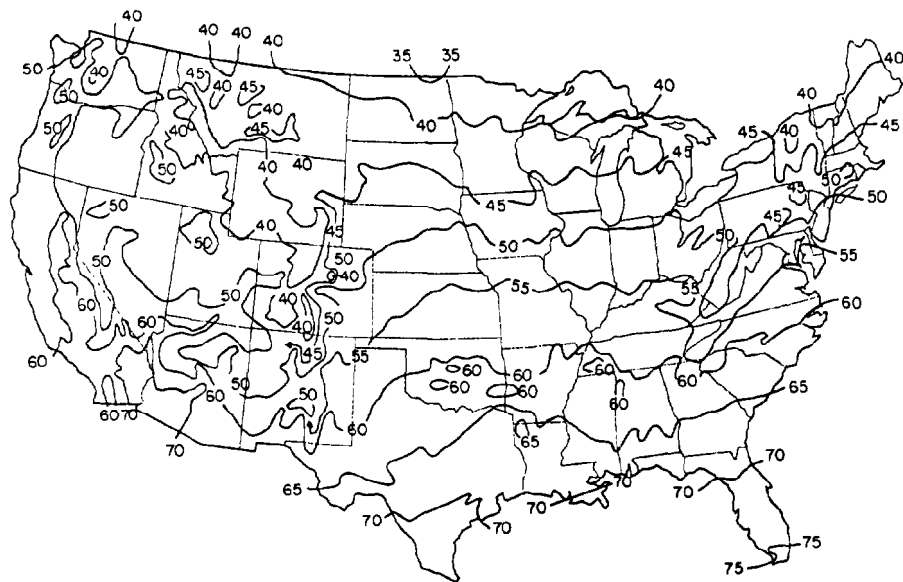


Fig. 31.1—Average annual temperature, °F, for the period 1899 to 1938. Isolines are drawn through points of approximate equal values.

begins, but considerable time, usually several months, is required to approach temperature equilibrium. In temperature surveys of wells, such temperature irregularities can be confused with an anomaly caused by some operating condition. Normally, however, the irregularities in the gradient resulting from normal operating conditions are small and the abnormal condition being investigated, such as a hole in the casing, fluid migration behind the pipe, or cement top, is of such size

or character that there is no uncertainty as to cause.

The actual temperature at depth is very important in many problems in drilling, production, and reservoir work. Drilling mud is often adversely affected by high temperature. The type of cement and additives are determined by the temperature at the casing seat or zone of interest. In oil reservoirs, the amount of gas in solution, the bubblepoint, and the viscosity are all related to the temperature, as is the amount of condensate formed and

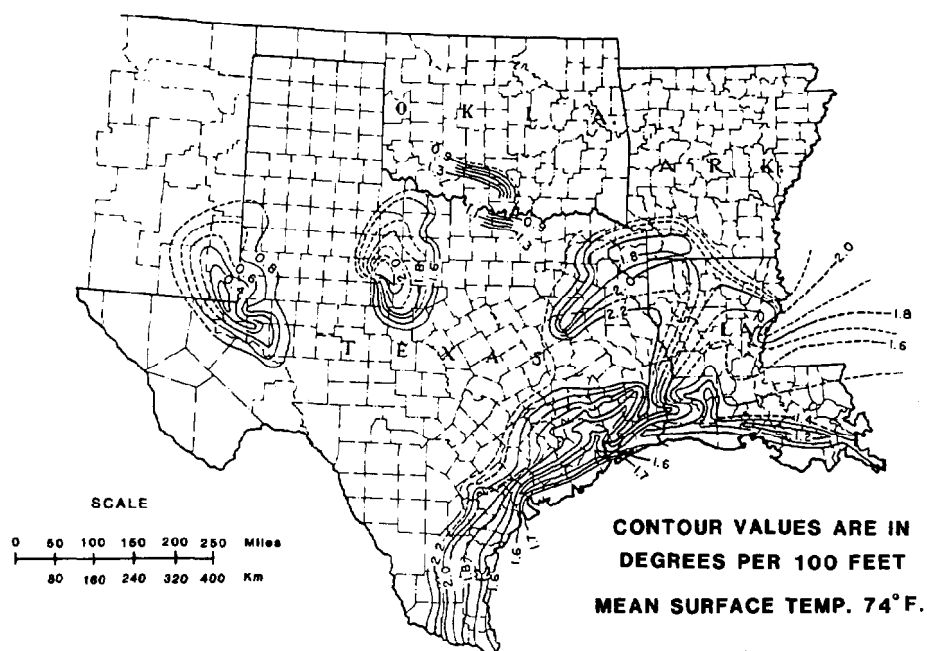


Fig. 31.2—Contour map of geothermal gradients in southwest U.S.

TABLE 31.1—AVERAGE HEAT CONDUCTIVITY OF COMMON SEDIMENTS (Btu/hr-sq ft-°F)

Rock salt	36
Anhydrite	32
Dense lime	20
Sand	16
Shale	12

the amount that remains as a liquid wetting the reservoir rock. The volume of gas per unit of reservoir rock and the supercompressibility of the gas are also related to the actual temperature.

Temperature Surveys

A temperature survey of a well is made either by running the thermometer continuously at a slow speed or by stopping it for a short time at regular intervals. For a survey through a long interval of hole, a continuous run is often preferred, while for a short interval numerous stops of 1 to 2 minutes are made. Temperature readings should be taken through the interval of interest, while running the thermometer in and while pulling up. Both runs should be at the same speed or at the same stops to determine more accurately the depth of any anomaly. On runs made very slowly, 2 to 5 ft/min, the actual thermal lag may be too small to warrant surveying the opposite direction. When a survey is started at a given rate, that rate should not be changed during the survey. To do so will cause a change in gradient or anomaly on the chart that may mask an actual anomaly or change in gradient in the well. Since the temperature chart is not available until the survey is completed and the thermometer is removed from the well, thorough notes that record time and depth of the instrument are required to correlate temperature and depth.

The location of a temperature change on a temperature survey is, in most cases, much more significant than the actual temperature or the amount of change in temperature. Normally, the temperature gradient in a well is reasonably uniform, and any deviation is indicative of an abnormal condition at that depth. The deviation may be an irregularity or anomaly in an otherwise uniform gradient, or it may be merely a change in the gradient. The primary causes of temperature change in a wellbore are expansion of gas, hydration of cement, and migration of fluid. Expansion of liquids in producing wells and heat of solution and chemical reaction are often present, especially in drilling wells, but the net effect on the temperature in the borehole is normally too small to be recognized. Gas expansion will cause an anomaly on the gradient, and migration of fluid will cause a change in gradient.

Gas expanding as it enters the borehole from the reservoir formation is much cooler than the adjacent formations, and therefore the particular intervals from which the gas is flowing can be identified by a temperature survey (Fig. 31.3A). A typical temperature survey conducted in a well producing minimal or no gas can be identified by a temperature survey (Fig. 31.3B). Greater detail will be recorded if the thermometer is run across the open hole or perforated sections while the well is pro-

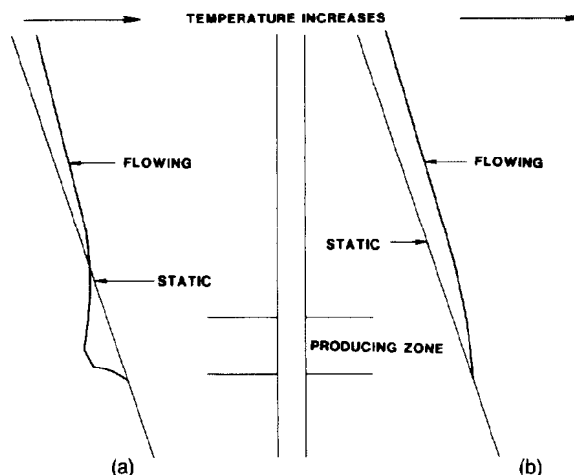


Fig. 31.3—(a) Example gradient gas flow. (b) Example gradient fluid flow.

ducing. When the tubing tail is below the producing interval, any gas produced that travels downward to the bottom of the tubing, then up the tubing past the thermometer, mixed with any other fluid that may be flowing into the wellbore, will mask anomalies that exist at the producing interval. With this type of completion, the tubing must be shut in and the annulus allowed to produce with the thermometer being run in the tubing. If a packer is set or, for other reasons, the well cannot be produced through the annulus, the survey can be run after the well is shut in. A temperature survey on a shut-in well relies on gas cooling by expansion to lower the temperature of that part of the formation producing gas below that of the formation not producing gas. Some time is required for the temperature to equalize, and a temperature survey run long enough after shut-in to complete afterflow will record lower temperatures in the principal intervals of gas production. A sequence of runs through the interval will permit a more reliable interpretation.

The lowest interval producing gas can be identified from a temperature survey by the cooling effect through the intervals producing the free gas and the return to the normal gradient below. Water-producing intervals can be determined only if enough free gas is produced with the oil to give a change in gradient at the lowest interval producing oil.

A hole in the casing through which fluid is moving can usually be found by running a temperature survey. In addition to the depth of the hole in the casing, the depth of the formation, which is the source of the migrating fluid, and the depth of the formation into which the fluid is moving must be determined when a hole is known or suspected to exist.

A permeability or injectivity profile of a water-injection well can be determined from a temperature survey. A typical temperature survey of a water-injection well with a homogeneous formation shows a cooling across the injection interval (Fig. 31.4). Two procedures are used to obtain injection-well temperature surveys. After injecting water for a period of time, injection is discontinued and, after a few hours, the survey is run. A more reliable answer would be expected from a series of

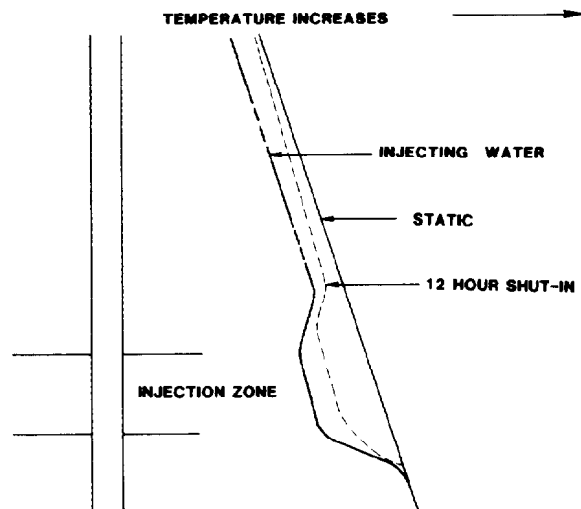


Fig. 31.4—Water-injection gradient.

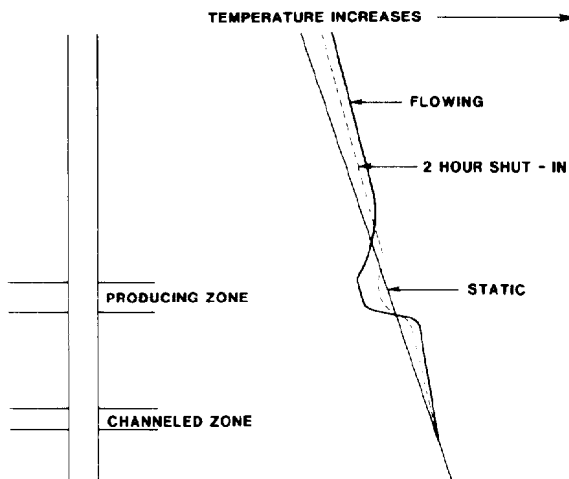


Fig. 31.5—Fluid channel gradient.

surveys at intervals of a few hours. Continued injection for many months can cool the entire formation and make it difficult to identify the relative injection capacity of the different parts. Under some conditions, another method that may give more detail is to discontinue injection for a day or more, then run a survey while injecting water at a very low rate, such as 1 to 5 bbl/hr. Because of the residual variations of temperature from normal water-injection operations, a survey before injection is recommended for comparison.

If water were channeling from below, the temperature survey would show a warmer anomaly at the base of the producing interval (Fig. 31.5). Fig. 31.6 shows ideal-temperature curves for various conditions of migration of fluid through a hole in the casing. Certain assumptions were made in drawing these ideal curves. Where gas is migrating, some expansion and, therefore, cooling is presumed as the gas leaves the formation. Also, it is assumed there will be a drop in pressure and, therefore, expansion and cooling at the depth of the hole in the casing. If there is no expansion at either point, the curves for gas would have the same appearance as the curves for

liquid. In cases where both formations are either above or below the casing hole, the movement of fluid from the hole to the farthest formation will mask any gradient between the hole and the nearest formation.

There are times when the volume of migrating fluids is not sufficient to affect the temperature. Gas leaking through a small hole in the casing will cause a very sharp temperature drop, but the volume may be too small to affect the gradient. Migration of fluids behind the casing will create a lower rate of temperature change than the normal gradient. If the flow is upward the gradient temperature will be higher than the normal gradient, and for downward flow the gradient temperature will be lower.

Preparation of the well is essential for a successful and reliable interpretation of the survey results. Usually the maximum anomaly is of the order of 2°F, and under less than optimal conditions the anomaly may be so small or so masked that a reliable interpretation is impossible. In these instances, the use of an electrical surface-recording differential thermometer may be the only method of obtaining a successful survey.

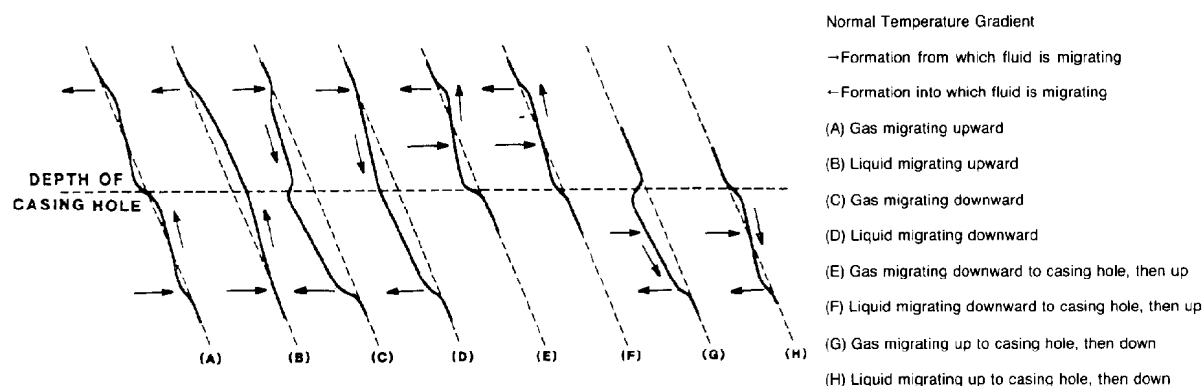


Fig. 31.6—Ideal-temperature curves of fluid migrating through casing hole.

Casing-leak and channeling-of-fluid temperature surveys are run with the well shut in. The shut-in time must be long enough for the entire wellbore to approach an even temperature gradient. A minimum of 24 hours should be allowed. However, the shut-in time required should be determined from past experience, type of problem to be identified, and location. Gas production and water production intervals are located with the well flowing at the maximum practical rate. If the survey cannot be run while flowing the well, the time interval between shutting in the well and running the survey may be critical. All afterflow must have ceased, but not so long as to allow the temperature to approach the normal gradient, which would mask any anomaly.

A temperature anomaly can be created by injection of fluid, usually oil or water, when normal conditions will not give a temperature change. Examples of this are identifying a channel below the producing interval and locating a packer or tubing leak by pumping cool fluids.

Drilling Wells

In drilling deep wells or wells that encounter high temperatures, especially in excess of 250°F, a representative bottomhole temperature (BHT) is required for selection of a proper mud program, cement, and additives to ensure proper cementing of the casing. In development drilling, temperature data from neighboring wells can be used in estimating the BHT of a new well. In exploration drilling, an estimation of the BHT may be all that is available. Unless offset data are available a

geothermal gradient must be assumed that will permit estimation of the BHT.

A technique exists for determining static BHT's by plotting on semilog paper T_{ws} vs. $(t_k + \Delta t)/\Delta t$ where

T_{ws} = bottomhole shut-in temperature measured at Δt , °F,

t_k = circulation time, hours, and

Δt = time after circulation ceases or shut-in time, hours.

The data required for this graph usually are obtained on successive openhole logging runs and allow an approximation of static BHT.⁵ Although this Horner-type analysis is not mathematically correct, when assuming short circulating times the technique provides reliable estimates of static temperature. This technique is most applicable in regions of high geothermal gradient, where log-recorded temperatures can be significantly lower than the static temperature.

The hydration of cement is an exothermic reaction, and sufficient heat is generated that the presence of cement behind a string of casing can be determined by a temperature survey for up to several days after cementing. The character of the anomaly at the top of cement in a particular field is fairly uniform but varies greatly in different fluids. The anomaly may be a large, sharp increase (Fig. 31.7A) in some cases 35 to 45°F, or it may be a very slight increase in gradient (Fig. 31.7B).

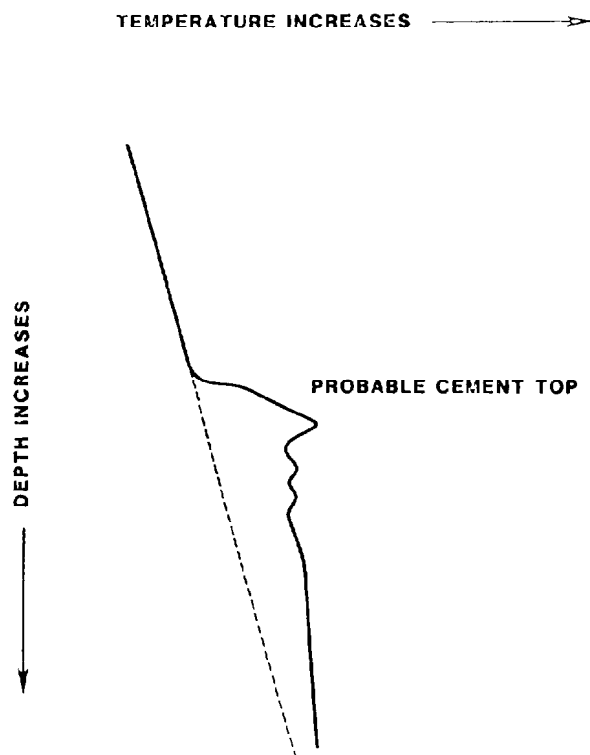


Fig. 31.7A—Effect of cement behind casing on temperature gradient.

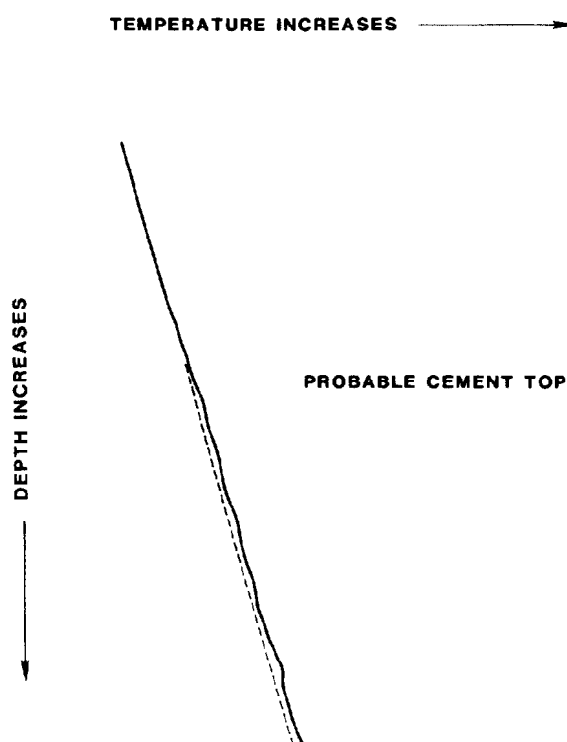


Fig. 31.7B—Effect of cement behind casing on temperature gradient.

The principal influence on the survey is the time elapsed between placement of the cement and running the survey. Other influential conditions include fineness of cement, chemical composition, rate of hydration, mass of cement in place, and the thermal conductivity of the adjacent formation. The maximum temperature usually occurs 4 to 9 hours after cementing, but reliable data can be determined in most areas after 48 hours. Any temperature change is affected more by the rate of hydration than by the total amount of heat liberated. Although hydration continues indefinitely, the rate decreases rapidly from the peak. A washed-out section of hole may be responsible for a large, sharp increase in temperature and can indicate a false cement top. A small temperature change or slight change in gradient could be caused by a small annular area or dilution of the cement with drilling mud. These factors, which influence the size of the temperature anomaly at the top of the cement in a given well, vary widely in their effect. However, even under an unfavorable combination enough heat is generated to permit a determination of the cement top.

A new cased-hole logging method exists for detecting vertical flow outside the casing resulting from faulty cement. The radial differential temperature (RDT) log measures variations in temperature in the plane of the casing radius on the inside of the casing.⁶ Normally, two sensors are used, placed 180° apart; one sensor may be used at the wall of the casing and the other sensor in the body of the tool. An anchor spring at the top of the logging tools prevents the entire tool from turning as the sensors rotate. A motor rotates the tool at a speed of one revolution every 4 minutes. The RDT logging tools are designed to allow attachment of a perforating gun, which can be adjusted to perforate into the suspected channel or abnormality located by logging.

If a channel is suspected in a perforated well, the well should be produced long enough to ensure that channel fluid is being produced before running the RDT log. The RDT sonde is placed at depths in the well where the channel is suspected. The arms are extended and the instrument revolves once or twice. Before moving to another depth the arms are retracted. As many measurements as required to delineate the channel can be made on one run. In some cases better results are obtained by injecting fluids at the surface to cool the channel.

Temperature surveys can be used to locate depth of lost circulation in an area where formations above the depth of drilling are known to have taken fluid. The

temperature survey will show a sharp increase in temperature immediately below the point of loss of fluid. The temperature break will be even greater if slow losses are occurring while running the survey. At times when the hole is considered dangerous, the survey can be run through open-ended drillpipe over the suspected interval.

Summary

Wellbore temperature surveys are an inexpensive method to determine problem well conditions. The data obtained from a temperature survey are often the only data available and usually are accurate and reliable. When an anomaly occurs, one of these conditions must exist: (1) expansion of gas, (2) migration of fluid, or (3) some type of chemical reaction. With the exception of measuring the actual temperature at a point in a wellbore, temperature surveying is highly qualitative. In the majority of surveys, consistency of procedures, past experience, and the engineer's ingenuity allow reliable information to be collected and unique analyses to be performed. Since no quantitative relationship between temperature and depth exists that covers all areas and sedimentary basins, an assumed gradient of 1 to 2°F/100 ft depth is appropriate.

References

1. Heald, K.C.: "Study of Earth Temperatures in Oil Fields on Anticlinal Structures," *Bull.* 205, API, Dallas (1930) 1.
2. Leonardon, E.G.: "The Economic Utility of Thermometric Measurements in Drill Holes in Connection with Drilling and Cementing Problems," *Geophysics* (1936) 1, 115.
3. Van Orstrand, C.E.: "Normal Geothermal Gradient in the United States," *Bull.*, AAPG (1935) 19, 79.
4. Nichols, E.A.: "Geothermal Gradients in Midcontinent and Gulf Coast Oil Fields," *Trans. AIME* (1947) 170, 44-50.
5. Dowdle, W.L. and Cobb, W.M.: "Static Formation Temperature From Well Logs—An Empirical Method," *J. Pet. Tech.* (Nov. 1975) 1326-30.
6. Cooke, C.E. Jr.: "Radial Differential Temperature (RDT) Logging — A New Tool for Detecting and Treating Flow Behind Casing," *J. Pet. Tech.* (June 1979) 676-82.

General References

- Romero-Juarez, A.: "A Simplified Method for Calculating Temperature Changes in Deep Wells," *J. Pet. Tech.* (June 1979) 763-68; *Trans.*, AIME, 267.
- Smith, R.C. and Steffensen, R.J.: "Interpretation of Temperature Profiles in Water-Injection Wells," *J. Pet. Tech.* (June 1975) 777-84; *Trans.*, AIME, 259.
- Wooley, G.R.: "Computing Downhole Temperature in Circulation, Injection, and Production Wells," *J. Pet. Tech.* (Sept. 1980) 1509-22.

Chapter 32

Potential Tests of Oil Wells

J.D. Kimmel, Oilcovery Inc.*

Richard N. Dalati, Cockrell Oil Corp.

A potential test is a simple production test under stabilized flowing conditions to determine the ability of a well to produce. Potential or production tests are used to determine the rate of production through a given size of choke. This production rate and GOR then are used to determine if the well is capable of producing the assigned daily allowable production rates.

Production-rate tests are conducted on a well so that its producing capabilities can be determined and a record of its producing abilities maintained. The results of these tests are used in diagnosing and evaluating a producing well. Their importance cannot be overemphasized since they are used in every phase of reservoir and equipment analysis in which a knowledge of the productivity of the reservoir is essential. The test results aid in determining the parameters shown in Table 32.1.

Production tests usually are considered part of routine field operations. Because they are performed on every type of producing well, a standard method of procedure that would cover every well cannot be set forth in detail. In many cases, the method or procedure for obtaining the results desired is left to the engineer's initiative and judgment and, in many cases, ingenuity.

In every production test an initial understanding of the equipment employed and the method of completion, and a general knowledge of the producing reservoir and the results of previous tests on the well or on comparable wells will greatly simplify the testing procedure and aid in obtaining the desired results.

Potential or production rate tests generally are required periodically by most state regulatory bodies in the U.S., such as the Texas Railroad Commission and the Louisiana Dept. of Conservation. The state regulatory bodies, authorized by the various states to control the production of oil and gas, set up a daily allowable or maximum rate at which each individual well may be produced. The well and reservoir conditions are considered

in setting up this maximum producing rate. Usually one other condition is involved in setting the producing allowable: *the produced or refined oil and gas storage or market capacity*. These regulatory bodies meet periodically and set a maximum number of producing days for a given period. The allowable is specified in two ways: the maximum amount of oil that can be produced each day and the maximum number of days each set period (usually 1 month) that this maximum daily allowable may be produced.

It is a responsibility of the engineer or person in charge to set up and supervise the proper testing of all producing wells. When the production is controlled by state regulatory bodies, it is also the responsibility of the engineer or person in charge to find out the requirements set up by these regulatory bodies as to the proper method for testing and reporting the tests on producing wells.

The importance of testing and information required to be supplied to the state regulatory agencies cannot be overlooked. Form W-2 of the Texas Railroad Commission's Oil and Gas Div. is an example of the information required (see Fig. 32.1).

As a general rule in Texas and Louisiana, the daily allowable is determined by the producing horizon of the well, but there are exceptions to this rule. The reservoir characteristics, previous reservoir performances, and completion procedures are considered before a definite allowable is set for the well. The general case in Texas is covered by a depth allowable set up in 1947. These allowables are set up for wells completed in proven areas and known reservoirs.

Texas Allowable Rule

The Texas Allowable Rules of 1947 and 1965 were based on producing depth and well spacing. These are normally referred to as "yardsticks." In 1966, another yardstick was established for offshore only (Table 32.2).

*This author also wrote the original chapter on this topic in the 1962 edition.

TABLE 32.1—DETERMINATIONS FROM TEST RESULTS

1. Optimal or maximum efficient production rates.
2. Correlation and identification of producing horizons.
3. Results of recovery methods.
4. Estimates of oil and gas reserves; for example, gauged rate production decline vs. time.
5. Decline trends and performance productions in the ability of the reservoir to produce.
6. Qualitative determinations of gas and/or liquid contacts.
7. Determinations relative to artificially imposed harmful wellbore or reservoir conditions such as gas or water coning, sanding or bridging action, and paraffin depositions.
8. Analyses and comparisons of well-completion practices and equipment.
9. Performance of and comparison between subsurface well equipment and installation principles.
10. Analyses and comparisons of artificial lifting practices and equipment.
11. Determining the necessity of and evaluating the results of remedial measures.

The allowable given a well completed in a new field or new reservoir is called the "Discovery Allowable." It is usually set up on a producing-depth basis. This allowable is for a certain period of time or until a certain number of wells are completed into the reservoir. For example, in Texas the onshore discovery allowable is for a 24-month period or until the 11th well is completed into the reservoir. The offshore discovery allowable is for an 18-month period or until the sixth well is completed into the reservoir. The discovery allowable in Texas is set up as in Table 32.3.

The allowables set up by the state regulatory bodies are not necessarily the proper rate to produce the wells. The producer should work very closely with the reservoir engineers and geologists to see that the test data, along with all other information available, are used to determine the most efficient producing rate of the well or reservoir.

When several companies produce from the same reservoir, it is common procedure to combine their knowledge and arrive at a maximum efficient producing rate (MER).

It is permissible for a company to request a change of allowables to conform more closely to the MER as determined by the company's engineers. Before any change in the allowables is made by the regulatory bodies, a meeting or hearing of all the companies involved in producing from the reservoir is proposed. At this time all the information available is evaluated to determine if a new and different allowable is warranted. This new allowable (to conform more to the MER) usually involves a reduction in the normal allowable set up by the regulatory body.

Productivity Index (PI)

It is desirable to be able to assign to a producing well a quantity that indicates the well's ability to produce. It was once a common occurrence "to open the well up" and measure the amount of production under wide-open flow. Today it is realized that wide-open flow of an oil or gas well can be very harmful to future well conditions.

RAILROAD COMMISSION OF TEXAS
Oil and Gas Division

Form W-2
Rev. 4/1/83
45-55

Type or print only

Oil Well Potential Test, Completion or Recompletion Report, and Log

1. FIELD NAME (See also REC Records or Wellbore) 2. LEASE NAME 3. OPERATOR'S NAME (Establish as shown on Form P-3 Organization Report) 4. ADDRESS 5. If Operator has changed within last 90 days name former operator 6. Location (Section, Block and Survey) 7. REC District No. 8. REC Lease No. 9. REC Well No. 10. Location of well site 11. Purpose of filing 12. If wellbore or recompletion, give former field (with recompletion) or gas ID or oil lease no. 13. If wellbore or recompletion, give former field (with recompletion) or gas ID or oil lease no. 14. Completion or recompletion date 15. Type of electric or other log run

SECTION I: POTENTIAL TEST DATA IMPORTANT: Test should be for 24 hours unless otherwise specified in field rules.

16. Date of test 17. Production started (Pumping Gas, Lifting, Pumping) 18. Test rate 19. Production during test 20. Calculated 24 hour rate 21. Was well shut during test? 22. Oil produced prior to test (See P-3 Recombination well) 23. Injection Gas-Oil Ratio

INSTRUCTIONS: File as original and one copy of the completed Form W-2 to the appropriate REC District Office within 30 days after completing a well and within 10 days after a potential test. If an operator does not properly report the results of a potential test within the 10-day period, the effective date of the allowable assigned to the well will not extend back more than 10 days before the W-2 was received in the District Office (Statute Rules 16 and 31). To report a completion or recompletion, fill in both sides of this form. To report a retest, fill in only the front side.

WELL TESTER'S CERTIFICATION
I declare under penalties prescribed in Sec. 91.143 Texas Natural Resources Code that I conducted or supervised this test by observation of (a) meter readings on (b) the top and bottom gauges of each tank into which production was run during the test. I further certify that the pressure test data shown above is true, correct, and complete to the best of my knowledge.

Signature: Well Tester Date of Completion REC Representative

OPERATOR'S CERTIFICATION
I declare under penalties prescribed in Sec. 91.143 Texas Natural Resources Code that I am authorized to make this report. That this report was prepared by me or under my supervision and direction, and that data and facts stated herein are true, correct, and complete to the best of my knowledge.

Typed or printed name of operator's representative Title of Person Telephone Area Code Number Date Signature

SECTION II: DATA ON WELL COMPLETION AND LOG (Not Required on Retest)

24. Type of Completion 25. Permit to Drill 26. Number of Interventions to Drill this well since first or last 27. Number of producing wells on this lease in this field (including this well) 28. Total number of acres in this lease 29. Lease Plug Back (Lifting, Pumping, or Drilling) 30. Interventions to produce well (Name, Lease, or Permit) 31. Location of well relative to nearest lease boundaries of lease on which this well is located 32. Elevation (OF, BBL, BT, CA, FT) 33. Well directional survey made other than on completion (Factor W-12) 34. Top of Pay 35. Total Depth 36. P in Layer 37. Surface casing (Determined by) 38. Is well multiple completion? 39. If multiple completion, list all intervals (completion or layer) 40. Is well recompletion? 41. Name of drilling contractor 42. Is recompleting Affiliates also used? 43. Casing Record (Report All Stringers Set in Well) 44. Tubing Record 45. Producing Interval (this completion) Indicate depth of perforation or open hole 46. Formation Record (List Depths of Principal Geological Formations and Formation Types)

REMARKS:

Fig. 32.1—Sample regulatory agency form.

TABLE 32.2—ALLOWABLE “YARDSTICK” SCHEDULE

Depth (ft)	47 Yardstick			65 Yardstick*					66 Offshore**		
	10	20	40	10	20	40	80	160	40	80	160
0 to 1,000	18	28	—	21	39	74	129	238	200	330	590
1,000 to 1,500	27	37	57	21	39	74	129	238	200	330	590
1,500 to 2,000	36	46	66	21	39	74	129	238	200	330	590
2,000 to 3,000	45	55	75	22	41	78	135	249	245	360	640
3,000 to 4,000	54	64	84	23	44	84	144	265	245	400	705
4,000 to 5,000	63	73	93	24	48	93	158	288	275	445	785
5,000 to 6,000	72	82	102	26	52	102	171	310	305	490	865
6,000 to 7,000	81	91	111	28	57	111	184	331	340	545	950
7,000 to 8,000	91	101	121	31	62	121	198	353	380	605	1,050
8,000 to 8,500	103	113	133	34	68	133	215	380	420	665	1,150
8,500 to 9,000	112	122	142	36	74	142	229	402	420	665	1,150
9,000 to 9,500	127	137	157	40	81	157	250	435	465	730	1,260
9,500 to 10,000	152	162	182	43	88	172	272	471	465	730	1,260
10,000 to 10,500	190	210	230	48	96	192	300	515	515	800	1,380
10,500 to 11,000	—	225	245	—	106	212	329	562	515	800	1,380
11,000 to 11,500	—	225	275	—	119	237	365	621	565	875	1,500
11,500 to 12,000	—	290	310	—	131	262	401	679	565	875	1,500
12,000 to 12,500	—	330	350	—	144	287	436	735	620	950	1,625
12,500 to 13,000	—	375	395	—	156	312	471	789	620	950	1,625
13,000 to 13,500	—	425	445	—	169	337	506	843	675	1,030	1,750
13,500 to 14,000	—	480	500	—	181	362	543	905	675	1,030	1,750
14,000 to 14,500	—	540	560	—	200	400	600	1,000	735	1,115	1,880
14,500 to 15,000	—	—	—	—	—	—	—	—	735	1,115	1,880

*1965 yardstick effective if field discovered after Jan. 1, 1965.

**1966 offshore yardstick effective Jan. 1, 1966.

Wide-open flow may cause water or gas coning, influx of sand into the wellbore, collapse of tubing or casing, and/or many other harmful results.

The ability of a well to produce usually is determined by use of the PI. The use of the PI was first mentioned by Moore in 1930.¹ In a 1936 paper M.L. Harder states that the relative ability of a well to produce shows the PI to be superior.²

API states in *Recommended Practice for Determining Productivity Indices*³ that the PI is calculated from the observed production rates and subsurface pressure measurements obtained. Special applications and modifications by the user to conform to individual requirements and conditions are normally used. The following discussion of PI is not meant to cover all applications but only to show how the PI may be used.

By definition, the PI is equal to the barrels per day of stock-tank oil production per pound force of pressure differential between the wellbore opposite the producing horizon and the static reservoir pressure, which is the average pressure of the well drainage area. Therefore, the PI is, in barrels of oil produced per day per psi decrease in reservoir pressure, the difference between the average pressure in the drainage area of the well and the flowing bottomhole pressure (BHP) of the well. According to the accepted concepts of flow, the rate of flow in a system containing a single fluid under steady-state conditions should be directly proportional to the pressure drop. Using this concept, the PI would be the slope of the line resulting from plotting the rate of flow against pressure drop. On such a plot the wide-open flow quantity or well potential would be measured at the maximum pressure drop available. Such a case is referred to as the “ideal PI.” Observed values of production rates vs. pressure differentials do not give straight lines. PI data on nonflowing wells are usually more linear than the data

on flowing wells. Experience has shown that the line will be curved. This is because PI is defined to occur under steady or pseudosteady-state flow conditions. The curvature results because μB is not constant if the flow is single phase and/or gas evolution or water coning exists around the wellbore — i.e., relative permeability effects. PI is higher than theoretical when calculated erroneously before pseudosteady-state flow exists. PI is meaningless unless the radius of wellbore damage is fixed — i.e., pseudosteady-state flow is established. The flow of compressible fluids (oil and water) into a wellbore after the drainage area has been established is, strictly speaking, described by a pseudosteady-state flow equation.

TABLE 32.3—DISCOVERY ALLOWABLES

Interval of Depth (ft)	Daily Well Allowable (bbl)
0 to 1,000	20
1,000 to 2,000	40
2,000 to 3,000	60
3,000 to 4,000	80
4,000 to 5,000	100
5,000 to 6,000	120
6,000 to 7,000	140
7,000 to 8,000	160
8,000 to 9,000	180
9,000 to 10,000	200
10,000 to 10,500	210
10,500 to 11,000	225
11,000 to 11,500	255
11,500 to 12,000	290
12,000 to 12,500	330
12,500 to 13,000	375
13,000 to 13,500	425
13,500 to 14,000	480
14,000 to 14,500	540

However, some people in the oil industry describe the flow by a Darcy-type equation, which is referred to as steady-state flow. The difference in the flow rates determined from the two equations is very small. We discuss PI by use of both the steady-state and pseudosteady-state flow equations.

Steady-State Flow

For a radial system under steady-state flow, the equation giving the flow rate is

$$q_o = \frac{7.08 \times 10^{-3} kh(p_e - p_{wf})}{\mu_o B_o [\ln(r_e/r_w) + s]}, \dots\dots\dots (1)$$

where

- q_o = oil production rate, STB/D,
- k = permeability of formation, md,
- h = thickness of formation, ft,
- p_e = pressure at the effective drainage radius r_e
normally approximated by \bar{p}_R ,
- \bar{p}_R = average reservoir pressure in drainage area, psi,
- p_{wf} = flowing BHP, psi,
- μ_o = oil viscosity, cp,
- B_o = oil formation volume factor, RB/STB,
- r_e = effective drainage radius, ft,
- r_w = wellbore radius, ft, and
- s = skin effect (zone of reduced or improved permeability), dimensionless

The term equivalent to the PI is

$$J = \frac{q_o}{\Delta p} = \frac{7.08 \times 10^{-3} kh}{\mu_o B_o [\ln(r_e/r_w) + s]}, \dots\dots\dots (2)$$

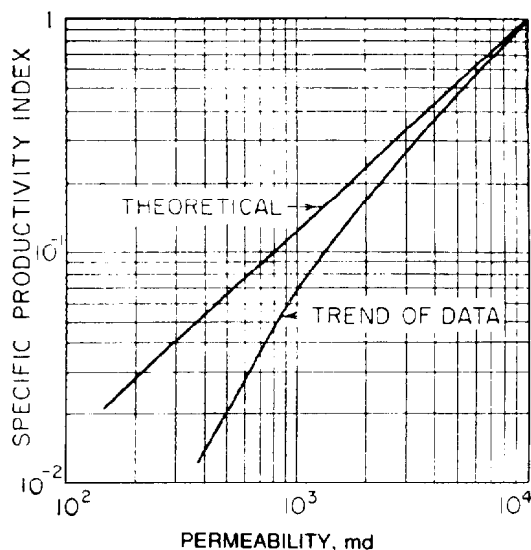


Fig. 32.2—PI—permeability correlation.

where J is the PI, STB/D-psi, and Δp is the pressure difference between p_e and p_{wf} , psi.

In analyzing the PI, it can be seen that it is a function of the formation characteristics, k and h , the fluid characteristics, μ_o and B_o , and the system characteristics, h , r_e , r_w , and s .

Specific PI

The term "specific PI" is frequently used and usually means the PI per foot of pay. When the term "specific" is used, it is necessary to state why. The productivity could just as well have been made specific to any other variable in Eq. 2.

Well systems do not operate at any time under steady-state conditions, but they do under pseudosteady-state conditions. Oil, water, and gas are compressible fluids; therefore, only pseudosteady-state occurs. Thus, we cannot expect Eq. 2 to yield exact correlation. The primary correlation sought has been with permeability so that the PI could be predicted from core analysis. An example of an early correlation is given by Fig. 32.2.⁴

Oil flowing into a wellbore will practically always seem to enter the wellbore from a formation of lower permeability than the homogeneous fluid value determined in the laboratory. In many cases the relative permeability to oil at interstitial water saturation is one. What actually happens is that the permeability measured in the laboratory is too high because the confining pressure is lower than in the reservoir.

Muskat⁵ states that the PI should not be used to predict production of high differential pressures by simply multiplying the PI by the pressure drop of interest. He states that it is doubtful that calculated potential tests would agree with actual tests. The relative comparison should reflect the comparative production capacity with fair approximation. The PI times reservoir pressure equals the open flow potential.

Muskat also states that the productivity index is an excellent tool to determine well problems such as:

1. Comparison before and after well treatments to evaluate these treatments. J should increase.
2. Stable GOR, R , with a declining J indicates plugging of wellbore.
3. R increasing markedly without decline in J indicates entry of extraneous gas. This would be the same if R changes with various production rates and J stays constant.
4. Rapid increase in water production should bring a decline in J if water is entering through typical strata within oil pay. If J is maintained, this should indicate the water is not coming through the oil-producing strata.
5. Decline of J should take place during normal reservoir depletion and parallel the normal growth of GOR or water/oil ratio (WOR). If not, plugging of the wellbore should be considered.

These are guidelines for further investigation.

Theoretical PI

Muskat and Evinger⁶ first showed that a theoretical PI could be worked out using the steady-state formula as developed for a radial system flowing oil and gas. By

such a system it can be shown that the J for a given well system can be expressed in terms of three parameters: (1) the producing GOR, (2) the pressure gradient in the well system, and (3) the absolute reservoir pressure.

It can be shown that for the steady-state flow of oil and gas in a radial system, the following equation expresses the rate of oil flow.

$$q_o = \frac{7.08 \times 10^{-3} kh}{\ln r_e/r_w + s} \int_{p_{wf}}^{\bar{p}_R} \frac{k_o/k}{\mu_o B_o} dp, \dots\dots\dots (3)$$

where k_o is effective permeability to oil.

The integral

$$\int_{p_{wf}}^{\bar{p}_R} \frac{k_o/k}{\mu_o B_o} dp$$

can be evaluated using Fig. 32.3.

The PI is, therefore,

$$J = \frac{q_o}{p_e - p_{wf}} = \frac{7.08 \times 10^{-3} kh A_c}{(p_e - p_{wf})[\ln(r_e/r_w) + s]}, \dots\dots\dots (4)$$

where A_c is the area under the curve.

By using Fig. 32.3 and the definition of the PI, it can be seen that J will not double if $(p_e - p_{wf})$ is doubled because the area under the curve will not double. Also p_e is determined by reservoir conditions and cannot be varied. Note that for a definite value of $(p_e - p_{wf})$ taken at a high absolute pressure, J will be greater than for the same $(p_e - p_{wf})$ taken at a lower pressure because the area under the curve will be greater.

It is not readily apparent, but can be shown, that J depends on the producing GOR, R . A simple explanation is that an increase in R means that the oil saturation is less, thus k_o is smaller. In Fig. 32.3, the curves labeled R_1 , R_2 , and R_3 are for different GOR's with $R_1 > R_2 > R_3$.

Pseudosteady-State Flow

The steady-state equation is used frequently; however, this would only apply if the pressure at the outer radius stayed constant, which would only happen if a complete pressure maintenance program were maintained. If the well has a closed boundary or is operating with an established drainage radius, then pseudosteady-state flow occurs. The pseudosteady-state equation is

$$q_o = \frac{7.08 \times 10^{-3} kh (\bar{p}_R - p_{wf})}{\mu_o B_o [\ln(r_e/r_w) - 0.75 + s]} \dots\dots\dots (5)$$

for a circular drainage area and

$$q_o = \frac{7.08 \times 10^{-3} kh (\bar{p}_R - p_{wf})}{\mu_o B_o (\ln x - 0.75 + s)} \dots\dots\dots (6)$$

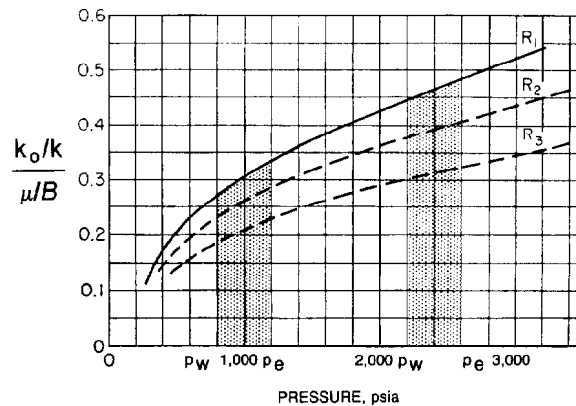


Fig. 32.3—Plot for determining PI for different GOR's.

for a non-circular drainage area.⁷

From Eq. 6 the actual PI is

$$J = \frac{7.08 \times 10^{-3} kh}{\mu_o B_o (\ln x - 0.75 + s)},$$

where x is a factor for noncircular drainage area and well location.

Most reservoir engineering flow equations assume radial geometry. This assumes the drainage area of the well is circular and the well is located in the center. Experience has shown that in many cases the drainage area of the well is rectangular, triangular, or other shapes. As stated previously, the PI, J , is a function of the system characteristics, which can be applied to the productivity index. Shape functions can be determined by reservoir limit tests.⁸

Van Everdingen originally defined the skin effects as the additional resistance concentrated around the wellbore that result from the drilling and completion techniques employed.⁹ This skin effect detracts considerably from a well's capacity to produce. More recently the skin effect is also used to indicate improved permeability around the wellbore that results from acidizing and/or fracturing. The skin effect can be defined as

$$s = \ln \frac{r_s}{r_w} \left(\frac{k - k_s}{k_s} \right), \dots\dots\dots (7)$$

where

- r_s = radius of area around the wellbore affected by skin effect, ft,
- k = formation permeability, md, and
- k_s = permeability of area around the wellbore affected by skin effect, md.

The skin effect, s , normally is determined from pressure transient analysis. The reader is referred to Chap. 35, Well Performance Equations, for a detailed treatment of skin effect.

The aim of the production engineer is to make the PI, J , as high as possible; the equation for J indicates this may be done by several ways that include¹⁰:

1. Remove the skin effect through acid treatment or the use of various completion or drilling fluids, depending on the formation.
2. Increase the effective permeability by fracturing or propping.
3. Reduce the viscosity by formation heating.
4. Reduce formation volume factor, B_o , by production techniques and surface separation system.
5. Increase the well penetration, h , by completing across the entire producing formation. Care should be taken not to complete across a zone of excessive gas or water production.
6. Reduce the ratio r_e/r_w . Since it appears as a logarithmic term, this has little influence. Underreaming is seldom considered as a means of well stimulation.

The above equations should indicate that the most important step in determining and analyzing the performance of any well, especially flowing wells, is to determine the well production rate for any given flowing BHP.

It is now readily apparent that to compare a PI of a well it is necessary to know what is being compared, which includes the permeability, sand thickness, well radius, drainage radius, fluid characteristics, and flow relations. A comparison should also be made on reservoir pressure and pressure drawdown for a similar GOR.

The standard procedure for conducting PI tests mainly consists of following the directions that have been set forth in the procedures for conducting static and flowing reservoir pressures and gauged-rate production tests. The most popular wireline pressure gauge is the Amerada recording pressure gauge.

In some cases, the use of artificial-lift equipment prevents the passage of subsurface gauges; therefore, other means must be found for determining these pressures. It is possible with the use of sounding devices—i.e., Ecometer or Sonolog—to determine the liquid level. Knowing the liquid level, the static or flowing pressures can be approximated by gradient and depth calculations.

Care should be exercised in determining the static and flowing pressures to be sure they are the equilibrium pressures. If there is any doubt regarding the equilibrium conditions, two or more pressure readings should be made several hours apart to be sure they are the same. Some formations stabilize in one hour but most take four to 24 hours. Tight formation could take several days. In determining the actual J , the flowing rates should have wide enough variation to compensate for any errors in measurement.

When artificial-lift equipment is used, the gauged production tests for determining the J must be lower than the production limitations of the lift equipment.

Methods of determining production rates are: (1) stock-tank measurement; (2) portable well testers, including batch-type meters, positive-displacement meters, turbine meters, and flow meters; and (3) stationary test equipment.

Stock-Tank Measurement

The oldest and most widely accepted means of determin-

ing the amount of liquid produced by an oil or gas well is the manual gauging of the production in stock tanks. A single well producing into a tank battery presents no testing problems, as it is a simple process to measure the liquid in the stock tanks at the start of the test and the liquid in the stock tanks at the end of the test. Most tank batteries are arranged so that one well may be tested at the battery while the other wells are being produced. This requires, of course, the addition of a test separator in addition to the production separator and also sufficient stock-tank volume so that no commingling of the production is required. A separate gas run and meter would also be required for measurement of the gas produced while the well is on test. If this meter run is not available, a portable orifice well tester could be used.

If testing facilities are not available at the lease, it is necessary to shut in the entire lease while individual wells are being tested into the tank battery. In the latter case, it is usually better to use portable test equipment to determine the production rate.

Before the production test is started, with stock tanks as a means of measurement, it is necessary to determine the amount of basic sediment and water (BS&W) at the bottom of the tank, in addition to the liquid level at the start of the test. If at all possible, stock tanks should be clean, since errors may be introduced in determining BS&W. Dirty stock tanks can cause the tank tables to be in error. If possible, produced water should be produced and gauged in separate stock tanks.

After gauging the test tank or gun barrel, the usual procedure would be to proceed to the separator, check and record the operating pressure, and on large-volume separators, if the well being tested has a low productivity, record the liquid level in the separator. The choke size at the wellhead should be carefully determined and if there is a question, the choke should be checked and calibrated.

If a treater or heater is used, its operating characteristics should be noted so that any conditions not uniform may be considered on the gauged production test. All tests should be made after the production has stabilized and under conditions that are as uniform as possible. No change should be made at the wellhead or tank battery during the duration of the test.

Standard tests should range from 24 to 168 hours in length, depending on the well and reservoir characteristics. All data should be observed and recorded at less frequent intervals. The time between intervals will vary depending on the length of test. In cases where short tests (6 to 8 hours' duration) are necessary, consecutive data recordings should be made hourly.

Tests should be for 24 to 168 hours' duration so that fluctuations in the GOR, as a result of heading tendencies and temperature variations, may be considered and the test results averaged. It is not uncommon to observe a 40 to 50°F temperature variation between night and day atmosphere and to observe a 10 to 20% variation in the gas/liquid ratio. Recognizing these facts, it becomes necessary to measure the temperature of either the liquid or vapor section of the separator.

The preferred location to obtain the temperature would be in the flow line immediately before the separator. This latter temperature would more nearly reflect the ac-

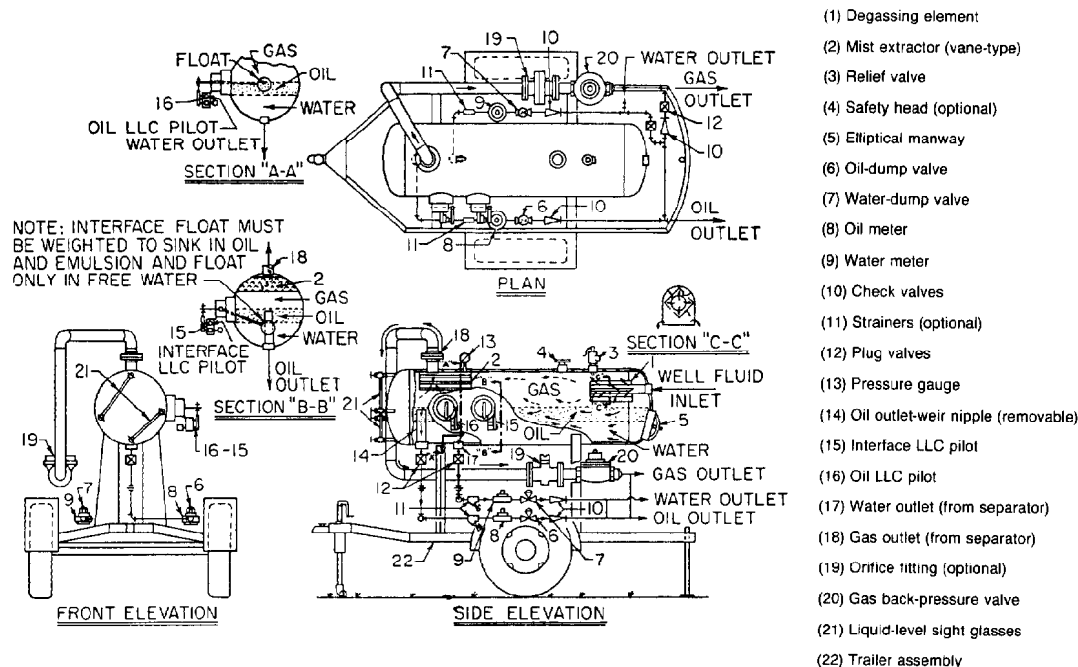


Fig. 32.4—Trailer-mounted three-phase well tester with PD meters.

tual liquid-phase temperature prior to the flash liberation process.

The production should be sampled each time the data are recorded during the production test. This interval sampling is very necessary if storage facilities are such that the water produced must be disposed of as it is produced. Refer to Chap. 17 for sampling information. Wells that produce with a high WOR should always be tested at length because of the usual uneven oil-producing rate.

Depending on the separation pressure and the characteristics of the crude for shrinkage, some consideration should be given to determining the amount of gas produced that is not measured by the gas meter but is vented from the stock tanks.

Points to check to ensure the accuracy of stock-tank gauges include:

1. Correct and accurate strapping table is used with the test tank.
2. No dents or damage has occurred to the stock tank since strapping table was made.
3. Tank is clean with no encrustations or deposits on the walls.
4. If foamy crude is being produced the liquid level will be almost impossible to determine correctly with a gauge tape. Chemical addition or settling time may be required to minimize the foam.
5. BS&W at bottom of tank is determined as accurately as possible before and after the test.
6. Gauge tape must not be kinked and plumb bob must be carefully touched at the bottom of tank.
7. Temperature of oil in the stock tank must be considered.
8. The oil level must be steady and undisturbed while a gauge reading is taken.

Portable Well Testers

The trend toward unitization and centralization of tank batteries has increased the demand for a means of determining production rates without requiring the installation of additional expensive stock tanks and test separators. The requirements are being solved by the use of well testers.

The well tester is a combination separating and measuring unit for oil, water, and gas. The well tester can be either two or three phase, can be used for permanent installation, or can be skid or trailer mounted for portable operation (see Figs. 32.4 through 32.8). The well tester may utilize several types of meters for both liquid and gas measurement. Note that the two-phase testers (Figs. 32.5 and 32.8) are not fitted with liquid level controllers (LLC's), but are blanked so LLC's can be added in the field for three-phase testing.

Each established class of metering equipment has survived and advanced in the petroleum industry today because it fits a definite need in the metering field. Each type has won its place in the petroleum industry by fulfilling the requirements of certain applications better than any other type. Selection of the type of meter used on a well tester may be determined by the user, based on the application of the well tester and the limitations and capabilities of the meters available (see Table 32.4 for various sizes and working pressures of standard well testers). Remember that it is better to have a unit that has the capacity to test (pressure and flow capacity) so that modifications to the test can be minimized.

Capacities are based on steady continuous flow for a 24-hour period. Fluid retention time is as follows.

- 0 to 600 psi = 1 minute.
- 600 to 1,000 psi = 50 seconds.
- More than 1,000 psi = 30 seconds.

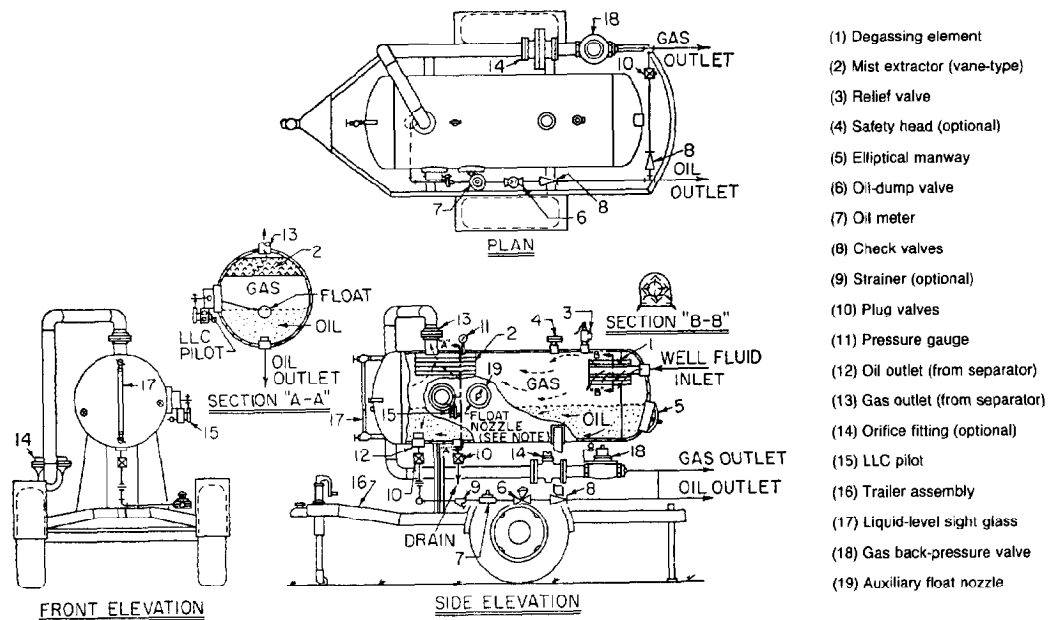


Fig. 32.5—Trailer-mounted two-phase well tester with PD meter.

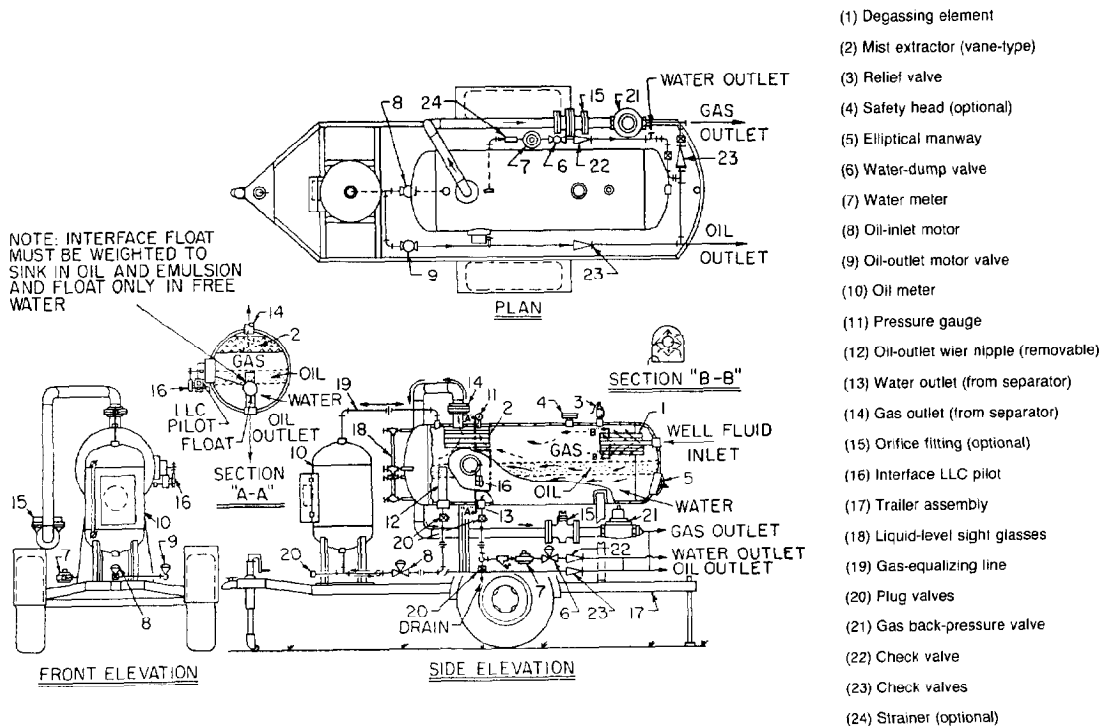


Fig. 32.6—Trailer-mounted three-phase well tester with oil-volume meter and PD meter.

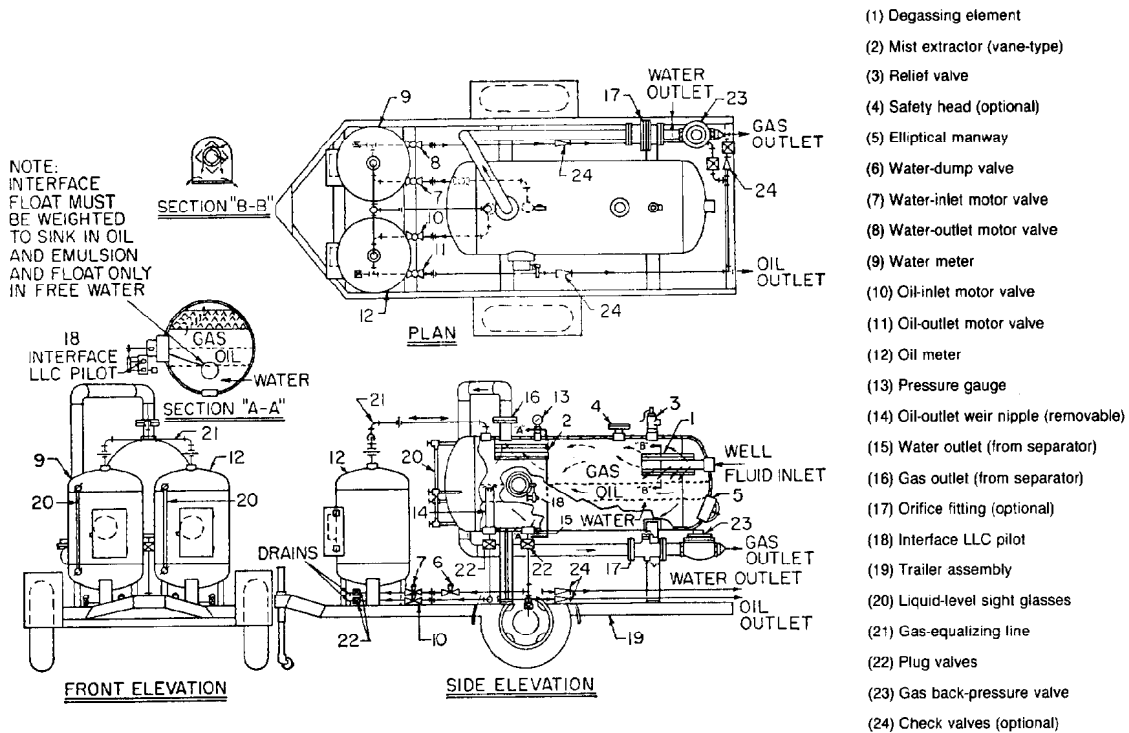


Fig. 32.7—Trailer-mounted three-phase well tester with batch-type meters.

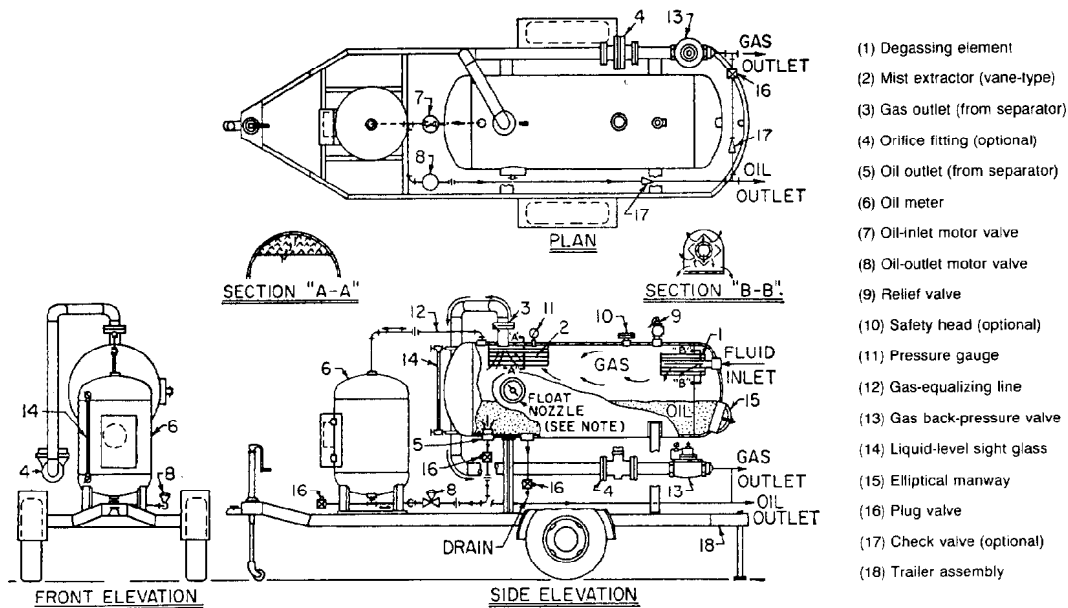


Fig. 32.8—Trailer-mounted two-phase well tester with volume meters.

TABLE 32.4—WELL-TESTER SPECIFICATIONS

			Rated Separator Capacities						
Separator Size			Two-Phase Separation		Three-Phase Separation				Approximate Weight (lbm)
Shell OD (in.)	Shell Length Seam to (ft)	Maximum Working Pressure (psi)	Oil Plus Water (B/D)	Gas (MMscf/D)	Oil (B/D)	Water (B/D)	Total Liquid Oil Plus Water (B/D)	Gas (MMscf/D)	
16	6	125	500	1.6	500	250	500	1.0	1,200
24	6	125	1,200	3.6	1,200	600	1,200	2.2	1,500
30	6	125	1,800	5.5	1,800	900	1,800	3.5	1,700
36	7	125	2,800	8.0	2,800	1,400	2,800	5.1	2,300
48	7	125	4,800	14.0	4,800	2,400	4,800	8.7	4,600
16	6	300	500	3.5	500	250	500	2.1	1,900
24	6	300	1,200	7.7	1,200	600	1,200	4.9	2,200
30	6	300	1,800	12.5	1,800	900	1,800	7.5	2,400
36	7	300	2,800	17.0	2,800	1,400	2,800	11.0	2,800
16	7	600	500	5.5	500	250	500	3.3	2,600
20	7	600	850	8.3	850	425	850	5.0	2,800
24	7	600	1,200	12.5	1,200	600	1,200	7.5	3,000
30	7	600	1,800	19.0	1,800	900	1,800	12.0	3,200
14	7	1,200	400	6.1	400	200	400	3.8	2,900
16	7	1,200	500	7.7	500	250	500	5.0	3,100
20	7	1,200	850	11.4	850	425	850	6.5	3,400
24	7	1,200	1,200	16.5	1,200	600	1,200	9.1	3,600
12	7	1,800	300	5.5	300	150	300	3.5	3,000
14	7	1,800	400	6.8	400	200	400	4.3	3,400
16	7	1,800	500	8.0	500	250	500	5.5	3,800
20	7	1,800	850	12.2	850	425	850	7.0	4,100
12	7	2,400	300	5.3	300	150	300	3.4	3,500
14	7	2,400	400	6.5	400	200	400	4.2	4,000
16	7	2,400	500	8.0	500	250	500	5.3	4,500
20	7	2,400	850	12.4	850	425	850	7.0	4,800

The type of fluid to be tested must be considered in determining the retention time. If the crude foams, the necessary retention time for the gas to break out of solution may be 5 minutes or longer. For three-phase separation, additional retention time may be required for the oil and water separation depending on the type of emulsion produced. Many times the addition of heat and/or chemicals is required to produce proper separation of the oil and water or gas and oil. Well testers are available in low working pressures that utilize either electric or gas-fired heaters to heat the well fluid and improve the separation processes. The meter used must be of sufficient metering capacity not to limit the capacity of the well tester. Working pressures are available up to 4,000 psi.

The listing in Table 32.4 of sizes and capacities of standard well testers is not complete but may be used as a guide to determine the approximate size and capacity of the unit required for your specific testing purpose.

The types of meter available for use on well testers are (1) batch-type meters, (2) positive-displacement meters, and (3) flow meters, including standard and mass flow meters.

Batch-Type Meters

The batch-type meter works by means of cyclic accumulation, isolation, and discharge of predetermined volumes. Each dump volume is registered on a counter. The counter reading is then multiplied by the dump volume to determine the total measured volume.

When metering vessels such as batch meters are used to measure liquid hydrocarbons, four factors must be ob-

tained and maintained:

1. An unchanging volume in the metering vessel must be maintained consistently. This means that there can be no foreign material deposited in the vessel and that the vessel itself must not change shape or size.

2. Exact upper and lower dumping levels must be obtained and maintained in the metering vessel. These dumping levels must be the same for each cycle.

3. Proper valve arrangement must be maintained so that no liquid may slip through the vessel without being metered. The valve or valves should be arranged so that there is a period of time at the beginning and end of each cycle during which both the inlet and outlet to the metering vessel are closed at the same time. This assures that no unmetered fluid will slip through the metering vessel.

4. An appropriate and accurate "meter factor" must be used to compensate for temperature change of the liquid, shrinkage (volume reduction) of the liquid resulting from pressure reduction, mechanical metering error of the metering vessel, and BS&W content of the liquid.

These various factors are usually combined into one factor known as the "meter factor" or "meter multiplier." These meter factors are usually less than 1.0. In other words, the meter normally reads higher than the net stock-tank volume.

Advantages and Disadvantages of Batch-Type Meters

1. A metering vessel can be used as its own meter proving tank if the vessel is inspected for encrustation, the dumping levels are observed during operations, and valves are checked for leakage.

TABLE 32.5—NOMINAL RATED CAPACITY OF VOLUME-TYPE DUMP METERS

Barrels per discharge	0.25	0.5	1.0	2.0	5.0	10.0	20.0	30.0
Metering capacity, bbl/24-hr day	300	500	720	1,440	2,000	4,000	8,000	15,000

2. A metering vessel will handle more sand and other foreign material without causing trouble than the positive-displacement (PD) meter.

3. A metering vessel will meter from zero flow to maximum rated rate of flow with the same degree of accuracy.

4. Weight-type (hydrostatic-head) metering controls may be used to meter foaming oil.

5. The unit may be adjusted while in operation.

6. Free gas will not register as liquid if the controls should fail to function.

7. Initial and installation cost is slightly higher than with the PD meter.

8. The meter delivers an intermittent discharge of liquid.

9. Gas is required to displace the liquid from the vessel.

10. Paraffin buildup on the vessel wall will cause inaccuracies.

11. The meter requires more space and is heavier than a PD meter.

12. With heavy viscous crudes a larger inlet or differential pressure arrangement between the separator and metering vessel may be required to maintain the rated capacity.

Nominal rated metering capacity of various sizes of volume-type dump meters under normal field conditions is given in Table 32.5. Pressure ratings are up to 3,000 psi. Volume meters are not used for gas measurement.

PD Meters

PD meters are quantitative instruments. They are termed "positive-displacement" because some sensing element is forcibly or positively displaced through a measuring cycle by the hydraulic action of the fluid on the element.¹¹ For a completed measuring cycle a known quantity is displaced by the sensing element. It is necessary to count the number of cycles and multiply them by the displacement volume to get the total liquid quantity that has passed through the meter. This latter function is carried out by the meter's gear train and register.

Fig. 32.9 shows the basic types of PD meters: nutating disk, oscillating piston, oval gear, rotary vane, reciprocating piston, and bi-rotor.

Probably 80 to 90% of all PD meters in service today are of the nutating-disk type. They are most popular because of the relative simplicity of the construction, ruggedness, accuracy over a wide range, and low cost. The accuracy of the nutating-disk type meter is not as high as that of the PD meters of the other types.

Advantages and Disadvantages of PD Meters

1. Discharge of the metered liquid is continuous.
2. PD meters can be used to meter exceptionally viscous liquids.

3. PD meters do not require gas to displace the fluid through the meters.

4. Initial and installation cost is lower.

5. Temperature compensation can be applied with certain types of PD meters less expensively than with batch-type meters.

6. Paraffin may not reduce metering accuracy.

7. Liquids metered must be free of gas, since slugs of gas may damage or wreck the meter. Gas will register as fluid when passing through a PD meter.

8. Sand, mud, salt, or other foreign particles will cause wear on the PD meter and cause inaccurate meter readings.

9. Some type of meter-proving process is required to prove PD meters periodically. Actual stock-tank gauges are used in many cases to determine the accuracy of the meter.

10. Meters must be operated between a minimum and maximum specified rate of flow. High or low rates of flow may affect the accuracy of the PD meter.

PD meters are available in pressure ratings to 5,000 psi. Capacities of PD meters depend on the size and type of meter. If possible the manufacturer of the PD meter should be requested to furnish information regarding the capacity.

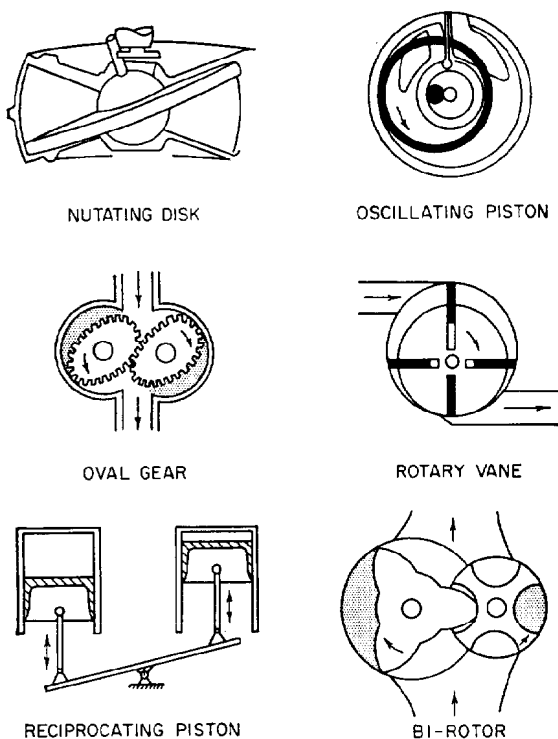


Fig. 32.9—Basic types of PD meters.

**TABLE 32.6—AVERAGE CAPACITY
FOR NUTATING-DISK-TYPE PD
METERS**

Size (in.)	Capacity (B/D)	
	Minimum	Maximum
5/8 to 3/4	68	340
3/4	102	510
1	170	850
1 1/2	342	1,710
2	548	2,740

Average Capacity for Nutating-Disk Type PD Meters. The average rates shown in Table 32.6 are based on oil as the fluid being metered. The manufacturer should always furnish information about recommended capacity. When PD meters are used downstream of separators or vessels that are not continually dumping, it is necessary to size the meter on the maximum "rate" of discharge while the vessel is dumping.

PD meters are used in some cases for gas measurement. The types used are the bellows and birotor. High cost and size have held the use of PD meters for gas measurement to a minimum.

Turbine Meter

Today most liquid measurement is done by the use of turbine meters. A turbine meter is a flow rate measuring device which has a rotating element that senses the velocity of the flowing liquid.¹² This liquid causes the rotating device to rotate at a velocity proportional to the volumetric flow. The movement of the rotating device is sensed either mechanically or electrically and is registered. The actual volume is then compared to the registered readout to arrive at a meter or register factor (see Figs. 32.10 and 32.11).

The turbine meter is used because of its simplicity and costs. Each meter application will require different meter or register factors.

Considerations in the selection of turbine meters include (1) properties of the liquid to be metered—viscosity, density, vapor pressure, corrosiveness, and lubricating ability; (2) operating conditions, including pressure, flow rates and whether continuous or intermittent, temperatures (some meters have temperature compensators), and quantity and size of abrasive particles in the fluid; and (3) space availability (see Fig. 32.12). Items or conditions that normally affect the meter factor are shown in Table 32.7. Both turbine and PD meters should be connected so that meter factors may be periodically determined.

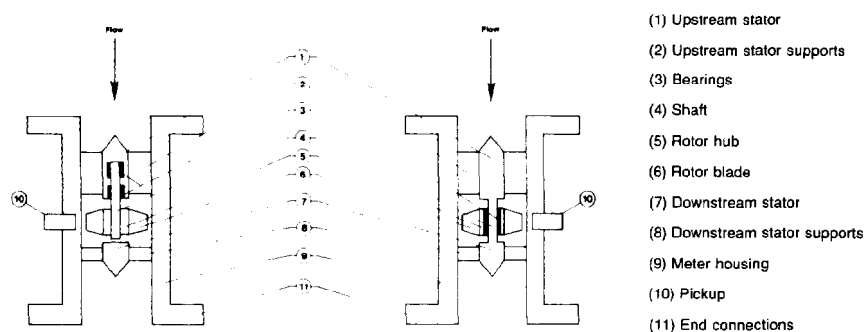


Fig. 32.10—Names of typical turbine meter parts.

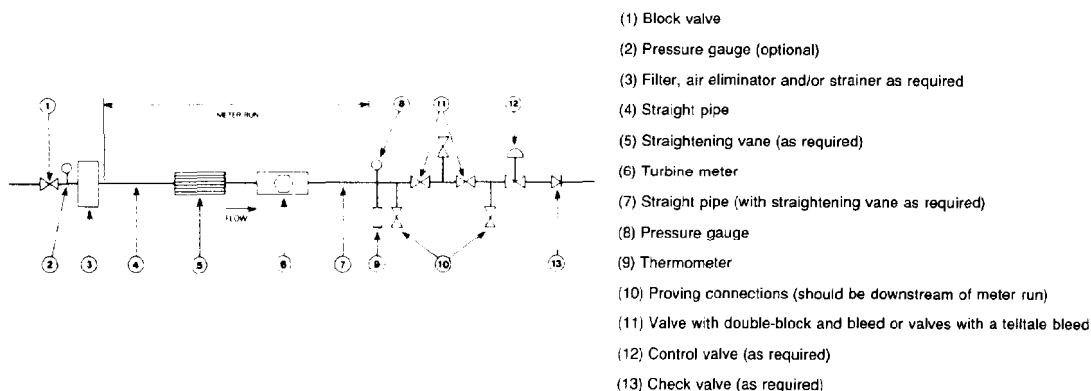


Fig. 32.11—Turbine meter system schematic.

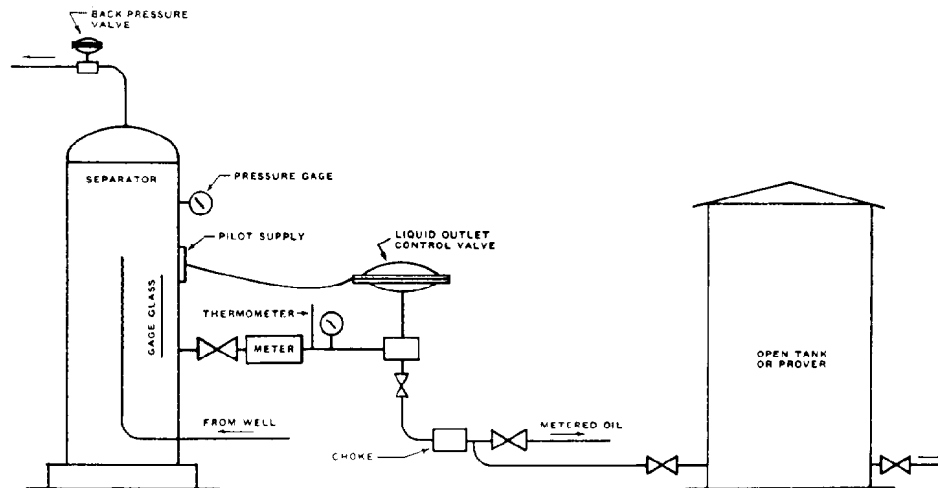


Fig. 32.12—Schematic operation diagram of oilwell production meter installation with stock tank or open prover.

Flowmeters

The standard-type flowmeters are: orifice plate, Venturi tubes, flow nozzle, Pitot tube, drag body, and lift surface. These meters or devices are used to create a flowing differential pressure. This flowing differential pressure is used to solve the flow equation for the rate of flow.

Orifice plate, Venturi tube, flow nozzle, and Pitot tube are commonly used. Drag body and lift surface are not as familiar. The net force resulting from a pressure difference is measured. This pressure difference is used to solve the flow equation. If the force is parallel to the flow direction, the force is called "drag body." If the force is perpendicular to the flow direction, the force is called a "lifting surface."

In addition to differential pressure drop, six other factors must be considered and included in the integration to determine a basic flow rate or quantity. They are (1) static pressure, (2) flowing temperature, (3) specific gravity of the flowing quantity, (4) size of orifice run, (5) size of the orifice plate if orifice plate is used to create the differential pressure, and (6) supercompressibility, if applicable.

These factors may be considered by the solving of the flow equation or they may be applied as a multiplying factor applied to the meter reading.

Mass Flowmeter. In about 1942, W.J.D. VanDijk of The Netherlands constructed and evaluated the first mass flowmeter, as such. The mass flowmeter measures the quantity of matter passed through the meter. This mass is independent of all ambient conditions, which is not true of volumetric meters discussed previously. If any type of flowmeter mentioned above is compensated in any way (electrically, mechanically, or a combination of both) for fluid density, it is a mass flowmeter. As early as 1930, pressure and temperature compensators could be attached to a standard orifice meter. They were mass flowmeters, in a true definition of mass flowmetering, although they were not called by that name.

On well testers, and for measurement of produced

water, oil, and gas, it is most common to use turbine, PD, and batch meters for liquid measurement and the standard orifice meter for gas measurement. Mass flowmeters may be used for both gas and liquid measurement. Because of the cost and special requirements for technicians to operate and maintain these meters, they are seldom used in field operations.

Automation and remote readout requirements can be accomplished with the use of well testers in much the same way as with automatic custody units. The liquid measurement may be relayed by pneumatic or electrical impulses to a transmitter. These impulses in turn may actuate some type of recording unit at a central location. The gas measurement would require some type of pressure transducer to convert the differential pressure to an electrical signal. More often, when remote recording of gas flow is required, an integrating flowmeter is used and the transmitted signal will read in volumetric units.

Fig. 32.13 shows a well tester installed at a tank battery for permanent test or lease automation.

Stationary Metering Installation

Stationary metering installations are those that include metering separators, metering treaters, and any other

TABLE 32.7—CONDITIONS AFFECTING THE METER FACTOR

1. Mechanics of meter as to tolerances.
2. Change in clearance due to wear or damage.
3. Flow rates and variations in flow.
4. Temperatures of liquids.
5. Viscosity of liquids.
6. Pressure of liquids.
7. Pressure drop across the meter as a resistance to flow.
8. Foreign material lodged or deposited in the meter or connecting piping.
9. Inlet condition changes, such as changes in the entrance to the meter, which change the flowing fluid profile.
10. Lubricating properties of the liquid.
11. Accuracy and conditions of meter-proving system and meter-factor test.

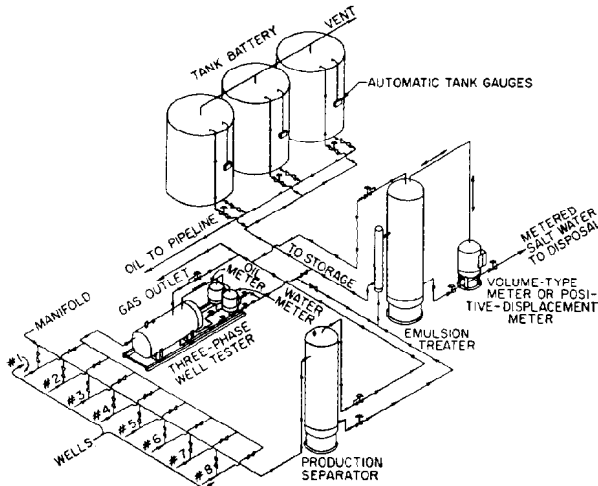


Fig. 32.13—Unitized or automatic tank battery.

type of meter used in conjunction with test separators or emulsion treaters. These units are installed as an integral part of the tank battery.

The metering separator combines two functions of separating and metering the produced fluid (see Figs. 32.14 and 32.15). The metering separator is divided into one compartment for separating the liquid and the gas and into one or two other compartments for metering the

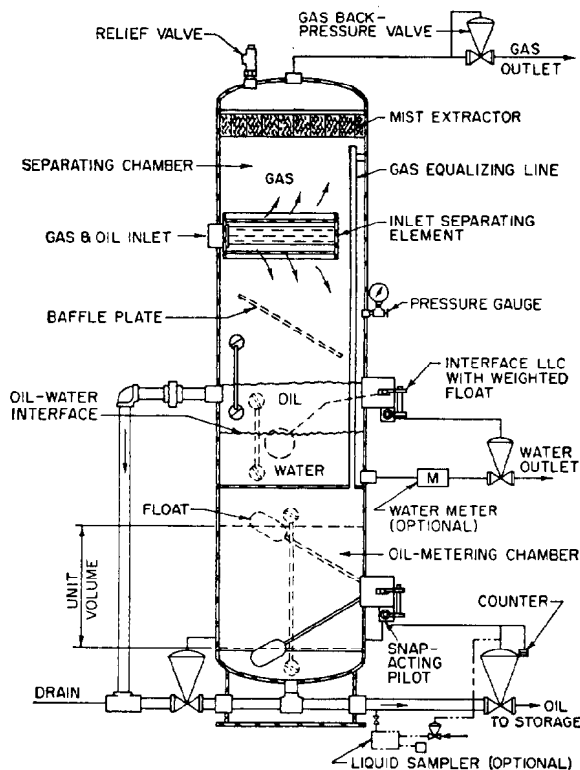


Fig. 32.14—Metering separator with free water knockout.

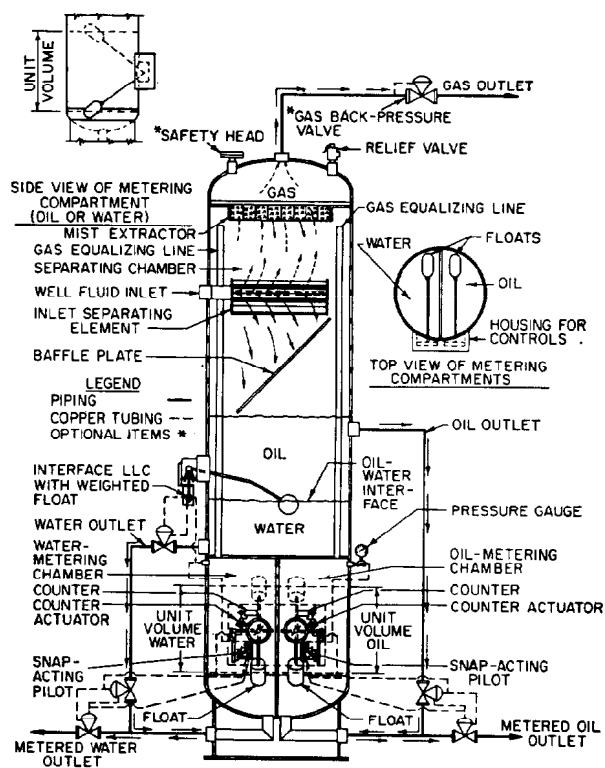


Fig. 32.15—Three-phase metering separator with integral metering compartments. Gauge glasses and valves are furnished for separating chamber and both metering chambers. Automatic BS&W samples can be furnished as an option.

oil and water. PD meters may be used for metering all produced fluids.

Pressure ratings range to 3,000 psi. Capacities will be the same as shown for standard oil and gas separators in Chapter 12. The metering capacity will be as shown for the type of meter used.

GOR

The GOR may be defined as the rate of gas production divided by the rate of oil production. It is usually expressed as standard cubic feet of gas per barrel of stock-tank oil produced under stabilized flowing conditions for a 24-hour period.

The term "cubic feet of gas" or "standard cubic feet of gas" means the volume of gas contained in one cubic foot of space at a standard pressure base and standard temperature base. This standard base is normally 14.65 psia and 60°F. Most tables published for orifice well testers, Pitot tubes, flow provers, and other gas measurement means are referred to a base pressure of 14.65 psia and 60°F temperature. Whenever the conditions of pressure and temperature vary they may be converted to a standard or base condition by the use of the real gas law.

The volume of gas used should be the total gas produced from the reservoir through either the casing or tubing. Any gas that is injected back into the reservoir for artificial lifting purposes such as gas lift should be subtracted from this total gas produced.

The volume of oil produced should be determined by any of the means discussed in the first part of this chapter.

Procedures for Well Testing

Flowing Wells. The oil flow should be stabilized during the 24-hour period immediately preceding the test. This stabilized flow should be very close to the assigned allowable or the daily producing rate. If the well being tested is a discovery well, the producing rate should be as close to the assigned discovery allowable as possible. Any adjustments should be made during the first 12 hours of the stabilization period and no adjustment made during the last 12 hours or during the time the well is on test. All gas withdrawn from the reservoir must be included as produced gas. If the oil has a great deal of shrinkage after it is placed in the stock tanks, some means should be considered for measurement of the gas that breaks out of solution. Any gas used for operation of machinery or for any other purpose must be considered as produced gas. Tests should range from 24 to 168 hours' duration to consider any uneven flow.

Intermittent Flowing Wells (Stopcocked). The procedure for testing should be as outlined for flowing wells, except the shut-in casing and tubing pressures should be approximately equal to the pressures recorded at the beginning of the test. The Texas Railroad Commission states, "The closed-in casing pressure at the end of the 24-hour test period shall not exceed the closed-in casing pressure at the beginning of the test by more than six-tenths (0.6) pounds per square inch per barrel of oil produced during the test." This rule also applies to flowing wells. This is true because of the "loading" characteristic of some wells while shut-in. Before an accurate test can be made the flow must be stabilized and stabilization cannot occur while producing from a loaded annulus or tubing.

Gas-Lift or Jetting Wells. The volume of gas used should be the net produced gas or formation gas. Formation gas will be equal to the total gas produced minus the injection gas.

Pumping Wells. In computing the GOR for pumping wells, the total volume of gas produced during the 24-hour period, ending with the closing in of the well at the conclusion of the tests, and the total barrels of oil that are produced in order to obtain the daily allowable must be used regardless of the actual pumping time in the 24-hour period. If the gas produced is not enough to measure accurately, this should be indicated on the test report as gas "too low to measure."

In some states the regulatory agencies will lower the assigned allowable of the well if the daily or producing allowable is not produced while making GOR tests.

Average GOR

To obtain an average GOR for several wells or for all the wells in a field, one cannot take the arithmetic average value of the ratios. For example, two wells with GOR's of 2,000 and 4,000 would not necessarily have an

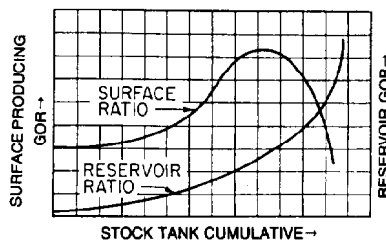


Fig. 32.16—Typical performance curve for an internal gas-driven reservoir.

average ratio of 3,000. For the average ratio to be 3,000 the wells would have to produce the same amounts of oil. The average GOR of several wells must be obtained by dividing the total gas production of all wells involved. For example, if the 2,000-ratio well produced 50 B/D oil and the 4,000-ratio well produced 200 B/D oil, the average GOR for the two wells would be

$$\bar{R} = \frac{(2,000 \times 50) + (4,000 \times 200)}{50 + 200} = 3,600 \text{ cu ft/bbl.}$$

For a large number of wells, the average ratio can be figured as

$$\bar{R} = \frac{\sum (R_{iw} \times q_{iw})}{\sum q_{iw}} \quad \dots \dots \dots (8)$$

where

\bar{R} = average GOR, cu ft/bbl,

R_{iw} = individual well GOR, cu ft/bbl, and

q_{iw} = individual well daily production, STB/D.

Cumulative GOR

The cumulative GOR is defined as the total amount of gas produced and kept from the reservoir up to a certain time divided by the cumulative oil produced up to the same time. Therefore,

$$R_p = \frac{G_p - G}{N_p}, \quad \dots \dots \dots (9)$$

where

R_p = cumulative GOR, cu ft/bbl,

G_p = total gas produced, cu ft,

G = gas reinjected, cu ft, and

N_p = total oil produced, bbl.

GOR as a Criterion of Reservoir Performance

The producing GOR is often used as an indication of the efficiency of a producing well, and the increase in the ratio is looked on as a danger signal in the control of the reservoir performance. The GOR should be kept as low as possible (see Fig. 32.16). The area under the curve, shown as the surface ratio, will be the total amount of produced gas. This is by the previous definition of

GOR. This shows that maintaining the GOR as low as possible will increase the cumulative production for the same amount of produced gas.

Consider the internal-gas-drive reservoir. As oil is produced from the reservoir the space is taken over by gas volume. The presence of gas within the reservoir decreases the ability of oil to flow and increases the ability of gas to flow. After a certain minimum gas saturation (about 5 to 10%) is exceeded, the ease with which gas flows increases to such an extent that it flows concurrently with the oil. This process continues until finally the only flow is almost all gas. This allows the reservoir energy to escape and causes the reservoir to cease production by natural means. Fig. 32.16 shows how the stock-tank cumulative production almost ceases as the reservoir/GOR increases.

Key Equations in SI Metric Units

$$q_o = \frac{5.427 \times 10^{-4} kh(p_e - p_{wf})}{\mu_o B_o [\ln(r_e/r_w) + s]}, \dots\dots\dots (1)$$

$$J = \frac{q_o}{\Delta p} = \frac{5.427 \times 10^{-4} kh}{\mu_o B_o [\ln(r_e/r_w) + s]}, \dots\dots\dots (2)$$

where

- q_o = oil production rate, m³/d
- k = permeability of formation, m²
- h = thickness of formation, m
- p_e = pressure at the effective drainage radius r_e , normally approximated by p_R , kPa
- p_{wf} = flowing bottomhole pressure, kPa
- μ_o = oil viscosity, Pa·s

B_o = oil formation volume factor, res m³/STm³

r_e = effective drainage radius, m

r_w = wellbore radius, m

s = skin effect (zone of reduced or improved permeability), dimensionless

J = productivity index (PI), m³/(d·kPa)

References

1. Moore, T.V.: "Definitions of Potential Productions of Wells Without Open Flow Tests," *Bull.*, API, Dallas (1930) 205.
2. Harder, M.L.: "Productivity Index," API, Dallas (May 1936).
3. *API Recommended Practice for Determining Productivity Indices*, API RP 36, first edition, API, Dallas (June 1958).
4. Calhoun, J.C. Jr.: *Fundamentals of Reservoir Engineering*, revised edition, U. of Oklahoma Press, Norman (1953).
5. Muskat, M.: "Physical Principles of Oil Production," Intl. Human Resources Development Corp., Boston (1981).
6. Muskat, M. and Evinger, H.H.: "Calculation of Theoretical Productivity Factor," *Trans.*, AIME (1942) **146**, 126-39.
7. Odeh, A.S.: "Pseudosteady-State Flow Equation and Productivity Index for a Well With Noncircular Drainage Area," *J. Pet. Tech.* (Nov. 1978) 1630-32.
8. Earlougher, R.C. Jr.: "Estimating Drainage Shapes From Reservoir Limit Tests," *J. Pet. Tech.* (Oct. 1971) 1266-75; *Trans.*, AIME, **251**.
9. van Everdingen, A.F.: "The Skin Effect and Its Influence on the Productive Capacity of a Well," *J. Pet. Tech.* (June 1953) 171-76; *Trans.*, AIME, **198**.
10. Dake, L.P.: *Fundamentals of Reservoir Engineering*, Elsevier Scientific Publishing Co., New York City (1978).
11. *Measurement of Petroleum Liquid Hydrocarbons by Positive Displacement Meter*, API Standard 1101, first edition, API, Dallas (Aug. 1960).
12. *Manual of Petroleum Measurement Standards*, API, Dallas (1961) Chap. 5.

Chapter 33

Open Flow of Gas Wells

R. V. Smith, Petroleum Consultant*

Introduction

The gauging or testing of gas wells arose from the need to measure the productive capacity of a well. The earliest response to this need was to open the well to flow to the atmosphere and then to measure the flow rate. However, it soon became apparent that such practices were wasteful of gas, dangerous for personnel and well equipment, and frequently damaging to the reservoir. In addition, such tests provided very little information for estimating production rates into a pipeline. As a result, the practice of gauging gas wells by opening the well to flow to the atmosphere decreased and now is almost completely confined to stripper gas areas where pressures are very low and the rates of flow are small.

Pitot-Tube Gauging of Low-Pressure Wells

The pitot tube is one of the simplest instruments for measuring the rate of flow of gas. As such, the pitot has been used extensively to obtain an approximate gauge of the open-flow capacity of low-pressure gas wells. The well is opened to flow to the atmosphere through a flow nipple, and the producing rate is measured with a pitot tube. The producing rate is influenced by the hydrostatic head of the column of flowing gas and the friction between the flowing gas and the walls of the flow string. Thus the observed rate of flow to the atmosphere may be a very close measure of the ability of shallow low-capacity reservoirs to deliver gas into the wellbore. However, it may be more nearly a measure of the flow capacity of the flow string in the case of a well producing from a high-capacity reservoir. This is especially true where the flow is through a small-diameter flow string.

Historically, gauging of wells with pitot-tube measurements has been useful in the drilling and completion of low-pressure gas wells. During the drilling of many wells in the Hugoton field of Kansas, Oklahoma, and Texas, it was the practice to take pitot gauges after

every bailer run or at the end of each 5 ft of formation drilled. Upon completion, data were available to construct a chart showing a relationship between the rate of flow and depth. The chart is useful in determining the depth of the major gas-producing zones. Such data were valuable in planning remedial work that may be necessary during the life of the well. Pitot-tube gauges were useful in determining rate-of-flow increases resulting from each stage of acid treatment. In many cases the pitot-tube gauge after acid treatment provided data from which the desired flow rates for a backpressure test could be selected.

Fig. 33.1 shows a pitot-tube and flow nipple arrangement that is suitable for gas measurement. The pitot tube should be made of 1/8-in.-ID pipe shaped to measure impact pressure at the center and in the plane of the opening of the flow nipple. The flow nipple should be at least eight pipe diameters long, free from burrs or other obstructions, and must be round. The impact pressures are measured with water or mercury manometers or a pressure gauge, depending on the pressure to be measured.

The impact pressure is converted to rate of flow by suitable equations or tables such as those published by Reid.¹ Subsequent experimental work by the USBM² is in reasonable agreement with the Reid data. The equations published by Reid were investigated by Binckley,³ who concluded that they were based on sound theoretical principles. Reid's equations and tables have been adjusted to a pressure base of 14.65 psia for the purposes of this handbook. The adjusted equations for impact pressures less than 15 psig are

$$q_g = 34.81 d_i^2 \sqrt{h_w}, \dots\dots\dots (1)$$

$$q_g = 128.4 d_i^2 \sqrt{h_m}, \dots\dots\dots (2)$$

and

$$q_g = 183.2 d_i^2 \sqrt{p_i}, \dots\dots\dots (3)$$

*This author also wrote the original chapter on this topic in the 1962 edition.

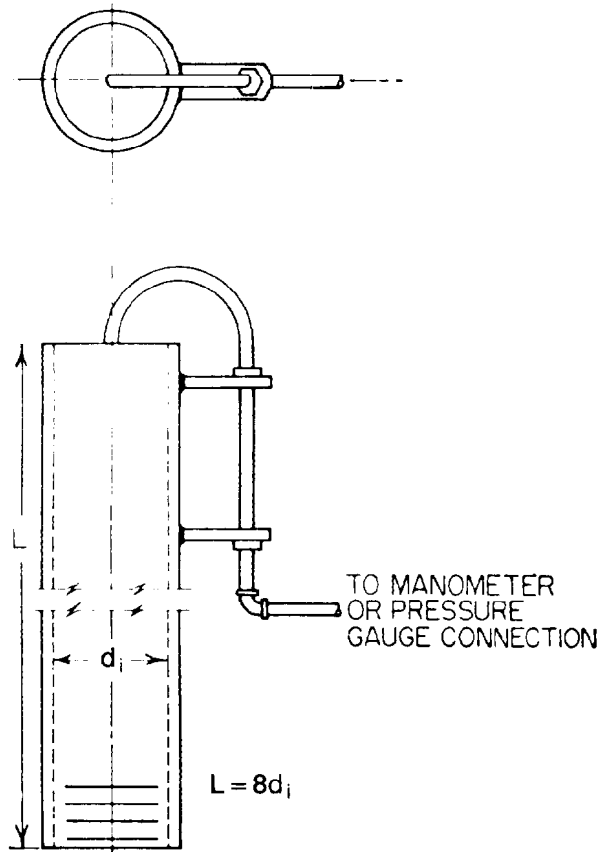


Fig. 33.1—Typical flow nipple and pitot tube for gas measurement.

where

- q_g = rate of gas flow, Mcf/D (14.65 psia and 60°F),
- d_i = ID of flow nipple, in.,
- h_w = height (manometer reading), in. water,
- h_m = height (manometer reading), in. mercury, and
- p_i = impact pressure, psig.

For impact pressures more than 15 psig, the adjusted Reid equation is

$$q_g = 23.89 d_i^2 p_1, \dots (4)$$

where p_1 is impact pressure, psia. Values of rates of flow for various impact pressures are given in Table 33.1 for a flow nipple with an ID of 1.000 in. Rates of flow in Table 33.1 were computed by Eqs. 1 through 3. The range of impact pressures is from 0.1 in. of water to 15 psig. Rates of flow for impact pressures from 15 to 200 psig were computed by Eq. 4 and are given in Table 33.2 for a flow nipple with an ID of 1.000 in. Impact pressures measured on larger flow nipples can be converted to rates of flow by multiplying the rate of flow from the table corresponding to the impact pressure by the square of the ID (in.) of the larger nipple.

Rates of flow taken from Tables 33.1 and 33.2 or computed by Eqs. 1, 2, 3, and 4 are for gases with a specific gravity of 0.600 (air = 1.000), flowing temperatures of

60°F, and for discharge into an atmospheric pressure of 14.65 psia. Corrections can be made when desirable by multiplying values from the equations or tables by the following factors.

$$F_g = \sqrt{\frac{0.600}{\gamma_g}}$$

and

$$F_T = \sqrt{\frac{520}{(460 + T_f)}},$$

where

F_g = specific gravity correction factor,

γ_g = specific gravity of gas being measured, air = 1.000,

F_T = flowing-temperature correction factor, and

T_f = temperature of flowing gas, °F.

The atmospheric-pressure correction factor for values from Table 33.1 and Eqs. 1, 2, and 3 is

$$F_{bar} = \sqrt{\frac{p_a}{14.65}},$$

where F_{bar} is barometric correction factor and p_a is atmospheric pressure, psia. The value of pressure used for p_i in Eq. 4 is the absolute pressure and is computed by adding the barometric pressure to the gauge pressure. The correction factor for barometric pressure for Table 33.2 is

$$F_{bar} = \frac{p_i + p_a}{p_i + 14.65}.$$

In ordinary usage, rates of flow are taken from pitot tables or formulas without correction.

Example Problem 1. Given an impact pressure of 27.2 in. of water on a flow nipple with ID = 2.441 in., determine the rate of flow.

Rate of flow from Table 33.1 for ID = 1.000 = 182 Mcf/D.

Rate of flow for ID = 2.441 in. is

$$q_g = 182(2.441)^2 = 182 \times 5.958 = 1,080 \text{ Mcf/D.}$$

Or, by Eq. 1, the rate of flow is

$$\begin{aligned} q_g &= 34.81(2.441)^2 \sqrt{27.2} \\ &= (34.81)(5.958)(5.215) = 1,080 \text{ Mcf/D.} \end{aligned}$$

Example Problem 2. Given an impact pressure of 65 psig on a flow nipple with ID = 4.082 in. with discharge into a barometric pressure of 13.2 psia, determine the rate of flow.

Rate of flow from Table 33.2 for ID of 1.000 and atmospheric pressure of 14.65 psia is 1,904 Mcf/D.

For ID of 4.082 in. and barometric pressure of 13.2 psia, the rate of flow is

$$\begin{aligned} q_g &= 1,904(4.082)^2 (65 + 13.2) / (65 + 14.7) \\ &= (1,904)(16.663)(0.9812) = 31,100 \text{ Mcf/D.} \end{aligned}$$

Or by Eq. 4,

$$q_g = 23.89(4.082)^2(65 + 13.2) \\ = 31,100 \text{ Mcf/D.}$$

Backpressure Testing

Before the development of the backpressure method for testing gas wells, the open-flow capacities of gas wells were determined by actual "open-flow" tests. The flowing of wells at their wide-open rate results in waste and possible damage to the well. In addition, the open-flow

test yields very little information regarding the capacity of a well to deliver gas into a pipeline system.

The backpressure method of testing gas wells was developed by Rawlins and Schellhardt.² Results of tests on 582 wells as reported in their study and other work on many wells reported elsewhere show that when the rates of flow are plotted on logarithmic coordinates against corresponding values of $(\bar{p}_R^2 - p_{wf}^2)$ —the difference of squares of the shut-in pressure \bar{p}_R and the flowing sand-face (bottomhole) pressure (BHP) p_{wf} —the relationship may be represented empirically by a straight line.

TABLE 33.1—RATES OF FLOW FOR IMPACT PRESSURES LESS THAN 15 PSIG MEASURED WITH A PITOT TUBE FOR FLOW NIPPLE WITH ID = 1.000 in.*

Impact Pressure			$q_g, 10^3 \text{ cu ft/D}$ (14.65 psia and 60°F)	Impact Pressure			$q_g, 10^3 \text{ cu ft/D}$ (14.65 psia and 60°F)
Water (in.)	Mercury (in.)	psig		Water (in.)	Mercury (in.)	(psig)	
0.1	—	—	11.0	10.9	0.80	—	115
0.2	—	—	15.6	12.0	0.88	—	121
0.3	—	—	19.1	12.2	0.90	—	122
0.4	—	—	22.0	13.9	1.02	0.5	130
0.5	—	—	24.6	15.0	1.1	—	135
0.6	—	—	27.0	16.3	1.2	—	140
0.7	—	—	29.1	17.7	1.3	—	146
0.8	—	—	31.1	19.0	1.4	—	152
0.9	—	—	33.0	20.4	1.5	—	157
1.0	—	—	34.8	21.8	1.6	—	162
1.25	—	—	38.9	24.5	1.8	—	172
1.36	0.10	—	40.6	27.2	2.0	1.0	182
1.6	0.12	—	44.0	29.9	2.2	—	190
1.8	0.13	—	46.7	32.6	2.4	—	199
2.0	0.15	—	49.2	—	2.6	—	207
2.2	0.16	—	51.6	—	2.8	—	215
2.4	0.18	—	53.9	—	3.0	1.5	222
2.7	0.20	—	57.2	—	3.2	—	230
3.0	0.22	—	60.3	—	3.4	—	237
3.5	0.26	—	65.1	—	3.6	—	244
4.1	0.30	—	70.5	—	3.8	—	250
4.5	0.33	—	73.8	—	4.0	2.0	257
5.0	0.37	—	77.8	—	4.2	—	263
5.4	0.40	—	80.9	—	4.4	—	269
6.0	0.44	—	85.2	—	4.6	—	275
6.8	0.50	—	90.8	—	4.8	—	281
8.2	0.60	—	99.7	—	5.0	2.5	287
9.0	0.66	—	104.4	—	5.2	—	293
9.5	0.70	—	107.3	—	5.4	—	298
10.0	0.74	—	110.1	—	5.6	—	304
5.8	—	—	309	—	15.3	7.5	502
6.0	3.0	—	314	—	16.3	8.0	518
6.5	—	—	327	—	17.3	8.5	522
7.0	3.5	—	340	—	18.3	9.0	549
7.5	—	—	352	—	19.3	9.5	564
8.0	4.0	—	363	—	20.4	10	580
8.5	—	—	374	—	22.4	11	608
9.0	4.5	—	385	—	24.4	12	634
9.5	—	—	396	—	26.5	13	661
10.0	—	—	406	—	28.5	14	677
10.2	5.0	—	410	—	30.5	15	710
11.2	5.5	—	430				
12.2	6.0	—	448				
13.2	6.5	—	466				
14.3	7.0	—	486				

*Multiply rate of flow from table by the square of the diameter for flow nipples with ID's more than 1,000 in.

TABLE 33.2—RATES OF FLOW FOR IMPACT PRESSURES, 15 TO 200 PSIG, MEASURED WITH A PITOT TUBE FOR FLOW NIPPLE WITH ID = 1.000 in.*

Impact Pressure (psig)	$q_g, 10^3$ cu ft/D (14.65 psia and 60°F)	Impact Pressure (psig)	$q_g, 10^3$ cu ft/D (14.65 psia and 60°F)
15	710	40	1,307
16	733	45	1,426
17	757	50	1,546
18	781	55	1,665
19	805	60	1,785
20	829	65	1,904
21	853	70	2,023
22	877	75	2,143
23	901	80	2,262
24	925	90	2,501
25	948	100	2,740
26	972	110	2,979
27	996	120	3,218
28	1,020	130	3,457
29	1,044	140	3,697
30	1,068	150	3,935
32	1,116	160	4,174
34	1,163	170	4,412
36	1,211	180	4,651
38	1,259	190	4,890
		200	5,129

*Multiply rate of flow from table by the square of the diameter for flow nipples with ID's more than 1.000 in.

The backpressure method of testing wells requires that a series of flow rates and corresponding pressure measurements be obtained under stabilized conditions or at certain fixed time intervals. Testing under stabilized pressure and rate-of-flow conditions or according to a fixed time interval has become known as multipoint or "flow-after-flow" backpressure testing.

As the original backpressure or multipoint method came into general use, it became evident that the method of testing was applicable to those wells that approached stabilized producing conditions within a relatively short time. However, performance characteristics could not be determined by this method for wells that approached stabilized producing conditions slowly over a considerable period. This characteristic of slow stabilization has been associated generally with wells producing from reservoirs with low permeability and resulted in the development of the isochronal method of backpressure testing by Cullender.⁴

The procedure used to obtain the necessary performance data for the isochronal testing method is to open the well from a shut-in condition and allow the well to flow without disturbing the rate by changing the mechanical adjustment of chokes or valves for a specific period of time. The well is then shut in and allowed to return to a shut-in pressure comparable with that existing before the well was first opened, after which the well is again opened at a different rate of flow. In isochronal testing, each rate of flow starts from a comparable shut-in condition, which provides a means of maintaining a simple pressure gradient throughout the drainage area of the well during testing. The isochronal method of testing

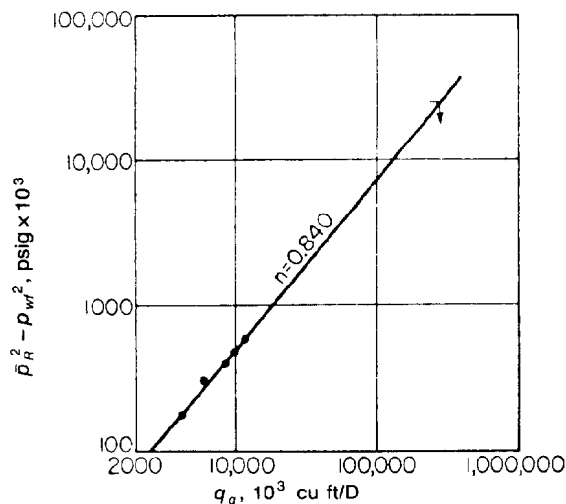


Fig. 33.2—Multipoint test showing bottomhole performance for Well B.

is especially suitable for determining the performance characteristics of wells producing from reservoirs with low permeability.

High-Pressure Gas and Gas-Condensate Wells

All the instructions for testing wells in this chapter apply to gas wells that produce a single-phase gas into the wellbore or to wells that are predominantly gas wells and the fluid flowing in the reservoir has a high in-place gas/liquid ratio (GLR). However, these methods for testing gas wells have been applied to high-ratio oil wells with some degree of success.

The chief difference between testing methods for high-pressure gas and gas-condensate wells and low-pressure wells is the care used in taking the data and methods used in computing the results. The effect of liquids is usually more pronounced in high-pressure than in low-pressure wells. Consequently, special care should be used to measure GLR's in high-pressure wells. Often it is necessary to determine the GLR at each rate of flow during a backpressure test. If the ratio was not constant during testing, the well probably was accumulating liquid in the wellbore during testing or unloading liquid. In either case the test is probably not acceptable and the well should be cleaned by flowing at a high rate and retested at rates of flow high enough to keep the well free of liquid.

Temperature effects during testing of high-pressure wells may be troublesome in interpreting test results. For example, Well B (Fig. 33.2) has a shut-in wellhead pressure of 4,173 psia at a wellhead temperature of 117°F. Maximum wellhead pressure was observed 3 minutes after the well was shut in. If wellhead pressure has been observed for an extended period of time, the wellhead pressure would have decreased to about 4,140 psia. The decrease in wellhead pressure is caused by the cooling of the gas in the well. In general, better tests can be obtained on such large-capacity wells if the testing is done after a preflow period. The preflow period should be run long enough to bring wellhead temperatures to a normal operating range of temperature. Wellhead

temperatures should be recorded during testing at periodic intervals so that actual measured temperatures can be used in computing subsurface pressures by methods outlined under Example 3 in the section on computing subsurface pressures.

Official Testing

Official testing of gas wells for state *regulatory bodies* is usually a multipoint test of short duration. In addition to the multipoint test, a single rate of flow for a period of 24 to 72 hours is required in some cases. The tester is referred to the test manuals of the various states, provinces of Canada, or appropriate countries for exact procedures, and no attempt is made here to outline official testing.

Backpressure Equations

In either multipoint or isochronal backpressure testing, the rates of flow and the corresponding values of the difference of squares of the average formation (reservoir) pressure \bar{p}_R and the sandface pressure [bottomhole flowing pressure (BHFP)] p_{wf} are plotted on logarithmic coordinates and a straight line is drawn through the points. The equation for the relationship is

$$q_g = C(\bar{p}_R^2 - p_{wf}^2)^n, \dots\dots\dots (5)$$

where the performance coefficient is represented by C and the exponent of the backpressure curve by n . The industry by common usage has referred to n as the "slope" of the backpressure curve, even though n is the reciprocal of the mathematical slope of the line. Here n is referred to as the "exponent" of the backpressure curve. Eq. 5 is an empirical relationship for both the multipoint test and the isochronal test and has resulted from the study of results of many tests. Values of the exponent vary for individual wells in the range of 0.5 to 1.0. Tests that result in exponents less than 0.5 or more than 1.0 should be rerun. Exponents of less than 0.5 resulting from multipoint tests may be caused by the slow-stabilization characteristics of the reservoir or by the accumulation of liquids in the wellbore. Exponents greater than 1.0 may be caused by the removal of liquid from the well during testing or by a cleaning of the formation around the well, such as the removal of drilling mud or stimulation fluids. Also, a multipoint test run in decreasing rate sequence may have an exponent of more than 1.0 for wells in slow-stabilizing reservoirs. Erratic exponents in isochronal testing are caused by either accumulation or cleaning of liquids from around the well. Erratic alignment of data points from multipoint or isochronal testing is usually caused by changes in actual well capacity during testing. Such changes may be caused by accumulation of liquids or the cleaning of the wells. The effects of the liquids in the well on multipoint testing have been given in detail by Rawlins and Schellhardt.²

Eq. 5 represents the capacity of a well to deliver gas into the wellbore, and it is useful especially in evaluating reservoir conditions. The capacity of a well to deliver gas at the wellhead may be represented by

$$q_g = C(p_{ts}^2 - p_{wf}^2)^n, \dots\dots\dots (6)$$

where C , the performance coefficient, and n , the exponent, are different from those in Eq. 5 for a given well. p_{ts} and p_{wf} represent wellhead shut-in (static tubing) pressure and working (flowing tubing) pressure on the flowing-gas column at the wellhead, respectively. Eq. 6 is useful especially in estimating the capacity of a well to deliver gas into a pipeline under specified conditions.

Gas Well Inflow Equation, Pseudosteady State

Reservoir engineers have realized for many years that interpretation of multipoint and isochronal tests by means of Eq. 5 gave no insight into the effect of reservoir or gas properties on the rate of flow into a well. Thus, Eq. 5 proved inadequate for reservoir engineering purposes. An equation that describes the pseudosteady-state flow of gas into a well has been presented in the literature.⁵⁻⁸ It is

$$q_g = \frac{703 \times 10^{-6} k_g h (\bar{p}_R^2 - p_{wf}^2)}{\mu_g T_R z (\ln r_e/r_w - 0.75 + s + F_{nD} q_g)}, \dots\dots\dots (7)$$

where

- q_g = gas-production rate, 10^3 cu ft/D,
- k_g = permeability, effective to gas, md,
- h = formation thickness, ft,
- \bar{p}_R = average reservoir pressure, psia,
- p_{wf} = flowing bottomhole pressure, psia,
- μ_g = gas viscosity, cp,
- T_R = reservoir temperature, °R,
- z = compressibility factor of gas,
- r_e = effective drainage radius, ft,
- r_w = wellbore radius, ft,
- s = skin factor, and
- F_{nD} = non-Darcy flow factor.

If we let

$$\frac{703 \times 10^{-6} k_g h (\bar{p}_R^2 - p_w^2)}{\mu_g T z} = C_1,$$

and

$$\ln r_e/r_w - 0.75 + s = C_2,$$

Eq. 7 becomes

$$q_g = \frac{C_1}{C_2 + F_{nD} q_g},$$

or

$$F_{nD} q_g^2 + C_2 q_g - C_1 = 0.$$

From this we get

$$q_g = \frac{-C_2 + \sqrt{C_2^2 + 4F_{nD} C_1}}{2F_{nD}}, \dots\dots\dots (8)$$

The maximum rate of flow [open-flow potential (OFP)] is given when C_1 is a maximum—that is, when $p_{wf} = 0$. Eq. 7 incorporates the properties of the reservoir and the gas and can be extended to noncircular areas as given in Ref. 5.

Determination of Absolute Open Flow (AOF)

The terms "calculated absolute open flow" (CAOF) and OFP are the rate of flow in thousands of cubic feet of gas per 24 hours that would be produced by a well if the pressure against the face of the producing formation in the wellbore were zero. The value of the OFP is usually determined graphically by plotting rates of flow q_g against the corresponding values of $\bar{p}_R^2 - p_{wf}^2$. The straight-line relationship between q_g and $\bar{p}_R^2 - p_{wf}^2$ is extended so the rate of flow q_g corresponding to the value of \bar{p}_R^2 can be read by extrapolation. Then q_g is the AOF of the well in cubic feet per 24 hours. The AOF can be computed from Eq. 5 or read directly from plotted relationships.

In wells producing from reservoirs with low permeability, the reported AOF must be identified further by the time involved in the test and the type of test. For example, the OFP of such a well as determined by a 3-hour multipoint test (each rate of flow lasting 3 hours) would be less than that determined by a 2-hour multipoint test. The open flow determined by an isochronal test of 3 hours would be different from that determined by a multipoint test. A good example of the relationship between AOF and type of test is given by Cullender.⁴ Reported OFP's on wells in low-permeability reservoirs are more or less meaningless without an indication of the type of test involved.

Determination of the Exponent n

The calculation of the exponent n is based on Eq. 5 and the relationship

$$n = \frac{\log q_{g2} - \log q_{g1}}{\log(\bar{p}_R^2 - p_{wf}^2)_2 - \log(\bar{p}_R^2 - p_{wf}^2)_1} \quad \dots \dots (9)$$

Values of q_g and corresponding values of $\bar{p}_R^2 - p_{wf}^2$, either actual experimental points or values read from the straight-line relationship, are substituted in Eq. 9. Usually the data points do not fall exactly on a straight line; so the best practice is to read values of q_g and $\bar{p}_R^2 - p_{wf}^2$ directly from the straight line.

Determination of the Performance Coefficient C

After the value of the exponent n has been determined, the value of the performance coefficient C may be determined by substitution of a corresponding set of values for q_g and $\bar{p}_R^2 - p_{wf}^2$ and the value of n into Eq. 5. The value of C is found by solution of the resulting equation. Graphically the value of C may be determined by extension of the straight-line relationship to $\bar{p}_R^2 - p_{wf}^2 = 1$ and reading the corresponding q_g . When $\bar{p}_R^2 - p_{wf}^2$ is unity, C is equal to q_g . In practice, a determination of the value of C is seldom necessary for routine analysis of backpressure tests.

Preparation of Well for Testing

The wellbore should be cleaned of liquids by flowing at a high rate to a pipeline for a period of 24 hours. If the well does not have a pipeline connection, it may be blown to the air for a short period of time, provided blowing is considered safe. Extra precautions should be taken on new wells to remove drilling mud, solids, and stimulation fluids from the wellbore. The well should be shut in

for 24 hours or longer to equalize the reservoir pressure in the vicinity of the well. Wells with slow pressure-buildup characteristics should be shut in 48 to 72 hours, if possible.

While the well is shut in, the gas-measurement equipment should be prepared for use. If the gas is to be measured with an orifice meter, the meter should be calibrated, the diameters and condition of the run and plate verified, and the differential pen should be zeroed in accordance with good meter practice. If a critical-flow prover (see later section on gas measurement) is used, it should be placed in a vertical position at the wellhead or downstream from the separator so that the gas will flow up and away from the test area. If a separator is used, control the rate of flow with a production choke and maintain pressure on the separator with a critical-flow prover or backpressure regulator when an orifice meter is used. If a separator is not used, control rate of flow and pressure at the wellhead with the critical-flow prover. Always install thermometer wells at the wellhead and at gas-measuring equipment so that temperatures may be measured with a thermometer or calibrated recording device. The thermometer wells should be filled with water or oil to obtain accurate temperature measurement.

Shut-In Pressure

All shut-in or flowing pressures should be measured with a dead-weight or piston gauge, because spring gauges are usually not accurate enough for backpressure tests. Determine and record the pressure at the end of the shut-in period, prepare the well for testing, and redetermine the shut-in pressure as a check on the first measurement and to obtain the rate of pressure buildup. Report each pressure and time the well was shut in prior to each pressure measurement. After the second pressure measurement, either the isochronal or multipoint test may be started.

Subsurface pressures in gas wells may be measured directly with pressure gauges or computed from wellhead pressures. Subsurface-pressure gauges are very useful in wells where liquids accumulate in the wellbore during shut-in. However, the use of subsurface gauges limits the rates of flow during the backpressure test to velocities that will not lift the gauge in the flow string. The use of subsurface gauges is limited to rather low rates of flow in 2 3/8-in. OD tubing, but there is practically no limitation on their use in 7-in. casing. The use of subsurface gauges in the annular spaces of dual completions is practically impossible. In cases where large-capacity wells are being tested, correction must be made for the effect of hysteresis on gauge readings, or the BHP must be measured at each rate of flow by a separate run of the gauge.

The accumulation of liquid in the wellbore is probably the most serious cause of erroneous calculated BHP's. Other sources of error are uncertainties in temperature gradients and specific gravities of the fluids flowing in the well. Before a backpressure test is begun, special care should be taken to remove the liquids from the wellbore by flowing at rates large enough to lift the liquid. If possible, each rate of flow used in the backpressure test should be large enough to lift continuously any liquid that may move into the wellbore during production. Temperature gradients can be

established for a new area only by actual measurement. Usually a flowing-temperature gradient can be estimated by assuming a straight-line gradient between flowing wellhead temperature and bottomhole temperature. Uncertainty in the specific gravity of the fluid flowing in the well can be eliminated to a large degree by careful measurement of gas/hydrocarbon liquid ratio and determination of the specific gravity of the separator gas, separator liquid, and stock-tank liquid.

Multipoint Test and Example

A four-point multipoint test of constant duration for each rate taken in increasing rate sequence is normally satisfactory for establishing the performance of a well. In the case of high-liquid-ratio wells or high-flowing-temperature conditions, a decreasing-rate-sequence test may be used if an increasing-rate-sequence test would not result in alignment of points. In the case of high-liquid-ratio wells, the low flow rates will not clean the wellbore of liquids that accumulate during production. In the case of wells with exceptionally high flowing temperature, it may be desirable to start the test at the highest rate of flow that will result in more nearly constant wellhead temperatures during the test rather than starting at the lowest rate of flow. However, a test in decreasing-rate sequence should not be run unless it is known that an increasing-rate-sequence test will not give a satisfactory test.

The four rates of flow for the test should be evenly distributed over the test range. For average- to low-capacity gas wells, the first rate of flow should lower the pressure at the wellhead about 5%, and the pressure reduction for the fourth rate should be 25%. The rate of flow required to reduce the working pressure to 5% for the first test rate can be approximated from pressure readings obtained while the well is being cleaned before the well is shut in. These recommended pressure reductions may not be possible for large-capacity wells with large flow strings.

After the well is opened for the first rate of flow, the test rate should be continued for 3 hours but no more than 4 hours. Each succeeding flow rate should be for the same period of time. During each flow rate, the wellhead working pressure and temperature, meter or prover pressure and differential, and temperature should be reported at the end of each 15-minute period. If separator and tanks are used during testing, the rate of liquid accumulation, both hydrocarbon and water, should be reported. If a critical-flow prover alone is used, the presence or absence of liquids in the gas stream should be noted and reported. The specific gravity of the separator gas or the specific gravity of the gas flowing from the critical-flow prover should be measured and reported, or a gas sample should be taken for analysis and calculation of the specific gravity. More representative gas specific gravities can be obtained after the well has been flowing at least an hour.

Table 33.3 is an actual copy of the field data sheet for a multipoint backpressure test for Well A in the Guymon Hugoton gas field in Texas County, OK.* The form on which the data are reported has proved convenient for recording test data. The times at which each plate was

changed and when the well opened on each rate of flow were carefully reported. The "remarks" column gives the results of the specific-gravity measurement and the condition of the flow with regard to whether the well was producing water. All the observations recorded in Table 33.3 are necessary for accurate analysis of test results.

Computation of the results of a backpressure test on a gas well involves the following steps.

1. Compute rates of flow and pressures at the face of the producing formation from pressure and volume observations made at the wellhead.
2. Determine values of $p_{ts}^2 - p_{wf}^2$ and $\bar{p}_R^2 - p_{wf}^2$ and rates of flow corresponding to these pressure factors. Then, p_R and \bar{p}_{wf} are calculated at the midpoint of the sandface in wells without tubing. If the well has tubing, they are determined at the entrance to the tubing, provided the entry to the tubing is no more than 100 ft from the midpoint of the sandface.
3. Plot values of q_g and corresponding values of $\bar{p}_R^2 - p_{wf}^2$ and $p_{ts}^2 - p_{wf}^2$ on logarithmic coordinates.
4. Determine values of the exponent n and the performance coefficient C of the flow equations

$$q_g = C(\bar{p}_R^2 - p_{wf}^2)^n$$

and

$$q_g = C(p_{ts}^2 - p_{wf}^2)^n.$$

For most routine analyses of backpressure tests, determination of the value of C is not necessary.

5. Determine the CAOF. Computations for rate of flow and pressures at the producing formation are explained in separate sections.

A convenient form for reporting the results of a multipoint test is illustrated in Table 33.4 for the test data taken on Well A and reported in Table 33.3. Table 33.4 shows general well information, a summary of test data, calculation of rates of flow, data for determining compressibility, and the difference of squares of pressures for wellhead and bottomhole conditions. The calculated OFP of $25,000 \times 10^3$ cu ft/D was determined in Fig. 33.3 where the rate of flow is the abscissa and $\bar{p}_R^2 - p_{wf}^2$ (in thousands) is the ordinate on logarithmic coordinates. The data points were connected by a straight line and extrapolated to a value of $\bar{p}_R^2 - p_{wf}^2$, where p_{wf}^2 is zero. In this case, the value is $\bar{p}_R^2 = 230.9$ (thousands). The corresponding rate of flow is $25,000 \times 10^3$ cu ft/D. The AOF of $25,000 \times 10^3$ cu ft/D for Well A is for a 3-hour four-point test. If the test were for a lesser-time four-point test, the resulting AOF would have been more than $25,000 \times 10^3$ cu ft/D.

The exponent n was determined by taking values of q_g and $\bar{p}_R^2 - p_{wf}^2$ from the straight line in Fig. 33.3 and Eq. 7 as follows.

$q_g, 10^3 \text{ cu ft/D}$	$\bar{p}_R^2 - p_{wf}^2 \text{ (thousands)}$
20,000	168
4,000	16.8

$$n = \frac{\log 20,000 - \log 4,000}{\log 168 - \log 16.8} = \frac{\log 5.00}{\log 10.0} = \frac{0.699}{1.000}$$

$$= 0.699.$$

* This test, used in the 1962 edition of the handbook, was run many years ago. It still stands as a classic multipoint test example today.

TABLE 33.3—FIELD DATA SHEET FOR MULTIPOINT TEST (WELL A)

DATE		WELLHEAD WORKING PRESSURE				METER OR PROVER				REMARKS
Time	Hrs.	Tbg. Psig	Csig. Psig	Annulus Psig	Temp. F	Psig	Diff.	Temp. F	Orifice	
6-17-47										
Well shut in for 20 days										
4:30 a		-	435.3	-						SIP
2" Prover installed on wellhead										
5:00 a	0	-	435.3			430.9			3/4	SIP
5:30	.5	-	418.9			414.5		66		Gas Dry
6:00	1.0	-	415.8			411.4		68		
6:30	1.5	-	413.9			409.2		68		
7:00	2.0	-	412.6			408.2		69		Gas Dry
7:30	2.5	-	411.4			407.0		69		Sp. Gravity 0.719
8:00	3.0	-	410.5			406.1		70		1st Point
Plate changed, opened at 8:03										
8:33	.5	-	402.8			399.4		70	7/8	
9:03	1.0	-	401.1			392.7		71		Gas Dry
9:33	1.5	-	399.7			391.3		71		
10:03	2.0	-	398.7			390.3		71		Gas Dry
10:33	2.5	-	397.9			389.5		72		
11:03	3.0	-	397.3			388.9		72		2nd Point
Plate changed, opened at 11:06										
11:36	.5	-	387.2			374.1		73	1	Gas Dump
12:06 p	1.0	-	385.6			372.5		73		
12:36	1.5	-	384.2			371.1		73		
1:06	2.0	-	383.3			370.2		73		Gas Dry
1:36	2.5	-	382.4			369.3		73		
2:06	3.0	-	381.5			368.4		73		3rd Point
Plate changed, opened at 2:09										
2:39	.5	-	370.4			350.2		73	1 1/8	
3:09	1.0	-	368.5			348.3		73		Gas Dry
3:39	1.5	-	367.2			347.0		73		
4:09	2.0	-	366.2			346.0		73		Gas Dry
4:39	2.5	-	365.2			345.0		73		
5:09	3.0	-	364.3			344.1		73		4th Point

PAGE 1 OF 1 DATA BY J. R. J.

The performance coefficient C was determined from the exponent $n=0.699$, Eq. 5, and one of the corresponding values of q_g and $\bar{p}_R^2 - p_{wf}^2$ as follows.

$$\begin{aligned}
 20,000 &= C(168)^{0.699} \\
 C &= 20,000/(168)^{0.699} \\
 \log C &= \log 20,000 - 0.699 \log 168 \\
 \log C &= 4.3010 - 1.5555 \\
 C &= 557.
 \end{aligned}$$

The value of 557 may be checked by extrapolating the straight line on Fig. 33.3 to $\bar{p}_R^2 - p_{wf}^2 = 1$ and reading the corresponding value of q_g . Note that the value of $C=557$ is for q_g in units of 10^3 cu ft/D and for $\bar{p}_R^2 - p_{wf}^2$ in units of thousands.

The backpressure equation for the results of the multipoint test on Well A given in Table 33.4 and illustrated in Fig. 33.3 is

$$q_g = 557(\bar{p}_R^2 - p_{wf}^2)^{0.699}.$$

The wellhead performance of Well A as determined by the test results given in Table 33.4 is illustrated in Fig.

33.4 where q_g and corresponding $p_{ts}^2 - p_{tf}^2$ values are plotted on logarithmic coordinates. The straight line has been extended to show a wellhead OFP of $22,000 \times 10^3$ cu ft/D. The exponent is 0.672 and C is 627. The backpressure relationship corresponding to Eq. 6 is

$$q_g = 627(p_{ts}^2 - p_{tf}^2)^{0.672}.$$

This wellhead performance equation for Well A, illustrated in Fig. 33.4, is a measure of the ability of Well A to deliver gas at the wellhead through 5½-in. casing as indicated by the multipoint test given in Table 33.4. The relationship is influenced by the size of the flow string and hydrostatic head of the gas column as well as the productive capacity of the well.

An example of the bottomhole performance as indicated by a multipoint test is given in Fig. 33.2 for an extremely large-capacity well. Well B (Fig. 33.4) had a shut-in pressure \bar{p}_R of 5,169 psia at a depth of 10,658 ft and a wellhead pressure of 4,173 psia. The calculated OFP was $280,000 \times 10^3$ cu ft/D. The corresponding wellhead performance for Well B producing through 2½-in.-OD, 6.5-lbm/ft tubing is illustrated in Fig. 33.5 where the data points for the test are plotted as circles.

TABLE 33.4—RESULTS OF MULTIPOINT BACKPRESSURE TEST (WELL A)

COMPANY _____ LEASE _____ WELL NO. A
 ADDRESS _____ DATE 6-17 1947
 DISTRICT _____ FIELD Hugoton RESERVOIR Hugoton
 LOCATION Texas County, Oklahoma
 CASING SIZE 5 1/2" WT. 14# I.D. 5.012 SET AT 2630 PERF. 2465-2620
 TUBING SIZE _____ WT. _____ I.D. _____ SET AT _____ PERF. _____
 PRODUCING SECTION FROM 2465 TO 2620 H. 2542 BOTTOMHOLE TEMPERATURE 90 @ 2540
 ELEVATION _____ DATE OF COMPLETION _____ PRODUCING THROUGH TBG. _____ CASING x
 F_r 0.0016105 BAROMETER 13.2 psi ACRES _____
 REMARKS: _____

FLOW DATA					TUBING DATA		CASING DATA		Duration of Flow Hr.
NO.	Prover Line Size	Choke X Orifice Size	Press. psig	Diff. h _w	Temp. F	Press. psig	Temp. F	Press. psig	
1	2"	3/4	406.1	-	70	-	-	435.3	66
2		7/8	388.9	-	72	-	-	410.5	70
3		1	368.4	-	73	-	-	397.3	72
4		1 1/8	344.1	-	73	-	-	381.5	73
5								364.3	73

NO.	Coefficient (24-Hour)	$\sqrt{h_w P_r}$	Pressure p _i	Flow Temp. Factor F _t	Gravity Factor F _g	Compress. Factor F _{pv}	Rate of Flow q _g , 10 ³ cu ft/D
1	9.694		419.3	0.9905	1.179	1.038	4928
2	13.33		402.1	0.9887	1.179	1.037	6479
3	17.53		381.6	0.9877	1.179	1.035	8062
4	22.45		357.3	0.9877	1.179	1.032	9640
5							

NO.	P _i	Temp. R	T _r
1	0.65	530	1.46
2	.62	532	1.46
3	.59	533	1.46
4	.55	533	1.46
5			

Gas Liquid Hydrocarbon Ratio _____ Mcf/bbl.
 Gravity of Liquid Hydrocarbons _____ deg.
 Specific Gravity Separator Gas _____
 Specific Gravity Flowing Fluid 0.719
 Critical Pressure 668 - 21 = 647 psia.
 Critical Temperature 398 - 34 = 364 R.
 H₂S _____ % CO₂ 0.1 % N₂ 12.0 %

P_r 448.5 psia P_r² 201.15 × 10³ P_r 480.5 P_r² 230.92 × 10³

NO.	P _{wf}	p _i ²	Δp ²	P _{wf}	P _{wf} ²	Δp ²
1	423.7	179.52	21.63	456.3	208.23	22.69
2	410.5	168.51	32.64	444.0	197.15	33.77
3	394.7	155.79	45.36	429.7	184.64	46.28
4	377.5	142.51	58.64	414.9	172.15	58.77
5						

Potential 25,000 10³ cu ft/D
 n 0.699
 Commission _____
 Company _____
 Others _____

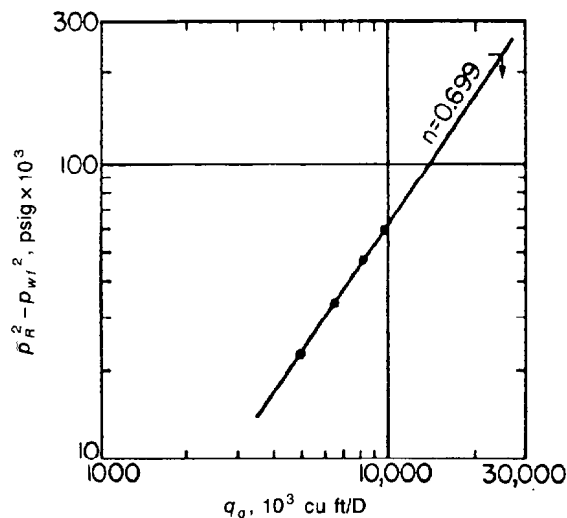


Fig. 33.3—Multipoint test showing bottomhole performance for Well A.

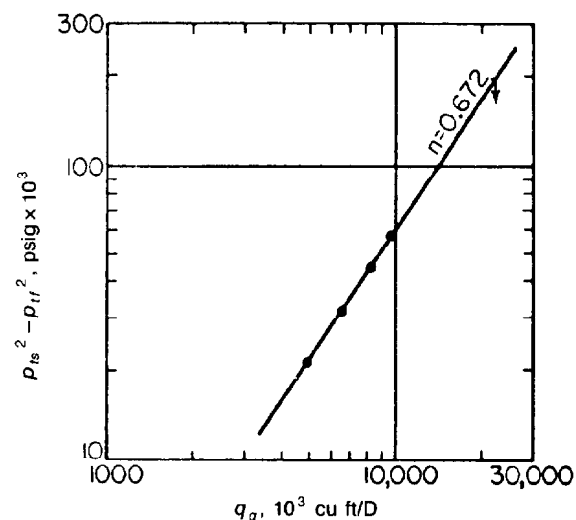


Fig. 33.4—Multipoint test showing wellhead performance for Well A.

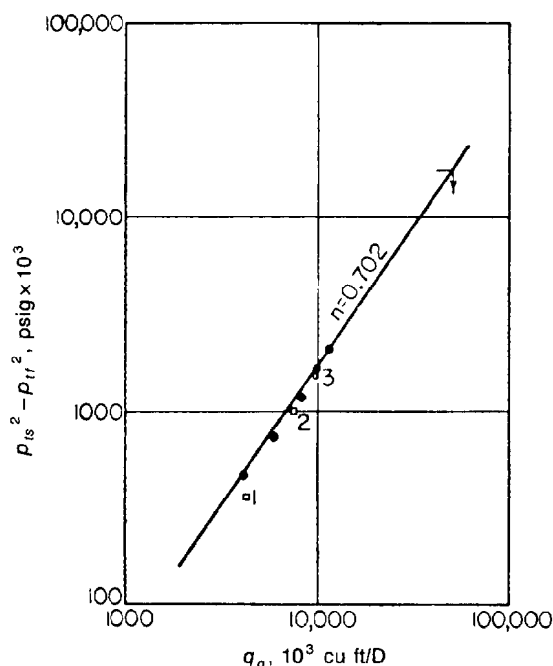


Fig. 33.5—Multipoint test showing wellhead performance for Well B.

Data points represented as squares (Fig. 33.5) are flow tests of several days' duration with Point 1 taken shortly after production started and Point 3 taken over a year later. The position of the data points in Fig. 33.5 indicated that the performance of Well B improved after the well was placed on production, which was probably caused by the removal of drilling fluids from the area around the wellbore.

The wellhead OFP of Well B was $41,000 \times 10^3$ cu ft/D, which was the approximate capacity of the tubing. A different wellhead performance curve would result if the tubing were changed in Well B. The wellhead performance for a different string of tubing can be calculated by starting with the bottomhole performance curve in Fig. 33.2 and calculating the pressure drop caused by friction for the different string of tubing.

Isochronal Test and Example

The isochronal method of backpressure testing as defined by Cullender⁴ considers the performance coefficient C in Eqs. 5 and 6 to be a variable with respect to time until the well stabilizes but a constant with respect to a specific time. Thus the backpressure performance of a well producing from a reservoir with low permeability is a series of parallel curves. Each curve represents the performance of the well at the end of a given time interval. Isochronal performance curves for wells producing from reservoirs with relatively higher permeability are closely spaced. For example, the isochronal curves for various times for Well B (Fig. 33.5) are for all practical purposes one curve, and Well B is said to stabilize rapidly.

The isochronal method of testing permits the determination of the true exponent n of the performance curve for a given gas well. This is accomplished by the

establishment of a simple pressure gradient around a producing well during the test period, which prevents the variation of the performance coefficient with time from obscuring the true value of the exponent. The determination of the relationship between performance coefficient and time permits the estimation of the rate of flow of a given well into a pipeline over long periods of time.

The term "isochronal" was adopted as being descriptive of the method, because only those conditions existing as a result of a single disturbance of constant duration are considered as being related to each other by Eqs. 5 and 6. The expression "single disturbance of constant duration" is defined as those conditions existing around a well as a result of a constant flow rate for a specific period of time from shut-in conditions. Under actual test conditions this requirement is rarely satisfied. However, this condition may be approximated by starting a well on production and allowing the well to produce without further outside or mechanical adjustments in rate of flow. Thus a simple pressure gradient is established around the wellbore as opposed to a complex pressure gradient resulting from a multipoint backpressure test.

The presentation of isochronal test data as a series of parallel curves with a constant exponent n and a constant performance coefficient C for a specific time interval involves certain assumptions. The exponent of the performance curves for a gas well is assumed independent of the drainage area. It is established immediately after the well is opened. The variations of the performance coefficient with respect to time are believed to be independent of the rate of flow and the pressure level under simple gradient conditions.

The procedure employed to obtain the necessary performance data for an isochronal test is to open a well from shut-in conditions and obtain rate-of-flow and pressure data at specific time intervals during the flow period without disturbing the rate of flow. After sufficient data have been obtained, the well is shut in and allowed to return to a shut-in condition comparable with that existing at the time the well was first opened. The well is again opened at a different rate of flow with data being obtained at the same time intervals as before. The procedure may be repeated as many times as necessary to obtain the desired number of data points.

With the exception of starting each rate of flow from shut-in conditions, the procedure for running isochronal tests is the same as that for the multipoint test. The necessity for cleaning the well, calibrating the gas-measuring equipment, and accurately measuring pressures and temperatures remains the same. At least four rates of flow should be taken; the lowest rate should reduce the pressure at the wellhead about 5% and the highest rate of flow should reduce the pressure about 25%.

The results of an isochronal test are computed in the same manner as those for a multipoint test. The data points are plotted on logarithmic coordinates as illustrated in Figs. 33.6 and 33.7. The isochronal curves are drawn so that the points taken at a constant time for the various rates of flow are joined by a straight line. For example, all the points on the line labeled "Time, 3 hr" in Fig. 33.6 represent the performance of Well A after flowing at the various rates of flow for 3 hours from shut-in conditions.

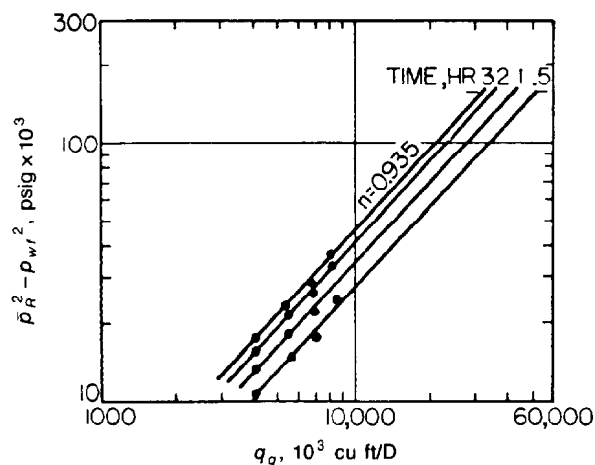


Fig. 33.6—Isochronal test showing bottomhole performance for Well A.

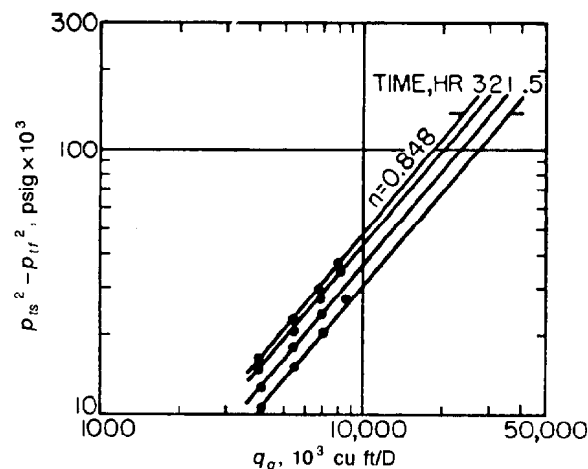


Fig. 33.7—Isochronal test showing wellhead performance for Well A.

The results of isochronal tests can be analyzed in two ways. One way is to use Eqs. 7 and 8 and the properties of the gas to determine the properties of the reservoir and the skin factor. The second way is to use the results as a basis for comparison of well performance at the time of the test with performance as measured previously or to set a base against which future performance is to be compared.

The isochronal type curves shown on Fig. 33.6 can be used to estimate the pressures that would have been observed if the test had been a constant-rate drawdown test. Test periods longer than the 3-hour periods on Fig. 33.6 are much more desirable for this purpose. With this information the $k_g h$ value for the reservoir and the total skin value ($s_t = s + F_{nD} q_g$) are calculated as given in Chap. 35. This results in several values for the total skin, s_t , as a function of the rate of flow, q_g , from which s and F_{nD} can be obtained for use in Eq. 7.⁶ The multipoint test can be analyzed to obtain $k_g h$, s , and F_{nD} as indicated by Ref. 7. A discussion of the performance-comparison method follows.

A copy of actual field data for an isochronal test is given in Table 33.5 for Well A, which is the same well used in the example of a multipoint test.* Four rates of flow of 3 hours' duration were used with each flow starting from shut-in conditions. Shut-in pressures reported varied from 359.6 psig after 48 hours for the first rate of flow to 357.6 psig, which was just previous to the fourth rate of flow. The results of the isochronal test are summarized in Table 33.6. Bottomhole and wellhead performance curves are illustrated on Figs. 33.6 and 33.7, respectively.

The isochronal test on Well A (Fig. 33.6) shows that the calculated OFP for a BHP of 399.1 psia was 51,500, 41,500, 35,000, and 31,500 $\times 10^3$ cu ft/D at the end of 0.5, 1.0, 2.0, and 3.0 hours, respectively. The calculated potential after 3 hours' flow was only 61% of the potential after 0.5 hour of flow. A similar figure for the wellhead performance of Well A is 66% (Fig. 33.7). If Well A were opened into a pipeline with a constant

pressure, the rate of flow at the end of 3 hours would be 66% of the rate of flow at 0.5 hour. Experimental data not given here show that the production at the end of 72 hours has decreased to about 48% of that at 0.5 hour. The figures showing change-of-performance characteristics with time illustrate the need for isochronal test data for estimating the delivery from a particular well into a pipeline. Accurate estimation of pipeline deliveries from wells producing from reservoirs with low permeability is practically impossible without isochronal test data.

Examination of the field notes under the "Remarks" column in Table 33.5 indicates that Well A started to produce water during the flow test taken on Dec. 20, 1951, which was the largest rate of flow. The effect of water production on well performance is illustrated by the irregularities in the corresponding data in Figs. 33.6 and 33.7. Water production and accumulation of water or liquids in the wellbore cause the performance characteristics of a well to deteriorate.

The data represented as squares in Fig. 33.5 are isochronal points taken after Well B has been flowing from 5 to 30 days. Their close agreement with the data from the multipoint test indicates that the performance of Well B does not vary appreciably with time. Well B produces from a reservoir with high permeability and the radius of drainage is established quickly after the well is opened to flow.

Comparison of Multipoint With Isochronal Test

Either the multipoint or the isochronal test is suitable for wells producing from reservoirs with high permeability. The isochronal method of testing is especially suitable for testing wells in low-permeability reservoirs. However, for wells producing from extremely low-permeability reservoirs where the unsteady-state effects last for days or even weeks, economic considerations may limit the testing to only one point of the isochronal type (starting flow from a shut-in condition). Multipoint tests should be limited to reservoirs where the unsteady-state effects are of very short duration. Otherwise the results of the multipoint test are difficult to analyze.

*This test, used in the 1962 edition, was run many years ago. It still stands as a classic isochronal test example today.

TABLE 33.5—FIELD DATA SHEET FOR ISOCHRONAL TEST (WELL A)

DATE		WELLHEAD WORKING PRESSURE				METER OR PROVER				REMARKS
Time	Hrs.	Tbg. Psig	Csg. Psig	Annulus Psig	Temp. F	Psig	Diff.	Temp. F	Orifice	
Well shut in for 48 hours										
12-17-51										
12:20 p	0	-	359.6	-	-	-	-	-	-	SIP
12:50	.5	-	345.1	-	-	341.4	-	67	3/4	Gas Dry
1:20	1.0	-	342.0	-	-	338.4	-	68	-	Gas Dry
1:50	1.5	-	340.2	-	-	336.6	-	68	-	Gas Dry
2:20	2.0	-	338.8	-	-	335.2	-	69	-	Gas Dry
2:50	2.5	-	337.7	-	-	334.2	-	70	-	Gas Dry
3:20	3.0	-	336.7	-	-	333.2	-	70	-	Gas Dry
12-18-51										
12:05 p	0	-	358.8	-	-	-	-	-	-	SIP
12:35	.5	-	337.8	-	-	331.4	-	67	7/8	Gas Damp
1:05	1.0	-	333.8	-	-	327.6	-	68	-	Gas Damp
1:35	1.5	-	331.5	-	-	325.0	-	70	-	Gas Damp
2:05	2.0	-	329.6	-	-	323.5	-	70	-	Gas Damp
2:35	2.5	-	328.3	-	-	322.3	-	70	-	Gas Damp
3:05	3.0	-	327.1	-	-	321.1	-	70	-	Gas Damp
12-19-51										
11:59 a	0	-	358.8	-	-	-	-	-	-	SIP
12:29 p	.5	-	330.0	-	-	318.7	-	68	1	Gas Damp
12:59	1.0	-	324.8	-	-	313.8	-	69	-	Gas Damp
1:29	1.5	-	321.6	-	-	310.8	-	70	-	Gas Damp
1:59	2.0	-	319.4	-	-	308.7	-	71	-	Gas Damp
2:29	2.5	-	317.7	-	-	307.1	-	72	-	Gas Damp
2:59	3.0	-	316.3	-	-	305.7	-	72	-	Gas Damp
12-20-51										
8:22 a	0	-	357.6	-	-	-	-	-	1 1/8	SIP
8:52	.5	-	317.8	-	-	301.3	-	67	-	Gas Wet
9:22	1.0	-	312.6	-	-	-	-	69	-	Connection frozen
9:52	1.5	-	309.2	-	-	292.4	-	70	-	Gas Wet
10:22	2.0	-	306.6	-	-	289.6	-	70	-	Gas Wet
10:52	2.5	-	304.6	-	-	287.7	-	71	-	Gas Wet
11:22	3.0	-	302.8	-	-	286.0	-	71	-	Gas Wet

PAGE 1 OF 1 DATA BY J. R. J.

TABLE 33.6—RESULTS OF ISOCHRONAL TEST ON WELL A

Date	p_{is} (psia)	Flow Duration (hr)	q_g (Mcf/D)	$\bar{p}_R^2 - p_{wf}^2$	$p_{is}^2 - p_{if}^2$
Dec. 17, 1951	372.8	0.5	4,159	10.60	10.60
		1.0	4,120	13.19	12.82
		2.0	4,078	15.79	15.08
		3.0	4,047	17.63	16.55
Dec. 18, 1951	372.0	0.5	5,552	14.85	15.18
		1.0	5,485	18.10	17.97
		2.0	5,461	21.58	20.87
		3.0	5,423	23.56	22.58
Dec. 19, 1951	372.0	0.5	7,019	17.93	20.59
		1.0	6,982	22.17	24.14
		2.0	6,847	26.48	27.76
		3.0	6,777	28.88	29.81
Dec. 20, 1951	370.8	0.5	8,599	24.96	27.93
		1.0	-	-	-
		2.0	8,153	34.10	35.22
		3.0	8,048	37.00	37.63

The results of the 3-hour multipoint test and the 3-hour isochronal test on Well A are shown together in Fig. 33.8 as wellhead performance curves. The exponent (0.672) for the multipoint test is less than the exponent (0.848) of the isochronal test. In general, exponents of multipoint curves run in increasing rate sequence are less than those for isochronal curves for the same well. The first data point on the multipoint test ($q_k = 4,928$ Mcf/D) is on the isochronal curve (Fig. 33.8) because the first rate of flow for the multipoint curve was started from shut-in conditions. Thereafter, the position of each succeeding point of the multipoint test is influenced not only by the rate of flow but also by each preceding point.

The initial points of each multipoint test on wells producing from reservoirs with low permeability represent the formation characteristics, while other points represent complex conditions that are almost impossible to interpret. The characteristic exponent of the isochronal curve still applies to the complex points, with the only difference in performance being in the performance coefficient C . If the exponent of 0.848 is applied to the complex points of the multipoint test (Fig. 33.8), it can be

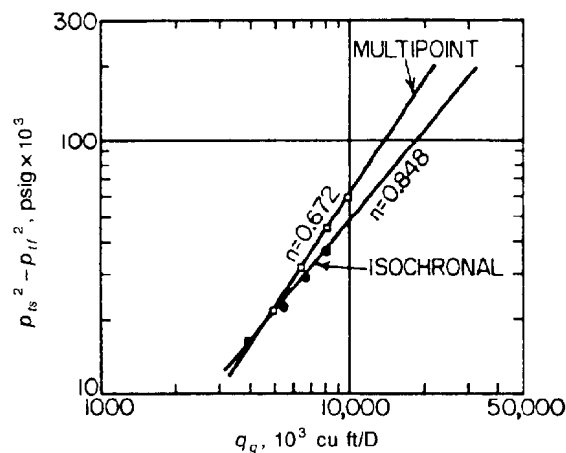


Fig. 33.8—Comparison of multipoint with isochronal test for Well A.

seen that the coefficient obtained in each case can be considered the result of an "effective" time, which has no permanent significance because it is not equal to the elapsed time or to the elapsed time since the last change in flow rate.

An examination of the multipoint and isochronal data presented in Fig. 33.5 for Well B shows that there are certain gas wells that stabilize so rapidly that there is no necessity for obtaining isochronal performance data. As the time required for stabilization increases, the differences between data obtained by the isochronal test and the multipoint test increase.

Gas Measurement

Orifice Meters

The recommended specifications for orifice meters and methods for computing rates of flow are those published by the American Gas Assn.⁹ It should be noted that the basic orifice factors are for a pressure base of 14.73 psia. Multiplying the basic orifice factors in Ref. 9 by 1.0055 changes volumes to a pressure base of 14.65 psia. Basic orifice factors for a pressure base of 14.65 psia have been published in the test manual of the Corporation Commission of the State of Kansas¹⁰ and the Interstate Oil Compact Commission.¹¹

Critical-Flow Provers

The following method for measurement and computation of rates of flow for critical-flow provers is a modification of the method published by Rawlins and Schellhardt.² The equation computing rates of flow from measurements with a critical-flow prover is

$$q_g = p_s F_p F_g F_T F_{pv}, \quad (10)$$

where p_s is static pressure on critical-flow prover, psia. Basic orifice factors, F_p , for 2- and 4-in. critical-flow provers are given in Table 33.7. These factors apply only to plates designed according to USBM specifications.

The adjustment factor (Table 33.8) to correct for an assumed specific gravity of 1.000 to the actual specific gravity of the gas flowing through the prover may be computed by

TABLE 33.7—BASIC ORIFICE FACTORS FOR CRITICAL-FLOW PROVER (USBM plate design) F_p —Mcf/D

Base temperature, °F		60	
Base pressure, psia		14.65	
Flowing temperature, °F		60	
Specific gravity		1.000	
2-in. Prover		4-in. Prover	
Orifice Diameter (in.)	Factor (F_p)	Orifice Diameter (in.)	Factor (F_p)
1/16	0.06569	1/4	1.074
3/32	0.1446	3/8	2.414
1/8	0.2716	1/2	4.319
3/16	0.6237	5/8	6.729
7/32	0.8608	3/4	9.643
1/4	1.115	7/8	13.11
5/16	1.714	1	17.08
3/8	2.439	1 1/8	21.52
7/16	3.495	1 1/4	26.57
1/2	4.388	1 3/8	31.99
5/8	6.638	1 1/2	38.12
3/4	9.694	1 3/4	52.07
7/8	13.33	2	68.80
1	17.53	2 1/4	88.19
1 1/8	22.45	2 1/2	110.6
1 1/4	28.34	2 3/4	136.9
1 3/8	34.82	3	168.3
1 1/2	43.19		

$$F_g = \sqrt{\frac{1}{\gamma_g}}, \quad (11)$$

where γ_g is specific gravity of the flowing gas, air = 1.000.

Factors to correct for an assumed flowing temperature of 60°F to the actual flowing temperature of the gas at the point of measurement are given in Table 33.9 and may be computed by

$$F_T = \sqrt{\frac{520}{T_f}}, \quad (12)$$

where T_f is actual flowing temperature of the gas, (°F+460).

The supercompressibility factor to correct for the effect of gas compressibility is computed from the compressibility by

$$F_{pv} = \sqrt{\frac{1}{z}}, \quad (13)$$

where z is compressibility of the gas at p_s and T_f or the pressure and temperature at point of measurement.

Methods for estimating gas compressibilities are given in Chap. 20.

Calculation of Subsurface Pressures

Specific Gravity of Flowing Fluid

Calculation of either shut-in or flowing pressures in gas wells requires a knowledge of the specific gravity of the fluid in the wellbore. In the case of a gas-condensate well, the specific gravity of the separator gas and the gravity of the stock-tank liquid are measured, and it is

TABLE 33.8—SPECIFIC-GRAVITY ADJUSTMENT FACTOR

$$F_g = \sqrt{\frac{1}{\gamma_g}}$$

Specific Gravity	0.000	0.001	0.002	0.003	0.004	0.005	0.006	0.007	0.008	0.009
0.550	1.348	1.347	1.346	1.345	1.344	1.342	1.341	1.340	1.339	1.338
0.560	1.336	1.335	1.334	1.333	1.332	1.330	1.329	1.328	1.327	1.326
0.570	1.325	1.323	1.322	1.321	1.320	1.319	1.318	1.316	1.315	1.314
0.580	1.313	1.312	1.311	1.310	1.309	1.307	1.306	1.305	1.304	1.303
0.590	1.302	1.301	1.300	1.299	1.298	1.296	1.295	1.294	1.293	1.292
0.600	1.291	1.290	1.289	1.288	1.287	1.286	1.285	1.284	1.282	1.281
0.610	1.280	1.279	1.278	1.277	1.276	1.275	1.274	1.273	1.272	1.271
0.620	1.270	1.269	1.268	1.267	1.266	1.265	1.264	1.263	1.262	1.261
0.630	1.260	1.259	1.258	1.257	1.256	1.255	1.254	1.253	1.252	1.251
0.640	1.250	1.249	1.248	1.247	1.246	1.245	1.244	1.243	1.242	1.241
0.650	1.240	1.239	1.238	1.237	1.237	1.236	1.235	1.234	1.233	1.232
0.660	1.231	1.230	1.229	1.228	1.227	1.226	1.225	1.224	1.224	1.223
0.670	1.222	1.221	1.220	1.219	1.218	1.217	1.216	1.215	1.214	1.214
0.680	1.213	1.212	1.211	1.210	1.209	1.208	1.207	1.206	1.206	1.205
0.690	1.204	1.203	1.202	1.201	1.200	1.200	1.199	1.198	1.197	1.196
0.700	1.195	1.194	1.194	1.193	1.192	1.191	1.190	1.189	1.188	1.188
0.710	1.187	1.186	1.185	1.184	1.183	1.183	1.182	1.181	1.180	1.179
0.720	1.179	1.178	1.177	1.176	1.175	1.174	1.174	1.173	1.172	1.171
0.730	1.170	1.170	1.169	1.168	1.167	1.166	1.166	1.165	1.164	1.163
0.740	1.162	1.162	1.161	1.160	1.159	1.159	1.158	1.157	1.156	1.155
0.750	1.155	1.154	1.153	1.152	1.152	1.151	1.150	1.149	1.149	1.148
0.760	1.147	1.146	1.146	1.145	1.144	1.143	1.143	1.142	1.141	1.140
0.770	1.140	1.139	1.138	1.137	1.137	1.136	1.135	1.134	1.134	1.133
0.780	1.132	1.132	1.131	1.130	1.129	1.129	1.128	1.127	1.127	1.126
0.790	1.125	1.124	1.124	1.123	1.122	1.122	1.121	1.120	1.119	1.119
0.800	1.118	1.117	1.117	1.116	1.115	1.115	1.114	1.113	1.112	1.112
0.810	1.111	1.110	1.110	1.109	1.108	1.108	1.107	1.106	1.106	1.105
0.820	1.104	1.104	1.103	1.102	1.102	1.101	1.100	1.100	1.099	1.098
0.830	1.098	1.097	1.096	1.096	1.095	1.094	1.094	1.093	1.092	1.092
0.840	1.091	1.090	1.090	1.089	1.089	1.088	1.087	1.087	1.086	1.085
0.850	1.085	1.084	1.083	1.083	1.082	1.081	1.081	1.080	1.080	1.079
0.860	1.078	1.078	1.077	1.076	1.076	1.075	1.075	1.074	1.073	1.073
0.870	1.072	1.072	1.071	1.070	1.070	1.069	1.068	1.068	1.067	1.067
0.880	1.066	1.065	1.065	1.064	1.064	1.063	1.062	1.062	1.061	1.061
0.890	1.060	1.059	1.059	1.058	1.058	1.057	1.056	1.056	1.055	1.055
0.900	1.054	1.054	1.053	1.052	1.052	1.051	1.051	1.050	1.049	1.049
0.910	1.048	1.048	1.047	1.047	1.046	1.045	1.045	1.044	1.044	1.043
0.920	1.043	1.042	1.041	1.041	1.040	1.040	1.039	1.039	1.038	1.038
0.930	1.037	1.036	1.036	1.035	1.035	1.034	1.034	1.033	1.033	1.032
0.940	1.031	1.031	1.030	1.030	1.029	1.029	1.028	1.028	1.027	1.027
0.950	1.026	1.025	1.025	1.024	1.024	1.023	1.023	1.022	1.022	1.021
0.960	1.021	1.020	1.020	1.019	1.019	1.018	1.017	1.017	1.016	1.016
0.970	1.015	1.015	1.014	1.014	1.013	1.013	1.012	1.012	1.011	1.011
0.980	1.010	1.010	1.009	1.009	1.008	1.008	1.007	1.007	1.006	1.006
0.990	1.005	1.005	1.004	1.004	1.003	1.003	1.002	1.002	1.001	1.001

usually necessary to compute the specific gravity of the fluid flowing in the wellbore. The shrinkage of the liquid between the separator and the stock tank is usually unknown and apparently can be neglected. The equation for computing the specific gravity of the flowing fluid, γ_{ff} , is:

$$\gamma_{ff} = \frac{R_{gL}\gamma_g + 4603 \gamma_L}{R_{gL} + V_L}, \dots\dots\dots (14a)$$

where

R_{gL} = gas to hydrocarbon liquid ratio, cu ft/bbl,

γ_L = specific gravity of hydrocarbon liquid referred to water, and

V_L = vapor volume equivalent of 1 bbl (60°F) of hydrocarbon liquid, cu ft/bbl.

The specific gravity and the approximate vapor volume of the hydrocarbon liquid can be calculated from the API gravity by

$$\gamma_L = \frac{141.5}{131.5 + \gamma_{API}} \dots\dots\dots (14b)$$

and

TABLE 33.9—FLOWING-TEMPERATURE ADJUSTMENT FACTOR

$$F_T = \sqrt{\frac{520}{T_f}}$$

Observed Temperature (°F)	0	1	2	3	4	5	6	7	8	9
0	1.063	1.062	1.061	1.060	1.059	1.057	1.056	1.055	1.054	1.053
10	1.052	1.051	1.050	1.049	1.047	1.046	1.045	1.044	1.043	1.042
20	1.041	1.040	1.039	1.038	1.037	1.035	1.034	1.033	1.032	1.031
30	1.030	1.029	1.028	1.027	1.026	1.025	1.024	1.023	1.022	1.021
40	1.020	1.019	1.018	1.017	1.016	1.015	1.014	1.013	1.012	1.011
50	1.010	1.009	1.008	1.007	1.006	1.005	1.004	1.003	1.002	1.001
60	1.000	0.9990	0.9981	0.9971	0.9962	0.9952	0.9943	0.9933	0.9924	0.9915
70	0.9905	0.9896	0.9887	0.9877	0.9868	0.9859	0.9850	0.9840	0.9831	0.9822
80	0.9813	0.9804	0.9795	0.9786	0.9777	0.9768	0.9759	0.9750	0.9741	0.9732
90	0.9723	0.9715	0.9706	0.9697	0.9688	0.9680	0.9671	0.9662	0.9653	0.9645
100	0.9636	0.9628	0.9619	0.9610	0.9602	0.9594	0.9585	0.9577	0.9568	0.9560
110	0.9551	0.9543	0.9535	0.9526	0.9518	0.9510	0.9501	0.9493	0.9485	0.9477
120	0.9469	0.9460	0.9452	0.9444	0.9436	0.9428	0.9420	0.9412	0.9404	0.9396
130	0.9388	0.9380	0.9372	0.9364	0.9356	0.9349	0.9341	0.9333	0.9325	0.9317
140	0.9309	0.9302	0.9294	0.9286	0.9279	0.9271	0.9263	0.9256	0.9248	0.9240
150	0.9233	0.9225	0.9217	0.9210	0.9202	0.9195	0.9187	0.9180	0.9173	0.9165
160	0.9158	0.9150	0.9143	0.9135	0.9128	0.9121	0.9112	0.9106	0.9099	0.9092
170	0.9085	0.9077	0.9069	0.9063	0.9055	0.9048	0.9042	0.9035	0.9028	0.9020
180	0.9014	0.9007	0.9000	0.8992	0.8985	0.8979	0.8972	0.8965	0.8958	0.8951
190	0.8944	0.8937	0.8931	0.8923	0.8916	0.8910	0.8903	0.8896	0.8889	0.8882
200	0.8876	0.8870	0.8863	0.8856	0.8849	0.8843	0.8836	0.8830	0.8823	0.8816
210	0.8810	0.8803	0.8797	0.8790	0.8784	0.8777	0.8770	0.8764	0.8758	0.8751
220	0.8745	0.8738	0.8732	0.8725	0.8719	0.8713	0.8706	0.8700	0.8694	0.8687
230	0.8681	0.8675	0.8668	0.8662	0.8656	0.8650	0.8644	0.8637	0.8631	0.8625
240	0.8619	0.8613	0.8606	0.8600	0.8594	0.8588	0.8582	0.8576	0.8570	0.8564

$$V_L = 369 + 5\gamma_{API} + 0.04(\gamma_{API})^2, \dots (14c)$$

where γ_{API} is stock-tank oil gravity, °API. The derivations of Eqs. 14a and 14c were given by Smith.¹²

Equations for Computing Subsurface Pressures

Pressures at the sandface or at the inlet to the tubing in shut-in or flowing gas wells may be measured with BHP gauges or computed from wellhead pressures. However, most subsurface pressures in gas wells are calculated by equations. The most usable and realistic equations available are those of Cullender and Smith,¹³ which have been adopted by the Kansas Corp. Commission, the Interstate Oil Compact Commission, and the New Mexico Conservation Commission, and by the Railroad Commission of Texas for certain fields. The equations were revised¹² recently for use with programmable calculators and small computers.

The revised flow equation for gas wells is

$$\frac{1,000 \gamma_g L}{53.356} = \int_{p_2}^{p_1} \frac{\left(\frac{p}{T_z} - 2.082 \frac{\gamma_g q_g^2}{d_i^4 p} \right) dp}{F^2 + \frac{H}{L} \frac{(p/T_z)^2}{1,000}}, \dots (15)$$

where

L = length of flowstring in well corresponding to H , ft,

H = vertical depth in well, ft, and

q_g = rate of gas flow at 14.65 psia and 60°F, 10^6 scf/D.

$$F^2 = \frac{2.6665 f q_g^2}{d_i^5} = (F_r q_g)^2 \dots (16a)$$

and

$$\sqrt{\frac{1}{f}} = \frac{4 \log 7.4 r_i}{K}, \dots (16b)$$

where

f = coefficient of friction (friction factor),

r_i = internal radius of pipe, in.,

K = absolute roughness characteristic = 0.0006 in., and

r/K = relative roughness.

Refer to Ref. 12 for the background of Eqs. 15, 16a, and 16b. The second term in the numerator on the right side of Eq. 15 is the kinetic energy term that heretofore has been set at zero because the computations were made manually. Although the kinetic energy term can be neglected without appreciable error in the majority of cases, there is no need to do so when programmable

TABLE 33.10— F_r VALUES FOR VARIOUS FLOW STRING ($K = 0.0006$ in.)

Nominal Size (in.)	d_o (in.)	(lbm/ft)	d_i (in.)	Minimum N_{Re}	F_r	Nominal Size (in.)	d_o (in.)	(lbm/ft)	d_i (in.)	Minimum N_{Re}	F_r
Tubing											
1	1.315	1.80	1.049	139,000	0.09505						
1¼	1.660	2.40	1.380	189,000	0.04643						
1½	1.990	2.75	1.610	224,000	0.03105						
2	2.375	4.70	1.995	284,000	0.01776						
2½	2.875	6.50	2.441	355,000	0.01050						
3	3.500	9.30	2.992	445,000	0.006180						
3½	4.000	11.00	3.476	525,000	0.004184						
4	4.500	12.70	3.958	605,000	0.002985						
4½	4.750	16.25	4.082	626,000	0.002755						
	4.750	18.00	4.000	612,000	0.002905						
4¾	5.000	18.00	4.276	659,000	0.002442						
	5.000	21.00	4.154	638,000	0.002633						
Casing						Casing					
	5.000	13.00	4.494	696,000	0.002146		7.625	45.00	6.445	1,033,000	0.0008417
	5.000	15.00	4.408	681,000	0.002257		8.000	26.00	7.386	1,199,000	0.0005911
5¾	5.500	14.00	5.012	784,000	0.001617	7½	8.125	28.00	7.485	1,216,000	0.0005710
							8.125	32.00	7.385	1,199,000	0.0005913
	5.500	15.00	4.976	778,000	0.001647		8.125	35.50	7.285	1,181,000	0.0006126
	5.500	15.50	4.950	773,000	0.001670						
	5.500	17.00	4.892	764,000	0.001722		8.125	39.50	7.185	1,163,000	0.0006349
	5.500	20.00	4.778	744,000	0.001830	8¼	8.625	17.50	8.249	1,353,000	0.0004438
	5.500	23.00	4.670	726,000	0.001942		8.625	20.00	8.191	1,342,000	0.0004520
							8.625	24.00	8.097	1,326,000	0.0004658
							8.625	28.00	8.003	1,309,000	0.0004801
5½	5.500	25.00	4.580	710,000	0.002043						
	6.000	15.00	5.524	872,000	0.001256		8.625	32.00	7.907	1,292,000	0.0004953
	6.000	17.00	5.450	860,000	0.001301		8.625	36.00	7.825	1,277,000	0.0005089
	6.000	20.00	5.352	843,000	0.001363		8.625	38.00	7.775	1,268,000	0.0005174
	6.000	23.00	5.240	823,000	0.001440		8.625	43.00	7.651	1,246,000	0.0005394
6¼	6.000	26.00	5.140	806,000	0.001514						
	6.625	20.00	6.049	964,000	0.0009922	8½	9.000	34.00	8.290	1,360,000	0.0004382
	6.625	22.00	5.989	953,000	0.001018		9.000	38.00	8.196	1,343,000	0.0004513
	6.625	24.00	5.921	941,000	0.001049		9.000	40.00	8.150	1,335,000	0.0004579
	6.625	26.00	5.855	930,000	0.001080		9.000	45.00	8.032	1,314,000	0.0004756
	6.625	28.00	5.791	919,000	0.001111	9	9.625	36.00	8.921	1,473,000	0.0003623
	6.625	31.80	5.675	899,000	0.001171		9.625	40.00	8.835	1,458,000	0.0003715
	6.625	34.00	5.595	885,000	0.001215		9.625	43.50	8.755	1,444,000	0.0003804
6½	7.000	20.00	6.456	1,035,000	0.0008380		9.625	47.00	8.681	1,430,000	0.0003888
	7.000	22.00	6.398	1,025,000	0.0008579		9.625	53.50	8.535	1,404,000	0.0004063
	7.000	23.00	6.366	1,019,000	0.0008691		9.625	58.00	8.435	1,386,000	0.0004189
	7.000	24.00	6.336	1,014,000	0.0008798						
	7.000	26.00	6.276	1,003,000	0.0009018	9¾	10.000	33.00	9.384	1,557,000	0.0003178
	7.000	28.00	6.214	992,000	0.0009253		10.000	55.50	8.908	1,471,000	0.0003637
	7.000	30.00	6.154	982,000	0.0009489		10.000	61.20	8.790	1,450,000	0.0003764
7¼	7.000	40.00	5.836	926,000	0.001089	10	10.750	32.75	10.192	1,704,000	0.0002566
	7.626	26.40	6.969	1,125,000	0.0006872		10.750	35.75	10.136	1,694,000	0.0002602
	7.625	29.70	6.875	1,108,000	0.0007119		10.750	40.00	10.050	1,678,000	0.0002660
	7.625	33.70	6.765	1,089,000	0.0007423		10.750	45.50	9.950	1,660,000	0.0002730
	7.625	38.70	6.625	1,064,000	0.0007837		10.750	48.00	9.902	1,651,000	0.0002765
							10.750	54.00	9.784	1,630,000	0.0002852

calculators or computers are used. Eq. 15 is based on the assumptions that the flow is completely turbulent, the coefficient of friction, f , is a constant, the compressibility of the gas at base pressure and temperature conditions (14.65 psia and 60°F) is 1.000, and only a gas phase is flowing.

Eq. 15 has a subtle but important concept in the value of the quantity H/L at the wellhead, where both H and L are zero. For a vertical wellbore, $H = L$ and

$$\frac{H}{L} = \lim_{H \rightarrow 0} \left(\frac{H}{L} \right) = 1.000.$$

In a deviated wellbore, H is less than L , and for a horizontal pipeline, $H = 0$, and as a result the term for the head of gas drops out of Eq. 15. For a complete guide to the algebraic convention for H and L , refer to Ref. 12.

TABLE 33.11— F_r VALUES FOR VARIOUS ANNULI ($K = 0.001$ in.)

Casing ID (in.)	Tubing OD (in.)							
	1.900	2.375	2.875	3.500	4.000	4.500	4.750	5.000
4.154	0.005082	0.006901	0.01093					
4.276	0.004576	0.006087	0.009268					
4.408	0.004107	0.005356	0.007867					
4.494	0.003838	0.004948	0.007119					
4.580	0.003593	0.004583	0.006473	0.01250				
4.670	0.003361	0.004242	0.005886	0.01086				
4.778	0.003109	0.003880	0.005281	0.009289				
4.892	0.002872	0.003544	0.004738	0.007980				
4.950	0.002761	0.003390	0.004492	0.007419				
4.976	0.002713	0.003324	0.004389	0.007187				
5.012	0.002649	0.003235	0.004251	0.006883	0.01245			
5.140	0.002438	0.002946	0.003809	0.005947	0.01012			
5.240	0.002289	0.002746	0.003509	0.005343	0.008738			
5.352	0.002137	0.002545	0.003213	0.004770	0.007506			
5.450	0.002016	0.002385	0.002983	0.004342	0.006634			
5.524	0.001931	0.002274	0.002825	0.004055	0.006074	0.01098		
5.595	0.001854	0.002175	0.002684	0.003806	0.005601	0.009783		
5.675	0.001773	0.002070	0.002538	0.003552	0.005133	0.008658		
5.791	0.001663	0.001930	0.002346	0.003226	0.004552	0.007351	0.01017	
5.836	0.001623	0.001880	0.002277	0.003111	0.004354	0.006924	0.009455	
5.855	0.001607	0.001859	0.002249	0.003065	0.004274	0.006755	0.009176	
5.921	0.001551	0.001790	0.002155	0.002911	0.004012	0.006215	0.008301	
5.989	0.001497	0.001722	0.002064	0.002764	0.003768	0.005726	0.007528	
6.049	0.001452	0.001665	0.001988	0.002643	0.003570	0.005341	0.006935	0.009582
6.154	0.001376	0.001572	0.001865	0.002450	0.003260	0.004757	0.006057	0.008132
6.214	0.001336	0.001522	0.001799	0.002349	0.003100	0.004466	0.005630	0.007451
6.276	0.001296	0.001472	0.001735	0.002251	0.002947	0.004193	0.005235	0.006837
6.336	0.001259	0.001427	0.001676	0.002161	0.002810	0.003952	0.004892	0.006313
6.366	0.001241	0.001405	0.001647	0.002119	0.002745	0.003839	0.004734	0.006074
6.398	0.001222	0.001382	0.001618	0.002074	0.002678	0.003724	0.004573	0.005835
6.445	0.001195	0.001349	0.001576	0.002012	0.002584	0.003565	0.004352	0.005508
6.456	0.001189	0.001342	0.001566	0.001998	0.002563	0.003529	0.004302	0.005436
6.625	0.001099	0.001234	0.001429	0.001796	0.002266	0.003041	0.003639	0.004486
6.765	0.001032	0.001153	0.001327	0.001651	0.002057	0.002710	0.003201	0.003879
6.875	0.0009830	0.001095	0.001255	0.001549	0.001912	0.002486	0.002910	0.003486
6.969	0.0009439	0.001049	0.001198	0.001469	0.001800	0.002316	0.002692	0.003196
7.185	0.0008619	0.0009524	0.001079	0.001306	0.001577	0.001987	0.002276	0.002655
7.285	0.0008273	0.0009120	0.001030	0.001240	0.001487	0.001857	0.002116	0.002450
7.385	0.0007946	0.0008739	0.0009839	0.001178	0.001405	0.001740	0.001972	0.002268
7.386	0.0007943	0.0008736	0.0009834	0.001177	0.001404	0.001739	0.001970	0.002266

Eq. 15 does not lend itself to mathematical integration without making assumptions regarding T and z , but it may be integrated over definite limits by the trapezoidal rule.

If we let

$$\int_{p_1}^{p_n} \frac{\left[\frac{p}{Tz} - 2.082 \frac{\gamma_g q_g^2}{d_i^4 p} \right] dp}{F^2 + \frac{H}{L} \frac{(p/Tz)^2}{1,000}} = \int_{p_1}^{p_n} Idp = \frac{1,000 \gamma_g L}{53.356}$$

$$= \frac{1}{2} [(p_2 - p_1)(I_2 + I_1) + (p_3 - p_2)(I_3 + I_2) + \dots + (p_n - p_{n-1})(I_n + I_{n-1})], \dots (17)$$

then

$$37.484 \gamma_g L = [(p_2 - p_1)(I_2 + I_1) + (p_3 - p_2)(I_3 + I_2) + \dots + (p_n - p_{n-1})(I_n + I_{n-1})], \dots (18)$$

where $I_1, I_2, I_3 \dots I_n$ is the trapezoidal rule interval corresponding to the respective pressure. If we make the assumptions that the kinetic energy term is zero or that the temperature, T , and the gas compressibility factor, z , are constant, the equations given in Chap. 30 of this handbook can be derived. However, the numerical examples that follow will make use of Eqs. 15 through 18.

The details of computations of a BHFP and a shut-in BHP by Eqs. 16a, 16b, 17, and 18 are illustrated by Example Problem 3 on Page 33-18. To utilize the equations, it is necessary to evaluate the factor F_r for various flow strings. The value may be determined by several correlations; however, the values given in Tables 33.10 and

TABLE 33.12—WORK SHEET FOR CALCULATION OF SUBSURFACE FLOWING PRESSURE BY EQS. 15, 16a, AND 16b

Company				Lease				Well No.				B				Date of Test			
γ_g	0.615	%CO ₂	2.5	%N ₂	—	p_{pc}	679	T_{pc}	361	Equations Used				15, 16a, 16b					
q_g	11.299	H	10,658	L	10,490	d_i	2.441 in.	Temperature Gradient				5°F/1,000 ft							
					10,658		1.995												
H	L	d_i	p_n	T	z	l_n	Δp	$\frac{(\Delta p) \times}{(l_n + l_{n-1})}$	$\frac{\Sigma(\Delta p) \times}{(l_n + l_{n-1})}$	$37.484 \times$					Line				
0	0	2.441	3,913.0	117	0.8776	104.719	0	—	—	0	0	0	0	0	1				
1,000	1,000	2.441	4,023.1	122	0.8894	104.346	110.1	23,018	23,018	23,053	2				2				
1,000	1,000	2.441	4,023.3	122	0.8894	104.343	110.3	23,059	23,059		3				3				
2,000	2,000	2.441	4,134.0	127	0.9012	103.992	110.7	23,063	46,121	46,105	4				4				
3,000	3,000	2.441	4,245.0	132	0.9129	103.659	111.0	23,049	69,170	69,158	5				5				
4,000	4,000	2.441	4,356.3	137	0.9244	103.337	111.3	23,039	92,209	92,211	6				6				
5,000	5,000	2.441	4,468.0	142	0.9359	103.036	111.7	23,052	115,261	115,263	7				7				
6,000	6,000	2.441	4,580.0	147	0.9472	102.743	112.0	23,047	138,308	138,316	8				8				
7,000	7,000	2.441	4,692.3	152	0.9584	102.464	112.3	23,045	161,352	161,369	9				9				
8,000	8,000	2.441	4,805.0	157	0.9695	102.196	112.7	23,065	184,417	184,421	10				10				
9,000	9,000	2.441	4,917.9	162	0.9805	101.943	112.9	23,047	207,464	207,473	11				11				
10,000	10,000	2.441	5,031.1	167	0.9913	101.693	113.2	23,052	230,516	230,526	12				12				
10,490	10,490	2.441	5,086.7	169.5	0.9966	101.583	55.6	11,302	241,818	241,822	13				13				
10,490	10,490	1.995	5,086.7	169.5	0.9966	76.546	0	—	241,818	241,822	14				14				
10,658	10,658	1.995	5,112.0	170.3	0.9989	76.446	25.3	3,871	245,689	245,695	15				15				

33.11 were calculated by the methods published by Smith.¹²

To compute subsurface pressures where the well is equipped with tubing set without a packer, the preferred practice is to calculate the flowing subsurface pressure from the wellhead pressure measured on the static gas column by means of the static column equations. If the well has a packer, it is necessary to calculate the flowing subsurface pressure by means of the equations for flowing gas columns.

Depths for calculating or measuring subsurface pressures in wells are determined in practice by the equipment installed in the well. Where a well is equipped without tubing or with tubing set without a packer, the proper depth for pressure determinations is the distance to the midpoint of the productive sandface. If the well has tubing set with a packer, the pressures are determined at the entrance to the tubing provided the entry to the tubing is no more than 100 ft from the midpoint of the productive sandface. Otherwise, appropriate corrections would be made to determine the pressure at the midpoint of the sandface.

An explanation of the computational procedures used in Tables 33.12 and 33.13 will be helpful before going into the details of the calculations. The recent advances in computing equipment or, more realistically, the dramatic decrease in the cost of computations have given the average engineer access at least to a handheld programmable calculator or more likely a microcomputer. Therefore, the emphasis in the past has been to simplify equations by making assumptions regarding pressure, temperature, and gas compressibility, but that has not been done here. Now the factor F_r and compressibility factor, z , become subroutines, the results of which are never seen by the user. In this case, Tables 33.10 and 33.11 may seem redundant. The compressibility factors given in Tables 33.12 and 33.13 were calculated by the equation of state published by Hall and Yarborough¹⁴ and Yarborough and Hall.¹⁵ The results of the computations in Tables 33.10 through 33.13 have been rounded,

and the rules for rounding vary from one piece of computing equipment to another. The algorithm used for solving Eqs. 15, 17, and 18 seems to work for all cases, but users may wish to devise their own algorithm.

Example Problem 3—Flowing Well. Details of the method for calculating a flowing subsurface pressure for Well B are given in Table 33.12.

The wellhead flowing pressure for Well B was 3,913 psia at a flow rate of 11.299×10^6 cu ft/D. The annular space between the tubing and casing was packed off and filled with mud so that it is necessary to calculate the flowing subsurface pressure at a depth of 10,658 ft down the flowing column of gas. Gas properties are those given in Table 33.12.

The flow string measures 10,490 ft of 2½-in.-OD, 6.50-lbm/ft tubing with 168 ft of 2½-in.-OD, 4.70-lbm/ft tubing at bottom of flow string. Also, $H = L$, or the flow string is vertical.

Computation of the required pressure is done in two major steps because of the change in size of the flow string at a depth of 10,490 ft. Computations are given in the following steps.

Step 1. Obtain the ID's from Table 33.10 and enter at top of Table 33.12

2½ in. OD—ID = 2.441 in.

2½ in. OD—ID = 1.995 in.

Step 2. Determine the temperature gradient applicable to the problem. In this example, the flowing temperature of the gas at the wellhead was 117°F, and the subsurface temperature at 10,658 ft was 170°F. The temperature was assumed to be a straight-line relationship between 117°F at $H = 0$ and 170°F at $H = 10,658$ ft for a temperature gradient of 5°F per 1,000 ft.

TABLE 33.13—WORK SHEET FOR CALCULATION OF SUBSURFACE SHUT-IN PRESSURE BY EQS. 15, 16a, AND 16b

Company		Lease		Well No.		B		Date of Test			
γ_g	0.615	%CO ₂	2.5	%N ₂	—	p_{pc}	679	T_{pc}	361	Equations Used	15, 16a, 16b
q_g	0	H	10,658	L	10,658	d_i	N.A.	Temperature Gradient		5°F/1,000 ft	
								$(\Delta p) \times (I_n + I_{n-1})$	$\Sigma(\Delta p) \times (I_n + I_{n-1})$	$37.484 \times \gamma_g L$	Line
H	L	d_i	p_n	T	z	I_n	Δp				
0	0	N.A.	4,173.0	117	0.8963	123.931	0	—	—	0	1
1,000	1,000	N.A.	4,266.0	122	0.9071	123.753	93.0	23,036	23,036	23,053	2
1,000	1,000	N.A.	4,266.1	122	0.9071	123.751	93.1	23,059	23,059		3
2,000	2,000	N.A.	4,359.3	127	0.9177	123.573	93.2	23,051	46,110	46,105	4
3,000	3,000	N.A.	4,452.6	132	0.9282	123.410	93.3	23,043	69,153	69,158	5
4,000	4,000	N.A.	4,546.1	137	0.9385	123.245	93.5	23,062	92,215	92,211	6
5,000	5,000	N.A.	4,639.7	142	0.9486	123.081	93.6	23,056	115,271	115,263	7
6,000	6,000	N.A.	4,733.4	147	0.9586	122.929	93.7	23,051	138,322	138,316	8
7,000	7,000	N.A.	4,827.2	152	0.9685	122.788	93.8	23,048	161,370	161,369	9
8,000	8,000	N.A.	4,921.1	157	0.9782	122.645	93.9	23,046	184,416	184,421	10
9,000	9,000	N.A.	5,015.1	162	0.9877	122.500	94.0	23,044	207,460	207,474	11
10,000	10,000	N.A.	5,109.3	167	0.9971	122.362	94.2	23,066	230,526	230,526	12
10,658	10,658	N.A.	5,171.3	170.3	1.0033	122.286	62.0	15,168	245,694	245,695	13

Step 3. Enter wellhead data on Line 1 where H and L are zero. Calculate I_1 from definition of I in Eq. 17.

From Eq. 17, I is:

$$\frac{p}{Tz} - 2.082 \left(\frac{\gamma_g q_g^2}{d_i^4 p} \right) \\ F^2 + \frac{H}{L} \frac{(p/Tz)^2}{1,000}$$

$$\frac{p}{Tz} = (3913)/(577)(0.8776) = 7.72747.$$

Note that z was calculated by methods given in Refs. 14 and 15 (see also Chap. 20).

$$2.082(\gamma_g q_g^2 / d_i^4 p) = \frac{2.082(0.615)(11.299)^2}{(2.441)^4 (3913)} \\ = 0.00118.$$

$$[p/Tz - 2.082(\gamma_g q_g^2 / d_i^4 p)] = 7.72629.$$

Using Eqs. 16a and 16b:

$$F^2 = 2.6665(q_g)^2 / \{ (d_i)^5 [4 \log(d_i/K) + 2.27281]^2 \} \\ = 2.6665(11.299)^2 / \{ (2.441)^5 \cdot [4 \log(2.441/0.0006) + 2.27281]^2 \} \\ = 340.425/24,200 = 0.014067,$$

or, from Table 33.10:

$$F^2 = (F, q_g)^2 = (0.01050 \times 11.299)^2 = 0.014075.$$

This value of F^2 will be used later for comparison.

$$(p/Tz)^2 / 1,000 = (7.72747)^2 / 1,000 = 0.059714.$$

At the wellhead, where $H=0$ and $L=0$ for a vertical wellbore $H=L$, then

$$H/L = \lim_{H \& L \rightarrow 0} (H/L) = 1.000.$$

For a deviated wellbore, H is less than L , and for a horizontal pipeline, $H = 0$, and the term for the head of gas drops out of the term for I .

$$F^2 + \frac{H}{L} (p/Tz)^2 / 1,000$$

$$= 0.014067 + (1.000)(0.059714)$$

$$= 0.073781.$$

Then

$$I = (7.72629) / (0.073781) = 104.719.$$

If the F^2 value determined from F_r (taken from Table 33.10) is substituted above, I becomes 104.708, which compares well with 104.719.

Step 4. Determine trial Δp (Line 2) for a depth of 1,000 ft by

$$\Delta p_1 = \frac{37.484 \times \gamma_g \times L}{2 I_1} = \frac{37.484(0.615)(1,000)}{2(104.719)} \\ = 110.1 \text{ psi.}$$

Step 5. Complete calculation of first trial I_2 (104.346) on Line 2 where the temperature is 122°F, and the first trial pressure is 3913.0 + 110.1 = 4023.1 psia. At these conditions, the compressibility factor, z , is 0.8894. Estimate the second trial Δp by:

$$\Delta p_2 = \frac{37.484(0.615)(1,000)}{104.719 + 104.346} = 110.3.$$

Step 6. Complete calculation of second trial I_2 (104.343) on Line 3 where the temperature remains at 122°F, and the second trial pressure is $3913.0 + 110.3 = 4023.3$ psia. Under these conditions, the compressibility factor, z , remains at 0.8894. Estimate the third trial Δp by

$$\Delta p_3 = \frac{37.484(0.615)(1,000)}{104.719 + 104.343} = 110.3.$$

Since the third trial Δp is the same to within 0.04 psi, the pressure at a depth of 1,000 ft was determined by trial and error to be $3,913.0 + 110.3 = 4,023.3$ psia. (Note that the third trial was not entered in Table 33.12.)

Step 7. Repeat Steps 4 through 6 to calculate the pressure at a depth of 2,000 ft. Only the final step was given in Table 33.12.

Table 33.13 illustrates the calculation of subsurface shut-in pressures in a gas well by Eqs. 15, 16a, and 16b by the same procedure used in Example 1. The only difference is that for the shut-in well the rate of flow, q_g , is zero and, as a result, the pressure loss caused by friction is zero. Therefore, the inside diameter of the pipe has no effect on the calculations.

Size of Integration Interval

The integration interval was 1,000 ft in Tables 33.12 and 33.13 for a moderately high-pressure well and, for the flowing example (Table 33.12), the rate of 11.299×10^3 cu ft/D gave an effective or average velocity of 14.7 ft/sec near the wellhead. Also, the compressibility factor, z , of the gas at wellhead conditions is in that portion of the z vs. pressure curve where z is very nearly a linear function of pressure. At this low velocity and the nearly linear relationship of z with pressure, an integration interval of 1,000 ft is probably more than enough. Likewise, at low pressures where z is again almost a straight-line function of pressure and at low velocities, the integration interval could be extended to 3,000 ft without undue error. However, even moderate computational facilities eliminate the necessity for expanding the integration interval to more than 1,000 ft.

Application of Backpressure Tests to Producing Problems

Backpressure tests taken properly are useful in predicting delivery rates into a pipeline and in reconditioning studies. For these purposes, either the multipoint or the isochronal test is suitable for wells producing from reservoirs with high permeability such as Well B (Fig. 33.5). The isochronal-type test is necessary for an accurate analysis of producing problems for wells producing from low-permeability reservoirs such as Well A (Fig. 33.7). Although multipoint tests can be used, such analyses are much more difficult.

Well performance at the bottom of the well is a measure of the capacity of the reservoir to deliver gas into the wellbore and is useful in analysis of reservoir problems. A wellhead performance curve is a measure of the capacity of the well to deliver gas into a pipeline and is useful in equipment and reconditioning problems. Usually, an analysis of producing problems can be completed with wellhead backpressure data.

Production Rate

Estimation of the steady production rate of a well into a pipeline operating at a relatively constant pressure requires both test data and a general knowledge of the producing characteristics of the well. For example, an estimate is required of the capacity of Well A (Fig. 33.7) to deliver gas into a pipeline operating at a pressure so that $p_{ts}^2 - p_{tf}^2$ in thousands equals 20. Starting from shut-in conditions, the delivery rates would be 6,950, 6,000, 5,150, and $4,730 \times 10^3$ cu ft/D. The rate at 72 hours would be $3,340 \times 10^3$ cu ft/D from data given in the text. The steady production rate would be about $2,000$ to $2,400 \times 10^3$ cu ft/D. Although theoretical methods have been published for estimation of stabilized production rates, they would require more data than is available for the well.

Well B (Fig. 33.5) would produce about $4,300 \times 10^3$ cu ft/D into a pipeline when

$$p_{ts}^2 - p_{tf}^2 = 500$$

as long as the well remained in good condition. Actually, the performance of Well B increased during production and the rate of flow would have increased. The performance of Well B did not deteriorate with time.

Estimation of the sustained production rate of a particular well against fixed pipeline conditions requires a general knowledge of well performance and a definite knowledge of the performance characteristics of the particular well. The accuracy of such estimations is dependent to a large extent on the amount of proper test data available for study.

Causes of Deterioration in Performance

The principal causes of deterioration in gas-well performance are hydrates, liquids, cavings, deposition of salts, equipment leaks, foreign objects, and damage to the producing formation. Any one or a combination of these causes may result in loss of productive capacity and in decreased income. The determination of the cause of deterioration in performance and the recommendation of remedial measures require a history of the performance of the particular well.

The tests illustrated in Fig. 33.8 for Well A give a history of the performance between the date (June 17, 1947) of the multipoint test and the date (Dec. 17, 1951) of the isochronal test. The performance indicated by the first point of the multipoint test ($q_g = 4,928 \times 10^3$ cu ft/D) is the same as that of the isochronal test. Thus it is concluded that the performance of Well A was maintained for about 4½ years. Nothing occurred that harmed the well. Similar conclusions regarding Well B are indicated for the time interval represented by the data on Fig. 33.5.

A regular program of testing gas wells is essential to planning remedial action.

Hydrates

The formation of gas hydrates in the flow string or in the reservoir may cause a well to cease flowing. The author knows of no remedial action to remove hydrates from the producing formation except that of allowing the natural heat of the reservoir to melt the hydrates. The formation of hydrates in the flow string may be prevented by use of

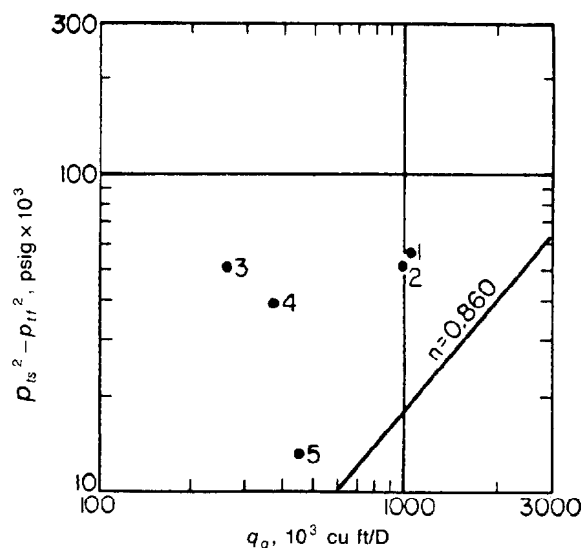


Fig. 33.9—Effect of tubing installation on performance of Well C; Points 1 through 4 are before tubing installation, Point 5 is after.

bottomhole chokes, injection of chemicals such as the alcohols or glycols into the flow string, or by the installation of downhole heating equipment. The accumulation of hydrates in the flow strings may be alleviated to some extent by elimination of obstructions in the flow string, use of proper valve sizes at the surface, elimination of sharp bends in surface lines, and proper placement of chokes in surface lines. Remedial action consists in lowering of hydrate-formation temperatures by chemicals or by maintaining the temperature of the flowing gas above the hydrate-formation temperature. Heating of the flow string in a well is usually accomplished by the circulation of hot oil in the casing around the tubing of the well. However, it must be emphasized that hydrate troubles are very easily confused with liquid troubles in low-temperature wells. A careful study should be made of flowing temperatures in a well before recommendations are made for hydrate prevention.

Liquids

Most performance difficulties in gas wells are caused by the accumulation of liquids in the wellbore. Liquid troubles may be caused by hydrocarbons (condensate and crude oil), salt water, or brines coming into the wellbore from the producing formation, brines from foreign sources through casing leaks, or fresh water. Occasionally, the production of formation water or crude oil may be eliminated by plugback operations. Liquids in wellbores may be removed by tubing strings of proper design, siphon strings (tubing with jet holes or gas-lift valves), and plunger lifts. Periodic flowing of the well at high rates to the pipeline may eliminate liquid troubles.

Remedial action for water troubles requires an identification of the source of the water. This is done by water analyses. If it is decided from analyses that the water is native to the formation, there is a choice between plugback work and water removal by various means. Salt water that is foreign to the producing forma-

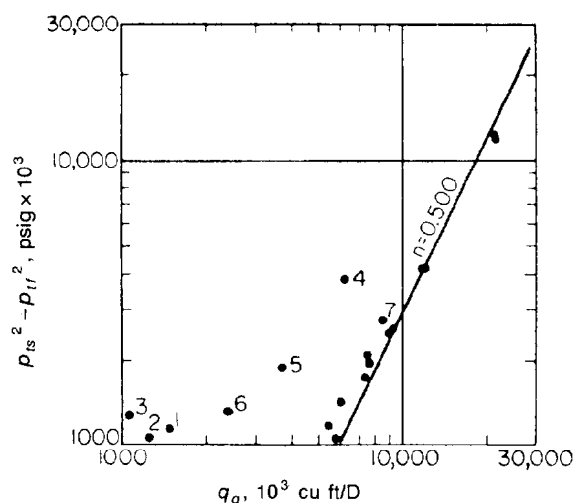


Fig. 33.10—Effect of obstruction in tubing on performance of Well D; Points 1 through 6 are before removal, Point 7 is after.

tion or fresh water in excessive amounts indicates a casing leak that should be repaired. However, moderate amounts of fresh water usually condense in the flow strings of gas wells. Fresh water that occurs naturally should not be confused with fresh water from a foreign source.

Cavings

Cavings that consist of shale and pieces of the formation are usually most troublesome in openhole completions. The presence of cavings in wells without tubing can be determined easily by comparison of measured depth with drilled depth. Remedial action consists of cleaning out, installation of liners in openhole, and acid washes where the formation is soluble in acid.

Unconsolidated sand is troublesome in many Gulf Coast wells. Sand may damage the performance of a well in addition to causing severe damage to equipment. Remedial action consists of cleaning out, installation of special liners, or consolidation treatment for the formation.

Deposition of Salts

Salts (sodium chloride or other chemical compounds) may be deposited in the flow strings or wellbores of gas wells. Sodium chloride and water-soluble salts often may be removed by water or light acid washes. Occasionally it is necessary to replace the flow string with clean pipe. Heavy crude oil (not a salt) may be removed from the flow string and to a limited extent from the face of the wellbore by washing with kerosene.

Casing and Tubing Leaks

Casing leaks usually permit the migration of gas into another formation, but occasionally in low-pressure areas water may come into the wellbore through leaks. The migration of gas into another formation is wasteful. Casing leaks, depending on their size in relation to well

capacity, cause deterioration in well performance. Positive identification usually can be made with subsurface temperature surveys or special techniques supplied by service companies.

Tubing leaks, where there is no packer, tend to defeat the purpose of the tubing. Liquid removal becomes difficult if the hole in the tubing is large. Small leaks in tubing are usually the result of corrosion. In wells where the annular space is packed off, tubing leaks may allow casing pressures to build up to dangerous levels.

Foreign Objects

Foreign objects such as swab rubbers, stud bolts, or pieces of metal may remain in the flow string of a well after completion. Such objects should be removed from the flow string because they can seriously affect the delivery capacity of a well. The removal of foreign objects from the upstream side of chokes is common.

Examples of Remedial Operations

The effect of water production and the installation of tubing on the performance of Well C in the Texas Hugoton field is illustrated in Fig. 33.9. The curve ($n=0.860$) shows the 3-hour isochronal test results taken immediately after completion. Numbered points are 72-hour isochronal tests taken at yearly intervals, except for Points 4 and 5, which were immediately before and after installation of tubing. Point 1, taken after completion, and Point 2, taken about a year after completion, represent good performance. Points 3 and 4 show poor performance with the result that Well C was producing about 30% of its assigned allowable. A study of Well C indicated that salt water was causing the poor performance. A string of 1 1/4-in. tubing with a 3/32-in. jet hole 100 ft from the bottom of the tubing was installed. The well was then produced continuously through the tubing string. At the time Point 5 was taken, the performance of the well had not only been restored but it had been improved over what it had been originally, which is shown by the relative positions of Points 1, 2, and 5 with respect to the 3-hour isochronal curve. Conclusions regarding Well C are that there was a minor water problem from completion through the time that performance data were taken for Points 1 and 2 (Fig. 33.9). Water movement into the wellbore had seriously damaged the performance of the well at the times Points 3 and 4 were taken. The installation of tubing after Point 4 permitted the removal of water from the well and even allowed the water saturation to be reduced in the formation around the wellbore. The position of Point 5 indicates better 72-hour performance than the well had originally as it is closer to the 3-hour isochronal curve than Points 1 and 2.

An example of the effect of a tubing obstruction on the performance of a well is illustrated in Fig. 33.10 for Well D, where the performance points (indicated by circles with and without numbers) were taken at intervals of a month after start of production. Well D was an extremely high-capacity well as indicated by the position of the original multipoint test. As the numbered points were of long-time-flow duration, it was thought that position of Points 1, 2, and 3 indicated some sort of liquid blockage in the reservoir. However, the tubing appeared to be free of liquids when the well was shut in and pressures were normal. Water-gas and condensate-gas

ratios were normal. Thus it was concluded that liquids were not the source of trouble. After Points 4, 5, and 6 were taken, it was decided to blow the well. Shortly after the well was opened, a swab rubber and several pieces of metal were blown from the well. Afterward, the performance of Well D returned to normal, as indicated by the positions of Point 7 and later performance points that are not numbered on Fig. 33.10.

Space does not permit a complete description of reconditioning procedures. However, it is hoped that this brief outline does illustrate the importance of adequate performance tests in the maintenance of well productivity and planning reconditioning procedures.

Nomenclature

- C = performance coefficient
- d_i = internal diameter, in.
- f = coefficient of friction (friction factor)
- F = term in Eq. 16a
- F_g = specific-gravity adjustment factor
- F_{nD} = non-Darcy flow factor
- F_p = basic orifice factor for critical-flow prover, 10^3 cu ft/D at 14.65 psia, 60°F, specific gravity = 1.000
- F_{pv} = supercompressibility adjustment factor
- F_r = factor defined by Eq. 16a
- F_T = flowing-temperature adjustment factor
- h_m = height (manometer reading), in. mercury
- h_w = height (manometer reading), in. water
- H = vertical depth in a well, ft (in untubed wells H is the vertical depth to the midpoint of the productive formation; in tubed wells H is the vertical depth to the entrance to the tubing)
- I = terms in Eq. 17
- K = absolute roughness characteristic, in.
- L = length of flow string in well corresponding to H , ft
- n = exponent of the backpressure equation or slope of the backpressure curve
- p = pressure, psia
- p_i = impact pressure on a pitot tube, psig
- p_1 = impact pressure on a pitot tube, psia
- p_{pc} = pressure, pseudocritical, psia
- \bar{p}_R = average pressure in the reservoir at vertical depth H
- p_s = static pressure on critical flow prover, psia
- p_{wf} = flowing pressure at wellhead measured on a flowing column of gas, psia
- p_{is} = shut-in pressure at wellhead, psia
- p_{wf} = subsurface (bottomhole) flowing pressure in the wellbore at vertical depth H , psia
- q_g = rate of flow, 10^3 cu ft/D or 10^6 cu ft/D (14.65 psia and 60°F)
- r_i = internal radius of pipe, in.
- R_{gL} = gas to hydrocarbon liquid ratio, cu ft/bbl
- T = temperature, °F+460
- T_f = temperature of flowing gas, °F+460

- T_{pc} = temperature, pseudocritical, °F+460
 T_R = reservoir temperature
 V_L = vapor volume equivalent of 1 bbl (60°F) of hydrocarbon liquid, cu ft/bbl
 z = compressibility factor for gas
 Δ = difference between two values
 γ_g = specific gravity of separator gas or gas being measured, air = 1.000
 γ_{ff} = specific gravity of the flowing fluid, air = 1.000
 γ_L = specific gravity of hydrocarbon liquid referred to water

Key Equations in SI Metric Units

$$q_g = 0.1533 d_i^2 p_1 \dots \dots \dots (4)$$

$$\gamma_{ff} = \frac{R_{gL} \gamma_g + 819.8 \gamma_L}{R_{gL} + V_L} \dots \dots \dots (14a)$$

$$\gamma_L = \frac{141.5}{131.5 + \gamma_{API}} \dots \dots \dots (14b)$$

$$V_L = 65.7 + 0.89 \gamma_{API} + 0.007(\gamma_{API})^2 \dots (14c)$$

$$\frac{1000 \gamma_g L}{31.509} = \int_{p_2}^{p_1} \frac{\left(\frac{p}{Tz} - 0.091 \frac{\gamma_g q_g^2}{d_i^4 p} \right) dp}{F^2 + \frac{H}{L} \frac{(p/Tz)^2}{1,000}} \dots \dots (15)$$

$$F^2 = \frac{5.3280 f q_g^2}{d_i^5} \dots \dots \dots (16a)$$

$$\sqrt{\frac{1}{f}} = 4 \log \frac{7.4 r_i}{K} \dots \dots \dots (16b)$$

$$63.473 \gamma_g L = [(p_2 - p_1)(I_2 + I_1) + (p_3 - p_2) \cdot (I_3 + I_2) + \dots (p_n - p_{n-1})(I_n + I_{n-1})] \dots \dots \dots (18)$$

where

- q_g is in m³/d,
 d_i is in mm,
 p is in kPa,
 V_L is in m/m,
 L is in m,
 T is in K,
 H is in m,
 r_i is in mm, and
 K is in mm.

References

1. Reid, W.: "Open Flow Measurement of Gas Well," *Western Gas* (Nov. 1929) 32.
2. Rawlins, E.L. and Schellhardt, M.A.: "Back-pressure Data on Natural Gas Wells and Their Application to Production Practices," USBM Monograph (1935) Washington, DC.
3. Binckley, C.W.: "Methods of Approximating Open Flow of Gas," *Proc., Southwestern Gas Measurement Short Course* (1954) 304.
4. Cullender, M.H.: "The Isochronal Performance Method of Determining the Flow Characteristics of Gas Wells," *J. Pet. Tech.* (Sept. 1955) 137-42; *Trans., AIME*, 204.
5. Odeh, A.S.: "Pseudosteady-State Flow Equation and Productivity Index for a Well With Noncircular Drainage Area," *J. Pet. Tech.* (Nov. 1978) 1630-32.
6. Ramey, H.J. Jr.: "Non-Darcy Flow and Wellbore Storage Effects in Pressure Build-Up and Drawdown of Gas Wells," *J. Pet. Tech.* (Feb. 1965) 223-33; *Trans., AIME*, 234.
7. Odeh, A.S., Moreland, E.E., and Schueler, S.: "Characterization of a Gas Well From One Flow-Test Sequence," *J. Pet. Tech.* (Dec. 1975) 1500-04; *Trans., AIME*, 259.
8. Smith, R.V.: "Unsteady-State Gas Flow into Gas Wells," *J. Pet. Tech.* (Nov. 1961) 1151-59; *Trans., AIME*, 222.
9. "Orifice Metering of Natural Gas," *Gas Measurement Committee Report 3*, American Gas Assn., New York City (April 1955).
10. *Manual of Back Pressure Testing of Gas Wells*, State of Kansas, Topeka (1959).
11. *Manual of Back Pressure Testing of Gas Wells*, Interstate Oil Compact Commission, Oklahoma City (1962).
12. Smith, R.V.: *Practical Natural Gas Engineering*, Pennwell Publishing Co., Tulsa (1983).
13. Cullender, M.H. and Smith, R.V.: "Practical Solution of Gas-Flow Equations for Wells and Pipelines with Large Temperature Gradients," *J. Pet. Tech.* (Dec. 1956) 281-87; *Trans., AIME*, 207.
14. Hall, K.R. and Yarborough, L.: "A New Equation of State for Z-Factor Calculations," *Oil and Gas J.* (June 18, 1973) 71, No. 25, 82-85.
15. Yarborough, L. and Hall, K.R.: "How to Solve Equation of State for Z-Factors," *Oil and Gas J.* (Feb. 18, 1974) 72, 86-88.

Chapter 34

Wellbore Hydraulics

A.F. Bertuzzi, Phillips Petroleum Co.*

M.J. Fetkovich, Phillips Petroleum Co.

Fred H. Poettmann, Colorado School of Mines*

L.K. Thomas, Phillips Petroleum Co.

Introduction

Wellbore hydraulics is defined here as the branch of production engineering that deals with the motion of fluids (oil, gas, and water) in tubing, casing, or the annulus between tubing and casing. Consideration is given to the relationship among fluid properties, fluid motion, and the well system. More specifically, the material presented is intended to describe methods for solving problems associated with the determination of the relationship among pressure drop, fluid rates, and pipe diameters and length.

To maintain the scope of this section within prescribed limits, some material and data that are pertinent to the solving of wellbore problems, but which can be found conveniently elsewhere, are not presented. The material not covered includes (1) methods of measurement and (2) complete data on fluid properties (See Chaps. 13, 16–19, 24).

The theoretical discussion that follows provides a basis for the development of correlations and calculation procedures in subsequent parts of the section.

Theoretical Basis

Fluids in Motion

Energy Relationships. The energy relationships for a fluid flowing through tubing, casing, or annulus may be obtained by an energy balance. Energy is carried with the flowing fluid and also is transferred from the fluid to the surroundings or from the surroundings to the fluid. Energy carried with the fluid includes (1) internal energy, U , (2) energy of motion or kinetic energy ($mv^2/2g_c$), (3) energy of position (potential energy mgZ/g_c), and (4) pressure energy, pV . Energy transferred between a fluid and

its surroundings includes (1) heat absorbed or given up, Q , and (2) work done by the flowing fluid or on the flowing fluid, W .

The conservation of mass, or the first law of thermodynamics, states that the change in internal energy plus kinetic energy plus potential energy plus pressure energy is equal to zero. The following energy balance between points 1 and 2 in Fig. 34.1 and the surroundings illustrates the relationship for the previously listed energy terms for unit mass of fluid.

$$U_2 + \frac{v_2^2}{2g_c} + \frac{g}{g_c}Z_2 + p_2V_2 = U_1 + \frac{v_1^2}{2g_c} + \frac{g}{g_c}Z_1 + p_1V_1 + Q - W, \dots\dots\dots (1)$$

where

U = internal energy,

v = velocity,

g_c = conversion factor of 32.174,

g = acceleration of gravity,

Z = difference in elevation,

p = pressure,

V = specific volume,

Q = heat absorbed by system from surroundings, and

W = work done by the fluid while in flow.

This energy-balance equation is based on a unit mass of fluid flowing and assumes no net accumulation of material or energy between points 1 and 2 in the system.

*Authors of the original chapter on this topic in the 1962 edition included these authors and J.K. Welchon (deceased).

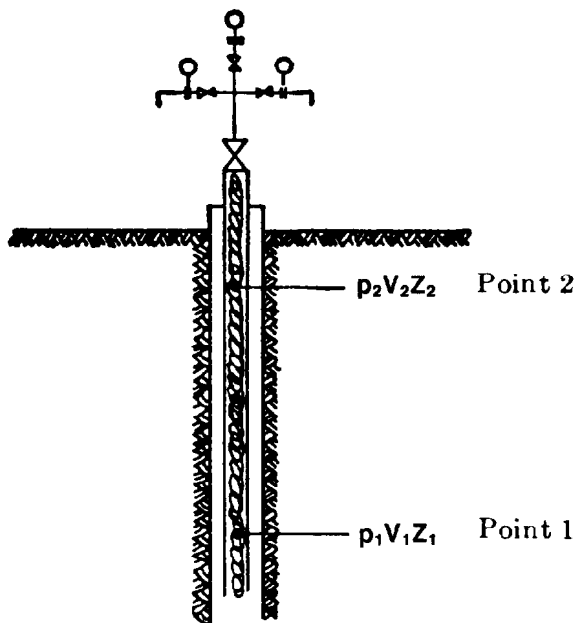


Fig. 34.1—Illustration of energy-balance relationship.

Eq. 1 also can be put in the form

$$\Delta U + \frac{\Delta v^2}{2g_c} + \frac{g}{g_c} \Delta Z + \Delta(pV) = Q - W. \quad (2)$$

since

$$\Delta U = \int_{S_1}^{S_2} T dS + \int_{V_1}^{V_2} p(-dV)$$

and

$$\int_{S_1}^{S_2} T dS = Q + E_t$$

where

T = temperature,
 S = entropy, and
 E_t = irreversible energy losses, and

$$\Delta(pV) = \int_{V_1}^{V_2} p dV + \int_{p_1}^{p_2} V dp.$$

Eq. 2 can be put in the more familiar form

$$\int_{p_1}^{p_2} V dp + \frac{\Delta v^2}{2g_c} + \frac{g}{g_c} \Delta Z = -W - E_t. \quad (3)$$

Since, in the system shown in Fig. 34.1, there is no work done by or on the flowing fluid, W is equal to zero and the following equation results.

$$\int_{p_1}^{p_2} V dp + \frac{\Delta v^2}{2g_c} + \frac{g}{g_c} \Delta Z = -E_t. \quad (4)$$

If flow is isothermal and the fluid is incompressible, Eq. 4 may be simplified to

$$\frac{\Delta p}{\rho} + \frac{\Delta(v^2)}{2g_c} + \frac{g}{g_c} \Delta Z = -E_t, \quad (5)$$

where ρ = density.

The dimensions of the energy terms in Eq. 5 are energy per unit mass of fluid, such as foot-pounds per pound. Quite often the force term is canceled (incorrectly) with that of the mass term resulting in the dimensions of length as of a column of fluid. For this reason, these terms frequently are referred to as "head," such as feet of the fluid. For most practical cases, the ratio g/g_c is essentially unity. Although the terms in Eq. 5 are sometimes expressed as feet of fluid, no serious error is involved. In fact, one can derive a very similar expression where the terms are expressed in feet of "head."

Eqs. 4 and 5 are the energy relationships that provide the basis for the computational methods of the sections to follow.

Irreversibility Losses. The use of Eqs. 4 and 5 requires a knowledge of E_t , the term that accounts for irreversibilities (such as friction) in the system. The term E_t can be expressed as follows¹:

$$E_t = \frac{fLv^2}{2g_cd}, \quad (6)$$

where f commonly is referred to as a friction factor, L is length, and d is pipe diameter. The friction factor, f , usually is expressed in terms of the physical variables of the system by correlations of experimental data.

For single-phase flow, the dimensionless friction factor, f , has been correlated in terms of the dimensionless Reynolds number $dv\rho/\mu$ with μ being viscosity. A relationship is also suggested by application of dimensional analysis to the variables involved. In either case the result is

$$f = F_1 \frac{(dv\rho)}{\mu}, \quad (7)$$

where F_1 is a function of Reynolds number.

Eq. 7 has been the basis for correlation of considerable experimental data for single-phase flow over the past years. Eqs. 5, 6, and 7 have been adapted to multiphase flow. Consideration of the character of pipe surfaces as absolute roughness, ϵ (that is, the distance from peaks to valleys in pipe-wall irregularities), which may be expressed as a dimensionless relative roughness factor, ϵ/d , has led to improvements in correlations of single-phase flow experimental data

$$f = F_2 \left[\left(\frac{dv\rho}{\mu} \right) \left(\frac{\epsilon}{d} \right) \right], \quad (8)$$

where F_2 is a function of Reynolds number and relative roughness.

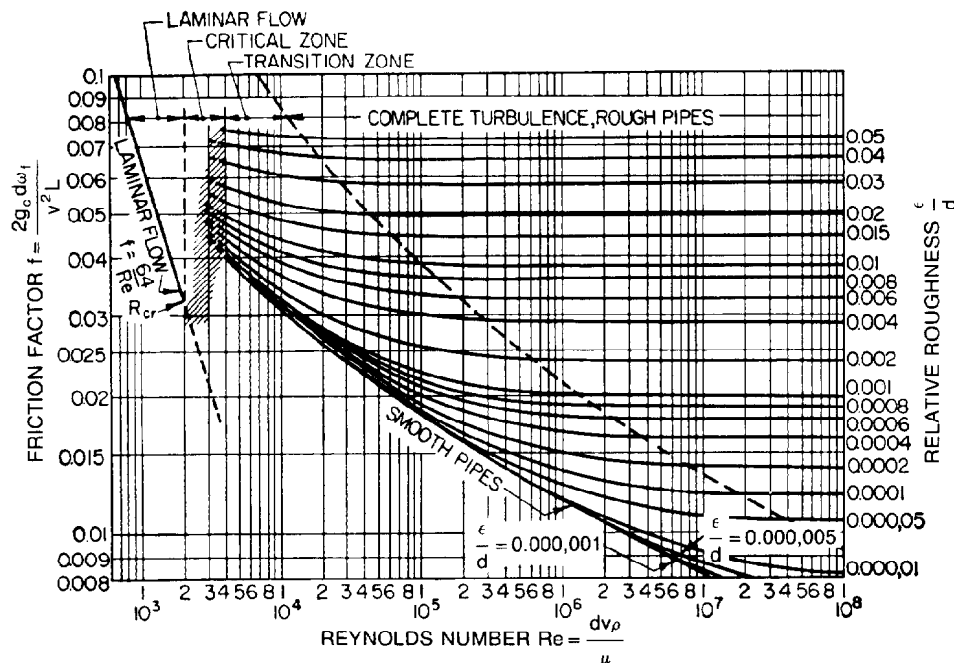


Fig. 34.2—Friction factor as a function of Reynolds number with relative roughness as a parameter.

Fig. 34.2 shows the correlation for single-phase flow according to Eq. 8.² Similar plots are found in the literature in which other friction factors are plotted as a function of Reynolds number. Care must be taken to avoid confusion, as the same name and symbol are used for various multiples of f as plotted in Fig. 34.2.

The laminar-flow region, which extends up to a Reynolds number of 2,000, is represented by a straight-line relationship $f = 64/N_{Re}$ on Fig. 34.2. Between 2,000 and 4,000, flow is unstable. Above 4,000, turbulence prevails and the influence of the physical properties decreases as the Reynolds number increases. In fact, it is shown that at very high Reynolds numbers the friction factor depends solely on the relative roughness factor ϵ/d .

The preceding theoretical discussion concerning irreversibility losses is based on considerations involving single-phase flow. Nevertheless, the material presented will provide a basis for considerations involving both single- and multiphase flow that appear in the following sections.

Static Fluids

Many wellbore problems are associated with static-fluid columns, either oil, water, or gas, or combinations thereof. In the case of static-fluid columns, Eq. 4 is applicable in general and reduces to

$$\int_{p_1}^{p_2} V dp + \frac{g}{g_c} \Delta Z = 0 \quad (9)$$

or

$$\int_{p_1}^{p_2} \frac{dp}{\rho} + \frac{g}{g_c} \Delta Z = 0, \quad (10)$$

since $v^2/2g_c$ and E_t are equal to zero. Since g/g_c is assumed to be unity,

$$\int_{p_1}^{p_2} \frac{dp}{\rho} + \Delta Z = 0. \quad (11)$$

For the case of a static-liquid column, it is usually satisfactory to use an average density for the column of liquid. Eq. 11 then can be expressed in the more convenient and familiar form as

$$\Delta p = \rho \Delta Z. \quad (12)$$

The preceding equations will provide a basis for the calculation procedures of the following sections for static-fluid columns.

Producing Wells

Gas Wells

Calculation of Static Bottomhole Pressures (BHP's).

Static BHP's are used to determine the deliverability of gas wells (backpressure curve) and to develop reservoir information for predicting reservoir performance and deliverability. Several methods for calculating static BHP's have appeared in the literature.³⁻⁶ The methods differ primarily as a result of the assumptions made. All start with Eq. 9 assuming g/g_c is unity for a static column:

$$\int_{p_1}^{p_2} V dp + \Delta Z = 0.$$

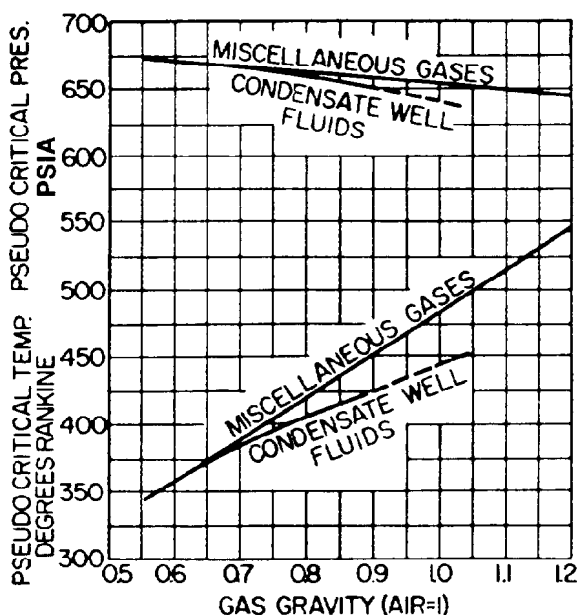


Fig. 34.3—Pseudocritical properties of condensate well fluids and miscellaneous natural gases.

If the column is vertical, $\Delta Z = L$, where L is the length of the pipe string, and Eq. 9 can be put in the form

$$\int_{p_2}^{p_1} V dp = L. \quad (13)$$

If the column is not vertical, but inclined with the vertical by an angle θ ,

$$\Delta Z = L \cos \theta$$

and again using L , Eq. 9 becomes

$$\int_{p_2}^{p_1} V dp = L \sin \theta. \quad (14)$$

Subsequently, only the vertical column will be considered and Eq. 13 will be used. Since

$$V = \frac{zRT}{Mp}, \quad (15)$$

where

z = compressibility factor,
 R = gas constant, and
 M = molecular weight,

Eq. 13, upon substitution, becomes

$$\int_{p_2}^{p_1} \frac{zRT}{M} \frac{dp}{p} = L. \quad (16)$$

For a particular gas, R/M , which is equal to $53.241/\gamma_g$ where γ_g is the gas gravity (air=1.0), is a constant. Therefore, Eq. 16 can be simplified to

$$\frac{53.241}{\gamma_g} \int_{p_2}^{p_1} zT \frac{dp}{p} = L. \quad (17)$$

It is at this point where certain assumptions are made and calculation procedures differ. Assumptions are made in regard to z and T .

For any calculation procedure, four "surface" properties must be known: well-effluent composition, well depth, wellhead pressure, and well temperature. The gas composition is used to calculate the pseudocritical properties p_{pc} and T_{pc} of the gas, from which is estimated the value of the compressibility factor z used in the calculations. Quite often, gas composition is not available and gas gravity must be used to estimate the pseudocritical properties (Fig. 34.3).⁴

A recommended method assumes constant and average temperature T and allows z to vary with pressure. With temperature being constant, Eq. 17 becomes

$$\frac{53.241 \bar{T}}{\gamma_g} \int_{p_2}^{p_1} \frac{z}{p} dp = L. \quad (18)$$

The method using Eq. 18 was suggested by Fowler.³ Poettmann⁴ made the solution of Eq. 18 practical by presenting tables of the function

$$\int_{0.2}^{p_{pr}} \frac{z}{p_{pr}} dp_{pr}$$

in terms of p_{pr} and T_{pr} . The tables are presented here as Table 34.1.

It can be shown that

$$\int_{p_2}^{p_1} \frac{z}{p} dp = \int_{(p_{pr})_2}^{(p_{pr})_1} \frac{z}{p_{pr}} dp_{pr} = \int_{0.2}^{(p_{pr})_1} \frac{z}{p_{pr}} dp_{pr} - \int_{0.2}^{(p_{pr})_2} \frac{z}{p_{pr}} dp_{pr}. \quad (19)$$

An advantage of this method is that it is a *direct method of calculating BHP*. No trial and error is involved. In terms of p_{pr} and T_{pr} Eq. 18 becomes

$$L = \frac{53.241 \bar{T}}{\gamma_g} \left[\int_{0.2}^{(p_{pr})_1} \frac{z}{p_{pr}} dp_{pr} - \int_{0.2}^{(p_{pr})_2} \frac{z}{p_{pr}} dp_{pr} \right]. \quad (20)$$

By rearranging,

$$\int_{0.2}^{(p_{pr})_1} \frac{z}{p_{pr}} dp_{pr} = \frac{L \gamma_g}{53.241 \bar{T}} + \int_{0.2}^{(p_{pr})_2} \frac{z}{p_{pr}} dp_{pr}. \quad (21)$$

Eq. 21 permits a direct solution for the static BHP.

TABLE 34.1—VALUES OF $\int_{0.2}^{p_{pr}} \frac{z}{p_{pr}} dp_{pr}$

Pseudo-reduced Pressure p_{pr}	Pseudoreduced Temperature, T_{pr}							Pseudo-reduced Pressure p_{pr}	Pseudoreduced Temperature, T_{pr}						
	1.05	1.10	1.15	1.20	1.25	1.30	1.35		1.40	1.45	1.50	1.60	1.70	1.80	1.90
0.2	0	0	0	0	0	0	0	0.2	0	0	0	0	0	0	0
0.3	0.350	0.350	0.350	0.350	0.350	0.350	0.350	0.3	0.350	0.350	0.350	0.350	0.350	0.350	0.350
0.4	0.615	0.619	0.623	0.626	0.628	0.630	0.632	0.4	0.633	0.634	0.635	0.636	0.637	0.638	0.639
0.5	0.905	0.916	0.926	0.934	0.939	0.944	0.948	0.5	0.951	0.954	0.956	0.960	0.962	0.964	0.966
0.6	0.955	0.971	0.985	0.998	1.011	1.022	1.032	0.6	1.040	1.045	1.048	1.049	1.049	1.050	1.050
0.7	1.078	1.100	1.124	1.145	1.162	1.178	1.190	0.7	1.199	1.203	1.207	1.210	1.211	1.213	1.214
0.8	1.175	1.207	1.239	1.264	1.285	1.300	1.313	0.8	1.322	1.332	1.340	1.347	1.352	1.357	1.359
0.9	1.256	1.300	1.335	1.365	1.386	1.403	1.417	0.9	1.429	1.440	1.450	1.462	1.472	1.480	1.485
1.0	1.327	1.375	1.420	1.455	1.479	1.500	1.515	1.0	1.530	1.541	1.551	1.568	1.580	1.590	1.598
1.1	1.380	1.438	1.485	1.528	1.552	1.573	1.591	1.1	1.606	1.616	1.631	1.653	1.667	1.676	1.684
1.2	1.433	1.500	1.550	1.600	1.625	1.645	1.666	1.2	1.682	1.690	1.710	1.737	1.753	1.761	1.770
1.3	1.463	1.545	1.602	1.657	1.684	1.709	1.731	1.3	1.746	1.758	1.779	1.810	1.828	1.836	1.845
1.4	1.492	1.590	1.654	1.713	1.742	1.772	1.795	1.4	1.810	1.825	1.847	1.882	1.903	1.911	1.920
1.5	1.510	1.620	1.690	1.757	1.791	1.824	1.848	1.5	1.867	1.884	1.906	1.938	1.962	1.973	1.984
1.6	1.527	1.649	1.726	1.800	1.839	1.875	1.900	1.6	1.923	1.943	1.964	1.995	2.021	2.035	2.047
1.7	1.544	1.670	1.754	1.834	1.876	1.917	1.943	1.7	1.969	1.991	2.012	2.043	2.072	2.089	2.102
1.8	1.560	1.690	1.782	1.867	1.913	1.958	1.985	1.8	2.014	2.038	2.060	2.093	2.123	2.142	2.157
1.9	1.575	1.708	1.808	1.896	1.944	1.993	2.022	1.9	2.054	2.079	2.100	2.136	2.165	2.187	2.204
2.0	1.590	1.725	1.833	1.924	1.975	2.027	2.059	2.0	2.093	2.119	2.140	2.178	2.207	2.231	2.250
2.1	1.604	1.743	1.854	1.947	2.003	2.057	2.092	2.1	2.126	2.153	2.176	2.215	2.248	2.272	2.292
2.2	1.617	1.761	1.876	1.971	2.031	2.086	2.125	2.2	2.160	2.187	2.212	2.252	2.288	2.313	2.334
2.3	1.631	1.779	1.897	1.994	2.059	2.116	2.157	2.3	2.193	2.222	2.249	2.288	2.329	2.354	2.375
2.4	1.644	1.797	1.919	2.018	2.087	2.145	2.190	2.4	2.227	2.256	2.285	2.325	2.369	2.395	2.417
2.5	1.658	1.815	1.940	2.041	2.115	2.175	2.223	2.5	2.260	2.290	2.321	2.362	2.410	2.436	2.459
2.6	1.672	1.830	1.958	2.061	2.137	2.198	2.249	2.6	2.288	2.318	2.350	2.392	2.442	2.469	2.492
2.7	1.685	1.845	1.976	2.081	2.159	2.221	2.275	2.7	2.316	2.347	2.379	2.423	2.474	2.502	2.525
2.8	1.699	1.860	1.994	2.101	2.180	2.245	2.302	2.8	2.344	2.375	2.407	2.453	2.506	2.534	2.557
2.9	1.712	1.875	2.012	2.121	2.202	2.268	2.328	2.9	2.372	2.404	2.436	2.484	2.538	2.567	2.590
3.0	1.726	1.890	2.030	2.140	2.224	2.291	2.354	3.0	2.400	2.432	2.465	2.514	2.570	2.600	2.623
3.1	1.740	1.904	2.046	2.157	2.243	2.311	2.376	3.1	2.423	2.455	2.489	2.540	2.597	2.628	2.652
3.2	1.754	1.918	2.062	2.175	2.261	2.331	2.397	3.2	2.446	2.478	2.512	2.565	2.623	2.657	2.681
3.3	1.767	1.932	2.078	2.192	2.280	2.350	2.419	3.3	2.469	2.502	2.536	2.591	2.650	2.685	2.709
3.4	1.781	1.946	2.094	2.210	2.298	2.370	2.440	3.4	2.492	2.525	2.559	2.616	2.676	2.714	2.738
3.5	1.795	1.960	2.110	2.227	2.317	2.390	2.462	3.5	2.515	2.548	2.583	2.642	2.703	2.742	2.767
3.6	1.808	1.974	2.125	2.243	2.333	2.407	2.480	3.6	2.535	2.568	2.603	2.664	2.726	2.766	2.792
3.7	1.822	1.988	2.140	2.259	2.349	2.424	2.498	3.7	2.556	2.588	2.624	2.686	2.748	2.791	2.817
3.8	1.835	2.002	2.155	2.275	2.365	2.440	2.517	3.8	2.576	2.609	2.644	2.708	2.771	2.815	2.843
3.9	1.849	2.016	2.170	2.291	2.381	2.457	2.535	3.9	2.597	2.629	2.665	2.730	2.793	2.840	2.868
4.0	1.862	2.030	2.186	2.306	2.397	2.474	2.553	4.0	2.617	2.649	2.685	2.752	2.816	2.864	2.893
4.1	1.875	2.044	2.201	2.321	2.413	2.490	2.569	4.1	2.634	2.667	2.703	2.771	2.836	2.885	2.915
4.2	1.889	2.058	2.216	2.336	2.429	2.506	2.586	4.2	2.651	2.685	2.721	2.789	2.856	2.907	2.937
4.3	1.902	2.073	2.230	2.351	2.444	2.523	2.602	4.3	2.669	2.702	2.740	2.808	2.875	2.928	2.958
4.4	1.916	2.087	2.245	2.366	2.460	2.539	2.619	4.4	2.686	2.720	2.758	2.826	2.895	2.950	2.980
4.5	1.929	2.101	2.260	2.381	2.476	2.555	2.635	4.5	2.703	2.738	2.776	2.845	2.915	2.971	3.002
4.6	1.942	2.115	2.274	2.395	2.491	2.570	2.651	4.6	2.719	2.754	2.793	2.863	2.933	2.990	3.022
4.7	1.955	2.128	2.288	2.409	2.507	2.586	2.666	4.7	2.735	2.770	2.810	2.881	2.952	3.009	3.041
4.8	1.969	2.142	2.301	2.423	2.522	2.601	2.682	4.8	2.752	2.786	2.826	2.899	2.970	3.027	3.061
4.9	1.982	2.155	2.315	2.437	2.538	2.617	2.697	4.9	2.768	2.802	2.843	2.917	2.989	3.046	3.080
5.0	1.995	2.169	2.329	2.451	2.553	2.632	2.713	5.0	2.784	2.818	2.860	2.935	3.007	3.065	3.100
5.1	2.009	2.183	2.342	2.465	2.567	2.646	2.728	5.1	2.799	2.834	2.876	2.952	3.024	3.082	3.118
5.2	2.024	2.197	2.355	2.479	2.581	2.661	2.743	5.2	2.814	2.850	2.892	2.968	3.042	3.099	3.136
5.3	2.038	2.210	2.369	2.492	2.595	2.675	2.758	5.3	2.830	2.865	2.908	2.985	3.059	3.117	3.153
5.4	2.053	2.224	2.382	2.506	2.609	2.690	2.773	5.4	2.845	2.881	2.924	3.001	3.077	3.134	3.171
5.5	2.067	2.238	2.395	2.520	2.623	2.704	2.788	5.5	2.860	2.897	2.940	3.018	3.094	3.151	3.189
5.6	2.079	2.251	2.408	2.533	2.636	2.718	2.801	5.6	2.874	2.912	2.955	3.037	3.110	3.168	3.206
5.7	2.091	2.264	2.421	2.547	2.650	2.731	2.815	5.7	2.888	2.926	2.970	3.049	3.125	3.185	3.224
5.8	2.102	2.277	2.435	2.560	2.663	2.744	2.828	5.8	2.902	2.941	2.985	3.065	3.141	3.201	3.241
5.9	2.114	2.290	2.448	2.574	2.677	2.758	2.842	5.9	2.916	2.955	3.000	3.080	3.156	3.218	3.259
6.0	2.126	2.303	2.461	2.587	2.690	2.772	2.855	6.0	2.930	2.970	3.015	3.096	3.172	3.235	3.276

TABLE 34.1—VALUES OF $\int_{0.2}^{p_{pr}} \frac{z}{p_{pr}} dp_{pr}$ (continued)

Pseudo-reduced Pressure p_{pr}	Pseudoreduced Temperature, T_{pr}							Pseudo-reduced Pressure p_{pr}	Pseudoreduced Temperature, T_{pr}						
	1.05	1.10	1.15	1.20	1.25	1.30	1.35		1.40	1.45	1.50	1.60	1.70	1.80	1.90
6.1	2.139	2.316	2.474	2.600	2.703	2.785	2.869	6.1	2.943	2.984	3.029	3.111	3.187	3.250	3.292
6.2	2.152	2.328	2.486	2.612	2.716	2.799	2.882	6.2	2.956	2.997	3.043	3.125	3.202	3.266	3.308
6.3	2.165	2.341	2.499	2.625	2.729	2.812	2.896	6.3	2.970	3.011	3.056	3.140	3.218	3.281	3.323
6.4	2.178	2.353	2.511	2.637	2.742	2.826	2.909	6.4	2.983	3.024	3.070	3.154	3.233	3.297	3.339
6.5	2.191	2.366	2.524	2.650	2.755	2.839	2.923	6.5	2.996	3.038	3.084	3.169	3.248	3.312	3.355
6.6	2.204	2.379	2.536	2.662	2.768	2.852	2.936	6.6	3.009	3.051	3.098	3.183	3.262	3.327	3.370
6.7	2.217	2.391	2.548	2.675	2.781	2.864	2.949	6.7	3.022	3.064	3.112	3.197	3.276	3.341	3.384
6.8	2.229	2.404	2.560	2.687	2.794	2.877	2.963	6.8	3.034	3.077	3.126	3.210	3.291	3.356	3.399
6.9	2.242	2.416	2.572	2.700	2.807	2.889	2.976	6.9	3.047	3.090	3.140	3.224	3.305	3.370	3.414
7.0	2.255	2.429	2.584	2.712	2.820	2.902	2.989	7.0	3.060	3.103	3.154	3.238	3.319	3.385	3.429
7.1	2.268	2.442	2.597	2.724	2.832	2.915	3.002	7.1	3.073	3.116	3.167	3.251	3.332	3.399	3.443
7.2	2.281	2.454	2.609	2.737	2.844	2.928	3.014	7.2	3.085	3.129	3.180	3.264	3.345	3.413	3.457
7.3	2.294	2.467	2.622	2.749	2.856	2.941	3.027	7.3	3.098	3.141	3.194	3.278	3.359	3.427	3.472
7.4	2.307	2.479	2.634	2.762	2.868	2.954	3.039	7.4	3.110	3.154	3.207	3.291	3.372	3.441	3.486
7.5	2.320	2.492	2.647	2.774	2.880	2.967	3.052	7.5	3.123	3.167	3.220	3.304	3.385	3.455	3.500
7.6	2.333	2.505	2.660	2.786	2.892	2.979	3.065	7.6	3.135	3.180	3.233	3.317	3.398	3.468	3.514
7.7	2.346	2.517	2.672	2.799	2.904	2.991	3.077	7.7	3.147	3.192	3.246	3.330	3.411	3.482	3.528
7.8	2.359	2.530	2.685	2.811	2.916	3.003	3.090	7.8	3.160	3.205	3.260	3.344	3.424	3.495	3.541
7.9	2.372	2.542	2.697	2.824	2.928	3.015	3.102	7.9	3.172	3.217	3.274	3.357	3.437	3.509	3.555
8.0	2.385	2.555	2.710	2.836	2.940	3.027	3.115	8.0	3.184	3.230	3.287	3.370	3.450	3.522	3.569
8.1	2.398	2.568	2.723	2.848	2.952	3.039	3.127	8.1	3.197	3.242	3.299	3.382	3.462	3.534	3.581
8.2	2.411	2.580	2.736	2.861	2.964	3.051	3.139	8.2	3.209	3.254	3.311	3.394	3.474	3.546	3.594
8.3	2.424	2.593	2.748	2.873	2.977	3.064	3.151	8.3	3.222	3.266	3.323	3.407	3.486	3.559	3.606
8.4	2.437	2.605	2.761	2.886	2.989	3.076	3.163	8.4	3.234	3.278	3.335	3.419	3.498	3.571	3.619
8.5	2.450	2.618	2.774	2.898	3.001	3.088	3.175	8.5	3.247	3.290	3.347	3.431	3.510	3.583	3.631
8.6	2.462	2.631	2.787	2.910	3.013	3.100	3.187	8.6	3.259	3.302	3.359	3.443	3.523	3.595	3.643
8.7	2.475	2.643	2.799	2.923	3.025	3.112	3.199	8.7	3.270	3.313	3.370	3.456	3.535	3.607	3.655
8.8	2.487	2.656	2.812	2.935	3.038	3.124	3.211	8.8	3.282	3.325	3.382	3.468	3.548	3.619	3.668
8.9	2.500	2.668	2.824	2.948	3.050	3.136	3.223	8.9	3.293	3.340	3.393	3.481	3.560	3.631	3.679
9.0	2.512	2.681	2.837	2.960	3.062	3.148	3.235	9.0	3.305	3.352	3.405	3.493	3.573	3.643	3.690
9.1	2.524	2.693	2.849	2.972	3.074	3.159	3.246	9.1	3.317	3.364	3.417	3.505	3.585	3.655	3.702
9.2	2.536	2.706	2.861	2.985	3.087	3.172	3.257	9.2	3.329	3.376	3.429	3.517	3.597	3.667	3.714
9.3	2.549	2.718	2.872	2.997	3.097	3.182	3.268	9.3	3.340	3.388	3.440	3.530	3.608	3.678	3.725
9.4	2.561	2.731	2.884	3.010	3.108	3.193	3.279	9.4	3.352	3.400	3.452	3.542	3.620	3.690	3.737
9.5	2.573	2.743	2.896	3.022	3.120	3.204	3.290	9.5	3.364	3.412	3.464	3.554	3.632	3.702	3.749
9.6	2.585	2.755	2.908	3.034	3.131	3.216	3.302	9.6	3.376	3.424	3.475	3.565	3.644	3.713	3.760
9.7	2.597	2.767	2.919	3.045	3.142	3.228	3.314	9.7	3.388	3.435	3.487	3.576	3.656	3.724	3.772
9.8	2.610	2.780	2.931	3.057	3.153	3.239	3.326	9.8	3.399	3.447	3.498	3.588	3.667	3.736	3.783
9.9	2.622	2.792	2.942	3.068	3.164	3.251	3.338	9.9	3.411	3.458	3.510	3.599	3.679	3.747	3.795
10.0	2.634	2.804	2.954	3.080	3.175	3.263	3.350	10.0	3.423	3.470	3.521	3.610	3.691	3.758	3.806
10.1	2.646	2.816	2.966	3.092	3.187	3.274	3.361	10.1	3.434	3.482	3.532	3.622	3.702	3.769	3.817
10.2	2.658	2.828	2.978	3.103	3.199	3.286	3.372	10.2	3.446	3.494	3.544	3.633	3.714	3.780	3.828
10.3	2.671	2.840	2.989	3.115	3.211	3.297	3.382	10.3	3.457	3.506	3.555	3.645	3.725	3.790	3.838
10.4	2.683	2.852	3.001	3.126	3.223	3.309	3.393	10.4	3.469	3.518	3.567	3.656	3.737	3.801	3.851
10.5	2.695	2.864	3.013	3.138	3.235	3.320	3.404	10.5	3.480	3.530	3.578	3.668	3.748	3.812	3.862
10.6	2.707	2.876	3.025	3.150	3.246	3.332	3.416	10.6	3.492	3.541	3.588	3.679	3.758	3.823	3.873
10.7	2.719	2.888	3.037	3.161	3.258	3.343	3.428	10.7	3.504	3.552	3.598	3.689	3.769	3.834	3.884
10.8	2.732	2.900	3.048	3.173	3.269	3.355	3.440	10.8	3.515	3.562	3.609	3.700	3.779	3.844	3.894
10.9	2.744	2.912	3.060	3.184	3.281	3.366	3.452	10.9	3.527	3.573	3.619	3.710	3.790	3.855	3.905
11.0	2.756	2.924	3.072	3.196	3.292	3.378	3.464	11.0	3.539	3.584	3.629	3.721	3.800	3.866	3.916
11.1	2.768	2.936	3.084	3.208	3.304	3.389	3.475	11.1	3.551	3.595	3.639	3.732	3.811	3.877	3.926
11.2	2.780	2.948	3.096	3.220	3.315	3.401	3.486	11.2	3.562	3.605	3.650	3.743	3.822	3.888	3.937
11.3	2.793	2.960	3.108	3.231	3.327	3.412	3.497	11.3	3.574	3.616	3.660	3.753	3.832	3.899	3.947
11.4	2.805	2.972	3.120	3.243	3.338	3.424	3.508	11.4	3.585	3.626	3.671	3.764	3.843	3.910	3.958
11.5	2.817	2.984	3.132	3.255	3.350	3.435	3.519	11.5	3.597	3.637	3.681	3.775	3.854	3.921	3.969
11.6	2.829	2.996	3.144	3.267	3.361	3.446	3.529	11.6	3.607	3.648	3.692	3.786	3.865	3.932	3.980
11.7	2.841	3.008	3.156	3.279	3.373	3.456	3.540	11.7	3.617	3.658	3.702	3.797	3.876	3.943	3.991
11.8	2.854	3.020	3.168	3.290	3.384	3.467	3.550	11.8	3.628	3.669	3.713	3.808	3.886	3.953	4.001
11.9	2.866	3.032	3.180	3.302	3.396	3.477	3.561	11.9	3.638	3.679	3.723	3.819	3.897	3.964	4.012
12.0	2.878	3.044	3.192	3.314	3.407	3.488	3.571	12.0	3.648	3.690	3.734	3.830	3.908	3.977	4.025

TABLE 34.1—VALUES OF $\int_{0.2}^{p_{pr}} \frac{z}{p_{pr}} dp_{pr}$ (continued)

Pseudo-reduced Pressure p_{pr}	Pseudoreduced Temperature, T_{pr}						Pseudo-reduced Pressure p_{pr}	Pseudoreduced Temperature, T_{pr}					
	2.00	2.20	2.40	2.60	2.80	3.00		2.00	2.20	2.40	2.60	2.80	3.00
0.2	0	0	0	0	0	0	6.1	3.321	3.362	3.409	3.442	3.466	3.477
0.3	0.350	0.350	0.350	0.350	0.350	0.350	6.2	3.337	3.379	3.426	3.459	3.483	3.494
0.4	0.639	0.640	0.640	0.640	0.640	0.640	6.3	3.354	3.395	3.443	3.476	3.501	3.511
0.5	0.867	0.868	0.869	0.869	0.869	0.869	6.4	3.370	3.412	3.460	3.493	3.518	3.528
							6.5	3.387	3.429	3.477	3.510	3.536	3.545
0.6	1.050	1.051	1.051	1.052	1.052	1.052							
0.7	1.216	1.218	1.219	1.220	1.220	1.220	6.6	3.402	3.444	3.493	3.526	3.551	3.561
0.8	1.360	1.363	1.364	1.364	1.364	1.364	6.7	3.417	3.459	3.508	3.542	3.567	3.577
0.9	1.489	1.492	1.494	1.495	1.495	1.495	6.8	3.432	3.475	3.524	3.557	3.582	3.592
1.0	1.602	1.607	1.608	1.609	1.610	1.610	6.9	3.447	3.490	3.539	3.573	3.598	3.608
							7.0	3.462	3.505	3.555	3.589	3.613	3.624
1.1	1.691	1.699	1.702	1.706	1.709	1.711	7.1	3.477	3.520	3.570	3.604	3.628	3.639
1.2	1.780	1.790	1.795	1.802	1.808	1.812	7.2	3.491	3.534	3.584	3.618	3.643	3.654
1.3	1.858	1.868	1.875	1.883	1.890	1.896	7.3	3.506	3.549	3.599	3.633	3.659	3.670
1.4	1.935	1.945	1.954	1.964	1.972	1.980	7.4	3.520	3.563	3.613	3.647	3.674	3.685
1.5	1.997	2.010	2.019	2.027	2.036	2.045	7.5	3.535	3.578	3.628	3.662	3.689	3.700
1.6	2.059	2.074	2.083	2.090	2.100	2.110	7.6	3.548	3.591	3.642	3.676	3.703	3.714
1.7	2.116	2.131	2.141	2.148	2.159	2.169	7.7	3.562	3.605	3.656	3.690	3.718	3.728
1.8	2.172	2.188	2.198	2.205	2.217	2.227	7.8	3.575	3.618	3.670	3.704	3.732	3.742
1.9	2.219	2.237	2.247	2.256	2.267	2.279	7.9	3.589	3.632	3.684	3.718	3.747	3.756
2.0	2.265	2.285	2.295	2.307	2.317	2.330	8.0	3.602	3.645	3.698	3.732	3.761	3.770
2.1	2.307	2.326	2.337	2.350	2.361	2.375	8.1	3.615	3.658	3.711	3.745	3.774	3.783
2.2	2.349	2.366	2.380	2.394	2.404	2.420	8.2	3.627	3.671	3.723	3.758	3.788	3.796
2.3	2.391	2.407	2.422	2.437	2.448	2.465	8.3	3.640	3.684	3.736	3.771	3.801	3.810
2.4	2.433	2.447	2.465	2.481	2.491	2.510	8.4	3.652	3.697	3.748	3.784	3.815	3.823
2.5	2.475	2.488	2.507	2.524	2.535	2.555	8.5	3.665	3.710	3.761	3.797	3.828	3.836
2.6	2.508	2.523	2.544	2.562	2.574	2.593	8.6	3.677	3.722	3.773	3.810	3.840	3.849
2.7	2.541	2.559	2.581	2.599	2.612	2.630	8.7	3.690	3.734	3.786	3.823	3.853	3.862
2.8	2.575	2.594	2.617	2.637	2.651	2.668	8.8	3.702	3.746	3.798	3.835	3.865	3.875
2.9	2.608	2.630	2.654	2.674	2.689	2.705	8.9	3.715	3.758	3.811	3.848	3.878	3.888
3.0	2.641	2.665	2.691	2.712	2.728	2.743	9.0	3.727	3.770	3.823	3.861	3.890	3.901
3.1	2.670	2.694	2.722	2.744	2.759	2.775	9.1	3.739	3.782	3.835	3.873	3.902	3.913
3.2	2.700	2.723	2.753	2.775	2.790	2.806	9.2	3.750	3.794	3.847	3.885	3.915	3.925
3.3	2.729	2.752	2.783	2.807	2.821	2.838	9.3	3.762	3.806	3.859	3.897	3.927	3.938
3.4	2.759	2.781	2.814	2.838	2.852	2.869	9.4	3.773	3.818	3.871	3.909	3.940	3.950
3.5	2.788	2.810	2.845	2.870	2.883	2.901	9.5	3.785	3.830	3.883	3.921	3.952	3.962
3.6	2.813	2.836	2.872	2.910	2.911	2.929	9.6	3.797	3.842	3.895	3.933	3.964	3.974
3.7	2.839	2.862	2.899	2.950	2.938	2.957	9.7	3.809	3.854	3.907	3.945	3.976	3.986
3.8	2.864	2.888	2.925	2.990	2.966	2.984	9.8	3.820	3.865	3.918	3.957	3.987	3.999
3.9	2.890	2.914	2.952	3.030	2.993	3.012	9.9	3.832	3.877	3.930	3.969	3.999	4.011
4.0	2.915	2.940	2.979	3.070	3.021	3.040	10.0	3.844	3.889	3.942	3.981	4.011	4.023
4.1	2.938	2.963	3.002	3.081	3.045	3.064	10.1	3.855	3.900	3.953	3.992	4.023	4.035
4.2	2.960	2.985	3.025	3.092	3.069	3.088	10.2	3.867	3.911	3.965	4.004	4.035	4.046
4.3	2.983	3.008	3.049	3.103	3.094	3.112	10.3	3.878	3.923	3.976	4.015	4.046	4.058
4.4	3.005	3.030	3.072	3.114	3.118	3.136	10.4	3.890	3.934	3.988	4.027	4.058	4.069
4.5	3.028	3.053	3.095	3.125	3.142	3.160	10.5	3.901	3.945	3.999	4.038	4.070	4.081
4.6	3.048	3.074	3.117	3.147	3.164	3.182	10.6	3.912	3.956	4.010	4.049	4.081	4.092
4.7	3.068	3.095	3.139	3.168	3.186	3.203	10.7	3.923	3.967	4.021	4.060	4.093	4.104
4.8	3.088	3.115	3.161	3.190	3.209	3.225	10.8	3.933	3.978	4.031	4.071	4.104	4.115
4.9	3.108	3.136	3.183	3.211	3.231	3.246	10.9	3.944	3.989	4.042	4.082	4.116	4.127
5.0	3.128	3.157	3.205	3.233	3.253	3.268	11.0	3.955	4.000	4.053	4.093	4.127	4.138
5.1	3.146	3.177	3.225	3.253	3.274	3.288	11.1	3.966	4.011	4.064	4.104	4.138	4.149
5.2	3.164	3.196	3.244	3.273	3.295	3.308	11.2	3.977	4.022	4.075	4.116	4.150	4.160
5.3	3.182	3.216	3.264	3.294	3.315	3.328	11.3	3.988	4.033	4.087	4.127	4.161	4.172
5.4	3.200	3.235	3.283	3.314	3.336	3.348	11.4	3.999	4.044	4.098	4.139	4.173	4.183
5.5	3.218	3.255	3.303	3.334	3.357	3.368	11.5	4.010	4.055	4.109	4.150	4.184	4.194
5.6	3.235	3.273	3.321	3.352	3.375	3.386	11.6	4.022	4.067	4.121	4.161	4.195	4.205
5.7	3.252	3.291	3.339	3.370	3.393	3.405	11.7	4.034	4.079	4.132	4.172	4.206	4.216
5.8	3.270	3.309	3.356	3.389	3.412	3.423	11.8	4.045	4.090	4.144	4.183	4.217	4.227
5.9	3.287	3.327	3.374	3.407	3.430	3.442	11.9	4.057	4.102	4.155	4.194	4.228	4.238
6.0	3.304	3.345	3.392	3.425	3.448	3.460	12.0	4.069	4.114	4.167	4.205	4.239	4.249

Example Problem 1.⁴ Calculate the static BHP of a gas well having a depth of 5,790 ft; the gas gravity is 0.60, and the pressure at the wellhead is 2,300 psia. The average temperature of the flow string is 117°F.

From Fig. 34.3,

$$T_{pc} = 358^\circ\text{R},$$

$$p_{pc} = 672 \text{ psia},$$

$$T_{pr} = \frac{T}{T_{pc}} = \frac{117 + 460}{358} = 1.612, \text{ and}$$

$$(p_{pr})_z = \frac{2,300}{672} = 3.423.$$

From Table 34.1,

$$\int_{0.2}^{(p_{pr})_z} \frac{z}{p_{pr}} dp_{pr} = 2.629$$

and

$$\frac{L\gamma_g}{53.241\bar{T}} = \frac{(5,790)(0.60)}{(53.241)(577)} = 0.113.$$

Therefore, from Eq. 21

$$\int_{0.2}^{(p_{pr})_z} \frac{z}{p_{pr}} dp_{pr} = 2.629 + 0.113 = 2.742.$$

From Table 34.1, 2.742 at a T_{pr} of 1.612 corresponds to a p_{pr} of 3.918. Then

$$p = 3.918(672) = 2,633 \text{ psia}.$$

If temperature is linear with depth,

$$T = aL + b \quad \dots\dots\dots (22)$$

and

$$dT = a \, dL, \quad \dots\dots\dots (23)$$

where a and b are constants. By substituting Eq. 23 in Eq. 17 and putting in the differential form, the following is obtained:

$$\frac{dT}{aT} = \frac{53.241z}{\gamma_g} \frac{dp}{p}, \quad \dots\dots\dots (24)$$

Integrating,

$$\frac{1}{a} \ln \frac{T_1}{T_2} = \frac{53.241}{\gamma_g} \int_{p_2}^{p_1} z \frac{dp}{p}, \quad \dots\dots\dots (25)$$

Since $a = (T_1 - T_2)/L$,

$$\frac{L/(T_1 - T_2)}{\ln T_1/T_2} = \frac{L}{T_{LM}} = \frac{53.241}{\gamma_g} \int_{p_2}^{p_1} z \frac{dp}{p}, \quad \dots\dots\dots (26)$$

then

$$L = \frac{53.241 T_{LM}}{\gamma_g} \int_{p_2}^{p_1} z \frac{dp}{p}, \quad \dots\dots\dots (27)$$

where

$$T_{LM} = \frac{T_1 - T_2}{\ln T_1/T_2};$$

T_1 and T_2 are, respectively, bottomhole and wellhead temperatures. It can be seen that Eq. 27 differs from Eq. 18 only in that here a log mean temperature T_{LM} is used, whereas Eq. 18 uses the arithmetic average temperature, \bar{T} .

Referring to the example as an illustration of the calculation procedure using the log-mean-temperature concept, T_{LM} merely is substituted for \bar{T} .

Another method of calculating static BHP in gas wells is based on the following equation.

$$p_1 = p_2 e^{0.01877 \gamma_g L / (\bar{T} \bar{z})}, \quad \dots\dots\dots (28)$$

Eq. 28 can be derived from Eq. 17 if an arithmetic average temperature \bar{T} and an arithmetic average compressibility factor \bar{z} are used. *The method using Eq. 28 is a trial-and-error procedure.* Values of p_1 are assumed to obtain a value of \bar{z} . p_1 then is calculated. The procedure is repeated until the values of p_1 are in agreement.

Example Problem 2. (Data used are from Ref. 5.) Given:

Well A

$$p_2 = 2,600 \text{ psia},$$

$$\gamma_g = 0.744,$$

$$L = 7,500 \text{ ft},$$

$$\bar{T} = 152.5^\circ\text{F} = 612.5^\circ\text{R},$$

$$p_{pc} = 663.8 \text{ psia (from Fig. 34.3), and}$$

$$T_{pc} = 385.6^\circ\text{R (from Fig. 34.3)}.$$

First Trial. Assume:

$$p_1 = 3,100 \text{ psia},$$

$$\bar{p} = 2,850 \text{ psia},$$

$$p_{pr} = 2,850/663.8 = 4.30,$$

$$T_{pr} = 612.5/385.6 = 1.59, \text{ and}$$

$$\bar{z} = 0.820.$$

Therefore,

$$\begin{aligned} e^{0.01877 \gamma_g L / (\bar{T} \bar{z})} &= e^{[(0.01877)(0.744)(7,500)] / [(612.5)(0.820)]} \\ &= e^{0.2082} \\ &= 1.2239. \end{aligned}$$

$$p_1 = (2,600)(1.2239) = 3,182 \text{ calculated.}$$

Second Trial. Assume:

$$\begin{aligned} p_1 &= 3,182 \text{ psia,} \\ \bar{p} &= 2,891 \text{ psia,} \\ p_{pr} &= 2,891/663.8 = 4.36, \\ T_{pr} &= 1.59, \text{ and} \\ \bar{z} &= 0.821. \end{aligned}$$

Therefore,

$$\begin{aligned} p_1 &= (2,600)(e^{0.2082}), \\ &= (2,600)(1.2239) \\ &= 3,182 \text{ psia calculated check.} \end{aligned}$$

Measured pressure at 7,500 ft equals 3,193 psia.

Calculation of Flowing BHP's: Flow in Tubing. Flowing BHP (BHFP) of a gas well when used with the known static formation pressure provides the basis for evaluating the well's deliverability. In wells that produce through tubing and have no packer, the static column of gas in the tubing-casing annulus is exposed to the producing formation. In this case, BHFP, or sandface pressure, can be determined by the relatively simple procedure of calculating the pressure at the bottom of the static column of gas in the annular space. The preceding section describes this calculation procedure. Where a gas well is equipped with a tubing-casing packer, it becomes necessary to use the flowing-gas column in calculating the BHFP.

Use of the flowing-gas column means that energy changes resulting from frictional effects, as well as the energy differences caused by the compressional effects and potential-energy changes, enter into the calculations.

Several methods have been developed for calculating the pressure drop in flowing-gas columns.^{4,6,7} Sukkar and Cornell's method⁶ is described in detail. Raghaven and Ramey⁸ extended Sukkar and Cornell's method to cover reduced temperatures to 3.0 and reduced pressures to 30. In a subsequent section that deals with gas flow in injection wells, Poettmann's⁴ method is described. Poettmann's method can be used for upward flow also.

The basic energy equation, Eq. 3, for any flowing fluid in differential form is

$$Vdv + \frac{g}{g_c} dZ - dE_f - dW = 0. \quad (29)$$

Assuming that the kinetic-energy term is small and can be taken as zero, and recognizing that dW , work done by or on the fluid, is zero, Eq. 29 reduces to

$$Vdv + \frac{g}{g_c} dZ + dE_f = 0. \quad (30)$$

For vertical gas flow, $dZ = dL$. Since

$$V = \frac{zRT}{Mp} \quad (15)$$

and

$$\frac{g}{g_c} = 1.0$$

and

$$dE_f = \frac{fv^2 dL}{2g_c d}, \quad (31)$$

Eq. 30, upon substitution, becomes

$$\frac{RzTd p}{Mp} + \left(1 + \frac{fv^2}{2g_c d}\right) dL = 0. \quad (32)$$

Velocity can be expressed in terms of volumetric flow rate and pipe diameter. Pressure can be expressed in terms of reduced pressure. Substituting these terms in Eq. 32, integrating the equation, and converting to common units results in

$$\int_{(p_{pr})_1}^{(p_{pr})_2} \frac{(z/p_{pr}) dp_{pr}}{1 + B(z/p_{pr})^2} = -0.01877 \gamma_g \int_{L_1}^{L_2} \frac{dL}{T} \quad (33)$$

where

$$B = \frac{667 f q_g^2 \bar{T}^2}{d_i^5 p_{pc}^2},$$

γ_g = gas gravity (air=1.0),

L = length of flow string, ft,

T = temperature, °R,

\bar{T} = average temperature, °R,

f = friction factor, dimensionless,

q_g = flow rate, 10⁶ cu ft/D referred to 14.65 psia and 60°F,

d_i = inside diameter of pipe, in.,

p_{pc} = pseudocritical pressure, psia, and

p_{pr} = pseudoreduced pressure p/p_{pc} .

At this point, it is further assumed that temperature is constant at some average value. This permits direct integration of the right side of Eq. 33, as

$$\int_{(p_{pr})_2}^{(p_{pr})_1} \frac{(z/p_{pr}) dp_{pr}}{1 + B(z/p_{pr})^2} = \frac{0.01877}{\bar{T}} \gamma_g L, \quad (34)$$

where the limits of the integral are inverted to change the sign. If the temperature is linear with depth, the use of log mean temperature as the average temperature provides a rigorous solution to the right side of Eq. 34. This use of log mean temperature confines the effect of the assumption of constant temperature to the left side of the equation, where, for practical purposes, it is extremely small. Thus, errors introduced by the assumption of constant temperature are negligible.

(continued on Page 34-23)

TABLE 34.2—EXTENDED SUKKAR-CORNELL INTEGRAL FOR BHP CALCULATION

$$\int_0^{p_{pr}} \frac{(z/p_{pr}) dp_{pr}}{1 + B(z/p_{pr})^2}$$

Pseudoreduced temperature for $B = 0.0$

p_{pr}	1.1	1.2	1.3	1.4	1.5	1.6	1.7	1.8	1.9	2.0	2.2	2.4	2.6	2.8	3.0
0.20	0.0000	0.0000	0.0000	0.0000	0.0000	0.000	0.000	0.000	0.000	0.0000	0.0000	0.0000	0.0000	0.0000	0.0000
0.50	0.8387	0.8582	0.8719	0.8824	0.8897	0.8966	0.9017	0.9079	0.9082	0.9108	0.9147	0.9177	0.9194	0.9206	0.9218
1.00	1.3774	1.4440	1.4836	1.5129	1.5334	1.5514	1.5654	1.5781	1.5823	1.5889	1.5986	1.6059	1.6111	1.6148	1.6184
1.50	1.6048	1.7373	1.8078	1.8565	1.8911	1.9192	1.9422	1.9609	1.9693	1.9798	1.9951	2.0063	2.0151	2.0211	2.0274
2.00	1.7149	1.9116	2.0157	2.0842	2.1331	2.1709	2.2023	2.2273	2.2397	2.2536	2.2744	2.2893	2.3013	2.3100	2.3184
2.50	1.7995	2.0298	2.1631	2.2507	2.3138	2.3607	2.3996	2.4307	2.4469	2.4641	2.4900	2.5081	2.5234	2.5347	2.5452
3.00	1.8750	2.1255	2.2778	2.3813	2.4570	2.5125	2.5583	2.5947	2.6148	2.6354	2.6654	2.6863	2.7050	2.7189	2.7314
3.50	1.9473	2.2101	2.3746	2.4898	2.5762	2.6390	2.6909	2.7325	2.7561	2.7798	2.8138	2.8382	2.8589	2.8752	2.8896
4.00	2.0178	2.2822	2.4603	2.5845	2.6793	2.7480	2.8052	2.8515	2.8784	2.9050	2.9426	2.9699	2.9928	3.0114	3.0274
4.50	2.0889	2.3622	2.5390	2.6698	2.7715	2.8449	2.9065	2.9569	2.9867	3.0158	3.0571	3.0871	3.1119	3.1322	3.1496
5.00	2.1547	2.4330	2.6128	2.7484	2.8558	2.9330	2.9982	3.0523	3.0645	3.1158	3.1605	3.1930	3.2195	3.2413	3.2597
5.50	2.2214	2.5013	2.6833	2.8222	2.9341	3.0146	3.0828	3.1400	3.1742	3.2074	3.2552	3.2899	3.3178	3.3408	3.3600
6.00	2.2872	2.5577	2.7512	2.8926	3.0079	3.0911	3.1616	3.2215	3.2575	3.2924	3.3428	3.3795	3.4085	3.4325	3.4524
6.50	2.3522	2.6329	2.8171	2.9603	3.0781	3.1635	3.2360	3.2980	3.3355	3.3720	3.4245	3.4629	3.4931	3.5176	3.5381
7.00	2.4165	2.6971	2.8814	3.0258	3.1452	3.2324	3.3065	3.3704	3.4092	3.4470	3.5012	3.5411	3.5722	3.5973	3.6181
7.50	2.4802	2.7602	2.9442	3.0893	3.2100	3.2985	3.3740	3.4393	3.4792	3.5180	3.5738	3.6148	3.6467	3.6723	3.6934
8.00	2.5432	2.8233	3.0058	3.1512	3.2727	3.3623	3.4387	3.5052	3.5460	3.5857	3.6486	3.6847	3.7173	3.7432	3.7646
8.50	2.6057	2.8836	3.0664	3.2118	3.3338	3.4239	3.5012	3.5685	3.6101	3.6504	3.7144	3.7512	3.7844	3.8108	3.8323
9.00	2.6676	2.9441	3.1260	3.2713	3.3934	3.4838	3.5617	3.6297	3.6718	3.7126	3.7775	3.8148	3.8484	3.8750	3.8969
9.50	2.7289	3.0039	3.1847	3.3296	3.4516	3.5422	3.6204	3.6889	3.7315	3.7727	3.8382	3.8760	3.9099	3.9357	3.9588
10.00	2.7896	3.0630	3.2427	3.3870	3.5087	3.5993	3.6776	3.7465	3.7894	3.8308	3.8969	3.9350	3.9690	3.9961	4.0182
10.50	2.8499	3.1215	3.2999	3.4436	3.5647	3.6552	3.7336	3.8026	3.8456	3.8872	3.9538	3.9921	4.0262	4.0533	4.0755
11.00	2.9096	3.1794	3.3565	3.4993	3.6198	3.7100	3.7883	3.8573	3.9004	3.9421	4.0090	4.0473	4.0814	4.1086	4.1309
11.50	2.9690	3.2369	3.4126	3.5543	3.6741	3.7640	3.8420	3.9108	3.9540	3.9958	4.0627	4.1010	4.1351	4.1622	4.1845
12.00	3.0280	3.2940	3.4681	3.6086	3.7277	3.8171	3.8948	3.9634	4.0065	4.0432	4.1150	4.1532	4.1872	4.2143	4.2366
12.50	3.0867	3.3506	3.5231	3.6623	3.7806	3.8694	3.9467	4.0150	4.0579	4.0994	4.1660	4.2041	4.2380	4.2650	4.2872
13.00	3.1452	3.4068	3.5777	3.7154	3.8328	3.9211	3.9977	4.0557	4.1084	4.1495	4.2158	4.2537	4.2875	4.3144	4.3365
13.50	3.2033	3.4627	3.6319	3.7680	3.8644	3.9721	4.0480	4.1155	4.1580	4.1989	4.2845	4.3021	4.3357	4.3625	4.3846
14.00	3.2612	3.5183	3.6857	3.8200	3.9354	4.0224	4.0977	4.1547	4.2067	4.2472	4.3122	4.3494	4.3829	4.4095	4.4316
14.50	3.3189	3.5735	3.7391	3.8716	3.9859	4.0722	4.1400	4.2131	4.2546	4.2947	4.3589	4.3957	4.4289	4.4555	4.4775
15.00	3.3763	3.6285	3.7922	3.9228	4.0349	4.1215	4.1950	4.2609	4.3018	4.3414	4.4047	4.4410	4.4741	4.5005	4.5224
15.50	3.4335	3.6832	3.8450	3.9736	4.0855	4.1702	4.2428	4.3080	4.3483	4.3874	4.4497	4.4855	4.5183	4.5446	4.5663
16.00	3.4906	3.7376	3.8974	4.0240	4.1346	4.2185	4.2900	4.3546	4.3942	4.4327	4.4939	4.5291	4.5617	4.5878	4.6094
16.50	3.5474	3.7919	3.9497	4.0740	4.1833	4.2663	4.3388	4.4007	4.4395	4.4773	4.5374	4.5720	4.6042	4.6302	4.6518
17.00	3.6041	3.8459	4.0016	4.1237	4.2316	4.3138	4.3830	4.4462	4.4843	4.5213	4.5802	4.6141	4.6461	4.6719	4.6933
17.50	3.6606	3.8996	4.0533	4.1731	4.2795	4.3608	4.4289	4.4913	4.5285	4.5648	4.6223	4.6555	4.6872	4.7129	4.7341
18.00	3.7170	3.9532	4.1048	4.2221	4.3271	4.4075	4.4743	4.5359	4.5722	4.6077	4.6638	4.6963	4.7276	4.7532	4.7743
18.50	3.7732	4.0066	4.1560	4.2709	4.3744	4.4538	4.5193	4.5801	4.6154	4.6501	4.7048	4.7365	4.7675	4.7928	4.8138
19.00	3.8293	4.0599	4.2071	4.3195	4.4214	4.4998	4.5640	4.6239	4.6582	4.6921	4.7451	4.7761	4.8067	4.8319	4.8527
19.50	3.8853	4.1129	4.2579	4.3678	4.4681	4.5455	4.6053	4.6574	4.7006	4.7335	4.7850	4.8151	4.8454	4.8704	4.8911
20.00	3.9411	4.1658	4.3086	4.4158	4.5145	4.5909	4.6522	4.7104	4.7425	4.7746	4.8244	4.8536	4.8835	4.9083	4.9288
20.50	3.9969	4.2186	4.3590	4.4636	4.5606	4.6360	4.6959	4.7531	4.7841	4.8152	4.8633	4.8916	4.9211	4.9457	4.9661
21.00	4.0525	4.2712	4.4094	4.5112	4.6065	4.6808	4.7392	4.7955	4.8253	4.8554	4.9017	4.9291	4.9582	4.9827	5.0029
21.50	4.1080	4.3237	4.4595	4.5586	4.6522	4.7254	4.7822	4.8376	4.8662	4.8953	4.9397	4.9662	4.9949	5.0192	5.0392
22.00	4.1634	4.3760	4.5095	4.6058	4.6976	4.7697	4.8250	4.8794	4.9068	4.9348	4.9774	5.0029	5.0311	5.0552	5.0751
22.50	4.2187	4.4282	4.5594	4.6528	4.7428	4.8138	4.8675	4.9209	4.9470	4.9739	5.0146	5.0391	5.0670	5.0908	5.1105
23.00	4.2739	4.4803	4.6091	4.6996	4.7879	4.8577	4.9098	4.9621	4.9869	5.0128	5.0514	5.0750	5.1024	5.1260	5.1455
23.50	4.3291	4.5323	4.6587	4.7463	4.8327	4.9014	4.9518	5.0031	5.0265	5.0513	5.0879	5.1104	5.1374	5.1608	5.1802
24.00	4.3841	4.5842	4.7081	4.7928	4.8773	4.9449	4.9935	5.0438	5.0659	5.0895	5.1241	5.1455	5.1720	5.1953	5.2144
24.50	4.4391	4.6360	4.7575	4.8391	4.9217	4.9882	5.0351	5.0843	5.1050	5.1275	5.1599	5.1803	5.2063	5.2294	5.2483
25.00	4.4940	4.6877	4.8067	4.8853	4.9660	5.0312	5.0764	5.1245	5.1438	5.1651	5.1955	5.2147	5.2403	5.2631	5.2819
25.50	4.5488	4.7392	4.8558	4.9314	5.0101	5.0741	5.1176	5.1646	5.1824	5.2025	5.2307	5.2488	5.2739	5.2965	5.3151
26.00	4.6036	4.7907	4.9048	4.9772	5.0541	5.1169	5.1585	5.2044	5.2208	5.2397	5.2656	5.2826	5.3073	5.3296	5.3480
26.50	4.6583	4.8421	4.9536	5.0230	5.0979	5.1594	5.1993	5.2440	5.2589	5.2766	5.3003	5.3162	5.3403	5.3624	5.3806
27.00	4.7129	4.8934	5.0024	5.0686	5.1415	5.2019	5.2398	5.2834	5.2968	5.3132	5.3347	5.3494	5.3730	5.3950	5.4129
27.50	4.7675	4.9447	5.0511	5.1142	5.1850	5.2441	5.2802	5.3227	5.3345	5.3497	5.3588	5.3823	5.4054	5.4272	5.4450
28.00	4.8220	4.9958	5.0997	5.1595	5.2284	5.2862	5.3204	5.3817	5.3720	5.3859	5.4027	5.4150	5.4376	5.4591	5.4767
28.50	4.8764	5.0469	5.1482	5.2048	5.2716	5.3282	5.3605	5.4006	5.4094	5.4219	5.4363	5.4475	5.4695	5.4908	5.5082
29.00	4.9308	5.0979	5.1966	5.2500	5.3147	5.3700	5.4004	5.4393	5.4465	5.4577	5.4697	5.4796	5.5012	5.5223	5.5394
29.50	4.9851	5.1488	5.2450	5.2950	5.3577	5.4117	5.4401	5.4779	5.4834	5.4933	5.5029	5.5116	5.5326	5.5535	5.5704
30.00	5.0394	5.1997	5.2932	5.3400	5.4005	5.4532	5.4797	5.5163	5.5202	5.5287	5.5359	5.5433	5.5638	5.5844	5.6011

TABLE 34.2—EXTENDED SUKKAR-CORNELL INTEGRAL FOR BHP CALCULATION (continued)

$$\int_{0.2}^{p_{pr}} \frac{(z/p_{pr}) dp_{pr}}{1+B(z/p_{pr})^2}$$

Pseudoreduced temperature for $B = 5.0$

p_{pr}	1.1	1.2	1.3	1.4	1.5	1.6	1.7	1.8	1.9	2.0	2.2	2.4	2.6	2.8	3.0
0.20	0.0000	0.0000	0.0000	0.0000	0.0000	0.0000	0.0000	0.0000	0.0000	0.0000	0.0000	0.0000	0.0000	0.0000	0.0000
0.50	0.0226	0.0220	0.0216	0.0214	0.0212	0.0210	0.0209	0.0207	0.0207	0.0206	0.0205	0.0205	0.0204	0.0204	0.0204
1.00	0.1036	0.0983	0.0954	0.0934	0.0921	0.0909	0.0901	0.0894	0.0890	0.0886	0.0881	0.0877	0.0874	0.0871	0.0869
1.50	0.2121	0.2052	0.1995	0.1954	0.1924	0.1901	0.1882	0.1668	0.1859	0.1850	0.1838	0.1829	0.1822	0.1816	0.1811
2.00	0.3002	0.3125	0.3102	0.3066	0.3034	0.3007	0.2983	0.2965	0.2954	0.2943	0.2926	0.2914	0.2904	0.2896	0.2889
2.50	0.3741	0.4046	0.4126	0.4133	0.4124	0.4107	0.4090	0.4076	0.4066	0.4056	0.4041	0.4030	0.4020	0.4012	0.4005
3.00	0.4419	0.4854	0.5032	0.5105	0.5137	0.5144	0.5143	0.5140	0.5138	0.5134	0.5125	0.5118	0.5112	0.5108	0.5103
3.50	0.5074	0.5594	0.5847	0.5983	0.6065	0.6101	0.6123	0.6138	0.6147	0.6152	0.6154	0.6155	0.6155	0.6157	0.6156
4.00	0.5715	0.6291	0.6594	0.6785	0.6915	0.6982	0.7029	0.7064	0.7087	0.7104	0.7121	0.7133	0.7140	0.7149	0.7154
4.50	0.6346	0.6957	0.7294	0.7530	0.7702	0.7797	0.7868	0.7927	0.7964	0.7994	0.8027	0.8051	0.8068	0.8084	0.8094
5.00	0.6966	0.7601	0.7960	0.8229	0.8440	0.8560	0.8653	0.8734	0.8785	0.8827	0.8879	0.8916	0.8941	0.8965	0.8980
5.50	0.7579	0.8225	0.8601	0.8895	0.9138	0.9280	0.9393	0.9493	0.9558	0.9611	0.9682	0.9732	0.9765	0.9795	0.9815
6.00	0.8185	0.8836	0.9222	0.9536	0.9803	0.9965	1.0095	1.0213	1.0289	1.0354	1.0441	1.0504	1.0544	1.0580	1.0604
6.50	0.8784	0.9437	0.9829	1.0156	1.0442	1.0620	1.0764	1.0896	1.0984	1.1060	1.1162	1.1236	1.1284	1.1324	1.1351
7.00	0.9378	1.0030	1.0423	1.0758	1.1058	1.1249	1.1406	1.1552	1.1649	1.1734	1.1848	1.1932	1.1987	1.2031	1.2060
7.50	0.9967	1.0614	1.1005	1.1346	1.1656	1.1857	1.2024	1.2182	1.2286	1.2379	1.2504	1.2597	1.2657	1.2704	1.2737
8.00	1.0551	1.1191	1.1578	1.1921	1.2237	1.2447	1.2621	1.2788	1.2900	1.2999	1.3167	1.3234	1.3299	1.3349	1.3383
8.50	1.1131	1.1761	1.2142	1.2486	1.2805	1.3020	1.3201	1.3374	1.3492	1.3596	1.3773	1.3845	1.3914	1.3967	1.4003
9.00	1.1706	1.2325	1.2698	1.3041	1.3361	1.3579	1.3764	1.3943	1.4066	1.4173	1.4357	1.4434	1.4506	1.4561	1.4599
9.50	1.2275	1.2883	1.3248	1.3587	1.3907	1.4125	1.4313	1.4497	1.4623	1.4733	1.4922	1.5008	1.5077	1.5135	1.5174
10.00	1.2841	1.3435	1.3791	1.4126	1.4443	1.4661	1.4851	1.5037	1.5165	1.5278	1.5472	1.5555	1.5630	1.5689	1.5729
10.50	1.3403	1.3983	1.4328	1.4658	1.4970	1.5187	1.5377	1.5564	1.5694	1.5808	1.6006	1.6090	1.6167	1.6226	1.6267
11.00	1.3961	1.4526	1.4860	1.5182	1.5490	1.5705	1.5894	1.6081	1.6211	1.6326	1.6526	1.6611	1.6687	1.6747	1.6789
11.50	1.4515	1.5065	1.5387	1.5701	1.6002	1.6214	1.6401	1.6587	1.6718	1.6833	1.7034	1.7118	1.7195	1.7254	1.7296
12.00	1.5067	1.5601	1.5910	1.6214	1.6509	1.6717	1.6901	1.7085	1.7215	1.7330	1.7530	1.7613	1.7689	1.7749	1.7790
12.50	1.5616	1.6133	1.6429	1.6721	1.7010	1.7213	1.7393	1.7575	1.7704	1.7817	1.8015	1.8097	1.8172	1.8231	1.8271
13.00	1.6163	1.6662	1.6944	1.7224	1.7505	1.7704	1.7879	1.8057	1.8184	1.8295	1.8489	1.8569	1.8644	1.8701	1.8742
13.50	1.6708	1.7188	1.7456	1.7722	1.7995	1.8188	1.8358	1.8532	1.8656	1.8765	1.8954	1.9032	1.9105	1.9161	1.9201
14.00	1.7250	1.7711	1.7965	1.8216	1.8480	1.8667	1.8830	1.9001	1.9121	1.9227	1.9410	1.9485	1.9556	1.9612	1.9651
14.50	1.7791	1.8232	1.8470	1.8706	1.8960	1.9142	1.9298	1.9463	1.9580	1.9681	1.9858	1.9920	1.9998	2.0053	2.0091
15.00	1.8330	1.8750	1.8973	1.9192	1.9436	1.9612	1.9760	1.9920	2.0032	2.0128	2.0298	2.0364	2.0432	2.0485	2.0523
15.50	1.8867	1.9266	1.9472	1.9675	1.9909	2.0077	2.0217	2.0372	2.0478	2.0570	2.0730	2.0792	2.0857	2.0910	2.0946
16.00	1.9402	1.9780	1.9970	2.0154	2.0377	2.0538	2.0669	2.0818	2.0918	2.1005	2.1155	2.1212	2.1275	2.1326	2.1362
16.50	1.9936	2.0292	2.0465	2.0631	2.0842	2.0996	2.1117	2.1260	2.1353	2.1434	2.1574	2.1626	2.1686	2.1736	2.1770
17.00	2.0469	2.0802	2.0958	2.1104	2.1303	2.1450	2.1561	2.1697	2.1783	2.1858	2.1987	2.2032	2.2090	2.2138	2.2172
17.50	2.1000	2.1311	2.1449	2.1575	2.1762	2.1900	2.2000	2.2131	2.2209	2.2276	2.2394	2.2433	2.2488	2.2535	2.2567
18.00	2.1530	2.1817	2.1937	2.2043	2.2217	2.2347	2.2437	2.2560	2.2630	2.2690	2.2795	2.2828	2.2880	2.2925	2.2956
18.50	2.2059	2.2323	2.2424	2.2509	2.2670	2.2791	2.2869	2.2985	2.3046	2.3100	2.3191	2.3217	2.3266	2.3309	2.3339
19.00	2.2587	2.2826	2.2909	2.2973	2.3120	2.3233	2.3299	2.3407	2.3459	2.3505	2.3582	2.3600	2.3646	2.3688	2.3717
19.50	2.3113	2.3329	2.3393	2.3434	2.3567	2.3671	2.3725	2.3825	2.3868	2.3906	2.3969	2.3979	2.4022	2.4062	2.4089
20.00	2.3639	2.3830	2.3875	2.3893	2.4012	2.4107	2.4148	2.4241	2.4273	2.4303	2.4350	2.4353	2.4392	2.4431	2.4456
20.50	2.4164	2.4329	2.4355	2.4350	2.4455	2.4541	2.4568	2.4653	2.4675	2.4696	2.4728	2.4723	2.4758	2.4795	2.4819
21.00	2.4688	2.4828	2.4834	2.4806	2.4895	2.4972	2.4986	2.5062	2.5074	2.5086	2.5101	2.5088	2.5119	2.5155	2.5177
21.50	2.5210	2.5325	2.5311	2.5259	2.5333	2.5400	2.5401	2.5468	2.5470	2.5472	2.5471	2.5449	2.5477	2.5510	2.5531
22.00	2.5733	2.5822	2.5788	2.5711	2.5770	2.5827	2.5814	2.5872	2.5862	2.5855	2.5837	2.5806	2.5830	2.5861	2.5881
22.50	2.6254	2.6317	2.6263	2.6161	2.6204	2.6252	2.6224	2.6273	2.6252	2.6235	2.6199	2.6159	2.6179	2.6209	2.6226
23.00	2.6774	2.6811	2.6736	2.6610	2.6637	2.6674	2.6632	2.6672	2.6639	2.6612	2.6558	2.6508	2.6524	2.6552	2.6568
23.50	2.7294	2.7304	2.7209	2.7057	2.7068	2.7095	2.7038	2.7068	2.7023	2.6986	2.6913	2.6854	2.6866	2.6892	2.6906
24.00	2.7813	2.7796	2.7680	2.7503	2.7497	2.7514	2.7441	2.7462	2.7405	2.7357	2.7266	2.7197	2.7204	2.7229	2.7241
24.50	2.8332	2.8288	2.8151	2.7947	2.7924	2.7981	2.7843	2.7854	2.7784	2.7726	2.7615	2.7536	2.7540	2.7562	2.7573
25.00	2.8849	2.8778	2.8620	2.8390	2.8351	2.8346	2.8243	2.8244	2.8161	2.8092	2.7961	2.7872	2.7872	2.7892	2.7901
25.50	2.9367	2.9268	2.9088	2.8832	2.8775	2.8760	2.8640	2.8532	2.8536	2.8456	2.8305	2.8205	2.8200	2.8219	2.8226
26.00	2.9883	2.9757	2.9556	2.9272	2.9198	2.9172	2.9037	2.9018	2.8908	2.8818	2.8646	2.8536	2.8526	2.8543	2.8548
26.50	3.0399	3.0245	3.0022	2.9711	2.9620	2.9583	2.9431	2.9402	2.9279	2.9177	2.8985	2.8864	2.8850	2.8864	2.8867
27.00	3.0915	3.0733	3.0488	3.0149	3.0040	2.9993	2.9824	2.9785	2.9648	2.9534	2.9320	2.9189	2.9170	2.9182	2.9184
27.50	3.1429	3.1220	3.0953	3.0586	3.0459	3.0400	3.0215	3.0165	3.0014	2.9889	2.9654	2.9512	2.9488	2.9498	2.9497
28.00	3.1944	3.1706	3.1417	3.1022	3.0877	3.0807	3.0604	3.0544	3.0379	3.0242	2.9985	2.9832	2.9803	2.9811	2.9809
28.50	3.2458	3.2191	3.1880	3.1457	3.1294	3.1212	3.0992	3.0922	3.0742	3.0593	3.0314	3.0149	3.0116	3.0122	3.0117
29.00	3.2971	3.2676	3.2343	3.1891	3.1710	3.1616	3.1379	3.1297	3.1103	3.0942	3.0641	3.0465	3.0426	3.0430	3.0424
29.50	3.3484	3.3160	3.2804	3.2324	3.2124	3.2019	3.1764	3.1672	3.1463	3.1289	3.0966	3.0778	3.0735	3.0736	3.0728
30.00	3.3997	3.3644	3.3265	3.2756	3.2537	3.2421	3.2148	3.2045	3.1821	3.1635	3.1288	3.1089	3.1040	3.1040	3.1029

TABLE 34.2—EXTENDED SUKKAR-CORNELL INTEGRAL FOR BHP CALCULATION (continued)

$$\int_{0.2}^{p_{pr}} \frac{(z/p_{pr}) dp_{pr}}{1 + B(z/p_{pr})^2}$$

Pseudoreduced temperature for $B = 10.0$

p_{pr}	1.1	1.2	1.3	1.4	1.5	1.6	1.7	1.8	1.9	2.0	2.2	2.4	2.6	2.8	3.0
0.20	0.0000	0.0000	0.0000	0.0000	0.0000	0.0000	0.0000	0.0000	0.0000	0.0000	0.0000	0.0000	0.0000	0.0000	0.0000
0.50	0.0115	0.0112	0.0110	0.0108	0.0107	0.0107	0.0106	0.0105	0.0105	0.0105	0.0104	0.0104	0.0104	0.0103	0.0103
1.00	0.0561	0.0525	0.0507	0.0494	0.0486	0.0479	0.0474	0.0470	0.0468	0.0465	0.0462	0.0460	0.0458	0.0456	0.0455
1.50	0.1292	0.1187	0.1132	0.1098	0.1074	0.1056	0.1041	0.1031	0.1024	0.1018	0.1009	0.1003	0.0997	0.0994	0.0990
2.00	0.2028	0.1968	0.1891	0.1837	0.1797	0.1767	0.1743	0.1725	0.1713	0.1703	0.1687	0.1676	0.1667	0.1660	0.1653
2.50	0.2684	0.2723	0.2677	0.2624	0.2578	0.2543	0.2513	0.2490	0.2475	0.2461	0.2440	0.2426	0.2413	0.2403	0.2394
3.00	0.3300	0.3422	0.3427	0.3399	0.3364	0.3332	0.3302	0.3278	0.3263	0.3248	0.3225	0.3210	0.3195	0.3184	0.3174
3.50	0.3897	0.4080	0.4130	0.4135	0.4123	0.4102	0.4080	0.4061	0.4047	0.4035	0.4014	0.3999	0.3985	0.3974	0.3964
4.00	0.4485	0.4708	0.4793	0.4832	0.4846	0.4841	0.4830	0.4820	0.4812	0.4803	0.4787	0.4776	0.4764	0.4755	0.4746
4.50	0.5065	0.5315	0.5423	0.5492	0.5533	0.5545	0.5547	0.5549	0.5549	0.5546	0.5538	0.5532	0.5523	0.5517	0.5511
5.00	0.5638	0.5904	0.6029	0.6122	0.6189	0.6217	0.6233	0.6248	0.6256	0.6260	0.6262	0.6263	0.6258	0.6256	0.6252
5.50	0.6204	0.6480	0.6617	0.6729	0.6818	0.6861	0.6891	0.6919	0.6934	0.6946	0.6959	0.6967	0.6967	0.6968	0.6967
6.00	0.6765	0.7045	0.7190	0.7316	0.7424	0.7481	0.7522	0.7563	0.7586	0.7605	0.7629	0.7645	0.7650	0.7654	0.7655
6.50	0.7321	0.7602	0.7752	0.7888	0.8010	0.8079	0.8131	0.8182	0.8214	0.8240	0.8273	0.8297	0.8307	0.8314	0.8317
7.00	0.7873	0.8153	0.8304	0.8447	0.8580	0.8659	0.8720	0.8781	0.8819	0.8852	0.8895	0.8925	0.8940	0.8950	0.8955
7.50	0.8421	0.8697	0.8846	0.8994	0.9134	0.9221	0.9290	0.9360	0.9404	0.9443	0.9494	0.9531	0.9550	0.9562	0.9568
8.00	0.8965	0.9236	0.9381	0.9531	0.9676	0.9770	0.9845	0.9921	0.9971	1.0015	1.0092	1.0115	1.0138	1.0152	1.0160
8.50	0.9506	0.9769	0.9909	1.0059	1.0207	1.0305	1.0385	1.0467	1.0522	1.0569	1.0653	1.0681	1.0706	1.0723	1.0732
9.00	1.0043	1.0296	1.0431	1.0580	1.0729	1.0829	1.0912	1.0999	1.1057	1.1108	1.1197	1.1228	1.1256	1.1275	1.1286
9.50	1.0575	1.0819	1.0947	1.1094	1.1242	1.1342	1.1428	1.1518	1.1579	1.1633	1.1726	1.1760	1.1790	1.1810	1.1822
10.00	1.1104	1.1338	1.1458	1.1601	1.1747	1.1847	1.1935	1.2027	1.2090	1.2145	1.2242	1.2278	1.2309	1.2331	1.2343
10.50	1.1630	1.1852	1.1964	1.2102	1.2245	1.2344	1.2432	1.2525	1.2589	1.2645	1.2746	1.2783	1.2814	1.2836	1.2850
11.00	1.2153	1.2363	1.2466	1.2598	1.2736	1.2834	1.2920	1.3013	1.3078	1.3135	1.3238	1.3275	1.3307	1.3329	1.3343
11.50	1.2674	1.2871	1.2964	1.3089	1.3222	1.3317	1.3402	1.3494	1.3559	1.3616	1.3719	1.3756	1.3788	1.3810	1.3824
12.00	1.3192	1.3376	1.3458	1.3574	1.3702	1.3794	1.3876	1.3967	1.4032	1.4088	1.4190	1.4227	1.4258	1.4280	1.4294
12.50	1.3708	1.3877	1.3949	1.4056	1.4178	1.4266	1.4345	1.4433	1.4497	1.4552	1.4653	1.4688	1.4719	1.4740	1.4753
13.00	1.4222	1.4377	1.4437	1.4533	1.4649	1.4733	1.4807	1.4893	1.4955	1.5008	1.5106	1.5140	1.5169	1.5193	1.5202
13.50	1.4734	1.4873	1.4921	1.5006	1.5115	1.5194	1.5264	1.5346	1.5406	1.5457	1.5551	1.5582	1.5611	1.5630	1.5642
14.00	1.5244	1.5368	1.5403	1.5476	1.5577	1.5652	1.5716	1.5794	1.5851	1.5899	1.5988	1.6016	1.6043	1.6062	1.6074
14.50	1.5753	1.5860	1.5883	1.5942	1.6035	1.6104	1.6163	1.6237	1.6290	1.6335	1.6417	1.6443	1.6468	1.6486	1.6497
15.00	1.6261	1.6351	1.6360	1.6405	1.6490	1.6553	1.6605	1.6575	1.6723	1.6764	1.6840	1.6862	1.6885	1.6902	1.6912
15.50	1.6767	1.6839	1.6835	1.6865	1.6941	1.6999	1.7043	1.7108	1.7151	1.7181	1.7256	1.7274	1.7296	1.7311	1.7320
16.00	1.7271	1.7326	1.7308	1.7323	1.7389	1.7440	1.7477	1.7537	1.7575	1.7607	1.7666	1.7679	1.7699	1.7713	1.7722
16.50	1.7775	1.7811	1.7778	1.7778	1.7834	1.7878	1.7906	1.7961	1.7993	1.8020	1.8070	1.8078	1.8096	1.8109	1.8116
17.00	1.8277	1.8294	1.8247	1.8230	1.8275	1.8314	1.8333	1.8382	1.8407	1.8429	1.8469	1.8472	1.8487	1.8499	1.8505
17.50	1.8778	1.8777	1.8714	1.8680	1.8714	1.8746	1.8756	1.8799	1.8818	1.8833	1.8862	1.8859	1.8872	1.8883	1.8888
18.00	1.9278	1.9257	1.9179	1.9127	1.9151	1.9175	1.9175	1.9212	1.9224	1.9232	1.9251	1.9242	1.9252	1.9261	1.9265
18.50	1.9777	1.9737	1.9643	1.9573	1.9585	1.9602	1.9592	1.9622	1.9626	1.9628	1.9634	1.9619	1.9626	1.9634	1.9637
19.00	2.0276	2.0215	2.0105	2.0017	2.0016	2.0026	2.0005	2.0029	2.0025	2.0020	2.0013	1.9992	1.9996	2.0002	2.0004
19.50	2.0773	2.0692	2.0566	2.0458	2.0446	2.0447	2.0416	2.0433	2.0420	2.0408	2.0388	2.0359	2.0360	2.0365	2.0366
20.00	2.1269	2.1167	2.1026	2.0898	2.0873	2.0867	2.0824	2.0833	2.0812	2.0792	2.0759	2.0723	2.0721	2.0724	2.0723
20.50	2.1765	2.1642	2.1484	2.1336	2.1298	2.1284	2.1229	2.1232	2.1201	2.1173	2.1126	2.1082	2.1077	2.1079	2.1077
21.00	2.2260	2.2116	2.1941	2.1773	2.1722	2.1699	2.1632	2.1627	2.1587	2.1551	2.1489	2.1438	2.1429	2.1429	2.1425
21.50	2.2754	2.2588	2.2396	2.2207	2.2143	2.2112	2.2033	2.2020	2.1970	2.1926	2.1848	2.1789	2.1777	2.1775	2.1770
22.00	2.3248	2.3060	2.2851	2.2641	2.2563	2.2523	2.2432	2.2411	2.2350	2.2298	2.2204	2.2137	2.2121	2.2118	2.2111
22.50	2.3741	2.3531	2.3304	2.3073	2.2981	2.2932	2.2828	2.2799	2.2728	2.2667	2.2557	2.2481	2.2462	2.2457	2.2449
23.00	2.4233	2.4001	2.3757	2.3503	2.3397	2.3340	2.3222	2.3185	2.3103	2.3033	2.2906	2.2822	2.2799	2.2792	2.2783
23.50	2.4725	2.4470	2.4208	2.3932	2.3812	2.3745	2.3615	2.3569	2.3476	2.3397	2.3253	2.3160	2.3133	2.3124	2.3113
24.00	2.5216	2.4938	2.4659	2.4360	2.4226	2.4149	2.4005	2.3951	2.3847	2.3758	2.3597	2.3494	2.3463	2.3453	2.3440
24.50	2.5706	2.5406	2.5108	2.4787	2.4637	2.4552	2.4394	2.4331	2.4215	2.4117	2.3937	2.3826	2.3791	2.3779	2.3765
25.00	2.6196	2.5873	2.5557	2.5212	2.5048	2.4953	2.4761	2.4709	2.4581	2.4473	2.4275	2.4155	2.4115	2.4102	2.4086
25.50	2.6685	2.6339	2.6005	2.5637	2.5457	2.5353	2.5166	2.5085	2.4946	2.4827	2.4611	2.4481	2.4437	2.4422	2.4404
26.00	2.7174	2.6805	2.6452	2.6060	2.5865	2.5751	2.5550	2.5459	2.5308	2.5179	2.4944	2.4804	2.4756	2.4739	2.4719
26.50	2.7663	2.7269	2.6898	2.6482	2.6272	2.6148	2.5932	2.5832	2.5668	2.5529	2.5275	2.5124	2.5073	2.5053	2.5032
27.00	2.8151	2.7734	2.7343	2.6904	2.6677	2.6543	2.6312	2.6203	2.6027	2.5877	2.5603	2.5443	2.5386	2.5365	2.5342
27.50	2.8638	2.8197	2.7788	2.7324	2.7082	2.6938	2.6691	2.6573	2.6384	2.6223	2.5929	2.5758	2.5698	2.5675	2.5650
28.00	2.9125	2.8660	2.8232	2.7743	2.7485	2.7331	2.7069	2.6941	2.6739	2.6567	2.6253	2.6072	2.6007	2.5982	2.5955
28.50	2.9612	2.9123	2.8675	2.8162	2.7887	2.7723	2.7446	2.7307	2.7092	2.6909	2.6575	2.6383	2.6314	2.6286	2.6258
29.00	3.0098	2.9585	2.9118	2.8579	2.8288	2.8114	2.7821	2.7673	2.7444	2.7250	2.6895	2.6692	2.6618	2.6589	2.6558
29.50	3.0584	3.0046	2.9560	2.8996	2.8689	2.8504	2.8194	2.8036	2.7794	2.7589	2.7212	2.6999	2.6920	2.6889	2.6857
30.00	3.1069	3.0507	3.0001	2.9412	2.9088	2.8892	2.8567	2.8399	2.8143	2.7926	2.7528	2.7304	2.7221	2.7187	2.7153

TABLE 34.2—EXTENDED SUKKAR-CORNELL INTEGRAL FOR BHP CALCULATION (continued)

$$\int_{0.2}^{p_{pr}} \frac{(z/p_{pr}) dp_{pr}}{1 + B(z/p_{pr})^2}$$

Pseudoreduced temperature for $B = 15.0$

p_{pr}	1.1	1.2	1.3	1.4	1.5	1.6	1.7	1.8	1.9	2.0	2.2	2.4	2.6	2.8	3.0
0.20	0.0000	0.0000	0.0000	0.0000	0.0000	0.0000	0.0000	0.0000	0.0000	0.0000	0.0000	0.0000	0.0000	0.0000	0.0000
0.50	0.0077	0.0075	0.0074	0.0073	0.0072	0.0071	0.0071	0.0071	0.0070	0.0070	0.0070	0.0070	0.0069	0.0069	0.0069
1.00	0.0385	0.0359	0.0345	0.0336	0.0330	0.0325	0.0322	0.0319	0.0317	0.0316	0.0313	0.0311	0.0310	0.0309	0.0308
1.50	0.0939	0.0838	0.0793	0.0765	0.0746	0.0732	0.0721	0.0713	0.0708	0.0703	0.0696	0.0692	0.0687	0.0685	0.0682
2.00	0.1571	0.1453	0.1371	0.1319	0.1282	0.1257	0.1236	0.1220	0.1211	0.1202	0.1189	0.1180	0.1172	0.1167	0.1161
2.50	0.2162	0.2093	0.2008	0.1943	0.1892	0.1857	0.1827	0.1804	0.1790	0.1777	0.1758	0.1745	0.1733	0.1724	0.1716
3.00	0.2725	0.2710	0.2648	0.2587	0.2533	0.2493	0.2458	0.2431	0.2413	0.2397	0.2374	0.2357	0.2342	0.2331	0.2320
3.50	0.3275	0.3302	0.3267	0.3222	0.3176	0.3138	0.3102	0.3074	0.3055	0.3038	0.3012	0.2994	0.2978	0.2964	0.2952
4.00	0.3818	0.3874	0.3862	0.3837	0.3805	0.3774	0.3743	0.3717	0.3699	0.3683	0.3657	0.3639	0.3622	0.3608	0.3596
4.50	0.4355	0.4430	0.4435	0.4431	0.4415	0.4393	0.4369	0.4349	0.4335	0.4320	0.4298	0.4281	0.4265	0.4252	0.4240
5.00	0.4887	0.4975	0.4992	0.5004	0.5006	0.4994	0.4978	0.4966	0.4956	0.4945	0.4928	0.4914	0.4900	0.4888	0.4877
5.50	0.5413	0.5508	0.5535	0.5561	0.5579	0.5577	0.5570	0.5566	0.5561	0.5554	0.5543	0.5534	0.5522	0.5512	0.5503
6.00	0.5936	0.6034	0.6066	0.6103	0.6135	0.6143	0.6144	0.6149	0.6149	0.6147	0.6143	0.6138	0.6129	0.6121	0.6113
6.50	0.6454	0.6553	0.6590	0.6634	0.6676	0.6694	0.6703	0.6715	0.6720	0.6724	0.6726	0.6727	0.6721	0.6715	0.6708
7.00	0.6969	0.7068	0.7105	0.7155	0.7205	0.7230	0.7246	0.7265	0.7276	0.7284	0.7293	0.7299	0.7296	0.7291	0.7286
7.50	0.7482	0.7577	0.7613	0.7666	0.7722	0.7754	0.7776	0.7802	0.7817	0.7829	0.7844	0.7854	0.7855	0.7852	0.7848
8.00	0.7991	0.8082	0.8114	0.8170	0.8230	0.8266	0.8293	0.8324	0.8344	0.8360	0.8391	0.8395	0.8398	0.8397	0.8394
8.50	0.8497	0.8582	0.8611	0.8666	0.8729	0.8768	0.8799	0.8835	0.8858	0.8878	0.8914	0.8920	0.8926	0.8927	0.8925
9.00	0.9000	0.9078	0.9102	0.9157	0.9220	0.9261	0.9295	0.9334	0.9360	0.9382	0.9423	0.9432	0.9440	0.9442	0.9441
9.50	0.9500	0.9570	0.9588	0.9641	0.9704	0.9746	0.9782	0.9824	0.9852	0.9876	0.9920	0.9932	0.9941	0.9944	0.9944
10.00	0.9998	1.0059	1.0071	1.0121	1.0181	1.0223	1.0260	1.0304	1.0334	1.0359	1.0407	1.0420	1.0430	1.0434	1.0435
10.50	1.0492	1.0544	1.0549	1.0595	1.0653	1.0694	1.0731	1.0776	1.0806	1.0833	1.0883	1.0897	1.0908	1.0913	1.0914
11.00	1.0985	1.1026	1.1024	1.1065	1.1119	1.1159	1.1195	1.1239	1.1271	1.1298	1.1349	1.1364	1.1375	1.1380	1.1381
11.50	1.1475	1.1506	1.1496	1.1530	1.1580	1.1618	1.1653	1.1696	1.1728	1.1755	1.1807	1.1822	1.1832	1.1837	1.1839
12.00	1.1963	1.1983	1.1964	1.1992	1.2037	1.2072	1.2105	1.2147	1.2178	1.2205	1.2256	1.2270	1.2281	1.2285	1.2287
12.50	1.2449	1.2458	1.2430	1.2449	1.2490	1.2522	1.2551	1.2592	1.2622	1.2648	1.2698	1.2711	1.2720	1.2724	1.2725
13.00	1.2934	1.2931	1.2893	1.2903	1.2939	1.2967	1.2993	1.3031	1.3060	1.3084	1.3131	1.3143	1.3152	1.3155	1.3156
13.50	1.3417	1.3402	1.3354	1.3354	1.3384	1.3408	1.3430	1.3465	1.3492	1.3514	1.3558	1.3567	1.3575	1.3578	1.3578
14.00	1.3899	1.3870	1.3812	1.3862	1.3825	1.3845	1.3862	1.3894	1.3918	1.3938	1.3977	1.3984	1.3991	1.3993	1.3992
14.50	1.4380	1.4337	1.4268	1.4247	1.4263	1.4278	1.4290	1.4319	1.4339	1.4356	1.4390	1.4395	1.4400	1.4401	1.4400
15.00	1.4860	1.4803	1.4722	1.4689	1.4698	1.4708	1.4714	1.4739	1.4756	1.4769	1.4797	1.4798	1.4802	1.4802	1.4800
15.50	1.5338	1.5266	1.5174	1.5129	1.5130	1.5135	1.5134	1.5155	1.5168	1.5177	1.5198	1.5196	1.5197	1.5197	1.5194
16.00	1.5815	1.5728	1.5625	1.5566	1.5559	1.5558	1.5551	1.5567	1.5575	1.5580	1.5594	1.5587	1.5587	1.5585	1.5582
16.50	1.6291	1.6189	1.6073	1.6001	1.5985	1.5979	1.5964	1.5976	1.5978	1.5979	1.5984	1.5973	1.5971	1.5968	1.5964
17.00	1.6766	1.6649	1.6520	1.6434	1.6409	1.6397	1.6374	1.6381	1.6378	1.6373	1.6370	1.6354	1.6350	1.6346	1.6341
17.50	1.7241	1.7107	1.6966	1.6865	1.6830	1.6812	1.6781	1.6783	1.6773	1.6764	1.6750	1.6730	1.6723	1.6718	1.6712
18.00	1.7714	1.7564	1.7410	1.7293	1.7249	1.7225	1.7186	1.7181	1.7166	1.7150	1.7127	1.7100	1.7091	1.7085	1.7078
18.50	1.8187	1.8020	1.7853	1.7720	1.7666	1.7635	1.7587	1.7577	1.7554	1.7533	1.7499	1.7466	1.7455	1.7447	1.7439
19.00	1.8659	1.8475	1.8294	1.8146	1.8081	1.8043	1.7986	1.7970	1.7940	1.7912	1.7866	1.7828	1.7814	1.7805	1.7796
19.50	1.9130	1.8929	1.8734	1.8569	1.8493	1.8449	1.8382	1.8360	1.8322	1.8288	1.8280	1.8186	1.8169	1.8158	1.8148
20.00	1.9600	1.9382	1.9173	1.8991	1.8904	1.8853	1.8776	1.8747	1.8702	1.8661	1.8590	1.8540	1.8519	1.8508	1.8496
20.50	2.0070	1.9834	1.9611	1.9412	1.9314	1.9255	1.9168	1.9132	1.9079	1.9031	1.8947	1.8889	1.8866	1.8853	1.8840
21.00	2.0539	2.0285	2.0048	1.9831	1.9721	1.9655	1.9557	1.9515	1.9453	1.9397	1.9300	1.9235	1.9209	1.9195	1.9180
21.50	2.1007	2.0736	2.0484	2.0248	2.0127	2.0054	1.9944	1.9895	1.9824	1.9761	1.9650	1.9578	1.9549	1.9532	1.9517
22.00	2.1475	2.1185	2.0918	2.0665	2.0531	2.0450	2.0330	2.0273	2.0193	2.0122	1.9997	1.9917	1.9884	1.9867	1.9850
22.50	2.1943	2.1634	2.1352	2.1080	2.0934	2.0845	2.0713	2.0649	2.0560	2.0481	2.0341	2.0253	2.0217	2.0198	2.0179
23.00	2.2410	2.2082	2.1785	2.1494	2.1335	2.1239	2.1095	2.1024	2.0924	2.0837	2.0681	2.0586	2.0546	2.0525	2.0506
23.50	2.2876	2.2529	2.2217	2.1906	2.1735	2.1631	2.1475	2.1396	2.1286	2.1191	2.1019	2.0916	2.0872	2.0850	2.0829
24.00	2.3342	2.2976	2.2648	2.2318	2.2134	2.2021	2.1853	2.1766	2.1646	2.1542	2.1355	2.1242	2.1196	2.1171	2.1149
24.50	2.3807	2.3422	2.3079	2.2728	2.2531	2.2410	2.2229	2.2135	2.2005	2.1891	2.1687	2.1567	2.1516	2.1490	2.1466
25.00	2.4272	2.3867	2.3509	2.3138	2.2927	2.2798	2.2604	2.2502	2.2361	2.2238	2.2017	2.1888	2.1834	2.1806	2.1780
25.50	2.4736	2.4312	2.3937	2.3546	2.3322	2.3184	2.2978	2.2867	2.2715	2.2583	2.2345	2.2207	2.2149	2.2119	2.2092
26.00	2.5200	2.4756	2.4366	2.3953	2.3716	2.3569	2.3350	2.3230	2.3067	2.2927	2.2671	2.2523	2.2461	2.2430	2.2401
26.50	2.5664	2.5200	2.4793	2.4360	2.4109	2.3953	2.3720	2.3592	2.3418	2.3268	2.2994	2.2837	2.2771	2.2738	2.2707
27.00	2.6127	2.5643	2.5220	2.4766	2.4501	2.4336	2.4089	2.3953	2.3767	2.3607	2.3315	2.3149	2.3078	2.3044	2.3011
27.50	2.6590	2.6086	2.5646	2.5170	2.4891	2.4718	2.4457	2.4312	2.4115	2.3944	2.3634	2.3458	2.3384	2.3347	2.3313
28.00	2.7053	2.6528	2.6072	2.5574	2.5281	2.5098	2.4824	2.4670	2.4460	2.4280	2.3951	2.3765	2.3687	2.3648	2.3612
28.50	2.7515	2.6969	2.6497	2.5977	2.5669	2.5478	2.5189	2.5026	2.4805	2.4614	2.4266	2.4070	2.3987	2.3947	2.3909
29.00	2.7977	2.7410	2.6921	2.6380	2.6057	2.5856	2.5553	2.5382	2.5148	2.4947	2.4579	2.4373	2.4286	2.4244	2.4205
29.50	2.8438	2.7851	2.7345	2.6781	2.6444	2.6234	2.5916	2.5736	2.5489	2.5278	2.4890	2.4674	2.4583	2.4538	2.4497
30.00	2.8899	2.8291	2.7769	2.7182	2.6830	2.6610	2.6278	2.6088	2.5829	2.5607	2.5200	2.4974	2.4878	2.4831	2.4788

TABLE 34.2—EXTENDED SUKKAR-CORNELL INTEGRAL FOR BHP CALCULATION (continued)

$$\int_{0.2}^{p_{pr}} \frac{(z/p_{pr}) dp_{pr}}{1 + B(z/p_{pr})^2}$$

Pseudoreduced temperature for $B = 20.0$

p_{pr}	1.1	1.2	1.3	1.4	1.5	1.6	1.7	1.8	1.9	2.0	2.2	2.4	2.6	2.8	3.0
0.20	0.0000	0.0000	0.0000	0.0000	0.0000	0.0000	0.0000	0.0000	0.0000	0.0000	0.0000	0.0000	0.0000	0.0000	0.0000
0.50	0.0058	0.0056	0.0055	0.0055	0.0054	0.0054	0.0053	0.0053	0.0053	0.0053	0.0052	0.0052	0.0052	0.0052	0.0052
1.00	0.0294	0.0272	0.0262	0.0255	0.0250	0.0246	0.0243	0.0241	0.0240	0.0239	0.0237	0.0236	0.0235	0.0234	0.0233
1.50	0.0740	0.0649	0.0610	0.0587	0.0572	0.0561	0.0551	0.0545	0.0541	0.0537	0.0532	0.0528	0.0525	0.0522	0.0520
2.00	0.1295	0.1156	0.1077	0.1030	0.0998	0.0976	0.0958	0.0945	0.0937	0.0930	0.0918	0.0911	0.0905	0.0900	0.0895
2.50	0.1832	0.1712	0.1614	0.1547	0.1498	0.1465	0.1438	0.1417	0.1404	0.1393	0.1376	0.1364	0.1354	0.1346	0.1339
3.00	0.2350	0.2264	0.2172	0.2099	0.2040	0.1999	0.1964	0.1937	0.1920	0.1904	0.1882	0.1867	0.1853	0.1842	0.1832
3.50	0.2860	0.2801	0.2725	0.2657	0.2597	0.2553	0.2514	0.2484	0.2463	0.2445	0.2419	0.2401	0.2384	0.2371	0.2359
4.00	0.3365	0.3326	0.3264	0.3208	0.3154	0.3111	0.3073	0.3041	0.3020	0.3000	0.2972	0.2952	0.2934	0.2919	0.2906
4.50	0.3865	0.3841	0.3790	0.3747	0.3703	0.3664	0.3629	0.3599	0.3578	0.3559	0.3531	0.3510	0.3492	0.3476	0.3462
5.00	0.4360	0.4346	0.4305	0.4273	0.4240	0.4208	0.4177	0.4151	0.4132	0.4114	0.4088	0.4068	0.4050	0.4034	0.4021
5.50	0.4852	0.4843	0.4809	0.4787	0.4765	0.4740	0.4714	0.4594	0.4678	0.4662	0.4639	0.4622	0.4604	0.4589	0.4577
6.00	0.5341	0.5335	0.5305	0.5291	0.5279	0.5261	0.5241	0.5226	0.5213	0.5201	0.5182	0.5167	0.5151	0.5137	0.5125
6.50	0.5827	0.5821	0.5794	0.5786	0.5783	0.5771	0.5756	0.5747	0.5738	0.5729	0.5714	0.5703	0.5689	0.5676	0.5665
7.00	0.6310	0.6304	0.6277	0.6274	0.6276	0.6270	0.6261	0.6257	0.6252	0.6246	0.6236	0.6228	0.6216	0.6205	0.6194
7.50	0.6791	0.6782	0.6755	0.6754	0.6761	0.6760	0.6755	0.6756	0.6754	0.6752	0.6746	0.6741	0.6732	0.6722	0.6712
8.00	0.7269	0.7257	0.7227	0.7228	0.7238	0.7241	0.7240	0.7245	0.7247	0.7247	0.7251	0.7244	0.7237	0.7227	0.7219
8.50	0.7745	0.7728	0.7695	0.7696	0.7708	0.7714	0.7716	0.7725	0.7729	0.7732	0.7740	0.7735	0.7730	0.7727	0.7714
9.00	0.8219	0.8196	0.8159	0.8160	0.8172	0.8179	0.8184	0.8195	0.8202	0.8207	0.8218	0.8216	0.8212	0.8205	0.8198
9.50	0.8690	0.8661	0.8620	0.8618	0.8631	0.8638	0.8644	0.8658	0.8666	0.8673	0.8687	0.8687	0.8684	0.8678	0.8672
10.00	0.9159	0.9123	0.9077	0.9073	0.9083	0.9091	0.9098	0.9113	0.9123	0.9131	0.9147	0.9148	0.9146	0.9141	0.9135
10.50	0.9626	0.9582	0.9530	0.9523	0.9531	0.9538	0.9545	0.9561	0.9571	0.9580	0.9599	0.9601	0.9599	0.9595	0.9589
11.00	1.0091	1.0039	0.9981	0.9969	0.9975	0.9980	0.9987	1.0002	1.0014	1.0023	1.0043	1.0045	1.0043	1.0039	1.0034
11.50	1.0554	1.0494	1.0429	1.0412	1.0414	1.0418	1.0423	1.0438	1.0450	1.0459	1.0479	1.0481	1.0479	1.0475	1.0470
12.00	1.1016	1.0946	1.0874	1.0851	1.0849	1.0851	1.0855	1.0868	1.0879	1.0888	1.0908	1.0909	1.0908	1.0903	1.0898
12.50	1.1476	1.1397	1.1317	1.1288	1.1282	1.1280	1.1282	1.1294	1.1304	1.1312	1.1331	1.1331	1.1328	1.1323	1.1318
13.00	1.1935	1.1846	1.1758	1.1721	1.1710	1.1706	1.1704	1.1714	1.1723	1.1730	1.1746	1.1745	1.1742	1.1736	1.1731
13.50	1.2392	1.2293	1.2197	1.2151	1.2136	1.2128	1.2122	1.2130	1.2137	1.2142	1.2156	1.2153	1.2149	1.2143	1.2136
14.00	1.2849	1.2739	1.2633	1.2579	1.2558	1.2547	1.2537	1.2542	1.2547	1.2549	1.2559	1.2554	1.2549	1.2542	1.2535
14.50	1.3304	1.3183	1.3068	1.3005	1.2977	1.2962	1.2948	1.2949	1.2952	1.2952	1.2957	1.2949	1.2943	1.2935	1.2928
15.00	1.3759	1.3625	1.3501	1.3428	1.3394	1.3375	1.3355	1.3353	1.3352	1.3349	1.3349	1.3339	1.3331	1.3322	1.3315
15.50	1.4212	1.4067	1.3933	1.3849	1.3808	1.3784	1.3759	1.3754	1.3749	1.3743	1.3736	1.3723	1.3713	1.3704	1.3695
16.00	1.4665	1.4507	1.4363	1.4267	1.4220	1.4191	1.4150	1.4151	1.4142	1.4132	1.4118	1.4101	1.4090	1.4080	1.4071
16.50	1.5116	1.4945	1.4792	1.4684	1.4629	1.4595	1.4558	1.4544	1.4531	1.4517	1.4496	1.4475	1.4462	1.4451	1.4441
17.00	1.5567	1.5383	1.5219	1.5099	1.5036	1.4997	1.4953	1.4935	1.4916	1.4898	1.4869	1.4844	1.4829	1.4817	1.4806
17.50	1.6017	1.5820	1.5645	1.5512	1.5441	1.5397	1.5345	1.5323	1.5298	1.5275	1.5238	1.5208	1.5191	1.5178	1.5166
18.00	1.6467	1.6256	1.6069	1.5924	1.5844	1.5794	1.5735	1.5708	1.5678	1.5649	1.5603	1.5568	1.5549	1.5534	1.5522
18.50	1.6916	1.6691	1.6493	1.6334	1.6245	1.6190	1.6123	1.6090	1.6054	1.6020	1.5964	1.5924	1.5902	1.5887	1.5873
19.00	1.7364	1.7125	1.6915	1.6742	1.6644	1.6583	1.6508	1.6470	1.6427	1.6388	1.6321	1.6275	1.6252	1.6235	1.6220
19.50	1.7811	1.7558	1.7336	1.7149	1.7042	1.6975	1.6891	1.6847	1.6797	1.6752	1.6675	1.6623	1.6597	1.6579	1.6563
20.00	1.8258	1.7990	1.7757	1.7555	1.7438	1.7364	1.7271	1.7222	1.7165	1.7114	1.7025	1.6967	1.6938	1.6919	1.6902
20.50	1.8705	1.8421	1.8176	1.7959	1.7832	1.7752	1.7650	1.7595	1.7530	1.7473	1.7372	1.7308	1.7276	1.7256	1.7238
21.00	1.9150	1.8852	1.8594	1.8362	1.8225	1.8139	1.8027	1.7965	1.7893	1.7829	1.7716	1.7645	1.7611	1.7589	1.7570
21.50	1.9596	1.9282	1.9012	1.8763	1.8616	1.8523	1.8401	1.8334	1.8254	1.8183	1.8056	1.7979	1.7942	1.7918	1.7898
22.00	2.0041	1.9711	1.9429	1.9164	1.9006	1.8906	1.8774	1.8700	1.8612	1.8534	1.8394	1.8310	1.8270	1.8245	1.8223
22.50	2.0485	2.0140	1.9844	1.9563	1.9395	1.9288	1.9146	1.9065	1.8968	1.8882	1.8730	1.8638	1.8595	1.8568	1.8545
23.00	2.0929	2.0568	2.0259	1.9962	1.9782	1.9668	1.9516	1.9428	1.9322	1.9229	1.9062	1.8963	1.8916	1.8889	1.8864
23.50	2.1372	2.0995	2.0674	2.0359	2.0168	2.0047	1.9684	1.9789	1.9674	1.9573	1.9392	1.9286	1.9235	1.9206	1.9180
24.00	2.1815	2.1422	2.1087	2.0756	2.0553	2.0425	2.0250	2.0149	2.0025	1.9916	1.9719	1.9605	1.9551	1.9521	1.9493
24.50	2.2258	2.1849	2.1500	2.1151	2.0937	2.0801	2.0615	2.0507	2.0373	2.0256	2.0044	1.9922	1.9865	1.9832	1.9804
25.00	2.2700	2.2274	2.1912	2.1546	2.1319	2.1176	2.0979	2.0863	2.0719	2.0594	2.0367	2.0237	2.0176	2.0142	2.0112
25.50	2.3142	2.2700	2.2324	2.1939	2.1701	2.1550	2.1341	2.1218	2.1064	2.0930	2.0687	2.0549	2.0484	2.0449	2.0417
26.00	2.3584	2.3124	2.2735	2.2332	2.2082	2.1923	2.1702	2.1571	2.1408	2.1265	2.1005	2.0858	2.0790	2.0753	2.0720
26.50	2.4025	2.3549	2.3145	2.2724	2.2461	2.2295	2.2062	2.1923	2.1749	2.1598	2.1321	2.1166	2.1094	2.1055	2.1020
27.00	2.4466	2.3973	2.3565	2.3115	2.2840	2.2665	2.2420	2.2274	2.2089	2.1929	2.1636	2.1471	2.1395	2.1355	2.1318
27.50	2.4907	2.4396	2.3964	2.3505	2.3218	2.3035	2.2778	2.2623	2.2428	2.2258	2.1948	2.1774	2.1695	2.1652	2.1614
28.00	2.5347	2.4819	2.4373	2.3895	2.3595	2.3404	2.3134	2.2971	2.2765	2.2586	2.2258	2.2075	2.1992	2.1948	2.1908
28.50	2.5707	2.5243	2.4781	2.4204	2.3971	2.3772	2.3409	2.3110	2.3100	2.2912	2.2566	2.2375	2.2287	2.2241	2.2200
29.00	2.6228	2.5664	2.5189	2.4672	2.4446	2.4119	2.3848	2.3664	2.3435	2.3217	2.2873	2.2675	2.2580	2.2552	2.2600
29.50	2.6666	2.6085	2.5596	2.5060	2.4720	2.4504	2.4195	2.4008	2.3768	2.3560	2.3178	2.2967	2.2871	2.2822	2.2777
30.00	2.7106	2.6507	2.6003	2.5447	2.5094	2.4870	2.4547	2.4352	2.4100	2.3882	2.3481	2.3261	2.3161	2.3109	2.3063

TABLE 34.2—EXTENDED SUKKAR-CORNELL INTEGRAL FOR BHP CALCULATION (continued)

$$\int_{0.2}^{p_{pr}} \frac{(z/p_{pr}) dp_{pr}}{1 + B(z/p_{pr})^2}$$

Pseudoreduced temperature for $B = 25.0$

p_{pr}	1.1	1.2	1.3	1.4	1.5	1.6	1.7	1.8	1.9	2.0	2.2	2.4	2.6	2.8	3.0
0.20	0.0000	0.0000	0.0000	0.0000	0.0000	0.0000	0.0000	0.0000	0.0000	0.0000	0.0000	0.0000	0.0000	0.0000	0.0000
0.50	0.0047	0.0045	0.0044	0.0044	0.0043	0.0043	0.0043	0.0042	0.0042	0.0042	0.0042	0.0042	0.0042	0.0042	0.0042
1.00	0.0237	0.0219	0.0211	0.0205	0.0201	0.0198	0.0196	0.0194	0.0193	0.0192	0.0191	0.0187	0.0189	0.0188	0.0187
1.50	0.0611	0.0529	0.0496	0.0477	0.0464	0.0454	0.0446	0.0441	0.0438	0.0435	0.0430	0.0427	0.0424	0.0422	0.0420
2.00	0.1106	0.0961	0.0888	0.0846	0.0818	0.0798	0.0783	0.0771	0.0764	0.0758	0.0749	0.0742	0.0737	0.0733	0.0729
2.50	0.1598	0.1453	0.1352	0.1287	0.1241	0.1211	0.1186	0.1168	0.1156	0.1146	0.1131	0.1121	0.1111	0.1104	0.1098
3.00	0.2079	0.1952	0.1846	0.1769	0.1711	0.1670	0.1637	0.1612	0.1596	0.1581	0.1561	0.1547	0.1534	0.1524	0.1515
3.50	0.2554	0.2444	0.2346	0.2267	0.2202	0.2156	0.2117	0.2087	0.2067	0.2049	0.2024	0.2007	0.1991	0.1978	0.1967
4.00	0.3025	0.2930	0.2840	0.2766	0.2702	0.2654	0.2613	0.2579	0.2557	0.2537	0.2508	0.2488	0.2470	0.2455	0.2442
4.50	0.3492	0.3408	0.3325	0.3260	0.3200	0.3154	0.3112	0.3078	0.3055	0.3034	0.3004	0.2982	0.2962	0.2946	0.2932
5.00	0.3957	0.3879	0.3803	0.3745	0.3693	0.3650	0.3610	0.3578	0.3555	0.3534	0.3503	0.3481	0.3461	0.3444	0.3429
5.50	0.4418	0.4345	0.4274	0.4223	0.4178	0.4139	0.4103	0.4073	0.4052	0.4031	0.4002	0.3980	0.3961	0.3963	0.3929
6.00	0.4878	0.4806	0.4739	0.4694	0.4656	0.4622	0.4589	0.4563	0.4543	0.4525	0.4498	0.4477	0.4458	0.4441	0.4428
6.50	0.5335	0.5263	0.5198	0.5158	0.5126	0.5097	0.5068	0.5045	0.5028	0.5012	0.4988	0.4969	0.4951	0.4935	0.4922
7.00	0.5790	0.5718	0.5653	0.5616	0.5589	0.5564	0.5539	0.5520	0.5506	0.5492	0.5471	0.5454	0.5437	0.5422	0.5409
7.50	0.6243	0.6169	0.6104	0.6069	0.6045	0.6024	0.6003	0.5987	0.5975	0.5964	0.5946	0.5932	0.5917	0.5902	0.5890
8.00	0.6694	0.6618	0.6550	0.6516	0.6495	0.6477	0.6459	0.6447	0.6437	0.6428	0.6415	0.6401	0.6388	0.6374	0.6362
8.50	0.7143	0.7063	0.6993	0.6960	0.6940	0.6924	0.6908	0.6899	0.6892	0.6884	0.6874	0.6862	0.6850	0.6837	0.6826
9.00	0.7591	0.7506	0.7433	0.7399	0.7380	0.7365	0.7351	0.7344	0.7338	0.7333	0.7325	0.7315	0.7304	0.7292	0.7282
9.50	0.8036	0.7946	0.7870	0.7834	0.7814	0.7800	0.7788	0.7783	0.7778	0.7774	0.7769	0.7760	0.7750	0.7739	0.7730
10.00	0.8480	0.8384	0.8303	0.8266	0.8245	0.8231	0.8219	0.8215	0.8212	0.8208	0.8205	0.8183	0.8189	0.8178	0.8169
10.50	0.8922	0.8820	0.8735	0.8695	0.8671	0.8657	0.8645	0.8641	0.8639	0.8636	0.8635	0.8628	0.8619	0.8609	0.8600
11.00	0.9362	0.9254	0.9163	0.9120	0.9094	0.9078	0.9056	0.9063	0.9061	0.9058	0.9058	0.9052	0.9043	0.9033	0.9024
11.50	0.9801	0.9686	0.9590	0.9542	0.9514	0.9496	0.9483	0.9479	0.9477	0.9475	0.9475	0.9468	0.9459	0.9449	0.9440
12.00	1.0239	1.0117	1.0014	0.9961	0.9930	0.9910	0.9896	0.9891	0.9889	0.9886	0.9885	0.9879	0.9869	0.9859	0.9850
12.50	1.0676	1.0545	1.0437	1.0378	1.0343	1.0321	1.0304	1.0298	1.0295	1.0292	1.0290	1.0283	1.0273	1.0262	1.0253
13.00	1.1111	1.0973	1.0857	1.0792	1.0753	1.0729	1.0709	1.0701	1.0698	1.0693	1.0689	1.0681	1.0670	1.0659	1.0650
13.50	1.1547	1.1398	1.1276	1.1204	1.1161	1.1134	1.1111	1.1101	1.1095	1.1089	1.1083	1.1073	1.1062	1.1050	1.1040
14.00	1.1979	1.1823	1.1693	1.1614	1.1566	1.1535	1.1509	1.1496	1.1489	1.1481	1.1472	1.1459	1.1447	1.1435	1.1425
14.50	1.2412	1.2246	1.2109	1.2021	1.1968	1.1934	1.1904	1.1889	1.1879	1.1868	1.1855	1.1840	1.1827	1.1815	1.1804
15.00	1.2844	1.2668	1.2523	1.2427	1.2368	1.2331	1.2296	1.2278	1.2265	1.2252	1.2234	1.2217	1.2202	1.2189	1.2177
15.50	1.3275	1.3089	1.2936	1.2830	1.2766	1.2725	1.2685	1.2663	1.2647	1.2631	1.2608	1.2588	1.2572	1.2558	1.2546
16.00	1.3705	1.3509	1.3347	1.3232	1.3161	1.3116	1.3071	1.3046	1.3026	1.3007	1.2978	1.2954	1.2937	1.2922	1.2909
16.50	1.4135	1.3928	1.3757	1.3632	1.3555	1.3505	1.3455	1.3426	1.3402	1.3379	1.3343	1.3316	1.3298	1.3291	1.3268
17.00	1.4564	1.4346	1.4166	1.4031	1.3947	1.3892	1.3836	1.3803	1.3775	1.3748	1.3705	1.3674	1.3653	1.3637	1.3623
17.50	1.4992	1.4763	1.4574	1.4428	1.4336	1.4278	1.4215	1.4178	1.4145	1.4114	1.4062	1.4028	1.4005	1.3987	1.3973
18.00	1.5420	1.5180	1.4981	1.4823	1.4724	1.4661	1.4591	1.4550	1.4512	1.4476	1.4417	1.4377	1.4353	1.4334	1.4318
18.50	1.5847	1.5595	1.5387	1.5217	1.5111	1.5042	1.4965	1.4920	1.4876	1.4835	1.4767	1.4723	1.4697	1.4677	1.4660
19.00	1.6274	1.6010	1.5792	1.5610	1.5496	1.5422	1.5338	1.5287	1.5238	1.5192	1.5114	1.5065	1.5036	1.5015	1.4998
19.50	1.6700	1.6424	1.6196	1.6002	1.5879	1.5800	1.5708	1.5653	1.5597	1.5546	1.5458	1.5404	1.5373	1.5351	1.5332
20.00	1.7126	1.6837	1.6599	1.6392	1.6261	1.6176	1.6076	1.6016	1.5954	1.5897	1.5799	1.5739	1.5706	1.5692	1.5663
20.50	1.7551	1.7250	1.7001	1.6781	1.6641	1.6551	1.6443	1.6377	1.6308	1.6246	1.6137	1.6071	1.6035	1.6011	1.5990
21.00	1.7975	1.7662	1.7403	1.7169	1.7020	1.6924	1.6808	1.6736	1.6660	1.6592	1.6472	1.6400	1.6362	1.6336	1.6314
21.50	1.8400	1.8073	1.7803	1.7556	1.7398	1.7296	1.7171	1.7094	1.7011	1.6936	1.6804	1.6726	1.6685	1.6658	1.6635
22.00	1.8824	1.8484	1.8203	1.7942	1.7775	1.7667	1.7532	1.7450	1.7359	1.7278	1.7134	1.7049	1.7005	1.6977	1.6953
22.50	1.9247	1.8895	1.8603	1.8327	1.8150	1.8036	1.7892	1.7804	1.7705	1.7617	1.7460	1.7370	1.7322	1.7293	1.7267
23.00	1.9670	1.9304	1.9001	1.8711	1.8524	1.8404	1.8251	1.8156	1.8049	1.7955	1.7785	1.7687	1.7637	1.7606	1.7579
23.50	2.0093	1.9714	1.9399	1.9094	1.8898	1.8771	1.8608	1.8507	1.8392	1.8290	1.8107	1.8002	1.7949	1.7916	1.7889
24.00	2.0516	2.0122	1.9797	1.9477	1.9270	1.9136	1.8964	1.8856	1.8733	1.8623	1.8427	1.8315	1.8258	1.8224	1.8195
24.50	2.0938	2.0531	2.0193	1.9858	1.9641	1.9501	1.9318	1.9204	1.9072	1.8955	1.8744	1.8625	1.8565	1.8530	1.8499
25.00	2.1360	2.0938	2.0590	2.0239	2.0011	1.9864	1.9671	1.9550	1.9409	1.9285	1.9060	1.8933	1.8870	1.8833	1.8801
25.50	2.1761	2.1346	2.0985	2.0618	2.0380	2.0226	2.0023	1.9895	1.9745	1.9613	1.9373	1.9238	1.9172	1.9133	1.9100
26.00	2.2202	2.1753	2.1380	2.0998	2.0749	2.0588	2.0373	2.0239	2.0079	1.9939	1.9684	1.9542	1.9472	1.9431	1.9397
26.50	2.2623	2.2159	2.1775	2.1376	2.1116	2.0948	2.0723	2.0581	2.0412	2.0264	1.9994	1.9843	1.9769	1.9728	1.9692
27.00	2.3044	2.2566	2.2169	2.1754	2.1483	2.1307	2.1071	2.0923	2.0744	2.0587	2.0301	2.0142	2.0065	2.0022	1.9984
27.50	2.3464	2.2971	2.2562	2.2131	2.1848	2.1666	2.1418	2.1263	2.1074	2.0909	2.0607	2.0440	2.0359	2.0314	2.0275
28.00	2.3885	2.3377	2.2955	2.2507	2.2213	2.2024	2.1764	2.1601	2.1403	2.1229	2.0911	2.0735	2.0650	2.0603	2.0563
28.50	2.4305	2.3782	2.3348	2.2883	2.2578	2.2380	2.2110	2.1939	2.1730	2.1548	2.1213	2.1028	2.0940	2.0891	2.0849
29.00	2.4724	2.4186	2.3740	2.3258	2.2941	2.2736	2.2454	2.2276	2.2056	2.1865	2.1513	2.1320	2.1228	2.1178	2.1134
29.50	2.5144	2.4591	2.4132	2.3632	2.3304	2.3091	2.2797	2.2611	2.2381	2.2181	2.1812	2.1610	2.1514	2.1462	2.1417
30.00	2.5563	2.4995	2.4523	2.4006	2.3666	2.3446	2.3139	2.2946	2.2705	2.2496	2.2110	2.1898	2.1798	2.1744	2.1698

TABLE 34.2—EXTENDED SUKKAR-CORNELL INTEGRAL FOR BHP CALCULATION (continued)

$$\int_{0.2}^{p_{pr}} \frac{(z/p_{pr}) dp_{pr}}{1 + B(z/p_{pr})^2}$$

Pseudoreduced temperature for $B = 30.0$

p_{pr}	1.1	1.2	1.3	1.4	1.5	1.6	1.7	1.8	1.9	2.0	2.2	2.4	2.6	2.8	3.0
0.20	0.0000	0.0000	0.0000	0.0000	0.0000	0.0000	0.0000	0.0000	0.0000	0.0000	0.0000	0.0000	0.0000	0.0000	0.0000
0.50	0.0039	0.0038	0.0037	0.0037	0.0036	0.0036	0.0036	0.0035	0.0035	0.0035	0.0035	0.0035	0.0035	0.0035	0.0035
1.00	0.0199	0.0184	0.0176	0.0172	0.0168	0.0166	0.0164	0.0162	0.0162	0.0161	0.0159	0.0158	0.0158	0.0157	0.0157
1.50	0.0521	0.0447	0.0418	0.0401	0.0390	0.0382	0.0375	0.0371	0.0368	0.0365	0.0361	0.0358	0.0356	0.0355	0.0353
2.00	0.0967	0.0823	0.0755	0.0718	0.0692	0.0676	0.0662	0.0652	0.0646	0.0640	0.0632	0.0626	0.0621	0.0618	0.0615
2.50	0.1422	0.1264	0.1164	0.1103	0.1060	0.1033	0.1010	0.0993	0.0983	0.0974	0.0960	0.0951	0.0943	0.0937	0.0931
3.00	0.1870	0.1719	0.1608	0.1531	0.1474	0.1436	0.1404	0.1381	0.1366	0.1353	0.1334	0.1321	0.1309	0.1300	0.1292
3.50	0.2314	0.2174	0.2063	0.1980	0.1914	0.1869	0.1831	0.1801	0.1782	0.1765	0.1741	0.1725	0.1710	0.1697	0.1687
4.00	0.2756	0.2625	0.2519	0.2436	0.2367	0.2318	0.2275	0.2242	0.2219	0.2199	0.2172	0.2152	0.2135	0.2120	0.2108
4.50	0.3195	0.3071	0.2970	0.2891	0.2823	0.2778	0.2729	0.2693	0.2669	0.2647	0.2617	0.2594	0.2575	0.2559	0.2545
5.00	0.3632	0.3513	0.3416	0.3343	0.3278	0.3229	0.3186	0.3149	0.3124	0.3101	0.3069	0.3046	0.3025	0.3008	0.2993
5.50	0.4067	0.3951	0.3858	0.3789	0.3729	0.3683	0.3641	0.3605	0.3580	0.3558	0.3525	0.3501	0.3480	0.3462	0.3448
6.00	0.4500	0.4386	0.4295	0.4230	0.4175	0.4132	0.4092	0.4059	0.4035	0.4013	0.3981	0.3957	0.3937	0.3919	0.3904
6.50	0.4931	0.4817	0.4728	0.4667	0.4616	0.4576	0.4539	0.4508	0.4486	0.4465	0.4435	0.4412	0.4392	0.4374	0.4359
7.00	0.5361	0.5247	0.5158	0.5099	0.5052	0.5015	0.4981	0.4952	0.4932	0.4913	0.4884	0.4863	0.4843	0.4826	0.4812
7.50	0.5789	0.5674	0.5584	0.5527	0.5483	0.5449	0.5417	0.5391	0.5372	0.5355	0.5329	0.5309	0.5291	0.5274	0.5260
8.00	0.6216	0.6098	0.6007	0.5951	0.5909	0.5877	0.5848	0.5824	0.5808	0.5792	0.5767	0.5749	0.5732	0.5716	0.5703
8.50	0.6642	0.6521	0.6428	0.6372	0.6331	0.6301	0.6273	0.6252	0.6237	0.6223	0.6200	0.6184	0.6168	0.6152	0.6139
9.00	0.7066	0.6941	0.6846	0.6789	0.6749	0.6719	0.6693	0.6674	0.6660	0.6647	0.6627	0.6612	0.6597	0.6582	0.6570
9.50	0.7488	0.7360	0.7261	0.7204	0.7163	0.7134	0.7109	0.7091	0.7078	0.7066	0.7048	0.7034	0.7020	0.7006	0.6994
10.00	0.7909	0.7776	0.7674	0.7615	0.7573	0.7544	0.7520	0.7503	0.7491	0.7480	0.7463	0.7451	0.7436	0.7423	0.7411
10.50	0.8329	0.8191	0.8085	0.8024	0.7980	0.7951	0.7926	0.7910	0.7899	0.7888	0.7873	0.7861	0.7847	0.7833	0.7822
11.00	0.8747	0.8604	0.8494	0.8430	0.8384	0.8354	0.8329	0.8313	0.8302	0.8292	0.8277	0.8265	0.8251	0.8238	0.8227
11.50	0.9165	0.9016	0.8901	0.8833	0.8785	0.8754	0.8728	0.8711	0.8700	0.8690	0.8676	0.8664	0.8650	0.8637	0.8626
12.00	0.9581	0.9426	0.9306	0.9234	0.9183	0.9150	0.9123	0.9106	0.9095	0.9084	0.9070	0.9057	0.9043	0.9030	0.9019
12.50	0.9996	0.9835	0.9710	0.9633	0.9579	0.9544	0.9515	0.9497	0.9485	0.9474	0.9459	0.9446	0.9431	0.9417	0.9406
13.00	1.0411	1.0242	1.0112	1.0030	0.9973	0.9936	0.9904	0.9884	0.9872	0.9860	0.9842	0.9828	0.9813	0.9799	0.9787
13.50	1.0824	1.0649	1.0513	1.0425	1.0364	1.0324	1.0290	1.0268	1.0254	1.0241	1.0222	1.0206	1.0191	1.0176	1.0164
14.00	1.1237	1.1054	1.0912	1.0818	1.0753	1.0710	1.0673	1.0649	1.0634	1.0618	1.0596	1.0579	1.0563	1.0547	1.0535
14.50	1.1649	1.1459	1.1310	1.1209	1.1139	1.1094	1.1054	1.1027	1.1009	1.0992	1.0966	1.0947	1.0930	1.0914	1.0901
15.00	1.2060	1.1862	1.1707	1.1598	1.1524	1.1475	1.1431	1.1402	1.1382	1.1362	1.1332	1.1311	1.1293	1.1276	1.1263
15.50	1.2471	1.2264	1.2102	1.1986	1.1907	1.1855	1.1806	1.1774	1.1751	1.1729	1.1694	1.1670	1.1651	1.1633	1.1620
16.00	1.2881	1.2666	1.2497	1.2372	1.2287	1.2232	1.2179	1.2144	1.2117	1.2092	1.2052	1.2026	1.2005	1.1987	1.1972
16.50	1.3291	1.3067	1.2890	1.2757	1.2666	1.2607	1.2549	1.2511	1.2481	1.2453	1.2407	1.2377	1.2354	1.2335	1.2320
17.00	1.3700	1.3467	1.3282	1.3140	1.3044	1.2981	1.2917	1.2876	1.2842	1.2810	1.2757	1.2724	1.2700	1.2680	1.2665
17.50	1.4109	1.3866	1.3674	1.3522	1.3419	1.3352	1.3283	1.3238	1.3200	1.3164	1.3105	1.3067	1.3042	1.3021	1.3005
18.00	1.4517	1.4264	1.4064	1.3903	1.3794	1.3722	1.3647	1.3598	1.3555	1.3515	1.3449	1.3407	1.3380	1.3358	1.3341
18.50	1.4924	1.4662	1.4454	1.4282	1.4167	1.4091	1.4009	1.3956	1.3908	1.3864	1.3789	1.3744	1.3714	1.3692	1.3674
19.00	1.5332	1.5059	1.4843	1.4661	1.4538	1.4457	1.4370	1.4312	1.4259	1.4211	1.4127	1.4077	1.4045	1.4022	1.4003
19.50	1.5738	1.5456	1.5231	1.5038	1.4908	1.4823	1.4728	1.4666	1.4608	1.4554	1.4462	1.4407	1.4373	1.4349	1.4329
20.00	1.6145	1.5852	1.5618	1.5414	1.5277	1.5187	1.5085	1.5019	1.4954	1.4896	1.4794	1.4734	1.4698	1.4672	1.4652
20.50	1.6551	1.6247	1.6005	1.5789	1.5644	1.5549	1.5440	1.5369	1.5298	1.5235	1.5123	1.5058	1.5019	1.4993	1.4971
21.00	1.6956	1.6642	1.6391	1.6163	1.6011	1.5910	1.5794	1.5718	1.5641	1.5572	1.5449	1.5379	1.5338	1.5310	1.5288
21.50	1.7361	1.7037	1.6776	1.6537	1.6376	1.6270	1.6146	1.6065	1.5981	1.5906	1.5773	1.5697	1.5654	1.5625	1.5601
22.00	1.7766	1.7431	1.7160	1.6909	1.6740	1.6629	1.6497	1.6410	1.6320	1.6239	1.6095	1.6013	1.5967	1.5937	1.5912
22.50	1.8171	1.7824	1.7544	1.7281	1.7103	1.6987	1.6846	1.6754	1.6657	1.6570	1.6414	1.6326	1.6277	1.6246	1.6220
23.00	1.8575	1.8217	1.7928	1.7651	1.7465	1.7343	1.7194	1.7096	1.6992	1.6899	1.6731	1.6636	1.6585	1.6552	1.6525
23.50	1.8979	1.8610	1.8311	1.8021	1.7826	1.7698	1.7541	1.7437	1.7325	1.7226	1.7046	1.6945	1.6890	1.6856	1.6828
24.00	1.9383	1.9002	1.8693	1.8390	1.8186	1.8053	1.7886	1.7777	1.7657	1.7551	1.7358	1.7250	1.7193	1.7158	1.7128
24.50	1.9786	1.9393	1.9075	1.8759	1.8546	1.8406	1.8230	1.8115	1.7987	1.7874	1.7669	1.7554	1.7494	1.7457	1.7426
25.00	2.0189	1.9785	1.9456	1.9127	1.8904	1.8758	1.8573	1.8452	1.8316	1.8196	1.7977	1.7855	1.7792	1.7754	1.7722
25.50	2.0592	2.0176	1.9837	1.9493	1.9262	1.9110	1.8915	1.8788	1.8644	1.8516	1.8284	1.8155	1.8088	1.8048	1.8015
26.00	2.0995	2.0566	2.0217	1.9860	1.9618	1.9460	1.9256	1.9123	1.8970	1.8835	1.8589	1.8452	1.8382	1.8341	1.8306
26.50	2.1397	2.0957	2.0597	2.0226	1.9974	1.9810	1.9596	1.9456	1.9294	1.9152	1.8891	1.8747	1.8674	1.8631	1.8595
27.00	2.1799	2.1346	2.0976	2.0591	2.0330	2.0159	1.9934	1.9788	1.9618	1.9468	1.9192	1.9040	1.8964	1.8920	1.8882
27.50	2.2201	2.1736	2.1355	2.0955	2.0684	2.0507	2.0272	2.0119	1.9940	1.9782	1.9492	1.9332	1.9252	1.9206	1.9167
28.00	2.2603	2.2125	2.1734	2.1319	2.1038	2.0854	2.0609	2.0449	2.0261	2.0095	1.9790	1.9622	1.9538	1.9491	1.9451
28.50	2.3005	2.2514	2.2112	2.1682	2.1391	2.1200	2.0945	2.0779	2.0580	2.0407	2.0086	1.9910	1.9823	1.9774	1.9732
29.00	2.3406	2.2903	2.2490	2.2045	2.1743	2.1546	2.1280	2.1107	2.0899	2.0717	2.0380	2.0196	2.0105	2.0055	2.0012
29.50	2.3807	2.3291	2.2868	2.2407	2.2095	2.1891	2.1614	2.1434	2.1216	2.1026	2.0673	2.0481	2.0386	2.0334	2.0289
30.00	2.4208	2.3679	2.3245	2.2769	2.2446	2.2235	2.1947	2.1760	2.1533	2.1334	2.0965	2.0764	2.0666	2.0612	2.0566

TABLE 34.2—EXTENDED SUKKAR-CORNELL INTEGRAL FOR BHP CALCULATION (continued)

$$\int_{0.2}^{p_{pr}} \frac{(z/p_{pr}) dp_{pr}}{1 + B(z/p_{pr})^2}$$

Pseudoreduced temperature for $B = 35.0$

p_{pr}	1.1	1.2	1.3	1.4	1.5	1.6	1.7	1.8	1.9	2.0	2.2	2.4	2.6	2.8	3.0
0.20	0.0000	0.0000	0.0000	0.0000	0.0000	0.0000	0.0000	0.0000	0.0000	0.0000	0.0000	0.0000	0.0000	0.0000	0.0000
0.50	0.0033	0.0032	0.0032	0.0031	0.0031	0.0031	0.0031	0.0030	0.0030	0.0030	0.0030	0.0030	0.0030	0.0030	0.0030
1.00	0.0171	0.0158	0.0152	0.0148	0.0145	0.0143	0.0141	0.0139	0.0139	0.0138	0.0137	0.0136	0.0136	0.0135	0.0135
1.50	0.0454	0.0387	0.0361	0.0346	0.0336	0.0329	0.0323	0.0320	0.0317	0.0315	0.0311	0.0309	0.0307	0.0305	0.0304
2.00	0.0861	0.0720	0.0657	0.0623	0.0601	0.0585	0.0573	0.0564	0.0559	0.0554	0.0546	0.0542	0.0537	0.0534	0.0531
2.50	0.1283	0.1119	0.1022	0.0965	0.0925	0.0900	0.0879	0.0864	0.0855	0.0847	0.0834	0.0826	0.0819	0.0813	0.0808
3.00	0.1703	0.1538	0.1425	0.1350	0.1295	0.1259	0.1230	0.1208	0.1194	0.1182	0.1165	0.1153	0.1142	0.1134	0.1127
3.50	0.2120	0.1960	0.1844	0.1759	0.1694	0.1650	0.1613	0.1585	0.1567	0.1550	0.1528	0.1513	0.1499	0.1487	0.1478
4.00	0.2536	0.2382	0.2266	0.2179	0.2108	0.2059	0.2017	0.1984	0.1962	0.1942	0.1916	0.1897	0.1880	0.1866	0.1855
4.50	0.2950	0.2800	0.2688	0.2601	0.2529	0.2477	0.2433	0.2396	0.2372	0.2350	0.2320	0.2298	0.2279	0.2263	0.2250
5.00	0.3362	0.3216	0.3106	0.3023	0.2951	0.2899	0.2854	0.2816	0.2790	0.2766	0.2734	0.2710	0.2690	0.2672	0.2658
5.50	0.3773	0.3630	0.3522	0.3442	0.3373	0.3321	0.3276	0.3238	0.3211	0.3187	0.3153	0.3128	0.3107	0.3089	0.3074
6.00	0.4183	0.4040	0.3934	0.3857	0.3791	0.3742	0.3698	0.3660	0.3634	0.3610	0.3576	0.3550	0.3529	0.3510	0.3495
6.50	0.4591	0.4449	0.4344	0.4270	0.4207	0.4159	0.4117	0.4080	0.4055	0.4032	0.3998	0.3972	0.3951	0.3932	0.3918
7.00	0.4999	0.4856	0.4752	0.4679	0.4618	0.4573	0.4532	0.4498	0.4473	0.4451	0.4418	0.4394	0.4373	0.4354	0.4339
7.50	0.5405	0.5261	0.5156	0.5085	0.5026	0.4983	0.4944	0.4912	0.4889	0.4867	0.4836	0.4812	0.4792	0.4774	0.4759
8.00	0.5810	0.5665	0.5558	0.5487	0.5431	0.5390	0.5352	0.5322	0.5300	0.5280	0.5247	0.5227	0.5208	0.5190	0.5175
8.50	0.6214	0.6066	0.5959	0.5888	0.5832	0.5792	0.5756	0.5727	0.5707	0.5688	0.5657	0.5638	0.5619	0.5602	0.5588
9.00	0.6617	0.6466	0.6357	0.6285	0.6230	0.6191	0.6156	0.6129	0.6109	0.6091	0.6062	0.6044	0.6026	0.6009	0.5996
9.50	0.7018	0.6865	0.6753	0.6681	0.6625	0.6586	0.6552	0.6526	0.6507	0.6490	0.6462	0.6445	0.6428	0.6412	0.6398
10.00	0.7419	0.7262	0.7147	0.7073	0.7017	0.6978	0.6945	0.6919	0.6901	0.6885	0.6858	0.6842	0.6825	0.6809	0.6796
10.50	0.7818	0.7657	0.7539	0.7464	0.7406	0.7367	0.7334	0.7308	0.7291	0.7275	0.7250	0.7234	0.7217	0.7201	0.7189
11.00	0.8217	0.8051	0.7930	0.7852	0.7793	0.7753	0.7719	0.7694	0.7677	0.7661	0.7637	0.7621	0.7604	0.7589	0.7576
11.50	0.8614	0.8444	0.8319	0.8239	0.8177	0.8136	0.8102	0.8076	0.8059	0.8043	0.8019	0.8004	0.7987	0.7971	0.7958
12.00	0.9011	0.8836	0.8707	0.8623	0.8559	0.8517	0.8481	0.8455	0.8438	0.8422	0.8398	0.8381	0.8364	0.8349	0.8336
12.50	0.9407	0.9227	0.9094	0.9006	0.8939	0.8895	0.8858	0.8831	0.8813	0.8797	0.8771	0.8755	0.8737	0.8721	0.8708
13.00	0.9803	0.9617	0.9479	0.9386	0.9317	0.9271	0.9232	0.9204	0.9185	0.9168	0.9141	0.9124	0.9106	0.9089	0.9076
13.50	1.0197	1.0006	0.9863	0.9765	0.9693	0.9645	0.9604	0.9574	0.9554	0.9535	0.9507	0.9483	0.9470	0.9453	0.9439
14.00	1.0591	1.0394	1.0246	1.0143	1.0067	1.0017	0.9973	0.9941	0.9920	0.9900	0.9869	0.9848	0.9829	0.9812	0.9798
14.50	1.0985	1.0781	1.0627	1.0519	1.0439	1.0386	1.0340	1.0305	1.0282	1.0261	1.0226	1.0205	1.0184	1.0167	1.0153
15.00	1.1377	1.1167	1.1008	1.0893	1.0809	1.0754	1.0704	1.0667	1.0642	1.0618	1.0580	1.0557	1.0536	1.0517	1.0503
15.50	1.1770	1.1552	1.1388	1.1266	1.1178	1.1120	1.1066	1.1027	1.0999	1.0973	1.0931	1.0905	1.0883	1.0864	1.0849
16.00	1.2162	1.1937	1.1767	1.1638	1.1545	1.1484	1.1426	1.1384	1.1354	1.1325	1.1278	1.1249	1.1226	1.1206	1.1191
16.50	1.2553	1.2321	1.2144	1.2008	1.1911	1.1846	1.1784	1.1739	1.1705	1.1674	1.1622	1.1590	1.1566	1.1545	1.1529
17.00	1.2944	1.2705	1.2521	1.2378	1.2275	1.2207	1.2140	1.2092	1.2055	1.2020	1.1962	1.1928	1.1901	1.1880	1.1864
17.50	1.3334	1.3087	1.2898	1.2746	1.2638	1.2566	1.2494	1.2443	1.2402	1.2364	1.2300	1.2262	1.2234	1.2212	1.2195
18.00	1.3725	1.3470	1.3273	1.3113	1.2999	1.2923	1.2846	1.2792	1.2747	1.2705	1.2634	1.2592	1.2563	1.2540	1.2522
18.50	1.4114	1.3851	1.3648	1.3479	1.3359	1.3280	1.3197	1.3139	1.3089	1.3044	1.2966	1.2920	1.2889	1.2865	1.2847
19.00	1.4504	1.4232	1.4022	1.3844	1.3718	1.3634	1.3546	1.3484	1.3430	1.3380	1.3294	1.3245	1.3212	1.3187	1.3168
19.50	1.4893	1.4613	1.4395	1.4208	1.4075	1.3988	1.3893	1.3828	1.3769	1.3714	1.3620	1.3566	1.3531	1.3506	1.3485
20.00	1.5281	1.4993	1.4768	1.4571	1.4432	1.4340	1.4239	1.4170	1.4105	1.4046	1.3944	1.3885	1.3848	1.3822	1.3800
20.50	1.5670	1.5373	1.5140	1.4933	1.4788	1.4691	1.4584	1.4510	1.4440	1.4376	1.4265	1.4201	1.4162	1.4135	1.4112
21.00	1.6058	1.5752	1.5511	1.5294	1.5142	1.5041	1.4927	1.4849	1.4773	1.4704	1.4583	1.4515	1.4473	1.4445	1.4422
21.50	1.6446	1.6130	1.5882	1.5655	1.5495	1.5390	1.5269	1.5186	1.5104	1.5030	1.4900	1.4826	1.4782	1.4752	1.4728
22.00	1.6833	1.6509	1.6252	1.6014	1.5848	1.5738	1.5609	1.5522	1.5434	1.5355	1.5214	1.5134	1.5088	1.5057	1.5032
22.50	1.7220	1.6887	1.6622	1.6373	1.6199	1.6084	1.5948	1.5856	1.5762	1.5677	1.5525	1.5440	1.5391	1.5360	1.5333
23.00	1.7607	1.7264	1.6991	1.6732	1.6550	1.6430	1.6286	1.6189	1.6088	1.5998	1.5835	1.5744	1.5693	1.5660	1.5632
23.50	1.7994	1.7641	1.7360	1.7089	1.6900	1.6755	1.6623	1.6521	1.6413	1.6317	1.6143	1.6046	1.5992	1.5957	1.5929
24.00	1.8381	1.8018	1.7729	1.7446	1.7249	1.7118	1.6959	1.6851	1.6736	1.6634	1.6448	1.6345	1.6288	1.6253	1.6223
24.50	1.8767	1.8394	1.8097	1.7802	1.7597	1.7461	1.7294	1.7180	1.7058	1.6950	1.6752	1.6642	1.6583	1.6546	1.6515
25.00	1.9153	1.8771	1.8464	1.8158	1.7944	1.7803	1.7627	1.7508	1.7379	1.7264	1.7054	1.6937	1.6875	1.6837	1.6805
25.50	1.9539	1.9146	1.8831	1.8513	1.8291	1.8144	1.7960	1.7835	1.7698	1.7577	1.7354	1.7231	1.7165	1.7126	1.7093
26.00	1.9924	1.9522	1.9198	1.8867	1.8637	1.8484	1.8291	1.8161	1.8016	1.7888	1.7652	1.7522	1.7454	1.7413	1.7378
26.50	2.0310	1.9897	1.9564	1.9221	1.8982	1.8824	1.8622	1.8486	1.8333	1.8198	1.7949	1.7812	1.7740	1.7698	1.7662
27.00	2.0695	2.0272	1.9930	1.9574	1.9326	1.9163	1.8951	1.8810	1.8649	1.8506	1.8244	1.8100	1.8025	1.7981	1.7944
27.50	2.1080	2.0647	2.0295	1.9927	1.9670	1.9501	1.9280	1.9133	1.8963	1.8814	1.8537	1.8386	1.8308	1.8262	1.8224
28.00	2.1465	2.1021	2.0661	2.0279	2.0014	1.9838	1.9608	1.9454	1.9277	1.9119	1.8829	1.8670	1.8589	1.8542	1.8502
28.50	2.1850	2.1395	2.1025	2.0631	2.0356	2.0175	1.9935	1.9775	1.9589	1.9424	1.9119	1.8953	1.8868	1.8820	1.8779
29.00	2.2234	2.1769	2.1390	2.0983	2.0698	2.0511	2.0261	2.0094	1.9900	1.9726	1.9408	1.9234	1.9146	1.9096	1.9053
29.50	2.2619	2.2142	2.1754	2.1333	2.1040	2.0846	2.0587	2.0414	2.0210	2.0030	1.9696	1.9513	1.9422	1.9370	1.9327
30.00	2.3003	2.2516	2.2118	2.1684	2.1381	2.1180	2.0912	2.0732	2.0519	2.0331	1.9982	1.9791	1.9696	1.9643	1.9598

TABLE 34.2—EXTENDED SUKKAR-CORNELL INTEGRAL FOR BHP CALCULATION (continued)

$$\int_{0.2}^{p_{pr}} \frac{(z/p_{pr}) dp_{pr}}{1 + B(z/p_{pr})^2}$$

Pseudoreduced temperature for $B = 40.0$

p_{pr}	1.1	1.2	1.3	1.4	1.5	1.6	1.7	1.8	1.9	2.0	2.2	2.4	2.6	2.8	3.0
0.20	0.0000	0.0000	0.0000	0.0000	0.0000	0.0000	0.0000	0.0000	0.0000	0.0000	0.0000	0.0000	0.0000	0.0000	0.0000
0.50	0.0029	0.0028	0.0028	0.0027	0.0027	0.0027	0.0027	0.0027	0.0027	0.0026	0.0026	0.0026	0.0026	0.0026	0.0026
1.00	0.0150	0.0139	0.0133	0.0129	0.0127	0.0125	0.0123	0.0122	0.0122	0.0121	0.0120	0.0119	0.0119	0.0118	0.0118
1.50	0.0403	0.0341	0.0318	0.0305	0.0296	0.0290	0.0284	0.0281	0.0279	0.0276	0.0273	0.0271	0.0270	0.0268	0.0267
2.00	0.0776	0.0640	0.0582	0.0551	0.0530	0.0517	0.0505	0.0497	0.0493	0.0488	0.0482	0.0477	0.0473	0.0471	0.0468
2.50	0.1170	0.1005	0.0912	0.0858	0.0821	0.0798	0.0779	0.0765	0.0756	0.0749	0.0738	0.0730	0.0724	0.0718	0.0714
3.00	0.1565	0.1393	0.1281	0.1208	0.1156	0.1122	0.1095	0.1074	0.1061	0.1050	0.1034	0.1023	0.1013	0.1005	0.0999
3.50	0.1958	0.1787	0.1668	0.1584	0.1520	0.1477	0.1442	0.1416	0.1398	0.1383	0.1362	0.1348	0.1335	0.1324	0.1315
4.00	0.2351	0.2182	0.2062	0.1973	0.1901	0.1853	0.1812	0.1780	0.1758	0.1740	0.1714	0.1696	0.1681	0.1667	0.1656
4.50	0.2743	0.2576	0.2457	0.2367	0.2292	0.2240	0.2195	0.2159	0.2135	0.2113	0.2084	0.2063	0.2045	0.2029	0.2017
5.00	0.3133	0.2969	0.2851	0.2762	0.2686	0.2633	0.2586	0.2548	0.2521	0.2498	0.2465	0.2442	0.2422	0.2405	0.2391
5.50	0.3523	0.3360	0.3244	0.3156	0.3081	0.3028	0.2980	0.2941	0.2913	0.2889	0.2854	0.2829	0.2808	0.2790	0.2775
6.00	0.3912	0.3750	0.3634	0.3549	0.3476	0.3423	0.3376	0.3336	0.3308	0.3283	0.3247	0.3221	0.3199	0.3181	0.3166
6.50	0.4300	0.4138	0.4032	0.3939	0.3868	0.3816	0.3770	0.3731	0.3703	0.3678	0.3642	0.3616	0.3594	0.3575	0.3560
7.00	0.4687	0.4525	0.4410	0.4328	0.4258	0.4208	0.4163	0.4124	0.4097	0.4073	0.4037	0.4011	0.3989	0.3970	0.3955
7.50	0.5073	0.4910	0.4795	0.4714	0.4646	0.4597	0.4553	0.4516	0.4490	0.4466	0.4431	0.4405	0.4383	0.4365	0.4350
8.00	0.5458	0.5294	0.5179	0.5097	0.5031	0.4983	0.4941	0.4905	0.4879	0.4856	0.4819	0.4797	0.4776	0.4758	0.4743
8.50	0.5843	0.5677	0.5560	0.5479	0.5413	0.5367	0.5325	0.5290	0.5266	0.5244	0.5208	0.5187	0.5166	0.5148	0.5133
9.00	0.6227	0.6059	0.5940	0.5859	0.5793	0.5747	0.5707	0.5673	0.5650	0.5628	0.5593	0.5573	0.5553	0.5535	0.5521
9.50	0.6609	0.6439	0.6319	0.6237	0.6171	0.6125	0.6085	0.6052	0.6030	0.6009	0.5975	0.5955	0.5936	0.5918	0.5904
10.00	0.6991	0.6818	0.6696	0.6612	0.6546	0.6500	0.6461	0.6429	0.6407	0.6386	0.6353	0.6334	0.6315	0.6298	0.6284
10.50	0.7372	0.7196	0.7071	0.6987	0.6919	0.6873	0.6833	0.6802	0.6780	0.6760	0.6728	0.6710	0.6690	0.6673	0.6660
11.00	0.7753	0.7573	0.7446	0.7359	0.7290	0.7243	0.7203	0.7172	0.7150	0.7130	0.7099	0.7081	0.7062	0.7045	0.7031
11.50	0.8132	0.7949	0.7819	0.7729	0.7659	0.7611	0.7571	0.7539	0.7517	0.7498	0.7466	0.7448	0.7429	0.7412	0.7398
12.00	0.8511	0.8324	0.8190	0.8098	0.8026	0.7977	0.7936	0.7903	0.7882	0.7862	0.7830	0.7812	0.7792	0.7775	0.7762
12.50	0.8890	0.8696	0.8561	0.8466	0.8391	0.8341	0.8299	0.8265	0.8243	0.8223	0.8190	0.8171	0.8152	0.8134	0.8121
13.00	0.9268	0.9072	0.8931	0.8832	0.8755	0.8703	0.8659	0.8624	0.8602	0.8580	0.8547	0.8527	0.8507	0.8490	0.8476
13.50	0.9645	0.9445	0.9299	0.9196	0.9117	0.9063	0.9017	0.8981	0.8957	0.8935	0.8900	0.8879	0.8859	0.8841	0.8827
14.00	1.0022	0.9816	0.9667	0.9559	0.9477	0.9421	0.9373	0.9335	0.9310	0.9287	0.9250	0.9228	0.9207	0.9188	0.9174
14.50	1.0398	1.0188	1.0034	0.9921	0.9835	0.9778	0.9727	0.9688	0.9661	0.9636	0.9596	0.9572	0.9551	0.9532	0.9517
15.00	1.0774	1.0558	1.0400	1.0282	1.0193	1.0133	1.0079	1.0037	1.0009	0.9982	0.9939	0.9914	0.9891	0.9872	0.9856
15.50	1.1149	1.0928	1.0765	1.0641	1.0548	1.0486	1.0429	1.0385	1.0355	1.0326	1.0279	1.0251	1.0228	1.0208	1.0192
16.00	1.1525	1.1297	1.1129	1.1000	1.0903	1.0837	1.0777	1.0731	1.0698	1.0667	1.0616	1.0586	1.0561	1.0541	1.0525
16.50	1.1899	1.1666	1.1492	1.1357	1.1255	1.1187	1.1123	1.1075	1.1039	1.1005	1.0949	1.0917	1.0891	1.0870	1.0853
17.00	1.2274	1.2034	1.1855	1.1713	1.1607	1.1536	1.1468	1.1417	1.1378	1.1341	1.1280	1.1245	1.1218	1.1196	1.1179
17.50	1.2648	1.2402	1.2217	1.2068	1.1958	1.1884	1.1811	1.1757	1.1714	1.1675	1.1630	1.1570	1.1541	1.1519	1.1501
18.00	1.3021	1.2769	1.2579	1.2422	1.2307	1.2230	1.2152	1.2095	1.2049	1.2006	1.1934	1.1892	1.1862	1.1839	1.1820
18.50	1.3395	1.3136	1.2940	1.2776	1.2655	1.2574	1.2492	1.2432	1.2382	1.2336	1.2256	1.2211	1.2180	1.2155	1.2136
19.00	1.3768	1.3502	1.3300	1.3128	1.3002	1.2918	1.2831	1.2767	1.2713	1.2663	1.2577	1.2528	1.2494	1.2469	1.2450
19.50	1.4140	1.3868	1.3659	1.3480	1.3349	1.3261	1.3168	1.3101	1.3042	1.2988	1.2894	1.2842	1.2806	1.2780	1.2760
20.00	1.4513	1.4233	1.4019	1.3831	1.3694	1.3602	1.3504	1.3433	1.3369	1.3311	1.3210	1.3153	1.3116	1.3089	1.3068
20.50	1.4885	1.4598	1.4377	1.4181	1.4038	1.3942	1.3838	1.3763	1.3695	1.3633	1.3523	1.3462	1.3422	1.3395	1.3373
21.00	1.5257	1.4963	1.4735	1.4530	1.4381	1.4281	1.4171	1.4093	1.4019	1.3952	1.3834	1.3768	1.3727	1.3698	1.3675
21.50	1.5629	1.5327	1.5093	1.4879	1.4723	1.4620	1.4503	1.4421	1.4341	1.4270	1.4143	1.4072	1.4028	1.3999	1.3975
22.00	1.6001	1.5691	1.5450	1.5227	1.5065	1.4957	1.4834	1.4747	1.4662	1.4586	1.4449	1.4373	1.4328	1.4297	1.4272
22.50	1.6372	1.6054	1.5807	1.5574	1.5406	1.5293	1.5164	1.5072	1.4982	1.4900	1.4754	1.4673	1.4625	1.4593	1.4567
23.00	1.6743	1.6417	1.6163	1.5920	1.5746	1.5629	1.5492	1.5396	1.5300	1.5213	1.5057	1.4970	1.4920	1.4887	1.4860
23.50	1.7114	1.6780	1.6519	1.6266	1.6085	1.5963	1.5820	1.5719	1.5617	1.5525	1.5358	1.5265	1.5213	1.5178	1.5151
24.00	1.7485	1.7143	1.6874	1.6612	1.6423	1.6297	1.6146	1.6041	1.5932	1.5834	1.5657	1.5559	1.5503	1.5468	1.5439
24.50	1.7855	1.7505	1.7229	1.6947	1.6761	1.6630	1.6472	1.6362	1.6246	1.6143	1.5954	1.5850	1.5792	1.5755	1.5725
25.00	1.8226	1.7867	1.7584	1.7301	1.7098	1.6962	1.6797	1.6682	1.6559	1.6450	1.6249	1.6139	1.6078	1.6041	1.6010
25.50	1.8596	1.8229	1.7938	1.7645	1.7434	1.7293	1.7120	1.7000	1.6871	1.6755	1.6543	1.6427	1.6363	1.6324	1.6292
26.00	1.8966	1.8591	1.8292	1.7988	1.7770	1.7624	1.7443	1.7318	1.7181	1.7059	1.6836	1.6713	1.6646	1.6606	1.6572
26.50	1.9336	1.8952	1.8645	1.8331	1.8105	1.7954	1.7765	1.7634	1.7491	1.7362	1.7126	1.6997	1.6927	1.6886	1.6851
27.00	1.9705	1.9313	1.8999	1.8673	1.8439	1.8283	1.8086	1.7950	1.7799	1.7664	1.7415	1.7279	1.7207	1.7164	1.7128
27.50	2.0075	1.9674	1.9352	1.9015	1.8773	1.8612	1.8406	1.8265	1.8106	1.7965	1.7703	1.7560	1.7484	1.7440	1.7403
28.00	2.0444	2.0034	1.9704	1.9356	1.9107	1.8940	1.8726	1.8579	1.8412	1.8264	1.7989	1.7839	1.7760	1.7715	1.7676
28.50	2.0813	2.0394	2.0057	1.9697	1.9439	1.9267	1.9044	1.8892	1.8717	1.8562	1.8274	1.8116	1.8035	1.7988	1.7948
29.00	2.1182	2.0755	2.0409	2.0038	1.9771	1.9594	1.9362	1.9204	0.9021	1.8859	1.8557	1.8393	1.8308	1.8259	1.8218
29.50	2.1551	2.1114	2.0761	2.0378	2.0103	1.9920	1.9680	1.9516	1.9325	1.9155	1.8840	1.8667	1.8579	1.8529	1.8487
30.00	2.1920	2.1474	2.1112	2.0717	2.0434	2.0246	1.9996	1.9826	1.9627	1.9460	1.9120	1.8940	1.8849	1.8797	1.8754

TABLE 34.2—EXTENDED SUKKAR-CORNELL INTEGRAL FOR BHP CALCULATION (continued)

$$\int_{0.2}^{p_{pr}} \frac{(z/p_{pr}) dp_{pr}}{1 + B(z/p_{pr})^2}$$

Pseudoreduced temperature for $B = 45.0$

p_{pr}	1.1	1.2	1.3	1.4	1.5	1.6	1.7	1.8	1.9	2.0	2.2	2.4	2.6	2.8	3.0
0.20	0.0000	0.0000	0.0000	0.0000	0.0000	0.0000	0.0000	0.0000	0.0000	0.0000	0.0000	0.0000	0.0000	0.0000	0.0000
0.50	0.0026	0.0025	0.0025	0.0024	0.0024	0.0024	0.0024	0.0024	0.0024	0.0024	0.0023	0.0023	0.0023	0.0023	0.0023
1.00	0.0134	0.0124	0.0119	0.0115	0.0113	0.0111	0.0110	0.0109	0.0108	0.0108	0.0107	0.0106	0.0106	0.0105	0.0105
1.50	0.0362	0.0305	0.0284	0.0272	0.0264	0.0258	0.0254	0.0250	0.0248	0.0247	0.0244	0.0242	0.0240	0.0239	0.0238
2.00	0.0707	0.0576	0.0522	0.0494	0.0475	0.0462	0.0452	0.0445	0.0440	0.0436	0.0430	0.0426	0.0423	0.0420	0.0418
2.50	0.1076	0.0912	0.0823	0.0772	0.0738	0.0716	0.0699	0.0586	0.0678	0.0671	0.0661	0.0654	0.0648	0.0644	0.0640
3.00	0.1449	0.1273	0.1163	0.1093	0.1043	0.1012	0.0986	0.0967	0.0955	0.0944	0.0930	0.0919	0.0910	0.0903	0.0897
3.50	0.1821	0.1643	0.1523	0.1441	0.1378	0.1338	0.1304	0.1279	0.1263	0.1248	0.1229	0.1215	0.1203	0.1193	0.1185
4.00	0.2193	0.2015	0.1892	0.1803	0.1732	0.1685	0.1645	0.1614	0.1594	0.1576	0.1552	0.1534	0.1520	0.1507	0.1496
4.50	0.2565	0.2388	0.2264	0.2172	0.2096	0.2045	0.2001	0.1966	0.1942	0.1921	0.1893	0.1872	0.1855	0.1840	0.1828
5.00	0.2936	0.2760	0.2637	0.2544	0.2466	0.2412	0.2366	0.2327	0.2301	0.2278	0.2246	0.2223	0.2204	0.2187	0.2174
5.50	0.3306	0.3131	0.3009	0.2917	0.2838	0.2783	0.2735	0.2695	0.2667	0.2643	0.2608	0.2583	0.2562	0.2544	0.2530
6.00	0.3676	0.3501	0.3380	0.3289	0.3211	0.3156	0.3107	0.3066	0.3038	0.3012	0.2976	0.2949	0.2928	0.2909	0.2895
6.50	0.4045	0.3871	0.3750	0.3660	0.3583	0.3528	0.3480	0.3439	0.3410	0.3384	0.3347	0.3319	0.3297	0.3278	0.3264
7.00	0.4414	0.4239	0.4118	0.4029	0.3954	0.3900	0.3852	0.3811	0.3782	0.3757	0.3719	0.3692	0.3669	0.3650	0.3635
7.50	0.4782	0.4607	0.4486	0.4397	0.4323	0.4270	0.4223	0.4182	0.4154	0.4129	0.4092	0.4064	0.4042	0.4023	0.4008
8.00	0.5150	0.4973	0.4852	0.4763	0.4690	0.4638	0.4592	0.4552	0.4525	0.4500	0.4459	0.4436	0.4414	0.4395	0.4380
8.50	0.5517	0.5339	0.5216	0.5128	0.5055	0.5004	0.4959	0.4920	0.4893	0.4869	0.4828	0.4806	0.4785	0.4766	0.4751
9.00	0.5883	0.5704	0.5580	0.5492	0.5419	0.5368	0.5323	0.5286	0.5259	0.5235	0.5196	0.5174	0.5153	0.5135	0.5120
9.50	0.6248	0.6067	0.5942	0.5853	0.5780	0.5730	0.5686	0.5649	0.5623	0.5599	0.5561	0.5540	0.5519	0.5501	0.5486
10.00	0.6613	0.6430	0.6304	0.6214	0.6140	0.6090	0.6046	0.6009	0.5984	0.5961	0.5923	0.5903	0.5882	0.5864	0.5850
10.50	0.6978	0.6792	0.6664	0.6573	0.6498	0.6447	0.6404	0.6367	0.6342	0.6320	0.6283	0.6262	0.6242	0.6224	0.6210
11.00	0.7342	0.7153	0.7023	0.6930	0.6854	0.6803	0.6759	0.6723	0.6698	0.6676	0.6639	0.6619	0.6598	0.6580	0.6566
11.50	0.7705	0.7514	0.7381	0.7286	0.7209	0.7157	0.7113	0.7076	0.7051	0.7029	0.6993	0.6972	0.6952	0.6934	0.6920
12.00	0.8068	0.7874	0.7738	0.7641	0.7562	0.7509	0.7464	0.7427	0.7402	0.7380	0.7343	0.7323	0.7302	0.7284	0.7270
12.50	0.8430	0.8233	0.8094	0.7994	0.7914	0.7860	0.7814	0.7776	0.7751	0.7728	0.7690	0.7670	0.7649	0.7630	0.7616
13.00	0.8792	0.8591	0.8449	0.8347	0.8264	0.8209	0.8161	0.8122	0.8097	0.8073	0.8035	0.8013	0.7992	0.7974	0.7959
13.50	0.9153	0.8949	0.8804	0.8698	0.8613	0.8556	0.8507	0.8467	0.8440	0.8416	0.8376	0.8354	0.8332	0.8313	0.8299
14.00	0.9514	0.9306	0.9157	0.9048	0.8961	0.8902	0.8851	0.8809	0.8782	0.8756	0.8715	0.8691	0.8669	0.8650	0.8635
14.50	0.9875	0.9663	0.9510	0.9396	0.9307	0.9246	0.9193	0.9150	0.9121	0.9094	0.9050	0.9025	0.9002	0.8983	0.8968
15.00	1.0235	1.0019	0.9863	0.9744	0.9652	0.9589	0.9533	0.9489	0.9458	0.9429	0.9382	0.9356	0.9332	0.9312	0.9297
15.50	1.0595	1.0374	1.0214	1.0091	0.9995	0.9931	0.9872	0.9825	0.9793	0.9762	0.9712	0.9684	0.9660	0.9639	0.9623
16.00	1.0955	1.0729	1.0565	1.0437	1.0338	1.0271	1.0209	1.0160	1.0125	1.0093	1.0039	1.0009	0.9984	0.9963	0.9946
16.50	1.1315	1.1084	1.0915	1.0782	1.0679	1.0609	1.0544	1.0494	1.0456	1.0422	1.0364	1.0331	1.0305	1.0283	1.0266
17.00	1.1674	1.1438	1.1265	1.1126	1.1019	1.0947	1.0878	1.0825	1.0785	1.0748	1.0685	1.0650	1.0623	1.0600	1.0583
17.50	1.2032	1.1791	1.1614	1.1469	1.1358	1.1283	1.1211	1.1155	1.1112	1.1072	1.1005	1.0967	1.0938	1.0915	1.0897
18.00	1.2391	1.2145	1.1962	1.1811	1.1696	1.1619	1.1542	1.1484	1.1437	1.1394	1.1321	1.1281	1.1250	1.1227	1.1208
18.50	1.2749	1.2497	1.2310	1.2153	1.2033	1.1953	1.1872	1.1811	1.1761	1.1715	1.1636	1.1592	1.1560	1.1536	1.1517
19.00	1.3107	1.2850	1.2658	1.2494	1.2370	1.2286	1.2200	1.2136	1.2082	1.2033	1.1948	1.1901	1.1867	1.1842	1.1823
19.50	1.3465	1.3202	1.3005	1.2834	1.2705	1.2618	1.2528	1.2460	1.2403	1.2350	1.2258	1.2207	1.2172	1.2146	1.2126
20.00	1.3823	1.3554	1.3351	1.3173	1.3039	1.2949	1.2854	1.2783	1.2721	1.2665	1.2566	1.2511	1.2474	1.2447	1.2426
20.50	1.4180	1.3905	1.3697	1.3512	1.3373	1.3279	1.3179	1.3105	1.3038	1.2978	1.2871	1.2812	1.2774	1.2746	1.2724
21.00	1.4538	1.4256	1.4043	1.3850	1.3706	1.3608	1.3503	1.3425	1.3354	1.3290	1.3175	1.3112	1.3071	1.3043	1.3020
21.50	1.4895	1.4607	1.4388	1.4187	1.4038	1.3937	1.3825	1.3744	1.3668	1.3599	1.3477	1.3409	1.3367	1.3337	1.3314
22.00	1.5251	1.4958	1.4733	1.4524	1.4369	1.4264	1.4147	1.4062	1.3981	1.3908	1.3776	1.3704	1.3660	1.3629	1.3605
22.50	1.5608	1.5308	1.5077	1.4860	1.4699	1.4591	1.4468	1.4379	1.4292	1.4215	1.4074	1.3997	1.3951	1.3919	1.3894
23.00	1.5965	1.5658	1.5421	1.5196	1.5029	1.4916	1.4788	1.4694	1.4603	1.4520	1.4371	1.4288	1.4239	1.4207	1.4181
23.50	1.6321	1.6008	1.5765	1.5531	1.5358	1.5242	1.5106	1.5009	1.4912	1.4824	1.4665	1.4577	1.4526	1.4493	1.4466
24.00	1.6677	1.6357	1.6108	1.5866	1.5687	1.5566	1.5424	1.5323	1.5219	1.5127	1.4958	1.4865	1.4811	1.4776	1.4748
24.50	1.7033	1.6706	1.6451	1.6200	1.6015	1.5890	1.5741	1.5635	1.5526	1.5428	1.5249	1.5150	1.5094	1.5058	1.5029
25.00	1.7389	1.7055	1.6794	1.6534	1.6342	1.6212	1.6057	1.5947	1.5831	1.5728	1.5538	1.5434	1.5375	1.5338	1.5308
25.50	1.7745	1.7404	1.7136	1.6867	1.6668	1.6535	1.6373	1.6247	1.6136	1.6027	1.5826	1.5716	1.5655	1.5617	1.5585
26.00	1.8100	1.7752	1.7478	1.7200	1.6995	1.6856	1.6697	1.6567	1.6439	1.6324	1.6112	1.5996	1.5933	1.5893	1.5861
26.50	1.8456	1.8101	1.7820	1.7532	1.7320	1.7177	1.7001	1.6876	1.6741	1.6621	1.6397	1.6275	1.6209	1.6168	1.6134
27.00	1.8811	1.8449	1.8162	1.7864	1.7645	1.7498	1.7314	1.7184	1.7042	1.6916	1.6681	1.6552	1.6483	1.6441	1.6406
27.50	1.9166	1.8797	1.8503	1.8195	1.7969	1.7817	1.7626	1.7491	1.7343	1.7210	1.6963	1.6828	1.6756	1.6712	1.6677
28.00	1.9521	1.9144	1.8844	1.8526	1.8293	1.8136	1.7937	1.7798	1.7642	1.7503	1.7244	1.7102	1.7027	1.6982	1.6945
28.50	1.9876	1.9492	1.9184	1.8857	1.8617	1.8455	1.8248	1.8103	1.7940	1.7795	1.7523	1.7375	1.7297	1.7251	1.7212
29.00	2.0231	1.9839	1.9525	1.9187	1.8940	1.8773	1.8558	1.8408	1.8238	1.8086	1.7801	1.7646	1.7565	1.7518	1.7478
29.50	2.0586	2.0186	1.9865	1.9517	1.9262	1.9091	1.8868	1.8712	1.8534	1.8376	1.8078	1.7916	1.7832	1.7783	1.7742
30.00	2.0941	2.0533	2.0205	1.9847	1.9584	1.9408	1.9176	1.9016	1.8830	1.8664	1.8354	1.8184	1.8097	1.8047	1.8005

TABLE 34.2—EXTENDED SUKKAR-CORNELL INTEGRAL FOR BHP CALCULATION (continued)

$$\int_0^{p_{pr}} \frac{(z/p_{pr}) dp_{pr}}{1 + B(z/p_{pr})^2}$$

Pseudoreduced temperature for $B = 50.0$

p_{pr}	1.1	1.2	1.3	1.4	1.5	1.6	1.7	1.8	1.9	2.0	2.2	2.4	2.6	2.8	3.0
0.20	0.0000	0.0000	0.0000	0.0000	0.0000	0.0000	0.0000	0.0000	0.0000	0.0000	0.0000	0.0000	0.0000	0.0000	0.0000
0.50	0.0023	0.0023	0.0022	0.0022	0.0022	0.0022	0.0021	0.0021	0.0021	0.0021	0.0021	0.0021	0.0021	0.0021	0.0021
1.00	0.0121	0.0111	0.0107	0.0104	0.0102	0.0100	0.0099	0.0098	0.0098	0.0097	0.0096	0.0096	0.0095	0.0095	0.0095
1.50	0.0328	0.0276	0.0257	0.0246	0.0238	0.0233	0.0229	0.0226	0.0224	0.0222	0.0220	0.0218	0.0217	0.0216	0.0215
2.00	0.0649	0.0524	0.0474	0.0447	0.0430	0.0418	0.0409	0.0402	0.0398	0.0395	0.0389	0.0385	0.0382	0.0380	0.0378
2.50	0.0997	0.0835	0.0750	0.0702	0.0670	0.0650	0.0634	0.0622	0.0615	0.0608	0.0599	0.0593	0.0587	0.0583	0.0579
3.00	0.1350	0.1173	0.1066	0.0998	0.0951	0.0921	0.0897	0.0879	0.0868	0.0858	0.0844	0.0835	0.0827	0.0820	0.0814
3.50	0.1703	0.1521	0.1402	0.1322	0.1261	0.1222	0.1191	0.1167	0.1151	0.1138	0.1119	0.1106	0.1095	0.1085	0.1078
4.00	0.2057	0.1873	0.1749	0.1660	0.1591	0.1545	0.1507	0.1477	0.1457	0.1440	0.1417	0.1401	0.1387	0.1375	0.1365
4.50	0.2410	0.2226	0.2101	0.2008	0.1933	0.1882	0.1839	0.1804	0.1781	0.1761	0.1734	0.1714	0.1697	0.1683	0.1671
5.00	0.2763	0.2579	0.2454	0.2359	0.2281	0.2227	0.2181	0.2143	0.2117	0.2094	0.2063	0.2040	0.2022	0.2006	0.1993
5.50	0.3116	0.2933	0.2807	0.2712	0.2632	0.2577	0.2529	0.2488	0.2461	0.2436	0.2402	0.2377	0.2357	0.2339	0.2326
6.00	0.3469	0.3285	0.3161	0.3066	0.2985	0.2929	0.2880	0.2838	0.2809	0.2784	0.2747	0.2721	0.2700	0.2681	0.2667
6.50	0.3821	0.3638	0.3513	0.3419	0.3339	0.3282	0.3233	0.3190	0.3161	0.3135	0.3097	0.3069	0.3048	0.3029	0.3014
7.00	0.4173	0.3990	0.3865	0.3772	0.3692	0.3636	0.3587	0.3544	0.3514	0.3488	0.3450	0.3421	0.3399	0.3380	0.3365
7.50	0.4525	0.4341	0.4216	0.4123	0.4044	0.3989	0.3940	0.3897	0.3868	0.3841	0.3803	0.3774	0.3752	0.3733	0.3718
8.00	0.4876	0.4692	0.4567	0.4474	0.4395	0.4340	0.4292	0.4250	0.4221	0.4194	0.4151	0.4128	0.4105	0.4086	0.4071
8.50	0.5227	0.5042	0.4916	0.4823	0.4745	0.4690	0.4643	0.4601	0.4573	0.4547	0.4504	0.4481	0.4458	0.4439	0.4424
9.00	0.5577	0.5391	0.5264	0.5171	0.5093	0.5039	0.4992	0.4951	0.4923	0.4897	0.4855	0.4832	0.4810	0.4791	0.4777
9.50	0.5927	0.5739	0.5612	0.5518	0.5440	0.5386	0.5340	0.5299	0.5271	0.5246	0.5204	0.5182	0.5160	0.5142	0.5127
10.00	0.6277	0.6087	0.5959	0.5864	0.5786	0.5732	0.5685	0.5645	0.5618	0.5593	0.5552	0.5530	0.5508	0.5490	0.5475
10.50	0.6626	0.6435	0.6304	0.6209	0.6130	0.6076	0.6029	0.5990	0.5962	0.5938	0.5897	0.5875	0.5854	0.5835	0.5821
11.00	0.6974	0.6781	0.6649	0.6553	0.6473	0.6418	0.6372	0.6332	0.6305	0.6280	0.6240	0.6219	0.6197	0.6179	0.6164
11.50	0.7323	0.7127	0.6994	0.6896	0.6815	0.6759	0.6712	0.6672	0.6645	0.6621	0.6581	0.6559	0.6537	0.6519	0.6505
12.00	0.7670	0.7473	0.7337	0.7237	0.7155	0.7099	0.7051	0.7011	0.6984	0.6959	0.6919	0.6897	0.6875	0.6857	0.6842
12.50	0.8018	0.7818	0.7680	0.7578	0.7494	0.7437	0.7388	0.7347	0.7320	0.7295	0.7254	0.7232	0.7210	0.7192	0.7177
13.00	0.8365	0.8163	0.8022	0.7917	0.7832	0.7774	0.7724	0.7682	0.7654	0.7629	0.7587	0.7565	0.7542	0.7523	0.7509
13.50	0.8712	0.8507	0.8363	0.8256	0.8169	0.8109	0.8058	0.8015	0.7987	0.7960	0.7917	0.7894	0.7872	0.7852	0.7838
14.00	0.9059	0.8850	0.8704	0.8594	0.8504	0.8443	0.8391	0.8347	0.8317	0.8290	0.8245	0.8221	0.8198	0.8178	0.8163
14.50	0.9405	0.9193	0.9044	0.8930	0.8839	0.8776	0.8722	0.8676	0.8645	0.8617	0.8570	0.8545	0.8521	0.8502	0.8486
15.00	0.9751	0.9536	0.9384	0.9266	0.9172	0.9108	0.9051	0.9004	0.8972	0.8942	0.8893	0.8866	0.8842	0.8822	0.8806
15.50	1.0097	0.9878	0.9722	0.9601	0.9504	0.9438	0.9379	0.9331	0.9297	0.9265	0.9213	0.9185	0.9160	0.9139	0.9123
16.00	1.0442	1.0220	1.0061	0.9935	0.9836	0.9768	0.9706	0.9656	0.9620	0.9586	0.9531	0.9501	0.9475	0.9454	0.9438
16.50	1.0788	1.0561	1.0399	1.0269	1.0166	1.0096	1.0031	0.9979	0.9941	0.9906	0.9847	0.9814	0.9788	0.9766	0.9749
17.00	1.1133	1.0902	1.0736	1.0601	1.0495	1.0423	1.0355	1.0301	1.0260	1.0223	1.0160	1.0125	1.0097	1.0075	1.0058
17.50	1.1477	1.1243	1.1073	1.0933	1.0824	1.0749	1.0678	1.0621	1.0578	1.0538	1.0471	1.0434	1.0405	1.0382	1.0364
18.00	1.1822	1.1583	1.1409	1.1264	1.1151	1.1074	1.0999	1.0940	1.0894	1.0852	1.0779	1.0740	1.0709	1.0686	1.0668
18.50	1.2167	1.1923	1.1745	1.1595	1.1478	1.1398	1.1320	1.1258	1.1209	1.1164	1.1086	1.1043	1.1012	1.0988	1.0969
19.00	1.2511	1.2263	1.2081	1.1925	1.1804	1.1721	1.1639	1.1575	1.1522	1.1474	1.1390	1.1345	1.1312	1.1287	1.1268
19.50	1.2855	1.2602	1.2416	1.2254	1.2129	1.2044	1.1957	1.1890	1.1834	1.1783	1.1693	1.1644	1.1609	1.1584	1.1564
20.00	1.3199	1.2942	1.2751	1.2583	1.2453	1.2365	1.2274	1.2204	1.2144	1.2090	1.1993	1.1941	1.1905	1.1878	1.1858
20.50	1.3542	1.3280	1.3085	1.2911	1.2777	1.2686	1.2590	1.2517	1.2453	1.2395	1.2292	1.2236	1.2198	1.2171	1.2149
21.00	1.3886	1.3619	1.3419	1.3238	1.3100	1.3005	1.2905	1.2829	1.2761	1.2699	1.2589	1.2528	1.2489	1.2461	1.2439
21.50	1.4229	1.3957	1.3753	1.3565	1.3422	1.3324	1.3219	1.3140	1.3067	1.3001	1.2884	1.2810	1.2778	1.2749	1.2726
22.00	1.4573	1.4295	1.4086	1.3892	1.3743	1.3643	1.3532	1.3449	1.3372	1.3302	1.3177	1.3108	1.3065	1.3035	1.3011
22.50	1.4916	1.4633	1.4419	1.4218	1.4064	1.3960	1.3844	1.3758	1.3676	1.3602	1.3468	1.3395	1.3350	1.3319	1.3295
23.00	1.5259	1.4971	1.4752	1.4543	1.4385	1.4277	1.4155	1.4066	1.3979	1.3900	1.3758	1.3680	1.3633	1.3601	1.3576
23.50	1.5602	1.5308	1.5084	1.4868	1.4704	1.4593	1.4466	1.4372	1.4280	1.4197	1.4046	1.3964	1.3914	1.3881	1.3855
24.00	1.5944	1.5646	1.5416	1.5193	1.5024	1.4908	1.4775	1.4678	1.4581	1.4493	1.4333	1.4245	1.4193	1.4160	1.4133
24.50	1.6287	1.5983	1.5748	1.5517	1.5342	1.5223	1.5084	1.4983	1.4880	1.4788	1.4618	1.4525	1.4471	1.4436	1.4408
25.00	1.6629	1.6319	1.6079	1.5841	1.5660	1.5537	1.5392	1.5287	1.5178	1.5081	1.4902	1.4803	1.4747	1.4711	1.4682
25.50	1.6972	1.6656	1.6410	1.6164	1.5978	1.5851	1.5700	1.5590	1.5476	1.5373	1.5184	1.5080	1.5021	1.4984	1.4954
26.00	1.7314	1.6992	1.6741	1.6487	1.6295	1.6164	1.6006	1.5892	1.5772	1.5664	1.5465	1.5355	1.5294	1.5256	1.5225
26.50	1.7656	1.7329	1.7072	1.6809	1.6611	1.6476	1.6312	1.6194	1.6068	1.5954	1.5744	1.5629	1.5565	1.5526	1.5494
27.00	1.7998	1.7665	1.7403	1.7131	1.6927	1.6788	1.6617	1.6494	1.6362	1.6243	1.6022	1.5901	1.5835	1.5794	1.5761
27.50	1.8340	1.8001	1.7733	1.7453	1.7243	1.7100	1.6922	1.6794	1.6656	1.6531	1.6299	1.6172	1.6103	1.6061	1.6027
28.00	1.8682	1.8337	1.8063	1.7775	1.7558	1.7410	1.7226	1.7094	1.6948	1.6818	1.6574	1.6441	1.6369	1.6326	1.6291
28.50	1.9024	1.8672	1.8393	1.8096	1.7872	1.7721	1.7529	1.7392	1.7240	1.7104	1.6849	1.6709	1.6634	1.6590	1.6553
29.00	1.9366	1.9008	1.8722	1.8416	1.8187	1.8030	1.7831	1.7690	1.7531	1.7309	1.7122	1.6976	1.6898	1.6853	1.6815
29.50	1.9707	1.9341	1.9052	1.8737	1.8500	1.8340	1.8133	1.7987	1.7821	1.7673	1.7394	1.7241	1.7160	1.7114	1.7076
30.00	2.0049	1.9678	1.9381	1.9057	1.8814	1.8649	1.8435	1.8284	1.8111	1.7956	1.7664	1.7505	1.7421	1.7373	1.7333

TABLE 34.2—EXTENDED SUKKAR-CORNELL INTEGRAL FOR BHP CALCULATION (continued)

$$\int_{0.2}^{p_{pr}} \frac{(z/p_{pr}) dp_{pr}}{1 + B(z/p_{pr})^2}$$

Pseudoreduced temperature for $B = 60.0$

p_{pr}	1.1	1.2	1.3	1.4	1.5	1.6	1.7	1.8	1.9	2.0	2.2	2.4	2.6	2.8	3.0
0.20	0.0000	0.0000	0.0000	0.0000	0.0000	0.0000	0.0000	0.0000	0.0000	0.0000	0.0000	0.0000	0.0000	0.0000	0.0000
0.50	0.0019	0.0019	0.0019	0.0018	0.0018	0.0018	0.0018	0.0018	0.0018	0.0018	0.0018	0.0018	0.0017	0.0017	0.0017
1.00	0.0101	0.0093	0.0089	0.0087	0.0085	0.0084	0.0083	0.0082	0.0081	0.0081	0.0080	0.0080	0.0080	0.0079	0.0079
1.50	0.0277	0.0232	0.0215	0.0206	0.0200	0.0195	0.0192	0.0189	0.0188	0.0186	0.0184	0.0183	0.0181	0.0181	0.0180
2.00	0.0559	0.0443	0.0399	0.0376	0.0361	0.0351	0.0343	0.0338	0.0334	0.0331	0.0326	0.0323	0.0321	0.0319	0.0317
2.50	0.0870	0.0715	0.0637	0.0594	0.0566	0.0549	0.0535	0.0524	0.0518	0.0512	0.0504	0.0499	0.0494	0.0490	0.0487
3.00	0.1189	0.1014	0.0913	0.0851	0.0808	0.0781	0.0760	0.0745	0.0734	0.0726	0.0714	0.0705	0.0698	0.0692	0.0687
3.50	0.1509	0.1325	0.1211	0.1135	0.1079	0.1043	0.1014	0.0993	0.0979	0.0966	0.0950	0.0939	0.0928	0.0920	0.0913
4.00	0.1831	0.1642	0.1521	0.1435	0.1369	0.1326	0.1291	0.1263	0.1245	0.1229	0.1209	0.1194	0.1181	0.1170	0.1161
4.50	0.2153	0.1962	0.1837	0.1745	0.1672	0.1624	0.1583	0.1551	0.1529	0.1510	0.1485	0.1466	0.1451	0.1438	0.1428
5.00	0.2475	0.2283	0.2157	0.2062	0.1984	0.1931	0.1887	0.1850	0.1826	0.1804	0.1775	0.1753	0.1736	0.1721	0.1709
5.50	0.2798	0.2606	0.2479	0.2382	0.2301	0.2245	0.2198	0.2158	0.2132	0.2108	0.2075	0.2051	0.2032	0.2016	0.2003
6.00	0.3120	0.2928	0.2801	0.2703	0.2620	0.2563	0.2515	0.2472	0.2444	0.2419	0.2383	0.2357	0.2337	0.2320	0.2306
6.50	0.3443	0.3251	0.3124	0.3026	0.2942	0.2884	0.2834	0.2791	0.2761	0.2735	0.2697	0.2670	0.2648	0.2630	0.2616
7.00	0.3766	0.3574	0.3446	0.3348	0.3264	0.3206	0.3156	0.3111	0.3081	0.3054	0.3015	0.2986	0.2964	0.2946	0.2932
7.50	0.4088	0.3896	0.3769	0.3671	0.3587	0.3529	0.3478	0.3433	0.3403	0.3375	0.3336	0.3306	0.3284	0.3265	0.3251
8.00	0.4411	0.4219	0.4091	0.3994	0.3910	0.3851	0.3801	0.3756	0.3725	0.3697	0.3651	0.3628	0.3605	0.3586	0.3572
8.50	0.4734	0.4541	0.4413	0.4316	0.4232	0.4174	0.4123	0.4079	0.4048	0.4020	0.3974	0.3951	0.3928	0.3909	0.3894
9.00	0.5056	0.4863	0.4735	0.4637	0.4554	0.4496	0.4445	0.4401	0.4370	0.4343	0.4297	0.4273	0.4251	0.4231	0.4217
9.50	0.5378	0.5185	0.5056	0.4958	0.4875	0.4817	0.4767	0.4722	0.4692	0.4665	0.4619	0.4596	0.4573	0.4554	0.4539
10.00	0.5701	0.5507	0.5377	0.5279	0.5195	0.5137	0.5087	0.5043	0.5013	0.4985	0.4940	0.4917	0.4894	0.4875	0.4861
10.50	0.6023	0.5828	0.5698	0.5599	0.5515	0.5457	0.5407	0.5363	0.5333	0.5305	0.5260	0.5237	0.5215	0.5196	0.5181
11.00	0.6344	0.6149	0.6018	0.5918	0.5833	0.5775	0.5725	0.5681	0.5651	0.5624	0.5579	0.5556	0.5534	0.5515	0.5500
11.50	0.6666	0.6469	0.6337	0.6237	0.6151	0.6093	0.6042	0.5998	0.5968	0.5941	0.5896	0.5873	0.5851	0.5832	0.5818
12.00	0.6987	0.6790	0.6656	0.6555	0.6469	0.6409	0.6359	0.6314	0.6284	0.6257	0.6212	0.6189	0.6166	0.6148	0.6133
12.50	0.7309	0.7110	0.6975	0.6872	0.6785	0.6725	0.6674	0.6629	0.6599	0.6571	0.6526	0.6503	0.6480	0.6461	0.6446
13.00	0.7630	0.7429	0.7293	0.7189	0.7101	0.7040	0.6986	0.6943	0.6912	0.6884	0.6838	0.6815	0.6792	0.6773	0.6758
13.50	0.7951	0.7749	0.7611	0.7505	0.7415	0.7354	0.7301	0.7255	0.7224	0.7196	0.7149	0.7125	0.7101	0.7032	0.7067
14.00	0.8272	0.8068	0.7929	0.7820	0.7730	0.7667	0.7613	0.7566	0.7534	0.7505	0.7457	0.7432	0.7409	0.7389	0.7374
14.50	0.8592	0.8387	0.8246	0.8135	0.8043	0.7979	0.7924	0.7876	0.7843	0.7813	0.7764	0.7738	0.7714	0.7694	0.7679
15.00	0.8913	0.8705	0.8562	0.8449	0.8355	0.8291	0.8233	0.8184	0.8151	0.8120	0.8069	0.8042	0.8017	0.7997	0.7982
15.50	0.9233	0.9024	0.8879	0.8763	0.8667	0.8601	0.8542	0.8492	0.8457	0.8425	0.8371	0.8343	0.8318	0.8298	0.8282
16.00	0.9554	0.9342	0.9195	0.9076	0.8978	0.8911	0.8850	0.8798	0.8762	0.8728	0.8672	0.8643	0.8617	0.8596	0.8580
16.50	0.9874	0.9660	0.9510	0.9389	0.9288	0.9219	0.9156	0.9103	0.9065	0.9030	0.8971	0.8940	0.8914	0.8892	0.8876
17.00	1.0194	0.9977	0.9826	0.9701	0.9598	0.9527	0.9462	0.9408	0.9368	0.9331	0.9269	0.9236	0.9208	0.9186	0.9170
17.50	1.0514	1.0295	1.0141	1.0012	0.9907	0.9835	0.9767	0.9711	0.9668	0.9630	0.9564	0.9529	0.9501	0.9478	0.9461
18.00	1.0834	1.0612	1.0455	1.0323	1.0215	1.0141	1.0070	1.0013	0.9968	0.9928	0.9858	0.9820	0.9791	0.9768	0.9751
18.50	1.1153	1.0929	1.0769	1.0634	1.0523	1.0447	1.0373	1.0313	1.0267	1.0224	1.0150	1.0110	1.0080	1.0056	1.0038
19.00	1.1473	1.1246	1.1083	1.0944	1.0830	1.0752	1.0675	1.0613	1.0564	1.0519	1.0440	1.0398	1.0366	1.0342	1.0324
19.50	1.1792	1.1562	1.1397	1.1253	1.1137	1.1056	1.0976	1.0912	1.0860	1.0812	1.0728	1.0683	1.0651	1.0626	1.0607
20.00	1.2112	1.1879	1.1711	1.1562	1.1443	1.1360	1.1277	1.1210	1.1155	1.1104	1.1015	1.0967	1.0933	1.0908	1.0889
20.50	1.2431	1.2195	1.2024	1.1871	1.1748	1.1663	1.1576	1.1507	1.1449	1.1395	1.1301	1.1250	1.1214	1.1188	1.1168
21.00	1.2750	1.2511	1.2337	1.2179	1.2053	1.1965	1.1875	1.1803	1.1741	1.1685	1.1584	1.1530	1.1493	1.1466	1.1446
21.50	1.3069	1.2827	1.2650	1.2487	1.2357	1.2267	1.2173	1.2099	1.2033	1.1974	1.1867	1.1809	1.1770	1.1743	1.1721
22.00	1.3388	1.3143	1.2962	1.2795	1.2661	1.2568	1.2470	1.2393	1.2324	1.2261	1.2147	1.2086	1.2046	1.2018	1.1995
22.50	1.3707	1.3458	1.3274	1.3102	1.2964	1.2869	1.2766	1.2687	1.2614	1.2547	1.2427	1.2361	1.2319	1.2291	1.2268
23.00	1.4026	1.3774	1.3586	1.3409	1.3267	1.3169	1.3062	1.2979	1.2902	1.2832	1.2705	1.2635	1.2592	1.2562	1.2538
23.50	1.4344	1.4089	1.3898	1.3715	1.3569	1.3469	1.3357	1.3271	1.3190	1.3116	1.2981	1.2908	1.2862	1.2832	1.2807
24.00	1.4663	1.4404	1.4210	1.4021	1.3871	1.3768	1.3652	1.3563	1.3477	1.3399	1.3256	1.3179	1.3131	1.3100	1.3074
24.50	1.4982	1.4719	1.4521	1.4327	1.4173	1.4066	1.3945	1.3853	1.3763	1.3681	1.3530	1.3448	1.3399	1.3366	1.3340
25.00	1.5300	1.5034	1.4832	1.4632	1.4474	1.4364	1.4238	1.4143	1.4048	1.3962	1.3803	1.3716	1.3664	1.3631	1.3604
25.50	1.5619	1.5349	1.5143	1.4937	1.4774	1.4662	1.4531	1.4432	1.4332	1.4242	1.4074	1.3983	1.3929	1.3895	1.3867
26.00	1.5937	1.5664	1.5454	1.5242	1.5075	1.4959	1.4823	1.4721	1.4616	1.4521	1.4344	1.4248	1.4192	1.4157	1.4128
26.50	1.6255	1.5978	1.5765	1.5547	1.5374	1.5255	1.5114	1.5008	1.4898	1.4799	1.4613	1.4512	1.4454	1.4417	1.4388
27.00	1.6574	1.6292	1.6075	1.5851	1.5674	1.5552	1.5405	1.5295	1.5180	1.5076	1.4881	1.4775	1.4714	1.4677	1.4646
27.50	1.6892	1.6607	1.6385	1.6155	1.5973	1.5847	1.5695	1.5582	1.5461	1.5353	1.5148	1.5036	1.4973	1.4935	1.4903
28.00	1.7210	1.6921	1.6695	1.6459	1.6272	1.6143	1.5985	1.5868	1.5742	1.5628	1.5413	1.5296	1.5231	1.5191	1.5159
28.50	1.7528	1.7235	1.7005	1.6762	1.6570	1.6438	1.6274	1.6153	1.6021	1.5903	1.5678	1.5555	1.5487	1.5447	1.5413
29.00	1.7846	1.7549	1.7315	1.7065	1.6868	1.6732	1.6563	1.6436	1.6300	1.6176	1.5941	1.5813	1.5742	1.5701	1.5666
29.50	1.8164	1.7863	1.7625	1.7368	1.7166	1.7076	1.6851	1.6722	1.6579	1.6449	1.6204	1.6070	1.5997	1.5954	1.5918
30.00	1.8482	1.8177	1.7934	1.7671	1.7463	1.7320	1.7139	1.7005	1.6856	1.6722	1.6465	1.6325	1.6249	1.6205	1.6168

TABLE 34.2—EXTENDED SUKKAR-CORNELL INTEGRAL FOR BHP CALCULATION (continued)

$$\int_{0.2}^{p_{pr}} \frac{(z/p_{pr}) dp_{pr}}{1 + B(z/p_{pr})^2}$$

Pseudoreduced temperature for $B = 70.0$

p_{pr}	1.1	1.2	1.3	1.4	1.5	1.6	1.7	1.8	1.9	2.0	2.2	2.4	2.6	2.8	3.0
0.20	0.0000	0.0000	0.0000	0.0000	0.0000	0.0000	0.0000	0.0000	0.0000	0.0000	0.0000	0.0000	0.0000	0.0000	0.0000
0.50	0.0017	0.0016	0.0016	0.0016	0.0016	0.0015	0.0015	0.0015	0.0015	0.0015	0.0015	0.0015	0.0015	0.0015	0.0015
1.00	0.0087	0.0080	0.0077	0.0074	0.0073	0.0072	0.0071	0.0070	0.0070	0.0070	0.0069	0.0069	0.0068	0.0068	0.0068
1.50	0.0240	0.0199	0.0185	0.0177	0.0172	0.0168	0.0165	0.0163	0.0161	0.0160	0.0158	0.0157	0.0156	0.0155	0.0154
2.00	0.0491	0.0385	0.0345	0.0325	0.0312	0.0303	0.0296	0.0291	0.0288	0.0285	0.0281	0.0278	0.0276	0.0274	0.0273
2.50	0.0772	0.0625	0.0554	0.0515	0.0490	0.0475	0.0462	0.0453	0.0448	0.0443	0.0435	0.0431	0.0426	0.0423	0.0420
3.00	0.1063	0.0894	0.0799	0.0742	0.0703	0.0679	0.0660	0.0646	0.0637	0.0629	0.0618	0.0611	0.0604	0.0599	0.0595
3.50	0.1356	0.1175	0.1066	0.0994	0.0943	0.0910	0.0884	0.0864	0.0851	0.0840	0.0825	0.0815	0.0806	0.0798	0.0792
4.00	0.1651	0.1464	0.1346	0.1264	0.1202	0.1162	0.1129	0.1104	0.1087	0.1073	0.1054	0.1040	0.1029	0.1018	0.1010
4.50	0.1947	0.1756	0.1634	0.1545	0.1475	0.1429	0.1391	0.1360	0.1340	0.1322	0.1299	0.1282	0.1268	0.1256	0.1246
5.00	0.2243	0.2050	0.1926	0.1833	0.1756	0.1706	0.1664	0.1629	0.1606	0.1585	0.1558	0.1538	0.1522	0.1508	0.1497
5.50	0.2540	0.2347	0.2221	0.2125	0.2045	0.1991	0.1946	0.1907	0.1881	0.1859	0.1827	0.1805	0.1787	0.1772	0.1760
6.00	0.2838	0.2644	0.2517	0.2420	0.2337	0.2281	0.2233	0.2192	0.2164	0.2140	0.2106	0.2081	0.2061	0.2045	0.2032
6.50	0.3135	0.2941	0.2815	0.2716	0.2632	0.2574	0.2525	0.2482	0.2453	0.2427	0.2390	0.2363	0.2343	0.2326	0.2313
7.00	0.3433	0.3239	0.3113	0.3014	0.2929	0.2870	0.2820	0.2775	0.2745	0.2718	0.2680	0.2652	0.2630	0.2613	0.2599
7.50	0.3732	0.3538	0.3411	0.3312	0.3226	0.3167	0.3116	0.3071	0.3040	0.3013	0.2973	0.2944	0.2922	0.2904	0.2890
8.00	0.4030	0.3836	0.3710	0.3611	0.3525	0.3465	0.3414	0.3368	0.3337	0.3309	0.3262	0.3239	0.3217	0.3198	0.3184
8.50	0.4328	0.4135	0.4009	0.3909	0.3824	0.3764	0.3713	0.3667	0.3635	0.3607	0.3560	0.3536	0.3514	0.3495	0.3481
9.00	0.4627	0.4434	0.4307	0.4208	0.4122	0.4063	0.4011	0.3965	0.3934	0.3905	0.3858	0.3834	0.3812	0.3793	0.3779
9.50	0.4926	0.4733	0.4606	0.4507	0.4421	0.4362	0.4310	0.4264	0.4233	0.4204	0.4157	0.4133	0.4110	0.4092	0.4077
10.00	0.5225	0.5031	0.4905	0.4805	0.4720	0.4660	0.4609	0.4563	0.4531	0.4503	0.4456	0.4432	0.4409	0.4390	0.4376
10.50	0.5523	0.5330	0.5203	0.5104	0.5018	0.4958	0.4907	0.4861	0.4830	0.4801	0.4754	0.4730	0.4708	0.4689	0.4675
11.00	0.5822	0.5629	0.5502	0.5402	0.5316	0.5256	0.5204	0.5159	0.5127	0.5099	0.5052	0.5028	0.5005	0.4987	0.4972
11.50	0.6121	0.5927	0.5800	0.5700	0.5613	0.5553	0.5502	0.5456	0.5424	0.5396	0.5349	0.5325	0.5303	0.5284	0.5270
12.00	0.6420	0.6226	0.6098	0.5997	0.5910	0.5850	0.5798	0.5752	0.5721	0.5692	0.5645	0.5621	0.5599	0.5580	0.5566
12.50	0.6718	0.6524	0.6396	0.6294	0.6207	0.6146	0.6094	0.6047	0.6016	0.5987	0.5940	0.5916	0.5893	0.5875	0.5860
13.00	0.7017	0.6822	0.6693	0.6591	0.6503	0.6442	0.6389	0.6342	0.6311	0.6282	0.6234	0.6210	0.6187	0.6168	0.6154
13.50	0.7316	0.7121	0.6991	0.6887	0.6798	0.6737	0.6683	0.6636	0.6604	0.6575	0.6527	0.6502	0.6479	0.6460	0.6445
14.00	0.7615	0.7419	0.7288	0.7183	0.7093	0.7031	0.6977	0.6929	0.6897	0.6867	0.6818	0.6793	0.6770	0.6750	0.6736
14.50	0.7913	0.7717	0.7585	0.7479	0.7388	0.7325	0.7270	0.7222	0.7189	0.7158	0.7108	0.7062	0.7039	0.7024	0.7010
15.00	0.8212	0.8014	0.7881	0.7774	0.7682	0.7619	0.7562	0.7513	0.7479	0.7448	0.7397	0.7370	0.7346	0.7326	0.7311
15.50	0.8510	0.8312	0.8178	0.8069	0.7976	0.7911	0.7854	0.7804	0.7769	0.7737	0.7684	0.7656	0.7632	0.7612	0.7597
16.00	0.8809	0.8609	0.8474	0.8363	0.8269	0.8203	0.8145	0.8094	0.8058	0.8025	0.7969	0.7941	0.7916	0.7896	0.7880
16.50	0.9107	0.8907	0.8770	0.8658	0.8562	0.8495	0.8435	0.8383	0.8345	0.8311	0.8254	0.8224	0.8198	0.8178	0.8162
17.00	0.9406	0.9204	0.9066	0.8951	0.8854	0.8786	0.8724	0.8671	0.8632	0.8597	0.8537	0.8505	0.8479	0.8458	0.8442
17.50	0.9704	0.9501	0.9362	0.9245	0.9146	0.9076	0.9013	0.8958	0.8918	0.8881	0.8818	0.8765	0.8758	0.8737	0.8721
18.00	1.0002	0.9798	0.9657	0.9538	0.9437	0.9366	0.9300	0.9245	0.9203	0.9164	0.9098	0.9064	0.9036	0.9014	0.8997
18.50	1.0300	1.0095	0.9953	0.9831	0.9728	0.9656	0.9588	0.9530	0.9486	0.9446	0.9377	0.9340	0.9311	0.9289	0.9272
19.00	1.0599	1.0392	1.0248	1.0123	1.0018	0.9945	0.9874	0.9815	0.9769	0.9727	0.9654	0.9615	0.9586	0.9563	0.9545
19.50	1.0897	1.0689	1.0543	1.0415	1.0308	1.0233	1.0160	1.0099	1.0051	1.0007	0.9930	0.9889	0.9858	0.9835	0.9817
20.00	1.1195	1.0985	1.0837	1.0707	1.0597	1.0521	1.0445	1.0383	1.0332	1.0286	1.0204	1.0161	1.0129	1.0105	1.0087
20.50	1.1493	1.1282	1.1132	1.0999	1.0886	1.0808	1.0730	1.0665	1.0612	1.0564	1.0478	1.0432	1.0398	1.0374	1.0355
21.00	1.1791	1.1578	1.1426	1.1290	1.1175	1.1095	1.1014	1.0947	1.0892	1.0841	1.0749	1.0701	1.0666	1.0641	1.0622
21.50	1.2089	1.1874	1.1721	1.1581	1.1463	1.1381	1.1297	1.1229	1.1170	1.1116	1.1020	1.0968	1.0933	1.0907	1.0887
22.00	1.2387	1.2170	1.2015	1.1871	1.1751	1.1667	1.1580	1.1509	1.1448	1.1391	1.1289	1.1235	1.1198	1.1171	1.1151
22.50	1.2685	1.2466	1.2309	1.2162	1.2039	1.1953	1.1862	1.1789	1.1724	1.1665	1.1558	1.1500	1.1461	1.1434	1.1413
23.00	1.2982	1.2762	1.2602	1.2452	1.2326	1.2238	1.2144	1.2069	1.2000	1.1938	1.1825	1.1763	1.1723	1.1695	1.1674
23.50	1.3280	1.3058	1.2896	1.2742	1.2613	1.2522	1.2425	1.2347	1.2276	1.2210	1.2090	1.2026	1.1984	1.1955	1.1933
24.00	1.3578	1.3354	1.3190	1.3031	1.2899	1.2807	1.2706	1.2625	1.2550	1.2482	1.2355	1.2287	1.2243	1.2214	1.2191
24.50	1.3876	1.3650	1.3483	1.3321	1.3185	1.3090	1.2986	1.2903	1.2824	1.2752	1.2619	1.2546	1.2501	1.2471	1.2447
25.00	1.4173	1.3946	1.3776	1.3610	1.3471	1.3374	1.3265	1.3180	1.3097	1.3022	1.2881	1.2805	1.2758	1.2727	1.2702
25.50	1.4471	1.4241	1.4069	1.3899	1.3757	1.3657	1.3544	1.3456	1.3369	1.3290	1.3142	1.3062	1.3013	1.2981	1.2956
26.00	1.4769	1.4537	1.4362	1.4187	1.4042	1.3940	1.3823	1.3732	1.3641	1.3558	1.3403	1.3318	1.3267	1.3235	1.3209
26.50	1.5066	1.4832	1.4655	1.4476	1.4327	1.4222	1.4101	1.4007	1.3912	1.3825	1.3662	1.3573	1.3520	1.3487	1.3460
27.00	1.5364	1.5127	1.4948	1.4764	1.4611	1.4504	1.4379	1.4282	1.4182	1.4092	1.3920	1.3827	1.3772	1.3738	1.3710
27.50	1.5661	1.5423	1.5240	1.5052	1.4895	1.4786	1.4656	1.4556	1.4452	1.4357	1.4178	1.4079	1.4023	1.3987	1.3959
28.00	1.5959	1.5718	1.5533	1.5340	1.5179	1.5067	1.4933	1.4829	1.4721	1.4622	1.4434	1.4331	1.4272	1.4235	1.4206
28.50	1.6256	1.6013	1.5825	1.5627	1.5463	1.5348	1.5209	1.5102	1.4989	1.4886	1.4690	1.4581	1.4520	1.4483	1.4452
29.00	1.6554	1.6308	1.6117	1.5915	1.5747	1.5629	1.5485	1.5375	1.5257	1.5150	1.4944	1.4831	1.4768	1.4729	1.4698
29.50	1.6851	1.6603	1.6410	1.6202	1.6030	1.5909	1.5761	1.5647	1.5524	1.5412	1.5198	1.5079	1.5014	1.4974	1.4942
30.00	1.7148	1.6898	1.6702	1.6489	1.6313	1.6189	1.6036	1.5919	1.5791	1.5675	1.5450	1.5327	1.5259	1.5218	1.5185

The integral function on the left side of Eq. 34 can be evaluated by use of Table 34.2 from Ref. 8. These tables were prepared by using an arbitrary reference point of p_{pr} of 0.2. Evaluation of the integral is based on the following relationships:

$$\int_{(p_{pr})_1}^{(p_{pr})_2} \frac{(z/p_{pr}) dp_{pr}}{1+B(z/p_{pr})^2} = \left[\int_{0.2}^{(p_{pr})_1} \frac{(z/p_{pr}) dp_{pr}}{1+B(z/p_{pr})^2} \right] - \left[\int_{0.2}^{(p_{pr})_2} \frac{(z/p_{pr}) dp_{pr}}{1+B(z/p_{pr})^2} \right] = \frac{0.01877 \gamma_g L}{\bar{T}} \quad \dots (35)$$

Since the tables and charts provide numerical values for the bracketed terms in Eq. 35, a calculation of flowing BHP can be obtained directly, with only simple mathematics being involved.

In the previous and subsequent calculation procedures, the diameter of the flow string enters into the calculations as the fifth power. It is important, therefore, that the exact dimensions of the flow string be used rather than nominal flow-string sizes. Table 34.3 lists the pertinent information on various flow-string sizes.

The effect of assuming a constant average temperature over the entire gas column in Eqs. 17, 21, and 35 can be mitigated by taking only small increments of depth from top to bottom and using a constant temperature for each increment of depth. Assuming a linear temperature gradient, the average temperature for each depth increment can be calculated. The larger the number of depth increments taken in calculating the pressure traverse, the closer one approximates the rigorous integration of the equations.

Example Problem 3. Calculate the BHP of a flowing-gas well. Given:

length of vertical pipe, $L = 10,000$ ft,
tubing ID, $d_{ti} = 2.00$ in.,
gas-flow rate, $q_g = 4.91 \times 10^6$ cu
ft/D,

flowing wellhead pressure, $p_2 = 1,980$ psia,
average flowing temperature, $\bar{T} = 636^\circ\text{R}$,
gas gravity (air=1.0), $\gamma_g = 0.750$,
 $p_{pc} = 660$ psia,
 $T_{pc} = 400^\circ\text{R}$, and
 $f = 0.016$.

Solution.

1. Calculate B .

$$B = \frac{667 f q_g^2 \bar{T}^2}{d_{ti}^5 p_{pc}^2} = \frac{(667)(0.016)(4.91)^2 (636)^2}{(2.00)^5 (660)^2} = 7.48.$$

2. Calculate $\frac{0.01877 \gamma_g L}{\bar{T}}$.

$$\frac{0.01877 \gamma_g L}{\bar{T}} = \frac{(0.01877)(0.750)(10,000)}{636} = 0.2213.$$

TABLE 34.3—FLOW STRING WEIGHTS AND SIZES

Nominal Size (in.)	API Rating (in.)	Weight per Foot (lbm/ft)	OD (in.)	ID (in.)
1 3/4	...	2.3 or 2.4	1.660	1.380
1 3/2	...	2.9 or 2.748	1.900	1.610
2	2 3/4	4.00	2.375	2.041
2	2 3/8	4.5 or 4.7	2.375	1.995
2 1/2	2 3/8	5.897	2.875	2.469
2 3/2	2 3/8	6.25 or 6.5	2.875	2.441
3	3 1/2	7.694	3.500	3.068
3	3 1/2	8.50	3.500	3.018
3	3 1/2	9.30	3.500	2.992
3	3 1/2	10.2	3.500	2.922
3 1/2	4	9.26 or 9.50	4.000	3.548
3 1/2	4	11.00	4.000	3.476
4	4 1/2	10.98	4.500	4.026
4	4 1/2	11.75	4.500	3.990
4	4 1/2	12.75	4.500	3.958
4 1/2	4 3/4	16.00	4.750	4.082
4 1/2	4 3/4	16.50	4.750	4.070
4 3/4	5	12.85	5.000	4.500
4 3/4	5	13.00	5.000	4.494
4 3/4	5	15.00	5.000	4.408
4 3/4	5	18.00	5.000	4.276
4 3/4	5	21.00	5.000	4.154
...	5 1/2	16.00	5.250	4.648
5 1/2	5 1/2	17.00	5.500	4.892
5 1/2	5 1/2	20.00	5.500	4.778
...	5 3/4	14.00	5.750	5.290
...	5 3/4	17.00	5.750	5.190
...	5 3/4	19.50	5.750	5.090
...	5 3/4	22.50	5.750	4.990
5 3/4	6	20.00	6.000	5.350
6 1/4	6 3/4	20.00	6.625	6.049
6 1/4	6 3/4	24.00	6.625	5.921
6 1/4	6 3/4	26.00	6.625	5.855
6 1/4	6 3/4	28.00	6.625	5.791
6 1/4	6 3/4	29.00	6.625	5.761
6 3/4	7	20.00	7.000	6.456
6 3/4	7	22.00	7.000	6.398
6 3/4	7	24.00	7.000	6.336
6 3/4	7	26.00	7.000	6.276
6 3/4	7	28.00	7.000	6.214
6 3/4	7	30.00	7.000	6.154
API	7 3/8	34.00	7.625	6.765
7 3/8	8	26.00	8.000	7.386
API	8 1/8	28.00	8.125	7.485
API	8 1/8	32.00	8.125	7.385
API	8 1/4	35.50	8.125	7.285
API	8 1/4	39.5 or 40.00	8.125	7.185
API	8 1/4	42.00	8.125	7.125
8 1/4	8 3/4	24.00	8.625	8.097
8 1/4	8 3/4	28.00	8.625	8.017
8 1/4	8 3/4	32.00	8.625	7.921
8 1/4	8 3/4	32.00	8.625	7.907
8 1/4	8 3/4	36.00	8.625	7.825
8 1/4	8 3/4	38.00	8.625	7.775
8 1/4	8 3/4	43.00	8.625	7.651
8 3/4	8 3/4	44.85	8.625	7.625
8 3/4	9	34.00	9.000	8.290
8 3/4	9	38.00	9.000	8.196
8 3/4	9	40.00	9.000	8.150
8 3/4	9	45.00	9.000	8.032
8 3/4	9	54.00	9.000	7.812
API	9 5/8	43.80	9.625	8.755
API	9 5/8	47.20	9.625	8.681
API	9 5/8	53.60	9.625	8.535
API	9 5/8	57.40	9.625	8.451
9 1/4	9 5/8	36.00	9.625	8.921
9 5/8	10	33.00	10.000	9.384
9 5/8	10	60.00	10.000	8.780
10	10 3/4	32.75	10.750	10.192
10	10 3/4	35.75	10.750	10.136
10	10 3/4	40.00	10.750	10.054
API	10 3/4	40.50	10.750	10.050
10	10 3/4	45.00	10.750	9.960
API	10 3/4	45.50	10.750	9.950
10	10 3/4	48.00	10.750	9.902
API	10 3/4	51.00	10.750	9.850
10	10 3/4	54.00	10.750	9.784

3. Calculate pseudoreduced wellhead pressure and pseudoreduced average temperature,

$$(p_{pr})_1 = \frac{1,980}{660} = 3.0$$

and

$$\bar{T}_{pr} = \frac{636}{400} = 1.59.$$

4. For $\bar{T}_{pr} = 1.59$, read from Table 34.2.

$$\int_{0.2}^{(p_{pr})_1} \frac{(z/p_{pr}) dp_{pr}}{1 + B(z/p_{pr})^2} = 0.4246.$$

$$5. \text{ Add } \frac{0.01877\gamma_g L}{\bar{T}} \text{ to } \int_{0.2}^{(p_{pr})_1} \frac{(z/p_{pr}) dp_{pr}}{1 + B(z/p_{pr})^2}.$$

$$0.4246 + 0.2213 = 0.6459.$$

6. From Table 34.2 find the pseudoreduced pressure corresponding to

$$\int_{0.2}^{(p_{pr})_1} \frac{(z/p_{pr}) dp_{pr}}{1 + B(z/p_{pr})^2} = 0.6459.$$

$$(p_{pr})_1 = 4.358.$$

7. Multiply $(p_{pr})_1$ by p_{pc} to obtain BHP.

$$p_1 = 4.358 \times 660 = 2,876 \text{ psia.}$$

Another procedure for calculating the BHP of flowing gas wells that has found widespread use since its adoption by various state regulatory agencies is that of Cullender and Smith.⁷ The method avoids the assumption of a constant average temperature by including the temperature within the integral.

$$18.75\gamma_g L = \int_{p_2}^{p_1} \frac{[p/(Tz)] dp}{F^2 + 0.001[p/(Tz)]^2}, \quad (36)$$

where

$$F^2 = (2.6665 f_f q_g^2) / d_i^5, \quad (37)$$

f_f is the Fanning friction factor and is equal to $f_f = f/4$, and f is the Moody friction factor from Fig. 34.2

Eq. 37 can be simplified by using the Nikuradse friction factor equation for fully turbulent flow and for an absolute roughness of 0.0006 in.:

$$F = F_r q_g = \frac{0.10797 q_g}{d_i^{2.612}}, \quad (38)$$

where $d_i < 4.277$ in. and

$$F = F_r q_g = \frac{0.10337 q_g}{d_i^{2.582}}, \quad (39)$$

where $d_i > 4.277$ in. Values of F_r are presented in Table 34.4 for various tubing and casing sizes.⁷

The right side of Eq. 36 may be integrated numerically by employing a two-step trapezoidal integration:

$$18.75\gamma_g L = \frac{(p_m - p_2)(I_m + I_2)}{2} + \frac{(p_1 - p_m)(I_1 + I_m)}{2}, \quad (40)$$

where

$$I = \frac{p/(Tz)}{F^2 + 0.001[p/(Tz)]^2}$$

and

$$p_m = p_1 + (p_1 + p_2)/2.$$

Eq. 40 may be separated into two expressions, one for each half of the flow string.

$$18.75\gamma_g L = (p_m - p_2)(I_m + I_2) \quad (41)$$

for the upper half, and

$$18.75\gamma_g L = (p_1 - p_m)(I_1 + I_m) \quad (42)$$

for the lower half.

By trial and error, p_m is calculated from Eq. 41. p_1 then is calculated in a similar manner by using the value of I_m from Eq. 41 and substituting in Eq. 42.

Simpson's rule then is employed to obtain a more accurate value of the BHP.

$$18.75\gamma_g L = \left(\frac{p_2 - p_1}{6} \right) (I_2 + 4I_m + I_1). \quad (43)$$

Rather than using the two-step trapezoidal integration to make the first estimate of the BHP, Simpson's rule may be used directly and the BHP calculated by trial and error.

As this indicates, the Cullender and Smith method involves tedious trial and error solution if hand calculated. The method is best solved by computer. Quoting Ref. 8,

Because the Cullender and Smith method considers both temperature and Z to be functions of pressure, it might appear that this method is somewhat more accurate than the Sukkar-Cornell approach. This is only an apparent advantage. If temperature is known in the gas column, it is possible to break the depth into several increments, each with one appropriate mean temperature.

This was alluded to previously. The Sukkar-Cornell method is an accurate, fast hand calculation procedure that avoids trial and error calculations. It is also amenable to computer solution.

Example Problem 4.⁹ Calculate the flowing BHP by the method of Cullender and Smith from the following well data:

gas gravity, $\gamma_g = 0.75$,
length of vertical pipe, $L = 10,000$ ft,
wellhead temperature, $T_2 = 570^\circ\text{R}$,
formation temperature, $T_1 = 705^\circ\text{R}$,
wellhead pressure, $p_2 = 2,000$ psig,
flowrate, $q_g = 4.915 \times 10^6$ cu
ft/D,
tubing ID, $d_{ti} = 2.441$ in.,
pseudocritical temperature, $T_{pc} = 408^\circ\text{R}$, and
pseudocritical pressure, $p_{pc} = 667$ psi.

$$\bar{T} = \frac{T_1 + T_2}{2} = \frac{570 + 705}{2} = 638^\circ\text{R},$$

$$\text{wellhead } T_{pr} = \frac{T_2}{T_{pc}} = \frac{570}{408} = 1.397,$$

$$\text{midpoint } T_{pr} = \frac{\bar{T}}{T_{pc}} = \frac{638}{408} = 1.564,$$

$$\text{bottom } T_{pr} = \frac{T_1}{T_{pc}} = \frac{705}{408} = 1.728,$$

$$\text{wellhead } p_{pr} = \frac{p_2}{p_{pc}} = \frac{2,000}{667} = 2.999,$$

$$F = \frac{(0.10797)(4.915)}{(2.441)^{2.612}} = 0.05158,$$

and $F^2 = 0.00266$.

Left side of Eq. 36,

$$18.75 \gamma_g L = (18.75)(0.75)(10,000) \\ = 140,625.$$

Calculate I_2 . From the compressibility factor chart (see Chap. 20) $z_2 = 0.705$. Therefore,

$$\frac{p_2}{T_2 z_2} = \frac{2,000}{(570)(0.705)} = 4.977$$

and

$$I_2 = \frac{4.977}{0.00266 + 0.001(4.977)^2} = 181.44.$$

Assume $I_2 = I_m$. Solving Eq. 41 for p_m ,

$$140,625 = (p_m - 2,000)(181.44 + 181.44),$$

$$p_m = 2,388 \text{ psia.}$$

TABLE 34.4—VALUES OF F_r FOR VARIOUS TUBING AND CASING SIZES

$F_r = \frac{0.10797}{d_i^{2.612}}$				
Nominal Size (in.)	OD (in.)	lbm/ft	ID (in.)	F_r
1	1.315	1.80	1.049	0.095288
1 1/4	1.660	2.40	1.380	0.046552
1 1/2	1.990	2.75	1.610	0.031122
2	2.375	4.70	1.995	0.017777
2 1/2	2.875	6.50	2.441	0.010495
3	3.500	9.30	2.992	0.006167
3 1/2	4.000	11.00	3.476	0.004169
4	4.500	12.70	3.958	0.002970
4 1/2	4.750	16.25	4.082	0.002740
	4.750	18.00	4.000	0.002889
4 3/4	5.000	18.00	4.276	0.002427
	5.000	21.00	4.154	0.002617
$F_r = \frac{0.01337}{d_i^{2.582}}$				
4 3/4	5.000	13.00	4.494	0.0021345
	5.000	15.00	4.408	0.0022437
5 1/8	5.500	14.00	5.012	0.0016105
	5.500	15.00	4.976	0.0016408
	5.500	17.00	4.892	0.0017145
	5.500	20.00	4.778	0.0018221
	5.500	23.00	4.670	0.0019329
	5.500	25.00	4.580	0.0020325
5 3/8	6.000	15.00	5.524	0.0012528
	6.000	17.00	5.450	0.0012972
	6.000	20.00	5.352	0.0013595
	6.000	23.00	5.240	0.0014358
	6.000	26.00	5.140	0.0015090
6 1/4	6.625	20.00	6.049	0.0009910
	6.625	22.00	5.989	0.0010169
	6.625	24.00	5.921	0.0010473
	6.625	26.00	5.855	0.0010781
	6.625	28.00	5.791	0.0011091
	6.625	31.80	5.675	0.0011686
	6.625	34.00	5.595	0.0012122
6 3/8	7.000	20.00	6.456	0.0008876
	7.000	22.00	6.398	0.0008574
	7.000	24.00	6.336	0.0008792
	7.000	26.00	6.276	0.0009011
	7.000	28.00	6.214	0.0009245
	7.000	30.00	6.154	0.0009479
	7.000	40.00	5.836	0.0010871
7 1/4	7.625	26.40	6.969	0.0006875
	7.625	29.70	6.875	0.0007121
	7.625	33.70	6.765	0.0007424
	7.625	38.70	6.625	0.0007836
	7.625	45.00	6.445	0.0008413
	8.000	26.00	7.386	0.0005917
7 3/8	8.125	28.00	7.485	0.0005717
	8.125	32.00	7.385	0.0005919
	8.125	35.50	7.285	0.0006132
	8.125	39.50	7.185	0.0006354
8 1/4	8.625	17.50	8.249	0.0004448
	8.625	20.00	8.191	0.0004530
	8.625	24.00	8.097	0.0004667
	8.625	28.00	8.003	0.0004810
	8.625	32.00	7.907	0.0004962
	8.625	36.00	7.825	0.0005098
	8.625	38.00	7.775	0.0005183
	8.625	43.00	7.651	0.0005403
8 3/8	9.000	34.00	8.290	0.0004392
	9.000	38.00	8.196	0.0004523
	9.000	40.00	8.150	0.0004589
	9.000	45.00	8.032	0.0004765
9	9.625	36.00	8.921	0.0003634
	9.625	40.00	8.835	0.0003726
	9.625	43.50	8.755	0.0003814
	9.625	47.00	8.681	0.0003899
	9.625	53.50	8.535	0.0004074
	9.625	58.00	8.435	0.0004200
9 3/8	10.000	33.00	9.384	0.0004167
	10.000	55.50	8.908	0.0003648
	10.000	61.20	8.790	0.0003775
10	10.750	32.75	10.192	0.0002576
	10.750	35.75	10.136	0.0002613
	10.750	40.00	10.050	0.0002671
	10.750	45.50	9.950	0.0002741
	10.750	48.00	9.902	0.0002776
	10.750	54.00	9.784	0.0002863

* Use only for internal diameters less than 4.277 in.

** Use only for internal diameters greater than 4.277 in.

Second trial:

$$p_{pr} = \frac{p_m}{p_{pc}} = \frac{2,388}{667} = 3.580,$$

$$z_m = 0.800 \text{ at } T_{pr} = 1.564, p_{pr} = 3.580,$$

$$\frac{p_m}{T_m z_m} = \frac{2,388}{(638)(0.800)} = 4.679,$$

and

$$I_m = \frac{4.679}{(0.00266) + 0.001(4.679)^2} = 190.57.$$

Solving Eq. 41 for p_m ,

$$140,625 = (p_m - 2,000)(190.57 + 181.44)$$

and

$$p_m = 2,378 \text{ psia.}$$

Third trial:

$$p_{pr} = \frac{p_m}{p_{pc}} = \frac{2,378}{667} = 3.565,$$

$$z_m = 0.800 \text{ at } T_{pr} = 1.564, p_{pr} = 3.565,$$

$$\frac{p_m}{T_m z_m} = \frac{2,378}{(638)(0.800)} = 4.659,$$

and

$$I_m = \frac{4.659}{0.00266 + 0.001(4.659)^2} = 191.21.$$

Solving Eq. 41 for p_m ,

$$140,625 = (p_m - 2,000)(191.21 + 181.44),$$

therefore

$$p_m = 2,377 \text{ psia.}$$

For the lower half of the flow string assume $I_1 = I_m = 191.21$. Solving Eq. 42 for p_1 ,

$$140,625 = (p_1 - 2,377)(191.21 + 191.21),$$

$$p_1 = 2,745 \text{ psia.}$$

Second trial:

$$p_{pr} = \frac{p_1}{p_{pc}} = \frac{2,745}{667} = 4.115,$$

$$z_1 = 0.869 \text{ at } T_{pr} = 1.728, p_{pr} = 4.115,$$

$$\frac{p_1}{T_1 z_1} = \frac{2,745}{(705)(0.869)} = 4.481$$

and

$$I_1 = \frac{4.481}{0.00266 + 0.001(4.481)^2} = 197.06.$$

Solving Eq. 42 for p_1 ,

$$140,625 = (p_1 - 2,377)(197.06 + 191.21),$$

$$p_1 = 2,739 \text{ psia.}$$

Third trial:

$$p_{pr} = \frac{p_1}{p_{pc}} = \frac{2,739}{667} = 4.106,$$

$$z_1 = 0.869 \text{ at } T_{pr} = 1.728, p_{pr} = 4.106,$$

$$\frac{p_1}{T_1 z_1} = \frac{2,739}{(705)(0.869)} = 4.471,$$

and

$$I_1 = \frac{4.471}{0.00266 + 0.001(4.471)^2} = 197.40.$$

Solve Eq. 42 for p_1 .

$$140,625 = (p_1 - 2,377)(197.40 + 191.21),$$

$$p_1 = 2,739 \text{ psia.}$$

Using Simpson's rule from Eq. 43,

$$140,625 = \frac{(p_1 - p_2)}{6} \times [181.44 + 4(191.21) + 197.40],$$

$$p_1 - p_2 = 738,$$

and

$$p_1 = 738 + 2,000 = 2,738 \text{ psia.}$$

A simplified method for calculating flowing BHP of gas wells results if an effective average temperature and an effective average compressibility are used over the length of the flow string. Low-pressure wells at shallow depths or wells where pressure drop is small are especially well suited for this method. With the usual assumptions that kinetic energy is negligible, g/g_c equals unity, etc., the following equation for vertical gas flow has been developed by Smith¹⁰:

$$p_{bh}^2 - e^s p_{th}^2 = \frac{25 f q_g^2 \bar{T}^2 \bar{z}^2 (e^s - 1)}{0.0375 d_i^5}, \dots \dots \dots (44)$$

where

$$\begin{aligned} p_{bh} &= \text{BHP, psia,} \\ p_{th} &= \text{tophole pressure, psia,} \\ f &= \text{friction factor, dimensionless, from Fig. 34.2,} \\ q_g &= \text{gas flow rate, } 10^6 \text{ cu ft/D referred to 14.65 psia and } 60^\circ\text{F,} \\ s &= \text{exponent of } e = \frac{0.0375\gamma_g L}{T\bar{z}}, \\ \gamma_g &= \text{gas gravity (air=1.0),} \\ L &= \text{length of vertical flow string, ft,} \\ \bar{T} &= \text{average temperature, } ^\circ\text{R,} \\ \bar{z} &= \text{average compressibility of gas, dimensionless,} \\ d_i &= \text{internal diameter of flow string, in., and} \\ e &= \text{natural logarithm base=2.71828.} \end{aligned}$$

The method using Eq. 44 is also a trial and error procedure.

In evaluating the friction factor for commercial pipe, Smith¹⁰ and Cullender and Binckley¹¹ have shown from an analysis of flow data that average absolute values of roughness, 0.00065 and 0.0006 in., respectively, are the correct values to use for clean commercial pipe. For an absolute roughness of 0.0006 in., Cullender and Binckley¹¹ derived an expression for the friction factor as defined in Fig. 34.2, as a power function of the Reynolds number and pipe diameter. In terms of field units,

$$f = 30.9208 \times 10^{-3} \frac{q_g^{-0.065} d_i^{-0.058} \gamma_g^{-0.065}}{\mu_g^{-0.065}}, \quad (45)$$

where

$$\begin{aligned} q_g &= \text{gas flow rate, } 10^6 \text{ cu ft/D,} \\ d_i &= \text{internal diameter of flow string, ft,} \\ \gamma_g &= \text{gas gravity (air=1.0), and} \\ \mu_g &= \text{gas viscosity, lbm/ft-sec.} \end{aligned}$$

Flow Through a Tubing-Casing Annulus. The flow equations that relate to flow through a circular pipe, when properly modified, can be used for conditions where flow is through an annular space. This modification involves determining the hydraulic radius of the annular cross section and using the friction factor obtained for an "equivalent" (i.e., having the same hydraulic radius) circular pipe. The hydraulic radius is defined as the area of flow cross section divided by the wetted perimeter. For a circular pipe,

$$r_H = \frac{\pi d_i^2 / 4}{\pi d_i} = \frac{d_i}{4}. \quad (46)$$

For a tubing-casing annulus,

$$r_H = \frac{(\pi/4)(d_{ci}^2 - d_{to}^2)}{\pi(d_{ci} + d_{to})} = \frac{d_{ci} - d_{to}}{4}, \quad (47)$$

where

$$\begin{aligned} d_{ci} &= \text{inside diameter of casing, ft,} \\ d_{to} &= \text{outside diameter of tubing, ft, and} \\ r_H &= \text{hydraulic radius, ft.} \end{aligned}$$

The diameter of an equivalent circular pipe, thus, would be

$$d_{eq} = d_{ci} - d_{to}. \quad (48)$$

Modification of Eq. 32 for annular flow involves only substituting d_{eq} for d_i . Likewise d_{eq} replaces d_i when determining friction factor (from the Reynolds-number plot, Fig. 34.2). However, the simplification of Eq. 32 includes velocity expressed as a function of diameter and volumetric flow rate, and so d_i^5 in B of Eq. 33 and in Eq. 44 becomes

$$d_i^5 = (d_{ci} + d_{to})^2 (d_{ci} - d_{to})^3. \quad (49)$$

Gas/Water Flow

The effect of water production on calculated pressure drop for gas wells operating in mist flow can be included by using an average density assuming zero slip velocity and by using total rate in the friction loss term. The volumetric average density can be calculated as

$$\bar{\rho} = \frac{q_g \rho_g + q_w \rho_w}{q_g + q_w}$$

where $\bar{\rho}$ is the average density at flowing conditions and q is the volumetric flow rate at flowing conditions. To include the effect of water in the Cullender and Smith calculation, modify the integrand, I , as follows (see Page 24):

$$I = \frac{[p/(Tz)](\bar{\rho}/\rho_g)}{F^2 \left(\frac{q_g + q_w}{q_g} \right)^2 + 0.001[p/(Tz)]^2 (\bar{\rho}/\rho_g)^2}$$

Gas-Condensate Wells

Calculation of BHP. Calculations of BHP on gas-condensate wells are based on equations previously presented for gas wells. The application of these equations may be limited somewhat by the amount of liquid present in the flow string.

Upon shutting in a gas-condensate well, part of the liquids that were being carried in the flow stream may fall back and accumulate in the bottom of the wellbore. For this reason, it is advisable to determine whether or not such a static liquid level exists in a gas-condensate well before relying on a BHP calculated from surface measurements. When the location of the static liquid level is known, the gas calculations can be used to determine the pressure at the gas-liquid interface and the length of the liquid column. An estimated liquid density will provide the additional pressure needed to determine pressure at formation level.

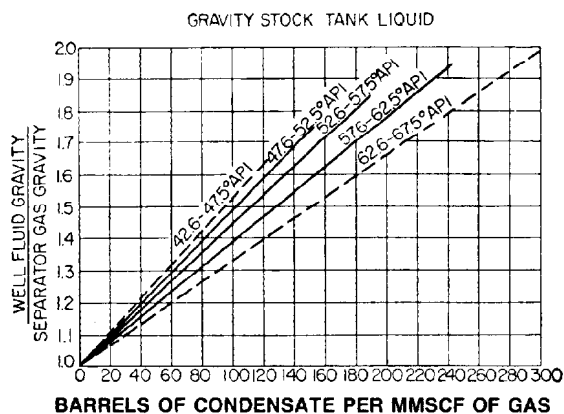


Fig. 34.4—Gas/gravity ratio vs. condensate/gas ratio as a function of condensate gravity.

In the flow equations for gas, the gas gravity is the flow-stream gravity. This is calculated for condensates from the following¹²:

$$\gamma_g = \frac{(\gamma_g)_{sp} + (4,591\gamma_L/R_{gL})}{1 + (1.123/R_{gL})}, \quad (50)$$

where

$(\gamma_g)_{sp}$ = separator gas gravity (air=1),
 γ_L = specific gravity of condensate, and
 R_{gL} = gas-liquid ratio, cu ft/bbl.

Nisle and Poettmann¹³ published a simple correlation based on field data (Fig. 34.4) that can be used to calculate the flow-stream gravity of the entrained mixture such as occurs in the case of a flowing gas-condensate well.

Accuracy of the flow equations for gas, as modified for gas-condensate wells, is influenced by the amount of liquid in the flow stream. The higher the gas-liquid ratio, the more accurate the calculated results will be.

Injection Wells

Petroleum-production operations often involve the injection of fluids into the subsurface formation, as is the case in waterflooding, pressure maintenance, gas cycling, and designing gas lift installations. Therefore, it becomes desirable to have a means of predicting the variation of pressure with depth for the vertical downward flow of fluids. Eqs. 29 and 30, previously discussed, form the basis of any specific fluid-flow relationship. They contain no limiting assumptions other than those arrived at in deriving Eq. 30 from Eq. 29. The only difference in applying Eq. 30 to vertical downward flow when compared with upward flow is that the integration limits are changed; that is, the sign of the *absolute values* of potential energy then changes and, depending on the rate of injection in the case of gas injection, the absolute value of the compressional energy change may vary from positive to negative. In other words, at low flow rates, the BHP is greater than the surface pressure; whereas, at high flow rates, the BHP is less than the surface pressure.

Liquid Injection

Calculation of Injection BHP. For isothermal flow of incompressible fluid, assuming $g/g_c = 1$, and integrating between limits of the top and bottom of the hole, Eq. 30 may be written as follows:

$$\frac{\Delta p}{\rho} + \Delta Z + E_f = 0, \quad (51)$$

(Since the datum plane is at the surface, ΔZ will be a negative number.) Then

$$p_2 = p_1 - \Delta Z \rho - E_f \rho, \quad (52)$$

since $-\Delta Z = D$, the depth. Therefore,

$$p_2 = p_1 + D\rho - E_f \rho. \quad (53)$$

Since $E_f = fv^2 D / 2g_c d_i$ (Fig. 34.2),

$$p_2 = p_1 + D\rho - \frac{fv^2 D \rho}{2g_c d_i}. \quad (54)$$

Converting pressure units to pounds per square inch,

$$p_2 = p_1 + \frac{D\rho}{144} - \frac{fv^2 D \rho}{288g_c d_i}, \quad (55)$$

where

p_2 = bottomhole pressure, psia, at depth D ,
 p_1 = surface pressure, psia,
 D = depth of well, ft,
 ρ = density of injected fluid, lbm/cu ft,
 f = friction factor (Fig. 34.2),
 v = fluid velocity, ft/sec,
 d_i = internal diameter of pipe, ft, and
 g_c = 32.2 conversion factor.

Eq. 55 reveals that the BHP for the case of incompressible flow as assumed for liquid injection into a wellbore is simply the surface pressure plus the pressure from the "weight of the liquid column" minus the pressure drop caused by frictional effects. For no flow, it reduces to the well-known expression for a static-fluid column

$$p_2 = p_1 + \frac{D\rho}{144}. \quad (56)$$

Gas Injection

Calculation of Injection BHP. Starting with the general differential equation, Eq. 30, Poettmann⁴ derived an expression for calculating the sandface pressure of flowing-gas wells in which the variation of the compressibility factor of the gas with pressure is taken into consideration. The same integral factor as given in Table 34.1 is employed for the calculation of static BHP in Table 34.5.

By following the same reasoning as in the previous section, the equation can be rearranged so that the pressure traverse for vertical flow downward can be calculated as follows:

$$D = \frac{D_s}{\{0.9521 \times 10^{-6} [f q_g^2 \gamma_g^2 D_s^2 / d_{ti}^5 (\Delta p)^2]\} - 1}, \quad (57)$$

where

$$\begin{aligned} D &= \text{depth of well, ft,} \\ \Delta p &= p_2 - p_1, \text{ psia,} \\ d_{ti} &= \text{ID of tubing, ft,} \\ q_g &= \text{gas flow, } 10^6 \text{ cu ft/D at 14.65 psia and } 60^\circ\text{F,} \\ f &= \text{friction factor (Fig. 34.2), and} \\ D_s &= D \text{ under static conditions (static equivalent depth for pressures encountered at flowing conditions)} \\ &= \frac{53.241 \bar{T}}{\gamma_g} \end{aligned}$$

$$\times \left[\int_{0.2}^{(p_{pr})} \frac{z}{p_{pr}} dp_{pr} - \int_{0.2}^{(p_{pr})} \frac{z}{p_{pr}} dp_{pr} \right].$$

Using the expression for the friction factor as derived by Cullender and Binckley¹¹ (Eq. 45) and substituting in Eq. 57 gives

$$D = \frac{D_s}{\{2.944 \times 10^{-8} [q_g^{1.935} \gamma_g^{1.935} D_s^2 / (d_{ti}^{5.058} \mu^{0.065}) (\Delta p)^2]\} - 1}, \quad (58)$$

Cullender and Smith's Eq. 36 also can be rearranged to calculate the BHP for the case of gas injection as follows:

$$18.75 \gamma_g D = \int_{p_1}^{p_2} \frac{[p/(Tz)] dp}{0.001 \left(\frac{p}{Tz} \right)^2 - F^2}. \quad (59)$$

The solution of this equation is identical to that previously described for flowing gas wells. D , depth of well, can be used interchangeably with L , length of flow string, when the well is vertical.

Similarly, by considering the downward flow of gas, the simplified equation developed by Smith¹⁰ for upward flow (Eq. 44) can be rearranged so that the pressure traverse for vertical flow downward can be calculated.

$$e^s p_{th}^2 - p_{bh}^2 = \frac{25 f q_g^2 \bar{T}^2 z (e^s - 1)}{0.0375 d_i^5}. \quad (60)$$

The nomenclature is the same as used in the corresponding Eq. 44.

In the case of gas injection down the annulus of a well, d_{ti}^5 of Eq. 57 (or d_i^5 of Eq. 60) is replaced as defined in Eq. 49; that is,

$$d_i^5 = (d_{ci} + d_{to})^2 (d_{ci} - d_{to})^3.$$

In the case of annulus injection using Eq. 58, $d_{ti}^{5.058}$ is replaced as follows:

$$d_i^{5.058} = (d_{ci} + d_{to})^{1.935} (d_{ci} - d_{to})^{3.123}. \quad (61)$$

Eqs. 57 through 60 provide a basis for calculating the BHP in a gas-injection well. In solving Eqs. 57 and 58, the calculating procedure is to assume a pressure p_2 and solve for the corresponding depth, D . The depth, D , so found will be the depth at which pressure p_2 occurs. By calculating several such points, a pressure-depth traverse can be plotted from which the pressure at the desired depth can be determined.

It is apparent that BHP during gas injection can be either greater or less than tophole pressure depending on the energy losses encountered. At low rates of flow, the pressure gradient is positive, whereas at high flow rates, the pressure gradient is negative. This is because, as flow rate increases, energy or frictional losses increase and they can be overcome only by a decrease in the change of compression energy or pV energy of the system. The decrease in potential energy resulting from elevation is constant and the change in kinetic energy is negligible. This can be illustrated by examining and rearranging Eq. 4 and considering the kinetic energy negligible.

$$\int_{p_1}^{p_2} V dp + E_f = - \frac{g}{g_c} \Delta Z. \quad (62)$$

For low flow rates,

$$\int_{p_1}^{p_2} V dp$$

is positive and E_f is always positive; thus, the sum of the compression energy and energy losses must equal the change in potential energy, which for a given depth is constant (the absolute value of $-\Delta Z$ is positive for gas injection since the absolute value of ΔZ is negative).

As E_f increases with flow rate, the

$$\int_{p_1}^{p_2} V dp$$

must decrease for the sum to remain constant. When E_f is equal to $(g/g_c) \Delta Z$, the pressure at the top and bottom of the hole is the same. This means that the decrease in potential energy is equal to the frictional losses. As E_f further increases, the added energy to overcome friction losses must come from the compressional energy since $-(g/g_c) \Delta Z$ is constant. This then means that the pressure gradient is negative.

TABLE 34.5—SAMPLE CALCULATIONS

Δp	p	p_{pr}	$\int_{0.2}^{(p_{pr})} \frac{z}{p_{pr}} dp_{pr}$	$\int_{(p_{wf})}^{(p_{pr})} \frac{z}{p_{pr}} dp_{pr}$	D_s	D	Depth corresponding to p of column (2)
(1)	(2)	(3)	(4)	(5)	(6)	(7)	(8)
	680	1.015	1.586				0
20	700	1.045	1.611	0.025	1.278	-1.460	1,460
20	720	1.074	1.636	0.025	1.278	-1.460	2,920
20	740	1.104	1.662	0.026	1.329	-1.532	4,452

Example Problem 5. Calculate the pressure at 4,000 ft in a gas injection well. Given:

tubing ID, $d_{ti} = 0.1663$ ft,
gas flow rate, $q_g = 0.783 \times 10^6$ cu
ft/D,

average temperature, $T = 600^\circ\text{R}$,
wellhead injection pressure, $p_1 = 680$ psia,
gas gravity, $\gamma_g = 0.625$, and
gas viscosity, $\mu_g = 8.74 \times 10^{-6}$
lbm/ft-sec.

Solution.

1. Substitute given values in Eq. 58.

$$D = \frac{D_s}{\frac{2.944 \times 10^{-8} (0.783)^{1.935} (0.625)^{1.935} D_s^2}{(0.1663)^{5.058} (8.75 \times 10^{-6})^{-0.065} (\Delta p)^2} - 1}$$

$$= \frac{D_s}{\frac{(3.00 \times 10^{-5}) D_s^2}{(\Delta p)^2} - 1}$$

and

$$D_s = \frac{53.241(600)}{0.625} \left[\int_{0.2}^{(p_{pr})} \frac{z}{p_{pr}} dp_{pr} - \int_{0.2}^{(p_{pr})} \frac{z}{p_{pr}} dp_{pr} \right] = 51,100 \left[\int_{0.2}^{(p_{pr})} \frac{z}{p_{pr}} dp_{pr} - \int_{0.2}^{(p_{pr})} \frac{z}{p_{pr}} dp_{pr} \right]$$

2. Determine p_{pc} and T_{pc} (Fig. 34.3).

$$p_{pc} = 670 \text{ psia}$$

and

$$T_{pc} = 365^\circ\text{R},$$

therefore,

$$T_{pr} = \frac{\bar{T}}{T_{pc}} = \frac{600}{365} = 1.64.$$

3. Assume values for Δp and solve for D (Table 34.5).
4. From plot of Col. 2 vs. Col. 8 read pressure at 4,000 ft to be 734 psia.

Oil Wells

Inflow Performance

The simplest and most widely used inflow performance or backpressure equation used to determine stabilized or pseudosteady-state flow at any backpressure p_{wf} is given by the productivity index (PI) equation as

$$q_o = J(\bar{p}_R - p_{wf}), \quad (63)$$

In terms of measured data the PI is represented as

$$J = \frac{q_o}{\bar{p}_R - p_{wf}}, \quad (64)$$

where

J = stabilized productivity index, STB/D-psi,

q_o = measured stabilized surface oil flow rate, STB/D,

p_{wf} = wellbore stabilized flowing pressure, psia, and

\bar{p}_R = average reservoir pressure, psia.

J is defined specifically as a PI determined from flow rate and pressure drawdown measurements. It normally varies with increasing drawdown (i.e., is not a constant value). In terms of reservoir variables, the stabilized or pseudosteady-state PI J^* at zero drawdown or as $p_{wf} \rightarrow p_R$ can be written as

$$J^* = \frac{7.08kh}{\left[\ln \left(\frac{r_e}{r_w} \right) - \frac{3}{4} + s \right]} \left(\frac{k_{ro}}{\mu_o B_o} \right)_{p_R}, \quad (65)$$

where

J^* = stabilized PI at zero drawdown, STB/D-psi,

k = effective permeability, darcy,

k_{ro} = relative permeability to oil, fraction,

h = formation thickness, ft,

μ_o = oil viscosity, cp (evaluated at \bar{p}_R),

B_o = oil formation volume factor, RB/STB (evaluated at \bar{p}_R),

r_e = external boundary radius, ft,

r_w = wellbore radius, ft, and

s = skin effect, dimensionless.

J^* is the special definition of PI J at a vanishing pressure drawdown (i.e., as p_{wf} approaches \bar{p}_R). PI for a well is defined uniquely only at a zero drawdown.

Although this discussion will be limited to the pseudo-steady state, a transient form of the flow coefficient $J_{(t)}^*$ also is given for completeness.

$$J_{(t)}^* = \frac{7.08kh}{\left(\ln \sqrt{\frac{14.23kt}{\phi \mu c_t r_w^2}} + s\right)} \left(\frac{k_{ro}}{\mu_o B_o}\right)_{p_R}, \dots (66)$$

where t is time, days, ϕ is porosity, fraction, and c_t is total compressibility, psi^{-1} .

The above equations are perfectly valid for single-phase flow (i.e., p_R and p_{wf} are always greater than the reservoir bubblepoint pressure, p_b). However, it has long been recognized that in reservoirs existing at or below the bubblepoint pressure, producing wells do not follow the simple PI Eqs. 63 and 64. Actual field tests indicate that oil flow rates obtained at increasing drawdowns decline much faster than would be predicted by Eq. 63.

Evinger and Muskat¹⁴ first derived a theoretical PI for steady-state radial flow in an attempt to account for the observed nonlinear flow behavior of oil wells. They arrived at the following equation:

$$q_o = \frac{7.08kh}{\ln\left(\frac{r_e}{r_w}\right)} \int_{p_{wf}}^{p_e} f(p) dp, \dots (67)$$

where p_e is the reservoir pressure at the external boundary, psia, and

$$f(p) = \left(\frac{k_{ro}}{\mu_o B_o}\right).$$

Calculations using Eq. 67 with typical reservoir and fluid properties indicated that PI at a fixed reservoir pressure p_e decreases with increasing drawdown. This apparently complex form of an inflow-performance-relationship (IPR) equation found little use in the field.

In a computer study by Vogel,¹⁵ results based on two-phase flow theory were presented to indicate that a single empirical IPR equation might be valid for most solution-gas-drive reservoirs. He found that a single dimensionless IPR equation approximately held for several hypothetical solution-gas drive reservoirs even when using a wide range of oil PVT properties and reservoir relative permeability curves. The fact that his study covered a wide range of fluid properties and relative permeability curves to obtain a single reference curve cannot be overemphasized. Vogel proposed that his simple equation be used in place of the linear PI relationship for solution-gas-drive reservoirs when the reservoir pressure is at or below the bubblepoint pressure.

The proposed equation (IPR) in dimensionless form was given as

$$\frac{q_o}{q_{o(\max)}} = 1 - 0.20 \left(\frac{p_{wf}}{\bar{p}_R}\right) - 0.80 \left(\frac{p_{wf}}{\bar{p}_R}\right)^2, \dots (68)$$

where $q_{o(\max)}$ is the maximum producing rate at $p_{wf}=0$ psia.

Fetkovich,¹⁶ in an attempt to verify the Vogel IPR relationship, obtained isochronal and flow-after-flow multipoint backpressure test field data on some 40 different oil wells. The reservoirs in which oilwell multipoint backpressure tests were obtained ranged from highly undersaturated, to saturated at initial reservoir pressure, to a partially depleted field with a gas saturation existing above the critical (equilibrium) gas saturation. A form of an IPR equation similar to that used for gas wells was found to be valid for tests conducted in all three reservoir fluid states, even for the conditions where flowing pressures were well above the bubblepoint pressures. Permeabilities of the reservoirs ranged from 6 to >1,000 md.

In all cases, oilwell backpressure curves were found to follow the same general form as that used to express the rate-pressure relationship of a gas well:

$$q_o = J'(\bar{p}_R^2 - p_{wf}^2)^n, \dots (69)$$

For the 40 oilwell backpressure tests examined, the exponent n was found to lie between 0.568 and 1.000—that is, within the limits commonly accepted for gas well backpressure curves.

In terms of measured data, J' is defined by

$$J' = \frac{q_o}{(\bar{p}_R^2 - p_{wf}^2)^n}, \dots (70)$$

where J' is the stabilized PI, STB/D $(\text{psi}^2)^n$. The exponent n usually is determined from a multipoint or isochronal backpressure test and is an indicator of the existence of non-Darcy flow. If $n=1$, non-Darcy flow is assumed not to exist.

With PI expressed in terms of pressures squared, \bar{p}_R^2 and p_{wf}^2 ,

$$J' = \frac{J^*}{2\bar{p}_R}, \dots (71)$$

Expressing the pseudosteady state J' in terms of reservoir variables,

$$J' = \frac{7.08kh}{2\bar{p}_R \left[\ln\left(\frac{r_e}{r_w}\right) - \frac{3}{4} + s \right]} \left(\frac{k_{ro}}{\mu_o B_o}\right)_{p_R}, \dots (72)$$

or

$$q_o = \frac{7.08kh}{\left[\ln\left(\frac{r_e}{r_w}\right) - \frac{3}{4} + s \right]} \left(\frac{k_{ro}}{\mu_o B_o}\right)_{p_R} \cdot \frac{(\bar{p}_R^2 - p_{wf}^2)^{1.0}}{2\bar{p}_R}, \dots (73)$$

Expressed in a form with reservoir variables and a non-Darcy flow term, F_{Da} , where the resulting n would be less than 1.0 and a function of F_{Da} ,

$$q_o = \frac{7.08kh}{\left[\ln\left(\frac{r_e}{r_w}\right) - \frac{3}{4} + s + F_{Da} \right]} \left(\frac{k_{ro}}{\mu_o B_o} \right)_{p_R} \cdot \frac{(\bar{p}_R^2 - p_{wf}^2)}{2\bar{p}_R} \quad (74)$$

When \bar{p}_R is equal to or less than the bubblepoint pressure p_b and n is less than 1, a non-Darcy flow factor, F_{Da} , is indicated. When $F_{Da}=0$, $n=1$. The term F_{Da} normally is developed from multipoint test data. As shown in a later example, it is possible to have $F_{Da}=0$ and n less than 1.0 for undersaturated wells producing at flowing pressures below the bubblepoint pressure. (See Fig. 8 of Ref. 16.) This is strictly a result of the shape of the $k_{ro}/(\mu_o B_o)$ pressure function.

Expressing the backpressure form of the IPR equation in terms similar to that of Vogel's equation (instead of Vogel's equation in terms of the backpressure curve), we have, from Eq. 69,

$$q_o = J'(p_R^2 - p_{wf}^2)^n$$

and

$$q_{o(max)} = J'(p_R^2)^n$$

or

$$J' = \frac{q_{o(max)}}{(p_R^2)^n} \quad (75)$$

Substituting and rearranging yields

$$\frac{q_o}{q_{o(max)}} = \left(\frac{p_R^2 - p_{wf}^2}{p_R^2} \right)^n = \left[1 - \left(\frac{p_{wf}}{p_R} \right)^2 \right]^n \quad (76)$$

For $n=1$, we have the simplest possible form of a multiphase IPR equation based on results obtained from actual field data:

$$\frac{q_o}{q_{o(max)}} = 1 - \left(\frac{p_{wf}}{p_R} \right)^2 \quad (77)$$

Comparing Eq. 77 to Vogel's Eq. 68, which was derived only from computer simulation data, we see that the coefficient for p_{wf}/\bar{p}_R is 0, and the coefficient for $(p_{wf}/p_R)^2$ is equal to 1. This results in an IPR Eq. 77 that yields a slightly more conservative answer than given by Vogel's original equation. (Actually, Vogel's Fig. 7 shows computer model calculated IPR results less than obtained from his reference equation.¹⁵) Not included in any of Vogel's simulation runs were effects of non-Darcy flow in the reservoir or perforation restrictions, which in the field result in n values less than 1.0 and an even more severe IPR rate reduction relationship.

Example Problem 6 (IPR). The following example illustrates the various possible methods of computing inflow rates.

An oil well is producing at a stabilized rate of 70 STB/D at a flowing BHP $p_{wf}=1,147$ psia. The average reservoir shut-in static pressure, $p_R=1,200$ psia. Calculate the maximum possible flow rate, q_o , at 0 psig, and the producing rate if artificial lift were installed to lower the flowing BHP to 550 psia. Make the calculations using the PI Eq. 63, Vogel's method, and the backpressure curve method with $n=1.0$ and $n=0.650$. (The data are from an actual IPR test reported in Ref. 16.)

Productivity Index (PI)

$$J = \frac{70}{1,200 - 1,147} = 1.32 \text{ STB/D-psi;}$$

$$q_o (15 \text{ psi}) = J(\bar{p}_R - p_{wf})$$

$$= 1.32 (1,200 - 15) = 1,564 \text{ STB/D;}$$

$$q_o (550 \text{ psi}) = 1.32(1,200 - 550) = 858 \text{ STB/D.}$$

Vogel IPR

$$q_o = 70 \text{ BOPD; } \frac{p_{wf}}{p_R} = \frac{1,147}{1,200} = 0.9558;$$

$$\left(\frac{p_{wf}}{\bar{p}_R} \right)^2 = 0.9136;$$

$$\frac{q_o}{q_{o(max)}} = 1 - 0.20 \left(\frac{p_{wf}}{\bar{p}_R} \right) - 0.80 \left(\frac{p_{wf}}{\bar{p}_R} \right)^2$$

$$= 1 - 0.19116 - 0.73088 = 0.07796;$$

$$q_{o(max)} = \frac{70}{0.07796} = 898 \text{ BOPD;}$$

and q_o at $p_{wf}=15$ psia.

$$\frac{q_o(15 \text{ psi})}{q_{o(max)}} = 1 - 0.20 \left(\frac{15}{1,200} \right)$$

$$- 0.80 \left(\frac{15}{1,200} \right)^2 = 0.99738;$$

$$q_o(15 \text{ psi}) = q_{o(max)}(0.99738)$$

$$= 898(0.99738) = 896 \text{ BOPD;}$$

q_o at $p_{wf}=550$ psia.

$$\frac{q_o(550 \text{ psi})}{q_{o(max)}} = 1 - 0.20 \left(\frac{550}{1,200} \right)$$

$$-0.80 \left(\frac{550}{1,200} \right)^2 = 0.740277;$$

$$q_o(550 \text{ psi}) = q_{o(\max)}(0.740277)$$

$$= 898(0.740277) = 665 \text{ BOPD.}$$

Backpressure Curve ($n=1.0$) IPR

$$q_o = 70 \text{ BOPD}; \bar{p}_R^2 = (1,200)^2 = 1,440,000;$$

$$p_{wf}^2 = (1,147)^2 = 1,315,609;$$

$$J' = \frac{70}{(1,200)^2 - (1,147)^2}$$

$$= \frac{70}{124,391} = 0.00056274 \text{ STB/D-psi}^2;$$

$$q_o(15 \text{ psi}) = J'(\bar{p}_R^2 - p_{wf}^2)$$

$$= 0.00056274 (1,440,000 - 225) = 810 \text{ BOPD};$$

$$q_o(550 \text{ psi}) = 0.00056274 (1,440,000 - 302,500)$$

$$= 640 \text{ BOPD.}$$

Using the dimensionless backpressure curve form in terms of $q_o/q_{o(\max)}$ and p_{wf}/\bar{p}_R with $n=1.0$,

$$q_o = 70 \text{ BOPD}; \left(\frac{p_{wf}}{\bar{p}_R} \right)^2 = \left(\frac{1,147}{1,200} \right)^2 = 0.9136;$$

$$\frac{q_o}{q_{o(\max)}} = 1 - \left(\frac{p_{wf}}{\bar{p}_R} \right)^2 = 1 - 0.9136 = 0.0864;$$

$$q_{o(\max)} = \frac{70}{0.0864} = 810 \text{ BOPD};$$

q_o at $p_{wf}=550$ psia.

$$\frac{q_o(550 \text{ psi})}{q_{o(\max)}} = 1 - \left(\frac{550}{1,200} \right)^2$$

$$= 1 - 0.168056 = 0.78993;$$

$$q_o(550 \text{ psi}) = 810(0.78993) = 640 \text{ BOPD.}$$

Backpressure Equation ($n=0.650$) IPR

$$q_o = 70 \text{ BOPD}; \bar{p}_R^2 = (1,200)^2 = 1,440,000;$$

$$p_{wf}^2 = (1,147)^2 = 1,315,609;$$

$$J' = \frac{70}{(1,440,000 - 1,315,609)^{0.650}} = \frac{70}{2,049.3}$$

$$= 0.0341580 \text{ STB/D-psi}^{2n};$$

$$q_o(15 \text{ psi}) = J'(\bar{p}_R^2 - p_{wf}^2)^{0.650}$$

$$= 0.0341580(1,440,000 - 225)^{0.650};$$

$$q_o(15 \text{ psi}) = 0.0341580(10,066.8) = 344 \text{ BOPD};$$

$$q_o(550 \text{ psi}) = 0.0341580(1,440,000 - 302,500)^{0.650}$$

$$= 295 \text{ BOPD.}$$

Using the dimensionless backpressure curve form in terms of $q_o/q_{o(\max)}$, p_{wf}/\bar{p}_R , and $n=0.650$,

$$q_o = 70 \text{ BOPD}; \left(\frac{p_{wf}}{\bar{p}_R} \right)^2 = \left(\frac{1,147}{1,200} \right)^2 = 0.9136;$$

$$\frac{q_o}{q_{o(\max)}} = \left[1 - \left(\frac{p_{wf}}{\bar{p}_R} \right)^2 \right]^{0.650}$$

$$= (1 - 0.9136)^{0.650} = 0.203579;$$

$$q_{o(\max)} = \frac{70}{0.203579} = 344 \text{ BOPD};$$

q_o at $p_{wf}=550$ psia.

$$\frac{q_o(550 \text{ psi})}{q_{o(\max)}} = \left[1 - \left(\frac{550}{1,200} \right)^2 \right]^{0.650} = 0.857892;$$

$$q_o = 344(0.857892) = 295 \text{ BOPD.}$$

Again, this example is based on field data where several rates were measured to establish the real IPR relationship of the well. The real absolute open flow of the well was 340 BOPD. This is 38% of the rate predicted by Vogel's IPR equation and 42% of the rate predicted by the backpressure equation with $n=1$. A value of $n=0.650$ as illustrated in this example is required to match the field data. A non-Darcy flow factor F_{Dd} is indicated for this test.

Single-Phase and Two-Phase IPR Equation. Fetkovich¹⁶ gives a general equation that treats flow both above and below the bubblepoint pressure for an undersaturated oil well.

$$q_o = J^*(\bar{p}_R - p_b) + J'(p_b^2 - p_{wf}^2), \dots \dots \dots (78)$$

where

$$J' = J^*(\mu_o B_o)_{p_R, p_b} \left(\frac{a_2}{2} \right), \dots \dots \dots (79)$$

Assuming $(\mu_o B_o)$ is a constant value above the bubblepoint pressure equal to $(\mu_o B_o)_b$ (the basis of the constant PI assumption for flow above the bubblepoint pressure, p_b), then $a_2 = 1/[p_b(\mu_o B_o)_b]$ (see Appendix of Ref. 16).

Then

$$J' = \frac{J^*(\mu_o B_o)_b}{2p_b(\mu_o B_o)_b} = \frac{J^*}{2p_b} \quad \dots \dots \dots (80)$$

Substituting Eq. 80 into 78 we obtain the final form of the single-phase and two-phase IPR equation:

$$q_o = J^*(\bar{p}_R - p_b) + \frac{J^*}{2p_b}(p_b^2 - p_{wf}^2) \quad \dots \dots \dots (81)$$

Example Problem 7. The following example illustrates the method of computing inflow rates for flows both above and below the bubblepoint pressure of an undersaturated oil well.

An oil well is producing at a rate of 50 STB/D at a flowing BHP of 2,100 psia. The reservoir average shut-in pressure is 3,200 psia with a bubblepoint pressure of 1,800 psia.

Calculate the maximum possible flow rate, q_o , at $p_{wf}=0$ psig and the producing rate at 550 psia flowing BHP. (For flows above p_b , $J=J^*$.)

$$J = J^* = \frac{q_o}{(\bar{p}_R - p_{wf})},$$

therefore,

$$J^* = \frac{50}{(3,200 - 2,100)} = \frac{50}{1,100}$$

$$= 0.045454 \text{ STB/D-psi}$$

and

$$q_o(15 \text{ psi}) = J^*(\bar{p}_R - p_b) + \frac{J^*}{2p_b}(p_b^2 - p_{wf}^2),$$

$$= 0.045454(3,200 - 1,800)$$

$$+ \frac{0.045454}{2(1,800)}(1,800^2 - 15^2),$$

$$= 64 + 0.000012626(3,240,000 - 225),$$

$$= 64 + 41 = 105.$$

This compares to 145 BOPD if the regular PI equation is assumed valid to 15 psia.

q_o at $p_{wf}=550$ psia

$$q_o(550 \text{ psi}) = J^*(\bar{p}_R - p_b) + \frac{J^*}{2p_b}(p_b^2 - p_{wf}^2)$$

$$= 0.045454(3,200 - 1,800)$$

$$+ \frac{0.045454}{2(1,800)}(1,800^2 - 550^2),$$

$$= 64 + 0.000012626(3,240,000 - 302,500),$$

$$= 64 + 37 = 101 \text{ BOPD.}$$

The additional 535-psi pressure drop from 550 psia to 15 psia results in only 4 BOPD increase. It is significant to point out that if several flows, all with flowing pressure p_{wf} below the bubblepoint pressure p_b , were calculated using the above equation and example and then plotted as a backpressure curve but with $\bar{p}_R^2 - p_{wf}^2$, it would indicate a value of $n=0.820$. We would have an indicated n less than 1.0 without a non-Darcy flow term F_{Da} . With the uncertainty involved in really knowing the *true* bubblepoint pressure of a particular well, we could obtain test n values less than 1.0 without non-Darcy flow existing.

To illustrate more clearly a case of drawdown data obtained at flowing pressures below the bubblepoint pressure to obtain J^* , we will use the 550 psia rate obtained above and the previously specified data. Actual unrounded calculated rate is 100.73 BOPD.

$$q_o = J^* \left[(\bar{p}_R - p_b) + \frac{(p_b^2 - p_{wf}^2)}{2p_b} \right]$$

$$J^* = \frac{q_o}{\left[(\bar{p}_R - p_b) + \frac{(p_b^2 - p_{wf}^2)}{2p_b} \right]},$$

$$= \frac{100.73}{\left[(3,200 - 1,800) + \frac{(1,800^2 - 550^2)}{2(1,800)} \right]},$$

$$= \frac{100.73}{(1,400 + 816)} = \frac{100.73}{2,216}$$

$$= 0.045450 \text{ STB/D-psi (good check).}$$

Future Inflow Performance. Standing¹⁷ presented a method for adjusting IPR by using Vogel's equation from a measured condition to a future reservoir pressure \bar{p}_R . It is based on the fact that PI can be defined uniquely only at a zero drawdown, $p_{wf} \rightarrow \bar{p}_R$.

$$J^* = \lim_{\Delta p \rightarrow 0} J \quad \dots \dots \dots (82)$$

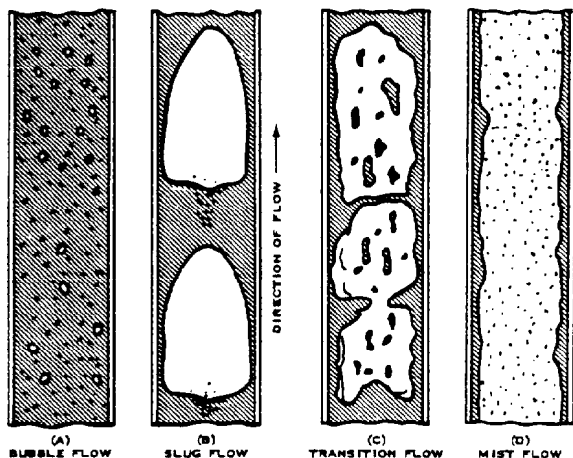


Fig. 34.6—Flow regime classifications for vertical two-phase flow.

Multiphase flow may be categorized into four different flow configurations or flow regimes, consisting of bubble flow, slug flow, slug-mist transition flow, and mist flow. In bubble flow, the liquid is continuous with the gas phase existing as bubbles randomly distributed (Fig. 34.6). The gas phase in bubble flow is small and contributes little to the pressure gradient except by its effect on the density. A typical example of bubble flow is the liberation of solution gas from an undersaturated oil at and above the point in the flow string where its bubblepoint pressure is reached.

In slug flow, both the gas and liquid phases significantly contribute to the pressure gradient. The gas phase in slug flow exists as large bubbles almost filling the pipe and separated by slugs of liquid. The gas bubbles are rounded on their leading edge, fairly flat on their trailing edge, and are surrounded on their sides by a thin liquid film. Liquid entrainment in the gas phase occurs at high flow velocities and small gas bubbles occur in the liquid slug. The velocity of the gas bubbles is greater than that of the liquid slugs, thereby resulting in a liquid holdup that not only affects well friction losses but also flowing density. Liquid holdup is defined as the in-situ flowing volume fraction of liquid. Slug flow accounts for a large percentage of two-phase production wells and, as a result, a good deal of research has been concentrated on this flow regime.

In transition flow, the liquid slugs between the gas bubbles essentially disappear, and at some point the liquid phase becomes discontinuous and the gas phase becomes continuous. The pressure losses in transition flow are partly a result of the liquid phase, but are more the result of the gas phase.

Mist flow is characterized by a continuous gas phase with liquid occurring as entrained droplets in the gas stream and as a liquid film wetting the pipe wall. A typical example of mist flow is the flow of gas and condensate in a gas condensate well.

Complete sets of pressure traverses for specific flow conditions and oil and gas properties have been published by service companies and others. These pressure gradient curves can be used for quick hand calculations.

Theoretical Considerations

As discussed in the Theoretical Basis section, the basis of any fluid-flow calculation consists of an energy balance on the fluid flowing between any two points in the system under consideration. The energy entering the system by virtue of the flowing fluid must equal the energy leaving the system plus the energy interchanged between the fluid and its surroundings.

The pressure drop in a vertical pipe associated with either single- or multiphase flow is given by

$$-dp = \frac{\tau_f dD}{144} + \frac{g\rho}{144g_c} dD + \frac{g v}{144g_c} dv, \quad (87)$$

where

p = pressure, psia.

τ_f = friction loss gradient, lbf/sq ft-ft.

D = depth, ft.

g = acceleration of gravity, ft/sec².

g_c = gravitational constant, (ft-lbm)/(lbf sec²).

ρ = fluid density, lbm/cu ft, and

v = fluid velocity, ft/sec.

Eq. 87 states that the fluid pressure drop in a pipe is the combined result of friction, potential energy, and kinetic energy losses.

The friction loss gradient and average density term for multiphase flow are evaluated using specific relationships for each flow regime. The kinetic energy term is usually small except for large flow rates. Duns and Ros¹⁸ have shown that for two-phase flow the kinetic energy term is significant only in the mist flow regime. Under this flow condition, $v_g \gg v_L$, and the kinetic energy term can be expressed as

$$\frac{\rho v}{g_c} dv = -\frac{w_t q_g}{g_c A^2} \frac{dp}{p}, \quad (88)$$

where

A = pipe area, sq ft,

w_t = total mass flow rate, lbm/sec, and

q_g = gas volumetric flow rate, cu ft/sec.

Eq. 87 now can be written in difference form for any depth increment, i , by assuming an average temperature and pressure exists over the increment. Making this assumption we have

$$\Delta p_i = \frac{1}{144} \left(\frac{\bar{\rho} + \tau_f}{1 - \frac{w_t q_g}{4637 A^2 \bar{p}}} \right) \Delta D_i, \quad (89)$$

where

$\bar{\rho}$ = average fluid density, lbm/cu ft.

Δp_i = pressure drop for increment i , psi.

\bar{p} = average pressure, psia, and

ΔD_i = the i th depth increment, ft.

Eq. 89 can be solved incrementally either by setting Δp_i and solving for ΔD_i or by setting ΔD_i and solving for Δp_i . Since pressure usually has more effect on average fluid properties than temperature and since temperature can be expressed as a function of depth, Δp_i should be set and ΔD_i calculated. The calculation procedure described here is an iterative process for each section and generally is programmed for solution on a computer.

Correlations

Since the original work in this area, which was presented by Poettmann and Carpenter,³³ several studies have been undertaken to collect additional experimental multiphase flow data and to develop new multiphase pressure drop correlations.¹⁸⁻²⁹ Also, various statistical studies have been performed comparing recent multiphase flow correlations³⁰⁻³² for large sets of flowing and gas lift cases.

Espanol *et al.*³⁰ selected the Hagedorn and Brown,²⁴ Duns and Ros,¹⁸ and Orkiszewski²⁵ methods as three of the best correlations for calculating multiphase pressure drops. An analysis of results calculated on 44 wells was used to determine the best overall correlation. This work concluded that the Orkiszewski correlation was the most accurate method over a large range of well conditions and it was the only correlation of the three considered suitable for evaluating three-phase flow for wells producing significant quantities of water.

Lawson and Brill³² point out that the Poettmann and Carpenter method is still a base line for comparing new multiphase flow correlations. Their original work is based on flow conditions similar to those found in many gas lift conditions and, therefore, is briefly discussed.

Poettmann and Carpenter.³³ Poettmann and Carpenter used data on flowing and gas lift wells to correlate the combined energy losses resulting from liquid holdup, frictional effects caused by the surface of the tubing, and other energy losses as a function of flow variables.

No attempt was made to evaluate the various components making up the total energy loss. The flowing fluid was treated as a single homogeneous mass, and the energy loss was correlated on this basis. A total flowing density or specific volume was used rather than an in-situ density or specific volume. That is, the energy of the fluid entering and leaving the tubing is a function of the pressure-volume properties of the total fluid entering and leaving the tubing, and not of the pressure-volume properties of the fluid in place, which would be different because of slippage or liquid-holdup effects. Lastly, in calculating flowing density or flowing specific volume, mass transfer between phases as the fluid flows up the tubing was taken into consideration, as well as the entire mass of the gas and liquid phases.

Viscosity as a correlating function was neglected. The degree of turbulence is of such a magnitude, in general, for a two-phase flowing oil well that the portion of the total energy loss resulting from viscous shear is negligible. This is not surprising since it is also true for single-phase turbulent flow. There the energy loss is independent of the physical properties of the flowing fluid. A

number of others* working on the same problem of multiphase flow have made the same observation.

Baxendell extended Poettmann and Carpenter's correlation by using large-volume flow data from wells on casing flow.³⁴ A detailed discussion of the Poettmann and Carpenter development can be found in the original 1962 edition of this handbook and in Ref. 33. The Poettmann and Carpenter correlation has served as the take-off point for many of the newer multiphase flow correlations.

Orkiszewski. To obtain a set of calculation procedures covering all flow regimes in two-phase flow, Orkiszewski²⁵ made a thorough review of the literature, tested various methods against a few sets of experimental data by hand calculations, and then selected the two methods, Griffith and Wallis¹⁹ and Duns and Ros,¹⁸ for his final evaluation. Orkiszewski programmed both methods and tested them against data from 148 wells. Neither method was accurate over the entire set of flow conditions. Griffith and Wallis's method, however, appeared to provide the better foundation for a general solution in slug flow, and, thus, Orkiszewski elected to modify their work.

Orkiszewski called his calculation procedures the Modified Griffith and Wallis method since their work was involved strictly with fully developed slug flow and since 95% of the 148 wells used by Orkiszewski in developing his method were in slug flow. Duns and Ros' method was used for mist flow and partly for transition flow since it appeared to be more fundamental than the Lockhart and Martinelli³⁵ method recommended by Griffith.

Orkiszewski's method essentially establishes which flow regime is present and then applies (1) Griffith's procedure for bubble flow, (2) Griffith's procedure modified by a liquid distribution coefficient parameter based on field data for slug flow, (3) a combination of the modified Griffith method and the Duns and Ros method for transition flow, or (4) Duns and Ros' method for mist flow. Accuracy claimed for this correlation is about $\pm 10\%$ for a wide range of flow conditions.

The determination of which flow regime applies for a given pipe segment is accomplished by checking the various dimensionless groups that define the boundaries of each flow regime (Fig. 34.7). Griffith and Wallis are responsible for defining the boundary between the bubble and slug flow regimes. Duns and Ros have defined the boundaries between the slug and transition flow regimes and between the transition and mist flow regimes. These boundaries are given by the inequalities listed below.

1. For the bubble flow regime, the boundary limits are $q_g/q_t < L_B$.
2. For the slug flow regime, the boundary limits are $q_g/q_t > L_B$, $v_{gD} < L_S$.
3. For the transition flow regime, the boundary limits are $L_M > v_{gD} > L_S$.
4. For the mist flow regime, the boundary limits are $v_{gD} > L_M$.

In these equations the subscripts *B*, *M*, and *S* indicate bubble, mist, and slug flow, respectively.

*Early investigators of this problem were T.V. Moore and H.D. Wilde Jr., "Experimental Measurement of Slippage in Flow Through Vertical Pipes," *Trans., AIME* (1931) 92, 296-313; and T.V. Moore and R.J. Schilthuis, "Calculation of Pressure Drops in Flowing Wells," *Trans., AIME* (1933) 103, 170-86.

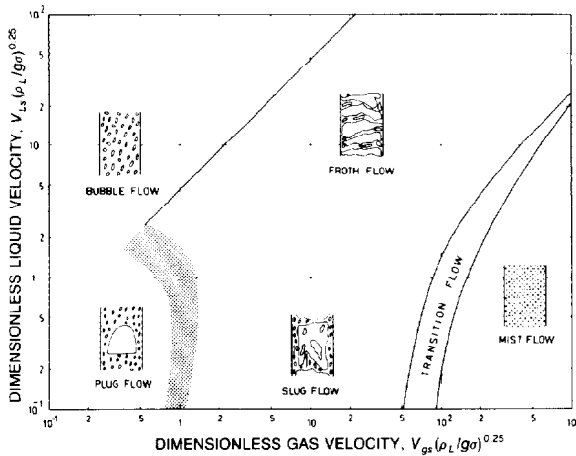


Fig. 34.7—Flow regime map.

These dimensionless groups are given by the following set of equations.

$$v_{gD} = \frac{q_g [\rho_L / (g\sigma)]^{0.25}}{A}, \quad (90)$$

at the bubble-slug boundary

$$L_B = 1.071 - \frac{0.2218 v_t^2}{d_H}, \quad (91)$$

but

$$L_B \geq 0.13,$$

at the slug-transition boundary

$$L_S = 50 + \frac{36 v_{gD} q_L}{q_g}, \quad (92)$$

and at the transition-mist boundary

$$L_M = 75 + 84 \left(\frac{v_{gD} q_L}{q_g} \right)^{0.75}, \quad (93)$$

where

- v_{gD} = dimensionless gas velocity,
- v_t = total fluid velocity (q_t/A), ft/sec,
- ρ_L = liquid density, lbm/cu ft,
- σ = liquid surface tension, lbm/sec²,
- L = flow regime boundary, dimensionless,
- d_H = hydraulic pipe diameter, ft,
- q_g = gas flow rate, cu ft/sec,
- g = acceleration of gravity, ft/sec², and
- A = flow area of pipe, sq ft.

The average density and friction loss gradient is defined later for each of the four possible flow regimes. These terms are evaluated for each pipe segment and are then substituted into Eq. 89 to calculate the pressure drop over the segment.

Bubble Flow. The average flowing density in *bubble flow* is calculated from the following equation, which volumetrically weights the gas and liquid densities.

$$\bar{\rho} = \rho_g f_g + (1 - f_g) \rho_L. \quad (94)$$

The flowing gas fraction, f_g , in bubble flow is given by

$$f_g = \frac{1}{2} \left[1 + \frac{q_t}{v_s A} - \sqrt{\left(\frac{1 + q_t}{v_s A} \right)^2 - \frac{4 q_g}{v_s A}} \right], \quad (95)$$

where the slip velocity, v_s , is the difference between the average gas and liquid velocities. Griffith suggests the use of an approximate value of $v_s = 0.8$ ft/sec for bubble flow.

The friction loss gradient for bubble flow is based on single-phase liquid flow.

$$\tau_f = \frac{f \rho_L v_L^2}{2 g_c d_H \cos \theta}, \quad (96)$$

where

$$v_L = \frac{q_L}{A(1 - f_g)}. \quad (97)$$

The friction factor, f , in Eq. 96 is the standard Moody² friction factor, which is a function of Reynolds number and relative roughness factor. The Reynolds number that is used for bubble flow is the liquid Reynolds number.

$$N_{Re} = \frac{1488 \rho_L d_H v_L}{\mu_L}, \quad (98)$$

where d_H is the hydraulic pipe diameter ($4A/\text{wetted perimeter}$), ft, and μ_L is the liquid viscosity, cp.

Slug Flow. The average density term for *slug flow* is expressed as

$$\bar{\rho} = \frac{w_t + \rho_L v_b A}{q_t + v_b A} + \delta \rho_L. \quad (99)$$

Eq. 99, with the exception of its last term, is equivalent to the average density term derived by Griffith and Wallis. The last term of Eq. 99 was added by Orkiszewski and contains a parameter, δ , that was correlated from oil-field data. The slip or bubble rise velocity, v_b , for slug flow was correlated by Griffith and Wallis and is given by

$$v_b = C_1 C_2 \sqrt{g d_H}. \quad (100)$$

The coefficient C_1 is the bubble-rise coefficient for bubbles rising in a static column of liquid. Values of C_1 have been determined theoretically by Dumitrescu³⁶ and experimentally by Griffith and Wallis¹⁹ as a function of bubble Reynolds number, Fig. 34.8, where

$$N_{Re_b} = \frac{1488 \rho_L d_H v_b}{\mu_L}. \quad (101)$$

The coefficient C_2 is a function of liquid velocity and, when multiplied by C_1 , represents the bubble-rise coefficient for bubbles rising in a flowing liquid. The coefficient C_2 has been determined experimentally by Griffith and Wallis¹⁹ and is correlated as a function of both bubble Reynolds number, N_{Re_b} , and liquid Reynolds number (Fig. 34.9), where

$$N_{Re} = \frac{1488 \rho_L d_H v_L}{\mu_L} \quad (102)$$

When Reynolds numbers larger than 6,000 are encountered, v_b can be evaluated from the following equations, which were developed by Orkiszewski and based on the work of Nicklin *et al.*²⁰ For bubble Reynolds numbers, N_{Re_b} , less than 3,000,

$$v_b = [0.546 + 8.74(10^{-6})N_{Re}] \sqrt{gd_H} \quad (103)$$

When bubble Reynolds number is between 3,000 and 8,000,

$$v_b = 0.5v_{bi} + 0.5 \left(v_{bi}^2 + \frac{13.59 \mu_L}{\rho_L \sqrt{d_H}} \right)^{0.5} \quad (104)$$

where

$$v_{bi} = [0.251 + 8.74(10^{-6})N_{Re}] \sqrt{gd_H} \quad (105)$$

For bubble Reynolds numbers greater than 8,000,

$$v_b = [0.35 + 8.74(10^{-6})N_{Re}] \sqrt{gd_H} \quad (106)$$

The friction loss gradient term for slug flow is the result of Orkiszewski's work and is given by

$$\tau_f = \frac{f \rho_L v_L^2}{2g_c d_H \cos \theta} \left(\frac{q_L + v_b A}{q_t + v_b A} + \delta \right) \quad (107)$$

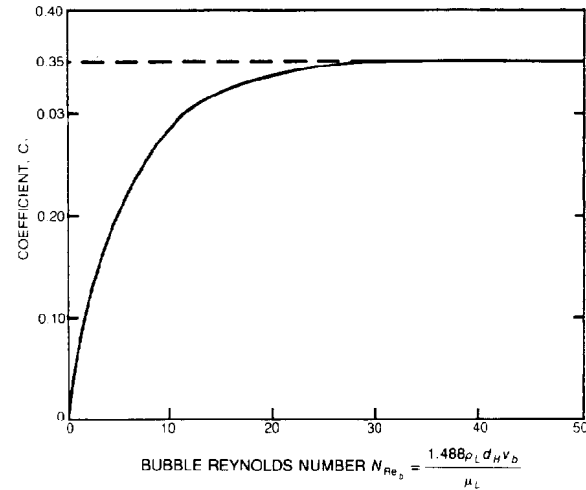


Fig. 34.8—Bubble-rise coefficient for bubbles rising in a static liquid column vs. bubble Reynolds number.

The friction factor in Eq. 107 is a function of relative roughness and the Reynolds number given by Eq. 102.

Orkiszewski defined the parameter δ , which appears in Eqs. 99 and 107 as a liquid distribution coefficient. This coefficient implicitly accounts for the following physical phenomena.

1. Liquid is distributed not only in the slug and as a film around the gas bubble but also as entrained droplets inside the gas bubble.
2. The friction loss has essentially two contributions, one from the liquid slug and the other from the liquid film.
3. The bubble rise velocity approaches zero as mist flow is approached.

Liquid distribution coefficient, δ , was correlated as a function of liquid viscosity, hydraulic radius, and total velocity and may be evaluated by one of the following empirical equations.

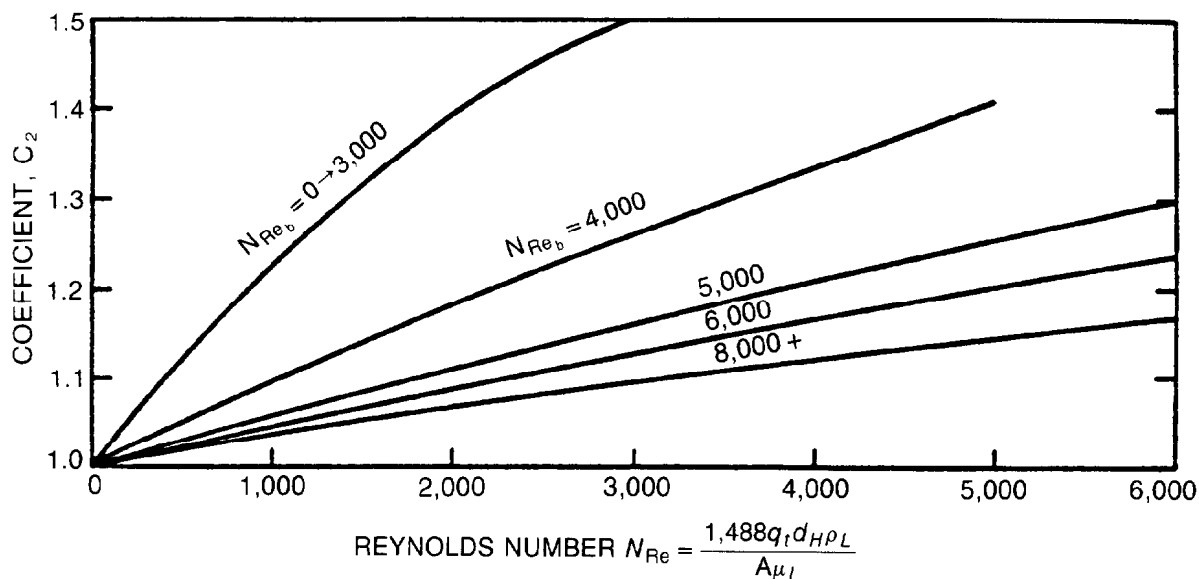


Fig. 34.9—Bubble-rise coefficient accounting for bubbles rising in a flowing liquid vs. Reynolds number.

Continuous Oil Phase. When $v_t < 10$,

$$\delta = \frac{0.0127}{d_H^{1.415}} \log(\mu_L + 1) - 0.284 + 0.167 \log v_t + 0.113 \log d_H \quad (108)$$

When $v_t > 10$,

$$\delta = \frac{0.0274}{d_H^{1.371}} \log(\mu_L + 1) + 0.161 + 0.569 \log d_H - \log v_t \left[\frac{0.01}{d_H^{1.571}} \log(\mu_L + 1) + 0.397 + 0.63 \log d_H \right] \quad (109)$$

Continuous Water Phase. When $v_t < 10$,

$$\delta = \frac{0.013}{d_H^{1.38}} \log \mu_L - 0.681 + 0.232 \log v_t - 0.428 \log d_H \quad (110)$$

When $v_t > 10$,

$$\delta = \frac{0.045}{d_H^{0.799}} \log \mu_L - 0.709 - 0.162 \log v_t - 0.888 \log d_H \quad (111)$$

Eqs. 108 through 111 are constrained by the following limits, which eliminate pressure discontinuities between flow regimes. When $v_t < 10$, $\delta \geq -0.065v_t$, and when $v_t > 10$,

$$\delta \geq -\frac{v_b A(1 - \rho/\rho_t)}{q_t + v_b A}$$

Transition Flow. The Duns and Ros method for calculating average flowing density and friction loss gradient in *transition flow* is used. They evaluated $\bar{\rho}$ and τ_f by linearly weighting the values obtained from slug and mist flow with dimensionless gas velocity, v_{gD} , and the dimensionless boundaries defining transition flow, L_M and L_S . The average density term is defined as

$$\bar{\rho} = \left(\frac{L_M - v_{gD}}{L_M - L_S} \right) \bar{\rho}_S + \left(\frac{v_{gD} - L_S}{L_M - L_S} \right) \bar{\rho}_M \quad (112)$$

where subscripts M and S are mist and slug flow conditions, respectively. Similarly, the friction loss gradient is defined as

$$\tau_f = \left(\frac{L_M - v_{gD}}{L_M - L_S} \right) \tau_{fS} + \left(\frac{v_{gD} - L_S}{L_M - L_S} \right) \tau_{fM} \quad (113)$$

Mist Flow. In *mist flow* the slip between the gas and liquid phases is essentially zero. The fraction of gas flowing can be expressed, therefore, as

$$f_g = \frac{q_g}{q_g + q_L} \quad (114)$$

Average flowing density is given by

$$\bar{\rho} = (1 - f_g)\rho_L + f_g\rho_g \quad (115)$$

The friction loss gradient for mist flow is primarily a result of the gas phase and is given by

$$\tau_f = \frac{f\rho_g v_{gs}^2}{2g_c d_H \cos\theta} \quad (116)$$

where v_{gs} is the superficial gas velocity and f is a function of the gas Reynolds number,

$$N_{Re} = 1488 \frac{\rho_g d_H v_{gs}}{\mu_g} \quad (117)$$

and a modified relative roughness factor, ϵ/d_H , which was developed by Duns and Ros. The roughness factor for mist flow is a function of the liquid film wetting the pipe walls and is given by the following set of equations and constraints. Let

$$N = 4.52(10^{-7})(v_{gs}\mu_L/\sigma)^2(\rho_g/\rho_L) \quad (118)$$

where N is a dimensionless number. Then for $N < 0.005$,

$$\frac{\epsilon}{d_H} = \frac{34\sigma}{\rho_g v_{gs}^2 d_H} \quad (119)$$

and for $N > 0.005$,

$$\frac{\epsilon}{d_H} = \frac{174.8\sigma(N)^{0.302}}{\rho_g v_{gs}^2 d_H} \quad (120)$$

Eqs. 119 and 120 are limited by upper and lower bounds for ϵ/d_H of 0.001 and 0.05.

Camacho³¹ studied 111 wells with high gas/liquid ratios and concluded that Orkiszewski's method performed better when mist flow calculations were used for gas/liquid ratios greater than 10,000. Obviously, if this approach is taken, an appropriate transition zone between slug and mist flow should be used to avoid abrupt pressure gradient changes. In another study, Gould *et al.*²⁷ also indicate that the onset of mist flow should occur at lower dimensionless gas velocities, especially for dimensionless liquid velocities less than 0.1.

Continuous-Flow Gas Lift Design Procedures

Gas lift^{28,33,37} is a method of artificial lift that uses the compressional energy of a gas to lift the reservoir fluid (see Chap. 5). The prime requisite is an adequate source of gas at a desired pressure and volume.

Wells having high water/oil ratios (WOR) and high productivity indices (that is, producing large volumes of fluid with high sustaining reservoir pressures) can be efficiently gas lifted through the tubing or the well annulus. Quite often it is necessary to produce very large volumes of water to obtain economic rates of oil production. Situations are known where it is possible to gas lift economically as much as 5,000 to 10,000 B/D total fluid, with the oil present being 1% of the total fluid produced and the rest being water. In applying the correlations to gas lift design calculations, the following procedure is recommended.

1. Establish the flow characteristics of the well—i.e., productivity index, WOR, gas/oil ratio (GOR), fluid properties, tubing size, etc.
2. Calculate the pressure traverses below the injection point for the range of flow rates.
3. Calculate the pressure traverses above the point of injection for different injection GOR's, holding the surface tubing or casing pressure constant.

From these three steps, as illustrated in Fig. 34.10, the horsepower requirements, pressure at injection point, depth of injection, and injection GOR's for a given rate of production, tubing size, and tubing or casing pressure can be calculated.

For a given set of well conditions and fluid production, there is an optimum depth and injection pressure that result in minimum horsepower requirements. In some cases, the optimal injection depth will be at the total depth of the well. There are two ranges of operation in gas lifting a reservoir fluid. One is an inefficient range characterized by high GOR and high horsepower requirements, and the other is an efficient range characterized by low GOR and low horsepower requirements. A plot of GOR vs. injection pressure is shown in Fig. 34.11.

In the inefficient range of operation, gas literally is "blown" through the flow string. The efficient range is to the left of the minimum injection pressure, and the inefficient range to the right. Inefficient and efficient ranges of operation have been observed in the laboratory on experimental gas lift involving short lengths of tubing.³⁸⁻⁴⁰ One investigator used a large amount of field data from a California field to develop empirically curves similar to those shown in Fig. 34.11 but had no way of predicting these curves for other fields where the physical properties of the fluids and the production data were different.⁴¹ In a plot of horsepower requirement vs. injection pressure (Fig. 34.12) the horsepower generally passes through a minimum value, which represents the maximum efficiency of the operation. Another interesting result of these gas lift calculations has been to show that the lower the surface pressure of the flow string that can be maintained consistent with efficient surface operations, the less will be the horsepower required to lift the reservoir fluid.

The use of the calculation procedure can best be expressed by use of a typical example problem.⁴²

Example Problem 9. It is desired to gas lift a well by flowing through the annulus. The well has a productivity index of 10.0 bbl total liquid per day per psi pressure drop. The static reservoir pressure is 3,800 psia at a well depth of 10,000 ft. The WOR is 18.33. Other pertinent information is as follows.

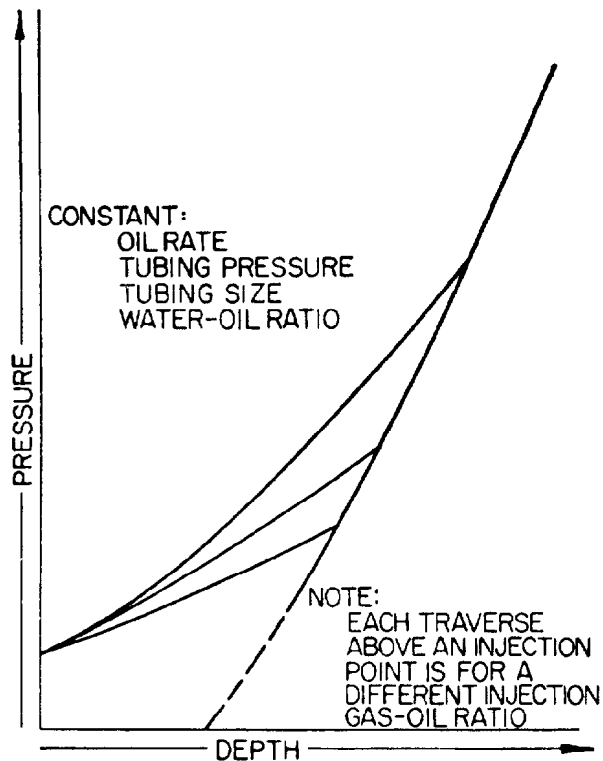


Fig. 34.10—Pressure traverse in gas-lift well.

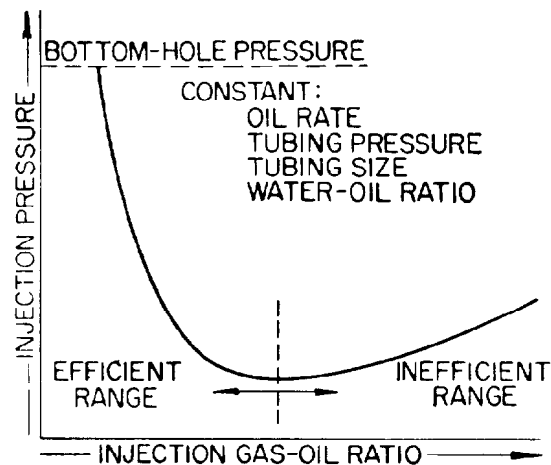


Fig. 34.11—Effect of injection pressure on injection GOR.

Tubing ID (2½ in. nominal, 6.5 lbm/ft)=2.441 in.; tubing OD (2½ in. nominal, 6.5 lbm/ft)=2.875 in.; casing ID (7 in. nominal, 26 lbm/ft)=6.276 in.; casing pressure=100 psia; average flowing temperature in annulus above injection depth=155°F; average flowing temperature in annulus below injection depth=185°F; average flowing temperature in tubing=140°F; gravity of stock-tank oil at 60°F=0.8390; gravity of separator gas (air=1.0)=0.625; gravity of produced water=1.15; $B=0.0000723p+1.114$; $R_s=0.1875p+17$; and $R=600$ cu ft/bbl oil.

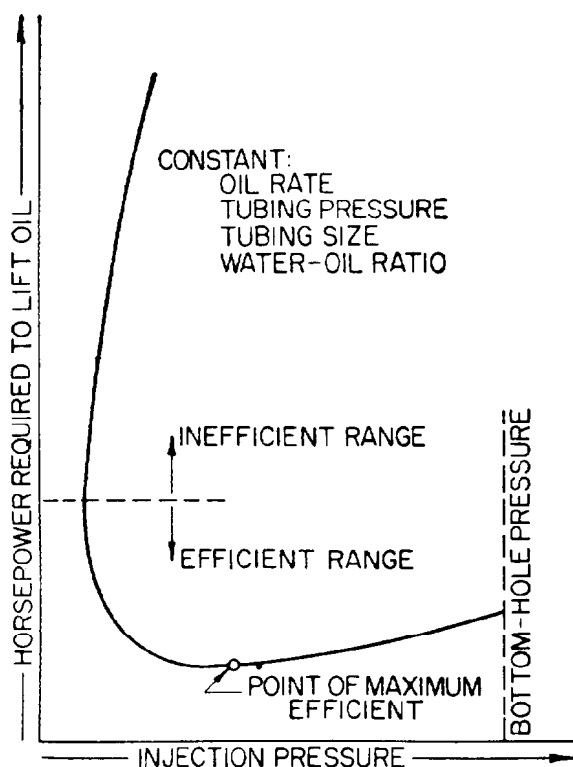


Fig. 34.12—Effect of injection pressure on horsepower requirements.

Calculate the variation of injection GOR with injection pressure and injection depth for a total liquid production rate of 4,000 B/D. Calculate the horsepower requirements to lift the oil as a function of injection pressure.

The solution of the problem involves the following steps.

1. Calculate the pressure traverse below the point of gas injection.
2. Calculate the pressure traverses above the point of gas injection for various GOR's.
3. Solve 1 and 2 simultaneously to determine the depth of injection for various injection GOR's and a casing pressure of 100 psia.
4. Calculate the theoretical adiabatic horsepower required to compress the gas from 100 psia to the injection-point pressure.

The first step in the solution of this problem is the calculation of the flowing density of the three-phase fluid produced into the well as a function of the pressure. Using Fig. 34.13, the differential pressure gradients were determined as a function of fluid density and, therefore, pressure. These calculations are illustrated in Table 34.6. These results then were placed on a plot of dD/dp vs. p . The depth traveled by the fluid flowing from the BHP to any lower pressure was determined by integrating this curve. In this way, Curve A in Fig. 34.14 was determined.

The second step of the solution was carried out mechanically the same as the first step, with the exceptions that the fluid densities were calculated for injection GOR's of 3,000, 3,500, 4,000, 5,000, and 7,500 scf/bbl, and that the integrations were carried out from the wellhead casing pressure of 100 psia to the pressures farther down the casing. The results of these calculations are shown in Fig.

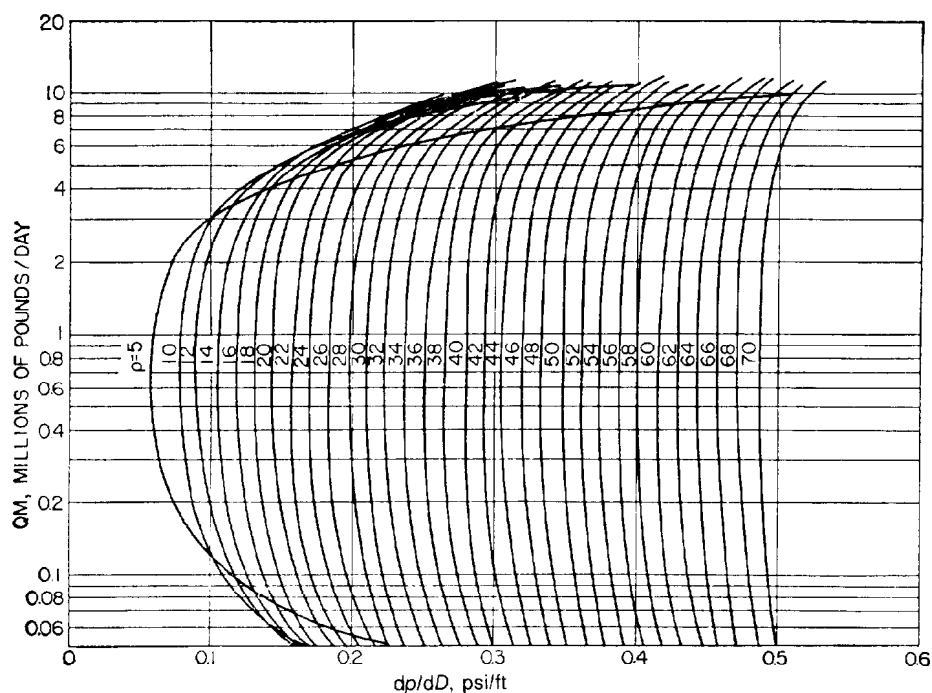


Fig. 34.13—Calculation of pressure traverses for flow in annulus. Tubing size is 2½ in. nominal (6.5 lbm/ft, 2.441-in. ID, 2.875-in. OD). Casing size is 7.0 in. nominal (26 lbm/ft, 6.276-in. ID).

TABLE 34.6—CALCULATION OF THE PRESSURE TRAVERSE BELOW THE POINT OF GAS INJECTION

$$q_o = \frac{4,000}{19.33} = 206.9 \text{ B/D}$$

$$q_o m = 1.594 \times 10^6 \text{ lbm/D}$$

$$\rho = \frac{m}{V_m} = \frac{7701.5}{5.61B + \frac{18.29(600 - R_s)}{p/z} + 102.8} \text{ lbm/cu ft}$$

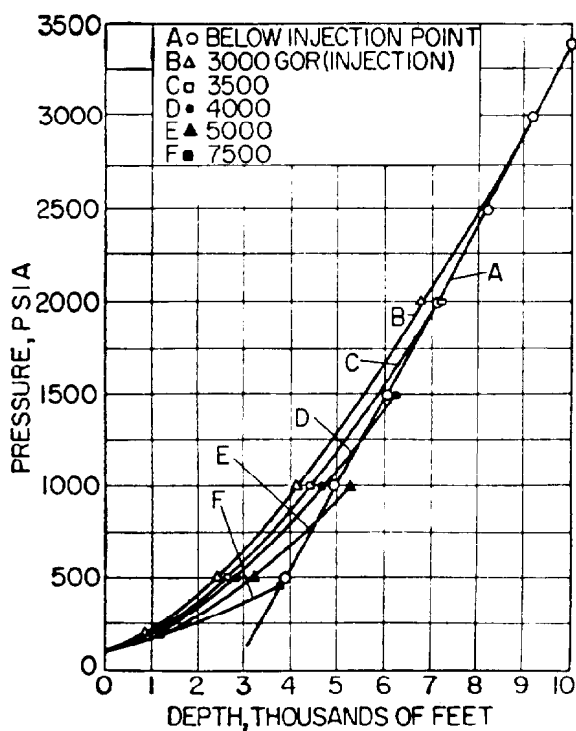
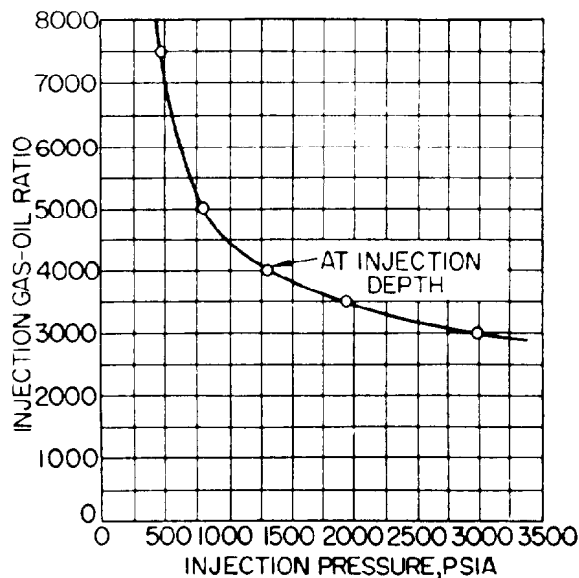
Flowing BHP = 3,400 psia

Establishing p vs. $1/dp/dD$

p	B	R_s	p/z	ρ	dp/dD	$1/dp/dD$
3,400	1.339	—	3,800	69.8	0.487	2.053
3,000	1.331	588	3,440	69.8	0.487	2.053
2,000	1.259	392	2,270	69.0	0.481	2.079
1,000	1.286	205	1,078	66.3	0.460	2.174
500	1.150	110.8	520.8	60.9	0.425	2.353

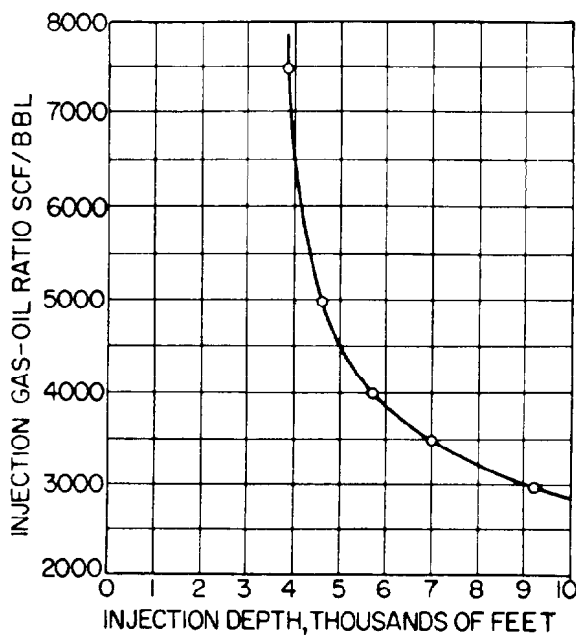
$$\int_{3,400}^{p_2} \frac{dp}{dp/dD}$$

p	$Dp_1 - Dp_2$	ΔD	D (ft)
3,400	—	0	10,000
3,000	821.2	821.2	9,179
2,500	1,028.5	1,849.7	8,150
2,000	1,035.0	2,884.7	7,115
1,500	1,048.5	3,933.2	6,066
1,000	1,071.5	5,004.7	4,995
500	1,121.0	6,125.7	3,874

**Fig. 34.14—Pressure vs. depth.****Fig. 34.15—Injection GOR vs. injection pressure.**

34.14 as curves B, C, D, E, and F. The intersections of these curves with Curve A represent the injection points for these flow rates and injection GOR's.

The injection GOR is plotted as a function of the injection pressure at injection depth in Fig. 34.15. For the conditions of this example problem, it will be noted that the injection pressure continually decreases as the GOR is increased from 3,000 to 7,500 scf/bbl. Fig. 34.16 shows the relationship between injection depth and injection GOR. This plot shows that, as the injection GOR is decreased, the point of injection is moved down the hole.

**Fig. 34.16—Injection depth vs. injection GOR.**

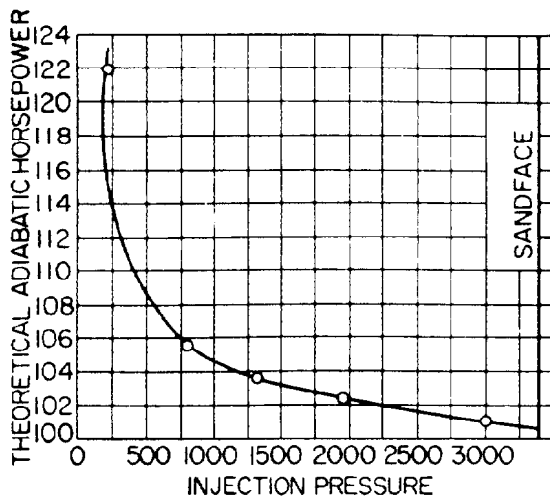


Fig. 34.17—Horsepower vs. injection pressure.

Fig. 34.17 shows the theoretical adiabatic horsepower required to compress the injected gas from the surface pressure to the injection pressure. For the conditions of this problem, the minimum horsepower is required when the injection point is at the bottom of the well, although, as pointed out in the earlier discussion, it is theoretically possible to obtain minimum horsepower requirements at points other than at the bottom of the hole.

The literature reports an interesting series of well tests in which curves calculated by the procedure described above completely characterize the gas lift performance

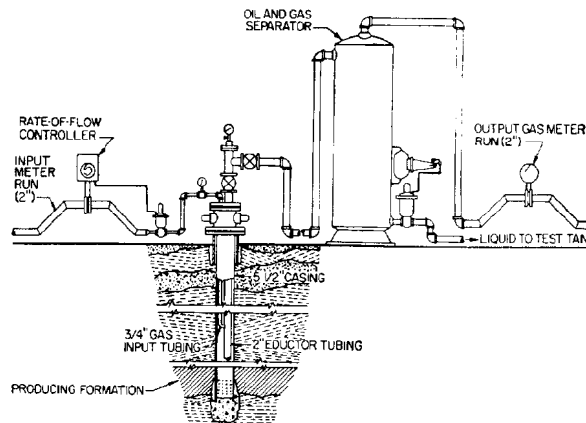


Fig. 34.18—Equipment arrangement.

of the well tested.⁴³ Fig. 34.18 shows the physical installation of the well tested. Tests were conducted at two points of gas injection, 3,800 and 4,502 ft. Detailed descriptions of the tests are available from Ref. 43.

Figs. 34.19 and 34.20 show a comparison of the observed and calculated pressure traverses above the point of gas injection. The comparison indicates good agreement.

Fig. 34.21 shows a comparison of observed data with curves calculated for average well conditions of total liquid flow vs. rate of gas injection.

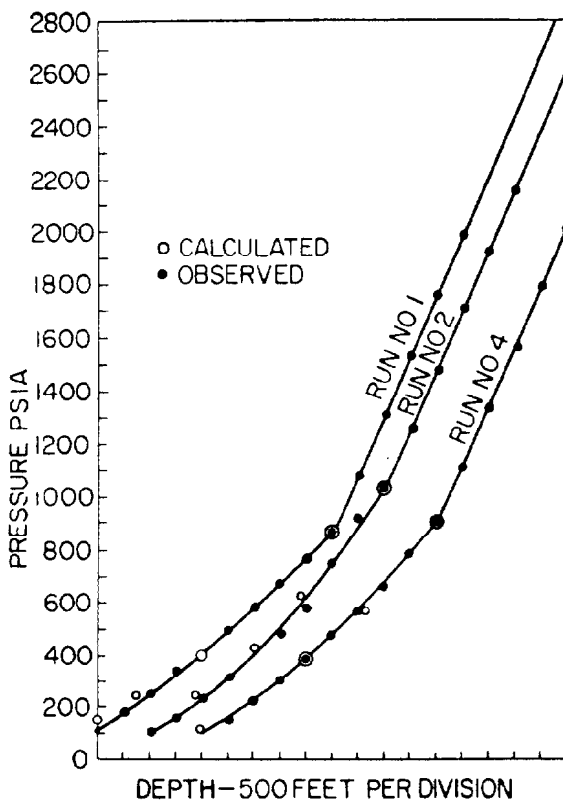


Fig. 34.19—Calculated and field-measured pressure traverses— injection depth is 4,502 ft.

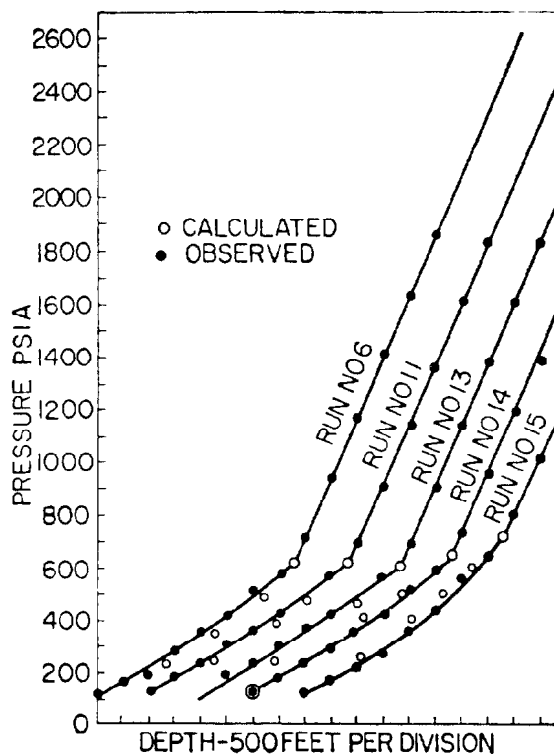


Fig. 34.20—Calculated and field-measured pressure traverses— injection depth is 3,810 ft.

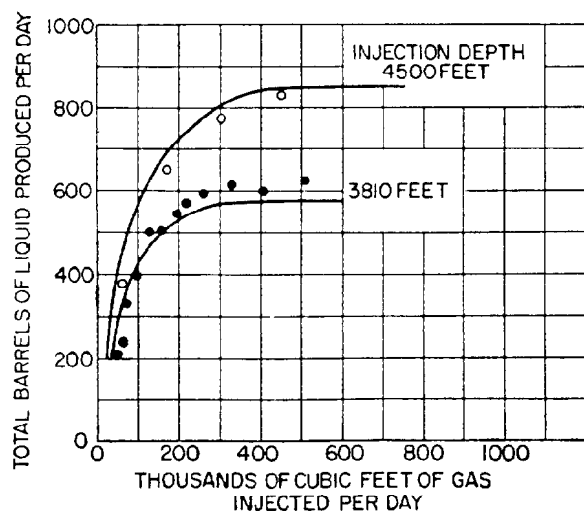


Fig. 34.21—Total liquid flow vs. rate of gas injection.

Fig. 34.22 is an example of a very useful type of plot that can be calculated for the optimum conditions of lift. It is a plot of ideal adiabatic horsepower per barrel per day of total fluid produced vs. total barrels of fluid produced per day under the conditions as indicated. Horsepower as used here is the horsepower required to compress the injected gas between the tubing pressure and injection pressure.

Flow Through Chokes

A wellhead choke or "bean" is used to control the production rate from a well. In the design of tubing and well completions (perforations, etc.), one must ensure that neither the tubing nor perforations control the production from the well. The flow capacity of the tubing and perforations always should be greater than the inflow performance behavior of the reservoir. It is the choke that is designed to control the production rate from a well. Wellhead chokes usually are selected so that fluctuations in the line pressure downstream of the choke have no effect on the well flow rate. To ensure this condition, flow through the choke must be at critical flow conditions; that is, flow through the coke is at the acoustic velocity. For this condition to exist, downstream line pressure must be approximately 0.55 or less of the tubing or upstream pressure. Under these conditions the flow rate is a function of the upstream or tubing pressure only.

For single-phase gas flow through a choke, the following equation is used:

$$q_g = \frac{Cp}{\sqrt{\gamma_g T}} \quad (121)$$

where

p = upstream pressure, psia,

γ_g = gas gravity,

T = upstream or wellhead temperature, °R,

C = coefficient, and

q_g = flow rate measured at either 14.4 or 14.7 psia and 60°F, 10^3 cu ft/D.

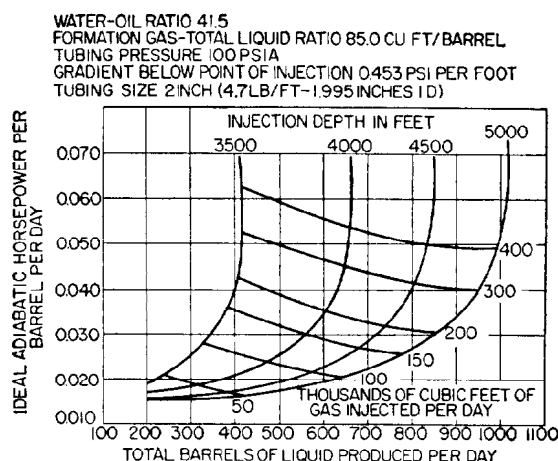


Fig. 34.22—Horsepower requirements vs. total fluid produced.

The coefficient, C , will vary depending on the base pressure.

Table 34.7 presents values of C taken from Rawlins and Schellhardt.⁴⁴ These values are for a standard pressure of 14.4 psia. Rawlins and Schellhardt did not make corrections for deviation from ideal gas. Correction can be made to Eq. 121 by multiplying the right side of the equation by $\sqrt{1/z}$, where z is the compressibility factor of the gas at the upstream pressure p and temperature T .

In the case of multiphase flow, Gilbert developed the following empirical equation based on data from flowing wells in the Ten Section field of California relating oil flow, GOR, tubing pressure, and choke size.⁴⁵

$$p_{tf} = \frac{435 R_{gL}^{0.546} q_l}{S^{1.89}} \quad (122)$$

where

p_{tf} = tubing flowing pressure, psig,

R_{gL} = gas/liquid ratio, 10^3 scf/bbl,

q_l = gross liquid rate (oil and water), B/D, and

S = choke size in 1/64 in.

Gilbert's equation may be written in the form:

$$p_{tf} = A q_l \quad (123)$$

TABLE 34.7—
COEFFICIENTS FOR
CHOKE NIPPLE

Orifice size (in.)	C
1/8	0.125
3/16	0.188
1/4	0.250
5/16	0.313
3/8	0.375
7/16	0.438
1/2	0.500
5/8	0.625
3/4	0.750

where $A = 435R_{gL}^{0.546}/S^{1.89}$ and where the tubing pressure is proportional to the production rate. This is true only under conditions of acoustic flow through the choke. At low flow rates, the rate is also a function of the downstream pressure and Eq. 123 no longer holds.

Ros presented a theoretical analysis on the mechanism of simultaneous flow of gas and liquid through a restriction at acoustic velocity.^{46,47} The result was a complex equation relating mass flow of gas and liquid, restriction size, and upstream pressure. Ros' equation was checked against oilfield data under critical flow conditions with good results. However, the equation is expressed in a form not really amenable to use by oilfield personnel.

Using Ros' analysis, Poettmann and Beck converted Ros' equation to oilfield units and reduced it to graphical form.⁴⁸ The result was Figs. 34.23 through 34.25 for oil gravities of 20, 30, and 40°API. The 20° gravity chart should be used for gravities ranging from 15 to 24°API; similarly, the 30° chart should be used for gravities ranging from 25 to 34°, and the 40° chart for gravities ranging from 35° on up. The charts are not valid if there is appreciable water production with the oil.

The charts can be entered from either the top or bottom scale. When entering from the GOR scale, go first to the tubing pressure curve and then horizontally to the choke size curve and then read the oil flow rate from the top scale. Conversely, when entering the chart at the oil flow rate scale, the reverse order is followed. Reliable estimates of gas rates, oil rates, tubing pressures, and choke sizes can be made by using these charts.

Chokes are subject to sand and gas cutting as well as asphalt and wax deposition, which changes the shape and size of the choke. This, then, could result in considerable error when compared to calculated values of flow for a standard choke size. A small error in choke size caused by a worn choke can effect a considerable error in the predicted oil rate. Thus, a cut choke could result in estimated oil rates considerably lower than measured.

From the inflow performance relationship of a well and by knowing the tubing size in the well, the tubing pressure curve for various flow rates can be calculated. The intersection of the choke performance curve for different choke sizes with the tubing pressure curve then gives one the wellhead pressures and flow rates for any choke size, as illustrated in Fig. 34.26.

Example Problem 10.⁴⁸

1. Determine the flow rate from a well flowing through a $\frac{5}{64}$ -in. choke at a flowing tubing pressure of 1,264 psia and a producing GOR of 2,250 cu ft/bbl. Stock-tank gravity is 44.4°. From Fig. 34.25, the solution is 60 B/D oil.

2. For this example, estimate the free gas present in the tubing. The solution gas at a tubing pressure of 1,264 psia from Fig. 34.25 is $R_s = 310$ cu ft/bbl. Then, the free gas present is $R - R_s = 2,250 - 310$ or 1,940 cu ft/bbl of oil at the wellhead.

3. It is desired to produce a well at 100 B/D oil. The producing GOR is 4,000 cu ft/bbl. At this rate the tubing pressure is 1,800 psia. Estimate choke size.

All three charts show estimated choke size to be $\frac{5}{64}$ in. Gilbert's charts also give $\frac{5}{64}$ in.⁴⁵

A number of other choke design correlations have been suggested. However, Poettmann and Beck's adaption of the Ros equation is recommended when no water is pro-

duced with the oil, and Gilbert's equation can be used when water is present.

Liquid Loading in Wells

Liquid loading in wells occurs when the gas phase does not provide sufficient transport energy to lift the liquids out of the well. This type of well does not produce at a flow rate large enough to keep the liquids moving at the same velocity as the gas. The accumulation of liquid will impose an additional backpressure on the formation that can affect the production capacity of the well significantly. Initially, the occurrence of liquid holdup may be reflected in the backpressure data obtained on a well wherein at the lower flow rates its performance, expressed as a backpressure curve, is worse than expected. Eventually, the well is likely to experience "heading" (fluctuating flow rates) followed by "load up" and cease to produce. Methods sometimes used to continue production from "loading" wells are pumping units, plunger lifts, smaller-diameter tubing, soap injection, and flow controllers.

This section is directed mainly toward relating loading to flow conditions within the well. In the simplest context, loading, as reflected on a deterioration of flow performance at lower flow rates on a backpressure curve, is related to the superficial velocity of the gas in the conduit at wellhead conditions. Duggan⁴⁹ found that a velocity of 5 ft/sec would keep wells unloaded whereas Lisbon and Henry⁵⁰ found that 1,000 ft/min (16.7 ft/sec) could be required.

R.V. Smith⁵¹ reported that experience with low-pressure wells in the West Panhandle and Hugoton fields showed that a velocity of 5 to 10 ft/sec is necessary to remove hydrocarbon liquids consistently and a velocity of 10 to 20 ft/sec is required for water.

Turner *et al.*⁵² analyzed the problem of liquid holdup on the basis of two proposed physical models: (1) liquid film movement along the walls of the pipe and (2) liquid droplets entrained in the high-velocity core. They concluded, on the basis of comparisons with field data, that the entrained drop movement was the controlling mechanism for removal of liquids. Their results indicated that in most instances wellhead conditions were controlling and the fluid velocity required to remove liquids could be expressed by the following equation.

$$v_f = \frac{20.4\sigma^{0.25}(\rho_L - \rho_g)^{0.25}}{\rho_g^{0.5}}, \dots\dots\dots (124)$$

where

v_f = terminal velocity of free-falling particle,
ft/sec,

σ = interfacial tension, dynes/cm,

ρ_g = gas phase density, lbm/cu ft, and

ρ_L = liquid phase density, lbm/cu ft.

Using simplifying assumptions with respect to gas, condensate, and water properties as given in Table 34.8, Eq. 124 can be expressed for water as

$$v_{gw} = \frac{5.62(67 - 0.0031p)^{0.25}}{(0.0031p)^{0.5}} \dots\dots\dots (125)$$

(continued on Page 34-50)

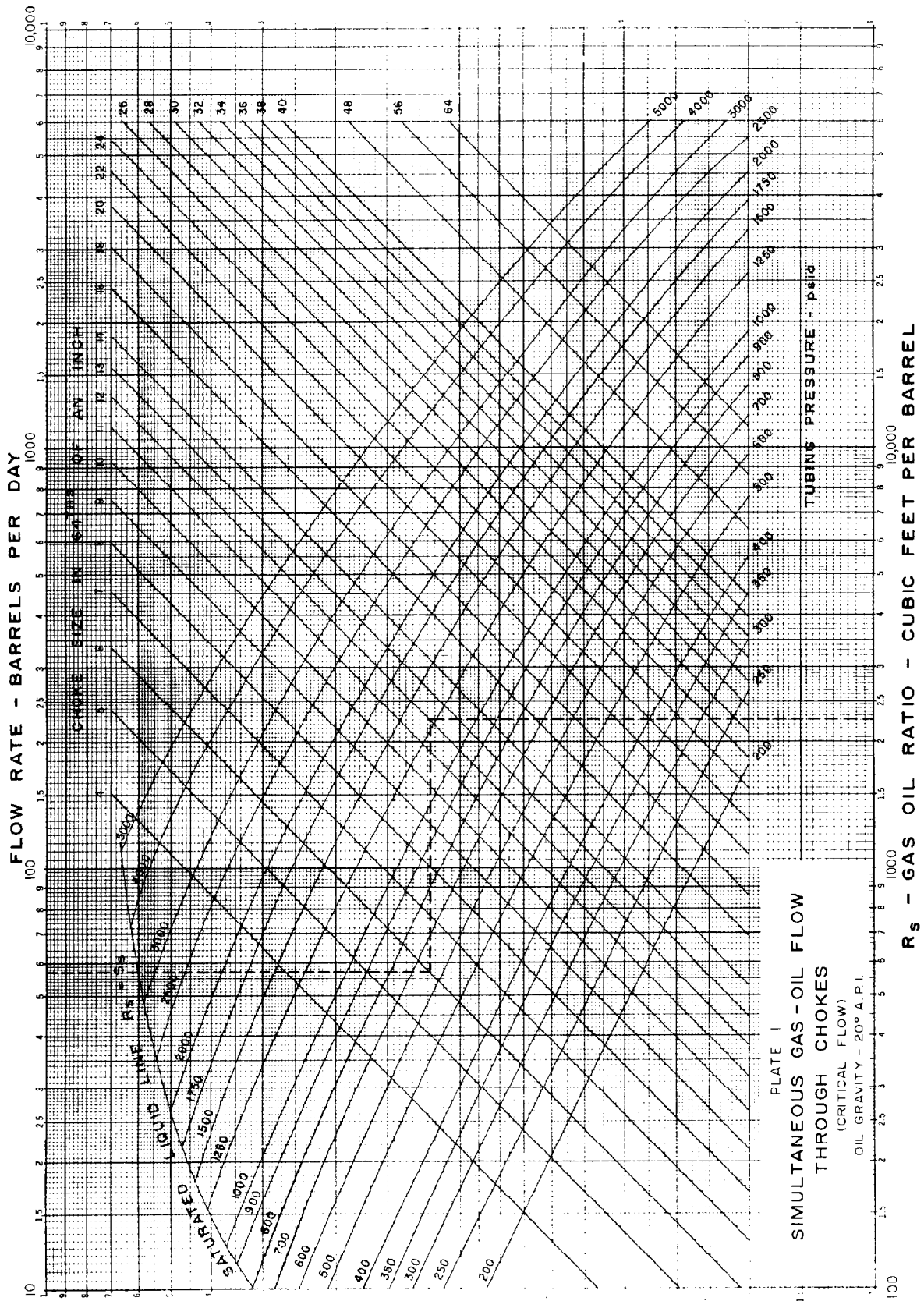
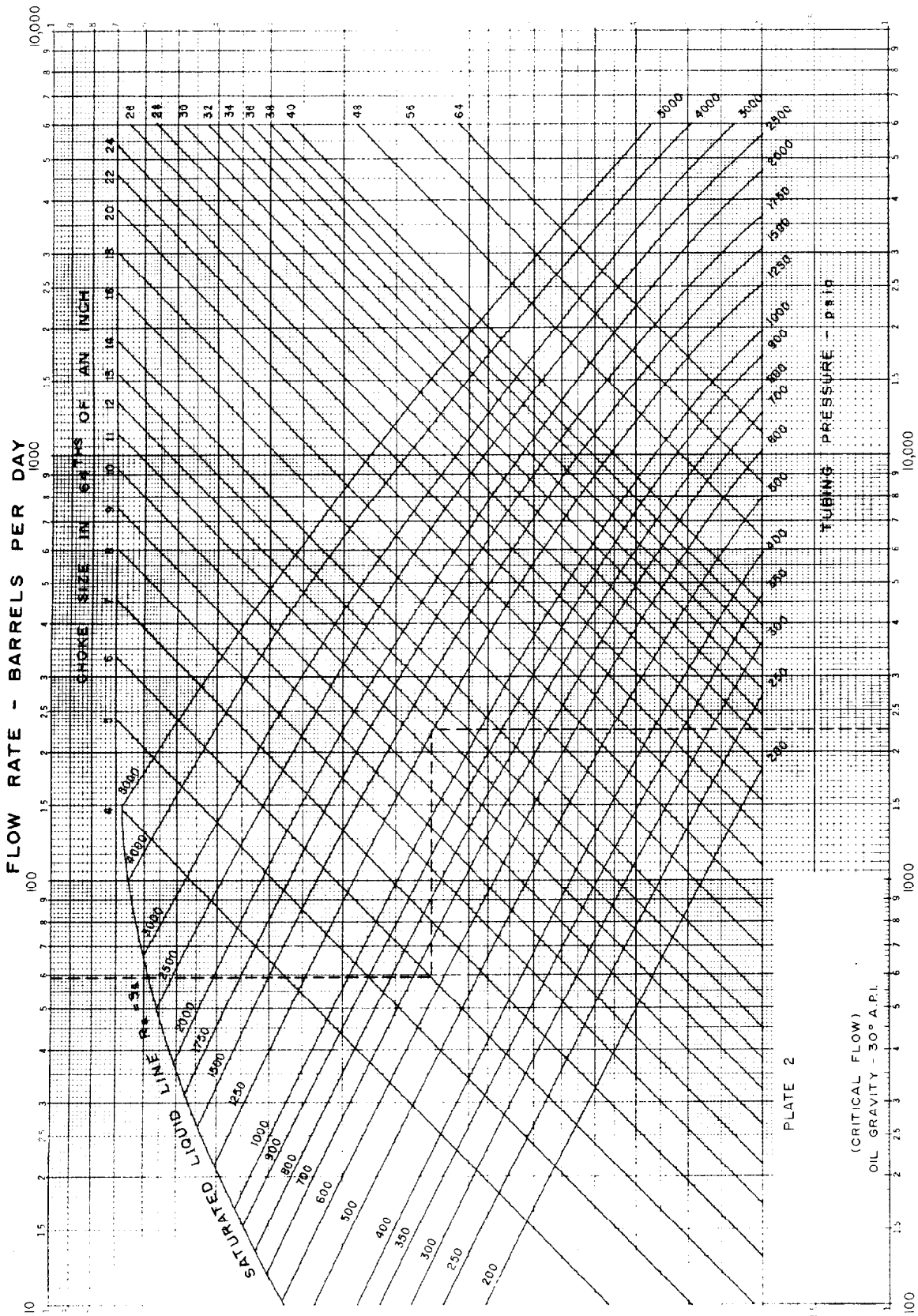


Fig. 34.23—Simultaneous gas/oil flow through chokes.



R_s - GAS OIL RATIO - CUBIC FEET PER BARREL

Fig. 34.24—Simultaneous gas/oil flow through chokes.

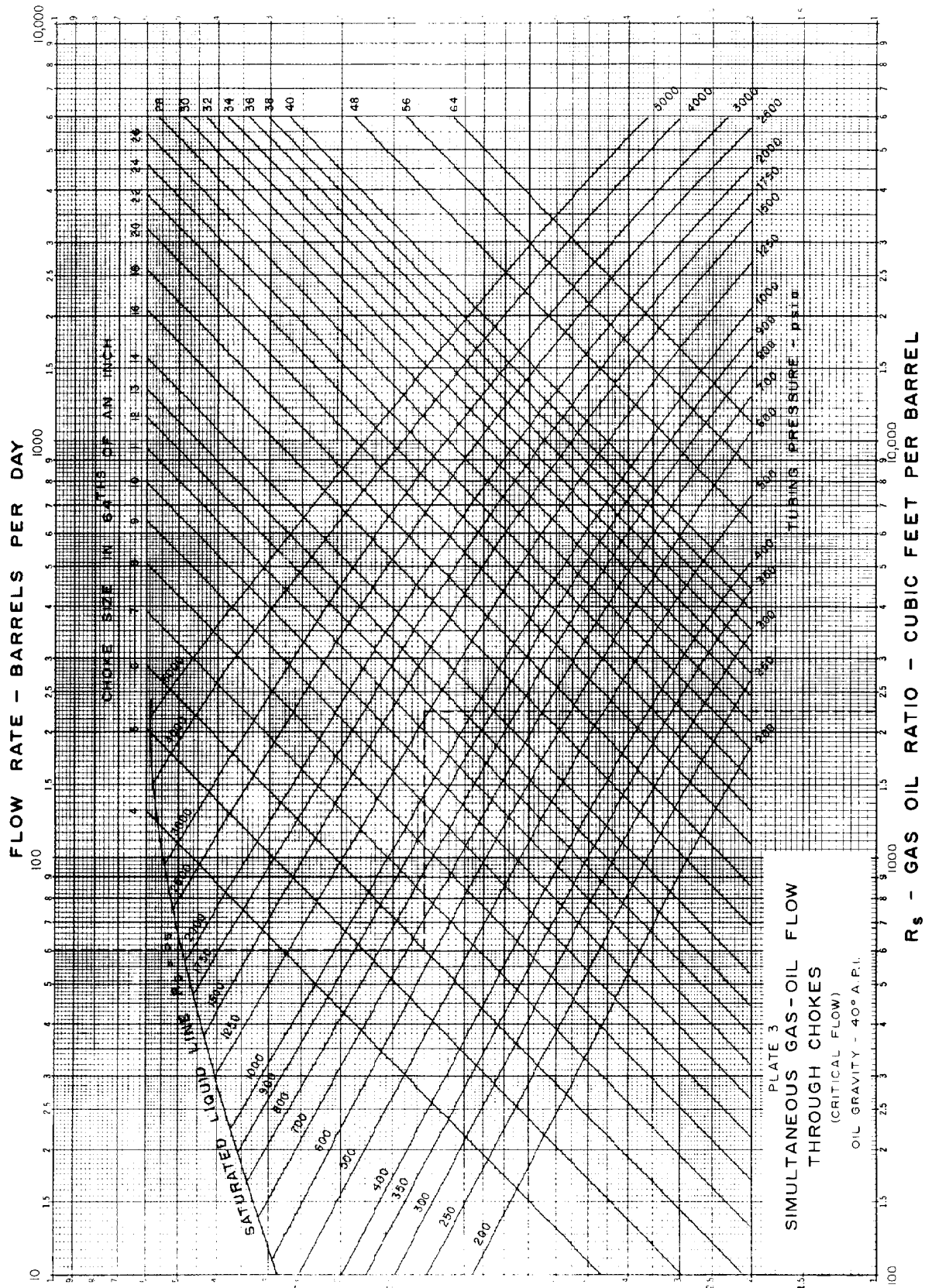


Fig. 34.25—Simultaneous gas/oil flow through chokes.

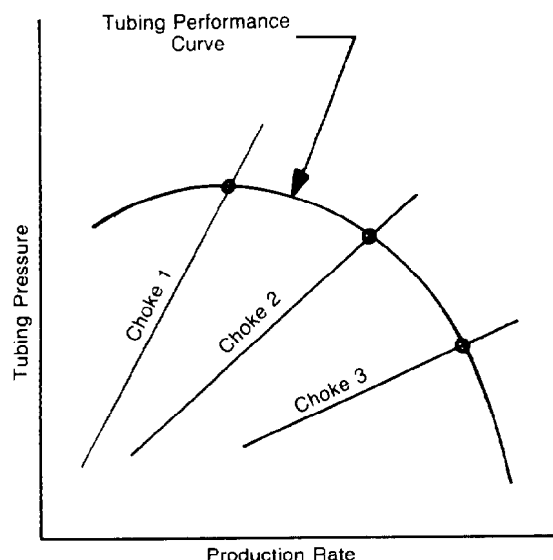


Fig. 34.26—Tubing and choke performance curves.

and for condensate as

$$v_{gc} = \frac{4.02(45 - 0.0031p)^{0.25}}{(0.0031p)^{0.5}}, \dots\dots\dots (126)$$

where

v_{gw} = gas velocity for water, ft/sec,
 v_{gc} = gas velocity for condensate, ft/sec, and
 p = pressure, psi.

Further, a minimum flow rate for a particular set of conditions (pressure and conduit geometry) can be calculated using Eqs. 125 through 127.

$$q_g = \frac{3.06pv_gA}{Tz}, \dots\dots\dots (127)$$

where

q_g = gas flow rate, 10^6 scf/D,
 A = flow area of conduit, sq ft,
 T = temperature, °R, and
 z = gas deviation factor.

Tek *et al.*⁵³ introduced a concept called “the lifting potential” to explain loading, unloading, heading, and dying of wells. Further, the concept relates the inflow behavior of the well with the multiphase flow in the well. Accordingly, it appears possible to address engineering considerations directed toward performance analysis or design of well equipment. Calculation procedures described earlier in this chapter with respect to well inflow performance and multiphase flow in the well should be adaptable to use the lifting potential concept.

TABLE 34.8—GAS, CONDENSATE, AND WATER PROPERTIES

	Gas	Condensate	Water
Interfacial tension, dynes/cm	—	20	60
Liquid phase density, lbm/cu ft	—	45	67
Gas gravity	0.6		
Gas temperature, °F	120		

Nomenclature

a, b = constants

A = flow area of conduit

A_c = area under curve

$$B = \frac{667f_g^2 \bar{T}^2}{d_i^5 p_{pc}^2} \text{ (see Eq. 33)}$$

C_1 = bubble-rise coefficient

C_2 = coefficient, function of liquid velocity

d_{ci} = inside diameter of casing

d_{eq} = diameter of an equivalent circular pipe

d_H = hydraulic pipe diameter

d_{ti} = ID of tubing

d_{to} = OD of tubing

ΔD_i = the i th depth increment

D_s = D under static conditions (static equivalent depth for pressures encountered at flowing conditions)

E_f = irreversible energy losses

f = friction factor (Fig. 34.2)

f_f = Fanning friction factor

$$F = F_r q_g = \frac{0.10797 q_g}{d_i^{2.612}} \text{ (see Eq. 38)}$$

F_{Da} = non-Darcy flow term

$$F_r = \frac{E}{q_g} \text{ (see Eq. 38)}$$

F_1 = function of Reynolds number

F_2 = function of Reynolds number and relative roughness

g_c = conversion factor of 32.174

$$I = \frac{p/(Tz)}{F^2 + 0.001[p/(Tz)]^2} \text{ (see Eqs. 40-43)}$$

J^* = stabilized PI at zero drawdown

J' = stabilized PI

J_f^* = stabilized PI at zero drawdown, from future flow data

J_p^* = stabilized PI at zero drawdown, from present flow data

J_t^* = a transient form of the flow coefficient

L = length of the pipe string (subscripts B , M , and S indicate bubble, mist, and slug flow)

L = flow regime boundary, dimensionless

n = exponent, usually determined from multipoint or isochronal backpressure test

N_{Re_b} = bubble Reynolds number

p_b = bubblepoint pressure

p_{bh} = BHP

p_e = reservoir pressure at the external boundary

Δp_i = pressure drop for increment i

$$p_m = p_1 + \frac{p_1 + p_2}{p_2}$$

p_{tf} = tubing flowing pressure

p_{th} = tophole pressure

p_1 = surface pressure

p_2 = bottomhole pressure at depth D

q_{of} = future oil rate

$q_{o(max)}$ = maximum producing rate at $p_{wf}=0$

Q = heat absorbed by system from surroundings

r_H = hydraulic radius

R_{gL} = gas-liquid ratio

s = skin effect, dimensionless

s = exponent of

$$e = \frac{0.0375 \gamma_g L}{\bar{T} \bar{z}} \quad (\text{see Eq. 44})$$

S = choke size in $\frac{1}{64}$ in.

T_{LM} = log mean temperature

T_1, T_2 = respectively, bottomhole and wellhead temperatures

U = internal energy

v_b = slip or bubble rise velocity

v_{gc} = gas velocity for condensate

v_{gD} = dimensionless gas velocity

v_{gs} = superficial gas velocity

v_{gw} = gas velocity for water

v_{Ls} = superficial liquid velocity

v_t = terminal velocity of free-falling particle

v_t = total fluid velocity (q_t/A)

w_t = total mass flow rate

z = compressibility factor or gas deviation factor

Z = difference in elevation

$(\gamma_g)_{sp}$ = separator gas gravity (air=1)

γ_L = specific gravity of condensate

δ = liquid distribution coefficient

ϵ = absolute roughness

σ = liquid surface tension

τ_f = friction loss gradient

Metric Conversion for Key Equations

Eq. 21

Customary.

$$\int_{0.2}^{(p_{pr})_1} \frac{z}{p_{pr}} dp_{pr} = \frac{L \gamma_g}{53.241 \bar{T}} + \int_{0.2}^{(p_{pr})_2} \frac{z}{p_{pr}} dp_{pr}.$$

SI.

$$\int_{0.2}^{(p_{pr})_1} \frac{z}{p_{pr}} dp_{pr} = \frac{L \gamma_g}{29.27 \bar{T}} + \int_{0.2}^{(p_{pr})_2} \frac{z}{p_{pr}} dp_{pr},$$

where

p = kPa,

L = m, and

T = °K.

Eq. 28

Customary.

$$p_i = p_2 e^{0.01877 \gamma_g L / (\bar{T} \bar{z})}.$$

SI.

$$p_1 = p_2 e^{0.0342 \gamma_g L / (\bar{T} \bar{z})},$$

where

p = kPa,

L = m, and

T = °K.

Eq. 35

Customary.

$$\int_{0.2}^{(p_{pr})_1} \frac{\left(\frac{z}{p_{pr}}\right) dp_{pr}}{1 + B \left(\frac{z}{p_{pr}}\right)^2} = \int_{0.2}^{(p_{pr})_2} \frac{\left(\frac{z}{p_{pr}}\right) dp_{pr}}{1 + B \left(\frac{z}{p_{pr}}\right)^2}$$

$$= \frac{0.01877 \gamma_g L}{\bar{T}}.$$

SI.

$$\int_{0.2}^{(p_{pr})_1} \frac{\left(\frac{z}{p_{pr}}\right) dp_{pr}}{1 + B \left(\frac{z}{p_{pr}}\right)^2} = \int_{0.2}^{(p_{pr})_2} \frac{\left(\frac{z}{p_{pr}}\right) dp_{pr}}{1 + B \left(\frac{z}{p_{pr}}\right)^2}$$

$$= \frac{0.0342 \gamma_g L}{\bar{T}}.$$

$$B = \frac{1.354 f q_g^2 \bar{T}^2}{d^5 p_{pc}^2},$$

where

q_g = 10^6 m³/d,

T = °K,

d = m, and

p_{pc} = kPa.

Eq. 36***Customary.**

$$18.75\gamma_g L = \int_{p_2}^{p_1} \frac{[p/(Tz)]dp}{F^2 + 0.001[p/(Tz)]^2}$$

SI.

$$34.4704\gamma_g L = \int_{p_2}^{p_1} \frac{[p/(Tz)]dp}{F^2 + 0.001[p/(Tz)]^2}$$

Eq. 37***Customary.**

$$F^2 = (2.6665f_f q_g^2)/d_i^5$$

SI.

$$F^2 = (0.0054150f_f q_g^2)/d_i^5,$$

where

 f_f = Fanning friction factor, dimensionless,** q_g = 10^6 m³/d, T = °K, p = kPa, d_i = m, and L = m.**Eq. 44****Customary.**

$$p_{bh}^2 - e^s p_{th}^2 = \frac{25f q_g^2 T^2 \bar{z}^2 (e^s - 1)}{0.0375 d_i^5}$$

SI.

$$p_{bh}^2 - e^s p_{th}^2 = \frac{1.354f q_g^2 T^2 \bar{z}^2 (e^s - 1)}{d_i^5},$$

where

 p = kPa, q_g = 10^6 m³/d, f = from Fig. 34.2, T = °K, d = m, $s = \frac{0.0683\gamma_g L}{Tz}$, and L = m.

*In using SI units, Table 34.4 and Eqs. 38 and 39 are not applicable.

** f_f is the Fanning friction factor equal to $f_t/4$, where f_t is the Moody friction factor from Fig. 34.2.**Eq. 56****Customary.**

$$p_2 = p_1 + \frac{D\rho}{144}$$

SI.

$$p_2 = p_1 + 9.8 \times 10^{-3} D\rho,$$

where

 p = kPa, D = m, and ρ = kg/m³.**Eq. 65****Customary.**

$$J^* = \frac{7.08kh}{\left[\ln\left(\frac{r_e}{r_w}\right) - \frac{3}{4} + s\right]} \cdot \frac{k_{ro}}{(\mu_o B_o) p_R}$$

SI.

$$J^* = \frac{0.0005427kh}{\left(\ln\frac{r_e}{r_w} - \frac{3}{4} + s\right)} \cdot \frac{k_{ro}}{(\mu_o B_o) p_R},$$

where

 J^* = m³/d-kPa, h = m, and μ_o = Pa·s.**Eq. 66****Customary.**

$$J_{(i)}^* = \frac{7.08kh}{\left(\ln\sqrt{\frac{14.23kt}{\phi\mu c_t r_w^2}} + s\right)} \left[\left(\frac{k_{ro}}{\mu_o B_o}\right)_{p_R}\right]$$

SI.

$$J_{(i)}^{**} = \frac{0.0005427kh}{\left(\ln\sqrt{\frac{0.009115kt}{\phi\mu c_t r_w^2}} + s\right)} \left[\left(\frac{k_{ro}}{\mu_o B_o}\right)_{p_R}\right],$$

where

 h = m, t = d, μ = Pa·s, c_t = 1/kPa, and r_w = m.

Eq. 87**Customary.**

$$-dp = \frac{\tau_f dD}{144} + \frac{g\rho}{144g_c} dD + \frac{gv}{144g_c} dv.$$

SI.

$$-dp = \tau_f dD + \frac{1000g\rho}{g_c} dD + \frac{1000\rho v}{g_c} dv,$$

where

$$\begin{aligned} p &= \text{kPa}, \\ \tau_f &= \text{kPa/m}, \\ D &= \text{m}, \\ \rho &= \text{g/cm}^3, \\ g &= 9.80 \text{ m/s}^2, \\ g_c &= 1000 \text{ kg/m} \cdot \text{kPa} \cdot \text{s}^2, \text{ and} \\ v &= \text{m/s}. \end{aligned}$$

Eq. 89**Customary.**

$$\Delta p_i = \frac{1}{144} \frac{\rho + \tau_f}{1 - \frac{w_i q_g}{4637 A^2 p}} \Delta D_i.$$

SI.

$$\Delta p_i = \frac{9.806\rho + \tau_f}{1 - \frac{w_i q_g}{1000 A^2 p}} \Delta D_i,$$

where

$$\begin{aligned} w_i &= \text{kg/s}, \\ q_g &= \text{m}^3/\text{s}, \text{ and} \\ A &= \text{m}^2. \end{aligned}$$

Eq. 90**Customary.**

$$v_{gD} = \frac{q_g}{A} \left(\frac{\rho_L}{g\sigma} \right)^{0.25}$$

SI.

$$v_{gD} = \frac{q_g}{A} \left(\frac{10^6 \rho_L}{g\sigma} \right)^{0.25},$$

where

$$\begin{aligned} q_g &= \text{m}^3/\text{s}, \\ A &= \text{m}^2, \\ \rho_L &= \text{g/cm}^3, \\ g &= 9.8 \text{ m/s}^2, \text{ and} \\ \sigma &= \text{g/s}^2. \end{aligned}$$

Eq. 91**Customary.**

$$L_B = 1.071 - \frac{0.2218 v_t^2}{d_H}.$$

SI.

$$L_B = 1.071 - \frac{0.7277 v_t^2}{d_H},$$

where

$$\begin{aligned} v_t &= \text{m/s and} \\ d_H &= \text{m}. \end{aligned}$$

Eq. 98**Customary.**

$$N_{\text{Re}} = \frac{1,488 \rho_L d_H v_L}{\mu_L}.$$

SI.

$$N_{\text{Re}} = \frac{1000 \rho_L d_H v_L}{\mu_L},$$

where

$$\begin{aligned} \rho_L &= \text{g/m}^3, \\ d_H &= \text{m}, \\ v_L &= \text{m/s}, \text{ and} \\ \mu_L &= \text{Pa} \cdot \text{s}. \end{aligned}$$

Eq. 101**Customary.**

$$N_{\text{Re}} = \frac{1,488 \rho_L d_H v_b}{\mu_L}$$

SI.

$$N_{\text{Re}} = \frac{1000 \rho_L d_H v_b}{\mu_L}.$$

Eq. 102**Customary.**

$$N_{\text{Re}} = \frac{1,488 \rho_L d_H v_t}{\mu_L}.$$

SI.

$$N_{\text{Re}} = \frac{1000 \rho_L d_H v_t}{\mu_L}.$$

Eq. 117**Customary.**

$$N_{Re} = \frac{1,488 \rho_g d_H v_{gs}}{\mu_g}.$$

SI.

$$N_{Re} = \frac{1000 \rho_g d_H v_{gs}}{\mu_g}.$$

Eq. 118**Customary.**

$$N = 4.52(10^{-7}) \left(\frac{v_{gs} \mu_L}{\sigma} \right)^2 \left(\frac{\rho_g}{\rho_L} \right).$$

SI.

$$N = 10^6 \left(\frac{v_{gs} \mu_L}{\sigma} \right)^2 \left(\frac{\rho_g}{\rho_L} \right),$$

where

$$\begin{aligned} v_{gs} &= \text{m/s}, \\ \mu_L &= \text{Pa} \cdot \text{s}, \text{ and} \\ \sigma &= \text{g/s}^2. \end{aligned}$$

Eq. 119**Customary.**

$$\frac{\epsilon}{d_H} = \frac{34\sigma}{\rho_g v_{gs}^2 d_H}.$$

SI.

$$\frac{\epsilon}{d_H} = \frac{1.115(10^{-4})\sigma}{\rho_g v_{gs}^2 d_H},$$

where

$$\begin{aligned} \sigma &= \text{g/s}^2, \\ v_{gs} &= \text{m/s}, \text{ and} \\ \rho_g &= \text{g/cm}^3. \end{aligned}$$

Eq. 120**Customary.**

$$\frac{\epsilon}{d_H} = \frac{174.8\sigma(N)^{0.302}}{\rho_g v_{gs}^2 d_H}.$$

SI.

$$\frac{\epsilon}{d_H} = \frac{5.735(10^{-4})\sigma(N)^{0.302}}{\rho_g v_{gs}^2 d_H},$$

where

$$\begin{aligned} \sigma &= \text{g/s}^2, \\ v_{gs} &= \text{m/s}, \text{ and} \\ \rho_g &= \text{g/cm}^3. \end{aligned}$$

Eq. 121**Customary.**

$$q_g = \frac{Cp}{\sqrt{\gamma_g T}}.$$

SI.

$$q_g = \frac{3.0169 Cp}{\sqrt{\gamma_g T}},$$

where

$$\begin{aligned} q_g &= \text{m}^3/\text{d}, \\ T &= {}^\circ\text{K}, \text{ and} \\ p &= \text{kPa}. \end{aligned}$$

Eq. 122**Customary.**

$$p_{if} = \frac{435 R_{gL}^{0.546} q_t}{S^{1.89}}.$$

SI.

$$p_{if} = \frac{2.50 R_{gL}^{0.546} q_t}{S^{1.89}},$$

where

$$\begin{aligned} p_{if} &= \text{kPa}, \\ R_{gL} &= \text{m}^3/\text{m}^3, \\ q_t &= \text{m}^3/\text{d}, \text{ and} \\ S &= \text{cm}. \end{aligned}$$

Eq. 125**Customary.**

$$v_{gw} = \frac{5.62(67 - 0.0031p)^{0.25}}{(0.0031p)^{0.5}}.$$

SI.

$$v_{gw} = \frac{1.713(67 - 0.00045p)^{0.25}}{(0.00045p)^{0.5}}.$$

Eq. 126**Customary.**

$$v_{gc} = \frac{4.02(45 - 0.0031p)^{0.25}}{(0.0031p)^{0.5}}.$$

SI.

$$v_{gc} = \frac{1.225(45 - 0.00045p)^{0.25}}{(0.00045p)^{0.5}},$$

where

$$p = \text{kPa and}$$

$$v_g = \text{m/s.}$$

Eq. 127

Customary.

$$q_g = \frac{3.06pv_gA}{T_z}.$$

SI.

$$q_g = \frac{0.24628pv_gA}{T_z},$$

where

$$p = \text{kPa,}$$

$$v_g = \text{m/s,}$$

$$A = \text{m}^2,$$

$$T = \text{°K, and}$$

$$q_g = 10^6 \text{ m}^3/\text{d.}$$

*Based on standard conditions of 520°R and 14.7 psia.

References

1. Brown, G.G. *et al.*: *Unit Operations*, John Wiley & Sons Inc., New York City (1950).
2. Moody, L.F.: "Friction Factors for Pipe Flow," *Trans., ASME* (1944) **66**, 671.
3. Fowler, F.C.: "Calculations of Bottom Hole Pressures," *Pet. Eng.* (1947) **19**, No. 3, 88.
4. Poettmann, F.H.: "The Calculation of Pressure Drop in the Flow of Natural Gas Through Pipe," *Trans., AIME* (1951) **192**, 317-24.
5. Rzasas, M.J. and Katz, D.L.: "Calculation of Static Pressure Gradients in Gas Wells," *Trans., AIME* (1945) **160**, 100-06.
6. Sukkar, Y.K. and Cornell, D.: "Direct Calculation of Bottom Hole Pressures in Natural Gas Wells," *Trans., AIME* (1955) **204**, 43-48.
7. Cullender, M.A. and Smith, R.V.: "Practical Solution of Gas-Flow Equations for Wells and Pipelines with Large Temperature Gradients," *J. Pet. Tech.* (Dec. 1956) 281-87; *Trans., AIME*, **207**.
8. Messer, P.H., Raghaven, R., and Ramey, H. Jr.: "Calculation of Bottom-Hole Pressures for Deep, Hot, Sour Gas Wells," *J. Pet. Tech.* (Jan. 1974) 85-94.
9. *Theory and Practice of the Testing of Gas Wells*, third edition, Energy Resources and Conservation Board, Calgary, Alberta, Canada (1978).
10. Smith, R.V.: "Determining Friction Factors for Measuring Productivity of Gas Wells," *Trans., AIME* (1950) **189**, 73.
11. Cullender, M.H. and Binckley, C.W.: Phillips Petroleum Co. Report presented to the Railroad Commission of Texas Hearing, Amarillo (Nov. 9, 1950).
12. *Back Pressure Test for Natural Gas Wells*, Railroad Commission of Texas, State of Texas.
13. Nisley, R.G. and Poettmann, F.H.: "Calculation of the Flow and Storage of Natural Gas in Pipe," *Pet. Eng.* (1955) **27**, No. 1, D-14; No. 2, C-36; No. 3, D-37.
14. Evinger, H.H. and Muskat, M.: "Calculation of Theoretical Productivity Factor," *Trans., AIME* (1942) **146**, 126.
15. Vogel, J.V.: "Inflow Performance Relationships for Solution-Gas Drive Wells," *J. Pet. Tech.* (Jan. 1968) 83-92.
16. Fetkovich, M.J.: "The Isochronal Testing of Oil Wells," *Pressure Transient Testing Methods*, Reprint Series, SPE, Richardson (1980).
17. Standing, M.B.: "Concerning the Calculation of Inflow Performance of Wells Producing From Solution Gas Drive Reservoirs," *J. Pet. Tech.* (Sept. 1971) 1141-50.
18. Duns, H. Jr. and Ros, N.C.J.: "Vertical Flow of Gas and Liquid Mixtures from Boreholes," *Proc., Sixth World Pet. Congress*, Frankfurt (June 19-26, 1963) Section II, Paper 22-106.
19. Griffith, P. and Wallis, G.B.: "Two-Phase Slug Flow," *J. Heat Transfer* (Aug. 1961) 307-20, *Trans., ASME*.
20. Nicklin, D.J., Wilkes, J.O., and Davidson, J.F.: "Two-Phase Flow in Vertical Tubes," *Trans., AIChE* (1962) **40**, 61-68.
21. Baxendell, P.B. and Thomas, R.: "The Calculation of Pressure Gradients in High-Rate Flowing Wells," *J. Pet. Tech.* (Oct. 1961) 1023-28.
22. Fancher, G.H. Jr. and Brown, K.E.: "Prediction of Pressure Gradients for Multiphase Flow in Tubing," *Soc. Pet. Eng. J.* (March 1963) 59-69.
23. Hagedorn, A.R. and Brown, K.E.: "The Effect of Liquid Viscosity on Two-Phase Flow," *J. Pet. Tech.* (Feb. 1964) 203-10.
24. Hagedorn, A.R. and Brown, K.E.: "Experimental Study of Pressure Gradients Occurring During Continuous Two-Phase Flow in Small Diameter Vertical Conduits," *J. Pet. Tech.* (April 1965) 475-84.
25. Orkiszewski, J.: "Predicting Two-Phase Pressure Drops in Vertical Pipe," *J. Pet. Tech.* (June 1967) 829-38; *Trans., AIME*, **240**.
26. Beggs, H.D. and Brill, J.P.: "A Study of Two-Phase Flow in Inclined Pipes," *J. Pet. Tech.* (May 1973) 607-17; *Trans., AIME*, **255**.
27. Gould, T.L., Tek, M.R., and Katz, D.L.: "Two-Phase Flow Through Vertical, Inclined, or Curved Pipe," *J. Pet. Tech.* (Aug. 1974) 915-26; *Trans., AIME*, **257**.
28. Brown, K.E.: *The Technology of Artificial Lift Methods*, Petroleum Publishing Co., Tulsa (1977).
29. Chierici, G.L., Ciucci, G.M., and Selocchi, G.: "Two-Phase Vertical Flow in Oil Fields—Prediction of Pressure Drop," *J. Pet. Tech.* (Aug. 1974) 927-38; *Trans., AIME*, **257**.
30. Espanol, J.H., Holmes, C.S., and Brown, K.E.: "A Comparison of Existing Multiphase Flow Methods for the Calculation of Pressure Drop in Vertical Wells," *Artificial Lift*, Reprint Series, SPE, Richardson (1975).
31. Camacho, C.A.: "A Comparison of Correlations for Predicting Pressure Losses in High Gas-Liquid Ratio Vertical Wells," M.S. thesis, U. of Tulsa (1970).
32. Lawson, J.D. and Brill, J.P.: "A Statistical Evaluation of Methods Used to Predict Pressure Losses for Multiphase Flow in Vertical Oil Well Tubing," *J. Pet. Tech.* (Aug. 1974) 903-13; *Trans., AIME*, **257**.
33. Poettmann, F.H. and Carpenter, P.G.: "Multiphase Flow of Gas, Oil, and Water Through Vertical Flow Strings with Application to the Design of Gas-Lift Installations," *Drill. and Prod. Prac.*, API, Dallas (1952) 257-317.
34. Baxendell, P.B.: "Producing Wells on Casing Flow—An Analysis of Flowing Pressure Gradients," *Trans., AIME* (1958) **213**, 202-06.
35. Lockhart, R.W. and Martinelli, R.C.: "Proposed Correlation of Data for Isothermal Two-Phase, Two-Component Flow in Pipes," *Chem. Eng. Progress* (Jan. 1949) 39-48.
36. Dumitrescu, D.T.: "Strömung an einer Luftblase in senkrechtem Rohr," *Zamm* (1943) **23**, No. 3, 139-49.
37. Pittman, R.W.: "Gas Lift Design and Performance," paper SPE 9981 presented at the 1982 SPE Technical Conference and Exhibition, Beijing, China, March 18-26.
38. Davis, G.J. and Weidner, C.R.: "Investigation of the Air Lift Pump," *Bull., Eng. Series*, U. Wisconsin (1911) **6**, No. 7.
39. Gosline, J.E.: "Experiments on the Vertical Flow of Gas-Liquid Mixtures in Glass Pipe," *Trans., AIME* (1936) **118**, 56-70.
40. Shaw, S.F.: "Flow Characteristics of Gas Lift in Oil Production," *Bull., Texas A&M U.* (1947) 113.
41. Babson, E.C.: "Range of Application of Gas Lift Methods," *Drill. and Prod. Prac.*, API, Dallas (1939) 266.
42. Benham, A.L. and Poettmann, F.H.: "Gas Lifting Through the Annulus of a Well," *Pet. Eng.* (July 1959) B25-B30.
43. Bertuzzi, A.F., Welch, J.K., and Poettmann, F.H.: "Description and Analysis of an Efficient Continuous-Flow Gas-Lift Installation," *J. Pet. Tech.* (Nov. 1953) 271-78; *Trans., AIME*, **198**.
44. Rawlins, E.L. and Schellhardt, M.A.: *Back-Pressure Data on Natural Gas Wells and Their Application to Production Practices*, Monograph Series, U.S. Bureau of Mines (1936) 7.

45. Gilbert, W.E.: "Flowing and Gas Lift Well Performance," *Drill. and Prod. Prac.*, API, Dallas (1954).
46. Ros, N.C.J.: "An Analysis of Critical Simultaneous Gas-Liquid Flow Through a Restriction and its Application to Flow Metering," *Appl. Sci. Res.* (1960) **9**, 374.
47. Ros, N.C.J.: "Letter to Editor Flow Meter Formula for Critical Gas-Liquid Flow Through a Restriction," *Appl. Sci. Res.* (1961) A-10, 295.
48. Poettmann, F.H. and Beck, R.L.: "New Charts Developed to Predict Gas-Liquid Flow Through Chokes," *World Oil* (March 1963) 95-101.
49. Duggan, J.O.: "Estimating Flow Rates Required to Keep Gas Wells Unloaded," *J. Pet. Tech.* (Dec. 1961) 1173-76.
50. Libson, T.N. and Henry, J.R.: "Case Histories: Identification of and Remedial Action for Liquid Loading in Gas Wells—Intermediate Shelf Gas Play," *J. Pet. Tech.* (April 1980) 685-93.
51. Smith, R.V.: *Practical Natural Gas Engineering*, PennWell Publishing Co., Tulsa (1983) **205**.
52. Turner, R.G., Hubbard, M.G., and Dukler, A.E.: "Analysis and Prediction of Minimum Flow Rate for the Continuous Removal of Liquids from Gas Wells," *J. Pet. Tech.* (Nov. 1969) 1475-80; *Trans.*, AIME, **246**.
53. Tek, M.R., Gould, T.L., and Katz, D.L.: "Steady and Unsteady-State Lifting Performance of Gas Wells Unloading Produced or Accumulated Liquids," paper SPE 2552 presented at the 1969 SPE Annual Fall Meeting, Denver, Sept. 28-Oct. 1.

Chapter 35

Well Performance Equations

R.A. Wattenbarger, Texas A&M U.*

Introduction

This chapter summarizes the equations that apply to the performance of a well in a reservoir. The equations are used to calculate the relationship between rate and pressure of a well and the properties of the fluids and formation. These equations apply only in the "drainage area" of the well and do not describe the entire reservoir performance, except for the case of a single-well depletion reservoir. For more complete treatment of the entire reservoir performance, refer to Chap. 37—Solution-Gas-Drive Oil Reservoirs, Chap. 38—Waterdrive Oil Reservoirs, or Chap. 39—Gas Condensate Reservoirs.

There have been several excellent references developed over the past few years on well pressure behavior.¹⁻⁷ These are much more detailed than this chapter and the reader should be aware of them. This chapter is a brief summary of this technology.

Diffusivity Equation

The equations that relate pressure and rates for a well are solutions of the diffusivity equation. This equation can be written as

$$\nabla^2 p = \frac{1}{0.000264} \frac{\phi \mu c_t}{k} \frac{\partial p}{\partial t}, \quad \dots \dots \dots (1)$$

where

- p = pressure, psi,
- ϕ = porosity of reservoir rock, fraction,
- μ = fluid viscosity, cp,
- c_t = total compressibility of system (see Eq. 5),
psi⁻¹,
- k = permeability of reservoir rock, md, and
- t = time, hours.

The vector notation used on the left side of the equation has the following meaning. In one dimension (1D),

$$\frac{\partial^2 p}{\partial x^2} = \frac{1}{0.000264} \frac{\phi \mu c_t}{k} \frac{\partial p}{\partial t}, \quad \dots \dots \dots (2a)$$

where x is the distance coordinate in a one-dimensional flow system, ft. In two dimensions (2D),

$$\frac{\partial^2 p}{\partial x^2} + \frac{\partial^2 p}{\partial y^2} = \frac{1}{0.000264} \frac{\phi \mu c_t}{k} \frac{\partial p}{\partial t}, \quad \dots \dots \dots (2b)$$

where x and y are distance coordinates in a 2D flow system, ft. In radial coordinates,

$$\frac{\partial^2 p}{\partial r^2} + \frac{1}{r} \frac{\partial p}{\partial r} = \frac{1}{0.000264} \frac{\phi \mu c_t}{k} \frac{\partial p}{\partial t}, \quad \dots \dots \dots (2c)$$

where r is the radius in radial flow system, ft.

Eq. 2c gives the most useful solution of the diffusivity equation for reservoir and well performance.

The geometry of the reservoir is in cylindrical coordinates with an inner radius, r_w , into which the fluid flows at a constant rate and an outer boundary, r_e , which is closed and represents the outer boundary of the reservoir. The solutions of this cylindrical coordinate problem have been presented by van Everdingen and Hurst⁸ and are presented again in Chap. 38.

Eq. 1 is a linear partial differential equation that models how pressure changes with location and time. Theoretically, solutions of Eq. 1 are valid only for reservoirs where the fluid and rock properties are constant. The application of the solutions of Eq. 1, then, are literally applicable for fluids with constant compressibility and

* Author of the original chapter on this topic in the 1962 edition was Ralph F. Neilsen.

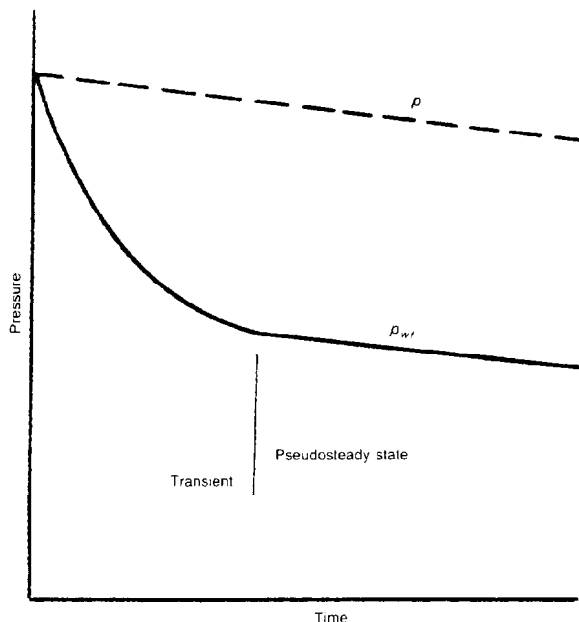


Fig. 35.1—Pressure behavior for constant rate in a closed reservoir.

viscosity and for formations with constant permeability. These conditions are very nearly met in the case of aquifer flow or for oil reservoir flow at pressures above the bubblepoint. The solutions of Eqs. 1 and 2 can be extended to multiphase reservoir flow for most practical cases.

Multiphase Flow

When more than one phase exists in the reservoir, it is still possible to write the differential equation in a form similar to Eq. 1. This equation was presented by Martin⁹ as

$$\nabla \left(\frac{k}{\mu} \right) \nabla p = \frac{1}{0.000264} \phi c_t \frac{\partial p}{\partial t} \quad (3)$$

This equation shows that the conditions of homogeneity are not necessarily met. The concepts of total mobility, $(k/\mu)_t$, and total compressibility, c_t , are introduced.

The total mobility is the sum of the individual phase mobility as follows.

$$\left(\frac{k}{\mu} \right)_t = \frac{k_o}{\mu_o} + \frac{k_g}{\mu_g} + \frac{k_w}{\mu_w} \quad (4)$$

TABLE 35.1—ANALOGIES OF SINGLE-PHASE VALUE TO MULTIPHASE EQUIVALENT

Single-Phase Value	Multiphase Equivalent
k/μ	$(k/\mu)_t$
c	c_t
qB	$q_t B_t$

where

- k_o = effective permeability to oil, md,
- k_g = effective permeability to gas, md,
- k_w = effective permeability to water, md,
- μ_o = oil viscosity, cp,
- μ_g = gas viscosity, cp, and
- μ_w = water viscosity, cp.

The total compressibility is the volumetrically weighted average of the compressibilities of the fluids and pore space as follows.

$$c_t = c_f + S_o c_o + S_g c_g + S_w c_w \quad (5)$$

where

- c_f = formation compressibility, psi^{-1} ,
- S_o = oil saturation, fraction of pore volume (PV),
- c_o = oil compressibility, psi^{-1} ,
- S_g = gas saturation, fraction of PV,
- c_g = gas compressibility, psi^{-1} ,
- S_w = water saturation, fraction of PV, and
- c_w = water compressibility, psi^{-1} .

The flow rate also must be expressed in terms of the equivalent total flow rate for multiphase flow. The expression for total reservoir flow rate is

$$q_t B_t = q_o B_o + (1,000 q_g - R_s q_o) B_g / 5.615 + q_w B_w \quad (6)$$

where

- q_t = total reservoir flow rate, STB/D,
- B_t = total formation volume factor, RB/STB,
- q_o = oil flow rate, STB/D,
- B_o = oil formation volume factor, RB/STB,
- q_g = gas flow rate, Mscf/D,
- R_s = solution gas-oil ratio, scf/STB,
- B_g = gas formation volume factor, res cu ft/scf
- q_w = water flow rate, STB/D, and
- B_w = water formation volume factor, RB/STB.

Martin's equation is a nonlinear partial differential equation. Therefore the general case does not have analytical solutions. However, for practical purposes, Eqs. 3 through 6 can be used for most well performance equations if the meaning of the mobility, compressibility, and flow rate are taken in this general three-phase sense. The single-phase solutions of Eq. 1 can be applied to the multiphase case by using the analogies given in Table 35.1.

Oil Well Performance

Well Pressure Performance—Closed Reservoir

The performance of a constant-rate well in a closed reservoir (of any geometry or heterogeneity) has the general form shown in Fig. 35.1.

The lower curve of Fig. 35.1 shows that the wellbore flowing pressure, p_{wf} , goes through a rapid pressure drop

at early (transient) times and then flattens out until it reaches a constant slope. On this coordinate plot, the closed-reservoir, constant-rate case has the properties

$$\frac{\partial p_{wf}}{\partial t} < 0$$

and

$$\frac{\partial^2 p_{wf}}{\partial t^2} \geq 0.$$

When p_{wf} reaches a straight line on the coordinate plot, the period of *pseudosteady state* has been reached. Every pressure point in the reservoir declines at the same constant rate of depletion after that time. Of particular importance is the decline of the average reservoir pressure, \bar{p}_R , which assumes the pseudosteady-state depletion rate from the very beginning of production.

The constant slope of Fig. 35.1 is valid only for constant-compressibility single-phase fluid. However, the general concept of the transient period and the pseudosteady-state period is the same for a multiphase flow with changing compressibilities. The \bar{p}_R slope would be changing according to the changes in compressibility, and the \bar{p}_R curve after a pseudosteady-state would not be exactly parallel to the p_{wf} curve. This nonideal behavior would be typical of a solution gas drive reservoir or a dry gas reservoir where the compressibility and mobilities are continually changing. The infinite-acting solutions and the pseudosteady-state solutions to follow are still ap-

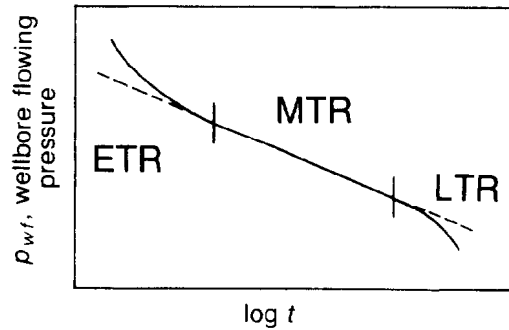


Fig. 35.2—Typical constant-rate drawdown test graph.

plicable for the multiphase flow case by using the analogies in Table 35.1. The value of \bar{p}_R , however, must be calculated by the material balance method that applies for this case.

Infinite-Acting Solution (MTR)

The pressure behavior of constant-rate flow in a closed reservoir goes through several periods: the early-time region (ETR), middle-time region (MTR), and late-time region (LTR). These periods are illustrated on a semilog plot of p_{wf} vs. $\log t$ in Fig. 35.2. The MTR solution is discussed first.

Eq. 1 can be solved for the infinite-reservoir case, which is useful for application at early times. The solution applies to a well producing at constant rate, beginning at $t=0$, and a homogeneous reservoir of constant thickness.

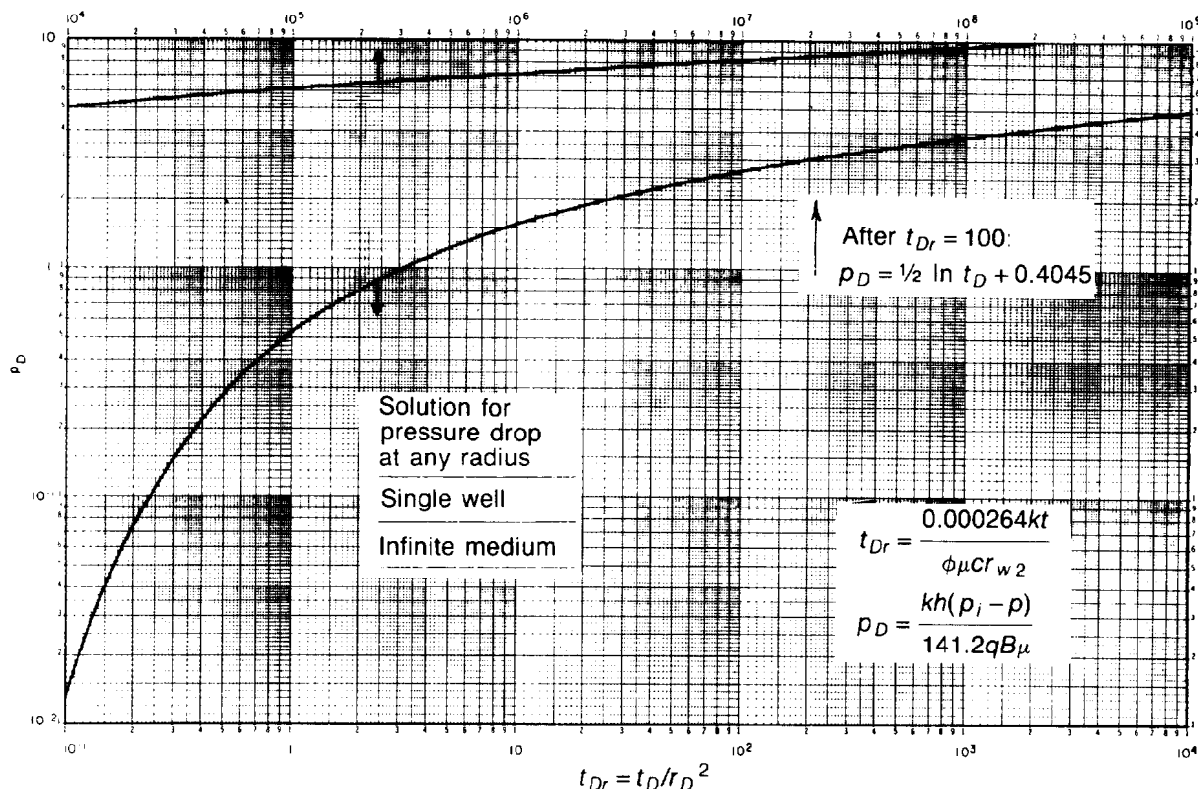


Fig. 35.3—Dimensionless pressure for a single well in an infinite system, no wellbore storage, no skin. Exponential-integral solution.

There are two important solutions for the infinite-reservoir case. One solution⁸ assumes that the wellbore has a finite radius, r_w . This solution is used mostly for aquifer behavior with the oil field being the inner radius rather than a wellbore. This solution is given in Chap. 38 for the infinite-aquifer case.

A simpler solution applies for well behavior. This solution, called the "line-source" or "exponential-integral" solution, assumes that the wellbore radius, r_w , approaches zero. This solution has the form

$$p_D(r_D, t_D) = -\frac{1}{2} Ei\left(\frac{-r_D^2}{4t_D}\right), \quad \dots\dots\dots (7)$$

where

$$\begin{aligned} p_D &= kh(p_i - p)/(141.2 qB\mu) = \text{dimensionless pressure,} \\ r_D &= r/r_w = \text{dimensionless radius,} \\ t_D &= (0.000264kt)/\phi\mu c_i r_w^2 = \text{dimensionless time,} \\ h &= \text{formation thickness, ft,} \\ p_i &= \text{initial pressure, psi, and} \\ r_w &= \text{wellbore radius, ft.} \end{aligned}$$

The exponential-integral function, Ei , is a special function that results from the solution of the line-source problem. A more practical solution to the problem is the plot of the dimensionless p_D vs. t_D/r_D^2 , which is shown in Fig. 35.3. The t_D term is the dimensionless time based on external radius, r_e . Fig. 35.3 can be used to determine the pressure at any time and radius from the producing well. This solution is valid as long as the radius at which the pressure is calculated is greater than $20 r_w$ or at the wellbore of the producing well (at r_w) at a value of $t_D/r_D^2 > 10$.

Fig. 35.3 is used mostly to determine the pressure at distances away from the well such as at a nearby well location during an interference test.

The more common solution of the exponential integral solution is the "semilog straight line solution," which applies after t_D is greater than 100. After this time, Eq. 8 applies at the wellbore:

$$p_D = \frac{1}{2} \ln t_D + 0.4045. \quad \dots\dots\dots (8)$$

In customary oilfield units, this equation has the form

$$p_{wf} = p_i - m \left(\log \frac{kt}{\phi\mu c_i r_w^2} - 3.23 \right), \quad \dots\dots\dots (9)$$

where m equals $(162.6qB\mu)/kh$ and p_{wf} is the flowing bottomhole pressure, psi. This equation results in a semilog plot of p_{wf} vs. $\log t$ with a slope of $-m$ psi/cycle (the MTR of Fig. 35.2.)

Eqs. 7 through 9 are used for infinite-acting solutions before the effects of boundaries affect the pressure transient behavior. When the closest boundary begins affecting the behavior at the wellbore, this time is the end of the semilog straight line, t_{end} . The last column in Table 35.2 shows t_{end} for various drainage shapes (shape factors).

Skin Effect

The solutions to Eq. 1 are modified to account for formation damage near the wellbore. The damage near the wellbore can be considered concentrated into a very thin radius around the wellbore such that the thickness of the damage is insignificant but a finite pressure drop results from this damage.

Fig. 35.4 shows a sketch of the physical concept of the damaged region and Fig. 35.5 shows the pressure profile resulting from this damage.

The magnitude of the pressure drop caused by the skin effect Δp_s is

$$\Delta p_s = 0.87ms, \quad \dots\dots\dots (10)$$

where s is the skin effect, defined in terms of dimensionless pressure such that it would have the following effect on Eq. 8.

$$p_D = \frac{1}{2} \ln t_D + 0.4045 + s. \quad \dots\dots\dots (11)$$

The value of the skin effect is calculated from transient well test data such as a buildup test or a drawdown test. The exact nature of the cause of the skin effect might not be known but might be caused by a combination of several factors. Some of these factors are (1) mud filtrate or mud damage near the wellbore, (2) the cement bond, (3) limited perforations through the casing and cement bond, and (4) partial penetration (completion). On the other hand, the value of the skin effect, s , might be negative. This would indicate an improved wellbore condition, which might be caused by (1) improved permeability in the vicinity of the wellbore because of acidizing or other well treatments, (2) a vertical or horizontal hydraulic fracture at the wellbore, or (3) a wellbore at an angle rather than normal to the bedding plane.

The determination of the skin effect is important in determining the need for a workover or the benefits of a workover. The effect of the skin can be stated as a modification to the wellbore radius by calculating an effective wellbore radius, r'_w , calculated by

$$r'_w = r_w e^{-s}. \quad \dots\dots\dots (12)$$




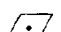






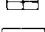
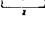
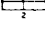
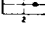
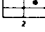

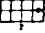
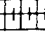
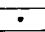
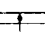
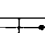
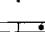

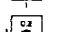
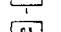
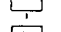

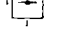


This effective wellbore radius, r'_w , can be considered the equivalent wellbore radius in an undamaged or unimproved formation, which would have the same flow characteristics as the actual well with the skin effect.

Wellbore Storage Effect (ETR)

At very early times the fluid production tends to come from the expansion of the fluid in the wellbore rather than the formation. This tends to delay the production rate from the formation. The relationship between the surface production rate, the expansion of the wellbore fluids, and the formation production rate are shown in Eq. 13:

$$q_{sf} = q + \frac{24C_s}{B} \frac{\partial p}{\partial t}, \quad \dots\dots\dots (13)$$

TABLE 35.2—SHAPE FACTORS FOR VARIOUS CLOSED SINGLE-WELL DRAINAGE AREAS

In Bounded Reservoirs	C_A	$\ln C_A$	$\frac{1}{2} \ln \left(\frac{2.2458}{C_A} \right)$	$(t_{DA})_{DSS}$ Exact For $t_{DA} >$	Less Than 1% Error For $t_{DA} >$	$(t_{DA})_{DSS}$ and Use Infinite System Solution With Less Than 1% Error For $t_{DA} <$
	31.62	3.4538	-1.3224	0.1	0.06	0.10
	31.6	3.4532	-1.3220	0.1	0.06	0.10
	27.6	3.3178	-1.2544	0.2	0.07	0.09
	27.1	3.2995	-1.2452	0.2	0.07	0.09
	21.9	3.0865	-1.1387	0.4	0.12	0.08
	0.098	-2.3227	+1.5659	0.9	0.60	0.015
	30.8828	3.4302	-1.3106	0.1	0.05	0.09
	12.9851	2.5638	-0.8774	0.7	0.25	0.03
	4.5132	1.5070	-0.3490	0.6	0.30	0.025
	3.3351	1.2045	-0.1977	0.7	0.25	0.01
	21.8369	3.0836	-1.1373	0.3	0.15	0.025
	10.8374	2.3830	-0.7870	0.4	0.15	0.025
	4.5141	1.5072	-0.3491	1.5	0.50	0.06
	2.0769	0.7390	+0.0391	1.7	0.50	0.02
	3.1573	1.1497	-0.1703	0.4	0.15	0.005
	0.5813	-0.5425	+0.6758	2.0	0.60	0.02
	0.1109	-2.1991	+1.5041	3.0	0.60	0.005
	5.3790	1.6825	-0.4367	0.8	0.30	0.01
	2.6896	0.9894	-0.0902	0.8	0.30	0.01
	0.2318	-1.4619	+1.1355	4.0	2.00	0.03
	0.1155	-2.1585	+1.4838	4.0	2.00	0.01
	2.3606	0.8589	-0.0249	1.0	0.40	0.025
In Vertically-Fractured Reservoirs*						
	2.6541	0.9761	-0.0835	0.175	0.08	Cannot use
	2.0348	0.7104	+0.0493	0.175	0.09	Cannot use
	1.9986	0.6924	+0.0583	0.175	0.09	Cannot use
	1.6620	0.5080	+0.1505	0.175	0.09	Cannot use
	1.3127	0.2721	+0.2685	0.175	0.09	Cannot use
	0.7887	-0.2374	+0.5232	0.175	0.09	Cannot use
In Waterdrive Reservoirs						
	19.1	2.95	-1.07	—	—	—
In Reservoirs of Unknown Production Character						
	25.0	3.22	-1.20	—	—	—

*Use $(x_e/x_f)^2$ in place of A/r_w^2 for fractured systems.

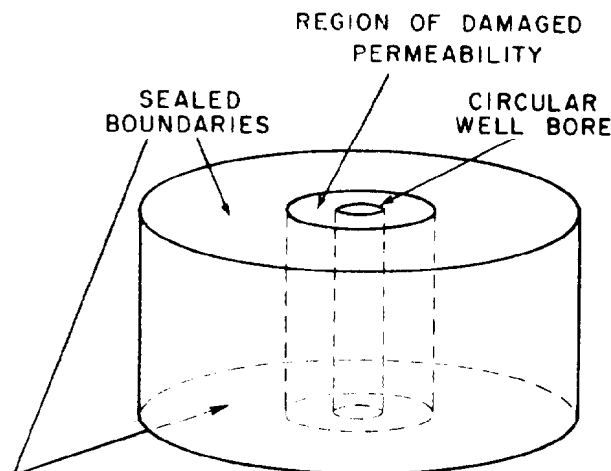


Fig. 35.4—Radial flow model showing damaged zone.

where C_s equals $V_w c_{wf}$ and q_{sf} is the flow rate at the "sandface," STB/D and C_s is the wellbore storage constant, equal to the volume of the wellbore, V_w , times the wellbore fluid compressibility, c_{wf} .

The effect of the wellbore storage is to make the very early transient pressure behave as though it were reflecting production only from the wellbore fluid expansion. This pressure drop can be calculated from

$$p_i - p_{wf} = \frac{qB}{24C_s} t. \quad (14)$$

Note that this shows a linear relationship between Δp and time. Consequently, a p vs. t plot will be linear during the wellbore storage period. Also, a plot of $\log \Delta p$ vs. $\log t$ is a straight line with a slope of unity. This wellbore storage effect may last for just a few seconds or it may last for many hours—i.e., for a deep, low-permeability gas well that has a large storage volume in the wellbore, a high-compressibility gas, and great resistance to flow from the formation.

After a period of time, this wellbore storage solution gives way to the semilog straight line (for the radial flow case). The period between the linear relationship and the semilog straight line is from one to one and one-half cycles of $\log t$. Fig. 35.6 shows that Eq. 12 applies during ETR, then gives way to Eq. 11 during MTR.¹⁰ This log-log dimensionless plot has the same shape as a plot of $\log (p_i - p_{wf})$ vs. $\log t$. This is sometimes called a "type curve."

Pseudosteady-State Behavior (LTR)

After a well produces at constant rate for a period of time, the boundary effects interrupt the infinite-acting pressure behavior. If the well is in an irregularly shaped drainage area, the closest boundary to the well causes the earliest departure from the infinite-acting pressure solution. After a transition period, the well begins pseudosteady-state behavior. The pseudosteady-state behavior begins after the effects of the farthest boundary have been felt at the wellbore.

When pseudosteady-state behavior begins (see Fig. 35.2) the rate of pressure decline, $(\partial p / \partial t)_{pss}$, is constant

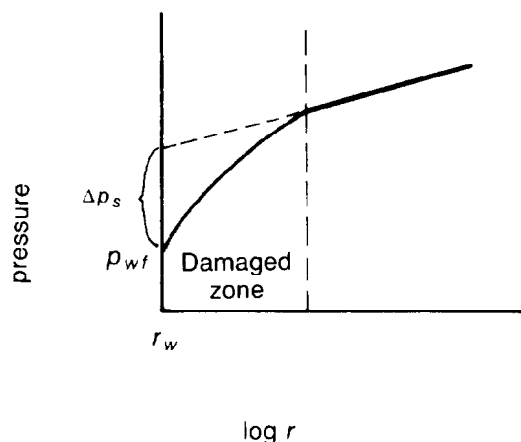


Fig. 35.5—Schematic of pressure distribution near wellbore.

at every point throughout the reservoir. This is a depletion period at which every point of the reservoir drops at a rate according to the pore volume, V_p , and compressibility of the drainage area, c_t .

$$\left(\frac{\partial p}{\partial t} \right)_{pss} = \frac{-0.234qB}{V_p c_t} \quad (15)$$

During pseudosteady-state behavior, wellbore pressure is related to the average reservoir pressure, \bar{p}_R , by a productivity index (PI), J , as follows.

$$q = J(\bar{p}_R - p_{wf}). \quad (16)$$

This PI equation relates the pressure drawdown to the production rate. For a circular drainage area we can write out the complete expression for the PI equation as

$$q = \left[\frac{7.08 \times 10^{-3} kh / (B\mu)}{\ln r_e / r_w - 0.75 + s} \right] (\bar{p}_R - p_{wf}), \quad (17)$$

where r_e is the exterior boundary radius, ft. Note that the quantity in brackets is equivalent to J in Eq. 16 for the circular drainage area. J is a constant if the viscosity and formation volume factor of the producing fluid are constant. If these fluid properties are not constant, Eqs. 16 and 17 still apply but the PI value changes with the changing fluid properties. For multiphase flow these equations still can be used by substituting the definition in Table 35.1 into Eqs. 16 and 17.

Eq. 17 has to be modified if the drainage area is not circular with the well in the center. A general form of the pseudosteady-state equation has been worked out by Dietz¹¹ and has been cited by other authors.¹⁻⁵ The generalized pseudosteady-state equation has the form

$$q = \left[\frac{7.08 \times 10^{-3} kh / (B\mu)}{\frac{2.2458}{C_A} \frac{A}{r_w^2} + s} \right] (\bar{p}_R - p_{wf}), \quad (18)$$

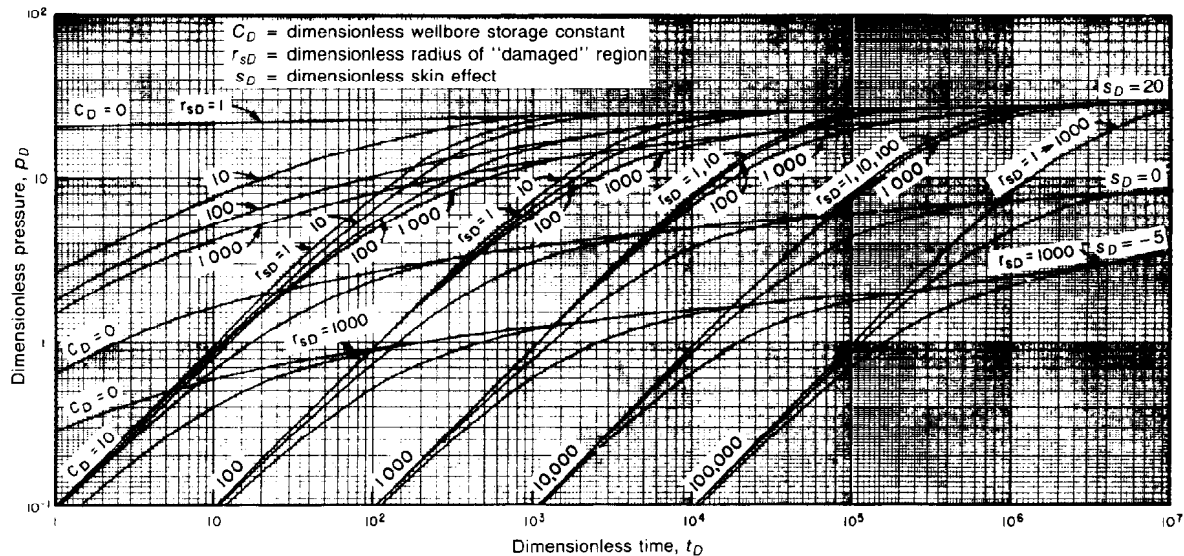


Fig. 35.6—Dimensionless pressure for a single well in an infinite reservoir including wellbore storage and a finite skin—composite reservoir.

where A is the drainage area, sq ft, and C_A is the shape factor (Table 35.2). This equation can be applied by using the values for C_A in Table 35.2 or by moving the terms in the denominator to the form

$$q = \left[\frac{7.08 \times 10^{-3} kh / (B\mu)}{\frac{1}{2} \ln \frac{2.2458}{C_A} + \frac{1}{2} \ln \frac{A}{r_w^2} + s} \right] (\bar{p}_R - p_{wf}) \quad (19)$$

This form is easier to use because the first term of the denominator also is tabulated in Table 35.2.

In Table 35.2, x_e is the distance from the well to the side of the square drainage area, and x_f is the distance from the well to either end of the vertical fracture. Table 35.2 also shows the dimensionless time, t_{DA} , at which the infinite-acting solution ends, and also the time at which pseudosteady state begins, $(t_{DA})_{pss}$.

Example Problem 1 (Transient and Pseudosteady State). A well is centered in an approximately square drainage area. The following data are given.

$$\begin{aligned} A &= 1.74 \times 10^6 \text{ sq ft (40 acres),} \\ h &= 21 \text{ ft,} \\ s &= 1.6, \\ r_w &= 0.25 \text{ ft,} \\ k_o &= 45 \text{ md,} \\ \mu_o &= 1.5 \text{ cp,} \\ \phi &= 0.18, \\ c_o &= 8.5 \times 10^{-6} \text{ psi}^{-1}, \\ c_w &= 3.2 \times 10^{-6} \text{ psi}^{-1}, \\ c_f &= 3.0 \times 10^{-6} \text{ psi}^{-1}, \\ S_w &= 0.25, \\ B_o &= 1.12, \text{ and} \\ p_i &= 5,100 \text{ psi.} \end{aligned}$$

Calculate the bottomhole pressure (BHP), p_{wf} , after 12 hours and after 120 days for a constant oil production rate of 80 STB/D.

Solution. From Eq. 5,

$$\begin{aligned} c_t &= c_f + S_o c_o + S_w c_w \\ &= [3.0 + (0.75)(8.5) + (0.25)(3.2)] \times 10^{-6} \\ &= 10.2 \times 10^{-6} \text{ psi}^{-1}. \end{aligned}$$

Calculate the time required to reach pseudosteady state. From Table 35.2,

$$(t_{DA})_{pss} = 0.1 = \frac{0.000264(45)t_{pss}}{(0.18)(1.5)(10.2 \times 10^{-6})(1.74 \times 10^6)},$$

where t_{pss} is 40.3 hours. So the well is infinite acting after 12 hours. By using Eq. 11,

$$p_D = \frac{1}{2} \ln t_D + 0.4045 + s.$$

By using the definitions of p_D and t_D in Eq. 8, we have

$$\begin{aligned} &\frac{(45)(21)(5,100 - p_{wf})}{141.2(80)(1.12)(1.5)} \\ &= \frac{1}{2} \ln \frac{0.000264(45)(12)}{(0.18)(1.5)(10.2 \times 10^{-6})(0.25)^2} + 0.4045 + 1.6; \\ &0.0498(5,100 - p_{wf}) = \frac{1}{2} \ln (8.28 \times 10^5) + 0.4045 + 1.6; \\ &5,100 - p_{wf} = (8.82)/(0.0498) = 177; \text{ and} \\ &p_{wf} = 4,923 \text{ psi at 12 hours.} \end{aligned}$$

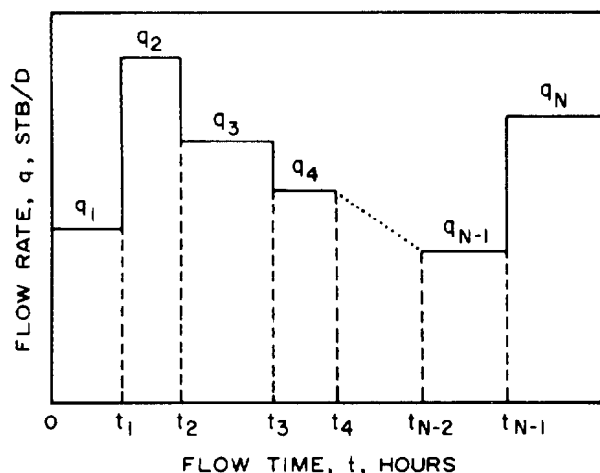


Fig. 35.7—Schematic representation of a variable production-rate schedule.

At 120 days, the well is in pseudosteady state (greater than 40.3 hours). First, calculate \bar{p}_R . Using Eq. 15, the rate of pressure decline can be calculated.

$$\left(\frac{\partial p}{\partial t}\right)_{pss} = \frac{-0.234qB}{V_p c_t}$$

$$= \frac{-0.234(80)(1.12)}{(21)(0.18)(1.74 \times 10^{-6})(10.2 \times 10^{-6})}$$

$$= -0.313 \text{ psi/hr.}$$

$$\bar{p}_R = 5,100 - 0.313(120)(24)$$

$$= 4,199 \text{ psi.}$$

Now, using Eq. 19,

$$q_o = \left[\frac{7.08 \times 10^{-3} kh/(B\mu)}{\frac{1}{2} \ln \frac{2.2458}{C_A} + \frac{1}{2} \ln \frac{A}{r_w^2} + s} \right]$$

$$\cdot (\bar{p}_R - p_{wf});$$

$$(80) = \left[\frac{7.08 \times 10^{-3} (45)(21)/(1.12 \times 1.5)}{-1.3224 + \frac{1}{2} \ln \frac{1.74 \times 10^{-6}}{(0.25)^2} + 1.6} \right]$$

$$\cdot (4,199 - p_{wf});$$

$$(80) = \left[\frac{3.982}{-1.3224 + 8.571 + 1.6} \right] (4,199 - p_{wf});$$

$$4,199 - p_{wf} = 178; \text{ and}$$

$$p_{wf} = 4,021 \text{ psi at 120 days.}$$

Production Rate Variation (Superposition)

These solutions have included only the constant-rate case. Of general interest, of course, are the cases where rate changes with time. These cases are best handled by using the principle of superposition.

The principle of superposition amounts to dividing the production history into a sequence of rate changes such as that shown in Fig. 35.7. The total effect of the production on the pressure response, Δp , is the additive effects of each of the rate changes. In Fig. 35.7, rate q_1 applies from $t=0$ to the current time. At t_1 the rate increases to q_2 . The effect of this rate change can be viewed as an incremental rate, $q_2 - q_1$, which has been in effect for a period of time $t - t_1$. Then q_3 would also be seen as a rate change, $q_3 - q_2$, which has been in effect for a period of time $t - t_2$. The effect of all these rate changes is computed by superposing the solutions that applied to each rate change and its corresponding time that it has been in effect. The equation for computing the total pressure drop, Δp_i , is

$$p_i - p_{wf} = \sum_{i=1}^N (q_i - q_{i-1}) f(t - t_{i-1}) \dots \dots \dots (20)$$

when $q_{i-1} = 0$ when $i = 1$.

The function $f(t)$ can be called the *unit response function*. The unit response function is the pressure drop, $p_i - p_{wf}$, which occurs at time t for a unit production rate ($q=1$). The unit response functions may be quantified by the cases described such as the wellbore storage equation at early times (ETR), the semilog straight line solution at MTR, and finally the pseudosteady-state solution at later times (LTR). For example, if q_1 had been in effect for a time longer than t_{pss} , its contribution to the pressure drop at time t would be calculated from the pseudosteady-state equations, which would comprise the calculation of the reduction in \bar{p} from Eq. 15 and the pressure drop from \bar{p}_R to p_{wf} in Eq. 16. The effect of the second rate might be still in the transient period, which would call for Eq. 11 to be applied.

Note that the calculation of the pressure decline of \bar{p}_R can be calculated with Eq. 15 only for the constant-compressibility case. For the general case, such as a solution gas drive reservoir, the appropriate material balance equations would be applicable to calculate \bar{p}_R . If the last rate change has been in effect for a time greater than t_{pss} and the system has constant compressibility, the following simplification can be made for Eq. 15.

$$\bar{p}_R = p_i - \frac{5.615 N_p B_o}{V_p c_t} \dots \dots \dots (21)$$

The following example problem shows how superposition can be applied for a case where both pseudosteady-state and transient pressure drops are added.

Example Problem 2 (Superposition). The well in Example Problem 1 produces according to the following schedule.

time (hours)	q_o (STB/D)
0 to 2	300
2 to 8	120
thereafter	80

Calculate p_{wf} at 12 hours and at 120 days.

Solution. As we observed in Example Problem 1, the well was infinite acting after 12 hours, so we use Eq. 20.

$$p_i - p_{wf} = \sum_{i=1}^N (q_i - q_{i-1}) f(t - t_{i-1}).$$

We first need $f(t)$, the unit response function. We can use Eq. 11 to find Δp in terms of t for $q=1$:

$$p_D = \frac{1}{2} \ln t_D + 0.4045 + s,$$

$$\frac{(45)(21)\Delta p}{141.2(1)(1.12)(1.5)}$$

$$= \frac{1}{2} \ln \frac{0.000264(45)t}{(0.18)(1.5)(10.2 \times 10^{-6})(0.25)^2}$$

$$+ 0.4045 + 1.6,$$

$$3.98\Delta p = \frac{1}{2} \ln 6.90 \times 10^4 t + 2.004, \text{ and}$$

$$\Delta p = 0.1256 \ln(6.90 \times 10^4 t) + 0.504,$$

so

$$f(t) = \Delta p = 0.1256 \ln(6.90 \times 10^4 t) + 0.504.$$

Substituting into Eq. 20,

$$p_i - p_{wf} = (q_1 - q_0)f(t - t_0)$$

$$+ (q_2 - q_1)f(t - t_1)$$

$$+ (q_3 - q_2)f(t - t_2);$$

$$p_i - p_{wf} = (300 - 0)f(12 - 0)$$

$$+ (120 - 300)f(12 - 2)$$

$$+ (80 - 120)f(12 - 8),$$

so the values of $f(12)$, $f(10)$, and $f(4)$ are used, giving

$$5,100 - p_{wf} = (300)[0.1256 \ln(6.9 \times 10^4 \times 12) + 0.504]$$

$$- (180)[0.1256 \ln(6.9 \times 10^4 \times 10) + 0.504]$$

$$- (40)[0.1256 \ln(6.9 \times 10^4 \times 4) + 0.504]$$

$$= (300)(2.22)$$

$$- (180)(2.19)$$

$$- (40)(2.08)$$

$$= 189;$$

$$p_{wf} = 4,911 \text{ psi at 12 hours.}$$

At 120 days, the well has a cumulative production of

$$N_p = 300 \text{ STB/D} \times (2/24 \text{ days})$$

$$+ 120 \text{ STB/D} \times (6/24 \text{ days})$$

$$+ 80 \text{ STB/D} \times (119.5 \text{ days})$$

$$= 9,615 \text{ STB.}$$

Using Eq. 21,

$$\bar{p}_R = p_i - \frac{5.615 N_p B_o}{V_p C_t}$$

$$= (5,100) - \frac{5.615(9,615)(1.12)}{(21)(0.18)(1.74 \times 10^6)(10.2 \times 10^{-6})}$$

$$= 5,100 - 901 = 4,199.$$

Using Eq. 19 (the same as Example Problem 1), we calculate

$$\bar{p}_R - p_{wf} = 178,$$

and again,

$$p_{wf} = 4,199 - 178 = 4,021 \text{ psi at 120 days.}$$

The effect of the early rate variation is “forgotten” after the rate is constant for $t_{pss} = 40.3$ hours, except for the slight increase in cumulative barrels (15 STB), which is negligible in this case.

Gas Well Performance

The performance of gas wells is similar to oil wells (liquid reservoirs) except for two major differences: (1) the fluid properties of gas change dramatically with pressure and (2) flow can become partially turbulent near the wellbore, resulting in a rate-dependent skin factor. These two factors are discussed and alternative forms of gas performance equations are presented.

The application of these principles to gas flow is only slightly more complicated than to liquid flow, but there is often much confusion about gas wells. There are several reasons for this. One reason is that there are many versions of gas flow equations in the literature. Some are in terms of p , some in terms of p^2 , and some in terms of a real gas pseudopressure, $m(p)$. All these equations can be used and are valid forms. Another reason for confusion is the different coefficients in the equations, which sometimes arise from the assumed temperature and pressure base of a standard cubic foot of gas. The following equations use only the symbols T_{sc} and p_{sc} , since the pressure base in different areas does vary significantly.

Still another reason for confusion is that deliverability testing has been customary with gas wells because of government requirements. Deliverability testing, based on a $\log(p_R^2 - p_{wf}^2)$ vs. $\log q_g$ plot, is largely an empirical approach. The deliverability plot approach was developed mainly for low-pressure gas wells and does not work well with the deeper, higher-temperature, and higher-pressure wells that are more common today.

The Effect of Gas Properties

In the derivation of the diffusivity equation, the form of Eq. 1 is not achieved because the values of z and μ vary with pressure. Consequently the following form occurs in the derivation.

$$\nabla \frac{p}{z\mu} \nabla p = \frac{1}{0.000264} \frac{\phi}{k} \frac{\partial p}{\partial t}, \quad \dots \quad (22)$$

where z is the dimensionless gas-law deviation factor. This equation is a nonlinear partial differential equation and cannot be solved analytically by the methods applied to Eq. 1.

A method for "linearizing" the partial differential equation was developed by Al-Hussainy *et al.*¹² They introduced a *real gas pseudopressure*, which may be defined as

$$m(p) = 2 \int_0^p \frac{p}{z\mu} dp. \quad \dots \quad (23)$$

This pressure-dependent function integrates the variations of p , z , and μ with pressure. When this function is introduced into the derivation of the diffusivity equation, the diffusivity equation for a real gas takes the form

$$\nabla^2 m(p) = \frac{1}{0.000264} \frac{\phi \mu c_g}{k} \frac{\partial m(p)}{\partial t}. \quad \dots \quad (24)$$

This equation still is not quite a linear differential equation because μ and c_g vary significantly with pressure.

The gas compressibility, c_g , can be expressed in terms of z as

$$c_g = \frac{1}{p} - \frac{1}{z} \frac{dz}{dp}. \quad \dots \quad (25)$$

For practical purposes, however, Eq. 23 can be taken as a linear differential equation in terms of $m(p)$. This was confirmed by the result of computer simulations performed by Wattenbarger and Ramey.¹³ They showed that the pressure transient equations can be used, with very good approximation, in terms of $m(p)$. After pseudo-steady-state, PI equations similar to Eqs. 16 through 19 can be used.

The application of the $m(p)$ solutions is not difficult. The values of $m(p)$ vs. p can be determined by graphical integration or can be calculated with computer programs that use built-in correlations to estimate the variation of z and μ with pressure.

Since our equations and graphical techniques depend on equations of a straight line of p either on a linear plot or a semilog plot, it is worth analyzing how the slopes of $m(p)$ are related to the slopes of p plots, or p^2 plots; we can show that the derivative of $m(p)$ with respect to, for example, $\log t$ is as follows.

$$\frac{\partial m(p)}{\partial(\log t)} = \left(\frac{2p}{z\mu} \right) \frac{\partial p}{\partial(\log t)} = \left(\frac{1}{z\mu} \right) \frac{\partial p^2}{\partial(\log t)}. \quad \dots \quad (26)$$

These relationships indicate that an $m(p)$ plot, or a p plot, or a p^2 plot can be used and then the relationships in Eq. 26 applied. The $m(p)$ plot is preferable because it is most likely to have the proper semilog straight line. The p and p^2 plots can be used as shortcuts if the proper MTR slope is identified. For example, the slope of a p vs. $\log t$ plot can be determined from a plot and then the value of the slope of $m(p)$ vs. $\log t$ can be calculated by using Eq. 26 without ever actually plotting values of $m(p)$.

Non-Darcy Flow

Darcy's law applies to gases at lower rates (laminar flow), which are found throughout the reservoir. However, near the wellbore the rates can become extremely high because of the converging flow as the gas approaches the wellbore. At these rates *inertial effects* can become important and Darcy's law no longer applies. The inertial effects take the form of distorted flow paths and also turbulence in different locations in the pore structure. Although the exact nature of this microscopic flow is not known in the reservoir, the net effect is a higher pressure gradient when these inertial effects become important.

For laminar flow we can rearrange Darcy's law to the following form.

$$-\frac{\partial p}{\partial x} = \frac{\mu}{k} v, \quad \dots \quad (30)$$

where $\partial p / \partial x$ is the pressure gradient and v is the macroscopic (Darcy) fluid velocity. At the higher rates, when

inertial effects become important, the Forchheimer equation is used:

$$-\frac{\partial p}{\partial x} = \frac{\mu}{k} v + F_t \rho v |v|, \quad \dots \quad (31)$$

where ρ is the fluid density and F_t is the turbulence factor. The right side of Eq. 31 contains a term for viscous forces and a term for inertial forces, both of which contribute to the pressure loss.

Although a number of workers have correlated the value of F_t with rock properties, for practical purposes the velocity varies too much in the vertical direction near a wellbore to predict the effect of non-Darcy flow in a particular well. One practical approach is to consider the nonDarcy effect near the wellbore as a rate-dependent part of the skin effect:

$$s' = s + F_{Da} |q_g|, \quad \dots \quad (32)$$

where F_{Da} is the non-Darcy (turbulence) factor, $(10^3 \text{ cu ft/D})^{-1}$, $|q_g|$ is the absolute value of gas rate, 10^3 cu ft/D , and s' is the effective skin effect of a well flowing at a rate q_g . Fig. 35.8 shows how s' varies with rate. The value of F_{Da} varies with pressure but for simplicity can be considered constant. The value of F_{Da} must be evaluated by transient testing of the well at several rates and determining corresponding values of s' .

The transient equations (MTR) and pseudosteady-state equations (LTR) are modified for gas wells as shown in the following.

Infinite-Acting Gas Reservoir (MTR)

The transient solution for the infinite-acting gas reservoir is analogous to the liquid case shown in Eq. 11. Eq. 11 then must be modified for the effect of non-Darcy flow and fluid property variation with pressure. This results in the following equation.

$$m_D = \frac{1}{2} \ln t_D + 0.4045 + s + F_{Da} |q_g|, \quad \dots \quad (33)$$

where

$$m_D = 1.987 \times 10^{-5} \left(\frac{T_{sc}}{p_{sc} T_R} \right) \frac{kh}{q_g} \left[m(p_i) - m(p_{wf}) \right]$$

and

$$\begin{aligned} m_D &= \text{dimensionless } m(p), \\ t_D &= \text{dimensionless time,} \\ T_{sc} &= \text{standard condition temperature, } ^\circ\text{R,} \\ p_{sc} &= \text{standard condition pressure, psia,} \\ T_R &= \text{reservoir temperature, } ^\circ\text{R,} \\ m(p_i) &= m(p) \text{ at initial pressure } p_i, \text{ psia}^2/\text{cp, and} \\ m(p_{wf}) &= m(p) \text{ at wellbore flowing pressure } p_{wf}, \\ &\quad \text{psia}^2/\text{cp.} \end{aligned}$$

The value of t_D is evaluated with $\phi\mu c$ evaluated at the initial pressure.

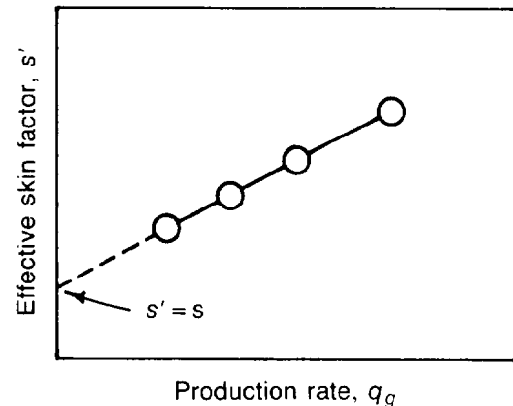


Fig. 35.8—Skin factor determination.

Before putting Eq. 33 into a more practical form, consider that the pressure drop term, $m(p_i) - m(p_{wf})$, can be stated as $\Delta m(p)$ and can be related to Δp and Δp^2 by the relationships

$$\Delta m(p) = \left(\frac{2p}{z\mu} \right)_{\bar{p}} \Delta p = \left(\frac{1}{z\mu} \right)_{\bar{p}} \Delta p^2. \quad \dots \quad (34)$$

The average values shown in parentheses are the integrated average values over the pressure range. For practical purposes it is accurate to evaluate these average quantities at the midpoint pressure. In other words, $2p/z\mu_{\bar{p}}$ is evaluated at \bar{p} , where \bar{p} is equal to $(\bar{p}_R + p_{wf})/2$ and $(1/z\mu)_{\bar{p}}$ is evaluated at \bar{p} , where \bar{p} is equal to $(\bar{p}_R + p_{wf})/2$, or $\sqrt{(\bar{p}_R^2 + p_{wf}^2)/2}$ for the p^2 equation. For the infinite-acting reservoir, the average reservoir pressure, \bar{p}_R , is the same as p_i .

These relationships are important because they allow us to account for the variation of fluid properties, within engineering accuracy, and still express equations simply in terms of p and p^2 . Eq. 33, when put in more practical form, can be expressed in terms of $m(p)$, p , or p^2 , as

$$\begin{aligned} &1.987 \times 10^{-5} \left(\frac{kh}{q_g} \right) \left[m(p_i) - m(p_{wf}) \right] \\ &= \frac{2.303}{2} \log \frac{0.000264kt}{(\phi\mu c)_i r_w^2} \\ &+ 0.4045 + s + F_{Da} |q_g|, \quad \dots \quad (35a) \end{aligned}$$

$$\begin{aligned} &1.987 \times 10^{-5} \left(\frac{kh}{q_g} \right) \left(\frac{2p}{z\mu} \right)_{\bar{p}} (p_i - p_{wf}) \\ &= \frac{2.303}{2} \log \frac{0.000264kt}{(\phi\mu c)_i r_w^2} \\ &+ 0.4045 + s + F_{Da} |q_g|, \quad \dots \quad (35b) \end{aligned}$$

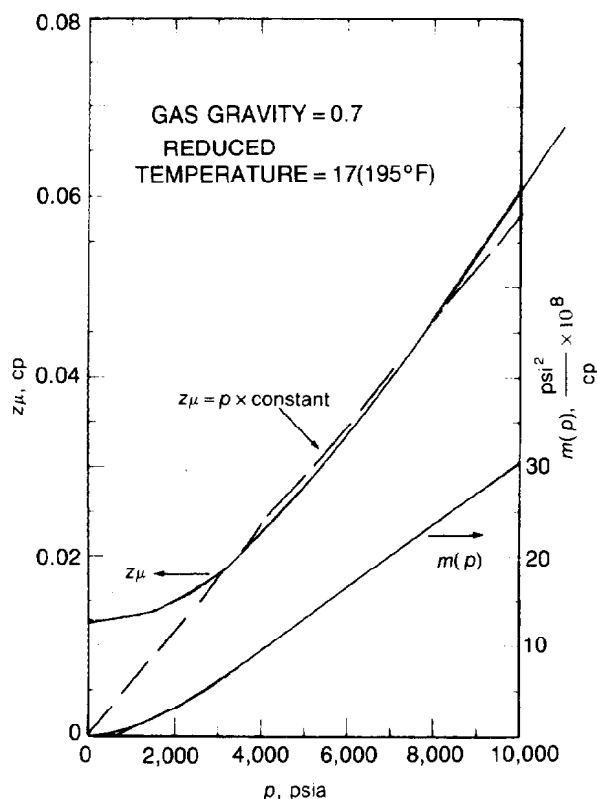


Fig. 35.9—Typical variation of $m(p)$ and $z\mu$ with pressure.

and

$$1.987 \times 10^{-5} \left(\frac{kh}{q_g} \right) \left(\frac{1}{z\mu} \right)_{\bar{p}} (p_i^2 - p_{wf}^2) \\ = \frac{2.303}{2} \log \frac{0.000264kt}{(\phi\mu c)_i r_w^2} \\ + 0.4045 + s + F_{Da} | q_g |, \dots (35c)$$

where $(\phi\mu c)_i = \phi\mu c$ evaluated at p_i . Eq. 35 can be used to predict p_{wf} for the infinite-acting period (MTR) between the wellbore storage period and the beginning of pseudosteady state.

Fig. 35.9 shows a typical relationship of $z\mu$ with pressure. The value of $z\mu$ is almost constant when p is below 2,000 psia. This makes the p^2 type of equation fairly accurate below 2,000 psi because $z\mu$ can be taken out of the integral in Eq. 23 if $z\mu$ is constant. p^2 plots and equations tend to work well in reservoir pressures less than 2,000 psia.

Fig. 35.9 also shows that $m(p)$ tends to be linear with p at higher pressures (above 3,000 psia). This means that p plots and equations tend to work well for higher-pressure reservoirs. If there is a doubt about whether these p^2 or p simplifications apply to a particular reservoir, then $m(p)$ plots and equations should be used.

Pseudosteady-State Solutions (LTR)

The pseudosteady-state solutions are analogous to the liquid solutions and can be put in essentially the same form. The only changes are to allow for the changes of fluid properties with pressure and non-Darcy flow. The inclusion of these effects is the same as discussed above. The result is the following form of the pseudosteady-state equations, in terms of $m(p)$, p , and p^2 .

$$q_g = 1.987 \times 10^{-5} \left(\frac{T_{sc}}{p_{sc} T_R} \right) \cdot \frac{kh}{\frac{1}{2} \ln \frac{2.2458A}{C_A r_w^2} + s + F_{Da} | q_g |} \cdot [m(\bar{p}) - m(p_{wf})], \dots (36a)$$

where $m(\bar{p}) = m(p)$ at p_R , psia²/cp, and C_A = shape factor from Table 35.2.

$$q_g = 1.987 \times 10^{-5} \left(\frac{T_{sc}}{p_{sc} T_R} \right) \cdot \frac{kh}{\frac{1}{2} \ln \frac{2.2458A}{C_A r_w^2} + s + F_{Da} | q_g |} \cdot \left(\frac{2p}{z\mu} \right)_{\bar{p}} (\bar{p} - p_{wf}), \dots (36b)$$

and

$$q_g = 1.987 \times 10^{-5} \left(\frac{T_{sc}}{p_{sc} T_R} \right) \cdot \frac{kh}{\frac{1}{2} \ln \frac{2.2458A}{C_A r_w^2} + s + F_{Da} | q_g |} \cdot \left(\frac{1}{z\mu} \right)_{\bar{p}} (\bar{p}^2 - p_{wf}^2). \dots (36c)$$

Eqs. 36 have general application for pseudosteady-state gas flow. Note that these forms of the pseudosteady-state equations are considerably different from the gas deliverability approach that is used extensively. The gas deliverability approach is empirical and based on a log-log plot of $\bar{p}^2 - p_{wf}^2$ vs. q_g . The comparison between Eqs. 36 and the deliverability plot approach is discussed by Lee.⁵

Long-Term Forecast

Long-term forecasting can be accomplished in a fairly straightforward manner using Eqs. 36 along with a \bar{p}_R/z plot. The \bar{p}_R/z plot, of course, is simply a material balance for a closed gas reservoir. Through this plot the value of \bar{p}_R can be determined for any value of cumulative production, G_p . Given this value of \bar{p}_R , one of the forms of Eqs. 36 then can be used to determine q_g .

Note that in deep, high-pressure reservoirs, the influence of formation and water compressibility can become important compared with gas compressibility. At these high pressures, greater than about 6,000 psig, the \bar{p}_R/z plot should be modified to account for the formation and water compressibilities. A technique for this modified \bar{p}_R/z plot is presented by Ramagost and Farshad.¹⁴

A complete forecast of production rate vs. time can be generated by converting the cumulative production to a time scale. The value of p_{wf} might be fixed as a condition of the production forecast, or it may be solved simultaneously with wellbore hydraulic relationships, such as given in Chap. 34.

Example Problem 3. A gas well produces from a drainage area that approximates a 4:1 rectangle with the well in the center. The following data apply.

$$\begin{aligned} A &= 6.96 \times 10^6 \text{ sq ft (160 acres),} \\ h &= 34 \text{ ft,} \\ s &= 2.3, \\ F_{Da} &= 0.0052 (10^3 \text{ cu ft/D})^{-1}, \\ r_w &= 0.23 \text{ ft,} \\ k_g &= 0.52 \text{ md,} \\ z\mu_g &= \text{see Fig. 35.9,} \\ \phi &= 0.11, \\ T_R &= 210^\circ\text{F} + 460 = 670^\circ\text{R,} \\ T_{sc} &= 60^\circ\text{F} + 460 = 520^\circ\text{R,} \\ p_{sc} &= 14.7 \text{ psia, and} \\ \bar{p}_R &= 4,150 \text{ psia.} \end{aligned}$$

Calculate the pseudosteady-state rate, q_g , if $p_{wf} = 1,500$ psia.

Solution. Use Eq. 36b—the simplest form of the pseudosteady-state equation.

$$\bar{p} = (\bar{p}_R + p_{wf})/2$$

$$= (4,150 + 1,500)/2$$

$$= 2,825 \text{ psia.}$$

From Fig. 35.9, we estimate $z\mu_g$ at 2,825 psia as

$$z\mu_g = 0.0165.$$

So,

$$\left(\frac{2p}{z\mu}\right)_{\bar{p}} = \frac{2(2,825)}{0.0165} = 3.42 \times 10^5.$$

From Table 35.2,

$$C_A = 5.3790.$$

Eq. 36b is

$$\begin{aligned} q_g &= 1.987 \times 10^{-5} \left(\frac{T_{sc}}{p_{sc} T_R} \right) \\ &\quad \cdot \frac{kh}{\frac{1}{2} \ln \frac{2.2458A}{C_A r_w^2} + s + F_{Da} |q_g|} \\ &\quad \cdot \left(\frac{2p}{z\mu} \right)_{\bar{p}} (\bar{p}_R - p_{wf}); \\ q_g &= 1.987 \times 10^{-5} \frac{(520)}{(14.7)(670)} \\ &\quad \cdot \frac{(0.52)(34)}{\frac{1}{2} \ln \frac{2.2458(6.96 \times 10^6)}{(5.379)(0.23)^2} + 2.3 + 0.0052 |q_g|} \\ &\quad \cdot (3.42 \times 10^5)(4,150 - 1,500) \\ &= 1.987 \times 10^{-5} (0.0528) \frac{17.68}{8.91 + 2.3 + 0.0052 |q_g|} \\ &\quad \cdot (3.42 \times 10^5)(2,650) \\ &= \frac{1.68 \times 10^4}{11.21 + 0.0052 |q_g|}. \end{aligned}$$

$$(11.21 + 0.0052 |q_g|) q_g = 1.68 \times 10^4.$$

This equation can be solved as a quadratic equation, or simply by trial and error, by using estimates of $|q_g|$ starting with $|q_g| = 0$:

$$(11.21 + 0) q_g = 1.68 \times 10^4$$

$$q_g = 1,499.$$

Next, try

$$(11.21 + 0.0052 \times 1,499) q_g = 1.68 \times 10^4;$$

$$q_g = 884.$$

Next, try

$$(11.21 + 0.0052 \times 884) q_g = 1.68 \times 10^4;$$

$$q_g = 1,063.$$

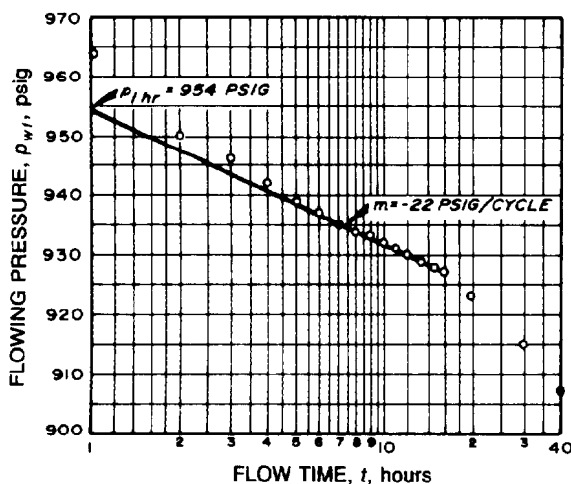


Fig. 35.10—Semilog data plot for drawdown test.

Next, try

$$(11.21 + 0.0052 \times 1,063)q_g = 1.68 \times 10^4;$$

$$q_g = 1,004,$$

until the solution converges at

$$q_g = 1,018 \times 10^3 \text{ cu ft/D.}$$

Transient Well Test Analysis

The subject of transient well test analysis can be very complicated and has been covered very thoroughly in the literature.¹⁻⁵ These references show not only the straightforward cases of transient well test analysis but also go into many exceptions, alternative techniques for analysis, and other complications. It is the intent here to cover only the most straightforward and routine methods for analysis of oil and gas wells.

The most common values to calculate from a transient well test analysis are kh , s , and \bar{p}_R . With these three values plus a knowledge of the drainage area and shape of the drainage area (values of C_A and A), the flow rate can be calculated or forecast for a particular BHP, p_{wf} , by using the pseudosteady-state equations. The method of analyzing kh and s for a drawdown test and a buildup test are summarized now.

Drawdown Test

The drawdown test is accomplished simply by putting a well on a constant production rate after the well has been shut in. Variations of the drawdown test involve analysis of variable rates, but only the constant-rate case is covered here. The analysis is based on the infinite-acting solution (MTR). The data are plotted on a pressure vs. log time semilog plot and the slope of the plot, m , is determined graphically in units of psi/cycle (see Fig. 35.10). The equations for determining kh for an oil well or a gas well are as follows.

For oil wells,

$$k_o h = -\frac{162.6 q_o B_o \mu_o}{m}, \quad \dots (37a)$$

and for gas wells,

$$k_g h = \frac{-5.792 \times 10^4 q_g (p_{sc} T_R / T_{sc})}{m^*}, \quad \dots (37b)$$

where m^* is the slope of $m(p)$ plot,

$$k_g h = \frac{-5.792 \times 10^4 q_g (p_{sc} T_R / T_{sc}) \left(\frac{z \mu_g}{2p} \right)_{wb}}{m'}, \quad \dots (37c)$$

where m' is the slope of p plot, or

$$k_g h = \frac{-5.792 \times 10^4 q_g (p_{sc} T_R / T_{sc}) (z \mu_g)_{wb}}{m''}, \quad \dots (37d)$$

where m'' is the slope of p^2 plot and subscript wb refers to wellbore. The values of $z \mu / 2p$ in Eq. 37c and $z \mu$ in Eq. 37d are evaluated at p_{wf} rather than $(\bar{p}_R + p_{wf})/2$, which is used in the pseudosteady-state equations.

The value of the skin effect, s , is determined from one of the following equations for oil and gas wells.

For oil wells,

$$s = 1.151 \left(\left| \frac{p_i - p_1}{m} \right| - \log \frac{k}{\phi \mu c_i r_w^2} + 3.23 \right), \quad \dots (38a)$$

where p_1 is the pressure at $\Delta t = 1$ hour; and for gas wells,

$$s = 1.151 \left(\left| \frac{m(p_i) - m(p_1)}{m^*} \right| - \log \frac{k}{\phi \mu c_i r_w^2} + 3.23 \right), \quad \dots (38b)$$

$$s = 1.151 \left(\left| \frac{p_i - p_1}{m'} \right| - \log \frac{k}{\phi \mu c_i r_w^2} + 3.23 \right), \quad \dots (38c)$$

or

$$s = 1.151 \left(\left| \frac{p_i^2 - p_1^2}{m''} \right| - \log \frac{k}{\phi \mu c_i r_w^2} + 3.23 \right), \quad \dots (38d)$$

The disadvantage of this equation (compared to buildup testing) is that p_i must be known to calculate s .

It is important to evaluate the proper semilog straight line. In many cases it is difficult to tell whether an apparent semilog straight line is in the MTR solution or is still being affected by wellbore effects (ETR). It is often helpful to make a log-log plot of $p_i - p_{wf}$ vs. flowing time, t , to analyze when the wellbore effects are finished. A straight line with a slope of unity on this log-log plot indicates that the pressure behavior is being totally dominated by wellbore storage. The semilog straight line then can be expected to begin at about 1.5 log cycles after the data points leave the log-log straight line of unity slope.

Buildup Testing

Buildup testing is more common than drawdown testing. The main reason for this is that the well rate is known when the well is shut in ($q=0$). The analysis of a buildup test is based on the assumption that a constant flow rate is maintained for a producing time, t_p , and then the well is shut in. Variations of the buildup test include analysis of variation in production rate before shut-in, but only the constant-rate production period is covered here. The pressure, p_{wf} ($\Delta t=0$), is measured just before shut-in and then at different shut-in times, Δt , after the time of shut-in.

A plot is made of the shut-in pressures, p_{wf} , vs. a time scale based on the shut-in time, Δt . The time scale is either $\log \Delta t$ or $\log (t_p + \Delta t)/\Delta t$. The first of these plots (Fig. 35.11) is called an "MDH plot" (Miller, Dyes, and Hutchinson¹⁵). The second type of plot (Fig. 35.12) is called a "Horner plot."¹⁶ Both plots give the same semilog straight line slope, which is also the same as measured in the drawdown test.

The kh for an oil or gas well can be determined from the slope of this semilog straight line by the following equations (identical to Eqs. 37, except for the sign).

For oil wells,

$$k_o h = \frac{162.6 q_o B_o \mu_o}{m}, \quad \dots \dots \dots (39a)$$

and for gas wells,

$$k_g h = \frac{5.792 \times 10^4 q_g (p_{sc} T_R / T_{sc})}{m^*}, \quad \dots \dots \dots (39b)$$

$$k_g h = \frac{5.792 \times 10^4 q_g (p_{sc} T_R / T_{sc})}{m'} \left(\frac{z \mu_g}{2p} \right)_{wb}, \quad \dots \dots (39c)$$

or

$$k_g h = \frac{5.792 \times 10^4 q_g (p_{sc} T_R / T_{sc})}{m''} (z \mu_g)_{wb}, \quad \dots \dots (39d)$$

Note that the signs are reversed for the Horner plot.

The skin factor, s , can be determined from one of the following equations.

For oil wells,

$$s = 1.151 \left(\left| \frac{p_1 - p_{wf}}{m} \right| - \log \frac{k_o}{\phi \mu_o c_t r_w^2} + 3.23 \right), \quad \dots \dots \dots (40a)$$

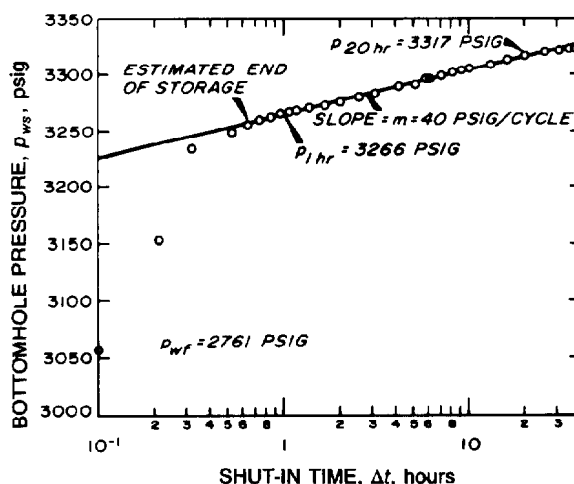


Fig. 35.11—MDH plot for buildup test.

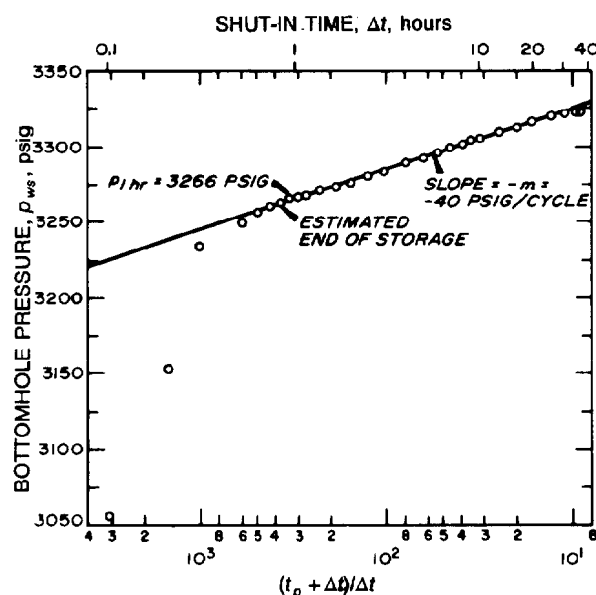


Fig. 35.12—Horner plot of pressure buildup data from Fig. 35.11.

and for gas wells,

$$s = 1.151 \left(\left| \frac{m(p_1) - m(p_{wf})}{m^*} \right| - \log \frac{k_g}{\phi \mu_g c_t} + 3.23 \right), \quad \dots \dots \dots (40b)$$

$$s = 1.151 \left(\left| \frac{p_1 - p_{wf}}{m'} \right| - \log \frac{k_g}{\phi \mu_g c_t r_w^2} + 3.23 \right), \quad \dots \dots \dots (40c)$$

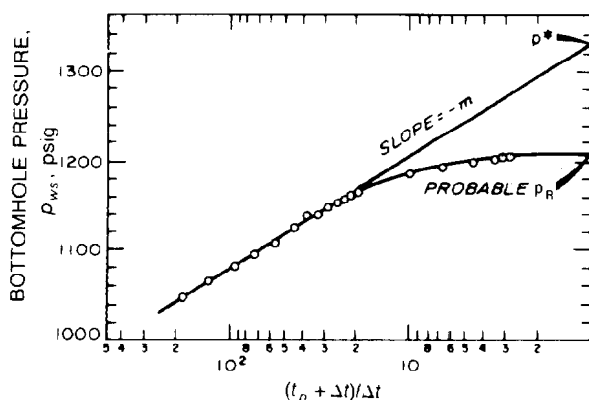


Fig. 35.13—Horner plot of typical pressure buildup data from a well in a finite reservoir.

or

$$s = 1.151 \left(\left| \frac{p_1^2 - p_{wf}^2}{m''} \right| - \log \frac{k_g}{\phi \mu_g c_t r_w^2} + 3.23 \right) \quad (40d)$$

The slope refers to the corresponding semilog straight line. p_{wf} is the last p_{wf} at $\Delta t = 0$. These equations are based on the equation of the semilog straight line. Therefore, if p_{ws} does not fall on the extrapolated semilog straight line at $\Delta t = 1$ hour, then p_1 is read on the semilog straight line rather than at the actual data.

Again, be reminded that transient well test analysis can be very complicated and can depart in many ways from the simple analysis presented here. These equations are presented only for quick reference and to show the proper interpretation of the real gas formulas for the normal cases. The reader should refer to Refs. 1 through 5 for more details and explanation of departures from these simple cases.

Determination of \bar{p}_R

The value of \bar{p}_R represents the average reservoir pressure in the drainage area of the well. It is important to determine \bar{p}_R from a buildup test so that \bar{p}_R can be used for material balance calculations, history matching in reservoir simulation, or in pseudosteady-state performance equations.

There are several methods for determining \bar{p}_R from a buildup test but the most general is the MBH (Matthews, Brons, and Hazebroek¹⁷). This method is generally applicable because a number of different reservoir drainage area shapes are available for analysis. These reservoir shapes are the same as those used for evaluating shape factors in Table 35.2.

Fig. 35.13 shows how the method is applied. The buildup test has a semilog straight line, which begins bending at the later shut-in times because of the effect of the boundaries. The data normally will bend down and become flat from this curve, but for unusual cases the data actually can bend up from the semilog straight line before it eventually becomes horizontal.

Asymptotically, the data approach the correct value of \bar{p}_R as Δt approaches infinity. Since our shut-in time normally is limited, the MBH method is based on extrapolating the semilog straight line to $\Delta t = \infty$, or $(t_p + \Delta t)/\Delta t = 1.0$. This value is called p^* . The method then provides a correction to calculate the correct value of \bar{p}_R from the extrapolated value of p^* .

The MBH method assumes that the well flowed at a constant rate for t_p and that the drainage area A is known for the well. The dimensionless producing time, t_{pDA} , is calculated. If t_{pDA} is greater than $(t_{pDA})_{pss}$, the later value can be used as t_{pDA} . In other words, it is not important what the rate history was before pseudosteady state was achieved.

Now that p^* has been extrapolated from the data and t_{pDA} has been calculated, then the correction between p^* and \bar{p}_R is made by using the MBH correction curve that best represents the drainage shape. The MBH correction curves are presented in Figs. 35.14 through 35.17. A stepwise procedure to determine \bar{p}_R can be summarized as follows.

1. Make a Horner plot.
2. Extrapolate the semilog straight line to the value of p^* at $(t_p + \Delta t)/\Delta t = 1.0$.
3. Evaluate m , the slope of the semilog straight line.
4. Calculate $t_{pDA} = (0.000264kt_p)/\phi\mu c_t A$.
5. Find the closest approximation to the drainage shape in Figs. 35.14 through 35.17. Choose a correction curve.
6. Read the value of $2.303(p^* - \bar{p}_R)/m$ from the correction curve at t_{pDA} .
7. Calculate the value of \bar{p}_R .

This procedure gives the value of \bar{p}_R in the drainage area of one well. If a number of wells are producing from the reservoir, each well can be analyzed separately to give a \bar{p}_R for its own drainage area. This is done, assuming that all wells are producing in pseudosteady state, by dividing the reservoir up into drainage areas for each well by constructing no-flow boundaries between the wells. Fig. 35.18 shows an illustration of such a segmentation of a reservoir. These no-flow boundaries represent the "watersheds" of the different drainage areas. The drainage areas are calculated so that each drainage area has the same reservoir flow rate compared to its PV. Thus,

$$(q_t/V_p)_1 = (q_t/V_p)_2 = (q_t/V_p)_3 = (q_t/V_p)_i \dots (41)$$

This relationship divides the drainage area (or PV) according to the producing rate of the well. As the well's rates change, then the drainage area changes for the well. If $q = 0$, for example, then no area would be allocated to that well. This procedure of calculating the drainage area and approximating drainage shape is repeated at the time of each pressure survey. The drainage areas and shapes keep changing as rates change.

There is often confusion about the meaning of p^* in the Horner plot. The value of p^* has no physical meaning except in the special case of an infinite-acting well ($r_e = \infty$). This is the case that Horner¹⁶ originally addressed in determining the initial pressure, p_i , in a newly discovered well. In this special infinite-acting case, $p^* = \bar{p}_R = p_i$. Otherwise, p^* has no physical meaning.

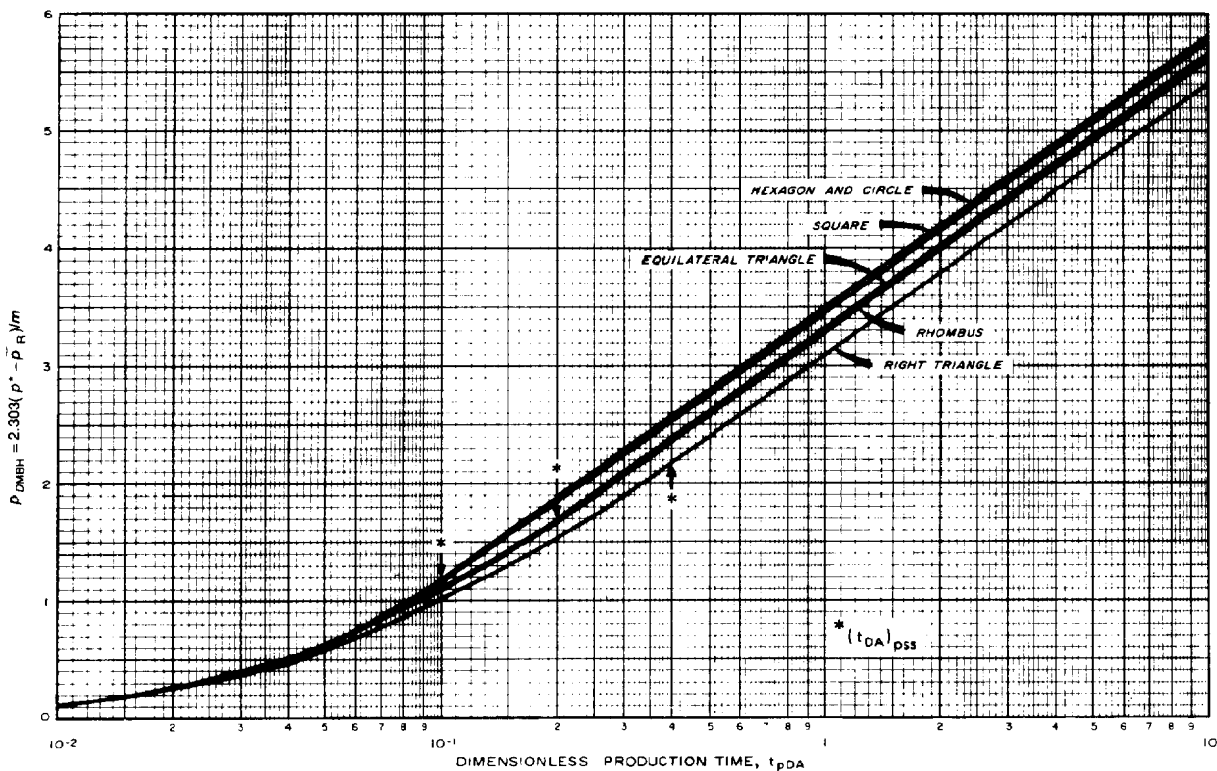


Fig. 35.14—MBH dimensionless pressure for a well in the center of equilateral drainage areas.

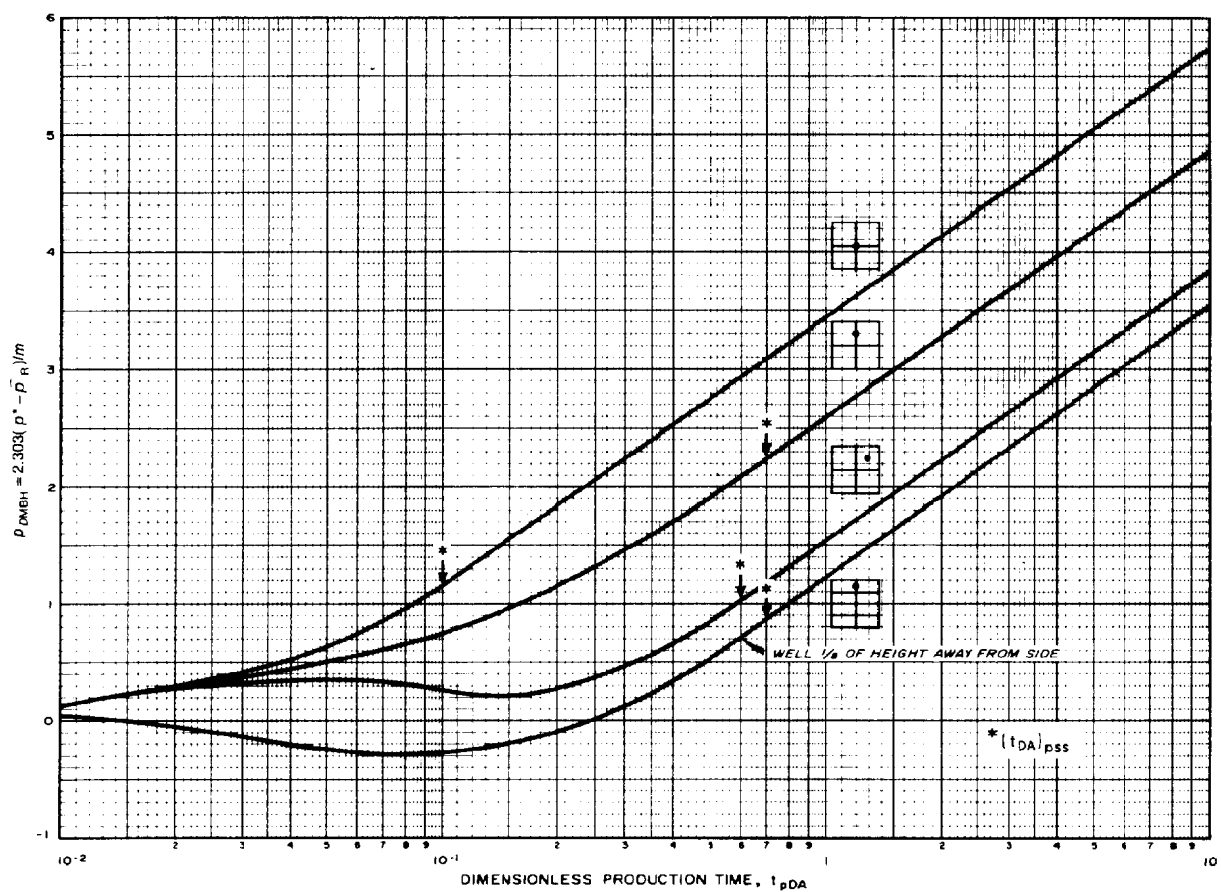


Fig. 35.15—MBH dimensionless pressure for different well locations in a square drainage area.

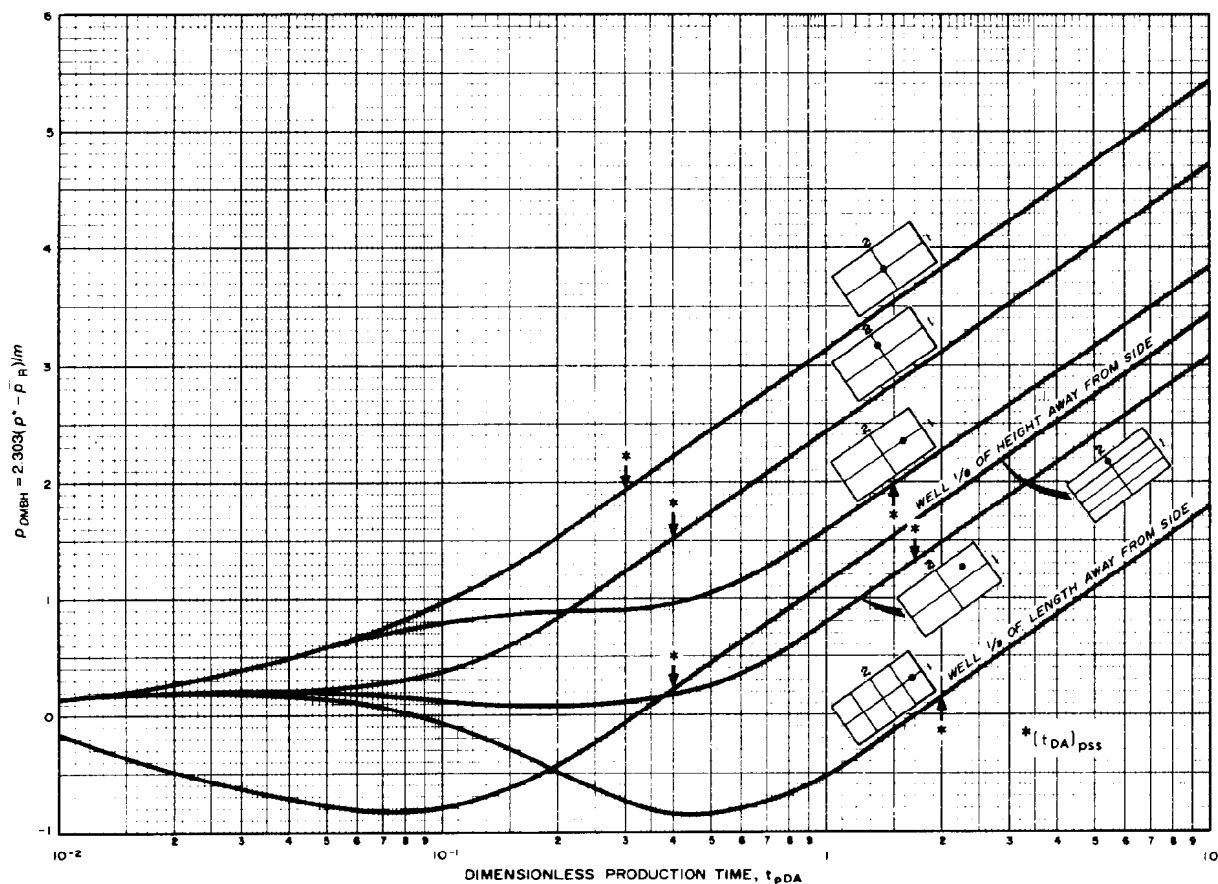


Fig. 35.16—MBH dimensionless pressure for different well locations in a 2:1 rectangular drainage area.

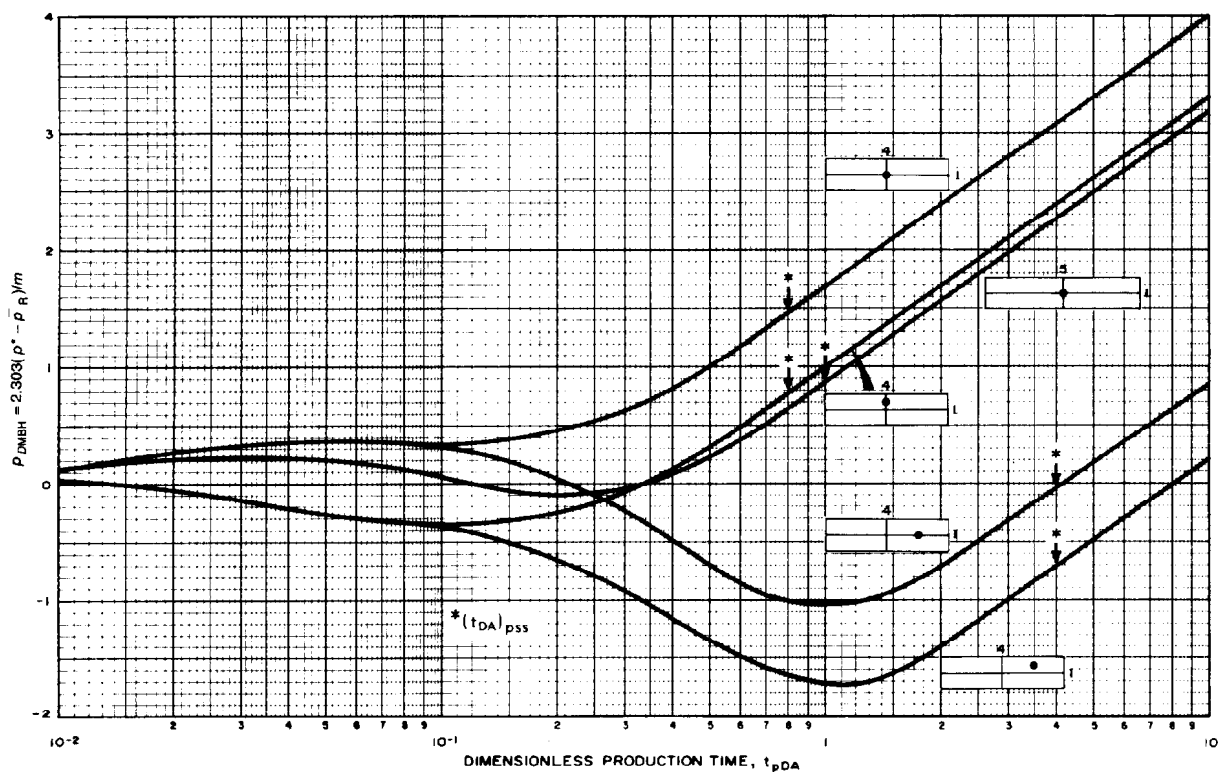


Fig. 35.17—MBH dimensionless pressure for different well locations in 4:1 and 5:1 rectangular drainage area.

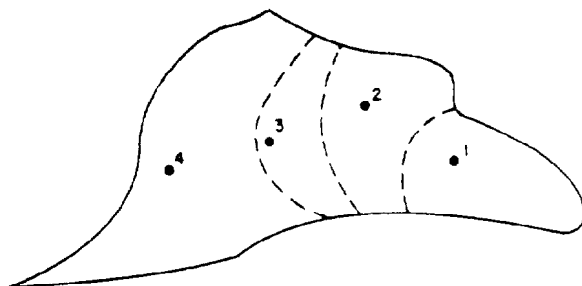


Fig. 35.18—Reservoir map showing approximate no-flow boundaries.

Example Problem 4 (Pressure Buildup Analysis) (after Earlougher²). *Pressure Buildup Test Analysis—Horner Method.* Table 35.3 shows pressure buildup data from an oil well with an estimated drainage radius of 2,640 ft. Before shut-in the well had produced at a stabilized rate of 4,900 STB/D for 310 hours. Known reservoir data are

$$\begin{aligned} D &= 10,476 \text{ ft}, \\ r_w &= (4.25/12) \text{ ft}, \\ c_r &= 22.6 \times 10^{-6} \text{ psi}^{-1}, \\ q_o &= 4,900 \text{ STB/D}, \\ h &= 482 \text{ ft}, \\ p_{wf}(\Delta t=0) &= 2,761 \text{ psig}, \\ \mu_o &= 0.20 \text{ cp}, \\ \phi &= 0.09, \\ B_o &= 1.55 \text{ RB/STB}, \\ \text{casing } d_i &= (6.276/12) \text{ ft, and} \\ t_p &= 310 \text{ hours.} \end{aligned}$$

Solution. The Horner plot is shown as Fig. 35.12. Residual wellbore storage or skin effects at shut-in times of less than 0.75 hour are apparent. The straight line, drawn after $\Delta t = 0.75$ hour, has a slope of -40 psig/cycle, so $m = 40$ psig/cycle.

Eq. 37a is used to estimate permeability:

$$k_o = \frac{162.6(4,900)(1.55)(0.20)}{(40)(482)} = 12.8 \text{ md.}$$

Skin factor is estimated from Eq. 40a using $p_{1hr} = 3.266$ psig from Fig. 35.12:

$$\begin{aligned} s &= 1.1513 \left\{ \frac{3,266 - 2,761}{40} \right. \\ &\quad \left. - \log \left[\frac{(12.8)(12)^2}{(0.09)(0.20)(22.6 \times 10^{-6})(4.25)^2} \right] \right. \\ &\quad \left. + 3.2275 \right\} = 8.6. \end{aligned}$$

TABLE 35.3—PRESSURE BUILDUP TEST DATA FOR EXAMPLE 4, $t_p = 310$ HOURS

Δt (hours)	$t_p + \Delta t$ (hours)	$(\Delta t_p + \Delta t)$ Δt	p_{ws} (psig)	$p_{ws} - p_{wf}$ (psig)
0.0	—	—	2,761	—
0.10	310.10	3,101	3,057	296
0.21	310.21	1,477	3,153	392
0.31	310.31	1,001	3,234	473
0.52	310.52	597	3,249	488
0.63	310.63	493	3,256	495
0.73	310.73	426	3,260	499
0.84	310.84	370	3,263	502
0.94	310.94	331	3,266	505
1.05	311.05	296	3,267	506
1.15	311.15	271	3,268	507
1.36	311.36	229	3,271	510
1.68	311.68	186	3,274	513
1.99	311.99	157	3,276	515
2.51	312.51	125	3,280	519
3.04	313.04	103	3,283	522
3.46	313.46	90.6	3,286	525
4.08	314.08	77.0	3,289	528
5.03	315.03	62.6	3,293	532
5.97	315.97	52.9	3,297	536
6.07	316.07	52.1	3,297	536
7.01	317.01	45.2	3,300	539
8.06	318.06	39.5	3,303	542
9.00	319.00	35.4	3,305	544
10.05	320.05	31.8	3,306	545
13.09	323.09	24.7	3,310	549
16.02	326.02	20.4	3,313	552
20.00	330.00	16.5	3,317	556
26.07	336.07	12.9	3,320	559
31.03	341.03	11.0	3,322	561
34.98	344.98	9.9	3,323	562
37.54	347.54	9.3	3,323	562

We can estimate Δp across the skin from Eq. 10:

$$\Delta p_s = 0.87(40)(8.6) = 299.$$

Average Drainage-Region Pressure—MBH. We use the pressure-buildup test data of Table 35.3. Pressure buildup data are plotted in Figs. 35.12. Other data are

$$\begin{aligned} A &= \pi r_e^2 \\ &= \pi(2,640)^2 \text{ sq ft.} \end{aligned}$$

To see if we should use $t_p = 310$ hours, we estimate t_{pss} using $(t_{DA})_{pss} = 0.1$ from Table 35.2.

$$\begin{aligned} t_{pss} &= \frac{(0.09)(0.2)(22.6 \times 10^{-6})(\pi)(2,640)^2(0.1)}{(0.0002637)(12.8)} \\ &= 264 \text{ hours.} \end{aligned}$$

Thus, we could replace t_p by 264 hours in the analysis. However, since t_p is only about $1.17 t_{pss}$, we expect no difference in \bar{p}_R from the two methods, so we use $t_p = 310$ hours. As a result, Fig. 35.12 applies.

Fig. 35.12 does not show p^* since $(t_p + \Delta t)/\Delta t$ does not go to 1.0. However, we may compute p^* from p_{ws} at $(t_p + \Delta t)/\Delta t = 10$ by extrapolating one cycle:

$$\begin{aligned} p^* &= 3,325 + (1 \text{ cycle})(40 \text{ psi/cycle}) \\ &= 3,365 \text{ psig.} \end{aligned}$$

Using the definition of t_{pDA} :

$$t_{pDA} = \frac{(0.0002637)(12.8)(310)}{(0.09)(0.20)(22.6 \times 10^{-6})(\pi)(2,640)^2}$$

$$= 0.117.$$

From the curve for the circle in Fig. 35.14, $p_{DMBH}(t_{pDA}=0.117)=1.34$. Then, from our step-wise procedure,

$$\bar{p}_R = 3,365 - \frac{40}{2.303}(1.34)$$

$$= 3.342 \text{ psig.}$$

This is 19 psi higher than the maximum pressure recorded.

Nomenclature

- A = drainage area of well
- c_{ti} = total compressibility evaluated at p_i
- c_{wf} = wellbore fluid compressibility
- C_A = shape factor from Table 35.2
- C_s = wellbore storage constant
- $f(t)$ = unit response function
- F_{Da} = non-Darcy (turbulence) factor
- F_t = turbulence factor
- m = $(162.6qB\mu)/kh$
- m_D = dimensionless $m(p)$
- $m(p) = 2 \int_0^p \frac{p}{z\mu} dp$ = real gas pseudopressure
- $m(\bar{p}) = m(p)$ at \bar{p}_R
- $m(p_i) = m(p)$ at initial pressure p_i
- $m(p_{wf}) = m(p)$ at wellbore flowing pressure p_{wf}
- m^* = slope of $m(p)$ plot
- m' = slope of p plot
- m'' = slope of p^2 plot
- p^* = MTR pressure trend extrapolated to infinite shut-in time
- $p_D = kh(p_i - p)/(141.2qB\mu)$ = dimensionless pressure
- $p_{DMBH} = 2.303(p^* - \bar{p}_R)/m$, dimensionless pressure, MBH method
- Δp_s = additional pressure drop across altered zone
- $|q_g|$ = absolute value of gas rate
- q_{sf} = flow rate at the sandface
- $r_D = r/r_w$ = dimensionless radius
- r_e = external drainage radius
- r_w' = effective wellbore radius
- s' = effective skin effect
- t_D = dimensionless time
- t_{DA} = dimensionless time based on drainage area, A
- $(t_{DA})_{pss}$ = time required to reach pseudosteady state, dimensionless
- t_{end} = end of MTR in drawdown test
- t_{pDA} = dimensionless producing time

t_{pss} = time required to achieve pseudosteady state

v = macroscopic (Darcy) fluid velocity

V_w = volume of the wellbore

x_e = distance from well to side of square drainage area

x_f = distance from well to either end of a vertical fracture

Subscript

wb = wellbore

Key Equations in SI Metric Units

$$\nabla^2 p = \frac{1}{3.557 \times 10^{-9}} \frac{\phi \mu c_t}{k} \frac{\partial p}{\partial t}, \dots \dots \dots (1)$$

where

p is in kPa,
 ϕ is a fraction,
 μ is in Pa·s,
 c_t is in kPa^{-1} ,
 k is in md, and
 t is in hours.

$$q_i B_i = q_o B_o + (q_g - R_s q_o) B_g + q_w B_w, \dots \dots \dots (6)$$

where

q_o, q_i, q_w are in std m^3/d ,
 B_o, B_i, B_w are in res $\text{m}^3/\text{std m}^3$,
 q_g is in std m^3/d , and
 B_g is in res $\text{m}^3/\text{std m}^3$.

$$p_D(r_D, t_D) = -\frac{1}{2} Ei \left(\frac{-r_D^2}{4t_D} \right), \dots \dots \dots (7)$$

where

$p_D = [kh(p_i - p)/(1866qB\mu)]$,

$$r_D = \frac{r}{r_w},$$

$$t_D = \frac{3.557 \times 10^{-9} kt}{\phi \mu c_t r_w^2},$$

h, r, r_w are in m,

k is in md,

p, p_i are in Pa,

q is in m^3/d ,

B is in res $\text{m}^3/\text{std m}^3$,

μ is in Pa·s,

t is in hours,

ϕ is a fraction, and

c_t is in kPa^{-1} .

$$p_{wf} = p_i - m \left(\log \frac{kt}{\phi \mu c_t r_w^2} - 8.10 \right), \dots \dots \dots (9)$$

where $m = 2.149 \times 10^6 qB\mu/(kh)$. See Eq. 7, for other units.

$$\left(\frac{\partial p}{\partial t} \right)_{pss} = \frac{-4.168 \times 10^{-2} qB}{V_p c_t}, \dots \dots \dots (15)$$

where V_p is in m^3 . See Eq. 7 for other units.

$$q = \left(\frac{5.356 \times 10^{-1} \frac{kh}{B\mu}}{\ln \frac{r_e}{r_w} - 0.75 + s} \right) (\bar{p}_R - p_{wf}), \quad \dots \quad (17)$$

where

$r_e = m$,
 s is dimensionless, and
 \bar{p}_R, p_{wf} are in kPa.
 See Eq. 7 for other units.

$$\bar{p}_R = p_i - \frac{N_p B_o}{V_p c_t}, \quad \dots \quad (21)$$

where

N_p is in m^3 ,
 V_p is in m^3 ,
 B_o is in res m^3 /std m^3 ,
 c_t is in kPa^{-1} , and
 \bar{p}_R, p_i are in kPa.

$$\nabla^2 m(p) = \frac{1}{3.557 \times 10^{-9}} \frac{\phi \mu c_g}{k} \frac{\partial m(p)}{\partial t}, \quad \dots \quad (24)$$

where $m(p)$ is in kPa^2 and c_g is in kPa^{-1} . See Eq. 7 for other units.

$$m_D = \frac{1}{2} \ln t_D + 0.4045 + s + F_{Da} |q_g|, \quad \dots \quad (33)$$

where

$$m_D = 2.708 \times 10^{-10} \left(\frac{T_{sc}}{p_{sc} T_R} \right) \frac{kh}{q_g} \cdot [m(p_i) - m(p_{wf})],$$

$$t_D = \frac{3.557 \times 10^{-9} kt}{\phi \mu c_t r_w^2},$$

s is dimensionless,
 F_{Da} is dimensionless,
 q_g is in m^3/d ,
 T_{sc}, T_R are in K,
 p_{sc} is in kPa,
 k is in md,
 h is in m, and
 $m(p_i), m(p_{wf})$ are in $kPa^2/Pa \cdot s$.
 See Eq. 7 for other units.

$$k_o h = - \frac{2.149 \times 10^6 q_o B_o \mu_o}{m}, \quad \dots \quad (37a)$$

See Eqs. 7 and 9 for units.

$$k_g h = \frac{4.250 \times 10^9 q_g \left(\frac{p_{sc} T_R}{T_{sc}} \right)}{m^*}, \quad \dots \quad (37b)$$

where m^* is in $kPa^2/Pa \cdot s \cdot cycle$. See Eq. 33 for other units.

$$s = 1.151 \left(\left| \frac{p_i - p_1}{m} \right| - \log \frac{k}{\phi \mu c_t r_w^2} + 8.10 \right), \quad \dots \quad (38a)$$

where m is in $kPa/cycle$. See Eq. 7 for other units.

References

1. Matthews, C.S. and Russell, D.G.: *Pressure Buildup and Flow Tests in Wells*, Monograph Series, SPE, Richardson, TX (1967) 1.
2. Earlougher, R.C. Jr.: *Advances in Well Test Analysis*, Monograph Series, SPE, Richardson, TX (1977) 5.
3. Dake, L.P.: *Fundamentals of Reservoir Engineering*, Elsevier Scientific Publishing Co., Amsterdam (1978).
4. Gas Well Testing—Theory and Practice, fourth ed., Energy Resources and Conservation Board, Calgary, Alta., Canada (1979).
5. Lee, John: *Well Testing*, Textbook Series, SPE, Richardson, TX (1982).
6. *Pressure Analysis Methods*, Reprint Series No. 9, SPE, Richardson, TX (1967).
7. *Pressure Transient Testing Methods*, Reprint Series No. 14, SPE, Richardson, TX (1980).
8. van Everdingen, A.F. and Hurst, W.: "The Application of the Laplace Transformation of Flow Problems in Reservoirs," *Trans. AIME* (1949) **186**, 305-24.
9. Martin, J.C.: "Simplified Equations of Flow in Gas Drive Reservoirs and the Theoretical Foundation of Multiphase Pressure Buildup Analyses," *Trans., AIME* (1959) **216**, 309-11.
10. Wattenbarger, R.A. and Ramey, H.J. Jr.: "An Investigation of Wellbore Storage and Skin Effect in Unsteady Liquid Flow: II. Finite Difference Treatment," *Soc. Pet. Eng. J.* (Sept. 1970) 291-97; *Trans., AIME*, **249**.
11. Dietz, D.N.: "Determination of Average Reservoir Pressure From Buildup Surveys," *J. Pet. Tech.* (Aug. 1965) 955-59; *Trans., AIME*, **234**.
12. Al-Hussainy, R., Ramey, H.J. Jr., and Crawford, P.B.: "The Flow of Real Gases Through Porous Media," *J. Pet. Tech.* (May 1966) 624-36; *Trans., AIME*, **237**.
13. Wattenbarger, R.A. and Ramey, H.J. Jr.: "Gas Well Testing With Turbulence, Damage and Wellbore Storage," *J. Pet. Tech.* (Aug. 1968) 877-87; *Trans., AIME*, **243**.
14. Ramagost, B.P. and Farshad, F.F.: "p/z Abnormally Pressured Gas Reservoirs," paper SPE 10125 presented at the 1981 SPE Annual Technical Conference and Exhibition, San Antonio, Oct. 4-7.
15. Miller, C.C., Dyes, A.B., and Hutchinson, C.A. Jr.: "The Estimation of Permeability and Reservoir Pressure From Bottom Hole Pressure Build-Up Characteristics," *Trans., AIME* (1950) **189**, 91-104.
16. Horner, D.R.: "Pressure Build-Up in Wells," *Proc., Third World Pet. Cong., The Hague* (1951) Sec. II, 503-23.
17. Matthews, C.S., Brons, F., and Hazebroek, P.: "A Method for Determination of Average Pressure in a Bounded Reservoir," *Trans., AIME* (1954) **201**, 182-91.

Chapter 36

Development Plan for Oil and Gas Reservoirs

Steven W. Poston, Texas A&M U.*

Introduction

The following discussion on the determination of the proper development plan for oil reservoirs or gas reservoirs is a summation of the current thinking in the oil industry. Conditions have changed dramatically since R.C. Craze wrote this chapter for the original book in 1962. At that time, the price of crude oil and gas was so low that the industry was concerned mainly with recovering the gross reserves from a field.

Today's economics have changed our outlook to such a degree that the need for a logical and efficient plan for the orderly development of an oil or gas field is of utmost importance. The bidding competition for reserves often has caused successful field development to be at least partially dependent on getting the most out of the ground with the minimum number of wells.

The oil business was originally an endeavor that allowed one to explore for hydrocarbons in relatively unexplored areas. The probability of finding large fields was quite high, and an excellent return on investment resulted when a new field was found. A majority of the large oil and gas fields have been found after 25 years of intensive exploration. The number of companies searching for hydrocarbons has increased while at the same time the fields are harder to locate. Now we are a very competitive industry in which there is little room for error. In other words, the rules of the game have changed.

New technology and thinking about logical field development has evolved during the last 20 years. Continuity of producing intervals between wells is now known to be much more important than previously thought. Advances in well test analysis have allowed the engineer and geologist to estimate reservoir size and intrawell continuity. Improved seismic techniques have allowed geophysics to play an increasingly important role in allocating well locations for efficient reservoir drainage.

A person interested in developing an oil or a gas field must use a basic understanding of geology, engineering, and economics. Other, more sophisticated techniques may have to be used at times to arrive at a realistic development plan. However, when one begins to develop a field, a number of questions need to be mulled over and should be discussed with colleagues. The thinking process occurs as follows.

Is the Well Being Drilled to Develop Proved, Probable, or Possible Reserves? The drilling of a development well in the middle of a field for proved reserves is considerably different than drilling an outpost well to help define the field limits. Greater reserves must be assigned to well questing for probable or possible reserves than for an infield development well. The drilling for known reserves often allows for a low return on investment. However, the reward must be greater if the risk of drilling and not finding the hydrocarbon accumulation increases. The benchmark for the go/no-go decision for the drilling of a well is a function of not only the return on investment but also the degree of risk to be incurred.

Answering these questions requires a combination of all disciplines in the petroleum industry. The greater the certainty of the reserves, the less the need for geological and engineering opinions.

What Are the Reservoir Rock and Fluid Characteristics? Field development is conducted far differently in a clean, well-developed sand than it is in a place such as the low-porosity and low-permeability Austin chalk region of Texas. High porosities and permeabilities and low oil viscosities permit high offtake rates and wide well spacing. These large "per well" recoveries often preclude the need for the serious study of the minimum economic reserves requirements.

*Author of the original chapter on this topic in the 1962 edition was Rupert C. Craze.

Development drilling will continue at a different pace for a continuous and homogeneous sand than for a field composed of a series of productive intervals sandwiched between shale layers of unknown lateral extent. A well completed in a series of sand stringers of uncertain areal extent should be placed on production for a time to see how much it actually will produce. Extensive drilling in such a field should wait until the economic worth of the total effort is determined from field production figures.

Any knowledge concerning the geology of the prospect attained before the well is drilled would furnish insight into the probable number of completion zones and where the completion intervals should be. The proper well spacing would be predicated on this knowledge.

The type of drive mechanism often will predicate the placement of the development wells. If a water drive is expected, the wells should be placed in the most updip locations possible. However, the updip placement of the wells would be a disaster if there is an expanding gas cap drive. The information is derived from reservoir engineering evaluations.

What Is the Surface Environment? Development considerations are completely different when drilling in a shallow well in west Texas or a Jurassic well in the North Sea. Platform rigs often are used to drill offshore wells. The number of drilling slots is limited, and, once the rig is moved off, it is often prohibitively expensive to move back on if new ideas arise.

What Surface Production Facilities Are Required? There is no sense in drilling an offshore development well if there are no facilities available for production hookup. The production facilities could cost much more than the value of the reserves. Drilling on land in an area where costs may be reduced considerably could allow the production facility costs to be only a fraction of the reserves' worth.

By What Method is the Product to be Sold? Gas must be transmitted by pipeline, whereas oil must be trucked or lightered to a receiving facility. For an oil well, revenue usually begins upon completion, while a gas well must wait for the installation of a pipeline. The cash flow situation for development of either an oil or a gas field is usually different because of the type of product.

What Is the Relationship Between the Costs and the Profit Margin? The margin of profit for an operator will vary considerably according to geographical location and the type of lease. Also, overhead costs may be greater for a large company than for a smaller company. The cost of money may be less for a large company because of a significant and established cash flow. Foreign profit margins are generally much less than margins from U.S. oil and gas sales.

Readers will see other areas of uncertainty in addition to those discussed here. However, the following discussion will shed light on some of the more important points that one should remember concerning the formulation of a development plan for either an oil reservoir or a gas reservoir. There are no handy formulas to use nor are there any tried-and-true rules to follow. Proper field development for a particular set of conditions requires a combination of a variety of oil field disciplines.

Oil and Gas Differences

Method of Sales

Development plans for oil or gas reservoirs generally follow different paths not only because of the optimal depletion characteristics but because of the method of sales.

Crude oil is a reasonably stable substance and, being liquid, may be loaded easily into some type of container for transportation to a sales point. The container is often at or very near atmospheric pressure. The container may be a truck, barge, or pipeline. On most land locations, sales may begin from a well as soon as the production equipment is installed. Also, since oil is contained and moved easily, the buyer of the crude oil may not always be constant.

Natural gas must be kept in some type of container so it will not dissipate into the atmosphere. The high compressibility of the gas permits a smaller container to be used with increased confining pressures. Economics dictates that gas is to be transported through pipelines. The pipeline company must be assured that sufficient reserves are present to justify the expense of installing the pipeline. These capital expenditures often require long-term commitments from all the interested parties.

Sufficient reserves must be proved to justify the expense of laying a pipeline. A number of wells may have to be drilled before any income is derived from the initial discovery. The operator must drill sufficient wells to ensure the quantities of gas required to be delivered over the contract period.

The oil may be transported out by barge or tank truck if the reserves do not justify the expense of installing a pipeline in the case of oil production. Operating expenses are greater when oil is moved by tank truck or barge, but the capital investment is negligible when compared to pipeline installation.

Development drilling in an oil field often may be conducted in a more growth-oriented manner than that in a gas field. Generally speaking, the capital investment required to develop a gas field is greater than for developing the same reserves in an oil field because a pipeline always is required to transport the gas. Non-capital-intensive barges or trucks may be used to transport oil.

The Best Depletion Technique

There are fundamental differences between developing and depleting an oil reservoir and a gas reservoir. These differences are discussed next.

Oil Reservoirs. Every effort should be made to maintain reservoir pressure as high as possible during the depletion of an oil reservoir. A high reservoir pressure helps to preclude the installation of some type of artificial lift system or some method to aid in recovery. High reservoir pressures usually result from an active water drive or gas cap encroachment, both of which displace oil and help to push it toward the wellbore. These displacement mechanisms result in a reduced oil saturation at a relatively high abandonment pressure.

Gas Reservoirs. The compressibility of gas may be up to 1,000 times greater than relatively incompressible oils. These high compressibilities can allow the majority

of the reserves in a gas reservoir to be depleted by simple gas expansion. In fact, ultimate recoveries of 80% of the original gas in place (OGIP) may be achieved by pressure depleting a gas reservoir, even though the remaining gas saturation may be quite high. Conversely, if a gas is trapped behind an advancing water front with a correspondingly lower residual saturation, the remaining gas left behind will be greater because the high compressibility of the gas allows a much greater quantity of gas to be trapped at these higher reservoir pressures.

Example Problem 1—Dry Gas Reservoir. The example given in Table 36.1 indicates the effect of the type of drive mechanism on ultimate recovery from a theoretical dry gas reservoir. Water is assumed to invade the reservoir uniformly in the water influx case. The assumption is not necessarily true in the operational context, but the illustration is made to show the necessity of abandoning gas reservoirs at low pressures.

The effect of the gas FVF in the lower-pressure reaches of the reservoir allow the pressure depletion case to recover more gas.

The previous discussion shows how the development of an oil reservoir may be conducted in a piecemeal and leisurely manner while development of a gas reservoir should be carried out with an eye toward maximizing the reservoir offtake rate to aid in the occurrence of pressure depletion conditions. To arrive at a development plan two basic steps need to be accomplished. These are (1) the characterization of the reservoir and (2) the prediction of the performance of the reservoir under various exploitation schemes and operating conditions.

Characterization of the Reservoir

Geology

Interpretation of Paleo-Environments. The limits of a reservoir and the possible variation of the porosity and permeability within the reservoir may be inferred by studying the well logs and cores taken from wildcat and appraisal wells. The knowledge gained from these studies would be of great help in setting wellsite locations early in the life of a development drilling project. Usually the reservoir productive characteristics are known only after the field or reservoir is maturely developed.

The nature of the reservoir rock often is reflected in the sedimentary record. The sedimentary section is penetrated during the drilling for oil and gas. The character of the sediments may be inferred by logs or by core analyses. For a number of years, geologists have been studying and relating currently occurring sedimentary processes to reservoir rock paleo-environments. Each sedimentary process has been shown to have a particular porosity and permeability distribution and to have a reasonably predictable areal extent.

The interpretation of the probable paleo-environment by log and core analysis of a sedimentary section could be of inestimable value early in the life of field development. The following discussion gives a brief overview of geological interpretive work.

The literature contains an overabundance of work on the evolution of clastic sediments. The reservoir characteristics of a clastic sediment (mainly sandstones) often is related largely to its depositional history.

TABLE 36.1—EXAMPLE OF EFFECTS OF DRIVE MECHANISM ON RECOVERY

$$V_R = 6,400 \text{ acre-ft}$$

$$\phi = 22\%$$

$$S_w = 23\%$$

$$S_{rg} = 34\%$$

$$G = 8.878 \times 10^9 \text{ scf}$$

Pressure (psia)	B_g (scf/cu ft)	Cumulative Production (10^9 scf)	
		Volumetric Reservoir	Waterdrive Reservoir
3,150	188	—	—
2,500	150	1.8	5.8
2,000	120	3.2	6.4
500*	28	7.6	—

*Low reservoir pressures will not be obtained because of the additional energy supplied by the encroaching water; therefore, B_g will be at a higher value at abandonment.

Therefore, a predictive interpretation may be done with some degree of certainty.

Less is known of carbonates. The chemical nature of the depositional processes to form carbonate reservoirs and the usually extensive diagenetic history cloud the true nature of the reservoir character. A large amount of data—i.e., a considerable number of wells—is required before the nature of a carbonate reservoir may be discerned.

Clastic Reservoirs. The depositional environment may be estimated by studying electric log sections that pass through the zone of interest and by analyzing core samples taken from the zone.¹⁻³ The interpretation of these paleo-environments is derived from the study of modern depositional environments. The character of modern streams, deltas, and beaches has been well documented.⁴⁻⁶

Bernard and LeBlanc⁷ divided the major depositional environments into continental, transitional, and deep marine classifications. Continental and deep marine deposits do not contain widespread oil or gas accumulations and are not discussed further. Transitional sediments may be divided into coastal interdeltaic and deltaic environments. The coastal interdeltaic area usually consists of linear, relatively narrow sand beaches, which extend seaward into a normal and then a deep-water environment. The sands composing the normal marine environment are usually very fine grained and are deposited in conjunction with a high percentage of clay. The generally low permeabilities displayed by normal marine sediments preclude a high incidence of commercial oil and gas deposits.⁸ Deepwater marine sediments are composed mostly of shales and are on the whole nonproductive.

The most common and important hydrocarbon-bearing sandstone reservoirs are of deltaic origin. These sediments usually are deposited in a high-energy, often fluctuating atmosphere. In deltaic environments encountered most often during oil and gas drilling operations, delta-bar and distributary channel sediments are the two most prevalent sedimentary environments found, while offshore bars may be found in the delta front areas.

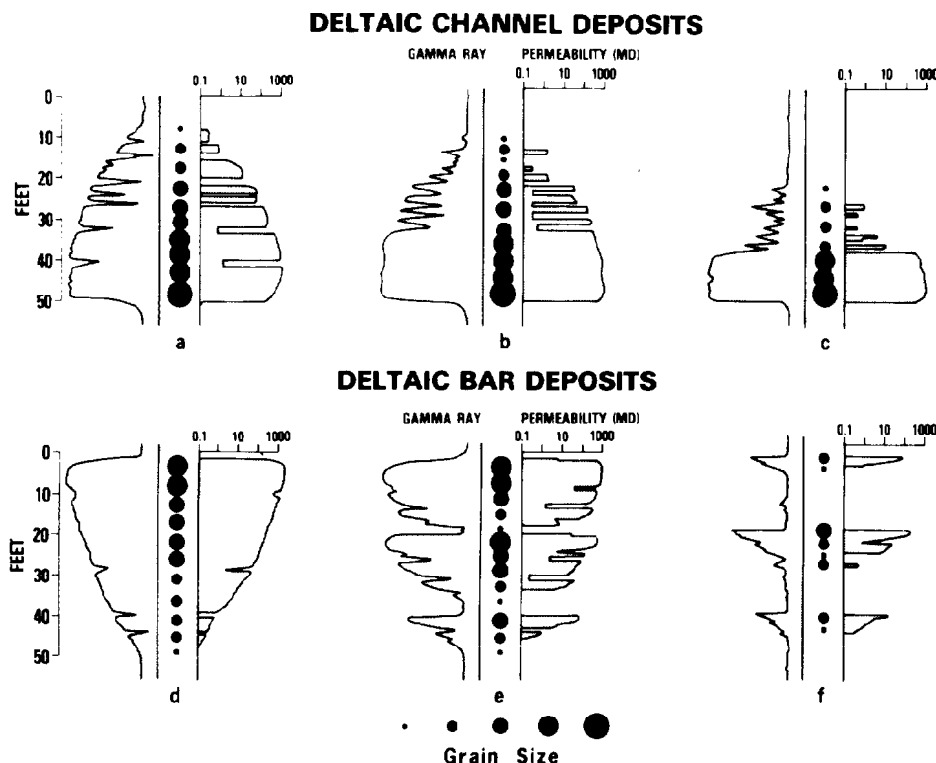


Fig. 36.1—Idealized porosity and permeability profiles—bar and channel deposits.

The delta-bar sequence is typified by an upward gradation from shallow, marine clays at the base through a section that shows an increasing grain size. The progressive upward coarsening of the sand-grain size is the result of the delta advancing over the marine clays. A high-energy regime is seen to increase in the vertical direction. A typical electric log section grades upward from a shale section (deeper water) to gradually increasing amounts of sand⁹ (see Fig. 36.1). The section contains crossbeds, ripple laminations, and modest amounts of quartz. Delta-bar sands grade downdip into pro-delta silts and clays and grade updip into the organic-rich, fresh- and brackish-water clays. Delta sands often are limited in areal extent, even though encompassing a thick sedimentary sequence. Vertical reservoir continuity may be restricted because of the large number of shale stringers present in the delta front sequence.

Distributary (river) channels transport sediments to the delta front. Distributary channels cut through deltas in a variety of meandering ways. Even though they comprise only a small portion of sedimentary record, these sediments often transect deltaic or offshore bar sand reservoirs and incur reservoir discontinuities in an otherwise homogeneous system. Fig. 36.2 is an example of such a discontinuity in the South Pass 27 field located in the offshore waters of south Louisiana.¹⁰ The field is included in the sand/shale sequence generated by prior deposition of the Mississippi River. Notice how the channel cut through the previously deposited sediments and formed a reservoir separate from the original.

Distributary channel sediments initially are deposited in a higher-energy atmosphere, and, hence, display a

coarser grain size toward the bottom of the section. The effect of grain size gradation may be seen in Fig. 36.1. These deposits are characterized by boxy log shapes with a very high sand content. The gradation of the sands is typified by an abrupt change from a shale to a very clean sand and then to a gradual increase in shale/sand ratio in the upward direction. Deposition is parallel to the source of the sediments.

Shoreline or barrier-island sandstones are represented by a sequence of normal marine muds grading upward into laminated sandstones. The section may be overlain by aeolian dune sandstones, which are the emergent portion of the shoreline. Sand gradation is generally coarsening upward. The sand grains are well sorted, and the quartz content of the sand is quite high. Wave action has reduced the less resistant feldspars to clay-sized particles, which have been transported to lower-energy regimes. Deposition is normal to the source of the sediments.¹¹ The sand bodies contain very few shale laminations and they are characterized by excellent lateral continuity.¹² The lowermost layer of a barrier bar sand comprises interbedded sand, silts, and shales. The second layer is made up of a bioturbated thick sand sequence. The penultimate layer consists of laminated sands laid down on the beach or the upper shore face of the barrier bar. The uppermost layer usually consists of oxidized aeolian deposits.¹³

Barrier bar reservoirs offer an excellent opportunity for hydrocarbon exploration. The reservoirs usually are overlain by lagoonal clays, which form an excellent trap. Barrier sands usually exhibit a high degree of internal continuity and are deposited parallel to the coastline.

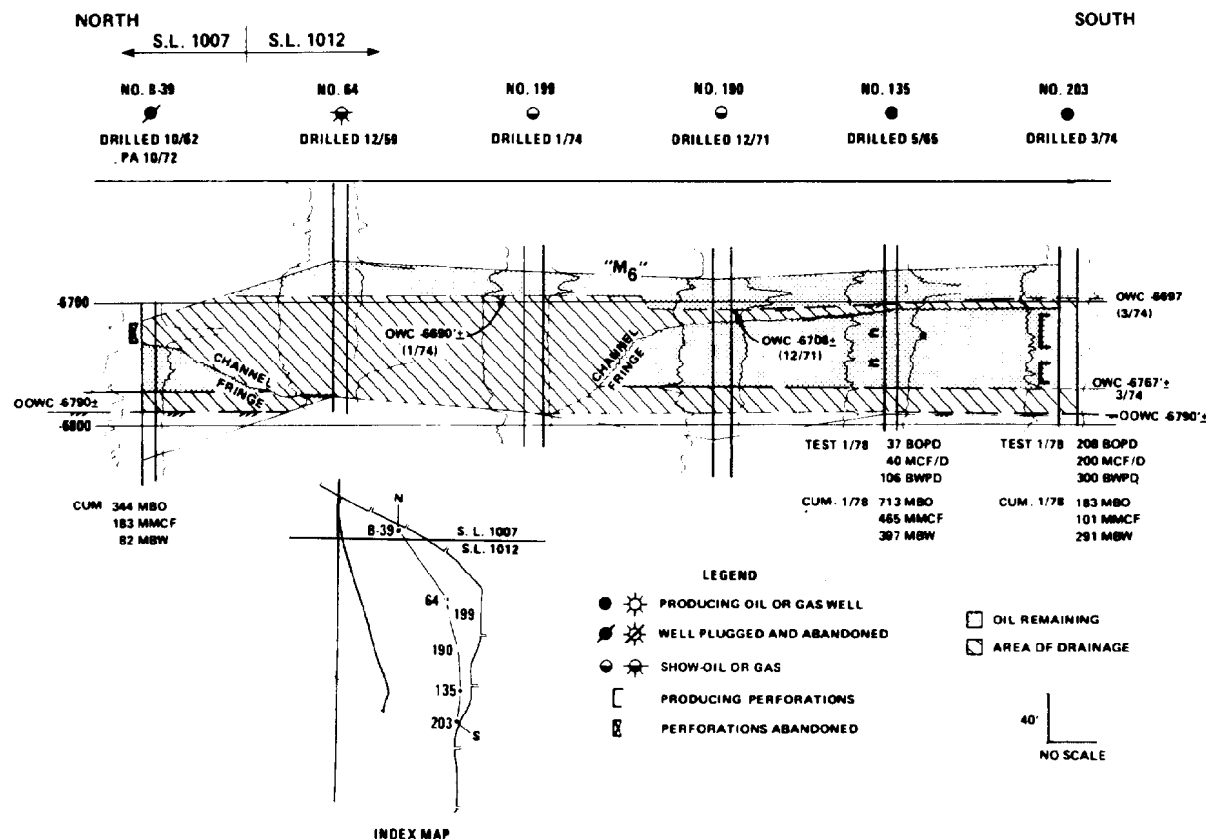


Fig. 36.2—Reservoir discontinuity—channel and fringe sands.

Carbonate Reservoirs. Carbonate reservoirs are completely different in nature from sandstone reservoirs. The composition of sandstone reservoirs is largely a product of the depositional environment; carbonate reservoirs are a product of not only the depositional environment but also mechanical processes that occur after deposition.¹⁴ The heterogeneities caused by the variety of formative processes may form extremely complex fields such as the Means field shown in Fig. 36.3.¹⁵ Note the field heterogeneity. Carbonates may be deposited in both shallow- and deepwater marine environments. The fields may range from a few acres (pinnacle reefs) to regional in size (carbonate banks). Jardine¹⁶ has discussed how

carbonate fields may be formed in a variety of settings.

Bioherm Reefs. Bioherm or pinnacle reefs usually are characterized by their relatively small size with a high degree of relief. The reefs contain a high percentage of skeletal material at the outermost portions of the accumulation. The interior of the reef is composed of finer-grained material and has less porosity and permeability than the outer limits.

Biostrome Reefs. Biostrome reefs were formed in less rapidly subsiding basins and may extend for hundreds of square miles. Like the bioherm reefs, the biostrome reefs contain a high percentage of skeletal material. Horizontal stratification is present.

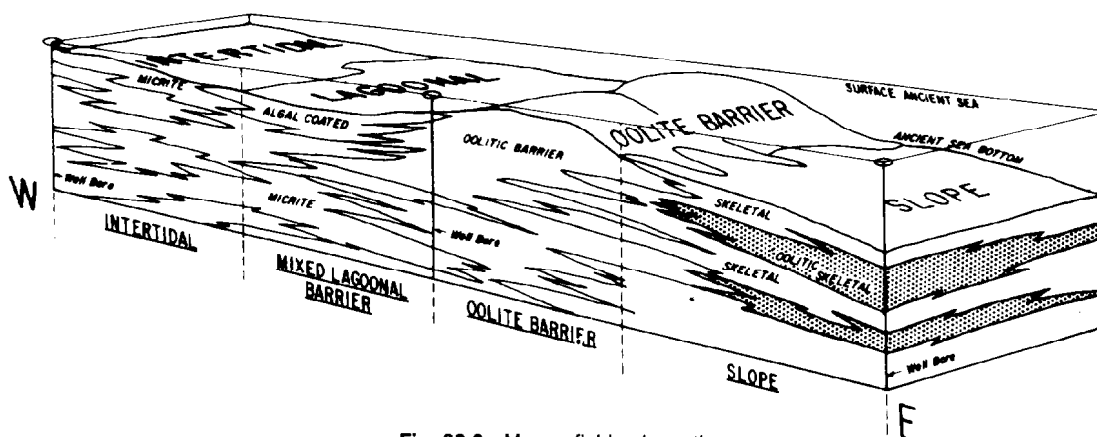


Fig. 36.3—Means field schematic.

PRIMARY POROSITY

SECONDARY POROSITY

DEPOSITIONAL TYPES	CONFIGURATION	GRAIN SIZE	POROSITY TYPE	PROCESS	FAVORABLE EFFECTS	UNFAVORABLE EFFECTS
BIOHERM REEF		C M F	VUG CELL I.O. CHALKY	FRACTURING JOINTS BRECCIA	INCREASE K	INCREASE CHANNELING
BIOSTROME REEF		C M F	VUG CELL I.O. CHALKY	LEACHING	INCREASE K & ϕ	
BANK (SHELF)		C M F	VUG CELL I.O. CHALKY	DOLOMITIZATION	INCREASE K	CAN ALSO DECREASE ϕ & K
SHOAL		C M F	VUG CELL I.O. CHALKY	RECRYSTALLIZATION	MAY INCREASE PORE SIZE AND K	DECREASE ϕ & K
NEAR-SHORE		C M F	VUG CELL I.O. CHALKY	CEMENTATION BY CALCITE DOLOMITE ANHYDRITE PYROBITUMEN QUARTZ		

Fig. 36.4—Distribution of porosity within various types of carbonate reservoirs.

Shelf Carbonates. Shelf carbonates are usually sheet-like or tabular bodies composed of a high percentage of skeletal material, enclosed by surrounding fine-grained material.

Nearshore Deposits. Nearshore deposits are usually of a thin and restricted nature and are generally fine grained. This type of deposit is of minor significance in oil and gas production.

Fig. 36.4¹⁶ summarizes the characteristics of the variety of carbonate deposits. Note the different types of porosity and the processes that affect the reservoir quality.

The development of oil and gas fields in carbonate sediments requires the study of the fossil content, any postdepositional alterations, and characterization of the pore space. This type of reservoir often displays two dissimilar porosity-permeability systems.

Extent of Shale Stringers. The knowledge of the probable lateral composition of a sandstone body soon after

discovery would be of considerable aid for planning of the future development drilling program. Weber¹⁷ combined studies done principally by Zeito,¹⁸ Verrien *et al.*,¹⁹ and Snider *et al.*²⁰ to arrive at Fig. 36.5. The figure summarizes a number of efforts to estimate the effect of depositional environment on the extent of shale stringers on sandstone reservoirs. Note how the marine sands possess the most extensive shale barriers, while the more poorly sorted point bars and distributary channels possess the shale members of least extent. Of course, the more widely correlative a producing interval is, the easier it is to predict future productive patterns. Many channels and point bars have been laid down in such a widely fluctuating atmosphere that correlation between wells is often difficult if not impossible. The recognition of the possible extent of the shale intercalations early in the life of development in the field would be of tremendous aid in the spotting of well locations.

Engineering

Intrawell continuity of the producing zone is one of the main ingredients for successfully depleting an oil or gas reservoir of the majority of the potential reserves. Additional development drilling often is required in a field when sand stringers are found to be discontinuous between producing wells.

The differential movement of fluids within a reservoir caused by rock heterogeneities was noted first in the engineering sense by Stiles.²¹ Poor response to the installation of many of the waterflood projects installed in some of the west Texas carbonate reservoirs in the 1950's and 1960's produced a spate of studies investigating the often discontinuous nature of the reservoirs. Refs. 15 and 22 through 25 are good reviews of some of these investigations. The determination of the degree of noncommunication between adjacent wells may be quantified to a certain degree by geological and reservoir engineering studies. The better-known techniques for estimating the degree of reservoir continuity are discussed next.

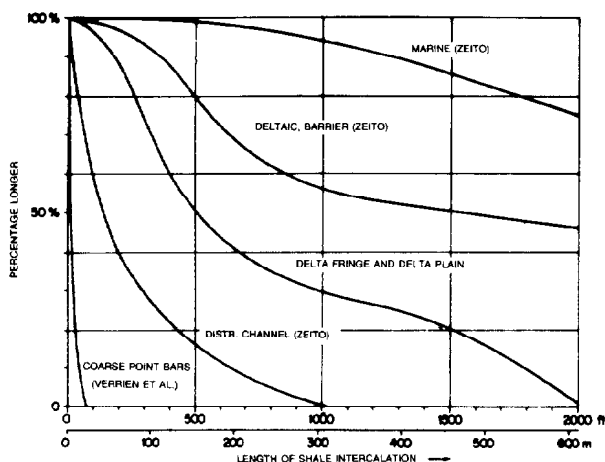


Fig. 36.5—Continuity of shale intercalations.

Net Pay/Net Connected Pay Ratio. Irregularities within sedimentary rocks often cause discontinuous productive horizons between wells. The degree of these discontinuities may be discerned by correlating the individual pay zones between adjacent wells. If a particular sand stringer is seen in one well but not in the other then it is called discontinuous. Sands are known to become more discontinuous with distance. A method to estimate the degree of producing-sand-interval intrawell communication is discussed in a paper by Stiles.²³ The continuity between wells is defined as the fraction of the total pay sand volume that is connected to another well.

A productive stringer is defined as continuous when correlatable between two wells. The stringer is classed as discontinuous if it is not correlative. Well pairs are compared, and eventually a figure may be drawn that summarizes the decline in reservoir continuity with distance. Fig. 36.6 is the result of one of these studies.²⁶ Notice the decline of continuity with distance between wells. The figure shows that the number of producing zone discontinuities was found to be much greater than expected when additional infill drilling was carried out in the Means field. A similar type of investigation by Stiles²³ in the Fullerton-Clearfork Unit had indicated a degree of reservoir continuity of 0.72. The estimate compares quite favorably with a material balance of the field.

A more recently published paper indicated that the material balance and the volumetric in-place estimate for a number of reservoirs in the Meren field compared very favorably.²⁷ A sand-by-sand correlation of these same reservoirs in the Meren field indicated a degree of continuity approaching that of unity. One could gather from these studies that communication was uniform throughout the reservoirs and additional infield drilling in all likelihood would not discover many discontinuous sand members. However, infield drilling in the Fullerton-Clearfork Unit could prove fruitful because of the good probability of penetrating previously undrained sand members.

Material Balance Studies. The results of volumetric reserves estimates may be compared to the material balance estimate. The material balance estimate is a function of production, which is derived from the movement of fluid through connected producing zones. Volumetric calculations are determined from net sand maps, which often do not take into account the effect of sand discontinuities on production. The difference between the results of the calculations gives an idea of the degree of discontinuity of a particular reservoir. Stiles²³ used the idea when studying the Fullerton-Clearfork Unit. The material balance method indicated 738 million bbl OIP. A volumetric estimate showed 1.03 billion bbl OIP. The ratio of the material balance estimate to volumetric estimate is 0.72. The low degree of communication would be an indicator of the successful outcome of an infield drilling project.

Computer Simulation Methods. Reservoir simulation studies are simply an extension of the material balance technique. However, the reservoir simulator allows one to take into account the producing and rock characteristics of individual areas within the reservoir.

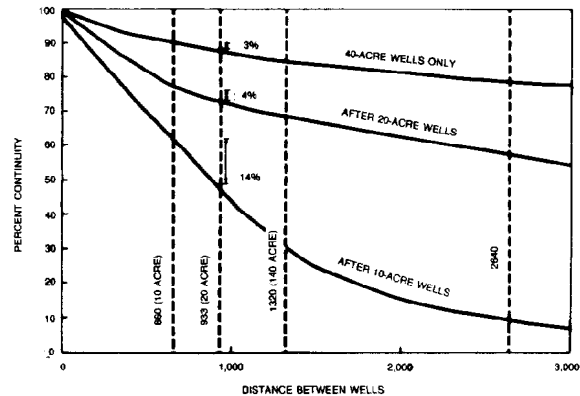


Fig. 36.6—Continuous pay—Means field.

Details of reservoir simulation are given in Chap. 48.

A study by Weber²⁸ is an excellent example of the use of core and log interpretation principles to aid in determining the paleo-environment. These interpretations then were used in a computer simulation program, which was able to typify the D 1.30 reservoir in the Obigbo field with a high degree of accuracy. Fig. 36.7 is the type log of the reservoir. Note the differentiation of the producing interval into four discrete depositional environments. Each of the environments is represented by an interval of differing productive characteristics. The variations of these environments were noted in the section of each well penetrating the D 1.30 sand interval. Core analyses indicated the range of permeabilities that each of the units would exhibit. A permeability distribution map was drawn for the reservoir as a whole from these machinations. Subsequent modeling of the drainage patterns within the reservoir could be carried out with a high degree of certainty since the pattern of deposition had been replicated.

Interference Testing. The analysis of reservoir pressures has been an age-old reservoir evaluation tool in the petroleum industry. The similarity of pressures within a group of wells usually helps prove or disprove the interwell communication. An abnormally different pressure from a particular well is often the first indication of reservoir separation. Further analysis may disclose a previously undetected fault separating the wells in question. Sometimes wells are seen to display similar static bottomhole pressures even though there is a known fault separation. The similarity of pressures is caused by the production from each well being sufficient to draw the reservoir pressure down to the same degree. A transient pressure test must be run between the well pairs to estimate the degree of interwell communication.

The alteration in the producing or injection rate of a well will have an effect on the pressure in a connected observation well. The study of these effects is called "transient-pressure" or "interference" testing. Interference testing may be done by either a long-term production or injection change in a well (interference testing) or by very short-term rate alterations (pulse testing). Ref. 29 presents a detailed description of the two methods.

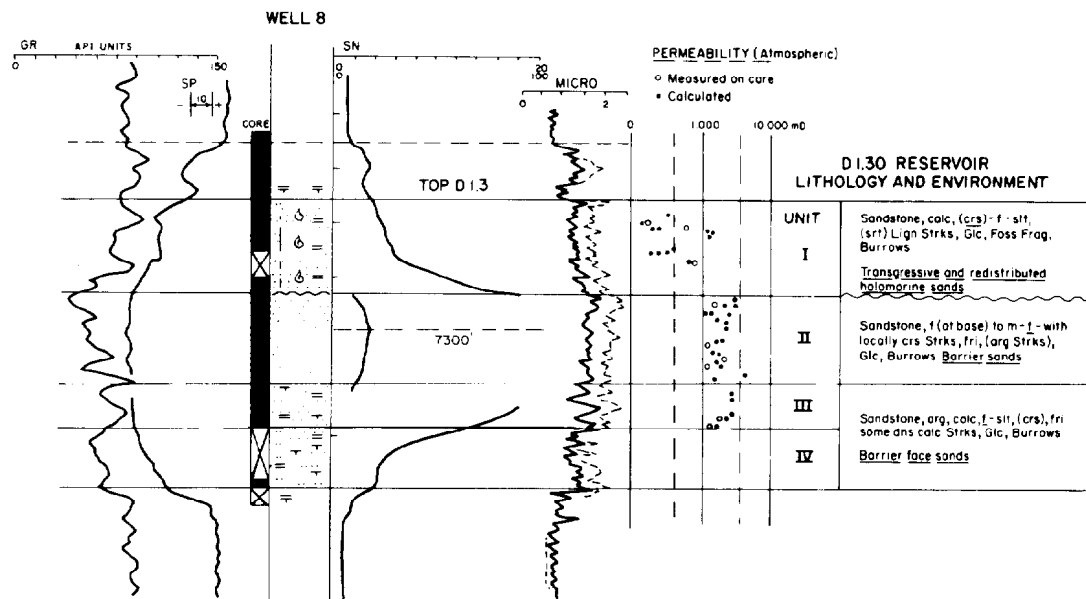


Fig. 36.7—Type log—D 1.30 sand, Obigbo field.

Interference tests comprise a relatively long-term rate alteration. The effect of the rate alteration will be noted in the observation well when there is interwell continuity. Of course, one would assume the presence of a discontinuity if the pressure fluctuation is not seen in the observation well.

The field application of an interference test is well documented in Ref. 30. A fieldwide spacing rule of 40 acres per well had been instituted in the North Anderson Ranch field in Lea County, NM. The engineering effort

was designed to estimate the true drainage area with the field. Four wells were produced and the resulting pressure decline was noted in a central observation well. (See Fig. 36.8 for the plan of the well layout.) The production from the four offsetting wells declined 11 psi after 165 hours' production. The diffusivity equation was used to calculate the expected pressure drop for similar conditions. The theoretically predicted pressure drop was 12 psi. The use of interference tests indicated a well drainage area greatly in excess of the initial 40-acre estimate. An 80-acre drilling pattern would effect a similar recovery with a greatly reduced number of wells.

Pulse testing is often more convenient than interference testing.³¹ The use of very precise pressure gauges coupled with individual design characteristics often allows pulse tests to be carried out within 1 or 2 days. Minor variations in production or injection volumes are able to send a pulse to observation wells. The variation of rates provides a "footprint," which may be noted by precision gauges placed in the observation wells. A pulse test is able to discern reservoir heterogeneities in a manner similar to the previously discussed interference test. However, the test may be carried out in a much shorter time because of the precision of the equipment. Ramey³² discusses the use of the pulse testing technique to determine reservoir anisotropy.

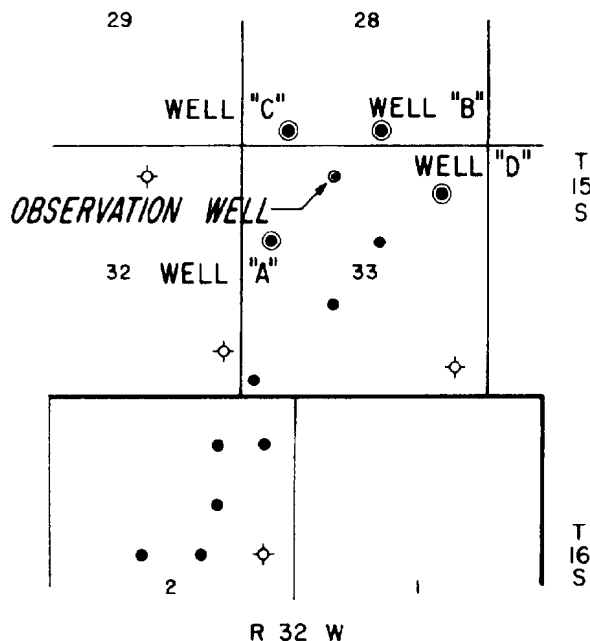


Fig. 36.8—Interference test plan.

Geophysics

3D Seismic Techniques. The three-dimensional (3D) seismic technique is a system of seismic data collection and processing that permits the proper vertical images to be developed and displayed by solving three orthogonal-wave equation migrations. The 3D method is a useful technique to map subsurface structures and to define the field configuration better previous to development. The detailed results allow the fault boundaries and

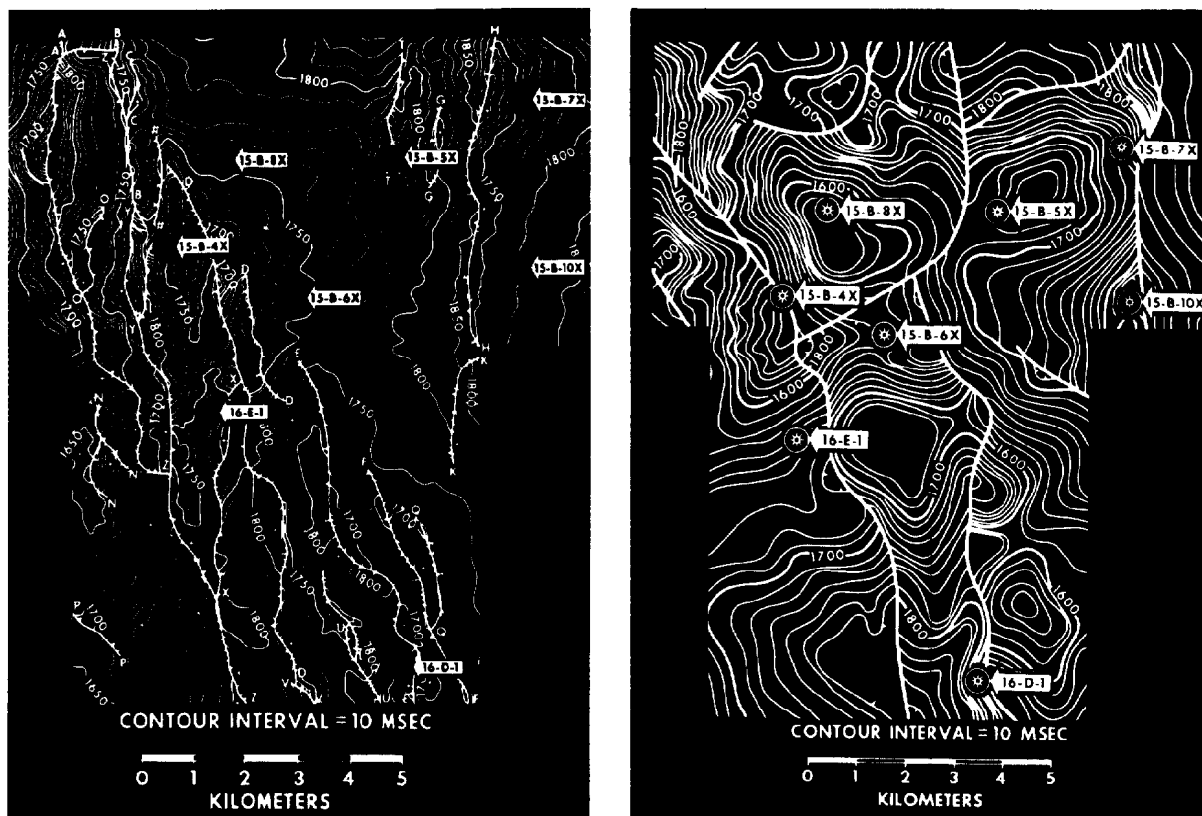


Fig. 36.9—Comparison of 2- and 3D seismic surveys.

stratigraphic limits of a reservoir to be mapped accurately soon after discovery. The number of appraisal wells would be reduced, and a more reliable estimate of the reserves could be obtained early in the life of the prospect. The knowledge of these two important facts would materially affect the overall drilling program.

The method is considerably more expensive than the more mundane seismic techniques, but it has been estimated that 100 sq miles of seismic coverage may be obtained for the cost of one appraisal well.³³ The 3D method provides greater structural definition than the better-known two-dimensional (2D) techniques for the following reasons.³⁴⁻³⁸

1. The placement of the vertical and horizontal reflection images is more accurate. Additionally, both vertical and horizontal sections may be presented for any depth and for any direction.
2. Diffraction events are eliminated.
3. The signal strength normally lost because of scattering problems is restored.
4. The increased control point density permits more accurate mapping.
5. The greater amount of data improves the statistical base for estimating near-surface corrections and velocities.

A particularly interesting example of using the 3D seismic method to evaluate a prospect and to help plan the drilling program may be seen in a study conducted in the Gulf of Thailand.³⁹ Three wildcat wells had disclosed the presence of probably commercial quantities of

gas. However, the prospect appeared to be faulted and a number of appraisal wells would be required to evaluate the potential in this relatively unexplored region. A region of 120 km² was subjected to a 3D seismic reconnaissance shot at 100-m intervals. The program afforded a greater definition of the megastructure, indicated faulting was much more prevalent than previously indicated, and also helped prove the viability of the prospect.

Figs. 36.9a and 36.9b compare the structural interpretations obtained by conventional 2D results with those obtained by 3D vertical migration. Note the increase in the complexity of the structure. The clarity of the 3D subsurface structural interpretation results from the more sharply focused nature of the process. The 2D interpretations give a more blurred or distorted picture because of the coarser sampling, which results in a statistically poorer presentation.

A survey conducted in offshore Trinidad⁴⁰ resulted in a change in the platform location and drilling plan of one prospect and the deletion of another prospect from development until additional exploration in other faultblocks was conducted.

Prediction of Reservoir Performance

After the reservoir has been characterized adequately, as described previously, a development plan must be selected. Performance of the reservoir under various exploitation schemes needs to be determined before selecting the final development plan. The modern tools used

by the reservoir engineer to predict the performance of the reservoir are reservoir simulators or mathematical models (see Chap. 48). A general description of the simulation steps and the results from simulation follows.

Simulation Steps

Data Preparation.

1. Select the appropriate simulator to use in the study—i.e., black oil, compositional, 2D, 3D, etc.
2. Divide the reservoir into a number of cells—i.e., establish a grid system for the reservoir.
3. Assign rock properties, geometry, initial fluid distribution, and fluid properties for each cell. The rock properties include permeability, porosity, relative permeability, capillary pressure, etc. The cell geometry includes depth, thickness, and location of wells. Fluid properties are specified by the usual PVT data and phase behavior if required.
4. Assign the production and/or injection schedule for wells and the well constraints that need to be maintained.

Performance Prediction. If no historical data are available, the next step is to make the necessary computer runs to obtain the performance of the wells and the reservoir as a function of time and various plans of development.

If historical data are available, the first step is to match the historical performance. The reservoir performance is calculated and the results are compared with the field-recorded histories of the wells. If the agreement is not satisfactory, adjustments in the data (such as the relative permeability, the specific permeability, the porosity, the aquifer, etc.) are made until a satisfactory match is achieved. The model then is used to predict the performance for alternative plans of operating the reservoir.

In summary, the reservoir engineer obtains from the simulators the reservoir performance for different development plans, including various displacement mechanisms (such as water or gas injection, miscible displacement, etc.), different number and location of wells, and effect of flow rates. The reservoir performance then is used in the appropriate economic analysis to decide on the optimal development plan.

References

1. Krueger, W.C. Jr.: "Depositional Environments of Sandstones as Interpreted from Electrical Measurements—An Introduction," *Trans., Gulf Coast Assoc. Geol. Soc.* (1968) **XVIII**, 226–41.
2. Selly, R.C.: "Subsurface Environmental Analysis of North Sea Sediments," *AAPG* (Feb. 1976) **60**, No. 2, 184–95.
3. Berg, R.R.: "Point Bar Origin of Fall River Sandstone Reservoirs, Northeastern Wyoming," *AAPG* (1968) 2116–22.
4. *Sedimentary Environments and Facies*, H.G. Reading (ed.), Elsevier Press, New York City (1978).
5. Reineck, H.E. and Singh, I.B.: *Depositional Sedimentary Environments*, second edition, Springer-Verlag Inc., New York City (1975).
6. Scholle, P.A. and Spearing, D.: "Sandstone Depositional Environments," *AAPG* (1982) Memoir 31.
7. Bernard, H.A. and LeBlanc, R.J.: *Resume of Quaternary Geology of the Northwestern Gulf of Mexico Province*, Princeton U. Press, Princeton, N.J. (1965) 137–85.
8. Berg, R.A.: *Studies of Reservoir Sandstones*, Prentice Hall, Englewood Cliffs, N.J. (1985).
9. Snider, R.M., Tinker, C.N., and Meckel, L.D.: "Deltaic Environmental Reservoir Types and Their Characteristics," *J. Pet. Tech.* (Nov. 1978) 1538–46.
10. Hartman, J.A. and Paynter, D.D.: "Drainage Anomalies in Gulf Coast Tertiary Sandstones," *J. Pet. Tech.* (Oct. 1979) 1313–22.
11. Pryor, W.A. and Fulton, K.: "Geometry of Reservoir-Type Sandbodies in the Holocene Rio Grande Delta and Comparison With Ancient River Analogs," paper SPE 7045 presented at the 1978 SPE/DOE Enhanced Oil-Recovery Symposium, Tulsa, April 16–19.
12. Poston, S.W., Berry, P., and Molokowu, F.W.: "Meren Field—The Geology and Reservoir Characteristics of a Nigerian Offshore Field," *J. Pet. Tech.* (Nov. 1983) 2095–2104.
13. LeBlanc, R.J.: "Distribution and Continuity of Sandstone Reservoirs—Parts 1 and 2," *J. Pet. Tech.* (July 1977) 776–804.
14. Harris, D.G. and Hewitt, C.H.: "Synergism in Reservoir Management—The Geologic Perspective," *J. Pet. Tech.* (July 1977) 761–70.
15. Kunkel, G.C. and Bagley, J.W. Jr.: "Controlled Waterflooding, Means Queen Reservoir," *J. Pet. Tech.* (Dec. 1965) 1385–90.
16. Jardine, D., et al.: "Distribution and Continuity of Carbonate Reservoirs," *J. Pet. Tech.* (July 1977) 873–85.
17. Weber, K.J.: "Influence of Common Sedimentary Structures on Fluid Flow in Reservoir Models," *J. Pet. Tech.* (March 1982) 665–72.
18. Zeito, G.A.: "Interbedding of Shale Breaks and Reservoir Heterogeneities," *J. Pet. Tech.* (Oct. 1965) 1223–28; *Trans., AIME*, **234**.
19. Verrien, J.P., Courand, G., and Montadert, L.: "Applications of Production Geology Methods to Reservoir Characteristics Analysis From Outcrops Observations," *Proc., Seventh World Pet. Cong., Mexico City* (1967) 425.
20. Snider, R.M., et al.: "Predicting Reservoir Rock Geometry and Continuity in Pennsylvanian Reservoir, Elk City Field, Oklahoma," *J. Pet. Tech.* (July 1977) 851–66.
21. Stiles, W.E.: "Use of Permeability Distribution in Waterflood Calculations," *Trans., AIME* (1949) **189**, 9–14.
22. Driscoll, V.J. and Howell, R.G.: "Recovery Optimization Through Infill Drilling—Concepts, Analysis, and Field Results," paper SPE 4977 presented at the 1974 SPE Annual Fall Meeting, Houston, Oct. 6–9.
23. Stiles, L.H.: "Optimizing Waterflood Recovery in a Mature Waterflood, The Fullerton Clearfork Unit," paper SPE 6198 presented at the 1976 SPE Annual Fall Meeting, Houston, Oct. 3–6.
24. George, C.J. and Stiles, L.H.: "Improved Techniques for Evaluating Carbonate Waterfloods in West Texas," *J. Pet. Tech.* (Nov. 1978) 1547–54.
25. "Application for Waterflood Response Allowable for Wasson Denver Unit," Shell Oil Co., testimony presented before Texas Railroad Commission, Austin (March 21, 1972) Docket 8-A-61677.
26. Barber, A.H. Jr. et al.: "Infill Drilling to Increase Reserves—Actual Experience in Nine Fields in Texas, Oklahoma and Illinois," *J. Pet. Tech.* (Aug. 1983) 1530–38.
27. Poston, S.W., Lubojacky, R.W. and Aruna, M.: "Meren Field—An Engineering Review," *J. Pet. Tech.* (Nov. 1983) 2105–12.
28. Weber, K.J. et al.: "Simulation of Water Injection in a Barrier-Bar-Type, Oil-Rim Reservoir in Nigeria," *J. Pet. Tech.* (Nov. 1978) 1555–65.
29. Earlougher, R.C. Jr.: *Advances in Well Test Analysis*, Monograph Series, SPE, Richardson (1977) 5, 264.
30. Matthies, E.P.: "Practical Application of Interference Tests," *J. Pet. Tech.* (March 1964) 249–52.
31. Johnson, C.R., Greenkorn, R.A., and Woods, E.G.: "Pulse-Testing: A New Method for Describing Reservoir Flow Properties Between Wells," *J. Pet. Tech.* (Dec. 1966) 1599–1602; *Trans., AIME*, **237**.
32. Ramey, H.J. Jr.: "Interference Analysis for Anisotropic Formations—A Case History," *J. Pet. Tech.* (Sept. 1975) 1290–98.
33. Brown, A.R.: "Three-D Seismic Surveying for Field Development Comes of Age," *Oil & Gas J.* (Nov. 17, 1980) 63–65.
34. Johnson, J.P. and Bone, M.P.: "Understanding Field Development History Utilizing 3D Seismic," paper OTC 3849 presented at the 1980 Offshore Technology Conference, Houston, May 5–8.
35. Graebner, R.J., Steel, G., and Wason, C.B.: "Evolution of Seismic Technology in the 80's," *APEA J.* (1980) **20**, 110–20.

36. French, W.S.: "Two Dimensional and Three Dimensional Migration of Model-Experiment Reflection Profiles," *Geophysics* (April 1974) **39**, No. 4, 265-77.
37. Hilterman, F.J.: "Interpretation Lessons From Three-Dimensional Modeling," *Geophysics* (May 1982) **47**, No. 5, 784-808.
38. McDonald, J.A., Gardner, G.H.F., and Kotcher, J.S.: "Areal Seismic Methods For Determining the Extent of Acoustic Discontinuities," *Geophysics* (Jan. 1981) **46**, No. 1, 2-16.
39. Dahm, C.G. and Graebner, R.J.: "Field Development with Three Dimensional Seismic Methods—Gulf of Thailand—A Case History," *Geophysics* (Feb. 1982) **47**, No. 2, 149-76.
40. Galbraith, M. and Brown, R.B.: "Field Appraisal with Three-Dimensional Seismic Surveys—Offshore Trinidad," *Geophysics* (Feb. 1982) **47**, No. 2, 177-95.

Chapter 37

Solution-Gas-Drive Reservoirs

Roger J. Steffensen, Amoco Production Co.*

Introduction

An oil reservoir is a solution-gas-drive reservoir if it undergoes primary depletion with the main reservoir energy supplied by the release of gas from the oil and the expansion of the in-place fluids as reservoir pressure drops. This excludes reservoirs affected significantly by fluid injection or water influx. Also, reservoirs that have vertical segregation of the gas and oil by gravity drainage merit special analysis. (In combination with appropriate production practices, gravity drainage can increase oil recovery significantly.) Reservoirs with an initial free-gas cap are sometimes included in the category of solution-gas-drive reservoirs; the gas-cap drive (gas expansion) supplements the solution-gas drive.

Solution-gas drive also is called dispersed-gas drive or internal- (as opposed to injected) gas drive because the gas comes out of solution throughout the portion of the oil zone that has a pressure below the bubblepoint. Initially, pore space in a solution-gas-drive reservoir contains interstitial water plus oil that contains gas in solution because of pressure. No free gas is assumed to be present in the oil zone. As reservoir pressure drops below the bubblepoint because of production, the oil shrinks. Part of the pore space is filled by gas that comes out of solution. The water expansion, a much smaller effect, is often neglected. The drive mechanism (gas evolution and expansion) is dispersed or scattered throughout the oil zone.

The evolved gas (less any produced gas) fills the pore space vacated by produced oil and by shrinkage of the remaining oil. The amount of oil recovered depends on the amount of pore space occupied by gas (the gas saturation S_g) and the oil shrinkage (B_o vs. pressure). Gas/oil relative-permeability characteristics and viscosities of oil and gas are important because they determine the flowing GOR at a given S_g (and thus the amount of free gas produced along with the oil).

Abundant literature is available on solution-gas-drive reservoir performance and prediction methods¹⁻²² and on production-rate computations for wells in those reservoirs.²³⁻³⁰ Special methods have been developed for predicting the behavior of volatile oil reservoirs.³¹⁻³⁸

Definitions

Bubblepoint pressure is the saturation pressure of the oil; as pressure drops below bubblepoint, gas starts coming out of solution from the oil. Critical gas saturation is the minimum saturation at which gas starts to flow. Gravity drainage refers to vertical segregation of gas and oil by countercurrent flow because of gravity (i.e., density difference); gas moves up and oil moves down. In differential gas separation, the evolved gas is continuously removed as pressure is lowered, so that the gas does not remain in contact with the liquid. Flash gas separation occurs when the evolved gas remains in contact with the liquid as pressure is lowered.

Typical Performance

Fig. 37.1 shows typical performance for a solution-gas-drive reservoir with an initial pressure above the bubblepoint. During the early production, pressure is above bubblepoint but is dropping rapidly. Gas saturation is zero, and the only gas produced was in solution in the produced oil at reservoir conditions (producing GOR, $R=R_{si}$). The rapid pressure decline is caused by the relatively low compressibility of the system. The only sources of pressure support are fluid and rock expansion.

Once the reservoir pressure reaches bubblepoint, solution-gas drive begins, and pressure declines less rapidly. The additional pressure support is a result of the liberation of gas as pressure declines and the expansion of this gas as it undergoes further pressure reduction.

As pressure drops below bubblepoint, the evolved gas is immobile until the gas saturation exceeds the critical

*Original chapter in 1962 edition was written by Vincent J. Sikora, now retired.

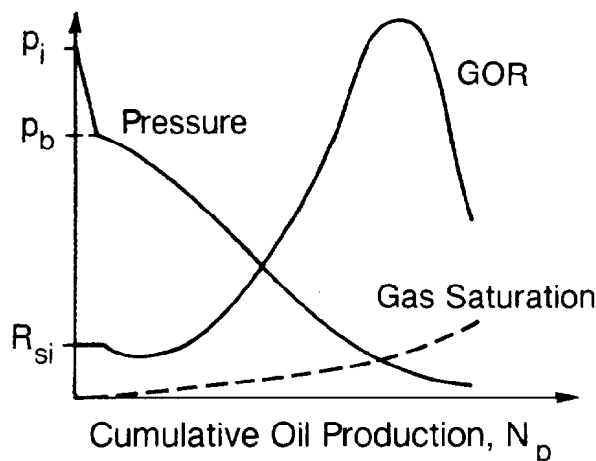


Fig. 37.1—Typical solution-gas-drive reservoir performance.

value, S_{gc} . For this period, there is no free-gas production, and the produced GOR declines because the produced oil now contains less gas in solution (lower R_s). Once S_{gc} is exceeded, free-gas production begins, and the total (free plus solution) produced GOR increases. This ratio rises to a peak much higher than the solution GOR (most of the gas produced at that time is free gas), then drops at low pressures. This drop is caused by insufficient additional gas evolution to sustain the high gas production. Solution-gas-drive reservoir performance is characterized by (1) relatively rapid pressure decline (faster than with fluid injection); (2) low initial producing GOR (equal to solution GOR) rising to a much higher GOR; (3) oil production rates declining because of both 1 and 2; (4) little or no water production; and (5) relatively low oil recovery—typically 15 to 20% of original oil in place (OOIP), but occasionally as low as 5% or as high as 30% OOIP.

A notable exception is that reservoirs benefiting from gravity drainage may have sustained production at a lower GOR and, consequently, a higher oil recovery. This is particularly true if the oil production is taken from the lower part of the oil column where the gas saturation and GOR are lower.

Types of Models Used

Performance prediction methods can be divided into two categories: tank-type models and gridded reservoir models. Tank-type models are simpler; gridded models can consider more details. Each is useful when used appropriately. Tank-type models for solution-gas-drive reservoirs are described in this chapter, and gridded models are discussed in Chap. 48.

Before gridded models were made practical by the introduction of modern computers, the main methods available for reservoir performance calculations were the tank-type models. These treat the reservoir as a single tank or region that is described by the average pressure and average saturations at a given time. This is equivalent to assuming that the reservoir is at equilibrium (i.e., has uniform pressure and saturation). Variations with time are considered, but variations with position are not. The field production rate vs. time for tank-type models is predicted

by calculating the rate for an average or representative well and then multiplying by the number of active wells.

Gridded reservoir models subdivide the reservoir into a number of gridblocks, each having its own PV, pressure, and saturations. Some blocks contain wells. Gridded models enable consideration of such details as reservoir heterogeneity, individual well locations and characteristics, and fluid migration between regions.

Tank-type models are adequate—in certain cases even preferable—for answering some questions, while being simpler and quicker to use than the gridded models. Understanding tank-type models aids the understanding of gridded simulators because both use basic continuity (material balance) principles. Even for reservoirs that ultimately may be studied with a gridded model, the calculated tank-type primary performance can provide useful, quick information and can serve as a reference point for comparison.

Also, a very important use of tank-type models is in interpretation of a reservoir's pressure/production history to determine the OIP and whether the reservoir is volumetric or has water influx. Havlena and Odeh¹⁵ presented particularly useful techniques for doing this with the material-balance equation rearranged as the equation of a straight line. They noted that OIP calculated by this equation is the oil that contributes to the pressure/production history (i.e., is communicating with wells). This may or may not agree with the volumetrically calculated OIP because of uncertainties in volumes and/or incomplete communication.

This chapter focuses on tank-type material balances and their application to solution-gas-drive reservoirs. Gridded simulator studies that are used to evaluate the range of applicability of tank-type models are also discussed. Calculation methods for ordinary (nonvolatile) oils are given first. These are normally adequate for oils having B_o less than roughly 2.0 RB/STB. The last part of the chapter discusses performance prediction methods for volatile oil reservoirs.

Basic Assumptions of Tank-Type Material Balance

1. The reservoir PV is constant (except in some cases where nonzero rock compressibility is considered).
2. The reservoir temperature is constant.
3. The reservoir has uniform porosity and uniform relative-permeability characteristics.
4. Equilibrium conditions exist throughout the reservoir at all times. Pressure is assumed to be uniform throughout the reservoir; consequently, fluid properties at any time (i.e., any pressure) do not vary with position in the reservoir. The effects of pressure drawdown around wells are neglected. The liquid saturation is assumed to be uniform throughout the oil zone. Thus, at a particular time, the value of the gas/oil relative-permeability ratio (k_{rg}/k_{ro}) is regarded as constant throughout the oil zone. This includes the assumption of no gravity segregation. For reservoirs having an initial gas cap, this includes the assumption of no gas coning at wells. Gas cap and oil zone volumes are assumed not to change with time. Any gas leaving the cap because of gas expansion is assumed to be distributed uniformly throughout the oil zone.

5. The PVT properties are representative of reservoir conditions. The fluid sample from which the PVT data are determined is assumed to be representative of the fluid in the reservoir, and the gas liberation mechanism in the reservoir is assumed the same as that used to determine the PVT data. Usually, differential vaporization is assumed to be most representative of conditions in the reservoir. With the possible exception of volatile oils, the fluid properties are assumed to be functions of only pressure—i.e., any effects of composition change are neglected.

6. The recovery is independent of rate.

7. Production is assumed to result entirely from liberation of solution gas and the expansion of the liberated gas of any initial gas cap and of oil as reservoir pressure decreases. This includes assumptions that there is no fluid injection; that water is immobile and there is no water production and no water influx; and that reservoir water and rock compressibility can be neglected (note that this assumption is used only below bubblepoint and that these effects should be considered above the bubblepoint).

8. A relationship is assumed for specifying oil production rate as a function of reservoir pressure and saturation.

9. Reservoir performance data, if used, are assumed to be reliable. This refers, for example, to average pressure vs. cumulative oil production used to determine OIP, and producing GOR vs. pressure used to determine or check the curve of k_{rg}/k_{ro} vs. saturation.

Basic Data Required

OIP

Two sources of OIP data are volumetric calculations and values determined from the reservoir's pressure/production history. Often, only the volumetric estimate is available. When there is enough solution-gas-drive history (reservoir average pressure vs. oil produced), this volumetric value can be checked by a comparison with the history-derived OIP. A convenient method for determining the OIP from pressure/production history is given by Havlena and Odeh¹⁵ and will be described in a later section.

A frequently given rule of thumb is that 5 to 10% of the fluid in place must be produced before the performance history is sufficient for calculation of OIP. For a solution-drive reservoir, this would be a large fraction of the ultimate recovery, which is typically 15 to 20%. While the amount of production is important, good values for average reservoir pressure at a sequence of times (based on well pressure tests) are equally important. If you have a sequence of pressure points that were determined from field measurements, try Havlena and Odeh's method; if several points form an essentially straight line, you probably have enough data to confirm the OIP (even at less than 5% recovery).

PVT

As reservoir pressure drops below the bubblepoint, the first gas liberation is by the flash vaporization process (the gas is not yet mobile and therefore stays in contact with the oil). Once the critical gas saturation is exceeded, some of the gas flows. Thereafter, the gas liberation process is somewhere between differential vaporization (gas is continuously removed from the oil) and flash vaporization.

As the gas saturation increases above critical, the gas mobility increases rapidly, the gas becomes more mobile than the oil, and the gas moves faster than the oil. Because the evolved gas moves ahead of the oil, the process is closer to differential. Overall, the process in the reservoir is approximated more closely by the laboratory differential PVT data than by the laboratory flash data. This is particularly true for high-solubility crudes. Use of the differential PVT data is recommended. Even for the pressure range just below bubblepoint, where flash PVT data are more appropriate, the differential data do not cause significant errors because flash and differential data are almost identical in this pressure range.

If laboratory data are not available, reasonable estimates sometimes may be obtained from published correlations (see Chap. 22).

Gas liberation in the separators is closer to a flash vaporization process and frequently is at a temperature much lower than the reservoir temperature. Because differential PVT data are used in the material-balance computations, the computed recoveries could be adjusted to account for the different process (and particularly the different temperature of gas separation) from bottomhole to stock-tank conditions (see Chap. 22 and Page 64 of Dake³⁹). For typical crudes, however, this adjustment is often within the range of other data and model limitations and consequently not warranted.

Initial Fluid Saturations

Because saturations are assumed to be uniform, a single value is used for initial water saturation, S_{wi} . The initial oil saturation is then $S_{oi} = 1.0 - S_{wi}$. The preferred data are initial fluid saturations obtained from a laboratory analysis of representative cores or from a combination of core analysis and well log analysis. Alternatively, these values can be based on logs or on other reservoirs in the same or similar formations.

Relative-Permeability Data

Generally, laboratory-determined k_g/k_o and k_{ro} data are averaged to obtain a single representative set for the reservoir that is consistent with the interstitial water saturation. If laboratory data are not available, estimates may be based on other reservoirs in the same or similar formations.

For reservoirs having sufficient solution-gas-drive history, the calculated k_g/k_o values vs. saturation can be compared with the averaged laboratory or estimated k_g/k_o data. These values may be calculated¹¹ with Eqs. 1 and 2, and the laboratory data can be adjusted slightly to match more closely the observed history of producing GOR (R) vs. reservoir pressure if necessary.

$$\frac{k_g}{k_o} = (R - R_s) \frac{\mu_g B_g}{\mu_o B_o} \quad (1)$$

$$S_o = \frac{(N - N_p) B_o S_{oi}}{N B_{oi}} \quad (2)$$

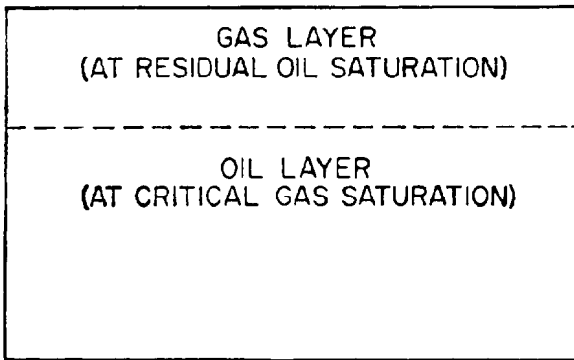


Fig. 37.2—Vertical saturation distribution for complete segregation.

where

- k_g = effective permeability to gas, md,
- k_o = effective permeability to oil, md,
- R = producing GOR, scf/STB,
- R_s = solution GOR, scf/STB,
- μ_g = gas viscosity, cp,
- μ_o = oil viscosity, cp,
- B_g = gas formation volume factor, RB/scf,
- B_o = oil formation volume factor, RB/STB,
- B_{oi} = value of B_o at initial pressure, RB/STB,
- S_o = oil saturation, fraction PV,
- S_{oi} = initial oil saturation, fraction PV,
- N_p = cumulative oil production, STB, and
- N = initial OIP, STB.

To use the above equations, you need estimates of the initial OIP (N) and of the current reservoir pressure. The fluid properties (μ_o , μ_g , B_o , and B_g) are evaluated at this pressure.

Pseudo-Relative-Permeability Data for Complete Segregation

This refers to reservoirs that have enough vertical communication for gravity segregation to occur, with evolved gas moving upward and oil draining downward. The literature on tank-type-model predictions includes description of relative-permeability modifications to obtain pseudo-relative-permeability curves to account for complete gravity segregation within the reservoir. Consequently, the suitability of such pseudocurves in the tank-type material-balance computations should be discussed. For reasons given below, this approach is potentially misleading and should be avoided.

The laboratory-measured relative-permeability data apply to an unsegregated situation (no change in saturation with height). This case is most consistent with the basic

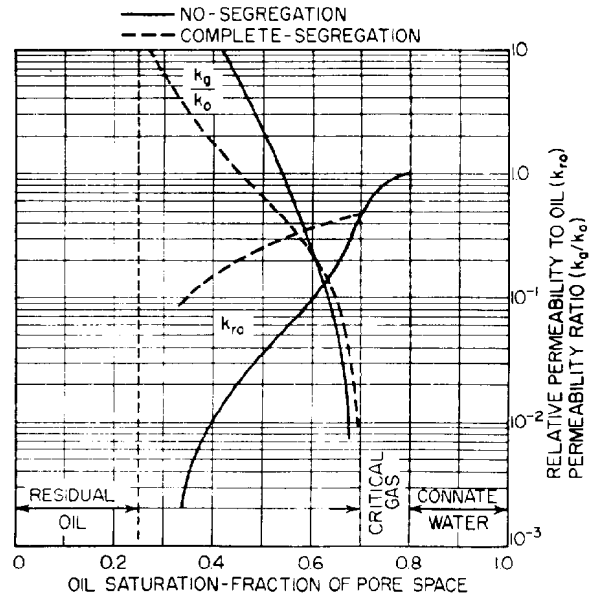


Fig. 37.3—Comparison of no-segregation and complete-segregation relative-permeability data.

assumptions of the tank-type model, and the tank-type model is most suitable for it. It is also possible to calculate¹³ pseudo or effective k_g/k_o and k_{ro} data for the case of a reservoir that has complete gravity segregation, as shown in Fig. 37.2, and flow from the total net pay thickness (i.e., assuming wells are completed in the total net pay).

The entire reservoir shown in Fig. 37.2 contains interstitial water saturation. Complete segregation means that the upper part of the reservoir contains gas and immobile oil at residual oil saturation, S_{or} , while the lower part contains oil and immobile gas at the critical gas saturation, S_{gc} . Vertical communication is assumed to be high enough that, as gas evolves in the lower region, any gas saturation above S_{gc} moves upward rapidly and leaves that region, while in the upper region any oil above S_{or} drains downward and moves into the lower region. The flow to wells is assumed to be horizontal and to consist of only gas in the upper region and of only oil in the lower region. On the basis of these assumptions, the effective k_g/k_o and k_{ro} are given by Eqs. 3 and 4.

$$\frac{k_g}{k_o} = \frac{(S_g - S_{gc})(k_{rg})_{or}}{(S_o - S_{or})(k_{ro})_{gc}} \quad \dots \dots \dots (3)$$

$$k_{ro} = \frac{S_o - S_{or}}{1 - S_w - S_{gc} - S_{or}} (k_{ro})_{gc} \quad \dots \dots \dots (4)$$

where

$(k_{rg})_{or}$ = relative permeability to gas at residual oil saturation,

$(k_{ro})_{gc}$ = relative permeability to oil at critical gas saturation,

S_g = gas saturation, fraction PV,

S_{gc} = critical gas saturation, fraction PV,

S_{or} = residual oil saturation, fraction PV, and

S_w = water saturation, fraction PV.

Fig. 37.3 compares ordinary k_r/k_o and k_{ro} curves for an unsegregated reservoir with the adjusted curves for the completely segregated assumption.

Pseudo-relative-permeability data calculated with Eqs. 3 and 4 are consistent with the above assumptions. And one might be tempted to assume that results computed for no segregation (unmodified relative-permeability data) and for complete segregation (the above pseudo-relative-permeability data) bracket the results to be expected for cases with partial segregation. What is wrong with this approach? The problem is that perforating the entire pay thickness is not the best way to operate such a reservoir. Producing gas at high GOR from the upper part of the pay thickness reduces reservoir energy (pressure support). It is much better to produce such a reservoir only from the lower part of the oil column, thereby reducing the producing GOR and maintaining reservoir energy. Consequently, the assumption of production from the entire pay thickness is inappropriate for this case. The tank-type model with pseudorelative permeabilities seriously underestimates the oil recovery compared to a good gravity-drainage project. Results of this model will lead to incorrect conclusions about the benefits of gravity drainage and about how to operate the field.

If a reservoir has enough vertical communication to benefit from gravity drainage, consider use of a gridded model (Chap. 48) for primary performance predictions. With the gridded model, you can study the benefits of selective perforation low in the pay, possible benefits of producing mainly from downdip wells if the reservoir has dip, and possible sensitivity of oil recovery to production rate and to the amount of vertical permeability.

Material-Balance Equation

The material-balance equation keeps inventory on all material entering, leaving, and accumulating within a region. Sometimes called the Schilthuis¹ equation when applied to a reservoir, it states that because reservoir volume is constant, the algebraic sum of volume changes (including production and injection) of the oil, free gas, and water must equal zero. In other words, expansion equals voidage; the net voidage (production minus injection minus influx) must be made up by expansion of the in-place materials. Van Everdingen *et al.*⁴⁰ stated the material balance in reservoir volumes as follows:

“(Cumulative oil produced and its original dissolved gas) + (Cumulative free gas produced) + (Cumulative water produced) – (Cumulative expansion of oil and dissolved gas originally in reservoir) – (Cumulative expansion of free gas originally in reservoir) = (Cumulative water entering original oil and water reservoir).”

Water and gas injection could also be considered in the material balance by replacing cumulative production with cumulative production minus cumulative injection.

For an oil reservoir having an initial gas cap, with m denoting the ratio of gas-cap-volume/oil-zone-volume, the material balance expressed in reservoir volumes is given by Eq. 5.

$$\begin{aligned}
 & N(B_o - B_{oi}) \text{ (expansion of initial oil)} \\
 & + N(R_{si} - R_s)B_g \text{ (volume occupied by liberated solution gas)} \\
 & + mNB_{oi} \left(\frac{B_g - B_{gi}}{B_{gi}} \right) \text{ (gas-cap gas expansion)} \\
 & + \frac{NB_{oi}(1+m)}{1-S_w} S_w c_w (p_{iR} - p_R) \text{ (water expansion)} \\
 & + \frac{NB_{oi}(1+m)}{1-S_w} c_f (p_{iR} - p_R) \text{ (rock expansion)} \\
 & = N_p B_o \text{ (oil production)} \\
 & + (G_{ps} - N_p R_s) B_g \text{ (liberated solution gas production)} \\
 & + G_{pc} B_g \text{ (gas-cap gas production)} \\
 & - G_i B_g \text{ (gas injection)} \\
 & + W_p B_w \text{ (water production)} \\
 & - W_i B_w \text{ (water injection)} \\
 & - W_e B_w \text{ (water influx), } \dots \dots \dots (5)
 \end{aligned}$$

where

R_s = solution GOR, scf/STB,

R_{si} = value of R_s at initial pressure, scf/STB, and

m = PV of gas cap/PV of oil zone, dimensionless.

Solving Eq. 5 for N yields the general material-balance equation for initial OIP:

$$\begin{aligned}
 N = & \frac{N_p B_o + (G_p - N_p R_s) B_g + (W_p - W_i - W_e) B_w - G_i B_g}{(B_o - B_{oi}) + (R_{si} - R_s) B_g + m B_{oi} \left(\frac{B_g - B_{gi}}{B_{gi}} \right) + \frac{B_{oi}}{1-S_w} (1+m) (S_w c_w + c_f) (p_{iR} - p_R)} \\
 & \dots \dots \dots (6)
 \end{aligned}$$

where $G_p = G_{ps} + G_{pc}$ = cumulative gas production, in standard cubic feet.

By considering a case only above bubblepoint or only below bubblepoint, some terms are zero or negligible, and the general equation can be simplified. These cases are discussed in the following sections.

Material Balance Above Bubblepoint

For an undersaturated reservoir (i.e., above bubblepoint), no gas will be released from solution, the produced GOR will remain constant at R_{si} , and there would not be any gas cap. Thus $(R_{si} - R_s) = 0$, $m = 0$, and $(G_p - N_p R_s) = 0$.

With these simplifications and the assumption of no gas injection, Eq. 6 reduces to

$$N = \frac{N_p B_o + (W_p - W_i - W_e) B_w}{B_o - B_{oi} + \frac{B_{oi}}{1 - S_{wi}} (S_w c_w + c_f) (p_{iR} - p_R)} \quad (7)$$

Because for the single-phase oil $B_o - B_{oi} = B_{oi} c_o (p_{iR} - p_R)$, the material-balance equation above bubblepoint becomes

$$N = \frac{N_p B_o + (W_p - W_i - W_e) B_w}{B_{oi} c_e (p_{iR} - p_R)} \quad (8)$$

where the effective compressibility (c_e) is

$$c_e = c_o + \frac{S_w c_w}{1 - S_w} + \frac{c_f}{1 - S_w} \quad (9)$$

Although water and rock compressibility are often neglected below bubblepoint because their effect is small compared with gas evolution and expansion, they should be included above bubblepoint. For example, consider a case with the following data:

$$c_o = 15 \times 10^{-6} \text{ vol/}(\text{vol-psi})$$

$$c_w = 3 \times 10^{-6} \text{ vol/}(\text{vol-psi})$$

$$c_f = 4 \times 10^{-6} \text{ vol/}(\text{PV-psi})$$

and

$$S_w = 0.20.$$

By use of Eq. 9,

$$\begin{aligned} c_e &= 15 \times 10^{-6} + \frac{(0.20)(3 \times 10^{-6})}{1 - 0.2} + \frac{4 \times 10^{-6}}{1 - 0.2} \\ &= 15 \times 10^{-6} + 0.75 \times 10^{-6} + 5 \times 10^{-6} \\ &= 20.75 \times 10^{-6} \text{ vol/}(\text{vol-psi}) \end{aligned}$$

For this example, the water and rock compressibility contribute more than one-fourth of the total compressibility. Their omission would cause the OIP calculated by Eq. 8 to be too high by a factor of $20.75/15 = 1.383$ (i.e., 38% too high). The error would be even greater for larger S_w .

Calculation of Oil Production Above Bubblepoint. For an initially undersaturated reservoir with negligible water production, injection, or influx, rearrangement of Eq. 8 yields the following expression for cumulative oil production:

$$N_p = \frac{N B_{oi} c_e (p_{iR} - p_R)}{B_o} \quad (10)$$

Calculation of oil recovery to bubblepoint is straightforward, with bubblepoint pressure as the value of p_R in Eq. 10. The remaining OIP is then $N - N_p$. This value is often used in computations of the additional recovery below bubblepoint.

Material Balance Below Bubblepoint

Below bubblepoint, the net expansion of hydrocarbons (gas evolution plus gas expansion minus oil shrinkage) is much greater than the expansion of rock and water. Consequently, the rock and water expansion terms can be omitted without serious error. By neglecting these terms and by assuming no water influx, no gas injection, and no net water production, we simplify Eq. 6 to Eq. 11.

$$N = \frac{N_p B_o + (G_p - N_p R_s) B_g}{(B_o - B_{oi}) + (R_{si} - R_s) B_g + m B_{oi} \left(\frac{B_g - B_{gi}}{B_{gi}} \right)} \quad (11)$$

Even if the initial pressure was above bubblepoint, Eq. 11 can be used to compute the performance below bubblepoint. In this case, the value used for N is the OIP at bubblepoint; N_p and G_p are the incremented oil and gas production below bubblepoint; and the "initial" fluid properties B_{oi} and B_{gi} are values at bubblepoint.

Another expression for N , often found in the literature and equivalent to Eq. 11, is given by Eq. 12.

$$N = \frac{N_p [B_i + B_g (R_p - R_{si})]}{B_i - B_{ii} + m B_{oi} \left(\frac{B_g}{B_{gi}} - 1 \right)} \quad (12)$$

where

$$R_p = \text{cumulative produced GOR, scf/STB.}$$

$$R_p = \frac{G_p}{N_p} \quad (13)$$

B_i is the two-phase (i.e., total hydrocarbon) FVF—reservoir barrels occupied by one barrel of stock-tank oil plus the gas that was initially dissolved in that oil at reservoir conditions.

$$B_i = B_o + B_g (R_{si} - R_s) \quad (14)$$

Material Balance as Equation of Straight Line for Determination of OIP and of Gas-Cap Size

Havlena and Odeh¹⁵ show how to use the material-balance equation along with a reservoir's pressure/production history to get information about whether the reservoir is volumetric or has water influx, plus the initial OIP (N) and the ratio of gas-cap-volume/oil-zone-volume (m) for a volumetric reservoir. Water influx is discussed in Chap. 38; only the volumetric case will be considered here.

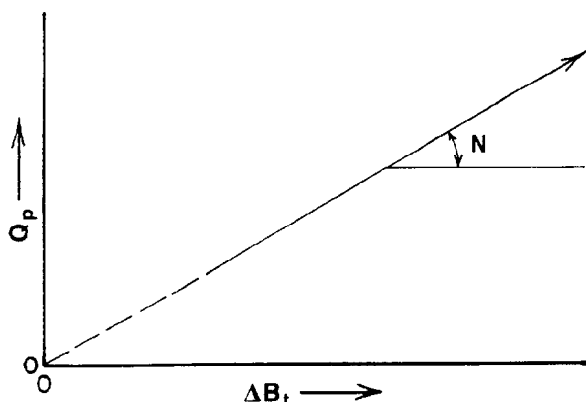


Fig. 37.4A—Straight-line material balance for reservoir without gas cap. Q_p from Eq. 15 vs. $\Delta B_t = B_t - B_{ti}$.

Havlena and Odeh rearranged Eq. 12 as the equation of a straight line, grouping terms as follows:

$$Q_p = N_p [B_t + B_g (R_p - R_{si})], \quad (15)$$

$$\Delta B_t = B_t - B_{ti}, \quad (16)$$

and

$$\Delta B_g = B_g - B_{gi}, \quad (17)$$

where

Q_p = net fluid production, RB,

ΔB_t = oil expansion per STB of initial OIP.
RB/STB, and

ΔB_g = expansion of initial free gas (the gas cap)
per scf of initial free gas in place,
RB/scf.

Eq. 12 can be rearranged as

$$Q_p = N \Delta B_t + N m \frac{B_{ti}}{B_{gi}} \Delta B_g. \quad (18)$$

A plot of Q_p vs. $\Delta B_t + m(B_{ti}/B_{gi}) \Delta B_g$ should result in a straight line going through the origin. The slope of this line represents N , the initial OIP. Similarly, in the absence of a gas cap, $Q_p = N \Delta B_t$; a plot of Q_p vs. ΔB_t should be a straight line of slope N , going through the origin. This is illustrated by Fig. 37.4A.

When field performance (Q_p vs. ΔB_t) is plotted, if it yields an approximately straight line, the slope indicates the value of the initial OIP (N). The data needed are fluid properties vs. pressure and the reservoir performance data at several times or pressures. The performance data are N_p , G_p , and average reservoir pressure (for determination of fluid properties). If the plot of Q_p vs. ΔB_t is not a straight line, possible reasons include (1) erroneous average pressures and/or fluid properties, (2) water influx (see Chap. 38), (3) gas cap is present and expand-

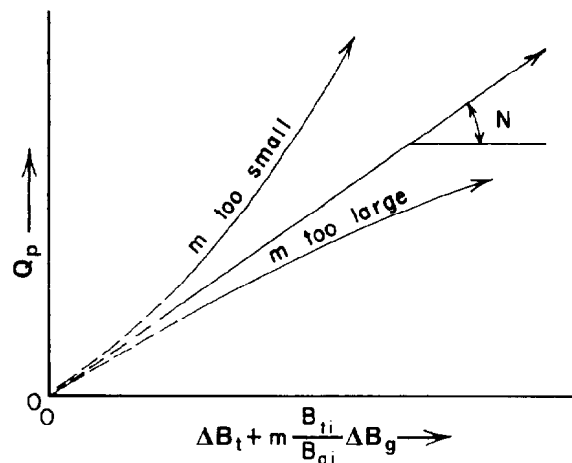


Fig. 37.4B—Straight-line material balance for reservoir with gas cap.

ing, and (4) gravity drainage that is affecting reservoir performance (R_p lower than for solution-gas drive alone).

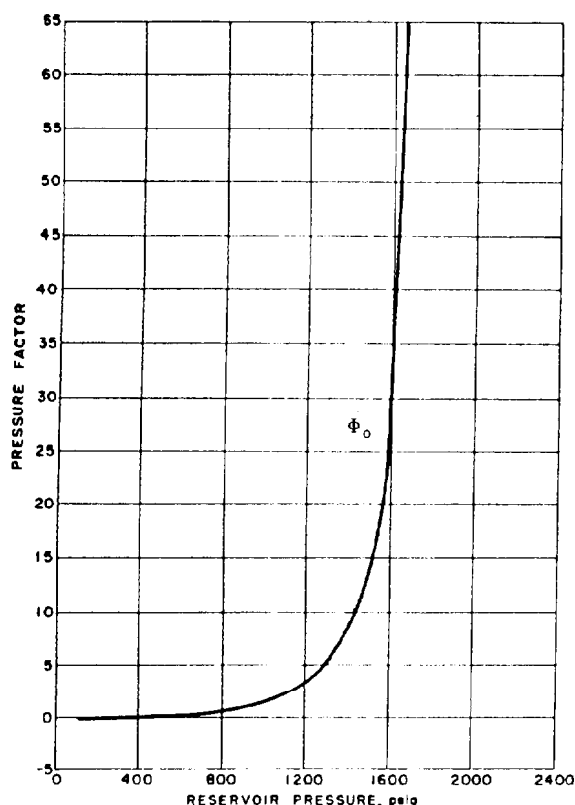
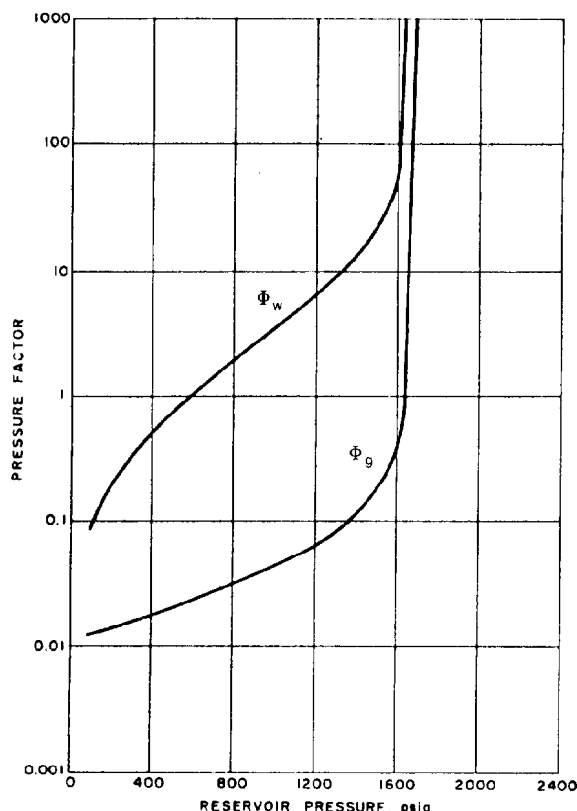
For a reservoir with an initial gas cap but no water influx, values of both N and m can be determined from the field performance data, as illustrated in Fig. 37.4B. By trial and error, the value of m yielding a straight line can be determined; N is the slope of this line.

For cases with a gas cap, Havlena and Odeh recommended that a second method also be used as a check, even though the first method (given above) "is a more powerful method" because "it specifies that the line must go through the origin." The second method plots values of $Q_p/\Delta B_t$ on the vertical (y) axis vs. values of $\Delta B_g/\Delta B_t$ on the horizontal (x) axis. If both sides of Eq. 18 are divided by ΔB_t , we can see that the plotted points should approximate a straight line with slope equal to NmB_{ti}/B_{gi} . Also, if this line is extrapolated so that it intercepts the y axis, the y value at that intercept is equal to N . Consequently, the slope and the y intercept of this plot enable calculation of both N and m . Comparison of these values with those determined by the first method is a desirable check, and also may aid selection of the best value of m for use in the first method.

Having values of N and m that are based on reservoir performance and/or on other information or estimates, we are now ready to consider predictions of future performance by solution-gas drive. Techniques for this have been published by Muskat,⁴ Tarner,² and Tracy.⁶ All three methods yield essentially the same results when small enough intervals of pressure or time are used. Because Tracy's method is the most convenient to use, it will be described first.

Material-Balance Calculations Using Tracy's Method

Prediction of solution-gas-drive performance involves the use of a material-balance equation such as Eq. 11, plus enough additional relationships (equation for producing GOR, and for relating saturations to N_p) to enable computation of N_p and G_p vs. pressure. The computations are performed for a sequence of pressure decrements. The

Fig. 37.5A—Oil pressure function Φ_o vs. reservoir pressure.Fig. 37.5B—Gas and water pressure functions Φ_g and Φ_w vs. reservoir pressure.

incremental oil production ΔN_p and the incremental gas production ΔG_p for the pressure decrement from p_{n-1} to p_n are determined by an iterative method, and the cumulative production values are then given by Eqs. 19 and 20.

$$(N_p)_n = (N_p)_{n-1} + \Delta N_p \quad \dots \dots \dots (19)$$

and

$$(G_p)_n = (G_p)_{n-1} + \Delta G_p \quad \dots \dots \dots (20)$$

Tracy simplified the use of Eq. 11 by introducing pressure functions Φ_g and Φ_o :

$$\Phi_g = \frac{1}{\left(\frac{B_o - B_{oi}}{B_g} \right) - (R_s - R_{si}) + mB_{oi} \left(\frac{1}{B_{gi}} - \frac{1}{B_g} \right)} \quad \dots \dots \dots (21)$$

and

$$\Phi_o = \left(\frac{B_o}{B_g} - R_s \right) \Phi_g \quad \dots \dots \dots (22)$$

Actually, Eq. 21 is a slight modification of Tracy's original equation. Tracy gave an example problem that

started at bubblepoint and used B_o at bubblepoint pressure instead of the B_{oi} used in Eq. 21. As discussed in the next section, use of B_{oi} in Eq. 21 makes Tracy's method also applicable above bubblepoint (in which case m is zero). Tracy also used R_s at bubblepoint instead of R_{si} , but these are equivalent because R_s is constant above bubblepoint.

Examples of Φ_g and Φ_o vs. pressure are shown in Figs. 37.5A and 37.5B. At the initial pressure, the denominator in Eq. 21 is zero; consequently, Φ_g and Φ_o are infinite. This, however, does not cause any difficulty because the only Φ values used are the finite values at lower pressures.

With Tracy's Φ functions, Eq. 11 becomes

$$N = N_p \Phi_o + G_p \Phi_g \quad \dots \dots \dots (23)$$

This form of the material-balance equation is particularly convenient because the Φ values are functions only of gas-cap size and of pressure. For each pressure level, the Φ values need to be calculated only once.

Material-Balance Equation 23 is applied to the pressure decrement from p_{n-1} to p_n :

$$\begin{aligned} N &= N_p \Phi_o + G_p \Phi_g \\ &= [(N_p)_{n-1} + \Delta N_p](\Phi_o)_n + [(G_p)_{n-1} + \Delta G_p](\Phi_g)_n, \quad \dots \dots \dots (24) \end{aligned}$$

where the average producing GOR is given by

$$\bar{R} = \frac{\Delta G_p}{\Delta N_p} = \frac{R_{n-1} + R_n}{2} \quad (25)$$

Solving Eq. 24 for ΔN_p ,

$$\Delta N_p = \frac{N - (N_p)_{n-1}(\Phi_o)_n - (G_p)_{n-1}(\Phi_g)_n}{(\Phi_o)_n + \bar{R}(\Phi_g)_n} \quad (26)$$

The producing GOR, R_n , at pressure p_n is the sum of up to three terms: the solution GOR $(R_s)_n$, the flowing (i.e., free) GOR, and the ratio $(R_{gc})_n$ of gas production directly from gas-cap/oil production:

$$R_n = (R_s)_n + \left(\frac{k_g}{k_o}\right)_n \left(\frac{\mu_o B_o}{\mu_g B_g}\right)_n + (R_{gc})_n \quad (27)$$

The term $(\mu_o B_o / \mu_g B_g)_n$ is a function only of pressure and is computed using values at pressure p_n . The value of $(k_g / k_o)_n$ is a function of the total liquid saturation, $S_o + S_w$, in the oil zone. The current oil saturation, $(S_o)_n$, is given by Eq. 28:

$$(S_o)_n = (1.0 - S_w) \frac{[N - (N_p)_n](B_o)_n}{NB_{oi}} \quad (28)$$

If the liquid saturation is known, the value of (k_g / k_o) can be read from a curve or calculated by interpolation in a table of values. The incremental material balance for each pressure step involves iterations to satisfy Eqs. 23 through 28. This determines ΔN_p , ΔG_p , S_o , and R_n .

For this iterative solution, either of two approaches could be used: (1) estimate the incremental oil production, ΔN_p , and solve for the corresponding GOR, R_n , or (2) estimate R_n and solve for ΔN_p . With either approach, the iterations are continued until the calculated results converge to the material-balance solution (i.e., until the value of N calculated using Eq. 23 agrees with the initially specified value of N). Tracy⁶ indicated that the more effective approach is to estimate R_n and to solve for ΔN_p .

Thus, Tracy's method for iterative solution of Material-Balance Equation 24 at each pressure level consists of the following steps.

1. Estimate the average GOR, \bar{R} , for the pressure decrement from p_{n-1} to p_n .
2. Compute estimated ΔN_p from Eq. 26.
3. Compute estimated $(N_p)_n$ by using $(N_p)_n = (N_p)_{n-1} + \Delta N_p$.
4. Compute oil saturation $(S_o)_n$ from Eq. 28.
5. Determine (k_g / k_o) corresponding to the liquid saturation.
6. Compute R_n from Eq. 27.
7. Compute new estimate of \bar{R} from Eq. 25.
8. Compute new estimate of ΔN_p as in Step 2 and of $(N_p)_n$ as in Step 3.
9. Compute $(G_p)_n$ from $(G_p)_n = (G_p)_{n-1} + \bar{R}\Delta N_p$.

10. Compute the estimated OIP (N) from Eq. 23 or 24.

11. To test GOR, check whether the new value of R computed at Step 7 is arbitrarily close to the previous estimate of \bar{R} for this same pressure decrement, denoted \bar{R}_{old} . An adequate test is

$$0.999 \leq \frac{\bar{R}}{\bar{R}_{old}} \leq 1.001.$$

If this criterion is satisfied, go on to Step 12. Otherwise, go back to Step 4 and continue the iterative solution for this pressure level by using the most recently calculated estimate of $(N_p)_n$. Usually, a few iterations suffice.

12. To test material balance, the computed value of N should agree with the initially specified value of N . An adequate test is

$$0.999 \leq \frac{N_c}{N_s} \leq 1.001,$$

where N_c is the computed initial OIP and N_s is the specified initial OIP.

If this is satisfied, an adequate material balance is considered to have been obtained for that pressure. The production for the pressure decrement has been computed with sufficient accuracy. If the above criterion is not satisfied, go back to Step 4 and continue the iterations until a material balance is obtained for this pressure decrement. This material-balance test will almost always be satisfied once the GOR test of Step 11 has been satisfied.

This completes the material-balance computation at the selected pressure p_n . The values computed are the incremental oil and gas production, the oil and gas saturations, and the producing GOR. Rates and time have not been considered because the tank-type material-balance performance was assumed to be independent of rate and time. Computations of rates and time are covered in a later section.

After results for one pressure decrement are obtained, the next pressure decrement is selected and the iterative computations are done for that pressure step. Because of a strong nonlinearity in the k_g / k_o vs. S_g relationship, results are sensitive to the size of the pressure step used (which influences the change in S_g and thus in k_g / k_o and GOR). Typically, until the pressure has dropped to 1,000 psi below bubblepoint, the pressure steps should not exceed 200 psi, and 100 psi is sometimes better. At lower pressures, larger pressure steps can be used. A good practice is to use pressure steps small enough that the GOR does not increase by more than a factor of two in a single step.

Applicability of Tracy's Method Above Bubblepoint

Historically, two reasons were given for not using Tracy's method above bubblepoint pressure: (1) use of Eq. 10 is simpler, and (2) according to the literature, Tracy's method is not applicable above bubblepoint. The purpose of this section is to show how Tracy's method can be used both above and below bubblepoint. Heretofore, the approach for calculating the total oil production N_p for initially undersaturated reservoirs has been to calculate N_p

to the bubblepoint with Eq. 10, to calculate incremental oil production below bubblepoint by Tracy's method or another method, and to add these two produced volumes together to obtain the total oil recovery. The new alternative is to use Tracy's method for the entire pressure range. Existing computer programs that use Tracy's method only below bubblepoint can be applied for the entire pressure range if data are modified as described below.

The literature contends that Tracy's method cannot be used above bubblepoint pressure because the Φ functions are infinite at bubblepoint. This is true for Tracy's equations in Ref. 6 that used B_o at the bubblepoint (Tracy's initial condition) instead of B_{oi} as in Eq. 21. However, if B_{oi} is used in Eq. 21, Tracy's method becomes more general. It can be used for all pressure intervals because the Φ functions (Eqs. 21 and 22) are infinite only at the initial pressure, which does not have to be the bubblepoint. Values of the Φ functions at the initial pressure are not used in Tracy's formulation; only the finite values at lower pressures are used. Consequently, if B_{oi} is used in Eq. 21, Tracy's method can predict performance for the entire pressure range from any initial pressure down to abandonment. When used above bubblepoint, Tracy's method does not require iteration because an accurate initial estimate can be made for R ($R=R_s$). When Tracy's method is used for the full pressure range of an initially undersaturated oil, however, three considerations are pertinent: (1) the computed recovery will be a fraction of the initial OIP, not of the OIP at bubblepoint; (2) bubblepoint pressure should be one of the pressure levels for proper consideration of gas evolution that starts at bubblepoint; and (3) the effects of rock and water compressibility must be considered for realistic computation of pressure decline above bubblepoint. A technique for considering the third point by adjusting the B_o data is given below.

Because rock and water compressibilities are relatively unimportant below bubblepoint, they were not included in the Tracy material-balance formulation. They can be included indirectly, however, by use of pseudovalues of the oil formation volume factor at pressures below the initial pressure. These pseudovalues, B_o^* , are given by Eq. 29.

$$B_o^* = B_o + B_{oi} \left(\frac{S_w c_w + c_f}{1 - S_w} \right) (p_{iR} - p_R). \quad (29)$$

These pseudovalues include the additional pressure support of water and rock compressibilities in the material-balance computations.

Comparison of Tarner's and Tracy's Methods

Tarner² and Tracy⁶ solved the same material-balance equation for a sequence of pressure decrements. Although Tracy's method is more convenient, Tarner's method is often referenced and consequently will be described.

For each pressure in the Tarner method, several estimates are made of the cumulative oil production, N_p . For each N_p , the corresponding cumulative gas production, G_p , is calculated two ways: from Material Balance Equation 11, or on the basis of relative permeability. To calculate G_p from relative permeability, first calculate S_o

(Eq. 28) and determine k_{rg}/k_{ro} . Second, calculate the GOR, R_n (Eq. 27). Third, calculate the incremental gas production ΔG_p (Eq. 25). Then the cumulative gas production is calculated by $G_p = (G_p \text{ at previous pressure}) + \Delta G_p$.

The correct value of N_p is the value at which both methods above yield identical values of G_p . Tarner suggested plotting both sets of calculated G_p values vs. N_p . The intersection of the two curves then yields the correct G_p and N_p .

Tarner's method works if the plotting is done accurately. It should yield the same results as Tracy's method because the same relationships are used. Tarner's method is time-consuming because you have to calculate and plot the two curves of G_p vs. N_p and then determine their intersection. While this graphical interpolation approach can be implemented on digital computers, Tracy's iterative approach is more straightforward to implement and usually converges within a few iterations.

Material-Balance Calculations Using Muskat and Taylor's Method

Muskat and Taylor's method⁴ is applicable to the tank-type depletion performance of a volumetric reservoir with no initial gas cap. It is intended mainly for below-bubblepoint pressure. For a sequence of pressure steps, Δp , the change in oil saturation, ΔS_o , during each step is calculated by use of the following depletion equation in differential form.

$$\frac{\Delta S_o}{\Delta p} = \frac{S_o \frac{B_g}{B_o} \frac{dR_s}{dp_R} + S_g B_g \frac{d(1/B_g)}{dp_R} + \frac{S_o k_{rg} \mu_o}{B_o k_{ro} \mu_g} \frac{dB_o}{dp_R}}{1 + \frac{k_{rg} \mu_o}{k_{ro} \mu_g}} \quad (30)$$

The stepwise solution of this depletion equation yields the reservoir oil saturation, S_o , vs. reservoir pressure, p_R . For each pressure at which S_o has been calculated, the cumulative recovery as a fraction of the original OIP can be calculated by use of Eq. 31.

$$\frac{N_p}{N} = 1 - \left(\frac{S_o}{1 - S_w} \right) \frac{B_{oi}}{B_o} \quad (31)$$

Having the value of S_o , k_{rg}/k_{ro} can be determined from the plot of k_{rg}/k_{ro} vs. S_o or vs. $S_o + S_w$, which is required data. The producing GOR is then

$$R = R_s + \frac{k_{rg}}{k_{ro}} \left(\frac{\mu_o B_o}{\mu_g B_g} \right) \quad (32)$$

Because this method assumes uniform oil saturation throughout the reservoir, it is not applicable when there is appreciable segregation of gas and oil.

Eq. 30 can be solved either explicitly or implicitly. Explicit means each term on the right side of Eq. 30 is evaluated on the basis of the pressure and saturation at the start of the pressure step. Each pressure step must be small so that these values are representative of conditions during the step. While this approach has the advantage of not requiring iteration, it is not self-checking. Significant cumulative errors may occur unless the pressure intervals are sufficiently small. In the implicit (iterative) solution, the terms on the right side of Eq. 30 are evaluated on the basis of estimated conditions (p_R and S_o) at either the middle or the end of the pressure step. This requires making an initial estimate of these conditions, computing the pressure step, checking agreement between estimated and computed values, and, if necessary, recomputing the step with the most recently computed values as the new estimates. This iterative solution involves more work but can handle larger pressure steps suitably.

Comparison With Gridded Simulator Equations

Because Eq. 30 looks rather formidable and mysterious, it may be helpful to show where the terms come from. This will also show the relationship of Eq. 30 to the equations used in gridded multiphase reservoir simulators; tank-type models and gridded models use similar continuity (material-balance) principles. For a two-phase (gas/oil) gridded model omitting gravity and capillary forces, the oil phase partial differential equation that combines Darcy-law flow and continuity is Eq. 33. This equation is in Darcy units.

$$\nabla \cdot \left(\frac{kk_{ro}}{\mu_o B_o} \nabla p \right) = \phi \frac{\partial}{\partial t} \left(\frac{S_o}{B_o} \right) - q_{ov}, \dots \dots \dots (33)$$

where ∇ denotes the gradient,

$$\nabla = \frac{\partial}{\partial x} + \frac{\partial}{\partial y} + \frac{\partial}{\partial z},$$

and $\partial(S_o/B_o)/\partial t$ is the partial derivative of the quantity S_o/B_o with respect to time.

The left side of Eq. 33 represents Darcy-law flow of oil in the reservoir (between blocks in a gridded model) and would be zero for a tank-type (one-block) model. The right-side terms represent oil accumulation and production. The corresponding equation for total (free+solution) gas is Eq. 34.

$$\begin{aligned} \nabla \cdot \left[\left(\frac{kk_{rg}}{\mu_g B_g} + R_s \frac{kk_{ro}}{\mu_o B_o} \right) \nabla p \right] \\ = \phi \frac{\partial}{\partial t} \left(\frac{S_g}{B_g} + R_s \frac{S_o}{B_o} \right) - q_{gv}, \dots \dots \dots (34) \end{aligned}$$

The corresponding equations for a tank-type model are obtained by noting that the left sides of Eqs. 33 and 34 are zero for the tank-type model. Deleting the left side

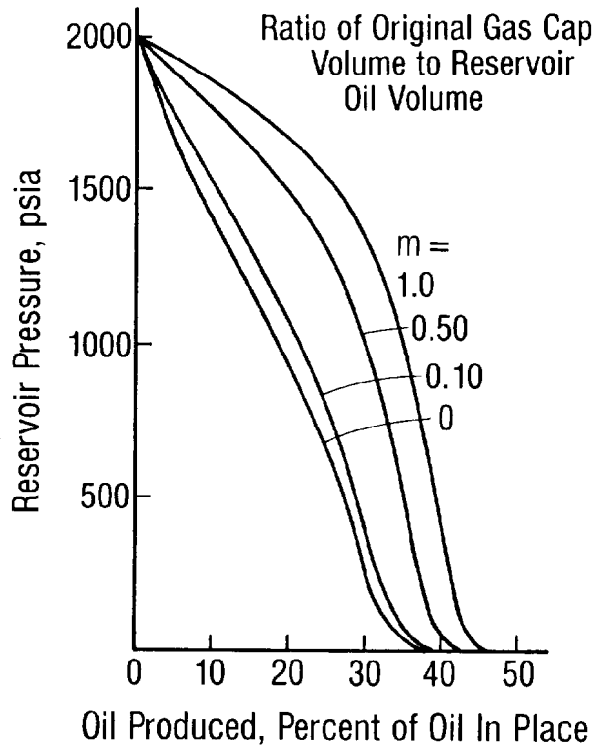


Fig. 37.6—Reservoir pressure vs. percent oil recovery for several values of m .

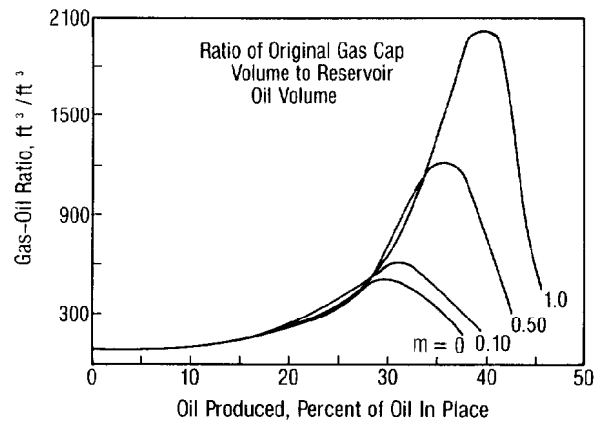


Fig. 37.7—Producing GOR vs. percent oil recovery for several values of m .

of each equation, multiplying by the bulk volume, and changing to oilfield units yields

$$V_p \frac{\partial}{\partial t} \left(\frac{S_o}{B_o} \right) = q_o \dots \dots \dots (35)$$

and

$$V_p \frac{\partial}{\partial t} \left(\frac{S_g}{B_g} + R_s \frac{S_o}{B_o} \right) = q_g \dots \dots \dots (36)$$

This total gas rate q_g is the sum of the free-gas production rate and the solution-gas production rate.

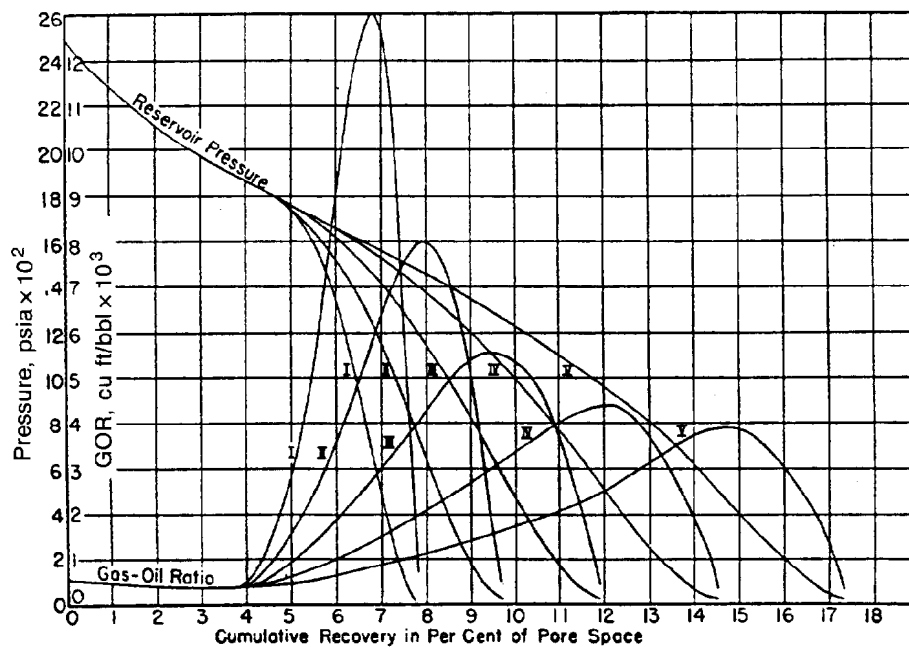


Fig. 37.8—Pressure and GOR histories of solution-gas-drive reservoirs producing oil of different viscosities.

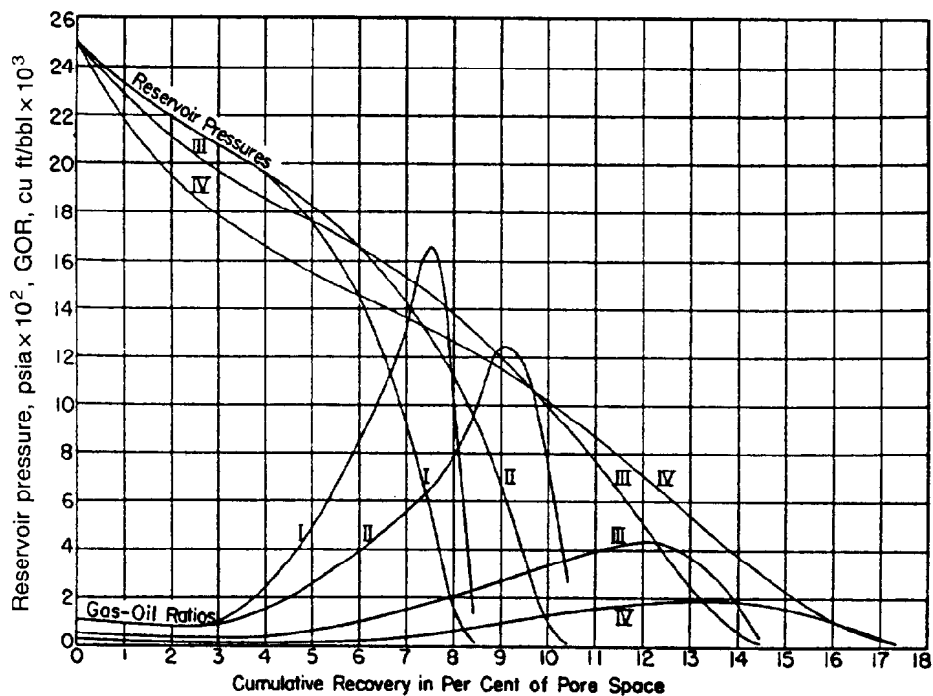


Fig. 37.9—Pressure and GOR histories of solution-gas-drive reservoirs producing oil of different gas solubilities and oil viscosities.

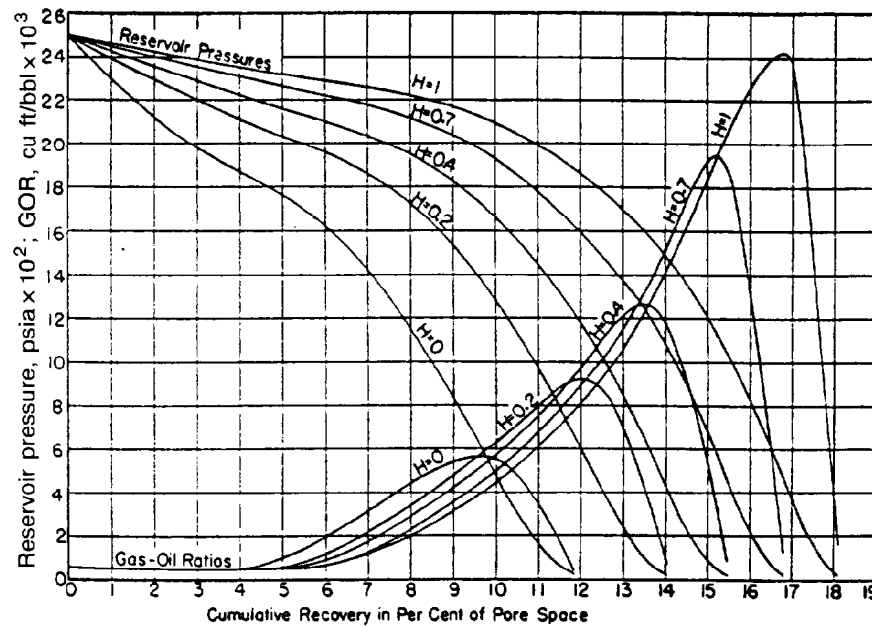


Fig. 37.10—Reservoir pressure and GOR histories of gas-drive reservoirs with various ratios of gas-cap volume to oil-zone volume (H = thickness of gas cap/thickness of oil zone).

The producing GOR (R), scf/STB, is given by

$$R = \frac{q_g}{q_o} = \frac{k_g/\mu_g B_g}{k_o/\mu_o B_o} + R_s = \frac{k_g \mu_o B_o}{k_o \mu_g B_g} + R_s \quad (37)$$

The producing GOR can also be expressed by use of q_o from Eq. 35 and q_g from Eq. 36:

$$R = \frac{q_g}{q_o} = \frac{V_p \frac{\partial}{\partial t} \left(\frac{S_g}{B_g} + R_s \frac{S_o}{B_o} \right)}{V_p \frac{\partial}{\partial t} \left(\frac{S_o}{B_o} \right)} \quad (38)$$

From the chain rule for derivatives,

$$\frac{dx}{dt} = \frac{dx}{dp} \frac{dp}{dt}$$

Eq. 38 becomes

$$R = \frac{S_g \frac{d(1/B_g)}{dp_R} + \frac{1}{B_g} \frac{dS_g}{dp_R} + \frac{R_s}{B_o} \frac{dS_o}{dp_R} + \frac{S_o}{B_o} \frac{dR_s}{dp_R} + R_s S_o \frac{d(1/B_o)}{dp_R}}{S_o \frac{d(1/B_o)}{dp_R} + \frac{1}{B_o} \frac{dS_o}{dp_R}} \quad (39)$$

By equating the two expressions for R given by Eqs. 37 and 39, using $dS_g = -dS_o$, and rearranging we obtain Eq. 30. Thus, the Muskat material balance for a tank-type reservoir (Eq. 30) can be derived as a special case of the equations for a gridded multiphase simulator. Because we use compatible equations, the results from a gridded simulator using special data to match the Muskat method (e.g., no flow between gridblocks) should match those obtained by Muskat's method. Even for a gridded simulator with flow between blocks, Ridings *et al.*¹⁴ showed results agreeing with Muskat's method. More information is given in the section entitled Insights from Simulator Studies.

Sensitivity of Material-Balance Results

Several authors have discussed the sensitivity of material-balance results to data variations. Turner² showed the effect of gas-cap size on performance for values of m (gas-cap-volume/oil-reservoir-volume) of 0 (no cap), 0.1, 0.5, and 1.0. Oil recovery vs. pressure is shown in Fig. 37.6; Fig. 37.7 shows GOR vs. oil recovery. Turner discussed applicability of assumptions about the gas initially in the gas cap: (1) the gas cap and the oil zone are each assumed to remain constant in size, and (2) all gas leaving the gas cap is assumed to pass through the oil zone (i.e., no bypassing—such as by gas coning at wells). Turner stated that such assumptions are obviously in error but they in part will compensate each other. The assumption of no bypassing tends to overestimate oil recovery, while the assumption of a constant oil-zone size (corresponding to low gravity drainage) tends to underestimate oil recovery.

Muskat and Taylor³ provided informative results about the sensitivity of oil recovery to oil property variations

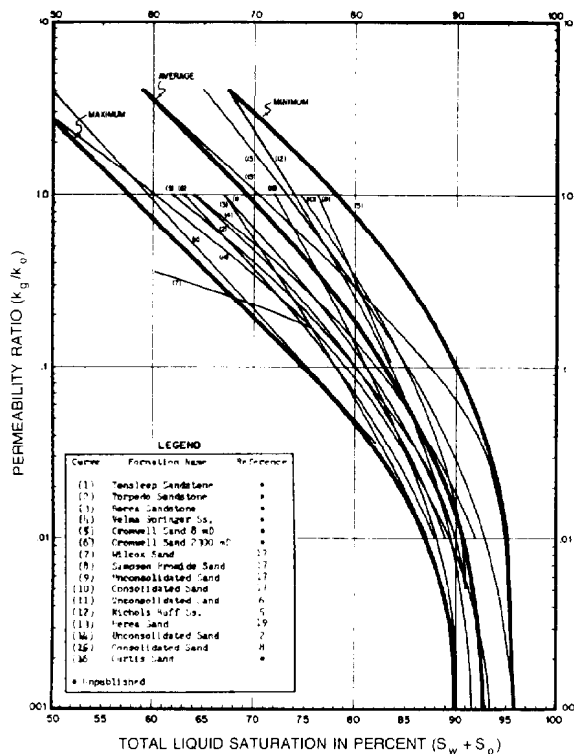


Fig. 37.11—Relative-permeability ratio for sands and sandstones vs. liquid saturation.

and to gas-cap size. Fig. 37.8 shows the reduction in oil recovery as oil viscosity is increased. It also shows the higher producing GOR's for cases with higher oil viscosity. Note the large variations in oil recovery, from less than 8% to more than 17%. Fig. 37.9 shows the combined effects of varying oil viscosity and solution GOR. Fig. 37.10 shows performance for several values of the gas-cap-volume/oil-zone-volume ratio, which Muskat and Taylor denoted by H . It can be seen that calculated oil recovery and peak GOR both increase with increasing gas-cap size. Muskat and Taylor emphasized the assumptions that gas-cap size remains constant throughout the production history and that depletion of the cap takes place by gas moving from the cap into the oil zone where it is assumed to be mixed or dispersed throughout the oil zone and produced along with the oil and gas originally in the oil zone.

Arps and Roberts⁸ plotted several sets of sandstone permeability ratio vs. liquid-saturation data and determined the three curves designated maximum, average, and minimum in Fig. 37.11. Maximum means highest oil recovery (lowest k_g/k_o at a given liquid saturation), while minimum means lowest oil recovery (highest k_g/k_o). For each k_g/k_o curve, they computed oil recovery [STB/(acre-ft)(percent porosity)] vs. pressure for several sets of oil fluid properties. Fig. 37.12 is for the minimum recovery (maximum k_g/k_o) case. Do not be confused by

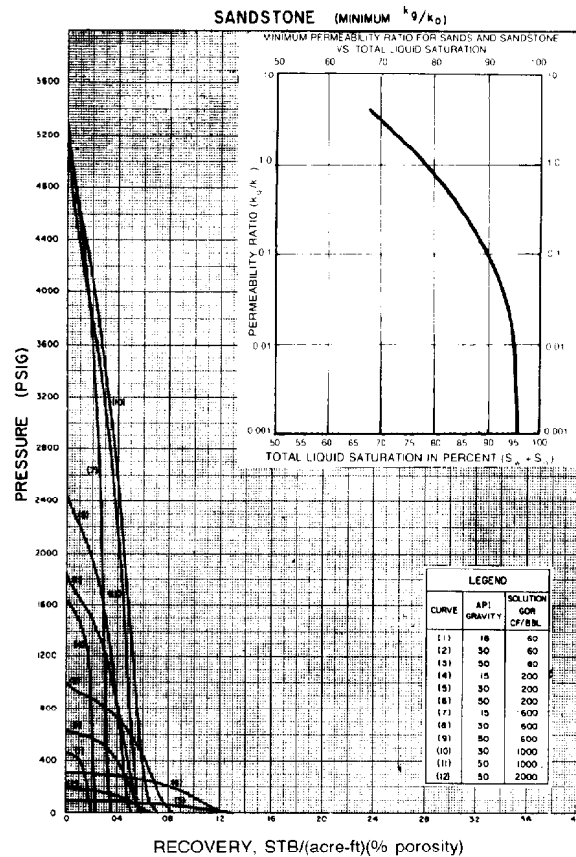


Fig. 37.12—Reservoir pressure vs. recovery factor, STB/acre-ft/percent porosity for sandstone with k_g/k_o giving minimum oil recovery.

the label of minimum k_g/k_o in this figure. Fig. 37.13 is the average case, and Fig. 37.14 shows results for the maximum recovery (minimum k_g/k_o) case. Again the label (maximum k_g/k_o) is misleading. Note the large variation in oil recovery, STB/acre-ft/percent porosity: 2 to 12 for the minimum case, 6 to 18 for the average case, and 9 to 26 for the maximum case. Arps and Roberts⁸ also presented results with limestone k_g/k_o curves. Computed recovery ranges were 1 to 7 for the minimum case, 3 to 16 for the average case, and 13 to 32 for the maximum recovery case.

Fig. 37.15 is the comparison by Sikora¹³ of reservoir performance for no segregation vs. complete segregation. The complete segregation case has a lower calculated oil recovery and a faster rise in producing GOR. This illustrates the adverse effects of assumed segregation on performance calculations in a tank-type model that, among other things, assumes production from the entire pay thickness. For a reservoir with high vertical communication, oil recovery could be increased by selective production from perforations in the lower part of the oil zone. The tank-type prediction with production from the entire pay thickness would be inapplicable and misleading. The limited applicability of the tank-type model to cases with segregation was discussed previously. Performance predictions that consider the selective production would require a more detailed model, such as a gridded simulator.

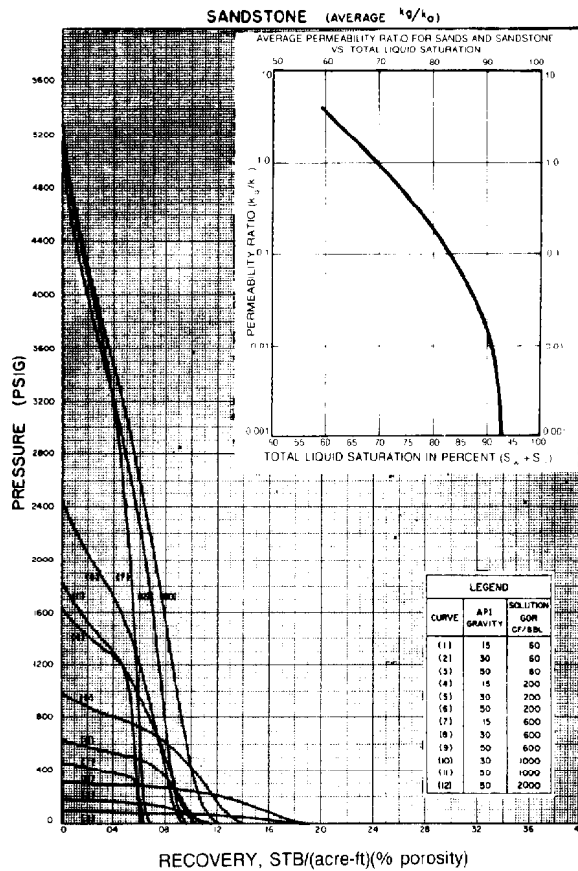


Fig. 37.13—Reservoir pressure vs. recovery factor, STB/acre-ft/percent porosity for sandstone with average k_g/k_o .

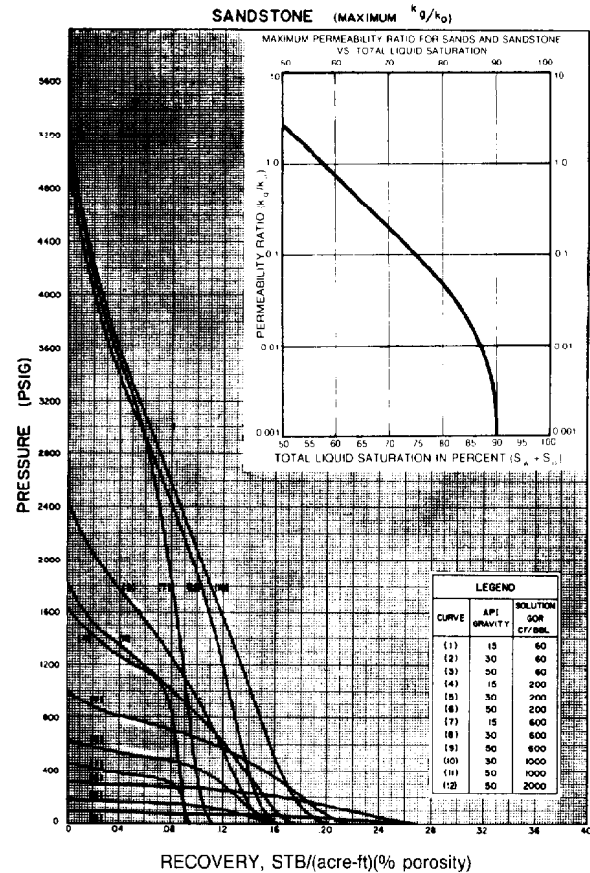


Fig. 37.14—Reservoir pressure vs. recovery factor, STB/acre-ft/percent porosity for sandstone with k_g/k_o giving maximum oil recovery.

Singh and Guerrero¹⁸ showed sensitivity of recovery to variations in gas-cap size (m), interstitial (connate) water saturation, permeability ratio (k_g/k_o), oil reservoir volume factor (B_o), solution GOR (R_s), and initial pressure (p_{iR}). Fluid properties are shown in Table 37.1 and Figs. 37.16 through 37.18. Singh and Guerrero used permeability-ratio data that approximated the sandstone average permeability ratio characteristics given by Arps and Roberts.⁸ Interstitial water saturation was 22%. They calculated performance from bubblepoint pressure of 2,500 psi down to a 100-psi abandonment pressure using 200-psi pressure decrements.

Fig. 37.19 shows oil recovery (below bubblepoint) vs. pressure for three base cases with m values of 0, 0.5, and 0.75. For each of the base cases, performance was computed for $\pm 30\%$ changes in each of the following: B_o , R_s or B_g , p_{iR} , interstitial water saturation, and k_g/k_o or μ_o/μ_g . The percentage change or error in oil recovery resulting from the $\pm 30\%$ change in these data items is shown in Table 37.2. Figs. 37.20 through 37.24 show the sensitivity of calculated performance to these $\pm 30\%$ changes in data values. These figures and Table 37.2 show that oil recovery percentage increased with reductions in B_o , p_{iR} , or k_g/k_o and with increases in R_s and S_{iw} . Table 37.2 shows that the changes in oil recovery were largest for cases with $m=0$ (no gas cap). The presence of a

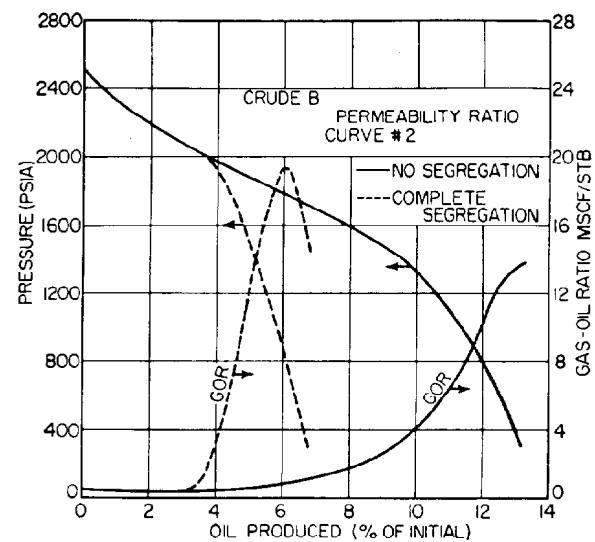


Fig. 37.15—Comparison of no-segregation and complete-segregation reservoir performance.

**TABLE 37.1—FLUID PROPERTY DATA FOR MATERIAL BALANCE
PERFORMANCE SENSITIVITY STUDIES**

Pressure (psia)	Oil Volume Factor (RB/STB)	Gas Volume Factor (RB/scf)	Solution GOR (scf/STB)	Viscosity of Oil (cp)	Viscosity of Gas (cp)
3,000	1.315	0.000726	650		
2,500	1.325	0.000796	650	1.200	0.02121
2,300	1.311	0.000843	618	1.260	0.02046
2,100	1.296	0.000907	586	1.320	0.01960
1,900	1.281	0.001001	553	1.386	0.01869
1,700	1.266	0.001136	520	1.455	0.01770
1,500	1.250	0.001335	486	1.530	0.01670
1,300	1.233	0.001616	450	1.615	0.01570
1,100	1.215	0.001998	412	1.714	0.01472
900	1.195	0.002626	369	1.826	0.01380
700	1.172	0.003481	320	1.954	0.01298
500	1.143	0.005141	264	2.103	0.01221
300	1.108	0.009027	194	2.281	0.01165
100	1.057	0.028520	94	2.539	0.01125

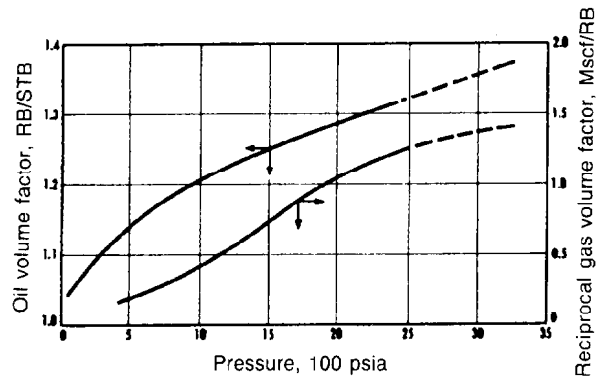


Fig. 37.16—FVF's vs. pressure used in performance sensitivity computations.

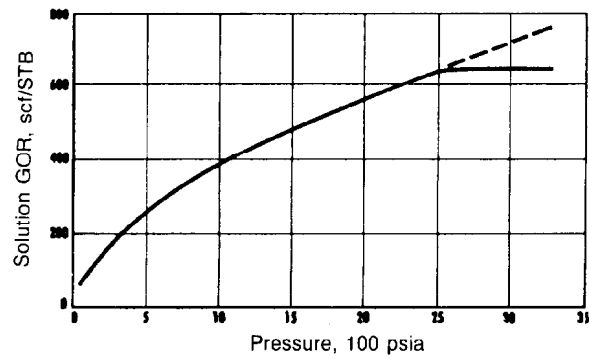


Fig. 37.17—Solution GOR vs. pressure used in performance sensitivity computations.

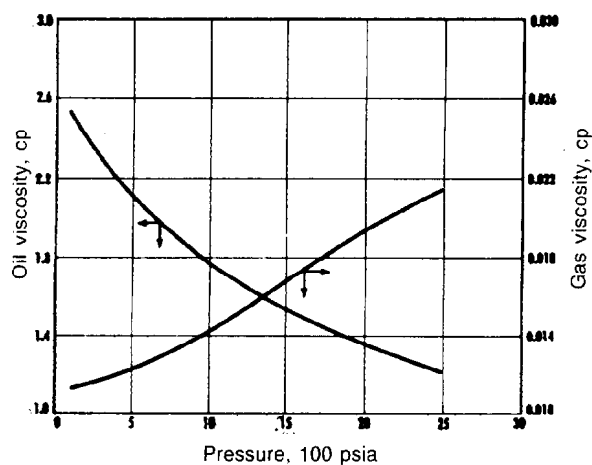


Fig. 37.18—Gas and oil viscosities vs. pressure used in performance sensitivity computations.

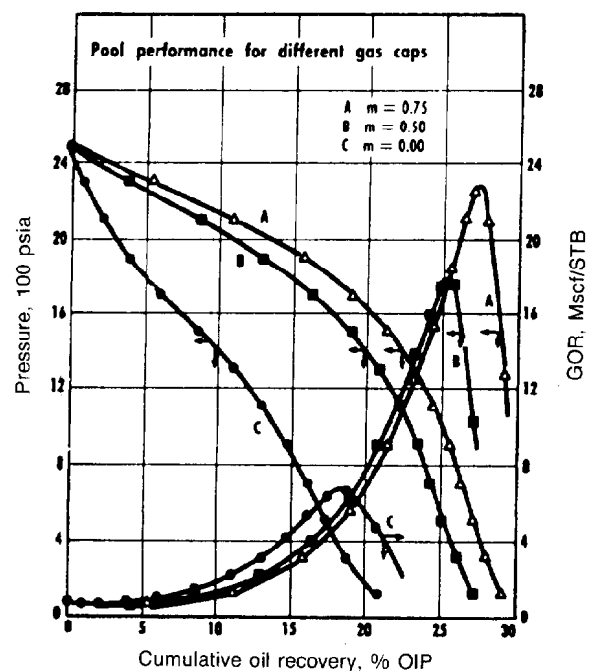


Fig. 37.19—Depletion-drive performance for three base cases with different gas-cap sizes.

TABLE 37.2—COMPUTED CHANGE OR ERROR IN OIL RECOVERY CAUSED BY $\pm 30\%$ CHANGE IN DATA

Factor	Percentage Factor Varied*					
	$m = 0$		$m = 0.50$		$m = 0.75$	
	-30.00	+30.00	-30.00	+30.00	-30.00	+30.00
B_o	+11.0553	-8.0781	+3.6011	-2.1059	+2.5361	-1.5338
B_g and R_s	-10.9920	+8.1900	-2.7845	+2.5720	-2.0157	+1.8088
ρ	+9.1756	-7.8326	+3.6844	-5.3114	+2.6490	-4.7911
S_w	-9.8654	+11.6368	-8.6772	+10.3622	-8.5560	+10.0768
k_g/k_o and μ_o/μ_g	+10.3020	-7.2521	+8.3833	-5.9272	+7.9464	-5.6907

*"Factor" denotes the type of data changed.

gas cap moderated performance sensitivity. This does not mean that the presence of a gas cap always reduces the overall uncertainty about future performance. For actual reservoirs, there will be additional uncertainties, such as gas-cap size and applicability of the tank-type model (e.g., no gravity drainage and no gas coning at wells).

Production Rate and Time Calculations

Rate and time were not considered in the material-balance computations described in the previous sections because performance (recovery vs. pressure) would be independent of rate and time for the assumed tank-type behavior with pressure equilibrium. Once the material-balance computations are completed, the incremental oil production for each pressure decrement has been calculated. The time required for this production can be calculated if the oil production rate can be determined.

All wells are assumed to have the same oil production rate at a given reservoir pressure (or equivalently an average well is considered). The production rate for the entire reservoir is calculated as the rate per well times the number of wells.

Two different approaches have been used for calculating the oil production rate, q_o , as a function of average reservoir pressure, \bar{p}_R , and well flowing BHP (p_{wf}). The simpler approach assumes a straight-line relationship shown in Fig. 37.25 and given by Eq. 40.

$$q_o = J(\bar{p}_R - p_{wf}) \quad (40)$$

The other approach does not assume a straight-line relationship. Curves that are called the well's inflow performance relationship (IPR) aid in calculation of q_o . Each approach is discussed below.

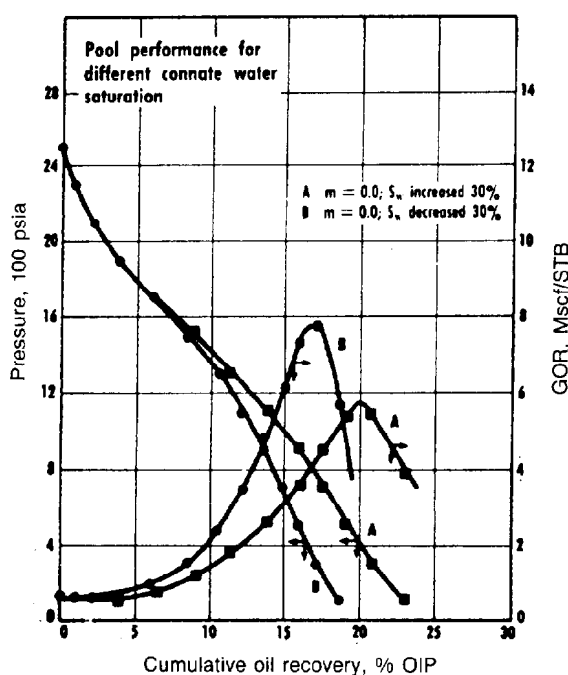


Fig. 37.20—Sensitivity of depletion-drive performance to $\pm 30\%$ change in interstitial water saturation.

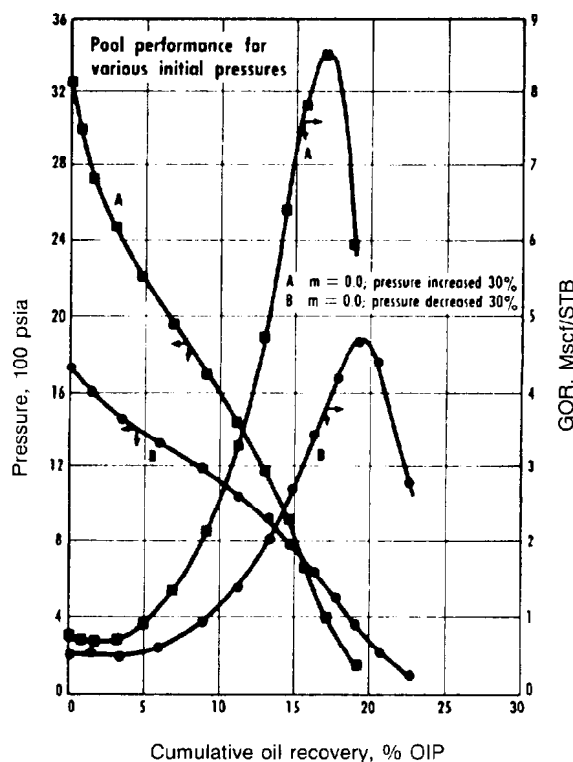


Fig. 37.21—Sensitivity of depletion-drive performance to $\pm 30\%$ change in initial pressure.

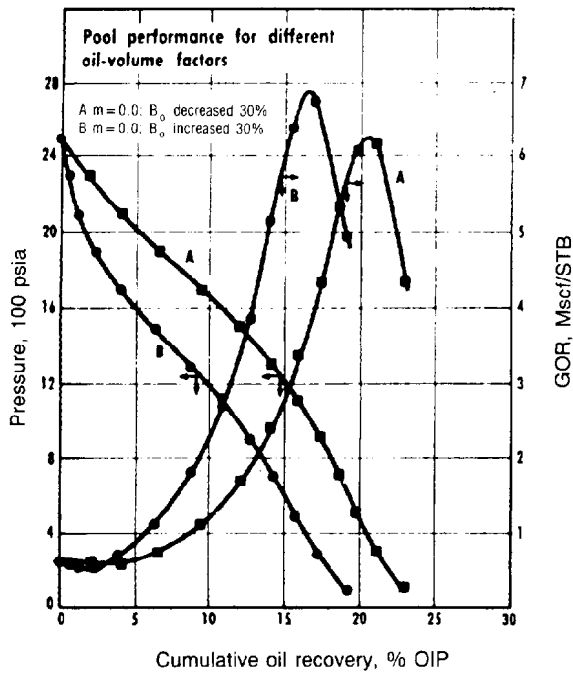


Fig. 37.22—Sensitivity of depletion-drive performance to $\pm 30\%$ change in B_o .

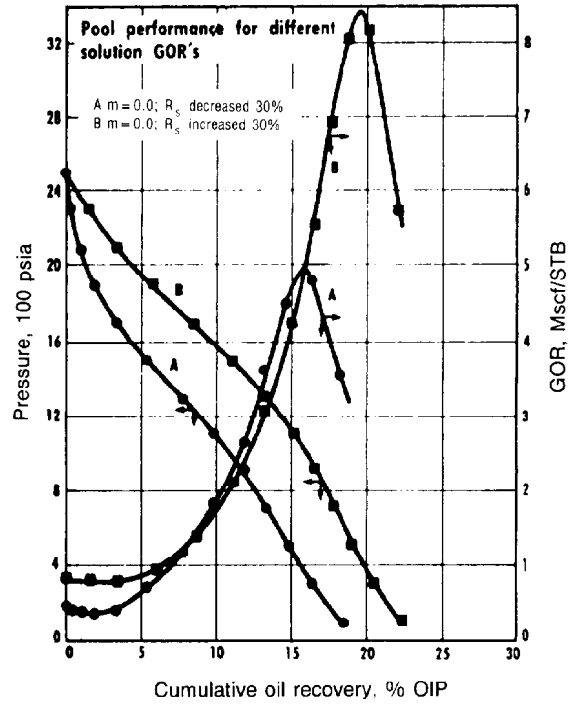


Fig. 37.23—Sensitivity of depletion-drive performance to $\pm 30\%$ change in R_s .

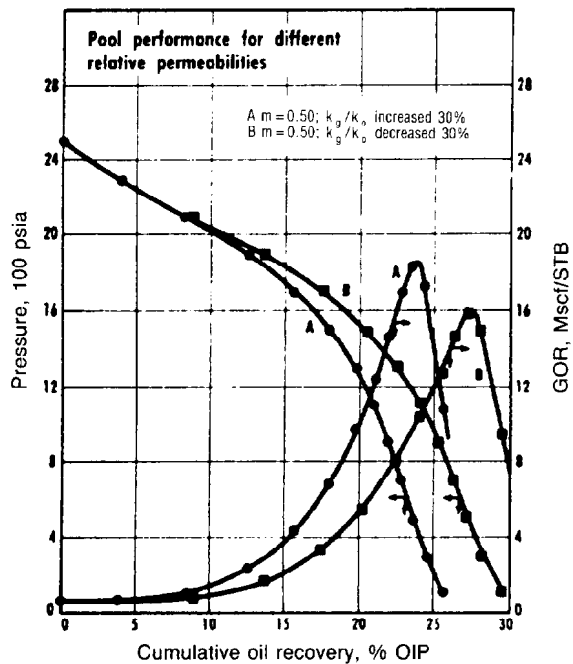


Fig. 37.24—Sensitivity of depletion-drive performance to $\pm 30\%$ change in permeability ratio k_g/k_o .

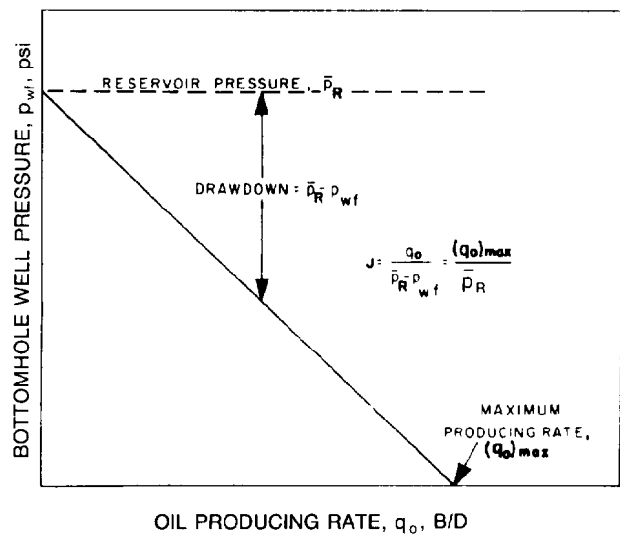


Fig. 37.25—Straight-line inflow performance (q_o vs. p_{wf}) relationship.

Rates Based on Productivity Index

Well production rates are often assumed to be directly proportional to the pressure drawdown (difference between reservoir and wellbore pressures), as shown by Eq. 40. The proportionality term is the productivity index, J , which is often based on the equation for pseudosteady-state flow in a bounded system. The generalized form of this equation presented by Odeh²⁷ has a shape factor or constant C_A to enable characterization of both noncircular and circular drainage areas:

$$q_o = \frac{0.00708k_{ro}kh(\bar{p}_R - p_{wf})}{\mu_o B_o \ln(C_A - \frac{3}{4} + s)} \quad (41)$$

For a radial system, the shape factor is $C_A = r_e/r_w$, where r_e is the external radius and r_w is the wellbore radius. The productivity index for a single well is then determined by combining Eqs. 40 and 41:

$$J = \frac{q_o}{\bar{p}_R - p_{wf}} = \frac{0.00708k_{ro}kh}{\mu_o B_o \ln(C_A - \frac{3}{4} + s)} \quad (42)$$

A well's productivity index is sometimes treated as a constant—at least for some limited time or pressure interval—because variations in μ_o , B_o , and k_{ro} are small. For performance predictions over larger pressure ranges, however, it is important to consider these variations.

The initial productivity index, J_i , can be determined two ways: (1) from well pressure and flow-rate tests (see Chap. 32), or (2) by Eq. 42 with $k_{ro} = 1.0$ at initial conditions.

The expression for J_i based on Eq. 42 is

$$J_i = \frac{0.00708kh}{\mu_{oi} B_{oi} \ln(C_A - \frac{3}{4} + s)} \quad (43)$$

No matter how J_i is determined, at a later time (i.e., a lower pressure), J is

$$J = J_i k_{ro} \left(\frac{\mu_{oi} B_{oi}}{\mu_o B_o} \right) \quad (44)$$

where k_{ro} is evaluated at the current liquid saturation and μ_o and B_o are evaluated at the current reservoir pressure. Eq. 44 assumes pseudosteady state flow conditions as the average reservoir pressure declines [i.e., $\partial/\partial t (S_o/B_o)$ is the same at all points]. J from Eq. 44 is used in Eq. 40 to calculate q_o . Consequently, the well's production rate is directly proportional to pressure drawdown ($\bar{p}_R - p_{wf}$), but the proportionality term (J) varies with pressure and saturation.

Rates Based on Inflow Performance Ratio (IPR)

The uniform saturation assumption of tank-type material balances is avoided in rate calculations using the IPR approach. The basic idea is that with increasing drawdown

(lower BHP), gas saturation will not be uniform. More gas will be evolved in the near-well region, causing higher gas saturations and more resistance to oil flow (lower k_{ro}). This increased flow resistance reduces the oil production rate at a given BHP.

The reader may be wondering why we would combine a tank-type material-balance computation that assumes uniform saturation with rate calculations based on a different assumption. Isn't it more consistent to stay with the uniform saturation assumption by using rates based on productivity index values? Although such questions are logical, note that the nonuniformity in near-well saturations tends to affect mainly rates. The overall material-balance results (oil recovery vs. average reservoir pressure) are more a function of average reservoir conditions than of near-well conditions. The IPR approach is also of interest for predicting oilwell productivity in other types of calculations for solution-gas-drive reservoirs.

Vogel²⁴ used a computer program to determine oil production rate (q_o) vs. BHP, p_{wf} , for each of a sequence of declining reservoir pressures. This was done for a circular reservoir with a completely penetrating well at its center using Weller's¹⁶ approximation described in the section entitled Insights from Simulator Studies.

Vogel simulated several circular reservoirs with different oil properties, relative-permeability characteristics, well spacings (i.e., sizes of the circular reservoir), and well skin conditions. His results for one case are shown in Fig. 37.26. Each line shows q_o vs. p_{wf} for a given cumulative oil recovery (or for a given reservoir pressure that is the pressure corresponding to zero q_o). Note that, in contrast to the straight line of Fig. 37.25, the lines in Fig. 37.26 have a downward curvature. This is a result of the greater resistance to oil flow with increasing gas saturation. Vogel pointed out the compatibility of his results with those of Evinger and Muskat,²³ who presented theoretical calculations to show that plots of q_o vs. p_{wf} for two-phase flow result in curved lines rather than straight lines.

Vogel found that in plotting dimensionless IPR curves, as shown in Fig. 37.27, the curves group closely. He approximated this group of curves by a single average or reference curve shown in Fig. 37.28. This curve can be an approximation for all wells. An equation for this curve is

$$\frac{q_o}{(q_o)_{\max}} = 1.0 - 0.2 \frac{p_{wf}}{\bar{p}_R} - 0.8 \left(\frac{p_{wf}}{\bar{p}_R} \right)^2 \quad (45)$$

where $(q_o)_{\max}$ = maximum oil production rate, STB/D.

Vogel did not provide a way to compute q_o given p_{wf} and \bar{p}_R . His approach required knowledge of q_o at some p_{wf} from a well test. Eq. 45 could then be used to calculate the q_o at any other value of p_{wf} . In 1971, Standing²⁶ provided the additional insights necessary to use Vogel's results in performance prediction models.

Standing noted that Eq. 45 can be rearranged to

$$\frac{q_o}{(q_o)_{\max}} = \left(1 - \frac{p_{wf}}{\bar{p}_R} \right) \left(1 + 0.8 \frac{p_{wf}}{\bar{p}_R} \right) \quad (46)$$

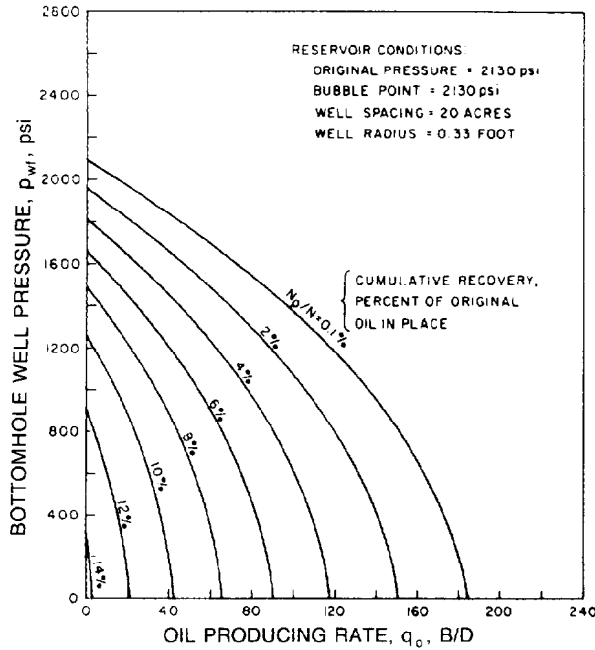


Fig. 37.26—Computed inflow performance relationships for a well in a solution-gas-drive reservoir.

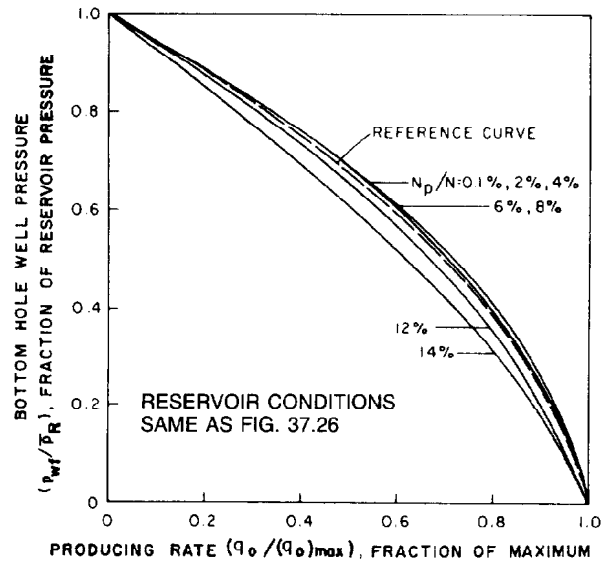


Fig. 37.28—Comparison of reference curve with computed IPR curves.

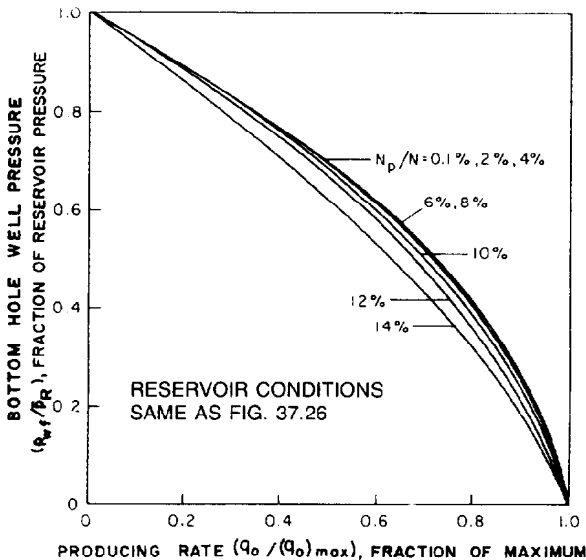


Fig. 37.27—Dimensionless inflow performance relationships for a well in a solution-gas-drive reservoir.

and that the productivity index of a well is defined by

$$J = \frac{q_o}{\bar{p}_R - p_{wf}} \quad (47)$$

Substituting Eq. 47 into Eq. 46 yields

$$J = \frac{(q_o)_{\max}}{\bar{p}_R} \left(1 + 0.8 \frac{p_{wf}}{\bar{p}_R} \right) \quad (48)$$

Standing noted that the physical conditions inherent in Eq. 48 are that reservoir gas and oil saturations, as well as reservoir pressure, vary with distance from the wellbore and that the well's skin factor is zero.

Standing also considered the situation in which fluid saturations are uniform within the reservoir. This would be the case for production with minimal drawdown. The well's productivity under these conditions of essentially uniform saturations and pressure was denoted by J^* . Note that J^* is based on the same conditions assumed for the productivity index, J , in Eq. 42; J^* is identical to the J of Eq. 42 and can be evaluated the same way:

$$J^* = \frac{0.00708 k_{ro} kh}{\mu_o B_o \ln \left(C_A - \frac{3}{4} + s \right)} \quad (49)$$

where k_{ro} is evaluated at the average fluid saturations in the reservoir, and μ_o and B_o are evaluated at the average reservoir pressure \bar{p}_R . Recall that for a radial system the shape factor C_A is simply r_e/r_w .

Standing used J to denote the true (or at least more accurate) value of the well's productivity index. The difference between J and J^* is an indication of the inaccuracy that occurs because J^* is based on uniform conditions.

Standing noted that J^* is the limiting value of J for very small drawdown (i.e., as p_{wf} approaches \bar{p}_R):

$$J^* = \lim_{p_{wf} \rightarrow \bar{p}_R} J = \frac{1.8(q_o)_{\max}}{\bar{p}_R} \quad (50)$$

Combining Eqs. 48 and 50 enables elimination of $(q_o)_{\max}/\bar{p}_R$, yielding

$$J = \frac{J^*}{1.8} \left(1 + 0.8 \frac{p_{wf}}{\bar{p}_R} \right) \quad (51)$$

Eqs. 49 and 51 enable calculation of the well's J once the average fluid saturations, p_{wf} , and p_R are known.

By combining Eqs. 45 and 50, Standing eliminated $(q_o)_{\max}$ and obtained Eq. 52, which is a general relationship for IPR curves at various average reservoir pressures.

$$q_o = \frac{J^* \bar{p}_R}{1.8} \left[1 - 0.2 \left(\frac{p_{wf}}{\bar{p}_R} \right) - 0.8 \left(\frac{p_{wf}}{\bar{p}_R} \right)^2 \right]. \quad (52)$$

Thus, Standing has shown how production rate in a solution-gas-drive performance model can be calculated by use of Vogel's IPR information. Because a value of J^* can be calculated with Eq. 49, all terms in Eq. 52 can be evaluated.

Later, Al-Saadoon²⁸ suggested that a different expression should be used for J . However, Rosbaco²⁹ clarified the situation by noting that although Standing²⁶ and Al-Saadoon²⁸ used different formulas for J and for J/J^* , both yield the same results for q_o vs. p_{wf} . Consequently, it is workable and acceptable to use Standing's equations.

Standing²⁵ discussed application of the IPR approach to damaged wells and Dias-Couto and Golan³⁰ developed a general IPR for wells in solution-gas-drive reservoirs that is applicable to wells with any drainage area shape, any completion flow efficiency, and at any stage of reservoir depletion.

Time Required for Oil Production

At this point, oil recovery vs. reservoir pressure is known from the material-balance calculations. The oil production rate per well, q_o , corresponding to a specified minimum p_{wf} can be calculated by use of either the productivity index approach (Eq. 42) or the IPR approach (Eqs. 49 and 52). This q_o is the calculated rate that the well is capable of producing. The well also may be subject to a scheduling constraint, such as an allowable production rate. Consequently, the well's oil production rate q_n at pressure p_n is the smaller of these two rates:

$$q_n = (q_o)_{\min}, \quad (53)$$

where $(q_o)_{\min}$ = minimum value of calculated and scheduled oil rate, STB/D.

The average oil production rate \bar{q}_o during the pressure decrement from p_{n-1} to p_n is given by Eq. 54.

$$\bar{q}_o = 0.5(q_n + q_{n-1}). \quad (54)$$

This average rate is used in Eq. 55 to calculate the time Δt_n required for the incremental oil production $(\Delta N_p)_n$ from p_{n-1} to p_n .

$$\Delta t_n = \frac{(\Delta N_p)_n}{\bar{q}_o n_w}. \quad (55)$$

The cumulative time, t_n , to reach pressure p_n is given by Eq. 56, with initial time $t_o = 0$.

$$t_n = t_{n-1} + \Delta t_n. \quad (56)$$

Insights from Simulator Studies

Because reservoir simulation is the topic of Chap. 48, we will not discuss it in detail here. For solution-gas-drive reservoirs, several comparisons have been made of gridded simulator results vs. simpler approaches, such as tank-type material balances. These comparisons help to confirm the range of applicability of the simpler approaches. The key questions addressed by these studies are the same questions Vogel²⁴ considered in getting the computed results on which he based the IPR method for well rate calculations. These questions are (1) to what extent is the saturation distribution nonuniform, and (2) how much does this influence performance.

The most informative study was by Ridings *et al.*,¹⁴ who compared laboratory vs. computed solution-gas-drive results for linear systems and obtained close agreement. Also, they used a gridded radial simulator to study the effect of rate and spacing on performance of solution-gas-drive reservoirs. Their conclusions concerning thin, homogeneous, horizontal solution-gas-drive reservoirs included the following.

1. "Ultimate recovery essentially is independent of rate and spacing, and agrees closely with recovery predicted by the conventional Muskat method."

2. "GOR depends somewhat on rate and spacing. For high rates or close spacings, GOR's initially are higher, but later become lower than a Muskat prediction would indicate. At low rates or wide spacings, GOR behavior approaches the Muskat prediction."

3. Computed depletion time agreed closely with conventional analysis (productivity index method) at low pressure drawdowns, but differed more for high drawdowns. This is in qualitative agreement with the results obtained by Vogel.²⁴

4. "Intermittent operation greatly affects instantaneous GOR behavior, but the cumulative GOR is not affected significantly. Also, oil recovery apparently is not affected." This refers to the cumulative oil recovery, not the amount of oil recovered in a given time period.

Note that Conclusions 1 and 2 support the use of tank-type models for predictions of recovery and of GOR (at least for low rates) for solution-gas-drive reservoirs. Although Muskat's method is mentioned, other tank-type approaches, such as Tracy's method, would be equally suitable.

Stone and Garder¹⁷ compared one-dimensional (1D) gridded simulator results vs. pressure and production data measured on a laboratory model produced by solution-gas drive. Computed and measured pressures vs. percent oil recovery were in close agreement.

In 1961, Levine and Prats¹² presented a comparison of solution-gas-drive results for an "exact method" (a 1D radial gridded simulator) vs. an "approximate method." The approximate method was based on assumptions of semisteady state—often called pseudosteady state (i.e., the stock-tank-oil desaturation rate is the same at all locations at any instant)—and "constant GOR," which actually meant uniform GOR (i.e., the total GOR is the same at all points at any instant). Levine and Prats showed close agreement between results of the simulator and the approximate method. These results, for various stages of depletion, were pressure and saturation vs. radius and the corresponding values of producing GOR and of percent

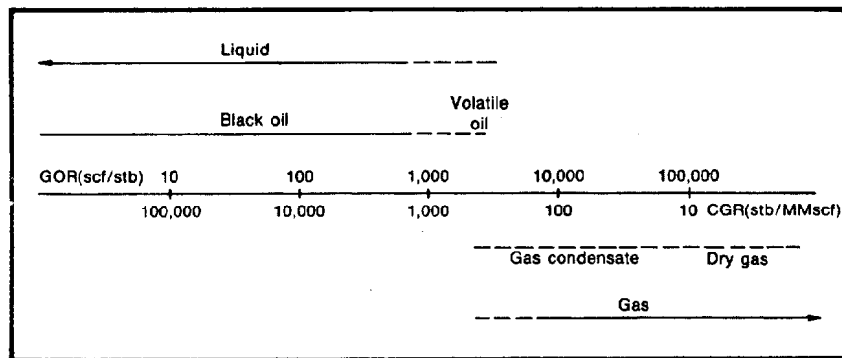


Fig. 37.29—Solution GOR range from black oil to gases. Volatile oils typically are in the range of 1,500 to 3,500 scf/STB.

oil recovery. Only limited information was given about the approximate method. This method would require derivation of additional equations and development of a computer program. Levine and Prats also discussed the extension of results to other sets of fluid and rock properties by use of dimensionless groups.

Later, Weller¹⁶ presented a different approach that retained the semisteady-state assumption but eliminated need for the "constant GOR" assumption. Weller showed that his method matched simulator results more closely than Levine and Prats' constant-GOR method. Weller developed equations for the radial distribution of saturation and pressure based on the combination of a transient period before the effects of a change in producing rate are felt at the drainage boundary with semisteady state (same rate of tank-oil desaturation everywhere) thereafter. Because these equations serve mainly as an alternative to a gridded simulator, details will not be given here (see Ref. 16).

Volatile Oil Reservoir Performance Predictions

Volatile oils are characterized by significant hydrocarbon liquid recovery from their produced reservoir gas. Also, volatile oils evolve gas and develop free-gas saturation in the reservoir more rapidly than normal black oils as pressure declines below the bubblepoint. This causes relatively high GOR's at the wellhead. Thus, performance predictions differ from those discussed for black oils mainly because of the need to account for liquid recovery from the produced gas. Conventional material balances with standard laboratory PVT (black-oil) data underestimate oil recovery. The error increases for increasing oil volatility.

A volatile oil can be defined as hydrocarbon that is liquid-phase oil at initial reservoir conditions but at pressures below bubblepoint evolves gas containing enough heavy components to yield appreciable condensate dropout at the separators. This is in contrast to black oils for which little error is introduced by the assumption that there is negligible hydrocarbon liquid recovery from produced gas.

Cronquist³⁸ used Fig. 37.29 to show the position of volatile oils in the GOR range between black oils and gases. Compared to black oils, volatile oils have higher solution GOR (1,500 to 3,500 scf/STB), generally higher

oil gravities (greater than 40 or 45° API), and higher B_o (above about 2.0 RB/STB). Volatile oils tend to shrink rapidly with pressure decline below bubblepoint. Cronquist used Fig. 37.30 to illustrate this behavior. The curves are made dimensionless (i.e., normalized to maximum values of unity) to facilitate comparisons. The ordinate b_{oD} is the dimensionless shrinkage:

$$b_{oD} = (B_{ob} - B_o) / (B_{ob} - B_{ou}).$$

The abscissa p_{RD} is a special form of dimensionless reservoir pressure:

$$p_{RD} = p_R / p_b,$$

where

p_{RD} = reservoir pressure, dimensionless,

p_R = reservoir pressure, psi, and

p_b = bubblepoint pressure, psi.

The curve labeled BO in Fig. 37.30 represents the typical behavior of a black oil. Shrinkage is almost proportional to pressure reduction below bubblepoint. In contrast, Curves E, F, and G are for progressively more volatile oils and show much greater shrinkage as pressure drops below bubblepoint.

This large shrinkage corresponds to substantial gas evolution (i.e., a large reduction in the solution GOR as pressure drops below bubblepoint). This is illustrated by Fig. 37.31, which shows dimensionless cumulative gas evolved, $R_{pD} = R_{rs} / R_{sb}$, vs. dimensionless pressure. R_{sb} is the solution GOR at bubblepoint, and R_{rs} is the reduction in solution GOR below bubblepoint: $R_{rs} = R_{sb} - R_s$. The trend line in Fig. 37.31 shows typical behavior for a black oil. Gas evolution is almost proportional to pressure reduction below the bubblepoint. Curves E, F, and G, which are for volatile oils, show much more gas evolution as pressure declines below bubblepoint.

Consequently, depletion performance of volatile oil reservoirs below bubblepoint is strongly influenced by the rapid shrinkage of oil and by the large amounts of gas evolved. This results in relatively high gas saturations, high producing GORs, and low to moderate production of reservoir oil. The produced gas can yield a substantial

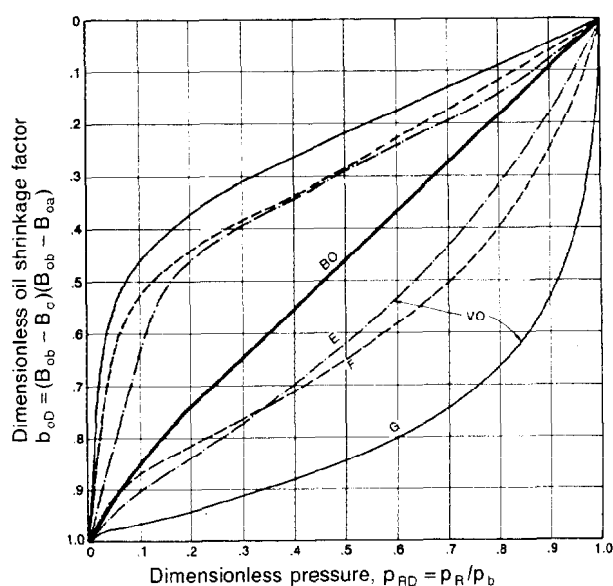


Fig. 37.30—Dimensionless shrinkage vs. dimensionless pressure. Curves E, F, and G are for progressively more volatile oils. Curve BO is for a black oil. Curve VO is for a volatile oil.

volume of hydrocarbon liquids in the processing equipment. This liquid recovery at the surface can equal or exceed the volume of stock-tank oil produced from the reservoir liquid phase.^{31,33,34,38} Depletion-drive recoveries are often between 15 and 25% of initial OIP. Improved recovery through injection of gas or water is sometimes considered but is beyond the scope of this chapter.

For volatile oil reservoir primary-performance prediction methods, the key requirements are correct handling of the oil shrinkage, gas evolution, gas and oil flow in the reservoir, and liquids recovery at the surface. For oil with a low volatility but a higher shrinkage than a typical black oil, simple corrections to differential shrinkage data are sometimes made.^{33,35,39} For volatile oils, however, it is essential to account for their special behavior more thoroughly. This includes determination of the composition of the gas evolved in the reservoir for a sequence of pressure steps below bubblepoint.

Methods for predicting volatile-oil reservoir-depletion performance that assume tank-type behavior (i.e., ignore pressure gradients) have been published by Cook *et al.*,³¹ Reudelhuber and Hinds,³³ and Jacoby and Berry.³⁴ In Refs. 31 and 33, laboratory data determined fluid compositions, while in Ref. 34, fluid compositions were computed from data for equilibrium constants. Cronquist³⁸ stated that there was no significant advantage of one method over the other two methods because "each method appears to yield acceptable results."

The multicomponent-flash method of Jacoby and Berry³⁴ is particularly appealing because a comparison of predicted vs. actual reservoir performance is available. Sections to follow describe the prediction method³⁴ and discuss a comparison of predicted vs. field performance.³⁶ The description of the multicomponent-flash method is from Sikora.¹³

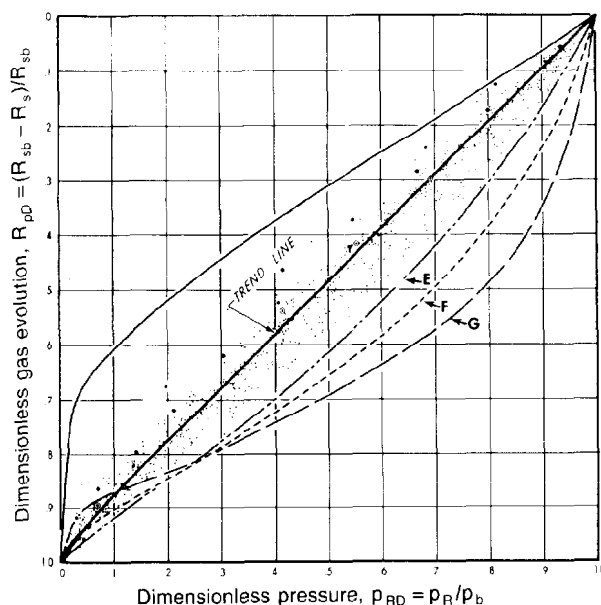


Fig. 37.31—Dimensionless evolved gas vs. dimensionless pressure. Curves E, F, and G are for progressively more volatile oils. The trend line typifies black-oil behavior.

Multicomponent-Flash Method of Jacoby and Berry

Data required to predict volatile-oil reservoir performance by the multicomponent-flash method include (1) the state and composition of the reservoir fluid at initial pressure; (2) appropriate sets of equilibrium vaporization ratios (K values) for the reservoir pressure range at the reservoir temperature and covering the temperature and pressure of surface separation; (3) some experimental liquid-phase densities at reservoir conditions to check correlations for calculating the required liquid densities during the depletion process; (4) experimental oil-phase viscosity data at reservoir temperature; and (5) relative-permeability-ratio data.

Calculation Procedure. Prediction of reservoir performance by the Multicomponent-Flash Method consists of the following steps, starting at pressure p_1 . For convenience, the calculation is made for a unit of hydrocarbon PV.

1. Select a pressure p_2 that is lower than p_1 .
2. Flash the number of moles of the reservoir composite fluid in the unit pore space at p_1 to the next lower pressure p_2 .
3. Assume a gas saturation at p_2 and calculate the average flowing bottomhole GOR with Eq. 57.

$$\bar{R} = \frac{k_g \mu_o}{k_o \mu_g} \quad (57)$$

4. Calculate the number of moles in each phase of the unit volume, the overall composition, and the number of moles of reservoir composite remaining in the unit volume at p_2 .

5. Determine the difference between the reservoir composite at p_1 and p_2 , which is the total amount and com-

TABLE 37.3—CALCULATED COMPOSITION (MOLE FRACTIONS) OF THE WELLSTREAM

Component	Reservoir Pressure (psia)							
	4,836	4,768	4,550	4,300	3,750	2,750	1,750	750
Nitrogen	0.0167*	0.0147	0.0170	0.0205	0.0235	0.0235	0.0215	0.0165
Methane	0.6051*	0.5718	0.6109	0.6711	0.7298	0.7582	0.7570	0.7001
Carbon dioxide	0.0218*	0.0215	0.0218	0.0224	0.0236	0.0250	0.0267	0.0274
Ethane	0.0752*	0.0764	0.0751	0.0737	0.0736	0.0775	0.0838	0.1004
Propane	0.0474*	0.0496	0.0470	0.0437	0.0411	0.0412	0.0451	0.0616
Butanes	0.0412*	0.0442	0.0407	0.0359	0.0315	0.0296	0.0308	0.0466
Pentanes	0.0297*	0.0325	0.0292	0.0246	0.0200	0.0171	0.0161	0.0246
Hexanes	0.0138*	0.0154	0.0135	0.0108	0.0082	0.0064	0.0057	0.0076
Heptanes plus	0.1491*	0.1739	0.1448	0.0973	0.0487	0.0215	0.0133	0.0152

*Original reservoir fluid composition; fractional analysis of bottomhole sample.

TABLE 37.4—CALCULATED RESERVOIR FLUID COMPOSITIONS (MOLE FRACTIONS)

Component	Reservoir Pressure (psia)									
	4,836	4,700	4,600	4,500	4,400	4,000	3,500	3,000	2,000	1,000
Composite or Overall Mixture in the Reservoir										
Nitrogen	0.0167*	0.0168	0.0168	0.0168	0.0167	0.0164	0.0160	0.0152	0.0128	0.0085
Methane	0.6051*	0.6060	0.6062	0.6062	0.6057	0.6001	0.5926	0.5766	0.5194	0.3937
Carbon dioxide	0.0218*	0.0218	0.0218	0.0218	0.0218	0.0217	0.0216	0.0214	0.0201	0.0163
Ethane	0.0752*	0.0752	0.0752	0.0752	0.0752	0.0753	0.0754	0.0754	0.0743	0.0674
Propane	0.0474*	0.0473	0.0473	0.0473	0.0474	0.0477	0.0480	0.0488	0.0510	0.0527
Butanes	0.0412*	0.0411	0.0411	0.0411	0.0412	0.0416	0.0422	0.0434	0.0476	0.0559
Pentanes	0.0297*	0.0296	0.0296	0.0296	0.0296	0.0301	0.0307	0.0319	0.0367	0.0475
Hexanes	0.0138*	0.0138	0.0137	0.0137	0.0138	0.0140	0.0144	0.0151	0.0179	0.0244
Heptanes plus	0.1491*	0.1484	0.1483	0.1483	0.1486	0.1531	0.1592	0.1722	0.2203	0.3336
Reservoir Oil Phase										
Nitrogen	0.0142	0.0131	0.0123	0.0115	0.0087	0.0066	0.0047	0.0025	0.0010	
Methane	0.5632	0.5447	0.5297	0.5146	0.4667	0.4205	0.3682	0.2662	0.1561	
Carbon dioxide	0.0214	0.0213	0.0212	0.0210	0.0202	0.0192	0.0177	0.0141	0.0090	
Ethane	0.0767	0.0772	0.0775	0.0776	0.0777	0.0776	0.0754	0.0681	0.0521	
Propane	0.0502	0.0512	0.0520	0.0528	0.0549	0.0568	0.0587	0.0600	0.0542	
Butanes	0.0449	0.0464	0.0476	0.0487	0.0520	0.0555	0.0592	0.0663	0.0706	
Pentanes	0.0332	0.0346	0.0358	0.0368	0.0404	0.0440	0.0485	0.0580	0.0679	
Hexanes	0.0159	0.0166	0.0174	0.0180	0.0199	0.0221	0.0246	0.0303	0.0371	
Heptanes plus	0.1803	0.1948	0.2065	0.2189	0.2595	0.2978	0.3430	0.4345	0.5520	
Reservoir Gas Phase										
Nitrogen	0.0256	0.0256	0.0256	0.0257	0.0262	0.0262	0.0253	0.0230	0.0198	
Methane	0.7546	0.7571	0.7575	0.7617	0.7700	0.7780	0.7770	0.7720	0.7492	
Carbon dioxide	0.0231	0.0230	0.0231	0.0231	0.0237	0.0243	0.0248	0.0261	0.0274	
Ethane	0.0698	0.0702	0.0705	0.0710	0.0722	0.0730	0.0754	0.0804	0.0902	
Propane	0.0376	0.0379	0.0380	0.0380	0.0384	0.0386	0.0393	0.0420	0.0504	
Butanes	0.0279	0.0281	0.0283	0.0282	0.0283	0.0278	0.0282	0.0290	0.0339	
Pentanes	0.0171	0.0173	0.0174	0.0173	0.0170	0.0163	0.0160	0.0155	0.0170	
Hexanes	0.0065	0.0067	0.0066	0.0065	0.0065	0.0061	0.0059	0.0055	0.0056	
Heptanes plus	0.0379	0.0341	0.0330	0.0285	0.0177	0.0098	0.0081	0.0066	0.0066	

*Original reservoir fluid at its bubblepoint; analysis of bottomhole sample.

position of the produced wellstream for this pressure decrement.

6. Calculate the bottomhole GOR by flashing the wellstream composition from p_1 to the average pressure $(p_1 + p_2)/2$, for this pressure decrement.

7. If the difference between the GOR from Step 6 and the average GOR from Step 3 exceeds the desired tolerance, select a new gas saturation and repeat Steps 3 through 7 to continue iterations for the current pressure decrement. If this difference is within the tolerance, the final answer has been obtained for this pressure decrement. For the next decrement, set $p_1 = p_2$ and select a

p_2 that is lower than the previous p_2 . Repeat Steps 1 through 7.

Example From Jacoby and Berry.³⁴

Reservoir temperature, 246°F

Initial pressure, 5,070 psia

Bubblepoint pressure, 4,836 psia

Initial GOR, 2 Mscf/STB

Oil gravity, 50°API

Conventional B_o , 4.7 RB/STB

Original reservoir fluid composition, Table 37.3 (column 1)

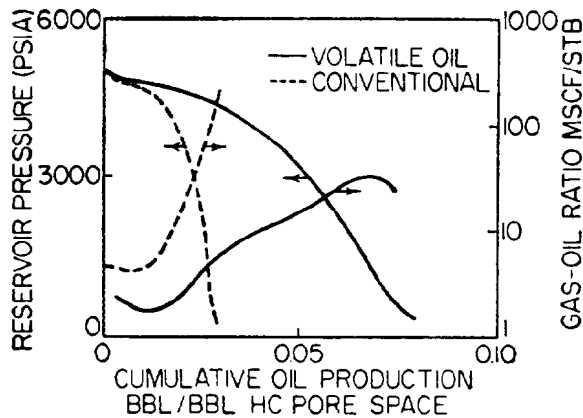


Fig. 37.32—Comparison of oil and gas production for volatile-oil material balance (multicomponent flash method) vs. conventional material balance.

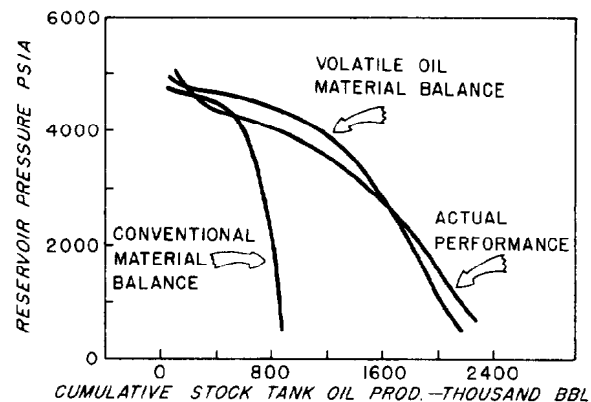


Fig. 37.34—Main Reservoir cumulative oil production vs. reservoir pressure.

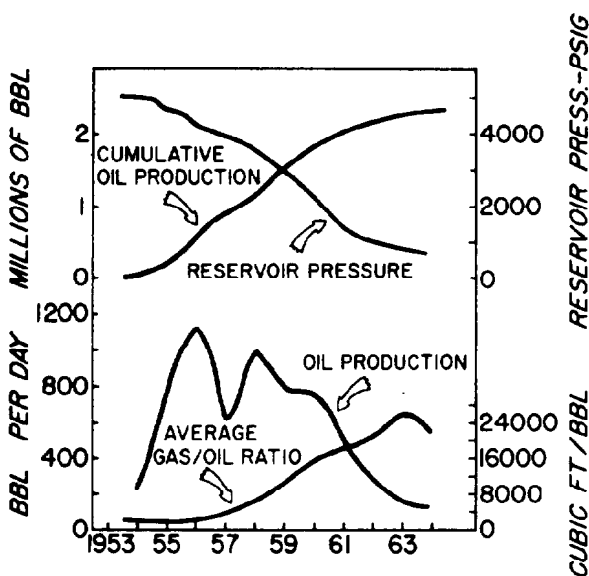


Fig. 37.33—Main Reservoir performance history.

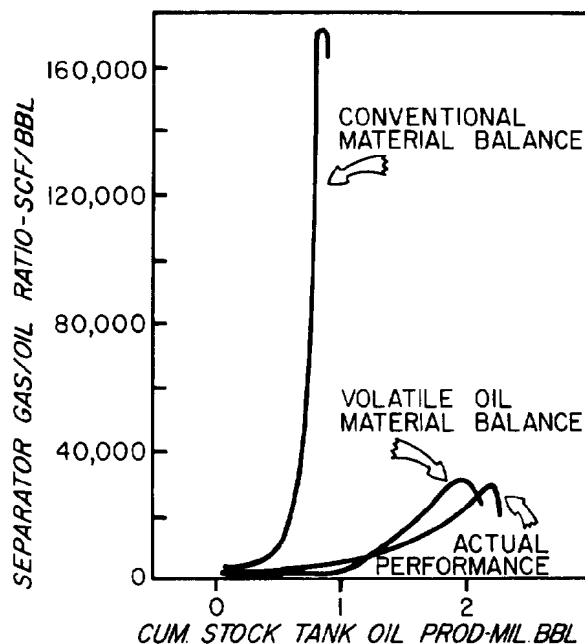


Fig. 37.35—Main Reservoir cumulative oil production vs. GOR.

Solution. Results calculated by Jacoby and Berry³⁴ with the above method are given in Tables 37.3 and 37.4 and in Fig. 37.32. Table 37.3 shows the calculated well-stream compositions, and Table 37.4 shows the fluid compositions in the reservoir. The oil and gas production in Fig. 37.32 was obtained by separating the wellstream data in Table 37.3 at separator conditions of 500 psia and 65°F and stock-tank conditions of 14.7 psia and 70°F. Fig. 37.32 also shows the comparison of oil and gas production with conventional performance predictions.⁶

Comparison of Predicted vs. Actual Reservoir Performance

Jacoby and Berry's example was a performance prediction published in 1957 for a volatile-oil reservoir in north Louisiana that was discovered in 1953 and produced from

the Smackover lime.³⁴ The reservoir was believed to be volumetric. The comparison vs. actual performance was published in 1965 by Cordell and Ebert.³⁶ They called this field the Main Reservoir. The field was completely developed with 11 wells on 160-acre spacing by 1956 and was 90% depleted by the time of their publication.

Fig. 37.33 shows performance history for the Main Reservoir.³⁶ Figs. 37.34 and 37.35 compare actual performance (cumulative stock-tank-oil production vs. reservoir pressure) vs. performance predicted by the volatile-oil material balance³⁴ and by conventional material balance.⁶ Cordell and Ebert stated that actual ultimate recovery would be 10% greater than predicted by the volatile-oil material balance and 175% greater than indicated by the conventional (black-oil) material-balance calculation.

Fig. 37.35 illustrates the large errors in applying a conventional black-oil material balance to volatile oils: oil recovery is underestimated, and producing GOR is overestimated. This emphasizes the importance of considering the varying reservoir and wellstream compositions in volatile-oil reservoir-performance predictions by use of a volatile-oil material-balance method.

Nomenclature

b_o = oil shrinkage factor	k_{ro} = relative permeability to oil
b_{oD} = oil shrinkage factor, dimensionless	$(k_{ro})_{gc}$ = relative permeability to oil at critical gas saturation
B_g = gas formation volume factor (gas FVF), RB/scf	K = reservoir vaporization ratio
B_{gi} = initial gas formation volume factor, RB/scf	m = PV of gas cap/PV of oil zone, dimensionless ratio
B_o = oil formation volume factor, RB/STB	n_w = number of wells
B_o^* = pseudovalues for formation volume factor, RB/STB	N = initial OIP, STB
$B_{ou} = B_o$ at atmospheric pressure and reservoir temperature, RB/STB	N_c = computed initial OIP, STB
$B_{ob} = B_o$ at bubblepoint pressure, RB/STB	N_p = cumulative oil production, STB
B_{oi} = initial oil formation volume factor, RB/STB	$(N_p)_n$ = cumulative oil production to pressure n , STB
B_t = two-phase FVF, RB/STB	$(N_p)_{n-1}$ = cumulative oil production to pressure $n-1$, STB
B_{ti} = initial two-phase FVF, RB/STB	ΔN_p = incremental oil production, STB
B_w = water formation volume factor, RB/STB	N_s = specified initial OIP, STB
ΔB_g = expansion of initial free gas in place, RB/scf	p_b = bubblepoint pressure, psi
ΔB_t = expansion of initial OIP, RB/STB	p_{iR} = initial reservoir pressure, psi
c_e = effective compressibility, vol/(vol-psi)	p_n = certain chosen pressure value, psi
c_f = formation compressibility, vol/(vol-psi)	p_{n-1} = pressure value one step below p_n , psi
c_o = oil compressibility, vol/(vol-psi)	p_R = reservoir pressure, psi
c_w = water compressibility, vol/(vol-psi)	\bar{p}_R = average reservoir pressure, psi
C_A = shape factor or constant, dimensionless	p_{RD} = reservoir pressure, dimensionless
G_i = cumulative gas injection, scf	p_{wf} = well flowing BHP, psi
G_p = cumulative gas production, scf	p_1, p_2 = intermediate pressure values in iterative equations, psi
G_{pc} = cumulative production of gas that was initially in the gas cap, scf	q_g = total gas production, scf/D
G_{ps} = cumulative production of gas that was initially solution gas, scf	q_{gv} = gas production rate/unit bulk volume, $\text{cm}^3/(\text{s} \cdot \text{cm}^3)$
$(G_p)_n$ = cumulative gas production to pressure n , scf	q_o = oil production rate, STB/D
$(G_p)_{n-1}$ = cumulative gas production to pressure $n-1$, scf	\bar{q}_o = average production rate, STB/D
ΔG_p = incremental gas production, scf	$(q_o)_{\max}$ = maximum oil production rate, STB/D
H = thickness of gas cap/thickness of oil-zone (Fig. 37.10)	$(q_o)_{\min}$ = minimum oil production rate, STB/D
J = productivity index, STB/D/psi	q_{ov} = oil production rate/unit bulk volume, $\text{cm}^3/(\text{s} \cdot \text{cm}^3)$
J^* = productivity index under conditions of uniform saturation and pressure, STB/D/psi	Q_p = net fluid produced, RB
J_i = initial productivity index, STB/D/psi	r_e = external radius, ft
k = permeability, md	r_w = wellbore radius, ft
k_g = effective permeability to gas, md	R = producing GOR, scf/STB
kh = formation flow capacity, md-ft	\bar{R} = average producing GOR, scf/STB
k_o = effective permeability to oil, md	R_{gc} = ratio of gas production directly from gas cap/oil production, scf/STB
k_{rg} = relative permeability to gas	R_n = producing GOR at pressure p_n , scf/STB
$(k_{rg})_{or}$ = relative permeability to gas at residual oil saturation	R_{old} = previous average producing GOR, scf/STB
	R_p = cumulative produced GOR, scf/STB
	R_{pD} = cumulative produced GOR, R_{sc}/R_{sb} , dimensionless
	R_{rs} = reduction in solution GOR below bubblepoint, $R_{sb} - R_s$, scf/STB
	R_s = solution GOR, scf/STB
	R_{sb} = solution GOR at bubblepoint, scf/STB
	R_{si} = initial solution GOR, scf/STB
	s = skin factor, dimensionless
	S_g = gas saturation, fraction PV
	S_{gc} = critical gas saturation, fraction PV
	S_{iw} = interstitial water saturation, fraction PV
	S_o = oil saturation, fraction PV
	S_{oi} = initial oil saturation, fraction PV

- S_{or} = residual oil saturation, fraction PV
 S_w = water saturation, fraction PV
 S_{wi} = initial water saturation, fraction PV
 t = time, days
 t_i = initial time, days
 t_n = cumulative time to reach pressure n , days
 Δt_n = incremental time for reservoir pressure to decline from p_{n-1} to p_n , days
 V_p = pore volume, RB
 W_e = cumulative water influx, STB
 W_i = cumulative water injected, STB
 W_p = cumulative water produced, STB
 μ_g = gas viscosity, cp
 μ_o = oil viscosity, cp
 μ_{oi} = initial oil viscosity, cp
 ϕ = porosity, fraction
 Φ_g = Tracy's pressure function for gas defined by Eq. 21, dimensionless
 Φ_o = Tracy's pressure function for oil defined by Eq. 22, dimensionless

References

- Schilthuis, R.J.: "Active Oil and Reservoir Energy," *Trans., AIME* (1936) **148**, 33-52.
- Turner, J.: "How Different Size Gas Caps and Pressure Maintenance Programs Affect Amount of Recoverable Oil," *Oil Weekly* (June 12, 1944) 32-44.
- Muskat, M. and Taylor, M.O.: "Effect of Reservoir Fluid and Rock Characteristics on Production Histories of Gas-Drive Reservoirs," *Trans., AIME* (1946) **165**, 78-93.
- Muskat, M.: *Physical Principles of Oil Production*, McGraw-Hill Book Co. Inc., New York City (1949).
- Dodson, C.R. et al.: "Application of Laboratory PVT Data to Reservoir Engineering Problems," *Trans., AIME* (1953) **198**, 287-98.
- Tracy, G.W.: "Simplified Form of the Material Balance Equation," *Trans., AIME* (1955) **204**, 243-46.
- Hawkins, M.F.: "Material Balances in Undersaturated Reservoirs Above Bubble Point," *Trans., AIME* (1955) **204**, 267-70.
- Arps, J.J. and Roberts, T.G.: "The Effect of the Relative Permeability Ratio, the Oil Gravity, and the Solution Gas-Oil Ratio on the Primary Recovery From a Depletion Type Reservoir," *Trans., AIME* (1955) **204**, 120-27.
- Wahl, W.L., Mullins, L.P., and Elfrink, E.B.: "Estimation of Ultimate Recovery from Solution Gas-Drive," *Trans., AIME* (1958) **213**, 132-38.
- Handy, L.L.: "A Laboratory Study of Oil Recovery by Solution Gas Drive," *Trans., AIME* (1958) **213**, 310-15.
- Craft, B.C. and Hawkins, M.F.: *Applied Petroleum Reservoir Engineering*, Prentice-Hall Inc., Englewood Cliffs, NJ (1959).
- Levine, J.S. and Prats, M.: "The Calculated Performances of Solution-Gas-Drive Reservoirs," *Soc. Pet. Eng. J.* (Sept. 1961) 142-52; *Trans., AIME*, **222**.
- Sikora, V.J.: "Solution-Gas-Drive Oil Reservoirs," *Petroleum Production Handbook*, T.C. Frick (ed.), SPE, Richardson, TX (1962).
- Ridings, R.L. et al.: "Experimental and Calculated Behavior of Dissolved-Gas-Drive Systems," *Soc. Pet. Eng. J.* (March 1963), 41-48; *Trans., AIME*, **228**.
- Havlena, D. and Odeh, A.S.: "The Material Balance Equation as an Equation of a Straight Line," *J. Pet. Tech.* (Aug. 1963) 896-900; *Trans., AIME*, **228**.
- Weller, W.T.: "Reservoir Performance During Two-Phase Flow," *J. Pet. Tech.* (Feb. 1966) 240-46; *Trans., AIME*, **237**.
- Stone, H.L. and Garder, A.O. Jr.: "Analysis of Gas-Cap or Dissolved Gas Drive Reservoirs," *Soc. Pet. Eng. J.* (June 1961) 92-104; *Trans., AIME*, **222**.
- Singh, D. and Guerrero, E.T.: "Material Balance Equation Sensitivity," *Oil and Gas J.* (Oct. 20, 1969) 95-102.
- Platt, C.R. and Lewis, W.M.: "Analysis of Unusual Performance Indicates High Solution-Gas-Drive Recovery—Stateline Ellenburger Field," *J. Pet. Tech.* (Dec. 1969) 1507-09.
- Dumore, J.M.: "Development of Gas Saturation During Solution-Gas Drive in an Oil Layer Below a Gas Cap," *Soc. Pet. Eng. J.* (Sept. 1970) 211-18; *Trans., AIME*, **249**.
- El-Khatib, N.A.F.: "A Modified Method for Performance Prediction of Depletion Drive Oil Reservoirs," preprint number 82-33-04 presented at the 1982 Annual CIM Petroleum Society Technology Meeting.
- El-Khatib, N.A.F.: "The Effect of Drainage Area and Production Rate on the Performance of Depletion Drive Oil Reservoirs," paper SPE 11019 presented at the 1982 SPE Annual Technical Conference and Exhibition, New Orleans, Sept. 26-29.
- Evinger, H.H. and Muskat, M.: "Calculation of Theoretical Productivity Factor," *Trans., AIME* (1942) **146**, 126-39.
- Vogel, J.V.: "Inflow Performance Relationships for Solution-Gas Drive Wells," *J. Pet. Tech.* (Jan. 1968) 83-92; *Trans., AIME*, **243**.
- Standing, M.B.: "Inflow Performance Relationships for Damaged Wells Producing by Solution-Gas Drive," *J. Pet. Tech.* (Nov. 1970) 1399-1400.
- Standing, M.B.: "Concerning the Calculation of Inflow Performance of Wells Producing from Solution-Gas-Drive Reservoirs," *J. Pet. Tech.* (Sept. 1971) 1141-42.
- Odeh, A.S.: "Pseudosteady-state Flow Equation and Productivity Index for a Well with Noncircular Drainage Area," *J. Pet. Tech.* (Nov. 1978) 1630-32.
- Al-Saadoon, F.T.: "Predicting Present and Future Well Productivities for Solution-Gas-Drive Reservoirs," *J. Pet. Tech.* (May 1980) 868-70.
- Rosbaco, J.A.: "Discussion of Predicting Present and Future Well Productivities for Solution-Gas-Drive Reservoirs," *J. Pet. Tech.* (Dec. 1980) 2265-66.
- Dias-Couto, L.E. and Golan, M.: "General Inflow Performance Relationship for Solution-Gas Reservoir Wells," *J. Pet. Tech.* (Feb. 1982) 285-88.
- Cook, A.B., Spencer, G.B., and Bobrowski, F.P.: "Special Considerations in Predicting Reservoir Performance of Highly Volatile Type Oil Reservoirs," *Trans., AIME* (1951) **192**, 37-46.
- Woods, R.W.: "Case History of Reservoir Performance of a Highly Volatile Type Oil Reservoir," *Trans., AIME* (1955) **204**, 156-59.
- Reudelhuber, F.O. and Hinds, R.F.: "A Compositional Material Balance Method for Prediction of Recovery from Volatile Oil Depletion Drive Reservoirs," *Trans., AIME* (1957) **210**, 19-26.
- Jacoby, R.H. and Berry, V.J. Jr.: "A Method for Predicting Depletion Performance of a Reservoir Producing Volatile Crude Oil," *Trans., AIME* (1957) **210**, 27-33.
- Brinkley, T.W.: "A Volumetric-Balance Applicable to the Spectrum of Reservoir Oils from Black Oils through High Volatile Oils," *J. Pet. Tech.* (June 1963) 589-94.
- Cordell, J.C. and Ebert, C.K.: "A Case History—Comparison of Predicted and Actual Performance of a Reservoir Producing Volatile Crude Oil," *J. Pet. Tech.* (Nov. 1965) 1291-93.
- Cronquist, C.: "Dimensionless PVT Behavior of Gulf Coast Reservoir Oils," *J. Pet. Tech.* (May 1973) 538-42.
- Cronquist, C.: "Evaluating and Producing Volatile Oil Reservoirs," *World Oil* (April 1979), 159-66 and 246.
- Dake, L.P.: *Fundamentals of Reservoir Engineering*, Elsevier Scientific Publishing Co., Amsterdam (1978).
- van Everdingen, A.F., Timmerman, E.H., and McMahon, J.J.: "Application of the Material Balance Equation to a Partial Water-Drive Reservoir," *Trans., AIME* (1953) **198**, 51-60.

Chapter 38

Water Drive Oil Reservoirs

Daylon L. Walton, Roebuck-Walton Inc.*

Introduction

Water drive reservoirs are those reservoirs in which a significant portion of volumetric withdrawals is replaced by water influx during the producing life of the reservoir. The total influx, and influx rates, will be governed by the aquifer characteristics together with the pressure-time behavior along the original reservoir/aquifer contact. Ordinarily, few wells are drilled into the aquifer and little or no information concerning the aquifer size, geometry, or rock properties is available. However, if sufficient reservoir pressure and production history is available, the aquifer properties may be inferred from solutions of Eq. 1, the radial form of the diffusivity equation.

$$\frac{\partial^2 p}{\partial r^2} + \frac{1}{r} \frac{\partial p}{\partial r} = \frac{\phi \mu c}{k} \frac{\partial p}{\partial t}, \dots \dots \dots (1)$$

where

- p = pressure,
- r = radius,
- ϕ = porosity,
- μ = viscosity,
- c = compressibility,
- t = time, and
- k = permeability.

These inferred aquifer properties then can be used to calculate the future effect of the aquifer on the reservoir performance.

Definitions

Aquifer Geometry

Radial—boundaries are formed by two concentric cylinders or sectors of cylinders.

Linear—boundaries are formed by two sets of parallel planes.

Nonsymmetrical—neither radial nor linear.

Exterior Boundary Conditions

Infinite—pressure disturbances do not affect the exterior boundary of the system, *during the time of interest*.

Finite closed—no flow occurs across the exterior boundary. Pressure disturbances reach the exterior boundary, *during the time of interest*.

Finite outcropping—aquifer is finite with pressure constant at exterior boundary (i.e., aquifer outcrops into lake, gulf, or other surface water source).

Basic Conditions and Assumptions

1. The reservoir is at the equilibrium average pressure at all times.
2. The water/oil (WOC) or water/gas contact (WGC) is an equipotential line.
3. The hydrocarbons behind the front are immobile.
4. The effects of gravity are negligible.
5. The difference between the average reservoir pressure and the pressure at the original WOC or WGC will be assumed to be zero if unknown.

Mathematical Analysis

Basic Equations

Van Everdingen and Hurst¹ obtained a general solution to Eq. 1 for two cases: (1) a constant water-influx rate (constant-terminal-rate case) and (2) a constant pressure drop (constant-terminal-pressure case). By using the principle of superposition, van Everdingen and Hurst extended these solutions to include variable water-influx rates and pressure drops. Mortada² further extended the solutions to include interference effects in homogeneous infinite radial aquifers.

Constant-Terminal-Rate Case. If time is divided into a finite number of intervals (Fig. 38.1), the average water influx in each interval can be used in Eq. 2 to calculate the pressure drop at the interior aquifer boundary. Eq. 2 shows that the relationship between the pressures and

* Author of the original chapter on this topic in the 1962 edition was Vincent J. Sikora.

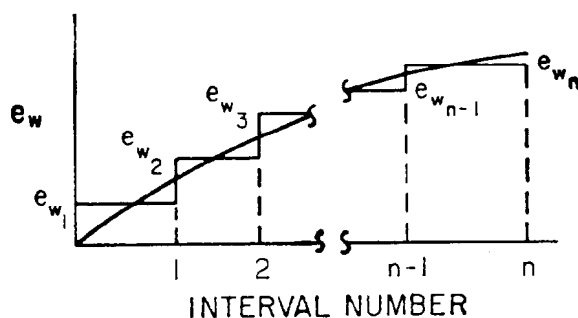


Fig. 38.1—Water influx rates—constant terminal rate case.

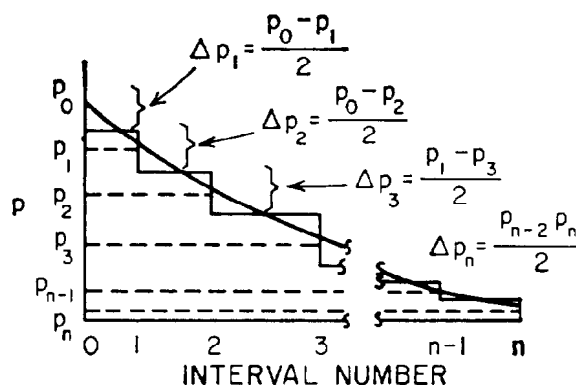


Fig. 38.2—Pressure drops—constant terminal pressure case.

water-influx rates is a function of a constant m_r and a variable p_D . The constant m_r is a function of the aquifer properties, whereas p_D is a function of aquifer properties and time.

$$\Delta p_{w_n} = m_r \sum_{j=1}^n [e_{w(n+1-j)} - e_{w(n-j)}] p_{D_j}, \quad \dots \quad (2)$$

where

p_{w_n} = cumulative pressure drop to the end of interval n ,

$e_{w(n+1-j)}$ = water-influx rate at interval $n+1-j$,

$$m_r = \frac{\mu_w}{0.001127kh\alpha} \quad \dots \quad (3)$$

for radial aquifers,

$$m_r = \frac{\mu_w}{0.001127kh} \quad \dots \quad (4)$$

for infinite linear aquifers,

$$m_r = \frac{\mu_w L}{0.001127khb} \quad \dots \quad (5)$$

for finite linear aquifers,

p_D = dimensionless pressure term,
 e_w = water influx rate, RB/D,
 p_w = pressure at the original WOC, psi,
 k = permeability, md,
 h = aquifer thickness, ft,
 b = aquifer width, ft,
 L = aquifer length, ft,
 μ_w = water viscosity, cp, and
 α = angle subtended by reservoir, radians.

For calculation convenience it is recommended that time be divided into equal intervals and Eq. 6 be used.

$$\Delta p_{w_n} = m_r \sum_{j=1}^n e_{w(n+1-j)} \Delta p_{D_j} \quad \dots \quad (6)$$

$$= m_r [e_{w_n} \Delta p_{D_1} + e_{w_{n-1}} \Delta p_{D_2} \dots$$

$$e_{w_2} \Delta p_{D_{(n-1)}} + e_{w_1} \Delta p_{D_n}], \quad \dots \quad (7)$$

where $\Delta p_{D_j} = p_{D_j} - p_{D_{j-1}}$.

Constant-Terminal-Pressure Case. If time is divided into a finite number of intervals (Fig. 38.2), Eq. 8 can be used to calculate the cumulative water influx for a given pressure history, using average pressure drops in each time interval.

$$W_{e_n} = m_p \sum_{j=1}^n \Delta \bar{p}_{(n+1-j)} W_{eD_j}, \quad \dots \quad (8)$$

where

W_{e_n} = cumulative water influx to end of interval,

$$m_p = 0.17811 \phi c_{wt} h \alpha r_w^2 \quad \dots \quad (9)$$

for radial aquifers,

$$m_p = 0.17811 \phi c_{wt} h b^2 \quad \dots \quad (10)$$

for infinite linear aquifers,

$\Delta \bar{p}_{(n+1-j)}$ = average pressure drop in interval $n+1-j$,

W_{eD} = dimensionless water-influx term,

r_w = field radius, ft, and

c_{wt} = total aquifer compressibility, psi^{-1} .

The solution of Eq. 8 requires the use of superposition, in a manner similar to that shown by the expansion of Eq. 6. A modification presented by Carter and Tracy³ permits calculations of W_e that approximate the values

obtained from Eq. 8 but does not require the use of superposition. This method is advantageous when the calculations are to be made manually, since fewer terms are required.

Using Carter and Tracy's method, Eq. 11, the cumulative water influx at time t_n is calculated directly from the previous value obtained at t_{n-1} .

$$W_{e_n} = W_{e_{(n-1)}} + \frac{[m_p \Delta p_n t_{D_n} - W_{e_{(n-1)}} p'_{D_n}] [t_{D_n} - t_{D_{(n-1)}}]}{p_{D_n} - t_{D_{(n-1)}} p'_{D_n}}, \quad (11)$$

where

$$p'_{D_n} = \frac{p_{D_n} - p_{D_{(n-1)}}}{t_{D_n} - t_{D_{(n-1)}}} \quad (12)$$

and

$$\Delta p_n = p_i - p_n \quad (13)$$

Reservoir Interference. Where two or more reservoirs² are in a common aquifer, it is possible to calculate the change in pressure at Reservoir A, for example, caused by water influx into another reservoir, B, using Eq. 14 or 15. These are Eqs. 2 and 3 with modified subscripts.

For unequal time intervals,

$$\Delta p_{o(A,B)_n} = m_r \sum_{j=1}^n [e_{wB_{(n+1-j)}} - e_{wB_{(n-j)}}] p_{D(A,B)_j}, \quad (14)$$

and for equal time intervals,

$$\Delta p_{o(A,B)_n} = m_r \sum_{j=1}^n e_{wB_{(n+1-j)}} \Delta p_{D(A,B)_j}, \quad (15)$$

where

$p_{D(A,B)}$ = dimensionless pressure term for Reservoir B with respect to Reservoir A,

$\Delta p_{o(A,B)}$ = pressure drop at Reservoir A caused by Reservoir B, and

e_{wB} = water influx rate at Reservoir B.

The total pressure drop at Reservoir A at any given time is the sum of the pressure drops caused by all reservoirs in the common aquifer, or

$$\Delta p_{oA_n} = \Delta p_{o(A,A)_n} + \Delta p_{o(A,B)_n} + \Delta p_{o(A,C)_n} + \dots \quad (16)$$

Since dimensionless pressure differences are available only for homogeneous infinite radial aquifers, pressure-interference calculations are limited at the present time to aquifers that can be approximated by a uniform, infinite, radial system.

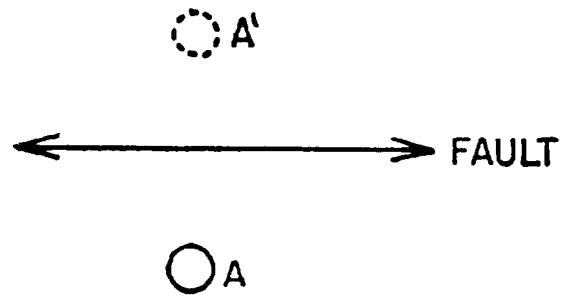


Fig. 38.3—Infinite aquifer bounded on one side by a fault.

Hicks *et al.*⁴ used the past pressure and production history in an analog computer to obtain influence-function curves for each pool in a multipool aquifer. The influence function $F(t)$ can be defined as the product of m_r and p_D ,

$$F(t) = m_r p_D, \quad (17)$$

and can be substituted in Eqs. 59 and 60 to calculate the future performance.

Nonsymmetrical Aquifers. By use of the images method,² the procedure for calculating reservoir interference can be extended to the case where one boundary of an infinite aquifer is a fault. For example, Fig. 38.3 shows Reservoir A located in this type of aquifer. To calculate the pressure performance at Reservoir A, first locate the mirror-image Reservoir A' across the fault. The water-influx history for the mirror-image Reservoir A' will be taken to be the same as Reservoir A. Next, assume that the fault does not exist so that there are two identical reservoirs in a single infinite aquifer, with Reservoir A' causing interference at Reservoir A. The pressure drop at Reservoir A now can be calculated by use of Eq. 19 (for equal time intervals).

$$\Delta p_{oA_n} = m_r \sum_{j=1}^n [e_{wA_{(n+1-j)}} \Delta p_{D_i}] + m_r \sum_{j=1}^n [e_{wA'_{(n+1-j)}} \Delta p_{D(A,A')_j}], \quad (18)$$

Because $e_{wA} = e_{wA'}$,

$$\Delta p_{oA_n} = m_r \sum_{j=1}^n e_{wA_{(n+1-j)}} [\Delta p_{D_j} - \Delta p_{D(A,A')_j}], \quad (19)$$

If other reservoirs in the aquifer also are causing reservoir interference at Reservoir A, each mirror image will cause reservoir interference at Reservoir A. The total pressure drop at Reservoir A, therefore, will be the sum of the pressure drops caused by each reservoir and each mirror image (see Fig. 38.4).

Nonsymmetrical aquifers will be discussed further under Methods of Analysis, Method 2.

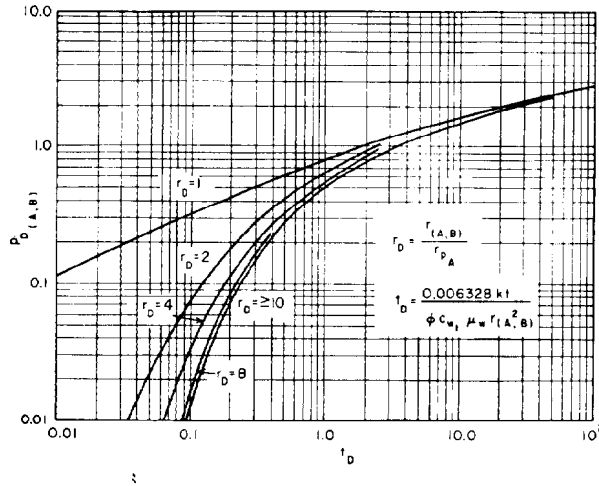


Fig. 38.4—Dimensionless pressure drop for infinite aquifer system for constant flow rate.^{3,8}

p_D and W_{eD} Values. Values of p_D , $p_{D(A,B)}$, and W_{eD} are functions of dimensionless time t_D (Eq. 20), aquifer geometry, and aquifer size (t_D for radial aquifers).

Table 38.1 gives the substitution for d in Eq. 20 to calculate t_D and the table, graph, or equation to obtain p_D , $p_{D(A,B)}$, or W_{eD} for various types of aquifers. The following equations are used in conjunction with Table 38.1.

$$t_D = \frac{0.006328kt}{\phi C_w \mu_w d^2}, \quad (20)$$

$$p_D = 1.1284\sqrt{t_D}, \quad (21)$$

$$p_D = 0.5(\ln t_D + 0.80907), \quad (22)$$

$$p_D = \ln r_D, \quad (23)$$

$$W_{eD} = 0.5(r_D^2 - 1), \quad (24)$$

$$\Delta p_D = \frac{2}{r_D^2} \Delta t_D, \quad (25)$$

and

$$p_D = t_D + 0.33333, \quad (26)$$

where

t_D = dimensionless time,

r_D = dimensionless radius = r_a/r_w ,

r_a = aquifer radius, ft,

r_w = field radius, ft, and

d = a geometry term obtained from Table 38.1.

Methods of Analysis

Reservoir Volume Known. Rigorous Methods. There are two methods for obtaining the coefficient m_r and Δp_D in Eq. 6 from the past pressures and the water-influx rates from a material balance on the reservoir. Method 1* is used whenever the aquifer can be approximated by a uniform linear or radial system; therefore, published values of p_D are used. If the aquifer can be approximated by a homogeneous, infinite, radial system, the method can be extended to handle reservoir interference. In Method 2,⁵ the product of m_r and p_D is replaced by Z (the resistance function).

$$\Delta p_{w_n} = \sum_{j=1}^n e_{w(n+1-j)} \Delta Z_j, \quad (27)$$

where $\Delta Z_j = Z_i - Z_{j-1}$.

Method 2 is not limited to homogeneous linear or radial aquifers because the final Z is obtained by adjusting previous approximations to Z . Techniques for applying Method 2 to the case where reservoir interference exists are not available at this time, except for unusual circumstances.

*Personal communication from Atlantic Refining Co.

TABLE 38.1—REFERENCE TABLE FOR OBTAINING W_{eD} AND p_D

Aquifer Type	Value of d in Eq. 20	p_D	W_{eD}
Infinite radial	r_w^*	Table 38.3	Table 38.3
Smaller t_D	r_w	Eq. 21	Eq. 21
Larger t_D	r_w	Eq. 22	
Finite outcropping radial	r_w	Table 38.7	Table 38.5
Smaller t_D	r_w	Table 38.7	
Larger t_D	r_w	Eq. 23	
Finite closed radial	r_w	Table 38.6	Table 38.6
Smaller t_D	r_w	Table 38.3	Table 38.3
Larger t_D	r_w	Eq. 25	Eq. 24
Infinite linear	b^{**}	Eq. 21	Eq. 21†
Finite closed linear	L^\ddagger	Table 38.8	
Larger t_D	L	Eq. 26	
Interference (infinite radial)	$r_{(A,B)}^{\S}$	Fig. 38.4, $p_{D(A,B)}$	
Larger t_D	$r_{(A,B)}$	Table 38.3, Eq. 22	

* r_w = radius of pool being analyzed, ft.

** b = width of aquifer, ft.

† $p_D = W_{eD}$.

‡ L = length of aquifer, ft.

§ $r_{(A,B)}$ = distance between centers of Reservoirs A and B, ft.

TABLE 38.2—COMPARISON OF RESULTS OF METHODS 1 AND 2 FOR SAMPLE CALCULATION

n Quarter or Interval No.	e_{w_n} Material Balance (B/D)	Δp_{f_n} Field (psi)	p_{D_n} $\Delta t_D = 10$ $r_D = \infty$	Z_n \sqrt{n} (psi/B/D)	Δp_{w_n} Method 1 (psi)	p_{w_n} Method 2 (psi)
1	500	55	1.651	1.000	55	55
2	1,100	136	1.960	1.414	136	135
3	3,400	318	2.147	2.732	318	317
4	3,400	478	2.282	2.000	478	477
5	3,700	581	2.389	2.236	581	584
6	3,900	663	2.476	2.449	663	672
7	3,000	616	2.550	2.646	616	630
8	2,700	599	2.615	2.828	599	614
9	3,100	652	2.672	3.000	652	664
10	3,600	733	2.723	3.162	733	739
11	3,500	761	2.770	3.317	761	761
12	3,600	803	2.812	3.464	803	807
13	3,800	858	2.851	3.606	858	860
14	4,100	928	2.887	3.742	928	934
15	3,900	949	2.921	3.873	949	946

The procedure for both methods can be illustrated best by an application to a single-pool aquifer. Assume that a reservoir has produced for 15 quarters and that Cols. 2 and 3 in Table 38.2 are, respectively, the pressures at the end of each quarter and the average water-influx rates obtained by material balance for each quarter.

Example Problem 1. Method 1. From the following assumed best set of aquifer properties, check Table 38.1 for the substitution of d in Eq. 20.

$$\begin{aligned}
 c_{wt} &= 5.5 \times 10^{-6} \text{ psi}^{-1}, \\
 \mu_w &= 0.6 \text{ cp}, \\
 h &= 50 \text{ ft}, \\
 \alpha &= 2\pi \text{ radians}, \\
 k &= 76 \text{ md}, \\
 \phi &= 0.16, \\
 r_w &= 3,270 \text{ ft},
 \end{aligned}$$

and the aquifer geometry is infinite radial.

Calculate a convenient value (to minimize interpolation) of dimensionless time interval (Δt_D) for the quarterly interval ($\Delta t = 91.25$ days) by varying the permeability (if necessary) in Eq. 20. In this case, $\Delta t_D = 10$, corresponding to $k = 91$ md, was selected. A check of Table 38.1 shows that p_D is to be obtained from Table 38.3 (also tabulated in Table 38.2, Col. 4).

$$m_{r_n} = \frac{\Delta p_{f_n}}{\sum_{j=1}^n e_{w_{n+1-j}} \Delta p_{D_j}}, \dots (28)$$

where Δp_D is the known field pressure drop at original WOC.

Calculate Δp_D as a function of interval number. Then calculate m_r as a function of interval number using Eq. 28 and plot m_r as a function of n (Curve 1, Fig. 38.5). Fig. 38.6 shows an example of the calculation procedure for $n=5$ using equal time intervals.

If the Δt_D selected is the correct value, m_r as a function of n will be constant. Variations from a constant can result from (1) incorrect Δt_D , (2) production and pressure errors, (3) incorrect aquifer size or shape, or (4) aquifer inhomogeneities. An examination of the m_r plot will aid in the analysis of the cause.

Value of m_r	Possible Remedy
increase with n	decrease with Δt_D
decrease with n	increase Δt_D
constant, then increasing	finite-closed aquifer
constant, then decreasing	finite-outcropping aquifer

For a finite-closed aquifer or finite-outcropping aquifer, Eq. 29 or 30 is used to find r_D .

$$r_D = 2.3(N_{it}\Delta t_D)^{0.518} \dots (29)$$

for $N_{it}\Delta t_D \leq 3.4$, and

$$r_D = 3(N_{it}\Delta t_D)^{0.301} \dots (30)$$

for $N_{it}\Delta t_D \leq 3.4$, where N_{it} is the time interval number where m_r vs. n increases from a constant value.

In this example, m_r increased with n (Fig. 38.5, $\Delta t_D = 10$). Therefore, Δt_D was decreased from 10 to 1 (large changes are recommended) and m_r for $\Delta t_D = 1$ was calculated (Curve 2). Now m_r is constant until about Interval 9 and then increases, indicating the possibility of a finite-closed aquifer. Using $N_{it} = 9$ and $\Delta t_D = 1$ in Eq. 29 gives a first approximation of 7 (rounded from 7.2) for r_D . The m_r calculated for $\Delta t_D = 1$ and $r_D = 7$ is reduced after Interval 9 (Curve 3) but is still too high and therefore indicates that the aquifer is still too large. An r_D of 6 is taken for the next approximation, and this results in a constant value of m_r (Curve 4). This shows that the past field behavior (Col. 3, Table 38.2) can be duplicated by assuming a finite-closed aquifer where $\Delta t_D = 1$ and $r_D = 6$ (Col. 6, Table 38.2). Because these aquifer properties gave the best match to the past field performance, they should be taken as the best set for predicting the future performance.

TABLE 38.3—DIMENSIONLESS WATER INFLUX AND DIMENSIONLESS PRESSURES FOR INFINITE RADIAL AQUIFERS

t_D	W_{eD}	P_D	t_D	W_{eD}	t_D	W_{eD}	t_D	W_{eD}
1.0×10^{-2}	0.112	0.112	1.5×10^3	4.136×10^2	1.5×10^7	1.828×10^6	1.5×10^{11}	1.17×10^{10}
5.0×10^{-2}	0.278	0.229	2.0×10^3	5.315×10^2	2.0×10^7	2.398×10^6	2.0×10^{11}	1.55×10^{10}
1.0×10^{-1}	0.404	0.315	2.5×10^3	6.466×10^2	2.5×10^7	2.961×10^6	2.5×10^{11}	1.92×10^{10}
1.5×10^{-1}	0.520	0.376	3.0×10^3	7.590×10^2	3.0×10^7	3.517×10^6	3.0×10^{11}	2.29×10^{10}
2.0×10^{-1}	0.606	0.424	4.0×10^3	9.757×10^2	4.0×10^7	4.610×10^6	4.0×10^{11}	3.02×10^{10}
2.5×10^{-1}	0.689	0.469	5.0×10^3	11.88×10^2	5.0×10^7	5.689×10^6	5.0×10^{11}	3.75×10^{10}
3.0×10^{-1}	0.758	0.503	6.0×10^3	13.95×10^2	6.0×10^7	6.758×10^6	6.0×10^{11}	4.47×10^{10}
4.0×10^{-1}	0.898	0.564	7.0×10^3	15.99×10^2	7.0×10^7	7.816×10^6	7.0×10^{11}	5.19×10^{10}
5.0×10^{-1}	1.020	0.616	8.0×10^3	18.00×10^2	8.0×10^7	8.866×10^6	8.0×10^{11}	5.89×10^{10}
6.0×10^{-1}	1.140	0.659	9.0×10^3	19.99×10^2	9.0×10^7	9.911×10^6	9.0×10^{11}	6.58×10^{10}
7.0×10^{-1}	1.251	0.702	1.0×10^4	21.96×10^2	1.0×10^8	10.95×10^6	1.0×10^{12}	7.28×10^{10}
8.0×10^{-1}	1.359	0.735	1.5×10^4	3.146×10^3	1.5×10^8	1.604×10^7	1.5×10^{12}	1.08×10^{11}
9.0×10^{-1}	1.469	0.772	2.0×10^4	4.679×10^3	2.0×10^8	2.108×10^7	2.0×10^{12}	1.42×10^{11}
1.0	1.570	0.802	2.5×10^4	4.991×10^3	2.5×10^8	2.607×10^7		
1.5	2.032	0.927	3.0×10^4	5.891×10^3	3.0×10^8	3.100×10^7		
2.0	2.442	1.020	4.0×10^4	7.634×10^3	4.0×10^8	4.071×10^7		
2.5	2.838	1.101	5.0×10^4	9.342×10^3	5.0×10^8	5.032×10^7		
3.0	3.209	1.169	6.0×10^4	11.03×10^3	6.0×10^8	5.984×10^7		
4.0	3.897	1.275	7.0×10^4	12.69×10^3	7.0×10^8	6.928×10^7		
5.0	4.541	1.362	8.0×10^4	14.33×10^3	8.0×10^8	7.865×10^7		
6.0	5.148	1.436	9.0×10^4	15.95×10^3	9.0×10^8	8.797×10^7		
7.0	5.749	1.500	1.0×10^5	17.56×10^3	1.0×10^9	9.725×10^7		
8.0	6.314	1.556	1.5×10^5	2.538×10^4	1.5×10^9	1.429×10^8		
9.0	6.861	1.604	2.0×10^5	3.308×10^4	2.0×10^9	1.880×10^8		
1.0×10^1	7.417	1.651	2.5×10^5	4.066×10^4	2.5×10^9	2.328×10^8		
1.5×10^1	9.965	1.829	3.0×10^5	4.817×10^4	3.0×10^9	2.771×10^8		
2.0×10^1	1.229×10^1	1.960	4.0×10^5	6.267×10^4	4.0×10^9	3.645×10^8		
2.5×10^1	1.455×10^1	2.067	5.0×10^5	7.699×10^4	5.0×10^9	4.510×10^8		
3.0×10^1	1.681×10^1	2.147	6.0×10^5	9.113×10^4	6.0×10^9	5.368×10^8		
4.0×10^1	2.088×10^1	2.282	7.0×10^5	10.51×10^4	7.0×10^9	6.220×10^8		
5.0×10^1	2.482×10^1	2.388	8.0×10^5	11.89×10^4	8.0×10^9	7.066×10^8		
6.0×10^1	2.860×10^1	2.476	9.0×10^5	13.26×10^4	9.0×10^9	7.909×10^8		
7.0×10^1	3.228×10^1	2.550	1.0×10^6	14.62×10^4	1.0×10^{10}	8.747×10^8		
8.0×10^1	3.599×10^1	2.615	1.5×10^6	2.126×10^5	1.5×10^{10}	1.288×10^9		
9.0×10^1	3.942×10^1	2.672	2.0×10^6	2.781×10^5	2.0×10^{10}	1.697×10^9		
1.0×10^2	4.301×10^1	2.723	2.5×10^6	3.427×10^5	2.5×10^{10}	2.103×10^9		
1.5×10^2	5.980×10^1	2.921	3.0×10^6	4.064×10^5	3.0×10^{10}	2.505×10^9		
2.0×10^2	7.586×10^1	3.064	4.0×10^6	5.313×10^5	4.0×10^{10}	3.299×10^9		
2.5×10^2	9.120×10^1	3.173	5.0×10^6	6.544×10^5	5.0×10^{10}	4.087×10^9		
3.0×10^2	10.58×10^1	3.263	6.0×10^6	7.761×10^5	6.0×10^{10}	4.868×10^9		
4.0×10^2	13.48×10^1	3.406	7.0×10^6	8.965×10^5	7.0×10^{10}	5.643×10^9		
5.0×10^2	16.24×10^1	3.516	8.0×10^6	10.16×10^5	8.0×10^{10}	6.414×10^9		
6.0×10^2	18.97×10^1	3.608	9.0×10^6	11.34×10^5	9.0×10^{10}	7.183×10^9		
7.0×10^2	21.60×10^1	3.684	1.0×10^7	12.52×10^5	1.0×10^{11}	7.948×10^9		
8.0×10^2	24.23×10^1	3.750						
9.0×10^2	26.77×10^1	3.809						
1.0×10^3	29.31×10^1	3.860						

If an infinite aquifer had been indicated, it may be desirable in some cases to predict the future performance assuming first an infinite aquifer and then a finite-closed aquifer having a calculated r_D based on the best estimate of Δt_D and setting N_{ii} equal to the last interval number in Eq. 20 or 30.

Note that, in general, the plot of m_r will not be a smooth plot because of errors in basic data. The first few values are particularly sensitive to errors and generally may be ignored.

If it is possible to obtain a relatively constant value of m_r , check the production and pressure data for errors. If the production and pressure data are correct, try Method

2. If it appears that the production and/or pressure data may be in error, refer to the following discussion of Errors in Basic Data.

Example Problem 2. Method 2. This method is based on the following principles: (1) the slope of Z (m_r times p_D) as a function of time is always positive and never increases; (2) a constant slope of Z vs. time indicates a finite aquifer (see Eqs. 25 and 26) and therefore the extrapolated slope is constant; and (3) a constant slope of Z vs. log time indicates an infinite radial aquifer (Eq. 22). Extrapolation of this constant slope continues to simulate an infinite aquifer.

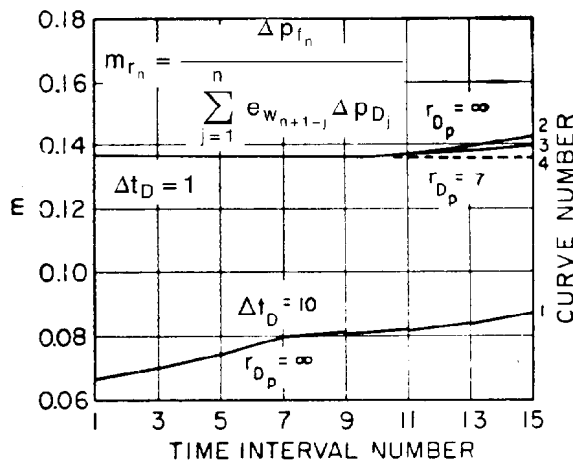


Fig. 38.5—Estimation of m_r , Δt_D , and r_{Dp} for data in Table 38.2 (Method 1).

As in the first procedure, time is divided into equal intervals. The first approximation to Z can be obtained as in Method 1 or by arbitrarily using the square root of the interval number (Col. 5, Table 38.2, and Trial 1, Fig. 38.7). A fitting factor m is calculated as a function of time for Trial 1 in exactly the same manner used to calculate m_r in Method 1.

$$m_n = \frac{\Delta p_{fn}}{\sum_{j=1}^n e_{w(n+1-j)} \Delta p_{Dj}} \quad (31)$$

However, instead of m being plotted, m is used to calculate the next approximation of Z by use of Eq. 32.

$$\text{New } Z_n = m_n(\text{old } Z_n) \quad (32)$$

The new values of Z are plotted as a function of n (Trial 2, Fig. 38.7), and a smooth curve is drawn through the points, making certain the slope is positive and never increases (Principle 1). This procedure is repeated with values of Z from this smoothed curve until the fitting factors are relatively constant and equal to 1 (Trial 3, Fig. 38.7).

The final Z curve then is extrapolated to calculate the future performance as follows.

1. If the final slope of Z as a function of time is constant, extrapolate Z at a constant slope (Principle 2).

2. If the final slope is not constant as a function of time but is constant as a function of log time, first assume that the aquifer is an infinite radial system and will continue to behave as such (Principle 3) and extrapolate Z as a straight line as a function of log time; then assume that the aquifer is immediately bounded and extrapolate Z as a straight line on a linear plot of time using the last known slope (Principle 2).

3. If the final slope is not constant for either time or log time, extrapolate Z as a straight line using half the last known slope.

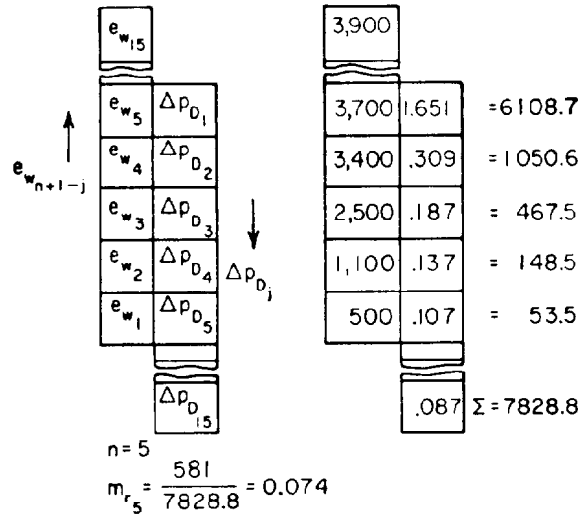


Fig. 38.6—Sample pressure-drop calculation.

Fig. 38.7 shows that three trials were needed to obtain a constant value of 1 for m . Col. 7, Table 38.2, shows that the final Z 's will duplicate the past pressure performance and therefore may be used to predict the future performance. Because Z becomes a straight line as a function of n , a finite-closed aquifer is indicated (Principle 2). Therefore, Z can be extrapolated as a straight line to calculate the future performance.

Errors in Basic Data. Good results were obtained for both methods, since accurate water influx and pressure data were used. In many cases a solution for m_r and Δp_D in Method 1 or Z in Method 2 is impossible because of errors in basic data. In these cases the errors may be eliminated by smoothing the basic data or may be adjusted somewhat by using Eqs. 33 and 34.⁵

$$\delta \Delta p_{fn} = -0.1 \frac{m_n - \bar{m}}{m_n} \Delta p_{fn} \quad (33)$$

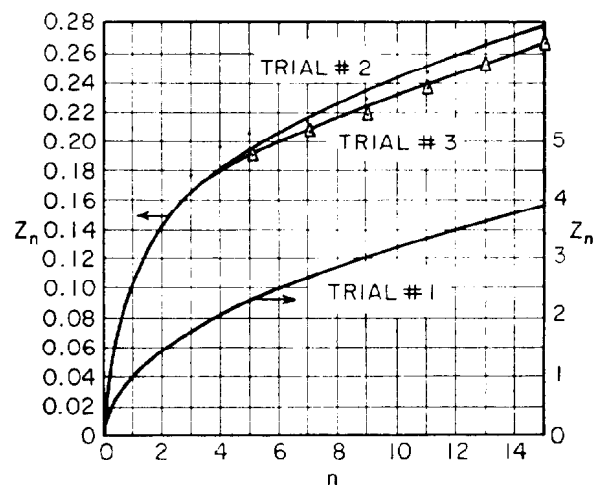


Fig. 38.7—Estimation of Z for data in Table 38.2 (Method 2).

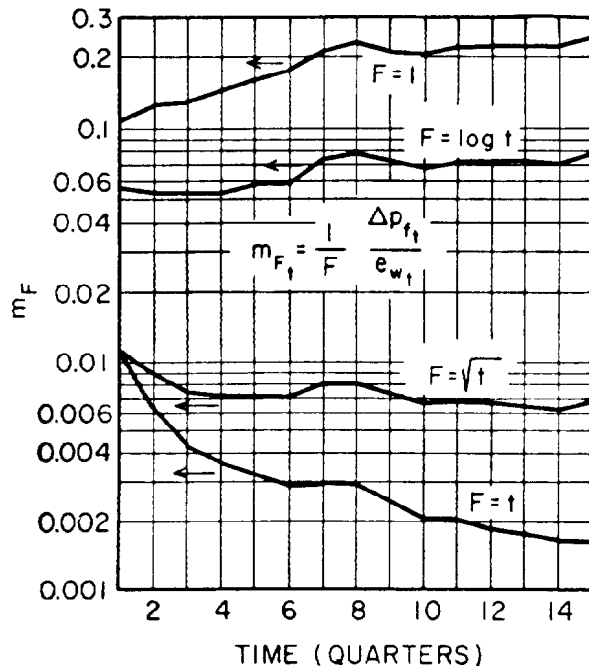


Fig. 38.8—Estimation of m_F and F function for approximate water drive analysis of data in Table 38.2.

and

$$\delta e_{w_f} = 0.4 \frac{m_n - \bar{m}}{m_n \bar{m} \Delta Z_1} \Delta p_{f_n} - \frac{1}{\Delta Z_1} \sum_{j=2}^n \delta e_{w_{(n+1-j)}} \Delta Z_j, \dots (34)$$

where

$$\begin{aligned} \delta p_{f_n} &= \text{correction to } \Delta p_{f_n}, \\ \delta e_{w_n} &= \text{correction to } e_{w_n}, \text{ and} \\ \bar{m} &= \text{average value of } m. \end{aligned}$$

In applying Eqs. 33 and 34 to Method 1, replace m by m_r and ΔZ by Δp_D . Note that, since Eqs. 33 and 34 imply that the last values of Z (or Δp_D) are reasonably correct, some judgment must be exercised when making these adjustments.

Approximate Methods. If the water influx rate is constant for a sufficiently long period of time, the following equations can be used to estimate water drive behavior roughly.

$$\Delta p_{wt_n} = m_F e_{wt_n} F \dots (35)$$

and

$$W_{e(t_1-t_2)} = \frac{1}{m_F} \int_1^2 \frac{\Delta p_{wt}}{F}, \dots (36)$$

where F is an approximation to p_D and a function of the type of aquifer and m_F is a proportionality factor. See Table 38.4 for function and aquifer type.

TABLE 38.4—WATER DRIVE BEHAVIOR EQUATIONS

Type Aquifer	F	Basis
Infinite radial	$\log t$	Eq. 22
Infinite linear	\sqrt{t}	Eq. 21
Finite outcropping	L	Eq. 23
Finite closed	t	Eq. 25 or 26

The equations for the infinite-radial and finite-outcropping aquifers are commonly referred to in the literature as the "simplified Hurst" and "Schilthuis" water drive equations.

The procedure consists of calculating m_F for the past history using Eq. 35 or 36, plotting m_F as a function of time, and extrapolating m_F to predict the future water drive performance. Since the method assumes a constant water influx rate, the use of these equations should be limited to short-term rough approximations of future water drive behavior. Large errors may be obtained if the method is used to predict the behavior for large changes in reservoir withdrawal rates.

Fig. 38.8 shows a comparison of m_F as a function of time for various values of F and the data in Table 38.2. These curves seem indicative of either an infinite linear or radial aquifer (the curves for these assumptions more nearly approach a constant value), whereas the more rigorous analyses indicated a finite aquifer. The selection of the best curve to use in predicting the future performance is difficult because of the fluctuations in the curves caused by variations in water influx rates. Note that this difficulty would be compounded if there were errors in the production and pressure data.

Fetkovitch⁷ presented a simplified approach that is based on the concept of a "stabilized" or pseudosteady-state aquifer productivity index and an aquifer material balance relating average aquifer pressure to cumulative water influx. This method is best suited for smaller aquifers, which may approach a pseudosteady condition quickly and in which the aquifer geometry and physical properties are known.

In a manner similar to single-well performance, the rate of water influx is expressed by Eq. 37.

$$e_w = J_a (\bar{p}_a - p_w), \dots (37)$$

where

$$\begin{aligned} e_w &= \text{water influx rate, B/D,} \\ J_a &= \text{aquifer productivity index, B/D-psi,} \\ \bar{p}_a &= \text{average aquifer pressure, psi, and} \\ p_w &= \text{pressure at the original WOC, psi.} \end{aligned}$$

Combining Eq. 37 with a material-balance equation for the aquifer, the increment of influx over a time interval $t_n - t_{n-1}$ is given by Eq. 38.

$$\Delta W_e = \frac{W_{ei} [\bar{p}_{a(n-1)} - \bar{p}_{wn} [1 - e^{(-J_a \Delta t_n)/(c_{wt} V_{wi})}]]}{P_{ai}}, \dots (38)$$

where

$W_{et} = W_{cwt} p_{ai}$, total aquifer expansion capacity, bbl,

V_{wi} = initial water volume in the aquifer, bbl,

p_{ai} = initial aquifer pressure, psi, and

c_{wt} = total aquifer compressibility, psi^{-1} .

$$\bar{p}_{a(n-1)} = p_{ai} \left[1 - \frac{w_{e(n-1)}}{W_{et}} \right], \dots\dots\dots (39)$$

$$J_a = \frac{7.08 \times 10^{-3} kh}{\mu_w (\ln r_D - 0.75)} \dots\dots\dots (40)$$

for a closed radial system, and

$$J_a = \frac{3(1.127 \times 10^{-3})kbh}{\mu_w L} \dots\dots\dots (41)$$

for a closed linear system.

Original Oil in Place (OOIP)

Occasionally, it may be necessary to estimate the OOIP and to make a water drive analysis simultaneously. In general, the methods available are very sensitive to errors in basic data so that it is necessary to have a large amount of accurate data. Also, since the expansion of the reservoir above the bubblepoint is relatively small, generally only the data obtained after the reservoir has passed through the bubblepoint will be significant in defining the OOIP. In the three methods to be discussed, the aquifer will be assumed to be infinite and radial.

Brownscombe-Collins Method. This method⁸ assumes that the OOIP and the aquifer permeability are unknown and that the reservoir and aquifer properties other than permeability are known.

The pressure performance and the variance are calculated using Eqs. 7 and 42 for a given assumed aquifer permeability and various estimates. The minimum variance from a plot of variance vs. OOIP (Fig. 38.9) will be the best estimate of OOIP for the selected permeability.

$$\sigma^2 = \frac{1}{n} \sum_{j=1}^n (\Delta p_{f_j} - \Delta p_{w_j}), \dots\dots\dots (42)$$

This procedure is repeated for various estimates of permeability until it is possible to obtain a minimum of the minimums. The permeability and the OOIP associated with this minimum should be the best estimates for the assumptions made.

It is possible to calculate the best estimate of OOIP for each selected permeability by the following procedure. Using the best available estimate of OOIP, calculate the reservoir voidage and expansion rates as a function of time. Select an aquifer permeability and use these rates in place of the water influx rates in Eq. 6 to calculate pressure drops Δp_{v_n} and Δp_{E_n} . The estimated OOIP mul-

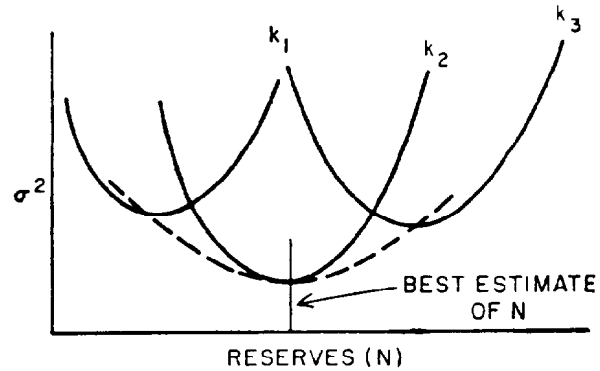


Fig. 38.9—Estimation of reservoir volume and water drive (Brownscombe-Collins method).

tiplied by the factor X calculated by Eq. 43 gives the best estimate of OOIP for the selected permeability. Eq. 44 gives the minimum variance for this permeability.

$$X = \frac{\sum_{j=1}^n (\Delta p_{v_j} - \Delta p_{f_j}) \Delta p_{E_j}}{\sum_{j=1}^n (\Delta p_{E_j})^2} \dots\dots\dots (43)$$

and

$$\sigma^2 = \frac{1}{n} \sum_{j=1}^n (\Delta p_{f_j} - \Delta p_{v_j} - X \Delta p_{E_j})^2, \dots\dots\dots (44)$$

where

Δp_f = total pressure drop at original WOC (field data), psi,

Δp_v = total pressure drop at WOC (calculated using reservoir voidage rates), psi, and

Δp_E = total pressure drop at WOC (calculated using reservoir expansion rates), psi.

van Everdingen, Timmerman, and McMahon Method.

This method⁹ assumes that the OOIP, aquifer conductivity $kh\alpha/\mu$, and diffusivity $k/(\phi\mu c)$ are unknown. Combination of the material-balance equation and Eq. 8 and solving for the OOIP yields Eq. 45.

$$N = A + m_p F(t), \dots\dots\dots (45)$$

where

$$A = \frac{1}{(F_V - 1)B_{oi}} [N_p F_V B_o + N_p (R_p - R_s) B_g + W_p], \dots\dots\dots (46)$$

$$F(t) = \frac{1}{(F_V - 1)B_{oi}} \left[\sum_{j=1}^n \Delta p_{(n+1-j)} W_{ed_j} \right], \dots\dots (47)$$

$$F_V = \frac{p_b - p}{pY} + 1, \dots\dots\dots (48)$$

TABLE 38.5—DIMENSIONLESS WATER INFLUX FOR FINITE OUTCROPPING RADIAL AQUIFERS

$r_D = 1.5$		$r_D = 2.0$		$r_D = 2.5$		$r_D = 3.0$		$r_D = 3.5$		$r_D = 4.0$		$r_D = 4.5$	
t_D	W_{eD}	t_D	W_{eD}	t_D	W_{eD}	t_D	W_{eD}	t_D	W_{eD}	t_D	W_{eD}	t_D	W_{eD}
5.0×10^{-2}	0.276	5.0×10^{-2}	0.278	1.0×10^{-1}	0.408	3.0×10^{-1}	0.755	1.00	1.571	2.00	2.442	2.5	2.835
6.0×10^{-2}	0.304	7.5×10^{-2}	0.345	1.5×10^{-1}	0.509	4.0×10^{-1}	0.895	1.20	1.761	2.20	2.598	3.0	3.196
7.0×10^{-2}	0.330	1.0×10^{-1}	0.404	2.0×10^{-1}	0.599	5.0×10^{-1}	1.023	1.40	1.940	2.40	2.748	3.5	3.537
8.0×10^{-2}	0.354	1.25×10^{-1}	0.458	2.5×10^{-1}	0.681	6.0×10^{-1}	1.143	1.60	2.111	2.60	2.893	4.0	3.859
9.0×10^{-2}	0.375	1.50×10^{-1}	0.507	3.0×10^{-1}	0.758	7.0×10^{-1}	1.256	1.80	2.273	2.80	3.034	4.5	4.165
1.0×10^{-1}	0.395	1.75×10^{-1}	0.553	3.5×10^{-1}	0.829	8.0×10^{-1}	1.363	2.00	2.427	3.00	3.170	5.0	4.454
1.1×10^{-1}	0.414	2.00×10^{-1}	0.597	4.0×10^{-1}	0.897	9.0×10^{-1}	1.465	2.20	2.574	3.25	3.334	5.5	4.727
1.2×10^{-1}	0.431	2.25×10^{-1}	0.638	4.5×10^{-1}	0.962	1.00	1.563	2.40	2.715	3.50	3.493	6.0	4.986
1.3×10^{-1}	0.446	2.50×10^{-1}	0.678	5.0×10^{-1}	1.024	1.25	1.791	2.60	2.849	3.75	3.645	6.5	5.231
1.4×10^{-1}	0.461	2.75×10^{-1}	0.715	5.5×10^{-1}	1.083	1.50	1.997	2.80	2.976	4.00	3.792	7.0	5.464
1.5×10^{-1}	0.474	3.00×10^{-1}	0.751	6.0×10^{-1}	1.140	1.75	2.184	3.00	3.098	4.25	3.932	7.5	5.684
1.6×10^{-1}	0.486	3.25×10^{-1}	0.785	6.5×10^{-1}	1.195	2.00	2.353	3.25	3.242	4.50	4.068	8.0	5.892
1.7×10^{-1}	0.497	3.50×10^{-1}	0.817	7.0×10^{-1}	1.248	2.25	2.507	3.50	3.379	4.75	4.198	8.5	6.089
1.8×10^{-1}	0.507	3.75×10^{-1}	0.848	7.5×10^{-1}	1.229	2.50	2.646	3.75	3.507	5.00	4.323	9.0	6.276
1.9×10^{-1}	0.517	4.00×10^{-1}	0.877	8.0×10^{-1}	1.348	2.75	2.772	4.00	3.628	5.50	4.560	9.5	6.453
2.0×10^{-1}	0.525	4.25×10^{-1}	0.905	8.5×10^{-1}	1.395	3.00	2.886	4.25	3.742	6.00	4.779	10	6.621
2.1×10^{-1}	0.533	4.50×10^{-1}	0.932	9.0×10^{-1}	1.440	3.25	2.990	4.50	3.850	6.50	4.982	11	6.930
2.2×10^{-1}	0.541	4.75×10^{-1}	0.958	9.5×10^{-1}	1.484	3.50	3.084	4.75	3.951	7.00	5.169	12	7.208
2.3×10^{-1}	0.548	5.00×10^{-1}	0.982	1.0	1.526	3.75	3.170	5.00	4.047	7.50	5.343	13	7.457
2.4×10^{-1}	0.554	5.50×10^{-1}	1.028	1.1	1.605	4.00	3.247	5.50	4.222	8.00	5.504	14	7.680
2.5×10^{-1}	0.559	6.00×10^{-1}	1.070	1.2	1.679	4.25	3.317	6.00	4.378	8.50	5.653	15	7.880
2.6×10^{-1}	0.565	6.50×10^{-1}	1.108	1.3	1.747	4.50	3.381	6.50	4.516	9.00	5.790	16	8.060
2.8×10^{-1}	0.574	7.00×10^{-1}	1.143	1.4	1.811	4.75	3.439	7.00	4.639	9.50	5.917	18	8.365
3.0×10^{-1}	0.582	7.50×10^{-1}	1.174	1.5	1.870	5.00	3.491	7.50	4.749	10	6.035	20	8.611
3.2×10^{-1}	0.588	8.00×10^{-1}	1.203	1.6	1.924	5.50	3.581	8.00	4.846	11	6.246	22	8.809
3.4×10^{-1}	0.594	9.00×10^{-1}	1.253	1.7	1.975	6.00	3.656	8.50	4.932	12	6.425	24	8.968
3.6×10^{-1}	0.599	1.00	1.295	1.8	2.022	6.50	3.717	9.00	5.009	13	6.580	26	9.097
3.8×10^{-1}	0.603	1.1	1.330	2.0	2.106	7.00	3.767	9.50	5.078	14	6.712	28	9.200
4.0×10^{-1}	0.606	1.2	1.358	2.2	2.178	7.50	3.809	10.00	5.138	15	6.825	30	9.283
4.5×10^{-1}	0.613	1.3	1.382	2.4	2.241	8.00	3.843	11	5.241	16	6.922	34	9.404
5.0×10^{-1}	0.617	1.4	1.402	2.6	2.294	9.00	3.894	12	5.321	17	7.004	38	9.481
6.0×10^{-1}	0.621	1.6	1.432	2.8	2.340	10.00	3.928	13	5.385	18	7.076	42	9.532
7.0×10^{-1}	0.623	1.7	1.444	3.0	2.380	11.00	3.951	14	5.435	20	7.189	46	9.565
8.0×10^{-1}	0.624	1.8	1.453	3.4	2.444	12.00	3.967	15	5.476	22	7.272	50	9.586
		2.0	1.468	3.8	2.491	14.00	3.985	16	5.506	24	7.332	60	9.612
		2.5	1.487	4.2	2.525	16.00	3.993	17	5.531	26	7.377	70	9.621
		3.0	1.495	4.6	2.551	18.00	3.997	18	5.551	30	7.434	80	9.623
		4.0	1.499	5.0	2.570	20.00	3.999	20	5.579	34	7.464	90	9.624
		5.0	1.500	6.0	2.599	22.00	3.999	25	5.611	38	7.481	100	9.625
				7.0	2.613	24.00	4.000	30	5.621	42	7.490		
				8.0	2.619			35	5.624	46	7.494		
				9.0	2.622			40	5.625	50	7.497		
				10.0	2.624								

and

$$Y = \frac{p_b - p}{p(F_V - 1)} \quad (49)$$

F_V = ratio of volume of oil and its dissolved original gas at a given pressure to its volume at initial pressure.

N = OOIP, STB,

N_p = cumulative oil produced, STB,

W_p = cumulative water produced, bbl,

R_p = cumulative produced GOR, scf/STB,

B_o = oil FVF, bbl/STB,

B_g = gas FVF, bbl/scf, and

p_b = bubblepoint pressure, psia.

Generally, Y is calculated with laboratory-determined values of $F_V - 1$. Because Y vs. p is generally a straight line, smoothed values of Y can be calculated with Eq. 50:

$$Y = b + m, \quad (50)$$

where b = intercept and m = slope.

The equations for obtaining the least-squares fit to Eqs. 46 and 47 for a given dimensionless time interval, Δt_D , and n data points are

$$nN = \sum_{j=1}^n A_j - m_p \sum_{j=1}^n F(t)_j \quad (51)$$

TABLE 38.5—DIMENSIONLESS WATER INFLUX FOR FINITE OUTCROPPING RADIAL AQUIFERS (continued)

$r_D = 5.0$		$r_D = 6.0$		$r_D = 7.0$		$r_D = 8.0$		$r_D = 9.0$		$r_D = 10.0$	
t_D	W_{eD}	t_D	W_{eD}	t_D	W_{eD}	t_D	W_{eD}	t_D	W_{eD}	t_D	W_{eD}
3.0	3.195	6.0	5.148	9.00	6.861	9	6.861	10	7.417	15	9.965
3.5	3.542	6.5	5.440	9.50	7.127	10	7.398	15	9.945	20	12.32
4.0	3.875	7.0	5.724	10	7.389	11	7.920	20	12.26	22	13.22
4.5	4.193	7.5	6.002	11	7.902	12	8.431	22	13.13	24	14.09
5.0	4.499	8.0	6.273	12	8.397	13	8.930	24	13.98	26	14.95
5.5	4.792	8.5	6.537	13	8.876	14	9.418	26	14.79	28	15.78
6.0	5.074	9.0	6.795	14	9.341	15	9.895	28	15.59	30	16.59
6.5	5.345	9.5	7.047	15	9.791	16	10.361	30	16.35	32	17.38
7.0	5.605	10.0	7.293	16	10.23	17	10.82	32	17.10	34	18.16
7.5	5.854	10.5	7.533	17	10.65	18	11.26	34	17.82	36	18.91
8.0	6.094	11	7.767	18	11.06	19	11.70	36	18.52	38	19.65
8.5	6.325	12	8.220	19	11.46	20	12.13	38	19.19	40	20.37
9.0	6.547	13	8.651	20	11.85	22	12.95	40	19.85	42	21.07
9.5	6.760	14	9.063	22	12.58	24	13.74	42	20.48	44	21.76
10	6.965	15	9.456	24	13.27	26	14.50	44	21.09	46	22.42
11	7.350	16	9.829	26	13.92	28	15.23	46	21.69	48	23.07
12	7.706	17	10.19	28	14.53	30	15.92	48	22.26	50	23.71
13	8.035	18	10.53	30	15.11	34	17.22	50	22.82	52	24.33
14	8.339	19	10.85	35	16.39	38	18.41	52	23.36	54	24.94
15	8.620	20	11.16	40	17.49	40	18.97	54	23.89	56	25.53
16	8.879	22	11.74	45	18.43	45	20.26	56	24.39	58	26.11
18	9.338	24	12.16	50	19.24	50	21.42	58	24.88	60	26.67
20	9.731	25	12.50	60	20.51	55	22.46	60	25.36	65	28.02
22	10.07	31	13.74	70	21.45	60	23.40	65	26.48	70	29.29
24	10.35	35	14.40	80	22.13	70	24.98	70	27.52	75	30.49
26	10.59	39	14.93	90	22.63	80	26.26	75	28.48	80	31.61
28	10.80	51	16.05	100	23.00	90	27.28	80	29.36	85	32.67
30	10.89	60	16.56	120	23.47	100	28.11	85	30.18	90	33.66
34	11.26	70	16.91	140	23.71	120	29.31	90	30.93	95	34.60
38	11.46	80	17.14	160	23.85	140	30.08	95	31.63	100	35.48
42	11.61	90	17.27	180	23.92	160	30.58	100	32.27	120	38.51
46	11.71	100	17.36	200	23.96	180	30.91	120	34.39	140	40.89
50	11.79	110	17.41	500	24.00	200	31.12	140	35.92	160	42.75
60	11.91	120	17.45			240	31.34	160	37.04	180	44.21
70	11.96	130	17.46			280	31.43	180	37.85	200	45.36
80	11.98	140	17.48			320	31.47	200	38.44	240	46.95
90	11.99	150	17.49			360	31.49	240	39.17	280	47.94
100	12.00	160	17.49			400	31.50	280	39.56	320	48.54
120	12.0	180	17.50			500	31.50	320	39.77	360	48.91
		200	17.50					360	39.88	400	49.14
		220	17.50					400	39.94	440	49.28
								440	39.97	480	49.36
								480	39.98		

and

$$N \sum_{j=1}^n F(t)_j = \sum_{j=1}^n A_j [F(t)]_j - m_p \sum_{j=1}^n [F(t)]_j^2. \quad (52)$$

The variance of this fit from field data can be calculated by Eq. 53.

$$\sigma^2 = \frac{1}{n} \sum_{j=1}^n \{A_j - N + m_p [F(t)]_j\}^2. \quad (53)$$

The minimum in a plot of variance vs. various assumed values of Δt_D will be the best estimate of Δt_D and can be used in Eqs. 51 and 52 to solve for the best estimate of N and m_p (see Fig. 38.10).

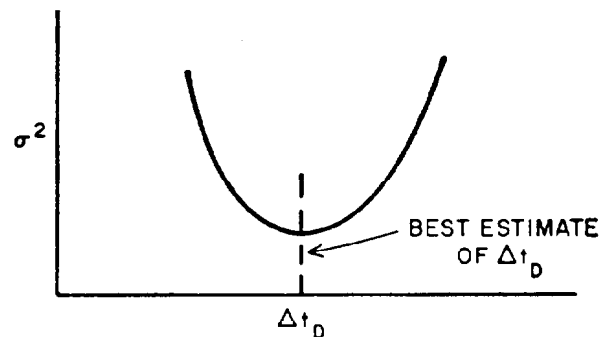


Fig. 38.10—Estimation of reservoir volume and water drive (van Everdingen-Timmerman-McMahon method).

TABLE 38.6—DIMENSIONLESS PRESSURES FOR FINITE CLOSED RADIAL AQUIFERS

$r_D = 1.5$		$r_D = 2.0$		$r_D = 2.5$		$r_D = 3.0$		$r_D = 3.5$		$r_D = 4.0$		$r_D = 4.5$	
t_D	p_D	t_D	p_D	t_D	p_D	t_D	p_D	t_D	p_D	t_D	p_D	t_D	p_D
6.0×10^{-2}	0.251	2.2×10^{-1}	0.443	4.0×10^{-1}	0.565	5.2×10^{-1}	0.627	1.0	0.802	1.5	0.927	2.0	1.023
8.0×10^{-2}	0.288	2.4×10^{-1}	0.459	4.2×10^{-1}	0.576	5.4×10^{-1}	0.636	1.1	0.830	1.6	0.948	2.1	1.040
1.0×10^{-1}	0.322	2.6×10^{-1}	0.476	4.4×10^{-1}	0.587	5.6×10^{-1}	0.645	1.2	0.857	1.7	0.968	2.2	1.056
1.2×10^{-1}	0.355	2.8×10^{-1}	0.492	4.6×10^{-1}	0.598	6.0×10^{-1}	0.662	1.3	0.882	1.8	0.988	2.3	1.072
1.4×10^{-1}	0.387	3.0×10^{-1}	0.507	4.8×10^{-1}	0.608	6.5×10^{-1}	0.683	1.4	0.906	1.9	1.007	2.4	1.087
1.6×10^{-1}	0.420	3.2×10^{-1}	0.522	5.0×10^{-1}	0.618	7.0×10^{-1}	0.703	1.5	0.929	2.0	1.025	2.5	1.102
1.8×10^{-1}	0.452	3.4×10^{-1}	0.536	5.2×10^{-1}	0.682	7.5×10^{-1}	0.721	1.6	0.951	2.2	1.059	2.6	1.116
2.0×10^{-1}	0.484	3.6×10^{-1}	0.551	5.4×10^{-1}	0.638	8.0×10^{-1}	0.740	1.7	0.973	2.4	1.092	2.7	1.130
2.2×10^{-1}	0.516	3.8×10^{-1}	0.565	5.6×10^{-1}	0.647	8.5×10^{-1}	0.758	1.8	0.994	2.6	1.123	2.8	1.144
2.4×10^{-1}	0.548	4.0×10^{-1}	0.579	5.8×10^{-1}	0.657	9.0×10^{-1}	0.776	1.9	1.014	2.8	1.154	2.9	1.158
2.6×10^{-1}	0.580	4.2×10^{-1}	0.593	6.0×10^{-1}	0.666	9.5×10^{-1}	0.791	2.0	1.034	3.0	1.184	3.0	1.171
2.8×10^{-1}	0.612	4.4×10^{-1}	0.607	6.5×10^{-1}	0.688	1.0	0.806	2.25	1.083	3.5	1.255	3.2	1.197
3.0×10^{-1}	0.644	4.6×10^{-1}	0.621	7.0×10^{-1}	0.710	1.2	0.865	2.50	1.130	4.0	1.324	3.1	1.222
3.5×10^{-1}	0.724	4.8×10^{-1}	0.634	7.5×10^{-1}	0.731	1.4	0.920	2.75	1.176	4.5	1.392	3.6	1.246
4.0×10^{-1}	0.804	5.0×10^{-1}	0.648	8.0×10^{-1}	0.752	1.6	0.973	3.0	1.221	5.0	1.460	3.8	1.269
4.5×10^{-1}	0.884	6.0×10^{-1}	0.715	8.5×10^{-1}	0.772	2.0	1.076	4.0	1.401	5.5	1.527	4.0	1.292
5.0×10^{-1}	0.964	7.0×10^{-1}	0.782	9.0×10^{-1}	0.792	3.0	1.328	5.0	1.579	6.0	1.594	4.5	1.349
5.5×10^{-1}	1.044	8.0×10^{-1}	0.849	9.5×10^{-1}	0.812	4.0	1.578	6.0	1.757	6.5	1.660	5.0	1.403
6.0×10^{-1}	1.124	9.0×10^{-1}	0.915	1.0	0.832	5.0	1.828			7.0	1.727	5.5	1.457
		1.0	0.982	2.0	1.215					8.0	1.861	6.0	1.510
		2.0	1.649	3.0	1.596					9.0	1.994	7.0	1.615
		3.0	2.316	4.0	1.977					10.0	2.127	8.0	1.719
		5.0	3.649	5.0	2.358							9.0	1.823
												10.0	1.927
												11.0	2.031
												12.0	2.135
												13.0	2.239
												14.0	2.343
												15.0	2.447

Havlena-Odeh Method. In this method,¹⁰ the material-balance equation is written as the equation of a straight line containing two unknown constants, N and m_p . Combination of the material-balance equation and Eq. 8 yields Eq. 54. (See Fig. 38.10.)

$$\frac{V_{R_n}}{E_{N_n}} = \frac{N + m_p \sum_{j=1}^n \Delta p_{(n-1-j)} W_{ed_j}}{E_{N_n}}, \dots \dots (54)$$

where

$$V_{R_n} = N_p [B_t + B_g(R_p - R_{si})] + (W_p - W_i)B_w - G_i B_{g_i},$$

$$E_{N_n} = B_t - B_{t_i} + \frac{B_{t_i}}{1 - S_w} (c_f + S_w c_w) (p_i - p_n) + m \frac{B_{t_i}}{B_{g_i}} (B_g - B_{g_i}),$$

V_{R_n} = cumulative voidage at the end of interval n , RB,

E_N = cumulative expansion per stock-tank barrel OOIP, RB,

B_t = two-phase FVF, bbl/STB,

W_p = cumulative water produced, STB,

W_i = cumulative water injected, STB,

G_i = cumulative gas injected, scf,

B_w = water FVF, bbl/STB,

c_f = formation compressibility, psi^{-1} ,

c_w = formation water compressibility, psi^{-1} ,

S_w = formation water saturation, fraction, and

m = fitting factor.

Eq. 54 is the equation of a straight line with a slope of m_p and a y intercept of N .

Estimates of r_D and Δt_D are made and the appropriate values of W_{ed} are obtained from Table 38.3 or 38.5, according to system geometry. The summation terms in Eq. 54 then may be calculated and a graph plotted, as shown in Fig. 38.11. If a straight line results, the values of m_p and N are obtained from the slope and intercept of the resulting graph. An increasing slope indicates that the summation terms are too small, while a decreasing slope indicates that the summation terms are too large. The procedure is repeated, using different estimates of r_D and/or Δt_D until a straight-line plot is obtained. It should be noted that more than one combination of r_D and Δt_D may yield a reasonable straight line—i.e., a straight-line result does not necessarily determine a unique solution for N and m_p .

Future Performance

The future field performance must be obtained from a simultaneous solution of the material-balance and water drive equations. If the reservoir is above saturation pressure, a direct solution is possible; however, if the reservoir is below saturation pressure, a trial-and-error procedure is necessary.

TABLE 38.6—DIMENSIONLESS PRESSURES FOR FINITE CLOSED RADIAL AQUIFERS (continued)

$r_D = 5.0$		$r_D = 6.0$		$r_D = 7.0$		$r_D = 8.0$		$r_D = 9.0$		$r_D = 10.0$	
t_D	p_D	t_D	p_D	t_D	p_D	t_D	p_D	t_D	p_D	t_D	p_D
3.0	1.167	4.0	1.275	6.0	1.436	8.0	1.556	10.0	1.651	12.0	1.732
3.1	1.180	4.5	1.322	6.5	1.470	8.5	1.582	10.5	1.673	12.5	1.750
3.2	1.192	5.0	1.364	7.0	1.501	9.0	1.607	11.0	1.693	13.0	1.768
3.3	1.204	5.5	1.404	7.5	1.531	9.5	1.631	11.5	1.713	13.5	1.784
3.4	1.215	6.0	1.441	8.0	1.559	10.0	1.653	12.0	1.732	14.0	1.801
3.5	1.227	6.5	1.477	8.5	1.586	10.5	1.675	12.5	1.750	14.5	1.817
3.6	1.238	7.0	1.511	9.0	1.613	11.0	1.697	13.0	1.768	15.0	1.832
3.7	1.249	7.5	1.544	9.5	1.638	11.5	1.717	13.5	1.786	15.5	1.847
3.8	1.259	8.0	1.576	10.0	1.663	12.0	1.737	14.0	1.803	16.0	1.862
3.9	1.270	8.5	1.607	11.0	1.711	12.5	1.757	14.5	1.819	17.0	1.890
4.0	1.281	9.0	1.638	12.0	1.757	13.0	1.776	15.0	1.835	18.0	1.917
4.2	1.301	9.5	1.668	13.0	1.801	13.5	1.795	15.5	1.851	19.0	1.943
4.4	1.321	10.0	1.698	14.0	1.845	14.0	1.813	16.0	1.867	20.0	1.968
4.6	1.340	11.0	1.757	15.0	1.888	14.5	1.831	17.0	1.897	22.0	2.017
4.8	1.360	12.0	1.815	16.0	1.931	15.0	1.849	18.0	1.926	24.0	2.063
5.0	1.378	13.0	1.873	17.0	1.974	17.0	1.919	19.0	1.955	26.0	2.108
5.5	1.424	14.0	1.931	18.0	2.016	19.0	1.986	20.0	1.983	28.0	2.151
6.0	1.469	15.0	1.988	19.0	2.058	21.0	2.051	22.0	2.037	30.0	2.194
6.5	1.513	16.0	2.045	20.0	2.100	23.0	2.116	24.0	2.090	32.0	2.236
7.0	1.556	17.0	2.103	22.0	2.184	25.0	2.180	26.0	2.142	34.0	2.278
7.5	1.598	18.0	2.160	24.0	2.267	30.0	2.340	28.0	2.193	36.0	2.319
8.0	1.641	19.0	2.217	26.0	2.351	35.0	2.499	30.0	2.244	38.0	2.360
9.0	1.725	20.0	2.274	28.0	2.434	40.0	2.658	34.0	2.345	40.0	2.401
10.0	1.808	25.0	2.560	30.0	2.517	45.0	2.817	38.0	2.446	50.0	2.604
11.0	1.892	30.0	2.846					40.0	2.496	60.0	2.806
12.0	1.975							45.0	2.621	70.0	3.008
13.0	2.059							50.0	2.746		
14.0	2.142										
15.0	2.225										

There are several methods of solution because there are several possible combinations of the various material-balance and water drive equations. However, only one combination will be used to illustrate the general application to (1) a reservoir above the bubblepoint pressure, and (2) a reservoir below the bubblepoint pressure. In either case, it will be necessary to know (1) the saturations behind the front from laboratory core data or other sources, (2) the water production as a function of frontal advance, and (3) the pressure gradient in the flooded portion of the reservoir.

Pressure Gradient Between New and Original Front Positions. Eq. 55 shows that the difference between the average reservoir pressure and the pressure at the original WOC is a function of water-influx rate, aquifer fluid and formation properties, and aquifer geometry.

$$\Delta p_{o_n} - \Delta p_{w_n} = \frac{\mu_w e_{w_n}}{k_w} F_G = p_{w_n} - p_{o_n}, \dots (55)$$

where F_G is the reservoir geometry factor. The linear frontal advance is given by

$$F_G = \frac{L_f}{0.001127hb} \dots (56)$$

and the radial frontal advance is given by

$$F_G = \frac{2\pi \ln(r_w/r_f)}{0.00708h\alpha}, \dots (57)$$

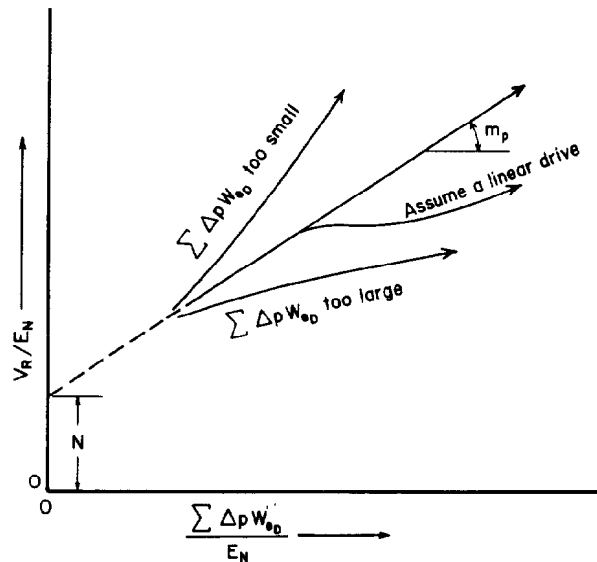
Fig. 38.11—Estimation of OOIP and m_p .

TABLE 38.7— DIMENSIONLESS PRESSURES FOR FINITE OUTCROPPING RADIAL AQUIFERS

$r_D = 1.5$		$r_D = 2.0$		$r_D = 2.5$		$r_D = 3.0$		$r_D = 3.5$		$r_D = 4.0$		$r_D = 6.0$	
t_D	p_D	t_D	p_D	t_D	p_D	t_D	p_D	t_D	p_D	t_D	p_D	t_D	p_D
5.0×10^{-2}	0.230	2.0×10^{-1}	0.424	3.0×10^{-1}	0.502	5.0×10^{-1}	0.617	5.0×10^{-1}	0.620	1.0	0.802	4.0	1.275
5.5×10^{-2}	0.240	2.2×10^{-1}	0.441	3.5×10^{-1}	0.535	5.5×10^{-1}	0.640	6.0×10^{-1}	0.665	1.2	0.857	4.5	1.320
6.0×10^{-2}	0.249	2.4×10^{-1}	0.457	4.0×10^{-1}	0.564	6.0×10^{-1}	0.662	7.0×10^{-1}	0.705	1.4	0.905	5.0	1.361
7.0×10^{-2}	0.266	2.6×10^{-1}	0.472	4.5×10^{-1}	0.591	7.0×10^{-1}	0.702	8.0×10^{-1}	0.741	1.6	0.947	5.5	1.398
8.0×10^{-2}	0.282	2.8×10^{-1}	0.485	5.0×10^{-1}	0.616	8.0×10^{-1}	0.738	9.0×10^{-1}	0.774	1.8	0.986	6.0	1.432
9.0×10^{-2}	0.292	3.0×10^{-1}	0.498	5.5×10^{-1}	0.638	9.0×10^{-1}	0.770	1.0	0.804	2.0	1.020	6.5	1.462
1.0×10^{-1}	0.307	3.5×10^{-1}	0.527	6.0×10^{-1}	0.659	1.0	0.799	1.2	0.858	2.2	1.052	7.0	1.490
1.2×10^{-1}	0.328	4.0×10^{-1}	0.552	7.0×10^{-1}	0.696	1.2	0.850	1.4	0.904	2.4	1.080	7.5	1.516
1.4×10^{-1}	0.344	4.5×10^{-1}	0.573	8.0×10^{-1}	0.728	1.4	0.892	1.6	0.945	2.6	1.106	8.0	1.539
1.6×10^{-1}	0.356	5.0×10^{-1}	0.591	9.0×10^{-1}	0.755	1.6	0.927	1.8	0.981	2.8	1.130	8.5	1.561
1.8×10^{-1}	0.367	5.5×10^{-1}	0.606	1.0	0.778	1.8	0.955	2.0	1.013	3.0	1.152	9.0	1.580
2.0×10^{-1}	0.375	6.0×10^{-1}	0.619	1.2	0.815	2.0	0.980	2.2	1.041	3.4	1.190	10.0	1.615
2.2×10^{-1}	0.381	6.5×10^{-1}	0.630	1.4	0.842	2.2	1.000	2.4	1.065	3.8	1.222	12.0	1.667
2.4×10^{-1}	0.386	7.0×10^{-1}	0.639	1.6	0.861	2.4	1.016	2.6	1.087	4.5	1.266	14.0	1.704
2.6×10^{-1}	0.390	7.5×10^{-1}	0.647	1.8	0.876	2.6	1.030	2.8	1.106	5.0	1.290	16.0	1.730
2.8×10^{-1}	0.393	8.0×10^{-1}	0.654	2.0	0.887	2.8	1.042	3.0	1.123	5.5	1.309	18.0	1.749
3.0×10^{-1}	0.396	8.5×10^{-1}	0.660	2.2	0.895	3.0	1.051	3.5	1.158	6.0	1.325	20.0	1.762
3.5×10^{-1}	0.400	9.0×10^{-1}	0.665	2.4	0.900	3.5	1.069	4.0	1.183	7.0	1.347	22.0	1.771
4.0×10^{-1}	0.402	9.5×10^{-1}	0.669	2.6	0.905	4.0	1.080	5.0	1.215	8.0	1.361	24.0	1.777
4.5×10^{-1}	0.404	1.0	0.673	2.8	0.908	4.5	1.087	6.0	1.232	9.0	1.370	26.0	1.781
5.0×10^{-1}	0.405	1.2	0.682	3.0	0.910	5.0	1.091	7.0	1.242	10.0	1.376	28.0	1.784
6.0×10^{-1}	0.405	1.4	0.688	3.5	0.913	5.5	1.094	8.0	1.247	12.0	1.382	30.0	1.787
7.0×10^{-1}	0.405	1.6	0.690	4.0	0.915	6.0	1.096	9.0	1.240	14.0	1.385	35.0	1.789
8.0×10^{-1}	0.405	1.8	0.692	4.5	0.916	6.5	1.097	10.0	1.251	16.0	1.386	40.0	1.791
		2.0	0.692	5.0	0.916	7.0	1.097	12.0	1.252	18.0	1.386	50.0	1.792
		2.5	0.693	5.5	0.916	8.0	1.098	14.0	1.253				
		3.0	0.693	6.0	0.916	10.0	1.099	16.0	1.253				

where

L_f = linear penetration of water front into reservoir, ft,

r_f = radius to water front after penetration, ft, and

α = angle subtended by reservoir, radians.

Note that F_G is a function of distance traveled by the front so that, if the pressure gradients between the reservoir and the original reservoir boundary are known for the past history, F_G may be evaluated as a function of frontal advance. Future values of F_G then can be obtained by extrapolating F_G as a function of frontal advance on some convenient plot (linear, semilog, etc.)

Reservoir Above Bubblepoint Pressure. Above the bubblepoint pressure the total compressibility can be assumed to be constant; so the material-balance equation

$$\Delta p_{on} = \frac{(q_{tn} - e_{wn}) \Delta t}{V_p c_{ot}} + \Delta p_{on-1}, \dots \dots \dots (58)$$

where

Δp_{on} = total reservoir pressure drop from initial pressure at end of interval n ,

q_{tn} = total production rate, RB/D,

V_p = total reservoir PV, bbl, and

c_{ot} = total reservoir compressibility, psi^{-1} ,

can be combined with Eqs. 6 and 55 and solved for the water-influx rate:

$$e_{wn} = \frac{\Delta p_{on-1} + (\Delta t q_{tn} / V_p c_{ot}) - m_r \sum_{j=2}^n e_{w(n+1-j)} \Delta p_{Dj}}{m_r \Delta p_{Dj} + (\Delta t / V_p c_{ot}) + (\mu_w F_g / k_w)} \dots \dots \dots (59)$$

The calculated water-influx rate now can be used in Eq. 58 to calculate Δp_{on} and the whole procedure is repeated for the next time interval. If Eq. 27 is used instead of Eq. 6, $m_r = 1$ and Δp_D is replaced by ΔZ in Eq. 59.

Reservoir Below Bubblepoint Pressure. To simplify the calculation procedure, it was assumed that (1) uniform saturations exist ahead of and behind the front, (2) the saturations do not change as any portion of the reservoir is bypassed, and (3) the changes in pressure are selected small enough that the changes in oil FVF's are very small. Fig. 38.12 shows the saturation changes as the front advances into the unflooded reservoir volume V_{n-1} during time interval n .

The following equations will be used in this method. Water influx rate:

$$e_{wn} = \frac{\Delta p_{on-1} - m_r \sum_{j=2}^n e_{w(n+1-j)} \Delta p_{Dj}}{m_r \Delta p_{Dj} - (\mu_w F_g / k_w)} \dots \dots \dots (60)$$

TABLE 38.7— DIMENSIONLESS PRESSURES FOR FINITE OUTCROPPING RADIAL AQUIFERS (continued)

$r_D = 8.0$		$r_D = 10$		$r_D = 15$		$r_D = 20$		$r_D = 25$		$r_D = 30$		$r_D = 40$	
t_D	p_D	t_D	p_D	t_D	p_D	t_D	p_D	t_D	p_D	t_D	p_D	t_D	p_D
7.0	1.499	10.0	1.651	20.0	1.960	30.0	2.148	50.0	2.389	70.0	2.551	12.0 × 10	2.813
7.5	1.527	12.0	1.730	22.0	2.003	35.0	2.219	55.0	2.434	80.0	2.615	14.0 × 10	2.888
8.0	1.554	14.0	1.798	24.0	2.043	40.0	2.282	60.0	2.476	90.0	2.672	16.0 × 10	2.953
8.5	1.580	16.0	1.856	26.0	2.080	45.0	2.338	65.0	2.514	10.0 × 10	2.723	18.0 × 10	3.011
9.0	1.604	18.0	1.907	28.0	2.114	50.0	2.388	70.0	2.550	12.0 × 10	2.812	20.0 × 10	3.063
9.5	1.627	20.0	1.952	30.0	2.146	60.0	2.475	75.0	2.583	14.0 × 10	2.886	22.0 × 10	3.109
10.0	1.648	25.0	2.043	35.0	2.218	70.0	2.547	80.0	2.614	16.0 × 10	2.950	24.0 × 10	3.152
12.0	1.724	30.0	2.111	40.0	2.279	80.0	2.609	85.0	2.643	16.5 × 10	2.965	26.0 × 10	3.191
14.0	1.786	35.0	2.160	45.0	2.332	90.0	2.658	90.0	2.671	17.0 × 10	2.979	28.0 × 10	3.226
16.0	1.837	40.0	2.197	50.0	2.379	10.0 × 10	2.707	95.0	2.697	17.5 × 10	2.992	30.0 × 10	3.259
18.0	1.879	45.0	2.224	60.0	2.455	10.5 × 10	2.728	10.0 × 10	2.721	18.0 × 10	3.006	35.0 × 10	3.331
20.0	1.914	50.0	2.245	70.0	2.513	11.0 × 10	2.747	12.0 × 10	2.807	20.0 × 10	3.054	40.0 × 10	3.391
22.0	1.943	55.0	2.260	80.0	2.558	11.5 × 10	2.764	14.0 × 10	2.878	25.0 × 10	3.150	45.0 × 10	3.440
24.0	1.967	60.0	2.271	90.0	2.592	12.0 × 10	2.781	16.0 × 10	2.936	30.0 × 10	3.219	50.0 × 10	3.482
26.0	1.986	65.0	2.279	10.0 × 10	2.619	12.5 × 10	2.796	18.0 × 10	2.984	35.0 × 10	3.269	55.0 × 10	3.516
28.0	2.002	70.0	2.285	12.0 × 10	2.655	13.0 × 10	2.810	20.0 × 10	3.024	40.0 × 10	3.306	60.0 × 10	3.545
30.0	2.016	75.0	2.290	14.0 × 10	2.677	13.5 × 10	2.823	22.0 × 10	3.057	45.0 × 10	3.332	65.0 × 10	3.568
35.0	2.040	80.0	2.293	16.0 × 10	2.689	14.0 × 10	2.835	24.0 × 10	3.085	50.0 × 10	3.351	70.0 × 10	3.588
40.0	2.055	90.0	2.297	18.0 × 10	2.697	14.5 × 10	2.846	26.0 × 10	3.107	60.0 × 10	3.375	80.0 × 10	3.619
45.0	2.064	10.0 × 10	2.300	20.0 × 10	2.701	15.0 × 10	2.857	28.0 × 10	3.126	70.0 × 10	3.387	90.0 × 10	3.640
50.0	2.070	11.0 × 10	2.301	22.0 × 10	2.704	16.0 × 10	2.876	30.0 × 10	3.142	80.0 × 10	3.394	10.0 × 10 ²	3.655
60.0	2.076	12.0 × 10	2.302	24.0 × 10	2.706	18.0 × 10	2.906	35.0 × 10	3.171	90.0 × 10	3.397	12.0 × 10 ²	3.672
70.0	2.078	13.0 × 10	2.302	26.0 × 10	2.707	20.0 × 10	2.929	40.0 × 10	3.189	10.0 × 10 ²	3.399	14.0 × 10 ²	3.681
80.0	2.079	14.0 × 10	2.302	28.0 × 10	2.707	24.0 × 10	2.958	45.0 × 10	3.200	12.0 × 10 ²	3.401	16.0 × 10 ²	3.685
		16.0 × 10	2.303	30.0 × 10	2.708	28.0 × 10	2.975	50.0 × 10	3.207	14.0 × 10 ²	3.401	18.0 × 10 ²	3.687
						30.0 × 10	2.980	60.0 × 10	3.214			20.0 × 10 ²	3.688
						40.0 × 10	2.992	70.0 × 10	3.217			25.0 × 10 ²	3.689
						50.0 × 10	2.995	80.0 × 10	3.218				
								90.0 × 10	3.219				

Flooded and unflooded volumes:

$$\Delta V_n = \frac{(e_{w_n} - q_{w_n}) \Delta t_n}{f_R(1 - S_{iw} - S_{or} - S_{gr})_{n-1}} \quad \dots \dots \dots (61)$$

and

$$V_n = V_{n-1} - \Delta V_n \quad \dots \dots \dots (62)$$

Oil saturation in V_n :

$$S_{o_n} = \frac{B_{o_n}}{V_n} \left\{ \frac{S_{o_{(n-1)}} V_n}{B_{o_{(n-1)}}} + \frac{f_R \Delta V_n [S_{o_{(n-1)}} - S_{or_n}] - q_{o_n} \Delta t_n}{B_{o_n}} \right\} \quad \dots \dots \dots (63)$$

Gas production:

$$\Delta G_{p_n} = \frac{V_n [S_{g_{(n-1)}} - S_{g_n}]}{B_{g_{(n-1)}}} + \frac{f_R \Delta V_n [S_{g_{(n-1)}} - S_{gr_n}]}{B_{g_n}} + q_{o_n} \Delta t_n \bar{R}_{s_n} \quad \dots \dots (64)$$

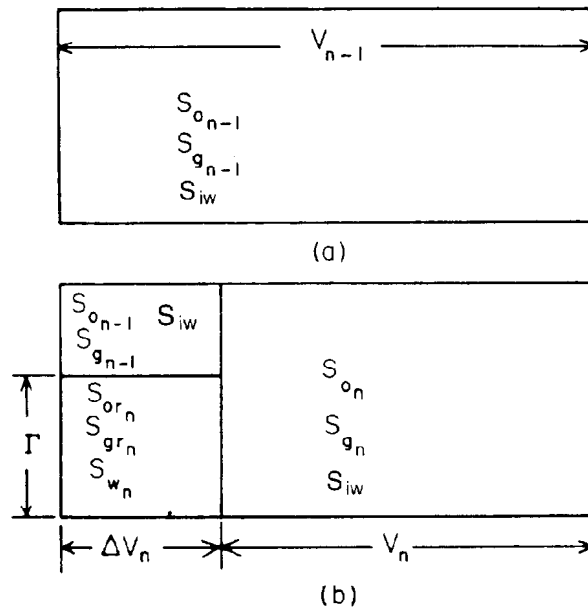


Fig. 38.12—Saturation change with frontal advance.

TABLE 38.7— DIMENSIONLESS PRESSURES FOR FINITE OUTCROPPING RADIAL AQUIFERS (continued)

$r_D = 50$		$r_D = 60$		$r_D = 70$		$r_D = 80$		$r_D = 90$		$r_D = 100$	
t_D	p_D	t_D	p_D	t_D	p_D	t_D	p_D	t_D	p_D	t_D	p_D
20.0 × 10	3.064	3.0 × 10 ²	3.257	5.0 × 10 ²	3.512	6.0 × 10 ²	3.603	8.0 × 10 ²	3.747	1.0 × 10 ³	3.859
22.0 × 10	3.111	4.0 × 10 ²	3.401	6.0 × 10 ²	3.603	7.0 × 10 ²	3.680	9.0 × 10 ²	3.806	1.2 × 10 ³	3.949
24.0 × 10	3.154	5.0 × 10 ²	3.512	7.0 × 10 ²	3.680	8.0 × 10 ²	3.747	1.0 × 10 ³	3.858	1.4 × 10 ³	4.026
26.0 × 10	3.193	6.0 × 10 ²	3.602	8.0 × 10 ²	3.746	9.0 × 10 ²	3.805	1.2 × 10 ³	3.949	1.6 × 10 ³	4.092
28.0 × 10	3.229	7.0 × 10 ²	3.676	9.0 × 10 ²	3.803	10.0 × 10 ²	3.857	1.3 × 10 ³	3.988	1.8 × 10 ³	4.150
30.0 × 10	3.263	8.0 × 10 ²	3.739	10.0 × 10 ²	3.854	12.0 × 10 ²	3.946	1.4 × 10 ³	4.025	2.0 × 10 ³	4.200
35.0 × 10	3.339	9.0 × 10 ²	3.792	12.0 × 10 ²	3.937	14.0 × 10 ²	4.019	1.5 × 10 ³	4.058	2.5 × 10 ³	4.303
40.0 × 10	3.405	10.0 × 10 ²	3.832	14.0 × 10 ²	4.003	15.0 × 10 ²	4.051	1.8 × 10 ³	4.144	3.0 × 10 ³	4.379
45.0 × 10	3.461	12.0 × 10 ²	3.908	16.0 × 10 ²	4.054	16.0 × 10 ²	4.080	2.0 × 10 ³	4.192	3.5 × 10 ³	4.434
50.0 × 10	3.512	14.0 × 10 ²	3.959	18.0 × 10 ²	4.095	18.0 × 10 ²	4.130	2.5 × 10 ³	4.285	4.0 × 10 ³	4.478
55.0 × 10	3.556	16.0 × 10 ²	3.996	20.0 × 10 ²	4.127	20.0 × 10 ²	4.171	3.0 × 10 ³	4.349	4.5 × 10 ³	4.510
60.0 × 10	3.595	18.0 × 10 ²	4.023	25.0 × 10 ²	4.181	25.0 × 10 ²	4.248	3.5 × 10 ³	4.394	5.0 × 10 ³	4.534
65.0 × 10	3.630	20.0 × 10 ²	4.043	30.0 × 10 ²	4.211	30.0 × 10 ²	4.297	4.0 × 10 ³	4.426	5.5 × 10 ³	4.552
70.0 × 10	3.661	25.0 × 10 ²	4.071	35.0 × 10 ²	4.228	35.0 × 10 ²	4.328	4.5 × 10 ³	4.448	6.0 × 10 ³	4.565
75.0 × 10	3.688	30.0 × 10 ²	4.084	40.0 × 10 ²	4.237	40.0 × 10 ²	4.347	5.0 × 10 ³	4.464	6.5 × 10 ³	4.579
80.0 × 10	3.713	35.0 × 10 ²	4.090	45.0 × 10 ²	4.242	45.0 × 10 ²	4.360	6.0 × 10 ³	4.482	7.0 × 10 ³	4.583
85.0 × 10	3.735	40.0 × 10 ²	4.092	50.0 × 10 ²	4.245	50.0 × 10 ²	4.368	7.0 × 10 ³	4.491	7.5 × 10 ³	4.588
90.0 × 10	3.754	45.0 × 10 ²	4.093	55.0 × 10 ²	4.247	60.0 × 10 ²	4.376	8.0 × 10 ³	4.496	8.0 × 10 ³	4.593
95.0 × 10	3.771	50.0 × 10 ²	4.094	60.0 × 10 ²	4.247	70.0 × 10 ²	4.380	9.0 × 10 ³	4.498	9.0 × 10 ³	4.598
10.0 × 10 ²	3.787	55.0 × 10 ²	4.094	65.0 × 10 ²	4.248	80.0 × 10 ²	4.381	10.0 × 10 ³	4.499	10.0 × 10 ³	4.601
12.0 × 10 ²	3.833			70.0 × 10 ²	4.248	90.0 × 10 ²	4.382	11.0 × 10 ³	4.499	12.5 × 10 ³	4.604
14.0 × 10 ²	3.862			75.0 × 10 ²	4.248	10.0 × 10 ³	4.382	12.0 × 10 ³	4.500	15.0 × 10 ³	4.605
16.0 × 10 ²	3.881			80.0 × 10 ²	4.248	11.0 × 10 ³	4.382	14.0 × 10 ³	4.500		
18.0 × 10 ²	3.892										
20.0 × 10 ²	3.900										
22.0 × 10 ²	3.904										
24.0 × 10 ²	3.907										
26.0 × 10 ²	3.909										
28.0 × 10 ²	3.910										

GOR (relative permeability):

$$R_n = \left(\frac{k_{rg} \mu_o}{k_{ro} \mu_g} \frac{\bar{B}_o}{\bar{B}_g} \right)_n + \bar{R}_{s_n} \quad (65)$$

GOR (production):

$$R_n = \frac{\Delta G_n}{q_{o_n} \Delta t_n} \quad (66)$$

For these equations,

- f_R = fraction of reservoir swept,
- S_o = oil saturation, fraction,
- S_g = gas saturation, fraction,
- S_w = water saturation, fraction, and
- S_{iw} = interstitial water saturation, fraction.

One method for solutions using equal time intervals is as follows.

1. Estimate the pressure drop during the next time interval.
2. Calculate the water-influx rate with Eq. 60.
3. Calculate ΔV_n and V_n with Eqs. 61 and 62.
4. Calculate the oil saturation in V_n for the predicted oil production during Interval n with Eq. 63.
5. Calculate gas production with Eq. 64.

6. Calculate the GOR with Eq. 65.

7. Calculate the GOR with Eq. 66 for average values of pressure and saturation.

8. Compare the GOR's obtained in Steps 6 and 7 and, if they agree, proceed to the next interval. If they do not agree, estimate a new pressure drop and repeat Steps 2 through 8.

If the water drive equation for unequal time intervals is used, the need for re-evaluating the pressure functions for each trial in a given interval can be eliminated. This procedure calls for selecting a given pressure drop and estimating the length of the next time interval in Steps 1 and 8 and this program. The remaining steps are unchanged.

Reservoir Simulation Models. The capability of mathematical simulation models to calculate pressure and fluid flow in nonhomogeneous and nonsymmetrical reservoir/aquifer systems has been thoroughly described in the literature since the early 1960's. Widespread availability of computers and models throughout the industry has helped to remove many of the idealizations and restrictions regarding geometry and/or homogeneity that are a practical requirement for analysis by traditional methods. These models have the capability to analyze performance for virtually any desired description of the physical system, including multipool aquifers. See Chap. 48 for more information.

TABLE 38.7— DIMENSIONLESS PRESSURES FOR FINITE OUTCROPPING RADIAL AQUIFERS (continued)

$r_D = 200$		$r_D = 300$		$r_D = 400$		$r_D = 500$		$r_D = 600$		$r_D = 700$	
t_D	p_D	t_D	p_D	t_D	p_D	t_D	p_D	t_D	p_D	t_D	p_D
1.5×10^3	4.061	6.0×10^3	4.754	1.5×10^4	5.212	2.0×10^4	5.356	4.0×10^4	5.703	5.0×10^4	5.814
2.0×10^3	4.205	8.0×10^3	4.898	2.0×10^4	5.356	2.5×10^4	5.468	4.5×10^4	5.762	6.0×10^4	5.905
2.5×10^3	4.317	10.0×10^3	5.010	3.0×10^4	5.556	3.0×10^4	5.559	5.0×10^4	5.814	7.0×10^4	5.982
3.0×10^3	4.408	12.0×10^3	5.101	4.0×10^4	5.689	3.5×10^4	5.636	6.0×10^4	5.904	8.0×10^4	6.048
3.5×10^3	4.485	14.0×10^3	5.177	5.0×10^4	5.781	4.0×10^4	5.702	7.0×10^4	5.979	9.0×10^4	6.105
4.0×10^3	4.552	16.0×10^3	5.242	6.0×10^4	5.845	4.5×10^4	5.759	8.0×10^4	6.041	10.0×10^4	6.156
5.0×10^3	4.663	18.0×10^3	5.299	7.0×10^4	5.889	5.0×10^4	5.810	9.0×10^4	6.094	12.0×10^4	6.239
6.0×10^3	4.754	20.0×10^3	5.348	8.0×10^4	5.920	6.0×10^4	5.894	10.0×10^4	6.139	14.0×10^4	6.305
7.0×10^3	4.829	24.0×10^3	5.429	9.0×10^4	5.942	7.0×10^4	5.960	12.0×10^4	6.210	16.0×10^4	6.357
8.0×10^3	4.894	28.0×10^3	5.491	10.0×10^4	5.957	8.0×10^4	6.013	14.0×10^4	6.262	18.0×10^4	6.398
9.0×10^3	4.949	30.0×10^3	5.517	11.0×10^4	5.967	9.0×10^4	6.055	16.0×10^4	6.299	20.0×10^4	6.430
10.0×10^3	4.996	40.0×10^3	5.606	12.0×10^4	5.975	10.0×10^4	6.088	18.0×10^4	6.326	25.0×10^4	6.484
12.0×10^3	5.072	50.0×10^3	5.652	12.5×10^4	5.977	12.0×10^4	6.135	20.0×10^4	6.345	30.0×10^4	6.514
14.0×10^3	5.129	60.0×10^3	5.676	13.0×10^4	5.980	14.0×10^4	6.164	25.0×10^4	6.374	35.0×10^4	6.530
16.0×10^3	5.171	70.0×10^3	5.690	14.0×10^4	5.983	16.0×10^4	6.183	30.0×10^4	6.387	40.0×10^4	6.540
18.0×10^3	5.203	80.0×10^3	5.696	16.0×10^4	5.988	18.0×10^4	6.195	35.0×10^4	6.392	45.0×10^4	6.545
20.0×10^3	5.227	90.0×10^3	5.700	18.0×10^4	5.990	20.0×10^4	6.202	40.0×10^4	6.395	50.0×10^4	6.548
25.0×10^3	5.264	10.0×10^4	5.702	20.0×10^4	5.991	25.0×10^4	6.211	50.0×10^4	6.397	60.0×10^4	6.550
30.0×10^3	5.282	12.0×10^4	5.703	24.0×10^4	5.991	30.0×10^4	6.213	60.0×10^4	6.397	70.0×10^4	6.551
35.0×10^3	5.290	14.0×10^4	5.704	26.0×10^4	5.991	35.0×10^4	6.214			80.0×10^4	6.551
40.0×10^3	5.294	15.0×10^4	5.704			40.0×10^4	6.214				

Nomenclature

A = constant described by Eq. 46	J_a = aquifer productivity index, B/D-psi
b = intercept	k = permeability, md
B_g = gas FVF, bbl/STB	L = aquifer length, ft
B_o = oil FVF, bbl/STB	L_f = linear penetration of water front into reservoir, ft
B_t = two-phase FVF, bbl/STB	m = fitting factor (see Page 38-7); ratio of initial reservoir free-gas volume to initial reservoir oil volume; slope
B_w = water FVF, bbl/STB	m_F = proportionality factor
c_f = formation compressibility, psi^{-1}	m_p = influx constant, bbl/psi (see Eqs. 9 and 10)
c_{ot} = total reservoir compressibility, psi^{-1}	m_r = rate constant, $\text{psi}/\text{bbl-D}$ (see Eqs. 3 through 5)
c_w = formation water compressibility, psi^{-1}	n = interval
c_{wt} = total aquifer compressibility, psi^{-1}	N = OOIP, STB
d = geometry term obtained from Table 38.1	N_{it} = time interval number
e_w = water influx rate, B/D	N_p = cumulative oil produced, STB
e_{wB} = water influx rate at Reservoir B, B/D	\bar{p}_a = average aquifer pressure, psi
$e_{w(n+1-j)}$ = water-influx rate at interval $n+1-j$, B/D	p_{a_i} = initial aquifer pressure, psi
e_{wt_n} = total water influx rate at interval n , B/D	p_b = bubblepoint pressure, psi
E_N = cumulative expansion per stock-tank barrel OOIP, bbl	p_D = dimensionless pressure term
f_R = fraction of reservoir swept	$p_{D(A,B)}$ = dimensionless pressure term for Reservoir B with respect to Reservoir A
F = approximation to p_D and a function of type of aquifer	p_w = pressure at original WOC, psi
F_G = reservoir geometry factor	p_{w_n} = cumulative pressure drop at the end of interval n , psi
$F(t)$ = influence function	Δp_D = known dimensionless field pressure drop at original WOC
F_V = ratio of volume of oil and its dissolved original gas at a given pressure to its volume at initial pressure	Δp_{D_i} = dimensionless pressure drop to time period i
G_i = cumulative gas injected, scf	
h = aquifer thickness, ft	
j = summation of time period $1 + o_n$	

TABLE 38.7— DIMENSIONLESS PRESSURES FOR FINITE OUTCROPPING RADIAL AQUIFERS (continued)

$r_D = 800$		$r_D = 900$		$r_D = 1,000$		$r_D = 1,200$		$r_D = 1,400$		$r_D = 1,600$	
t_D	p_D	t_D	p_D	t_D	p_D	t_D	p_D	t_D	p_D	t_D	p_D
7.0×10^4	5.983	8.0×10^4	6.049	1.0×10^5	6.161	2.0×10^5	6.507	2.0×10^5	6.507	2.5×10^5	6.619
8.0×10^4	6.049	9.0×10^4	6.108	1.2×10^5	6.252	3.0×10^5	6.704	2.5×10^5	6.619	3.0×10^5	6.710
9.0×10^4	6.108	10.0×10^4	6.161	1.4×10^5	6.329	4.0×10^5	6.833	3.0×10^5	6.709	3.5×10^5	6.787
10.0×10^4	6.160	12.0×10^4	6.251	1.6×10^5	6.395	5.0×10^5	6.918	3.5×10^5	6.785	4.0×10^5	6.853
12.0×10^4	6.249	14.0×10^4	6.327	1.8×10^5	6.452	6.0×10^5	6.975	4.0×10^5	6.849	5.0×10^5	6.962
14.0×10^4	6.322	16.0×10^4	6.392	2.0×10^5	6.503	7.0×10^5	7.013	5.0×10^5	6.950	6.0×10^5	7.046
16.0×10^4	6.382	18.0×10^4	6.447	2.5×10^5	6.605	8.0×10^5	7.038	6.0×10^5	7.026	7.0×10^5	7.114
18.0×10^4	6.432	20.0×10^4	6.494	3.0×10^5	6.681	9.0×10^5	7.056	7.0×10^5	7.082	8.0×10^5	7.167
20.0×10^4	6.474	25.0×10^4	6.587	3.5×10^5	6.738	10.0×10^5	7.067	8.0×10^5	7.123	9.0×10^5	7.210
25.0×10^4	6.551	30.0×10^4	6.652	4.0×10^5	6.781	12.0×10^5	7.080	9.0×10^5	7.154	10.0×10^5	7.244
30.0×10^4	6.599	40.0×10^4	6.729	4.5×10^5	6.813	14.0×10^5	7.085	10.0×10^5	7.177	15.0×10^5	7.334
35.0×10^4	6.630	45.0×10^4	6.751	5.0×10^5	6.837	16.0×10^5	7.088	15.0×10^5	7.229	20.0×10^5	7.364
40.0×10^4	6.650	50.0×10^4	6.766	5.5×10^5	6.854	18.0×10^5	7.089	20.0×10^5	7.241	25.0×10^5	7.373
45.0×10^4	6.663	55.0×10^4	6.777	6.0×10^5	6.868	19.0×10^5	7.089	25.0×10^5	7.243	30.0×10^5	7.376
50.0×10^4	6.671	60.0×10^4	6.785	7.0×10^5	6.885	20.0×10^5	7.090	30.0×10^5	7.244	35.0×10^5	7.377
55.0×10^4	6.676	70.0×10^4	6.794	8.0×10^5	6.895	21.0×10^5	7.090	31.0×10^5	7.244	40.0×10^5	7.378
60.0×10^4	6.679	80.0×10^4	6.798	9.0×10^5	6.901	22.0×10^5	7.090	32.0×10^5	7.244	42.0×10^5	7.378
70.0×10^4	6.682	90.0×10^4	6.800	10.0×10^5	6.904	23.0×10^5	7.090	33.0×10^5	7.24	44.0×10^5	7.378
80.0×10^4	6.684	10.0×10^5	6.801	12.0×10^5	6.907	24.0×10^5	7.090				
100.0×10^4	6.684			14.0×10^5	6.907						
				16.0×10^5	6.908						

Δp_{Dj} = dimensionless pressure drop to time period j

Δp_E = total pressure drop at WOC (calculated using reservoir expansion rates), psi

Δp_f = total pressure drop at original WOC (field data), psi

$\Delta \bar{p}_{(n+1-j)}$ = average pressure drop in interval, psi

$\Delta p_{o(A,B)}$ = pressure drop at Reservoir A caused by Reservoir B, psi

Δp_{oA_n} = total pressure drop at Reservoir A at end of interval n , psi

Δp_v = total pressure drop at WOC (calculated using reservoir voidage rates), psi

q_{on} = total oil production rate at end of interval n , B/D

q_{tn} = total production rate, B/D

r_a = aquifer radius, ft

r_D = dimensionless radius = r_a/r_w

r_f = radius to water front after penetration, ft

r_w = field radius, ft

R_p = cumulative produced GOR, scf/STB

R_{s_n} = average solution GOR at end of interval n , scf/STB

S_g = gas saturation, fraction

S_{iw} = interstitial water saturation, fraction

S_o = oil saturation, fraction

S_{or_n} = residual oil saturation at end of interval n , fraction

S_w = formation water saturation, fraction

t_D = dimensionless time

Δt_D = dimensionless time interval

V_p = total reservoir PV, bbl

V_R = cumulative voidage, bbl

V_{w_i} = initial water volume in the aquifer, bbl

w = aquifer width, ft

W_{eD} = dimensionless water-influx term

W_{e_n} = cumulative water influx at end of interval n , bbl

$W_{et} = W_{c_w} p_{ai}$, total aquifer expansion capacity, bbl

W_i = cumulative water injected, bbl

W_p = cumulative water produced, bbl

Y = constant described by Eqs. 49 and 50

Z = resistance function

Z_n = new values of Z

α = angle subtended by reservoir, radians

δe_{w_n} = correction to e_{w_n}

δp_{f_n} = correction to Δp_{f_n}

μ_w = water viscosity, cp

σ^2 = variance

ϕ = porosity, fraction

TABLE 38.8—DIMENSIONLESS PRESSURES FOR FINITE-CLOSED LINEAR AQUIFERS

t_D	p_D	t_D	p_D
0.005	0.07979	0.18	0.47900
0.01	0.11296	0.20	0.50516
0.02	0.15958	0.22	0.53021
0.03	0.19544	0.24	0.55436
0.04	0.22567	0.26	0.57776
0.05	0.25231	0.28	0.60055
0.06	0.27639	0.30	0.62284
0.07	0.29854	0.4	0.72942
0.08	0.31915	0.5	0.83187
0.09	0.33851	0.6	0.93279
0.10	0.35682	0.7	1.03313
0.12	0.39088	0.8	1.13326
0.14	0.42224	0.9	1.23330
0.16	0.45147	1.0	1.33332

TABLE 38.7— DIMENSIONLESS PRESSURES FOR FINITE OUTCROPPING RADIAL AQUIFERS (continued)

$r_D = 1,800$		$r_D = 2,000$		$r_D = 2,200$		$r_D = 2,400$		$r_D = 2,600$		$r_D = 2,800$		$r_D = 3,000$	
t_D	p_D	t_D	p_D	t_D	p_D	t_D	p_D	t_D	p_D	t_D	p_D	t_D	p_D
3.0×10^5	6.710	4.0×10^5	6.854	5.0×10^5	6.966	6.0×10^5	7.057	7.0×10^5	7.134	8.0×10^5	7.201	1.0×10^6	7.312
4.0×10^5	6.854	5.0×10^5	6.966	5.5×10^5	7.013	7.0×10^5	7.134	8.0×10^5	7.201	9.0×10^5	7.260	1.2×10^6	7.403
5.0×10^5	6.965	6.0×10^5	7.056	6.0×10^5	7.057	8.0×10^5	7.200	9.0×10^5	7.259	10.0×10^5	7.312	1.4×10^6	7.480
6.0×10^5	7.054	7.0×10^5	7.132	6.5×10^5	7.097	9.0×10^5	7.259	10.0×10^5	7.312	12.0×10^5	7.403	1.6×10^6	7.545
7.0×10^5	7.120	8.0×10^5	7.196	7.0×10^5	7.133	10.0×10^5	7.310	12.0×10^5	7.401	16.0×10^5	7.542	1.8×10^6	7.602
8.0×10^5	7.188	9.0×10^5	7.251	7.5×10^5	7.167	12.0×10^5	7.398	14.0×10^5	7.475	20.0×10^5	7.644	2.0×10^6	7.651
9.0×10^5	7.238	10.0×10^5	7.298	8.0×10^5	7.199	16.0×10^5	7.526	16.0×10^5	7.536	24.0×10^5	7.719	2.4×10^6	7.732
10.0×10^5	7.280	12.0×10^5	7.374	8.5×10^5	7.229	20.0×10^5	7.611	18.0×10^5	7.588	28.0×10^5	7.775	2.8×10^6	7.794
15.0×10^5	7.407	14.0×10^5	7.431	9.0×10^5	7.256	24.0×10^5	7.668	20.0×10^5	7.631	30.0×10^5	7.797	3.0×10^6	7.820
20.0×10^5	7.459	16.0×10^5	7.474	10.0×10^5	7.307	28.0×10^5	7.706	24.0×10^5	7.699	35.0×10^5	7.840	3.5×10^6	7.871
30.0×10^5	7.489	18.0×10^5	7.506	12.0×10^5	7.390	30.0×10^5	7.720	28.0×10^5	7.746	40.0×10^5	7.870	4.0×10^6	7.908
40.0×10^5	7.495	20.0×10^5	7.530	16.0×10^5	7.507	35.0×10^5	7.745	30.0×10^5	7.765	50.0×10^5	7.905	4.5×10^6	7.935
50.0×10^5	7.495	25.0×10^5	7.566	20.0×10^5	7.579	40.0×10^5	7.760	35.0×10^5	7.799	60.0×10^5	7.922	5.0×10^6	7.955
51.0×10^5	7.495	30.0×10^5	7.584	25.0×10^5	7.631	50.0×10^5	7.775	40.0×10^5	7.821	70.0×10^5	7.930	6.0×10^6	7.979
52.0×10^5	7.495	35.0×10^5	7.593	30.0×10^5	7.661	60.0×10^5	7.780	50.0×10^5	7.845	80.0×10^5	7.934	7.0×10^6	7.992
53.0×10^5	7.495	40.0×10^5	7.597	35.0×10^5	7.677	70.0×10^5	7.782	60.0×10^5	8.856	90.0×10^5	7.936	8.0×10^6	7.999
54.0×10^5	7.495	50.0×10^5	7.600	40.0×10^5	7.686	80.0×10^5	7.783	70.0×10^5	7.860	10.0×10^6	7.937	9.0×10^6	8.002
56.0×10^5	7.495	60.0×10^5	7.601	50.0×10^5	7.693	90.0×10^5	7.783	80.0×10^5	7.862	12.0×10^6	7.937	10.0×10^6	8.004
		64.0×10^5	7.601	60.0×10^5	7.695	95.0×10^5	7.783	90.0×10^5	7.863	13.0×10^6	7.937	12.0×10^6	8.006
				70.0×10^5	7.696			10.0×10^6	7.863			15.0×10^6	8.006
				80.0×10^5	7.696								

Key Equations With SI Units

The equations in this chapter may be used directly with practical SI units without conversion factors, except for certain equations containing numerical constants. These equations are repeated here with appropriate constants for SI units.

$$m_r = \frac{\mu_w}{8.527 \times 10^{-5} kh\alpha}, \quad (3)$$

$$m_r = \frac{\mu_w}{8.527 \times 10^{-5} kh}, \quad (4)$$

$$m_r = \frac{\mu_w L}{8.527 \times 10^{-5} khb}, \quad (5)$$

$$m_p = (1)\phi c_{wt} h\alpha r_w^2, \quad (9)$$

$$m_p = (1)\phi c_{wt} hb^2, \quad (10)$$

$$t_D = \frac{8.527 \times 10^{-5} kt}{\phi c_{wt} \mu_w d^2}, \quad (20)$$

$$J_a = \frac{5.36 \times 10^{-4} kh}{\mu_w (\ln r_D - 0.75)}, \quad (40)$$

$$J_a = \frac{3(8.527 \times 10^{-5})kbh}{\mu_w L}, \quad (41)$$

$$F_G = \frac{L_f}{8.527 \times 10^{-5} hb}, \quad (56)$$

and

$$F_G = \frac{2\pi \ln(r_w/r_f)}{5.36 \times 10^{-4} h\alpha}, \quad (57)$$

where

k is in md,

h is in m,

b is in m,

L is in m,

r_D is dimensionless,

r_w is in m,

μ_w is in mPa·s,

c_{wt} is in kPa⁻¹,

J_a is in m³/d·kPa,

m_r is in kPa/m³·d,

m_p is in m³/kPa,

F_G is in m⁻¹, and

α is in radians.

References

1. Van Everdingen, A.F. and Hurst, W.: "The Application of the Laplace Transformation to Flow Problems in Reservoirs," *Trans., AIME* (1949) **186**, 305-24.
2. Mortada, M.: "A Practical Method for Treating Oilfield Interference in Water-Drive Reservoirs," *J. Pet. Tech.* (Dec. 1955) 217-26; *Trans., AIME*, **204**.
3. Carter, R.D. and Tracy, G.W.: "An Improved Method for Calculating Water Influx," *J. Pet. Tech.* (Dec. 1960) 58-60; *Trans., AIME*, **219**.
4. Hicks, A.L., Weber, A.G., and Ledbetter, R.L.: "Computing Techniques for Water-Drive Reservoirs," *J. Pet. Tech.* (June 1959) 65-67; *Trans., AIME*, **216**.
5. Hutchinson, T.S. and Sikora, V.J.: "A Generalized Water-Drive Analysis," *J. Pet. Tech.* (July 1959) 169-78; *Trans., AIME*, **216**.
6. Schilthuis, R.J.: "Active Oil and Reservoir Energy," *Trans., AIME* (1936) **118**, 33-52.
7. Fetkovich, M.J.: "A Simplified Approach to Water Influx Calculations—Finite Aquifer Systems," *J. Pet. Tech.* (July 1971) 814-28.
8. Browncombe, E.R. and Collins, F.A.: "Estimation of Reserves and Water Drive from Pressure and Production History," *Trans., AIME* (1949) **186**, 92-99.
9. Van Everdingen, A.F., Timmerman, E.H., and McMahon, J.J.: "Application of the Material Balance Equation to a Partial Water-Drive Reservoir," *J. Pet. Tech.* (Feb. 1953) 51-60; *Trans., AIME*, **198**.
10. Havlena, D. and Odeh, A.S.: "The Material Balance as an Equation of a Straight Line," *J. Pet. Tech.* (Aug. 1963) 896-900; *Trans., AIME*, **228**.

General References

- Chatas, A.T.: "A Practical Treatment of Nonsteady-State Flow Problems in Reservoir Systems—I," *Pet. Eng.* (May 1953) B42-
- Chatas, A.T.: "A Practical Treatment of Nonsteady-State Flow Problems in Reservoir Systems—II," *Pet. Eng.* (June 1953) B38-
- Chatas, A.T.: "A Practical Treatment of Nonsteady-State Flow Problems in Reservoir Systems—III," *Pet. Eng.* (Aug. 1953) B46-

Closman, P.J.: "An Aquifer Model for Fissured Reservoirs," *Soc. Pet. Eng. J.* (Oct. 1975) 385-98.

Henson, W.L., Beardon, P.L., and Rice, J.D.: "A Numerical Solution to the Unsteady-State Partial-Water-Drive Reservoir Performance Problem," *Soc. Pet. Eng. J.* (Sept. 1961) 184-94; *Trans., AIME*, **222**.

Howard, D.S. Jr. and Rachford, H.H. Jr.: "Comparison of Pressure Distributions During Depletion of Tilted and Horizontal Aquifers," *J. Pet. Tech.* (April 1956) 92-98; *Trans., AIME*, **207**.

Hurst, W.: "Water Influx Into a Reservoir and Its Application to the Equation of Volumetric Balance," *Trans., AIME* (1943) **151**, 57-72.

Hutchinson, T.S. and Kemp, C.E.: "An Extended Analysis of Bottom-Water-Drive Reservoir Performance," *J. Pet. Tech.* (Nov. 1956) 256-61; *Trans., AIME*, **207**.

Lowe, R.M.: "Performance Predictions of the Murg Tex Oil Reservoir Using Unsteady-State Calculations," *J. Pet. Tech.* (May 1967) 595-600.

Mortada, M.: "Oilfield Interference in Aquifers of Non-Uniform Properties," *J. Pet. Tech.* (Dec. 1960) 55-57; *Trans., AIME*, **219**.

Mueller, T.D. and Witherspoon, P.A.: "Pressure Interference Effects Within Reservoirs and Aquifers," *J. Pet. Tech.* (April 1956) 471-74; *Trans., AIME*, **234**.

Nabor, G.W. and Barham, R.H.: "Linear Aquifer Behavior," *J. Pet. Tech.* (May 1964) 561-63; *Trans., AIME*, **231**.

Odeh, A.S.: "Reservoir Simulation—What Is It?" *J. Pet. Tech.* (Nov. 1969) 1383-88.

Stewart, F.M., Callaway, F.H., and Gladfelter, R.E.: "Comparisons of Methods for Analyzing a Water Drive Field, Torchlight Tensleep Reservoir, Wyoming," *J. Pet. Tech.* (Sept. 1954) 105-10; *Trans., AIME*, **201**.

Woody, L.D. Jr. and Moore, W.D.: "Performance Calculations for Reservoirs with Natural or Artificial Water Drives," *J. Pet. Tech.* (Aug. 1957) 245-51; *Trans., AIME*, **210**.

Chapter 39

Gas-Condensate Reservoirs

Phillip L. Moses, Core Laboratories Inc.*
Charles W. Donohoe, Core Laboratories Inc.

Introduction

The importance of gas-condensate reservoirs has grown continuously since the late 1930's. Development and operation of these reservoirs for maximum recovery require engineering and operating methods significantly different from crude-oil or dry-gas reservoirs. The single most striking factor about gas-condensate systems (fluids) is that they exist either wholly or preponderantly as vapor phase in the reservoir at the time of discovery (the critical temperature of the system is lower than the reservoir temperature). This key fact nearly always governs the development and operating programs for recovery of hydrocarbons from such reservoirs; the properties of the fluids determine the best program in each case. A thorough understanding of fluid properties together with a good understanding of the special economics involved is therefore required for optimum engineering of gas-condensate reservoirs. Other important aspects include geologic conditions, rock properties, well deliverability, well costs and spacing, well-pattern geometry, and plant costs.

Engineers have a wealth of literature on gas-condensate reservoirs available for reference. From this mass of material, Refs. 1 through 5 are especially recommended for fundamental background, and Refs. 6 through 8 are recommended for information on properties of pure compounds and their simple mixtures related to gas-condensate systems. For information regarding reservoir engineering processes and data, Refs. 5 and 9 through 16 are recommended.

The best single bibliography on gas-condensate reservoirs is that of Katz and Rzasa¹⁷; however, later pertinent literature listings will be found in Refs. 6 through 14. The collection of references in Refs. 11 and 12 is particularly recommended for case histories of various gas-condensate operations. Petroleum production papers pub-

lished by SPE (AIME)¹⁸ and API¹⁹ have been indexed separately through the years 1985 and 1953, respectively.

The practicing field engineers should have the following minimum library on gas-condensate systems available for their use: either Ref. 1, 2, or 3; Refs. 5, 9, 13, and 15; and selected volumes of Refs. 11 and 12.

Properties and Behavior of Gas-Condensate Fluids

Sloan²⁰ described the general occurrence of petroleum in the earth: "...think of all the hydrocarbons, beginning with the lightest, methane, to the heaviest asphaltic substances as a series of compounds of the same family, consisting of carbon and hydrogen in a limitless number of proportions. A hydrocarbon reservoir then, is a porous section of the sedimentary crust of the earth containing a group of hydrocarbons, which is probably unique and whose overall properties such as reservoir phase, gas/oil ratio, gasoline content, viscosity, etc., is the direct result of this composition, together with the temperature and pressure that happen to exist in this particular spot in the porous sediment.

"It is now easy to conceive of any possible combination of these hydrocarbons in a given reservoir, and it is also easy to visualize a reservoir fluid whose physical state may range from a completely dry gas in the reservoir, shading gradually through the wet gas, the condensate, the critical mixture, the highly compressible volatile liquid, the more stable light crude oil whose color is beginning to darken, the heavier crudes with decreasing solution gas, and ending with the semisolid asphalts and waxes with no measurable solution gas.

"The condensate reservoir that is the topic under discussion is therefore first a hydrocarbon reservoir. Due to the composition and proportion of the individual hydrocarbons in the mixtures, the content is gas phase at the temperature and pressure of the reservoir."

*Original chapter in 1962 edition was written by T.A. Pollard and Howard B. Bradley.

TABLE 39.1—HYDROCARBON ANALYSES AND PROPERTIES OF EXAMPLE CRUDE OILS AND GAS CONDENSATES

Component	Mole Fraction				
	Crude Oil A*	Crude Oil B*	Condensate 843**	Condensate 944**	Condensate 1143**
Carbon dioxide	—	—	0.00794	0.00130	0.00695
Nitrogen	—	—	0.01375	0.00075	0.01480
Methane	0.4404	0.5345	0.76432	0.89498	0.89045
Ethane	0.0432	0.0636	0.07923	0.04555	0.04691
Propane	0.0405	0.0466	0.04301	0.01909	0.01393
Butanes	0.0284	0.0379	0.03060	0.00958	0.00795
Pentanes	0.0174	0.0274	0.01718	0.00475	0.00424
Hexanes	0.0290	0.0341	0.01405	0.00385	0.00379
Heptanes and heavier	0.4011	0.2559	0.02992	0.02015	0.01098
Molecular weight C ₇ plus	287	247	120	144	143
Specific gravity C ₇ plus, 60°/60°F	0.9071	0.8811	0.7397	0.7884	0.7593
Viscosity C ₆ plus, Saybolt universal seconds at 100°F	100 [†]	42			
Tank-oil gravity, °API at 60°/60°F	27.4	34.5	73	53.2	61.1
Producing gas/oil ratio, cu ft/bbl	525	1,078	18,000 ±	43,000 ±	69,000 ±

*See Ref. 12, p. 327.

**See Ref. 2, Vol. I, Table 6.8, pp. 402-04.

†Viscosity of residual oil left in apparatus, approximating the hexanes-plus material.

Composition Ranges of Gas-Condensate Systems

Approximate composition indices for gas-condensate systems are the gas/liquid ratio of produced fluids (sometimes called the GOR) or its reciprocal, the liquid/gas ratio, and the gravity of the tank liquid separated out under various surface conditions. These two indices vary widely; they do not necessarily prove whether a hydrocarbon system is in the vapor phase in the reservoir.

Eilerts *et al.*² (Vol. 1, Chaps. 1 and 8) show in a survey that the liquid/gas ratios of gas-condensate systems can vary from more than 500 (very "rich") to less than 10 bbl/MMscf; tank condensate produced from the wells varied from less than 30 to more than 80°API, and more than 85% was within the range of 45 to 65°API. Eilerts *et al.*² (Vol. 1) also quote a rule of thumb that a gas-condensate system exists when the gas/liquid ratio exceeds 5,000 cu ft/bbl (200 bbl/MMscf and less) and the liquid is lighter than 50°API. This appears to be on the conservative side because there is evidence that systems exist as single-phase vapor in the reservoir when the surface gas/liquid ratio is less than 4,000 cu ft/bbl (more than 250 bbl/MMscf) and the API gravity of the liquid in the stock tanks is lower than 40°API.

A more accurate representation of the composition of gas-condensate fluids is provided by fractional analyses of the well streams coming from the reservoirs. The contrast of the fluid composition with the total stream coming from crude-oil reservoirs is fairly large for the relative amounts of the lighter vs. heavier ends of the paraffin-hydrocarbon series. For example, Eilerts *et al.*² (Vol. 1, Table 8.8) report a methane content from about 75 to 90 mol% for several gas-condensate systems, whereas Dodson and Standing²¹ report 44 and 53 mol%, respectively, for two crude-oil systems (see Table 39.1). The table, however, shows much lower heptanes-and-heavier content for the gas-condensate systems than for the crude oil. These are the two outstanding composition features of gas-condensate systems.

Pressure and Temperature Ranges of Gas-Condensate Reservoirs

Gas-condensate reservoirs may occur at pressures below 2,000 psi and temperatures below 100°F²⁰ and probably can occur at any higher fluid pressures and temperatures within reach of the drill. Most known retrograde gas-condensate reservoirs are in the range of 3,000 to 8,000 psi and 200 to 400°F. These pressure and temperature ranges, together with wide composition ranges, provide a great variety of conditions for the physical behavior of gas-condensate deposits. This emphasizes the need for very meticulous engineering studies of each gas-condensate reservoir to arrive at the best mode of development and operation.

Phase and Equilibrium Behavior

An understanding of the behavior of pure paraffin hydrocarbons and simple two-component or three-component systems (involving such compounds as methane, pentane, and decane) is of considerable benefit to the engineer working with gas-condensate reservoir problems. Excellent coverage is given this subject by Sage and Lacey¹ and a more condensed discussion by Burcik.³ Occasional review of such material will assist the engineer concerned with more complex hydrocarbon mixtures.

Chap. 23 describes the phase and equilibrium behavior of complex (multicomponent) hydrocarbon mixtures (see Fig. 23.14 and the accompanying discussion). Note that the critical state (critical point) is that state or condition at which the composition and all other intensive properties of the gas phase and the liquid phase become identical—i.e., the phases are indistinguishable. In gas-condensate reservoirs, the portion of the phase diagram to the left of and above the critical point will not be involved.

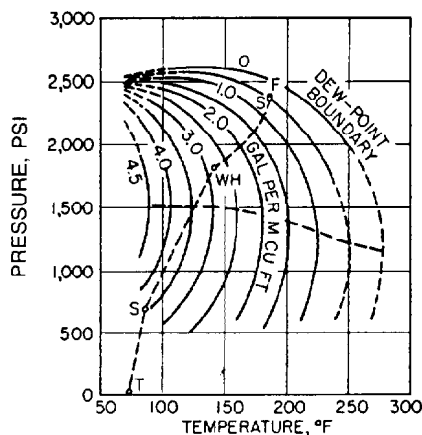


Fig. 39.1—Phase diagram of Eilerts' Fluid 843.

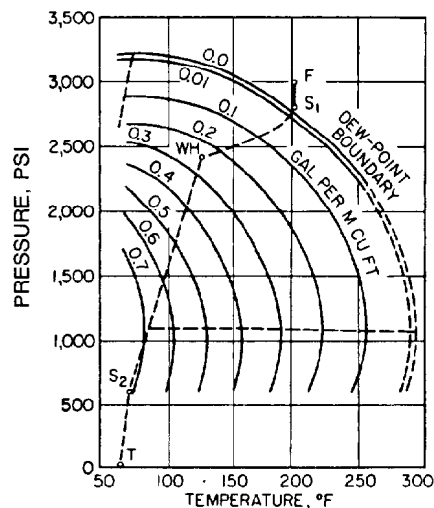


Fig. 39.2—Phase diagram of Eilerts' Fluid 1143.

The term “retrograde condensation” (discussed in Chap. 23) is used more loosely than implied by its rigorous definition.¹ In field practice, the term may imply any process where the amount of condensing liquid phase passes through a maximum, whether the process is isothermal or not.

While Fig. 23.14 provides a simplified picture of the phase diagram, reservoir engineers will find that very few quantitative phase diagrams on naturally occurring gas-condensate mixtures have been published. Figs. 39.1 through 39.3 come from extensive work² and represent quantitative measurements on the flow streams from wells in the Chapel Hill, Carthage, and Seeligson fields in Texas. The critical points are not shown because they are at temperatures below those of interest to field operations. This emphasizes that the compositions of gas-condensate systems vary widely and strongly affect the form of the phase diagrams encountered in actual gas-condensate reservoirs. These three phase diagrams represent a reasonable spread in the properties of gas-condensate systems, from a gas/liquid ratio of about 18,000 to 69,000 cu ft/bbl (56 to 14.5 bbl/MMscf). This does not mean, however, that all other gas-condensate systems would fall inside the limits of the properties suggested by these three phase diagrams.

The three cases in Figs. 39.1 through 39.3 imply that the dewpoint boundary approaches zero pressure at a relatively high temperature. Other condensate systems are believed to approximate the qualitative picture shown in Fig. 23.14 more closely. Note that all three systems exhibit both cricondentherm and cricondenbar points (maximum temperature and pressure, respectively, beyond which there is no liquid present in the vapor); the critical temperatures all fall to the left of each diagram at lower temperatures and pressures than the maxima for the dewpoint boundaries.

Liquid-content lines on phase diagrams can be represented by a number of different units. Figs. 39.1 through 39.3 use gallons per thousand cubic feet of separator gas.

The approximate behavior of condensate fluids while being produced from the reservoir into surface vessels can be represented advantageously on phase diagrams. In Fig. 39.2, for example, Line FT shows a flow path for fluids that starts at formation conditions (outside the dewpoint boundary, indicating that the formation fluids were all in vapor phase); proceeds to sandface pressure, Point S_1 , at the well; declines as the fluid rises from the bottom of the hole to the wellhead, Point WH; passes through the choke to separator conditions, Point S_2 ; and reaches Point T, representing tank conditions. The phase diagram is thus helpful to the engineer in visualizing what happens to gas-condensate fluids as they flow from the formation to the wellbore and from there to surface equipment.

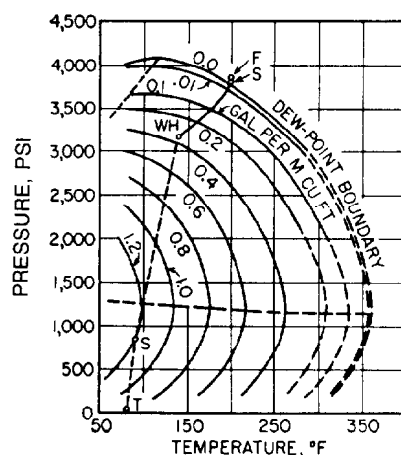


Fig. 39.3—Phase diagram of Eilerts' Fluid 944.

Methods have been proposed by Organick²² and Eilerts *et al.*² for predicting the critical temperatures and pressures of hydrocarbon mixtures and for computing the phase diagrams (including dewpoint curves) of gas-condensate fluids. The dependability of these methods for a wide range of gas-condensate compositions has not yet been established. For reservoir engineering work, direct laboratory measurements of phase diagrams or of pressure-depletion behavior are necessary because of the large recoveries at stake. Laboratory work may not be required for other problems.

Gas/Liquid Ratios and Liquid Contents of Gas-Condensate Systems

As discussed earlier, it is difficult to specify whether a hydrocarbon system is in the vapor phase in the reservoir from measurements of field gas/liquid ratio and tank-oil gravity. Fluid production with tank-oil gravities as low as 30° API and gas/liquid ratios as low as 3,000 cu ft/bbl may be from true gas-condensate systems; this possibility should always be checked by laboratory measurements of phase behavior for these and intermediate values.

"Liquid content" and "gas/liquid ratio" can be direct reciprocals, depending on the type of problem considered. The terms must be carefully defined in each case because gas-condensate systems in the field frequently undergo different types of separating procedures that involve several stages before the final liquid phase ("liquid" means hydrocarbon liquid unless otherwise specified) reaches the tanks at atmospheric pressure. To study the properties of gas-condensate fluids at reservoir conditions, it is convenient to define gas/liquid ratios and liquid contents on the basis of the gas and liquid outputs of the first-stage separator through which the fluids pass. These two output streams then represent the total composition of the gas-condensate fluid in the reservoir if sampling, producing, and measuring conditions have been properly set and maintained. Other gas/liquid ratios may be reported, however, including the total gas output of all stages of separation divided by the tank-liquid volumes corresponding to the gas output; note that the total gas output would include a measurement of tank vapors as well as separator gas to represent the full composition of the wellstream.

The gas/liquid ratio at stock-tank conditions may be roughly approximated when field facilities are not available for measurements. The gas and liquid flow rates from the high-stage separator are observed and a liquid sample collected from the separator in a stainless-steel cylinder of known volume. If all the cylinder contents are bled into a calibrated graduate at atmospheric pressure and the volume of the resultant liquid phase is compared with the original liquid volume, an approximate value of the liquid-phase shrinkage may be determined. From this, the high-stage gas/liquid ratio may be converted to stock-tank conditions. This procedure ignores the volume of gas liberated between high-stage separator and stock-tank conditions. This volume can be approximated by using a calibrated glass separator with gas meter attached in place of the graduate. Ignoring this gas volume adds further errors to those resulting from not simulating the existing field stage separation conditions. The higher the first-stage separation pressure, the greater the error in total gas volume of the gas/liquid ratio. This is only an approx-

imate method that may be used when there are no intermediate separator stages and stock tanks for individual well measurements and when the atmospheric temperature and pressure do not vary appreciably from stock-tank conditions.

Gas/liquid ratios usually are reported in cubic feet per barrel of liquid (or thousands of cubic feet per barrel) and liquid contents or liquid/gas ratios in barrels of liquid per million standard cubic feet of gas. The separator streams used in the ratio must be specified.

Properties of Separated Phases

The properties of both liquid and gas phases separated from gas-condensate streams can vary considerably. One of the dominant properties of the gas is high methane content. Eilerts *et al.*² (Vol. 1, Chap. 8) list the compositions of the gas and liquid phases of eight gas-condensate systems. Methane contents of the gas phases (simulated from field separators) varied from about 0.83 to 0.92 mole fraction; the hexanes and heavier ("hexanes plus") varied from 0.004 to about 0.008 mole fraction. The liquid phases varied from about 0.1 to nearly 0.3 mole fraction methane; hexanes plus varied from about 0.4 to 0.7 mole fraction.

In the absence of measured data, properties of the separated phases of gas-condensate systems (including volumetric and density behavior) can be approximated by methods described in Chaps. 20 through 23, especially Chaps. 20 and 22 (see also Refs. 9 and 14).

Viscosities of Gas-Condensate Systems

The viscosity of a gas-condensate system is of interest in various reservoir calculations, particularly with respect to cycling operations and the representation of such reservoirs in computer models. Whenever possible, viscosity of the vapor phase at reservoir conditions should be measured directly. Carr *et al.*²³ presented a method to estimate the viscosities of gas systems from a knowledge of compositions or specific gravities (see also Chap. 20 and Ref. 14).

Viscosities of separate gas and liquid phases at the surface conditions usually encountered can be obtained by direct measurement or by the use of the correlations for gas previously mentioned and the correlation of Chew and Connally²⁴ for liquid (see also Chap. 22). Viscosity information on separated materials is needed mainly for separator or plant residue gases to be injected during cycling and for some types of reservoir calculations.

Gas-Condensate Well Tests and Sampling

Proper testing of gas-condensate wells is essential to ascertain the state of the hydrocarbon system at reservoir conditions and to plan the best production and recovery program for the reservoir. Without proper well tests and samples, it would be impossible to determine the phase conditions of the reservoir contents at reservoir temperature and pressure accurately and to estimate the amount of hydrocarbon materials in place accurately.

Tests are made on gas-condensate wells for a number of specific purposes: to obtain representative samples for laboratory analysis to identify the composition and properties of the reservoir fluids; to make field determinations on gas and liquid properties; and to determine formation

and well characteristics, including productivity, producibility, and injectivity. The first consideration for selecting wells for gas-condensate fluid samples is that they be far enough from the "black-oil ring" (if present) to minimize any chance that the liquid oil phase will enter the well during the test period. A second and highly important consideration is the selection of wells with as high productivities as possible so that minimum pressure draw-down will be suffered when the reservoir fluid samples are acquired.

Well Conditioning

Proper well conditioning is essential to obtain representative samples from the reservoir. The best production rates before and during the sampling procedure have to be considered individually for each reservoir and for each well. Usually the best procedure is to use the lowest rate that results in smooth well operation and the most dependable measurements of surface products. Minimum draw-down of bottomhole pressure during the conditioning period is desirable and the produced gas/liquid ratio should remain constant (within about 2%) for several days; the less-permeable reservoirs require longer periods. The farther the well deviates from constant produced gas/liquid ratio, the greater the likelihood that the samples will not be representative.

Recombined separator samples from gas-condensate wells are considered more representative of the original reservoir fluid than subsurface samples.

Accurate measurements of hydrocarbon gas and liquid production rates during the well-conditioning and well-sampling tests are necessary because the laboratory tests will later be based on fluid compositions recombined in the same ratios as the hydrocarbon streams measured in the field. The original reservoir fluid cannot be simulated in the laboratory unless accurate field measurements of all the separator streams are taken. (Gas/liquid ratios may be reported and used in several different forms, as discussed previously.) If the produced gas/condensate (gas/liquid) ratio from field measurements is in error by as little as 5%, the dewpoint pressure determined in the laboratory may be in error by as much as 100 psi. Water production rates should be measured separately and produced water excluded as much as possible from hydrocarbon samples sent to the laboratory.

Separator pressure and temperatures should remain as constant as possible during the well-conditioning period; this will help maintain constancy of the stream rates and thus of the observed hydrocarbon gas/liquid ratio. If the well is being prepared during a period when atmospheric temperatures vary considerably from night to day, reasonably consistent average temperatures and pressures on the several vessels during the conditioning period should be adequate.

Field Sampling and Test Procedures

After the conditioning period has proceeded long enough to show that producing conditions are steady, exacting measurement methods must be used to obtain representative samples. The mechanics of well sampling is partially covered in Chaps. 12 through 14, 16, and 17. The help of experienced laboratory personnel is advisable in

acquiring gas and condensate-liquid samples. Certain minimum items of information in addition to all stream rates are essential, including regular readings of the pressures and temperatures of all vessels sampled, and of tubing heads and casing heads where available, and a recorded history of the well conditions before and during sampling, along with the actual mechanics of the sampling steps. Other information acquired during the sampling period that would help to explain reservoir and well conditions should also be recorded because it is useful in interpreting the results of the tests.

Care must be taken that the compositions of gas and liquid samples obtained are representative and are properly preserved for laboratory analyses. API RP 44²⁵ outlines appropriate sampling methods.

For cases when the liquid-phase sample is obtained at a low temperature (from low-temperature separation equipment), triethylene-glycol/water mixtures are convenient for collecting the samples. Ten percent or more of the cylinder volume for liquid-phase samples should be gas to prevent excessive pressure that could result from temperature rise during subsequent shipment. This 10% "gas cap" can be effected by closing the cylinder sample-inlet valve when 90% of the glycol/water mixture has been displaced and then carefully withdrawing nearly all the remaining mixture from the bottom of the cylinder without losing the oil phase.

The volumes of fluids requested for laboratory testing should be acquired during the sampling period, plus a reasonable amount (25% or more) of extra sample materials in separate containers for emergency use should some of the main samples be lost by leakage or other adversity between the field site and the laboratory.

At the end of actual sampling mechanics in the field, the well should remain on stream for a reasonable period of time, and its producing rate, gas/liquid ratio, and various pressures and temperatures should be observed to confirm that they are consistent with the information developed before and during the sampling period. Any radical changes should be analyzed carefully to decide whether resampling may be necessary to ensure accuracy of the samples and well statistics obtained during the sampling period.

Equipment is available for making some determinations of gas-condensate properties in the field.² Among these properties are the gas/liquid ratios of several vessels simulating various separation conditions (numbers of stages, pressures and temperatures of the stages, and other conditions) and the "gasoline content" of the overhead gas at each stage. If hydrogen sulfide and carbon dioxide are present in the production streams, special sampling procedures should be used and the samples should be taken in stainless-steel cylinders. These corrosive gases could react with the sample cylinders during shipment.

Field determinations of the hydrocarbon compositions of streams from gas-condensate wells can be made with appropriate fractionation equipment in mobile laboratories. Eilerts *et al.*² described such equipment and the test procedures for determining the effect of individual hydrocarbons on liquid/gas ratios at different separation pressures and temperatures. These tests can assist in determining optimum field separation conditions for given production objectives. They require special equipment and experienced personnel.

Measurements of gas-condensate well productivity, producibility, and injectivity are of considerable importance for planning overall field operations and size of plants for either gasoline recovery or condensate-liquids recovery and cycling, as bases for contracts for deliverability from a reservoir for pipeline purposes, and for various other needs. This topic is discussed more fully later; test procedures are described in Chap. 33 and in several published standards and regulations.²⁶⁻²⁹

Sample Collection and Evaluation

In taking samples for recombination to evaluate a gas-condensate reservoir, the samples of gas and samples of liquid usually are taken from the first stage of separation. A representative portion of all the hydrocarbons produced from the well will be contained in these two samples. The first step in the laboratory study is to evaluate the samples taken. The first test is to measure the bubblepoint of the separator liquid. The bubblepoint should correspond to the separator pressure at separator temperature at the time the samples were taken.

The hydrocarbon composition of the separator samples should then be determined by chromatography or low-temperature fractional distillation or a combination of both. An example of the composition of typical separator products are shown in Table 39.2. These compositions may be evaluated by calculation of the equilibrium ratio for each component (see Chap. 23). The equilibrium ratio for a component is the mole percent of that component in the vapor phase divided by the mole percent of the same component in the liquid phase. As an example, the equilibrium ratio for methane in Table 39.2 is calculated by the equation

$$K_1 = y_1/x_1 = 83.01/10.76 = 7.71,$$

where

- K_1 = the equilibrium ratio for methane,
 y_1 = methane in the vapor phase, mol%, and
 x_1 = methane in the liquid phase, mol%.

The experimental equilibrium ratio for methane is 7.71 for the temperature and pressure existing in the field separator at the time of sampling.

The equilibrium ratios for each of the hydrocarbons methane through hexane are calculated in a similar manner. These data can then be compared with equilibrium ratios, such as those published in Ref. 16. If the equilibrium ratios compare favorably, then the samples are in equilibrium and the study should continue. If they do not compare well, then new samples should be obtained before proceeding.

Recombination of Separator Samples

The samples are now ready to be recombined in the same ratio that they were produced. Because we have samples of first-stage separator gas and first-stage separator liquid, we must have the produced gas/liquid ratio in the same form. If the producing gas/liquid ratio was measured in the field in this form, then we can proceed directly with the recombination. If the ratio was measured in the field in the form of primary-separator gas per barrel of second-stage separator liquid or per barrel of stock-tank liquid, then a laboratory shrinkage test must be run to simulate field separation conditions. The shrinkage obtained can then be used to convert the field-measured ratio to the form necessary for the recombination. Once the separator products have been recombined, the composition can be measured and compared with the calculated composition. This will check the accuracy of the physical recombination.

TABLE 39.2—HYDROCARBON ANALYSES OF SEPARATOR PRODUCTS AND CALCULATED WELL STREAM

Component	Separator Liquid (mol %)	Separator Gas		Well Stream	
		mol %	gal/1,000 cf gas	mol %	gal/1,000 cf gas
Hydrogen sulfide	0.00	0.00		0.00	
Carbon dioxide	0.00	0.01		0.01	
Nitrogen	0.01	0.13		0.11	
Methane	10.76	83.01		68.93	
Ethane	6.17	9.23	2.454	8.63	2.295
Propane	8.81	4.50	1.231	5.34	1.461
iso-Butane	2.85	0.74	0.241	1.15	0.374
n-Butane	7.02	1.20	0.376	2.33	0.730
iso-Pentane	3.47	0.31	0.113	0.93	0.338
n-Pentane	3.31	0.25	0.090	0.85	0.306
Hexanes	8.03	0.21	0.085	1.73	0.702
Heptanes plus	49.57	0.41	0.185	9.99	6.006
Total	100.00	100.00	4.775	100.00	12.212

Properties of heptanes plus

API gravity at 60°F	39.0	
Density, g/cm ³ at 60°F	0.8293	0.827
Molecular weight	160	158

Calculated separator gas gravity (air = 1.000)	0.699
Calculated gross heating value for separator gas per cubic foot of dry gas at 14.65 psia and 60°F, Btu	1,230
Primary-separator-gas/separator-liquid ratio at 60°F, scf/bbl*	3,944
Primary-separator-liquid/stock-tank-liquid ratio at 60°F, bbl	1.191
Primary-separator-gas/well-stream ratio, Mscf/MMscf	805.19
Stock-tank-liquid/well-stream ratio, bbl/MMscf	171.4

*Primary separator gas and primary separator liquid collected at 440 psig and 87°F.

Dewpoint and Pressure/Volume Relations

The laboratory personnel will next measure the pressure/volume relations of the reservoir fluid at reservoir temperature with a visual cell. This is a constant-composition expansion and furnishes the dewpoint of the reservoir fluid at reservoir temperature and the total volume of the reservoir fluid as a function of pressure. The volume of liquid at pressures below the dewpoint as a percent of the total volume may also be measured. Phase diagrams can be developed by measuring the liquid volumes at several other temperatures. Table 39.3 is an example of the dewpoint determination and pressure/volume relations of a gas-condensate reservoir fluid.

Simulated Pressure Depletion

Pressure depletion of gas-condensate reservoirs may be simulated in the laboratory by use of high-pressure visual cells. In these depletion studies made in the laboratory, the assumption is that the retrograde liquid that condenses in the reservoir rock will not achieve a sufficiently high saturation to become mobile. This assumption appears to be valid except for very rich gas-condensate reservoirs. For very rich gas-condensate reservoirs where the retrograde liquid may achieve a high enough saturation to migrate to producing wells, the gas/liquid relative permeability data should be measured for the reservoir rock system. These data can then be used to adjust the predicted recovery from the reservoir.

Table 39.4 is an example of a depletion study on a gas-condensate reservoir fluid. Note from Table 39.4 that the dewpoint pressure of this reservoir fluid is 6,010 psig. The composition listed in the 6,010-psig-pressure column in Table 39.4 is the composition of the reservoir fluid at the dewpoint and exists in the reservoir in the gaseous state.

TABLE 39.3—PRESSURE/VOLUME RELATIONS OF RESERVOIR FLUID AT 256°F (Constant-Composition Expansion)

Pressure (psig)	Relative Volume	Deviation Factor, z
7,500	0.9341	1.328
7,000*	0.9523	1.264**
6,500	0.9727	1.199
6,300	0.9834	1.175
6,200	0.9891	1.163
6,100	0.9942	1.150
6,010†	1.0000	1.140‡
5,950	1.0034	
5,900	1.0076	
5,800	1.0138	
5,600	1.0267	
5,300	1.0481	
5,000	1.0749	
4,500	1.1268	
4,000	1.2024	
3,500	1.3096	
3,000	1.4689	
2,500	1.7169	
2,100	2.0191	
1,860	2.2747	
1,683	2.5150	
1,460	2.9087	
1,290	3.3173	
1,160	3.7153	
1,050	4.1342	

*Reservoir pressure.

**Gas expansion factor = 1.545 Mscf/bbl.

†Dewpoint pressure.

‡Gas expansion factor = 1.471 Mscf/bbl.

TABLE 39.4—DEPLETION STUDY AT 256°F

Component	Reservoir Pressure, psig							
	6,010	5,000	4,000	3,000	2,100	1,200	700	700*
Hydrocarbon Analysis of Produced Well Stream, mol %								
Carbon dioxide	0.01	0.01	0.01	0.01	0.01	0.01	0.01	Trace
Nitrogen	0.11	0.12	0.12	0.13	0.13	0.12	0.11	0.01
Methane	68.93	70.69	73.60	76.60	77.77	77.04	75.13	11.95
Ethane	8.63	8.67	8.72	8.82	8.96	9.37	9.82	4.10
Propane	5.34	5.26	5.20	5.16	5.16	5.44	5.90	4.80
iso-Butane	1.15	1.10	1.05	1.01	1.01	1.10	1.26	1.57
n-Butane	2.33	2.21	2.09	1.99	1.98	2.15	2.45	3.75
iso-Pentane	0.93	0.86	0.78	0.73	0.72	0.77	0.87	2.15
n-Pentane	0.85	0.76	0.70	0.65	0.63	0.68	0.78	2.15
Hexanes	1.73	1.48	1.25	1.08	1.01	1.07	1.25	6.50
Heptanes plus	9.99	8.84	6.48	3.82	2.62	2.25	2.42	63.02
	100.00	100.00	100.00	100.00	100.00	100.00	100.00	100.00
Molecular weight of heptanes plus	158	146	134	123	115	110	109	174
Density of heptanes plus	0.827	0.817	0.805	0.794	0.784	0.779	0.770	0.837
Deviation factor, z								
Equilibrium gas	1.140	1.015	0.897	0.853	0.865	0.902	0.938	
Two-phase	1.140	1.016	0.921	0.851	0.799	0.722	0.612	
Well stream produced, cumulative % of initial	0.000	6.624	17.478	32.927	49.901	68.146	77.902	

*Composition of equilibrium liquid phase.

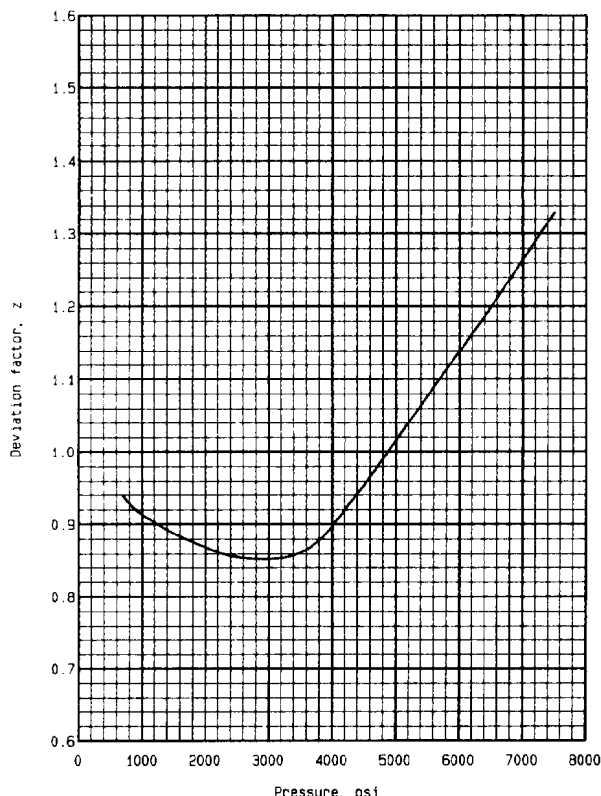


Fig. 39.4—Deviation factor, z , of well stream during depletion at 256°F.

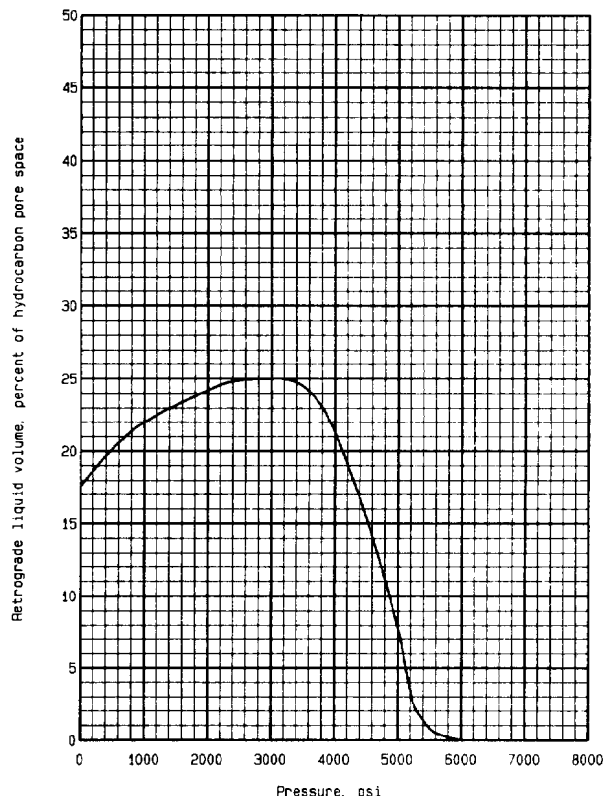


Fig. 39.5—Retrograde condensation during depletion.

The depletion study is performed by expanding the reservoir fluid in the cell by withdrawing mercury from the cell until the first depletion pressure is reached; this is 5,000 psig in the example. The fluid in the cell is brought to equilibrium and the volume of retrograde liquid is measured. The mercury is then reinjected into the cell and, at the same time, gas is removed from the top of the cell so that a constant pressure is maintained. Mercury is injected into the cell until the hydrocarbon or reservoir volume of the cell is the same as the volume when the test was begun at the dewpoint pressure. The gas volume removed from the cell is measured at the depletion pressure and reservoir temperature. The gas removed is charged to analytical equipment where its composition is determined and its volume is measured at atmospheric pressure and temperature. The composition determined is that listed in Table 39.4 under the heading 5,000 psig. The volume of gas produced in this manner is then divided by the standard volume of gas in the cell at the dewpoint pressure. The produced volume is presented in Table 39.4 as cumulative well stream produced.

As mentioned earlier, as the gas is removed from the top of the cell, its volume is measured at the depletion pressure and reservoir temperature. From this volume, the "ideal volume" of this displaced volume may be calculated with the ideal-gas law. When the ideal volume is divided by the actual volume of the gas produced at standard conditions, we get the deviation factor, z , for the produced gas. This is listed in Table 39.4 under

"Deviation Factor z , equilibrium gas" and plotted in Fig. 39.4. The actual volume of gas remaining in the cell at this point is the gas originally in the cell at the dewpoint pressure minus the gas produced at the first depletion level. If we divide the actual volume remaining in the cell into the calculated ideal volume remaining in the cell at this first depletion pressure, we obtain the two-phase deviation factor shown in Table 39.4. We call this value a two-phase deviation factor because the material remaining in the cell after the first depletion level is actually gas and retrograde liquid and the actual gas volume we calculated above is the gas volume plus the vapor equivalent of the retrograde liquid. The two-phase z factor is significant in that it is the z factor of all the hydrocarbon material remaining in the reservoir. It is the two-phase z factor that should be used when a p/z -vs.-cumulative-production plot is made in evaluating gas-condensate production.

This series of expansions and constant-pressure displacements is repeated at each depletion pressure until an arbitrary abandonment pressure is reached. The abandonment pressure is considered arbitrary because no engineering or economic calculations have been made to determine this pressure for the purpose of the reservoir-fluid study.

In addition to the composition of the produced well stream at the final depletion pressure, the composition of the retrograde liquid was also measured. These data are included as a control composition in the event the study is used for compositional material-balance purposes.

The volume of retrograde liquid measured during the course of the depletion study is shown in Fig. 39.5 and Table 39.5. The data are shown as a percent of hydrocarbon pore space. These are the data that should be used in conjunction with relative permeability data and water saturation data to determine the extent of retrograde liquid mobility. As mentioned earlier, this is a significant factor only with extremely rich gas-condensate reservoirs.

Also obtained from the reservoir fluid study is Table 39.6. This table was calculated with the results of the laboratory depletion study described previously applied to a unit-volume reservoir. The unit volume chosen was 1,000 Mscf in place at the dewpoint pressure (note the 1,000 Mscf in Table 39.6 in the first column of numbers). Equilibrium ratios were then used to calculate the amount of stock-tank liquid, primary-separator gas, second-stage gas, and stock-tank gas contained in the unit-volume reservoir. The equilibrium ratios used were for the separator conditions listed at the bottom of Table 39.6. The separator conditions used for these calculations should be the conditions in use in the field or those conditions anticipated for the field. The relative amounts of gas and liquid produced will be a function of the surface separation conditions, among other things. These calculations may be made at a variety of conditions to determine optimum separator pressures and temperatures. For the purpose of this table, production was begun at the dewpoint pressure. The amount of total well effluent (well stream) produced from this unit-volume reservoir as a function of pressure is listed in the table. The amount of stock-tank liquid produced as a function of pressure is also listed. The primary-separator gas, second-stage gas, and stock-tank gas are presented in a similar manner. Various other factors associated with the production of the gas and condensate from this reservoir are also presented in the table.

TABLE 39.5—RETROGRADE CONDENSATION DURING GAS DEPLETION AT 256°F

Pressure (psig)	Retrograde Liquid Volume (% hydrocarbon pore space)
6,010*	0.0
5,950	Trace
5,900	0.1
5,800	0.2
5,600	0.5
5,300	2.0
5,000**	7.8
4,000	21.3
3,000	25.0
2,100	24.4
1,200	22.5
700	21.0
0	17.6

*Dewpoint pressure.

**First depletion level.

Table 39.6 shows the initial stock-tank liquid in place to be 181.74 bbl for this unit-volume reservoir. After production to 700 psig, 51.91 bbl had been produced. The difference between these two numbers (181.74 - 51.91), 129.83 bbl, is the amount of retrograde loss or liquid still unproduced at 700 psig expressed in terms of stock-tank barrels. The value of 181.74 bbl may be considered the recovery by pressure maintenance, assuming 100% conformance and 100% displacement efficiency.

Table 39.7 furnishes the gravity of the stock-tank liquid that may be expected to be produced as a function of reservoir pressure. Also reported are the instantaneous gas/liquid ratios as a function of reservoir pressure.

TABLE 39.6—CALCULATED CUMULATIVE RECOVERY DURING DEPLETION PER MMscf OF ORIGINAL FLUID

	Initial in Place	Reservoir Pressure (psig)						
		6,010	5,000	4,000	3,000	2,100	1,200	700
Well stream, Mscf	1,000	0	66.24	174.78	329.27	499.01	681.46	779.02
Normal temperature separation*								
Stock-tank liquid, bbl	181.74	0	10.08	21.83	31.89	39.76	47.36	51.91
Primary separator gas, Mscf	777.15	0	53.18	145.16	283.78	440.02	608.25	696.75
Second-stage gas, Mscf	38.52	0	2.26	5.17	8.03	10.51	13.21	14.99
Stock-tank gas, Mscf	38.45	0	2.29	5.38	8.73	11.85	15.51	18.05
Total plant products in primary separator gas, gal								
Ethane	1,841	0	126	344	674	1,050	1,474	1,709
Propane	835	0	58	163	331	526	749	873
Butanes (total)	368	0	26	73	155	256	374	441
Pentanes plus	179	0	12	35	73	122	177	206
Total plant products in second-stage gas, gal								
Ethane	204	0	12	27	42	55	70	80
Propane	121	0	7	17	27	36	47	54
Butanes (total)	53	0	3	8	13	17	23	27
Pentanes plus	23	0	1	3	5	7	10	11
Total plant products in well stream, gal								
Ethane	2,295	0	153	404	767	1,171	1,626	1,880
Propane	1,461	0	95	250	468	707	979	1,137
Butanes (total)	1,104	0	70	178	325	486	674	789
Pentanes plus	7,352	0	408	890	1,322	1,680	2,037	2,249

*Primary separator at 450 psig and 75°F; second-stage separator at 100 psig and 75°F, stock tank at 75°F.

These data may be calculated without the benefit of rock properties or interstitial water values. The assumption is that the retrograde liquid does not achieve significant mobility. Because only one phase is flowing, water and hydrocarbon liquid saturations do not enter into the calculations. The assumption that the retrograde liquid does not flow in the reservoir except in the drawdown area immediately around the wellbore appears to be good. Only with very rich reservoirs does movement of retrograde liquid add significantly to well production.

It was mentioned earlier that the most popular form of material balance on a gas-condensate reservoir is the p/z -vs.-cumulative-production curve. It was stated that the z factor to be used must be the two-phase z factor. The cumulative production must be the total production from the well. This includes, in most instances, the first-stage separator gas, second-stage separator gas, tank vapors, and the vapor equivalent of the stock-tank liquid. The most accurate production figures from a gas-condensate field are usually the sales-gas volumes. This usually includes the first- and second-stage separator gas. To make the p/z -vs.-cumulative plot, the tank vapors and the vapor equivalent of the stock liquid must be accounted for. Without the benefit of laboratory data, the tank vapors must be estimated and the vapor equivalent of the stock-tank liquid calculated with an average or estimated number.

Table 39.7 furnishes the data to make these calculations. If sales gas is the primary- and second-stage gas, and the average reservoir pressure is 5,000 psig, then the total well-stream volume can be calculated by dividing the sales volume by 0.83704. This factor accounts for the tank vapors and the vapor equivalent of the tank liquid. If the sales gas is only the first-stage gas, then the appropriate factor would be 0.80285.

Operation by Pressure Depletion

Pressure-depletion gas-condensate reservoir behavior can be predicted from the laboratory data described previously, or if necessary, by various correlation and computation procedures that provide similar information (with less ac-

curacy) on the basis of the composition of the gas-condensate system. Whenever possible, the predictions should be made with actual laboratory data because the better accuracy obtained at the reservoir conditions is justified by the large gas and liquid reserves involved in reservoir calculations.

Predictions With Laboratory-Derived Data and Hydrocarbon Analysis

With the assumption that the liquid condensate in the reservoir during a pressure-depletion operation stays in place (does not build up sufficiently to provide liquid-phase permeability for flow), reservoir behavior can be predicted from the laboratory constant-composition depletion study discussed previously. Pertinent information is shown in Tables 39.3 through 39.6 and Figs. 39.4 and 39.5.

Liquid-phase change in the reservoir is shown in Fig. 39.5 derived from Table 39.5. Note that the amount of liquid remaining in the reservoir passes through a maximum but does not return to zero, indicating that pressure-depletion operations leave some liquid hydrocarbons behind at abandonment pressure. Economic analyses of pressure-depletion operations are necessary for estimating the magnitude of this loss and its effect on development and operating policy for the reservoir.

The ultimate recoveries by pressure depletion of wet gas, condensate, and plant products can be calculated for the reservoir described in Table 39.8 by use of the data given in Table 39.6.

Gas in place at original pressure:

$$(500 \times 10^6)(1.545)(178.1) = 137,582 \text{ MMscf.}$$

Gas in place at dewpoint pressure:

$$(500 \times 10^6)(1.471)(178.1) = 130,992 \text{ MMscf.}$$

Wet gas produced to dewpoint pressure:

$$137,582 - 130,992 = 6,590 \text{ MMscf.}$$

TABLE 39.7—CALCULATED INSTANTANEOUS RECOVERY DURING DEPLETION

	Reservoir Pressure (psig)						
	6,010	5,000	4,000	3,000	2,100	1,200	700
Normal temperature separation*							
Stock-tank liquid gravity at 60°F, °API	49.3	51.7	55.4	60.4	64.6	67.5	68.6
Separator-gas/well-stream ratio, Mscf/MMscf							
primary-separator gas only	777.15	802.85	847.45	897.28	920.44	922.04	907.14
primary and second-stage separator gases	815.67	837.04	874.26	915.77	935.04	936.84	925.38
Separator-gas/stock-tank-liquid ratio, scf/STB							
primary-separator gas only	4,276	5,277	7,828	13,774	19,863	22,121	19,475
primary and second-stage separator gases	4,488	5,502	8,076	14,058	20,178	22,476	19,867
Recovery from smooth well stream compositions, gal/min							
Ethane plus	12,212	10,953	9,175	7,509	6,851	6,970	7,574
Propane plus	9,917	8,648	6,856	5,164	4,469	4,479	4,963
Butanes plus	8,456	7,209	5,434	3,752	3,057	2,990	3,349
Pentanes plus	7,352	6,158	4,437	2,800	2,108	1,959	2,171

* Primary separator at 450 psig and 75°F; second-stage separator at 100 psig and 75°F; stock tank at 75°F.

Wet gas produced from dewpoint pressure to abandonment:

$$(130,992)(0.77902) = 102,045 \text{ MMscf.}$$

Total wet gas produced:

$$6,590 + 102,045 = 108,635 \text{ MMscf.}$$

Condensate produced to dewpoint pressure:

$$(6,590)(181.74) = 1,197,667 \text{ bbl.}$$

Condensate produced from dewpoint pressure to abandonment:

$$(130,992)(51.91) = 6,799,795$$

Total condensate produced:

$$1,197,667 + 6,799,795 = 7,997,462$$

Percent recoveries by pressure depletion from dewpoint pressure to abandonment:

$$\text{Wet gas} = \frac{102,045}{130,992} \times 100 = 77.9\%;$$

$$\text{Condensate} = \frac{6,799,795}{181.74 \times 130,992} \times 100 = 28.6\%.$$

The total plant products can be calculated in a similar manner, depending on the flow streams to be processed and the recovery efficiencies anticipated.

Predictions With Vapor/Liquid Equilibrium Calculation and Correlations

In the absence of direct laboratory data on a specific gas-condensate system, pressure-depletion behavior can be estimated with vapor/liquid equilibrium ratios (i.e., equilibrium constants, equilibrium factors or K values) to compute the phase behavior when the composition of the total gas-condensate system is known. Correlations for estimating phase volumes must also be available.

When multicomponent hydrocarbon gases and liquids exist together under pressure, part of the lighter hydrocarbons (light ends) are dissolved in the liquid phase, and part of the heavier hydrocarbons (heavy ends) are vaporized in the gas phase. A convenient concept to describe the behavior of specific components quantitatively is the equilibrium ratio. The ratios vary considerably with the pressure, temperature, and composition of the system involved.

The equilibrium ratio is defined as the mole fraction of a given constituent in the vapor phase divided by the mole fraction of the same constituent in the liquid phase, the two phases existing in equilibrium with each other. The equilibrium ratio is designated as K . The basis for this definition is discussed in Chap. 23 and by Standing.⁹ Fig. 23.21 illustrates the behavior of equilibrium ratios for a particular system and shows the rather wide variation possible for a given constituent at different pressures. The

TABLE 39.8—FORMATION AND FLUID DATA FOR A GAS-CONDENSATE RESERVOIR

Original reservoir pressure, psig	7,000
Dewpoint pressure, psig	6,010
Assumed abandonment pressure, psig	700
Average reservoir temperature, °F	256
Hydrocarbon pore space (by volumetrics), cu ft	500×10^6
Gas expansion factor (B_g) of produced fluid at original pressure, Mscf/bbl	1.545
Gas expansion factor (B_g) of produced fluid at dewpoint, Mscf/bbl	1.471

figure shows a tendency of the equilibrium ratios to converge isothermally to a value of $K=1$ at a specific pressure. The pressure is properly called the "apparent convergence pressure."⁹ The selection of equilibrium-ratio values for calculations usually is based on the system's apparent convergence pressure, which can change in a pressure-depletion process because of changing system composition with pressure decline.

Large inaccuracies can occur in pressure-depletion calculations with equilibrium ratios when the heavier hydrocarbons (e.g., heptanes and heavier) are not adequately described. To obtain satisfactory results in calculating pressure-depletion behavior of a gas-condensate system, an extended analysis of the C_{7+} fraction should be made. A determination of the molar distribution of C_{7+} through at least C_{25} is recommended. As can be observed in Table 39.4, the C_{7+} component of the subject gas-condensate fluid exhibited a change in molecular weight from 158 at a pressure of 6,010 psig to 109 at a pressure of 700 psig. The change in density of the C_{7+} component was from 0.827 to 0.778 over the same pressure range. Table 39.4 also shows that at 700 psig, the molecular weight of the C_{7+} in the liquid phase is 174, compared to 109 in the gas phase, and the density is 0.837 in the liquid phase, compared to 0.778 in the gas phase. This change in composition of the C_{7+} fraction with pressure reduction leads to large errors in the vapor/liquid split of the C_{7+} fraction when equilibrium ratios are used and in the resultant molecular weight and density of the calculated gas and liquid volumes.

Should such an extended analysis of the C_{7+} component not be available, then a statistical split should be made that maintains the integrity of the average molecular weight and density of the C_{7+} component. Once the C_{7+} component has been divided into multiple pseudocomponents, the physical properties required to make reservoir flash calculations must be developed.

Whitson³⁰ presents a method for determining the molar distribution of single-carbon-number (SCN) groups that are defined by their boiling points as a function of each group's molecular weight. To make the distribution, a three-parameter gamma probability function is used. Whitson also presents equations for calculating the required physical properties with the Watson³¹ characterization factor. This method can be easily programmed for a personal computer and permits rapid development of molar distribution and physical properties. A statistical expansion of the C_{7+} component of the gas-condensate fluid presented in Table 39.2 has been made with the technique Whitson described. The results of this expansion

are presented in Table 39.9. The ability to calculate accurately the pressure-depletion performance of a gas-condensate reservoir depends on proper characterization of the vapor/liquid equilibrium ratios (K values) of the hydrocarbon system.

Equilibrium ratios for nonhydrocarbon components and hydrocarbons C_1 through C_{10} can be found in the *Engineering Data Book*.¹⁶ Hoffman *et al.*³² and Cook *et al.*³³ have presented methods for developing K values for the pseudocomponents. Hoffman *et al.*'s procedure can be programmed easily for a personal computer for rapid development of equilibrium ratios. An alternative method is to plot the methane and normal pentane K values as a function of their boiling points on a semilog graph for each depletion pressure to be calculated. An equation can be determined for a straight line connecting these two points. The K value for each of the other components and pseudocomponents can then be calculated for each pressure point with their individual boiling points. This method of obtaining K values was used in the earlier example calculation. There are some limitations on the accuracy of the data derived by these methods unless some measured data on similar hydrocarbon systems are available. However, the data should be usable for the quick, rough approximations often needed in the preliminary reservoir evaluation stage. The C_1 through C_6 composition of the gas-condensate fluid presented in Table 39.2 was used to develop a K -value relationship for the extended C_{7+} compositions. The resultant relationship is presented in Fig. 39.6.

Chap. 23 describes the general techniques of the use of vapor/liquid equilibrium ratios to compute the phase compositions and magnitudes of hydrocarbon gas/liquid mixtures. Standing⁹ also has an excellent presentation of this usage, including a discussion of the serious errors that can result in calculating the phase behavior of gas-condensate systems. When these methods are used to estimate the pressure-depletion behavior of a gas-condensate reservoir, the following procedure is used.

1. Assume that the original (known) composition flashes from original pressure (and volume) to a lower pressure, at which the compositions and amounts (in moles) of the liquid and gas phases are computed with the best K values available.

2. Estimate the volume of each phase with the methods discussed below.

3. Assume that enough vapor-phase volume is removed (produced) at constant pressure to cause the remaining gas plus all the liquid to conform to the reservoir's original constant volume.

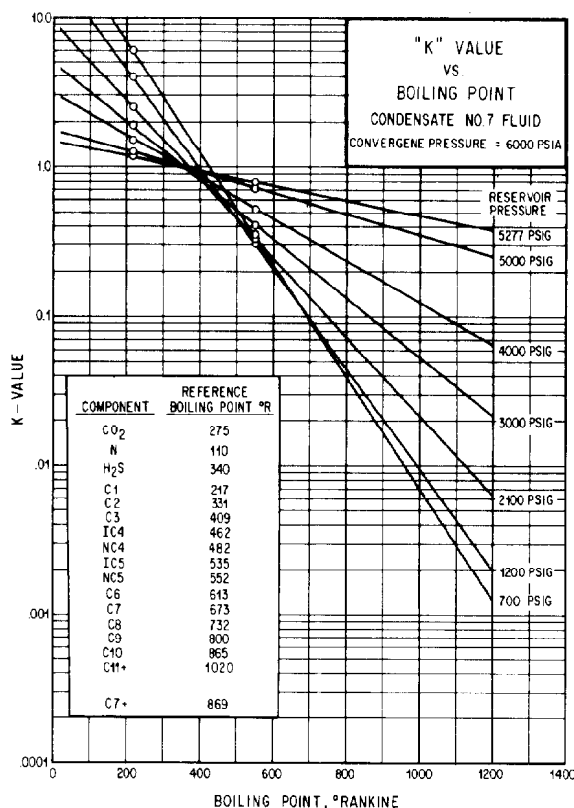


Fig. 39.6— K -value correlation for Condensate 7 depletion.

4. Subtract the number of moles of each component in the vapor represented by this gas removal from the original system composition.

5. With the new total composition from Step 4, consider the system flashed to the next lower pressure step and repeat the procedure. Removal of vapor phase alone is required by the assumption that fluid flowing into the wells will not be accompanied by any liquid phase at any step of the process.

As indicated previously, the calculations require knowledge of the volume occupied by each phase at each pressure step. Methods to estimate these volumes are described in Chaps. 20 and 22 and also by Standing.⁹ To estimate phase volumes, smoothed values should be used from curves drawn through the points computed from properties of the phase at each known composition.

TABLE 39.9—STATISTICAL EXPANSION OF C_{7+} COMPONENT, CONDENSATE 7

C_{7+} Mole fraction 0.0999
Molecular weight 158.0
Density, g/cm³ 0.827

Component	Mole Fraction	Mole Weight	Density (g/cm ³)	Boiling Point (°R)
C ₇	0.01685	100.9	0.7486	658
C ₈	0.01535	113.6	0.7648	702
C ₉	0.01235	126.9	0.7813	748
C ₁₀	0.00941	139.5	0.7960	791
C ₁₁₊	0.04594	205.1	0.8641	1,020

These calculations are intended to approximate the experimental procedure used in the PVT cell during a laboratory pressure-depletion study. The number of pressure steps used in making such calculations is arbitrary but probably should conform to about 500-psi intervals, with points usually closer together at the start and at the end of the calculations. The calculated depletion performance of Condensate 7 is presented in Table 39.10. The dewpoint pressure of 5,277 psig was calculated with an empirical relationship Nemeth and Kennedy³⁴ presented. The best method to determine the dewpoint pressure is by direct measurement, as in the laboratory PVT analysis. If these data are not available, then one must resort to estimation by empirical methods, such as that used in this example, or by gas/liquid production performance. In the latter choice, one must deplete the reservoir to a pressure below the dewpoint. In Table 39.10 a comparison of wet gas and condensate recoveries is made between the laboratory-measured and calculated depletion performance. As can be seen from the comparison, large errors are possible in the calculated data resulting from estimation of the dewpoint pressure and the physical properties of the reservoir fluid.

Hydrocarbon/Liquid Condensation; Effect on Gas-Condensate Behavior

For some gas-condensate systems, large amounts of liquid can be condensed during pressure depletion, resulting in high liquid saturations in the formation pores. When this probability is indicated by either laboratory tests or calculations, the possibility of hydrocarbon/liquid flow through and out of the reservoir must be examined. Relative permeability information (usually curves showing k_{rg}/k_{ro} vs. liquid saturation in the formation) should be combined with viscosity data (μ_o/μ_g) to estimate the volumetric proportion of liquid in the flowing stream (thus removed from the reservoir), thereby affecting the remaining reservoir phase compositions at each of the depletion steps. The best $k_{rg}\mu_o/k_{ro}\mu_g$ data to use are those determined in the laboratory with actual samples of the reservoir rock and hydrocarbon system in question. In the absence of such information, k_{rg}/k_{ro} can be estimated by the methods explained in Chap. 28; viscosity approximations may be made by the methods described by Carr *et al.*²³ After the amount of gas and liquid removed at each step has been estimated, the calculation procedures can be adjusted to obtain the desired behavior predictions.

Pressure Drawdown at Wells; Effect on Well Productivity and Recovery

The previous discussion has taken liquid condensation in the formation into account as though it occurred uniformly throughout the reservoir (uniform pressure at any instant of time). In low-permeability formations, however, there can be appreciable pressure drawdown at the producing wells because the pressures near the wellbores are much lower than in the main part of the reservoir. This tends to increase the early condensation of liquids around the wells considerably, thus decreasing the gas permeability and affecting the phase behavior of the system near the wells. This is important from at least two standpoints: (1) composition history of fluids produced from the reservoir may diverge from that predicted by assuming uniform pressure in the reservoir at any instant of time and

(2) adverse effects on the ability of the wells to produce may occur, potentially affecting the optimum well spacing and the rate of gas-condensate recovery from the zone as pressures decline.

The effects of well-pressure drawdown on the composition history (and ultimate liquid recoveries) of gas-condensate reservoir production have had little discussion in the literature. The general expectation would be that in lower-pressure areas around the wells, liquid hydrocarbons are precipitated earlier and in greater amounts than in the main volume of the reservoir. The main factors involved in this phenomenon are the richness of the gas condensate, the retrograde characteristics of the reservoir fluid, and the permeability of the reservoir rock. Normally, the area around the wellbore that is affected will be small and the condition will stabilize. Normal operating practices to restrict the pressure drawdown to reasonable values will alleviate the problem. In those reservoirs that exhibit extremely low permeability and contain fluids exhibiting condensable liquids of more than 200 bbl/MMscf, the problem can be severe. When separator samples are taken for the laboratory, the analysis procedure discussed previously should be followed to minimize the drawdown effect on the gas and liquid compositions.

The effects on well productivity of precipitated liquid in the vicinity of the wellbore theoretically can be appreciable. Normally, estimates of future well productivity ignore the drawdown effects of production on liquid-phase distribution in the reservoir. The greater liquid accumulations and lower gas permeabilities near the wells thus are ignored in theoretical predictions of well productivity (or extrapolations from early tests); these predictions then tend to show minimum decline rates. The operating engineer should be alert to this possibility whenever calculated well or reservoir rates approach undesirably close to the minimum necessary for the operating objectives of the project. Well productivity is discussed later.

Relative Merits of Measured vs. Calculated Pressure-Depletion Behavior

This chapter has emphasized that for purposes of reservoir analysis and prediction, measured properties and observed behavior of gas-condensate systems are much superior to the use of correlations or approximations. This applies in particular to the use of equilibrium ratios for simulating or predicting the pressure-depletion behavior of a reservoir. The problem is discussed and illustrated by Standing⁹ in his Vapor Liquid Equilibria and Gas-Condensate Systems chapters. In particular, Standing's Fig. 36 shows that serious errors (in excess of 40%) can be incurred in the computation of the liquid volume of a gas-condensate system from errors of less than 10% in the equilibrium ratios for heptanes-plus and methane.

The literature contains reports on the use of equilibrium ratios for calculating the reservoir behavior of gas-condensate systems. Allen and Roe³⁵ computed the pressure-depletion behavior of a gas-condensate reservoir and observed certain discrepancies with the actual behavior. These authors did not report laboratory-measured equilibrium ratios for the specific fluids involved, however; consequently, there were no means to compare computed fluid behavior with actual fluid behavior. All the observed discrepancies were assigned arbitrarily by Allen

TABLE 39.10—CALCULATED COMPOSITION OF PRODUCED STREAM, mol%

Component	Reservoir pressure (psig)							
	5,277	5,000	4,000	3,000	2,100	1,200	700	700*
Carbon dioxide	0.01	0.01	0.01	0.01	0.01	0.01	0.01	Trace
Nitrogen	0.11	0.11	0.13	0.13	0.13	0.12	0.12	0.01
Methane	68.93	70.74	74.77	77.09	78.05	77.55	75.53	12.29
Ethane	8.63	8.67	8.77	8.88	9.04	9.37	9.76	4.22
Propane	5.34	5.28	5.13	5.05	5.10	5.41	5.95	5.02
Iso-butane	1.15	1.12	1.06	1.01	1.01	1.08	1.22	1.62
n-butane	2.33	2.26	2.10	1.99	1.96	2.09	2.41	3.80
Iso-pentane	0.93	0.89	0.79	0.73	0.69	0.73	0.86	2.14
n-pentane	0.85	0.81	0.71	0.64	0.61	0.64	0.75	2.16
Hexanes	1.73	1.62	1.35	1.15	1.03	1.04	1.23	5.97
Fraction C ₇	1.685	1.55	1.21	0.97	0.82	0.78	0.90	7.33
Fraction C ₈	1.535	1.38	1.01	0.75	0.59	0.52	0.59	7.92
Fraction C ₉	1.235	1.09	0.73	0.49	0.35	0.28	0.31	7.34
Fraction C ₁₀	0.941	0.81	0.49	0.30	0.19	0.14	0.15	6.14
Fraction C ₁₁₊	4.594	3.66	1.74	0.81	0.42	0.24	0.21	34.04
	100.000	100.00	100.00	100.00	100.00	100.00	100.00	100.00
Heptanes-plus	9.990	8.49	5.18	3.32	2.37	1.96	2.16	62.77
mol%	158	155	146	137	129	124	121	166
molecular weight	0.825	0.822	0.812	0.802	0.793	0.784	0.780	0.832
density								
Deviation factor, z								
equilibrium gas	1.021	0.987	0.901	0.861	0.863	0.899	0.930	
two-phase	1.021	1.009	0.922	0.845	0.782	0.695	0.595	
Gas FVF, Mscf/scf	0.2561	0.2511	0.2201	0.1730	0.1211	0.0668	0.0380	
Retrograde liquid volume, % hydrocarbon pore space	0.000	15.3	26.96	27.89	26.43	23.85	21.95	
Cumulative recovery per MMScf of original fluid								
	Initial in place	Reservoir pressure (psig)						
		5,277	5,000	4,000	3,000	2,100	1,200	700
Well stream, Mscf	1,000	0.00	40.73	160.03	311.34	478.33	662.91	768.03
Normal temperature separation**								
Stock-tank liquid, bbl	183.13	0.00	6.91	21.98	34.00	42.98	50.71	55.05
Primary separator gas, Mscf	776.98	0.00	32.46	138.96	280.26	437.60	610.03	707.57
Second-stage gas, Mscf	37.01	0.00	1.42	4.76	7.74	10.21	12.58	14.08
Stock-tank gas, Mscf	38.31	0.00	1.50	5.26	8.92	12.19	15.60	17.93
Total separator gas, Mscf	852.30	0.00	35.38	148.98	296.92	460.00	638.21	739.58
Comparison of Recovery Calculations								
	Laboratory Depletion	Calculated Depletion						
Gas in place at original pressure, MMscf	137,582	137,582						
Gas in place at dewpoint pressure, MMscf	130,992	128,050						
Wet gas produced to dewpoint pressure, MMscf	6,590	9,532						
Wet gas produced from dewpoint to abandonment, MMscf	102,045	98,346						
Total wet gas produced, MMscf	108,635	107,878						
Condensate produced to dewpoint pressure, bbl	1,197,667	1,745,595						
Condensate produced from dewpoint to abandonment, bbl	5,297,156	5,413,947						
Total condensate produced, bbl	6,494,823	7,159,542						

*Composition of equilibrium liquid phase.

**Primary separator at 450 psig and 75°F; second stage separator at 100 psig and 75°F; stock tank at 75°F.

and Roe to factors other than the possible inaccuracies of equilibrium ratios from correlations compared with actual measured ratios for the particular system composition and reservoir conditions involved. Some of these discrepancies were probably attributable to the equilibrium ratios used.

Berryman³⁶ compared calculated gas-condensate fluid performance with that actually obtained in the laboratory; however, he made observations on actual vapor/liquid equilibrium in the laboratory cell and adjusted the literature equilibrium ratios to conform to this actual behavior. With the adjusted vapor/liquid equilibrium ratios, the calculated performance was found to match actual reservoir performance during early life satisfactorily.

Rodgers *et al.*³⁷ provided detailed laboratory data, vapor/liquid equilibrium calculations, and actual reservoir performance for a small gas-condensate reservoir in Utah. The pressure range involved was moderate compared with most cases. Even at these moderate pressures, however, the literature-derived equilibrium ratios for heptanes-plus did not agree favorably with measured values for the system. The authors commented that the "appearance of the data . . . clearly shows the need for improved techniques in establishing proper equilibrium data."

On the basis of this experience and for the reasons Standing stated, it would appear desirable to use measured values of phase and volumetric behavior for a gas-condensate system in predicting the pressure-depletion behavior of a gas-condensate reservoir. As more data are obtained and better correlating methods developed, it is possible that equilibrium ratios may achieve suitable accuracy for reservoir-type calculations in the future. Numerous equation-of-state (EOS) calculation techniques have been developed that produce phase equilibrium data that can be used to perform depletion calculations for gas-condensate reservoirs. Many are discussed in Refs. 38 through 40. The use of EOS methods, while more flexible and in many cases more accurate, requires sophisticated computer programs that may or may not be available or warranted. Continued improvement in techniques using EOS's may enhance the accuracy of calculated pressure-depletion performance.

Operation by Pressure Maintenance or Cycling

Pressure maintenance of a gas-condensate reservoir can exist by virtue of (1) an active water drive after moderate reduction of pressure from early production, (2) pressure maintenance through water injection operations, (3) injection of gas, or (4) combinations of all of these. From time to time, certain reservoirs may be encountered that have fluids near their critical points and that thereby may be candidates for special recovery methods, such as the injection of specially tailored gas compositions to provide miscibility and phase-change processes that could improve recovery efficiency. These usually are not regarded as gas-condensate cases.

Water Drive and Water Injection Pressure Maintenance

Very few cases of gas-condensate reservoirs operated under natural water drive have been reported in the litera-

ture. To be attractive economically, a water drive would have to be sufficiently strong to maintain pressure high enough to minimize condensed hydrocarbon losses in the formation. Under these conditions, expenditures for cycling or other pressure-maintenance operations might not be justified; a careful engineering and economic analysis should be made if this possibility seems imminent. The analysis should include a geologic review of conditions surrounding the reservoir to estimate whether any indicated early water drive is apt to last for the life of the operation. There are also other considerations to be studied carefully, including the expenses of dewatering or working over invaded producing wells, the displacement efficiency of water moving gas, and the potential bypassing and loss of condensate fluids when wells become watered-out prematurely through permeable stringers [invasion efficiency (see Pages 39-17 and 39-18) of the natural flood]. Should this last possibility exist, use of a natural water drive would be of doubtful value if the amount of hydrocarbons in place is large. In any case, predictions of recovery by natural water drive should take into account the factors for water injection discussed below.

The injection of water into a gas-condensate reservoir to maintain pressure is sometimes considered. A number of factors must be weighed carefully before a decision is reached. The mobility ratio (mobility of driving fluid over mobility of the driven fluid, water/gas) in this case is favorably low because of the very high mobility of the gas, thus tending to provide high areal sweep and pattern ($h\phi S$ -weighted) efficiencies. There is strong evidence, however, that displacement efficiency by the water is not high. While Buckley *et al.*⁴¹ indicated that the displacement efficiency of water driving out gas can be as high as 80 to 85%, experiments and field observations by Geffen *et al.*⁴² indicate that it may be as low as 50%. This is offset to some extent by the improved areal sweep efficiency enjoyed at a low mobility ratio. All things considered, the recovery of gas condensate in the vapor phase by water injection is likely to be appreciably lower than by cycling, and any consideration of water injection for gas-condensate recovery should be accompanied by detailed experimental work on cores from the specific reservoir involved. This will help to determine whether the water can, in fact, accomplish a high enough displacement efficiency to justify its use.

Should water injection be decided on, gas and liquid recovery predictions for the reservoir can be made by combining the pattern ($h\phi S$ -weighted), invasion, and displacement efficiencies with a knowledge of the condensable-liquids content of the gas-condensate system at the pressure chosen for pressure maintenance. As an example, an areal sweep efficiency of 90% (based on an extremely low mobility ratio for water displacing gas) might be applied to the case cited on Page 39-24. Taking into account the thickness variations of the reservoir, this might provide a pattern ($h\phi S$ -weighted) efficiency of about 95%. With an assumed invasion efficiency of 65% within the invaded volume, water injection for this case would have swept out about 55% (product of the above three efficiencies) of the vapor phase in place at the start of injection. This compares with the actual recovery of more than 86% of the wet vapor by cycling operations, as discussed on Page 39-22.

These estimates of possible gas recoveries by either a natural water drive or water injection can be affected materially by the permeability distribution in the reservoir. The presence of large differences in permeability will result in premature water breakthrough. Flowing gas wells tend to "load up" when producing water and, depending on the vertical flow velocity and bottomhole flowing pressure, may cease to flow. This inability to flow results from sufficient water dropping out in the tubing to form a hydrostatic water column that exerts a pressure equal to the bottomhole pressure. It is difficult to obtain economical flow rates by artificial lift. This loss of productivity may result in premature abandonment of the project. The problems would be particularly serious for deeper reservoirs where the cost of removing water would be a significant factor. Yuster⁴³ discusses possible remedial methods for drowned gas wells. Bennett and Auvenshine⁴⁴ discuss dewatering gas wells. Dunning and Eakin⁴⁵ describe an inexpensive method to remove water from drowned gas wells with foaming agents.

Generally, the use of water injection for maintaining pressure in a gas-condensate reservoir is unlikely to be attractive where a wide range of permeabilities exists in a layered reservoir and selective breakthrough of water into producing wells might be expected before an appreciable fraction of the gas condensate in place could be recovered.

Reservoir Cycling, Gas Injection

Dry-Gas Injection. Comparative economics determines whether a gas-condensate reservoir should be produced by pressure depletion or by pressure maintenance.

The objective of using dry-gas injection in gas-condensate reservoirs is to maintain the reservoir pressure high enough (usually above or near the dewpoint) to minimize the amount of retrograde liquid condensation. Dry field gases are miscible with nearly all reservoir gas-condensate systems; methane normally is the primary constituent of dry field gas. Dry-gas cycling of gas-condensate reservoirs is a special case of miscible-phase displacement of hydrocarbon fluids for improving recovery. Experimentation has shown that the displacement of one fluid by another that is miscible with it is highly efficient on a microscopic scale; usually the efficiency is considered 100% or very nearly so. This is one of the factors that explain the effectiveness and attractiveness of cycling. Another advantage of cycling is that it provides a means to obtain liquid recoveries from reservoirs at economical rates while at the same time avoiding waste of the produced gas when a market for that gas is not available; the operation provides at its termination a reservoir of dry gas with a potentially greater economic value.

Inert-Gas Injection. The demand for dry gas as a marketable commodity varies, and the economic aspects of retaining dry cycled gas in reservoirs for future use have a changing significance. Most conservation laws in the U.S. still provide for minimizing waste of condensable liquids that would result if gas-condensate reservoirs were depleted through the retrograde range in a manner that left large liquid volumes unrecoverable.

The use of inert gas to replace voidage during cycling of gas-condensate reservoirs can be an economical alternative to dry natural gas. One of the first successful inert-

gas injection projects was in 1949 at Elk Basin, WY,⁴⁶ where stack gas from steam boilers was used for injection. In 1959, the first successful use of internal combustion engine exhaust was seen in a Louisiana oil field.⁴⁷ The first use of pure cryogenic produced nitrogen to prevent the retrograde loss of liquids from a gas-condensate fluid was in the Wilcox 5 sand in the Fordoche field located in Pointe Coupee Parish, LA.⁴⁸ In the Fordoche field, the nitrogen was used as makeup gas. The nitrogen amounted to about 30% of the natural-gas/nitrogen mixture injected.

Moses and Wilson's⁴⁹ studies confirmed that the mixing of nitrogen with a gas-condensate fluid elevated the dewpoint pressure. Moses and Wilson also presented data to show that the mixing of a lean gas with a rich-gas condensate would also result in a fluid with a higher dewpoint pressure. The increase in dewpoint pressure was greater with nitrogen than with the lean gas. In the same study, results are presented from slim-tube displacement tests of the same gas-condensate fluid both by pure nitrogen and by a lean gas. In both displacements, more than 98% recovery of reservoir liquid was achieved. These test results were also observed by Peterson,⁵⁰ who used gas-cap gas material from the Painter field located in southwest Wyoming. The authors concluded that the observed results were obtained because of multiple-contact miscibility.

Cryogenic-produced nitrogen possesses many desirable physical properties.⁵¹ Those that make nitrogen most useful for a cycling fluid are that it is totally inert (non-corrosive) and that it has a higher compressibility factor than lean gas (requires less volume). The latter advantage is partially offset by increased compression requirements when compared with lean gas.

Until the mid 1970's, most inert-gas injection consisted of injection of combustion or boiler gas into oil zones. The need for an alternative source of gas for gas-condensate-cycling projects emerged because of the high cost of hydrocarbon gas needed to replace reservoir voidage. The combustion and boiler gas that had been used to displace oil miscibly contains byproducts (CO , O_2 , H_2O , and NO_x) that are highly corrosive⁵² and decrease cost effectiveness.

Economic parameters used to evaluate any process are by their nature representative only under the general economic conditions during which they are prepared. Therefore, there will be no attempt here to present representative economic data. However, one should be cognizant of and take into account those variables peculiar to a particular process when applying current economic parameters to compare different processes.

Many factors affect the economics of a gas-cycling project. The major factors are product prices, makeup gas costs, liquid content of reservoir gas, and degree of reservoir heterogeneity. When inert-gas injection is considered, some important additional factors should also be considered. Donohoe and Buchanan⁵³ and Wilson⁵² have discussed these factors.

The use of inert gas as a cycling fluid offers both advantages and disadvantages. The major advantages are that it permits early sale of residue gas and liquids, resulting in greater discounted net income and that a higher recovery of total hydrocarbons is achieved because the reservoir contains large volumes of nitrogen rather than hydrocarbon gas at abandonment.

Offsetting these advantages are some disadvantages: production problems and increased operating costs caused by corrosion if combustion or flue gas is used as cycling fluid; possible additional capital investments to remove the inert gas from the sales gas, to pretreat before compression, and/or to fund reinjection facilities; and early breakthrough of inert gas caused by high degrees of heterogeneity in the reservoir, resulting in excessive operating costs to obtain marketable sales gas.

All these factors should be evaluated properly when the depletion method is selected.

Calculation of Cycling Performance. Methods of calculating reservoir performance under gas-cycling operations generally fall into one of two categories: feasibility and/or sensitivity analysis or detailed design and evaluation. The calculation method selected usually is determined after consideration of the quality and quantity of data available and the ultimate use of the engineering study.

When the potential of a gas-condensate reservoir for cycling is first considered, it is generally desirable to make calculations that require the use of some reasonably simplifying assumptions. In this manner, relatively rapid and inexpensive results can be obtained that define the approximate cycling rate, cycling life, ultimate recovery, and profitability. If, at the conclusion of these studies, it appears that gas cycling is feasible, more detailed and exacting studies can be made with mathematical simulators to evaluate the earlier results and to design the most advantageous distribution of injection and producing wells.

Efficiency and Effectiveness of Cycling. The principal factors determining reservoir cycling efficiency have been used with interchangeable labels and definitions in the literature. It is therefore necessary to define the various efficiencies clearly. The engineer should define and explain terms carefully when reporting estimates on gas-condensate reservoir behavior.

Reservoir Cycling Efficiency. E_R is defined as the reservoir wet hydrocarbons recovered during cycling divided by the reservoir wet hydrocarbons in place in the productive volume of the reservoir at the start of cycling. Both figures must be computed at the same pressure and temperature; e.g., at reservoir conditions or at standard conditions. The reservoir cycling efficiency can be visualized as the product of three other efficiencies: pattern ($h\phi S$ -weighted), invasion, and displacement. A fourth efficiency factor, areal sweep, can be evaluated for various injection patterns using analog or mathematical models. All efficiency terms used (except "displacement efficiency") must be identified as to time—i.e., time of dry-gas breakthrough into first producing well, time of breakthrough into last well, end of cycling, or other suitable designation.

Areal Sweep Efficiency. E_A is the area enclosed by the leading edge of the dry-gas front (outer limit of injected gas) divided by the total area of reservoir that was productive at the start of cycling. (Black oil, if present, is usually excluded from these areas.) Area of sweep can be estimated closely from analog or mathematical model studies (discussed later) or by observing the locations of wells developing dry-gas content during actual operations. The areal sweep efficiency depends primarily on the injection and production well patterns and rates and the lateral

homogeneity of the formations from a permeability and porosity standpoint. Lesser factors affecting areal sweep efficiency include variations in water content of the pores; time of operation of the compression plant in relation to the input capacities of the wells and their locations in the reservoir; the activity, if any, of a natural water drive; and the presence and handling of black-oil wells if an oil ring exists in the reservoir. Mathematical model techniques (Chap. 48) provide a useful means for predicting the areal sweep efficiencies of gas-condensate reservoirs and, simultaneously, the rate of frontal advance of the injected dry gas. For such studies, a reasonable amount of subsurface data is needed on sand characteristics, reservoir fluid properties, properties of injected fluid, and geologic description.

Pattern ($h\phi S$ -Weighted) Efficiency. E_p is the hydrocarbon pore space enclosed by the projection (through full reservoir thickness) of the leading edge of the dry-gas front divided by the total productive hydrocarbon pore space of the reservoir at start of cycling. (Black oil, if present, is usually excluded from these volumes.) The hydrocarbon volume contained within the dry-gas-front projection can be determined by outlining the farthest-advanced position of the front (from model studies or field observations) on a hydrocarbon isovol map (isovol maps are developed from data on sand thickness, porosity, and interstitial water content), determining the hydrocarbon volume enclosed by this line, and comparing the volume with total reservoir productive hydrocarbon pore space. Note that the definition specifies "projection of the leading edge" and avoids stating whether either the entire gross or entire microscopic PV's are invaded or displaced by the injected gas. For the special cases in which productive thickness, porosity, interstitial water content, and effective permeability are each uniform, the pattern ($h\phi S$ -weighted) and areal sweep efficiencies are the same. The pattern ($h\phi S$ -weighted) efficiency in general depends on the same factors discussed for areal sweep efficiency. Expected pattern ($h\phi S$ -weighted) efficiencies of nearly 95% have been predicted under favorable conditions.⁵⁴

Invasion Efficiency. E_I is the hydrocarbon pore space invaded (contacted or affected) by the injected gas divided by the hydrocarbon pore space enclosed by the projection (through full reservoir thickness) of the leading edge of the dry-gas front. (Sometimes volumetric sweep efficiency, $E_v = E_p \times E_I$, is used.) The definition says nothing about the effectiveness of the invading fluid in forcing original fluid out of the pores contacted. The term "vertical sweep efficiency" has sometimes been used in the sense of invasion efficiency. This is misleading in that it uses a one-dimensional term ("vertical") when dealing with a three-dimensional problem. Invasion efficiencies can be as high as 90% under favorable conditions.⁵⁵ However, invasion is affected significantly by large variations in reservoir flow properties. These might be strictly lateral variations in horizontal permeability (and to a lesser extent in porosity and interstitial water content) of a single-bed reservoir that does not have any variations vertically at any location; strictly layering effects by which the reservoir may comprise several strata, each relatively uniform in properties but differing appreciably in permeability from all the others; or combinations of these extreme cases. Performance of cycling operations can vary ap-

TABLE 39.11—EFFICIENCY TERMS USED IN RESERVOIR CYCLING OPERATIONS

	Areal Sweep Efficiency	Pattern ($h\phi S$ -weighted) Efficiency	Invasion Efficiency	Displacement Efficiency	Reservoir Cycling Efficiency
Definitions	Area enclosed by leading edge of injected-gas (dry-gas) front divided by total area of reservoir productive at start of cycling.	Hydrocarbon pore space enclosed by the projection (through full reservoir thickness) of leading edge of dry-gas front divided by total productive hydrocarbon pore space of reservoir at start of cycling.	Hydrocarbon pore space invaded by (contacted or affected by) dry gas divided by hydrocarbon pore space enclosed by the projection (through full reservoir thickness) of leading edge of dry-gas front.	Wet hydrocarbon volume swept out of individual pores or small groups of pores divided by hydrocarbon volume in same pores at start of cycling (both volumes calculated at same temperature and pressure).	Reservoir wet hydrocarbons recovered during cycling divided by reservoir wet hydrocarbons in place at start of cycling (calculated at same temperature and pressure).
	$E_A = E_P$ for uniform thickness, porosity, interstitial water content, and effective permeability.		E_I is 100% for uniform effective permeability in a gas-condensate reservoir.	E_D is usually assumed 100% for gas-condensate cycling operations.*	$E_P \times E_I \times E_D$
Previous Usage	"Sweep efficiency" (Ref. 5, Pages 657, 771, and 777; Ref. 51, Pages 246 and 247, and Ref. 13, Pages 308-09)** "Pattern efficiency" (Ref. 57)** "Flood coverage" (Ref. 59, Pages 358 and 374)** "Areal sweep efficiency" or "pattern efficiency" (Ref. 62, Page 406)	"Sweep efficiency" (Ref. 5, Pages 755, 763, and 770, and Ref. 13, Pages 408-09)** "Invasion" or "percent of volume swept out" (Ref. 58, Page 67)** "Conformance factor" (Ref. 56, Pages 130 and 136) "Sweeping efficiency" (Ref. 57) "Pattern efficiency" (Ref. 60, Pages 63, 64, 98, and 99, and Ref. 54, Page 77) "Volumetric efficiency" (Ref. 55, Pages 9-11) "Reservoir sweep" or "reservoir coverage" (Ref. 61, Page 110)	Efficiency "caused by permeability stratification" (Ref. 13, Pages 408-09) "Conformance factor" (Ref. 57) "Flushing efficiency" (Ref. 41, Pages 246 and 247) "Displacement" or "sweep efficiency" (Ref. 63, Page 337) "Internal flushing efficiency" or "internal displacement efficiency" (Ref. 55, Pages 9-11) "Vertical sweep efficiency" (Ref. 62, Page 406)	"Displacement efficiency" (Ref. 56, Pages 130 and 136, and Ref. 13, Pages 408-09) "Flood efficiency" (Ref. 59, Pages 358 and 374) "Displacement" (Ref. 61, Page 110) "Displacement" or "sweep efficiency" (Ref. 63, Page 337)	"Sweep efficiency" (Ref. 5, Pages 612, 771, and 788) "Over-all instantaneous cycling efficiency" (Ref. 60, Pages 140, 141, 235, and 236) "Over-all displacement efficiency" (Ref. 62, Pages 9-11)

*But quite variable for nonmiscible flooding operations (such as water injection into gas-condensate reservoirs).
 **Arbitrarily defined as occurring at the time invading fluid first reaches the producing wells; first breakthrough.

preciably according to what combination of the two extremes may exist for a given reservoir. Mathematical models can handle reservoir heterogeneities, both horizontally and vertically, if the data are available. Maximum use of core analysis data, pressure buildup and drawdown analysis, and detailed analysis of downhole logs is required to ensure an accurate evaluation of a reservoir's potential as a cycling project.

Displacement Efficiency. E_D is the volume of wet hydrocarbons swept out of individual pores or small groups of pores divided by the volume of hydrocarbons in the same pores at the start of cycling; note that both volumes must be calculated at the same conditions of pressure and temperature. This term is used here because it has received wide acceptance in the literature (on immiscible as well as miscible processes) for the microscopic displacement of fluids. Displacement efficiency is controlled mainly by the miscibility of the driving and driven fluids and their mobilities. For a cycling operation in which the pressure is being maintained at or above the dewpoint, the displacement efficiency resulting from action of the dry gas against the wet-gas phase in the individual pores will be virtually 100% because of near-complete miscibility and the near-identical mobility ratios of the two fluids. If the pressure is well below the dewpoint, the displacement efficiency will be less than 100% because of the immobility of the condensed liquid and incompleteness of revaporization of the dry gas. Evaluation

of a case of this type requires trial calculations of vapor/liquid equilibrium to estimate the extent to which dry gas coming into contact with the condensed liquid would revaporize some of the components and carry them toward the producing wells.

Thus the reservoir cycling efficiency is the product of the pattern ($h\phi S$ -weighted), invasion, and displacement efficiencies, as summarized in Table 39.11, along with the previous discussion, and usage of terms appearing in some of the literature.

Permeability Distribution. Permeability variation, both laterally and vertically, can have a strong influence on recoveries by cycling. Vertical stratification of horizontal permeability is probably the primary factor controlling invasion efficiency. In reservoirs containing layers or regions of contrasting permeabilities, the leading edge of the dry-gas front (used in calculating invasion efficiency) is at a different position for each layer. Field observations usually establish the front on the basis of breakthrough in the most-permeable layer, whereas mathematical model studies may have been based on an average permeability of layers or a discrete number of layers, thus predicting later breakthrough. This possibility should be understood when model predictions of breakthrough time are compared with field observations. Detailed reservoir analysis is required in developing a mathematical model to ensure that the model used adequately reflects the properties of the reservoir.

TABLE 39.12—CALCULATIONS ILLUSTRATING THE DILUTION CAUSED BY WEIGHTED-AVERAGE PERMEABILITY PROFILE—BASED ON 16 WELLS (COTTON VALLEY BODCAW GAS-CONDENSATE RESERVOIR)

Layer	Permeability (md)	Sand Thickness (ft)	Permeability Thickness (Col. 2 times Col. 3)	Capacity ^a (%)	Porosity (%)	Porosity Thickness (Col. 3 times Col. 6)	Production When Layer Displaced (%)	Production Between Layer Displacements (%)	Production (mean value) ^c (%)	Cumulative Dry Gas Produced ^d (%)	Composition of Gas ("wet gas" minus Col. 11) (%)	Wet Gas Produced Between Layer Displacements (%)	Cumulative Wet Gas Produced (%)
1	250	2	500	3.14	19.30	38.60	67.6	2.5	68.80	3.14	96.86	2.42	67.6
2	240	2	480	3.02	19.20	38.40	70.1	2.7	71.50	6.16	93.84	2.53	70.0
3	230	4	920	5.79	19.10	76.40	72.8	1.4	73.60	11.95	88.05	1.23	72.6
4	225	2	450	2.83	19.05	38.10	74.2	1.6	75.00	14.78	85.22	1.36	73.8
5	220	8	1,760	11.06	19.00	152.00	75.8	1.6	76.60	25.83	74.17	1.19	75.1
6	215	2	430	2.70	18.95	37.90	77.4	1.5	78.10	28.53	71.47	1.07	76.3
7	210	4	840	5.29	18.90	75.60	78.9	1.5	79.60	33.82	66.18	0.99	77.4
8	205	2	410	2.58	18.85	37.70	80.4	3.9	82.30	36.40	63.60	2.48	78.4
9	195	6	1,170	7.35	18.72	112.32	84.3	1.9	85.30	43.76	56.24	1.07	80.9
10	190	4	760	4.79	18.66	74.64	86.2	2.0	87.20	48.55	51.45	1.03	81.9
11	185	2	370	2.33	18.60	37.20	88.2	2.2	89.30	50.88	49.12	1.08	83.0
12	180	4	720	4.52	18.55	74.20	90.4	9.6	95.20	55.40	44.60	4.28	84.0
13	160	2	320	2.01	18.25	36.50	100.0	5.7	102.80	57.41	42.50	2.43	88.3
14	150	10	1,500	9.43	18.10	181.00	105.7	3.5	107.40	66.84	33.16	1.16	90.8
15	145	4	580	3.65	18.05	72.20	109.2	3.3	110.90	70.49	29.51	0.97	91.9
16	140	8	1,120	7.05	18.00	144.00	112.5	3.7	114.30	77.54	22.46	0.83	92.9
17	135	2	270	1.70	17.90	35.80	116.2	3.8	118.10	79.24	20.76	0.79	93.7
18	130	6	780	4.91	17.80	106.80	120.0	4.5	122.20	84.15	15.85	0.71	94.5
19	125	4	500	3.14	17.75	71.00	124.5	4.5	126.70	87.29	12.71	0.57	95.2
20	120	4	480	3.02	17.65	70.60	129.0	5.2	131.60	90.31	9.69	0.50	95.8
21	115	2	230	1.45	17.60	35.20	134.2	10.8	139.60	91.76	8.24	0.89	96.3
22	105	4	420	2.54	17.40	69.60	145.0	6.7	148.30	94.40	5.60	0.38	97.2
23	100	6	600	3.77	17.30	103.80	151.7	15.0	159.20	98.17	1.88	0.27	97.6
24	90	2	180	1.13	17.10	34.20	166.7	217.3	275.30	99.30	0.70	1.52	97.8
25	35	2	70	0.44	15.35	30.70	384.0	239.0	503.50	99.74	0.26	0.62	99.4
26	20	2	40	0.26	14.20	28.40	623.0	—	—	100.00	0.00	—	100.0
Total		100	15,900	100.00		1,812.66							

Weighted-average permeability = 159.00 md, weighted-average porosity = 18.13%, and weighted-average sand thickness = 23.81 ft.

$$^a \text{Percent capacity of } x = \frac{k_x h_x}{\sum kh}$$

$$^b \text{Percent produced of } x \text{ (assumes uniform interstitial water content)} = \frac{(\phi_x \sum kh)}{(k_x \sum kh)} = (\text{weighted-average } k/k_x) / (\phi_x / \text{weighted-average } \phi)$$

^c Percent produced (mean value of x) = (percent produced of x + percent produced of $(x+1) - 2$.

^d Cumulative dry gas of x in flow stream = capacity _{x} + capacity _{$x+1$} + ... capacity _{n} .

^e Col. 9 minus the product of Cols. 9 and 11.

^f First value of Col. 8 plus cumulative of Col. 13.

There can be several sources of comparative permeability information for reservoir layers, including direct measurements of permeabilities on cores removed from wells, formation tests during drilling and completion, comparative transmissibilities from carefully run injection profiles, and flow, drawdown, and buildup tests on wells completed in different layers. If different kinds of information are to be used together, they should all be adjusted to the same units for calculating the effects of permeability variation on gas-condensate reservoir performance.

Much discussion has been published regarding the effects of permeability variation on the recoveries of hydrocarbons from reservoirs. Discussions with particular reference to gas-condensate reservoirs have been provided by Muskat,^{5,64} Standing *et al.*,⁶⁵ Miller and Lents,⁶⁶ and others.⁶⁷⁻⁷⁰ Generally, the proposals to account for the effect of permeability variations on gas-condensate reservoir performance use two different methods of well-to-well averaging of horizontal permeabilities. The first method averages all high permeabilities from all wells together (irrespective of vertical positions of the high-permeability samples in the section) and all low permeabilities from all wells in another group, with intermediate permeabilities classified into one or more subgroups. Each of the average permeabilities is regarded as a single stratum continuous throughout the reservoir. This type of averaging would appear to give maximum probability of computed early breakthroughs of dry gas to producing wells. In the second method, permeabilities are averaged from well to well according to vertical position in the sec-

tion. For example, permeabilities in the top 10% of each well's productive section might all be averaged together, the next 10% together, and so on to the bottom. This procedure maintains layers in their relative vertical positions in the reservoir, and thus, by averaging laterally, the effects of any individual high-permeability samples tend to be damped out unless high-permeability streaks are actually persistent in one or more layers of the section.

Either of these methods can be used in solutions presented by Muskat,^{5,64} who used the "stratification ratio" to develop mathematical means of evaluating the effects of vertical variation of permeability on cycling. "Stratification ratio" is the ratio of the permeability of the most-permeable recognizable layer in the section to that of the least-permeable layer in the same section (these permeabilities are the layer average in each case, determined by whatever means, rather than individual high or low permeabilities from single plugs or cores from the layer). The Muskat development also assumes simple parallel superposition of layers of different horizontal permeabilities with no crossflow between. The resultant correlations are presented graphically in the references.

Miller and Lents⁶⁶ used the second type of lateral permeability averaging in their analysis of the Cotton Valley Bodcaw reservoir. Their work should be reviewed for an understanding of the detailed procedure used. The table of permeabilities they developed (rearranged in descending order of magnitude) for illustrating the calculation of dilution behavior of the subject reservoir with time is shown here as Table 39.12. The calculation assumes no

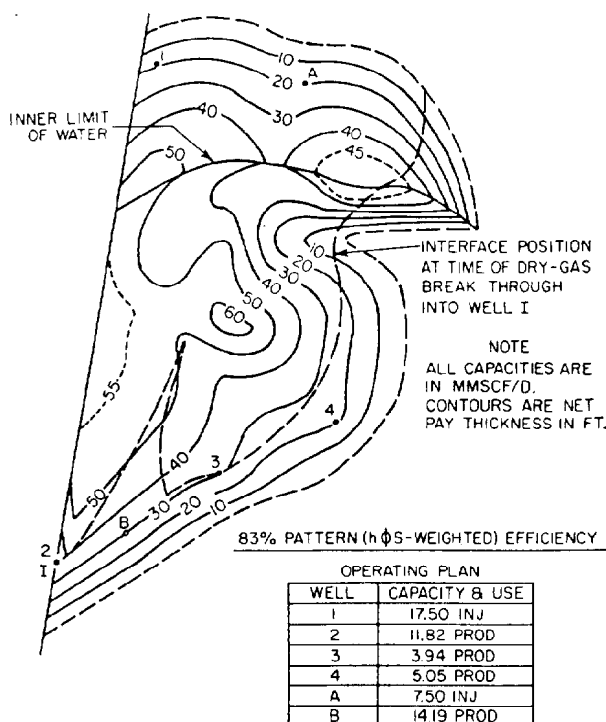


Fig. 39.7—Boundary of invaded area predicted by early potentiometric model studies.

crossflow, and the reservoir is treated as though it were composed of alternating layers of variable porosity and permeability. It is also assumed that parallel flow occurs simultaneously in the various layers with the same potential distribution throughout the layers. The injection wells are treated as a line source, and the producing wells as a "line sink." Hence, the calculations in the table predict the percentage of original reservoir hydrocarbon volume at constant pressure produced at the instant each layer has been displaced and the percentage of dry gas (and wet gas) in the producing stream as more and more layers are displaced (breakthrough). The recovery to any stage of dilution in the produced gas can then be predicted; the recovery Miller and Lents calculated (supported by later production history, as shown by Brinkley's⁵⁵ Fig. 7) is in good agreement with predictions from Muskat's correlations.

Very little has been published comparing the actual behavior and final recoveries of gas-condensate reservoirs with those predicted with the different methods of accounting for permeability variation. Stelzer⁶³ reports on the performance of the Paluxy gas-condensate reservoir of the Chapel Hill field, TX, the cycling behavior of which had been predicted earlier by Marshall and Oliver.⁵⁸ This analysis is discussed further later. In a discussion of Stelzer's paper, Hurst takes the position that permeability variation or stratification in a reservoir can be of minor significance in controlling the ultimate recovery by cycling:

The lithological nature of a reservoir is such that with the interspersing of shale throughout, it can virtually reproduce the configuration of a uniform sand if the

sweep is sufficiently great in length. . . Few reservoirs conform to a parallel deposition of lens, each of different uniform permeability, unless one wishes to subscribe to the worst possible consequences for cycling, which can condemn the application of such a program in a rich gas-condensate field.

Such unpublished information as has come to our attention tends to substantiate the belief that most reservoirs are not composed of continuous layers of contrasting permeabilities (with no crossflow) that would tend to produce quick breakthrough during injection operations. Hurst's viewpoint should therefore be considered seriously by the engineer predicting the behavior of cycling projects, because overemphasis on the permeability variation within a reservoir could produce too pessimistic a view of possible recoveries and thereby condemn cycling in gas-condensate reservoirs that might, in fact, yield profitable cycling performance.

The second method for lateral averaging of permeabilities is recommended, whether the Miller and Lents⁶⁶ analysis or other techniques are applied to the handling of permeability variation in gas-condensate reservoirs. Proper consideration for pattern ($h\phi S$ -weighted) efficiency must be given in each case.

Prediction of Cycling Operations with Model Studies—

Analog Techniques. The steady-state flow of fluids through porous media, when governed by Darcy's law, is analogous to the flow of current through an electrical conductor governed by Ohm's law. Thus steady-state electrical-model studies have been used quite successfully in the prediction of gas-condensate cycling operations.

The fundamental analogy between an electrical model of a gas-condensate reservoir and the flow system of the reservoir depends on the equivalence of electrical charge to reservoir fluid, current flow to fluid flow, specific conductivity to fluid mobility, and potential (voltage) distribution in the model to a function Φ_g (not to pressure distribution in the reservoir, as in an oil/water system) defined by Muskat⁴ as

$$\Phi_g = \frac{\rho_g}{\mu_g} dp,$$

where

ρ_g = gas density,

μ_g = gas viscosity, and

p = pressure.

This analogy holds, provided the sources, sinks, and boundary conditions are made equivalent in shape and distribution.

Steady-state models can be divided into two general classes: electronic and electrolytic. The former depends on the movement of electrons through resistive solids, such as metal sheets, carbon paper, and graphite-impregnated cloth or rubber sheeting. Electrons are introduced at one boundary and move into the model to displace free electrons throughout the entire body of the model. The electrons moving out of the model at the other boundary produce a current that causes a potential drop in the solid resistive medium in accordance with Ohm's

law. As a result, the movement of the equivalent fluid interface can be traced. In the case of a graphite-impregnated cloth model, the reservoir is represented by layers of cloth, the number of layers of which are some function of the permeability/net-thickness product (kh) of the producing strata. The shape of each layer of cloth conforms to the shape of the kh range it represents. Copper electrodes are fixed in the cloth model at positions corresponding to the wells in the reservoir and direct currents are passed through these electrodes in proportion to the well flow rates. The electrodes are not usually scaled to the actual well diameters.

Electrolytic models depend on the mobility of the ions in the medium. Because the velocity of an ion in an electrolyte system is proportional to the potential gradient, just as the velocity of a liquid particle in a porous medium is proportional to the pressure gradient, an electrolytic model can be set up that provides a good analogy to single-phase flow in a porous system. The ions are moved into the model across one or more boundaries and displace ions throughout the entire medium, causing ions to leave through other boundaries. The flowing current and potential drop are established in exactly the same way as in the electronic models.

Electrolytic models can be divided into three major types: gel, blotter, and liquid. Although the first two types can be used to determine the areal sweep patterns in two-dimensional uniform media, the potentiometric model that uses a liquid electrolyte is the most flexible and accurate. In this type, the fluid conductivity of the porous medium is usually represented by an open container that has its bottom shaped to produce electrolyte depths proportional to the kh of the producing strata and its sides shaped to conform to the productive limits of the strata. This construction implies that there is no vertical variation in permeability and no bedding at any location in the reservoir, as represented by the model. Copper electrodes (not scaled to well diameter) are fixed in the model at positions corresponding to the locations of the wells in the reservoir, and alternating currents of proper phase are passed through these electrodes. The magnitudes of these currents are made proportional to the production and injection rates to be used in the reservoir. The direction of current flow at every point in the model is considered analogous to the direction taken by the flowing fluid in the reservoir.

The general assumptions applicable to steady-state analog techniques are that (1) a vertical and discrete interface exists between the displacing and the displaced phases; (2) because the history of advance of only one front can be traced at any one time, if two interfaces or fronts are present (such as gas/gas and gas/water), one is considered a stationary boundary; (3) average reservoir pressure is constant regardless of the injection or production schedule (this avoids compressibility effects in the model study); and (4) gravitational effects are neglected. In addition, if the mobility ratio of the system is not (near) unity or infinity, the necessary procedures become tedious and costly.

An example case history by Marshall and Oliver⁵⁸ reported results of a potentiometric model study of the Paluxy sand reservoir of the Chapel Hill field, Smith County, TX. This gas-condensate reservoir is bounded on the north by a gas/water contact, on the west by a fault, and on the south and east by a pinchout. It was assumed

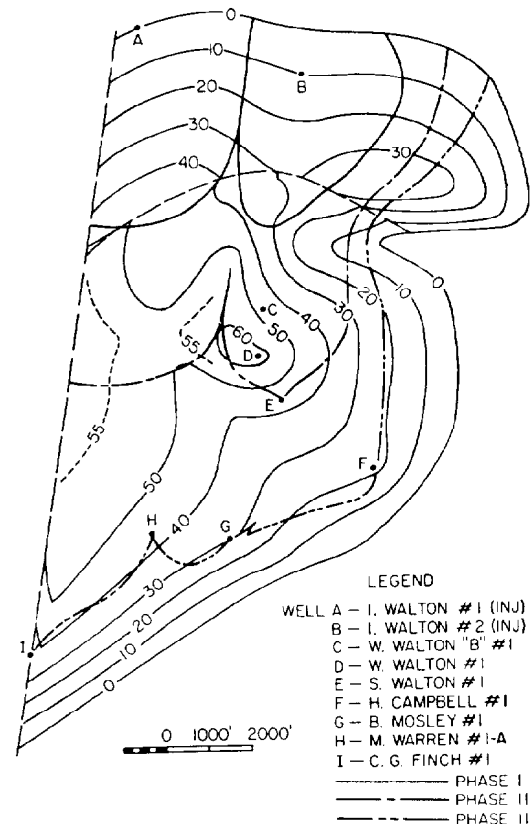


Fig. 39.8—Boundaries of invaded areas predicted by later potentiometric model studies.

that the gas/water contact was a fixed impermeable boundary; that the permeability, porosity, and interstitial water content were each uniform throughout the producing zone; that the reservoir volume rate of dry-gas injection was equal to the corresponding rate of gas-condensate production; and that gravity effects were negligible. Fig. 39.7 shows the final dry-gas/wet-gas interface position at time of breakthrough into Well 1 (determined after several trials of well arrangement and production- and injection-rate schedules) that yielded an optimum pattern ($h\phi S$ -weighted) efficiency prediction of 83%. Injection was into Wells 1 and A with production from Wells 2 through 4 and B as indicated in Fig. 39.7. This program provided a sustained capacity of 35 MMscf/D for the life of the operation.

Stelzer⁶³ reported a comparison of model study predictions with actual performance for this reservoir. Actual gas injection was begun in accordance with the north/south sweep indicated by the model study. During the initial period (first 15 months after cycling began) the production- and injection-rate program predicted by the initial model study was followed quite closely. New structural data revealed in the drilling of additional wells, however, required some changes in the isopach map of the Paluxy sand. The results from a second model study, which incorporated these changes plus injection into only Wells A and B, are shown in Fig. 39.8. Three interface boundaries (dry-gas fronts) are shown for three

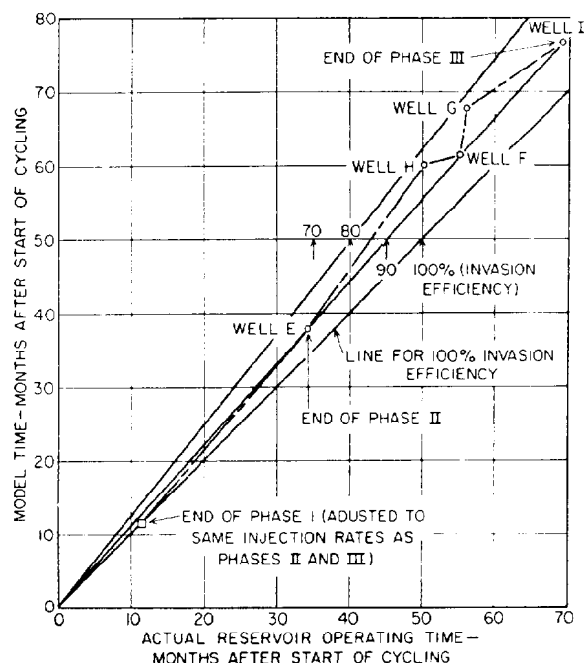


Fig. 39.9—Comparison of predicted with actual times of first dry-gas breakthrough, Paluxy gas-condensate reservoir, Chapel Hill field, TX.

production- and injection-rate schedules. The first schedule was maintained for the first 15 months of cycling; the second was continued until breakthrough of dry gas into Well E; the final schedule was maintained until first breakthrough at Well I. There was close agreement between the model rates used and actual reservoir rates.

The second model study indicated a pattern ($h\phi S$ -weighted) efficiency of 88%, a 5% increase over that obtained by the initial study. Stelzer estimated the amount of reservoir gas in place at start of cycling to be 78.4 Bscf. The new model study thus implies an additional 4 Bscf of predicted recoverable gas as a result of better reservoir definition and better operating schedules.

The data in Fig. 39.9 compare model (predicted) breakthrough times with the actual times to dry-gas appearance in corresponding field wells. (Phases 1, 2, and 3 of actual behavior correspond to Schedules 1, 2, and 3 of the model study.) Field data on breakthrough were taken from breaks in content curves of isobutanes-plus; the dashed line shows the cumulative well-by-well breakthrough behavior of the dry-gas flood. Because predicted and actual injection and production rates were nearly equal and constant during the period shown (except for Phase 1, which was adjusted to the same average rates), times on the plot are directly proportional to cumulative reservoir volumes of gas. Therefore, the lower light line represents a hypothetical invasion efficiency of 100% that would prevail if actual breakthrough times coincided with those predicted by the model [and the areal and pattern ($h\phi S$ -weighted) sweeps were identical with model predictions]. The upper light line represents an arbitrary invasion efficiency of 80% [assuming that predicted and actual pattern ($h\phi S$ -weighted) efficiencies are identical]. The straight heavy line from the origin through the last well to experience breakthrough

indicates an invasion efficiency a little greater than 90% and implies that more complete invasion of low-permeability regions behind the dry-gas front was accomplished during the later stages of cycling. The agreement of predicted breakthrough times within 10% of actual breakthrough times illustrates the great utility of potentiometric models in planning cycling operations. Small further improvement in the pattern ($h\phi S$ -weighted) and invasion efficiencies was to be expected before abandonment of the reservoir in this case.

Stelzer's⁶³ figures (at the start of cycling) of 78.4 Bscf of gas in place and 74 bbl of condensable liquids in the vapor phase of the reservoir per 1 MMscf of gas indicate that 5,800,000 bbl of condensable liquids is in the reservoir vapor phase at the start of cycling. Using the model-derived pattern ($h\phi S$ -weighted) efficiency of 88% (end of Schedule 3), 5,100,000 bbl of liquids was subject to removal by dry-gas invasion. Stelzer's Fig. 5 shows that about 4,640,000 bbl of liquid products were recovered between the start of cycling and the breakthrough of gas at Well 1. This provides an invasion efficiency of 91% at that time, based on 100% displacement efficiency. Thus the product of the pattern ($h\phi S$ -weighted) and invasion efficiencies represents a reservoir cycling efficiency of 80% at the time of breakthrough into Well 1. In addition, later operations increased the cumulative recovery during cycling to more than 5 million bbl of condensable liquids, thus bringing final reservoir cycling efficiency to more than 86%. This is considered very good.

Prediction of Cycling Operations With Mathematical Reservoir Simulators. The use of mathematical reservoir simulators to calculate reservoir performance during gas-cycling operations yields results superior to those obtained by the more simplified calculation procedures. Use of these simulators removes the necessity of making the assumptions required in an analog model. Some assumptions are required, however, which should be understood to perform a reservoir simulation study properly. The theory of reservoir simulation is presented in Chap. 48. Coats⁷¹ presents a good discussion of reservoir simulation studies of gas-condensate reservoirs. One must keep in mind that the results from a mathematical reservoir simulator depend on the quality of the data used to prepare the reservoir model. If good data are not available, one should consider whether the expense and time required to perform a mathematical reservoir simulation are justified.

Data Requirements for Gas-Condensate Cycling Study.

To evaluate properly the potential of cycling a gas-condensate reservoir, the following data are required.

1. Geologic data—maps and cross sections showing net effective sand thickness, structural contours on the top and base of the productive formation, location of gas/water interface originally and at the date the model study begins, and location of dry-gas/wet-gas interface at the start of study—and general information on lithology and lenticularity of the productive strata, such as extent of fissures, fractures, caverns, and other special conditions. If a black-oil ring is present, its size and extent should be shown.

2. Physical properties of the reservoir rock—isoporosity map (or average porosity), effective or specific isopermeability map (or average values), and interstitial water content.

3. Fluid characteristics (produced, and injected where applicable)—fluid composition, retrograde dewpoint pressure of reservoir fluids, gas FVF or specific volume vs. pressure, deviation factor, condensate content of reservoir fluid, viscosity, and densities of liquid and gas phases, all from original reservoir pressure through the range of interest (usually to abandonment conditions).

4. Amount of original fluids in place (derivable from data in Points 1 through 3).

5. Reservoir pressure history (volumetrically weighted) from discovery to present. If this is not available, isobaric contour maps at the various pressure survey dates should be supplied.

6. Condensate, gas, and water production data, from the date of discovery.

7. Proposed future production rates.

8. Gas- and/or water-injection data, past and future projections.

9. Productivity, injectivity, and backpressure test data on wells.

Ultimate Recovery of Gas and Condensate Liquids by Cycling. The same reservoir for which pressure-depletion calculations were made previously can be used to illustrate the effectiveness of a cycling operation. Table 39.8 lists the basic data for predicting the ultimate recoveries of wet gas, condensate, and plant products during cycling at original reservoir pressure (to avoid serious drawdown effects) followed by pressure depletion to abandonment pressure. Productive thickness, porosity, and interstitial water content are each assumed uniform. Consequently, the 79.0% areal sweep efficiency obtained by a potentiometric model study is also the pattern ($h\phi S$ -weighted) efficiency. The invasion efficiency is assumed to be 90% because permeability variations are moderate. Because a dry-gas/wet-gas cycling operation is a miscible flood, the displacement efficiency is essentially 100%. Therefore, the reservoir cycling efficiency would be 71.1%. To simplify the example, it is assumed that after cycling, the unswept pore space both inside and outside the dry-gas front will pressure deplete in the same manner as predicted previously for the noncycling case; it will also be assumed economical to recover the butanes-plus from the gas produced.

Reservoir wet gas produced during cycling period (original reservoir composition):

$$130,992 \times 0.711 = 93,135 \text{ MMscf.}$$

Reservoir wet gas produced by pressure depletion after cycling (changing composition, as shown in pressure-depletion example):

$$102,045 \times (1,000 - 0.711) = 29,491 \text{ MMscf.}$$

Reservoir wet gas produced at abandonment pressure, 700 psig:

$$93,135 + 29,491 = 122,626 \text{ MMscf.}$$

Total separator gas produced (see Table 39.6):
During cycling,

$$\frac{777.15 + 38.52 + 38.45}{1,000} \times 93,135$$

$$= 0.85412 \times 93,135 = 79,548 \text{ MMscf.}$$

During depletion,

$$\frac{696.75 + 14.99 + 18.05}{1,000} \times 29,491$$

$$= 0.72979 \times 29,491 = 21,522 \text{ MMscf.}$$

Total:

$$79,548 + 21,522 = 101,070 \text{ MMscf.}$$

Total condensate produced:
During cycling,

$$181.74 \times 93,135 = 16,926,355 \text{ bbl.}$$

During depletion,

$$51.91 \times 29,491 = 1,530,878 \text{ bbl.}$$

Total:

$$16,926,355 + 1,530,878 = 18,457,233 \text{ bbl.}$$

These figures represent a significant improvement over the recoveries previously estimated for pressure-depletion alone.

Noninjection-Gas Requirements in Cycling Operations.

The noninjection-gas requirements for cycling can affect the amount of gas available for injection. The amount of gas to be cycled is determined by the optimum pressure level to be maintained and the efficiency of reservoir fluid recovery to be achieved; the amount of gas readily available, including sources and costs; and the design and operating programs for surface facilities. The amount of gas that is economical to cycle through a gas-condensate reservoir varies with many factors, including richness of the vapor at reservoir cycling pressure, size and cost of the plant, and the price of the field products and of dry gas. Miller and Lents⁶⁶ expected to cycle the equivalent of about 115% of the gas in place to recover some 85% of the wet-gas reserve of the Cotton Valley Bodcaw reservoir. While Brinkley⁵⁵ indicated cycling-gas volumes of as much as 130% of original wet gas in place for various reservoirs, no general correlation has been presented on the amount of gas that is economically sound to cycle; this should be the subject of a detailed engineering analysis in each case. The makeup gas needed for constant-pressure cycling is mainly the volume required to replace shrinkage by liquid recovery and the amount consumed

for various fuel needs. For some composition, temperature, and pressure ranges, the removal of high-molecular-weight constituents from the produced wet gas may result in a higher compressibility factor for the injected dry gas; hence, the greater volume per mole injected may require little or no makeup gas for constant-pressure cycling.

The amount of gas not available for injection because of consumption for operating needs should be taken into account in determining makeup gas requirements if pressure is to be maintained. The amount of fuel for compression and treatment plants depends mainly on the total amount of gas to be returned to the reservoir and the discharge pressure for the plant. Discharge pressure, in turn, depends on the total rate of injection demanded and the number of injection wells and their intake capacities throughout the life of the operation. Other factors affecting the amount of gas required for overall operations are type of plant, type of liquid-recovery system used, and auxiliary field requirements (such as for drilling, completion, and well testing; camp fuel and power for maintenance shops, general service facilities, employee housing; and other factors that vary from one case to another).

Moore⁵⁴ reports that gas fuel consumption for the compression plant alone varies from 7 to 12 cu ft/bhp-hr; this is probably for gases with heat values of about 1,000 Btu/cu ft. Horsepower requirements per million standard cubic feet of gas compressed per day are correlated in Ref. 16 (Compressor section).

An example based on Refs. 16 and 52 shows that, with 8 cu ft/bhp-hr, a compression ratio of 15.0 (compressing from, say, 461 to 7,000 psia) requiring three stages of compression with a ratio per stage of 2.47, and a specific-heat ratio of 1.25, the cubic feet of compressor fuel used per million cubic feet of gas compressed can be calculated as follows.

For a gas of 0.65 specific gravity and a stage compression ratio of 2.5, the chart in Ref. 16 reads 22 bhp. The allowance factor for interstage pressure drop (three compression stages) is 1.1.

Fuel used per million cubic feet of gas compressed = bhp × cu ft of fuel/bhp-hr × ratio/stage × number of stages × allowance factor. Or compressor fuel consumption is

$$m_c = 22 \times 8 \times 24 \times 2.47 \times 3 \times 1.1 = 34.4 \text{ Mscf/MMscf.}$$

This compares favorably with the factor presented in Moore's⁵⁴ Fig. 8. For an example reservoir originally containing 130,992 MMscf of wet gas, which might be cycled the equivalent of 1 1/4 times, the approximate compressor fuel consumption would be

$$130,992 \times 1.25 \times 34.4 = 5.633 \text{ MMscf.}$$

This is approximately 3% of the gas handled through the plant.

Treatment plant fuel and other plant needs added to compressor fuel bring the range of consumption inside the plant fence to 3 to 7% of the gas handled by a cycling plant. In addition to these needs and others mentioned earlier, possible gas losses can occur in a cycling operation: gas used in "blowing down" wells, should this be necessary for cleaning or treating purposes; small gas leaks at compressor plants and in field lines; and gas leaks

resulting from imperfect seals or corrosion in well tubings, casings, and cement jobs. Remedial workover operations should be planned immediately when there is evidence of appreciable loss of gas between the compression plant and the reservoir sandface or between the outflow-well sandface and the plant intake.

Combination Recovery Procedures

Partial water drive—conditions of natural water influx at rates too low to maintain pressure completely at the desired production rates—can exist for gas-condensate reservoirs. In such cases, operation may be by partial water drive and depletion, supplemental water injection, or partial water drive and cycling.

Prediction of reservoir behavior and recovery under these conditions requires knowledge or assumptions about the aquifer and the water drive it supplies. This information can be deduced from a study of geologic conditions and early producing history of the reservoir; sometimes the deductions are accurate, sometimes not. Projections of water drive magnitude into the future at selected reservoir pressure levels can be made by methods developed in Refs. 72 and 73. If sufficient early producing history of a reservoir is available, it can usually be matched (simulated) by a mathematical reservoir simulation study. The future behavior of the reservoir can then be predicted under the following producing methods: (1) producing history and ultimate recovery of gas and liquids under partial water drive and pressure depletion at the selected production rate; (2) amount of supplemental water injection required to maintain reservoir pressure fully at the selected pressure level and production rate; and (3) size of cycling plant required to maintain pressure at the selected pressure level and production rate.

General Operating Problems: Well Characteristics and Requirements

As with any complex operation, gas-condensate recovery projects have many operating problems. Those pertaining to the plant, lines, and other surface facilities are best left to experienced plant and maintenance personnel, except as they affect reservoir operation (e.g., compressor-oil or corrosion-products carry-over into wells). Operating difficulties occurring at and below the wellhead are often concerns of the reservoir engineer and have an important bearing on the effectiveness of reservoir operation, whether by pressure depletion or by pressure maintenance. Among these are the maintenance of injection and production wells in good mechanical condition, the protection of wells against excessive corrosion, the general maintenance of well injectivity and well productivity (which are often interrelated), and the formation of hydrates that can interfere with the general injection and/or production operation.

Well Productivity and Testing

It is essential to maintain the producing capacities of gas-condensate wells above minimum levels for good economic performance. Much has been written about the productivities of gas and gas-condensate wells, their general producing characteristics, and the optimum methods for testing and reporting their productivities. Loss of productivity of gas-condensate wells can occur from reservoir

pressure decline (including possible effects from condensation of liquids in the reservoir and consequent reduction of effective gas permeability), from the invasion of water into producing wells, from solid precipitates in the pore space, from formation damage during well killing or workover operations, and from mechanical failure of downhole equipment. The engineer must have indices at his disposal that show the productivity histories of wells and whether productivity decline is excessive for prevailing producing conditions.

Productivity Testing. In making productivity tests on wells, orderly well-conditioning and overall test procedures should be used, as suggested in Chap. 33 or in standards recommended by Texas,²⁶ New Mexico,²⁷ Kansas,²⁸ and the Interstate Oil Compact Commission.²⁹

It is common to use wellhead pressures in determining well productivity (or injectivity) characteristics with arbitrary correction procedures for estimating BHP's from the observed surface pressures. No fully satisfactory methods have been devised for making accurate estimates of gas-condensate well BHP's, either static or flowing. Calculated static pressures can have serious uncertainties because of unknown amounts of liquid hydrocarbons or water in the wellbore and tubing and unknown temperature distribution. Calculated flowing pressures can have uncertainties because of inaccuracies in the detailed temperature distribution and the particular friction factor assumed for each specific case. Lessem *et al.*⁷⁴ provide helpful charts for approximating the temperature distribution in flowing gas wells. Errors and uncertainties of the above nature become worse as well depths increase. Consequently, for best results, downhole pressure measurements with accurate gauges should be used. Where this is not feasible, BHP's may be estimated from surface pressure readings for gas-condensate wells with better accuracy than is usually true for oil wells. Chaps. 33 and 34 discuss methods for making such estimates. For these methods, measured fluid properties (e.g., density) should be used whenever available in preference to calculated or correlation values.

For gas and gas-condensate wells, a plot of static and producing BHP's vs. producing rates (in millions of standard cubic feet per day) is not a straight line. Smooth curves with closer approximations to straight lines can be obtained by plotting squares of the static and producing well BHP's (absolute) vs. producing rate. A rough analogy to oilwell behavior is then obtained by plotting the differences in squares of the static and producing pressures vs. the corresponding producing rates (usually on log-log paper). If several pressures are obtained on a well at different rates, these procedures do not always yield straight-line relationships (see Chap. 33 and Ref. 75); however, they provide reasonable indices for limited extrapolation to future well behavior and for comparison of current with past well behavior. Estimation of future well productivity can be made by modifying initial well productivity to account for the changes in reservoir pressure and gas permeability as pressure declines and liquid is deposited in the pores. For no loss of gas permeability, a new productivity line can be drawn on the plot of pressure squared vs. rate, parallel to the original productivity line and through the square of the new static pressure selected; this yields an estimate of flowing rate for any

flowing pressure selected. If the original curve for rate vs. difference in squares of static and flowing pressures is used, rates can be estimated for any future flowing pressure by using the proper (future) static pressure; low-permeability wells would require special adjustment of earlier isochronal test data obtained (see Chap. 33 and Ref. 75). These methods yield approximations of future productivity as affected by pressure decline in the absence of fluid-phase and viscosity changes in the reservoir. If gas permeability, k_g , is likely to be seriously affected by condensation of liquids in the pores (and gas viscosity by pressure decline), then the change in gas mobility k_g/μ_g must be approximated and radial-flow calculations made (see Chap. 35) to estimate the new productivity curve corresponding to the static pressure selected for prediction.

Normally, the two aforementioned types of productivity estimates ignore the drawdown effects of production on liquid-phase distribution in the reservoir and any consequent additional reduction of gas permeability near the producing wells; minimum calculated reduction of productivity should, therefore, result from these two estimating methods. Large deviations from such estimates, based on a well's early characteristics, would indicate that the well should be analyzed for productivity troubles.

Excessive Productivity Loss. If the capacity of a producing well declines abnormally compared with that predicted from its original productivity (in the absence of excessive water production), and if appreciable liquid condensation around the wellbore within the formation is suspected, efforts to improve well productivity should be made. These could include the short-term injection of dry gas into the well (several days to several weeks) to evaporate part of the liquid, followed by immediate production to remove some of the vaporized liquid block.

Loss of well productivity caused by excessive water production has been discussed briefly. In some cases, well workover operations would be justified to reduce or to shut off water entry.

Other factors that can influence well productivity are deposits on the sandface or in the pores near the wellbore, perhaps caused by salts precipitated from reservoir water; any mechanical damage resulting from killing the well for pulling equipment or workover; mechanical failure of downhole equipment; and possible hydrates (see Chap. 33). In case of well productivity injury for mechanical reasons, conventional methods of well repair should be undertaken on the basis of the particular difficulty involved.

Various means are available for stimulating low-productivity wells; see Chaps. 54 and 55 and discussions by Clinkenbeard *et al.*⁷⁶

Well Injectivity

Maintenance of well injectivity is essential for the economic operation of cycling programs. Injectivity decline can be caused by sandface plugging or by buildup of reservoir pressure.

Injectivity Testing. The characterization of gas-injection wells is similar to that for gas-producing wells. In either case, analysis is made on the basis of plots of rates vs. the squares of BHP's or rates vs. differences of squares

of pressures. Consequently, after suitable well conditioning, as previously described, injectivity testing should consist of a series of injection rates at different pressures to establish the early injectivity performance of the well when well conditions are known to be good and the sandface is clean. If facilities are not available for obtaining a range of injection rates and pressures, it is sometimes acceptable to obtain production rates and pressures for the injection well through a reasonable range and use the pressure-squared relationship for extrapolating across the zero-rate axis into higher injection-pressure ranges to approximate well characteristics. Plots of production rate vs. difference in squares of pressure can also be adapted to estimate later well-injectivity behavior.

As in the case of producing wells, if injectivity declines with time, analysis of well conditions is required to decide whether corrective procedures should be used. If a gas-condensate reservoir is being operated essentially at constant pressure, then the obvious index of injectivity decline is whether the rate for each injection well remains constant at the injection-well pressure. Injection-rate decline at constant well pressure or injection-pressure rise at constant injection rate shows that injectivity is declining.

Injection-Well Plugging. Plugging of the sandface can occur in injection wells. This may result from liquid carry-over from the compressors (probably lubricating oil components) or from corrosion products from surface lines or well equipment.

Carry-over of lubricating oils from compressors can be serious. Usually, the remedy is to install high-efficiency aftercoolers, scrubbers, and/or mist extractors on the discharge side of the compressors. A particularly effective combination for this is the use of "drips" or collectors, followed by plate or screen impaction-type mist eliminators, followed by combination fibrous and wire-mesh filter elements.

When liquid-blocking of the sand around an injection wellbore cannot be relieved by backflowing (as mentioned later), consideration can be given to "slugging" the well with suitable volatile solvents. The solvent used should preferably be miscible with both the normal injection gas and the liquid that is suspected to be blocking the pores. While propane is a good solvent for many hydrocarbon liquids, some lubricating oils have constituents not soluble or miscible with propane. In these cases, other solvents (possibly nonhydrocarbons) should be used. Sometimes solvent injection is followed immediately by resumption of dry-gas injection. If successful, this dissolves part or all of the liquid block and spreads out the materials in the reservoir sufficiently to relieve the problem. In other cases, the solvent is injected into the formation for short periods and then produced back out to provide a type of washing intended to remove the liquid accumulation from the formation.

Corrosion products from steel lines between compressor discharge and the sandface can also provide serious well plugging. All well piping and casing and all surface lines should be cleaned thoroughly before they are installed to avert as much as possible the transportation of fine corrosion products to the sandface when injection starts. For continued protection during the life of injection equipment, liquid carry-over and mist-elimination measures should be combined with adequate control of corrosive

agents in the field gas. Sometimes the use of internally coated or lined pipe is justified. These and other corrosion-control procedures are best carried out with the help of a competent corrosion engineer.

Corrosion products that plug the sandface are sometimes removed by backflowing the injection well to blow the material off the sand and out of the well. Where this is feasible, such complete removal of the plugging agents from the borehole is believed to be the best for the well. Other remedies may include treating the well with inhibited hydrochloric acid to dissolve the corrosion products. Sometimes the acid is pushed back into the formation and injection is started immediately without backwashing or backflowing of the well. If repeated periodically, this procedure is questionable because it is possible to develop plugging farther away from the well face that could ultimately hinder injection and be difficult to correct.

Number of Wells Required

The number of wells used in exploiting gas-condensate reservoirs has varied from the equivalent of less than 160 acres/well to more than 640 acres/well. Bennett⁷⁷ discussed the general problem and pointed out that the first wells are "drilled to determine the upper and lower limits of condensate production; to determine the extent of the pool, the net pay, thickness, porosity, etc.; and to provide suitable production or injection wells to fit a final pattern," which will not necessarily have a regular geometrical design.

The number of wells to be drilled for gas-condensate operations must be analyzed for each specific case. Important factors to be considered are (1) contract commitments to deliver gas and products, (2) capacity of plant to be served, (3) productivities and injectivities of the wells, (4) maximum practical pattern (*h₀S*-weighted) efficiencies, controlled by number and location of wells (reservoir geometry is an important consideration), (5) amount of recoverable hydrocarbons and their value, and (6) project costs, including well-development costs. Items 3 through 5 must be balanced against Items 1, 2, and 6 to ensure that the economic objectives and contract commitments of the project are met. If wells are low in capacity, extra wells may be needed to meet production requirements during periods of well repair or workover.

Economics of Gas-Condensate Reservoir Operation

Arthur⁷⁸ and Boatright and Dixon⁷⁹ published discussions on the economics of cycling gas-condensate reservoirs. Arthur concluded that the most profitable method of operation depends on many factors, and the answer cannot be generalized. The following factors adapted from Arthur's list are considered important.

1. Reservoir formation and fluid characteristics, including occurrence or absence of black oil, size of reserves of products, properties and composition of reservoir hydrocarbons, productivities and injectivities of wells, permeability variation (controls the degree of bypassing of injected gas), and degree of natural water drive existing.
2. Reservoir development and operating costs.
3. Plant installation and operating costs.
4. Market demand for gas and liquid petroleum products.

5. Future relative value of the products.
6. Existence or absence of competitive producing conditions between operators in the same reservoir.
7. Severance, ad valorem, and income taxes.
8. Special hazards or risks (limited concession or lease life, political climate, and others).
9. Overall economic analysis.

In choosing between pressure depletion and pressure maintenance as operating methods for a gas-condensate reservoir, detailed analyses must be made for predicting optimum economics. Cycling and gas processing procedures require sizable plant expenditures. Possible processing methods, whether reservoir fluids are cycled or not, include stabilization, compression, absorption, and fractionation. The last two recover appreciably more condensables from wet gas than do the first two. If the removal of ethane from a gas stream is desirable for economic or other reasons, fractionation should be used.

When reservoir characteristics appear favorable for recovery of condensable hydrocarbons, it must be considered whether cycling would be economical. The primary comparison is between value of the estimated additional recovery of liquid products by cycling and the actual cycling costs, taking into account deferment of gas income and other factors. Economic analyses of cycling and noncycling are required and must be carried out in detail for maximum dependability with information factors and assumptions pertinent to each particular case. General information on valuation of oil and gas properties is given in Chap. 41.

Economic comparisons are of no value unless reasonably accurate predictions of physical reservoir behavior can be made. Consequently, in the gas-condensate reservoir case, the information given previously would have to be expanded to include schedules of annual production and injection volumes derived from the physical characteristics of the reservoir and from the external factors that would affect production rates. Schedules of investment, anticipated prices of products, operating costs, and taxes would also be required to complete the detailed information needed to make comparative economic analyses.

Nomenclature

- B_g = gas expansion factor (gas FVF)
 E_A = areal sweep efficiency
 E_D = displacement efficiency
 E_I = invasion efficiency
 E_p = pattern ($h\phi S$ -weighted) efficiency
 E_R = reservoir cycling efficiency
 E_V = volumetric sweep efficiency
 h = net pay thickness, ft
 k = permeability, md
 k_{rg} = relative permeability to gas, fraction
 k_{ro} = relative permeability to oil, fraction
 K = equilibrium ratio
 p = pressure, psi
 S = hydrocarbon fluid saturation of the pore space, %
 x = layer number
 z = deviation factor (compressibility factor)
 μ_g = gas viscosity, cp
 μ_o = oil viscosity, cp

ρ_g = gas density, g/cm³

ϕ = porosity, %

Φ_g = flow potential, psi

References

1. Sage, B.H. and Lacey, W.N.: *Volumetric and Phase Behavior of Hydrocarbons*, API Project 37, Stanford U. Press, Stanford, CA (1939).
2. Eilerts, C.K. et al.: *Phase Relations of Gas-Condensate Fluids, Test Results, Apparatus, and Techniques*, American Gas Assn., New York City (1957) 1 and 2.
3. Burcik, E.J.: *Properties of Petroleum Reservoir Fluids*, John Wiley & Sons Inc., New York City (1957).
4. Muskat, M.: *The Flow of Homogeneous Fluids Through Porous Media*, McGraw-Hill Book Co. Inc., New York City (1937).
5. Muskat, M.: *Physical Properties of Oil Production*, McGraw-Hill Book Co. Inc., New York City (1949).
6. Sage, B.H. and Lacey, W.N.: *Thermodynamic Properties of the Lighter Paraffin Hydrocarbons and Nitrogen*, API, New York City (1950).
7. Sage, B.H. and Lacey, W.N.: *Some Properties of the Lighter Hydrocarbons, Hydrogen Sulfide, and Carbon Dioxide*, API, New York City (1955).
8. *Fundamental Research on Occurrence and Recovery of Petroleum*, API, New York City (1943-55) 1-7.
9. Standing, M.B.: *Volumetric and Phase Behavior of Oil Field Hydrocarbon Systems*, SPE, Richardson, TX (1977).
10. Katz, D.L.: "Phase Relationships in Oil and Gas Reservoirs," *Bull.*, Texas Engineering Expt. Station (1949) 114.
11. *Trans.*, AIME (1931-present; 132-present) SPE, Richardson, TX (published annually).
12. *Drill. and Prod. Prac.* (1939-present) API, Dallas (published annually).
13. Craft, B.C. and Hawkins, M.F.: *Applied Petroleum Reservoir Engineering*, Prentice-Hall Inc., Englewood Cliffs, NJ (1959).
14. Katz, D.L. et al.: *Handbook of Natural Gas Engineering*, McGraw-Hill Book Co. Inc., New York City (1959).
15. *Equilibrium Ratio Data Book*, Natural Gas Assn. of America, Tulsa, OK (1955).
16. *Engineering Data Book*, ninth edition, Gas Processors Suppliers Assn. and Natural Gas Assn. of America, Tulsa, OK (1981).
17. Katz, D.L. and Rzasa, M.J.: *Bibliography for Physical Behavior of Hydrocarbons Under Pressure and Related Phenomena*, J.W. Edwards Publisher Inc., Ann Arbor (1946).
18. *General Index to Petroleum Publications of SPE-AIME*, SPE, Richardson, TX (1921-85) 1-5.
19. *Index of Division of Production Papers, 1927-1953*, API, New York City (1954).
20. Sloan, J.P.: "Phase Behavior of Natural Gas and Condensate Systems," *Pet. Eng.* (Feb. 1950) 22, No. 2, B-54-B-64.
21. Dodson, C.R. and Standing, M.B.: "Prediction of Volumetric and Phase Behavior of Naturally Occurring Hydrocarbon Systems," *Drill. and Prod. Prac.*, API (1941) 326-40.
22. Organick, E.L.: "Prediction of Critical Temperatures and Critical Pressures of Complex Hydrocarbon Mixtures," *Chem. Eng. Prog.* (1953) 49, No. 6, 81-97.
23. Carr, N.L., Kobayashi, R., and Burrows, D.B.: "Viscosity of Hydrocarbon Gases Under Pressure," *J. Pet. Tech.* (Oct. 1954) 47-55; *Trans.*, AIME, 201.
24. Chew, J.N. and Connally, C.A. Jr.: "A Viscosity Correlation for Gas-Saturated Crude Oils," *Trans.*, AIME (1959) 216, 23-25.
25. "API Recommended Practice for Sampling Petroleum Reservoir Fluids," API RP 44, first edition, Dallas (Jan. 1966).
26. *Back-Pressure Test for Natural Gas Wells*, Texas Railroad Commission, Austin (1985).
27. *Manual for Back Pressure Test for Natural Gas Wells*, New Mexico Oil Conservation Commission, Santa Fe (1966).
28. *Manual of Back Pressure Testing of Gas Wells*, Kansas State Corp. Commission, Topeka (1959).
29. *A Suggested Manual for Standard Back-Pressure Testing Methods*, Interstate Oil Compact Commission, Oklahoma City (1986).
30. Whitson, C.H.: "Characterizing Hydrocarbon Plus Fractions," paper EUR 183 presented at the 1980 SPE European Offshore Petroleum Conference and Exhibition, London, Oct. 21-24.
31. Watson, K.M., Nelson, E.F., and Murphy, G.B.: "Characterization of Petroleum Fractions," *Ind. Eng. Chem.* (1935) 27, 1460-64.

32. Hoffman, A.E., Crump, J.S., and Hocott, C.R.: "Equilibrium Constants for a Gas-Condensate System," *Trans., AIME* (1953) **198**, 1-10.
33. Cook, A.B., Walker, C.J., and Spencer, G.B.: "Realistic K Values of C_7+ Hydrocarbons for Calculating Oil Vaporization During Gas Cycling at High Pressures," *J. Pet. Tech.* (July 1969) 901-15; *Trans., AIME*, **246**.
34. Nemeth, L.K. and Kennedy, H.T.: "A Correlation of Dewpoint Pressure With Fluid Composition and Temperature," *Soc. Pet. Eng. J.* (June 1967) 99-104.
35. Allen, F.H. and Roe, R.P.: "Performance Characteristics of a Volumetric Condensate Reservoir," *Trans., AIME* (1950) **189**, 83-90.
36. Berryman, J.E.: "Predicted Performance of a Gas-Condensate System, Washington Field, Louisiana," *J. Pet. Tech.* (April 1957) 102-07; *Trans., AIME*, **210**.
37. Rodgers, J.K., Harrison, N.H., and Regier, S.: "Comparison Between the Predicted and Actual Production History of a Condensate Reservoir," *J. Pet. Tech.* (June 1958) 127-31; *Trans., AIME*, **213**.
38. Redlich, O. and Kwong, J.N.S.: "On the Thermodynamics of Solutions V. an Equation of State Fugacities of Gaseous Solutions," *Chem. Review* (1949) **44**, 233.
39. Peng, D.Y. and Robinson, D.B.: "A New Two-Constant Equation of State," *Ind. Eng. Chem. Fundamentals* (1976) **15**, 15-59.
40. Martin, J.J.: "Cubic Equations of State—Which?" *Ind. Eng. Chem. Fundamentals* (May 1979) **18**, 81.
41. *Petroleum Conservation*, S.E. Buckley *et al.* (eds.), AIME, New York City (1951).
42. Geffen, T.M. *et al.*: "Efficiency of Gas Displacement From Porous Media by Liquid Flooding," *Trans., AIME* (1952) **195**, 29-38.
43. Yuster, S.T.: "The Rehabilitation of Drowned Gas Wells," *Drill. and Prod. Prac.*, API (1946) 209-16.
44. Bennett, E.N. and Auvenshine, W.L.: "Dewatering of Gas Wells," *Drill. and Prod. Prac.*, API (1956) 224-30.
45. Dunning, H.N. and Eakin, J.L.: "Foaming Agents are Low-Cost Treatment for Tired Gassers," *Oil and Gas J.* (Feb. 2, 1959) **57**, No. 6, 108-10.
46. Bates, G.O., Kilmer, J.W., and Shirley, H.T.: "Eight Years of Experience with Inert Gas Equipment," paper 57-PET-34 presented at the 1957 ASME Petroleum Mechanical Engineering Conference, Sept.
47. Barstow, W.F.: "Fourteen Years of Progress in Catalytic Treating of Exhaust Gas," paper SPE 457 presented at the 1973 SPE Annual Meeting, Las Vegas, Sept. 30-Oct. 3.
48. Eckles, W.W. and Holden, W.W.: "Unique Enhanced Oil and Gas Recovery Project for Very High Pressure Wilcox Sands Uses Cryogenic Nitrogen and Methane Mixture," paper SPE 9415 presented at the 1980 SPE Annual Technical Conference and Exhibition, Dallas, Sept. 21-24.
49. Moses, P.L. and Wilson, K.: "Phase Equilibrium Considerations in Utilizing Nitrogen for Improved Recovery From Retrograde Condensate Reservoirs," paper SPE 7493 presented at the 1978 SPE Annual Technical Conference and Exhibition, Houston, Oct. 1-4.
50. Peterson, A.V.: "Optimal Recovery Experiments with N_2 and CO_2 ," *Pet. Eng. Intl.* (Nov. 1978) 40-50.
51. "Physical Properties of Nitrogen for Use in Petroleum Reservoirs," *Bull.*, Air Products and Chemical Inc., Allentown, PA (1977).
52. Wilson, K.: "Enhanced-Recovery Inert Gas Processes Compared," *Oil and Gas J.* (July 31, 1978) 162-72.
53. Donohoe, C.W. and Buchanan, R.D.: "Economic Evaluation of Cycling Gas-Condensate Reservoirs With Nitrogen," paper SPE 7494 presented at the 1978 SPE Annual Technical Conference and Exhibition, Houston, Oct. 1-4.
54. *Proc.*, Ninth Oil Recovery Conference, Symposium on Natural Gas in Texas, College Station, TX (1956).
55. Brinkley, T.W.: "Calculation of Rate and Ultimate Recovery from Gas Condensate Reservoirs," paper 1028-G presented at the 1958 SPE Petroleum Conference on Production and Reservoir Engineering, Tulsa, OK, March 20-21.
56. Patton, C.E. Jr.: "Evaluation of Pressure Maintenance by Internal Gas Injection in Volumetrically Controlled Reservoirs," *Trans., AIME* (1947) **170**, 112-55.
57. API Standing Subcommittee on Secondary Recovery Methods, Circ. D-294, API (March 1949) Appendix B.
58. Marshall, D.L. and Oliver, L.R.: "Some Uses and Limitations of Model Studies in Cycling," *Trans., AIME* (1948) **174**, 67-87.
59. Calhoun, J.C. Jr.: *Fundamentals of Reservoir Engineering*, U. of Oklahoma Press, Norman (1953) 358, 374.
60. Hock, R.L.: "Determination of Cycling Efficiencies in Cotton Valley Field Gas Reservoir," *Oil and Gas J.* (Nov. 4, 1948) **47**, No. 27, 63-99.
61. Calhoun, J.C. Jr.: "A Resume of the Factors Governing Interpretation of Waterflood Performance," paper presented at the 1956 SPE-AIME North Texas Section Secondary Recovery Symposium, Wichita Falls, Nov. 19-20.
62. Pirson, S.J.: *Oil Reservoir Engineering*, McGraw-Hill Book Co. Inc., New York City (1958) 406.
63. Stelzer, R.B.: "Model Study vs. Field Performance Cycling the Paluxy Condensate Reservoir," *Drill. and Prod. Prac.*, API (1956) 336-42.
64. Muskat, M.: "Effect of Permeability Stratification in Cycling Operations," *Trans., AIME* (1949) **179**, 313-28.
65. Standing, M.B., Linblad, E.N., and Parsons, R.L.: "Calculated Recoveries by Cycling from a Retrograde Reservoir of Variable Permeability," *Trans., AIME* (1948) **174**, 165-90.
66. Miller, M.G. and Lents, M.R.: "Performance of Bodcaw Reservoir, Cotton Valley Field Cycling Project, New Methods of Predicting Gas-Condensate Reservoir Performance Under Cycling Operations Compared to Field Data," *Drill. and Prod. Prac.*, API (1946) 128-49.
67. Law, J.: "A Statistical Approach to the Interstitial Heterogeneity of Sand Reservoirs," *Trans., AIME* (1945) **155**, 202-22.
68. Hurst, W. and van Everdingen, A.F.: "Performance of Distillate Reservoirs in Gas Cycling," *Trans., AIME* (1946) **165**, 36-51.
69. Cardwell, W.T. Jr. and Parsons, R.L.: "Average Permeabilities of Heterogeneous Oil Sands," *Trans., AIME* (1945) **160**, 34-42.
70. Sheldon, W.C.: "Calculating Recovery by Cycling a Retrograde Condensate Reservoir," *J. Pet. Tech.* (Jan. 1959) 29-34.
71. Coats, K.H.: "Simulation of Gas Condensate Reservoir Performance," paper SPE 10512 presented at the 1982 SPE Reservoir Simulation Symposium, New Orleans, Jan. 31-Feb. 3.
72. Hurst, W.: "Water Influx into a Reservoir and Its Application to the Equation of Volumetric Balance," *Trans., AIME* (1943) **151**, 57-72.
73. van Everdingen, A.F. and Hurst, W.: "Application of Laplace Transformation to Flow Patterns in Reservoirs," *Trans., AIME* (1949) **186**, 305-24.
74. Lesem, L.B. *et al.*: "A Method of Calculating the Distribution of Temperature in Flowing Gas Wells," *J. Pet. Tech.* (June 1957) 169-76; *Trans., AIME*, **210**.
75. Tek, M.R., Grove, M.L., and Poettmann, F.H.: "Method for Predicting the Back-Pressure Behavior of Low Permeability Natural Gas Wells," *J. Pet. Tech.* (Nov. 1957) 302-09; *Trans., AIME*, **210**.
76. Clinkenbeard, P., Bozeman, J.F., and Davidson, R.D.: "Gas Well Stimulation Increases Production and Profits," *J. Pet. Tech.* (Nov. 1958) 21-24.
77. Bennett, E.O.: "Factors Influencing Spacing in Condensate Fields," *Pet. Eng.* (1944) **15**, No. 10, 158-62.
78. Arthur, M.G.: "Economics of Cycling," *Drill. and Prod. Prac.*, API (1948) 144-59.
79. Boatright, B.B. and Dixon, P.C.: "Practical Economics of Cycling," *Drill. and Prod. Prac.*, API (1941) 221-27.

Chapter 40

Estimation of Oil and Gas Reserves

Forrest A. Garb, SPE, H.J. Gruy & Assocs. Inc.*
Gerry L. Smith,** H.J. Gruy & Assocs. Inc.

Estimating Reserves

General Discussion

Management's decisions are dictated by the anticipated results from an investment. In the case of oil and gas, the petroleum engineer compares the estimated costs in terms of dollars for some investment opportunity vs. the cash flow resulting from production of barrels of oil or cubic feet of gas. This analysis may be used in formulating policies for (1) exploring and developing oil and gas properties; (2) designing and constructing plants, gathering systems, and other surface facilities; (3) determining the division of ownership in unitized projects; (4) determining the fair market value of a property to be bought or sold; (5) determining the collateral value of producing properties for loans; (6) establishing sales contracts, rates, and prices; and (7) obtaining Security and Exchange Commission (SEC) or other regulatory body approvals.

Reserve estimates are just what they are called—estimates. As with any estimate, they can be no better than the available data on which they are based and are subject to the experience of the estimator. Unfortunately, reliable reserve figures are most needed during the early stages of a project, when only a minimum amount of information is available. Because the information base is cumulative during the life of a property, the reservoir engineer has an increasing amount of data to work with as a project matures, and this increase in data not only changes the procedures for estimating reserves but, correspondingly, improves the confidence in the estimates. Reserves are frequently estimated (1) before drilling or any subsurface development, (2) during the development drilling of the field, (3) after some performance data are available, and (4) after performance trends are well established. Fig. 40.1 demonstrates (1) the various periods in the life of an imaginary oil property, (2) the sequence

of appropriate recovery estimating methods, (3) the impact on the range of recovery estimates that usually results as a property ages and more data become available, (4) a hypothetical production profile, and (5) the relative risk in using the recovery estimates. Time is shown on the horizontal axis. No particular units are used in this chart, and it is not drawn to any specific scale. Note that while the ultimate recovery estimates may become accurate at some point in the late life of a reservoir, the reserve estimate at that time may still have significant risk. During the last week of production, if one projects a reserve of 1 bbl and 2 bbl are produced, the reserve estimate was 100% in error.

Reserve estimating methods are usually categorized into three families: analogy, volumetric, and performance techniques. The performance-technique methods usually are subdivided into simulation studies, material-balance calculations, and decline-trend analyses. The relative periods of application for these techniques are shown in Fig. 40.1.^{1,2} During Period AB, before any wells are drilled on the property, any recovery estimates will be of a very general nature based on experience from similar pools or wells in the same area. Thus, reserve estimates during this period are established by analogy to other production and usually are expressed in barrels per acre.

The second period, Period BC, follows after one or more wells are drilled and found productive. The well logs provide subsurface information, which allows an acreage and thickness assignment or a geologic interpretation of the reservoir. The acre-foot volume considered to hold hydrocarbons, the calculated oil or gas in place per acre-foot, and a recovery factor allow closer limits for the recovery estimates than were possible by analogy alone. Data included in a volumetric analysis may include well logs, core analysis data, bottomhole sample information, and subsurface mapping. Interpretation of these

*Original chapter in 1962 edition was written by Jan J. Arps.

**Deceased

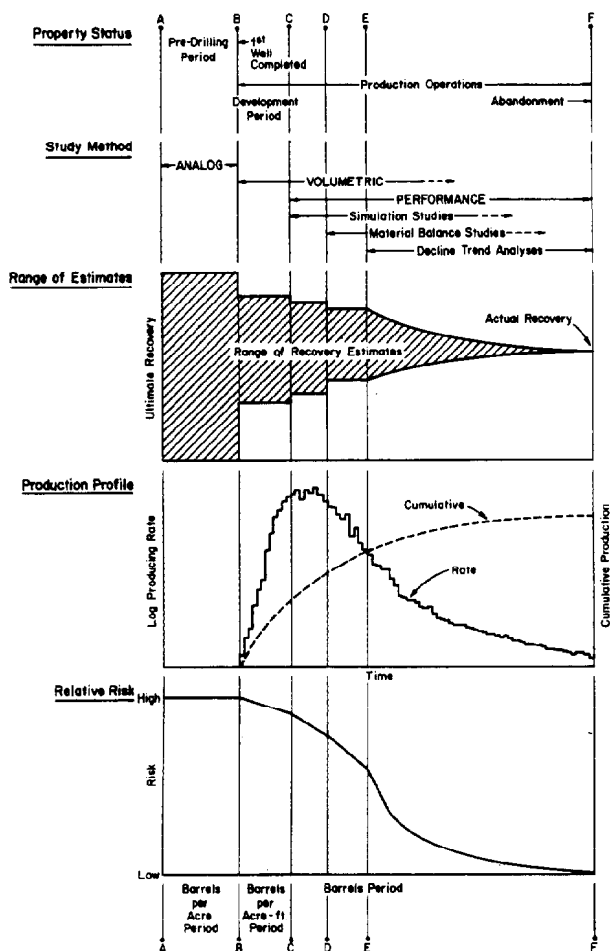


Fig. 40.1—Range in estimates of ultimate recovery during life of reservoir.

data, along with observed pressure behavior during early production periods, may also indicate the type of producing mechanism to be expected for the reservoir.

The third period, Period CD, represents the period after delineation of the reservoir. At this time, performance data usually are adequate to allow derivation of reserve estimates by use of numerical simulation model studies. Model studies can yield very useful reserve estimates for a spectrum of operating options if sufficient information is available to describe the geometry of the reservoir, any spatial distribution of the rock and fluid characteristics, and the reservoir producing mechanism. Because numerical simulators depend on matching history for calibration to ensure that the model is representative of the actual reservoir, numerical simulation models performed in the early life of a reservoir may not be considered to have high confidence.

During Period DE, as performance data mature, the material-balance method may be implemented to check the previous estimates of hydrocarbons initially in place. The pressure behavior studied through the material-balance calculations may also offer valuable clues regarding the type of production mechanism existent in the reservoir. Confidence in the material-balance calculations

depends on the precision of the reservoir pressures recorded for the reservoir and the engineer's ability to determine the true average pressure at the dates of study. Frequent pressure surveys taken with precision instruments have enabled good calculations after no more than 5 or 6% of the hydrocarbons in place have been produced.

Reserve estimates based on extrapolation of established performance trends, such as during Period DEF, are considered the estimates of highest confidence.

In reviewing the histories of reserve estimates over an extended period of time in many different fields, it seems to be a common experience that the very prolific fields (such as East Texas, Oklahoma City, Yates, or Redwater) have been generally underestimated during the early "barrels-per-acre-foot" period compared with their later performance, while the poorer ones (such as West Edmond and Spraberry) usually are overestimated during their early stages.

It should be emphasized that, as in all estimates, the accuracy of the results cannot be expected to exceed the limitations imposed by inaccuracies in the available basic data. The better and more complete the available data, the more reliable will be the end result. In cases where property values are involved, additional investment in acquiring good basic data during the early stages pays off later. With good basic data available, the engineer making the estimate naturally feels more sure of his results and will be less inclined to the cautious conservatism that often creeps in when many of the basic parameters are based on guesswork only. Generally, all possible approaches should be explored in making reserve estimates and all applicable methods used. In doing this, the experience and judgment of the evaluator are an intangible quality, which is of great importance.

The probable error in the total reserves estimated by experienced engineers for a number of properties diminishes rapidly as the number of individual properties increases. Whereas substantial differences between independent estimates made by different estimators for a single property are not uncommon, chances are that the total of such estimates for a large group of properties or an entire company will be surprisingly close.

Petroleum Reserves—Definitions and Nomenclature³

Definitions for three generally recognized reserve categories, "proved," "probable," and "possible," which are used to reflect degrees of uncertainty in the reserve estimates, are listed as follows. The proved reserve definition was developed by a joint committee of the SPE, American Assn. of Petroleum Geologists (AAPG), and American Petroleum Inst. (API) members and is consistent with current DOE and SEC definitions. The joint committee's proved reserve definitions, supporting discussion, and glossary of terms, are quoted as follows. The probable and possible reserve definitions enjoy no such official sanction at the present time but are believed to reflect current industry usage correctly.

Proved Reserves Definitions³

The following is reprinted from the *Journal of Petroleum Technology* (Nov. 1981, Pages 2113-14) proved reserve definitions, discussion, and glossary of terms.

Proved Reserves. Proved reserves of crude oil, natural gas, or natural gas liquids are estimated quantities that geological and engineering data demonstrate with reasonable certainty to be recoverable in the future from known reservoirs under existing economic conditions.*

Discussion. Reservoirs are considered proved if economic producibility is supported by actual production or formation tests or if core analysis and/or log interpretation demonstrates economic producibility with reasonable certainty. The area of a reservoir considered proved includes (1) that portion delineated by drilling and defined by fluid contacts, if any, and (2) the adjoining portions not yet drilled that can be reasonably judged as economically productive on the basis of available geological and engineering data. In the absence of data on fluid contacts, the lowest known structural occurrence of hydrocarbons controls the lower proved limit of the reservoir. Proved reserves are estimates of hydrocarbons to be recovered from a given date forward. They are expected to be revised as hydrocarbons are produced and additional data become available.

Proved natural gas reserves comprise nonassociated gas and associated/dissolved gas. An appropriate reduction in gas reserves is required for the expected removal of natural gas liquids and the exclusion of nonhydrocarbon gases if they occur in significant quantities.

Reserves that can be produced economically through the application of established improved recovery techniques are included in the proved classification when these qualifications are met: (1) successful testing by a pilot project or the operation of an installed program in that reservoir or one with similar rock and fluid properties provides support for the engineering analysis on which the project or program was based, and (2) it is reasonably certain the project will proceed.

Reserves to be recovered by improved recovery techniques that have yet to be established through repeated economically successful applications will be included in the proved category only after successful testing by a pilot project or after the operation of an installed program in the reservoir provides support for the engineering analysis on which the project or program was based.

Estimates of proved reserves do not include crude oil, natural gas, or natural gas liquids being held in underground storage.

Proved Developed Reserves. Proved developed reserves are a subcategory of proved reserves. They are those reserves that can be expected to be recovered through existing wells (including reserves behind pipe) with proved equipment and operating methods. Improved recovery reserves can be considered developed only after an improved recovery project has been installed.

Proved Undeveloped Reserves. Proved undeveloped reserves are a subcategory of proved reserves. They are those additional proved reserves that are expected to be recovered from (1) future drilling of wells, (2) deepening of existing wells to a different reservoir, or (3) the installation of an improved recovery project.

*Most reservoir engineers add the expression "considering current technology."

Glossary of Terms

Crude Oil

Crude oil is defined technically as a mixture of hydrocarbons that existed in the liquid phase in natural underground reservoirs and remains liquid at atmospheric pressure after passing through surface separating facilities. For statistical purposes, volumes reported as crude oil include: (1) liquids technically defined as crude oil; (2) small amounts of hydrocarbons that existed in the gaseous phase in natural underground reservoirs but are liquid at atmospheric pressure after being recovered from oilwell (casinghead) gas in lease separators*; and (3) small amounts of nonhydrocarbons produced with the oil.

Natural Gas

Natural gas is a mixture of hydrocarbons and varying quantities of nonhydrocarbons that exists either in the gaseous phase or in solution with crude oil in natural underground reservoirs. Natural gas may be subclassified as follows.

Associated Gas. Natural gas, commonly known as gas-cap gas, that overlies and is in contact with crude oil in the reservoir.**

Dissolved Gas. Natural gas that is in solution with crude oil in the reservoir.

Nonassociated Gas. Natural gas in reservoirs that do not contain significant quantities of crude oil.

Dissolved gas and associated gas may be produced concurrently from the same wellbore. In such situations, it is not feasible to measure the production of dissolved gas and associated gas separately; therefore, production is reported under the heading of associated/dissolved or casinghead gas. Reserves and productive capacity estimates for associated and dissolved gas also are reported as totals for associated/dissolved gas combined.

Natural Gas Liquids

Natural gas liquids (NGL's) are those portions of reservoir gas that are liquefied at the surface in lease separators, field facilities, or gas processing plants. NGL's include but are not limited to ethane, propane, butanes, pentanes, natural gasoline, and condensate.

Reservoir

A reservoir is a porous and permeable underground formation containing an individual and separate natural accumulation of producible hydrocarbons (oil and/or gas) that is confined by impermeable rock and/or water barriers and is characterized by a single natural pressure system.

*From a technical standpoint, these liquids are termed "condensate"; however, they are commingled with the crude stream and it is impractical to measure and report their volumes separately. All other condensate is reported as either "lease condensate" or "plant condensate" and included in natural gas liquids.

**Where reservoir conditions are such that the production of associated gas does not substantially affect the recovery of crude oil in the reservoir, such gas may be reclassified as nonassociated gas by a regulatory agency. In this event, reserves and production are reported in accordance with the classification used by the regulatory agency.

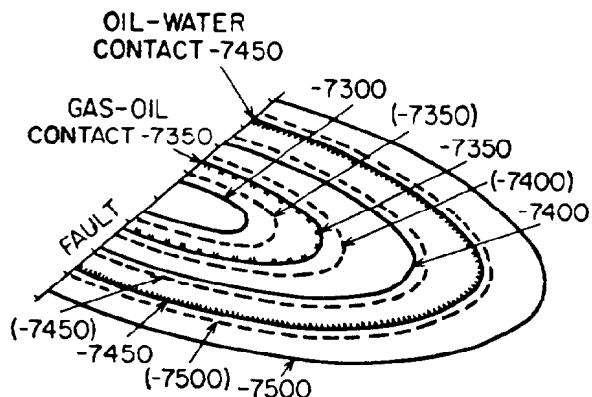


Fig. 40.2—Geological map on top (—) and base (---) of reservoir.

In most situations, reservoirs are classified as oil reservoirs or as gas reservoirs by a regulatory agency. In the absence of a regulatory authority, the classification is based on the natural occurrence of the hydrocarbon in the reservoir as determined by the operator.

Improved Recovery

Improved recovery includes all methods for supplementing natural reservoir forces and energy, or otherwise increasing ultimate recovery from a reservoir. Such recovery techniques include (1) pressure maintenance, (2) cycling, and (3) secondary recovery in its original sense (i.e., fluid injection applied relatively late in the productive history of a reservoir for the purpose of stimulating production after recovery by primary methods of flow or artificial lift has approached an economic limit). Improved recovery also includes the enhanced recovery methods of thermal, chemical flooding, and the use of miscible and immiscible displacement fluids.

Probable Reserves

Probable reserves of crude oil, natural gas, or natural gas liquids are estimated quantities that geological and engineering data indicate are reasonably probable to be recovered in the future from known reservoirs under existing economic conditions. Probable reserves have a higher degree of uncertainty with regard to extent, recoverability, or economic viability than do proved reserves.

Possible Reserves

Possible reserves of crude oil, natural gas, or natural gas liquids are estimated quantities that geological and engineering data indicate are reasonably possible to be recovered in the future from known reservoirs under existing economic conditions. Possible reserves have a higher degree of uncertainty than do proved or probable reserves.

Computation of Reservoir Volume⁴

When sufficient subsurface control is available, the oil- or gas-bearing net pay volume of a reservoir may be computed in several different ways.

1. From the subsurface data a geological map (Fig. 40.2) is prepared, contoured on the subsea depth of the top of the sand (solid lines), and on the subsea depth of the base of the sand (dashed lines). The total area enclosed by each contour is then planimeted and plotted as abscissa on an acre-feet diagram (Fig. 40.3) vs. the corresponding subsea depth as the ordinate. Gas/oil contacts (GOC's) and water/oil contacts (WOC's) as determined from core, log, or test data are shown as horizontal lines.* After the observed points are connected, the combined gross volume of oil- and gas-bearing sand may be determined by the following methods.

*If working in SI units, the depths will be expressed in meters and the planimeted areas enclosed by each contour will be expressed in hectares. The resultant hectare-meter plot can be treated exactly like the following acre-foot example to yield reservoir volumes in cubic meters. (1 ha · m = 10,000 m³.)

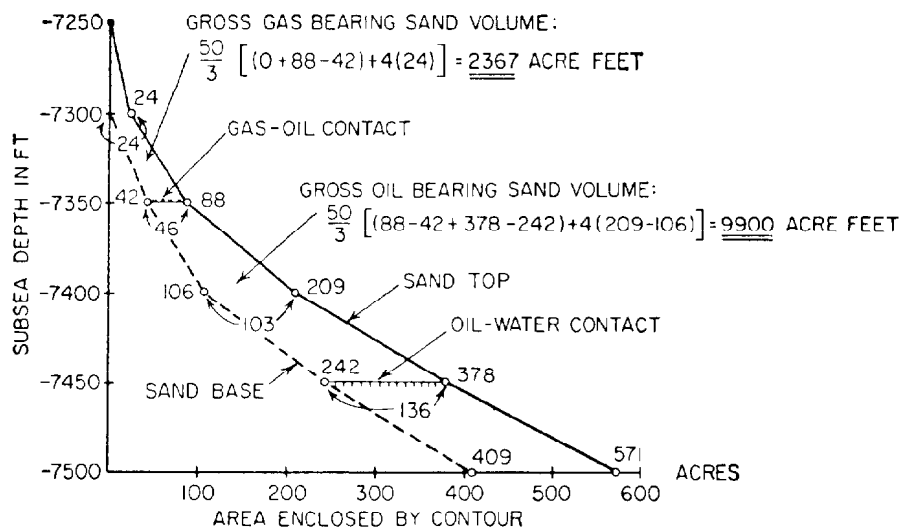


Fig. 40.3—Acre-feet diagram.

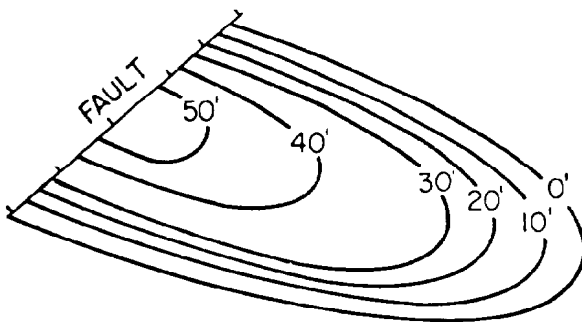


Fig. 40.4—Isopachous map—gas sand.

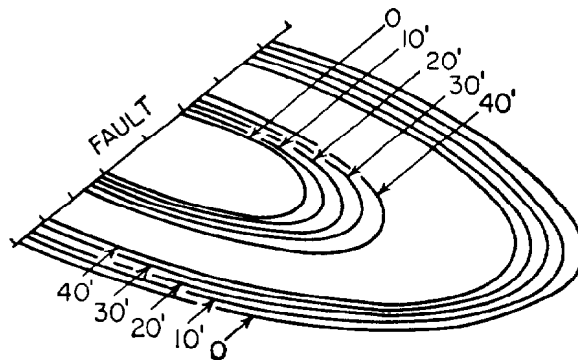


Fig. 40.5—Isopachous map—oil sand.

- a. Planimetered from the acre-feet diagram.
- b. If the number of contour intervals is even, computed by *Simpson's rule*:

$$^{50}_3[(0+136)+4(24+103)+2(46)]=12,267 \text{ acre-ft.}$$

(The separate calculations of the volume of gross gas-bearing sand and gross oil-bearing sand by means of Simpson's rule are shown in the diagram of Fig. 40.3.)

- c. With somewhat less accuracy, computed by the *trapezoidal rule*:

$$50[\frac{1}{2}(0+136)+(24+46+103)]=12,050 \text{ acre-ft.}$$

- d. Computed by means of the somewhat more complicated *pyramidal rule*:

$$^{50}_3[(0+136)+2(24+46+103)+\sqrt{24 \times 88}+\sqrt{88 \times 209} \\ +\sqrt{209 \times 378}-\sqrt{42 \times 106}-\sqrt{106 \times 242}] \\ =11,963 \text{ acre-ft.}$$

- e. If the sand is of uniform thickness, it will oftentimes suffice to multiply the average gross pay thickness \bar{h}_t by the area enclosed by the contour $\frac{1}{2}Z$ ft above the WOC.

- f. If the area within the top contour is circular (area A , height Z), then the top volume is $\frac{1}{6}\pi Z + \frac{1}{2}AZ$ if treated as a segment of a sphere, and $\frac{1}{3}AZ$ if treated as a cone.

From a study of the individual well logs or core data, it is then determined what fraction of the gross sand section is expected to carry and to produce hydrocarbons.

Multiplication of this net-pay fraction by the gross sand volume yields the net-pay volume. If, for example, in the case illustrated with Figs. 40.2 and 40.3, it is found that 15% of the gross section consisted of evenly distributed shale or dense impervious streaks, the net gas- and oil-bearing pay volumes may be computed as, respectively,

$$0.85 \times 2,367 = 2,012 \text{ net acre-ft of gas pay}$$

and

$$0.85 \times 9,900 = 8,415 \text{ net acre-ft of oil pay.}$$

2. From individual well-log data, separate isopachous maps may be prepared for the net gas pay (Fig. 40.4) or for the net pay (Fig. 40.5) and the total net acre-feet of oil- or gas-bearing pay computed as under Item 1a, b, or c.

3. If the nature of the porosity varies substantially from well to well, and if good log and core-analysis data are

available on many wells, it is sometimes justified to prepare an isopachous map of the number of porosity feet (porosity fraction times net pay in feet) and compute the total available void space in the net-pay section from such an isopachous map by the methods discussed under Item 1a, b, or c.

Computation of Oil or Gas in Place

Volumetric Method

If the size of the reservoir, its lithologic characteristics, and the properties of the reservoir fluids are known, the amount of oil or gas initially in place may be calculated with the following formulas:

Free Gas in Gas Reservoir or Gas Cap (no residual oil present). For standard cubic feet of free gas,

$$G_{Fi} = \frac{43,560 V_g \phi (1 - S_{iw})}{B_g}, \quad (1)$$

where

V_g = net pay volume of the free-gas-bearing portion of a reservoir, acre-ft,

ϕ = effective porosity, fraction,

S_{iw} = interstitial water saturation, fraction,

B_g = gas FVF, dimensionless, and

43,560 = number of cubic feet per acre-foot.

Values for the gas FVF or the reciprocal gas FVF, $1/B_g$, may be estimated for various combinations of pressure, temperature, and gas gravity (see section on gas FVF).*

Oil in Reservoir (no free gas present in oil-saturated portion). For stock-tank barrels of oil,

$$N = \frac{7,758 V_o \phi (1 - S_{iw})}{B_o}, \quad (2)$$

where

N = reservoir oil initially in place, STB,

V_o = net pay volume of the oil-bearing portion of a reservoir, acre-ft,

B_o = oil FVF, dimensionless, and

7,758 = number of barrels per acre-foot.

*Refer to Chaps. 20 through 25 for detailed coverage of oil, gas, condensate and water properties, and correlations.

TABLE 40.1—BARRELS OF STOCK-TANK OIL IN PLACE PER ACRE-FT

B_o	S_{iw}	Porosity, ϕ						
		0.05	0.10	0.15	0.20	0.25	0.30	0.35
1.0	0.10	349	698	1,047	1,396	1,746	2,095	2,444
	0.20	310	621	931	1,241	1,552	1,862	2,172
	0.30	272	543	815	1,086	1,358	1,629	1,901
	0.40	233	465	698	931	1,164	1,396	1,629
	0.50	194	388	582	776	970	1,164	1,358
1.5	0.10	233	465	698	931	1,164	1,396	1,629
	0.20	206	411	617	822	1,028	1,234	1,439
	0.30	182	365	547	729	912	1,094	1,276
	0.40	155	310	465	621	776	931	1,086
	0.50	128	256	384	512	640	768	896
2.0	0.10	175	349	524	698	873	1,047	1,222
	0.20	155	310	465	621	776	931	1,086
	0.30	136	272	407	543	679	815	950
	0.40	116	233	349	465	582	698	815
	0.50	97	194	291	388	485	582	679
3.0	0.10	116	233	349	465	582	698	815
	0.20	105	209	314	419	524	628	733
	0.30	89	178	268	357	446	535	625
	0.40	78	155	233	310	388	465	543
	0.50	66	132	198	264	330	396	462

Table 40.1 shows the number of barrels of stock-tank oil per acre-foot for different values of porosity, ϕ , interstitial water saturation, S_{iw} , and the oil FVF, B_o .

Solution Gas in Oil Reservoir (no free gas present).

For standard cubic feet of solution gas,

$$G_s = \frac{7,758 V_o \phi (1 - S_{iw}) R_s}{B_o}, \quad (3)$$

where G_s is the solution gas in place, in standard cubic feet, and R_s is the solution GOR, in standard cubic feet per stock-tank barrel.

Material-Balance Method⁵⁻⁸

In the absence of reliable volumetric data or as an independent check on volumetric estimates, the amount of oil or gas in place in a reservoir may sometimes be computed by the material-balance method.⁵ This method is based on the premise that the PV of a reservoir remains constant or changes in a predictable manner with the reservoir pressure when oil, gas, and/or water are produced. This makes it possible to equate the expansion of the reservoir fluids upon pressure drop to the reservoir voidage caused by the withdrawal of oil, gas, and water minus the water influx. Successful application of this method requires an accurate history of the average pressure of the reservoir, as well as reliable oil-, gas-, and water-production data and PVT data on the reservoir fluids. Generally, from 5 to 10% of the oil or gas originally in place must be withdrawn before significant results can be expected. Without very accurate performance and PVT data the results from such a computation may be quite erratic,⁶ especially when there are unknowns other than the amount of oil in place, such as the size of a free-gas cap, or when a water drive is present.

When the number of available equations exceeds the number of such unknowns, the solution should preferably be by means of the "method of least squares."⁷ Because of the sensitivity of the material-balance equation

to small changes in the two-phase FVF, B_t , an adjustment procedure, called the Y method, may be used for the pressure range immediately below the bubblepoint. The method consists of plotting values of

$$Y = \frac{(p_b - p_R) B_{oi}}{p_R (B_t - B_{oi})}, \quad (4)$$

where

p_b = bubblepoint pressure, psia,

p_R = reservoir pressure, psia,

B_t = two-phase FVF for oil, dimensionless, and

B_{oi} = initial oil FVF, dimensionless,

vs. reservoir pressure, p_R , and bringing a straight line through the plotted points, with particular weight given to the more accurate values away from the bubblepoint. This straight-line relationship is then used to correct the previous values for Y , from which the adjusted values for B_t are computed. Values of B_t computed with this method for pressures substantially below the bubblepoint should not be used if differential liberation is assumed to represent reservoir producing conditions.

When an active water drive is present, the cumulative water influx, W_e , should be expressed in terms of the known pressure/time history and a water drive constant,⁸ thus reducing this term to one unknown. A completely worked-out example of the use of material balance that uses this conversion and in which the amount of oil in place is determined for a partial water drive reservoir where 36 pressure points and equations were available at a time when about 9% of the oil in place had been produced is given in Ref. 7.

The material-balance equation in its most general form reads

$$N = \frac{N_p [B_t + 0.1781 B_g (R_p - R_{si})] - (W_e - W_p)}{B_{oi} \left\{ m \frac{B_g}{B_{gi}} + \frac{B_t}{B_{oi}} - (m+1) \left[1 - \frac{\Delta p_R (c_f + S_{iw} c_w)}{1 - S_{iw}} \right] \right\}}, \quad (5)$$

TABLE 40.2—CLASSIFICATION OF MATERIAL-BALANCE EQUATIONS

Reservoir Type	Material-balance Equation*	Unknowns	Equation
Oil reservoir with gas cap and active water drive	$N = \frac{Np[B_t + 0.1781B_g(R_p - R_{si})] - (W_e - W_p)}{mB_{oi}\left(\frac{B_g}{B_{gi}} - 1\right) + (B_t - B_{oi})}$	N, W_e, m	6
Oil reservoir with gas cap; no active water drive ($W_e = 0$)	$N = \frac{Np[B_t + 0.1781B_g(R_p - R_{si})] + W_p}{mB_{oi}\left(\frac{B_g}{B_{gi}} - 1\right) + (B_t - B_{oi})}$	N, m	7
Initially undersaturated oil reservoir with active water drive ($m = 0$): 1. Above bubblepoint	$N = \frac{\left[N_p(1 + \Delta p_R c_o) - \frac{W_e - W_p}{B_{oi}}\right](1 - S_{iw})}{\Delta p[(c_o + c_f - S_{iw}(c_o - c_w))]}$	N, W_e	8
2. Below bubblepoint	$N = \frac{N_p[B_t + 0.1781B_g(R_p - R_{si})] - (W_e - W_p)}{B_t - B_{oi}}$	N, W_e	9
Initially undersaturated oil reservoir; no active water drive ($m = 0$), ($W_e = 0$): 1. Above bubblepoint	$N = \frac{\left[N_p(1 + \Delta p_R c_o) - \frac{W_p}{B_{oi}}\right](1 - S_{iw})}{\Delta p_R[c_o + c_f - S_{iw}(c_o - c_w)]}$	N	10
2. Below bubblepoint	$N = \frac{N_p[B_t + 0.1781B_g(R_p - R_{si})] + W_p}{B_t - B_{oi}}$	N	11
Gas reservoir with active water drive	$G = \frac{G_p B_g - 5.615(W_e - W_p)}{B_g - B_{gi}}$	G, W_e	12
Gas reservoir; no active water drive ($W_e = 0$)	$G = \frac{G_p B_g + 5.615W_p}{B_g - B_{gi}}$	G	13

*The constant 0.1781 is 7,758 bbl/acre-ft = 43,560 sq ft/acre. This constant and 5.615, which converts barrels to cubic feet, may be omitted if all volumes are expressed in cubic meters.

where

- N_p = cumulative oil produced, STB,
- R_p = cumulative GOR, scf/STB,
- R_{si} = initial solution GOR, scf/STB,
- W_e = cumulative water influx, bbl,
- W_p = cumulative water produced, bbl,
- Δp_R = change in reservoir pressure, psi,
- B_{gi} = initial gas FVF, res cu ft/scf,
- m = ratio of initial reservoir free-gas volume and initial reservoir-oil volume,
- c_f = compressibility of reservoir rock, change in PV per unit PV per psi, and
- c_w = compressibility of interstitial water, psi⁻¹.

When a free-gas cap is present, this equation may be simplified to Eq. 6 of Table 40.2 by neglecting the reservoir formation compressibility c_f and the interstitial water compressibility c_w .

When such a reservoir has no active water drive ($W_e = 0$), Eq. 7 results.

For initially undersaturated reservoirs ($m = 0$) below the bubblepoint, Eqs. 6 and 7 reduce to Eqs. 9 and 11, depending on whether an active water drive is present.

For initially undersaturated reservoirs ($m = 0$) above the bubblepoint, no free gas is present ($R_p - R_{si} = 0$), while $B_t = B_{oi} + \Delta p_R c_o$ (where c_o is the compressibility of reservoir oil, volume per psi), so that general Eq. 5 reduces to Eqs. 8 and 10, depending on whether an active water drive is present.

For gas reservoirs the material-balance equation takes the form of Eq. 12 or 13, depending on whether an active water drive is present. The numerator on the right side in each case represents the net reservoir voidage by production minus water influx, while the denominator is the gas-expansion factor ($B_g - B_{gi}$) for the reservoir.

TABLE 40.3—CONDITIONS FOR UNIT-RECOVERY EQUATION, DEPLETION-TYPE RESERVOIR

	Initial Conditions*	Ultimate Conditions*
Reservoir pressure	p_i	p_a
Interstitial water, ϕS_{iw} , bbl/acre-ft	7,758	7,758
Free gas, ϕS_{gr} , bbl/acre-ft	0	7,758
Reservoir oil, bbl/acre-ft	$7,758 \phi (1 - S_{iw})$	$7,758 \phi (1 - S_{iw} - S_{gr})$
Stock-tank oil, bbl/acre-ft	$7,758 \phi \frac{1 - S_{iw}}{B_{oi}}$	$7,758 \phi \frac{1 - S_{iw} - S_{gr}}{B_{oa}}$

*Substitute 10 000 for the 7,758 constant if cubic meters per hectare-meter is used.

Saturated Depletion-Type Oil Reservoirs—Volumetric Methods

General Discussion

Pools without an active water drive that produce solely as the result of expansion of natural gas liberated from solution in the oil are said to produce under a depletion mechanism, also called an internal- or solution-gas drive. When a free-gas cap is present, this mechanism may be supplemented by an external or gas-cap drive (Page 40-13). When the reservoir permeability is sufficiently high and the oil viscosity low, and when the pay zone has sufficient dip or a high vertical permeability, the depletion mechanism may be followed or accompanied by gravity segregation (Page 40-14).

When a depletion-type reservoir is first opened to production, its pores contain interstitial water and oil with gas in solution under pressure. No free gas is assumed to be present in the oil zone. The interstitial water is usually not produced, and its shrinkage upon pressure reduction is negligible compared with some of the other factors governing the depletion-type recovery.

When this reservoir reaches the end of its primary producing life, and disregarding the possibility of gas-cap drive or gravity segregation, it will contain the same interstitial water as before, together with residual oil under low pressure. The void space vacated by the oil produced and by the shrinkage of the remaining oil is now filled with gas liberated from the oil. During the depletion process this gas space has increased gradually to a maximum value at abandonment time. The amount of gas space thus created is the key to the estimated ultimate recovery under a depletion mechanism. It is reached when the produced free GOR in the reservoir, which changes according to the relative permeability ratio relationship and the viscosities of oil and gas involved, causes exhaustion of the available supply of gas in solution.

Unit-Recovery Equation

The unit-recovery factor is the theoretically possible ultimate recovery in stock-tank barrels from a homogeneous unit volume of 1 acre-ft of pay produced by a given mechanism under ideal conditions.

The unit-recovery equation for a saturated depletion-type reservoir is equal to the stock-tank oil initially in place in barrels per acre-foot at initial pressure p_i minus the residual stock-tank oil under abandonment pressure p_a , as shown in Table 40.3.

By difference, the unit recovery by depletion or solution-gas drive is, in stock-tank barrels per acre-foot,

$$N_{ug} = 7,758 \phi \left(\frac{1 - S_{iw}}{B_{oi}} - \frac{1 - S_{iw} - S_{gr}}{B_{oa}} \right), \dots \dots (14)$$

where S_{gr} is the residual free-gas saturation under reservoir conditions at abandonment time, fraction, and B_{oa} is the oil FVF at abandonment, dimensionless. The key to the computation of unit recovery by means of this equation is an estimate of the residual free-gas saturation S_{gr} at the ultimate time. If a sufficiently large number of accurate determinations of the oil and water saturation on freshly recovered core samples is available, an approximation of S_{gr} may be obtained by deducting the average total saturation of oil plus water from unity. This method is based on the assumption that the depletion process taking place within the core on reduction of pressure by bringing it to the surface is somewhat similar to the actual depletion process in the reservoir. Possible loss of liquids from the core before analysis may cause such a value for S_{gr} to be too high. On the other hand, the smaller amount of gas in solution in the residual oil left after flushing by mud filtrate has a tendency to reduce the residual free-gas saturation. Those using this method hope that these two effects somewhat compensate for each other.

A typical S_{gr} value for average consolidated sand, a medium solution GOR of 400 to 500 cu ft/bbl, and a crude-oil gravity of 30 to 40°API is 0.25.

Either a high degree of cementation, a high shale content of the sand, or a 50% reduction in solution GOR may cut this typical S_{gr} value by about 0.05, while a complete lack of cementation or shaliness such as in clean, loose unconsolidated sands or a doubling of the solution GOR may increase the S_{gr} value by as much as 0.10.

At the same time, the crude-oil gravity generally increases or decreases the S_{gr} value by about 0.01 for every 3°API gravity.

Example Problem 1. A cemented sandstone reservoir has a porosity $\phi=0.13$, an interstitial water content $S_{iw}=0.35$, a solution GOR at bubblepoint conditions, $R_{sb}=300$ cu ft/bbl, an initial oil FVF $B_{oi}=1.20$, an oil FVF at abandonment $B_{oa}=1.07$, and a stock-tank oil gravity of 40°API. Based on the above considerations, the higher-than-average oil gravity would just about offset the effect of the somewhat lower-than-average GOR, and the residual free-gas saturation S_{gr} after a 0.05 reduction for the cementation can therefore be estimated at 0.20.

Solution. The unit recovery by depletion according to Eq. 14 would be

$$N_{ug} = (7.758)(0.13) \left(\frac{1-0.35}{1.20} - \frac{1-0.35-0.20}{1.07} \right) \\ = 122 \text{ STB/acre-ft } [157 \text{ m}^3/\text{ha} \cdot \text{m}],$$

where N_{ug} is the unit recovery by depletion or solution-gas drive, STB.

Muskat's Method.⁹ If the actual relationships between pressure and oil-FVF B_o , gas-FVF B_g , gas-solubility in oil (solution GOR) R_s , oil viscosity μ_o , and gas viscosity μ_g are available from a PVT analysis of the reservoir fluids, and if the relationship between relative permeability ratio k_{rg}/k_{ro} and the total liquid saturation, S_t , is known for the reservoir rock under consideration, the unit recovery by depletion can be arrived at by a stepwise computation of the desaturation history directly from the following depletion equation in differential form:

$$\frac{\Delta S_o}{\Delta p_R} = \frac{S_o \frac{B_g}{B_o} \frac{dR_s}{dp_R} + (1-S_o-S_{iw}) B_g \frac{d(1/B_g)}{dp_R} + S_o \frac{\mu_o}{\mu_g} \frac{k_{rg}}{k_{ro}} \frac{dB_o}{dp_R}}{1 + \frac{\mu_o}{\mu_g} \frac{k_{rg}}{k_{ro}}} \quad (15)$$

where

S_o = oil or condensate saturation under reservoir conditions, fraction,

μ_o = reservoir oil viscosity, cp,

μ_g = reservoir gas viscosity, cp,

k_{rg} = relative permeability to gas as a fraction of absolute permeability, and

k_{ro} = relative permeability to oil as a fraction of absolute permeability.

The individual computations are greatly facilitated by computing and preparing in advance in graphical form the following groups of terms, which are a function of pressure only,

$$\left(\frac{B_g}{B_o} \frac{dR_s}{dp_R} \right), \left[B_g \frac{d(1/B_g)}{dp_R} \right], \frac{\mu_o}{\mu_g}, \left(\frac{1}{B_o} \frac{dB_o}{dp_R} \right),$$

and the relative permeability ratio k_{rg}/k_{ro} , which is a function of total liquid saturation S_t only.

The accuracy of this type of calculation on a desk calculator falls off rapidly if the pressure decrements chosen are too large, particularly during the final stages when the GOR is increasingly rapidly.

With modern electronic computers, however, it is possible to use pressure decrements of 10 psi or smaller, which makes a satisfactory accuracy possible.

This stepwise solution of the depletion equation yields the reservoir oil saturation S_o as a function of reservoir pressure p_R . The results may be converted into cumulative recovery per acre-foot. In stock-tank barrels per acre-foot,

$$N_p = 7,758 \phi \left(\frac{1-S_{iw}}{B_{oi}} - \frac{S_o}{B_o} \right) \quad (16)$$

The results may be converted into cumulative recovery as a fraction of the original oil in place (OOIP) by

$$\frac{N_p}{N} = 1 - \left(\frac{S_o}{1-S_{iw}} \right) \left(\frac{B_{oi}}{B_o} \right) \quad (17)$$

while the GOR history, in standard cubic feet gas/stock-tank barrel, may be computed by

$$R = R_s + 5.615 \frac{B_o}{B_g} \frac{\mu_o}{\mu_g} \frac{k_{rg}}{k_{ro}} \quad (18)$$

where R is the instantaneous producing GOR, in standard cubic feet per stock-tank barrel, and the relative production rate in barrels per day by

$$q_o = \frac{k_o}{k_{oi}} \frac{\mu_{oi}}{\mu_o} \frac{p_R}{p_i} q_{oi} \quad (19)$$

where

q_o = oil-production rate, B/D,

k_o = effective permeability to oil, md,

k_{oi} = initial effective permeability to oil, md,

μ_{oi} = initial reservoir oil viscosity, cp, and

q_{oi} = initial oil-production rate, B/D.

It should be stressed that this method is based on the assumption of uniform oil saturation in the whole reservoir and that the solution will therefore break down when there is appreciable gas segregation in the formation. It is therefore applicable only when permeabilities are relatively low.

Another limitation of this method as well as of the Tarnier method, discussed hereafter, is that no condensation of liquids from the produced gas is assumed to take place in the tubing or in the surface extraction equipment. It should therefore not be applied to the high-temperature, high-GOR, and high-FVF "volatile" oil reservoirs to be discussed later.

Tarnier's Method. Babson¹⁰ and Tarnier¹¹ have advanced trial-and-error-type computation methods for the desaturation process that require a much smaller number of pressure increments and can therefore be more readily handled by a desk calculator. Both methods are based on a simultaneous solution of the material-balance equation (Eq. 11) and the instantaneous GOR (Eq. 18).

Tarnier's method is the more straightforward of the two. The procedure for the stepwise calculation of the cumulative oil produced $(N_p)_2$ and the cumulative gas produced $(G_p)_2$ for a given pressure drop from p_1 to p_2 is as follows.

TABLE 40.4—COMPUTED DEPLETION RECOVERY IN STB/ACRE-FT/PERCENT POROSITY FOR TYPICAL FORMATIONS

Solution GOR (cu ft/bbl) (R_{sb})	Oil Gravity, (°API) γ_o	Sand or Sandstone ($S_{iw} = 0.25$)			Limestone, Dolomite or Chert ($S_{iw} = 0.15$)	
		Unconsolidated	Consolidated	Highly Cemented	Vugular	Fractured
60	15	7.2	4.9	1.4	2.6	0.4
	30	12.0	8.5	4.9	6.3	1.8
	50	19.2	13.9	9.5	11.8	5.1
200	15	7.0	4.6	1.8	2.6	0.5
	30	11.6	7.9	4.4	5.8	1.5
	50	19.4	13.7	9.2	11.4	4.4
600	15	7.6	4.8	2.5	3.3	0.9
	30	10.5	6.5	3.6	4.7	(1.2)
	50	15.0	9.7	5.8	7.2	(2.1)
1,000	30	12.3	7.6	4.5	5.4	(1.6)
	50	12.0	7.2	4.1	4.8	(1.2)
2,000	50	10.6	6.4	4.0	(4.3)	(1.5)

1. Assume that during the pressure drop from p_1 to p_2 the cumulative oil production increases from $(N_p)_1$ to $(N_p)_2$. N_p should be set equal to zero at bubblepoint.

2. Compute the cumulative gas produced $(G_p)_2$ at pressure p_2 by means of the material-balance equation (Eq. 11), which for this purpose—and assuming $W_p = 0$ —is rewritten in the following form:

$$(G_p)_2 = (N_p)_2(R_p)_2 = N \left[(R_{si} - R_s) - 5.615 \times \frac{B_{oi} - B_o}{B_g} \right] - (N_p)_2 \left(5.615 \frac{B_o}{B_g} - R_s \right) \quad \dots (20)$$

3. Compute the fractional total liquid saturation $(S_l)_2$ at pressure p_2 by means of

$$(S_l)_2 = S_{iw} + (1 - S_{iw}) \frac{B_o}{B_{oi}} \left[1 - \frac{(N_p)_2}{N} \right] \quad \dots (21)$$

4. Determine the k_{rg}/k_{ro} ratio corresponding to the total liquid saturation $(S_l)_2$ and compute the instantaneous GOR at p_2 by means of

$$R_2 = R_s + 5.615 \frac{B_o}{B_g} \frac{\mu_o}{\mu_g} \frac{k_{rg}}{k_{ro}} \quad \dots (22)$$

5. Compute the cumulative gas produced at pressure p_2 by means of

$$(G_p)_2 = (G_p)_1 + \frac{R_1 + R_2}{2} [(N_p)_2 - (N_p)_1] \quad \dots (23)$$

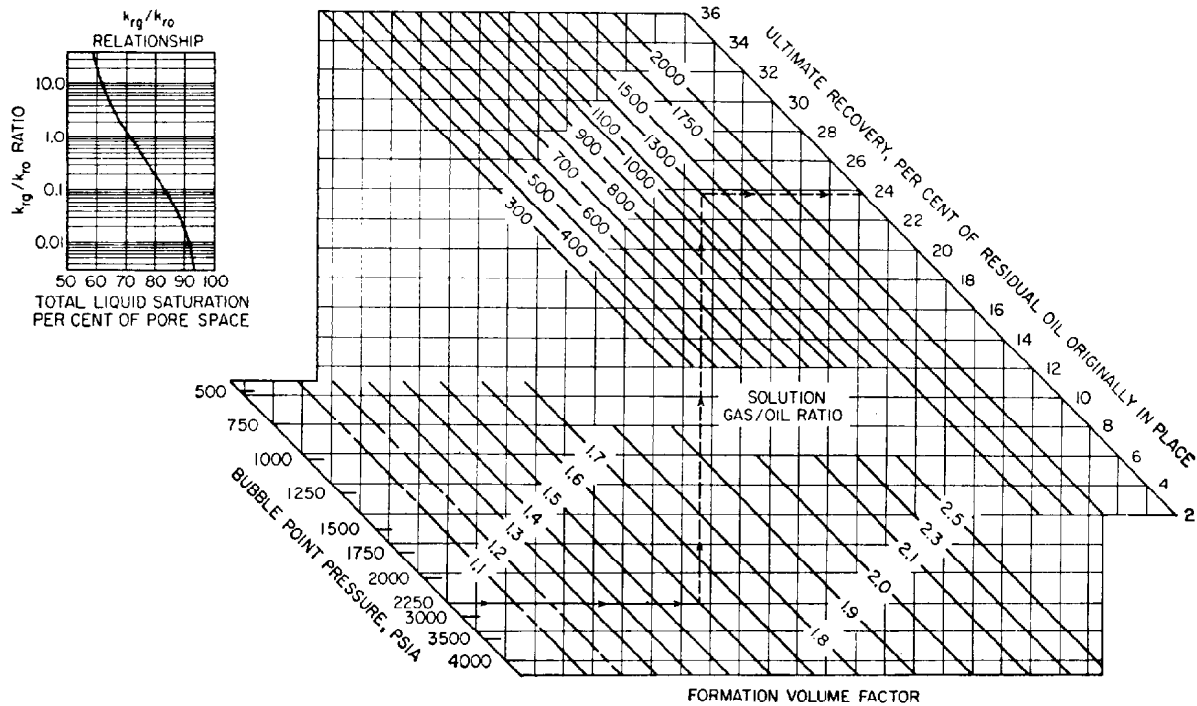
in which R_1 represents the instantaneous GOR computed previously at pressure p_1 .

Usually three judicious guesses are made for the value $(N_p)_2$ and the corresponding values of $(G_p)_2$ computed by both Steps 2 and 5. When the values thus obtained for $(G_p)_2$ are plotted vs. the assumed values for $(N_p)_2$, the intersection of the curve representing the results of Step 2 and the one representing Step 5 then indicates the cumulative gas and oil production that will satisfy both equations. In actual application, the method is usually simplified further by equating the incremental gas production $(G_p)_2 - (G_p)_1$, rather than $(G_p)_2$ itself. This

equality signifies that at each pressure step the cumulative gas, as determined by the volumetric balance, is the same as the quantity of gas produced from the reservoir, as controlled by the relative permeability ratio of the rock, which in turn depends on the total liquid saturation. Although the Tarner method was originally designed for graphical interpolation, it also lends itself well to automatic digital computers. The machine then calculates the quantity of gas produced for increasing oil withdrawals by both equations and subtracts the results of one from the other. When the difference becomes negative, the machine stops and the answer lies between the last and next to last oil withdrawals.

Tarner's method has been used occasionally to compute recoveries of reservoirs with a free-gas cap or to evaluate the possible results from injection of all or part of the produced gas. When a free-gas cap is present, or when produced gas is being reinjected, breakthrough of free gas into the oil-producing section of the reservoir is likely to occur sooner or later, thus invalidating the assumption of uniform oil saturation throughout the producing portion of the reservoir, on which the method is based. Since such a breakthrough of free gas causes the instantaneous GOR (Eq. 18) as well as the entire computation method to break down, the use of Tarner's method in its original form for this type of work is not recommended. It should also be used with caution when appreciable gas segregation in an otherwise uniform reservoir is expected.

Computed Depletion-Recovery Factors. Several investigators^{9, 12-14} have used the Muskat and Tarner methods to determine the effects of different variables on the ultimate recovery under a depletion mechanism. In one such attempt¹² the k_{rg}/k_{ro} relationships for five different types of reservoir rock representing a range of conditions for sands and sandstones and for limestones, dolomites, and cherts were developed. These five types of reservoir rock were assumed to be saturated under reservoir conditions with 25% interstitial water for sands and sandstones and 15% for the limestone group and with 12 synthetic crude-oil/gas mixtures representing a range of crude-oil gravities from 15 to 50°API and gas solubilities from 60 to 2,000 cu ft/STB. Their production performance and recovery factors to an abandonment pressure equal to 10% of the bubblepoint pressure were then computed by means of depletion (Eq. 15).

**Notes:**

Interstitial water is assumed to be 30% of pore space and dead-oil viscosity at reservoir temperature to be 2 cp.

Equilibrium gas saturation is assumed to be 5% of pore space.

As here used "ultimate oil recovery" is realized when the reservoir pressure has declined from the bubblepoint pressure to atmospheric pressure.

FVF units are reservoir barrels per barrel of residual oil.

Solution GOR units are standard cubic feet per barrel of residual oil.

Example 1:

Required: Ultimate recovery from a system having a bubblepoint pressure = 2,250 psia, FVF = 1.6, and a solution GOR.

Procedure: Starting at the left side of the chart, proceed horizontally along the 2,250-psi line to FVF = 1.6. Now rise vertically to the 1,300-scf/bbl line. Then go horizontally and read an ultimate recovery of 23.8%.

Example 2:

Required: Convert the recovery figure determined in Example 1 to tank oil recovered.

Data requirements: Differential liberation data given in Example 1. Flash liberation data: bubblepoint pressure = 2,250 psia, FVF = 1.485, FVF at atmospheric pressure = 1.080 for both flash and differential liberation.

Procedure: Calculate the oil saturation at atmospheric pressure by substituting differential liberation data in the equation as follows:

$$\left[\left(\frac{S_o}{B_o} \right)_b - \left(\frac{S_o}{B_o} \right)_a \right] (100) \div \left[\left(\frac{S_o}{B_o} \right)_b \right] = N_{ul}$$

$$\left(\frac{0.700}{1.600} - \frac{S_o}{1.080} \right) (100) \div \left(\frac{0.700}{1.600} \right) = 23.8$$

Oil saturation at atmospheric pressure = 0.360.

Next, substitute the calculated value of oil saturation and the flash liberation data into the previous equation and calculate the ultimate oil recovery as a percentage of tank oil originally in place.

$$\left(\frac{0.700}{1.485} - \frac{0.360}{1.080} \right) (100) \div \left(\frac{0.700}{1.485} \right) = N_{ul}$$

N_{ul} (ultimate oil recovery) = 29.3% of tank oil originally in place.

Fig. 40.6—Chart for estimating ultimate recovery from solution gas-drive reservoirs.

These theoretical depletion-recovery factors, expressed as barrels of stock-tank oil per percent porosity, will be found in Table 40.4 for the different types of reservoir rocks, oil gravities, and solution GOR's assumed.

In cases where no detailed data are available concerning the physical characteristics of the reservoir rock and its fluid content, Table 40.4 has been found helpful in estimating the possible range of depletion-recovery factors. It may be noted that the k_{rg}/k_{ro} relationship of the reservoir rock is apparently the most important single factor governing the recovery factor. Unconsolidated intergranular material seems to be the most favorable, while increased cementation or consolidation tends to affect recoveries unfavorably. Next in importance is crude-oil gravity with viscosity as its corollary. Higher oil gravi-

ties and lower viscosities appear to improve the recovery. The effect of GOR on recovery is less pronounced and shows no consistent pattern. Apparently the beneficial effects of lower viscosity and more effective gas sweep with higher GOR is in most cases offset by the higher oil FVF's.

In general, these data seem to indicate a recovery range from the poorest combinations of 1 to 2 bbl/acre-ft for each percent porosity to the best combinations of 19 to 20 bbl/acre-ft/percent porosity. An overall average seems to be around 10 bbl/acre-ft/percent porosity.

It is also of interest to note that when the reservoir is about two-thirds depleted, the pressure has usually dropped to about one-half the value at bubblepoint.

In another attempt¹⁵ nine nomographs were developed, each for a given combination of the k_{rg}/k_{ro} curve, "dead-oil" viscosity, and interstitial water content. The nomograph for an average k_{rg}/k_{ro} relationship, an interstitial water content of 0.30, and a dead-oil viscosity of 2 cp is reproduced as Fig. 40.6. Instructions for its use are shown opposite the figure.

The authors¹³ also introduced an interesting empirical relationship between the relative permeability ratio k_{rg}/k_{ro} , the equilibrium gas saturation S_{gc} , the interstitial water saturation S_{iw} , and the oil saturation S_o :

$$\frac{k_{rg}}{k_{ro}} = \xi(0.0435 + 0.4556\xi), \dots\dots\dots (24)$$

where $\xi = (1 - S_{gc} - S_{iw} - S_o)/(S_o - 0.25)$. A similar correlation¹⁵ for sandstones that show a linear relationship between $1/p_c^2$ (where p_c = critical pressure) and saturation is

$$\frac{k_{rg}}{k_{ro}} = \frac{(1 - S^*)^2 [1 - (S^*)^2]}{(S^*)^4}, \dots\dots\dots (25)$$

where effective saturation $S^* = S_o/(1 - S_{iw})$. This equation represents a useful expression for calculating relative permeability ratios in sandstone reservoirs for which an average water saturation has been obtained by either electrical log or core analysis.

API Estimation of Oil and Gas Reserves

In a statistical study of the actual performance of 80 solution gas-drive reservoirs, the API Subcommittee on Recovery Efficiency¹⁶ developed the following equation for unit recovery (N_{ug}) below the bubblepoint for solution gas-drive reservoirs, in stock-tank barrels per acre-foot*:

$$N_{ug} = 3,244 \left[\frac{\phi(1 - S_{iw})}{B_{ob}} \right]^{1.1611} \times \left(\frac{k}{\mu_{ob}} \right)^{0.0979} \times (S_{iw})^{0.3722} \times \left(\frac{p_b}{p_a} \right)^{0.1741}, \dots\dots\dots (26)$$

where

- k = absolute permeability, darcies,
- B_{ob} = oil FVF at bubblepoint, RB/STB,
- μ_{ob} = oil viscosity at bubblepoint, cp,
- p_a = abandonment pressure, psig, and
- p_b = bubblepoint pressure, psig.

The permeability distribution in most reservoirs is usually sufficiently nonuniform in vertical and horizontal directions to cause the foregoing depletion calculations on average material to be fairly representative.

However, when distinct layers of high and low permeability, separated by impervious strata, are known to be present, the depletion process may advance more rapidly in high-permeability strata than in low-permeability zones. In such cases separate performance calculations should

be made for each permeability bank that is known to be continuous and the results converted into rate/time curves for each by combining Eqs. 16 and 19. The estimated ultimate recovery will then be based on a superposition of such rate/time curves for the different zones.

If there is a wide divergence in permeabilities, one may find that at a time when the combined rate for all zones has reached the economic limit the more permeable banks will be depleted and have yielded their full unit recovery while the pressure depletion and the recovery from the tighter zones are still incomplete.

Undersaturated Oil Reservoirs Without Water Drive Above the Bubblepoint—Volumetric Method¹⁷⁻¹⁹

With progressively deeper drilling, a number of oil reservoirs have been encountered that, while lacking an active water drive, are in undersaturated condition. Because of the expansion of the reservoir fluids and the compaction of the reservoir rock upon pressure reduction, substantial recoveries may sometimes be obtained before the bubblepoint pressure p_b is reached and normal depletion sets in. Such recoveries may be computed as follows.

The oil initially in place in stock-tank barrels per acre-foot at pressure p_i is according to Eq. 2,

$$N = \frac{7,758 \times \phi_i (1 - S_{iw})}{B_{oi}},$$

where ϕ_i is initial porosity. By combining this expression with the material-balance equation (Eq. 10), the recovery factor above the bubblepoint in stock-tank barrels per acre-foot may be expressed as

$$N_p = \frac{7,758 \phi_i (p_i - p_b) [c_o + c_f - S_{iw}(c_o - c_w)]}{B_{oi} [1 + c_o(p_i - p_b)]}, \quad (27)$$

where c_w is the compressibility of interstitial water in volume per volume per psi.

Example Problem 2. Zone D-7 in the Ventura Avenue field, described by E.V. Watts,¹⁹ is an example of an undersaturated oil reservoir without water drive. Its reservoir characteristics are

- p_i = 8,300 psig at 9,200 ft,
- p_b = 3,500 psig,
- ϕ_i = 0.17,
- S_{iw} = 0.40,
- B_{ob} = 1.45,
- B_{oa} = 1.15,
- γ_o = 32 to 33° API,
- c_o = 13×10^{-6} ,
- c_w = 2.7×10^{-6} ,
- c_f = 1.4×10^{-6} ,
- S_{gr} = 0.22, and
- R_{sb} = 900 cu ft/bbl.

Solution. On the basis of these data, Watts computes the recovery by expansion above the bubblepoint at 47 bbl/acre-ft and by a depletion mechanism below the bubblepoint at 110 bbl/acre-ft (see Ref. 19 for details).

* Because Eq. 26 is empirically derived, conversion to metric units ($m^3/ha \cdot m$) requires multiplication of N_{ug} by 1.2889.

Volatile Oil Reservoirs— Volumetric Methods²⁰⁻²⁵

Deeper drilling, with accompanying increases in reservoir temperatures and pressures, has also revealed a class of reservoir fluids with a phase behavior between that of ordinary "black" oil and that of gas or gas condensate. These intermediate fluids are referred to as "high-shrinkage" or "volatile" crude oils because of their relatively large percentage of ethane through decane components and resultant high volatility. Volatile-oil reservoirs are characterized by high formation temperatures (above 200°F) and abnormally high solution GOR and FVF (above 2). The stock-tank gravity of these volatile crudes generally exceeds 45°API.

The inherent differences in phase behavior of volatile oils are sufficiently significant to invalidate certain premises implicit in the conventional material-balance methods. In such conventional material-balance work it is assumed that all produced gas, whether solution gas or free gas, will remain in the vapor phase during the depletion process, with no liquid condensation on passage through the surface separation facilities. Furthermore, the produced oil and gas are treated as separate independent fluids, even though they are at all times in compositional equilibrium. Although these basic assumptions simplify the conventional material-balance calculations, highly inaccurate predictions of reservoir performance may result if they are applied to volatile-oil reservoirs.

In highly volatile reservoirs, the stock-tank liquids recovered by condensation from the gaseous phase may actually equal or even exceed those from the associated liquid phase. This rather surprising occurrence is exemplified in a paper by Woods,²⁴ in which the case history of an almost depleted volatile-oil reservoir is presented.

Example Problem 3. Woods' reservoir data for this volatile-oil reservoir were

$$\begin{aligned} p_i &= 5,000 \text{ psig,} \\ p_b &= 3,940 \text{ psig,} \\ T_R &= 250^\circ\text{F,} \\ \phi &= 0.198, \\ k &= 75 \text{ md,} \\ S_{iw} &= 0.25, \\ R_{sb} &= 3,200 \text{ scf/bbl,} \\ \gamma_{oi} &= 44^\circ\text{API,} \\ \gamma_{oa} &= 62^\circ\text{API, and} \\ B_{ob} &= 3.23. \end{aligned}$$

Solution. At 80% depletion when $p_R = 1,450$ psig and $R = 23,000$ scf/bbl, the percentage recovery was 21% of which 5% was from expansion above the bubblepoint, 9% from the depletion mechanism, and 7% from liquids condensed out of the gas phase by conventional field separation equipment (see Ref. 24 for details).

In view of the increasing number and importance of volatile-oil reservoirs in recent years, appropriate techniques have been developed to provide realistic predictions of the anticipated production performance of these reservoirs.²⁰⁻²⁵ The depletion processes are simulated by an incremental computation method, using multicomponent flash calculations and relative-permeability data, as indicated in the following stepwise sequence for a chosen pressure decrement:

1. The change in composition of the in-place oil and gas is determined by a flash calculation.
2. The total volume of fluids produced at bottomhole conditions is determined by a volumetric material balance.
3. The relative volumes of oil and gas produced at bottomhole conditions are determined by a trial-and-error procedure that involves simultaneously satisfying the volumetric material balance and the relative-permeability relationship.
4. This total well-stream fluid is then flashed to actual surface conditions to obtain the producing GOR and the volume of stock-tank liquid corresponding to the selected pressure decrement.

When this calculation procedure is repeated for successive pressure decrements, the resultant tabulations represent the entire reservoir depletion and recovery processes. Since these stepwise calculations are rather tedious and time-consuming, the use of digital computers is recommended.

This method of reservoir analysis provides compositional data on all fluid phases, including the total well-stream. This information is then readily available for separator, crude-stabilization, gasoline-plant, or related studies at any desired stage of depletion.

In the case of small reservoirs with relatively limited reserves, such lengthy laboratory work and phase-behavior calculations may not be justified. An empirical correlation was developed²⁴ for prediction of the ultimate recovery in such cases, based only on the initial producing GOR, R , the reservoir temperature, T_R , and the initial stock-tank oil gravity, γ_{oi} .

$$N_{ul} = -0.070719 + \frac{143.50}{R} + 0.000120807T_R + 0.0011807\gamma_{oi}, \dots \dots \dots (28)$$

where N_{ul} = ultimate oil production from saturation pressure p_b to 500 psi, in stock-tank volume per reservoir volume of hydrocarbon pore space.

It is claimed that this correlation will give values within 10% of those calculated by the more rigorous procedure previously outlined.

Oil Reservoirs With Gas-Cap Drive— Volumetric Unit Recovery Computed by Frontal-Drive Method²⁶⁻²⁸

The Buckley-Leverett frontal-drive method may be used in calculating oil recovery when the pressure is kept constant by injection of gas in a gas cap but is also applicable to a gas-cap drive mechanism without gas injection when the pressure variation is relatively small so that changes in gas density, solubility, or the reservoir volume factor may be neglected. A reservoir with a very large gas-cap volume as compared with the oil volume can sometimes be considered to meet these qualifications even though no gas is being injected.

The two basic equations, Eqs. 29a and b, refer to a linear reservoir under constant pressure with a constant cross-sectional area exposed to fluid flow and with the free gas moving in at one end of the reservoir and fluids being produced at a constant rate at the other end. Interstitial water is considered as an immobile phase.

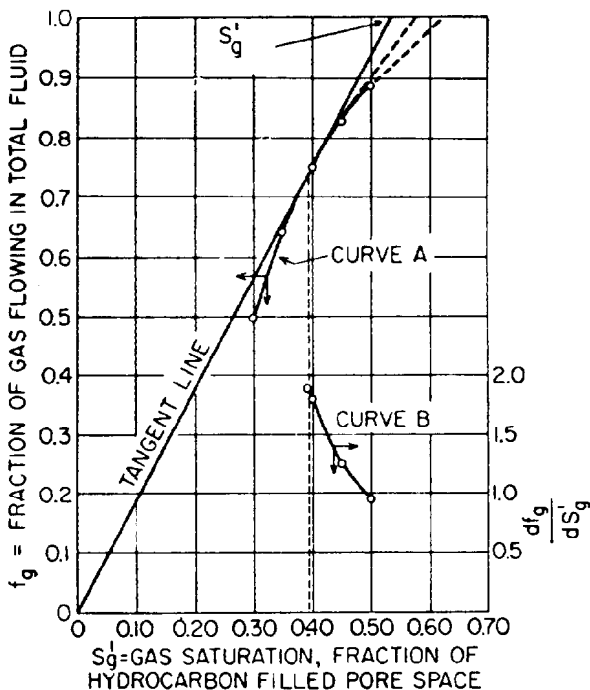


Fig. 40.7—Frontal-drive method in gas-cap drive.

If the capillary-pressure forces are neglected, the fractional-flow equation of gas is

$$f_g = \frac{1 - Ek_{ro}(\mu_g/\mu_o)}{1 + (k_{ro}/k_{rg})(\mu_g/\mu_o)} \quad (29a)$$

and

$$E = \frac{k \sin \Theta A (\rho_o - \rho_g)}{365 \mu_g q_t} \quad (29b)$$

where

- f_g = fractional flow of gas,
- E = parameter,
- Θ = dip angle, degrees,
- A = area of cross-section normal to bedding plane, sq ft,
- ρ_o = density of reservoir oil, g/cm³,
- ρ_g = density of reservoir gas, g/cm³, and
- q_t = total flow rate, reservoir cu ft/D.

Since the ratio of k_{ro}/k_{rg} is a function of gas saturation, and all other factors are constant, f_g can be determined by Eq. 29a as a function of gas saturation (see Fig. 40.7, Curve A).

The rate-of-frontal-advance equation may be rearranged to give the time in days for a given displacing-phase saturation to reach the outlet face of the linear sand body as a function of the slope of the fractional flow vs. saturation curve (Fig. 40.7, Curve B) as follows:

$$t = \frac{5.615NB_o}{q_t(df_g/dS_g)} \quad (30)$$

Note: S'_g as used in this section is gas saturation as a fraction of the hydrocarbon-filled pore space. When N is in cubic meters, q_t is in cubic meters per day.

The calculation procedure is first to calculate the fractional-flow curve (Fig. 40.7, Curve A). The average gas saturation in the swept area at breakthrough, which is equivalent to the fraction of oil in place recovered, may then be obtained from the fractional-flow curve by constructing a straight line tangent to the curve through the origin and reading \bar{S}'_g at $f_g = 1.0$. The time of breakthrough at the outlet face may be computed from the slope of the curve at the point of tangency. The subsequent performance history after breakthrough may then be calculated by constructing tangents at successively higher values of S'_g and obtaining \bar{S}'_g in a similar manner.

Example Problem 4. Welge²⁸ presents a typical calculation of gas-cap drive performance for the Mile Six Pool in Peru.

Given:

Reservoir volume = $1,902 \times 10^6$ cu ft,
distance from original GOC to average
withdrawal point = 1,540 ft,

$$\text{average cross-sectional area} = \frac{1,902 \times 10^6}{1,540}$$

$$= 1.235 \times 10^6 \text{ sq ft,}$$

$$k_o = 300 \text{ md,}$$

$$\Theta = 17.50,$$

$$\mu_g = 0.0134 \text{ cp,}$$

$$\mu_o = 1.32 \text{ cp,}$$

$$q_t = 64,000 \text{ res cu ft/D [18 125 res m}^3\text{/d],}$$

$$B_o = 1.25,$$

$$B_g = 0.0141$$

$$N = 44 \times 10^6 \text{ STB [6.996} \times 10^6 \text{ m}^3\text{],}$$

$$R_s = 400 \text{ cu ft/bbl [71.245 m}^3\text{/m}^3\text{],}$$

$$\rho_o = 0.78 \text{ g/cm}^3, \text{ and}$$

$$\rho_g = 0.08 \text{ g/cm}^3.$$

Solution. The performance history calculations are given in Table 40.5 in a slightly simplified form.

Oil Reservoirs Under Gravity Drainage²⁹⁻³⁷

Occurrence of Gravity Drainage

Gravity drainage is the self-propulsion of oil downward in the reservoir rock. Under favorable conditions it has been found to effect recoveries of 60% of the oil in place, which is comparable with or exceeding the recoveries normally obtained by water drive. Gravity is an ever-present force in oil fields that will drain oil from reservoir rock from higher to lower levels wherever it is not overcome by encroaching edge water or expanding gas.

Gravity drainage will be most effective if a reservoir is produced under conditions that allow flow of oil only or counterflow of oil and gas. This may be attained under pressure maintenance by crestal-gas injection, which keeps the gas in solution, or it may be attained by a gradual reduction in pressure, so that the oil and gas can segregate continuously by counterflow. It also may be obtained by

first producing the reservoir under a depletion-type mechanism until the gas has been practically exhausted, then by gravity drainage. A thorough discussion of the many aspects of gravity drainage will be found in the classic paper by Lewis.³²

Several investigators³³⁻³⁶ have attempted to formulate gravity drainage analytically, but the relationships are quite complicated and not readily adaptable to practical field problems. Most studies agree, however, that the occurrence of gravity drainage of oil will be promoted by low viscosities, μ_o , high relative permeability to oil, k_{ro} , high formation dips or lack of stratification, and high density gradients ($\rho_o - \rho_g$). Thick sections of unconsolidated sand with minimal surface area, large pore sizes, low interstitial water saturation, and consequently high k_{ro} appear to be especially favorable.

These factors usually are combined in a rate-of-flow equation, which states that such flow must be proportional to $(k_{ro}/\mu_o)(\rho_o - \rho_g) \sin \Theta$, in which Θ represents the angle of dip of the stratum. Smith³⁷ compared the values of this term for a dozen reservoirs, some of which had strong gravity-drainage characteristics and some of which lacked such characteristics.

When expressing k_{ro} in millidarcies, μ_o in centipoises, and ρ_o and ρ_g in g/cm³, it was found that for reservoirs exhibiting strong gravity-drainage characteristics the value of the term $(k_{ro}/\mu_o)(\rho_o - \rho_g) \sin \Theta$ ranged from 10 to 203 and that in reservoirs where gravity-drainage effects were not apparent, this function showed values between 0.15 and 3.4.

Case Histories of Gravity Drainage After Pressure Depletion

The most spectacular cases of gravity drainage have been of this kind. Following are the two best known.

1. *Lakeview Pool in Kern County, CA.*^{31,32} The discovery well in the Lakewood gusher area blew out in March 1910, flowed wild for 544 days, and ultimately produced 8¼ million bbl of oil, depleting the reservoir pressure. Gravity drainage thereafter controlled this reservoir. There was no appreciable water influx. The sand is relatively clean and poorly cemented. The average depth is 2,875 ft. The formation dip is 15 to 45°. There are 126 producing wells on 588 acres. The net sand thickness averages 71 ft, the height of the oil column is 1,285 ft, and there are 41,798 net acre-ft of pay.

Reservoir data for this reservoir are $p_i = p_b = 1,285$ psig, p_R on Jan. 1, 1957 = 35 psig, $T_R = 115^\circ\text{F}$, $\phi = 0.33$, k ranges up to 4,800 md and averages 3,600 md (70% of samples above 100 md, 37% above 1,000 md), $S_{iw} = 0.235$, $R_{sh} = 200$ cu ft/bbl, $B_{oi} = 1.106$,

$\gamma_o = 22.5^\circ\text{API}$, N_p for Jan. 1, 1957 = 44.6 million bbl of oil; estimated ultimate 47 million bbl or 1,124 bbl/acre-ft, corresponding to 63% of the initial oil in place.

During the first 20 years the oil level in the field receded almost exactly in proportion to the amount of oil produced, just as in a tank.

2. *Oklahoma City Wilcox Reservoir, OK.*^{29,32} The discovery well, Mary Sudik No. 1, blew out in March 1930, and flowed wild for 11 days.

The segregation of gas and development of gravity drainage began to be important in 1934, when the average pressure became less than 750 psig, and was virtually complete by 1936, when the average pressure had dropped to 50 psig.

Water influx played an effective role until 1936, when it came to a halt after invading the bottom 40% of the reservoir. Gravity has been the dominant mechanism since. The Wilcox sand consists of typical round frosted sand grains, clean and poorly cemented.

The average depth is 6,500 ft; the formation dip is 5 to 15°; 884 wells have been drilled on a total area of 7,080 acres. The net pay thickness is 220 ft. The 890,000 net acre-ft of Wilcox pay contained originally 1,083 million bbl of stock-tank oil, as confirmed by material balance.

Reservoir data for this reservoir are $p_i = p_b = 2,670$ psi at minus 5,260 ft, $T_R = 132^\circ\text{F}$, $\phi = 0.22$, k ranges from 200 to 3,000 md, $S_{iw} = 0.03$ (oil wet), $R_{sh} = 735$ cu ft/bbl, $B_{oi} = 1.361$, $\gamma_{oi} = 40^\circ\text{API}$, $\gamma_{oa} = 38$ to 39°API .

According to Katz,²⁹ oil saturations found in the gas zone were between 1 and 26%, while saturations between 53 and 93% were found in the oil-saturated zone below the GOC. The oil saturation below the WOC has been estimated at 43%, showing gravity to be more effective than water displacement in this reservoir.

Cumulative production, N_p , for Jan. 1, 1958, is estimated at 525 million bbl and the ultimate recovery at 550 million bbl. After an estimated 189 million bbl displaced by the water influx is deducted, the upper 60% of the Wilcox reservoir will yield under gravity drainage ultimately 361 million bbl or 696 bbl/acre-ft, corresponding to 57% of the oil in place.

Oil Reservoirs With Water Drive—Volumetric Methods³⁸

General Discussion

Natural-water influx into oil reservoirs is usually from the edge inward parallel to the bedding planes (edgewater drive) or upward from below (bottomwater drive). Bottomwater drive occurs only when the reservoir thickness exceeds the thickness of the oil column, so that the oil/water interface underlies the entire oil reservoir. It is

TABLE 40.5—PERFORMANCE-HISTORY CALCULATION

S'_g near Outlet Face	k_{ro}	k_{ro}/k_{rg}	f_g	df_g/ds'_g	t_{yr}	$S'_g =$ Recovery Fraction of Oil in Place	Flowing GOR = $[f_g/(1-f_g)](B_o/B_g)$ $\times 5.61 + R_s$
0.30	0.197	0.715	0.496	—	—	—	—
0.35	0.140	0.364	0.642	—	—	—	—
0.395	0.102	0.210	0.739	1.87	7.1	0.534	1.808
0.40	0.097	0.200	0.752	1.81	7.3	0.535	1.908
0.45	0.067	0.118	0.829	1.25	10.6	0.586	2.811
0.50	0.045	0.0715	0.885	0.94	14.1	0.622	4.227

TABLE 40.6—CONDITIONS FOR UNIT-RECOVERY EQUATION, WATER-DRIVE RESERVOIR

	Initial Conditions	Ultimate Conditions
Reservoir pressure	P_i	P_a
Interstitial water, bbl/acre-ft	$7,758\phi S_{iw}$	$7,758\phi S_{iw}$
Reservoir oil, bbl/acre-ft	$7,758\phi(1 - S_{iw})$	$7,758\phi S_{or}$
Stock-tank oil, bbl/acre-ft	$7,758\phi(1 - S_{iw})/B_{oi}$	$7,758\phi S_{or}/B_{oa}$

further possible only when vertical permeabilities are high and there is little or no horizontal stratification with impervious shale laminations.

In either case, water as the displacing medium moves into the oil-bearing section and replaces part of the oil originally present. The key to a volumetric estimate of recovery by water drive is in the amount of oil that is not removed by the displacing medium. This residual oil saturation (ROS) after water drive, S_{or} , plays a role similar to the final (residual) gas saturation, S_{gr} , in the depletion-type reservoirs.

To determine the unit-recovery factor, which is the theoretically possible ultimate recovery in stock-tank barrels from a homogeneous unit volume of 1 acre-ft of pay produced by complete waterflooding, the amount of interstitial water and oil with dissolved gas initially present will be compared with the condition at abandonment time, when the same interstitial water is still present but only the residual or nonfloodable oil is left. The remainder of the original oil has at that time been removed by water displacement.

Unit-Recovery Equation

The unit recovery for a water-drive reservoir is equal to the stock-tank oil originally in place in barrels per acre-foot minus the residual stock-tank oil at abandonment time (Table 40.6).

By difference, the unit recovery by water drive, in stock-tank barrels per acre-foot, is

$$N_{uw} = 7,758\phi \left(\frac{1 - S_w}{B_{oi}} - \frac{S_{or}}{B_{oa}} \right), \dots \dots \dots (31)$$

where N_{uw} is the unit recovery by water drive, in stock-tank barrels, and S_{or} is the residual oil saturation, fraction. The ROS at abandonment time may be found by actually submitting cores in the laboratory under simulated reservoir conditions to flooding by water (flood-pot tests). Another method commonly used is to consider the oil satu-

ration as found by ordinary core analysis after multiplying with the oil FVF at abandonment, B_{oa} , as the residual oil saturation in the reservoir to be expected from flooding with water. This is based on the assumption that water from the drilling mud invades the pay section just ahead of the core bit in a manner similar to the water displacement process in the reservoir itself.

Recovery-Efficiency Factor

The unit recovery should be multiplied by a permeability-distribution factor and a lateral-sweep factor before it may be applied to the computation of the ultimate recovery for an entire water-drive reservoir.

These two factors usually are combined in a recovery-efficiency factor. Baucum and Steinle³⁸ have determined this recovery-efficiency factor for five water-drive reservoirs in Illinois. Table 40.7 lists the recovery efficiencies for these reservoirs, together with some other pertinent data.

Average Recovery Factor From Correlation of Statistical Data

In 1945, Craze and Buckley,^{39,40} in connection with a special API study on well spacing, collected a large amount of statistical data on the performance of 103 oil reservoirs in the U.S. Some 70 of these reservoirs produced wholly or partially under water-drive conditions. Fig. 40.8 shows the correlation between the calculated ROS under reservoir conditions and the reservoir oil viscosities for these water-drive reservoirs. The deviation of the ROS from the average trend in Fig. 40.8, vs. permeability, is given by the average trend in Fig. 40.9. The deviation of the ROS from the average trend in Fig. 40.8, vs. reservoir pressure decline, is given by the average trend in Fig. 40.10.

Example Problem 5. In a case where the porosity, $\phi=0.20$, the average permeability, $k=400$ md, the interstitial water content, $S_{iw}=0.25$, the initial oil FVF, $B_{oi}=1.30$, the oil FVF under abandonment conditions, $B_{oa}=1.25$, the initial reservoir oil viscosity, $\mu_o=1.0$ cp, and the abandonment pressure, $p_a=90\%$ of the initial pressure, p_i , determine the average ROS.

Solution. S_{or} may be estimated as $0.35+0.03-0.04=0.34$ and the average water-drive recovery factor from Eq. 31 is

$$N_{uw} = (7,758)(0.20) \left(\frac{1-0.25}{1.30} - \frac{0.34}{1.25} \right) \\ = 473 \text{ STB/acre-ft.}$$

TABLE 40.7—RECOVERY-EFFICIENCY FOR WATER-DRIVE RESERVOIR

Reservoir Number	ϕ	S_{iw}	B_o	S_{or}^*	Unit-Recovery Factor (bbl/acre-ft)	Actual Recovery* (bbl/acre-ft)	Recovery Efficiency (%)
1	0.179	0.400	1.036	0.20	526	429	82
2	0.170	0.340	1.017	0.20	592	430	73
3	0.153	0.265	1.176	0.20	504	428	85
4	0.192	0.370	1.176	0.20	500	400	80
5	0.196	0.360	1.017	0.20	653	482	74
							Average = 79

*From flood-pot tests.

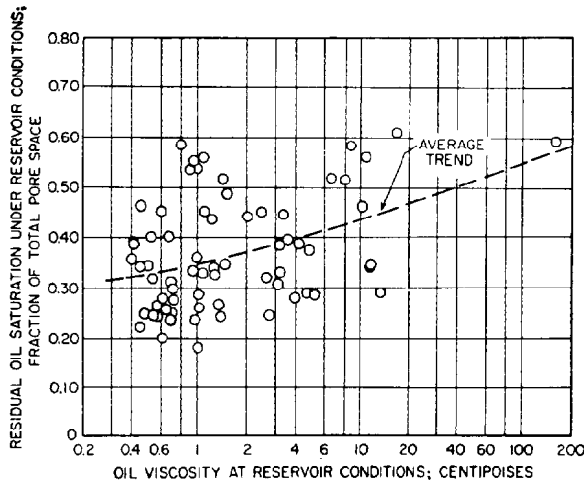


Fig. 40.8—Effect of oil viscosity on ROS water-drive sand fields.

In another statistical study of the Craze and Buckley data and other actual water-drive recovery data on a total of 70 sand and sandstone reservoirs, the API Subcommittee on Recovery Efficiency¹⁶ developed Eq. 32 for unit recovery for water-drive reservoirs, N_{uw} . In stock-tank barrels per acre-foot,*

$$N_{uw} = 4,259 \left[\frac{\phi(1-S_{iw})}{B_{oi}} \right]^{1.0422} \times \left(\frac{k\mu_{wi}}{\mu_{oi}} \right)^{0.0770} \times (S_{iw})^{-0.1903} \times \left(\frac{p_i}{p_a} \right)^{-0.2159}, \quad (32)$$

where symbols and units are as previously defined except permeability, k , is in darcies, and pressure, p , is in psig.

Example Problem 6. For the same water-drive reservoir used previously and assuming $\mu_{wi} = 0.5$ cp, the API statistical equation yields the following unit recovery factor:

$$\begin{aligned} N_{uw} &= 4,259 \left[\frac{(0.20)(1-0.25)}{1.30} \right]^{1.0422} \\ &\times \left[\frac{(0.4)(0.5)}{1.0} \right]^{0.0770} \times (0.25)^{-0.1903} \\ &\times \left(\frac{1.0}{0.9} \right)^{-0.2159} \\ &= 504 \text{ STB/acre-ft.} \end{aligned}$$

Because data were arrived at by comparing indicated recoveries from various reservoirs with the known parameters from each reservoir, the estimated residual oil and the average recovery factor based on these correlations allows for a recovery-efficiency factor (permeability-distribution factor times lateral-sweep factor) that is not present in the unit-recovery factor based on actual residual oil as found by flood-pot tests or in the cores.

*Because Eq. 32 is empirically derived, conversion to metric units ($\text{m}^3/\text{ha} \cdot \text{m}$) requires multiplication of N_{ug} by 1.2889.

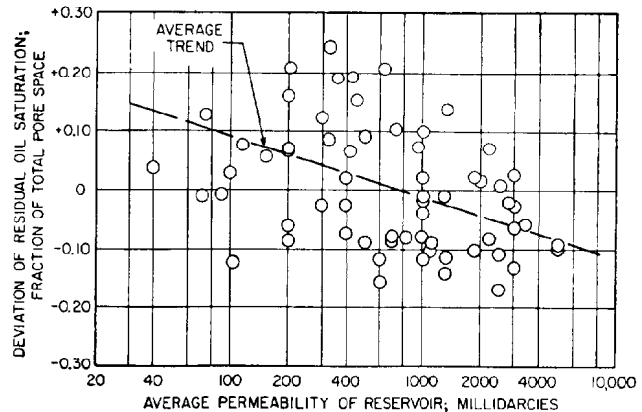


Fig. 40.9—Relation between deviation of ROS from average trend in Fig. 40.8 and permeability water-drive sand fields.

Water-Drive Unit Recovery Computed by Frontal-Drive Method²⁶⁻²⁸

The advance of a linear flood front can be calculated by two equations derived by Buckley and Leverett²⁶ and simplified by Welge²⁸ and by Pirson.²⁷ These are known as the fractional-flow equation and the rate-of-frontal-advance equation. This method assumes that (1) a flood bank exists, (2) no water moves ahead of this front, (3) oil and water move behind the front, and (4) the relative movement of oil and water behind the front is a function of the relative permeability of the two phases.

If the throughput is constant and the capillary-pressure gradient and gravity effects are neglected, the fractional-flow equation can be written as follows:

$$f_w = \frac{1}{1 + (k_{ro}/k_{rw})(\mu_w/\mu_o)}, \quad (33)$$

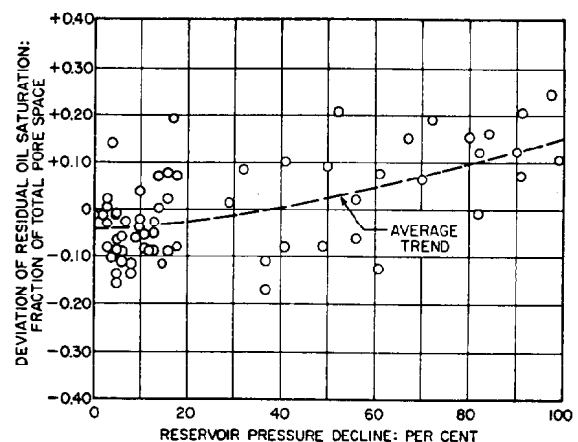


Fig. 40.10—Relation between deviation of ROS from average trend in Fig. 40.8 and pressure-decline water-drive sand fields.

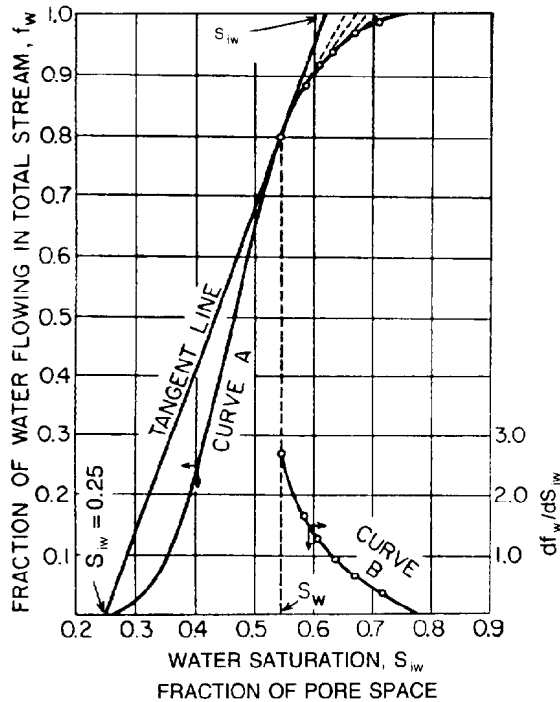


Fig. 40.11—Fraction of water flowing in total stream f_w and slope of f_w curve df_w/dS_w vs. water saturation S_w (example: frontal-water-drive problem).

where f_w is the fraction of water flowing in the reservoir at a given point, k_{rw} is the water relative permeability, fraction, and μ_w is the reservoir water viscosity, cp. Since k_{ro}/k_{rw} is a function of water saturation, f_w can be determined by Eq. 33 as a function of water saturation for a given water/oil viscosity ratio (see Fig. 40.11, Curve A).

The Buckley-Leverett rate-of-frontal-advance equation may be rearranged to give the time in days for a given displacing phase saturation to reach the outlet face of the linear sand body as a function of the slope of the fractional flow vs. saturation curve (Fig. 40.11, Curve B) as follows:

$$t = \frac{5.615 NB_o}{q_t(df_w/dS_w)} \quad (34)$$

where df_w/dS_w is the slope of the f_w vs. S_w curve; the time, t , is in days; and the total liquid flow rate, q_t , is in reservoir cubic feet per day.

The average water saturation behind the flood front at breakthrough, and therefore the oil recovery, may be obtained from the fractional-flow curve by constructing a straight line tangent to the curve through S_{iw} at $f_w=0$, and reading \bar{S}_{iw} at $f_w=1.0$. The time of breakthrough at the producing well may be computed from the slope of the curve at the point of tangency. The subsequent performance history after breakthrough may be calculated by constructing tangents at successively higher values of S_{iw} and obtaining \bar{S}_{iw} in a similar manner.

Table 40.8 illustrates the calculation procedure for a water drive at constant pressure in a homogeneous reservoir and with a water-influx rate equal to the production rate.

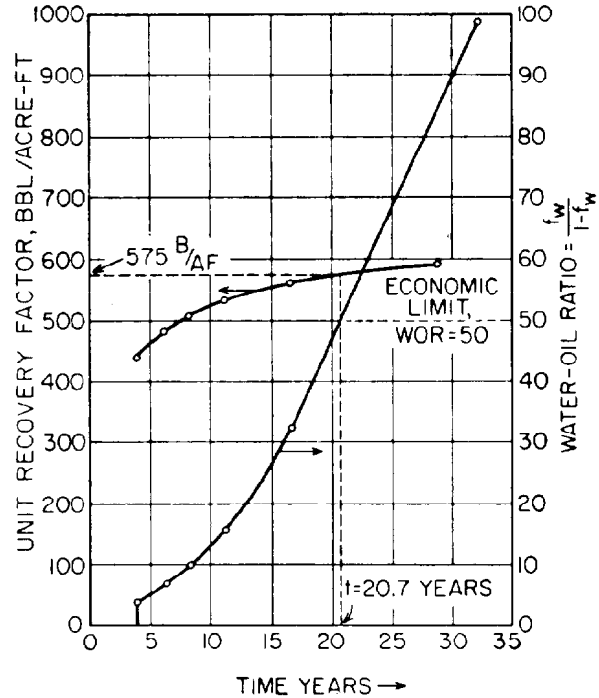


Fig. 40.12—Example of frontal-drive problem, unit-recovery factor, and WOR vs. time.

Fig. 40.12 is a plot of the results of the performance-history calculation from Table 40.8. If the economic limit is taken to be a WOR of 50, then it can be noted from Fig. 40.12 that the unit-recovery factor will be 575 bbl/acre-ft to be recovered in 20.7 years.

Effect of Permeability Distribution^{1,41-44}

In some reservoirs there may be distinct layers of higher and lower permeabilities separated by impervious strata, which appear to be more or less continuous across the reservoir. In such a case, water and oil will advance much more rapidly through the higher-permeability streaks than through the tighter zones, and therefore the recovery at the economic limit will be less than that indicated by the unit-recovery factor.

Methods for computing waterflood recoveries that take into account the permeability distribution were proposed by Dykstra and Parsons,⁴¹ Muskat,⁴² and Stiles.⁴³

In the Dykstra-Parsons paper⁴¹ it is assumed that individual zones of permeability are continuous from well to well, and a computation procedure as well as charts are presented for the coverage or fraction of the total volume of a linear system flooded with water for given values of (1) the mobility ratio $k_{rw}\mu_o/k_{ro}\mu_w$, (2) the produced WOR, and (3) the permeability variance.

This permeability variance is a statistical parameter that characterizes the type of permeability distribution. It is obtained by plotting the percentage of samples "larger than" the sample being plotted vs. the logarithm of permeability for that sample on log-probability graph paper and then dividing the difference between the median or 50% permeability and the 84.1% permeability by the median permeability. Although the Dykstra-Parsons method

TABLE 40.8—WATER-DRIVE PERFORMANCE-HISTORY CALCULATION*

S_{iw}	S_{ow}	f_w	df_w/dS_{iw}	Time (years)	Residual Oil Saturation ($1 - S_{iw}$)	Unit-Recovery Factor (bbl/acre-ft)	WOR = $f_w / (1 - f_w)$
0.545	0.619	0.800	2.70	3.94	0.381	441	4.0
0.581	0.655	0.875	1.69	6.29	0.345	484	7.0
0.605	0.675	0.910	1.29	8.24	0.325	507	10.1
0.634	0.697	0.940	0.95	11.19	0.303	534	15.7
0.673	0.720	0.970	0.64	16.61	0.280	561	32.3
0.718	0.748	0.990	0.33	32.21	0.252	594	99.0

* $N = 597,000$ STB. $B_{oi} = 1.30$. $\phi = 0.20$. $S_{iw} = 0.25$, and $q_f = 200$ B/D $\times 5$ 615 cu ft/bbl = 1,222 reservoir cu ft/D.

does not allow for variations in porosity, interstitial water, and floodable oil in the different permeability groups, it has apparently been used extensively and successfully on close-spaced waterfloods, mainly in California.

Johnson⁴⁴ in 1956 published a simplification of this method and presented a series of charts showing the fractional recovery of oil in place at a given produced WOR for a given permeability variance, mobility ratio, and water saturation. Reznik *et al.*⁴⁵ published an extension to the Dykstra-Parsons method that provides a discrete analytical solution to the permeability stratification problem on a real-time basis.

In the Stiles method⁴³ it again is assumed that individual zones of permeability are continuous from well to well and that the distance of penetration of the flood front in a linear system is proportional to the average permeability of each layer. Instead of representing the entire permeability distribution by one statistical parameter, Stiles tabulates the available samples in descending order of permeability and plots the results in terms of dimensionless permeability and cumulative capacity fraction as a function of cumulative thickness. From these data, Stiles computes the produced water cut of the entire system as the watering out progresses through the various layers, starting with those of the highest permeability. Stiles then assumes that at a given time each layer that has not had breakthrough will have been flooded out in proportion to the ratio of its average permeability to the permeability of the last zone that had just had breakthrough, and then constructs a recovery vs. thickness relationship. This then is combined with previous results to yield a recovery vs. water-cut graph. The Stiles method is used extensively and successfully, mainly in the midcontinent and Texas, for close-spaced waterfloods. It does not make allowance for the difference in mobility existing in the formation ahead of and behind the flood front, which the Dykstra-Parsons method allows for. It also does not provide for differences in porosity, interstitial water, and floodable oil in the various permeable layers.

Arps¹ introduced in 1956 a variation of the Stiles method, called the "permeability-block method." This method handles the computations by means of a straightforward tabulation and does make allowance for the differences in porosity, interstitial water, and floodable oil existing in the various permeable layers. Since it is designed primarily for the computation of recoveries from water-drive fields above their bubblepoint, no free-gas saturation

is assumed. The method further assumes that (1) no oil moves behind the front, (2) no water moves ahead of the front, (3) watering out progresses in order from zones of higher to zones of lower permeability, and (4) the advance of the flood front in a particular permeability streak is proportional to the average permeability.

This method, applied to a hypothetical pay section 100 ft thick, is illustrated in Table 40.9, which is based on data from a Tensleep sand reservoir in Wyoming where good statistical averages of more than 3,000 core analyses were available. Part of these cores were taken with water-base mud that yielded the residual-oil figures on Line 6. Another portion was taken with oil-base mud and yielded the interstitial-water figures of Line 7. An oil/water viscosity ratio of 12.5 was used in calculating the WOR of Line 13.

In Group 1 the recovery of 61.7 bbl/acre-ft for WOR=15.5 is the product of the fraction of samples in the group and the unit-recovery factor. In all other groups for WOR=15.5 the full recovery is reduced in the proportion of its average permeability to 100 md. The total recovery at WOR=15.5 is shown as 175.6 bbl/acre-ft. The cumulative recoveries for WOR's of 35.9, 76.5, 307.7, and infinity are calculated in a similar manner. Fig. 40.13 is a plot of WOR vs. recovery factor. From Fig. 40.13 it can be seen that, if the economic limit is taken to be a WOR of 50, the recovery factor would be 297 bbl/acre-ft.

It should be stressed that the permeability-block method is applicable only when the zones of different permeability are continuous across the reservoir, or between the source of the water and the producing wells. When the waterfront has to travel over large distances, nonuniformity of permeability distribution in lateral directions begins to dominate, and recoveries will approach those obtainable if the formation were entirely uniform (permeability distribution factor=1). In such a case, an estimate based on the permeability-block method may be considered as conservative, except for the fact that one of the basic assumptions of this method is that the WOC, or front, moves in pistonlike fashion through each permeability streak, sweeping clean all recoverable oil. In reality, part of this oil will be recovered over an extended period after the initial breakthrough, which may tend to make the estimate optimistic. Those using the permeability-block method hope that these two effects are more or less compensating.

TABLE 40.9—WATER DRIVE PERMEABILITY-BLOCK CALCULATIONS

Group	1	2	3	4	5	Total
(1) Permeability range, md	> 100	50 to 100	25 to 50	10 to 25	0 to 10	
(2) Percent of samples in group	8.5	10.9	14.5	21.2	44.9	100.0
(3) Average permeability, md	181.3	69.0	34.4	16.1	2.4	
(4) Capacity, darcy-ft $(2) \times (3) \div 1,000$	1.541	0.752	0.499	0.341	0.108	3.241
(5) Average porosity fraction ϕ	0.159	0.150	0.152	0.130	0.099	
(6) Average residual-oil fraction S_{gr}	0.173	0.195	0.200	0.217	0.222	
(7) Average interstitial-water fraction S_{iw}	0.185	0.154	0.131	0.107	0.185	
(8) Relative water permeability behind front k	0.65	0.63	0.60	0.56	0.54	
(9) Relative oil permeability ahead of front k_{ro}	0.475	0.53	0.61	0.66	0.47	
(10) Unit-recovery factor $(B_{oi} = 1.07)$	726	693	722	623	415	
(11) Cumulative "wet" capacity, $\Sigma(4)$	1.541	2.293	2.792	3.133	3.241	
(12) Cumulative "clean oil" capacity, $3.241 - (11)$	1.700	0.948	0.449	0.108	0	
(13) Water-oil ratio WOR $= (\mu_o/\mu_w)(8/9)(11/12)$	15.5	35.9	76.5	307.7	∞	
(14) Cumulative recovery at WOR = 15.5 bbl/acre-ft Min $k_{wet} = 100$ md	61.7	52.1	36.0	21.3	4.5	175.6
(15) Cumulative recovery at WOR = 35.9 bbl/acre-ft Min $k_{wet} = 50$ md	61.7	75.5	72.0	42.5	8.9	260.6
(16) Cumulative recovery at WOR = 76.5 bbl/acre-ft Min $k_{wet} = 25$ md	61.7	75.5	104.7	85.1	17.9	344.9
(17) Cumulative recovery at WOR = 307.7 bbl/acre-ft Min $k_{wet} = 10$ md	61.7	75.5	104.7	132.1	44.7	418.7
(18) Cumulative recovery at WOR = ∞ bbl/acre-ft Min $k_{wet} = 0$ md	61.7	75.5	104.7	132.1	186.3	560.3

Effect of Buoyancy and Imbibition

In limestone pools producing under a bottomwater drive, such as certain of the vugular D-3 reef reservoirs in Alberta, one finds an extreme range in the permeabilities, often running from microdarcies on up into the darcy range. Under those conditions the modified Stiles method heretofore described yields results that are decidedly too

low. The reason is that, in pools like the Redwater D-3, there is a substantial density difference between the rising salt water and the oil. While the water rises and advances through the highly permeable vugular material, it may at first bypass the low-permeability matrix material, leaving oil trapped therein. However, as soon as such bypassing occurs, a buoyancy gradient is set up across this tight material, which tends to drive the trapped oil out vertically into the vugular material and fractures. In the case of Redwater D-3, where the density difference between salt water and oil is 0.26, while the vertical permeabilities for matrix material are only a fraction of the horizontal permeabilities, a simple calculation based on Darcy's law applied to a vertical tube shows that during the anticipated lifetime of the field very substantial additional oil recovery may be obtained because of this so-called buoyancy effect.

To calculate the recovery under a buoyancy mechanism it is necessary first to determine by statistical analysis of a large number of cores the average interval between high-permeability zones or fractures. A separate computation is then made for each of the permeability ranges to determine what percentage of the matrix oil contained in a theoretical tube of such average length may be driven out during the producing life of the reservoir under the effect of the buoyancy phenomenon.

Surprisingly improved recoveries are sometimes indicated by this method over what one would expect from a Stiles type of calculation, and the results from recent studies of the rise in water table of the Redwater D-3 seem to confirm the validity of this concept.

In addition to this buoyancy phenomenon the effect of capillarity and preferential wetting of the reservoir rock by water also should be considered. Imbibition of water from fractures and vugular material into the low-permeability matrix as the water advances may materially aid the buoyancy mechanism but is much more difficult to evaluate quantitatively.

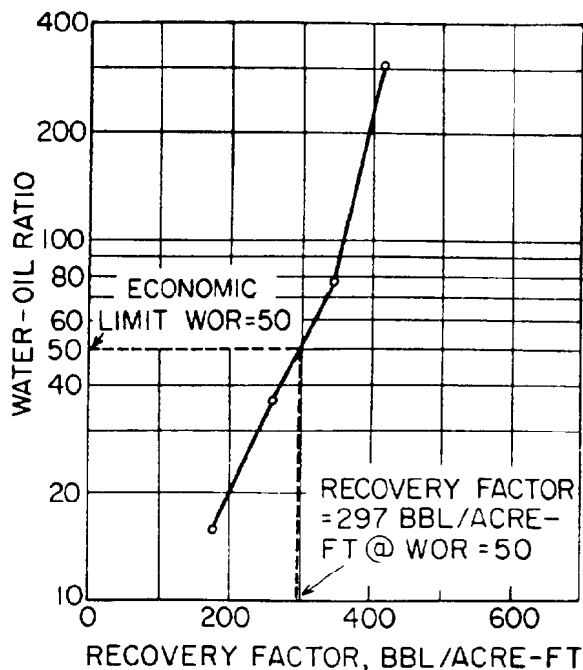


Fig. 40.13—Example of modified Stiles permeability-block method WOR vs. recovery factor.

TABLE 40.10—PSEUDOCRITICAL CALCULATIONS FROM GAS ANALYSIS

Component (1)	Volume % or Mol% (2)	Critical Temperature (°R) (3)	Critical Pressure (psia) (4)	2 × 3	2 × 4
				100 (5)	100 (6)
Methane	86.02	343.5	673	296	572
Ethane	7.70	550.1	708	42.4	54.5
Propane	4.26	666.2	617	28.4	26.3
Isobutane	0.57	733.2	530	4.2	3.0
Normal butane	0.87	765.6	551	6.7	4.8
Isopentane	0.11	830.0	482	0.9	0.5
Normal pentane	0.14	847.0	485	1.2	0.7
Hexanes	0.33	914.6	434	3.0	1.4
Total	100.00			382.8	663.2

Volumetric Recovery Estimates for Nonassociated Gas Reservoirs⁴⁶⁻⁵³

Compressibility Factor

The compressibility factor z is a dimensionless factor which, when multiplied by the reservoir volume of gas, as computed by the ideal-gas laws, yields the true reservoir volume. The reservoir volume occupied by 1 lbm-mole of gas (gas weight in pounds equal to molecular weight), in cubic feet, is

$$G = \frac{(10.73)z(460 + T_R)}{p_R}, \quad \dots \dots \dots (35)$$

where G is the total initial gas in place in reservoir, in standard cubic feet, and T_R is the reservoir temperature, °F. For example, 1 lbm-mole of methane (molecular

weight 16.04) under standard conditions ($p_R = 14.7$ psia, $T_R = 60^\circ\text{F}$) occupies 379.4 cu ft.

The compressibility factor may be determined in the following ways.

1. Experimentally by PVT analysis of a gas sample.
2. By computation from an analysis of the gas expressed in mol% or volume %. With this method a weighted-average or pseudocritical pressure and temperature are obtained for the gas by multiplying the individual critical pressure and temperature for each component, with the corresponding mol% of such component as shown in Table 40.10.

The gas whose composition is given in Table 40.10 has a pseudocritical temperature of 382.8°R and a pseudocritical pressure of 663.2 psia. The pseudoreduced temperature then is found at a temperature of 150°F as $(460 + 150)/382.8 = 1.59$ and its pseudoreduced pressure

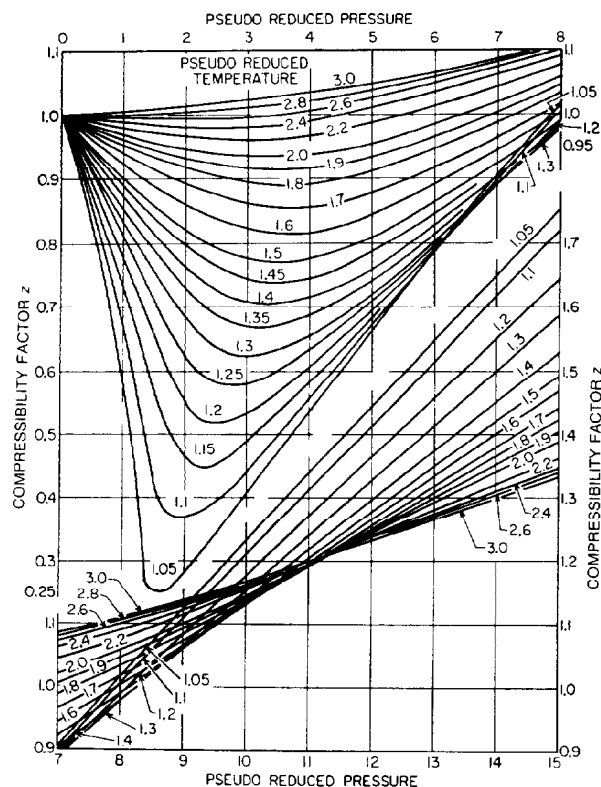


Fig. 40.14A—Compressibility factors for natural gases.

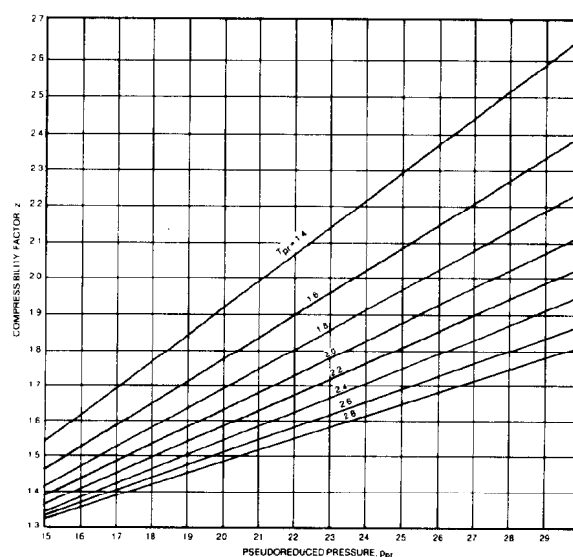


Fig. 40.14B—Compressibility factors for natural gases at pressures of 10,000 to 20,000 psia.

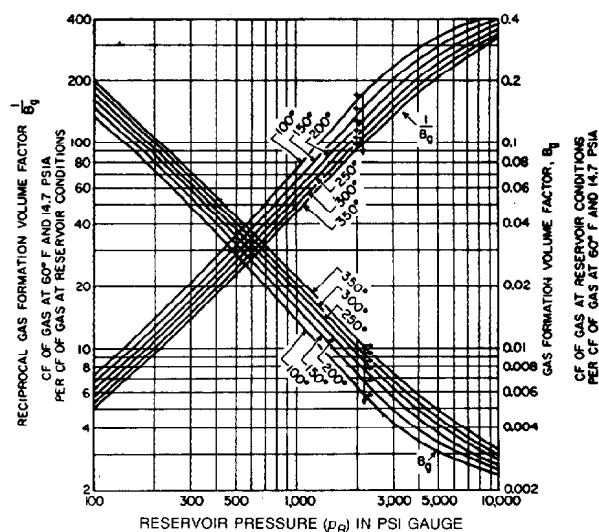


Fig. 40.15—Gas FVF $B_g = \frac{14.17}{p_R + 14.7} \frac{460 + T_R}{460 + 60} z$

and reciprocal gas FVF

$$\frac{1}{B_g} = \frac{p_R + 14.7}{14.7} \frac{460 + 60}{460 + T_R} \frac{1}{z}$$

vs. pressure, psig, and temperature, °F.
Gas gravity 0.6 (air 1.0).

at 750 psia as $750/663.2 = 1.13$. These ratios are entered into the chart of Fig. 40.14A to read $z = 0.91$. This correlation chart⁴⁶ and an extended correlation chart⁴⁷ for higher-pressure gas reservoirs up to 20,000 psia, Fig. 40.14B, are designed for gaseous mixtures containing methane and other natural gases but substantially free of nitrogen. For hydrocarbon gases containing substantial amounts of hydrogen sulfide or CO_2 , these correlations do not apply, and additional corrections are necessary as described in Ref. 48. (See Chap. 20 for complete coverage of gas properties and gas property correlations, some of which are specific to computer applications.)

TABLE 40.11—PSEUDOCRITICAL CALCULATIONS FROM SPECIFIC GRAVITY

Specific gravity of Gas (Air = 1.0)	Pseudocritical Temperature (°R) (460 + °F)	Pseudocritical Pressure (psia) (14.7 + psig)
0.55	348	674
0.60	363	672
0.70	392	669
0.80	422	665
0.90	451	660
1.00	480	654
1.10	510	648
1.20	540	641
1.30	570	632
1.40	600	623
1.50	629	612
1.60	658	600
1.65	673	593

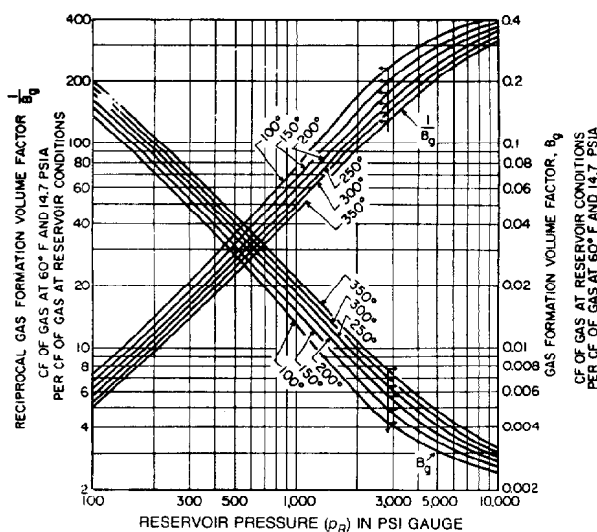


Fig. 40.16—Gas FVF $B_g = \frac{14.17}{p_R + 14.7} \frac{460 + T_R}{460 + 60} z$

and reciprocal gas FVF

$$\frac{1}{B_g} = \frac{p_R + 14.7}{14.7} \frac{460 + 60}{460 + T_R} \frac{1}{z}$$

vs. pressure, psig, and temperature, °F.
Gas gravity 0.7 (air 1.0).

3. By computation from the specific gravity of the gas. If only the specific gravity of the gas (air = 1.0) is known, another approximate correlation can be used, based on California natural gases,⁴⁹ which is expressed by Table 40.11.

For example, if the specific gravity of a gas is 0.66, the pseudocritical temperature can be estimated by interpolation as 381°R and pseudocritical pressure as 670 psia. The pseudoreduced values then are found as before and the z factor read from Fig. 40.14A.

Gas FVF

The gas FVF, B_g , is a dimensionless factor representing the volume of free gas at a reservoir temperature of $T^\circ\text{F}$ and a pressure of p psia per unit volume of free gas under standard conditions of 60°F and 14.7 psia. If the compressibility factor, z , is known, B_g may be computed by

$$B_g = \frac{14.7}{p_R} \frac{460 + T_R}{460 + 60} z = 0.02827 (460 + T_R) \frac{z}{p_R} \quad (36)$$

Typical values of the gas FVF, B_g , and the reciprocal gas FVF, $1/B_g$, for different temperatures and pressures and for gases of specific gravities between 0.6 and 1.0 will be found in Figs. 40.15 through 40.19.

In estimating gas reserves, the estimator should be careful to indicate clearly the pressure base at which the reserves are stated. Reserves at a base pressure of 14.4 psia will be approximately 16% greater than the same reserves stated at a base pressure of 16.7 psia.

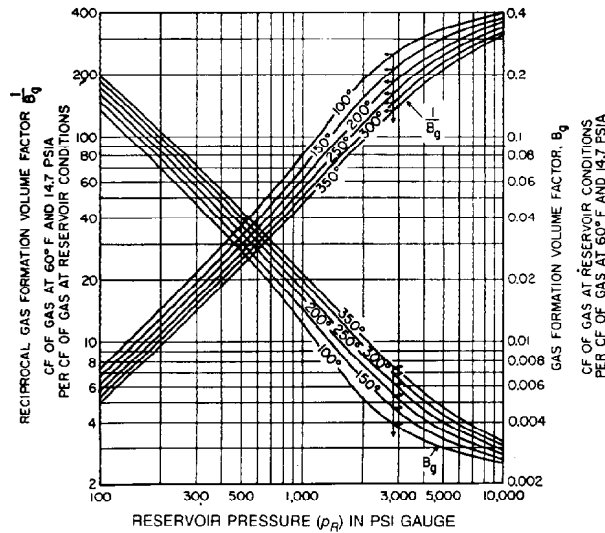


Fig. 40.17—Gas FVF $B_g = \frac{14.17}{p_R + 14.7} \frac{460 + T_R}{460 + 60} z$

and reciprocal gas FVF

$$\frac{1}{B_g} = \frac{p_R + 14.7}{14.7} \frac{460 + 60}{460 + T_R} \frac{1}{z}$$

vs. pressure, psig, and temperature, °F.
Gas gravity 0.8 (air 1.0).

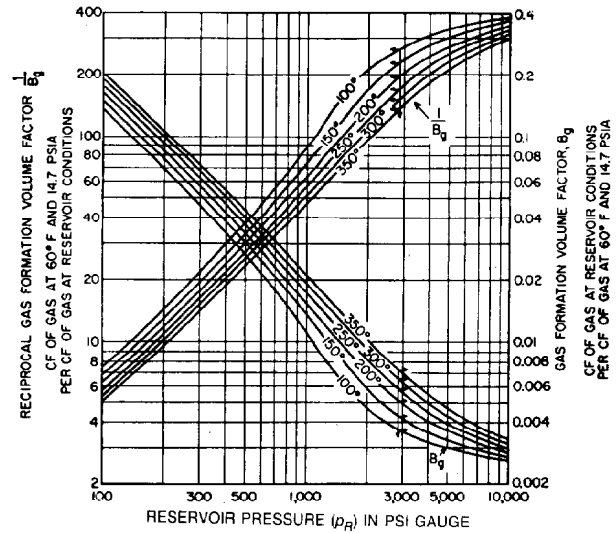


Fig. 40.18—Gas FVF $B_g = \frac{14.17}{p_R + 14.7} \frac{460 + T_R}{460 + 60} z$

and reciprocal gas FVF

$$\frac{1}{B_g} = \frac{p_R + 14.7}{14.7} \frac{460 + 60}{460 + T_R} \frac{1}{z}$$

vs. pressure, psig, and temperature, °F.
Gas gravity 0.9 (air 1.0).

The standard pressure base for the states of Texas, Oklahoma, and Kansas is 14.65 psia (14.4 lbm plus 4 oz/sq in.); for Colorado, Louisiana, Nebraska, Mississippi, Montana, New Mexico, and Wyoming it is 15.025 psia (14.4 lbm plus 10 oz/sq in.); and for California it is 14.73 psia).

Gas In Place

According to Eq. 1, the gas in place in a reservoir containing nonassociated gas and interstitial water, but no residual oil, in standard cubic feet of free gas, is

$$G_{Fi} = \frac{43,560 V_g \phi (1 - S_{iw})}{B_g}$$

Oftentimes the recoverable gas from a reservoir is estimated by multiplying the gas in place by an overall recovery factor.

For example, with a pressure gradient of 46.5 psi/100 ft of depth, a surface temperature of 74°F, a temperature gradient of 1.5°F/100 ft of depth, a specific gravity of the gas of 0.7, and a recovery factor for blanket high-permeability formations of around 80%, typical values of the recoverable gas in thousands of cubic feet per acre-foot is found in Table 40.12 for various combinations of porosity, ϕ , and interstitial-water content, S_{iw} .

The numbers in Table 40.12 are not directly applicable to wide-spaced low-permeability formations, such as those which require fracturing or other stimulation tech-

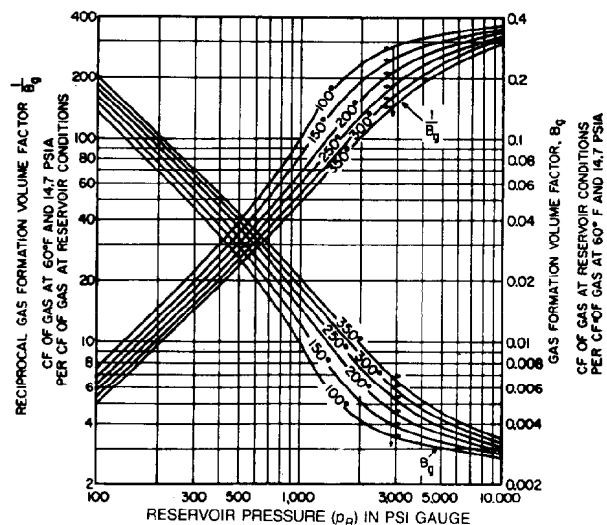


Fig. 40.19—Gas FVF $B_g = \frac{14.17}{p_R + 14.7} \frac{460 + T_R}{460 + 60} z$

and reciprocal gas FVF

$$\frac{1}{B_g} = \frac{p_R + 14.7}{14.7} \frac{460 + 60}{460 + T_R} \frac{1}{z}$$

vs. pressure, psig, and temperature, °F.
Gas gravity 1.0 (air 1.0).

TABLE 40.12—TYPICAL VALUES OF RECOVERABLE GAS, Mcf/acre-ft

Porosity ϕ	0.05	0.10	0.15	0.20	0.25	0.30	0.35
Interstitial water S_{iw}	0.35	0.30	0.30	0.25	0.25	0.20	0.15
Depth, ft							
1,000	37	80	121	172	216	276	342
2,000	77	166	249	355	444	569	705
3,000	122	263	395	565	706	903	1,120
4,000	159	342	512	732	915	1,171	1,451
6,000	215	463	695	993	1,241	1,589	1,970
8,000	255	549	823	1,176	1,470	1,882	2,333
10,000	277	598	896	1,281	1,601	2,049	2,540
12,000	294	634	951	1,359	1,699	2,175	2,695
15,000	311	671	1,006	1,437	1,797	2,300	2,851

niques to produce at commercial rates. In such cases allowance should be made for the fact that the economic limit of production may be reached before the entire spacing unit is depleted. Known or suspected lenticularity of the gas-bearing formation also should be taken into account in estimating the potential drainage area.

Unit Recovery for a Gas Reservoir Without Water Drive

Dry Gas. The unit-recovery factor (the theoretically possible ultimate recovery from a homogeneous unit volume of pay under ideal conditions) for a dry-gas reservoir without water influx is equal to the gas initially in place at pressure p_i , minus the gas remaining under abandonment pressure at ultimate recovery, p_a , both expressed in standard cubic feet per acre-foot of sand (Table 40.12). By difference, the unit recovery for a dry-gas reservoir, in standard cubic feet of gas per acre-foot, is

$$G_{ul} = 43,560\phi(1 - S_{iw}) \left(\frac{1}{B_{gi}} - \frac{1}{B_{ga}} \right), \quad (37)$$

where G_{ul} is the ultimate gas recovery from reservoir, in standard cubic feet, and B_{ga} is the gas FVF at abandonment, in reservoir cubic feet per standard cubic foot. The abandonment pressure (p_a) to be used depends on the operating pressure of the pipeline outlet, the availability of compressors to boost low-pressure gas to pipeline pressures, the depth of the reservoir, the size of the production tubing, and the permeability and pay thickness of the reservoir.

Gas Condensate. In gas-condensate reservoirs, condensation of hydrocarbon liquids may occur upon pressure drop in the reservoir and in the surface separation equipment. Condensation of liquids in the reservoir may cause the unit-recovery factor as computed for a dry-gas reservoir to be optimistic, because the volume of condensate in the reservoir at abandonment pressure is usually smaller than the reservoir volume of the gases at that pressure which condensed into liquid. Recovery of condensate in the surface separation equipment also reduces the amount of free gas available for sale. In rich gas-condensate reservoirs without water drive produced under pressure-depletion conditions, the recovery computations should therefore be based on an actual laboratory depletion study

of a recombined sample. If such an analysis is not available, an approximation may be made on the basis of the fact that the amount of free gas corresponding to 1 cu ft of condensate is usually about 150 to 200 scf. Based on an average figure of 175 cu ft (1 m³ of condensate on the average corresponds to 175 std m³ of gas), the unit recovery in terms of residue or sales gas, when the residual condensate saturation in the reservoir at abandonment time is S_{or} , and the average produced gas/condensate ratio is R_p scf/bbl, may be estimated, in standard cubic feet residue gas per acre-foot, as

$$G_{ul} = 43,560\phi \frac{R_p}{R_p + 175} \left(\frac{1 - S_{iw}}{B_{gi}} - \frac{1 - S_{iw} - S_{or}}{B_{ga}} - 175 S_{or} \right), \quad (38)$$

S_{or} may be estimated from a material-balance calculation on the condensate present in the reservoir gas under initial conditions, and the condensate to be recovered during the depletion of the reservoir in the surface separation equipment.

Effect of Permeability Distribution

Unless a gas reservoir is known to be permeable and homogeneous, the unit-recovery factor should be corrected for the fact that depletion may progress more rapidly in the high-permeability strata than in the low-permeability zones, particularly if these zones are separated by impervious strata. An uneconomic rate of production may be reached before the tighter zones are drained down to abandonment pressure. In many cases, nonuniformity of permeability in lateral directions provides a compensating influence. In very hard and tight formations, extensive fracturing may have the same result. A computation based on the assumption that the strata of different permeabilities are uniform and continuous across the reservoir is therefore in most cases too pessimistic. Such a computation does provide a means, however, to indicate the minimum recoverable reserves while the assumption of a completely homogeneous reservoir and the direct use of the unit-recovery factor indicate a maximum figure for the recoverable reserves.

A permeability-block method to compute such minimum reserves for a nonassociated dry gas reservoir is as follows.

According to Eqs. 13 and 14 of Sec. 11.15 in Ref. 50, the boundary pressure in a closed cylindrical gas reservoir, drained by a well in the center with zero pressure against the sandface, may be approximated as

$$p_R = \left(\frac{1}{p_i} + C_1 \frac{k_{rg}}{\phi_h} t \right)^{-1}, \dots \dots \dots (39)$$

while the gas production rate is

$$q_g = C_2 k_g h_e p^2, \dots \dots \dots (40)$$

in which C_1 and C_2 are constants and ϕ_h and h_e are effective hydrocarbon porosity and effective thickness, respectively.

It will be assumed that a large number of core analyses are available on a gas reservoir, which are divided in permeability groups as shown on Table 40.13. The average permeability, k , for each group is then corrected to the relative gas permeability, k_{rg} , at the given S_{iw} saturation. The average porosity, ϕ , for each group is corrected also to the effective hydrocarbon-bearing porosity, $\phi_h = \phi(1 - S_{iw})$.

It will further be assumed that each permeability group represents a separate and distinct homogeneous layer having a relative gas permeability k_{rg} and a hydrocarbon-filled porosity ϕ_h equal to the average for each group. Each layer is sealed off from the others and feeding into a common wellbore that is exposed to zero pressure.

To keep the computations as simple as possible it will further be assumed that the ideal-gas laws are applicable. The same method may be applied by taking the deviation from the ideal-gas laws into consideration, by assuming other than zero wellbore pressure, and by taking into account liquid condensation in gas-condensate reservoirs, but such computations soon become rather unwieldy.

By the time Group 1, comprising the highest permeability, is bled down to a pressure p_1 , a time t has expired, which according to Eq. 39 is equal to

$$t = \frac{(\phi_h)_1}{C_1(k_{rg})_1 p_i} \left(\frac{p_i}{p_1} - 1 \right), \dots \dots \dots (41)$$

The fractional pressure p_n/p_i in any layer n at this same time t is found by substituting the t value of Eq. 41 into Eq. 39.

$$\frac{p_n}{p_i} = \left[1 + \frac{(k_g)_n (\phi_h)_1}{(k_g)_1 (\phi_h)_n} \left(\frac{p_i}{p_1} - 1 \right) \right]^{-1}, \dots \dots \dots (42)$$

The combined production rate from all layers, q_n , at this time is, according to Eq. 40,

$$q_n = C_3 \sum_1^n (k_g)_n (h_e)_n \left(\frac{p_n}{p_i} \right)^2, \dots \dots \dots (43)$$

TABLE 40.13—CONDITIONS FOR UNIT RECOVERY EQUATION IN A DRY-GAS RESERVOIR

	Initial Conditions	Ultimate Conditions
Reservoir pressure	p_i	p_a
Interstitial water, cu ft/acre-ft	$43,560 \phi S_{iw}$	$43,560 \phi S_{iw}$
Free gas, scf/acre-ft	$\frac{43,560 \phi (1 - S_{iw})}{B_{gi}}$	$\frac{43,560 \phi (1 - S_{iw})}{B_{ga}}$

while the cumulative production from all layers, G_{pn} , at this time is

$$G_{pn} = C_4 \sum_1^n (\phi_h)_n (h_e)_n \left(1 - \frac{p_n}{p_i} \right), \dots \dots \dots (44)$$

in which C_3 and C_4 are constants.

The fractional production rate from all layers, f_{gn} , with respect to the initial production rate from all layers is, therefore,

$$f_{gn} = \frac{\sum_1^n (k_g)_n (h_e)_n (p_n/p_i)^2}{\sum_1^n (k_g)_n (h_e)_n}, \dots \dots \dots (45)$$

while the cumulative production from all layers as a fraction of the total gas in place in all layers is

$$\frac{G_{pn}}{G_n} = \frac{\sum_1^n (\phi_h)_n (h_e)_n [1 - (p_n/p_i)]}{\sum_1^n (\phi_h)_n (h_e)_n}, \dots \dots \dots (46)$$

Thus a rate-cumulative relationship may be established based on Eqs. 45 and 46, whereby the rate is expressed as a fraction or percentage of the initial rate, and the cumulative as a fraction or percentage of the gas in place. By selecting an appropriate economic limit rate the recovery factor can then be found. The computation procedure is illustrated with the example in Table 40.14.

Usually only three or four assumptions for the ratio p_i/p_1 are necessary to delineate the curve, which may then be plotted on semilog paper as shown in Fig. 40.20.

In this particular case, it could be estimated that the minimum recovery factor for this reservoir at a time when the production rate has declined to 1% of its initial value would be on the order of 74% of the gas in place.

TABLE 40.14—PERMEABILITY-BLOCK METHOD FOR GAS RESERVOIRS WITHOUT WATER DRIVE

Group (n)	1	2	3	4	Total	Percent of Initial rate and gas in place
(1) Permeability, range	$10 < k < 100$	$1 < k < 10$	$0.1 < k < 1$	$0.01 < k < 0.1$		
(2) \bar{k}_g	25.26	3.36	0.34	0.05		
(3) ϕ_h	0.070	0.068	0.045	0.022		
(4) k_g/ϕ_h	360.8	49.4	7.56	2.27		
(5) $(k_g/\phi_h)_n \div (k_g/\phi_h)_1$	1	0.13692	0.02095	0.00629		
(6) Number of samples, n'	170	530	889	622	2,211	
(7) $\bar{k}_g n'$	4,294	1,780	302.3	31.1	6,407.4	(= 100%)
(8) $(\phi_h) n'$	11.90	36.04	40.00	13.68	101.62	(= 100%)
Assume $(p_n/p_i) = 4$						
Pressure (p_n/p_i)						
$= [1 + 3(5)]^{-1}$	0.2500	0.7088	0.9408	0.9815		
Rate $= (7)(p_n/p_i)^2$	268.4	894.3	267.6	30.0	1,460.3	(= 22.8%)
Cumulative $= (8)[1 - (p_n/p_i)]$	8.92	10.49	2.37	0.25	22.03	(= 21.7%)
Assume $(p_n/p_i) = 25$						
Pressure (p_n/p_i)						
$= [1 + 24(5)]^{-1}$	0.0400	0.2333	0.6654	0.8688		
Rate $= (7)(p_n/p_i)^2$	6.9	96.9	133.8	23.5	261.1	(= 4.07%)
Cumulative $= (8)[1 - (p_n/p_i)]$	11.42	27.63	13.38	1.79	54.22	(= 53.4%)
Assume $(p_n/p_i) = 101$						
Pressure (p_n/p_i)						
$= [1 + 100(5)]^{-1}$	0.0099	0.0681	0.3231	0.6139		
Rate $= (7)(p_n/p_i)^2$	0.4	8.2	31.6	11.7	51.9	(= 0.81%)
Cumulative $= (8)[1 - (p_n/p_i)]$	11.78	33.59	27.08	5.28	77.73	(= 76.5%)

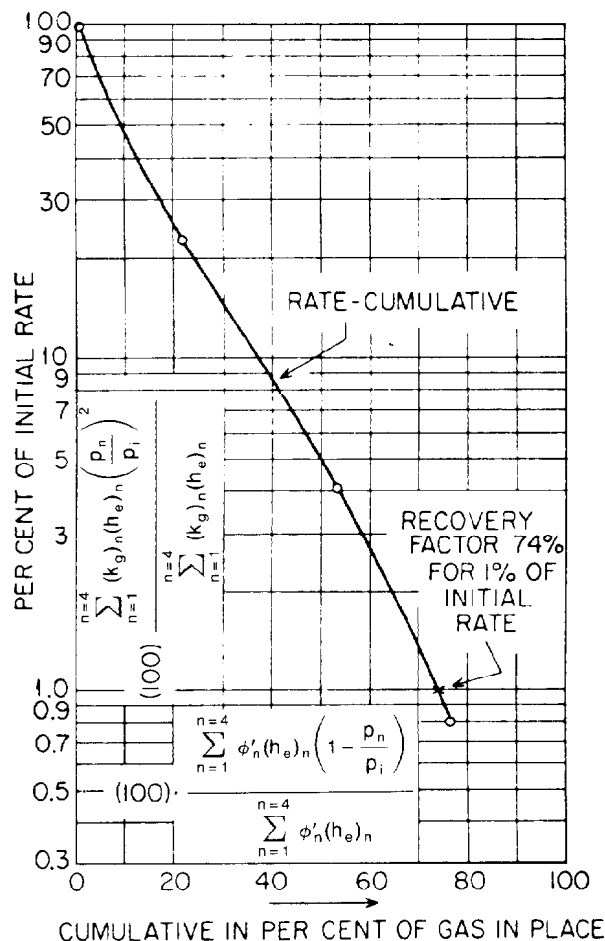


Fig. 40.20—Permeability-block method for gas reservoirs without water drive.

Recovery From Gas Reservoirs With Water Drive

In the case of gas reservoirs with effective water drive, the pressure will be wholly or partially maintained by the movement of water into the reservoir as gas is withdrawn, the magnitude of the pressure decline being dependent on the rate of gas withdrawal with respect to the rate of water influx. Because the portion of the reservoir that will be ultimately invaded by water is not always predictable, and because the amount of gas that as a nonwetting phase may be bypassed by the water is difficult to estimate, the recovery from gas reservoirs with water drive is usually estimated by applying a recovery factor to the volume of gas originally in place as calculated by Eq. 1. The selection of this recovery factor depends on the thickness and homogeneity of the sand, the relative permeability of the sand to gas and water at varying gas saturations, and the geometry and dip of the gas-bearing strata.

Because gas is trapped and bypassed by the advancing water and because of the associated water production problems, recovery factors are significantly lower for gas reservoirs with water drive than for those producing by volumetric expansion. Typical factors range from 50 to 70% for water-drive gas reservoirs as compared with 70 to 90% for expansion-drive gas reservoirs.

Production-Decline Curves^{35,54-58}

General Principles

All estimates of ultimate recovery by extrapolation of a performance trend fundamentally follow the same pattern. The two quantities one usually wishes to determine are either remaining oil reserves or remaining productive life. Cumulative production and time, therefore, normally are selected as independent variables and are plotted as abscissas. A varying characteristic of the well performance that can be measured easily and recorded then is selected

as a variable to produce a trend curve. For extrapolation purposes this variable has to meet two qualifications: (1) its value must be a more or less continuous function of the independent variable and change in a uniform manner; and (2) it must have a known endpoint.

By plotting the values of this continuously changing dependent variable as ordinates vs. the values of the independent variable (cumulative production or time) as abscissas, and graphically extrapolating the apparent trend until the known endpoint is reached, an estimate of the remaining reserves or remaining life can be obtained. The basic assumption in this procedure is that whatever causes controlled the trend of a curve in the past will continue to govern its trend in the future in a uniform manner.

This extrapolation procedure is therefore strictly of an empirical nature, and a mathematical expression of the trend curve based on physical considerations of the reservoir can be set up only for a few simple cases.⁵⁴

Among the many dependent variables that can be used in estimates based on performance trends, the rate of production is by far the most popular when production is not restricted. In that case one commonly refers to production-decline curves. The two main types are rate/time and rate/cumulative curves for each of the two independent variables. Rate of oil production as the dependent variable has the advantage of always being readily available and accurately recorded. The endpoint requirement is also easily met, since known or estimated operating costs usually make it possible to determine accurately the economic-limit rate and thus the endpoint of the curve.

Gradual changes in the production rate of a well may be caused by the following.

1. Decreasing efficiency or effectiveness of the lifting equipment.
2. Reduction of productive index, or completion factor,⁵⁷ or increase in the skin effect⁵⁸ as a result of physical changes in and around the wellbore such as deposition of wax, salt, or asphaltenes from the produced fluids or the accumulation of loose sand, silt, mud, or cavings.
3. Changes in bottomhole pressure, GOR, water percentage, or other reservoir conditions.

To be used for reserve estimation, production decline caused by reservoir conditions must be distinguished from that caused by wellbore conditions or by failure of the lifting equipment.

The efficiency of the lifting equipment may be checked by conventional inspection for tubing or valve leaks, and the volumetric pump efficiency by dynamometer, sonic fluid-level tests, etc. Such tests may indicate the need for a pulling job to replace the downhole pumping equipment or gas-lift valves.

A study of the completion factor, skin effect, or productive index over a period of time by means of bottomhole pressure-buildup analysis^{57,58} may indicate an adverse wellbore condition that can sometimes be corrected by appropriate stimulation methods.

Unless defective conditions of the wellbore are detected or cured, the reserve estimates obtained by decline-curve analysis will be limited to those recoverable under existing and sometimes only partially effective wellbore conditions.

When the lifting equipment is operating properly and wellbore conditions are found to be satisfactory, a declining production trend must reflect changing reservoir con-

TABLE 40.15—SAMPLE CALCULATION OF ECONOMIC LIMIT FOR A WELL*

Crude price per bbl	28.00
Gas revenue per bbl	2.00
Total	\$30.00
Less production taxes	1.43
Less royalty (12.5% after production taxes)	3.57
Leaves net income per gross bbl	\$25.00
Estimated direct operating cost at economic limit	\$2,500 per month
Estimated economic-limit rate	100 gross bbl/month

*The price and taxation of oil and gas has changed significantly in the history of the industry. The estimated price anticipated to be in effect at abandonment time are appropriate for this calculation.

ditions, and the extrapolation of such a trend can then be a reliable guide for prediction of the remaining recoverable reserves.

Economic Limit

The economic-limit rate is the production rate that will just meet the direct operating expenses of a well. In determining this economic limit it is often advisable to analyze closely the expenditures charged against a well, and determine how much actually would be saved if the well were abandoned. This saving yields the best yardstick of the economic limit of production, because certain expenses may have to be continued if other wells on the lease are kept in operation. Table 40.15 is a sample calculation of the economic limit for a well.

Nominal and Effective Decline

There are two types of decline.⁵⁵ The *nominal decline* rate, a , is defined as the negative slope of the curve representing the natural logarithm of the production rate of q vs. time t , or

$$a = - \frac{d \ln q}{dt} = - \frac{dq/dt}{q} \quad (47)$$

Nominal decline, being a continuous function, is used mainly to facilitate the derivation of the various mathematical relationships.

The *effective decline* rate d , being a stepwise function and therefore in better agreement with actual production recording practices, is the rate more commonly used in practice. It is the drop in production rate from q_i to q_1 over a period of time equal to unity (1 month or 1 year) divided by the production rate at the beginning of the period, or

$$d = \frac{q_i - q_1}{q_i} \quad (48)$$

The time period may be 1 month or 1 year for effective monthly or annual decline, respectively.

TABLE 40.16—CONSTANT-PERCENTAGE DECLINE (EFFECTIVE DECLINE ¼ to 4% PER MONTH)

Time (months)	Effective Decline ¼% per Month		Effective Decline ½% per Month		Effective Decline ¾% per Month		Effective Decline 1% per Month	
	Rate	Cumulative	Rate	Cumulative	Rate	Cumulative	Rate	Cumulative
1	0.9975000	0.9975000	0.9950000	0.9950000	0.9925000	0.9925000	0.9900000	0.9900000
2	0.9950063	1.9925063	0.9900250	1.9900250	0.9850562	1.9775563	0.9801000	1.9701000
3	0.9925187	2.9850250	0.9850750	2.9700999	0.9776683	2.9552246	0.9702990	2.9403990
4	0.9900274	3.9750624	0.9801495	3.9502494	0.9703358	3.9255604	0.9605960	3.9009950
5	0.9875623	4.9626248	0.9752488	4.9254981	0.9630583	4.8886187	0.9509900	4.8519851
6	0.9850934	5.9477182	0.9703725	5.8958706	0.9558354	5.8444541	0.9414801	5.7934652
7	0.9826307	6.9303489	0.9655206	6.8613913	0.9486666	6.9731207	0.9320653	6.7255306
8	0.9801741	7.9105230	0.9606931	7.8220843	0.9415516	7.7346722	0.9227447	7.6482753
9	0.9777237	8.8882467	0.9558896	8.7779739	0.9344900	8.6691622	0.9135173	8.5617925
10	0.9752794	9.8635261	0.9511101	9.7290840	0.9274813	9.5966435	0.9043821	9.4661746
11	0.9728412	10.8363673	0.9463546	10.6754386	0.9205252	10.5171686	0.8953383	10.3615128
12	0.9704091	11.8067763	0.9416228	11.6170614	0.9136212	11.4307899	0.8863849	11.2478977
24	0.9416938	23.2641790	0.8866535	22.5559511	0.8347038	21.8742023	0.7856781	21.2178644
36	0.9138282	34.3825469	0.8348932	32.8562594	0.7626031	31.4155252	0.6964132	30.0550922
48	0.8867872	45.1719121	0.7861544	42.5552644	0.6967304	40.1326804	0.6172901	37.8882772
60	0.8605463	55.6420099	0.7402610	51.6880687	0.6365477	48.0968584	0.5471566	44.8314939
72	0.8350820	65.8022881	0.6970466	60.2877255	0.5815635	55.3731006	0.4849910	50.9858562
84	0.8103711	75.6619141	0.6563550	68.3853585	0.5313287	62.0208300	0.4298890	56.4409899
96	0.7863915	85.2297847	0.6180388	76.0102745	0.4854332	68.0943366	0.3810471	61.2763380
108	0.7631215	94.5145332	0.5819595	83.1900692	0.4435021	73.6432212	0.3377544	65.5623173
120	0.7405400	103.5245374	0.5479863	89.9507277	0.4051929	78.7127999	0.2993804	69.3613447

Different Types of Production-Decline Curves

Three types of production-decline curves are commonly recognized.⁵⁴ With *constant-percentage decline* the nominal decline rate, a , is constant, or

$$a = -\frac{dq/dt}{q}, \quad (49)$$

which after integration leads to the rate/time relationship

$$q = q_i e^{-at}, \quad (50)$$

After integrating a second time, the cumulative production at time t is obtained as expressed by the rate/cumulative relationship:

$$N_p = \frac{q_i - q}{a}, \quad (51)$$

From Eq. 50, the remaining life to abandonment time may be obtained as

$$t_a = \frac{\ln F_q}{a}, \quad (52)$$

in which $F_q = q_i/q_a$, or, by elimination of decline a with Eq. 51,

$$t_a = \frac{N_{pa}}{q_i} \left(\frac{F_q \ln F_q}{F_q - 1} \right) \quad (53)$$

In other words, the future life under constant-percentage decline will be $(F_q \ln F_q)/(F_q - 1)$ times as long as the life required to produce the same ultimate N_{pa} at constant rate q_i .

With *hyperbolic decline* the nominal decline rate a is proportional to a fractional power n of the production rate, this power being between 0 and 1, or

$$a = -\frac{dq/dt}{q} = bq^n, \quad (54)$$

in which the constant b is determined under initial conditions by

$$b = \frac{a_i}{q_i^n}. \quad (55)$$

After integration the following rate/time relationship is obtained:

$$q = q_i (1 + na_i t)^{-1/n}. \quad (56)$$

After a second integration the cumulative production at time t is obtained as expressed by the rate/cumulative equation

$$N_p = \frac{q_i^n}{(1-n)a_i} (q_i^{1-n} - q^{1-n}). \quad (57)$$

Under certain conditions, production obtained by gravity drainage will follow this type of decline for the exponent $n = 1/2$ (Ref. 35). The rate/time relationship then reads

$$q = \frac{q_i}{[1 + (a_i/2)t]^2} \quad (58)$$

and the rate/cumulative relationship

$$N_p = \frac{2\sqrt{q_i}}{a_i} (\sqrt{q_i} - \sqrt{q}). \quad (59)$$

From Eq. 58 the remaining life to abandonment time for this special case of hyperbolic decline ($n = 1/2$) may be obtained as

$$t_a = \frac{2(\sqrt{F_q} - 1)}{a_i}, \quad (60)$$

TABLE 40.16—CONSTANT-PERCENTAGE DECLINE (EFFECTIVE DECLINE ¼ to 4% PER MONTH) (continued)

Time (months)	Effective Decline 1¼% per Month		Effective Decline 1½% per Month		Effective Decline 1¾% per Month		Effective Decline 2% per Month	
	Rate	Cumulative	Rate	Cumulative	Rate	Cumulative	Rate	Cumulative
1	0.9875000	0.9875000	0.9850000	0.9850000	0.9825000	0.9825000	0.9800000	0.9800000
2	0.9751562	1.9626563	0.9702250	1.9552250	0.9653062	1.9478063	0.9604000	1.9404000
3	0.9629668	2.9256230	0.9556716	2.9108966	0.9484134	2.8962196	0.9411920	2.8815920
4	0.9509297	3.8765528	0.9413366	3.8522332	0.9318162	3.8280358	0.9223682	3.8039602
5	0.9390431	4.8155959	0.9272165	4.7794497	0.9155094	4.7435452	0.9039208	4.7078810
6	0.9273051	5.7429009	0.9133083	5.6927580	0.8994880	5.6430331	0.8858424	5.5937233
7	0.9157137	6.6586147	0.8996086	6.5923666	0.8837469	6.5267801	0.8681255	6.4618489
8	0.9042673	7.5628820	0.8861145	7.4784811	0.8682814	7.3950614	0.8507630	7.3126119
9	0.8929640	8.4558460	0.8728228	8.3513039	0.8530864	8.2481478	0.8337478	8.1463597
10	0.8818019	9.3376479	0.8597304	9.2110343	0.8381574	9.0863053	0.8170728	8.9634325
11	0.8707794	10.2084273	0.8468345	10.0578688	0.8234897	9.9097949	0.8007313	9.7641638
12	0.8598947	11.0683220	0.8341320	10.8920008	0.8090786	10.7188735	0.7847167	10.5488805
24	0.7394118	20.5859132	0.6957761	19.9773671	0.6546082	19.3912851	0.6157803	18.8267637
36	0.6358223	28.7700393	0.5803691	27.5557615	0.5296295	26.4079477	0.4832131	25.3225570
48	0.5467402	35.8075257	0.4841044	33.8771427	0.4285119	32.0849793	0.3791854	30.4199145
60	0.4701390	41.8590228	0.4038070	39.1500088	0.3466998	36.6781441	0.2975531	34.4198961
72	0.4042700	47.0626730	0.3368283	43.5482749	0.2805074	40.3943754	0.2334949	37.5587485
84	0.3476296	51.5372641	0.2809593	47.2170094	0.2269525	43.4010986	0.1832274	40.0218585
96	0.2989248	55.3849412	0.2343571	50.2772181	0.1836224	45.8337740	0.1437816	41.9547020
108	0.2570438	58.6935382	0.1954848	52.8298360	0.1485650	47.8019996	0.1128278	43.4714366
120	0.2210306	61.5385833	0.1630601	54.9590562	0.1202007	49.3944488	0.0885379	44.6616435

or, after elimination of initial decline a_i by Eq. 59,

$$t_a = \frac{N_{pa}}{q_i} \sqrt{F_q} \quad (61)$$

In other words, the future life under hyperbolic decline ($n = 1/2$) will be $\sqrt{F_q}$ times as long as the life required to produce the same ultimate N_{pa} at constant rate q_i .

With harmonic decline, the nominal decline rate a is proportional to the production rate, or

$$a = -\frac{dq/dt}{q} = bq, \quad (62)$$

in which the constant b is determined under initial conditions by

$$b = \frac{a_i}{q_i} \quad (63)$$

After integration, the following rate/time relationship for harmonic decline is obtained:

$$q = \frac{q_i}{1 + a_i t} \quad (64)$$

After a second integration the cumulative production at time t is obtained as expressed by the rate/cumulative relationship

$$N_p = \frac{q_i}{a_i} \ln \frac{q_i}{q} = \frac{q_i}{a_i} \ln F_q \quad (65)$$

From Eq. 64, the remaining life to abandonment time may be obtained as

$$t_a = \frac{F_q - 1}{a_i} \quad (66)$$

or, after elimination of initial decline a_i with Eq. 65,

$$t_a = \frac{N_{pa}}{q_i} \left(\frac{F_q - 1}{\ln F_q} \right) \quad (67)$$

In other words, the future life under harmonic decline will be $(F_q - 1)/\ln F_q$ times as long as the life required to produce the same ultimate N_{pa} at constant rate q_i .

Relationship Between Effective and Nominal Decline. The effective decline rate d (or d_i for initial conditions) for the three types of production-decline curves is related to the nominal decline rate a (or a_i for initial conditions) as follows.

$$d = 1 - e^{-a} \quad (68)$$

and

$$a = -\ln (1 - d) \quad (69)$$

For hyperbolic decline,

$$d_i = 1 - (1 + na_i)^{-1/n} \quad (70)$$

and

$$a_i = \frac{1}{n} [(1 - d_i)^{-n} - 1] \quad (71)$$

For harmonic decline,

$$d_i = \frac{a_i}{1 + a_i} \quad (72)$$

and

$$a_i = \frac{d_i}{1 - d_i} \quad (73)$$

An analysis of a large number of actual production-decline curves assembled by Cutler⁵⁶ indicates that most decline curves normally encountered are of the hyperbolic type, with values for the exponent n between 0 and 0.7, while the majority fall between 0 and 0.4. Gravity-drainage production under certain conditions will have an exponent $n = 0.5$ (Ref. 59). The occurrence of harmonic decline ($n = 1$) is apparently rare.

TABLE 40.16—CONSTANT-PERCENTAGE DECLINE (EFFECTIVE DECLINE ¼ to 4% PER MONTH) (continued)

Time (months)	Effective Decline 2½% per Month		Effective Decline 3% per Month		Effective Decline 3½% per Month		Effective Decline 4% per Month	
	Rate	Cumulative	Rate	Cumulative	Rate	Cumulative	Rate	Cumulative
1	0.9750000	0.9750000	0.9700000	0.9700000	0.9650000	0.9650000	0.9600000	0.9600000
2	0.9506250	1.9256250	0.9409000	1.9109000	0.9312250	1.8962250	0.9216000	1.8816000
3	0.9268594	2.8524844	0.9126730	2.8235730	0.8986321	2.7948571	0.8847360	2.7563360
4	0.9036879	3.7561723	0.8852928	3.7088658	0.8671800	3.6620371	0.8493466	3.6156826
5	0.8810957	4.6372680	0.8587340	4.5675998	0.8368287	4.5988658	0.8153727	4.4310553
6	0.8590683	5.4963363	0.8329720	5.4005718	0.8075397	5.3064055	0.7827578	5.2138130
7	0.8375916	6.3339279	0.8079828	6.2085547	0.7792758	6.0856813	0.7514475	5.9652605
8	0.8166518	7.1505797	0.7837434	6.9922981	0.7520012	6.8376825	0.7213896	6.6866501
9	0.7962355	7.9468152	0.7602311	7.7525291	0.7256811	7.5633636	0.6925340	7.3791841
10	0.7763296	8.7231448	0.7374241	8.4899532	0.7002823	8.2636459	0.6648326	8.0440167
11	0.7569214	9.4800662	0.7153014	9.2052547	0.6757724	8.9394183	0.6382393	8.6822561
12	0.7379984	10.2180646	0.6938424	9.8990970	0.6521204	9.5915387	0.6127098	9.2949658
24	0.5446416	17.7589797	0.4814172	16.7675099	0.4252610	15.8463764	0.3754133	14.9900821
36	0.4019446	23.3241626	0.3340277	21.5331058	0.2773214	19.9252836	0.2300194	18.4795354
48	0.2966344	27.4312584	0.2317625	24.8396782	0.1808469	22.5852220	0.1409351	20.6175575
60	0.2189157	30.4622883	0.1608067	27.1339192	0.1179339	24.3198220	0.0863523	21.9275445
72	0.1615594	32.6991834	0.1115745	28.7257601	0.0769071	25.4509900	0.0529089	22.7301864
84	0.1192306	34.3500082	0.0774151	29.8302468	0.0501527	26.1886477	0.0324178	23.2219728
96	0.0879920	35.5683143	0.0537139	30.5965865	0.0327056	26.6696893	0.0198627	23.5232952
108	0.0649379	36.4674222	0.0372690	31.1283054	0.0213280	26.9833863	0.0121701	23.7079184
120	0.0479241	37.1309623	0.0258588	31.4972345	0.0139084	27.1879545	0.0074567	23.8210388

Decline Tables for Constant-Percentage Decline

Tables 40.16 and 40.17 will facilitate computations of future rates and cumulative production for constant effective decline percentages 100*d*, from ¼ to 10% per month. Hand-held calculator and computer programs are available for constant-percentage decline and other types of production-decline calculations.

With constant-percentage decline the production rate in successive months may be designated as a geometric series,

$$(1-d)(1-d)^2(1-d)^3 \dots (1-d)^t$$

in which the rate during the last month preceding the period studied equals unity. For each monthly decline percentage 100*d* the "Rate" column in the decline tables represents the production rate per month $(1-d)^t$ after the number of months *t* shown in the left and right time columns has expired. The cumulative production,

$$\frac{(1-d)[1-(1-d)^t]}{d},$$

after *t* months is shown in the columns labeled "Cumulative."

TABLE 40.17—CONSTANT-PERCENTAGE DECLINE (EFFECTIVE DECLINE 4½ to 10% PER MONTH)

Time (months)	Effective Decline 4½% per Month		Effective Decline 5% per Month		Effective Decline 5½% per Month		Effective Decline 6% per Month	
	Rate	Cumulative	Rate	Cumulative	Rate	Cumulative	Rate	Cumulative
1	0.9550000	0.9550000	0.9500000	0.9500000	0.9450000	0.9450000	0.9400000	0.9400000
2	0.9120250	1.8670250	0.9025000	1.8525000	0.8930250	1.8380250	0.8836000	1.8236000
3	0.8709839	2.7380089	0.8573750	2.7098750	0.8439086	2.6819336	0.8305840	2.6541840
4	0.8317896	3.5697985	0.8145063	3.5243813	0.7974937	3.4794273	0.7807490	3.4349330
5	0.7943591	4.3641576	0.7737809	4.2981622	0.7536315	4.2330588	0.7339040	4.1688370
6	0.7586129	5.1227705	0.7350919	5.0332541	0.7121818	4.9452406	0.6898698	4.8587068
7	0.7244753	5.8472458	0.6983373	5.7315914	0.6730118	5.6182523	0.6481776	5.5071844
8	0.6918739	6.5391198	0.6634204	6.3950118	0.6359961	6.2542485	0.6095689	6.1167533
9	0.6607396	7.1998594	0.6302494	7.0252612	0.6010163	6.8552648	0.5729948	6.6897481
10	0.6310063	7.8308657	0.5987369	7.6239982	0.5679604	7.4232253	0.5386151	7.2283632
11	0.6026111	8.4334768	0.5688001	8.1927983	0.5367226	7.9599479	0.5062982	7.7346614
12	0.5754936	9.0089703	0.5403601	8.7331584	0.5072029	8.4671508	0.4759203	8.2105817
24	0.3311928	14.1935746	0.2919890	13.4522087	0.2572548	12.7617140	0.2265001	12.1181642
36	0.1905993	17.1772810	0.1577792	16.0021952	0.1304804	14.9399289	0.1077960	13.9778620
48	0.1096887	18.8943847	0.0852576	17.3801062	0.0661800	16.0447258	0.0513023	14.8629300
60	0.0631251	19.8825668	0.0460698	18.1246743	0.0335667	16.6050820	0.0244158	15.2841517
72	0.0363281	20.4512592	0.0248943	18.5270092	0.0170251	16.8892962		
84	0.0209066	20.7785380	0.0134519	18.7444149				
96	0.0120316	20.9668849	0.0072689	18.8618923				
108	0.0069241	21.0752773	0.0039278	18.9253724				
120	0.0039848	21.1376564	0.0021224	18.9596745				

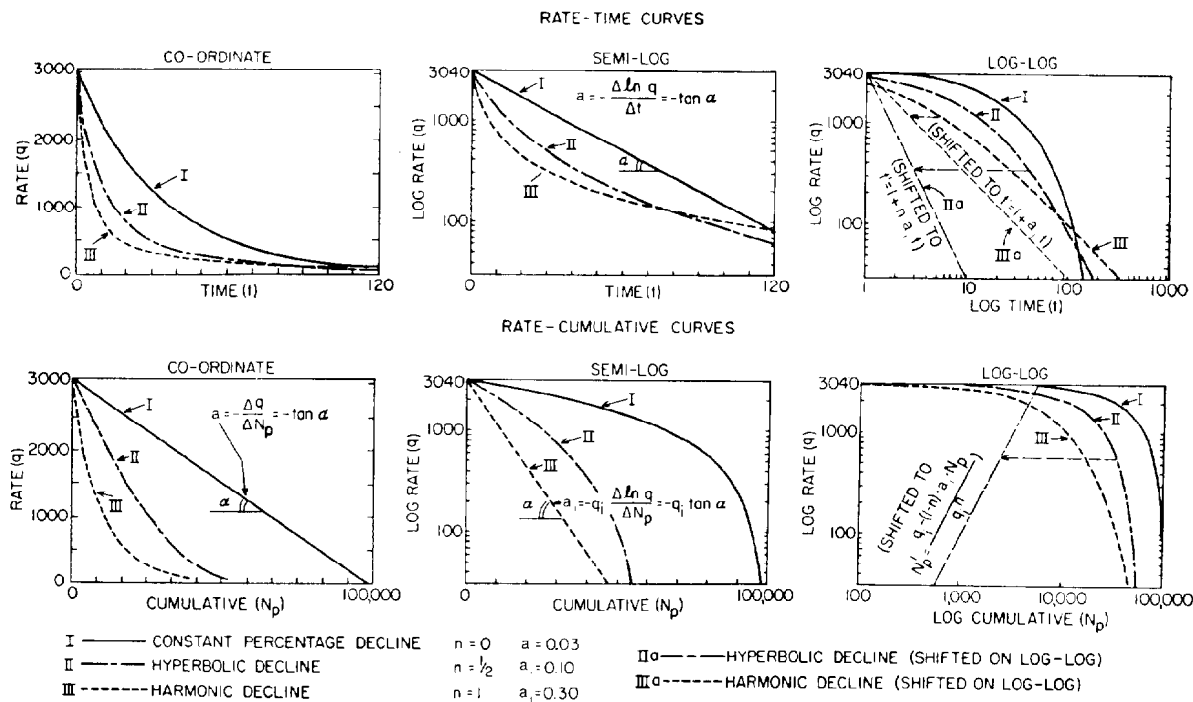


Fig. 40.21—Three types of production-decline curves on coordinate, semilog, and log-log graph paper.²

Example Problem 7. The production from a lease has declined from 4,286 to 3,000 bbl/month in 10 months. Assuming constant-percentage decline, what is the monthly decline and what will be the production rate 40 months later and the cumulative production over this 40-month period?

Solution. (See Table 40.16.)

$$3,000 \div 4,286 = 0.700.$$

Following the 10-month horizontal line, a rate of 0.700 is encountered in the table for 3½% decline per month. Rate 40 months later:

$$3,000 \times (\text{rate})_{36} \times (\text{rate})_4 = 3,000 \times 0.27732 \times 0.86718$$

$$= 721 \text{ bbl/month.}$$

Cumulative production over 40-month period:

$$3,000 \times [(\text{cum.})_{36} + (\text{rate})_{36} \times (\text{cum.})_4]$$

$$= 3,000 \times (19.92528 + 0.27732 \times 3.66204) = 62,822 \text{ bbl.}$$

Straightening Production-Dcline Curves

Fig. 40.21 shows the rate/time and rate/cumulative trends of the three types of production-decline curves on regular coordinate paper, semilog paper, and log-log paper.

Inspection of this chart shows that in the case of constant-percentage decline the rate/time curve becomes a straight line on semilog paper, while the rate/cumulative curve straightens out on regular coordinate paper. In either case the tangent of the angle of slope is equal to the nominal-decline fraction.

TABLE 40.17—CONSTANT-PERCENTAGE DECLINE (EFFECTIVE DECLINE 4½ to 10% PER MONTH) (continued)

Time (months)	Effective Decline 6½% per Month		Effective Decline 7% per Month		Effective Decline 7½% per Month		Effective Decline 8% per Month	
	Rate	Cumulative	Rate	Cumulative	Rate	Cumulative	Rate	Cumulative
1	0.9350000	0.9350000	0.9300000	0.9300000	0.9250000	0.9250000	0.9200000	0.9200000
2	0.8742250	1.8092250	0.8649000	1.7949000	0.8556250	1.7806250	0.8464000	1.7664000
3	0.8174004	2.6266254	0.8043570	2.5992570	0.7814531	2.5720781	0.7786880	2.5450880
4	0.7642694	3.3908947	0.7480520	3.3473090	0.7320941	3.3041723	0.7163930	3.2614810
5	0.7145919	4.1054866	0.6956884	4.0429974	0.6771871	3.9813594	0.6590815	3.9205625
6	0.6681434	4.7736300	0.6469902	4.6989876	0.6263981	4.6077574	0.6063550	4.5269175
7	0.6247141	5.3983440	0.6017009	5.2916884	0.5794182	5.1871756	0.5578466	5.0847641
8	0.5841076	5.9824517	0.5595818	5.8512702	0.5359618	5.7231375	0.5132189	5.5979830
9	0.5461407	6.5285923	0.5204111	6.3716813	0.4957647	6.2189022	0.4721614	6.0701443
10	0.5106415	7.0392338	0.4839823	6.8556636	0.4585823	6.6774845	0.4343885	6.5045328
11	0.4774498	7.5166836	0.4501035	7.3057672	0.4241887	7.1016732	0.3996374	6.9041701
12	0.4464156	7.9630992	0.4185963	7.7243635	0.3923745	7.4940477	0.3676664	7.2718365
24	0.1992869	11.5179507	0.1752229	10.9577534	0.1539578	10.4345211	0.1351786	9.9454463
36	0.0889648	13.1048917	0.0733476	12.3112384	0.0604091	11.5882879	0.0497006	10.9284428
48	0.0397153	13.8133270	0.0307031	12.8778022	0.0237030	12.0409966	0.0182732	11.2898575
60	0.0177295	14.1295835	0.0128522	13.1149637	0.0093004	12.2186280		

In the case of hyperbolic-type decline curves the rate/time relationship as well as the rate/cumulative relationship can be straightened out after shifting to become straight lines on log-log paper. The shifted rate/cumulative curve in this case assumes a reverse slope. Besides the extra work involved in shifting, this type of paper also has the disadvantage that the horizontal scale on which the unknown variable is plotted usually becomes rather crowded at the point where the answer is desired. For this reason, special graph paper for hyperbolic decline has been designed,⁵⁴ which makes it possible to plot either time or cumulative on a linear scale and still obtain the advantage of straight-line extrapolation.

In the case of harmonic decline it may be noted that the rate/time relationship can also be straightened out on log-log paper after shifting, and assumes a slope of 45°. It may be of interest that in this case a plot of the inverse of the production rate vs. time on a linear scale also yields a straight line. The rate/cumulative relationship for harmonic decline becomes a straight line on semilog paper. The nominal-decline fraction in this case is equal to the rate times the tangent of the slope angle.

As a matter of convenience the semilog paper most often is used for rate/time extrapolations, while regular coordinate paper is favored for rate/cumulative extrapolations. Because straight-line extrapolation on this paper requires constant-percentage decline, it will be obvious that such extrapolations may provide results that are too conservative. Experienced engineers usually allow for this by graphically flattening the decline slope in the later stages.

A geometric construction method for such extrapolation is described by Arps.⁵⁴

Loss-Ratio Method

The inverse of the nominal decline rate $q/(dq/dr)$ is called the "loss ratio" and may be used in tabular form for extrapolation purposes and for identification of the type of decline. In constant-percentage decline the loss ratio is constant, while in hyperbolic decline the first derivative of the loss ratio is constant and equal to the exponent n . In harmonic decline the first derivative of the loss ratio is constant and equal to one.

Extrapolation of various production-decline curves by difference tables with the loss-ratio method is described in Ref. 54.

Relationship Between Reserves and Decline

From the rate/cumulative equation for constant-percentage decline,⁵⁵ it may be noted that the remaining reserves, N_r , are equal to the difference between the present production rate and the production rate at the economic limit, divided by the nominal-decline fraction, provided the same time units are used for determining both the decline and the production rates.

This leads to the following short cut: when the nominal decline is 1% per month, the remaining reserves are 100 times the difference in monthly production rates; for a nominal decline of 2% per month this ratio equals 50; for 3% it is 33⅓; for 4% it is 25, etc.

When production rates are on a daily or annual basis the same formula holds, provided the decline is expressed on the same time basis.

Other Performance Curves

Oil Percentage in Total Fluid vs. Cumulative Oil

Another variable that is often substituted for the production rate in water-drive fields—particularly when the production of oil is restricted—is the oil percentage of the total fluid produced. Because projections of this oil percentage vs. time are not often required, one usually finds this oil-percentage variable plotted only vs. cumulative. An example of such a curve on semilog paper is shown for a Tar Springs sand reservoir in Illinois in Fig. 40.22. The endpoint in this case is the lowest oil percentage that, combined with the total fluid-producing capacity of the lease, will just cover operating expenses.

Cumulative Gas vs. Cumulative Oil

It is a characteristic of most depletion-type oil reservoirs that only a fraction of the oil in place is recoverable by primary production methods. Gas, on the other hand, moves much more freely through the reservoir, and it can generally be assumed that at abandonment time only the

TABLE 40.17—CONSTANT-PERCENTAGE DECLINE (EFFECTIVE DECLINE 4½ TO 10% PER MONTH) (continued)

Time (months)	Effective Decline 8½% per Month		Effective Decline 9% per Month		Effective Decline 9½% per Month		Effective Decline 10% per Month	
	Rate	Cumulative	Rate	Cumulative	Rate	Cumulative	Rate	Cumulative
1	0.9150000	0.9150000	0.9100000	0.9100000	0.9050000	0.9050000	0.9000000	0.9000000
2	0.8372250	1.7522250	0.8281000	1.7381000	0.8190250	1.7240250	0.8100000	1.7100000
3	0.7760609	2.5182859	0.7535710	2.4916710	0.7412176	2.4652426	0.7290000	2.4390000
4	0.7009457	3.2192316	0.6857496	3.1774210	0.6708020	3.1360446	0.6561000	3.0951000
5	0.6413653	3.8605969	0.6240321	3.8014528	0.6070758	3.7431204	0.5904900	3.6855900
6	0.5868493	4.4474462	0.5678693	4.3693220	0.5494036	4.2925239	0.5314410	4.2170310
7	0.5369671	4.9844133	0.5167610	4.8860830	0.4972102	4.7897342	0.4782969	4.6953279
8	0.4913249	5.4757381	0.4702525	5.3563356	0.4499753	5.2397094	0.4304672	5.1257951
9	0.4495623	5.9253004	0.4279298	5.7842654	0.4072276	5.6469370	0.3874205	5.5132156
10	0.4113495	6.3366499	0.3894161	6.1736815	0.3685410	6.0154780	0.3486784	5.8618940
11	0.3763848	6.7130346	0.3543687	6.5280502	0.3335296	6.3490076	0.3138106	6.1757046
12	0.3443920	7.0574267	0.3224755	6.8505257	0.3018443	6.6508519	0.2824295	6.4581342
24	0.1186059	9.4879483	0.1039904	9.0596524	0.0911100	8.6583736	0.07976644	8.2821020
36	0.0408469	10.3250006	0.0335344	9.7720416	0.0275010	9.2643325	0.02252840	8.7972445
48	0.0140673	10.6132747	0.0108140	10.0017697	0.0083010	9.4472378	0.00636269	8.9427359

solution gas in the remaining oil at the then-prevailing pressure plus the free gas at that same pressure are left in the reservoir. In other words, even though it is not known exactly how much oil may be recovered, a much firmer idea is generally available of the amount of gas that will be produced during the primary production period. This provides us with the possibility of an endpoint to a performance curve. The cumulative-gas/cumulative-oil method is illustrated in Fig. 40.23. Cumulative oil production is plotted on the horizontal scale, while the cumulative gas production is plotted on the vertical scale. As is normal in depletion-type fields, the trend of the curve appears to steepen with increasing GOR's.

For depletion-type reservoirs, the GOR sometimes is plotted on semilog paper vs. cumulative oil. Such a curve often shows a fairly good straight-line relationship, which may be used to predict the trend of the cumulative-gas/cumulative-oil curve.

From a volumetric calculation an estimate is made of the total gas to be released from the reservoir down to an assumed abandonment pressure. This figure, which in this case was 1.42 billion cu ft, is marked on Fig. 40.23 as a horizontal line and represents the ceiling of the cumulative-gas/cumulative-oil curve.

By extrapolating the current trend until it intersects the estimate for the total gas available, we can obtain an estimate for the total primary oil recovery.

Material-Balance Method for Nonassociated Gas Reservoirs

The best performance variable in the case of free-gas reservoirs is the static formation pressure. This pressure usually is measured periodically by bottomhole pressure

bomb, or if there are no liquids present in the tubing, it may be calculated from observed shut-in tubing pressures.

The general material-balance equation for a gas reservoir with active water drive may be rewritten as*

$$\frac{1}{B_g} = \frac{1}{B_{gi}} - \frac{G_p + (5.615W_p/B_g)}{GB_{gi}} + \frac{5.615W_e}{GB_g B_{gi}} \quad (74)$$

For a gas reservoir without active water drive ($W_e=0$), this equation converts to*

$$\frac{1}{B_g} = \frac{1}{B_{gi}} - \frac{G_p + (5.615W_p/B_g)}{GB_{gi}}, \quad \dots \dots \dots (75)$$

and the same equation for a gas reservoir without active water drive ($W_e=0$) and without significant water production ($W_p=0$) reads

$$\frac{1}{B_g} = \frac{1}{B_{gi}} - \frac{G_p}{GB_{gi}} \quad \dots \dots \dots (76)$$

By plotting the reciprocal of the gas FVF, $1/B_g$, on regular coordinate paper vs. cumulative gas produced, G_p , or in case of appreciable water production vs. the term $G_p + 5.615(W_p/B_g)$, a straight line should result if no active water-drive mechanism exists (Fig. 40.24, Curve a). This straight line intersects the vertical axis at the value $1/B_{gi}$ and its extrapolation to the horizontal axis indicates the amount of free gas in place, G . When an active water drive exists, the plotted data fall on a curve

*Delete 5.615 if all volumes are cubic meters.

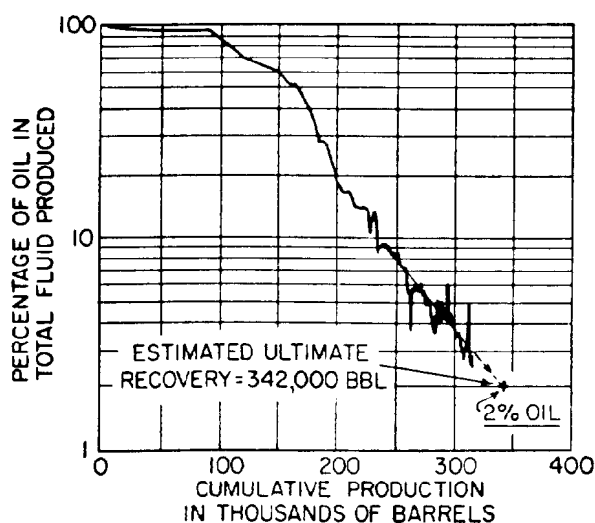


Fig. 40.22—Oil percentage vs. cumulative relationship on semi-log paper. Tar Springs sand production, Calvin Field, IL.

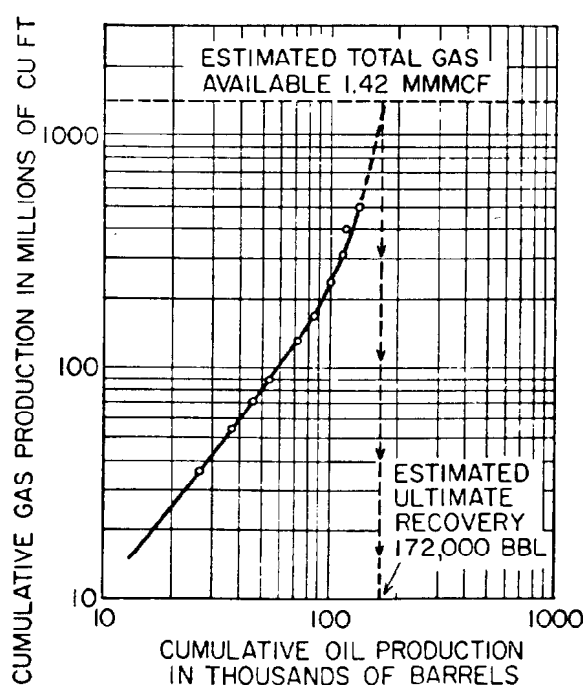


Fig. 40.23—Cumulative gas vs. cumulative oil recovery. Lake sand production, Bankline-Owen Field, TX.

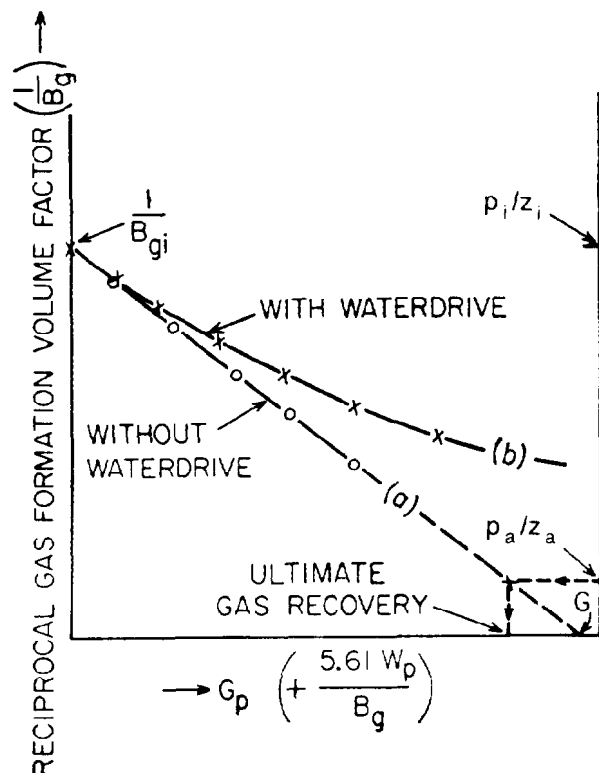


Fig. 40.24—Graphical evaluation of material-balance equation for gas reservoirs.

with a gradually diminishing slope (Curve *b*), which intersects the vertical axis at the value $1/B_{gi}$. Extrapolation of the initial tangent of this curve to its intersection with the horizontal axis also indicates the amount of free gas in place, G .

Instead of plotting the reciprocal gas FVF, $1/B_g$, it is often more convenient to plot p/z on the vertical axis, as shown on the right side of the scale in Fig. 40.24. The ultimate gas recovery at the abandonment pressure, p_a , is then found by the intersection of the curve with the value p_a/z_a at abandonment time.

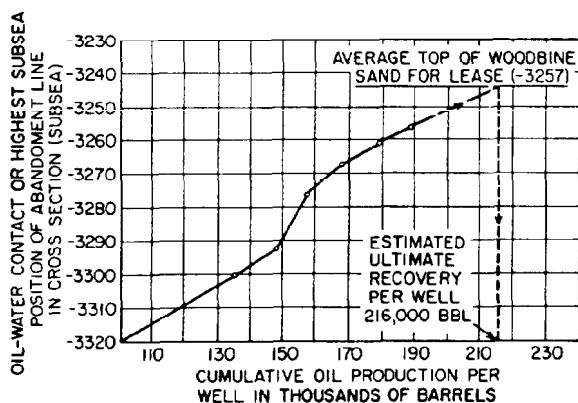


Fig. 40.25—Abandonment line (subsea) vs. cumulative oil recovery. Woodbine sand, East Texas field.

WOC or Abandonment Contour vs. Cumulative Oil

Another method that is sometimes practiced in the larger water-drive fields such as east Texas is to choose the depth of the WOC, or abandonment contour, as the dependent variable to be plotted vs. the cumulative oil recovery as the independent variable. The endpoint of this type of performance curve is the average depth of the top of the sand for a given lease. The method of extrapolation in this case is based on the simple assumption that whenever the abandonment contour progresses to the top of the sand the lease is ready for abandonment. An example of this is shown in Fig. 40.25.

Plotting this type of chart for many leases in the East Texas field indicates that the rise in the water table appears to be more or less proportional to the cumulative oil production.

A plot of p/z vs. cumulative gas production, such as Fig. 40.24, is theoretically sound and should give reliable results for normally pressured, constant-volume gas reservoirs. Typically, however, a plot of cumulative gas production for an overpressured gas reservoir (where reservoir pressure exceeds the normal hydrostatic or relaxation pressure) will yield two slopes. An initial slope will be observed above relaxation pressure, and a steeper slope will occur after reservoir pressure drops below relaxation pressure. The second slope will extrapolate correctly to yield initial gas in place and ultimate gas recovery. Solution of Eq. 77,⁶⁰ will yield results equivalent to extrapolation of the correct (second) slope if proper values of formation compressibility (c_f) and water compressibility (c_w) are entered:

$$G_p = G \left\{ \frac{\frac{p_i}{z_i} - \frac{p}{z} \left[1 - \frac{\Delta p_R (c_w S_{iw} + c_f)}{(1 - S_{iw})} \right]}{\frac{p_i}{z_i}} \right\} \dots (77)$$

Improved Recovery Reserves

Estimates of improved recovery reserves for conventional fluid injection and various enhanced recovery processes are often made by applying an overall reservoir recovery efficiency in a volumetric calculation. The overall reservoir recovery efficiency, E_R , may be expressed as the product of three efficiencies: the displacement (or microscopic) efficiency, E_D , the pattern sweep efficiency, E_P , and the invasion efficiency, E_I . The resulting volumetric equation for improved recovery reserves, N_{IR} , is

$$N_{IR} = E_R \left(\frac{7,758 A h \phi S_o}{B_o} \right), \dots (78)$$

where E_R is the recovery efficiency $= E_D \times E_P \times E_I$, fraction, S_o is the oil saturation at start of improved recovery process, fraction, and other symbols and units as previously defined.

Methods for estimating the various efficiency terms are presented earlier in this chapter and in Chap. 44. Reliable estimates of improved recovery reserves often require the use of reservoir simulation models (see Chap. 48) to account properly for process variables and reservoir heterogeneities.

Nomenclature

- a = nominal decline rate; the negative slope of the curve representing the natural logarithm of the production rate q vs. time t ; also the instantaneous rate of change of the production rate vs. time, divided by the instantaneous production rate q ; expressed as a decimal fraction with time in months or years
- A = area, in Eq. 29b in square feet, elsewhere in acres
- b = constant (in decline-curve analysis, Eq. 63)
- B_g = gas FVF, a dimensionless factor representing the volume of free gas at a reservoir temperature of T_R , °F, and a pressure of p_R , psia per unit volume of free gas under standard conditions of 60°F and 14.7 psia
- B_o = oil FVF; a dimensionless factor representing the volume of oil saturated with solution gas at reservoir temperature T_R and pressure p_R , per unit volume of stock-tank oil; it may be determined by PVT analysis of a bottomhole or recombined sample or obtained from appropriate correlation charts; a typical oil FVF relationship vs. gas solubility R_s would be of the type
- $$B_o = 1.05 + 0.0005R_s$$
- B_t = two-phase FVF for oil; a dimensionless factor representing the volume of oil and its original complement of dissolved gas at reservoir temperature T_R and pressure p_R per unit volume of stock-tank oil; this two-phase formation factor for oil, B_t , is related to the oil FVF B_o , the gas FVF B_g , the gas-solubility factor R_s , and the gas-solubility factor at the bubblepoint R_{sb} by
- $$B_t = B_o + 0.1781B_g(R_{sb} - R_s)$$
- c_f = compressibility of reservoir rock (formation); expressed as change in PV per unit PV per psi; c_f appears to vary inversely with rock porosity from 10×10^{-6} (10 microsips) for 2% porosity, to 4.8×10^{-6} (4.8 microsips) for 10% porosity, and 3.4×10^{-6} (3.4 microsips) for 25% porosity
- c_o = compressibility of reservoir oil; in volume per psi for undersaturated oil above the bubblepoint; typical values for c_o range from 5×10^{-6} (5 microsips) for low-gravity oils to 25×10^{-6} (25 microsips) for higher-gravity oils, with 10×10^{-6} (10 microsips) being a good average
- c_w = compressibility of interstitial water; in volume per volume per psi; although the water compressibility c_w varies somewhat with pressure, temperature, and the amount of salt or gas in solution, 3×10^{-6} (3 microsips) represents a good average value
- d = effective decline rate; the drop in production rate per unit of time (month or year) divided by the production rate at the beginning of the period; expressed as a decimal fraction
- E = parameter in Eqs. 29a and b
- E_R = recovery efficiency, fraction
- f_g = fractional flow of gas
- f_w = water fraction of flow stream in reservoir that consists of oil and water
- F_q = ratio of initial to final production rate q_i/q_a (in decline-curve analysis, Page 40-28)
- G = total initial gas in place in reservoir, scf
- G_{Fi} = free reservoir gas in place, scf
- G_p = cumulative gas produced, scf
- G_s = solution gas in place, scf
- G_{ul} = ultimate gas recovery from reservoir, scf
- h_e = effective thickness, ft
- h_l = average gross pay thickness, ft
- k = absolute permeability, md
- k_o = effective permeability to oil, md
- k_{rg} = relative permeability to gas as a fraction of absolute permeability
- k_{ro} = relative permeability to oil as a fraction of absolute permeability
- k_{rw} = relative permeability to water as a fraction of absolute permeability
- \ln = natural logarithm to the base e
- \log = common logarithm to the base 10
- m = ratio of initial reservoir free gas volume and initial reservoir oil volume; related to the amount of free initial reservoir gas G_{Fi} , the initial gas FVF B_{gi} , the amount of initial reservoir oil in place N , and the initial oil FVF B_{oi} by
- $$m = G_{Fi}B_{gi}/5.615NB_{oi}$$
- n = exponent (in decline-curve analysis)
- N = reservoir oil initially in place, STB
- N_{IR} = improved reserves, STB
- N_p = cumulative oil produced, STB
- N_r = remaining oil reserves as of date of study, STB
- N_{ug} = unit recovery by depletion or solution-gas drive, STB
- N_{ul} = ultimate recovery from reservoir, STB
- N_{uw} = unit recovery by water drive, STB
- p_c = critical pressure, psia
- p_R = reservoir pressure, psia; generally measured by bottomhole pressure bomb at a depth representative of the entire reservoir, e.g., the midpoint of the oil or gas column; although the vertical pressure gradient in oil fields may range from as low as 20 or 30 psi/100 ft to as high as 90 or 100 psi/100 ft of depth, typical hydrostatic gradients usually range from 44 to 52 psi/100 ft

q_a = production rate at abandonment, B/D

q_g = rate of gas production, scf/D

q_o = rate of oil production, B/D

q_t = rate of total fluid production, B/D (on Page 40-14 q_t designates the total flow rate of oil and free gas, on Page 40-18 the total flow rate of oil and water; both expressed in cubic feet per day under reservoir conditions)

R = instantaneous producing GOR, scf/STB

R_p = cumulative GOR, scf/STB, related to cumulative gas produced, G_p , and cumulative oil produced, N_p , by

$$R_p = G_p / N_p$$

R_s = solution GOR (gas-solubility factor); the number of standard cubic feet of gas, liberated under specified separator conditions, which are in solution in 1 bbl of stock-tank oil at reservoir temperature T_R and pressure p_R ; it may be determined by PVT analysis of a bottomhole or recombined sample or obtained from appropriate correlation charts. A typical gas-solubility relationship vs. pressure for medium-gravity crude, expressed in cubic feet per barrel, would be of the type

$$R_s = 135 + 0.25p_R$$

S^* = effective saturation, fraction

S_g = free-gas saturation under reservoir conditions, fraction of pore space

S'_g = free-gas saturation under reservoir conditions, fraction of hydrocarbon-filled pore space (Page 40-14):

$$S'_g = S_o / (1 - S_{iw})$$

S_{gc} = equilibrium (or critical) free-gas saturation, which is the maximum free-gas saturation reached when lowering the pressure below the bubblepoint, before the relative permeability to gas becomes measurable; expressed as a fraction of pore space under reservoir conditions

S_{gr} = residual free-gas saturation under reservoir conditions at abandonment time, fraction of pore space

S_{iw} = interstitial water saturation, fraction of pore space; generally determined by (1) analysis of water content of cores taken with a nonaqueous drilling fluid, (2) measurement of capillary pressure on cores, or (3) quantitative analysis of electrical logs

S_o = oil or condensate saturation under reservoir conditions, fraction of pore space

S_{or} = residual-oil saturation under reservoir conditions, fraction of pore space, generally determined by multiplying the residual oil saturation from core analysis by B_o

S_t = total liquid saturation under reservoir conditions, fraction of pore space:

$$S_t = 1 - S_g = S_o + S_w$$

t = time, days (Eq. 30) or months

T_R = reservoir temperature, °F, measured at a depth representative of the entire reservoir; e.g., at the midpoint of the oil or gas column. Vertical temperature gradients in oil fields range from 0.5 to 3°F/100 ft of depth with 1.5°F/100 ft being a good average

T_{sc} = standard temperature, 60°F

V = gross pay volume, acre-ft

V_g = net pay volume of the free-gas-bearing portion of a reservoir, acre-ft

V_o = net pay volume of the oil-bearing portion of a reservoir, acre-ft

W_e = cumulative water influx, bbl

W_p = cumulative water produced, bbl

z = compressibility factor for the free gas in the reservoir; a dimensionless factor, which, when multiplied by the reservoir volume of gas as computed by the ideal-gas laws, yields the true reservoir volume

Z = height, ft

γ_o = gravity of stock-tank liquid (oil or condensate), °API

Θ = angle of formation dip, degrees

μ_g = reservoir gas viscosity, cp, ranging from 0.01 cp at low temperatures and pressures to 0.06 cp for high gas gravities at very high temperatures and pressures, with 0.02 cp being a good average

μ_o = reservoir oil viscosity, cp, ranging from less than 0.1 cp for volatile oils under very high temperatures and pressures to very high values for low-gravity oils that will barely flow at all; most reservoir oils, however, fall between 0.4 and 2 cp

μ_w = reservoir water viscosity, cp, ranging from 0.2 cp at high temperatures to 1.5 cp at lower temperatures, with 0.5 cp being a good average

ρ_g = density of reservoir gas, g/cu cm

ρ_o = density of reservoir oil, g/cu cm

ϕ = effective porosity, as a fraction of bulk pay volume; generally determined by laboratory analysis of cores, side-wall samples, or cuttings; quantitative analysis of electrical, radioactivity, or sonic logs; typical values for ϕ range from as low as 0.03 in tight limestones, and from 0.10 to 0.20 in cemented and consolidated sandstones, to as high as 0.35 in unconsolidated sands

ϕ_h = effective hydrocarbon-bearing porosity, as a fraction of bulk pay volume, $= \phi(1 - S_{iw})$

Subscripts

a = abandonment time conditions
 b = bubblepoint conditions
 i = initial conditions

Key Equations in SI Metric Units

$$G_{Fi} = \frac{V_g \phi (1 - S_{iw}) 10\,000}{B_g}, \quad (1)$$

where

G_{Fi} is in std m³ of free gas,
 V_g is net pay volume of free gas-bearing portion of reservoir, in ha·m, and
 10 000 is m³/ha·m.

$$N = \frac{V_o \phi (1 - S_{iw}) 10\,000}{B_o}, \quad (2)$$

where N is reservoir oil initially in place, in m³, and V_o is net pay volume of the oil-bearing portion of a reservoir, in ha·m.

$$G_s = \frac{V_o \phi (1 - S_{iw}) R_s 10\,000}{B_o}, \quad (3)$$

where G_s is solution gas in place, in std m³, and R_s is solution GOR, in std m³/stock-tank m³ of oil.

$$N = \frac{N_p [B_i + B_w (R_p - R_{si})] - (W_i - W_p)}{B_{oi} \left\{ m \frac{B_o}{B_{oi}} + \frac{B_i}{B_{oi}} - (m+1) \left[1 - \frac{\Delta p_R (c_f + S_{wi} c_w)}{1 - S_{wi}} \right] \right\}}, \quad (5)$$

where

N_p is cumulative oil produced, in m³,
 R_p is cumulative GOR, in std m³/stock-tank m³,
 R_{si} is initial solution GOR, in std m³/stock-tank m³,
 W_e is cumulative water influx, in m³,
 W_p is cumulative water produced, in m³,
 Δp_R is change in reservoir pressure, in atm,
 c_f is compressibility of reservoir rock change, in PV per unit PV per atm, and
 c_w is compressibility of interstitial water, atm⁻¹.

$$N_p = \phi \left(\frac{1 - S_{iw}}{B_{oi}} - \frac{S_o}{B_o} \right) 10\,000, \quad (16)$$

where N_p is in m³/ha·m.

$$R = R_s + \frac{B_o \mu_o k_{rg}}{B_g \mu_g k_{ro}}, \quad (18)$$

where R is instantaneous producing GOR, in std m³/stock-tank m³, and R_s is solution GOR, in std m³/stock-tank m³.

$$E = \frac{0.009k \sin \Theta A (\rho_o - \rho_g)}{\mu_g q_t}, \quad (29b)$$

where A is area of cross section normal to bedding plane, in m², and q_t is total flow area, in res m³/d.

$$t = \frac{NB_o}{q_t (df_g/dS_g)}, \quad (30)$$

where N is in m³ and q_t is in m³/d.

$$G = \frac{82.057 z T_R}{p_R}, \quad (35)$$

where

G is reservoir volume, in cm³/g mol,
 T_R is reservoir temperature, in K, and
 p_R is reservoir pressure, in atm.

$$B_g = \frac{1}{p_R} \frac{(273.16 + T_R)}{(273.16 + T_{sc})} z = 0.00346 (273.16 + T_R) \frac{z}{p_R}, \quad (36)$$

where

T_{sc} is standard temperature, 15.56°C
 1 is standard pressure, in atm
 T_R is in °C, and
 p_R is in atm.

$$G_{ul} = 10\,000 \phi \frac{R_p}{R_p + 175} \times \left(\frac{1 - S_{iw}}{B_{gi}} - \frac{1 - S_{iw} - S_{or}}{B_{ga}} - 175 S_{or} \right), \quad (38)$$

where R_p is in std m³ gas/m³ condensate and G_{ul} is in std m³ residue gas/ha·m.

$$N_{IR} = E_R \left(\frac{10\,000 A h \phi S_o}{B_o} \right), \quad (78)$$

where A is in ha and h is in m.

References

- Garb, F.A.: "Oil and Gas Reserves Classification, Estimation, and Evaluation," *J. Pet. Tech.* (March 1985) 373-90.
- Arps, J.J.: "Estimation of Primary Oil Reserves," *J. Pet. Tech.* (Aug. 1956) 182-91; *Trans., AIME*, **207**.
- "Proved Reserves Definitions," Joint Committee of SPE, AAPG, and API, *J. Pet. Tech.* (Nov. 1981) 2113-14.
- Wharton, J.B. Jr.: "Isopachous Maps of Sand Reservoirs," *Bull., AAPG* (1948) **32**, No. 7, 1331.
- Schilthuis, R.J.: "Active Oil and Reservoir Energy," *Trans., AIME* (1936) **118**, 33-52.
- Woods, R.W. and Muskat, M.: "An Analysis of Material Balance Calculations," *Trans., AIME* (1945) **160**, 124-39.
- van Everdingen, A.F., Timmerman, E.H., and McMahon, J.J.: "Application of the Material Balance Equation to a Partial Water-Drive Reservoir," *J. Pet. Tech.* (Feb. 1953) 51-60; *Trans., AIME*, **198**.
- van Everdingen, A.F. and Hurst, W.: "The Application of the Laplace Transformation to Flow Problems in Reservoirs," *Trans., AIME* (1949) **186**, 305-24.

9. Muskat, M. and Taylor, M.O.: "Effect of Reservoir Fluid and Rock Characteristics on Production Histories of Gas Drive Reservoirs," *Trans., AIME* (1946) **165**, 78-93.
10. Babson, E.C.: "Prediction of Reservoir Behavior from Laboratory Data," *Trans., AIME* (1944) **155**, 120-32.
11. Turner, J.: "How Different Size Gas Caps and Pressure Maintenance Programs Affect Amount of Recoverable Oil," *Oil Weekly* (June 12, 1944) 32.
12. Arps, J.J. and Roberts, T.G.: "The Effect of the Relative Permeability Ratio, the Oil Gravity and the Solution Gas-Oil Ratio on the Primary Recovery from a Depletion Type Reservoir," *J. Pet. Tech.* (Aug. 1955) 120-27; *Trans., AIME*, **204**.
13. Wahl, W.L., Mullins, L.D., and Elfrink, E.B.: "Estimation of Ultimate Recovery from Solution Gas-Drive Reservoirs," *J. Pet. Tech.* (June 1958) 132-38; *Trans., AIME*, **213**.
14. Higgins, R.V.: "Calculating Oil Recoveries for Solution-gas Drive Reservoirs," RI 5226, USBM, Washington D.C. (April 1956).
15. Torcaso, M.A. and Wyllie, M.R.J.: "A Comparison of Calculated k_{rg}/k_{ra} Ratios With a Correlation of Field Data," *J. Pet. Tech.* (Dec. 1958) 57-58; *Trans., AIME*, **213**.
16. "A Statistical Study of Recovery Efficiency," *API Bull. D-14* (Oct. 1967).
17. Hawkins, M.F. Jr.: "Material Balances in Expansion Type Reservoirs Above Bubble Point," *J. Pet. Tech.* (Oct. 1955) 49-52; *Trans., AIME*, **204**.
18. Hobson, G.D. and Mrosovsky, I.: "Material Balance Above the Bubble Point," *J. Pet. Tech.* (Nov. 1956) 57-58; *Trans., AIME*, **207**.
19. Watts, E.V.: "Some Aspects of High Pressures in the D-7 Zone of the Venture Avenue Field," *Trans., AIME* (1948) **174**, 191-205.
20. Jacoby, R.H. and Berry, V.J. Jr.: "A Method for Predicting Depletion Performance of a Reservoir Producing Volatile Crude Oil," *J. Pet. Tech.* (Jan. 1957) 25-29; *Trans., AIME*, **210**.
21. Reudelhuber, F.O. and Hinds, R.F.: "A Compositional Material Balance Method for Prediction of Recovery from Volatile Oil Depletion Drive Reservoirs," *J. Pet. Tech.* (Jan. 1957) 19-26; *Trans., AIME*, **210**.
22. Cook, A.B., Spencer, G.B., and Bobrowski, F.P.: "Special Considerations in Predicting Reservoir Performance of Highly Volatile Type Oil Reservoirs," *Trans., AIME* (1951) **192**, 37-46.
23. Brinkman, F.H. and Weinaug, C.F.: "Calculated Performance of a Dissolved Gas Reservoir by a Phase Behavior Method," paper SPE 740-G presented at the 1956 SPE Annual Fall Meeting, Los Angeles, Oct. 14-17.
24. Woods, R.W.: "Case History of Reservoir Performance of a Highly Volatile Type Oil Reservoir," *J. Pet. Tech.* (Oct. 1955) 156-59; *Trans., AIME*, **204**.
25. Jacoby, R.H., Koeller, R.C., and Berry, V.J. Jr.: "Effect of Composition Temperature on Phase Behavior and Depletion Performance of Rich Gas-Condensate Systems," *J. Pet. Tech.* (July 1959) 58-63; *Trans., AIME*, **216**.
26. Buckley, S.E. and Leverett, M.C.: "Mechanism of Fluid Displacement in Sand," *Trans., AIME* (1942) **146**, 107-16.
27. Pirson, S.J.: *Elements of Oil Reservoir Engineering*, McGraw-Hill Book Co. Inc., New York City (1950) 285.
28. Welge, H.J.: "A Simplified Method for Computing Oil Recovery by Gas or Water Drive," *Trans., AIME* (1952) **195**, 91-98.
29. Katz, D.L.: "Possibilities of Secondary Recovery for the Oklahoma City Wilcox Sand," *Trans., AIME* (1942) **146**, 28-53.
30. Stahl, R.F., Martin, W.A., and Huntington, R.L.: "Gravitational Drainage Liquids from Unconsolidated Wilcox Sand," *Trans., AIME* (1943) **151**, 138-46.
31. Sims, W.P. and Frailing, W.G.: "Lakeview Pool, Midway-Sunset Field," *Trans., AIME* (1950) **189**, 7-18.
32. Lewis, J.O.: "Gravity Drainage in Oil Fields," *Trans., AIME* (1944) **155**, 133-54.
33. Cardwell, W.T. Jr. and Parsons, R.L.: "Gravity Drainage Theory," *Trans., AIME* (1949) **179**, 199-215.
34. Terwilliger, P.L. *et al.*: "An Experimental and Theoretical Investigation of Gravity Drainage Performance," *Trans., AIME* (1951) **192**, 285-96.
35. Matthews, C.S. and Lefkovits, H.C.: "Gravity Drainage Performance of Depletion Type Reservoirs in the Stripper Stage," *J. Pet. Tech.* (Dec. 1956) 265-74; *Trans., AIME*, **207**.
36. Essley, P.L. Jr., Hancock, G.L. Jr., and Jones, K.E.: "Gravity Drainage Concepts in a Steeply Dipping Reservoir," paper SPE 1029-G presented at the 1958 SPE Annual Fall Meeting, Tulsa.
37. Smith, R.H.: "Gravity Drainage," AIME Study Group Meeting, Los Angeles, Oct. 27, 1952.
38. Baucum, A.W. and Steinle, P.: "Efficiency of Illinois Water Drive Reservoirs," *Drill. and Prod. Prac.*, API (1946) 217.
39. Craze, R.C. and Buckley, S.E.: "A Factual Analysis of the Effect of Well Spacing on Oil Recovery," *Drill. and Prod. Prac.*, API, Dallas (1945) 144.
40. Guthrie, R.K. and Greenberger, M.H.: "The Use of Multiple Correlation Analyses for Interpreting Petroleum Engineering Data," API 901-31-G, API, Dallas (March 1955).
41. Dykstra, H. and Parsons, R.L.: "The Prediction of Oil Recovery by Water Flood," *Secondary Recovery of Oil in the United States*, second edition, API, Dallas (1950) 160.
42. Muskat, M.: "The Effect of Permeability Stratification in Complete Waterdrive Systems," *Trans., AIME*, **189** (1950) 349-58.
43. Stiles, W.E.: "Use of Permeability Distribution in Water-Flood Calculations," *Trans., AIME* (1949) **186**, 9-13.
44. Johnson, C.E. Jr.: "Prediction of Oil Recovery by Waterflood—A Simplified Graphical Treatment of the Dykstra-Parsons Method," *J. Pet. Tech.* (Nov. 1956) 55-56; *Trans., AIME*, **207**.
45. Reznik, A.A., Enick, R.M., and Panvelker, S.B.: "An Analytical Extension of the Dykstra-Parsons Vertical Stratification Discrete Solution to a Continuous, Real-Time Basis," *Soc. Pet. Eng. J.* (Dec. 1984) 643-55.
46. Brown, G.G. *et al.*: *Natural Gasoline and the Volatile Hydrocarbons*, Midwest Printing Co., Tulsa (1941).
47. Katz, D.L.: *Handbook of Natural Gas Engineering*, McGraw-Hill Book Co. Inc., New York City (1981).
48. Robinson, D.B., Macrygeorgos, C.A., and Govier, G.W.: "The Volumetric Behavior of Natural Gases Containing Hydrogen Sulfide and Carbon Dioxide," *Trans., AIME* (1960) **219**, 54-60.
49. Standing, M.B.: *Volumetric and Phase Behavior of Oil Field Hydrocarbons*, Reinhold Publishing Corp., New York City (1952) 25-26.
50. Muskat, M.: *Flow of Homogeneous Fluids Through Porous Media*, McGraw-Hill Book Co. Inc., New York City (1937) 711.
51. Gruy, H.J. and Crichton, J.A.: "A Critical Review of Methods Used in the Estimation of Natural Gas Reserves," *Trans., AIME* (1949) **179**, 249-63.
52. Calhoun, J.C.: *Fundamentals of Reservoir Engineering*, (revised edition) U. of Oklahoma Press, Norman (1953) 6-18.
53. Elfrink, E.B., Sandberg, C.R., and Pollard, T.A.: "A New Compressibility Correlation for Natural Gases and Its Application to Estimates of Gas in Place," *Trans., AIME* (1949) **186**, 219-23.
54. Arps, J.J.: "Analysis of Decline Curves," *Trans., AIME* (1945) **160**, 219-27.
55. Brons, F. and McGarry, M.W. Jr.: "Methods for Calculating Profitabilities," paper SPE 870-G presented at the 1957 SPE Fall Meeting, Dallas, Oct. 6.
56. Cutler, W.W. Jr.: "Estimation of Underground Oil Reserves by Well Production Curves," *Bull.*, USBM, Washington, DC (1924) **228**.
57. Arps, J.J.: "How Well Completion Damage Can Be Determined Graphically," *World Oil* (April 1955) 225-32.
58. van Everdingen, A.F.: "The Skin Effect and Its Influence on the Productive Capacity of a Well," *J. Pet. Tech.* (June 1953) 171-76; *Trans., AIME*, **198**.
59. "Proved Reserves of Crude Oil, Natural Gas Liquids and Natural Gas," American Gas Assn. and American Petroleum Inst. Annual Reports.
60. Ramagost, B.P. and Farshad, F.F.: "P/Z Abnormally Pressured Gas Reservoirs," paper SPE 10125 presented at the 1981 SPE Annual Technical Conference and Exhibition, San Antonio, Oct. 4-7.

General References

"U.S. Crude Oil, Natural Gas, and Natural Liquids," DOE Annual Report (1980).

"Reserves Definition," U.S. Securities and Exchange Commission, Regulation S-X.

World Pet. Cong., London (1983) *Oil and Gas J.* (Nov. 21) 58.

Chapter 41

Valuation of Oil and Gas Reserves

Forrest A. Garb, H.J. Gruy & Assocs.*
Timothy A. Larson, Ernst & Whitney

Types of Oil and Gas Property Ownership

The most common types of oil and gas property ownership in the U.S.¹ are mineral interests, working interests, royalties, overriding royalties, net-profits interests, and production payments.

A mineral interest in a property is a part of the "fee simple" interest. In most states, the mineral interest can be severed from the surface interest and transferred by a mineral deed (in Louisiana, the mineral and surface interest cannot be severed in perpetuity). The owner of the minerals, either through fee simple title or by a mineral deed, can execute a lease of the oil and gas rights. Consideration paid for a lease is called a lease bonus. During the primary term of the lease, it can be held by paying rentals, production, or drilling activities. The rentals, usually called delay rentals, are paid in lieu of drilling or production. From an income-tax standpoint, these rentals are ordinary income to the lessor and are deductible by the lessee. For tax purposes, a bonus must be capitalized as a part of the cost of the lease by the lessee. This bonus is income that is subject to depletion for the mineral-interest owner; although if the lease is not eventually productive, the depletion taken must be restored to income in the year the lease is proved worthless.

A "royalty" or "royalty interest" is the mineral owner's share of production free of the expense of production. It is distinguished from a mineral interest by the absence of operating rights. The basic royalty interest usually is expressed as a fraction of the total production, such as $\frac{1}{8}$ of $\frac{1}{8}$, $\frac{1}{8}$ of $\frac{1}{4}$. Royalty has historically been subject to production taxes, federal excise taxes [Windfall Profits Tax (WPT)], and in some states, *ad valorem* taxes.

An "overriding royalty interest" is an interest in oil and gas produced free of the expense of production and in addition to the usual landowner's royalty. It continues for the life of the lease and is subject to production taxes, WPT taxes, and in some states, *ad valorem* taxes. An

overriding royalty interest is commonly expressed as a fraction of the revenue accruing to the working interest; for example, $\frac{1}{8}$ of $\frac{1}{8}$ of the total oil and gas produced.

In some areas, such as the Rocky Mountains, overriding royalties are often expressed as a percentage of $\frac{1}{8}$ of the total oil and gas produced.

A "net-profits interest" is a share of the gross production measured by the lessee's net profits from the operation of a specific tract of land. It is normally carved out of the working interest.

A "carried interest" is a fractional interest in an oil and gas property that gives the owner no personal obligation for operating or development costs. The operating or development costs attributable to such fractional interest are borne and paid by the owners of the remaining fractional working interest, who recoup such expenditures or an agreed sum out of production from the property.

A "production payment" is a share of the oil, gas, and other minerals produced from a tract of land, free of the cost of production, that terminates when a specific sum from the sale of the oil, gas, and other minerals has been realized by the owner of the interest. There is no personal liability to pay the sum specified in the instrument creating the production payment; the owner looks only to production from the tract of land for the sum specified. A production payment is usually expressed in dollars and may carry an incremental payment computed in the manner of interest. A production payment is said to be "carved out" when it is transferred out of another oil and gas interest. It is "reserved" when the interest is retained by the seller upon the sale of another oil and gas interest. Production payments limited to oil or gas only are called "oil payment" or "gas payment," respectively.

A reversionary interest is usually a portion of the working interest that reverts to another party on the occurrence of some defined event. This event is often the payout of the investment or some multiple of the investment or may be the passing of some defined time period.

*Author of the original chapter was Jan J. Arps (deceased).

TABLE 41.1—REVENUE INTERESTS

A owns: $\frac{1}{8}$ of $\frac{8}{8}$ less $\frac{1}{4}$ of $\frac{1}{8}$ of $\frac{8}{8}$ less $\frac{1}{8}$ of $\frac{1}{8}$ of $\frac{8}{8}$ or $\frac{5}{64}$ (of $\frac{8}{8}$) or	RI=0.07812
B owns: $\frac{1}{4}$ of $\frac{1}{8}$ of $\frac{8}{8}$ or $\frac{1}{32}$ (of $\frac{8}{8}$) or	RI=0.03125
C owns: $\frac{1}{8}$ of $\frac{1}{8}$ of $\frac{8}{8}$ or $\frac{1}{64}$ (of $\frac{8}{8}$) or	RI=0.01562

All or any part of each of these oil and gas interests may be purchased, sold, or mortgaged at the owner's election.

Each economic interest in a property represents the right to a certain fraction of the gross income from the sales of oil and gas [revenue-interest fraction (RI)], and an obligation to pay a certain fraction of the cost of production [working-interest fraction (WI)]. In the case of royalty interests, overriding royalty interests, carried interests, and production payments, the WI is zero because these interests are free of the cost of production.

A "working interest" is the lessee's or operating interest under an oil and gas lease. The typical oil and gas lease provides for a royalty to be paid to the lessor or other royalty owners, free of the expenses of production; the balance of the production represents the working interest of the lessee, and this part of the production bears the entire expense of production. The working interest created by an oil and gas lease may be further divided by the creation of overriding royalties, production payments, net-profits interests, and carried working interests. When there is one lessee under an oil and gas lease, he must pay the entire cost of production and his WI is 100%. Where two or more lessees jointly own a lease, the WI of each lessee when totaled should add up to 100% of the working interest under such lease. The various co-owners of such a lease normally enter into an operating agreement and designate an operator of the property. For example, for a joint-interest owner who owns a quarter of the working interest, the WI equals 0.25. The WI is in effect equal to the fraction of the cost of production that a lessee has to pay.

An RI, also referred to as net interest or division-order interest, is a fractional interest in the total gross revenue from a tract of land that represents the actual quantity of total oil and gas produced from such land attributable to an oil and gas interest in such land. An RI is commonly expressed as a decimal fraction of % of the gross revenue from such production.

An example may clarify the system. Landowner A leases his land for oil and gas purposes to D, retaining the usual $\frac{1}{8}$ royalty interest. In order to hedge against non-

productive development, A sells $\frac{1}{4}$ of his $\frac{1}{8}$ royalty to B and $\frac{1}{8}$ of his $\frac{1}{8}$ to C. A, B, and C thus become the royalty owners under the land mentioned above. Their RI's are computed in Table 41.1.

D, the original lessee, then conveys the lease to E, retaining $\frac{1}{6}$ of $\frac{7}{8}$ overriding-royalty interest. The lease is now said to be burdened with a $\frac{1}{6}$ override. D now owns $\frac{1}{6}$ of $\frac{7}{8}$ or $\frac{7}{48}$, or RI=0.05469.

To support him with his development and operating costs, E now sells one-fourth of his interest in the lease to F. E now owns $\frac{3}{4}$ of ($\frac{7}{8}$ of $\frac{8}{8}$ less $\frac{1}{6}$ of $\frac{7}{8}$ of $\frac{8}{8}$) or $\frac{31}{512}$, or RI=0.61524, while paying $\frac{3}{4}$ of the costs or WI=0.75. F now owns $\frac{1}{4}$ of ($\frac{7}{8}$ of $\frac{8}{8}$ less $\frac{1}{6}$ of $\frac{7}{8}$ of $\frac{8}{8}$) or $\frac{10}{512}$, or RI=0.20508 while paying $\frac{1}{4}$ of the costs or WI=0.25.

The working- and revenue-interest fractions pertaining to the various economic interests in this example should now each add up to unity, as shown in Table 41.2.

Valuation²⁻¹³

Determination of Fair Market Value

Fair market value of an oil- or gas-productive property, as commonly understood, is the price at which the property would be sold after exposure to the market for a reasonable period of time by a willing seller to a willing buyer, neither being under compulsion to buy or to sell, and both being competent and having reasonable knowledge of the facts.

Fiske,³ presenting the viewpoint of the Internal Revenue Service in 1956, listed six methods used to determine the fair market value in order of preferential weight: (1) an actual sale of the property near the valuation date; (2) a bona fide offer to sell or purchase the property near the valuation date; (3) actual sales of similar properties in the same or nearby oil and gas fields near the valuation date; (4) valuations made for purposes other than federal taxation near the valuation date; (5) analytical appraisals; and (6) opinions of qualified oil or gas operators.

This section deals with the determination of the fair market value of oil and gas properties by the analytical- or engineering-appraisal method, enumerated by Fiske as

TABLE 41.2—WORKING AND REVENUE INTEREST FRACTIONS

	Fraction of Working Interest (decimal fraction of costs)	Revenue- Interest Fraction (decimal fraction of revenue)
Landowner (Lessor)	0	0.07812
Royalty Owner	0	0.03125
Royalty Owner	0	0.01562
Overriding-Royalty Owner	0	0.05469
Operator	0.75	0.61524
Nonoperator	0.25	0.20508
Total	1.00	1.00000

Item 5. With this method, the appraiser estimates the recoverable hydrocarbon reserves from the property and appraises the probable future net income or cash flow to be realized from the production and sale of these reserves. While fair market value for a hydrocarbon-producing property is not a precise number, it can be approximated within rather close limits by use of the engineering-appraisal method.⁴

Preparing a Cash-Flow Projection

For the purpose of determining future net income or cash flow, oil and gas production should be forecast on information about future demand for petroleum or on the basis of purchase contracts if these govern but should not exceed the physical ability of the well or wells to produce. Where proration or market curtailment is in force, trends in oil and gas allowables or market should be considered.

Usually, the gross income from oil and gas sales to be obtained from such production is based by the appraiser on current posted prices for crude oil and on predicted economic conditions.

The constant price projections are required for financing and Securities Exchange Commission filings, while the predicted prices that are based on economic studies are used for business decisions.

Gas prices should be based on gas-purchase contracts in force on the properties being appraised. The effect of escalation clauses in such gas-purchase contracts, which are subject to future approval by regulatory agencies, are usually set out separately.

In most states, oil and gas production is subject to state, county, and local taxes payable by the producer. The producer customarily charges the appropriate part of these taxes to the various interests in a given property. Tax rates on oil and gas production in the various states have historically varied and may be obtained from the state regulatory agency. The taxes are usually collected by the pipeline company by deduction from the runs.

Corporation or private income taxes are normally considered outside the scope of an oil and gas property valuation, but some valuation formulas make indirect allowance for them. Tax ramifications can totally change the economics of a proposed transaction and related evaluation. For certain purposes, such as bank evaluations, income taxes, as an inherent part of the future income, are sometimes specifically included in the forecast.

Operating or production costs comprise the expenses required to produce the oil and gas and to maintain the leases. These costs, usually called direct lifting costs, include the cost of labor, field supervision, power, fuel, repairs, stimulation and/or recompletion of wells, plant repairs, transportation, insurance, and other such items. As the age of the wells increases, additional expenditures may have to be made to keep the wells in operating condition and possibly for disposal of produced salt water.

Capital expenditures include the cost of construction of gasoline plants, repressuring systems, additional development wells, artificial lifting equipment, engines, tanks, and other durable items required to produce all the economically recoverable oil.

An owner of a working interest in oil or gas properties pays the full amount of his working-interest share of direct costs and capital expenditures, but he pays production and federal excise taxes only on the production to his net

revenue interest. Royalty or overriding royalty interests, however, ordinarily bear none of the normal lifting costs or capital expenditures but do bear production and federal excise taxes on their revenue-interest portion of the oil or gas produced.

The gross income to be realized from the production of the revenue-interest portion of the oil and gas reserves, when reduced by the amounts necessary for production and federal excise taxes, the working-interest share of operating expenses, repairs, recompletions, and additional capital expenditures, is the future net income or the net cash flow generated from the production of the estimated oil and gas reserves. Salvage value of equipment at the time of abandonment is ordinarily not included in the cash-flow projection because such income is usually offset by the cost of properly plugging and abandoning the property in compliance with state regulations. An exception is sometimes made where the life of the property is short and such salvageable equipment minus abandonment costs constitutes a major part of the value.

After the technical analysis of the properties has been made, which results in a determination of the volume and rate of production of oil and gas, and these data have been reduced to a projection of future operating net income or cash flow, it becomes necessary to establish the appraisal value.

Analytical Methods for Computation of Appraisal Value

Although there are many methods for computing appraisal value, only the most popular will be discussed. All these compute the appraisal value of a property by the discounted-cash-flow procedure and give proper weight to the time pattern of future income. Appraisal values that are based on a given fraction of the undiscounted future cash income or on payout in a given number of years do not meet this requirement and are not included.

The examples provided are from the original edition of this handbook and reflect the economic conditions current at that time. The methodology remains valid, however, and any values in the examples would be subject to change with time.

Appraisal value equal to a fraction of the present worth of the net cash flow before federal taxes computed at a safe rate of interest. Method 1 is relatively simple, easy to understand, and widely used. It is based on the premise that future income should only be discounted at an interest rate that reflects the current-time value of money and that such interest rate—which fluctuates with the prevailing cost of money—is not used as a vehicle for the risk factor. In its application, the combined present worth of the future operating net income or cash flow is calculated by discounting the future annual cash-flow increments at prevailing or projected compound interest rates. An example of such a present-worth computation at an interest rate of 10%/yr is shown in Table 41.3. While Table 41.3 is a hand calculation, most calculations are made with electronic data processing equipment, as shown in Table 41.4.

The total present worth of the future net operating income, which in this example is \$1,499,941, is not to be construed as the market value of the oil or gas property. The purchaser of such a property logically is entitled to

**TABLE 41.3—CASH-FLOW PROJECTION AND PRESENT-WORTH CALCULATION
FOR XYZ OIL COMPANY'S INTEREST IN PRODUCING OIL PROPERTY**

Operator: XYZ Co.
Revenue Interest: RI = 0.375
Working Interest: WI = 0.500

Oil Sales Price = \$29.00/bbl
Production Taxes = 4.6% plus \$0.0019/bbl
Estimated Operating Expenses = \$800.00/well-month

Lease: Mary Jones
Field: Rock Creek
State: Texas
Acres: 100
No. of Wells: 1

Date of Evaluation 1-1-85

Step	Estimated Future	Operation	1/1/85	1/1/86	1/1/87	1/1/88	1/1/89	1/1/90	1/1/91	Total
1	Gross lease production, bbl		50,301	42,570	30,738	24,180	19,490	13,847	4,506	185,632
2	Net production to XYZ, bbl	RI × Step 1	18,863	15,964	11,527	9,068	7,309	5,193	1,690	69,614
3	Oil revenue, dollars	Step 3 × Price	547,023	462,949	334,276	262,957	211,954	150,586	49,003	2,018,748
4	Production taxes, dollars	$[0.046 \times \text{Step 3}] + [0.0019 \times \text{Step 2}]$	25,199	21,326	15,399	12,113	9,764	6,937	2,258	92,996
5	Producing well-months	wells × months	12	12	12	12	12	12	12	84
6	Operating costs, dollars	Step 5 × \$800	9,600	9,600	9,600	9,600	9,600	9,600	9,600	67,200
7	Capital expenditures, dollars	—	—	—	—	—	—	—	—	—
8	XYZ share of operating plus capital costs, dollars	WI × [Step 6 + Step 7]	4,800	4,800	4,800	4,800	4,800	4,800	4,800	33,600
9	Net federal excise* (WPT), dollars		14,336	7,982	4,957	3,174	1,973	987	152	33,561
10	Future net revenue**, dollars	Step 3 – Step 4 – Step 8 – Step 9	502,688	428,841	309,120	242,870	195,417	137,862	41,793	1,858,591
11	10% annual deferment factor (Table 41.11)	$F_{LS} = (\text{Step } 1 + i)^{-12-t}$	0.9535	0.8668	0.7880	0.7164	0.6512	0.5920	0.5382	
12	Present worth of XYZ's cash flow		479,294	371,713	243,582	173,980	127,261	81,618	22,493	1,499,941

*Calculated externally according to regulations current at time of appraisal. Regulations may be obtained from tax accountants.

**Ad valorem taxes if any should be extracted at this step.

TABLE 41.4—PROJECTION OF ESTIMATED PRODUCTION AND REVENUE AS OF JAN. 1, 1985

XYZ Oil Co

Working Interest 0.500000
Net Oil Interest 0.375000
Net Gas Interest 0.375000

Oil
Proved
Primary
Producing

XYZ Oil Co
Mary Jones
Initial Wells 1
Rock Creek Field
Texas

		Future Production				Future Gross Revenue Before Production Taxes (dollars)					Future Net Revenue	Discounted Value at 10.00%
		Oil or Condensate		Gas		Oil Revenue	Gas Revenue	Total Revenue	Production Taxes	Costs		
Year	Number of Wells	Gross (bbl)	Net (bbl)	Gross (Mscf)	Net (Mscf)							
1985	1	50,301	18,863			547,023		547,023	25,199	19,136	502,688	479,294
1986	1	42,570	15,964			462,949		462,949	21,326	12,782	428,841	371,713
1987	1	30,738	11,527			334,276		334,276	15,399	9,757	309,120	243,582
1988	1	24,180	9,068			262,957		262,957	12,113	7,974	242,870	173,980
1989	1	19,490	7,309			211,954		211,954	9,764	6,773	195,417	127,261
1990	1	13,847	5,193			150,586		150,586	6,937	5,787	137,862	81,618
1991	1	4,506	1,690			49,003		49,003	2,258	4,952	41,793	22,493
Sub Total		185,632	69,614			2,018,748		2,018,748	92,996	67,161	1,858,591	1,499,941
Remaining	0	0	0			0		0	0	0	0	0
Total		185,632	69,614			2,018,748		2,018,748	92,996	67,161	1,858,591	1,499,941

The as-of-date gross oil price = \$29.00/bbl, tax tier 3.				Prices and Windfall Profit Taxes	Year	\$/bbl	\$/Mscf	WFPTX(\$)	Year	\$/bbl	\$/Mscf	WFPTX (\$)
					1985	29.00		14,336				
					1986	29.00		7,982				
					1987	29.00		4,957				
					1988	29.00		3,174				
					1989	29.00		1,973				
					1990	29.00		987				
					1991	29.00		152				

Total WFP Tax = \$33,561

TABLE 41.5—DISCOUNTED FUTURE NET CASH INCOME VS. PROPERTY LIFE

Average 5% Deferment Factor on Cash-Flow Projection	Equivalent Constant-Rate Production (years)	Number of Transactions	Percentage of 5% Discounted Value of Future Net Cash Income Paid	Average Percentage of 5% Discounted Value of Future Net Cash Income Paid
0.82 through 0.70	8 through 15	11	60 through 84	71
0.70 through 0.52	15 through 30	13	50 through 89	70
0.52 through 0.40	30 through 45	6	58 through 89	75
0.40 through 0.32	45 through 60	4	68 through 98	78

a profit above the bank interest rate. Also, when cash flow is computed by this method, the federal income taxes on the operating net income usually are not deducted, and allowance must be made for them. In addition, a risk-of-doing-business factor is usually included.

Depending on whether cost-depletion or percentage-depletion allowance is applicable and depending on the amounts of future intangible development expenditures and equipment depreciation, this federal income tax liability will vary on the basis of the tax rate applicable to the interest owner.

The profit margin required in the transaction may also vary widely because of risks inherent in the operation of the property and the respective trading ability of the parties to the transaction.

In addition, in the opinion of many operators, the long-term inflationary trend may put a premium on future income from sales of a basic raw material, such as crude oil or natural gas.

Prospective purchasers should, therefore, weigh all these factors with the federal taxes payable and the risks of the operations as negative factors and the inflationary effects and possible additional "romance" in the transaction as plus factors. Thus they can arrive at the proper fraction of the present worth at some safe interest rate that they are willing to pay.

In a speech presented at the Petroleum Engineers Club of Dallas, Oct. 17, 1952, H.J. Gruy considered as fair market value "two-thirds of future net cash income before amortization and federal taxes, discounted at 5%/yr." This methodology is still in use. However, the discount rate at the time of the evaluation is substituted for the 5%/yr rate.

A study by Garb *et al.*¹⁰ in 1981 indicated that, in spite of varying tax and economic conditions, one classic yardstick for estimating the value of oil in the ground had remained reasonably constant through the years. An analysis of 10 major transactions during the period 1979-81, a volatile oil-price period, indicated that oil reserves in the ground demonstrated a market value of approximately one-third of their posted wellhead price.

Dodson⁹ listed in 1959, among some seven different methods that may be used to determine the fair market value of oil and gas reserves, "percentages of the present worth, which may vary from 50 to 100% but which recently have been from 75 to 80%."

A study by Arps⁶ of 34 actual property transactions made during the postwar years in the mid-continent, gulf coast, and California showed that the percentage of the 5% discounted value of future net cash income (before amortization and federal taxes) paid for these properties varied with their future lives, as shown in Table 41.5.

These data show a tendency for the average percentages of the last column to increase when the estimated life of the properties becomes longer. In none of these transactions did the total consideration exceed two-thirds of the undiscounted future net cash income before federal taxes. Fagin¹¹ introduced an empirical "market-value yardstick" that is based on the trend in actual prices paid for producing properties during the postwar years in long-life fields such as East Texas (see Table 41.6). To find the market value by this yardstick for constant-rate production of a similar character, the percentage shown in Col. 3 of the market-value-yardstick table for the applicable number of years of constant-rate production of Col. 2 of this table is determined. This percentage is then multiplied with the average 5% deferment factor of Col. 1 and with the undiscounted future net cash flow to yield the estimated market value.

Example Problem 1. A property with an estimated future net cash flow of \$1,000,000 and a 10-year constant-rate life would have a market value of $0.73 \times 0.79 \times \$1,000,000 = \$577,000$.

Solution. When the given cash-flow projection does not show a constant rate, the appropriate percentage is found in Col. 3, which corresponds to the applicable average 5% deferment factor from Col. 1 of Table 41.6. This percentage is then multiplied by the average 5% deferment factor of Col. 1 and by the undiscounted future net cash flow to yield the estimated market value.

Example Problem 2. A property with an estimated future net cash flow of \$500,000, which has a 5% discounted value of \$375,000 (average deferment factor 0.75), would have a market value of $0.72 \times 0.75 \times \$500,000 = \$270,000$.

TABLE 41.6—FAGIN'S MARKET-VALUE YARDSTICK

Average 5% Deferment Factor on Cash Flow Projection	Equivalent Constant-Rate Projection (years)	Market Value as Percentage of 5% Discounted Value of Future Net Cash Flow
0.88	5	79
0.79	10	73
0.70	15	71
0.63	20	68
0.52	30	66
0.44	40	70
0.32	60	71

TABLE 41.7—MIDYEAR LUMP-SUM DEFERMENT FACTORS $F_{LS} = (1+i)^{-1/2}$

Year	2%	3%	3½%	4%	4½%	5%	5½%	6%	6½%	7%	7½%	8%	8½%
1	0.9901	0.9853	0.9829	0.9806	0.9782	0.9759	0.9736	0.9713	0.9690	0.9667	0.9645	0.9623	0.9600
2	0.9708	0.9566	0.9497	0.9429	0.9361	0.9295	0.9228	0.9163	0.9099	0.9035	0.8972	0.8909	0.8848
3	0.9517	0.9288	0.9176	0.9066	0.8958	0.8852	0.8747	0.8645	0.8543	0.8444	0.8346	0.8249	0.8155
4	0.9330	0.9017	0.8866	0.8717	0.8572	0.8430	0.8291	0.8155	0.8022	0.7891	0.7764	0.7639	0.7516
5	0.9147	0.8754	0.8566	0.8382	0.8203	0.8029	0.7859	0.7693	0.7532	0.7375	0.7222	0.7073	0.6927
6	0.8968	0.8500	0.8276	0.8060	0.7850	0.7646	0.7449	0.7258	0.7073	0.6893	0.6718	0.6549	0.6385
7	0.8792	0.8252	0.7996	0.7750	0.7512	0.7282	0.7061	0.6847	0.6641	0.6442	0.6249	0.6064	0.5884
8	0.8620	0.8012	0.7726	0.7452	0.7188	0.6936	0.6693	0.6460	0.6236	0.6020	0.5813	0.5615	0.5423
9	0.8451	0.7778	0.7465	0.7165	0.6879	0.6605	0.6344	0.6094	0.5855	0.5626	0.5408	0.5199	0.4999
10	0.8285	0.7552	0.7212	0.6889	0.6583	0.6291	0.6013	0.5749	0.5498	0.5258	0.5031	0.4814	0.4607
11	0.8123	0.7332	0.6968	0.6624	0.6299	0.5991	0.5700	0.5424	0.5162	0.4914	0.4680	0.4457	0.4246
12	0.7964	0.7118	0.6733	0.6370	0.6028	0.5706	0.5403	0.5117	0.4847	0.4593	0.4353	0.4127	0.3913
13	0.7807	0.6911	0.6505	0.6125	0.5768	0.5434	0.5121	0.4827	0.4551	0.4292	0.4049	0.3821	0.3607
14	0.7654	0.6710	0.6285	0.5889	0.5520	0.5175	0.4854	0.4554	0.4273	0.4012	0.3767	0.3538	0.3324
15	0.7504	0.6514	0.6072	0.5663	0.5282	0.4929	0.4601	0.4296	0.4013	0.3749	0.3504	0.3276	0.3064
16	0.7357	0.6324	0.5867	0.5445	0.5055	0.4694	0.4361	0.4053	0.3768	0.3504	0.3260	0.3033	0.2824
17	0.7213	0.6140	0.5669	0.5235	0.4837	0.4471	0.4134	0.3823	0.3538	0.3275	0.3032	0.2809	0.2603
18	0.7071	0.5961	0.5477	0.5034	0.4629	0.4258	0.3918	0.3607	0.3322	0.3060	0.2821	0.2601	0.2399
19	0.6932	0.5788	0.5292	0.4841	0.4429	0.4055	0.3714	0.3403	0.3119	0.2860	0.2624	0.2408	0.2211
20	0.6797	0.5619	0.5113	0.4654	0.4239	0.3862	0.3520	0.3210	0.2929	0.2673	0.2441	0.2230	0.2038
21	0.6664	0.5456	0.4940	0.4475	0.4056	0.3678	0.3337	0.3029	0.2750	0.2498	0.2271	0.2064	0.1878
22	0.6533	0.5297	0.4773	0.4303	0.3882	0.3503	0.3163	0.2857	0.2582	0.2335	0.2112	0.1912	0.1731
23	0.6405	0.5142	0.4612	0.4138	0.3714	0.3336	0.2998	0.2695	0.2425	0.2182	0.1965	0.1770	0.1595
24	0.6279	0.4993	0.4456	0.3979	0.3554	0.3177	0.2842	0.2543	0.2277	0.2039	0.1828	0.1639	0.1470
25	0.6156	0.4847	0.4305	0.3825	0.3401	0.3026	0.2693	0.2399	0.2138	0.1906	0.1700	0.1517	0.1355
26	0.6035	0.4706	0.4159	0.3678	0.3255	0.2882	0.2553	0.2263	0.2007	0.1781	0.1582	0.1405	0.1249
27	0.5917	0.4569	0.4019	0.3537	0.3115	0.2745	0.2420	0.2135	0.1885	0.1665	0.1471	0.1301	0.1151
28	0.5801	0.4436	0.3883	0.3401	0.2981	0.2614	0.2294	0.2014	0.1770	0.1556	0.1369	0.1205	0.1061
29	0.5687	0.4307	0.3751	0.3270	0.2852	0.2489	0.2174	0.1900	0.1662	0.1454	0.1273	0.1115	0.0978
30	0.5576	0.4181	0.3625	0.3144	0.2729	0.2371	0.2061	0.1793	0.1560	0.1359	0.1184	0.1033	0.0901
31	0.5466	0.4059	0.3502	0.3023	0.2612	0.2258	0.1953	0.1691	0.1465	0.1270	0.1102	0.0956	0.0831
32	0.5359	0.3941	0.3384	0.2907	0.2499	0.2150	0.1852	0.1595	0.1376	0.1187	0.1025	0.0885	0.0766
33	0.5254	0.3826	0.3269	0.2795	0.2392	0.2048	0.1755	0.1505	0.1292	0.1109	0.0953	0.0820	0.0706
34	0.5151	0.3715	0.3159	0.2688	0.2289	0.1951	0.1664	0.1420	0.1213	0.1037	0.0887	0.0759	0.0650
35	0.5050	0.3607	0.3052	0.2584	0.2190	0.1858	0.1577	0.1340	0.1139	0.0969	0.0825	0.0703	0.0599
36	0.4951	0.3502	0.2949	0.2485	0.2096	0.1769	0.1495	0.1264	0.1069	0.0905	0.0767	0.0651	0.0552
37	0.4854	0.3400	0.2849	0.2389	0.2006	0.1685	0.1417	0.1192	0.1004	0.0846	0.0714	0.0603	0.0509
38	0.4759	0.3301	0.2753	0.2297	0.1919	0.1605	0.1343	0.1125	0.0943	0.0791	0.0664	0.0558	0.0469
39	0.4665	0.3205	0.2659	0.2209	0.1837	0.1528	0.1273	0.1061	0.0885	0.0739	0.0618	0.0517	0.0432
40	0.4574	0.3111	0.2570	0.2124	0.1758	0.1456	0.1207	0.1001	0.0831	0.0691	0.0575	0.0478	0.0399
41	0.4484	0.3021	0.2483	0.2042	0.1682	0.1386	0.1144	0.0944	0.0780	0.0646	0.0535	0.0443	0.0367
42	0.4396	0.2933	0.2399	0.1964	0.1609	0.1320	0.1084	0.0891	0.0733	0.0603	0.0497	0.0410	0.0339
43	0.4310	0.2847	0.2318	0.1888	0.1540	0.1257	0.1027	0.0840	0.0688	0.0564	0.0463	0.0380	0.0312
44	0.4226	0.2764	0.2239	0.1816	0.1474	0.1197	0.0974	0.0793	0.0646	0.0527	0.0430	0.0352	0.0288
45	0.4143	0.2684	0.2163	0.1746	0.1410	0.1140	0.0923	0.0748	0.0607	0.0493	0.0400	0.0326	0.0265
46	0.4062	0.2606	0.2090	0.1679	0.1350	0.1086	0.0875	0.0706	0.0570	0.0460	0.0372	0.0301	0.0244
47	0.3982	0.2530	0.2020	0.1614	0.1291	0.1034	0.0829	0.0666	0.0535	0.0430	0.0346	0.0279	0.0225
48	0.3904	0.2456	0.1951	0.1552	0.1236	0.0985	0.0786	0.0628	0.0502	0.0402	0.0322	0.0258	0.0208
49	0.3827	0.2384	0.1885	0.1492	0.1183	0.0938	0.0745	0.0592	0.0472	0.0376	0.0300	0.0239	0.0191
50	0.3752	0.2315	0.1822	0.1435	0.1132	0.0894	0.0706	0.0559	0.0443	0.0351	0.0279	0.0222	0.0176

While the examples use a 5% discount factor that is no longer valid, the methodology remains valid. Users of this technique should use discount rates appropriate for the time of the evaluation.

Appraisal value equal to the present value of the net cash flow before federal taxes computed at a speculative rate of interest. Unlike Method 1, the profit margin over and above bank interest rates to take care of inherent risks and federal income tax liabilities is incorporated in Method 2 the higher discount rate. The possible range of such speculative rates of return is reflected by various quotations from the literature. This method is, again, fairly

simple in its application, because federal income taxes are not included in the computation.

Use of Method 2 leads to comparatively high market values for properties of very short life. Because experience shows that very few transactions are made where the total consideration exceeds two-thirds of the future net cash income, experienced engineers in such cases usually limit their appraisal value to this maximum. This formula also tends to discriminate against long-life transactions because high speculative rates of return compound rapidly and reduce the value of cash-flow increments 20 to 30 years, hence to very small amounts. For example, Table 41.7 shows that the midyear lump-sum deferment

TABLE 41.7—MIDYEAR LUMP-SUM DEFERMENT FACTORS $F_{LS} = (1+i)^{1/2-t}$ (continued)

Year	9%	9½%	10%	12%	15%	20%	25%	30%	35%	40%	45%	50%	60%	70%
1	0.9578	0.9556	0.9535	0.9449	0.9321	0.9129	0.8945	0.8770	0.8607	0.8452	0.8304	0.8165	0.7906	0.7670
2	0.8787	0.8727	0.8668	0.8437	0.8105	0.7607	0.7156	0.6747	0.6375	0.6037	0.5727	0.5443	0.4941	0.4512
3	0.8062	0.7970	0.7880	0.7533	0.7048	0.6340	0.5724	0.5190	0.4722	0.4312	0.3950	0.3629	0.3088	0.2654
4	0.7396	0.7279	0.7163	0.6726	0.6129	0.5283	0.4579	0.3992	0.3498	0.3080	0.2724	0.2419	0.1930	0.1561
5	0.6785	0.6647	0.6512	0.6005	0.5329	0.4402	0.3664	0.3071	0.2591	0.2200	0.1879	0.1613	0.1206	0.0918
6	0.6225	0.6070	0.5920	0.5362	0.4634	0.3669	0.2931	0.2362	0.1919	0.1571	0.1296	0.1075	0.0754	0.0540
7	0.5711	0.5544	0.5382	0.4787	0.4030	0.3057	0.2345	0.1817	0.1422	0.1122	0.0894	0.0717	0.0471	0.0318
8	0.5240	0.5063	0.4893	0.4274	0.3504	0.2548	0.1876	0.1398	0.1053	0.0802	0.0616	0.0478	0.0295	0.0187
9	0.4807	0.4624	0.4448	0.3816	0.3047	0.2123	0.1501	0.1075	0.0780	0.0573	0.0425	0.0319	0.0184	0.0110
10	0.4410	0.4222	0.4044	0.3407	0.2650	0.1769	0.1200	0.0827	0.0578	0.0409	0.0293	0.0212	0.0115	0.0065
11	0.4046	0.3856	0.3676	0.3042	0.2304	0.1474	0.0960	0.0636	0.0428	0.0292	0.0202	0.0142	0.0072	0.0038
12	0.3712	0.3522	0.3342	0.2716	0.2003	0.1229	0.0768	0.0489	0.0317	0.0209	0.0139	0.0094	0.0045	0.0022
13	0.3405	0.3216	0.3038	0.2425	0.1742	0.1024	0.0615	0.0376	0.0235	0.0149	0.0096	0.0063	0.0028	0.0013
14	0.3124	0.2937	0.2762	0.2165	0.1515	0.0853	0.0492	0.0290	0.0174	0.0106	0.0066	0.0042	0.0018	0.0008
15	0.2866	0.2682	0.2511	0.1933	0.1317	0.0711	0.0393	0.0223	0.0129	0.0076	0.0046	0.0028	0.0011	0.0005
16	0.2630	0.2450	0.2283	0.1726	0.1146	0.0593	0.0315	0.0171	0.0095	0.0054	0.0032	0.0019	0.0007	0.0003
17	0.2412	0.2237	0.2075	0.1541	0.0996	0.0494	0.0252	0.0132	0.0071	0.0039	0.0022	0.0012	0.0004	0.0002
18	0.2213	0.2043	0.1886	0.1376	0.0866	0.0411	0.0201	0.0101	0.0052	0.0028	0.0015	0.0008	0.0002	
19	0.2031	0.1866	0.1715	0.1229	0.0753	0.0343	0.0161	0.0078	0.0039	0.0020	0.0010	0.0006	0.0001	
20	0.1863	0.1704	0.1559	0.1097	0.0655	0.0286	0.0129	0.0060	0.0029	0.0014	0.0007	0.0004		
21	0.1709	0.1556	0.1417	0.0980	0.0570	0.0238	0.0103	0.0046	0.0021	0.0010	0.0005	0.0002		
22	0.1568	0.1421	0.1288	0.0875	0.0495	0.0198	0.0082	0.0035	0.0016	0.0007	0.0003	0.0002		
23	0.1438	0.1298	0.1171	0.0781	0.0431	0.0165	0.0066	0.0027	0.0012	0.0005	0.0002	0.0001		
24	0.1320	0.1185	0.1065	0.0697	0.0374	0.0138	0.0053	0.0021	0.0009	0.0004	0.0002			
25	0.1211	0.1082	0.0968	0.0623	0.0326	0.0115	0.0042	0.0016	0.0006	0.0003	0.0001			
26	0.1111	0.0988	0.0880	0.0556	0.0283	0.0096	0.0034	0.0012	0.0005	0.0002				
27	0.1019	0.0903	0.0800	0.0496	0.0246	0.0080	0.0027	0.0010	0.0004	0.0001				
28	0.0935	0.0824	0.0727	0.0443	0.0214	0.0066	0.0022	0.0007	0.0003					
29	0.0858	0.0753	0.0661	0.0396	0.0186	0.0055	0.0017	0.0006	0.0002					
30	0.0787	0.0688	0.0601	0.0353	0.0162	0.0046	0.0014	0.0004	0.0001					
31	0.0722	0.0628	0.0546	0.0315	0.0141	0.0038	0.0011	0.0003	0.0001					
32	0.0662	0.0573	0.0497	0.0282	0.0122	0.0032	0.0009	0.0003						
33	0.0608	0.0524	0.0452	0.0251	0.0106	0.0027	0.0007	0.0002						
34	0.0557	0.0478	0.0411	0.0224	0.0093	0.0022	0.0006	0.0002						
35	0.0511	0.0437	0.0373	0.0200	0.0080	0.0019	0.0005	0.0001						
36	0.0469	0.0399	0.0339	0.0179	0.0070	0.0015	0.0004							
37	0.0430	0.0364	0.0308	0.0160	0.0061	0.0013	0.0003							
38	0.0395	0.0333	0.0280	0.0143	0.0053	0.0011	0.0002							
39	0.0362	0.0304	0.0255	0.0127	0.0046	0.0009	0.0002							
40	0.0332	0.0277	0.0232	0.0114	0.0040	0.0007	0.0001							
41	0.0305	0.0253	0.0211	0.0102	0.0035	0.0006	0.0001							
42	0.0280	0.0231	0.0192	0.0091	0.0030	0.0005								
43	0.0257	0.0211	0.0174	0.0081	0.0026	0.0004								
44	0.0235	0.0193	0.0158	0.0072	0.0023	0.0004								
45	0.0216	0.0176	0.0144	0.0065	0.0020	0.0003								
46	0.0198	0.0161	0.0131	0.0058	0.0017	0.0002								
47	0.0182	0.0147	0.0119	0.0051	0.0015	0.0002								
48	0.0167	0.0134	0.0108	0.0046	0.0013	0.0002								
49	0.0153	0.0123	0.0098	0.0041	0.0011	0.0001								
50	0.0140	0.0112	0.0089	0.0037	0.0010	0.0001								

factor for income received in Year 30 amounts to 0.2371 for 5% interest, 0.0601 for 10% interest, and 0.0046 for 20% interest. Because of these shortcomings, the use of Method 2 is not recommended, particularly when long-life properties are involved with a high profit-to-investment ratio.

In a speech presented at the Oil and Gas Inst. in Dallas, March 26, 1949, E.L. DeGolyer commented, "It is rather surprising that more often than not the latter method, i.e. one-half of a 4% discounted future net revenue, is very close to the future net revenue (before amortization and federal taxes) discounted at 10½% per year."

Dodson⁹ listed in 1959 among some seven different methods that may be used to determine the fair market

value of oil and gas reserves, "rate of return on investment of apparently 14% or more."

From a study of five actual and representative valuations that have served as a basis for settlement for gift or *ad valorem* taxes, Reynolds⁷ concluded in 1959 that: "The range of from 13% to 21% annual rate of return before tax adjustments provides limits on which the engineer can operate." He also observed that the data from these appraisals "indicate that the project with a short life will demand a higher rate of return than one with a long life and low risk. This is probably caused by the investors' long-range faith in the oil industry, the belief that higher prices per unit are in the offing, and the fact that less money management is necessary for reinvesting earnings."

TABLE 41.7—MIDYEAR LUMP-SUM DEFERMENT FACTORS $F_{LS} = (1+i)^{-1/2-t}$ (continued)

Year	80%	90%	100%	110%	120%	130%	140%	150%	160%	170%	180%	190%	200%
1	0.7454	0.7255	0.7071	0.6901	0.6742	0.6594	0.6455	0.6325	0.6202	0.6086	0.5976	0.5872	0.5773
2	0.4141	0.3818	0.3536	0.3286	0.3065	0.2867	0.2690	0.2530	0.2385	0.2254	0.2134	0.2025	0.1924
3	0.2300	0.2010	0.1768	0.1565	0.1393	0.1246	0.1121	0.1012	0.0917	0.0835	0.0762	0.0698	0.0641
4	0.1278	0.1058	0.0884	0.0745	0.0633	0.0542	0.0467	0.0405	0.0353	0.0309	0.0272	0.0241	0.0214
5	0.0710	0.0557	0.0442	0.0355	0.0288	0.0236	0.0195	0.0162	0.0136	0.0115	0.0097	0.0083	0.0071
6	0.0394	0.0293	0.0221	0.0169	0.0131	0.0102	0.0081	0.0065	0.0052	0.0042	0.0035	0.0029	0.0024
7	0.0219	0.0154	0.0110	0.0080	0.0059	0.0045	0.0034	0.0026	0.0020	0.0016	0.0012	0.0010	0.0008
8	0.0122	0.0081	0.0055	0.0038	0.0027	0.0019	0.0014	0.0010	0.0008	0.0006	0.0004	0.0003	0.0003
9	0.0068	0.0043	0.0028	0.0018	0.0012	0.0008	0.0006	0.0004	0.0003	0.0002	0.0002	0.0001	
10	0.0038	0.0022	0.0014	0.0009	0.0006	0.0004	0.0002	0.0002	0.0001				
11	0.0021	0.0012	0.0007	0.0004	0.0003	0.0002	0.0001						
12	0.0012	0.0006	0.0003	0.0002	0.0001								
13	0.0006	0.0003	0.0002										
14	0.0004	0.0002											
15	0.0002												
16	0.0001												

The aforementioned rates of return were applied to the entire transaction, including the reserved production payment. Because of "leverage" afforded by the then-permitted ABC method of purchasing properties, the actual rate of return on the equity capital was higher than the rate of return for the transaction as a whole.

The calculated pretax internal rate of return remains a useful yardstick for establishing a fair market value. The acceptable rate of return at any time will be a function of comparative investment opportunities and the subjective assessment of the risk. At the time of this writing, pretax rate of return must fall between 20 and 30% to be competitive with other investment options.

Appraisal value equal to the present value of the net cash flow after federal income taxes computed at an intermediate rate of interest. Method 3 is the most sophisticated approach to the fair-market-value problem. It requires an actual computation of the federal tax liability for each year and is rather laborious. The method also requires tax and accounting information that may not be readily available to the evaluating engineer. Those favoring this method generally use electronic-data-processing facilities that reduce the actual work by the valuation engineer to the preparation of the basic input data. The rate of return in this type of computation comes close to the actual rate of return that, aside from price fluctuations and errors in estimating, may be realized on the purchase. If this method is followed, the fair market value may be defined as the cash value that, if paid for the property, would yield a satisfactory rate of return on the purchase price. A satisfactory rate of return or yield is one that is sufficient to induce the buyer to risk his funds in the particular project rather than in safer investments offering a lower yield. This rate must be commensurate with the physical hazards of producing and the economic hazards of future production. In principle, it is the same incentive recognized in the regulation of public utilities, where the reasonable rate of return upon the fair value of the property (the rate base) is held to be that sufficient to induce the investment of capital in establishing, maintaining, and expanding the property.

Check List of Data Required for Evaluation of Oil- and Gas-Producing Properties

Because the previously discussed evaluation procedures

are reflections of the pattern of future revenues, most evaluation methods are based on the predicted projections of oil and gas production. These projections are prepared either by extrapolating established trends in producing capacity or by academically estimating anticipated production on the basis of geologic interpretations and/or analogy (see Chap. 40).

To make a sound valuation of a given producing property, the appraiser requires certain basic data. The following check list may serve as a reminder when collecting such data.

Maps and Cross Sections. These include ownership maps, geological-structure maps, isopach maps, geological cross sections, etc.

Lease-Location Data. List leases to be included and show for each lease the lease name, number of producing wells, number of temporarily abandoned wells, total number of acres, field name, county, state, and legal description of lease.

Well Logs. These logs include all electrical, acoustic, and radioactivity logs that have been run in each well. Also, if available, geological-sample logs and directional well-survey reports should be included.

Core-Analysis Data. All core-analysis reports for the zones that have been cored and analyzed should be included.

Fluid-Sample-Analysis Data. This includes all bottom-hole fluid-sample-analysis reports and, for gas wells, gas-analysis, specific-gravity, or recombined-sample-analysis reports.

Well History. Chronological history of all well operations including original drilling and completion, recompletions, and remedial work to date should be included. If not otherwise included in a complete chronological well history, provide the following data for each well: conservation commission completion, potential test, and GOR reports; completion (and/or recompletion) date; elevation; kelly bushing, derrick floor, and ground level; total depth* and plugged-back depth; casing size and setting depth; tubing size and setting depth; drillstem test data including intervals tested, time open, fluid recovered, and bottomhole pressure (BHP) data; coring data, including intervals cored, footage recovered, and core description;

*All depths should be referred to a single datum for which the elevation above sea level is also given. The kelly bushing datum is preferred.

geological tops of all major formations encountered; well-location plats or location description; producing formation name, interval perforated, initial production and potential test data; depths to top, bottom, oil/water contact, and gas/oil contact; and pay thickness (gross feet and net feet).

Past-Production History. This history includes tabulation of oil, water, and gas production by months, by leases, by wells, and by pay zones since original completion. Also, include other past history reports, such as production methods (type and size of equipment and dates installed); BHP and wellhead pressure reports; open-flow potential test reports (gas wells); conservation commission (or USGS) production, allowable, and MER reports; pipeline run statements; water-disposal and treating reports; fluid-injection records; and production history of offset operations.

Current Production Data. Tabulate for each well the most current actual test of oil, water, and gas produced and include test date, choke size [or stroke length and strokes per minute (spm)], producing tubing pressure, and producing casing pressure. For gas wells, indicate latest shut-in tubing and casing pressures, including date well was shut in and duration of shut-in time.

Current-Allowable Data. Summarize allowable formula and current daily allowable rates for each well, per producing day, and per calendar day.

Gross Crude Price. For each lease, give the name of the crude purchaser, the average gravity of the oil, and the gross price paid. If the crude is trucked, show the trucking cost per barrel (may be obtained from pipeline run statements).

Gross Gas Price. For each lease, give the name of the gas purchaser and summarize the provisions of the gas contract such as the gross gas price per 1,000 cu ft, the contract pressure base, the minimum delivery pressure, the effective date and term of the contract, and escalation clauses (may be obtained from gas contracts and FPC approval certificates).

Severance and Local Taxes. Indicate the total value of both severance and local (state, county, school, etc.) taxes in terms of a percentage of the total gross income or as an amount per barrel of oil or Mcf of gas produced.

Federal Excise Tax (WPT) Information. This should include, where applicable, tier, company or entity classification for tax, natural gas classification, and price controls, if any.

Operating Expenses. Tabulate actual gross operating expenses per well per month for each lease during the past year. State whether such expenses include, in addition to all direct costs, such items as well-stimulation expenses, workover or recompletion expenses, a portion of district or division overhead expenses, or severance and *ad valorem* taxes.

Completion and Recompletion Costs. In case of undeveloped or nonproducing reserves, provide an estimate of completed well costs or recompletion costs for reserves behind the casing.

Division of Interests. Tabulate the working interest (fraction of $\%$ of the costs) and the revenue interest (fraction of $\%$ of the income) for each interest owner so that for each lease 100% of the working interest and 100% of the revenue interest lease is accounted for. Indicate the lease operator (copy of division orders for oil and gas).

Existing Production Payments or Liens. Tabulate the balance due on all production payments or liens as of a recent date and indicate provisions for the rate of payment.

Lease and Assignment Provisions. Summarize special provisions of all leases and assignments that may adversely affect the value of the leases. In particular, show special provisions concerning shallower or deeper rights and commitments or obligations for the drilling of wells (may be obtained from lease and assignment agreements).

Lease Facilities. Provide complete information concerning lease-facility wells, such as water wells, disposal wells, and injection wells. Provide specifications (size, capacity, etc.) for major lease-facility equipment, such as gas compressors, oil-treating plants, and water-injection plants.

Operating Agreements. In case of joint interest or unitized properties, provide a list of the basic provisions of the operating agreement, such as preferential rights to purchase other interests, obligations for development, basis of overhead allocation, and "call" on the oil (may be obtained from operating agreements and/or letter agreements).

Unitization Agreements. In case of unitized properties, provide a list of the basic provisions of the unitization agreement concerning the basis for calculation of participation percentages and future revisions of same owing to possible future adjustments in operating methods, unitized area, etc. (may be obtained from unitization agreements).

Special Reports. Provide a copy of all special geological and engineering reports that contain data pertinent to a current evaluation of the property. In particular, special engineering reports concerning plans for future development and secondary recovery operations may be helpful in projecting future production rates and future net operating income.

Income Tax Information. Include if applicable.

Forecast of Future Rate of Production¹²

Declining Production

When a property has a well-established performance history and the production rate shows a persistent decline, the appraiser should first make sure that this decline is not caused by either decreasing effectiveness of the lifting equipment or adverse wellbore conditions.

If he finds that the lifting equipment is operating properly and that the wellbore is clean, the past decline may be used as a guide for the projection of future production. First the type and rate of decline must be established.

Constant-Percentage Decline

When the drop in production rate per unit of time is a constant percentage of the production rate, the production curve is of the constant-percentage-decline type. This can best be demonstrated by plotting the production rate vs. time on semilogarithmic paper, with the production rate on the log scale, which should then show a straight-line trend. The production rate may also be plotted vs. cumulative production on regular coordinate paper, which should again show a straight-line trend for this type of decline (Fig. 40.1, Curve I). In either case, the slope of the curve represents the nominal decline fraction or percentage. The decline may also be found by observing the

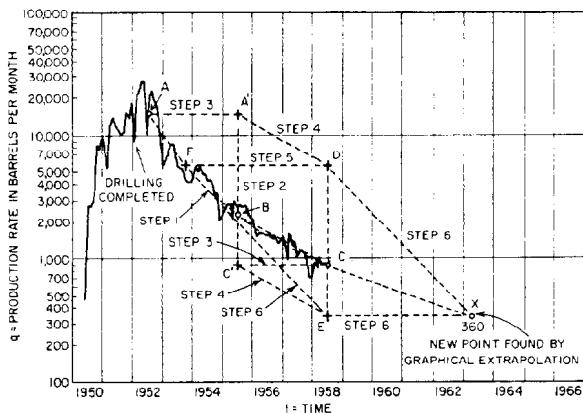


Fig. 41.1—Graphical extrapolation of hyperbolic and harmonic rate/time curves on semilog paper. Step 1: Smooth out the given production curve, and select three equidistant points on it (A, B, and C). Step 2: Draw a vertical line midway between A and C through Point B. Step 3: Project A and C horizontally on this middle line and find Points A' and C'. Step 4: Draw A'D parallel to BC. Step 5: Project D back horizontally on the curve and find Point F. Step 6: draw DX parallel to FE, and find the unknown extrapolated Point X at the intersection with the horizontal line through E.

ratio between the production at the end of a given period and at the beginning of that period and obtaining the effective decline by interpolation from Table 40.16 or 40.17. For example, if the production rate from a well or lease declined from 4,286 to 3,000 bbl/month in 10 months, the ratio between these two production rates is 0.70, and one may read from Table 40.16 that such a drop in rate in 10 months corresponds to an effective decline of $3\frac{1}{2}\%$ /month.

The forecast may then be made on that basis either by reading the future rates from an extrapolation of the straight-line trend on the semilog decline chart or by computing the future rates by means of Table 40.16 or 40.17. Such extrapolation is then continued until the economic-limit rate of production is reached.

Hyperbolic Decline

When the drop in production rate per unit of time expressed as a fraction of the production rate is proportional to a fractional power n of the production rate ($0 < n < 1$), the production curve is of the hyperbolic-decline type.

This is usually evident from a plot of the production rate vs. time on semilog paper, which for this case will not follow a straight line but will show a gradual flattening out.

A rate-cumulative graph on regular coordinate paper will show the same type of curvature (Fig. 40.21, Curve II).

Hyperbolic-decline curves may be straightened out for extrapolation by plotting on double logarithmic or log-log paper after the curves are shifted by adding or subtracting a constant amount to all time or cumulative values. This is a laborious and, with the development of computers, outdated procedure. Most appraisers prefer a graphical extrapolation of the rate/time curve on semilog paper. Such extrapolation may be supported by actually

computing a few points of the curve by means of Eq. 60 of Chap. 40 or by using the graphical extrapolation method on semilog paper shown in Fig. 41.1, which is based on the "three-point rule"¹²: "For any two points on a hyperbolic rate-time curve, for which the production rates are in a given ratio, the point midway in between will have a production rate which is a fixed number of times the rate of either the first or the last point, regardless of where the first two points are chosen."

For example, when the three equidistant points on the past-performance portion of the curve show production rates of 2,000, 1,300, and 1,000 bbl/month, then the future time interval between the ordinates of 1,000 and 650 bbl/month must be equal to the time interval between the ordinates of 650 and 500 bbl/month.

The future projection is then obtained by reading the production rates from the graphically extrapolated curve. Hyperbolic decline is the most common form of production-decline trend found with nonprorated or capacity production. The fractional power n is usually between 0 and 0.50, with the latter value applicable to gravity-drainage-type production under certain conditions.

Harmonic Decline

When the drop in production rate per unit of time expressed as a fraction of the production rate is proportional to the production rate itself, the production curve is of the harmonic-decline type.

Such a curve, plotted as a rate/time graph on semilog paper, does not follow a straight line but shows a rather persistent, pronounced curvature. The rate-cumulative graph on regular coordinate paper shows the same strong curvature (see Fig. 40.21, Curve III).

Harmonic decline may be identified graphically by plotting the inverse of the production rate vs. time on regular coordinate paper, which should then show a straight line. It may also be demonstrated by plotting the rate-cumulative relationship on semilog paper, which should also follow a straight line.

Harmonic decline for production-decline curves does not occur very often, and extrapolation on this basis usually provides a projection that is too optimistic. It is occasionally applicable to capacity production from depletion-type gas wells or to nonprorated production from reservoirs with a bottomwater drive where it is economically feasible to lift and to dispose of large volumes of water.

Extrapolation of the rate/time graph may best be carried out by plotting the inverse of the production rate vs. time on regular coordinate paper and extending the straight line obtained.

A rate/time graph on semilog paper may also be extended by the same construction on the basis of the three-point rule for hyperbolic decline illustrated in Fig. 41.1.

Part Constant Rate—Part Declining Production

In the above discussion, it was assumed that past performance showed the production to be declining, and in such cases the projection is merely based on a continuation of that decline trend.

When no past decline trend is available because the property is relatively new or under proration or market curtailment, however, the appraiser must base his projection on a volumetric estimate of the ultimate recovery and

try to match the future performance of the property against this estimate. This is usually done by assuming a rate of decline typical for this type of production and computing, by means of Eq. 55 of Chap. 40, the cumulative recovery to be obtained when the production is declining from the prorated rate to the economic limit. The number of months of constant-rate production preceding this decline period is then found by subtracting the cumulative production at the appraisal date as well as the estimated production to be obtained during the decline period from the estimated ultimate recovery and dividing the result by the assumed monthly production rate under proration.

Proration or Market Curtailment

Historically, production frequently has been limited by proration. Future operations may encounter proration to guard against loss of reserves through wasteful operations or may encounter curtailment of production because of low market demand. These considerations must be projected in a proper assessment of properties located in affected areas.

Produced Product Prices

The volatility of international energy markets has eliminated any confidence in estimating future product prices on the basis of plots of historical data. Most evaluations are currently performed over a range of assumptions. Constant oil and gas price evaluations are most frequently required for securities registration and for financing purposes. Projected economic conditions that assume maximum and minimum cost and price assumptions are usually applied in management decisions.

Development and Operating Costs¹³⁻¹⁵

Development Costs

Costs of development include the drilling and completion of wells and such improvements as roads, buildings, pipelines, tanks, natural-gasoline plants, and power installations. These costs are changing constantly owing to both economic conditions beyond the control of the operator and technical improvements in drilling and production methods.

The drilling and completion of wells usually constitutes the chief item of expense for development. Shallow wells that are drilled with a portable outfit may cost as little as \$20,000. In the hilly districts of Kentucky, it may require a greater outlay to move the drilling rig to the location than the cost of the well itself. Costs on the high side, apart from exceptional experiences with mishaps or long fishing jobs, may reach tens of millions of dollars for 18,000 to 25,000 ft.

The initial exploratory well generally costs much more than the development wells, and the continued development of a field almost always brings lowered costs with improved methods and increased competition among contractors.

Tangible and Intangible Costs. For income-tax purposes, development costs are divided into two categories: tangible and intangible. Tangible development costs represent the physical property that has salvage value, such as derrick, pipe, and smaller equipment. They are capitalized and retired through annual charges to depreciation.

Intangible drilling and development costs are labor, power, fuel, freight and hauling, water, repairs, and other items that provide no salvage return after completion of the well or that have no physical identity. This class of costs may either be capitalized and retired through annual charges or written off as an expense item in the income account during the year it was incurred. Generally, the latter course is followed. The intangible costs make up 60 to 70% of the entire well cost; the percentage is greater with the shallow wells or any other wells where the casing program requires less pipe than usual.

Well Spacing. An important consideration in appraising undeveloped properties is the prevailing well spacing. Properties that are already fully drilled present no problem, but those that are yet to be developed require consideration of this feature because the future profits will be controlled greatly by the number of wells required.

The number of development wells commonly required as a matter of practical necessity by reason of offset, competitive situations, and the specific lease requirements and obligations is generally much larger than the minimum number of wells required for proper drainage.

Operating Expenses

These expenses cover the field operations necessary to bring the oil and gas to the surface and to deliver a salable product to the stock tank or the gas pipeline.

Direct Lifting Expenses and Direct Expenses. The operating costs are generally divided into direct lifting expenses at the property, such as labor, power, fuel, repairs, renewals, and into-the-field organization; or district expenses, such as supervision, engineering, accounting, timekeeping, warehousing, and general transportation, which in turn are distributed over a number of property units on some ratable basis.

In the determination of a proper measure of production costs for use in estimates, the appraiser may first ascertain the definite record of the property under consideration, or else he may draw on his experience with similar properties elsewhere.

Cost per Well-Month. Operating expenses are preferably expressed on a per-well-month basis rather than per barrel of oil produced. The field cost of operating any given well is the same, within reasonable limits, whether the amount pumped is large or small. The pumping assembly that is installed for pumping an 80-B/D well continues in use when less than half that amount is being produced, but the cost of the operation continues practically unchanged.

Average Cost per Barrel. The use of an average cost per barrel may be acceptable when the production rates are so severely restricted that they are expected to continue at a uniform pace over a considerable period of time. When the production is declining, however, the assumption of an average cost per barrel that is based on a past-experience figure for the property under consideration may lead to erroneous results. The reason is that, with declining production and constant or nearly constant per-well costs, the operating cost per barrel must increase with time until it equals the gross income at the economic limit.

TABLE 41.8—FIELD OR DISTRICT OPERATING COST

Labor, including benefits and transportation furnished	20 to 30%
District expense, including insurance, professional services, damages, etc.	20 to 30%
Repairs and maintenance	30 to 50%
Power, water, waste disposal, and oil treating	5 to 15%

In the case of constant-percentage decline, allowance may be made for this increasing tendency by computing a weighted-average operating cost per barrel with the following relationship:

$$O_u = \frac{O_i \ln q_i/q_a}{q_i - q_a} \quad (1)$$

where

- O_u = weighted average operating cost, dollars,
- O_i = operating expenses per well-month, dollars,
- q_i = initial production rate, bbl/D, and
- q_a = production rate at abandonment, bbl/D.

Example Problem 3. If the operating cost per well-month, O_i , is estimated at \$300, and if the initial production rate, q_i , is 2,113 bbl/well/month, while the economic-limit production rate, q_a , is 113 bbl/well/month, the weighted-average operating cost/bbl over the life of the property is

$$\frac{300 \ln 2,113/113}{2,113 - 113} = \$0.44.$$

In the case of hyperbolic decline ($n = 1/2$), Eq. 1 takes the form

$$\bar{O}_u = \frac{O_i}{q_i} \sqrt{q_i/q_a} \quad (2)$$

In the case of harmonic decline, this relationship reads

$$\bar{O}_u = \frac{O_i}{q_i} \left(\frac{q_i/q_a - 1}{\ln q_i/q_a} \right) \quad (3)$$

In the case of constant-rate production, the average operating cost per gross barrel is simply the estimated operating cost per well-month divided by the rate of production.

The most desirable cost estimate and the one that is conclusive if it can be ascertained is the actually recorded experience at the property subject to such modifications as may appear to be warranted in the judgment of the appraiser.

Range of Costs. Operating costs per well for primary production range from almost insignificant amounts per well-month up to \$10,000 or more per well-month. The latter rate is found offshore or where heavy equipment handles large volumes of water with the oil and where power and maintenance charges are high. Many farms throughout the eastern U.S. contain wells that yield less than 1/2 B/D;

their profitable operation is possible only because repair expenses are negligible and the men who milk the cows also attend the wells.

For entire fields or districts, operating costs generally break down as shown in Table 41.8. Labor and district expense are of about equal magnitude and together comprise about half the total operating costs. The other half is for repairs, maintenance, power, water, waste disposal, and oil treating.

Stimulation Costs. Stimulation costs—such as reacidizing, reshooting, refracturing, and other stimulation treatments—should be considered as part of the operating costs. Fracturing costs have mounted in recent years to where such stimulation expenses may add from 10 to nearly 100% to the operating costs.

Recompletion Costs. Operating costs generally cover only those expenses necessary to keep a well on production for a given productive interval. The cost of recompleting a well into a different producing zone, therefore, is normally treated as a development expense.

Ad Valorem Taxes. To the direct operating expenses should be added the *ad valorem* or property taxes. These taxes show a wide variation in different states and counties and may range from almost nothing to as high as 15%.

Trucking Charges. In case the property is not connected to a pipeline and oil must be trucked out, such charges are usually charged directly against the gross income from oil and gas sales on a per-barrel basis.

The various forms of *production taxes* and WPT's directly levied against the oil and gas produced and commonly collected by the purchaser are not normally included under operating expenses but are charged directly against the gross income from oil and gas sales.

Administration and Supervision

Under this heading are charged direction, executives, central-office expense, accounting, insurance, supervision, personnel relations, and public relations. They are generally designated as overhead as distinguished from the field and district controllable expenses. In many company records, the charges vary widely because of both management ability and the differences in accounting methods.

Production Taxes

Taxes levied directly against oil and gas produced by the various states and usually collected by the pipeline company come under a variety of names—such as gross production taxes, severance tax, excise taxes, stream-pollution taxes, conservation taxes, maintenance taxes, license taxes, school taxes, state taxes, or gas-gathering taxes.

Federal Taxes¹⁶

General

When a projection of future cash net income is made in the appraisal method previously described, provision for estimated federal income taxes is made before discounting such future projection to present worth. In this

method, income taxes are considered an inherent part of the cost of doing business that must be provided for out of the producing operation.

The producing properties that often have difficulties are those whose owners failed to provide for future income taxes. An oil producer may be able to continue exploration and drilling activities at an increasing rate so that his exploration expenses and intangible drilling deductions will reduce income taxes for a number of years. But if such an operator eventually runs out of drilling locations or funds for further development, he may be forced to sell property to meet his taxes or loan obligations. According to this method, the correct approach is to include federal income taxes in the cash-flow projection and to consider any tax savings obtainable through exploration and drilling activities solely as a credit to those activities, reducing their net cost. Often, the appraiser allows indirectly for such income taxes by a higher than normal discount rate or by taking a fraction of the present worth before income taxes. Computation of the net operating income after federal taxes requires a thorough understanding of current tax provisions. Because of the volatility of taxation, the tax consequences on the property valuation at the time of the appraisal should be verified. The most important points of federal tax provisions are summarized below.

Depletion is generally considered to be the gradual exhaustion of a wasting asset through production. The objective of the depletion allowance is to permit the taxpayer owing an economic interest a reasonable deduction for the estimated cost of the reserves thus exhausted. The 1954 Code, Sec. 611, as amended provides that, in the case of oil and gas wells, the taxpayer will be allowed to deduct a reasonable allowance for depletion and depreciation of improvements.

Cost depletion under this provision is computed by multiplying the depletable basis in the property at the end of the tax period, unadjusted by current period depletion, by a fraction, the numerator being unit sales for the taxable period and the denominator unit reserves at the end of the period plus unit sales during the period. In contrast, percentage depletion for oil and gas wells is 15% of the taxpayer's gross income from the property but cannot exceed 50% of its taxable income. It is also limited to 65% of the total taxable income of the interest owner/taxpayer, with any amount disallowed by this limitation deductible in a future year when sufficient taxable income exists. The taxpayer is permitted to deduct, and is required to adjust basis for, either cost or percentage depletion, whichever is highest.

Although cost depletion is limited to the recovery of the taxpayer's basis in the property, percentage depletion is not so limited; if the taxpayer has no depletable basis in a property or if the entire basis has been recovered through prior depletion charges, he may still continue to claim depletion computed on a percentage basis.

Percentage depletion is permitted only as a deduction to independent producers and royalty owners on a maximum of 1,000 B/D of oil equivalent. The deduction is not allowed to integrated oil companies. Gas production for this purpose is converted to oil equivalent volumes at a rate of 6 Mcf to 1 bbl oil. It should also be noted that the transfer of a proven property to another interest owner will generally cause the loss of the percentage

depletion deduction to the transferee with respect to that property.

In determining taxable income from the property for percentage-depletion purposes, deduction must be made not only for ordinary operating expenses of the specific property, including equipment depreciation, but also for intangible drilling and development costs and for a proportionate amount of the overhead properly attributable to the producing function. In determining the overhead allocation, it is customary to allocate general overhead expenses between the producing operations and the other activities carried on by the taxpayer, frequently in proportion to the expenses directly attributable to each activity, and then further to allocate that portion of the overhead attributable to the producing function among specific properties usually in relation to the direct expense from such properties.

Capitalized Leasehold Costs. Ordinarily, a depletable basis in an oil or gas property is of no particular advantage to the taxpayer. The items that must be capitalized as leasehold costs are direct costs (such as lease bonuses or lease-purchase prices) and acquisition costs (such as title-examination fees, recording fees, documentary stamps if any), and geological and geophysical expenses incurred as a result of which the taxpayer either acquires or retains a property interest. Delay rentals paid on unproductive properties may be expensed or capitalized at the election of the taxpayer, and if the taxpayer has elected to capitalize intangible drilling and development costs, such items are added to the depletable basis in the property.

Intangibles. While expenditures for tangible items of well equipment and related items are capitalized and recovered by periodic depreciation allowances throughout their useful lives, in the case of expenditures for intangible drilling and development costs (intangibles), the taxpayer in the oil and gas industry may elect to deduct such items when they are paid or accrued or to capitalize them for recovery through depletion allowances. Because percentage depletion is allowed without reference to the basis of the property, it is apparent that only in infrequent cases would the taxpayer choose to capitalize intangibles.

This concept requires that all costs of drilling and developing an oil property be divided into the two categories—tangible and intangible, the former to be recovered through depreciation. In general, items with a salvage value are classed as tangibles while intangibles embrace all items without a salvage value. Examples of intangibles include labor, fuel, repairs, hauling, and supplies used in drilling, shooting, and cleaning of wells; any necessary site preparation, such as ground clearing, drainage road making, surveying, and geological work; and in the construction of derricks, tanks, pipelines, and other physical structures necessary for drilling and preparation for production.

The decision to expense intangibles must be made by the taxpayer for his first taxable year in which intangibles are paid or incurred. The choice is available only to the owner of an operating or working interest who undertakes the risk of drilling on the property.

Once the capitalized cost and applicable depletion methods have been determined, the allowable depletion, D_A , is the higher of cost depletion, D_C , or percentage

depletion, if applicable, with the latter equal to 15% of gross income, V_{DE} , but limited as stated above under cost depletion.

The allowable depletion selected will therefore be 15% of gross depletion, V_{DE} , when

$$D_A = V_{DE},$$

where

$$V_{TI} > V_{DE} > D_C$$

and

$$V_{DE} = (0.15 \times V) < (0.65 \times I_T), \quad \dots \dots \dots (4)$$

where

D_A = allowable depletion, highest of D_C or lesser of V_{DE} and V_{TI} ,

V_{DE} = "percent of gross" revenue, percentage depletion,

V_{TI} = "50% of net" percentage depletion, equal to 50% of taxable net income, dollars,

D_C = cost depletion; portion of leasehold cost proportional to reserves produced in a given year, dollars,

V = gross revenue (value); the total earned income from oil and gas sales, dollars, and

I_T = interest owner's taxable income, dollars.

The allowable depletion selected will be 50% of net percentage depletion, when

$$D_A = V_{TI},$$

where

$$V_{DE} > V_{TI} > D_C$$

and

$$V_{TI} = 0.50 O_G C_{PT} V O_a C_I D_P, \quad \dots \dots \dots (5)$$

where

O_G = general overhead expenses, dollars,

C_{PT} = local production tax, dollars,

O_a = operating expenses per well-month, dollars,

C_I = intangible drilling and development costs, dollars, and

D_P = depreciation, the decline in value of tangible assets with use of passage of time (obsolescence),

or cost depletion, D_C , when

$$D_A = D_C,$$

$$D_C > V_{DE} > V_{TI},$$

$$D_C > V_{TI} > V_{DE},$$

$$V_{DE} > D_C > V_{TI},$$

$$V_{TI} > D_C > V_{DE},$$

and

$$D_C = \frac{s}{N_r + s} \times C_{dl}, \quad \dots \dots \dots (6)$$

where

C_{dl} = depletable leasehold cost basis at beginning of tax period, dollars,

N_r = reserves at end of tax period, bbl or Mcf, and

s = unit sales during periods.

Example Problem 4. An operator owns half of the working interest ($WI=0.50$) in a two-well lease that produced 20,000 bbl of oil during the taxable year. His revenue interest is $\frac{1}{2}$ of $\frac{7}{8}$ ($RI=0.4375$). The remaining reserves (Q) on Jan. 1 are estimated to be 50,000 bbl. His depletion leasehold cost (LC) on Dec. 31 of the taxable year is \$20,000. The gross income per barrel of oil produced is \$30, plus \$2 from associated gas sales. Local production taxes are 5% of gross income, or \$1.60/net bbl, while operating expenses, including district expenses and *ad valorem* taxes, are \$2,000/well/month. General overhead (GO) is \$1/net bbl. Intangible development cost during the year was \$40,000, while equipment depreciation is \$2/net bbl of oil produced. What is the allowable depletion?

Solution.

$$V_{DE} = 0.15 \times 0.4375 \times 20,000 \times 32 = 42,000.$$

$$D_C = \frac{20,000}{50,000 + 20,000} \times 20,000 = \$5,714.$$

$$V_{TI} = 0.50 \times [0.4375 \times 20,000 \times (30 + 2 - 1.60 - 1 - 2)$$

$$- 0.50 \times 40,000 - 0.50 \times 2 \times 12 \times 2,000] = \$97,875.$$

In this case, apparently, $V_{TI} > V_{DE} > D_C$ and the allowable depletion is therefore $D_A = V_{DE} = \$7,700$.

Alternative Minimum Tax. The Internal Revenue Code of 1954 has been amended at various times to include provisions requiring that a taxpayer pay a specified rate of tax on certain defined tax preference items. These preference items currently include two oil- and gas-related expenses: percentage depletion deductions in excess of the depletable basis in a specific property and certain intangible drilling and development costs. The latter item is not applicable to corporate taxpayers.

While the percentage depletion preference item is fairly self-explanatory, the determination of the intangibles that must be included as a preference item requires computation:

$$C_{IP} = C_{IX} - I_a.$$

TABLE 41.9—TIER AND RATE STRUCTURE, WPT

	Independent Producer (%)	Other than Independent Producer (%)
Tier 1 (oil other than Tier 2 or 3)	50	70
Tier 2 (stripper oil and certain U.S. government interests)	30	50
Tier 3 (newly discovered, heavy and incremental tertiary oil)	30	30
Tier 3 (newly discovered oil subsequent to May 31, 1979)	15	15

where

C_{IP} = preference intangible drilling costs, dollars,
and

C_{IX} = intangible costs minus C_{IA} , dollars.

I_a is the net income from productive oil and gas properties, defined as the aggregate amount of gross income from all such properties, less deductions allocable to the properties reduced by C_{IX} as set forth above.

This preference item can be reduced if the taxpayer chooses to capitalize all or any portion of the intangibles paid or incurred during the year.

Windfall Profit Tax. In April 1980, Congress passed the Windfall Profit Tax Act that was designed to tax the oil and gas interest owner on the windfall profit that was to be received as a result of the deregulation of domestic crude-oil prices. The taxable profit is the excess of the selling price over what the price would have been were it sold before decontrol, adjusted by an inflation factor. An additional adjustment is allowed for severance taxes imposed on the difference between the controlled and decontrolled price. The tax base is also limited to 90% of the net income from the property.

Once the tax base is determined, the appropriate tax rate must then be applied. Three tiers have been specifically defined into which all taxable crude oil falls. The rates applicable to each tier depend on the classification of the interest owner and the nature of the oil produced. Exemptions for certain interest owners and oil types are also provided. The current tier and rate structure is given in Table 41.9.

Newly discovered oil, which falls within Tier 3, is subject to a tax rate schedule that declines from 22.5% in 1984 to 15% in 1986 and thereafter.

Tax Consequences Related to Conveyances. Oil and gas taxation of property conveyances has evolved into a complex set of rules that are necessary because of the many variations of transactions that involve oil and gas interests. Any appraiser who is valuing an interest that includes tax consequences should be aware of the types of various transactions.

There are four primary methods of disposing of oil and gas interests: sale, sublease, special sharing arrangements in a partnership, and production payments. The acquisition of interests may involve the reciprocal of these methods as well as the receipt of an interest for services.

The sale/purchase of an interest provides the easiest forum within which to determine the tax consequences. The

seller will recognize gain that will be characterized as capital or ordinary, depending on various factors that involve the classification of the seller and the tax history of the property. The buyer will merely have basis in the property that should be allocated between the mineral interest and lease and well equipment. Note that an interest owner will often look to the appraiser for guidance regarding the amount that should be allocated to lease and well equipment.

A sublease commonly arises where the transfer of a working interest is burdened with a nonoperating interest retained by the assignor. Consideration received by the assignor is ordinary income because it is characterized as a lease bonus. Any basis in the property is attributed to the nonoperating interest that is depletable; it is not allowed as an offset to the income. The assignee's purchase price will be allocated between leasehold cost and lease and well equipment, if applicable.

Special sharing arrangements are frequently used in a partnership context to allow special allocation of certain items of income and deduction. The partnership allocation rules explained in the Internal Revenue Code and the regulations published by the Dept. of the Treasury should be used as a guide to confirm the tax treatment of such allocations. A problem exists in the standard "third for a quarter" transaction outside the partnership context; the expenses paid by the assignee attributable to the seller's retained interest are considered leasehold cost. They are not deductible even if they are in the nature of intangibles.

A production payment is the right to a specific share of production from an oil and gas property. Where the production payment is used to finance a project, it is treated as a loan by the lender and the interest owner who carved it out of production. Where a working-interest owner retains a production payment and conveys his working interest, he is treated as having sold his interest and should report the proceeds as income realized from the sale of the property. In certain instances, the holder of the production payment may be treated as owning an economic interest. As indicated previously, this would allow the possible deduction of depletion, subject to the restrictions discussed.

The acquisition of an interest in an oil and gas property is frequently made through the performance of services. At one time, it was generally believed that, at the date of transfer, the party receiving the interest was not involved in a taxable event. He, along with the other vendors, dealers, and professionals involved in the property, was merely contributing capital to enable its development. This position, while originally accepted by the Internal Revenue Service, has recently come under

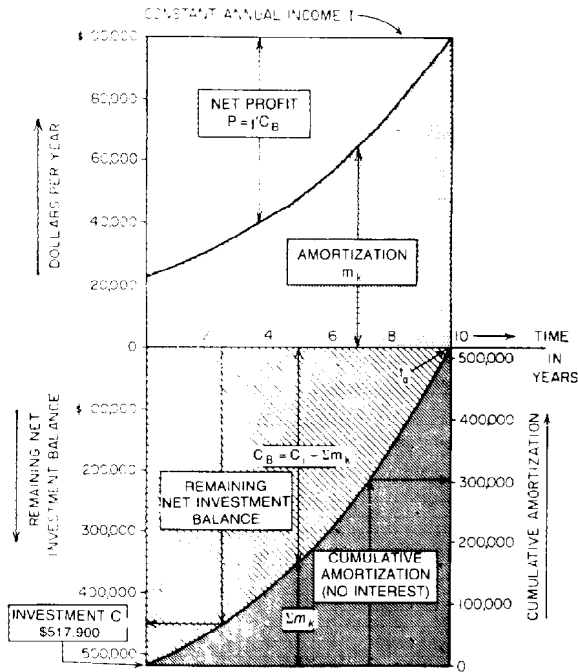


Fig. 41.2—Discounted-cash-flow method. Rate of return $j' = \Sigma P / \Sigma C_B = P / C_B = \text{constant}$. At abandonment time, $C_i = \Sigma m_k$ (no interest).

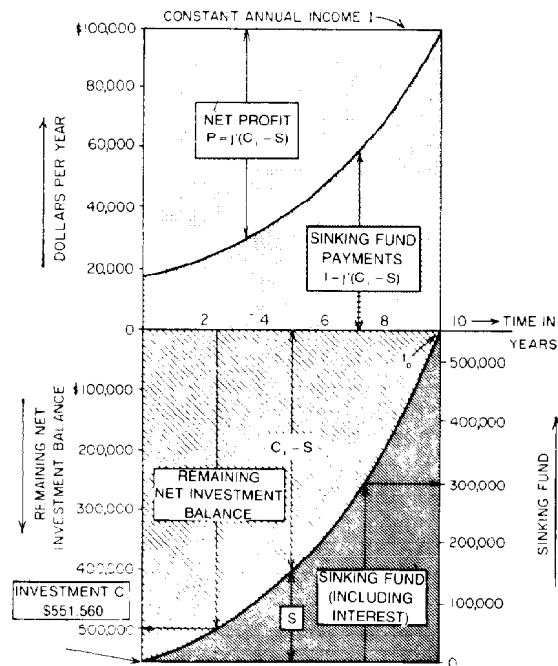


Fig. 41.4—Morkill method. Rate of return $j' = \Sigma P / \Sigma (C_i - S) = P / (C_i - S) = \text{constant}$. At abandonment time t_a , $C_i = S$ (including interest).

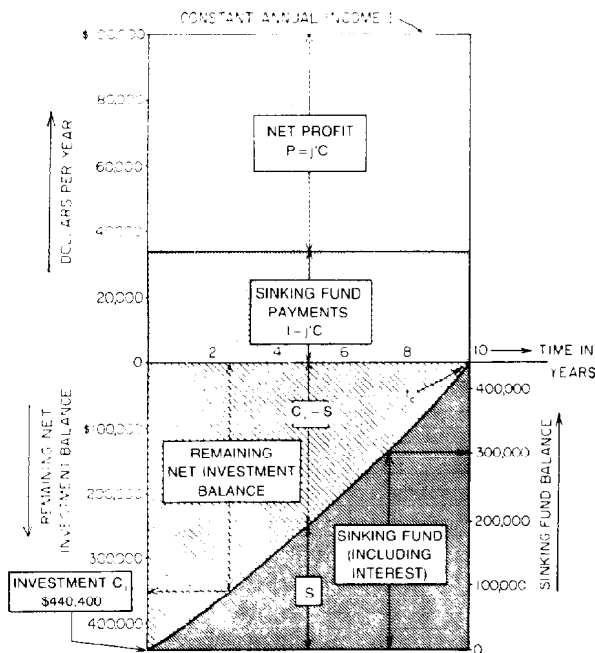


Fig. 41.3—Hoskold method. Rate of return $j' = P / C_i = \text{constant}$. At abandonment time t_a , $C_i = S$ (including interest).

attack and is being severely restricted. The government's current position is that in most instances, at the date of transfer, the taxpayer performing services recognizes taxable income. The issue is far from settled, and additional activity is expected to clarify the tax consequences of such transactions.

Different Concepts of Valuation

The literature includes many different methods that may be used to evaluate the known or estimated future projection of net income from a given venture.¹⁷⁻²⁰ One of them, the discounted-cash-flow method, illustrated in Fig. 41.2, simply reduces these future income payments to present worth or present value by a chosen rate of compound interest or rate of return. It represents the banker's approach to a stream of future income payments and is widely used in industrial work.

The *Hoskold method*, illustrated in Fig. 41.3, was specifically designed for ventures with a limited life, such as mines or oil or gas wells, and was first used in mine-evaluation work.

The *Morkill method*, illustrated in Fig. 41.4, is actually a refinement of the Hoskold method and is also mainly applicable to ventures with a limited life, such as mines and oil or gas wells.

The *accounting method*, illustrated in Fig. 41.5, represents the accounting approach to the valuation problem and takes into account the actual depletion pattern applicable to the given venture. It is particularly suited for those ventures where a specified total number of units of production is involved and where, as is the case in most extractive industries, the depletion applied to the original capital investment is on a unit-of-production basis.

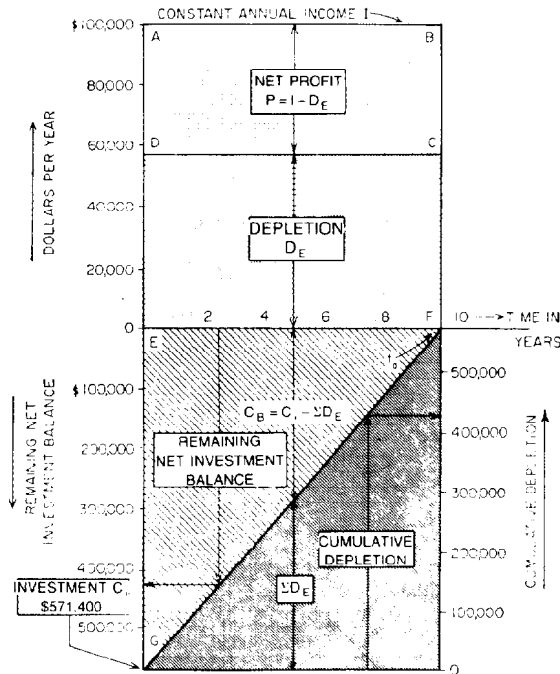


Fig. 41.5—Accounting method. Rate of return $j' = \Sigma P / \Sigma C_B$. At abandonment time t_a , $C_i = \Sigma D_E$ (no interest).

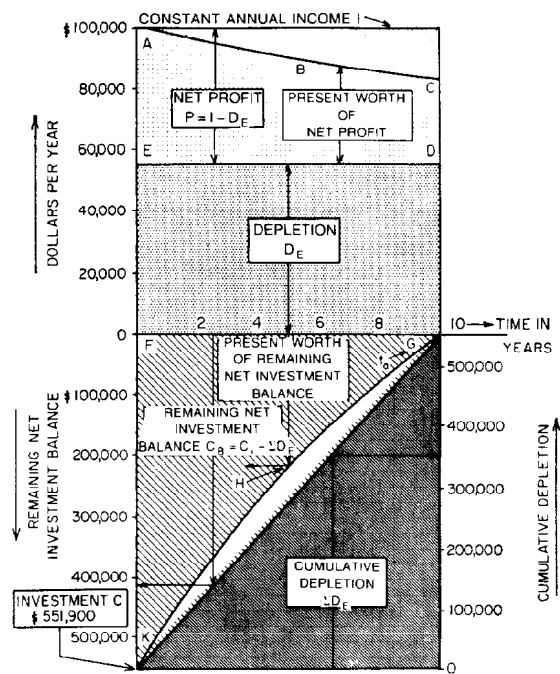


Fig. 41.6—Average-annual-rate-of-return method. Rate of return $j' = \text{present worth of } \Sigma P / \text{present worth of } \Sigma C_B = \text{Area } ABCDE / \text{Area } FGHK$. At abandonment time t_a , $C_i = \Sigma D_E$ (no interest).

The *average-annual-rate-of-return method*, illustrated in Fig. 41.6, is essentially a refinement of the accounting method and, by applying the present-worth concept to both the net annual profits and the net remaining investment balances, simplifies the computations and properly weighs the time pattern of the income.

A complete summary of the basic equations for these different methods and their appraisal and rate-of-return equations will be found in Table 41.10. The top part of this table shows the equations for continuous compounding and the solution for the constant-rate case. The bottom part shows the appraisal equations and the rate-of-return equations for the general case where the cash flow, I , varies from year to year.

Discounted-Cash-Flow Method

This method, also referred to as the investors method¹⁸ or internal-rate-of-return method,^{17,18} is the one most often used in appraisal work. It is based on the principle that, in making an investment outlay, the investor is actually buying a series of future annual operating-income payments. The rate of return (with this method) is the maximum interest rate that one could pay on the capital tied up over the life of the investment and still break even. The time pattern of these future income payments is, therefore, given proper weight.

No fixed amortization pattern needs to be adopted with this method because the annual amounts available for amortization are equal to the difference between the net income and the fixed profit percentage on the unreturned balance of the investment. The computations necessary for a property evaluation are, therefore, relatively simple. They usually involve only the discounting of the pro-

jected cash flow to present value by means of the desired rate of interest.

The appraisal value is then

$$C_i = I_1(1+i')^{-1/2} + I_2(1+i')^{-1} + \dots + I_t(1+i')^{-1/2-t},$$

$$C_i = \sum_{n=1}^{n=t_a} I_n(1+i')^{-1/2-n}, \dots \dots \dots (7)$$

in which I_1, I_2, \dots, I_t represents the projection of the cash income in successive years and the compound-interest factor for the speculative effective interest rate i' is computed for the assumption that the entire income for each year is received at mid-year. Appropriate midyear compound-interest factors $(1+i')^{-1/2-t}$ will be found in Table 41.11 for speculative effective interest rates from 2 to 200%. In the case of oil-producing properties, the computed earning power by this method is not necessarily the same as the average rate of return later shown on a company's books for the net investment in the property. Most oil companies amortize their investments in producing properties in proportion to the depletion of the reserves or on a unit-of-production basis. However, no provision for such amortization pattern is made in the discounted-cash-flow method. When the production rate and the income both follow constant-percentage decline and the ratio between initial and final production rates is substantial, no serious difference will result. However, when the rate of production and the income are constant for a long period of time, a substantial difference may develop and the average rate of return, as shown later on the company's books, may be appreciably higher than the rate of return used in the evaluation by the discounted-cash-flow method.

TABLE 41.10—SUMMARY OF EQUATIONS APPLICABLE TO DIFFERENT VALUATION METHODS

Method	Discounted Cash Flow		Hoskold	
For continuous compounding, basic equation	$I dt = j' C_B dt - dC_B$ where $t=0$ $C_B = C_i$ $t=t_a$ $C_B = 0$	(8)	$I dt + jS dt = j' C_i dt + dS$ where $t=0$ $S=0$ $t=t_a$ $S=C_i$	(14)

Appraisal equation for constant annual income of I dollars per year	$C_i = \frac{(1 - e^{-j't_a})I}{j'}$	(9)	$C_i = \frac{(1 - e^{-j't_a})I}{j' - (j' - j)e^{-j't_a}}$	(15)
---	--------------------------------------	-----	---	------

Rate-of-return equation for constant annual income of I dollars per year	Solution for j' which will satisfy Eq. 9		$j' = \frac{I}{C_i} \frac{je^{-j't_a}}{1 - e^{-j't_a}}$	
--	---	--	---	--

General case: Appraisal equation	$C_i = \sum_{n=1}^{n=t_a} I_n (1 + j')^{1/2 - n}$	(7)	$C_i = \frac{\sum_{n=1}^{n=t_a} I_n (1 + i)^{t_a - n}}{1 + \frac{j'}{i} [(1 + i)^{t_a - 1}]}$	(10)
-------------------------------------	---	-----	---	------

or

$C_i = \frac{F_{PV} \Sigma I}{\frac{j'}{i} - \left(\frac{j'}{i} - 1 \right) (1 + i)^{-t_a}}$	(11)
---	------

Rate-of-return equation	Solution for i' that will satisfy Eq. 7		$i' = \frac{i \left\{ \frac{1}{C_i} \left[\sum_{n=1}^{n=t_a} I_n (1 + i)^{t_a - n} \right] - 1 \right\}}{(1 + i)^{t_a - 1}}$	(12)
-------------------------	--	--	---	------

or

$i' = \frac{i \left[\frac{F_{PV} \Sigma I}{C_i} - (1 + i)^{-t_a} \right]}{1 - (1 + i)^{-t_a}}$	(13)
---	------

The method may be illustrated with the diagram of Fig. 41.2, which shows the application of the discounted-cash-flow method to a venture that is expected to yield an income of \$100,000/yr evenly over a period of 10 yrs and where a speculative nominal rate of return j' of 15%/yr is desired. Time in years is plotted on the horizontal axis, while the constant income is represented by the horizontal line for \$100,000/yr in the upper part of the diagram. The top portion of the diagram shows how the portion of the total income, I , allocated to amortization, m_k , increases, while the net-profit portion (P) decreases with time. The bottom portion of the chart illustrates the manner in which the cumulative Σm_k gradually reduces the unreturned balance of the investment, $C_B = C_i - \Sigma m_k$, from its initial value, C_i , to zero at abandonment of the venture.

The computation of the curves for this constant-rate case is based on the basic differential equation for discounted cash flow,

$$I dt = j' C_B dt - dC_B, \quad (8)$$

where

I = yearly net income, dollars,

j' = nominal annual speculative interest rate,
fraction, and

C_B = balance of unreturned portion of
investment, dollars.

Integration of this equation for constant-rate income between the limits $t=0$, $C_B = C_i$ and $t=t_a$, $C_B=0$ leads to the appraisal value C_i for a nominal rate of return $j'=0.15$:

$$C_i = (1 - e^{-j't_a}) \left(\frac{I}{j'} \right) = [1 - e^{-(0.15)(10)}] \left(\frac{100,000}{0.15} \right) = \$517,900. \quad (9)$$

TABLE 41.10—SUMMARY OF EQUATIONS APPLICABLE TO DIFFERENT VALUATION METHODS (continued)

Morkill	Accounting	Average annual rate of return
$I dt + jS dt = j'(C_i - S)dt + dS \quad (18)$ where $t=0 \quad S=0$ $t=t_a \quad S=C_i$	$j' = \frac{\left(\frac{\Sigma I}{C_i} - 1\right) \Sigma I}{\Sigma I t_a - \int_0^{t_a} dt \int_0^t I dt}$ where $\Sigma I = \int_0^{t_a} I dt$	$j' = \frac{\left(\frac{\Sigma I}{C_i} - 1\right) \int_0^{t_a} I (1+j)^{-t} dt}{\Sigma I \int_0^{t_a} (1+j)^{-t} dt - k}$ where $k = \int_0^{t_a} dt \int_0^t (1+j)^{-t} I dt$ and $\Sigma I = \int_0^{t_a} I dt$
$C_i = \frac{[e^{(i+j')t_a} - 1]I}{j + j'e^{(i+j')t_a}} \quad (19)$	$C_i = \frac{t_a I}{1 + \frac{j' \cdot t_a}{2}} \quad (23)$	$C_i = \frac{t_a I \cdot (1 - e^{-t_a j'})}{j' t_a - \left(\frac{j'}{j} - 1\right)(1 - e^{-t_a j'})} \quad (22)$
Solution for j' that will satisfy Eq. 19 $C_i = \frac{\sum_{n=1}^{n=t_a} I_n (1+i+j')^{t_a-n}}{1 + \frac{j'}{j+i+j'} [(1+i+j')^{t_a} - 1]} \quad (16)$	$C_i = \frac{\Sigma I}{1 + j' \sum_{n=1}^{n=t_a} \left[1 - \frac{(N_p)^{n-1/2}}{(N_p)_a} \right]} \quad (20)$	$C_i = \frac{F_{PV} \Sigma I}{\frac{j'}{j} - \left(\frac{j'}{j} - 1\right) F_{PV}} \quad (24)$
Solution for j' that will satisfy Eq. 16 $j' = \frac{\frac{\Sigma I}{C_i} - 1}{\sum_{n=1}^{n=t_a} \left[1 - \frac{(N_p)^{n-1/2}}{(N_p)_a} \right]} \quad (21)$	$j' = \frac{F_{PV}}{(1 - F_{PV})} \left(\frac{\Sigma I}{C_i} - 1 \right) \quad (25)$	

Legend:

- I_n = net annual operating income during n th year, dollars
 ΣI = total future net operating income, dollars
 C_B = balance of unreturned portion of investment, dollars
 S = balance of sinking fund, dollars
 C_i = initial capital investment or purchase price, dollars
 F_{PV} = average deferment factor on cash-flow projection at a safe rate of interest i ; as a decimal fraction
 j = nominal annual safe interest rate or rate of return; as a decimal fraction
 j' = nominal annual speculative interest rate or rate of return; as a decimal fraction
 j = effective annual safe interest rate or rate of return; as a decimal fraction
 j' = effective annual speculative interest rate or rate of return; as a decimal fraction
 t = time, years
 t_a = time until abandonment, years
 e = base natural logarithms
 $(N_p)_{n-1/2}$ = cumulative production at the midpoint of year n
 $(N_p)_a$ = cumulative production at abandonment time; the end of the last year t_a

TABLE 41.11—LUMP-SUM DEFERMENT FACTORS FOR EFFECTIVE ANNUAL INTEREST RATES FROM 2 TO 200%/yr, APPLICABLE TO PAYMENTS AT YEAR END

Year	2%	3%	4%	5%	6%	8%	10%	12%	15%	20%	25%	30%	35%	40%	45%
1	0.9804	0.9709	0.9615	0.9524	0.9434	0.9259	0.9091	0.8929	0.8696	0.8333	0.8000	0.7692	0.7407	0.7143	0.6897
2	0.9612	0.9426	0.9246	0.9070	0.8900	0.8573	0.8264	0.7972	0.7561	0.6944	0.6400	0.5917	0.5487	0.5102	0.4756
3	0.9423	0.9152	0.8890	0.8639	0.8396	0.7938	0.7513	0.7118	0.6575	0.5787	0.5120	0.4552	0.4064	0.3644	0.3280
4	0.9239	0.8885	0.8548	0.8227	0.7921	0.7350	0.6830	0.6355	0.5718	0.4823	0.4096	0.3501	0.3011	0.2603	0.2262
5	0.9057	0.8626	0.8219	0.7835	0.7473	0.6806	0.6209	0.5674	0.4972	0.4019	0.3277	0.2693	0.2230	0.1859	0.1560
6	0.8879	0.8375	0.7903	0.7462	0.7050	0.6302	0.5645	0.5066	0.4323	0.3749	0.2621	0.2072	0.1652	0.1328	0.1076
7	0.8705	0.8131	0.7599	0.7107	0.6651	0.5835	0.5132	0.4523	0.3759	0.2791	0.2097	0.1594	0.1224	0.0949	0.0742
8	0.8535	0.7894	0.7307	0.6768	0.6274	0.5403	0.4665	0.4039	0.3269	0.2326	0.1678	0.1226	0.0906	0.0678	0.0512
9	0.8368	0.7664	0.7026	0.6446	0.5919	0.5003	0.4241	0.3606	0.2843	0.1938	0.1342	0.0943	0.0671	0.0484	0.0353
10	0.8203	0.7441	0.6756	0.6139	0.5584	0.4632	0.3855	0.3220	0.2472	0.1615	0.1074	0.0725	0.0497	0.0346	0.0243
11	0.8042	0.7224	0.6496	0.5847	0.5268	0.4289	0.3505	0.2875	0.2149	0.1346	0.0859	0.0558	0.0368	0.0247	0.0168
12	0.7885	0.7014	0.6246	0.5568	0.4970	0.3971	0.3186	0.2567	0.1869	0.1122	0.0687	0.0429	0.0273	0.0176	0.0116
13	0.7730	0.6810	0.6006	0.5303	0.4688	0.3677	0.2897	0.2292	0.1625	0.0935	0.0550	0.0330	0.0202	0.0126	0.0080
14	0.7579	0.6611	0.5775	0.5051	0.4423	0.3405	0.2633	0.2046	0.1413	0.0779	0.0440	0.0254	0.0150	0.0090	0.0055
15	0.7430	0.6418	0.5553	0.4810	0.4173	0.3152	0.2394	0.1827	0.1229	0.0649	0.0352	0.0195	0.0111	0.0064	0.0038
16	0.7284	0.6232	0.5339	0.4581	0.3936	0.2919	0.2176	0.1631	0.1069	0.0541	0.0281	0.0150	0.0082	0.0046	0.0026
17	0.7142	0.6050	0.5134	0.4363	0.3714	0.2703	0.1978	0.1456	0.0929	0.0451	0.0225	0.0116	0.0061	0.0033	0.0018
18	0.7002	0.5874	0.4936	0.4155	0.3503	0.2503	0.1799	0.1300	0.0808	0.0376	0.0180	0.0089	0.0045	0.0023	0.0013
19	0.6864	0.5703	0.4747	0.3957	0.3305	0.2317	0.1635	0.1161	0.0703	0.0313	0.0144	0.0068	0.0033	0.0017	0.0009
20	0.6730	0.5537	0.4564	0.3769	0.3118	0.2145	0.1486	0.1037	0.0611	0.0261	0.0115	0.0053	0.0025	0.0012	0.0006
21	0.6598	0.5375	0.4388	0.3589	0.2942	0.1987	0.1351	0.0926	0.0531	0.0217	0.0092	0.0040	0.0018	0.0009	0.0004
22	0.6468	0.5219	0.4220	0.3418	0.2775	0.1839	0.1228	0.0826	0.0462	0.0181	0.0074	0.0031	0.0014	0.0006	0.0003
23	0.6342	0.5067	0.4057	0.3256	0.2618	0.1703	0.1117	0.0738	0.0402	0.0151	0.0059	0.0024	0.0010	0.0004	0.0002
24	0.6217	0.4919	0.3901	0.3101	0.2470	0.1577	0.1015	0.0659	0.0349	0.0126	0.0047	0.0018	0.0007	0.0003	0.0001
25	0.6095	0.4776	0.3751	0.2953	0.2330	0.1460	0.0923	0.0588	0.0304	0.0105	0.0038	0.0014	0.0006	0.0002	0.0001
26	0.5976	0.4637	0.3607	0.2812	0.2198	0.1352	0.0839	0.0525	0.0264	0.0087	0.0030	0.0011	0.0004	0.0002	0.0001
27	0.5859	0.4502	0.3468	0.2678	0.2074	0.1252	0.0763	0.0469	0.0230	0.0073	0.0024	0.0008	0.0003	0.0001	
28	0.5744	0.4371	0.3335	0.2551	0.1956	0.1159	0.0693	0.0419	0.0200	0.0061	0.0019	0.0006	0.0002	0.0001	
29	0.5631	0.4243	0.3206	0.2429	0.1846	0.1073	0.0630	0.0374	0.0174	0.0051	0.0015	0.0005	0.0002		
30	0.5521	0.4120	0.3083	0.2314	0.1741	0.0994	0.0573	0.0334	0.0151	0.0042	0.0012	0.0004	0.0001		
31	0.5412	0.4000	0.2965	0.2204	0.1643	0.0920	0.0521	0.0298	0.0131	0.0035	0.0010	0.0003	0.0001		
32	0.5306	0.3883	0.2851	0.2099	0.1550	0.0852	0.0474	0.0266	0.0114	0.0029	0.0008	0.0002	0.0001		
33	0.5202	0.3770	0.2741	0.1999	0.1462	0.0789	0.0431	0.0238	0.0099	0.0024	0.0006	0.0002			
34	0.5100	0.3660	0.2636	0.1904	0.1379	0.0730	0.0391	0.0212	0.0086	0.0020	0.0005	0.0001			
35	0.5000	0.3554	0.2534	0.1813	0.1301	0.0676	0.0356	0.0189	0.0075	0.0017	0.0004	0.0001			
36	0.4902	0.3450	0.2437	0.1727	0.1227	0.0626	0.0323	0.0169	0.0065	0.0014	0.0003	0.0001			
37	0.4806	0.3350	0.2343	0.1644	0.1158	0.0580	0.0294	0.0151	0.0057	0.0012	0.0003				
38	0.4712	0.3252	0.2253	0.1566	0.1092	0.0537	0.0267	0.0135	0.0049	0.0010	0.0002				
39	0.4620	0.3158	0.2166	0.1491	0.1031	0.0497	0.0243	0.0120	0.0043	0.0008	0.0002				
40	0.4529	0.3066	0.2083	0.1420	0.0972	0.0460	0.0221	0.0107	0.0037	0.0007	0.0001				
41	0.4440	0.2976	0.2003	0.1353	0.0917	0.0426	0.0201	0.0096	0.0032	0.0006	0.0001				
42	0.4353	0.2890	0.1926	0.1288	0.0865	0.0395	0.0183	0.0086	0.0028	0.0005					
43	0.4268	0.2805	0.1852	0.1227	0.0816	0.0365	0.0166	0.0076	0.0025	0.0004					
44	0.4184	0.2724	0.1780	0.1169	0.0770	0.0338	0.0151	0.0068	0.0021	0.0003					
45	0.4102	0.2644	0.1712	0.1113	0.0727	0.0313	0.0137	0.0061	0.0019	0.0003					
46	0.4022	0.2567	0.1646	0.1060	0.0685	0.0290	0.0125	0.0054	0.0016	0.0002					
47	0.3943	0.2493	0.1583	0.1009	0.0647	0.0269	0.0113	0.0049	0.0014	0.0002					
48	0.3865	0.2420	0.1522	0.0961	0.0610	0.0249	0.0103	0.0043	0.0012	0.0002					
49	0.3790	0.2350	0.1463	0.0916	0.0575	0.0230	0.0094	0.0039	0.0011	0.0001					
50	0.3715	0.2281	0.1407	0.0872	0.0543	0.0213	0.0085	0.0035	0.0009	0.0001					

To find the rate of return corresponding to a given purchase price by the discounted-cash-flow method, no straightforward solution is possible; one has to resort to a trial-and-error procedure.

The curve for the unreturned balance, C_B , for this case is shown in the bottom portion of the graph, together with the cumulative amortization ($\Sigma m_k = C_i - C_B$). The corresponding amortization portion, m_k , of the income, I , is shown in the top portion of the graph.

It may be noted from Fig. 41.2 that the rate of return, j' , is the constant ratio of net profit ($P = I - m_k$) and the unreturned balance of investment ($C_B = C_i - \Sigma m_k$), and the balance, C_B , is declining slowly at first and faster toward the end and does not keep pace with the actual depletion of the source of income.

Hoskold's Method

Most industries and manufacturing enterprises have an indeterminate life (apparently perpetual) and are therefore not called on to replace the original investment. This does not mean that such enterprises will continue forever; it means merely that, except for competition, nothing is apparent that might cause termination. Because of this uncertainty, appraisal by the discounted-cash-flow method is generally the best method for such ventures.

Oil, gas, mining, and other extractive industries, however, differ from the foregoing enterprises. When the oil reservoir is depleted or the ore body mined out, there is no value left except possibly some equipment salvage. It is desirable to return the original capital to the investor by the time the profitable life of the enterprise is ended.

TABLE 41.11—LUMP-SUM DEFERMENT FACTORS FOR EFFECTIVE ANNUAL INTEREST RATES FROM 2 TO 200%/yr, APPLICABLE TO PAYMENTS AT YEAR END (continued)

Year	50%	60%	70%	80%	90%	100%	110%	120%	130%	140%	150%	160%	170%	180%	190%	200%
1	0.6667	0.6250	0.5882	0.5556	0.5263	0.5000	0.4762	0.4545	0.4348	0.4167	0.4000	0.3846	0.3704	0.3571	0.3448	0.3333
2	0.4444	0.3906	0.3460	0.3086	0.2770	0.2500	0.2268	0.2066	0.1890	0.1736	0.1600	0.1479	0.1372	0.1276	0.1189	0.1111
3	0.2963	0.2441	0.2035	0.1715	0.1458	0.1250	0.1080	0.0939	0.0822	0.0723	0.0640	0.0569	0.0508	0.0456	0.0410	0.0370
4	0.1975	0.1526	0.1197	0.0953	0.0767	0.0625	0.0514	0.0427	0.0357	0.0301	0.0256	0.0219	0.0188	0.0163	0.0141	0.0123
5	0.1317	0.0954	0.0704	0.0529	0.0404	0.0313	0.0245	0.0194	0.0155	0.0126	0.0102	0.0084	0.0070	0.0058	0.0049	0.0041
6	0.0878	0.0596	0.0414	0.0294	0.0213	0.0156	0.0117	0.0088	0.0068	0.0052	0.0041	0.0032	0.0026	0.0021	0.0017	0.0014
7	0.0585	0.0373	0.0244	0.0163	0.0112	0.0078	0.0056	0.0040	0.0029	0.0022	0.0016	0.0012	0.0010	0.0007	0.0006	0.0005
8	0.0390	0.0233	0.0143	0.0091	0.0059	0.0039	0.0026	0.0018	0.0013	0.0009	0.0007	0.0005	0.0004	0.0003	0.0002	0.0002
9	0.0260	0.0146	0.0084	0.0050	0.0031	0.0020	0.0013	0.0008	0.0006	0.0004	0.0003	0.0002	0.0001			
10	0.0173	0.0091	0.0050	0.0028	0.0016	0.0010	0.0006	0.0004	0.0002	0.0001						
11	0.0116	0.0057	0.0029	0.0016	0.0009	0.0005	0.0003	0.0002	0.0001							
12	0.0077	0.0036	0.0017	0.0009	0.0005	0.0002	0.0001									
13	0.0051	0.0022	0.0010	0.0005	0.0002	0.0001										
14	0.0034	0.0014	0.0006	0.0003	0.0001											
15	0.0023	0.0009	0.0003	0.0001												
16	0.0015	0.0005	0.0002													
17	0.0010	0.0003	0.0001													
18	0.0007	0.0002														
19	0.0005	0.0001														
20	0.0003															
21	0.0002															
22	0.0001															
23	0.0001															
24	0.0001															

This leads to a somewhat different approach to the evaluation of enterprises in such extractive industries. One of the earliest methods, proposed by Hoskold in 1877¹⁹ for the mining industry, emphasizes complete return of the originally invested capital at abandonment time by means of a sinking fund. Hoskold's method presupposes a uniform rate of return at the speculative rate of interest i' on the original capital and provides for redemption of capital at abandonment time by annual reinvestment of the balance of the yearly earnings in a sinking fund at a safe rate of interest i . No fixed amortization pattern is used, but proper weight is given to the specific time pattern of the future cash-income payments.

The appraisal value by the Hoskold method is computed with

$$C_i = \frac{\sum_{n=1}^{n=t_a} I_n(1+i)^{t_a-n}}{1+(i'/i)[(1+i)^{t_a}-1]}, \quad \dots\dots\dots(10)$$

in which the numerator represents the combined value of the cash-income payments, I_n (no depreciation or depletion), computed at abandonment time (t_a) including compound interest at the safe rate (i) per year.

When the weighted average deferment factor or discount factor on the production rate and income projection (F_{PV}) is available at a safe interest rate of 5%/yr, this equation reduces to

$$C_i = \frac{F_{PV}\Sigma I}{(i'/i)-[(i'/i)-1](1+i)^{-t_a}}, \quad \dots\dots\dots(11)$$

The rate of return corresponding to a given purchase

price may be computed directly with the general rate-of-return equations.

$$i' = \frac{i \left\{ 1/C_i \left[\sum_{n=1}^{n=t_a} I_n(1+i)^{t_a-n} \right] - 1 \right\}}{(1+i)^{t_a} - 1}, \quad \dots\dots\dots(12)$$

or

$$i' = \frac{i[(\bar{F}_{PV}\Sigma I/C_i) - (1+i)^{-t_a}]}{1 - (1+i)^{-t_a}}, \quad \dots\dots\dots(13)$$

The interesting feature of this method is its concept of a safe or bank interest rate (i) that is used to build up the sinking fund to full return of the invested capital at the end of the project's life, while at the same time a constant speculative interest rate (i') is earned on the original capital investment (C_i) throughout the same period.

This speculative interest rate (i') is not comparable with the rate of return used in the discounted-cash-flow, accounting, or average-annual-rate-of-return methods because it applies strictly to the entire initial investment and not to the declining balances of such investment.

This method may be illustrated with Fig. 41.3, which shows what would happen to the net profit, the contributions to the sinking fund, and the sinking fund itself if the Hoskold method were applied to the same venture as before that yielded \$100,000/yr income evenly over 10 years. It was assumed that a speculative rate of return (j') of 15%/yr is desired, while the safe nominal interest rate (j) is 5%/yr. The constant-income rate (I) is again shown as the horizontal line in the top part of the diagram. This portion of the chart shows further that the net-profit portion of this annual income (P) is not declining as in the

previous case but is a constant percentage (15%) of the initial investment (C_i). The remaining portion of the income, which is diverted to the sinking fund, is also constant for this case.

The curve on the bottom part of Fig. 41.3 illustrates how the payments to the sinking fund plus interest at a safe rate build this fund up to where the entire initial investment (C_i) is available again at abandonment time.

Computation of the data for this constant-rate case is based on the basic differential equation for the Hoskold method:

$$Idt + jSdt = j'C_i dt + dS, \dots\dots\dots (14)$$

where

j = nominal annual speculative interest rate, fraction,

S = sinking fund balance, dollars, and

C_i = initial capital investment or purchase price, dollars.

Integration of this equation for constant-rate income between the limits $t=0$, $S=0$ and $t=t_a$, $S=C_i$ leads to the appraisal value C_i for a speculative interest rate ($j'=0.15$) and a safe nominal interest rate ($j=0.05$).

$$C_i = \frac{(1 - e^{-j't_a})I}{j' - (j' - j)e^{-j't_a}}$$

$$= \frac{[1 - e^{-(0.05)(10)}](100,000)}{0.15 - (0.10)[e^{-(0.05)(10)}]} = \$440,400. \dots (15)$$

Correspondingly, the constant-net-profit portion (P) of the annual income is $0.15 \times 440,400 = \$66,060$, while the annual sinking fund payment is $\$100,000 - \$66,060 = \$33,940$, as shown on the top portion of the diagram. The curve for the sinking fund (S) for this case is shown in the bottom portion of the figure together with the remaining unreturned portion of the investment ($C_i - S$).

It may be observed that the rate of return (j') is the ratio of the net annual profit (P) to the initial investment (C_i), and the remaining net investment balance ($C_i - S$) is declining somewhat more slowly in the beginning than in the end. Although the curvature is much less than in the discounted-cash-flow method, it still does not keep pace with the actual depletion of the source of income.

Morkill's Method

A variation of the Hoskold equation was proposed in 1918 by Morkill,²⁰ who felt that the risk or speculative rate of interest (i') should be expected only from the amount of capital remaining unreturned, while the security or safe rate of interest (i) should apply to the sinking fund.

The appraisal value by Morkill's method may be computed from

$$C_i = \frac{\sum_{n=1}^{n=t_a} I_n(1+i+i')^{t_a-n}}{1 + [i'/(i+i')][(1+i+i')^{t_a} - 1]}, \dots\dots\dots (16)$$

in which the numerator represents the combined value at abandonment time (t_a) of the annual cash-income payments, I_n (no depreciation), including compound interest at the total interest rate ($i+i'$).

It may be of interest to note that, if the safe interest rate (i) is zero, this equation reduces to the appraisal equation for the discounted-cash-flow method, if the compound-interest factors at the speculative rate (i') are applied at year end instead of midyear:

$$C_i = \sum_{n=1}^{n=t_a} I_n(1+i')^{-n}. \dots\dots\dots (17)$$

Appropriate year-end compound-interest factors $(1+i')^{-t}$ will be found in Table 41.11 for speculative interest rates from 2 to 200%.

To find the rate of return corresponding to a given purchase price for the Morkill method, no direct solution is possible, and one has to resort to a trial-and-error procedure. Morkill's method is illustrated in Fig. 41.4, which shows the net profit, contributions to the sinking fund, and growth of the sinking fund if this method were applied to the same venture as the other examples that yielded a \$100,000/yr income evenly over 10 years. As in the Hoskold method, it was assumed that a speculative nominal rate of return (j') of 15%/yr is desired, while the safe nominal interest rate (j) is 5%/yr.

The horizontal line in the top part of the diagram represents the constant-rate income (I) of \$100,000/yr. The other curves for this constant-rate case are computed from the basic differential equation for the Morkill method,

$$Idt + jSdt = j'(C_i - S)dt + dS. \dots\dots\dots (18)$$

Integration of this equation for constant-rate income between the limits $t=0$, $S=0$ and $t=t_a$, $S=C_i$ leads to the appraisal value (C_i) for a speculative nominal interest rate ($j'=0.15$) and a safe nominal interest rate ($j=0.05$).

$$C_i = \frac{[e^{(j+j')t_a} - 1]I}{j + j'e^{(j+j')t_a}}$$

$$= \frac{[e^{(0.20)(10)} - 1](100,000)}{0.05 + (0.15)[e^{(0.20)(10)}]} = \$551,560. \dots\dots (19)$$

The growth of the sinking fund is shown by the curve in the bottom portion of Fig. 41.4, together with the remaining unreturned portion of the investment ($C_i - S$). The net-profit portion (P) of the operating income (I) shown in the top portion is by definition equal to j' times the amount $C_i - S$. It may be noted from this chart that the rate of return (j') is the constant ratio of net profit (P) and the unreturned balance of the investment ($C_i - S$), and the sinking fund is growing slowly at first and faster toward the end and does not keep pace with the actual depletion of the source of income.

Accounting Method

This method, also referred to as the average-book method,¹⁸ is closely related to many of the concepts used in conventional oil-company accounting procedure and

computes the rate of return on a proposed investment as the ratio of the average net annual profits over the life of the venture (after depletion) to the average book investment over its life. It takes into account the actual depletion pattern and provides results that are compatible with the actual average rate of return later shown by a company's books. With amortization of an investment on a unit-of-production basis or in proportion to the depletion of the reserves, the appraisal value by this method may be expressed for the case where the net income per unit of production is constant as

$$C_i = \frac{\Sigma I}{1 + i' \sum_{n=1}^{n=t_a} \left[1 - \frac{(N_p)_{n-1/2}}{(N_p)_a} \right]}, \dots \dots \dots (20)$$

in which ΣI represents the total of the operating net income payments in successive years,

$$\sum_{n=1}^{n=t_a} I_n,$$

i' the desired speculative rate of return, $(N_p)_{n-1/2}$ the cumulative production at the midpoint of the n th year, and $(N_p)_a$ the cumulative production or estimated ultimate at abandonment time.

Although this method is comparatively simple, it has found only limited application.

The rate of return (i') for a given purchase price (C_i) may be computed directly by

$$i' = \frac{(\Sigma I/C_i) - 1}{\sum_{n=1}^{n=t_a} \left[1 - \frac{(N_p)_{n-1/2}}{(N_p)_a} \right]} \dots \dots \dots (21)$$

or for the constant-rate case by

$$j' = 2 \left(\frac{I}{C_i} - \frac{1}{t_a} \right) \dots \dots \dots (22)$$

Its principal features are illustrated in Fig. 41.5, which shows the net profit (P), the amounts reserved for depletion (D_E), and the cumulative depletion (ΣD_E) if the accounting method were applied to the same venture as before that yielded \$100,000/yr income evenly over 10 years. It was assumed that an average speculative rate of return (j') of 15%/yr is desired. The horizontal line in the top part of the figure represents the \$100,000/yr income rate. Because the income rate and the depletion of the reserves for this simplified case are assumed to be constant, the amounts reserved for depletion (D_E) are, therefore, also shown by a horizontal straight line. Simultaneously, the cumulative depletion in the bottom part of the diagram is a straight line running from zero in the beginning to the capital investment (C_i) at abandonment time (scale on right side).

By definition the rate of return (j') is the average net profit (P) divided by the average investment balance (C_B) and is also equal to the total of the annual net profits as represented by the area of Rectangle ABCD in the top

part of the diagram divided by the total of the annual investment balances as represented by the area of Triangle EFG in the bottom portion of the diagram or, algebraically,

$$t_a(I - D_E) = j' t_a \frac{C_i}{2},$$

while

$$D_E = \frac{C_i}{t_a},$$

so that, after substitution,

$$C_i = \frac{t_a I}{1 + \frac{j' t_a}{2}} = \frac{(10)(100,000)}{1 + \frac{(0.15)(10)}{2}} = \$571,400. \dots \dots \dots (23)$$

It may be noted that this method, in contrast to those previously discussed, allows for a depletion pattern that follows the actual depletion of the source of income. This is indicated for this constant-rate case by the diagonal straight line in the bottom portion of Fig. 41.5.

Average-Annual-Rate-of-Return Method

The average rate of return, computed by this method, is essentially the ratio of the present value of the future net profits (after depletion) to the present value of the net book investments over the life of a property.⁶ The method is particularly suited for investments in oil- and gas-producing properties, where amortization of the invested capital is customarily on a unit-of-production basis and, therefore, is proportional to the depletion of the reserves. The average annual rate of return used in this method corresponds closely to the one later shown by the company's books, while the time pattern of income payments is properly weighted. The equation is particularly simple in its application because the discounting to present worth needs to be done only for the safe interest rate (i). Because this interest rate is usually a fixed number, a series of weighted-average-deferment-factor charts for the most common types of production decline may be prepared in advance. Such charts for $i=0.05$ are shown in Figs. 41.7 and 41.8.

According to Arps,⁶ the appraisal value by the average-annual-rate-of-return method for the case where the net operating income per unit of production is constant may be computed from

$$C_i = \frac{\bar{F}_{PV} \Sigma I}{(i'/i) - [(i'/i) - 1] \bar{F}_{PV}} \dots \dots \dots (24)$$

where I represents the total of the operating net income payments in successive years,

$$\sum_{n=1}^{n=t_a} I_n,$$

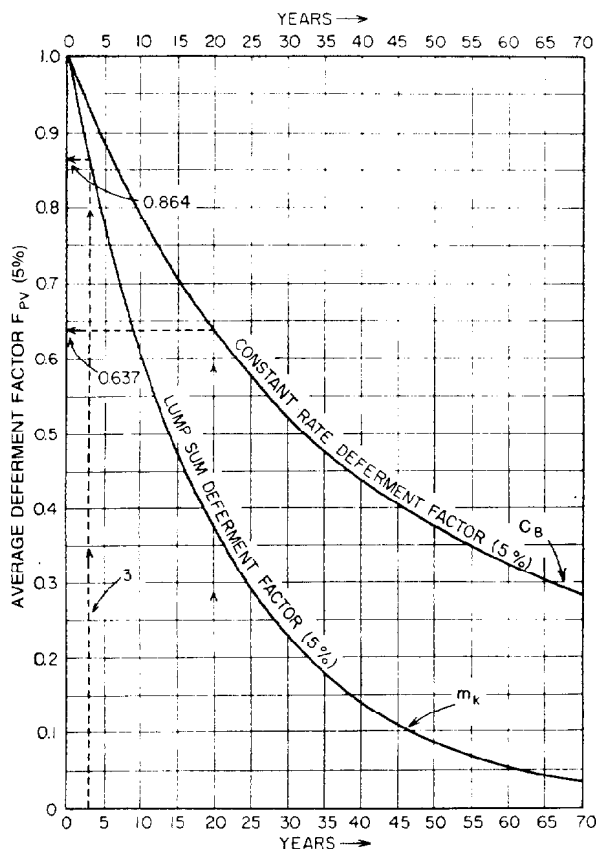


Fig. 41.7—Lump-sum and constant-rate deferment factors for 5% interest.

and i' and i are the speculative and safe interest rates, respectively. \bar{F}_{PV} is the weighted average deferment factor on production and income at the interest rate i .

The rate of return (i') for a given purchase price (C_i) may be computed directly by means of the equation

$$i' = \frac{i\bar{F}_{PV}}{1 - \bar{F}_{PV}} \left(\frac{\Sigma I}{C_i} - 1 \right) \quad (25)$$

The relative simplicity of these equations derives from the fact that, with amortization on a unit-of-production basis, the deferment factor (\bar{F}_{PV}) for the production rate and the net operating income will be identical to the average deferment factor applicable to the annual amounts set aside for amortization. For further details of the derivation and equations, refer to Ref. 21. In cases where the deferment factor on the net operating income is not exactly equal to the deferment factor applicable to the production rates, such as when the lifting costs per barrel are increasing with time, it is customary to use the weighted average deferment factor applicable to the net operating-income projection in the equation.

The principal features of this method are illustrated in Fig. 41.6, which shows the net profit (P), the amounts reserved for depletion (D_E), and the cumulative depletion (ΣD_E) if the average-annual-rate-of-return method

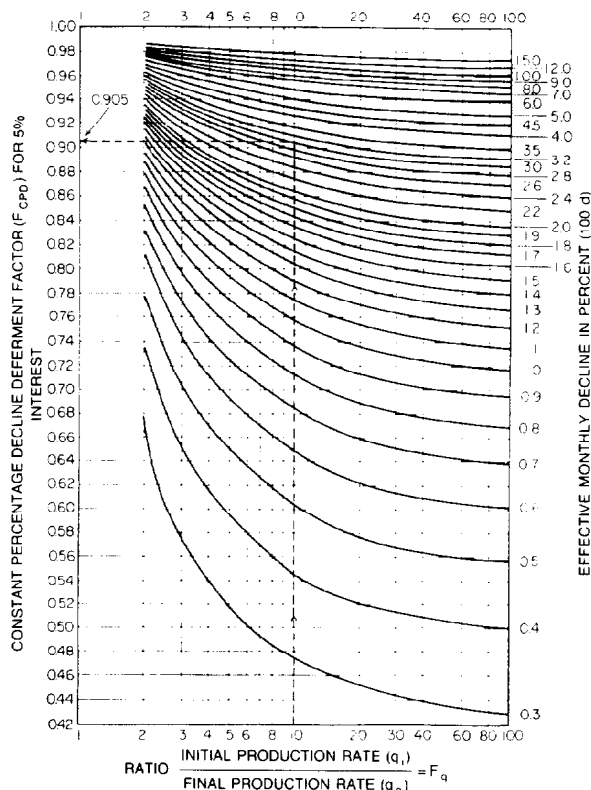


Fig. 41.8—Constant-percentage-decline deferment factor for 5% interest.

were applied to the same venture as before that yielded a \$100,000/yr income evenly over 10 years. It was again assumed that an average speculative rate of return (j') of 15%/yr is desired. The horizontal line in the top part of the figure representing the annual depletion rate, and the diagonal line in the bottom portion of the diagram, representing the cumulative depletion, are the same as previously discussed for the accounting method shown in Fig. 41.5.

The average constant-rate deferment factor for continuous compounding, a safe nominal interest rate ($j=0.05$), and a total life ($t=10$ yrs) may be read from Fig. 41.7 as $\bar{F}_{CR}=0.787$ so that the initial capital investment (C_i) may be computed by means of Eq. 25 as

$$C_i = \frac{(0.787)(10)(100,000)}{(0.15/0.05) - [(0.15/0.05) - 1](0.787)} = \$551,900.$$

The present worth of the net profit, discounted at the safe interest rate ($j=0.05$) is shown by Curve ABC, while the present worth of the net remaining investment balances at the same rate of interest is shown by Curve GHK in the bottom part of the diagram. The speculative rate of return (j') with this method is then graphically represented by the ratio of Area ABCDE and area FGHK.

Interest Tables and Deferment Factors¹⁷

Simple and Compound Interest

Interest rate is the ratio between the amount paid for or gained from the use of funds and the amount of funds used.

Simple Interest. In simple interest, the interest to be paid on repayment of a loan is proportional to the length of time the principal sum has been borrowed. For example, on a loan of \$100 at a nominal interest rate of 6%/yr for a period of 2 months, the interest due upon repayment of the loan would be $0.06 \times \$100 \times \frac{2}{12} = \1.00 . Loans are rarely made at simple interest for periods of more than 1 year.

Compound Interest. In compound interest, the loan is increased by an amount equal to the interest due at the end of the interest period—e.g., on a loan of \$1,000 at an interest rate of 5%/yr for a period of 4 years, the total amount due upon repayment of the loan would be $1.05^4 \times \$1,000 = \$1,216$.

Compounding can be annually, semiannually, quarterly, monthly, or continuously, depending on the length of the stipulated interest period.

Effective and Nominal Interest

The effective annual interest rate (i) is the total compound interest over a year's time, expressed as a fraction or percentage of the amount outstanding at the beginning of the year.

The nominal annual interest rate (j) applies when the interest is compounded over M periods in a year and is equal to M times the interest rate j/M for one period. When interest is compounded once a year, the nominal (j) and effective (i) interest rates are identical.

The relationships between effective (i) and nominal (j) annual interest rate are

$$i = \left(1 + \frac{j}{M}\right)^M - 1 \quad (26)$$

and

$$j = M[(1+i)^{1/M} - 1]. \quad (27)$$

When the nominal annual interest rate is $j=0.06$ or 6%/yr and compounding is on a monthly basis ($M=12$), the monthly interest rate is

$$\frac{j}{M} = \frac{0.06}{12} = 0.005, \text{ or } \frac{1}{2}\%,$$

and the effective annual interest rate is

$$i = (1 + 0.005)^{12} - 1 = 0.06168 \text{ or } 6.168\%/\text{yr}.$$

For the case where interest is compounded continuously ($M \rightarrow \infty$), these relations reduce to

$$i = e^j - 1 \quad (28)$$

and

$$j = \ln(1+i). \quad (29)$$

Table 41.12 expresses the relationships between effective annual interest rate i and nominal annual interest rate j for annual, semiannual ($M=2$), quarterly ($M=4$), monthly ($M=12$), and continuous ($M=\infty$) compounding.

Lump-Sum Deferment Factor

A deferment factor F_{PV} , also referred to as average discount factor or present-worth factor, is defined as the ratio of the present worth of one or a series of future payments and the total undiscounted amount of such future payments. The following deferment factors are commonly used in valuation work.

The lump-sum deferment factor \bar{F}_{LS} , also known as the single-payment present-worth factor, is the ratio of the present value or present worth of a single future payment made t years hence and the amount of the single payment.

For an effective annual interest rate (i), the lump-sum deferment factor for t years is

$$\bar{F}_{LS} = (1+i)^{-t}. \quad (30)$$

Tables 41.7 and 41.11 show lump-sum deferment factors for effective annual interest rates i from 2 to 200%/yr for payments falling either at year end $(1+i)^{-t}$ or at midyear $(1+i)^{1/2-t}$, respectively; e.g., the present worth of a lump-sum payment of \$200 to be made 10 years hence, if interest is computed at 5%/yr, is $\$200 \times 1.05^{-10} = \$200 \times 0.6139 = \$122.78$.

The midyear lump-sum deferment factors are used in the discounted-cash-flow method when a future-income projection by years is to be discounted to present value. It is then customary to assume that the entire year's income is received at the midyear point. For fractional years, the lump-sum deferment factor for an interest rate of 5%/yr may also be read directly from Fig. 41.7, Curve A.

For a nominal annual interest rate j , compounded M times a year, the corresponding equation is

$$F_{LS} = \left(1 + \frac{j}{M}\right)^{-tM}. \quad (31)$$

For continuous compounding ($M=\infty$) at a nominal annual interest rate (j) this equation reduces to

$$\bar{F}_{LS} = e^{-tj}. \quad (32)$$

The lump-sum deferment factor for continuous compounding may be read directly from the graph in Fig. 41.9 for given values of tj .

Constant-Rate Deferment Factor, F_{CR}

Also known as the equal-payment-series present-worth factor, this is the ratio of the present worth of a series of Mt equal payments, made at equal intervals of $12/M$ months over a period of t years in the future, and the total amount of such payments.

TABLE 41.12—RELATIONSHIP BETWEEN EFFECTIVE ANNUAL INTEREST RATE i AND NOMINAL INTEREST RATE j FOR SEMIANNUAL, QUARTERLY, MONTHLY, AND CONTINUOUS COMPOUNDING

Nominal annual interest rate j (Decimal)	Effective Annual Interest Rate i When the Nominal Rate j is Compounded			
	Semiannually $m = 2$	Quarterly $m = 4$	Monthly $m = 12$	Continuously $m = \infty$ $e^j = 1$
	$\left(1 + \frac{j}{2}\right)^2 - 1$	$\left(1 + \frac{j}{4}\right)^4 - 1$	$\left(1 + \frac{j}{12}\right)^{12} - 1$	
0.01	0.01002	0.01004	0.01004	0.01005
0.02	0.02010	0.02015	0.02018	0.02020
0.03	0.03022	0.03034	0.03042	0.03045
0.04	0.04040	0.04060	0.04074	0.04081
0.05	0.05062	0.05094	0.05117	0.05127
0.06	0.06090	0.06136	0.06168	0.06184
0.07	0.07122	0.07186	0.07299	0.07251
0.08	0.08160	0.08243	0.08300	0.08329
0.09	0.09202	0.09308	0.09381	0.09417
0.10	0.10250	0.10381	0.10471	0.10517
0.11	0.11302	0.11462	0.11572	0.11628
0.12	0.12360	0.12551	0.12682	0.12750
0.13	0.13422	0.13648	0.13803	0.13883
0.14	0.14490	0.14752	0.14934	0.15027
0.15	0.15562	0.15865	0.16075	0.16183
0.16	0.16640	0.16986	0.17227	0.17351
0.17	0.17722	0.18115	0.18389	0.18530
0.18	0.18810	0.19252	0.19562	0.19722
0.19	0.19902	0.20397	0.20745	0.20925
0.20	0.21000	0.21551	0.21939	0.22140
0.22	0.23210	0.23882	0.24360	0.24608
0.24	0.25440	0.26248	0.26824	0.27125
0.26	0.27690	0.28647	0.29333	0.29693
0.28	0.29960	0.31080	0.31888	0.32313
0.30	0.32250	0.33547	0.34489	0.34986
0.32	0.34560	0.36049	0.37137	0.37713
0.34	0.36890	0.38586	0.39832	0.40495
0.36	0.39240	0.41158	0.42576	0.43333
0.38	0.41610	0.43766	0.45369	0.46228
0.40	0.44000	0.46410	0.48213	0.49182
0.42	0.46410	0.49090	0.51107	0.52196
0.44	0.48840	0.51807	0.54053	0.55271
0.46	0.51290	0.54561	0.57051	0.58407
0.48	0.53760	0.57352	0.60103	0.61607
0.50	0.56250	0.60181	0.63209	0.64872
0.55	0.62562	0.67419	0.71218	0.73325
0.60	0.69000	0.74901	0.79586	0.82212
0.65	0.75562	0.82630	0.88326	0.91554
0.70	0.82250	0.90613	0.97456	1.01375
0.75	0.89062	0.98854	1.06989	1.11700
0.80	0.96000	1.07360	1.16942	1.22554
0.85	1.03062	1.16136	1.27333	1.33965
0.90	1.10250	1.25188	1.38178	1.45960
0.95	1.17562	1.34521	1.49495	1.58571
1.00	1.25000	1.44141	1.61304	1.71828
1.10	1.40250	1.64266	1.86471	2.00417
1.20	1.56000	1.85610	2.13843	2.32012
1.30	1.72250	2.08222	2.43693	2.66930
1.40	1.89000	2.32150	2.75909	3.05520
1.50	2.06250	2.57446	3.10989	3.48169
1.60	2.24000	2.84160	3.49047	3.95303
1.70	2.42250	3.12344	3.90311	4.47395
1.80	2.61000	3.42051	4.35025	5.04965
1.90	2.80250	3.73334	4.83448	5.68589
2.00	3.00000	4.06250	5.35860	6.38906

When the interest rate over the time interval between payments is j/M and the first payment occurs at the end of the first interest period, the constant-rate deferment factor is

$$\bar{F}_{CR} = \frac{1 - [1 + (j/M)]^{-Mt}}{tj} \quad (33)$$

When the payments are due at the end of each year, the equation reads

$$\bar{F}_{CR} = \frac{1 - (1+i)^{-t}}{ti} \quad (34)$$

When the annual payments are due at midyear, and the first payment is 6 months hence, the deferment factor is

$$\bar{F}_{CR} = (1+i)^{1/2} \frac{[1 - (1+i)^{-t}]}{ti} = \frac{(1+i)^{1/2} - (1+i)^{1/2-t}}{ti} \quad (35)$$

Constant-rate deferment factors for this case and effective interest percentages from 3 to 10% are listed in Table 41.13.

The pipeline income from oil or gas production and the operating expenses are normally accounted for on a monthly basis, and the constant-rate deferment factor for such monthly payments then takes the form

$$\bar{F}_{CR} = \frac{1 - [1 + (j/12)]^{-12t}}{tj} = \frac{1 - (1+i)^{-t}}{12t[(1+i)^{1/2} - 1]} \quad (36)$$

The constant-rate deferment factor according to this equation for an effective annual interest rate of 5%/yr, monthly payments, and monthly compounding may be read directly against the number of years t on Fig. 41.7, Curve B.

For continuous compounding ($M=\infty$) at a nominal interest rate (j) the equation reduces to

$$\bar{F}_{CR} = \frac{1 - e^{-tj}}{tj} \quad (37a)$$

The constant-rate deferment factor for such continuous compounding may be read directly from the graph in Fig. 41.9 for given values of tj . The constant-rate deferment factor for the equal monthly payments received at the end of each month during a specific interval of 1 year between $(t-1)$ and t years from now takes the form

$$\bar{F}_{CR} = \frac{(1+i)^{1-t} - (1+i)^{-t}}{12[(1+i)^{1/2} - 1]} \quad (37b)$$

This "annual deferment factor" is more accurate than the midyear lump-sum deferment factor of Eq. 30 and Table

41.7 for oil- and gas-appraisal work. Table 41.14 provides these factors for effective interest rates between 3 and 20%/yr.

Constant-Percentage-Decline

Deferment Factor \bar{F}_{CPD}

This is the ratio of the present value or present worth of a series of future payments that follow constant-percentage decline and the total amount of such income. When the pipeline income from oil and gas production and the operating expense are accounted for at the end of each month, and when the compounding of interest and the effective decline d are also on a monthly basis, the equation for the deferment factor takes the form

$$\bar{F}_{CPD} = \left\{ \frac{d}{[(1+i)^{1/2} - 1] + d} \right\} \left[\frac{F_q - (1-d)(1+i)^{t_a}}{F_q - (1-d)} \right] \quad (38)$$

where

\bar{F}_{CPD} = constant percentage-decline deferment factor; the average deferment factor applicable to a series of future payments that follow constant-percentage decline, fraction,

d = effective decline rate, drop in production rate per unit of time divided by the production rate at the beginning of the period, fraction,

F_q = ratio between initial and final production rates or payments,

i = effective annual compound safe interest rate, fraction, and

t_a = abandonment time or future life, years.

The constant-percentage-decline deferment factors according to this equation for an effective annual interest rate of 5%/yr or 0.4074%/month, monthly payments, and monthly compounding may be read directly from the graph in Fig. 41.8 for varying ratios F_q and different effective decline rates d .

For continuous compounding ($M=\infty$) at a nominal interest rate j , the equation reduces to

$$\bar{F}_{CPD} = \left(\frac{\ln F_q}{\ln F_q + tj} \right) \left(\frac{F_q - e^{-tj}}{F_q - 1} \right) \quad (39)$$

The constant-percentage-decline deferment factors for such continuous compounding may be read directly from the graph in Fig. 41.9 for given values of ratio F_q and tj .

Time t_a may be computed from Eq. 56 or 57 in Chap. 40:

$$t_a = \frac{\ln F_q}{a} = \frac{N_{pa}}{q_i} \frac{F_q \ln F_q}{(F_q - 1)}$$

TABLE 41.13—CONSTANT-RATE DEFERMENT FACTORS $F_{CR} = (1+i)^{1/2} - (1+i)^{-1/2} / ti$

Each Annual Income Received in One Payment at Midyear

Year	3%	3½%	4%	4½%	5%	5½%	6%	6½%	7%	7½%	8%	8½%	9%	9½%	10%	10½%	11%
1	0.9853	0.9829	0.9806	0.9782	0.9759	0.9736	0.9713	0.9690	0.9667	0.9645	0.9623	0.9600	0.9578	0.9556	0.9535	0.9513	0.9492
2	0.9710	0.9663	0.9617	0.9572	0.9527	0.9482	0.9438	0.9394	0.9351	0.9308	0.9266	0.9224	0.9183	0.9142	0.9101	0.9061	0.9021
3	0.9569	0.9501	0.9433	0.9367	0.9302	0.9237	0.9173	0.9111	0.9049	0.8988	0.8927	0.8868	0.8809	0.8751	0.8694	0.8638	0.8582
4	0.9431	0.9342	0.9254	0.9168	0.9084	0.9001	0.8919	0.8838	0.8759	0.8682	0.8605	0.8530	0.8456	0.8383	0.8311	0.8241	0.8172
5	0.9296	0.9187	0.9080	0.8975	0.8873	0.8772	0.8674	0.8577	0.8483	0.8390	0.8299	0.8209	0.8122	0.8036	0.7952	0.7869	0.7788
6	0.9163	0.9035	0.8910	0.8788	0.8668	0.8552	0.8438	0.8326	0.8218	0.8111	0.8007	0.7905	0.7806	0.7708	0.7613	0.7520	0.7429
7	0.9033	0.8887	0.8744	0.8605	0.8470	0.8339	0.8211	0.8086	0.7964	0.7845	0.7729	0.7617	0.7507	0.7399	0.7294	0.7192	0.7092
8	0.8905	0.8742	0.8583	0.8428	0.8279	0.8133	0.7992	0.7854	0.7721	0.7591	0.7465	0.7342	0.7223	0.7107	0.6994	0.6884	0.6777
9	0.8780	0.8600	0.8425	0.8256	0.8093	0.7934	0.7781	0.7632	0.7488	0.7349	0.7213	0.7082	0.6955	0.6831	0.6711	0.6595	0.6482
10	0.8657	0.8461	0.8272	0.8089	0.7912	0.7742	0.7578	0.7419	0.7265	0.7117	0.6973	0.6835	0.6700	0.6570	0.6444	0.6323	0.6205
11	0.8537	0.8325	0.8122	0.7926	0.7738	0.7556	0.7382	0.7214	0.7052	0.6895	0.6745	0.6599	0.6459	0.6324	0.6193	0.6067	0.5945
12	0.8419	0.8192	0.7976	0.7768	0.7568	0.7377	0.7193	0.7016	0.6847	0.6683	0.6526	0.6375	0.6230	0.6090	0.5955	0.5825	0.5700
13	0.8303	0.8063	0.7833	0.7614	0.7404	0.7203	0.7011	0.6827	0.6650	0.6481	0.6318	0.6162	0.6013	0.5869	0.5731	0.5598	0.5470
14	0.8189	0.7936	0.7695	0.7465	0.7245	0.7036	0.6836	0.6644	0.6462	0.6287	0.6120	0.5960	0.5806	0.5660	0.5519	0.5384	0.5254
15	0.8077	0.7811	0.7559	0.7319	0.7091	0.6873	0.6666	0.6469	0.6281	0.6101	0.5930	0.5767	0.5610	0.5461	0.5318	0.5182	0.5051
16	0.7968	0.7690	0.7427	0.7178	0.6941	0.6716	0.6503	0.6300	0.6107	0.5924	0.5749	0.5583	0.5424	0.5273	0.5128	0.4991	0.4859
17	0.7860	0.7571	0.7298	0.7040	0.6796	0.6564	0.6345	0.6138	0.5941	0.5754	0.5576	0.5407	0.5247	0.5094	0.4949	0.4810	0.4678
18	0.7755	0.7455	0.7172	0.6906	0.6655	0.6417	0.6193	0.5981	0.5781	0.5591	0.5411	0.5240	0.5078	0.4925	0.4779	0.4640	0.4508
19	0.7651	0.7341	0.7049	0.6776	0.6518	0.6275	0.6046	0.5831	0.5627	0.5435	0.5253	0.5081	0.4918	0.4764	0.4617	0.4479	0.4347
20	0.7549	0.7229	0.6930	0.6649	0.6385	0.6137	0.5905	0.5685	0.5479	0.5285	0.5102	0.4929	0.4765	0.4611	0.4465	0.4326	0.4195
21	0.7450	0.7120	0.6813	0.6525	0.6256	0.6004	0.5768	0.5546	0.5337	0.5141	0.4957	0.4783	0.4620	0.4465	0.4319	0.4182	0.4051
22	0.7352	0.7014	0.6699	0.6405	0.6131	0.5875	0.5635	0.5411	0.5201	0.5004	0.4819	0.4645	0.4481	0.4327	0.4182	0.4045	0.3915
23	0.7256	0.6909	0.6587	0.6288	0.6009	0.5750	0.5507	0.5281	0.5070	0.4872	0.4686	0.4512	0.4349	0.4195	0.4051	0.3915	0.3787
24	0.7162	0.6807	0.6479	0.6174	0.5891	0.5629	0.5384	0.5156	0.4943	0.4745	0.4559	0.4385	0.4223	0.4070	0.3926	0.3792	0.3665
25	0.7069	0.6707	0.6373	0.6063	0.5777	0.5511	0.5265	0.5035	0.4822	0.4623	0.4437	0.4264	0.4102	0.3950	0.3808	0.3675	0.3549
26	0.6978	0.6609	0.6269	0.5955	0.5665	0.5397	0.5149	0.4919	0.4705	0.4506	0.4321	0.4148	0.3987	0.3836	0.3695	0.3563	0.3440
27	0.6889	0.6513	0.6168	0.5850	0.5557	0.5287	0.5037	0.4806	0.4592	0.4394	0.4209	0.4037	0.3877	0.3728	0.3588	0.3458	0.3335
28	0.6801	0.6419	0.6069	0.5748	0.5452	0.5180	0.4929	0.4698	0.4484	0.4286	0.4102	0.3931	0.3772	0.3624	0.3486	0.3357	0.3237
29	0.6715	0.6327	0.5972	0.5648	0.5350	0.5077	0.4825	0.4593	0.4379	0.4182	0.3999	0.3829	0.3671	0.3525	0.3389	0.3261	0.3143
30	0.6631	0.6237	0.5878	0.5550	0.5251	0.4976	0.4724	0.4492	0.4279	0.4082	0.3900	0.3731	0.3575	0.3430	0.3296	0.3170	0.3053
31	0.6548	0.6149	0.5786	0.5456	0.5154	0.4879	0.4626	0.4394	0.4182	0.3986	0.3805	0.3638	0.3483	0.3340	0.3207	0.3083	0.2968
32	0.6466	0.6062	0.5696	0.5363	0.5060	0.4784	0.4531	0.4300	0.4088	0.3893	0.3714	0.3548	0.3395	0.3254	0.3122	0.3000	0.2887
33	0.6386	0.5978	0.5608	0.5273	0.4969	0.4692	0.4440	0.4209	0.3998	0.3804	0.3626	0.3462	0.3311	0.3171	0.3041	0.2921	0.2810
34	0.6308	0.5895	0.5522	0.5185	0.4880	0.4603	0.4351	0.4121	0.3911	0.3718	0.3542	0.3379	0.3230	0.3092	0.2964	0.2846	0.2736
35	0.6231	0.5814	0.5438	0.5100	0.4794	0.4517	0.4265	0.4036	0.3827	0.3636	0.3461	0.3300	0.3152	0.3016	0.2890	0.2774	0.2666
36	0.6155	0.5734	0.5356	0.5016	0.4710	0.4433	0.4181	0.3953	0.3745	0.3556	0.3382	0.3224	0.3078	0.2943	0.2819	0.2705	0.2598
37	0.6080	0.5656	0.5276	0.4935	0.4628	0.4351	0.4101	0.3874	0.3667	0.3479	0.3307	0.3150	0.3006	0.2873	0.2751	0.2638	0.2534
38	0.6007	0.5580	0.5198	0.4856	0.4549	0.4272	0.4022	0.3796	0.3591	0.3405	0.3235	0.3080	0.2937	0.2807	0.2686	0.2575	0.2473
39	0.5935	0.5505	0.5121	0.4778	0.4471	0.4195	0.3946	0.3722	0.3518	0.3334	0.3165	0.3012	0.2871	0.2742	0.2624	0.2515	0.2414
40	0.5865	0.5431	0.5046	0.4703	0.4396	0.4120	0.3873	0.3650	0.3448	0.3265	0.3098	0.2946	0.2808	0.2681	0.2564	0.2457	0.2358
41	0.5795	0.5359	0.4973	0.4629	0.4322	0.4048	0.3801	0.3580	0.3379	0.3198	0.3033	0.2883	0.2747	0.2622	0.2507	0.2401	0.2304
42	0.5727	0.5289	0.4903	0.4557	0.4251	0.3977	0.3732	0.3512	0.3313	0.3134	0.2971	0.2823	0.2688	0.2565	0.2452	0.2348	0.2252
43	0.5660	0.5220	0.4831	0.4487	0.4181	0.3909	0.3665	0.3446	0.3249	0.3072	0.2911	0.2765	0.2631	0.2510	0.2399	0.2296	0.2202
44	0.5594	0.5152	0.4763	0.4419	0.4113	0.3842	0.3600	0.3382	0.3187	0.3012	0.2852	0.2708	0.2577	0.2457	0.2348	0.2247	0.2155
45	0.5530	0.5086	0.4696	0.4352	0.4047	0.3777	0.3536	0.3321	0.3127	0.2953	0.2796	0.2654	0.2525	0.2407	0.2299	0.2200	0.2109
46	0.5466	0.5021	0.4630	0.4286	0.3983	0.3714	0.3475	0.3261	0.3069	0.2897	0.2742	0.2602	0.2472	0.2358	0.2252	0.2154	0.2065
47	0.5404	0.4957	0.4566	0.4223	0.3920	0.3653	0.3415	0.3203	0.3013	0.2843	0.2690	0.2551	0.2425	0.2311	0.2206	0.2111	0.2023
48	0.5342	0.4894	0.4503	0.4160	0.3859	0.3593	0.3357	0.3147	0.2959	0.2791	0.2639	0.2502	0.2378	0.2265	0.2162	0.2068	0.1982
49	0.5282	0.4833	0.4442	0.4100	0.3799	0.3535	0.3300	0.3092	0.2906	0.2740	0.2590	0.2455	0.2333	0.2222	0.2120	0.2028	0.1943
50	0.5223	0.4773	0.4382	0.4040	0.3741	0.3478	0.3246	0.3039	0.2855	0.2691	0.2543	0.2409	0.2289	0.2179	0.2080	0.1989	0.1905

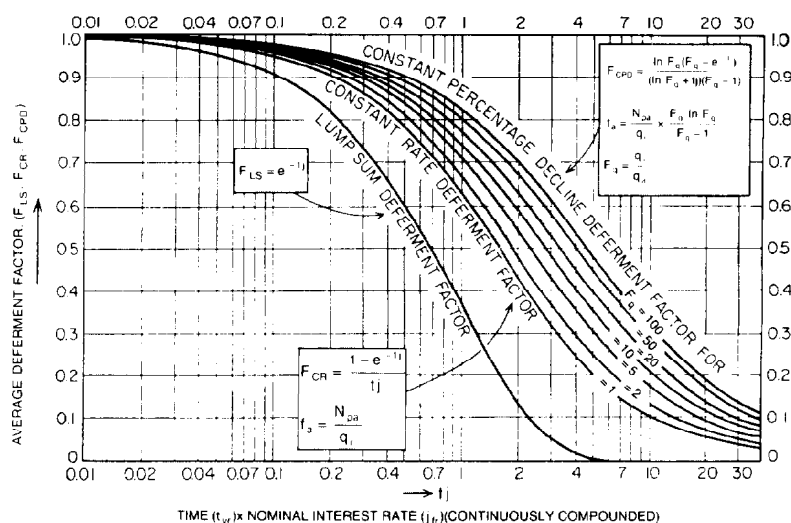


Fig. 41.9—Deferment factors for lump-sum, constant-rate, and constant-percentage decline.

TABLE 41.13—CONSTANT-RATE DEFERMENT FACTORS $F_{CR} = (1+i)^{1/2} - (1+i)^{1/2-t}/ti$ (continued)

Each Annual Income Received in One Payment at Midyear

Year	11½%	12%	12½%	13%	13½%	14%	14½%	15%	15½%	16%	16½%	17%	17½%	18%	18½%	19%	19½%	20%
1	0.9470	0.9449	0.9428	0.9407	0.9386	0.9366	0.9345	0.9325	0.9305	0.9285	0.9265	0.9245	0.9225	0.9206	0.9186	0.9167	0.9148	0.9129
2	0.8982	0.8943	0.8904	0.8866	0.8828	0.8791	0.8754	0.8717	0.8680	0.8644	0.8609	0.8573	0.8538	0.8504	0.8469	0.8435	0.8401	0.8368
3	0.8527	0.8473	0.8419	0.8366	0.8314	0.8263	0.8212	0.8162	0.8112	0.8063	0.8015	0.7967	0.7920	0.7873	0.7827	0.7781	0.7736	0.7692
4	0.8103	0.8036	0.7970	0.7905	0.7841	0.7777	0.7715	0.7654	0.7594	0.7534	0.7476	0.7418	0.7361	0.7305	0.7250	0.7196	0.7142	0.7090
5	0.7708	0.7630	0.7553	0.7478	0.7404	0.7331	0.7260	0.7190	0.7121	0.7053	0.6987	0.6921	0.6857	0.6794	0.6732	0.6671	0.6611	0.6552
6	0.7339	0.7252	0.7166	0.7082	0.7000	0.6920	0.6841	0.6764	0.6688	0.6614	0.6542	0.6470	0.6401	0.6332	0.6265	0.6199	0.6135	0.6072
7	0.6995	0.6900	0.6807	0.6716	0.6628	0.6541	0.6456	0.6374	0.6293	0.6214	0.6137	0.6061	0.5987	0.5915	0.5844	0.5775	0.5707	0.5641
8	0.6673	0.6572	0.6473	0.6376	0.6283	0.6191	0.6102	0.6015	0.5930	0.5848	0.5767	0.5688	0.5612	0.5537	0.5464	0.5392	0.5322	0.5254
9	0.6372	0.6265	0.6162	0.6061	0.5963	0.5868	0.5776	0.5686	0.5598	0.5513	0.5430	0.5349	0.5270	0.5194	0.5119	0.5046	0.4975	0.4906
10	0.6090	0.5980	0.5872	0.5768	0.5667	0.5569	0.5474	0.5382	0.5292	0.5206	0.5121	0.5039	0.4959	0.4882	0.4806	0.4733	0.4662	0.4593
11	0.5827	0.5713	0.5602	0.5496	0.5393	0.5293	0.5196	0.5102	0.5012	0.4924	0.4838	0.4756	0.4676	0.4598	0.4522	0.4449	0.4378	0.4309
12	0.5579	0.5463	0.5351	0.5242	0.5137	0.5036	0.4939	0.4844	0.4753	0.4665	0.4579	0.4496	0.4416	0.4339	0.4264	0.4191	0.4121	0.4052
13	0.5347	0.5229	0.5115	0.5006	0.4900	0.4798	0.4700	0.4606	0.4514	0.4426	0.4341	0.4259	0.4179	0.4102	0.4028	0.3956	0.3887	0.3819
14	0.5130	0.5010	0.4896	0.4785	0.4679	0.4577	0.4479	0.4385	0.4294	0.4206	0.4122	0.4040	0.3962	0.3886	0.3813	0.3742	0.3674	0.3608
15	0.4925	0.4805	0.4690	0.4580	0.4474	0.4372	0.4274	0.4180	0.4090	0.4003	0.3920	0.3839	0.3762	0.3687	0.3615	0.3546	0.3479	0.3414
16	0.4733	0.4613	0.4498	0.4388	0.4282	0.4181	0.4084	0.3991	0.3901	0.3816	0.3733	0.3654	0.3578	0.3505	0.3434	0.3366	0.3301	0.3238
17	0.4552	0.4432	0.4317	0.4208	0.4103	0.4003	0.3907	0.3815	0.3727	0.3642	0.3561	0.3483	0.3409	0.3337	0.3268	0.3202	0.3138	0.3077
18	0.4382	0.4262	0.4148	0.4039	0.3936	0.3836	0.3741	0.3651	0.3564	0.3481	0.3402	0.3325	0.3252	0.3182	0.3115	0.3050	0.2988	0.2929
19	0.4222	0.4103	0.3989	0.3882	0.3779	0.3681	0.3588	0.3498	0.3413	0.3332	0.3254	0.3179	0.3108	0.3039	0.2974	0.2911	0.2851	0.2793
20	0.4071	0.3952	0.3840	0.3734	0.3632	0.3536	0.3444	0.3356	0.3273	0.3193	0.3117	0.3044	0.2974	0.2907	0.2843	0.2782	0.2723	0.2667
21	0.3928	0.3811	0.3700	0.3595	0.3495	0.3400	0.3310	0.3224	0.3142	0.3063	0.2989	0.2918	0.2850	0.2785	0.2723	0.2663	0.2606	0.2552
22	0.3793	0.3677	0.3568	0.3464	0.3366	0.3272	0.3184	0.3100	0.3019	0.2943	0.2870	0.2801	0.2734	0.2671	0.2611	0.2553	0.2498	0.2445
23	0.3666	0.3551	0.3444	0.3341	0.3245	0.3153	0.3066	0.2983	0.2905	0.2830	0.2759	0.2692	0.2627	0.2566	0.2507	0.2451	0.2397	0.2345
24	0.3545	0.3433	0.3326	0.3226	0.3131	0.3041	0.2956	0.2875	0.2798	0.2725	0.2656	0.2590	0.2527	0.2467	0.2410	0.2355	0.2303	0.2253
25	0.3431	0.3320	0.3215	0.3117	0.3023	0.2935	0.2852	0.2773	0.2698	0.2627	0.2559	0.2495	0.2434	0.2375	0.2320	0.2267	0.2216	0.2168
26	0.3323	0.3214	0.3111	0.3014	0.2922	0.2836	0.2754	0.2677	0.2604	0.2534	0.2469	0.2406	0.2346	0.2290	0.2236	0.2184	0.2135	0.2088
27	0.3221	0.3113	0.3012	0.2917	0.2827	0.2742	0.2663	0.2587	0.2516	0.2448	0.2384	0.2323	0.2265	0.2210	0.2157	0.2107	0.2059	0.2014
28	0.3124	0.3018	0.2918	0.2825	0.2737	0.2654	0.2576	0.2502	0.2432	0.2366	0.2304	0.2244	0.2188	0.2134	0.2083	0.2035	0.1988	0.1944
29	0.3031	0.2927	0.2830	0.2738	0.2652	0.2571	0.2495	0.2422	0.2354	0.2290	0.2229	0.2171	0.2116	0.2064	0.2014	0.1967	0.1922	0.1879
30	0.2944	0.2842	0.2746	0.2656	0.2572	0.2492	0.2418	0.2347	0.2281	0.2218	0.2158	0.2102	0.2048	0.1996	0.1949	0.1903	0.1860	0.1818
31	0.2861	0.2760	0.2666	0.2578	0.2495	0.2418	0.2345	0.2276	0.2211	0.2150	0.2092	0.2037	0.1985	0.1935	0.1888	0.1844	0.1801	0.1761
32	0.2781	0.2683	0.2590	0.2504	0.2423	0.2347	0.2276	0.2209	0.2145	0.2085	0.2029	0.1975	0.1925	0.1876	0.1831	0.1787	0.1746	0.1707
33	0.2706	0.2609	0.2519	0.2434	0.2355	0.2280	0.2211	0.2145	0.2083	0.2025	0.1969	0.1917	0.1868	0.1821	0.1777	0.1734	0.1694	0.1656
34	0.2634	0.2539	0.2450	0.2367	0.2290	0.2217	0.2149	0.2085	0.2024	0.1967	0.1913	0.1862	0.1814	0.1769	0.1725	0.1684	0.1645	0.1608
35	0.2565	0.2472	0.2385	0.2304	0.2228	0.2157	0.2090	0.2027	0.1968	0.1913	0.1860	0.1810	0.1763	0.1719	0.1677	0.1637	0.1599	0.1562
36	0.2500	0.2408	0.2323	0.2244	0.2169	0.2100	0.2034	0.1973	0.1915	0.1861	0.1810	0.1761	0.1715	0.1672	0.1631	0.1592	0.1555	0.1519
37	0.2437	0.2348	0.2264	0.2186	0.2113	0.2045	0.1981	0.1921	0.1865	0.1812	0.1762	0.1714	0.1670	0.1627	0.1587	0.1549	0.1513	0.1479
38	0.2378	0.2290	0.2208	0.2131	0.2060	0.1993	0.1931	0.1872	0.1817	0.1765	0.1716	0.1670	0.1626	0.1585	0.1546	0.1509	0.1474	0.1440
39	0.2321	0.2234	0.2154	0.2079	0.2009	0.1944	0.1883	0.1825	0.1771	0.1721	0.1673	0.1628	0.1585	0.1545	0.1507	0.1470	0.1436	0.1403
40	0.2266	0.2181	0.2102	0.2029	0.1960	0.1897	0.1837	0.1781	0.1728	0.1678	0.1632	0.1588	0.1546	0.1507	0.1469	0.1434	0.1400	0.1368
41	0.2214	0.2130	0.2053	0.1981	0.1914	0.1851	0.1793	0.1738	0.1687	0.1638	0.1592	0.1549	0.1509	0.1470	0.1434	0.1399	0.1366	0.1335
42	0.2164	0.2082	0.2006	0.1935	0.1870	0.1808	0.1751	0.1697	0.1647	0.1600	0.1555	0.1513	0.1473	0.1436	0.1400	0.1366	0.1334	0.1303
43	0.2116	0.2035	0.1961	0.1892	0.1827	0.1767	0.1711	0.1659	0.1609	0.1563	0.1519	0.1478	0.1439	0.1402	0.1367	0.1334	0.1303	0.1273
44	0.2069	0.1991	0.1918	0.1850	0.1787	0.1728	0.1673	0.1621	0.1573	0.1528	0.1485	0.1445	0.1407	0.1371	0.1337	0.1304	0.1274	0.1244
45	0.2025	0.1948	0.1876	0.1810	0.1748	0.1690	0.1636	0.1586	0.1538	0.1494	0.1452	0.1413	0.1376	0.1340	0.1307	0.1275	0.1245	0.1217
46	0.1983	0.1907	0.1836	0.1771	0.1710	0.1654	0.1601	0.1552	0.1505	0.1462	0.1421	0.1382	0.1346	0.1311	0.1279	0.1248	0.1218	0.1190
47	0.1942	0.1867	0.1798	0.1734	0.1675	0.1619	0.1567	0.1519	0.1474	0.1431	0.1391	0.1353	0.1317	0.1283	0.1252	0.1221	0.1192	0.1165
48	0.1903	0.1829	0.1762	0.1699	0.1640	0.1586	0.1535	0.1488	0.1443	0.1401	0.1362	0.1325	0.1290	0.1257	0.1226	0.1196	0.1168	0.1141
49	0.1865	0.1793	0.1726	0.1665	0.1607	0.1554	0.1504	0.1457	0.1414	0.1373	0.1334	0.1298	0.1264	0.1231	0.1201	0.1171	0.1144	0.1118
50	0.1828	0.1758	0.1692	0.1632	0.1576	0.1523	0.1474	0.1429	0.1386	0.1345	0.1308	0.1272	0.1238	0.1207	0.1177	0.1148	0.1121	0.1095

Hyperbolic-Decline Deferment Factor, F_{Hy}

This is the ratio of the present value or present worth of a series of future payments that follow hyperbolic decline (decline proportional to a fractional power of the production rate) and the total amount of such payments.

For continuous compounding ($M=\infty$) at a nominal interest rate j the average deferment factor is¹⁹

$$F_{Hy} = \frac{\sqrt{F_q} - e^{-tj}}{\sqrt{F_q} - 1} - \frac{tj\sqrt{F_q} e^{(F_q-1)tj}}{(\sqrt{F_q} - 1)^2} \times \left[Ei\left(\frac{tj}{\sqrt{F_q} - 1}\right) - Ei\left(\frac{tj\sqrt{F_q}}{\sqrt{F_q} - 1}\right) \right], \dots (40)$$

where t =future life (in years) determined from Eq. 64 or 65 of Chap. 40.

$$t = \frac{N_{pa}}{q_i} \sqrt{F_q} = \frac{2(\sqrt{F_q} - 1)}{a_i}$$

The hyperbolic-decline deferment factors for such continuous compounding of interest may be read from the graph in Fig. 41.10 for given values of ratio F_q and product tj .

Harmonic-Decline Deferment Factor F_{Ha}

This is the ratio of the present value or present worth of a series of future payments that follow harmonic decline (decline proportional to the production rate) and the total

TABLE 41.14—ANNUAL DEFERMENT FACTORS $F_{CR} = (1+i)^{1-t} - (1+i)^{-t}/12[(1+i)^{1/2} - 1]$

Annual Deferral Factors are Applicable to Equal Payments Received at the End of Each Month
During a Specific Interval of 1 Year Between $(t-1)$ and t Years From Now

Year	3%	3½%	4%	4½%	5%	5½%	6%	6½%	7%	7½%	8%	8½%	9%	9½%	10%	10½%	11%	11½%
1	0.9842	0.9816	0.9790	0.9765	0.9740	0.9715	0.9691	0.9666	0.9642	0.9618	0.9594	0.9570	0.9547	0.9524	0.9500	0.9477	0.9455	0.9432
2	0.9555	0.9484	0.9414	0.9345	0.9276	0.9209	0.9142	0.9076	0.9011	0.8947	0.8883	0.8821	0.8759	0.8697	0.8637	0.8577	0.8518	0.8459
3	0.9277	0.9163	0.9052	0.8942	0.8835	0.8729	0.8625	0.8522	0.8422	0.8323	0.8225	0.8130	0.8035	0.7943	0.7852	0.7762	0.7674	0.7587
4	0.9006	0.8853	0.8704	0.8557	0.8414	0.8274	0.8136	0.8002	0.7871	0.7742	0.7616	0.7493	0.7372	0.7254	0.7138	0.7024	0.6913	0.6804
5	0.8744	0.8554	0.8369	0.8189	0.8013	0.7842	0.7676	0.7514	0.7356	0.7202	0.7052	0.6906	0.6763	0.6624	0.6489	0.6357	0.6228	0.6102
6	0.8489	0.8265	0.8047	0.7836	0.7632	0.7434	0.7241	0.7055	0.6875	0.6699	0.6530	0.6365	0.6205	0.6050	0.5899	0.5753	0.5611	0.5473
7	0.8242	0.7985	0.7738	0.7499	0.7268	0.7046	0.6832	0.6625	0.6425	0.6232	0.6046	0.5866	0.5692	0.5525	0.5363	0.5206	0.5055	0.4909
8	0.8002	0.7715	0.7440	0.7176	0.6922	0.6679	0.6445	0.6220	0.6005	0.5797	0.5598	0.5407	0.5222	0.5045	0.4875	0.4711	0.4554	0.4402
9	0.7769	0.7454	0.7154	0.6867	0.6593	0.6330	0.6080	0.5841	0.5612	0.5393	0.5183	0.4983	0.4791	0.4608	0.4432	0.4264	0.4103	0.3948
10	0.7543	0.7202	0.6879	0.6571	0.6279	0.6000	0.5736	0.5484	0.5245	0.5017	0.4799	0.4593	0.4396	0.4208	0.4029	0.3859	0.3696	0.3541
11	0.7323	0.6959	0.6614	0.6288	0.5980	0.5688	0.5411	0.5149	0.4901	0.4667	0.4444	0.4233	0.4033	0.3843	0.3663	0.3492	0.3330	0.3176
12	0.7110	0.6723	0.6360	0.6017	0.5695	0.5391	0.5105	0.4835	0.4581	0.4341	0.4115	0.3901	0.3700	0.3509	0.3330	0.3160	0.3000	0.2848
13	0.6903	0.6496	0.6115	0.5758	0.5424	0.5110	0.4816	0.4540	0.4281	0.4038	0.3810	0.3596	0.3394	0.3205	0.3027	0.2860	0.2703	0.2555
14	0.6702	0.6276	0.5880	0.5510	0.5165	0.4844	0.4543	0.4263	0.4001	0.3756	0.3528	0.3314	0.3114	0.2927	0.2752	0.2588	0.2435	0.2291
15	0.6506	0.6064	0.5654	0.5273	0.4919	0.4591	0.4286	0.4003	0.3739	0.3494	0.3266	0.3054	0.2857	0.2673	0.2502	0.2342	0.2193	0.2055
16	0.6317	0.5859	0.5436	0.5046	0.4685	0.4352	0.4044	0.3758	0.3495	0.3251	0.3024	0.2815	0.2621	0.2441	0.2274	0.2120	0.1976	0.1843
17	0.6133	0.5661	0.5227	0.4829	0.4462	0.4125	0.3815	0.3529	0.3266	0.3024	0.2800	0.2594	0.2405	0.2229	0.2068	0.1918	0.1780	0.1653
18	0.5954	0.5469	0.5026	0.4621	0.4250	0.3910	0.3599	0.3314	0.3052	0.2813	0.2593	0.2391	0.2206	0.2036	0.1880	0.1736	0.1604	0.1482
19	0.5781	0.5284	0.4833	0.4422	0.4047	0.3706	0.3395	0.3111	0.2853	0.2617	0.2401	0.2204	0.2024	0.1859	0.1709	0.1571	0.1445	0.1329
20	0.5612	0.5106	0.4647	0.4231	0.3855	0.3513	0.3203	0.2922	0.2666	0.2434	0.2223	0.2031	0.1857	0.1698	0.1553	0.1422	0.1302	0.1192
21	0.5449	0.4933	0.4468	0.4049	0.3671	0.3330	0.3022	0.2743	0.2492	0.2264	0.2058	0.1872	0.1703	0.1551	0.1412	0.1287	0.1173	0.1069
22	0.5290	0.4766	0.4296	0.3875	0.3496	0.3156	0.2851	0.2576	0.2329	0.2106	0.1906	0.1725	0.1563	0.1416	0.1284	0.1164	0.1056	0.0959
23	0.5136	0.4605	0.4131	0.3708	0.3330	0.2992	0.2689	0.2419	0.2176	0.1959	0.1765	0.1590	0.1434	0.1293	0.1167	0.1054	0.0952	0.0860
24	0.4987	0.4449	0.3972	0.3548	0.3171	0.2836	0.2537	0.2271	0.2034	0.1823	0.1634	0.1466	0.1315	0.1181	0.1061	0.0954	0.0857	0.0771
25	0.4841	0.4299	0.3819	0.3395	0.3020	0.2688	0.2393	0.2132	0.1901	0.1695	0.1513	0.1351	0.1207	0.1079	0.0965	0.0863	0.0772	0.0692
26	0.4700	0.4154	0.3673	0.3249	0.2876	0.2548	0.2258	0.2002	0.1777	0.1577	0.1401	0.1245	0.1107	0.0985	0.0877	0.0781	0.0696	0.0620
27	0.4563	0.4013	0.3531	0.3109	0.2739	0.2415	0.2130	0.1880	0.1660	0.1467	0.1297	0.1148	0.1016	0.0900	0.0797	0.0707	0.0627	0.0556
28	0.4431	0.3877	0.3395	0.2975	0.2609	0.2289	0.2010	0.1765	0.1552	0.1365	0.1201	0.1058	0.0932	0.0822	0.0725	0.0640	0.0565	0.0499
29	0.4302	0.3746	0.3265	0.2847	0.2485	0.2170	0.1896	0.1658	0.1450	0.1270	0.1112	0.0975	0.0855	0.0750	0.0659	0.0579	0.0509	0.0448
30	0.4176	0.3620	0.3139	0.2725	0.2366	0.2057	0.1788	0.1556	0.1355	0.1181	0.1030	0.0898	0.0784	0.0685	0.0599	0.0524	0.0458	0.0401
31	0.4055	0.3497	0.3019	0.2607	0.2254	0.1949	0.1687	0.1461	0.1267	0.1099	0.0953	0.0828	0.0720	0.0626	0.0544	0.0474	0.0413	0.0360
32	0.3936	0.3379	0.2902	0.2495	0.2146	0.1848	0.1592	0.1372	0.1184	0.1022	0.0883	0.0763	0.0660	0.0571	0.0495	0.0429	0.0372	0.0323
33	0.3822	0.3265	0.2791	0.2388	0.2044	0.1751	0.1502	0.1288	0.1106	0.0951	0.0817	0.0703	0.0606	0.0522	0.0450	0.0388	0.0335	0.0290
34	0.3711	0.3154	0.2683	0.2285	0.1947	0.1660	0.1417	0.1210	0.1034	0.0884	0.0757	0.0648	0.0556	0.0477	0.0409	0.0351	0.0302	0.0260
35	0.3602	0.3048	0.2580	0.2186	0.1854	0.1574	0.1336	0.1136	0.0966	0.0823	0.0701	0.0597	0.0510	0.0435	0.0372	0.0318	0.0272	0.0233
36	0.3498	0.2945	0.2481	0.2092	0.1766	0.1491	0.1261	0.1067	0.0903	0.0765	0.0649	0.0551	0.0468	0.0397	0.0338	0.0288	0.0245	0.0209
37	0.3396	0.2845	0.2386	0.2002	0.1682	0.1414	0.1189	0.1002	0.0844	0.0712	0.0601	0.0508	0.0429	0.0363	0.0307	0.0260	0.0221	0.0187
38	0.3297	0.2749	0.2294	0.1916	0.1602	0.1340	0.1122	0.0940	0.0789	0.0662	0.0556	0.0468	0.0394	0.0331	0.0279	0.0236	0.0199	0.0168
39	0.3201	0.2656	0.2206	0.1833	0.1525	0.1270	0.1059	0.0883	0.0737	0.0616	0.0515	0.0431	0.0361	0.0303	0.0254	0.0213	0.0179	0.0151
40	0.3107	0.2566	0.2121	0.1754	0.1453	0.1204	0.0999	0.0829	0.0689	0.0573	0.0477	0.0397	0.0331	0.0276	0.0231	0.0193	0.0161	0.0135
41	0.3017	0.2479	0.2039	0.1679	0.1384	0.1141	0.0942	0.0779	0.0644	0.0533	0.0442	0.0366	0.0304	0.0252	0.0210	0.0175	0.0145	0.0121
42	0.2929	0.2395	0.1961	0.1607	0.1318	0.1082	0.0889	0.0731	0.0602	0.0496	0.0409	0.0338	0.0279	0.0231	0.0191	0.0158	0.0131	0.0109
43	0.2844	0.2314	0.1885	0.1537	0.1255	0.1025	0.0839	0.0686	0.0562	0.0461	0.0379	0.0311	0.0256	0.0211	0.0173	0.0143	0.0118	0.0098
44	0.2761	0.2236	0.1813	0.1471	0.1195	0.0972	0.0791	0.0645	0.0526	0.0429	0.0351	0.0287	0.0235	0.0192	0.0158	0.0129	0.0106	0.0087
45	0.2681	0.2160	0.1743	0.1408	0.1138	0.0921	0.0746	0.0605	0.0491	0.0399	0.0325	0.0264	0.0215	0.0176	0.0143	0.0117	0.0096	0.0078
46	0.2602	0.2087	0.1676	0.1347	0.1084	0.0873	0.0704	0.0568	0.0459	0.0371	0.0301	0.0244	0.0198	0.0160	0.0130	0.0106	0.0086	0.0070
47	0.2527	0.2017	0.1612	0.1289	0.1032	0.0828	0.0664	0.0534	0.0429	0.0345	0.0278	0.0224	0.0181	0.0146	0.0118	0.0096	0.0078	0.0063
48	0.2453	0.1949	0.1550	0.1234	0.0983	0.0784	0.0627	0.0501	0.0401	0.0321	0.0258	0.0207	0.0166	0.0134	0.0108	0.0087	0.0070	0.0057
49	0.2382	0.1883	0.1490	0.1181	0.0936	0.0744	0.0591	0.0470	0.0375	0.0299	0.0239	0.0191	0.0153	0.0122	0.0098	0.0079	0.0063	0.0051
50	0.2312	0.1819	0.1433	0.1130	0.0892	0.0705	0.0558	0.0442	0.0350	0.0278	0.0221	0.0176	0.0140	0.0112	0.0089	0.0071	0.0057	0.0046

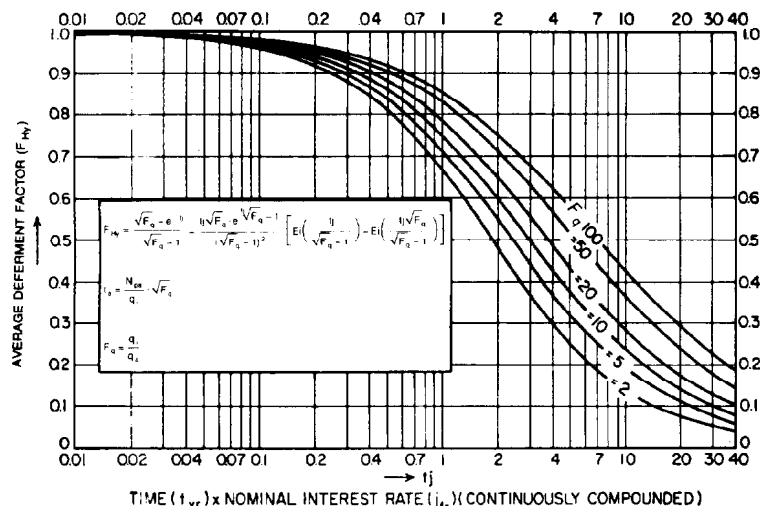
**Fig. 41.10—Deferment factors for hyperbolic decline ($n = 1/2$).**

TABLE 41.14—ANNUAL DEFERMENT FACTORS $F_{CR} = (1+i)^{1-t} - (1+i)^{-t}/12[(1+i)^{1/2} - 1]$ (continued)

Annual Deferment Factors are Applicable to Equal Payments Received at the End of Each Month
During a Specific Interval of 1 Year Between $(t-1)$ and t Years From Now

12%	12½%	13%	13½%	14%	14½%	15%	15½%	16%	16½%	17%	17½%	18%	18½%	19%	19½%	20%
0.9410	0.9387	0.9365	0.9343	0.9322	0.9300	0.9278	0.9257	0.9236	0.9215	0.9194	0.9173	0.9153	0.9132	0.9112	0.9092	0.9072
0.8401	0.8344	0.8288	0.8232	0.8177	0.8122	0.8068	0.8015	0.7962	0.7910	0.7858	0.7807	0.7757	0.7707	0.7657	0.7608	0.7560
0.7501	0.7417	0.7334	0.7253	0.7173	0.7094	0.7016	0.6939	0.6864	0.6790	0.6716	0.6644	0.6573	0.6504	0.6435	0.6367	0.6300
0.6698	0.6593	0.6491	0.6390	0.6292	0.6195	0.6101	0.6008	0.5917	0.5828	0.5741	0.5655	0.5571	0.5488	0.5407	0.5328	0.5250
0.5980	0.5860	0.5744	0.5630	0.5519	0.5411	0.5305	0.5202	0.5101	0.5003	0.4906	0.4813	0.4721	0.4631	0.4544	0.4459	0.4375
0.5339	0.5209	0.5083	0.4960	0.4841	0.4725	0.4613	0.4504	0.4397	0.4294	0.4194	0.4096	0.4001	0.3908	0.3818	0.3731	0.3646
0.4767	0.4630	0.4498	0.4370	0.4247	0.4127	0.4011	0.3899	0.3791	0.3686	0.3584	0.3486	0.3390	0.3298	0.3209	0.3122	0.3038
0.4256	0.4116	0.3981	0.3851	0.3725	0.3604	0.3488	0.3376	0.3268	0.3164	0.3063	0.2967	0.2873	0.2783	0.2696	0.2613	0.2532
0.3800	0.3659	0.3523	0.3393	0.3268	0.3148	0.3033	0.2923	0.2817	0.2716	0.2618	0.2525	0.2435	0.2349	0.2266	0.2186	0.2110
0.3393	0.3252	0.3118	0.2989	0.2866	0.2749	0.2637	0.2531	0.2429	0.2331	0.2238	0.2149	0.2064	0.1982	0.1904	0.1830	0.1758
0.3030	0.2891	0.2759	0.2634	0.2514	0.2401	0.2293	0.2191	0.2094	0.2001	0.1913	0.1829	0.1749	0.1673	0.1600	0.1531	0.1465
0.2705	0.2570	0.2441	0.2320	0.2206	0.2097	0.1994	0.1897	0.1805	0.1718	0.1635	0.1556	0.1482	0.1412	0.1345	0.1281	0.1221
0.2415	0.2284	0.2161	0.2044	0.1935	0.1832	0.1734	0.1642	0.1556	0.1474	0.1397	0.1325	0.1256	0.1191	0.1130	0.1072	0.1017
0.2156	0.2030	0.1912	0.1801	0.1697	0.1600	0.1508	0.1422	0.1341	0.1265	0.1194	0.1127	0.1064	0.1005	0.0950	0.0897	0.0848
0.1925	0.1805	0.1692	0.1587	0.1489	0.1397	0.1311	0.1231	0.1156	0.1086	0.1021	0.0959	0.0902	0.0848	0.0796	0.0751	0.0707
0.1719	0.1604	0.1497	0.1398	0.1306	0.1220	0.1140	0.1066	0.0997	0.0932	0.0872	0.0817	0.0764	0.0716	0.0671	0.0628	0.0589
0.1535	0.1426	0.1325	0.1232	0.1146	0.1066	0.0992	0.0923	0.0859	0.0800	0.0746	0.0695	0.0648	0.0604	0.0563	0.0526	0.0491
0.1370	0.1267	0.1173	0.1085	0.1005	0.0931	0.0862	0.0799	0.0741	0.0687	0.0637	0.0591	0.0549	0.0510	0.0474	0.0440	0.0409
0.1224	0.1127	0.1038	0.0956	0.0881	0.0813	0.0750	0.0692	0.0639	0.0590	0.0545	0.0503	0.0465	0.0430	0.0398	0.0368	0.0341
0.1093	0.1001	0.0918	0.0843	0.0773	0.0710	0.0652	0.0599	0.0551	0.0506	0.0466	0.0428	0.0394	0.0363	0.0334	0.0308	0.0284
0.0975	0.0890	0.0813	0.0742	0.0678	0.0620	0.0567	0.0519	0.0475	0.0434	0.0398	0.0365	0.0334	0.0306	0.0281	0.0258	0.0237
0.0871	0.0791	0.0719	0.0654	0.0595	0.0541	0.0493	0.0449	0.0409	0.0373	0.0340	0.0310	0.0283	0.0259	0.0236	0.0216	0.0197
0.0778	0.0703	0.0636	0.0576	0.0522	0.0473	0.0429	0.0389	0.0353	0.0320	0.0291	0.0264	0.0240	0.0218	0.0198	0.0181	0.0164
0.0694	0.0625	0.0563	0.0508	0.0458	0.0413	0.0373	0.0337	0.0304	0.0275	0.0248	0.0225	0.0203	0.0184	0.0167	0.0151	0.0137
0.0620	0.0556	0.0498	0.0447	0.0402	0.0361	0.0324	0.0291	0.0262	0.0236	0.0212	0.0191	0.0172	0.0155	0.0140	0.0126	0.0114
0.0554	0.0494	0.0441	0.0394	0.0352	0.0315	0.0282	0.0252	0.0226	0.0202	0.0181	0.0163	0.0146	0.0131	0.0118	0.0106	0.0095
0.0494	0.0439	0.0390	0.0347	0.0309	0.0275	0.0245	0.0218	0.0195	0.0174	0.0155	0.0139	0.0124	0.0111	0.0099	0.0089	0.0079
0.0441	0.0390	0.0345	0.0306	0.0271	0.0240	0.0213	0.0189	0.0168	0.0149	0.0133	0.0118	0.0105	0.0093	0.0083	0.0074	0.0066
0.0394	0.0347	0.0306	0.0270	0.0238	0.0210	0.0185	0.0164	0.0145	0.0128	0.0113	0.0100	0.0089	0.0079	0.0070	0.0062	0.0055
0.0352	0.0308	0.0271	0.0237	0.0209	0.0183	0.0161	0.0142	0.0125	0.0110	0.0097	0.0085	0.0075	0.0066	0.0059	0.0052	0.0046
0.0314	0.0274	0.0239	0.0209	0.0183	0.0160	0.0140	0.0123	0.0108	0.0094	0.0083	0.0073	0.0064	0.0056	0.0049	0.0043	0.0038
0.0280	0.0244	0.0212	0.0184	0.0160	0.0140	0.0122	0.0106	0.0093	0.0081	0.0071	0.0062	0.0054	0.0047	0.0041	0.0036	0.0032
0.0250	0.0217	0.0188	0.0162	0.0141	0.0122	0.0106	0.0092	0.0080	0.0070	0.0060	0.0053	0.0046	0.0040	0.0035	0.0030	0.0027
0.0224	0.0193	0.0166	0.0143	0.0123	0.0107	0.0092	0.0080	0.0069	0.0060	0.0052	0.0045	0.0039	0.0034	0.0029	0.0025	0.0022
0.0200	0.0171	0.0147	0.0126	0.0108	0.0093	0.0080	0.0069	0.0059	0.0051	0.0044	0.0038	0.0033	0.0028	0.0025	0.0021	0.0018
0.0178	0.0152	0.0130	0.0111	0.0095	0.0081	0.0070	0.0060	0.0051	0.0044	0.0038	0.0032	0.0028	0.0024	0.0021	0.0018	0.0015
0.0159	0.0135	0.0115	0.0098	0.0083	0.0071	0.0061	0.0052	0.0044	0.0038	0.0032	0.0028	0.0024	0.0020	0.0017	0.0015	0.0013
0.0142	0.0120	0.0102	0.0086	0.0073	0.0062	0.0053	0.0045	0.0038	0.0032	0.0028	0.0024	0.0020	0.0017	0.0015	0.0012	0.0011
0.0127	0.0107	0.0090	0.0076	0.0064	0.0054	0.0046	0.0039	0.0033	0.0028	0.0024	0.0020	0.0017	0.0014	0.0012	0.0010	0.0009
0.0113	0.0095	0.0080	0.0067	0.0056	0.0047	0.0040	0.0034	0.0028	0.0024	0.0020	0.0017	0.0014	0.0012	0.0010	0.0009	0.0007
0.0101	0.0084	0.0071	0.0059	0.0049	0.0041	0.0035	0.0029	0.0024	0.0020	0.0017	0.0014	0.0012	0.0010	0.0009	0.0007	0.0006
0.0090	0.0075	0.0062	0.0052	0.0043	0.0036	0.0030	0.0025	0.0021	0.0018	0.0015	0.0012	0.0010	0.0009	0.0007	0.0006	0.0005
0.0081	0.0067	0.0055	0.0046	0.0038	0.0032	0.0026	0.0022	0.0018	0.0015	0.0013	0.0010	0.0009	0.0007	0.0006	0.0005	0.0004
0.0072	0.0059	0.0049	0.0040	0.0033	0.0028	0.0023	0.0019	0.0016	0.0013	0.0011	0.0009	0.0007	0.0006	0.0005	0.0004	0.0004
0.0064	0.0053	0.0043	0.0036	0.0029	0.0024	0.0020	0.0016	0.0013	0.0011	0.0009	0.0008	0.0006	0.0005	0.0004	0.0004	0.0003
0.0057	0.0047	0.0038	0.0031	0.0026	0.0021	0.0017	0.0014	0.0012	0.0010	0.0008	0.0006	0.0005	0.0004	0.0004	0.0003	0.0002
0.0051	0.0042	0.0034	0.0028	0.0022	0.0018	0.0015	0.0012	0.0010	0.0008	0.0007	0.0006	0.0005	0.0004	0.0003	0.0003	0.0002
0.0046	0.0037	0.0030	0.0024	0.0020	0.0016	0.0013	0.0011	0.0009	0.0007	0.0006	0.0005	0.0004	0.0003	0.0003	0.0002	0.0002
0.0041	0.0033	0.0027	0.0021	0.0017	0.0014	0.0011	0.0009	0.0007	0.0006	0.0005	0.0004	0.0003	0.0003	0.0002	0.0002	0.0001
0.0036	0.0029	0.0023	0.0019	0.0015	0.0012	0.0010	0.0008	0.0006	0.0005	0.0004	0.0003	0.0003	0.0002	0.0002	0.0001	0.0001

amount of such payments. For continuous compounding ($M = \infty$) at a nominal interest rate (j), the average deferment factor is¹⁷

$$\bar{F}_{Ha} = \frac{e^{t_a j / (F_q - 1)}}{\ln F_q} \left[Ei \left(\frac{t_a j}{F_q - 1} \right) - Ei \left(\frac{t_a j F_q}{F_q - 1} \right) \right], \quad (41)$$

where

$$t_a = \frac{N_{pa} (F_q - 1)}{q_i \ln F_q}.$$

The harmonic-decline deferment factors for such continuous compounding of interest may be read directly from the graph in Fig. 41.11 for given values of ratio F_q and tj .

Calculation of Loan Payout

In the preparation of an engineering report, it is sometimes necessary to include a projection of future income and a payout schedule for a proposed loan. To prepare such a payout schedule, the balance of the loan at the end of each year or period must be determined.

A calculation procedure has been suggested by Wilson and Boyd²¹ based on the following assumptions: (1) the principal amount of the loan is growing by virtue of monthly compounding of interest; (2) the loan payments during any year are made in equal monthly installments that are deposited at the end of each calendar month; and (3) both the principal and the loan payments bear interest compounded monthly at the nominal annual interest rate of the loan.

Wilson and Boyd use two numerical factors to determine the balance at the end of each year. These are listed in Table 41.15.

Factor 1 is the total value of \$1, invested at the specified annual nominal interest rate, compounded monthly. Factor 2 is the total value of \$1, invested each month,

TABLE 41.15—LOAN PAYOUT CALCULATION FACTORS

Nominal Interest Rate	Months	Factor 1	Factor 2	Nominal Interest Rate	Months	Factor 1	Factor 2
4% ($\frac{1}{3}\%$ /month)	1	1.003333	1.000000	6½% ($\frac{1}{2}\frac{1}{4}\%$ /month)	1	1.005417	1.000000
	2	1.006678	1.001667		2	1.010863	1.002709
	3	1.010033	1.003337		3	1.016338	1.005426
	4	1.013400	1.005011		4	1.021843	1.008154
	5	1.016778	1.006689		5	1.027378	1.010892
	6	1.020167	1.008370		6	1.032943	1.013640
	7	1.023568	1.010056		7	1.038538	1.016397
	8	1.026980	1.011745		8	1.044164	1.019165
	9	1.030403	1.013438		9	1.049820	1.021943
	10	1.033838	1.015134		10	1.055506	1.024730
	11	1.037284	1.016834		11	1.061224	1.027528
	12	1.040742	1.018539		12	1.066972	1.030336
4½% ($\frac{3}{8}\%$ /month)	1	1.003750	1.000000	7% ($\frac{1}{2}\%$ /month)	1	1.005833	1.000000
	2	1.007514	1.001875		2	1.011701	1.002917
	3	1.011292	1.003755		3	1.017602	1.005845
	4	1.015085	1.005639		4	1.023538	1.008784
	5	1.018891	1.007528		5	1.029509	1.011735
	6	1.022712	1.009422		6	1.035514	1.014697
	7	1.026547	1.011321		7	1.041555	1.017671
	8	1.030397	1.013224		8	1.047631	1.020657
	9	1.034261	1.015132		9	1.053742	1.023654
	10	1.038139	1.017045		10	1.059889	1.026663
	11	1.042032	1.018963		11	1.066071	1.029683
	12	1.045940	1.020885		12	1.072290	1.032715
5% ($\frac{1}{2}\%$ /month)	1	1.004167	1.000000	7½% ($\frac{1}{2}\frac{1}{4}\%$ /month)	1	1.006250	1.000000
	2	1.008351	1.002083		2	1.012539	1.003125
	3	1.012552	1.004172		3	1.018867	1.006263
	4	1.016771	1.006267		4	1.025235	1.009414
	5	1.021008	1.008368		5	1.031643	1.012578
	6	1.025262	1.010475		6	1.038091	1.015756
	7	1.029534	1.012587		7	1.044579	1.018947
	8	1.033824	1.014705		8	1.051108	1.022151
	9	1.038131	1.016830		9	1.057677	1.025368
	10	1.042457	1.018960		10	1.064287	1.028599
	11	1.046800	1.021096		11	1.070939	1.031843
	12	1.051162	1.023238		12	1.077633	1.035101
5½% ($\frac{1}{2}\frac{1}{4}\%$ /month)	1	1.004583	1.000000	8% ($\frac{2}{3}\%$ /month)	1	1.006667	1.000000
	2	1.009188	1.002292		2	1.013378	1.003333
	3	1.013813	1.004590		3	1.020134	1.006681
	4	1.018460	1.006896		4	1.026935	1.010045
	5	1.023128	1.009209		5	1.033781	1.013423
	6	1.027817	1.011529		6	1.040673	1.016816
	7	1.032528	1.013856		7	1.047610	1.020224
	8	1.037260	1.016190		8	1.054595	1.023647
	9	1.042014	1.018531		9	1.061625	1.027086
	10	1.046790	1.020879		10	1.068703	1.030540
	11	1.051588	1.023235		11	1.075827	1.034009
	12	1.056408	1.025597		12	1.083000	1.037494
6% ($\frac{1}{2}\%$ /month)	1	1.005000	1.000000	8½% ($\frac{1}{2}\frac{1}{4}\%$ /month)	1	1.007083	1.000000
	2	1.010025	1.002500		2	1.014217	1.003542
	3	1.015075	1.005008		3	1.021401	1.007100
	4	1.020151	1.007525		4	1.028636	1.010675
	5	1.025251	1.010050		5	1.035922	1.014267
	6	1.030378	1.012584		6	1.043260	1.017876
	7	1.035529	1.015126		7	1.050650	1.021503
	8	1.040707	1.017676		8	1.058092	1.025146
	9	1.045911	1.020235		9	1.065586	1.028807
	10	1.051140	1.022803		10	1.073134	1.032485
	11	1.056396	1.025379		11	1.080736	1.036180
	12	1.061678	1.027964		12	1.088391	1.039893
9% ($\frac{3}{4}\%$ /month)	1	1.007500	1.000000	11% ($\frac{1}{2}\frac{1}{2}\%$ /month)	1	1.009167	1.000000
	2	1.015056	1.003750		2	1.018417	1.004583
	3	1.022669	1.007519		3	1.027753	1.009195
	4	1.030339	1.011306		4	1.037174	1.013834
	5	1.038067	1.015113		5	1.046681	1.018502
	6	1.045852	1.018939		6	1.056276	1.023199
	7	1.053696	1.022783		7	1.065958	1.027924
	8	1.061599	1.026647		8	1.075730	1.032678
	9	1.069561	1.030531		9	1.085591	1.037462
	10	1.077583	1.034434		10	1.095542	1.042275
	11	1.085664	1.038357		11	1.105584	1.047117
	12	1.093807	1.042299		12	1.115719	1.051989

TABLE 41.15—LOAN PAYOUT CALCULATION FACTORS (continued)

Nominal Interest Rate	Months	Factor 1	Factor 2	Nominal Interest Rate	Months	Factor 1	Factor 2
9½% (¾%/month)	1	1.007917	1.000000	11½% (2¾%/month)	1	1.009583	1.000000
	2	1.015896	1.003958		2	1.019259	1.004792
	3	1.023939	1.007938		3	1.029026	1.009614
	4	1.032045	1.011938		4	1.038888	1.014467
	5	1.040215	1.015959		5	1.048844	1.019351
	6	1.048450	1.020002		6	1.058895	1.024267
	7	1.056750	1.024066		7	1.069043	1.029214
	8	1.065116	1.028151		8	1.079288	1.034192
	9	1.073548	1.032259		9	1.089631	1.039203
	10	1.082047	1.036388		10	1.100074	1.044246
	11	1.090614	1.040538		11	1.110616	1.049321
	12	1.099248	1.044711		12	1.121259	1.054429
10% (⅔%/month)	1	1.008333	1.000000	12% (1%/month)	1	1.010000	1.000000
	2	1.016736	1.004167		2	1.020100	1.005000
	3	1.025209	1.008356		3	1.030301	1.010033
	4	1.033752	1.012570		4	1.040604	1.015100
	5	1.042367	1.016806		5	1.051010	1.020201
	6	1.051053	1.021066		6	1.061520	1.025336
	7	1.059812	1.025350		7	1.072135	1.030505
	8	1.068644	1.029658		8	1.082857	1.035709
	9	1.077549	1.033990		9	1.093685	1.040947
	10	1.086529	1.038346		10	1.104622	1.046221
	11	1.095583	1.042726		11	1.115668	1.051530
	12	1.104713	1.047131		12	1.126825	1.056875
10½% (7⁄8%/month)	1	1.008750	1.000000	12½% (1¼%/month)	1	1.010417	1.000000
	2	1.017577	1.004375		2	1.020942	1.005208
	3	1.026480	1.008776		3	1.031577	1.010453
	4	1.035462	1.013202		4	1.042322	1.015734
	5	1.044522	1.017654		5	1.053180	1.021051
	6	1.053662	1.022132		6	1.064150	1.026406
	7	1.062881	1.026636		7	1.075235	1.031798
	8	1.072182	1.031167		8	1.086436	1.037228
	9	1.081563	1.035724		9	1.097753	1.042695
	10	1.091027	1.040308		10	1.109188	1.048201
	11	1.100573	1.044919		11	1.120742	1.053745
	12	1.110203	1.049557		12	1.132416	1.059328
13% (1⅓%/month)	1	1.010833	1.000000	15% (1¼%/month)	1	1.012500	1.000000
	2	1.021784	1.005417		2	1.025156	1.006250
	3	1.032853	1.010872		3	1.037971	1.012552
	4	1.044043	1.016368		4	1.050945	1.018907
	5	1.055353	1.021903		5	1.064082	1.025314
	6	1.066786	1.027478		6	1.077383	1.031776
	7	1.078343	1.033093		7	1.090850	1.038291
	8	1.090025	1.038749		8	1.104486	1.044861
	9	1.101834	1.044447		9	1.118292	1.051486
	10	1.113770	1.050185		10	1.132271	1.058167
	11	1.125836	1.055966		11	1.146424	1.064903
	12	1.138032	1.061788		12	1.160755	1.071697
13½% (1⅝%/month)	1	1.011250	1.000000	15½% (17⁄24%/month)	1	1.012917	1.000000
	2	1.022627	1.005625		2	1.026000	1.006458
	3	1.034131	1.011292		3	1.039253	1.012972
	4	1.045765	1.017002		4	1.052676	1.019542
	5	1.057530	1.022755		5	1.066273	1.026169
	6	1.069427	1.028550		6	1.080046	1.032853
	7	1.081458	1.034390		7	1.093997	1.039595
	8	1.093625	1.040274		8	1.108128	1.046395
	9	1.105928	1.046201		9	1.122441	1.053254
	10	1.118370	1.052174		10	1.136939	1.060173
	11	1.130951	1.058192		11	1.151624	1.067152
	12	1.143674	1.064255		12	1.166500	1.074191
14% (1⅞%/month)	1	1.011667	1.000000	16% (1⅓%/month)	1	1.013333	1.000000
	2	1.023469	1.005833		2	1.026844	1.006667
	3	1.035410	1.011712		3	1.040536	1.013393
	4	1.047490	1.017637		4	1.054410	1.020178
	5	1.059710	1.023607		5	1.068468	1.027025
	6	1.072074	1.029624		6	1.082715	1.033932
	7	1.084581	1.035689		7	1.097151	1.040901
	8	1.097235	1.041800		8	1.111779	1.047932
	9	1.110036	1.047960		9	1.126603	1.055026
	10	1.122986	1.054167		10	1.141625	1.062184
	11	1.136088	1.060423		11	1.156846	1.069406
	12	1.149342	1.066729		12	1.172271	1.076692

TABLE 41.15—LOAN PAYOUT CALCULATION FACTORS (continued)

Nominal Interest Rate	Months	Factor 1	Factor 2	Nominal Interest Rate	Months	Factor 1	Factor 2
14½% (1½%/month)	1	1.012083	1.000000	16½% (1¾%/month)	1	1.013750	1.000000
	2	1.024313	1.006042		2	1.027689	1.006875
	3	1.036690	1.012132		3	1.041820	1.013813
	4	1.049216	1.018271		4	1.056145	1.020815
	5	1.061894	1.024460		5	1.070667	1.027881
	6	1.074726	1.030699		6	1.085388	1.035012
	7	1.087712	1.036989		7	1.100313	1.042208
	8	1.100855	1.043329		8	1.115442	1.049471
	9	1.114157	1.049721		9	1.130779	1.056801
	10	1.127620	1.056165		10	1.146327	1.064199
	11	1.141245	1.062661		11	1.162089	1.071665
	12	1.155035	1.069209		12	1.178068	1.079201
17% (1½%/month)	1	1.014167	1.000000	19% (1½%/month)	1	1.015833	1.000000
	2	1.028534	1.007083		2	1.031917	1.007917
	3	1.043105	1.014234		3	1.048256	1.015917
	4	1.057882	1.021451		4	1.064853	1.024002
	5	1.072869	1.028738		5	1.081714	1.032172
	6	1.088068	1.036093		6	1.098841	1.040429
	7	1.103482	1.043518		7	1.116239	1.048774
	8	1.119115	1.051013		8	1.133913	1.057207
	9	1.134969	1.058580		9	1.151866	1.065730
	10	1.151048	1.066219		10	1.170104	1.074343
	11	1.167354	1.073931		11	1.188631	1.083049
	12	1.183892	1.081716		12	1.207451	1.091847
17½% (1½%/month)	1	1.014583	1.000000	19½% (1½%/month)	1	1.016250	1.000000
	2	1.029379	1.007292		2	1.032764	1.008125
	3	1.044391	1.014654		3	1.049546	1.016338
	4	1.059622	1.022088		4	1.066602	1.024640
	5	1.075075	1.029595		5	1.083934	1.033032
	6	1.090753	1.037175		6	1.101548	1.041516
	7	1.106660	1.044829		7	1.119448	1.050092
	8	1.122798	1.052558		8	1.137639	1.058761
	9	1.139173	1.060362		9	1.156126	1.067526
	10	1.155785	1.068243		10	1.174913	1.076386
	11	1.172641	1.076202		11	1.194005	1.085343
	12	1.189742	1.084238		12	1.213408	1.094398
18% (1½%/month)	1	1.015000	1.000000	20% (1½%/month)	1	1.016667	1.000000
	2	1.030225	1.007500		2	1.033611	1.008333
	3	1.045678	1.015075		3	1.050838	1.016759
	4	1.061364	1.022726		4	1.068352	1.025279
	5	1.077284	1.030453		5	1.086158	1.033894
	6	1.093443	1.038258		6	1.104260	1.042604
	7	1.109845	1.046142		7	1.122665	1.051412
	8	1.126493	1.054105		8	1.141376	1.060319
	9	1.143390	1.062148		9	1.160399	1.069325
	10	1.160541	1.070272		10	1.179739	1.078433
	11	1.177949	1.078478		11	1.199401	1.087642
	12	1.195618	1.086768		12	1.219391	1.096955
18½% (1½%/month)	1	1.015417	1.000000				
	2	1.031071	1.007708				
	3	1.046967	1.015496				
	4	1.063107	1.023364				
	5	1.079497	1.031312				
	6	1.096139	1.039343				
	7	1.113038	1.047457				
	8	1.130197	1.055655				
	9	1.147621	1.063937				
	10	1.165314	1.072305				
	11	1.183279	1.080761				
	12	1.201521	1.089304				

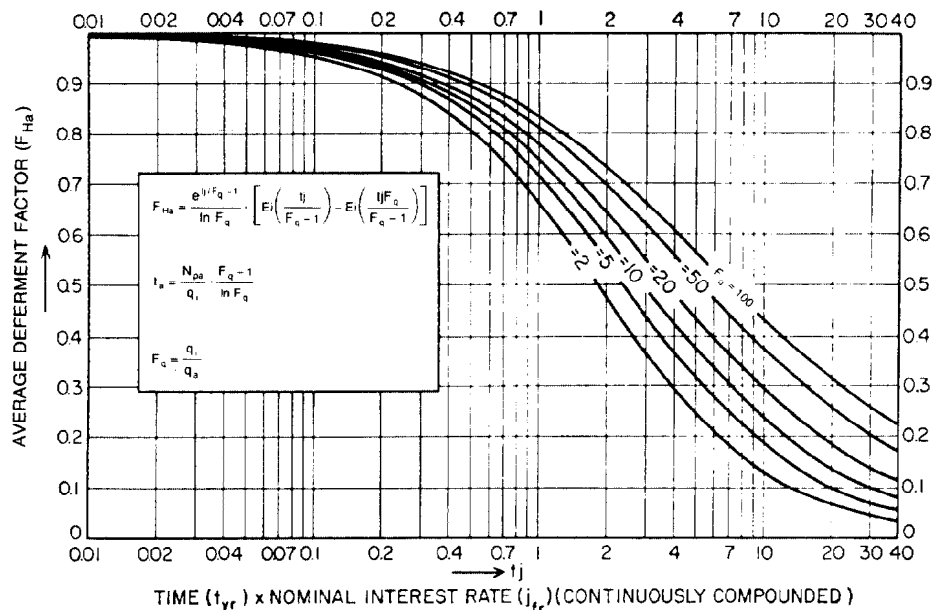


Fig. 41.11—Deferment factors for harmonic decline.

with monthly compounded interest, at the end of a given number of months, divided by the number of months. The equations for the factors are

$$F_1 = \left(1 + \frac{j}{12}\right)^t$$

and

$$F_2 = \frac{(F_1 - 1)}{\left(\frac{j}{12} \times t\right)}$$

where

F_1 = Factor 1,

F_2 = Factor 2,

j = annual nominal interest rate, and

t = time, months.

The calculation steps are (1) multiply the previous year-end balance of the loan by Factor 1; (2) multiply the total annual payment by Factor 2; (3) deduct the product of Step 2 from the product of Step 1 (the difference is then equivalent to the year-end balance of the loan); and (4) for a period of time less than 1 year, the appropriate factors for the number of months involved are used instead of the 12-month period for the entire year.

TABLE 41.16—SAMPLE LOAN-PAYOUT CALCULATION

Year	Working- Interest Revenue (1)	Total Payments to Loan 80% of (1) (2)	Loan Balance Start of Period (3)	Factor 1 (4)	Loan Balance x Factor 1 (3) x (4) (5)	Factor 2 (6)	Loan Payment x Factor 2 (2) x (6) (7)	Year-End Loan Balance (5) - (7) (8)	Allocation to Principal (3) - (8) (9)	Allocation to Interest (2) - (9) (10)
9 months 1957	\$ 675,240	\$ 540,192	\$2,000,000	1.042014	\$2,084,028	1.018531	\$550,202	\$1,533,826	\$ 446,174	\$ 74,018
1958	835,200	668,160	1,533,826	1.056408	1,620,346	1.025597	685,263	935,083	598,743	69,417
1959	776,100	620,880	935,083	1.056408	987,829	1.025597	636,733	351,096	584,027	36,853
1960	632,200	358,776*	351,056	*	*	*	*	0	351,056	7,720
1961	514,000							Payout = % ₆₀		
1962	714,240									
Thereafter	1,232,090									
Totals	\$5,082,070	\$2,188,008							\$2,000,000	\$188,008

*To determine the appropriate data for the last fractional year, the procedure is as follows:

- Determine the average monthly payment from 80% of revenue for 1960. In this case, \$42,147 per month.
- Calculate the number of months to pay out the principal balance without considering interest. In this case the number of months is 8.3.
- Calculate the loan balance at the end of the nearest whole month.
 - 8 months of payments = $8(42,147) = \$337,176$.
 - Loan balance x factor 1 for 8 months = $\$351,096 \times 1.037260 = \$364,136$.
 - 8 months of payments x factor 2 = $\$337,176 \times 1.016190 = \$342,635$.
 - Loan balance after 8 months = $\$364,136 - \$342,635 = \$21,501$.
- Calculate the total payment for the ninth month, and the last 9-month period (payout = Sept. 1960).
 - Payment for ninth month = loan balance x factor 1 for 1 month = $\$21,501 \times 1.004583 = \$21,600$.
 - Total payments for last 9 months = $\$21,600$ plus $\$337,176 = \$358,776$.

A sample calculation shown in Table 41.16 deals with the problem of determining the date of payout, the total payments required, and the annual amount of interest payments for a loan of \$2,000,000 at 5½% nominal interest per year, payable out of 80% of the net runs. The calculations are shown in considerably more detail than required solely for clarity.

Nomenclature

- a = nominal decline rate; instantaneous rate of change divided by the instantaneous production rate, decimal fraction
- C_B = balance of unreturned portion of investment, dollars
- C_{dl} = depletable leasehold cost basis at beginning of tax period, dollars
- C_i = initial capital investment or purchase price, dollars
- C_l = intangible drilling and development costs, dollars
- C_{IA} = deduction if intangibles were capitalized and amortized over 120 months or depleted by use of cost depletion rates, dollars
- C_{IP} = preference intangible drilling costs, dollars
- C_{IX} = intangible costs minus C_{IA} , dollars
- C_{PT} = local production tax, dollars
- C_{WI} = working interest, decimal fraction of gross costs
- d = effective decline rate, the drop in production rate per unit of time divided by the production rate at the beginning of the period, decimal fraction
- D_A = allowable depletion, highest of D_C or lesser of V_{DE} and V_{TI}
- D_C = cost depletion; portion of leasehold cost proportional to reserves produced in a given year, dollars
- D_E = depletion; the decline of a capital value as a result of intentional piecemeal removal or gradual consumption in use
- D_{KB} = depth measurement below kelly bushing
- D_p = depreciation; the decline in value of tangible assets with use or the passage of time (obsolescence)
- e = base of natural logarithms
- $Ei(x)$ = exponential integral of x
- F_1 = total value of dollars invested at specified annual interest compounded monthly, dollars
- F_2 = total value of dollars invested each month with monthly compounded interest at end of month divided by the number of months since investment, dollars
- \bar{F}_{CPD} = constant-percentage-decline deferment factor; the average deferment factor applicable to a series of future payments that follow constant-percentage decline, decimal fraction
- \bar{F}_{CR} = constant-rate deferment factor; the average deferment factor applicable to a series of equal future payments made at equal time intervals, decimal fraction
- \bar{F}_{Ha} = harmonic-decline deferment factor; the average deferment factor applicable to a series of future payments that follow harmonic decline, decimal fraction
- \bar{F}_{Hy} = hyperbolic-decline deferment factor; the average deferment factor applicable to a series of future payments that follow hyperbolic decline, decimal fraction
- \bar{F}_{LS} = lump-sum deferment factor; the average deferment factor applicable to one single future payment, decimal fraction
- \bar{F}_{PV} = deferment factor; a factor used to reduce revenue received in the future to a present value, decimal fraction
- F_q = ratio between initial and final production rates or payments
- i = effective annual compound safe interest rate, decimal fraction
- i' = effective annual compound speculative interest rate, decimal fraction
- i_R = revenue interest; decimal fraction of gross revenue
- I = yearly net income, dollars
- I_a = net operating income; the total earned income from oil and gas sales after deduction of lease operating expenses, federal excise taxes, and production taxes, dollars/yr
- I_n = net annual operating income during Year n , dollars
- I_T = interest owner's taxable income, dollars
- j = nominal annual safe interest rate; used when interest is compounded over M periods in a year and equal to M times the interest j/M over one period, decimal fraction
- j' = nominal annual speculative interest rate, decimal fraction
- m_k = amortization; extinguishment of an intangible asset or indebtedness
- M = number of times the interest is compounded per year
- n = number of yearly payments
- N_p = cumulative oil produced, bbl
- N_r = reserves at end of tax period, bbl or Mcf
- O_a = operating expenses, including *ad valorem* taxes, dollars
- O_G = general overhead expenses, dollars
- O_t = operating expenses per well-month, dollars
- O_u = weighted average operating costs per barrel, dollars
- P = net profit; the total net operating income after deduction of capital expenditures, dollars

- P_{PV} = future net revenue or cash flow; the projection of total annually earned income from oil and gas sales after deduction of production taxes, federal excise taxes, operating expenses, and incidental capital expenditures, dollars
- q = production rate, bbl/D/month, or bbl/yr
- s = unit sales during periods
- S = sinking fund balance
- t = time, months or years
- t_a = abandonment time or future life, years
- T_{wp} = Windfall Profit Tax (WPT)
- V = gross revenue (value); the total earned income from oil and gas sales, dollars
- V_{DE} = "percent of gross" revenue, percentage depletion
- V_{TI} = "50% of net" percentage depletion, equal to 50% of taxable net income, dollars
- ΣI = total future net operating income, dollars

Subscripts

- a = abandonment
- i = initial
- t = conditions at Time t

References

- Foster, V.: "The A-B-C's of Oil Loans," Louisiana State U., Baton Rouge (1958).
- Davis, R.E. and Stephenson, E.A.: "The Valuation of Natural Gas Properties," *J. Pet. Tech.* (July 1953) 9-13.
- Fiske, L.E.: *The Valuation of Oil and Gas Properties in Estates and Trusts*, second edition, Rocky Mountain Mineral Law Inst. (1956).
- Eggleston, W.S.: "Methods and Procedures for Estimating Fair-Market Value of Petroleum Properties," *J. Pet. Tech.* (May 1964) 481-86.
- DeGolyer, E.L. and MacNaughton, L.W.: "Valuation in the Petroleum Industry," *Oil and Gas Taxes*, Prentice-Hall Inc., Englewood Cliffs, NJ, 2003.1-2003.6.
- Arps, J.J.: "Profitability of Capital Expenditures for Development Drilling and Producing Property Appraisal," *J. Pet. Tech.* (July 1958) 13-20; *Trans.*, AIME, **213**.
- Reynolds, F.S.: "Discounted Cash Flow as a Measure of Market Value," *J. Pet. Tech.* (Nov. 1959) 15-19.
- Terry, L.F. and Hill, K.E.: "Valuation of Producing Properties for Loan Purposes," *J. Pet. Tech.* (July 1953) 23-26.
- Dodson, C.R.: "The Petroleum Engineer's Function in Oil and Gas Financing," *J. Pet. Tech.* (April 1960) 19-22.
- Garb, F.A., Gruy, H.J., and Wood, J.W.: "Determining the Value of Oil and Gas in the Ground," *World Oil* (March 1982) 105-08.
- Fagin, K.M.: "An Empirical Yardstick for Appraising the Present Fair Market Value of Steady Future Net Operating Income from Oil and Gas Producing Properties," Study Group Meeting, Dallas Section, SPE, Nov. 1, 1956.
- Arps, J.J.: "Analysis of Decline Curves," *Trans.*, AIME (1945) **160**, 228-47.
- Paine, P.: *Oil Property Valuation*, John Wiley & Sons Inc., New York City (1942).
- Morrissey, N.S.: "Active Fields Report Drilling Data," *Oil and Gas J.* (Oct. 6, 1958) 172.
- "Joint Association Survey of Industry Drilling Costs 1959," API, IPAA, and Mid-Continent Oil and Gas Assn. (March 1961).
- Breeding, C.W. and Herzfeld, J.R.: "Effect of Taxation on Valuation and Production Engineering," *J. Pet. Tech.* (Sept. 1958) 21-25.
- Brons, F. and McGarry, J.S. Jr.: "Methods of Calculating Profitabilities," paper SPE 870-G presented at the 1957 SPE Annual Meeting, Dallas, Oct. 6-9.
- Hill, H.G.: "A New Method of Computing Rate of Return on Capital Expenditures," paper presented at the Philadelphia Chapter of the Natl. Assn. for Business Budgeting, Aug. 1953.
- Hoskold, H.D.: *Engineer's Valuing Assistant*, Longmans, Green & Co. Inc., New York City (1877).
- Morkill, D.B.: *Formulas for Mine Valuation*, Mining and Scientific Press, 117, 276.
- Wilson, W.W. and Boyd, W.L.: "Simplified Calculations Determine Loan Payout," *World Oil* (May 1958).

General References

- Arps, J.J.: "Reason for Differences in Recovery Efficiency," paper SPE 2068 presented at the 1968 SPE Hydrocarbon Economics and Evaluation Symposium, Dallas, March 4-5.
- Campbell, J.M.: *Petroleum Evaluation for Financial Disclosures*, Campbell Petroleum Series, Norman, OK (1982).
- Campbell, J.M. and Hubbard, R.A.: "Price Forecasting and Project Evaluation in the 1980's," *J. Pet. Tech.* (May 1984) 817-25.
- Campbell, J.M. et al.: *Mineral Property Economics*, Campbell Petroleum Series, Norman, OK (1977).
- Chan, S.A.: "Financial and Engineering Considerations in Petroleum Property Acquisitions," paper SPE 11301 presented at the 1983 SPE Hydrocarbon Economics and Evaluation Symposium, Dallas, March 3-4.
- Cozzolino, J.M.: "A Simplified Utility Framework For the Analysis of Financial Risk," paper SPE 6359 presented at the 1977 SPE Hydrocarbon Economics and Evaluation Symposium, Dallas, Feb. 21-22.
- Economics and Finance*, Reprint Series, SPE, Richardson, TX (1980) **16**.
- Grossling, B.F.: "In Search of a Statistical Probability Model for Petroleum-Resource Assessment," U.S. Dept. of the Interior, Reston, VA (1975).
- Gentry, R.W. and McCray, A.W.: "The Effect of Reservoir Fluid Properties on Production Decline Curves," *J. Pet. Tech.* (Sept. 1978) 1327-41.
- Greenwalt, W.A.: "Determining Venture Participation," *J. Pet. Tech.* (Nov. 1981) 2189-95.
- Mintz, F.: "Reserve Based Financing—Specific Requirements and Alternatives," paper SPE 9578 presented at the 1981 SPE Hydrocarbon Economics and Evaluation Symposium, Dallas, Feb. 25-27.
- Newendorp, P.D.: "A Strategy for Implementing Risk Analyses," *J. Pet. Tech.* (Oct. 1984) 1791-96.
- Petrie, T.A. and Paasch, R.D.: "Implications of Evolving U.S. Oil Pricing Policy for Domestic Reserve Values," *J. Pet. Tech.* (Feb. 1981) 341-48.
- Standards Pertaining to the Estimating and Auditing of Oil and Gas Reserve Information*, SPE, Richardson, TX (1980).

Chapter 42

Injection Operations

W.P. Schultz, Core Laboratories Inc.*

H.M. Shearin, Suburban Propane Exploration Co. Inc.*

Introduction

The petroleum industry, like other industries, exists today because it markets desirable products at a profit. To do this, it is extremely important that every phase of an oil company's activity be conducted with this goal in mind. The specific goals and details of operation of a particular company may vary slightly or significantly from those of other companies—depending primarily on economic and marketing structure—but each desires to optimize economics of its detailed as well as its overall operations.

There are, of course, many facets to be considered in this program of optimization, and these may vary from one company to the next, from one locale to another, or even with time. No longer can companies analyze their economics considering only development and depletion of their reserves by primary means. World demand and availability of hydrocarbon products; economics of exploration, development, production, and transportation; obligations of drilling and regulation of production operations imposed by various governing authorities; taxation; and competition of other raw materials in the energy market all have had the combined effect on petroleum industry operations of demanding closer coordination and control of activities within a given company. Equally important, more detailed consideration and long-range planning must be devoted to specific projects undertaken. This chapter has been written with these general thoughts in mind.

Oilfield development and production operations constitute a major part of most oil companies' activities. More probably can be done to improve the overall economics of a company and actually shape its future by critical and thorough analysis of this phase of operations than can be done in any other activity. Every company is well aware of the high cost of finding oil, of developing a reserve, and of producing it. Experience has shown

that from most fields primary recovery is not an efficient process and that, usually, large volumes of oil are left underground as unrecoverable at the time of abandonment. The technology of oilfield operations has developed rapidly as a result of research, field application, and engineering and geological analysis. Today, in most field operations, new technology is adopted when the economics warrant it.

Petroleum reservoir engineering is by no means an exact science. Probably it never will be since so many parameters that cannot actually be measured or defined are involved; however, research and experience have yielded a substantial knowledge that is quite adequate to serve as a basis for providing management with sound recommendations regarding field development and operations, which on the basis of current technology should result in optimal economic recovery from a reservoir.

For many years it has been known that injection of either water or gas into a petroleum reservoir can improve recovery. The general history of field application of these processes is interesting to review. Many injection projects were initiated in fields before reservoir natural-energy-drive mechanisms were understood—even before there was a general awareness of what data were needed to evaluate properly either the possibilities or the results of such processes. It is not surprising, therefore, to find that some projects succeeded in substantially increasing recovery and others failed.

As the science of reservoir engineering developed, many injection projects were considered more carefully before they were actually initiated and, as a result, were on a sounder technological and economic basis from the start. Consequently, most injection operations are well engineered. In fact, the development plans of most new discoveries include the option of initiating injection operations right from the start, when feasible.

The solution of problems in any technical operation is

*These authors also wrote the original chapter on this topic in the 1962 edition.

always dependent on knowing the relevant facts. The oil industry is no exception to this rule, and many critical facts that engineers or geologists must use in their analysis of a reservoir can be obtained best early in the life of the reservoir. Some necessary facts can be obtained at later times, but only at a very large additional expense. It is therefore in keeping with sound business principles for an operator to think ahead when drilling wells and to begin planning ahead the very day a new reservoir is discovered. With this philosophy, engineers can be assured that sufficient and necessary information will be available for proper technical analysis when needed, that the best program for ultimate depletion of reserves is recognized early in the life of the reservoir, and that the development program for the reservoir is guided toward maximum use in the exploitation program best suited for optimal economic recovery. The thought process involved in this philosophy applied to development of a sound injection operation is discussed in this chapter.

Important Factors in the Design of Injection Operations

Objective

Individual oil and gas reservoirs, like human beings, are each different, and the reservoirs present a wide variety of properties for the engineer to consider. Of prime importance in making an analysis of these properties for the design of an injection program is establishing the objective of the operation.

The establishment of a proper objective for a given operator depends on the particular circumstances. An operator with limited investment opportunities might favor improvement in reserves. One with ample reserves for the current rate of production would favor an improvement or maintenance of production rate. Another, having insufficient rate and reserves, would favor improvement in each. The objective of the injection operation will likely be (1) sustaining the rate through pressure maintenance, (2) increasing ultimate recovery through a more efficient displacement process, or (3) combining improved rate and recovery to lead to the accumulation of maximum present worth.

In many instances, injection operations have been undertaken in reservoirs simply because nearby properties have responded favorably to injection. This same line of incomplete reasoning is then generally carried one step further, and it is concluded that the reservoir conditions are unknown because of variable physical properties and past production practices; therefore, no proper engineering analysis can be made and injection must be tried to see what will happen. Projects initiated with this reasoning are almost always injection operations without an objective. This "cart before the horse" philosophy is to see what will happen, then decide what is desired. Without an objective the engineering analysis will result in nebulous conclusions, for the objective influences both the timing and the choice of the injection process.

Timing

Care must be taken to ensure that the planning of the program is not delayed past the optimal time to start the injection physically. In all cases, it is desirable to

recognize the need for injection in a reservoir to obtain specific objectives as early in the life of the reservoir as possible. Early planning, even if not in great detail, will make it possible to obtain adequate basic data for proper engineering analysis at the only time such data are available. In many instances, such planning may dictate a modification of the development program so that wells will be located and completed to provide maximum efficiency to the injection program with a minimum amount of costly redrilling or workover expense.

The optimal time to start an injection project is often related to the best-suited process for the given field. For example, an immiscible displacement with gas might best be undertaken in some high-permeability sands after the reservoir reaches a low pressure, since at low pressures, the cost of compressing gas to replace a reservoir barrel of volume is low. Low-pressure waterflooding might perhaps be started when the optimal amount of free gas is present. Low-permeability reservoirs or those with high-shrinkage oil might call for the immediate use of a pressure-maintenance project in maintaining well productivity and in preventing high shrinkage losses. Some injection operations may require high reservoir pressures to accommodate the process.

For older fields, in which the optimal time to start a project may have long passed, the question becomes not one of optimal time but of the best process to employ. At times, the question is whether a change in the conditions of the reservoir, such as repressuring, can re-establish the opportunity for conducting an improved operation.

Injection Fluids

In any injection project, certain parameters are fixed and are beyond the control of engineers. These include fluid properties of the reservoir oil, rock properties, geologic stratifications, faulting, and depth. On the other hand, engineers can vary such items as injection fluid, injection pressure, pattern, and injection rate. Selection of the proper injection fluid for a given reservoir is probably the most difficult part of the design of any injection operation. Generally, air and water are the only materials considered inexpensive enough to use in large quantities for the displacement of crude oil. Current prices of natural gas make it an expensive injection fluid. However, when it exists in areas where there is no market, its greatest economic benefit may be as an injection fluid. It is in this area, however, that the knowledge, imagination, and ingenuity of the reservoir engineer can be used to develop injection programs that will greatly improve recovery and profit from most reservoirs. The project should be designed to allow for the possible use of small amounts of more expensive materials, such as propane, butane, liquefied petroleum gas, CO_2 , wetting agents, and polymers.

Projected Recovery

Data Required. Projecting oil recovery from a reservoir in which injection operations are to be conducted requires an estimation of (1) the amount of oil in place initially, (2) the recovery by any primary depletion that occurred before the start of injection, (3) the oil saturation at the start of injection and the residual oil saturation after the displacement process and how it is distributed

through the reservoir, (4) the fraction of the reservoir to be swept, and (5) the injection and production rates.

Sufficient data are needed to determine these quantities. Some sources of these data are listed in Table 42.1.

Engineering Analysis. The prediction of the performance of an injection operation is derived by (1) preparing an estimate of the oil moved as a function of the volume injected and (2) defining the injection and production rates and related volume injected to time. The details of the calculation procedures are presented in the six chapters that follow in this handbook. In general, the amount of oil recovered is determined from material-balance calculations applied to the fraction of the reservoir swept by the injected fluid. The potential injection and production rates are calculated from equations or measurements on models. The rate may be reduced through proration or through limitation in sizing equipment.

Optimizing an Injection Operation

The decision as to the optimal injection program for a given reservoir involves selection of the best process and of the best manner for conducting that process. The selection of the best process requires a study of (1) primary performance, (2) source of injection fluid, (3) cost of injecting various fluids, and (4) unit displacement efficiency of various fluids.

The selection of the best manner for carrying out the operation requires a study of (1) the time to start injection, (2) pressure maintenance, (3) partial pressure maintenance, (4) well stimulation, (5) additional drilling, and (6) pattern choice. After the best manner for conducting each process is developed, a comparison of the economics of the optimal plan for each process will show the most desirable program.

Analysis of a Reservoir for Injection Operations

Beginning the Analysis

Data Gathering and Testing. Some reservoirs may be similar in many respects but completely different in others. Because of this, it is necessary to obtain information that experienced geologists and engineers can use to define the character of each specific reservoir. Much of the information is obtained during the development portion of a reservoir's history. Some types of information are collected periodically throughout the producing life of the reservoir. Certain types of data are needed to evaluate the probable economics and producing characteristics of the reservoir by natural depletion, and additional information is necessary for proper analysis of potential recovery and economics under various injection programs. It is a responsibility of the engineer and geologist, as a team, to outline a long-range program of data requirements early in the life of every reservoir and a schedule of how and when these data are to be collected. The details of this program should be modified continuously as more knowledge of the reservoir is gained.

If conducted properly, the initial development program can contribute substantially to the early recognition of both primary and injection-operation potential of any

TABLE 42.1—DATA REQUIRED TO ESTIMATE RECOVERY FROM INJECTION OPERATIONS

<u>Oil Initially in Place</u>	
Adequate number of wells to define areal extent	
Well logs to define productive section and sometimes content	
Core measurements for porosity, interstitial water, oil saturation, and sometimes capillary properties; these data also serve as a basis for well-log calibration	
Material-balance calculations based on reservoir pressures and production history to confirm volumetric estimates of oil in place	
<u>Primary Performance</u>	
Production of oil, gas, and water by wells	
Pressures from periodic pressure-buildup tests	
Fluid properties	
Relative-permeability measurements on cores for displacing and displaced phases	
Geologic data from nonproductive wells outside the productive limits to assist in the determination of the primary drive mechanism	
<u>Fraction of the Reservoir to be Swept</u>	
Core measurements for variation in permeability and content	
Cross sections and pressure interference tests to determine the reservoir continuity between wells	
Stratification from core measurements and logs	
Orientation of permeability	
Selected injection pattern	
Fluid viscosities and relative permeabilities	
Areal sweep performance of injection pattern models	
<u>Injection Rate and Production Rate</u>	
Effective reservoir permeability from cores, pressure-buildup tests, and productivity-index tests	
Relative-permeability curves on displacing and displaced phases	
Wellbore conditions from pressure-buildup analysis	
Injection pressure	
Fluid properties	
Throughput rate from model performance or calculations	

reservoir. This program should be designed to yield (1) the broad specifications of the reservoir, such as general field limits, general reservoir geometry, (2) general rock properties of the producing formation, (3) approximate location of reservoir gas/oil and water/oil contacts if present, (4) characteristics of in-place reservoir fluids, (5) initial reservoir pressure and temperature conditions, and (6) general information pertaining to average well productivities. Quite obviously, if this program is to accomplish its economic and informative objectives, no consideration should yet be given to ultimate well spacing. In the case of large structures this initial program should consist of carefully planned, bold stepouts and, in all cases, obtaining as much information as needed to direct properly further field development and data-gathering techniques.

Often, sufficient information can be obtained from a well-planned data-gathering program conducted during the early portion of development of a reservoir to permit intelligent preliminary examination of the probable need for injection and the general feasibility of various types of injection. Early data-gathering efforts should result in the accumulation of sufficient information to permit selection of those techniques that will yield required and reliable information as other wells are drilled. Such information also can be used to refine the preliminary conclusions pertaining to probable reservoir potential under

various operating methods begun earlier on the basis of initial data. Recommendations concerning selection of the best program of operation for a particular reservoir normally should be based on behavior forecasts that involve detailed analysis of primary producing performance.

The economic potential of injection operations can suffer materially in many cases if such operations are not initiated early in the producing life of a reservoir. Thus an urgency exists to determine early the economic potential of various operating programs; one often cannot wait for primary performance information covering a majority of the reservoir's primary life and still reap the benefits that might have accrued by early initiation of some form of injection. Engineers, therefore, have quite a large responsibility to obtain sufficient information and to recognize when enough is available for making sound recommendations concerning future operations in any given reservoir. The relative timing for when this can be done in a reservoir's life may be considerably different for different reservoirs, depending primarily on the ability to recognize and define the natural forces contributing to production in each case. From a technical standpoint, full development of the field on some arbitrary spacing decided without regard to reservoir characteristics and potential should not be undertaken until it can be guided by the needs of the operating program best suited to the reservoir.

The initial-development portion of any reservoir's history is therefore a critical period. The information that should be obtained during this period includes the following.

1. Detailed routine core analysis in sufficient volume and with sufficient well logs of different types permits selection of those data-gathering techniques that when used on later wells will ensure obtaining necessary and accurate interpretations and measurements of rock properties such as porosity and permeability. Data about the initial wells should be adequate for general definition of such things as structure, gross formation thickness, net productive formation thickness, field limits, porosity, permeability, lithology, and the homogeneity and continuity of the producing formation.

2. Drillstem tests define the general productive characteristics of various zones and help establish the location of gas/oil and water/oil contacts if present.

3. Periodic static-subsurface-pressure surveys establish original reservoir pressure as well as subsequent pressure history.

4. Temperature surveys establish reservoir temperature.

5. Reservoir fluid samples establish the physical properties of hydrocarbons present in the reservoir as functions of pressure and temperature and the variation of these properties with depth and area. Also, formation-water samples establish chemical composition.

6. Controlled periodic production tests of wells provide such information as general production characteristics, GOR, and water cut.

7. Special well tests such as productivity-index measurements, pressure-buildup tests, and interference tests provide information regarding efficiency of completion techniques, average formation productivity, and formation continuity.

8. Special core-analysis tests on selected, and in some cases specially preserved, core samples help determine such things as interstitial water saturation, gas/oil and water/oil relative-permeability characteristics, residual oil saturation by waterflood, and permeability reduction caused by flooding with water of various salinities.

9. Monthly oil-, water-, and gas-production histories by well are also useful.

The engineer must use judgment with regard to exactly how much of each kind of basic data is required in any particular case. In general, the volume of data needed varies more with complexity of the reservoir system than with size. Complexity of reservoirs is often disregarded. Usually, more different types of data should be obtained early in the development period so that economy and reliability can be built into subsequent completion techniques and data-gathering programs.

Type of Injection

Many factors are involved in determining the data needed to analyze properly the potential of various injection programs for a specific reservoir. Experienced engineers with proper data at hand should be able to recognize early the types of injection programs that might prove worthy of detailed consideration. Often, new reservoirs are discovered in the same formation and in close proximity to existing fields for which detailed performance information already exists. Unless factors point to differences between the two, in his preliminary thoughts, the engineer usually can consider that the new field probably will behave in a manner similar to the other. If existing injection projects are successful or if they are failing, the preliminary thinking on a new reservoir, unless obvious differences exist, will be that similar projects in the new reservoir probably would behave in about the same manner. This thought process is a normal one but can be dangerous in that the results of a specific injection project many times are actually a function of the original thought, evaluation, and planning of the project as well as the engineering control exercised throughout its life. Proper engineering control of injection projects in practice varies considerably, and for this reason, thinking based on analogy is good for preliminary screening but should not be the prime consideration in evaluating the need for or the potential of various injection programs. Prime consideration should be given to the physical characteristics of the particular reservoir being evaluated.

Reservoir Fluid and Rock Characteristics. One of the first questions that should be answered by engineers concerns the technical feasibility of various forms of injection. This involves preliminary analysis of reservoir rock and fluid characteristics and early interpretations of reservoir geometry. Engineers should be on the lookout continuously for characteristics such as high interstitial water content, unfavorable water/oil or gas/oil relative-permeability properties, unfavorable mobility ratios, indications of natural formation fracture and fault systems, unusual areal and vertical variations of porosity and permeability, and lack of vertical and areal formation continuity. None of these situations rule out the technical possibilities of injection projects, but they are warning signals to engineers and may complicate their problems.

Engineers know, for example, that if (1) the reservoir appears to have fair continuity and shape, (2) permeability is reasonably distributed, and (3) relative-permeability relations and oil properties are favorable, then either water-, gas-, or enhanced-recovery injection projects are possibly feasible from a technical standpoint. If the reservoir oil is viscous, then mobility-ratio characteristics normally favor water over gas injection, and thermal processes might increase recovery. If a high interstitial water saturation exists, then under certain conditions this can be more of a disadvantage for water than for gas injection. Benefits often can be derived through enhanced-recovery operations in reservoirs containing highly undersaturated oils. Through experience engineers have learned that low formation permeability in itself is not a factor that eliminates injection possibilities but that often a more critical factor can be extreme variation of permeability. All these factors, along with others, can be available for the engineer's scrutiny early in the development period and, if used properly, can guide the early thinking about overall plans for a reservoir.

Availability of Injection Fluids. In viewing the possibilities of injection operations, engineers must also consider the availability of fluids for injection. This factor alone can sometimes eliminate further evaluation of some particular form of injection or, in other cases, materially affect the economics of a project. A water-injection operation might appear very attractive from a technical standpoint; yet if water cannot be made available in required quantities and at reasonable cost, further consideration of the process would be only academic. Engineers should certainly consider the possibilities of gas-injection and miscible-drive projects when gas or liquid plant products are available in the area. Of course it is impossible to set forth a checklist of factors that could be used early in the life of every reservoir to determine the absolute need or feasibility of injection projects. Each factor discussed here is important, and variations of any one or of all the pertinent parameters can affect results to various degrees.

Predicted Reservoir Performance During Primary Operations

Another important consideration that must be an integral part of the engineer's appraisal of possible injection projects is the need for the project. This can be a very complicated part of the overall analysis and should involve not only technical aspects of the project itself but also the effect that the project's results might have from an overall company standpoint. The latter is treated in more detail along with a discussion of economics in this chapter. Technical need for injection projects involves analysis of past reservoir performance, recognition and definition of the natural energy forces contributing to primary production, and evaluation of the efficiency and forecast of performance of the primary production operations.

Other chapters in this handbook deal with the types of drive mechanisms that can be present individually or in combination in any given reservoir. Engineers must have a detailed understanding of these natural processes before they can recognize the need for application of supplemental recovery processes to a reservoir. General-

ly speaking, the depletion- or solution-gas-drive process is an inefficient one, but coupled with good segregation and oil and gas counterflow, the process can be much more efficient. In general, better recovery efficiency is usually expected by a natural water drive than by any other natural process, and gas-cap expansion-drive processes are usually intermediate in effectiveness.

Engineers know, however, that these are generalizations and that the existence and effectiveness of each must be evaluated for each reservoir. They can make reasonable guesses of possible future primary performance on the basis of behavior of analogous fields and on preliminary evaluation of data acquired early in a reservoir's life, but these guesses can be translated into sound engineering conclusions only through a detailed study of the particular reservoir's performance. When they are able through intelligent use of available information concerning basic properties of the reservoir system to calculate accurately and match the actual past performance of a reservoir, then they gain confidence in any predictions they might make of future primary performance.

An experience factor is involved, however, that cannot be overlooked. Engineers must be able to recognize whether a match of calculated and actual performance is a real match such that the solution is reasonably unique and their understanding of the primary production process is good or whether there actually could be several widely different solutions that could result in equally good matches of performance. In the latter case there is either a lack of understanding of basic reservoir parameters and a need for more basic data, or there is insufficient production performance available for analysis at that time.

Often, it might be possible to plan early production from the reservoir in such a manner as to aid in reservoir evaluation. Extreme changes in production rate (upward or downward or both) and maintenance of those rates at reasonably constant levels for a period of time can often result in changes in observed reservoir pressure or well performance that are extremely useful in early recognition of prevailing natural-energy forces. Since treatment of the various methods of analysis appears in other chapters, there is no need to discuss them at this point. Emphasis, however, should again be placed on the urgency of early recognition and definition of the efficiency of the primary production process because it is of prime importance in ascertaining the need for injection.

Predicted Reservoir Performance During Injection Operations

The next step in the process of determining the best method of operation for a given reservoir is the prediction of performance for various injection programs that are considered technically and practically feasible on the basis of preliminary examination of available information. Normal methods of accomplishing this objective are discussed in later chapters; however, the following philosophy should be a normal part of engineers' thinking processes. An injection program is not to be designed for the reservoir at hand because a similar project appeared successful in some other reservoir; it is not developed simply because the process is one that has been used extensively in the past; it does not follow that,

just because a certain pattern of injection and production was good for one reservoir, it should also be the best or even good in another reservoir. Each reservoir must be examined in the light of its character and needs.

Many injection projects are hampered by inadequate programs borrowed from yesterday (a period when reservoir fluid-flow processes were not well understood) and applied to reservoirs without appreciation of differences in reservoir detail or other pertinent circumstances. Engineers should strive to be current in thinking and original in ideas. A surface map showing location of injection and production wells for a project might appear to be extremely radical on first examination; however, if sound technical procedures show that it could result in better economic recovery than any other scheme, the plan is not radical. Programs are developed for obtaining desired results in underground reservoirs and not to be symmetrical, uniform, or appealing with regard to topography or property lines. At the time engineers make detailed analyses of the potential of injection operations, they should have already answered, by means of the planned data-gathering program, as many pertinent details as possible about characteristics of the reservoir rock, reservoir fluids, reservoir geometry and continuity, and well-behavior characteristics.

Economics

Although technical analyses of possible future operations in a reservoir must be thorough and sound, an equally important consideration during overall evaluation is economics. Any project might be an outstanding success from a technical standpoint, but its real value is measured in terms of income and expense. In designing the general specifications of an injection program, engineers should first recognize or ascertain some of the overall objectives of their company. Usually engineers find that there is considerable latitude with regard to some important considerations in a study that are well within the limits of sound technology but that with varying assumptions could represent quite a spread in the economic results of a given project. This is particularly true of factors that influence production rate.

As stated earlier, it might be more desirable from an economic and marketing standpoint in one company to recover as much oil as possible and as fast as possible whereas in another company the interest may be for long-term maintenance of stabilized high production rates. Knowledge of this is important in designing an injection project. Engineers should be cautious in their economic analysis and not permit conclusions to be drawn that on the basis of the project alone might be reasonable but that with broader consideration could be invalid. An example of such a case might be the prediction of a water-injection project that would recover large volumes of additional oil. The economics of such a proj-

ect might appear to be very favorable; however, if the company cannot market the additional oil at the forecasted rates and values, such a project could not possibly result in the indicated benefits from an overall company standpoint.

Wells are often drilled that are not needed from the standpoint of producing reserves. The surplus wells are there because economic and marketing differences exist between companies, because of regulations concerning drilling requirements, because wells drilled for primary operations are not suitable for later operations, and in some cases because of false economic reasoning. Many wells have been drilled simply because they pay out in a fairly short period of time. Some of these wells may have benefited companies from a current-income standpoint, a lesser number from a present-worth standpoint, and probably very few from an ultimate-recovery standpoint. Unnecessary drilling is a waste of money and should be eliminated; engineers can be very instrumental in such a program through efforts to appraise the potential of reservoirs early in their life and to forestall complete development until the future plan for the reservoir is known. At that time only the necessary additional wells can be drilled and they can be located strategically according to need. The benefits of additional oil recovery and reduced costs that can be obtained through cooperative or unitized operations should be uppermost in engineers' minds.

Many times variables exist in the engineers' technical analyses that seem to defy definition. Engineers must know how critical reasonable variation of such parameters is in the overall analysis. Sometimes results pertaining to such cases can be derived only through pilot applications. These pilot operations serve the primary purpose of reducing risk that might be involved in a fieldwide program. This is particularly true for EOR projects where injection of expensive chemicals, steam, or oxygen is involved. In those cases where it is necessary to resort to a pilot program, it should first of all have specific objectives, detailed engineering control to ensure early attainment of the objectives, and planning to make it an integrated part of the expanded fieldwide program.

Petroleum engineers today are no longer just professionals with technical experience or background relating to oil production. They must also understand principles of finance. They not only must be able to know what "yardsticks" are used by their company and by others to evaluate the benefits of a specific project, but also must be able to design the project so that maximum benefits can result. Engineers can play a major role in the future of the oil industry. Rewards will certainly come to individuals who recognize the existing challenge and who, with "know-how," good judgment, and new ideas, are always striving to improve the specific facets as well as the overall complexion of the industry.

Chapter 43

Gas-Injection Pressure Maintenance In Oil Reservoirs

I.F. Roebuck Jr., Roebuck-Walton Inc.*

Introduction

The first recorded deliberate attempt to stimulate recovery from an oil reservoir by hydrocarbon gas injection was in the Macksburg field, Washington County, OH,¹ long before water injection was used for secondary recovery purposes. For almost 60 years, most secondary recovery projects included some form of immiscible gas injection, and its use continued even after the advent of new methods and materials. In spite of this, it was the late 1940's before serious attempts were made to develop quantitative techniques for describing reservoir performance under gas-injection operations, especially with regard to depleted oil reservoirs. Before then, such efforts were directed primarily toward describing the water displacement process.

As a result, techniques used to describe the performance characteristics of immiscible gas injection consist of modifications to methods originally developed for describing performance of water-injection operations, even though there is a fundamental difference in the basic displacement mechanisms of the two fluids. Such modifications, therefore, include the effects of gas solution in the reservoir oil, vaporization of lighter hydrocarbons from oil, or both.

Physical criteria for successful gas-injection operations are basically the same as for other types of fluid injection; the same physical and thermodynamic variables control the displacement process. As in all engineering investigations, pertinent variables must be defined, evaluated, and applied by the investigative techniques available and with a knowledge and awareness of the limitations of the techniques and the accuracy and reliability of the data and information at hand.

Gas injection has been used to maintain reservoir pressure at some selected level or to supplement natural

reservoir energy to a lesser degree by reinjection of a portion of the produced gas. Complete or partial pressure-maintenance operations can result in increased hydrocarbon recovery and improved reservoir production characteristics.

The quantity of additional liquid hydrocarbons that can be recovered from a reservoir is influenced by several characteristics of the particular reservoir, including reservoir rock properties, reservoir temperature and pressure, physical and compositional properties of the reservoir fluids, type of reservoir drive mechanism, reservoir geometry, sand continuity, structural relief, rates of production, and fluid saturation conditions.

Basically, increased hydrocarbon recovery can be attributed to the oil displacement and vaporization action of the injected gas and, in some cases, to the prevention of losses in recovery that would occur if pressure were not maintained. The conservation aspects of gas-injection pressure-maintenance operations can be particularly important with reservoirs containing volatile high-shrinkage crude oils and with gas-cap reservoirs containing large quantities of retrograde condensate gas. Gas injection has also been employed frequently to prevent migration of oil into a gas cap in oil reservoirs with natural water drives, with downdip water injection, or both. Other uses of gas injection in high relief reservoirs have been to enhance gravity drainage processes and to recover so-called attic oil residing above the uppermost oil-zone perforations.

Improvements in reservoir producing characteristics may, in some cases, be sufficient justification to initiate gas-injection operations even though a competitive recovery process might be used to achieve greater ultimate hydrocarbon recovery. Decreased depletion time resulting from pressure-maintenance operations can have a significant influence on the economic justification for gas injection. Decreased reservoir oil viscosity and gas saturation in the vicinity of the wellbore tend to

*Original chapter in 1962 edition, Part 1, *Gas-Injection Pressure Maintenance*, was written by I.F. Roebuck Jr. and Kenneth M. Garms. Part 2, *Miscible Displacement*, is now a separate chapter (see Chap. 45).

maintain individual well productivities, and producing wells are generally more able to maintain their desired producing rates or allowables. Further advantages can be obtained by elimination of penalties imposed by regulatory agencies for excessive net gas production where produced gas is not reinjected. Thus, many times it is possible to maintain full-field allowables over most of the producing life of the project, thereby reducing the depletion time of the reservoir, with attendant savings in operating costs and increased present value of future revenues.

Since 1978 and the passage of the Natural Gas Policy Act, the increasing value of sales gas has resulted in a decline in the numbers of new gas-injection projects. However, some opportunities still exist in remote areas where recovery considerations are augmented by the storage aspects of such projects and by specialized applications in connection with gravity drainage systems and attic oil recovery projects.

Concurrent with this, CO_2 and nitrogen injection for miscible displacement of crude oil have been of increasing interest and application. On the basis of both economic and technical considerations, it is not unreasonable to expect that immiscible nitrogen-injection projects will see increasing application in many oil reservoirs that in the past would have been subjected to hydrocarbon-gas injection. In general, calculation techniques previously developed for hydrocarbon-gas injection and displacement can be used for the design and application of nitrogen-injection projects under conditions of immiscible displacement.

It is the purpose of this chapter to point out the physical criteria for successful gas-injection operations, to describe the variables that must be defined and evaluated, and to demonstrate some of the techniques available for the prediction and evaluation of field performance under immiscible gas-injection operations.

Most of the calculations described are now accomplished with hand calculators or digital computers; many of them can be applied with relatively basic varieties of today's generation of microcomputers. At the same time, the physical and mathematical relationships described have been incorporated into a wide variety of mathematical reservoir simulation models. The formulation and application of such models is beyond the intended scope of this chapter, but a few selected references to technical articles describing models for gas-injection processes are included in Appendix B.

The calculation techniques described here are the classical methods for describing immiscible displacement with complete pre-equilibrium between the injected and displaced phases, gas and oil, while accounting for the effects of reservoir heterogeneities, injection/production well configurations, and differing physical characteristics of the fluids. The reservoir is treated in terms of the average properties of a unit volume of rock, and production performance is described on the basis of an average well.

The simplest types of so-called reservoir simulation models employ essentially these same techniques but, by means of one-, two-, or three-dimensional cell arrays, account for areal and vertical variations in rock and fluid properties, well-to-well gravity effects, and individual well characteristics.

More complex component or compositional models allow also for nonequilibrium conditions between injected and displaced fluids and can be used to describe individual well streams in terms of the compositions of the produced fluids.

The accuracy and reliability of the results obtained generally increase with each of these methods, or models, in the order described, depending on the quantity and quality of the reservoir and fluid data available, the internal variations in reservoir properties, the fluid characteristics, and the ability to describe the overall physical system. The time and worker requirements, and hence the cost of the study, also increase in the same order.

Therefore, the choice of a method for describing project performance is a matter of judgment, considering economics, the time available, and the requirements for accuracy in a practical sense. Obviously, these requirements will vary with the phase of work undertaken and the overall purpose of the study at hand. Certainly, early feasibility studies usually can and should be made with nothing more than the simple, classical techniques. Such is also the case for many detailed studies where the effects of gravity and phase equilibrium are negligible or when the quantity and quality of data are inadequate to support more complex full-scale simulation studies.

Types of Gas-Injection Operations

Gas-injection pressure-maintenance operations are generally classified into two distinct types depending on where in the reservoir, relative to the oil zone, the gas is introduced. Basically, the same physical principles of oil displacement apply to either type of operation; however, the analytical procedures for predicting reservoir performance, the overall objectives, and the field applications of each type of operation may vary considerably.

Dispersed Gas Injection

Dispersed gas-injection operations, frequently referred to as internal or pattern injection, normally use some geometric arrangement of injection wells for the purpose of uniformly distributing the injected gas throughout the oil-productive portions of the reservoir. In practice, injection-well/production-well arrays vary from the conventional regular pattern configurations (e.g., five-spot, seven-spot, nine-spot) to patterns seemingly haphazard in arrangement with relatively little uniformity over the injection area. The selection of an injection arrangement is usually based on considerations of reservoir configuration with respect to structure, sand continuity, permeability and porosity variations, and the number and relative positions of existing wells.

This method of injection has been found adaptable to reservoirs having low structural relief and to relatively homogeneous reservoirs having low specific permeabilities. Because of greater injection-well density, dispersed gas injection provides rapid pressure and production response—thereby reducing the time necessary to deplete the reservoir. Dispersed injection can be used where an entire reservoir is not under one ownership, particularly if the reservoir cannot be conveniently unitized.

Some limitations to dispersed-type gas injection are: (1) little or no improvement in recovery efficiency is derived from structural position or gravity drainage, (2)

areal sweep efficiencies are generally lower than for external gas-injection operations, (3) gas "fingering" caused by high flow velocities generally tends to reduce the recovery efficiency over that which could be expected from external injection, and (4) higher injection-well density contributes to greater installation and operating costs.

External Gas Injection

External gas-injection operations, frequently referred to as crestal or gas-cap injection, use injection wells in the the structurally higher positions of the reservoir—usually in the primary or secondary gas cap. This manner of injection is generally employed in reservoirs having significant structural relief and average to high specific permeabilities. Injection wells are positioned to provide good areal distribution of the injected gas and to obtain maximum benefit of gravity drainage. The number of injection wells required for a specific reservoir will generally depend on the injectivity of each well and the number of wells necessary to obtain adequate areal distribution.

External injection is generally considered superior to dispersed-type injection, since full advantage can usually be obtained from gravity drainage benefits. In addition, external injection ordinarily will result in greater areal sweep and conformance efficiencies than will similar dispersed injection operations.

Optimal Time to Initiate Gas Pressure-Maintenance Operations

Generalizations as to the optimal time to initiate gas pressure maintenance are of limited practical value because of the exceedingly large number of variables that must be considered from an economic and reservoir mechanics standpoint. Obviously, there is no method of calculating directly the optimal time from an economic standpoint; instead, several calculations of future performance, assuming initiation of injection at various stages of reservoir depletion, must be made and compared on an economic basis.

Considering only hydrocarbon recovery and improvements in producing characteristics, it can be stated that generally more favorable reservoir conditions for gas-injection operations are present when the reservoir is at or slightly below the reservoir fluid saturation pressure. Within this range of reservoir pressures, the initial free-gas saturation in the oil zone is at a minimum—a condition favorable to obtaining maximum recovery efficiency from the gas displacement process.

Efficiencies of Oil Recovery by Gas Displacement

It is convenient to analyze and evaluate the recovery efficiency obtainable by gas displacement operations in terms of three efficiency factors, generally referred to as (1) unit-displacement efficiency, (2) conformance efficiency, and (3) areal sweep efficiency. Each recovery efficiency may be considered as one component element that accounts for the influence of certain parameters on the overall recovery efficiency of the displacement process. The product of the three efficiency factors provides an estimate of the percentage oil recovery that can be expected with this recovery process in a particular reservoir

under specified conditions. Analytical procedures are available for evaluating each efficiency factor individually. In certain instances, such analytical procedures are combined to determine two or more of the factors as a unit; for example, the term "volumetric efficiency" is sometimes employed where the conformance and areal sweep efficiencies are combined into one factor. Similarly, the term "displacement efficiency" is sometimes used where the unit displacement and conformance efficiencies are evaluated in combination. For the purpose of this chapter, the three components describing the overall recovery process are defined as follows.

1. *Unit displacement efficiency* is the percentage of oil in place within a totally swept reservoir-rock volume that is recovered as a result of the displacement process.

2. *Conformance efficiency* is the percentage of the total rock or pore volume within the swept area that is contacted by the displacing fluid.

3. *Areal sweep efficiency* is the percentage of the total reservoir or pore volume that is within the swept area, the area contacted by the displacing fluid.

Each of the three efficiencies increases with continued displacement; therefore, each is a function of the number of displacement volumes injected. The rate of increase in recovery efficiency in a given portion of a reservoir diminishes as gas breakthrough occurs. Therefore, the maximum value of each component efficiency and, consequently, the ultimate recovery efficiency is limited by economic considerations.

Methods of Evaluating Unit-Displacement Efficiency

Equations

Unit-displacement efficiency is normally determined by analytical procedures developed from the two fundamental equations reported by Buckley and Leverett.² These equations essentially characterize the mechanics of steady-state, two-phase fluid flow encountered in oil displacement by an immiscible fluid. These equations were developed by means of relative-permeability concepts and are based on Darcy's law describing steady-state fluid flow through porous media.

The so-called *fractional-flow equation* describes quantitatively the fraction of gas flowing in terms of the physical characteristics of a unit element of porous media. In customary units, using a unit area, this equation is as follows.

$$f_g = \frac{1 + 1.127[k_o A / (\mu_o q_t)] \left[(\partial P_c / \partial L) - 0.433(\rho_o - \rho_g) \sin \alpha \right]}{1 + (k_{ro} / k_{rg})(\mu_g / \mu_o)} \quad \dots \dots \dots (1)$$

where

- f_g = fractional flow of gas,
- q_t = total flow rate, B/D,
- A = cross-sectional area, sq ft,
- P_c = oil/gas capillary pressure $(\rho_o - \rho_g)$, psi
- L = distance, ft,

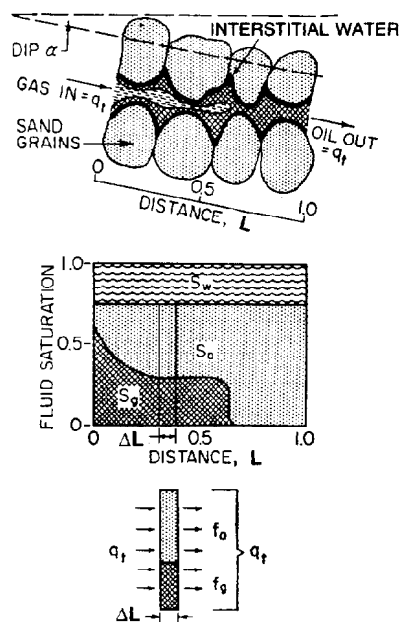


Fig. 43.1—Schematic representation of saturation distribution during gas-displacement process.

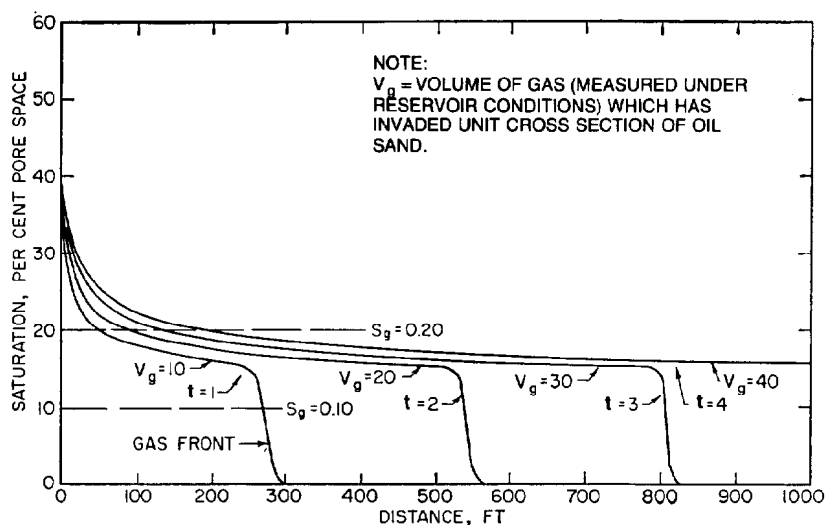


Fig. 43.2—Fluid saturation distribution at four time periods during gas displacement process.

- ρ_o = oil density, g/cm³,
 ρ_g = gas density, g/cm³,
 α = angle of dip, positive down-dip, degrees,
 k_o = effective permeability to oil, darcies,
 k_{ro} = relative permeability to oil, fraction,
 k_{rg} = relative permeability to gas, fraction,
 μ_o = oil viscosity, cp, and
 μ_g = gas viscosity, cp.

To relate the fraction of gas flowing to time, Buckley and Leverett developed the following material-balance equation.

$$L = \frac{5.615 q_i t}{\phi A} \left(\frac{\partial f_g}{\partial S_g} \right), \dots \dots \dots (2)$$

where

- t = time, days,
 ϕ = porosity, fraction, and
 S_g = gas saturation, fraction.

The value of the derivative $\partial(f_g)/\partial(S_g)$ may be obtained for any value of gas saturation by plotting f_g from Eq. 1 vs. S_g and determining slopes at various points on the resulting curve.^{3,4} This graphical procedure is generally considered to be sufficiently precise for most reservoir engineering calculations. It is especially suited where the calculations are to be made by hand calculators. A more precise mathematical procedure for evaluating the function $\partial(f_g)/\partial(S_g)$ was presented by Kern⁵ and is particularly adaptable for use with digital computers.

Figs. 43.1 and 43.2 illustrate the displacement process described by Eqs. 1 and 2. Calculated oil- and gas-saturation distributions for a hypothetical example of gas displacement after successive periods of injection are shown in Fig. 43.2. The area beneath any curve represents the gas-invaded zone, whereas the area to the right of the "gas front" at any time represents the uninvaded zone.

Modifications of Displacement Equations

Eqs. 1 and 2 were developed on the basis of the following simplifying assumptions.

1. Steady-state flow conditions prevail.
2. Displacement takes place at constant pressure.
3. The displacing and displaced phases are in compositional equilibrium.
4. None of the injected gas is dissolved in the oil.
5. There is no production of fluids from behind the gas front.
6. The advancing gas moves parallel to the bedding planes of the formation.
7. The gas front moves uniformly through laminated sands.
8. The interstitial water present is immobile.

The applicability of the basic displacement equations to a given reservoir is, of course, governed to a large extent by the restrictions imposed by the basic assumptions. Several authors have reported modifications to the displacement equations that eliminate the need for making certain of the assumptions. Modifications that take into consideration the swelling effects experienced from injection into an undersaturated reservoir and production of fluids from behind the gas front have been presented by Welge,³ Kern,⁵ Shreve and Welch,⁶ and others. Jacoby and Berry,⁷ Attra,⁸ and others have presented equations and analytical procedures for calculating per-

formance where there is significant compositional interchange of components between the displacing gas phase and the reservoir oil. The influence of deviations from the conditions described in Assumptions 6 and 7 is generally taken into consideration in the determination of conformance efficiencies.

Influencing Factors

Eqs. 1 and 2 provide a means for investigating the relative influence of the various parameters affecting unit-displacement efficiency. These factors are (1) initial saturation conditions, (2) fluid viscosity ratios, (3) relative-permeability ratios, (4) rate and formation dip, (5) capillary pressure, and (6) reservoir pressure and fluid properties.

Initial Saturation Conditions. Frequently, gas-injection operations are initiated after reservoir pressures have declined to such an extent as to permit the accumulation of free gas released from solution in the oil. If the free-gas saturation exceeds the breakthrough or critical saturation determined from the fractional-flow curve, an oil bank ahead of the front will not be formed; consequently, oil production will be accompanied by immediate and continually increasing free-gas production.² This influence of initial mobile gas saturation on gas displacement performance has been demonstrated by laboratory investigations and mathematical analyses.⁹ Fig. 43.3 shows a comparison of calculated and experimentally determined gas displacement performance. It will be noted that approximately 10% oil recovery was attained prior to gas breakthrough where the initial gas saturation was zero, whereas with an initial gas saturation of 18.1% PV, a period of gas-free production was not observed.

The magnitude of the interstitial water saturation present in a reservoir, of course, influences the quantity of oil subject to gas displacement. It apparently does not have an influence on the breakthrough unit-displacement efficiency as determined by the fractional-flow equations, however.¹⁰ If the interstitial water saturation is a mobile phase, the displacement equations are not directly applicable since they were developed from concepts of two-phase flow. Approximations of gas displacement performance can usually be made where three phases are mobile by treating the water and oil phases as a single liquid phase. Displacement calculations can then be made with k_{rg}/k_{ro} data determined from core samples containing interstitial water saturation. Oil recovery can be differentiated from total liquid recovery on the basis of k_{rw}/k_{ro} data or by material-balance calculations incorporating an estimated minimum interstitial water saturation.

Fluid Viscosity Ratios. The effects of variations in oil viscosity on calculated unit-displacement efficiency can be seen from an examination of the curves presented in Fig. 43.4. Note that the oil recovery is significantly improved as the viscosity of the oil approaches that of the displacing gas. This indicates that the most efficient displacement will occur where the oil-to-gas viscosity ratio is unity or less.

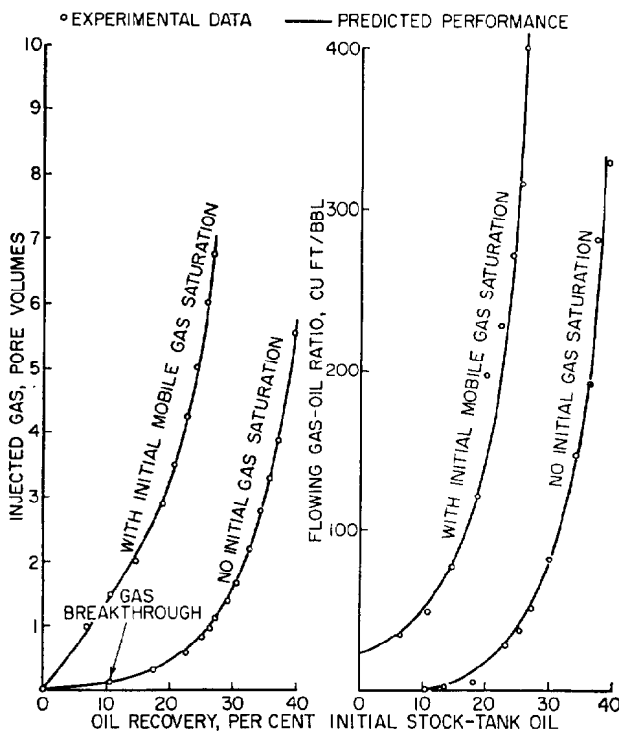


Fig. 43.3—Comparison of calculated and experimental gas-injection performance for two conditions of initial gas saturation.

Rate and Formation Dip. Note from Eq. 1 that several factors influence the magnitude of the gravity term. Since the fractional flow of gas decreases as the magnitude of the gravity term increases, maximum benefits from gravity segregation are obtained when the following occur.

1. Specific permeabilities and relative permeabilities to oil are high.
2. Reservoir oil viscosities are low and densities are high.
3. The cross-sectional area to flow is large.
4. The angle of dip is high (Fig. 43.5).
5. Injection and production rates are low.

Frequently, the design of a gas-injection program can have an appreciable effect on whether maximum advantage is obtained from gravity drainage in a given reservoir. For example, proper location and distribution of injection wells along the structurally high portions of the reservoir may in some cases increase the cross-sectional area to flow and take full advantage of maximum reservoir dip. Cap oil viscosities and relative oil permeabilities are favorable when pressures are highest. In addition, injection and production rates, in terms of reservoir withdrawals, are generally lowest at high reservoir pressures, indicating that maximum benefits from gravity drainage can be achieved by initiating gas-injection operations early in the life of a reservoir.

Relative-Permeability Ratios. It has been shown that the concepts of relative permeability can be applied equally well to complete or partial pressure-maintenance operations.¹¹ Since relative-permeability ratio, along

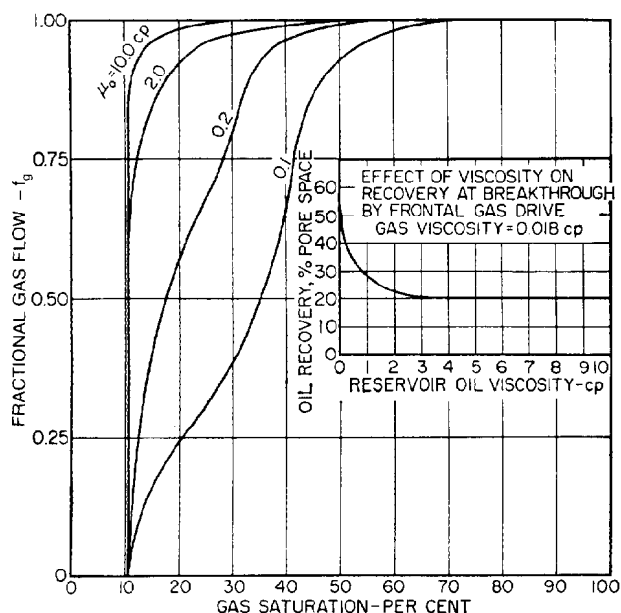


Fig. 43.4—Effect of oil viscosity on fractional flow of gas.

with viscosity ratio, fixes the relative portions of gas and oil flowing at any given saturation condition, it is one of the more important factors influencing unit-displacement efficiency. Relative permeability is a characteristic of the reservoir rock and is a function of fluid-saturation conditions; therefore, an operator has no control over the relative-permeability characteristics of a given reservoir. However, because of the significant influence that this factor has on the performance of gas-displacement operations, it is important that calculations be based on dependable data obtained from laboratory analyses of core samples. If possible, the laboratory-determined data should be supplemented by relative permeabilities calculated from field performance data.

Capillary Pressure. Capillary-pressure forces tend to oppose the forces of gravity drainage and, as a result, tend to decrease unit gas displacement efficiency. At extremely low rates of displacement where frictional factors become negligible, the saturation distribution may be controlled to a large extent by the balance between capillary and gravitational forces. However, at the rates of displacement normally employed in practice, it is generally considered that in most cases capillary forces, or capillary-pressure gradients, can be neglected without seriously detracting from the utility of the analysis.

Reservoir Pressures and Fluid Properties. In certain highly undersaturated reservoirs, particularly those containing high-gravity crude oils that are to some degree volatile, the unit-displacement efficiency can be increased by initiating pressure-maintenance operations at the highest pressure possible. Under the proper conditions of pressure and fluid composition and at the proper degree of undersaturation, a miscible-fluid displacement can be achieved by use of relatively "dry" injection gas. The mechanics of this process, which reportedly achieves unit-displacement efficiencies approaching

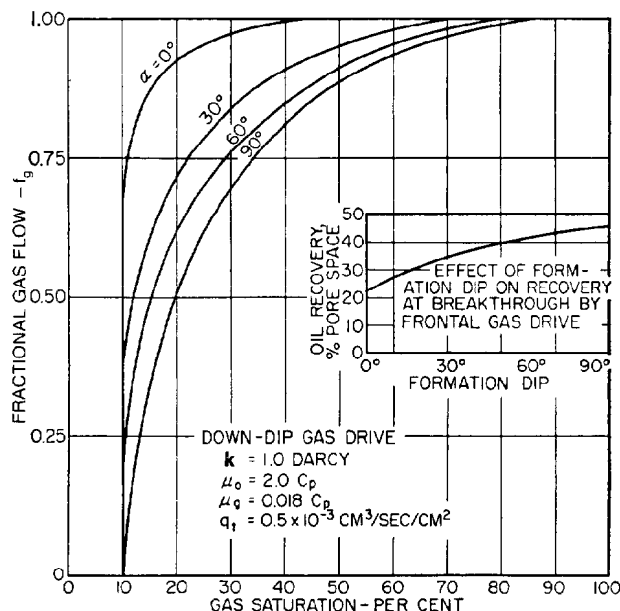


Fig. 43.5—Effect of formation dip on fractional flow of gas.

100%, will be considered more in detail in Chap. 45. Recovery efficiency often can be improved by gas injection at high reservoir pressures even though miscibility is not achieved. This improvement in recovery may be a result of (1) swelling or expansion of the undersaturated reservoir oil resulting from addition of dissolved gas, (2) reduction of the oil viscosity from addition of dissolved gas, and (3) vaporization of the residual oil and subsequent recovery from the produced gas.¹²

Laboratory data obtained from tests using samples of reservoir fluid and injection gas are necessary to evaluate quantitatively the degree of swelling and vaporization that will take place under specified reservoir conditions. These data may be used in conjunction with conventional material-balance, compositional-balance, and displacement equations to arrive at an estimate of unit-displacement efficiency.

Calculation Procedures

Example procedures for calculating displacement efficiency are included in Appendix A for the cases of horizontal and vertical (down dip) flow of displacing gas.

Methods of Evaluating Conformance Efficiency

Several methods have been advanced for evaluating the conformance efficiency for a given reservoir. Generally, all the methods are somewhat empirical and are based on either comparisons of calculated and observed past displacement performance or statistical analyses of core-analysis data.

If a displacement process such as gas-cap expansion or pilot injection operations has been operative in a reservoir long enough to yield sufficient and reliable data concerning the position of the gas front and recovery as a function of time, past reservoir performance can be used to calculate conformance efficiency. The basic premise

for this type of analysis is that the conformance efficiency is the predominant factor responsible for deviations between actual displacement performance and the ideal or theoretical. On this basis, the conformance efficiency is calculated by dividing the observed recovery at various time intervals by theoretical recovery for corresponding time periods. Theoretical recovery may be determined from unit-displacement-efficiency calculations including an appropriate areal sweep efficiency. The conformance efficiencies thus determined may then be empirically correlated with either rate of production or percent recovery to determine an average value or trend for use in making future performance predictions.

Several authors have presented methods for determining conformance efficiencies based on statistical treatments of core-analysis data. Perhaps the most frequently used is an adaptation of the method presented by Stiles¹³ for evaluating the effect of permeability variations on waterflood performance (see Chap. 44). Conformance-efficiency calculations for miscible-fluid displacement using this analytical technique are presented in Chap. 45. The same calculation procedures may be used when immiscible gas displacement is considered, except that the relative-permeability ratio k_{rg}/k_{ro} must be considered for immiscible gas displacement, whereas it is not applicable to miscible displacement. The relative-permeability ratio used in such calculations is considered to be constant and is generally taken to be the relative permeability to gas at residual oil saturation divided by the relative permeability to oil at initial gas saturation.

Influencing Factors

The conformance efficiency for a given reservoir is largely controlled by the influence of (1) variations in rock properties, (2) mobility ratios, and (3) gravity segregation.

Variations in Rock Properties. Reservoir-rock porosity and permeability vary from one pore channel to the next. In addition, reservoir rock almost universally is formed in layers—stratified—either to a small extent or over large distances. Stratification can be merely differences in porosity and permeability of layers in capillary equilibrium or can be separations caused by impermeable shale or other rock streaks. Variations in porosity and permeability can be both vertical and horizontal. All these rock heterogeneities tend to decrease the effective size of the reservoir as far as displacement operations are concerned. Therefore, the degree of heterogeneity controls to a large extent the conformance efficiency attainable from gas-injection operations in a given reservoir.

Mobility Ratios. The mobility of a fluid is an index of the ease with which the fluid will flow under specified conditions. Herein, mobility is defined as the relative permeability to a fluid at a given saturation divided by the fluid viscosity. Mobility ratio, M , is an index of the ease with which one fluid will flow relative to another fluid. It is defined herein as the ratio of the gas mobility to the oil mobility or, in equation form,

$$M = \frac{k_{rg}}{k_{ro}} \frac{\mu_o}{\mu_g}, \dots\dots\dots (3)$$

with permeabilities and viscosities as before.

If the mobility ratio is equal to unity, it indicates that, for a given pressure differential, oil and gas will flow with equal ease; values greater than unity indicate that gas will be the more mobile fluid, etc. During the gas displacement process, mobility ratio can vary from essentially zero during periods of low gas saturation to values approaching infinity during the periods of high gas saturation.

In heterogeneous reservoir-rock systems, relative-permeability characteristics may be extensively variable both laterally and vertically. As a result, the displacing gas will not form a uniform front as it advances but will tend to “finger” ahead in the layers or areas having higher mobility ratios. As the displacement progresses, the mobility ratio continues to increase in the portions of the reservoir previously contacted by displacing gas. As a result, there is a decreasing tendency for gas to enter regions of low permeability or regions of low gas saturation. These volumes are therefore bypassed and little or no oil is recovered from them. It can be seen that the factors tending to increase the mobility ratio also tend to accentuate the detrimental effects of sand heterogeneity on conformance efficiency.

High localized injection and production rates in the presence of adverse mobility ratios and sand heterogeneity can add to the severity of gas channeling and resultant bypassing of oil. The possibility of creating this adverse effect frequently can be reduced through proper selection of the number and location of injection wells and proper scheduling of fluid withdrawals so that minimum pressure drawdown is created in the vicinity of the advancing gas front.

Gravity Segregation. As was previously mentioned, gravity forces tend to improve unit-displacement efficiency. Gravity drainage has essentially the same influence on conformance efficiency, and its effectiveness is controlled by the same factors—i.e., rate, angle of dip, vertical permeability, etc. Under favorable conditions, gravity drainage tends to maintain a more uniform gas front and therefore tends to offset the effects of adverse mobility ratios and permeability variations.

Under certain conditions, gravity segregation of the displacing and displaced fluids has an adverse effect on the conformance efficiency. In reservoirs having relatively good vertical communication, low formation dips, and slow displacement rates, the gas tends to segregate to the top of the formation, bypassing oil in the lower portions and creating a so-called umbrella effect, which causes premature breakthrough of the gas and a lowering of conformance efficiency.

Methods of Evaluating Areal Sweep Efficiency

Several investigators have shown that the areal sweep efficiency for a given reservoir is controlled to a large extent by (1) injection/production well arrangements with respect to reservoir geometry, (2) mobility ratio of the fluids involved, and (3) number of displacement volumes injected.

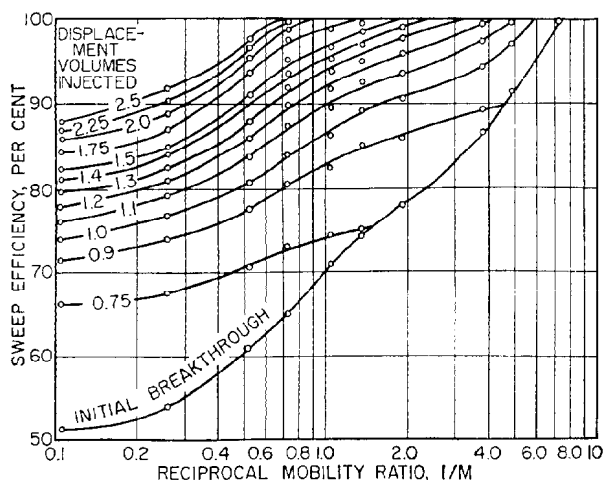


Fig. 43.6—Sweep efficiency as a function of mobility ratio.

Applied mathematical techniques have been used to investigate the influence of these factors on regular geometrical reservoir units of constant thickness. On the other hand, various types of laboratory and numerical models have been used to study the effects on areal sweep efficiencies of irregular reservoir boundaries, irregular well arrangements, variable formation thicknesses, and variable mobility ratios. From these investigations, it generally can be concluded that the areal sweep efficiency at gas breakthrough will be a maximum in a given reservoir when the mobility ratio is low and when the distance from injection to production well is large. After gas breakthrough, areal sweep efficiencies are improved as the number of injected displacement volumes increase. The influence of mobility ratio and displacement volumes injected on the areal sweep efficiency of a regular five-spot reservoir unit may be seen in Fig. 43.6. The data presented in this illustration were obtained from model studies that used miscible fluids of various viscosities to study the influence of various mobility ratios. These data are generally considered to be applicable to reservoir analyses for either water or gas displacement when actual model studies for a given reservoir are not available.

Areal sweep efficiencies, calculated at gas breakthrough and at successive periods thereafter until the economic limit is reached, are required for estimating reservoir performance under pressure-maintenance operations. If the injection/production well arrangements and the fluid mobility ratios for a given reservoir closely approximate those that have been studied in the laboratory, the data on this subject reported in the literature may be used as a basis for estimating the areal sweep efficiencies. Data reported by Dyes *et al.*¹⁴ have been found particularly useful since consideration was given to the influence of production after gas breakthrough. Note that the quantitative applicability of laboratory data is inherently questionable because of uncertainties in model scaling, laboratory techniques, and associated simplifying assumptions. Nevertheless, laboratory-model studies still offer the most convenient means of determining quantitative data concerning areal

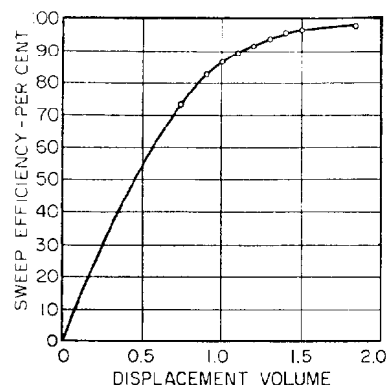


Fig. 43.7—Areal sweep efficiency as a function of injection fluid volume for a mobility ratio of unity.

sweep efficiencies. For this reason, if mathematical model studies are not practical for the particular reservoir under consideration, published data (tempered by experience) must generally be resorted to as a basis for predicting areal sweep efficiencies even though the well arrangements being investigated do not duplicate those reported in the literature.

For application to performance predictions, it is frequently desirable to construct a curve showing the areal sweep efficiency for a given mobility ratio as a function of the fractional gas flow, f_g , or the displacement volumes injected. For example, Fig. 43.7 shows a replot of the data presented in Fig. 43.6 for a mobility ratio of unity. If necessary, the trend established from these data may be adjusted up or down depending on the judgment of the engineer as to the applicability of the model to the reservoir under consideration.

As was discussed in a previous section of this chapter, during gas displacement operations there is a significant gradient in mobility ratios behind the gas front. Therefore, an average mobility ratio must be selected to determine areal sweep efficiencies from published data. Probably the most representative, and certainly the most conservative, value for this purpose is the mobility ratio determined at the average gas saturation behind the front according to the methods presented in connection with unit-displacement efficiencies.

Calculation of Gas Pressure-Maintenance Performance

Estimates of gas-injection performance are generally based on the simultaneous solution of one or more forms of the conventional material-balance equations and the displacement equations previously discussed. The manner in which these equations are applied will vary depending on the scope of the investigation, the type of reservoir under consideration, and whether dispersed or external injection is to be used for complete or for partial pressure maintenance. Rigorous treatment of all factors influencing production performance and the displacement processes in a given reservoir can result in the development of calculation procedures that are quite

complex. Specific analytical techniques and procedures as applied to various types of reservoirs have been the subject of numerous articles in the technical literature and several reservoir engineering textbooks. A selected bibliography of technical articles dealing with specific analytical techniques and procedures that can be used for estimating reservoir performance under gas-injection operations is included in Appendix B. Note that these references are indexed according to the type of reservoir under consideration, the major influencing factors, and the type of injection-well arrangement. These references can be used as a basis for developing suitable analytical techniques to estimate future pressure-maintenance performance in any given reservoir. However, since each petroleum reservoir is unique, in the final analysis engineers must rely upon imagination and experience to develop techniques, based on fundamental theory, for the particular reservoir under consideration.

Although the equation forms and specific details of estimating reservoir performance will vary somewhat for each reservoir considered, certain general analytical procedures are common to most investigations and can be used as a basis for developing specific calculation techniques. A complete engineering analysis of a reservoir for the purpose of evaluating gas-injection operations will usually consist of four major phases: (1) assembly, preparation, and analysis of basic data; (2) analysis of past performance; (3) projection of future performance of current operations; and (4) estimation of gas pressure-maintenance performance.

Basic Data

The need for adequate and comprehensive basic data has been emphasized in other chapters of this book and is apparent when it is realized that the validity and therefore the utility of any engineering analysis is determined primarily by the quality and quantity of basic data. The data requirements for analysis of gas-injection operations are, with few exceptions, the same as the requirements for analysis of other types of fluid-injection operations. Appendix C includes an outline of the usual data requirements for engineering analyses as presented by Patton,¹⁵ with certain additions and modifications.

Analysis of Past Performance

The methods used to evaluate past reservoir performance will, of course, vary depending on the active reservoir drive mechanisms present, the quantity of suitable basic data available, and the amount of detail or scope of the investigation. Procedures for analyzing past reservoir performance are discussed in detail in other chapters. The results of such analyses will determine to a large extent the methods used for predicting gas-injection pressure-maintenance performance and will provide the current reservoir pressure and saturation distribution conditions for use in such predictions. Further, proper analysis of past performance will aid in supplementing and establishing the reliability of data required for the projection of reservoir performance under injection operations.

Projection of Future Performance of Current Operations

Decisions regarding the installation of gas-injection

operations must be made on the basis of the relative benefits to be derived from such operations compared with competitive recovery techniques. Therefore, any complete analysis of gas-injection operations would include the projection of future reservoir performance under the current production operations. Methods of projecting future primary production performance and other types of injection operations are discussed in detail in other chapters.

Estimation of Gas Pressure-Maintenance Performance

Generally, projections of partial pressure-maintenance performance, for either external or dispersed-type gas injection, can be made by use of conventional material- and volumetric-balance techniques in combination with recovery efficiency determinations previously discussed. On the other hand, if complete pressure maintenance is being considered, the project performance can be estimated by only the displacement equations and other analytical procedures presented previously in connection with the discussions of unit displacement, conformance, and areal sweep efficiency.

Procedures for calculating the future performance of both external and dispersed-type gas-injection operations are included in Appendix A. These example calculations include the determination of displacement efficiency and pressure, producing gas/oil ratio, and recovery performance for primary operations and for various degrees of gas-injection pressure maintenance for two idealized reservoirs.

Performance-Time Predictions. Predictions of future gas-injection performance are necessary for making economic comparisons of various types of future operations. Such predictions will usually include estimates of functions of time such as (1) reservoir pressures; (2) oil-, gas-, and water-production rates; (3) gas- and water-injection rates; (4) GOR's; (5) cumulative oil, gas, and water recovery; (6) cumulative gas and water injected; (7) number of producing, injecting, and shut-in wells; and (8) recoverable plant products, if applicable.

To estimate these quantities, it is necessary to develop relationships between the hydrocarbon distribution of the subject reservoir and the positions of injection and production wells. Once this is done and with a given injection rate, Eq. 2 can be used to calculate the time necessary for the gas front to reach incrementally selected points in the reservoir.

In gas-cap-drive reservoirs and where external injection is being considered for reservoirs having significant structural relief, it is frequently convenient to relate hydrocarbon PV, cross-sectional area, and well completion intervals to subsea depth within the reservoir. If such relationships are used and if the advancing gas front is assumed to conform to structural depth, displacement equations and fluid inventory equations can be used to predict the rate of advance of the gas front, taking into consideration changes in cross-sectional area and reservoir productivity.

Until the gas front reaches the top of the perforations in the structurally highest well, oil and gas production is controlled by the productivities or allowables of the producing wells ahead of the front; and producing GOR's

TABLE 43.1—BASIC RESERVOIR DATA

Oil reservoir having no original gas cap	
Initial oil volume, N , STB	30,650,351
Average porosity, ϕ , %	29.5
Average rock permeability, k , md	300.0
Average interstitial water saturation, S_w , %	30.0
Initial bubblepoint pressure, p_b , psig	1,375
Oil reservoir with original gas cap	
Initial oil volume, N , STB	30,650,351
Initial gas-cap gas volume, Mcf	12,716,000
Area of gas/oil contact A , acres	842
Ratio of gas-cap to oil-zone volume, m , fraction	0.610
Average porosity, ϕ , %	29.5
Average rock permeability, k , md	300.0
Average oil-zone water saturation, S_{wo} , %	30.0
Average gas-cap water saturation, S_{wg} , %	25.0
Bubblepoint pressure at gas/oil level p_b , psig	1,375

are controlled by gas-saturation conditions ahead of the front. If it is assumed that each producing well is shut in as gas breakthrough occurs, the producing GOR will remain a function of oil-zone gas saturation, and the total oil-producing rate and gas-injection rate will decline as the front reaches each successively lower-producing well. The oil-producing rate at any position of the gas front can be determined from the productivities or allowables of the wells in the uninvaded portions of the reservoir. If it is assumed that each well is produced to an economically limiting GOR prior to being shut in, production from behind the front must be accounted for by use of the modified displacement equations referred to previously. In such cases, a comprehensive fluid inventory is required to account for the portion of the injected gas being produced at any time and the portion that is advancing down structure. If partial-pressure-maintenance operations are being considered, it is necessary to introduce material-balance equations to calculate, by trial-and-error methods, the pressure decline and relative positions of the advancing gas front.

With complete pressure maintenance in reservoirs having low structural relief or where the gas front is likely to advance parallel to the bedding planes of the formation,

the cumulative hydrocarbon distribution, cross-sectional area, and reservoir productivity can be related to distance from injection to production wells. Where dispersed gas injection is being considered, calculations can be made for a typical pattern element of the reservoir and the results applied to the total number of patterns present. Care should be taken to select a method of reservoir representation that will conform as nearly as possible to the anticipated frontal advance in a given reservoir.

APPENDIX A

Example Calculations of Future Performance

I. Basic Data

The basic reservoir rock and fluid data used throughout are presented in Tables 43.1 and 43.2 and in Figs. 43.8 and 43.9.

II. Unit Displacement

A. Horizontal Gas Flow

1. Equation

$$f_g = \frac{1}{1 + (k_{ro}/k_{rg})(\mu_g/\mu_o)}$$

where

- f_g = fractional gas flow,
- k_{ro} = relative permeability to oil at S_g ,
- k_{rg} = relative permeability to gas at S_g ,
- μ_o = oil viscosity at p , cp, and
- μ_g = gas viscosity at p , cp.

2. Procedure

a. Calculate and construct a fractional-flow curve for selected increments of gas saturation, S_g , as indicated in Table 43.3 and Fig. 43.10.

TABLE 43.2—SUMMARY OF RESERVOIR-FLUID PROPERTIES

Pressure p (psig)	Oil-Volume Factor B_o (bbl/STB)	Solution GOR R_s (scf/STB)	Gas-Volume Factor B_g (bbl/scf)	Oil Viscosity μ_o (cp)	Gas Viscosity μ_g (cp)	Oil Density ρ_o (g/cm ³)	Gas Density ρ_g (g/cm ³)
$p_b = 1,375$	1.210	430.1	0.00178	0.480	0.0148	0.765	0.084
1,300	1.200	414.9	0.00194	0.490	0.0146	0.766	0.082
1,200	1.186	397.0	0.00211	0.508	0.0143	0.767	0.079
1,100	1.173	379.0	0.00233	0.527	0.0140	0.769	0.076
1,000	1.160	361.0	0.00258	0.544	0.0137	0.771	0.073
900	1.147	342.0	0.00290	0.564	0.0134	0.773	0.068
800	1.134	321.7	0.00329	0.587	0.0132	0.775	0.062
700	1.120	301.0	0.00380	0.609	0.0129	0.779	0.056
600	1.106	277.9	0.00447	0.633	0.0126	0.783	0.050
500	1.091	254.9	0.00540	0.661	0.0124	0.788	0.043
400	1.076	230.2	0.00677	0.692	0.0121	0.794	0.035
300	1.060	202.1	0.00904	0.729	0.0119	0.801	0.027
200	1.043	167.9	0.01339	0.773	0.0117	0.809	0.018
100	1.024	125.2	0.02545	0.832	0.0116	0.819	0.009
0	1.001	0.0	0.19802	0.910	0.0114	0.835	0.001

b. Construct the tangent to the f_g curve from the equilibrium gas saturation, S_g (equal to zero in this case), and read the average gas saturation behind the front at breakthrough from the intercept where $f_g = 1.0$. This average gas saturation \bar{S}_g corresponds to the oil recovery as a fraction of total pore volume behind the front.

c. Construct other tangents as required to obtain the average gas saturations and oil recoveries at various other values of f_g or frontal gas saturations S_g .

B. Downdip Gas Flow

1. Equation

$$f_g = \frac{1 + 0.489[k_o(\rho_g - \rho_o)\sin \alpha / (q_t \mu_o)]}{1 + (k_{ro}/k_{rg})(\mu_g/\mu_o)}$$

where

- f_g = fractional gas flow,
- k_o = effective permeability to oil, darcies,
- ρ_g = gas density at p , g/cm³,
- ρ_o = oil density at p , g/cm³,
- α = angle of gas flow (-90°),
- q_t = rate of frontal gas movement, B/D-sq ft,
- k_{ro} = relative permeability to oil at S_g ,
- k_{rg} = relative permeability to gas at S_g ,
- μ_o = oil viscosity at p , cp, and
- μ_g = gas viscosity at p , cp.

2. Procedure

a. By using a unit flow, calculate and construct a fractional-flow curve for selected increments of gas saturation, S_g , as indicated in Table 43.4 and in Fig. 43.11.

b. Construct the tangent to the f_g curve from the equilibrium gas saturation, S_{ge} (equal to zero in this case), and read the average gas saturation behind the front at breakthrough from the intercept where $f_g = 1.0$. This average gas saturation \bar{S}_g corresponds to the oil recovery as a fraction of the total swept pore volume.

c. Construct the tangent to the f_g curve where f_g becomes asymptotic to 1.0 and read the ultimate or maximum value for \bar{S}_g .

III. Dispersed Gas-Injection Pressure Maintenance

A. Partial Pressure Maintenance

1. Equations

$$\Delta N_p = \frac{(1 - N_{pi}) \Delta[(B_o/B_g) - R_s] - B_{ob} \Delta(1/B_g)}{[(B_o/B_g) - R_s] + \bar{R}(1 - \Delta G_i)}$$

$$S_L = S_w + (1 - S_w) \left(\frac{B_o}{B_{ob}} \right) (1 - N_p),$$

and

$$R = R_s + \left(\frac{k_{rg}}{k_{ro}} \right) \left(\frac{\mu_o}{\mu_g} \right) \left(\frac{B_o}{B_g} \right),$$

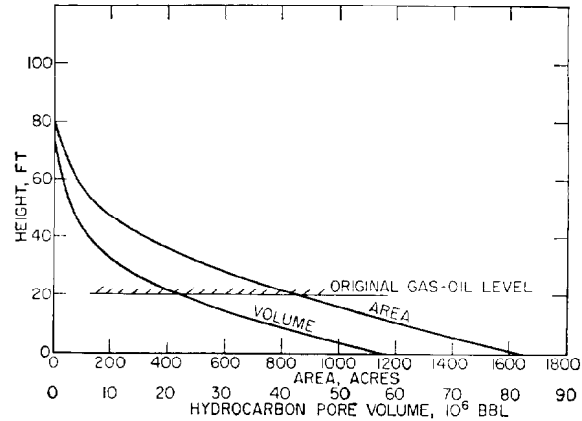


Fig. 43.8—Reservoir volume and area as functions of height.

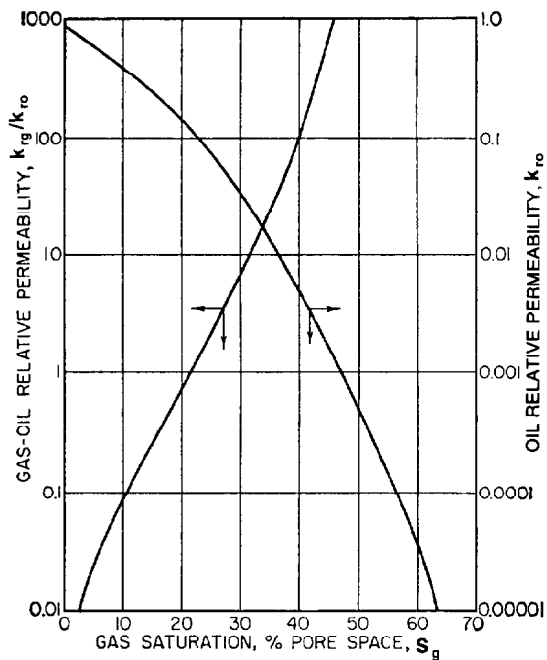


Fig. 43.9—Relative-permeability data.

where

- ΔN_p = incremental oil production, fraction of OIP,
- N_p = cumulative oil production, fraction of OIP,
- N_{pi} = cumulative oil produced from previous step, fraction of OIP,
- R = instantaneous GOR, scf/STB,
- \bar{R} = average GOR, scf/STB,
- R_s = solution GOR, scf/STB,
- S_L = total liquid saturation, fraction,
- S_w = interstitial water saturation, fraction,
- k_{rg} = relative permeability to gas at S_L ,
- k_{ro} = relative permeability to oil at S_L ,
- μ_g = gas viscosity at p , cp,
- μ_o = oil viscosity at p , cp,
- B_o = oil FVF, RB/STB,
- B_{ob} = oil FVF at p_b , RB/STB,
- B_g = gas FVF, bbl/scf, and
- ΔG_i = incremental gas injection, fraction of produced gas.

TABLE 43.3—FRONTAL-ADVANCE CALCULATION, HORIZONTAL FLOW

S_g (1)	k_{rg}/k_{ro} (2)	$(k_{ro}/k_{rg})(\mu_g/\mu_o)$ (3)	$1 + (3)$ (4)	$f_g = 1/(4)$ (5)
0	0.000	—	—	0
0.02	0.004	7.725	8.725	0.1146
0.05	0.025	1.236	2.236	0.4472
0.10	0.088	0.351	1.351	0.7402
0.15	0.265	0.117	1.117	0.8953
0.20	0.770	0.0400	1.0400	0.9614
0.25	2.300	0.0134	1.0134	0.9868
0.30	7.35	0.00420	1.00420	0.9958
0.35	25.15	0.00122	1.00122	0.9988
0.40	117.0	0.00026	1.00026	0.9997
0.45	755.0	0.00004	1.00004	1.0000

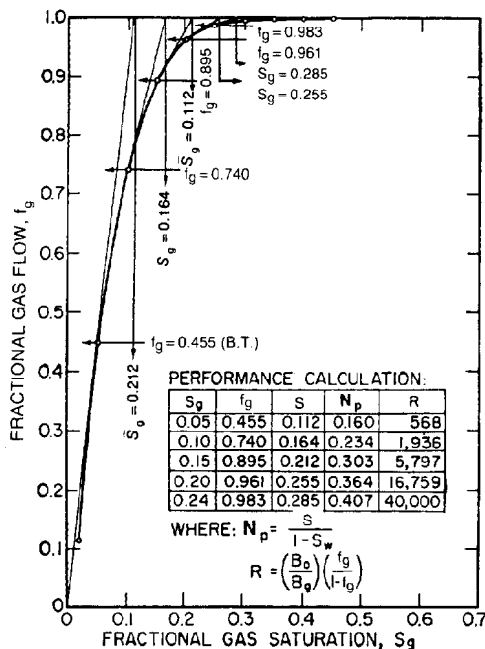
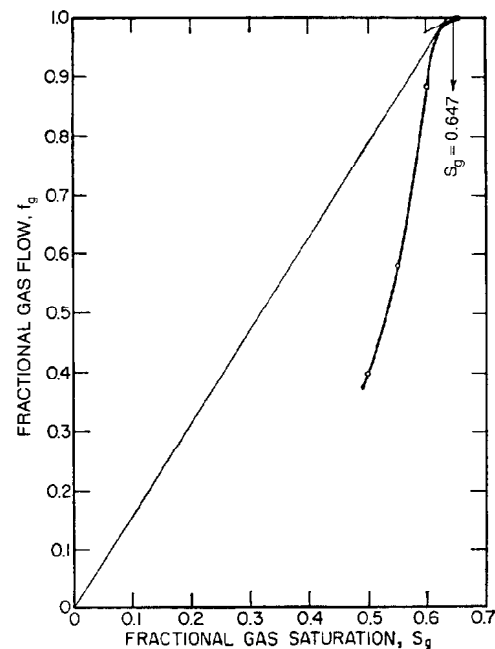
2. Procedure

a. Select pressure increments such that any one increment $\leq 10\%$ of the initial or bubble-point pressure and obtain fluid properties as indicated in Table 43.2.

b. Perform material-balance calculation as shown in Table 43.5, with no gas injection, by assuming an incremental oil production ΔN_p and verifying this value by the trial-and-error procedure indicated. This procedure can be shortened by use of previous calculated ΔN_p for the second and third trials at each pressure. (Note that subscript i in Col. 13 refers to previous step.)

c. Repeat this procedure for various values of gas injection as shown in Table 43.6.

d. Construct performance curves as indicated in Fig. 43.12.

**Fig. 43.10—Frontal-advance performance, horizontal gas flow.****Fig. 43.11—Frontal-advance performance, gas-cap expansion.****TABLE 43.4—FRONTAL-ADVANCE CALCULATION, GAS-CAP EXPANSION**

S_g (1)	k_{rg}/k_{ro} (2)	$(k_{ro}/k_{rg})(\mu_g/\mu_o)$ (3)	$1 + (3)$ (4)	$1/(4)$ (5)	k_{ro} (6)	$C_1 \times (6)^*$ (7)	$f_g = 1/(4)$ $[1 - (7)](5)$ (8)
0.20	0.770	0.04000	1.04000	0.9615	0.1320	366.6	-351.5
0.25	2.300	0.01340	1.01340	0.9868	0.0680	188.8	-185.3
0.30	7.35	0.00420	1.00420	0.9958	0.0320	88.9	-87.5
0.35	25.15	0.00122	1.00122	0.9988	0.0130	36.1	-35.06
0.40	117.0	0.00026	1.00026	0.9997	0.0048	13.3	-12.30
0.45	755.0	0.00004	1.00004	0.99996	0.0116	4.44	-3.40
0.50	—	0	1.00000	1.0000	0.0005	1.39	-0.400
0.55	—	0	1.00000	1.0000	0.00015	0.417	0.583
0.60	—	0	1.00000	1.0000	0.00004	0.111	0.889
0.65	—	0	1.00000	1.0000	0.00000	0.000	1.000

* $C_1 = 21,306 [k(\rho_g - \rho_o) \sin \alpha / (q, \mu_o)]$, where k is absolute permeability.

TABLE 43.5—DEPLETION DRIVE CALCULATION, FINITE-DIFFERENCE METHOD WITH NO REINJECTION OF PRODUCED GAS*

P (1)	ΔN_p (assumed) (2)	$N_p = \Sigma(2)$ (3)	$1 - N_p$ (4)	B_o/B_{ob} (5)	$S_o =$ $(1 - S_w)(4)(5)$ (6)	$S_i =$ $S_o + S_w$ (7)	$f_g =$ $(B_o/B_g)(\mu_o/\mu_g)$ (8)	k_{rg}/k_{ro} (9)	$(8) \times (9)$ (10)	R_s (11)
$P_b = 1,375$	0	0	1.0	1.0	0.700	1.000	22,035	0	0	430.1
1,300	0.0160	0.0160	0.9840	0.992	0.683	0.983	20,829	0.0001	2.1	414.9
1,200	0.0170	0.0330	0.9670	0.980	0.663	0.963	19,951	0.0160	319.2	397.0
1,100	0.0155	0.0485	0.9515	0.969	0.645	0.945	18,969	0.0275	521.6	379.0
1,000	0.0147	0.0632	0.9368	0.959	0.6289	0.9289	17,841	0.0431	768.9	361.0
900	0.0142	0.0774	0.9226	0.948	0.6122	0.9122	16,651	0.0653	1,087.3	342.0
800	0.0132	0.0906	0.9094	0.937	0.5965	0.8965	15,357	0.0960	1,474.3	321.7
700	0.0114	0.1020	0.8980	0.9256	0.5818	0.8818	13,919	0.1350	1,879.1	301.0
600	0.0110	0.1130	0.8870	0.9140	0.5675	0.8675	12,409	0.1890	2,345.3	277.9
500	0.0097	0.1227	0.8773	0.9017	0.5537	0.8537	10,777	0.2575	2,775.1	254.9
400	0.0093	0.1320	0.8680	0.8893	0.5403	0.8403	9,089	0.3420	3,108.4	230.2
300	0.0098	0.1418	0.8582	0.8760	0.5262	0.8262	7,184	0.4700	3,376.5	202.1
200	0.0112	0.1530	0.8470	0.8620	0.5111	0.8111	5,149	0.6560	3,377.7	167.9
100	0.0150	0.1680	0.8320	0.8463	0.4929	0.7929	2,882	0.9600	2,766.7	125.2
0	0.0590	0.2270	0.7730	0.8264	0.4472	0.7472	403	2.580	1,039.7	0.0

$R =$ $(11) + (10)$ (12)	$\bar{R} =$ $[(R_i + R_{i+1})/2]**$ (13)	$(B_o/B_g) - R_s$ (14)	$(13) + (14)$ (15)	$\Delta[(B_o/B_g) - R_s]$ (16)	$(4)(16)*$ (17)	$\Delta(1/B_g)$ (18)	$B_{ob} \Delta(1/B_g)$ (19)	$(17) - (19)$ (20)	$\Delta N_p =$ $(20)/(15)$ (21)
430.1	—	250.0	—	—	—	—	—	—	0
417.0	423.6	205.0	628.6	-45.0	-45.0	-45.5	-55.1	10.1	0.0161
716.2	566.6	165.0	731.6	-40.0	-39.4	-42.7	-51.7	12.3	0.0168
900.6	808.4	125.5	933.9	-39.5	-38.2	-43.8	-53.0	14.8	0.0158
1,129.9	1,015.2	88.4	1,103.6	-37.1	-35.3	-42.7	-51.7	16.4	0.0149
1,429.3	1,279.6	53.5	1,333.1	-34.9	-32.7	-42.6	-51.5	18.8	0.0141
1,796.0	1,612.6	23.4	1,636.0	-30.1	-27.8	-40.5	-49.0	21.2	0.0130
2,180.1	1,988.0	-6.1	1,981.9	-29.5	-26.8	-41.0	-49.6	22.8	0.0115
2,623.2	2,401.6	-30.7	2,370.9	-24.6	-22.1	-39.8	-48.2	26.1	0.0110
3,030.0	2,826.6	-52.7	2,773.9	-22.0	-19.5	-38.2	-46.2	26.7	0.0096
3,338.6	3,184.3	-71.3	3,113.0	-18.6	-16.3	-37.6	-45.5	29.2	0.0094
3,578.6	3,458.6	-84.9	3,373.7	-13.6	-11.8	-37.1	-44.9	33.1	0.0098
3,545.6	3,562.1	-90.0	3,472.1	-5.1	-4.4	-35.9	-43.4	39.0	0.0112
2,891.9	3,218.8	-85.0	3,133.8	+5.0	+4.2	-35.4	-42.8	47.0	0.0150
1,039.7	1,965.8	-5.05	1,960.8	+80.0	+66.6	-34.2	-41.4	108.0	0.0551

*Hand calculated values rounded off and will vary slightly from the computer-generated values given here.

**i = previous step.

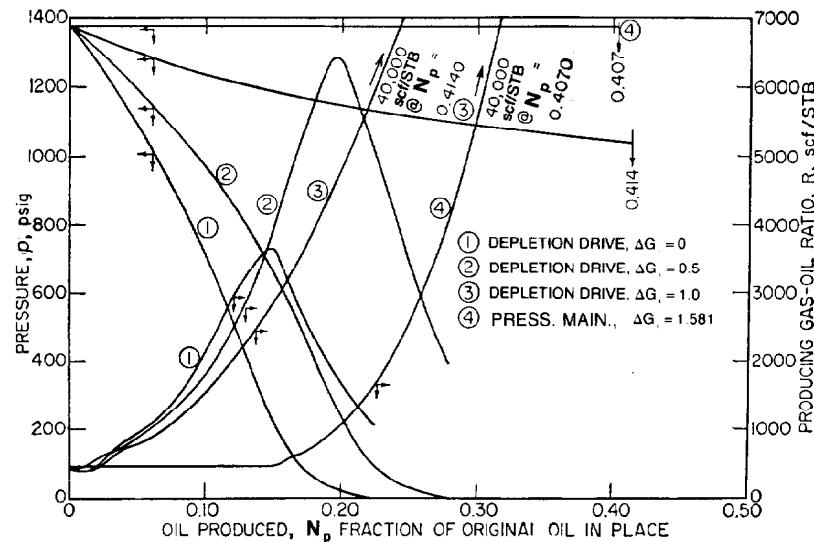


Fig. 43.12—Dispersed gas-injection pressure-maintenance performance.

**TABLE 43.6—DEPLETION DRIVE CALCULATION, FINITE-DIFFERENCE METHOD
WITH DISPERSED GAS INJECTION**

p (1)	ΔN_p (assumed) (2)	$N_p = \Sigma(2)$ (3)	$1 - N_p$ (4)	B_o/B_{ob} (5)	$S_o =$ $(1 - S_w)(4)(5)$ (6)	$S_L =$ $S_o + S_w$ (7)	$f_g =$ $(B_o/B_g)(\mu_o/\mu_g)$ (8)	k_{rg}/k_{ro} (9)	(8) \times (9) (10)	R_s (11)
$\Delta G_i = 0.5$										
$p_b = 1,375$	0	0	1.0	1.0	0.700	1.000	22,035	0	0	430.1
1,300	0.0230	0.0230	0.9770	0.992	0.677	0.977	20,829	0.009	187.5	414.9
1,200	0.0240	0.0470	0.9530	0.980	0.654	0.954	19,951	0.022	438.9	397.0
1,100	0.0245	0.0715	0.9285	0.969	0.629	0.929	18,969	0.044	834.6	379.0
1,000	0.0215	0.0930	0.9070	0.959	0.609	0.909	17,841	0.072	1,284.6	361.0
900	0.0200	0.1130	0.8870	0.948	0.589	0.889	16,651	0.112	1,864.9	342.0
800	0.0170	0.1300	0.8700	0.937	0.571	0.871	15,357	0.167	2,564.6	321.7
700	0.0150	0.1450	0.8550	0.9256	0.554	0.854	13,919	0.240	3,340.6	301.0
600	0.0135	0.1585	0.8415	0.9140	0.538	0.838	12,409	0.345	4,281.1	277.9
500	0.0115	0.1700	0.8300	0.9017	0.524	0.824	10,777	0.465	5,011.3	254.9
400	0.0110	0.1810	0.8190	0.8893	0.510	0.810	9,089	0.623	5,662.4	230.2
300	0.0114	0.1924	0.8076	0.8760	0.495	0.795	7,184	0.860	6,178.2	202.1
200	0.0126	0.2050	0.7950	0.8620	0.480	0.780	5,149	1.180	6,075.8	167.9
100	0.0167	0.2217	0.7783	0.8463	0.461	0.761	2,882	1.790	5,158.8	125.2
0	0.0573	0.2790	0.7210	0.8264	0.417	0.717	403	4.850	1,954.5	0.0
$\Delta G_i = 1.0$										
$p_b = 1,375$	0	0	1.0	1.0	0.700	1.000	22,035	0	0	430.1
1,300	0.051	0.051	0.949	0.992	0.659	0.959	20,829	0.019	395.8	414.9
1,200	0.083	0.134	0.866	0.980	0.594	0.894	19,951	0.100	1,995.1	397.0
1,100	0.150	0.284	0.716	0.969	0.486	0.786	18,969	1.030	19,538.1	379.0
1,000	0.284	0.568	0.432	0.959	0.290	0.590	17,841	170.0	3,032,970.0	361.0
$R =$ (11) + (10) (12)	$R =$ $[(R_i + R_{i+1})/2]$ (13)	$(1 - \Delta G_i) \bar{R}$ (14)	$(B_o/B_g) - R_s$ (15)	(14) + (15) (16)	$\Delta[(B_o/B_g) - R_s]$ (17)	(4)/(17) (18)	$\Delta(1/B_g)$ (19)	$B_{ob} \Delta(1/B_g)$ (20)	(18) - (20) (21)	$\Delta N_p =$ (21)/(16) (22)
430.1	—	—	250.0	—	—	—	—	—	—	0
602.4	516.2	258.1	205.0	463.1	-45.0	-45.0	-45.5	-55.5	10.5	0.0227
835.9	719.2	359.6	165.0	524.6	-40.0	-39.1	-42.7	-51.7	12.6	0.0240
1,213.6	1,024.8	512.4	125.5	637.9	-39.5	-37.6	-43.8	-53.0	15.4	0.0241
1,645.6	1,429.6	714.8	88.4	803.2	-37.1	-34.4	-42.7	-51.7	17.3	0.0215
2,206.9	1,926.2	963.1	53.5	1,016.6	-34.9	-31.7	-42.6	-51.5	19.8	0.0195
2,886.3	2,546.6	1,273.3	23.4	1,296.7	-30.1	-26.7	-40.5	-49.0	22.3	0.0172
3,641.6	3,264.0	1,632.0	-6.1	1,625.9	-29.5	-25.7	-41.0	-49.6	23.9	0.0147
4,559.0	4,100.3	2,050.2	-30.7	2,019.5	-24.6	-21.0	-39.8	-48.2	27.2	0.0135
5,266.2	4,912.6	2,456.3	-52.7	2,403.6	-22.0	-18.5	-38.2	-46.2	27.7	0.0115
5,892.6	5,579.4	2,789.7	-71.3	2,718.4	-18.6	-15.4	-37.6	-45.5	30.1	0.0110
6,380.3	6,136.4	3,068.2	-84.9	2,983.3	-13.6	-11.1	-37.1	-44.9	33.8	0.0113
6,243.7	6,312.0	3,156.0	-90.0	3,066.0	-5.1	-4.1	-35.9	-43.4	39.3	0.0128
5,284.0	5,763.8	2,881.9	-85.0	2,796.9	+5.0	+4.0	-35.4	-42.8	46.8	0.0167
1,954.5	3,619.2	1,809.6	-5.05	1,804.6	+80.0	+62.3	-34.2	-41.4	103.7	0.0575
430.1	—	—	250.0	—	—	—	—	—	—	0
810.7	620.4	0	205.0	205.0	-45.0	-45.0	-45.5	-55.5	10.5	0.051
2,392.1	1,601.4	0	165.0	165.0	-40.0	-38.0	-42.7	-51.7	13.7	0.083
19,917.1	11,154.6	0	125.5	125.5	-39.5	-34.2	-43.8	-53.0	18.8	0.150
3,033,331.0	1,526,624.0	0	88.4	88.4	-37.1	-26.6	-42.7	-51.7	25.1	0.284

TABLE 43.7—GAS-CAP EXPANSION CALCULATION, FINITE-DIFFERENCE METHOD WITHOUT COUNTERFLOW

p (1)	ΔN_p [from (11)] (2)	$N_p =$ $\Sigma(2)$ (3)	$1 - N_p$ (4)	$\Delta(B_o/B_g - R_s)$ (5)	$(4)/(5)$ (6)	$\Delta(1/B_g)$ (7)	$(1+m)B_{ob}(7)$ (8)	(6) - (8) (9)	$(B_o/B_g - R_s) +$ $\bar{R}(1 - \Delta G_i)$ (from dep. dr.) (10)	$\Delta N_p =$ (9)/(10) (11)
$\Delta G_i = 0$										
1,375	0	0	1.0000	—	—	—	—	—	—	0
1,300	0.0694	0.0694	0.9306	-45.0	-45.0	-45.5	-88.6	43.6	628.6	0.0694
1,200	0.0629	0.1323	0.8677	-40.0	-37.2	-42.7	-83.2	46.0	731.6	0.0629
1,100	0.0546	0.1869	0.8131	-39.5	-34.3	-43.8	-85.3	51.0	933.9	0.0546
1,000	0.0523	0.2392	0.7608	-37.1	-30.2	-42.7	-83.2	53.0	1,013.6	0.0523
900	0.0423	0.2815	0.7185	-34.9	-26.6	-42.6	-83.0	56.4	1,331.1	0.0423
800	0.0350	0.3165	0.6835	-30.1	-21.6	-40.5	-78.9	57.3	1,638.0	0.0350
700	0.0344	0.3509	0.6491	-17.3	-11.8	-41.0	-79.9	68.1	1,981.9	0.0344
$\Delta G_i = 0.5$										
1,375	0	0	1.0000	—	-45.0	—	—	—	—	0
1,300	0.0941	0.1046	0.8954	-45.0	-35.8	-45.5	-88.6	43.6	463.1	0.0941
1,200	0.0904	0.2103	0.7897	-40.0	-31.2	-42.7	-83.2	47.4	524.6	0.0904
1,100	0.0848	0.3124	0.6876	-39.5	-25.5	-43.8	-85.3	54.1	637.9	0.0848
1,000	0.0718	0.4092	0.5908	-37.1	—	-42.7	-83.2	57.7	803.2	0.0718
$\Delta G_i = 1.0$										
1,375	0	0	1.0000	—	—	—	—	—	—	0
1,300	0.2127	0.2127	0.7873	-45.0	-45.0	-45.5	-88.6	43.6	205.0	0.2127
1,200	0.3133	0.5260	0.4740	-40.0	-31.5	-42.7	-83.2	51.7	165.0	0.3133
$\Delta(B_g)$ (12)	$mN(B_{ob}/B_{gb})(12)$ (13)	S_g (from dep. dr.) (14)	S_g (from f_g vs. S_g) (15)	$\Delta N_p \bar{R} \Delta G_i$ (10 ⁶ bbl) (16)	$\Sigma(16)$ (10 ⁶ bbl) (17)	$(17)B_g$ (10 ³ bbl) (18)	$(17i)(12)$ (10 ³ bbl) (19)	$(13) + (18)$ + (19) (10 ³ bbl) (20)	$(20)/(15)$ (PV, 10 ³ bbl) (21)	h , ft (22)
—	—	0	0.750	0	0	0	—	—	—	20.0
0.00016	2,034,560	0.017	0.647*	0	0	0	0	2,034.6	3,145	17.8
0.00017	2,161,720	0.037	0.647	0	0	0	0	2,161.7	3,341	15.4
0.00022	2,797,520	0.055	0.647	0	0	0	0	2,797.5	4,324	12.7
0.00025	3,179,000	0.0711	0.647	0	0	0	0	3,179.0	4,913	10.0
0.00032	4,069,120	0.0878	0.647	0	0	0	0	4,069.1	6,289	6.9
0.00039	4,959,240	0.1035	0.645**	0	0	0	0	4,959.2	7,689	3.4
0.00051	6,485,160	0.1182	0.645	0	0	0	0	6,485.2	10,055	-1.0
—	—	0	0.750	0	0	0	—	—	—	20.0
0.00016	2,034,560	0.017	0.647*	827.5	827.5	1,605.4	0	3,640.0	5,626.0	16.3
0.00017	2,161,720	0.037	0.647	1,165.0	1,992.5	4,204.2	0.3	6,366.2	9,839.6	10.8
0.00022	2,797,520	0.055	0.647	1,603.5	3,596.0	8,378.7	0.9	11,177.1	17,275.3	3.7
0.00025	3,179,000	0.0711	0.647	2,120.8	5,716.8	14,749.3	2.1	17,930.4	27,713.1	-5.2
—	—	0	0.750	0	0	0	—	—	—	20.0
0.00016	2,034,560	0.017	0.647*	3,927.2	3,927.2	7,618.8	0	9,653.4	14,920.2	12.1
0.00017	2,161,720	0.037	0.647	15,378	19,305.2	40,734.0	1.3	42,897.0	66,301.4	-1.7

* Calculated at corresponding rate and pressure of 1,375 psig (9480.3 kPa).

** Calculated at corresponding rate and pressure of 900 psig (6205.3 kPa).

e. For cases where the gas saturation, S_g , exceeds the critical gas saturation as determined from an f_g vs. S_g curve at the appropriate pressure, performance from that point to abandonment must be determined by the frontal-advance method illustrated in III-B, which follows. Abandonment recovery to a limiting GOR can be determined directly from the f_g relationship.

B. Pressure Maintenance

1. Equation is same as II-A in preceding section.
2. Procedure
 - a. Construct f_g curve and tangents as shown in II-A.
 - b. Calculate performance as shown in Fig. 43.10.
 - c. Construct performance curves as indicated in Fig. 43.12.
 - d. Calculate injection requirements for complete pressure maintenance at the bubble-point by the equation

$$\Delta G_i = 1 + \frac{(B_o/B_g) - R_s}{R_s}$$

IV. External Gas-Injection Pressure Maintenance

A. Partial Pressure Maintenance

1. Equation

$$\Delta N_p =$$

$$\frac{(1 - N_{pi})\Delta[(B_o/B_g) - R_s] - (1 + m)B_{ob}\Delta(1/B_g)}{[(B_o/B_g) - R_s] + \bar{R}(1 - \Delta G_i)}$$

where

ΔN_p = incremental oil production, fraction of OIP,

N_{pi} = cumulative oil production from previous step, fraction of OIP,

\bar{R} = average GOR, scf/STB,

R_s = solution GOR, scf/STB,

B_o = oil FVF, RB/STB,

B_{ob} = oil FVF at p_b , RB/STB,

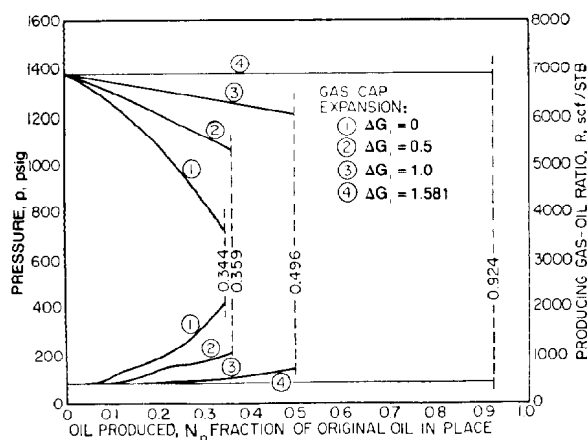


Fig. 43.13—External gas-injection pressure-maintenance performance.

B_g = gas FVF, bbl/scf,
 ΔG_i = incremental gas injection, fraction of
 produced gas, and
 m = ratio of gas-cap to original oil-zone volume,
 fraction.

(Note that subscript i refers to previous step.)

2. Procedure

- Select pressure increments such that any one increment $\leq 10\%$ of the initial or bubble-point pressure and obtain fluid properties as indicated in Table 43.2.
- Perform depletion drive material-balance calculation with $\Delta G_i = 0$, as described in III-A.
- Perform material-balance calculation as shown in Table 43.7, using \bar{R} as determined from depletion drive calculation in Point b and \bar{S}_g as determined from unit-displacement calculations.
- Determine positions of gas/oil level and abandonment conditions, using data in Fig. 43.8 and calculations in Table 43.7.
- Construct performance curves as indicated in Fig. 43.13.

B. Pressure Maintenance

- Equation is the same as II-B.
- Procedure
 - Construct f_g curve and tangents as in II-B.
 - Calculate recovery and construct performance curves as indicated in Fig. 43.13.
 - Calculate injection requirements for complete pressure maintenance at the bubble-point by the equation

$$\Delta G_i = 1 + \frac{[(B_o/B_g) - R_s]}{R_s}$$

APPENDIX B

Selected References Containing Equations, Calculation Procedures, and Example Calculations Related to Gas-Injection Performance Predictions

External Injection—Complete Pressure Maintenance

Emphasis on Gravity Drainage and Segregation

- Combs, G.D. and Knezek, R.B.: "Gas Injection for Upstructure Drainage," *J. Pet. Tech.* (March 1971) 361-72.
- Craig, F.F. Jr. et al.: "A Laboratory Study of Gravity Segregation in Frontal Drives," *J. Pet. Tech.* (Oct. 1957) 275-81; *Trans.*, AIME, 210.
- Martin, J.C.: "Reservoir Analysis for Pressure Maintenance Operations Based on Complete Segregation of Mobile Fluids," *Trans.*, AIME (1958) 213, 220-27.
- McCord, D.R.: "Performance Predictions Incorporating Gravity Drainage and Gas Cap Pressure Maintenance — LL-370 Area, Bolivar Coastal Field, *J. Pet. Tech.* (Sept. 1953) 231-48; *Trans.*, AIME, 198.
- Shreve, D.R. and Welch, L.W. Jr.: "Gas Drive and Gravity Drainage Analysis for Pressure Maintenance Operations," *J. Pet. Tech.* (June 1956) 136-43; *Trans.*, AIME, 207.
- Stewart, F.M., Garthwaite, D.L., and Krebill, F.K.: "Pressure Maintenance by Inert Gas Injection in the High Relief Elk Basin Field," *J. Pet. Tech.* (March 1955) 49-55; *Trans.*, AIME, 204.
- van Wingen, N., Barton, W.C. Jr., and Case, C.H.: "Coalinga Nose Pressure Maintenance Project," *J. Pet. Tech.* (Oct. 1973) 1147-52.

General Frontal-Advance Applications

- Buckley, S.E. and Leverett, M.C.: "Mechanism of Fluid Displacement in Sands," *Trans.*, AIME (1942) 146, 107-16.
- Craft, B.C. and Hawkins, M.F.: *Applied Petroleum Reservoir Engineering*, Prentice-Hall Inc., Englewood Cliffs, NJ (1959) 361-75.
- Dardaganian, S.G.: "The Application of the Buckley-Leverett Frontal Advance Theory to Petroleum Recovery," *J. Pet. Tech.* (April 1958) 49-52; *Trans.*, AIME (1958) 213, 365-68.
- Justus, J.B. et al.: "Pressure Maintenance by Gas Injection in the Brookhaven Field, Mississippi," *J. Pet. Tech.* (April 1954) 43-53; *Trans.*, AIME (1954) 201, 97-107.
- Kirby, J.E. Jr., Stamm, H.E. III, and Schnitz, L.B.: "Calculation of the Depletion History and Future Performance of a Gas-Cap-Drive Reservoir," *J. Pet. Tech.* (July 1957) 218-26; *Trans.*, AIME, 210.
- Pirson, S.J.: *Oil Reservoir Engineering*, McGraw-Hill Book Co. Inc., New York City (1958) 555-605.
- Snyder, R.W. and Ramey, H.J. Jr.: "Application of Buckley-Leverett Displacement Theory to Noncommunicating Layered Systems," *J. Pet. Tech.* (Nov. 1967) 1500-06; *Trans.*, AIME, 240.
- Stutzman, L.F. and Thodos, G.: "Frontal Drive Production Mechanisms—A New Method for Calculating the Displacing Fluid Saturation at Breakthrough," *J. Pet. Tech.* (April 1957) 67-69; *Trans.*, AIME, 210, 364-66.
- Welge, H.J.: "A Simplified Method for Computing Oil Recovery by Gas or Water Drive," *Trans.*, AIME (1952) 195, 91-98.

Gas Displacement Above the Bubble-Point and Production From Behind the Front

- Kern, L.R.: "Displacement Mechanisms in Multi-Well Systems," *Trans.*, AIME (1952) 195, 39-46.
- Shreve, D.R. and Welch, L.W. Jr.: "Gas Drive and Gravity Drainage Analysis for Pressure Maintenance Operations," *J. Pet. Tech.* (June 1956) 136-43; *Trans.*, AIME, 207.

Nonequilibrium Gas Displacement

- Attra, H.D.: "Nonequilibrium Gas Displacement Calculations," *Soc. Pet. Eng. J.* (Sept. 1961) 130-36; *Trans.*, AIME, 222.
- Jacoby, R.H. and Berry, V.J. Jr.: "A Method for Predicting Pressure Maintenance Performance for Reservoirs Producing Volatile Crude Oil," *J. Pet. Tech.* (March 1958) 59-69; *Trans.*, AIME, 213.

Gas Injection in Combination Drive Reservoirs

- Blair, E.A. et al.: "A Reservoir Study of the Friendswood Field," *J. Pet. Tech.* (June 1971) 685-94.
- Cotter, W.H.: "Twenty-Three Years of Gas Injection Into A Highly Undersaturated Crude Reservoir," *J. Pet. Tech.* (April 1962) 361-65.
- Wooddy, L.D. Jr. and Moscrip, R. III: "Performance Calculations for Combination Drive Reservoirs," *J. Pet. Tech.* (June 1956) 128-35; *Trans.*, AIME, 207.

Dispersed Gas Injection—Complete and Partial Pressure Maintenance

1. Craft, B.C. and Hawkins, M.F.: *Applied Petroleum Reservoir Engineering*, Prentice-Hall Inc., Englewood Cliffs, NJ (1959) 375-90.
2. Craig, F.F. Jr. and Geffen, T.M.: "The Determination of Partial Pressure Maintenance Performance by Laboratory Flow Tests," *J. Pet. Tech.* (Feb. 1956) 42-49; *Trans.*, AIME, **207**.
3. Craig, F.F. Jr., Geffen, T.M., and Morse, R.A.: "Oil Recovery Performance of Pattern Gas or Water Injection Operations from Model Tests," *J. Pet. Tech.* (Jan. 1955) 7-14; *Trans.*, AIME, **204**.
4. Hoss, R.L.: "Calculated Effect of Pressure Maintenance on Oil Recovery," *Trans.*, AIME (1948) **174**, 121-30.
5. Kelly, P. and Kennedy, S.L.: "Thirty Years of Effective Pressure Maintenance By Gas Injection in the Hilbig Field," *J. Pet. Tech.* (March 1965) 279-81.
6. Last, G.J., Craig, F.F. Jr., and Reader, P.J.: "Significance of Partial Pressure Maintenance by Fluid Injection," *J. Pet. Tech.* (Jan. 1964) 20-24.
7. Leibrock, R.M., Hiltz, R.G., and Huzarevich, J.E.: "Results of Gas Injection in the Cedar Lake Field," *Trans.*, AIME (1951) **192**, 357-66.
8. McGraw, J.H. and Lohec, R.E.: "The Pickton Field—Review of a Successful Gas Injection Project," *J. Pet. Tech.* (April 1964) 399-404; discussion, 405.
9. Meltzer, B.D., Hurdle, J.M., and Cassingham, R.W.: "An Efficient Gas Displacement Project—Raleigh Field, Mississippi," *J. Pet. Tech.* (May 1965) 509-14.
10. Muskat, M.: *Physical Principles of Oil Production*, McGraw Hill Book Co. Inc., New York City (1949) 437-53.
11. Patton, E.C. Jr.: "Evaluation of Pressure Maintenance by Internal Gas Injection in Volumetrically Controlled Reservoirs," *Trans.*, AIME (1947) **170**, 112-52; Discussion, 154-55.
12. Pirson, S.J.: *Oil Reservoir Engineering*, McGraw-Hill Book Co. Inc., New York City (1958) 484-532.
13. Shehabi, J.A.N.: "Effective Displacement of Oil by Gas Injection in a Preferentially Oil-Wet, Low-Dip Reservoir," *J. Pet. Tech.* (Dec. 1979) 1605-13.
14. Tracy, G.W.: "Simplified Form of the Material Balance Equation," *J. Pet. Tech.* (Jan. 1955), 53-56; *Trans.*, AIME, **204**, 243-46.

Mathematical Models for Reservoir Simulation

1. Coats, K.H.: "An Analysis for Simulating Reservoir Performance Under Pressure Maintenance by Gas and/or Water Injection," *Soc. Pet. Eng. J.* (Dec. 1968) 331-40.
2. Cook, R.E., Jacoby, R.H., and Ramesh, A.B.: "A Beta-Type Reservoir Simulator for Approximating Compositional Effects During Gas Injection," *Soc. Pet. Eng. J.* (Oct. 1974) 471-81.
3. McCulloch, R.C., Langton, J.R., and Spivak, A.: "Simulation of High Relief Reservoirs, Rainbow Field, Alberta, Canada," *J. Pet. Tech.* (Nov. 1969) 1399-1408.
4. McFarlane, R.C., Mueller, T.D., and Miller, F.G.: "Unsteady-State Distributions of Fluid Compositions in Two-Phase Oil Reservoirs Undergoing Gas Injection," *Soc. Pet. Eng. J.* (March 1967) 61-74; *Trans.*, AIME, **240**.
5. Price, H.S. and Donohue, D.A.T.: "Isothermal Displacement Processes With Interphase Mass Transfer," *Soc. Pet. Eng. J.* (June 1967) 205-20; *Trans.*, AIME, **240**.
6. Strickland, R.F. and Morse, R.A.: "Gas Injection for Upstructure Oil Drainage," *J. Pet. Tech.* (Oct. 1979) 1323-31.
7. Thomas, L.K., Lumpkin, W.B., and Reheis, G.M.: "Reservoir Simulation of Variable Bubble-Point Problems," *Soc. Pet. Eng. J.* (Feb. 1976) 10-16.

APPENDIX C

Data Requirements for Engineering Analysis of Gas-Injection Operations¹³

Analytical Data

1. Core analyses from a representative number of wells

- a. Porosity
 - b. Permeability
 - c. Water saturation
2. Special core analyses on a sufficient number of samples to cover permeability range of the reservoir
 - a. Capillary-pressure data (for determining interstitial saturations)
 - b. Gas/oil relative permeability, k_{rg}/k_{ro}
 - c. Relative permeability to oil, k_{ro}
 3. Hydrocarbon compositional analysis
 - a. Gas-cap, casing-head, and trap samples
 - b. Reservoir-fluid samples
 4. Reservoir-fluid property analyses
 - a. Solubility
 - (1) Flash
 - (2) Differential
 - b. Relative oil volume
 - (1) Flash
 - (2) Differential
 - c. Oil viscosity
 - d. Oil density
 - e. Gas viscosity
 - f. Gas density

Field Data

1. Development history
2. Abandonment history, if any
3. Production history
 - a. Oil
 - b. Water
 - c. Gas
4. Injection history, if any
 - a. Gas
 - b. Water
5. Pressure history
6. Well productivity data
7. Gas/oil and oil/water contacts (original and present)
8. Well and test data
 - a. Drillstem tests
 - b. Production tests
 - c. Sample cuttings
 - d. Core descriptions
 - e. Electrical and radioactivity logs
9. Average reservoir temperature
10. Well completion data

Interpretive Data (prepared from preceding data)

1. Structure maps
 - a. Top of zone
 - b. Base of zone
2. Isopachous maps
 - a. Total net sand
 - b. Net gas sand
 - c. Net oil sand
3. Reservoir volume distribution
 - a. Volume vs. subsea depth, and/or
 - b. Volumes by injection/production units
4. Cross-sectional area
 - a. Area vs. subsea depth, and/or
 - b. Area perpendicular to bedding planes for injection/production units

5. Volume-weighted reservoir datum
6. Average reservoir fluid properties (as functions of pressure)
 - a. Differential oil formation volume factor
 - b. Flash relative volume factor
 - c. Gas formation volume factor
 - d. Oil viscosity
 - e. Gas viscosity
 - f. Oil gravity
 - g. Gas gravity
 - h. Gas deviation factor
 - i. Differential gas solubility
 - j. Average oil and gas composition
 - k. Oil and water compressibility
7. Volume-weighted average pressures
8. Permeability distribution
9. Average reservoir-rock properties
 - a. Porosity
 - b. Permeability
 - c. Interstitial water saturation
 - d. Gas/oil relative permeability ratio, k_g/k_o
 - e. Oil relative permeability, k_o/k
10. Well productivities
 - a. As a function of subsea depth
 - h. By injection/production units
 - c. Productivity indices

Nomenclature

- A = cross-sectional area
 B_g = gas FVF
 B_o = oil FVF
 B_{ob} = oil FVF at p_b
 f_g = fractional gas flow
 ΔG_i = incremental gas injection
 k_o = effective permeability to oil
 k_{rg} = relative permeability to gas
 k_{ro} = relative permeability to oil
 L = distance
 m = ratio of gas-cap to original oil-zone volume
 M = mobility ratio
 N_p = cumulative oil production
 ΔN_p = incremental oil production
 p = pressure
 p_b = bubblepoint pressure
 p_c = oil/gas capillary pressure ($\rho_o - \rho_g$)
 q_t = total flow rate
 \bar{R} = instantaneous GOR
 \bar{R} = average GOR
 R_s = solution GOR
 S_g = gas saturation
 S_L = total liquid saturation
 S_w = interstitial water saturation
 t = time
 α = angle of dip, positive downdip
 μ_g = gas viscosity
 μ_o = oil viscosity
 ρ_g = gas density
 ρ_o = oil density
 ϕ = porosity, fraction

Key Equations in SI Metric Units

$$f_g = \frac{1 + (8.639 \times 10^{-5})[k_o A / (\mu q_t)] \left[\left(\frac{\partial P_c}{\partial L} \right) - 9.795(\rho_o - \rho_g) \sin \alpha \right]}{1 + \left(\frac{k_{ro}}{k_{rg}} \right) \left(\frac{\mu_o}{\mu_g} \right)} \quad \dots \dots \dots (1)$$

where

- f_g = fractional flow of gas,
 q_t = total flow rate, m³/d,
 A = cross-sectional area, m²,
 P_c = oil/gas capillary pressure, $\rho_o - \rho_g$, kPa,
 L = distance, m,
 ρ_o = oil specific gravity (water = 1) or density, g/cm³,
 ρ_g = gas specific gravity (water = 1) or density, g/cm³,
 α = angle of dip, positive downdip, degrees,
 k_o = effective permeability to oil, μm^2 ,
 k_g = effective permeability to gas, μm^2 ,
 μ_o = oil viscosity, Pa·s, and
 μ_g = gas viscosity, Pa·s.

$$L = \frac{q_t t}{\phi A} \left(\frac{\partial f_g}{\partial S_g} \right), \quad \dots \dots \dots (2)$$

where

- t = time, days,
 ϕ = porosity, fraction,
 S_g = gas saturation, fraction,

and others are as in Eq. 1.

$$f_g = \frac{1 + 0.848 \times 10^{-3} [k_o (\rho_g - \rho_o) \sin \alpha / (q_t \mu_o)]}{1 + \left(\frac{k_o}{k_g} \right) \left(\frac{\mu_g}{\mu_o} \right)} \quad \dots \dots \dots (\text{A.II.B})$$

where

- f_g = fractional gas flow,
 k_o = effective permeability to oil, μm^2 ,
 k_g = effective permeability to gas, μm^2 ,
 ρ_g = gas specific gravity at p (water = 1),
 ρ_o = oil specific gravity at p (water = 1),
 α = angle of gas flow (-90°),
 q_t = rate of frontal gas movement, m³/d·m²,
 μ_o = oil viscosity at p , Pa·s, and
 μ_g = gas viscosity at p , Pa·s.

Note: All other material-balance, saturation, and GOR equations that follow are correct for standard SI units, where B_o and B_g are volume factors (in m³/m³) and \bar{R} , R_s , and R_p are GOR's (in m³/m³).

References

1. Muskat, M.: *Physical Principles of Oil Production*, McGraw-Hill Book Co. Inc., New York City (1949) 709.
2. Buckley, S.E. and Leverett, M.C.: "Mechanism of Fluid Displacement in Sands," *Trans., AIME* (1942) **146**, 107-16.
3. Welge, H.J.: "A Simplified Method for Computing Oil Recovery by Gas or Water Drive," *Trans., AIME* (1952) **195**, 91-98.
4. Dardaganian, S.G.: "The Application of the Buckley-Leverett Frontal Advance Theory to Petroleum Recovery," *J. Pet. Tech.* (April 1958), 49-52; *Trans., AIME*, **213**, 365-68.
5. Kern, L.R.: "Displacement Mechanism in Multi-well Systems," *Trans., AIME* (1952) **195**, 39-46.
6. Shreve, D.R. and Welch, L.W. Jr.: "Gas Drive and Gravity Drainage Analysis for Pressure Maintenance Operations," *J. Pet. Tech.* (June 1956), 136-43; *Trans., AIME*, **207**.
7. Jacoby, R.H. and Berry, V.J. Jr.: "A Method for Predicting Pressure Maintenance Performance for Reservoirs Producing Volatile Crude Oil," *J. Pet. Tech.* (March 1958), 59-69; *Trans., AIME*, **213**.
8. Attra, H.D.: "Nonequilibrium Gas Displacement Calculation," *Soc. Pet. Eng. J.* (Sept. 1961) 130-36; *Trans., AIME*, **222**.
9. Craft, B.C. and Hawkins, M.F.: *Applied Petroleum Reservoir Engineering*, Prentice-Hall Inc., Englewood Cliffs, NJ (1959) 370.
10. Anders, E.L. Jr.: "Mile Six Pool—An Evaluation of Recovery Efficiency," *J. Pet. Tech.* (Nov. 1953) 279-86; *Trans., AIME*, **198**.
11. Craig, F.F. Jr. and Geffen, T.M.: "The Determination of Partial Pressure Maintenance Performance by Laboratory Flow Tests," *J. Pet. Tech.* (Feb. 1956) 42-49; *Trans., AIME*, **207**.
12. Slobod, R.L. and Koch, H.A. Jr.: "High Pressure Gas Injection—Mechanism of Recovery Increase," *Drill. and Prod. Prac.*, API (1953) 82.
13. Stiles, W.E.: "Use of Permeability Distribution in Water Flood Calculations," *Trans., AIME* (1949) **186**, 9-13.
14. Dyes, A.B., Caudle, B.H., and Erickson, R.A.: "Oil Production after Breakthrough as Influenced by Mobility Ratio," *J. Pet. Tech.* (April 1954), 27-32; *Trans., AIME* (1954) **201**, 81-86.
15. Patton, E.C. Jr.: "Evaluation of Pressure Maintenance by Internal Gas Injection in Volumetrically Controlled Reservoirs," *Trans., AIME* (1947) **170**, 112-52; Discussion 154-55.

Chapter 44

Water-Injection Pressure Maintenance and Waterflood Processes

C.E. Thomas, Core Laboratories Inc.*
Carroll F. Mahoney, Core Laboratories Inc.
George W. Winter, Core Laboratories Inc.

Introduction

Many factors that are important to waterflooding are also important in water-pressure maintenance, so it is difficult to define the point of separation between the two processes. Accordingly, a major portion of the information presented in this chapter applies to both waterflooding and water-pressure-maintenance operations. For our purposes, waterflooding and water-pressure maintenance are defined as follows.

Waterflooding is a secondary-recovery method by which water is injected into a reservoir to obtain additional oil recovery through movement of reservoir oil to a producing well, after the reservoir has approached its economically productive limit by primary-recovery methods.

Water-pressure maintenance is a process whereby water is injected into an oil-producing reservoir to supplement the natural energy that is indigenous to the reservoir and to improve the oil-producing characteristics of the field before the economically productive limits are reached.

General History and Development of Waterflooding

The first recognition of the benefits that can be obtained from water injection came as a result of accidental flooding when water was inadvertently admitted to producing oil sands through abandoned wells. In 1880, Carll¹ reported increased oil production following accidental flooding in the Pithole City (PA) area, and suggested the use of intentional flooding. Although waterflooding was illegal in Pennsylvania before 1921 and in New York before 1919, water-injection operations in these areas were reported as early as the 1890's.² Since it was illegal, limited information is available on operations before 1922;

however, increased production was noted in 1907 in Pennsylvania's Bradford field and in 1912 in New York.³ The linedrive pattern was introduced in 1922 and the five-spot pattern in 1924. The use of pattern injection programs, when combined with surface pressure injection, provided a more effective and efficient method of moving oil to the producing wells.

The initial success of waterflooding in the Bradford area can be attributed to a number of favorable factors. The Bradford sand generally had no natural water encroachment, contained a relatively low-viscosity crude, and had a low initial gas saturation. As a result, primary recovery was limited, and the oil recovery by water injection was significantly larger than that achieved by natural pressure depletion.

Waterflooding was slow to expand outside the Pennsylvania-New York area. The first waterflood was initiated in Oklahoma in 1931 in a shallow Bartlesville sand in Nowata County. In 1936, waterflooding was introduced in Texas when injection was applied to the Fry pool in Brown County. Within 10 years, waterflooding was in operation in most of the oil-producing areas. However, it was not until the early 1950's that the general applicability of waterflooding was recognized.⁴

There are no generally reliable records of water-injection operations in areas outside the U.S. during this developmental period, but sufficient data have been published to indicate a comparable growth pattern in other parts of the world.

Waterflooding currently is accepted worldwide as a reliable and economic recovery technique; almost every significant oil field that does not have a natural water drive has been, is being, or will be considered for waterflooding.

*Original chapter in the 1962 edition was written by H.C. Osborne, C.E. Thomas, J.F. Armstrong, L.L. Crain, C.F. Mahoney, F.C. Kelton, Bill Lafayette, and J.E. Smith.

Important Factors in Waterflooding or Water-Injection Pressure Maintenance

In determining the suitability of a given reservoir for waterflooding or pressure maintenance, these factors must be considered: (1) reservoir geometry, (2) lithology, (3) reservoir depth, (4) porosity, (5) permeability (magnitude and degree of variation), (6) continuity of reservoir rock properties, (7) magnitude and distribution of fluid saturations, (8) fluid properties and relative-permeability relationships, and (9) optimal time to waterflood.

Generally, the influence of all these factors on ultimate recovery, rate of return, and ultimate economic return must be considered collectively to evaluate the economic feasibility of conducting waterflood and/or water-pressure-maintenance operations in a particular reservoir. Factors other than reservoir characteristics also will have a great influence. These include the price of oil, marketing conditions, operating expenses, and availability of water.

Reservoir Geometry

One of the first steps in organizing reservoir information to determine whether water injection is feasible is to establish the geometry of the reservoir. The structure and stratigraphy of the reservoir control the location of the wells and, to a large extent, dictate the methods by which a reservoir may be produced through water-injection practices.

Structure is a principal factor in governing gravitational segregation. In the presence of high permeabilities, recovery by gravity segregation, particularly in old pools, may reduce oil saturation to a value at which the application of water injection may be uneconomical. If a suitable structure exists and the remaining oil saturation proves sufficient for secondary operations, the adaptation of a peripheral flood may result in a higher areal sweep efficiency than would the conventional pattern or linedrive floods. High relief also would suggest investigation of a companion gas-injection program. The shape of the field and the presence or absence of a gas cap would also influence this decision.

Most water-injection operations conducted to date have taken place in fields that exhibit only moderate structural relief. Many floods are located in pools where the oil accumulation occurs in reservoirs of the stratigraphic-trap type. Since these pools, as a rule, have been produced by dissolved-gas drive and have not received any benefits from natural-water encroachment or other displacement-energy mechanisms, high oil saturations usually remain after primary-recovery operations, making these reservoirs most attractive for secondary-recovery operations.

In such pools, the dip of the strata may be so slight as to have no noticeable effect on secondary-recovery operations. Thus, the location of the injection and producing wells may be made to conform to property lines and to known sand conditions. Whether such a practice would prove successful in pools where oil and gas distribution has been controlled by a high-relief structure is questionable.

An analysis of reservoir geometry and past reservoir performance is often important in defining the presence and strength of a natural-water drive and, thus, in defining the need for supplementing injection. If a natural-water

drive is determined to be strong, injection may be unnecessary. Structural features such as faults, or stratigraphic features such as shale-outs, or any other permeability barrier usually will influence these decisions. An otherwise suitable reservoir may be so highly faulted as to make any injection program economically unattractive.

Lithology

Lithology has a profound influence on the efficiency of water injection in a particular reservoir. Lithological factors that affect floodability are porosity, permeability, and clay content. In some complex reservoir systems, only a small portion of the total porosity, such as fracture porosity, will have sufficient permeability to be effective in water-injection operations. In these cases, a water-injection program will have only a minor impact on the matrix porosity, which might be crystalline, granular, or vugular in nature. Evaluation of such effects requires an extensive laboratory investigation and a somewhat comprehensive reservoir study. Evaluations can be supplemented by experimental pilot injection operations.

There is laboratory evidence that a difference between the mineralogical compositions of the sand grains and cementing material of various oil-producing formations may account for differences in the residual oil saturation (ROS) that have been observed subsequent to waterflooding. These differences in oil saturation are indicated to be dependent not only on the mineralogical composition of the reservoir rock but also on the composition of the hydrocarbons within the rock. Benner and Bartell⁵ have shown that, under certain conditions, the basic constituents of some types of petroleum cause quartz to become hydrophobic because of the adsorption of these constituents by the surface of the sand grains. In a similar manner, the acidic constituents of other types of petroleum render calcite hydrophobic. At present, there are not enough data available to permit valid predictions regarding the effects on recovery when the pore walls are made wet to various degrees by water and petroleum, but it appears probable that there is some effect.

Although there is evidence that the clay minerals that are present in some oil sands may clog the pores by swelling and deflocculating when waterflooding is used, no exact data are available as to the extent to which this may occur. The effect depends on the nature of the clay minerals; however, an approximation of the pore-clogging impact may be determined through laboratory investigations. The montmorillonite group is most likely to cause a reduction in permeability by swelling; kaolinite is least likely to cause a reaction. The extent to which such a reduction in permeability will occur also depends on the salinity of the water that is injected. Brines are usually preferable to fresh water for flooding purposes.

Reservoir Depth

The depth of the reservoir is another factor that should be considered in waterflooding. If the depth of the reservoir is too great to permit redrilling economically and if old wells have to be used as injection and producing wells, lower recoveries may be expected than in cases in which new wells can be drilled. This is particularly true in old fields where regular well spacings were not observed and where infill development was not as extensive as lease-line development. Also, after primary operations, ROS's

in most deep pools probably are lower than in shallow pools, because a greater volume of solution gas was generally available to expel the oil and because shrinkage factors are higher. Therefore, less oil remains. Greater depth, on the other hand, permits the use of higher pressures and wider well spacings, provided the reservoir rock possesses a sufficient degree of lateral uniformity.

Caution should be exercised in shallow-depth fields since the maximum pressure that can be applied in a secondary-recovery operation is limited by the depth of the reservoir. In waterflood operations, it has been found that there is a critical pressure (usually approximating that of the static pressure of the column of rock overlying the productive sand, or about 1 psi/ft of sand depth) which, if exceeded, apparently permits the penetrating water to expand openings along fractures or other planes of weakness, such as joints and, possibly, bedding planes. This results in the channeling of the injected water or the bypassing of large portions of the reservoir matrix. Consequently, an operational pressure gradient of 0.75 psi/ft of depth normally is allowed to provide a sufficient margin of safety to prevent pressure parting. However, to remove as much doubt as possible, information regarding fracture pressures or breakdown pressures in a given locality should be studied. Either pressure should be considered as an upper limit for injection. These considerations will also influence equipment selection and plant design, as well as the number and location of injection wells.

Porosity

The total recovery of oil from a reservoir is a direct function of the porosity, because the porosity determines the amount of oil that is present for any given percent of oil saturation. Since the fluid content of reservoir rock varies from 775.8 to 1,551.6 bbl/acre-ft for porosities of 10 and 20%, respectively, it is important that reliable porosity data be assembled. Porosities sometimes vary from 10 to 35% in an individual zone. In limestones and dolomites, pinpoint and fractured porosities may vary from 2 to 11%; honeycombed and cavernous porosities may vary from 15 to 35%. In establishing an average porosity, the arithmetic average of the porosities determined from core samples has proved acceptable. If there are sufficient data, isoporosity maps are used when the distribution of porosity is important—as, for instance, when some fields are unitized. These maps may be areally or volumetrically weighted to give a very good total porosity value. If enough core data are available, statistical analyses of porosity and permeability may be used to improve the use of these data.

To date, the most satisfactory method of measuring this important property has been through laboratory measurements of core samples. Various logging methods have been quite satisfactory in many cases. The logs may include a "microlog" or "contact log," neutron log, density log, or sonic log.

Permeability (Magnitude and Degree of Variation)

The magnitude of the permeability of the reservoir rock controls, to a large degree, the rate of water injection that can be sustained in an injection well for a specific pressure at the sandface. Therefore, in determining the suitability of a given reservoir for waterflooding, it is necessary to determine (1) the maximum permissible injection pres-

sure from depth considerations, and (2) the rate vs. spacing relationships from the pressure/permeability data. This should indicate roughly the additional drilling that would be required to complete the proposed flood program in a reasonable length of time. An approximation of the expected recovery then can be compared with the monetary expenditure for this development program, so as to indicate quickly the suitability of the reservoir as a flood prospect. If the project profitability is favorable, more detailed work may be warranted.

The degree of variation in permeability has justifiably received much attention in recent years. Reasonably uniform permeability is essential for a successful waterflood, because this determines the quantities of injected water that must be handled. If great variations in the permeability of the individual strata within the reservoir are noted, and if these strata maintain continuity over substantial areas, injected water will break through early in high-permeability streaks and will transport large quantities of injected water before the low-permeability streaks have been swept effectively. This, of course, will influence the economics of the project and thus the suitability of the reservoir for flooding. Not to be overlooked is that continuity of these streaks or strata is as important as the permeability variation. If there is no correlation between the permeability profiles of the individual wells, the chances are good that the high-permeability zones are not continuous and that the channeling of injected fluids will be less severe than indicated by performance calculations.

Continuity of Reservoir-Rock Properties

The importance of reservoir-rock continuity in relation to permeability and vertical uniformity in determining the suitability of a reservoir for waterflooding has been mentioned previously. Since the flow of fluids in a reservoir is essentially in the direction of bedding planes, horizontal (along bedding planes) continuity is of primary interest. If the reservoir body is split into layers by partings of shale or dense rock, a study of a cross section of the producing horizon should indicate whether individual layers have a tendency to shale out in relatively short lateral distances, or whether sand development is uniform. Also, evidence of crossbedding and fracturing should be collected from core data. These features should be considered in determining well-spacing and flood patterns, and in estimating the volume of the reservoir that will be affected during the injection program. The presence of shale partings is not necessarily detrimental, provided the individual layers of reservoir rock exhibit a reasonable degree of continuity and uniformity with respect to permeability, porosity, and oil saturation. When vertical discontinuities exist (i.e., when there is a water- or gas-bearing stratum in the producing formation), shale partings will sometimes permit a selective completion; such a completion allows the exclusion or reduction of water or gas production and permits selective water injection.

Fluid Saturations and Distributions

In determining the suitability of a reservoir for waterflooding, a high oil saturation certainly would be considered more suitable than a low oil saturation. Usually, the higher the oil saturation at the beginning of flood operations, the higher the recovery efficiency will be. Also, ultimate

recovery will be higher, the bypassing of water will be less, and the economic return per dollar risked will be greater. Also involved in the suitability determination is the ROS after passage of the water front. Methods for ascertaining this saturation are discussed later in this chapter. The more this value can be reduced, the greater the ultimate oil recovery and economic gain. Most of the newer, more specialized displacement techniques that are currently under development and experimentation are aimed solely at reducing the value of ROS behind the displacing medium (see Chap. 42).

Also of great interest is the initial saturation measurement of the interstitial water. A knowledge of this quantity is essential in determining the initial oil saturation. Leverett and Lewis⁶ and other investigators^{7,8} have shown experimentally that, as a fraction of PV, oil recovery by solution-gas drive is essentially independent of connate-water saturations. Therefore, the amount of residual oil after the solution-gas depletion varies inversely with the water saturation. Worthy of mention here is the effect that initial water saturation has on the formation of an oil bank in front of the advancing water front. If the water saturation exceeds some critical value, an oil bank may not form; although substantial oil recovery may be achieved, oil will be produced at high water cuts. The water saturation that would preclude the formation of an oil bank may be determined from the fractional-flow equation, as illustrated later. This value may vary greatly from field to field. The fractional-flow equation also will indicate the amount of water that may be expected in the total flow stream at any particular saturation.

In the U.S. midcontinent area, waterflood programs have resulted in substantial oil recoveries being obtained from sands that have water saturations ranging from 22 to 40%. The average saturation in the Bartlesville sand of Oklahoma is about 30%. In the Bradford field, gas injection has proved unprofitable with oil saturations of 40% and water saturations of 30%; however, waterflooding has been very successful.

The Venango fields of Pennsylvania have responded more favorably to gas injection than to waterflooding because of high interstitial-water saturations. Oil saturations in cores range from 20 to 35%, with interstitial water varying from 40 to 60%. Waterflood oil recoveries have been uneconomical in these fields, but gas injection has resulted in additional recoveries of up to 100 bbl/acre-ft.⁹

An exception to the rule concerning the uneconomical flooding of sands with high water content occurred in the Woodsen Shallow field, Throckmorton County, TX; a successful waterflood program was carried out in this field where the sands have an average water saturation of 54%.¹⁰

Interstitial water content may be estimated from cores that are obtained with an oil-based mud system, through electrical log interpretations, laboratory restored-state floods, or capillary-pressure tests.

Another factor that is instrumental in determining the susceptibility of a reservoir to waterflood operations is the free-gas saturation. The pore space occupied by free gas in the reservoir is dependent on the voidage created by the produced stock-tank oil and gas, provided no influx of edge water has occurred. If accurate production data are known, the pore space depleted by the produced oil and gas may be determined. For solution-gas-drive

reservoirs, the portion of pore space occupied by gas may be determined by

$$S_g = (100 - S_w) \frac{NB_{oi} - (N - N_p)B_o}{NB_{oi}}, \dots\dots\dots (1)$$

where

- S_g = gas saturation, fraction,
- S_w = water saturation, fraction,
- N = initial oil in place, STB,
- N_p = oil produced, STB,
- B_{oi} = initial oil FVF, RB/STB, and
- B_o = oil FVF, RB/STB.

Several authors have shown through experiments that, for a given oil saturation, the percent of recovery by waterflood increases as gas saturations increase to about 30%, but the benefits decline as gas saturations go beyond the 30% level. The effect of free gas has been to cause lower ROS's behind the front than could be obtained by waterflooding the same systems in the absence of such gas. The increased recovery obtained because of the presence of gas during a waterflood has been variously attributed to changes in the physical characteristics of the oil, to the selective plugging action of the gas, to inclusion of oil mist in the free-gas phase, and to replacement of residual oil by residual gas. The degree of improvement in recovery has not been established in the field; however, an investigation¹¹ into the influence of a free-gas saturation on recovery by water drive indicated that the optimal gas saturation could be determined for maximum oil recovery by water displacement. Some operators who have injected gas ahead of water have reported that floods have benefited in one way or another. Besides the advantages of increased oil and gas production, benefits such as increased water-injection rates, more efficient flooding, and decreased paraffin problems have been reported.

The effects of free-gas saturations on oil recovery in waterflooding remain an academic problem. Until the merits of injecting gas ahead of (or with) water can be proved practicable in both the laboratory and in the field, caution should be used in applying this method to any large field operation.

Fluid Properties and Relative-Permeability Relationships

The physical properties of the reservoir fluids also have pronounced effects on the advisability of waterflooding a given reservoir. Of major importance among these effects is the viscosity of the oil. The viscosity of the oil affects the mobility ratio. The relative permeability of the reservoir rock to the displacing and displaced fluids is also a factor in the mobility ratio, as is the viscosity of the displacing fluid—water, in this case (refer to Chap. 43). The mobility of any single phase (e.g., oil) is the ratio of the permeability of that phase to its viscosity, k_o/μ_o . The mobility ratio, M , is the ratio of the mobility of the displacing fluid to that of the displaced fluid. The larger the mobility ratio, the lower will be recovery at breakthrough; hence, more water must be produced to recover a fixed amount of oil. This is because (1) a smaller area is swept at breakthrough, and (2) the stratification effect is enhanced.

With high-viscosity (low-gravity) crudes, primary recovery normally is lower and shrinkage is less than with low-viscosity crudes. This tends to offset the bad effects of high-viscosity crudes since it often results in higher oil saturations at the beginning of water-injection operations.

Optimal Time to Waterflood

The optimal time to waterflood a particular reservoir depends on the operator's primary objective in waterflooding. Among these objectives might be (1) maximum oil recovery, (2) maximum number of dollars of future net income, (3) maximum number of dollars of future net income per dollar invested, (4) stabilized rate of monetary return, or (5) maximum discounted present worth. Certainly all these objectives are desirable, and all seem to call for an early beginning of water-injection operations; however, that is not always the case. The most common way to determine the optimal time to begin flooding is to compute the anticipated oil recovery, production rate, monetary investment, and income for several assumed times of initiation—and then observe the effect of these factors on the most desirable goal.

In a homogeneous reservoir, maximum oil recovery can be expected if flooding is begun at the precise time bubblepoint pressure is reached. This is because residual oil after waterflooding will have the maximum amount of gas in solution and, at the bubblepoint, oil viscosity is most favorable. If the effect of a free-gas saturation on ROS is ignored, heterogeneity causes the optimal pressure for highest recovery to be lower than the bubblepoint pressure. If the bubblepoint pressure is quite low, production rates may have substantially declined and the operator may prefer an earlier flood. Water-injection operations initiated above the bubblepoint in a heterogeneous recovery may ultimately result in less oil recovery but may be justified economically.

Objective 1, maximum oil recovery, is important to all operators or agencies who are concerned primarily with the best interests of the public. Objectives 2, 3, and 5, involving certain financial goals, are most important to privately owned companies, either independent or major; in these cases, the choice would depend on a company's size and financial position and on whether it is planning to sell the property. Objective 4, stabilized rate of monetary return, becomes important when financing, such as production loans and oil payments, and federal taxes are considered. This last point, federal taxes, is particularly important to small operators who are subject to large variations in a tax rate that depends on their tax bracket. Also, some money-lending agencies are particularly interested in properties that are anticipated to have long producing lives—i.e., to have a production rate that has been stabilized somewhat below the attainable rate. Other agencies are more interested in a fast return on investment.

In summary, then, the optimal time to begin water-injection operations depends on which of the objectives is of primary concern.

Determination of Residual Oil After Waterflooding

Perhaps the most commonly used technique for calculating total waterflood recovery is to subtract the ROS after waterflooding from the oil saturation before flooding, then

to multiply the difference by the appropriate factors to convert the displaced portion to barrels of stock-tank oil, after making adjustments for such things as areal pattern efficiency and vertical conformance. If original reservoir saturation conditions and fluid properties are known or can be determined, current saturation conditions may be computed at any time from the pressure and production history. The determination of the ROS resulting from displacement by an advancing water front can be determined satisfactorily only from laboratory measurements made on representative samples of the reservoir rock. These samples must be subjected to a displacement process that is similar to that expected under waterflood. Such tests of waterflood susceptibility, or potential, are run on both fresh cores and on restored-state samples. Interpretation of the data is often difficult, particularly when fresh-core techniques are used or when there are not enough data available to establish its reliability.

Fresh-Core Techniques

The fresh-core technique has the advantage of being quicker and cheaper than the restored-state technique. In applying this technique, a core sample that is fresh from the field is subjected to waterflooding and the residual oil is determined. This procedure is meaningful only when coring conditions have ensured that flushing and contamination by drilling fluid has been virtually eliminated, as is the case when a depleted sand is cored with cable tools. Contamination of cores by the drilling fluid, which often contains surface-active agents and other chemicals as well as contaminating solids, can drastically change wettability characteristics and reduce ROS's to considerably below the naturally occurring value. Any ROS that has been determined in this manner should be regarded suspiciously and be used only if the reported values can be verified by other means.¹²

Interpretation of Conventional Core-Analysis Data

In the absence of more dependable data, some authors recommend that the oil saturation measurement that is derived from conventional core analysis of cores taken with water-based drilling fluids be used as a reasonable estimate of the ROS after waterflooding. This procedure is valid only after the saturation value is increased by the FVF at the existing reservoir pressure. The resulting measurement is believed to be more dependable than the saturation value that is determined from further flooding this same core sample with more water, as is done with the fresh-core technique.

Laboratory tests¹³ indicate that an additional correction should be made for the reduction in oil saturation that results from gas expansion as the core is being pulled. The actual reservoir ROS would be represented by the term $S_{or} B_{oR} C_{ge}$, where S_{or} is the residual oil measured at the surface, B_{oR} is the oil FVF at current reservoir conditions, and C_{ge} is the correction for gas expansion. (A value for C_{ge} of 10.0% is acceptable in the absence of measured data.)

Restored-State Technique

Probably the most dependable means of determining the ROS behind an advancing front is to study the results of waterflood susceptibility tests that are performed by the

restored-state technique on representative samples of the reservoir rock. This requires the obtaining of enough data to establish dependably that the core samples represent all the permeability ranges contained in the reservoir. This ideal situation is very rarely available to the engineer, so interpretations must be made with less than the ideal data. In the restored-state technique, the sample is first extracted and then dried in an effort to remove all contaminants. Then, the irreducible water saturation is determined by the capillary-pressure method. After this, the sample is saturated with brine, which is usually of approximately the same composition as that of the reservoir. All mobile water then is displaced with an oil of about the same viscosity as the reservoir oil, leaving the core sample in its original condition. Then the core sample is subjected to a water-displacement process until the effluent is essentially 100% water. At this point, the oil saturation is determined in the normal manner and called the ROS.

Relative-Permeability Curves

ROS's also may be determined from relative-permeability curves, but the normal purpose of these curves is to give more data for the area that lies between the two extreme conditions of interstitial water and ROS. Since the measurements for the area between those two conditions are made on rather small samples of the reservoir rock, they are normally performed with an oil of substantially greater viscosity than that of the reservoir oil. The more viscous oil facilitates accurate measurement of the pressure gradients that are necessary for dependable relative-permeability determination. Therefore, relative-permeability curves should be used primarily for fractional-flow and rate/pressure calculations, with more weight being given to the middle saturation range than to those on either end. This view seems to support the practice of arbitrarily reshaping the experimental k_{rw} curve in the vicinity of the ROS and the experimental k_{ro} curve in the vicinity of the irreducible water saturation so as to confirm more dependable determinations of these saturations. Further, it seems to indicate that considerable error might be introduced by using an ROS taken from relative-permeability measurements alone.

Effect of Initial Saturations

Initial saturations of water, oil, and gas on reservoir suitability have been discussed previously in this chapter. The effect of these saturations on the ROS behind the water front will be considered here.

As previously mentioned in the discussion of fluid saturation and distributions, an initial water saturation that is above the "critical" value will cause the displacement mechanism to be of the "subordinate-phase" variety that normally prevails after breakthrough. This means that a frontal displacement will be impossible; still, considerable quantities of oil may be recovered if it is economical to use large volumes of water. For predictions of this type of performance, a fractional flow evaluation is necessary—rather than reliance on the concept of an ROS behind an advancing front, or "piston," of water.

The effect of an initial gas saturation has been investigated by several authors, most of whom report increasing beneficial results in reducing the ROS left by the displacing water when an initial gas saturation up to 30% has been found.¹⁴⁻¹⁶ Some authors^{14,17} have reported

substantial benefits from an initial gas saturation of more than 30%; however, these benefits begin to decline as the gas saturation increases. True benefits were also found to vary with the properties of the reservoir rock as well as with the properties of the reservoir fluids. All authors report substantial increases in ROS's as the oil/water viscosity ratio increased. Accurate predictions of the amount by which the ROS may be reduced as a result of any initial gas saturation is a matter for laboratory determination or for calculation from field performance data.¹⁷ Craft and Hawkins¹² state that the total residual hydrocarbon saturation will be about the same value, whether for oil or gas, or a combination of oil and gas. This view is not rigidly supported by laboratory data but the value may be used as an approximation.

Influence of Wettability

It has been shown that wettability has an influence on the interstitial water saturation, ROS, capillary pressure, relative permeability, waterflood performance, and the resistivity index of oilfield cores. In short, any property that is influenced by saturation conditions and/or interfacial relationships also will be influenced by wettability. This indicates the importance of assuring that all measurements of such properties are made under the correct conditions. Any laboratory measurements that are made under improper wettability conditions will give results that will differ to a potentially large degree from the true magnitude of the property as it exists in the reservoir. The importance of wettability in reservoir-rock-fluid behavior has been increasingly emphasized in recent literature.¹²⁻¹⁵

In most cases, the laboratory data, engineering calculations, and field experience will indicate that water is generally more efficient than gas in displacing oil from reservoir rocks. There are two primary reasons for this: (1) the viscosity of water is much nearer that of oil than is the viscosity of gas, and (2) the water occupies the less conductive portions of the pore spaces whereas the gas occupies the more conductive portions. Thus, in water displacement, the oil is left to the central and more conductive portions of the pore channels. This circumstance is true only for reservoir rocks that are preferentially water-wet (hydrophilic), as is the case for most reservoir rocks. Where the rock is preferentially oil-wet (hydrophobic), the displacing water will invade the more conductive portions first (just as the gas does), thus resulting in lower displacement efficiencies. However, the efficiency by water displacement still exceeds that by gas displacement because of the viscosity advantage. This effect is accounted for in capillary-pressure and relative-permeability measurements only if the rock samples in the laboratory exhibit the same number and degree of hydrophilic and/or hydrophobic qualities as those that prevail in the reservoir. Waterflood oil-recovery predictions that were based on core-analysis data have shown recoveries from water-wet rock to exceed recoveries from oil-wet rock by as much as 15% of the original oil in place (OOIP).¹⁸ Apparently, coring fluids and core-handling techniques can disturb the native wettability characteristics of reservoir rock surfaces and may render undependable the laboratory measurements that are made on any particular core. However, a few coring fluids, brine in particular, have been found not to affect core wettability, and core handling and preserving procedures have been

TABLE 44.1—EXAMPLES OF THE STILES CALCULATION

Line =	Permeability Range (md)	Number Feet in Group (2)	$h =$ Cumulative Feet (3)	Capacity in Group (md-ft) (4)	$kh =$ Cumulative Capacity (md-ft) (5)	Average Permeability of Group (md) = (4)/(2) (6)	Permeability at End of Group = $\bar{k} = (6) + (6) + 1$ (7)	$khM_{wo} = (5)M_{wo}$ (8)	$(kh)_i - kh = (kh)_i - (5)$ (9)	$khM_{wo} + (kh)_i - kh = (8) + (9)$ (10)	Water Cut (fraction) = (8)/(10) (11)	$kh_i - kh/\bar{k} = (9)/(7)$ (12)	Recovery (ft) = (3) + (12) (13)	Recovery (fraction) = (13)/ h_i (14)
1	220 to 250	1	1	225	225	225.0	210.0	247.5	7.725	7.972.5	0.031	36.8	37.8	0.310
2	190 to 220	1	2	195	420	195.0	186.2	462.0	7.530	7.992.0	0.057	40.4	42.4	0.348
3	170 to 190	2	4	355	775	177.5	167.1	852.5	7.175	8.027.5	0.106	42.9	46.9	0.384
4	150 to 170	3	7	470	1,245	156.7	148.4	1,369.5	6.705	8.074.5	0.170	45.2	52.2	0.428
5	130 to 150	3	10	420	1,665	140.0	129.5	1,831.5	6.285	8,116.5	0.226	48.5	58.5	0.480
6	110 to 130	5	15	595	2,260	119.0	108.9	2,486.0	5.690	8,176.0	0.304	52.2	67.2	0.551
7	90 to 110	9	24	890	3,150	98.9	90.5	3,465.0	4.800	8,265.0	0.419	53.0	77.0	0.631
8	75 to 90	14	38	1,150	4,300	82.1	75.1	4,730.0	3.650	8,380.0	0.564	48.6	86.6	0.710
9	60 to 75	20	58	1,360	5,600	68.0	60.5	6,226.0	2.290	8,516.0	0.731	37.9	95.9	0.786
10	45 to 60	23	81	1,220	6,880	53.0	45.5	7,568.0	1.070	8,638.0	0.876	23.5	104.5	0.857
11	30 to 45	17	98	645	7,525	37.9	31.5	8,277.5	425	8,702.5	0.951	13.5	111.5	0.914
12	15 to 30	14	112	350	7,875	25.0	16.3	8,662.5	75	8,737.5	0.991	4.6	116.6	0.956
13	0 to 15	10	122	75	7,950	7.5	—	8,745.0	0	8,745.0	1.000	0.0	122.0	1.000

 $h_i = 122$ $C_i = 7,950$

$$M_{wo} = \frac{k_{rw}}{k_{ro}} \frac{\mu_o}{\mu_w} (B) = \frac{0.200}{0.800} \times \frac{3.60}{0.90} (1.100) = 1.100.$$

developed to preserve wettability characteristics during storage and laboratory testing.

Predicting Water Injection Oil Recovery and Performance

Predictions of future oil recovery and reservoir performance for waterflood and water injection projects provide the basis for the economic evaluation of the profitability of proposed projects. These performance and recovery projections should be made in sufficient detail to define the economic viability of the project. This definition should be made after consideration is given to the investment requirements, cost of operations, projected recovery, and the return that is expected on the investment. In some cases, an estimate of the ultimate oil recovery that is expected from the operation may be sufficient; in fact, it may be the only estimate possible if basic reservoir and past production data are limited or are of questionable reliability. However, in most cases, detailed projections are required for making economic evaluations. These include the projection of future well requirements and recompletions, individual well injection and producing rates, reservoir and injection pressures, producing WOR's, and oil recovery throughout the course of the project. Detailed projections require complex predictive methods and complete and detailed reservoir data. It is the responsibility of the reservoir engineer to choose the detail and complexity of the performance projections—following consideration of the management requirements, the cost of developing the projections, and the amount and reliability of the basic reservoir and economic data that are available.

Displacement Calculation Procedures

There are a number of methods presented in the literature for calculating the performance of a waterflood project. Two of the early methods that were developed for application in stratified reservoirs are the Stiles¹⁹ and Dykstra-Parsons.¹⁵ The Stiles method is based on the assumptions that fluid displacement occurs in a piston-like manner, in a linear bed of a specific permeability, and that the rate of advance of the flood front is proportional to the permeability of the bed. The Dykstra-Parsons method for predicting waterflood performance includes

consideration of actual fluid mobilities rather than an assumption of equal mobility for the displacing and displaced fluids. With this exception, the basic assumptions made in the development of both techniques are essentially the same.

For the description of water/oil displacement in homogeneous reservoirs, two methods are of primary importance: the Buckley-Leverett²⁰ frontal advance theory, and a subsequent extension of this work by Welge.²¹ These two techniques provide the fundamental basis for describing the water/oil displacement characteristics of a linear reservoir segment with homogeneous properties.

Stiles Calculation. In the Stiles¹⁹ method, the following assumptions are made. The rate of flood advance in a linear bed is proportional to the permeability of that bed. After breakthrough, the water/oil production rates are governed by, respectively, the water and the oil mobility ratios of the beds that produce the water and oil in the output well. This latter point is equivalent to the assumption that the rate of fluid movement in each bed is proportional to the oil mobility if breakthrough has not occurred, or proportional to the water permeability if breakthrough has occurred, and that there is no crossflow between beds. The Stiles method involves a calculation procedure that gives recovery values for a "unit" of the total reservoir.

The data needed for the calculations are the individual, measured, permeability values for the reservoir unit being considered, the water/oil mobility ratio, and the oil FVF at flood conditions. The Stiles calculations give the values of produced watercut vs. oil recovery as a fraction of the total recoverable oil. In practical applications, the total recoverable oil is determined independently, as the difference between the amount of oil in the reservoir at the start of the waterflood and the amount of oil remaining after the flood has been completed (to 100% water cut); this difference is then adjusted by an areal coverage factor for the flood unit.

For convenience in calculating, the permeability values are arranged in a numerically descending sequence. If there are a great many values, they may be grouped by permeability ranges and the total millidarcy-foot capacity and footage for each range is computed. In the case of such grouped values, it is preferable to set the ranges

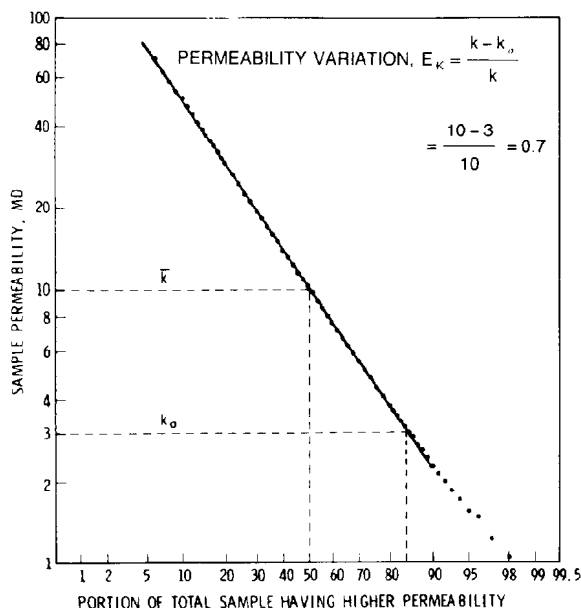


Fig. 44.1—Log-normal permeability distribution.

so that there will be approximately equal capacities in the middle permeability ranges and somewhat smaller capacities in the high and low permeability ranges.

Values for cumulative capacity and cumulative thickness, as well as the average permeability for each group, then are calculated. The fractional cumulative capacity may be plotted vs. fractional cumulative thickness; the result of this procedure is referred to as a capacity-distribution curve. In the original Stiles method, the permeability data are plotted at the midpoint values of cumulative thickness, a smooth curve is drawn through the points, and a new set of permeability values are read at the thickness values to be used in the final calculations. In the equivalent calculation method presented in this chapter, the plotting may be eliminated because the smoothing of permeability values is accomplished by forward interpolation between successive permeability values. The calculation of fractional capacity and thickness also may be eliminated if the capacity-distribution curve is not required.

An example of a water-cut recovery calculation is shown in Table 44.1. In that table, the letters h and kh , in Cols. 3 and 5, represent cumulative foot and millidarcy-foot capacity, respectively; h_i and $(kh)_i$, in Cols. 2 and 4, represent the corresponding totals; and \bar{k} , in Col. 7, designates the interpolated average permeability in millidarcies. The equations for the fractional water cut and recovery, at the time when h feet are producing water, are as follows.

$$f_w = \frac{khM_{wo}}{khM_{wo} + (kh)_i - kh} \quad (2)$$

and

$$N_{pa} = \frac{1}{h_i} \left[h + \frac{(kh)_i - kh}{\bar{k}} \right] \quad (3)$$

where M_{wo} equals the water/oil mobility ratio multiplied by the FVF of the reservoir oil at the time of flooding:

$$M_{wo} = \frac{k_{rw}}{k_{ro}} \frac{\mu_o}{\mu_w} \times B,$$

where

k_{rw}/k_{ro} = water/oil relative permeability ratio,

μ_o/μ_w = oil/water viscosity ratio,

B = FVF,

N_{pa} = recovery to depletion (abandonment),

kh = capacity of flowing water, and

$1 - kh$ = capacity of flowing oil.

The resulting recovery vs. water-cut data may be used as the starting point for further calculations in connection with the flood unit. For example, if the unit is a five-spot in a depleted field and an estimate of the gas space in the reservoir is available, calculations of the time behavior of the flood may be made for an assumed injection-rate schedule. These calculations would involve determination of the fill-up time and a subsequent application of the water-cut recovery curve so as to calculate the oil production rate vs. time.

As noted previously, the Stiles method gives recovery vs. water-cut data for a hypothetical flood unit, in which breakthrough into various producing wells of the unit occurs at the same time. The information could be expected to approximate that for the behavior of a five-spot pattern or that for a group of five-spots, provided an appropriate areal coverage factor is applied.

Dykstra-Parsons Calculation. Dykstra and Parsons¹⁵ performed a series of laboratory waterflooding tests on field core samples and concluded that oil recovery by waterflooding is a function of both mobility ratio and permeability distribution, with the mobility ratio being defined as follows.

$$M = \frac{k_w}{\mu_w} \frac{\mu_o}{k_o}, \quad (4)$$

where k_w is the permeability to water in the water-contacted portions of the reservoirs, and k_o is the permeability to oil ahead of the waterfront (or mobility of swept to unswept region).

On the basis of the laboratory test results, and calculations made on a layered linear model in which it was assumed there was no crossflow, a correlation that related waterflood recovery to both mobility ratio and permeability distribution was developed. Permeability distribution was measured by the efficiency of permeability variation E_K , as follows.

$$E_K = \frac{\bar{k} - k_o}{\bar{k}}, \quad (5)$$

where \bar{k} is the mean permeability and k_o is the permeability value at 84.1% of the cumulative sample, as shown in Fig. 44.1.⁴

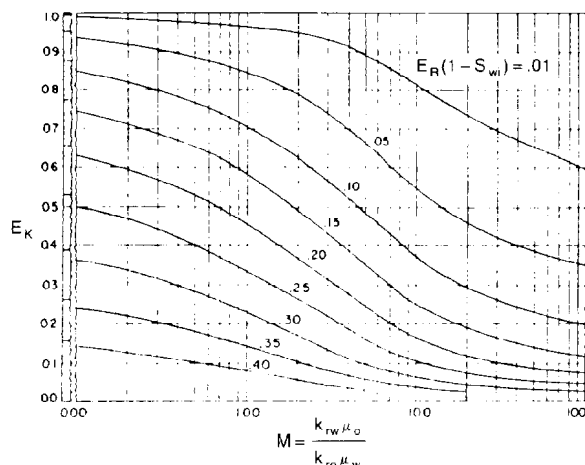


Fig. 44.2—Permeability variation vs. mobility ratio, showing lines of constant $E_R(1 - S_{wi})$ for a producing WOR of 1.

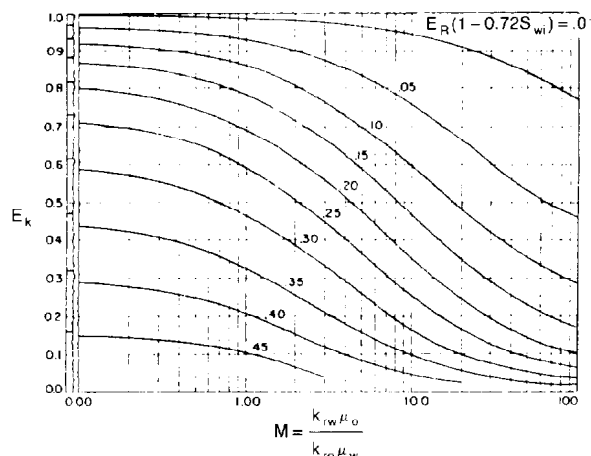


Fig. 44.3—Permeability variation vs. mobility ratio, showing lines of constant $E_R(1 - 0.72S_{wi})$ for a producing WOR of 5.

The correlations developed by Dykstra and Parsons were for WOR's of 1, 5, 25, and 100, with recovery related to permeability variation, interstitial water saturation, ROS, and mobility ratio. The basic equations used in developing the correlations were based on the following approach.

At the beginning of injection, the mobility in a layer is determined by the oil and gas phases. As water advances into a layer, the mobility is a composite of oil, gas, and water mobilities; after fill-up, the mobility is determined by the relative permeability and the viscosity ratios. The varying nature of the overall mobility results in a continuously changing injectivity. This method assumes that the permeability distribution is log-normal.

By use of the linear Darcy flow equation for incompressible fluids, the following equations for "coverage" or "conformance efficiency" and WOR were developed:

$$E_C = \left\{ n_{BT} + \frac{(n - n_{BT})M}{(M - 1)} - \frac{1}{(M - 1)} \sum_{i=(n_{BT}+1)}^n \left[\sqrt{M^2 + \frac{k_i}{k_x}(1 - M^2)} \right] \right\} \div n \quad (6)$$

and

$$F_{wo} = \frac{\sum_{i=1}^{n_{BT}} k_i}{\sum_{i=(n_{BT}+1)}^n \left[\frac{k_i}{\sqrt{M^2 + \frac{k_i}{k_x}(1 - M^2)}} \right]} \quad (7)$$

where

- E_C = fractional coverage or conformance efficiency,
- F_{wo} = WOR,
- n = number of layers,
- k_i = permeability of layer,
- k_x = permeability of x layer, or the layer that has just been flooded,
- M = mobility ratio, and
- n_{BT} = number of layers in which water has broken through (varies from 1 to n).

When the coverage and F_{wo} are known, it is possible to predict oil recovery and water cut as a function of time, provided the injection rates can be determined adequately.

To develop the relationship between the producing WOR and coverage, or fractional oil recovery, the equations must be solved for breakthrough conditions in each layer of the system, or at least for a substantial number of layers. This method is laborious for hand calculations and, in a later paper, Johnson²² presented a graphical technique for applying the Dykstra-Parsons method that was based on the plots shown in Figs. 44.2 through 44.5, where E_R is the fractional recovery of OIP at a given producing WOR. An example of the manner in which these plots were used in applying the Dykstra-Parsons technique was presented by Craig.⁴

Both the Stiles and the Dykstra-Parsons methods were developed for linear, piston-like displacement in a stratified system, and the results that are obtained when applying these techniques must be interpreted within the context of the limitations imposed by the basic assumptions. However, the concepts established as a result of this early work provided the basis for a number of predictive techniques that have since been developed.

Frontal Advance Calculation. The frontal advance calculation was derived from the concept of fractional flow presented by Leverett²³ in his classic 1941 paper. The fractional flow equation was developed from Darcy's law for water and oil and, in generalized form, it is as follows.

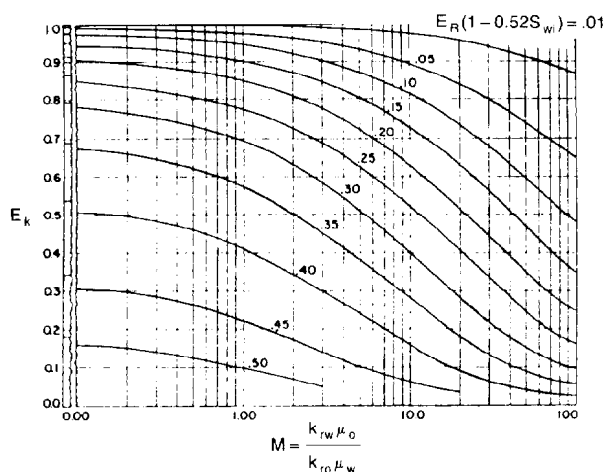


Fig. 44.4—Permeability variation vs. mobility ratio, showing lines of constant $E_R(1 - 0.52S_{wi})$ for a producing WOR of 25.

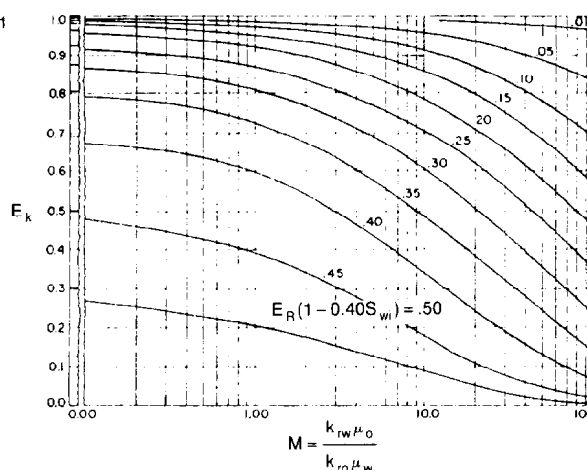


Fig. 44.5—Permeability variation vs. mobility ratio, showing lines of constant $E_R(1 - 0.40S_{wi})$ for a producing WOR of 100.

$$f_w = \frac{1 - (k_o/\mu_o q) \left(\frac{\partial P_c}{\partial L} - g \Delta \rho \sin \theta \right)}{1 + \frac{\mu_w}{\mu_o} \frac{k_o}{k_w}}, \quad \dots \dots (8)$$

where

- f_w = fraction of water in the flowing stream,
- k_o, k_w = effective formation permeability to the specific phase, kk_{ro} and kk_{rw} ,
- μ_o = oil viscosity,
- μ_w = water viscosity,
- q = fluid volumetric flow rate per unit cross-sectional area,
- P_c = capillary pressure, $p_o - p_w$,
- L = distance along direction of measurement,
- $\Delta \rho$ = density difference between water and oil, $\rho_w - \rho_o$,
- θ = angle of formation dip referenced to horizontal, and
- g = acceleration caused by gravity.

In practical units, the equation becomes

$$f_w = \frac{1 + 0.001127 \frac{k_o A}{q_i \mu_o} \left(\frac{\partial P_c}{\partial L} - 0.434 \Delta \rho \sin \theta \right)}{1 + \frac{\mu_w}{\mu_o} \frac{k_o}{k_w}}, \quad \dots \dots (9)$$

where

- f_w = fractional flow of the displacing fluid,
- k_o = effective permeability to oil, md,
- k_w = effective permeability to water, md
- A = cross-sectional area of flow, sq ft,
- q_i = total flow rate, $(q_w + q_o)$, B/D,
- P_c = capillary pressure, $p_o - p_w$, psi,
- $\Delta \rho$ = density difference, g/cm^3 , $\rho_w - \rho_o$,
- θ = dip angle, positive updip,
- μ = phase viscosity, cp, and
- L = distance, ft.

In the case of a water drive, neglecting the effects of the capillary pressure gradient and the dip of the reservoir, the terms $\partial P_c / \partial L$ and $g \Delta \rho \sin \theta$ become insignificant. The fractional flow equation then reduces to

$$f_w = \frac{1}{1 + (k_o/k_w)(\mu_w/\mu_o)}, \quad \dots \dots (10)$$

which states that the fraction of water in the flow stream is a function of the relative-permeability relationships in which μ_o and μ_w are constant for a given reservoir pressure. Since k_o/k_w is a function of saturation, Buckley and Leverett²⁰ derived the following frontal-advance equation on the basis of relative-permeability concepts.

$$L = \frac{5.615 q_i}{\phi A} \left(\frac{\partial f_w}{\partial S_w} \right)_{S_w}, \quad \dots \dots (11)$$

where

- L = distance, ft,
- q_i = total flow rate, B/D,
- ϕ = porosity,
- A = cross-sectional area, sq ft, and
- t = time, days.

This states that the distance a plane of constant saturation (S_w) advances is directly proportional to time and to the derivative $(\partial f_w / \partial S_w)$ at that saturation. The value of the derivative may be obtained for any value of water saturation by plotting f_w from Eq. 9 vs. S_w and graphically taking the slopes at values of S_w . Fig. 44.6 shows a plot of f_w vs. S_w in addition to the resultant df_w/dS_w vs. S_w relationships for the S_w vs. k_o/k_w data at a viscosity ratio of water to oil of 0.50 (see Table 44.2).

If the df_w/dS_w values found in Fig. 44.6 are substituted into Eq. 11, the distance that a given water-saturation plane or front will advance for any time t can be calculated for the known throughput q in barrels per day, fractional porosity, and cross-sectional area (in sq ft).

Fig. 44.7 represents the water-saturation profile or frontal-advance curves for a bed that is 1,320 ft wide and 20 ft thick, and has a porosity of 20% and a throughput of 900 B/D for 60, 120, and 240 days with the f_w , $\partial f_w / \partial S_w$ vs. S_w relationship shown in Fig. 44.6 The curves shown in Fig. 44.7 are characteristically double-valued or triple-valued. For example, the water saturation after 240 days at 400 ft is 20, 36, and 60%. The saturation can have only one value at any place and time, and the difficulty is resolved by dropping perpendiculars so that the areas to the right (A) equal the areas to the left (B).

Fig. 44.8 represents the initial water and oil distributions in the example reservoir and also the distributions after 240 days. The area to the right is the flood front or "oil bank," and the area to the left is the water-invaded zone. The area above the 240-day curve and below the 90% water-saturation curve represents oil that may be recovered by the displacement of additional volumes of water through the area. The area above the 90% water saturation curve represents unrecoverable oil because the ROS is 10%.

Welge Calculations. In 1952, Welge²¹ extended the earlier work of Buckley and Leverett²⁰ to derive a simplified method for calculating fractional flow and recovery performance after water breakthrough. The basic equations developed by Welge are as follows:

$$\bar{S}_w - S_{w2} = W_i f_{o2} \quad (12)$$

and

$$W_i = \frac{1}{\left(\frac{dS_w}{dS_w} \right)_{S_{w2}}} \quad (13)$$

where

\bar{S}_w = average water saturation, fraction of PV,

S_{w2} = water saturation at the producing end of the system,

W_i = cumulative PV's of water injected,

fraction, and

f_{o2} = fraction of oil flowing at the producing end of the system.

An example of the use of the Welge technique for calculating waterflood displacement performance was presented by Craig.⁴ Basic data used in the example calculation are average permeability, 50 md; porosity, 20%; irreducible water saturation, 10% of PV; oil viscosity, 1.0 cp; and water viscosity, 0.5 cp (see Table 44.3).

By Eq. 10,

$$f_w = \frac{1}{1 + \frac{k_{ro} \mu_w}{k_{rw} \mu_o}}$$

The fractional flow vs. water saturation relationship is calculated from basic data, such as those given in Table 44.4.

TABLE 44.2— S_w vs. k_o/k_w DATA AT A VISCOSITY RATIO OF WATER TO OIL OF 0.50

S_w	k_o/k_w
0.20	∞
0.30	17.0
0.40	5.5
0.50	1.70
0.60	0.55
0.70	0.17
0.80	0.0055
0.90	0.0000

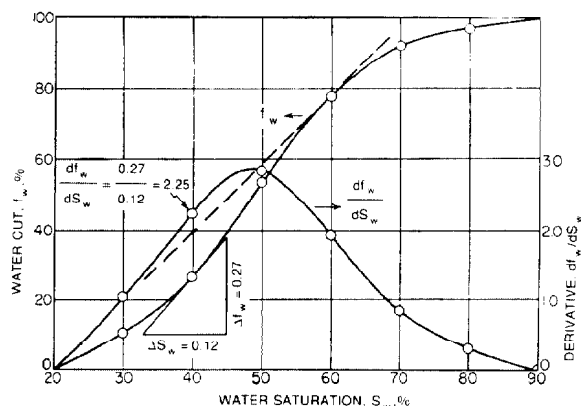


Fig. 44.6—Plot of f_w vs. S_w .

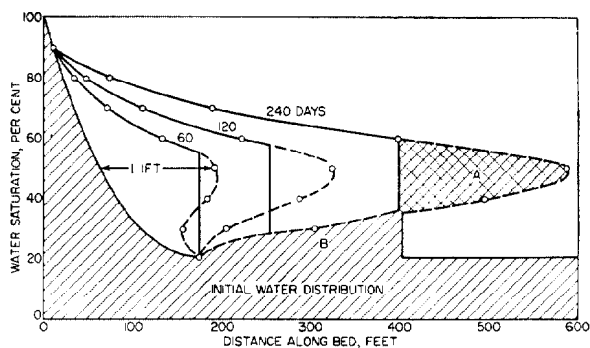


Fig. 44.7—Fluid distribution at initial conditions and at 60, 120, and 240 days.

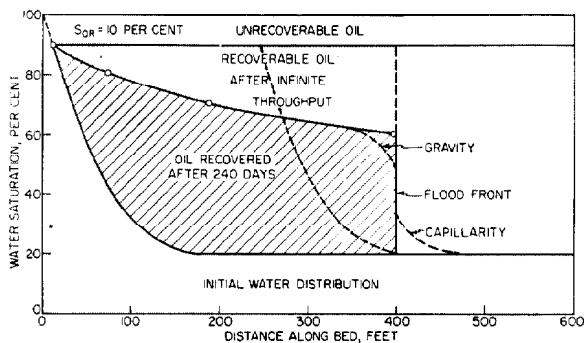


Fig. 44.8—Water saturation distributions as a function of distance.

TABLE 44.3—RELATIVE PERMEABILITY CHARACTERISTICS

Water Saturation, S_w (fraction)	Relative Permeability	
	Oil, k_{ro} (fraction)	Water, k_{rw} (fraction)
0.10	1.000	0.000
0.30	0.373	0.070
0.40	0.210	0.169
0.45	0.148	0.226
0.50	0.100	0.300
0.55	0.061	0.376
0.60	0.033	0.476
0.65	0.012	0.600
0.70	0.000	0.740

TABLE 44.4—FRACTIONAL FLOW DATA

Water Saturation, S_w (% PV)	Fractional Flow of Water, f_w
10	0.0000
30	0.2729
40	0.6168
45	0.7533
50	0.8571
55	0.9250
60	0.9665
65	0.9901
70	1.0000

The fractional flow curve from this calculation is shown in Fig. 44.9. For water breakthrough, the tangent to the fractional flow curve from the point of irreducible water saturation defines (1) \bar{S}_w , the average water saturation behind the front, (2) S_{w2} , the water saturation at the producing end of the system, and (3) f_w , the fractional flow of water at the downstream end of the system.

$$\bar{S}_w = 0.563 \text{ PV,}$$

S_{wBT} = average water saturation at water breakthrough, % PV,

S_{wsz} = water saturation at upstream end of the stabilized zone, % PV,

S_{w2} = 0.469 PV, and

f_{w2} = 0.798.

From the fractional flow curve, df_w/dS_w is determined for water saturations that are higher than S_{w2} at water

breakthrough conditions, and the df_w/dS_w vs. S_w curve is developed, as shown by Fig. 44.10. From Eq. 13, W_i is calculated for increasing values of S_{w2} and f_{w2} and corresponding values of \bar{S}_w are calculated from Eq. 12.

The results for the calculations of the example problem are shown in Table 44.5.

Areal Sweep and Pattern Efficiency

The previous discussion dealt with fundamental techniques for defining water/oil displacement characteristics in linear reservoir segments in stratified reservoirs and in homogeneous reservoir rock systems. However, from a practical standpoint, a truly linear displacement is never used in waterflood operations. In practice, water is injected into some wells and oil and water are produced from others, and often portions of the reservoir are never contacted by the injected water. Therefore, it is necessary to consider the areal sweep efficiency so as to make esti-

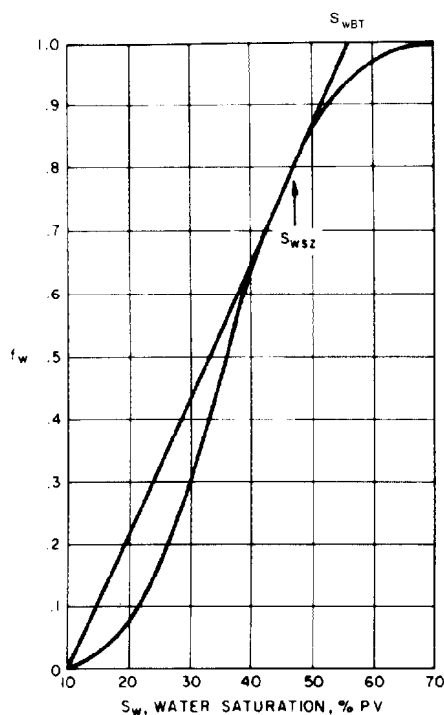
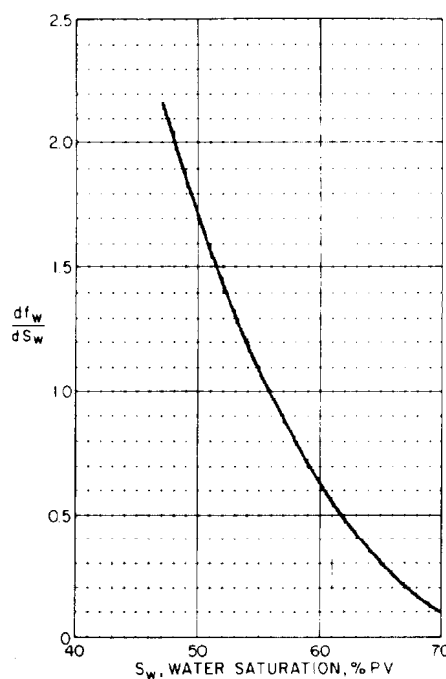
**Fig. 44.9—Fractional flow curve, example problem.****Fig. 44.10—Plot of df_w/dS_w example problem.**

TABLE 44.5—WATERFLOOD DISPLACEMENT PERFORMANCE
(Example Problem)

S_{w1} Exit-End Water Saturation (fraction PV)	f_{w2} Exit-End Flowing Stream Consisting of Water (fraction)	df_w/dS_{w1} Slope of Fractional Flow Curve	W_{i1} PV of Cumulative Injected Water	S_{w1} Average Water Saturation (fraction PV)
0.469	0.798	2.16	0.463	0.563
0.495	0.848	1.75	0.572	0.582
0.520	0.888	1.41	0.711	0.600
0.546	0.920	1.13	0.887	0.617
0.572	0.946	0.851	1.176	0.636
0.597	0.965	0.649	1.540	0.652
0.622	0.980	0.477	2.100	0.666
0.649	0.990	0.317	3.157	0.681
0.674	0.996	0.195	5.13	0.694
0.700	1.000	0.102	9.80	0.700

mates of recoverable oil for a particular project and to predict reservoir performance for waterflood operations.

The purpose of this section is (1) to present methods for determining areal sweep efficiency for pattern flood projects, (2) to discuss factors that affect areal floodout patterns, and (3) to present correlating factors that are used to define areal sweep efficiency.

Methods of Determining Areal Sweep Efficiency. To conduct waterflood operations in a continuous reservoir with a relatively large areal extent, it is common practice to locate injection and producing wells in a regular geometric pattern so that a symmetrical and interconnective network is formed. Five of these basic patterns will be discussed: (1) direct line drive, (2) staggered line drive, (3) five-spot, (4) seven-spot, and (5) nine-spot.^{24,25} Figs. 44.11A through 44.11E are diagrammatic representations of these basic waterflood patterns. The dashed areas represent the basic symmetrical elements that are used in both analytical and model determinations of sweepout patterns.

It is often impractical or even impossible to design waterflood operations that correspond to one of the standard geometrical flood patterns. In such a case, the operator must select a less sophisticated well network—the choice being either a peripheral or random injection pattern.

The random flood pattern will not be considered specifically in this work because that type of flood is required only in certain explicit cases; it is used only when it is impossible to arrive at an arrangement of the peripheral or geometric type of pattern. Most of the material dealing with peripheral floods will apply generally to random waterflood networks. Fig. 44.12 is an illustration of the typical peripheral flood network.²⁶ It is obvious from this figure that there is no symmetrical element that could be considered for analysis, and that reservoir simulation techniques are necessary to obtain reliable future performance predictions for random or peripheral injection patterns.²⁷

Mathematical Analysis of Areal Pattern Efficiency.

Most practical mathematical analyses of flood coverage are based on Darcy's law when it is assumed that steady-state single-phase flow occurs through large areas of homogeneous reservoir rock.

Muskat²⁴ presents a comprehensive review of this theory in his early discussions of the steady-state flow ca-

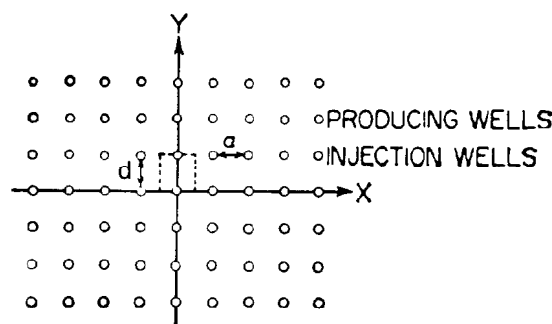


Fig. 44.11A—A diagrammatic representation of a direct-line-drive well network. Dashed segment represents basic symmetry element.

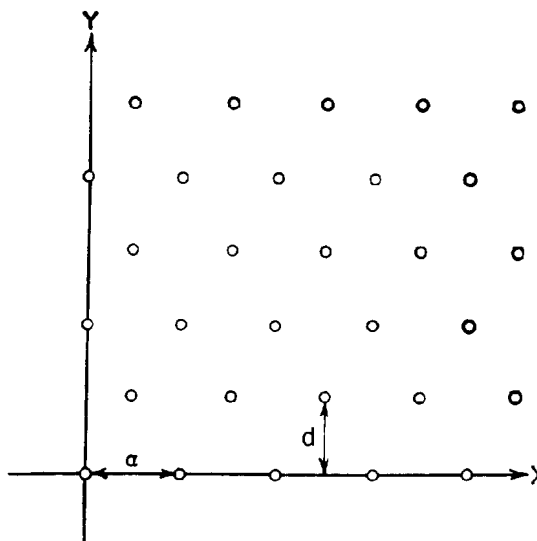


Fig. 44.11B—A diagrammatic representation of the staggered-line-drive network.

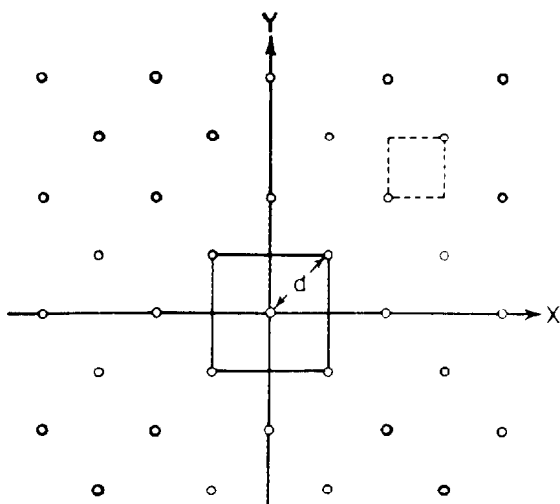


Fig. 44.11C—The five-spot well network. Dashed segment represents basic symmetry element.

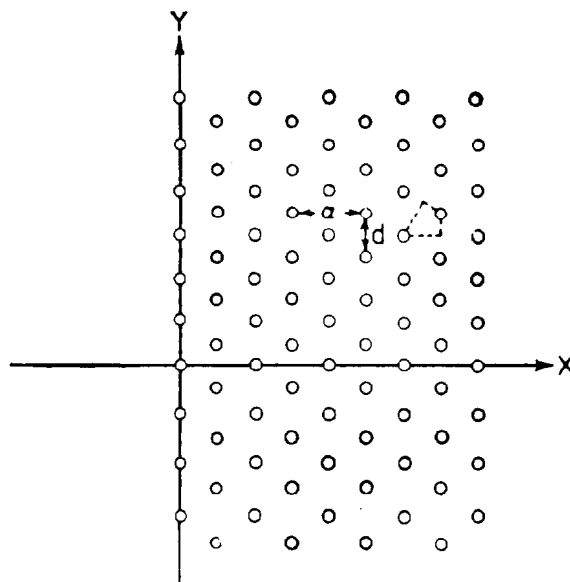


Fig. 44.11D—The seven-spot well network. Dashed segment represents basic symmetry element.

capacity of the various pattern networks. As early as 1934, Muskat and Wyckoff²⁸ presented a theoretical means of calculating areal sweep efficiency for basic flood patterns. Fig. 44.13 is taken from their early work and it shows the variation in calculated steady-state homogeneous-fluid sweep efficiencies for linedrive networks with different values of d/a , where d is the distance between rows of

wells and a is the difference between adjacent wells in a single row. The graph shows a curve for both direct linedrive and staggered linedrive patterns with d/a values from 0.45 to 4.0. Even though the absolute values of pattern efficiency presented in this illustration apply to a simplified system, there are two conclusions that can be drawn from the information: (1) at breakthrough, the staggered

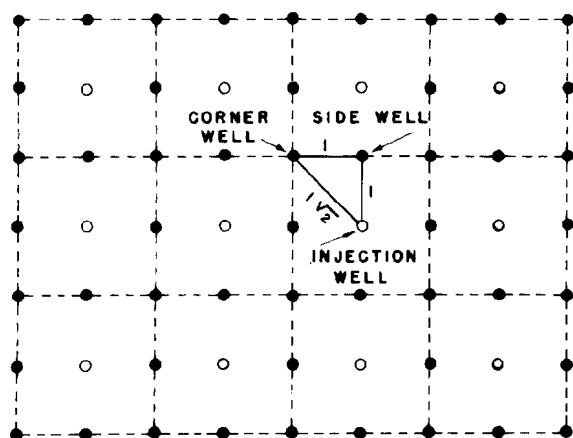


Fig. 44.11E—Nine-spot injection system showing the reservoir element represented by the model.

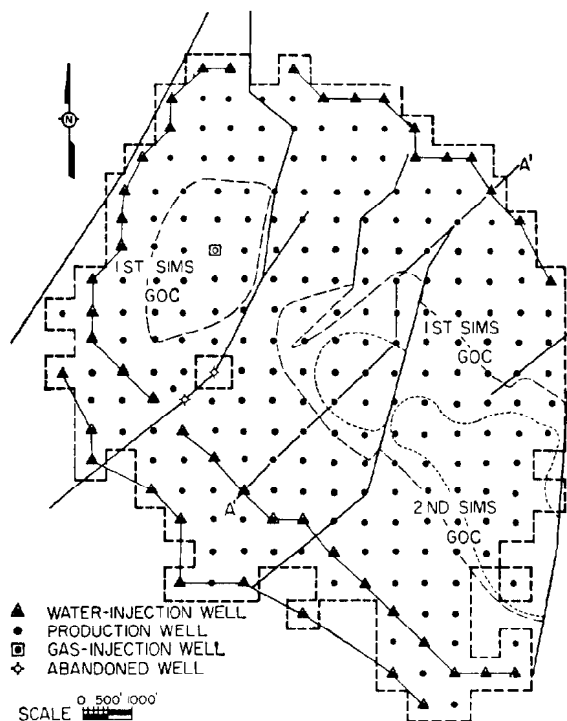


Fig. 44.12—Typical random flood network.

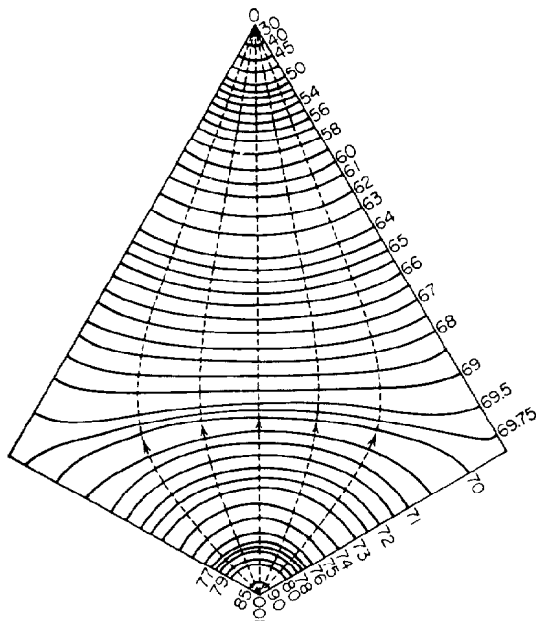


Fig. 44.17—The steady-state, homogeneous-fluid equipressure contours and streamlines in a segment of a seven-spot-network element. Numbers represent percentages of the total pressure drop.

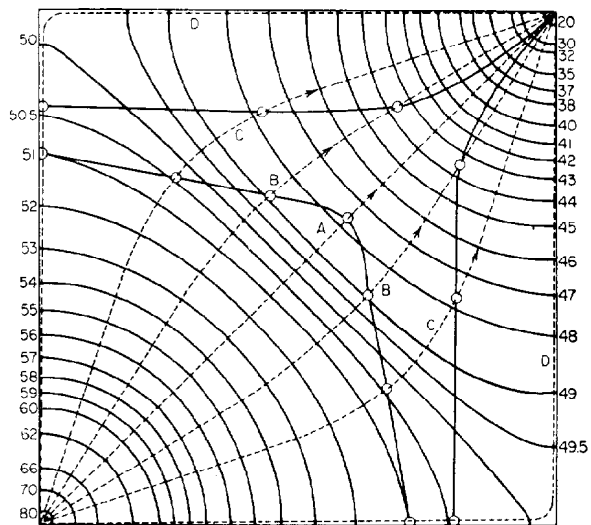


Fig. 44.18—Potentiometric model study of the five-spot network, showing the isopotential lines, the flow lines, and two flood fronts.

techniques. Figs. 44.14 through 44.17 are taken from Muskat and Wyckoff²⁸ and represent steady-state isopotential contours and streamlines for systems with homogeneous fluids that have direct linedrive, staggered linedrive, five-spot, and seven-spot networks, respectively. When the isopotential lines and streamlines are known,

it is easy to determine the fluid interface position at any time during the flood by using the methods described by Craft and Hawkins.¹² In the particular case analyzed for a five-spot pattern and a mobility ratio of 1.0, depicted by Fig. 44.18, the calculated breakthrough sweep efficiency is 72%. This corresponds to a value of 71.5% that

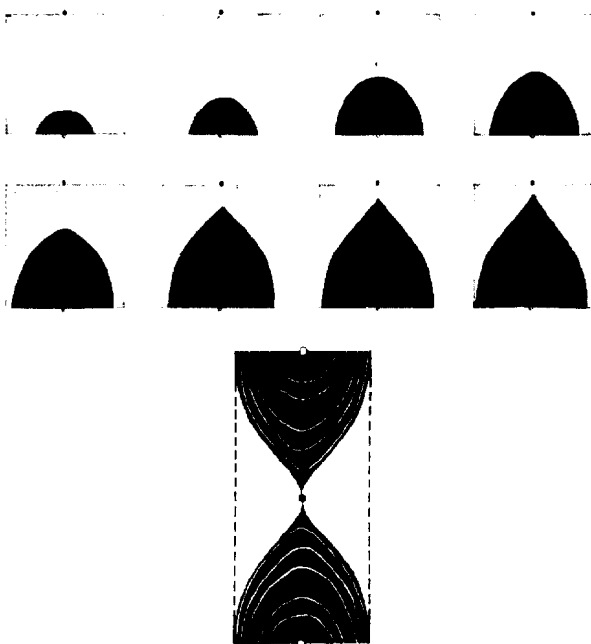


Fig. 44.19—Flood between alternate lines of input and output wells.

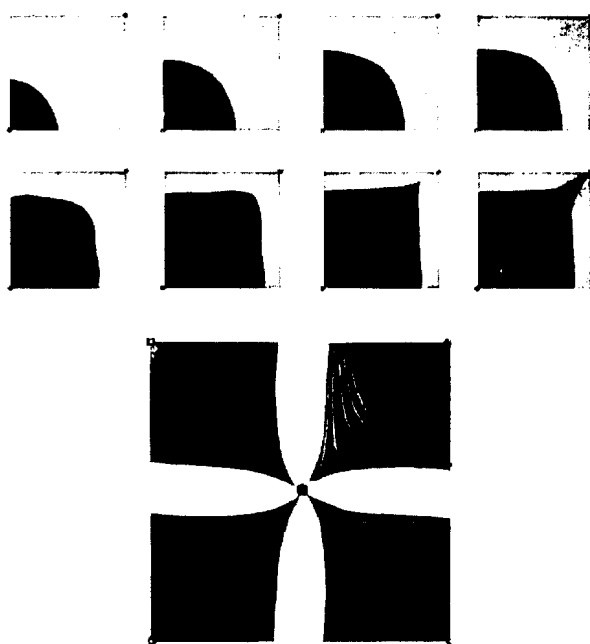


Fig. 44.20—Flood in five-spot array.

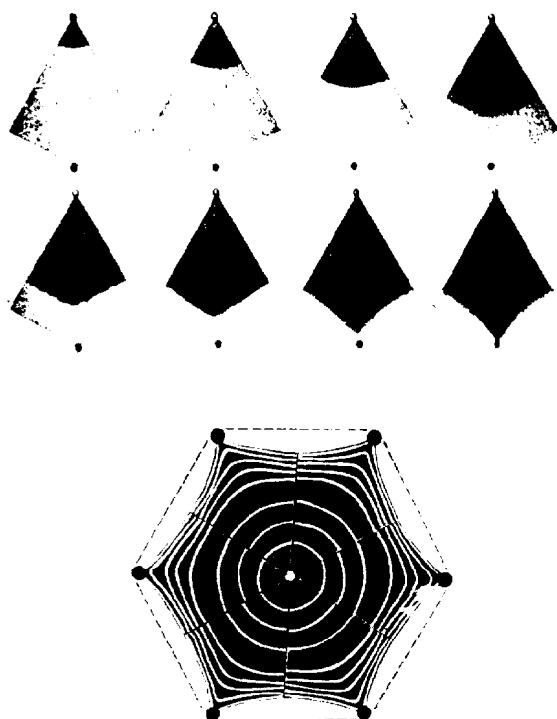


Fig. 44.21—Flood in inverted seven-spot array.

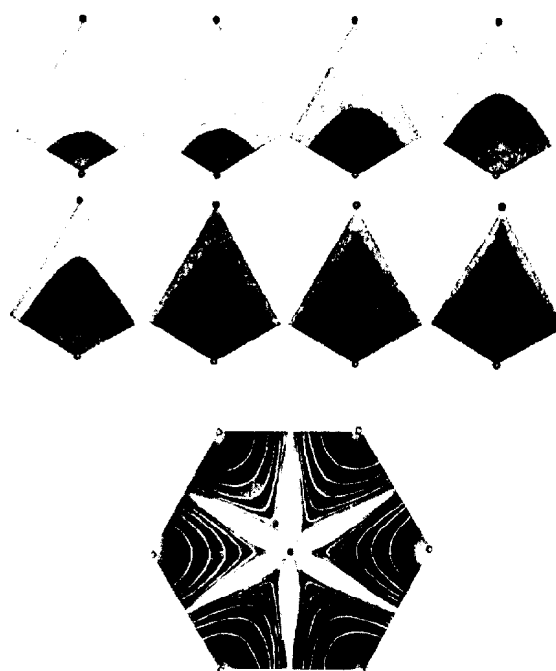


Fig. 44.22—Flood in seven-spot array.

was computed by Muskat as the steady-state breakthrough sweep efficiency for the five-spot pattern at a mobility ratio of 1.0.

Analog Methods for Investigating Areal Sweep Efficiency. Several types of analog models have been used in the petroleum industry to study the shape of injection-fluid fronts and to evaluate areal sweep efficiencies. All the models depend on the analogy between Darcy's law and Ohm's law for a conductive medium that is scaled to represent the reservoir geometry. One of the earliest of these analogs is an electrolytic model designed by Wyckoff *et al.*²⁹ Its operation is based on the movement of copper ammonium and zinc ammonium ions in a medium such as blotting paper or gelatin. Figs. 44.19 through 44.22 are photographic histories of various pattern floods under steady-state, homogeneous-fluid flow conditions, as obtained by using a blotter-type electrolytic model. Fig. 44.23 shows the same type of photographic history but it represents an irregular well network and was obtained with the gelatin type of electrolytic model.³⁰

The potentiometric model was introduced to the industry in 1939 by Swearingen³¹ as a method for studying sweep efficiency in gas-cycling operations; the model has been further refined for waterflood studies by Hurst and McCarty³² and Lee.³³ The potentiometric model is based on the same basic principle as the electrolytic model except that electron flow, rather than ionic flow, is measured.

Porous Reservoir Models. The approach presented by Slobod and Caudle³⁴ is another that has been used by the petroleum industry for studying areal pattern efficiency; this involves scaled porous models of the reservoir element. The model initially is saturated with a fluid that rep-

resents the reservoir oil. Injected fluid in this case contains an X-ray-absorbing material and the displacing front can be followed on a fluorescent screen or X-ray film. Fig. 44.24 is an X-ray shadowgraph study of the five-spot model by Slobod and Caudle.³⁴ An areal sweep efficiency at breakthrough for the 1:1 mobility system is indicated as 69%.

Two-Dimensional (2D) Numerical Models. In an early paper describing the use of numerical models in predicting flood coverage for a peripheral, or random, water injection program, McCarty and Barfield²⁶ presented results obtained for two typical field studies, as shown in Figs. 44.25 and 44.26. In this approach, the computer is used to perform essentially the same calculations as those described by Muskat, with the reservoir defined by a grid network. A valid method of numerical analysis is used to allow solution of the basic differential equations that describe the simultaneous flow of oil and water. As is true of the methods described by Muskat and Wyckoff,²⁸ Stahl,³⁵ and Craft and Hawkins,¹² the digital computer calculates the pressure distribution in the reservoir and then tracks the progress of the interface between the displacing and displaced phases.

This calculation can be done for any combination of injection and producing rates. The approach will allow the calculation of the optimal sweep efficiency under a particular pattern as a function of reservoir injection and producing rate distribution.

Mobility-Ratio Effects. In the previous discussion of various methods of studying areal sweep efficiency, it is important to realize that each technique is based on the assumption that isopotential lines remain fixed during the advance of the front; that is, that the mobility of the dis-

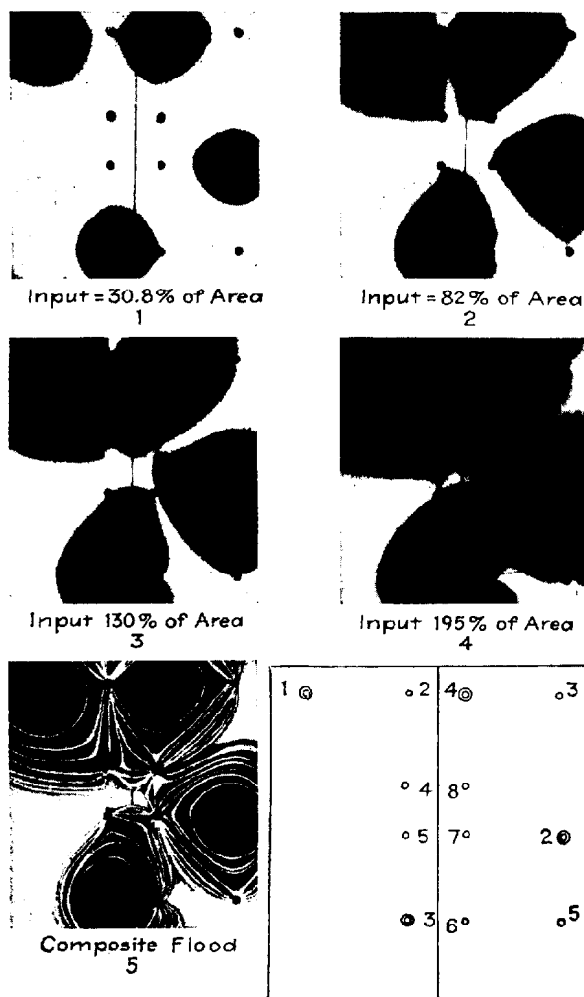


Fig. 44.23—The photographic history of the injection-fluid fronts in an injection project of limited area and with an irregular well distribution, under steady-state, homogeneous-fluid-flow conditions as obtained with a gelatin electrolytic model. Double circles indicate injection wells.

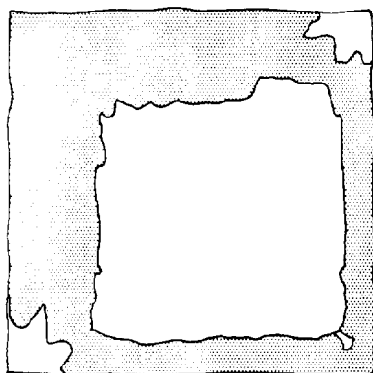


Fig. 44.24—Typical radiograph showing areal sweepout efficiency for the five-spot well spacing. Mobility ratio = 1.

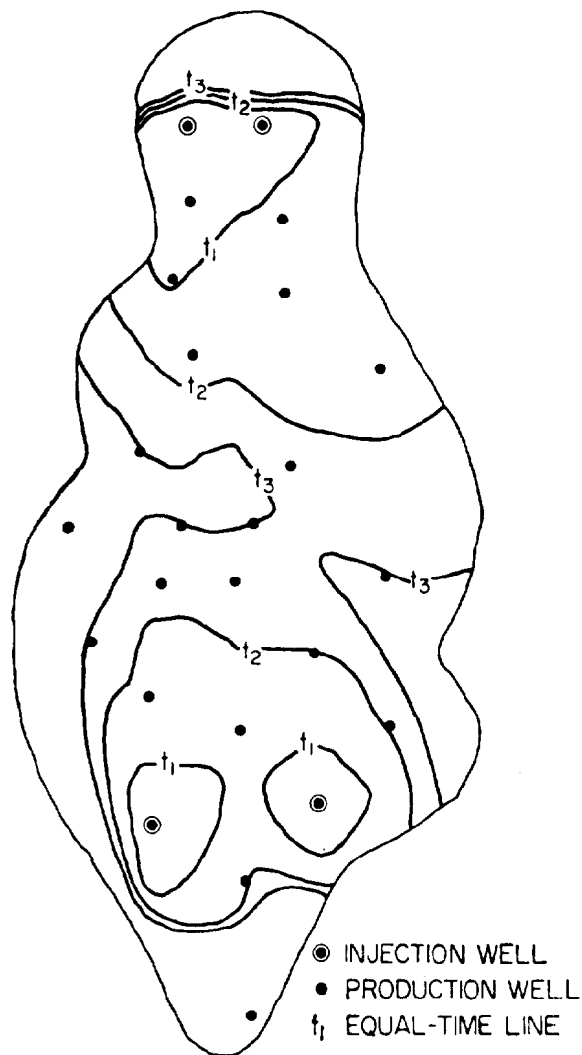


Fig. 44.25—Typical flood pattern resulting from field study.

placing fluid is the same as that of the displaced phase. However, it is well known that isopotential lines change constantly during most injection operations. Consequently, the actual pattern efficiency that will result in the reservoir can be quite different from that indicated by a simplified analysis that assumes a mobility ratio of 1.

The mobility ratio is probably the most important factor involved in determining pattern efficiency. Even though the methods previously cited were based on the assumption of a mobility ratio of unity, it does not mean that they are not of practical use, and the resulting information has served as a basis for further experimental investigations of certain geometrical characteristics that come into play during waterflood operations.

Although the early analog models that were used for studying pattern efficiency did not take into consideration the mobility-ratio effects, later investigations have made use of ingenious ideas to circumvent this restriction. Burton and Crawford³⁶ described an electrolytic model that has been used to estimate flood coverage by mobility ratios of 0.5, 0.85, 1.2, and 3. In that work, the

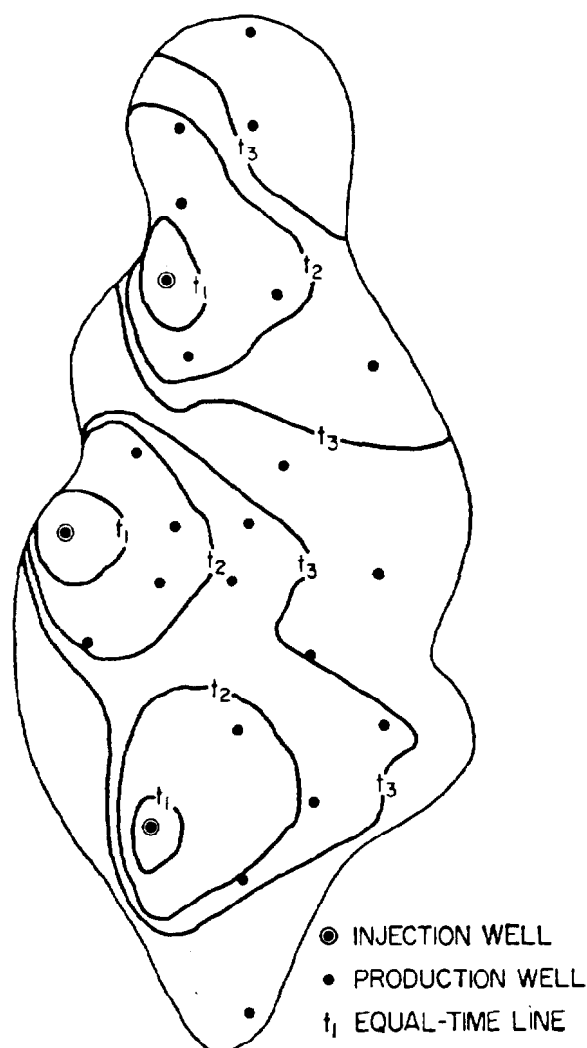


Fig. 44.26—Typical flood pattern resulting from field study.

adjustment for mobility ratios was accomplished through the use of metallic complex ammonium ions other than the copper and zinc compounds used by Wyckoff *et al.*²⁹ Aronofsky³⁷ has been able to include mobility ratios other than unity in a special adaptation of the potentiometric model. Nobles and Janzen³⁸ have presented a variation of the potentiometric model by replacing the liquid with a system of interconnecting resistors; by changing the values of these resistors, they were able to introduce mobility-ratio effects.

The most logical model with which to study mobility-ratio effects is a porous model, or, specifically, a porous model that uses X-ray shadowgraph techniques. In this type of analysis, the injection and displaced phases may be selected so that almost any mobility ratio can be fixed in the reservoir model. Experimental studies by Slobod and Caudle³⁴ take advantage of this feature of the X-ray shadowgraph technique, so that liquids of different viscosities can be used as the displaced and displacing phases and the effect of mobility ratios can be evaluated. Their original work has been extended by Caudle *et al.*³⁹ Fig.

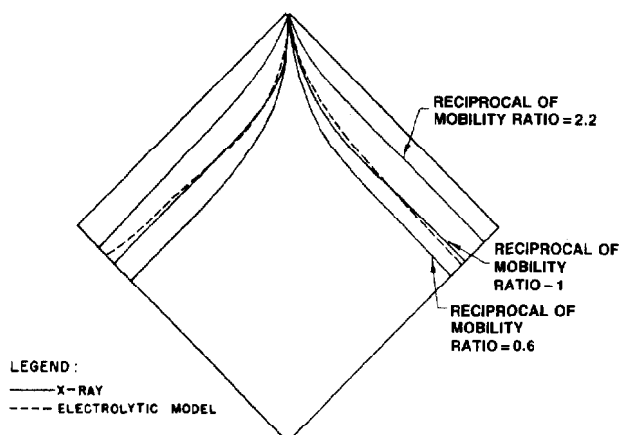


Fig. 44.27—Areal sweepout patterns, five-spot well spacing.

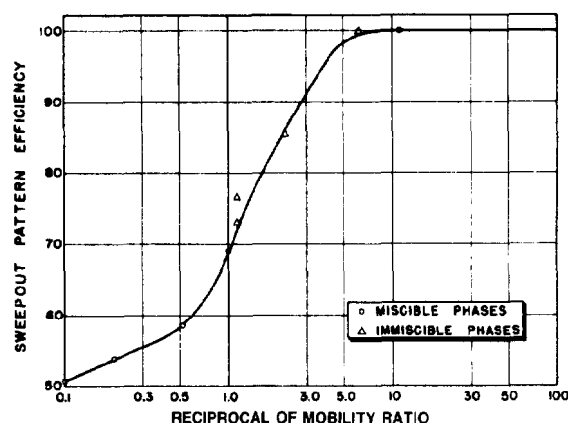


Fig. 44.28—Sweepout pattern efficiency vs. reciprocal of mobility ratio for the five-spot well spacing.

44.27 is an X-ray shadowgraph that shows the effects of the reciprocal of mobility ratio on sweep efficiency at breakthrough for three different reciprocals of mobility ratios. Fig. 44.28 is a plot of the reciprocal mobility ratio vs. five-spot pattern sweepout efficiency at breakthrough. It is apparent from these illustrations that there is little change in breakthrough efficiency for reciprocal mobility ratios that are greater than 7.

In his monograph, Craig⁴ has summarized the areal sweep efficiency studies that have been presented in the literature for various flooding patterns. These summaries are listed in Tables 44.6 through 44.12.

Fig. 44.29 is a plot of the areal sweep efficiencies at breakthrough that were developed as a function of mobility ratio by the various investigations referenced in Table 44.7. As indicated, there is good agreement in the region below a mobility ratio of 1.0; however, considerable deviation exists at higher mobility ratios. Craig⁴ points out that potentiometric model data obtained for high mobility ratios may yield high sweep efficiency values and that miscible displacement methods may give low re-

TABLE 44.6—AREAL SWEEP EFFICIENCY STUDIES—LINEDRIVE PATTERNS

Date	Author(s)	Method	Line Drive	d/a	Mobility Ratio	Reference
1933	Wyckoff <i>et al.</i>	electrolytic model	direct	1.0	1.0	29
1934	Muskat and Wyckoff	electrolytic model	direct	0.5 to 4.0	1.0	28
			staggered	0.5 to 4.0		
1952	Aronofsky	numerical and potentiometric model	direct	1.5	0.1, 1.0, 10	37
1952	Slobod and Caudle	X-ray shadowgraph using miscible fluids	direct	1.5	0.1 to 10	34
1954	Dyes <i>et al.</i> *	X-ray shadowgraph using miscible fluids	direct	1.0	0.1 to 17	40
			staggered	1.0		
1955	Cheek and Menzie	fluid mapper	direct	2.0	0.04 to 11.0	41
1956	Prats	numerical approach	staggered	1.0 to 6.0	1.0	42
1956	Burton and Crawford	gelatin model	direct	1.0	0.5 to 3.0	36

* After-breakthrough performance also presented in these references.

TABLE 44.7—AREAL SWEEP EFFICIENCY STUDIES—DEVELOPED FIVE-SPOT

Date	Author(s)	Method	Mobility Ratio	Reference
1933	Wyckoff <i>et al.</i>	electrolytic model	1.0	29
1934	Muskat and Wyckoff	electrolytic model	1.0	28
1951	Fay and Prats	numerical	4.0	43
1952	Slobod and Caudle	X-ray shadowgraph using miscible fluids	0.1 to 10	34
1953	Hurst	numerical	1.0	44
1954	Dyes <i>et al.</i> *	X-ray shadowgraph using miscible fluids	0.6 to 10	40
1955	Craig <i>et al.</i> *	X-ray shadowgraph using immiscible fluids	0.16 to 5.0	45
1955	Cheek and Menzie	fluid mapper	0.04 to 10.0	41
1956	Aronofsky and Ramey	potentiometric model	1.0 to 10.0	37
1958	Nobles and Janzen	resistance network	0.1 to 6.0	38
1960	Habermann	fluid flow model using dyed fluids	0.037 to 130	46
1961	Bradley <i>et al.</i>	potentiometric model using conductive cloth	0.25 to 4	47

* After-breakthrough performance also presented in these references.

TABLE 44.8—AREAL SWEEP EFFICIENCY STUDIES—NORMAL AND INVERTED FIVE-SPOT PILOT*

Date	Author(s)	Method	Type	Mobility Ratio	Areal Sweep Efficiency at Breakthrough (%)	Reference
1958	Paulsell**	fluid mapper	inverted	0.319	117.0	48
				1.0	105.0	
				2.01	99.0	
1959	Moss <i>et al.</i>	potentiometric	inverted	∞	92.0	49
1960	Caudle and Loncaric**	X-ray shadowgraph	normal	0.1 to 10.0	†	50
1962	Neilson and Flock	rock flow model	inverted	0.423	110.0	51

*(Note: base area = a^2 , where a is the distance between adjacent producing wells.)

** After-breakthrough performance also presented in these references.

† Depends on ratio of injection rate to producing rate.

sults because of mixing. As a result, he concluded that the most probable value of sweep efficiency at high mobility ratios for the five-spot pattern is represented by the solid line of Fig. 44.29. Breakthrough sweep efficiencies obtained later, from investigations with numerical methods conducted in 1979 by Martin and Wegner,⁵⁶ are in agreement with this conclusion.

There are insufficient data for patterns other than the five-spot to allow a comparison of the results obtained by various investigators; however, the correlations shown

in Figs. 44.30 through 44.48 are standards in the industry for determining areal sweep efficiency relationships for the normal patterns. In these figures,

V_d = displaceable PV's injected, fraction,
 f_s = fraction of total flow coming from the swept portion of the pattern,
 f_{icw} = corner well producing water cut, and
 f_{isw} = side well producing water cut.

**TABLE 44.9—AREAL SWEEP EFFICIENCY STUDIES—DEVELOPED
NORMAL SEVEN-SPOT PATTERN**

Date	Author(s)	Method	Mobility Ratio	Areal Sweep Efficiency at Breakthrough (%)	Reference
1933	Wyckoff <i>et al.</i>	electrolytic model	1.0	82.0	29
1934	Muskat and Wyckoff	electrolytic model	1.0	74.0	28
1956	Burton and Crawford*	gelatin model	0.33	80.5	36
			0.85	77.0	
			2.0	74.5	
1961	Guckert*	X-ray shadowgraph using miscible fluids	0.25	88.1 to 88.2	52
			0.33	88.4 to 88.6	
			0.5	80.3 to 80.5	
			1.0	72.8 to 73.6	
			2.0	68.1 to 69.5	
			3.0	66.0 to 67.3	
			4.0	64.0 to 64.6	

*After-breakthrough performance also presented in these references.

**TABLE 44.10—AREAL SWEEP EFFICIENCY STUDIES—DEVELOPED INVERTED (SINGLE
INJECTION WELL) SEVEN-SPOT PATTERN**

Date	Author(s)	Method	Mobility Ratio	Areal Sweep Efficiency at Breakthrough (%)	Reference
1933	Wyckoff <i>et al.</i>	electrolytic model	1.0	82.2	29
1956	Burton and Crawford*	gelatin model	0.5	77.0	36
			1.3	76.0	
			2.5	75.0	
1961	Guckert*	X-ray shadowgraph using miscible fluids	0.25	87.7 to 89.0	52
			0.33	84.0 to 84.7	
			0.50	79.0 to 80.5	
			1.0	72.8 to 73.7	
			2.0	68.8 to 69.0	
			3.0	66.3 to 67.2	
			4.0	63.0 to 63.6	

*After-breakthrough performance also presented in these references.

**TABLE 44.11—AREAL SWEEP EFFICIENCY STUDIES—
DEVELOPED NORMAL NINE-SPOT PATTERN**

Date	Author	Method	Mobility Ratio	Reference
1939	Krutter	Electrolytic model		
1961	Guckert*		1.0	53
		X-ray shadowgraph using miscible fluids	1.0 and 2.0	52

*After breakthrough performance also presented in this reference.

**TABLE 44.12—AREAL SWEEP EFFICIENCY STUDIES—INVERTED
(SINGLE INJECTION WELL) NINE-SPOT PATTERN**

Date	Author	Method	Mobility Ratio	Reference
1964	Kimbler <i>et al.</i> *	X-ray shadowgraph using miscible fluids	0.1 to 10.0	25
1964	Watson <i>et al.</i> *	fluid flow model using dyed fluid	0.1 to 10.0	54

*After-breakthrough performance also presented in these references.

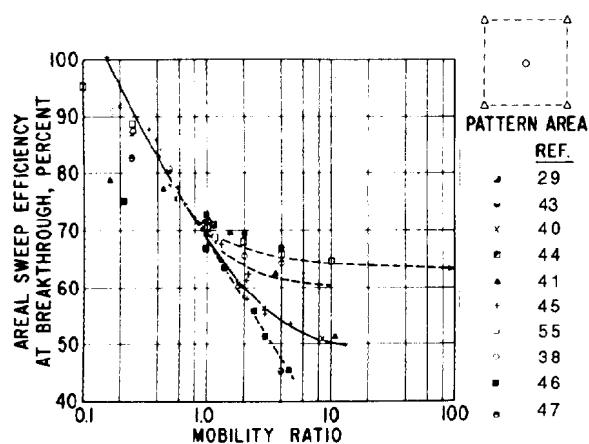


Fig. 44.29—Areal sweep efficiency at breakthrough, developed five-spot pattern.

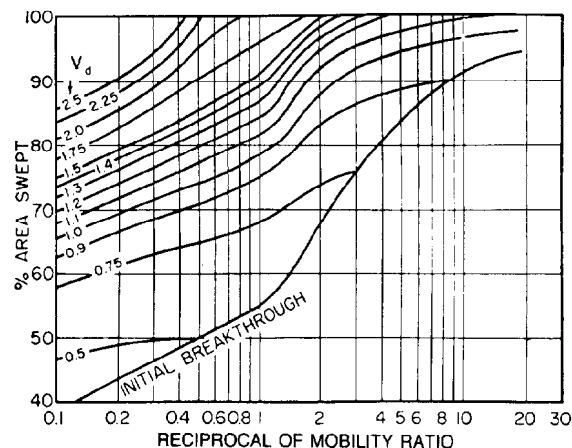


Fig. 44.32—Effect of reciprocal mobility ratio on the displaceable volumes injected for the direct line drive (square pattern); $d/a = 1$.

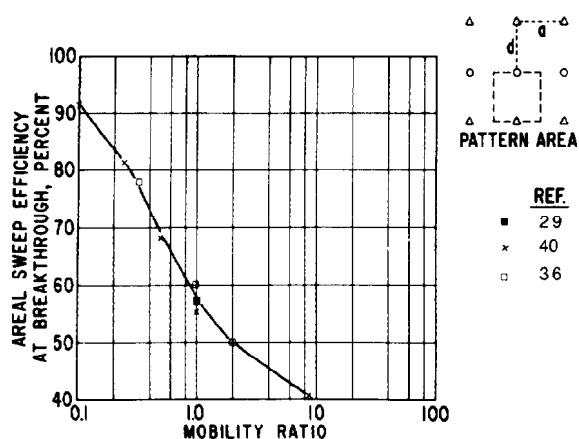


Fig. 44.30—Areal sweep efficiency at breakthrough, developed direct line drive, $d/a = 1.0$.

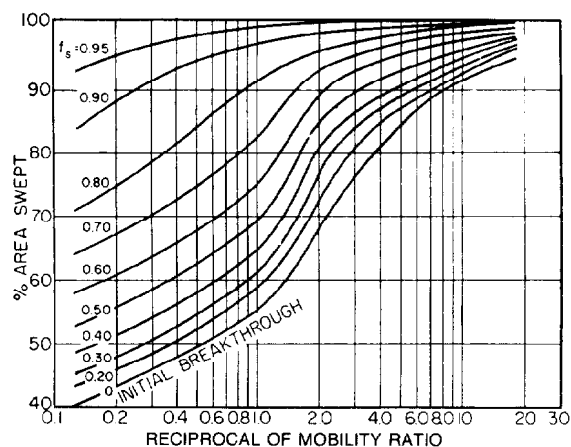


Fig. 44.33—Effect of reciprocal mobility ratio on oil production for the direct line drive (square pattern); $d/a = 1$.

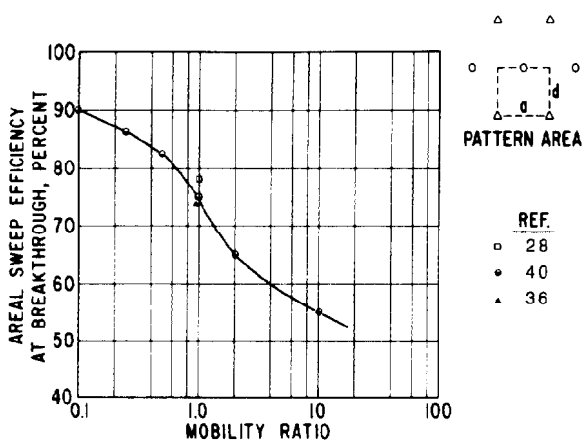


Fig. 44.31—Areal sweep efficiency at breakthrough, developed staggered line drive, $d/a = 1.0$.

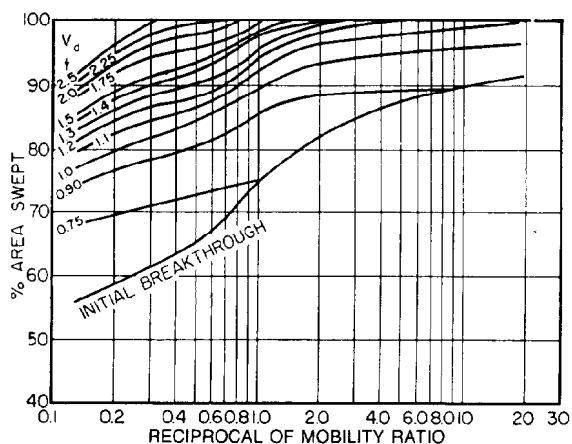


Fig. 44.34—Effect of reciprocal mobility ratio on the displaceable volumes injected for the staggered line drive; $d/a = 1$.

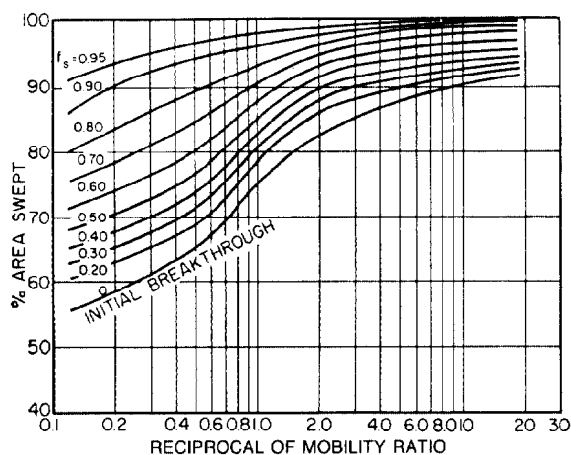


Fig. 44.35—Effect of reciprocal mobility ratio on oil production for the staggered line drive; $d/a = 1$.

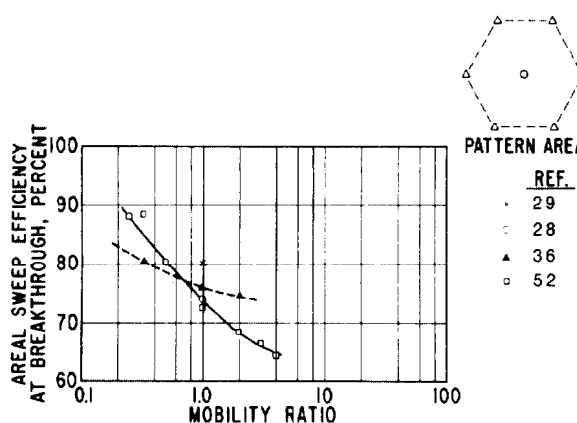


Fig. 44.38—Areal sweep efficiency at breakthrough, developed normal seven-spot pattern.

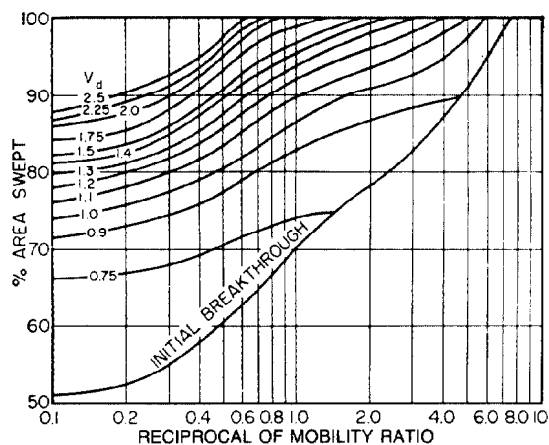


Fig. 44.36—Effect of reciprocal mobility ratio on the displaceable volumes injected for the five-spot pattern.

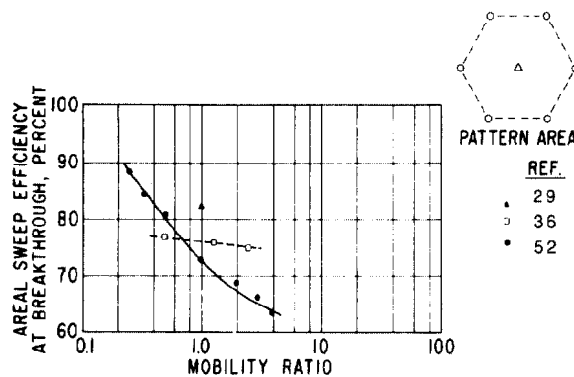


Fig. 44.39—Areal sweep efficiency at breakthrough, developed inverted seven-spot pattern.

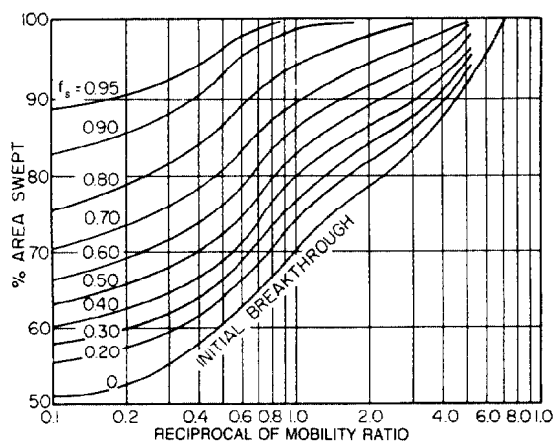


Fig. 44.37—Effect of reciprocal mobility ratio on oil production for the five-spot pattern.

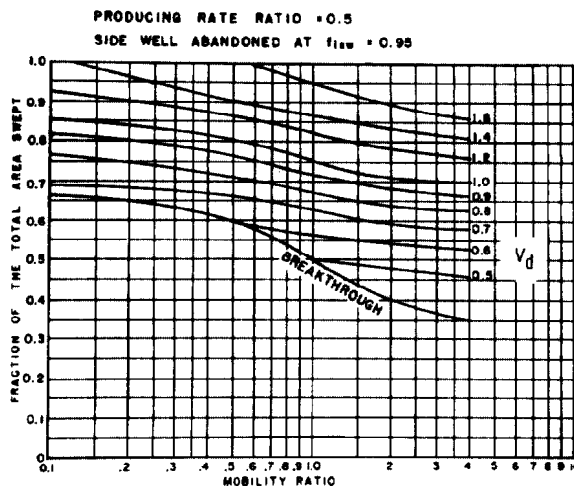


Fig. 44.40—Sweepout pattern efficiency as a function of mobility ratio for the nine-spot pattern at various displaceable volumes injected.

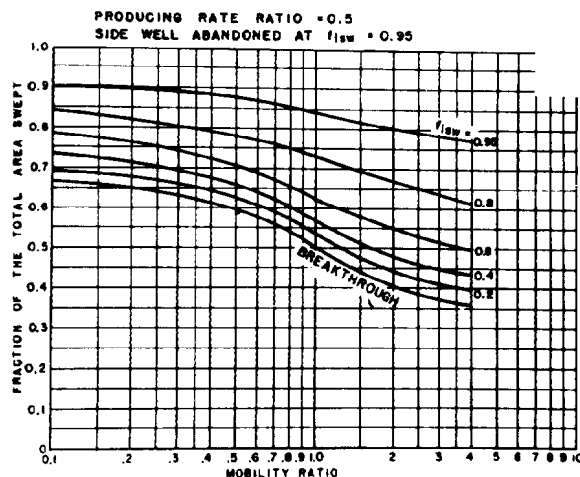


Fig. 44.41—Sweepout pattern efficiency as a function of mobility ratio for the nine-spot pattern at various side-well producing cuts (f_{isw}).

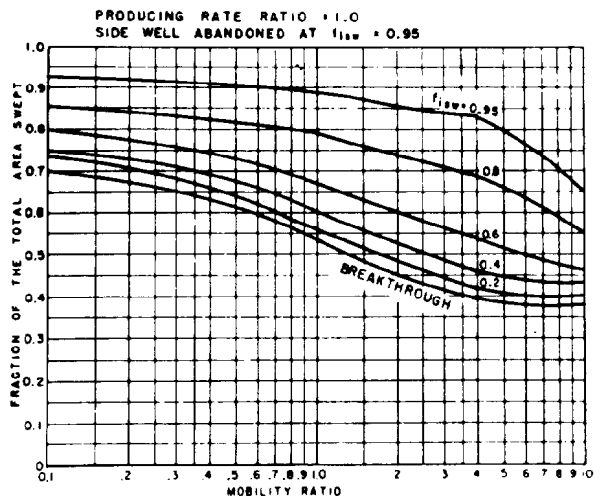


Fig. 44.44—Sweepout pattern efficiency as a function of mobility ratio for the nine-spot pattern at various side-well producing cuts (f_{isw}).

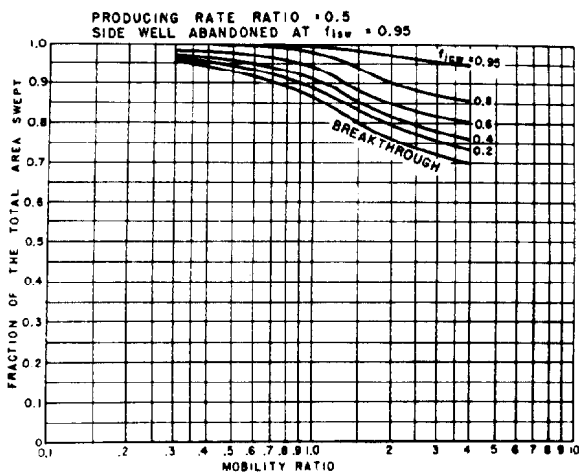


Fig. 44.42—Sweepout pattern efficiency as a function of mobility ratio for the nine-spot pattern at various corner-well producing cuts (f_{icw}).

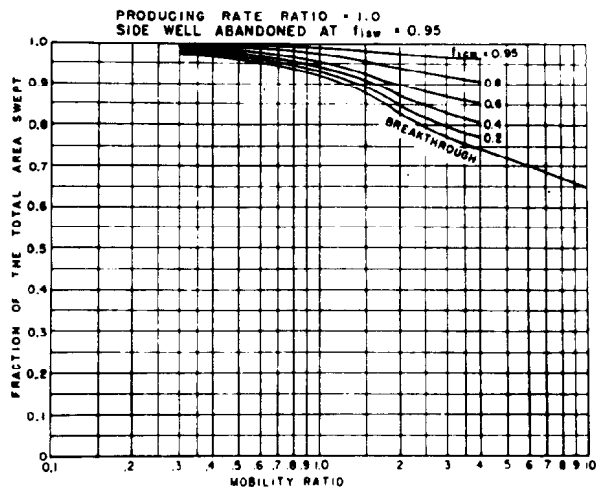


Fig. 44.45—Sweepout pattern efficiency as a function of mobility ratio for the nine-spot pattern at various corner-well producing cuts (f_{icw}).

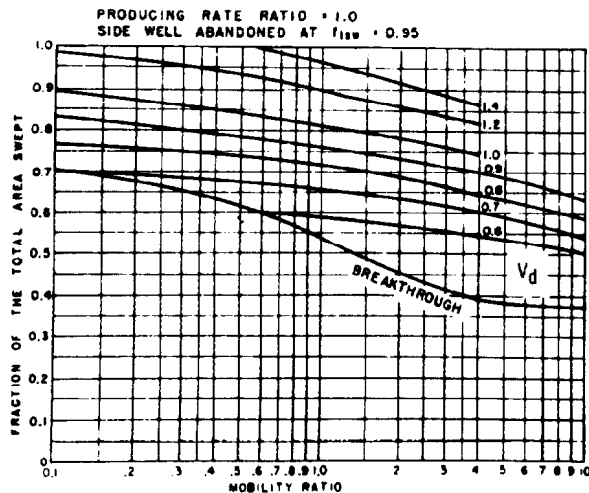


Fig. 44.43—Sweepout pattern efficiency as a function of mobility ratio for the nine-spot pattern at various displaceable volumes injected.

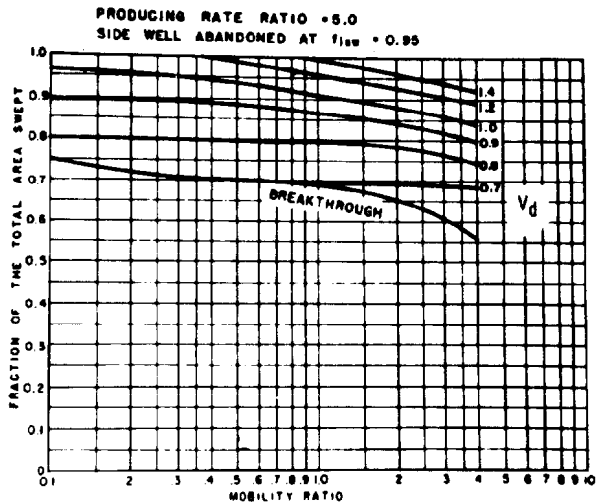


Fig. 44.46—Sweepout pattern efficiency as a function of mobility ratio for the nine-spot pattern at various corner-well producing cuts (f_{icw}).

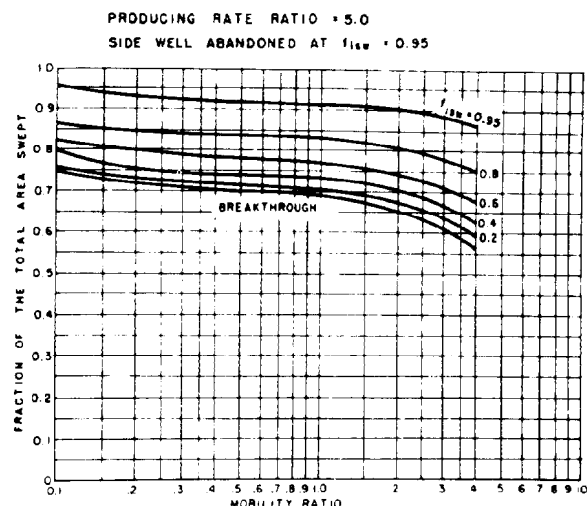


Fig. 44.47—Sweepout pattern efficiency as a function of mobility ratio for the nine-spot pattern at various side-well producing cuts (f_{isw}).

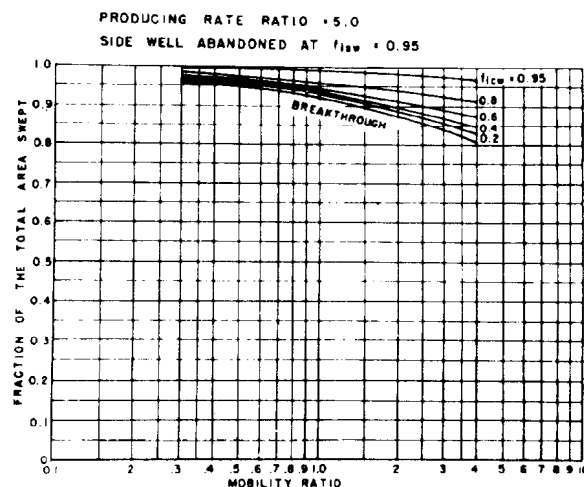


Fig. 44.48—Sweepout pattern efficiency as a function of mobility ratio for the nine-spot pattern at various corner-well producing cuts (f_{icw}).

Effect of Reservoir Dip. The effect of reservoir dip on five-spot sweep patterns has been investigated by Matthews and Fischer.⁵⁷ It was found that distortion would occur in the normal sweepout patterns in dipping reservoirs. Most of this distortion was attributed to gravitational effects. The conclusion reached in this study was that pattern flooding is practical for dipping reservoirs but that the pattern should be shifted to allow for dip. Figs. 44.49 through 44.52 are charts that show how to locate wells correctly for pilot and field five-spot floods in reservoirs that have substantial dip. In these figures,

N = ratio of square root of production rates,

S_F = position of center of unflooded area at moment of fill-up (correct drilling location) fraction of length of side or diagonal,

F_F = ratio of viscous to gravity forces defined by

$$F_F = \frac{(F_{og} + 1)q\mu khL}{g\Delta\rho \sin \alpha}$$

μ = fluid viscosity, poise,

q = injection rate before interference,

$$F_{og} = \frac{S_o - S_{or}}{S_g - S_{gr}},$$

S_o = oil saturation at start of flood, fraction,

S_{or} = ROS, fraction,

S_g = gas saturation at start of flood, fraction, and

S_{gr} = residual gas saturation, fraction.

Prats *et al.*⁵⁸ have made analytical studies of the same problem. Van der Poel and Killian⁵⁹ have made analytical and analog studies to investigate the area that can be swept out in dipping reservoirs by using water drive around the structurally highest wells.

Effect of Directional Permeability. Some formations exhibit differences in reservoir permeability in one horizontal direction relative to another. When this situation is encountered, it is apparent that pattern sweep efficiencies will be affected adversely when the direction of high permeability is between an injector and a producing well. The initial study to determine the effect of directional permeability on the areal sweep performance of a five-spot pattern flood was made by Hutchinson.⁶⁰ If the X-ray shadowgraph technique is used and a directional permeability difference of 16 to 1 is considered, the data shown in Figs. 44.53 and 44.54 are obtained for mobility ratios varying from 0.1 to 10. It is apparent from these data that improved sweep efficiency results when the pattern is oriented with the direction of maximum permeability, parallel to a line passing through the injection wells. In later investigations, Landrum and Crawford⁶¹ and Mortada and Nabor⁶² also studied the effects of directional permeability on five-spot and linedrive patterns. The results of their studies confirm the data obtained by Hutchinson.⁶⁰

Effect of Reservoir Fractures

In 1958, Dyes *et al.*⁶³ presented one of the most comprehensive studies of the effect of vertical fractures on sweepout pattern efficiencies. Their investigations showed that relatively long and highly conductive vertical fractures, not usually obtained from fracturing operations, are required to affect sweep efficiencies substantially. Other investigations⁶⁴⁻⁶⁷ have confirmed the results of Dyes *et al.*; these show that vertical fracturing can affect breakthrough sweep efficiency significantly, but that sweep efficiency at higher water cuts is influenced to a much lesser degree. Table 44.13 is a summary of the results obtained by Dyes *et al.*⁶³

Landrum and Crawford⁶⁸ have investigated the effect of horizontal fractures on sweep efficiency in thick reservoirs. The results of their studies, along with those of other investigators,^{36,69,70} show that the adverse effect

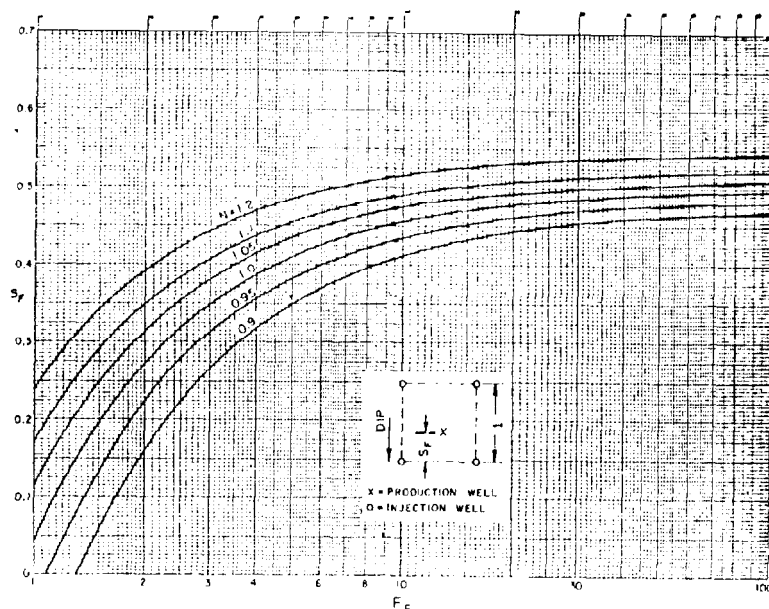


Fig. 44.49—Correct location of production well in pilot five-spot—side along strike.

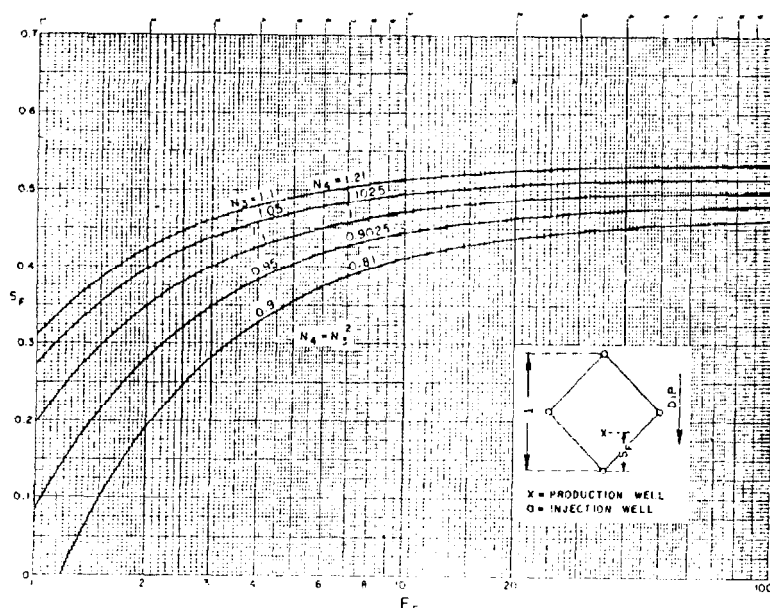


Fig. 44.50—Correct location of production well in pilot five-spot—diagonal along strike.

of horizontal fractures on areal sweep efficiency is a direct function of fracture radii; that is, only small effects were observed on sweep efficiency when the fractures had small radii. However, as the fracture radius increases, sweep efficiency will be reduced drastically.

Methods for Predicting Waterflood Performance

There are many papers and articles in the petroleum industry literature that present or discuss methods for predicting waterflood or water-injection performance. Most

of the classic prediction techniques that have been developed since the early work by Muskat,²⁴ Stiles,¹⁹ Buckley-Leverett,²⁰ Dykstra-Parsons,¹⁵ and others have been modifications, enhancements, or extensions of those pioneering techniques, which were discussed in the initial part of this section. In many cases, those techniques, when combined with data obtained from areal sweep investigations, provided the basis from which several of the methods were conceived and developed.

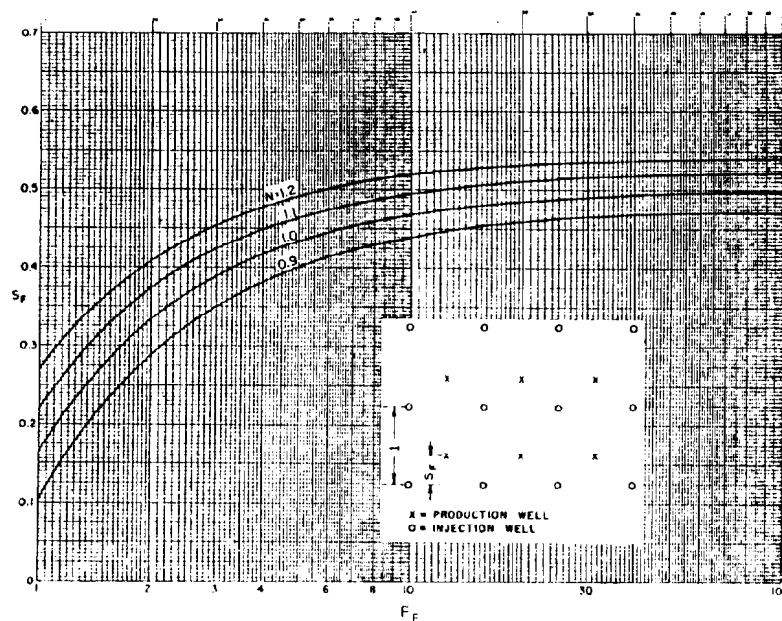


Fig. 44.51—Correct location of production wells in a field of five-spots—side along strike.

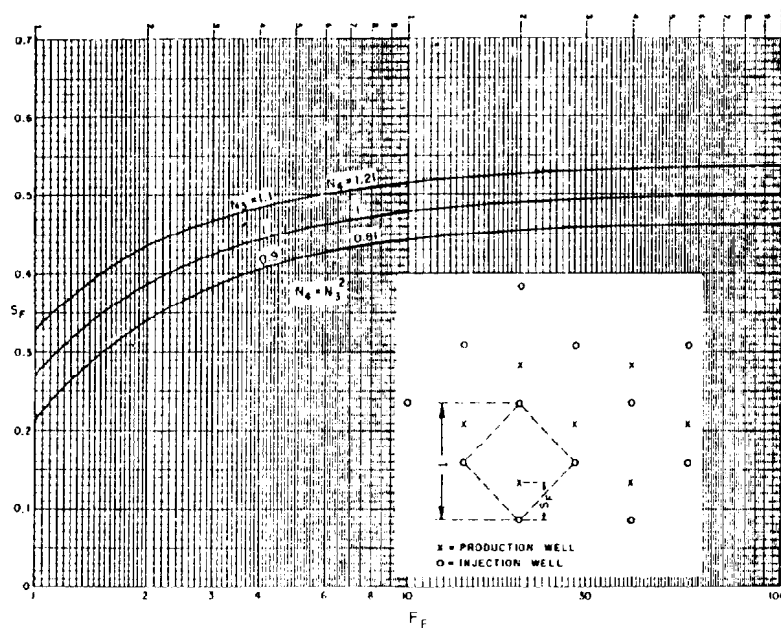


Fig. 44.52—Correct location of production wells in a field of five-spots—diagonal along strike.

In his monograph, Craig⁴ has described and compared the classic prediction methods that were presented before 1971, and has included recommendations for selecting the appropriate waterflood prediction technique to obtain the desired results. The methods that were considered were categorized into five groups, which may be summarized as follows: (1) reservoir heterogeneity (Refs. 15, 19, 22, and 71 through 80), (2) areal sweep methods (Refs. 25, 28, 34, 37, 40, 50, 55, and 81 through 85), (3) displacement mechanism (Refs. 20, 21, 45, and 86 through 97), (4) numerical methods (Refs. 98 through 103), and (5) empirical approaches (Refs. 104 through 107).

Craig's monograph is certainly the most comprehensive review and evaluation of the techniques for predicting waterflood performance that has appeared in the petroleum industry literature.

Craig compared the capabilities of each method that was evaluated to the capabilities of the "perfect method," in which the calculation procedures would allow consideration of all pertinent fluid-flow, well-pattern, and heterogeneity effects—i.e., the influence of relative permeability characteristics, wettability, pore size distribution, and initial and final water and oil saturations; the effect of different well arrangements and mobility ratio on injection rate

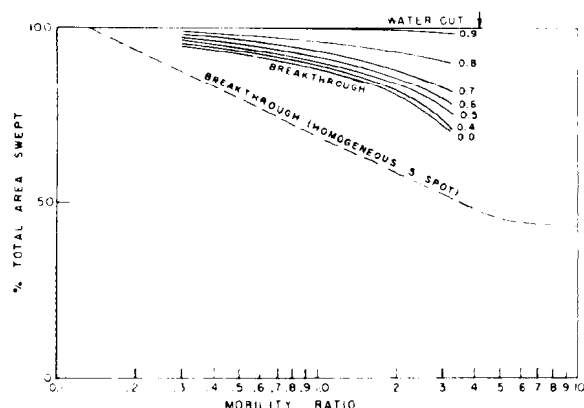


Fig. 44.53—Sweepout pattern efficiency in a five-spot pattern of anisotropic horizontal permeability. The most favorable arrangement has the direction of maximum permeability parallel to lines through injection wells, as illustrated here.

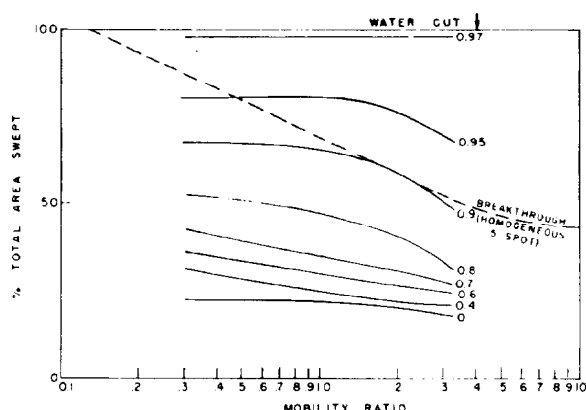


Fig. 44.54—Sweepout pattern efficiency in a five-spot pattern operating under the least favorable arrangement; i.e., with the direction of maximum permeability parallel to a line from an injection well direct to a producing well.

and areal sweep efficiency; and the effect of the heterogeneity of the reservoir rock recovery and performance.

Table 44.14 shows Craig's evaluation of these techniques, as compared to the "perfect method."

Of the many classic methods that were evaluated, Craig has concluded that the three that most closely meet the requirements of the "perfect method" are Higgins-Leighton,^{93-95,97} Craig *et al.*^{4,108} and Prats *et al.*^{58, 108}

The Higgins-Leighton method can be used for various flooding patterns or for irregular well patterns, while the other two can be applied only for the five-spot pattern. Computer programs for the Higgins-Leighton and Craig *et al.* techniques are available in the literature. Examples of the calculation procedures and complete descriptions of the techniques also can be found in the literature. The

best, detailed description of the Higgins-Leighton technique is given in Ref. 97. Complete and detailed calculations for an example waterflooding problem that was solved by the Craig *et al.* technique are presented in Craig's monograph⁴ and by Timmerman.¹⁰⁸ An example of the use of the Prats *et al.* technique is also presented by Timmerman.¹⁰⁸

Other authors have compared results obtained by a number of the classic methods with actual field performance. Abernathy¹⁰⁹ compared the observed performance of five-spot waterfloods in three carbonate reservoirs in west Texas with the performance predicted by the Stiles,¹⁹ Craig *et al.*,⁴⁵ and Hendrickson⁹⁰ techniques. Figs. 44.55 through 44.57 show these comparisons.

TABLE 44.13—EFFECT OF VERTICAL FRACTURES ON FIVE-SPOT PATTERN SWEEP PERFORMANCE: FRACTURES IN LINE WITH INJECTION-PRODUCTION WELL DIRECTION

Fractured	Fracture Length (Fraction of Distance Between Injector and Producer)	M	Areal Sweep Efficiency (%)		Throughput at 90% Watercut (Displaceable PV)
			Breakthrough	90% Watercut	
Unfractured		0.1	99	99	1.0
		1.1	72	99	1.8
		3.0	56	92	2.2
Injection	1/4	0.1	93	98	1.0
	1/4	1.1	45	96	1.7
	1/4	3.0	39	92	2.2
	1/2	0.1	88	98	1.1
	1/2	1.1	37	96	1.8
	1/2	3.0	28	92	2.7
	3/4	0.1	33	97	1.2
	3/4	1.1	14	93	2.3
	3/4	3.0	10	83	3.8
Production	1/4	0.1	78	98	1.1
	1/4	1.1	43	95	1.6
	1/4	3.0	40	88	1.9
	1/2	0.1	38	98	1.2
	1/2	1.1	24	96	1.7
	1/2	3.0	22	92	2.1
	3/4	0.1	18	98	1.8
	3/4	1.1	13	94	2.3
	3/4	3.0	9	87	3.3

TABLE 44.14—COMPARISON OF WATERFLOOD PREDICTION METHODS

Method and Modification	Date Presented	Fluid Flow Effects				Pattern Effects				Heterogeneity Effects				
		Consider Initial Gas Saturation?	Consider Saturation Gradient?	Consider Varying Injectivity?	Applies to		Applicable Mobility Ratio?	Consider Areal Sweep?	Sweep Increase Breakthrough?	Require Published Lab Data?	Require Additional Lab Data?	Consider Stratified Reservoir?	Consider Crossflow?	Consider Spatial Variations?
					Linear System?	Five-spot Pattern?								
Perfect Method	1944	yes	yes	yes	yes	yes	any	yes	yes	no	no	yes	yes	yes
	1950	yes	no	yes	—	yes	1.0	no	no	no	no	yes	no	no
	1959	yes	no	yes	—	yes	any	no	no	yes	yes	no	yes	no
	1950	yes	no	yes	—	yes	any	no	no	yes	yes	no	yes	no
Johnson	1956	yes	no	no	yes	no	any	no	no	no	no	yes	no	no
	1962	yes	no	no	yes	no	any	no	no	no	no	yes	no	no
	1949	no	no	no	yes	no	any	no	no	no	no	yes	no	no
	1950	no	no	no	yes	no	1.0	no	no	no	yes	no	yes	no
Schmalz-Rahme	1956	no	no	no	yes	no	1.0	no	no	no	yes	no	yes	no
	1957	no	no	no	—	yes	1.0	no	no	no	no	yes	no	no
	1961	yes	no	yes	—	yes	1.0	no	no	no	no	yes	no	no
	1965	no	no	no	yes	no	1.0	no	no	no	no	yes	no	no
Muskat	1946	no	no	no	—	yes	1.0	yes	yes	no	no	no	no	no
	1953	no	no	no	—	yes	1.0	yes	yes	yes	no	yes	no	no
	1952 to 1959	no	no	yes	—	yes	any	yes	yes	yes	no	yes	no	no
	1952 to 1956	no	no	yes	—	yes	any	yes	yes	yes	no	yes	no	no
Deppa-Hauber	1961 to 1964	yes	no	yes	—	yes	any	yes	yes	yes	no	yes	no	no
	1942	no	yes	no	yes	no	—	no	no	no	no	no	no	no
	Buckley-Leverett	1959	no	yes	yes	no	—	—	no	yes	no	yes	no	no
	Roberts	1959	no	yes	no	yes	—	—	no	yes	no	yes	no	no
Kufus and Lynch	1959	no	yes	no	yes	no	any	no	no	no	no	yes	no	no
	1967	no	yes	no	yes	no	any	no	no	no	no	yes	no	no
	1955	yes	yes	yes*	—	yes	any	yes	yes	yes	no	yes*	no	no
	1961	no	yes	no	—	yes	any	yes	yes	yes	no	yes	no	no
Wasson and Schrider	1968	yes	yes	yes*	—	yes	any	yes	yes	yes	yes	yes*	no	no
	Rapoport <i>et al.</i>	1958	no	yes	yes	yes	any	yes	yes	yes	yes	yes	no	no
	Higgins-Leighton	1962 to 1964	yes	yes	yes	yes	any	yes	yes	yes	no	yes	no	no
	4 Douglas-Blair-Wagner	1958	no	yes	yes	—	any	any	yes	yes	yes	no	yes	no
Hiatt	1958	no	yes	no	yes	no	any	any	yes	yes	no	yes	yes	no
	1959	no	yes	yes	—	yes	any	any	yes	no	no	yes	no	no
	1964	no	yes	no	yes	no	—	—	no	no	no	yes	yes	no
	Moret-Seytoux	1965 to 1966	no	yes	yes	—	any	any	yes	yes	no	yes	yes	no
Guthrie-Greenberger	1955	no	yes	no	—	—	any	any	yes	no	no	yes	no	no
	Schauer	1957	yes	no	no	—	any	any	yes	yes	no	yes	yes	yes
	Guerrero-Earlougher	1961	yes	no	no	—	any	—	no	no	no	yes	no	no
	API	1967	no	yes	no	—	any	any	yes	yes	no	yes	yes	yes

*Using Caudle and Witte injectivity correlation.

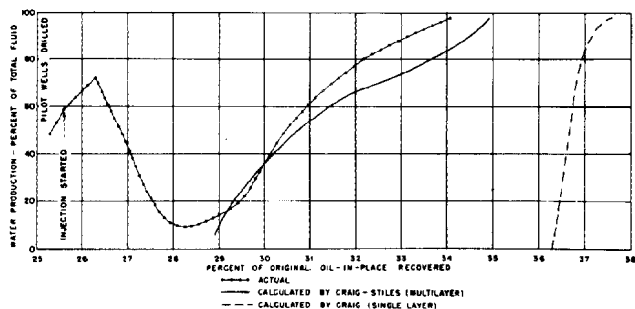


Fig. 44.55—Calculated vs. actual performance of Panhandle field.

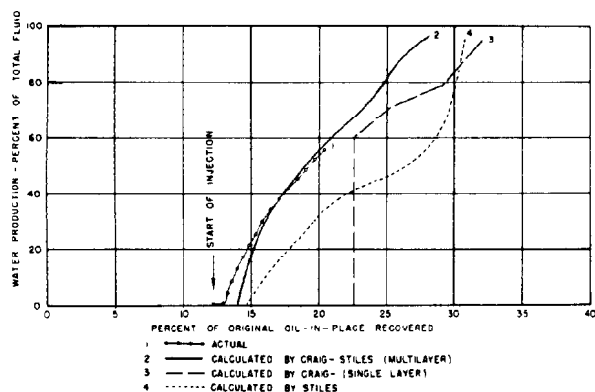


Fig. 44.56—Calculated vs. actual performance of Foster field pilot.

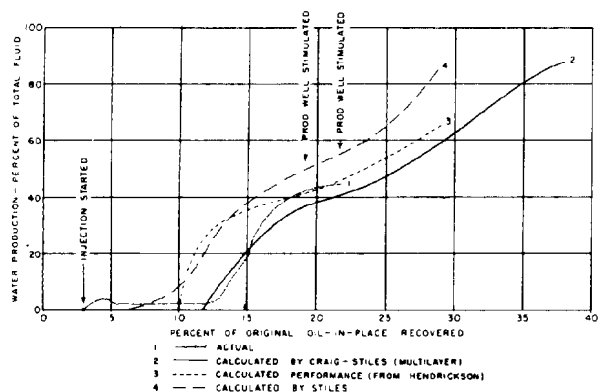


Fig. 44.57—Calculated vs. actual performance of Welch field pilot.

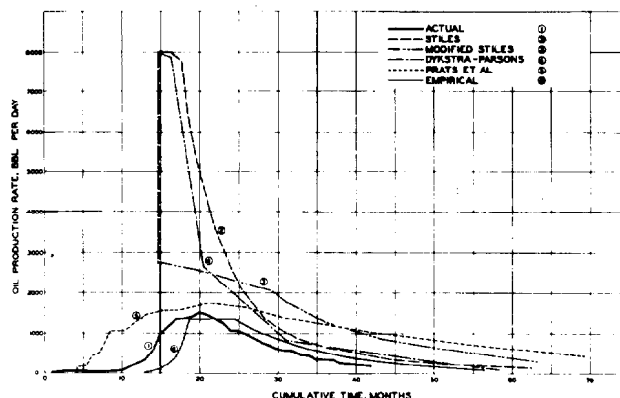


Fig. 44.58—Comparison of actual and predicted recovery history, Flood 1.

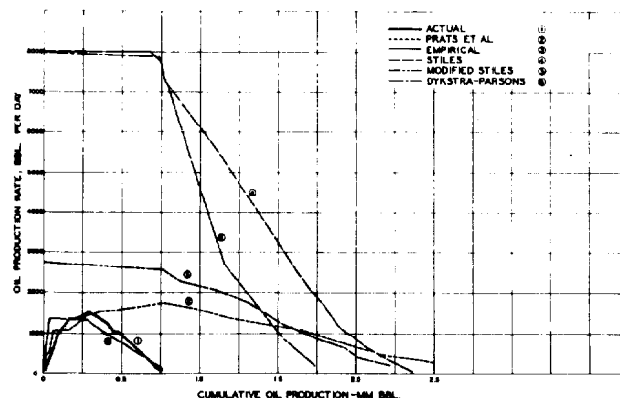


Fig. 44.59—Comparison of actual and predicted oil recovery, Flood 1.

Guerrero and Earlougher¹⁰⁶ compared the actual and predicted performance of two floods. The predictive methods that were compared included Stiles', modified Stiles', Dykstra-Parsons', Prats *et al.*'s, and the empirical approach developed by Guerrero and Earlougher. The results of these comparisons are shown in Figs. 44.58 through 44.61. (Also see Ref. 4, Figs. 8.16 through 8.19.) Higgins and Leighton⁹⁴ compared the results obtained by using their method with actual field performance and with predicted performance obtained by the methods of Prats *et al.* and Slider.⁷⁴ This comparison is shown in Fig. 44.62. (Also see Ref. 4, Fig. 8.20.)

It is obvious from these comparisons that the fields do not always perform as predicted regardless of the method that is used to estimate future performance. This is true for many reasons, including (1) an incorrect or inadequate description of the reservoir rock, fluid, and water/oil flow properties, (2) a prediction technique that does not have the capability to consider all the factors that affect water-flood performance, and (3) the fact that there is always a question of the reliability of the estimates of the interwell character of the reservoir rock and the vertical and horizontal variations that exist in reservoir rock and fluid properties.

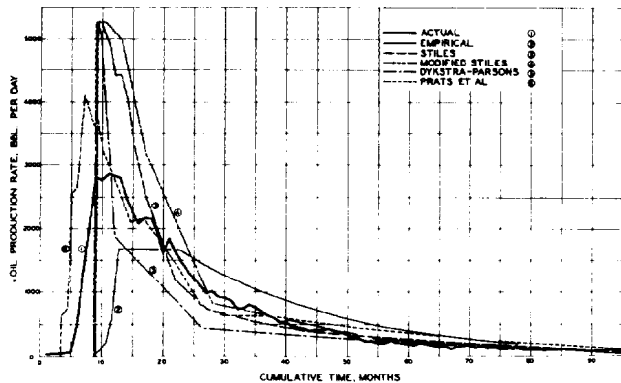


Fig. 44.60—Comparison of actual and predicted recovery history, Flood 2.

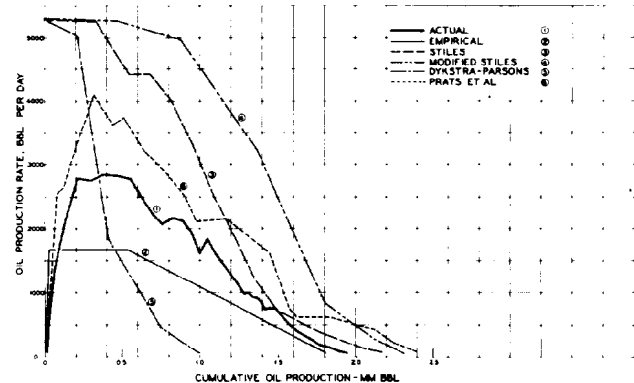


Fig. 44.61—Comparison of actual and predicted oil recovery, Flood 2.

The prediction techniques selected as most promising by Craig⁴ appear to deserve primary consideration when one of the classic techniques is being selected for projecting future reservoir performance under waterflood operations. The comparisons made by Abernathy¹⁰⁹ show the Craig-Stiles multilayer method to be capable of making predictions that yield a good match with actual reservoir performance. In the Guerrero and Earlougher comparison, the Prats *et al.* method performed very well in the case of Flood 2 but erred badly with respect to oil recovery in the prediction of the behavior of Flood 1. The Higgins and Leighton method gave a good comparison with respect to actual performance in the case presented.

Since the time when Craig made his evaluation and comparison of the classic prediction methods that were available, reservoir simulation models have continued to be improved and expanded to the point that, today, there are models available for prediction of waterflood or water-injection performance under a variety of conditions. The reservoir simulation models that are available to the industry at present are capable of considering any type of flooding pattern, as well as gravity, capillary, and viscous forces, with virtually any type of three-dimensional (3D) reservoir description. The initial developments of the numerical methods were made by Douglas *et al.*⁹⁸ in 1958, and this work was later extended to two dimensions by Douglas *et al.*¹⁰⁰ in 1959. Since that time, numerical models and reservoir simulation techniques have improved continuously, in step with the increased speed and storage capacity of the computing systems that have become available.

Although the subject of reservoir simulator development and application has been covered in another section of this handbook, it is important to emphasize that the simulation models and techniques that are presently available to the industry are capable of modeling the most complex reservoir systems. With the use of these tools, predictions of waterflood and water-injection performance can be made in such detail that almost every factor that affects reservoir and individual well behavior can be considered and simulated.

Selection of the Waterflood Prediction Method

When choosing the appropriate waterflood prediction method, the engineer must bear in mind the objective in

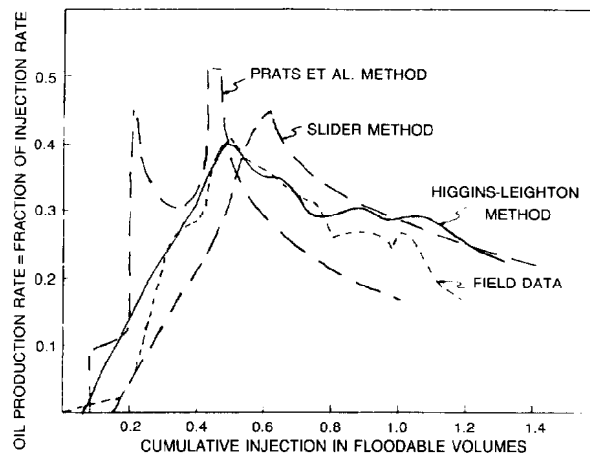


Fig. 44.62—Comparison of field behavior with predicted performances by the Prats *et al.*, Slider, and Higgins-Leighton methods.

making the recovery predictions, the amount and quality of basic data that are available, and the resources that are available for performing the calculations in light of both the manpower that will be necessary and the actual costs for computer use or data processing. In some instances, a simple estimate of ultimate oil recovery may be sufficient and, in fact, it may be the only reliable estimate possible because of data limitations. However, in most cases, more detailed projections will be required to evaluate the economic potential of the proposed project; and a method must be used that will allow the estimation of future well requirements, producing WOR's, producing rates, oil recovery, injection well requirements, and injection rates and distribution, all as functions of time.

The methods available to the reservoir engineer range in complexity from those that provide an estimate of ultimate recovery to those that use sophisticated reservoir simulation models that are capable of predicting both reservoir and individual well performance for water injection operations. However, the time requirements and costs for making the calculations are in direct proportion

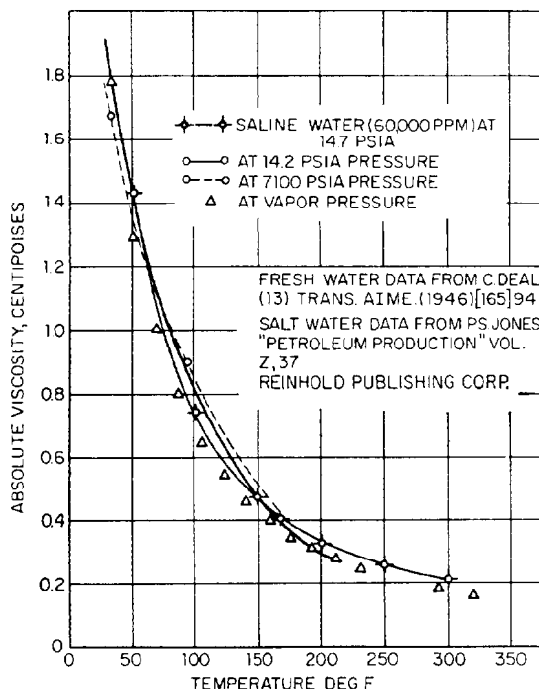


Fig. 44.63—Viscosity of water at oilfield temperatures and pressures.

to the complexity of the technique used. The engineer must choose the method for predicting performance while taking into account the availability of time and resources and the reliability and quantity of the basic data at hand.

The most basic evaluation is that of defining the ultimate oil recovery to be expected from the project. This can be determined by using the Welge²¹ technique or by estimating ROS's and conformance. Empirical approaches are also available to provide these estimates if data are limited. Guthrie and Greenberger¹⁰⁴ have developed an equation, based on waterflooding experience in a number of sandstone reservoirs, that has proven effective for estimating the ultimately recoverable oil. The equation is as follows:

$$E_R = 0.2719 \log k + 0.25569 S_w - 0.1355 \log \mu_o - 1.5380\phi - 0.0003488h + 0.11403, \dots (14)$$

where E_R is the oil recovery efficiency, fraction, and h is the formation thickness, ft.

Another equation that is applicable in estimating the ultimate recoverable oil was developed by an API committee.¹⁰⁷ The relationship developed by this committee is as follows.

$$E_R = 0.54898 \left[\frac{\phi(1-S_w)}{B_{oi}} \right]^{0.0422} \left(\frac{k\mu_{wi}}{\mu_{oi}} \right)^{0.077} \times (S_w)^{-0.1903} \left(\frac{p_i}{p_a} \right)^{-0.2159}, \dots (15)$$

where p_i is the initial pressure and p_a is the pressure at depletion (abandonment).

When a projection of producing WOR as a function of oil recovery is required, the basic methods that are available are those developed by Stiles,¹⁹ Slider,⁷⁴ and others. These procedures allow a prediction of the water-cut performance of the waterflood as well as the ultimate recovery. The published correlation charts of Johnson,²² based on the data developed by Dykstra-Parsons,¹⁵ will allow a quick prediction of future waterflood performance.

For a more detailed projection of future performance, Craig⁴ has suggested the techniques proposed by Higgins-Leighton,⁹³⁻⁹⁷ Craig *et al.*,⁴⁵ and Prats *et al.*⁸⁰ These techniques require considerably more engineering time and more reservoir data than do the basic calculations, but they will enable projections to be made in sufficient detail so that an economic analysis of the project can be made for comparison with the projected return that might be expected as a result of alternative operational programs.

The complex reservoir simulation models that are available to the industry today can produce projections of water injection performance that consider all the factors that influence the behavior of the injection operation. Their use requires a detailed description of the reservoir rock, fluid, and fluid-flow properties, as well as the characterization of individual wells. When the basic data are available for future performance predictions, there is no doubt that the simulation approach will produce the highest confidence level that is attainable with today's technology. When compared to the other alternatives that are available, reservoir simulation approaches are expensive; however, if used properly, these techniques will enable a complete evaluation of the potential of a proposed water injection project.

The engineer has many choices available in selecting the approach that he will use to evaluate a prospective water injection operation. To repeat, the selection should be made while bearing in mind the overall objectives of the evaluation, the resources that are available, and the data that are either immediately available or that can be obtained within the imposed time or monetary limitations.

Water-Injection Well Behavior

The initial water-injection rate of a well depends on the (1) effective permeability, (2) oil and water viscosity, (3) sand thickness, (4) effective well radius, (5) reservoir pressure, and (6) injection pressure at the sandface. As water begins to fill the reservoir, other factors are introduced to affect the behavior of the injection well. These factors are influenced by the increase in flow resistance as water extends into the reservoir and by the quality of the injection water.

The fundamental equation²⁴ for the rate of water injection into a well is expressed as

$$i_w = \frac{0.00708 k_w h (p_{iwf} - p_e)}{\mu_w \ln(r_e/r_w)}, \dots (16)$$

There are numerous uncertainties that make quantitative applications of the equation difficult. They do not, however, impair its usefulness in explaining the relative importance of each of the factors.¹¹⁰

1. **Effective Permeability.** The symbol k_w denotes the effective permeability (millidarcies) of the sand to water. According to laboratory work on clean sands, the relative permeability to water ranges from 30 to 60% of the dry permeability as the water saturation varies from 70 to 85%. Tests on virgin and artificially oil-saturated cores show that the effective permeability of the sand to water is often less than one-tenth of the dry permeability. Whenever possible, the effective permeability to water should be determined on representative cores from the field.

2. **Viscosity.** The viscosity (centipoise) of the injected water, μ_w , can be measured, or a value approximated, from Fig. 44.63.

3. **Sand Thickness.** The sand thickness, h , is the net effective sand thickness (feet) of the interval that is open for injection.

4. **Pressure.** The bottomhole flowing injection pressure, p_{iwf} , (pounds per square inch) at the sand face can be estimated from the wellhead pressure, the depth of the well, the density of the water, and the flowing pressure gradients. p_e is the effective reservoir pressure (external boundary pressure).

5. **Well Radius.** The effective radius of a well, r_w , (feet) may vary from a few inches to several feet, depending on the type of completion.

6. **Pressure Radius.** The pressure radius (external boundary radius), r_e , can be estimated, at least roughly, from the amount of water that is injected and from the available pore space, and is the distance from the injection well where the pressure is p_e . The available pore space is defined as the total PV less that occupied by interstitial water and oil. As more and more water is injected, the pressure radius, r_e , in Eq. 16 increases and, therefore, the injection rate, i_w , must decrease with time.

The pressure radius, r_e , depends on the cumulative volume of water that is injected into the space that is available, in accordance with the equation

$$r_e = \left(\frac{5.61 W_i}{\pi h \phi S_g} \right)^{1/2}, \quad (17)$$

where W_i is the cumulative water injected, bbl.

The oil may or may not be moved by the advancing water. If the oil is not moved, the water will fill the gas space. If the oil is moved ahead of the water bank, the volume of injected water that is required to fill the reservoir with liquids (oil and water), for a given distance (to external radius), will still be the same as that which was originally necessary to fill the gas space.

If a large percentage of oil is being moved, Eq. 16 does not hold strictly true, and a more exact expression prior to interference is

$$i_w = \frac{0.00708 h k_w (p_{iwf} - p_e)}{(\mu_w/k_w) \ln(R_w/r_w) + (\mu_o/k_o) \ln(R_e/R_w)}, \quad (18)$$

where R_w is the outer radius of the waterflood front and R_e is the outer radius of the oil bank.

As a rule, the width of the oil bank is small in comparison to the radius of the encroached water so that very little error will be introduced by considering the simpler

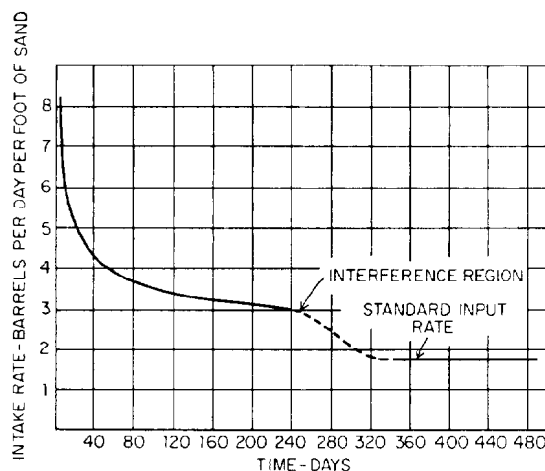


Fig. 44.64—Five-spot pattern computed input well history.

case. The change in intake rate with time can be calculated by Eq. 19.

$$\frac{0.0253 k \Delta p t}{\mu_w \phi S_g (r_w)^2} = 1 + \left(\frac{0.0142 k h \Delta p}{\mu_w i_w} - 1 \right) \times 10^{0.00617 k h \Delta p / (\mu_w i_w)} \quad (19)$$

Eqs. 16, 18, and 19 can be applied to a single-well system (radial flow); however, they are not valid for pattern floods after interference has occurred between injection wells. When interference occurs, the advancing liquid converges on the producing well and, for mobility ratios near unity, finally stabilizes at the steady-state conductivity of the specific pattern. The effect of interference on a five-spot pattern for a system with a favorable mobility ratio ($M \leq 1$) is as shown in Fig. 44.64.

Muskat²⁴ and Deppe⁸⁴ have developed equations for calculating the steady-state injectivities for the normal flooding patterns when a mobility ratio of one is considered. These equations are as follows.

Five-spot pattern²⁴:

$$i_w = \frac{0.001538 k_w h \Delta p}{\mu_w \left(\log \frac{d}{r_w} - 0.2688 \right)} \quad (20)$$

Direct line drive²⁴:

$$\text{for } \frac{d}{a} \geq 1,$$

$$i_w = \frac{0.001538 k_w h \Delta p}{\mu_w \left(\log \frac{a}{r_w} + 0.682 \frac{d}{a} - 0.798 \right)} \quad (21)$$

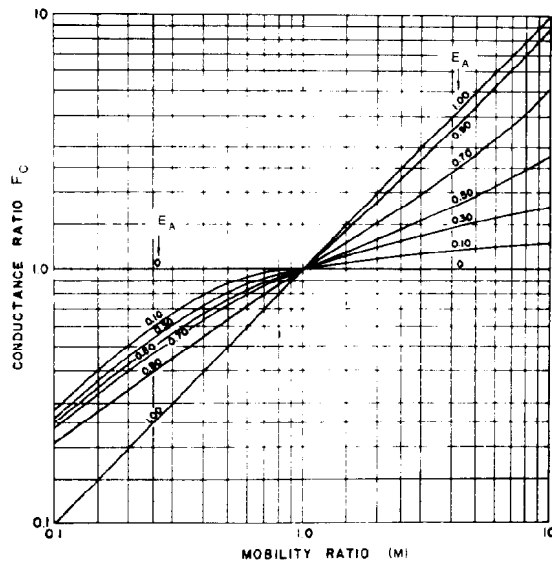


Fig. 44.65—Conductance ratio as a function of mobility ratio and the pattern area swept (E_A), five-spot pattern.

Staggered line drive²⁴:

for $\frac{d}{a} \geq 1$,

$$i_w = \frac{0.001583k_w h \Delta p}{\mu_w \left(\log \frac{a}{r_w} + 0.682 \frac{d}{a} - 0.798 \right)}, \quad \dots (22)$$

where d is the distance between rows of wells, ft and a is the distance between wells in a row, ft.

Seven-spot pattern⁸⁴:

$$i_w = \frac{0.002051k_w h \Delta p}{\mu_w \left(\log \frac{d}{r_w} - 0.2472 \right)}, \quad \dots (23)$$

Inverted nine-spot pattern⁸⁴:

$$i_w = \frac{0.001538k_w h \Delta p_{ic}}{\mu_w \left(\frac{1+F_p}{2+F_p} \right) \left(\log \frac{d}{r_w} - 0.1183 \right)}, \quad \dots (24)$$

$$= \frac{0.003076k_w h \Delta p_{is}}{\mu_w \left[\left(\frac{3+F_p}{2+F_p} \right) \left(\log \frac{d}{r_w} - 0.1183 \right) - \frac{0.301}{2+F_p} \right]}, \quad \dots (25)$$

where

d = distance between rows of wells,

F_p = corner-to-side-well producing-rate ratio,

Δp_{ic} = pressure differential between injection well and corner well, and

Δp_{is} = pressure differential between injection well and side well.

These equations allow the determination of the steady-state injectivities for the normal patterns if it is assumed the system is completely filled with liquid and has a mobility ratio of one.

There are a number of papers that report the results of investigations to define the variation of injectivities for the five-spot pattern at mobility ratios that are other than one. Various techniques were used. Deppe⁸⁴ and Aronofsky and Ramey⁵⁵ used potentiometric model techniques; Caudle and Witte⁸² used the X-ray shadowgraph technique and a porous model of the reservoir element. In the Caudle and Witte study,⁸² one-eighth of the five-spot pattern was modeled. Nobles and Janzen³⁸ used resistance networks to simulate mobility differences, and Prats *et al.*⁸⁰ used an analytical solution. Qualitatively, all investigators arrived at the same conclusion—i.e., if the mobility ratio is favorable ($M \leq 1$), injectivities will decline continuously during the entire operation; however, if the mobility ratio is unfavorable ($M > 1$), injectivities will increase continuously.

In their work, Caudle and Witte determined the variation in injectivity for the five-spot pattern as a function of the mobility ratio that exists before and after water breakthrough. Fig. 44.65 shows the results of their studies, in the form of the relationships between the conductance ratio, the mobility ratio, and the fractional areas of the reservoir that are contacted by the injected fluid.

Craig⁴ points out that, subsequent to fill-up, the relationships developed by Caudle and Witte can be used along with Eq. 20 to calculate water injection rates for the five-spot pattern:

$$i_w = F_C \times i_b,$$

where

i_w = water-injection rate,

F_C = Caudle and Witte conductance ratio, and

i_b = the injection rate of fluid that has the same mobility as the reservoir oil in a liquid-filled (base) pattern, as calculated from Eq. 20.

As the intake rate declines in the early stages of injection, it is important to be able to tell whether the decline results from the plugging of the sand (a situation that requires remedial work), from natural reservoir fill-up, or from mobility ratio effects. Consequently, a method is required to determine the intake capacity of the well itself without regard to the conductivity of the well system surrounding it. Such a method would be achieved by conducting periodic tests on certain selected wells scattered across the flood area. A close check of the efficiency of the input of the wells could then be maintained.

One practical method of determining the efficiency of the input wells is to use the calculated injectivity index

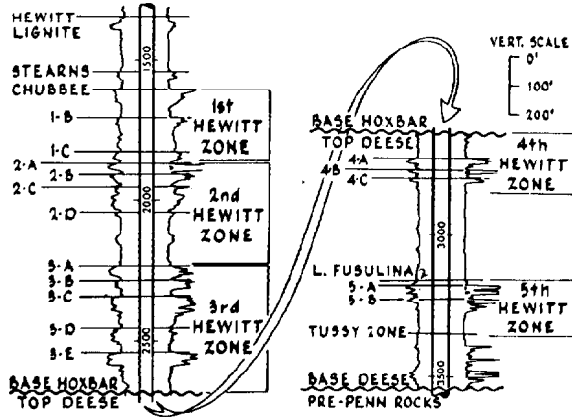


Fig. 44.66—Composite type log, Hewitt field, Carter County, OK.

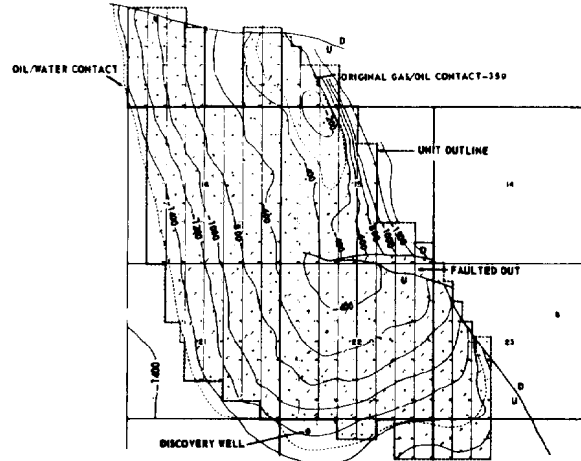


Fig. 44.67—Hewitt unit, Chubbee structure map.

of the well. The injectivity index is defined as the number of barrels per day of gross liquid that is pumped into an injection well per pound per square inch of pressure differential between the mean injection pressure and the mean formation pressure associated with a specific subsurface datum, usually the mean formation depth. To be most valuable in a study of the behavior of the individual input wells, use of the injectivity-index concept should be restricted to defining the conductivity of an individual well; it should not be used to determine the general conductivity of the well system. This restricted injectivity index, which may be called a "localized injectivity index," is best used in measuring the conductivity of the cylinder of sand surrounding the well—most of the pressure drop takes place in this cylinder, whose inside wall is the sandface.

The localized injectivity index can be calculated from a modified Eq. 16:

$$i_w = \frac{0.00708 k_w h (p_{iwf} - p_{bp})}{\mu_w \ln(r_i/r_w)} \quad (26)$$

where p_{bp} is the transient backpressure and r_i is the distance from the well to the point of pressure equalization at p_{bp} .

Differentiating, the localized injectivity index, with p_{bp} being constant, is expressed as

$$I = \frac{di_w}{dp_{iw}} = \frac{0.00708 k_w h}{\mu_w \ln(r_i/r_w)} \quad (27)$$

Experimentally, it has been found that, for small volumes of injected water, di_w/dp_{iw} is constant. If small volumes of water are injected during the course of a test, r_i changes only slightly; r_i is considerably greater than r_w and the logarithm of r_i/r_w is practically constant. If, however, larger volumes are injected during the course of the test, the $\ln r_i/r_w$ will no longer be constant and the localized injectivity index, di_w/dp_{iw} , will not be constant. If large enough volumes are injected so that equi-

librium conditions are obtained, the corresponding pattern formula is applicable. In the case of a five-spot pattern, the change in intake rate for each change in pressure can be approximated by

$$I = \frac{di_w}{dp_{iw}} = \frac{0.00354 k_w h}{\mu_w [\ln(d/r_w) - 0.6190]} \quad (28)$$

where d is the distance between unlike wells.

The transient backpressure, p_{bp} , is a pressure phenomenon that occurs when the intake rate of an injection well is changed. Theoretically, the flow of water from a well into the surrounding formation will continue until the intensity of the sandface pressure is reduced to that of the reservoir pressure. In practice, if the pressure on an input well suddenly is reduced to the atmospheric pressure at the surface, the well backflows for a period of time that varies from a few minutes to several hours. The pressure that caused the backflow of water from the well is defined as the transient backpressure. This pressure, which occurs near the wellbore, is greater than the average reservoir pressure and has been attributed qualitatively to the compressibility of water and gas near the wellbore. When the injection is terminated, the backflow is caused by the expansion of the water and gas that results from the decrease in pressure. Quantitative treatment of this phenomenon has been given by Nowak and Lester¹¹¹ and Hazebroek *et al.*¹¹² The transient backpressure gradually dissipates and approaches the reservoir pressure. The localized injectivity index should be determined after the transient pressure has started falling very slowly or is in equilibrium with the reservoir pressure.

A comparison of the injectivity indices for injection wells in the waterflood will give an indication as to the wells that are not performing satisfactorily, and investigations should be made to determine whether the remedial measures are necessary to improve the injectivity rate. The intake rate of a normal well declines during its life, at least until a constant steady-state pressure distribution is established in the part of the reservoir affected by the well. In addition to the normal well decline, the sandface

TABLE 44.15—HEWITT UNIT RESERVOIR DATA

General	
Unit area, acre	2,610
Floodable net sand volume, acre-ft	284,700
Average composite thickness, ft	109
Original oil in place, MMbbl	350.8
Rock Properties	
Permeability, md	184
Porosity, %	21.0
Interstitial water, %	23.0
Lorenz coefficient	0.49
Permeability variation	0.726
Fluid Properties	
Mobility ratio	4.0
Original reservoir pressure, psig	905
Reservoir temperature, °F	96
Original FVF, RB/STB	1.13
Flood start FVF, RB/STB	1.02
Oil stock-tank gravity, °API	35
Oil viscosity, cp	8.7
Original dissolved GOR, cu ft/STB	253
Primary recovery mechanism	solution gas drive gravity drainage

TABLE 44.16—SUMMARY OF ROCK AND FLUID PROPERTIES, RESERVOIR PROPERTIES, AND PRODUCTION-INJECTION DATA, JAY/LITTLE ESCAMBIA CREEK (LEC) WATERFLOOD

Rock and Fluid Properties	
Porosity, %	14.0
Permeability, md	35.4
Water saturation, %	12.7
Oil FVF, RB/STB	1.76
Oil viscosity, cp	0.18
Oil gravity, °API	51
Solution GOR, scf/STB	1,806
Hydrogen sulfide content, mol%	8.8
Mobility ratio (water/oil)	0.3
Reservoir Properties	
Datum, ft subsea	15,400
Original pressure, psia	7,850
Current pressure, psia	5,750
Saturation pressure, psia	2,830
Temperature, °F	285
Production area, acres	14,415
Net thickness, ft	95
OOIP, MMSTB	728
Production/Injection (Jan. 1, 1981)	
Oil production rate, MSTB/D	90
Cumulative oil production, MMSTB	296
Water injection rate, Mbbl	250
Cumulative water injection, MMbbl	524

gradually becomes plugged by suspended solids in the injected water. These suspended solids include materials like clay, silt, iron oxide, and hydroxides. In addition to suspended solids, dissolved and organic growths may contribute to the plugging of the formation sandface. Plugging of the sandface by these materials may be minimized with the proper treatment of the injection water. This treatment is covered in this chapter under the heading Water Treating.

By means of rate/pressure curves established at intervals of a few months, it is possible to distinguish between the decrease in intake rate caused by plugging and that caused by fill-up of the reservoir as mobility ratio effects. Rate/pressure curves are helpful also in indicating the value of the critical breakthrough pressure at which rupture of the formation occurs. If plugging is occurring and the injection rate declines, backflow of the well may be induced to remove the material from the sandface. Or if the plugging material on the sandface cannot be removed by backflowing, then perhaps it can be dissolved through the use of various types of acids. If necessary, fracturing may be used to increase the injectivity rate in the well.

Water-Injection Case Histories

Many examples of field case histories of water-injection projects can be found in the literature. Seven case histories of waterfloods in both sandstone and limestone reservoirs, using pattern as well as peripheral injection, are detailed in SPE Reprint Series No. 2a, *Waterflooding* (1973). SPE Reprint Series Nos. 4 (1962) and 4a (1975), *Field Case Histories* and *Oil and Gas Reservoirs*, also describe the history of several typical waterflood and pressure-maintenance projects.

For this chapter, three recently reported water-injection-project case histories were selected from the literature as a means of illustrating the use of contemporary technolo-

gy and reservoir engineering methods to solve some of the more complex problems encountered in many oil fields today. Summarized in the following discussion are results of projects involving (1) an older field with multiple sands, (2) a deep carbonate reservoir, and (3) an offshore field.

The effects of extensive waterflooding operations in the Hewitt field unit, Carter County, OK, were reported in 1982 by Ruble.¹¹³ The project described in that paper is a pattern waterflood in multiple sands that had been essentially depleted through 50 years of primary operations. The project is a good example of a simultaneous waterflooding of numerous sands containing relatively high-viscosity oil at shallow depths, as shown in Fig. 44.66. A structure map of the Hewitt unit is shown in Fig. 44.67. A summary of the reservoir performance data is given in Table 44.15. The additional oil recovery by waterflooding has been estimated to be 34.9×10^6 STB (123 bbl/acre-ft) as compared to a primary recovery of 109.6×10^6 STB (385 bbl/acre-ft). These numbers represent approximately 10 and 31% of the OOIP, respectively. Among the outstanding features of this project are (1) the use of triple completion injection wells with tubing and packer installations for control of the water that is injected into as many as 22 individual sands, (2) the plugging of 680 old wells and drilling of 149 new wells, and (3) the use of surveillance and selective injection programs to optimize oil recovery.

Langston *et al.*¹¹⁴ have reported on a large-scale water-injection project in the Jay/Little Escambia Creek field in Florida and Alabama. The project is a good example of a pressure- and rate-maintained project in a deep, undersaturated, carbonate reservoir. A summary of the production performance data for the field is presented in Table 44.16. The injection pattern is a 3:1 staggered line drive, as shown in Fig. 44.68. Reservoir pressure and

oil production rates, shown in Fig. 44.69, were maintained at constant levels for 6 years before they began to decline. Ultimate oil recovery is expected to be 346×10^6 STB, or 47.5% of the OOIP. This represents 222×10^6 STB more recovery than from primary operations—i.e., water-injection procedures will account for 64% of the total anticipated recovery. A great number of rock and fluid property data were acquired during the early development phase of the field. Use of these data provided the basis for decisions concerning unitization and the subsequent injection program.

Although water injection programs are being carried out in many offshore fields, primarily in the Persian Gulf area, in the North Sea, on the Louisiana-Texas gulf coast, and on the California coast, case histories have been reported on only a few. Jordan *et al.*¹¹⁵ reported on injection operations in the Bay Marchand field, offshore Louisiana, in April 1969.

Initial reservoir pressures in individual sands of the Bay Marchand field ranged from 4,600 to 5,291 psig. Reservoir temperatures varied from 182 to 197°F. Initial GOR's averaged 450 scf/STB and oil gravities were between 21 and 30° API. PVT properties varied with depth and the oil columns were undersaturated at their volumetric midpoints. Oil viscosities ranged from 1.1 to 1.9 cp, indicating favorable mobility ratios.

Porosities were rather uniform and averaged 29%. However, permeabilities exhibited wide variations; three reservoirs had geometric-mean air permeabilities of less than 100 md, while the remaining sands had values up to 2,000 md. Initial water saturations exhibited a corresponding variation, from 40 to 15%.

Pressure maintenance using seawater for injection began in 1963. According to McCune,¹¹⁶ who reported on operations in the Bay Marchand field in Oct. 1982, successful injection operations have been carried out over a 20-year period in six major sand reservoirs. A typical sand unit structure map and pressure-production history are illustrated in Figs. 44.70a and 44.70b, respectively.

The techniques used to test, treat, filter, and pump seawater are discussed in detail in the papers by Jordan *et al.*¹¹⁵ and McCune.¹¹⁶ The basic methods used in the Bay Marchand field, which include both coarse and fine filtration of solids, oxygen removal, and chemical treatment for control of corrosion and bacteria, have since been adopted in many other seawater injection projects.

Pilot Floods

A pilot waterflood is conducted to provide a means of evaluating the feasibility of a full-field implementation of the waterflood process. Both reservoir performance and operational procedures can be evaluated during the pilot flood. This experience is helpful in performing the engineering and economic studies that are necessary in deciding whether expanded waterflood operations should be carried out.

It is important to understand that a pilot flood should be designed to assure engineering success rather than economic success. Any small economic loss sustained by the pilot flood can be weighed directly against the much greater economic loss that would result from expanded waterflood operations that are undertaken without accurate pilot performance data. Such economic losses can result

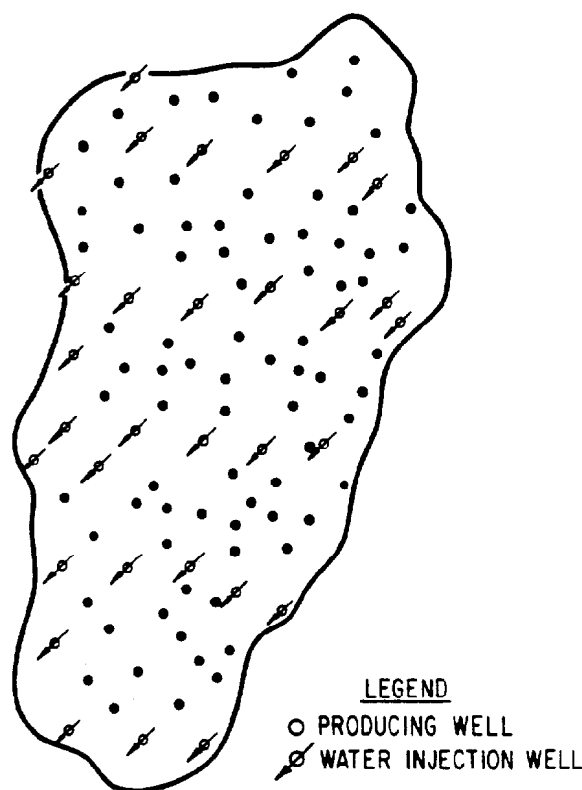


Fig. 44.68—Jay/Little Escambia Creek waterflood well location map.

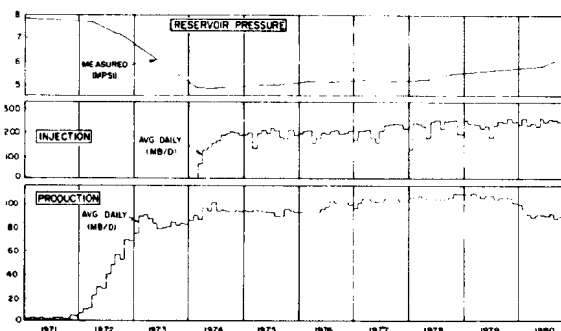


Fig. 44.69—Jay/Little Escambia Creek unit performance.

from the project capital investments or from a reduction in the ultimately recoverable oil reserves.

Caudle and Loncaric⁵⁰ has suggested several aspects of field pilot operations that need to be considered to achieve the greatest amount of useful data from the project. Fluid movement is most critical; one cannot isolate a segment (pilot area) of a reservoir and confine assessments of fluid movement to that segment.

A commonly used pilot flood pattern is the inverted five-spot, in which there is one injection well and four producing wells; all other nearby wells are shut in. The popularity of this pattern is mostly because only one injection well is required. The inherent problem with this pattern is that

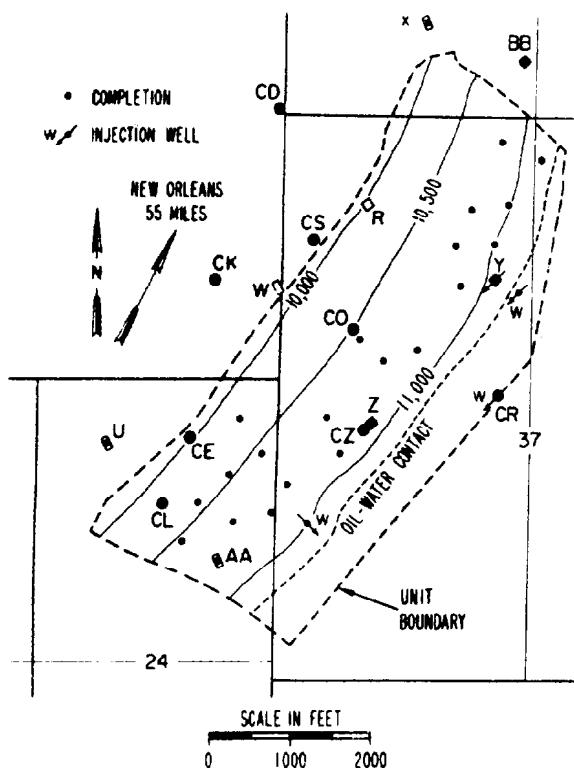


Fig. 44.70A—Typical unit structure map, Bay Marchand field.

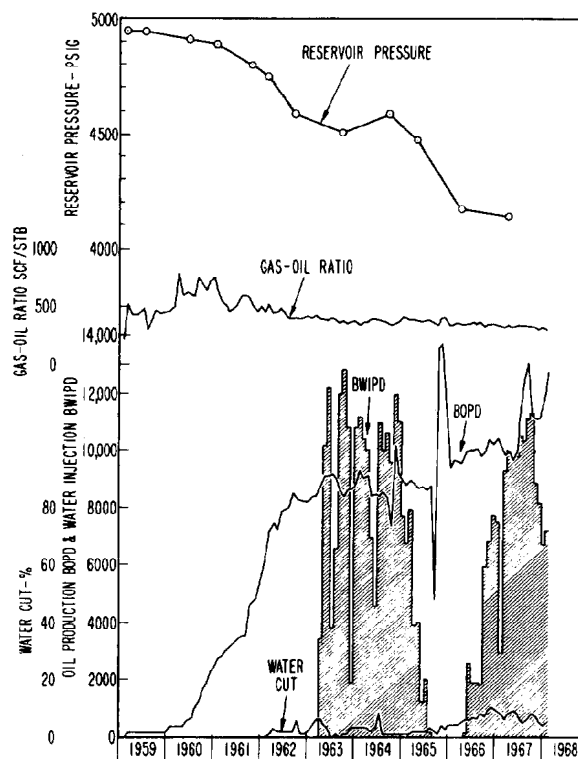


Fig. 44.70B—Pressure production history vs. time. Typical unit reservoir, Bay Marchand field.

three-fourths of the produced fluid comes from outside the "pilot area" while, at the same time, fluid leaves the pilot area from the regions between the producing wells. The relative volumes are affected by the ratio of production rates to injection rates.

A "volumetric balance" can be maintained in the pilot area by allocating only one-fourth the rate of the injection well to each production well. Although the volumes are balanced, the production history will still reflect the fact that only one-fourth of the oil that is produced actually comes from inside the pilot area. Therefore, no reliable estimate of the amount of recoverable oil in the pilot area can be made. Computer model studies show that the production history for this pilot pattern is so greatly affected by conditions outside the pilot area that correction factors are probably inadequate to compensate for the errors. This is especially true if there is a gas saturation in the reservoir at the start of injection.

The considerations noted previously suggest that a reversal of that pattern, in which one producing well is surrounded by four injection wells, could be a more accurate mechanism for evaluating the performance of a pilot flood. This pattern would minimize the escape of the oil originally contained in the pilot area as well as the entry of outside oil into the pilot area. The conventional five-spot pattern, as it is known, is probably the most simple and useful pilot pattern. While it is true that three-fourths of the injected fluid will not enter the pilot area, the production from the center producer will be much more useful for predicting total fluid recoveries.

The purpose of the pilot flood is to facilitate an evaluation of the performance of a small section of the reservoir so that the resulting information can be used to estimate the behavior of a much more extensive operation. If the production history of the individual pilot well does not generate data that are representative of the entire area to be flooded, a correction factor can be used to adjust the actual production history in order that the potential production of a fully developed or "confined" pattern flood element can be estimated.

Such a pilot (or pilot production well) must operate as if it were in a confined area (i.e., in one that is surrounded by many similar areas). In reality, such a situation could occur only if the pilot area composed the entire proposed flood project. However, if a sufficient number of similar elements are operated around the pilot, results that would closely approximate those of the confined case could be achieved. The number of similar elements around the pilot area that are necessary to generate results that are usable without correction depends on the mobility ratio and initial gas saturation.

Model studies^{117,118} have shown that, in general, the single conventional five-spot pilot is adequate for mobility ratios below one. More complex pilot patterns are necessary at higher mobility ratios.

Certain considerations should be weighed in deciding the location of the pilot area. Knowledge of the reservoir's geometrical configuration, its structural data, and its stratigraphic data are necessary to make the selection. A partially confined or bounded area will increase the value

of the pilot in predicting the behavior of an expanded flood. The boundaries to be sought are as follows: (1) oil/water contacts with respect to monoclinical or anticlinal structures, (2) fault planes, (3) small fault blocks, (4) structural or permeability pinchouts, and (5) shale-outs to the side.

Reservoir and well conditions must be evaluated before initiation of the pilot flood. In selecting the portion of the reservoir in which the pilot flood is to begin, it is important to be informed concerning these elements: (1) the pattern and spacing of injection and producing wells with respect to the formation structure and the distribution of formation properties, (2) the type of well completions, completion intervals, and the repair and workovers that have occurred in the past, and (3) the productivity factors that have been measured for producing oil wells.

Reservoir conditions and other related data provide information that is necessary before, and at the initiation of, the pilot flood. Some characteristics and categories of data that are valuable in determining the magnitude and distribution of oil, water, and gas saturations before the start of the pilot flood are (1) the development and production history, (2) total oil recoveries during primary operations, (3) encroachment of water or gas, (4) reservoir pressures within and surrounding the selected pilot flood area, and (5) distribution of fluids through gravity drainage.

The behavior of the reservoir and the wells should be evaluated continually throughout the life of the pilot flood. The records of this monitoring should include information about the following matters: (1) water-injection history on each well, including the time the injection began; (2) cumulative volumes of water and the rate of injection, by well, for the flood; (3) injection pressures and the identities of the sections taking water; (4) fluid production history, by well, for the total area within the flood region and for wells in the surrounding area; included should be the rate of production and the cumulative volumes of oil, water, and gas; (5) WOR and GOR trends; (6) reservoir pressure distribution inside, and surrounding, the flood area; (7) the frontal advance and associated displacement efficiency of water, as evidenced by the time and location at which water appears in individual wells; (8) workover history of both injection and producing wells; and (9) any pertinent changes in the pilot flood program.

There are two efficiency factors that may be calculated and used in evaluating the effectiveness of the pilot flood. One involves a displacement efficiency, determined on the basis of the ratio of the volume of total fluids produced to the volume of water injected. This ratio will indicate whether the injected water is effectively moving fluids from the injection well to the producing well (or wells) within the pilot area. The second factor involves the sweep efficiency within the flood pattern and the fractional depletion of the oil zone, which determine the economic life of the reservoir as well as the ultimate oil recovery.

Production data in the form of production-decline curves may be used to evaluate the pilot flood performance. The usual procedure in presenting the history of oil production in pilot flood operations has been to plot the logarithm of oil production vs. time or the logarithm of time. The advantages of using production-decline curves are that

they indicate the time of fill-up and the current oil-production response with respect to the injection program. However, there are limitations in using production-decline curves to evaluate injection efficiencies and the future behavior of the pilot. Among these limitations is the fact that true decline conditions seldom exist because fluid production is controlled by water-injection rates. There is no basis for assuming any particular shape with regard to a production-decline curve because the oil rate does not necessarily vary with time; the oil production rate is directly dependent on the rate at which water is injected and on the physical characteristics of the reservoir rock and the fluids it contains.

During the development and operation of the pilot test, certain conclusions regarding the performance of an expanded waterflood may be drawn. For example, if the reservoir has a high water saturation, the water may be more mobile than the oil, which would soon result in a high WOR in the pilot area. Because of the permeability reductions around the wellbores of the input wells, the formation itself might not take a satisfactory injection rate without exceeding the maximum pressure. Again, excessive pressure would produce adverse conditions. Water-cut data, used in conjunction with the Stiles calculation¹⁹ or other similar conformance calculations, will indicate whether the pilot is performing as expected.

Surface-Active Agents in Waterflooding

Surface-active agents in waterflooding are used to improve oil recovery by (1) improving mobility, (2) reducing interfacial tension, and (3) altering the rock wettability.

Laboratory investigations and field tests in which various surface-active agents and other chemicals are used will be discussed in Chap. 45, "Miscible Displacement," and Chap. 47, "Chemical Flooding." The large number of technological advances that have taken place during the past decade and the voluminous publications on the use of surface-active agents allow only a brief reference to the subject in this chapter.

Mobility Improvement

Control of the mobility of the injected water, along with the use of surface-active agents and chemicals to alter the wettability characteristics of the reservoir rock, are among the techniques now being used in certain waterflood projects to improve oil displacement efficiencies. The addition of an acrylamide polymer or some similar chemical to increase the viscosity of water causes areal and vertical coverage in the reservoir to be increased as a result of a reduction in the mobility ratio between the displaced and displacing fluids. This addition of a polymer also reduces the volume of injected fluids required in the oil displacement process that lowers the saturation in the swept portion of the reservoir to its residual value. The first field studies involving the use of polymers for mobility control were reported by Sandiford in 1964.¹¹⁹

The injection of a high-molecular-weight polyacrylamide polymer to increase waterflood sweep efficiencies through improved mobility ratios was considered to be unprofitable in two reported case histories^{120,121} that are summarized below. In the Wilmington field, CA,¹²⁰ a large-scale injection program was initiated during 1969 in relatively unconsolidated sands that contained an

18° API gravity crude oil with a reservoir oil viscosity of 30.8 cp. The mobility ratio of brine/oil was 14.2, compared to a mobility ratio of 1.33 for a 250-ppm polymer/oil. After injection of 1,300,000 lbm of polymer over a period of 2.5 years at an average concentration of 213 ppm, the injection of polymer was discontinued because no increase in oil recovery could be attributed to the polymer injection. The poor response was believed to be caused by (1) a polymer concentration that was too low; (2) injection rates that decreased by an average of 25% (as a result of scale formation), accumulation of undissolved polymer on the face of the formation, and possible reduction in the reservoir permeability from adsorption of the polymer (85 lbm/acre-ft); and (3) a premature breakthrough of the polymer solution through highly permeable intervals.

A pilot project¹²¹ in the Pembina field of Alberta, Canada, was started in Nov. 1971 with two 160-acre, five-spot patterns composed of six injection wells and two producing wells. The producing interval consisted of a conglomerate zone underlain by a sandstone, and these zones had average permeabilities of 63.6 and 25.3 md, respectively.

The viscosity of the 37° API crude oil, at reservoir conditions, was 1.05 cp. A total of 217,400 lbm of polymer was injected, with the first 124,750 lbm being injected at a concentration of 1,000 ppm and the remaining 92,650 lbm being injected at decreasing concentrations from 1,000 to 100 ppm. The conclusions reached from the Pembina pilot project were as follows.

1. The overall performance of the producing wells in the pilot area showed no permanent improvement.
2. Early breakthrough of polymer through the conglomerate zone indicated that the polymer did not significantly reduce the effects of the highly permeable interval.
3. Water/rock interaction and formation water commingling reduced the effective viscosity level of the polymer solution to approximately 25% of the designed value.
4. There was a significant reduction in the injection rates of two injection wells during polymer injection.
5. Adsorption of the polyacrylamide polymer was about 2 mg/m² of surface area.

The injection of polymer solutions to improve oil recovery through mobility control has not yet been well established for general application. Laboratory displacement tests should be performed on reservoir rock samples, and the reservoir crude oil and formation water should be used as a guide in selecting the type of polymer and the concentrations necessary for scaling the formulation to field conditions. Of particular significance is the effect of the formation water's salinity on reducing both the viscosity of the polymer solution and its adsorption by the reservoir rock.

Published reports¹²²⁻¹²⁴ about various field applications of polymer solutions have indicated improvements in oil recovery efficiencies of 5 to 15% above recoveries from conventional waterfloods.

Reduction in Interfacial Tension

Early laboratory tests¹²⁵⁻¹²⁷ indicated that dilute solutions of surfactants would remove more oil from sandstone cores than would untreated water. The economic feasibility of using this process in a waterflood has been ques-

tioned because of the loss of the surfactant by adsorption at the rock/liquid interfaces. The adsorption is especially problematical with both anionic and cationic surfactants, and it occurs to a lesser degree with nonionic surfactants. In one field project, the results of which were published¹²⁸ in 1968, a nonionic surfactant was injected at concentrations of 25 to 250 ppm into a sandstone reservoir at an advanced stage of waterflooding; an additional oil recovery of approximately 9% was attributed to the use of the surfactant.

Alteration of Rock Wettability

Recognition of the use of alkaline salts to improve oil recovery was first disclosed by Squires¹²⁹ and patented by Atkinson¹³⁰ in 1927. Wagner and Leach,¹³¹ in 1959, presented laboratory results that showed improved oil recovery through the injection of water containing chemicals that altered the pH of the injected water. Acidic injection water resulted in an improvement in WOR and a corresponding increase in recovery; however, its use as an injection medium has not proved practical because of chemical reactions with most reservoir rocks. Subsequent laboratory tests¹³² established similarly improved oil recovery results with sodium hydroxide.

Laboratory tests have indicated that the injection of caustic solutions can result in improved oil recovery, primarily as a result of lowering the water relative permeability,¹³³ pH control,¹³⁴ and the oil/water interfacial tension.¹³⁵ These effects, though, are dependent on the water salinity,¹³⁴ the temperature,¹³⁶ and the type of crude oil.

In 1974, there was a report¹³⁴ of a field trial in which a solution containing 3.2 wt% sodium carbonate was injected into a previously waterflooded Miocene sand in southeast Texas. The test involved two wells located 36 ft apart. Some improvement in oil cuts was noted at the producing well before alkaline water breakthrough, suggesting the formation of a low-mobility water-in-oil emulsion bank. No economic evaluation of the test was reported.

The first field test of the caustic flooding process was mentioned by Nutting¹³⁷ in 1925. A report¹³² published in 1962 of a field trial in which sodium hydroxide was used in the Muddy "J" sand, Harrisburg field, West Harrisburg Unit, Banner County, NE. The injection of a 40,000-bbl slug of 2.0 wt% sodium hydroxide resulted in a recovery of approximately 8,700 bbl of oil from an area that previously had been flooded out by normal water injection operations. In another case, an 8% PV slug of 2.0 wt% sodium hydroxide was injected into a portion of the Singleton field, Banner County, NE. The test was in an area under waterflood that had not been completely watered out. Increased oil recovery, reported¹³⁸ in 1970, amounted to 17,600 bbl, or 2.34% PV.

The only description of a large-scale field trial of caustic flooding that has been published¹³⁹ involved a 63-acre area in the Whittier field, CA. The area had been under waterflood for 2.5 years before caustic was injected. A 0.2 wt% sodium hydroxide slug, equal in volume to 23% PV, was injected. The slug was followed by plain water. The increase in oil recovery beyond that by waterflooding was estimated to be from 350,000 to 470,000 bbl, or 5.03 to 6.75% PV.

Water Source and Requirements

During the planning stages of a waterflood program, these basic steps must be taken: (1) the water requirements should be determined as accurately as the data will permit; (2) all possible water sources should be surveyed with special attention given to satisfying the quantitative requirements; and (3) the selected source should be developed in the most economical manner permitted by good engineering practice.

Waterflood Requirements

Daily Water-Injection Rates. The largest daily demand for water from the water source occurs during the fill-up period when there is no return water available. During the early life of the reservoir's injection program, or during the fill-up period, it is usually advantageous to maintain a high rate of injection so as to accomplish an early fill-up (a rate between 1 and 2 B/D/acre-ft is desirable). One author¹⁴⁰ states that after fill-up has been achieved, the injection rate should be maintained at about 1 B/D and not less than ½ B/D/acre-ft. Flood pattern, well spacing, and injection pressures should be designed to meet these requirements.

Ultimate Water Requirements. The PV method has been found to give a good approximation of the ultimate water requirements for a waterflood. The volume of water required should range from 150 to 170% of the total pore space, and the measurement of such space should include the PV of any adjacent overlying gas sand or basal water sand. The ultimate water requirements, together with the average water-injection rate, will serve as a basis for estimating the total life of the waterflood.

Makeup Water. The volume of return water becomes an increasingly significant percentage of the required injection rate as a flood progresses; therefore, it is an economic necessity that produced water be injected unless the treating cost of the produced water is higher than that of the makeup water. If gas or water sands are not present, the produced water will compose 40 to 50% of the ultimate water requirements. If gas or water sands are present, less return water will be available—thus, the ultimate makeup water requirement will increase to as much as 60 to 70% of the total quantity of water that is injected. In recent years, federal and state agencies have enacted regulations that limit or prohibit disposal of oilfield waters in surface systems. Environmental regulations should be reviewed carefully when studies of the treatment and disposal of produced water are being made.

Water Sources

There are three principal freshwater sources and two sources of salt water that can be used for waterflooding purposes. Freshwater supplies include surface waters, municipal water, waters from alluvium beds, and some subsurface waters. Saltwater sources include some subsurface waters and the oceans. Where economically permitted, salt water usually is preferable to fresh water.

Fresh Water—Surface Sources. Surface waters, including ponds, lakes, streams, and rivers, have been used throughout the history of oilfield waterflooding projects,

and these are the sources for which competition from other industries and from municipalities is highest. There are a number of other factors that limit the availability of this resource. For example, there is a continuing growth in the demand for fresh water, and droughts have resulted in water shortages in some areas during recent years. In addition, some states have taken legislative action to control freshwater supplies. Therefore, when fresh water is to be used in a waterflood project, it may be necessary to obtain approval from the appropriate state agency before proceeding with development of such a source. If salt water is chosen as the injection medium, legal approval for the withdrawal of the water may not be necessary.

Small ponds and streams are very unreliable as a constant source of supply for all seasons of the year. Large lakes and rivers are preferable; however, these also may have limited capacity during drought periods. The principal disadvantages of surface sources are the unreliability of their quality and quantity, the high cost of treating equipment, and the cost of the chemicals that are necessary to obtain a satisfactory water.

Fresh Water—Alluvium Beds. A more favored method of using river or stream waters calls for the alluvium beds near the river to be tested with shallow wells. Use of this source in some of the world's largest waterfloods—the Salem unit in Illinois,¹⁴¹ the Burbank unit,¹⁴² and the Olympic pool in Oklahoma—indicates the high productivity that can be achieved from alluvium beds. If closed injection systems are used, chemical treatment (with the possible exception of a bactericide) normally is not required. Filtration usually is unnecessary because of the natural filtration of the alluvium beds.

Sulfate-reducing bacteria are anaerobic and thrive within a few feet of the surface, so waters from alluvium beds frequently can be highly contaminated with these bacteria. However, low-cost chemical treatment can control these organisms. Having noted this minor problem, it is safe to say that the quality of water from alluvium wells is more dependable than that from direct surface sources. Wells are not subject to extreme turbidity changes during rainy seasons or to the variable organic content of the surface waters.

The reliability of alluvium beds as a continuing source of water is slightly better than the reliability of an adjacent river or stream. The water table will drop steadily when a river dries up, but wells should go on supplying water for some time after the surface waters are depleted.

The principal advantages of alluvium-bed sources are their low development cost, low pumping cost, and the possibility that they will not need filtration. If bacteria are not a problem, corrosion rates should be low and chemical treatment unnecessary.

Fresh Water—Subsurface Formations. In certain areas, subsurface sand or carbonate formations may be tested for water production with good results. Good-quality water often is produced from certain formations whose depths range from close to the surface to 1,000 ft or more. As in the case of the alluvium wells, closed systems usually are used, thus eliminating chemical treatment and filtration requirements. When a well is completed in a freshwater subsurface formation, drawdown tests should

TABLE 44.17—RESERVOIR ENGINEERING

Dissolved Gas	Test	Effects	Remedial Treatment	pH Control	Tolerance Suggested
Hydrogen sulfide, H ₂ S	Odor or taste. If lab analysis desired, sample is preserved by addition of zinc acetate and sodium hydroxide.	Very corrosive in the presence of moisture, particularly if oxygen is present.	1. Open aeration (poor) 2. Synthetic or natural combustion exhaust gases flowing counter-current to water in packed towers. 3. Forced-draft aerators.	A decrease in pH will increase rate of corrosion, but the corrosion rate also depends on the composition of the contacted metal and the alkalinity of the solution.	50 ppm. ¹⁵⁷ Corrosion rate is rapid up to 15 ppm. High H ₂ S concentrations may act to inhibit corrosion.
Carbon dioxide, CO ₂	Determine the stability of the carbonate-bicarbonate balance, titrate for free CO ₂ at source point.	1. Corrosion increases with increasing percentages of CO ₂ . 2. Removal of CO ₂ may cause precipitation of metallic carbonates or bicarbonates.	1. Aeration by the three methods mentioned above. 2. Increase the alkalinity. 3. Chemical inhibitors.	An increase in pH also will decrease the free CO ₂ that is present. Free CO ₂ may not exist in water with pH values which are greater than 8.3.	Function of the carbonate and bicarbonate stability vs. corrosive activity is caused directly by the CO ₂ . Not as corrosive as equal portions of O ₂ or H ₂ S.
Oxygen	Determine if the Fe ⁺⁺ ion is being oxidized. Dissolved O ₂ meter and membrane probe is used when H ₂ S is absent.	1. It is largely responsible for corrosion of equipment. 2. Its reaction with metallic ions (Fe ⁺⁺ mostly) will cause plugging in the reservoir.	1. Use of closed systems will minimize oxygen use. 2. Open systems—vacuum aeration has been used. 3. Counterflow (in bubble tower) of natural gas with low oxygen content.	No effect is to be found in either acidic or alkaline water.	Limits of detection—i.e., 10 ppb (Note: iron bacteria can grow in waters containing 0.3 ppm. ¹⁵³ SRB can also live in aerobic conditions.) Soluble O ₂ is approximately four times as corrosive as equal mole volumes of CO ₂ .

be made to determine the initial productivity. The test should be conducted for a sufficient length of time to determine the static working fluid level, which will indicate the rate at which the well can be produced.

Optimal spacing in the water-supply wells may vary from 25 ft for sand points to as much as 1,320 ft for deep wells. The productivity will indicate how many wells are necessary to meet the daily water requirements. Where a number of deep wells are required to develop the fresh-water source, the economic viability of drilling the additional wells should be carefully considered.

Pumping equipment for water wells may include surface-driven or submersible, centrifugal (or rod) pumps. If a high-pressure gas source is available, gas-lifting methods should be considered also. Selection of the pumps should be governed by economic considerations, and these are influenced by the static fluid level, the drawdown, and the desired productivity. The advantages of freshwater wells in subsurface formations include low corrosion rates and the possible elimination of the need for chemical treating and filtration.

Salt Water—Subsurface. In most oil fields, either above or below the oil zones, there are saltwater formations that are potential sources of water supply.¹⁴³ The relatively shallow saltwater wells are similar in most respects to the shallow freshwater wells.^{144,145} The saltwater wells are completed in the same manner and have the same advantages of being adaptable to closed injection systems. Many producing areas have deep saltwater formations that have extensive areal coverage and a thickness of up to several hundred feet. These prolific saltwater-producing formations frequently have high working fluid levels. Such formations may contain waters with high mineral content, and have wellhead temperatures in the range of 100 to

173°F. Hydrogen sulfide may or may not be present. If the water contains significant amounts of hydrogen sulfide, open systems that incorporate aeration, sedimentation, and filtration capabilities should be used. Examples of prolific formations are the Arbuckle¹⁴⁶ and Mississippi limestones in Kansas and Oklahoma, the Ellenburger lime in Texas, the Tar Springs in Illinois, and the Madison lime in Wyoming. The drilling and completion costs of deep supply wells may range up to, and exceed, \$500,000; however, they frequently are the most economical source of large volumes of water because of small fluid-level drawdowns. The advantages of the deep saltwater wells include their adaptability to closed systems, their high and reliable productivity, the compatibility of salt water with the oil sand, and, where high hydrostatic fluid levels are found, the relatively low lifting costs.

Salt Water—Ocean. Use of ocean water for injection purposes is confined to coastal regions and offshore fields.^{116,147-149} Closed systems in which shallow wells on the shore are used as the source of supply are preferred. A moderately high corrosion rate should be expected, and ocean water probably will require a bactericide. The advantages of oceanwater supply include an inexhaustible source and low development and pumping costs.

Salt Water—Return Water. During the life of a flood, the return water may represent a total volume of from 30 to 60% of the injection requirements. The use of the return water for injection may improve the economic condition of the overall project. In open systems, return water generally is added to the makeup water and injected. The mixing of the waters in a pond or settling tank permits precipitation and sedimentation of the incompatible constituents. In recent years, however, it has been determined

TABLE 44.18—WATER-INJECTION PRESSURE MAINTENANCE

Organisms	Genus	Phylum	Environment	Agents Used for Treating	Effect of Agents in Reducing Growth	Purpose in Treating
Sulfate reducers	Desulfouibrio	—	Anaerobic (though they cannot grow in the presence of free oxygen, they can live; will not grow in highly saline waters.) Low-pH waters also stifle growth.	Chlorine* Quaternary ammonium compounds Other bactericides**	Partially effective Effective	1. To prevent corrosive activity as a result of H ₂ S formation. 2. To prevent plugging of sandface.
Organisms	Pseudomonas	—	Aerobic or facultative (usually require free oxygen for growth)	Chlorine* Quaternary ammonium compounds	Effective Effective. (Note: change bactericide if immunization occurs.)	1. To prevent plugging of equipment. 2. To prevent plugging of sandface.
Iron bacteria	Leptothrix Crenothrix Gallienella	—	Bacteria withdraw ferrous iron (Fe ⁺⁺) that is present in their aqueous habitat and deposit it in the form of Fe(OH).	Bactericides Chlorine*	Effective Effective. (Note: slug injection is usually sufficient.)	1. To prevent plugging of equipment. 2. To prevent plugging of sandface.
Algae	—	Thallophyta	Chlorophyll-containing plants (require presence of sunlight and moisture for growth).	Copper sulfate Sodium pendachlorphenate	Effective, depending on water alkalinity. Effective, depending on water alkalinity.	1. To prevent plugging of equipment. 2. To prevent plugging of sandface.
Fungi	—	Thallophyta	Oxygen (require presence of free oxygen).	Closed system Chlorine* Closed system	Effective Effective Effective	1. To prevent plugging of equipment. 2. To prevent plugging of sandface.

* Limited to iron-free waters.

** Mercuric and phenolic compounds; fatty and resin amines; formaldehyde.

that the mixing of the produced water and makeup water results in increased scale deposition and corrosion in the surface system and injection wells. Also, scale deposition in the perforations, and the transport of suspended solids (a product of corrosion) into the formation, reduce the well injectivity and necessitate frequent backwashing and acid treatments. Therefore, in many of the major waterfloods, the waters are isolated in the surface system and are injected separately into the reservoir.

In closed systems, the compatibility of the return and makeup waters is more critical than it is in an open system, but the two waters can be mixed satisfactorily in most cases. Complete analysis of the water should be made, with special attention being given to the detection of any combinations of ions that may precipitate on being mixed. The effect of the more common precipitates and the treatment of them is covered in this chapter under Water Treating.

Water Treating

During the early days of waterflooding, only the quantity, not the quality, of the water was given consideration. However, it was soon noted that when the quality was poor, higher injection pressures were required to maintain suitable injection rates and corrosion problems mounted. As a result, the operators of the early waterfloods began to realize that the quality of the water was equally as important as the quantity, and that poor water treating was proving disastrous to waterfloods that otherwise might have been successful. Water-treating practices have improved greatly as the waterflood industry has matured, a point that is substantiated in the literature by the many contributions on this subject.^{145,150-164} API has published recommendations for analysis of oilfield waters¹⁵⁰ and biological analysis of injection waters.¹⁵¹ Successful results normally can be achieved when these recommended

procedures are followed. Standardized procedures for membrane-filterability tests,¹⁵² a useful tool in water testing, also have been adopted by the industry.

After the water source is known, a water analysis is required to determine these matters: (1) compatibility of the injection water with the reservoir water (the test should include actual blends as well as theoretical combinations); (2) whether an open or closed injection facility would be the most suitable; and (3) what treatment is necessary to have an acceptable water for the reservoir and to minimize corrosion of the equipment.

Prudent operation of the waterflood requires that water analyses be conducted periodically to determine the presence of dissolved gases, certain minerals (discussed later), and microbiological growth—undesirable constituents of water. Samples of the injected water should be collected at several points in the system—for example, at any point in the system where a change in water quality could or should occur, and at the injection wells.

Sampling

The importance of good sampling practices cannot be overemphasized. An extremely accurate chemical analysis of a water sample followed by a brilliant assessment of the problems indicated by the analysis is worthless if the sample does not represent the water in the system.

Dissolved Gases

To eliminate the loss of dissolved gases through changes in temperature and pressure, testing of such gases should be carried out in the field soon after a water sample is taken. The three dissolved gases to be considered are hydrogen sulfide, CO₂, and oxygen. Table 44.17 lists the test, the effects of the gas when present, remedial treatment, pH control, and tolerance permitted in ppm.

Microbiological Growth

Static control of colonies of one-celled animals and plants is of much concern to operators attempting to maintain a suitable water for injection. Aerobic, anaerobic, fungal, and algal growths will cause reservoir and equipment plugging and corrosion. Table 44.18 lists the various organisms, their environment, the various treating agents that have been used, the results that may be expected, and the purpose of the treatment.

Special attention and control are required for sulfate-reducing bacteria (SRB). The presence of the sulfate ion is essential to the growth and reproduction of these particular bacteria. Sulfate, in turn, causes plugging. The reaction of the sulfate ion with the SRB forms the sulfide ion, which then reacts with iron. Iron sulfide is serious plugging agent and H_2S is an extremely corrosive agent.

Early studies of SRB involved the plate-count method,^{153,154} a clinical practice derived for the purpose of isolating and identifying bacteria. But this technique is of little value in assessing sulfate-reducing bacteria activity, which is what really counts.

The objective of studies of SRB in a water system is to determine whether practical problems exist, and to be able to execute effective countermeasures if such problems are found. The concept of bacterial activity was developed to meet this objective. The procedures for conducting these studies are presented in the API RP 38 publication.¹⁵¹

Many organic and inorganic bactericides are now available to control this problem.

Minerals

Appearance. A notation concerning the appearance of the water at the time it is sampled is important for future reference. Frequently, organic growths and precipitated material can be detected visually.

Temperature. The temperature of the water sample is important in estimating the solubilities of various materials. For example, calcium carbonate solubility decreases with increasing temperature, as does calcium sulfate and all sulfates.

Significance of pH. Simply put, pH is a measure of the acidity or caustic intensity of water. Two important points to remember are that calcium carbonate and iron solubilities both decrease with increasing pH value; therefore, the higher the pH the more difficult it is to hold iron in solution and to keep calcium scale from forming. However, if iron is being removed in the water-treating program, then a high pH may be beneficial. The pH value is very important when corrosion control is considered.

Turbidity. A turbidity test measures the suspended material in a water and it is based on the intensity of light scattered by the sample in comparison with light scattered by a known concentration of a standard solution. The higher the scattered light, the higher the turbidity. Standards are compared to Formazin polymer, which has gained acceptance as the turbidity reference standard suspension for water.

The generally accepted method of measurement is conducted with a nephelometer. Results are reported in nephelometric turbidity units (NTU), which correspond

with Formazin turbidity units (FTU) and Jackson candle units (JCU). Normal turbidity measurements are within the 0- to 50-NTU range.

Iron. Some form of iron is probably the most common plugging agent encountered in injection wells. Ferrous iron (Fe^{++}) is soluble to 100+ ppm, while ferric iron (Fe^{+++}) is insoluble except at low pH levels (3 ppm or less). Low iron contents are desirable in any water. The retention of soluble iron in solution is the prime objective in closed systems. In properly operated iron-removal plants, the iron content in the finished water should be less than 0.2 ppm. In many cases, it is possible to reduce the iron so that it is consistently less than 0.1 ppm. There should be no significant increase in iron content as the water travels from the pressure source to the injection wells.

Manganese. Soluble manganese in water reacts somewhat as iron does, except that it is more difficult to remove. In most waters, good manganese removal requires a pH level of 9.5 to 10 ppm. Manganese problems in the Appalachian oil fields have been very severe. Only in a few isolated cases has it been troublesome in the Illinois basin; it has been of little concern in most floods in that area, or farther west. Low to moderate manganese contents are found in many waters and can be tolerated as long as the pH values remain low enough to keep it in solution.

Alkalinity. The alkalinity of water is defined by the measure of its acid-neutralizing capacity. Since the occurrence of hydroxide is quite unusual in flood waters, alkalinity generally can be taken as a measure of carbonates and bicarbonates. Calcium carbonate solubility depends on alkalinity; however, other factors, such as pH, calcium content, temperature, and total dissolved solids, influence the reaction.

Sulfates. Sulfates are of most interest from a deposition standpoint. Three generalizations may be made with regard to this class of substances.

1. An abnormally low or zero sulfate value in a brine suggests the possibility of the presence of barium and strontium. It requires practice and experience to evaluate a low-sulfate-content water.
2. In general, high-sulfate water should not be mixed with water containing appreciable amounts of barium or strontium.
3. A high-sulfate brine indicates there is a possibility of exceeding the calcium sulfate solubility. The solubility of $SrSO_4$ or $CaSO_4$ is governed by the limiting factor of either SO_4 or Ca or Sr and the ionic strength or foreign salt concentration of the brine.

Chlorides. Chlorides are the primary indication of the salinity of a water, or the ionic strength of a brine, or the presence of a fresh water. Chloride tests can be useful in tracing the progress of a waterflood.

Hardness. The term hardness refers to a measure of the amounts of calcium and magnesium that are present in the water and is expressed in ppm of calcium carbonate. Since calcium is involved, the hardness of the water is of importance in relation to calcium carbonate stability.

Calcium and Magnesium. These two minerals are grouped together because they are the principal contributors to a water's hardness. The calcium salts are less soluble than magnesium under most practical conditions. Also, the presence of an appreciable quantity of calcium is necessary for calcium sulfate and calcium carbonate scale to form. It is important to note that other factors, beyond the calcium value, must be considered in assessing calcium carbonate formation.

Suspended Solids. Suspended solids are a mixture of fine, nonsettling particles, or precipitated material in the water. Unless suspended solids are removed, difficulties involving plugging of the injection or disposal wells can be expected.

Dissolved Solids. It is necessary to prevent precipitation of those soluble salts that are dissolved in the water, so that there will be no plugging of the sandface.

Total Solids. Technically, the term "total solids" means the combination of dissolved and suspended solids. Long experience in operating water injection systems has established that good water-quality control requires knowledge of not only the general content of the water but the constituents of the undissolved (suspended) material that exist under in-line conditions. It is this suspended material that may cause well and reservoir plugging. The suspended solids often are the result of the precipitation of constituents of the water, but the quantity and type of solids that actually are precipitating cannot be ascertained from the water analysis alone.

The Millipore™ filter test has been developed to provide a means of measuring suspended material under injection system conditions. This test is conducted with the MF-Millipore filter of mixed esters of cellulose and a uniform pore size of, generally, 0.45- μm opening. The filter diameter may be of several sizes; however, 90-mm-diameter filters are recommended because a greater volume of throughput water can be handled, thus giving a more representative test for the system being examined.

A small stream of water is taken, through suitable connections and the test apparatus, from the selected point in a system. The test apparatus that holds the filter will trap all the suspended material flowing through the sample line. The water effluent that passes through the filter is measured and recorded, for use in the later analysis, as volume throughput in milliliters of water. After sufficient water has passed through it and/or the initial pressure of about 10 psig has increased sufficiently to indicate plugging, the filter is removed and placed in a protective screwcap tube (preferably containing distilled water to prevent the drying out of the filter) and submitted to the laboratory for either comprehensive or selective analysis. As a safety precaution, it is highly recommended that duplicate samples be obtained through the use of a parallel-apparatus hookup.

Identification of the solids and particle size distribution (with Coulter counter) is useful for designing facilities to treat and to remove solids from the water.

Barium. Barium ions have been quite troublesome in many cases because of the extremely low solubility of the most common form of their deposition, barium sulfate.

It is generally undesirable to mix a water with appreciable amounts of barium with a water containing high sulfates or strontium.

Strontium. This is another alkaline earth metal that occurs in small quantities and is associated with calcium and barium minerals. It is found principally in the form of celestite (SrSO_4) and strontianite (SrCO_3) ores; its solubility in both forms is considerably greater than its barium counterpart but much less than CaSO_4 .

Sequestering and Chelating Agents. The use of sequestering and chelating agents in injection waters plays an important role in preventing the precipitation of salts of calcium, barium, strontium, iron, copper, nickel, manganese, etc.¹⁵⁵ The definition of each term is given as: (1) *sequester*: to set apart, to put aside, or to separate, and (2) *chelate*: pertaining to or designating a group or compound which, by means of two valences (principal or residual, or both), attaches itself to a central metallic atom so as to form a heterocyclic ring.

The sequestering agent will separate the metallic cation from the anion by chelation. This will prevent the metallic ion from reacting with the anions to form precipitates that will cause plugging of the reservoir. If precipitation of the metallic salt ions does occur, reverse flow of the injection well and acid treatments usually will correct the situation so that normal injection rates can be continued and maintained. The requirements for desirable sequestering agents are that they¹⁵⁵ (1) form chelates in the presence of other ions such as calcium, magnesium, strontium, barium, and others that are common to waters used for secondary recovery, (2) form stable water-soluble chelates or complexes with iron, (3) be compatible with other chemical compounds used for water treatment, (4) be economically feasible, and (5) be easy and safe to handle.

The most widely used sequestering agents are "Ver-sentates" (trademark for certain salts of ethylenediaminetetraacetic acid and related compounds), citric acid, gluconic acid, organic phosphonates, and the polyphosphates. Of these, the citric acid sequestrants have been most successful.

Corrosion Inhibitors. Corrosion inhibitors are chemicals that are used to control the corrosive activity between the metallic alloys and water. "The current interest in chemical inhibition is largely a result of the availability of organic treating compounds that possess both corrosion-inhibiting and biocidal properties. Field and laboratory tests made with organic inhibitors such as quaternary, rosin, and fatty amine compounds have indicated favorable results in minimizing corrosion caused by dissolved acidic gases."¹⁵⁶

Selection and Sizing of Waterflood Plants

The selection and the sizing of waterflood plant facilities normally are unique to each waterflood because of the many variable parameters. The primary parameters might be the volume and pressure, while secondary parameters might include the treating requirements and the economic position of the investor. A variation in any single one of these parameters might drastically modify or completely change the selection and sizing of a waterflood plant.

The volumes of injection water to be handled will, of course, be the most important basic item of information to learn for determining the size of the plant. Here, too, there are several parameters on which the calculation is based. Essentially, the water volume is a function of the gross size of the reservoir to be flooded, the porosity of the reservoir rock, the anticipated conformity or efficiency of the flood, and the ROS at both the initiation and completion of the flood. These data will be applied to the actual reservoir calculations, and only the final gross volume and the required daily injection rate must be known by the plant designer. As a general rule of thumb, 8 to 15 bbl of injected water per barrel of secondary oil, or $1\frac{1}{4}$ to 2 PV of injected water, will provide a reasonable estimate of the ultimate water-handling requirements. Daily injection rates may vary from 5 to 25 bbl/ft of pay. The producing-equipment capacity may be a limiting factor in determining the maximum injection rates. A relatively high ratio between the amount of fluid that is injected and the amount of fluid that is produced can be anticipated before fill-up.

There are certain other factors that should be considered in designing the proper capacity of the plant facilities. If the available quantity of supply water is relatively small, it is usually necessary to consider produced brine along with other supply waters so that an adequate injection volume is provided. Where the original source water is not compatible with the produced water, or where the produced water is best handled in a closed system and original source water is best handled in an open or semi-open system, flexibility in capacity design will be required. This flexibility is necessary to adjust or to balance capacities between two separate injection systems (one with a constantly increasing load, the other with a constantly diminishing load).

The pressure required to inject water into a formation is a function of formation depth, rock permeability, water quality, and the injection rate that is required. The basic reservoir data and secondary-recovery study will have defined the rock properties so that the anticipated surface pressures can be defined closely, if no adverse effects are anticipated as a result of poor-quality or incompatible water. Poor quality might be because the water contains a large quantity of solids as a result of poor filtration, inadequate settling, precipitation in an unstable water, or the growth of bacteria. Incompatibility might result from mixing injection water with formation water, from the swelling of clay particles, or from chemical reactions between the rock minerals and the injected water. In general, it has been found that the pressures than initially are encountered are less than might be anticipated when the only governing factors are depth and permeability; however, increasing pressures should be expected if there is no plan to reduce the injection rate as fill-up is approached. A final factor in predicting injection rates is the method of production. If the reservoir is to be produced by natural flow, the injection pressure must be sufficient to overcome dynamic hydraulic forces and to support a flowing rate of production. If, on the other hand, production is to be by mechanical means, with producing fluid levels at or near reservoir depth, a considerable reduction in injection-pressure requirements is possible. Consideration should be given to what the maximum allowable injection pressures should be. As a rule of thumb, pres-

sure at the surface should not exceed 0.5 psi for every foot of reservoir depth. The maximum wellhead injection pressure will limit the resulting pressure at the perforations, which is less than the parting or fracture pressure. This pressure can be determined by an injectivity test conducted before or during pilot flood operations. Breakdown pressures are often encountered below the 0.5-psi value, and in such circumstances the maximum pressure will be defined by the breakdown pressure. In older fields, or in reservoirs located at considerable depth, the mechanical strength of the injection-well casing may be the deciding factor concerning the pressure limit. This limitation can be overcome by installation of competent tubing set on a packer.

The source and the condition of the supply water will be the most important factors in determining a treating method. It is generally good practice to plan originally on using a closed system that requires little or no treating. Subsequently, the closed system may evolve into one in which the mixing of produced water will require custom-tailoring for conditions that are unique to the particular flood being considered. By starting with a basic treating system, the unit may be expanded into a complete version that may include aeration, chemical treating, flocculation, settling, corrosion inhibition, and bacteria control.

In developing the proper treating system for a particular plant, the economic factors that are unique to the situation should be given close attention. If the flood is to be of relatively short duration, it may be profitable to use a system that is less than adequate and to anticipate more than normal maintenance demands. In other circumstances, it might prove most profitable to install corrosion-resistant equipment and to reduce the use of corrosion-inhibiting treatment. Consideration should be given to installing fiberglass tubing or internally plastic-lined tubing in injection wells. Also, if new injection wells are to be drilled, a full or partial string of fiberglass casing should be considered to minimize corrosion and scale buildup, especially in the area across the producing formation. A paper published in 1980 discusses the use of fiberglass liners and injection tubing in a west Texas waterflood.¹⁶⁵

Possibly the last item to be considered by many design engineers, and yet the most important item in many companies, is the financial position of the investor. It is quite possible that a particular operator may have limited investment capital and would find it desirable to keep this sum to a minimum, at the expense of higher future operation costs or additional future investment. The capital investment situation might also affect the choice of injection rate. The operator might be in a financial position in which a low, long-term, constant income would be most advantageous; in other circumstances, a short-term, high-income situation might be most desirable. Under either of these conditions, the normal approach to determining injection rates and plant design would be modified to produce the most desirable income vis-à-vis investment conditions.

When the most desirable injection rate as well as the pressure and treating technique have been determined, the plant must be designed to fit the prescribed conditions. For a closed system, the plant design may be extremely simple and yet completely automatic. With in-line, high-

pressure filtration equipment and a relatively high-discharge head source well pump, it is possible to use the supply pump as the injection pump and to inject directly from the supply well to the injection well. In this plan, individual cartridge-type well filters may be used if the supply water is relatively free of solids.

The next stage in increasing the capacity of the injection plant would be to install a booster pump downstream from the filters, so that the supply pump and filters would not have to operate at injection pressures. The step after that would be to place a gas- or oil-blanketed water surge tank between the supply and filter system and the injection pumps. With this arrangement, low-pressure equipment can be used for supply and filtration; if the supply water and produced water are found compatible, produced water can be commingled in the surge tank. Where the systems are separated, it is also possible to use injection pumps with maximum pressure capacities. Further flexibility is also possible in that both source and injection rates can be varied independently, as long as the supply rate is at least as great as the injection rate. Corrosion frequently is minimized in the low-pressure side of this type of system by use of plastics, which also results in reduced fabrication costs.

If a supply water is naturally aerated, the operation of a closed system becomes pointless. Also, because of excessive amounts of dissolved acid gases and/or a high content of dissolved iron, it may be desirable to aerate the water as a treating technique. When an open treating system is being designed, consideration should be given to using natural elevation or substructures to obtain gravity flow through the system. Under these circumstances, open gravity filters are often the most economical and practical.

When a complete chemical-treating program is planned, the most common approach is to have the prefabricated mixing and sludge tank placed immediately ahead of the filters. In certain circumstances, it has been found desirable to deaerate the treated water before using it for injection. Chemical treatments can be used; however, chemicals are too costly except for the removal of very small quantities of oxygen. Counterflow, bubble-tray towers that use natural gas or a vacuum are sometimes used for oxygen removal. However, oxygen is not removed if it can be avoided, because of the relatively high cost of the process; the price must be weighed against the deleterious effects of the entrained oxygen.

Centrifugal pumps have proved most satisfactory for low-pressure supply water and for injection at low pressures. Among the advantages of this type of pump are the small number of its moving parts and its excellent adaptability to volume control; however, in cases in which an appreciable amount of power is to be used, the relatively low efficiencies of centrifugal pumps (particularly when they are operated at other than design conditions) may preclude their use. In selecting centrifugal pumps, the proper metals should be chosen carefully for both the case and the trim to ensure the best performance. The greatest economy may be achieved with a cheaper pump that is subject to some corrosion rather than with a much more expensive pump, even though it might not be susceptible to corrosion. The positive-displacement type of injection pump is the most common one in use. Some use has been made of multistage centrifugal pumps; however,

they have not yet been widely accepted because of some limitations in flexibility and efficiency.

The most generally accepted type of pump for medium- to high-pressure water injection is of either vertical or horizontal multicylinder design. These pumps are relatively simple to operate and to maintain, and they can be purchased with a variety of corrosion-resistant parts and accessories. The selection of the proper number of pumps and their capacity is contingent on the present and future requirements for the project. It is, of course, a good practice to provide a standby capacity that is sufficient to maintain continuous injection in case one pump has a mechanical failure. This can be accomplished by distributing the maximum design load over two or more units so that at least half the injection capacity can be maintained.

A considerable number of filtering techniques are now used in the oil field. These involve ceramic-, metallic-, paper-, and cloth-element pressure filters with sand, gravel, or coal media; and rapid sand pressure filters with sand, coal, or graphite media. The choice of filters is a function of the raw water quality and volume of water required for injection. If solids in the water must be reduced to submicrometer size, one of the element-type or diatomaceous-earth filters, or a combination of the two, is recommended. For less rigorous filtration, the gravity or rapid sand pressure filters are most widely used. In general, filtration rates are considered normal at about 2 gal/min-sq ft of filter area; however, this figure will vary considerably depending on the quality of the influent and the desired quality of the effluent. Decreased rates also may be desirable if very frequent backwashing is necessary. The rates and techniques for backwashing are prescribed by the manufacturers of the various types of filters; this function should be considered in plant design to ensure adequate clear-water storage for both backwashing and continuous injection. It may be desirable to install additional filter capacity so that filtration will not stop during backwashing. The addition of standby filtration facilities also offers a guarantee against a total shutdown in which a filter requires a complete change of the filter medium.

Refs. 116, 144, 145, 147, 148, and 149 discuss waterflood plant facilities. Also, Ref. 163 discusses waterflood plant facilities for a North Sea waterflood project.

For a more detailed discussion on plant design criteria, design calculations, etc., the reader is directed to Chap. 15, Surface Facilities for Waterflooding and Saltwater Disposal.

Nomenclature

- a = distance between wells in a row, ft
- A = cross-sectional area, sq ft
- B = FVF, RB/STB
- B_o = oil FVF, RB/STB
- B_{oi} = initial oil FVF, RB/STB
- B_{oR} = oil FVF at current reservoir conditions, RB/STB
- C_{ge} = correction for gas expansion
- d = distance between rows of wells, ft
- E_C = fractional coverage or conformance efficiency

- E_K = efficiency of permeability variation, fraction
 E_R = oil recovery efficiency, fraction
 f_{icw} = corner well producing water cut, fraction
 f_{isw} = side well producing water cut, fraction
 f_{o2} = fraction of oil flowing at the producing end of the system
 f_s = fraction of total flow coming from the swept portion of the pattern
 f_w = fractional flow of water
 F_C = Caudle and Witte conductance ratio
 F_F = ratio of viscous to gravity forces
 F_{og} = oil/gas saturation ratio
 F_P = corner-to-side-well producing-rate ratio
 F_{wo} = WOR
 g = acceleration caused by gravity, ft/sec²
 h = formation thickness, ft
 i_b = injection rate of fluid that has same mobility as the reservoir oil in a liquid-filled (base) pattern, as calculated from Eq. 20, RB/D
 i_w = water-injection rate, RB/D
 k_o = effective permeability to oil, md
 k_w = effective permeability to water, md
 k_x = permeability of x layer, or the layer that has just been flooded, md
 \bar{k} = mean permeability, md
 k_o = permeability value at 84.1% of cumulative sample, md
 L = distance, ft
 M = mobility ratio
 M_{wo} = water/oil mobility ratio multiplied by the FVF of the reservoir oil at the time of flooding
 n = number of layers
 n_{BT} = number of layers in which water has broken through (varies from 1 to n)
 N = initial oil in place, STB, or ratio of square root of production rates
 N_p = oil produced, STB
 N_{pu} = recovery to depletion (abandonment), fraction
 p_a = pressure at depletion (abandonment), psi
 p_{bp} = transient backpressure, psi
 p_e = effective reservoir pressure (external boundary pressure), psi
 p_i = initial pressure, psi
 Δp_{ic} = pressure differential between injection well and corner well, psi
 Δp_{is} = pressure differential between injection well and side well, psi
 P_c = capillary pressure, $p_o - p_w$, psi
 q_i = total flow rate ($q_w + q_o$), B/D
 r_e = pressure radius (external boundary radius), ft
 r_i = distance from well to the point of pressure equalization at p_{bp} , ft
 r_w = effective radius of a well, ft
 R_o = outer radius of oil bank, ft
 R_w = outer radius of waterflood front, ft
 S_F = position of center of unflooded area at moment of fill-up (correct drilling location), fraction of length of side or diagonal
 S_g = gas saturation at start of flood, fraction
 S_{gr} = residual gas saturation, fraction
 S_o = oil saturation at start of flood, fraction
 S_{or} = ROS, fraction
 S_w = water saturation, fraction
 S_{w2} = water saturation at the producing end of the system, fraction
 S_{wBT} = average water saturation at water breakthrough, % PV
 S_{wsc} = water saturation at upstream end of stabilized zone, % PV
 t = time, days
 V_d = displaceable PV's injected, fraction
 W_i = cumulative PV's of water injected, fraction
 θ = angle of formation dip referenced to horizontal
 μ_o = oil viscosity, cp
 μ_w = water viscosity, cp
 $\Delta\rho$ = density difference between water and oil, $\rho_w - \rho_o$, g/cm³
 ϕ = porosity

Key Equations in SI Metric Units

$$E_R = 0.2719 \log k + 0.25569 S_w - 0.1355 \log \mu_o - 1.5380 \phi - 0.0011444 h + 0.52478 \dots (14)$$

$$E_R = 93.5399 \left[\frac{\phi(1-S_w)}{B_{oi}} \right]^{0.0422} \left(\frac{k\mu_{wi}}{\mu_{oi}} \right)^{0.077} \times (S_w)^{-0.1903} \left(\frac{p_i}{p_a} \right)^{-0.2159} \dots (15)$$

$$i_w = \frac{5.427 \times 10^{-4} k_w h (p_{iwf} - p_e)}{\mu_w \ln \left(\frac{r_e}{r_w} \right)} \dots (16)$$

$$\frac{3.4542 \times 10^{-4} k \Delta p t}{\mu_w \phi S_g r_w^2} = 1 + \left(\frac{1.0885 \times 10^{-3} k h \Delta p}{\mu_w i_w} - 1 \right) \times 10^{4.7297 \times 10^{-4} k h \Delta p / (\mu_w i_w)} \dots (19)$$

$$i_w = \frac{1.178966 \times 10^{-4} k_w h \Delta p}{\mu_w \left(\log \frac{d}{r_w} - 0.2688 \right)} \quad \dots \dots \dots (20)$$

$$i_w = \frac{1.572211 \times 10^{-4} k_w h \Delta p}{\mu_w \left(\log \frac{d}{r_w} - 0.2472 \right)} \quad \dots \dots \dots (23)$$

$$I = \frac{2.714382 \times 10^{-4} k_w h}{\mu_w \left(\ln \frac{d}{r_w} - 0.6190 \right)} \quad \dots \dots \dots (28)$$

where

B_{oi} is in m^3/m^3 ,
 d, h, r_e, r_w are in m,
 I is in m^3/d ,
 i_w is in m^3/d ,
 k, k_w are in μm^2 ,
 p_{iwf}, p_e are in kPa,
 S_g, S_w are in fraction,
 t is in days,
 μ_o, μ_w are in Pa·s, and
 ϕ is a fraction.

References

- Carll, J.F.: "The Geology of the Oil Regions of Warren, Venango, Clarion and Butler Counties," *Second Geological Survey of Pennsylvania 1875-79* (1880) 268.
- Lewis, J.O.: "Methods of Increasing the Recovery from Oil Sands," *Bull. 148*, U.S. Bureau of Mines (1917) 108-14.
- Torrey, P.D.: "A Review of Secondary Recovery of Oil in the United States," *Secondary Recovery of Oil in the United States*, API, Dallas (1950) 1.
- Craig, F.F. Jr.: "The Reservoir Engineering Aspects of Waterflooding," Monograph Series, SPE, Richardson, TX (1971) 3, 112-23.
- Benner, F.C. and Bartell, F.E.: "The Effect of Polar Impurities Upon Capillary and Surface Phenomena in Petroleum Production," *Drill and Prod. Prac.*, API, Dallas (1941) 341.
- Leverett, M.C. and Lewis, W.B.: "Steady Flow of Gas-oil-water Mixtures Through Unconsolidated Sands," *Trans.*, AIME (1941) **142**, 107-16.
- Pirson, S.J.: *Oil Reservoir Engineering*, second edition, McGraw-Hill Book Co. Inc., New York City (1958) 360.
- Muskat, M. and Botset, H.G.: "Effect of Pressure Reduction upon Core Saturation," *Trans.*, AIME (1939) **132**, 172-83.
- Dickey, P.A.: "Influence of Fluid Saturation on Secondary Recovery of Oil," *Secondary Recovery of Oil in the United States*, second edition, API, Dallas (1950) 17.
- Dean, P.C.: "Case History of Water Flooding in Throckmorton County, Texas," *Oil and Gas J.* (April 12, 1947) 78.
- Land, C.S.: "The Optimum Gas Saturation for Maximum Oil Recovery from Displacement by Water," paper SPE 2216 presented at the 1968 SPE Annual Meeting, Houston, Sept. 29-Oct. 2.
- Craft, B.C. and Hawkins, M.J. Jr.: *Applied Petroleum Reservoir Engineering*, Prentice-Hall Inc., Englewood Cliffs, NJ (1959) **107**, 357, 412-13.
- Rathmell, J.J., Braun, P.H., and Perkins, T.K.: "Reservoir Waterflood Residual Oil Saturation from Laboratory Tests," *J. Pet. Tech.* (Feb. 1973) 175-85; *Trans.*, AIME, **255**.
- Holmgren, C.R. and Morse, R.A.: "Effect of Free Gas Saturation on Oil Recovery by Waterflooding," *Trans.*, AIME (1951) **192**, 135-40.
- Dykstra, H. and Parsons, R.L.: "The Prediction of Oil Recovery by Waterflood," *Secondary Recovery of Oil in the United States*, API, Dallas (1950) 160-74.
- Dyes, A.B.: "Production of Water-Driven Reservoirs Below Their Bubble Point," *J. Pet. Tech.* (Oct. 1954) 31-35; *Trans.*, AIME, **201**.
- Kyte, J.R. et al.: "Mechanism of Waterflooding in the Presence of Free Gas," *J. Pet. Tech.* (Sept. 1956) 215-21; *Trans.*, AIME, **207**.
- Bobek, J.E., Mattax, C.C., and Denekas, M.O.: "Reservoir Rock Wettability—Its Significance and Evaluation," *J. Pet. Tech.* (July 1958) 155-60; *Trans.*, AIME, **213**.
- Stiles, W.E.: "Use of Permeability Distribution in Water-flood Calculations," *Trans.*, AIME (1949) **186**, 9-13.
- Buckley, S.E. and Leverett, M.C.: "Mechanism of Fluid Displacement in Sands," *Trans.*, AIME (1942) **146**, 107-16.
- Welge, H.J.: "A Simplified Method for Computing Oil Recoveries by Gas or Water Drive," *Trans.*, AIME (1952) **195**, 91-98.
- Johnson, C.E. Jr.: "Prediction of Oil Recovery by Waterflood—A Simplified Graphical Treatment of the Dykstra-Parsons Method," *J. Pet. Tech.* (Nov. 1956) 55-56; *Trans.*, AIME, **207**.
- Leverett, M.C.: "Capillary Behavior in Porous Solids," *Trans.*, AIME (1941) **142**, 152-69.
- Muskat, M.: *Physical Principles of Oil Production*, McGraw-Hill Book Co. Inc., New York City (1949).
- Kimbler, O.K., Caudle, B.H., and Cooper, H.E. Jr.: "Areal Sweepout Behavior in a Nine-Spot Injection Pattern," *J. Pet. Tech.* (Feb. 1964) 199-202; *Trans.*, AIME, **231**.
- McCarty, D.G. and Barfield, E.C.: "The Use of High-Speed Computers for Predicting Flood-Out Patterns," *Trans.*, AIME (1958) **213**, 139-45.
- Henley, D.H.: "Method for Studying Waterflooding Using Analog, Digital, and Rock Models," paper presented at the 1953 Technical Conference on Petroleum, Pennsylvania State U., University Park, Oct. 1953.
- Muskat, M. and Wyckoff, R.C.: "A Theoretical Analysis of Water-flooding Networks," *Trans.*, AIME (1934) **107**, 62-76.
- Wyckoff, R.D., Botset, H.G., and Muskat, M.: "The Mechanics of Porous Flow Applied to Water-flooding Problems," *Trans.*, AIME (1933) **103**, 219-49.
- Botset, H.G.: "The Electrolytic Model and Its Application to the Study of Recovery Problems," *Trans.*, AIME (1946) **165**, 15-25.
- Swearingen, J.W.: "Predicting Wet-Gas Recovery in Recycling Operations," *Oil Weekly* (1939) **96**.
- Hurst, W. and McCarty, G.M.: "The Applications of Electrical Models to the Study of Recycling Operations," *Drill and Prod. Prac.*, API, Dallas (1941).
- Lee, B.D.: "Potentiometric-model Studies of Fluid Flow in Petroleum Reservoirs," *Trans.*, AIME (1948) **174**, 41-66.
- Slobod, R.L. and Caudle, B.H.: "X-Ray Shadowgraph Studies of Areal Sweepout Efficiencies," *Trans.*, AIME (1952) **195**, 265-70.
- Stahl, C.D.: "Coverage of Flood Patterns," *Prod. Monthly* (May 1957).
- Burton, M.B. and Crawford, P.B.: "Application of the Gelatin Model for Studying Mobility Ratio Effects," *J. Pet. Tech.* (Oct. 1956) 63-67; *Trans.*, AIME, **207**.
- Aronofsky, J.S.: "Mobility Ratio—Its Influence on Flood Patterns during Water Encroachment," *Trans.*, AIME (1952) **195**, 15-24.
- Nobles, M.A. and Janzen, H.B.: "Application of a Resistance Network for Studying Mobility Ratio Effects," *J. Pet. Tech.* (Feb. 1958) 60-62; *Trans.*, AIME, **213**.
- Caudle, B.H., Erickson, R.A., and Slobod, R.L.: "The Encroachment of Injected Fluids Beyond the Normal Well Pattern," *J. Pet. Tech.* (May 1955) 79-85; *Trans.*, AIME, **204**.
- Dyes, A.B., Caudle, B.H., and Erickson, R.A.: "Oil Production after Breakthrough as Influenced by Mobility Ratio," *J. Pet. Tech.* (April 1954) 27-32; *Trans.*, AIME, **201**, 81-86.
- Check, R.E. and Menzie, D.E.: "Fluid Mapper Model Studies of Mobility Ratio," *Trans.*, AIME (1955) **204**, 278-81.
- Prats, M.: "The Breakthrough Sweep Efficiency of the Staggered Line Drive," *J. Pet. Tech.* (Dec. 1956) 67-68; *Trans.*, AIME, **207**.
- Fay, C.H. and Prats, M.: "The Application of Numerical Methods to Cycling and Flooding Problems," *Proc.*, Third World Pet. Cong. (1951) **2**, 555-63.
- Hurst, W.: "Determination of Performance Curves in Five-Spot Waterflood," *Pet. Eng.* (1953) **25**, B40-46.

45. Craig, F.F., Geffen, T.M., and Morse, R.A.: "Oil Recovery Performance of Pattern Gas or Water Injection Operations From Model Tests," *J. Pet. Tech.* (Jan. 1955) 7-15; *Trans.*, AIME, **204**.
46. Habermann, B.: "The Efficiency of Miscible Displacement As A Function of Mobility Ratio," *J. Pet. Tech.* (Nov. 1960) 264-72; *Trans.*, AIME, **219**.
47. Bradley, H.B., Heller, J.P., and Odeh, A.S.: "A Potentiometric Study of the Effects of Mobility Ratio on Reservoir Flow Patterns," *Soc. Pet. Eng. J.* (Sept. 1961) 125-29; *Trans.*, AIME, **222**.
48. Paulsell, B.L.: "Areal Sweep Performance of Five-Spot Pilot Floods," MS thesis, Pennsylvania State U., University Park (Jan. 1958).
49. Moss, J.T., White, P.E., and McNiel, J.S.: "In-Situ Combustion Process—Result of a Five-Well Field Experiment in Southern Oklahoma," *J. Pet. Tech.* (April 1959) 55-64; *Trans.*, AIME, **216**.
50. Caudle, B.H. and Loncaric, I.G.: "Oil Recovery in Five-Spot Pilot Floods," *J. Pet. Tech.* (June 1960) 132-36; *Trans.*, AIME, **219**.
51. Neilson, I.D.R. and Flock, D.L.: "The Effect of a Free Gas Saturation on the Sweep Efficiency of an Isolated Five-Spot," *Bull.* 55, CIM (1962) 124-29.
52. Guckert, L.G.: "Areal Sweepout Performance of Seven and Nine-Spot Flood Patterns," MS thesis, Pennsylvania State U., University Park (Jan. 1961).
53. Krutter, H.: "Nine-Spot Flooding Program," *Oil and Gas J.* (Aug. 17, 1939) **38**, No. 14, 50.
54. Watson, R.E., Silberberg, I.H., and Caudle, B.H.: "Model Studies of Inverted Nine-Spot Injection Pattern," *J. Pet. Tech.* (July 1974) 801-04.
55. Aronofsky, J.S. and Ramey, H.J. Jr.: "Mobility Ratio—Its Influence on Injection or Production Histories in Five-Spot Waterflood," *J. Pet. Tech.* (Sept. 1956) 205-10; *Trans.*, AIME, **207**.
56. Martin, J.C. and Wegner, R.E.: "Numerical Solution of Multiphase, Two-Dimensional Incompressible Flow Using Stream-Tube Relationships," *Soc. Pet. Eng. J.* (Oct. 1979) 313-23.
57. Matthews, C.S. and Fischer, M.J.: "Effect of Dip on Five-Spot Sweep Patterns," *J. Pet. Tech.* (May 1956) 111-17; *Trans.*, AIME, **207**.
58. Prats, M., Strickler, W.R., and Matthews, C.S.: "Single-Fluid Five-Spot Floods in Dipping Reservoirs," *J. Pet. Tech.* (Oct. 1955) 160-67; *Trans.*, AIME, **204**.
59. Van der Poel, C. and Killian, J.W.: "Attic Oil," paper SPE 919-G presented at the 1957 SPE Annual Meeting, Dallas, Oct. 6-9.
60. Hutchinson, C.A. Jr.: "Reservoir Inhomogeneity Assessment and Control," *Pet. Eng.* (Sept. 1959) B19-26.
61. Landrum, B.L. and Crawford, P.B.: "Effect of Directional Permeability on Sweep Efficiency and Production Capacity," *J. Pet. Tech.* (Nov. 1960) 67-71; *Trans.*, AIME, **219**.
62. Mortada, M. and Nabor, G.W.: "An Approximate Method for Determining Areal Sweep Efficiency and Flow Capacity in Formations with Anisotropic Permeability," *Soc. Pet. Eng. J.* (Dec. 1961) 277-86; *Trans.*, AIME, **222**.
63. Dyes, A.B., Kemp, C.E., and Caudle, B.H.: "Effect of Fractures on Sweep-Out Patterns," *J. Pet. Tech.* (Oct. 1958) 245-49; *Trans.*, AIME, **213**.
64. Crawford, P.B. and Collins, R.E.: "Estimated Effect of Vertical Fractures on Secondary Recovery," *J. Pet. Tech.* (Aug. 1954) 41-45; *Trans.*, AIME, **201**.
65. Simmons, J. et al.: "Swept Areas After Breakthrough in Vertically Fractured Five-Spot Patterns," *Trans.*, AIME (1959) **216**, 73-77.
66. Crawford, P.B. et al.: "Sweep Efficiencies of Vertically Fractured Five-Spot Patterns," *Pet. Eng.* (March 1956) **28**, B95-102.
67. Hartsock, J.H. and Slobod, R.L.: "The Effect of Mobility Ratio and Vertical Fractures on the Sweep Efficiency of a Five-Spot," *Prod. Monthly* (Sept. 1961) **26**, No. 9, 2-7.
68. Landrum, B.L. and Crawford, P.B.: "Estimated Effect of Horizontal Fractures in Thick Reservoirs on Pattern Conductivity," *J. Pet. Tech.* (Oct. 1957) 50-52; *Trans.*, AIME, **210**.
69. Crawford, P.B. and Collins, R.E.: "Analysis of Flooding Horizontally Fractured Thin Reservoirs," *World Oil* (1954: Aug.-139, Sept.-173, Oct.-214, Nov.-212, Dec.-197).
70. Pinson, J. et al.: "Effect of Large Elliptical Fractures on Sweep Efficiencies in Water Flooding or Fluid Injection Programs," *Prod. Monthly* (Nov. 1963) **28**, No. 11, 20-22.
71. Schmalz, J.P. and Rahme, H.D.: "The Variation of Waterflood Performance with Variation in Permeability Profile," *Prod. Monthly* (Sept. 1950) **15**, No. 9, 9-12.
72. Arps, J.J.: "Estimation of Primary Oil Reserves," *J. Pet. Tech.* (Aug. 1956) 182-91; *Trans.*, AIME, **207**.
73. Ache, P.S.: "Inclusion of Radial Flow in Use of Permeability Distribution in Waterflood Calculations," paper SPE 935-G presented at the 1957 SPE Annual Meeting, Dallas, Oct. 6-9.
74. Slider, H.C.: "New Method Simplifies Predicting Waterflood Performance," *Pet. Eng.* (Feb. 1961) **33**, B68-78.
75. Johnson, J.P.: "Predicting Waterflood Performance by the Graphical Representation of Porosity and Permeability Distribution," *J. Pet. Tech.* (Nov. 1965) 1285-90.
76. Felsenthal, M., Cobb, T.R., and Heuer, G.J.: "A Comparison of Waterflood Evaluation Methods," paper SPE 332 presented at the 1962 SPE Fifth Biennial Secondary Recovery Symposium, Wichita Falls, TX, May 7-8.
77. Yuster, S.T. and Calhoun, J.C. Jr.: "Behavior of Water Injection Wells," *Oil Weekly* (Dec. 18 and 25, 1944) 44-47.
78. Suder, F.E. and Calhoun, J.C. Jr.: "Waterflood Calculations," *Drill. and Prod. Prac.*, API, Dallas (1949) 260-70.
79. Muskat, M.: "The Effect of Permeability Stratification in Complete Water-Drive Systems," *Trans.*, AIME (1950) **189**, 349-58.
80. Prats, M. et al.: "Prediction of Injection Rate and Production History for Multifluid Five-Spot Floods," *J. Pet. Tech.* (May 1959) 98-105; *Trans.*, AIME, **216**.
81. Muskat, M.: *Flow of Homogeneous Fluids Through Porous Systems*, J.W. Edwards Inc., Ann Arbor, MI (1946).
82. Caudle, B.H. and Witte, M.D.: "Production Potential Changes During Sweepout in a Five-Spot System," *J. Pet. Tech.* (Dec. 1959) 63-65; *Trans.*, AIME, **216**.
83. Caudle, B.H., Hickman, B.M., and Silberberg, I.H.: "Performance of the Skewed Four-Spot Injection Pattern," *J. Pet. Tech.* (Nov. 1968) 1315-19; *Trans.*, AIME, **243**.
84. Deppe, J.C.: "Injection Rates—The Effect of Mobility Ratio, Area Swept and Pattern," *Soc. Pet. Eng. J.* (June 1961) 81-91; *Trans.*, AIME, **222**.
85. Hauber, W.C.: "Prediction of Waterflood Performance for Arbitrary Well Patterns and Mobility Ratios," *J. Pet. Tech.* (Jan. 1964) 95-103; *Trans.*, AIME, **231**.
86. Felsenthal, M. and Yuster, S.T.: "A Study of the Effect of Viscosity On Oil Recovery by Waterflooding," paper SPE 163-G presented at the 1951 SPE West Coast Meeting, Los Angeles, Oct. 25-26.
87. Roberts, T.G.: "A Permeability Block Method of Calculating a Water Drive Recovery Factor," *Pet. Eng.* (1959) **31**, B45-48.
88. Kufus, H.B. and Lynch, E.J.: "Linear Frontal Displacement in Multilayer Sands," *Prod. Monthly* (Dec. 1959) **24**, No. 12, 32-35.
89. Snyder, R.W. and Ramey, H.J. Jr.: "Application of Buckley-Leverett Displacement Theory to Noncommunicating Layered Systems," *J. Pet. Tech.* (Nov. 1967) 1500-06; *Trans.*, AIME, **240**.
90. Hendrickson, G.E.: "History of the Welch Field San Andres Pilot Waterflood," *J. Pet. Tech.* (Aug. 1961) 745-49.
91. Wasson, J.A. and Schrider, L.A.: "Combination Method for Predicting Waterflood Performance for Five-Spot Patterns in Stratified Reservoirs," *J. Pet. Tech.* (Oct. 1968) 1195-1202; *Trans.*, AIME, **243**.
92. Rapoport, L.A., Carpenter, C.W., and Leas, W.J.: "Laboratory Studies of Five-Spot Waterflood Performance," *Trans.*, AIME (1958) **213**, 113-20.
93. Higgins, R.V. and Leighton, A.J.: "A Computer Method to Calculate Two-Phase Flow in Any Irregularly Bounded Porous Medium," *J. Pet. Tech.* (June 1962) 679-83; *Trans.*, AIME, **225**.
94. Higgins, R.V. and Leighton, A.J.: "Computer Prediction of Water Drive of Oil and Gas Mixtures Through Irregularly Bounded Porous Media—Three-Phase Flow," *J. Pet. Tech.* (Sept. 1962) 1048-54; *Trans.*, AIME, **225**.
95. Higgins, R.V. and Leighton, A.J.: "Waterflood Prediction of Partially Depleted Reservoirs," paper SPE 757 presented at the 1963 SPE California Regional Meeting, Santa Barbara, Oct. 24-25.
96. Higgins, R.V., Boley, D.W., and Leighton, A.J.: "Aids to Forecasting the Performance of Waterfloods," *J. Pet. Tech.* (Sept. 1964) 1076-82; *Trans.*, AIME, **231**.
97. Higgins, R.V. and Leighton, A.J.: "Computer Techniques for Predicting Three-Phase Flow in Five-Spot Waterfloods," RI 7011, U.S. Bureau of Mines (Aug. 1967).
98. Douglas, J. Jr., Blair, P.M., and Wagner, R.J.: "Calculation of Linear Waterflood Behavior Including the Effects of Capillary Pressure," *Trans.*, AIME (1958) **213**, 96-102.

99. Hiatt, W.N.: "Injected-Fluid Coverage of Multi-Well Reservoirs With Permeability Stratification," *Drill. and Prod. Prac.*, API, Dallas (1958) 165-94.
100. Douglas, J. Jr., Peaceman, D.W., and Rachford, H.H. Jr.: "A Method for Calculating Multi-Dimensional Immiscible Displacement," *Trans.*, AIME (1959) 216, 297-306.
101. Warren, J.E. and Cosgrove, J.J.: "Prediction of Waterflood Behavior in a Stratified System," *Soc. Pet. Eng. J.* (June 1964) 149-57; *Trans.*, AIME, 231.
102. Morel-Seytoux, H.J.: "Analytical-Numerical Method in Waterflooding Predictions," *Soc. Pet. Eng. J.* (Sept. 1965) 247-58; *Trans.*, AIME, 234.
103. Morel-Seytoux, H.J.: "Unit Mobility Ratio Displacement Calculations for Pattern Floods in Homogeneous Medium," *Soc. Pet. Eng. J.* (Sept. 1966) 217-27; *Trans.*, AIME, 237.
104. Guthrie, R.K. and Greenberger, M.H.: "The Use of Multiple-Correlation Analyses for Interpreting Petroleum Engineering Data," *Drill. and Prod. Prac.*, API, Dallas (1955) 130-37.
105. Schauer, P.E.: "Application of Empirical Data in Forecasting Waterflood Behavior," paper SPE 934-G presented at the 1957 SPE Annual Fall Meeting, Dallas, Oct. 6-9.
106. Guerrero, E.T. and Earlougher, R.C.: "Analysis and Comparison of Five Methods Used to Predict Waterflooding Reserves and Performance," *Drill. and Prod. Prac.*, API, Dallas (1961) 78-95.
107. Arps, J.J. et al.: "A Statistical Study of Recovery Efficiency," *Bull. 14D*, API, Dallas (1967).
108. Timmerman, E.H.: *Practical Reservoir Engineering—Part II*, PennWell Publishing Co., Tulsa (1982) 170-90.
109. Abernathy, B.F.: "Waterflood Prediction Methods Compared to Pilot Performance in Carbonate Reservoirs," *J. Pet. Tech.* (March 1964) 276-82.
110. Dickey, P.A. and Andresen, K.H.: "The Behavior of Water-Input Wells," *Secondary Recovery of Oil in The United States*, API, Dallas (1950) 30.
111. Nowak, T.J. and Lester, G.W.: "Analysis of Pressure Fall-off Curves Obtained in Water Injection Wells to Determine Injective Capacity and Formation Damage," *J. Pet. Tech.* (June 1955) 96-102; *Trans.*, AIME, 204.
112. Hazebroek, P., Rainbow, H., and Matthews, C.S.: "Pressure Fall-off in Water Injection Wells," *Trans.*, AIME (1958) 213, 250-60.
113. Ruble, D.B.: "Case Study of a Multiple Sand Waterflood, Hewitt Unit, OK," *J. Pet. Tech.* (March 1982) 621-27.
114. Langston, E.P., Shirer, J.A., and Nelson, D.E.: "Innovative Reservoir Management—Key to Highly Successful Jay/LEC Waterflood," *J. Pet. Tech.* (May 1981) 783-91.
115. Jordan, C.A., Edmondson, T.A., and Jeffries-Harris, M.J.: "The Bay Marchand Pressure Maintenance Project—Unique Challenges of an Offshore Sea-Water Injection System," *J. Pet. Tech.* (April 1969) 389-96.
116. McCune, C.: "Seawater Injection Experience—An Overview," *J. Pet. Tech.* (Oct. 1982) 2265-70.
117. Bernard, W.J. and Caudle, B.H.: "Model Studies of Pilot Waterfloods," *J. Pet. Tech.* (March 1967) 404-10; *Trans.*, AIME, 240.
118. Craig, F.F. Jr.: "Laboratory Model Study of Single Five-Spot and Single Injection-Well Pilot Waterflooding," *J. Pet. Tech.* (Dec. 1965) 1454-60; *Trans.*, AIME, 234.
119. Sandiford, B.B.: "Laboratory and Field Studies of Water Floods Using Polymer Solutions to Increase Oil Recoveries," *J. Pet. Tech.* (Aug. 1964) 917-22; *Trans.*, AIME, 231.
120. Krebs, H.J.: "Wilmington Field California Polymer Flood—A Case History," *J. Pet. Tech.* (Dec. 1976) 1473-80.
121. Groeneveld, H., Melrose, J.C., and George, R.A.: "Pembina Field Polymer Pilot Flood," *J. Pet. Tech.* (May 1977) 561-70.
122. "Polymer Flood Shows Promise as Recovery Tool," *Oil and Gas J.* (July 4, 1966) 56.
123. Sloat, B.: "Polymer Treatment Boosts Production on Four Floods," *World Oil* (March 1969) 44-47.
124. Sloat, B.: "Polymer Treatment Should Be Started Early," *Pet. Eng.* (July 1970) 64-72.
125. Taber, J.J.: "The Injection of Detergent Slugs in Water Floods," *Trans.*, AIME (1958) 213, 186-92.
126. Dunning, H.N. and Hsiao, L.: "Laboratory Experiments with Detergents as Water-Flooding Additives," *Prod. Monthly* (Nov. 1953) 591-96.
127. Johansen, R.T., Dunning, H.N., and Beaty, J.W.: "Petroleum Displacement by Detergent Solutions," *Prod. Monthly* (Feb. 1959) 26-34.
128. Inks, C.G. and Lahring, R.I.: "Controlled Evaluation of a Surfactant in Secondary Recovery," *J. Pet. Tech.* (Nov. 1968) 1320-24; *Trans.*, AIME, 243.
129. Squires, F.: "Method of Recovering Oil and Gas," U.S. Patent No. 1,238,355 (Aug. 28, 1917).
130. Atkinson, H.: "Recovery of Petroleum From Oil Bearing Sands," U.S. Patent No. 1,651,311 (Nov. 29, 1927).
131. Wagner, O.R. and Leach, R.O.: "Improving Oil Displacement by Wettability Adjustment," *J. Pet. Tech.* (April 1959) 65-72; *Trans.*, AIME, 216.
132. Leach, R.O. et al.: "A Laboratory and Field Study of Wettability Adjustment in Water Flooding," *J. Pet. Tech.* (Feb. 1962) 206-12; *Trans.*, AIME, 225.
133. Mungan, N.: "Certain Wettability Effects In Laboratory Waterfloods," *J. Pet. Tech.* (Feb. 1966) 247-52; *Trans.*, AIME, 237.
134. Cooke, C.E. Jr., Williams, R.E., and Kolodzie, P.A.: "Oil Recovery by Alkaline Waterflooding," *J. Pet. Tech.* (Dec. 1974) 1365-74.
135. Ehrlich, R.: "Wettability Alteration During Displacement of Oil by Water from Petroleum Reservoir Rock," paper presented at the 1974 Natl. Colloid Symposium, Austin, June 24.
136. Cooper, R.J.: "The Effect of Temperature on Caustic Displacement of Crude Oil," paper SPE 3685 presented at the 1971 SPE California Regional Meeting, Los Angeles, Nov. 4-5.
137. Nutting, P.G.: "Chemical Problems in the Water Driving of Petroleum in Oil Sands," *Ind. and Eng. Chem.* (Oct. 1925) 17, 1035-36.
138. Emery, L.W., Mungan, N., and Nicholson, R.W.: "Caustic Slug Injection in the Singleton Field," *J. Pet. Tech.* (Dec. 1970) 1569-76.
139. Graue, D.J. and Johnson, C.E. Jr.: "A Field Trial of the Caustic Flooding Process," *J. Pet. Tech.* (Dec. 1974) 1353-58.
140. Kornfeld, J.A.: "Illinois' Largest Waterflood Recovers Two Million Barrels in 25 Months," *Waterflooding*, technical manual reprinted from *Oil and Gas J.*, Petroleum Publishing Co., Tulsa (Aug. 4, 1952) 68-71, 91-92.
141. Enright, R.J.: "Giant Salem Flood in Full Swing," *Waterflooding*, technical manual reprinted from *Oil and Gas J.*, Petroleum Publishing Co., Tulsa (Dec. 7, 1953) 71-73.
142. Barnes, K.B.: "Community Water Pipeline Serves Four Producing Areas," *Waterflooding*, technical manual reprinted from *Oil and Gas J.*, Petroleum Publishing Co., Tulsa (Oct. 13, 1952) 189-91.
143. Walters, J.D.: "Prolific Waterflood in East Kansas," *Waterflooding*, technical manual reprinted from *Oil and Gas J.*, Petroleum Publishing Co., Tulsa (May 4, 1953) 96-97, 100.
144. Wheeler, D.: "Treating and Monitoring 450,000 B/D Injection Water," *Pet. Eng.* (Nov. 1975) 68-80.
145. Gates, G.L. and Parent, C.F.: "Water-Quality Control Presents Challenge in Giant Wilmington Field," *Oil and Gas J.* (Aug. 16, 1976) 115-26.
146. Stiles, W.E.: "Olympic Pool Waterflood," *Waterflooding*, Reprint Series, SPE, Richardson, TX (1973) 2a, 44-50.
147. Morrison, J.B. and Jorque, M.A.: "How the World's Largest Injection System was Designed," *Pet. Eng.* (July 1981) 122-34.
148. Brown, J.N., Dubrevil, L.R., and Schneider, R.D.: "Seawater Project in Saudi Arabia—Early Experience of Plant Operation, Water Quality, and Effect on Injection Well Performance," *J. Pet. Tech.* (Oct. 1980) 1709-10.
149. El-Hattab, M.I.: "GUPCO's Experience in Treating Gulf of Suez Seawater for Waterflooding the El Morgan Oil Field," *J. Pet. Tech.* (July 1982) 1449-60.
150. "Analysis of Oil Field Waters," second edition, API RP 45 (Nov. 1968), reissued July 1981.
151. "Biological Analysis of Subsurface Injection Waters," third edition, API RP 38 (Dec. 1975), reissued March 1982.
152. "Methods for Determining Water Quality for Subsurface Injection Using Membrane Filters," Natl. Assn. of Corrosion Engineers Standard TM-01-73 (Feb. 1973).
153. Ellenberger, A.R. and Holbren, J.H.: "Flood Water Analyses and Interpretations," *J. Pet. Tech.* (June 1959) 22-25.
154. Clayton, J.M., Ellenberger, A.R., and Sloat, B.: "Water Treatment in Water Flooding," *Prod. Monthly* (April 1957) 38-42.
155. Bell, W.E. and Shaw, J.K.: "Evaluation of Iron Sequestering Agents in Water Flooding," *Prod. Monthly* (March 1958) 20-23.
156. Watkins, T.W.: "New Trends in Treating Waters for Injection," *World Oil* (Jan. 1958) 143-50.
157. Hockaday, D. et al.: "Experts Answer Questions on Waterflooding," *World Oil* (Sept. 1958) 106-08.

158. Torrey, P.D.: "Preparation of Water for Injection into Oil Reservoirs," *Waterflooding*, Reprint Series, SPE, Richardson, TX (1959) 2, 22-29.
159. Bilhartz, H.L.: "Are We Making Water Systems Too Complex?" *Waterflooding*, Reprint Series, SPE, Richardson, TX (1959) 2, 33-36.
160. Patton, C.C.: "Oilfield Water Systems," Campbell Petroleum Series (1977).
161. Ostroff, A.G.: "Introduction to Oilfield Water Technology," second edition, Natl. Assn. of Corrosion Engineers (1979).
162. Mitchell, R.W. and Finch, E.M.: "Water Quality Aspects of North Sea Injection Water," *J. Pet. Tech.* (June 1981) 1141-52.
163. Vetter, O.J., Kandarpa, V., and Harouaka, A.: "Prediction of Scale Problems Due to Injection of Incompatible Waters," *J. Pet. Tech.* (Feb. 1982) 273-84.
164. Shen, J. and Crosby, C.C.: "Insight Into Strontium and Calcium Sulfate Scaling Mechanisms in a Wet Producer," *J. Pet. Tech.* (July 1983) 1249-55.
165. Ghauri, W.K.: "Production Technology Experience in a Large Carbonate Waterflood, Denver Unit, Wason San Andres Field," *J. Pet. Tech.* (Sept. 1980) 1493-1502.

General References

- Callaway, F.H.: "Evaluation of Waterflood Prospects," *J. Pet. Tech.* (Oct. 1959) 11-16.
- Dalton, R.L. Jr., Rapoport, L.A., and Carpenter, C.W.: "Laboratory Studies of Pilot Waterfloods," *J. Pet. Tech.* (Feb. 1960) 24-30; *Trans.*, AIME, 219.
- Jordan, J.K.: "Reliable Interpretation of Waterflood Production Data," *J. Pet. Tech.* (Aug. 1958) 18-24.
- Justen, J.J. and Hoenmans, P.J.: "Pembina Pilot Waterflood Proving Successful," *J. Pet. Tech.* (June 1958) 21-23.
- Rosenbaum, M.J.F. and Matthews, C.S.: "Studies on Pilot Waterflooding," *J. Pet. Tech.* (Nov. 1959) 316-23; *Trans.*, AIME, 216.
- Wright, F.F.: "Field Results Indicate Significant Advances in Water Flooding: Effect of Rates on Performance in Browning Unit Water Flood," *J. Pet. Tech.* (Oct. 1958) 12-14.

Chapter 45

Miscible Displacement

LeRoy W. Holm, Union Oil Co. of California*

Introduction

Through research efforts and pilot testing over the past 25 years, miscible-phase-displacement processes have been developed as a successful means of obtaining greater oil recovery in many reservoirs. To understand these processes, it is first necessary to provide a definition of miscibility, particularly as distinguished from solubility. "Solubility" is the ability of one substance (fluid) to mix with a fluid or fluids and form a single homogeneous phase. "Miscibility" is the ability of two or more fluid substances (gases or liquids) to form a single homogeneous phase when mixed in all proportions.

For petroleum reservoirs, miscibility is defined as that physical condition between two or more fluids that permits them to mix in all proportions without the existence of an interface. If two fluid phases form after some proportion of one fluid is added, the fluids are considered immiscible. Figs. 45.1, 45.2, and 45.3 illustrate the difference in immiscible and miscible relations between certain fluids.¹

Low-molecular-weight (MW) hydrocarbons such as ethane, propane, butane, or mixtures of liquefiable petroleum gas (LPG) are the injected fluids (solvents) that have been used for *first-contact miscible* flooding. These solvents in any amount will form a single phase with the oil in the reservoir, so are miscible upon first contact with the oil. Heavier hydrocarbons such as C_5 to C_{12} also are miscible with reservoir oils but have not been used as injectants because of their higher costs. However, since solvents like ethane and LPG are abundant in most reservoir oil, they can promote miscible displacement when nonoil-miscible fluids such as methane, natural gas, CO_2 , flue gas, or nitrogen are injected to vaporize or extract C_2 to C_{12} in situ from the

oil. This mechanism of in-situ transfer of light hydrocarbons from the reservoir oil to the injected fluid that forms a mixture miscible with reservoir oil is known as *dynamic miscibility* or *multiple-contact miscibility*.

There are, as a result of extensive research and development efforts by the petroleum industry and various universities (much of which was funded by the U.S. DOE during 1973–81), several forms of miscible displacement operations currently in use or under consideration. The processes include (1) miscible-slug drive for first-contact miscibility, (2) condensing-gas drive for dynamic miscibility, (3) vaporizing-gas drive for dynamic miscibility, and (4) extracting-liquid or critical-fluid drive for dynamic miscibility. A brief discussion of the theoretical aspects and limiting factors of each of these types of miscible displacement, in addition to an outline of engineering study basic requirements, are presented on the following pages. Engineering examples are presented in the Appendix in conjunction with a discussion of alternative procedures.

Theoretical Aspects of Miscible-Phase Displacement

Miscible-Slug Process

The simplest type of miscible drive is the "liquid slug" process.²⁻⁴ In this type of miscible drive, a slug of material such as propane or LPG (liquefied petroleum gases C_2 to C_4) is injected into the reservoir and followed by a dry gas.* The slug miscibly displaces oil from the contacted portion of the reservoir by virtue of a

*Originally, in 1962 edition, this chapter was a part of Chap. 40, Gas-Injection Pressure Maintenance and Miscible-Phase Displacement in Oil Reservoirs, written by James L. Moore and Richard F. Hinds.

*Other naphthohydrocarbon fluids, such as certain alcohols, can be miscible with reservoir oil.⁵ However, these alcohols tend to promote miscible displacement between oil and in-situ water so that complex phase and mobility relationships occur. Prohibitively large volumes of these alcohols are required to maintain a miscible displacement in the reservoir. As injected, soluble oils or oil external microemulsions also are miscible with the reservoir oil.^{6,7} Since complex phase relationships also occur between these fluids and both the oil and water in the reservoir, and because other chemicals are used in conjunction with them, discussion of this displacement process is found in Chap. 47—Chemical Flooding.

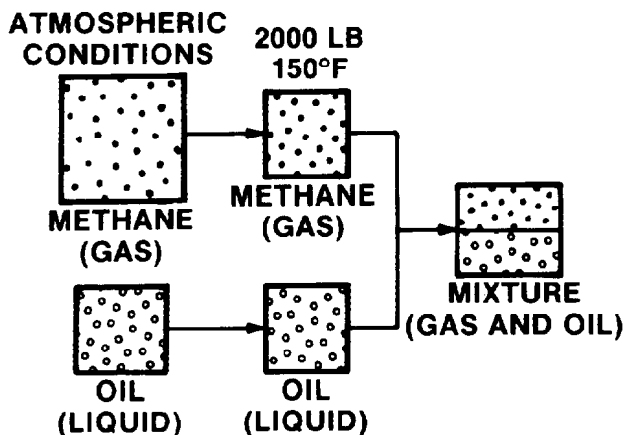


Fig. 45.1—Immiscibility of methane (gas) and oil (liquid) at reservoir conditions of temperature and pressure.

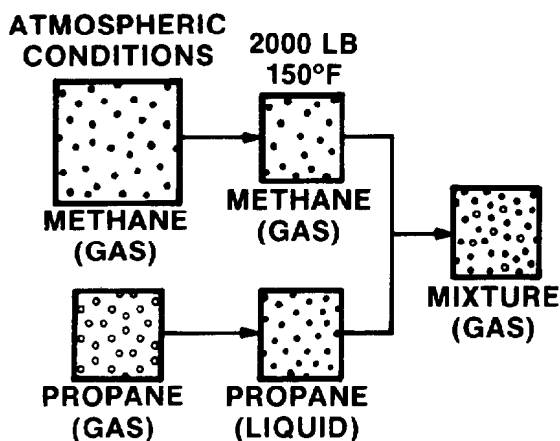


Fig. 45.2—Miscibility of methane (gas) and propane (or LPG) liquid at reservoir conditions of temperature and pressure. Here propane (or LPG) is a gas in presence of gas.

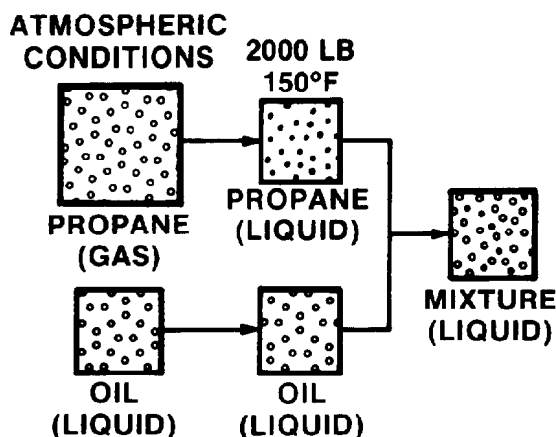


Fig. 45.3—Miscibility of propane (or LPG) liquid and oil liquid at reservoir conditions of temperature and pressure. Here propane (or LPG) is a liquid in the presence of a liquid.

solvent cleaning action. For the purposes of discussion, LPG will be used to denote the slug material. In practice, LPG solvents that are first-contact miscible with reservoir fluids are too expensive to inject continuously. Instead, the solvent is injected in a limited volume, or slug, that is small relative to the reservoir PV, and the slug, in turn, is miscibly displaced with a less expensive fluid such as methane, natural gas, or flue gas. Ideally with such a process scheme, solvent miscibly displaces reservoir oil while drive gas miscibly displaces the solvent, propelling the small solvent slug through the reservoir.

Pressure and Composition Requirements. The basic requirement for miscible displacement by the slug process is that the solvent slug be miscible with both the reservoir oil and the drive gas, which is mostly methane. Miscibility between the LPG slug and the displacing gas requires a certain minimum pressure,⁸ which can be estimated from published data on the cricondenbars of mixtures of pure components (Fig. 45.4). For example, this pressure may be as low as 1,100 psia at the reservoir temperature of 150°F.⁹ It is important to note that for temperatures between the critical temperature of LPG and methane, the critical pressure (miscible pressure) is usually much higher than the critical pressure of either fluid. Where additional data are required, these values should be determined in the laboratory.

Equilibrium phase diagrams, previously discussed in Chap. 20, are convenient representations of the ranges of temperature, pressure, and composition within which combinations of phases coexist.

Fig. 45.5 is a triangular phase diagram that illustrates the phase behavior requirement for first-contact miscibility.¹⁰ For the pressure and temperature at which this pseudoternary diagram was determined, all mixtures of LPG (C_2 to C_4) and oil (C_{5+}) lie entirely within the single-phase region. As indicated on the diagram, an LPG slug could be diluted with methane to Composition A and the resulting mixtures would remain first-contact miscible with Reservoir Oil B. Composition A is the intersection of the right side of the triangle (methane/LPG compositions) and the tangent to the phase boundary curve that passes through the oil composition.

As the concentration of methane in the injection fluid increases, the pressure (cricondenbar) increases and ultimately becomes impractically high for first-contact miscibility. When this happens, dynamic miscibility can be achieved by the condensing- or vaporizing-gas drive mechanisms.

Condensing-Gas Drive (or Enriched-Gas Drive)

A condensing-gas drive is that process of oil displacement by gas that makes use of an injected gas containing low-MW hydrocarbon (C_2 to C_6) components, which condense in the oil being displaced. To effect conditions of miscible displacement, sufficient quantities of low-MW components must be condensed into the oil to generate a critical mixture at the displacing front.

This process was brought to the attention of the industry in the late 1950's by laboratory investigations,^{11,12} which showed that the use of condensing gas drives would result in increased oil recovery from many reservoirs during either primary or secondary phases of

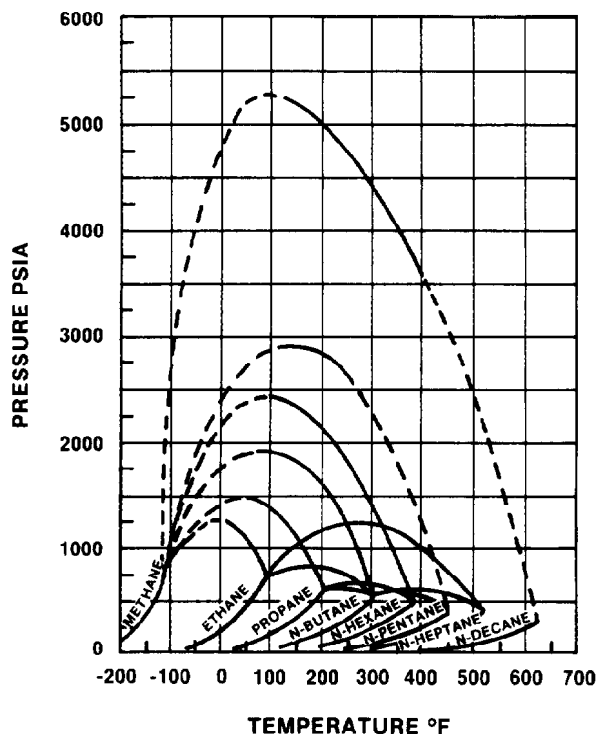


Fig. 45.4—Critical loci of binary n-paraffin systems.

production. Laboratory tests were conducted with a wide composition range of injection gases and reservoir fluids, at pressures greater than, equal to, or less than the saturation pressure (bubblepoint pressure) of the displaced fluid. One of the principal conclusions from these tests was that high oil recoveries could be obtained regardless of whether the oil was originally saturated or unsaturated with natural hydrocarbon gases at the displacement pressure.

The phase relations governing this process are illustrated by a triangular diagram in Fig. 45.6. Initially, a rich gas of Composition C is injected into Reservoir Oil A. As indicated by a line joining these two points, some mixture compositions fall in the two-phase region and thus these two components are not immediately miscible. However, after several consecutive steps of Gas C contacting the oil, the C_2 -to- C_6 components condensed out of the gas at each contact are absorbed by the oil until a critical Mixture B is obtained at the miscible front. It is noteworthy that, had Gas C initially fallen to the left of the immiscible-miscible (I-M) line, it would have been impossible to enrich the oil to B. There would not be sufficient amounts of the gas-enriching components in the injected gas to reach the Miscible Point B. The I-M line is referred to as the limiting tie line of the phase diagram.

Limiting Factors (Phase Behavior)

Control of Injection-Gas Composition. As indicated in the definition of miscible displacement by condensing-gas drive, the quantity of low MW components in the injection gas is critical.¹² Also, the actual dynamic or multiple-contact phase behavior may be more complicated than shown in the simple pseudoternary diagram

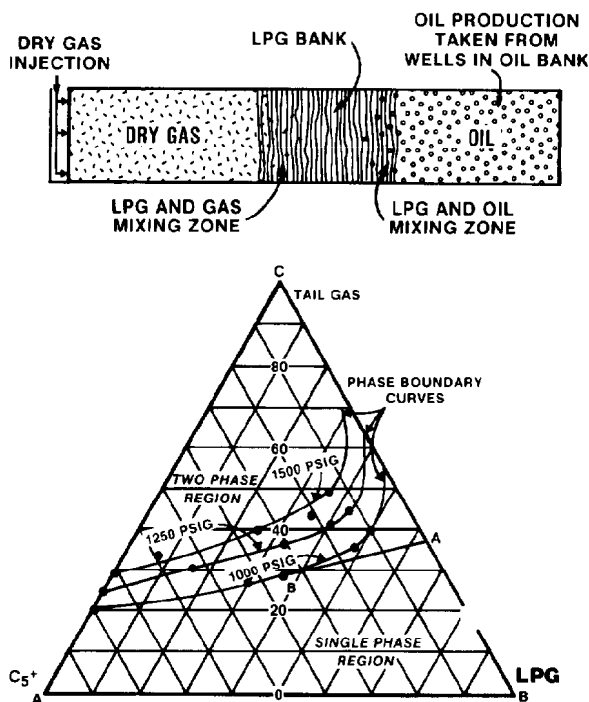


Fig. 45.5—Phase boundary curves for the system reservoir oil/LPG/tail gas; 180°F—volume percent basis.

of Fig. 45.6. Contiguous zones of miscible compositions of bubble- and dewpoint fluids can exist. The bubble-point curve represents the composition of a fluid where the last vapor disappears at a fixed pressure and temperature; the dewpoint curve represents the composition where the first liquid appears at these same conditions. Regions of liquid/liquid, liquid/liquid/vapor and liquid/vapor/solid (asphalt) equilibrium have been found in more recent studies. For this reason it is important that

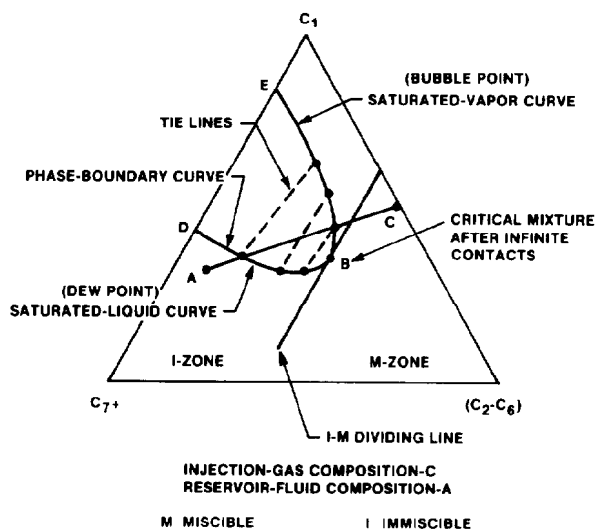


Fig. 45.6—Illustration of miscible displacement (condensing-gas drive).

3. The reservoir fluid must be sufficiently undersaturated with respect to the injection pressure. This factor is very critical. The requirement that the oil composition lies to the right of the limiting tie line also implies that only oils that are undersaturated with respect to methane can be miscibly displaced by methane or natural gas. Thus, oil of Composition F on the bubblepoint curve of Fig. 45.7 could not develop vaporizing-gas drive miscibility with methane/natural gas. Inspection of Fig. 45.7 shows that as the concentration of low-MW hydrocarbons in the reservoir oil decreases, the oil Composition A moves toward the left side of the pseudoternary diagram and higher pressures are required to shrink the size of the two-phase region and to develop miscibility. Increasing pressure both decreases the size of the two-phase region and changes the slopes of tie lines by increasing the vaporization of low-MW hydrocarbons into the vapor phase.

4. The density of the reservoir fluid must be sufficiently low, as reflected in stock-tank gravities of approximately 40° API and greater.

Laboratory studies would provide quantification for these requirements.

Extracting-Liquid or Supercritical Fluid Drive

CO₂ Miscible Process. A fourth mechanism for achieving dynamic or multiple-contact miscibility involves the injection of a solvent gas (such as CO₂, ethane, N₂O, or H₂S), which is not first-contact miscible with reservoir oils but is highly soluble in them. Table 45.1 shows the critical temperatures and solubilities of some of these solvent gases for comparison with methane.

The critical temperatures of these gases are close to reservoir temperatures and the gases are very compressible at these conditions (Fig. 45.8).²³ CO₂, from the standpoint of availability, cost, and operational handling, is the most practical of these fluids. As a liquid, or as a dense, critical fluid solvent, CO₂ extracts from the oil hydrocarbons of higher MW than the predominantly C₂ to C₄ hydrocarbons that methane vaporizes.²⁴ In addition to the C₂ to C₄ hydrocarbons, these fluids include C₅ to C₁₂ hydrocarbons from the gasoline fraction of the crude and even C₁₃ to C₃₀ gas-oil fractions of the crude.

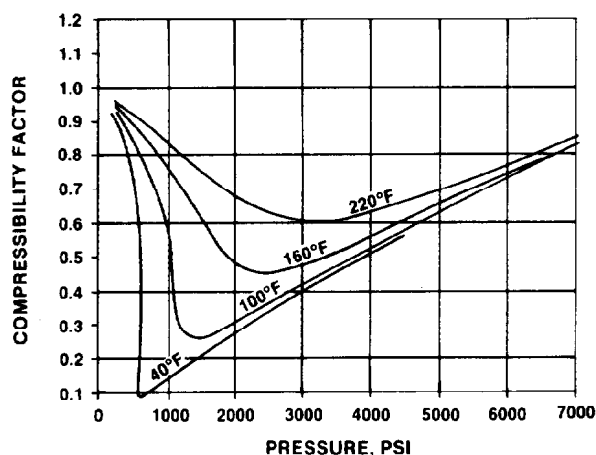


Fig. 45.8—Compressibility factors for CO₂.

TABLE 45.1—CRITICAL TEMPERATURES AND SOLUBILITIES OF SOLVENT GASES

	Critical Temperature		Solubility of Gas in a Crude Oil at 1,000 psi and 135°F (scf/bbl)
	(°F)	(°C)	
Carbon dioxide	88	31	634
Ethane	90	32	640
Hydrogen sulfide	213	100	522
Methane	-117	-82	209

In fact, the C₂ to C₄ hydrocarbons are not needed to achieve miscibility, so reservoir oils, which are depleted in methane and the low-MW hydrocarbons (dead oils), are still candidates for CO₂ miscible flooding.²⁵ This greatly increases the application potential for miscible displacement. After multiple contacts with the reservoir oil, the hydrocarbon-enriched-CO₂ phase miscibly displaces reservoir oil.^{26,27}

The phase behavior representation of this process is more complicated than the previous hydrocarbon injection processes. Fig. 45.9 indicates the enrichment in C₅ to C₃₀ hydrocarbons required to achieve the miscible displacement fronts.

Pressure-Composition Requirement. The reservoir pressures at which miscible displacement can occur are similar to those for the first-contact or enriched-gas processes (1,000 to 2,000 psi) because of the high solvency of the dense, supercritical CO₂ at these pressures and most reservoir temperatures (<200°F). Lower miscibility pressures are achieved at lower temperatures. Also, like the dependence of the vaporizing gas process on the C₂ to C₆ content of the in-situ oil, the CO₂ miscible process is dependent on the C₅ to C₃₀ content of the oil. At a given reservoir temperature, miscibility displacement with CO₂ is achieved at lower pressures where the C₅ to C₃₀ content is higher (Fig. 45.10).²⁸

Recent data indicate that the C₅ to C₁₂ content of the oil has the greatest effect on the miscibility pressure. The heavy portion (C₃₁+) of the oil also affects this

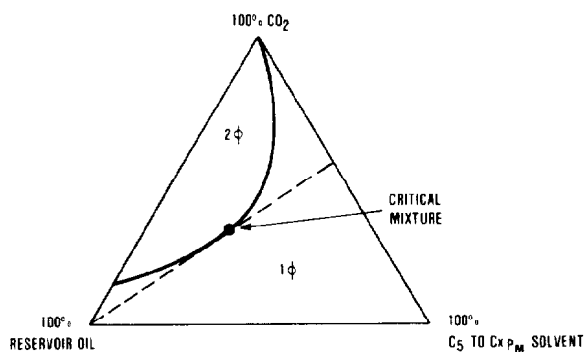


Fig. 45.9—Postulated phase diagram for fluids at displacement front after CO₂ has extracted hydrocarbons in-situ from reservoir oil, contacted at miscible pressure p_M .

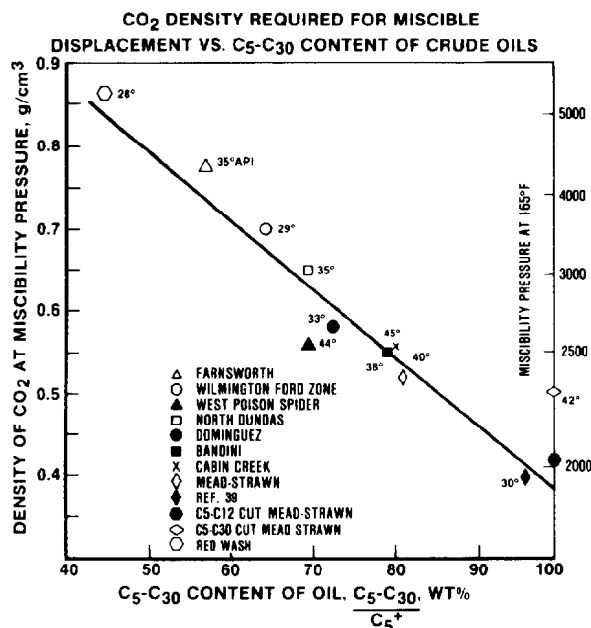


Fig. 45.10—CO₂ density required for miscible displacement vs. C₅ to C₃₀ content of various crude oils. MMP's at 165°F for same crude oils.

miscibility pressure. Increased heavy oil components, usually accompanied by lesser amounts of C₅ to C₁₂ components, require higher pressure to compress the CO₂ to a more dense fluid and promote adequate enrichment at the displacement front. This means a greater mass of CO₂ would be required for miscible recovery of heavy oil with accompanying increased costs.

Process Considerations. To effect a true miscible displacement process, CO₂ should be injected continuously, or a CO₂ slug should be driven by a gas that is miscible with the CO₂. Methane, flue gas, or nitrogen can be used for this purpose. However, because of the improved mobility achieved, water is often used as the drive fluid. Although CO₂ is soluble in the water, it is not miscible with it, so that the water-driven CO₂ slug dissipates by leaving a residual phase. This residual is one of the factors controlling the CO₂ slug size required.

CO₂ often is available in mixtures with other gases. The effect of these impurities is either to raise or lower

the pressure required to achieve miscible displacement in a reservoir.^{14,29,30} Gases such as nitrogen and methane raise the minimum miscibility pressure (MMP); ethane, propane, or hydrogen sulfide tend to lower the pressure requirement.

Factors Affecting Displacement Efficiency

Under the conditions of miscible displacement, nearly all the oil in place within the pore channels contacted will be displaced by virtue of the elimination of interfacial forces between the gas and oil³¹ and by the absence of relative-permeability effects. As the enriched gas and oil approach their critical mixture, there is a marked reduction in their IFT. Even though miscibility (defined by zero IFT and no interface) has not been reached at this point, improved oil recovery over immiscible displacement has been observed in laboratory flooding using such two-phase fluids. Such displacement has been described as near-miscible (incorrectly as partial-miscible) displacement. The actual recovery from the reservoir by miscible and near-miscible floods will be considerably less than that obtained in laboratory floods because of factors affecting pattern and conformance efficiency and dispersion of the miscible slug in the reservoir. The following discussion of factors which affect displacement efficiency applies to all forms of miscible and near-miscible processes.

Dispersion

Mixing zones form between the reservoir oil and LPG slug (or multiple-contact miscible slug) and between the injected drive gas and the slug. Three mechanisms that contribute to this mixing are molecular diffusion, microscopic convective dispersion, and macroscopic convective dispersion.^{32,33,35} Microscopic dispersion is pore-size mixing in excess of that from the random motion of molecules and is caused by convection in the tortuous flow through porous media. Further mixing of fluids by macroscopic convective dispersion can be caused by permeability heterogeneities over a larger area of the porous rock³⁴ (Fig. 45.11).

In a relatively homogeneous reservoir, the length of these mixing zones determines the minimum slug size. The slug should not be diluted to such an extent that miscibility is lost before most of the reservoir area is contacted. On the other hand, viscosity and density differences between solvent and oil, which also affect the slug, may be moderated by diffusion and dispersion, with a decrease in fingering, gravity override, and resultant slug-stabilization tendencies.

Laboratory studies have indicated that in linear-flow systems the mixing zone grows rapidly at first, decreases in rate of growth as displacement continues, and eventually stabilizes in length. A survey of the literature shows that a difference of opinion exists about the stabilizing effect that diffusion and dispersion have on the mixing zone in the reservoir. It is generally agreed, however, that the length of the mixing zone varies proportionately with the viscosity of the driven fluid.^{4,36-39} As the viscosities of the injected gases and liquid, and even the vaporized or extracted hydrocarbon enriched slugs, are low (less than 1 cp), field applications generally have been restricted to reservoirs with oil viscosity of less than 5 cp.

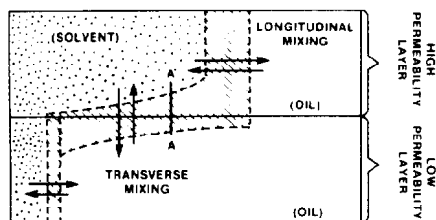


Fig. 45.11—Mixing of solvent and oil by longitudinal and transverse dispersion.

Two correlations, based on laboratory data, have been presented in the literature as a means to estimate the minimum slug size required for miscible drive in a homogeneous reservoir. One correlation⁴ states that the mixing-zone length is related to the ratio of the viscosity difference to the viscosity ratio. The other correlation³ says that the slug size required for a given path length varies inversely as the square root of the path length. Laboratory tests^{3,4} have indicated that, under ideal conditions, a bank of solvent with a volume as low as a few percent of the hydrocarbon pore space is all that might be required to maintain miscibility. However, experience has shown that slug volumes required for practical field operation range from 10 to 30% HCPV in a pattern area to counter the effects of dispersion, gravity segregation, reservoir-rock heterogeneities, well-pattern arrangements, etc.^{8,21}

Mobility Ratio

Despite the fact that displacement of nearly 100% of the oil in the contacted area occurs, the overall efficiency of miscible displacement may be lowered by the effect of an unfavorable mobility ratio (defined here as the ratio of the displacing to the displaced mobilities). The sweep pattern in a miscible-slug operation is controlled by the ratio of the displacing gas to the displaced oil mobilities,⁴⁰ which in the swept area will reduce itself to the viscosity ratio of oil to gas⁴¹ (Fig. 45.12).

This ratio, of course, is unfavorable when compared with conventional waterflood operations. Laboratory tests have indicated that viscous fingering occurs at unfavorable mobility ratios (Fig. 45.13). This phenomenon has been described as dendritic fingers of solvent (or drive gas) forming and growing in length until they break through the penetrated LPG slug or oil bank. These viscous fingers result in earlier solvent breakthrough and poorer oil recovery after breakthrough for a given volume of solvent injected than would be the case if the displacing front remained stable. The breakthrough oil recovery of miscible floods will be governed principally by the mobility ratio of the injected fluids and reservoir oil, and by the reservoir geometry.

Conformance Efficiency

Assuming that miscible displacement can be achieved by one of the foregoing processes, the greatest single factor that controls maximum recovery of oil from a reservoir is conformance efficiency. For the purpose of this chapter, conformance efficiency is defined as the fraction of the total PV within the pattern area that is contacted by the displacing fluid. The dominating factors that control conformance are the gross sand heterogeneity and size distribution of the rock interstices, which usually are defined in terms of permeability variation or stratification.⁴² These factors become particularly critical when effecting the displacement of the higher-viscosity oils. The associated unfavorable mobility ratio, in conjunction with a wide variance in permeability, results in a low conformance. In addition, gravity segregation can take place in formations possessing vertical permeability.⁴³ This adverse effect occurs when the light injection gases or liquids rise to the top of the formation or

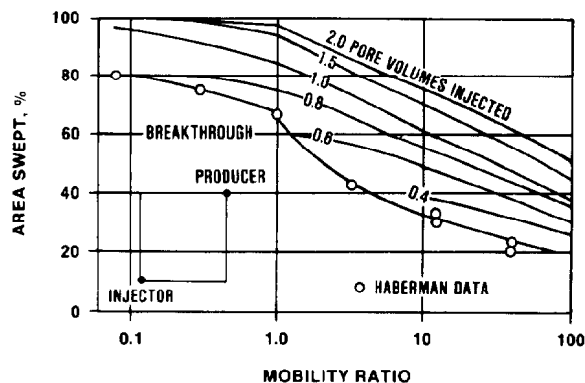


Fig. 45.12—Displacement behavior for developed five-spot, data from 0.0047-in. model.

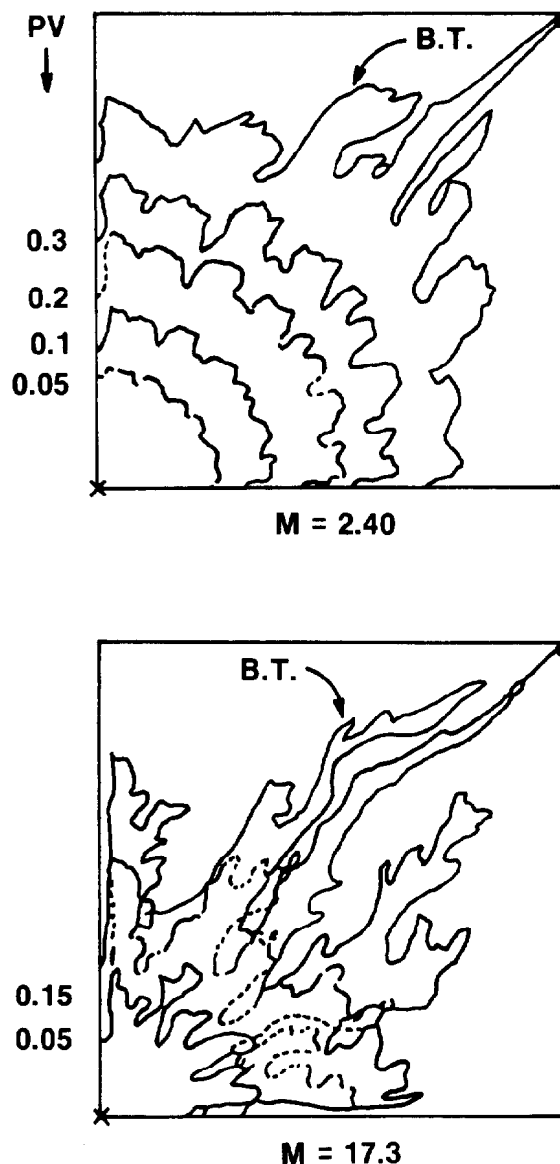


Fig. 45.13—Displacement fronts for different mobility ratios and injected PV until breakthrough, quarter of a five-spot.

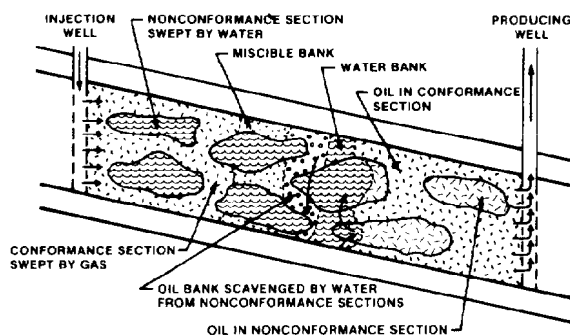


Fig. 45.14—Combination water-drive/miscible-drive project in low-conformance reservoir provides high oil recovery by water in the nonconformance sections and by miscible displacement from the conformance sections.

permeable zone and override or bypass the denser reservoir oil. The combination of these factors in a miscible displacement operation can yield an overall recovery efficiency that is much lower than that of waterflood. This problem has been a principal deterrent to the use of miscible processes.

Improving Pattern and Volumetric Sweep Efficiencies With Water During Miscible Displacement

In 1957, a method for improving pattern and volumetric sweep (conformance) in miscible displacement operations was proposed.⁴⁰ The method consists of injecting LPG, followed by a bank of natural gas to displace the LPG miscibly, and then natural gas and water simultaneously. The injection of the water reduces the relative permeability to gas in the region swept by the LPG slug and increases the viscosity of part of the displacing phase. These two factors combine to lower total mobility of this system, resulting in improved sweep (Fig. 45.14). Further research and field pilot tests have extended this technique to both the slug and/or drive gas in all types of miscible displacement.⁴⁴ Water usually is injected alternately with the drive gas and/or the miscible slug (termed WAG). The injection of water with an LPG or CO₂ slug can trap a portion of the oil mobilized by the miscible gas, particularly in reservoirs having strong water-wetting characteristics. A low water-to-gas ratio (0.5:1) is recommended if WAG is required. Also, this type operation is limited to reservoirs in which sufficient injection capacity is available. A tight reservoir would require too many injection wells to inject the necessary volumes of gas and water to meet desirable oil production rates.

Two other potential problems with this technique are (1) segregation of the injected fluids into different strata and (2) trapping of oil by mobile water.⁴⁵ Fluid injection into selected strata and proportioning of the injected fluids within strata may be helpful in such cases. In laboratory studies it is important to use the actual reservoir fluids and rock to determine the effects of rock wettability on oil mobilization and trapping in the presence of water. Refined oils or single hydrocarbons such as decane do not wet rock to the degree that crude oil does

and, consequently, tend to be trapped to a greater extent by water.

Improving Recovery Efficiency by Gravity Stabilization

In reservoirs with dip, gravity segregation of fluids can be used advantageously to prevent viscous fingering or gravity override. This is achieved by injecting the solvent and/or gas updip and producing downdip at a rate low enough for gravity to keep the fluids segregated. Fingers of solvent or gas are suppressed and sweepout is improved. Field applications of this method have been successful.

Improving Recovery Efficiency with Foams or Emulsions

The mobility of solvents and gas in porous media can be decreased by foaming or emulsifying them with water containing surfactants.⁴⁶ Laboratory studies have shown that these foams form selectively in the highly permeable porous channels and thereby tend to reduce fluid channeling.^{47,48} Further field testing of this technique is in progress.

Engineering Study

Basic Requirements

A detailed engineering investigation is necessary to select and to design the miscible displacement operation properly and to ensure that it will be successful. The following information is generally necessary or desirable as a basis for selecting the operation that will be most economically feasible.

Detailed Geology. Core analyses from enough wells are needed to provide adequate areal and vertical distribution of rock properties, fluid saturations, capillary pressure, and waterflood susceptibility data.

Information regarding the reservoir structure, size, shape, and dip with particular emphasis on the definition of stratification or zoning conditions is needed also. If the latter is known to exist, an isometric fence diagram of the reservoir (Fig. 45.15) should be constructed that shows all the details of porosity development, shale conditions, etc., which can be obtained from well logs, core analysis, pressure transient tests, and individual well performance. This diagram aids in relating well performances and spacing with reservoir geometry.

Phase Behavior of Reservoir Fluids. Laboratory analysis of reservoir oil and gas should be conducted to determine such information as differential and flash vaporization data, liquid and gas viscosities, and hydrocarbon compositions over a wide range of pressures. In many instances, it is necessary to know the PVT relationships of the mixtures comprising the reservoir fluids as well as the possible materials that might be injected.

Laboratory displacement tests should be conducted in sandpacked columns (Berea or native cores) to determine: (1) the pressure required for miscible displacement [although correlations such as Fig. 45.10 and those in other references are available, laboratory tests (Fig. 45.16) are the most accurate method to find the MMP]⁴⁹; (2) the displacement efficiencies expected in

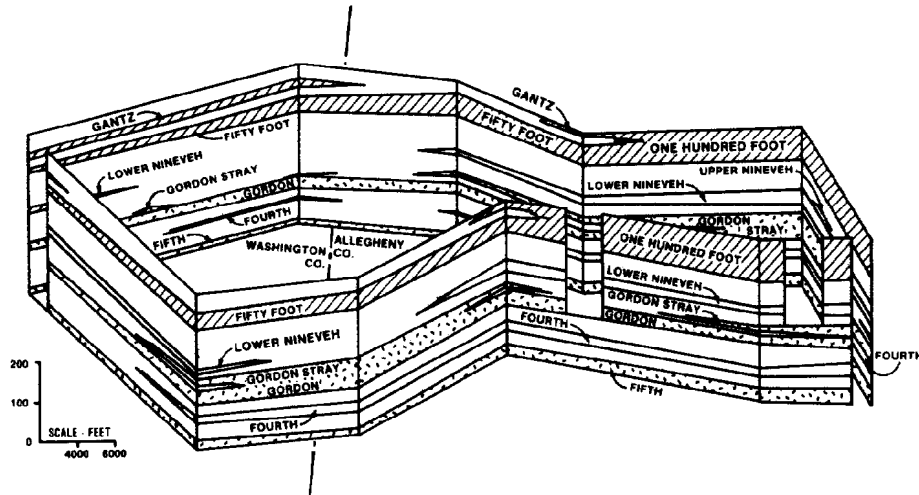


Fig. 45.15—Three-dimensional (fence) diagram illustrating general reservoir complexity.

the conforming areas for the LPG, condensing gas, high-pressure gas, etc; and (3) injection techniques at the desired operating pressure, temperatures, and for varying concentrations (or compositions) of injected materials.

Compatibility of injected materials with reservoir fluids should be determined. CO_2 , LPG products, or other light hydrocarbons will precipitate heavy paraffinic or asphaltic material in certain types of crude oil and may cause a reduction in permeability and a viscosity change in the oil.

Past Reservoir Behavior and Estimation of Primary and/or Conventional Secondary Recovery. The natural reservoir recovery mechanism should be evaluated to permit a reliable estimate of future primary recovery. Evaluation of any secondary recovery application in the reservoir is needed also.

Existing reservoir conditions should be determined. Past performance in connection with reservoir fluid and core analysis will provide an estimation of the state of the reservoir at the initiation of the miscible displacement project. This will include such essential items as reservoir pressure, fluid saturation distribution, and modeling or simulation of secondary-flooding history.

General Applicability of Miscible-Displacement Techniques. Knowledge of the previously mentioned factors, such as reservoir geometry and pressure conditions, can lead to the selection of the miscible process best suited to the reservoir.

Availability of injection materials and proximity of CO_2 , N_2 , or gasoline-plant facilities may dictate, in the final analysis, the selection of a specific miscible process.

Recovery by Miscible Displacement. Pattern efficiency is defined here as that areal coverage of the reservoir through which the displacing fluid moves from its source to the producing wells. This factor may be estimated from laboratory model studies or from the literature.^{50,51}

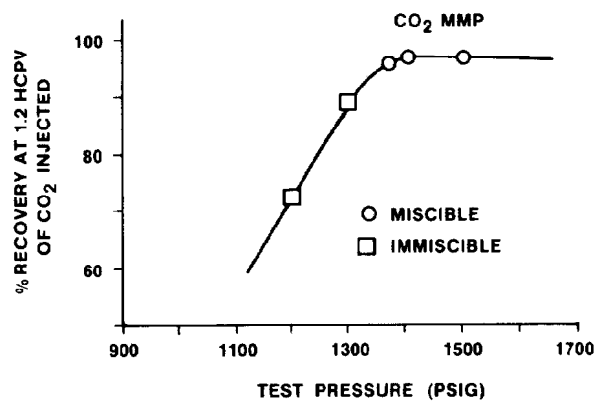


Fig. 45.16—Laboratory test results for fixed oil composition and fixed temperature in slim tubes.

It must be noted, however, that in the assumption of a pattern efficiency, the effect of unconformities and stratification must be considered.

Volumetric sweep efficiency, defined previously, is calculated from the knowledge of the stratification, vertical and areal variation of the rock properties, and mobility ratios of the displacing fluids to that of the displaced oil. There are several methods being used by engineers.⁵² One of these methods is illustrated in the example calculation (see Appendix) with reference to alternative procedures.

Displacement efficiency should be determined from laboratory studies. This factor represents the percent recovery from the conforming volume of the reservoir and may range from 80 to 100%. As mentioned previously, it is important to study the actual reservoir rock and fluids when possible to determine the rock wetting characteristics and their effect on displacement efficiency.

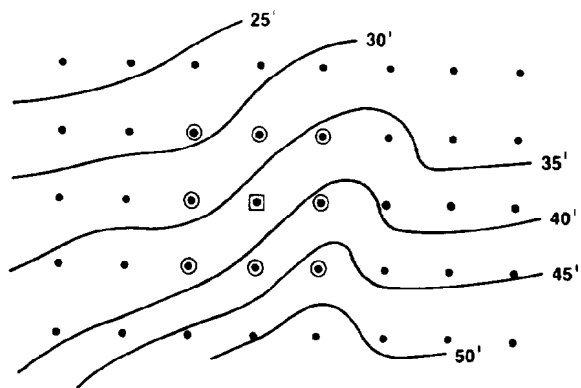


Fig. 45.17—Assumed reservoir for gas injection (inverted nine-spot pattern).

TABLE 45.2—CALCULATION OF CAPACITY DISTRIBUTION FOR EXAMPLE RESERVOIR

Cumulative Thickness (ft)	h	k	C	C_{cum}
1	0.029	83.0	0.198	0.198
2	0.057	41.0	0.098	0.296
3	0.086	39.0	0.093	0.389
4	0.114	31.0	0.074	0.463
5	0.143	26.0	0.062	0.525
6	0.171	23.0	0.055	0.580
7	0.200	19.0	0.045	0.625
8	0.229	17.0	0.040	0.665
9	0.257	17.0	0.040	0.705
10	0.286	14.0	0.033	0.738
11	0.314	13.0	0.031	0.769
12	0.343	10.0	0.024	0.793
13	0.371	7.9	0.019	0.812
14	0.400	7.0	0.017	0.829
15	0.429	6.5	0.015	0.844
16	0.457	6.4	0.015	0.859
17	0.486	6.2	0.015	0.874
18	0.514	4.8	0.011	0.885
19	0.543	4.7	0.011	0.896
20	0.571	4.5	0.011	0.907
21	0.600	4.5	0.011	0.918
22	0.629	4.1	0.010	0.928
23	0.657	3.6	0.009	0.937
24	0.686	3.5	0.008	0.945
25	0.714	3.4	0.008	0.953
26	0.743	2.9	0.007	0.960
27	0.771	2.9	0.007	0.967
28	0.800	2.6	0.006	0.973
29	0.829	2.5	0.006	0.979
30	0.857	2.1	0.005	0.984
31	0.886	2.0	0.005	0.989
32	0.914	1.3	0.003	0.992
33	0.943	1.3	0.003	0.995
34	0.971	1.2	0.003	0.998
35	1.000	0.8	0.002	1.000
Total		419.7		

All the oil that is displaced in a miscible flood may not be produced. The ability of producing wells to capture the mobilized oil must be considered.

Total recovery factor, or percent recovery of oil from the entire reservoir, represents the product of the pattern, conformance, displacement, and capture efficiencies.

Injectivity and Productivity of Wells. These affect project life and have a significant effect on economics. Injectivity tests in the field or extensive relative permeability measurements may be necessary.

Mathematical Simulation. This may be used in projecting reservoir performance. Finite-difference,⁵³ modified black-oil,⁵⁴ finite-element and compositional simulators^{55,56} have been developed for predicting or history matching flood performance. Streamtube models^{57,58} and scaled physical models⁵⁹ also have been developed and may be informative.

Program Design. Design of production and injection facilities should be coordinated and used with current operations to the fullest advantage.

Economic Evaluation and Comparison. The miscible drive operation and other competitive methods^{60,61} should be evaluated and compared on an economic basis. This analysis generally governs the final decision.

Pilot Operation and Evaluation of Results. In many cases where waterflood operations appear very competitive with miscible drive, a pilot injection program is recommended if a suitable area in the field can be located. The selection of the ultimate program of operation may be delayed pending the results of the pilot, thus reducing the risks inherent in such operations.

Field Experience

Since the first miscible flooding projects of the early 1950's, there have been many applications throughout the world of all the miscible processes. Some of the best documented of each of these processes and their variations are listed under General References for Applications of Miscible Processes. More complete information on these is found in the publications listed under General References for Field Tests of Miscible Processes.

APPENDIX

Engineering Examples

As indicated in the previous sections, oil recovery and related performance in miscible drive operations will depend mainly on the degree of stratification and permeability distribution existing in the reservoir. Consequently, engineering calculations generally will be reduced to a function of estimating conformance efficiency.

In the following examples we have assumed a reservoir under an inverted nine-spot well pattern (see Fig. 45.17), with an average permeability profile and capacity distribution as indicated in Table 45.2. The procedure followed is a modification of a standard water-cut recovery calculation,⁶² which is based on the vertical distribution of productive capacity. The calculations for

these examples are carried out assuming (1) linear fluid flow with no crossflow, (2) distance of penetration of the miscible front being proportional to permeability, (3) constant pressure drop between the injection and producing wells, (4) S_{or} (residual oil saturation) behind front equals zero, (5) S_{gF} (free-gas saturation) equals zero, (6) k_{rg}/k_{ro} (relative-permeability ratio) equals one, thereby defining the mobility ratio as the viscosity ratio of reservoir oil to the displacing gas, and (7) abandonment at a GOR of 100,000/1.

High-Pressure Gas Injection and Condensing-Gas Drive

For comparison these two processes are calculated together using the basic reservoir data presented in Table 45.3. High-pressure gas injection is assumed to take place at the initial reservoir pressure, whereas the injection pressure for the condensing-gas-drive process is assumed to be at saturation pressure. The calculation of the recovery and producing GOR data are presented in Table 45.4. From this table the fraction of cumulative

TABLE 45.3—BASIC RESERVOIR DATA FOR HIGH-PRESSURE-GAS-INJECTION AND CONDENSING-GAS-DRIVE EXAMPLES

Original reservoir pressure, psig	4,356
Saturation pressure, psig	2,446
Reservoir temperature, °F	197
Original solution GOR, scf/bbl	1,130
Formation volume factor (reservoir oil)	
At original pressure	1.675
At saturation pressure	1.734
Reservoir oil viscosity, cp	
At original pressure	0.26
At saturation pressure	0.22
Injection-gas viscosity, cp	
At original pressure	0.029
At saturation pressure	0.022
Formation volume factor for injection gas, bbl/Mscf	
At original pressure	0.74
At saturation pressure	1.15
k_{rg}/k_{ro} at displacing front	1.0

TABLE 45.4—CALCULATION OF RECOVERY AND PRODUCING GOR DATA (High-Pressure Gas Injection and Condensing-Gas Drive)

h_i Curve (1)	Δh (2)	C Curve (3)	ΔC (4)	k_D (4)/(2) (5)	\bar{h} (6)	k_D Curve (7)	$1 - C$ $1 - (3)$ (8)	$k_D h_i$ (7) × (1) (9)	$k_D h_i + (1 - C)$ (9) + (8) (10)
0.00	—	0.000	—	—	—	9.00	1.000	0.000	1.000
0.01	0.01	0.080	0.080	8.00	0.005	6.20	0.920	0.062	0.982
0.02	0.01	0.135	0.055	5.50	0.015	5.30	0.865	0.106	0.971
0.05	0.03	0.280	0.145	4.83	0.035	3.80	0.720	0.190	0.910
0.10	0.05	0.435	0.155	3.10	0.075	2.61	0.565	0.261	0.826
0.20	0.10	0.630	0.195	1.95	0.150	1.50	0.370	0.300	0.670
0.30	0.10	0.755	0.125	1.25	0.250	0.95	0.245	0.285	0.530
0.40	0.10	0.830	0.075	0.75	0.350	0.64	0.170	0.256	0.426
0.50	0.10	0.880	0.050	0.50	0.450	0.43	0.120	0.215	0.335
0.60	0.10	0.917	0.037	0.37	0.550	0.33	0.083	0.198	0.281
0.70	0.10	0.946	0.029	0.29	0.650	0.25	0.054	0.175	0.229
0.80	0.10	0.972	0.026	0.26	0.750	0.18	0.028	0.144	0.172
0.90	0.10	0.990	0.018	0.18	0.850	0.15	0.010	0.135	0.145
0.95	0.05	0.997	0.007	0.14	0.925	0.13	0.003	0.124	0.127
1.00	0.05	0.000	0.003	0.06	0.975	0.00	0.000	0.000	0.000

High-pressure gas injection at original pressure $F = 1.0 \times 0.26/0.029 \times 1.675/0.74 = 20.3$ Mcf/STB.

Condensing-gas drive at saturation pressure $F = 1.0 \times 0.22/0.022 \times 1.734/1.15 = 15.1$ Mcf/STB.

N_p (10)/(7) (11)	CF at Original Pressure (12)	CF at Saturation Pressure (13)	GOR at Original Pressure (12)/(8) + 1.13 (14)	GOR at Saturation Pressure (13)/(8) + 1.13 (15)
0.111	—	—	1.130	1.130
0.158	1.624	1.206	2.911	2.441
0.183	2.740	2.036	4.324	3.534
0.239	5.683	4.222	9.063	7.058
0.316	8.829	6.559	16.784	12.768
0.447	12.787	9.499	35.711	26.830
0.558	15.324	11.384	63.687	47.596
0.666	16.847	12.515	100.230	75.848
0.779	17.861	13.269	149.979	111.706
0.852	18.612	13.827		
0.916	19.201	14.264		
0.955	19.729	14.656		
0.967	20.094	14.927		
0.977	20.236	15.033		
1.000	20.297	15.078		

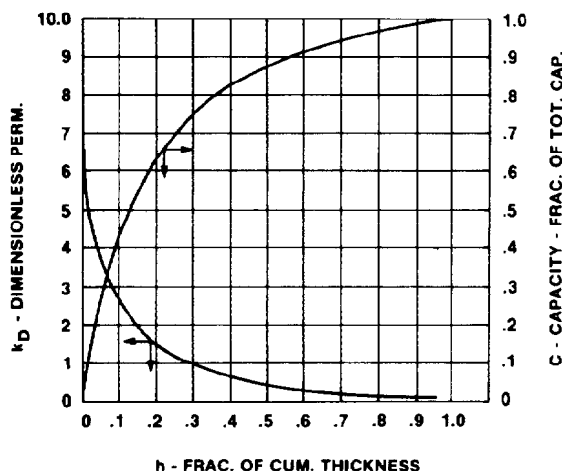


Fig. 45.18—Permeability and capacity distribution vs. sand-thickness fraction.

thickness, h , is plotted as a function of dimensionless permeability, k_D , and fraction of total capacity, C . These data are illustrated in Fig. 45.18. The recovery and GOR data are shown in Fig. 45.19. Note that, at an assumed abandonment ratio of 100,000 scf/bbl. recovery by condensing-gas drive was indicated to be 74.2% of the oil existing in the pattern area. The corresponding recovery for high-pressure gas injection was found to be only 66.5%. The difference in recovery between these two methods is essentially a result of the difference in the compressibility factors of the displacing gas at the two pressures.

Time-Rate Performance. Time-rate performance was not calculated for all the examples presented since it would be a function of the well productivity. However, it must be pointed out that the excess pressure available in the high-pressure gas-injection process would yield higher well productivity and a shorter life, which could lead to more favorable economics.

Recovery of LPG Products. Recovery of LPG products contained initially in the injected gas under the condensing-gas-drive process was not illustrated. This item, however, would be a function of the following factors: (1) percent recovery from the reservoir (estimated

TABLE 45.5—BASIC RESERVOIR DATA FOR MISCIBLE-SLUG INJECTION EXAMPLE

Reservoir pressure, psig	1,500
Saturation pressure, psig	1,500
Reservoir temperature, °F	197
Formation volume factor for reservoir oil, RB/STB	1.218
Solution GOR, scf/bbl	330
Stock-tank oil gravity, °API	35
Reservoir oil viscosity at 1,500 psig, cp	0.70
Injection gas viscosity at 1,500 psig, cp	0.015
Formation volume factor for injection gas, RB/Mcf	1.966
k_{rg}/k_{ro} at displacing front	1.0
Reservoir-gas saturation, %	15
Interstitial water saturation, %	22
Producing GOR at initiation of injection, scf/bbl	3,000
Estimated LPG slug volume for sweep pattern area, % HCPV	5

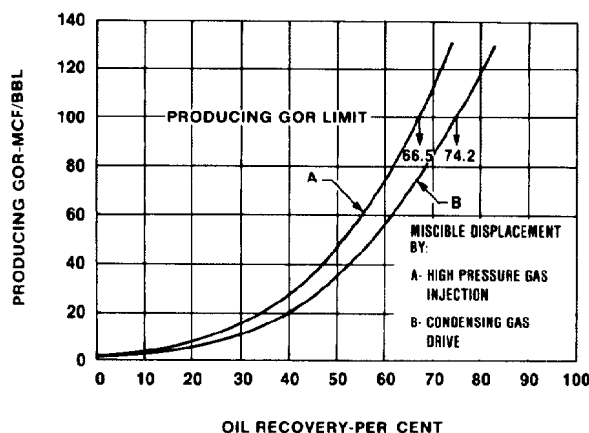


Fig. 45.19—Comparison of oil recoveries by high-pressure gas injection and condensing-gas drive vs. producing GOR.

from GOR and oil-recovery data), (2) gasoline-plant recovery efficiency, and (3) plant ownership of recoverable liquids.

These factors, in addition to the high cost of LPG, become critical in an economic comparison of recovery processes.

Volume of Gas Injected. The volume of gas injected is estimated on a reservoir volume in/reservoir volume produced basis. The volume of rich gas injected in condensing-gas-drive operations will depend on an evaluation of performance as related to the zones of stratification. To achieve the maximum effect from miscible displacement it is necessary to inject sufficient rich gas to establish a miscible front in the least permeable zone.

Miscible-Slug Injection

To illustrate the miscible-slug process the reservoir in the previous examples was assumed to have been depleted to 1,500 psig. Table 45.5 presents a list of the pertinent reservoir data that existed for this condition.

The recovery and GOR performance was calculated using the capacity distribution data (Cols. 1 through 11) in Table 45.4 and the A factor, as calculated from the fluid data. These results are summarized in Table 45.6 and illustrated in Fig. 45.20. It is noted that the recovery at a GOR of 100,000/1 was found to be 58.2% of the oil existing in the pattern area. This is a somewhat lower value than those indicated for high-pressure gas injection and condensing-gas drive. The difference is attributed to the more unfavorable mobility ratio at the lower pressure.

In this example, the GOR has decreased to approximately solution ratio as breakthrough was approached. It was assumed that all the free-gas saturation was produced during this interval.

The size of the LPG slug injected was assumed to be 5% of the HCPV in the pattern area. This volume is within the range (2 to 10%) dictated by economics but does not include a substantial safety factor. The volume of LPG slug produced was not calculated for this exam-

TABLE 45.6—CALCULATION OF RECOVERY AND PRODUCING GOR DATA MISCIBLE-SLUG-INJECTION EXAMPLE

C Curve*	1 - C*	N_p *	CF**	R_p †
0.000	1.000	0.111	—	0.330
0.080	0.920	0.158	2.312	2.843
0.135	0.865	0.183	3.902	4.841
0.280	0.720	0.239	8.092	11.569
0.435	0.565	0.316	12.572	22.581
0.630	0.370	0.447	18.207	49.538
0.755	0.245	0.558	21.820	89.391
0.830	0.170	0.666	23.987	141.430
0.880	0.120	0.779	25.432	
0.917	0.083	0.852	26.501	
0.946	0.054	0.916	27.339	
0.972	0.028	0.955	28.091	
0.990	0.010	0.967	28.611	
0.997	0.003	0.977	28.813	
1.000	0.000	1.000	28.900	

*From Table 45.4

** $F = 1 \times 0.70/0.015 \times 1.218/1.966 = 28.9$ Mcf/STB

† R_p = Fourth Col./Second Col. + 330/1.000

ple, but it can be estimated by multiplying the conformance efficiency at abandonment by the volume of slug injected. The net recoverable LPG, similar to that of condensing-gas-drive operations, would be reduced by the gasoline-plant recovery efficiency and plant-ownership percentage.

The volume of dry gas injected is estimated on a reservoir volume in/reservoir volume out basis.

Alternative Calculation Procedures

Alternative procedures for predicting performance of miscible drive operations are found in the literature. Several investigators have presented solutions to the permeability-stratification problem in the analysis of waterflooding which may be modified to fit miscible-drive processes.⁶³⁻⁶⁸ Other authors have presented their treatments with respect to gas cycling, which in itself is an example of miscible displacement.⁶⁹⁻⁷² For direct application to miscible drive operations, theoretical analyses and equations for linear displacement have been presented that offer a direct means for describing performance.^{68,73}

An excellent example that compares the results of calculated and actual performance of a pilot LPG flood has been published.²¹ In this example the reservoir was divided into several zones of varying permeability with radial-flow forms of Darcy's law used to calculate performance.

Mathematical simulators commonly are used today for designing and predicting reservoir performance of miscible floods. Two examples are (1) a vaporizing gas drive in a moderately stratified reservoir by use of a compositional simulator^{74,75} and (2) a condensing gas drive in a downward displacement in a reef by use of a black-oil simulator.⁷⁶

Nomenclature

C = capacity, fraction of total capacity

C_{cum} = cumulative capacity, fraction of total capacity

CF = equivalent gas production

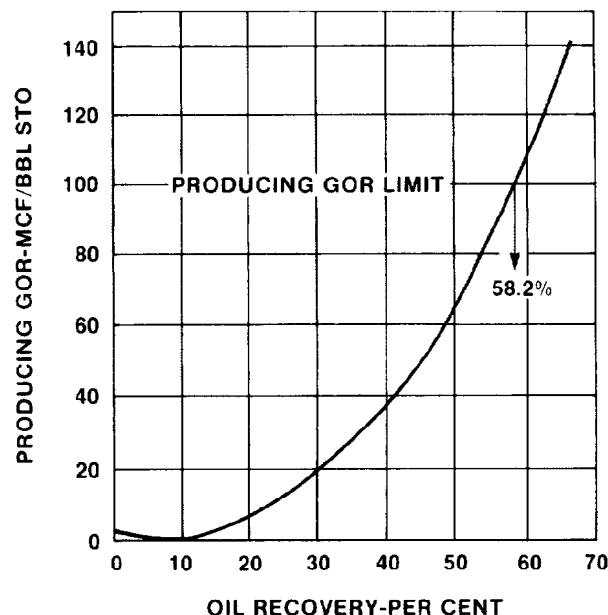


Fig. 45.20—Oil recovery vs. producing GOR for LPG slug injection.

$$F = k_{rg}/k_{ro} \times \mu_o/\mu_g \times B_o/B_g$$

h = cumulative thickness, fraction of total thickness

\bar{h} = average cumulative thickness, fraction of total thickness

k = permeability, millidarcies

$k_D = \Delta C/\Delta h$ = dimensionless permeability

$N_p = [k_D h + (1 - C)]/k_D$ = fraction of total oil recovery

p_M = miscible pressure, psia

$R_p = CA/(1 - C) + R_s$ = producing gas-oil ratio, Mcf/STB

R_s = solution GOR

$1 - C$ = equivalent oil production

References

- Clark, N.J. et al.: "Miscible Drive—Its Theory and Application." *J. Pet. Tech.* (June 1958) 11-20.
- Morse, R.A.: British Patent No. 696524 (1953).
- Koch, H.A. Jr. and Slobod, R.L.: "Miscible Slug Process," *Trans., AIME* (1957) **210**, 40-47.
- Hall, H.N. and Geffen, T.M.: "A Laboratory Study of Solvent Flooding," *Trans., AIME* (1957) **210**, 48-57.
- Gatlin, C. and Slobod, R.L.: "The Alcohol Slug Process for Increasing Oil Recovery," *Trans., AIME* (1960) **219**, 46-53.
- Gogarty, W.B. and Tosch, W.D.: "Miscible-Type Waterflooding: Oil Recovery With Micellar Solutions," *J. Pet. Tech.* (Dec. 1968) 1407-14; *Trans., AIME*, **243**.
- Holm, L.W.: "Use of Soluble Oils for Oil Recovery," *J. Pet. Tech.* (Dec. 1971) 1475-83; *Trans., AIME*, **251**.
- Craig, F.F. Jr. and Owens, W.W.: "Miscible Slug Flooding—A Review," *J. Pet. Tech.* (April 1960) 11-15.
- Brown, G.G. et al.: "Natural Gasoline and the Volatile Hydrocarbons," Natural Gasoline Assn. of America (1948).
- Hutchinson, C.A. Jr. and Braun, P.H.: "Phase Relations of Miscible Displacement in Oil Recovery," *AIChE J.* (1961) **7**, 64.
- Stone, H.L. and Crump, J.S.: "Effect of Gas Composition Upon Oil Recovery by Gas Drive," *Trans., AIME* (1956) **207**, 105-10.

12. Kehn, D.M., Pyndus, G.T., and Gaskell, M.H.: "Laboratory Evaluation of Prospective Enriched Gas Drive Projects," *Trans., AIME* (1958) **213**, 382-85.
13. Clark, N.J., Schultz, W.P., and Shearin, H.M.: "New Injection Method Affords Total Oil Recovery," *Pet. Engr.* (Oct. 1956) B-45.
14. Whorton, L.P. and Kieschnick, W.F. Jr.: "Oil Recovery by High Pressure Gas Injection," *Oil and Gas J.* (April 1950) **48**, 78-89.
15. Katz, D.L.: "Possibility of Cycling Deep Depleted Oil Reservoirs after Compression to a Single Phase," *Trans., AIME* (1952) **195**, 175-82.
16. Griffith, B.L. and Hollrah, V.M.: "Report on Field Trial of High Pressure Gas," *Oil and Gas J.* (June 1952) 86-93.
17. Slobod, R.L. and Koch, H.A. Jr.: "High Pressure Gas Injection—Mechanism of Recovery Increase," *Drill and Prod. Prac.*, API (1953) 82.
18. Wilson, J.F.: "Miscible Displacement—Flow Behavior and Phase Relationships for a Partially Depleted Reservoir," *Trans., AIME* (1960) **219**, 223-28.
19. Koch, H.A. Jr. and Hutchinson, C.A.: "Miscible Displacements of Reservoir Oil Using Flue Gas," *J. Pet. Tech.* (Jan. 1958) 7-19; *Trans., AIME* (1958) **213**.
20. Blackwell, R.J., Rayne, J.R., and Terry, W.M.: "Factors Influencing Efficiency of Miscible Displacement," *J. Pet. Tech.* (Jan. 1959) 1-8; *Trans., AIME* (1959) **216**.
21. Justen, J.J. et al.: "The Pembina Miscible Displacement Pilot and Analysis of Its Performance," *J. Pet. Tech.* (March 1960) 38-45; *Trans., AIME*, **29**.
22. Rushing, M.D. et al.: "Miscible Displacement with Nitrogen," *Pet. Eng.* (Nov. 1977) 26-30.
23. Sage, B.H. and Lacey, W.N.: *Some Properties of the Lighter Hydrocarbons, Hydrogen Sulfide, and Carbon Dioxide*, Monograph, Research Project 37, API, Dallas (1955).
24. Holm, L.W. and Josendal, V.A.: "Mechanisms of Oil Displacement by Carbon Dioxide," *J. Pet. Tech.* (Dec. 1974) 1427-35; *Trans., AIME*, **257**.
25. Holm, L.W. and Josendal, V.A.: "Discussion of Determination and Prediction of CO₂ Minimum Miscibility Pressure," *J. Pet. Tech.* (May 1980) 870-71.
26. Orr, F.M. Jr. and Silva, M.K.: "Equilibrium Phase Compositions of CO₂/Hydrocarbon Mixtures—Part 1: Mixtures Measurement by Continuous Multiple Contact Experiment," *Soc. Pet. Eng. J.* (April 1983) 272-80.
27. Shelton, J.L. and Yarbrough, L.: "Multiple Phase Behavior in Porous Media During CO₂ or Rich Gas Flooding," *J. Pet. Tech.* (Sept. 1977) 1171-78.
28. Holm, L.W. and Josendal, V.A.: "Effect of Oil Composition on Miscible-Type Displacement by Carbon Dioxide," *Soc. Pet. Eng. J.* (Feb. 1982) 87-98.
29. Metcalfe, R.S.: "Effects of Impurities on Minimum Miscibility Pressures and Minimum Enrichment Levels for CO₂ and Rich-Gas Displacements," *Soc. Pet. Eng. J.* (April 1982) 219-25.
30. Jacoby, R.H. and Rzas, M.J.: "Equilibrium Vaporization Ratios for Nitrogen, Methane, Carbon Dioxide, Ethane and Hydrogen Sulfide in Absorber Oil-Natural Gas and Crude Oil-Natural Gas Systems," *Trans., AIME* (1952) **195**, 99-110.
31. Simon, R., Rosman, A., and Zana, E.: "Phase Behavior Properties of CO₂—Reservoir Oil Systems," *Soc. Pet. Eng. J.* (Feb. 1978) 20-26.
32. Perkins, T.K. and Johnston, O.C.: "A Review of Diffusion and Dispersion in Porous Media," *Soc. Pet. Eng. J.* (March 1963) 70-84; *Trans., AIME*, **228**.
33. Blackwell, R.J.: "Laboratory Studies of Microscopic Dispersion Phenomena," *Soc. Pet. Eng. J.* (March 1962) 1-8; *Trans., AIME*, **225**.
34. Warren, J.E. and Skiba, F.F.: "Macroscopic Dispersion," *Soc. Pet. Eng. J.* (Sept. 1964) 215-30; *Trans., AIME*, **231**.
35. van der Poel, C.: "Effect of Lateral Diffusivity on Miscible Displacement in Horizontal Reservoirs," *Soc. Pet. Eng. J.* (Dec. 1962) 317-26; *Trans., AIME*, **225**.
36. Lacey, J.W., Draper, A.L., and Binder, G.G. Jr.: "Miscible Fluid Displacement in Porous Media," *J. Pet. Tech.* (April 1958) 76-79; *Trans., AIME*, **213**.
37. von Rosenberg, D.V.: "Mechanics of Steady State Single Phase Fluid Displacement from Porous Media," *J. Am. Chem. Soc.* (March 1956) **2**, 55-59.
38. Offeringa, J., and van der Poel, C.: "Displacement of Oil from Porous Media by Miscible Liquids," *J. Pet. Tech.* (Dec. 1954) 37-43; *Trans., AIME*, **201**.
39. Everett, J.P., Gooch, F.W. Jr., and Calhoun, J.C. Jr.: "Liquid-Liquid Displacement in Porous Media as Affected by the Liquid-Liquid Viscosity Ratio and Liquid-Liquid Miscibility," *Trans., AIME* (1950) **189**, 215-24.
40. Caudle, B.H. and Dyes, A.B.: "Improving Miscible Displacement by Gas-water Injection," *Trans., AIME* (1958) **213**, 281-84.
41. Habermann, B.: "The Efficiency of Miscible Displacement as a Function of Mobility Ratio," *Trans., AIME* (1960) **219**, 264-72.
42. Dykstra, H. and Parsons, R.L.: "The Prediction of Oil Recovery by Water Flood," *Secondary Recovery of Oil in the United States*, second edition, API, New York City (1950) 160.
43. Gardner, G.H., Downie, J., and Kendall, H.A.: "Gravity Segregation of Miscible Fluids in Linear Models," *Soc. Pet. Eng. J.* (June 1962) 95-104; *Trans., AIME*, **225**.
44. Blackwell, R.J. et al.: "Recovery of Oil by Displacement With Water-Solvent Mixtures," *Trans., AIME* (1960) **219**, 293-300; *Miscible Processes*, Reprint Series, SPE, Dallas (1965) **8**.
45. Tiffin, D.L. and Yellig, W.F.: "Effects of Mobile Water on Multiple-Contact Miscible Gas Displacements," *Soc. Pet. Eng. J.* (June 1983) 447-55.
46. Fried, A.N.: "The Foam Drive Process for Increasing the Recovery of Oil," RI 5866, USBM (1961).
47. Bernard, G.G.: "Effect of Foam on Recovery of Oil by Gas Drive," *Prod. Monthly* (1963) **27**, No. 1, 18-21.
48. Holm, L.W.: "Foam Injection Test in the Siggins Field, Illinois," *J. Pet. Tech.* (Dec. 1970) 1499-1506.
49. Yellig, W.F. and Metcalfe, R.S.: "Determination and Prediction of CO₂ Minimum Miscibility Pressures," *J. Pet. Tech.* (Jan. 1980) 160-68.
50. Dyes, A.B., Caudle, B.H., and Erickson, R.A.: "Oil Production After Breakthrough as Influenced by Mobility Ratio," *Trans., AIME* (1954) **201**, 81-86.
51. Muskat, M.: *Flow of Homogeneous Fluids Through Porous Media*, McGraw-Hill Book Co. Inc., New York City (1937).
52. Claridge, E.L.: "CO₂ Flooding Strategy in a Communicating Layered Reservoir," *J. Pet. Tech.* (Dec. 1982) 2746-56.
53. Aziz, K. and Settari, A.: *Petroleum Reservoir Simulation*, Applied Science Publishers Ltd., London (1979).
54. Peaceman, D.W. and Rachford, H.H. Jr.: "Numerical Calculation of Multidimensional Miscible Displacement," *Soc. Pet. Eng. J.* (Dec. 1962) 327-39; *Trans., AIME*, **225**.
55. Price, H.S. and Donohue, D.A.T.: "Isothermal Displacement Processes with Interphase Mass Transfer," *Soc. Pet. Eng. J.* (June 1967) 205-20; *Trans., AIME*, **240**.
56. Coats, K.H.: "An Equation of State Compositional Model," *Soc. Pet. Eng. J.* (Oct. 1980) 363-76.
57. Higgins, R.V. and Leighton, A.J.: "A Computer Method to Calculate Two-Phase Flow in Any Irregularly Bounded Porous Medium," *J. Pet. Tech.* (June 1962) 679-83; *Trans., AIME*, **225**.
58. Faulkner, B.L.: "Reservoir Engineering Design of a Tertiary Miscible Gas Drive Pilot Project," paper SPE 5539 presented at the 1975 SPE Annual Technical Conference and Exhibition, Dallas, Sept. 28-Oct. 1.
59. Pozzi, A.L. and Blackwell, R.J.: "Design of Laboratory Models for Study of Miscible Displacement," *Soc. Pet. Eng. J.* (March 1963) 28-40; *Trans., AIME*, **228**.
60. Stalkup, F.I. Jr., *Miscible Displacement*, Monograph Series, SPE, Dallas (1983) **8**.
61. *Miscible Processes*, Reprint Series, SPE, Dallas (1983) **8**.
62. Stiles, W.E.: "Use of Permeability Distribution in Waterflood Calculations," *Trans., AIME* (1949) **186**, 9-13.
63. Calhoun, J.C. Jr.: *Fundamentals of Reservoir Engineering*, U. of Oklahoma Press, Norman (1953) 360.
64. Muskat, M.: "The Effect of Permeability Stratification in Complete Water Drive Systems," *Trans., AIME* (1950) **189**, 349-58.
65. Dykstra, H. and Parsons, R.L.: *The Prediction of Oil Recovery by Waterflooding Secondary Recovery of Oil in the United States*, second edition, API, New York City (1950) 160.
66. Johnson, C.E. Jr.: "Prediction of Oil Recovery by Water Flood—A Simplified Graphical Treatment of the Dykstra-Parsons Method," *Trans., AIME* (1956) **207**, 345-46.
67. Suder, F.E. and Calhoun, J.C. Jr.: "Waterflood Calculations," *Drill. and Prod. Prac.*, API (1949) 260.
68. Johnson, E.F. and Welge, H.J.: "An Analysis of the Linear Displacement of Oil by Gas Driven Solvent," paper 906-G presented at the 1957 SPE Annual Meeting, Dallas, Feb. 24-28.

69. Muskat, M.: "Effect of Permeability Stratification in Cycling Operations," *Trans.*, AIME (1949) **179**, 313-28.
70. Lindbad, E.N., Standing, M.B., and Parsons, R.L.: "Calculated Recoveries by Cycling from a Retrograde Reservoir of Variable Permeability," *Trans.*, AIME (1948) **174**, 165-90.
71. Hurst, W., and van Everdingen, A.F.: "Performance of Distillate Reservoirs in Gas Cycling," *Trans.*, AIME (1946) **165**, 36-51.
72. Sheldon, W.C.: "Calculating Recovery by Cycling a Retrograde Condensate Reservoir," *J. Pet. Tech.* (Jan. 1959) 29-34.
73. Gardner, G.H.F.: "Equations of Motion for A Linear Miscible Displacement," PAPER 902-G presented at the 1957 SPE Annual Meeting, Dallas, Feb. 24-28.
74. Warner, H.R. Jr. *et al.*: "University Block 31 Field Study: Part 1—Middle Devonian Reservoir History Match," *J. Pet. Tech.* (Aug. 1979) 962-70.
75. Warner, H.R. Jr., Hardy, J.H., and Davidson, C.D.: "University Block 31 Field Study: Part 2—Reservoir and Gas Plant Performance Predictions," *J. Pet. Tech.* (Aug. 1979) 971-78.
76. Gillund, G.N. and Patel, C.: "Depletion Studies of Two Contrasting D-2 Reefs," paper 80-31-37 presented at the 1980 Annual Technical Meeting of the Petroleum Soc. of CIM, Calgary, May 25-28.

General References

Applications of Miscible Processes

- Baugh, E.G.: "Performance of Seeligson Zone 20-B Enriched Gas-Drive Project," *J. Pet. Tech.* (March 1960) 29-33.
- Blanton, J.R., McCaskill, N., and Herbeck, E.F.: "Performance of a Propane Slug Pilot in a Watered-Out Sand—South Ward Field," *J. Pet. Tech.* (Oct. 1970) 1209-14.
- Christian, L.D. *et al.*: "Planning a Tertiary Oil-Recovery Project for Jay/LEC Fields Unit," *J. Pet. Tech.* (Aug. 1981) 1535-44.
- DesBrisay, C.L. *et al.*: "Miscible Flood Performance of the Intisar 'D' Field, Libyan Arab Republic," *J. Pet. Tech.* (Aug. 1975) 935-43.
- DesBrisay, C.L. *et al.*: "Review of Miscible Flood Performance, Intisar 'D' Field, Socialist People's Libyan Arab Jamahiriya," *J. Pet. Tech.* (Aug. 1982) 1651-60.
- Hansen, P.W.: "A CO₂ Tertiary Recovery Pilot, Little Creek Field, Mississippi," paper SPE 6747 presented at the 1977 SPE Annual Technical Conference and Exhibition, Denver, Oct. 9-12.
- Herbeck, D.F., and Blanton, J.R.: "Ten Years of Miscible Displacement in Block 31 Field," *J. Pet. Tech.* (June 1961) 543-49.
- Holm, L.W. and O'Brien, L.J.: "Carbon Dioxide Test at the Mead-Strawn Field," *J. Pet. Tech.* (April 1971) 431-42.
- Holm, L.W.: "Propane-Gas-Water Miscible Floods in Watered-Out Areas of the Adena Field, Colorado," *J. Pet. Tech.* (Oct. 1972) 1264-70.
- Jenks, L.H., Campbell, J.B., and Binder, G.G. Jr.: "A Field Test of Gas-Driven Liquid Propane Method of Oil Recovery," *Trans.*, AIME (1957) **210**, 34-39.
- Kane, A.V.: "Performance Review of a Large Scale CO₂-WAG Enhanced Recovery Project, SACROC Unit—Kelly Snyder Field," *J. Pet. Tech.* (Feb. 1979) 217-31.
- Lackland, S.D. and Hurford, G.T.: "Advanced Technology Improves Recovery at Fairway," *J. Pet. Tech.* (March 1973) 354-58.
- Marrs, D.G.: "Field Results of Miscible Displacement Program Using Liquid Propane Driven by Gas, Parks Field Unit, Midland County, Texas," *J. Pet. Tech.* (April 1961) 327-32.
- Pontious, S.B. and Tham, M.J.: "North Cross (Devonian) Unit CO₂ Flood—Review of Flood Performance and Numerical Simulation," *J. Pet. Tech.* (Dec. 1978) 1706-14.
- Sessions, R.E.: "Small Propane Slug Proving Success in Slaughter Field Lease," *J. Pet. Tech.* (Jan. 1963) 31-36.
- ### Field Tests of Miscible Processes
- Bleakley, W.B.: "Journal Survey Shows Recovery Projects Up," *Oil and Gas J.* (March 1974) 69-78.
- Brannan, G. and Whittington, H.M. Jr.: "Enriched Gas Miscible Flooding—A Case History of the Levelland Unit Secondary Miscible Project," *J. Pet. Tech.* (Aug. 1977) 919-24.
- Burt, R.A. Jr.: "High Pressure Miscible Gas Displacement Project, Bridger Lake Unit, Summit County," paper SPE 3487 presented at the 1971 SPE Annual Meeting, New Orleans, Oct. 3-6.
- Gernet, J.M. and Brigham, W.E.: "Meadow Creek Unit Lakota 'B' Combination Water-Miscible Flood," *J. Pet. Tech.* (Sept. 1964) 993-97.
- Glasser, S.R.: "History and Evaluation of an Experimental Miscible Flood in the Rio Bravo Field," *Prod. Monthly* (Jan. 1964) 17-20.
- Griffith, J.D., Baiton, N., and Steffensen, R.J.: "Ante Creek—A Miscible Flood Using Separator Gas and Water Injection," *J. Pet. Tech.* (Oct. 1970) 1232-41.
- Griffith, J.D. and Cyca, L.G.: "Performance of South Swan Hills Miscible Flood," *J. Pet. Tech.* (July 1981) 1319-26.
- Griffith, J.D. and Home, A.L.: "South Swan Hills Solvent Flood," *Proc.*, Ninth World Pet. Cong., Tokyo (1975) **4**, 269-78.
- Harvey, M.T., Shelton, J.L. and Kelm, C.H.: "Field Injectivity Experiences with Miscible Recovery Projects Using Alternate Rich Gas and Water Injection," *J. Pet. Tech.* (Sept 1977) 1051-55.
- Kloepfer, C.V. and Griffith, J.D.: "Solvent Placement Improvement by Pre-Injection of Water, Lobstick Cardium Unit Pembina Field," paper SPE 948 presented at the 1964 SPE Annual Meeting, Houston, Oct. 11-14.
- Lane, L.C., Teubner, W.G., and Campbell, A.W.: "Gravity Segregation in a Propane Slug-Miscible Displacement Project, Baskington Field," *J. Pet. Tech.* (June 1965) 661-63.
- Macon, R.S.: "Design and Operation of the Levelland Unit CO₂ Injection Facility," paper SPE 8410 presented at the 1979 SPE Annual Technical Conference and Exhibition, Las Vegas, Sept. 23-26.
- Meltzer, B.D., Hurdle, J.M., and Cassingham, R.W.: "An Efficient Gas Displacement Project—Ralcigh Field, Mississippi," *J. Pet. Tech.* (May 1965) 509-14.
- Palmer, F.S., Nute, A.J., and Peterson, R.L.: "Implementation of a Gravity-Stable Miscible CO₂ Flood in the 8000-Foot Sand, Bay St. Elaine Field," *J. Pet. Tech.* (Jan. 1984) 101-10.
- Pottier, J. *et al.*: "The High Pressure Injection of Miscible Gas at Hassi-Messaoud," *Proc.*, Seventh World Pet. Cong., Mexico City (1967) **3**, 533-44.
- Thrash, J.C.: "Twofreds Field—Tertiary Oil Recovery Project," paper SPE 8382 presented at the 1979 SPE Annual Technical Conference and Exhibition, Las Vegas, Sept. 23-26.
- Tittle, R.M. and From, K.T.: "Success of Flue Gas Program at Neale Field," paper SPE 1907 presented at the 1960 SPE Annual Meeting, Houston, Oct. 1-4.

Chapter 46

Thermal Recovery

Chieh Chu, Getty Oil Co.*

Introduction

Thermal recovery generally refers to processes for recovering oil from underground formations by use of heat. The heat may be supplied externally by injecting a hot fluid such as steam or hot water into the formations, or it may be generated internally by combustion. In combustion, the fuel is supplied by the oil in place and the oxidant is injected into the formations in the form of air or other oxygen-containing fluids. The most commonly used thermal recovery processes are steam injection processes and in-situ combustion.

Two Forms of Steam Injection Processes

In principle, any hot fluid can be injected into the formations to supply the heat. The fluids used most extensively are steam or hot water because of the general availability and abundance of water. Hot water injection has been found to be less efficient than steam injection and will not be discussed here. A schematic view of the steam injection process is shown in Fig. 46.1, together with an approximate temperature distribution inside the formation.¹

There are two variations of steam injection processes—steam stimulation and steam displacement.

Steam Stimulation

This method has been known as the huff 'n' puff method, since steam is injected intermittently and the reservoir is allowed to produce after each injection. In this process the main driving force for oil displacement is provided by reservoir pressure, gravitational force, rock and fluid expansion, and, possibly, formation compaction. In the steam stimulation process only the part of the reservoir adjacent to the wellbore is affected. After a number of cycles of injection and production, the near-wellbore region in reservoirs having little or no dip becomes so depleted of oil that further injection of steam is futile. In this case, wells must be drilled at very close spacing to obtain a high oil recovery.

Steam Displacement

This process, usually referred to as steamflood or steam-drive, has a much higher oil recovery than steam stimulation alone. Whereas steam stimulation is a one-well operation, steamflood requires at least two wells, one serving as the injector and the other serving as the producer. The majority of steamflood projects use pattern floods. In many cases, steam stimulation is required at the producers when the oil is too viscous to flow before the heat from the injector arrives. Because of the high oil recovery achievable through steamflooding, many reservoirs that were produced by steam stimulation previously now are being steamflooded.

Three Forms of In-Situ Combustion

In-situ combustion usually is referred to as fireflood. There are three forms of in-situ combustion processes—dry forward combustion, reverse combustion, and wet combustion.

Dry Forward Combustion

In the earlier days, this was the most commonly used form of the combustion processes. It is dry because no water is injected along with air. It is forward because combustion starts at the injector and the combustion front moves in the direction of the air flow.

Fig. 46.2 gives a schematic view of the dry forward combustion process.² The upper part of the figure shows a typical temperature distribution along a cross section leading from the injector at the left to the producer at the right. Two things need to be pointed out. First, the region near the producer is cold, at the original temperature of the reservoir. If the unheated oil is highly viscous, it cannot be pushed forward by the heated oil at its back that has been made mobile by the high temperature of the combustion zone. This phenomenon is called "liquid blocking." Second, the temperature of the region in the back of the combustion zone is high, indicating a great amount of heat being stored in the region, not used efficiently.

*Now with Texaco Inc.

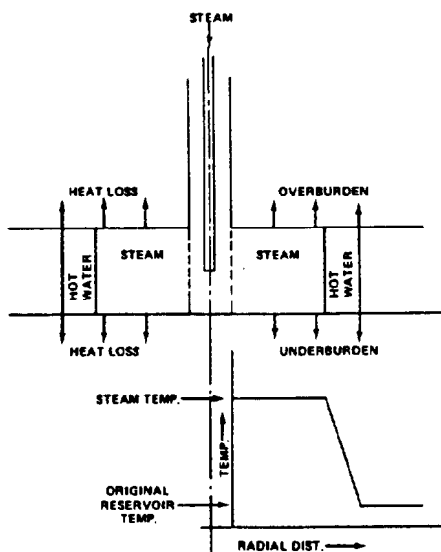


Fig. 46.1—Steam injection processes.

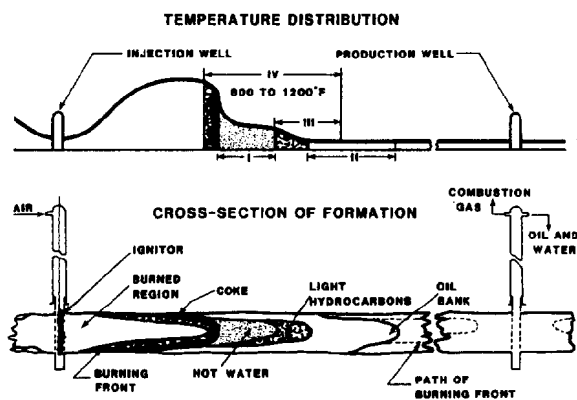


Fig. 46.2—Dry forward combustion.

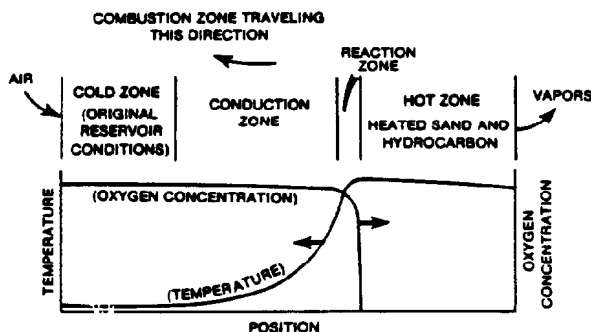


Fig. 46.3—Reverse combustion.

The lower part of Fig. 46.2 shows the fluid saturation distributions inside the formation under the combustion process. One should note the clean sand in the burned-out region. Being able to burn the undesirable fraction of the oil (the heavier portion) is one advantage of the forward combustion process over the reverse combustion process.

Reverse Combustion

Strictly speaking, it should be called dry reverse combustion, because normally only air is injected, no water. A simple example will help to explain how reverse combustion works. In ordinary cigarette smoking, one ignites the tip of the cigarette and inhales. The burning front will travel from the tip of the cigarette toward one's mouth, along with the air. This is forward combustion. The cigarette also can be burned if one exhales. This way, the burning front still moves from the tip of the cigarette toward one's mouth, but the air flow is in the opposite direction. This is, then, reverse combustion.

Fig. 46.3 shows the various zones inside the formation, with the cold zone near the injector at the left and the hot zone near the producer.³ Since the region around the producer is hot, the problem of liquid blocking mentioned earlier in connection with the dry forward process has been eliminated.

In principle, there is no upper limit for oil viscosity for the application of the reverse combustion process. However, this process is not as efficient as the dry forward combustion because a desirable fraction of the oil (the lighter portion) is burned and an undesirable fraction of the oil (the heavier portion) remains in the region behind the combustion front. Besides, spontaneous ignition could occur at the injector.⁴ If this happens, the oxygen will be used up near the injector and will not support combustion near the producer. The process then reverts to forward combustion.

No reverse combustion project has ever reached commercial status. Nevertheless, this process should not be written off because, in spite of the difficulties facing this process, it could offer some hope of recovering extremely viscous oil or tar.

Wet Combustion

The term "wet combustion" actually refers to wet forward combustion. This process was developed to use the heat contained behind the combustion zone. In this process, water is injected either alternately or simultaneously with air. Because of its high heat capacity and latent heat of vaporization, water is capable of moving the heat behind the combustion front forward, and helping to displace the oil in front of the combustion zone.

Fig. 46.4 shows the temperature distributions of the wet combustion process as the water/air ratio (WAR) increases.⁵ The curve for WAR=0 refers to dry combustion. With an increase in WAR, the high-temperature zone behind the combustion zone shortens (WAR=moderate). With a further increase in WAR, the combustion will be partially quenched as shown by the curve for WAR=large.

The wet combustion process also is known as the COFCAW process, which is an acronym for "combination of forward combustion and waterflood." This process also can be construed as steamflood with in-situ steam

generation. It should be noted that this method cannot prevent liquid blocking and its application is limited by oil viscosity, as is the dry forward combustion.

Historical Development

The following lists chronologically some of the major events that occurred in the development of the thermal recovery methods.

- 1931 A steamflood was conducted in Woodson, TX.⁶
- 1949 A dry forward combustion project was started in Delaware-Childers field, OK.⁷
- 1952 A dry forward combustion project was conducted in southern Oklahoma.⁸
- 1955 A reverse combustion project was initiated in Belamy, MO.⁹
- 1958 The steam stimulation process was accidentally discovered in Mene Grande Tar Sands, Venezuela.¹⁰
- 1960 Steam stimulation was started in Yorba Linda, CA.¹¹
- 1962 Wet combustion phase of a fireflood project was started in Schoonebeek, The Netherlands.¹²

Current Status

U.S. Oil Production by Enhanced Recovery Methods

The significance of the thermal recovery processes can be seen from the April 1982 survey of the *Oil and Gas J.*¹³ As shown in Table 46.1, of the daily U.S. oil production with EOR processes, 76.9% comes from steam injection and 2.7% comes from in-situ combustion, totaling 79.6% obtained by thermal recovery processes. The combustion process, although dwarfed by the steam injection processes, accounts for more than double the production of all the chemical floods combined, which amounts to 1.2%.

Geographical Distribution of Thermal Recovery Projects

Table 46.2, based largely on the 1982 survey,¹³ shows the geographical distribution of the steam injection projects in the world. Of the daily oil production from steam injection processes, 71.7% comes from the U.S., 15.4%

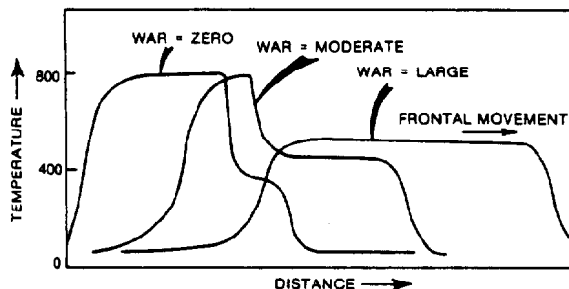


Fig. 46.4—Wet combustion.

from Indonesia, 7.0% from Venezuela, and 3.0% from Canada. In the U.S., California accounts for nearly all the production, with small percentages coming from Louisiana, Arkansas, Texas, Oklahoma, and Wyoming.

The daily oil production by in-situ combustion is shown in Table 46.3. Here, the U.S. accounts for 40.0% of the total production, followed by Romania (26.0%), Canada (22.1%), and Venezuela (10.8%). Of the U.S. production, nearly one-half comes from California, one-third from Louisiana, with the rest from Mississippi, Texas, and Illinois.

Major Thermal Recovery Projects

The major thermal recovery projects, again based largely on the 1982 survey,¹³ are listed in Table 46.4.

Reservoirs Amenable to Thermal Recovery

Table 46.5 shows the ranges of reservoir properties in which the technical feasibility of steamflood and fireflood has been proven.¹⁴

Potential for Incremental Recovery

According to Johnson *et al.*,¹⁵ vast energy resources exist in the tar sands in Venezuela and Colombia (1,000 to 1,800 billion bbl), Canada (900 billion bbl), and the U.S. (30 billion bbl). These tar sands should be a major target

TABLE 46.1—U.S. EOR PRODUCTION (1982)

	B/D	%
Steam	288,396	76.9
Combustion	10,228	2.7
Total thermal	298,624	79.6
Micellar/polymer	902	0.2
Polymer	2,587	0.7
Caustic	580	0.2
Other chemicals	340	0.1
Total chemicals	4,409	1.2
CO ₂ miscible	21,953	5.9
Other gases	49,962	13.3
Total	71,915	19.2
Grand Total	374,948	100.0

TABLE 46.2—OIL PRODUCTION BY STEAM INJECTION PROCESSES (1982)

	B/D	%
U.S.	288,396	71.7
Arkansas	800	
California	284,093	
Louisiana	1,600	
Oklahoma	617	
Texas	711	
Wyoming	575	
Canada (Alberta)	12,180	3.0
Brazil	1,920	0.5
Trinidad	3,450	0.9
Venezuela	28,030	7.0
Congo	2,500	0.6
France	360	0.1
Germany	3,264	0.8
Indonesia	62,000	15.4
Total	402,100	100.0

TABLE 46.3—PRODUCTION BY IN-SITU COMBUSTION (1982)

	B/D	%
U.S.	10,228	40.0
California	4,873	
Illinois	179	
Kansas	2	
Louisiana	2,940	
Mississippi	1,300	
Texas	934	
Canada	5,690	22.1
Alberta	150	
Saskatchewan	5,540	
Brazil	284	1.1
Venezuela	2,799	10.8
Romania	6,699	26.0
Total	25,760	100.0

TABLE 46.4—MAJOR THERMAL RECOVERY PROJECTS

	Field, Location (Operator)	Enhanced Oil Production (B/D)
Steamflood	Kern River, CA (Getty)	83,000
	Duri, Indonesia (Caltex)	40,000
	Mount Poso, CA (Shell)	22,800
	San Ardo, CA (Texaco)	22,500
	Tia Juana Este, Venezuela (Maraven)	15,000
Steam stimulation	Lagunillas, Venezuela (Maraven)	40,850
	Duri, Indonesia (Caltex)	22,000
	Cold Lake, Alberta (Esso)	10,000
Fireflood	Suplacu de Barcau, Romania (IFP/IPCCG)	6,552
	Batrum No. 1, Saskatchewan (Mobil)	2,900
	Bellevue, LA (Getty)	2,723
Thermal	Jobo, Venezuela (Lagoven)	13,000

TABLE 46.5—RESERVOIRS AMENABLE TO STEAMFLOOD AND FIREFLOOD

	Steamflood	Fireflood
Depth, ft	160 to 5,000	180 to 11,500
Net pay, ft	10 to 1,050	4 to 150
Dip, degrees	0 to 70	0 to 45
Porosity, %	12 to 39	16 to 39
Permeability, md	70 to 10,000	40 to 10,000
Oil gravity, °API	-2 to 44	9.5 to 40
Oil viscosity at initial temperature, cp	4 to 10 ⁶	0.8 to 10 ⁶
Oil saturation at start, %	15 to 85	30 to 94
OOIP at start, bbl/acre-ft	370 to 2,230	430 to 2,550

for development of thermal recovery methods, since the results will be most rewarding if a percentage of these resources can be tapped economically.

Based on an assumed oil price of \$22.00/bbl, Lewin and Assocs. Inc.¹⁶ estimated that the ultimate recovery in the U.S. by thermal recovery methods will amount to 5.6 to 7.9 billion bbl. This includes 4.0 to 6.0 billion bbl by steamfloods and 1.6 to 1.9 billion bbl by firefloods.

Production Mechanisms

The production mechanisms in steam injection processes have been identified by Willman *et al.*¹⁷ as (1) hot water-flood, including viscosity reduction and swelling, (2) gas drive, (3) steam distillation, and (4) solvent extraction effect. The relative importance of these mechanisms on light and heavy oil, represented by 37.0 and 12.2 °API, respectively, is given in Table 46.6.

In firefloods, the above mechanisms are also important. In addition, the breaking up of heavy oil fractions into light oil fractions through cracking should have at least two effects: increase in volume and more drastic reduction in viscosity. The gas drive effect also should be increased because of the large amount of air injected and combustion gas produced.

Theoretical Considerations

Surface Line and Wellbore Heat Losses

In current field practice, downhole steam generators are still in the developmental stage. Surface steam generators are being used in almost all of the steam injection projects. Steam from a generator normally is sent to the injector wellhead through a surface line. Some heat will be lost to the surrounding atmosphere by convection and radiation. As steam travels from the wellhead through the wellbore to the sandface at the pay zone, heat will be lost to the overburden, mainly by conduction. The method of calculating surface line and wellbore heat losses is discussed below.

Surface Line Heat Losses

The steam lines in most of the steam injection projects are insulated. The heat loss from such a line, Btu/hr, is:

$$Q_{rl} = 2\pi r_{in} U_{ti} (T_s - T_{at}) \Delta L, \dots \dots \dots (1)$$

where

r_{in} = outside radius of the insulation surface, ft,

T_s = steam temperature, °F,

T_{at} = atmospheric temperature, °F, and

ΔL = pipe length, ft.

In the above, U_{ti} is the overall heat transfer coefficient (based on inside radius of the pipe or tubing), Btu/hr-ft-°F, and can be calculated as follows.

$$U_{ti} = \left[\frac{r_{in} \ln \left(\frac{r_{in}}{r_{to}} \right)}{k_{hin}} + \frac{1}{h+I} \right]^{-1}, \dots \dots \dots (2)$$

where r_{to} is the outside radius of pipe, ft, and k_{hin} is the thermal conductivity of insulation material, Btu/hr-sq ft-°F.

The convection heat transfer coefficient, h , Btu/hr-sq ft-°F, can be calculated thus¹⁸:

$$h = 0.75 v_w^{0.6} / r_{in}^{0.4}, \dots\dots\dots (3)$$

where v_w is the wind velocity, mi/hr. The radiation heat transfer coefficient, I , normally can be neglected.

If the pipe is bare, that is, uninsulated, then $r_{io} = r_{in}$ and

$$U_{ii} = h. \dots\dots\dots (4)$$

If the steam is superheated, T_s will vary along the line as heat is being lost to the atmosphere. When the pipe is long, it needs to be broken up into segments and the heat loss calculated segment by segment. In each segment,

$$T_{s2} = T_{s1} - Q_{rl} / w_s C_s, \dots\dots\dots (5)$$

where

T_{s1}, T_{s2} = steam temperatures at the beginning and the end of the segment, °F,

Q_{rl} = heat loss along the segment, Btu/hr,

w_s = mass rate of steam, lbm/hr, and

C_s = heat capacity of steam, Btu/lbm-°F.

If the steam is saturated, the heat loss will cause reduction in steam quality.

$$f_{s2} = f_{s1} - Q_{rl} / w_s L_s, \dots\dots\dots (6)$$

where f_{s1} and f_{s2} equal the steam quality at the beginning and the end of the pipe segment, fraction, and L_s is the latent heat of steam, Btu/lbm.

Wellbore Heat Losses

In most of the steam injection projects, saturated steam at a certain quality is injected into the formation. Here, we assume a more general case in which the steam first enters the wellbore as superheated steam, becomes saturated with a gradually diminishing quality, and is further cooled after its complete condensation into hot water.

Superheated Steam. Assume that when the depth D is 0, the temperature of the steam is T_s and varies with time. Also assume that a linear geothermal gradient exists so that

$$T_f = g_G D + T_{su}, \dots\dots\dots (7)$$

where T_f is the temperature of the formation. Suppose one starts with the temperature of the steam at a depth D_1 , and desires to calculate the temperature at depth D_2 with the length of the depth interval $\Delta D = D_2 - D_1$. Since the formation temperature at D is $g_G D_1 + T_{su}$, Ramey's equation for the gas case¹⁹ becomes

$$\begin{aligned} T(D_2, t) = & g_G D_2 + T_{su} - g_G A - AB \\ & + [T(D_1, t) - g_G D_1 - T_{su} + g_G A + AB] e^{-\Delta D/A}. \end{aligned} \dots\dots\dots (8)$$

A is defined as

$$A = \frac{w_s C_s [k_{hf} + r_{ii} U_{ii} f(t)]}{2\pi r_{ii} U_{ii} k_{hf}} \dots\dots\dots (9)$$

and

$$B = \frac{1}{778 C_s}, \dots\dots\dots (10)$$

where

k_{hf} = thermal conductivity of the formation, Btu/D-ft-°F,

r_{ii} = inside radius of the tubing, ft,

U_{ii} = overall heat transfer coefficient for the annular space between inside of the tubing and outside of the casing based on r_{ii} , Btu/D-ft-°F,

$f(t)$ = transient heat conduction time function for earth, dimensionless, shown in Fig. 46.5,

C_s = heat capacity of steam, Btu/lbm-°F,

g_G = geothermal gradient, °F/ft, and

T_{su} = surface temperature, °F.

For $t > 7$ days,

$$f(t) = \ln \frac{2\sqrt{\alpha t}}{r_{co}} - 0.29, \dots\dots\dots (11)$$

where α is the thermal diffusivity, sq ft/D, and r_{co} is the outside radius of casing, ft.

Saturated Steam. When the steam is saturated, the wellbore heat loss will cause changes in the steam quality whereas the steam temperature, T_s , is kept constant. If

TABLE 46.6—MECHANISMS CONTRIBUTING TO STEAM RECOVERY

	Recovery (% Initial Oil in Place)			
	Torpedo Sandstone Core 37°API Crude		Torpedo Sandstone Core 12.2°API Crude	
	800 (520°F)	84 (327°F)	800 (520°F)	84 (327°F)
	71.0	68.7	68.7	66.0
Steam injection pressure, psig				
Hot waterflood recovery (includes viscosity reduction and swelling)	3.0	3.0	3.0	3.0
Recovery from gas drive	18.9	15.6	9.3	4.9
Extra recovery from steam distillation	4.7	4.6	3.0	3.7
Recovery improvements from solvent/extraction effects				
Total recovery by steam	97.6	91.9	84.0	77.6

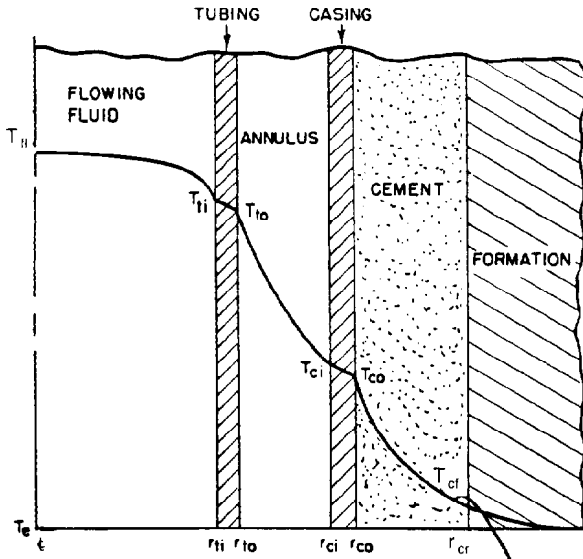


Fig. 46.5—Transient heat conduction in an infinite radial system.

the steam quality at D is $f_s = f_s(D_1, t)$, the steam quality at D_2 can be calculated by Satter's equation²⁰:

$$f_s(D_2, t) = f_s(D_1, t) + \frac{A'B' + aD_1 + b - T_s}{A'} \Delta D + \frac{a(\Delta D)^2}{2A'} \quad (12)$$

In Eq. 12,

$$A' = \frac{w_s L_s [k_{hf} + r_{ii} U_{ii} f(t)]}{2\pi r_{ii} U_{ii} k_{hf}} \quad (13)$$

and

$$B' = \frac{1}{778 L_s} \quad (14)$$

Hot Water. For cooling of the hot water, Ramey's equation for the liquid phase¹⁹ applies. To advance from depth D_1 to D_2 ,

$$T(D_2, t) = g_G D_2 + T_{su} - g_G A + [T(D_1, t) - g_G D_1 + T_{su} + g_G A] e^{-\Delta D/A} \quad (15)$$

Overall Heat Transfer Coefficient. The temperature distribution in an annular completion is shown in Fig. 46.6.²¹ To evaluate the overall heat transfer coefficient, U_{to} , based on the outside tubing surface, the following procedure developed by Willhite²¹ can be used.

1. Select U_{to} based on outside tubing surface.
2. Calculate $f(t)$, as defined previously.
3. Calculate T_{cf} at cement/formation interface.

$$T_{cf} = \frac{T_{fl} f(t) + \frac{k_{hf}}{r_{io} U_{to}} T_f}{f(t) + \frac{k_{hf}}{r_{io} U_{to}}} \quad (16)$$

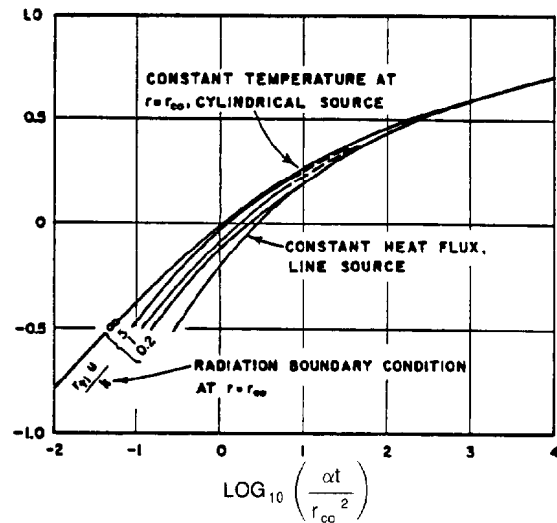


Fig. 46.6—Temperature distribution in an annular completion.

where T_{fl} = temperature of fluid, °F.

4. Calculate T_{ci} at casing inside surface.

$$T_{ci} = T_{cf} + \left(\frac{\ln \frac{r_{cf}}{r_{co}}}{k_{hce}} + \frac{\ln \frac{r_{co}}{r_{ci}}}{k_{hca}} \right) r_{to} U_{to} (T_{fl} - T_{cf}) \quad (17)$$

where

r_{cf} = radius to cement/formation interface, ft,

r_{ci} = inside radius of casing, ft,

k_{hce} = thermal conductivity of the cement, Btu/hr-ft-°F, and

k_{hca} = thermal conductivity of the casing material, Btu/hr-ft-°F.

5. Estimate I for radiation and h for natural convection.

6. Calculate U_{to} .

$$U_{to} = \left(\frac{1}{h + I} + \frac{r_{to} \ln \frac{r_{cf}}{r_{co}}}{k_{hce}} \right)^{-1} \quad (18)$$

With commercial insulation of thickness Δr ,

$$U_{to} = \left[\frac{r_{to} \ln \frac{r_{in}}{r_{to}}}{k_{hin}} + \frac{r_{to}}{r_{in}(h' + I')} + \frac{r_{to} \ln \frac{r_{cf}}{r_{co}}}{k_{hce}} \right]^{-1} \quad (19)$$

where h' and I' are based on insulation outside surface.

Calculations Including Pressure Changes. A more sophisticated calculation procedure proposed by Earlougher²² includes the effect of pressure changes inside the wellbore. The wellbore is divided into a sequence

of depth intervals. The conditions at the bottom of each interval are calculated, on the basis of the conditions at the top of that interval. The procedure is as follows.

1. Calculate the pressure at the bottom of the interval, p_2 .

$$p_2 = p_1 + 1.687 \times 10^{-12} (v_{t1} - v_{t2}) \frac{w_s^2}{r_{ti}^4} + 6.944 \times 10^{-3} \frac{\Delta D}{v_{t1}} - \Delta p, \dots (20)$$

where

v_t = specific volume of the total fluid, cu ft/lbm (condition 1 is top of interval and 2 is bottom),

ΔD = length of depth interval, ft, and

Δp = frictional pressure drop over interval, psi.

The Beggs and Brill correlation²³ for two-phase flow can be used to calculate the Δp in the above equation.

2. Calculate the heat loss over the interval.

$$Q_l = \frac{2\pi k_{hf} r_{co} U_{co} \Delta D}{k_{hf} + r_{co} U_{co} f(t)} \times [0.5(T_{s1} + T_{s2}) - 0.5(T_{f1} + T_{f2})], \dots (21)$$

where U_{co} is the overall heat transfer coefficient based on outside casing surface, Btu/hr-sq ft-°F.

3. Calculate the steam quality at the bottom of the interval.

$$f_{s2} = \frac{f_{s1} L_{v1} + H_{w1} - H_{w2} - Q_l / w_s}{L_{v2}}, \dots (22)$$

where H_{w1} and H_{w2} are the enthalpy of liquid water at top and bottom of the interval, Btu/lbm, and L_{v1} and L_{v2} are the latent heat of vaporization at top and bottom of the interval, Btu/lbm.

More Recent Developments. A new model has been developed by Farouq Ali²⁴ that treats wellbore heat losses rigorously by using a grid system to represent the surrounding formation. In addition, the pressure calculation accounts for slip and the prevailing flow regime, based on well-accepted correlations.

Analytical Models for Steam Injection

For predicting reservoir performance under steam injection processes, the usual practice is to use three-dimensional (3D), three-phase numerical simulators. Where the simulators are unavailable or a quick estimate of the performance is needed, one can resort to simple analytical methods. Usually these methods take into account the thermal aspects of the process only, without regard to the fluid flow aspects.

Front Displacement Models

Marx-Langenheim Method.²⁵ Consider that heat is injected into a pay zone bounded by two neighboring for-

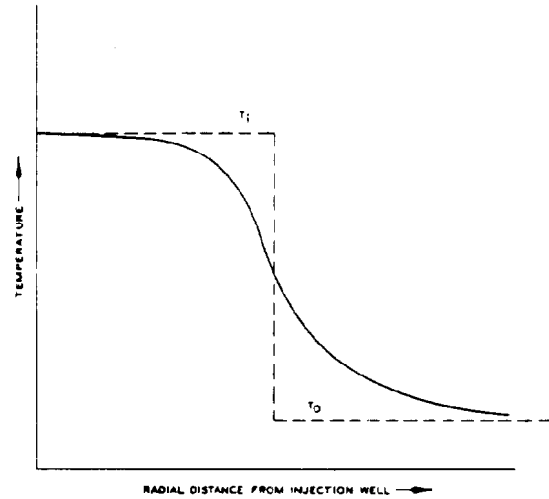


Fig. 46.7—Temperature distribution in Marx-Langenheim model.

mations. The heat-carrying fluid is supposed to advance with a sharp front perpendicular to the boundaries of the formation (Fig. 46.7). The heat balance gives: heat injected into the pay zone equals heat loss to the overburden and underlying stratum plus heat contained in the pay zone.

The heated area at any time t can be calculated

$$A = \frac{Q_{ri} M h \alpha_o}{4 k_{ho}^2 \Delta T} \left(e^{t_D} \operatorname{erfc} \sqrt{t_D} + 2 \sqrt{\frac{t_D}{\pi}} - 1 \right), \dots (23)$$

where

A = heated area at time t , sq ft,

t = time since injection, hr,

Q_{ri} = heat injection rate, Btu/hr,

M = volumetric heat capacity of the solid matrix containing oil and water, Btu/cu ft-°F

$$= (1 - \phi) \rho_r C_r + S_{wi} \phi \rho_w C_w + S_{oi} \phi \rho_o C_o,$$

$$\dots (24)$$

ϕ = porosity, fraction,

ρ_r, ρ_o, ρ_w = density of rock grain, oil, water, lbm/cu ft,

C_r, C_o, C_w = heat capacity of rock, oil, water, Btu/lbm-°F,

S_{oi}, S_{wi} = initial saturation of oil, water, fraction,

h = pay thickness, ft,

α_o = overburden thermal diffusivity, sq ft/hr,

k_{ho} = overburden thermal conductivity, Btu/hr-ft-°F,

$\Delta T = T_{inj} - T_{fi}$, °F,

T_{inj} = injection temperature, °F,

T_{fi} = initial formation temperature, °F,

t_D = dimensionless time

$$= \left(\frac{4 k_{ho}^2}{M^2 h^2 \alpha_o} \right) t, \dots (25)$$

and

$$\sqrt{t_D} = \left(\frac{2k_{ho}}{Mh\sqrt{\alpha_o}} \right) t^{1/2} \quad (26)$$

The complementary error function is:

$$\operatorname{erfc} x = 1 - \operatorname{erf} x = 1 - \frac{2}{\pi} \int_0^x e^{-\beta^2} d\beta, \quad (27)$$

where β is a dummy variable.

To evaluate $e^{t_D} \operatorname{erfc} \sqrt{t_D}$, one can use the following approximation,²⁶

$$\text{Let } y = \frac{1}{1 + 0.3275911\sqrt{t_D}}, \quad (28)$$

$$\begin{aligned} e^{t_D} \operatorname{erfc} \sqrt{t_D} &= 0.254829592y - 0.284496736y^2 \\ &+ 1.42143741y^3 - 1.453152027y^4 + 1.061405429y^5 \\ &\dots \dots \dots (29) \end{aligned}$$

Assume that all the movable oil is displaced in the heated area. If we assume that all the displaced oil is produced, we can calculate the cumulative steam/oil ratio (SOR):

$$F_{so}^* = \frac{i_s t}{4.275 A h \phi (S_{oi} - S_{io})}, \quad (30)$$

where

i_s = steam injection rate, B/D, cold water equivalent,

S_{oi} = initial oil saturation, and

S_{io} = irreducible oil saturation.

Differentiation of the expression for A with t gives the rate of expansion of the heated area. The oil displacement rate, q_{od} , in B/D, is

$$q_{od} = 4.275 \left[\frac{Q_{ri} \phi (S_{oi} - S_{or})}{M \Delta T} \right] e^{t_D} \operatorname{erfc} \sqrt{t_D} \quad (31)$$

From this one can calculate the instantaneous SOR:

$$F_{so} = \frac{i_s}{q_{od}} \quad (32)$$

The thermal (heat) efficiency, E_h , is defined as

$$E_h = \frac{Q_{hz}}{Q_{it}} \quad (33)$$

where

Q_{hz} = heat remaining in the heated zone, Btu,

Q_{it} = total heat injection, Btu, and

$$E_h = \frac{A h M \Delta T}{Q_{ri} T} \quad (34)$$

It can easily be shown that

$$E_h = \frac{1}{t_D} \left(e^{t_D} \operatorname{erfc} \sqrt{t_D} + 2 \sqrt{\frac{t_D}{\pi}} - 1 \right) \quad (35)$$

Ramey's Generalization of the Marx-Langenheim Method.²⁷ The Marx-Langenheim method can be extended to the case where a series of constant injection rates is maintained over various time periods. If the heat injection rate is $(Q_{ri})_i$ over the period $0 < t < t_1$, and $(Q_{ri})_n$ over the period $t_{n-1} < t < t_n$,

$$\begin{aligned} A &= \frac{M h \alpha_o}{4 k_{ho}^2 \Delta T} \left\{ (Q_{ri})_n F(t_{Dn}) \right. \\ &+ \sum_{i=1}^{i=n-1} [(Q_{ri})_i - (Q_{ri})_{i+1}] F(t_{Di}) \left. \right\}, \quad (36) \end{aligned}$$

where

$$F(t_{Di}) = e^{t_{Di}} \operatorname{erfc} \sqrt{t_{Di}} + 2 \sqrt{\frac{t_{Di}}{\pi}} - 1 \quad (37)$$

and $F(t_{Dn}) = F(t_{Di})$ with $i = n$. The oil displacement rate at t_i depends on the heat injection rate at that time, independent of the previous heat injection rates.

Mandl-Volek's Refinement of the Marx-Langenheim Method.²⁸ Mandl and Volek observed that the heated area measured in laboratory experiments tends to be lower than that predicted by the Marx-Langenheim method after a certain critical time, t_c . For $t \geq t_c$,

$$\begin{aligned} A &= \frac{Q_{ri} M h \alpha_o}{4 k_{ho}^2 \Delta T} \left[e^{t_D} \operatorname{erfc} \sqrt{t_D} + 2 \sqrt{\frac{t_D}{\pi}} - 1 - \sqrt{\frac{t_D - t_{cD}}{\pi}} \right. \\ &\times \left(\frac{1}{1 + \frac{L_s f_s}{C_w \Delta T}} + \frac{t_D - t_{cD}^{-3}}{3} e^{t_D} \operatorname{erfc} \sqrt{t_D} \right. \\ &\left. \left. - \frac{t_D - t_{cD}}{3 \sqrt{\pi t_D}} \right) \right] \quad (38) \end{aligned}$$

t_c is determined by this equation:

$$e^{t_{cD}} \operatorname{erfc} \sqrt{t_{cD}} = \frac{1}{1 + \frac{L_s f_s}{C_w \Delta T}} \quad (39)$$

The relationship between t_c and t_{cD} is again

$$t_{cD} = \left(\frac{4 k_{ho}^2}{M^2 h^2 \alpha_o} \right) t_c \quad (40)$$

Myhill and Stegemeier²⁹ used a slightly different version of the Mandl-Volek model and calculated oil/steam ratio (OSR) for 11 field projects. They found that the actual OSR's range from 70 to 100% of the calculated ratios.

Steam Chest Models

In contrast to the front displacement models discussed previously, Neuman³⁰ visualized that steam rises to the top and grows both horizontally outward and vertically downward. Doscher and Ghassemi³¹ took a view even more drastic than Neuman's. They theorized that steam rises to the top instantly and the only direction of the steam zone movement is vertically downward. Vogel³² followed the same reasoning and developed the following simple equation for thermal efficiency:

$$E_h = \frac{1}{1 + \sqrt{\frac{4}{\pi} t_D}} \quad (41)$$

Table 46.7 compares the thermal efficiencies calculated by the Marx-Langenheim method and the Vogel method. This table shows that the Vogel method predicts a thermal efficiency that lies between 80 and 100% of that calculated by the Marx-Langenheim method.

Steam Stimulation

Steam stimulation usually is carried out in a number of cycles. Each cycle consists of three stages: steam injection, soaking, and production. The basic concept of this process follows.

Without stimulation, the oil production rate is

$$q_{oc} = \frac{0.00708kk_{ro}h}{\mu_{oc} \ln \frac{r_e}{r_w}} (p_e - p_w), \quad (42)$$

where

- q_{oc} = cold oil production rate, B/D,
- k = absolute permeability, md,
- k_{ro} = relative permeability to oil, fraction,
- μ_{oc} = cold oil viscosity, cp,
- p_e = static formation pressure at external radius r_e , psia, and
- p_w = bottomhole pressure, psia.

After steam injection, the oil inside the heated region, $r_w < r < r_h$, will have a lower viscosity, μ_{oh} . The hot oil production, q_{oh} , is:

$$q_{oh} = \frac{0.00708kk_{ro}h}{\mu_{oh} \ln \frac{r_h}{r_w} + \mu_{oc} \ln \frac{r_e}{r_h}} (p_e - p_w), \quad (43)$$

TABLE 46.7—COMPARISON BETWEEN MARX-LANGENHEIM AND VOGEL METHODS

t_D	Thermal Efficiency		Ratio Vogel/ML
	Marx-Langenheim	Vogel	
0.01	0.930	0.900	0.967
0.1	0.804	0.737	0.917
1.0	0.556	0.470	0.845
10.0	0.274	0.219	0.799
100.0	0.103	0.081	0.787

where r_h equals the radius of the heated region, ft. The ratio between q_{oh} and q_{oc} is

$$\frac{q_{oh}}{q_{oc}} = \frac{1}{\frac{\mu_{oh}}{\mu_{oc}} \frac{\ln \frac{r_h}{r_w}}{\ln \frac{r_e}{r_h}} + \frac{\ln \frac{r_e}{r_h}}{\ln \frac{r_e}{r_w}}} \quad (44)$$

As the reservoir fluids are produced, energy associated with the fluids are removed from the reservoir. This causes a reduction in r_h and a reduction in temperature, which increases μ_{oh} .

Several methods have been developed for calculating reservoir performance under steam stimulation. One of the methods, which has enjoyed wide acceptance, is the Boberg and Lantz method.³³ This method assumes a constant r_h , with a changing \bar{T} inside the heated zone. The method consists of the following steps.

1. Calculate the size of the heated region using the Marx-Langenheim method.
2. Calculate the average temperature in this region.
3. Calculate the oil production rate, taking into account the reduced oil viscosity in this region.
4. Repeat Steps 1 through 3 for succeeding cycles, by including the residual heat left from preceding cycles.

The average temperature of the heated region is calculated by

$$\bar{T} = T_R + (T_s - T_R)[\bar{V}_r \bar{V}_z (1 - \delta) - \delta], \quad (45)$$

where

- \bar{T} = average temperature of the heated region, $r_w < r < r_h$, at any time t , °F,
- T_R = original reservoir temperature, °F,
- T_s = steam temperature at sandface injection pressure, °F,
- \bar{V}_r, \bar{V}_z = average values of V_r, V_z for $0 < r < r_h$ and all h_j ,*
- V_r, V_z = unit solution for the component conduction problems in the r and z directions, and
- δ = energy removed with the produced fluids, dimensionless.

The quantities \bar{V}_r and \bar{V}_z can be obtained from Fig. 46.8 as functions of dimensionless time, t_D . For \bar{V}_r ,

$$t_D = \frac{\alpha_o(t - t_i)}{r_h^2}, \quad (46)$$

*These symbols have no physical connotation. They are simply mathematical symbols.

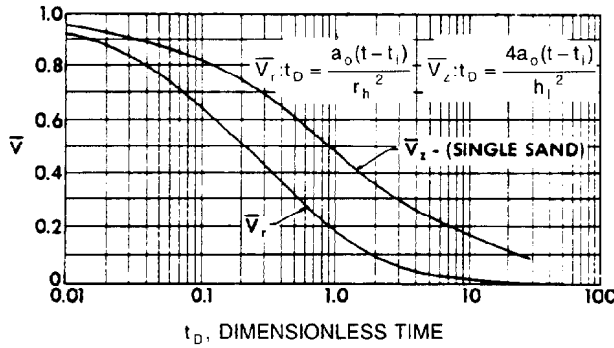


Fig. 46.8—Solutions for V_r and V_s , single sand.

where

- α_o = overburden thermal diffusivity, sq ft/D,
 t = time since start of injection for the current cycle, D,
 t_i = time of injection for the current cycle, D,
 and
 r_h = radius of region originally heated, ft.

For \bar{V}_z ,

$$t_D = \frac{\alpha_o(t-t_i)}{\bar{H}_1^2}, \quad (47)$$

where

$$\bar{H}_1 = \frac{m_{sit}(f_s L_s + H_{ws} - H_{wR})}{\pi(r_h^2 M)(T_s - T_R)N_s}, \quad (48)$$

and

- m_{sit} = total mass of steam injected, lbm,
 N_s = number of sands,
 H_{ws}, H_{wR} = enthalpy, Btu/lbm, of water at steam and reservoir temperatures, °F, and
 M = volumetric heat capacity, Btu/cu ft-°F.

The energy removed with produced fluids, δ , can be calculated thus:

$$\delta = \frac{1}{2} \int_{t_i}^t \frac{Q_{rt} dt}{h_t \pi r_h^2 M (T_s - T_R)}, \quad (49)$$

where

- h_t = total thickness of all sands, ft,
 Q_{rt} = heat removal rate at time t , Btu/D,

$$Q_{rt} = q_{oh}(H_{og} + H_w), \quad (50)$$

$$H_{og} = (5.6146M_o + R_t C_g)(\bar{T} - T_R), \quad (51)$$

and

$$H_w = 5.6146\rho_w[F_{wot}(h_f - H_{wR}) + R_t L_s], \quad (52)$$

where h_f is the enthalpy of liquid water at T above 32°F (see steam tables), Btu/lbm, H_{og} is the enthalpy of oil and gas based on a STB of oil, Btu/STB oil, and H_w is

the enthalpy of water carried by oil based on a STB of oil, Btu/STB oil. Also, L_s is h_{fg} in the steam tables.

If $p_w > p_s$ and $F_{so} < F_{wot}$

$$F_{so} = 0.0001356 \left(\frac{p_s}{p_w - p_s} \right) R_t, \quad (53)$$

bbl liquid water at 60°F/STB oil.

If F_{so} (calculated) $> F_{wot}$,

$$F_{so} = F_{wot}. \quad (54)$$

In the above,

- R_t = total produced GOR, scf/STB,
 F_{wot} = total produced WOR, STB/STB,
 F_{so} = steam/oil ratio, STB/STB,
 p_w = producing bottomhole pressure, psia, and
 p_s = saturated vapor pressure of water at \bar{T} , psia.

The rate of hot oil production can be calculated thus:

$$q_{oh} = F_J J_c \Delta p, \quad (55)$$

where F_J is the ratio of stimulated to unstimulated productivity indexes, dimensionless,

$$F_J = \frac{1}{\frac{\mu_{oh}}{\mu_{oc}} C_1 + C_2}, \quad (56)$$

and J_c is the unstimulated (cold) productivity index, STB/D/psi,

$$J_c = \frac{0.000708 k k_{ro} h}{\mu_{oc} \ln \frac{r_e}{r_w}}. \quad (57)$$

If p_e is constant,

$$C_1 = \frac{\ln \frac{r_h}{r_w}}{\ln \frac{r_e}{r_w}} \quad (58)$$

and

$$C_2 = \frac{\ln \frac{r_e}{r_h}}{\ln \frac{r_e}{r_w}}. \quad (59)$$

Thus Eq. 55 is identical with Eq. 43 in this case. If p_e is declining,

$$C_1 = \frac{\ln \frac{r_h}{r_w} - \frac{r_h^2}{2r_e^2}}{\ln \frac{r_e}{r_w} - \frac{1}{2}} \quad (60)$$

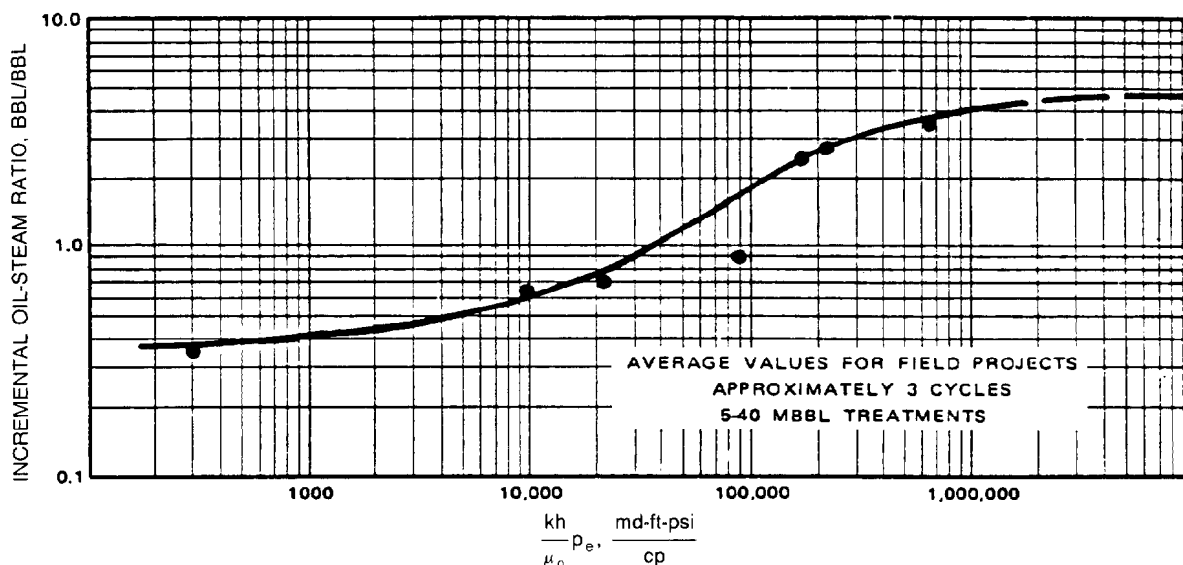


Fig. 46.9—Correlation of steam stimulation results.

and

$$C_2 = \frac{\ln \frac{r_e}{r_h} - \frac{1}{2} + \frac{r_h^2}{2r_e^2}}{\ln \frac{r_e}{r_w} - \frac{1}{2}} \quad \dots \dots \dots (61)$$

This method of calculating oil production rate is probably the weakest part of the Boberg-Lantz method.

1. It assumes a monotone decline between p_e and p_w . Actually, because the injected steam is at a high pressure, there could be a high pressure p_s near r_h and the pressure declines toward both p_w and p_e .

2. Only the change in μ_o is accounted for in changing from cold oil productivity to hot oil productivity. Left unaccounted for is the change in k_{ro} , which should change with changing S_o .

Based on the Boberg-Lantz method, a correlation was developed by Boberg and West³⁴ that allows one to estimate incremental OSR with known reservoir properties (Fig. 46.9).

Numerical Simulation

The analytical models for thermal recovery processes usually are concerned with the thermal aspects of the processes only. The fluid flow aspects are neglected. To account adequately for the fluid flow inside porous media under a thermal recovery process, numerical simulators will be needed. In these simulators, the reservoir is divided into a number of blocks arranged in one, two, or three dimensions. A detailed study is made of the reservoir by applying fundamental equations for flow in porous media to each one of the blocks.

Numerical reservoir simulators are no substitute for field pilots. They have several advantages, however, over field pilots. Field conditions are irreversible. It took millions of years for the field to develop to the present state. Once disturbed, it cannot revert to the original conditions and start over again. Furthermore, it takes a long time, in terms of months or even years, before the pilot results

can be evaluated. The cost for pilots is, of course, enormous. In comparison, a simulated reservoir can be produced many times, each time starting at the existing state. This can be done within a short period of time, in terms of seconds, once the reservoir model is properly set up. The cost for reservoir simulation is much less than that of a pilot. However, simulated reservoirs may never duplicate field performance. Modern practice is to use reservoir simulation to help design a pilot before launching a large-scale field development.

Numerical models and physical models are complementary to each other. As will be detailed later, physical models can be classified into two types: elemental models and partially scaled models. In an elemental model, experiments are conducted with actual reservoir rock and fluids. The results can help explain various fluid flow and heat transfer mechanisms as well as chemical reaction kinetics. In a partially scaled model, reservoir dimensions, fluid properties, and rock properties are scaled for the laboratory model so that the ratios of various forces in the reservoir and the physical model are nearly the same. One can only build partially scaled models because fully scaled models are difficult or impossible to construct. One of the advantages of a numerical model over a physical model is that there is no scaling problem in numerical simulation. However, in many cases, a numerical model needs physical models to validate the formulation or to provide necessary input data for the simulation.

Steam Injection Model

Numerical simulation models for steam injection processes have been developed by Coats *et al.*³⁵ and Coats.^{36,37} A steam injection model consists of a number of conservation equations.

1. *Mass balance of H_2O .* Both water and steam are included.

2. *Mass balances of hydrocarbons.* Only one equation will be necessary for nonvolatile oil. For volatile oil, two or more pseudocomponents will be needed to describe the vaporization/condensation phenomenon of the oil and two or more equations will be needed.

3. **Energy balance.** The energy balance accounts for heat conduction, convection, vaporization/condensation phenomenon, and heat loss from the pay zone to its adjacent formations. The need to include an energy balance in the model sets the thermal recovery processes apart from isothermal processes for oil recovery.

In addition to the conservation equations, the model needs to include the following auxiliary equations.

1. If both water and steam coexist, temperature is the saturated steam temperature for a given pressure. An equation is needed to describe this relationship between temperature and pressure.

2. The sum of saturations for the oil, water, and gas phases equals unity.

3. The mol fractions of hydrocarbon components in the liquid and gas phases are related through equilibrium vaporization constants (K -values).

4. The sum of gas-phase mol fractions equals unity. This includes steam and any volatile components of hydrocarbons.

5. The sum of liquid-phase mol fractions for hydrocarbons equals unity.

In-Situ Combustion Model

Numerical simulation models have been developed by Crookston *et al.*,³⁸ Youngren,³⁹ Coats,⁴⁰ and Grabowski *et al.*⁴¹ The in-situ combustion model is more complicated than the model for steam injection. The conservation equations are as follows.

1. **Mass balance of H_2O .** This equation includes the water produced from combustion.

2. **Mass balances of hydrocarbons.** This includes consumption of certain hydrocarbons through cracking and combustion. It also may include the production of certain other components through cracking.

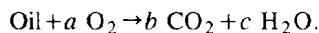
3. **Mass balance of oxygen.** This accounts for the consumption of oxygen by combustion.

4. **Mass balance of inert gas.** If air is used, the conservation of nitrogen should be accounted for. CO_2 produced from combustion may be included in the equation for the inert gas or be treated separately.

5. **Mass balance of coke.** This includes the formation and burning of coke.

6. **Energy balance.** This equation now includes the heat of reaction for the reactions involved in the in-situ combustion process. These reactions may include low-temperature oxidation of hydrocarbons, high-temperature oxidation or burning of hydrocarbons, thermal cracking (which produces coke and other products), and combustion of coke.

This model also needs a number of auxiliary equations, which include (1) steam/water equilibrium, (2) vaporization equilibrium of hydrocarbons, (3) phase saturation constraints, (4) mol fraction constraints, and (5) chemical stoichiometry. An example is:



This says that one mol of oil reacts with a mols of oxygen to form b mols of CO_2 and c mols of H_2O .

This model also requires a chemical reaction kinetics equation. For each reaction involved in the process, an equation can be written to denote that the reaction rate varies as a function of temperature and concentrations of

the various reactants. One possible form of the reaction rate equation is the following Arrhenius equation:

$$w = k'(C_o)^m (C_{O_2})^n \exp\left(-\frac{E}{RT}\right) \dots \dots \dots (62)$$

This equation says that the reaction rate, w , is proportional to the concentration of oil, C_o , raised to the m th power times the concentration of oxygen, C_{O_2} , raised to the n th power. The temperature dependence of the reaction rate is in the given exponential form, where E is the activation energy, the energy barrier the reactants need to overcome before being converted to the products, R is the gas constant, and T is the absolute temperature. The proportionality constant, k' , usually is called the pre-exponential factor.

The models developed so far are believed to be adequate as far as the formulation of the process mechanisms is concerned. However, problems abound.

1. Artificial breakdown of the crude oil into two components may not be sufficient to describe faithfully the vaporization/condensation phenomena and the chemical reactions involved in the combustion process. More components mean more equations to be solved and hence higher computer costs.

2. The grid size problem could be severe. A grid size large enough for economic computation could greatly distort the temperature distributions in the simulated reservoir. This would lead to erroneous predictions of the chemical reaction rates and thus of reservoir performance under combustion.

Laboratory Experimentation

The thermal numerical models have been used widely for screening thermal prospects, designing field projects, and formulating production strategies. Still, we cannot completely dispense with laboratory experiments for several reasons. First, the numerical models need data that can be measured only experimentally. These data include relative permeabilities, chemical kinetics, adsorption of chemicals on rocks, etc. Second, the numerical models are valid only when all the pertinent mechanisms are accounted for. The currently available models cannot handle adequately situations such as injection of chemicals along with steam, swelling of clays, which reduces the permeability, etc.

As previously mentioned, physical models for thermal recovery processes may be classified into two types, namely, elemental models and partially scaled models. The elemental models are used to study the physico-chemical changes inside a rock-fluid system under certain sets of operating conditions and are normally zero-dimensional (0D) or one-dimensional (1D). The partially scaled models are used to simulate the performance of a reservoir under thermal recovery operations and are normally 3D. Although the intent is to scale every physico-chemical change that takes place in the processes, the models usually are partially scaled because of the extreme difficulty in achieving full scaling.

Elemental Models

Elemental models used for steamflooding can be exemplified by those used by Willman *et al.*¹⁷ In their classic work, they used glass bead packs and natural cores

of different lengths to study the recovery of oil under hot waterflood and steamflood at different temperatures. The oils used included crudes of different gravities and oil fractions.

Fireflood pots and combustion tubes are also elemental models. In another classic work, Alexander *et al.*⁴² used fireflood pots (0D) to study fuel laydown and air requirement, as affected by crude oil characteristics, porous medium type, oil saturation, air flux, and time-temperature relationships. The combustion tube (1D) used by Showalter⁴³ enabled him to delineate the temperature profiles at various times, thus giving the combustion front velocity. More recently, combustion tubes were used to study the use of water along with air⁴⁴⁻⁴⁶ and the use of oxygen-enriched air in combustion.⁴⁷

Partially Scaled Models

Partially scaled models have been used to simulate steamfloods in $\frac{1}{8}$ of a five-spot pattern, $\frac{1}{4}$ of a five-spot pattern, etc.⁴⁸⁻⁵³ Similar attempts have also been made for firefloods.⁵⁴ However, it is certainly much more difficult to include chemical kinetics along with the fluid flow and heat transfer aspects of the combustion process.

Partially scaled models for steamfloods fall into two types, namely, high-pressure models and vacuum or low-pressure models.

High-Pressure Models. All experimental studies on steamflooding had used high-pressure models until vacuum models came along and offered an alternative approach. The scaling laws of Pujol and Boberg⁵⁵ normally were followed in the design. If the dimensions are scaled down by a factor of F in the model, the steam injection rate will be scaled down by the same factor and so will the pressure drop between the injector and the producer. The permeability will be scaled up by a factor of F , and the model time will be scaled down by a factor of F^2 . Because of the necessity of increasing the permeability in the model to a great extent, reservoir rock material cannot be used. Nevertheless, the experiments will be conducted with the actual crude. Also, the steam pressure and steam quality to be employed in the field will be used in the model.

Vacuum Models. In a small-scale physical model, the thickness is reduced greatly as compared with that in the field. To obtain the same gravitational effects as in the field, the pressure drop from the injector to the producer also must be reduced greatly. The vaporization/condensation phenomenon of water and hydrocarbons is governed by the Clausius-Clapeyron equation, which involves $d \ln p$, or dp/p . Thus, a decrease in the pressure drop (dp) necessitates a corresponding decrease in the pressure (p) itself. This is the rationale behind the vacuum-model approach developed by the Shell group as reported by Stegemeier *et al.*⁵⁶

To see the differences between a high-pressure model and the vacuum model, Table 46.8 has been prepared for using both models to simulate a hypothetical field element with a hypothetical oil. The entries for the high-pressure models were based on the scaling laws of Pujol and Boberg⁵⁵ and the entries for the vacuum model were based on the work of Stegemeier *et al.*⁵⁶

TABLE 46.8—COMPARISON OF HIGH-PRESSURE AND VACUUM MODELS FOR STEAMFLOODS

	Field	High-Pressure Model	Vacuum Model
Length, ft	229	1	1
Permeability, darcies	2	458	1,527
Time	5 yrs	50 min	120 min
Steam rate	300 B/D	144.7 cm ³ /min	263.1 cm ³ /min
Pressure 1, psia	400	400	2.70
Steam quality	0.80	0.80	0.082
Oil viscosity, cp	3.0	3.0	23.6
Temperature, °F	445	445	137.5
Pressure 2, psia	100	100	1.24
Steam quality	0.80	0.80	0.108
Oil viscosity, cp	6.3	6.3	38.2
Temperature, °F	328	328	108.9

The following observations can be made on the high-pressure and vacuum models.

1. Neither the high-pressure model nor the vacuum model can accurately simulate the capillary forces and the relative permeability curves of the actual rock/fluid system because, to obtain a very high permeability, actual rock material is not being used.

2. The high-pressure model does not observe the Clausius-Clapeyron equation, whereas the vacuum model follows it to a large extent but not exactly.

3. To use the vacuum model, an oil has to be reconstituted to obtain the required oil viscosity/temperature relationship. This is completely different from the actual crude in many physicochemical aspects, including its vaporization/condensation behavior and chemical kinetics. In contrast, a high-pressure model normally uses actual crudes.

Field Projects

Screening Guides

In dealing with oil prospects, the first step is to find out whether the field in question can be produced by certain recovery methods. Screening guides are useful for this purpose. Screening guides for steamflood and fireflood processes have been proposed by various authors including Farouq Ali,⁵⁷ Geffen,⁵⁸ Lewin *et al.*,⁵⁹ Iyoho,⁶⁰ Chu,⁶¹⁻⁶³ and Poettmann.⁶⁴ These screening guides are listed in Table 46.9.

A perusal of the various screening guides listed in Table 46.9 shows that some of the earlier screening guides were quite restrictive in selecting oil prospects. Such a guide tends to minimize the error of the second kind, that is, the risk of excluding some undesirable prospects. In so doing, it tends to increase the error of the first kind, that is, the risk of missing some desirable prospects. Recent changes in the price structure of the crude oil and improved technology helped to widen the range of applicability for the steamflood and fireflood processes. This is reflected in the less restrictive screening guides developed in more recent years. However, in minimizing the error of the first kind (erroneous rejection), the newer guides may possibly increase the error of the second kind (erroneous acceptance). This should be borne in mind when applying these guides to oil prospects.

TABLE 46.9—SCREENING GUIDES FOR STEAMFLOOD AND FIREFLOOD PROJECTS

References	Year	h	D	ϕ	k	ρ	S_o	$^{\circ}\text{API}$	μ	kh/μ	ϕS_o	γ^*	Remarks
Steamfloods													
Farouq Ali ⁵⁷	1973	≥ 30	$< 3,000$	0.30	$\sim 1,000$			12 to 15	$< 1,000$		0.15 to 0.22		
Geffen ⁵⁸	1973	> 20	$< 4,000$					> 10		> 20	> 0.10		
Lewin and Assocs. ⁵⁹	1976	> 20	$< 5,000$				> 0.50	> 10		> 100	> 0.065		
Iyoho ⁶⁰	1979	30 to 400	2,500 to 5,000	> 0.30	$> 1,000$		> 0.50	10 to 20	200 to 1,000	> 50	> 0.065		
Chu ⁶¹	1983	> 10	> 400	> 0.20			> 0.40	< 36			> 0.08		
Firefloods													
Poettmann ⁶⁴	1964			> 0.20	> 100						> 0.10		
Geffen ⁵⁸	1973	> 10	> 500			> 250		< 45		> 100	> 0.05		for COFCAW only
Lewin and Assocs. ⁵⁹	1976	> 10	> 500				> 0.50	10 to 45		> 20	> 0.05		
Chu ⁶²	1977			≥ 0.22			≥ 0.50	≤ 24	$< 1,000$		> 0.13		confidence limits approach
	1977											> 0.27	regression analysis approach
Iyoho ⁶⁰	1978	5 to 50	200 to 4,500	≥ 0.20	> 300		> 0.50	10 to 40	$< 1,000$	> 20	> 0.077		for dry combustion (well spacing ≤ 40 acres)
	1978	10 to 120		≥ 0.20			> 0.50	< 10	no upper limit		> 0.064		for reverse combustion
	1978	> 10	> 500	≥ 0.25			> 0.50	< 45	$< 1,000$		> 0.064		for wet combustion
Chu ⁶³	1982			> 0.16	> 100		> 0.35	< 40		> 10	> 0.10		

$$\gamma^* = -0.12 + 0.00262h + 0.000114k + 2.23S_o + 0.000242kh/\mu - 0.000189D - 0.0000652\mu$$

Reservoir Performance

Performance Indicators Common to Both Steamfloods and Firefloods. Sweep Efficiency. The areal and vertical sweep of the steam front or burning front has pronounced influence on the economics of the steamflood or fireflood projects. Some reported sweep efficiencies of the steamflood and fireflood projects are given in Table 46.10.⁶⁵⁻⁸¹ Whereas the volumetric sweep of steamfloods varies from 24 to 99%, that of firefloods appears to be lower, ranging from 14 to 60%.

TABLE 46.10—SWEEP EFFICIENCY OF STEAMFLOOD AND FIREFLOOD PROJECTS

Field, Location (Operator)	Areal	Vertical	Volumetric
Steamfloods			
Inglewood, CA ⁶⁵ (Chevron-Socal)	60.0	50.0	30.0
Kern River, CA ^{66,67} (Chevron)	—	—	80.0
Kern River, CA ⁶⁸⁻⁷⁰ (Getty)	~ 100.0		62.8 to 98.8
Midway Sunset, CA ^{71,72} (Tenneco)	—	—	60.0 to 70.0
El Dorado, KA ⁷³ (Cities)	—	—	< 50.0
Deerfield, MO ⁷⁴ (Esso-Humble)	85.0	40.0	34.0
Schoonebeek, The Netherlands ⁷⁵ (Nederlandse)	—	—	24.3 to 41.9
Firefloods			
South Belridge, CA ⁷⁶ (General Petroleum)			
Within Pattern Area (2.75 acres)	100	59.6	59.6
Within Total Burned Area (7.90 acres)	100	50.4	50.4
Sloss, NE ⁷⁷⁻⁷⁹ (Amoco)	50	28	14
South Oklahoma ⁸⁰ (Magnolia)	85	—	26
Shannon Pool, WY ⁸¹ (Pan American/Casper)	43	100	43

Oil Recovery. Table 46.11 lists some of the reported oil recoveries of steamflood and fireflood projects.⁸²⁻¹²¹

For the estimation of the oil recovery obtainable in a steam injection project, the analytical methods discussed previously can be used. As steam injection continues, the thermal efficiency will gradually diminish and the instantaneous SOR will increase gradually. When this ratio reaches a certain limit, further injection of steam will become uneconomical and needs to be stopped. The cumulative oil production at that time divided by the original oil in place (OOIP) will give the oil recovery.

The oil recovery from a fireflood project can be calculated with the recognition that oil production comes from both the burned and unburned regions (Nelson and McNeil¹²²). Let E_{vb} equal the volumetric sweep efficiency of the burning front and E_{Ru} equal the recovery efficiency in the unburned region. The overall oil recovery is:

$$E_R = \left(1 - \frac{C_m}{62.4\phi S_o}\right) E_{vb} + (1 - E_{vb}) E_{Ru}, \dots (63)$$

where C_m is the fuel content, lbm/cu ft. In this equation, the fuel consumed is taken to be a 10° API oil with a density of 62.4 lbm/cu ft.

The equation developed by Satman *et al.*¹²³ can be used to calculate the oil recovery from a dry combustion project.

$$Y = 47.0 \left[0.427S_o - 0.00135h - 2.196 \left(\frac{1}{\mu_o} \right)^{0.25} \right] X, \dots (64)$$

where

$$Y = \frac{\Delta N_p + V_{fh}}{N} \times 100 \dots (65)$$

and

$$X = \frac{i_{at} E_{O_2}}{[N_{sp}/(\phi S_o)](1 - \phi)} \dots (66)$$

TABLE 46.11—OIL RECOVERY OF STEAMFLOOD AND FIREFLOOD PROJECTS

Field, Location (Operator)	Thermal Oil Recovery (% OOIP)
Steamfloods	
Smackover, AR (Phillips) ^{82,83}	25.7*
Kern River, CA (Chevron) ⁸⁴	69.9*
Kern River, CA (Getty) ^{68,70}	46.6 to 72.6
Midway Sunset, CA (CWOD) ⁸⁵	63.0*
Mount Poso, CA (Shell) ^{86,87}	34.6*
San Ardo, CA (Texaco) ⁸⁸	47.5, 51.2
Slocum, TX (Shell) ^{89,90}	55.8*
Winkelman Dome, WY (Amoco) ^{91,92}	28.1*
Tia Juana Estes, Venezuela (Maraven) ⁹³⁻⁹⁵	26.3*
Firefloods	
Brea-Olinda, CA (Union) ^{96,97}	25.1*
Midway Sunset, CA (Mobil) ⁹⁸	20.0
Midway Sunset, CA (CWOD) ⁹⁹	52.8
South Belridge, CA (General Petroleum) ⁷⁶	56.7
South Belridge, CA (Mobil) ¹⁰⁰	14.5
Robinson, IL (Marathon) ¹⁰¹⁻¹⁰⁶	31.9
Bellevue, LA (Cities) ^{107,108}	41.5*
Bellevue, LA (Getty) ¹⁰⁹⁻¹¹²	44.6*
May Libby, LA (Sun) ¹¹³	68.0
Heidelberg, MS (Gulf) ^{114,115}	22.4*
Sloss, NE (Amoco) ^{77,79}	14.3
Glen Hummel, TX (Sun) ^{116,117}	31.0
Gloriana, TX (Sun) ^{116,118}	29.7
North Tisdale, WY (Continental) ¹¹⁹	23.0
Suplacu de Barceau, Romania (IFP/ICPPG) ¹²⁰	47.5
Miga, Venezuela (Gulf) ¹²¹	11.6

* Anticipated.

In the above equation,

ΔN_p = cumulative incremental oil production, bbl,

V_{fb} = fuel burned, bbl,

N = OOIP, bbl,

i_{at} = cumulative air injection, 10^3 scf,

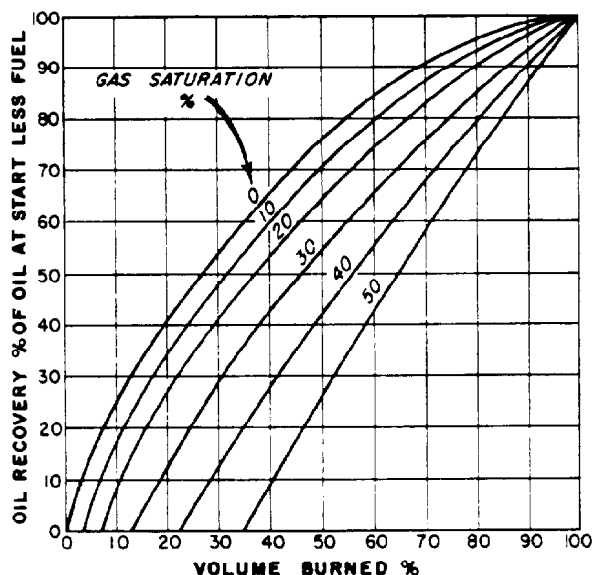
E_{O_2} = oxygen utilization efficiency, fraction, and

N_{sp} = oil in place at start of project, bbl.

Gates and Ramey¹²⁴ developed a correlation between oil recovery and PV burned at various initial gas saturation, on the basis of field data taken from the South Belridge fireflood project⁷⁶ and laboratory combustion-tube data. This correlation, shown in Fig. 46.10, should be useful in predicting current oil recovery as the fireflood proceeds.

Changes in Oil Property. At the temperatures and pressures prevailing in steamfloods, no changes in the oil property are expected to occur because of any chemical reactions. However, the properties of the recovered oil could have been changed as a result of steam distillation. In firefloods, of course, oil properties change considerably because of thermal cracking and combustion, as well as steam distillation. Changes in oil property in some of the reported steamfloods and firefloods are shown in Table 46.12.¹²⁵⁻¹³⁰

Performance Indicator Pertaining to Steamfloods Only. Steam Oil Ratio (SOR). The SOR, F_{so} , is the most important factor characterizing the success or failure of a steamflood project. Its reciprocal, the OSR, F_{os} , also is used commonly. In projects where oil is used as fuel

**Fig. 46.10—Estimated oil recovery vs. volume burned.**

for steam generation, 1 bbl of oil normally can generate 13 to 14 bbl (cold-water equivalent) of steam. Thus, the highest SOR that is tolerable without burning more oil than that produced is 13 to 14. For steamflood operation, there are other costs than fuel alone. Because of this, steam injection is normally terminated when the instantaneous SOR reaches the level of eight or so. Ideally the overall SOR should be around four. This corresponds to 3 to 4 bbl of oil produced per barrel of oil burned.¹³¹ This ideal case is, unfortunately, not normally achievable. The SOR of the majority of the steamflood field projects falls into the range of 5 to 7.

The following set of regression equations developed by Chu⁶² can be used to estimate the SOR with known reservoir and crude properties.

1. For $F_{so} > 5.0$ ($F_{os} < 0.20$),

$$F_{so} = 1 / (-0.011253 + 0.00002779D + 0.0001579h - 0.001357\theta + 0.000007232\mu_o + 0.00001043kh/\mu_o + 0.5120\phi S_o) \quad (67)$$

2. For $F_{so} \leq 5.0$ ($F_{os} \geq 0.20$),

$$F_{so} = 18.744 + 0.001453D - 0.05088h - 0.0008864k - 0.0005915\mu_o - 14.79S_o - 0.0002938kh/\mu_o, \dots (68)$$

where

D = depth, ft,

h = reservoir thickness, ft,

θ = dip angle, degrees,

μ_o = oil viscosity, cp,

k = permeability, md, and

S_o = oil saturation at start, fraction.

Another method of estimating F_{so} has been given by Myhill and Stegemeier,²⁹ based on the Mandl-Volek model.

TABLE 46.12—CHANGES IN OIL PROPERTY IN STEAMFLOOD AND FIREFLOOD PROJECTS

Field, Location (Operator)	°API		Temperature (°F)	Viscosity (cp)	
	Before	After		Before	After
Steamflood					
Brea, CA ¹²⁵ (Shell)*	23.5	25.9	—	—	—
Fireflood					
South Belridge, CA ⁷⁶ (General Petroleum)	12.9	14.2	87 120	2,700 540	800 200
West Newport, CA ^{126,127} (General Crude)	15.2	20.0	160 60 100	120 4,585 777	54 269 71
East Venezuela ¹²⁸ (Mene Grande)	9.5 then 10.5	12.2	210	32	10
Kyrook, KY ¹²⁹ (Gulf)	10.4	14.5	60 210	90,000 120	2,000 27
South Oklahoma ⁸⁰ (Magnolia)	15.4	20.4	66	5,000 after a month	800 5,000
Asphalt Ridge, UT ¹³⁰ (U.S. DOE)**	14.2	20.3			

*Changes in % C₄ - C₁₂; before—21, after—28.

**Changes in other properties:

	Before	After
Pour point, °F	140	25
Residue boiling above 1,000°F, wt%	62	35

Performance Indicators Pertaining to Firefloods Only.

Fuel Content. Fuel content (lbm/cu ft of burned volume) is the amount of coke available for combustion that is deposited on the rock as a result of distillation and thermal cracking. It is the most important factor influencing the success of a fireflood project. If the fuel content is too low, combustion cannot be self-sustained. A high fuel content, however, means high air requirement and power cost. Besides, oil production also may suffer.

Fuel content can be determined by laboratory tube runs. Gates and Ramey¹²⁴ presented a comparison of the estimated fuel content by use of various methods including laboratory experiments and field project data from the South Belridge project.⁷⁶ Their comparison shows that fuel content determined from the tube runs can provide reasonably good estimation of the fuel content obtainable in the field.

In the absence of experimental data, the correlation of Showalter⁴³ relating the fuel content to API gravity can be used. Fig. 46.11 shows a comparison of the Showalter data and field project data.⁶³ In addition, the following regression equation developed by Chu⁶² based on data from 17 field projects can be used to calculate the fuel content:

$$C_m = -0.12 + 0.00262h + 0.000114k + 2.23S_o \\ + 0.000242kh/\mu_o - 0.000189D - 0.0000652\mu_o, \quad (69)$$

where C_m is the fuel content, lbm/cu ft.

Both laboratory experiments and field projects indicate that, for a specific reservoir, fuel content decreases as WAR increases. However, no statistically significant correlation was found to exist between fuel content and WAR in the presence of widely varying reservoir properties.⁶³

Air Requirement. As pointed out by Benham and Poettmann,¹³² air requirement, a , in 10⁶ scf/acre-ft of burned volume, can be calculated on the basis of stoichiometric considerations:

$$a = \frac{\left(\frac{2F_{cc} + 1}{F_{cc} + 1} + \frac{F_{HC}}{2} \right) C_m}{0.001109(12 + F_{HC})E_{O_2}} \times 0.04356, \quad (70)$$

where F_{cc} is the CO₂/CO ratio in produced gas and F_{HC} is the atomic H/C ratio. In the absence of necessary data for Eq. 70, the Showalter correlation⁴³ relating air requirement to API gravity can be used. A comparison of the Showalter data and field project data is given in Fig. 46.12.⁶³ It can be seen that all the field points fall on the upper side of the Showalter curve. Air requirement in the fields can exceed laboratory values because of air channeling and migration. In addition, the following regression equation developed by Chu⁶³ can be used:

$$a = 4.72 + 0.03656h + 9.996S_o + 0.000691k, \quad (71)$$

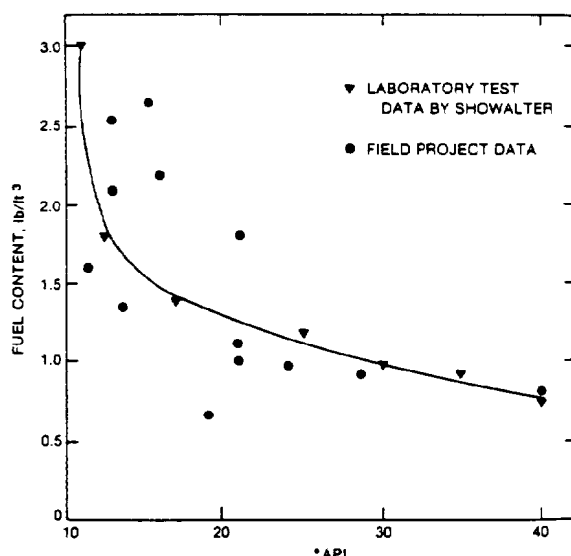


Fig. 46.11—Effect of oil gravity on fuel content.

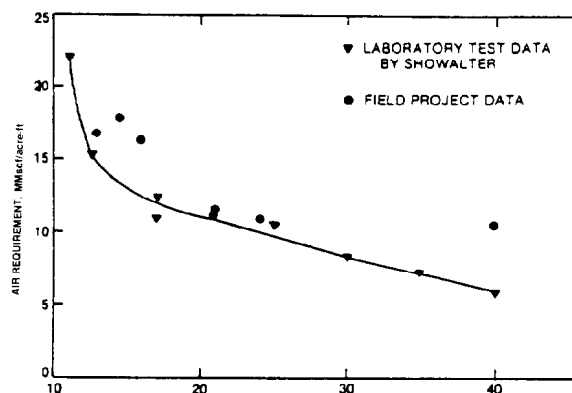


Fig. 46.12—Effect of oil gravity on air requirement.

Air-Oil Ratio (AOR). This important ratio relates air injection to oil production and usually is expressed in terms of 10^3 scf/bbl. Oil recovery comes from both the burned and unburned regions. The AOR can be calculated thus¹²²:

$$F_{ao} =$$

$$\frac{a}{\left[\left(\frac{\phi S_o}{5.6146} - \frac{C_m}{350} \right) E_{vb} + \frac{\phi S_o}{5.6146} (1 - E_{vb}) E_{Ru} \right]} 43.56 \quad (72)$$

In the absence of E_{vb} and E_{Ru} , the following regression equation developed by Chu⁶² based on 17 field projects can be used.

$$F_{ao} = 21.45 + 0.0222h + 0.001065k + 0.002645\mu_o - 76.76\phi S_o \quad (73)$$

Besides, the correlation between oil recovery and PV burned developed by Gates and Ramey¹²⁴ can be used for estimating the current AOR as the fireflood proceeds.

Both laboratory experiments and field projects indicate that, for a specific reservoir, AOR decreases as WAR increases. No statistically significant correlation, however, has been found between AOR and WAR in the presence of widely varying reservoir properties.⁶³

Project Design

Design Features Common to Both Steamfloods and Firefloods

Pattern Selection. For any oil recovery process with fluid injection, a cardinal rule of pattern selection is that, to achieve a balance between fluid injection and production,

the ratio of the number of producers to the number of injectors should be equal to the ratio of well injectivity to well productivity (Caudle *et al.*¹³³). Because of the high mobility of air or steam compared to that of the oil, the injectivity/productivity ratio is high, favoring a high producer/injector ratio. This rule generally has been followed by the various reported steamflood and fireflood projects. The use of inverted 13-spot, 9-spot, 7-spot, and 6-spot patterns, unconfined five-spot patterns, down-the-center line of injectors, and single well injection has been reported.

Aside from the injectivity/productivity ratios, other factors also should enter into consideration in pattern selection. These factors include: heat loss considerations, utilization of existing wells, reservoir dip, difficulty in producing hot wells, etc. Based on these and other considerations, repeated five-spot patterns, updip and crest injections and line drive also were used. The choice of pattern or nonpattern floods in the various steamflood and fireflood projects is shown in Table 46.13.¹³⁴⁻¹³⁸

Completion Intervals. In most of the steamflood and fireflood projects, the producers usually are completed for the entire sand interval to maximize production. The injectors usually are completed at the lower third or lower half of the interval, to minimize the override of the steam or air. In wet combustion projects, it is advisable to complete the lower part for air injection and upper part for water injection. This is to minimize the underflow of water as well.

Producer Bottomhole Pressure (BHP). In their study for a steamflood, Gomaa *et al.*¹³⁹ found that decreasing the producer BHP lowers the average reservoir pressure, increases steam volume, and increases predicted oil recovery. It is, therefore, important to keep the producers pumped off all the time. Without any reason to believe otherwise, keeping the producers pumped off should benefit a fireflood as well as a steamflood.

TABLE 46.13—PATTERN TYPES OF STEAMFLOODS AND FIREFLOODS

Pattern Types	Steamfloods	Firefloods
Inverted 13-spot	Slocum, TX ^{89,90} (Shell)	
Inverted 9-spot	San Ardo, CA ⁸⁸ (Texaco) Yorba Linda, CA ¹¹ (Shell)	Bellevue, LA ^{107,108} (Cities Service) Bellevue, LA ¹⁰⁹⁻¹¹² (Getty)
Inverted 7-spot	Kern River, CA ⁸⁴ (Chevron) Slocum, TX ^{89,90} (Shell) Tia Juana, Venezuela ¹³⁵ (Shell)	Silverdale, Alta. ¹³⁴ (General Crude)
Unconfined inverted 5-spot		West Newport, CA ^{126,127} (General Crude)
Down-the-center-line of injectors		Trix-Liz, TX ^{116,136} (Sun) Glen Hummel, TX ^{116,117} (Sun)
Single well injection		Miga, Venezuela ¹²¹ (Gulf)
Repeated 5-spot	East Coalinga, CA ¹³⁷ (Shell) Kern River, CA ⁸⁴ (Chevron) Kern River, CA ⁶⁸⁻⁷⁰ (Getty) Winkelman Dome, WY ^{91,92} (Pan American)	Sloss, NE ⁷⁷⁻⁷⁸ (Amoco)
Updip or crest injection	Brea, CA ¹²⁵ (Shell) Midway Sunset, CA ^{71,72} (Tenneco)	Midway Sunset, CA ⁹⁸ (Mobil) Heidelberg, MS ^{114,115} (Gulf)
Downdip injection	South Belridge, CA ¹³⁸ (Mobil)	
Updip and downdip injection	Mount Poso, CA ^{86,87} (Shell)	
Line drive		Suplacu de Barcau, Romania (IPF/ICPPG) ¹²⁰

Design Features Pertaining to Steamfloods Only

Steam Injection Rate. According to Chu and Trimble,¹⁴⁰ the optimal choice of a constant steam injection rate is relatively independent of sand thickness. As sand thickness decreases, the total oil content in the reservoir decreases. This calls for a lower steam rate. At the same time, a higher steam rate is needed to compensate for the increased percentage heat loss with a decrease in thickness. These two counteracting factors result in only a small variation in the optimal steam rate as thickness is changed from 90 to 30 ft.

The same study with five-spot patterns shows that the optimal choice of a constant steam rate is proportional to the pattern size. Furthermore, varying steam rates appear to be preferable to constant steam rates. An optimal steam rate schedule calls for a high steam rate in the initial stage and a decrease in the steam rate with time.

Steam Quality. Steam quality refers to the mass fraction of water existing in vapor form. Gomaa *et al.*¹³⁹ reported that increasing steam quality increases oil recovery vs. time but had little effect on recovery vs. Btu's injected. This indicates that heat injection is the important parameter in determining steamflood performance.

Just as with steam injection rates, the optimal choice of steam quality should be studied. High-quality steam could cause excessive steam override. This may be remedied by using lower-quality steam at one stage of a steamflood.

Design Features Pertaining to Fireflood Only

Dry vs. Wet Combustion. The choice between dry combustion and wet combustion is an important decision to be made in conducting a field project. Laboratory experiments indicated that the use of water either simultaneously

or alternately with air does reduce the AOR, although the oil recovery may not be improved significantly. As was mentioned previously, a correlation between AOR and WAR, based on data from 21 field projects, was found to be statistically insignificant in the presence of widely varying reservoir properties.⁶³

Cities Service conducted a field comparison test of dry and wet combustion in the Bellevue field, LA,¹⁴¹ in which possible interference by variations in reservoir properties was essentially circumvented by using two contiguous patterns, one with dry combustion and another with wet combustion. This test found that, with wet combustion, the volumetric sweep was improved to a great extent. This indirectly implies an increase in oil recovery. Furthermore, the air requirement for a specific volume of reservoir was reduced. This reduced the operating cost and improved the economics. Because of these encouraging results, the possible advantages of using wet combustion should be explored.

Air Injection Rate. According to Nelson and McNeil,¹²² the air injection rate depends on the desired rate of advance of the burning front. A satisfactory burning rate was stated to be 0.125 to 0.5 ft/D. In the design method proposed by these authors, a maximum air rate is first determined, based on the minimum burning rate of 0.125 ft/D. They recommended a time schedule such that the air rate would be increased gradually to the maximum rate, held at this rate for a definite period, and then reduced gradually to zero. The Midway Sunset, CA, project of Chanslor-Western⁹⁹ used a burning rate of 1 in./D (0.08 ft/D). Gates and Ramey¹²⁴ found that the air rate should provide a minimum rate of burning front advance of 0.15 ft/D or an air flux of at least 2.15 scf/hr-sq ft at the burning front.

WAR. The reported WAR in various field projects ranged from 0 (for dry combustion) to 2.8 bbl/10³ scf. The choice of WAR depends on water availability, quality of the water available, well injectivity, and economic considerations. Combustion tube experiments, properly designed and executed, should be helpful.

Well Completion

Special well completions are needed for injectors and producers to withstand the high temperatures in steamfloods, and to withstand the corrosive environment as well in firefloods.

According to Gates and Holmes,¹⁴² wells used in steam operations should be completed with due consideration of heat loss with thermal stresses. In deep wells, tubular goods with high qualities, such as the normalized and tempered P-105 tubing and P-110 casing, should be used if the tubing and casing are not free to expand. Thermal stress can be minimized by the proper use of expansion joints. Thermal packers should be used on steam injection wells and deep wells undergoing cyclic steaming. The cement should include a thermal strength stabilizing agent, an insulating additive and a bounding additive.

For firefloods, Gates and Holmes¹⁴² felt that steel casing and tubing such as J-55 is suitable for injectors. These wells can be completed with normal Portland ce-

ment, with high-temperature cement placed opposite and about 100 ft above the pay zone. The high-temperature cement recommended for the injectors is calcium aluminate cement (with or without silica flour), pozzolan cement, or API Class G cement (with 30% silica flour). If spontaneous ignition occurs, the use of cemented and perforated liners is required to prevent well damage resulting from burnback into the borehole. The producers should be completed to withstand relatively high temperatures and severe corrosion and abrasion. These authors recommended the use of gravel-flow pack, and stainless steel 316 for both liner and tubing opposite the pay zone.

The well completion methods for injectors and producers in the various steamflood and fireflood projects, detailed by Chu^{61,63} previously, are given in Table 46.14.

Field Facilities

Steamflood Facilities

Steam Generation and Injection. Most of the steam injection projects use surface steam generators. The major difference between oilfield steam generators and industrial multitube boilers is the ability to produce steam from saline feedwater with minimum treatment. Other features include unattended operation, portability, weatherproof construction, and ready accessibility for repairs. The ability to use a wide variety of fuels including lease crude is also an important requirement. The capacity of steam generators used in steamflood projects usually ranges from 12 to 50×10⁶ Btu/hr, with 50×10⁶ Btu/hr becoming the industry standard in California.

With surface steam generators, the steam goes from the generators to the injection wells through surface lines. Most surface steam lines are insulated with a standard insulation with aluminum housings. The steam is split into individual injectors through a header system using chokes to reach critical flow. This procedure requires that the steam achieve sonic velocity, which, under one field condition,⁶⁸ calls for a pressure drop of about 55% across the choke. The chokes are sized to each other to give the desired flow rate into each injector. As long as the pressure drop is greater than 55%, the flow rate will be independent of the actual wellhead injection pressure.

A recent development is the use of downhole steam generators to eliminate wellbore heat losses in deep wells. There are two basic designs, which differ on the method of transferring heat from the hot combustion gases to produce steam.¹⁴³ In one design, the combustion gas mixes directly with feed water and the resulting gas/steam mixture is injected into the reservoir. Because of this, the combustion process takes place at the injection pressure. In another design, there is no direct contact between the combustion gas and water, just as in the surface generators. The combustion gas returns to the surface to be released after giving up much of the heat to generate steam. A lower pressure than injection pressure can be used in this case.

Still another new development is cogeneration of steam and electricity.¹⁴⁴ The effluent gas from a combustor is used in a gas turbine, which drives an electrical generator. The exhaust gas from the turbine is then used in steam generators to produce steam for thermal recovery purposes.

TABLE 46.14—WELL COMPLETION FOR STEAMFLOODS AND FIREFLOODS

Injectors	Steamfloods	Firefloods
Casing	Grades: J-55, K-55, and N-80 Sizes: 4½, 5½, 6¾, 7, and 9¾ in. Tensile prestressing of casing in deep wells	Grades: J-55 and K-55 Sizes: 4½, 5½, 7, and 8½ in. across the pay zone
Openhole or perforated completions	Both openhole completions with slotted liners and solid-string completion with jet perforations have been reported. Liner sizes: 4½, 5½, or 7 in. Perforations: ¼ or ½ in., one or two per foot, or one-half per foot Some with stainless steel wire-wrapped screens.	Perforated completion more prevalent than openhole completion with or without liners. Liner sizes: 3½ or 5½ in. Perforations: ¼ or ½ in. (two or four per foot)
Cement	Class A, G, and H cement with silica flour (30 to 60% of dry cement).	Use of high-temperature cement prevalent.
Gravel packing	Use not prevalent.	Use not prevalent.
Tubing	Tubing insulations used in deep wells: asbestos with calcium silicate, plus aluminum radiation shield; or jacketed tubing with calcium silicate.	Tubing used for air injection or as a thermowell. In wet combustion, various ways have been used for injection of air and water.
Producers		
Casing	Grade: K-55 Sizes: 4½, 5½, 6¾, 7, and 8¾ in. Tensile prestressing of casing in deep wells	Grades: H-40, J-55, and K-55 Sizes: 5½, 7, 8¾, and 9¾ in.
Openhole or perforated completions	Both openhole completion with slotted liners and solid-string completion with jet perforations have been reported. Liner sizes: 4½, 4¾, or 6¾ in. Slot sizes: 40, 60, or 60/180 mesh Perforations: ½ in., four per foot Some with stainless steel wire-wrapped screens.	Openhole completion with or without slotted liners and perforated completion are equally prevalent. Liner sizes: 4¾, 5½, or 6¾ in. Slot sizes: 60-mesh, 0.05, 0.07, or 0.08 in. Perforations: ½ in. (two or four per foot)
Cement	Class G and H cement with silica flour (30 to 60% of dry cement).	Use of high-temperature cement was reported.
Gravel packing	Use more prevalent than in injectors. Gravel size: 6/9 mesh flow-packed.	Use more prevalent than in injectors. Gravel sizes: 20/40 or 6/9 mesh, flow- or pressure-packed.
Tubing	Tubing for rod pump.	Tubing for rod pump, to serve as a thermowell, or for cooling water injection.

Water Treatment. The feedwater treatment for steam generation consists mainly of softening, usually through zeolite ion exchange. Some feedwaters may require filtration and deaeration to remove iron. Still others may need to use KCl for control of clay swelling and chlorine to combat bacteria. Facilities for oil removal also will be needed if the produced water is to be reused as feedwater for steam generation.

Fireflood Facilities

Ignition Devices. In many fields, the reservoir temperature is so high that spontaneous ignition would occur only a few days after starting air injection. In some projects, steam, reactive crude, or other fuels will be added to help ignition.

Many other fields need artificial ignition devices, which include electrical heaters, gas burners, and catalytic ignition systems. The various ignition methods, including equipment and operational data, have been discussed by Strange.¹⁴⁵

Air Compressors. The air compressors can be gas engine or electrical motor driven. Depending on the total

injection rate the compressor needs to supply and the output pressure needed, the capacity of the compressors can range from 1.0 to 20.0×10^6 scf/D, and the power rating can range from 300 to 3,500 hp.

Monitoring and Coring Programs

Monitoring Programs

A thermal recovery project could be a complete failure economically and still be considered a success if it could provide useful information on the reservoir performance under steamflood or fireflood. A properly designed monitoring program carried out during the project and coring programs during and after the project are important in providing the information necessary for evaluating steamflood or fireflood performance.

The Sample, Control, and Alarm Network (SCAN) automation system installed by Getty in the Kern River field¹⁴⁶ illustrates how a large steam injection operation can be monitored. This system consists of a devoted central computer that monitors 96 field sites. At these sites, the production rates of more than 2,600 producers and the operating rates of 129 steam generators are gathered. The SCAN performs several functions.

1. It automatically schedules and controls well production tests at each site.
2. It monitors results of well production tests, steam generator operating rates, flow status, and injection status of producers, valve positions during well tests, and various status contact checks.
3. It sounds the alarm upon any malfunctioning at a field site or a steam generator.
4. It reports necessary operating information routinely on a daily, weekly, or monthly basis, and other special reports on demand from the operator.

The Silverdale, Alta., fireflood project of General Crude¹³⁴ also uses an automatic data collection system. Differential pressure transducers, thermocouple-amplifier transducers, pressure transducers, and motor load transducers are used to measure and record data at each well. These data are transmitted to a central system, which can be interrogated and can indicate any alarm situation when pressures, temperatures, or flow rates fall outside certain specified ranges.

Not all thermal projects call for elaborate automatic monitoring programs. The following program used in the Bodcau, LA, fireflood project of Cities Service-DOE¹⁴⁷ typifies one needed for a small-scale pilot.

1. Gas production rates, useful for mass balance calculations, were measured monthly. Monthly analysis of the produced gas gave data for the calculation of the oxygen utilization efficiency.
2. Oil and water production rates were measured at least twice each month.
3. Flow line temperatures were measured daily. These temperatures, in conjunction with the gas production rates, were useful in determining the amount of quench water needed at the producers.
4. Downhole temperature profiles were taken monthly at the observation wells. These profiles helped to delineate the development of the burned volume.

Coring Program

Drilling core holes could be very expensive, depending on the depths of the pay zones. However, a judiciously designed and properly executed coring program, either during a thermal project or afterward, could provide valuable information on the project performance. Such a program can give the following information: (1) residual oil saturation (ROS) after steamflood or fireflood, (2) vertical sweep of the injected steam or burned volume, (3) areal sweep of the steam front or burning front, (4) maximum temperature distribution, both areally and vertically, and (5) effective permeability of the rock, and whether any deposits formed during the process could have reduced the flow capacity.

A typical coring program, used for postmortem evaluation in the Sloss, NE, fireflood project,⁷⁹ is summarized next.

Core Analyses. Porosity, permeability, and oil saturations were measured on each foot of the recovered cores. Oil saturations were determined by the routine Dean-Stark extraction and weight loss method, and the infrared absorption method.

Log Analyses. Compensated formation density and dual-induction laterolog logs were run in the core holes to determine porosity and oil saturation.

Photographs and Visual Examination. Whereas black-and-white photographs were found to be rather useless, ultraviolet photographs gave an excellent picture as to where the oil was removed by the burning process. The absence of oil also could be seen by visual examination. In some intervals, the reddish color of the core indicated that the core had been subjected to a temperature high enough for iron oxidation.

Mineral Analyses of the Cores. Various minerals, including glauconite, illite, chlorite, and kaolinite, underwent permanent changes with the temperature increase. The maximum temperature to which the core samples had been exposed could be determined from the form and color of these minerals.

Microscopic Studies. The scanning electron microscope was used to study anhydrite formation and clay alteration in the core samples, which had been subjected to high temperatures.

Tracers

The use of tracers helped to monitor fluid movement and interpret areal coverage in individual steamflood patterns. According to Wagner,¹⁴⁸ preferred aqueous-phase or gaseous-phase tracers include radioisotopes, salts with detectable cations and anions, fluorescent dyes, and water-soluble alcohols. Radioactive tracers include tritium, tritiated water, and krypton-85. Other tracers include ammonia, air, sodium nitrite, sodium bromide, and sodium chloride.

Operational Problems and Remedies

Operational problems plaguing steamflood and fireflood projects and their remedies, previously detailed by Chu,^{61,63} are summarized next.

Problems Common to Steamfloods and Firefloods

Well Productivity. Production of the highly viscous crude may be extremely low before the arrival of the steam front or burning front. The production rate can be improved by injecting light oil as a diluent, hot oil treatment, cyclic steam injection, or burning at the producers.

When producer temperature exceeds 250°F, pump efficiency decreases to a great extent because of hot produced fluids flashing to steam or direct breakthrough of the injected steam or flue gas. The best remedy is to plug off the hot zone and redirect the steam or flue gas to the oil section before entering the wellbore.

Sanding. Sanding can be severe even in steamflood projects. The remedies include the HypercleanTM technique, foamed-in tight-hole slotted liners, a sodium aluminate sand consolidation technique, and the use of phenolic-resin gravel packing.

In firefloods, sanding is particularly severe if the sand is extremely unconsolidated. The erosion can be aggravated further by coke particles and high gas rates. Sandblasting could require frequent pulling of wells and replacement of pumps.

Emulsions. In steamfloods, emulsions sometimes can be broken easily by chemical treatment. The problem could

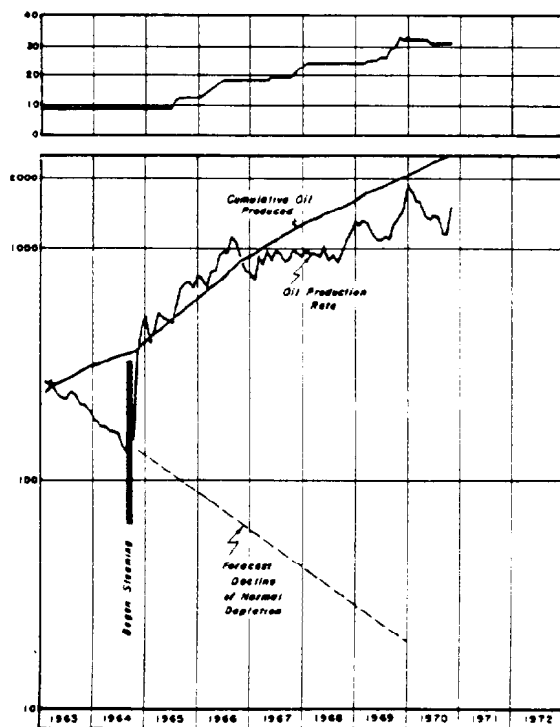


Fig. 46.13—Production history of cyclic steam stimulation, TM sand, Huntington Beach offshore field, CA.

become severe if the emulsion is complicated with the solids produced and with the continuously changing nature of the produced fluids.

Emulsions found in fireflood projects are formed of heavy oil, cracked light ends, quench and formation water, solids, and possibly, corrosion products. They can become a continual and major problem in some projects, and require expensive emulsion breakers.

Problems Plaguing Steamfloods Only

Steam Placement. The lack of control of steam placement during steam stimulation is a major problem in producers with liner completions. The use of solid string completions will help reduce the problem.

Steam Splitting. The uneven splitting of steam in a two-phase regime can cause significant differences in steam quality into different injectors. This can be corrected by modifying the layout of the steam line branching system.

TABLE 46.15—RESERVOIR ROCK AND FLUID PROPERTY DATA, TM SAND, HUNTINGTON BEACH OFFSHORE FIELD, CA

Depth, ft	2,000 to 2,300
Thickness, ft	
Gross	115
Net	40 to 58
Porosity, %	35
Permeability, md	400 to 800
Oil gravity, °API	12 to 15
Reservoir temperature, °F	125
Reservoir pressure at start, psig	600 to 800
Oil viscosity at 125°F, cp	682
Oil saturation at start, %	75

Problems Plaguing Firefloods Only

Poor Injectivity. Various substances can cause losses in injectivity for the air injectors. If identifiable, these problems can be remedied by appropriate means. Injector plugging by iron oxide can be reduced by injecting air into the casing and bleeding it through the tubing. Asphaltene buildup can be reduced by squeeze washing with asphaltene solvent. Emulsion formed in situ can be reduced by emulsion breakers. Scale formation caused by barium and strontium sulfate can be reduced by an organic phosphate. The injection of NuTri™ (trichloromethylene) and acidizing are useful in improving the injectivity.

Corrosion. Corrosion can be mild or serious and is caused by simultaneous injection of air and water, production of acids, sulfur, oxygen, and CO₂. Corrosion inhibitors are needed regularly.

Exploration Hazards. To minimize explosion hazards in the air injection system, an explosion-proof lubricant should be used. Flushing of the interstage piping with a nitrox solution is necessary.

Case Histories

Many thermal recovery projects have been reported in the literature. The following describes a number of selected projects and gives the reasons for their selection.

Steam Stimulation Operations

Huntington Beach, CA (Signal)¹⁴⁹—Typical Operation. The steam stimulation project was conducted in the TM sand, in the Huntington Beach offshore field, Orange County, CA. This project typifies the behavior of a heavy-oil reservoir under cyclic steam stimulation. The reservoir properties are given in Table 46.15.

Steam injection was started in nine producers in Sept. 1964, resulting in a large increase in oil production. This early success prompted the expansion of the project by drilling wells on 5-acre spacing. The number of wells increased from 9 in 1964 to 35 in 1969. The performance of the steam stimulation project during the 1964–70 period is shown in Fig. 46.13. With steam stimulation and with the almost quadrupling of the number of wells, the oil rate increased more than 10-fold, from 125 B/D oil in 1964 to about 1,500 B/D oil in 1970.

The performance of steam stimulation normally deteriorates as the number of cycles increases. As shown in Table 46.16, the OSR changed from the range of 3 to 3.8 bbl/bbl for the first two cycles to the range of 2.4 to 2.5 bbl/bbl for the third and fourth cycles.

Fig. 46.14 shows how oil production in one well decreases during a cycle and how it varies from one cycle to another.

Paris Valley, CA (Husky)¹⁵⁰—Co-Injection of Gas and Steam. A wet combustion project was initiated at Paris Valley, which is located in Monterey County, CA. Before the arrival of the heat front, the producers were stimulated with steam. A special feature that made this project interesting was the co-injection of air and steam in three of the stimulation cycles. The reservoir properties are given in Table 46.17.

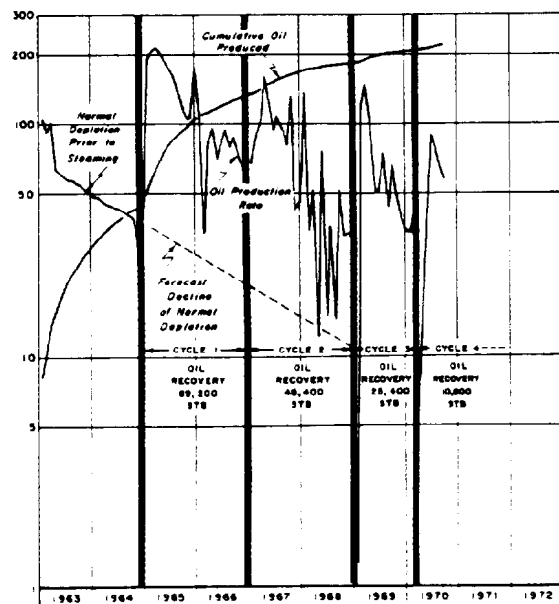


Fig. 46.14—Oil production rate, Well J-128, Huntington Beach offshore field.

In Table 46.18, Cycles 3 and 5 of Well 20 and Cycle 7 of Well 3 used air-steam injection. For Well 20, oil production in Cycle 3 was 4,701 bbl while that in Cycle 2 was 2,449 bbl. Thus, with air-steam injection, oil production increased by 92%. A similar increase was noticeable for Cycle 5 of Well 20 and Cycle 7 of Well 3 when compared with their respective preceding cycles, which used steam only.

Steamflood Projects

Kern River, CA (Getty)⁶⁸⁻⁷⁰—Largest Steamflood. The Kern River field is located northeast of Bakersfield, CA, in the southeastern part of the San Joaquin Valley. Getty Oil Co.'s steam displacement operation in this field is the largest in the world, based on a 1982 survey.¹³ According to this survey, the thermal oil production rate was 83,000 B/D in an area of 5,070 acres.

The Kern River formation consists of a sequence of alternating sand and shale members. The reservoir properties are given in Table 46.19.

The Kern River field was discovered in the late 1890's. In the mid-1950's, bottomhole heaters were used to improve the oil productivity. In Aug. 1962, a 2.5-acre normal five-spot hot waterflood was started. Results showed that this process was technically feasible but economically unattractive. In June 1964, the hot waterflood pilot was converted to a steam displacement test and the number of injectors was increased from the original 4 wells to 47 wells. Continued expansion through the years has increased the number of injectors to 1,788 wells, with 2,556 producers by 1982. The original Kern project and some later expansions are shown in Fig. 46.15. The steam displacement operation was in general conducted in 2.5-acre five-spot patterns.

Getty Oil Co.'s steam displacement operation includes many projects. For illustration purposes, the Kern project is presented here with a map showing the well patterns (Fig. 46.16) and a figure showing the injection and

TABLE 46.16—SUMMARY OF PERFORMANCE THROUGH FOUR "HUFF 'N' PUFF" CYCLES AS OF OCTOBER 1, 1970; TM SAND, HUNTINGTON BEACH OFFSHORE FIELD, CA

	Cycle 1	Cycle 2	Cycle 3	Cycle 4
Number of wells	24	18	11	4
Average cycle length, months	14	18	15.3	14.5
Average oil recovery per well, STB	28,900	30,900	24,650	29,225
Average quality of steam injected, %	71.4	69.3	75.1	78.5
Average volume of steam injected, bbl	9,590	8,130	10,190	11,760
Ratio of oil recovered to steam injected, STB/bbl	3	3.8	2.4	2.5

TABLE 46.17—RESERVOIR ROCK AND FLUID PROPERTY DATA, ANSBERRY RESERVOIR, PARIS VALLEY FIELD, CA

Depth, ft	800	
Net thickness, ft	50	
Dip, degrees	15	
Porosity, %	32	
Permeability, md	3,750	
Oil gravity, °API	10.5	
Reservoir temperature, °F	87	
Initial pressure, psig	220	
Saturation at start, %		
Oil	64	
Water	36	
Oil viscosity, cp		
	<u>Upper Lobe</u>	<u>Lower Lobe</u>
87°F	227,000	23,000
100°F	94,000	11,000
200°F	340	120

TABLE 46.18—RESPONSE TO CYCLIC AIR/STEAM

	Well 20				Well 3	
	Cycle 2	Cycle 3	Cycle 4	Cycle 5	Cycle 6	Cycle 7
Steam volume, 10 ³ bbl	13.2	16.2	15.7	10.4	8.2	9.2
Air volume, 10 ⁶ scf	0	1.5	0	3.7	0	3.6
Air/steam ratio, scf/bbl	0	91	0	355	0	394
Comparable producing days	161	161	90	90	97	97
Oil produced, bbl	2,449	4,701	270	503	2,375	4,203
Steam/oil ratio, bbl/bbl	5.4	3.4	58	21	3.5	2.2
Oil/steam ratio, bbl/bbl	0.19	0.29	0.02	0.05	0.29	0.45
Peak oil production test, B/D	51	81	24	38	60	141

TABLE 46.19—RESERVOIR ROCK AND FLUID PROPERTY DATA, KERN RIVER FIELD, CA

Depth, ft	500 to 1,300
Thickness, ft	30 to 90
Dip, degrees	4
Porosity, %	28 to 33
Permeability, md	1,000 to 5,000
Oil gravity, °API	12.0 to 16.5
Reservoir temperature, °F	90
Reservoir pressure at start, psig	100
Oil viscosity, cp	
90°F	4,000
250°F	15
Oil saturation at start, %	35 to 52

production history of the four-pattern pilot (Fig. 46.17). In this project, the cumulative SOR was 3.8 bbl/bbl and the production rate reached 100 B/D of oil per pattern. Core hole data before and after the steamflood showed an oil recovery of 72% and also a very high areal sweep efficiency.

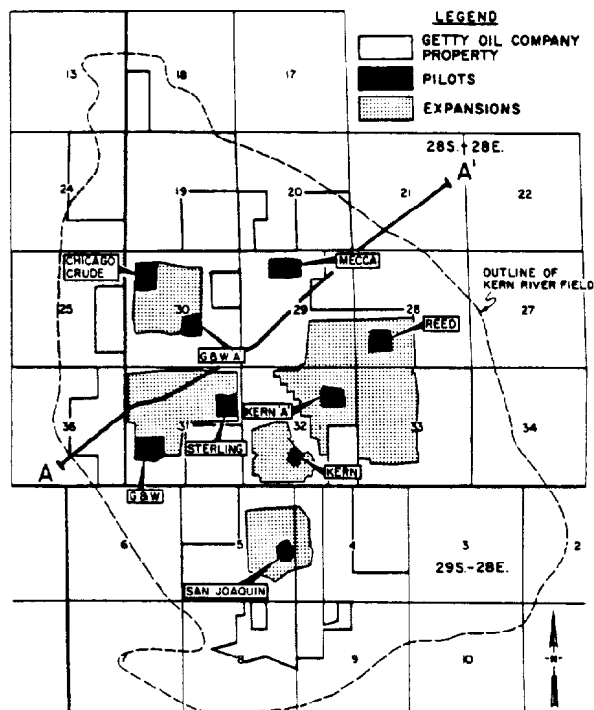
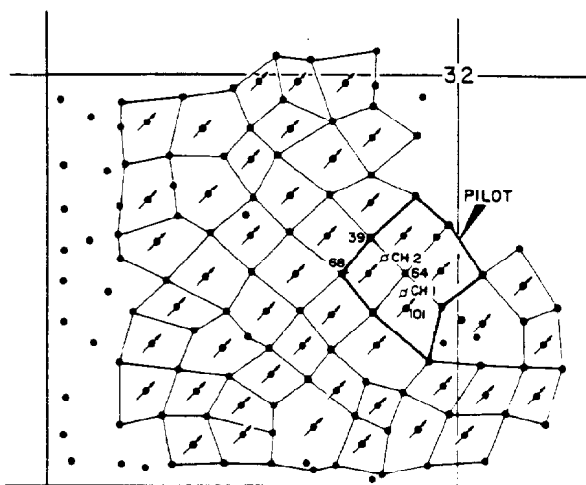
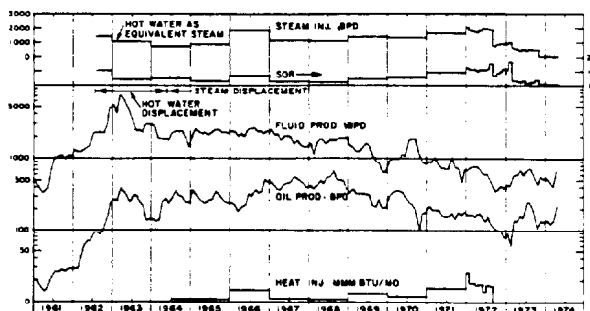
Brea, CA (Shell)¹²⁵—Steam Distillation Drive, Deep Reservoir, Steeply Dipping. A steam distillation drive was initiated in 1964 in the Brea field, which is located about 25 miles east of Los Angeles. This project is interesting because the oil is relatively light with low viscosity, and the reservoir is steeply dipping at a great depth. The reservoir properties are summarized in Table 46.20.

The dipping reservoir is seen clearly in Fig. 46.18. The injectors are located updip, as shown in Fig. 46.19. Because of the depth, insulated tubing was used for the injectors. This figure also shows the area of temperature response and production response. The injection and production rates are given in Table 46.20. As of Dec. 1971, the steam rate was 1,010 B/D water and the oil rate was 230 B/D, giving an estimated SOR of 4.4 bbl/bbl.

Smackover, AR (Phillips)^{82,83}—Reservoir With Gas Cap. The Smackover field is located in Ouachita County, AR. The steamflood pilot, conducted in the Nacatoch sand, is worth mentioning because the reservoir has a gas cap thicker than the oil sand itself. This gas cap can be seen readily in the log and coregraph of Sidum Well W-35 (Fig. 46.21). The reservoir properties are given in Table 46.21.

TABLE 46.20—RESERVOIR ROCK AND FLUID PROPERTY DATA, BREA FIELD, CA

Depth, ft	4,600 to 5,000
Gross stratigraphic thickness, ft	300 to 800
Ratio of net to gross sand, %	63
Dip, degrees	66
Porosity, %	22
Permeability, md	77
Oil gravity, °API	24
Reservoir temperature, °F	175
Reservoir pressure at start, psi	110
Oil viscosity at 175°F, cp	6
Saturation at start, %	
Oil	49
Gas	18

**Fig. 46.15—Kern River field, CA.****Fig. 46.16—Kern steam displacement project, Kern River field.****Fig. 46.17—Injection and production history, Kern hot water and steam displacement project (four patterns) Kern River field.**

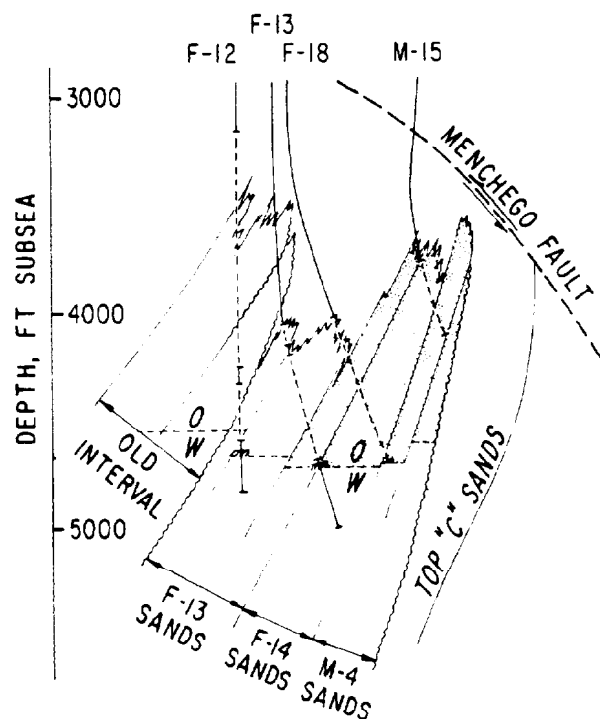


Fig. 46.18—Cross section through the lower "B" sands, Brea field.

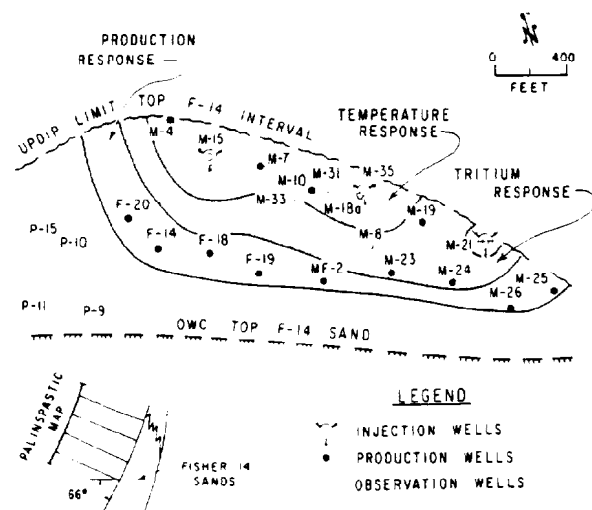


Fig. 46.19—Well locations and area of temperature, tritium, and production responses, Brea field, CA.

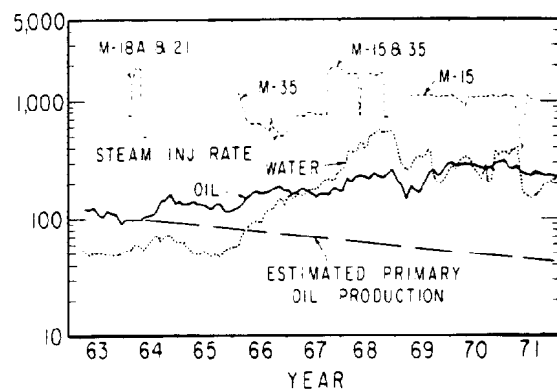


Fig. 46.20—Injection and production history, Brea steam distillation pilot.

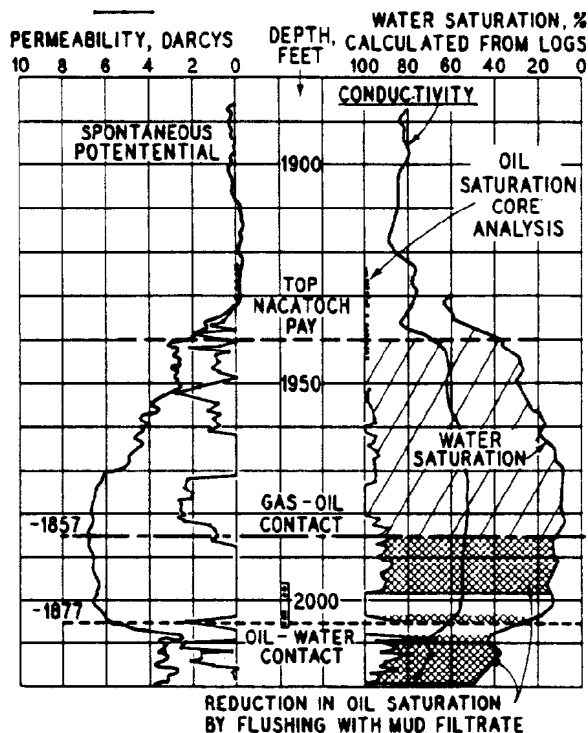


Fig. 46.21—Log and coregraph, Sidum Well W-35, Smackover field, AR.

Fig. 46.22 is a map of the 10-acre five-spot pilot, which was later expanded to a 22-acre nine-spot pattern by adding four more producers. As shown in Fig. 46.23, steam injection started in Nov. 1964 and stopped in Oct. 1965. The oil production continued long after steam injection stopped. As of Aug. 1970, the additional oil produced by steamflood was 207,000 bbl. With total steam injection of 860,000 bbl, the cumulative SOR was 4.14 bbl/bbl.

The temperature log in Fig. 46.24 shows that steam goes to the gas cap. It can be concluded that the increase in oil production was not caused by frontal displacement. Rather, the oil zone temperature increased because of conduction and convection from the gas cap, thus reducing the oil viscosity and increasing the oil production.

TABLE 46.21—RESERVOIR ROCK AND FLUID PROPERTY DATA, SMACKOVER FIELD, AR

Depth, ft	1,920
Thickness, ft	
Gross	130
Net	25
Dip, degrees	0 to 5
Porosity, %	35
Permeability, md	2,000
Oil gravity, °API	20
Reservoir temperature, °F	110
Reservoir pressure at start, psia	5
Oil viscosity, cp	
60°F	180
110°F	75
Saturation at start, %	
Oil	50
Water	50

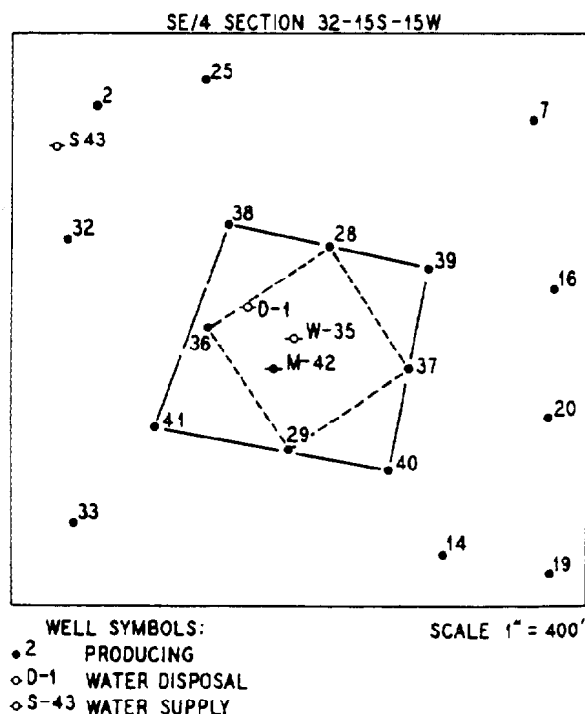


Fig. 46.22—Sidum steam injection pilot, Smackover field.

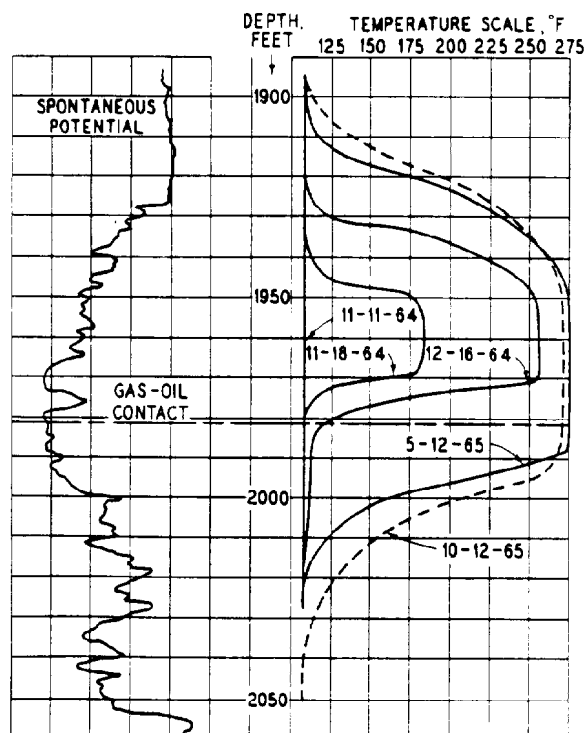


Fig. 46.24—Temperature log, Sidum Well W-42, Smackover field.

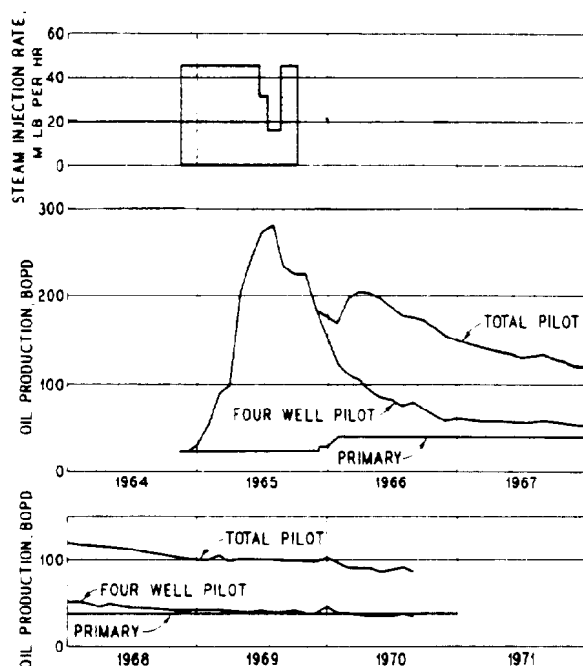


Fig. 46.23—Injection and production history, Sidum steam injection pilot, Smackover field.

Slocum, TX (Shell)^{89,90}—Reservoir With Water Sand. The Slocum field is located in southern Anderson County in northeast Texas. The steamflood project interests us since it is conducted in an oil reservoir underlain by a water sand, as shown in the type log (Fig. 46.25). The reservoir properties are given in Table 46.22.

The field was discovered in 1955. Only about 1% of OOIP was produced by primary operation. A small steamflood pilot using a $\frac{1}{4}$ -acre normal five-spot pattern showed encouraging results. A full-scale seven-pattern project was initiated in 1966–67, with 5.65-acre, 13-spot patterns (Fig. 46.26).

Both injectors and producers were completed a few feet into the water sand. Steam moves horizontally through the water layer, rises vertically into the oil layer, and displaces oil that had been heated and mobilized. The oil then falls down and subsequently is swept toward the producers. The injection and production history is shown in Fig. 46.27.

Street Ranch, TX (Conoco)¹⁵¹—Extremely Viscous Tar, Fracture-Assisted Steamflood. The Street Ranch pilot was conducted in the San Miguel-4 tar sand reservoir located in Maverick County, TX. This pilot proved the technical feasibility of the fracture-assisted steamflood technology (FAST) in recovering extremely viscous heavy oils and tars. The reservoir properties are given in Table 46.23. The pilot used a 5-acre inverted five-spot pattern. The four producers were fractured horizontally with cold water, steam stimulated, perforated, and resteamed. The injector then was fractured horizontally to establish communication with the producers. The pilot consisted of three

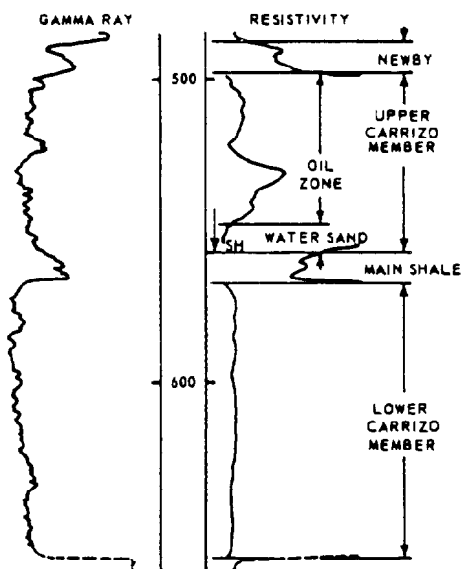


Fig. 46.25—Type log, Slocum field, TX.

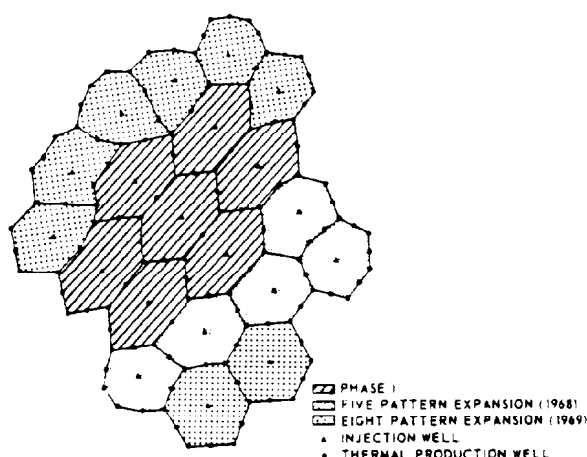


Fig. 46.26—Slocum thermal recovery project.

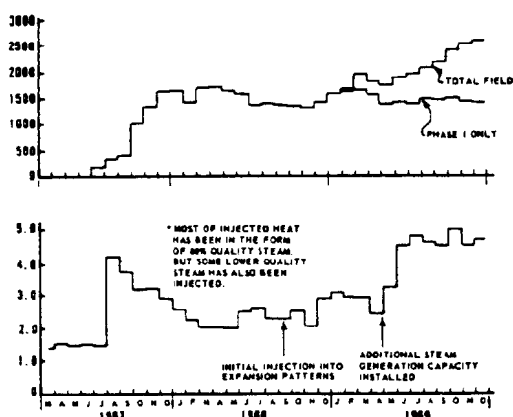


Fig. 46.27—Injection and production history, Slocum thermal recovery project.

TABLE 46.22—RESERVOIR ROCK AND FLUID PROPERTY DATA, SLOCUM FIELD, TX

Depth, ft	520
Thickness, ft	
Gross	34
Net	32
Dip, degrees	0 to 5
Porosity, %	34
Permeability, md	>2,000
Oil gravity, °API	18 to 19
Reservoir temperature, °F	80
Initial reservoir pressure, psig	110
Oil viscosity, cp	
60°F	1,000 to 3,000
400°F	3 to 7
Oil saturation at start, %	68

phases: (1) fracture preheat, (2) matrix steam injection, and (3) heat scavenging with water injection. The tar production and steam/tar ratio during the 31-month history are shown in Figs. 46.28 and 46.29, respectively. The average tar production rate was 185 B/D and the cumulative steam/tar ratio was 10.9 bbl/bbl. Postpilot core holes showed residual tar saturations as low as 8% and an average recovery efficiency of 66%.

Lacq Supérieur, France (Elf Aquitaine)¹⁵²—Carbonate Reservoir. The Lacq Supérieur field is on the north side of the Pyrenees Mts. in southwest France. The steam-flood pilot is unique because it was conducted in a carbonated, dolomitized, and highly fractured reservoir. The reservoir properties are given in Table 46.24.

The pilot was located in the central part of the fractured limestone zone, near the top of an anticline. The pattern area is 35 acres, defined by six old producers, as shown in Fig. 46.30. The injector was the only one drilled for the pilot. Steam injection started in Oct. 1977. Oil production started to increase, only 3 months after steam injection began. The production history is shown in Fig. 46.31. By June 1980, incremental oil production amounted to 176,000 bbl with a cumulative steam injection of 926,000 bbl. The cumulative SOR is 5.26 bbl/bbl. This

TABLE 46.23—RESERVOIR ROCK AND FLUID PROPERTY DATA, STREET RANCH PILOT, TX

Depth, ft	1,500
Thickness, ft	
Gross	52
Net	40.5
Dip, degrees	2
Porosity, %	26.5 and 27.5
Permeability, md	250 to 1,000
Tar gravity, °API	~2.0
Reservoir temperature, °F	95
Tar viscosity at 95°F, cp (est.)	20,000,000
Tar kinematic viscosity, cSt	
175°F	520,000
200°F	61,000
250°F	2,900
300°F	870
Pour point, °F	170 to 180
Total sulfur, wt%	9.5 to 11.0
Initial boiling point, °F	500
Tar saturation at start, %	54.7 and 38.9

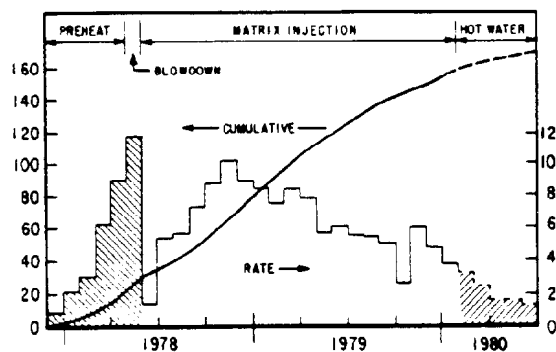


Fig. 46.28—Tar production history, Street Ranch pilot, TX.

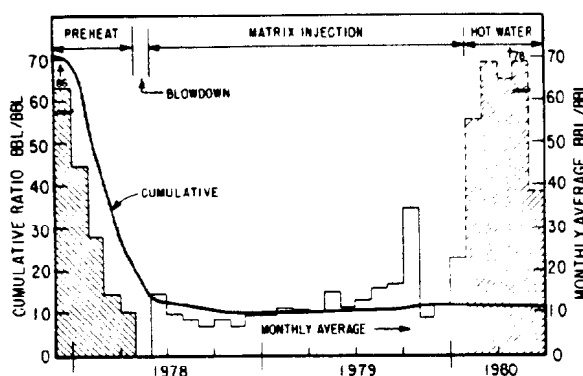


Fig. 46.29—Steam/tar ratios, Street Ranch pilot.

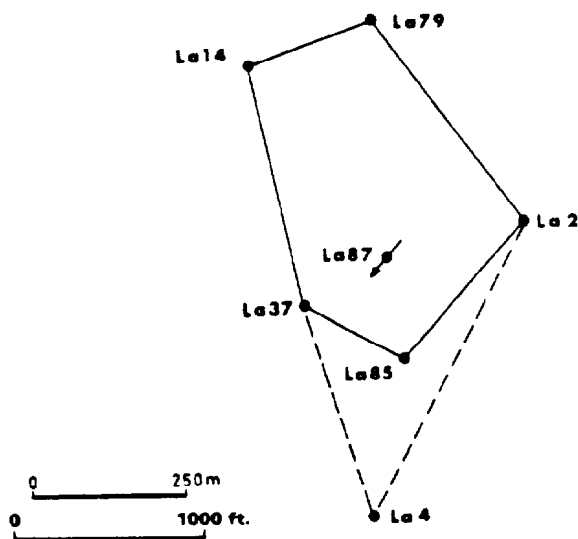


Fig. 46.30—Pilot area, Lacq Supérieur field, France.

TABLE 46.24—RESERVOIR ROCK AND FLUID PROPERTY DATA, LACQ SUPERIEUR FIELD, FRANCE

Depth, ft	1,970 to 2,300	
Thickness, ft	400	
Oil gravity, °API	21.5	
Reservoir temperature, °F	140	
Reservoir pressure, psi	870	
Oil viscosity at 140°F, cp	17.5	
	Matrix Blocks	Fissure Network
Porosity, %	12	0.5
Permeability, md	1	5,000 to 10,000
Water saturation at start, %	60	100

pilot showed that a strongly fissured reservoir can be exploited efficiently by the steamflood process, as if it were a homogeneous reservoir. The dissociation of the carbonate rocks by steam apparently produced no unfavorable effects. Rather, the CO_2 evolved might have some positive effect on the process efficiency.

Fireflood Projects

Suplacu de Barcau, Romania (IFP-ICPP)¹²⁰—Largest Fireflood. The Suplacu de Barcau field lies in northwestern Romania. This is reportedly the largest fireflood project in the world, producing nearly 6,563 B/D of 15.9°API oil. The reservoir properties are given in Table 46.25.

The project started with a pilot in 1964 using a 1.24-acre inverted five-spot pattern that was later expanded into a 4.94-acre inverted nine-spot pattern. This was followed by a semicommercial operation in the period 1967–71 with eight 9.88-acre inverted nine-spot patterns. This operation further expanded into full commercial operation, first retaining the nine-spot patterns with the same spacing, and later changing to linedrive operation. The original pilot and later expansions are shown in Fig. 46.32. Injection wells numbered 38 in 1979 with 20 using alternate air and water injection and the balance using straight air. The production history is given in Fig. 46.33. The WAR was 0.089 to 0.178 bbl/ 10^3 scf. As of 1979, the air injection rate was $63,600 \times 10^3$ scf/D. With an oil rate of 6,563 B/D, the AOR was estimated to be 9.7×10^3 scf/bbl.

West Heidelberg, MS (Gulf)^{114,115}—Deepest Fireflood. The West Heidelberg field is located in Jasper County in eastern Mississippi. With a depth exceeding 2 miles, it is the deepest fireflood project, or the deepest thermal project, for that matter. The Cotton Valley formation has eight sands. The fireflood was conducted in Sand No. 5. The reservoir properties are given in Table 46.26.

As shown in the structure map of Sand No. 5 (Fig. 46.34), only one injector was used, near the top of the structure, with seven producers located downdip. The injection and production history is given in Fig. 46.35. It can be estimated from this figure that, during the period 1973–76, the average air injection rate was about 900×10^3 scf/D whereas the average oil production rate was about 400 B/D. This gives an AOR of only 2.25×10^3 scf/bbl.

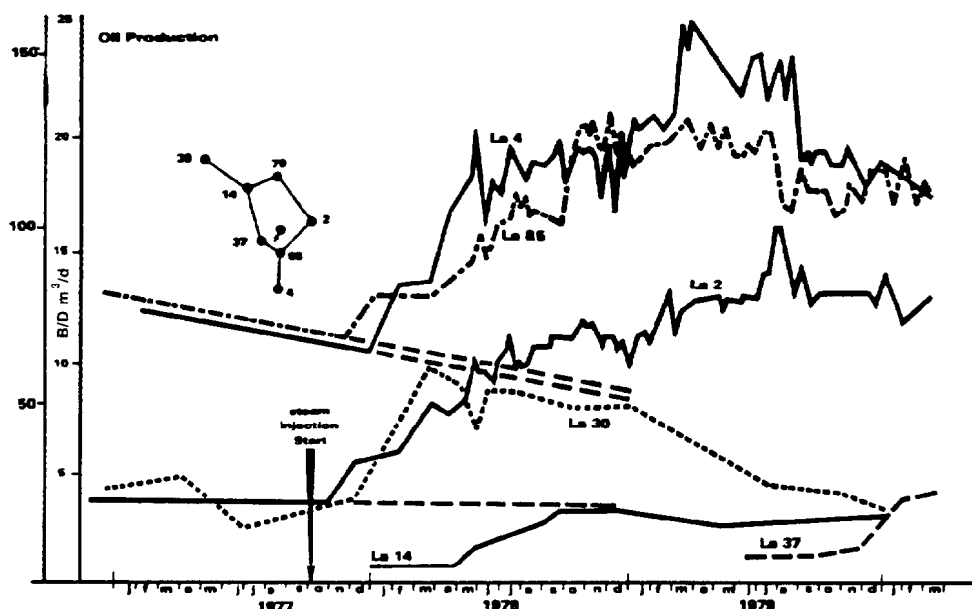


Fig. 46.31—Production history, Lacq Supérieur field.

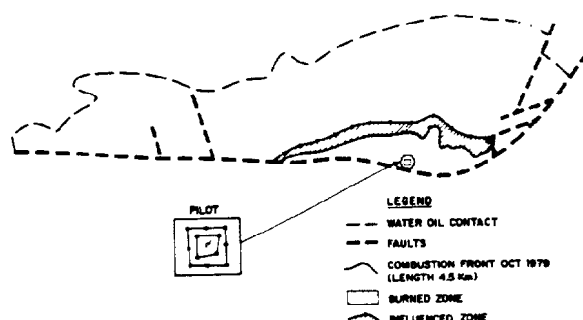


Fig. 46.32—Suplacu de Barcau field, Romania.

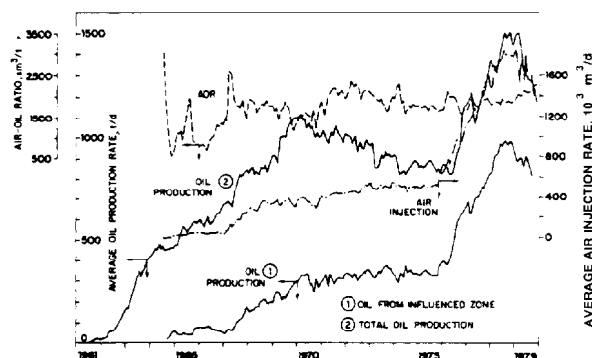


Fig. 46.33—Injection and production history, Suplacu de Barcau field.

TABLE 46.25—RESERVOIR ROCK AND FLUID PROPERTY DATA, SUPLACU DE BARCAU FIELD, ROMANIA

Depth, ft	164 to 656
Net thickness, ft	32.8
Porosity, %	32
Permeability, md	1,722
Oil gravity, °API	15.9
Reservoir temperature, °F	64
Oil viscosity at 64°F, cp	2,000
Oil saturation at start, %	85

TABLE 46.26—RESERVOIR ROCK AND FLUID PROPERTY DATA, WEST HEIDELBERG FIELD, MS

Depth, ft	11,500
Thickness, ft	
Gross	20 to 40
Net	30
Dip, degrees	5 to 15
Porosity, %	16.4
Permeability, md	39
Oil gravity, °API	24
Reservoir temperature, °F	221
Oil viscosity at 221°F, cp	4.5
Oil saturation at start, %	77.8

Gloriana, TX (Sun)^{116,118}—Thinnest Reservoir Produced by a Fireflood. The Gloriana field is in Wilson County, TX. The fireflood took place in the Poth "A" Sand. It is possibly the thinnest reservoir that has ever been produced by a fireflood. The reservoir properties are given in Table 46.27.

The field originally was developed on 40-acre spacing. A new well, Well 2-8, was ignited in May 1969. Well 2-5, a producer, burned out and was converted to air injection in May 1971. These wells, along with other wells,

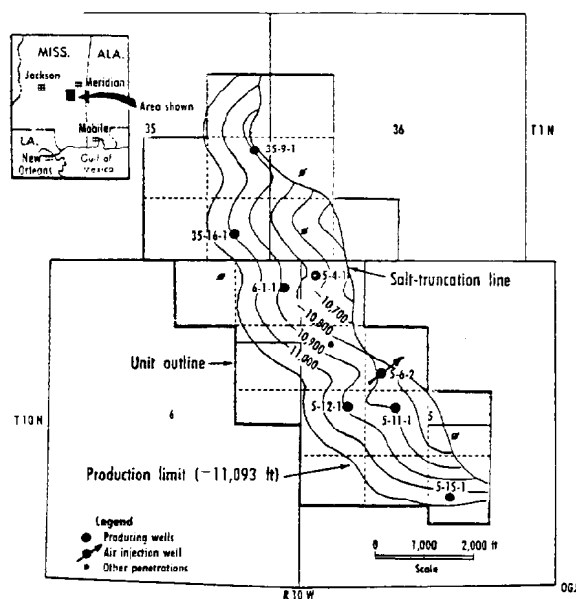


Fig. 46.34—Structure map of Sand No. 5, West Heidelberg field, MS.

are shown in the isopachous map in Fig. 46.36. The injection and production histories are given in Figs. 46.37 and 46.38, respectively. Air injection stopped in Dec. 1974 when the oil production rate declined to the economic limit.

Sloss, NE (Amoco) 77-79—Wet Combustion, Tertiary Recovery. The Sloss field is located in Kimball County, NE. The pilot used a wet combustion process in a previously waterflooded reservoir. Here, the pay is thin and deep, the oil is light, the viscosity is low, and the oil satu-

TABLE 46.27—RESERVOIR ROCK AND FLUID PROPERTY DATA, GLORIANA FIELD, TX

Depth, ft	1,600
Thickness, ft	
Gross	10
Net	4
Dip, degrees	0 to 5
Porosity, %	35
Permeability, md	1,000
Oil gravity, °API	20.8
Reservoir temperature, °F	112
Oil viscosity, cp	
112°F	70 to 150
80°F	250 to 500
Oil saturation at start, %	58.5

ration at the start of the flood was low. The reservoir properties are given in Table 46.28.

The fireflood started in 1967 with six 80-acre five-spots. Additional wells were included so that it covered 960 acres in its final stage. The pilot area is shown in Fig. 46.39. The injection and production data in the 4½-year period of its operation are given in Figs. 46.40 and 46.41, respectively. Between Feb. 1967 and July 1971, total air injected was $13,754 \times 10^6$ scf and water injected was $10,818 \times 10^3$ bbl, giving a WAR of 0.79 bbl/ 10^3 scf. The total oil production was 646,776 bbl. This gives an AOR of 21.3×10^3 scf/bbl. The areal sweep by the greater-than-350°F zone was 50%. Combining with a vertical sweep of 28%, the volumetric sweep was only 14%.

Asphalt Ridge, UT (DOE) 130—Extremely Viscous Tar, Combination Reverse/Forward Combustion. The Northwest Asphalt Ridge deposit is located in northeast Utah, near the city of Vernal. The fireflood conducted

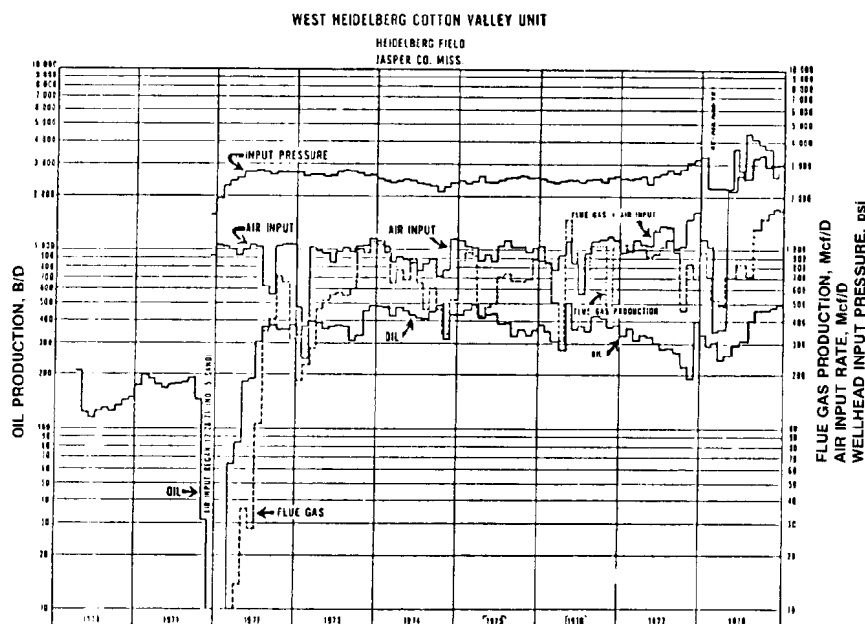


Fig. 46.35—Injection and production history, West Heidelberg field.

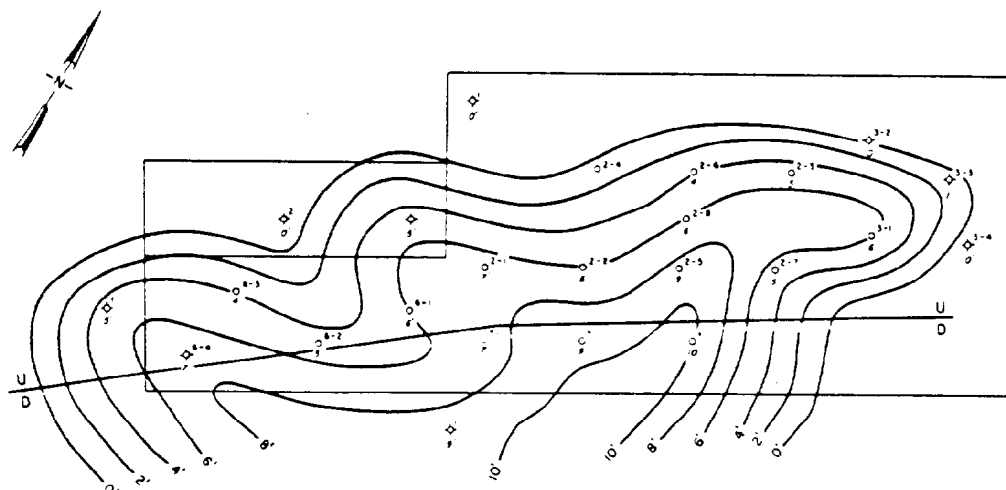


Fig. 46.36—Isopachous map, net oil, Poth "A" sand, Gloriana field, TX.

in this deposit is interesting because it attempted to use a combination of reverse and forward combustion for the recovery of oil from tar sands. The reservoir properties are given in Table 46.29.

The U.S. DOE conducted two fireflood tests in the Asphalt Ridge area. The first, conducted in 1975, demonstrated the feasibility of using reverse combustion to recover oil in the tar sand. The second tested a combination of reverse combustion and forward combustion during the period from Aug. 1977 to Feb. 1978. The location of the test sites and well arrangements are shown in Fig. 46.42. In both tests, the line drive was on a small area of 120×40 ft, covering only 0.11 acres. In the second test, several echoings of reverse and forward combustion phases were noticed in the northwest area, as seen from the temperature variations at observation Well 203 (Fig. 46.43). The reverse combustion phase had an areal sweep of 95% and vertical sweep of 91%, giving a volumetric sweep of 86%. The echoing forward combustion phase had an areal sweep of 75% and vertical sweep of 44%, giving a volumetric sweep of only 33%. The produced oil was of better quality than the original bitumen, with the pour point reduced from 140 to 25°F and the amount of residue lowered from 62 to 35 wt%.

Forest Hill, TX (Air Products-Greenwich)¹⁵³—**Oxygen-Enriched Air.** The Forest Hill field is located in Wood County, TX. The significance of the field test lies in the use of oxygen-enriched air for the fireflood. The reservoir properties are given in Table 46.30.

The field was on primary production in 1964. Air injection started in 1976. One of the air injectors was switched to oxygen-enriched air in 1980. The test site is shown in Fig. 46.44. As seen in Fig. 46.45, during a 2-year period, the oxygen concentration in the injected gas ranged from 21 to 90%. The test showed that essentially pure oxygen can be handled and injected safely in a typical oilfield environment. Short of any definitive comparison, the test only hinted that using enriched air might produce oil faster than using air only.

Thermal Properties

Only some selected thermal properties of the rock/fluid systems encountered in the thermal recovery projects will be presented briefly. A more complete compilation of tables and figures has been included in Appendix B of Ref. 154.

Oil Viscosities

The viscosity-temperature relationships for representative heavy-oil deposits are shown in Fig. 46.46. Oil viscosities should be measured experimentally. In the absence of experimental data, the viscosities can be estimated by charts (Fig. 46.47 to 46.49)¹⁵⁵⁻¹⁵⁷ and equations.¹⁵⁸

Beggs and Robinson¹⁵⁸ suggested the following equations for estimating viscosities of live oils. Dead-oil viscosity is first calculated:

$$\mu_{od} = 10^X - 1, \dots\dots\dots (74)$$

where μ_{od} equals the viscosity of dead oil (gas-free oil) at T , cp.

$$X = YT^{-1.163}, \dots\dots\dots (75)$$

$$Y = 10^Z, \dots\dots\dots (76)$$

and

$$Z = 3.0324 - 0.02023 \gamma_o, \dots\dots\dots (77)$$

where γ_o equals the oil gravity, °API, and T is the temperature, °F. Live-oil viscosity is calculated next.

$$\mu = A\mu_{od}B, \dots\dots\dots (78)$$

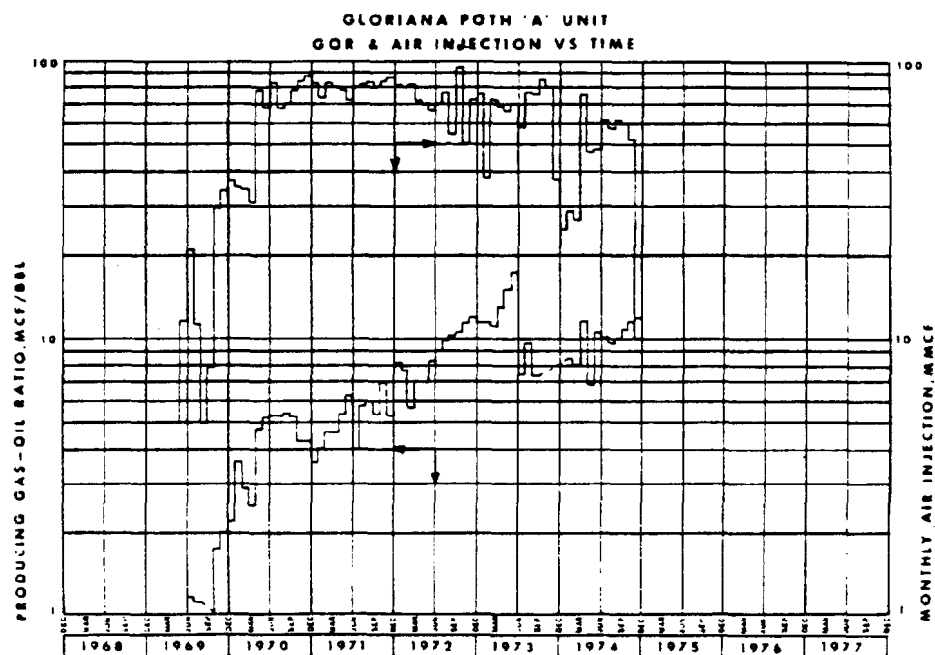


Fig. 46.37—GOR and air injection history, Gloriana field.

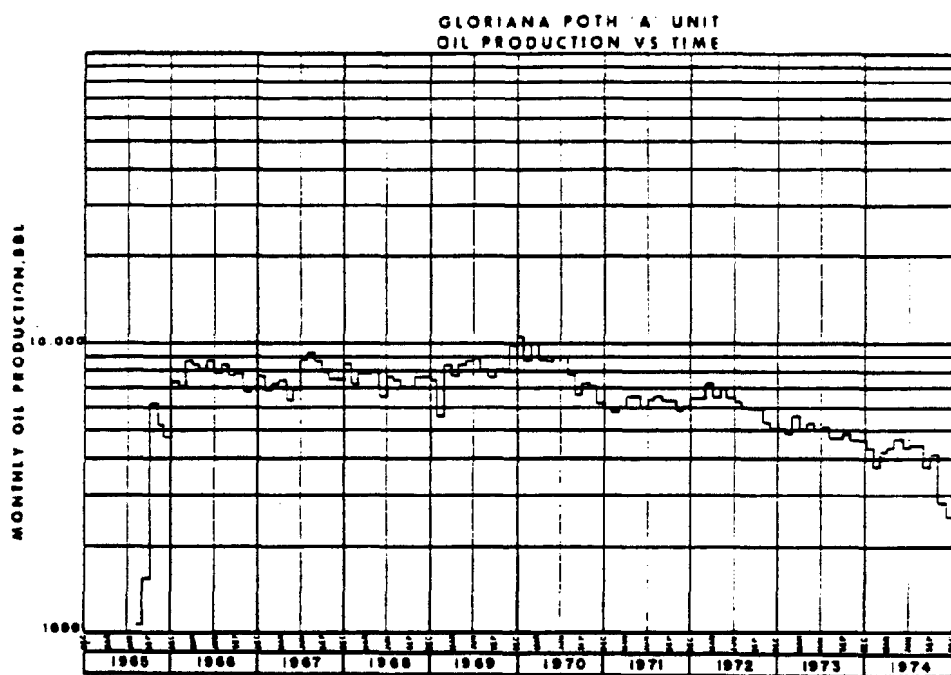


Fig. 46.38—Oil production history, Gloriana field.

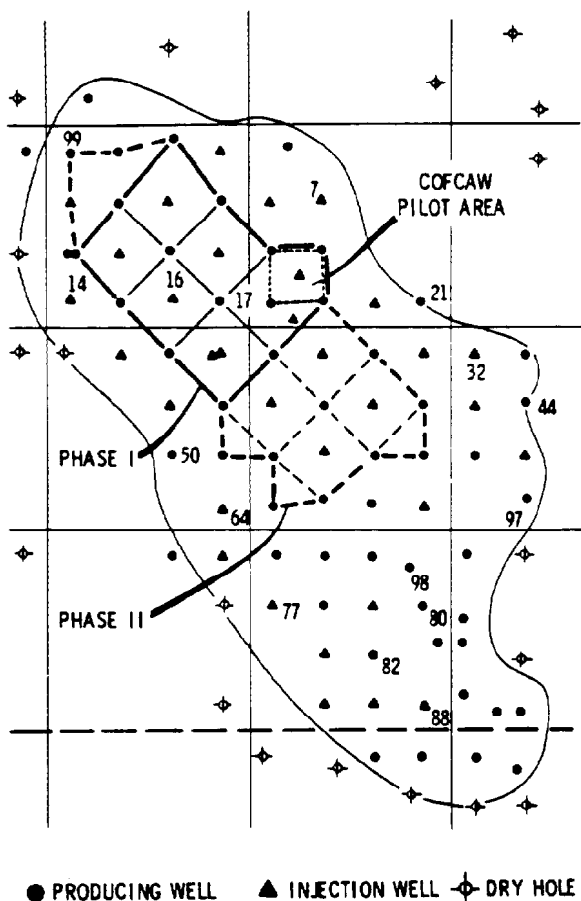


Fig. 46.39—Sloss unit, NE.

TABLE 46.28—RESERVOIR ROCK AND FLUID PROPERTY DATA, SLOSS FIELD, NE

Depth, ft	6,200
Net thickness, ft	14.3
Porosity, %	19.3
Permeability, md	191
Oil gravity, °API	38.8
Reservoir temperature, °F	200
Reservoir pressure, psig	2,274
Oil viscosity at 200°F, cp	0.8
Oil saturation at start, %	20 to 40

TABLE 46.29—RESERVOIR ROCK AND FLUID PROPERTY DATA, ASPHALT RIDGE FIELD, UT

Depth, ft	350
Net thickness, ft	13.1
Porosity, %	31.1
Permeability, md	
Saturated	85
Extracted	675
Oil gravity, °API	14
Reservoir temperature, °F	52
Oil viscosity at 60°F, cp	>1,000,000
Pour point, °F	140
Saturations at start, %	
Oil	65
Water	2.4

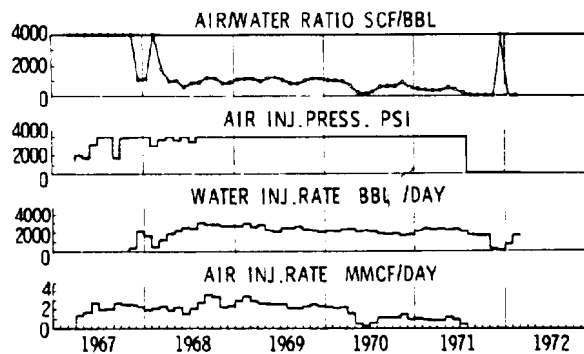


Fig. 46.40—Injection history, Sloss field COFCAW pilot.

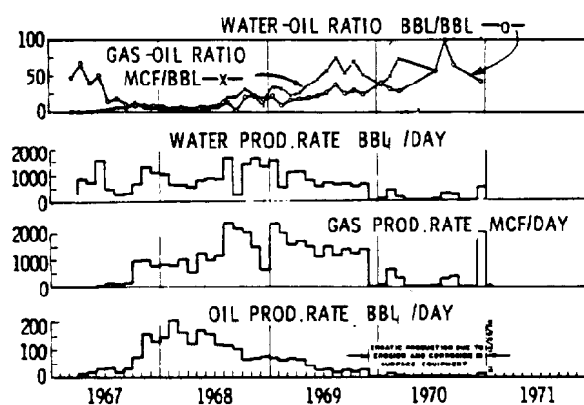


Fig. 46.41—Production history, Sloss field COFCAW pilot.

MAJOR UTAH TAR SAND DEPOSITS

- ① ASPHALT RIDGE
- ② SUNNYSIDE
- ③ HILL CREEK
- ④ P.B. SPRING
- ⑤ TAR SAND TRIANGLE
- ⑥ CIRCLE CLIFFS

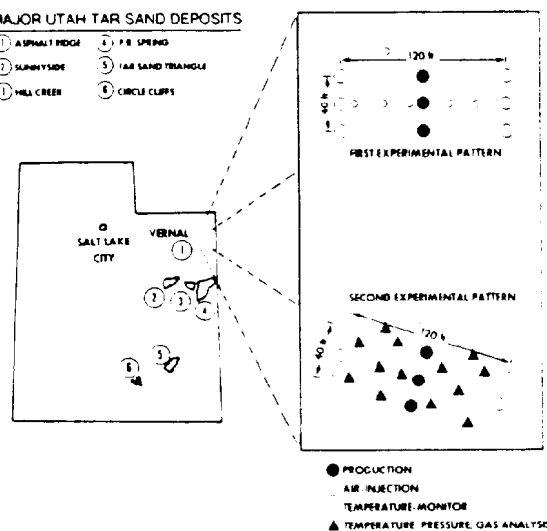


Fig. 46.42—LETC field site, Asphalt Ridge deposit, UT.

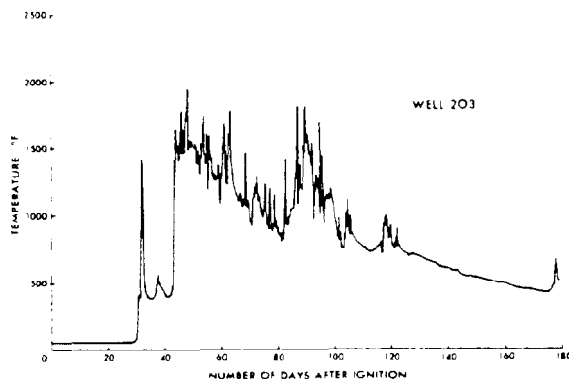


Fig. 46.43—Maximum temperature vs. time, Well 203, Asphalt Ridge deposit.

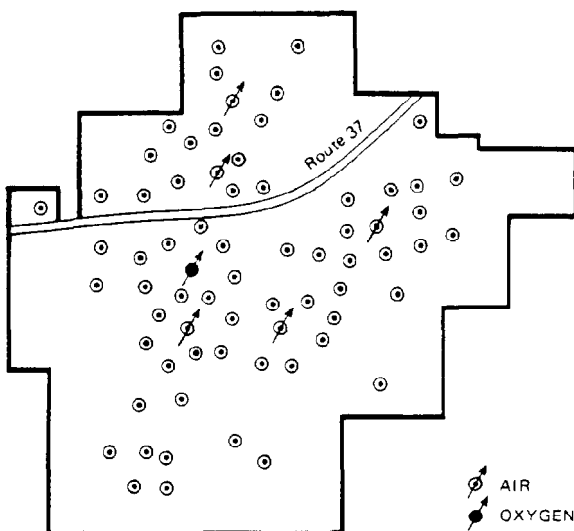


Fig. 46.44—Forest Hill field, TX.

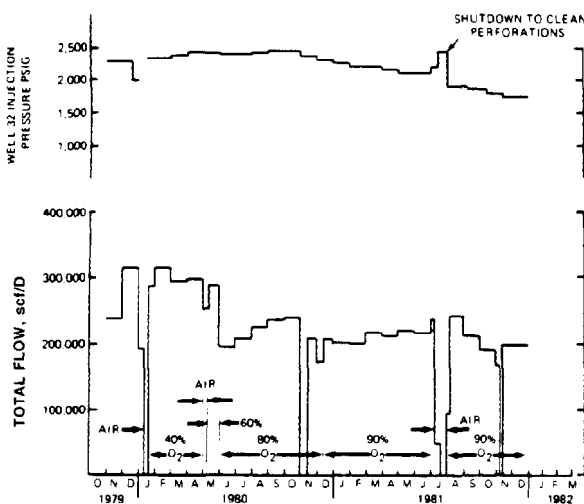


Fig. 46.45—Injection history, Well 32, Forest Hill field.

TABLE 46.30—RESERVOIR ROCK AND FLUID PROPERTY DATA, FOREST HILL FIELD, TX

Depth, ft	4,800
Net thickness, ft	15
Porosity, %	27.7
Permeability, md	626
Oil gravity, °API	10
Reservoir temperature, °F	185
Oil viscosity at 185°F, cp	1,002
Saturations at start, %	
Oil	64
Water	36

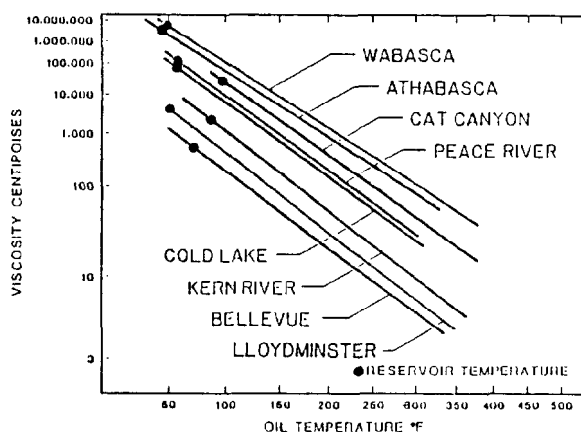


Fig. 46.46—Viscosity/temperature relationships for representative heavy oil deposits.

where

$$A = 10.715(R_s + 100)^{-0.515}, \quad (79)$$

$$B = 5.44(R_s + 150)^{-0.338}, \quad (80)$$

and R_s is the solution gas/oil ratio, scf/STB.

Relative Permeability Curves

Relative permeability data should be determined experimentally. In the absence of experimental data, the following equations may be used for rough estimation. According to Brooks and Corey,¹⁵⁹

$$k_{rw} = (S_w^*)^5, \quad (81)$$

$$k_{ro} = (1 - S_w^*)^2 (1 - S_w^{*2}), \quad (82)$$

and

$$S_w^* = \frac{S_w - S_{iw}}{1 - S_{iw}}, \quad (83)$$

where S_{iw} is the irreducible water saturation, percent.

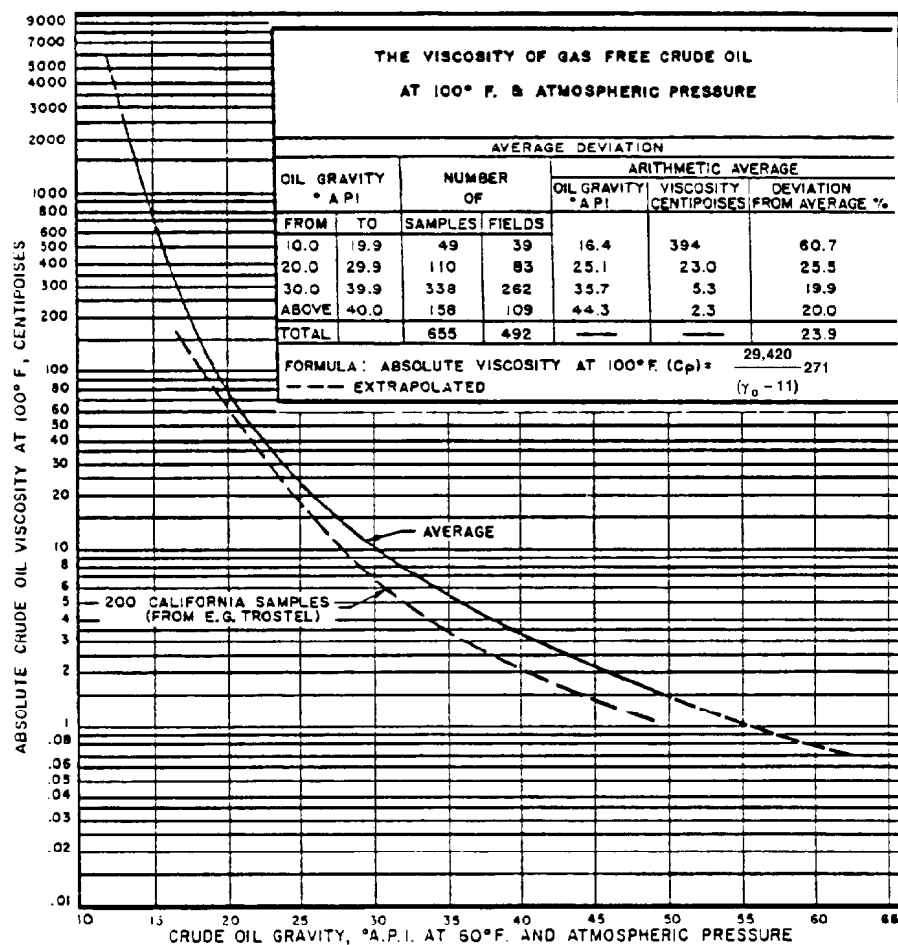


Fig. 46.47—Dead oil viscosity.

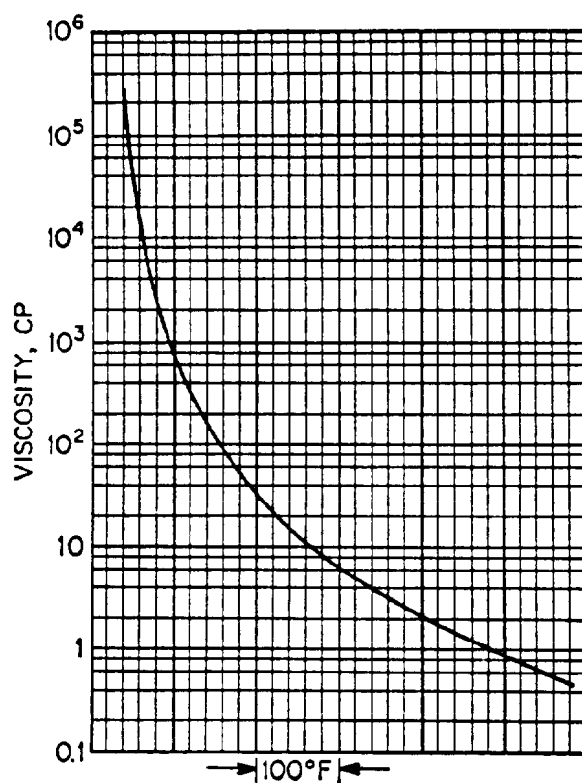


Fig. 46.48—Universal temperature/viscosity chart.

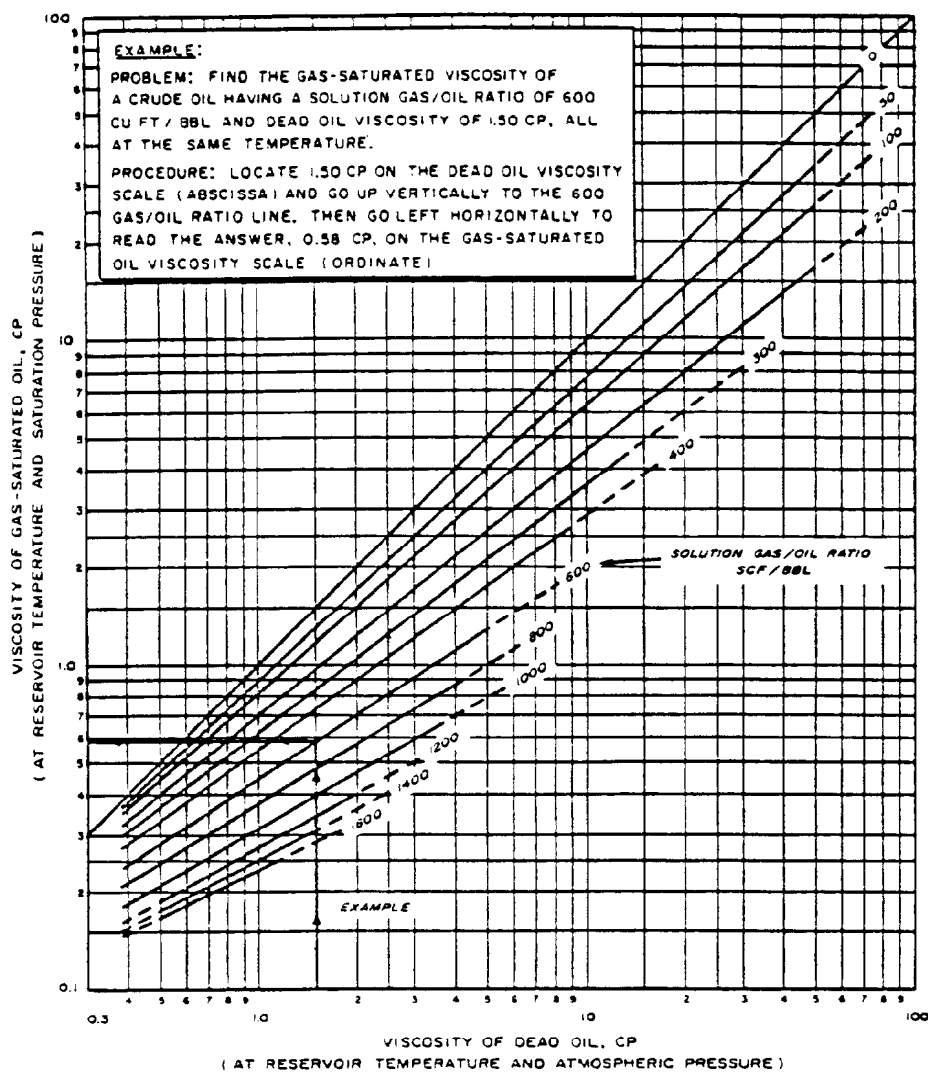


Fig. 46.49—Live oil viscosity.

According to Somerton,¹⁶⁰ for unconsolidated sand,

$$S_{iw} = 0.211 + 2.0 \times 10^{-4} T + 1.1 \times 10^{-6} T^2, \dots (84)$$

where T is the temperature, °F.

The effect of temperature on irreducible water saturation and relative permeability of unconsolidated sands has been studied by Poston *et al.*¹⁶¹ Some of their results are given in Figs. 46.50 through 46.52. The effect of temperature on relative and absolute permeabilities of consolidated sandstones has been studied by Weinbrandt *et al.*¹⁶² Some of their results are given in Figs. 46.53 through 46.56.

PV Compressibility

The compressibility of unconsolidated, Arkosic sands was measured by Sawabini *et al.*¹⁶³ Fig. 46.57 shows that the effective PV compressibility lies in the range between 10^{-4} and 10^{-3} psi⁻¹, about 2 to 3 orders of magnitude higher than the normally accepted figure of 10^{-6} psi⁻¹ for consolidated sandstones. In Fig. 46.57, p_{to} is the total overburden pressure, psi, and p_p is the pore pressure, psi.

Thermal Conductivity

Thermal behavior of unconsolidated oil sands was studied by Somerton *et al.*¹⁶⁴ Fig. 46.58 shows how thermal conductivity of Kern River oil sands varies with brine saturation.

Vaporization Equilibrium

Vaporization equilibrium of an oil fraction is described by the equilibrium vaporization constant, K , which is defined as

$$K = \frac{y}{x}, \dots (85)$$

where y is the mol fraction in vapor phase and x is the mol fraction in liquid phase.

Poettmann and Mayland¹⁶⁵ in 1949 published a series of charts on equilibrium constants of various oil fractions with normal boiling points of 300°F, 400°F, etc., up to 1,000°F. To illustrate how K values vary with temperature and pressure, the figure for normal boiling point=500°F is shown in Fig. 46.59.

More recently, Lee *et al.*¹⁶⁶ presented equilibrium constants of oil fractions with 100°F boiling ranges. For example, Fraction 1 has the boiling range up to 300°F, Fraction 2 boiling between 300 and 400°F, and Fraction 6 boiling above 700°F. Figs. 46.60 and 46.61 show the effects of pressure and temperature, respectively, on the K values for these oil fractions as well as N₂, CH₄, and CO₂.

Chemical Kinetics

Chemical reactions taking place in an in-situ combustion process are considered to fall into three types: (1) low-temperature oxidation, (2) fuel deposition or coke formation, and (3) combustion. The kinetic data of these three types of reactions reported by various authors have been summarized in the paper by Fassihi *et al.*¹⁶⁷ and will not be reproduced here.

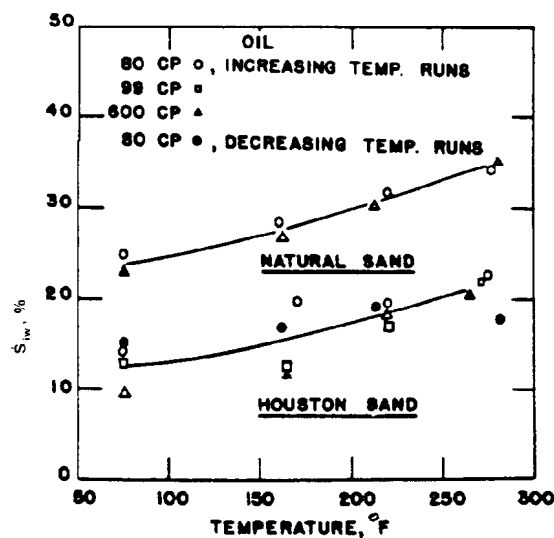


Fig. 46.50—Effect of temperature on irreducible water saturation, Houston sand, and natural sand.

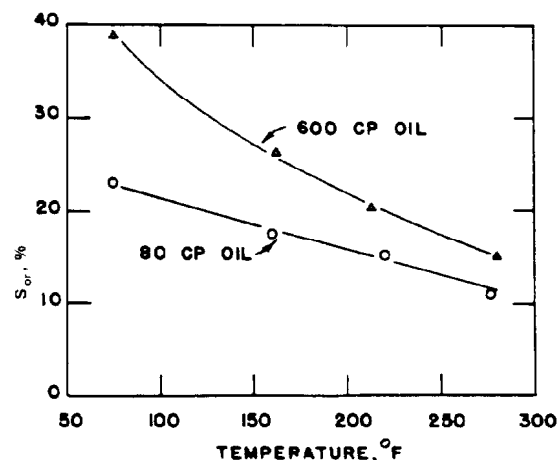


Fig. 46.51—Effect of temperature on ROS, natural sand.

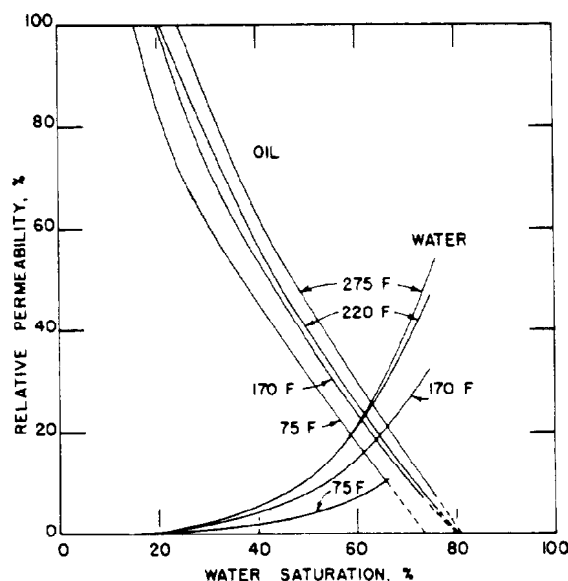


Fig. 46.52—Water and oil relative permeability at four temperatures, Houston sand, 80-cp oil.

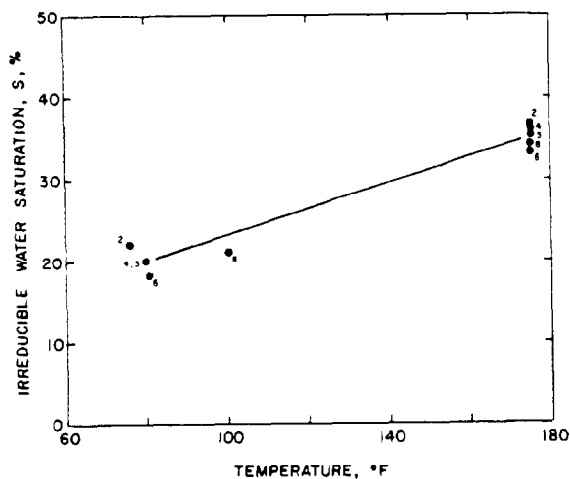


Fig. 46.53—Effect of temperature on irreducible water saturation, sandstone cores.

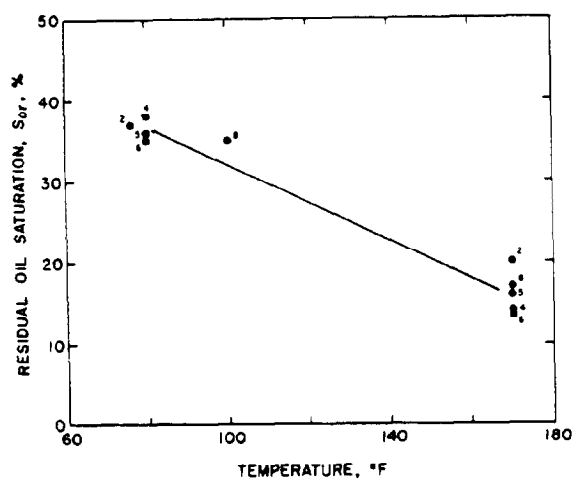


Fig. 46.54—Effect of temperature on ROS, sandstone cores.

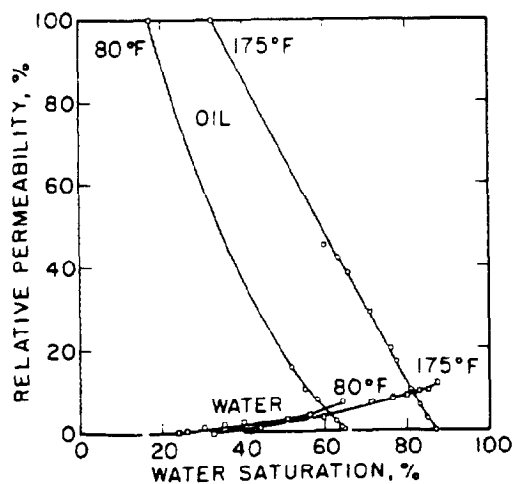


Fig. 46.55—Water and oil relative permeability at two temperatures, Core 4, Boise sandstone.

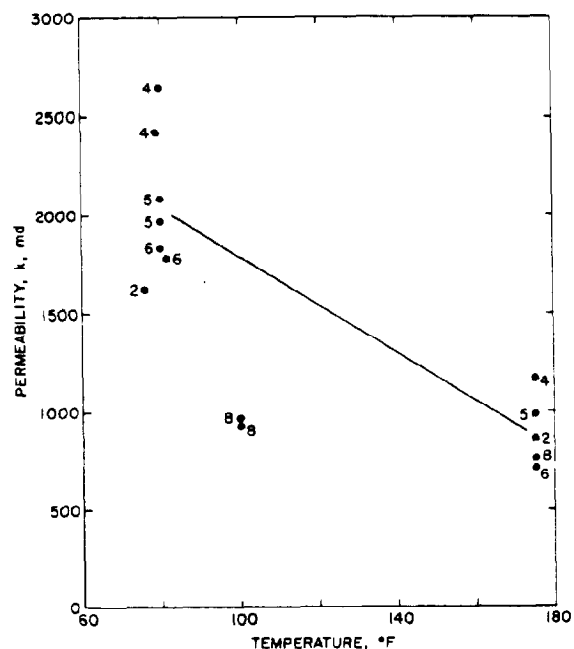


Fig. 46.56—Effect of temperature on absolute permeability, sandstone cores.

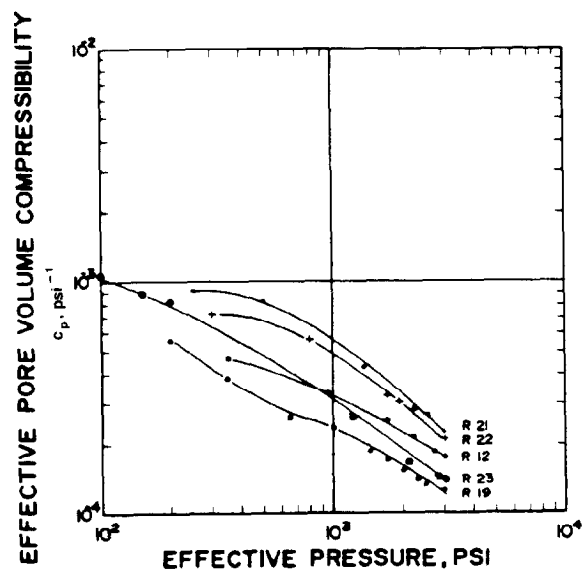


Fig. 46.57—Effective PV compressibility, unconsolidated Arkosic oil sand.

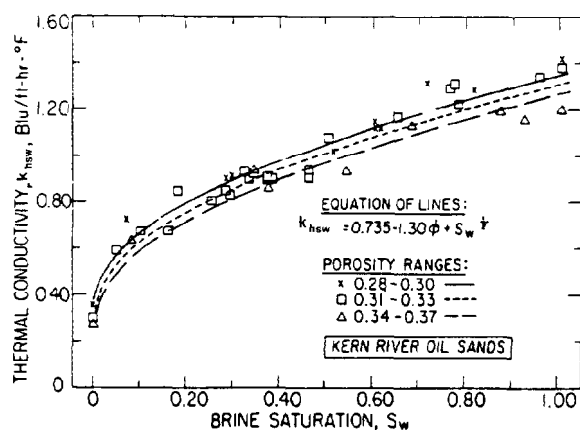


Fig. 46.58—Thermal conductivity of Kern River oil sands.

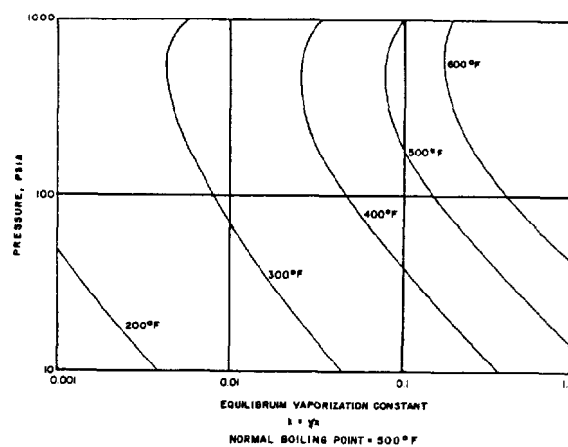


Fig. 46.59—Equilibrium vaporization constant, normal boiling point—500°F.

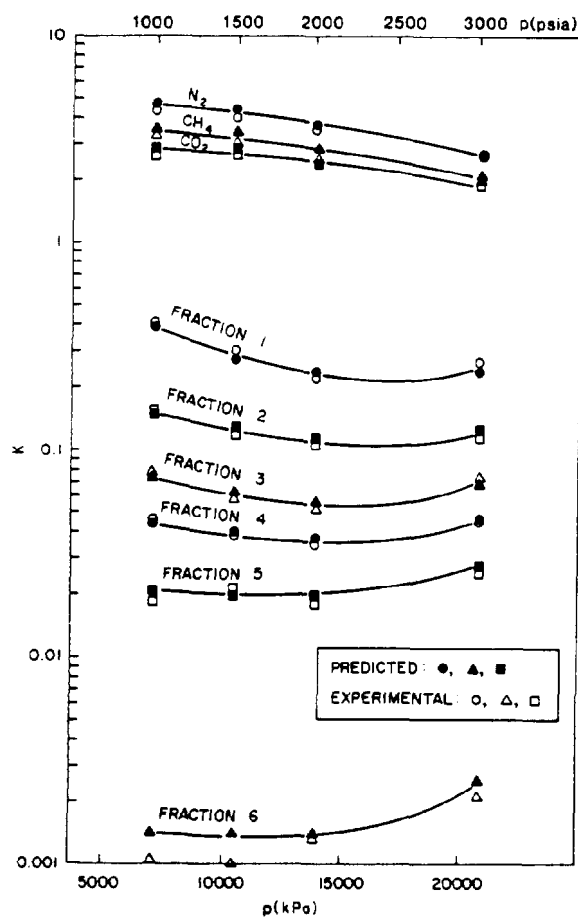


Fig. 46.60—Effect of pressure on equilibrium K values for Crude A at 260°C.

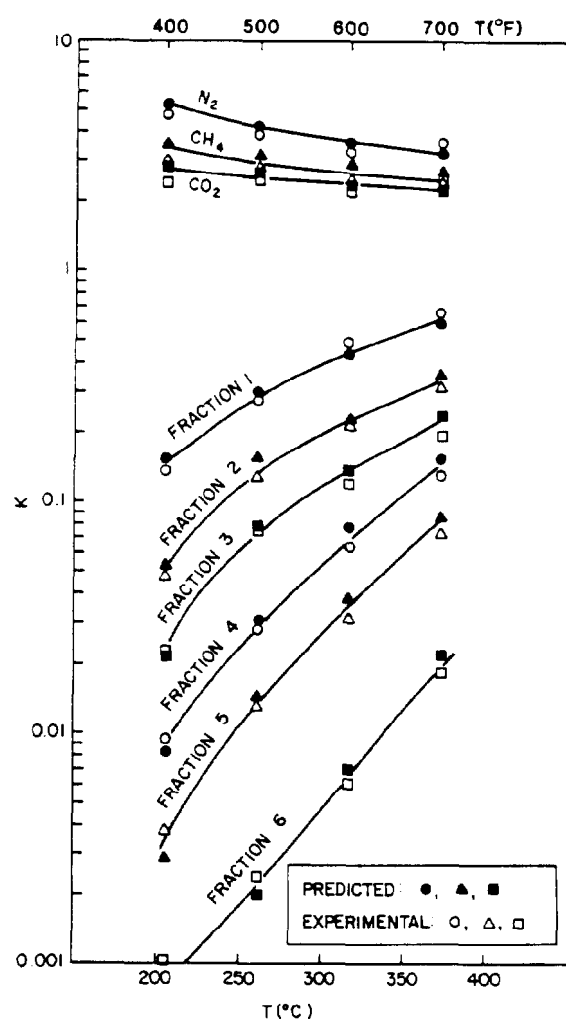


Fig. 46.61—Effect of temperature on equilibrium K values of Crude B at 1,514.7 psia.

TABLE 46.31—SATURATED STEAM TABLE

Absolute Pressure, p (psia)	Temperature T (°F)	Specific Volume, cu ft/lbm			Enthalpy, Btu/lbm		
		Saturated Liquid, v_L	Evaporate, v_{fg}	Saturated Vapor, v_g	Saturated Liquid, H_L	Evaporate, L_s	Saturated Vapor, H_g
0.08865	32.018	0.016022	3,302.4	3,302.4	0.0003	1,075.5	1,075.5
14.696	212.00	0.016719	26.782	26.799	180.17	970.3	1,150.5
50.0	281.02	0.017274	8.4967	8.5140	250.2	923.9	1,174.1
100.0	327.82	0.017740	4.4133	4.4310	298.5	888.6	1,187.2
150.0	358.43	0.01809	2.9958	3.0139	330.6	863.4	1,194.1
200.0	381.80	0.01839	2.2689	2.2873	355.5	842.8	1,198.3
250.0	400.97	0.01865	1.82452	1.84317	376.1	825.0	1,201.1
300.0	417.35	0.01889	1.52384	1.54274	394.0	808.9	1,202.9
400.0	444.60	0.01934	1.14162	1.16095	424.2	780.4	1,204.6
500.0	467.01	0.01975	0.90787	0.92762	449.5	755.1	1,204.7
600.0	486.20	0.02013	0.74962	0.76975	471.7	732.0	1,203.7
700.0	503.08	0.02050	0.63505	0.65556	491.6	710.2	1,201.8
800.0	518.21	0.02087	0.54809	0.56896	509.8	689.6	1,199.4
900.0	531.95	0.02123	0.47968	0.50091	526.7	669.7	1,196.4
1,000.0	544.58	0.02159	0.42436	0.44596	542.6	650.4	1,192.9
1,200.0	567.19	0.02232	0.34013	0.36245	571.9	613.0	1,184.8
1,400.0	587.07	0.02307	0.27871	0.30178	598.8	576.5	1,175.3
1,600.0	604.87	0.02387	0.23159	0.25545	624.2	540.3	1,164.5
1,800.0	621.02	0.02472	0.19390	0.21861	648.5	503.8	1,152.3
2,000.0	635.80	0.02565	0.16266	0.18831	672.1	466.2	1,138.3
2,200.0	649.45	0.02669	0.13603	0.16272	695.5	426.7	1,122.2
2,400.0	662.11	0.02790	0.11287	0.14076	719.0	384.8	1,103.7
2,600.0	673.91	0.02938	0.09172	0.12110	744.5	337.6	1,082.0
2,800.0	684.96	0.03134	0.07171	0.10305	770.7	285.1	1,055.8
3,000.0	695.33	0.03428	0.05073	0.08500	801.8	218.4	1,020.3
3,208.2*	705.47	0.05078	0.00000	0.05078	906.0	0.0	906.0

Steam Properties

An abbreviated steam table¹⁶⁸ is given in Table 46.31.

Nomenclature

a = air requirement, 10^6 , scf/acre-ft
 A = heated area at time t , sq ft, or
quantities defined by Eqs. 9 and 79
 A' = quantity defined by Eq. 13
 B = quantities defined by Eqs. 10 and 80
 B' = quantity defined by Eq. 14
 C_m = fuel content, lbm/cu ft
 C_o = heat capacity of oil, Btu/lbm-°F, or
concentration of oil, lbm mol/cu ft
 C_r = heat capacity of rock, Btu/lbm-°F
 C_s = heat capacity of steam, Btu/lbm-°F
 C_w = heat capacity of water, Btu/lbm-°F
 C_{O_2} = concentration of oxygen, lbm mol/cu ft
 C_1 = quantity defined by Eqs. 58 and 60
 C_2 = quantity defined by Eqs. 59 and 61
 D = depth, ft
 E = activation energy, Btu/lbm mol
 E_h = thermal (heat) efficiency, fraction
 E_{O_2} = oxygen utilization efficiency, fraction
 E_r = overall oil recovery
 E_{Ru} = recovery efficiency in the unburned
region, fraction
 E_{vb} = volumetric sweep efficiency of the
burning front, fraction
 f_{s1} = steam quality at the beginning of the
pipe segment, fraction

f_{s2} = steam quality at the end of the pipe
segment, fraction
 $f(t)$ = transient heat conduction time function
for earth, dimensionless
 F_{ao} = AOR
 F_{cc} = CO₂/CO ratio in produced gas
 F_{HC} = atomic H/C ratio
 F_J = ratio of stimulated to unstimulated
productivity indices, dimensionless
 F_{so} = steam/oil ratio, STB/STB
 F_{wor} = total produced WOR, STB/STB
 h = pay thickness, ft, or convection heat
transfer coefficient, Btu/hr-sq ft-°F
 h' = convection heat transfer coefficient
based on insulation outside surface,
Btu/hr-sq ft-°F
 h_f = enthalpy of liquid water at T above
32°F, Btu/lbm
 h_t = total thickness of all sands, ft
 H_{og} = enthalpy of oil and gas Btu/lbm
 H_w = enthalpy of water carried by oil based
on a STB of oil, Btu/STB oil
 H_{wR} = enthalpy of water at reservoir tempera-
ture, Btu/lbm
 H_{ws} = enthalpy of water at steam tempera-
ture, Btu/lbm
 i_{at} = cumulative air injection, 10^3 scf
 i_s = steam injection rate, B/D
 I = radiation heat transfer coefficient,
Btu/hr-sq ft-°F

I' = radiation heat transfer coefficient based on insulation outside surface, Btu/hr-sq ft-°F	r_{to} = outside radius of pipe, ft
J_c = unstimulated (cold) productivity index, STB/D-psi	r_w = well radius, ft
k = absolute permeability, md	R = gas constant
k' = pre-exponential factor	R_s = solution GOR, scf/STB
k_{hca} = thermal conductivity of the casing material, Btu/hr-sq ft-°F	R_t = total produced GOR, scf/STB
k_{hce} = thermal conductivity of the cement, Btu/hr-ft-°F	S_g = gas saturation, fraction
k_{hcf} = thermal conductivity of the formation, Btu/D-ft-°F	S_{io} = irreducible oil saturation, fraction
k_{hin} = thermal conductivity of insulation material, Btu/hr-ft-°F	S_{iw} = irreducible water saturation, percent
k_{ho} = overburden thermal conductivity, Btu/hr-ft-°F	S_o = oil saturation at start, fraction
k_{ro} = relative permeability to oil, fraction	S_{oi} = initial oil saturation, fraction
k_{rw} = relative permeability to water, fraction	S_{wi} = initial water saturation, fraction
K = equilibrium vaporization constant	S_w^* = normalized water saturation, fraction
L = pipe length, ft	t = time since injection, hours
L_s = latent heat of steam, Btu/lbm	t_c = critical time, hours
L_{v1} = latent heat of vaporization at top of interval, Btu/lbm	t_D = dimensionless time
L_{v2} = latent heat of vaporization at bottom of interval, Btu/lbm	t_i = time of injection for the current cycle, days
m_{sit} = total mass of steam injected, lbm	\bar{T} = average temperature of the heated region, $r_w < r < r_h$, at any time t , °F
M = volumetric heat capacity, Btu/cu ft-°F	T_{at} = atmospheric temperature, °F
N = OOIP, bbl	T_{cf} = temperature at cement/formation interface, °F
N_s = number of sands	T_{ci} = temperature at casing inside surface, °F
N_{sp} = oil in place at start of project, bbl	T_{fi} = initial formation temperature, °F
ΔN_{sp} = cumulative incremental oil production, bbl	T_{ff} = temperature of fluid, °F
p_e = static formation pressure at external radius, psia	T_{inj} = injection temperature, °F
p_p = pore pressure, psi	T_R = original reservoir temperature, °F
p_s = saturated vapor pressure of water at \bar{T} , psia	T_s = steam temperature, °F
p_{to} = total overburden pressure, psi	T_{su} = formation temperature at ground surface, °F
p_w = bottomhole pressure, psia	U_{co} = overall heat transfer coefficient based on outside casing surface, Btu/hr-sq ft-°F
p_1 = pressure at top of interval, psia	U_{ti} = overall heat transfer coefficient based on inside radius of pipe or tubing, Btu/hr-sq ft-°F
p_2 = pressure at bottom of interval, psia	U_{to} = overall heat transfer coefficient based on outside tubing surface, Btu/D-sq ft-°F
Δp = frictional pressure drop over interval, psia	v_t = specific volume of total fluid, cu ft/lbm
q_o = oil displacement rate, B/D	v_w = wind velocity, mile/hr
q_{oc} = cold oil production rate, B/D	V_{fb} = fuel burned, bbl
q_{oh} = hot oil production rate, B/D	V_r, V_z = unit solution for component conduction problems in the r and z directions*
Q_{hz} = heat remaining in heated zone, Btu	\bar{V}_r, \bar{V}_z = average values of V_r and V_z for $0 < r < r_h$
Q_{it} = total heat injection, Btu	w = Arrhenius reaction rate
Q_{ri} = heat injection rate, Btu/hr	w_s = mass rate of steam, lbm/hr
Q_{rt} = heat loss along the segment, Btu/hr	x = mole fraction in liquid phase
Q_{rt} = heat removal rate at time t , Btu/D	X = quantity defined by Eq. 66
r_{cf} = radius to cement/formation interface, ft	y = mole fraction in vapor phase
r_{ci} = inside radius of casing, ft	Y = quantity defined by Eq. 65
r_{co} = outside radius of casing, ft	α = thermal diffusivity, sq ft/D
r_e = external radius, ft	α_o = overburden thermal diffusivity, sq ft/D
r_h = radius of region originally heated, ft	
r_{in} = outside radius of insulation surface, ft	
r_{ti} = inside radius of tubing, ft	

*These symbols have no physical connotation. They are simply mathematical symbols.

β = dummy variable in Eq. 27
 δ = energy removed with the produced fluids, dimensionless
 Θ = dip angle, degrees
 μ_o = oil viscosity, cp
 μ_{oc} = cold oil viscosity, cp
 μ_{od} = viscosity of dead oil (gas-free oil) at T , cp
 μ_{oh} = hot oil viscosity, cp
 ρ_o, ρ_r, ρ_w = density of oil, rock grain, and water, lbm/cu ft
 ϕ = porosity, fraction

Key Equations in SI Units

$$h = 7.165 v_w^{0.6} / r_{in}^{0.4} \quad (3)$$

$$p_2 = p_1 + 7.816 \times 10^{-12} (v_{t1} - v_{t2}) \frac{w_s^2}{r_{ti}^4} + 9.806 \times 10^{-3} \frac{\Delta D}{v_{t1}} - \Delta p \quad (20)$$

$$F_{so}^* = \frac{Q_s t}{Ah\phi(S_{oi} - S_{io})} \quad (30)$$

$$q_{oc} = \frac{0.0005427 k k_{ro} h}{\mu_{oc} \ln \frac{r_e}{r_w}} (p_e - p_w) \quad (42)$$

$$Y = 0.2639 \left[0.427 S_o - 0.004429 h - 0.3905 \left(\frac{1}{\mu_o} \right)^{0.25} \right] X \quad (64)$$

where

$$X = \frac{i_{at} E_{O_2}}{[N_{sp}/(\phi S_o)](1 - \phi)}$$

$$F_{so} \text{ (in m}^3/\text{m}^3\text{)} = 1 / \left(-0.011253 + 0.00009117D + 0.0005180h - 0.07775\Theta + 0.007232\mu_o + 0.00003467 \frac{kh}{\mu_o} + 0.5120\phi S_o \right) \quad (67)$$

$$F_{so} \text{ (in m}^3/\text{m}^3\text{)} = 18.744 + 0.004767D - 0.16693h - 0.89814k - 0.5915\mu_o - 14.79S_o - 0.0009767 \frac{kh}{\mu_o} \quad (68)$$

$$C_m \text{ (in kg/m}^3\text{)} = -1.9222 + 0.137695h + 1.85029k + 35.72S_o + 0.012887 \frac{kh}{\mu_o} - 0.00993D - 1.0444\mu_o \quad (69)$$

$$a = \frac{\left(\frac{2F_{cc} + 1}{F_{cc} + 1} + \frac{F_{HC}}{2} \right) C_m}{0.01776(12 + F_{HC})E_{O_2}} \quad (70)$$

$$a \text{ (in std m}^3/\text{m}^3\text{)} = 108.356 + 2.75367h + 229.477S_o + 16.073k \quad (71)$$

$$F_{ao} = \frac{a}{\left[\left(\phi S_o - \frac{C_m}{1,000} \right) E_{vb} + \phi S_o (1 - E_{vb}) E_{Ru} \right]} \quad (72)$$

$$F_{ao} \text{ (in std m}^3/\text{m}^3\text{)} = 3820.4 + 12.97h + 192.20k + 471.1\mu_o - 13671.5\phi S_o \quad (73)$$

where

a is in std m³/m³,
 A is in m²,
 C_m is in kg/m³,
 D is in m,
 F_{ao} is in std m³/m³,
 F_{so} is in m³/m³,
 F_{so}^* is in m³/m³,
 h is in kJ/m² · h · K (Eqs. 2 through 4),
 h is in m,
 i_{at} is in std m³,
 k is in μm²,
 N_{sp} is in m³,
 ρ 's are in kPa,
 q_{oc} is in m³/d,
 Q_s is in m³/h,
 r_{in} is in m,
 r_{ti} is in m,
 t is in h,
 v_t is in m³/kg,
 v_w is in kg/h,
 w_s is in kg/h,
 μ_o is in Pa · s, and
 μ_{oc} is in Pa · s.

References

1. Farouq Ali, S.M.: "Steam Injection," *Secondary and Tertiary Oil Recovery Processes*, Interstate Oil Compact Commission, Oklahoma City (Sept. 1974) Chap. 4.
2. McNeil, J.S. and Moss, J.T.: "Oil Recovery by In-Situ Combustion," *Pet. Eng.* (July 1958) B-29-B-42.
3. Berry, V.J. Jr. and Parrish, D.R.: "A Theoretical Analysis of Heat Flow in Reverse Combustion," *Trans., AIME* (1960) **219**, 124-31.
4. Dietz, D.N. and Weijdemans, J.: "Reverse Combustion Seldom Feasible," *Producers Monthly* (May 1968) 10.
5. Smith, F.W. and Perkins, T.K.: "Experimental and Numerical Simulation Studies of the Wet Combustion Recovery Process," *J. Can. Pet. Tech.* (July-Sept. 1973) 44-54.
6. Stovall, S.L.: "Recovery of Oil from Depleted Sands by Means of Dry Steam," *Oil Weekly* (Aug. 13, 1934) 17-24.
7. Grant, B.R. and Szasz, S.E.: "Development of Underground Heat Wave for Oil Recovery," *Trans., AIME* (1954) **201**, 108-18.
8. Kuhn, C.S. and Koch, R.L.: "In-Situ Combustion—Newest Method of Increasing Oil Recovery," *Oil and Gas J.* (Aug. 10, 1953) **52**, 92-96, 113, 114.
9. Trantham, J.C. and Marx, J.W.: "Bellamy Field Tests: Oil from Tar by Counterflow Underground Burning," *J. Pet. Tech.* (Jan. 1966) 109-15; *Trans., AIME*, **237**.
10. Giusti, L.E.: "CSV Makes Steam Soak Work in Venezuela Field," *Oil and Gas J.* (Nov. 4, 1974) 88-93.
11. Stokes, D.D. and Doscher, T.M.: "Shell Makes a Success of Steam Flood at Yorba Linda," *Oil and Gas J.* (Sept. 2, 1974) 71-76.
12. Dietz, D.N.: "Wet Underground Combustion, State-of-the-Art," *J. Pet. Tech.* (May 1970) 605-17; *Trans., AIME*, **249**.
13. "Steam Dominates Enhanced Oil Recovery," *Oil and Gas J.* (April 5, 1982) 139-59.
14. "Experts Assess Status and Outlook for Thermal, Chemical, and CO₂ Miscible Flooding Processes," *J. Pet. Tech.* (July 1983) 1279-92.
15. Johnson, L.A. Jr. et al.: "An Echoing In-Situ Combustion Oil Recovery Project in the Utah Tar Sand," *J. Pet. Tech.* (Feb. 1980) 295-304.
16. *Enhanced Oil Recovery Potential in the United States*, Report by Lewin and Assocs. for Office of Technology Assessment (Jan. 1978) 40-41.
17. Willman, B.T. et al.: "Laboratory Studies of Oil Recovery by Steam Injection," *Trans., AIME* (1961) **222**, 681-90.
18. McAdams, W.H.: *Heat Transmission*, third edition, McGraw-Hill Book Co. Inc., New York City (1954) 261.
19. Ramey, H.J. Jr.: "Wellbore Heat Transmission," *J. Pet. Tech.* (April 1962) 427-35.
20. Satter, A.: "Heat Losses During Flow of Steam Down a Wellbore," *J. Pet. Tech.* (July 1965) 845-51.
21. Willhite, G.P.: "Overall-All Heat Transfer Coefficients in Steam and Hot Water Injection Wells," *J. Pet. Tech.* (May 1967) 607-15.
22. Earlougher, R.C. Jr.: "Some Practical Considerations in the Design of Steam Injection Wells," *J. Pet. Tech.* (Jan. 1969) 79-86.
23. Beggs, H.D. and Brill, T.P.: "A Study of Two-Phase Flow in Inclined Pipes," *J. Pet. Tech.* (May 1973) 607-14.
24. Farouq Ali, S.M.: "A Comprehensive Wellbore Steam/Water Flow Model or Steam Injection and Geothermal Applications," *Soc. Pet. Eng. J.* (Oct. 1981) 527-34.
25. Marx, J.W. and Langenheim, R.N.: "Reservoir Heating by Hot Fluid Injection," *Trans., AIME* (1959) **216**, 312-15.
26. Evans, J.G.: "Heat Loss During the Injection of Steam Into a 5-Spot," paper presented as term project in PNG 515, Pennsylvania State U., University Park (June 1960).
27. Ramey, H.J. Jr.: "Discussion of Reservoir Heating of Hot Fluid Injection," *Trans., AIME* (1959) **216**, 364-65.
28. Mandl, G. and Volek, C.W.: "Heat and Mass Transport in Steam-Drive Processes," *Soc. Pet. Eng. J.* (March 1969) 59-79.
29. Myhill, N.A. and Stegemeier, G.L.: "Steam Drive Correlations and Prediction," *J. Pet. Tech.* (Feb. 1978) 173-82.
30. Neuman, C.H.: "A Gravity Override Model of Steamdrive," *J. Pet. Tech.* (Jan. 1985) 163-69.
31. Doscher, T.M. and Ghassemi, F.: "The Influence of Oil Viscosity and Thickness on the Steam Drive," *J. Pet. Tech.* (Feb. 1983) 291-98.
32. Vogel, J.V.: "Simplified Heat Calculations for Steamfloods," *J. Pet. Tech.* (July 1984) 1127-36.
33. Boberg, T.C. and Lantz, R.B.: "Calculation of the Production Rate of a Thermally Stimulated Well," *J. Pet. Tech.* (Dec. 1966) 1613-23.
34. Boberg, T.C. and West, R.C.C.: "Correlation of Steam Stimulation Performance," *J. Pet. Tech.* (Nov. 1972) 1367-68.
35. Coats, K.H. et al.: "Three-Dimensional Simulation of Steamflooding," *Soc. Pet. Eng. J.* (Dec. 1974) 573-92.
36. Coats, K.H.: "Simulation of Steamflooding with Distillation and Solution Gas," *Soc. Pet. Eng. J.* (Oct. 1976) 235-47.
37. Coats, K.H.: "A Highly Implicit Steamflood Model," *Soc. Pet. Eng. J.* (Oct. 1978) 369-83.
38. Crookston, R.B., Culham, W.E., and Chen, W.H.: "Numerical Simulation Model for Thermal Recovery Processes," *Soc. Pet. Eng. J.* (Feb. 1979) 37-58.
39. Youngren, G.K.: "Development and Applications of an In-Situ Combustion Reservoir Simulator," *Soc. Pet. Eng. J.* (Feb. 1980) 39-51.
40. Coats, K.H.: "In-Situ Combustion Model," *Soc. Pet. Eng. J.* (Dec. 1980) 533-54.
41. Grabowski, J.W. et al.: "A Fully Implicit General Purpose Finite-Difference Thermal Model for In-Situ Combustion and Steam," paper SPE 8396 presented at the 1979 SPE Annual Technical Conference and Exhibition, Las Vegas, Sept. 23-26.
42. Alexander, J.D., Martin, W.L., and Dew, J.N.: "Factors Affecting Fuel Availability and Composition During In-Situ Combustion," *J. Pet. Tech.* (Oct. 1962) 1154-64.
43. Showalter, W.E.: "Combustion-Drive Tests," *Soc. Pet. Eng. J.* (March 1963) 53-58.
44. Parrish, D.R. and Craig, F.F. Jr.: "Laboratory Study of a Combination of Forward Combustion and Waterflooding—The COF-CAW Process," *J. Pet. Tech.* (June 1969) 753-61.
45. Burger, J.G. and Sahuquet, B.C.: "Laboratory Research on Wet Combustion," *J. Pet. Tech.* (Oct. 1973) 1137-46.
46. Garon, A.M. and Wygal, R.J. Jr.: "A Laboratory Investigation of Firewater Flooding," *Soc. Pet. Eng. J.* (Dec. 1974) 537-44.
47. Moss, J.T. and Cady, G.V.: "Laboratory Investigation of the Oxygen Combustion Process for Heavy Oil Recovery," paper SPE 10706 presented at the 1982 SPE California Regional Meeting, San Francisco, March 24-26.
48. Pursley, S.A.: "Experimental Simulation of Thermal Recovery Processes," *Proc., Heavy Oil Symposium*, Maracaibo, Venezuela (1974).
49. Huygen, H.H.A.: "Laboratory Steamfloods in Half of a Five-Spot," paper SPE 6171 presented at the 1976 Annual Technical Conference and Exhibition, New Orleans, Oct. 3-6.
50. Ehrlich, R.: "Laboratory Investigation of Steam Displacement in the Wabasca Grand Rapids 'A' Sand," *Oil Sands of Canada-Venezuela 1977*, CIM (1978) Special Vol.
51. Prats, M.: "Peace River Steam Drive Scaled Model Experiments," *Oil Sands of Canada-Venezuela 1977*, CIM (1978) Special Vol.
52. Doscher, T.M. and Huang, W.: "Steam-Drive Performance Judged Quickly from Use of Physical Models," *Oil and Gas J.* (Oct. 22, 1979) 52-57.
53. Singhal, A.K.: "Physical Model Study of Inverted Seven-Spot Steamfloods in a Pool Containing Conventional Heavy Oil," *J. Can. Pet. Tech.* (July-Sept. 1980) 123-34.
54. Binder, G.G. et al.: "Scaled-Model Tests of In-Situ Combustion in Massive Unconsolidated Sands," *Proc., 7th World Pet. Cong.*, Mexico City (1967).
55. Pujol, L. and Boberg, T.C.: "Scaling Accuracy of Laboratory Steamflooding Models," paper SPE 4191 presented at the 1972 SPE California Regional Meeting, Bakersfield, Nov. 8-10.
56. Stegemeier, G.L., Laumbach, D.D., and Volek, C.W.: "Representing Steam Processes with Vacuum Models," *Soc. Pet. Eng. J.* (June 1980) 151-74.
57. Farouq Ali, S.M.: "Current Status of Steam Injection as a Heavy Oil Recovery Method," *J. Can. Pet. Tech.* (Jan.-March 1974) 1-15.
58. Geffen, T.M.: "Oil Production to Expect from Known Technology," *Oil and Gas J.* (May 7, 1973) 66-76.
59. Lewin and Assocs. Inc.: *The Potentials and Economics of Enhanced Oil Recovery*, Federal Energy Administration (April 1976) Report B76/221, 2-6.
60. Iyoho, A.W.: "Selecting Enhanced Oil Recovery Processes," *World Oil* (Nov. 1978) 61-64.
61. Chu, C.: "State-of-the-Art Review of Steamflood Field Projects," paper SPE 11733 presented at the 1983 SPE California Regional Meeting, Ventura, March 23-25.

62. Chu, C.: "A Study of Fireflood Field Projects," *J. Pet. Tech.* (Feb. 1977) 171-79.
63. Chu, C.: "State-of-the-Art Review of Fireflood Field Projects," *J. Pet. Tech.* (Jan. 1982) 19-36.
64. Poettmann, F.H.: "In-Situ Combustion: A Current Appraisal," *World Oil*, Part 1 (April 1964), 124-28; Part 2 (May 1964) 95-98.
65. Blevins, T.R., Aseltine, R.J., and Kirk, R.S.: "Analysis of a Steam Drive Project, Inglewood Field, California," *J. Pet. Tech.* (Sept. 1969) 1141-50.
66. Blevins, T.R. and Billingsley, R.H.: "The Ten-Pattern Steamflood, Kern River Field, California," *J. Pet. Tech.* (Dec. 1975), 1505-14; *Trans.*, AIME, **259**.
67. Oglesby, K.D. et al.: "Status of the Ten-Pattern Kern River Field, California," *J. Pet. Tech.* (Oct. 1982) 2251-57.
68. Bursell, C.G.: "Steam Displacement—Kern River Field," *J. Pet. Tech.* (Oct. 1970) 1225-31.
69. Bursell, C.G. and Pittman, G.M.: "Performance of Steam Displacement in the Kern River Field," *J. Pet. Tech.* (Aug. 1975) 977-1004.
70. Greaser, G.R. and Shore, R.A.: "Steamflood Performance in the Kern River Field," paper SPE 8834 presented at the 1980 SPE/DOE Symposium on Enhanced Oil Recovery, Tulsa, April 20-23.
71. McBean, W.N.: "Attic Oil Recovery by Steam Displacement," paper SPE 4170 presented at the 1972 SPE California Regional Meeting, Bakersfield, Nov. 8-10.
72. Rehkopf, B.L.: "Metson Attic Steam Drive," paper SPE 5855 presented at the 1976 SPE California Regional Meeting, Long Beach, April 8-9.
73. Hearn, C.L.: "The El Dorado Steam Drive—A Pilot Tertiary Recovery Test," *J. Pet. Tech.* (Nov. 1972) 1377-84.
74. Valleroy, V.V. et al.: "Deerfield Pilot Test of Oil Recovery by Steam Drive," *J. Pet. Tech.* (July 1967) 956-64.
75. van Dijk, C.: "Steam-Drive Project in the Schoonebeek Field, The Netherlands," *J. Pet. Tech.* (March 1968) 295-302.
76. Gates, C.F. and Ramey, H.J. Jr.: "Field Results of South Belridge Thermal Recovery Experiment," *Trans.*, AIME (1958) **213**, 236-44.
77. Parrish, D.R. et al.: "A Tertiary COFCAW Pilot Test in the Sloss Field, Nebraska," *J. Pet. Tech.* (June 1974) 667-75; *Trans.*, AIME, **257**.
78. Parrish, D.R., Pollock, C.E., and Craig, F.F. Jr.: "Evaluation of COFCAW as a Tertiary Recovery Method, Sloss Field, Nebraska," *J. Pet. Tech.* (June 1974) 676-86; *Trans.*, AIME, **257**.
79. Buxton, T.S. and Pollock, C.B.: "The Sloss COFCAW Project—Further Evaluation of Performance During and After Air Injection," *J. Pet. Tech.* (Dec. 1974) 1439-48; *Trans.*, AIME, **257**.
80. Moss, J.T., White, P.D., and McNeil, J.S.: "In-Situ Combustion Process—Results of a Five-Well Field Experiment in Southern Oklahoma," *Trans.*, AIME (1959) **216**, 55-64.
81. Parrish, D.R. et al.: "Underground Combustion in the Shannon Pool, Wyoming," *J. Pet. Tech.* (Feb. 1962) 197-205; *Trans.*, AIME, **225**.
82. Smith, R.V. et al.: "Recovery of Oil by Steam Injection in the Smackover Field, Arkansas," *J. Pet. Tech.* (Aug. 1973) 833-89.
83. "Smackover Field," *Improved Oil Recovery Field Reports* (1975) **1**, No. 1, 135-43; *Enhanced Oil Recovery Field Reports*, SPE, Richardson, TX (1982) **8**, No. 1, 685-88.
84. "Kern River Field, Standard Oil Company of California," *Improved Oil Recovery Field Reports*, SPE, Richardson, TX (1975) **1**, No. 1, 83-92; *Enhanced Oil Recovery Field Reports*, SPE, Richardson, TX (1980) **6**, No. 1, 23-24.
85. "Midway-Sunset Field, Chanslor-Western Oil and Development Company," *Improved Oil Recovery Field Reports*, SPE, Richardson, TX (1976) **2**, No. 3, 445-54; *Enhanced Oil Recovery Field Reports*, SPE, Richardson, TX (1982) **8**, No. 1, 729-32.
86. Stokes, D.D. et al.: "Steam Drive as a Supplemental Recovery Process in an Intermediate Viscosity Reservoir, Mount Poso Field, California," *J. Pet. Tech.* (Jan. 1978) 125-31.
87. "Mount Poso Field," *Improved Oil Recovery Field Reports*, SPE, Richardson, TX (1975) **1**, No. 2, 277-86; *Enhanced Oil Recovery Field Reports*, SPE, Richardson, TX (1982) **8**, No. 1, 701-03.
88. Traverse, E.F., Deibert, A.D., and Sustek, A.J.: "San Ardo—A Case History of a Successful Steamflood," paper SPE 11737 presented at the 1983 SPE California Regional Meeting, Ventura, March 23-25.
89. Hall, A.L. and Bowman, R.W.: "Operation and Performance of a Slocum Thermal Recovery Project," *J. Pet. Tech.* (April 1973) 402-08.
90. "Slocum Field," *Improved Oil Recovery Field Reports*, SPE, Richardson, TX (1976) **2**, No. 1, 119-28; *Enhanced Oil Recovery Field Reports*, SPE, Richardson, TX (1979) **5**, No. 2, 291-97.
91. Pollock, C.B. and Buxton, T.S.: "Performance of a Forward Steamdrive Project—Nugget Reservoir, Winkelman Dome Field, Wyoming," *J. Pet. Tech.* (Jan. 1969) 35-40.
92. "Winkelman Dome Field," *Improved Oil Recovery Field Reports*, SPE, Richardson, TX (1975) **1**, No. 1, 155-62; *Enhanced Oil Recovery Field Reports*, SPE, Richardson, TX (1980) **6**, No. 1, 41-44.
93. Herrera, A.J.: "The M6 Steam Drive Project Design and Implementation," *J. Cdn. Pet. Tech.* (July-Sept. 1977) 62-83.
94. Herrera, A.J.: "Steam-Drive Recovery Being Used on Lake Maracaibo Coastal Field," *Oil and Gas J.* (July 17, 1978) 74-80.
95. "Tia Juana Este Field, Maraven, S.A.," *Enhanced Oil Recovery Field Reports*, SPE, Richardson, TX (1978) **3**, No. 4, 751-62; *Enhanced Oil Recovery Field Reports*, SPE, Richardson, TX (1982) **8**, No. 1, 751-53.
96. Showalter, W.E. and MacLean, M.A.: "Fireflood at Brea-Olinda Field, Orange County, California," paper SPE 4763 presented at the 1974 SPE Symposium on Improved Oil Recovery, Tulsa, April 22-24.
97. "Brea Olinda Field," *Improved Oil Recovery Field Reports*, SPE, Richardson, TX (1975) **1**, No. 1, 15-18; *Enhanced Oil Recovery Field Reports*, SPE, Richardson, TX (1981) **7**, No. 1, 407-08.
98. Gates, C.F. and Sklar, L.: "Combustion as a Primary Recovery Process—Midway Sunset Field," *J. Pet. Tech.* (Aug. 1971) 981-86; *Trans.*, AIME, **251**.
99. Counihan, T.M.: "A Successful In-Situ Combustion Pilot in the Midway Sunset Field, California," paper SPE 6525 presented at the 1977 SPE California Regional Meeting, Bakersfield, April 13-15.
100. Gates, C.F., Jung, K.D., and Surface, R.A.: "In-Situ Combustion in the Tulare Formation, South Belridge Field, Kern County, CA," *J. Pet. Tech.* (May 1978) 798-806; *Trans.*, AIME, **265**.
101. Hewitt, C.H. and Morgan, J.T.: "The Fry In-Situ Combustion Test—Reservoir Characteristics," *J. Pet. Tech.* (March 1965) 337-42; *Trans.*, AIME, **234**.
102. Clark, G.A. et al.: "The Fry In-Situ Combustion Test—Field Operations," *J. Pet. Tech.* (March 1965) 343-47; *Trans.*, AIME, **234**.
103. Clark, G.A. et al.: "The Fry In-Situ Combustion Test—Field Operations and Performance," *J. Pet. Tech.* (March 1965) 348-53; *Trans.*, AIME, **234**.
104. Earlougher, R.C. Jr., Galloway, J.R., and Parsons, R.W.: "Performance of the Fry In-Situ Combustion Project," *J. Pet. Tech.* (May 1970) 551-57.
105. Bleakley, W.B.: "Fry Unit Fireflood Surviving Economic Pressures," *Oil and Gas J.* (May 3, 1971) 92-97.
106. Howell, J.C. and Peterson, M.E.: "The Fry In Situ Combustion Project Performance and Economic Status," paper SPE 8381 presented at the 1979 SPE Annual Technical Conference and Exhibition, Las Vegas, Sept. 23-26.
107. Little, T.P.: "Successful Fireflooding of the Bellevue Field," *Pet. Eng. Intl.* (Nov. 1975) 55-56.
108. "Bellevue Field, Cities Service Oil Co.," *Improved Oil Recovery Field Reports*, SPE, Richardson, TX (1975) **1**, No. 3, 471-80; *Enhanced Oil Recovery Field Reports*, SPE, Richardson, TX (1982) **8**, No. 1, 713-15.
109. Cato, R.W. and Frnka, W.A.: "Getty Oil Reports Fireflood Pilot is Successful Project," *Oil and Gas J.* (Feb. 12, 1968) 93-97.
110. "Getty Expands Bellevue Fire Flood," *Oil and Gas J.* (Jan. 13, 1975) 45-49.
111. Bleakley, W.B.: "Getty's Bellevue Field Still Going and Growing," *Pet. Eng. Intl.* (Nov. 1978) 54-68.
112. "Bellevue Field, Getty Oil Co.," *Improved Oil Recovery Field Reports*, SPE, Richardson, TX (1976) **2**, No. 2, 275-84; *Enhanced Oil Recovery Field Reports*, SPE, Richardson, TX (1982) **8**, No. 1, 717-19.
113. Hardy, W.C. et al.: "In-Situ Combustion Performance in a Thin Reservoir Containing High-Gravity Oil," *J. Pet. Tech.* (Feb. 1972) 199-208; *Trans.*, AIME, **253**.
114. Mace, C.: "Deepest Combustion Project Proceeding Successfully," *Oil and Gas J.* (Nov. 17, 1975) 74-81.
115. "West Heidelberg Field," *Improved Oil Recovery Field Reports*, SPE, Richardson, TX (1975) **1**, No. 2, 351-59; *Enhanced Oil Recovery Field Reports*, SPE, Richardson, TX (1980) **7**, No. 1, 451-54.

116. Buchwald, R.W. Jr., Hardy, W.C., and Neinast, G.S.: "Case Histories of Three In-Situ Combustion Projects," *J. Pet. Tech.* (July 1973) 784-86.
117. "Glen Hummel Field," *Improved Oil Recovery Field Reports*, SPE, Richardson, TX (1975) 1, No. 1, 45-46; *Enhanced Oil Recovery Field Reports*, SPE, Richardson, TX (1978) 4, No. 1, 39-42.
118. "Gloriana Field," *Improved Oil Recovery Field Reports*, SPE, Richardson, TX (1975) 1, No. 1, 57-69; *Enhanced Oil Recovery Field Reports*, SPE, Richardson, TX (1978) 4, No. 1, 43-46.
119. Martin, W.L. *et al.*: "Thermal Recovery at North Tisdale Field, Wyoming," *J. Pet. Tech.* (May 1972) 606-16.
120. Gabelle, C.P. *et al.*: "Heavy Oil Recovery by In-Situ Combustion—Two Field Cases in Romania," *J. Pet. Tech.* (Nov. 1981) 2057-66.
121. Terwilliger, P.L. *et al.*: "Fireflood of the P₂₃ Sand Reservoir in the Miga Field of Eastern Venezuela," *J. Pet. Tech.* (Jan. 1975) 9-14.
122. Nelson, T.W. and McNeil, J.S.: "How to Engineer an In-Situ Combustion Project," *Oil and Gas J.* (June 5, 1961) 59, No. 23, 58-65.
123. Satman, A., Brigham, W.E., and Ramey, H.J. Jr.: "In-Situ Combustion Models for the Steam Plateau and for Fieldwide Oil Recovery," DOE/ET/12056-11, U.S. DOE (June 1981).
124. Gates, C.F. and Ramey, H.J. Jr.: "A Method for Engineering In-Situ Combustion Oil Recovery Projects," *J. Pet. Tech.* (Feb. 1980) 285-94.
125. Volek, C.W. and Pryor, J.A.: "Steam Distillation Drive, Brea Field, California," *J. Pet. Tech.* (Aug. 1972) 899-906.
126. Burke, R.E.: "Combustion Project is Making a Profit," *Oil and Gas J.* (Jan. 18, 1965) 44-46.
127. Koch, R.L.: "Practical Use of Combustion Drive at West Newport Field," *Pet. Eng.* (Jan. 1965) 72-81.
128. Bowman, C.H.: "A Two-Spot Combustion Recovery Project," *J. Pet. Tech.* (Sept. 1965) 994-98.
129. Terwilliger, P.L.: "Fireflooding Shallow Tar Sands—A Case History," *J. Can. Pet. Tech.* (Oct.-Dec. 1976) 41-48.
130. Johnson, L.A. *et al.*: "An Echoing In-Situ Combustion Oil-Recovery Project in a Utah Tar Sand," *J. Pet. Tech.* (Feb. 1980) 295-305.
131. Perry, C.W., Hertzberg, R.H., and Stosur, J.J.: "The Status of Enhanced Oil Recovery in the United States," *Proc.*, Tenth World Pet. Congress, Bucharest (1980) 3, 257-66.
132. Benham, A.L. and Poettmann, F.H.: "The Thermal Recovery Process—An Analysis of Laboratory Combustion Data," *Trans.*, AIME (1958) 213, 83-85.
133. Caudle, B.H., Hickman, B.M., and Silberberg, I.H.: "Performance of the Skewed Four-Spot Injection Pattern," *J. Pet. Tech.* (Nov. 1968) 1315-19.
134. Cady, G.V., Hoffman, S.J., and Scarborough, R.M.: "Silverdale Combination Thermal Drive Project," paper SPE 8904 presented at the 1980 SPE California Regional Meeting, Los Angeles, April 9-11.
135. de Haan, M.J. and Schenk, L.: "Performance Analysis of a Major Steam Drive Project in the Tia Juana Field, Western Venezuela," *J. Pet. Tech.* (Jan. 1969) 111-19.
136. "Texas Fireflood Looks Like a Winner," *Oil and Gas J.* (Feb. 17, 1969) 52.
137. Afoju, B.I.: "Conversion of Steam Injection to Waterflood, East Coalinga Field," *J. Pet. Tech.* (Nov. 1974) 1227-32.
138. Gates, C.F. and Brewer, S.W.: "Steam Injection into the D and E Zone, Tulare Formation, South Belridge Field, Kern County, California," *J. Pet. Tech.* (March 1975) 343-48.
139. Gomaa, E.E., Duerksen, J.H., and Woo, P.T.: "Designing a Steamflood Pilot in the Thick Monarch Sand of the Midway-Sunset Field," *J. Pet. Tech.* (Dec. 1977) 1559-68.
140. Chu, C. and Trimble, A.E.: "Numerical Simulation of Steam Displacement—Field Performance Applications," *J. Pet. Tech.* (June 1975) 765-74.
141. Joseph, C. and Pusch, W.H.: "A Field Comparison of Wet and Dry Combustion," *J. Pet. Tech.* (Sept. 1980) 1523-28.
142. Gates, C.F. and Holmes, B.G.: "Thermal Well Completions and Operation," paper PD11 presented at the Seventh World Pet. Cong., Mexico City (1967).
143. Fox, R.L., Donaldson, A.B., and Mulac, A.J.: "Development of Technology for Downhole Steam Production," paper SPE 9776 presented at the 1981 SPE/DOE Joint Symposium on Enhanced Oil Recovery, Tulsa, April 5-8.
144. Carraway, P.M., Kloth, T.L., and Bull, A.D.: "Co-Generation: A New Energy System to Generate Both Steam and Electricity," paper SPE 9907, presented at the 1981 California Regional Meeting, Bakersfield, March 25-26.
145. Strange, L.K.: "Ignition: Key Phase in Combustion Recovery," *Pet. Eng.* (Nov. 1964) 105-09; (Dec. 1964) 97-106.
146. Shore, R.A.: "The Kern River SCAN Automation System Sample, Control and Alarm Network," paper SPE 4173 presented at the 1972 SPE California Regional Meeting, Bakersfield, Nov. 8-10.
147. "Bodcau In-Situ Combustion Project," first annual report, DOE Publications SAN-1189-2, U.S. DOE (Sept. 1977).
148. Wagner, O.R.: "The Use of Tracers in Diagnosing Interwell Reservoir Heterogeneities—Field Results," *J. Pet. Tech.* (Nov. 1977) 1410-16.
149. Yoelin, S.D.: "The TM Sand System Stimulation Project," *J. Pet. Tech.* (Aug. 1971) 987-94.
150. Meldau, R.F., Shipley, R.G., and Coats, K.H.: "Cyclic Gas/Steam Stimulation of Heavy-Oil Wells," *J. Pet. Tech.* (Oct. 1981) 1990-98.
151. Britton, M.W. *et al.*: "The Street Ranch Pilot Test of Fracture-Assisted Steamflood Technology," *J. Pet. Tech.* (March 1983) 511-21.
152. Sahuquet, B.C. and Ferrier, J.J.: "Steam-Drive Pilot in a Fractured Carbonate Reservoir: Lacq Supérieur Field," *J. Pet. Tech.* (April 1982) 873-80.
153. Hvizdos, L.J., Howard, J.V., and Roberts, G.W.: "Enhanced Oil Recovery Through Oxygen-Enriched In-Situ Combustion: Test Results from the Forest Hill Field in Texas," *J. Pet. Tech.* (June 1983) 1061-70.
154. Prats, M.: *Thermal Recovery*, Monograph Series, SPE, Richardson, TX (1983) 201-38.
155. Beal, C.: "The Viscosity of Air, Water, Natural Gas, Crude Oil and Its Associated Gases at Oil Field Temperatures and Pressures," *Trans.*, AIME (1946) 165, 103.
156. *Petroleum Production Handbook*, T.C. Frick (ed.), Vol. II, McGraw-Hill Book Co. Inc., New York City (1962) 19-39.
157. Chew, J. and Connally, C.A. Jr.: "A Viscosity Correlation for Gas-Saturated Crude Oils," *Trans.*, AIME (1959) 216, 23-25.
158. Beggs, H.D. and Robinson, J.R.: "Estimating the Viscosity of Crude Oil Systems," *J. Pet. Tech.* (Sept. 1975) 1140-41.
159. Brooks, R.H. and Corey, A.T.: "Properties of Porous Media Affecting Fluid Flow," *Proc.*, ASCE, Irrigation and Drainages Div. (1966) 92, No. IR2.
160. Somerton, W.H. and Udell, K.S.: "Thermal and High Temperature Properties of Rock-Fluid Systems," paper presented at the 1981 OASTRA Workshop on Computer Modeling, Edmonton, Alta., Jan. 28-30.
161. Poston, S.W. *et al.*: "The Effect of Temperature on Irreducible Water Saturation and Relative Permeability of Unconsolidated Sands," *Soc. Pet. Eng. J.* (June 1970) 171-80.
162. Weinbrandt, R.M., Ramey, H.J. Jr., and Cassé, F.J.: "The Effect of Temperature on Relative and Absolute Permeability of Sandstones," *Soc. Pet. Eng. J.* (Oct. 1975) 376-84.
163. Sawabini, C.T., Chilingar, G.V., and Allen, D.R.: "Compressibility of Unconsolidated, Arkosic Oil Sands," *Soc. Pet. Eng. J.* (April 1974) 132-38.
164. Somerton, W.H., Keese, J.A., and Chu, S.L.: "Thermal Behavior of Unconsolidated Oil Sands," *Soc. Pet. Eng. J.* (Oct. 1974) 513-21.
165. Poettmann, F.H. and Mayland, B.J.: "Equilibrium Constants for High Boiling Hydrocarbon Fractions of Varying Characterization Factors," *Pet. Refiner* (July 1949) 101-12.
166. Lee, S.T. *et al.*: "Experimental and Theoretical Studies on the Fluid Properties Required for Simulation of Thermal Processes," *Soc. Pet. Eng. J.* (Oct. 1981) 535-50.
167. Fassihi, M.R., Brigham, W.E., and Ramey, H.J. Jr.: "The Reaction Kinetics of In-Situ Combustion," *Soc. Pet. Eng. J.* (Aug. 1984) 408-16.
168. "1967 ASTM Steam Tables," ASME, New York City (1967).

General References

- "Bibliography of Thermal Methods of Oil Recovery," *J. Can. Pet. Tech.* (April-June 1975) 55-65.

- Chu, C. and Crawford, P.B.: "In Situ Combustion." *Improved Oil Recovery*, Interstate Oil Compact Commission, Oklahoma City (1983) Chap. 6.
- Crawford, P.B.: "In-Situ Combustion." *Secondary and Tertiary Oil Recovery Processes*, Interstate Oil Compact Commission, Oklahoma City (1974) Chap. 5.
- Farouq Ali, S.M.: "Steam Injection." *Secondary and Tertiary Oil Recovery Processes*, Interstate Oil Compact Commission, Oklahoma City (1974) Chap. 6.
- Farouq Ali, S.M. and Meldau, R.F.: "Steamflooding." *Improved Oil Recovery*, Interstate Oil Compact Commission, Oklahoma City (1983) Chap. 7.
- Prats, M.: *Thermal Recovery*, Monograph Series, SPE, Richardson, TX (1982) 7.
- Thermal Recovery Processes*, Reprint Series, SPE, Richardson, TX (1965, 1985) 7.
- Thermal Recovery Techniques*, Reprint Series, SPE, Richardson, TX (1972) 10.

Chapter 47

Chemical Flooding

Larry W. Lake, U. of Texas

Introduction

Chemical flooding is any isothermal EOR process whose primary goals are to recover oil by (1) reducing the mobility of the displacing agent (mobility control process), and/or (2) lowering the oil/water interfacial tension (low-IFT process).

These classifications do not exclude processes where both effects are important, such as micellar/polymer (MP) flooding, nor do they imply that other effects, such as wettability alteration, extraction, or oil swelling, are not present.

Mobility control processes inject a low-mobility displacing agent to increase volumetric and displacement sweep efficiency. The two main techniques are (1) polymer flooding, whereby a small amount of polymer is added to thicken brine and (2) foam flooding, through which low mobilities are attained by injecting a stabilized dispersion of gas in water. Polymer or mobility buffer "drives" also are used to displace micellar and high-pH slugs. Foams have been used or proposed as driving agents for micellar, solvent, and steam slugs also. For these reasons foam flooding could be discussed easily in the chapters on solvent and thermal EOR processes; however, foam stabilization requires surfactants, whose discussion belongs in this chapter.

Low-IFT methods rely on injecting or forming in-situ a surface-active agent (surfactant) which lowers oil/water IFT and, ultimately, residual oil saturation (ROS). Processes that inject the surfactant are called "MP" floods because of the tendency for surfactants to form micelles in aqueous solutions and the inevitable need to drive the micellar solution with polymer. High-pH or alkaline processes produce a surfactant in situ, since these processes rely on reactions with acidic components of the crude to generate the surfactant.

This chapter is divided into sections corresponding to mobility control and low-IFT processes. Each section begins with a general discussion of how the particular mechanism recovers oil, followed by material on the individual

processes, and concludes with typical oil displacement results. The chapter concludes by giving comparative screening parameters for each chemical flooding process.

Mobility Control Processes

Effect of Low Mobility on Oil Recovery

Mobility control processes are most applicable to reservoirs that have substantial movable oil [oil in place (OIP) minus ROS] since they displace oil only in excess of ROS. The mobility ratio concept illustrates how lowering the mobility improves oil recovery.

The mobility ratio, M , between a displacing agent and a displaced fluid is

$$M = \lambda_D / \lambda_d, \dots\dots\dots (1)$$

where λ_D is the mobility of displacing agent(s) and λ_d is the mobility of displaced fluid(s). Practical use of Eq. 1 requires specific definitions of the quantities in the numerator and denominator and of the conditions at which these quantities are evaluated.

For two-phase waterflooding, common specializations of Eq. 1 are the endpoint mobility ratio, M^o , the average mobility ratio, M , and the shock mobility ratio, M^* . Each definition has been used in particular applications in the literature: M has been used to correlate areal sweep relations, M^* is the most direct indicator of viscous instability, and M^o is the most widely cited value in the literature for waterfloods.^{1,2} For the special case of a piston-like displacement all three definitions are identical. From the general definition of Eq. 1, lowering the mobility of the displacing fluid is equivalent to lowering any of the mobility ratios. This recovers oil by increasing both volumetric and displacement sweep efficiency.

Volumetric sweep efficiency, E_V , is the PV of a reservoir contacted by a displacing agent divided by the total PV. E_V is composed of two parts: areal, E_A , and invasion (vertical) sweep efficiency, E_I .

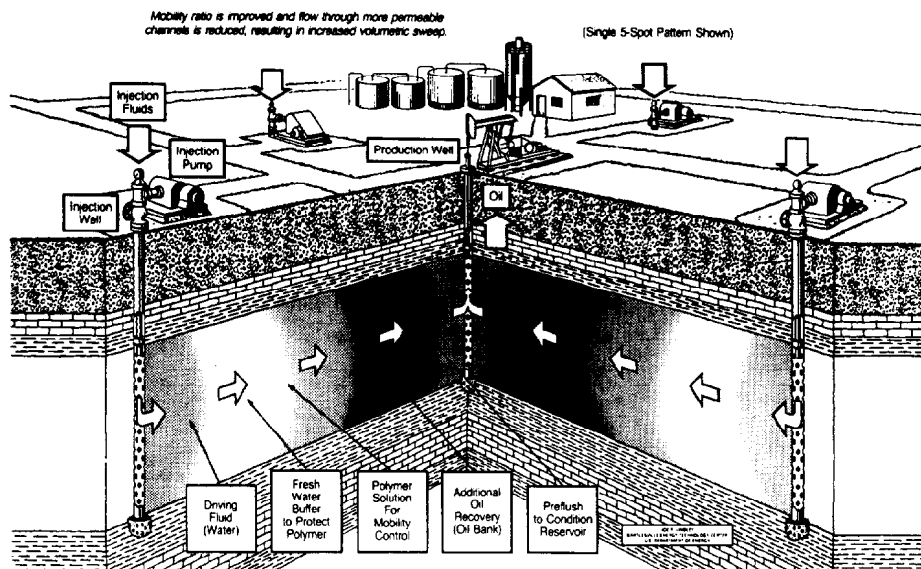


Fig. 47.1—Schematic of polymer flooding.

For more detailed discussions of E_A and E_I see Chaps. 39, 43, and 44 and Refs. 1 through 11. Both quantities depend on throughput and on several fluid, petrophysical, and geometric factors, usually expressed as dimensionless groups. However, E_A and E_I both increase as M decreases—i.e., as the mobility of the displacing agent, λ_D , decreases.

When the displacement is piston-like in a homogeneous, isotropic, horizontal medium and $M > 1$ (an *unfavorable* mobility ratio), the displacement front forms small perturbations, called “viscous fingers,” which grow during propagation. Such fingers also form when $M < 1$, but they are damped out by the *favorable* mobility ratio. The growing viscous fingers can contribute substantially to poor oil recovery because of large-scale bypassing. Mobility control agents prevent viscous fingering either in a conventional waterflood (polymer flooding) or as a part of an otherwise inherently unstable EOR process.

Displacement efficiency, E_D (local or microscopic sweep efficiency), is the volume of oil recovered in a displacement divided by the oil volume just before the displacement, the displacement having maximum volumetric sweep efficiency. The classical solution by Buckley and Leverett can be used to describe the effect of mobility lowering on E_D .¹² Because of the dependence on several factors there is no unique correspondence between M and E_D ; however, lowering M or λ_D results in improved oil recovery through larger E_D .

Lowering M , then, results in improved oil recovery by increasing areal, vertical, and displacement sweep efficiencies. Since it is the products of these factors that determine overall oil recovery, this implies that an increase in any one may not result in a large overall increase in oil recovery, particularly if one of the other efficiencies were low. Even with the combination of the three efficiencies, the incremental oil recovered with a mobility control process must be balanced against the additional expense required to inject the viscous mobility control agent.

Polymer Flooding

Polymers have been used in oil production in three modes.

1. They have been used as near-well treatments to improve the performance of water injectors or high-watercut producers by blocking off high-conductivity zones.

2. Polymers also are used as agents that may be cross-linked in situ to plug high-conductivity zones at depth in the reservoir.¹³ These processes require that polymer be injected with an inorganic metal cation, which will cross-link subsequently injected polymer molecules with ones already bound to solid surfaces.

3. The other mode is use as agents to lower M or λ_D .

The first mode is not truly a chemical flooding process, since the actual oil-displacing agent is not the polymer. The overwhelming majority of polymer EOR projects have been in the third mode, which is the one emphasized here.

Fig. 47.1 is a schematic of a typical polymer flood injection sequence: a preflush, usually consisting of a low-salinity brine; an oil bank; the polymer solution itself; a freshwater buffer to protect the polymer solution from backside dilution; and, finally, chase or drive water. Many times the freshwater buffer contains polymer in decreasing amounts (a grading or taper) to lessen the effects of unfavorable mobility ratio between the chase water and the polymer solution. Because of the driving nature of the process, polymer floods always are performed through separate sets of injection and production wells.

M is lowered in a polymer flood by injecting water that contains a high-molecular-weight, water-soluble polymer. Since the water is usually a dilution of an oilfield brine, interactions with salinity are important, particularly for certain classes of polymers. Salinity in this chapter is the total dissolved solids (TDS) content of the aqueous phase. Typical values are shown in Fig. 47.2.¹⁴ Virtually all chemical flooding properties depend on the concentrations of specific ions rather than salinity only. It is particularly important to monitor the aqueous phase's total divalent

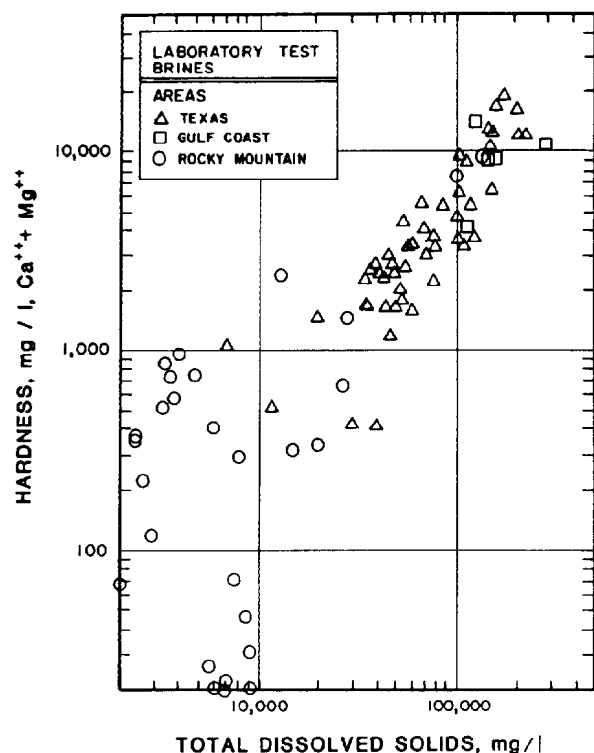


Fig. 47.2—Salinities from representative oilfield brines.

cation content (hardness) separately, since the latter are usually more critical to chemical flood properties than the same TDS concentration. Fig. 47.2 also shows typical brine hardnesses.

Because of the high molecular weight (1 to 3 million is typical) only a small amount (typically about 500 ppm) of polymer will bring about a substantial increase in water viscosity. Furthermore, several types of polymers lower mobility by lowering water relative permeability (permeability reduction effect) in addition to increasing the water viscosity. How polymer lowers mobility, and the interactions with salinity may be qualitatively illustrated with some discussion of polymer chemistry.

Polymer Types. Several polymers have been considered for polymer flooding: xanthan gum, hydrolyzed polyacrylamide (HPAM), copolymers of acrylic acid and acrylamide, copolymers of acrylamide and 2-acrylamide-2 methyl propane sulfonate (AM/AMPS), hydroxyethylcellulose (HEC), carboxymethylhydroxyethylcellulose (CMHEC), polyacrylamide (PAM), polyacrylic acid, glucan, dextran polyethyleneoxide (PEO), and polyvinyl alcohol (PA). Only the first three have actually been field tested; however, the variety of entries in this partial listing emphasizes that there are many potentially suitable chemicals, some of which may prove more effective than those currently used. Nevertheless, virtually all of the commercially attractive polymers fall into two generic classes: polyacrylamides and polysaccharides (biopolymer or xanthan gum). The remainder of this discussion deals with these exclusively. Representative molecular structures are given in Fig. 47.3.¹⁵

POLYACRYLAMIDE

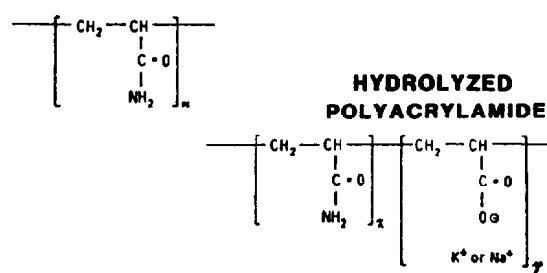


Fig. 47.3A—Molecular structure for partially hydrolyzed polyacrylamide.

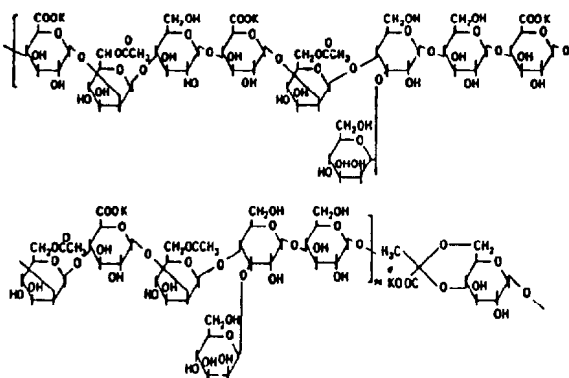


Fig. 47.3B—Molecular structure for polysaccharide (biopolymer).

Polyacrylamides. PAM's are polymers whose monomeric unit is the acrylamide molecule. As used in polymer flooding, PAM's have undergone partial hydrolysis, which causes anionic (negatively charged) carboxyl groups ($-\text{COO}^-$) to be scattered along the chain. The polymers are called partially hydrolyzed polyacrylamides (HPAM's) for this reason. Typical degrees of hydrolysis are 30% or more of the acrylamide monomers; hence, the HPAM molecule is quite negatively charged, which accounts for many of its physical properties. The viscosity-increasing feature of HPAM lies in its large molecular weight, which is accentuated by the anionic repulsion between polymer molecules and also between segments on the same molecule. The repulsion causes the molecule in solution to elongate or uncoil and snag on others similarly elongated, an effect that accentuates the mobility reduction at higher concentrations.

If the brine salinity and/or hardness is high, however, this repulsion is decreased greatly through ionic shielding as the freely rotating carbon/carbon bonds allow the molecule to ball up or coil. (Fig. 47.3 shows the molecular structure of hydroxyethylcellulose.) This causes a corresponding decrease in the effectiveness of the polymer, since the snagging effect is reduced greatly. Virtually all HPAM properties show a large sensitivity to salinity and hardness. This is an obstacle to using HPAM in many reservoirs. On the other hand, HPAM is inexpensive, relatively resistant to bacterial attack, and exhibits permeability reduction.

Polysaccharides. A second major class of polymers are the polysaccharides, which are formed from the polymeri-

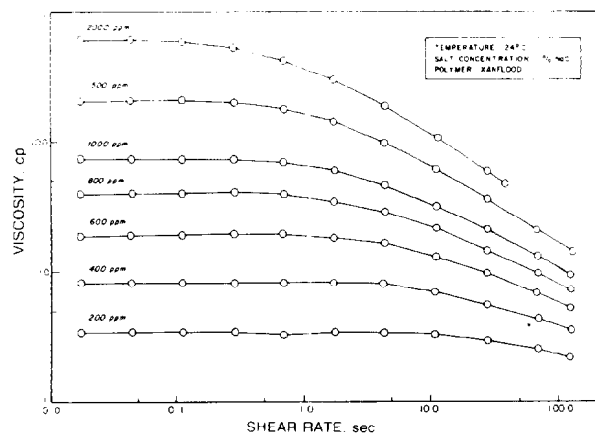


Fig. 47.4—Polymer solution viscosity vs. shear rate and polymer concentration.

zation of saccharide molecules (Fig. 47.3). Polysaccharides or biopolymers are formed from a bacterial fermentation process. This process leaves substantial debris in the polymer product that must be removed before the polymer is injected.¹⁶ The polymer is also susceptible to bacterial attack after it has been introduced into the reservoir. These disadvantages are offset by the insensitivity of polysaccharide properties to brine salinity and hardness. The origin of this insensitivity is seen in Fig. 47.3, which shows the polysaccharide molecule to be relatively nonionic and, therefore, free of the ionic shielding effects of HPAM. Polysaccharides are more branched than are HPAM's and the oxygen-ringed carbon bond does not rotate fully; hence, the molecule increases brine viscosity by snagging and by adding a more rigid structure to the solution. Polysaccharides do not exhibit permeability reduction, however.

At the present time HPAM is less expensive per unit amount than polysaccharides; however, when compared on a unit amount of mobility reduction, particularly at high salinities, the costs are close enough so that the preferred polymer for a given application is site-specific. Historically, HPAM's have been used in about 95% of the reported field polymer floods.¹⁷ Both classes of polymers tend to degrade chemically at elevated temperatures.

Polymer Properties. Because of the complexity of the subject, a comprehensive treatment of polymer properties is not possible. However, qualitative trends, a few quantitative relations and representative data are presented on these properties: viscosity relations, non-Newtonian effects, retention, permeability reduction, and chemical, biological, or mechanical degradation.

Viscosity Relations and Non-Newtonian Effects. Fig. 47.4 shows polymer solution viscosity, μ_p , vs. shear rate measured in a laboratory viscometer at fixed salinity.¹⁸ At low shear rates, μ_p is independent of shear rate, $\dot{\epsilon}(\mu_p = \mu_p^\infty)$, and the solution is a Newtonian fluid. At higher $\dot{\epsilon}$, μ_p decreases, approaching a limiting ($\mu_p = \mu_p^\infty$) value not much greater than the water viscosity, μ_w , at some critical high shear rate (not shown on Fig. 47.4). A fluid whose viscosity decreases with increasing $\dot{\epsilon}$ is *shear thinning*. The shear thinning behavior of the polymer solution is caused by the uncoiling and

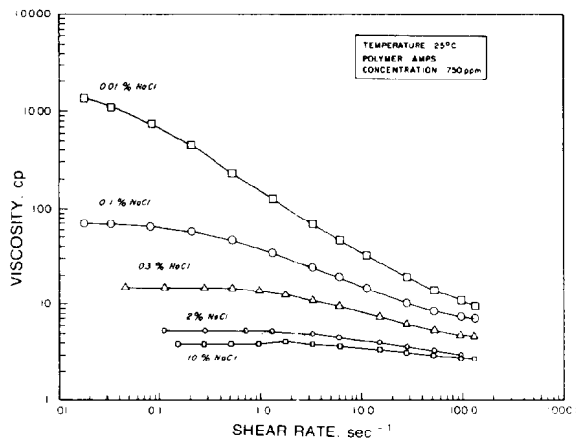


Fig. 47.5—Polymer solution viscosity vs. shear rate at various brine salinities.

unsnagging of the polymer chains when they are placed in a shear flow. Below the critical shear rate the curve is reversible.

Fig. 47.5 shows a viscosity/shear-rate plot at fixed polymer concentration with variable NaCl concentration for an AMPS polymer.¹⁹ Note the profound sensitivity of the viscosity to salinity: as a rule of thumb the polymer solution viscosity decreases a factor of 10 for every factor-of-10 increase in NaCl concentration. The viscosity of HPAM polymers and HPAM derivatives is even more sensitive to hardness, but viscosities of polysaccharide solutions are relatively insensitive to both.

The behavior in Figs. 47.4 and 47.5 is favorable because for the bulk of a reservoir's volume, $\dot{\epsilon}$ is usually low (about 1 to 5 seconds⁻¹), making it possible to attain a design M with a minimal amount of polymer. Near the injection wells, however, $\dot{\epsilon}$ can be quite high, which causes the polymer injectivity to be greater than that expected on the basis of μ_p^∞ . The relative magnitude of this enhanced injectivity effect can be estimated once quantitative definitions of shear rate in permeable media and shear-rate/viscosity relations are given.²⁰

The polymer solution viscosity/shear-rate relationship may be described by a power law model.²¹

$$\mu_p = K(\dot{\epsilon})^{n-1}, \quad \dots \dots \dots (2)$$

where K and n are the power-law coefficient and exponent, respectively. Eq. 2 applies only over a limited range of shear rates: below some low shear rate the polymer solution viscosity is constant at μ_p^∞ , and above the critical shear rate the polymer solution viscosity is also constant μ_p^∞ . The truncated nature of the power law is awkward in calculations; hence, another useful relationship is the Meter model.²²

$$\mu_p = \mu_p^\infty + \frac{\mu_p^\circ - \mu_p^\infty}{1 + \left(\frac{\dot{\epsilon}}{\dot{\epsilon}_{1/2}}\right)^{\alpha-1}}, \quad \dots \dots \dots (3)$$

where α is an empirical coefficient and $\dot{\epsilon}_{1/2}$ is the shear rate at which μ_p is the average of μ_p° and μ_p^∞ . As with all polymer properties, all empirical parameters are functions of salinity, hardness, and temperature.

When applied to permeable media flow these general trends and equations continue to apply. μ_p is usually called the "apparent" viscosity and the effective shear rate, $\dot{\epsilon}_e$, is based on capillary tube concepts.

$$\dot{\epsilon}_e = \frac{u_w}{4\sqrt{\phi k_w S_w}} \quad (4)$$

where

- u_w = superficial flux of polymer-rich (water) phase,
- k_w = permeability to polymer-rich (water) phase,
- S_w = saturation of polymer-rich (water) phase, fraction, and
- ϕ = porosity of medium, fraction.

Polymer Retention. All polymers experience retention on solid surfaces because of adsorption or mechanical trapping within a permeable medium. Polymer retention varies with polymer type, molecular weight, rock composition, brine salinity and hardness, flow rate, and temperature. Field-measured values of retention range from 20 to 400 lbm polymer/acre-ft bulk volume with desirable retention level being less than about 50 lbm/acre-ft. Retention causes the loss of polymer from solution, which can cause the mobility control effect to be destroyed—an effect that is particularly pronounced at low polymer concentrations. Polymer retention also causes a delay in the rate of polymer propagation.

Offsetting the delay caused by retention is an acceleration of the polymer solution through the permeable medium, which is caused by inaccessible PV (IPV). The most common explanation for IPV is that the smaller portions of the pore space will not allow polymer molecules to enter because of their size. Thus, a portion of the total pore space is uninvaded or inaccessible to polymer, and accelerated polymer flow results. Large as they are, however, most polymer molecules will fit easily into all but the smallest pore throats. Hence, a second explanation of IPV is based on a wall exclusion effect whereby the polymer molecules aggregate in the center of a narrow channel.²³ The polymer pore fluid layer near the wall has a lower viscosity than the fluid in the center, which causes an apparent fluid slip.

IPV depends on polymer molecular weight, media permeability, porosity, and pore size distribution, becoming more pronounced as molecular weight increases and the ratio of permeability to porosity (characteristic pore size) decreases. IPV can be 30% of the total pore space or greater.

Permeability Reduction. As mentioned previously HPAM polymers can cause lowered mobility through a permeability reduction effect. This phenomenon has been described through three factors.²⁴ The *resistance factor*, F_R , is the ratio of the injectivity of a single-phase polymer solution to that of brine flowing under the same conditions:

$$F_R = \frac{\lambda_w}{\lambda_p} = \frac{k_w/\mu_w}{k_p/\mu_p} \quad (5)$$

where

- k_p = permeability to polymer solution,
- λ_w = mobility of water-rich phase, and
- λ_p = mobility of polymer solution.

For constant-flow-rate experiments, F_R is the inverse ratio of pressure drops; for constant-pressure-drop experiments, F_R is the ratio of flow rates. F_R is an indication of the total mobility-lowering contribution of a polymer. To describe the permeability reduction effect alone, a *permeability reduction factor*, F_{rk} , is defined as

$$F_{rk} = \frac{k_w}{k_p} = \frac{\mu_w}{\mu_p} F_R \quad (6)$$

A final definition is the *residual resistance factor*, F_{Rr} , which is the mobility of a brine solution before and after polymer injection.

$$F_{Rr} = \frac{\lambda_{wb}}{\lambda_{wa}} \quad (7)$$

where λ_{wb} is the mobility of water-rich phase before polymer injection and λ_{wa} is the mobility of water-rich phase after polymer injection. F_{Rr} is a measure of the permanence of the permeability reduction effect caused by the polymer solution. It is the primary measure of the performance of a channel-blocking application of polymer solutions. For many cases, F_{rk} and F_{Rr} are nearly equal; however, F_R is usually much larger than F_{rk} because the former contains the viscosity-enhancing effect as well as the permeability-reduction effect.

The most common measure of permeability reduction is F_{rk} . F_{rk} is sensitive to polymer type, molecular weight, degree of hydrolysis, shear rate, and permeable media pore structure. Polymers that have undergone even a small amount of mechanical degradation seem to lose most of their permeability reduction effect. For this reason, qualitative tests based on screen factor devices are common to estimate polymer quality.²⁴ F_{rk} has been correlated to polymer adsorption and rheological properties by Hirasaki and Pope.²⁵

Chemical and Biological Degradation. The average polymer molecular weight can be decreased, to the detriment of the overall process, by chemical, biological, or mechanical degradation. Chemical degradation can be minimized by restricting polymer usage to low-temperature applications, and by adding oxygen scavengers (e.g., sodium sulfate or sodium sulfite) to the polymer solution. Biological degradation can be eliminated by adding oxygen scavengers and biocides (e.g., formaldehyde or isopropyl alcohol). In fact, nearly all applications contain some of these chemicals, usually in very small quantities (see Ref. 16 or 26).

Mechanical Degradation. Mechanical degradation, on the other hand, is potentially present under all applications. Mechanical degradation occurs when polymer solutions are exposed to high-velocity flows. These can be present in surface equipment (valves, orifices, pumps, or tubing), downhole conditions (perforations or screens), or in the sandface itself. Perforated completions, particularly, are a cause for concern, since large quantities of

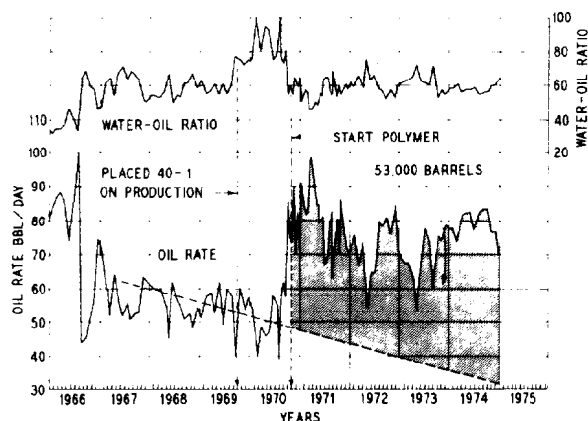


Fig. 47.6—Tertiary polymer flood response from North Burbank Unit, Osage County, OK.

polymer solution are being forced through a number of small holes. For this reason, most polymer injections are done through openhole or gravel-pack completions. Because flow velocity falls off quickly with distance from an injector, little mechanical degradation occurs within the reservoir itself.

All polymers mechanically degrade under high enough flow rates. However, HPAM's are most susceptible under normal operating conditions, particularly if the salinity or hardness of the brine is large. Evidently, the ionic coupling of these anionic molecules is relatively fragile compared with the polysaccharide chains. Also, elongational stress is as destructive to polymer solutions as is shear stress, although the two generally accompany each other. Maerker and others have correlated permanent viscosity of a polymer solution loss to an elongational stretch rate times length product.^{27,28} On a viscosity/shear-rate plot (purely shear flow), mechanical degradation usually begins at shear rates greater than the minimum-viscosity critical shear rate.

Field Results. Fig. 47.6 shows a tertiary polymer flooding field response from the North Burbank unit, Osage

County, OK.²⁹ The figure shows WOR and oil rate before and immediately after polymer injection. Polymer injection began in late 1970, which quickly arrested a declining oil rate and an increasing WOR. The oil rate then resumed its prepolymer decline but at a substantially higher level. The polymer oil or incremental oil recovery (IOR) from a polymer flood is the difference between the cumulative oil actually produced and that which would have been produced by a continuing waterflood. Thus, for a technical analysis of the project it is important to establish a polymer flood oil rate decline and an accurate waterflood decline rate. The IOR for North Burbank is the shaded area in Fig. 47.6.

Table 47.1 summarizes other field results on more than 250 polymer floods on the basis of a comprehensive survey by Manning *et al.*¹⁷ The table emphasizes oil recovery data and screening parameters used for polymer flooding. Approximately one-third of the statistics are from commercial or field-scale floods. The oil recovery statistics in Table 47.1 show average polymer flood recoveries of 3.56% remaining (after waterflood) oil in place, and 2.69 STB of IOR for each pound of polymer injected, with wide variations in both numbers. The large variability reflects the emerging nature of polymer flooding in the previous decades. Considering the STB IOR per pound of polymer average and the average costs of crude and polymer, it appears that polymer flooding could be a highly attractive EOR process. However, such costs always should be compared on a discounted basis reflecting the time value of money, which will decrease the apparent attractiveness of polymer flooding because of the decreased injectivity of the polymer solutions.

Foam Flooding

Gas/liquid foams offer an alternative to polymers for providing mobility control in chemical floods, and have been both proposed and field tested as mobility control agents in steamfloods.

Foams are dispersions of gas bubbles in liquids. Gas/liquid dispersions are normally unstable and usually will break in less than 1 second. If surfactants are added to the liquid, however, stability is improved greatly so that some foams can persist indefinitely. To understand foam

TABLE 47.1—POLYMER FLOOD STATISTICS

	Number of Projects*	Mean	Minimum	Maximum	Standard Deviation
Oil recovery, % remaining OIP	50	3.56	0	25.3	5.63
Oil recovery, STB/lbm	80	2.69	0	36.5	4.86
Oil recovery, STB/acre-ft	88	24.0	0	188.7	36.65
Permeability variation, fraction	118	0.70	0.06	0.96	0.19
Mobile oil saturation, fraction	62	0.27	0.03	0.51	0.12
Oil viscosity, cp	153	36	0.072	1,494	110.2
Resident brine salinity, g TDS/L	10	40.4	5.0	133.0	33.4
Water-to-oil mobility ratio, dimensionless	87	5.86	0.1	51.8	11.05
Average polymer concentration, ppm	93	339	51	3,700	343
Temperature, °F	172	115	46	234	85
Average permeability, md	187	349	1.5	7,400	720
Average porosity, fraction	193	0.20	0.07	0.38	0.20

*Partial data available on most projects

properties requires some discussion of surfactants and their classifications. Most of the discussion applies to MP surfactants as well.

Surfactant Chemistry. A typical surfactant monomer is composed of a nonpolar portion (lipophile—i.e., having strong affinity for oil) and a polar portion (hydrophile—i.e., strong affinity for water); the entire monomer is an amphiphile (has affinity for both oil and water) because of this dual nature. Fig. 47.7 shows the molecular structure of two common surfactants (top two panels) and illustrates (lowest panel) a shorthand notation for surfactant monomers: the monomer is represented by a “tadpole” symbol with the nonpolar portion being the tail and the polar head. Surfactants are classified into four groups that depend on their polar portions (see Table 47.2).³⁰

Anionics. As required by electroneutrality, the anionic surfactant molecule is uncharged with an inorganic metal cation (usually sodium) associated with the monomer. In an aqueous solution the molecule ionizes to free cations and the anionic monomer. Anionic surfactants are the most common in EOR because they are good surfactants, relatively resistant to retention, stable, and relatively inexpensive.

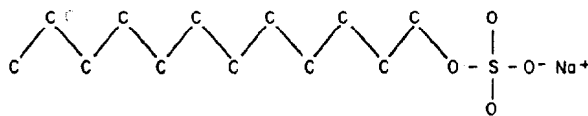
Cationics. In this case the surfactant molecule contains a cationic hydrophile and an inorganic anion to balance the charge. Cationic surfactants have little use in EOR because they are adsorbed highly by the anionic surfaces of interstitial clays.

Nonionics. These surfactants do not form ionic bonds, but when dissolved in aqueous solutions, they exhibit surfactant properties simply by electronegativity contrasts between their constituents. Nonionics are much less sensitive to high salinities than anionics or cationics.

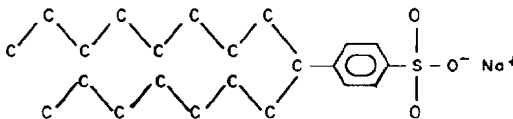
Amphoterics. A final class of surfactants are those that contain aspects of two or more of the previous classes. For example, an amphoteric may contain both an anionic group and a nonpolar group. These surfactants have not been used in EOR.

Within any one class there is a huge variety of possible surfactants. Fig. 47.7 illustrates differences in lipophile molecular weight [C_{12} for the sodium dodecyl sulfate (SDS) vs. C_{16} for Texas No. 1], hydrophile identity (sulfate vs. sulfonate), and tail branching (straight chain for SDS vs. two tails for Texas No. 1) all within the same class of anionic surfactants. In addition to these, there are variations in the position of the hydrophile attachment and the number of hydrophiles (monosulfonates vs. disulfonates, for example). Even small variations can change surfactant properties drastically (e.g., sulfates tend to be less thermally stable than sulfonates). For details on the

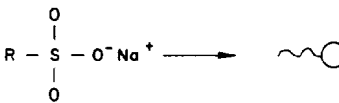
SODIUM DODECYL SULFATE



TEXAS NO. 1 SULFONATE



COMMERCIAL PETROLEUM SULFONATES



R – HYDROCARBON GROUP
(non – polar)

Fig. 47.7—Typical surfactant molecular structures.

effect of structure on surfactant properties see Refs. 31 and 32.

Most commercial surfactants contain distributions of surfactants and surfactant types that further add to their complexity. In the following, distinctions between surfactant types are ignored by simply treating the surfactant as the tadpole structure of Fig. 47.7.

Foam Stability. The stability of a foam may be understood by viewing the liquid film separating two gas bubbles in cross section as in the lower panel of Fig. 47.8.³³ The hydrophiles of the surfactant are oriented into the interior of the film and the lipophiles toward the bulk gas phase. Suppose that some external force causes the film to thin as in the lower panel. Since capillary pressure is inversely proportional to interfacial curvature, the pressure in the thinned portion of the film is lower than in the adjacent flat portion. This causes a pressure difference within the film, liquid flow, and healing. The pressure in the gas phase is assumed constant because of its relatively low density if the foam is static, or low viscosity if in motion.

Table 47.2—CLASSIFICATION OF SURFACTANTS AND EXAMPLES

● ⁻ M Anionics	● ⁺ M Cationics	● ⁺ Amphoterics	● ⁻ Nonionics
Sulfonates	Quaternary ammonium	Aminocarboxylic	Alkyl-
Sulfates	Pyridinium	acids	Alkyl-aryl
Carboxylates	Imidazolinium	Others	Acyl
Phosphates	Piperidinium		Acylamindo-
Others	Sulfonium		Acylaminepolyglycol ethers
	Compounds		Polyol ethers
	Others		Alkanolamides
			Others

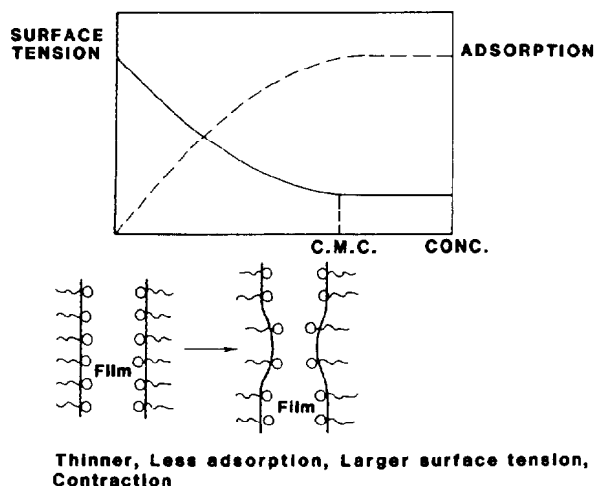


Fig. 47.8—Upper panel shows surface tension and adsorption of a surfactant vs. concentration. Lower panel is the Gibbs-Marangoni effect.

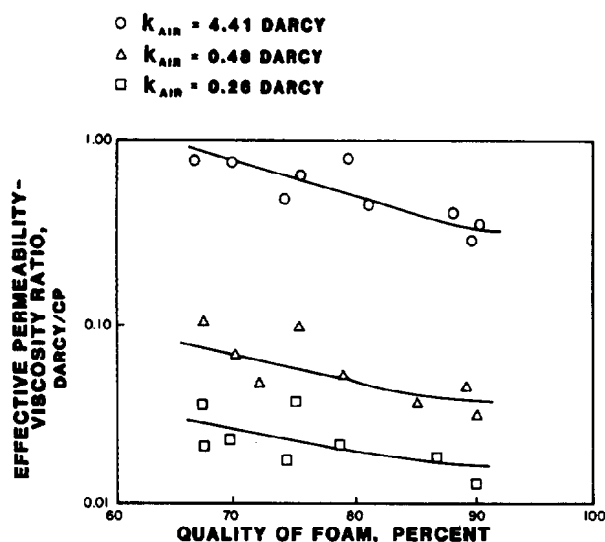


Fig. 47.9—Effective permeability-viscosity ratio vs. foam quality for consolidated porous media.

The upper panel in Fig. 47.8 shows that the gas/liquid surface tension is a decreasing function of surface adsorption as required by the Gibbs theory. According to this view the thinned portion of the film will have less specific adsorption (since the surface area is locally greater) and greater surface tension. This locally high surface tension also causes healing.

Clearly, the surface tension at the gas/liquid interfaces play an important role in film stability. Very low surface tension would not be favorable; fortunately gas/liquid surface tensions are rarely lower than 20 dynes/cm even with the best foaming agents. In the absence of external forces, the film is at an equilibrium thickness caused by a balance between the repulsion forces of the electrical dou-

ble layer on the interior of the film boundary and the attractive Van der Waal forces between the molecules in the film. If the film becomes substantially smaller than the equilibrium thickness, the free energy barrier between the repulsive and attractive contributions is breached and the film will collapse.

Such thinning can be caused spontaneously by diffusion of the gas from small to large bubbles and by gravity drainage. Patton *et al.*³⁴ reported on the rate of spontaneous collapse of a large number of foams as a function of surfactant type, temperature, and pH.³⁴ The half-life of the foam heights reported in their static tests ranges from 1 to about 45 minutes. They report that anionic surfactants have greater stability than nonionics, and that the stability of sulfonate foams is affected greatly by water hardness. Foams were generally more unstable at high temperatures, and many could be stabilized by adding a second surfactant.

External effects that may cause the foam to collapse are the presence of a foam breaker (oil or a high electrolyte concentration could do this), local heating, or contact with a hydrophobic surface.

Foam Physical Properties. Physically, foams are characterized by three measures.

Quality. Foam quality, Γ , is the percentage of the total (bulk) foam volume that is gas volume. The quality can increase with increasing temperature and decreasing pressure both because the gas volume can increase, and also because gas dissolved in the bulk liquid phase can evolve from solution. Foam qualities can be quite high, approaching 97% in many cases. A foam with quality greater than 90% is a *dry* foam.

Texture. This measure is the average bubble size. The texture determines how the foam will flow through a permeable medium. If the average bubble size is larger than the average pore diameter, the foam flows as a progression of films separating individual gas bubbles. Given typical foam textures and pore sizes, this condition is most nearly realized in permeable flow, particularly for high foam qualities.

Bubble Size Range. Foams with a large distribution range are more likely to be unstable because of the gas diffusion from large to small bubbles.

Mobility Lowering. Foams can reduce the mobility of a gas phase drastically. Fig. 47.9 shows the steady-state mobility of foams of differing quality in Berea cores at three different permeabilities as a function of quality.³⁵ On the extreme right of this figure ($\Gamma \rightarrow 100\%$), the mobility should approach the respective air permeability divided by the air viscosity; this mobility is two to three factors of 10 greater than any of the experimental points on the figure. When $\Gamma \rightarrow 0$ the mobility should approach the water permeability divided by μ_w . Thus, the mobility of the foam is lower than that of either of its constituents alone. The mobility of the foam decreases with increasing quality until the films between the gas bubbles begin to break and the foam collapses (not shown on Fig. 47.9). Foams are effective in reducing the mobility at all three permeabilities in Fig. 47.9, but the effect of foam quality is more pronounced at the highest permeability. This is a consequence of the contrast between the texture of the foam and the mean pore size of the medium.³⁶

The mobility reduction caused by the foam can be viewed as an increase in a single-phase viscosity or as a decrease in the gas-phase permeability. Representative data of the second type are in Fig. 47.10, which shows the gas-phase permeability, both with and without foam, and gas saturation plotted against the liquid injection rate.³⁷ Note that the foam causes a great decrease in gas permeability at the same rate and even at the same gas saturation compared to the nonfoaming displacement. The analogous analysis performed on the aqueous-phase relative permeability shows that neither the gas saturation nor the presence of the foaming agent affects the aqueous-phase relative permeability.³⁸

The low foam mobilities in permeable media flow are postulated to be caused by at least two different mechanisms: (1) the formation of or the increase in a trapped residual gas phase saturation and (2) a blocking of pore throats caused by the gas films. From Fig. 47.10 the effect of a trapped gas saturation, which would lower the gas mobility through a relative-permeability lowering, is much smaller than the pore-throat-blocking effect. The trapped gas-phase saturation effect may become important, however, during the later stages of a displacement where the lower pressures could cause more gas to come out of solution.

The mobility reduction of foams, viewed as a viscosity enhancement, has been studied in capillary tubes.³⁹ General observations on these data are that foams are generally shear-thinning fluids whose power law coefficient increases with the capillary tube radius. Using theoretical arguments based on a Newtonian fluid and an inviscid gas, Hirasaki and Lawson showed that the film thickness of a single moving bubble increases as the bubble velocity to the two-thirds power.⁴⁰ Since shear stress in a capillary is inversely proportional to film thickness, the apparent viscosity of a foam in a capillary tube decreases with increasing velocity. Thus, the shear-thinning effect observed in capillary tubes is actually a consequence of the film thickening as velocity increases. A second implication in the Hirasaki-Lawson theory is that foam texture occupies as great an importance in determining rheological behavior as does foam quality.

Field Results. Field tests of foam injection alone have been scarce. Holm reports on the injection of an air/brine foam into a single well in the Siggins field.⁴¹ Though there was no measureable oil response, the mobility to both air and brine were reduced significantly, and the injection profile into the central well became more uniform.

Low-IFT Processes

In addition to stabilizing gas dispersions, surfactants used in MP flooding or generated in situ can recover oil by lowering oil/water IFT.

Lowering ROS

The basic tool for illustrating how lowering IFT reduces ROS is the capillary desaturation curve (CDC) shown in Fig. 47.11. The CDC is a plot of nonwetting- or wetting-phase residual saturation on the y axis vs. a dimensionless ratio of viscous to local capillary forces on a logarithmic x axis. On Fig. 47.11, S_{orw} is the residual oil (assumed nonwetting), and S_{iw} is the irreducible water-(wetting)-phase saturation. The CDC has been calculat-

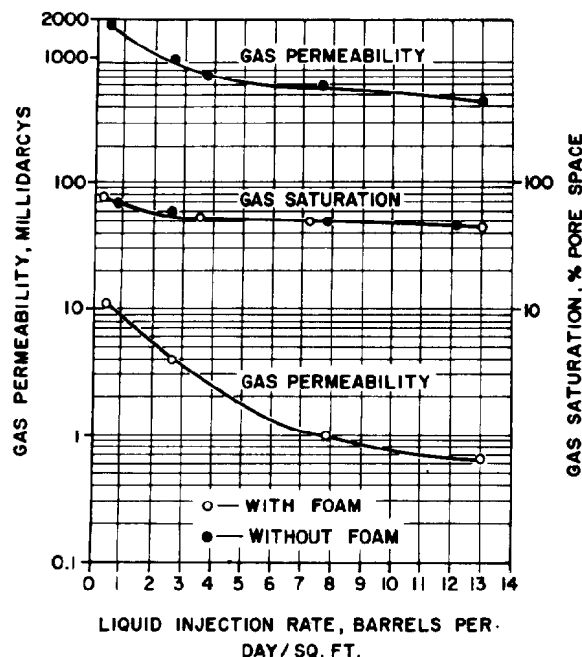


Fig. 47.10—Effect of liquid flow rate and gas saturation on gas permeability with and without foam.

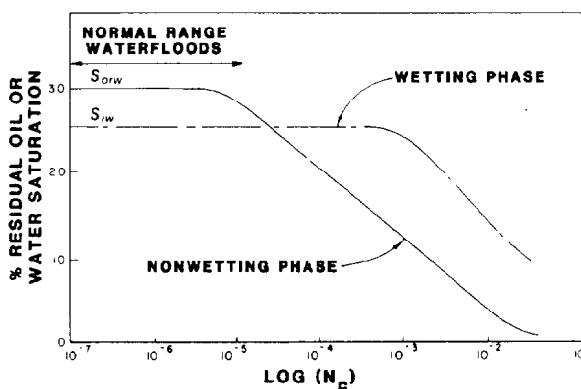


Fig. 47.11—Schematic capillary desaturation curves.

ed theoretically,⁴²⁻⁴⁴ but the most common source of this curve is experimental measurement.^{45,46} The ratio of viscous to local capillary forces is the capillary number, N_c , one form of which is

$$N_c = u_w \mu_w / \sigma_{wo} \quad (8)$$

For a waterflood, u_w and μ_w are the superficial flux and viscosity of the displacing water, and σ_{wo} is the IFT between the water and oil phases. For a MP flood a more general definition is appropriate, but Eq. 8 and the CDC can illustrate this case also.

The CDC is a nearly horizontal plateau at small N_c until a critical value above which both residual phase saturations decrease. At a second critical N_c , the residual phase saturations are zero and complete recovery of the

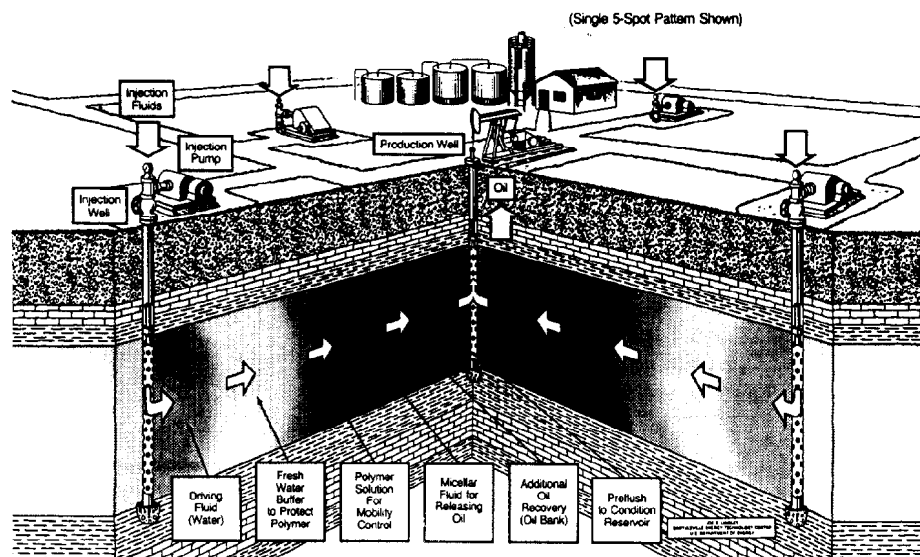


Fig. 47.12—Schematic of an MP flooding process.

originally trapped phase occurs. The shape of the CDC is determined by the pore geometry of the medium and the wetting behavior of the two phases. The wetting phase requires a larger N_c for complete recovery. To a lesser extent, the CDC shape is affected by the mean pore size and pore size distribution of the medium, and the initial saturations. Typical N_c 's for waterflooding are quite small, which indicates that ROS and S_{iw} may be assumed constant for this purpose (see Fig. 47.11). Because of the logarithmic x axis, a decrease by several factors of 10 in N_c is necessary to significantly change either residual phase saturation. Of the three quantities in Eq. 8 only the IFT can be changed this drastically; a typical value for causing good ROS reduction is in the range of 10^{-3} dyne/cm, a value that can be obtained only with a good surfactant.

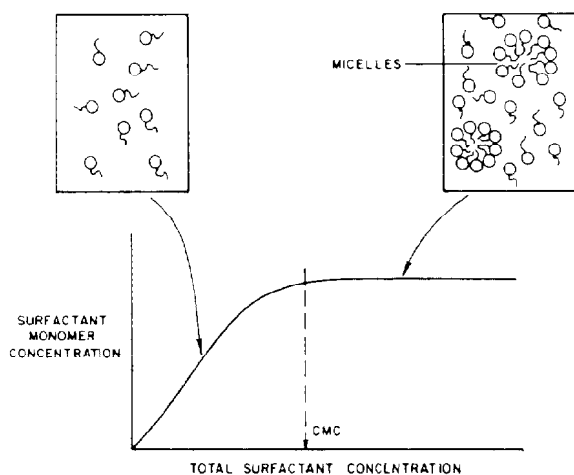


Fig. 47.13—Schematic of the CMC.

MP Flooding

MP flooding has appeared in the technical literature under many names: detergent, surfactant, low-tension, soluble oil, microemulsion, and chemical flooding. There are also several company names that imply a specific sequence and type of injected fluids as well as the specific nature of the oil-recovering MP slug itself. Though there are differences among company processes, the common aspects are more numerous and important.

An idealized version of a MP flooding sequence is in Fig. 47.12. The process is applied invariably to tertiary floods (those producing at high WOR's) and is always implemented in the drive mode (not cyclic or huff 'n' puff). The complete process consists of the following.

Preflush. A volume of brine whose purpose is to change (usually lower) the salinity and hardness of the resident brine so that mixing with the surfactant will not cause the loss of interfacial activity. Preflushes have ranged in size from 0 to 100% of the reservoir PV. In some processes a sacrificial agent is added to lessen the subsequent surfactant retention and also to precipitate divalent cation.⁴⁷

MP Slug. This volume, ranging from 5 to 40% PV in field applications, contains the main oil-recovering agent, the *primary* surfactant, in concentrations ranging from 1 to 20 vol%. Several other chemicals (cosurfactants, alcohols, oil, polymer, biocide, and oxygen scavenger) are usually necessary for good oil recovery.

Mobility Buffer. This fluid is a dilute solution of a water-soluble polymer whose purpose is to drive the MP slug and banked-up fluids to the production wells. Much of polymer flooding technology carries over to designing and implementing the mobility buffer.⁴⁸

Freshwater Buffer. This is a volume of brine containing a concentration of polymer grading between that of the mobility buffer at the front end and zero at the back. The gradual concentration decrease mitigates the effect of the unfavorable mobility ratio between the chase water and mobility buffer.

Chase Water. The purpose of the chase water is simply to reduce the expense of continually injecting polymer. If the mobility and freshwater buffers have been designed properly, the MP slug will be depleted before it is penetrated by the chase water.

Surfactant Solutions. If an anionic surfactant is dissolved in brine, the surfactant disassociates into a cation and a monomer. If the surfactant concentration then is increased, the lipophilic portions of the surfactant begin to associate among themselves to form aggregates or *micelles* containing several monomers each. A plot of surfactant monomer concentration vs. total surfactant concentration (Fig. 47.13) is a curve that begins at the origin, increases with unit slope, then levels off at the critical micelle concentration (CMC). Above the CMC all further increases in surfactant concentration cause increases only in the micelle concentration. CMC's are typically quite small (about 10^{-5} to 10^{-4} mol/L). At nearly all practical concentrations for MP flooding the surfactant is predominantly in the micelle form; hence, the name micellar/polymer flooding. The representations of the micelles in Fig. 47.13 and elsewhere are schematic. The actual micelle structures can take on various forms, which can fluctuate with time.

When this solution contacts an oleic phase (the term "oleic" indicates that this phase can contain more than oil) the surfactant tends to accumulate at the intervening interface. The lipophilic tail dissolves in the oleic phase, and the hydrophilic in the aqueous phase. The accumulation at the interface causes the IFT between the two phases to lower. The extent of the IFT lowering is proportional to the excess surface concentration of the surfactant—the difference between the surface and bulk surfactant concentration—from Gibbs' theory, as was the case in Fig. 47.8. The surfactant itself and the attending conditions should be adjusted to maximize the excess surface concentration; however, in doing so the solubility of the surfactant in the bulk oleic and aqueous phases also is affected. Since this solubility also impinges on the mutual solubility of brine and oil, which also affects IFT's, this discussion leads naturally to the topic of surfactant/brine/oil phase behavior. Curiously, and this is true of many micellar properties, the surfactant concentration itself plays a rather minor role in what follows, compared with the temperature, brine salinity, and hardness.

Surfactant/Brine/Oil Phase Behavior. Surfactant/brine/oil phase behavior is illustrated conventionally on a ternary diagram. A ternary diagram is an equilateral triangle whose apexes represent pure components, boundaries represent two-component mixtures, and interior represents three-component mixtures. For complicated mixtures the three apexes must represent "pseudocomponents" whose composition remains constant throughout the diagram. The pressure and temperature are also fixed. The diagram can represent both the overall composition of a surfactant/brine/oil mixture, and the equilibrium composition of each phase if the mixture forms more than one phase. Ternaries and their accompanying definitions are discussed in Chap. 23.

MP phase behavior is affected strongly by the salinity of the brine pseudocomponent. Consider the sequence of phase diagrams (Figs. 47.14 through 47.16) as the brine salinity is increased. The phase behavior about to be de-

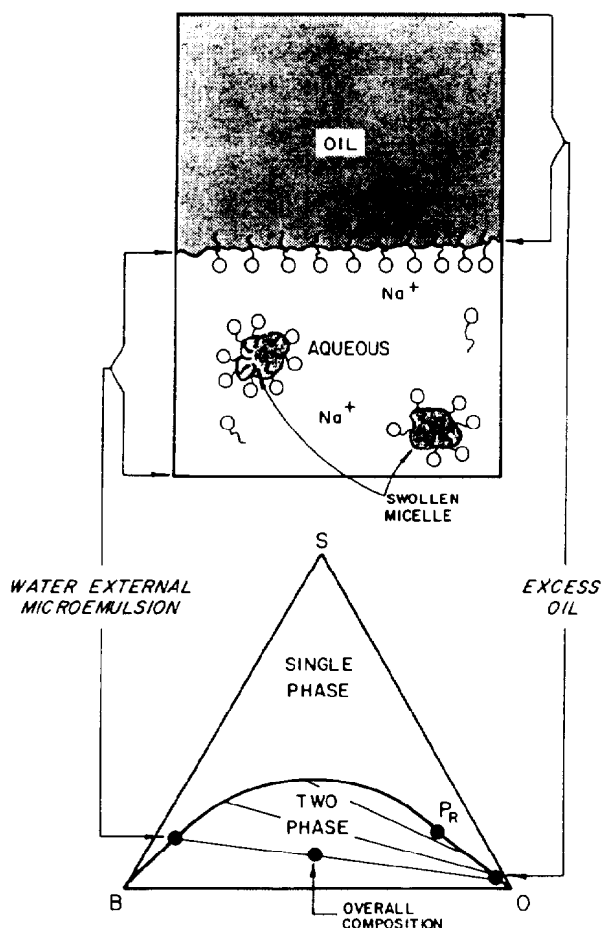


Fig. 47.14—Schematic of low-salinity surfactant/brine/oil phase behavior.

scribed was presented originally by Winsor⁴⁹ and adapted to MP flooding later.^{50,51}

At low brine salinity, a typical MP surfactant will exhibit good aqueous (water-rich) phase solubility and poor oleic (oil-rich) phase solubility. Thus, an overall composition near the brine/oil boundary of the ternary will split into two phases: an *excess oil* phase that is essentially pure oil and a (water-external) *microemulsion* phase that contains brine surfactant, and some solubilized oil. The solubilized oil occurs when globules of oil occupy the central core of the *swollen* micelles. The tie lines within the two-phase region have a negative slope. This type of phase environment is called variously a Winsor Type I system, a lower-phase microemulsion (because it is more dense than the excess oil phase), or a Type II system. The latter terminology is adopted here—II means that no more than two phases can (not necessarily will) form and (–) means that the tie lines have negative slope (Fig. 47.14). The right plait point in such a system, P_R , usually is located quite close to the oil apex. Any overall composition above the binodal curve is single phase.

For high brine salinities (Fig. 47.15) electrostatic forces drastically decrease the surfactant's solubility in the aqueous phase. An overall composition within the two-phase region now will split into an *excess brine* phase and an

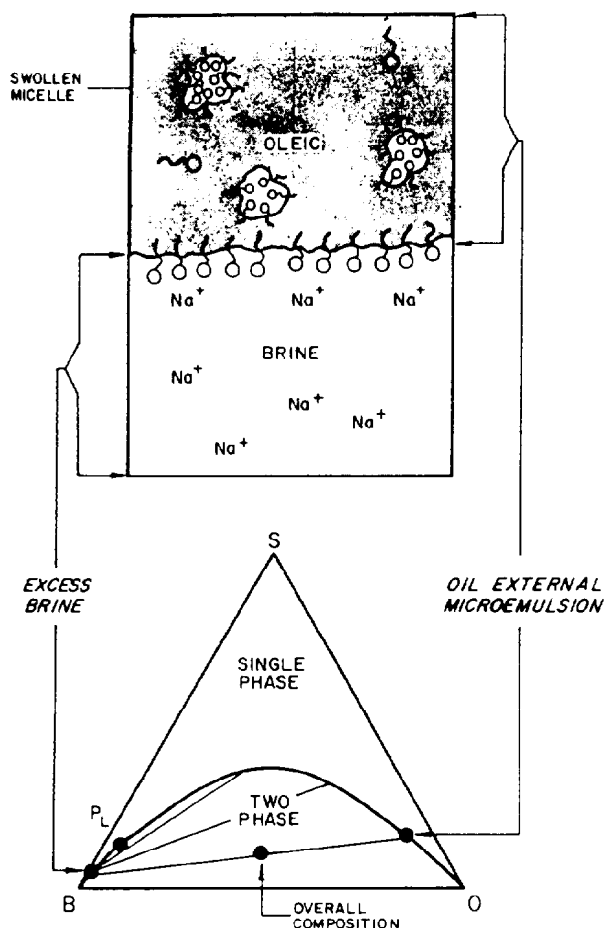


Fig. 47.15—Schematic of surfactant/brine/oil high-salinity phase behavior.

(oil-external) microemulsion phase, which contains most of the surfactant and some solubilized brine. The brine is solubilized through the formation of inverted swollen micelles (Fig. 47.15) with brine globules at their cores. The phase environment is a Winsor Type II system, an upper-phase microemulsion, or a Type II(+) system. The plait point, P_L , is now close to the brine apex.

The two extremes presented thus far are roughly mirror images; note that the microemulsion phase is water-continuous in the Type II(−) systems and oil-continuous in Type II(+) systems. The induced solubility of oil in a brine-rich phase, Type II(−), suggests an extraction mechanism in oil recovery. Though extraction does play some role, it is dwarfed by the IFT effect discussed later, particularly when phase behavior at intermediate salinities is considered.

At salinities between those of Figs. 47.14 and 47.15, there is a continuous change between Type II(−) and II(+) systems and a third surfactant-rich phase is formed, as shown in Fig. 47.16. An overall composition within the three-phase region separates into excess oil and brine phases as in the Type II(−) and II(+) environments, and into a microemulsion phase whose composition is represented by an invariant point. This environment is called

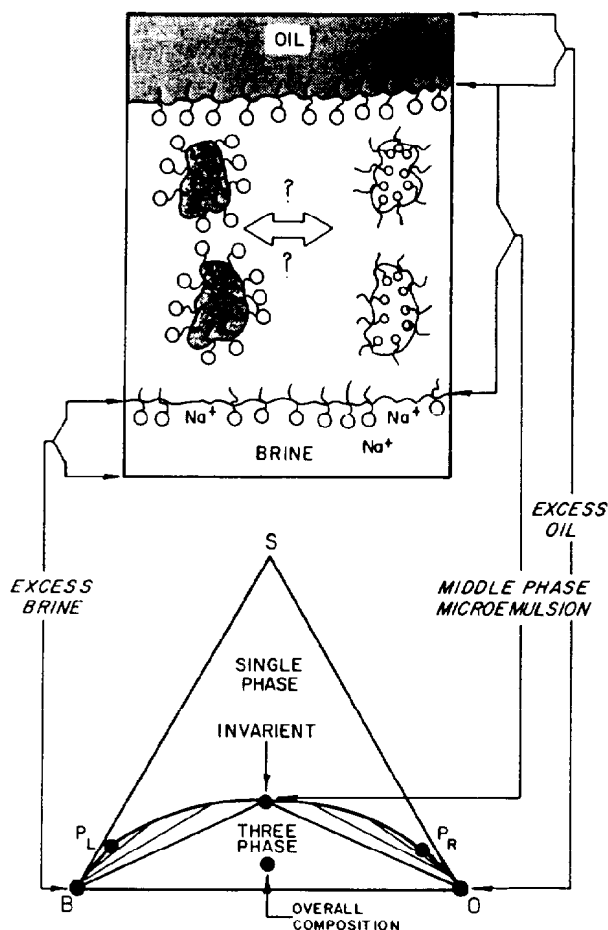


Fig. 47.16—Schematic of surfactant/brine/oil phase behavior at optimal salinity.

a Winsor Type III, a middle-phase microemulsion, or a Type III system. Above and to the right and left of the three-phase region are Type II(−) and II(+) lobes wherein two phases will form as before. Below the three-phase region there is a third two-phase region (as required by thermodynamics) whose extent is usually so small that it is neglected.⁵² In the three-phase region there are now two IFT's between the microemulsion and oil, σ_{mo} , and the microemulsion and water, σ_{mw} .

Fig. 47.17, a prism diagram, shows the entire progression of phase environments from Type II(−) to II(+). The Type III region forms through the splitting of a critical tie line that lies close to the brine/oil boundary as the salinity increases to C_{el} (low effective salinity limit for Type III phase environment).⁵³ A second critical tie line also splits at C_{eu} (high effective salinity limit for Type III phase environment) as salinity is decreased from a Type II(+) environment. Over the Type III salinity range the invariant point, M , migrates from near the oil apex to near the brine apex before disappearing at the appropriate critical tie lines. The migration of the invariant point implies essentially unlimited solubility of brine and oil in a single phase, which has generated an intense research interest into the nature of the Type III microemulsion.⁵⁴

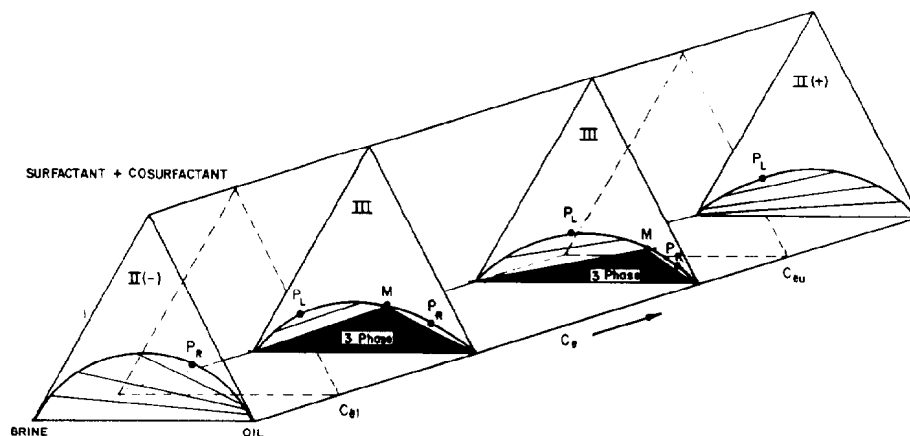


Fig. 47.17—Prism diagram showing sequence of phase environment transition.

Several variables other than salinity can bring about the Fig. 47.17 phase environment shifts. In general, changing any condition that enhances the surfactant's oil solubility will cause the shift from Type II(−) to II(+). Some of the more important are: (1) decreasing temperature,⁵¹ (2) increasing surfactant molecular weight,³¹ (3) decreasing tail branching,³¹ (4) decreasing oil specific gravity⁵⁵⁻⁵⁷ and (5) increasing concentration of high-molecular-weight alcohols.⁵⁸ Decreasing the surfactant's oil solubility will cause the reverse change. Thus, Fig. 47.17 could be redrawn with any of the above variables (and several others) on the base of the prism with the variable C_e (effective salinity) increasing in the direction of increased oil solubility.

Nonideal Effects. In much the same manner as the ideal gas law approximates the behavior of real gases, Fig. 47.17 is an approximation to actual MP phase behavior. Some of the more important nonidealities are as follows.

1. At high surfactant concentrations and/or at low temperatures^{54,59} or even in the presence of pure surfactants,⁶⁰ phases other than those on Fig. 47.17 have been observed. These phases tend to be high-viscosity liquid crystals or other condensed phases. The large viscosities are detrimental to oil recovery since they can cause local viscous instabilities during a displacement. Frequently, low- to medium-molecular-weight alcohols (cosolvents) are added to MP formulations to "melt" these undesirable viscosities. When the brine contains polymer, a condensed phase can be observed at low surfactant concentration because of exclusion of the polymer from the microemulsion phase. Cosurfactants can be used to eliminate this polymer/surfactant incompatibility.⁶¹

2. When cosurfactants are present it is frequently inappropriate to lump all of the chemicals into the surfactant apex of the Fig. 47.17 prism. If the cosurfactants do not partition with the primary surfactant during a displacement the benefit of adding the chemical is lost; hence, surfactant/cosurfactant separation effects are important. Efforts to account for the preferential partitioning of the cosurfactant include a quaternary phase behavior representation and a pseudophase theory.^{62,63}

3. The Type III salinity limits (C_{el} and C_{eu}) are func-

tions of surfactant concentration. This dependency may be visualized by tilting the vertical triangular planes in Fig. 47.17 about their bases. This dilution effect^{64,65} forms the basis for the salinity requirement diagram design procedure.^{66,67} The dilution effect is particularly pronounced when the brine contains significant quantities of divalent ions.

4. The Fig. 47.17 phase-behavior shifts are specific to the exact ionic composition of the brine, not simply to the total salinity. For anionic surfactants, other anions in solution have little effect on the MP phase behavior; however, cations readily cause phase-environment changes. Divalent cations (calcium and magnesium are the most common) are usually 5 to 20 times as potent as monovalent cations (usually sodium). Divalents are usually present in oilfield brines in smaller quantities than monovalents as shown in Fig. 47.2, but their effect is so pronounced that it is necessary, as a minimum, to separately account for salinity and hardness. Nonconstant monovalent/divalent ratios also will cause electrolyte interactions with clay minerals through cation exchange. The disproportionate effects of the salinity and hardness are accounted for by defining a weighted sum of the monovalent and divalent concentrations as an effective salinity. The C_e 's in Fig. 47.17 imply effective salinities.

Phase Behavior and IFT. Early MP flooding literature contains considerable information about the techniques of measuring IFT's and what causes them to be low.⁶⁸ IFT's were found to vary with the types and concentration of surfactant, cosurfactant, electrolyte, oil, and polymer and with temperature. However, in what was surely one of the most significant advances in all of MP technology, all IFT's were shown to correlate directly with the MP phase behavior. The correlation was proposed originally by Healy and Reed,⁵⁹ theoretically substantiated by Huh,⁶⁹ and since verified experimentally by several others.^{31,70} The practical benefit of this correlation is that relatively difficult measurements of IFT's can be largely supplanted by simple phase behavior measurements. Indeed, in the recent literature, the behavior of IFT's has been inferred by a narrower subset of phase-behavior studies based on the solubilization parameter.⁶⁵

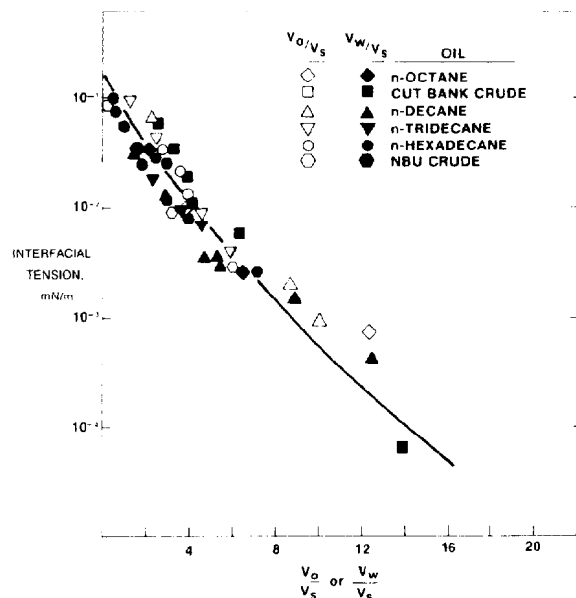


Fig. 47.18—Correlation of solubilization ratios with IFT.

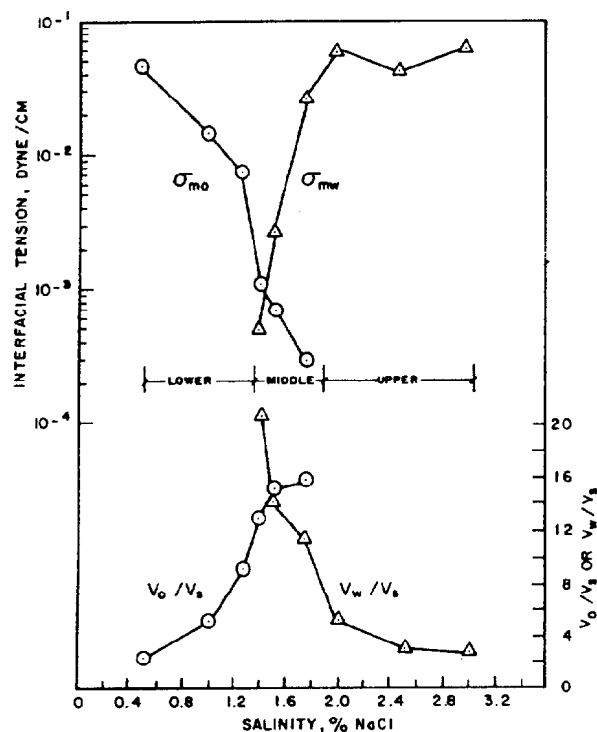


Fig. 47.19—IFT and solubilization ratios.

To investigate further the relation between IFT's and phase behavior, let V_o , V_w , and V_s be the volume fractions of oil, brine, and surfactant in the microemulsion phase, respectively. According to Figs. 47.14 through 47.16, the microemulsion phase is present at all salinities; hence, all three quantities are well-defined and continuous. Considering the Type II(-) behavior of Fig. 47.14, for example, V_o , V_w , and V_s are the coordinates of the microemulsion phase composition on the binodal curve.

Solubilization parameters between the microemulsion-oil phases, F_{mo} , for Type II(-) and III phase behavior, and between the microemulsion-aqueous phases, F_{mw} , for Type II(+) and III are defined as

$$F_{mo} = V_o / V_s \quad \dots \dots \dots (9a)$$

and

$$F_{mw} = V_w / V_s \quad \dots \dots \dots (9b)$$

The IFT's between the corresponding phases, σ_{mo} and σ_{mw} , are functions only of F_{mo} and F_{mw} . Fig. 47.18 shows a typical correlation.⁷⁰

The corresponding behavior of the solubilization parameters and IFT's are shown in Fig. 47.19 in a different manner. Consider a locus at constant oil, brine, and surfactant overall concentrations in Fig. 47.17 but with a variable salinity. If the nonideal effects are unimportant and the locus is at low surfactant concentration and intermediate brine/oil ratios, σ_{mo} will be defined from low salinity up to C_{eu} , and σ_{mw} from C_{el} to high salinities. Both IFT's are the lowest in the three-phase Type III region, between C_{el} and C_{eu} , where both solubilization parameters are also large. There is, further, a precise salinity where both IFT's are equal at values low enough ($\sim 10^{-3}$ dyne/cm) for good oil recovery. This salinity is the *optimal salinity* for this particular surfactant/brine/oil combination and the common IFT is the *optimal IFT*. Optimal salinities have been defined on the basis of equal IFT's, as in Fig. 47.19, equal solubilization parameters, maximum oil recovery in corefloods, and equal contact angles.^{50,71,72} All definitions of optimal salinity give roughly the same value; hence, since optimal phase behavior salinity is the same as maximum oil recovery salinity, generating an interfacially active MP slug translates into generating this optimal salinity in situ in the presence of the surfactant material.

Generating Optimal Conditions. Historically there have been three techniques for generating optimal conditions in an MP displacement.

1. The MP system's optimal salinity can be raised to that of the resident brine salinity in the candidate reservoir. This procedure philosophically is the most satisfying of the three design procedures given here and usually the most difficult. Though it has been the subject of intensive research, surfactants that have high optimal salinities that are not (at the same time) thermally unstable at reservoir conditions, excessively retained by the solid surfaces, or expensive have not yet been discovered. Field successes with synthetic surfactants have demonstrated the technical feasibility of this approach, however.⁷³ A sec-

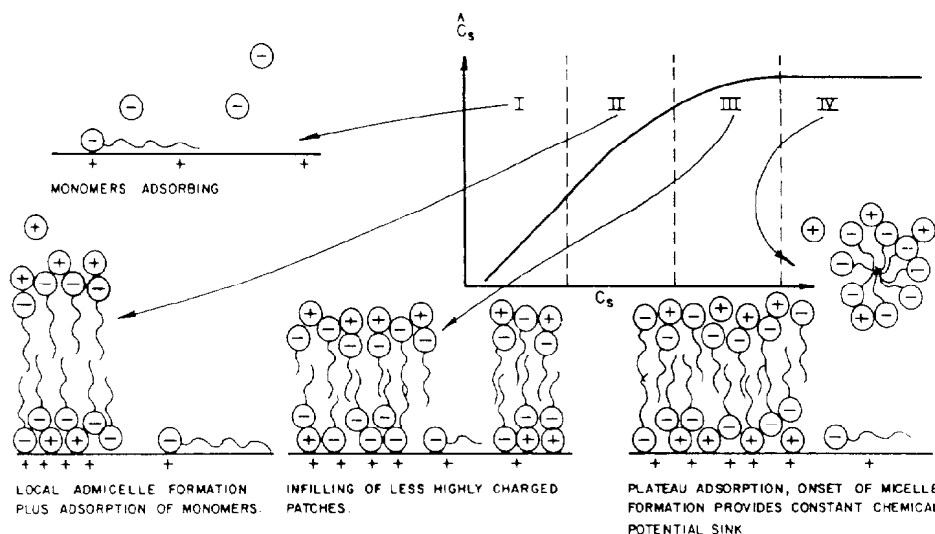


Fig. 47.20—Schematic of surfactant adsorption on metal oxide surface.

ond way to make the optimal salinity of the MP formulation equal to the resident brine salinity is to add cosurfactant.

2. Resident salinity of a candidate reservoir can be lowered to match the MP slug's optimal salinity. This is the main purpose of the preflush step illustrated in Fig. 47.12. A successful preflush is appealing because, with the resident salinity lowered, the MP slug would displace oil wherever it goes in the reservoir. Preflushes generally require quite large volumes to lower the resident salinity significantly owing to mixing effects and cation exchange.^{74,75} With some planning, the function of the preflush could be accomplished during the waterflood preceding the MP flood.

3. The salinity gradient design attempts to dynamically lower the resident salinity to an optimum during the displacement by sandwiching the MP slug between the overoptimal resident brine and an underoptimal mobility-buffer salinity.^{66,67} The success of this procedure relies on it being necessary that only a portion of the MP slug be in the active region for good oil recovery. For salinity gradient floods the salinity of the mobility buffer is the most significant factor in bringing about good oil recovery.⁷⁶ The salinity gradient design has several other advantages in being resilient to design and process uncertainties, in providing a favorable environment for the polymer in the mobility buffer, minimizing retention, and being relatively indifferent to the surfactant dilution effect.

Surfactant Retention. Surfactants are retained through one of at least four mechanisms.

1. On metal oxide surfaces (Fig. 47.20) the surfactant monomer will adsorb physically through hydrogen bonding and micelle-like associations with the monomer tails, and ionically bond with cationic surface sites (I).⁷⁷ At higher surfactant concentrations, C_s , this association includes tail-to-tail interactions with the solution monomers with proportionally greater adsorption (II and III). At and above the CMC (IV), the supply of monomers becomes

constant as does the retention (\hat{C}_s is the adsorbed surfactant concentration).

2. In hard brines the prevalence of divalent cations causes the formation of surfactant/divalent complexes, which have a low solubility in brine.⁷⁸ Precipitation of this surfactant/divalent complex will lead to retention. When oil is present this effect is lessened by the surfactant's solubility in the oleic phase.

3. At hardness levels somewhat lower than those required for precipitation, the preferred multivalent/surfactant complex will be a monovalent cation that can exchange chemically with cations originally bound to the reservoir clays just as inorganic cations do.⁷⁹

4. In the presence of oil in a II(+) phase environment the surfactant will reside in the oil-external microemulsion phase. Because this region is above the optimal salinity, the IFT is relatively large (Fig. 47.18) and this phase and its dissolved surfactant can be trapped.⁶⁴ A similar phase trapping effect does not occur in the II(−) environment because the aqueous mobility buffer miscibly displaces the trapped aqueous-external microemulsion phase without permanent retention.

Most studies of surfactant retention have not made the previously mentioned mechanistic distinctions; therefore, which mechanism predominates in a given application is not obvious. All mechanisms retain more surfactant at high salinity and hardness, which, in turn, can be attenuated by adding cosurfactants. Precipitation and phase trapping can be eliminated by lowering the mobility buffer salinity, at which conditions the chemical adsorption mechanism on the reservoir clays is predominant. Therefore, there should be some correlation of surfactant retention with reservoir clay content. Fig. 47.21 is an attempt to make this correlation by plotting laboratory and field surfactant retention data against clay fraction.⁸⁰ The correlation is by no means perfect since it ignores variations in MP formulation and clay type distribution as well as salinity effects. However, the figure does capture a general trend that is useful for a first-order estimate of retention in a given reservoir.

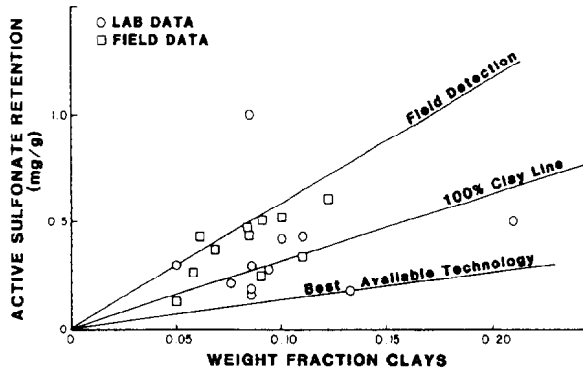


Fig. 47.21—Surfactant retention and weight fraction of clays.

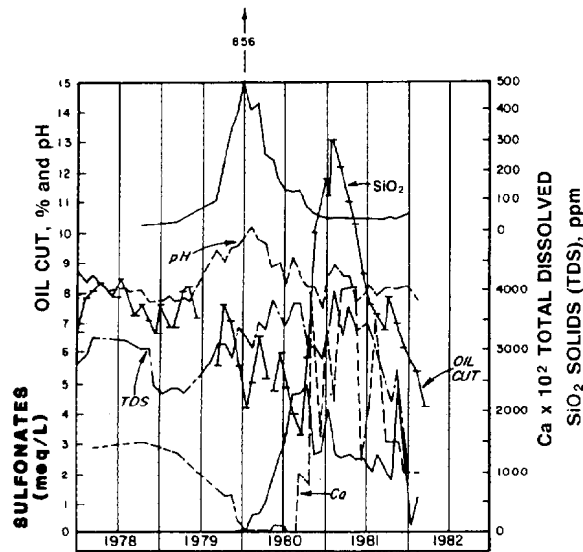
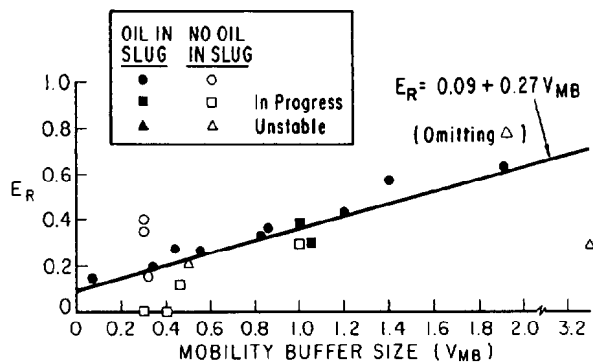


Fig. 47.22—MP production response from Well 12-1, Bell Creek Pilot.



Recovery Efficiency vs. Mobility Buffer Size

Fig. 47.23—Recovery efficiencies from 21 MP field tests.

A useful way to estimate the volume of surfactant required for an MP slug is through the dimensionless frontal advance lag, F_D .⁸¹

$$F_D = \frac{1 - \phi}{\phi} \frac{\rho_r}{\rho_s} \frac{\hat{C}_s}{C_s} \quad (10)$$

where

F_D = frontal advance lag, dimensionless,

ρ_r = density of rock, mass/volume rock,

ρ_s = density of surfactant slug, mass/volume solution,

C_s = concentration of surfactant, mass surfactant/mass solution, and

\hat{C}_s = retained surfactant concentration, mass surfactant/mass rock (includes all forms of surfactants).

F_D expresses the volume of surfactant retained at its injected concentration as a fraction of the PV. For best surfactant usage, the volume of surfactant injected should be large enough to contact all of the PV, but small enough to prevent excessive production of the surfactant. Therefore, the MP slug size, V_{ps} , should be equal to or somewhat larger than F_D .

Field Response. Fig. 47.22 shows the produced fluid analyses of Well 12-1 in the Bell Creek (Carter and Powder River Counties, MT) MP flood. This flood used a high oil content MP slug preceded by a preflush that contained sodium silicate to lessen surfactant retention and reduce divalent cation concentration. Well 12-1 was a producer in the center of a unconfined single 40-acre, five-spot pattern. Further details on the flood are available in Refs. 47 and 82.

Before MP slug injection in Feb. 1979, Well 12-1 was experiencing low and declining oil cuts. MP oil response beginning in late 1980 is superimposed on this decline, reaching peak cuts of about 13% about 6 months later. Note that, just as in polymer flooding, the pre-MP decline must be clearly established for accurate evaluation of the MP oil recovery. The surfactant is preceding the oil in Fig. 47.22 because of an excessively large content of water-soluble, inactive disulfonate in the MP slug. Simultaneous oil and surfactant production is a persistent feature of field MP floods, probably because of heterogeneities and dispersive mixing. Other significant features in Fig. 47.22 are the evident presence of the preflush preceding the MP slug, inferred from the maxima in the pH and silicate concentrations, and the very efficient removal of the calcium cations ahead of the surfactant.

Fig. 47.23 shows oil recovery efficiency, E_R (incremental oil recovered/OIP at start of MP process), from a survey of more than 40 MP field tests correlated as a function of mobility-buffer slug size. As of the date of the survey there were no commercial projects reported. Similar analyses on other process variables showed no or weak correlation.⁸³ The strong correlation in Fig. 47.23 indicates the importance of mobility control in MP design.⁴⁸ Note also from this figure that ultimate oil recovery efficiency averages about 30% in field tests.

Performance Prediction. Generally, three things must be achieved for efficient oil recovery.⁸⁴ (1) the MP surfactant slug must be propagated in an interfacially active mode, (2) enough surfactant must be injected so that some of it is unretained by the permeable media surfaces, and (3) the MP displacement must be designed so that the active surfactant sweeps a large portion of the reservoir without excessive dissipation (because of dispersion) or channeling.

Attaining the first goal is the result of formulation work based on the phase-behavior concepts discussed previously. The extent to which the second and third goals are satisfied depends on prevailing economics, which, in turn, depends on the oil-recovering ability of the entire process. The next few paragraphs describe a simple procedure by which oil recovery and oil rate-time curves may be estimated for an interfacially active MP process. Since there are innumerable ways in which interfacial activity may be lost, the procedure is most accurate for processes that clearly satisfy the first design goal.

Recovery Efficiency. This procedure has two steps: estimating the recovery efficiency of an MP flood and then proportioning this recovery according to injectivity and fractional flow to give an oil rate-time curve. Space considerations will limit many of the details, which may be found in Ref. 80.

The recovery efficiency, E_R , of an MP flood is the product of a volumetric sweep efficiency, E_V , a displacement efficiency, E_D , and a mobility buffer efficiency, E_{MB} .

$$E_R = E_D E_V E_{MB} \quad (11)$$

Each quantity must be calculated independently.

Displacement Efficiency. The displacement efficiency of an MP flood is the ultimate (time-independent) volume of oil displaced divided by the volume of oil contacted.

$$E_D = 1 - \frac{S'_{or}}{S_{orw}} \quad (12)$$

where S'_{or} and S_{orw} are the ROS to an MP and waterflood, respectively. S_{orw} must be known, but S'_{or} can be obtained from a large slug (free from the effects of surfactant retention) laboratory coreflood. Low values of S'_{or} indicate successful attainment of good interfacial activity in the MP slug. If coreflood results aren't available, S'_{or} may be estimated from a CDC by using a "field" capillary number.⁸³

$$N_c = 0.565 q \mu_o \gamma_o / (h \sqrt{A}), \quad (13)$$

where

- N_c = capillary number, dimensionless,
- q = injection/production rate,
- μ_o = oil viscosity,
- h = net thickness, and
- A = pattern area.

Eq. 13 is in consistent units. For screening purposes, assume a controlling IFT of 10^{-3} dyne/cm [$1 \mu\text{N/m}$]; the CDC curve chosen to estimate S'_{or} should be consistent,

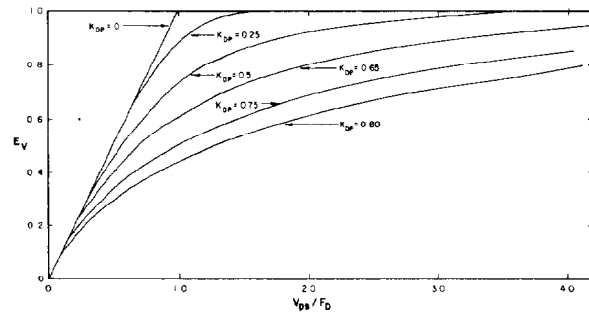


Fig. 47.24—Relationship between MP volumetric sweep efficiency, heterogeneity, and slug-size retention ratio.

as much as possible, with conditions of the candidate reservoir.

Volumetric Sweep Efficiency. Volumetric sweep efficiency, E_V , is the volume of oil contacted divided by the volume of target oil. E_V is a function of MP slug size, V_{PS} , retention, F_D , and heterogeneity based on the Dykstra-Parsons coefficient, K_{DP} . Fig. 47.24 shows this relationship. K_{DP} may be estimated from geologic study, from matching the previous waterflood, or from core data (a typical value would be 0.6). The F_D is estimated from Eq. 10 on the basis of the retention level, \hat{C}_s , surfactant slug concentration, C_s , porosity, and rock and fluid densities. \hat{C}_s can come from a laboratory coreflood, Fig. 47.21 (if clay fraction is known), or by using $\hat{C}_s = 0.4$ mg/g as a default. V_{PS} and C_s are from the proposed design.

Mobility Buffer Efficiency. The mobility buffer efficiency, E_{MB} , is a function of E_V and K_{DP} .

$$E_{MB} = (1 - E_{MBe}) [1 - \exp(0.4 V_{MB} / E_V^{1.2})] + E_{MBe}$$

and

$$E_{MBe} = 0.71 - 0.6 K_{DP} \quad (14a)$$

where E_{MBe} is the mobility buffer efficiency extrapolated to $V_{MB} = 0$ and V_{MB} is the mobility buffer volume, fraction V_p . Eq. 14a was obtained from a numerical simulation.

The recovery efficiency now may be calculated from Eqs. 11 through 14a. The reasonableness of the value may be checked with Fig. 47.23.

Calculation of q_o vs. t Plot. The production function (oil rate vs. time) is based on E_R and the following procedure. The dimensionless production function is assumed to be triangular with oil production beginning at oil bank arrival time, increasing linearly to a peak (maximum) oil cut when the surfactant breaks through, and decreasing linearly to sweepout time. The triangular shape is imposed by the reservoir heterogeneity.

The first step is to calculate the dimensionless oil bank and surfactant breakthrough times for a homogeneous laboratory coreflood.

$$t_{Dob} = \left(\frac{S_{ob} - S_{oi}}{f_{ob} - f_{oi}} \right) t_{DS} \quad (14b)$$

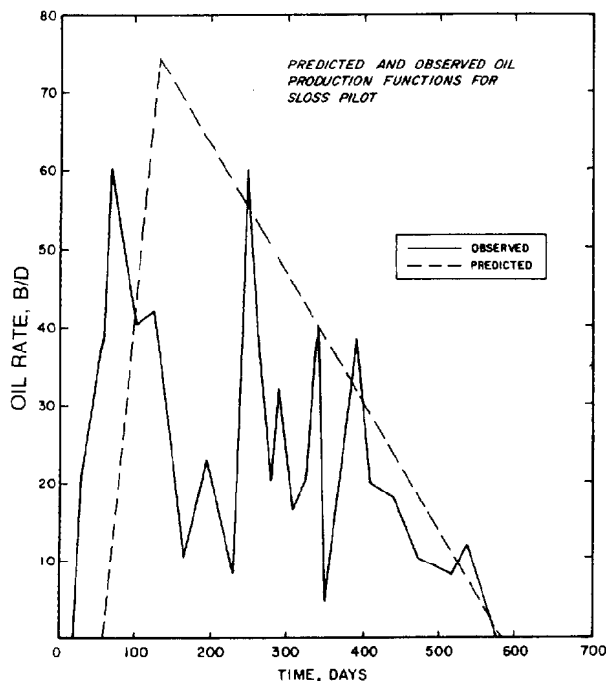


Fig. 47.25—Comparison between predicted and observed oil rate-time responses for the Sloss MP pilot.

and

$$t_{Ds} = 1 + F_D - S'_{or} \quad (14c)$$

where

- t_{Dob} = oil bank arrival time, dimensionless,
- S_{ob} = oil bank saturation, fraction,
- S_{oi} = initial oil saturation, fraction,
- f_{ob} = oil bank oil fractional flow, fraction,
- f_{oi} = initial oil fractional flow, fraction, and
- t_{Ds} = surfactant arrival time, dimensionless.

S_{ob} and f_{ob} may be estimated from the oil/water relative permeability curve as described previously in Refs. 80 and 85, or from laboratory experiment.

The second step is to correct these values for the heterogeneity of the candidate reservoir by using an effective mobility ratio, M_e , where

$$\log(M_e) = \frac{K_{DP}}{(1 - K_{DP})^{0.2}} \quad (15)$$

The corrected breakthrough times are now

$$t'_{Dob} = t_{Dob}/M_e \quad (16a)$$

and

$$t'_{Ds} = t_{Ds}/M_e \quad (16b)$$

where t'_{Dob} is the corrected oil bank arrival time, dimensionless, t'_{Ds} is the corrected surfactant arrival time,

dimensionless, and the peak oil cut, f_{opk} , is

$$f_{opk} = \frac{M_e - M_e \left(\frac{t_{Dob}}{t_{Ds}} \right)^{1/2}}{(M_e - 1)} f_{ob} \quad (17)$$

The final step is to convert the dimensionless production function to oil rate, q_o , vs. time, t . This follows from

$$q_o = q f_o \quad (18a)$$

and

$$t = V_p t_D / q \quad (18b)$$

where f_o is the oil cut, t_D is the dimensionless time, and f_o and t_D are any points on the triangular oil recovery curve, which begins at (t'_{Dob}, f_{oi}) , peaks at (t'_{Dob}, f_{opk}) , and ends at $(t'_{Dsw}, 0)$. The dimensionless time at complete sweepout, t'_{Dsw} , is selected to make the area under the $f_o - t'_D$ curve equal to E_R ,

$$t'_{Dsw} = t'_{Dob} + 2E_R S_{orw} / f_{opk} \quad (19)$$

A comparison of the results of this procedure with the Sloss field MP pilot is in Fig. 47.25. Details of this match and other matches are in the original references.

High-pH Processes

The final chemical flooding EOR process is high-pH flooding (Fig. 47.26). As in polymer and MP flooding, there is usually a brine preflush to precondition the reservoir, a finite volume of the oil-displacing chemical, a graded mobility buffer driving agent, and the entire process is driven by chase water. Moreover, for both high-pH and MP flooding the oil-displacing chemical is a surfactant; however, for MP flooding the surfactant is injected while in high-pH flooding it is generated in situ.

High-pH Chemistry

High pH's indicate large concentrations of the hydroxide anions (OH^-). The pH of an ideal aqueous solution is defined as

$$\text{pH} = -\log_{10} C_{\text{H}^+} \quad (20)$$

where the concentration of hydrogen ions, C_{H^+} , is in mol/L. As the concentration of OH^- is increased, the concentration of H^+ decreases, since the two concentrations are related through the dissociation of water,

$$K_w = \frac{(C_{\text{OH}^-})(C_{\text{H}^+})}{C_{\text{H}_2\text{O}}} \quad (21)$$

and the water concentration is nearly constant. These considerations suggest two means for introducing high pH's into a reservoir: dissociation of a hydroxyl-containing species or adding chemicals that preferentially bind hydrogen ions.

Many chemicals could be used to generate high pH, but the most commonly used are sodium hydroxide (caustic, NaOH), sodium orthosilicate, and sodium carbonate (Na_2CO_3). NaOH generates OH^- by dissociation; the

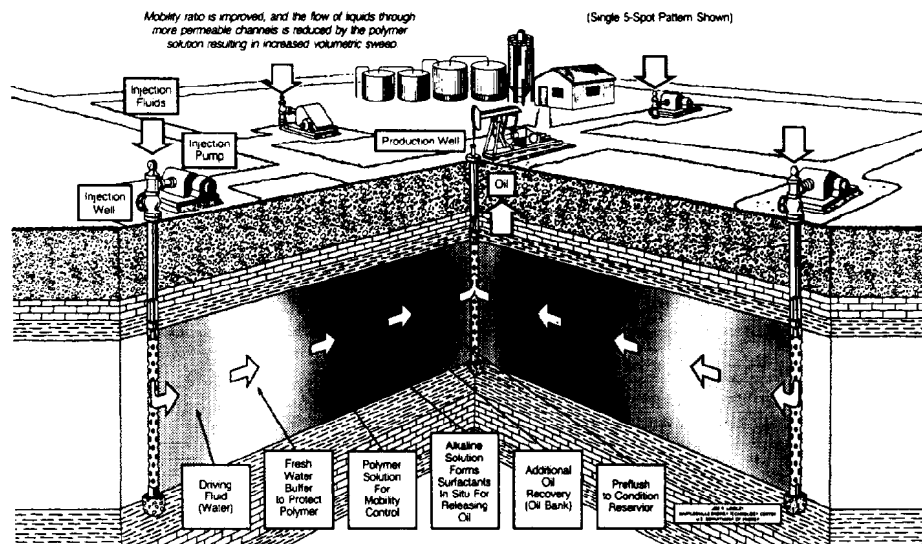
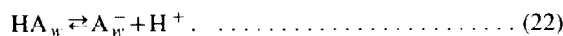


Fig. 47.26—Schematic of high-pH flooding process.

latter two through the formation of weakly dissociating acids (silicic and carbonic acid, respectively) that remove free H^+ ions from solution. High-pH chemicals generally have been used in field applications in concentrations ranging up to 5 wt% (injected pH's of 11 to 13) and with slug sizes up to 20% PV. The resulting amounts of chemicals are quite comparable with the surfactant usage in MP flooding; however, high-pH chemicals are substantially less costly. This cost advantage must be discounted by the historically lower oil recoveries in high-pH flooding.

OH^- by itself is not a surfactant, since the absence of a lipophilic tail makes it exclusively water-soluble. If the crude oil contains an acidic hydrocarbon component, HA_o , some of this, HA_w , can partition to the aqueous phase where it can react.⁸⁶



The exact nature of HA_o is unknown and probably highly dependent on crude oil type. The deficiency of hydrogen ions in the aqueous phase will cause the extent of this reaction to be to the right. The anionic species A_w^- is a surfactant that can have many of the properties and enter into most of the phenomena described above for MP flooding.

If there is no HA_o originally present in the crude, little surfactant can be generated. A useful procedure for characterizing crudes for their attractiveness to high-pH flooding is through the *acid number*. The acid number is the milligrams of potassium hydroxide (KOH) required to neutralize 1 gram of crude oil. To make this measurement, the crude is extracted with water until the acidic species HA is removed. The aqueous phase containing HA_w , A_w^- , and H^+ is then brought to pH=7 by adding the KOH. For a meaningful value, the crude must be free of acidic additives (e.g., scale inhibitor) and acidic gases (CO_2 or H_2S). A good high-pH flooding crude will have an acid number of 0.5 mg/g or greater, but acid numbers as low as 0.2 mg/g may be candidates, since only a small

amount of surfactant is required to saturate oil/brine interfaces. Fig. 47.27 presents a histogram of acid numbers based on the work of Jennings.^{87,88}

Displacement Mechanisms

Oil recovery mechanisms in high-pH flooding have been attributed to eight separate phenomena.⁸⁹ This chapter concentrates on only three: IFT lowering, wettability reversal, and emulsion formation. The last two mechanisms also are present in MP flooding but are dwarfed by the low-IFT effect. With smaller ultimate oil recoveries, the distinction among effects becomes important in high-pH flooding.

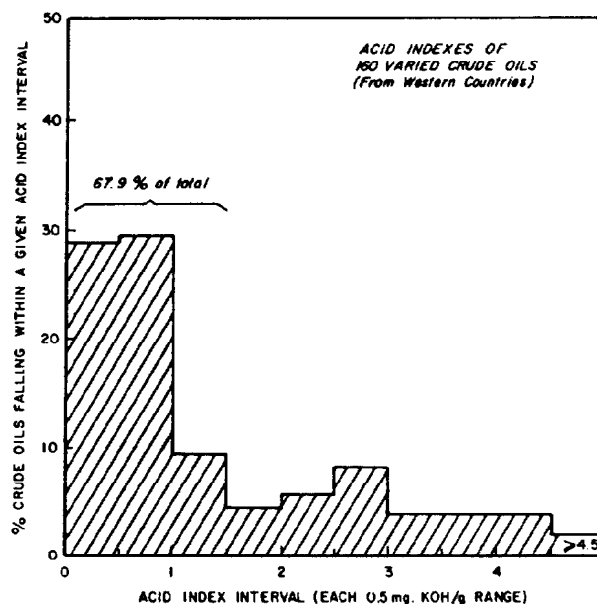


Fig. 47.27—Histogram of acid numbers.

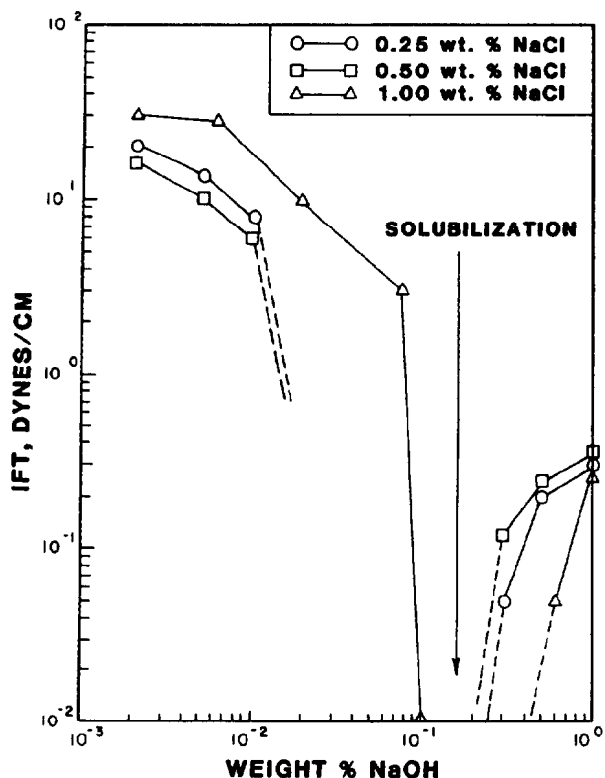


Fig. 47.28—IFT's for caustic/crude/brine systems.

The generated surfactant, A_w^- , aggregates at oil/water interfaces, which can lower IFT.⁸⁶ In general, such lowering is not as pronounced as in MP flooding but, under certain conditions, can be large enough to produce good oil recovery. Fig. 47.28 shows IFT measurements of caustic solutions against Long Beach crude oil at various brine salinities. The IFT's are sensitive to both NaOH concentration and salinity, showing minima in the NaOH concentration range of 0.01 to 0.1 wt%. The decrease in IFT in these experiments is limited by the spontaneous emulsification of the oil/water mixture when the IFT reaches a minimum.

There are many similarities in the low-IFT effects in MP and high-pH flooding. The data in Fig. 47.28 show a clear resemblance to the data in the upper plot of Fig. 47.19 except they are plotted vs. NaOH concentration (presumed proportional to A_w^- concentration) instead of salinity. This suggests an optimal salinity of about 1.0 wt% NaCl for a 0.03 wt% NaOH solution. Indeed, the work of Jennings *et al.*⁸⁷ has shown that there is an optimal NaOH concentration for a given salinity in oil recovery experiments. Moreover, the presence of the emulsification effect when IFT's are low is exactly what one would expect from Fig. 47.17 at a surfactant concentration above the invariant point surfactant concentration. This suggests that the data in Fig. 47.28 showing a Type II(-) phase environment at low NaOH concentrations are Type II(+) at high (similar to what would be expected from the dilution effect in MP flooding). Further work is necessary to establish the connection to MP phase-behavior definitively, since the actual surfactant concentration A_w^- is likely to be much lower in a high-

pH system. However, Nelson *et al.*⁹⁰ show that a cosurfactant can increase the optimal salinity in a high-pH system much like in MP systems.

See Chap. 28 for a discussion of wettability and its effects on petrophysical properties. Owens and Archer⁹¹ showed that increasing the water wetness increased ultimate oil recovery, where the wettability was reported as decreasing the water/oil contact angle measured on polished synthetic surfaces. This has also been shown by others using high-pH chemicals.^{92,93} The increased oil recovery is the result of two mechanisms: a relative permeability effect, which causes the mobility ratio of a displacement to decrease, and a shifting of the CDC (see Fig. 47.11).

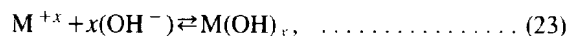
Cooke *et al.*⁹⁴ have reported improved oil recovery with increased oil wetness. Other data show that oil recovery is a maximum when the wettability of a permeable medium is neither strongly water- nor oil-wet.⁹⁵ Given the latter information, the important factor may be the change in the wettability rather than the actual wettability of the final state of the medium. In the original wetting state of the medium, the nonwetting phase occupies large pores and the wetting phase small pores. If the wettability of a medium is reversed, there will be nonwetting fluid in small pores and wetting fluid in large pores. The resulting fluid redistribution, as the phases attempt to return to their natural state, would make both phases vulnerable to recovery through viscous forces.

High-pH chemicals can cause improved oil recovery through the formation of emulsions. The emulsification produces additional oil in at least two ways: through a mobility ratio lowering since many of these emulsions have a substantially increased viscosity and through solubilization and entrainment of oil in a flowing aqueous stream. The first mechanism improves displacement and volumetric sweep as do the mobility control agents discussed previously. Local formation of highly viscous emulsions should be discouraged, however, as these would promote viscous fingering from the less viscous oil-free high-pH solution. The solubilization and entrainment mechanism would be more important when the IFT between the swollen water phase and the remaining crude is low. Fig. 47.28 shows that for certain conditions, emulsification and low IFT's occur simultaneously. McAuliffe showed that emulsions injected in a core and those formed in situ give comparable oil recoveries.^{96,97}

Rock/Fluid Interactions

Interactions of the high-pH chemicals and the permeable media minerals can cause excessive retardation in the propagation of these chemicals throughout the permeable medium. This chapter discusses three aspects of rock-fluid interactions: formation of divalent/hydroxide compounds, cation exchange, and mineral dissolution.

OH^- ions themselves are not appreciably bound to the solid surfaces; however, in the presence of multivalent cations they can form hydroxyl compounds,



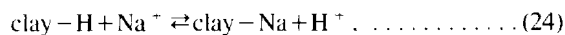
which, being relatively insoluble, can precipitate from solution. This reaction, in turn, lowers the pH of the solution, and also can cause formation damage through pore

blockage and fines migration. The anionic surfactant species A_w^- can interact with the inorganic cations in solution just as in MP flooding; however, the interaction with the divalent cations usually takes precedence, particularly in hard brines (see Fig. 47.3) or where there are substantial quantities of soluble multivalent minerals. Because of these interactions and those involving the surfactants A_w^- , high-pH processes are as sensitive to brine salinity and hardness as are MP processes.

Other high-pH rock/fluid interactions are intimately associated with the clay minerals. Clays are hydrous aluminum/silicate compounds that occupy the smallest (less than 2 microns) particle size in typical media. Macroscopically, clays occur as segregated streaks of variable degree of continuity throughout a typical reservoir, or as distributed clays, which can line pore walls or fill pore throats. Distributed clays are of most concern here, since these have quite large surface areas (15 to 40 m²/g clay), and therefore can exhibit considerable reactivity.⁹⁸ Chemically, clays can take on a variety of formulas that differ substantially in their reactivity even though the differences in their molecular formulas are apparently minor.

The ability of a clay mineral to exchange divalent cations with an aqueous solution can drastically change the ionic environment of a solution with which it is in contact. Clays have excess negative charges caused by the substitution of +2-valence minerals for +3-valence minerals within the octahedral or tetrahedral crystal lattice.⁹⁹ The cation exchange capacity, Z_V , is a measure of this excess negative charge; typical Z_V 's are 1 to 10 meq/100 g clay for kaolinite and 100 to 180 meq/100 g clay for montmorillonite. These free anionic sites are covered with cations from the solution, each of which has a specific degree of selectivity for the particular clay site. In general, H^+ has high clay selectivity, and divalent cations are bound more strongly than are monovalents. This means that the anionic sites can be occupied predominantly by H^+ and/or divalents even when clays are in contact with relatively soft brines. Any subsequent change in the electrolyte environment of the contacting solution can cause the clays to take or give up these cations with a possible detrimental effect on high-pH (and MP) flooding.

H^+ cations can exchange on the clay sites with the injected sodium according to



where "clay" represents a mineral exchange site.¹⁰⁰ The reversible reaction Eq. 24 will clearly cause the H^+ concentration to increase with a resulting pH decline. Fig. 47.29 shows the extent of the OH^- retardation caused by cation exchange in laboratory floods. Note that many of the lower pH's may require more than 3 PV of fluid injection to attain the injected pH.

Unlike MP flooding, high-pH chemicals can react directly with clay minerals and the silica substrate to cause consumption of OH^- ions. The reactions with clays are manifest by the elution of soluble aluminum and silica species from core displacements.¹⁰¹ The resulting soluble species subsequently can cause precipitates through hydroxyl reactions as in Eq. 24.¹⁰² The rate of hydroxyl consumption from this slow reaction (cation exchange is generally fast enough so that local equilibrium applies)

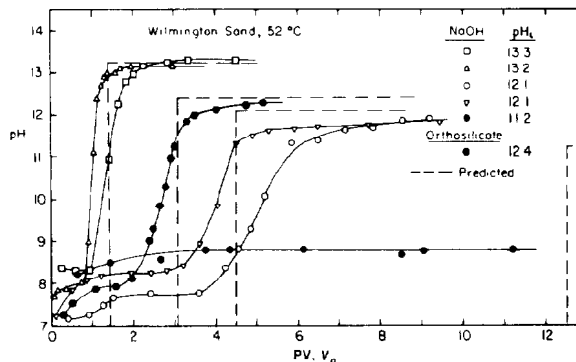


Fig. 47.29—Effluent histories pH from laboratory corefloods. Experimental curves are solid lines with points, theoretical results are dashed lines.

is determined by a dimensionless Damköhler number, N_{Da} ,

$$N_{Da} = \phi k L / u_w, \quad (25)$$

where k is the reaction rate constant, time⁻¹, and L is the medium length for a first-order reaction. N_{Da} is the ratio of the reaction rate to the bulk fluid rate. If all conditions are equivalent between a laboratory experiment and a prototype field flood, N_{Da} clearly will be much larger in the field than in the laboratory owing to the much larger length scale. A larger N_{Da} implies more reaction relative to the residence time within the system. Thus, it follows that the penetration distance—the distance traveled by full-strength OH^- ions—will be considerably smaller in the field than in the laboratory. Bunge and Radke, who illustrate this with several numerical calculations, caution against extrapolating laboratory-measured values of OH^- consumption to field cases unless the discrepancies in N_{Da} have been taken into account.¹⁰¹

Field Results

High-pH field tests of particular interest include a wettability reversal test,⁹⁴ an emulsion flood,⁹⁶ and a polymer-driven flood.¹⁰³ Fig. 47.30 shows the production data from a high-pH flood conducted in the Whittier field.¹⁰⁴ The crude oil was 20°API with a 40-cp viscosity, and the 0.2 wt% NaOH chemical was injected as a 0.23-PV slug.

There are many features in these data that are common to the responses of the other chemical flooding processes in Figs. 47.6 and 47.22. The oil production rate declines as the total fluid production increases, indicating a declining oil cut. The oil rate response to the caustic injection is again superimposed on the waterflood decline, which is extrapolated to estimate the IOR. (There are two waterflood decline curves in Fig. 47.28, one based on the actual decline and one based on computer simulation.) The 350,000 to 470,000 STB of oil produced by the caustic injection was considered a success by the operators.

Table 47.3 shows a summary of data from completed high-pH field floods. Note the wide range in reservoir and oil characteristics and in oil saturation at the start of the flood.¹⁰⁵ IOR, expressed as a fraction of PV, ranges from 0.0006 to 8.0, which translates into recoveries, expressed as a fraction of the OIP at the project start, that

TABLE 47.3—SUMMARY OF HIGH-pH FIELD TESTS

Field, Location, Operator	μ_o at Residual Reservoir Temperature (cp)	Residual Reservoir Temperature (°F)	Oil Saturation at Project Start (%)	Porosity (%)	Net Thickness (ft)	Injection Water Salinity (ppm TDS)	Depth (ft)
Bradford, PA (Several tests by several operators)	—	—	60	16 to 20	30	—	—
Southeast Texas (Exxon)	75	112	40	33 to 35	—	saline	1,250
Harrisburg, NE (Amoco)	1.5	200	watered out	15	10	300	5,900
Northward-Estes, TX (Gulf)	2.28	115	64	206	36	850	3,140
Singleton, NE (Sinclair)	15	—	40 (estimated) watered out	16	—	—	—
Whittier, CA (Chevron)	40	120	51	30	137	fresh hardness (1)	1,500
Brea-Olinda, CA (Union)	90	135	Watered out	—	—	—	—
Orcutt Hill, CA (Union)	17 to 60	140	50	22.5	155	15,000	2,200

are comparable with but slightly smaller than those reported from polymer floods (Table 47.1). Of equal importance is the STB of IOR produced per pound of chemical injected (0.015 to 0.43 in Table 47.3). This is substantially lower than the polymer flood values; however, the cost of the high-pH chemical is also substantially lower.

Summary

Fig. 47.31 presents screening guides for the three major chemical flooding processes presented in this chapter based on the work of Taber and Martin.¹⁰⁶ Though there are many other possible guidelines, the figure focuses on three common reservoir parameters: oil viscosity at reservoir conditions, permeability, and depth. The guides are intended as rules of thumb for candidate reservoir selection and are not substitutes for detailed reservoir evaluation.

Chemical flooding application usually is limited to moderate to low oil viscosities because of economics. As the oil viscosity increases, more of the respective chemical is required to attain good mobility control. This causes a direct penalty in chemical cost and an indirect penalty in increased project life. Similar considerations place a

lower limit on the reservoir permeability, although in the case of polymers used in polymer or MP flooding there is a technical limit imposed by the inability to propagate large molecules through very small pore spaces. Deep reservoirs usually imply the ability to apply larger surface pressures with accompanying increase in injection rates. This beneficial effect is offset by the susceptibility of polymers to chemical degradation at elevated temperatures. High-pH processes are also more reactive at high temperature, which causes excessive consumption.

The information in Fig. 47.31 suggest the avenues of future development for chemical flooding EOR processes: (1) the development of more cost-effective chemicals such as surfactants and polymers that are more salinity resistant, have minimal retention, can be manufactured onsite, or can be recycled, (2) development of more efficient design procedures such as applying MP technology to high-pH flooding design, (3) removing technical limitations on the use of water-soluble polymers, particularly as they relate to temperature sensitivity, and (4) more reliable prediction techniques, particularly as they relate to risk estimates. Each general area will continue to prompt considerable research so that the economic viability of chemical flooding will become commonplace.

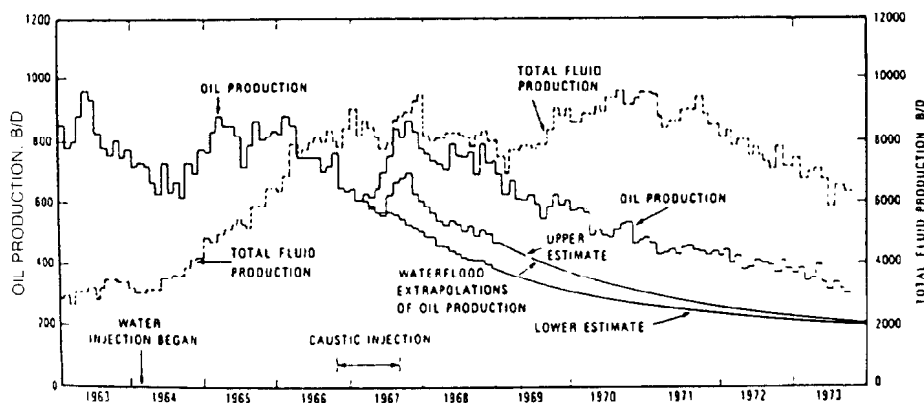


Fig. 47.30—Production response from the Whittier field high-pH flood.

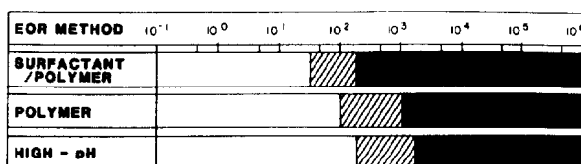
TABLE 47.3—SUMMARY OF HIGH-pH FIELD TESTS (continued)

Type of Chemical Material	Acid number (mg KOH/g)	Chemical Concentration Injection (wt%)	Slug Size (% V_p)	lbm chemical (bbl/bbl V_p)	Recovery, Fraction PV	bbl Incremental Oil per lbm Chemical
Na_2CO_3	—	—	—	—	—	—
Na_2CO_3	2.4	3.2	—	—	—	—
NaOH	low	2.0	0.013	0.093	0.003	0.03
NaOH	0.22	5.0	15	2.55	8.0	0.03
NaOH	low	2.0	8	0.55	0.023	0.042
NaOH	—	0.2	20	0.16	0.05 to 0.07	0.32 to 0.43
ortho-silicate	—	0.12	—	—	—	—
ortho-silicate	0.6	0.42	0.017	0.028	0.0006	0.015 to 0.030

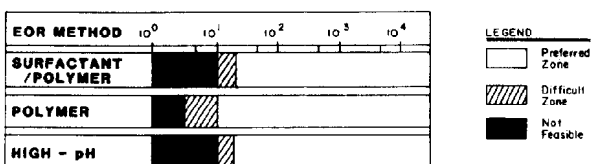
Nomenclature

- A = pattern area
 C_{el} = low effective salinity limit
 C_{eu} = high effective salinity limit
 C_s = concentration of surfactant, mass surfactant/mass solution
 \hat{C}_s = retained surfactant concentration, mass surfactant/mass rock (includes all of the previously mentioned forms of surfactants)
 $\dot{\epsilon}_e$ = effective shear rate
 $\dot{\epsilon}_{1/2}$ = shear rate when polymer solution viscosity is 1/2 of high and low values, Eq. 3
 E_{MB} = mobility buffer efficiency
 E_{MBe} = mobility buffer efficiency extrapolated
 f_{ob} = oil bank oil fractional flow, fraction
 f_{oi} = initial oil fractional flow, fraction
 f_{opk} = peak oil cut
 F_D = frontal advance lag, dimensionless
 F_{mo} = solubilization ratios between the microemulsion/oleic phases
 F_{mw} = solubilization ratios between the microemulsion/aqueous phases
 F_{rk} = permeability reduction factor
 F_R = resistance factor
 F_{Rr} = residual resistance factor
 k_p = permeability to polymer solution
 k_w = permeability to polymer-rich (water) phase
 K = power-law coefficient
 K_{DP} = Dykstra-Parsons coefficient
 K_w = dissociation coefficient of water
 M_e = effective mobility ratio
 M^* = shock mobility ratio
 M° = endpoint mobility ratio

OIL VISCOSITY - CENTIPOISE AT RESERVOIR CONDITION



PERMEABILITY, md



DEPTH, FEET

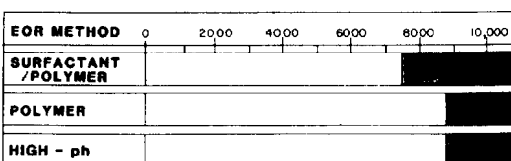


Fig. 47.31—Comparative evaluation of reservoir parameters for chemical flooding.

- n = power-law exponent
 N_c = capillary number, dimensionless
 P_L = left plait-point designation
 P_R = right plait-point designation
 S_{ob} = oil bank saturation, fraction
 S_{oi} = initial oil saturation, fraction
 S'_{or} = ROS to an MP flood
 S'_{orw} = ROS to a waterflood
 S_w = saturation of polymer-rich (water) phase
 t_{Dob} = oil bank arrival time, dimensionless
 t'_{Dob} = corrected oil bank arrival time, dimensionless
 t_{Ds} = surfactant arrival time, dimensionless
 t'_{Ds} = corrected surfactant arrival time, dimensionless
 t'_{Dsw} = dimensionless time at complete sweepout
 u_w = superficial flux of polymer-rich (water) phase, L/t
 v_w = superficial velocity of water phase
 V_{MB} = mobility buffer volume, fraction
 V_{ps} = MP slug size
 Z_V = cation exchange capacity
 λ_d = mobility of displaced fluid(s)
 λ_D = mobility of displacing agent(s)
 λ_p = mobility of polymer solution
 λ_w = mobility of water-rich phase
 λ_{wa} = mobility of water-rich phase after polymer injection
 λ_{wb} = mobility of water-rich phase before polymer injection
 μ_p = apparent viscosity of polymer solution
 μ_p^o = polymer solution viscosity below some low shear rate
 μ_p^∞ = polymer solution viscosity above the critical shear rate
 μ_w = viscosity of the displacing water
 ρ_r = density of rock, mass/volume rock
 ρ_s = density of surfactant slug, mass/volume solution
 σ_{mo} = IFT between the microemulsion phase and oil
 σ_{mw} = IFT between the microemulsion phase and water
 σ_{wo} = IFT between the water and oil phases

Acknowledgments

Several useful discussions with R.S. Schechter and G.A. Pope are gratefully acknowledged.

References

- Craig, F.F. Jr.: "The Reservoir Engineering Aspects of Waterflooding," Monograph Series, SPE, Richardson, TX (1971) 3, 48-75.
- Hagoort, J.: "Displacement Stability of Water Drives in Water-Wet Connate-Water-Bearing Reservoirs," *Soc. Pet. Eng. J.* (Feb. 1974) 63-67; *Trans.*, AIME, 257.
- Morel-Seytoux, H.J.: "Analytical-Numerical Method in Waterflooding Prediction," *Soc. Pet. Eng. J.* (Sept. 1965) 247-58; *Trans.*, AIME, 234.
- Dyes, A.B., Caudle, B.H., and Erickson, R.A.: "Oil Production after Breakthrough as Influenced by Mobility Ratio," *J. Pet. Tech.* (April 1954) 27-32; *Trans.*, AIME, 201.
- Claridge, E.L.: "Prediction of Recovery in Unstable Miscible Flooding," *Soc. Pet. Eng. J.* (April 1972) 143-55.
- Reznik, A.A., Enick, R.M., and Panvelker, S.B.: "An Analytical Extension of the Dykstra-Parsons Vertical Stratification Discrete Solution to a Continuous, Real-Time Basis," *Soc. Pet. Eng. J.* (Dec. 1984) 643-56.
- Dykstra, H. and Parsons, R.L.: "The Prediction of Oil Recovery by Waterflood: Secondary Recovery of Oil in the United States," *Bull.*, API, Dallas (1950).
- Johnson, C.E. Jr.: "Prediction of Oil Recovery by Water Flood—A Simplified Graphical Treatment of the Dykstra-Parsons Method," *J. Pet. Tech.* (Nov. 1956) 55-56; *Trans.*, AIME, 207.
- Zapata, V.J.: "The Effects of Viscous Crossflow on Sharp Front Displacements in Two-Layered Porous Media," MS thesis, U. of Texas, Austin (1979).
- Hearn, C.L.: "Simulation of Stratified Waterflooding by Pseudo Relative Permeability Curves," *J. Pet. Tech.* (July 1971) 805-13.
- Dietz, D.N.: *A Theoretical Approach to the Problem of Encroaching on By-Passing Edge Water*, Proc., Akad. van Wetenschappen, Amsterdam (1953) 83-91.
- Buckley, S.E. and Leverett, M.S.: "Mechanism of Fluid Displacement in Sands," *Trans.*, AIME (1942) 146, 107-16.
- Needham, R.B., Threlkeld, C.B., and Gall, J.W.: "Control of Water Mobility Using Polymers and Multivalent Cations," paper SPE 4747 presented at the 1974 SPE Improved Oil Recovery Symposium, Tulsa, OK, April 22-24.
- Gash, B.H., Griffith, T.D., and Chan, A.F.: "Phase Behavior Effects on the Oil Displacement Mechanisms of Broad Equivalent Weight Surfactant Systems," paper SPE 9812 presented at the 1981 SPE Enhanced Oil Recovery Symposium, Tulsa, OK, April 5-8.
- Willhite, G.P. and Domínguez, J.G.: "Mechanisms of Polymer Retention in Porous Media," *Improved Oil Recovery by Surfactant and Polymer Flooding*, D.O. Shah and R.S. Schechter (eds.), Academic Press Inc., New York City (1977) 511-55.
- Wellington, S.L.: "Biopolymer Solution Viscosity Stabilization—Polymer Degradation and Antioxidant Use," *Soc. Pet. Eng. J.* (Dec. 1983) 901-12.
- Manning, R.K., Pope, G.A., and Lake, L.W.: "A Technical Survey of Polymer Flooding Projects," Contract No. DOE/BETC/10327-19, U.S. DOE (Sept. 1983).
- Tsaur, K.: "A Study of Polymer/Surfactant Interactions for Micellar/Polymer Flooding Applications," MS thesis, U. of Texas, Austin (1978).
- Martin, F.D., Donaruma, L.G., and Hatch, M.J.: "Development of Improved Mobility Control Agents for Surfactant/Polymer Flooding," second annual report, Contract No. DOE/BC/00047-13, U.S. DOE (Oct. 1980).
- Tinker, G.E., Bowman, R.W., and Pope, G.A.: "Determination of In-Situ Mobility and Wellbore Impairment From Polymer Injectivity Data," *J. Pet. Tech.* (May 1976) 586-96.
- Savins, J.G.: "Non-Newtonian Flow Through Porous Materials," *Ind. and Eng. Chem.* (1969) 61, No. 10, 18-47.
- Meter, D.M., and Bird, R.B.: "Tube Flow of Non-Newtonian Polymer Solutions, Parts 1 and 2—Laminar Flow and Rheological Models," *AIChE J.* (Nov. 1964) 878-81 and 1143-50.
- Duda, J.L., Klaus, E.E., and Fan, S.K.: "Influence of Polymer Molecule-Wall Interactions on Mobility Control," *Soc. Pet. Eng. J.* (Oct. 1981) 613-22.
- Jennings, R.R., Rogers, J.H., and West, T.J.: "Factors Influencing Mobility Control By Polymer Solutions," *J. Pet. Tech.* (March 1971) 391-401; *Trans.*, AIME, 251.
- Hirasaki, G.J. and Pope, G.A.: "Analysis of Factors Influencing Mobility and Adsorption in the Flow of Polymer Solution Through Porous Media," *Soc. Pet. Eng. J.* (Aug. 1974) 337-46.
- Shupe, R.D.: "Chemical Stability of Polyacrylamide Polymers," *J. Pet. Tech.* (Aug. 1981) 1513-29.
- Maerker, J.M.: "Mechanical Degradations of Partially Hydrolyzed Polyacrylamide Solutions in Unconsolidated Porous Media," *Soc. Pet. Eng. J.* (Aug. 1976) 172-74.
- Seright, R.S.: "The Effects of Mechanical Degradation and Viscoelastic Behavior on Injectivity of Polyacrylamide Solutions," *Soc. Pet. Eng. J.* (June 1983) 475-85.
- Clampitt, R.L. and Reid, T.B.: "An Economic Polymerflood in the North Burbank Unit, Osage County, Oklahoma," paper SPE 5552 presented at the 1975 SPE Annual Technical Conference and Exhibition, Dallas, Sept. 28-Oct. 1.

30. Akstinat, M.H.: "Surfactants for WOR Process in High-salinity Systems: Product selection and evaluation," *Enhanced Oil Recovery*, Elsevier Scientific Publishing Co., New York City (1981).
31. Graciaa, A., et al.: "Criteria for Structuring Surfactants to Maximize Solubilization of Oil and Water: Part 1—Commercial Non-Ionics," *Soc. Pet. Eng. J.* (Oct. 1982) 743-49.
32. Barakat, Y., et al.: "Criteria for Structuring Surfactants to Maximize Solubilization of Oil and Water," *J. Colloid Interface Sci.* (1983) **92**, No. 2, 561-74.
33. Overbeek, J. Th. G.: "Colloids and Surface Chemistry, A Self-Study Subject Guide, Part 2, Lyophobic Colloids," *Bull.*, Center for Advanced Engineering Study and Dept. of Chemical Engineering, Massachusetts Inst. of Technology, Cambridge, MA (1972).
34. Patton, J.T., et al.: "Enhanced Oil Recovery by CO₂ Foam Flooding," final report, Contract No. DOE/MC/03259-15, U.S. DOE (April 1982).
35. Khan, S.A.: "The Flow of Foam Through Porous Media," MS thesis, Stanford U., Stanford, CA (1965).
36. Fried, A.N.: "The Foam-Drive Process for Increasing the Recovery of Oil," Report of Investigations 5866, U.S. Dept. of the Interior (1960).
37. Bernard, G.G. and Holm, L.W.: "Effect of Foam on Permeability of Porous Media to Gas," *Soc. Pet. Eng. J.* (Sept. 1964) 267-72; *Trans.*, AIME, **231**.
38. Bernard, G. G., Holm, L.W., and Jacobs, W.L.: "Effect of Foam on Trapped Gas Saturation and on Permeability of Porous Media to Water," *Soc. Pet. Eng. J.* (Dec. 1965) 295-300; *Trans.*, AIME, **234**.
39. Holbrook, S.T., Patton, J.T., and Hsu, W.: "Rheology of Mobility-Control Foams," *Soc. Pet. Eng. J.* (June 1983) 456-60.
40. Hirasaki, G.J. and Lawson, J.B.: "Mechanisms of Foam Flow in Porous Media: Apparent Viscosity in Smooth Capillaries," *Soc. Pet. Eng. J.* (April 1985) 176-90.
41. Holm, L.W.: "Foam Injection Test in the Siggins Field, Illinois," *J. Pet. Tech.* (Dec. 1970) 1499-1508.
42. Larson, R.G., Scriven, L.E., and Davis, H.T.: "Percolation Theory of Residual Phases in Porous Media," *Nature* (1977) **268**, 409-13.
43. Stegemeier, G.L.: "Mechanisms of Entrapment and Mobilization of Oil in Porous Media, *Improved Oil Recovery by Surfactant and Polymer Flooding*," D.O. Shah and R.S. Schechter (eds.), Academic Press, New York City (1977) 55-93.
44. Mohanty, K.K. and Salter, S.J.: "Multiphase Flow in Porous Media: Part 3—Oil Mobilization, Transverse Dispersion, and Wettability," paper SPE 12127 presented at the 1983 SPE Annual Technical Conference and Exhibition, San Francisco, Oct. 5-8.
45. Larson, R.G.: "From Molecules to Reservoirs: Problems in Enhanced Oil Recovery," PhD dissertation, U. of Minnesota, Minneapolis (1980).
46. Camilleri, D.: "Micellar/Polymer Flooding Experiments and Comparison with an Improved 1-D Simulator," MS thesis, U. of Texas, Austin (1983).
47. Holm, L.W.: "Design, Performance and Evaluation of the Uniflood Micellar-Polymer Process—Bell Creek Field," paper SPE 11196 presented at the 1982 SPE Annual Technical Conference and Exhibition, New Orleans, Sept. 26-29.
48. Gogarty, W.B., Meabon, H.P., and Milton, H.W. Jr.: "Mobility Control Design for Miscible-Type Waterfloods Using Micellar Solutions," *J. Pet. Tech.* (Feb. 1970) 141-47.
49. Winsor, P.A.: *Solvent Properties of Amphiphilic Compounds*, Butterworths, London (1954).
50. Healy, R.N., Reed, R.L., and Stenmark, D.G.: "Multiphase Microemulsion Systems," *Soc. Pet. Eng. J.* (June 1976) 147-60.
51. Nelson, R.C., and Pope, G.A.: "Phase Relationships in Chemical Flooding," *Soc. Pet. Eng. J.* (Oct. 1978) 325-38.
52. Anderson, D.F., et al.: "Interfacial Tension and Phase Behavior in Surfactant-Brine-Oil Systems," paper SPE 5811, presented at the 1976 SPE Symposium on Improved Oil Recovery, Tulsa, March 22-24.
53. Bennett, K.E., et al.: "Microemulsion Phase Behavior—Observations, Thermodynamic Essentials, Mathematical Simulation," *Soc. Pet. Eng. J.* (Dec. 1981) 747-62.
54. Scriven, L.E.: "Equilibrium Bi-Continuous Structures," *Micellization, Solubilization, and Microemulsions*, K.L. Mittal (ed.), Plenum Press, New York City (1976).
55. Puerto, M.C. and Reed, R.L.: "Three-Parameter Representation of Surfactant/Oil/Brine Interaction," *Soc. Pet. Eng. J.* (Aug. 1983) 669-82.
56. Cayias, J.L., et al.: "Modelling Crude Oils for Low Interfacial Tension," *Soc. Pet. Eng. J.* (Dec. 1976) 351-57.
57. Nelson, R.C.: "The Effect of Live Crude on Phase Behavior and Oil-Recovery Efficiency of Surfactant Flooding Systems," *Soc. Pet. Eng. J.* (June 1983) 501-10.
58. Salter, S.J.: "The Influence of Type and Amount of Alcohol on Surfactant-Oil-Brine Phase Behavior and Properties," paper SPE 6843 presented at the 1977 SPE Annual Technical Conference and Exhibition, Denver, Oct. 9-12.
59. Healy, R.N. and Reed, R.L.: "Physicochemical Aspects of Microemulsion Flooding," *Soc. Pet. Eng. J.* (Oct. 1974) 491-501; *Trans.*, AIME, **257**.
60. Salter, S.J.: "Optimizing Surfactant Molecular Weight Distribution: I. Sulfonate Phase Behavior and Physical Properties," paper SPE 12036 presented at the 1983 SPE Annual Technical Conference and Exhibition, San Francisco, Oct. 5-8.
61. Trushenski, S.P.: "Micellar Flooding: Sulfonate-Polymer Interaction," *Improved Oil Recovery by Surfactant and Polymer Flooding*, D.O. Shah and R.S. Schechter (eds.), Academic Press, New York City (1977) 555-75.
62. Salter, S.J.: "Selection of Pseudo-Components in Surfactant-Oil-Brine-Alcohol Systems," paper SPE 7056 presented at the 1978 SPE Improved Oil Recovery Symposium, Tulsa, OK, April 16-19.
63. Hirasaki, G.J.: "Interpretation of the Change in Optimal Salinity with Overall Surfactant Concentration," *Soc. Pet. Eng. J.* (Dec. 1982) 971-82.
64. Glover, C.J., et al.: "Surfactant Phase Behavior and Retention in Porous Media," *Soc. Pet. Eng. J.* (June 1979) 183-93.
65. Bourrel, M., et al.: "Properties of Amphiphile/Oil/Water Systems at an Optimum Formulation for Phase Behavior," paper SPE 7450 presented at the 1978 SPE Annual Technical Conference and Exhibition, Houston, Oct. 1-4.
66. Nelson, R.C.: "The Salinity Requirement Diagram—A Useful Tool in Chemical Flooding Research and Development," *Soc. Pet. Eng. J.* (April 1982) 259-70.
67. Hirasaki, G.J., van Domselaar, H.R., and Nelson, R.C.: "Evaluation of the Salinity Gradient Concept in Surfactant Flooding," *Soc. Pet. Eng. J.* (June 1983) 486-500.
68. Cayias, J.L., Schechter, R.S., and Wade, W.H.: "The Measurement of Low Interfacial Tension via the Spinning Drop Technique," *Adsorption at Interfaces*, L.K. Mittal (ed.), Symposium Series, ACS (1975) No. 8, 1231-39.
69. Huh, C.: "Interfacial Tensions and Solubilizing Ability of a Microemulsion Phase that Coexists with Oil and Brine," *J. Colloid Interface Sci.* (1979) **71**, No. 2, 408-26.
70. Glinsmann, G.R.: "Surfactant Flooding with Microemulsions Formed In-situ—Effect of Oil Characteristics," paper SPE 8326 presented at the 1979 SPE Annual Technical Conference and Exhibition, Las Vegas, Sept. 23-26.
71. Reed, R.L. and Healy, R.N.: "Some Physico-Chemical Aspects of Microemulsion Flooding: A Review," *Improved Oil Recovery by Surfactant and Polymer Flooding*, D.O. Shah and R.S. Schechter (eds.), Academic Press, New York City (1977) 383-438.
72. Reed, R.L. and Healy, R.N.: "Contact Angles for Equilibrated Microemulsion Systems," *Soc. Pet. Eng. J.* (June 1984) 342-50.
73. Bragg, J.R., et al.: "Loudon Surfactant Flood Pilot Test," paper SPE 10862 presented at the 1982 SPE Enhanced Oil Recovery Symposium, Tulsa, April 4-7.
74. Lake, L.W. and Helfferich, F.: "Cation Exchange in Chemical Flooding Part 2—The Effect of Dispersion, Cation Exchange, and Polymer/Surfactant Adsorption in Chemical Flood Environment," *Soc. Pet. Eng. J.* (Dec. 1978) 435-44.
75. Pope, G.A., Lake, L.W., and Helfferich, F.G.: "Cation Exchange in Chemical Flooding, Part 1—Basic Theory Without Dispersion," *Soc. Pet. Eng. J.* (Dec. 1978) 418-34.
76. Paul, G.W. and Froning, H.R.: "Salinity Effects of Micellar Flooding," *J. Pet. Tech.* (Aug. 1973) 957-58.
77. Harwell, J.H.: "Surfactant Adsorption and Chromatographic Movement with Application in Enhanced Oil Recovery," PhD dissertation, U. of Texas, Austin (1983).

78. Somasundaran, M.C., Goyal, A., and Manev, E.: "The Role of the Surfactant Precipitation and Redissolution in the Adsorption of Sulfonate on Minerals," paper SPE 8263 presented at the 1979 SPE Annual Technical Conference and Exhibition, Las Vegas, Sept. 23-26.
79. Hill, H.J. and Lake, L.W.: "Cation Exchange in Chemical Flooding: Part 3—Experimental," *Soc. Pet. Eng. J.* (Dec. 1978) 445-56.
80. Paul, G.W. *et al.*: "A Simplified Predictive Model for Micellar/Polymer Flooding," paper SPE 10733 presented at the 1982 SPE California Regional Meeting, San Francisco, March 24-26.
81. Lake, L.W., Stock, L.G., and Lawson, J.B.: "Screening Estimation of Recovery Efficiency and Chemical Requirements for Chemical Flooding," paper SPE 7069 presented at the 1978 SPE Improved Oil Recovery Symposium, Tulsa, OK, April 16-19.
82. Aho, G.E. and Bush, J.: "Results of the Bell Creek Unit 'A' Micellar Polymer Pilot," paper SPE 11195 presented at the 1982 SPE Annual Technical Conference and Exhibition, New Orleans, Sept. 26-29.
83. Lake, L.W. and Pope, G.A.: "Status of Micellar-Polymer Field Tests," *Pet. Eng. Intl.* (Nov. 1979) 51, 38-60.
84. Gilliland, H.E. and Conley, F.R.: "Surfactant Waterflooding," paper presented at the 1975 Symposium on Hydrocarbon Exploration, Drilling, and Production, Paris, France, Dec. 10-12.
85. Pope, G.A.: "The Application of Fractional Flow Theory to Enhanced Oil Recovery," *Soc. Pet. Eng. J.* (June 1980) 191-205.
86. Ramakrishnan, T.S. and Wassan, D.T.: "A Model for Interfacial Activity of Acidic Crude Oil/Caustic Systems for Alkaline Flooding," *Soc. Pet. Eng. J.* (Aug. 1983) 602-12.
87. Jennings, H.Y. Jr., Johnson, C.E. Jr., and McAuliffe, C.D.: "A Caustic Waterflooding Process for Heavy Oils," *J. Pet. Tech.* (Dec. 1974) 1344-52.
88. Minssieux, L.: "Waterflood Improvement by Means of Alkaline Water," *Enhanced Oil Recovery by Displacement with Saline Solutions*, Gulf Publishing Co., Houston (1979) 75-90.
89. DeZabala, E.F. *et al.*: "A Chemical Theory for Linear Alkaline Flooding," *Soc. Pet. Eng. J.* (April 1982) 245-58.
90. Nelson, R.C. *et al.*: "Cosurfactant-Enhanced Alkaline Flooding," paper SPE 12672 presented at the 1984 SPE Enhanced Oil Recovery Symposium, Tulsa, April 15-18.
91. Owens, W.W. and Archer, D.L.: "The Effect of Rock Wettability on Oil-Water Relative Permeability Relationships," *J. Pet. Tech.* (July 1971) 873-78; *Trans.*, AIME, 251.
92. Wagner, O.R. and Leach, R.O.: "Improving Oil Displacement by Wettability Adjustment," *J. Pet. Tech.* (April 1959) 65-72; *Trans.*, AIME, 216.
93. Ehrlich, R., Hasiba, H.H., and Raimondi, P.: "Alkaline Waterflooding for Wettability Alteration—Evaluating a Potential Field Application," *J. Pet. Tech.* (Dec. 1974) 1335-43.
94. Cooke, C.E. Jr., Williams, R.E., and Kolodzie, P.A.: "Oil Recovery by Alkaline Waterflooding," *J. Pet. Tech.* (Dec. 1974) 1344-52.
95. Lorenz, P.B., Donaldson, E.C., and Thomas, R.D.: "Use of Centrifugal Measurements of Wettability to Predict Oil Recovery," *Bull. RI 7873*, U.S. Dept. of Interior (1974).
96. McAuliffe, C.D.: "Oil-in-Water Emulsions and Their Flow Properties in Porous Media," *J. Pet. Tech.* (June 1973) 727-33.
97. McAuliffe, C.D.: "Crude-Oil-in-Water Emulsions To Improve Fluid Flow in an Oil Reservoir," *J. Pet. Tech.* (June 1973) 721-26.
98. Grim, R.E.: *Clay Mineralogy*, McGraw-Hill Book Co. Inc., New York City (1968).
99. Brownlow, A.H.: *Geochemistry*, Prentice-Hall, Inc., Englewood Cliffs, NJ (1979).
100. Somerton, W.H. and Radke, C.J.: "Role of Clays in the Enhanced Recovery of Petroleum from Some California Sands," *J. Pet. Tech.* (March 1983) 643-54.
101. Bunge, A.L. and Radke, C.J.: "Migration of Alkaline Pulses in Reservoir Sands," *Soc. Pet. Eng. J.* (Dec. 1982) 998-1012.
102. Sydansk, R.D.: "Elevated-Temperature Caustic/Sandstone Interaction: Implications for Improving Oil Recovery," *Soc. Pet. Eng. J.* (Aug. 1982) 453-62.
103. Sloat, B. and Zlomke, D.: "The Isenhour Unit—A Unique Polymer-Augment Alkaline Flood," paper SPE 10719 presented at the 1982 SPE Enhanced Oil Recovery Symposium, Tulsa, OK, April 4-7.
104. Graue, D.J. and Johnson, C.E. Jr.: "Field Trial of Caustic Flooding Process," *J. Pet. Tech.* (Dec. 1974) 1353-58.
105. Mayer, E.H., *et al.*: "Alkaline Injection for Enhanced Oil Recovery—A Status Report," *J. Pet. Tech.* (Jan. 1983) 209-21.
106. Taber, J.J. and Martin, F.D.: "Technical Screening Guides for Enhanced Oil Recovery" paper SPE 12069 presented at the 1983 SPE Annual Technical Conference and Exhibition, San Francisco, Oct. 5-8.

Chapter 48

Reservoir Simulation

K.H. Coats, Scientific Software-Intercom

Introduction

Webster's dictionary defines *simulate* as *to assume the appearance of without the reality*. Simulation of petroleum reservoir performance refers to the construction and operation of a model whose behavior assumes the appearance of actual reservoir behavior. The model itself is either physical (for example, a laboratory sandpack) or mathematical. A mathematical model is simply a set of equations that, subject to certain assumptions, describes the physical processes active in the reservoir. Although the model itself obviously lacks the reality of the oil or gas field, the behavior of a valid model simulates (assumes the appearance of) that of the field.

The purpose of simulation is estimation of field performance (e.g., oil recovery) under one or more producing schemes. Whereas the field can be produced only once, at considerable expense, a model can be produced or run many times at low expense over a short period of time. Observation of model performance under different producing conditions aids selection of an optimal set of producing conditions for the reservoir.

The tools of reservoir simulation range from the intuition and judgment of the engineer to complex mathematical models requiring use of digital computers. The question is not whether to simulate but, rather, which tool or method to use. This chapter attempts to summarize the evolution and current status of reservoir simulation practice involving usage of the mathematical, computerized models. The relatively modern nature of this practice is indicated by the first edition of this handbook (1962) not including a chapter on reservoir simulation.

The nearly exponential growth in annual rate of simulation-related publications from the mid-1960's to the present indicates the industry's widespread acceptance of mathematical simulation as an engineering tool. This acceptance has been and remains qualified by questioning and improvement of accuracy in simulation model results. Thus a significant portion of the extensive literature deals

with model (1) evaluation or validation through comparison of field (laboratory) and model results and (2) improvement by use of new techniques related to model mathematics and representation of reservoir fluid and rock description parameters.

The volume and increasing complexity of publications related to the latter item preclude a detailed mathematical description of current simulation technology in this chapter. Rather, emphasis is given to a general description of reservoir simulation models, how and why they are used, choice of different types of models for different reservoir problems, and reliability of simulation results in the face of model assumptions and uncertainty in reservoir fluid and rock description parameters. The chapter concludes with an abbreviated description of simulation model technology consisting of comments on a number of highly technical publications. Various texts¹⁻⁴ give detailed descriptions of simulation technology through the late 1970's, including finite-difference approximations, model formulations, iterative solution techniques, and stability analyses.

A Brief History

In a broad sense, reservoir simulation has been practiced since the beginning of petroleum engineering in the 1930's. Before 1960, engineering calculations consisted largely of analytical methods,^{5,6} zero-dimensional material balances,^{7,8} and one-dimensional (1D) Buckley-Leverett^{9,10} calculations.

The term *simulation* became common in the early 1960's, as predictive methods evolved into relatively sophisticated computer programs. These programs represented a major advancement because they allowed solution of large sets of finite-difference equations describing two- and three-dimensional (2D and 3D), transient, multiphase flow in heterogeneous porous media. This advancement was made possible by the rapid evolution of

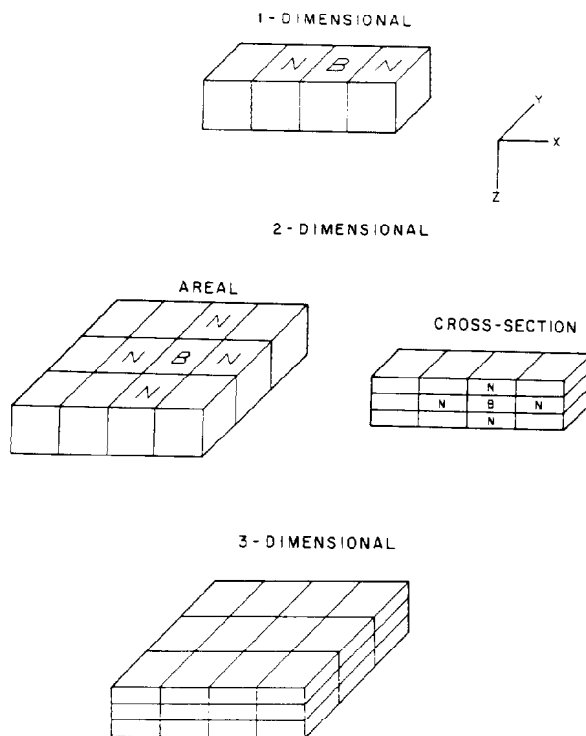


Fig. 48.1—1-, 2-, and 3D grids.

large-scale, high-speed digital computer, and development of numerical mathematical methods for solving large systems of finite-difference equations.

During the 1960's, reservoir simulation efforts were devoted largely to two-phase gas/water and three-phase black-oil reservoir problems. Recovery methods simulated were limited essentially to depletion or pressure maintenance. It was possible to develop a single simulation model capable of addressing most reservoir problems encountered. This concept of a single, general model always has appealed to operating companies because it significantly reduces the cost of training and usage and, potentially, the cost of model development and maintenance.

During the 1970's, the picture changed markedly. The sharp rise in oil prices and governmental trends toward deregulation and partial funding of field projects led to a proliferation of enhanced-recovery processes. This led to simulation of processes that extended beyond conventional depletion and pressure maintenance to miscible flooding, chemical flooding, CO₂ injection, steam or hot-water stimulation/flooding, and in-situ combustion. A relatively comfortable understanding of two-component (gas and oil) hydrocarbon behavior in simple immiscible flow was replaced by a struggle to unravel and characterize the physics of oil displacement under the influence of temperature, chemical agents, and complex multicomponent phase behavior. In addition to simple multiphase flow in porous media, simulators had to reflect chemical absorption and degradation, emulsifying and interfacial tension (IFT) reduction effects, reaction kinetics, and other thermal effects and complex equilibrium phase behavior. This proliferation of recovery methods in the

1970's caused a departure from the single-model concept as individual models were developed to represent each of these new recovery schemes.

Research during the 1970's resulted in many significant advances in simulation model formulations and numerical solution methods. These advances allowed simulation of more complex recovery processes and/or reduced computing costs through increased stability of the formulations and efficiency of the numerical solution methods.

General Description of Simulation Models

A number of papers¹¹⁻¹⁴ present general, largely non-mathematical discussions of reservoir simulation. Odeh¹¹ gives an excellent description of the conceptual simplicity of a simulation model. He illustrates the subdivision of a reservoir into a 2- or 3D network of gridblocks and then shows that the simulation model equations are basically the familiar volumetric material balance equation^{7,8} written for each phase for each gridblock. The phase flow rates between each gridblock and its two, four, or six (in 1D, 2D, or 3D cases, respectively) adjacent blocks are represented by Darcy's law modified by the relative permeability concept. Fig. 48.1 illustrates 1-, 2-, and 3D grids representing a portion of a reservoir. The block and its two or four neighbors are denoted by B and N in the 1D and 2D grids. One can visualize an interior block of the 3D grid with its six neighbors, two on either side of the block in the x, y, and z directions.

The subsea depths to the top surface of each grid in Fig. 48.1 vary with areal position, reflecting reservoir formation dip. Reservoir properties such as permeability and porosity, and fluid properties such as pressure, temperature, and composition, are assumed uniform throughout a given gridblock. However, reservoir and fluid properties vary from one block to another; fluid properties for each gridblock also vary with time during the simulation period.

A simulation model is a set of partial-difference equations requiring numerical solution as opposed to a set of partial differential equations amenable to analytical solution. The reasons for this are (1) reservoir heterogeneity—variable permeability and porosity and irregular geometry, (2) nonlinearity of relative permeability and capillary pressure vs. saturation relationships, and (3) nonlinearity of fluid PVT properties as functions of pressure, composition, and temperature. The models require high-speed digital computers because of the large amount of arithmetic associated with the solutions.

The large amount of arithmetic performed by a simulation model stems from the large number of gridblocks representing the reservoir and from the number and complexity of equations describing the oil-recovery process. Total arithmetic or computing expense for a given model run is at least linearly proportional to the total number of gridblocks, $N_x N_y N_z$, where N_x , N_y , and N_z are the numbers of gridblocks specified in the x, y and z directions, respectively.

The individual gridblocks are customarily identified by subscripts i, j, k , where blocks are numbered $i=1,2,\dots,N_x$ in the x direction, $j=1,2,\dots,N_y$ in the y direction, and $k=1,2,\dots,N_z$ in the z direction. Most simulators use no-flow or closed boundary conditions at the exterior boundaries [$x=(0,L_x)$, $y=(0,L_y)$ and $z=(0,L_z)$] with provision

for aquifer influx along the areally exterior boundary. The nonrectangular, areal ($x-y$) shapes of most reservoirs are represented by zero gridblock porosity and permeability in the appropriate areal portions of the $x-y$ grid.

Preceding statements described the simulation model as a set of equations expressing conservation of mass for each phase for each gridblock. More precisely, the model equations express conservation of mass of each reservoir fluid *component* for each block. The number and identity of these components depend on the nature of the original reservoir fluid and the particular oil-recovery process, as discussed in the following. The total number of mass conservation equations is then $N_x N_y N_z N$, where N is the number of components necessary to describe the reservoir fluids.

Each conservation equation states that the mass rate of flow into a gridblock minus the mass rate of flow out must equal the rate of change or accumulation of mass within the block. These N mass-balance equations (one for each component) apply to each gridblock. The block is an open system, in the thermodynamic sense, because of fluid flow between the block and its six neighbors and fluid injection or production if a well is perforated in the block.

The center of gridblock (i, j, k) is located at (x_i, y_j, z_k) . This block has six neighboring blocks $(i \pm 1, j, k)$, $(i, j \pm 1, k)$ and $(i, j, k \pm 1)$. For brevity and clarity, the interblock flow rates are written here in terms of only x -direction flow between blocks $(i-1, j, k)$ and (i, j, k) , the indices j and k are suppressed, and the general symbol C_I denotes concentration (mass/volume) of component I in the various phases. The three immiscible phases (water, oil, and gas) are denoted by subscripts w , o , and g , respectively.

The interblock flow rate of component I , according to Darcy's law modified by relative permeability, is

$$q_I = \frac{kA}{L} \left[\frac{k_{rw}}{\mu_w} C_{Iw} (\Delta p_w - \gamma_w \Delta Z) + \frac{k_{ro}}{\mu_o} C_{Io} (\Delta p_o - \gamma_o \Delta Z) + \frac{k_{rg}}{\mu_g} C_{Ig} (\Delta p_g - \gamma_g \Delta Z) \right], \quad (1)$$

where

- q_I = component I interblock flow rate, mass/time,
- k = absolute permeability,
- $A = \Delta y_i \Delta z_k$ = cross-sectional area normal to flow,
- L = distance between adjacent block centers, $(\Delta x_{i-1} + \Delta x_i)/2$,
- k_{rp} = relative permeability to phase P ($P = w, o, g$),
- μ_P = viscosity of phase P
- C_{IP} = concentration of component I in phase P , mass/volume,
- Δp_P = pressure of phase P
- γ_P = specific weight of phase P
- $\Delta_x = x_{i-1} - x_i$, where x is p or Z , and
- Z = subsea depth, measured positively downward.

If subscript $J=1,2,3$ is used to denote phases w, o, g respectively, then Eq. 1 simplifies to

$$q_I = \left(\sum_{J=1}^3 \frac{kA}{L} \frac{k_{rJ}}{\mu_J} C_{IJ} \right) (\Delta p_J - \gamma_J \Delta Z). \quad (2)$$

The first term in parentheses is the interblock *transmissibility*, T_{IJ} , for flow of component I in phase J , requiring evaluation here at $(i-1/2, j, k)$ —i.e., between blocks $i-1$ and i . The kA/L portion of T is normally calculated as the harmonic or series-resistance mean value using block $i-1$ and block i properties. The remaining portion of T normally is evaluated at the upstream gridblock—i.e., the block from which the phase is flowing. Thus Eq. 2 becomes simply

$$q_I = \sum_{J=1}^3 (T_{IJ})_{i-1/2} (\Delta p_J - \gamma_J \Delta Z), \quad (3)$$

representing interblock flow of component I from gridblock $i-1$ to gridblock i .

The right-hand or accumulation terms of the mass balances are

$$\frac{V}{\Delta t} \left[\phi \sum_{J=1}^3 (S_J C_{IJ}) \right], \quad (4)$$

where

- V = grid block volume, $\Delta x_i \Delta y_j \Delta z_k$
- $\bar{\delta}$ = time difference operator, $\delta X \equiv X_{n+1} - X_n$,
- n = time level, $t_{n+1} = t_n + \Delta t$,
- Δt = timestep,
- ϕ = porosity, fraction, and
- S_J = saturation of phase J , fraction of pore space.

Eqs. 3 and 4 give the final form of the component I mass-balance equation for gridblock (i, j, k) as

$$\sum_{J=1}^3 \Delta [T_{IJ} (\Delta p_J - \gamma_J \Delta Z)] - q_{pI} = \frac{V}{\Delta t} \sum_{J=1}^3 \bar{\delta} (\phi S_J C_{IJ}), \quad (5)$$

where q_{pI} is the mass rate of production of component I from the block resulting from any well perforated in the block and the Laplacian term of type $\Delta(T\Delta p)$ is defined as

$$\Delta(T\Delta p) \equiv \Delta_x (T_x \Delta_x p) + \Delta_y (T_y \Delta_y p) + \Delta_z (T_z \Delta_z p)$$

and

$$\Delta_x (T_x \Delta_x p) \equiv T_{i+1/2, j, k} (p_{i+1, j, k} - p_{i, j, k}) - T_{i-1/2, j, k} (p_{i, j, k} - p_{i-1, j, k}).$$

For the general case where each component is present (soluble) in all three phases, Eq. 5 is N equations in $3N+6$ unknowns. The unknowns are $3N$ C_{IJ} values, 3 phase saturations, and 3 phase pressures. Thus an additional $2N+6$ equations are required for a determinate or solvable model having equal numbers of equations and unknowns. The N Eqs. 5 are referred to as *primary* equations while the additional $2N+6$ equations are denoted *constraint* equations. The constraint equations are manipulated in the model programming to eliminate $2N+6$ variables (unknowns) in terms of the remaining N (primary) unknowns. The result is then the set of N primary Eqs. 5 in N primary unknowns. The constraint equations are relations between unknowns pertaining only to the particular gridblock (i,j,k) to which Eqs. 5 apply. The N primary Eqs. 5, however, involve unknowns (e.g., p_J) at the gridblock (i,j,k) and its six neighboring blocks, owing to the nature of the interblock flow terms on the left-hand side.

The $2N+6$ constraint equations are illustrated here for the case of an isothermal, compositional model where the N components are H_2O and $N-1$ hydrocarbon components (e.g., methane, ethane... C_7). The first three constraints are

$$S_w + S_o + S_g = 1.0, \dots\dots\dots (6)$$

$$p_o - p_w = P_{cwo}(S_w), \dots\dots\dots (7)$$

and

$$p_g - p_o = P_{cgo}(S_g), \dots\dots\dots (8)$$

where P_{cwo} = water/oil capillary pressure and P_{cgo} = gas/oil capillary pressure.

These constraints express the requirement that the phase saturations sum to unity and also eliminate the water and gas phase pressures in terms of the unknown oil pressure phase using capillary pressure curves. For this compositional case, concentration $C_{IJ} = \rho_J x_{IJ}$ where ρ_J is the molar density of phase J (mols/volume) and x_{IJ} is mol fraction of component I in phase J . The next three constraints require that the mol fractions of all components sum to unity in each of the three phases,

$$\sum_{I=1}^N x_{IJ} = 1.0 \dots\dots\dots (9)$$

where $J = w, o, g$ or 1, 2, 3. The remaining $2N$ constraints express equilibrium of each component among the three phases,

$$f_{Iw} = f_{Io} \dots\dots\dots (10a)$$

and

$$f_{Io} = f_{Ig} \dots\dots\dots (10b)$$

where f_{IJ} is the fugacity of component I in phase J . These fugacities can be expressed in terms of mol fractions and pressure by use of an equation of state (EOS). Alternatively, they can be replaced by equilibrium K -value relation-

ships (e.g., $y = Kx$) with K -values given as functions of pressure or of pressure and composition.

The $2N+6$ constraint Eqs. 6 through 10 are manipulated to eliminate one-phase saturation, two-phase pressures and $2N-3$ mole fractions (x_{IJ}) from the N primary Eqs. 5. The final result is a model consisting of the N Eq. 5 in N unknowns consisting of two saturations, one pressure, and $N-3$ mole fractions. Each coefficient or term remaining in the N primary equations is then either one of the N primary unknowns or a function of one or more of the primary unknowns.

Types of Models

Different types of simulation models are used to describe different mechanisms associated with different oil-recovery processes. The most widely used types are black oil, compositional, thermal, and chemical flood. The four basic recovery mechanisms for recovering oil from reservoirs are (1) fluid expansion, (2) displacement, (3) gravity drainage, and (4) capillary imbibition. Simple fluid expansion with pressure decline results in oil expulsion from and subsequent flow through the porous matrix. Oil is displaced by gas and injected or naturally encroaching water. Gravity drainage, caused by positive (water/oil and oil/gas) density differences, aids oil recovery by causing upward drainage of oil from below an advancing bottom-water drive and downward drainage from above a declining gas/oil contact. Finally, imbibition, generally normal to the flow direction, can be an important recovery mechanism in lateral waterfloods in heterogeneous sands with large vertical variation of permeability.

Accommodation of compositional and the enhanced-recovery processes in this discussion requires the addition of a fifth mechanism, oil *mobilization*. This loosely defined term includes widely differing phenomena that create or mobilize recoverable oil. Some of these phenomena are not really distinct from the first four.

The black-oil model accounts for the four basic mechanisms in simulation of oil recovery by natural depletion or pressure maintenance (e.g., waterflooding). This isothermal model applies to reservoirs containing immiscible water, oil, and gas phases with a simple pressure-dependent solubility of the gas component in the oil phase. The two-component representation of the hydrocarbon content¹⁵ presumes constant (pressure-independent) compositions of the oil component and the gas component, no volatility of the oil component in the gas phase, no solubility of the oil and gas components in the water phase, and no volatility of water (H_2O) in the oil and gas phases. The oil component is stock-tank oil and its unit of mass is 1 STB (1 bbl at stock-tank pressure and temperature). The gas component is surface system gas and its unit of mass is 1 standard cubic foot (scf). The water component unit of mass is 1 STB. For water and gas, components and phases are identical while the oil phase is a mixture of the oil component and the gas component.

The number of components (N) and therefore the number of Eqs. 5 per gridblock is three for the black-oil model. Table 48.1 gives the definitions of component concentrations, C_{IJ} , for this model. The water phase, gas phase, and saturated oil phase, reciprocal formation volume factors, b_w (STB/RB), b_g (scf/RB), and b_o (STB/RB), respectively, are given single-valued functions of pressure. For undersaturated oil, b_o is dependent on

pressure and solution gas (R_s , scf/STB). As discussed later original work in formulations¹⁶⁻¹⁸ led to a number of papers¹⁹⁻²⁴ describing black-oil models during the 1960's.

The remaining model types discussed here account for some mobilization mechanisms in addition to the four basic recovery mechanisms. The isothermal compositional model represents reservoir fluids by N components, including water and $N-1$ hydrocarbon components. Generally, but not necessarily, solubilities of water in the oil and gas phases and of hydrocarbon components in the water phase are considered negligible. For water, then, the concentration in Eqs. 5 is as given in Table 48.1. The hydrocarbon component I concentration C_{IJ} is $\rho_J x_{IJ}$, as mentioned earlier, for $J=o, g$ or 2, 3. Gas/oil phase equilibrium and phase densities within each gridblock are calculated using equilibrium K -values from pressure- and composition-dependent correlations or, more recently, from EOS's.²⁵⁻²⁸ Unlike the black-oil model, the compositional model can represent the mobilization of oil by outright (single-contact) or dynamic (multicontact) miscibility, oil swelling and viscosity reduction by solution of an injected nonequilibrium gas (e.g., CO_2), and stripping or vaporization of an oil's lighter ends by injection of a dry gas. With one exception,²⁹ recent papers²⁹⁻³³ describing compositional models are based on equilibrium K -values obtained from EOS's.

A thermal simulation model is a set of N conservation equations, similar to Eq. 5, which expresses conservation of mass of H_2O and $N-2$ hydrocarbon components and conservation of energy. With energy designated as "component" N , the last ($I=N$) of Eqs. 5 becomes the energy balance upon addition of terms representing heat conduction and overburden heat loss. An additional requirement is the use of $\rho_J H_J$ for C_{NJ} in the well and interblock flow terms and $\rho_J U_J$ for C_{NJ} in the right side accumulation term. H_J and U_J are enthalpy and internal energy, respectively, energy/mole. If the in-situ combustion capability is included then the mass conservation equations include source (sink) terms represented by Arrhenius reaction rate expressions for cracking and oxidation of hydrocarbon components and the energy balance includes heat of reaction terms. For the same number of fluid components, a thermal model has one more (energy) conservation equation than the compositional model and one additional unknown, temperature T .

For steam-injection processes, thermal model components are typically H_2O , heavy (nonvolatile) and light (solution gas or distillable) hydrocarbon components and energy. For in-situ combustion studies, typical components are H_2O , heavy-oil component, a lighter (distillable) oil component, solid coke, O_2 , CO_2 , N_2 , and energy. Frequently CO_2 and N_2 are lumped as one component to reduce computing expense. The steam tables and/or an EOS are used to calculate liquid H_2O (water phase) properties and the H_2O gas/water phase K -value as functions of pressure and temperature. In most applications, H_2O is assumed insoluble in the oil phase. In most current models, the distribution of other (non- H_2O) components among all phases is represented by user-provided K -values dependent on only pressure and temperature.

Thermal simulators are applied to steam-injection or in-situ combustion processes in heavy-oil reservoirs where oil is mobilized primarily by (1) reduction of oil viscosi-

TABLE 48.1—DEFINITIONS OF CONCENTRATIONS C_{IJ} FOR THE BLACK-OIL MODEL

I	Component	Phase		
		$J=1$ Water	$J=2$ Oil	$J=3$ Gas
1	water	b_w	0	0
2	oil	0	b_o	0
3	gas	0	$b_o R_s$	b_g

ty with increased temperature, (2) distillation of intermediate hydrocarbon components from the oil phase to the more mobile gas phase, and (3) cracking of the oil phase [usually above 500°F (260°C)] with subsequent distillation. Thermal models developed from 1965 to 1982³⁴⁻⁴⁰ generally exhibit a trend toward inclusion of more dimensions, more components and dual capability of steamflood and in-situ combustion.

Chemical flood models include polymer, micellar (surfactant), and alkaline (caustic). Polymer waterflooding improves oil recovery by lowering the oil/water mobility ratio, by reducing the effective permeability to water, and/or by increasing water viscosity. In micellar flooding, surfactants greatly reduce oil/water IFT, thereby solubilizing oil into the micelles and forming an oil bank.⁴¹ The surfactant slug and mobilized oil normally are propelled toward the production well by a graded bank of polymer-thickened water. The mechanisms responsible for improved oil recovery in alkaline flooding are thought to include low IFT, wettability alteration, and emulsification.⁴² Chemical flooding processes involve complicated fluid/fluid and rock/fluid interactions such as adsorption, ion exchange, viscous shear, and three- (or more) phase flow. Several recent papers⁴³⁻⁴⁵ describe implementation of these complex chemical flood mechanisms in numerical simulators.

The four types of models described above are defined or distinguished by the recovery process and the nature of the original reservoir fluid. Considering the nature of the reservoir formation leads to a fifth, *fractured-matrix* type of simulation model. While in theory any recovery process can be implemented in a fractured-matrix reservoir, most simulation work reported to date is concerned with black oil fractured-matrix models. Three-dimensional models are described by Thomas *et al.*⁴⁶ for the three-phase case and by Gilman and Kazemi⁴⁷ for two-phase water-oil flow. Their models consider a discontinuous array of matrix blocks in a continuous 3D fracture network. Flow throughout the reservoir and to the wells occurs in the fracture system and the matrix blocks are treated as sink/source terms in that system. Their model equations include the set of N conservation Eqs. 6 written for each gridblock in the fracture system. Each *gridblock* may contain a number of similarly behaving *matrix blocks*. However, additional terms are added to Eqs. 6, representing matrix-fracture flow. Also, for each gridblock additional equations are required to express mass conservation of each component in the matrix blocks included in the gridblock. These additional equations can be eliminated or combined with the basic N (fracture system) flow equations^{46,47} so that the final model includes only N equations (per block) possessing interblock flow terms. Blaskovich *et al.*⁴⁸ describe a fractured-matrix model

which allows for reservoir-wide flow through the matrix as well as the fracture system. This extension leads to a model including $2N$ equations (per block) possessing interblock flow terms.

Model Input Data and Calculated Results

A simulation model requires three types of input data. First, reservoir description data include (1) overall geometry, (2) grid size specification, (3) permeability, porosity, and elevation for each gridblock, and (4) relative permeability and capillary pressure vs. saturation functions or tables. Geological and petrophysical work, which involves logs and core analyses, is necessary for Items 1 and 3. Laboratory tests on core samples yield estimates of relative permeability and capillary pressure relationships. Second, fluid PVT properties, such as formation volume factors, solution gas or component equilibrium K -values, and viscosities are obtained by laboratory tests. Finally, well locations, perforated intervals, and productivity indices (PI's) must be specified. Each well must be assigned a production (injection) rate schedule and/or a limiting producing (injecting) pressure for use in calculating well deliverability (injectivity).

Model output or calculated results include spatial distributions of fluid pressure, saturations and compositions, and producing GOR and WOR and injection/production rate (for wells on injectivity/productivity) for each well at the end of each timestep of the computations. Internal manipulation of these results gives average reservoir pressure and instantaneous rates and cumulative injection/production of oil, gas, and water by well and total field vs. time.

Current models offer various levels of visual output display features that ease the engineer's assimilation and interpretation of simulator results. Example features are contour maps of pressure, saturations, compositions and temperature, concise tabular summaries of individual well or well-group performance, and field or well timeplots of quantities such as production rates and WOR's and GOR's.

Purpose of Reservoir Simulation

Reservoir simulation is used to estimate recovery for a given existing producing scheme (forecasting) to evaluate the effects on recovery of altered operating conditions, and to compare economics of different recovery methods. Black-oil models have been widely applied to forecast oil recovery and to estimate the effects on oil recovery of (1) well pattern and spacing, (2) well completion intervals, (3) gas and/or water coning as a function of rate, (4) producing rate, (5) augmenting a natural water drive by water injection and desirability of flank or peripheral as opposed to pattern waterflooding, (6) infill drilling, and (7) gas vs. water vs. water-alternating-gas (WAG) injection.

A few of many reported studies are briefly mentioned here. Henderson *et al.*⁴⁹ applied a single- (gas) phase model to optimize the locations and numbers of wells necessary to meet peak deliverability requirements in a gas storage field. Mann and Johnson⁵⁰ showed good agreement between model-predicted and actual field performance. Thomas and Driscoll⁵¹ applied a black-oil model in estimating locations of bypassed oil for the purpose of designing an infill drilling plan. Two studies^{52,53}

report extensive results related to rate-sensitivity of various Alberta reservoirs subjected to water-oil displacements. Thakur *et al.*⁵⁴ applied a black-oil model to characterize (through history matching) offshore Nigerian reservoirs and estimate incremental recovery of waterflooding over natural depletion, with infill drilling and removal of allowable rates.

Compositional models also are used for most of Purposes 1 through 7 listed previously, but only in cases where the black-oil assumption of constant composition oil and gas components is invalid. Example compositional model applications include (1) depletion of a volatile oil or gas condensate reservoir where hydrocarbon phase compositions and properties vary significantly with pressure below bubble- or dewpoint, (2) injection of non-equilibrium gas (dry or enriched) into an oil reservoir to mobilize oil by vaporization into the more mobile gas phase or by attainment of outright (single-contact) or dynamic (multicontact) miscibility, and (3) injection of CO₂ into an oil reservoir to mobilize oil by stripping of light ends, oil viscosity reduction, and oil swelling.

Compositional simulation has been performed to estimate (1) loss of recovery caused by liquid dropout during depletion of retrograde gas condensate reservoirs and the reduction of this loss by full or partial cycling (re-injection of gas from surface facilities) and (2) effects of pressure level, injected gas composition, and CO₂ or N₂ injection on oil recovery by vaporization or miscibility. Graue and Zana⁵⁵ describe application of a compositional model in estimating Rangely (CO) field oil recovery by CO₂ injection as a function of injected composition and pressure level. Results of compositional simulation of a CO₂ project include CO₂ breakthrough time and rate and composition of produced fluids. These are required to design production facilities and CO₂ recycling strategies.⁵⁶ Modeling is also useful to optimize pattern size and CO₂/water-injection rates to overcome the effects of reservoir heterogeneity.⁵⁷

Thermal models are applied in reservoir studies of in-situ combustion and are used to simulate performance of cyclic steam simulation and steamflooding. In steam injection, questions addressed by simulation relate to effects of injected steam quality and injection rate, operating pressure level, and inclusion of gas with the injected steam. One question in cyclic stimulation concerns the optimal time periods per cycle for steam injection, soak, and production. The flooding case introduces the issues of well pattern and spacing. A number of steam-injection field studies using models have been published. Herrera and Hanzlik⁵⁸ compare field data and model results for a cyclic stimulation operation. Williams⁵⁹ discusses field performance and model results for stimulation and flooding, and Meldau⁶⁰ discusses field and model results related to addition of gas to the injected steam. Gomaa *et al.*⁶¹ and Moughamian *et al.*⁶² applied steamflood simulation in identifying and optimizing operating parameters in pilot and field drive operations.

Numerical simulation has been used to estimate chemical flood performance in a reservoir environment where the processes are very complex and many reservoir parameters affect the results. Chemical flood simulation has been used to construct a screening algorithm for the selection of reservoirs suitable for micellar/polymer flooding⁶³ and to examine competing EOR strategies—

e.g., CO₂ vs. surfactant flooding.⁶⁴ For caustic⁶⁵ and polymer⁶⁶ applications, as well as for the micellar process, chemical flood modeling is useful to discern controlling process mechanisms and to identify laboratory data required for process description.

In recent years, simulation has been used increasingly to estimate and compare recoveries from a given reservoir under alternative enhanced-recovery processes, such as CO₂ injection, thermal methods (steam injection and in-situ combustion), and several types of chemical flooding.

Considerations in Practical Application of Simulation Models

This section describes the procedure followed and certain questions faced by the engineer conducting a reservoir simulation study. The engineer must select the appropriate type of simulation model, select the grid network, and specify rock and fluid description data. Then the engineer must attempt to reduce or at least estimate inaccuracies in simulation results which stem from uncertain rock/fluid description data and from spatial truncation error.

Selection of Model Type

As mentioned earlier, selection of model type may depend on both the nature of the original reservoir fluid and upon the recovery process(es) to be studied. As a rough guide, an original reservoir oil solution gas or GOR value, R_s , below 2,000 scf/STB indicates a black oil, whereas a higher value indicates a volatile oil or retrograde gas condensate requiring compositional treatment.

For a black-oil reservoir, a black-oil model may be used to study natural depletion, water injection and/or equilibrium gas injection operations. However, a compositional model is generally necessary to estimate recovery by injection of dry or enriched gas, solvent, or CO₂. An exception here is the applicability of a modified black-oil model⁶⁷ in simulation of CO₂ or solvent injection where outright (single-contact) miscibility occurs.

Compositional simulation is generally employed for volatile oil reservoirs. However, a less expensive black-oil model study is adequate for simulating above-bubblepoint waterflooding performance. Compositional models have generally been employed to study retrograde gas condensate reservoirs. The compositional model is necessary in the case of below-dewpoint cycling. However, in some cases natural depletion or above-dewpoint cycling can be simulated at less expense using a black-oil model modified to account for volatility of the oil (condensate) component in the gas phase.⁶⁸⁻⁷⁰

The alkaline and surfactant-flood processes generally require use of the complex chemical flood simulation model. However, some (augmented) black-oil models offer the capability to simulate polymer and alkaline flooding.

Selection of Model Grid

Selection of the x - y - z gridblock network involves many factors, including available budget and the engineer's judgment and experience. For any type of model, the arithmetic or computing expense per timestep is at least linearly proportional to the total number of gridblocks

employed. The computing expense of a single model run is proportional to the product of the number of gridblocks and the number of timesteps required by the model to cover the total time period of interest. In many cases, the timestep size is controlled by the maximum rate of change (overall gridblocks) in one or more calculated quantities such as pressure and saturations. This maximum rate of change generally occurs at or near a well or in the vicinity of a flood front. A doubling of the number of gridblocks can result approximately in a doubling of this maximum rate of change since each gridblock is (on the average) one-half as large. The average timestep size, then, might decrease by a factor of two if the number of blocks were doubled. The final result is a computing expense per model run which can approach a proportionality to the square of the total number of gridblocks. This indicates the importance of selecting the smallest number of gridblocks consistent with reservoir/well description, recovery process characteristics, and the questions asked regarding reservoir performance.

The number of gridblocks and resultant study computing expense are the lowest in cases where the engineer can justify use of a representative element of the total field as the basis for the model study. This may be possible in reservoirs developed with repeated well patterns, for any recovery process—waterflooding, CO₂ injection, steamflooding, etc. In such cases, the representative element ideally should be a *symmetrical* element of the reservoir. In strict terms, this requires (1) a repeated, regular pattern of identically completed and operated wells, (2) a horizontal, areally homogeneous reservoir formation of uniform thickness, and (3) areally uniform initial fluid saturation distributions. If these conditions were met, then questions regarding total field optimization, forecasting and comparative evaluation of recovery processes could be addressed inexpensively by simulation of the single pattern (element).

While actual reservoirs never satisfy these conditions exactly, representative-element simulation studies are frequently performed for repeated pattern processes. In some cases, a substantial portion of the reservoir may exhibit only moderate areal heterogeneity and thickness variation. Resultant variation in performance from one pattern to another may be sufficiently small for engineering purposes to justify scale-up of single-pattern results to total field performance.

Representative-element simulation is often performed where the study purpose is comparative evaluation of alternative recovery processes as opposed to forecasting of total field performance for a specific process and operating scheme. The justification of single-element simulation implied in such cases is that the resultant ranking of alternative processes is unaffected by the variations in pattern (element) properties over the field. This justification can be and frequently is checked by repeating the various process simulations for two or more patterns of different properties representative of different portions of the reservoir.

Finally, the relatively inexpensive single-element simulation applies to design or optimization studies of a specific recovery process operated in a repeated pattern mode. For a repeated-pattern steamflood, single-pattern model runs have been performed to "optimize" pattern type (e.g., five-, seven- or nine-spot) and size, injected

steam quality and rate, well completions, etc. Occasional publications describe single-pattern simulation studies using a one-quarter five-spot or one-quarter nine-spot as the symmetrical element of the respective pattern. Actually, a one-eighth five-spot or nine-spot (and $\frac{1}{2}$ seven-spot) are the smallest symmetrical elements and should be used to minimize computing expense.⁷¹

Currently, a major portion of the industry-wide effort and computing expense in simulation studies is associated with total-field forecasting of black-oil reservoir performance under a sequence of recovery processes. Typically, the engineer must select a 3D grid for a large reservoir with significant heterogeneity, large areal variation in dip and thickness, irregular well locations and increasing numbers of wells with successive development stages. The engineer may face a several- to many-year period of historical performance under natural depletion, frequently with some natural water encroachment. Study objectives may include history matching, followed by matching and forecasting for a waterflood period, in turn followed by forecasting for some tertiary scheme such as CO₂ injection.

The total number of gridblocks is the product of the number of areal blocks, $N_x N_y$, and the number of grid layers, N_z . Different considerations enter into selection of these two numbers of spacings. Factors indicating a need for fine areal grid spacing are high well density and sharp or rapid changes (areally) in permeability, porosity, thickness, and dip. Since these factors frequently vary over the field, the x - and y -direction grid spacings are often nonuniform. Grid spacings generally increase toward the downdip reservoir boundaries and increase greatly with distance into the aquifer if the latter is present and included in the grid.

In general, of course, the number of areal gridblocks required increases with the size of the reservoir and the number of wells. However, grid spacings ranging from very fine to very coarse may be appropriate for different reservoirs of comparable size. The smallest numbers of areal blocks (coarsest areal spacings) are associated with reservoir studies limited to natural depletion and crestal or flank gas and/or water injection. In such a case, a coarse grid may result in a number of areal blocks that include two or more similar type (e.g., production) wells, with little loss in engineering significance of the simulator results. Large numbers of areal blocks may be required in cases of pattern waterfloods or enhanced recovery processes. A rough guide in this case is the need for at least two, preferably three or more, gridblocks separating each injection-production well pair. However, recent studies describe estimation of pseudorelative-permeability curves, which allow adjacent-block placement of an injector/producer well pair.^{72,73}

The major factors affecting the number of grid layers (vertical gridblocks) required are the formation stratification, vertical communication, and total thickness. Many reservoirs possess a number of formation layers, which correlate from well to well over much of or all the field. Variations of layer thickness, permeability, and porosity may be significant areally and even greater from one layer to another. The vertical communication (vertical permeability) between adjacent layer-pairs may vary from zero to very high, both areally and from one layer-pair to another. In general, at least one grid layer should be

used for each correlatable formation layer. However, common sense and budget constraints argue against definition of a large number of very thin grid layers. Three-dimensional reservoir studies typically employ 4 to 12 grid layers, and one or more of these grid layers may be a lumped representation of several thin formation layers.

The need for subdivision of one formation layer into two or more grid layers depends on the layer thickness and fluid-segregation characteristics of the recovery process and operating rates. Most recovery processes result in moderate to severe gravity segregation of oil and injected fluids; injected water or gas tend to underrun or override oil, respectively; many steamflood projects exhibit severe override of oil by the steam. A formation layer that has significant thickness and zero to poor vertical communication with layers above and below may exhibit a pronounced phase segregation and require two or more grid layers. In the idealized example of a fieldwide, pronounced gravity override in a vertically homogeneous reservoir, a variable grid spacing increasing from top to bottom might be specified. That is, four layers of thicknesses 5, 10, 20, and 25 ft might give more accurate results than four layers of equal 15-ft thickness.

A customary approach to determining N_z involves use of the simulation model itself in 2D cross-sectional (x - z slice) mode. For the particular recovery process of interest, x - z model runs are performed by using different numbers of grid layers. Pseudorelative-permeability curves reflecting phase segregation are calculated from model runs performed with fine vertical grid spacing.⁷⁴⁻⁷⁶ These pseudocurves are then used in equivalent x - z model runs using fewer grid layers to obtain coarse (vertical) definition results similar to the fine-spacing "correct" results. The fewer grid layers of the coarse definition are then employed in the 3D reservoir study grid. This concept of generating pseudocurves for coarse vertical grids that reproduce vertical fine-grid results (using rock or laboratory relative permeabilities) has been extended to the areal spacing problem,^{72,75} as mentioned earlier.

Obviously, a minimum computing expense follows from use of a single grid layer representing the entire formation thickness. This results in a 2D x - y areal grid as opposed to a 3D grid and occasionally is justified in the two extremes of a very high vertical permeability and a layered formation with zero vertical permeability. Pseudorelative permeability and capillary pressure curves are discussed for the former case in papers describing the vertical equilibrium (VE) concept^{21,77} and for the latter case by Hearn.⁷⁸

Specification of Reservoir Rock and Fluid Description Data

Geological and petrophysical work based on logs and core analyses yields maps of structure, net ϕh , and kh products for each of the several reservoir layers. The kh and ϕh data often are augmented or modified by results of drillstem, pressure buildup, and pulse tests. For each layer, the engineer can overlay his areal x - y grid spacing network on these maps and read off the values of subsea depth, ϕh , and kh at the center of each gridblock. These values along with gross thickness of each block are then transposed to a data file in a format compatible with that

required by the simulation model. Current research effort is directed toward developing computer programs that accept digitized core analysis, log and geological data, the selected grid network, and, through mapping and interpolation techniques, automatically prepare the simulation input data file.

Laboratory core analysis work includes measurement of relative-permeability, k_r , and capillary-pressure, P_c , curves for a number of field cores. Variations in rock lithology may result in different sets of k_r and P_c curves for different layers and/or different areal portions of the reservoir. Most simulation models allow multiple sets of such data in tabular form with assignment of each set to a user-specified layer/portion of the reservoir. If the rock water/oil (gas/oil) capillary pressure values are small, the water/oil (gas/oil) transition zone in the reservoir may be a very small fraction of total formation thickness. In such cases, pseudocapillary-pressure curve(s) should be used.⁷⁷

For black-oil studies, laboratory tests are performed to determine gas compressibility factor and saturated oil and gas viscosities vs. pressure. Differential and/or constant-composition expansion tests on oil samples yield the saturated oil pressure-dependent formation volume factor, B_o (RB/STB), and solution gas, R_s (scf/STB). The resulting oil and associated gas properties vs. pressure are entered in the data file in tabular form compatible with simulator input requirements. For gas condensate depletion studies, constant-volume and constant-composition expansion tests yield the required pressure-dependent liquid content, C_L (STB/scf), and condensate density values.

A wide variety of laboratory tests are performed for compositional model studies that involve injection of a nonequilibrium fluid (dry or enriched gas, CO_2 , N_2 , etc.). Swelling tests yield relative volumes, saturation pressures, and equilibrium phase compositions for each of a sequence of mixtures of, say, 1 mole of original reservoir oil and injected fluid.⁷⁹ Various single- and multicontact tests may be augmented by 1D corefloods and/or slim-tube displacements. Orr *et al.*^{80,81} discuss a variety of CO_2 -oil laboratory tests. Much of the laboratory PVT test data must be processed to yield correlations or a calibrated EOS⁸²⁻⁸⁵ for simulator input requirements.

History Matching

In most simulation studies, reservoirs have some period of historical performance data that include WOR, GOR, individual phase rates and cumulatives, and pressure measurements by well. Ideally, periodic (e.g., monthly), accurate measurements of all these data would be recorded and available for all wells. In the typical case, many of these data are unrecorded or unavailable and some of the reported values may be of questionable accuracy.

The reservoir description based on log and core analysis data reflects a very small (volumetric) sampling of the reservoir. The historical reservoir-performance data reflect the reservoir description, and its impact on pressure/fluid movement behavior, on a much larger scale. The previously mentioned geological and petrophysical work yields an initial reservoir description. History matching yields a refinement of that description, which improves agreement between model results and observed reservoir behavior. The history-match phase of

the simulation study entails a sequence of model runs in which input reservoir description parameters are altered to improve this agreement. This is a trial-and-error procedure frequently requiring considerable engineering judgment and experience. The description parameters obtained from the geological/petrophysical work often are used to establish legitimate ranges of parameter variation in the history-match model runs.

This history-match phase can consume half or more of the total simulation study (match plus prediction) computing effort and expense, depending on the length of the history period, complexity of the reservoir, and amount of available performance data.

Refs. 86 through 90 describe methods and applications of inverse simulation or automatic history matching. This concept requires user-specification of a finite set of reservoir description parameters to be determined (e.g., zonal permeability, porosity values), a finite set of observed reservoir performance data to be matched, and a regression procedure coded interactively with the simulator. A single computer submittal is then performed, which in turn executes many model history runs. The regression procedure automatically varies description-parameter values from run to run to determine that set of description-parameter values that maximize agreement between model results and the set of observed data. This concept is especially appealing to the engineers who have experienced the frequently high frustration levels associated with trial-and-error matching of complex reservoir behavior. However, to date the trial-and-error procedure still predominates with isolated successes reported with automatic history matching. Two factors complicating the latter approach are (1) the expense of the required single computer submittal can be very large, (2) the a priori choice of description parameters (or zonation) can be difficult, subjective, and lead to a questionable reservoir description.

Validity of Simulation Results

Uncertainties or errors in simulation model results may arise from (1) questionable assumptions or mechanisms not represented in the differential form of the model, (2) spatial and time truncation error introduced by replacement of the model differential equations by finite-difference approximations, and (3) inadequately known reservoir rock and/or fluid description data. In addition, the exact solution of the difference equations is not attained because of round-off error introduced by the finite word length of the computer. Round-off error is generally negligible compared with errors from the other three sources. With some exceptions, the above sources of error are listed in order of increasing importance. However, successful history matching can reverse the importance of the second and third sources.

Comparisons of model and laboratory experiment results can indicate model validity in the absence of the Uncertainty 3 above. Several such comparisons show good model-experiment agreement for gas/oil systems,^{91,92} water/oil coning,⁹³ and fractured-matrix imbibition.⁹⁴

Model Assumptions

An assumption common to many black-oil models is complete re-solution of free gas in accordance with the

saturated $R_s(p)$ curve during repressurization. This may be a poor assumption in a case where gridblock thickness is large and gas/oil gravity (vertical) segregation is pronounced. Prior to repressurization in a given block, the free gas may exist as a high gas saturation in only the upper portion of the block. This contradicts its representation in the model as a lower saturation distributed throughout the entire block volume. In the segregated state, the gas will redissolve only in the lower or residual oil saturation in the upper, gas-occupied portion of the block volume. However, the model will allow re-solution in the entire block's oil volume. Pressure hysteresis in the $R_s(p)$ curve has been used to cope with this problem; an alternative remedy where the computing budget permits is the use of more grid layers.

An assumption common in early black-oil models was that the reservoir oil obeyed a single pair of $B_o(p)$ and $R_s(p)$ curves. Some black-oil reservoirs exhibit a significant variation of oil API gravity and PVT behavior with depth or with depth and areal location. In some such cases, this variation can be represented in a black-oil model by simply allowing initial solution gas R_{si} to vary with depth in the undersaturated oil column, retaining a single set of $B_o(p)$ and $R_s(p)$ curves. In other cases, multiple sets of these curves and two oil components are necessary and the single oil-type assumption in a black-oil model can lead to appreciable error.

Mechanisms or phenomena that are significant in some reservoirs and may not be represented in the model include compaction, hysteresis in wetting and nonwetting relative permeabilities, and interlayer wellbore crossflow. The latter is a particularly difficult modeling problem and the subject of continuing research. A production well completed in a number of layers may exhibit production from some layers and, simultaneously, injection (backflow or recirculation) into others. Factors that promote this possibility are low-pressure drawdown (high PI and/or low rate) and poor vertical communication between the reservoir layers in the vicinity of the well. A rigorous treatment of this problem requires modeling of wellbore multiphase hydraulics and phase segregation combined with calculation of correct phase mixtures for the layers undergoing injection.

Spatial Truncation Error

Spatial and time truncation error theoretically can be reduced to any desired low level by sufficiently reducing gridblock dimensions and timestep size. However, the resultant increased number of blocks and timesteps frequently lead to prohibitive computer expense and memory storage requirements.

Time truncation error is generally insignificant. In most applications timestep size is restricted by considerations other than time truncation error, such as model stability, frequencies of printout, and frequencies of changes in well data (rates, completions, new wells, etc.). In any given case, the level of time truncation error can be estimated by repeating a run or portion of a run with a smaller (or larger) timestep. Insensitivity of results to timestep size indicates low-time truncation error.

Spatial truncation error appears in the forms of numerical dispersion, grid-orientation effects, and error in calculated well WOR and GOR values. Spatial truncation error can be expressed in mathematical terms through

complex manipulation of the model differential equations and Taylor series expansions. In simpler terms, this error can be viewed as a consequence of replacing the physical continuum (reservoir formation) by a 3D network of mixing cells (gridblocks). This consequence is the contradictory requirements that any variable value (pressure, saturation, temperature, concentration) simultaneously represents the value at the grid point (e.g. block center) and the entire block's volumetric average value. This requirement is not met (1) during a frontal displacement as a sharp front enters the gridblock, (2) when gravity forces result in phase segregation within the block's thickness, and/or (3) when areal cusping or coning causes sharp localized saturation gradients within the block volume.

Numerical dispersion generally appears as falsely smeared spatial gradients of water saturation in waterflooding, temperature in steamflooding, solvent in miscible flooding, and chemical agent in chemical flooding. This excessive smearing occurs primarily in the areal (x or y) directions and, if uncontrolled, results in too early calculated breakthrough times of water (heat, solvent, etc.) at production wells. This numerical dispersion generally increases with increasing areal gridblock size (Δx and Δy). Lantz⁹⁵ quantitatively related the difference equation truncation error term to an artificial, second-order diffusion term in the differential equation.

The engineer can anticipate possibly significant numerical dispersion effects in simulating two types of miscible displacement. The first type is slug or bank, as opposed to continuous, injection of solvent or CO_2 . Numerical dispersion erodes the calculated solvent concentration within the bank. If miscibility requires maintenance of solvent bank integrity or a certain solvent peak concentration, then this numerical dispersion can result in a calculated (false) loss of miscibility. The second type is multicontact miscibility. For continuous solvent injection in 1D simulations, several studies^{31,96,97} report the need for 100 to 300 gridblocks to reduce the effect of numerical dispersion on miscible front velocity.

Kyte and Berry⁷⁵ describe control of numerical dispersion in simulation of waterflooding through large areal gridblocks. They use pseudorelative-permeability curves obtained from detailed (fine-grid) cross-sectional simulations. Harpole and Hearn⁹⁸ used their method in a 3D black-oil study. To date, steamflood simulation generally has been confined to pattern studies for which a sufficient number of gridblocks between unlike wells is used to minimize numerical dispersion effects. Killough *et al.*⁷³ describe their reduction of numerical dispersion in a stratified, heterogeneous, repeated pattern black-oil reservoir study. They performed fine-grid, 3D single-pattern simulations and then used regression to determine pseudorelative permeabilities for a 2×2 four-block areal grid representation of the pattern. Agreement between the 3D fine-grid results and four-block pattern results was good enough to allow fieldwide simulation by use of the latter coarse, areal definition. Several recent papers⁹⁹⁻¹⁰¹ describe local grid refinement, the method of characteristics, and other methods to reduce numerical dispersion effects.

Pronounced grid-orientation effects have been noted in simulation of adverse mobility ratio floods with models incorporating the commonly used five-point difference scheme and single-point upstream weighting. The value

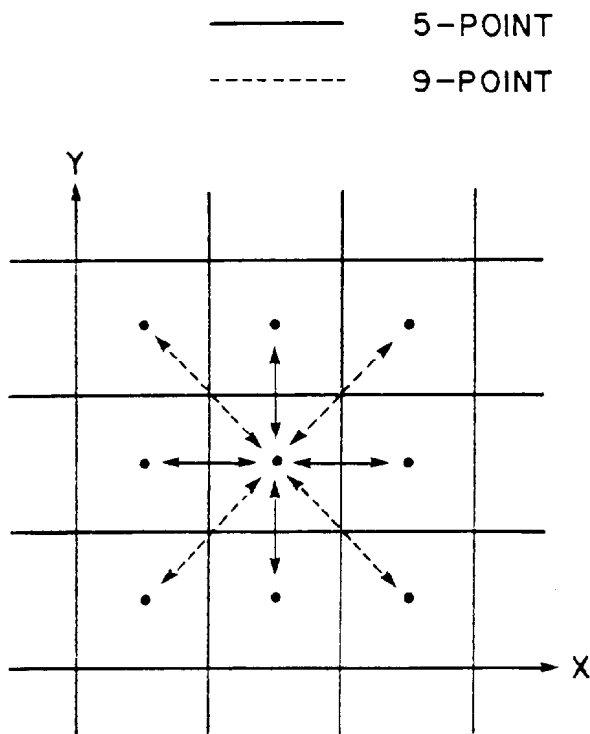


Fig. 48.2—Five-point and nine-point difference schemes.

of the coefficient $k_{rj}C_{Hj}/\mu_j$ in Eq. 2 obviously affects the interblock Darcy flow rate from gridblock $i-1$ to block i . Intuition might dictate evaluation of this coefficient at some average of variable values (pressure, saturations, etc.) in the two blocks. However, considerations of stability and numerical dispersion frequently have led to its evaluation at conditions existing in the block from which the flow occurs—i.e., the upstream block. This is referred to as single-point upstream weighting. The five-point difference scheme is reflected in the form of terms of type $\Delta(\tau\Delta p)$ in Eq. 5 for the case of 2D flow. These terms represent the interblock Darcy flow rates in the mass balance equation for each gridblock. The solid arrows of Fig. 48.2 illustrate these flow rates between the gridblock and each of its four neighbors.

A strong grid-orientation effect was first reported by Todd *et al.*¹⁰² for highly adverse mobility waterfloods and later observed for pattern steamfloods.¹⁰³ An areal grid with the usual perpendicular x and y axes may be placed over a five-spot pattern with the x axis either parallel to or at a 45° angle to the line connecting the injector to a producer (Fig. 48.3). These parallel and diagonal grids¹⁰² can result in markedly different calculated shapes of the water or steam front and the breakthrough times. This difference was reduced by the nine-point finite difference formulation described by Yanosik and McCracken,¹⁰⁴ illustrated by the four extra dashed-line diagonal flow terms in Fig. 48.2. The nine-point scheme has been programmed into many simulators treating adverse mobility ratio waterfloods, steamfloods, and CO_2 solvent displacements.

As an example of this grid orientation effect, Fig. 48.3 shows a 3-acre nine-spot steamflood pattern with the diagonal grid and 45° -shifted parallel grid. This pattern

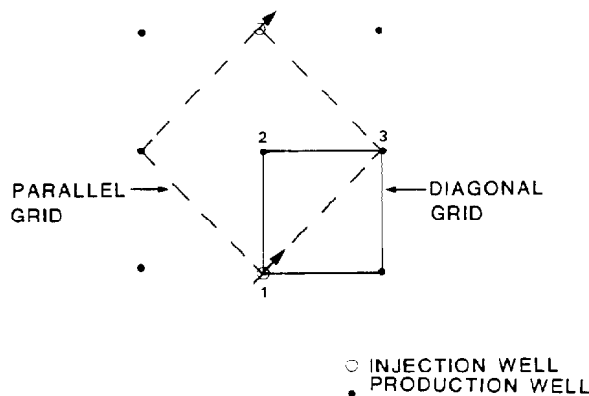


Fig. 48.3—Nine-spot grids.

has three types of wells—labeled 1 (injector), 2 (near producer), and 3 (far producer). Reservoir formation and fluid properties and well rates used in the simulation model are reported elsewhere.¹⁴ The calculated results in Table 48.2 show the pronounced effect of grid orientation on steam breakthrough times calculated by use of the five-point difference scheme. Obviously, steam should arrive at the near producer, Well 2, before it reaches the far producer, Well 3. The parallel grid with the five-point scheme actually gives breakthrough at Well 3 at 117 days, before breakthrough at Well 2 (204 days). Table 48.2 shows that the nine-point difference scheme virtually eliminates the effect of grid orientation for this problem. Figure 48.4 uses parallel and diagonal grids to show calculated steam-front shapes at 80 days for the two different schemes. The difference between the nine-point fronts for two grids is small and about equal to the error of manual interpolation.

A two-point, upstream weighting method¹⁰² was proposed to reduce both numerical dispersion and grid-orientation effects. Abou-Kassem and Aziz¹⁰¹ discuss this and other methods¹⁰⁶⁻¹⁰⁸ for reducing the orientation effect. They conclude that the nine-point scheme is the most effective in reducing steamflood grid-orientation effects. Two studies¹⁰⁵⁻¹⁰⁹ show very significant reduction of grid-orientation effects in pattern steamflood simulation results when areally homogeneous, square grids ($\Delta x = \Delta y = \text{constant}$) are used with the Yanosik and McCracken nine-point scheme. However, the effects persist for a non-square, uniform grid ($\Delta x = 2\Delta y$)¹⁰⁹ and the latter scheme yields physically unreasonable results for the cases of heterogeneity and nonuniform grids where Δx (or Δy) varies with x (y). The latter shortcoming is addressed by several recent papers¹¹⁰⁻¹¹² that propose new or altered nine-point schemes. Frauenthal *et al.*¹¹³ describe a modified five-point difference scheme and Pruess *et al.*¹¹⁴ present a seven-point, hexagonal gridblock scheme for reducing grid-orientation effects.

The engineer can anticipate possibly significant grid-orientation effects in simulating single- or repeated-pattern, adverse mobility ratio displacements. Preliminary areal, single-pattern model runs allow estimation of the level of such effects and the need for use of a nine-point scheme or other remedy.

The discussion and references cited obviously indicate the current concern regarding effects of numerical-dispersion and grid-orientation effects on the validity of

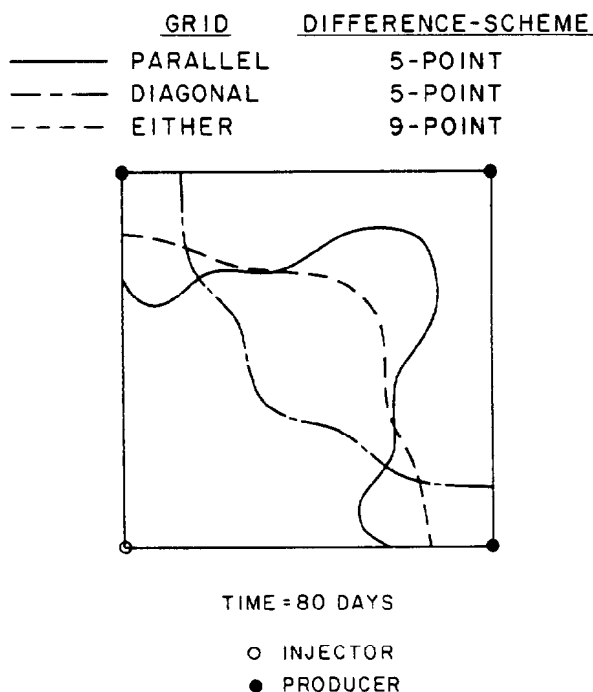


Fig. 48.4—Calculated shape of steamflood front in a nine-spot pattern.

simulation results. However, these numerical effects are not serious in many simulation studies. Numerical-dispersion effects are generally demonstrated as smearing of theoretically sharp fronts in 1- or 2D horizontal displacements in homogeneous formations. Actual reservoir behavior frequently reflects strong gravity effects such as a gas or solvent override or a water underrun. These gravity effects combined with reservoir structure (areal variation in dip angle) can have an influence on fluid movement patterns, which dominates the numerical effects just discussed. In addition, reservoir heterogeneity can play the same relatively dominant role as gravity forces. In highly stratified or layered reservoirs, the different rates of travel of injected fluid through different layers can dominate the numerical dispersion effect at the leading edges of the individual layer displacement fronts. Finally, a given level of numerical-dispersion or grid-orientation effect is acceptable if its impact on calculated reservoir performance is inconsequential in an engineering sense—i.e., in light of the questions being asked.

The model itself often can be used to estimate the level of these numerical errors and the degree of their acceptability. Before selecting the full study grid, preliminary model runs using grids of varying coarseness can be performed for a representative cross-section or 3D portion

of the reservoir. The results can be helpful in selecting the coarsest grid spacing compatible with acceptably low numerical dispersion.

In fieldwide simulation, spatial truncation error may affect calculated values of well productivity, wellbore producing pressure, and WOR and GOR. Without special measures, the model calculates the well behavior with only the gridblock's average values of pressure, saturations, etc. However, the actual well behavior may reflect near-well coning, liquid dropout, or gas evolution effects. The dimensions of this near-well region may be two orders of magnitude smaller than the areal block dimensions (Δx , Δy). Thus the block's average conditions may provide a poor basis for calculating well behavior. This problem can be significant for a well completed throughout formation thickness and even more significant for a partially penetrating well.

The simplest remedy to this problem is applicable in some cases where good vertical communication results in a high degree of vertical phase segregation. In this case, well pseudorelative-permeability curves have been used.^{115,116} These curves reflect the location of the completion interval and relate well behavior to average block conditions. A more complicated approach requires use of multivariable correlations relating well WOR and GOR to average block conditions.^{117,118} These correlations are developed from a number of single-well r - z (radial-depth) model runs with fine grid spacing near the wellbore. The most rigorous treatment of this problem incorporates individual 1D radial or 2D r - z simulations for each well simultaneously within the fieldwide 3D simulation.^{119,120} Again, in any given case, the model itself can be used to estimate the severity of this problem through comparison of single-well, r - z and representative 3D (portion of reservoir) model results.

Uncertain Reservoir Description Data

Errors in reservoir description data clearly contribute to errors in simulation model results. Since the description data are never exactly known, one might infer that model results are necessarily erroneous and unreliable. A number of considerations contribute, in contradiction of this inference, to model results being widely used to select and to design oil-recovery processes and to forecast oil recovery.

Accurate determination of all reservoir description data is not necessary for reliability of model results. The required accuracy of any description parameter is proportional to its influence on computed results (reservoir performance). The simulation model should be used to perform preliminary sensitivity runs to determine which description data are important. Expense and effort should then be concentrated on obtaining or refining only those "sensitive" description data. The particular parameters found to be important will vary from study to study, depending on the nature of the reservoir, the recovery process(es) of interest, and study objectives or questions. For example, if computed oil recovery is insensitive to wide variations in the gas relative-permeability curve, then the accuracy of this curve might deserve little attention. In a case where the gravity drainage mechanism is dominant, the oil relative-permeability curve at low and midrange oil saturations has a large effect on oil recovery and deserves effort of definition. Gas viscosity, relative

TABLE 48.2—CALCULATED STEAM BREAKTHROUGH TIMES (DAYS) FOR A NINE-SPOT PATTERN

	Well 2		Well 3	
	Diagonal	Parallel	Diagonal	Parallel
Five-point	47.8	204	1,400	117
Nine-point	87.7	75.5	900	1,000

permeability, and capillary pressure may play virtually no role and their accuracies are irrelevant. All phase relative permeabilities may be unimportant in a natural or flank waterflood of a relatively clean, thick high-relief sand where gravity forces are dominant with pronounced phase segregation. Only relative-permeability curve endpoints may be important in such cases. However, thinner sand or stratification, lower permeability and/or higher rates can increase the importance of water and oil relative-permeability curve shapes. While capillary pressure is unimportant in many reservoir studies, it can provide the dominant, cross-imbibition, mechanism in waterflooding thin, heterogeneous water-wet sands.

In some studies, the engineer is less concerned with the absolute accuracies of both model results and description data than with the sensitivity of calculated results to variations in those data. An example is a study performed to compare oil recoveries under alternative recovery processes. Model runs performed for each process, with reservoir description data varied over estimated ranges of uncertainty, may yield substantially invariant process rankings and incremental oil recovery differences. If so, any significant history-matching effort may be unnecessary and the only concern regarding accuracy of description data should be the estimated ranges of uncertainty. Another example is a design study of a given recovery process performed to optimize pattern type and size, well completions, and rates. Model runs, as just described, may show that minimal history-match and/or laboratory efforts for reservoir description are necessary to meet the study objective.

As previously mentioned, reservoir description data are altered through history matching to improve agreement between model results and reservoir performance data. Frequently, the study objectives involve estimation of reservoir performance under displacement conditions not present or recovery processes not active during the history period. In such cases, some description parameters that significantly influence future performance may not be reflected in the historical performance. An example is a heavy-oil reservoir that was produced for nearly 40 years under natural depletion with no water drive. Solution gas was very low and interstitial water saturation was immobile. A 50% water cut developed in time as a large pressure decline caused water mobility through water expansion and porosity reduction. Performance data included WOR, GOR, and pressure data for a number of wells. The only description parameters influencing these data were formation permeability, compressibility, critical gas saturation, water relative permeability at saturations slightly above S_{wc} , and gas relative permeability at saturations slightly above S_{gc} . The history-match effort gave a good match of performance with a unique set of these parameter values. However, it provided no information regarding the full-range relative-permeability curves necessary to estimate oil recovery under waterflood and steam stimulation or flooding. Laboratory relative-permeability measurements and waterflood and thermal pilots were conducted in this case.

Laboratory work and well pressure testing can be performed to estimate values of some reservoir description parameters that are not reflected in performance data. These parameters, together with others determined by history matching, can be used in model runs to estimate

oil recovery under the various alternative recovery schemes within the study scope. Field pilot tests then may be planned for one or more of the recovery processes, subject to the model results and engineering judgment.

Argument has persisted for years regarding uniqueness of the reservoir description obtained by history matching. A thorough treatment of this question requires length and mathematical complexity beyond the scope of this chapter. Any such treatment requires careful definition of terms. For example, define a reservoir description as a bounded set of m numbers $\{x_i\}$ representing selected zonal permeabilities and porosities and parameters characterizing relative permeability curves. Let the sets of N numbers $\{d_j^*\}$, $\{d_j\}$ represent observed and model calculated performance data where $d_j = d_j(x_1, x_2, \dots, x_m)$. If $N > m$, each x_i affects one or more d_j , and the d_j are independent functions of $\{x_i\}$ (in a mathematical sense undefined here), then with rare exceptions a unique set of parameter values $\{x_i\}$ will minimize the difference between the observed and calculated data. An altered zonation gives a physically different parameter set $\{\hat{x}_i\}$. Again, a unique set of values of $\{\hat{x}_i\}$ generally will minimize the difference between observed and calculated data. However, for this two-parameter set "experiment," comparable matches of observed data would allow a claim of non-uniqueness.

As a practical matter, study budget and time constraints prevent exhaustive trials of different parameter sets and even limit the number of model runs with different combinations of parameter values within a given set. Generally, difficulty encountered in a history-match effort is that of finding any reasonable description that gives good agreement with history. The effort rarely ends with difficulty in selecting among significantly different reservoir descriptions that give comparably good matches. In any event, the pertinent question regarding reservoir-description data is not related to correctness or uniqueness in an absolute sense. The pertinent question concerns the engineering significance of variations in parameter values within ranges of uncertainty. As discussed previously, the model itself is useful in estimating this significance.

Simulation Technology

Simulation technology can be divided roughly into the categories of model definition, model formulation, solution techniques, and special techniques related to numerical dispersion control, viscous fingering, and grid-orientation effects. Model definition includes specification of the problem (process) addressed, component identities, mass transport laws or expressions, fluid PVT and rock property relationships and, finally, the set of finite-difference equations expressing conservation of mass for each gridblock. These equations are generally nonlinear. Before they can be solved for pressures, saturations, etc., they must be linearized and manipulated into a set of simultaneous linear algebraic equations. The term *formulation* refers to these manipulations and the final form of this set of linearized equations. In a general sense, this set of equations can be expressed in the matrix form $AP = b$ where A is a very sparse, banded $N_b \times N_b$ matrix and the known b and unknown P are column vectors of dimension N_b . A rapidly expanding portion of the simulation literature describes increasingly efficient, iterative solution techniques for this problem.

Model Formulations

In 1959, Douglas *et al.*¹⁶ proposed *leap-frog* and *simultaneous* formulations for incompressible 2D two-phase flow. During 1960–69 a number of authors^{21–24} described two- and three-phase, 2D and 3D black-oil models based on this simultaneous formulation. In 1960, Stone and Garder¹⁸ and Sheldon *et al.*¹⁷ introduced the concept of eliminating saturation derivatives among the black-oil model equations to obtain a single difference equation in pressure. Fagin and Stewart¹⁹ in 1966 and Breitenbach *et al.*²⁰ in 1968 described three-phase black-oil models based on this implicit-pressure/explicit-saturation (IMPES) formulation. The IMPES formulation is explicit in saturation and composition in that relative permeabilities and concentrations are expressed explicitly in the interblock flow terms. Solution of the pressure equations over the grid is followed by an explicit updating of phase saturations and compositions in each gridblock.

In 1969, Blair and Weinaug¹²¹ published a fully *implicit* formulation which expresses all terms in the interblock flow and well production expressions implicitly. This requires simultaneous solution of all N model equations. A number of later papers describe implementation of the implicit formulation in black-oil,¹²² compositional³¹ and thermal³⁹ models.

In 1970, MacDonald¹²³ improved the stability of the IMPES method for the two-phase water/oil case by following the pressure equation solution with solution of a water-saturation equation over the grid using implicit (new-time-level or end-of-timestep) values of relative permeabilities in the interblock flow terms. Spillette *et al.*¹²⁴ extended this concept to the three-phase case and called the formulation *sequential*.

The IMPES formulation can become unstable if the volumetric flow through a gridblock in a timestep exceeds a small fraction of the block PV. The more stable sequential formulation remains stable to much larger ratios of gridblock volumetric throughput/PV. The tolerable throughput ratio for the implicit formulation is significantly larger than that of the sequential method. Arithmetic (or computing cost) per timestep and timestep size both increase from IMPES to sequential to implicit formulations. Since the total cost of simulating a given time period is proportional to the product of arithmetic per timestep and timestep size, all three formulations are used widely today.

The sequential formulation can fail to preserve material balances in some problems where adjacent gridblock compositions differ greatly.¹²⁵ Meijerink¹²⁶ described a *stabilized* IMPES formulation, which improves the stability of IMPES to a lesser extent than the sequential method but reduces material balance error in regions of steep composition gradients.

Thomas and Thurnau¹²⁷ describe an *adaptive implicit* formulation, which allows different levels of implicitness in different gridblocks. These various levels may change with timestep number and with iteration number within a given timestep. As previously mentioned, the implicit formulation¹²¹ requires simultaneous solution of N equations for each block over the entire grid. The corresponding arithmetic effort of solution is proportional to N^3 . Since $N=1$ for IMPES, the implicit formulation obviously requires considerably more computing time per timestep

than does IMPES. For each gridblock, the adaptive implicit method internally senses (without user intervention) which dependent variables (e.g., saturations, pressure, mole fractions) require implicit dating for stability. For most practical reservoir problems this results in one equation per gridblock for a major fraction of the grid and an overall average number of equations per block considerably less than N . Thus the method can attain the stability of the implicit formulation with considerably less computing expense. Also, computer storage requirements are reduced significantly. Future implementations of this formulation may contribute to increased model reliability (stability) and efficiency in simulations of all types of recovery processes.

Single-well coning studies generally involve radial grid spacings, resulting in very small gridblocks near the well and large throughput ratios. For these studies, the IMPES formulation is unsuitable, and the implicit formulation is generally the most efficient.¹²⁸ For field-scale, 3D black-oil studies, the overall computing time is frequently less with the sequential than with the IMPES or implicit formulation. The typical black-oil simulator applied today in 1,000- or more gridblock, field-scale studies is an IMPES model with a user-specified option of sequential solution. Smaller black-oil studies and preliminary cross-sectional, coning, and sensitivity studies associated with the large problems frequently employ the implicit formulation. Recent thermal models involve implicit formulations. With one exception³¹ recent compositional models^{29–33} are based on the IMPES formulation.

The popular IMPES and more recent implicit formulations are illustrated here for the case of 3D two-phase flow of water and undersaturated oil. This illustration is in the form of the Newton-Raphson procedure, which Blair and Weinaug¹²¹ used in describing their implicit formulation. For clarity, rock compressibility, gravity, and capillary pressure are neglected, and phase (component) production rates are fixed, independent of pressure and saturations. The terms *explicit* and *implicit* refer to the time level of evaluation for variables or terms in the left side, interblock flow terms of Eqs. 5. Explicit dating denotes evaluation at the beginning of the timestep, t_n (level n), while implicit dating denotes evaluation at the end of the timestep, t_{n+1} (level $n+1$). The implicit formulation of Eq. 5, then, appears for each gridblock as

$$\Delta(T_w \Delta_p) - q_{pw} - \frac{V_p}{\Delta t} [b_w S_w - (b_w S_w)_n] \\ \equiv f(S_w, p) = 0 \quad \dots \dots \dots (11a)$$

and

$$\Delta(T_o \Delta p) - q_{po} - \frac{V_p}{\Delta t} [b_o S_o - (b_o S_o)_n] \\ \equiv g(S_w, p) = 0, \quad \dots \dots \dots (11b)$$

where

T = interblock transmissibility,

p = pressure,

q_{pP} = production rate of phase P, oil or water

V_p = PV of gridblock,

Δt_P = timestep
 b_P = reciprocal formation volume factor of
 phase P, ST vol/res vol,
 S_P = saturation of phase P, and
 f, g = function of.

Gridblock indices i, j , and k on all terms are suppressed for clarity. All terms at time level n are known from the previous timestep's calculations. The absence of time level subscript denotes the implicit level, $n+1$. Thus all terms $T_w, T_o, b_w, b_o, S_w, S_o, p$ in Eq. 11 represent unknown values at time level $n+1$. For all N_b gridblocks, Eqs. 11 are $2N_b$ equations in the $2N_b$ unknowns $\{S_{wi,j,k,n+1}, p_{i,j,k,n+1}\}$. For a particular gridblock, Eqs. 11 are two equations in the 14 unknowns consisting of (S_w, p) pairs in the block and its six neighbors. These six neighbor pairs are introduced by the Laplacian interblock flow terms. Oil saturations are not additional unknowns since $S_o = 1 - S_w$; the transmissibilities T and reciprocal formation volume factors (b) are functions of S_w and p .

Application of the well-known Newton-Raphson iterative procedure to Eq. 11 gives

$$f(S_w, p) \equiv f(S_w^\ell, p^\ell) + \left(\frac{\delta f}{\delta S_w} \right)^\ell \delta S_w + \left(\frac{\delta f}{\delta p} \right)^\ell \delta p = 0 \quad (12a)$$

and

$$g(S_w, p) \equiv g(S_w^\ell, p^\ell) + \left(\frac{\delta g}{\delta S_w} \right)^\ell \delta S_w + \left(\frac{\delta g}{\delta p} \right)^\ell \delta p = 0, \quad (12b)$$

where ℓ is iteration number, superscript ℓ denotes evaluation at (S_w^ℓ, p^ℓ) , $\delta p \equiv p^{\ell+1} - p^\ell$, and S_w^ℓ, p^ℓ approach the desired S_w, p values as ℓ increases. The terms containing derivatives are actually sums of seven terms because of the previously mentioned functional dependence on neighboring block unknowns. Substituting from Eqs. 11 into Eqs. 12, performing the differentiation and rearranging the result gives

$$\Delta(T_{11}^\ell \Delta \delta S_w) + \Delta(T_{12}^\ell \Delta \delta p) - \frac{V_p}{\Delta t} b_w^\ell \delta S_w - \frac{V_p}{\Delta t} (S_w b_w c_w)^\ell \delta p + f(S_w^\ell, p^\ell) = 0 \quad (13a)$$

and

$$\Delta(T_{21}^\ell \Delta \delta S_w) + \Delta(T_{22}^\ell \Delta \delta p) + \frac{V_p}{\Delta t} b_o^\ell \delta S_w - \frac{V_p}{\Delta t} (S_o b_o c_o)^\ell \delta p + g(S_w^\ell, p^\ell) = 0, \quad (13b)$$

or in condensed matrix form,

$$\Delta(T \Delta P) - C P + R = 0, \quad (14)$$

where T and C are 2×2 matrices and P and R are 2×1 column vectors:

$$T = \begin{Bmatrix} T_{11} & T_{12} \\ T_{21} & T_{22} \end{Bmatrix} \quad C = \begin{Bmatrix} c_{11} & c_{12} \\ c_{21} & c_{22} \end{Bmatrix} \quad P = \begin{Bmatrix} \delta S_w \\ \delta p \end{Bmatrix} \quad R = \begin{Bmatrix} f^\ell \\ g^\ell \end{Bmatrix} \quad (15)$$

The coefficients T_{11}, T_{21} arise from saturation derivatives of relative permeabilities in the transmissibilities. The C matrix elements are obvious upon inspection of Eqs. 13 (e.g., $c_{12} = V_p / \Delta t (S_w b_w c_w)$). The compressibilities (c_w, c_o) appear through the definition $c = (1/b) db/dp$.

Eq. 14 written for all gridblocks is a set of N_b linear parabolic difference equations in the N_b unknowns $\{P_{i,j,k}\}$. Following solution by a direct or iterative technique, the new iterates are calculated as $S_w^{\ell+1} = S_w^\ell + \delta S_w, p^{\ell+1} = p^\ell + \delta p$. Coefficients are recalculated at $(S_w^{\ell+1}, p^{\ell+1})$ for all blocks and Eq. 14 is solved again. These *outer* or *Newton* iterations are continued until the maximum values over the grid of $\{|\delta S_w|, |\delta p|\}$ are less than some prescribed tolerances. The term *inner* iterations refers to iterations performed by an iterative solution technique in solving Eq. 14 for a given Newton iteration.

The IMPES formulation treats transmissibilities explicitly so that the first terms in Eqs. 11 are $\Delta(T_{wn} \Delta p)$ and $\Delta(T_{on} \Delta p)$, where T_{wn} and T_{on} are calculated from known saturations at time level n . This results, upon application of Eq. 12, in zero values for transmissibility derivatives with respect to neighboring block saturations and Eq. 16 replaces Eq. 13:

$$\Delta(T_{wn} \Delta \delta p) - \frac{V_p}{\Delta t} b_w^\ell \delta S_w - \frac{V_p}{\Delta t} (S_w b_w c_w)^\ell \delta p + f(S_w^\ell, p^\ell) = 0 \quad (16a)$$

and

$$\Delta(T_{on} \Delta \delta p) + \frac{V_p}{\Delta t} b_o^\ell \delta S_w - \frac{V_p}{\Delta t} (S_o b_o c_o)^\ell \delta p + g(S_w^\ell, p^\ell) = 0 \quad (16b)$$

The single saturation unknown, δS_w , can be eliminated by multiplying Eqs. 16a and 16b by B_w^ℓ and B_o^ℓ , respectively, and adding to obtain

$$B_w^\ell \Delta(T_{wn} \Delta \delta p) + B_o^\ell \Delta(T_{on} \Delta \delta p) - \frac{V_p}{\Delta t} (S_w c_w + S_o c_o)^\ell \delta p + B_w^\ell f^\ell + B_o^\ell g^\ell = 0, \quad (17)$$

where B is the formation volume factor, $1/b$.

This is a set of N_b single or scalar, linear parabolic difference equations in the N_b pressure unknowns $\{\delta p_{ijk}\}$. As described before, a number of outer or Newton iterations are performed with pressure updated and coefficients

recalculated after each iteration. After convergence, saturation S_w is explicitly calculated, block by block, from Eq. 11a (with T_{wn} in the first term). Eq. 17 can be written more simply for the section to follow as

$$\Delta(T\Delta\delta p) - c\delta p + r = 0, \dots\dots\dots (18)$$

where T , δp , c , and r are scalars.

Solution Techniques

Eq. 18 written for all N_b gridblocks can be expressed in matrix form as

$$AP = b, \dots\dots\dots (19)$$

where A is a nonsymmetric, sparse $N_b \times N_b$ matrix and P is the $N_b \times 1$ column vector $\{\delta p_{ijk}\}$. Direct solution (Gaussian elimination) or iterative methods can be used to solve Eq. 19. The arithmetic effort required in direct solution strongly depends on the pattern of nonzero elements in the A matrix. This pattern in turn depends upon the particular linear ordering or numbering of the N_b gridblocks. An ordering is simply a one-to-one correspondence between a linear index $m = 1, 2, \dots, N_b$ and the gridblock indices $\{i, j, k\}$, $i = 1, 2, \dots, N_x$, $j = 1, 2, \dots, N_y$, $k = 1, 2, \dots, N_z$. Here the term *natural* ordering denotes numbering the blocks consecutively first in the shortest direction, then in the next shortest direction, and finally in the longest direction. For example, if $N_x > N_y > N_z$, then

$$m = k + (j-1)N_z + (i-1)N_yN_z. \dots\dots\dots (20)$$

Breitenbach *et al.*,¹²⁹ Peaceman,¹ and others illustrate the diagonal-band form of the A matrix and minimum direct solution effort which result from this natural ordering.

The half bandwidth of the A matrix is N_yN_z and the arithmetic effort (number of multiplications) of direct solution is roughly proportional to $N_b(N_yN_z)^2$. Iterative methods require an arithmetic effort roughly proportional to N_b . Thus increasing problem size, N_b , renders iterative solution increasingly preferable to direct solution. For large problems, computer storage requirement is also significantly less for iterative than direct solution.

Price and Coats¹³⁰ described reduced bandwidth direct solution methods based on diagonal (D2) and alternate-diagonal (D4) gridblock orderings. For certain test problems and iterative methods, they showed a D4 direct/iterative work ratio less than unity for half bandwidths up to about 30. Compared with natural ordering, D4 ordering can reduce direct solution computational effort by factors up to four and six for the 2D and 3D cases, respectively. Woo *et al.*¹³¹ described other techniques that take advantage of matrix sparsity to reduce direct solution effort. In spite of these advancements in direct solution, iterative methods remain preferable for large reservoir studies.

Successive-overrelaxation (SOR) iterative methods described by Young^{132,133} have been used in simulators from the early 1960's. Block SOR (BSOR) methods, including line (LSOR), two-line, and planar SOR, have proved especially popular. The BSOR methods require direct solution within each block, which means that direct

solution must be performed for tridiagonal matrices in LSOR and pentadiagonal matrices in planar SOR. As the block size is increased the arithmetic work per iteration increases because of the increased arithmetic associated with this direct solution within each block. However, convergence rate generally increases and the total number of iterations correspondingly decreases with increasing block size. To some extent, optimal block size can be determined by mathematical analysis^{133,134} of this tradeoff between work per iteration and number of iterations. The SOR methods remain popular because of ease of coding, low computer storage requirement and automatic determination of the optimum value of the single iteration parameter. Varga¹³⁴ describes the *power method* for this parameter determination and Breitenbach *et al.*¹²⁹ illustrate its application.

In 1971, Watts¹³⁵ presented an additive correction method which improves LSOR convergence rate in highly anisotropic problems. A highly anisotropic problem is one where, throughout the grid, transmissibilities in one direction are much greater than those in other direction(s). Set-tari and Aziz¹³⁶ extended Watts' method to other iterative solution techniques.

Alternating-direction iterative methods (ADI) were developed for 2D by Peaceman and Rachford¹³⁷ in 1955 and for 3D by Douglas and Rachford¹³⁸ in 1956. These methods were widely used in simulation throughout the 1960's and into the 1970's. The ADI methods require a sequence or set of iteration parameters. While mathematical analysis yields an optimal parameter set for certain cases,^{1,137} actual reservoir cases frequently require some trial-and-error effort.

In 1968, Stone¹³⁹ described the *strongly-implicit procedure* (SIP); Weinstein *et al.*¹⁴⁰ described SIP in 3D. Again, a set of iteration parameters is required. Parameter estimation methods associated with ADI have proved useful for SIP¹ but, again, some trial-and-error effort is required or beneficial in many reservoir studies.

A number of studies^{129,136,139,141} compare direct solution, LSOR, ADI, and SIP methods for a variety of test and reservoir problems. There is no simple answer to which method is best. The ranking of the methods is problem-dependent in that it depends on the range of variation in coefficient (transmissibility) values in the A matrix and the pattern (e.g., highly anisotropic), if any, of their variation. In general, the more difficult reservoir problems have a very large range from the smaller to larger transmissibilities and this large ratio is not uniformly associated with a particular direction throughout the grid. SIP became widely used throughout the 1970's and remains in use today because it frequently outperforms the other methods in these difficult cases.

A new class or type of iterative methods is the subject of a number of papers¹⁴¹⁻¹⁵⁰ published since the mid 1970's. Basically, the methods involve approximate factorization of the A matrix into an LU product, followed by an iterative sequence

$$LU(\underline{p}^{k+1} - \underline{p}^k) = \underline{r}^k, \dots\dots\dots (21)$$

where

L = a lower triangular matrix (all entries $\ell_{ij} = 0$ for $j > i$),

U = an upper triangular matrix (all entries u_{ij}
 $= 0$ for $j < i$),
 k = iterate number, and
 $r^k = b - Ap^k$.

Convergence is accelerated by the conjugate gradient,¹⁴¹ orthomin,¹⁴³ or other techniques. Because of the sparse, banded nature of the lower and upper triangular matrices L and U , the arithmetic work per iteration of solving Eq. 21 is a very small fraction of that required in direct solution of the original problem, Eq. 19.

These new methods seem very attractive in that they require no iteration parameter and are more robust than previous methods. That is, they generally exhibit fast or reasonable convergence rates, even for difficult reservoir problems where older methods fail or converge slowly. Two studies^{148,150} showed convergence for the difficult thermal (steamflood) problem where negative transmissibilities can occur.¹⁵¹ The interested reader should consult the reference sections of Refs. 141 through 150 for a number of equally good papers dealing with these new iterative methods.

Code Vectorization

The computational speed, storage, and vectorization capabilities of computer hardware have increased sharply in the past few years. As an example, the Cray-1S computer provides up to 4,000,000 decimal-words of storage, compared with a typically available 100,000 words on most machines used until 1975. Recently introduced computers offer sharp increases in computational speeds and speed/cost ratios. In addition, vector processing capabilities of Control Data Corp. and Cray supercomputers significantly increase the efficiency of simulators coded to use this vectorization.

This increased machine size, speed, and vector processing contribute to the feasibility of larger reservoir studies. Until the middle 1970's, most black-oil studies involved grids of 3,000 or fewer blocks. In 1980, Mrosovsky *et al.*¹⁵² described a Prudhoe Bay field study with more than 16,000 active gridblocks. Studies on the supercomputers with grids of more than 30,000 blocks have been performed recently.

The vector-processing capability has had a strong impact on simulation technology. The resultant increase in feasible study size has spurred the development of new, faster iterative solution techniques. Several papers¹⁵²⁻¹⁵⁶ describe the contribution of code vectorization to reduced computing expense and the need to develop or redesign model code to take advantage of the vectorization.

Nomenclature

A = a nonsymmetric, sparse $N_b \times N_b$ matrix
 $A = \Delta y_i \Delta z_k$ = cross-sectional area normal to flow
 b_P = reciprocal formation volume factor of phase P , ST vol/res vol
 C = 2×2 matrix
 C_{IJ} = concentration of component I in phase J
 C_{IP} = concentration of component I in phase P
 C_{NJ} = concentration of component N in phase J
 f_{IJ} = fugacity of component I in phase J

H_J = enthalpy, energy/mole
 k_{rP} = relative permeability to phase P ($P=w,o,g$)
 L = a lower triangular matrix (all entries $\ell_{ij}=0$ for $j > i$), see Eq. 21
 L = distance between adjacent block centers, $(\Delta x_{i-1} + \Delta x_i)/2$, see Eq. 1
 $m = 1, 2, \dots, N_b$, linear index
 N_b = total number of gridblocks, $N_x N_y N_z$
 N_x = number of gridblocks in x direction
 N_y = number of gridblocks in y direction
 N_z = number of gridblocks in z direction
 n = time level, $t_{n+1} = t_n + \Delta t$
 P = $N_b \times 1$ column vector $\{\delta p_{ijk}\}$, see Eq. 19
 P_{cgo} = gas/oil capillary pressure
 P_{cwo} = water/oil capillary pressure
 q_I = component I interblock flow rate, mass/time
 q_{pl} = mass rate of production of component I
 q_{pP} = production rate of phase P (water or oil)
 R = 2×1 column vector
 S_{gc} = critical gas saturation
 S_J = saturation of phase J
 S_{wc} = critical water saturation
 T = interblock transmissibility and $T=2 \times 2$ matrix
 T_{IJ} = interblock transmissibility for flow of component I in phase J
 T_{on} = oil transmissibility at time level n
 T_{wn} = water transmissibility at time level n
 U = an upper triangular matrix (all entries $u_{ij}=0$ for $j < i$)
 U_J = internal energy, energy/mole
 V = grid block volume, $\Delta x_i \Delta y_j \Delta z_k$
 $\Delta x = x_{i-1} - x_i$, where x is p or Z
 x_{IJ} = mol fraction of component I in phase J
 γ_P = specific weight of phase P
 δ = time difference operator, $\delta X \equiv X_{n+1} - X_n$
 μ_P = viscosity of phase P

Subscripts

i, j, k = gridblock indices
 J = w, o, g or $1, 2, 3$,
 n = step number

Superscripts

k = iteration number
 ℓ = iteration number

References

1. Peaceman, D.W.: *Fundamentals of Numerical Reservoir Simulation*, Elsevier Scientific Pub. Co., New York City (1977).
2. Crichlow, H.G.: *Modern Reservoir Engineering—A Simulation Approach*, Prentice-Hall, Inc., Englewood Cliffs, NJ (1977).
3. Aziz, K. and Settari, A.: *Petroleum Reservoir Simulation*, Applied Science Publishers, London (1979).
4. Thomas, G.W.: *Principles of Hydrocarbon Reservoir Simulation*, second edition, Intl. Human Resources Dev. Corp., Boston (1982).
5. Muskat, M.: *The Flow of Homogeneous Fluids Through Porous Media*, J.W. Edwards, Inc., Ann Arbor, MI (1946).
6. Muskat, M.: *Physical Properties of Oil Production*, McGraw-Hill Book Co. Inc., New York City (1949).

7. Muskat, M.: "The Production Histories of Producing Gas-Drive Reservoirs," *J. Applied Phys.* (1945) **16**, 147.
8. Katz, D.L.: "Methods of Estimating Oil and Gas Reserves," *Trans., AIME* (1936) **118**, 18-32.
9. Buckley, S.E. and Leverett, M.C.: "Mechanism of Fluid Displacement in Sands," *Trans., AIME* (1942) **146**, 107-17.
10. Welge, H.J.: "A Simplified Method for Computing Oil Recoveries by Gas or Water Drive," *Trans., AIME* (1952) **195**, 91-98.
11. Odeh, A.S.: "Reservoir Simulation—What Is It?" *J. Pet. Tech.* (Nov. 1969) 1383-88.
12. Staggs, H.M. and Herbeck, E.F.: "Reservoir Simulation Models—An Engineering Overview," *J. Pet. Tech.* (Dec. 1971) 1428-36.
13. O'Dell, P.M.: "Numerical Reservoir Simulation: Review and State of the Art," paper presented at the 1974 National AIChE Meeting, Tulsa, OK, March 11-13.
14. Coats, K.H.: "Reservoir Simulation: State of the Art," *J. Pet. Tech.* (Aug. 1982) 1633-42.
15. Craft, B.C. and Hawkins, M.F. Jr.: *Applied Petroleum Reservoir Engineering*, Prentice-Hall, Inc., Englewood Cliffs, NJ (1959).
16. Douglas, J. Jr., Peaceman, D.W., and Rachford, H.H., Jr.: "A Method for Calculating Multi-Dimensional Immiscible Displacement," *Trans., AIME* (1959) **216**, 297-308.
17. Sheldon, J.W., Harris, C.D., and Bavy, D.: "A Method for General Reservoir Behavior Simulation on Digital Computers," paper SPE 1521-G presented at the 1960 SPE Annual Meeting, Denver, Oct. 2-5.
18. Stone, H.L. and Garder, A.O. Jr.: "Analysis of Gas-Cap or Dissolved-Gas Drive Reservoirs," *Soc. Pet. Eng. J.* (June 1961) 92-104; *Trans., AIME*, **222**.
19. Fagin, R.G. and Stewart, C.H. Jr.: "A New Approach to the Two-Dimensional Multiphase Reservoir Simulator," *Soc. Pet. Eng. J.* (June 1966) 175-82; *Trans., AIME*, **237**.
20. Breitenbach, E.A., Thurnau, D.H., and Van Poolen, H.K.: "The Fluid Flow Simulation Equations," paper SPE 2020 presented at the 1968 SPE Symposium on Numerical Simulation of Reservoir Performance, Dallas, April 22-23.
21. Coats, K.H. *et al.*: "Simulation of Three-Dimensional, Two-Phase Flow in Oil and Gas Reservoirs," *Soc. Pet. Eng. J.* (Dec. 1967) 377-88; *Trans., AIME*, **240**.
22. Peery, J.H. and Herron, E.H. Jr.: "Three-Phase Reservoir Simulation," *J. Pet. Tech.* (Feb. 1969) 211-20; *Trans., AIME*, **246**.
23. Snyder, L.J.: "Two-Phase Reservoir Flow Calculations," *Soc. Pet. Eng. J.* (June 1969) 170-82.
24. Sheffield, M.: "Three-Phase Fluid Flow Including Gravitational, Viscous and Capillary Forces," *Soc. Pet. Eng. J.* (June 1969) 255-69; *Trans., AIME*, **246**.
25. Zudkevitch, D. and Joffe, J.: "Correlation and Prediction of Vapor-Liquid Equilibria with the Redlich-Kwong Equation of State," *AIChE J.* (Jan. 1970) **16**, 112-19.
26. Soave, G.: *Chem. Eng. Sci.* (1972) **27**, 1197.
27. Peng, D.Y. and Robinson, D.B.: "A New Two-Constant Equation of State," *Ind. Eng. Chem. Fund.* (1976) **15**, 59.
28. Martin, J.J.: "Cubic Equations of State—Which?" *Ind. Eng. Chem. Fund.* (May 1979) **18**, 81.
29. Kazemi, H., Vestal, C.R., and Shank, G.D.: "An Efficient Multicomponent Numerical Simulator," *Soc. Pet. Eng. J.* (Oct. 1978) 355-68.
30. Fussell, L.T. and Fussell, D.D.: "An Iterative Technique for Compositional Reservoir Models," *Soc. Pet. Eng. J.* (Aug. 1979) 211-20.
31. Coats, K.H.: "A Equation of State Compositional Model," *Soc. Pet. Eng. J.* (Oct. 1980) 363-76.
32. Nghiem, L.X., Fong, D.K., and Aziz, K.: "Compositional Modeling With an Equation of State," *Soc. Pet. Eng. J.* (Dec. 1981) 688-98.
33. Young, L.C. and Stephenson, R.E.: "A Generalized Compositional Approach for Reservoir Simulation," *Soc. Pet. Eng. J.* (Oct. 1983) 727-42.
34. Gottfried, B.S.: "A Mathematical Model of Thermal Oil Recovery in Linear Systems," *Soc. Pet. Eng. J.* (Sept. 1965) 196-210; *Trans., AIME*, **234**.
35. Shutler, N.D.: "Numerical Three-Phase Model of the Two-Dimensional Steamflood Process," *Soc. Pet. Eng. J.* (Dec. 1970) 405-17; *Trans., AIME*, **249**.
36. Weinstein, H.G., Wheeler, J.A., and Woods, E.G.: "Numerical Model for Thermal Process," *Soc. Pet. Eng. J.* (Feb. 1977) 65-78; *Trans., AIME*, **263**.
37. Crookston, H.B., Culham, W.E., and Chen, W.H.: "A Numerical Simulation Model for Thermal Recovery Processes," *Soc. Pet. Eng. J.* (Feb. 1979) 37-58; *Trans., AIME*, **267**.
38. Youngren, G.K.: "Development and Application of an In-Situ Combustion Reservoir Simulator," *Soc. Pet. Eng. J.* (Feb. 1980) 39-51.
39. Coats, K.H.: "In-Situ Combustion Model," *Soc. Pet. Eng. J.* (Dec. 1980) 533-53.
40. Hwang, M.K., Jines, W.R., and Odeh, A.S.: "An In-Situ Combustion Process Simulator With a Moving-Front Representation," *Soc. Pet. Eng. J.* (April 1982) 271-79.
41. Gogarty, W.B.: "Status of Surfactant or Micellar Methods," *J. Pet. Tech.* (Jan. 1976) 93-102.
42. Johnson, C.E. Jr.: "Status of Caustic and Emulsion Methods," *J. Pet. Tech.* (Jan. 1976) 85-92.
43. Pope, G.A. and Nelson, R.C.: "A Chemical Flooding Compositional Simulator," *Soc. Pet. Eng. J.* (Oct. 1978) 339-54.
44. Todd, M.R. and Chase, C.A.: "A Numerical Simulator for Predicting Chemical Flood Performance," *Proc., Fifth SPE Symposium on Reservoir Simulation* (1979) 161-74.
45. Fleming, P.D. III, Thomas, C.P., and Winter, W.K.: "Formulation of a General Multiphase, Multicomponent Chemical Flood Model," *Soc. Pet. Eng. J.* (Feb. 1981) 63-76.
46. Thomas, L.K., Dixon, T.N., and Pierson, R.G.: "Fractured Reservoir Simulation," *Soc. Pet. Eng. J.* (Feb. 1983) 42-54.
47. Gilman, J.R. and Kazemi, H.: "Improvements in Simulation of Naturally Fractured Reservoirs," *Soc. Pet. Eng. J.* (Aug. 1983) 659-707.
48. Blaskovich, F.T. *et al.*: "A Multicomponent Isothermal System for Efficient Reservoir Simulation," paper SPE 11480 presented at the 1983 SPE Middle East Oil Show, Manama, March 14-17.
49. Henderson, J.H., Dempsey, J.R. and Tyler, J.C.: "Use of Numerical Models to Develop and Operate Gas Storage Reservoirs," *J. Pet. Tech.* (Nov. 1969) 1239-46.
50. Mann, L.D. and Johnson, G.A.: "Predicted Results of Numeric Grid Models Compared With Actual Field Performance," *J. Pet. Tech.* (Nov. 1970) 1390-98.
51. Thomas, J.E. and Driscoll, V.J.: "A Modeling Approach for Optimizing Waterflood Performance, Slaughter Field Chickenwire Pattern," *J. Pet. Tech.* (July 1973) 757-63.
52. "A Study of the Sensitivity of Oil Recovery to Production Rate," *Proc., Alberta Energy Resources Conservation Board*, No. 7511 (Feb. 1974) Schedule 1, Shell Canada Ltd.
53. Stright, D.H. Jr., Bennion, D.W., and Aziz, K.: "Influence of Production Rate on the Recovery of Oil From Horizontal Waterfloods," *J. Pet. Tech.* (May 1975) 555-63.
54. Thakur, G.C., *et al.*: "G-2 and G-3 Reservoirs, Delta South Field, Nigeria: Part 2—Simulation of Water Injection," *J. Pet. Tech.* (Jan. 1982) 148-58.
55. Graue, D.J. and Zana, E.T.: "Study of a Possible CO₂ Flood in Rangely Field, Colorado," *J. Pet. Tech.* (July 1981) 1312-18.
56. Bloomquist, C.W., Fuller, K.L., and Moranville, M.B.: "Miscible Gas Enhanced Oil Recovery Economics and the Effects of the Windfall Profit Tax," paper SPE 10274 presented at the 1981 SPE Annual Technical Conference and Exhibition, San Antonio, Oct. 5-7.
57. Todd, M.R., Cobb, W.M., and McCarter, E.D.: "CO₂ Flood Performance Evaluation for the Cornell Unit, Wasson San Andres Field," *J. Pet. Tech.* (Oct. 1982) 1583-90.
58. Herrera, J.Q. and Hanzlik, E.J.: "Steam Stimulation History Match of Multiwell Pattern in the S1-B Zone, Cat Canyon Field," paper SPE 7969 presented at the 1979 California Regional Meeting, Ventura, April 18-20.
59. Williams, R.L.: "Steamflood Pilot Design for a Massive, Steeply Dipping Reservoir," paper SPE 10321 presented at the 1981 SPE Annual Technical Conference and Exhibition, San Antonio, Oct. 5-7.
60. Meldau, R.F., Shipley, R.G., and Coats, K.H.: "Cyclic Gas/Steam Stimulation of Heavy-Oil Wells," *J. Pet. Tech.* (Oct. 1981) 1990-98.
61. Gomaa, E.E., Duerksen, J.H., and Woo, P.T.: "Designing a Steamflood Pilot in the Thick Monarch Sand of the Midway-Sunset Field," *J. Pet. Tech.* (Dec. 1977) 1559-68.
62. Moughamian, J.M., *et al.*: "Simulation and Design of Steam Drive in a Vertical Reservoir," *J. Pet. Tech.* (July 1982) 1546-54.
63. "Selection of Reservoirs Amenable to Micellar Flooding," First Annual Report, Dept. of Energy (Dec. 1980) BC/00048-20.
64. Fayers, F.J., Hawes, R.I., and Mathews, J.D.: "Some Aspects

- of the Potential Application of Surfactants or CO₂ as EOR Processes in North Sea Reservoirs," *J. Pet. Tech.* (Sept. 1981) 1617-27.
65. deZabala, E.F., et al.: "A Chemical Theory for Linear Alkaline Flooding," *Soc. Pet. Eng. J.* (April 1982) 245-58.
 66. Patton, J.T., Coats, K.H., and Colegrove, G.T.: "Prediction of Polymer Flood Performance," *Soc. Pet. Eng. J.* (March 1971) 72-84; *Trans.*, AIME, 251.
 67. Todd, M.R. and Longstaff, W.J.: "The Development, Testing, and Application of a Numerical Simulator for Predicting Miscible Flood Performance," *J. Pet. Tech.* (July 1972) 874-82; *Trans.*, AIME, 253.
 68. Cook, R.E., Jacoby, R.H., and Ramesh, A.B.: "A Beta-Type Reservoir Simulator for Approximating Compositional Effects During Gas Injection," *Soc. Pet. Eng. J.* (Oct. 1974) 471-81.
 69. Patton, J.T., Coats, K.H., and Spence, K.: "Carbon Dioxide Well Simulation: Part 1—A Parametric Study," *J. Pet. Tech.* (Aug. 1982) 1798-1804.
 70. Coats, K.H.: "Simulation of Gas Condensate Reservoir Performance," paper SPE 10512 presented at the 1982 SPE Reservoir Simulation Symposium, New Orleans, Feb. 1-3.
 71. Coats, K.H.: "Simulation of 1/8 Five-/Nine-Spot Patterns," *Soc. Pet. Eng. J.* (Dec. 1982) 902.
 72. Killough, J.E., et al.: "The Kuparek River Field: A Regression Approach to Pseudorelative Permeabilities," paper SPE 10531, presented at the 1982 SPE Symposium on Reservoir Simulation, New Orleans, Feb. 1-3.
 73. Killough, J.E., et al.: "The Prudhoe Bay Field: Simulation of a Complex Reservoir," *Proc.*, Intl. Petroleum Exhibition and Technical Symposium, Beijing (1982) 777-94.
 74. Jacks, H.H., Smith, O.E., and Mattax, C.C.: "The Modeling of a Three-Dimensional Reservoir With a Two-Dimensional Reservoir Simulator—The Use of Dynamic Pseudo Functions," *Soc. Pet. Eng. J.* (June 1973) 175-85.
 75. Kyte, J.R. and Berry, D.W.: "New Pseudo Functions to Control Numerical Dispersion," *Soc. Pet. Eng. J.* (Aug. 1975) 269-76.
 76. Killough, J.E. and Foster, H.P. Jr.: "Reservoir Simulation of the Empire Abo Field: The Use of Pseudos in a Multilayered System," *Soc. Pet. Eng. J.* (Oct. 1979) 279-88.
 77. Coats, K.H., Dempsey, J.R., and Henderson, J.H.: "The Use of Vertical Equilibrium in Two-Dimensional Simulation of Three-Dimensional Reservoir Performance," *Soc. Pet. Eng. J.* (March 1971) 63-71; *Trans.*, AIME, 251.
 78. Hearn, C.L.: "Simulation of Stratified Waterflooding by Pseudo Relative Permeability Curves," *J. Pet. Tech.* (July 1971) 805-13.
 79. Simon, R., Rosman, A., and Zana, E.T.: "Phase-Behavior Properties of CO₂-Reservoir Oil System," *Soc. Pet. Eng. J.* (Feb. 1978) 20-26.
 80. Orr, F.M. and Silva, M.K.: "Equilibrium Phase Compositions of CO₂/Hydrocarbon Mixtures—Part 1: Measurement by a Continuous Multiple-Contact Experiment," *Soc. Pet. Eng. J.* (April 1983) 272-80.
 81. Orr, F.M., Silva, M.K., and Lien, C.: "Equilibrium Phase Compositions of CO₂/Crude Oil Mixtures—Part 2: Comparison of Continuous Multiple-Contact and Slim-Tube Displacement Tests," *Soc. Pet. Eng. J.* (April 1983) 281-91.
 82. Katz, D.L. and Firoozabadi, A.: "Predicting Phase Behavior of Condensate/Crude-Oil Systems Using Methane Interaction Coefficients," *J. Pet. Tech.* (Nov. 1978) 1649-55; *Trans.*, AIME, 265.
 83. Yarbrough, L.: "Application of a Generalized Equation of State to Petroleum Reservoir Fluids," *Equations of State in Engineering, Advances in Chemistry Series*, K.C. Chao and R.L. Robinson (eds.), American Chemical Society, Washington, D.C. (1979), 182, 385-435.
 84. Whitson, C.H. and Torp, S.B.: "Evaluating Constant-Volume Depletion Data," *J. Pet. Tech.* (March 1983) 610-20.
 85. Coats, K.H. and Smart, G.T.: "Application of a Regression-Based EOS PVT Program to Laboratory Data," paper SPE 11197, presented at the 1982 SPE Annual Technical Conference and Exhibition, New Orleans, Sept. 26-29.
 86. Coats, K.H., Dempsey, J.R., and Henderson, J.H.: "A New Technique for Determining Reservoir Description from Field Performance Data," *Soc. Pet. Eng. J.* (March 1970) 66-74; *Trans.*, AIME, 249.
 87. Thomas, L.K. and Hellums, L.J.: "A Nonlinear Automatic History Matching Technique for Reservoir Simulation Models," *Soc. Pet. Eng. J.* (Dec. 1972) 508-14; *Trans.*, AIME, 253.
 88. Wasserman, M.L., Emanuel, A.S., and Seinfeld, J.H.: "Practical Application of Optimal-Control Theory to History-Matching Multiphase Simulator Models," *Soc. Pet. Eng. J.* (Aug. 1975) 347-55; *Trans.*, AIME, 259.
 89. Boberg, T.C., et al.: "Application of Inverse Simulation to a Complex Multireservoir System," *J. Pet. Tech.* (July 1974) 801-08; *Trans.*, AIME, 257.
 90. Watson, A.T., et al.: "History Matching Two-Phase Petroleum Reservoirs," *Soc. Pet. Eng. J.* (Dec. 1980) 521-32.
 91. Blair, P.M. and Peaceman, D.W.: "An Experimental Verification of a Two-Dimensional Technique for Computing Performance of Gas-Drive Reservoirs," *Soc. Pet. Eng. J.* (March 1963) 19-27; *Trans.*, AIME, 228.
 92. Ridings, R.L., et al.: "Experimental and Calculated Behavior of Dissolved-Gas-Drive Systems," *Soc. Pet. Eng. J.* (March 1963) 41-48; *Trans.*, AIME, 228.
 93. Mungan, N.: "A Theoretical and Experimental Coning Study," *Soc. Pet. Eng. J.* (June 1975) 247-54; *Trans.*, AIME, 259.
 94. Kazemi, H. and Merrill, L.S.: "Numerical Simulation of Water Imbibition in Fractured Cores," *Soc. Pet. Eng. J.* (June 1979) 175-82.
 95. Lantz, R.B.: "Quantitative Evaluation of Numerical Diffusion (Truncation Error)," *Soc. Pet. Eng. J.* (Sept. 1971) 315-20; *Trans.*, AIME, 251.
 96. Van-Quy, N., Simandoux, P., and Corteville, J.: "A Numerical Study of Diphasic Multicomponent Flow," *Soc. Pet. Eng. J.* (April 1972) 171-84; *Trans.*, AIME, 253.
 97. Fussell, D.D., Shelton, J.L., and Griffith, J.D.: "Effect of 'Rich' Gas Composition on Multiple-Contact Miscible Displacement—A Cell-to-Cell Flash Model Study," *Soc. Pet. Eng. J.* (Dec. 1976) 310-16; *Trans.*, AIME, 261.
 98. Harpole, K.J. and Hearn, C.L.: "The Role of Numerical Simulation in Reservoir Management of a West Texas Carbonate Reservoir," *Proc.*, Intl. Exhibition and Technical Symposium, Beijing (1982) 759-76.
 99. Heinemann, Z.E., et al.: "Using Local Grid Refinement in a Multiple-Application Reservoir Simulator," *Proc.*, SPE Symposium on Reservoir Simulation, San Francisco (1983) 205-18.
 100. Ewing, R.E., Russell, T.F., and Wheeler, M.F.: "Simulation of Miscible Displacement Using Mixed Methods and a Modified Method of Characteristics," *Proc.*, SPE Symposium on Reservoir Simulation, San Francisco (1983) 71-82.
 101. Carr, A.H. and Christie, M.A.: "Controlling Numerical Diffusion in Reservoir Simulation Using Flux-Corrected Transport," *Proc.*, SPE Symposium on Reservoir Simulation, San Francisco (1983) 25-32.
 102. Todd, M.R., O'Dell, P.M., and Hirasaki, G.J.: "Methods for Increased Accuracy in Numerical Reservoir Simulators," *Soc. Pet. Eng. J.* (Dec. 1972) 515-30; *Trans.*, AIME, 253.
 103. Coats, K.H., et al.: "Three-Dimensional Simulation of Steamflooding," *Soc. Pet. Eng. J.* (Dec. 1974) 573-92; *Trans.*, AIME, 257.
 104. Yanosik, J.L. and McCracken, T.A.: "A Nine-Point, Finite-Difference Reservoir Simulator for Realistic Prediction of Adverse Mobility Ratio Displacements," *Soc. Pet. Eng. J.* (Aug. 1979) 253-62; *Trans.*, AIME, 267.
 105. Abou-Kassem, J.H. and Aziz, K.: "Grid Orientation During Steam Displacement," paper SPE 10497 presented at the 1982 SPE Symposium on Reservoir Simulation, New Orleans, Feb. 1-3.
 106. Holloway, C.C., Thomas, L.K., and Pierson, R.G.: "Reduction of Grid Orientation Effects in Reservoir Simulation," paper SPE 5522 presented at the 1975 SPE Annual Technical Conference and Exhibition, Dallas, Sept. 28-Oct. 1.
 107. Robertson, G.E. and Woo, P.T.: "Grid-Orientation Effects and the Use of Orthogonal Curvilinear Coordinates in Reservoir Simulation," *Soc. Pet. Eng. J.* (Feb. 1978) 13-19.
 108. Vinsome, P.K.W. and Au, A.D.K.: "One Approach to the Grid Orientation Problem in Reservoir Simulation," paper SPE 8247 presented at the 1979 SPE Annual Technical Conference and Exhibition, Las Vegas, Sept. 23-26.
 109. Coats, K.H. and Ramesh, A.B.: "Effects of Grid Type and Difference Scheme on Pattern Steamflood Simulation Results," paper SPE 11079 presented at the 1982 SPE Annual Technical Conference and Exhibition, New Orleans, Sept. 26-29.
 110. Bertiger, W.I. and Padmanabhan, L.: "Finite-Difference Solutions to Grid Orientation Problems Using IMPES," paper SPE 12250 presented at the 1983 SPE Symposium on Reservoir Simulation, San Francisco, Nov. 16-18.
 111. Shah, P.C.: "A Nine-Point Finite Difference Operator for Reduction of the Grid Orientation Effect," paper SPE 12251 presented

- at the 1983 SPE Symposium on Reservoir Simulation, San Francisco, Nov. 16-18.
112. Coats, K.H. and Modine, A.D.: "A Consistent Method for Calculating Transmissibilities in Nine-Point Difference Equations," paper SPE 12248 presented at the 1983 SPE Symposium on Reservoir Simulation, San Francisco, Nov. 16-18.
 113. Frauenthal, J.C., Towler, B.F., and diFranco, R.: "Reduction of Grid-Orientation Effects in Reservoir Simulation By Generalized Upstream Weighting," paper SPE 11593 presented at the 1983 SPE Symposium on Reservoir Simulation, San Francisco, Nov. 16-18.
 114. Pruess, K. and Bodvarsson, G.S.: "A Seven-Point Finite-Difference Method for Improved Grid Orientation Performance in Pattern Steamfloods," paper SPE 12252 presented at the 1983 SPE Symposium on Reservoir Simulation, San Francisco, Nov. 16-18.
 115. Emmanuel, A.S. and Cook, G.W.: "Pseudo-Relative Permeability for Well Modeling," *Soc. Pet. Eng. J.* (Feb. 1974) 7-9.
 116. Chappellear, J.E. and Hirasaki, G.J.: "A Model of Oil-Water Coning for Two-Dimensional, Areal Reservoir Simulation," *Soc. Pet. Eng. J.* (April 1976) 65-72; *Trans.*, AIME, 261.
 117. Woods, E.G. and Khurana, A.K.: "Pseudofunctions for Water Coning in a Three-Dimensional Reservoir Simulator," *Soc. Pet. Eng. J.* (Aug. 1977) 251-62.
 118. Addington, D.V.: "An Approach to Gas-Coning Correlations for a Large Grid Cell Reservoir Simulator," *J. Pet. Tech.* (Nov. 1981) 2267-74.
 119. Akbar, A.M., Arnold, M.D., and Harvey, A.H.: "Numerical Simulation of Individual Wells in a Field Simulation Model," *Soc. Pet. Eng. J.* (Aug. 1974) 315-20.
 120. Mrosovsky, I. and Ridings, R.L.: "Two-Dimensional Radial Treatment of Wells Within a Three-Dimensional Reservoir Model," *Soc. Pet. Eng. J.* (April 1974) 127-31.
 121. Blair, P.M. and Weinaug, C.F.: "Solution of Two-Phase Flow Problems Using Implicit Difference Equations," *Soc. Pet. Eng. J.* (Dec. 1969) 417-24; *Trans.*, AIME, 246.
 122. Bansal, P.P. et al.: "A Strongly Coupled, Fully Implicit, Three-Dimensional, Three-Phase Reservoir Simulator," paper SPE 8329 presented at the 1979 SPE Annual Technical Conference and Exhibition, Las Vegas, Sept. 23-26.
 123. MacDonald, R.C. and Coats, K.H.: "Methods for Numerical Simulation of Water and Gas Coning," *Soc. Pet. Eng. J.* (Dec. 1970) 425-36; *Trans.*, AIME, 249.
 124. Spillette, A.G., Hillestad, J.G., and Stone, H.L.: "A High-Stability Sequential-Solution Approach to Reservoir Simulation," paper SPE 4542 presented at the SPE 1973 Annual Meeting, Las Vegas, Sept. 30-Oct. 3.
 125. Coats, K.H.: "A Highly Implicit Steamflood Model," *Soc. Pet. Eng. J.* (Oct. 1978) 369-83.
 126. Meijerink, J.A.: "A New Stabilized Method for Use in IMPES-Type Numerical Reservoir Simulators," paper SPE 5247 presented at the 1974 SPE Annual Meeting, Houston, Oct. 6-9.
 127. Thomas, G.W. and Thurnau, D.H.: "Reservoir Simulation Using an Adaptive Implicit Method," *Soc. Pet. Eng. J.* (Oct. 1983) 759-68.
 128. Trimble, R.H. and McDonald, A.E.: "A Strongly Coupled, Fully Implicit, Three-Dimensional, Three-Phase Well Coning Model," *Soc. Pet. Eng. J.* (Aug. 1981) 454-58.
 129. Breitenbach, E.A., Thurnau, D.H., and Van Poolen, H.K.: "Solution of the Immiscible Fluid Flow Simulation Equations," *Soc. Pet. Eng. J.* (June 1969) 155-69.
 130. Price H.S. and Coats, K.H.: "Direct Methods in Reservoir Simulation," *Soc. Pet. Eng. J.* (June 1974) 295-308; *Trans.*, AIME, 257.
 131. Woo, P.T., Roberts, S.J., and Gustavson, F.G.: "Application of Sparse Matrix Techniques in Reservoir Simulation," *Sparse Matrix Computations*, J.R. Bunch and D.E. Rose (eds.), Academic Press Inc., Washington, D.C. (1976) 427-38.
 132. Young, D.M.: "The Numerical Solution of Elliptic and Parabolic Partial Differential Equations," *Survey of Numerical Analysis*, J. Todd (ed.), McGraw-Hill Book Co. Inc., New York City (1963) 380-438.
 133. Young, D.M.: *Iterative Solution of Large Linear Systems*, Academic Press Inc., Washington, D.C. (1971).
 134. Varga, R.S.: *Matrix Iterative Analysis*, Prentice-Hall, Inc., Englewood Cliffs, N.J. (1962) 322.
 135. Watts, J.W.: "An Iterative Matrix Solution Method Suitable for Anisotropic Problems," *Soc. Pet. Eng. J.* (March 1971) 47-51; *Trans.*, AIME, 251.
 136. Settari, A. and Aziz, K.: "A Generalization of the Additive Correction Methods for the Iterative Solution of Matrix Equations," *Soc. Ind. Appl. Math. J. Number Analysis* (1973) 10, 506-21.
 137. Peaceman, D.W. and Rachford, H.H.: "The Numerical Solution of Parabolic and Elliptic Differential Equations," *Soc. Ind. Appl. Math. J.* (1955) 3, 28-41.
 138. Douglas, J. and Rachford, H.H.: "On the Numerical Solution of Heat Conduction Problems in Two and Three Space Variables," *Trans.*, American Math. Soc. (1956) 82, 421-39.
 139. Stone, H.L.: "Iterative Solution of Implicit Approximation of Multidimensional Partial Differential Equations," *Soc. Ind. Appl. Math. J. Number Analysis* (1968) 5, 530-58.
 140. Weinstein, H.G., Stone, H.L., and Kwan, T.V.: "Iterative Procedure for Solution of Systems of Parabolic and Elliptic Equations in Three Dimensions," *IEC Fundamentals* (1969) 8, 281-87.
 141. Watts, J.W. III: "A Conjugate Gradient-Truncated Direct Method for the Iterative Solution of the Reservoir Simulation Pressure Equation," *Soc. Pet. Eng. J.* (June 1981) 345-53.
 142. Hestenes, M.R. and Stiefel, E.: "Methods of Conjugate Gradients for Solving Linear Systems," *J. of Research* (1952) 49, 509-36.
 143. Concus, P. and Golub, G.H.: "A Generalized Conjugate Gradient Method for Nonsymmetric Systems of Linear Equations," Report STAN-CS-76-535, Stanford U., Stanford, CA (Jan. 1976).
 144. Vinsome, P.K.W.: "Orthomin, an Iterative Method for Solving Sparse Banded Sets of Simultaneous Linear Equations," paper SPE 5729 presented at the 1976 SPE Symposium on Numerical Simulation of Reservoir Performance, Los Angeles, Feb. 19-20.
 145. Meijerink, J.A. and Van Der Worst, H.A.: "An Iterative Solution Method for Linear Systems of Which the Coefficient Matrix is a Symmetric M-Matrix," *Math. of Comp.* (Jan. 1977) 148-62.
 146. Kershaw, D.S.: "The Incomplete Cholesky-Conjugate Gradient Method for the Iterative Solution of Systems of Linear Equations," *J. Comput. Physics* (1978) 26, 43-65.
 147. Young, D.M. and Je, N.C.: "Generalized Conjugate Gradient Acceleration of Nonsymmetric Iterative Methods," *Linear Algebraic Applications* (1980) 34, 159-94.
 148. Tan, T.B.S. and Letkeman, J.P.: "Application of D4 Ordering and Minimization in an Effective Partial Matrix Inverse Iterative Method," paper SPE 10493 presented at the 1982 SPE Symposium on Reservoir Simulation, New Orleans, Feb. 1-3.
 149. Behie, A. and Forsyth, P.A.: "Practical Considerations for Incomplete Factorization Methods in Reservoir Simulation," paper SPE 12263 presented at the 1983 SPE Symposium on Reservoir Simulation, San Francisco, Nov. 16-18.
 150. Wallis, J.R.: "Incomplete Gaussian Elimination as a Preconditioning for Generalized Conjugate Gradient Acceleration," paper SPE 12265 presented at the 1983 SPE Symposium on Reservoir Simulation, San Francisco, Nov. 16-18.
 151. Coats, K.H.: "Reservoir Simulation: A General Model Formulation and Associated Physical/Numerical Sources of Instability," *Boundary and Interior Layers—Computational and Asymptotic Methods*, J.J. Miller (ed.), Boole Press, Dublin (1980) 62-76.
 152. Mrosovsky, I., Wong, J.Y., and Lampe, H.W.: "Construction of a Large Field Simulator on a Vector Computer," *J. Pet. Tech.* (Dec. 1980) 2253-64.
 153. Woo, P.T.: "Application of Array Processor to Sparse Elimination," *Proc.*, paper SPE 7674 presented at the 1979 SPE Symposium on Reservoir Simulation, Denver, Jan. 31-Feb. 2.
 154. Nolen, J.S., Kuba, D.W., and Kasic, M.J. Jr.: "Application of Vector Processors to Solve Finite Difference Equations," *Soc. Pet. Eng. J.* (Aug. 1981) 447-53.
 155. Calahan, D.A.: "Performance of Linear Algebra Codes on the CRAY-1," *Soc. Pet. Eng. J.* (Oct. 1981) 558-64.
 156. Killough, J.E. and Levesque, J.M.: "Reservoir Simulation and the In-House Vector Processor: Experience for the First Year," paper SPE 10521 presented at the 1982 SPE Symposium on Reservoir Simulation, New Orleans, Feb. 1-3.

General Reference

- Mattox, C.C. and Dalton, R.L.: *Reservoir Simulation*, Monograph Series, SPE, Dallas; to be published in 1986.

Chapter 49

Electrical Logging

M.P. Tixier, Consulting Engineer *

Fundamentals

Well logging is an operation involving a continuous recording of depth vs. some characteristic datum of the formations penetrated by a borehole. The record is called a log. In addition, a magnetic tape is usually made.

Many types of well logs are recorded by appropriate downhole instruments called *sondes*, lowered into the wellbore on the end of a cable. The winch of the logging cable is generally brought to the well on a special logging truck (Fig. 49.1), which also carries the recorders, power sources, and auxiliary equipment. The parameters being logged are measured in situ as the sonde is moved along the borehole. The resulting signals from the sonde are transmitted through electrical conductors in the cable to the surface, where the continuous recording, or log, is made.

Electrical logging is an important branch of well logging. Essentially, it is the recording, *in uncased sections of a borehole*, of the *resistivities* (or their reciprocals, the *conductivities*) of the subsurface formations, generally along with the *spontaneous potentials* (SP) generated in the borehole.

Electrical logging has been accepted as one of the most efficient tools in oil and gas exploration and production. When a hole has been drilled, or at intervals during the drilling, an electrical survey is run to obtain quickly and economically a complete record of the formations penetrated. This recording is of immediate value for geological correlation of the strata and detection and evaluation of possibly productive horizons. The information derived from the electrical logs may at the same time be supplemented by sidewall samples of the formations taken from the wall of the hole or by still other types of borehole investigations that can be performed by using additional wireline equipment available for use with the logging truck [deviation surveys, caliper (hole-diameter) surveys, dipmeter surveys, temperature surveys, radioactivity (gamma ray, density, neutron, and nuclear

spectrometry) surveys, acoustic surveys, wireline formation tester, etc.].

As explained later, several types of resistivity-measuring systems are used that have been designed to obtain the greatest possible information under diverse conditions—e.g., conventional devices (normals and laterals), induction log (IL), Laterolog™ (LL), microresistivity devices, and electromagnetic propagation logs. Table 49.1 gives the service company nomenclature for various logging tools.

The typical appearance of a standard electrical log is illustrated in Fig. 49.2. The left track of the log contains the SP curve. The middle track contains a 16-in. short normal (shallow-investigation resistivity curve), recorded on both regular and amplified sensitivity scales as solid curves, and a 64-in. normal (medium-investigation resistivity curve, dashed curve). The right track contains an 18-ft 8-in. lateral (deep-investigation curve).

Logs recorded with other combinations of resistivity-measuring devices have a similar general appearance, although the corresponding devices differ in principle and performance. Microresistivity logs generally include a microcaliper curve (hole-diameter recording), which is useful in the location of permeable zones. Of late, four-logarithmic tracks are often replacing the two-arithmetic track mentioned previously.

The curves are recorded on the most appropriate of several available sensitivity scales. The usual depths of scales are 2 in.=100 ft (regular) and 5 in.=100 ft (detail). Less frequently a scale of 1 in.=100 ft is used. For cases where great detail is involved, as in micrologging and dipmeter logging, special expanded scales are available. In many parts of the world, metric depth scales are used instead of English scales.

Earth Resistivities

Formation resistivities are important clues to probable lithology and fluid content. With a few exceptions that are rare in oilfield practice, such as metallic sulfides and

*Authors of the original chapter on this topic in the 1962 edition included this author, H.G. Doll, M. Martin, and F. Segesman.

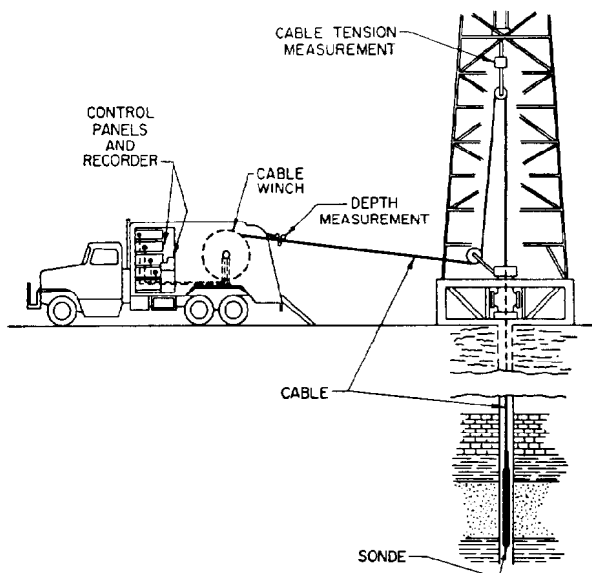


Fig. 49.1—Setup for wireline logging operations in wells (schematic).

graphite, dry rocks are very good insulators but, when their pores are impregnated with water, they conduct electric current. Subsurface formations in general have finite measurable resistivities because of the water contained in their pores or adsorbed on their interstitial clay. Formation resistivity also depends on the shape and the interconnection of the pore spaces occupied by the water. These depend on the formation lithology and, in the case of reservoir rocks, on the presence of nonconductive oil or gas.

Units of Resistivity and Conductivity. In electrical logging, the resistivity is usually measured. An exception is induction logging, in which the conductivity is recorded along with its reciprocal, the resistivity. Measurements made with electromagnetic propagation are discussed later.

The resistivity (specific resistance) of a substance to the flow of electrical current, at any given temperature, is the resistance measured between opposite faces of a unit cube of that substance. In electrical-logging work,

TABLE 49.1—SERVICE COMPANY NOMENCLATURE

Schlumberger	Gearhart	Dresser Atlas	Welex
Electrical Log	Electrical Log	Electrolog	Electric Log
Induction Electric Log (IEL)	Induction Electric Log	Induction Electrolog	Induction Electric Log
Induction Spherically Focused Log (ISF)			
Dual Induction Spherically Focused Log	Dual Induction-Laterolog	Dual Induction Focused Log	Dual Induction Log
Laterolog-3 (LL3)	Laterolog-3	Focused Log	Guard Log
Dual Laterolog	Dual Laterolog	Dual Laterolog	Dual Guardlog
Microlog (ML)	Micro Electric Log	Minilog	Contact Log
Microlaterolog (MLL)	Microlaterolog	Microlaterolog	$F_o R_{xo}$ Log
Proximity Log (PL)		Proximity Log	
Microspherically Focused Log (MSFL)			
Borehole Compensated Sonic Log	Borehole Compensated Sonic Log	Borehole Compensated Sonic Log	Acoustic Velocity Log
Long Spaced Sonic Log		Long Spacing BHC Acoustilog	
Cement Bond/Variable Density Log	Sonic Cement Bond System	Acoustic Cement Bond Log	Microseismogram
Gamma Ray Neutron	Gamma Ray Neutron	Gamma Ray Neutron	Gamma Ray Neutron
Sidewall Neutron Porosity Log	Sidewall Neutron Porosity Log	Sidewall Epithermal Neutron Log	Sidewall Neutron Log
Compensated Neutron Log (CNL)	Compensated Neutron Log	Compensated Neutron Log	Dual Spaced Neutron Log
Thermal Neutron Decay Time Log		Neutron Lifetime Log	
Dual Spacing TDT		Dual Detector Neutron	
Compensated Formation Density Log	Compensated Density Log	Compensated Densilog	Density Log
Litho-Density Log			
High Resolution Dipmeter	Four Electrode Dipmeter	Diplog	Diplog
Formation Interval Tester		Formation Tester	Formation Tester
Repeat Formation Tester	Selective Formation Tester	Formation Multi Tester	
Sidewall Sampler	Sidewall Core Gun	Corgun	Sidewall Coring
Electromagnetic Propagation Log			
Bore Hole Geometry Tool	X-Y Caliper	Caliper Log	Caliper Log
Ultra Long Spacing Electric Log			
Natural Gamma Ray Spectrometry		Spectralog	
General Spectroscopy Tool		Carbon/Oxygen Log	
Well Seismic Tool			
Fracture Identification Log	Fracture Detection Log		

the meter was chosen as the unit of length; so the unit of resistivity is taken as the $(\Omega \cdot \text{m})^2/\text{m}$, or more simply, the ohm-meter, $\Omega \cdot \text{m}$.

Since conductivity is the reciprocal of resistivity ($C=1/R$), a possible unit of conductivity would be $1/(\Omega \cdot \text{m})$, or \mathcal{U}/m . However, since this unit would necessitate extensive use of decimal fractions, a unit one-thousandth as large, the millimho/meter ($\text{m}\mathcal{U}/\text{m}$), is employed. Thus, formations having resistivities of 10, 100, or 1,000 $\Omega \cdot \text{m}$ have conductivities of 100, 10, or 1 $\text{m}\mathcal{U}/\text{m}$, respectively.

Dependence of Water Resistivity on Salinity and Temperature. The resistivity of an electrolytic solution decreases as the amount of chemicals therein increases. At any given temperature the electrical conductivity of a formation water or a drilling mud will depend on the concentration and nature of the dissolved chemicals.

In most cases the predominant solute is sodium chloride (NaCl); therefore, the NaCl conversion chart (Fig. 49.3) may generally be used to obtain resistivity from concentration. If other chemicals are present in relatively large amounts, it is possible to convert the concentrations of such chemicals into equivalent concentrations of NaCl to find the resistivity. To make the conversion, apply the appropriate multipliers given in Table 49.2 for the concentration of each separate ion [in parts per million (ppm) or (m^3/m^3) by weight, or in grains per gallon (gr/gal) or (kg/m^3)], and add the products.¹ Note that concentrations expressed in milligrams per liter (mg/L) and in ppm may be appreciably different at high concentrations. Below about 50,000 ppm, however, measurements at room temperature in the two units may be used interchangeably without serious error.

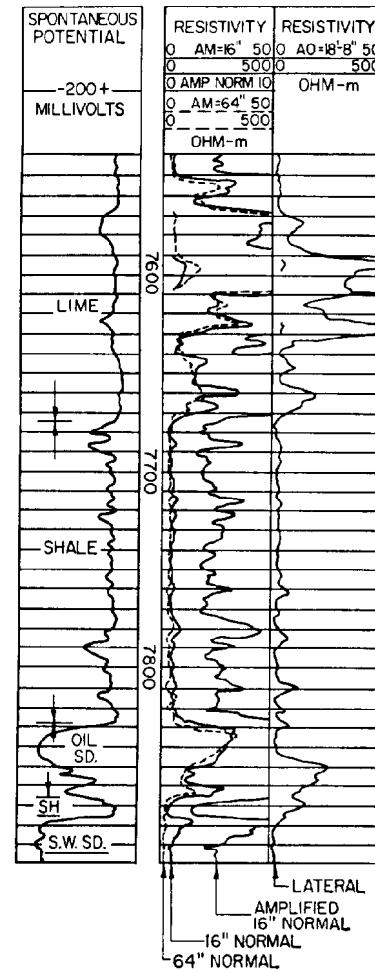


Fig. 49.2—Typical electrical log.

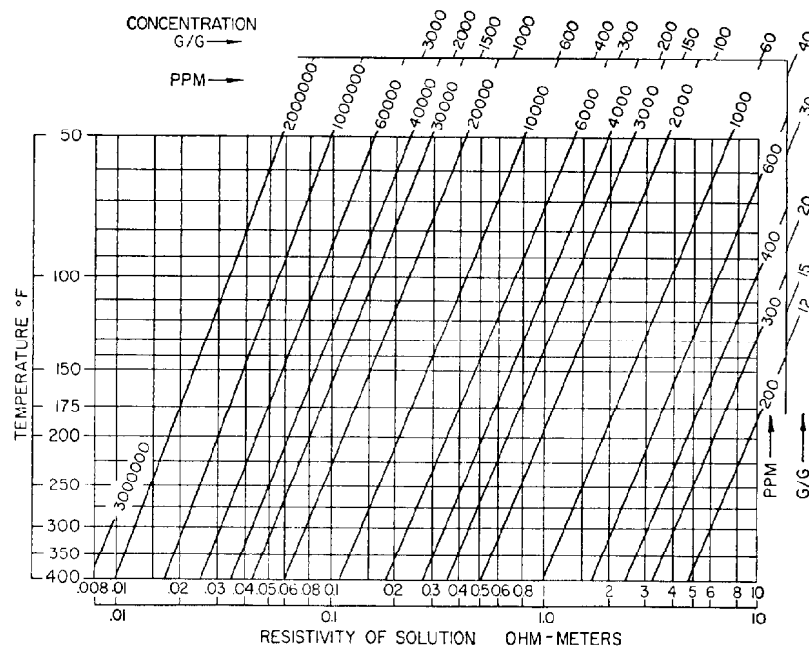


Fig. 49.3—Resistivity vs. concentration for NaCl solutions at various temperatures.

The resistivity of an electrolytic solution decreases as its temperature increases. This is of great importance, since temperature in the earth increases with depth.

Before the resistivity of the drilling mud (measured at surface temperature) can be compared with that of a formation (measured at a much higher temperature in a deep well) the resistivities must be converted to values that would have been observed at a common temperature. The temperature conversion is accomplished by means of Fig. 49.3, which shows for NaCl solutions the effects of both salinity and temperature on resistivity. Downhole temperatures may be estimated from a so-called "bottomhole temperature" (BHT) obtained by means of a maximum-reading thermometer inserted in the body of the sonde.

Resistivities of Formation Waters. Formation waters can vary remarkably with geographic location, depth, and geological age. Shallow groundwaters are usually fresh (not saline), with resistivities sometimes exceeding 20 to 50 $\Omega \cdot m$ at room temperature. They also may contain appreciable amounts of calcium and magnesium salts, which make them "hard." At great depths, formation waters generally tend to be more saline. In deep wells, formation-water resistivities sometimes may correspond to complete saturation (0.014 $\Omega \cdot m$ at 200°F).

A knowledge of R_w , the formation-water resistivity, is important in electrical-log interpretation. R_w may be obtained from the readings of the SP curve (Eq. 9) or from resistivity measurements on samples of formation water recovered from production or in drillstem tests. It also may be estimated from measurements of the resistivity of the permeable formations of interest when they are 100% water-saturated, R_0 , if the porosity or formation factor is known (Eqs. 1 and 2). R_w may be computed, as has been explained, from analyses of formation waters. Resistivity of formation waters is discussed further in Chap. 24.

Mud, Mudcake, and Mud-Filtrate Resistivities. Resistivities of the mud, R_m , the mudcake, R_{mc} , and the mud filtrate, R_{mf} , are all important in log interpretation. R_m is obtained by direct measurement on a mud sample. R_{mf} and R_{mc} are obtained by direct measurements on filtrate and mudcakes pressed from a sample of the mud, or they can be estimated from average statistical data on the basis of mud resistivity.²⁻⁴ Correction for the variation of these resistivities with temperature is made by use of Fig. 49.3.

Formation Resistivity Factor. If R_0 is the resistivity of a clean (nonshaly) formation completely saturated with water of resistivity R_w , the ratio R_0/R_w will be a constant that depends on the lithologic structure of the for-

mation and not on the resistivity, R_w , of the saturating water. This constant is the *formation resistivity factor*, F_R , commonly called "formation factor."

$$F_R = \frac{R_0}{R_w} \quad (1)$$

Dependence of Formation Factor on Porosity and Lithology. The formation factor, F_R , of a clean formation can be related to its porosity, ϕ , by an empirical formula of the form $F_R = a/\phi^m$, where a and m are constants. The exponent m , sometimes called the cementation exponent or factor, varies with the lithology.

In the construction of many graphs for log interpretation,² the "Humble formula" proposed by Winsauer *et al.*⁵ has been generally adopted:

$$F_R = \frac{0.62}{\phi^{2.15}} \quad (2)$$

An early formula proposed by Archie, which fits particularly well for consolidated formations such as hard sandstones and limestones, is

$$F_R = \frac{1}{\phi^2} \quad (3)$$

Limestones often contain vugs, interconnected with fissures, which add their porosity to that of the matrix. When the vugs and fissures are spaced closely, compared with the spacings of the resistivity-measuring devices, Eq. 3 often can be used as in the case of sandstones or limestones with only granular porosity. Nevertheless, it is sometimes advisable to use values of m greater than two as required to fit local observations.

Shaly (Dirty) Formations. Shales and clays are themselves porous and are generally impregnated with mineralized water. Therefore, they have appreciable conductivity, which is enhanced by ion-exchange conduction through the shale matrix. (This shale conduction is sometimes, though not quite properly, referred to as resulting from "conductive solids.") On the other hand, the size of the shale pores is so small that practically no movement of fluid is possible. Accordingly, shale, whether deposited in thin laminations or dispersed in the interstices of the sand, contributes to the conductivity of the formation without contributing to its effective porosity.

The relation between formation resistivity and porosity becomes more complex for shaly formations than for clean formations. Because of the additional shale conductance, the ratio of formation resistivity to water resistivity (i.e., the formation factor) is not constant when the resistivity of the impregnating water changes.⁶ Nevertheless, if the shale content is not too great, experimental observations show that for low enough values of water resistivity this ratio is almost constant, as though the conductance of the shale were then negligible in comparison with that of the water; and a limiting formation factor is found, which is related approximately to the effective porosity in the same way as the formation factor of a clean sand.

TABLE 49.2—CONVERSIONS FOR CATIONS AND ANIONS

Cations		Anions	
Na	1.0	Cl	1.0
Ca	0.95	SO ₄	0.5
Mg	2.0	CO ₃	1.26
		HCO ₃	0.27

Relation Between Formation Resistivity and Saturation. When a part of the pore space is occupied by an insulating material such as oil or gas, the resistivity of the rock, R_t , is greater than the resistivity that it has when 100% water-bearing, R_0 . The resistivity of such rock is a function of the fraction of the PV occupied by water.

For substantially clean formations, the water saturation, S_w , is related to R_t (resistivity of formation containing hydrocarbons and formation water, with a water saturation S_w) and R_0 (resistivity of same formation when 100% saturated with the same water) by an empirical relation known as the Archie equation.⁷

$$S_w = \left(\frac{R_0}{R_t} \right)^{1/n} \quad \dots \dots \dots (4)$$

Empirically determined values of n range between 1.7 and 2.2, depending on the type of formation. Experience shows that $n=2$ should give a sufficiently good approximation. Then, combining Eqs. 4 and 1 gives

$$S_w = \left(\frac{R_0}{R_t} \right)^{1/2} = \left(\frac{F_R R_w}{R_t} \right)^{1/2} \quad \dots \dots \dots (5)$$

The ratio R_t/R_0 is sometimes designated as the resistivity index, I_R ; accordingly, $S_w = (I_R)^{-1/n}$.

The relation between formation resistivity and water saturation is more complex when the formations contain some shale or clay because of the additional conductance resulting from the interstitial shale.^{8,9}

Ranges of Resistivity—Formation Classifications. Clays and shales are porous, practically impervious formations and are often very uniform throughout their mass. Their resistivity is comparatively low and practically constant over wide intervals. Compact and impervious rocks, such as gypsum, anhydrite, dense calcareous formations, or certain kinds of coal, are highly resistive because of their very small interstitial water content.

Resistivities of porous and permeable formations, such as sands, vary widely, depending on their lithology and fluid content. In electrical logging it is convenient to classify reservoir rocks as follows.

Soft Formations. These formations are chiefly poorly consolidated sand/shale series. The porosity of the sands is intergranular and exceeds 20%. Resistivities range from 0.3 $\Omega \cdot m$ for saltwater-bearing sands to several $\Omega \cdot m$ for oil-saturated sands.

Intermediate Formations. These are chiefly moderately consolidated sandstones but frequently limestones and/or dolomites. Reservoir porosity is generally intergranular, ranging from about 15 to 20%. The reservoir formations are interbedded with shales and very often with tight rocks. Resistivities range from 1 to about 100 $\Omega \cdot m$.

Hard Formations. These are chiefly limestones and/or dolomites, and also consolidated sandstones. They consist mostly of tight rocks containing porous and permeable zones, and shale streaks. The porosity of reservoirs is less than 15%. Most often, the porous and

permeable zones contain fissures and vugs. Resistivity range is from 2 to 3 $\Omega \cdot m$ to several hundred. For the completely tight formations, such as salt and anhydrite, the resistivity may be practically infinite.

Anisotropy. In many sedimentary strata, the mineral grains have a flat or plate-like shape with an orientation parallel to the sedimentation. Current travels with great facility along the water-filled interstices, which are mostly parallel to the stratification. These strata, therefore, do not possess the same resistivity in all directions. Such *microscopic anisotropy* is observed mostly in shales.

Moreover, in electrical logging, the distance between electrodes or coils on the measuring devices is great enough that the volume of formation involved in the measurements very often includes sequences of interbedded resistive and conductive streaks. Since current flows more easily along the beds than perpendicular to them, the formation has *macroscopic anisotropy*.

Both kinds of anisotropy may add their respective effects to influence the apparent resistivity. The longitudinal, or horizontal, resistivity, R_H , measured along the bedding planes is always less than the transverse, or vertical (perpendicular) resistivity, R_V .

Resistivity-measuring devices whose readings are not appreciably affected by the borehole [the deep induction log (ILD), and under certain conditions, the laterolog (LL), and the long lateral when the ratio R_H/R_m is low or moderate] will read R_H . Because of the borehole effect, the short-spacing-electrode devices usually read values greater than R_H .¹⁰

Distribution of Fluids and Resistivities in Permeable Formations Invaded by Mud Filtrate. Inasmuch as the hydrostatic pressure of the mud is usually maintained greater than the natural pressure of the formations, mud filtrate (forced into the permeable beds) displaces the original formation fluids in the region close to the borehole. Solid materials from the mud deposited on the wall of the hole form a mudcake, which tends to impede and reduce further infiltration.

The thickness and the nature of the mudcake depend on the kind of mud and on the drilling conditions rather than on the formations. The thickness, h_{mc} , is usually between $\frac{1}{8}$ and 1 in. For water-based muds the mudcake resistivity, R_{mc} , is about equal to one or two times the mud resistivity, R_m . In some oil-emulsion muds, R_{mc} may be somewhat greater.

Fig. 49.4a represents a schematic cross section of an oil-bearing permeable bed penetrated by a borehole. Fig. 49.4b and 49.4c show the corresponding radial distribution of fluids in formation and resistivities.

As indicated in Fig. 49.4a, the zones of different resistivity may be divided into the drilling mud within the borehole (of resistivity R_m); the mudcake R_{mc} , the flushed zone R_{xo} ; a transition zone; in some cases an "annulus," R_{an} (present only in certain oil- or gas-bearing formations); and the uncontaminated zone (of resistivity R_t). The invaded zone (of "average" resistivity, R_i) includes the flushed zone and the transition zone.

Invaded Zone. This zone is behind and close to the wall of the hole; it is believed that most of the original interstitial fluids have been flushed out by the mud

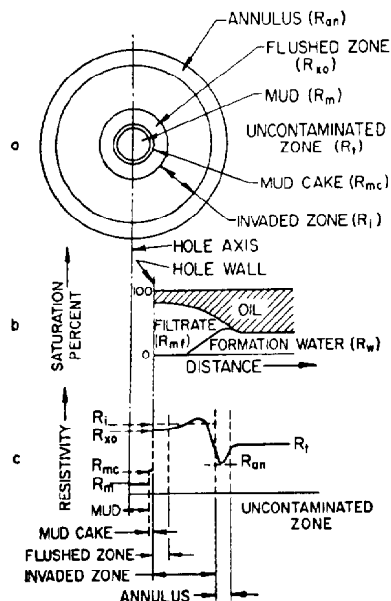


Fig. 49.4—*a*. Horizontal section through a permeable oil-bearing bed ($S_w < 60\%$); *b*. radial distribution of fluids in formation (qualitative); *c*. radial distribution of resistivities.

filtrate. This flushed zone, of resistivity R_{xo} , is considered to extend, under usual conditions of invasion, at least 3 in. from the wall. Exceptions to this rule can occur.

If the bed is water bearing, the pores in the flushed zone are completely filled with the mud filtrate, and for clean formations R_{xo} is nearly equal to $F_R R_{mf}$; F_R being the formation factor and R_{mf} the mud-filtrate resistivity.

If the bed is oil bearing, the flushed zone contains some residual oil saturation, S_{or} . From Eq. 5, S_{xo} , the water saturation in the flushed zone is

$$S_{xo} = \left(\frac{F_R R_{mf}}{R_{xo}} \right)^{1/2}$$

or

$$R_{xo} = \frac{F_R R_{mf}}{S_{xo}^2}, \quad \dots \dots \dots (6)$$

where $S_{xo} = 1 - S_{or}$.

Beyond the region of maximum flushing, R_{xo} , there is a more or less extended transition region, the nature of which depends on the characteristics of the formation, the speed of invasion, and the hydrocarbon content. The invaded zone includes the flushed zone and the part of the transition zone invaded by filtrate. In the case of water-bearing sands and oil-bearing sands of high water saturation, the invaded zone extends up to the uncontaminated zone, R_f .

There can be no exact definition of the depth of the invaded zone, but it is convenient to introduce a factor d_i , called the "electrically equivalent diameter of invasion," corresponding to an average invaded zone of resistivity R_i , which has the same effect as the actual in-

vaded zone on measurements made in the borehole. The depth of invasion is variable. It depends on the plastering properties of the mud, pressure differences between the mud column and the formation, time elapsed since the formation was drilled, porosity of the formation, proportion and nature of the fluids (water, oil, gas) present in the pores, reaction of any interstitial clays with the mud filtrate, etc.

All other conditions being the same, the greater the porosity, the smaller the depth of invasion. With usual muds, d_i seldom exceeds $2d_h$ (d_h = hole diameter) in high-porosity sands, but it may exceed $5d_h$ and even $10d_h$ in low-porosity formations such as consolidated sandstones or limestones. In some cases, invasion can be extremely shallow in very permeable formations and in gas-bearing formations.

In very permeable beds, when there is an appreciable difference between the specific gravities of the mud filtrate and the salt-laden interstitial water, gravity-segregation effects may occur, with the fresher filtrate tending to accumulate at the top boundary of the bed, resulting in a decrease in the depth of invasion in the lower part of the bed.¹¹

In fissured formations, the permeability is quite often enormous because of the fissures—much greater than the permeability of the matrix material surrounding them. Suppose that a formation is composed of a porous but relatively impermeable material, broken by networks of roughly parallel fissures. Mud filtrate penetrates the fissures easily and deeply, driving out much of the original fluids (oil and formation water). On the other hand, the matrix itself may be penetrated hardly at all by the filtrate. Since the fissures constitute a small part of the total PV, only a very small portion of the total original fluids is displaced. As a result, R_{xo} is little different from R_f , and the ratio R_{xo}/R_{mf} is no longer representative of the formation factor.

Annulus. When the formation contains hydrocarbons, the process of invasion is complex. The distribution of fluids is then affected by the two-phase permeabilities, relative densities (gravities) and viscosities of the fluids, capillary forces, etc.

When the initial water saturation is low (less than about 50%), one important feature is the existence of an *annular region* just inside the uncontaminated zone, containing mainly formation water and some residual oil. This annulus is explained as follows. The mud filtrate penetrates the formation radially, sweeping the removable oil and formation water ahead of it. For large oil saturation, the relative permeability to oil is appreciably greater than that to water. Therefore, the oil moves faster, leaving a zone (the annulus) enriched in formation water behind it.

It seems likely that, because of the effects of diffusion, capillary pressure, gravity, etc., the existence of a well-defined annulus is a transitory phenomenon. Field log experience nevertheless seems to show that the annulus does very often exist at the time the logs are run. Computations have shown that the presence of the annulus has a practically negligible effect on the response of the devices with electrodes (normals, laterals, and laterolog). It may have an effect on the induction log, but this can be taken care of for practical purposes by means of appropriate interpretation charts.²

Uncontaminated Zone. For clean formations, from Eq. 5,

$$R_t = \frac{F_R R_w}{S_w^2} \dots \dots \dots (7)$$

In the usual case, R_{mf} is 10 to 25 times as large as R_w . Thus, comparing Eqs. 6 and 7 with usual values of S_w and S_{xo} , R_t , even in oil-bearing formations, is often less than R_{xo} , as represented in Fig. 49.4c.

Apparent Resistivity. Since any resistivity measurement is affected in some degree by the resistivities of all the media in the immediate vicinity of the sonde (i.e., mud, different parts of the formation that vary in resistivity, adjacent formations if the bed measured is thin), any given device records an apparent resistivity. Each resistivity device is calibrated so that when the sonde is in a homogeneous medium (or in some other condition appropriate to practice, specified for the particular device) the apparent resistivity reading is equal to the actual resistivity.

Requirements for and Types of Resistivity Devices. Inspection of basic relations in Eqs. 1, 2, 5, and 6 shows that a determination of S_w and ϕ requires a knowledge of R_t and R_{xo} (or R_i , in certain cases where R_{xo} is not easily determined). Thus, for the reservoir-evaluation problem, it is necessary to have resistivity-measuring devices with different depths of investigation to obtain values indicative of the resistivities of the invaded zone and the uncontaminated zone. The readings of the deep- and shallow-investigation curves may often be used to correct each other, through correction charts or departure curves, to obtain better values of R_t and R_i .

Another function of resistivity recording is to provide an accurate definition of bed boundaries, particularly of permeable beds. Finally, it is desirable that the readings not be influenced by the effect of the mud column or, in case of thin beds, by the adjacent formations.

These requirements are only partly satisfied with the "conventional" resistivity devices. The introduction of microdevices and focused devices has brought about an appreciable improvement.

Currently used resistivity devices may be classified in two categories.

1. Macrodevices, which derive their reading from about 10 to 100 cu ft of material around the sonde (useful for R_t and R_i evaluation), and include unfocused-electrode devices, focused-electrode devices, and induction logging devices.

2. Microdevices (also called wall-resistivity devices), which derive their readings from a few cubic inches of material behind or close to the wall of the hole. Since the electrodes are mounted on an insulating rubber pad pressed against the wall of the hole, measurements are affected only marginally by the mud column. Microdevices are of unfocused and focused types.

Resistivity devices that have electrodes may be used in holes filled with water or water-based drilling mud, which provides the electrical contact necessary between electrodes and formation. The induction log can also be used in empty holes or in holes filled with nonconductive oil-based mud. The various resistivity devices are described later.

Spontaneous Potential (SP) Log

The SP log is a record of the naturally occurring potentials in the mud at different depths in a borehole. The measurement is made in uncased holes containing water-based or oil-emulsion muds between an exploratory electrode on the sonde in the borehole and a stationary reference electrode at the surface.

Usually the SP curve (Fig. 49.2) consists of a more or less straight baseline (corresponding to the shales) having excursions or peaks to the left (opposite the permeable strata). The shapes and the amplitudes of the excursions may be different, according to the formations, but there is no definite correspondence between the magnitudes of the excursions and the values of permeability or porosity of the formation.

The principal uses of the SP curve are to (1) detect the permeable beds, (2) locate their boundaries (except when the formations are too resistive), (3) correlate such beds, and (4) obtain good values for R_w , the formation-water resistivity.

Origin of the SP. The character of the potentials measured in the mud results from ohmic drops produced by the flow of SP currents through the mud resistance. If the mud is extremely conductive, these ohmic drops may be insignificant, and the variations in the SP curve may be too small to be useful.*

The SP currents flow as a result of electromotive forces (EMF's) existing within the formations or at the boundaries between formations and mud. One phenomenon that could cause an EMF to appear across the mudcake opposite a permeable bed is *electrofiltration*. The mud filtrate, in being forced through the mudcake, would tend to produce an EMF, positive in the direction of flow. According to experiments,¹² the EMF across the mudcake may be quite sizable, but there is also an electrofiltration EMF generated across the adjacent shales. Thus, the net effect of electrofiltration in causing variations of SP is small and in most cases negligible for all practical purposes—a conclusion verified by field experience.**

Most important are the EMF's of electrochemical origin, which occur at the contacts between the drilling mud (or its filtrate) and the formation water, in the pores of the permeable beds, and across the adjacent shales.¹⁶ In a clean sand lying between shale beds, all penetrated by a borehole containing conductive (water-based) mud, the total electrochemical EMF, E_c , is produced in the chain (Fig. 49.5): Mud/mud filtrate/formation water/shale/mud. The EMF of the junction, mud/mud filtrate, is taken to be practically nil because, although the resistivities of the mud and its filtrate may differ, their electrochemical activities should be the same.

The part of the chain consisting of "formation water/shale/mud" gives rise to the shale-membrane EMF, E_M . The part "mud filtrate/formation water" gives rise to the liquid-junction EMF, E_J . For NaCl (monovalent-ion) solutions, at 75°F,

$$E_M = 59 \log_{10} \frac{a_w}{a_{mf}}$$

*In such a case the gamma ray log, which distinguishes shales from nonshale beds, is sometimes recorded as a substitute for the SP.

**Further information on the electrofiltration EMF, or streaming potential, may be found in Refs. 13 through 15.

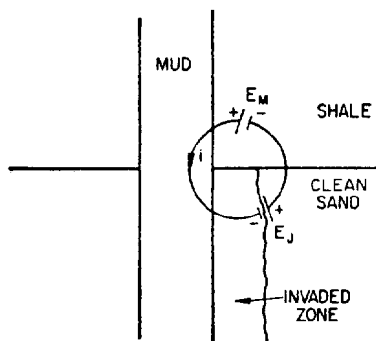


Fig. 49.5—Schematic representation of electrochemical chain and SP current path at boundary between permeable bed and adjacent shale.

and

$$E_J = 12 \log_{10} \frac{a_w}{a_{mf}},$$

where a_w and a_{mf} are the chemical activities of the formation water and mud filtrate, respectively (at 75°F), and E_M and E_J are in millivolts. The total E_c is the sum of E_M and E_J :

$$E_c = K_c \log_{10} \frac{a_w}{a_{mf}}, \quad \dots \dots \dots (8)$$

where K_c is the electrochemical coefficient and is equal to 71 at 75°F.

Eq. 8 is general, provided that both formation water and mud filtrate are essentially NaCl solutions of any concentration. The values of K_c are directly proportional to the absolute temperature. Thus, at 150°F the coefficient K_c in Eq. 8 becomes 81 instead of 71, and at 300°F it becomes 101 (see Fig. 49.6).

From Eq. 8, in the usual case of a_w greater than a_{mf} , E_c is positive. However, if a_{mf} is greater than a_w , corresponding to mud more saline than formation water, then E_c is negative and the SP deflections corresponding to permeable beds are then reversed on the log.

Effect of Invasion on Generation of the EMF. In the explanation of the electrochemical potential, it has been assumed that no shale-type potential is created by the mudcake. In the normal case, mud filtrate bathes both sides of the mudcake and no shale-type potential can arise. In some formations, there is only a little filtrate behind the mudcake. Such small amount of filtrate will be contaminated easily by the formation water. In this case, one face of the mudcake is wetted by the filtrate in the hole, the other face by contaminated filtrate of different activity. This will give rise to a shale-type potential of the same polarity as the main shale potential, and the SP curve will be decreased. This explains the decreasing of the SP curve with time in very highly permeable beds.¹⁷ The filtrate is evacuated by gravity

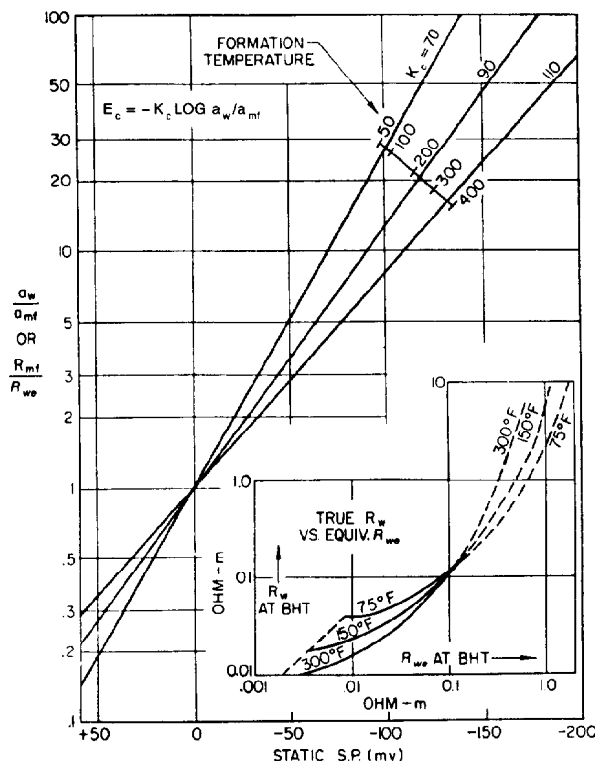


Fig. 49.6— R_w determination from the SP. The inset chart of true R_w vs. R_{wv} applies to formation waters of average composition.

segregating forces and the formation fluids tend to come back toward the hole with time.

Conversely, an increase in SP with time is observed often in low-permeability water-bearing formations. Very little filtrate invades the formation in a freshly drilled hole and the filtrate is contaminated by the formation water. As the invasion proceeds, more and more filtrate goes into the formation and the mudcake is wetted on both faces by the mud filtrate. When the mudcake does not contribute any shale-type potential, the SP curve, recorded on the front of a thick permeable sand, is said to be fully developed.

Effect of Interstitial Shales on the SP. Increasing amounts of shale or clay in a permeable bed effectively result in a reduction of the SP curve. At the limit, for 100% shaliness, E_c becomes zero; that is, the "sand" is then all shale and indistinguishable from the surrounding shales.

The presence of oil in a shaly sand tends to enhance the effect of the shale. All other conditions being the same, the total E_c of a shaly sand will be smaller if oil bearing than if water bearing.

The effect of interstitial shale is also greater in low-porosity formations. In these cases, only a small amount of shale reduces the SP deflection appreciably. Conversely, the E_c of shaly water-bearing sands of high porosity remains practically equal to the E_c of a clean sand, as long as the shale content is reasonably low—i.e., does not exceed a few percent.

Geometric Effect Influencing the SP Curve

Circulation of the SP Current. The various EMF's add their effects to generate the SP currents, which follow the paths represented schematically in Fig. 49.7 (right) by solid lines. Each current line encircles the junction of mud, invaded zone, and uncontaminated zone. In the usual case where the formation waters are saltier than the mud, E_c is positive and the current circulates in the direction of the arrows. The potential of a point in the mud column opposite the sand is negative with respect to one opposite the shale.

Along its path, the SP current forces its way through a series of resistances, both in the ground and in the mud. Along a closed line of current flow, the total of the ohmic-potential drops is necessarily equal to the algebraic sum of the EMF's encountered. Moreover, the total potential drop is divided between the different formations and the mud in proportion to the resistance of the path through each respective medium.

Static SP (Clean Formations) and Pseudostatic SP (Shaly Formations). It is convenient to use an idealized representation in which the SP current is prevented from flowing by means of insulating plugs placed across hole and invaded zones, as shown in Fig. 49.7a (right). Under these conditions, a plot of the potential in the mud column would appear as the dashed cross-hatched curve on the left of Fig. 49.7a, with a maximum negative deflection opposite the permeable bed equal to the algebraic sum of all the EMF's of various origins. This is the maximum SP that could be measured. It is therefore convenient to use this theoretical value as a reference. In the case of a clean sand, it is called the static SP, E_{SSP} . If the sand is shaly, it is called the pseudostatic SP, E_{pSP} .

For given values of the activities of mud and formation water, the pseudostatic SP of a shaly sand is smaller than the static SP of a clean sand. The ratio E_{pSP}/E_{SSP} is called the reduction factor or ratio and is designated by the symbol α_{SP} .

The SP log records only that portion of the potential drop occurring in the mud. When the bed is sufficiently thick the amplitude of the SP deflection approaches the static SP (or E_{pSP} in case of shaly formations), because then the resistance offered to the current by the bed itself is negligible compared with the resistance of the path through the mud in the borehole.

Factors Influencing the Shape and Amplitude of SP Deflections. As seen in Fig. 49.7b, the current circulates in the hole not only opposite the permeable formation but also a short distance beyond its boundaries. As a result, although on the static SP diagram the boundaries of a permeable bed are indicated by sharp breaks, those on the actual SP curve show a more gradual change in potential. An analysis of the circulation of the current¹⁸ shows that, for uniform resistivity in the formations, the bed boundaries are located at the inflection points on the SP log. This fact provides a means of determining the thickness of a bed from the SP log.

Both the shape of the SP deflection and its relative amplitude (in fractional parts of the E_{SSP} or E_{pSP}) are influenced by four factors, which determine the conditions for the circulation of SP currents: (1) bed thickness, (2) resistivities of the bed, the adjacent formations, and the

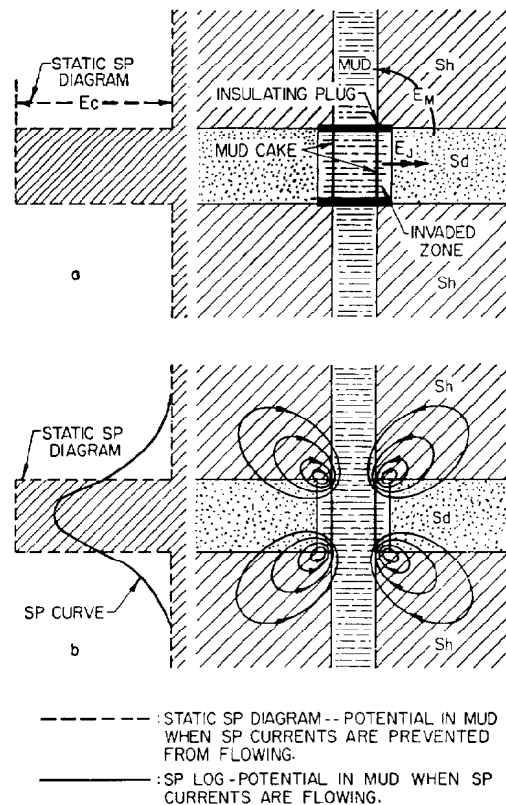


Fig. 49.7—a. Static SP diagram (left) that would be observed in hole when current is prevented from flowing by means of insulating plugs (right); b. actual SP diagram (solid curve, left) and schematic representation of SP current distribution in and around permeable bed (right).

mud, (3) borehole diameter, and (4) depth of invasion. All other factors remaining the same, a change of the total EMF's affects the amplitude but does not modify the general shape of the SP log.

Influence of Mud Resistivity and Hole Diameter. The mud resistivity has a predominant influence on the SP curve. If the mud is of about the same degree of salinity as the formation water, electrochemical EMF's are small. If the mud is more saline than the formation water, the SP may be reversed (sand deflections toward the positive side of the log). Moreover, the lower the mud resistivity (compared with the formation resistivity) the broader the deflection above and below the permeable bed and, because the ohmic drops in the mud are decreased, the smaller the amplitude of the deflection.

An increase in hole diameter acts approximately like an increase in the ratio of formation resistivity to mud resistivity. It tends to round off the deflections on the SP log and reduce the amplitude of the deflections opposite thin beds. A decrease in hole diameter has the same effect as a decrease in the ratio of formation resistivity to mud resistivity.

The SP log would also be influenced by a lack of homogeneity of the mud—a change in salinity of the mud

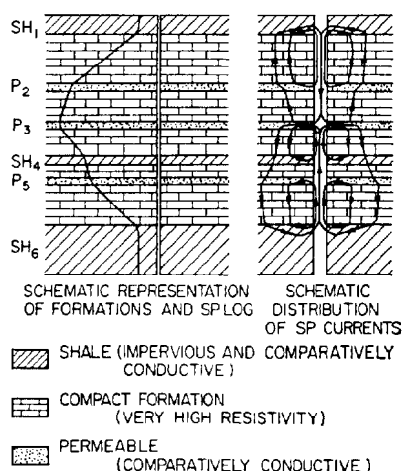


Fig. 49.8—SP phenomena in highly resistive formations (schematic).

at a certain level would result in an SP baseline shift at that level. However, it has been found in practice that such changes in salinity are rare.

Effect of Invasion. Permeable beds in general are invaded by mud filtrate. Because the boundary between mud filtrate and interstitial water is somewhere inside the formation, a fraction of the SP current flows directly from the shale into the invaded zone, without penetrating the mud column. As a result, the presence of the invaded zone has an effect on the SP log similar to that of an increase in hole diameter.

SP in Soft Formations. Theory and field experience have shown that the amplitude of the SP deflection is practically equal to the static SP (of a clean sand) or to the pseudostatic SP (of a shaly sand) when the permeable beds are thick and the resistivities of the formations are not too great compared with that of the mud. Moreover, the SP curves define the boundaries of the bed with great accuracy. The amplitude of the deflection is less than the static SP or pseudostatic SP for thin beds, and the thinner the bed, the smaller the deflection.

On the other hand, when the resistivity of the formation, R_f , is considerably greater than that of the mud, R_m , the SP curves are rounded off, the boundaries are marked less accurately, and all other conditions being the same, the amplitude of the peak is less than when the ratio R_f/R_m is close to unity.

For the case of shaly sands, the SP curve may also be affected by the presence of oil. A change in the magnitude of the SP deflection occurs very often when passing an oil/water contact in a shaly sand. This change is not a positive criterion for the detection of oil because the same effect would be obtained if the salinity of the interstitial water were reduced or if the percentage of shale were increased.

SP in Hard Formations. Hard formations are highly resistive except for permeable beds, whether oil- or water-bearing, and shales, which are impervious. The SP currents generated by the different EMF's flow into the hole out of the shale sections and out of the hole into

the permeable sections. In between, they flow through the mud rather than through resistive sections close to the borehole, because of the large resistances the latter paths offer. However, within the formation at a distance from the borehole, where the paths through the resistive beds have larger cross sections and hence lower resistances, the SP currents can complete their circuits from permeable beds to shale. They cannot return to the mud through adjacent permeable beds because there they encounter EMF's opposing them.

Opposite a given resistive bed, the SP current in the mud column remains essentially constant along the borehole. This means that the potential drop per unit length of hole is also constant, thus giving a constant slope on the SP log as shown by the straight-line portions of the SP in Fig. 49.8. At the level of each conductive bed, some SP current will enter or leave the mud column, thus modifying the slope of the SP log. For instance, the slope of the SP log changes at the level of the permeable bed, P_2 , because part of the current leaves the hole and flows into the bed.¹⁸

As a general rule, in hard formations the permeable beds are characterized on the SP log by slope changes or curvatures that are convex toward the negative side of the log. Shales are characterized by curvatures that are convex toward the positive side of the log. Highly resistive beds correspond to essentially straight parts of the SP log.

Determination of Static SP (SSP). The SP deflection is measured with respect to the shale baseline, a reference line which can generally be traced along the extreme positive edges of the SP curve. Usually the shale line is straight and vertical.*

In any given well, since the mud salinity is constant and the interstitial waters may tend to be constant, there is often a definite tendency for the maximum SP deflections to be the same for the same types of permeable formations at comparable depths. Thus, it is usually possible to draw, parallel to the shale line, a sand line on the log along the maximum negative deflections of the clean sands of sufficient thickness.

It is very likely that, for all the beds where the SP peaks reach the sand line, (1) the formation-water resistivity is practically the same, (2) the beds are virtually free from shaly material, and (3) the amplitude of the deflection is equal to the SSP. For thin beds in cases where the SSP cannot be determined as above (or for a thin shaly sand), the SP reading from the log must be corrected by means of appropriate charts in order to obtain the E_{SSP} or E_{pSP} .²

Determination of R_w from SSP

Since the variations of electrofiltration potential from sand to shale can generally be neglected, the SSP is taken in practice as equal to the corresponding value of $-E_c$ as long as the SP is "fully developed."

It is convenient to replace Eq. 8 by

$$E_{SSP} = -K_c \log \frac{R_{mf}}{R_{we}}, \dots \dots \dots (9)$$

*Field experience has shown that in certain regions there may be shifts of the shale line. Sometimes these shifts are found systematically at the same places in the geological column and can be used as markers.

where R_{we} is an equivalent formation-water resistivity. The computation of R_{we} is given in the chart of Fig. 49.6, and R_w is derived from R_{we} by means of the auxiliary chart at the lower right of Fig. 49.6. The solid curves on this auxiliary chart correspond to highly saline formation waters, where the presence of salts different from NaCl is negligible in practice. They are derived from the known activity/resistivity relationships for pure NaCl solutions. The dashed curves correspond to formation waters of low salinity, where the presence of other salts (calcium and magnesium chlorides, sulfates, and bicarbonates) have an important bearing on the activity values. These curves are derived from empirical observations and cover formation waters of average composition.¹⁹ Note that, for intermediate salinities ($0.08 < R_w < 0.3$ at 75°F), the value of R_{we} is practically equal to R_w .

The mud filtrate is taken here as an NaCl solution, and this is generally done in practice, except for muds containing gypsum, CaCl_2 , or NaOH. In such cases, the determination of R_w from the SP curve requires the measurement of the activity of the mud. A field instrument is provided for this purpose.

Resistivity Logging Devices*

A general classification of the types of resistivity logging devices was given previously.

Electrical Survey (ES). During the first 25 years of logging practice, the standard ES (Fig. 49.2) usually included, in addition to the SP, three conventional (unfocused) resistivity curves; namely, a *short normal* curve (distance between electrodes A and M is 16 in.), a *long normal* (AM=64 in.) or a *short lateral* (distance between electrodes A and O is 6 to 9 ft), and a *standard lateral* (AO=18 ft, 8 in. in general), all recorded simultaneously. In some regions, such as the Permian basin (west Texas and New Mexico), the short-normal spacing was reduced to 10 in., and the limestone sonde was recorded instead of the long normal. The ES log is rarely run today, but it was the standard log for many decades.

Induction-Electrical Surveys (IES) (Figs. 49.9 and 49.10). The simultaneous recording of induction (conductivity and resistivity) curves, 16-in. normal, and SP curve, is a good combination for the logging of formations of low to moderate resistivities in fresh muds. Of late, the 16-in. normal has been replaced by a focused electrode system, and two induction logs of different investigations may also replace the single induction.

Focused Electrode Devices. In wells drilled with very saline mud, or in high resistivity formations, a laterolog or dual laterolog is used with a gamma ray tool. Fulltest benefit of these combinations usually is derived if a microresistivity survey is also run. Microresistivity surveys generally include a microcaliper curve (hole-diameter recording) (see Figs. 49.9 and 49.10). To avoid multiple runs, many of the above devices are combined with porosity logs—acoustic, density, and neutron logs. These porosity logs are discussed in other chapters.

*See Table 49.6 for the names of the various service companies' tools.

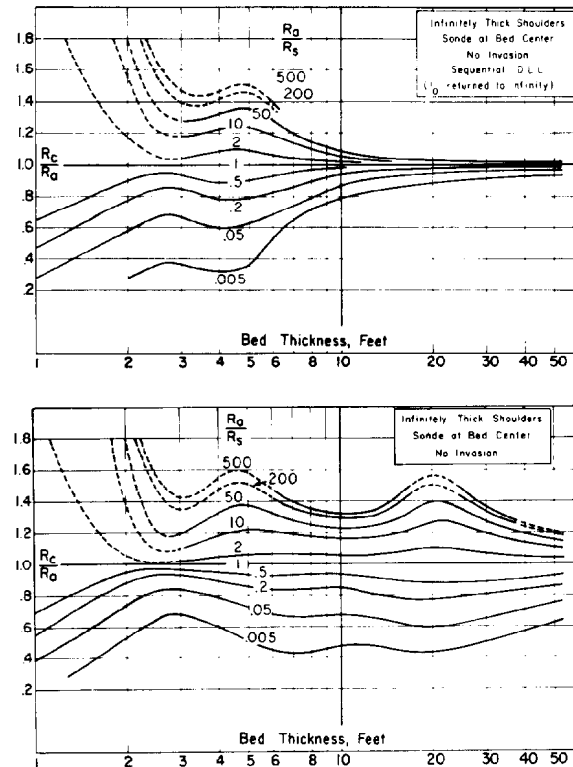


Fig. 49.9—Shoulder-bed corrections, LLS (top) and LLD (bottom).

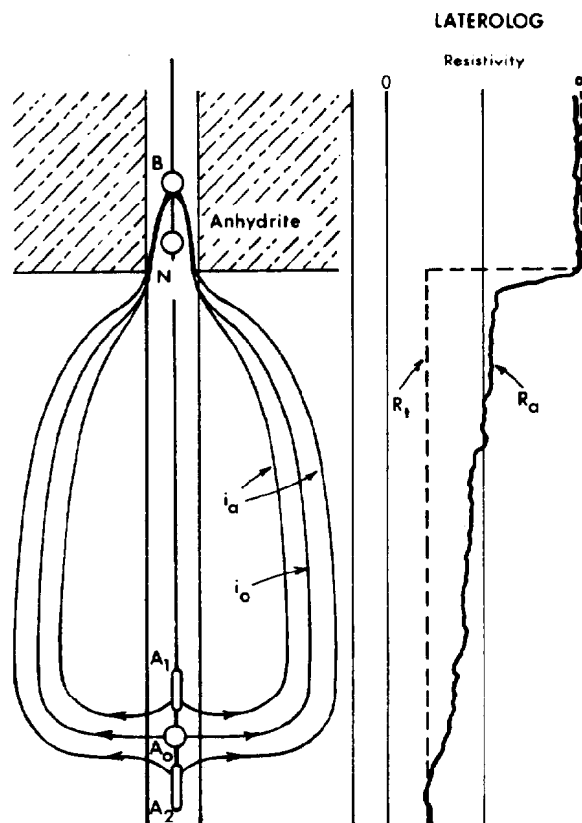


Fig. 49.10—Principle of Delaware effect.

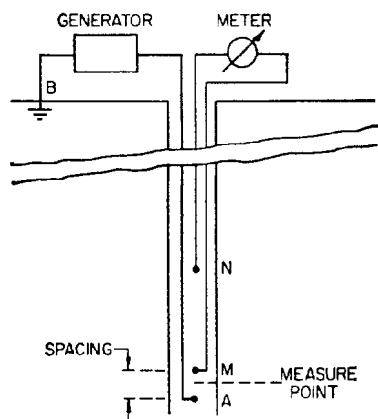


Fig. 49.11—Normal device (schematic).

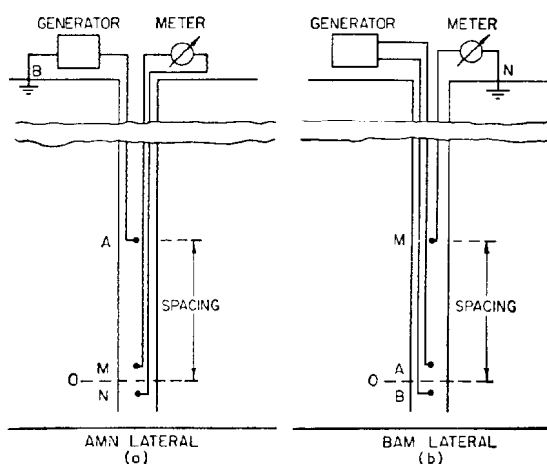


Fig. 49.12—Lateral device (schematic).

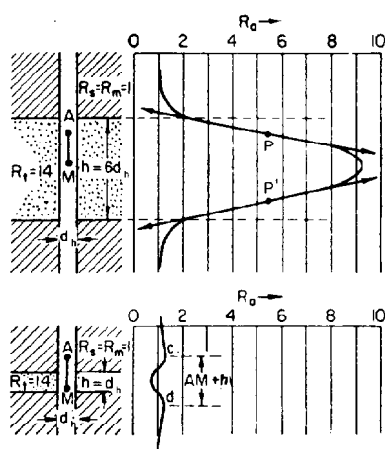


Fig. 49.13—Laboratory curves for normal sonde of spacing $AM=2d$ through uninvaded beds more resistive than adjacent formations.

Conventional Resistivity Devices

During the first quarter century of well logging, the only electrical surveys available were the conventional resistivity logs plus the SP. Thousands of them were run each year in holes drilled all over the world. Since then, new logging methods have been developed to measure values much closer to R_{xo} and R_t , which are the values sought. Nevertheless, the conventional ES (consisting of SP, 16-in. normal, 64-in. normal, and 18-ft 8-in. lateral) still is being run in some parts of the world. For this reason, and also because new information can often be obtained by reinterpreting old ES logs, this chapter includes discussion on the principles and responses of the ES measurements.

Principles: Normal and Lateral Devices. In conventional resistivity logging a current of known intensity is sent between two electrodes, A and B (A on the sonde, B on the sonde or at the surface), and the resulting potential difference is measured between other electrodes M and N. The apparent resistivity is proportional to the measured potential difference.

For normal devices, the distance AM is small (1 to 6 ft) compared with MN, MB, and BN. In practice N or B may be placed in the hole at a large distance above A and M (Fig. 49.11). The voltage measured is practically the potential of M (because of current from A), referred to an infinitely distant point. The distance AM of a normal device is its *spacing*. The point of measurement is midway between A and M.

For lateral devices, measuring electrodes M and N are close to each other and located several feet below current electrode A. Current-return electrode B is at a great distance above A or at the surface. The voltage measured is approximately equal to the potential gradient at the point of measurement O, midway between M and N. The distance AO is the spacing of the lateral device. The two arrangements shown in Fig. 49.12 (in which current and measuring electrodes are interchanged) are equivalent as regards measured potentials (and resistivities).

Curve Shapes—Laboratory Results. Fig. 49.13 shows laboratory curves from a normal device for homogeneous resistive layers between adjacent beds of low resistivity. The curves are symmetrical with respect to the center planes of the layers. The same curves are recorded if M is above A instead of, as in the figure, A above M.

The upper part of Fig. 49.13 shows a resistive bed thicker than the spacing (bed thickness, h , is $6d_h$; spacing AM is $2d_h$; where d_h is the hole diameter). At the boundaries of the bed the curve tends to be rounded off owing to the influence of the borehole. Moreover, the indicated bed thickness (distance between the inflection points P and P') is less than the actual thickness. Normal curves tend to show resistive beds thinner than they actually are (and conductive beds thicker than they actually are) by an amount equal to the spacing AM. The error in picking the boundaries of thick resistive beds is small for short-spacing normals, which is one reason for the recording of a short normal.

As shown in the lower part of Fig. 49.13, for a resistive layer thinner than the spacing, the curve shows

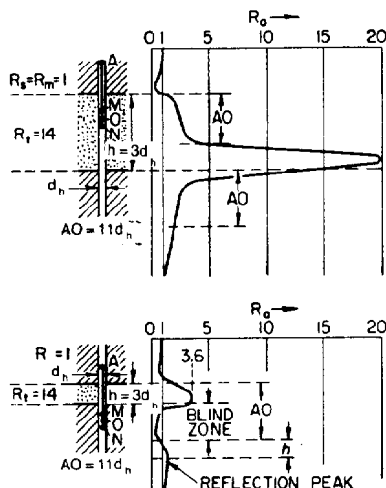


Fig. 49.14—Laboratory curves for lateral sonde of spacing $AO = 11d$ through uninvaded beds more resistive than adjacent formations.

a depression opposite the layer with two symmetrical small peaks, c and d, on either side. The main disadvantage of the normal device is that beds thinner than the spacing, no matter how resistive they may be, appear on the log as being conductive.

Fig. 49.14 shows similar curves for a lateral. The lateral curves are markedly dissymmetrical, and their features are more complex. Again the transitions in the curves at the boundaries have been rounded off by the effect of the borehole. When the bed is thicker than the spacing, the upper boundary of the bed is not well defined on the lateral curve, and, as a whole, the bed appears as being displaced downward by a distance equal to the spacing AO .

In the lower part of Fig. 49.14 the lateral indicates a resistive layer thinner than the spacing by a sharp peak of relatively low apparent resistivity. Below the layer is a low-resistivity "blind zone," followed by a "reflection peak" at a distance AO below the bottom boundary of the layer. The blind zone is recorded when the resistive streak is located between the current electrode and the measuring electrodes.

The lateral is useful for the location of thin, highly resistive streaks, although interpretation may be difficult if several resistive streaks are close together. A lower streak located in the blind zone of an upper resistive streak may be missed, and the reflection peaks may be mistaken for actual resistive streaks in the formation. For a resistive layer of thickness approximately equal to the spacing (*critical thickness*), the lateral is almost completely flattened.

Similar generalizations are possible for lateral curves recorded for beds more conductive than the surrounding formations. Whether the layer is thick or thin, the shape of the curve is dissymmetrical and the anomalies are spread downward, outside the bottom boundaries. The apparent increase of bed thickness is roughly equal to AO .

Normals and Laterals in Hard Formations. Fig.

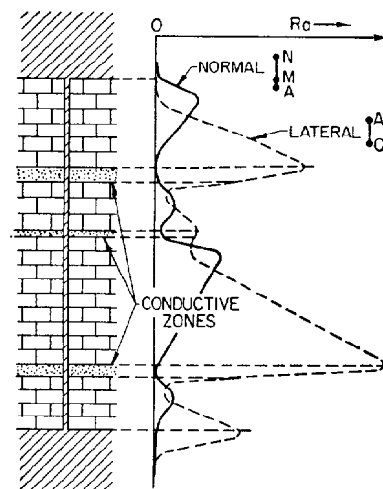


Fig. 49.15—Responses of normals and laterals in hard formations (qualitative).

49.15 shows schematically the behavior of the normals and laterals in thick, highly resistive formations containing porous or shaly (that is, more conductive) zones. In a highly resistive formation most of the current from electrode A flows up or down the borehole, dividing in inverse proportion to the resistances of the two paths, which are determined mostly by the resistance of the mud column in the hole between the current electrode and the nearest conductive beds. At the conductive beds, depending on their thickness and conductivity, the current has low-resistance paths from the hole. The lopsided appearance of the normal and lateral curves is explainable in terms of the unequal division of current flowing up and down the hole.

The normal, for example, has M and N above the current electrode. The voltage measured is the ohmic potential drop in the hole resulting from current flowing in the mud between M and N. When the device is near the bottom of a resistive bed, most of the current flows down to the conductive bed just below, and there is little potential drop between M and N because the current up is small. When the device has moved farther up in the bed, the current down decreases because the resistance of that path has increased. Also, since the resistance of the upward path has decreased, the current up increases. Therefore, the potential drop between M and N increases as the device moves upward until electrode N reaches the next conductive bed, where the upward current is diverted from the hole. Above that level the normal reading decreases.

The explanation of the shape of the lateral curve is similar. The direction of the lopsidedness for either device depends on whether the measuring electrodes are above or below the current electrode. The depressions read on the curves opposite the conductive beds are smooth and, in the case of the lateral, much broadened and displaced downward. Accurate determinations of bed boundaries from the curves are practically impossible.

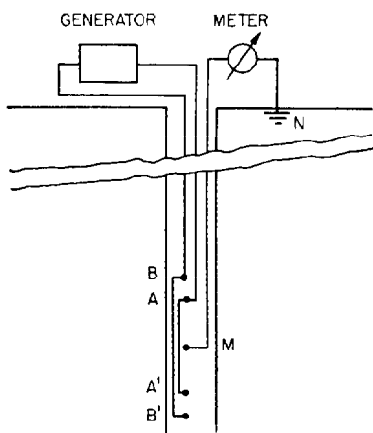


Fig. 49.16—Limestone sonde (schematic).

Limestone Sonde. Four current electrodes (A, A', B, and B'), connected as shown in Fig. 49.16 by insulated wires of negligible resistance, are symmetrically arranged so that $AB = A'B'$. A measuring electrode, M, is placed in the middle of the device. Depths are measured from electrode M. In practice $AM = A'M = 30$ or 35 in., and $AB = A'B' = 4$ or 5 in. The device is therefore a symmetrical double lateral.

Opposite a thick, highly resistive layer (upper part of Fig. 49.17) practically all the flow of current is confined to the spaces between A and B and between A' and B'. No current flows from B or B', up or down the hole away from the device. Hence, from Ohm's law, B and B' are at zero potential. Similarly M is at the same potential as A and A'.

The potential of M is, therefore, equal to the potential drop in the mud, because of the flow of current, between A and B (or A' or B'). As long as all the electrodes of the devices are opposite the resistive formation this potential difference is dependent only on hole size and mud resistivity; if these are constant, a constant apparent resistivity is recorded.

If the device is located just above a conductive streak (as in the lower part of Fig. 49.17), the streak is effectively a low resistance connecting adjacent portions of the device to points at zero potential. Part of the current now flows in the paths indicated by the arrows, and the potential of electrode M is correspondingly decreased. The conductive streak is indicated on the log by a relatively sharp, symmetrical depression.

The limestone sonde gives clearer and simpler logs in hard formations, but measurements with the limestone sonde are strongly affected by the mud column. When the formations are much more resistive than the mud, the readings are appreciably lower than the formation resistivities.

Application of Conventional Resistivity Logs. The three devices that are generally recorded in the conventional electrical log (16-in. normal, 64-in. normal, and 18-ft, 8-in. lateral) were designed to provide the most complete information with a system of nonfocused macrodevices.

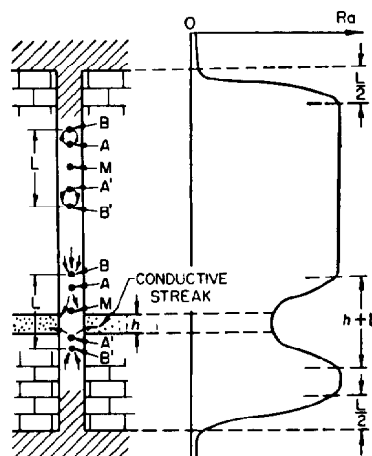


Fig. 49.17—Principle of limestone sonde (schematic).

The short normal is well adapted for bed definition, boundary determination, and correlation of formations of low or moderate resistivities (sand-shale series). The lateral generally shows sharp peaks at the level of thin resistive beds, but the definition of these beds is often obscured by blind zones and spurious peaks.

The precision of the normal and lateral curves for bed definition is limited in hard formations and is quite poor when salty muds are used. Somewhat better resolution is obtained with the limestone sonde. In all cases, formation delineation is more detailed and accurate with the IL and focused devices (LL) and with the microdevices. In hard formations the 16-in. normal and the limestone sonde can provide an approximation to the value of R_i and hence an approach for formation factor evaluation. The capabilities of the conventional tools for the determination of R_i are discussed later in this chapter.

Induction Logging

The IL was first developed to measure formation resistivity in boreholes containing oil-based muds.²⁰ Electrode devices do not work in these nonconductive muds, and attempts to use wall-scratcher electrodes proved unsatisfactory. Experience soon demonstrated that the induction tools had many advantages over the conventional ES for logging wells drilled with water-based muds.²¹

Induction logging devices are focused to minimize the influence of the borehole and of the surrounding formations. They are designed for deep investigation and reduction of the influence of the invaded zone.

Principle

Practical induction sondes include a system of several transmitter and receiver coils. However, the principle can be understood by considering a sonde with only one transmitter coil and one receiver coil (Fig. 49.18).

High-frequency AC of constant intensity is sent through the transmitter coil. The alternating magnetic field thus created induces secondary currents in the formations. These currents flow in circular ground-loop paths coaxial with the transmitter coil. These ground-loop currents, in turn, create magnetic fields that induce

signals in the receiver coil. The induced receiver signals are essentially proportional to the conductivity of the formations. Any signal produced by direct coupling of transmitter and receiver coils is balanced out by the measuring circuits.

The IL operates to advantage when the borehole fluid is an insulator—even air or gas. But when properly designed the tool also will work very well when the borehole contains conductive mud, provided that the mud is not too salty, the formations are not too resistive, and the borehole diameter is not too large.

Equipment

Four types of induction equipment are now in use.

1. **The 6FF40 IES** tool includes a six-coil induction device of 40-in. normal spacing, a 16-in. normal, and an SP electrode. The induction array provides the greatest lateral depth of investigation presently available with induction tools.

2. **The 6FF28 IES** is a small-diameter (2½ in.) tool for use in slim holes. It is a scaled-down version of the 6FF40, having a 28-in. coil spacing, and incorporates a standard 16-in. normal and an SP.

3. **The Dual Induction-Laterolog 8 (DIL™) or Spherically Focused Log (SFL)** system uses a deep-reading induction device (ID, similar to the 6FF40), a medium induction device (IM), an LL8 (or an SFL), and an SP electrode. The IM device has vertical resolution similar to that of the 6FF40 tool but about half the depth of investigation. It is much more affected by large hole diameters and/or salty muds. The DIL log, with its three focused resistivity readings of different depths of investigation, is superior to the IES log for determination of R_t and R_{xo} in extreme ranges of invasion depths and in cases of annulus.

4. **The ISF/Sonic** combination incorporates an ID measurement similar to that from the 6FF40 tool, the new ISF log, an SP curve that may be electronically corrected for noise, a borehole compensated (BHC) sonic log, and an optional gamma ray curve. Of late, the BHC sonic tool can be replaced in this tool string by a combination neutron/density device.

Log Presentation and Scales

The SP and/or gamma ray curve are recorded in Track 1 for all tools; they can be recorded simultaneously with ISF/sonic equipment. A gamma ray curve may also be run with 6FF40 or DIL equipment.

Fig. 49.19 illustrates the standard IES presentation. The induction conductivity curve is sometimes recorded over both Tracks 2 and 3. The linear scale is in millimhos per meter (mΩ/m), increasing to the left. In Track 2 both the 16-in. normal and the reciprocated induction curves are recorded on the conventional linear resistivity scale.

The DIL introduced the logarithmic grid for resistivity presentations. The current form is the "log-linear" grid shown in Fig. 49.20. In this, the resistivity curves on the detail log (5 in./100 ft) have a split 4-decade logarithmic scale. On the correlation log (1 or 2 in./100 ft), the scale is linear. This presentation offers several advantages over the other alternatives. The detail log has good readability in low resistivities, a wide range without backup traces, and the ease of reading resistivity ratios

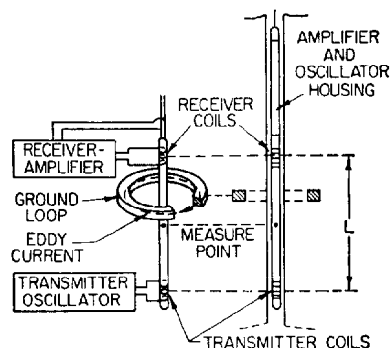


Fig. 49.18—Induction-logging equipment (schematic).

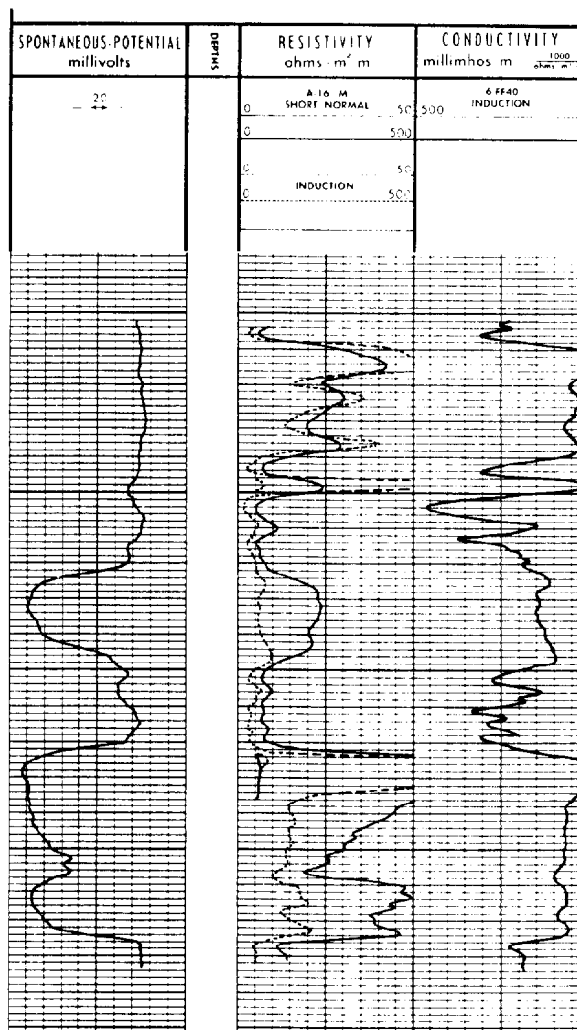


Fig. 49.19—Induction-electrical log presentation.

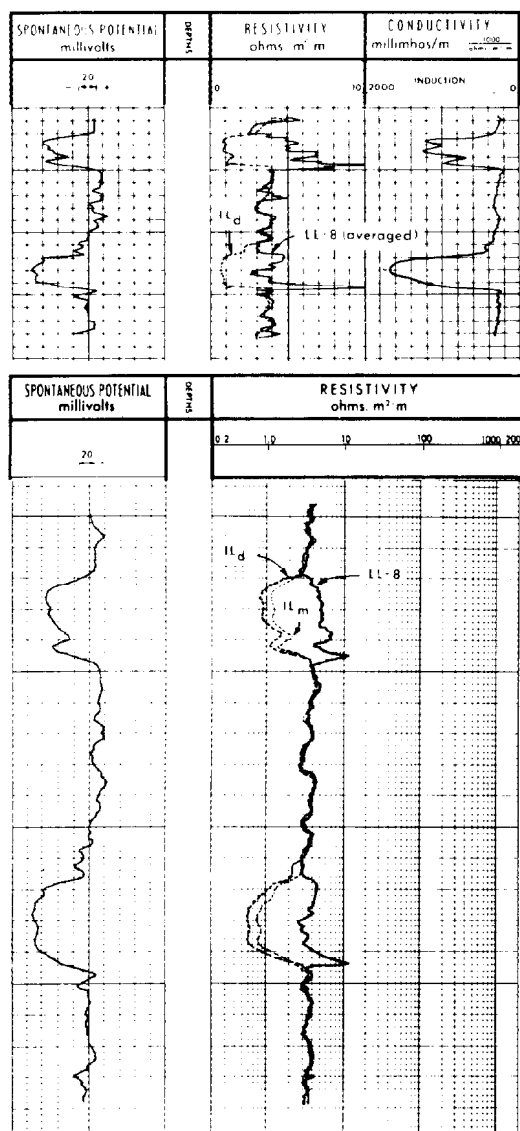


Fig. 49.20—Dual Induction Laterolog 8 presentation.

directly from the logarithmic scale. The linear scale is more easily correlated with earlier logs. This format has gained acceptance as the standard for resistivity logs.

The ISF log in combination with the sonic log requires a modification of this grid usage because Track 3 is needed for the sonic Δt curve. The grid selected is shown in Fig. 49.21.

Skin Effect

In very conductive formations the induced secondary currents are large, and their magnetic fields are important. The magnetic fields of their ground loops induce additional EMF's in other ground loops. This interaction between the loops causes a reduction of the conductivity signal recorded by the induction log. This signal reduction is known as "skin effect."

Induction logs usually are automatically corrected for skin effect during recording. The correction is based on the magnitude of the uncorrected tool response treated as

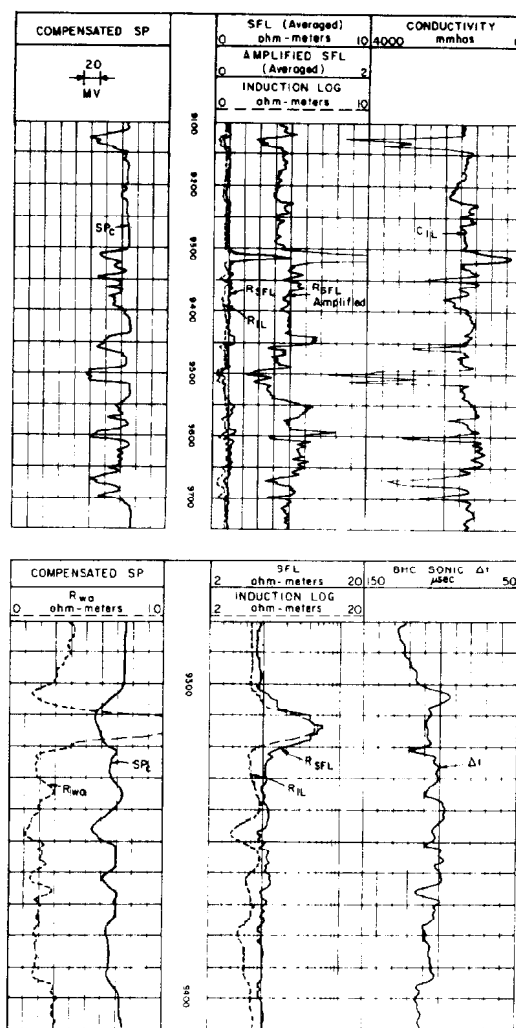


Fig. 49.21—ISF/sonic presentation.

if it were from a homogeneous medium. A secondary skin-effect correction may be required when the media surrounding the sonde are not of uniform conductivity. Such corrections are incorporated in various interpretation charts.

Geometrical Factor

When conductivities are not high, skin effect may be neglected, and the response of induction logs can be described in terms of conductivities and "geometrical factors" of the volumes surrounding the tool. The geometrical factor, G , of a volume having a specific geometrical orientation with the sonde is simply the fraction of the total signal that would originate with that volume in an infinite homogeneous medium. For computation of geometrical factor to be practical, it is necessary to assume that the volumes conform to symmetry of revolution about the sonde.

The magnitude of the signal in conductivity units is the product of the geometrical factor and the conductivity of the material, and the total signal sensed by the tool is the

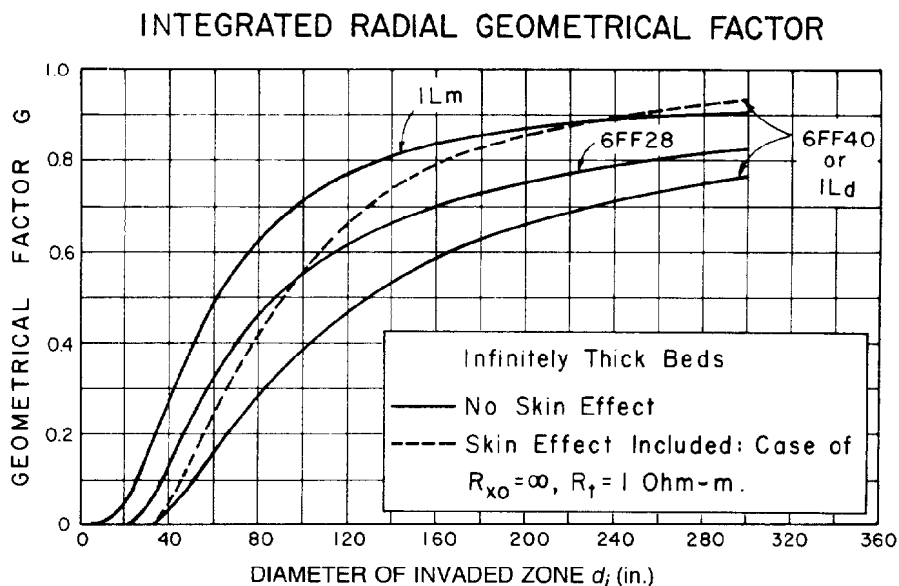


Fig. 49.22—Geometrical factor. Dashed curve includes skin effect under conditions shown, for the ILd device.

sum of these products for all volumes within range (which extends to infinity, but can be circumscribed to practical limits). Since the G 's add up to unity by definition, this can be stated:

$$C_{IL} = C_1 G_1 + C_2 G_2 + C_3 G_3 + \dots + C_N G_N, \dots (10)$$

where C and G refer to the zones of differing conductivity and N is the total number of such zones.

The chief significance of this concept is the fact that a volume of space defined only by its geometry relative to the sonde has a fixed and computable geometrical factor. This permits the construction of mathematically sound correction charts to account for the effects of borehole mud, the invaded zone, and adjacent beds on the R_t measurement, providing symmetry of revolution exists.² These charts incorporate the secondary skin effect correction mentioned above.

Invasion Effects

Fig. 49.4 illustrates an invaded formation. It includes volumes having several conductivities, C_m , C_{xo} , C_i , and C_t (corresponding to R_m , R_{xo} , R_i , and R_t). The total conductivity signal, C_T , received from this zone by the induction tool is

$$C_T = C_m G_m + C_{xo} G_{xo} + C_i G_i + C_t G_t, \dots (11)$$

If the zone were infinitely thick, this would be the only signal received, and $C_T = C_{IL}$. If the tool is a 6FF40, the hole size moderate, and the mud relatively fresh, the borehole signal is negligible, and the C_{xo} and C_i zones can be merged into one for this example.

If a moderate diameter of invasion, say 65 in., is assumed, Fig. 49.22 reveals that the geometrical factor of all material within the 65-in. diameter is 0.2. If R_{xo} is taken equal to $4 R_t$, then $C_{xo} = C_t/4$, and the induction tool response is

$$\begin{aligned} C_{IL} &= C_{xo} G_{xo} + C_t G_t, \\ &= (C_t/4) (0.2) + C_t (0.8), \\ &= 0.85 C_t. \end{aligned}$$

In the same conditions, but using salty mud so that $R_{xo} = R_t/4$, the response is

$$\begin{aligned} C_{IL} &= 4 C_t (0.2) + C_t (0.8), \\ &= 1.6 C_t, \end{aligned}$$

which illustrates the "conductivity-seeking" characteristic of the induction devices, and shows why they must be used with discretion in salt-mud environments. As a rule of thumb, R_t should be less than about $2.5 R_{xo}$ and d_i (diameter of invaded zone) no greater than 100 in. for satisfactory R_t determination from 6FF40-type induction logs.

Annulus

In oil-bearing formations of low S_w and high permeability, an annulus of low resistivity, R_{an} , may exist between the flushed zone, R_{xo} , and the virgin formation. When R_{xo} is greater than R_t , R_{an} is less than R_t , and the effects of the two on the induction log tend to cancel. However, the high conductivity of the annulus has more effect in medium invasion ranges ($2d_h < d_i < 4$ or $5d_h$), and it may cause a single ID to read resistivities lower than either R_{xo} or R_t . The DIL 8 tool is often capable of detecting the presence of annuli, since in these circumstances the IM measurement reads lower than either the LL8 or the ID values.

Thin Bed Corrections

The skin-effect correction accomplished automatically in the induction tools assumes infinitely thick beds. Skin effect in thin beds may require additional corrections, and these are provided in Ref. 2.

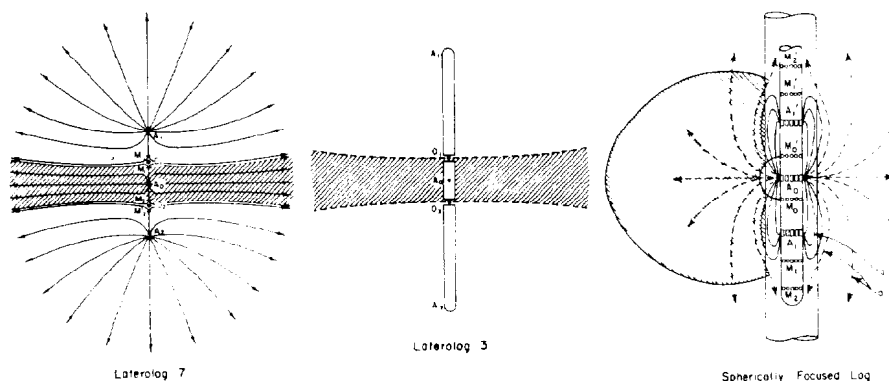


Fig. 49.23—Schematic of focusing-electrode devices.

Borehole Corrections

Conductivity signals from the mud can be evaluated using geometrical factors. Chart Rcor-4 (Ref. 2) gives corrections for the various induction tools and standoffs. On the basis of bit size the nominal borehole signal is sometimes removed from the recorded log. When the hole signal is significant, log headings should always be consulted to ascertain whether this was done. This precaution applies most frequently to the IM measurement of the DIL tool.

For hole diameters in the range of 7 to 13 in. there is an uncertainty of about ± 0.0003 on the geometrical factor of the borehole for the 6FF40 sonde. This results from several factors, including diameter and shape of the borehole, mudcake thickness, standoff, and sonde tilt. To preclude the possibility of cumulative errors exceeding 20% of the 6FF40 reading, the tool should not be used where the resistivity to be measured is greater than about $500 R_m$.

Very Resistive Formations

There is an uncertainty of about $\pm 2 \text{ m}\Omega/\text{m}$ on the zero of the present induction sondes (6FF40, ID, and IM), and consequently the resistivity error may be great as conductivity approaches zero. To preclude an error of more than 20%, the formation conductivity should be greater than $10 \text{ m}\Omega/\text{m}$ (i.e., the resistivity less than $100 \Omega \cdot \text{m}$). This error can sometimes be practically eliminated by downhole calibration techniques if suitable formations are present.

Calibration

Primary calibration is performed by placing a test loop around the sonde. The conductive loop has a resistance, which has been adjusted to produce a certain conductivity signal in the sonde. An additional calibration procedure has a signal produced internally in the sonde to adjust the control-panel sensitivity for proper galvanometer deflections. The "zero errors" of the electronics in the equipment are also checked and balanced out. "Calibrate tails," usually attached to the log, serve as a record of the calibration tests made before and after the logging run.

In some regions it is possible to check the calibration of the IL by observing that the conductivity reading op-

posite an impervious formation of exceedingly high resistivity (such as anhydrite) represents the sum of all spurious signals. If the hole diameter is known, it is then possible to correct the IL reading so that the range of uncertainty is reduced and greater accuracy is obtained in formations of practical interest.

Summary

1. The IL can be used most effectively in holes filled with moderately conductive drilling muds, nonconductive muds, and in empty holes.
2. Vertical focusing is good, making possible reliable evaluation of beds down to about 5 ft thick with 6FF40, ID, and IM devices, and down to about $3\frac{1}{2}$ ft thick with 6FF28 tools.
3. The deep induction logs (ILD) are only moderately affected by invasion in relatively fresh muds, and good R_t determinations are possible where R_t is less than about $2.5 R_{xo}$ and d_i is less than 100 in.
4. The three curves of the DIL give more precise knowledge of invasion profiles and hence better R_t values in the cases of deep invasion or annulus.
5. The log-linear presentation of the DIL and other IL's meets most log requirements better than alternative displays.

Focused-Electrode Logs

The responses of conventional ES can be greatly affected by the borehole and adjacent formations. These influences are minimized by a family of resistivity tools that use focusing currents to control the path taken by the measure current. These currents are supplied from special electrodes on the sondes.

Equipment

The focused-electrode tools include the Laterologs (LL) and SFL's. These tools are much superior to the ES devices for large R_t/R_m values (salt muds and/or highly resistive formations) and for large resistivity contrasts with adjacent beds (R_t/R_s or R_s/R_t). They are much better for resolution of thin to moderately thick beds. Focusing-electrode systems are available with deep, medium, and shallow depths of investigation.

Devices using this principle have as quantitative applications the determination of R_t and of R_{xo} . The R_t tools are Laterolog 7 (LL7), Laterolog 3 (LL3), and

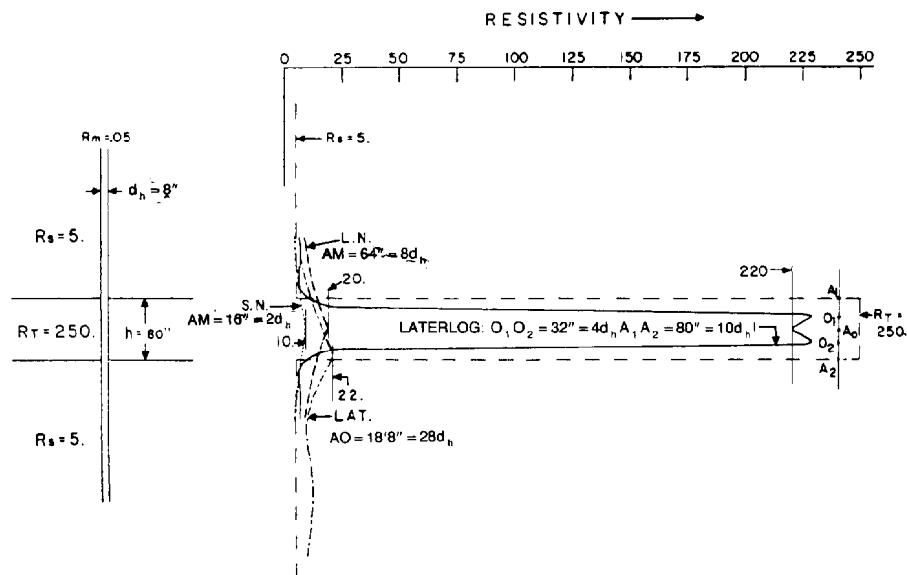


Fig. 49.24—Response of Laterolog 7 and ES opposite a thin, resistive, noninvaded bed, with very-salty mud (laboratory determination).

LLD of the deep dual laterolog. The medium-to-shallow-reading devices, all integral with combination tools, are Laterolog 8 (LL8) of the DIL, LLS of the shallow dual laterolog, and the SFL of the ISF/sonic combination.

Laterolog 7. This device²² comprises a center electrode A_0 , and three pairs of electrodes: M_1 and M_2 ; M'_1 and M'_2 ; and A_1 and A_2 (Fig. 49.23). The electrodes of each pair are symmetrically located with respect to A_0 and are connected to each other by a short-circuiting wire.

A constant current I_0 is sent through electrode A_0 . Through bucking electrodes A_1 and A_2 , an adjustable current is developed; the bucking current intensity is adjusted automatically so that the two pairs of monitoring electrodes, M_1 and M_2 and M'_1 and M'_2 , are brought to the same potential. The potential drop is measured between one of the monitoring electrodes and an electrode at the surface (i.e., at infinity). With a constant I_0 current, this potential varies directly with formation resistivity.

Since the potential difference between the M_1 - M_2 pair and the M'_1 - M'_2 pair is maintained at zero, no current from A_0 is flowing in the hole between M_1 and M'_1 or between M_2 and M'_2 . Therefore, the current from A_0 must penetrate horizontally into the formations.

Fig. 49.23 shows the distribution of current lines when the sonde is in a homogeneous medium; the "sheet" of I_0 current, indicated by the hatched area, retains a fairly constant thickness up to a distance from the borehole somewhat greater than the total length $A_1 A_2$ of the sonde. Experiments have shown that the sheet of I_0 current retains substantially the same shape opposite thin resistive beds. The thickness of the I_0 current sheet is 32 in. (distance $O_1 O_2$ on Fig. 49.23), and the length $A_1 A_2$ of the sonde is 80 in.

Fig. 49.24 compares the curves obtained experimen-

tally opposite a thin resistive bed using the conventional devices (16- and 64-in. normals and 18-ft, 8-in. lateral) with the corresponding LL7 recording. The conventional devices give poor results; the LL7, in spite of difficult conditions (R_T/R_m is 5,000), shows the bed very clearly and reads close to R_T . An SP curve may be recorded on depth simultaneously with the LL7.

Laterolog 3

Like LL7, LL3 also uses currents from bucking electrodes to focus the measuring current into a horizontal sheet penetrating into the formation. However, as seen in Fig. 49.23, large electrodes are used. Symmetrically placed, on either side of the central A_0 electrode, are two very long (about 5-ft) electrodes, A_1 and A_2 , which are shorted to each other. A current, I_0 , flows from the A_0 electrode whose potential is fixed. From A_1 and A_2 flows a bucking current, which is automatically adjusted to maintain A_1 and A_2 at the potential of A_0 . All electrodes of the sonde are thus held at the same constant potential. The magnitude of the I_0 current is then proportional to formation conductivity.

The I_0 current sheet is constrained to the shaded, approximately disk-shaped area in Fig. 49.23. The thickness, $O_1 O_2$, of the I_0 current sheet is usually about 12 in., much thinner than for LL7. As a result, LL3 has a better vertical resolution and shows more detail than LL7. Furthermore, the influences of the borehole and of the invaded zone are slightly less.

The simultaneous recording of an SP curve is possible, but the SP has to be displaced in depth, usually by about 25 ft, because of the large mass of metal in the sonde. However, a gamma ray curve is normally run simultaneously with the LL3 for lithology definition, since the SP has very little character in the salt muds where the LL is used. There is also available a simultaneous LL3-neutron/gamma ray combination tool.

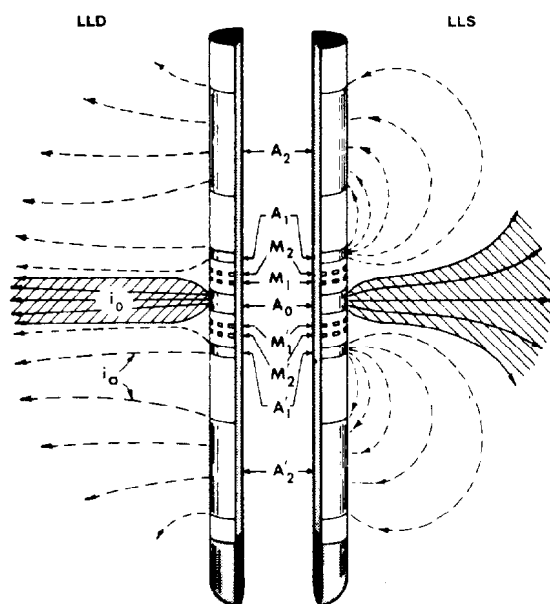


Fig. 49.25—Schematic of the dual laterolog.

Guard-Electrode Device. In the guard-electrode system, the surveying current flows into the adjacent formations from a measuring electrode disposed between relatively long upper and lower guard electrodes from which current also flows. The guard electrodes tend to confine the current from the measuring electrode to a generally horizontal path. The measuring and guard electrodes are connected through a very low impedance, as necessary to measure the surveying current supplied to the measuring electrode.

A resistivity value is obtained by recording the ratio of the voltage of an electrode in the assembly (referred to a distant point) to the current emitted from the measuring electrode. The guard-electrode device is used mostly in hard-rock territories for detailed bed definition, correlation, and as a help in reservoir evaluation. For the determination of R_t , it is preferable that R_{mf}/R_w be small (less than 4), as in the case of salty muds.

Laterolog 8. The shallow-investigation LL8 device is recorded with small electrodes on the DIL sonde. It is similar in principle to LL7 device except for its shorter spacings. The thickness of the I_0 current sheet is 14 in., and the distance between the two bucking electrodes is somewhat less than 40 in. The current-return electrode is located a relatively short distance from A_0 . With this configuration, the LL8 tool gives sharp vertical detail, and the readings are more influenced by the borehole and the invaded zone² than are those for LL7 and LL3. The LL8 data are recorded with the DIL on a split 4-decade logarithmic scale.

Dual Laterolog. Since the measure current of an LL has to traverse mud and invaded zone to reach the undisturbed formation, the measurement is necessarily a combination of effects. With only one resistivity measurement, the invasion profile and R_{xo} had to be known or

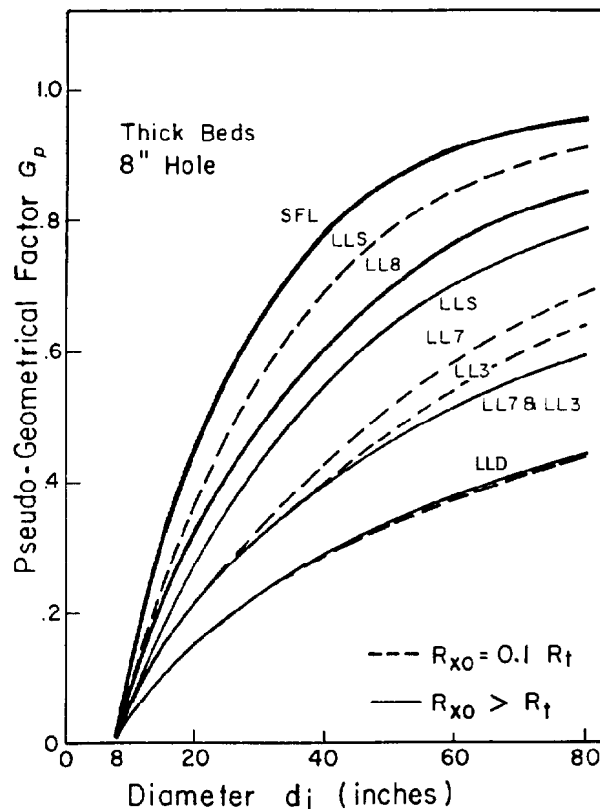


Fig. 49.26—Radial pseudogeometrical factors, fresh muds (solid) and salty muds (dashed).

estimated in order to calculate R_t . The need for a second measurement at a different depth of investigation resulted in the dual laterolog/gamma ray tools (Fig. 49.25).

One version of the tool records the two laterologs sequentially; another does it simultaneously and has added a shallow MICROSF (MSFL) for R_{xo} information. Both can record a gamma ray curve on depth, simultaneously with the resistivity curves. An SP can also be run.

By use of effectively longer bucking electrodes and a longer spacing, the LLD (deep laterolog) has been given a deeper investigation than either LL7 or LL3 devices. The LLS (shallow laterolog) uses the same electrodes in a different manner (Fig. 49.25 right) to achieve a current beam equal in thickness to that of LLD, 24 in., but having a much shallower penetration. The LLS depth of investigation lies between those of the LL7 and LL8 devices (Fig. 49.26).

Spherically Focused Log. The SFL log is part of the ISF/sonic combination, and it was developed as an improvement over both the 16-in. normal and the LL8 as a short-spacing companion to the deep induction log.

Normal resistivity devices rely on the concept of equal intensity of current radiation in all directions, as would happen in a homogeneous isotropic medium. When the current distribution is distorted from the spherical model, as by the presence of a borehole, the readings must be corrected by departure curves. The SFL device uses focusing currents to enforce an approximately spherical

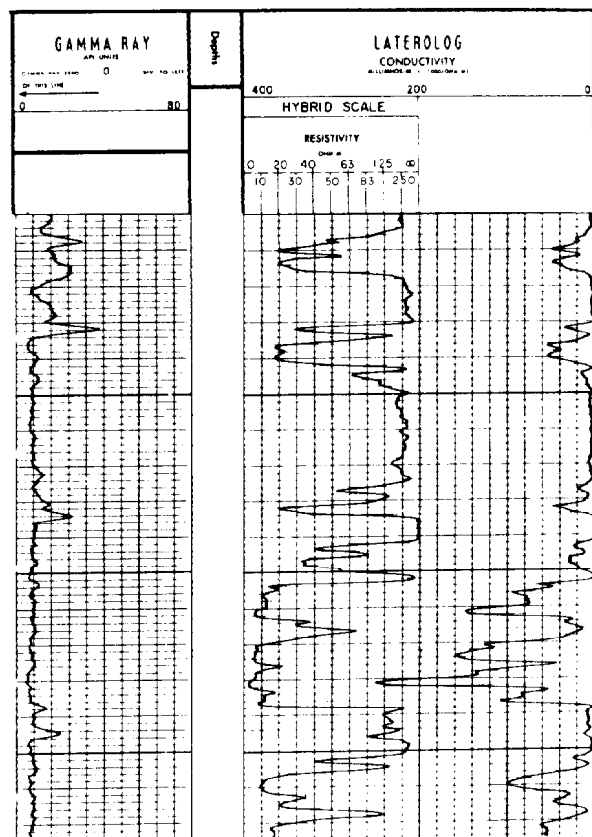


Fig. 49.27—Laterolog recorded on hybrid scale.

shape on the equipotential surfaces over a wide range of wellbore variables. The borehole effect is virtually eliminated where $d_h \leq 10$ in., yet most of the response is from the invaded zone in all but extreme conditions.

Scales. The linear resistivity scales originally used for LL data were poorly adapted to record the wide range of measurements characteristic of these tools. Although linear scales are still used occasionally, compressed scales of either the hybrid or logarithmic type have supplanted the linear for quantitative work.

The hybrid scale, first used on the LL3 log, presented linear resistivity on the first half of the grid track and linear conductivity on the last half. Thus, one galvanometer could record all resistivities from zero to infinity. (See Fig. 49.27.)

The logarithmic scale was used first with the dual induction tool, and it has also been adapted for the LL and the SFL devices (Fig. 49.28). It combines readability and detail in low resistivities with a wide range of values, and it also offers the advantage of graphic (quick-look) interpretations.

Influence of Wellbore Variables

These logging devices can be significantly affected by the borehole mud, the invaded zone, and adjacent beds. Charts Rcor-1 and Rcor-2 of Ref. 2 provide needed corrections. Where only one measurement is available, some knowledge or assumption of depth of invasion must be used for deriving R_t . Readings must be corrected for borehole effect before the shoulder-bed charts are entered. (See Figs. 49.29 and 49.9.) These figures

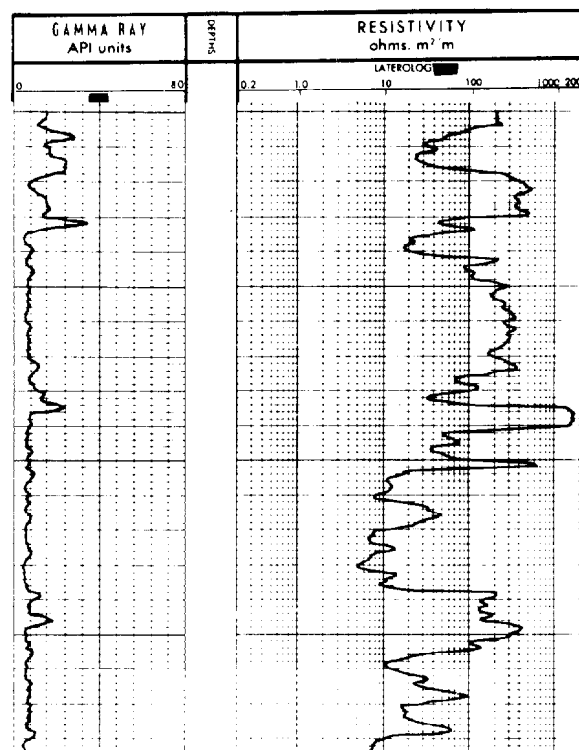


Fig. 49.28—Laterolog over same interval as Fig. 49.22, recorded on logarithmic scale.

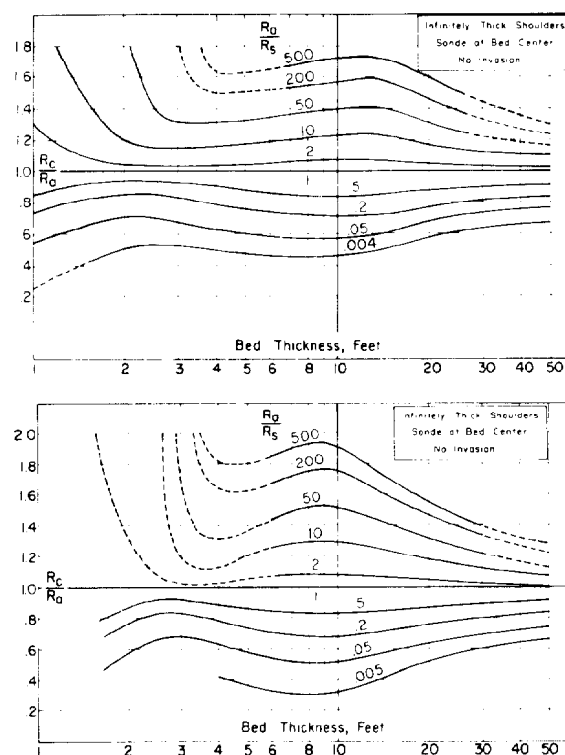


Fig. 49.29—Shoulder-bed corrections, LL3 (top) and LL7 (bottom).

give R_c/R_a as a function of bed thickness, R_c being the corrected resistivity and R_a the apparent resistivity corrected for borehole effect.

Pseudogeometrical Factors

Geometrical factor may be defined as that fraction of the total signal that would originate from a volume having a specific geometrical orientation with the sonde in an infinite homogeneous medium.

The only well-logging devices for which this concept is sound are the induction tools, because only with these is the measuring geometry independent of variations in R_{xo}/R_t . However, it is useful to construct charts based on "pseudogeometrical factors" for other resistivity devices, for purposes of comparative evaluation. Such a chart is shown in Fig. 49.26 in which the integrated pseudogeometrical factors of progressively larger cylinders are plotted vs. the diameters of the cylinders. The apparent resistivity, R_a , measured in a thick bed is given approximately by

$$R_a = R_{xo} G_{pi} + R_t (1 - G_{pi}), \quad \dots \dots \dots (12)$$

where G_{pi} is the pseudogeometrical factor. It must be emphasized that a pseudogeometrical factor relating to an electrode-type resistivity device is applicable in only one set of conditions, and therefore charts of this type are not valid as general-purpose invaded-zone correction charts. The most useful feature of the Fig. 49.26 chart is its graphic comparison of the relative contribution of invaded zones to the responses of the various tools.

The Delaware Effect

If both B and N electrodes are placed downhole as in Fig. 49.10, LL data may exhibit "Delaware effect"* (or "gradient") in sections located just below thick nonconductive beds such as anhydrite. It appears as abnormally high resistivity for 80 ft or so below the resistive bed. The LL3 is the only field tool now using this arrangement.

Fig. 49.10 illustrates the effect and its causes. As B enters the thick anhydrite, the current flow is confined to the borehole, and if the bed is thick enough (several hundred feet) practically all the current will flow in that part of the hole below B. Then when N enters the bed, it can no longer remain near zero potential as intended. It is exposed to an increasing negative potential as it rises farther from the bed boundary. This potential appears at the surface as an increase in the resistivity measurement.

LL7 and LLD devices normally use surface electrodes for current return, so they are not subject to Delaware effect. However, a small anti-Delaware effect has been observed, which produces resistivities that are too low just below the resistive beds.

Conclusions

Resistivity devices with the focusing electrode principle meet certain logging requirements better than other types now available. These requirements are (1) to take measurements leading to determination of R_t in conditions for which the induction tools are not well suited—i.e., R_t values in excess of 100 Ω -m and/or mud resistivities of the same order or lower than those of the

formation waters—and (2) to provide correlation and R_{xo} determinations in conjunction with deeper-reading R_t devices.

Microresistivity Devices

Microresistivity devices are used to measure R_{xo} (resistivity of the flushed zone) and to delineate permeable beds by detecting the presence of mudcake. In the discussion that follows, the microlog (ML) will be treated in considerable detail, not because of its relative importance—the microlaterolog (MLL), the proximity log (PL), and the MSFL are superior tools for obtaining R_{xo} —but because its principle is fundamental, and it is still the best of the three microresistivity devices for delineating permeable-bed boundaries, hence for making "sand counts."

Measurements of R_{xo} are important for several reasons. When invasion is moderate to deep, knowledge of the R_{xo} value makes possible more accurate determinations of true resistivity and hence of saturation. Also, some methods for computing saturation are entered with the ratio R_{xo}/R_t . Also, in clean formations, a value of F may be computed from R_{xo} and R_{mf} , if S_{xo} is known or estimated. From F , a value for porosity may be found.

To measure R_{xo} a shallow-investigation tool is desirable, since the R_{xo} zone may sometimes extend only a few inches beyond the hole wall. Also, the reading should preferably not be affected by the borehole.

A sidewall-pad tool is indicated. The pad, carrying short-spacing electrode devices, is pressed against the mudcake, thus reducing the short-circuiting effect of the mud. Currents from the electrodes on the pad must pass through the mudcake to reach the R_{xo} zone.

Microresistivity readings are more or less affected by mudcake, depending on its resistivity, R_{mc} , and thickness, h_{mc} . Moreover, mudcakes can be anisotropic, with mudcake resistivity parallel to the borehole wall less than that across the mudcake. Mudcake anisotropy increases the mudcake effect on microresistivity readings, so that the effective, or electrical, mudcake thickness is greater than that indicated by a caliper. The microresistivity tools incorporate two-arm calipers, which show the size and condition of the borehole.

Equipment

Present equipment includes a combination tool with two pads mounted on opposite sides. One is the ML pad, and the other may be for either the MLL or the PL, as required by mudcake conditions. The measurements are recorded simultaneously. The MSFL is a combination tool, which can be run with either formation density or dual laterolog equipment.

Log Presentation

The microresistivity logs are scaled, of course, in resistivity units. When recorded by itself, the ML data are usually recorded over Tracks 2 and 3 on a linear resistivity scale. The microcaliper data are in Track 1. The MML or PL is recorded on a four-decade logarithmic scale on the right of the depth track (Fig. 49.30). The caliper is recorded in Track 1. When the ML data are also recorded, they are in Track 1 on a linear scale. The MSFL data are also recorded on the

* So-called because it was first observed in the Delaware sand of the Delaware basin (west Texas). This sand underlies a very thick anhydrite bed.

logarithmic grid. When run with the dual laterolog, it is presented on the same film as the LL curves. With the Compensated Formation Density (FDC™) log, it must be presented on a separate film, since the FDC log uses a linear grid; the two logs are normally recorded simultaneously.

Microlog

With the microlog tool,²³ two short-spacing devices with different depths of investigation provide resistivity measurements of a very small volume of mudcake and formation immediately adjoining the borehole. They readily detect the presence of any mudcake, indicating invaded (hence permeable) formations.

Principle. Arms and springs press a rubber pad against the hole wall. In the face of the pad are inserted three small electrodes in line, spaced 1 in. apart. With these electrodes a 1- \times 1-in. microinverse, $R_{1 \times 1}$, and a 2-in. micronormal, R_2 , are recorded simultaneously.

As drilling mud filters into the permeable formations, mud solids accumulate on the hole wall, forming a mudcake. The resistivity of the mudcake is about equal to, or slightly greater than, the resistivity of the mud. Mudcake resistivity is usually considerably smaller than the resistivity of the invaded zone near the borehole.

The 2-in. micronormal has a greater depth of investigation than the 1- \times 1-in. microinverse. It is therefore less influenced by the mudcake and reads a higher resistivity, producing "positive" curve separation. In the presence of the low-resistivity mudcake, both devices will measure moderate resistivities, usually ranging from about 2 to 10 times R_m .

Interpretation. Positive separation in a permeable zone is illustrated in Fig. 49.30, at Level A. The caliper shows evidence of mudcake. However, quantitative inferences of permeability are not possible from the ML data. When no mudcake exists, for whatever reason, the ML data may yield useful information as to borehole condition or lithology, but the log is not quantitatively interpretable.

Under favorable circumstances, R_{xo} values can be derived from the ML by use of Fig. 49.31. R_{mc} values for this purpose can be measured directly or estimated from Ref. 2, and h_{mc} is obtained from the caliper. Limitations of the method are (1) the ratio R_{xo}/R_{mc} must be lower than about 15 (porosity more than 15%), (2) h_{mc} must be no greater than $\frac{1}{2}$ in., and (3) depth of invasion has to be over about 4 in., otherwise the ML readings are affected by R_f . Eqs. 6 or 14 permit the porosity derivation from the ML measurements. For this, the value of S_{xo} must be reasonably well known.

Mud Log

The ML sonde is lowered into the hole with arms closed. Except in holes smaller than 8 in., the measuring pad will randomly face away from the wall part of the time, and its reading then will be determined mostly by the mud. A recording of these readings, conveniently made going down, serves as a "mud log," on which the lowest resistivities correspond to the upper limit of the in-situ value of R_m . This log has several potential applications, including crosschecking the surface R_m measurement, detecting mud-system changes, and identifying downhole water flows.

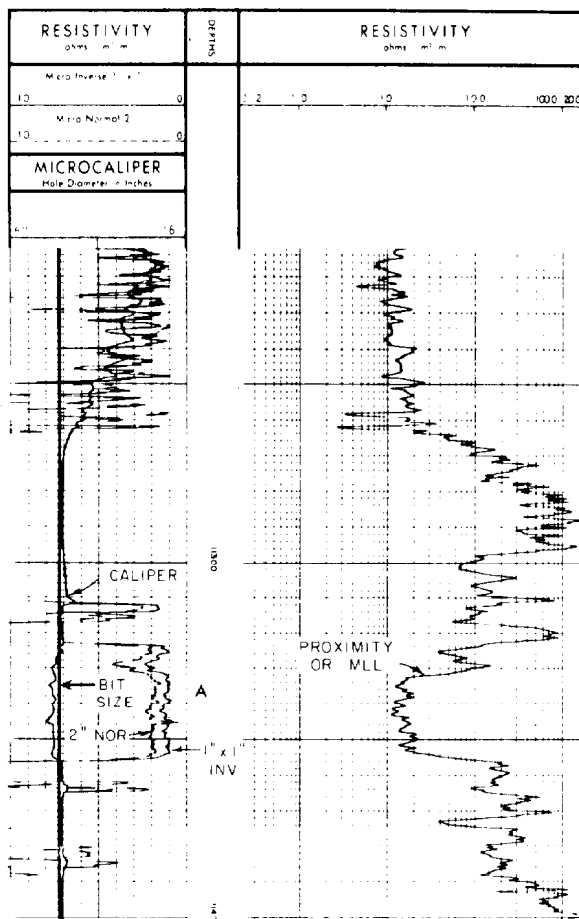


Fig. 49.30—Presentation of proximity log-microlog.

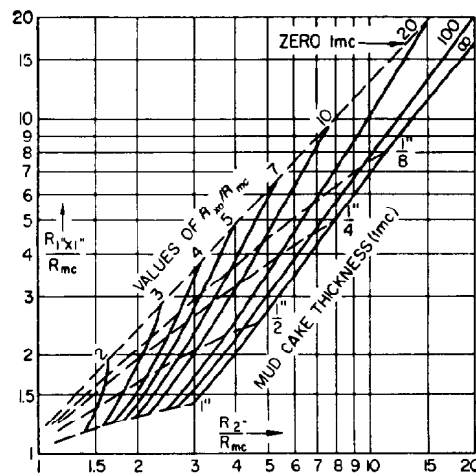


Fig. 49.31—Interpretation chart for 8-in.-hole series C microlog for which adjacent electrodes are 1 in. apart. $R_{2 \text{ in.}}$ designates reading of 2-in. micronormal ($AM_2 = 2$ in.) and $R_{1 \times 1 \text{ in.}}$ is 1- by 1-in. microinverse ($AM_1 = 1$ in., $M_1, M_2 = 1$ in.). Type I hydraulic pad, noninsulated sonde.

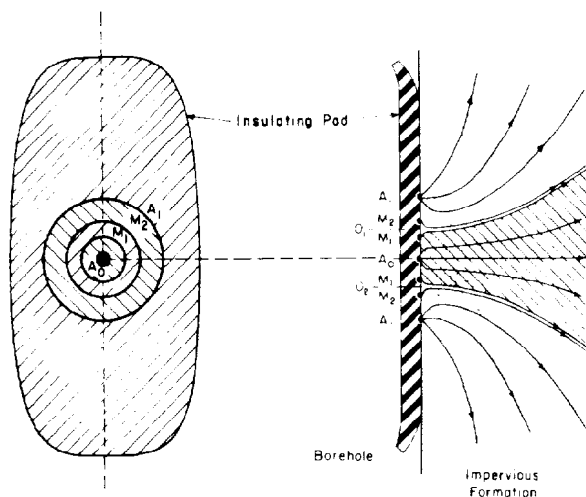


Fig. 49.32—Microlaterolog pad showing electrodes (left) and schematic current lines (right).

Microlaterolog (MLL)

On ML (Fig. 49.31) for values of R_{xo}/R_{mc} greater than about 15, the curves for constant values of R_{xo}/R_{mc} are crowded; as a result, the accuracy of the determination of R_{xo} from the ML is poor in this region. With the MLL method, it is possible to determine R_{xo} accurately for higher values of R_{xo}/R_{mc} , provided, however, that the mudcake thickness does not exceed $\frac{3}{8}$ in.

Principle. The MLL pad is shown in Fig. 49.32.²⁴ A small electrode, A₀, and three concentric circular electrodes are embedded in a rubber pad applied against the hole wall. A constant current, I₀, is emitted through electrode A₀. Through the outer electrode, A₁, is sent a current automatically adjusted so that the potential difference between the two monitoring electrodes is maintained essentially equal to zero. The I₀ current flowing past the M₁ electrode cannot reach M₂ and is forced to flow in a beam into the formations. The current lines are shown on the figure. The I₀ current near the pad forms a narrow beam, which opens up rapidly at a few inches from the face of the pad. The MLL reading is influenced mostly by the formation within this narrow beam.

Fig. 49.33 compares qualitatively the current-line distributions of the MLL and the ML when the corresponding pad is applied against a permeable formation. The greater the value of R_{xo}/R_{mc} the greater the tendency for the microlog I₀ current to escape through the mudcake to reach the mud in the borehole. Consequently, for high R_{xo}/R_{mc} values, the readings of the ML respond very little to variations of R_{xo} . On the contrary, all the MLL I₀ current flows into the formation and the MLL reading will depend mostly on the value of R_{xo} .

Response. Laboratory tests have shown that the virgin formation has practically no influence on the MLL readings if the invasion depth is more than 3 or 4 in. The influence of mudcake is negligible up to $h_{mc} = \frac{3}{8}$ in. but increases rapidly with greater thicknesses. Chart Rxo-2 in Ref. 2 gives appropriate corrections; however, if mudcakes thicker than $\frac{3}{8}$ in. are anticipated, the PL is preferred for R_{xo} determination.

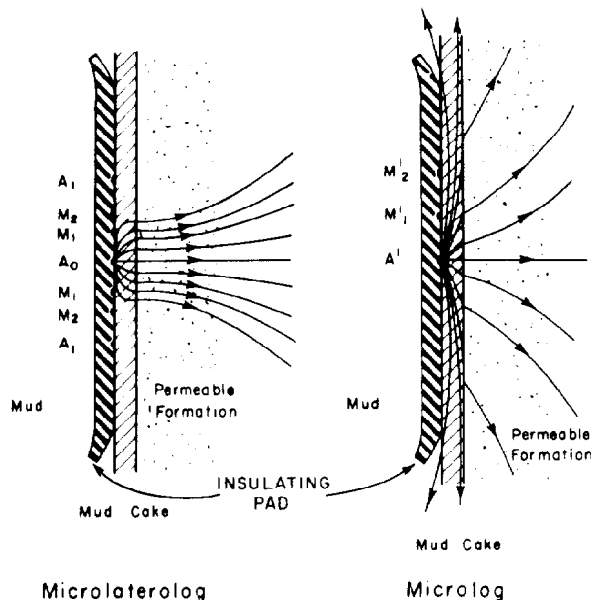


Fig. 49.33—Comparative distribution of current lines of Microlaterolog and Microlog.

Proximity Log (PL)

Principle. The proximity tool is similar in principle to the MLL tool. The electrodes are mounted on a somewhat wider pad, which is applied to the wall of the borehole; the system is automatically focused by monitoring electrodes.

Response. Pad and electrode design are such that isotropic mudcakes up to $\frac{3}{8}$ in. have very little effect on the measurements (see Chart Rxo-2 in Ref. 2). If the invasion is shallow, the reading of the proximity device is influenced by R_t . The resistivity measured can be expressed as

$$R_{PL} = G_{pi} R_{xo} + (1 - G_{pi}) R_t, \quad \dots \dots \dots (13)$$

where G_{pi} is the pseudogeometrical factor of the invaded zone. The value of G_{pi} as a function of invasion diameter d_i is given in Fig. 49.34; this chart gives only an approximate value of G_{pi} , which in fact also depends to some extent on the diameter of the borehole and on the ratio R_{xo}/R_t .

If d_i is greater than 40 in., G_{pi} is very close to 1 and, accordingly, R_{PL} will differ little from R_{xo} . If d_i is less than 40 in., R_{PL} is somewhere between R_{xo} and R_t , usually much closer to R_{xo} than to R_t . R_{PL} can be fairly close to R_t only if the invasion is very shallow (of course when R_{xo} and R_t are nearly equal, the value of R_{PL} will depend very little on d_i).

MICROSFL (MSFL)

This is a pad-mounted SFL device. It embodies two distinct advantages over other microresistivity devices: (1) it is compatible with other logging tools, specifically the FDC and the simultaneous dual laterolog (SDL), which eliminates the need for a separate logging run to obtain R_{xo} information, and (2) it responds to shallow R_{xo} zones in the presence of mudcake. The MSFL gives good R_{xo} resolution in thick-mudcake conditions, but

does not require as great an invasion depth as does the PL. This characteristic makes it useful in a wider range of conditions than either the PL or the MLL. The effect of mudcake on the MSFL data is shown in Ref. 2.

Principle. Spherical focusing is the shaping of the equipotential surfaces produced by the resistivity device to approximately spherical form. The focusing is accomplished by auxiliary electrodes, as in the MLL and PL; but, instead of being forced into a narrow beam, the measure current is merely prevented from following the borehole mud or mudcake paths. A careful selection of electrode spacings achieves an optimal compromise between too much and too little depth of investigation.

Conclusions

The ML permits a very accurate delineation of permeable beds in all types of formations. It can also provide satisfactory R_{xo} and porosity determinations under favorable conditions, which are (1) $R_{xo}/R_{mc} \leq 15$, (2) $h_{mc} \leq \frac{1}{2}$ in., and (3) depth of invasion greater than about 4 in.

The focused microresistivity tools can provide good R_{xo} values under a much wider range of conditions. The MLL is limited chiefly by mudcake thickness, but is well adapted to salt-base muds. When h_{mc} exceeds $\frac{3}{8}$ in., the PL or the MSFL log is preferable.

Uses and Interpretation of Well Logs

Bed Detection and Definition

Formations encountered in uncased boreholes may be detected and their boundaries defined by a number of different logs. The SP and short-investigation curves are most commonly used. For great detail, the microdevices are superior—ML in fresh muds and MLL in very salty muds. A substitute for the SP in salt muds is the gamma ray log, which distinguishes shales from nonshale beds. Also, the sonic and density logs could be used in all types of formations, with any type of mud.

In holes filled with nonconductive muds, or in empty holes, the induction, radiation, temperature, sonic (not applicable in empty holes), and perhaps section-gauge logs can provide useful information. Sometimes conventional devices with wall scratchers, for contact with the formation, may be run.

Porous and Permeable Beds—Sand Count. Porous and permeable beds are of primary interest since they are the potential oil and gas reservoirs. A sand-count determination of the total effective thickness of a permeable section, excluding shale streaks and other impermeable zones, can be derived from electrical logs.

Fresh Muds. The SP and microresistivity devices are the principle curves for locating and defining permeable beds. The SP has a good resolving power in formations of low and moderate resistivity. In very resistive formations it can still detect shales and permeable beds, but it cannot define their boundaries accurately. In most types of formations the ML is best for establishing the detailed location of the boundaries of permeable beds.

The microcaliper helps in the location of permeable beds because it can usually detect the mudcakes, particularly if the adjacent formations are approximately at bit size. Shales, on the other hand, generally tend to cave

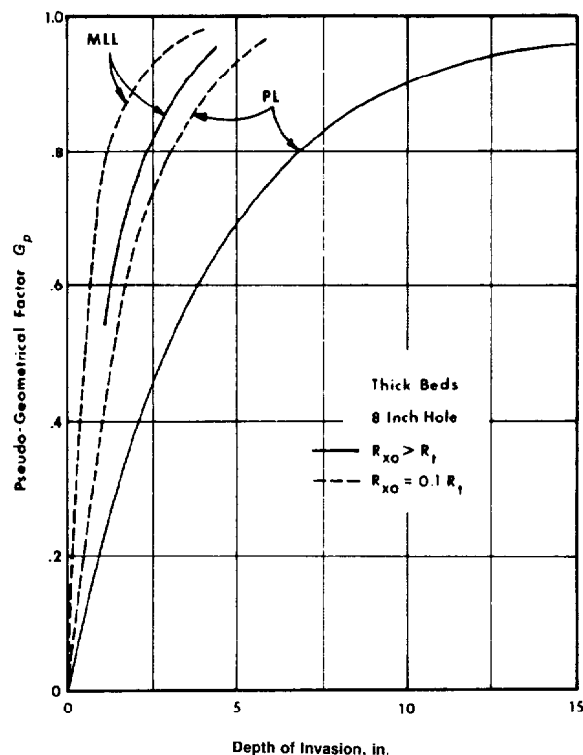


Fig. 49.34—Pseudogeometrical factors, MLL and PL.

or erode more than the permeable or hard impervious beds. Very often, and mostly in sand-shale series, the difference between the readings of a short-investigation and a long-investigation device is a clear indication of the presence of a permeable bed.

Salt Muds. The combination of very salty mud with moderate-to-high formation resistivity adversely affects the conventional (nonfocused) devices and the SP curve. Also, mudcakes are thin; as a consequence, the microcaliper (or also the section gauge) is not of great help for the detection of permeable sections but detects clearly the caved shales. In conjunction with the LL and MLL the gamma ray log distinguishes between shales and nonshales, and the neutron, sonic log, and density log provide indications of porosity.

Correlation

The process of correlating two (or more) logs in different wells depends essentially on the similarity in shapes or outlines of the curves (Fig. 49.35). In some regions such correlations may be easily made for wells miles apart; in other cases (where serious faulting, lenticular deposits, or unconformities are present) it may be difficult to correlate logs from wells only a few hundred feet apart. The knowledge of formation dip from dipmeter determinations assists in correlation.

Correlations are facilitated when the curves show characteristic "markers" such as a well-known chalk or shale section. Thin resistive beds such as lignites or evaporites frequently furnish valuable correlation points. For long-range correlation, the devices that investigate large volumes of formation are best. However, when the

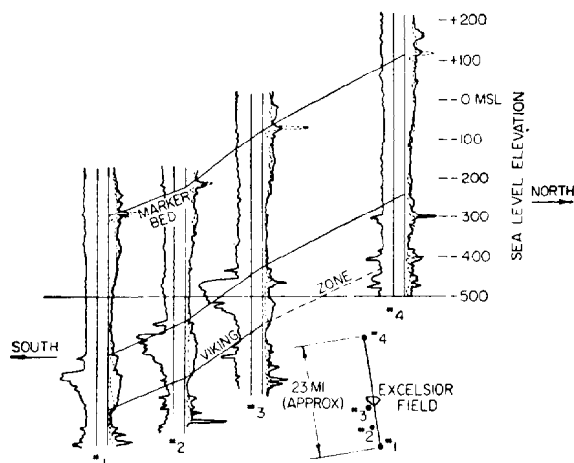


Fig. 49.35—Example of long-distance correlation.

pay zones are known in a field, they can be correlated in great detail from well to well by comparing the ML or MLL; thus, the geometry of the reservoir can be obtained.

Investigation of Porosity

Evaluation of formation porosity from electrical logs is based on determination of the formation factor, F_R , which is related to porosity, ϕ , by Eq. 2. F_R can be found from the value of R_{xo} as determined from the ML or MLL with Eq. 6 rewritten as

$$F_R = \frac{R_{xo}}{R_{mf}} (S_{xo})^2, \quad (14)$$

where $S_{xo} = 1 - S_{or}$.

To determine R_{xo} from microresistivity measurements, it is necessary that invasion be deep enough that the measurements are not affected by the formation resistivities beyond the flushed zone. An exceedingly great mudcake thickness may also limit the accuracy of the R_{xo} determination. For reliable porosity interpretation from ML data the porosity should be greater than about 12 to 15%.

In an oil-bearing sand, the residual oil saturation (ROS) must be surmised for use in Eq. 14. Taking a value of 20% for the ROS would not usually entail too great an error in most cases, at least in formations with granular porosity and containing light oils. Greater ROS's are frequent, however, chiefly in the cases of highly viscous oil. Gas-bearing formations also seem to display high residual gas saturations in the flushed zone if the permeability is high. This is because of segregation effects resulting from a combination of gravity and capillary forces. Because of these residual saturations, the ML may show water contacts.

To check the results of the microresistivity devices, or to replace them in case they are not available, F_R may be determined as equal to R_0/R_w , R_0 being the true resistivity of the formation at a level where it is 100% water bearing. Extrapolation of a value of F_R determined at a water-bearing level to the oil-bearing section within the same formation implies that the lithological

characteristics are approximately constant, which is not always the case, however.

Still another approach often used in hard formations is based on the value of R_i , the average resistivity of the invaded zone estimated from the readings of the limestone sonde or the short normal.^{25,26} This procedure has proved valuable in many cases.

Other Tools for Obtaining Porosity. The sonic log, the neutron log, and the density log are increasing in importance as auxiliaries to the electrical logs for improved porosity determination.* In addition, with the present sample taker, reliable determination of formation factor and porosity are often possible from sidewall cores.

Investigation of Fluid Content

Quite often good qualitative judgments about a formation as a potential producing zone can be had by direct visual inspection of the log. Basically such judgments usually depend on (1) identification of a permeable formation by means of the SP, mudcake indications on microcaliper, positive separation on ML, indication of invasion by separation between shallow- and deep-investigation macroresistivity curves, etc., and (2) indication by the deep-investigation resistivity devices that R_i in the permeable formation is appreciably larger than the resistivity, R_0 , that the formation would be expected to have if water bearing.

When it can be assumed that there is no abrupt change in the salinity of the formation waters, the radius of invasion, etc., qualitative evaluations of saturation may be made by comparing a porosity log with a resistivity log over a large enough section of formations. Such a method, in which the neutron log was the source of the porosity data, was proposed several years ago.²⁷ Also, the possibility of accurate measurements of porosity with the sonic and density logs has prompted similar qualitative interpretation procedures.²⁸

When invasion is not too deep, so that the deep-investigation resistivity devices read fairly close to R_i , the following procedures are applicable.

1. Sonic** transit time may be plotted vs. a deep IL resistivity (in case of fresh muds) or vs. the LLD resistivity (in case of salty muds).²⁹ By a proper choice of scales, lines of constant resistivity index, I_R , become straight lines on the chart, as in Fig. 49.36. The line of 100% water saturation ($I_R = 1$) is constructed as the line bounding the leftmost plotted points and passing through the point corresponding to infinite resistivity and zero sonic log porosity. Lines for other values of I_R may then be constructed. It is possible to distinguish between oil- or gas-bearing and water-bearing zones by the relative positions of the plotted points. For a zone to be oil- or gas-productive the plotted point should fall appreciably to the right of and below the line of 100% saturation. This method is useful even if the formation-water resistivity is not initially well known.

2. By use of porosity derived from the sonic or neutron log and the resistivity from the deep-investigation log, apparent values of the formation-water resistivity

*The short-interval sonic velocity log (sonic log) is discussed in Chap. 50. The neutron log is discussed in Chap. 51.

**With some precautions, density or neutron data may be employed in place of sonic data in a similar crossplot technique.

$R_{wa} = R_t / F_R$ may be computed (using Eqs. 2 or 3 to obtain F_R). When tabulated in terms of depth, those apparent values that stand definitely above the average trend indicate the presence of hydrocarbon saturation. This procedure is rapid and applicable in shaly sands. It is also applicable when formation-water salinity varies appreciably with depth, provided that the variation is gradual and continuous.

3. The readings of a short-investigation resistivity log should give indications of the variations in the formation factor (and porosity). Accordingly, hydrocarbon saturation can also be qualitatively determined by examining the ratios of the readings of a short-investigation device (such as a short normal, LLS, or PL) to those of the deep induction log (ILD) or LLD. The two sets of readings may be used to locate points on a graphic plot, as described previously, or to construct a continuous curve of the ratio vs. depth. In either case the comparison is facilitated if the logs have been recorded on a logarithmic sensitivity scale.

The following procedure is helpful when, because of deep invasion, the value of the true resistivity is in doubt. The porosity from the sonic log is compared with the porosity computed from a shallow-investigation resistivity log (such as short normal, limestone sonde, LLS or PL). The latter porosity is affected by any residual oil saturation, whereas the sonic log porosity is not. Zones where the two porosities differ should accordingly indicate potentially productive formations.

Also, in hard formations (where permeability is generally low) a resistivity gradient (corresponding to a saturation gradient) is observed on the logs between the zone of lowest water saturation and the level of 100% water saturation. The existence of this gradient is the basis of a method for the delineation of intervals saturated with hydrocarbons.³⁰

Quantitative Interpretation*

Quantitative determinations of the hydrocarbon saturation from electrical logs are essentially determinations of the water saturation, S_w , in the uncontaminated zone. Recalling Eq. 5

$$S_w = \left(\frac{R_0}{R_t} \right)^{1/2} = \left(\frac{F_R R_w}{R_t} \right)^{1/2}$$

The evaluation of R_t is a major step in the determination. Evaluation of F_R is equivalent to an evaluation of porosity, as already discussed. R_0 may be determined in a 100% water-saturated section of the same sand or in a lithologically similar sand.

Some interpretation procedures do not require explicit evaluation of R_t and F_R . Along with a knowledge of the SSP, or equivalently the ratio R_{mf}/R_w , they are based on the ratios of readings taken with deep- and shallow-investigation devices [e.g., R_{xo}/R_t method, induction-electrical log (IEL) interpretation, Rocky Mountain method]. A special approach is applied in case of shaly formations.

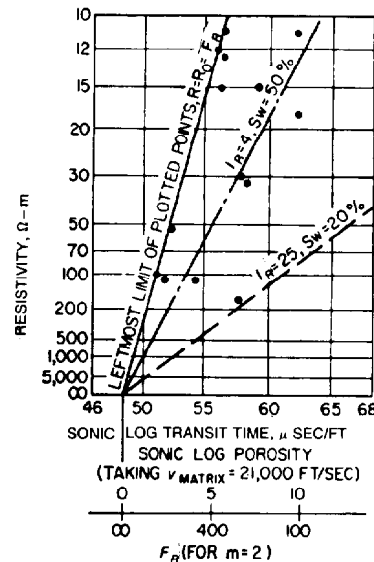


Fig. 49.36—Qualitative method for differentiating water-bearing and oil- or gas-bearing zones by plotting deep-investigation resistivity values against sonic-log transit times. The ordinate scale is proportional to $(1/R)^{1/2}$.

Determination of R_t . Conventional resistivity logs can provide for the value of R_t only for thick beds, since the readings in general cannot be reasonably corrected for the effect of adjacent formations. The long lateral, because of its large radius of investigation, is practically unaffected by the mud column and the invaded zone and gives a good approximation of R_t when the beds are reasonably uniform over a thickness of at least 30 ft. Such favorable conditions are seldom met in practice.

The long-normal reading usually requires a correction for the borehole effect. This correction is sufficiently accurate in fresh mud. The reading is close to R_t when the bed thickness is at least 10 to 15 ft and invasion is shallow. The effect of deep invasion can be accounted for, to some extent, by means of departure curves.^{31,32} Correction for invasion requires the help of other devices with shorter radii of investigation (ML and/or short normal), which provide values of the invaded-zone resistivity.

The advantage of the ILD and the LLD is that under usual conditions of application their readings are practically unaffected by the mud column or by the adjacent formations for bed thicknesses greater than about 5 to 6 ft.

The ILD, with the present technique, is appropriate for logging in fresh mud. Its accuracy is excellent for formations reading up to 50 Ω-m and reasonable up to 200 Ω-m. Above that figure the accuracy is not so good. The ILD gives R_t when the invasion diameter does not exceed 25 to 40 in. and can be corrected for deep invasion. The auxiliary readings are the ML and/or the short normal, or better, the LL8 or SFL, particularly in case of consolidated formations.

*Only computations that can be made by hand will be studied here. Latest interpretation techniques are made by computers and are explained under The Digital Age.

The LL is the essential tool for the logging of hard formations in salty mud. It gives R_t for shallow invasion (d_i less than 15 to 25 in.). Correction for invasion is made with the help of the MLL or MSFL. The most efficient way to correct for invasion and thus obtain R_t is the use of a three-log combination: (1) DIL or dual induction/SFL in fresh muds and in soft and intermediate formations and (2) dual laterolog/ R_{xo} in hard formations or salty muds. The so-called "butterfly or tornado charts" in Ref. 2 provide a simple procedure to obtain R_t .

Maximum Producing Oil Index

If the porosity, ϕ , of a formation is uniform and intergranular, the quantities $S_{xo}\phi$ and $S_w\phi$ represent the amounts of water per unit of bulk volume present in the pores of the flushed and uncontaminated zones, respectively. The difference $Y = (S_{xo} - S_w)\phi$ is the amount of oil per bulk volume displaced by the mud filtrate. Y is called "maximum producible oil index" because it approximates the maximum amount of oil per bulk volume producible with water drive. Y is given approximately by the equation²⁹

$$Y = \left(\frac{R_{mf}}{R_{xo}} \right)^{1/2} - \left(\frac{R_w}{R_t} \right)^{1/2} \quad (15)$$

Evaluation of Y by this equation does not require a direct knowledge of porosity, ϕ , formation saturation, S_w , or flushed-zone saturation, S_{xo} (or ROS).

Ratio Methods

It is impossible, in the space available, to present all log-interpretation techniques or to present all charts and tabulations made up thereof. For the practicing log interpreter most of the charts needed are included in Ref. 2.

The R_{xo}/R_t Method. For clean formations, saturations can be computed from the empirical relationship found by combinations Eqs. 5 and 6,

$$S_w = S_{xo} \left(\frac{R_{xo}}{R_t} \cdot \frac{R_w}{R_{mf}} \right)^{1/2} \quad (16)$$

Any method which gives correct values for R_{xo} , R_t , R_{mf} , and R_w may be used to determine S_w , provided S_{xo} is known or can be reasonably surmised.

The chart of Fig. 49.37 provides a convenient way for solving Eq. 16. The ratio R_{mf}/R_w is entered in abscissas (upper scale) and the ratio R_{xo}/R_t in ordinates. From the point so plotted, an oblique line is extended up to its intersection with the edge of the chart; from this intersection, a horizontal line is drawn which gives the values of S_w for different values of S_{xo} .

The value of S_w found directly by interpolation between the two nearby oblique lines is based on the assumption that S_{xo} , on the average, is related to S_w through the empirical equation $S_{xo} = \sqrt[3]{S_w}$. Within the limits where $R_w \approx R_{we}$ (i.e., R_w between 0.08 and 0.3 Ω -m at 75°F), the E_{SSP} can be entered, instead of R_{mf}/R_w , using the lower grid.

Microlog Shaly-Sand Method. The amplitudes of both the SP deflection and the resistivities are reduced by the presence of interstitial shale in a formation. In some ex-

SATURATION DETERMINATION

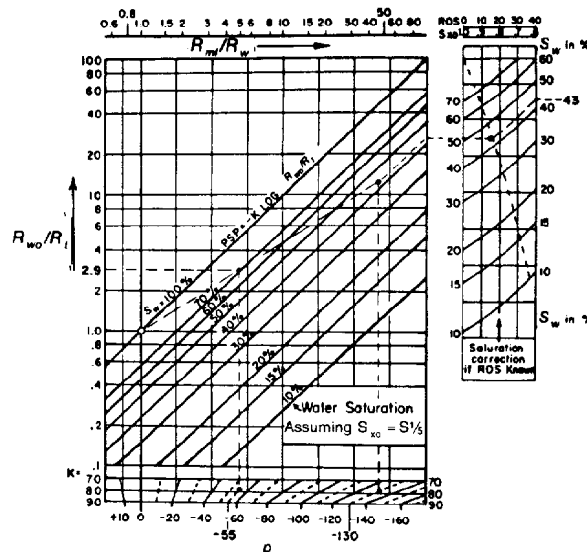


Fig. 49.37—Interpretation chart for R_{xo}/R_t and shaly-sand methods. (Working lines illustrate example of Fig. 49.38).

treme cases shaly oil sands are hardly differentiated from the adjacent shales on the logs. Furthermore, the ML does not show much separation between the curves. Interpretations in shaly sands, therefore, are generally made under comparatively unfavorable conditions. The practical method of interpretation described hereafter is quite approximate and is applicable only when the amount of shaliness is not too great.*

The practical method of interpretation in shaly formations³³ is based on the observations made on field logs that in 100% water-saturated shaly sands the PSP (pseudostatic SP) is given by

$$E_{PSP} = -K_c \log \frac{R_{xo}}{R_0} \quad (17)$$

For an interlaminated sand-shale formation containing oil and/or gas, the PSP can be expressed by the equation

$$E_{PSP} = -K_c \log \frac{R_{xo}}{R_t} - 2\alpha_{SP} K_c \log \frac{S_{xo}}{S_w} \quad (18)$$

where α_{SP} is the SP reduction factor and is defined as E_{PSP}/E_{SSP} . For clean sands, $\alpha_{SP} = 1$ and Eq. 18 reduces to Eq. 17 as a special case.

According to Eq. 18 the determination of S_w in a shaly sand requires the knowledge of R_{xo} , S_{xo} , R_t , E_{PSP} , and E_{SSP} . The E_{SSP} can be determined from clean sands reasonably close to the shaly formations considered. The E_{PSP} is given by the deflection of the SP curve at the level of the bed, after correction for bed thickness, if necessary. The value of $S_{xo} = 1 - S_{or}$ again must be surmised.

The solution of the equation for S_w is given by Fig. 49.37, which applies to both clean and shaly formations. For a shaly sand, the PSP and R_{xo}/R_t are first entered in abscissa and ordinate, respectively. This gives us the ap-

*Some other shaly-sand references are Refs. 8 and 9.

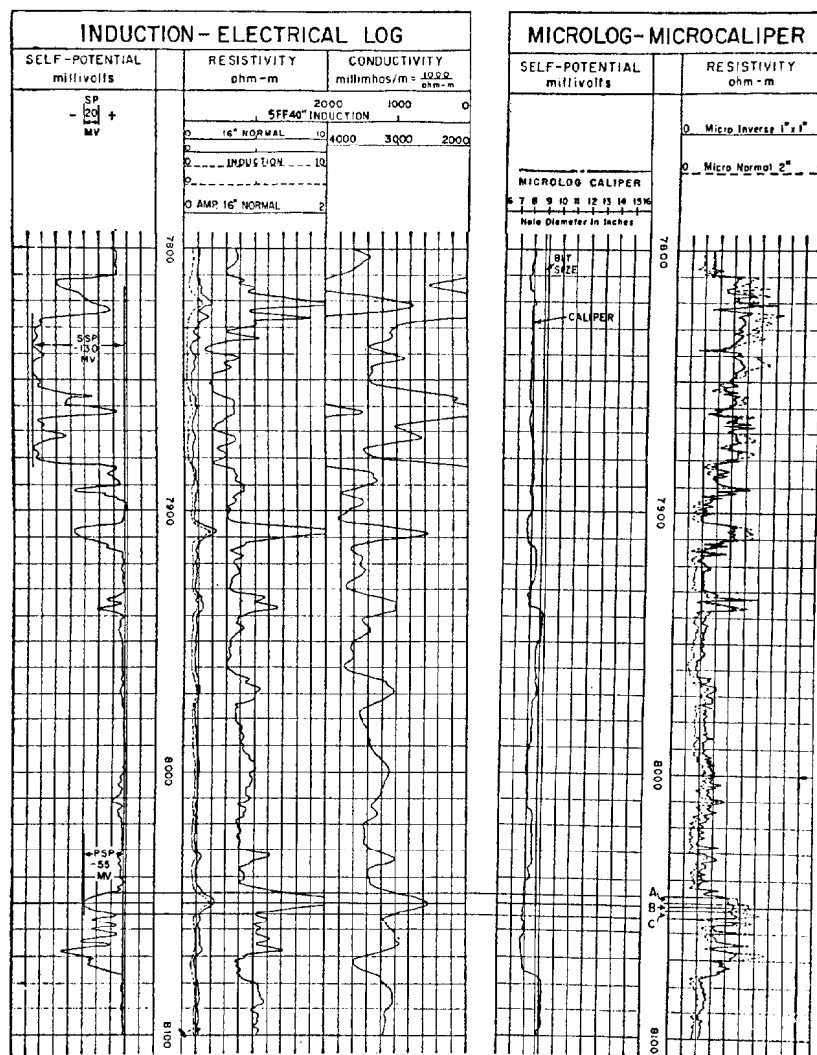


Fig. 49.38—Shaly-sand example: induction-electrical survey and microlog-microcaliper survey in well on Louisiana Gulf Coast. $R_m = 1.45$, $R_{mf} = 1.2$, and $R_{mc} = 1.3$ at BHT (140°F). $d = 8\frac{3}{4}$ in.

parent saturation. To find the true saturation, a line is drawn through the origin (circled), and the point representing the apparent saturation; and this line is extended until it intercepts the E_{SSP} or the corresponding value of R_{mf}/R_w . The saturation at this point is treated in the same manner as in the R_{xo}/R_t method above.

If the E_{SSP} is not known and R_w is unobtainable, it is not possible to determine the water saturation, S_w . Nevertheless, plotting the ratio R_{xo}/R_t vs. PSP on Fig. 49.37 will show whether or not the sand falls on the 100% water-saturation line. If it falls some distance below this line, there is a chance for production.

Note that in sand-shale laminations the value of S_w is the water saturation of the sand itself. In sands containing disseminated shale, it is the water bound by the quartz grains and does not include the water held by the colloids.

Example Problem 1. Fig. 49.38 shows the IEL and the ML over a portion of a well in Jefferson Davis Parish, LA. The shaly sand from 8,046 to 8,054 ft will

be interpreted. The mud resistivity at formation temperature of 140°F is 1.45 Ω -m, $R_{mc} = 1.3$ Ω -m, and $R_{mf} = 1.2$ Ω -m at 140°F. Bit size is 8 $\frac{3}{4}$ in.

From the IEL, the E_{PSP} is -55 mV. The E_{SSP} (sand at 7,830 to 7,850 ft) is -130 mV. Thus α_{SP} is 0.42. The short-normal resistivity R_{16} is 2.2 Ω -m, and the induction-log resistivity R_{IL} is 1.9 Ω -m. Invasion is known to be quite shallow, as further substantiated by the readings of the microlog. Therefore R_{IL} may be taken as equal to R_t .

As shown by the positive separation on the ML, three distinct porous intervals, A, B, and C, appear between 8,046 and 8,054 ft. The values of R_{xo} and h_{mc} for each interval are found by use of Fig. 49.31. Thus, for Interval A R_{xo} is 4.0, for Interval B it is 5.6, and for Interval C it is 6.8. The average R_{xo} is 5.5, and for all three intervals the mudcake thickness is $\frac{1}{2}$ in. Note that the microcaliper indicates a hole diameter of 7 $\frac{3}{4}$ in., exactly 1 in. smaller than bit size, corresponding to a $\frac{1}{2}$ -in. mudcake, thus verifying the h_{mc} values from Fig. 49.31.

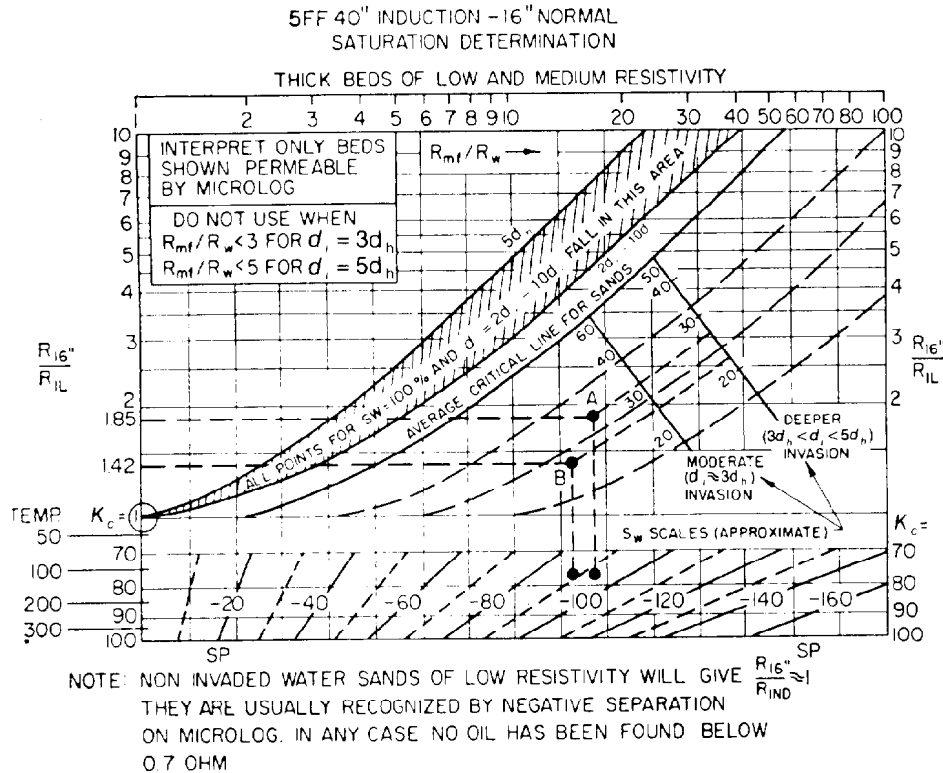


Fig. 49.39—40-in. induction log, 16-in. normal interpretation chart. (Working lines illustrate example of Fig. 49.40.)

All necessary data are now at hand:

$$\begin{aligned} R_{xo} &= 5.5 \Omega\text{-m} \\ R_t (=R_{IL}) &= 1.9 \Omega\text{-m} \\ E_{PSP} &= -55 \text{ mV} \\ E_{SSP} &= -130 \text{ mV} \\ \alpha_{SP} &= 0.42 \\ K_c &= (\text{for the SP}) \text{ at } 140^\circ\text{F} \text{ is close to } 79 \\ R_{xo}/R_t &= 2.9, \text{ and} \\ R_{xo}/R_{mf} &= 4.6 \end{aligned}$$

Fig. 49.37 is entered with $R_{xo}/R_t = 2.9$ and $PSP = -55$ at $K_c = 79$, locating a point on the chart. Then a line is drawn through this point from the origin and extended until it intersects the vertical line erected at $E_{SSP} = -130$ mV for $K_c = 79$. This intersection gives a value of S_w equal to 43%, assuming that S_{or} is 15%, which is reasonable. The sand was perforated from 8,046 to 8,050 ft and made 75 BOPD and 280,000 cu ft/D gas through a 7/64-in. choke.

IEL Interpretation Method. A chart for practical interpretation of fluid saturation from the readings of the IEL combination is shown in Fig. 49.39, Ref. 2. The conditions limiting valid use of the chart are: (1) the invasion diameter d_i must be between $2d_h$ and $10d_h$ (d_h is the hole diameter), (2) R_{xo} must be greater than R_t , which is generally fulfilled if R_{mf}/R_w is greater than three to five, as for fresh muds and saline formation waters, and (3) the beds must be fairly homogeneous—i.e., the short-

normal reading must not be perturbed by the presence of resistive streaks.

The chart incorporates approximate compensation for the presence of an annulus, assuming equal viscosities for the oil and water and an S_{or} in the flushed zone of 15 to 30%. To use the chart the value of the ratio $R_{16''}/R_{1L}$ (resistivity from 16-in. normal divided by the IL resistivity), corrected, if necessary, for effect of borehole and adjacent formations, is plotted either vs. the SSP (lower grid) entered opposite the appropriate formation temperature or vs. R_{mf}/R_w (upper scale).

Points falling within the shaded area correspond to water-bearing sands. Points falling below the shaded area correspond to oil saturation. Approximate saturation scales are provided for d_i values of $3d_h$ and $5d_h$. The dashed lines represent lines of equal saturation on the chart. The critical saturation corresponds to $S_w = 60\%$ in soft formations and 50% in consolidated sandstones. These may not be the correct critical saturations for many limestones.

For shaly formations a construction like that used in the shaly-sand method can be used in Fig. 49.39. Although not rigorously correct, this procedure should give acceptable results if the shaliness is not too great.

Since it is not always known beforehand whether the interpretation chart (Fig. 49.39) is within its limits of applicability, it is useful to employ the value of porosity or formation factor, when known from independent sources, to check the results by means of Eq. 5. Details of this "porosity balance" check are given in Ref. 34.

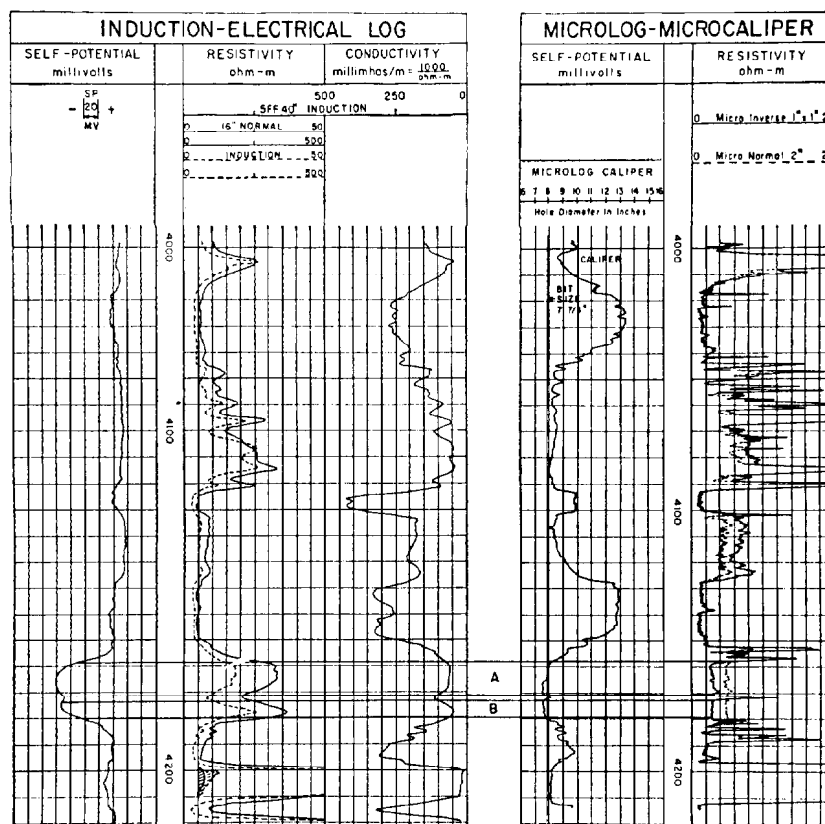


Fig. 49.40—Induction-electrical log and microlog-microcaliper log on a well in Young County, TX. $R_m = 0.95$ and $R_{mf} = 0.61$ at BHT (117°F). $d = 7\frac{7}{8}$ in.

Example Problem 2. Fig. 49.40 shows part of the induction-electrical log and ML on a well in Young County, TX. The sand at the bottom of the figure is divided into two parts, A and B, by a thin, hard streak, as shown on the ML. A and B will be interpreted separately. Necessary well data are $R_m = 0.95$ and $R_{mf} = 0.61$, at BHT of 117°F ; hole diameter, d_h , is $7\frac{7}{8}$ in.

Interval A. From the induction-electrical log, $R_{IL} = 17.5 \Omega\text{-m}$, $R_{16} = 32.5 \Omega\text{-m}$, $\text{SP} = -95 \text{ mV}$, and BHT is 117°F . Applying Fig. 49.39, the ratio $R_{16}/R_{IL} = 32.5/17.5 = 1.85$. The SP is -95 mV , so the point is fixed on the chart, giving an average S_w of about 30%.

Interval B. Here the $R_{IL} = 26.0 \Omega\text{-m}$ and $R_{16} = 37.0 \Omega\text{-m}$. $R_{16}/R_{IL} = 37.0/26.0 = 1.42$. The SP is -90 mV at 117°F . This fixes a point on Fig. 49.39, which gives a value of S_w of about 25%. Drillstem tests on the two intervals showed that the sand contained gas and distillate, with a higher flowing pressure over Interval B.

Rocky Mountain Method. The Rocky Mountain method²⁵ was developed for the interpretation of conventional electrical logs to yield values of S_w and ϕ in invaded, clean, hard formations when they are sufficiently thick and homogeneous. It is necessary that the invasion be such that the average resistivities recorded by the short normal and the lateral (when corrected for borehole effect) approximate the average values of R_i and R_t , respectively. For this to be true, the short-

normal readings should be at least 10 times the mud resistivity. Only average values, over thick intervals, can be obtained with this method.

$$R_i = \frac{F R_{wi}}{S_i^2}, \quad \dots \dots \dots (19)$$

where:

1. R_{wi} is the resistivity of the water found in the invaded zone. It is usually made up of filtrate and interstitial (connate) water mixed in such proportion that

$$\frac{1}{R_{wi}} = \frac{f_w}{R_w} + \frac{(1-f_w)}{R_{mf}}, \quad \dots \dots \dots (20)$$

where f_w is the fraction of interstitial (connate) water in the total mixture (usually 5 to 10%).

2. S_i is the water saturation in the invaded zone. It has been found by experience that $S_i^2 \approx S_w$; so $R_i = F R_{wi} / S_w$. Inasmuch as $R_t = F R_w / S_w^2$, we obtain $S_w = (R_i / R_t) / (R_{wi} / R_w)$.

Since $R_w / R_{wi} = f_w + (1-f_w) R_w / R_{mf}$, it follows that R_{wi} / R_w is a function of the SP value. The upper part of Fig. 49.41 gives a graphical solution of the equation for S_w . The SP is entered in ordinate and the ratio R_i / R_t on oblique lines. The intersection gives the abscissa S_w .

The lower part of the chart is used to obtain the porosity by using the water saturation, S_w , just found, with the

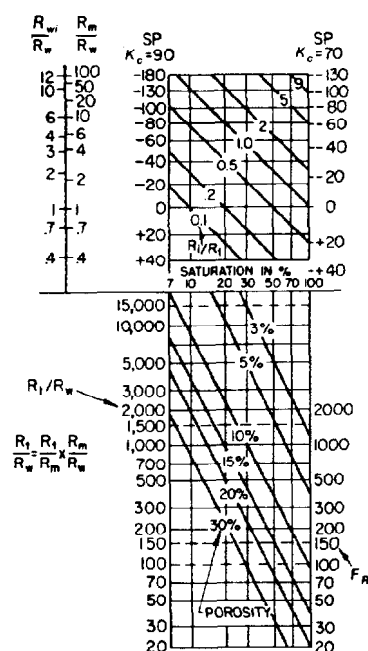


Fig. 49.41—Interpretation chart for Rocky Mountain method.

value of R_t/R_w . The intersection falls on or between oblique lines that are graduated into porosity values, according to the Humble formula, Eq. 2. This method should not be used in salt muds.

Electromagnetic Propagation Tool

Principle. The EPT[™] (electromagnetic propagation tool³⁵) measures the travel time and attenuation rate of an electromagnetic wave through the formation near the borehole. In addition, a caliper and a ML can also be recorded. The tool can be combined with the gamma ray, neutron, or density instruments.

The propagation time of water differs sharply from those of gas, oil, or matrix rock and is, moreover, little affected by the salinity of the water. This tool permits the evaluation of water saturation that is relatively independent of water resistivity (salinity) and, in fact, is most accurate in the fresher waters.

Dielectric permittivity is one of the main factors determining electromagnetic propagation in a material. Dielectric permittivity of any medium is proportional to the electric dipole moment per unit volume. The electric

dipole moment is made up of one or more effects: electronic, ionic, interfacial, and dipolar. Since each of these dominates over a certain range of the electromagnetic spectrum, they can be separated experimentally.

The electronic contribution results from the displacement of electron clouds, and is the only one that operates at optical frequencies. The ionic and interfacial contributions come from displacement and movement of ions, hence are confined to low frequencies. The dipolar contribution is from permanent electric dipoles, which orient themselves in the direction of an applied electric field. With the exception of water, there are very few materials abundantly found in nature that have permanent electric dipoles. A borehole dielectric measurement in the 10^9 -Hz frequency region, where the dipole polarization of water dominates, should lead to a measurement of water content that is independent of salinity.

Table 49.3 gives laboratory-measured values of propagation time and dielectric permittivity (relative to air) of typical reservoir materials.

Tool. The tools now in the field carry two transmitters and two receivers on a wall-contact pad, configured as shown in Figs. 49.42 and 49.43. These transmitters and receivers must be antennas to operate as they do in the microwave frequency range. The tool uses a differential measurement based on the signals detected by near and far receivers, similar in principle to the widely used method of measuring Δt with a two-receiver sonic tool. In a similar manner, the two receivers produce cancellation of any effects caused by mudcake or variations in signal coupling (so long as both receivers are affected equally).

To reduce any error caused by sonde tilt, the EPT uses an antenna configuration similar to the transducer array used in a borehole-compensated sonic tool. Transmitting antennas are placed above and below the receiver pair and are pulsed alternately. Simple geometric considerations show that if these two transmission modes are averaged, the first-order effects of pad tilt will be eliminated.

The basic principle of the tool involves a surface or lateral electromagnetic wave launched along the surface of a conducting pad. In the absence of mudcake, the electromagnetic wave would move along the pad face past two receiving antennas, but in the normal borehole case with mudcake present, propagation takes place on the surface between mudcake and formation. The phase shift and attenuation per unit distance along the surface of the pad are proportional to ϵ and C (as shown in theory) for a plane wave.

It has been demonstrated both theoretically and experimentally that for mud cakes up to $\frac{3}{8}$ in. the travel time measured by the EPT is essentially the same as the travel time in the invaded zone without any mud cake. Above such thickness the measurement deteriorates rapidly until the tool responds only to the mud. Limited experience with air- and oil-based mud-filled tools indicates that even very thin layers of these fluids between the pad and the formation cause the tool to respond only to the fluid and not the formation. This is because of the short travel time of these fluids. The tool contains a 1.1-GHz microwave transceiver. The transmitter is capable of generating more than 2 W of output power

TABLE 49.3—ELECTROMAGNETIC PROPAGATION VALUES

	Relative Dielectric Permittivity, ϵ	Loss-Free Propagation Time, t_{po}
Gas or air	1.0	3.3
Oil	2.2	4.9
Water	56–80	25–30
Quartz	4.7	7.2
Limestone	7.5	9.1
Dolomite	6.9	8.7
Anhydrite	6.5	8.4

while the receiver can process a 0.3 pico watt (pW) signal. This allows accurate measurements in formations when R_{ad} approaches $0.3 \Omega\text{-m}$.

Assuming a plane wave varying sinusoidally in time, the electric field, E , at the second receiver is given by

$$E = E_0 e^{-\gamma L + j\omega t} \quad (21)$$

where E_0 is the electric field at the first receiver; L is the distance between the two receivers; j is the vectorial operator $\sqrt{-1}$; ω is the angular frequency; t is the time of travel of the waves over a distance L in the formation; and γ is the complex propagation factor given by

$$\gamma = \alpha + j\beta \quad (22)$$

where α is the attenuation factor (coefficient) in neper/m, and β is the phase factor in rad/m.

For a "lossless" formation,* $\alpha = 0$. From Eq. 21, the phase velocity v_{po} is given by

$$v_{po} = \frac{L}{t} = \frac{\omega}{\gamma_d} = \frac{1}{t_{pd}} \quad (23)$$

where the subscript o indicates loss-free conditions and t_{pd} is the loss-free propagation time of a given medium in ns/m.

From Maxwell's equations, it can be shown that

$$\gamma_d = j\omega\sqrt{\mu\epsilon} = j\omega t_{po} \quad (24)$$

where μ is the magnetic permeability (H/m). Since most formations of interest are nonmagnetic, μ of the formation is the same as that of free space ($\mu_0 = 4\pi \times 10^{-7}$ H/m), and ϵ is the dielectric permittivity (F/m). When the formation is lossy, γ and α are complex.

*Formation with no electromagnetic energy losses

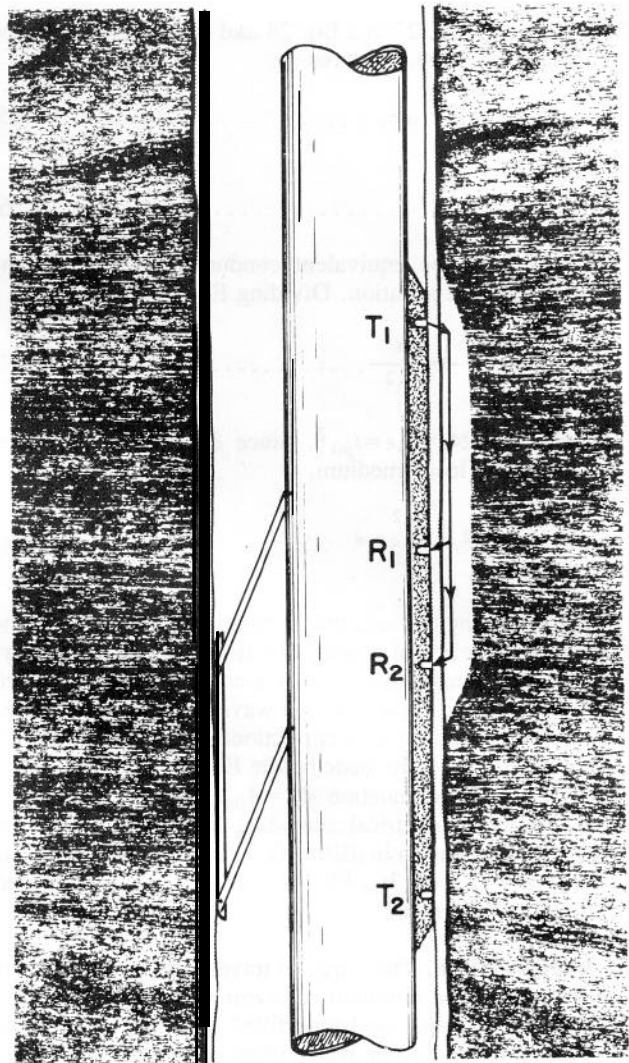


Fig. 49.42—Schematic of EPT antenna pad, showing principle of 2-receiver measurement of transit time.

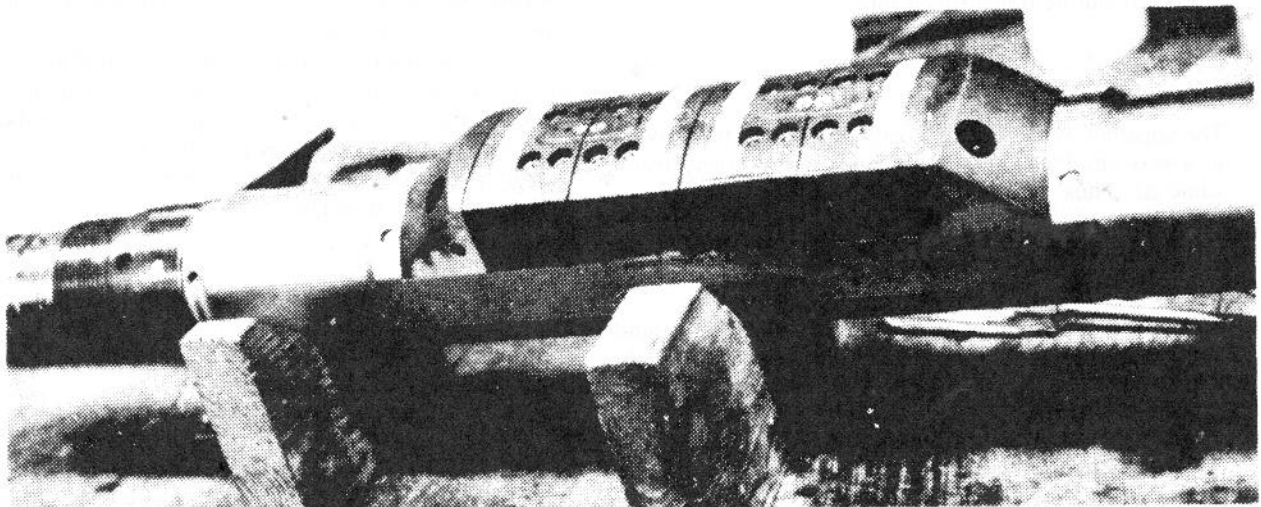


Fig. 49.43—The EPT antenna pad.

Squaring Eq. 22 and Eq. 24 and equating the real and imaginary terms, we have

$$\omega^2 \mu_o \epsilon = \beta^2 - \alpha^2, \quad \dots \quad (25)$$

and

$$\omega \mu_o C = 2\alpha\beta, \quad \dots \quad (26)$$

where C is the equivalent conductivity (Ω/m) of the losses in the formation. Dividing Eq. 25 by ω^2 ,

$$\mu_o \epsilon = \frac{\beta^2}{\omega^2} - \frac{\alpha^2}{\omega^2}. \quad \dots \quad (27)$$

From Eq. 24, $\phi_o \epsilon = t_{po}^2$. Since $\beta/\omega = t_{pl}$ is the travel time in the lossy medium,

$$t_{po}^2 = t_{pl}^2 - \frac{\alpha^2}{\omega^2} \cdot * \quad \dots \quad (28)$$

Remembering that α is the attenuation factor, Eq. 28 implies that the actual propagation time in a conductive formation is longer than that of a corresponding loss-free formation. If the propagation wave is not a plane wave, suitable spreading-loss corrections to the measured attenuation (A_{log}) are made before Eq. 28 is applied. Thus the corrected attenuation $A_c = A_{log} - G_{sl}$ (dB/m) where G_{sl} is the geometrical spreading loss and A_{log} the recorded attenuation in dB/m. G_{sl} is about 50 dB/m in air or $G_{sl} = 45.0 + 1.3t_{pl} + 0.18t_{pl}^2$. Here t_{pl} is the recorded travel time in ns/m.

Interpretation. The range of travel time encountered in the borehole in common reservoir rock varies from 6.3 ns/m for a 40-pu sandstone filled with hydrocarbons to 17.2 ns/m for a 40-pu water-filled limestone. In terms of phase shift, this corresponds to angles between 100 and 270° when computed over a 4-cm receiver spacing.

The EPT log responds primarily to the bulk volume of water in the formation. Since the tool has a relatively shallow depth of investigation—about 1 to 6 in. depending on the conductivity—it normally responds to the flushed zone of an invaded section.

Eq. 28 can be transformed into

$$t_{po} = \left(t_{pl}^2 - \frac{A_c}{3604} \right)^{1/2} \quad \dots \quad (29)$$

The apparent water-filled porosity (ϕ_{EPT}) can be derived in a way similar to the derivation of the porosity from sonic Δt . Thus

$$\phi_{EPT} = \frac{t_{po} - t_{pm}}{t_{pwo} - t_{pm}} \quad \dots \quad (30)$$

t_{pwo} , the loss-free propagation time of water, varies with the temperature and slightly with pressure and can be obtained as

$$t_{pwo} = 20 \left(\frac{710 - T/3}{444 + T/3} \right),$$

where T is the temperature, °F. Knowledge of water salinity is not required to obtain t_{pwo} .

* α in neper/m and A_{log} is dB/m. Since 1 neper = 8.686 dB, $A_{log} = 8.686\alpha$.

The loss-free propagation time of matrix, t_{pm} , is indicated on Table 49.2. The nature of the matrix can be determined by the knowledge of the apparent matrix density and interpolating between lithology density values. The water saturation S_{xo} is given by

$$t_{po} = S_{xo} \phi t_{pwo} + (1 - S_{xo}) \phi t_{ph} + (1 - \phi) t_{pm} \quad \dots \quad (31)$$

or

$$S_{xo} = \frac{t_{po} - t_{pm} + \phi(t_{pm} - t_{ph})}{\phi(t_{pwo} - t_{ph})}, \quad \dots \quad (32)$$

where t_{ph} is the propagation time for hydrocarbon and ϕ is the porosity of the formation. Since t_{pm} and t_{ph} are fairly close, we can estimate S_{xo} roughly as

$$S_{xo} = \frac{\phi_{EPT}}{\phi} \quad \dots \quad (33)$$

Example Problem 3. Fig. 49.44 is an example of the log presentation currently in use. Track 1 contains a conventional caliper curve, taken from the motion of the backup pad, and the attenuation curve, scaled in dB/m. Tracks 2 and 3 are given to the principal measurement, travel time (t_{pl}), in ns/m. Track 3 also presents the signal levels from the two receivers. The chief use of these curves is to monitor the primary signal detection at the receivers, which provides an indication of the relative reliability of the log parameters at any level.

A self-evident and very real advantage may be inferred from the 4-cm spacing between receivers; the tool has excellent vertical resolution. The log of Fig. 49.44 actually looks overactive in spots, but its repeatability testifies that the recording is valid. In fact, the data recorded by the tool are too detailed for direct merging with other logs by means of computer. Averaging (smoothing) subroutines are thus required preliminaries for programs using EPT data.

Example Problem 4. Fig. 49.45 shows an ISF log and the porosity computed from density, neutron, and EPT logs. Zone A is obviously gas bearing, as evidenced by the neutron porosity reading much less than the density. The EPT porosity is a little higher than the neutron porosity and much less than the density porosity, confirming the presence of hydrocarbons.

Zone B exhibits a different porosity profile. Once again the neutron porosity is less than the density porosity, indicating the presence of some light hydrocarbons, but now the EPT porosity is less than both neutron and density porosities. Since the total porosity from neutron and density logs is roughly

$$\phi = \frac{\phi_N + \phi_D}{2},$$

and the hydrocarbon volume is

$$\phi_{HC} = \phi - \phi_{EPT},$$

the volume of hydrocarbons affecting the three porosity tools is about the same for Zones A and B as determined from the EPT data. However, there is a much stronger light hydrocarbon effect on the neutron and density logs in Zone A. Thus, it would be expected that Zone B contains more condensate or oil than Zone A.

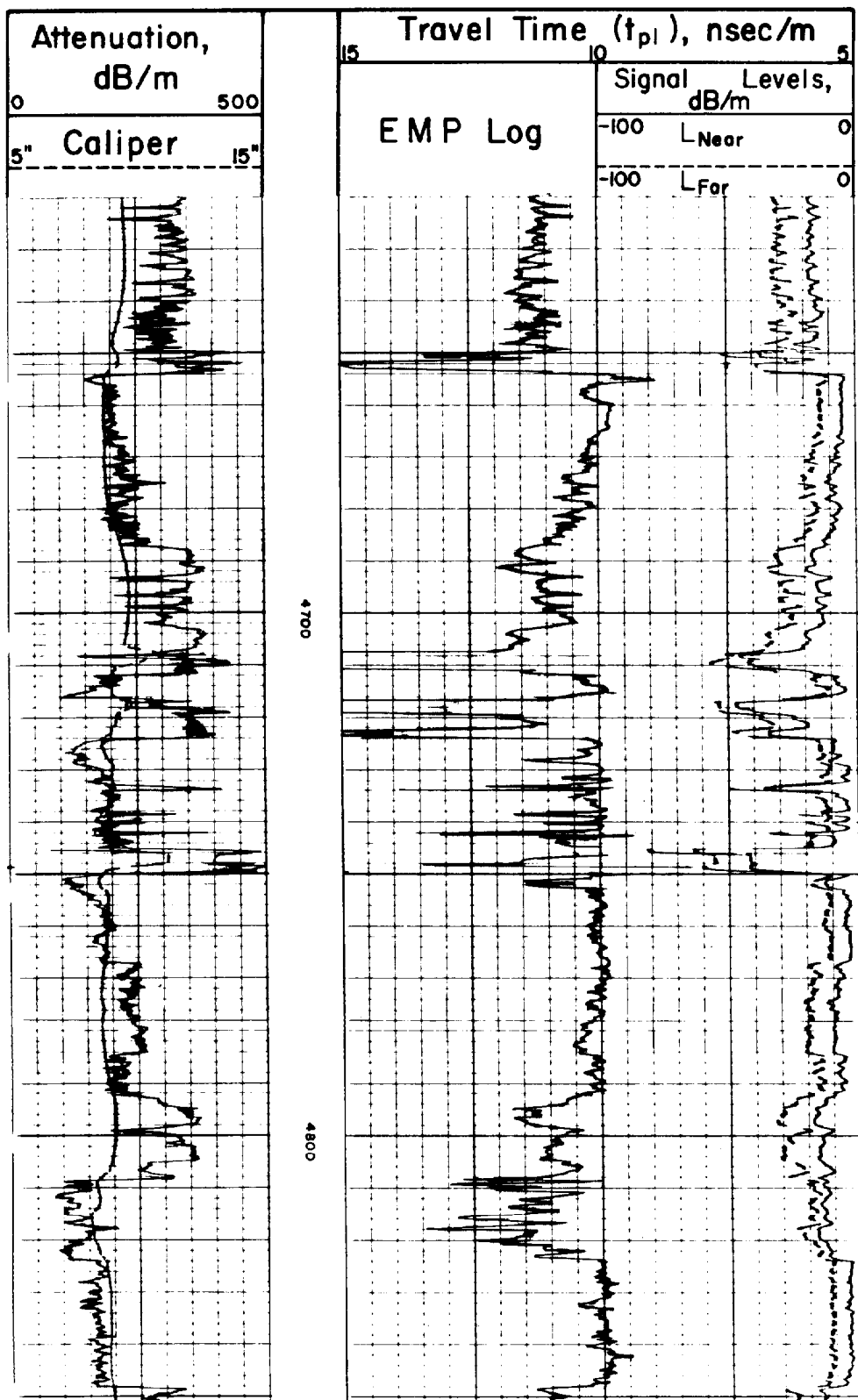


Fig. 49.44—An unaveraged EPT log shows fine detail. Repeat sections (faint curves) of the attenuation and t_{pl} curves show excellent repeatability.

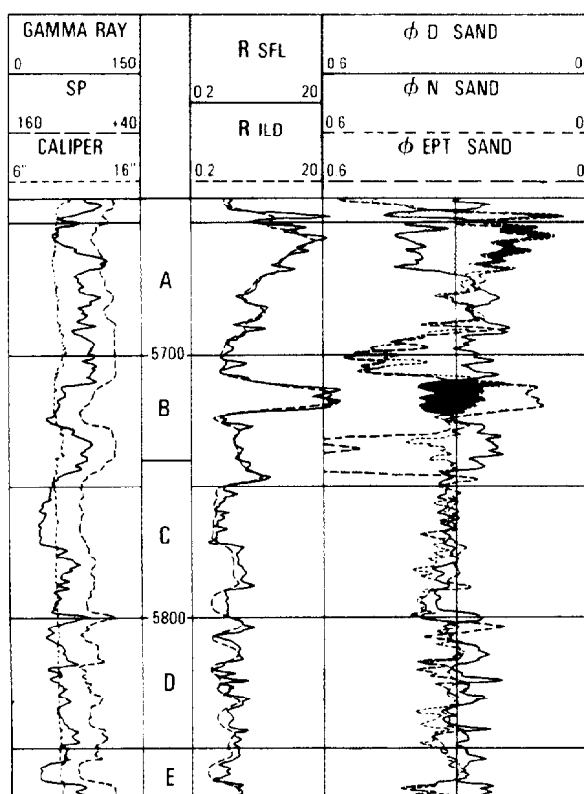


Fig. 49.45—ISF and EPT/CNL/FDC logs.

Zone C appears to contain some residual hydrocarbons, since the EPT porosity is often slightly less than the neutron and density porosities. There is a little more hydrocarbon in the shalier bottom part of Zone C than in the cleaner top portion.

The very top of Zone D contains oil since the EPT measurement is much lower than the neutron and density porosities, which read about the same. Water-bearing zones are identified when the EPT porosity is about the same or higher than the neutron and density porosity. Thus, Zone E is clearly water bearing, as is the bottom of Zones B and D.

Machine programs are available to give complete quantitative interpretation of all these logs. This is especially important in the study of tar sands or crude oils where the hydrocarbon is not flushed by the mud filtrate and where S_{xo} is very near S_w . These studies are also of great interest to provide values of residual oil saturations.

The Digital Age

Before 1960, all logs were recorded in analog form on film or paper. Magnetic tape recording was introduced in 1960 to record dipmeter. Shortly thereafter, various other logs were also recorded on tape, thus permitting the use of computers for various purposes. Before long, computers were made an intrinsic part of the recording systems on the logging trucks. This has revolutionized the capacity for data acquisition at the wellsite. At the same time, many computer-processed products have become available in real time or only a short time after logging is completed at the wellsite.

TABLE 49.4—WELLSITE ANALYSIS AVAILABLE IN REAL TIME

Generic Name	Derivation	Log Input Required	Presentation	Schlumberger	Gearhart	Dresser	Welex
R_{wa}	Assumes all formations contain 100% water. Computes apparent R_w . $R_{wa} = R_t/F$	Simultaneous resistivity and porosity. Usually sonic and induction	Single curve in Track 1 on logarithmic scale.	R_{wa}	R_{wa}	R_{wa}	R_{wa}
R_{xo}/R_t	Uses deep resistivity and shallow focused resistivity to estimate R_{xo}/R_t ratio.	Simultaneous deep resistivity and shallow focused resistivity	Single curve in Track 1 compatibly scaled as a pseudo SP curve.	R_{xo}/R_t	R_{xo}/R_t	R_{xo}/R_t	R_{xo}/R_t
"F" overlay or " R_o " overlay	Derives F from a porosity curve that is played onto logarithmic resistivity as R_o .	Deep resistivity and porosity	Single dashed curve in Tracks 2 and 3 on logarithmic scale.	R_o	R_o	"F" Curve	"F" Curve
Compatible porosity scales	Any combination of porosity logs with same lithology assumptions to compute porosity.	Simultaneous porosity logs	Coded curves in Tracks 2 and 3 with gamma ray and caliper in Track 1.	Compatible porosity scales	Compatible porosity scales	Compatible porosity scales	Compatible porosity scales
Hole volume	Uses caliper logs to compute hole volume for cement calculation.	Caliper curve—preferably 2 curves at 90° such as 4-arm dipmeter	Pips or tic marks in depth column at every 10 cu ft and 100 cu ft.	Borehole volume	Borehole volume	Borehole volume	Borehole volume
Fracture locating log	Uses differences in adjacent pad readings from 4-arm dipmeter to infer fractures.	4-arm dipmeter	Adjacent pad readings are superimposed and any separation is coded.	Fracture identification log	Fracture detector log	Fracture location log	Dipmeter fracture log

TABLE 49.5—WELLSITE ANALYSIS AVAILABLE IN REPLAY* TIME

Generic Name	Derivation	Log Input Required	Presentation	Schlumberger	Gearhart	Dresser	Welex
Merged and depth shifted data	Replays all logs, shifts depths and makes simple calculations such as R_{wa} , R_{xo} , R_{xo}/R_t , compatible porosity scales or cross plot porosities.	Any logs run on tape.	Usually 3 to 5 tracks. Varies by service company, displays only log data.	Cyberlook Pass 1	Cross-plot (X-plot)	Prolog	Computer Van
Wellsite evaluation log	Uses all logs to provide a first order computer analysis.	Resistivity and porosity	Usually 3 or 4 tracks. Has reservoir data derived from log data.	Cyberlook	Well evaluation log	Prolog	CAL
Formation dip computations	Computes formation dip from 4-arm dipmeter	4-arm dipmeter	Formation dip, hole deviation, calipers.	Cyberdip	FED DDL	Pro-Dip	
True vertical depth log	Computes TVD of any point from dipmeter orientation data	Continuous dipmeter plus any log to be converted to TVD	Replay of any log on TVD scale	TVD	TVD	TVD	

*All logs available in real time are also available in replay time if recorded on magnetic tape

Without any doubt, the digital age is responsible for the creation of new equipment deemed impossible before. Many interpretation techniques and studies today could not be made without the use of computers. Finally, electronic transmission of log data is a present reality, facilitating exchange between wells and offices, towns and continents. An overview of this vast field is necessary.

Magnetic Tapes

API-recommended standard format permits logging service company tapes to be read by most computers. More exhaustive treatment of the subject is available directly from the service companies. Quality control of the magnetic tape is ensured in real time in integrated logging systems having on-board computers.

Computed Log Products

Log analysis performed by a computer is available to the log user at three different levels.

1. Real-time "quick-look" products, summarized in Table 49.4, run at the same time the log is being run. Many of these curves, such as R_{wa} and F curves, are recorded on the standard logs and are often placed in the SP or resistivity tracks.

2. Wellsite log analysis products, summarized in Table 49.5, are generally available at the wellsite in replay time. Wellsite analysis is made after the logging is completed. The process involves playing back taped logs and using an appropriate log analysis program, such as a shaly-sand analysis or a dipmeter computation.

3. Computing center products are provided well after the logging is finished (days or weeks later) and are generally more comprehensive than either of the wellsite products. In general, these computations fall into three categories: shaly-sand analysis, complex lithology study, and dipmeter processing. The most-used products are summarized in Table 49.6. Other, less frequently used products such as tar sand analysis or mechanical properties are not included; details on these may be obtained directly from the service company.

TABLE 49.6—LOG ANALYSIS AVAILABLE FROM COMPANY COMPUTING CENTERS

Generic Name	Derivation	Log Input Required	Presentation	Schlumberger	Gearhart	Dresser	Welex
Advanced sandstone analysis	Uses most sophisticated analytical and statistical methods to correct and compute logs in sandstones and shaly sandstones.	Resistivity, density, neutron, gamma ray with sonic desirable	Usually 4 tracks presentation of lithology, saturation, porosity and bulk volume.	SARABAND VOLAN	Comsand "F" Pairs	EPILOG Sandstone Analysis	CAL
Advanced carbonate analysis	Uses most sophisticated analytical and statistical methods to correct and compute logs in carbonate and lithologically complex reservoirs	Resistivity, density, neutron, gamma ray with sonic and microresistivity desirable	Usually 4 tracks presentation of lithology, saturation, porosity, and bulk volume.	CORIBAND GLOBAL	Comlith Frax	EPILOG Complex Reservoir Analysis	CAL
Advance dipmeter computations	Uses most advanced correlation logic to compute dips followed by a statistical sorting to retain the most reliable data.	4-arm dipmeter	Arrow plot with caliper, correlation curve and hole deviation. Also available: azimuth frequency, modified Schmidt plots, histograms, and listings.	CLUSTER (structural) and GEODIP (stratigraphic)	NEXUS	Dresser computed dipmeter	Diplog analysis

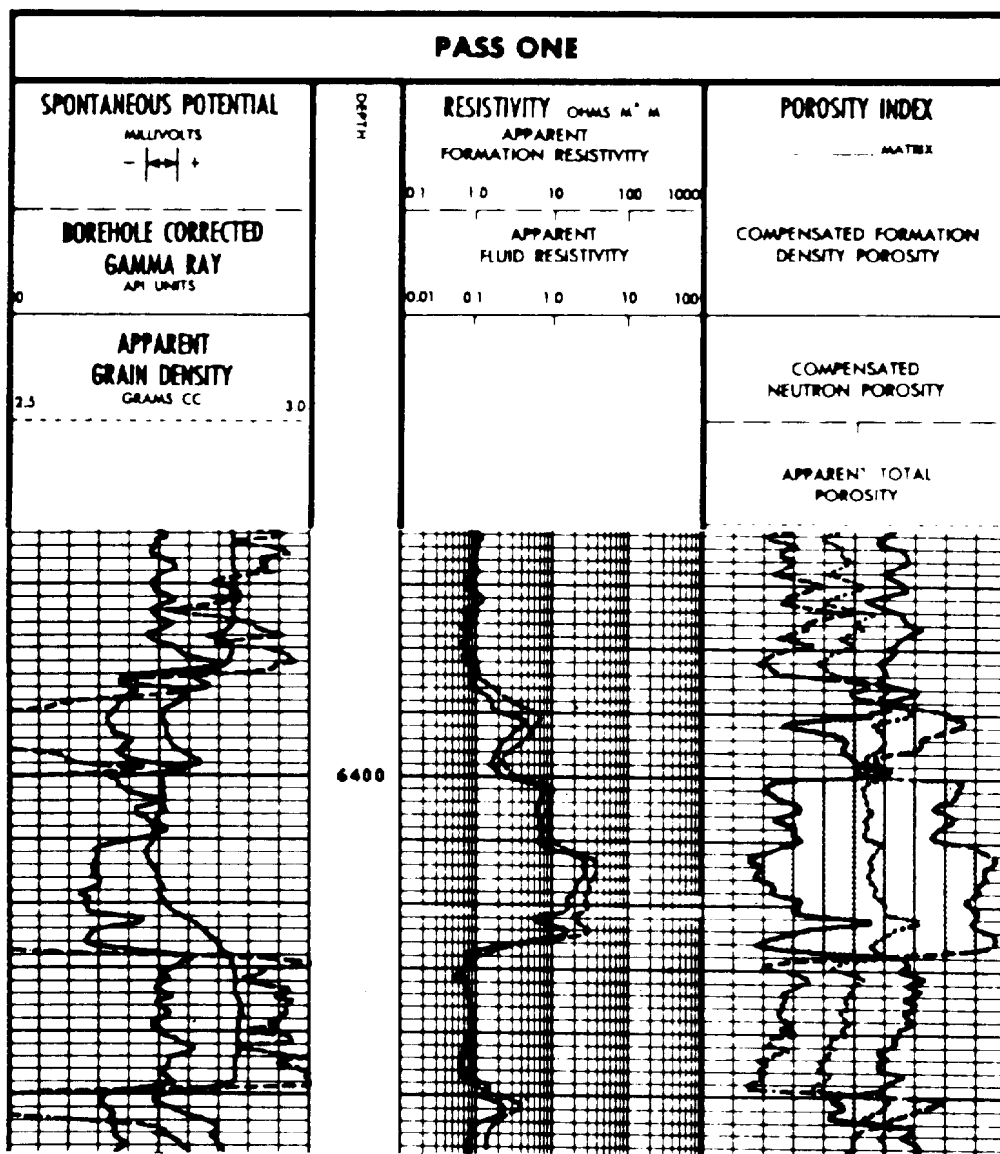


Fig. 49.46—CYBERLOOK Pass One log.

An example of wellsite log analysis is the CYBERLOOK™ program,³⁶ which requires as a minimum suite of logs a deep investigation resistivity, CNL™-FDC™ (compensated neutron/density logs), a gamma ray, or SP curve. The CYBERLOOK computation is based on the dual-water model and is normally made in two passes.

On the Pass One log (Fig. 49.46), the SP curve is on Track 1 with the gamma ray. On Track 2, in four cycles, are found the R_t curve, the R_{wa} (computed from R_t), and the porosity given by the CNL. Track 3 shows the porosity given by the density, ϕ_D , the porosity given by the neutron, ϕ_N , and a crossplot porosity computed from ϕ_D and ϕ_N .

On Pass Two log (Fig. 49.47), the Track 1 gives the shale index, which is the minimum shale index of several shale indicators obtained from the SP curve, the gamma ray, and the maximum and minimum neutron readings. Track 2 shows R_t as a dashed curve and R_0 as a solid

curve. The left half of Track 3 has the water saturation and the right half has the porosity and bulk volume free water. A differential caliper is presented as a dotted curve with bit size in the middle of Track 3. A gas flag appears in the depth track when a large hydrocarbon correction was necessary to obtain the porosity from neutron/density logs.

VOLAN™ is an example of a complex analysis program (Fig. 49.48). It is based on the dual-water model, as is the CYBERLOOK program mentioned previously, but the computations are far more refined and the results more accurate. For a detailed study of the dual-water model, see Refs. 37 and 38. The dual water model simply says that in a shaly sand, its equivalent formation water conductivity is dependent on the relative amount of "bound" water and "free" water.

The conductivity of the bound water is found by the use of the nearby shale resistivity and the total porosity given by the average of CNL. In a like manner, the free

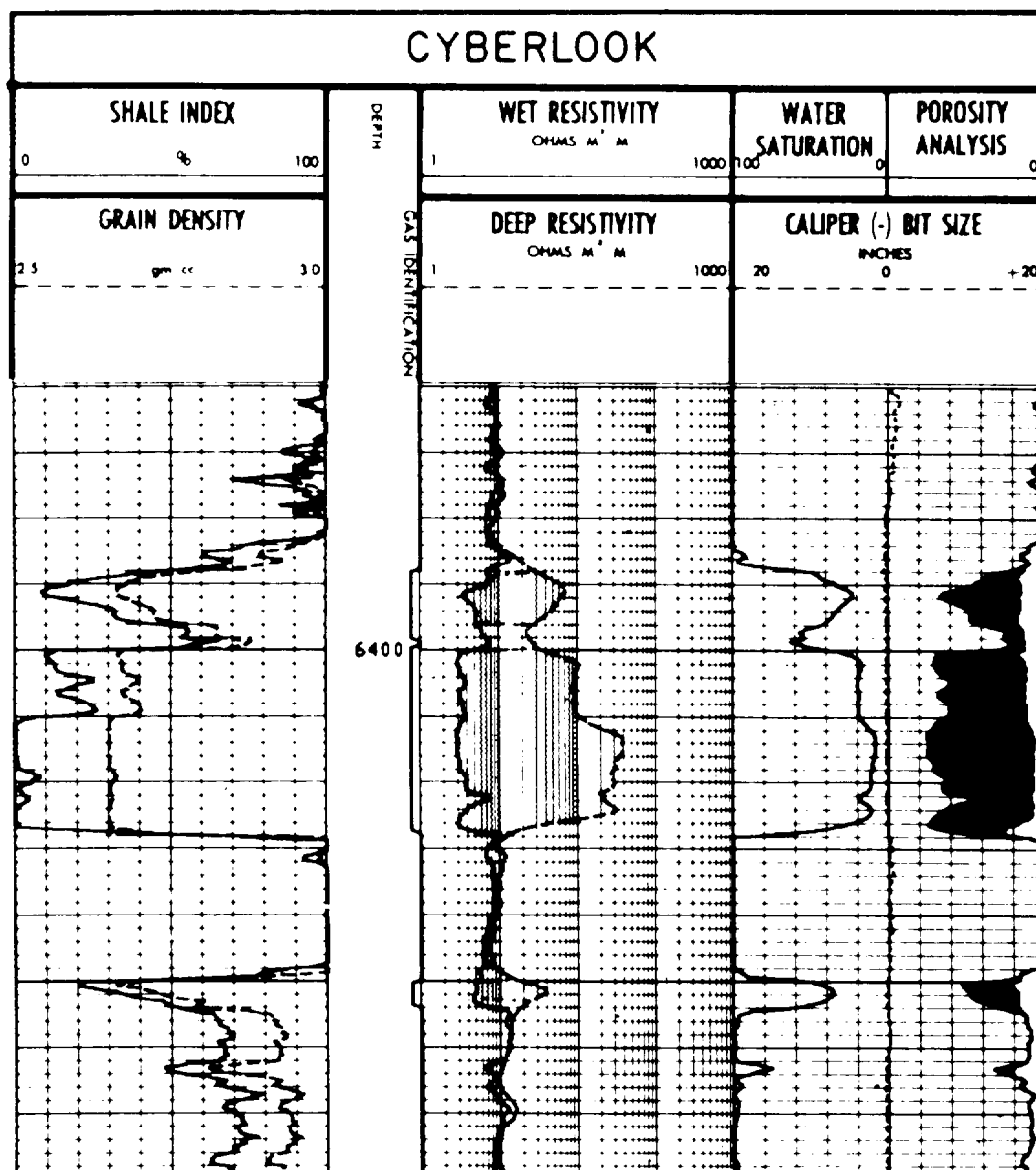


Fig. 49.47—CYBERLOOK Pass Two log.

water conductivity is found by use of the resistivity of the clean water sand and its total porosity. In a shaly water sand, the equivalent water conductivity is found in the same way by using the resistivity of the shaly water sand and its total porosity. Knowing the bound and free water conductivities, it is easy to compute their fractions of the total porosity that are necessary to obtain the same equivalent water conductivity of the shaly water sand.

The fractions of bound and free water can be related to the relative deflections of the gamma ray or SP curve, etc., thus permitting the use of such calibrations when analyzing hydrocarbon saturated zones. The analysis is done by using a dispersed-clay-type equation.

Nomenclature

a_{mf} = chemical activity of mud filtrate
 a_w = chemical activity of formation water

A_c = corrected attenuation of a formation
 A_{log} = recorded attenuation of a formation
 C = equivalent conductivity of losses in the formation
 C_{IL} = conductivity as given by induction log
 C_T = total conductivity signal
 C_i = conductivity of invaded zone
 C_m = conductivity of mud
 C_t = true conductivity of formation
 C_{xo} = conductivity of flushed zone
 E = electric field
 E_c = total electrochemical EMF
 E_j = liquid-junction EMF
 E_M = shale-membrane EMF
 E_{PSP} = pseudostatic SP
 E_{SSP} = static SP

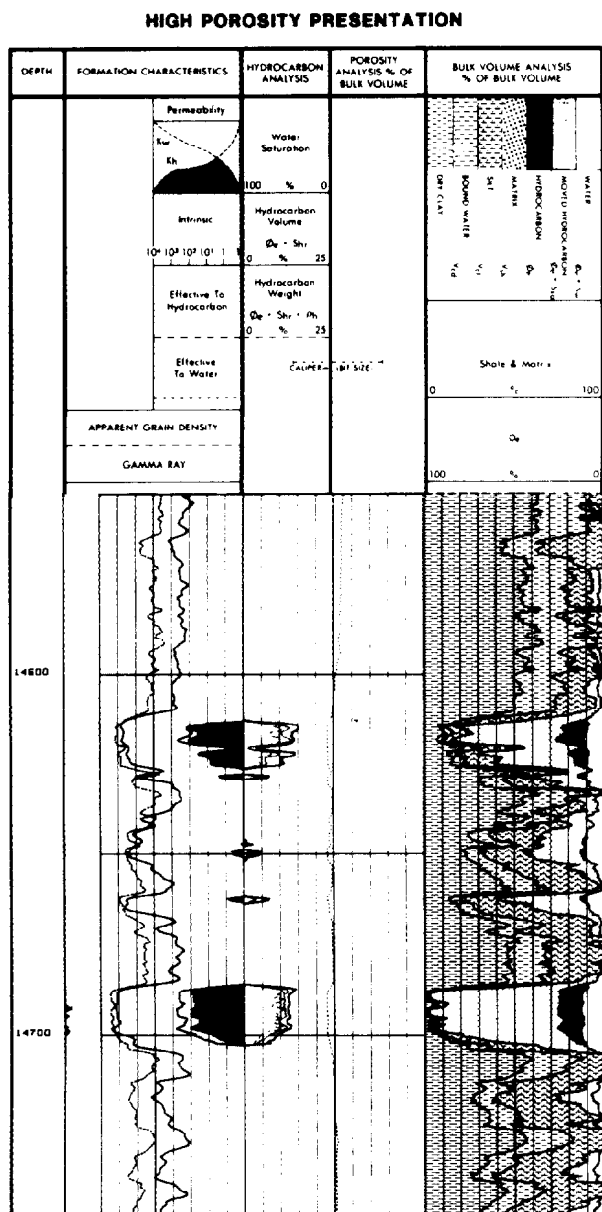


Fig. 49.48—High-porosity presentation.

- E_0 = electric field at the first receiver
 F_R = formation resistivity factor
 F_{R_w} = resistivity factor of formation water
 $F_{R_{wi}}$ = resistivity factor of water in invaded zone
 f_w = fraction of interstitial (connate) water in the total mixture
 G_i = geometrical factor of invaded zone
 G_m = geometrical factor of mud
 G_{pi} = pseudogeometrical factor of the invaded zone
 G_{sl} = geometrical spreading loss
 G_t = geometrical factor, true formation
 G_{xo} = geometrical factor of flushed zone
 I_R = resistivity index
 j = vectorial operator $\sqrt{-1}$

- K_c = electrochemical coefficient
 m = cementation exponent or factor
 n = saturation exponent
 R_a = apparent resistivity
 R_{an} = annulus resistivity
 R_c = corrected resistivity
 R_{IL} = induction-log resistivity
 R_{PL} = proximity-log resistivity
 R_i = resistivity of invaded zone
 R_{mc} = resistivity of mudcake
 R_{mf} = resistivity of mud filtrate
 R_t = true formation resistivity
 R_w = formation-water resistivity
 R_{we} = equivalent formation-water resistivity
 R_{wi} = resistivity of the water found in the invaded zone
 R_{xo} = resistivity of flushed zone
 R_0 = resistivity of a clean (nonshaly) formation saturated with 100% water
 $R_{1 \times 1}$ = resistivity of 1- \times 1-in. microinverse
 R_2 = resistivity of 2-in. micronormal
 R_{16} = short-normal resistivity
 S_i = water saturation in the invaded zone
 S_{or} = residual oil saturation
 S_w = formation water saturation
 S_{xo} = water saturation in the flushed zone
 t_{ph} = propagation time for hydrocarbon
 t_{pl} = travel time in the lossy medium
 t_{pm} = loss-free propagation time of matrix
 t_{po} = loss-free propagation time
 t_{pwo} = loss-free propagation time of water
 Y = maximum producible oil index
 α_{SP} = SP reduction factor
 γ = complex propagation factor
 ϵ = relative dielectric permittivity
 μ = magnetic permeability
 ϕ_D = density porosity
 ϕ_{EPT} = electromagnetic propagation tool porosity
 ϕ_{HC} = hydrocarbon porosity
 ϕ_N = neutron porosity
 ω = angular frequency

Abbreviations

- CNLTM = compensated neutron log
 DIL = dual induction-laterolog 8
 EPT = electromagnetic propagation tool
 ES = electrical survey
 FDCTM = compensated density log
 ID = deep-reading induction device
 IEL = induction-electrical log
 IES = induction-electrical survey
 IL = induction log
 ILd = deep induction log
 IM = medium-reading induction device
 ISF = induction spherically-focused log
 LL = laterolog
 LLD = deep laterolog
 LLS = shallow laterolog
 ML = microlog

MLL = microlaterolog
 MSFI = shallow MICROSL
 PL = proximity log
 SDL = simultaneous dual laterolog
 SFL = spherically focused log
 SSP = static SP

References

- Dunlap, H.F. and Hawthorne, H.R.: "Calculation of Water Resistivities from Chemical Analysis," *J. Pet. Tech.* (July 1957) 202-17; *Trans.*, AIME, 192.
- a. "Log Interpretation Charts," Schlumberger Well Services (1979).
 b. "Log Interpretation Charts," Dresser-Atlas (1981).
 c. "Charts for the Interpretation of Well Logs," Welex (1979) EL-1002.
 d. "Chart Book," Gearhart (1982).
- Lamont, N.: "Relationships Between the Mud Resistivity, Mud Filtrate Resistivity, and the Mud Cake Resistivity of Oil Emulsion Mud Systems," *J. Pet. Tech.* (Aug. 1957) 51-52; *Trans.*, AIME, 210.
- Mounce, W.D. and Rust, W.M. Jr.: "Natural Potentials in Well Logging," *Pet. Tech.* (Sept. 1943); *Trans.*, AIME, 6.
- Winsauer, W.O., et al.: "Resistivity of Brine-saturated Sands in Relation to Pore Geometry," *Bull.*, AAPG (Feb. 1952) 253-77.
- Patnode, H.W. and Wyllie, M.R.J.: "Presence of Conductive Solids in Reservoir Rocks as a Factor in Electric Log Interpretation," *J. Pet. Tech.* (Feb. 1950) 47-52; *Trans.*, AIME, 189.
- Archie, G.E.: "Classification of Carbonate Reservoir Rocks and Petrophysical Considerations," *Bull.*, AAPG (Feb. 1952) 36, 278-98.
- Waxman, M.H. and Thomas, E.C.: "Electrical Conductivities in Shaly Sands—I. The Relation Between Hydrocarbon Saturation and Resistivity Index; II. The Temperature Coefficient of Electrical Conductivity," *J. Pet. Tech.* (Feb. 1974) 213-23; *Trans.*, AIME, 257.
- Waxman, M.H. and Smits, L.J.M.: "Electrical Conductivities in Oil-Bearing Shaly Sands," *Soc. Pet. Eng. J.* (June 1968) 107-22; *Trans.*, AIME, 243.
- Kunz, K. and Moran, J.: "Some Effects of Anisotropy on Resistivity Measurements in Boreholes," *Geophysics* (Oct. 1958) 23, 770-94.
- Doll, H.G.: "Filtrate Invasion in Highly Permeable Sands," *Pet. Engr.* (Jan. 1955) 27, B53-66.
- Gondouin, M. and Scala, C.: "Streaming Potential and the SP Log," *J. Pet. Tech.* (Aug. 1958) 170-79; *Trans.*, AIME, 213.
- Hill, H.J. and Anderson, A.E.: "Streaming Potential Phenomena in SP Log Interpretation," *J. Pet. Tech.* (Aug. 1959) 203-08; *Trans.*, AIME, 216.
- Wyllie, M.R.J.: "Investigation of Electrokinetic Component of the Self-Potential Curve," *J. Pet. Tech.* (Jan. 1951) 1-18; *Trans.*, AIME, 192.
- Wyllie, M.R.J., de Witte, A.J., and Warren, J.E.: "On the Streaming Potential Problem in Well Logging," *Trans.*, AIME (1958) 213, 409-17.
- Wyllie, M.R.J.: "Quantitative Analysis of the Electrochemical Component of the SP Curve," *J. Pet. Tech.* (Jan. 1949) 17-26; *Trans.*, AIME, 186.
- Segesman, F. and Tixier, M.P.: "Some Effects of Invasion on the SP Curve," *J. Pet. Tech.* (June 1959) 138-46; *Trans.*, AIME, 216.
- Doll, H.G.: "SP Log: Theoretical Analysis and Principles of Interpretation," *J. Pet. Tech.* (Sept. 1948) 146-85; *Trans.*, AIME, 179.
- Goudouin, M., Tixier, M.P., and Simard, G.L.: "Experimental Study on Influence of Chemical Composition of Electrolytes on SP Curve," *J. Pet. Tech.* (Feb. 1957) 58-72; *Trans.*, AIME, 210.
- Doll, H.G.: "Introduction to Induction Logging and Application to Logging of Wells Drilled with Oil-base Mud," *J. Pet. Tech.* (June 1949) 148-62; *Trans.*, AIME, 186.
- Dumanoir, J.L., Tixier, M.P., and Martin, M.: "Interpretation of the Induction-Electrical Log in Fresh Mud," *J. Pet. Tech.* (July 1957) 202-17; *Trans.*, AIME, 210.
- Doll, H.G.: "Laterolog—A New Resistivity Logging Method with Electrodes Using an Automatic Focusing System," *J. Pet. Tech.* (Nov. 1951) 305-16; *Trans.*, AIME, 192.
- Doll, H.G.: "Micro Log—A New Electrical Logging Method for Detailed Determinations of Permeable Beds," *J. Pet. Tech.* (June 1950) 155-64; *Trans.*, AIME, 189.
- Doll, H.G.: "The MicroLaterolog," *J. Pet. Tech.* (Jan. 1953) 17-32; *Trans.*, AIME, 198.
- Tixier, M.P.: "Electrical Log Analysis in the Rocky Mountains," *Oil and Gas J.* (June 1949) 48, 143-48.
- Tixier, M.P.: "Porosity Index in Limestone from Electrical Logs," *Oil and Gas J.* (Nov. 1951) 140-42, 169-73.
- Wyllie, M.R.J.: "Procedures for the Direct Employment of Neutron Log Data in Electric Log Interpretation," *Geophysics* (Oct. 1952) 17, 790-805.
- Tixier, M.P., Alger, R.P., and Tanguy, D.R.: "New Development in Induction and Sonic Logging," *J. Pet. Tech.* (May 1960) 79; *Trans.*, AIME, 219.
- Doll, H.G. and Martin, M.: "How to Use Electric Log Data to Determine Maximum Producing Oil Index in a Formation," *Oil and Gas J.* (July 1954) 53, 120-26.
- Tixier, M.P.: "Evaluation of Permeability from Electric Log Resistivity Gradient," *Oil and Gas J.* (June 1949) 48, 113-23.
- a. "Resistivity Departure Curves," *Bull.*, Schlumberger Well Surveying Corp. (1949).
 b. "Interpretation Charts for Electric Logs and Contact Logs," *Bull.*, Welex Inc., A-101.
- a. "Resistivity Departure Curves (Beds of Infinite Thickness)," *Bull.*, Schlumberger Well Surveying Corp. (1955).
 b. "Fundamentals of Quantitative Analysis of Electric Logs," *Bull.*, Welex Inc., A-132.
- Poupon, A., Loy, M.E., and Tixier, M.P.: "A Contribution to Electrical Log Interpretation in Shaly Sands," *J. Pet. Tech.* (June 1954) 138-45; *Trans.*, AIME, 201.
- Tixier, M.P.: "Porosity Balance Verifies Water Saturation Determined From Logs," *J. Pet. Tech.* (July 1958) 161-69; *Trans.*, AIME, 213.
- Wharton, R.P., et al.: "Electromagnetic Propagation Logging: Advances in Technique and Interpretation," paper SPE 9267 presented at the 1980 SPE Annual Technical Conference and Exhibition, Dallas, Sept. 21-24.
- Best, D.L., Gardner, J.S., and Dumanoir, J.L.: "A Computer-Processed Wellsite Log Computation," paper presented at the 1978 SPWLA Annual Logging Symposium, June 13-16.
- Coates, G.R., Schulze, R.P., and Throop, W.H.: "Volan*—An Advanced Computational Log Analysis," paper presented at the 1982 SPWLA Annual Logging Symposium, July 6-9.
- Clavier, C., Coates, G.R., and Dumanoir, J.: "Theoretical and Experimental Bases for the Dual-Water Model for Interpretation of Shaly Sands," *Soc. Pet. Eng. J.* (April 1984) 153-68.

General References

- Alger, R.P.: "Interpretation of Electrical Logs in Fresh Water Wells in Unconsolidated Formations," paper presented at the 1966 SPWLA Annual Logging Symposium, Tulsa, OK, May 8-11.
- "Departure Curves for Laterolog," *Bull.*, Schlumberger Well Surveying Corp. (Aug. 1952).
- DeWitte, L.: "A Study of Electric Log Interpretation Methods in Shaly Formations," *J. Pet. Tech.* (July 1955) 103-10; *Trans.*, AIME, 204.
- Doll, H.G.: "SP Log in Shaly Sands," *J. Pet. Tech.* (July 1950) 205-14; *Trans.*, AIME, 189.
- Guyod, H.: "Electric Analog of Resistivity Logging," *Geophysics* (1955) 615-29.
- Guyod, H.: "Electric Log Interpretation," *Oil Weekly* (Dec. 1955).
- "Guyod's Electrical Well Logging," *Bull.*, Wellex Inc., A-132.
- "Interpretation Handbook for Resistivity Logs," *Bull.*, Schlumberger Well Surveying Corp. (1949).

- Johnson, H.M.: "A History of Well Logging," *Geophysics* (1962) 507-27.
- Jorden, J.R. and Campbell, F.L.: *Well Logging I—Rock Properties, Borehole Environment, Mud and Temperature Logging*, Monograph Series, SPE, Dallas (1984).
- Keller, G.V.: "Modified Mono-Electrodes for Improved Resistivity Logging," *Prod. Monthly* (July 1950) 14, 13-16.
- Kerver, J.K. and Prokop, C.L.: "Effect of the Presence of Hydrocarbons on Well Logging Potential," *Oil and Gas J.* (Dec. 1955) 102-06.
- Lipson, L.B. and Overton, H.L.: "The Effect of Treating Agents on the Electrochemical Activities of Drilling Mud Filtrates," paper SPE 867G presented at the 1957 SPE Annual Meeting, Dallas, Oct. 7-10.
- "Log Interpretation, Vol. I—Principles, Vol. II—Applications," *Bull.*, Schlumberger Well Services (1974).
- Mayer, C. and Sibbit, A.: "Global, A New Approach to Computer Processed Log Interpretation," paper SPE 9341 presented at the 1980 SPE Annual Technical Conference and Exhibition, Dallas, Sept. 21-24.
- Millican, M.L., Raymer, L.L., and Alger, R.P.: "Wellsite Recordings of the Movable Oil Plot," paper presented at the 1964 SPWLA Annual Logging Symposium, Midland, TX, May 13-15.
- Morris, R.L. and Biggs, W.P.: "Using Log-Derived Values of Water Saturation and Permeability," paper presented at the 1967 SPWLA Annual Logging Symposium.
- Pirson, S.J.: "Formation Evaluation by Log Interpretation," *World Oil* (May 1957) 170-83.
- Tixier, M.P., Morris, R.L., and Connell, J.G.: "Log Evaluation of Low Resistivity Pay Sands in the Gulf Coast," *Log Analyst* (Nov./Dec. 1968).
- Wyllie, M.R.J.: *The Fundamentals of Electric Log Interpretation*, second edition, Academic Press Inc., New York City (1957).

Chapter 50

Nuclear Logging Techniques

Darwin V. Ellis, Schlumberger-Doll Research *

Introduction

In this chapter, the use of nuclear radiation in wireline logging will be presented. To avoid repetition, the reader is referred to Chap. 49 for a basic introduction to the principles of wireline logging in terms of the operation and general types of devices used in the area of electrical logging; Chap. 51 discusses the third major area—acoustic well logging.

To introduce the general subject of nuclear logging, it is appropriate to provide a motivation for the use of nuclear measurement techniques in well logging. This can be done best by constructing a list of petrophysical parameters of interest in the evaluation of hydrocarbon-bearing formations. In the most straightforward application, the purpose of well logging is to provide measurements that can be related to the volume fraction and type of hydrocarbon present in porous formations. In the case of openhole logging (as distinguished from measurements made in a production well with steel casing), there are four principal parameters of interest: (1) presence of hydrocarbons, (2) porosity, ϕ , (3) water saturation, S_w , and (4) permeability, k . To this list, additional parameters or descriptors can be added: (5) lithology, (6) clay identification, and (7) pore fluid identification. For cased-hole logging the same list of petrophysical parameters of interest may hold, but with perhaps more emphasis on fluid identification.

Relationship of Petrophysical Parameters and Physical Parameters

These petrophysical parameters of interest are derived normally from a number of measurements provided by logging services. For the moment, we will concentrate on some bulk physical parameters associated with them that may be amenable to measurement through the use of nuclear techniques.

Presence of Hydrocarbons. An obvious method for the detection of hydrocarbons is based on their chemical compositions. Since there is no oxygen in most hydrocarbons, the ratio of the atomic concentration of carbon to oxygen for a hydrocarbon is significantly different from the ratio for most sedimentary rocks and formation fluids. Thus, a measurement of the ratio of the number of carbon atoms to oxygen atoms (C/O) contained in a formation would indicate directly the presence of hydrocarbons when no carbon is present in the matrix. This is to be contrasted with the method of electrical measurements, where detection of hydrocarbons is based on the contrast of conductivities between saline water and hydrocarbon in a porous medium.

Porosity. The porosity or nonmatrix portion of a rock sample can be determined from a measurement of its bulk density. The fundamental equation that relates the bulk density, ρ_b , to the solid matrix, which has a density ρ_{ma} , and the porosity or volume fraction, ϕ , which contains a fluid of density ρ_f , is

$$\rho_b = \phi \rho_f + (1 - \phi) \rho_{ma} \quad \dots \dots \dots (1)$$

From this relationship, the porosity, ϕ , can be determined from a measurement of bulk density, assuming that the matrix density and fluid density are known. These will be known with any precision only if the fluid type and properties and the lithology are known. In practical terms, the density range of fluids is between 0.8 and 1.2 g/cm³ (although calcium chloride solutions may reach 1.4 g/cm³), and most matrix densities are between 2.60 and 2.96 g/cm³.

Another means of detection and quantification of porosity is based on the fact that the formation porosity is filled with liquid or gas, all of which contain disproportionate amounts of hydrogen. This hydrogen may be

*Author of the original chapter on this topic in the 1962 edition was John L.P. Campbell.

associated with the brackish formation water or with the hydrocarbons. Thus, detection of hydrogen is a means of inferring porosity in an otherwise solid rock matrix.

Hydrocarbon Saturation. The determination of hydrocarbon saturation can proceed once the porosity of a formation has been determined. It can be done (1) by the direct measurement of C/O and comparison to the value expected for fully oil- and water-saturated cases, or (2) by a more indirect measurement of the effective salinity of the formation in question.

Permeability. There is no clear-cut physical parameter amenable to nuclear measurements that will predict formation permeability accurately. However, there is one measurement technique—nuclear magnetic resonance—that can be related to permeability; it is discussed in Chap. 53.

Lithology, Clay Types, and Fluid Identification. These parameters have been grouped together because of a common approach for their determination, which is basically some aspect of their chemical composition.

There are two principal interests in identifying the lithology. One is for a reasonable matrix density to be assigned to a formation so that porosity can be extracted from the density measurement. The other is to provide identification of formations for use in well-to-well correlation. Since the neutron properties of rocks are somewhat dependent on the type of lithology, it is possible to determine the three principal lithological matrices by comparison of the gamma ray attenuation and neutron-slowing-down properties of the medium. Well-to-well correlation often is done most simply by comparison of the natural radioactivity of the formations.

However, a more direct approach for the identification of the lithology (i.e., sandstone, limestone, or dolomite) is not based on the density but rather on the unique chemical composition of each of these matrices. One method of identifying the lithology would be to make a chemical identification of the various elements associated with the matrix. Another slightly more refined approach to the determination of the lithology depends on another bulk property of the material: its average atomic number. The average atomic number of the formation, which reflects to some extent the lithological composition, can be obtained by measuring the low-energy gamma ray absorption properties of the material.

Identification and quantification of clays are much more difficult, since the chemical compositions of clays are so varied. Hence, the chemical composition of clays is a key to their detection. A measurement of the presence of elements such as Al, Si, Fe, and K must be counted as a means to their identification. An earlier technique, which measured the total natural gamma ray activity of earth formations, was based on the fact that the naturally occurring radioactive daughter products (subsequent products of radioactive decay of an element) of uranium, thorium, and potassium were associated with clay minerals. Sometimes, however, one or more of these elements (U, Th, K) is present in a formation containing no clay. Examples of this include the case of potassium feldspar in the rock matrix or uranium dissolved in the formation water.

A third property of clays is the great abundance of hydrogen associated with the clay mineral structure. Thus, detection of the presence of hydrogen is another means of clay identification.

Pore fluid identification is based on indirect measurements and inferences. The presence of gas in the formation pores will have a significant impact on the bulk density for reasonable porosities as well as on the neutron-slowing-down properties. The distinction between oil and water again is measured most directly by the atomic C/O density ratio or based on the thermal neutron absorption properties of the water phase, which generally contains chlorides.

Fig. 50.1 summarizes the relationships between petrophysical descriptors and physical parameters, which can be determined quantitatively through the use of nuclear radiation and measurement techniques. A third column has been added to indicate the additional information necessary to interpret the suggested bulk property measured to obtain the desired petrophysical descriptor.

Physical Parameters and Nuclear Radiation

Before presenting the basic nuclear phenomena necessary to describe the operation of most of the common nuclear logging devices, we need to link, in general terms, the physical parameters discussed previously to the types of general nuclear techniques that will be described later in more detail. To be specific, it should be pointed out that the types of nuclear radiation used in well logging are gamma radiation and neutrons. These two types of penetrating radiation are the only ones that are able to traverse the pressure housings of the logging tools and the formation of interest and still return a measurable signal. It is for this reason that α and β radiation are of no particular interest for exploring formation characteristics; their penetration ranges are much too small to be of any practical use.

In the preceding section, it is clear that many of the proposed parameters to be measured are, in fact, no more than the chemical composition of the earth formation. Instead of the obvious but time-consuming and expensive chemical analysis of formation samples, a technique of gamma ray spectroscopy can be used. This is based on the fact that the nucleus of any atom, after having been put into an excited state by a previous nuclear reaction, can emit gamma rays of characteristic energies, which uniquely identify the atom in question. Gamma ray spectroscopy refers to the detection and identification of these characteristic gamma rays.

Another use of gamma rays is in conjunction with the measurement of bulk density. The bulk density of a material has a significant influence on the scattering and transmission of gamma rays through it. At very low energies, the transmission of gamma rays is influenced additionally by the chemical composition. This additional absorption is related to the atomic number, Z , of the absorber.

The interest in using neutrons in well logging techniques comes from several properties of their interaction with matter. First, the transmission and moderation of neutrons are influenced by the bulk properties of the medium and, in particular, by the amount of hydrogen present. The scattering of neutrons by hydrogen is very

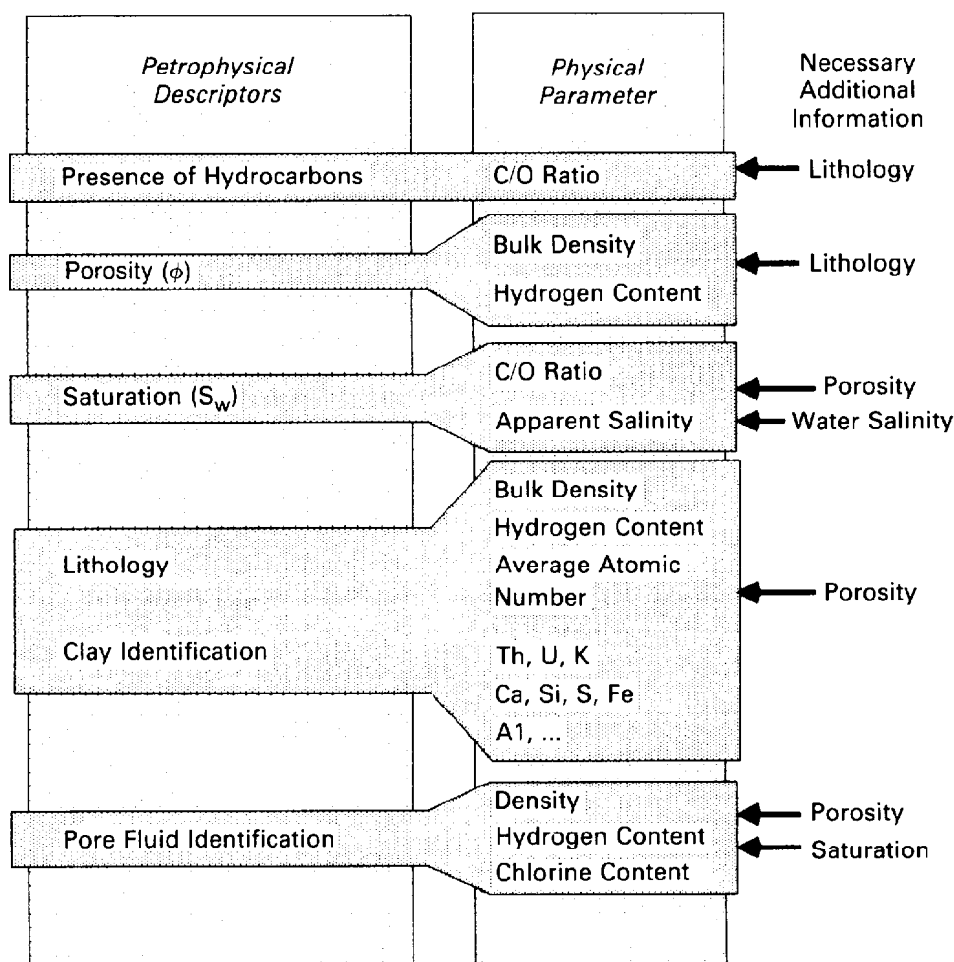


Fig. 50.1—Relationship between petrophysical descriptors and measurable physical parameters.

efficient in reducing the neutron energy. Second, interaction of high-energy neutrons with certain nuclei can excite characteristic gamma rays for subsequent elemental identification by gamma ray spectroscopy. At very low energies, neutrons can be absorbed, thereby reducing the flux, and as a byproduct, another set of characteristic gamma rays may be emitted. Some of these capture gamma rays are emitted after some delay and are referred to as activation gamma rays. So there are two types of measurements that can be based on the use of neutrons: the scattering or slowing-down properties of formations and neutron production of gamma rays (either by absorption or inelastic high-energy reactions with elements) of characteristic energies for use in spectroscopic identification. Fig. 50.2 illustrates the types of nuclear measurement techniques that can be used to measure physical parameters related to the relevant petrophysical descriptors sought.

Nuclear Physics for Logging Applications

Nuclear Radiation

Nuclear radiation refers to the transport of energy by a nuclear particle. In the earliest investigation of radioactive materials, three types of radiation were identified

and named, quite unimaginatively, α , β , and γ radiation. It subsequently was discovered that α radiation consisted of fast-moving He particles stripped of their electrons and that β radiation consisted of energetic electrons. The gamma rays were found to be packets of electromagnetic radiation, also referred to as photons.

The discovery of this radiation then provoked its quantification, namely the measurement of the amount of energy transported. The unit chosen is known as the electron-volt (eV), which is equal to the kinetic energy acquired by an electron accelerated through an electric potential of 1 V. For the types of radiation discussed in the following sections, the range of energies is between fractions of an eV and millions of electrons volts (MeV). Another convenient multiple for discussing gamma ray energies is the kiloelectron volt (keV).

Since α and β radiation consist of energetic charged particles, their interaction with matter is primarily ionization. That is, they interact with the electrons of material by losing energy rapidly during their passage and transferring it to electrons. In most materials their range is rather limited and is a function of the material properties (Z , the atomic charge or number of electrons per atom, and its density) and the energy of the particle. They consequently have not been of any practical impor-

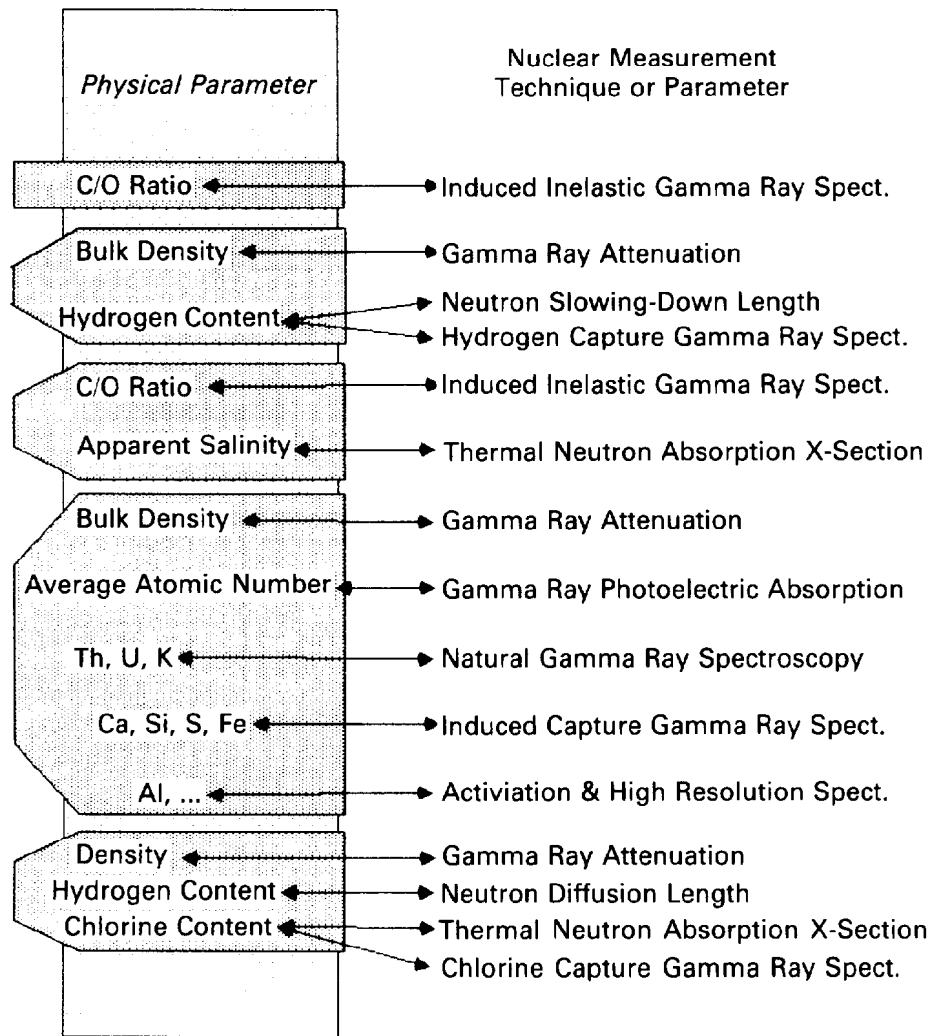


Fig. 50.2—Nuclear measurement techniques linked to measurable physical parameters of petrophysical interest.

tance for well logging applications. Gamma rays, on the other hand, are extremely penetrating radiation, which makes them of great importance for well logging applications.

Radioactive decay of certain naturally occurring substances such as radium was responsible for the developments mentioned and needs further discussion. Radioactive decay is a time-varying property of nuclei whereby a transition from one nuclear energy state to another lower one is made spontaneously. The result is that the excess energy is shed by the nucleus by one or more of the types of radiation previously mentioned. The basic experimental fact of radioactivity is that the probability of any one nucleus decaying, within an interval of time dt , is proportional to dt —i.e., it is independent of external influences, including the decay of another nucleus. This probability is proportional only to the time interval of observation. So for a *single* radioactive atom the probability $P(dt)$ of decaying in the interval of time dt is expressed as

$$P(dt) = \lambda dt, \quad (2)$$

where λ is the decay constant. For a *collection* of N_p particles, the number decaying, dN , is just

$$dN = -\lambda dt N_p, \quad (3)$$

resulting in the expression for radioactive decay, namely

$$\frac{dN}{N_p} = -\lambda dt \rightarrow N_p = N_i e^{-\lambda t}, \quad (4)$$

where N_p now is the number of particles remaining at time t , of the initial number of particles N_i . The constant of proportionality, λ , is related to the better-known parameter, the half-life, $t_{1/2}$, by

$$t_{1/2} = \frac{0.693}{\lambda}. \quad (5)$$

No physical quantity can ever be measured exactly, but in the case of nuclear processes where the number of events observed is small, randomness is important. The practical complication of this statistical process of nuclear decay is that only the bulk or average properties can be predicted with any certainty. We can talk only about the measurement of a group of particles together and the distribution of the measured value about some mean.

To understand one important property of nuclear radiation, it is necessary to digress a moment for a quick review of the binomial distribution, which was discovered in the 18th century by Bernoulli. It describes the probability, P_x , that an event that has a probability P of occurring will occur x times when the observation is repeated z times. The probability thus specified was identified with the binomial expansion of $(P+q)^z$, where

$$q = 1 - P, \dots\dots\dots (6)$$

so that the general term of the expansion is

$$P_x = \frac{z!}{x!(z-x)!} P^x (1-P)^{z-x}, \dots\dots\dots (7)$$

which gives the probability of x occurrences in z trials.

This expression can be applied to radioactive decay, in which P_x represents the probability of having x nuclei decay in time dt when there are z atoms present. For this case, generally the probability P is very small but the number of particles observed (z) is very large so that Eq. 7 simplifies to

$$P_x = \mu^x \frac{e^{-\mu}}{x!}, \dots\dots\dots (8)$$

which is known as the Poisson distribution. It gives the probability of observing x decays in a given time where an average of $\bar{\mu}$ decays is to be expected. Fig. 50.3 shows the general form of the Poisson distribution with the maximum probability at the mean value, which was taken as 100 for this example. The curve resembles the usual bell-shaped distribution curve with a width specified by a parameter σ , the standard deviation.

The practical importance of this discussion is that the appropriate σ for the Poisson distribution that characterizes the statistics of counting random nuclear events is not an independent parameter (as is the case for most measurements) but is related to the mean value $\bar{\mu}$ by

$$\sigma = \sqrt{\bar{\mu}}, \dots\dots\dots (9)$$

This means that if N_r counts from a radiation detector are expected per time interval, then, in repeated observations, about 32% of the measurements will deviate beyond the value of $N_r \pm \sqrt{N_r}$. This is a quantitative description of the statistics associated with all nuclear logging techniques.

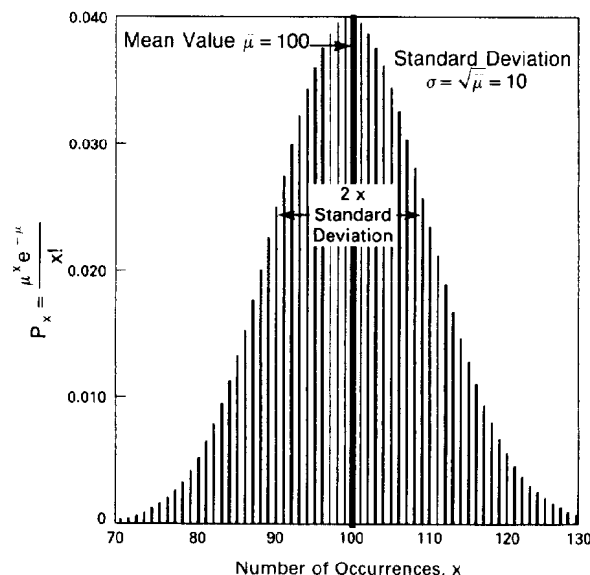


Fig. 50.3—The Poisson distribution for the case of mean value ($\bar{\mu}$) of 100. The probability, P_x , is shown for values of x around the expected mean value.

There have been a number of clever techniques for dealing with the statistical fluctuations inherent in nuclear counting rates. Probably best known is the R-C circuit, which has a time constant associated with it and permits the recording of a continuous moving average. There are now more modern digital signal processing techniques (such as Kalman filtering) to provide more refined filtered counting rates or outputs derived from statistically varying counting rates. However, the only sure approach to reduce the fluctuations is to increase the average number measured, either by using higher-output sources, more efficient counters, or longer counting times per sample.

Particle Reactions. There are certain nuclear particle interactions of interest to well logging. To discuss these as necessary in the following sections, a few mathematical definitions are presented here to help the mechanisms of the reactions.

As in radioactive decay, the process of nuclear reactions is also statistical in nature. The question of interest is how readily these reactions will take place. Fig. 50.4 shows the idealization of the nuclear reaction process. A beam of radiation (it may be gamma rays or neutrons) of an intensity Ψ_i is seen to enter the slab of material. The intensity of the radiation, Ψ_i , is called the flux and has units of numbers of particles per unit surface area per unit time.

The slab of material is characterized by N_p , the number of particles per unit volume with which the flux of radiation may interact. The experimental fact observed is that after passing through a slab of material of thickness δh , a certain fraction of the incident particles have undergone interactions, and that number is proportional to the thickness and the number of target nuclei and the incident flux. This is expressed mathematically as

$$\delta \Psi = \sigma \Psi N_p \delta h, \dots\dots\dots (10)$$

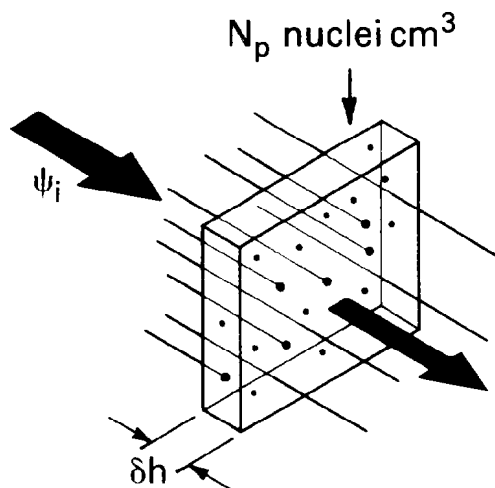


Fig. 50.4—Idealized view of nuclear radiation interacting with matter showing the reduction in flux traversing a thickness of material characterized by the number of interacting particles per cubic centimeter.

where the constant of proportionality, σ , is called the cross section of the interaction. The units of this microscopic cross section σ are area/interacting target nucleus. Cross section is used because in a classical sense it is the apparent area each target nucleus presents to the incoming beam. In effect, it collects all the nuclear interaction details into one useful number. The practical unit is called the "barn" and is equal to 10^{-24} cm^2 . The macroscopic cross section, Σ , is the product of σ and N_p and has the dimension of area/particle times particles/volume or inverse length. In practical terms, Σ can be calculated easily because N_p is related to Avogadro's number, N_A , and the material density, ρ_b , by

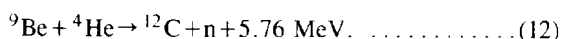
$$N_p = \frac{N_A}{M} \rho_b, \quad (11)$$

where M is the molecular weight of the target for a single particle per molecule.

In general, the cross sections for most reactions must be determined experimentally and are often available in graphical or tabular form. The quantity $\sigma \Psi N_p$ in Eq. 10 has dimensions of $(\text{cm}^3 \cdot \text{sec})^{-1}$ and has the interpretation of the reaction rate per unit volume resulting from the incident flux.

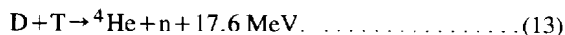
Nuclear Reactions. To discuss the second type of radiation of great importance to well logging applications—neutrons, which are not the result of naturally occurring radioactive decay schemes—a brief discussion of artificial or induced radioactivity is given here.

The classic reaction that inspired the discovery of the neutron was the bombardment of beryllium by alpha particles and can be written as



This forms the basis for the cheapest, easiest, and most reliable method for neutron production. The physical explanations of this reaction are beyond the scope of interest of the present work and may be found in Refs. 1 and 2. The practical construction of a neutron source consists of finding a naturally occurring α emitter and mixing it with an appropriate light element having a large $(\alpha, n)^*$ cross section. Some possibilities for α emitters are Pu, Ra, Am, and Po. Three target elements are Be, B, and Li. The actual spectrum (energy distribution) of emitted neutrons is quite complicated and depends somewhat on the geometric details of the α emitter and target; but generally speaking, the peak of the neutron distribution is around 4 MeV.

Another method of exploiting particle-induced reactions is by use of charged particle accelerators. In one realization currently used in well logging, deuterium and tritium ions are accelerated toward a target impregnated with the hydrogen isotopes deuterium (D) and tritium (T). The reaction is written as



The cross section for this reaction has a maximum at about 100 keV of D projectile energy, which dictates the accelerating voltages in such a device.

Despite the engineering difficulties of constructing such a device, the advantages for logging are many. One is the relative high energy of the produced neutrons. They are emitted at 14.1 MeV (not 17.6 MeV, because some of the energy of this reaction is given up to the alpha particle). These high-energy neutrons are useful for producing other interesting nuclear reactions in the formation, as discussed later. The other advantage is that a source of this type can be controlled—i.e., switched off and on at will. This provides a degree of safety unparalleled for radioactive sources as well as opening the door to measurements involving timing as a means of determining some interesting nuclear properties of the formation.

Now that we have covered the two types of nuclear radiations currently used in logging devices, let us examine how gamma rays and neutrons interact with matter and define some macroscopic properties of matter that can be used to characterize this behavior.

Fundamentals of Gamma Ray Interactions

For the purposes of our discussion there are three types of gamma ray interactions that are of interest: the photoelectric effect, Compton scattering, and pair production. The type of interaction a gamma ray will undergo depends on the properties of the material and the energy of the gamma ray. The ordering of these three interactions reflects the transition of the dominant process as the gamma ray energy increases.

The photoelectric effect concerns the interaction of a gamma ray with an atomic electron in the material. In this process the incident gamma ray disappears and transfers its energy to the bound electron. Depending on

*This shorthand (α, n) indicates a reaction of an α particle with an unspecified nucleus, n , resulting in the production of a neutron and another unspecified nucleus.

the energy of the incident gamma ray, generally the electron is freed from its nucleus and begins collisions with the adjacent material. Normally the ejected electron is replaced by another electron with the accompanying emission of a characteristic fluorescence X-ray with an energy dependent on the atomic number of the material and generally below 100 keV.

The cross section for the photoelectric effect, σ_{pe} , varies strongly with energy, falling off as nearly the cube of the gamma ray energy (E_{GR}). It is also highly dependent on the atomic number (Z) of the absorbing medium. In the energy range of 40 to 80 keV, the cross section per atom of atomic number Z is given by

$$\sigma_{pe} \propto \frac{Z^{4.6}}{E_{GR}^{3.15}} \quad (14)$$

For most earth formations the photoelectric effect becomes the dominant process for gamma ray energies below about 100 keV.

The photoelectric effect is an important process in understanding one of the conventional gamma ray detection devices and a well logging tool³ that is sensitive to the lithology of the scattering formation. The tool in question makes a measurement of the photoelectric absorption factor, F_{pe} , which is proportional to the photoelectric cross section per electron.

Since this quantity is very sensitive to the average atomic number of the medium, Z , it can be used to obtain a direct measurement of the lithology of the scattering medium. This is because the principal rock matrices (sandstone, limestone, and dolomite) have considerably different photoelectric absorption characteristics and the pore fluids play only a minor role because of their low Z 's.

The Compton scattering process involves the interaction of a gamma ray and an electron. It is a process in which only part of the gamma ray energy is imparted to the electron and the energy of the gamma ray, consequently, is reduced. Unlike the photoelectric effect, the probability for Compton scattering changes relatively slowly with energy.

To see the bulk effect of Compton scattering in a material consisting of nuclei of atomic mass A and atomic number Z , one can use the linear absorption coefficient, which is just the Compton cross section, σ_{Co} , multiplied by the number of electrons per cubic centimeter:

$$\Sigma_{Co} = \sigma_{Co} \frac{N_A}{A} \rho_b Z. \quad (15)$$

The final Z factor in this equation takes into account that there are Z electrons per atom. Consequently, the attenuation of gamma rays resulting from Compton scattering will be some function of the bulk density (ρ_b) and the ratio of $Z/A \approx 1/2$ for most elements of interest is the basis for the determination of bulk density from gamma ray scattering devices.

The third and final gamma ray interaction is that of pair production. It, like the photoelectric process, is one of absorption rather than scattering. In this case the gam-

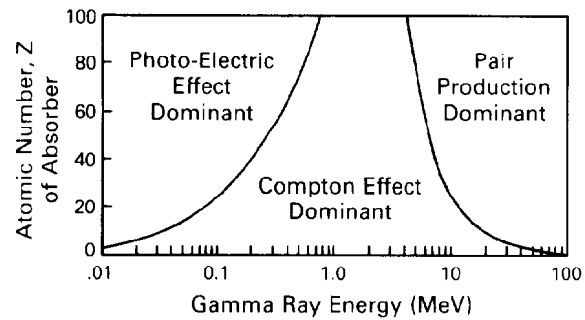


Fig. 50.5—Regions of dominance of the three major gamma ray interactions in terms of the gamma ray energy, E_{GR} , and the atomic number, Z , of the target material. The two lines separating the three regions indicate where the two adjacent interactions occur with equal probability.

ma ray interacts with the electric field of the nucleus, and if the gamma ray energy is above the threshold energy of 1.022 MeV, it disappears and an electron/positron pair is formed. The subsequent annihilation of the positron (positively charged electron) results in the emission of two gamma rays of 511 keV each. The cross section of this process is somewhat energy-dependent and is zero below the required threshold energy of 1.022 MeV. In addition, it also depends on the charge of the nucleus.

To establish the regions of dominance of the three types of interactions, refer to Fig. 50.5. It shows, as a function of gamma ray energy and atomic number of the absorber, the regions in which the probabilities of the various processes are equal. The regions of dominance are quite clear.

From the earlier definition of cross section, the fundamental law of gamma ray attenuation can be stated as

$$\Psi = \Psi_i e^{-n\sigma h}, \quad (16)$$

where Ψ_i is the flux incident on a scatterer of thickness h , n is the number of scatterers per unit volume, and σ is the cross section for scattering per scatterer.

In the case of gamma-gamma density devices, the source of gamma rays is chosen to have an energy for which the primary interaction is Compton scattering. In this case the scatterers are electrons and σ refers to the Compton cross section per electron. This results in the following expression for the attenuation of the source energy gamma rays:

$$\Psi = \Psi_i e^{-\rho_b (Z/A) N_A \sigma h}, \quad (17)$$

where h , in this case, is very nearly the source-to-detector spacing.

It is convenient to define the electron density index as

$$\rho_e = 2 \frac{Z}{A} \rho_b, \quad (18)$$

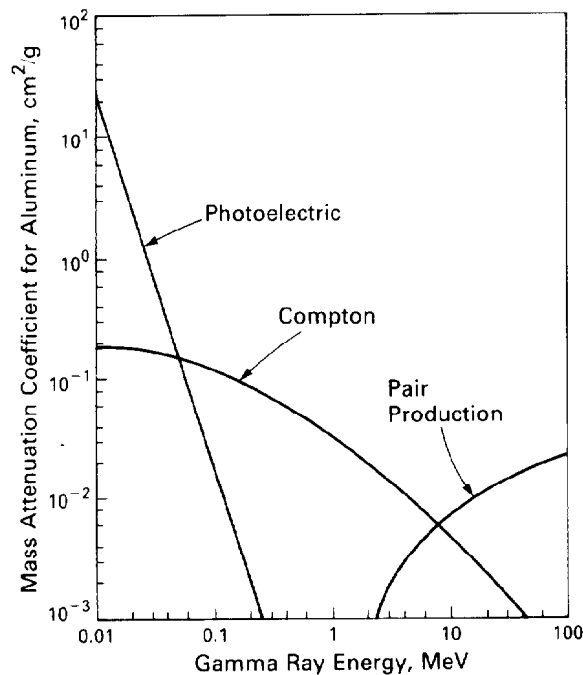


Fig. 50.6—The mass absorption coefficient for gamma ray interactions in aluminum.

so that the attenuation of the gamma rays is seen to be proportional to the spacing, h , between source and detector and the electron density index, which in turn can be related to the bulk density if the properties (specifically Z/A) of the scattering material are known. For most sedimentary rocks the ratio of Z/A is nearly $1/2$ so that ρ_e is very nearly equal to ρ_b .

Another unit for measuring the gamma ray attenuation properties of a material is the mass absorption coefficient, K_a ,* which regroups the constants in Eq. 17—i.e.,

$$K_a = \frac{Z}{A} N_A \sigma, \dots \dots \dots (19)$$

so that the gamma ray attenuation equation can be written as

$$\Psi = \Psi_i e^{-K_a \rho_b x}, \dots \dots \dots (20)$$

The convenience of the mass absorption coefficient for Compton scattering is that it is remarkably similar for all materials since $Z/A \approx 1/2$ and the density dependence has been eliminated. Fig. 50.6 shows the mass attenuation coefficients (in cm^2/g) for aluminum. This element, with a density of 2.7 g/cm^3 and atomic number of 13, is quite typical of earth formations. The average atomic number ranges from 11 to 16 between quartz and limestone, while the grain densities are between 2.65 and 2.71 g/cm^3 .

Fundamentals of Neutron Interactions

As in the case of gamma rays, the interaction of neutrons with materials can be categorized by the types of interactions with the appropriate cross sections that describe

*The symbol used in physics for mass absorption coefficient is μ .

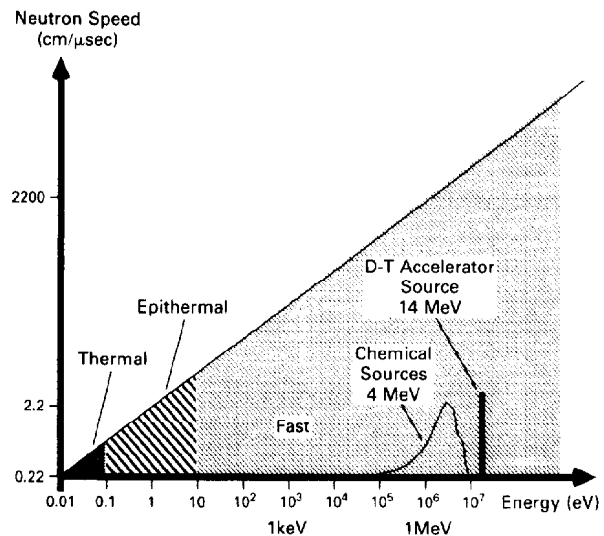


Fig. 50.7—The relationship between neutron energy and speed for the three broad classifications of neutron energies.

each one. The reactions of neutrons with matter are much more varied and complex than those of the gamma rays. For simplification we will confine ourselves to four principal types of interactions of neutrons with matter.

Fig. 50.7 defines in broad terms the energy range of interest for neutrons. For logging applications it can be seen that the energy range of interest is over about 9 decades: from source neutrons of 5 to 15 MeV in the broad fast neutron range above 10 eV, to epithermal neutrons in the range of 0.2 to 10 eV and thermal neutrons, which are distributed around 0.025 eV at room temperature.

To have an idea of the time scale for later discussions of the thermalization process, it is useful to note the relationship between neutron energy and its associated velocity. To evaluate the velocity of a neutron, we can use (at low energies) the classical relationship between kinetic energy, E_k , velocity, v , and mass, m ,

$$E_k = \frac{1}{2}mv^2, \dots \dots \dots (21)$$

so that the velocity, v , is given by

$$v = \sqrt{\frac{2E_k}{m}}, \dots \dots \dots (22)$$

If this expression for velocity is evaluated for thermal energies (0.025 eV), the result is 2200 m/s or 0.22 cm/μs. Thus, the velocity at any energy E (in eV) is given by

$$v = 0.22 \sqrt{\frac{E}{0.025}}, \dots \dots \dots (23)$$

where v is the velocity, cm/ μ s. Therefore, the speed of an epithermal neutron of 2.5 eV is 2.2 cm/ μ s, and for a near-source energy neutron of 2.5 MeV the velocity is 2200 cm/ μ s. These velocities are also noted on Fig. 50.7.

Of the four principal types of interactions, the first two generally are referred to as moderating interactions, or interactions in which the energy (or speed) of the neutron is reduced. One of these is known as elastic scattering and the other, inelastic scattering. Classical mechanics (elastic billiard ball analysis) can describe the moderating power of the struck nucleus. The energy of the neutron is reduced more efficiently as the mass of the struck nucleus approaches the mass of the neutron. Thus, hydrogen and other low-atomic-mass elements are quite efficient in reducing fast-neutron energy. Fig. 50.8 illustrates, for elastic neutron scattering with several elements, the range of reduction in neutron energy available for a single collision. It is seen that for the most common earth formation elements the maximum energy reduction per collision for the heavy elements is about 10 to 25%. However, for the case of hydrogen it is seen that the entire neutron energy can be lost in a single collision.

In the case of inelastic scattering, a portion of the energy of the incident neutron goes into exciting the target nucleus. This reduces the energy of the incident neutron and, in addition, the target nucleus usually will produce a characteristic gamma ray upon de-excitation. This type of reaction always has a threshold energy (below which it will not happen) associated with it and is exploited in the measurement of the C/O ratio in earth formations.

The second general category of neutron interactions is known as absorptive interactions. The two general types are radiative capture and reactions in general. In radiative capture, unlike the moderating interactions considered above, the neutron (usually near thermal energies) is absorbed by the target nucleus and then disappears, and subsequent characteristic gamma rays are produced. The general category of neutron reactions is quite broad; it will be sufficient to say that the interaction of neutrons with other nuclei can provoke the emission of other particles such as alphas, protons, β 's, or even several subsequent neutrons. All these reactions, although common, have a very small probability for happening relative to the other interactions of interest to us and usually occur over a restricted and high-energy range.

To show the complexity of the cross sections for neutron interactions see Fig. 50.9, which schematically indicates the variations with energy. The top figure refers to the total cross section as a function of neutron energy, E_N , and the four following figures indicate how this can be decomposed. The first line (n,n) refers to elastic scattering, which is shown to be rather constant with energy except for some resonances at low energies. The next line shows inelastic interactions (n,n') showing some characteristic threshold below which this reaction is not possible; the fourth line is one of the many particle reactions possible (n,α); and the final line (although there could be others) is the radiative capture (n,γ), which is seen to increase in probability at low energies.

Despite these complexities, there are some gross properties that can be assigned to materials on the basis of

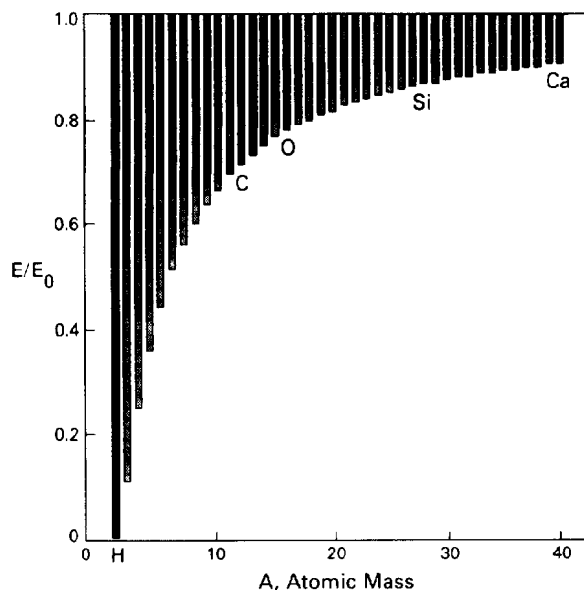


Fig. 50.8—The range of energy reduction possible for neutron elastic scattering with several important elements for formation evaluation. E_0 is the energy before scattering, and E is the energy after scattering. Hydrogen is seen to provide the greatest possible energy reduction for a single collision.

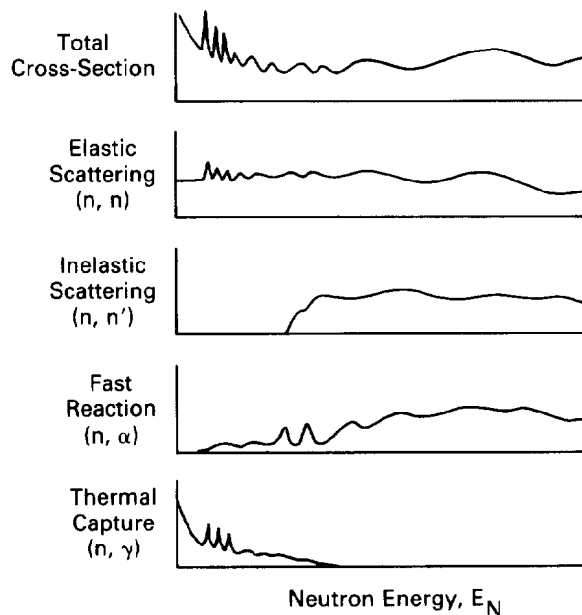


Fig. 50.9—A schematic illustration of the components involved for the total neutron cross section as a function of energy. The characteristics of four specific cross sections are shown.

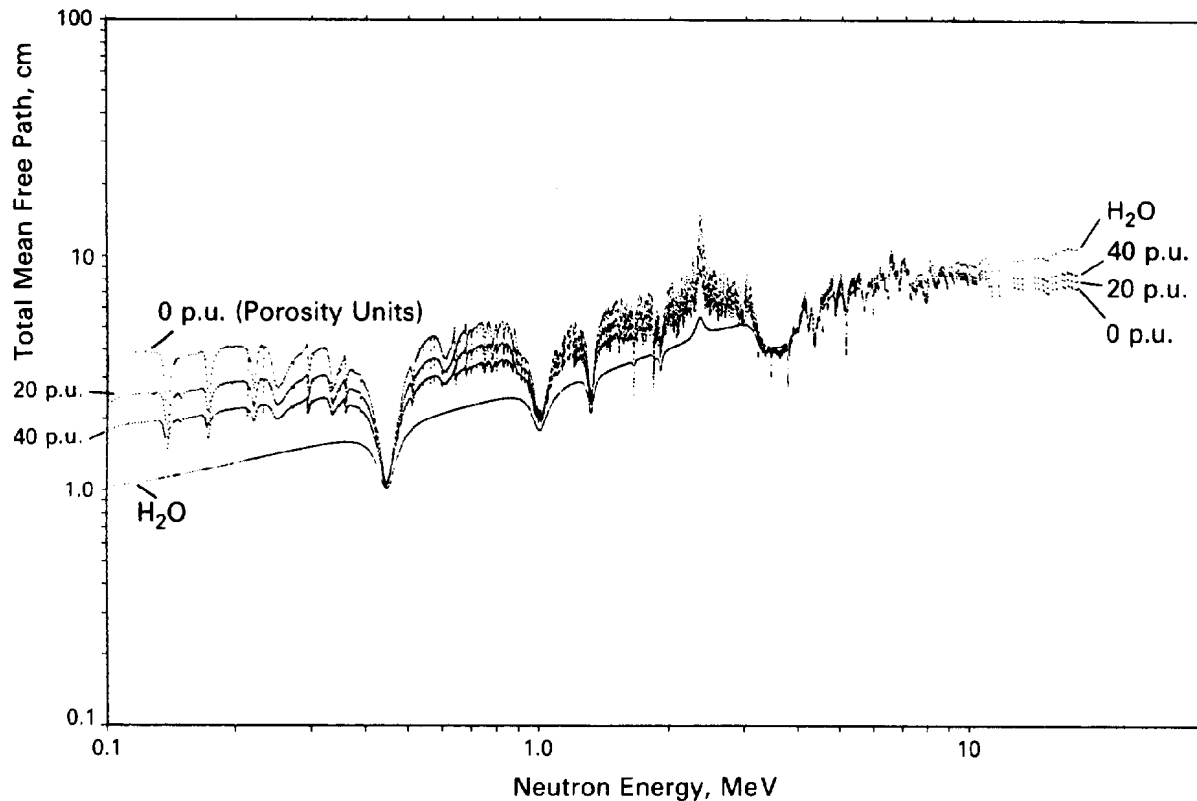


Fig. 50.10—The mean free path of fast neutrons in water and water-filled limestone at several porosities as a function of energy.

their neutron cross sections. The first is the macroscopic cross section, which is defined as the product of the cross section in question times the number of atoms per cubic centimeter, N_p —i.e.,

$$\Sigma_i = N_p \sigma_i = \frac{N_A \rho_b}{A} \sigma_i \quad (24)$$

The dimensions of the macroscopic cross section Σ_i are inverse centimeters and the interpretation is that its reciprocal is the mean-free-path length in centimeters between interactions of Type i . Frequently in logging, use is made of the macroscopic absorption cross section at thermal energies. The units of this (so-called capture units, c.u.) are just 1,000 times the Σ_i defined previously, where σ_i refers to the thermal absorption cross section, which is dominant at thermal energies for most elements. Fig. 50.10 shows the total mean free path in limestone of 0, 20, 40, and 100 porosity units (PU) as a function of energy for fast neutrons. At the energy of chemical source emission (2 to 4 MeV), it is seen that there is very little porosity dependence. It is only as the neutrons are slowed down that the mean free path becomes strongly porosity-dependent.

As mentioned earlier, in the case of elastic scattering, low-mass nuclei are more efficient in reducing the energy of the scattered neutron. As can be inferred from Fig. 50.8, the result of a collision can be considered, on average, as a percentage decrease of the neutron energy. This

usually is expressed as the average logarithmic energy decrement, ξ :

$$\bar{\xi} = \overline{\ln(E_i) - \ln(E)} = -\overline{\ln(E/E_i)} \quad (25)$$

It can be shown from classic mechanics that the average log energy decrement is simply related to the atomic mass, A , of the struck nucleus by

$$\bar{\xi} \approx \frac{2}{A+2/3} \quad (26)$$

for large values of atomic mass A . The average log energy decrement allows an estimation of the average number of collisions, n , to reduce the neutron from an initial energy E_i to some lower energy E from the following reasoning. If the sequence $E_1, E_2 \dots E_n$ represents the average energy after each collision, then we can write

$$\ln\left(\frac{E_i}{E_n}\right) = \ln\left(\frac{E_i}{E_1} \frac{E_1}{E_2} \dots \frac{E_{n-1}}{E_n}\right) \quad (27)$$

$$= \ln\left(\frac{E_i}{E_1}\right)^n = n \ln\left(\frac{E_i}{E_1}\right) \quad (28)$$

$$= n\bar{\xi} \quad (29)$$

TABLE 50.1—NEUTRON SLOWING-DOWN PARAMETERS

Moderator	ξ	\bar{n}^*
H	1.0	14.5
C	0.158	91.3
O	0.12	121
Ca	0.05	305
H ₂ O	0.92	15.8
20-PU limestone	0.514	29.7
0-PU limestone	0.115	132

*Average number of collisions from 4.2 MeV to 1 eV.

Thus, the average number of collisions is given by

$$\bar{n} = \frac{1}{\xi} \ln \left(\frac{E_i}{E_n} \right) \dots \dots \dots (30)$$

The constant ξ can be computed for a mixture of elements by weighting the value of each ξ_i for element i with the appropriate total scattering cross section σ_i . Table 50.1 shows some typical values for the average logarithmic energy decrement and the number of collisions necessary to reduce source energy neutrons (4.2 MeV) to 1 eV.

There are two more parameters that help to characterize neutron interactions with bulk material. One parameter is known as the slowing-down length, L_s , and the other as the diffusion length, L_d . L_s can be described as roughly proportional to the average distance a neutron (in an infinite homogeneous medium) travels from its emission at high energy until it arrives at the lower edge of the epithermal energy region. This distance can be calculated⁴ with a detailed knowledge of the cross sections of the constituent elements. Fig. 50.11 shows the variation of L_s as a function of water-filled porosity for limestone, sandstone, and dolomite.

L_d can be thought of as the distance a thermal energy neutron travels between the point at which it became thermal until its final capture. This distance is given by

$$L_d = \sqrt{D/\Sigma}, \dots \dots \dots (31)$$

where D is the thermal diffusion coefficient and Σ is the macroscopic thermal absorption cross section of the material. The diffusion coefficient, D , also can be calculated from the knowledge of the cross sections of the material and is shown in Fig. 50.12 as a function of porosity for the three principle matrices.

Since thermal neutrons will be affected strongly by the presence of thermal absorbers, it is interesting to look at an abbreviated list of elements that frequently are found in formations that have large macroscopic thermal absorption cross sections. This is found in Table 50.2, where the units are capture cross section (c.u.) per gram of material. Of particular interest is chlorine, the implication being that salt water will have some measurable effect on the thermal neutron population as well as iron and boron, which frequently are associated with clays.

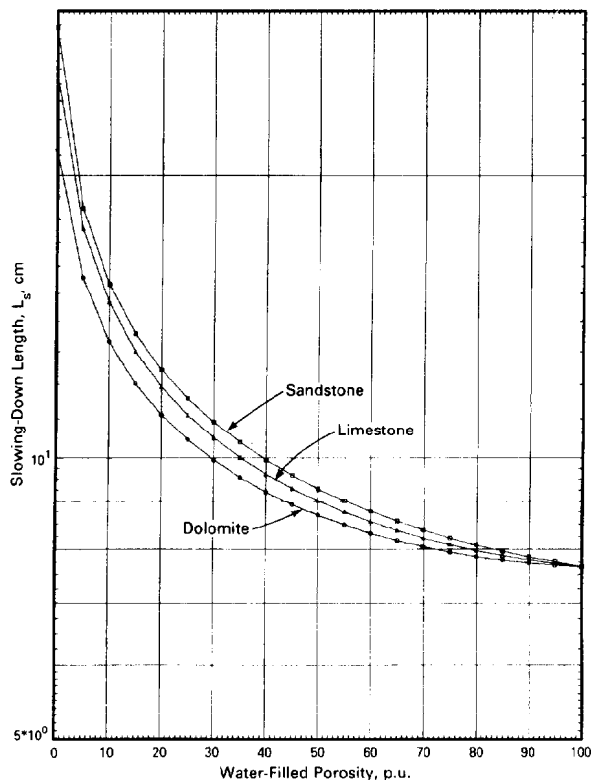


Fig. 50.11—The calculated slowing-down length, L_s , as a function of water-filled porosity for three rock matrices: sandstone, limestone and dolomite.

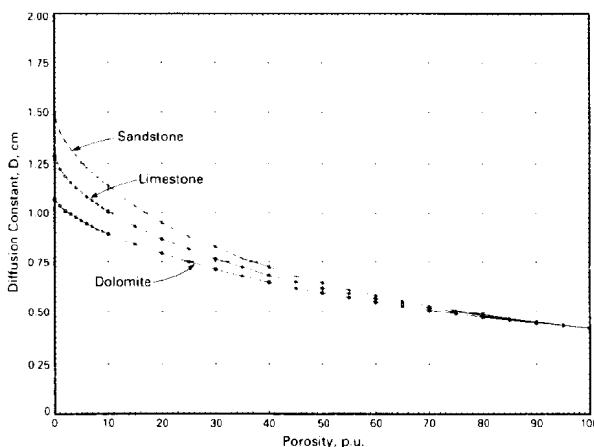


Fig. 50.12—The calculated thermal diffusion coefficient, D , as a function of water-filled porosity for three rock matrices: sandstone, limestone, and dolomite.

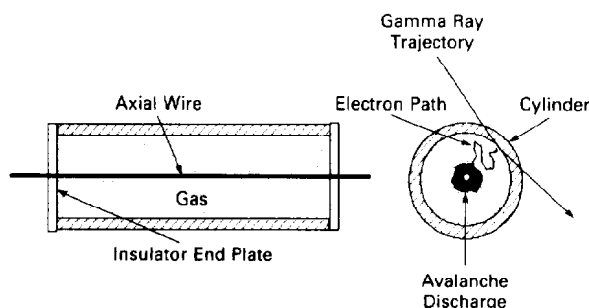


Fig. 50.13—Components of a gas-discharge radiation detector.

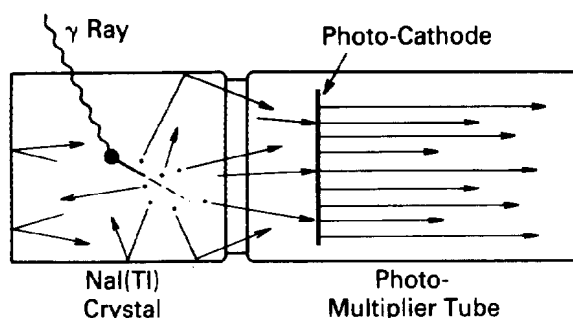


Fig. 50.14—Schematic of the steps involved in gamma ray detection by the production of a measurable electrical signal in a photomultiplier coupled to an NaI crystal.

Another auxiliary parameter, the migration length (L_m), has been defined as

$$L_m^2 = L_s^2 + L_d^2 \quad (32)$$

It can be viewed as a distance that represents the combination of the path traveled during the slowing-down phase (L_s) and the distance traveled in the thermal phase before being captured (L_d). The use of this parameter provides a convenient way of predicting the response of a thermal neutron porosity device, which is discussed in more detail in a later section.

Nuclear Radiation Detectors

Gamma Ray Detectors. The devices for the detection of gamma rays involve the exploitation of one or more of the three processes of gamma ray interactions with matter described earlier. Three general types of gamma ray detectors in current use will be described next. The first variety, the ionized-gas counter, is a direct descendant of the earliest efforts in nuclear radiation detection. The second and most common present-day gamma ray detector used in well logging applications is the scintillation detector. The third type of device, the solid-state detector, is just beginning to be used in logging applications.

The common form of the ionized-gas or gas-discharge counter consists of a metal cylinder with an axial wire passing through it (Fig. 50.13) and insulated from it. The cylinder is filled with a gas that is normally nonconduc-

tive, and some moderate (several hundreds of volts) electrical potential is maintained between the central wire and the cylinder. The detection process is initiated by the formation of some ionized gas molecules. These freed electrons are accelerated by the radial electric field and in successive collisions produce additional free electrons, which finally results in a measurable charge collection on the central wire.

For gamma rays to be detected with such a device, the gas somehow must be ionized initially. Since the gas density is moderate, even at rather high pressure available in commercial tubes, and the atomic number of useful gases is relatively low, there is little possibility of the gamma rays interacting directly with the gas. The main detection mechanism is photoelectric absorption or recoil electron ejection from Compton scattering in the metal shield. For the gamma rays absorbed near the inner radius of the cylinder, there is some probability of the ejected electron escaping into the gas and providing the initial ionization. This also is illustrated in Fig. 50.13.

It should be evident from the foregoing discussion that the detection efficiency of such detectors is not high. It can be improved somewhat by the incorporation of conductive high-atomic-number gamma absorbers, such as silver, as an inner lining of the cylinder. Although they can be operated in a proportional mode, the energy resolution of these detectors is not of great practical use. The most positive aspects of gas-discharge counters are their simplicity, ruggedness, and reliability for functioning in the hostile environment of well logging. Because of their poor efficiency and inapplicability to spectroscopic gamma ray detection, they are being replaced rapidly by a newer generation of scintillation detectors.

A more common type of gamma ray detector uses a scintillation crystal. Once again, the active detector element is sensitive to ionizing radiation, such as energetic electrons. When these particles travel within the crystal lattice, they impart their energy to a cascade of secondary electrons, which finally are trapped by impurity atoms. As the electrons are trapped, visible or near-visible light is emitted. The light flashes are then detected by a photomultiplier tube optically coupled to the crystal and transformed into an electrical pulse. This is indicated schematically in Fig. 50.14. The output pulse height can be related to the total energy deposited in the crystal by the initial high-energy electron. The great advantage of such a detection scheme is the possibility of performing gamma ray spectroscopy—that is, to detect the actual energy of the incident gamma ray, which, in some cases, will identify uniquely the source of the emitted gamma ray, as in the case of induced gamma ray logging.

However, a scintillation detector is a detector of gamma rays only to the extent that an electron is produced in the crystal through one or more of the three basic gam-

TABLE 50.2—MACROSCOPIC THERMAL ABSORPTION CROSS SECTIONS
{ $\Sigma[c.u./(g/cm^3)]$ }

Boron	42 300
Chlorine	564
Hydrogen	198
Manganese	146
Iron	27.5

gamma ray interaction mechanisms: photoelectric absorption, Compton scattering, and pair production. Thus, the gamma ray detection efficiency of a scintillator will depend on its size, density, and average atomic number (for photoelectric absorption). A scintillator in common use is a crystal of sodium iodide doped with a thallium impurity, NaI (Tl), which has good gamma ray absorption properties and a fairly rapid scintillation decay time (~ 0.23 μsec) to allow for high-counting-rate spectroscopy.

The use of such a device for gamma ray spectroscopy implies that the output light pulse is proportional to the incident gamma ray energy; however, this is possible only for the case of total absorption of the gamma ray. Some of the difficulties that can complicate the detected spectrum are shown in Fig. 50.15, for the case of a tool designed to look for the unique gamma rays emitted by inelastic neutron reactions with carbon and oxygen. The figure illustrates what might happen to an inelastic carbon gamma ray that is produced at the site marked (IS) with an initial energy of 4.44 MeV. It first makes a Compton scattering in the borehole fluid (CS) and loses 90 keV of energy before traversing the tool housing and entering the NaI detector with an energy of 4.05 MeV. At the point marked (PP) it suffers a pair-production interaction, producing one electron and one positron with energies of 2.00 and 1.03 MeV, respectively, the missing 1.02 MeV having gone into the creation of the electron/positron pair. Both particles impart their energy to the scintillation process indicated by the dashed lines. When the positron has given up all its kinetic energy, it annihilates with an electron to produce two gamma rays, each of 0.51 MeV energy. One of the gamma rays undergoes Compton scattering at (CS), and the reduced-energy gamma ray (0.41 MeV) is finally absorbed photoelectrically within the crystal at point (Ph.A). The other 0.51-MeV gamma ray is shown escaping the crystal, to the right, and being absorbed in the tool housing without contributing to the total energy transferred to the crystal. The energy recorded by the crystal for the event depicted is 3.54 MeV ($4.05 \text{ MeV} - 1.02 \text{ MeV pair-production} + 0.511 \text{ MeV annihilation}$) instead of the 4.44 MeV that we would like to be measuring.

Thus, the degradation of the structure of the incident gamma ray spectrum is seen to be inherent in the physics of the many processes involved in the detection. Only if the gamma ray is absorbed totally by the detector is the light output of the scintillator proportional to the incident gamma ray energy. This would be the case for the photoelectric absorption, for example. Fig. 50.16 shows the energy deposited in this case as the single line to the right marked E_γ .

If only a Compton interaction occurs, then a fraction of the energy will be registered. The possible range of energy deposition in this case follows the distribution shown in Fig. 50.16 from zero to the Compton edge, which corresponds to the maximum energy being transferred from the gamma ray to the electron. Additionally, if the gamma ray is of sufficiently high energy there may be a pair-production reaction, and if one or more of the 511-keV photons escapes the detector without interaction, the so-called first and second escape peaks will be produced in the detected spectrum. Fig. 50.17 indicates the additional distortion introduced by this process.

In addition to the distortions in the measured spectrum produced by the possible interactions within the detector,

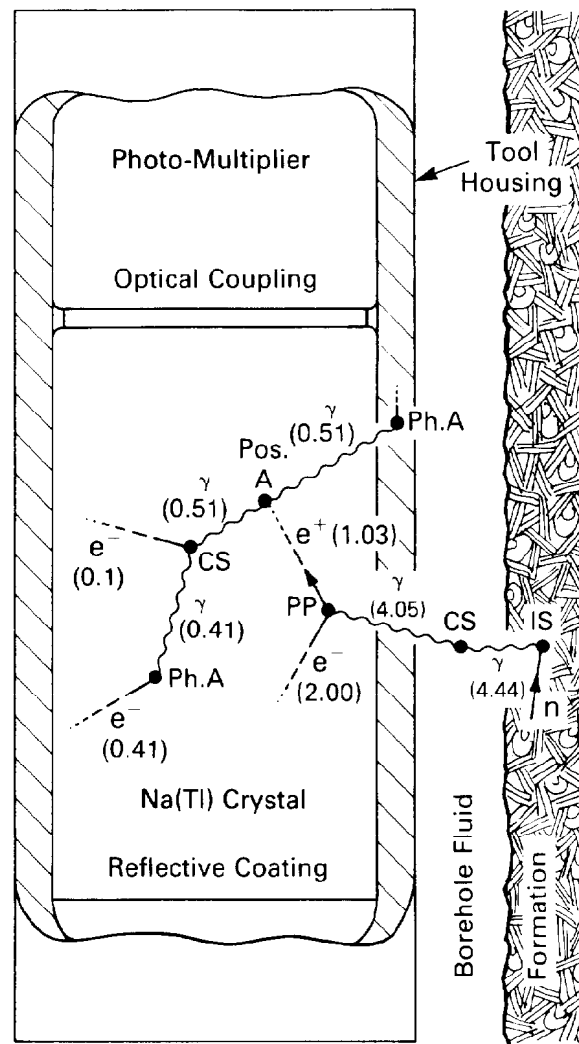


Fig. 50.15—Illustration of the possible sources of gamma ray energy degradation in an NaI detector system.

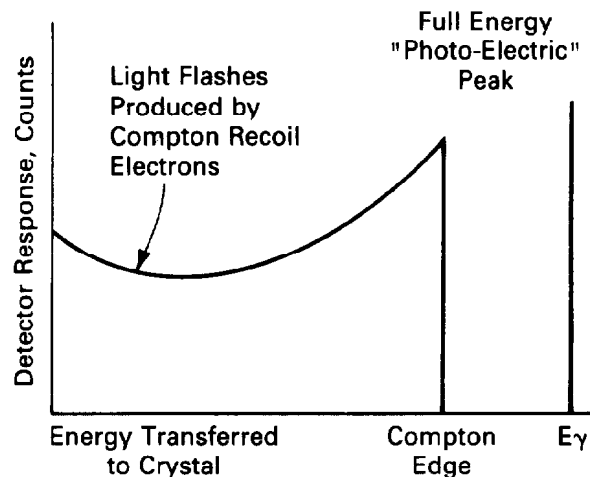


Fig. 50.16—Idealized response from a scintillation detector to mono-energetic gamma rays of energy E_γ , showing the photo-peak and the Compton tail.

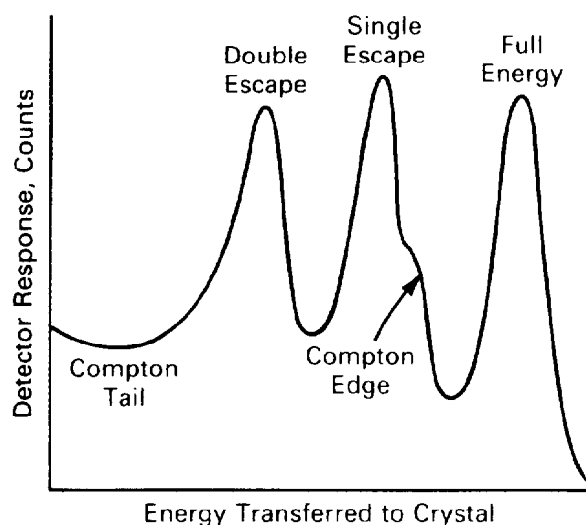


Fig. 50.17—Idealized spectrum distortion in a scintillator caused by pair-production. The highest energy peak corresponds to photoelectric absorption or the full energy of the incident monoenergetic gamma ray, and the two lower energy escape peaks correspond to escape from the crystal of one or two of the annihilation gamma rays of 511 keV.

a dominant perturbation to the measurement is the detector resolution. This refers to the broadening of the line spectra, as can be observed clearly in Fig. 50.17. The width of the observed gamma ray lines is, in the case of an NaI detector, primarily a function of the gamma ray energy, the size of the crystal, and the optical coupling between the crystal and photomultiplier, as well as the characteristics of the photomultiplier. One of the major drawbacks of the scintillation detectors is their poor energy resolution. The reason is that detection in this type of device requires a number of inefficient steps, the result being that the energy required to produce one information carrier (a photo-electron in the photo-multiplier) is about 1,000 eV. Thus, the number of carriers for a typical radiation detection is rather small; the statistical fluctuations on such a small number place an inherent limitation on the energy resolution.

The use of semiconductor materials as radiation detectors can produce many more information carriers per detected event and, thus, can achieve a very-high-energy resolution. In a solid-state device such as the germanium detector, the semiconductor properties are used to transfer the charged-particle energy into a usable electrical pulse in a much more direct manner. When a gamma ray interacts with the detector, charged particles are produced. These, in turn, transfer energy to electrons bound (by only 0.7 eV for Ge) in the crystal lattice, enabling many of them to become free. Each free electron leaves a positive hole in the electron structure of the crystal. Under a strong electrical field applied to the detector crystal, the free electrons and holes migrate quickly to the electrodes and create an electrical impulse.

The excellent resolution arises because the band gap is so small. About 3.5×10^5 electrons are freed by the detection of a 1-MeV gamma ray to contribute to the resulting pulse with no intervening inefficient steps. The

result is sharp energy resolution. Another result is that the detector must be operated at extremely low temperatures. This is because at room temperatures the electrons have sufficient energy to cross the 0.7-eV band gap and camouflage those freed by gamma ray interactions. Although the gamma ray spectra obtained with Ge detectors are superb, their overall counting rates are less than those obtained by NaI detectors. Application of solid-state detectors is limited to devices concerned with precise spectroscopic elemental definition or in-situ chemical analysis.

Neutron Detectors. Neutrons are detected through nuclear reactions in which energetic charged particles are produced. Thus, most neutron detectors consist of a target material for this conversion coupled with a conventional detector, such as a proportional counter or scintillator, to achieve the measurement. Since the cross section for neutron interactions in most materials is a strong function of neutron energy, different techniques have been developed for different energy regions. For well logging applications, at present, it is the detection of thermal and epithermal neutrons that is of interest. The detection schemes considered in this section are appropriate for these low-energy neutrons.

The determination of useful nuclear reactions for neutron detectors involves satisfying several criteria: the cross section for reaction must be very large, the target nuclide should be of high isotopic abundance, and the energy liberated in the reaction following the neutron capture should be high for subsequent ease of detection by conventional means. Three target nuclei have been found generally to satisfy these conditions: ^{10}B , ^6Li , and ^3He . In the case of the first two targets, the (n, α) reaction is used, and for ^3He it is the (n, p) reaction.

The boron reaction is exploited widely in the form of BF_3 in a proportional tube. In this case the boron trifluoride serves as the target and as the proportional tube gas. For this application the gas is enriched in ^{10}B , to attain a high detection efficiency. Another approach is to use boron as the inner coating of a proportional counter, which may use some other proportional gas more suitable than BF_3 for applications involving fast timing, for example.

Since a suitable lithium compound gas does not exist, the lithium reaction is not exploited in a proportional counter. However, lithium scintillators, similar to those of sodium iodide for gamma ray detection, are available. Because of the large amount of energy released by the (n, α) reaction, neutrons are registered at an energy of about 4.1 MeV, which provides a means of discriminating against the gamma rays, which also will be detected readily by the LiI crystal.

The most common neutron detector in well logging, however, is based on the ^3He (n, p) reaction. In this case ^3He is used as the target and proportional gas in a counter. It is preferred to BF_3 because it has a higher cross section than the boron reaction and the gas pressure can be made much higher without degradation of its proportional operation. The overall simplicity of a proportional tube is preferred to the additional complications associated with a scintillator.

For the three reactions discussed, the cross sections vary inversely with the square root of the neutron energy so that the detection efficiency for neutrons will vary in the same manner. The detectors using these reactions, then,

are basically thermal neutron detectors. For some logging applications, it is desirable to measure the epithermal neutron flux while being insensitive to thermal neutrons. This can be achieved by making a minor modification to any of the three types of detectors previously mentioned. It consists of using an exterior thermal-neutron-absorbing material with a large cross section, such as cadmium, to shield the detector. Thermal neutrons will be absorbed in the shield, but the reaction particles, whose range is small (on the order of tenths of millimeters), will not reach the counter. The higher-energy neutrons that manage to penetrate the shield will be detected by the thermal neutron detector with somewhat reduced efficiency.

Nuclear Radiation Logging Devices

The logging devices discussed in the following section fall under two general categories: those that measure natural radiation fields and those that produce radiation fields and measure some aspect of their interaction with the formation. The first group contains tools that measure the natural gamma ray activity of earth formations resulting from the spontaneous decay of radioactive materials. The second category can be broken down into the type of radiation used—gamma rays or neutrons. The latter may be subdivided further into the use of chemical or steady-state neutron sources or pulsed particle accelerator-based sources described earlier.

Rather than trace the historical development, which has been well documented by Segesman,⁵ only the most recent logging devices will be discussed. Both neutron porosity and gamma-gamma density devices have undergone substantial evolution since their respective introductions as commercial services. The earliest devices invariably used a single detector. As the use of these types of measurements grew, more emphasis was put on improving the quantitative nature of the measurements and a better appreciation of environmental effects was gained. This led to the development of borehole-compensated devices generally using a second detector at a lesser spacing from the source that, because of its larger sensitivity to environmental effects, provides a correction to be applied to the principal detector.

Gamma Ray Devices

There are two series of naturally occurring radioactive isotopes that occur in significant quantities in sedimentary rocks: the uranium and thorium series. The only other significant naturally occurring radioisotope is that of potassium (⁴⁰K). Clay minerals that are formed during the decomposition of igneous rocks in general have a very high cation exchange capacity. Because of this property they are able to retain trace amounts of radioactive minerals that originally may have been components of the feldspars and micas that go into the production of clay minerals. This process generally results in a higher concentration of radioactive elements in shales than in sandstones or carbonate rocks not produced by weathering. However, some radioactivity can be associated with carbonate rock and sandstones because of transport of radioactive minerals in solution in the formation waters.

The principal use of the gamma ray log is to distinguish between the shales and the nonshales. Historically, the first gamma ray devices measured only the total gamma

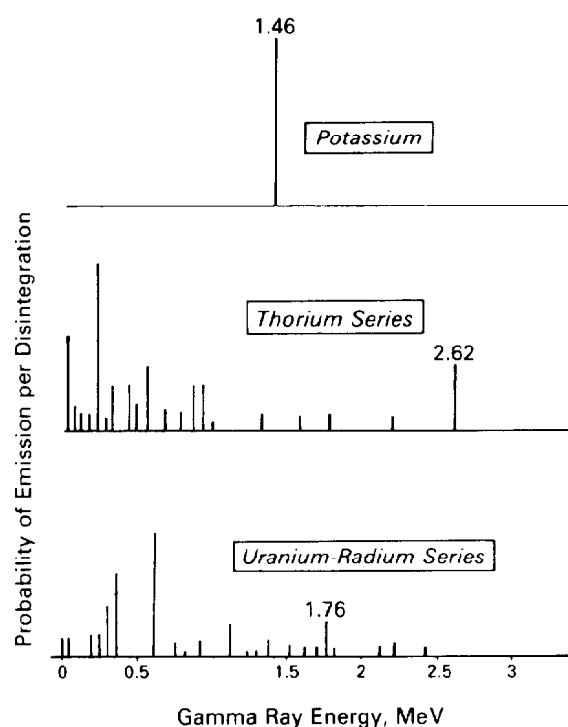


Fig. 50.18—Theoretical gamma ray emission spectra from the three naturally occurring radioactive products.

ray flux emanating from the formation. However, it is now known that different types of shale have different total gamma ray activity because of the Th, U, and K concentrations. Fig. 50.18 shows the various gamma ray line emissions associated with each. This indicates that by determining the intensity of the particular gamma ray energies it is possible to identify the quantity of each radioactive emitter in the formation. With the development of improved spectroscopic-quality gamma ray detectors, it became natural to refine the gamma ray measurement into a measurement of the actual concentrations of the three components.

The measurement element for recent gamma ray or spectral gamma ray logging devices is the NaI detector. The gamma ray devices measure the total number of gamma rays above some practical lower limit (on the order of 100 keV). This total counting rate will be (1) a function of the distribution and quantity of radioactive material in the formation and (2) influenced by the size and efficiency of the detector used. For this reason some calibration standards have been established by the API, and all total-intensity gamma ray logs are recorded in API units.

The definition of the API unit of radioactivity comes from the artificially radioactive formation constructed at the U. of Houston facility. A formation containing approximately 4% K, 24 ppm Th, and 12 ppm U was constructed and defined to be 200 API units. The details of this calibration facility can be found in Ref. 6.

Spectral gamma ray devices basically use the same type of detection system as the total gamma ray devices, but instead of one broad energy region for detection, the gamma rays are analyzed into several different energy bins.

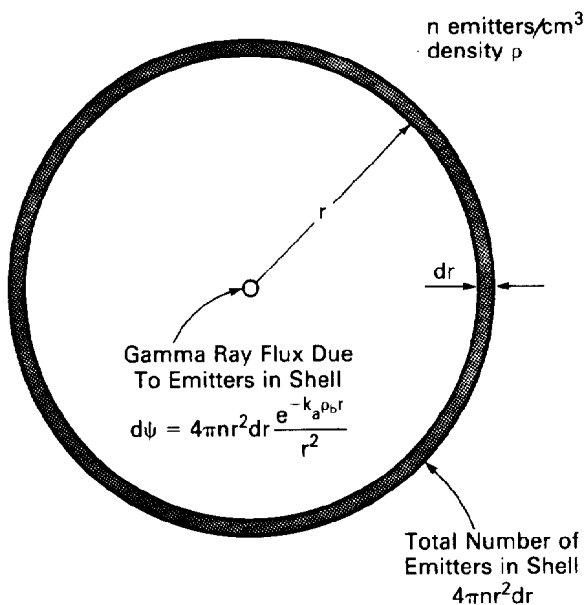


Fig. 50.19—Geometry for the gamma ray flux at a point from uniformly distributed sources in an infinite medium.

This allows for the determination (after comparing to normalized standard formations where the concentrations of K, U, and Th are known) of the concentrations of these elements present in the measured formation. These log output quantities usually are expressed as a percent by weight of the total material.

It is of interest to note that the gamma ray intensity from a uniformly distributed source (whose concentration is maintained at a constant value when expressed in weight percent of the medium in which it is embedded) is independent of the formation density, even though the attenuation is a direct function of the formation density. This can be seen from the following argument.

Consider an infinite homogeneous medium containing n gamma ray emitters per cubic centimeter, each with a source strength of emission of one gamma ray per second. To calculate the total gamma ray flux that would be seen by a detector at a given point in this medium, refer to Fig. 50.19. The contribution to the total counting rate from a spherical shell of thickness dr at a distance r from the detector would be the number of emitters contained in this shell multiplied by the attenuation over the path length r to the detector,

$$d\Psi = 4\pi r^2 n dr \frac{e^{-K_a \rho_b r}}{4\pi r^2}, \dots \dots \dots (33)$$

and the total counting rate is just the integral

$$\Psi = n \int_0^\infty e^{-K_a \rho_b r} dr, \dots \dots \dots (34)$$

$$\Psi = n \frac{1}{K_a \rho_b}, \dots \dots \dots (35)$$

This simply says that the total counting rate is proportional to n/ρ_b , which can be expressed as the weight percent of the material that is radioactive. Consequently, the utility of expressing the radioactive contents as weight fractions is seen.

One of the fundamental difficulties in the interpretation of the gamma ray device measurements is inherent in its very concept. There are nonradioactive clays and there are "hot" dolomites. The use of spectral gamma ray devices can often point out an anomaly such as a "hot" dolomite or other formation with some unusual excess of U, or in other cases K or Th.

Both types of devices suffer to some small degree from the borehole environment. Because of mud in the borehole and varying hole diameters, the gamma rays emitted from the formation must pass through different amounts of gamma ray absorbers to reach the detector. Additional complications can arise because of mud additives such as barite or KCl. In the first case, the barium content of the mud becomes a very efficient absorber of low-energy gamma rays emanating from the formation. In the second case, the borehole fluid is also a source of radioactive potassium, which is contained in the KCl additive. Ref. 7 discusses a method for correcting for these effects.

Gamma-Gamma Density Devices

As noted in an earlier section, the transmission of gamma rays through matter can be related to the electron density if the predominant interaction is Compton scattering. Thus, a gamma ray transmission-type measurement through a formation can be used to determine its density and with some information on the material composition (lithology and pore fluids) the porosity can be determined.

The gamma ray source usually used in density devices is ^{137}Cs , which emits gamma rays at 662 keV, well below the limit for pair production. This isotope has a half life of about 30 years, which provides a usable, stable intensity during a reasonable period. Some devices use ^{60}Co , which emits two gamma rays at 1332 and 1173 keV.

The earliest devices consisted of the gamma ray source and a single detector, which initially was called a Geiger-Müller tube. However, to compensate for the frequent occurrence of intervening mudcake, modern devices incorporate two detectors (generally both NaI) in a housing that shields them from direct radiation from the source and is forced up against the formation with a hydraulically operated arm. This arm provides a force of application as well as a measurement of the diameter (along one axis) of the borehole.

The measurement principle derives from the fact that the counting rate of a detector will vary exponentially with the density of the formation. Consequently, the formation density can be determined simply from an observed counting rate. However, in the case of intervening mudcake of unknown density and thickness, there will be a disturbance of the counting rate. Fig. 50.20 shows the usual logging situation. To correct for this intervening mudcake, the apparent density of the long- and short-spacing devices can be derived. Laboratory measurements then are used to define the correction, $\Delta\rho$, that must be applied to the apparent density from the long-spacing detector to read the value of the formation density behind it.

In at least one device the shape of the gamma ray spectrum is measured and correlated with the photoelectric absorption parameters of the formation, which, in turn, can be linked with the lithology of the formation. The photoelectric factor, F_{pe} , is proportional to the photoelectric cross section per electron. Fig. 50.21 shows the utility of such a measured parameter for distinguishing between the three principal matrices.

Since the F_{pe} of mixtures does not combine volumetrically, a new parameter, U , which has the property of combining linearly, has been developed for interpretation purposes. The definition of U is the product of F_{pe} and electron density,

$$U = F_{pe} \rho_e, \dots \dots \dots (36)$$

and corresponds to the macroscopic photoelectric cross section. This follows from the definition of F_{pe} , which is the photoelectric cross section per electron, and ρ_e , which is proportional to the number of electrons per cubic centimeter. Thus, the value of U for any mixture can be computed by making a simple volumetric addition of the U associated with each of the pure components of the mixture. Table 50.3 lists some useful lithology parameters for a number of commonly encountered minerals. Fig. 50.22 shows the use of U and density in the determination of lithology once the effect of porosity has been eliminated.

Examination of Table 50.3 shows the enormous sensitivity of the parameter U or F_{pe} to elements with a large atomic number. In particular, note the values of F_{pe} for the several iron compounds and for barium. In the case of iron, this sensitivity can be exploited to make a determination of shale content of the formation if there is iron associated with the clay mineral. This is discussed in the section on interpretation. However, the sensitivity to barite makes the F_{pe} measurement difficult in heavily weighted barite muds. If there is a substantial thickness of barite mudcake between the tool skid and the formation or if there is invasion of BaSO_4 particles into the formation, the resultant photoelectric absorption can seriously disturb the measurement.

Neutron Porosity Devices

Historically, the neutron device was the first nuclear device to be used to obtain an estimate of formation porosity. The principle of operation is based on the fact that hydrogen, with its relatively large scattering cross section and small mass, is very efficient in the slowing of fast neutrons. Thus, a measurement of the flux of epithermal neutrons resulting from the interaction of high-energy source neutrons with a formation will be related to its hydrogen content. If the hydrogen (in the form of water or hydrocarbons) is contained within the pore space, then the measurement will yield porosity. The simplest version of the device consists of a source of fast neutrons such as Pu-Be or Am-Be with average source energies of several MeV and a detector of much lower-energy neutrons at some distance from the source. Two general categories will be considered on the basis of the types of neutrons detected—epithermal or thermal.

To be a little more quantitative about the response of neutron porosity devices, we can use the results of two-group diffusion theory,⁸ which show that the flux of

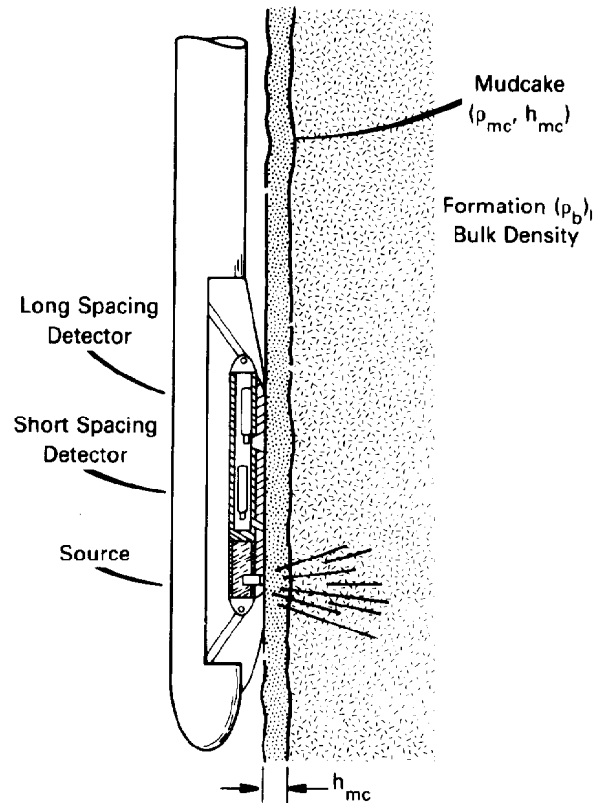


Fig. 50.20—Schematic of a compensated density device in a borehole with mudcake.

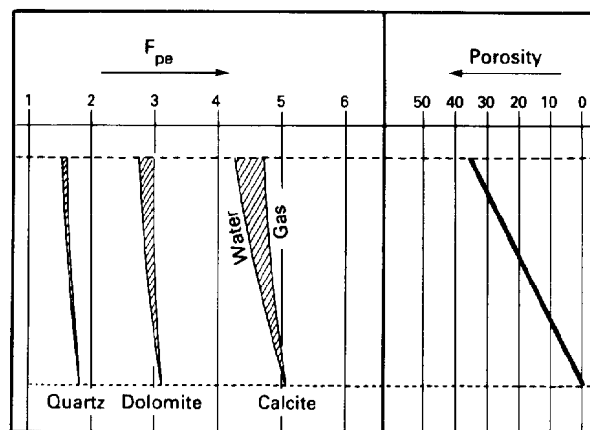


Fig. 50.21—Values of the photoelectric factor, F_{pe} , for the three principal matrices showing the relative insensitivity to porosity.

TABLE 50.3—LITHOLOGY PARAMETERS FOR VARIOUS MATERIALS

Elements	Formula	Molecular Weight	Z	F_{pe}	ρ_b	ρ_e^{**}	U^\dagger
Hydrogen	H	1.008	1	0.00025			
Carbon	C	12.011	6	0.15898			
Oxygen	O	16.000	8	0.44784			
Sodium	Na	22.991	11	1.4093			
Magnesium	Mg	24.32	12	1.9277			
Aluminum	Al	26.98	13	2.5715	2.700	2.602	
Silicon	Si	28.09	14	3.3579			
Sulfur	S	32.066	16	5.4304	2.070	2.066	
Chlorine	Cl	35.457	17	6.7549			
Potassium	K	39.100	19	10.081			
Calcium	Ca	40.08	20	12.126			
Titanium	Ti	47.90	22	17.089			
Iron	Fe	55.85	26	31.181			
Strontium	Sr	87.63	38	122.24			
Zirconium	Zr	91.22	40	147.03			
Barium	Ba	137.36	56	493.72			
Minerals							
Anhydrite	CaSO ₃	136.146		5.055	2.960	2.957	14.95
Barite	BaSO ₄	233.366		266.8	4.500	4.011	1070.0
Calcite	CaCO ₃	100.09		5.084	2.710	2.708	13.77
Carnallite	KCl·MgCl ₂ ·6H ₂ O	277.88		4.089	1.61	1.645	6.73
Celestine	SrSO ₄	183.696		55.13	3.960	3.708	204.0
Corundum	Al ₂ O ₃	101.90		1.552	3.970	3.894	6.04
Dolomite	CaCO ₃ ·MgCO ₃	184.42		3.142	2.870	2.864	9.00
Gypsum	CaSO ₄ ·2H ₂ O	172.18		3.420	2.320	2.372	8.11
Halite	NaCl	58.45		4.65	2.165	2.074	8.65
Hematite	Fe ₂ O ₃	159.70		21.48	5.210	4.987	107.0
Ilmenite	FeO·TiO ₂	151.75		16.63	4.70	4.46	74.2
Magnesite	MgCO ₃	84.33		0.829	3.037	3.025	2.51
Magnetite	Fe ₃ O ₄	231.55		22.08	5.180	4.922	109.0
Marcasite	FeS ₂	119.98		16.97	4.870	4.708	79.9
Pyrite	FeS ₂	119.98		16.97	5.000	4.834	82.0
Quartz	SiO ₂	60.09		1.806	2.654	2.650	4.79
Rutile	TiO ₂	79.90		10.08	4.260	4.052	40.8
Sylvite	KCl	74.557		8.510	1.984	1.916	16.3
Zircon	ZrSiO ₄	183.31		69.10	4.560	4.279	296.0
Liquids							
Water	H ₂ O	18.016		0.358	1.000	1.110	0.40
Salt water	(120,000 ppm)			0.807	1.086	1.185	0.96
Oil	CH _{1.6}			0.119	0.850*	0.948*	0.11
	CH ₂			0.125	0.850*	0.970*	0.12
Miscellaneous							
Clean sandstone	*			1.745	2.308	2.330	4.07
Dirty sandstone	*			2.70	2.394	2.414	6.52
Average shale				3.42	2.650*	2.645*	9.05
Anthracite	C:H:O—			0.161	1.700*	1.749*	0.28
coal	93:3:4						
Bituminous	C:H:O—			0.180	1.400*	1.468*	0.26
coal	82:5:13						

*Variable; values shown are illustrative.

** ρ_e is electron density = $\rho_b \times 2Z/A$. $U = F_{pe} \rho_e$.

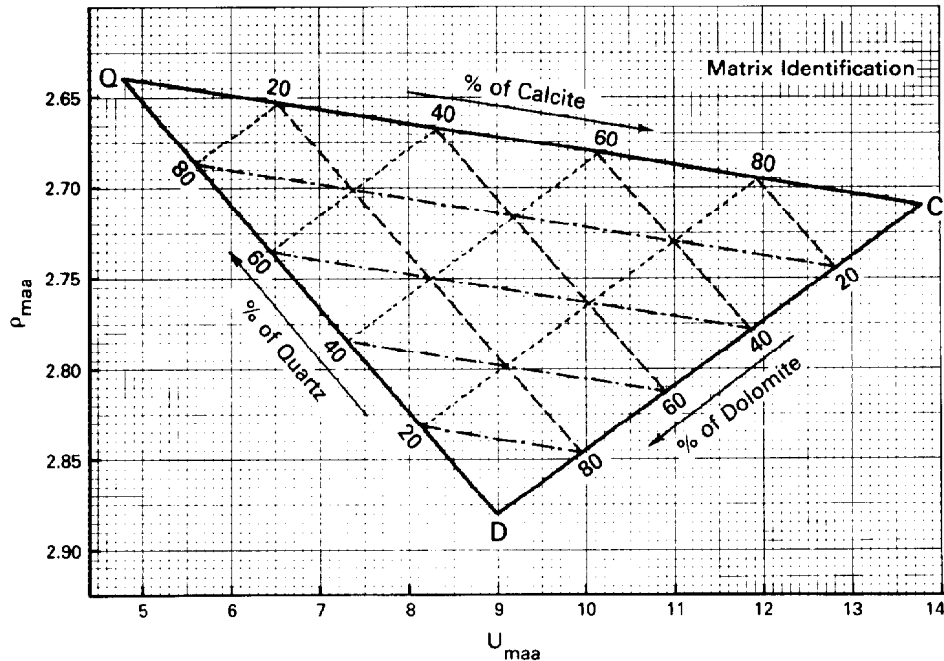


Fig. 50.22—Matrix identification chart from U and density once the effect of porosity has been eliminated.

epithermal neutrons, in an infinite medium containing a point source of fast neutrons, falls off exponentially with the distance from the source, L , with a characteristic length, L_s , which is determined by the constituents of the medium:

$$\Psi_{\text{epi}} \propto \frac{1}{D} \frac{e^{-L/L_s}}{L}, \quad \dots \dots \dots (37)$$

where D is the epithermal diffusion coefficient, which is related to the transport mean free path of neutrons. At a fixed spacing, counting rates should vary nearly exponentially with the slowing-down length of the formation. An indication of this type of behavior can be seen in Fig. 50.23, which shows, on the left, the counting rate of one of the early epithermal neutron devices as a function of porosity, and on the right as a function of slowing-down length. The matrix effect is much reduced in the

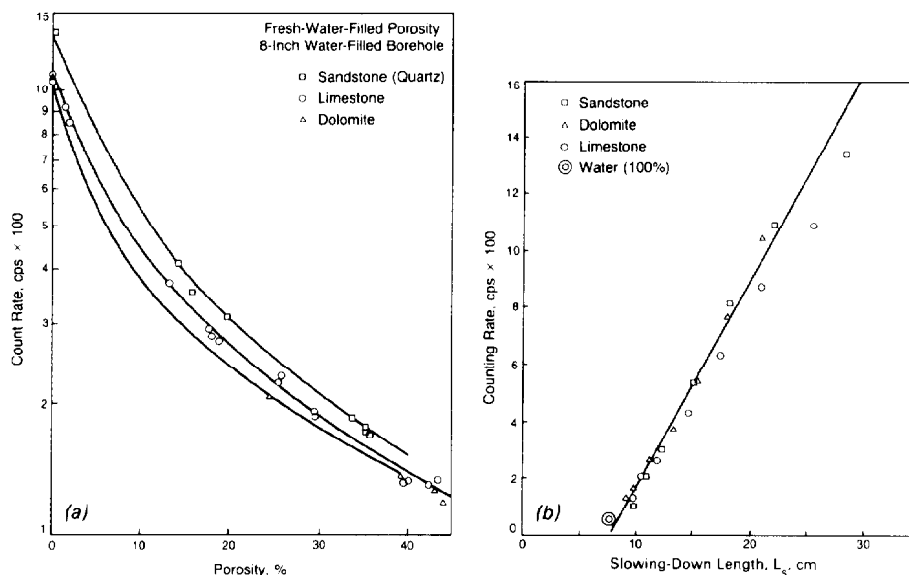


Fig. 50.23—Counting rates for a long-spacing epithermal detector in test formations of various porosities. On the left, the data are plotted as a function of the formation porosity with three data trends resulting that correspond to the three matrices of the test formations. On the right, the same data have been replotted as a function of the corresponding slowing-down length for each of the test formations.

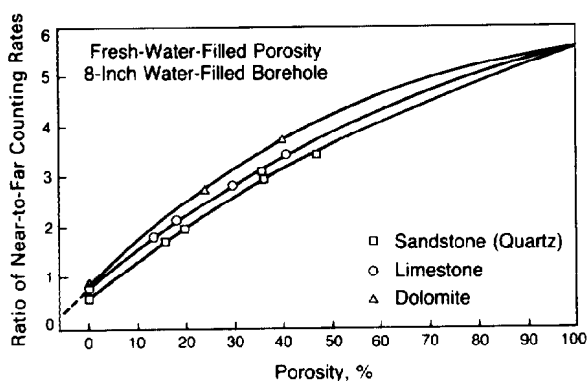


Fig. 50.24—The ratio of near to far detector counting rates as a function of porosity for a thermal neutron porosity device.

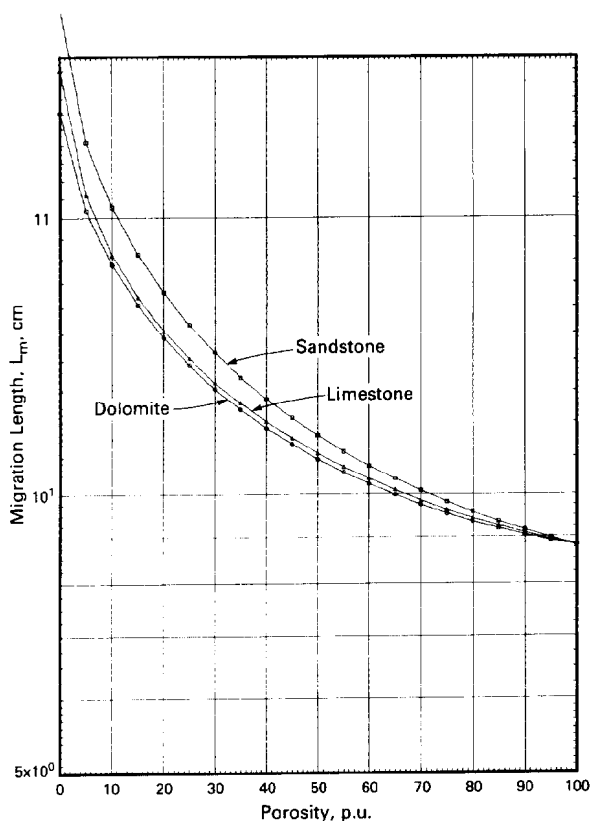


Fig. 50.25—The calculated migration length, L_m , as a function of porosity for the three principal matrices: sandstone, limestone, and dolomite.

second presentation. It also shows how the counting rate in any other material, once its slowing-down length has been calculated, then can be estimated or, conversely, how the slowing-down length of the formation can be determined from a measurement of the epithermal flux. It was seen in Fig. 50.11 that the slowing-down length is strongly dependent on the amount of hydrogen present in the mixture for which it is calculated.

Fig. 50.11 also shows the slowing-down length as a function of porosity for three common matrix materials: limestone, dolomite, and sandstone. From this presentation, it can be seen that if the matrix is known, the appropriate true porosity can be determined. As an operational expedient it has been convenient to convert the epithermal counting rate into porosity directly, assuming a limestone matrix with a slight correction to be made for the other two matrices. The separation of the three curves in the previous figure suggests how such a correction is made.

One of the first really quantitative devices of this type used a single epithermal detector in a skid applied mechanically against the borehole wall. This sidewall epithermal neutron device had the advantage of minimizing borehole effects, although it is sensitive to the actual size of the borehole and can be disturbed by the presence of mud-cake between the pad surface and the borehole wall.

A more recent development is the dual-detector compensated neutron device. This type of device uses a pair of thermal detectors for increased counting rate to improve the statistical uncertainty of the derived porosity values at high porosity. The second detector, the nearer to the source, is used to provide compensation for borehole effects. Although thermal neutron detection is used, it can be shown⁸ that if the source-to-detector spacings are appropriately chosen, the ratio of the two counting rates should vary exponentially as the inverse of the slowing-down length just as in the case of the single epithermal detector. In practice, however, it is found that some additional corrections must be made to the measurements, which can deviate from expected values if the thermal capture properties of the borehole and formation are significantly different. These generally are provided by the service companies in the forms of charts or nomographs. More recently they have been provided as a part of computerized interpretation.

The migration length, discussed in an earlier section, provides a convenient way to characterize the response of the thermal neutron device. Fig. 50.24, taken from Edmundson,⁹ shows the ratio of the near to the far counting rate of such a device for three types of lithologies as a function of porosity. If the porosity values on the points of this plot are converted through the use of Fig. 50.25, which shows the migration length, L_m , as a function of porosity, then the counting rates for the three lithologies lie on a single line, as seen in Fig. 50.26. This demonstrates that the response characteristics of the neutron porosity tools are given by some function of the slowing-down length and diffusion length rather than porosity.

Although the API committee⁶ that set up the gamma ray calibration standards also took some steps to standardize neutron log responses, their recommendations for API units have not been implemented. The conventional approach to neutron log output is to calibrate the tool in limestone primary formations and to report all readings

in apparent limestone porosity. Conversion charts are then necessary to correct the apparent limestone porosity for the matrix in which the measurement actually was made. (As noted previously, some consideration should be given to using the slowing-down length and diffusion length as the units for reporting the log measurements.) These measurements would be converted to porosity by use of charts similar to Figs. 50.11 and 50.25, lying entirely in the realm of interpretation.

One of the biggest limitations of the thermal porosity device is the disturbance on the measurement that can be caused by shale, either from its iron or potassium content or associated trace elements with high thermal capture cross section. However, even without the additional disturbance of thermal absorbers, clays and shales present a problem for all neutron porosity interpretation because of the hydroxyls associated with the clay mineral structure. Fig. 50.27 illustrates this point by showing the variation of slowing-down length of a sand/illite and sand/kaolinite mixture as a function of porosity. In both cases the sand and shale volumes are in equal proportions. It is clear that if the presence of clay in addition to the sand is not taken into account, large errors in porosity can result. Also note that the apparent porosity of kaolinite is much larger than that of illite. The examples shown in the figures indicate that a 20-PU sand/illite mixture will appear to be about 25 PU, whereas the 20-PU sand/kaolinite mixture will have an apparent porosity of about 36 PU. This will be seen in a later section to be caused by the differing hydroxyl content of these two clay minerals.

It is also of note that the most recent neutron porosity device consists of a pair of thermal and a pair of epithermal detectors. This enables measuring an apparent porosity unaffected by thermal absorbers and simultaneously obtaining a measurement of the macroscopic thermal absorption coefficient, Σ , which additionally describes the formation.

Pulsed Neutron Logging Devices

Pulsed neutron logging devices respond to the macroscopic thermal absorption capture cross section. The macroscopic thermal absorption cross section depends on the chemical constituents of the matrix and pore fluids. Chlorine, which is nearly always a constituent of formation waters, has a large absorption cross section. Thus, a measurement of the absorption cross section can provide the means of identifying salt water and measuring formation fluid saturation.

To determine the macroscopic thermal cross section, the actual phenomenon being measured is the lifetime of thermal neutrons in an absorptive medium. In a manner analogous to radioactive decay, we can predict the time-dependent behavior of thermal neutrons. The reaction rate for thermal neutron absorption is given by the product of the macroscopic cross section Σ and the velocity of the neutron, v . So for a system of N_N neutrons the rate of thermal absorption is given by

$$dN_N = -\Sigma v dt, \quad \dots \dots \dots (38)$$

which when integrated yields

$$N_N = N_i e^{-\Sigma v t}, \quad \dots \dots \dots (39)$$

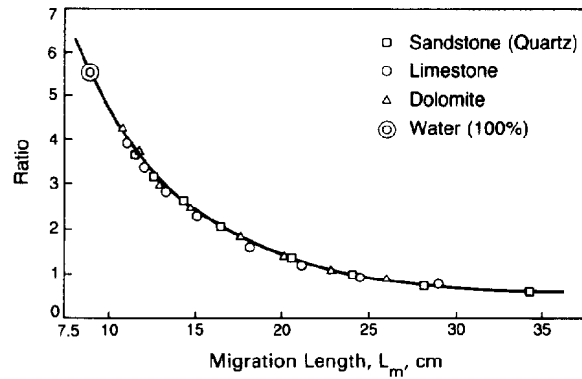


Fig. 50.26—The ratio data of Fig. 50.24 plotted as a function of the migration length, L_m , corresponding to the matrix and porosity of the test formation measurements.

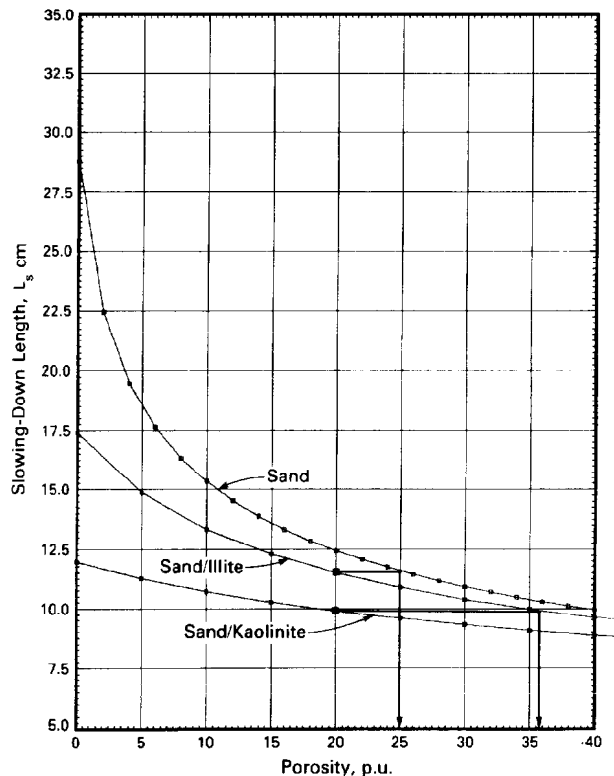


Fig. 50.27—The calculated slowing-down length as a function of porosity for sand and sand/clay mixtures. For the two lower lines the matrix is composed of equal mixtures, by volume, of sand and kaolinite or illite.

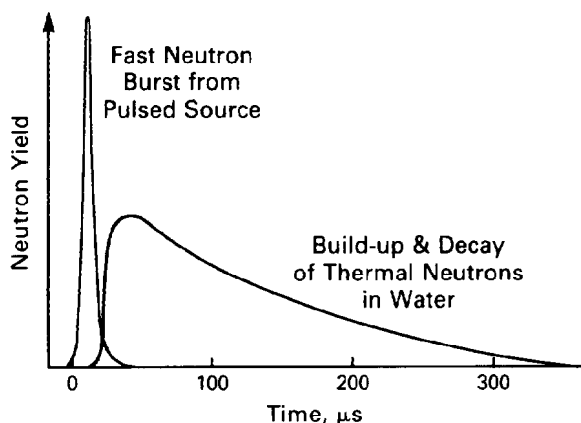


Fig. 50.28—Schematic timing diagram of a pulsed neutron capture/gamma ray device.

which relates the number present at time t to an initial number N_i at time zero. The exponential decay constant is seen to depend inversely on the desired quantity Σ .

The practical realization of such a pulsed neutron logging device depends on a pulsed source of high-energy neutrons. Such a device was discussed previously. The basic mode of operation consists of pulsing the source of 14-MeV neutrons for a brief period. This forms a cloud of high-energy neutrons in the borehole and formation, which then becomes thermalized through multiple collisions. This process is illustrated in Fig. 50.28. Only at thermal energies does the absorption become important and the neutrons begin to disappear in accordance with Eq. 39. As each neutron is captured, whether it be by hydrogen or chlorine, gamma rays are emitted, and the decay of the gamma ray counting rate is the actual measurement that reflects the decay of the neutron population.

As seen from Eq. 39, the decay constant for a particular formation is given by $1/v\Sigma$. The value of the capture cross section Σ is listed in Table 50.4 for a number of pertinent cases. Included in the table is the decay time associated with the particular matrix, which was computed from the relationship

$$\tau_d = \frac{K}{\Sigma_{\text{abs}}}, \quad (40)$$

where K is 4550 μsec , because v for thermal neutrons is 0.22 $\text{cm}/\mu\text{sec}$ and Σ_{abs} , the thermal absorption cross section, is in capture units.

TABLE 50.4—CAPTURE CROSS SECTIONS AND DECAY TIMES

	Σ (c.u.)	τ_d (μsec)
Quartz	4.26	1086
Dolomite	4.7	968
Lime	7.07	643
20-PU lime	10.06	452
Water	22	206
Salt water (26% NaCl)	125	36

Since the derivation of the decay-time measurement is based on the simple model of a cloud of thermal neutrons being present and then decaying, it is of some interest to see just how long it is after the burst of 14-MeV neutrons that they become thermalized. To estimate this time we need only to refer to the section on neutron physics, where the average number of collisions for thermalization and the mean free path were discussed. The simplest estimate of the time required is to suppose that between each collision the average distance traveled is the mean free path ($1/\Sigma_t$). The time between one collision and the next, Δt , is then given approximately by

$$\Delta t \approx \frac{1}{\Sigma_t} \frac{1}{v}, \quad (41)$$

where Σ_t is the total cross section and v is given in terms of the energy E by Eq. 23. The $1/v$ factor can be replaced by using Eq. 23 in conjunction with the expression (Eq. 30) for the average number of collisions, \bar{n} , yielding

$$\frac{1}{v} \propto e^{\bar{n}\xi/2}, \quad (42)$$

where ξ is the average logarithmic energy decrement defined in Eq. 25.

The value of an average mean free path for formations of interest can be estimated from Fig. 50.10. From the above information, the total time, t_t (μsec), from emission to thermal energies is given by

$$t_t = \int \Delta t = \frac{1}{\Sigma} 3.6 \times 10^{-4} \int_0^{\bar{n}} e^{\bar{n}\xi/2} d\bar{n}. \quad (43)$$

Evaluation of this expression for 20%-porosity limestone gives an estimate of about 2.8 μsec and in water it is only 0.5 μsec , both of which are much smaller than the decay times shown in Table 50.4.

Numerous measurement schemes are used for controlling the period during which the 14-MeV neutrons are produced and the period during which the gamma rays are measured. Some devices use dual-detector systems in an attempt to correct for the small disturbance that can be introduced by the borehole size and salinity as well as to provide some measure of the porosity.

Inelastic and Capture Gamma Ray Spectrometry

The primary motivation for the development of induced gamma ray spectroscopy devices was the possibility of performing in-situ chemical analysis of the formation constituents. The tantalizing possibility of directly measuring the ratio of the number of carbon atoms to oxygen atoms and thus providing the first direct downhole measurement of the presence of hydrocarbons spurred the development of a number of technologically sophisticated devices. This is to be contrasted with a traditional approach that depends on the analysis of a core or side-wall sample.

Tools of this type are based on a type of chemical analysis that can be performed through the use of neutrons and gamma ray spectroscopy. Neutrons are used to excite the nuclei, which then emit gamma rays of precise

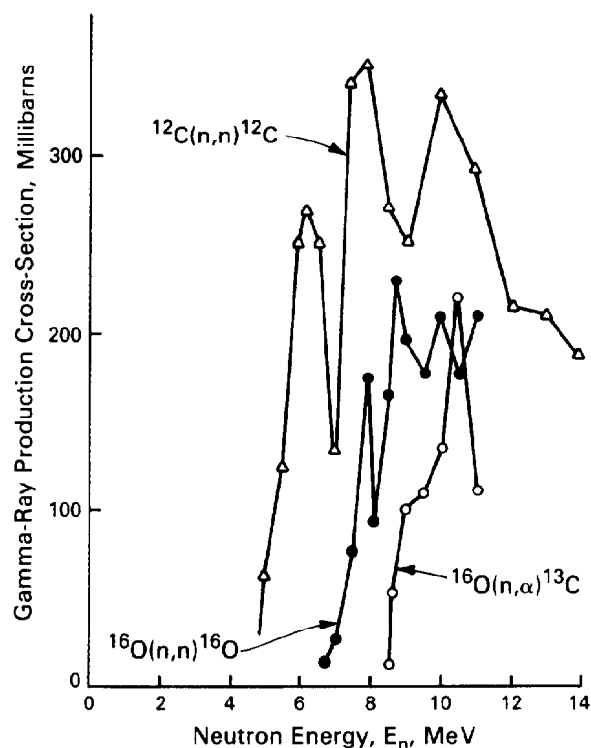


Fig. 50.29—Cross sections for the production of inelastic gamma rays by carbon and oxygen as a function of the incident neutron energy.

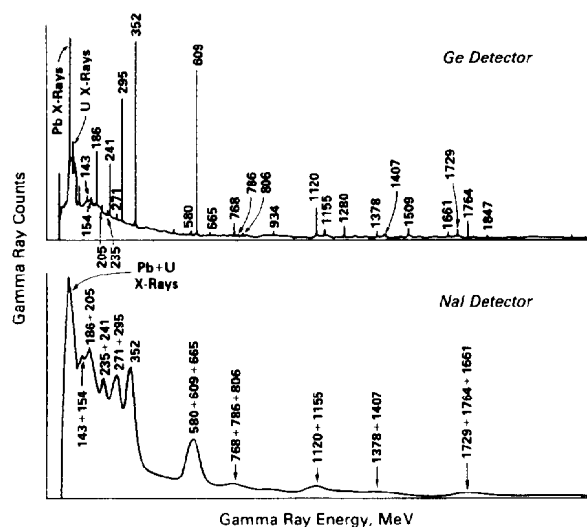


Fig. 50.30—Comparison spectra from a high-resolution solid-state detector (Ge) compared to the gamma ray spectrum detected with a more conventional NaI detector.

energies uniquely identifying the isotope in question. There are two neutron reactions that can produce such gamma ray emissions: inelastic scattering, which can occur with very-high-energy neutrons, and capture reactions with thermalized neutrons as exploited in pulsed neutron logging.

Few elements for well-logging applications have large inelastic cross sections, but fortunately carbon and oxygen do. Fig. 50.29 shows the cross sections for the production of gamma rays from inelastic scattering from carbon and oxygen. These inelastic induced gamma rays are observed not only by spectroscopic gamma ray detection but also in conjunction with timing. To avoid confusion with gamma rays produced from thermal capture, the inelastic gamma rays are detected during the burst of 14-MeV neutrons. At some later time, gamma rays arising from thermal absorption are detected, providing sensitivity to a large number of elements such as H, Fe, Cl, Si, Ca, S, etc. At least two different neutron pulsing and gamma ray detection sequences are currently in use. One method¹⁰ uses a fixed time of about 50 to 100 μ sec between neutron bursts, and another method,¹¹ which collects information on the capture gamma rays, uses a variable neutron-pulse interval that is controlled by the characteristic decay time of the thermalized neutrons.

Tool design differences can optimize the detection of the inelastic or capture gamma rays. Some designs incorporate the measurement of both through appropriate timing cycles. In addition to the measurement of the gamma ray yields of the various elements, the macroscopic cross section Σ can be determined from an analysis of the decay of the total gamma ray signal, which is also measured. The only practical limitation on the number of elements is determined by counting statistics and the inherent detector resolution.

An experimental tool that uses a high-resolution Ge detector has measured more than two dozen different elements in borehole logging. This type of detector must be operated at very low temperatures (-196°C), which introduces a number of technological problems for borehole measurements. However, the advantage that it brings is in the much improved resolution, which increases the number of distinct gamma rays that can be distinguished in the spectrum. Fig. 50.30 shows the dramatic improvement compared to a conventional NaI detector for the examination of a natural uranium sample. Two elements that are readily detectable with such a device are aluminum, which is very useful in the classification and quantification of in-situ clays, and vanadium, which can be correlated¹² with the API gravity of the associated oil.

Interpretation of Nuclear Logs

The following section discusses how the previously mentioned nuclear logging tools are used in interpretation. However, it should be stated at the outset that this is not intended to be a self-contained log interpretation course. A number of references¹³⁻¹⁷ of such works should be consulted for further information.

The approach taken here is more or less a stand-alone interpretation of each tool. An examination of all the combination measurements and the interpretation techniques used with each tool is beyond the scope of this chapter. Nonetheless, several of the more standard tool combination interpretation approaches are discussed. Fig. 50.31

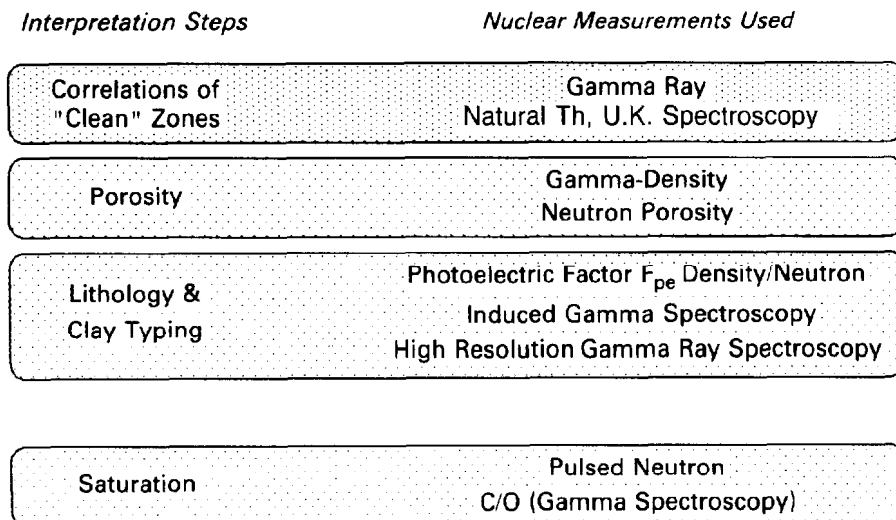


Fig. 50.31—Four interpretation tasks and the nuclear measurements associated with them.

indicates four of the steps in the interpretation process and the nuclear measurements used to obtain the desired results. The indicated list of measurement devices or techniques is in the order of the discussion that follows.

Interpretation of Gamma Ray Measurements

The gamma ray log traditionally has been used for correlating zones from well to well, crude lithology identification, and rough volume of shale estimation. With the current state of knowledge of clay composition and other more refined lithology determinations, it is clear that the surest use of the gamma ray is, indeed, for correlation.

For estimating the volume of shale, the approach is to scan the log for minimum and maximum gamma ray readings, γ_{\min} and γ_{\max} . The minimum reading then is assumed to be the clean point and the maximum reading is taken as the shale point. Then the gamma ray reading in API units at any other point in the well, γ_{\log} , is scaled accordingly:

$$V_{sh} \propto \frac{\gamma_{\log} - \gamma_{\min}}{\gamma_{\max} - \gamma_{\min}} \quad (44)$$

This ratio usually is referred to as the gamma ray index and can be scaled into percent shaliness according to charts¹³ depending on rock type. This method is sometimes appropriate, if in fact the maximum gamma ray reading corresponds to the same type of shale as the values that are being interpreted.

Numerous examples show the deficiencies of this method, and for this reason the spectral gamma ray tool was developed. Tools of this type measure, in fact, the relative concentration of three radioactive components of the total gamma ray signal. It is interesting to point out the relationship between the concentration of the three radioactive components and the total gamma ray signal in API units. It is given by

$$\gamma_{API} = A \times Th + B \times U + C \times K \quad (45)$$

When thorium and uranium are measured in ppm and potassium in weight percent, it is found that ratios of the coefficients (A:B:C) are 1:2:4; i.e., 1 wt% K contributes four times more to γ_{API} than 1 ppm of thorium. It is obvious from this that in a shaly sand, if a mineral rich in potassium (such as mica) is present, the total gamma ray signal will increase and give a false indication of percentage shale when, in fact, this additional radioactivity is caused by the mica.

There are two solid reasons for using a spectral gamma ray measurement over the standard gamma ray, which is really reliable only for correlation. The first is for the detection of radioactive anomalies, such as referred to previously, and the second is to make some estimation of the clay types by classifying them in terms of the relative contributions of the three radioactive components. For this second point the reader is referred to publications on spectral gamma ray interpretation.¹⁸⁻²⁰

Fig. 50.32 shows a log example from the North Sea in a micaceous sand. At 10,612 to 10,620 ft, a shale is indicated that has a total gamma ray signal of about 90 API units. With just the total gamma ray as an indicator it appears that the zone 10,568 to 10,522 ft contains about half the amount of shale estimated for the lower zone. However, the decomposition of the gamma ray signal shows quite clearly that the amounts of U, Th, and K in these two zones are quite different. In fact, the upper zone is a mixture of sand and mica, whereas the lower zone is, indeed, shale.

In the next example, Fig. 50.33, the gamma ray alone would indicate that below the lower boundary of the shale bed at 12,836 ft, there is a relatively clean sand. It can be seen, however, from the K trace that the high level of potassium in the shale zone persists several feet below 12,836. This excess potassium was found to be caused by feldspar, which has considerable impact on the grain density to be used in the interpretation of density logs.

The third example, Fig. 50.34, shows how a uranium-rich formation would be misinterpreted (in simple gamma ray interpretation) as being shale. The sudden increase

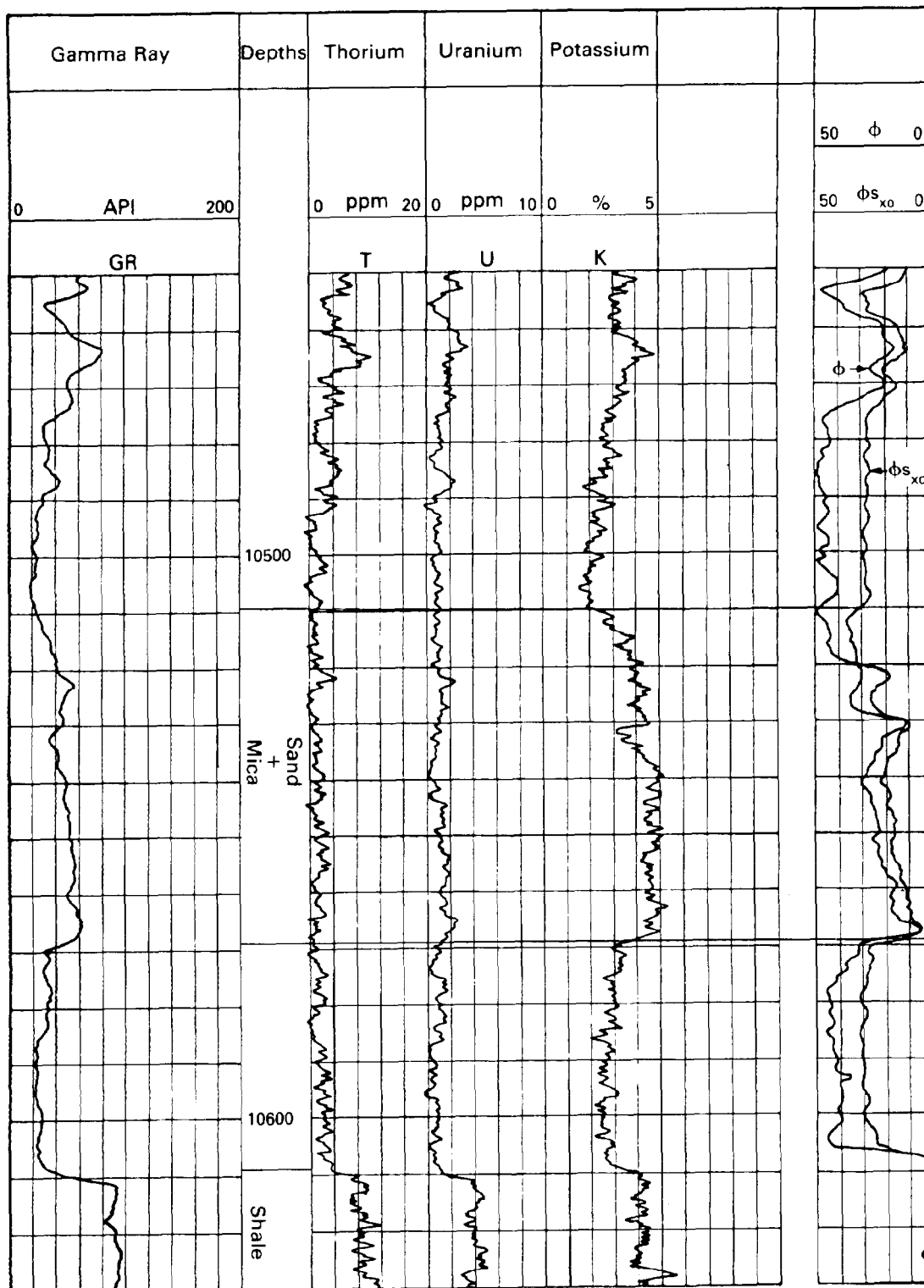


Fig. 50.32—A spectral gamma ray log from the North Sea in a micaceous sand.

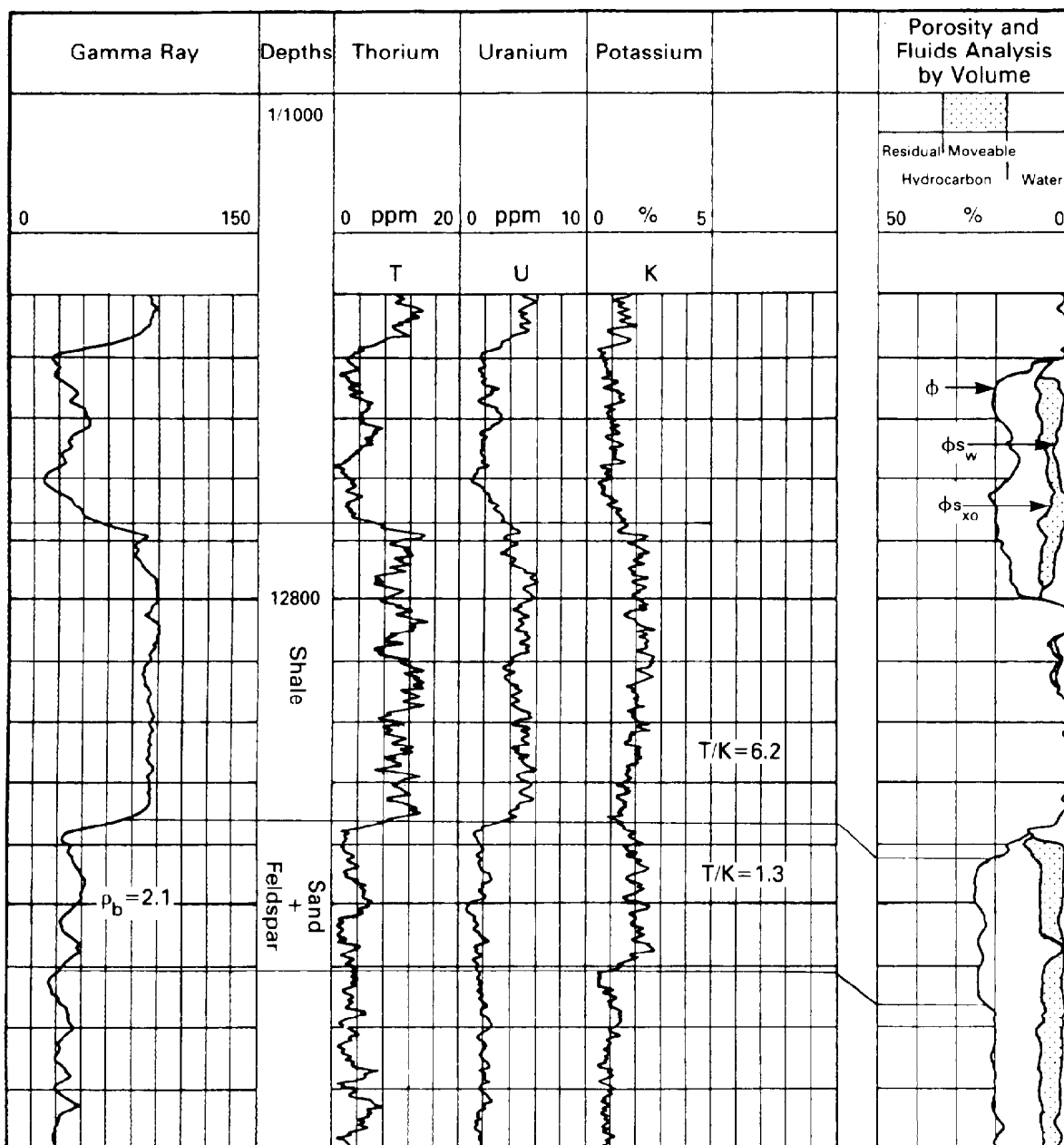


Fig. 50.33—A spectral gamma ray log from Nigeria where a continuing trace of K is attributed to the presence of feldspar.

in uranium content alone signals that this is not a simple shale of the variety in the adjacent levels. Core analysis showed this zone, however, to be rich in organic material and U is often trapped in organic complexes.

Porosity Determination

Gamma-Gamma Density Devices. The basic output of the gamma-gamma density device, bulk density, is conceptually the simplest measured parameter to interpret in terms of porosity. The basic relation (Eq. 1) is

$$\rho_b = \phi \rho_f + (1 - \phi) \rho_{ma}$$

which volumetrically links the density of the pore fluid, ρ_f , and the rock matrix density, ρ_{ma} , to the bulk density, ρ_b .

However, there are a few difficulties to overcome to interpret the output of such a density device, especially the matter of electron density index, ρ_e . It was shown in an earlier discussion that the gamma-gamma density device is measuring the electron density index. Table 50.3 shows a comparison between bulk density and electron density index. It is in close correspondence for nearly all the compounds listed except for water and hydrocarbons. This is because the average value of Z/A is about $1/2$ for all elements except hydrogen. It is seen that because of

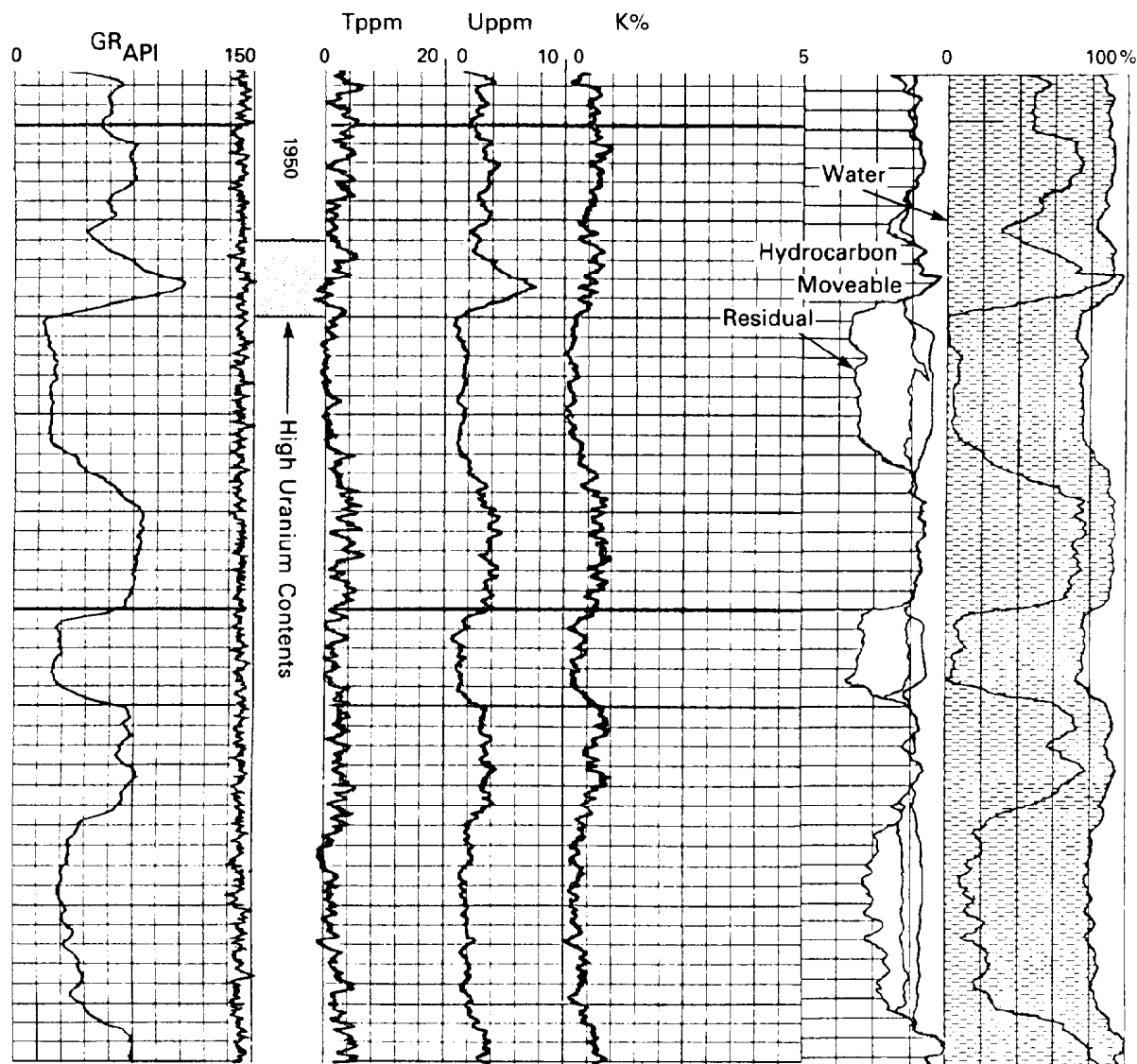


Fig. 50.34—A spectral gamma ray log showing a zone of anomalous U concentration.

this discrepancy for hydrogen, the bulk density and electron density index of water differ by about 11%.

To compensate for this fact, a simple transform of the electron density index is made so that in water-filled limestone the transformed or log density, ρ_{\log} , agrees with the bulk density. Fig. 50.35 shows this simple transform where the bulk density for 0-PU limestone and water are plotted against the electron density values. The equation of the straight line connecting these two points,

$$\rho_b = 1.0704\rho_e - 0.188, \quad (46)$$

corresponds to the published transform¹⁴ used by the logging companies. It is worthwhile to point out that this transformed density, ρ_{\log} , will also agree to within 0.004 g/cm³ for the other principal matrix materials listed in the table.

Returning to the interpretation problem, the solution of Eq. 1 for porosity yields

$$\phi = \frac{\rho_{ma} - \rho_b}{\rho_{ma} - \rho_f}, \quad (47)$$

so the problem rests on knowing the values to insert for fluid and matrix density. Before examining the means for determining these values, it is perhaps of some interest to know to what precision these two parameters must be known.

It is interesting to look at the uncertainty that can be tolerated on the value used for the matrix density, ρ_{ma} . From the previous equation we can write

$$\partial\phi = \left[\frac{\rho_b - \rho_{ma}}{(\rho_f - \rho_{ma})^2} - \frac{1}{\rho_f - \rho_{ma}} \right] \partial\rho_{ma} \quad (48)$$

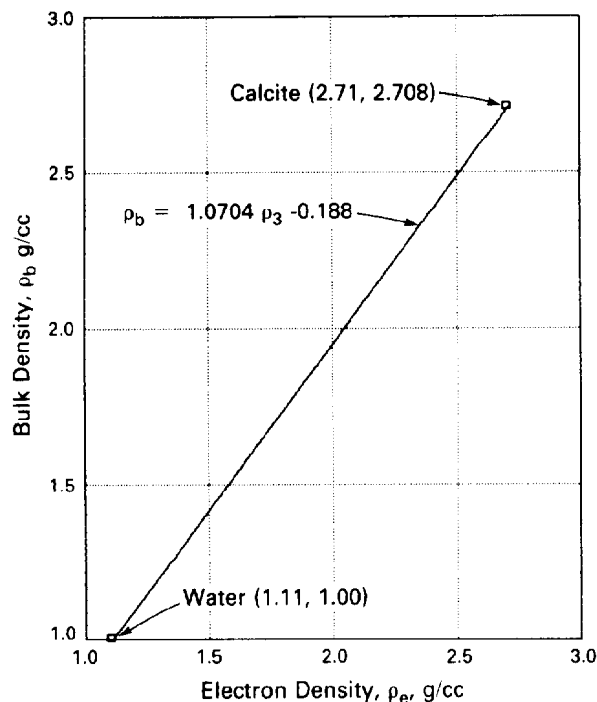


Fig. 50.35—The transform between the measured electron density index, ρ_e , and bulk density, ρ_b .

If this is evaluated for the case of a sand of about 30% porosity we can use the values $\rho_b = 2.16$, $\rho_f = 1.00$, and $\rho_{ma} = 2.65$ and obtain

$$d\phi = 0.43d\rho_{ma} \quad (49)$$

Thus, for the uncertainty in ϕ to be less than 0.02, the uncertainty in ρ_{ma} must be less than 0.05 g/cm^3 . A more detailed analysis of the uncertainty in grain density that can be tolerated can be found in Ref. 21.

For values of fluid density it is necessary to know the type of fluid in the pores. The fluid density for hydrocarbon may range from 0.2 to 0.8. Salt-saturated water (NaCl) may be as high as 1.2 g/cm^3 , and with the presence of CaCl_2 , values even as great as 1.4 g/cm^3 may occur. However, the uncertainty that can be tolerated in ρ_f is much greater than that for ρ_{ma} . An error analysis of Eq. 47 for the values chosen above shows that $\partial\phi = 0.18\partial\rho_f$, which allows about double the margin of error.

The value for matrix density in simple cases can be taken from Table 50.3, which shows a rather narrow variation between 2.65 g/cm^3 for quartz and 2.96 g/cm^3 for anhydrite. Grain densities for shales are an entirely separate matter and will not be covered here. The obvious problem left is assigning a matrix density, which can only be done with a knowledge of the lithology. In essence, all density interpretation aimed at porosity determination revolves on this.

Before going on to the determination of lithology and thus an estimate of grain density, quality control of the density measurement should be discussed.

As mentioned earlier, the modern gamma-gamma density devices are compensated measuring devices. They use two detectors at different spacings from the gamma ray source to compensate for the possible intervening presence of mudcake or drilling fluid. Normally, in addition to the density curve the log will also show a trace of the compensation, generally referred to as the $\Delta\rho$ curve. This curve represents the correction made to the apparent density seen by the long-spacing detector (ρ_{ls}) based on the discrepancy between the long- and short-spacing measurements.

The counting rate from either detector can be converted to an apparent density after a series of laboratory calibrations.²² If there is not any intervening material between the tool surface and the formation being measured, then the two values will be equal. As the mudcake thickness increases, the two density values will diverge for some reasonable value of thickness (generally less than 1 in.). The quantity $\Delta\rho$ is determined by experimentation, as a function of the density differences, to be the amount to be added to the apparent long-spacing density, ρ_{ls} , to match the bulk density of the formation—i.e.,

$$\rho_b = \rho_{ls} + \Delta\rho \quad (50)$$

Although it commonly is thought that $\Delta\rho$ is a measure of the mudcake thickness, h_{mc} , it is, in fact, proportional to the product of mudcake thickness and the density contrast between the mudcake, ρ_{mc} , and the formation density—i.e.,

$$\Delta\rho \propto h_{mc}(\rho_b - \rho_{mc}) \quad (51)$$

Beyond some thickness (~ 1 in.), the compensation scheme will break down and the ρ_b value will be in doubt. However, this point cannot be identified simply by use of a cutoff value of $\Delta\rho$. A very small gap of water ($\rho_{mc} = 1$) in front of a low-porosity formation would yield a large value of $\Delta\rho$ and yet be perfectly compensated for, whereas a 1-in.-thick mudcake of medium density in front of a high-porosity zone may yield a small $\Delta\rho$ with some residual error in the compensation. Nonetheless, it is certain that the $\Delta\rho$ curve will be used as quality control on the bulk density with some fixed cutoff value despite this caution.

Neutron Porosity Devices. Modern neutron porosity devices are of two types, depending on the energy range of detection: thermal or epithermal. By convention, the log output usually is scaled in equivalent limestone porosity units. Under appropriate circumstances, this would correspond to the true porosity of a clean, water-filled limestone formation. In the following discussion it is assumed that the log reading already has been corrected for the various environmental effects. In addition to the environmental corrections that must be made before the porosity values are interpreted, there are three effects that must be considered in more detail.

Matrix Effect. As in density logging, it is necessary to know the rock matrix to make any practical use of the apparent limestone porosity value measured. Fig. 50.36 shows, for a thermal and an epithermal device, the matrix correction necessary to transform the measured units into the appropriate porosity units. It should be noted that these

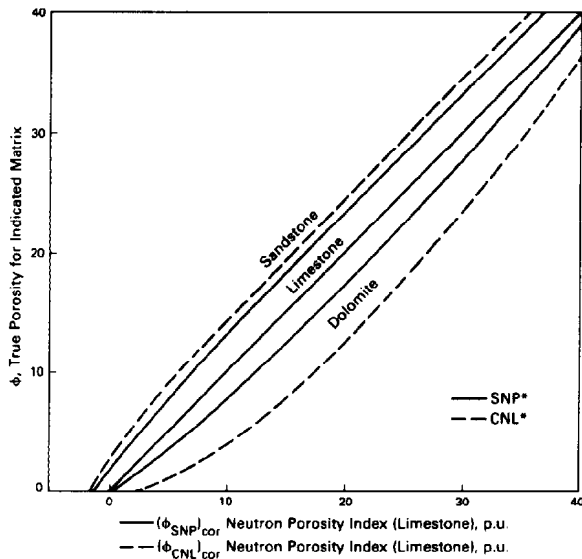


Fig. 50.36—Matrix correction chart for two specific neutron porosity tools.

two charts are for two very specific tools (CNL* and SNP*). When such tools are involved, the appropriate chart for the corresponding tool should be used, since some of the so-called matrix effect is tool-design dependent. However, a large part of the matrix effect can be understood in terms of the two basic parameters used to describe the bulk parameters of the formation (i.e., the slowing-down length and the migration length).

First consider the case of epithermal detection. To demonstrate the construction of the matrix-effect correction curves, there are four steps to consider.

1. The first step is the link between the measurement (for this case we take the simple case of using the ratio of near- to far-detector counting rate) and porosity in the primary laboratory calibration standards. This is a freshwater-filled limestone with 8-in. borehole. Fig. 50.37 shows the behavior of the ratio, $F = N_{Nn}/N_{Nf}$, as a function of limestone porosity, ϕ_{ls} . From this plot a fit can be established to ascribe a functional relationship between the measured parameter F and the limestone porosity ϕ_{ls} ,

$$F = f(\phi_{ls}). \quad (52)$$

2. In the second step, the relationship between the measured parameter F and the slowing-down length, L_s , must be established for measurement in all three of the principal matrices. That this can be done easily is shown in Fig. 50.38, where measurements in quartz, dolomite, and limestone are shown for a range of porosities. From this plot a new fit can be found,

$$F = f(L_s), \quad (53)$$

*Mark of Schlumberger.

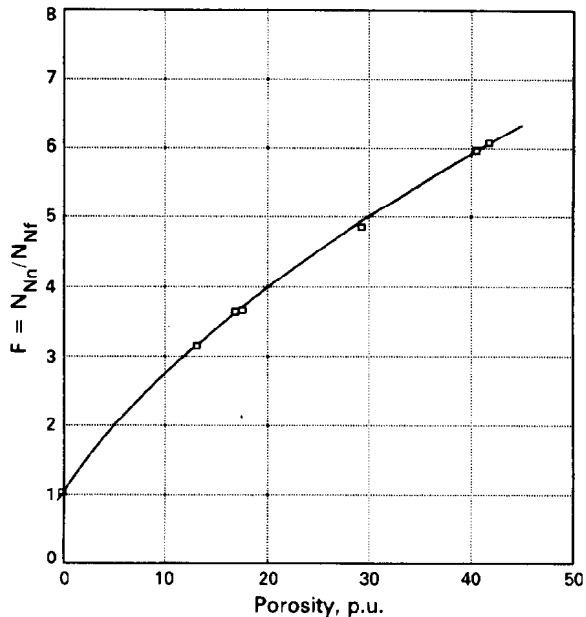


Fig. 50.37—Experimental values for the ratio of epithermal counting rates as a function of porosity in limestone calibration formations.

that allows the prediction of the measured ratio from the known slowing-down length of the formation.

3. The next step is to establish the connection between the slowing-down length, L_s , and porosity for limestone as shown in Fig. 50.39 and seen earlier in Fig. 50.11. This curve now represents the limestone “transform” of Eq. 52 and the porosity axis represents true porosity.

4. The slowing-down lengths of sandstone and dolomite now are calculated as a function of porosity and are shown also in Fig. 50.39. They fall on either side of the limestone response because of their different chemical compositions, which influence their slowing-down lengths.

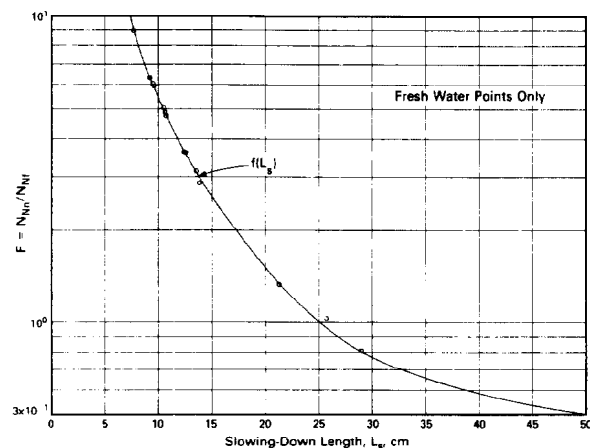


Fig. 50.38—Data of Fig. 50.37 plotted as a function of the equivalent slowing-down length, L_s , of the corresponding formations.

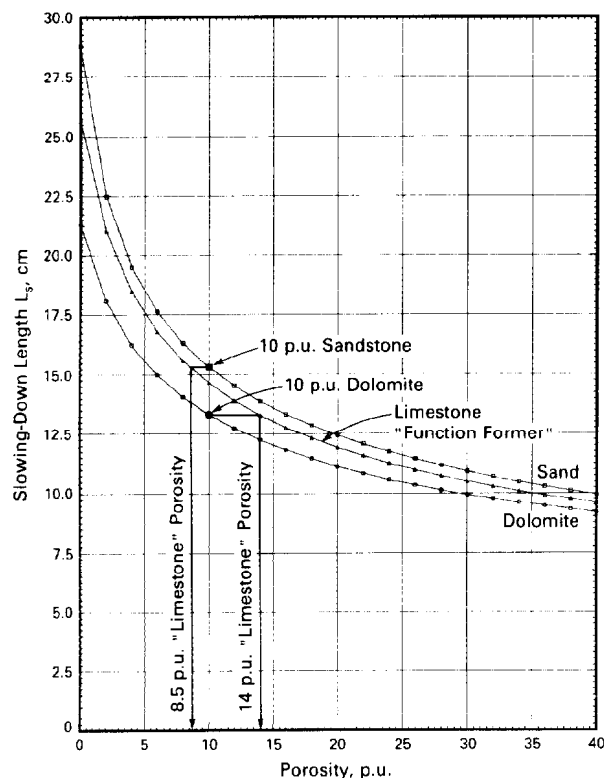


Fig. 50.39—Estimation of the epithermal matrix effect from slowing-down length, L_s , as a function of porosity for sandstone and dolomite.

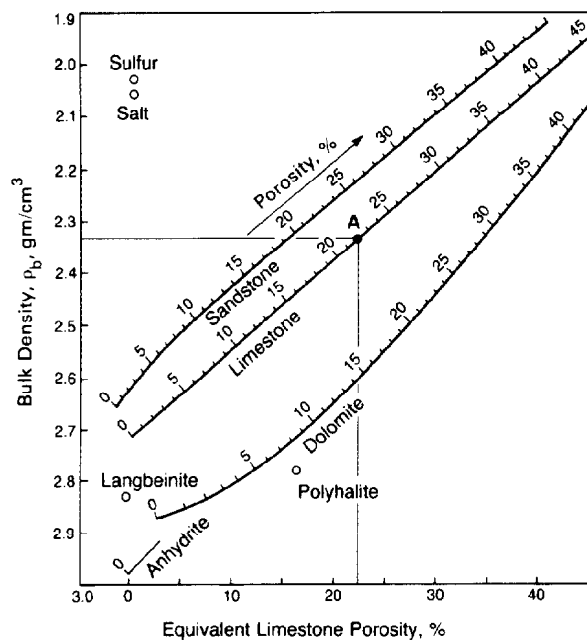


Fig. 50.40—A neutron/density cross plot for a thermal neutron porosity device. The lithology of a formation can be identified by plotting points representing ϕ_n (in limestone porosity units) and ρ_b . Point A may represent a 22-p.u. limestone or, less likely, a mixture of sandstone and dolomite.

The apparent limestone porosity for either formation can be found by selecting a porosity, 10-PU sandstone for example, and finding the corresponding slowing-down length (approximately 15.5 cm). The apparent limestone porosity then is obtained by finding the porosity associated with the limestone formation of the same L_s value. In this case it is 8.5 PU. The same case for dolomite indicates 14 PU instead of 10 PU.

A similar procedure can be used for a thermal neutron porosity device. As shown earlier, it has been found useful to cast the results in terms of the migration length L_m .⁹ Because the L_m contains some information concerning the macroscopic thermal absorption cross section, the results are qualitatively similar to the preceding but differ slightly in magnitude. This can be seen by performing the preceding exercise on the plots of L_m vs. porosity of Fig. 50.25.

Fig. 50.40 shows the neutron/density crossplot for a dual-detector thermal device. The matrix effect can be observed by comparing the equiporosity points on the individual lithology lines with the apparent limestone porosity scale on the abscissa. These discrepancies are the same as indicated in the portion of Fig. 50.36 indicated as "thermal." Ref. 23 discusses the effect of absorbers on the thermal tool response.

Gas Effect. Neutron porosity devices have been calibrated for liquid-filled porosity. However, the replacement of the liquid in the pores by gas will have a considerable impact on the slowing-down length of the formation and thus on the apparent porosity. In general terms, partial replacement of the water component of the mixture by a much lighter gas will increase the neutron slowing-down length and thus the apparent porosity will decrease. The actual apparent porosity decrease will be a function primarily of the true porosity, the water saturation, the gas density, and, to some extent, the lithology. In a situation such as this, replacement of fluid in the pores by a less-dense gas will decrease the bulk density of the formation. These two effects have been exploited in well logging by making the density and neutron porosity measurements in a single measurement pass. On the log presentation these two effects cause the density and neutron traces to separate, which can be recognized easily as being caused by the presence of gas, if the invasion is less than 6 in.

To quantify the traditional neutron-density gas separation indication and to illustrate the possibility of estimating gas saturation from an epithermal neutron measurement and a density measurement, consider Figs. 50.41 and 50.42. In both these figures the slowing-down length of a sand formation has been computed between zero and 40 PU at 2-PU increments. These values of slowing-down length have been plotted as a function of the corresponding bulk density of the formation for the five gas saturations indicated on the figures. In the case of Fig. 50.41, the gas density, ρ_g , has been taken to be 0.001 g/cm³, and in Fig. 50.42, the gas density has been taken to be about 0.25 g/cm³, which covers the entire range possible under normal reservoir conditions. In either case it is clear that, for the presence of gas at a fixed porosity, the slowing-down length is larger than that associated with the water-filled porosity. The interpretation of this larger value of L_s is an apparent decrease in porosity. In the case of the total gas saturation curve of

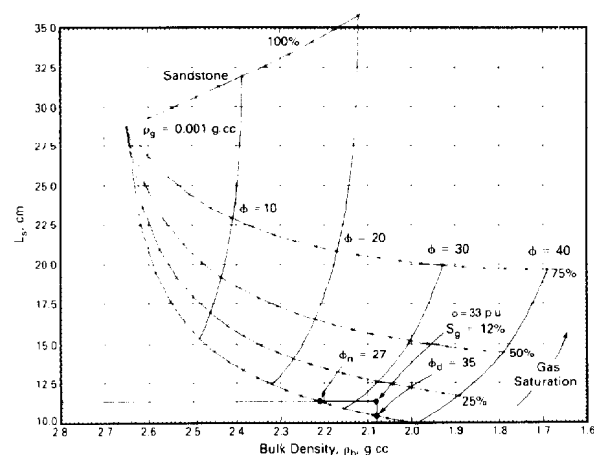


Fig. 50.41—A plot of slowing-down length, L_s , vs. bulk density, ρ_b , for sandstone formations with varying gas saturation. Invasion of borehole fluid is assumed to be negligible and the gas density is taken to be 0.001 g/cm³.

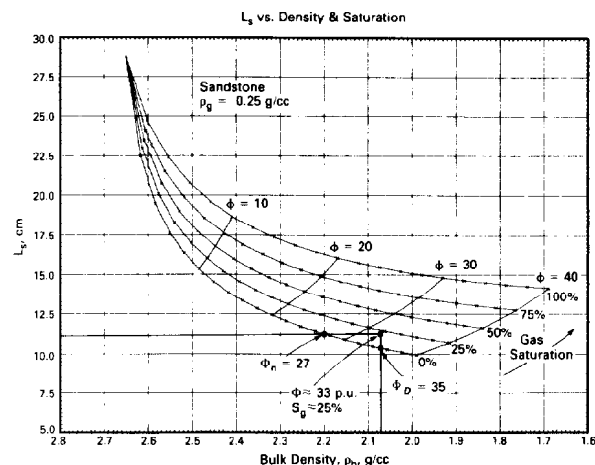


Fig. 50.42—Effect of gas saturation in sandstone for a gas density of 0.25 g/cm³.

Fig. 50.41, L_s values greater than ~ 28 cm would correspond to zero or negative apparent porosities on the log readings.

On the plots of L_s vs. ρ_b , a pair of points (L_s , ρ_b) will yield the saturation and porosity corresponding to the conditions of gas density specified. For both figures the assumption for the calculation is that the matrix is sandstone with no shale. The gas density difference for the two plots spans the range of expected gas densities. The saturation referred to on the figures is with reference to a gas/water mixture. For the lowest curve on both figures, the porosity is entirely filled with water.

Since the slowing-down length normally is not presented on a neutron porosity log, an example taken from the log of Fig. 50.43 can serve as a guide. From the gas zone clearly indicated on this figure we can use the following values for the illustration: ϕ_N , neutron porosity (sand) = 27 PU and ϕ_D , density porosity (sand) = 35 PU.

The lowermost curves on Figs. 50.41 and 50.42 serve to determine the correspondence between ϕ_N and the slowing-down length, L_s . It is indicated by the horizontal line to be about 11 cm for this example. The density porosity of 35 PU can be seen to correspond to a density of about 2.07 g/cm³, as indicated by the vertical line. The intersection of these two points at the coordinate (2.07, 11), shown in the figure, indicates about 25% gas saturation in the case of a gas density of 0.25 g/cm³ (Fig. 50.42), and a saturation of about 12.5% if the gas density is taken to be nearly zero. The porosity of the formation can be found by following the slope of the equiporosity lines from the example coordinate to the lower liquid-saturated line and is seen to indicate a value of about 33 PU for both cases.

With more information concerning the gas properties of a reservoir, this interpretation can be used instead to yield an indication of the invasion of the drilling fluid into the zone of investigation of the neutron and density devices.

Shale Effect. Generally, the presence of shale tends to increase the neutron porosity values. The reason for this lies in two effects: additional hydrogen resulting from the

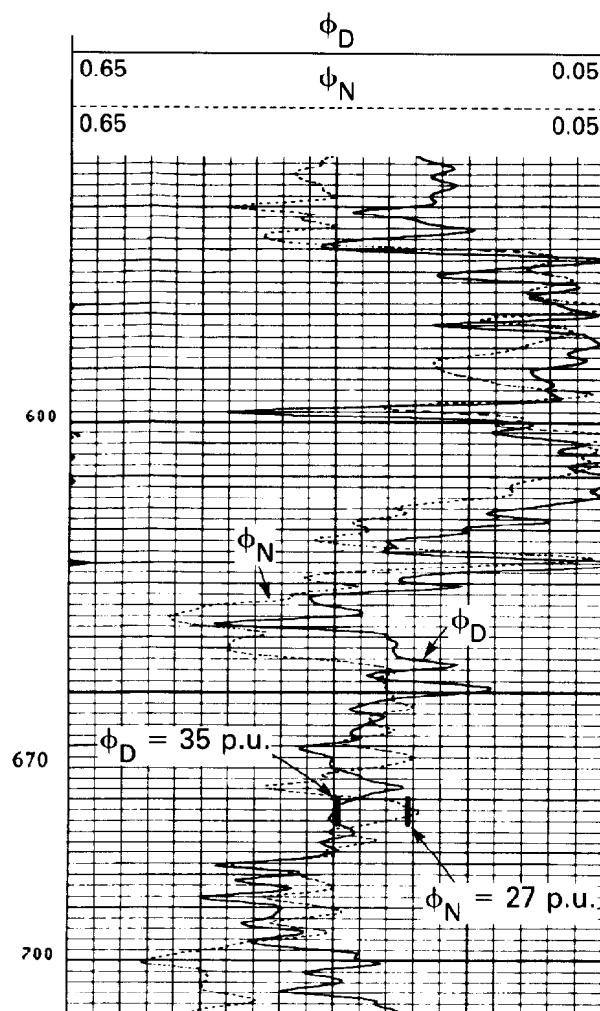


Fig. 50.43—Log example of the neutron/density combination exhibiting the characteristic crossover behavior in a gas zone.

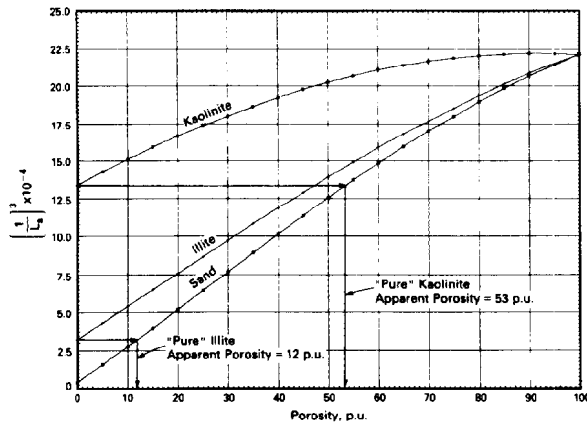


Fig. 50.44—Comparison of $(1/L_s)^3$ for sandstone, kaolinite, and illite as a function of porosity. The apparent porosity of pure illite is seen to be about 53 p.u. and for illite, 12 p.u.

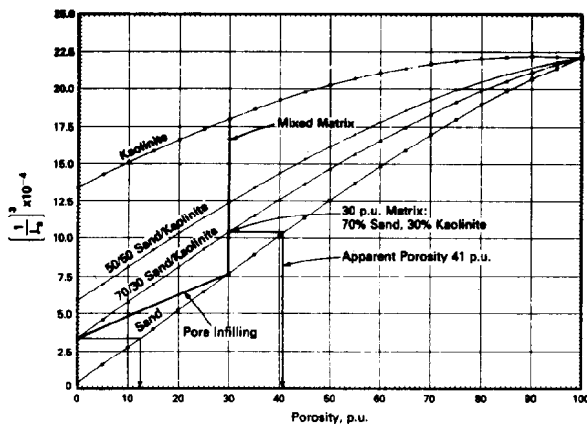


Fig. 50.45—Variation of $(1/L_s)^3$ vs. porosity for sand and sand/kaolinite mixtures. A line at 30 p.u. indicates the effect of changing the matrix from sand to kaolinite, and another indicates the change in $(1/L_s)^3$ expected when the 30 p.u. is filled progressively with kaolinite.

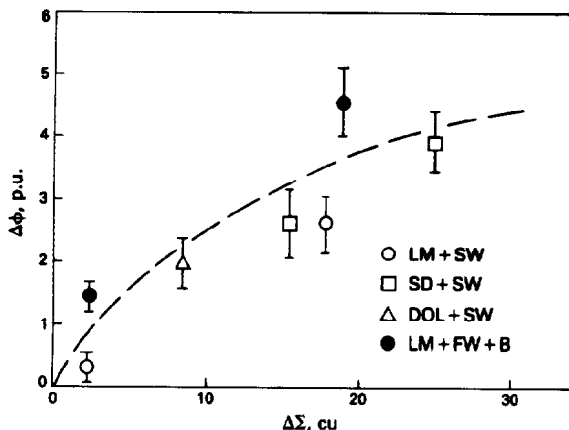


Fig. 50.46—Correction for a thermal neutron porosity tool as a function of the formation, Σ .²⁴

hydroxyls in the clay minerals, and in the case of thermal porosity devices, the possibility of additional thermal neutron absorbers such as boron associated with the clay minerals.

Initially, consider the case of thermal absorbers and consider just two types of clay minerals, kaolinite and illite. For these two clays (and many others) we refer to the data compiled by Edmundson *et al.*⁹ The chemical formula for kaolinite is $\text{Al}_4\text{Si}_4\text{O}_{10}(\text{OH})_8$ and the formula for illite is $\text{K}_2\text{Si}_6\text{Al}_3\text{Fe}_3\text{O}_{20}(\text{OH})_4$.

The important point to note about these formulations is the differing amount of (OH). A rough calculation indicates that kaolinite has about one-third the hydrogen density of water and that illite, with a lesser amount of hydroxyls, has about one-tenth the hydrogen density of water. In the case of either of these "pure" clay minerals, a neutron porosity device will detect some large value of porosity, since the slowing-down length will be influenced greatly by the presence of the (OH) components.

That the slowing-down length is considerably affected can be seen in Fig. 50.44, which shows the value of L_s of sand, illite, and kaolinite from 0 to 100 PU. The ordinate in this figure is $(1/L_s)^3$, which has been chosen because it tends to vary linearly with the combination of two materials of differing values of L_s . Values for the two pure clay minerals are indicated at 0 PU. From the figure, the apparent porosity would be about 53 PU for pure kaolinite and about 12 PU for illite. This is consistent with the trend expected from the hydrogen density. For the slowing-down length, the choice of the replacement of three Fe atoms for three Al atoms is immaterial, but it will have an impact on the thermal neutron absorption because of capture by the iron.

By using a plot similar to Fig. 50.44, the expected response of an epithermal neutron porosity device to a mixture of kaolinite and sand can be predicted. Fig. 50.45 shows an example of this. In the case of a true 30 PU (that is, 30% of the volume is water-filled), the mixed-matrix line indicates the change of L_s with a change in the sand/kaolinite matrix. Following the indicated line, a matrix of 70% sand and 30% kaolinite would have an apparent porosity of about 41% compared to the actual value of 30%.

On the other hand, we can take the case of 30 PU, or more precisely the case of 70 vol% being sand, and ask what happens to the value of L_s as the porosity is filled with kaolinite. This process also is indicated by the porosity-infilling line in Fig. 50.45. It is clear that the endpoint of this line must lie on the line of the 30/70 kaolinite mixture. As indicated in this case, the minimum apparent porosity as deduced from the slowing-down length will be about 12 PU where, in fact, there will be no porosity available for fluids.

The impact on thermal neutron porosity devices is somewhat more difficult to predict and will depend in detail on the tool design and consequent response. A similar type of graphical construction using the migration length instead of the slowing-down length can be used to see that for the normal neutron absorbers, such as iron, in the clay minerals there is not a large effect. However, if boron is present in any substantial quantity, this will not be the case. To deal with this problem Arnold *et al.*²⁴ have determined experimentally a correction for the apparent porosity of a dual-detector thermal neutron porosity

device as a function of the macroscopic absorption cross section $\Delta\Sigma$ of the formation. It is shown in Fig. 50.46.

Despite the foregoing discussion, it must be recognized that neutron porosity devices do, in fact, respond to porosity, among other things. The dynamic range of the measurement at low porosity is excellent because of the sensitivity of the slowing-down length in this range. The problems of interpretation caused by the influence of shale are tractable when the neutron measurements are combined with other tools.

Lithology Determination

Neutron/Density Combination. One of the traditional methods of lithology interpretation is the neutron/density combination. The useful property of combining these two measurements can be seen in Fig. 50.40: the three principal lithologies form three different response lines. The grain density, ρ_{ma} , increases in an almost linear fashion from sand to dolomite, so that it is tempting to draw lines of equal grain density for intermediate points that do not lie on any of the three lines. This type of presentation is shown in Fig. 50.47. With this approach, the particular lithology mixture is not of great importance but a fair estimation of the appropriate grain density is obtained despite the fact that ρ_{ma} is not a characterizing parameter for neutron logs.

The combination of the neutron and density measurements in this fashion can solve only simple binary mineral combinations. To interpret the results unambiguously, the two minerals must be known. For example, one can imagine a result, marked as Point A on Fig. 50.40, arising from a formation consisting of a sand and dolomite mixture. In this case, with no additional knowledge, the interpretation of the indicated point, intermediate between dolomite and sandstone, would be limestone.

Photoelectric Factor. Discrepancies such as these can be resolved by the use of additional information. In particular, one such nuclear measurement is the photoelectric factor, F_{pe} . It is convenient for purposes of interpretation to use the quantity U (Eq. 36). It has the property of combining volumetrically for the case of several substances being present in the scattering region whose individual absorption characteristics can be computed. For a two-component system (fluid and matrix) of porosity ϕ this can be written as

$$U = U_f \phi + U_{ma}(1 - \phi). \quad (54)$$

F_{pe} for this mixture then can be determined from Eq. 36, where

$$\rho_e = (\rho_e)_f \phi + (\rho_e)_{ma}(1 - \phi). \quad (55)$$

The results of this type of computation are shown in the crossplot of Fig. 50.48, which shows how F_{pe} varies as a function of density for the three principal matrices: limestone, dolomite, and sandstone. The interesting thing about this presentation is the order in which the three lines fall; dolomite now is bracketed by limestone and sandstone. It is obvious that in the hypothetical case of the sandy dolomite, given previously, the ambiguity about the presence of limestone would be removed when inspecting the corresponding value of F_{pe} . In this case it would clearly indicate a sand/dolomite mixture.

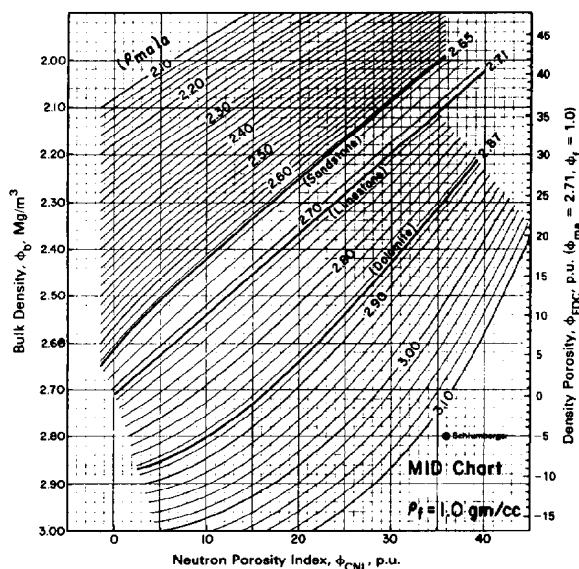


Fig. 50.47—Extracting apparent grain density, ρ_{ma} , from the neutron/density cross plot.

One elementary use of the F_{pe} curve in conjunction with density is to make a simple two-mineral model. This is no more than formalization of the relationships seen in the preceding figure. This is done by solving the following set of equations for U and ρ , and using the fact that the volumes sum to unity:

$$U_{log} = U_1 V_1 + U_2 V_2 + U_f \phi,$$

$$\rho_{log} = \rho_1 V_1 + \rho_2 V_2 + \rho_f \phi, \quad (56)$$

and

$$1 = V_1 + V_2 + \phi.$$

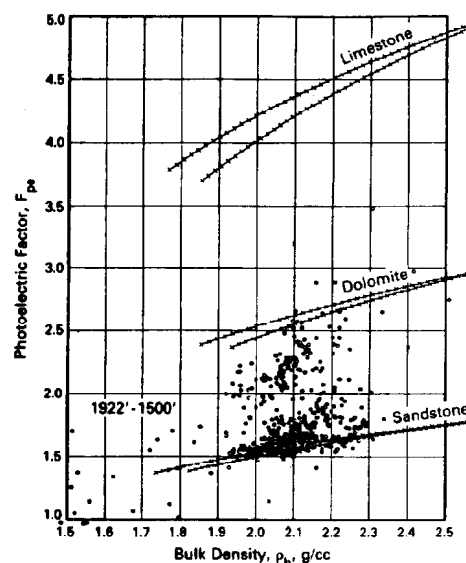


Fig. 50.48—A cross plot of the photoelectric factor vs. density. Lines for the three principal matrices are indicated. The points represent the sampled log data.

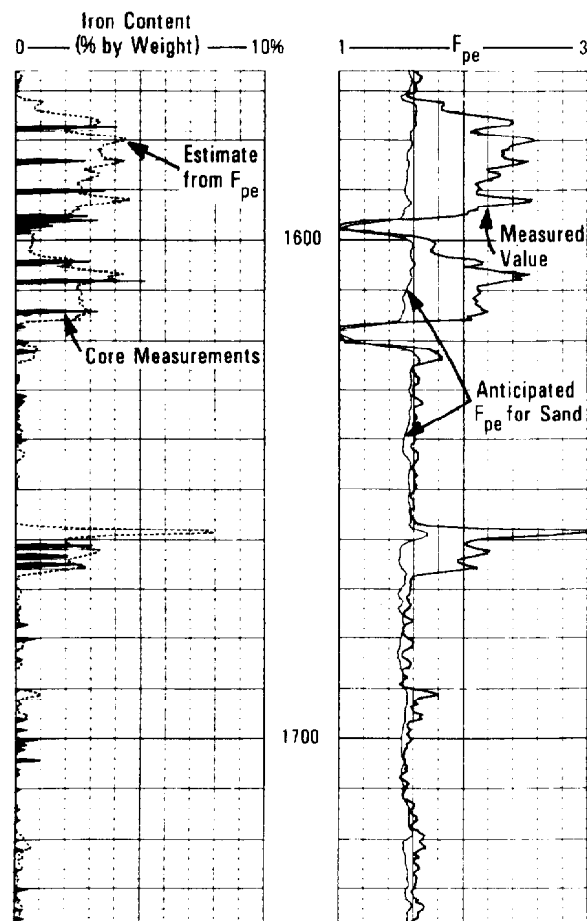


Fig. 50.49—A log example showing the conversion of the excess F_{pe} in a shaly sand to the weight fraction of iron. In Track 1, the estimate from F_{pe} (Eq. 61) is compared to values obtained by core analysis.

The indicated parameters for the two suspected minerals can be inserted in this equation to solve for the appropriate porosity and lithology mix.

However, there is no reason to limit this type of analysis to two minerals. It can be expanded to many more with the addition of supplementary measurements such as Th, U, K, Al, Fe, and Si. The natural combination with the gamma ray spectral information has been shown useful for complex mineralogy in which two different three-mineral combinations can be treated.²⁵

Another interesting use of F_{pe} can be to get an estimation of shale in sand. The F_{pe} values measured in shales are related primarily to their iron content. For an example of this application, refer to Fig. 50.48. The data points shown on the crossplot are from some sand and shale sequences. The clean-sand points are evident by their placement with respect to the indicated sand line. The shale points are those scattered to higher values of F_{pe} . In this case the lithology measurement is responding to the photoelectric absorption resulting from the iron associated with the shale. In this particular case the shale is known to be a mixture of kaolinite and illite and the iron is associated with the illite.

To demonstrate the quantitative nature of the F_{pe} measurement, consider the following argument for the determination of the weight percent of a trace photoelectric absorber in an otherwise two-component system. If F_{pex} represents the photoelectric factor of the trace absorber and the associated volume fraction is V_x (which is considered to be much smaller than unity), the following approximate equation applies:

$$U \approx U_f \phi + U_{ma}(1 - \phi) + U_x V_x, \quad (57)$$

where $V_x \ll 1$ and

$$U_x = \rho_{ex} F_{pex}. \quad (58)$$

Note that the third term in this equation represents the product of the trace element absorption factor and its associated mass contained in 1 cm^3 :

$$U_x V_x = F_{pex} \rho_x V_x. \quad (59)$$

Thus, the weight per cubic centimeter of the absorber can be determined from the measured parameter (i.e., from the product of the measured ρ and F_{pe}) U from the following:

$$\rho_x V_x = \frac{U - U_f \phi - U_{ma}(1 - \phi)}{F_{pex}}. \quad (60)$$

The fraction by weight of the solid fraction, f_x , is then given by

$$f_x = \frac{U - U_f \phi - U_{ma}(1 - \phi)}{F_{pex} \rho_{ma}(1 - \phi)}. \quad (61)$$

An interesting application of this idea is shown for the log data of Fig. 50.48. The measured F_{pe} curve is shown in Track 2 of Fig. 50.49 along with the curve of the anticipated F_{pe} based on pure sandstone. The shading represents the "excess" photoelectric factor, which can be converted to percent weight of iron by use of the above argument. The resulting curve of the iron concentration is found in Track 1 of Fig. 50.49, along with a series of discrete measurements of the iron concentration made on the core samples. The good agreement demonstrates the validity of the supposition that, in this case, the F_{pe} measurement is responding primarily to the iron concentration in the shale and the volume of shale present. A similar procedure could be followed for any other suspected trace element of sufficient concentration and photoelectric absorption factor.

Induced-Gamma-Ray Spectroscopy. The induced gamma spectroscopy tools are very important for lithology determination in complex situations. In the case of induced capture gamma rays a large number of elements can be identified: hydrogen, silicon, calcium, iron, sulfur, and chlorine. Lithology identification can be made by comparing the yields of particular elements. For example, anhydrite is identified easily by the strong gamma ray yield from sulfur and calcium associated with this mineral.

**TABLE 50.5—ATOMIC DENSITIES IN UNITS OF
AVOGADRO'S NUMBER (6.023×10^{23})**

	Density (g/cm ³)	Oxygen (atoms/cm ³)	Carbon (atoms/cm ³)
Limestone	2.71	0.081	0.027
Dolomite	2.87	0.094	0.031
Quartz	2.65	0.088	—
Anhydrite	2.96	0.087	—
Oil	0.85	—	0.061
Water	1.0	0.056	—

Limestone can be distinguished from sandstone by comparing the silicon and calcium yields. Numerous references^{26,27} show examples of these types of procedures as well as interpretation schemes proposed by some service companies.

High-resolution spectroscopic devices will provide enormous advances in mineralogical identification. Such devices use solid-state gamma ray detectors instead of the conventional NaI detectors, which suffer from poor resolution. One of the most promising applications of such devices is the possibility of making aluminum activation measurements. Because aluminum is a common constituent of clay minerals, it is well adapted to quantitative clay content determination. As an example of the type of information that is obtainable from a high-resolution gamma ray spectroscopy device, refer to Fig. 50.50, which shows the gamma ray spectrum obtained after irradiation of the formation with a ²⁵²Cf source. Along with the gamma rays from the naturally occurring thorium, uranium, and potassium, the artificially produced radiation from manganese, sodium, aluminum, and vanadium is seen.

The gamma ray intensities from the aluminum and vanadium isotopes can be used to produce a log calibrated in weight percent of the two elements. In the case of the aluminum, the measurement is a continuous one made at about 400 ft/hr and is shown in Fig. 50.51 along with core measurements from the same well. To detect the vanadium, since it is present in rather small amounts, stationary readings were taken. These values are indicated along with error bars representing the uncertainty of the measurement caused by counting statistics. These two traces illustrate the type of detailed evaluations that can be made by logging devices, which previously could be made only with extensive core analysis.

Saturation Determination

Inelastic Gamma Ray Spectroscopy. Two nuclear tools are well adapted for the determination of saturation. The first is based on the determination of the ratio of carbon to oxygen atoms in the formation. The use of such a ratio is shown clearly in Table 50.5, where it is seen that there is a significant difference between the atomic C/O ratios of oil, water, and the common matrix minerals.

Fig. 50.52 shows how the atomic C/O ratio changes as a function of porosity and water saturation for the three principal matrices. From this figure it is clear that for clean formations of a given lithology the interpretation is relatively straightforward. An inherent difficulty in the measurement is immediately obvious. At low porosities the dynamic range of the C/O ratio as a function of water

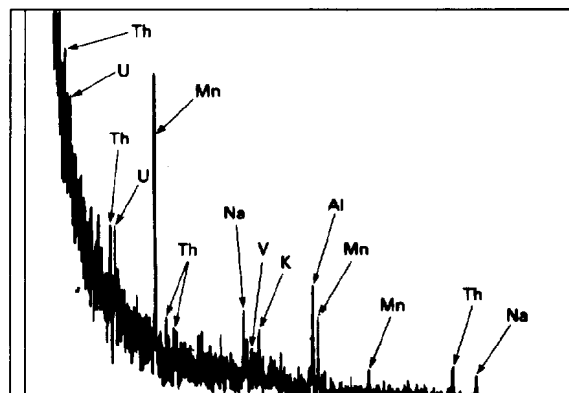


Fig. 50.50—Gamma ray spectrum obtained with a high resolution Ge gamma ray spectrometer and Cf neutron source.

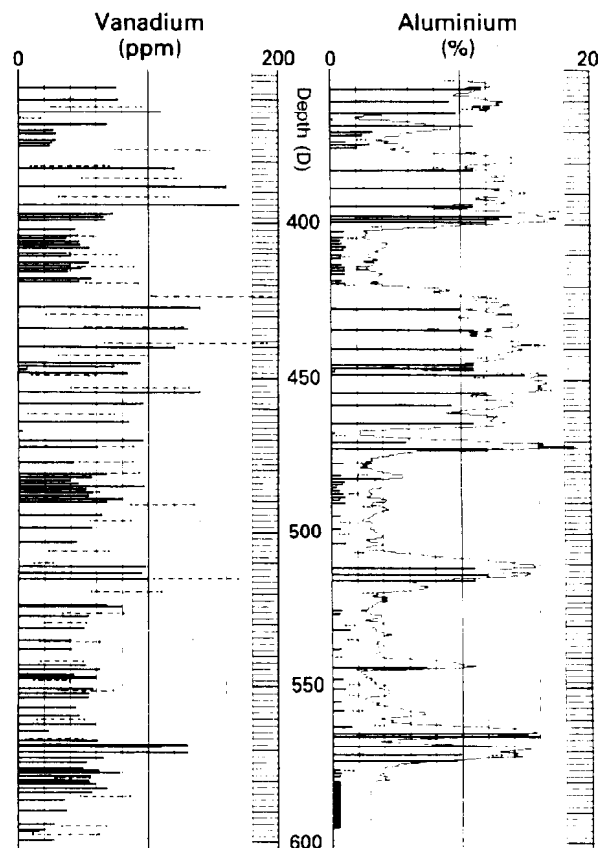


Fig. 50.51—Aluminum and vanadium logs of an oil-bearing shaly sand derived from a high-resolution gamma ray spectrometer. The solid bars represent the results of core analysis. The dashed bars indicate the log value of vanadium and its statistical uncertainty.

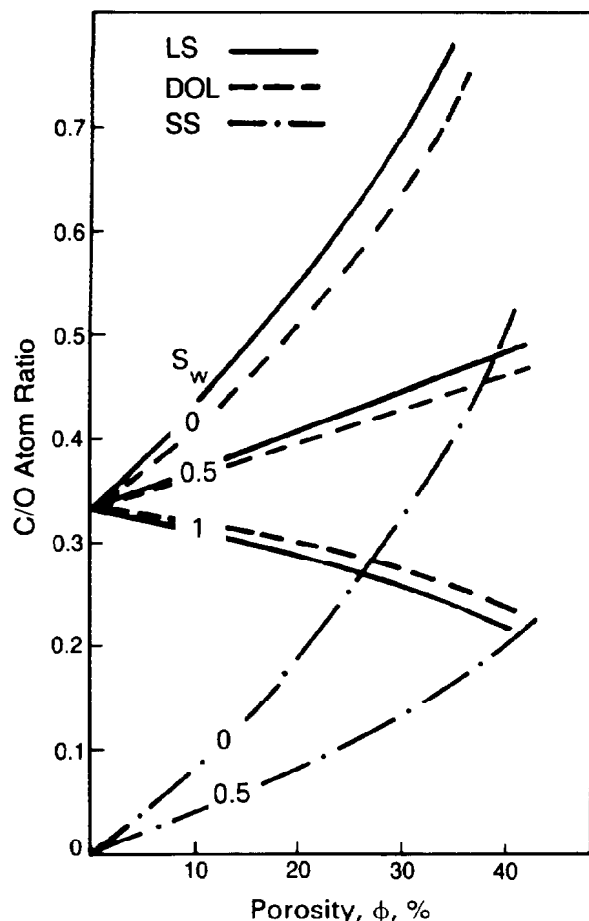


Fig. 50.52—Variation of C/O as a function of porosity and water saturation.

saturation shrinks to zero. Examples of interpretation of this ratio in more complex situations can be found in the references.^{28,29}

Pulsed Neutron Logging. The second type of nuclear device used for the determination of water saturation, particularly in cased wells, is the pulsed neutron device. This log responds primarily to the time taken for the thermal neutrons to be absorbed by the formation. The most common important thermal neutron absorber is chlorine, which is present in most formation waters. Hence, the response of the pulsed neutron tool resembles the usual openhole resistivity measurements.

The advantage, however, of the pulsed neutron technique is the ability to log in cased hole. It can distinguish between oil and salt water contained in the pores. If the porosity is known, gas/oil interfaces can be distinguished. Under ideal conditions of salinity, porosity, and lithology, the water saturation, S_w , can be computed.

In the simplest case of a single mineral, the measured value of Σ_{\log} can be thought of as consisting of two components, one from the matrix and the other from the formation fluid:

$$\Sigma_{\log} = (1 - \phi)\Sigma_{ma} + \phi\Sigma_f \quad (62)$$

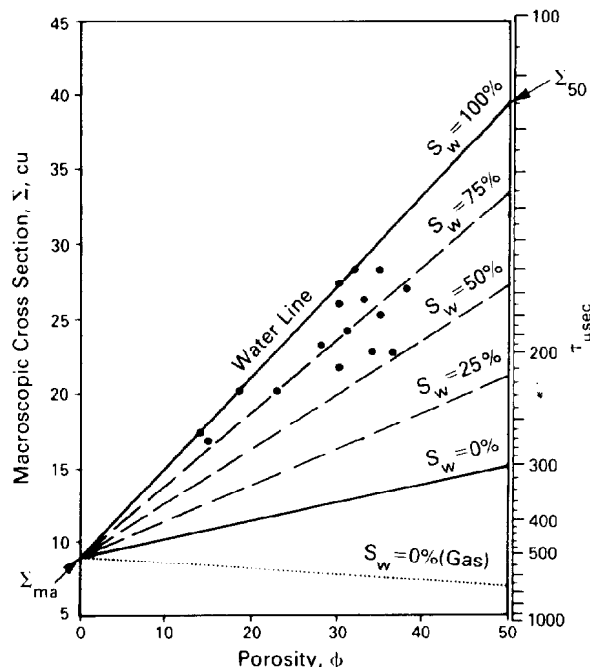


Fig. 50.53—Solution of S_w with Σ .

In terms of water saturation, the fluid component is broken into water and hydrocarbon components:

$$\Sigma_{\log} = (1 - \phi)\Sigma_{ma} + \phi S_w \Sigma_w + \phi(1 - S_w)\Sigma_h \quad (63)$$

The graphical solution of this equation for S_w is shown in Fig. 50.53. To use this approach the values of Σ_w and Σ_h must be known.

The presence of shale, which may contain thermal absorbers such as boron, will seriously disturb this simple interpretation scheme, but a number of references³⁰ indicate methods for dealing with the problem. For saturation determination, the results of a single measurement run are questionable if the water salinity is less than 50,000 ppm and if the porosity is below 15%, particularly in shaly zones.

Perhaps the greatest successful application of this type of device is in the time-lapse technique. In this procedure the change in saturation between two runs in a producing reservoir can be determined simply from the difference of the two measured Σ values, the porosity, and the difference in Σ_w and Σ_h —i.e.,

$$S_{w1} - S_{w2} = \frac{\Sigma_1 - \Sigma_2}{\phi(\Sigma_w - \Sigma_h)} \quad (64)$$

Uncertainties in the quantity (such as Σ_{ma} , Σ_{cl} , and clay volume) disappear in this differential measurement technique.

Future Interpretation Models

New interpretation models will evolve from a more fundamental approach to the interpretation of complex lithologies in which relationships are formed between the geochemistry of the formation, as determined from core analysis, and log measurements.

The premise of this approach is that the total geochemical signature of a formation may yield valuable information on the minerals present, including clays, the grain size, and other indications of the environment of deposition and diagenetic alteration. This information may be related to the types and abundances of clay minerals present, to the electrical properties of the clays and, perhaps, even to the location of the clays. It seems reasonable, for example, that chemical data can not only distinguish kaolinite from illite, but also that the chemical properties of a detrital kaolinite will differ from those of a kaolinite grown slowly in pore spaces.

One of the primary tools for the penetration into this area of interpretation is the high-resolution spectroscopic tool, which was described previously. It will enable us to obtain a precise mineral identification at each location of interest. However, other devices, such as the induced gamma ray spectroscopy tool, the gamma-gamma density device with a direct measurement of lithology, and the combination thermal and epithermal neutron device, are being examined for their responses to particular minerals of interest, for incorporation into this interpretation scheme.

In addition to the possibility of obtaining grain-size estimates from this approach and thus an additional input to permeability transforms, one result will be the real possibility of the detection, quantification, and classification of the clay minerals from log measurements.³¹ One of the primary benefits of such an interpretation output will be a reservoir damage risk assessment. This will be based on the knowledge that has been acquired through unfortunate experience concerning potential damage to a reservoir that can occur when the clay mineral content is not considered in production planning. For example, acidization of a formation containing chlorite, an iron-rich clay mineral, can produce an iron oxide gel that fills pores, ruining a potentially valuable formation. Another example is that diagenetic pore-lining kaolinite particles will remain in place at low production rates. At higher rates, however, the particles may break loose, lodge in pore throats, and damage production.

Although geochemical interpretation is in its infancy, initial experience with clay type and grain-size prediction from core analysis data and log data has been very encouraging. Refinement of this type of interpretation model may lead to a new cycle of future tool development. One can imagine measuring specific geochemical parameters with an entire range of new tools rather than inferring them from perturbations on measurements designed for other purposes.

Nomenclature

A = atomic mass
 D = thermal diffusion coefficient
 E = energy
 E_{GR} = gamma ray energy
 E_i = initial energy
 E_k = kinetic energy
 E_N = neutron energy
 E_o = energy before scattering
 E_γ = energy of mono-energetic gamma rays
 f_s = fraction by weight of solid fraction
 F = measured parameter

F_{pe} = photoelectric absorption factor
 F_{pex} = photoelectric factor of trace absorber
 h = thickness
 h_{mc} = mudcake thickness
 K = conversion constant between τ_d and Σ_{abs}
 K_a = mass absorption coefficient
 L = distance from the source
 L_d = diffusion length
 L_m = migration length
 L_s = slowing-down length
 m = mass
 M = molecular weight
 n = number of scatterers per unit volume
 \bar{n} = average number of collisions
 N_A = Avogadro's number
 N_i = initial number of particles
 N_N = number of neutrons
 N_{Nf} = neutron counting rate at far detector
 N_{Nn} = neutron counting rate at near detector
 N_p = number of particles
 N_r = counts from a radiation detector
 P = probability
 P_x = probability of having x nuclei decay in time dt
 q = probability of nonoccurrence
 r = path length (radius) to the detector
 S_w = water saturation
 t = time
 $t_{1/2}$ = half-life
 U = product of F_{pe} and electron density
 U_f = fluid parameter
 U_{ma} = matrix parameter
 U_x = trace element parameter
 v = velocity
 V_{sh} = volume of shale
 V_x = associated volume fraction
 x = number of decays
 z = particles observed
 Z = atomic number
 α = emitter
 γ_{log} = gamma ray reading in API units at any point in the well
 γ_{max} = maximum gamma ray reading
 γ_{min} = minimum gamma ray reading
 δh = thickness of slab material
 λ = decay constant
 $\bar{\mu}$ = average value of Poisson distribution
 ξ = average logarithmic energy decrement
 ρ_b = bulk density
 ρ_e = electron density index
 ρ_f = fluid density
 ρ_g = gas density
 ρ_{log} = log density
 ρ_{ls} = apparent long-spacing density
 ρ_{ma} = solid matrix density
 ρ_{mc} = mudcake density
 σ = microscopic cross section or standard deviation
 σ_{Co} = Compton cross section

σ_{pe} = cross section for the photoelectric effect
 Σ = macroscopic thermal absorption cross section
 Σ_{abs} = thermal absorption cross section
 Σ_{Co} = macroscopic Compton cross section
 Σ_f = formation fluid cross section
 Σ_h = hydrocarbon cross section
 Σ_i = macroscopic cross section
 Σ_{log} = observed formation cross section
 Σ_{ma} = matrix cross section
 Σ_t = total cross section
 Σ_w = water cross section
 τ_d = decay time
 ϕ = porosity
 ϕ_D = density porosity
 ϕ_{ls} = limestone porosity
 ϕ_N = neutron porosity
 Ψ = radiation flux
 Ψ_i = intensity of radiation
 Ψ_{epi} = flux of epithermal neutrons

References

- Evans, R.D.: *The Atomic Nucleus*, McGraw-Hill Book Co., New York City (1967) 426-38.
- Weidner, R.T. and Sells, R.L.: *Elementary Modern Physics*, Allyn and Bacon, Boston (1960) 372-78.
- Bertozzi, W., Ellis, D.V., and Wahl, J.S.: "The Physical Foundation of Formation Lithology Logging with Gamma Rays," *Geophysics* (Oct. 1981) **46**, No. 10.
- Kreft, A.: "Calculation of the Neutron Slowing Down Length in Rocks and Soils," *Nukleonika* (1974) **XIX**.
- Segesman, F.F.: "Well-logging Method," *Geophysics* (Nov. 1980) **45**, No. 11.
- Belknap, W.B. *et al.*: "API Calibration Facility for Nuclear Logs," *Drill. and Prod. Prac.*, API, Dallas (1959).
- Ellis, D.V.: "Correction of NGT Logs for the Presence of KCl and Barite Muds," paper presented at the 1982 SPWLA Annual Logging Symposium, Corpus Christi, July 6-8.
- Allen, L.S. *et al.*: "Dual-Spaced Neutron Logging for Porosity," *Geophysics* (Feb. 1967) **32**, No. 1.
- Edmundson, H. and Raymer, L.L.: "Radioactive Logging Parameters for Common Minerals," paper presented at the 1979 SPWLA Annual Logging Symposium, Tulsa, June 3-6.
- Culver, R.B., Hopkinson, E.C., and Youmans, A.H.: "Carbon/Oxygen (C/O) Logging Instrumentation," *Soc. Pet. Eng. J.* (Oct. 1974) 463-70.
- Hertzog, R.C. and Plasek, R.E.: "Neutron-Excited Gamma-Ray Spectrometry for Well Logging," *IEEE Trans. Nuc. Sci.* (Feb. 1979) NS-26, No. 1.
- The Role of Trace Metals in Petroleum*, T.F. Yen (ed.), Ann Arbor Science Publishers Inc., Ann Arbor (1975).
- Well Logging and Interpretation Techniques*, Dresser Atlas, Houston (1982).
- Log Interpretation—Vol. 1, Principles*, Schlumberger, Ridgefield, CN (1974).
- Desbrandes, R.: *Theorie et Interpretation des Diagraphies*, Editions Technip, Paris (1968).
- Serra, O.: "Diagraphies Differéces—Bases de l'Interpretation," *Bull., Cent. Rech. Explor.-Prod. Elf-Aquitaine*, Editions Technip, Paris (1979).
- Hilchie, D.W.: *Applied Openhole Log Interpretation*, Douglas W. Hilchie Inc., Golden, CO (1978).
- Hassan, M., Hossin, A., and Combaz, A.: "Fundamentals of the Differential Gamma Ray Log—Interpretation Technique," *Trans., SPWLA* (1976) paper H.
- Fertl, W.H.: "Gamma Ray Spectral Data Assists in Complex Formation Evaluation," *The Log Analyst* (Sept.-Oct. 1979) **20**, No. 5, 3-38.
- Serra, O., Baldwin, J., and Quirein, J.A.: "Theory, Interpretation and Practical Applications of Natural Gamma Ray Spectroscopy," *Trans., SPWLA* (July 1980) paper Q.
- Granberry, R.J., Jenkins, R.E., and Bush, D.C.: "Grain Density Values of Cores from some Gulf Coast Formations and their Importance in Formation Evaluation," paper presented at the 1968 SPWLA Annual Logging Symposium, New Orleans, June 23-26.
- Ellis, D.V. *et al.*: "Litho-Density Tool Calibration," *Soc. Pet. Eng. J.* (Aug. 1985) 515-23.
- Ellis, D.V. and Case, C.R.: "CNT—A Dolomite Response," paper S presented at the 1983 SPWLA Annual Logging Symposium, Calgary, June 27-30.
- Arnold, D.M. and Smith, H.D. Jr.: "Experimental Determination of Environmental Corrections for a Dual-Spaced Neutron Porosity Log," paper W presented at the 1981 SPWLA Annual Logging Symposium, Mexico City, June 23-26.
- Quirein, J.A., Gardner, J.S., and Watson, J.T.: "Combined Natural Gamma Ray Spectral/Litho-Density Measurements Applied to Complex Lithologies," paper SPE 11143 presented at the 1982 SPE Annual Technical Conference and Exhibition, New Orleans, Sept. 26-29.
- Flaum, C. and Pirie, G.: "Determination of Lithology from Induced Gamma Ray Spectroscopy," paper H presented at the 1981 SPWLA Annual Logging Symposium, Mexico City, June 23-26.
- Gilchrist, W.A. Jr. *et al.*: "Application of Gamma Ray Spectroscopy to Formation Evaluation," paper presented at the 1982 SPWLA Annual Logging Symposium, Corpus Christi, July 5-9.
- Westaway, P., Hertzog, R.C., and Plasek, R.E.: "The Gamma Spectrometer Tool Inelastic and Capture Gamma-Ray Spectroscopy for Reservoir Analysis," *Soc. Pet. Eng. J.* (June 1983) 553-64.
- Oliver, D.W., Frost, E., and Fertl, W.H.: "Continuous Carbon/Oxygen Logging—Instrumentation, Interpretive Concepts and Field Applications," paper TT presented at the 1981 SPWLA Annual Logging Symposium, Mexico City, June 23-26.
- Pulsed Neutron Logging*, W.A. Hoyer (ed.), SPWLA Reprint Volume (1979).
- Herron, M.M.: "Mineralogy from Geochemical Well Logging," paper presented at the 1984 Annual Meeting of the Clay Minerals Society, Baton Rouge, Oct. 1-4.

Chapter 51

Acoustic Logging

A. (Turk) Timur, Chevron Corp.

Introduction

Acoustic wave propagation methods have become an integral part of formation evaluation since the first downhole measurement of velocities was conducted in 1927.¹ These early measurements were conducted to obtain time/depth curves to use in interpreting seismic data.² In the 1930's, proposals were made to conduct velocity measurements in a fashion similar to electric logging, by using an acoustic transmitter and one or more receivers. First successful implementation of this technology was in the late 1940's and early 1950's.³⁻⁵ Commercial acoustic velocity logs were first introduced in 1954 by Seismograph Service Corp. in the U.S. and by United Geophysical in Canada.

Since then, technology involving borehole measurements of acoustic wave propagation properties has developed significantly and has become established as a major formation evaluation method. These acoustic wave propagation methods used in well logging can be broadly classified into two groups: transmission and reflection. Properties measured in each method and their applications in formation evaluation are listed in Table 51.1

Compressional wave velocities measured by acoustic logging were found to be related to porosity so closely that the acoustic log became a standard porosity tool, which it still is in many areas. The second most common use of borehole acoustic measurements is in evaluating cement jobs by measurements inside casing.

This chapter describes the use of acoustic wave propagation properties in formation evaluation after a brief description of elasticity, acoustic wave propagation properties in rocks, and methods of recording these in the borehole.

Elasticity

Introduction

The theory of elasticity investigates relationships between external forces applied to a body and resulting

changes in its size and shape.⁶ In this theory, it is assumed that displacements are small and the body returns to its original condition after the forces are removed. Applied forces and the resulting deformations are described by stresses and strains.

Stress is the force, F , per unit area, A , applied; strain, ϵ , is deformation per unit length, L , or volume, V , as illustrated in Fig. 51.1.

Within the elastic limit, as shown in Fig. 51.2, stresses are found to be proportional to strains (Hooke's law). The ratio of stress to strain is a different constant for different loading conditions. These proportionality constants are defined as elastic moduli, which are fundamental properties of a material.

Young's Modulus, E . This is the ratio of tensile or compressive stress (F_L/A) to the resultant strain ($\epsilon_L = \Delta L/L$):

$$E = \frac{F_L/A}{\Delta L/L}$$

Shear (or Torsion) Modulus, G . The ratio of shearing stress (F_s/A) to the shearing strain $\epsilon_s = (\Delta L/L)$ is

$$G = \frac{F_s/A}{\epsilon_s}$$

Bulk Modulus, K . Bulk modulus describes the change of V under hydrostatic pressure, p :

$$K = \frac{p}{\Delta V/V}$$

where K is also the reciprocal of compressibility, c .

TABLE 51.1—ACOUSTIC WAVE PROPAGATION METHODS

Property	Application
Transmission	seismic and geological interpretation
Compressional- and shear-wave velocities	porosity lithology hydrocarbon content geopressure detection mechanical properties of rocks
Compressional- and shear-wave attenuations	cement bond quality location of fractures rock consolidation permeability indication
Reflection	location of vugs and fractures
Transit time and amplitude of reflected waves	orientation of fractures and bed boundaries channeling and microannulus casing quality

Poisson's Ratio, μ . This is a measure of the geometric change of shape under uniaxial stress. It is expressed as the ratio of the fractional change in diameter, d , (transverse strain, ϵ_T) to the fractional change in length (longitudinal strain, ϵ_L):

$$\mu = \frac{\Delta d/d}{\Delta L/L}$$

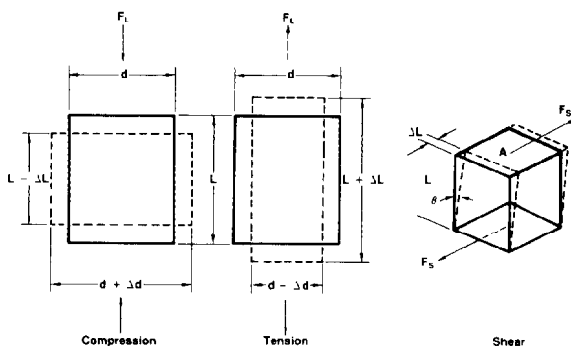
Relationships Among Elastic Parameters. These four elastic parameters are not independent; any one parameter can be expressed in terms of two others:

$$E = 2(1 + \mu)G$$

$$K = E/3(1 - 2\mu)$$

Acoustic Waves

Acoustic waves propagate mechanical energy. For instance, if an elastic material is subjected to an instantaneous force at one end, it is compressed (Fig. 51.3).

**Fig. 51.1—Longitudinal, transverse, and shear deformations.**

This disturbance is then transmitted along the material by a series of compressions and rarefactions. The disturbance travels at a constant velocity that is a fundamental property of the material. The elastic moduli and the density determine the velocity of propagation for each material.

Two types of mechanical wave propagation will be described qualitatively. Detailed discussions of acoustic wave propagation are given in Refs. 7 through 11.

Compressional Waves. Compressional waves are those in which the mechanical disturbance is transmitted by a particle motion parallel to the direction of wave propagation (Fig. 51.3). They are also called longitudinal, pressure, primary, or P-waves. Particles of the material oscillate around this rest position in simple harmonic motion. As they move from equilibrium, they push or pull their neighbors, thereby transmitting the disturbance through the material. The velocity of this compressional wave motion, v_p , is a constant for a given material:

$$v_p = \frac{1}{\rho} (K + \frac{4}{3}G)^{1/2}, \dots \dots \dots (1)$$

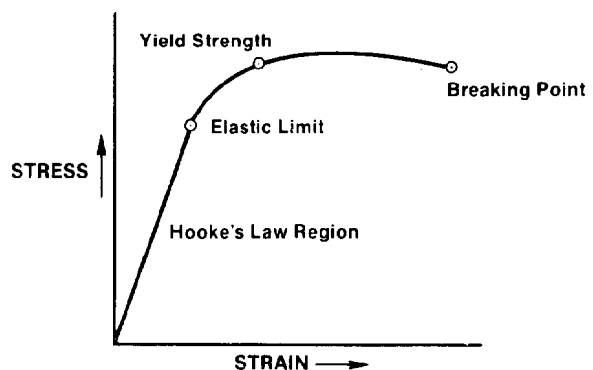
where ρ is the density.

Shear Waves. Shear waves, also called transverse, torsional, or S-waves, are those where particle motion is perpendicular to the direction of wave propagation (Fig. 51.4).

Particles in the material again move about their rest position with simple harmonic motion. For this motion to be transmitted, however, each particle must have a force of attraction to its neighbor. Whereas compressional waves can be propagated simply by elastic collision of one molecule with the next, attractive forces must exist between adjacent molecules to transmit shear waves. Since these forces are very small in gases and liquids, fluids do not transmit shear waves.

The velocity of shear waves, v_s , is also a constant for a given material:

$$v_s = \left(\frac{G}{\rho} \right)^{1/2} \dots \dots \dots (2)$$

**Fig. 51.2—Stress/strain diagram for an elastic material.**

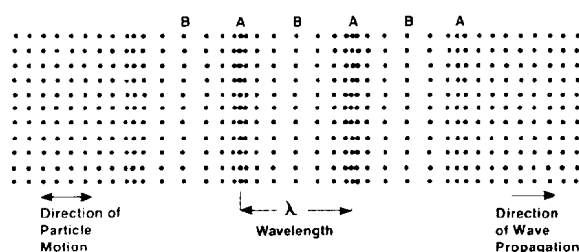


Fig. 51.3—Compressional wave.

Characteristics of Acoustic Waves

Acoustic waves have many characteristics similar to light waves. They undergo interference, diffraction, reflection, and refraction. At a boundary separating materials of two different velocities, they are mode converted, reflected, and refracted according to Snell's law.

For either compressional or shear waves, velocities are related to frequency, f , by

$$v = \lambda f,$$

where λ is the wave length.

Motion of either compressional or shear waves in an extended medium is characterized by an infinite number of particles, each vibrating in simple harmonic motion. A simple description of this wave propagation is given by a plane wave solution of the wave equation:

$$u = A \cos(2\pi ft - 2\pi \frac{s}{\lambda}),$$

where u is the particle motion at a given point, s , away from the source and at any given time, t . At any given time, $t=0$, the displacement along the wave varies as $\cos(2\pi s/\lambda)$; hence, the u is equal to signal amplitude A , where s is equal to even multiples of wavelength—i.e., $s=0, \lambda, 2\lambda$. Motion of each particle, on the other hand, is described by a simple harmonic motion given by

$$u = A \cos(2\pi ft).$$

An additional feature of acoustic waves to be considered is attenuation. As one moves away from the source, the intensity of sound decreases. This decrease of acoustic waves results from (1) geometric spread of energy, reflection, refraction, and scattering, and (2) absorption, whereby mechanical energy is converted into heat.

The decrease in intensity because of absorption is given by

$$I = I_0 e^{-2\alpha s},$$

where I_0 is the acoustic intensity at the source, I is intensity at a distance, s , from the source, and α is the coefficient of absorption.

The acoustic intensity is proportional to the square of the amplitude; therefore, the amplitude, A , of a wave at a

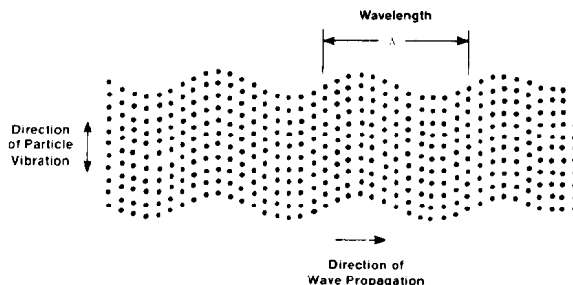


Fig. 51.4—Shear wave.

distance, s , from the source is

$$A = A_0 e^{-\alpha s},$$

where A_0 is the amplitude at the source.

A schematic diagram of an experimental apparatus is given in Fig. 51.5 to illustrate the measurement of acoustic properties. Two piezoelectric elements are attached to the specimen as shown. A pulser provides the electric pulse to the transmitting piezoelectric element and also triggers the oscilloscope trace. The transmitter vibrates according to the change of voltage with time, generating a mechanical pulse in the specimen. As it travels through the specimen, the mechanical pulse is attenuated. The receiving piezoelectric element converts this attenuated pulse into an electric pulse that is displayed on the oscilloscope screen.

The travel time of the mechanical pulse through the specimen is read on the horizontal scale of the oscilloscope, and the velocity is calculated from

$$v = \frac{L}{t}.$$

By using a set of either P-wave or S-wave transducers, both velocities, v_p and v_s , can be measured as described. These velocities, assuming an infinite, isotropic, homogeneous, and elastic medium, are related to elastic moduli by

$$v_p^2 \rho = P = K + \frac{4}{3} G, \quad \dots \dots \dots (3)$$

$$v_s^2 \rho = G, \quad \dots \dots \dots (4)$$

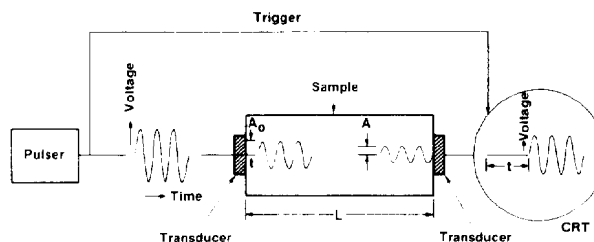


Fig. 51.5—Experimental apparatus for measurement of velocity and attenuation.

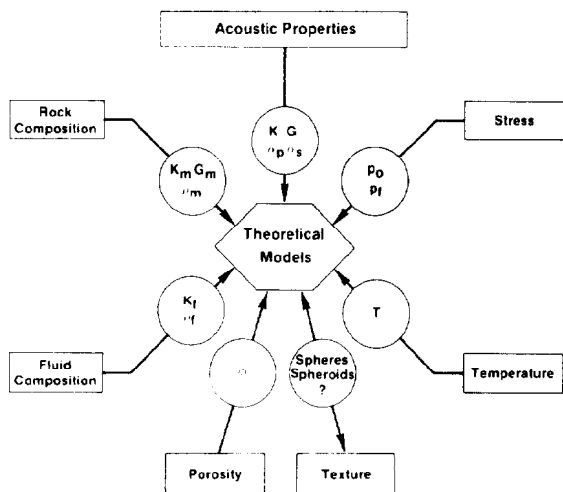


Fig. 51.6—Factors affecting acoustic properties of rocks.

and

$$\mu = \frac{0.5(v_p/v_s)^2 - 1}{(v_p/v_s)^2 - 1}, \dots \dots \dots (5)$$

where P , K , and G are P-wave, bulk, and shear moduli, respectively, μ is Poisson's ratio, and ρ is density.

As mentioned earlier, these same elastic constants can be obtained directly by measuring lateral and longitudinal strains as functions of stress. Elastic constants measured in this manner are referred to as static elastic constants in contrast to dynamic elastic constants measured through the use of acoustic wave propagation techniques.

One method for measurement of attenuation requires specimens of two different lengths from the same material. Assuming that the voltage amplitude of the received signal from the specimen of length L_1 is A_1 and from the specimen of length L_2 is A_2 , and that voltage amplitudes are proportional to the amplitudes of mechanical pulses, the two amplitudes can be expressed as

$$A_1 = A_0 e^{-\alpha L_1}$$

and

$$A_2 = A_0 e^{-\alpha L_2}$$

Hence, the coefficient of absorption, nepers/cm, is obtained from

$$\alpha = \frac{1}{L_2 - L_1} \ln \frac{A_1}{A_2}.$$

Or, in more common units, attenuation is given in decibels per unit length, defined as

$$\alpha = \frac{20}{L_2 - L_1} \log \frac{A_1}{A_2}.$$

Other parameters defining attenuation are the quality factor, Q , and the logarithmic decrement, δ . Coefficients of compressional and shear wave attenuation (α_p , α_s) are related to the respective quality factors (Q_p , Q_s) and the logarithmic decrements (δ_p , δ_s) by

$$\frac{1}{Q} = \frac{\alpha v}{\pi f} = \frac{\delta}{\pi}, \dots \dots \dots (6)$$

where v is velocity and f is frequency.

Acoustic Wave Propagation in Rocks

Introduction

Acoustic wave propagation properties of rocks are known to depend on porosity, rock matrix composition, stress (overburden and pore fluid pressures), temperature, fluid composition, and texture (structural framework of grains and pore spaces), as illustrated in Fig. 51.6.¹² A unified approach involving measurements of compressional and shear-wave velocities, analyses of rock composition, and use of theoretical models to interpret these data was described in Refs. 13 through 16.

Acoustic Properties

Acoustic wave propagation properties were described in the preceding section for homogeneous, elastic media. Applications of these relationships to rocks, however, are complicated by the presence of pores and cracks, and fluids contained in them. A simplified, theoretical development is described in the Appendix to illustrate some of these complications by incorporating rock-frame, pore-fluid, and rock-grain compressibilities into the velocity equations.

As indicated earlier, acoustic wave properties in rocks are functions of numerous independent variables. Therefore, evaluation of various theories of acoustic wave propagation requires laboratory experiments conducted on rock samples under controlled pressure, temperature, and saturation conditions.

Various experimental methods have been developed for measuring acoustic wave propagation properties of rock samples. Detailed description of one of the laboratory systems is given by Timur.¹⁷ It is designed to conduct sequential measurements of properties of both the compressional and the shear waves on rock samples subjected to simulated subsurface conditions. A typical experimental setup is shown in Fig. 51.7, where a rock sample is assembled between two transducers in a sample holder. This assembly is placed in a pressure vessel and subjected to varying overburden and pore fluid pressures and temperatures. A minicomputer digitally records the compressional and shear-wave pulses transmitted through the rock samples, as well as sample temperature, overburden and pore fluid pressures, and sample length changes.

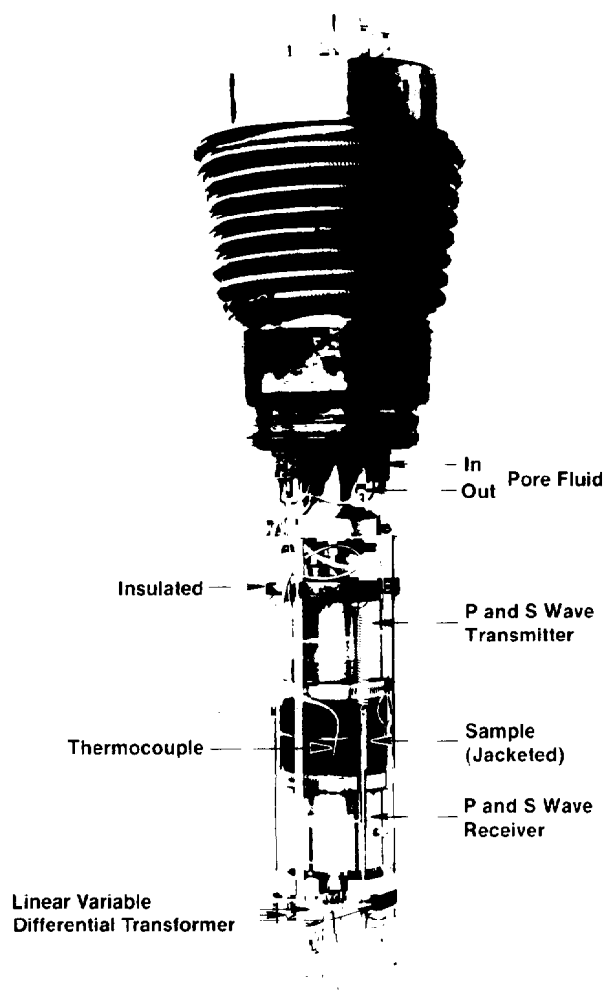


Fig. 51.7—A typical sample ($d = 8.9$ cm, $L = 5.1$ cm) assembled for acoustic measurements.

A typical set of compressional and shear-wave velocity data obtained with this apparatus is shown in Fig. 51.8. The rate of change of porosity in this sample with varying overburden and pore fluid pressures is shown in Fig. 51.9. These data were obtained from concurrent measurements of changes in the sample pore and bulk volumes during acoustic measurements.

Fig. 51.10 illustrates typical compressional and shear-wave attenuation data, obtained from the amplitude spectra of transmitted pulses.

Porosity

Porosity dependence of v_p in rocks has been intensively investigated.¹⁸⁻²³ This forms the basis for estimating porosities from in-situ measurements with an acoustic velocity log.

Results of early laboratory measurement of compressional-wave velocities determined on water-saturated sandstones are plotted vs. porosities in Fig. 51.11.²⁴ The porosity/velocity relationship is within the indicated statistics as long as the lithology remains relatively constant.

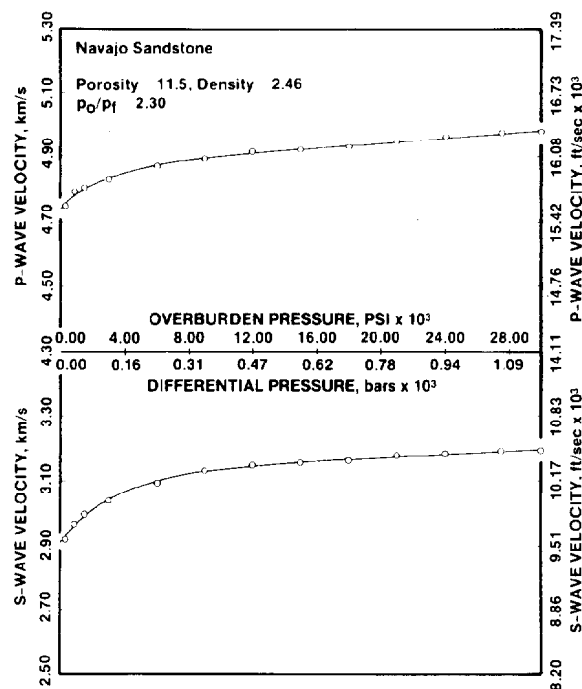


Fig. 51.8—Pressure dependence of compressional- and shear-wave velocities in a Navajo sandstone.

Porosity dependence of v_s has also been investigated to some extent.²⁵⁻²⁸ A change in shear-wave travel times ($1/v_s$) per unit change in porosity (ϕ) is found to be almost twice the corresponding change in $1/v_p$.

Rock Composition

Rock composition affects the velocities in significant ways, as illustrated in Fig. 51.12.²⁹ Laboratory data plotted in this figure are for cores saturated with brine and subjected to an overburden pressure of 3,000 psi. The two principal minerals in the rock were quartz, in the form of tripolite, and calcite. They were mixed in relative proportions ranging from approximately 50% calcite/50% quartz to 80% calcite/20% quartz. The samples with lower porosity had a continuous calcite matrix, whereas the samples with a higher porosity had a continuous quartz matrix.

Effects of rock composition usually are taken into account by establishing velocity/porosity relationships for each group of rocks of similar composition through correlations of both the laboratory and the field data. This is illustrated in Fig. 51.12 by two separate groupings, one for calcite matrix and the other for quartz.

Rock composition plays a significant role in acoustic wave propagation properties. A procedure for comprehensive analyses needed for this purpose was described by Jones *et al.*¹³ First, they conducted a combination of measurements of X-ray diffraction, elemental analysis, clay analysis, and grain density measurements. Each of these then was assigned an experimental error, and linear programming was used to establish the rock mineral composition, as shown in Table 51.2.

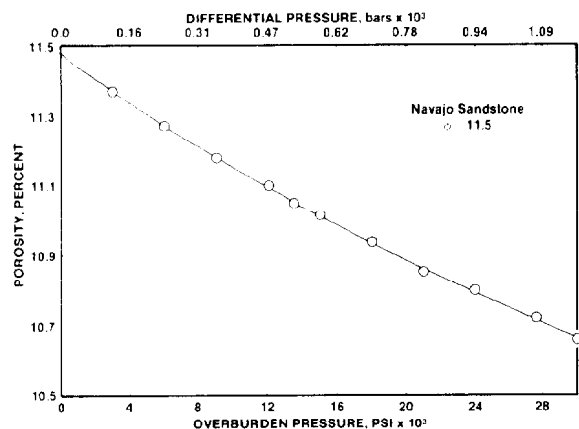


Fig. 51.9—Pressure dependence of porosity of Navajo sandstone.

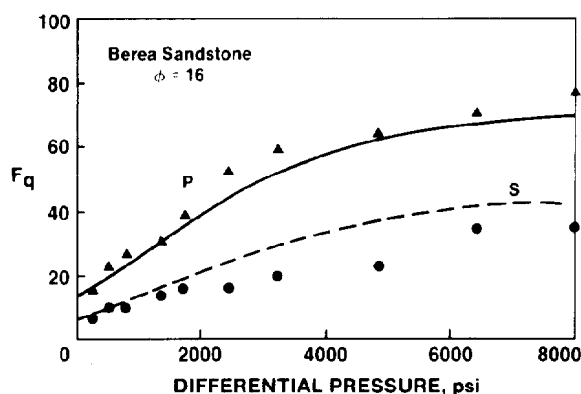


Fig. 51.10—Pressure dependence of compressional and shear attenuation in a Berea sandstone saturated with brine.

Stress

Pressure dependence of velocities of compressional and shear waves also has been the subject of numerous studies. Velocities of elastic waves traveling in a porous medium are known to be functions of both the external (overburden) pressure, p_o , and the internal (pore fluid) pressure, p_f . Some of the experimental results indicating dependence of compressional-wave velocity on confining pressure are given in Fig. 51.13 for various rock

samples including dolomite, limestone, and sandstone and for a sandpack.²⁹ In general, velocities increase with increasing p_o and decrease with increasing p_f .

From a theoretical analysis of elastic wave propagation in sphere packs, Brandt³⁰ predicted velocities to be functions of $(p_o - np_f)$, where n is a number between 0 and 1. Experimental data of Hicks and Berry³¹ and Wyllie *et al.*¹⁹ indicated n to be close to unity, whereas data obtained by Banthia *et al.*³² indicated values of n to

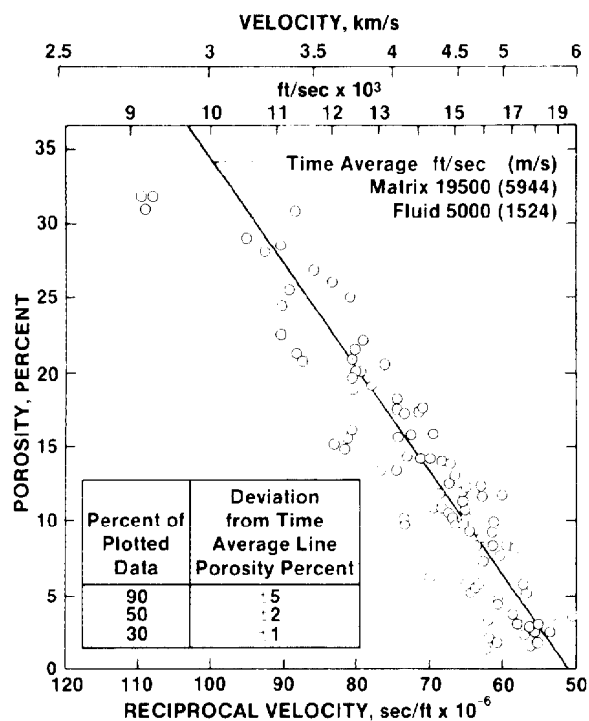


Fig. 51.11—Velocity/porosity data determined in laboratory for water-saturated sandstones compared with time-average relation for quartz/water system.

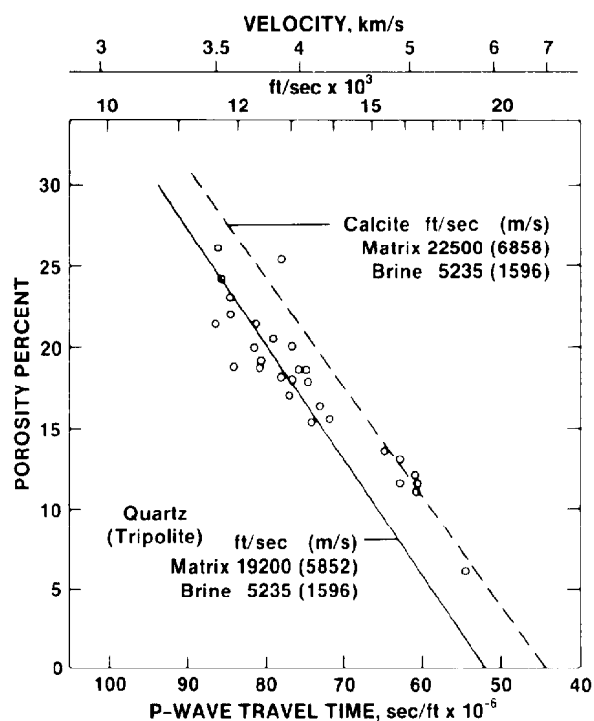


Fig. 51.12—Comparison of compressional-wave velocities as function of porosity for brine-saturated tripolite samples under confining pressure of 3,000 psi.

TABLE 51.2—ROCK COMPOSITION

Sample	Navajo sandstone
Petrography	medium-porosity, well-sorted quartzite
Grain density	2.60
Grain porosity	19.4
X-ray, wt%	
Quartz	93.0
Calcite	1
Dolomite	—
Clay	1.7
Feldspar	0.7
Pyrite	—
Anhydrite	0.4
NAA and AAS, wt%	
Si	42.60
Al	1.20
Ti	0.79
Fe	0.20
Mg	0.02
Ca	0.20
Na	0.00
K	0.16
O	54.00
Phyllo-silicate	6.00
Computed volume, %	
Quartz	68.37
Calcite	—
Dolomite	—
Clay	4.73
Feldspar	0.57
Pyrite	—
Anhydrite	—
Silica	6.93
Siderite	—

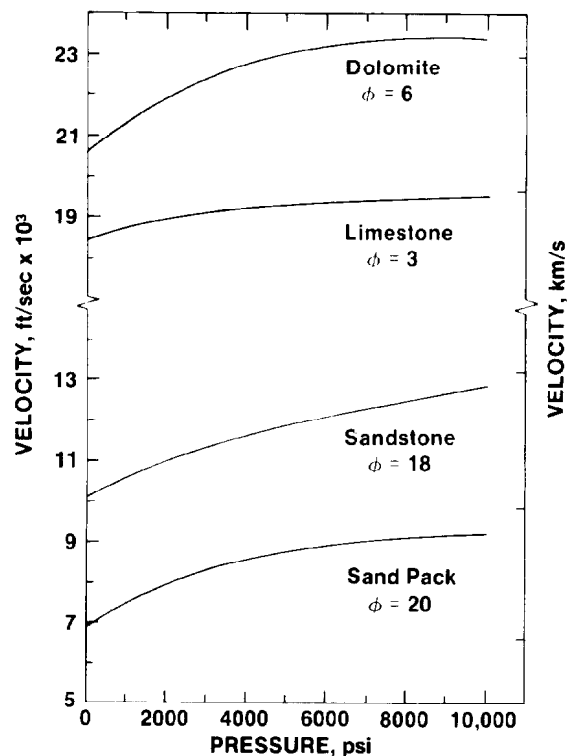


Fig. 51.13—Compressional-wave velocity vs. confining pressure for brine-saturated carbonates, sandstone and sand pack.

be significantly less than 1. To investigate this discrepancy, Gardner *et al.*³³ conducted experiments taking into account the past pressure history of samples. They found that p_o and p_f are equally effective in changing velocities—i.e., $n=1$, provided that the differential pressure ($p_d = p_o - p_f$) follows a pressure cycle previously imposed on the sample (Fig. 51.14).

Temperature

The effect of temperature on elastic wave velocities is considered to be of second order and usually is neglected in seismic exploration and acoustic log interpretations. To study this effect, early laboratory experiments³⁴⁻³⁸ were conducted by measuring velocity as a function of overburden pressure at constant values of temperature instead of as a function of temperature at constant pressure. Also, the effects of pore fluid pressure were not considered. Later, the effects of temperature on the velocities were investigated through laboratory measurements on rock samples subjected to simulated subsurface pressure conditions¹⁷ (Fig. 51.15). On the average, the compressional wave velocities were found to decrease by 1.7% and the shear-wave velocities by 0.9% for 100°C increase in temperature.

Below freezing temperatures, however, the effect of temperature on elastic wave velocities become much more significant. An increase of 50% or more in compressional wave velocities is observed upon freezing the pore fluid in some rock samples.³⁹ Below freezing, compressional wave velocity in water-saturated rocks was found to increase with decreasing temperature, whereas it was nearly independent of temperature in dry

rocks. The shapes of the velocity vs. temperature curves were functions of rock composition, pore structure, and the pore fluids. Some of the velocity vs. porosity data at subfreezing temperature is illustrated in Fig. 51.16.³⁹⁻⁴³

Fluid Composition

An understanding of the effects of fluid composition on elastic wave properties has become much more significant with the increasing interest in detection of hydrocarbons with seismic measurements. As a result, these effects have been the subject of many studies, both theoretical and experimental, in the recent literature. The

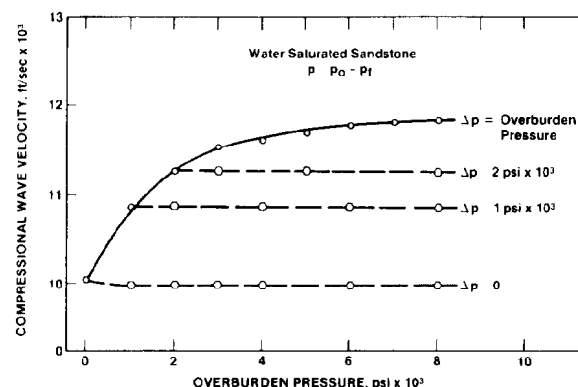


Fig. 51.14—Compressional-wave velocity as a function of differential pressure.

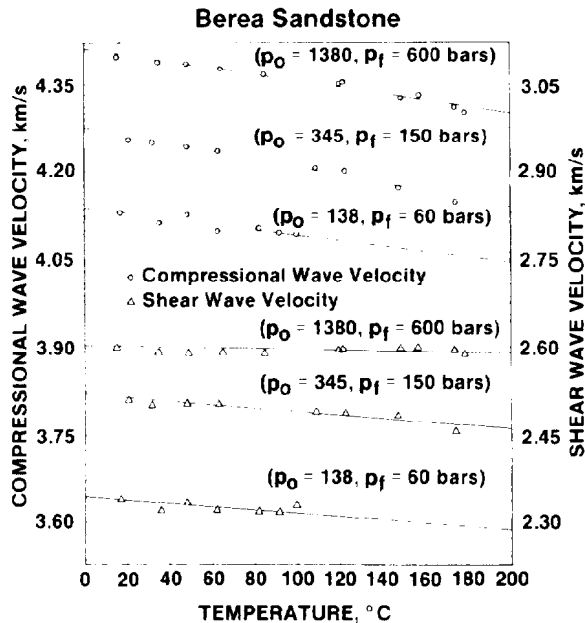


Fig. 51.15—Temperature dependence of compressional- and shear-wave velocities in brine-saturated Berea sandstone.

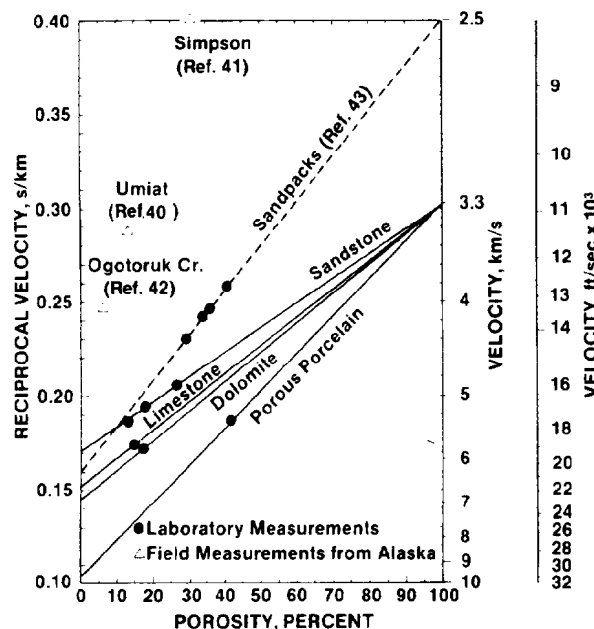


Fig. 51.16—Compressional-wave velocity of frozen rocks as a function of porosity.

first important theoretical contribution was made by Gassmann,⁴⁴ who described the relationships between pore fluid, rock skeleton (or frame), and the rock grains by starting with first principles of the theory of elasticity. Later, Biot^{45,46} developed a more comprehensive theory of elastic wave propagation in a fluid-saturated, isotropic and microhomogeneous porous solid over a wide frequency range. Biot's theory, which reduces to that of Gassmann at low frequencies, incorporates the effects of fluid composition through the density and compressibility of the saturant fluid (see Appendix).

Geertsma⁴⁷ investigated the applications of Biot's theory to the interpretation of acoustic logs and estimated expected range of velocity dispersion by comparing velocities at zero and infinitely high frequencies. Since the estimated velocity dispersion was found to be generally less than 3%, the low frequency approximation of Biot's theory and, hence, Gassmann's theory is useful for most applications. Brown and Korringa⁴⁸ further generalized Gassmann's theory and succeeded in removing the requirement of macrohomogeneity.

The experimental data of King,⁴⁹ shown in Fig. 51.17 for brine-, kerosene-, and air-saturated (dry) Boise sandstone ($\phi=25\%$), illustrated the predicted behavior; compressional-wave velocity is greater in brine-saturated rocks than in comparable gas-saturated rocks, with the reverse true for shear-wave velocity.

On the other hand, experimental data of Gregory⁵⁰ in Fig. 51.18 indicate that for some rocks, shear-wave velocity behavior upon the change of saturation from gas to brine is opposite to the predictions of the Biot theory. This may be due to the presence of isolated microcracks in these rocks, whereas the Biot/Gassmann theories assume the pore structure to be open and interconnected.

Texture

Texture in this context is the structural framework of the rock consisting of solid matrix and pore structure. Its importance in elastic wave propagation has been dramatically illustrated in Fig. 51.19. The data in this figure are the compressional and shear-wave velocities in dry and water-saturated Troy granite with a porosity of 0.3%.⁵¹ Velocities were measured as functions of confining pressure by maintaining pore fluid pressure (p_f) at 1 bar. Compressional-wave velocities are higher when the rock is water-saturated, whereas the shear-wave velocities are unchanged between the two states. What is most interesting, however, is that a porosity of only 0.3% is affecting the velocities by 20% or more.

Classical bounding theories⁵²⁻⁵⁵ obviously cannot account for these large changes in the respective moduli because of large differences between the properties of rock matrix and fluid in the pores. This is because they used the total porosity without considering how it is distributed.

Scanning electron micrographs (SEM's) shown in Fig. 51.20 show pore space in Troy granite to consist mainly of thin cracks, typical of most granites.⁵⁶

The effects of these cracks on elastic wave propagation properties have been investigated extensively, and many theoretical models have been developed.^{14,57} The theoretical curves shown in Fig. 51.19 were obtained by fitting the velocity data with the noninteractive scattering theory.¹⁴ For these theoretical formulations, the rock is

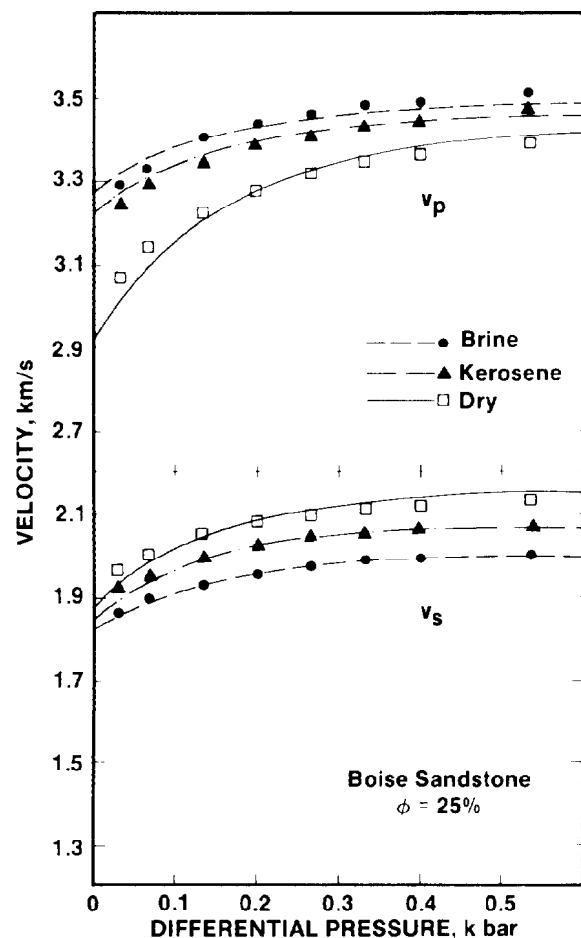


Fig. 51.17—Observed and theoretical compressional- and shear-wave velocities in Boise sandstone as a function of pressure for three saturation fluids. The circles, triangles, and squares are laboratory data from King for brine-, kerosene- and air-saturated (dry) samples.

assumed to consist of a solid matrix and pores of spherical and oblate spheroidal shapes. Using the SEM's as a guide and the porosity as a constraint, the pore space was modeled by a spectrum of pore shapes ranging from spheres to very fine cracks. Theoretical velocities were calculated as a function of pressure by first determining the ranges in pore shapes at each pressure condition. Depending on the fit, the pore aspect ratio (ratio of minor to major axis of an ellipsoid) spectra were adjusted and calculations were repeated until good fits were obtained to all velocities. Theoretical curves plotted on Fig. 51.19 are based on the final model.

Effects of various pore shapes on acoustic velocities as predicted by the noninteractive scattering theory are illustrated in Fig. 51.21. The effects shown in this figure are for a rock with matrix properties of $K_m=0.44$ megabar, $G=0.37$ megabar, and $\rho_m=2.7$ g/cm³; for water with $K_w=23.2$ kilobar and $\rho_w=1$ g/cm³; and for gas with $K_g=1.5 \times 10^{-3}$ kilobar and $\rho_g=10^{-3}$ g/cm³. As indicated, for a given porosity, the thinner (smaller aspect ratio) pores affect the velocities much more than the spherical pores.

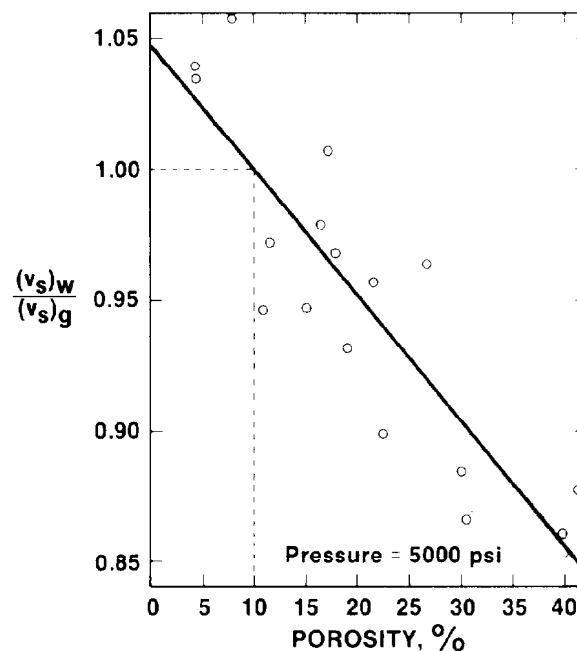


Fig. 51.18—S-wave velocity ratio vs. porosity for dry, $(v_s)_g$, and fully water-saturated, $(v_s)_w$, rocks.

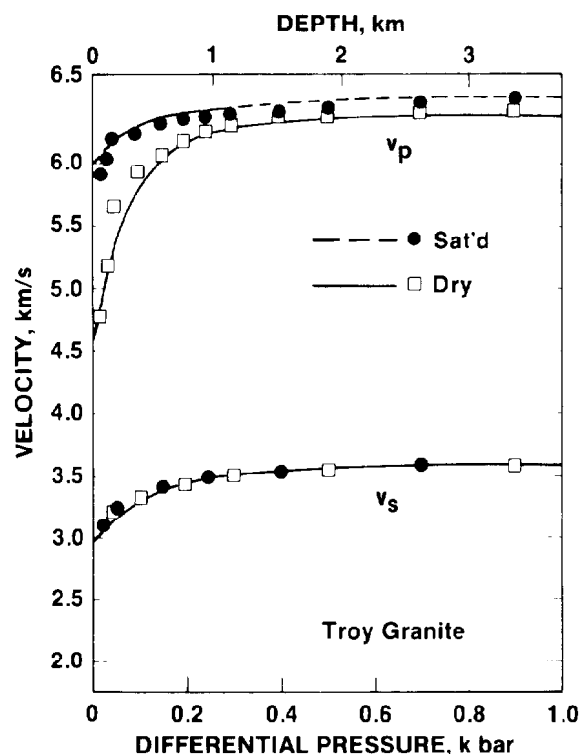


Fig. 51.19—Observed and theoretical compressional (v_p) and shear (v_s) velocities in dry and water-saturated Troy granite as a function of differential pressure. The data (points) are from Ref. 51.

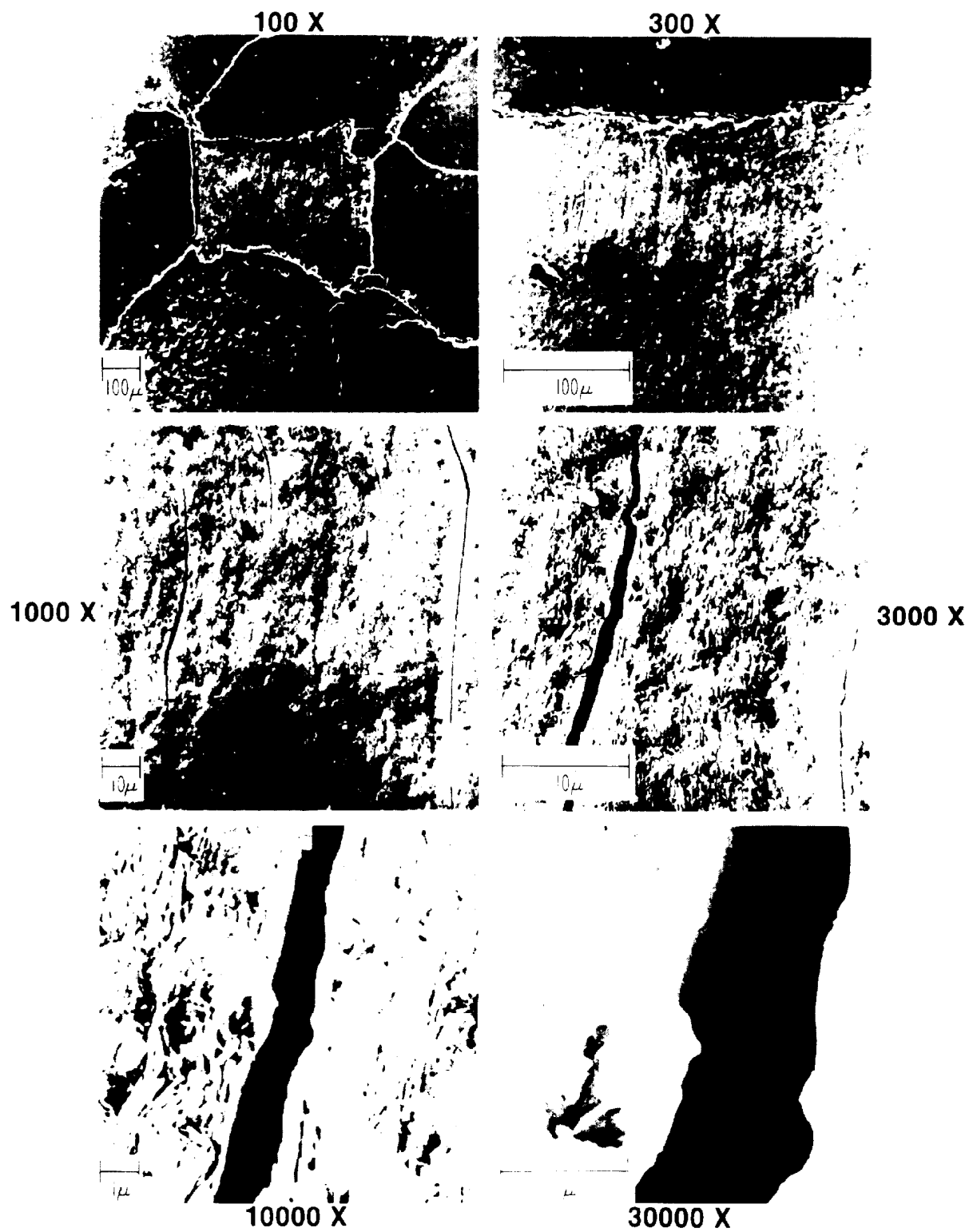


Fig. 51.20—Scanning electron micrographs of pore system in Troy granite.

This theory also was used to analyze the "well-behaved" (according to Biot/Gassmann) experimental data of Fig. 51.17, where the results are plotted as solid and long- and short-dashed curves. Additionally, however, it also can explain the "unexpected" behavior of the experimental data of Fig. 51.18, as illustrated in Fig. 51.21 by its predictions for the S-wave velocities in rocks with pores of various shapes.

Modeling of the real rock can be achieved by approximating the regular pores by spheres and rounded spheroids and by approximating the grain boundary spaces and flat pores by low-aspect-ratio cracks. However, there is no practical way to measure a pore aspect-ratio spectrum independently. An extensive study by Hadley⁵⁸ involved counting hundreds of cracks on three SEM's, each covering about 1 mm² of rock surface. These results are being used for testing "crack" theories. So far, these theories have added much to our understanding of acoustic wave propagation; their practical applications, however, have not yet materialized.

Summary

Factors affecting acoustic wave propagation properties of rocks were illustrated in a qualitative fashion with emphasis on compressional and shear-wave velocities, mostly because attenuation properties are much less understood. Among the factors influencing velocities, porosity, lithology (mineral composition and structural framework), saturation and differential pressure are considered primary, and the others, with certain qualifications, secondary. As the previous discussion indicates, significant advances have been made in understanding the properties of acoustic wave propagation in rocks. Further advances will be made because of the significance of this work, not only in formation evaluation, but also in seismic exploration.

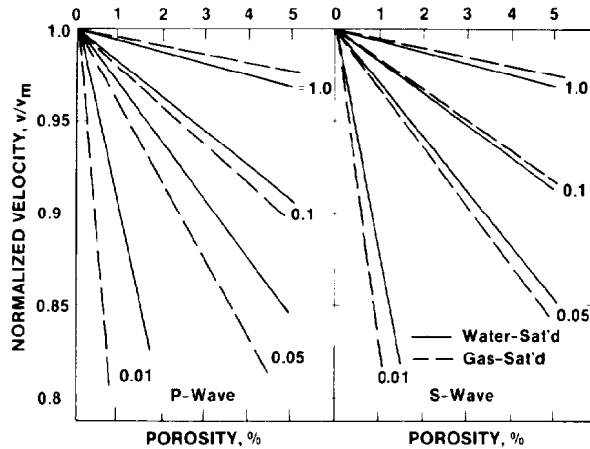


Fig. 51.21—Normalized P- and S-wave velocities vs. column concentration of inclusions (porosity) of different aspect ratios for water- and gas-saturated pores, respectively.

Acoustic Wave Propagation Methods

Introduction

Acoustic wave propagation methods used in well logging can be classified into two groups: transmission and reflection (Table 51.1). In the transmission method, one or more transmitters emit acoustic energy, which is transmitted by formation and/or casing and is detected by one or more receivers. In the reflection method, one or more transducers emit acoustic energy, part of which is reflected by the borehole wall and/or casing and is detected by the same transducer.

In this section, both the transmission and reflection methods will be described, starting with a description of acoustic wave propagation in a borehole and followed by various methods of recording acoustic data.

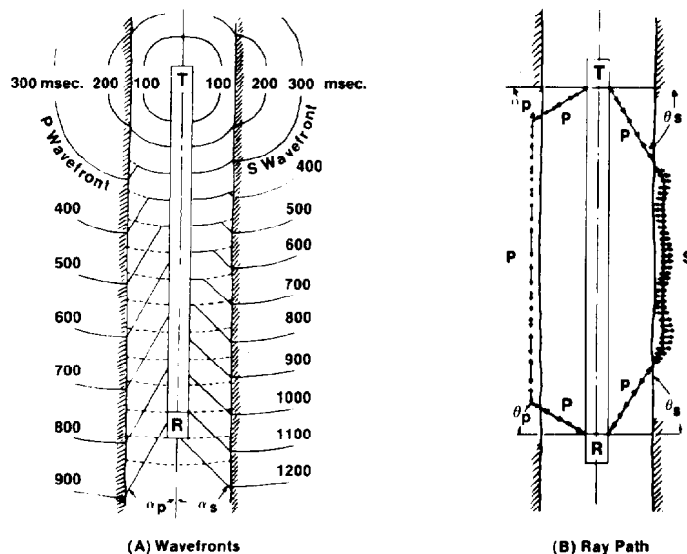


Fig. 51.22—Compressional, P, and shear, S, wave propagation in or around a fluid-filled borehole.

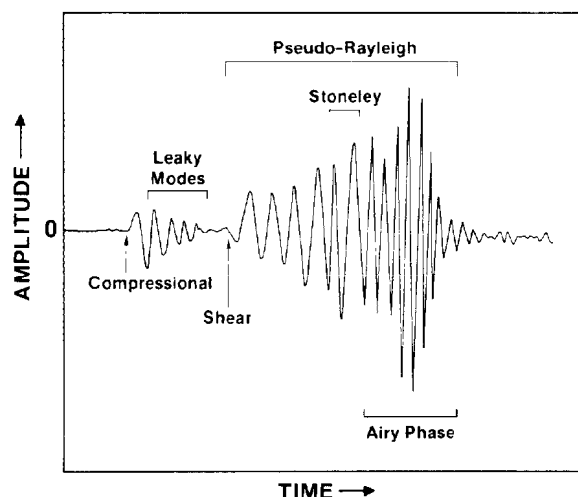


Fig. 51.23—Acoustic waveform.

Acoustic Wave Propagation in a Fluid-Filled Borehole

The propagation of elastic waves in a borehole filled with liquid has been studied extensively.⁶⁰⁻⁷⁰ Only a qualitative description of the phenomenon will be given here for identifying the components of an acoustic pulse recorded in a borehole.

The general geometry for the transmission method is illustrated in Fig. 51.22, which shows a single receiver logging sonde. Two pressure transducers are spaced on an acoustically insulated body, the upper one to generate compressional waves in the borehole fluid and the lower one to detect compressional waves reaching it. The receiver converts these waves to electrical signals. These are transmitted to the surface and displayed on an oscilloscope as a record of received-signal amplitude vs. time and recorded either in analog form on film or digitally on magnetic tape.

This received signal, which is referred to as the acoustic waveform, represents several acoustic waves and is illustrated by the synthetic waveform trace shown in Fig. 51.23. For the usual case of a liquid-filled borehole in a formation with both the compressional- and shear-wave velocities higher than borehole fluid velocity, two body (or head) waves and two guided waves are propagated. These waves are shown in Fig. 51.23 in the order of their arrival time at the receiver: (1) compressional wave, (2) shear wave, (3) pseudo-Rayleigh waves, and (4) Stoneley waves.

Compressional and shear waves, which are also called P, primary, and S, secondary waves, respectively, are head or body waves because they travel in the body of the formation. Pseudo-Rayleigh and Stoneley waves, which also are called reflected conical (or normal mode) and tube wave (or water arrival), respectively, are guided waves because they require the presence of the borehole for their existence.

A description of the various ray paths of these waves may help further in understanding elastic wave propagation in and around the borehole. The acoustic transmitter shown in Fig. 51.22 generates compressional waves

traveling with a velocity, v_f , in the mud. When these waves reach the borehole face, they are both reflected and refracted. For angles of incidence less than the P-wave critical angle θ_p ,

$$\theta_p = \sin^{-1} \left(\frac{v_f}{v_p} \right),$$

part of the energy is transmitted into the formation in the form of compressional wave and another part as a shear wave, and the remainder is reflected back into the mud as a compressional wave, all according to Snell's law.

At or near the P-wave critical angle, a shear wave is still transmitted into the formation and P-wave reflected back into the mud, but a P-wave is critically refracted and travels with the v_p in the formation, close and parallel to the borehole wall, while continuously radiating P-wave energy back into the mud at the same P-wave critical angle (Fig. 51.22).

At the S-wave critical angle (θ_s),

$$\theta_s = \sin^{-1} \left(\frac{v_f}{v_s} \right),$$

the S-wave is critically refracted and travels with the v_s in the formation along a path similar to that of the refracted P-wave. It also continuously radiates P-wave energy back into the mud at the S-wave critical angle (Fig. 51.22). Beyond the S-wave critical angle, all the incident energy is reflected back into the mud to form the guided pseudo-Rayleigh waves (Fig. 51.24).

To summarize, the compressional wave travels as a P-wave between the transmitter and the formation, in the formation, and also between the formation and the receiver (PPP); the shear wave travels as a P-wave between the transmitter and the formation, an S-wave in the formation, and again as a P-wave between the formation and the receiver (PSP). If the formation shear-wave velocity is slower than borehole fluid velocity, shear waves cannot be refracted along the borehole wall; therefore, no shear head wave is generated.

As described earlier, compressional and shear waves travel at velocities determined by the elastic moduli and the density of the formation:

$$v_p = \frac{1}{t_p} = \frac{1}{\rho_b^{1/2}} \left(K + \frac{4}{3} G \right)^{1/2} \dots \dots \dots (7)$$

and

$$v_s = \frac{1}{t_s} = \left(\frac{G}{\rho_b} \right)^{1/2} \dots \dots \dots (8)$$

ρ_b is the bulk density of formation, and t_p and t_s are compressional- and shear-wave transit times.

The body waves travel at all frequencies at speeds given by Eqs. 8 and 9. They are nondispersive (variation of velocity with frequency is negligible), and undergo attenuation and geometric spreading. Attenuation, α , of the body waves is proportional to the logarithmic ratio of the amplitudes, A_1 and A_2 , at distances s_1 and s_2 from the source^{15,16}:

$$\alpha = \frac{20}{s_2 - s_1} \log \left[\frac{A_1}{A_2} \cdot \frac{F_{gs2}}{F_{gs1}} \right],$$

where α is in decibel/ft and F_{gs} is a geometrical spreading factor.

The ringy packet shown between the compressional and shear waves is called the leaky or PL mode.⁶⁶ It is a guided wave generated by the interaction of the formation with totally reflected compressional waves between the compressional and shear critical angles. Paillet and White⁶⁹ have shown that the leaky mode propagates at a velocity close to that of compressional waves in the formation and its phase velocity decreases with increasing frequency. They also have shown that the leaky mode amplitude, and hence the shape of the compressional wave train, varies with a change of Poisson's ratio.

Pseudo-Rayleigh and Stoneley waves are the two main guided waves. They both arrive after the shear wave, have larger amplitudes and longer durations than either the compressional or the shear wave, and are dispersive.⁶⁷ The pseudo-Rayleigh wave is generated by the total internal reflection of the acoustic energy at the borehole face beyond the shear critical angle. It travels within the borehole by multiple internal reflections without loss of energy into the formation; therefore, it is a guided wave. Its amplitude decays exponentially in the formation away from the borehole face, but is oscillatory in the fluid. A pseudo-Rayleigh wave is not generated unless $v_s > v_f$ and it travels with a velocity v_r such that $v_f < v_r \leq v_s$ with an Airy phase traveling slower than v_f .

Fig. 51.25 shows the dispersion characteristics for the phase and group velocities of the guided waves in a fluid-filled borehole.⁶⁷ The parameters used are (1) for the formation, P-wave velocity = 15×10^3 ft/sec, S-wave velocity = 9×10^3 ft/sec, density = 2.3 g/cm^3 , and (2) for the borehole fluid, P-wave velocity = 6×10^3 ft/sec, density = 1.2 g/cm^3 ; the borehole diameter is 8 in. The phase and group velocities plotted are normalized to the P-wave velocity of the borehole fluid.

As shown in this figure, the pseudo-Rayleigh waves are very dispersive. At the low-frequency end, there is a cutoff frequency below which these waves are not generated. At this frequency, the pseudo-Rayleigh wave phase velocity is equal to the shear-wave velocity of the formation and it steeply decreases with increasing frequency and asymptotically approaches at high frequencies the velocity of the fluid in the mud. Group velocity of pseudo-Rayleigh wave has an Airy phase that travels more slowly than the borehole fluid velocity (Fig. 51.25). Pseudo-Rayleigh waves have large amplitudes and arrive after the refracted shear wave, often making identification of the smaller-amplitude S-wave arrival difficult. However, only a small error is made if the velocity estimates are made by using the pseudo-Rayleigh arrivals.

The second type of guided waves is the Stoneley wave, which is the true surface wave coupled between the borehole fluid and the formation. The particular motion of these waves is shown in Fig. 51.26,⁷¹ where r is the borehole radius. Their amplitudes decay exponentially both in the fluid and in the formation away from the borehole face. As shown in Fig. 51.24, they are slightly dispersive, have no geometric spreading, and travel at

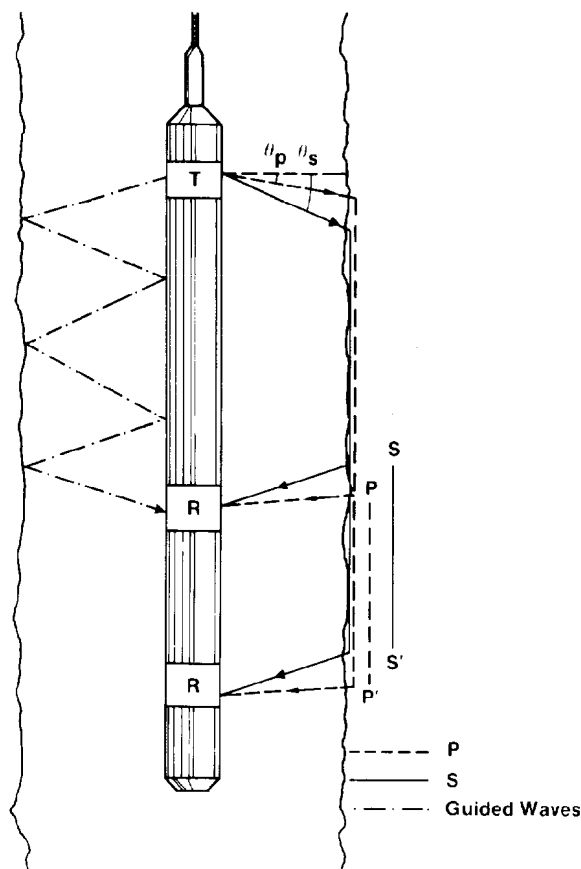


Fig. 51.24—Two-receiver sonde and the ray paths of body and guided waves.

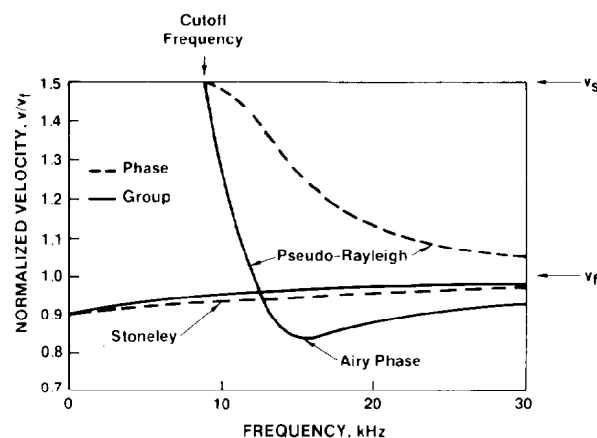


Fig. 51.25—Dispersion characteristics of the pseudo-Rayleigh and Stoneley waves.

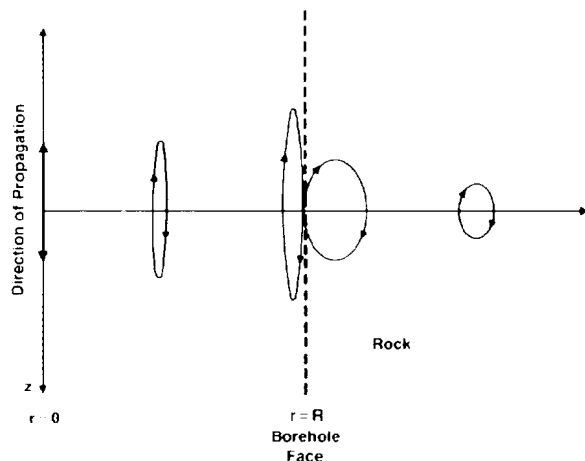


Fig. 51.26—Stoneley (or tube) wave particle motions.

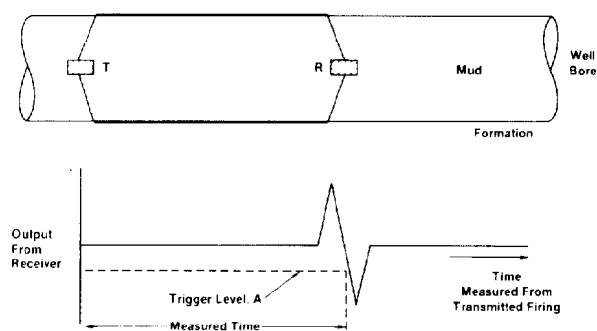


Fig. 51.27—Transit time measurement by a single-receiver tool.

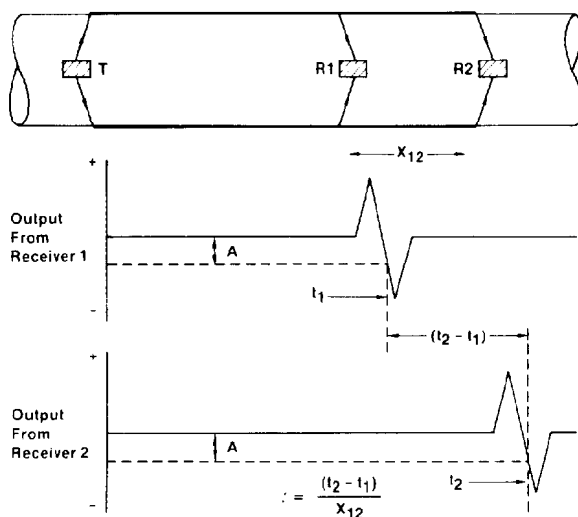


Fig. 51.28—Transit time measurement by a two-receiver tool.

velocities slightly slower than that of the borehole fluid or formation shear wave velocity, whichever is less.

Unlike the formation shear wave or pseudo-Rayleigh waves, Stoneley waves always are present, whether or not v_s is greater than v_f . They arrive as a compact pulse slightly later than that for a direct fluid arrival or shear arrival if $v_s < v_f$. Stoneley wave amplitudes are high at low frequencies and decay rapidly with increasing frequency.⁷² In the low-frequency end, the Stoneley waves are called tube waves and travel with a velocity, v_t , given by⁸

$$v_t = \frac{v_f}{\left(1 + \frac{K_f}{G}\right)^{1/2}}, \quad \dots \dots \dots (9)$$

where K_f is the bulk modulus of the fluid, given by

$$K_f = \rho_f v_f^2,$$

and

$$G = \rho_b v_s^2.$$

Therefore, in formations with $v_s < v_f$, so that neither shear nor pseudo-Rayleigh waves are present, the Stoneley wave can be used to estimate formation shear-wave velocity if formation bulk density is available from a density log.

The dispersion characteristics described so far (of the pseudo-Rayleigh and the Stoneley waves) are for a borehole containing a point source. The effects of the logging sonde on dispersion behavior also have been investigated by Cheng and Toksöz.⁶⁷ Their study indicated, first, that the dispersion curves for the pseudo-Rayleigh wave are shifted to lower frequencies as the borehole radius increases. They further found that for a relatively rigid tool, presence of a logging sonde simply makes the borehole diameter appear smaller, thus shifting the dispersion curves to higher frequencies.

As stated at the beginning of this section, only a qualitative description was given of the elastic wave propagation in a fluid-filled borehole. Ray theory is only an approximation when describing elastic wave properties in a cylindrical geometry. Accurate description of this phenomenon requires solution of the wave equation for cylindrical boundary conditions. The reader is referred to the references given at the beginning of this section for a more quantitative treatment.

Methods of Recording Acoustic Data

As described in the previous section, an acoustic waveform is rich in information. It may have four component waves: compressional, shear, pseudo-Rayleigh, and Stoneley. Each of these, in turn, has four measurable properties: velocity, amplitude, amplitude attenuation, and frequency.²⁷

Various methods of logging were developed to record one or more of these properties. A brief description of some of these logging techniques, with emphasis on those in more common use, follows.

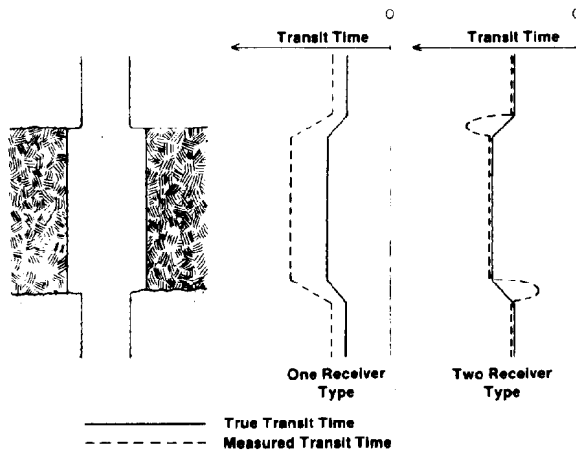


Fig. 51.29—The effect of hole enlargement on the response of acoustic velocity logging tools: (a) one-receiver type and (b) two-receiver type.

Conventional Acoustic Logging

The most commonly used property of acoustic waves in a borehole is the velocity of compressional waves. In conventional acoustic logging, the time, t , required for a compressional wave to travel through 1 ft of formation is recorded as a function of depth. This parameter, t , referred to as the interval transit time, transit time, or travel time, is the reciprocal of the velocity of the compressional waves:

$$t = t_p = \frac{1}{v_p}$$

Transit time also is referred to as compressional-wave slowness and is identified as t_p to differentiate it from shear wave transit time:

$$t_s = \frac{1}{v_s}$$

Velocities observed in acoustic logging vary from 4,000 to 25,000 ft/sec; hence, the travel times range from 40 to 250 μ s/ft.

Tool Characteristics. The original acoustic logging tool, as mentioned earlier, used one transmitter and one receiver (Fig. 51.27). Values of t recorded in this arrangement, however, also include travel time of sound in mud in the borehole.⁷³ To remove this component, a dual-receiver commercial tool was introduced⁷⁴ to measure the time difference between the arrival of the signal at the first receiver and at the second receiver (Fig. 51.28).

Two-receiver systems, however, also were found to be unsatisfactory, especially at boundaries of hole irregularity,⁷⁵ as illustrated in Fig. 51.29.

To improve accuracy of t measurement further, a borehole-compensated sonde (Fig. 51.30) with two

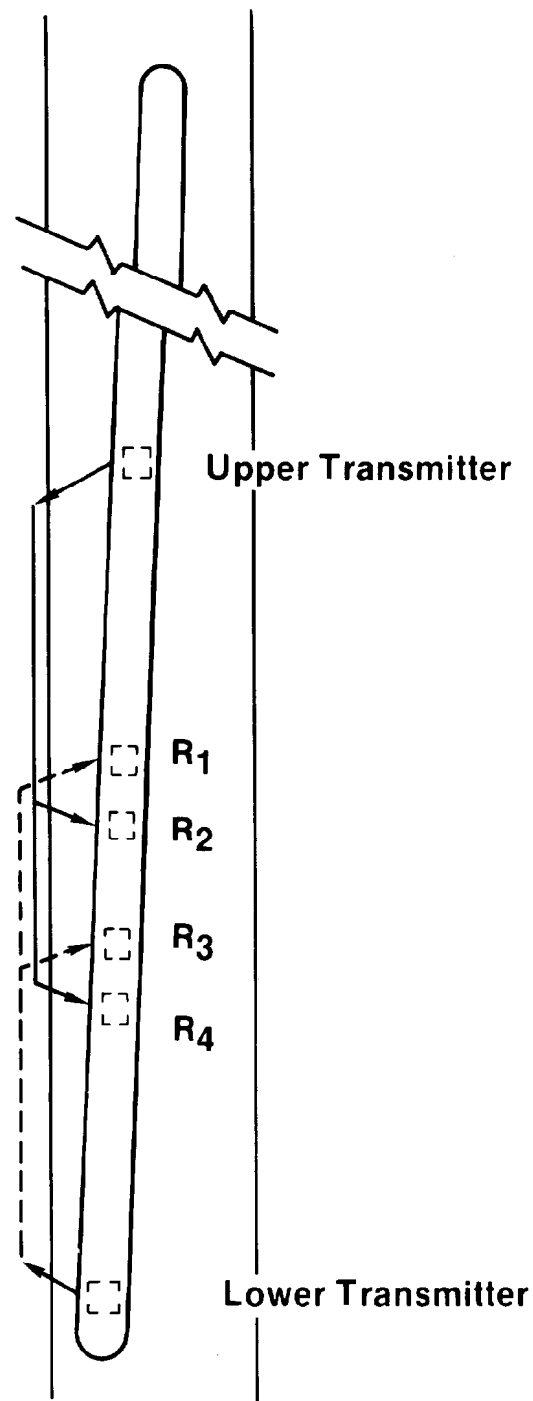


Fig. 51.30—Borehole-compensated acoustic log.

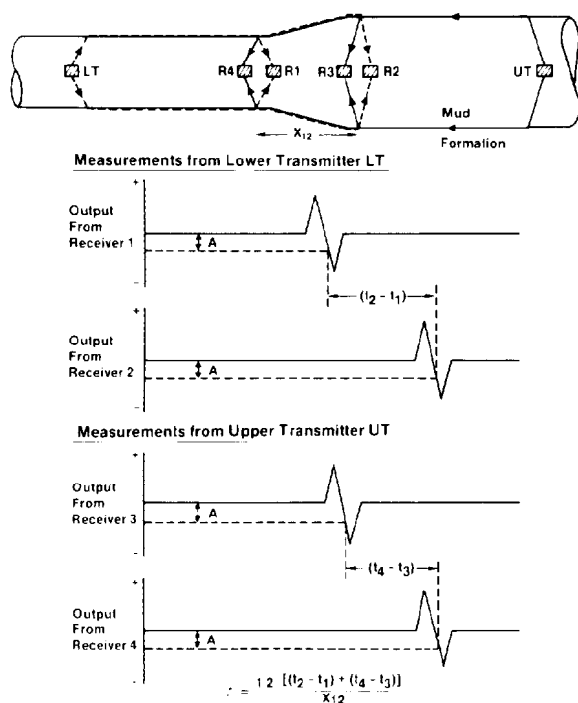


Fig. 51.31—Travel time measurement with the borehole-compensated acoustic log.

transmitters and four receivers was developed.⁷⁶ This borehole-compensated tool may be considered to be composed of two separate two-receiver systems. As illustrated by the measurement scheme in Fig. 51.31, perturbations caused by hole irregularities are oppositely directed; therefore, they cancel. These sondes usually have a 2-ft span between the receivers with a 3-ft spacing between each transmitter and its near receiver.

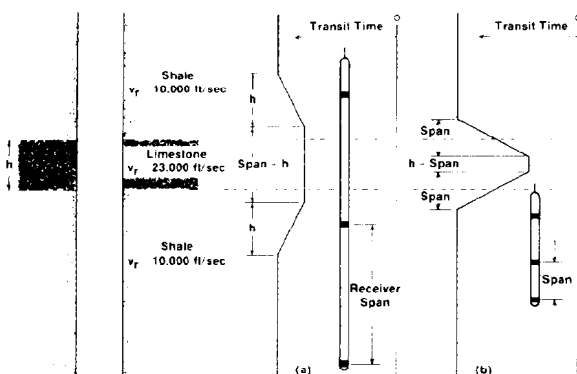


Fig. 51.33—The effect of bed thickness on the response of an acoustic velocity logging device: (a) bed thinner than the span and (b) bed thicker than the span.

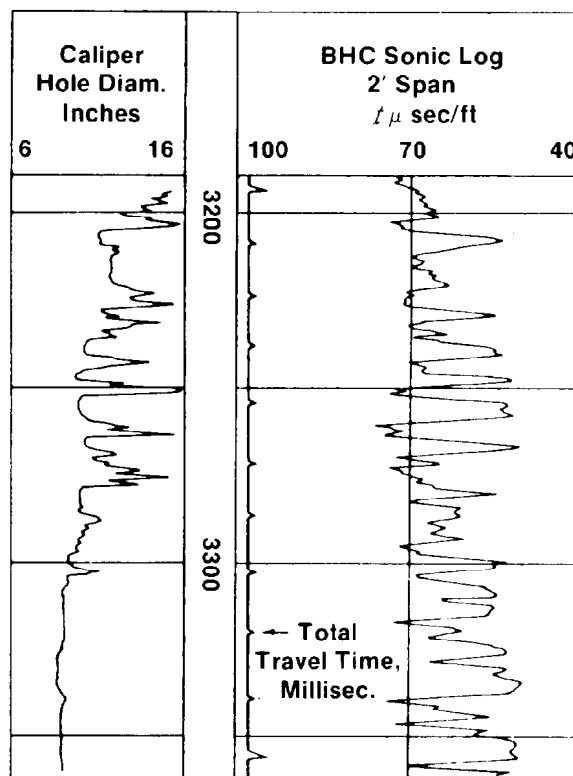


Fig. 51.32—Presentation of acoustic log.

Log Presentation. Transit time t measured by acoustic velocity logs is recorded as a function of depth across Tracks 2 and 3 in units of microseconds per foot ($\mu\text{sec/ft}$). The typical example shown in Fig. 51.32 also has the integrated travel time recorded at the left edge of Track 2 as a series of pips, placed at 1-millisecond intervals.

Additional Curves Recorded. A three-arm caliper and a gamma ray curve can be recorded simultaneously in Track 1 of the conventional acoustic logs (Fig. 51.32). The gamma ray curve can be replaced or supplemented by a spontaneous-potential (SP) curve; however, this SP should be used only for qualitative interpretation because of proximity of the electrode to the metal in the sonde.

Tool Span. The usual span for the acoustic log receivers is 2 ft; however, tools with receiver spacings of 3 in.⁷⁷ to 1 m⁷⁸ or longer also have been developed for special applications.

The shorter the span, of course, the more detail given by the tool. The relative effects of bed thickness, h , and tool span on measured transit times are illustrated in Fig. 51.33. The log measures only the formation between the receivers. The measured transit time is the weighted average of transit times in formations between the receivers.

Cycle Skipping and Triggering on the Noise. In transit time logging, the first arrival of the acoustic pulse must trigger both receivers of the sonde to yield correct values

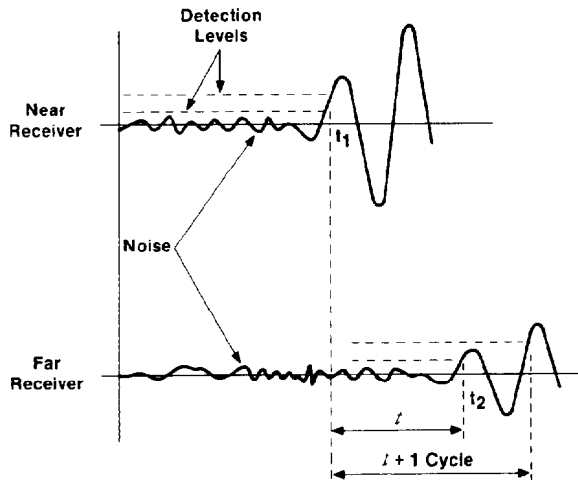


Fig. 51.34—Cycle skip and triggering on the noise.

of t . Under certain conditions, even though the first arrival is strong enough to trigger the first receiver, it may be attenuated to such an extent that by the time it reaches the far receiver it may be too weak to trigger it (Fig. 51.34). Instead, the far receiver may be triggered by a later arrival in the same acoustic pulse. This causes large and abrupt increases in the recorded transit time values. This phenomenon, known as "cycle skipping," may occur when the signal is strongly attenuated by (1) gas sands, especially if they cause gas in the mud; (2) poorly consolidated formations; (3) recently drillstem-tested intervals, because of the release of gas; (4) fractured formations; and (5) aerated mud.

If the detection levels are set too low, however, either one or both receivers may be triggered by noise, which is always present as the tool is being dragged up the hole. Depending on the receivers involved, triggering may cause t spikes either too short or too long. Examples of cycle skipping and triggering by noise are illustrated in Figs. 51.35 and 51.36.⁷⁹

Calibration. The precision of measurement of acoustic transit time with the acoustic log is determined by the precision of the timing circuitry, which, in turn, is controlled by the frequency of the quartz crystal used. For the usual crystals of 2.5 MHz, the potential resolution of the transit time measurement is $\pm 0.4 \mu\text{sec}/\text{ft}$.

The accuracy of the transit time measurement, however, depends on many other factors in addition to the precision of the timing circuitry. A discussion of some of the factors affecting the measurement of transit time is given by Thomas.⁷³

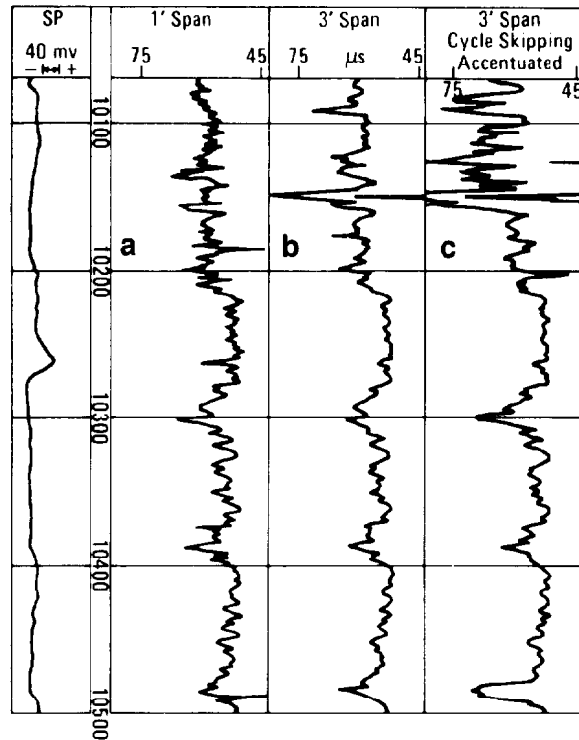


Fig. 51.35—Sonic log run in Edwards limestone: (a) 1-ft span, (b) 3-ft span, and (c) 3-ft span with intentionally accentuated cycle-skipping.

An essential factor is to ensure the proper calibration of the logging system. Calibration procedures of each commercially available acoustic velocity system are described in respective service company manuals. These should be required before and after logging to ensure the accuracy of the surface equipment. It is important to emphasize, however, that most calibration procedures do

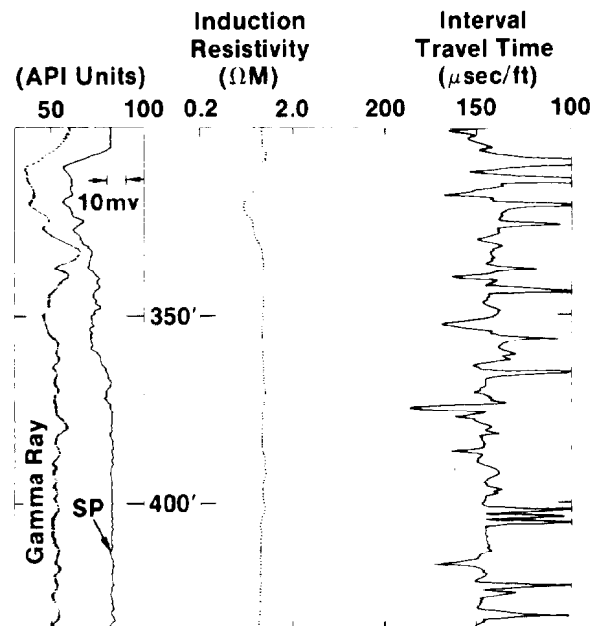


Fig. 51.36—Cycle skip and noise on acoustic log.

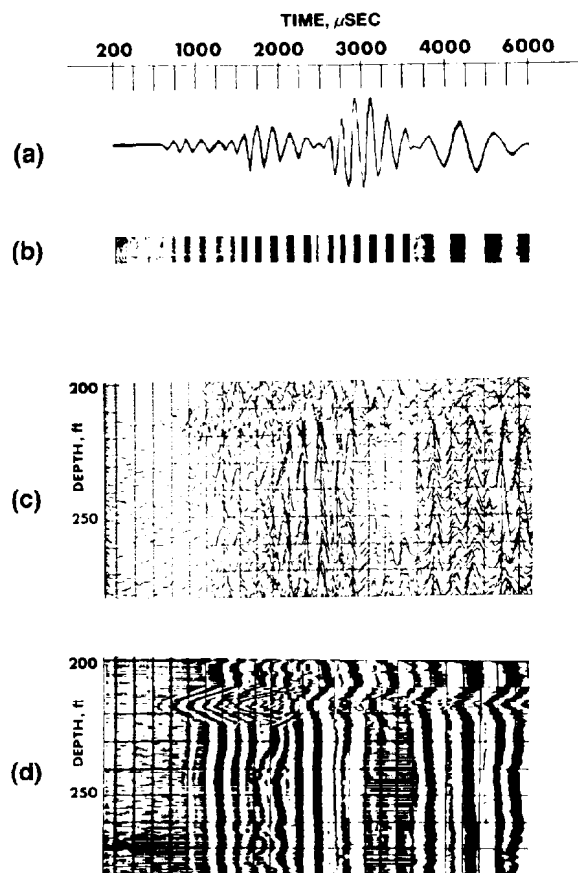


Fig. 51.37—Acoustic waveform recording.

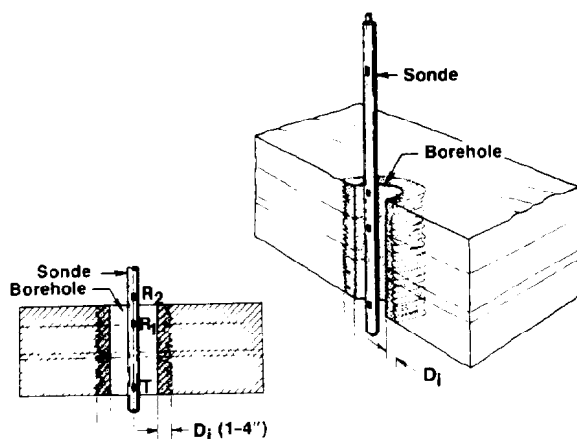


Fig. 51.38—Approximate volume of investigation of conventional acoustic logs.

just that. They merely check linearity of some of the circuitry in the surface instrumentation without any input from the downhole sonde.

A true calibration requires measuring the response of the complete system, surface instrumentation, and sonde in a standard environment. For this purpose, the tool is placed in a fluid-filled steel sleeve and transit time is checked against the known value of $57 \mu\text{sec}/\text{ft}$. In addition, some free pipe in the surface casing should be logged while going in and coming out of the hole, and checked against the value for steel of $57 \mu\text{sec}/\text{ft}$. Anhydrite beds, with a transit time of $50 \mu\text{sec}/\text{ft}$, and other formations with known transit times sometimes can be used to check the accuracy of the log; however, these methods are useful only if the downhole velocities in naturally occurring rocks are known not to vary from location to location or with depth of burial.

Amplitude/Time Recording

As described earlier, the acoustic wave (Fig. 51.37a) contains information other than compressional wave velocity. One of the methods developed to record some of this formation is the amplitude/time recording. In this method, which is also called the "X-Y mode," the amplitude of acoustic energy is recorded as a function of time at preassigned depths along the wellbore (Fig. 51.37c). Usually, this is achieved by analog recording of the output of one of the receivers on film.

Within the last few years, however, the introduction of wellsite and downhole computers has made possible the digital recording of waveforms from an array of acoustic receivers. For example, with one of these tools, a waveform is digitized at every $\frac{1}{2}$ -in. depth interval of the borehole to obtain more than 500 data points. Processing of this wealth of new information is a current area of research that is expected to increase significantly the usefulness of borehole acoustic measurements.

Intensity/Time Recording

For most applications, analog recordings of waveforms at $\frac{1}{2}$ -in. depth intervals are rather cumbersome to use. Hence, for routine use, to obtain a continuous recording or a log, waveforms are recorded in the intensity/time mode. In this presentation, each waveform is reduced to a series of dashes of varying width and intensity, depending on its frequency and amplitude (Fig. 51.37b). The process can be visualized by rotating the acoustic waveform of Fig. 51.37b by 90° on its horizontal axis and then recording the positive-going portions of the wave train as series of dashes and leaving the negative-going portions as blank spaces, as shown in Fig. 51.37c. The intensity/time log (Fig. 51.37d) is obtained by stacking these dashed lines from each depth interval.

Unfortunately, this process has not been standardized. Some service companies have the negative part of the waveform as the dark dashes and the positive part as the light blanks; other companies, vice versa. Also, some service companies have the time increasing from left to right, while other companies increase in the opposite direction. The various trade names for this presentation are Variable Density LogTM (VDL) by Schlumberger and Dresser, 3-D LogTM by Birdwell, and Micro-Seismogram LogTM by Welex.

Long-Spaced Acoustic Logging

Introduction. Conventional acoustic logs have a relatively shallow depth of investigation, D_i . The approximate bulk volume of the rock investigated by conventional acoustic logs is illustrated in Fig. 51.38.⁸⁰

This region is most subject to alterations because of stress relief, mechanical damage caused by drilling, and chemical alteration (clay hydration) caused by drilling fluid. An important early study by Hicks⁸¹ clearly demonstrated that acoustic velocities in certain formations sensitive to damage were significantly lower when measured near the borehole face than when measured deeper in the formation. Hicks⁸¹ clearly demonstrated that these borehole effects on acoustic velocities diminish with increased transmitter-to-receiver spacing. Since then, many investigators have observed drastically poor logging data caused by borehole enlargement and formation alteration around the borehole.

Borehole Size. Effects of borehole geometry on log measurements can be considered in terms of hole rugosity and hole enlargement. Borehole rugosity, which can cause significant errors in pad-type tools (such as density, sidewall neutron porosity, microresistivity, and high-frequency dielectric measurements) can produce diffractions in acoustic waves propagating along the borehole. In general, these should not affect the first-arrival compressional transit time measurements but can affect the

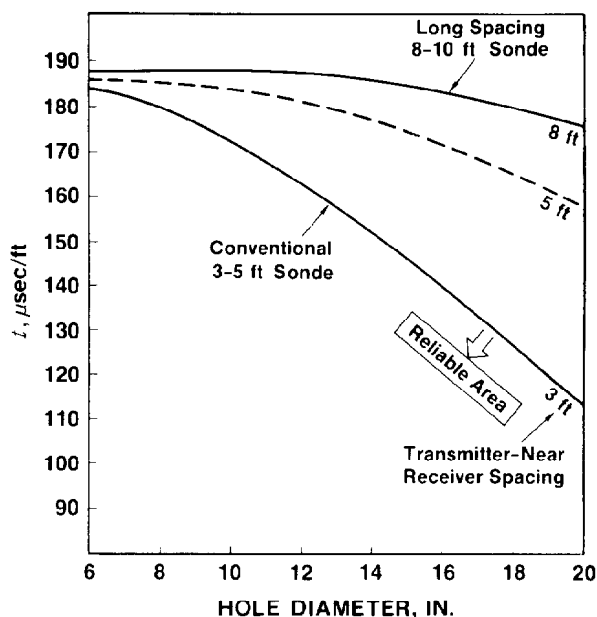


Fig. 51.39—Maximum detectable formation transit time, various transmitter-to-near-receiver spacing.

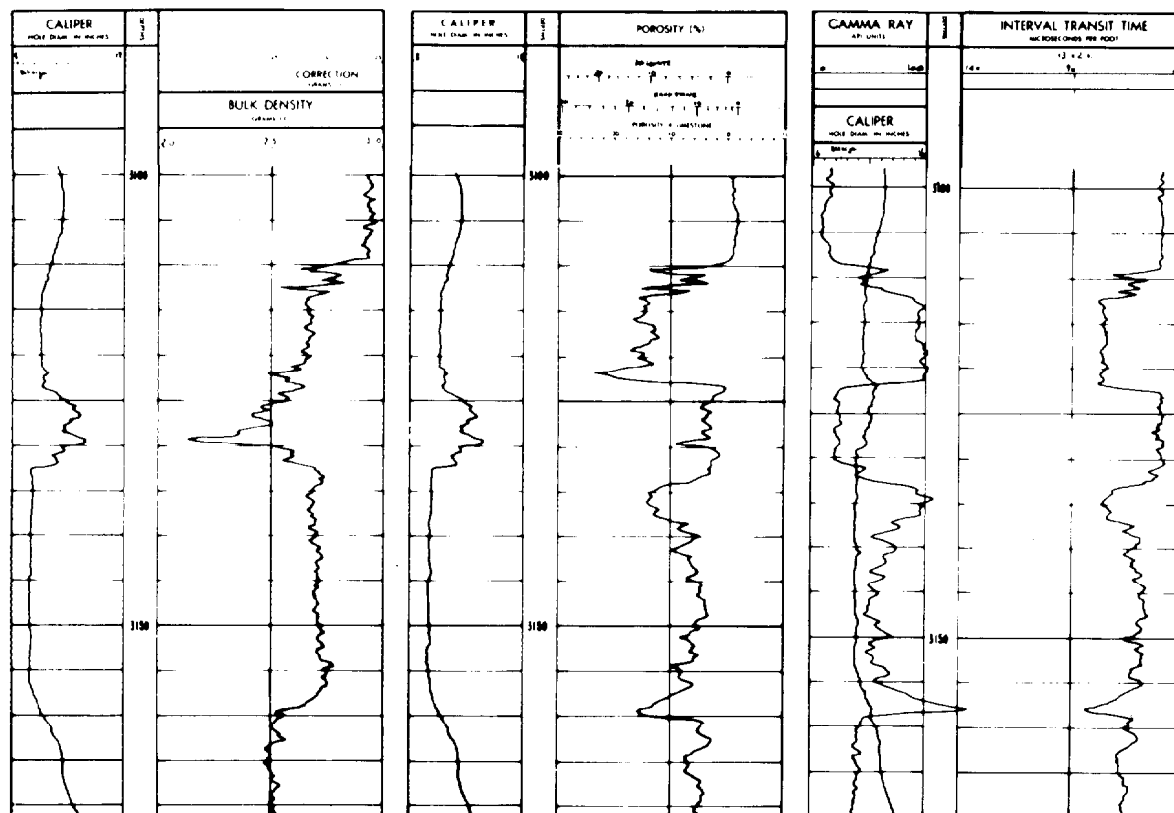


Fig. 51.40—Effects of cavity on density, sidewall neutron, and acoustic logs.

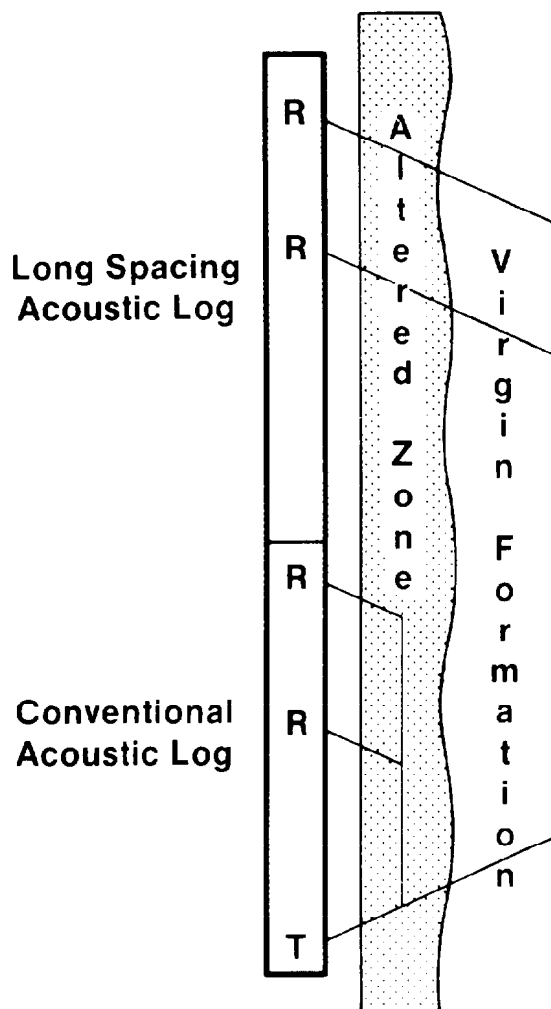


Fig. 51.41—Comparison of depth of investigations of conventional and long-spacing acoustic logs.

amplitudes. The hole size, however, can have a significant effect on the transit time measurements if the hole is large enough and the tool is centralized because the acoustic energy traveling directly down the hole in the mud might arrive at the receiver before the formation compressional wave.

Hole size effects on acoustic measurements have been investigated extensively.^{73,82} For a centralized tool, Goetz *et al.*⁸² computed the travel times along the direct mud path and the refracted path in the formation, for various hole sizes. Some of their results are illustrated in Fig. 51.39 in terms of t vs. borehole diameter. Below the line labeled conventional 3- to 5-ft sonde, a centered tool will read the formation transit time. Between this line and the dashed line (computed for a receiver with a 5-ft spacing from the transmitter), a centered tool will record a value intermediate between formation and mud transit times. Above the dashed line, a conventional acoustic log measures the velocity of compressional waves in the mud. The upper solid line is for a longer-spacing acoustic log with 8- to 10-ft receiver spacing. Below this

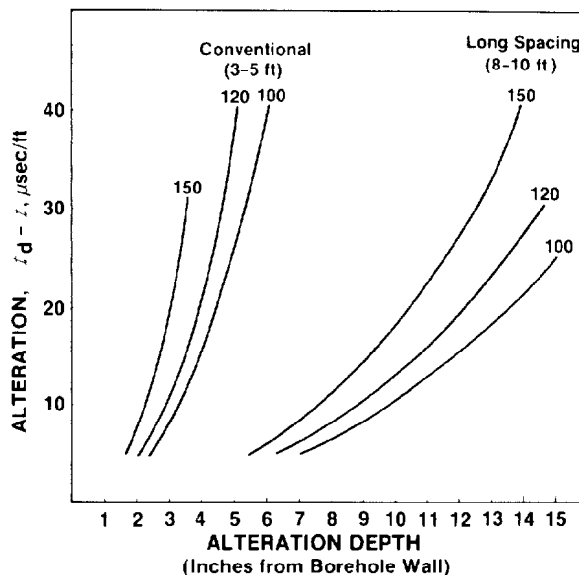


Fig. 51.42—Effects of formation alteration on measurements with conventional (3 to 5 ft) and long-spacing (8 to 10 ft) acoustic sondes.

line, the long-spaced tool measures high formation transit times in larger-diameter holes in the range where conventional tools would record incorrectly low formation travel times.

Even though these borehole size effects are important, conventional borehole-compensated acoustic logs can record reliable measurements under much more adverse borehole conditions than other porosity tools, such as density and neutron tools. The influence of a cavity on the density, sidewall neutron, and conventional acoustic tools is compared in Fig. 51.40.⁸³ In this figure, over the elliptical cavity indicated by the calipers on the density and acoustic logs, both the density and sidewall neutron curves are useless, whereas the acoustic log provides reliable data. This feature of the acoustic log is used to complement density and neutron porosity that are not reliable because of poor hole conditions.

Formation Alteration. A more important factor affecting the borehole acoustic measurements is formation alteration or damage around the borehole (Fig. 51.41). This can occur because of stress relaxation near the borehole wall, mechanical damage caused by prolonged exposure to drilling, or chemical alteration of the formation by interaction of drilling fluid with sensitive clays in the formation. Under these conditions, accurate measurements of acoustic velocities depend on hole size and transmitter receiver spacing, as well as velocities of both altered and unaltered zones around the borehole.

Formation alteration was investigated by Goetz *et al.*⁸² by assuming a step profile transit time around the borehole, with the altered or damaged zone having a transit time t_d that is greater than the undisturbed formation t and a mud transit time of 200 $\mu\text{sec/ft}$. They computed the depths of investigation of conventional acoustic (3- to 5-ft) and long-spacing (8- to 10-ft) acoustic logs in a 10-in.-diameter borehole. They also

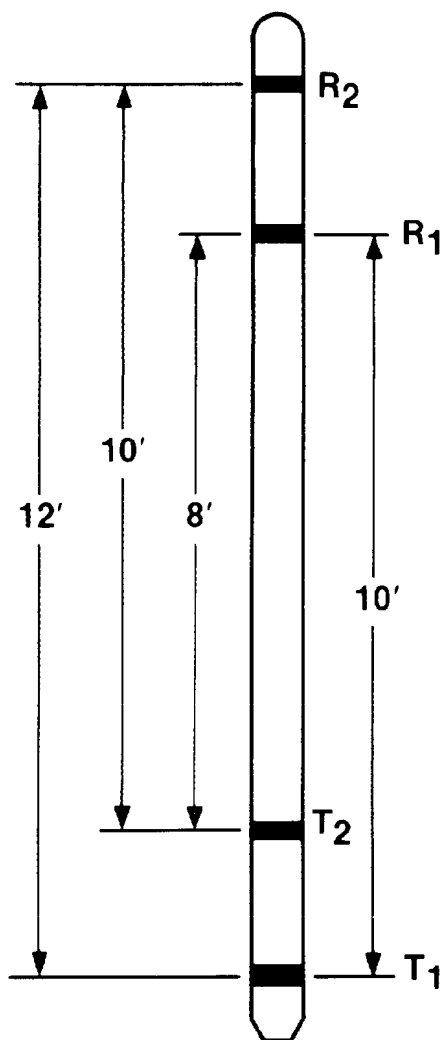


Fig. 51.43—Schlumberger long-spacing sonic log.

calculated formation alteration ($t_d - t$) as a function of alteration depth for unaltered formation transit times of 100, 120, and 150 $\mu\text{sec}/\text{ft}$. Their results, plotted in Fig. 51.42, illustrate the ability of the longer-spacing tool to overcome the effects of formation damage. In this figure, the area to the left of each curve represents the conditions for reliable measurements. For example, at an alteration of 20 $\mu\text{sec}/\text{ft}$, a conventional tool can handle an alteration of 5 in. if the formation transit time, t , is 100 $\mu\text{sec}/\text{ft}$, but only 3 in. if $t = 150 \mu\text{sec}/\text{ft}$.

Long-Spacing Acoustic Logging Tool. Both the borehole enlargement and the formation alteration effects can be accommodated by acoustic tools with longer transmitter-to-receiver spacings. A schematic diagram of one such tool, the Long Spacing Sonic™ by Schlumberger,⁸⁴ is shown in Fig. 51.43. Two transmitters, 2 ft apart, are at the bottom, and two receivers, 2 ft apart, are at the top, with 8-ft spacing between the two sections. Two long-spacing logs are recorded concurrently, one with 8- to 10-ft spacing and the other with 10-

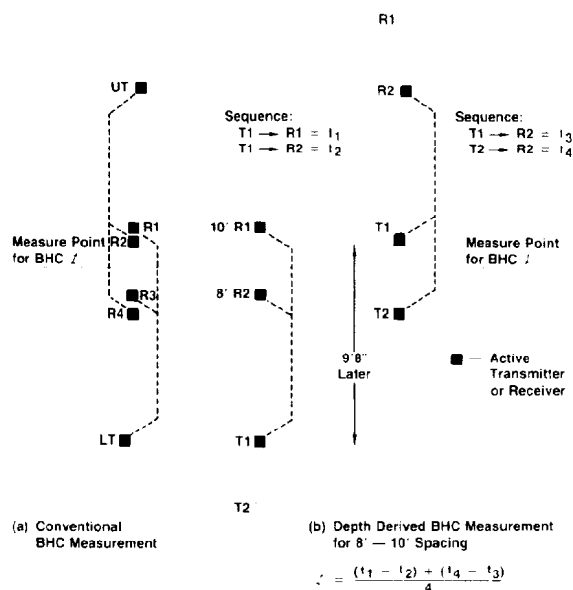


Fig. 51.44—Borehole-compensated transit time measurements: (a) conventional and (b) depth derived.

to 12-ft spacing. Borehole compensation is accomplished by a depth-derived measurement scheme illustrated in Fig. 51.44b, rather than the inverted array technique shown in Fig. 51.44a, which was described earlier (Fig. 51.31). To obtain the transit time at depth level, first the transmitter T_1 is pulsed twice and the respective times $t_1 = T_1 \rightarrow R_1$, $t_2 = T_1 \rightarrow R_2$ are recorded. The transit time for this case is given by

$$t_1 = \frac{t_1 - t_2}{2} \mu\text{sec}/\text{ft},$$

which is subject to errors discussed earlier if the hole size is different at the two receiver positions.

After the tool has moved 9 ft 8 in. up hole, the transmitters will be spanning the same depth interval between the points of refraction. This time they are each pulsed, and the travel times, $t_3 = T_1 \rightarrow R_2$ and $t_4 = T_2 \rightarrow R_2$ are recorded by the second receiver (R_2). For this second case, the transit time is given by

$$t_2 = \frac{t_4 - t_3}{2} \mu\text{sec}/\text{ft},$$

which is subject to the same errors as t_1 but in an opposite direction. The depth-derived transit time for the 8- to 10-ft spacing is obtained by averaging these two measurements:

$$t = \frac{t_1 + t_2}{2}.$$

A similar borehole compensation is obtained for the 10- to 12-ft spacing by using the second transmitter T_2 in the first position, instead of T_1 , and the first receiver R_1 in the second position, instead of R_2 .

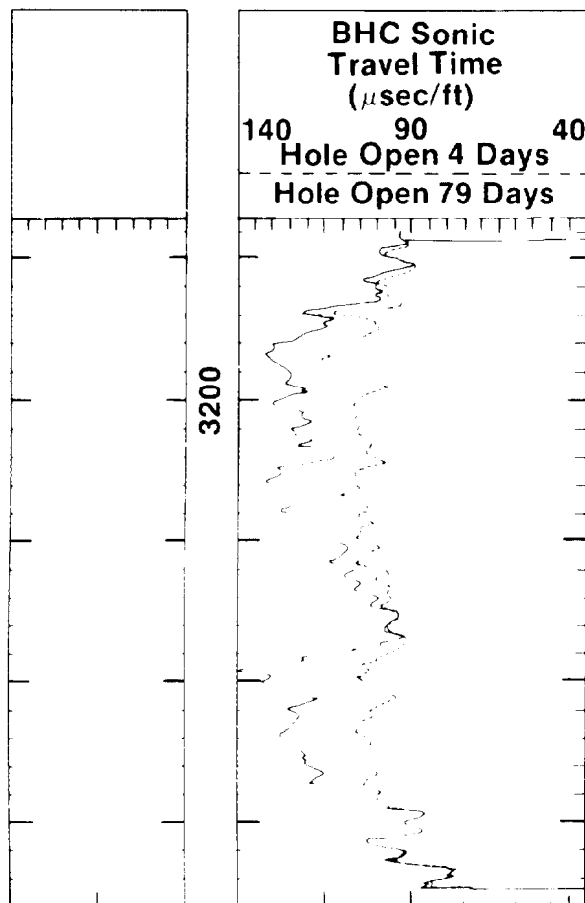


Fig. 51.45—Formation alteration caused by exposure to mud; bit size 12¼ in.

Effects of prolonged exposure to drilling and drilling mud on acoustic velocities measured with a conventional borehole-compensated acoustic log are illustrated in example logs in Fig. 51.45 taken from the reference by Misk *et al.*⁸⁵ The dashed curve is obtained after the hole has been exposed to drilling for 4 days with the borehole relatively undamaged; the solid curve is after 79 days of exposure. During this period, the formation over much of the interval has been damaged enough to increase the t by 30 $\mu\text{sec}/\text{ft}$ or more.

As described previously, long-spacing acoustic logs are less affected by altered zones. A comparison of conventional and long-spaced acoustic logs is shown in Fig. 51.46 for a sand/shale section.⁷³ In the upper section, the conventional log is reading higher values of t than those by the long-spacing tool, probably because of shale alteration. In Sand Z, both logs are in agreement, whereas in sections directly above and below Sand Z, the conventional log is reading significantly higher values of t , probably because of hole washouts.

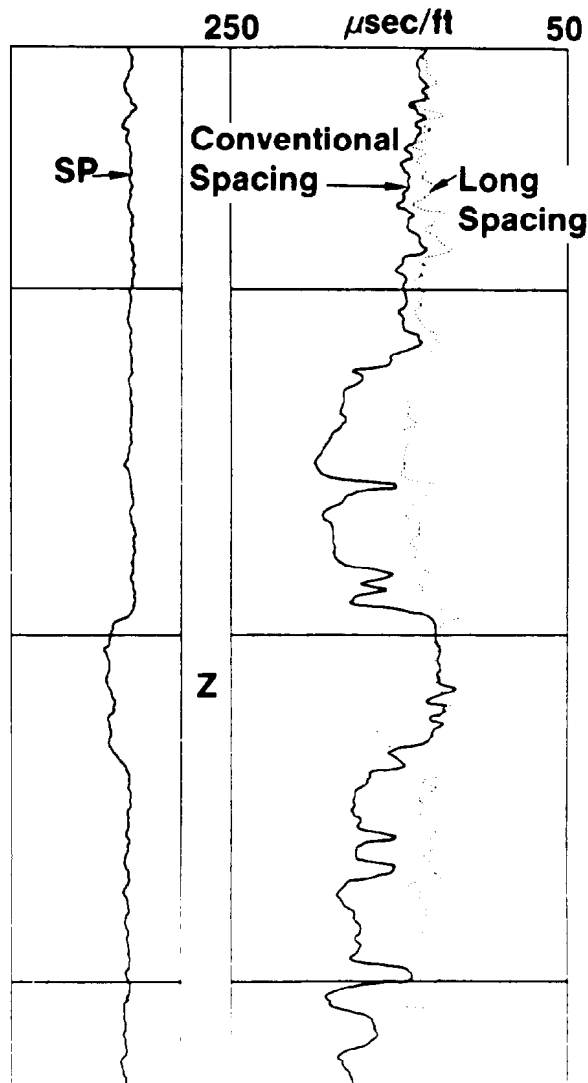


Fig. 51.46—Conventional and long-spacing acoustic logs in a sand/shale section.

The example in Fig. 51.47 is a comparison of the two acoustic tools in shallow and deeper Louisiana gulf coast sand/shale sequences.⁸⁶ Physical characteristics of both the shale at 3,470 ft and the sand at 3,500 ft have been altered by drilling and interaction with mud filtrate. The conventional spaced tool is reading 15 $\mu\text{sec}/\text{ft}$ higher because of this alteration. This is also reflected by a 10-millisecond difference between the respective transit time integration curves shown in the depth tract. In the deeper section, as the formations become more compacted, the formation alteration is reduced; hence, the conventional and long-spacing measurements are in agreement within the interval 8,500 to 8,600 ft.

Even though, in most instances, the t values from 8- to 10-ft and 10- to 12-ft spaced receivers are in agreement, very deep formation alteration can sometimes affect the t values recorded by the 8- to 10-ft receivers. The example in Fig. 51.48 is from a shallow well with modified depths.⁸⁴ In the upper zone, the 8- to 10-ft spacing is reading values higher by 10 $\mu\text{sec}/\text{ft}$ than those given by

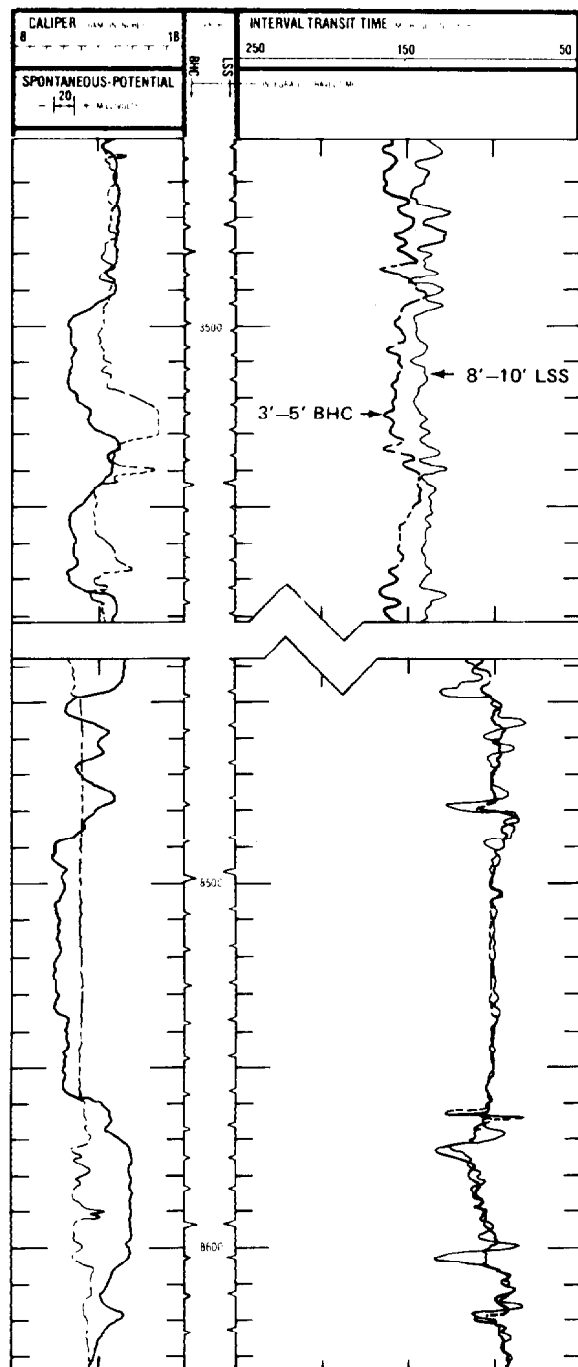


Fig. 51.47—Conventional (BHC) and long-spacing (LSS) acoustic logs in a Louisiana gulf coast sand/shale sequence.

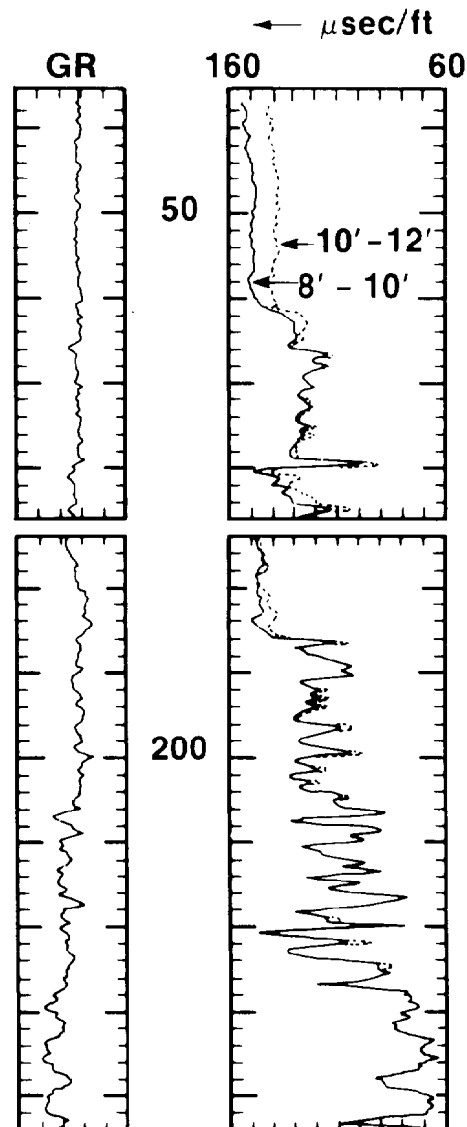


Fig. 51.48—Very deep formation alteration.

the 10- to 12-ft spacing, because of very deep formation alteration. In the lower section, the 8- to 10-ft spacing still reads a few microseconds higher down to the compacted formations below depth 227 ft.

In the final example shown in Fig. 51.49, the better response of the long-spaced logs in enlarged boreholes is illustrated. In the upper section, the conventional spaced tool is reading the mud transit time in a hole washed out

to 20 in. In the lower section, the borehole is not washed out but the conventional tool is reading up to 60 $\mu\text{sec}/\text{ft}$ too high because of formation alteration. Below 8,700 ft, all three curves (i.e., the 3- to 5-ft, 8- to 10-ft, and 10- to 12-ft curves), are in agreement.

Summary. Borehole size and formation alteration can significantly affect the properties of acoustic waves

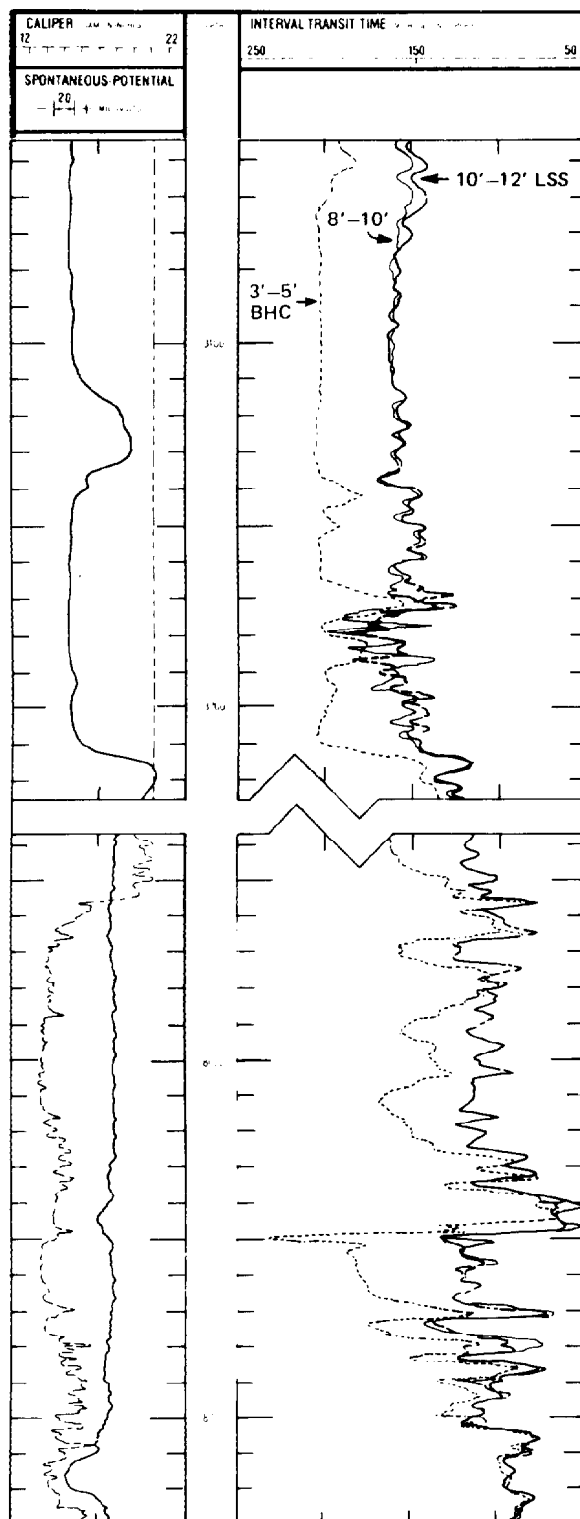


Fig. 51.49—Response of conventional and long-spacing acoustic logs in an enlarged borehole.

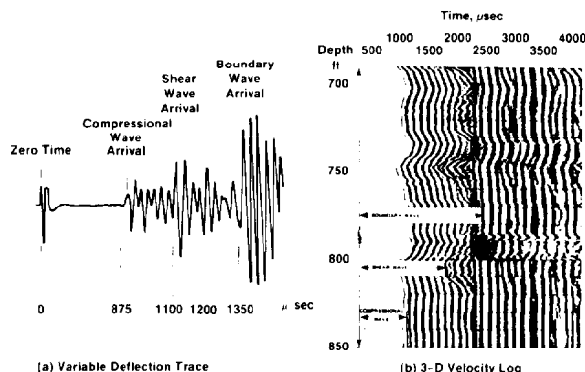


Fig. 51.50—Identification of shear arrivals on analog recording of (a) acoustic waveforms and (b) variable-density (3D) presentations.

traveling in a borehole. The long-spaced acoustic tools are much less affected by borehole conditions and yield more reliable values of compressional-wave transit times under borehole conditions in which conventional tools would be grossly in error. The vertical bed boundary resolution of the long-spaced tool is the same as that of the conventional tool since the receiver spacing is 2 ft for both. Because of the longer transmitter-to-receiver spacing, the acoustic energy has to travel farther; therefore, it is attenuated more. This has caused more frequent spiking and cycle skipping on the long-spaced acoustic logs; however, this technology is improving through the introduction of more powerful transmitters, more sensitive receivers, downhole digitizing, and surface processing of waveforms.

Shear-Wave Logging

The borehole acoustic measurement methods described so far have been for obtaining compressional wave velocities. The desirability of obtaining other information contained in the acoustic waveform has long been recognized.²⁷ Most of the effort has been directed toward obtaining the velocity of shear waves.

Early attempts involved hand-picking the shear-wave arrivals on the analog recording of either waveforms or variable-density—microseismogram or three-dimensional (3-D)—presentations as illustrated in Fig. 51.50⁶³

Another method involves automatic recording of shear-wave travel times by a bias technique.⁸⁷⁻⁹⁰ In this method, a high-amplitude event following the compressional-wave arrivals is assumed to be the shear wave arrival. The transit time of these waves is measured by setting the voltage bias level higher than the compressional-wave amplitudes.

A thorough investigation of conventional methods for determining shear-wave velocities from long- and short-spaced acoustic logs was conducted by Koerperich.⁹¹ In this study, borehole experiments were conducted by using a conventional Schlumberger Borehole Compensated Sonic Log® (BHC) with two transmitters and four receivers at 3- and 5-ft spacing and a Schlumberger experimental long-spaced tool with a single transmitter and four receivers located at 10, 12, 14, and 16 ft from the

transmitter. Waveforms recorded with these tools in a carbonate section are shown in Fig. 51.51 for several transmitter-to-receiver spacings. As indicated in this figure, it is easier to identify the later arrivals on the longer-spacing waveforms because of the greater separation in arrival times.

Some measurement results from this study are shown in Figs. 51.52 and 51.53 for a carbonate and a sand/shale section, respectively. For both compressional and shear waves, long spacings generally yield slightly lower travel times (higher velocities) than short spacings. Another important aspect of this study involved laboratory measurements of acoustic velocities on core samples. Compressional and shear-wave velocities were measured on core plugs subjected to simulated subsurface overburden and pore pressure conditions. These results are plotted as circles in Figs. 51.52 and 51.53. Koerperich⁹¹ states that average agreement between the laboratory and log shear velocities (for both the long- and short-spaced tools) is within 2% for carbonates and 8% in sandstones, and that it is slightly better for the compressional waves. He states further that these differences between the laboratory and the log values are nonsystematic.

The foregoing discussion demonstrates that determination of shear transit times in a borehole by hand-picking the arrival times from waveforms or from variable-density presentations is at best a tedious and not very accurate process. Further, attempts to automate this process by threshold detection have been subject to errors when using an axial transmitter/receiver logging technology designed primarily for measurement of compressional-wave travel times. The reasons for these errors are explained by some of the recent modeling studies of acoustic wave propagation in a fluid-filled borehole.⁶⁵⁻⁶⁷ These studies demonstrate that the shear-wave arrival is indistinguishable from the onset of the reflected conical waves on the synthetic acoustic waveforms. However, the phase and group velocities of the reflected conical wave at its low-frequency cutoff are equal to the formation shear-wave velocity (see Fig. 51.25). Hence, if the onset of the reflected conical wave is measured in error, the transit time will be close to that of the shear wave. This might be the case in some of the previously discussed studies.

Acoustic Array Logging

Borehole modeling of acoustic wave propagation has demonstrated the need for a new generation of acoustic logging technology to extract more information from acoustic waveforms. Acoustic logging tools having arrays of transmitters and receivers, and complex digital signal processing capabilities have been developed to analyze the data obtained.

One such tool is shown in Fig. 51.54.⁹² It has a lower-frequency transmitter (11 kHz vs. the conventional 20 kHz), an array of four receivers placed at a longer spacing from the transmitter, and a downhole digitizer to record waveforms without cable distortions. Surface instrumentation records the signals digitally. The processing method, using a four-fold correlation algorithm, analyzes waveforms from the four receivers simultaneously to obtain compressional and shear-wave transit times (Fig. 51.55).

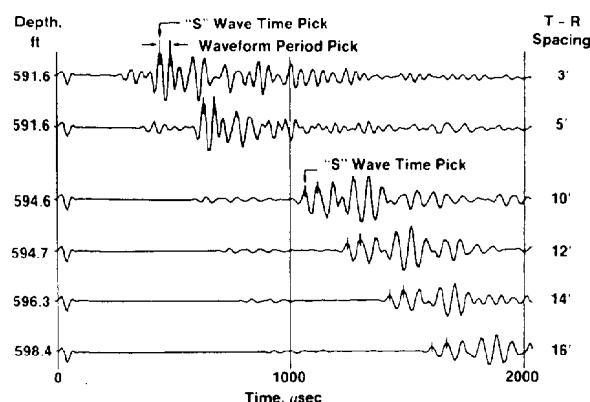


Fig. 51.51—Acoustic waveforms recorded at various transmitter-to-receiver spacings in a carbonate section.

Another acoustic array log is a 12-receiver experimental sonde developed by Schlumberger.⁷⁷ It has a single 10 kHz transmitter and an array of 12 receivers. The receivers have been arranged both in a nonuniform array spanning 4 ft with spacings of 0, 6, 9, 12, 15, 18, 21, 24, 27, 30, 36, 42, and 48 in. and in a uniform array spanning 5.5 ft with 6 in. between the receivers. The spacing between the transmitter and a receiver array is adjustable between 5 and 25 ft.

An experimental tool developed by Elf Aquitaine uses an array of transmitters and an array of receivers.⁷⁸ The transmitting array has five transmitters uniformly spaced at 0.25 m apart; hence, it has a span of 1 m. The receiving array has 12 receivers uniformly spaced at 1-m intervals. The distance between the receiving and the transmitting arrays is set at 1 m.

Finally, the prototype sonde by Schlumberger (shown in Fig. 51.56) has an eight-receiver array and two transmitters.⁹³ In addition, it has two additional receivers spaced at 3 and 5 ft from the transmitter to simulate conventional tools. It also has the capability to measure the compressional-wave velocity of the borehole fluid. Again, waveforms are digitized downhole and transmitted to the surface for recording and analysis.

As apparent from the previous discussion, this is a very active area of development. Tools are constantly being developed to explore the extraction of additional information, such as pseudo-Rayleigh and Stoneley wave velocities, from acoustic waveforms. Capabilities are being developed to record large amounts of data. For example, more data are obtained with one of these array tools in a 1-mile-deep well than are recovered in a 1-mile seismic section.

A parallel and complementary area of development is signal processing methods for analyzing these data. Processing methods such as direct phase determination,⁹⁴ slowness time coherence,⁹³ and semblance^{77,95} have been developed to permit automated analysis of shear-wave transit times. Array processors are being added to wellsite data acquisition systems to permit real-time signal processing.

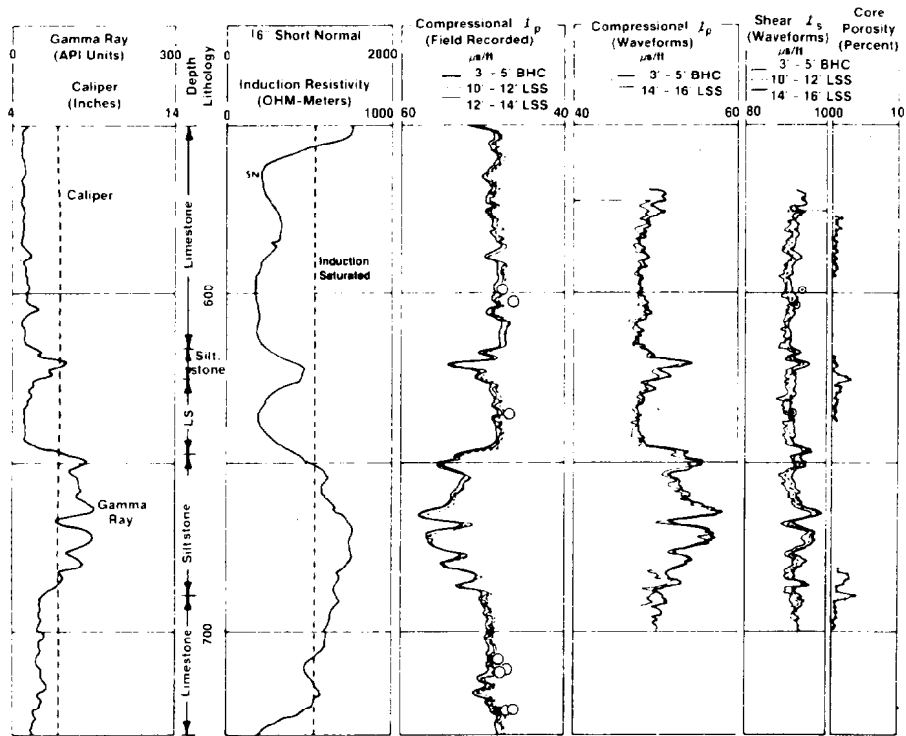


Fig. 51.52—Borehole and laboratory measurements of compressional- and shear-wave transit times in a carbonate section.

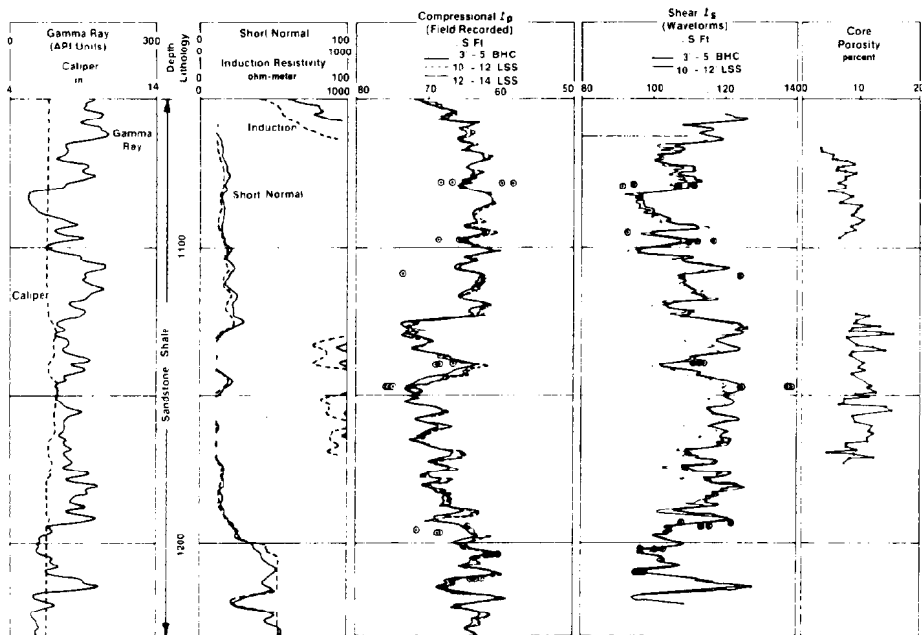


Fig. 51.53—Borehole and laboratory measurements of compressional- and shear-wave transit times in a sand/shale section.

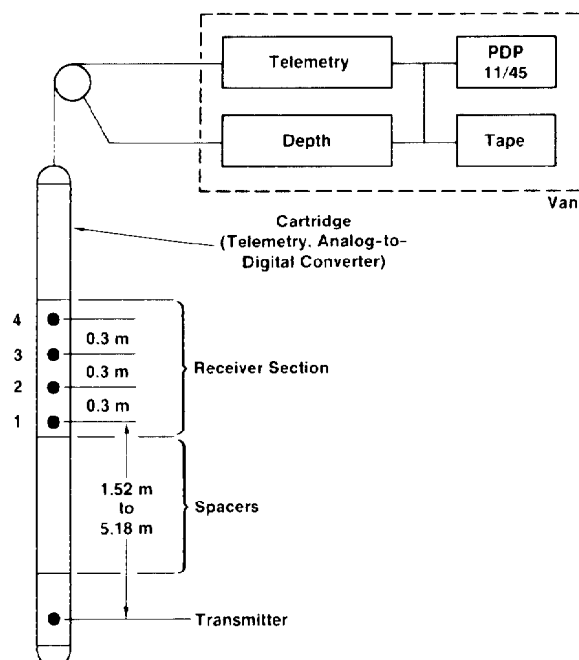


Fig. 51.54—A four-receiver acoustic array log with a downhole digitizer.

So far, emphasis has been on extraction of shear-wave velocity from acoustic waveforms. With continued improvement in tool design and signal processing, it is expected that in the not too distant future, acoustic logs will record not only the velocities of compressional, shear, pseudo-Rayleigh and Stoneley waves, but their attenuations as well.

Reflection Method

The reflection method of acoustic wave propagation logging is basically similar to sonar. A single transducer rotates at constant speed, emitting acoustic pulses in the megahertz range and recording their echoes from the borehole face (Fig. 51.57). As in the transmission method, both travel times and amplitudes are used. The azimuth of the beam also is recorded.

The first such logging tool, the borehole televiewer,⁹⁶ used only the amplitude of the reflected signals to

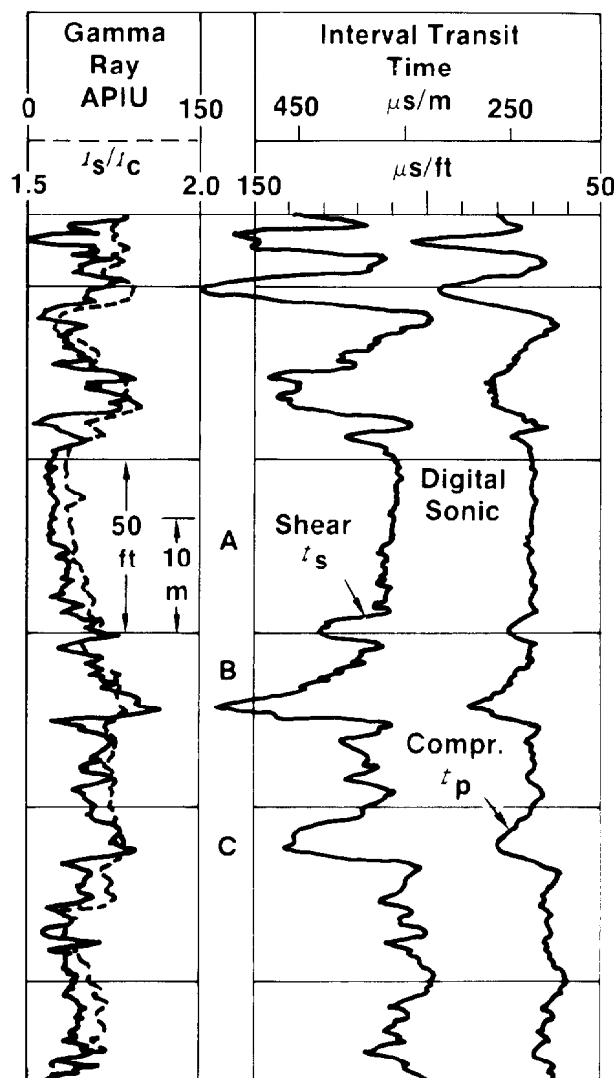


Fig. 51.55—Compressional- and shear-wave transit time log obtained by analysis of the waveforms recorded with the sonde in Fig. 51.54.

generate a picture of the borehole wall. When the borehole wall is smooth, the amplitude of the reflected signal is high; it is recorded as a light spot. Low-amplitude reflections from fractured or vuggy walls are recorded as dark spots. The resulting log is essentially a black and white picture of the borehole wall, split vertically along magnetic north and flattened (Figs. 51.58 through 51.60).

For the borehole televiewer (BHTV) log, the vertical scale is depth and the horizontal scale corresponds to azimuth of the borehole wall. An isometric view of a vertical fracture intersecting the wellbore in an east-west direction is shown on the left in Fig. 51.58.⁹⁷ The corresponding BHTV log on the right shows the fracture as two vertical dark lines 180° apart. Similarly, an isometric of a south-dipping fracture or bedding plane is shown with the corresponding BHTV log in Fig. 51.59.

An example of a BHTV log (Seisviewer® by Birdwell⁹⁸) based on amplitude imaging is shown in Fig.

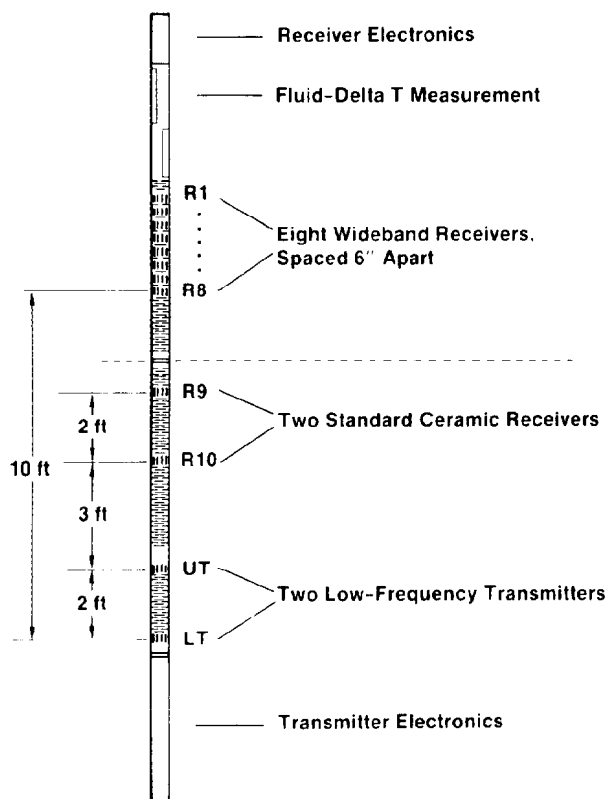


Fig. 51.56—An eight-receiver acoustic array sonde.

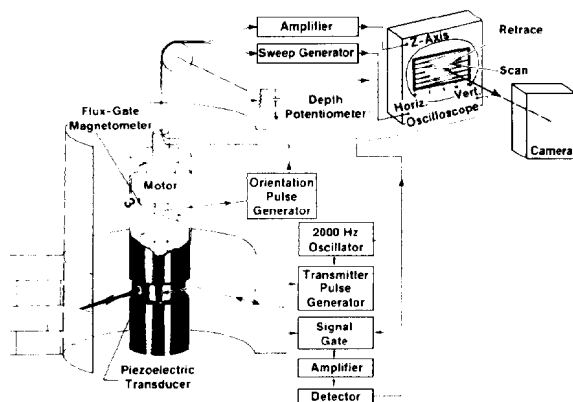


Fig. 51.57—Block diagram of BHTV logging system.

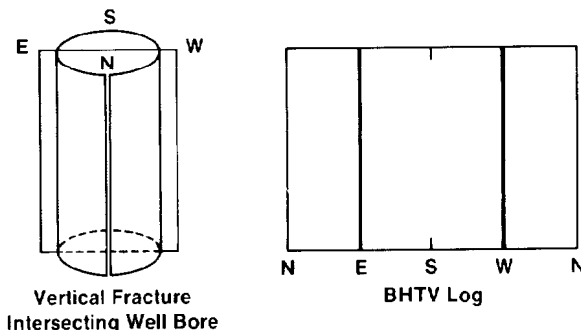


Fig. 51.58—Isometric of a vertical fracture intersecting a borehole and corresponding BHTV log.

51.60 for a borehole intersected by two fractures. The corresponding isometric on the right describes the two different dips and strikes.

Significant hardware and signal processing improvements have been made to early BHTV technology.^{97,99-101} Current technology uses transit time information to obtain an image, in addition to the image obtained from the amplitudes of the reflected signals. Transit time images complement amplitude images in many ways. Transit time measurement is essentially a near-perfect borehole geometry tool with a resolution of 0.05 in. BHTV images developed from the transit time measurements can be considered as two-dimensional (2D) relief maps of the borehole.

Further use of transit time measurements is made in generating tilted polar scan displays.⁹⁹ These are essentially 3D casts of the borehole, which can be viewed from all directions. The tilted polar scan of Fig. 51.61 shows a damaged section of a casing viewed from two angles, which also can be viewed from any desired angle.

Applications

Introduction

Some present and possible future applications of acoustic logging will be presented to illustrate the use of borehole acoustic measurements described earlier and listed in Table 51.1. Discussion here will emphasize the more important uses, and only references will be given to more routine and less significant ones.

Seismic and Geological Interpretation

Borehole measurements of acoustic properties were developed originally to obtain time/depth curves to use in seismic interpretation.¹⁰² In addition to recording transit times of the compressional waves as functions of depth, acoustic logs also integrate these data and record a tick mark on the log for each millisecond of elapsed time. These marks are then used in conjunction with check-shot surveys for seismic interpretation.^{79,103}

Recent advances in borehole shear-wave velocity recording also have allowed this technology to be used with surface seismic shear surveys in a way similar to the compressional-wave velocity log use with the seismic compressional surveys.¹⁰⁴

An important geological application of acoustic logs has been for correlating geologic sections. As described earlier (see Fig. 51.39), acoustic log response is much less affected by borehole irregularities than are some of the other porosity logs. As a result, acoustic logs provide valid data over a large proportion of the borehole.

Further, acoustic logs usually show much character and detail. Therefore, they have been useful for locating bed boundaries, identifying gas/oil interfaces, and determining subsurface geology. An example of geological correlation is shown in Fig. 51.62; even though the two wells in this figure are 10 miles apart, the character of the compressional transit time curves is quite similar.

Porosity

Borehole measurements of acoustic velocities were instrumental in the development of quantitative formation evaluation in the 1950's, although they were developed initially to aid seismic interpretation. Over the years, the primary use of acoustic logs in formation evaluation has been the determination of porosity from measurements of compressional-wave transit time ($t = 1/v_p$). Earlier in this chapter, factors affecting acoustic properties were described through both theoretical and experimental studies of elastic wave propagation in porous media. On the basis of these discussions, it would be at best naive to expect a simple linear relationship between porosity and compressional-wave transit time. However, empirical observations have indeed demonstrated the validity of such a relationship under certain special conditions.

Consolidated Rocks. A commonly used linear relationship for estimating porosity from acoustic measurements (based on laboratory measurements of acoustic velocity and porosity in porous rocks and other materials) was proposed by Wyllie *et al.*^{18,19} Commonly referred to as the Wyllie time-average equation, it is expressed as

$$\frac{1}{v_p} = \frac{\phi}{v_L} + \frac{(1-\phi)}{v_m}, \quad \dots \dots \dots (10)$$

or in terms of transit times, as

$$t = \phi t_L + (1-\phi)t_m, \quad \dots \dots \dots (11)$$

where

- $t (=1/v_p)$ = transit time of the compressional waves for the liquid-saturated porous medium,
- $t_L (=1/v_L)$ = transit time for saturant liquid that forms the solid frame of the porous medium,
- $t_m (=1/v_m)$ = transit time for rock matrix that forms the solid frame of the porous medium, and
- ϕ = porosity.

This relationship can be rearranged as

$$t = (t_L - t_m)\phi + t_m \quad \dots \dots \dots (12)$$

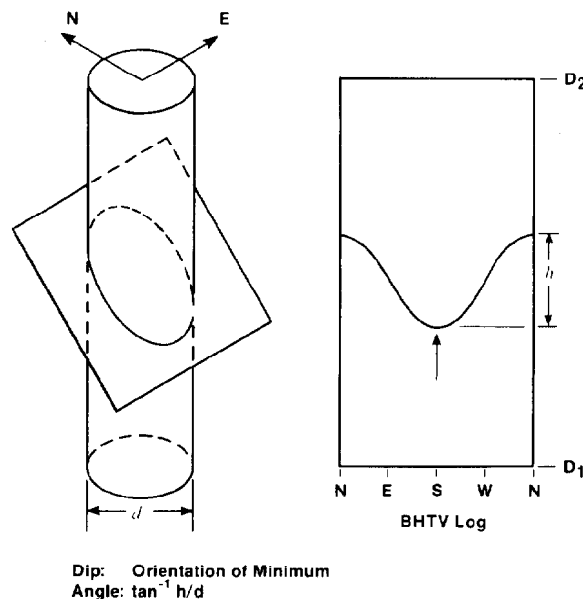


Fig. 51.59—Isometric of fracture or bedding plane intersecting borehole at moderate dip angle, and corresponding BHTV log.

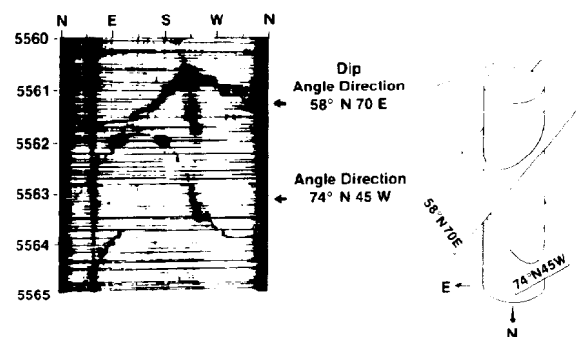


Fig. 51.60—BHTV indicating two fractures of different dips and strikes.

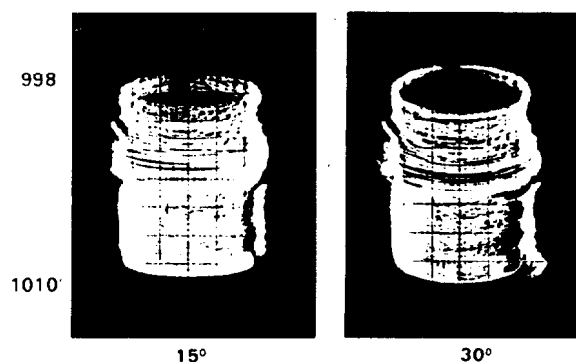


Fig. 51.61—BHTV tilted polar image of a section of a damaged casing.

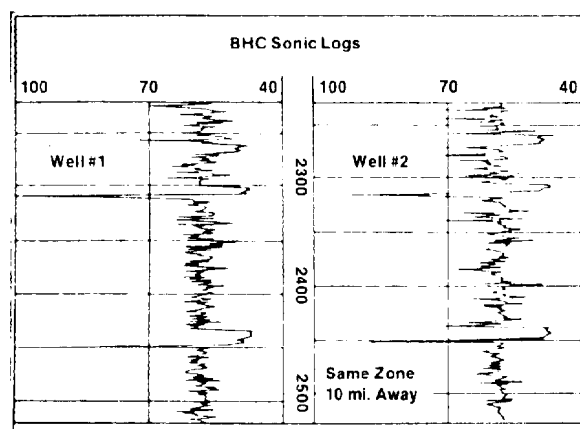


Fig. 51.62—Acoustic log correlation between two wells.

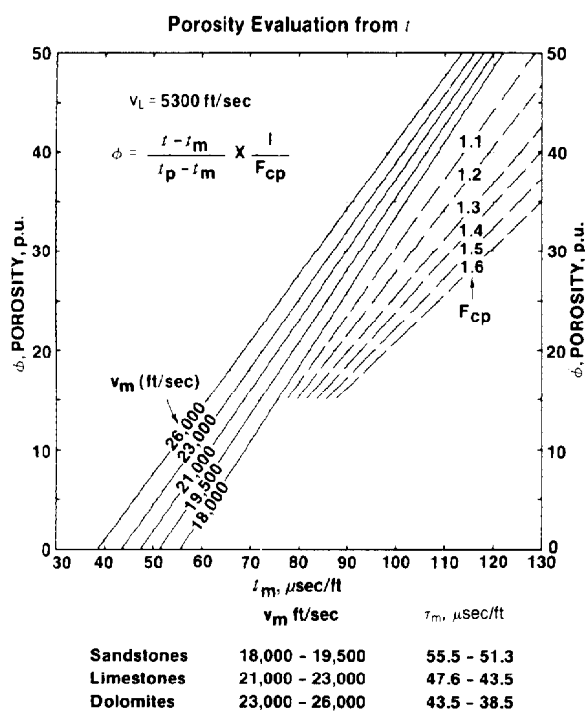


Fig. 51.63—Porosity evaluation from acoustic log.

or

$$t = m\phi + b, \quad (13)$$

where the slope is $m = t_L - t_m$ and the intercept is $b = t_m$.

The most attractive feature of Eq. 12 is its simplicity. It states that the transit time of an acoustic wave in a porous rock is the porosity-weighted average of its transit times in the matrix and the liquid in its pores. Also, it extrapolates to correct values for 0 and 100% porosities—i.e., t_m and t_L , respectively.

This simplicity coupled with pedagogically pleasing qualities made Eq. 12 popular and, more importantly, established acoustic logging as an important tool in formation evaluation. As stated, however, there is no theoretical justification for such a simple relationship. In the Appendix, the linear relationship, Eq. 13, is shown to be a second-order approximation of a comprehensive relationship, Eq. A-9, with the intercept b approximately equal to the matrix transit time and the slope m strongly dependent on elastic properties of the porous rock frame and the compressibility of pore fluid. Nevertheless, under the right conditions, a linear dependence of transit time on porosity has been established through literally hundreds of empirical observations.

A graphical representation of the time-average equation, Eq. 11, is given in Fig. 51.63.¹⁰⁵ This is a good beginning for determining porosity from acoustic log measurements when no other information is available. It provides acceptable values of porosity for well-compacted rocks with uniform pore size distribution and under effective stress (difference between the overburden stress and pore fluid pressure) of at least 4,000 psi.

In most applications, the linear relationship of Eq. 13 has been found to be more useful than the time-average equation, Eq. 11, provided that the values of b and m can be determined. As indicated in the Appendix, the parameter b is approximately equal to $(1/v_m)$; therefore, it depends on rock matrix properties. Published values for b range from 50 to 60 $\mu\text{sec}/\text{ft}$ for sandstones, from 45 to 50 for limestones, and from 40 to 48 for dolomites.

Velocities of compressional and shear waves for a large number of materials are given in handbooks by Clark¹⁰⁶ and by Simmons and Wang.¹⁰⁷ An extensive list of compressional and shear transit times have been compiled by Wells *et al.*¹⁰⁸ for minerals and rocks encountered in oil and mineral exploration. Probably the most comprehensive compilation of compressional and shear-wave velocities for marine sediments, rock-forming minerals, and rocks is given, for various pressures and temperatures, in a recent handbook by Carnichael.¹⁰⁹ A set of compressional and shear-wave velocity data from the literature is listed in Table 51.3¹¹ for selected materials, to illustrate the range of velocities encountered in and around the borehole.

The values of m depend on the elastic moduli of the rock frame, which in turn are controlled by the effective stress and pore structure and by the compressibility of the pore fluid. Changes in velocities have been observed to become smaller with increasing effective stress. Therefore, pressure dependence of m may be small enough to be neglected in normally pressured sections below 7,000 ft. Effects of pore structure might be

TABLE 51.3—ACOUSTIC VELOCITIES

Material		v_p (ft/sec)	v_s (ft/sec)
Nonporous solids			
anhydrite		20,000	11,400
calcite		20,100*	—
cement (cured)		12,000	—
dolomite		23,000	12,700
granite		19,700	11,200
gypsum		19,000	—
limestone		21,000	11,100
quartz		18,900*	12,000
salt		15,000*	8,000
steel		20,000	9,500
Water-saturated porous rocks in situ			
	Porosity (%)		
dolomites	5 to 20	20,000 to 15,000	11,000 to 7,500
limestones	5 to 20	18,500 to 13,000	9,500 to 7,000
sandstones	5 to 20	16,000 to 11,500	9,500 to 6,000
sands (unconsolidated)	20 to 35	11,500 to 9,000	—
shales		7,000 to 17,000	—
Liquids**			
water (pure)		4,800	
water (100,000 mg NaCl/L)		5,200	
water (200,000 mg NaCl/L)		5,500	
drilling mud		6,000	
petroleum		4,200	
Gases			
air (dry or moist)		1,100	
hydrogen		4,250	
methane		1,500	

*Arithmetic average of values along axes.

**At normal temperature and pressure.

described qualitatively by stating that the magnitude of m increases with decreasing grain contact areas. Thus, m is small for crystalline rocks and larger for granular and shalier rocks, ranging from 0.5 to 1.5 $\mu\text{sec}/\text{ft}$ for carbonates and from 1 to 3 $\mu\text{sec}/\text{ft}$ for sandstones.

Compressibility of the pore fluid depends on whether it is gas, oil, or water and becomes significant in poorly consolidated rocks (see Eq. A-7). In well-consolidated rocks under high effective stress, the relative contribution of pore fluid compressibility to the overall rock elastic moduli is small; therefore, variations of m because of pore fluid content may be neglected.

The large range in values of b and m necessitates the use of core analysis data to calibrate the acoustic log for estimating porosity. For this purpose, porosities and travel times are measured on core samples under the equivalent subsurface pressure conditions, and the linear relationship between the two is established by statistical analysis. If laboratory measurements of t are not available, restored pressure measurements of porosity, or porosity corrected for equivalent subsurface conditions can be correlated to t from the acoustic log to establish the linear relationship, provided that adequate depth correspondence between core and log data can be established.

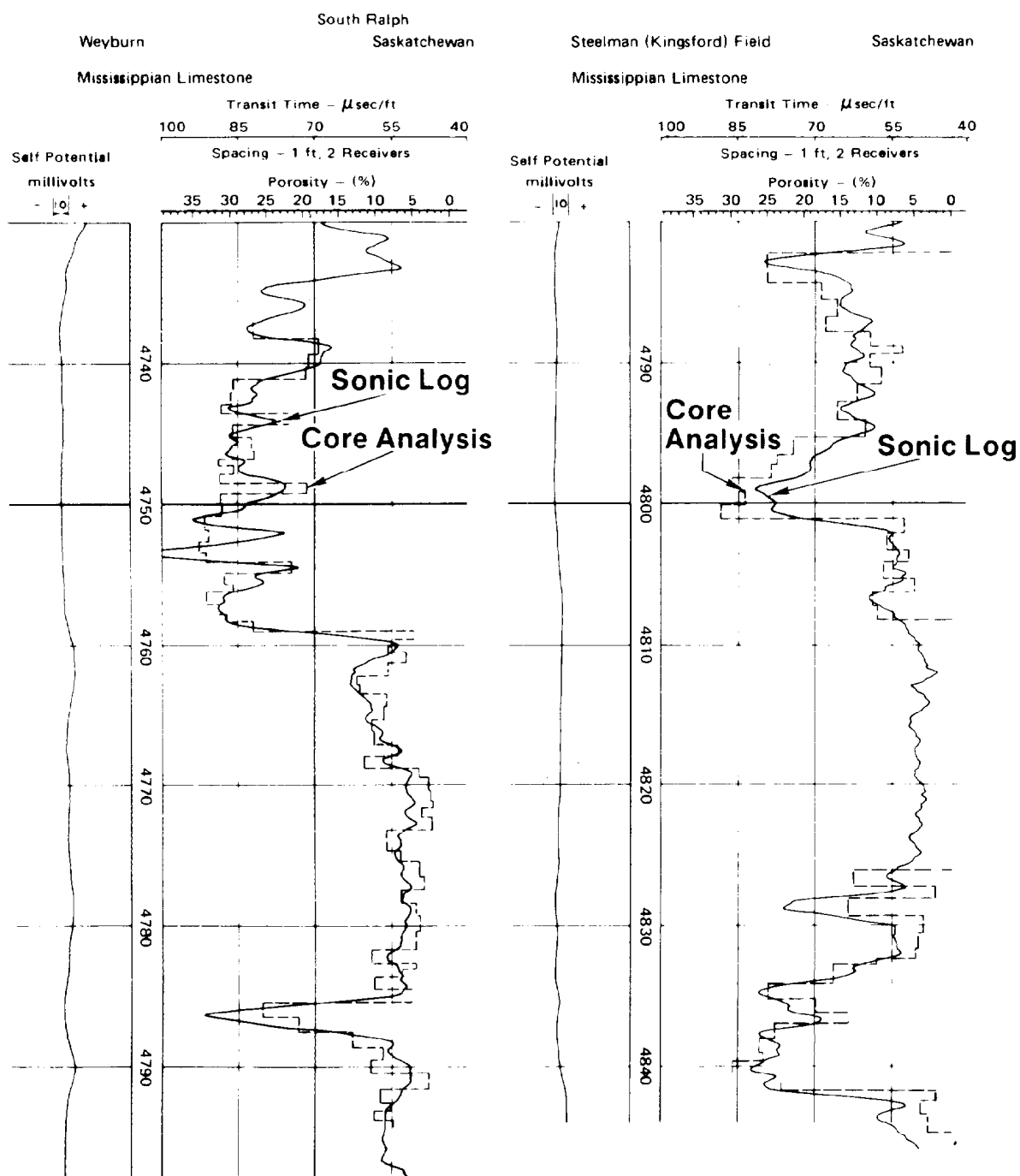
There are numerous field examples of acoustic log measurements yielding reliable estimates of porosity in well-compacted, clean sandstones and carbonates, provided that the lithology is known. Fig. 51.64 illustrates

the close agreement between acoustic-log-measured transit times and core-measured porosities for carbonate sections in two wells.

In fact, the acoustic log in certain areas is the most consistently reliable porosity device. To reiterate, the conditions required are (1) lithology is accurately known, (2) porosity is largely intergranular, and (3) rocks are well compacted and subjected to a differential stress of at least 4,000 psi.

As with other conventional porosity logs, variations in lithology make porosity estimates from compressional-wave transit times unreliable. To overcome this, acoustic logs are used with density and/or neutron logs, or with measurements of shear-wave transit times described in the next section.

Secondary Porosity. Another application of the acoustic log is for estimation of "secondary porosity" in vugular and/or fractured rocks. For this, it is assumed that compressional wave velocity is affected only by the primary or intergranular porosity. The density and neutron logs are assumed to respond to total porosity. Hence, any difference between these is assumed to be secondary porosity consisting of vugs and/or fractures. An example of this is shown in Fig. 51.65, where the section contains anhydrite with fracture porosity.¹¹⁰ Notice that while the transit time t remains approximately constant over the entire section, density ρ_b decreases from 2.97 to 2.83



Note: Porosity Scale Based on Matrix Velocity, $v_m = 23,000$ ft/sec

Fig. 51.64—Acoustic log vs. core analysis porosity.

g/cm^3 , and the neutron porosity ϕ_N increases from 0 to 4%, thereby indicating a secondary porosity of 4%.

Poorly Consolidated Rocks. In poorly consolidated sandstones, reliability of porosity estimates from acoustic logs is rather poor. In these cases, usually a combination of density and neutron logs is preferred. One significant advantage of the acoustic log is that it is much less affected by the hole conditions, such as washouts and rugosity. This was illustrated in Fig. 51.39 where the density and sidewall neutron logs were responding to hole conditions whereas the acoustic log was found to yield reliable estimates of porosity.

Several methods have been developed to obtain porosity information from acoustic logs in poorly compacted sands.^{21,111} One approach²¹ involves adjustment of porosity calculated from the time-average equation using a compaction correction factor F_{cp} . First, the apparent porosity ϕ_a is computed from

$$\phi_a = \frac{t - t_m}{t_L - t_m} \quad (14)$$

Then this value is corrected by F_{cp} to obtain the corrected porosity, ϕ_c , from

$$\phi_c = \frac{\phi_a}{F_{cp}} \quad (15)$$

The values of F_{cp} (Fig. 51.63) range from 1 to 1.6 or higher. One method used to estimate F_{cp} is based on estimating the compaction of sands from the compaction of adjacent shales. If the transit time of adjacent shales is 100 $\mu\text{sec}/\text{ft}$ or less, they are assumed to be compacted. Hence, to obtain the correction factor, the transit time t_{sh} observed in the nearby shales is divided by 100.

$$F_{cp} = \frac{t_{sh}}{100} \quad (16)$$

Other methods for determining F_{cp} include determination of porosity either from a resistivity log in a water-bearing sand or from other porosity logs such as density and/or neutron, and then comparing the value with ϕ_a obtained from the acoustic log.

More recently another empirical relationship for estimating porosity from compressional-wave velocity was developed by Raymer *et al.*¹¹¹ on the basis of extensive field observations of transit time vs. porosity. The relationship reported is for the full porosity range from 0 to 100%; however, for the porosity range of interest, 0 to 37%, it is expressed as

$$v = \phi v_f + (1 - \phi)^2 v_m,$$

where v_m is 17,850 ft/sec for sandstone, 20,500 ft/sec for limestone, and 22,750 ft/sec for dolomite, respectively; and v_f is velocity of sound in the pore fluid.

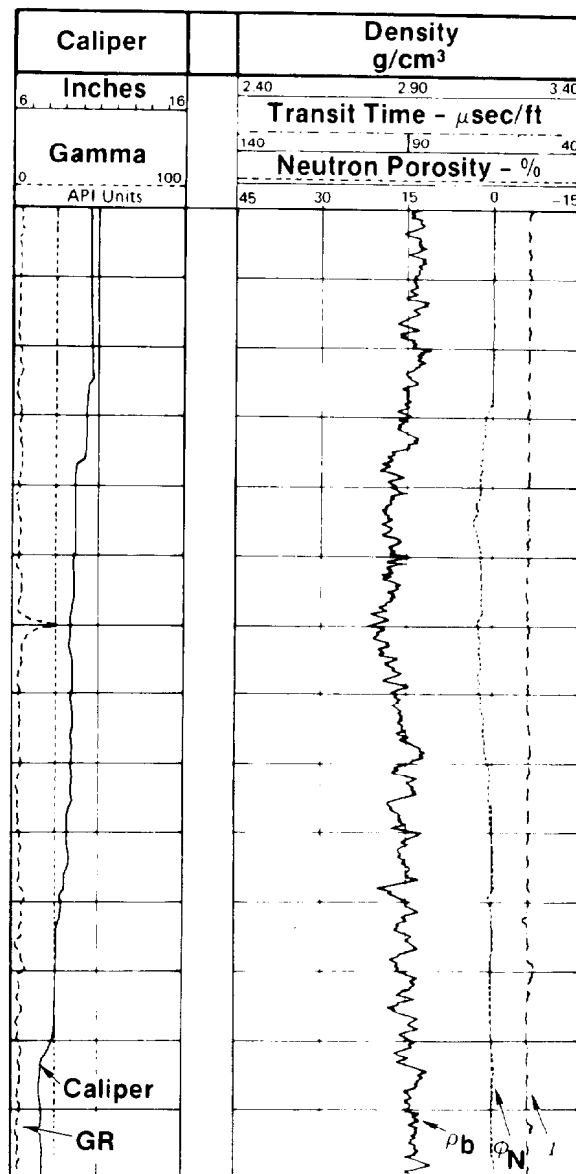


Fig. 51.65—Secondary porosity in the Auquilco formation, Neuquen basin, Argentina.

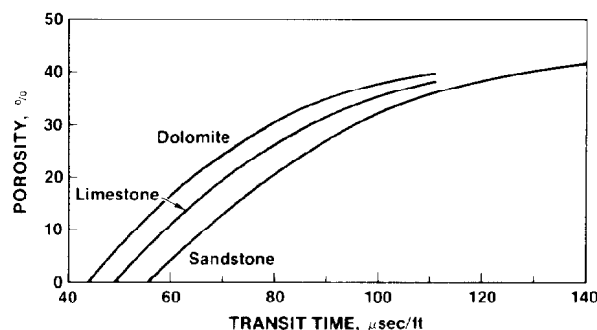


Fig. 51.66—An empirical relationship for estimating porosity in sandstone, limestone, and dolomite.

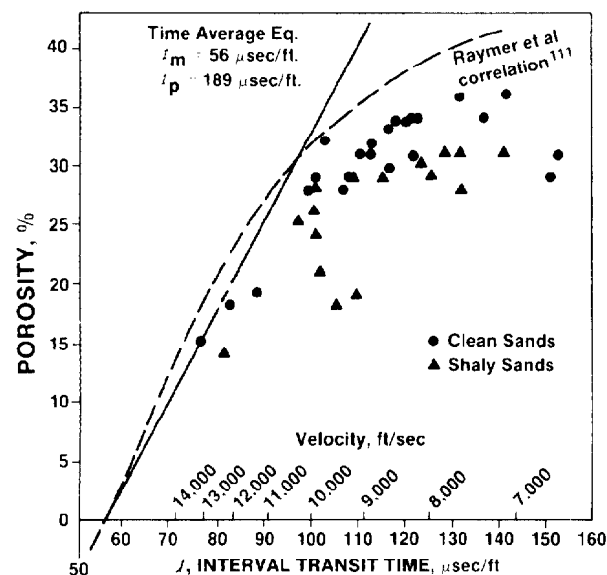


Fig. 51.67—Velocity/porosity correlations for moderately consolidated to unconsolidated sands.

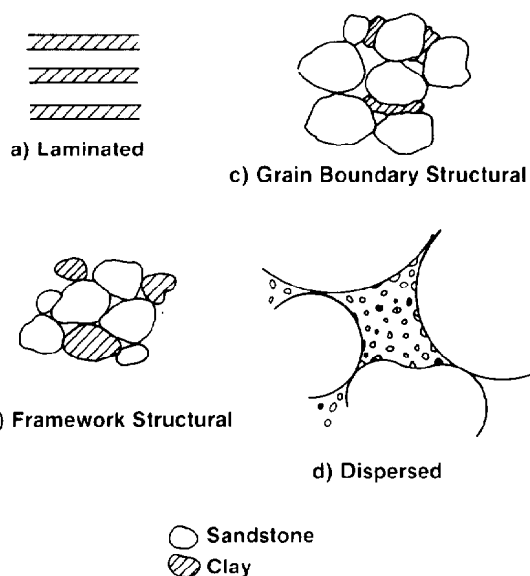


Fig. 51.68—Shaly sand models for acoustic wave propagation studies.

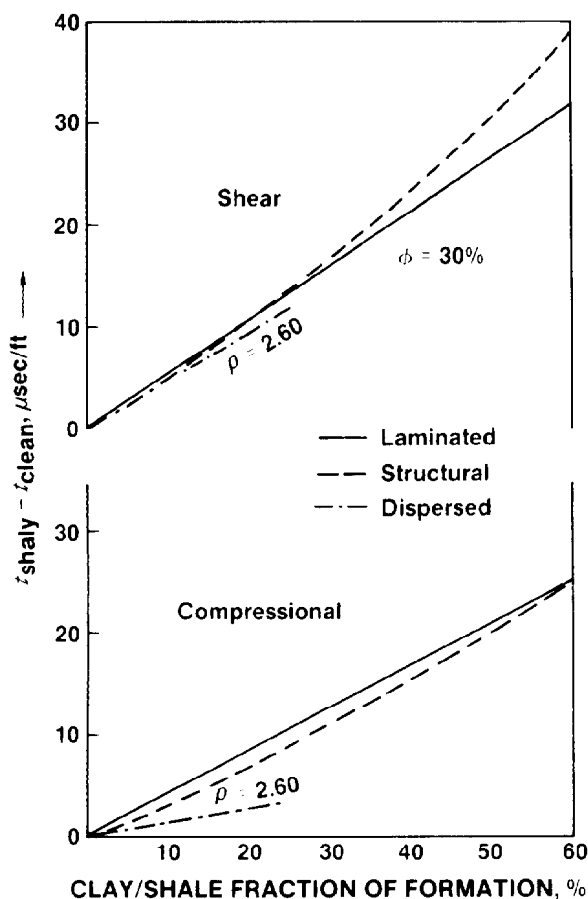


Fig. 51.69—Estimated shale effects on compressional and shear velocities.

A graphical representation of this empirical relationship is given in Fig. 51.66. Raymer *et al.*¹¹¹ found this relationship to be a better estimator of porosity than the time-average equation. They also reported that it is applicable to both consolidated and unconsolidated rocks.

Predictions from this relationship and from the time-average equations were investigated by Hartley¹¹² for the moderately consolidated to unconsolidated sands of the Gulf of Mexico. The lack of agreement indicated in Fig. 51.67 led Hartley to the universally applicable conclusion that empirical relationships "may provide erroneous porosities if they are applied outside of the data set from which they were developed."

Shaly Sands. Another aspect of Hartley's study¹¹² considers the effects of shaliness in porosity interpretation. In Fig. 51.67, porosity predictions from the empirical relations are worse for the shaly sands. Effects of shales on acoustic velocities are not very well understood; as a result, they are difficult to account for. A recent theoretical study by Minear¹¹³ shed much light on this problem by relating clay effects to their distribution within the rock framework. Minear used the Kuster-Toksöz¹¹⁴ model of porous media and divided clay distributions into four groups. As illustrated in Fig. 51.68, these four groups are (1) the laminated model (Fig. 51.68a), in which clay-mineral-rich and shaly layers alternate with clean sandstone layers, (2) the framework structural model (Fig. 51.68b), in which shale grains substitute for quartz grains randomly, (3) the grain boundary structural model (Fig. 51.68c), in which shale grains occur at some, but not all, boundaries between the quartz grains, and (4) the dispersed clay model (Fig. 51.68d), in which clays occur dispersed in the pore fluid or lining the pores but not between the grain contacts.

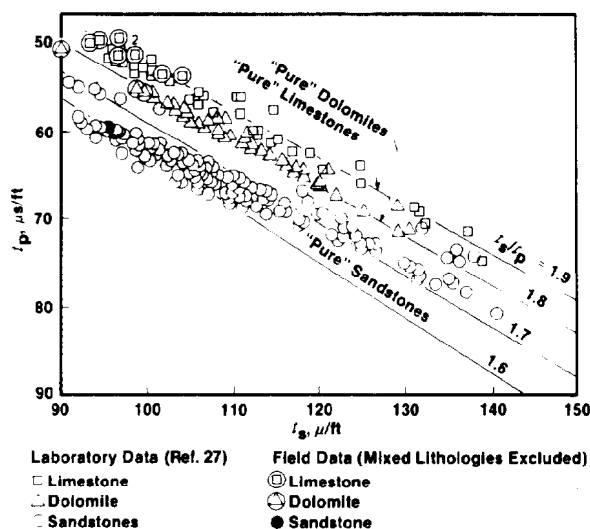


Fig. 51.70—Compressional-wave transit time vs. shear-wave transit time.

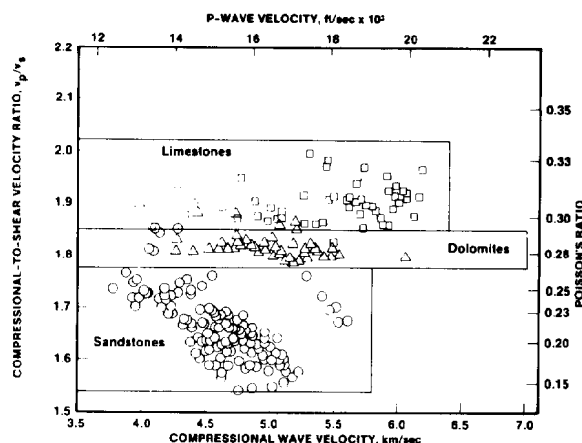


Fig. 51.71—Compressional- to shear-wave velocity ratio vs. compressional-wave velocity. Data from Fig. 51.70.

One of the obvious conclusions in this study is that the time-average equation is applicable to the laminated model. A more interesting conclusion, however, states that the framework (Fig. 51.68b) and grain-boundary (Fig. 51.68c) shales seem to have the same effect on acoustic velocities. Further results of this study are summarized in Fig. 51.69. The differences, $t_{\text{shaly}} - t_{\text{clean}}$, between the transit times of the shaly and clean formation for both the compressional and shear waves are plotted vs. the clay or shale fraction for a sandstone with a porosity of 30%. Structural and laminated shales have approximately the same effect on t_p and t_s but increase t_s more than t_p . Dispersed clay, if it has a density close to that for sandstone, has about the same effect on t_s as the structural and the laminated clays; however, its effect on t_p is only about one-third of that by the other two.

Lithology

Estimation of lithology from conventional acoustic log measurements may be made by solving for the matrix travel time from the time-average equation if the porosity is known from another source. Even though this technique has been used under certain conditions, matrix transit times of the most common rock types determined in this fashion are not distinct enough to make this a very useful method.

A more deterministic method for establishing lithology from acoustic log measurements is based on the relationships shown in Fig. 51.70. In this figure, laboratory- and borehole-measured values of compressional-wave transit times are plotted against shear-wave transit times. Laboratory data cover a porosity range of 5 to 30% for sandstones and 5 to 25% for carbonates, and an effective stress range of 0 to 6,000 psi.²⁷ As indicated, each lithology has a well-defined trend, regardless of porosity or effective stress (depth). Lines of equal velocity ratio

(v_p/v_s) are closely spaced for dolomites and limestones—1.8 and 1.9, respectively. The sandstones range from 1.6 for low-porosity sands to 1.75 for high-porosity sands under low effective stress.

Lithology identification is also illustrated in Fig. 51.71 by replotting the velocity ratio data of Fig. 51.70 vs. compressional wave velocities.

Use of borehole measurements of compressional and shear transit times is described by Nations⁸⁸ for determining porosity and lithology in mixed-lithology rocks. He assumes that velocity ratio is a constant for a "pure" rock type: 1.6 for sandstones, 1.8 for dolomites, and 1.9 for limestones. He further assumes that mixed-lithology rocks will exhibit a ratio that is directly proportional to the content of the two minerals and that porosity is distributed equally between the two. From the velocity ratio, he first determines the mineralogical composition; then, on the basis of this information, assigns the appropriate matrix transit time for calculating porosity. An example of the results of this technique is illustrated in Fig. 51.72 for dolomite/sandstone and dolomite/limestone mixtures.

Hydrocarbon Content

Acoustic signals on microseismogram or variable-density logs are known to disappear sometimes in oil and gas zones in unconsolidated formations. This property is used to locate oil/water contacts, as well as gas caps, but is not completely reliable. Sometimes, even within the same zone, signal disappearance may or may not be indicative of presence of hydrocarbons.

Laboratory studies conducted by Gardner and Harris¹¹⁵ on sandpacks indicate that shear-wave velocities decrease when liquid is added to sandpacks, whereas the compressional-wave velocity increases (Fig. 51.73).

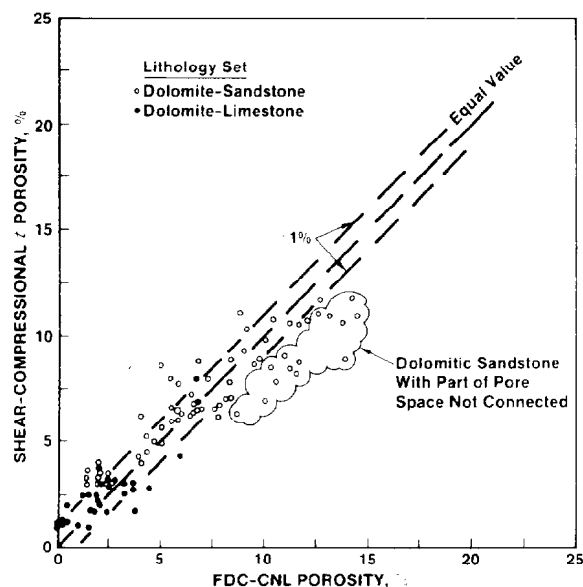


Fig. 51.72—Porosity from compressional-wave transit time corrected for lithology by the velocity ratio vs. porosity from density/neutron crossplot for complex lithologies.

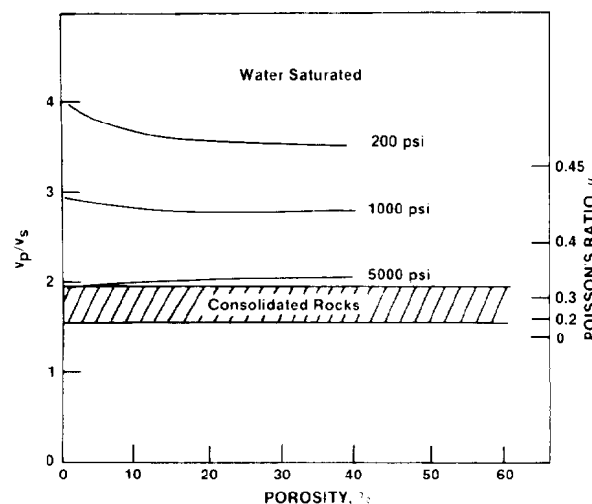


Fig. 51.74—Ratio of compressional-wave to shear-wave velocity for sands and consolidated rock.

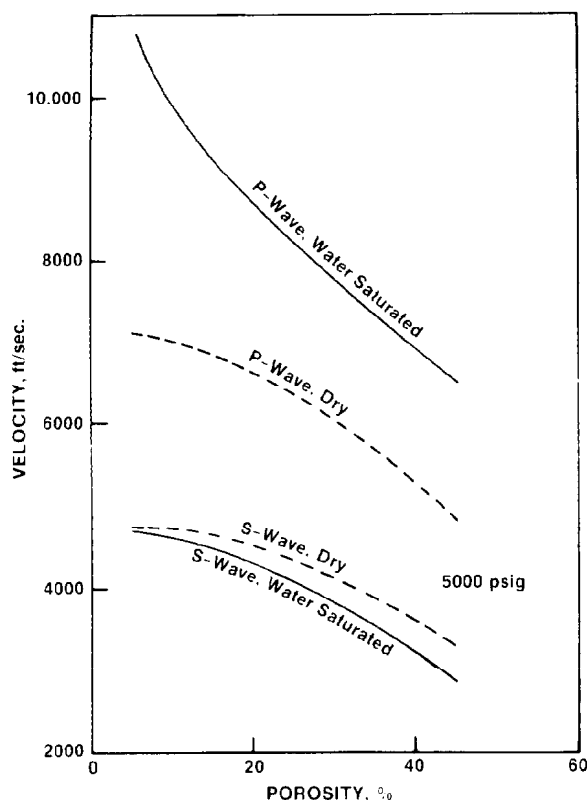


Fig. 51.73—Variation of compressional-wave and shear-wave velocities of wet and dry sands with porosity at 5,000 psig differential pressure.

These observed differences between compressional and shear-wave velocities are illustrated by plotting velocity ratio as a function of porosity and pressure (Fig. 51.74). Also shown in this figure is the velocity ratio range of 1.75 ± 0.20 for the consolidated sedimentary rocks. A velocity ratio greater than two indicates an unconsolidated sand saturated with liquid. Below this value it may be either an unconsolidated sand containing gas or a consolidated rock.

For the consolidated rocks, the ranges of velocity ratios for liquid and gas saturation were obtained by Gregory⁵⁰ through laboratory measurements. The results of his study are summarized in Fig. 51.75.

Additional experimental data obtained on a sandpack are shown in Fig. 51.76.¹¹⁶ Laboratory measurements of compressional- and shear-wave velocities are measured as a function of water saturation and plotted on this figure together with measured values of density.

These data and the previous observations may be interpreted in general terms through use of the Gassmann-Biot theory described in the Appendix. Taking the square roots of Eqs. A-1 and A-2 gives, respectively,

$$v_p = \frac{1}{\rho_b^{1/2}} \left[P_d + f(K_f) \right]^{1/2}$$

and

$$v_s = \left(\frac{G}{\rho_b} \right)^{1/2}.$$

Predictions of these equations also are plotted on Fig. 51.76 as dashed lines. One of the predictions of Eq. A-1 is that for 100% gas saturation, incompressibility of pore

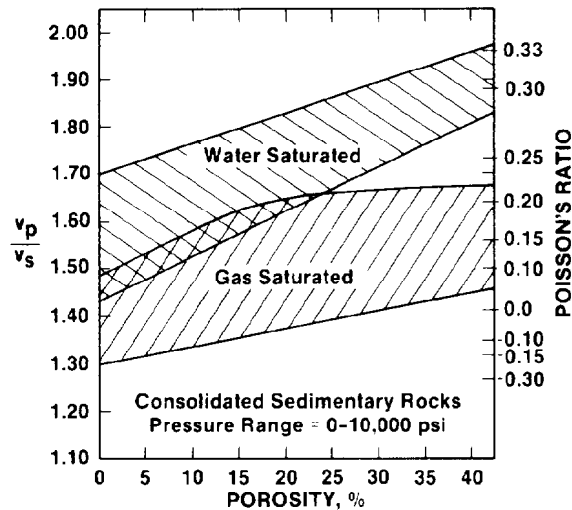


Fig. 51.75—Variations of velocity ratio with porosity for water-saturated and gas-saturated rocks.

fluid (K_f) is much smaller than that of the rock matrix (K_m); hence, $f(K_f)$ becomes negligibly small (see Eq. A-4). Therefore, P-wave velocities calculated from this equation for the gas-saturated rocks are smaller than those for the liquid-saturated rocks.

The S-wave velocity, however, becomes the function of gas saturation through dependence on the bulk density because the shear modulus G is the same for the rock whether it contains gas or liquid. Hence, as indicated in Eq. A-2, shear-wave velocity increases upon introduction of gas to the extent that the bulk density decreases.

Returning to the P-wave velocities, since the compressibility of gas is much larger than that of water, a small amount of gas reduces pore fluid compressibility essentially to that of gas as predicted by Eq. A-7 (see Appendix).

$$c_f = S_w c_w + (1 - S_w) c_g,$$

where c_g is gas compressibility. Hence, a small amount of gas reduces compressional-wave velocities significantly, but additional gas saturation has little further effect. This was illustrated by the laboratory data and theoretical prediction plotted in Fig. 51.76. A field example shown in Fig. 51.77 confirms this by demonstrating that compressional-wave transit time does not differentiate the upper zone at 90% gas saturation from the lower one containing 20% gas, because the t curve essentially is responding to the velocity of the mud in both intervals.

Effects of gas saturation on the compressional to shear-wave velocity ratio is illustrated in Fig. 51.78 for a deep dolomite reservoir.¹¹⁷ Over the 18,500 to 18,520-ft interval the v_p/v_s ratio is 1.8; this is as expected for a dolomite lithology. Over the gas zone below 18,520 ft, however, this ratio is reduced to 1.6, and clearly differentiates the gas zone. A similar gas effect is shown in Fig. 51.79 for a sandstone reservoir. In this case, the v_p/v_s ratio is reduced from 1.67 to 1.51, again clearly delineating the gas zone.

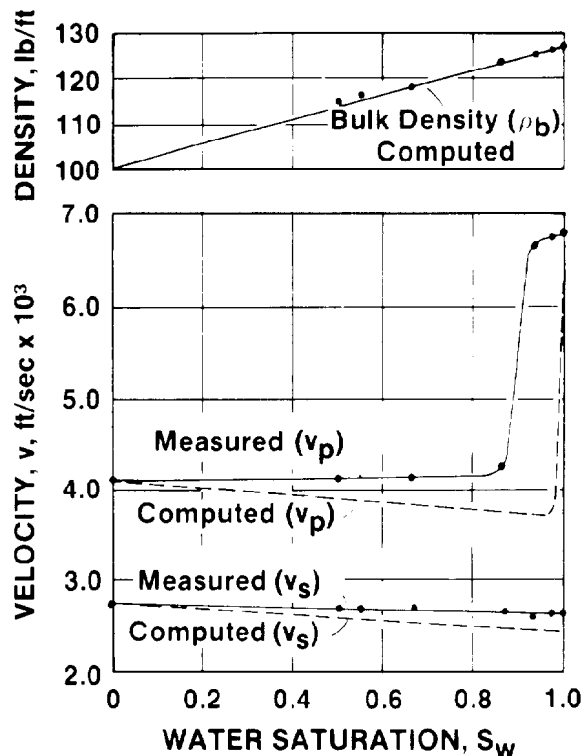


Fig. 51.76—Compressional- and shear-wave velocity and bulk density vs. saturation for a sand pack.

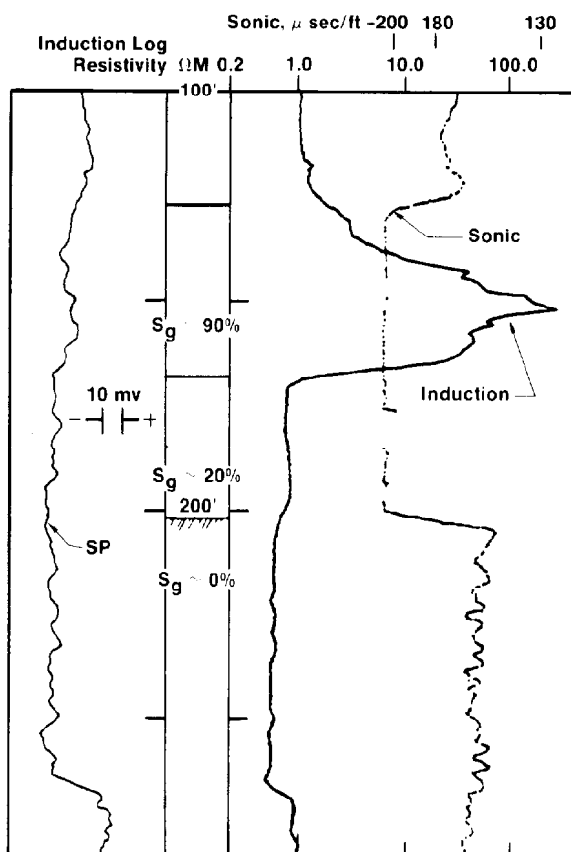


Fig. 51.77—Gas effect on acoustic log.

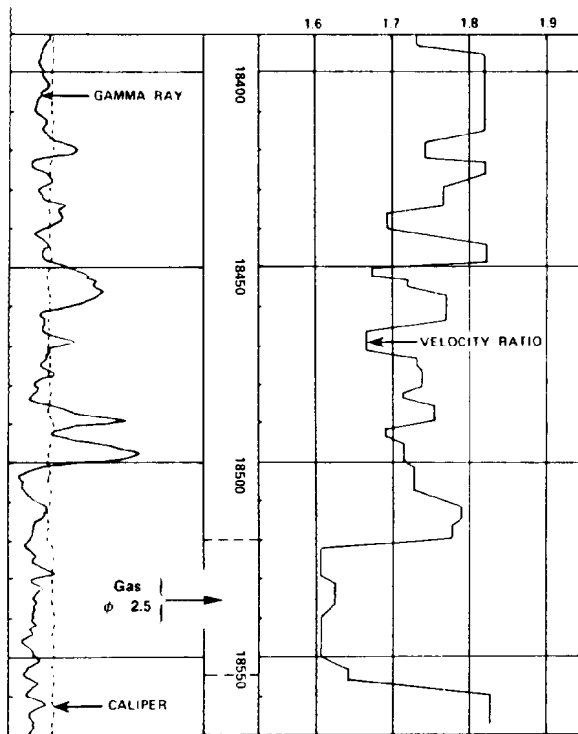


Fig. 51.78—Gas effect on compressional- to shear-wave velocity ratio in a dolomite reservoir.

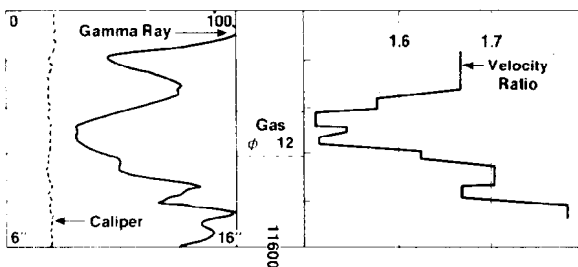


Fig. 51.79—Gas effect on compressional- to shear-wave velocity ratio in sandstone reservoir.

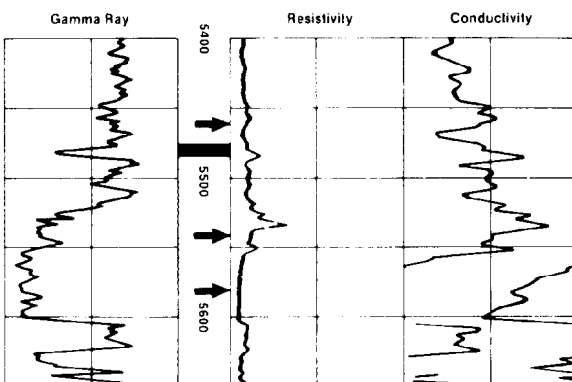


Fig. 51.80—Typical gulf coast induction log indicating two gas sands.

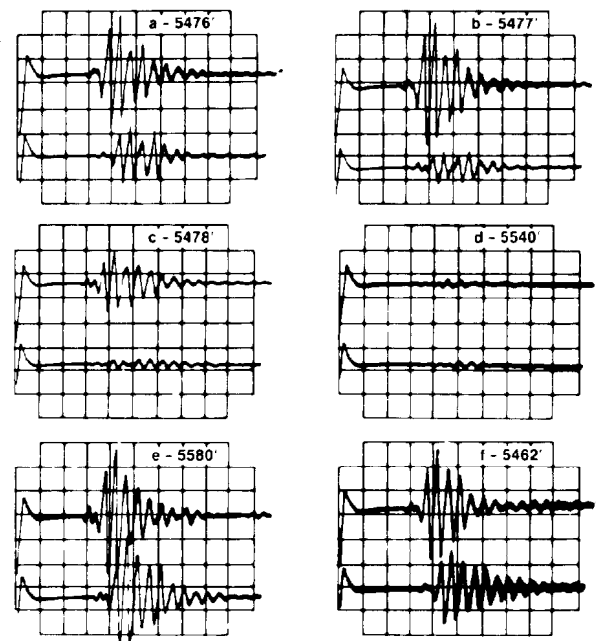


Fig. 51.81—Scope pictures from selected levels in the log on Fig. 51.80.

In general, the effects of gas saturation on acoustic velocities in rock may be summarized as follows.

1. Compressional-wave velocity is greater in liquid-saturated rocks than in comparable gas-saturated rocks, whereas the reverse is true for shear-wave velocities.

2. The difference in compressional-wave velocity for the liquid- and gas-saturated states becomes negligibly small with increasing depth, whereas the equivalent difference for the shear-wave velocities remains constant.

3. Under equivalent pressure conditions, compressional-wave velocity decrease upon gas saturation (in poorly consolidated rocks) is much greater than that in well-consolidated rocks.

Attenuations of elastic waves are also used to identify gas zones.¹¹⁸ This is illustrated in the typical Gulf Coast sands shown in Figs. 51.80 and 51.81. In Fig. 51.80, the induction log indicates two gas zones: one in a thin stringer at 5,476 ft and the other in a massive sand at 5,520 ft underlain by water. Scope pictures in Fig. 51.81 were recorded with a single-transmitter, dual-receiver acoustic log while going into the hole described in the previous figure. In Fig. 51.81a, the lower-receiver signal is just becoming affected as it moves very close to the gas stringer. One foot lower, at 5,477 ft, the lower receiver is in the top of the gas zone. In Fig. 51.81c, the lower receiver is in the gas sand and the upper receiver is being affected. In the massive gas sand at 5,540 ft, both receivers are showing almost total compressional wave loss, whereas in the water sand at 5,580 ft, a strong signal is apparent at both receivers. For comparison, a typical shale response at 5,462 ft is given in Fig. 51.81f.

Geopressure Detection

Geopressure refers to a buried rock/fluid system in which the fluid pressure is greater than the hydrostatic pressure of a full column of formation water. Geopressure also is called abnormal pressure or overpressure. Abnormally high fluid pressures are found worldwide. Such pressures occur when fluid in the pore space begins to support more overburden than just fluids—i.e., not all the compressional forces are transmitted by the rock matrix only.

The ability to predict the occurrence and magnitude of abnormal pressures is a requirement in planning efficient drilling and, ultimately, completion procedures. Hottel and Johnson¹¹⁹ established a procedure for determining the first occurrence of geopressure and the precise depth vs. pressure relationship. They observed that for hydrostatic-pressure formations in a given geological province, a plot of the logarithm of compressional-wave travel time in shales, t_{sh} , vs. depth is generally a straight line. The divergence of the observed travel time t_{ob} from that obtained with the established normal trend t_n is a measure of the pore-fluid pressure in the shale and, hence, in the adjacent permeable formation (Fig. 51.82). They also established a trend of resistivity vs. depth for shales and used it similarly in conjunction with acoustic log data.

A field example showing acoustic log response in an abnormal pressure section in the North Sea is given on the right track of Fig. 51.83.¹²⁰ A remarkably accurate prediction of abnormal pressure by surface seismic measurements is shown for comparison in the left track.

A procedure for evaluation of formation pressure is summarized as follows.¹²¹

1. Plot shale velocity or transit time and establish a normal compaction trend line.
2. Locate the anomalous pressure top at the depth at which plotted data points diverge from the normal trend.
3. Take the difference between observed shale transit time and normal shale transit time.
4. Convert the difference to formation pressure gradient by means of an empirically derived curve for a given age and for a given area (Fig. 51.84 was used for the example shown in Fig. 51.83).
5. Multiply the pressure gradient obtained by depth to compute the formation fluid pressure at that depth.

Another approach for evaluating abnormal pressures is suggested by Eaton.¹²² He proposes the following empirical relationship for predicting pore fluid pressure (p_f):

$$\frac{p_f}{D} = \left[\frac{p_o}{D} - \left(\frac{p_f}{D} \right)_n \right] \left[\frac{t_n}{t_{ob}} \right]^m$$

where

D = depth, ft

p_f/D = pore fluid pressure gradient, psi/ft.

p_o/D = overburden stress gradient, psi/ft.

$(p_f/D)_n$ = normal hydrostatic pressure gradient (0.456 psi/ft for Gulf Coast, 0.434 for fresh waters),

t_n = transit time on the extrapolated normal curve at depth,

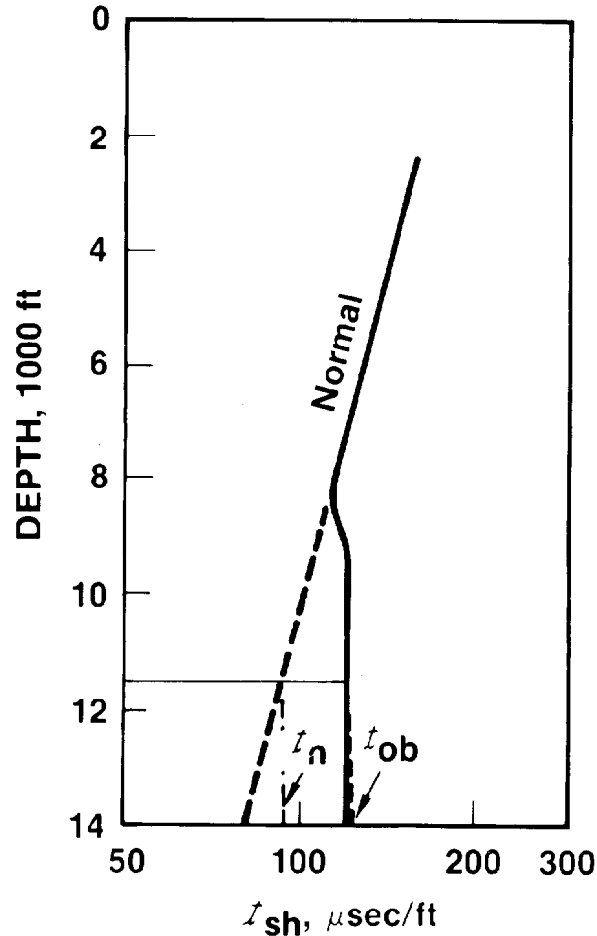


Fig. 51.82—Prediction of geopressure from shale transit time.

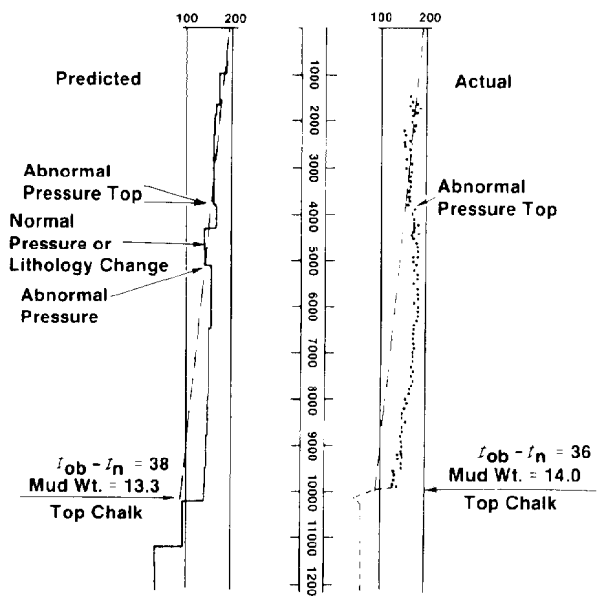


Fig. 51.83—Comparison of seismic prediction and actual down-hole pressure environment.

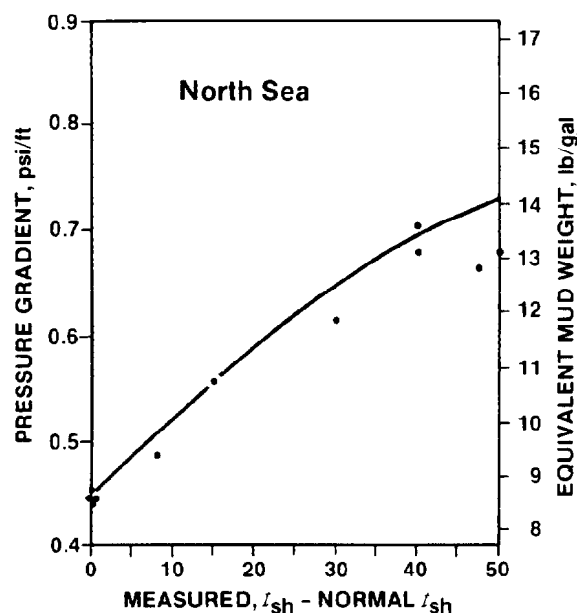


Fig. 51.84—Transit-time/pressure correlation, North Sea.

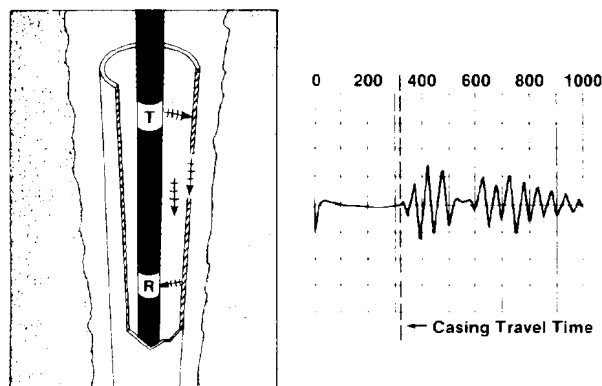


Fig. 51.85—Free pipe.

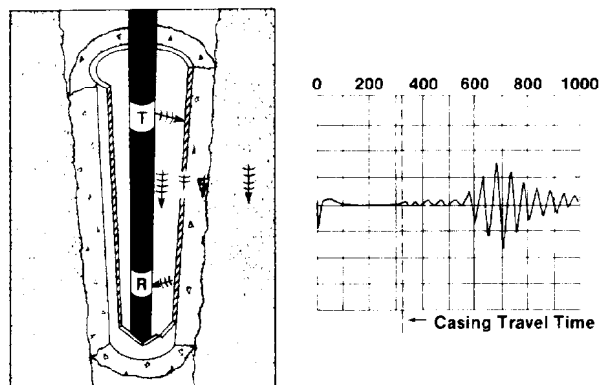


Fig. 51.86—Good bond to casing and formation.

t_{ob} = observed transit time at depth, and
 m = empirical exponent varying regionally
 around a value of three.

Cement Bond Quality

The primary purposes of oilwell cementing are to secure casing to prevent leakage to the surface and to isolate producing zones from water zones. With the increasing cost of completing wells, accurate determination of the quality of the casing cementation has become necessary to avoid costly recompletion and squeeze cementing jobs.

The successful cementing of a well is affected by many factors: cement setting time, pressure, temperature, hole size and deviation, formation and cement characteristics, casing surface, and damage to the cement bond by perforating or squeezing operations. These and many other factors must be considered when evaluating the effectiveness of a cement job.

Early in acoustic logging, it was observed that the amplitude of an acoustic signal in a firmly cemented pipe is only a fraction of that of a free pipe.¹²³ Since then, downhole acoustic measurements have been firmly established as the primary technology for determining cement bonding not only to the casing but to the formation as well.^{124,125} Under favorable conditions even the compressive strength of cement can be determined.¹²⁶

Free Pipe. A schematic axial transmitter and receiver configuration is shown in Fig. 51.85 for cement bond logging.¹²⁷ In a free pipe, most of the energy is confined to the casing and the borehole fluid, as indicated in Fig. 51.85. The resulting acoustic waveform as recorded by the receiver is also shown in this figure. The following observations characterize waveforms observed in free, unbonded casing.

1. The first arrival of the waveform is equal to the total travel time in casing between transmitter and receiver, plus the travel time in fluid between the tool and the pipe.
2. The amplitude of the entire waveform is high.
3. The waveform exhibits a highly uniform frequency.
4. The waveform is persistent and lasts a relatively long time.

Good Bond to Casing and Formation. When the cement is perfectly bonded to both the casing and the formation, a very favorable acoustic coupling is developed. As a result, maximum energy is transferred to the formation, and very little energy is transmitted through the casing and cement sheath. As shown in Fig. 51.86, the waveform shows practically no signal at the casing arrival time and very little amplitude until the formation arrival time.

Bond to Casing and to a High-Velocity Formation. In areas of high-velocity formations, signals from the formation arrive at the same time as or earlier than the casing signal, thereby complicating the interpretation significantly (Fig. 51.87).

Cement Bond to Casing Only. A commonly occurring condition is that the periphery of the casing is totally surrounded and bonded by a hardened sheath of cement that

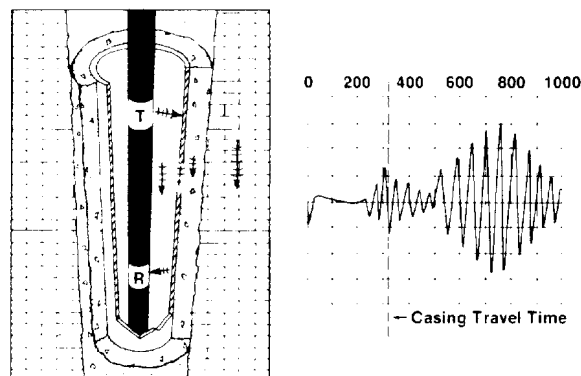


Fig. 51.87—Bond to casing and to a high-velocity formation.

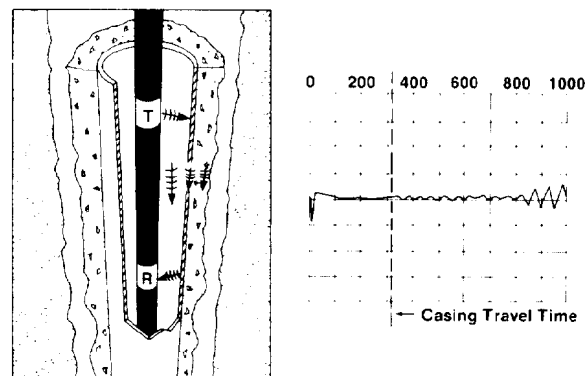


Fig. 51.88—Cement bond to casing only.

is not bonded to the formation (Fig. 51.88). This might happen because the cement does not bond with mudcake of poorly consolidated formations, or the mudcake dries and shrinks away from cement.

Under this condition, energy traveling through the casing is attenuated drastically because of the highly attenuating cement sheath. The annulus outside the cement sheath offers very unfavorable acoustic coupling; hence, very little energy is transferred to the annular fluid and virtually none into the formation. This is indicated by the lack of later-arriving formation energy in the waveform of Fig. 51.88. The energy observed at 870 μ sec is the beginning of the fluid wave for the transmitter-to-receiver spacing of 5 ft.

Partial Bonding. A most difficult situation in evaluating cement bond quality is the condition of partial bond (Fig. 51.89). A small gap may be formed between the casing and cement in an otherwise well-bonded casing. In this situation the waveform typically contains two distinct wave energies. The first wave energy arrives at casing time, since part of the casing is free to vibrate. The second wave energy arrives at a time indicated by the velocity of the formation. Hence, both a moderately strong casing arrival and a moderate-to-strong formation arrival exists.

The typical partial-bonding waveform is characteristic of either a microannulus or a channel in the cement. A microannulus is a very small separation between casing and cement. Normally, a hydraulic seal exists with a microannulus, but not with a channel in the cement. Thus, it is important to differentiate between the two. The best way is to rerun the bond log with pressure on the casing. If a microannulus exists, the casing will expand, decreasing the separation and transferring acoustic energy to and from the formation. The casing signal will decrease and formation signals will then become more evident. However, if only channeling exists, pressuring the casing will not greatly alter the log.

Another way to differentiate between microannulus and channeling is by noting the length of section over which the condition exists.¹²⁵ Since microannulus is thought to be caused by the condition of the exterior surface of the casing, such as the presence of grease or mill

varnish, the effect tends to appear over a long section of log. Channeling ordinarily occurs over shorter sections.

Examples of various bonding conditions are illustrated by the variable-density (3D) log shown in Fig. 51.90.¹²⁸ The interval from X552 to X614 ft shows a good pipe bond but no formation bond. Only a few formation arrivals can be seen, indicating a lack of acoustical coupling between the cement sheath and the formation itself. Above and below this interval are sections of poorly bonded pipe. This probably is due to channeling. This is suggested by the strong pipe signal overriding a weak formation signal. The interval from X468 to X518 ft is well bonded, as evidenced by the strong formation signal. However, there is evidence of a microannulus between X506 and X518 ft. Here the formation signal is distorted somewhat by a casing signal.¹²⁸

A recently introduced technology, the Cement Evaluation Tool by Schlumberger, shows great promise in differentiating between microannulus and channeling.¹²⁹ This tool is based on the acoustic reflection method; however, unlike the borehole televiewer with one rotating transducer, it has eight transducers placed on a centralized sonde at 45° from each other in a helical path. These transducers, emitter and receiver, are about

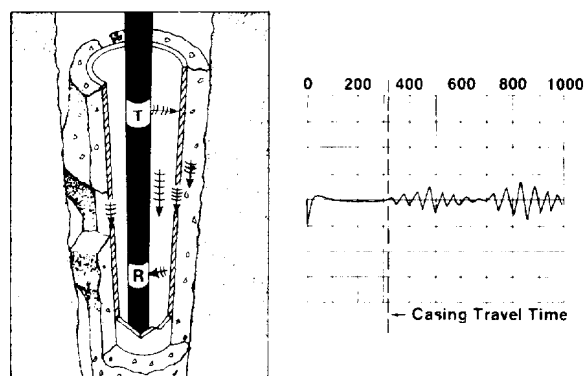


Fig. 51.89—Partial bonding.

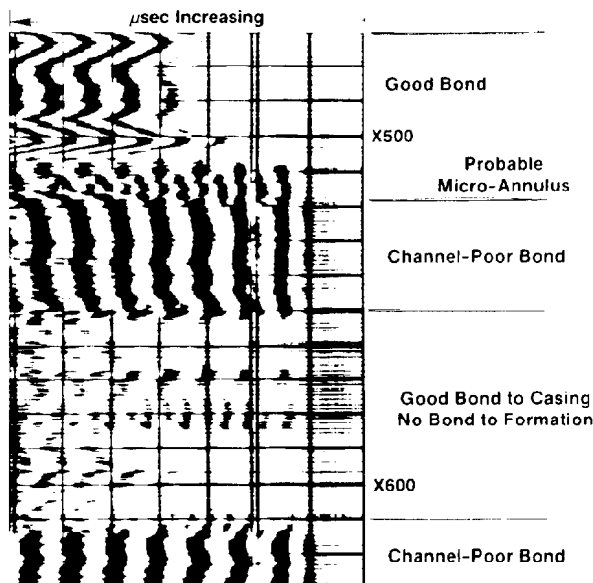


Fig. 51.90—Good bond to casing—no bond to formation.

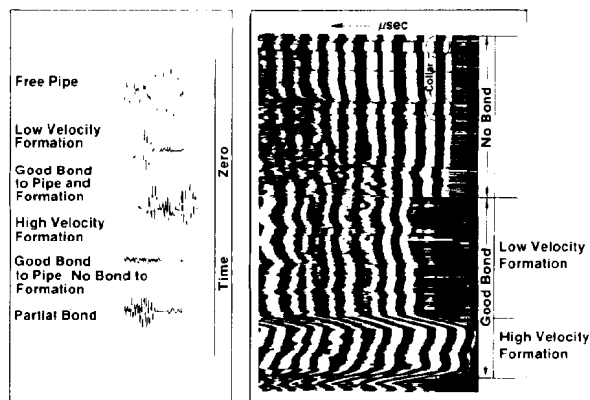


Fig. 51.92—Full waveforms and variable-density log for different bonding conditions.

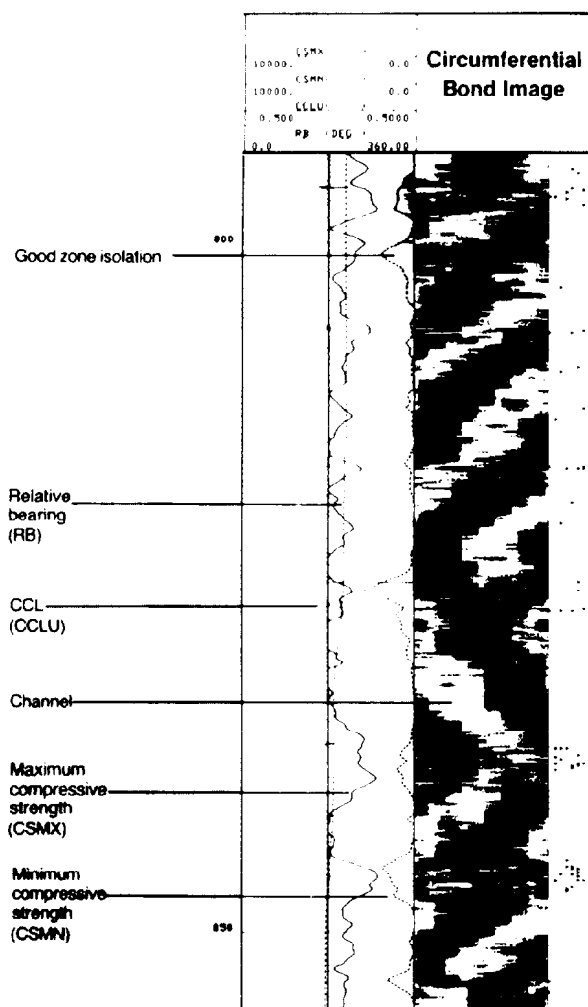


Fig. 51.91—Ultrasonic cement evaluation log.

1 in. in diameter and operate at 500 kHz. They repeatedly send a short ultrasonic pulse toward the casing to make it resonate in its thickness mode. Cement behind the casing is detected as a rapid damping of this resonance, whereas a lack of cement gives a longer resonance decay.

An example of a cement evaluation log is shown in Fig. 51.91.¹³⁰ The right track can be viewed as a map of cement behind the casing. It is divided into eight channels, each one representing one transducer with a shading from white (free pipe) to black (good cement). In this example, a channel is clearly visible as a white streak.

Summary of Bonding Conditions. Typical full waveforms for various bonding conditions are summarized in Fig. 51.92.¹²⁸

When there is no cement bonded to the casing, a free casing signal is indicated on the variable-density log as straight dark lines with distortion at the collars. This distortion occurs for a vertical distance equal to the spacing between the transmitter and receiver of the logging instrument (6 ft on the example shown in Fig. 51.92).

When there is good cement bonding both to the casing and to the formation, there is no casing signal, but there is a strong formation signal. The difference in response for the low- and high-velocity arrivals for a well-bonded section is clearly illustrated in the lower section of the variable-density log of Fig. 51.92.

Cased-Hole Evaluation

Most existing wells were completed before the advent of reliable porosity logging devices; therefore, accurate porosity data for planning of enhanced recovery operations must be obtained through existing casing. Radioactivity logging measurements commonly are used for this purpose; this information, however, can be supplemented by the acoustic log measurements in wells

where a good cement bond exists between casing and the formation.¹³¹ A recent study¹³² involving laboratory modeling and computer simulations has indicated that acoustic logging can be successful in both bonded and unbonded casing.

Through-casing acoustic logs have provided reliable measurements of compressional and shear-wave velocity data for evaluating porosity and lithology. An openhole and cased-hole comparison is shown in Fig. 51.93 for the compressional and shear-wave transit times t_p and t_s . The logs were obtained by analysis of the waveforms digitally recorded with the acoustic logging system shown in Fig. 51.54. The agreement between compressional and shear transit time logs run in open and cased holes is excellent. This further enhances the role of acoustic measurements in cased-hole evaluation.

Mechanical Properties

A knowledge of the mechanical properties of rocks is important in drilling, production, and formation evaluation. Mechanical properties include the elastic properties such as Young's modulus, shear modulus, Poisson's ratio, and bulk pore compressibilities, as well as the inelastic properties such as fracture pressure gradient and formation strength. Borehole measurements of acoustic properties in combination with density log measurements are being used more and more for in-situ determination of mechanical properties of rocks.

Elastic Moduli. Elastic constants describe the mechanical properties of matter: Young's modulus, shear modulus, bulk modulus, and Poisson's ratio. Knowledge of these moduli for rocks is needed in studying the propagation of acoustic waves, as well as in practical engineering problems connected with drilling, formation fracturing, and predicting reservoir performance.

A commonly used approach to gather this information is to obtain core samples and to conduct laboratory experiments. For meaningful results, these measurements must be made at equivalent subsurface conditions. Needless to say, these are time-consuming and costly. Even then the results are suspect because the process of coring removes the overburden stress from the sample and causes other disturbances that may not be reversible.

Numerous studies have been conducted that compared elastic moduli obtained by the static (from measurements of stress and strain) and the dynamic (from acoustic velocities and density) methods. In rocks subjected to lower effective stresses, the dynamic elastic moduli are higher than the static values; as the stress increases, however, these differences decrease.^{133,134} Theoretical studies by Walsh¹³⁵ predicted that this could be caused by the presence of cracks in rocks. In fact, Simmons and Brace¹³³ found the static and dynamic moduli to be in close agreement when rocks are subjected to higher stresses (30,000 psi) so that the cracks are closed.

The relationship of the in-situ-measured elastic moduli to those determined in the laboratory was investigated by Myung and Helander.¹³⁶ They made laboratory measurements of compressional- and shear-wave velocities on core samples under simulated subsurface pressure conditions and reported a close agreement between in-situ and laboratory-determined values of dynamic elastic moduli.

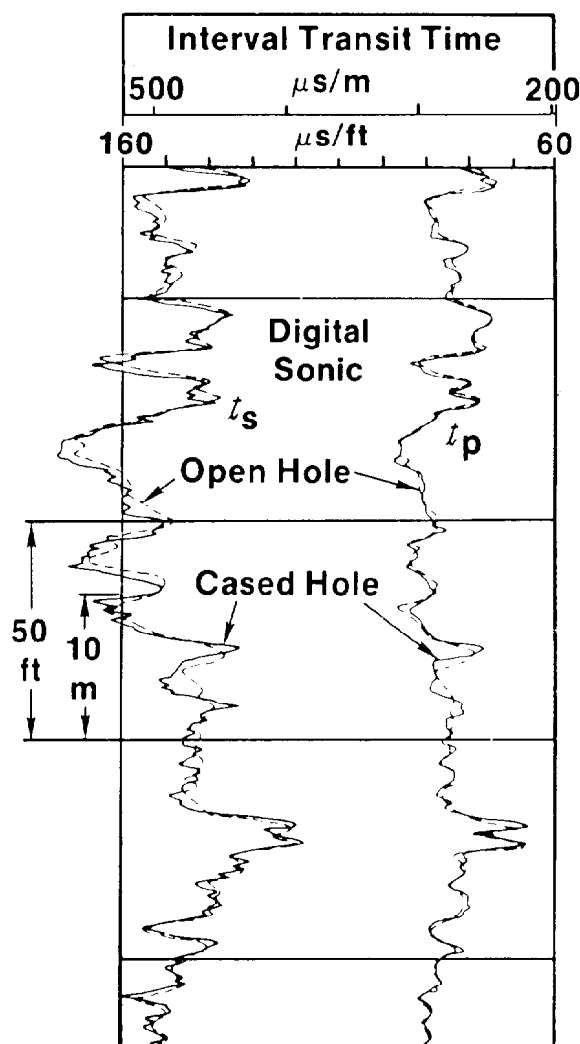


Fig. 51.93—Comparison of digital-sonic logs in a well before and after casing.

Since then, many other investigators have used borehole acoustic measurements to determine elastic moduli.^{89,137,138} Compressional- and shear-wave velocities obtained from the acoustic log measurements are used with values of density from a density log to calculate Young's modulus, shear modulus, bulk modulus, and Poisson's ratio by assuming an infinite, isotropic, homogeneous, and elastic medium (see Eqs. 3 through 6).

Applications of these in-situ-determined values of moduli include predicting sand production and subsidence, and determining fracturing characteristics of formations. An application involving fracture characteristics is shown in Fig. 51.94.⁶³ The core and log data are from a section of igneous and metamorphic rocks. The fracture characteristics of the core are shown graphically as well as plotted quantitatively as rock quality designation (RQD), which is the ratio of the cumulative length of unfractured core to the unit length of core. Elastic moduli curves are quite similar to the RQD curve.

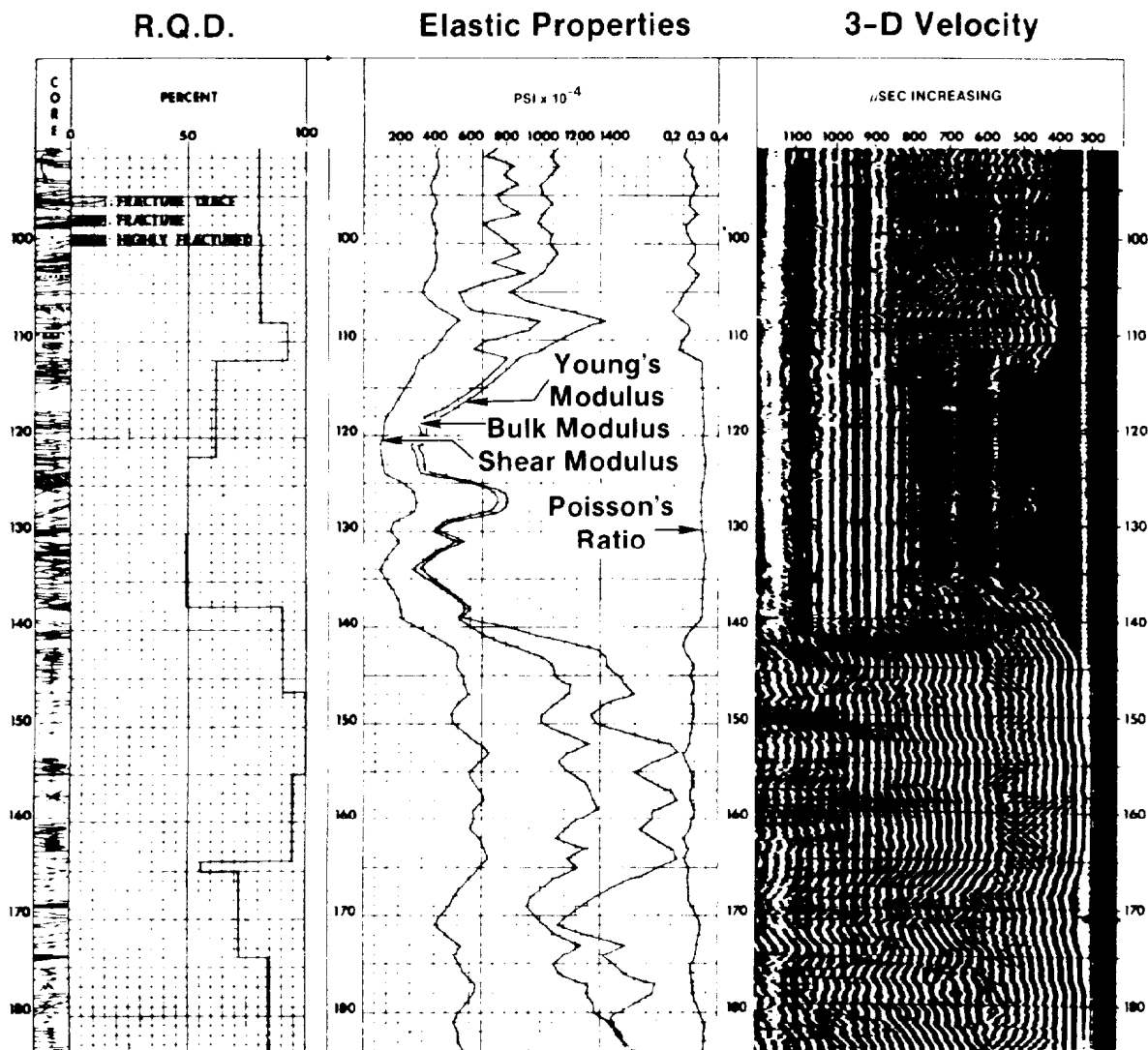


Fig. 51.94—Comparison of rock quality designation (R.Q.D.), elastic properties, and 3D velocity log.

Fracturing. Fracturing of formations is a commonly used well stimulation technique. To determine the best zones for fracturing, laboratory compressibility tests can be run on rock samples from the zones of interest. Fracture design requires a knowledge of elastic moduli, which can be obtained from borehole measurements.

An earlier use of borehole acoustic measurements was for the identification of zones favorable for fracturing. High-amplitude and high-velocity shear waves have been associated with zones that can be fractured successfully, whereas zones with low-velocity and low-amplitude S-waves were found to be quite plastic. In the example shown in Fig. 51.95, Anderson and Walker¹³⁹ indicate a well-defined shear wave in the zone from 4,600 to 4,545 ft and none above this zone.

During drilling, control of hydrostatic pressure in the borehole is necessary to not exceed fracturing pressure of the formations, thereby causing circulation loss.

However, a knowledge of fracture pressure is needed for proper design of fracturing operation to stimulate hydrocarbon production from tight formations. An estimate of fracture pressure (p_{fr}) is given by Hubbert and Willis:¹⁴⁰

$$\frac{p_{fr}}{D} = \left(\frac{p_o}{D} - \frac{p_f}{D} \right) \left(\frac{\mu}{1-\mu} \right) + \frac{p_o}{D},$$

where

p_o = overburden pressure,
 p_f = pore-fluid pressure,
 μ = Poisson's ratio, and
 D = depth.

Recent applications of this relationship are discussed by Atkinson.¹⁴¹

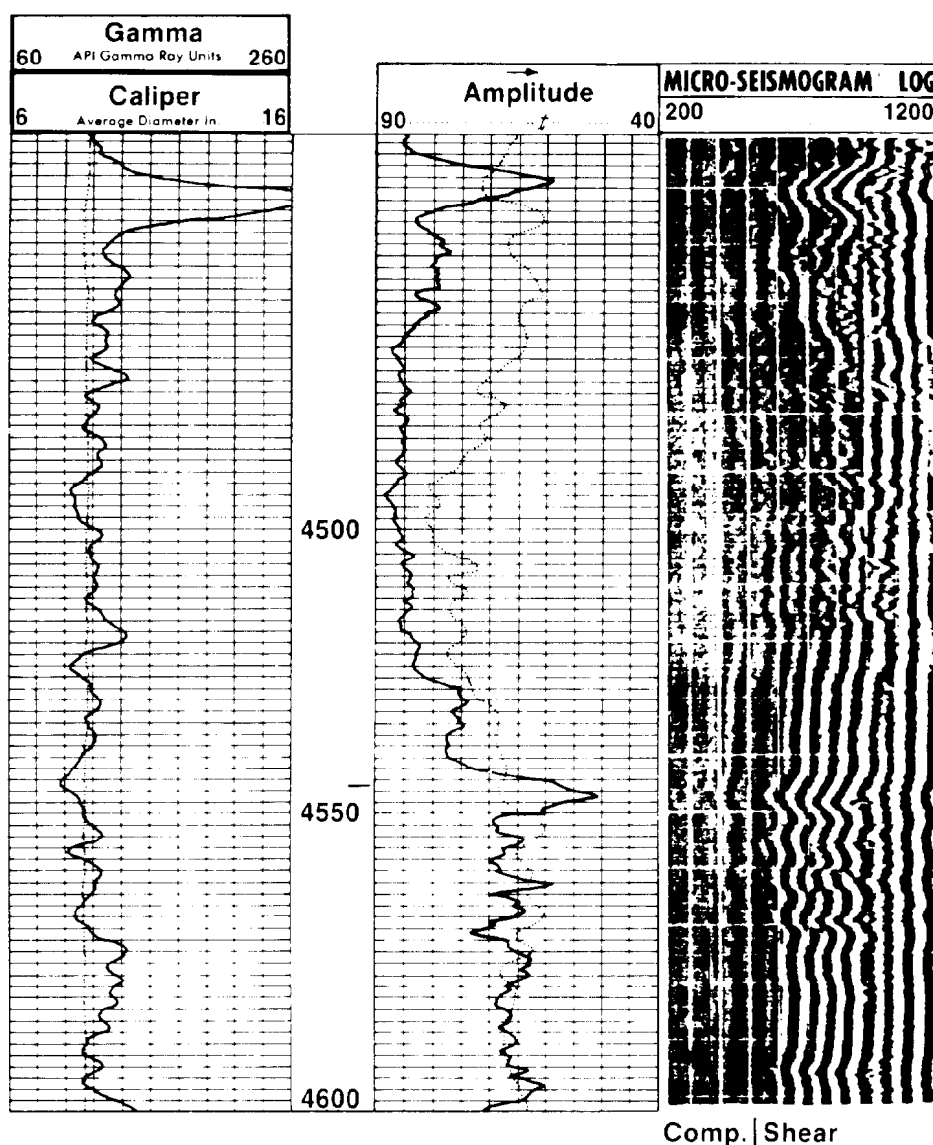


Fig. 51.95—Evaluation of fracturing prospects.

Sand Control. Sand-production control has been a costly problem affecting the economics of oil and gas production in many areas. To avoid unnecessary sand-control measures, various techniques have been developed that use borehole measurements of acoustic properties.^{138,142-144}

In the example shown in Fig. 51.96, the need for sand control is predicted by assuming that hydrocarbon effects on acoustic properties are predominant in poorly consolidated formations.¹⁴² In the oil zones shown, transit times are significantly higher than the value in the water zone, and the amplitudes are reduced, thereby indicating poorly consolidated rocks.

Fracture Evaluation

Many of the important reservoirs in the world produce from naturally occurring fractures, yet evaluating the

performance of these reservoirs is much less understood. Techniques for evaluating naturally fractured reservoirs are reviewed in the literature by Aguilera and van Poolen,¹⁴⁵ Suau and Gartner,¹⁴⁶ and Aguilera.¹⁴⁷ Among these, techniques based on measurements of acoustic properties are prominent. Cycle skipping observed on the transit time curve has been associated with fracturing in certain formations. Also, reduction of signal amplitude has been correlated with fractures. More successful applications, however, involve the use of variable-density or waveform logs.^{148,149} For these logs, when fractures occur, anomalies also occur in the acoustic wave banding pattern. Sometimes these are diagonal patterns, but more often they occur as sudden breaks in the banding.

Fig. 51.97 shows a variable-density log (3-D log) from a granite section in New Hampshire.¹⁴⁹ In Zone C,

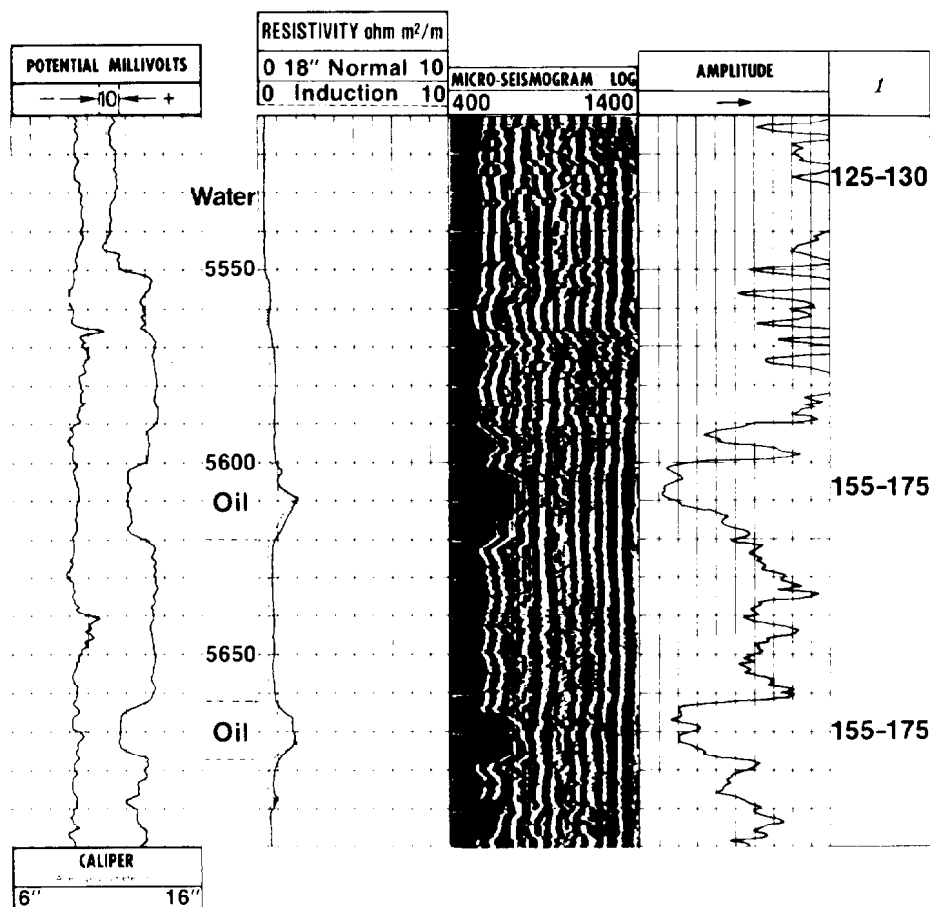


Fig. 51.96—Hydrocarbon effects indicate the need for sand control.

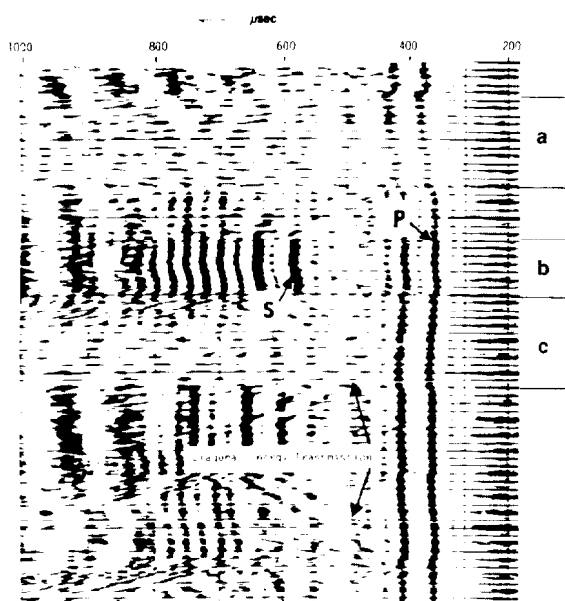


Fig. 51.97—Variable density (3D) log in fractured granite.

the compressional wave is not attenuated, whereas the shear-wave amplitude is reduced significantly. A theoretical study by Knopoff and McDonald¹⁵⁰ would predict this to be due to a low-angle (or horizontal) fracture. High-amplitude compressional and shear energies indicate that Zone B has no fractures. High attenuation of the compressional and shear waves in Zone A is interpreted to be caused by an oblique fracture. The diagonal energy pattern below Zone C is caused by the presence of a reflector (fracture) near the borehole.

In the foregoing analysis, fractures are considered to be thin reflectors causing distortion in wave propagation because of acoustic impedance mismatch with the surrounding rock. Since abrupt changes in lithology and porosity also can cause similar acoustic impedance mismatches, this simplified interpretation becomes much more complex.

When the hole conditions are favorable and there is no mudcake or heavy muds in the hole, the borehole reflection method provides a more straightforward technique for the evaluation of fractures. A borehole televiewer sonde operating in a circular borehole intersecting a vertical fracture is shown on the left in Fig. 51.98.¹⁰⁰ The borehole televiewer log obtained in this configuration, shown on the right, clearly depicts the vertical fracture as two dark lines.

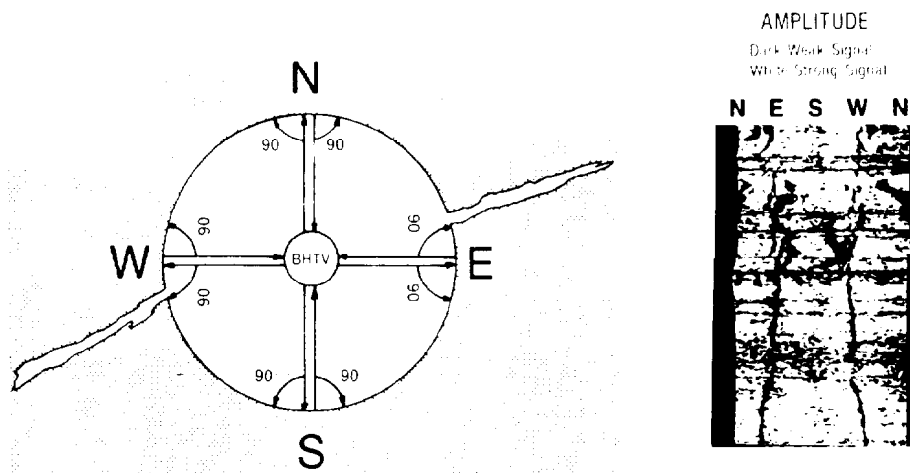


Fig. 51.98—Vertical fracture intersecting a circular borehole and its representation on BHTV amplitude log.

The amplitude image from the BHTV, however, cannot distinguish whether the fracture is open or filled. An open fracture produces an image on the amplitude log because little or no signal returns to the sonde. A filled fracture also can produce an image if there is sufficient acoustic impedance contrast between the filling material and the host rock to produce a weaker signal. Therefore, both open and filled fractures may produce similar dark images on the amplitude log.

Transit time imaging, however, responds not to variations of signal amplitude but rather to the travel time (and, hence, the distance) from the borehole wall. On the transit time log, the distance to the borehole face is represented by a gray scale designating white for far, dark for near, and black for no signal. Therefore, an open fracture produces a black image on the transit time image, whereas a filled fracture does not. Fig. 51.99 shows a vertical fracture on the amplitude log on the left. The similar black outline on the transit time log on the right confirms that this is an open fracture.

Permeability

Theoretical studies by Biot^{45,46} have indicated that changes in acoustic attenuation may reflect the fluid mobility (the ratio of permeability to viscosity). Later studies by Wyllie *et al.*²⁴ and Gardner and Harris¹¹⁵ considered the logarithmic decrement (Eq. 6) of acoustic energy to be a result of solid friction ("jostling" decrement) in the rock matrix and viscous drag ("sloshing" decrement) within the saturant fluid.

The solid matrix losses (jostling losses) were studied experimentally by Gardner and Harris,¹¹⁵ with respect to the effects of overburden pressure and fluid saturation. The results of their investigation indicate the jostling decrement of a sandstone under overburden pressures to be almost independent of fluid saturation and signal frequency. Hence, changes in the logarithmic decrement can be attributed to sloshing loss, which, according to Biot,^{45,46} reflects changes in fluid mobility.

Later, in a theoretical study, Rosenbaum⁶⁴ applied Biot's theory to the investigation of propagation of acoustic pulses in a fluid-filled borehole surrounded by a porous medium. He predicted that permeability could be estimated from an analysis of tube wave data contained in the acoustic waveform recorded in a borehole. He suggested that, for a sealed interface between the borehole and formation, maximum sensitivity to permeability was obtained in the interval between S-wave arrival and the fluid wave. For the open interface (no mudcake), the entire signal following the S-wave arrival could be used. The P-wave arrival was least sensitive to permeability and could be used for normalization.

Results of this study were first tested by Staal and Robinson¹⁵¹ in the Groningen gas field, The Netherlands. They recorded acoustic waveforms and analyzed them to obtain a permeability profile, which compared favorably with the core analysis data.

More recently, Rosenbaum's prediction⁶⁴ of the relationship between the energy loss of the tube (Stoneley) wave and permeability was investigated more extensively by Williams *et al.*¹⁵² Using a special long-spacing acoustic logging tool, they measured the tube wave transit time and energy ratio in wells located in different geographic locations with formations of varying lithology, permeability, saturating fluid, depth, and geological age. From these wells, they also obtained whole core samples for measurements of permeability. For these widely varying conditions, they report qualitative correlations between core-measured permeabilities and the tube wave data.

An example shown in Fig. 51.100 for a Cretaceous carbonate section is highly promising as it indicates that both tube amplitude ratio, A_{R2}/A_{R1} , and transit time correlate well with a permeability increase of three orders of magnitude in the center zone.

Conclusions

Borehole measurements of acoustic properties have a wide range of applications in exploration, production,

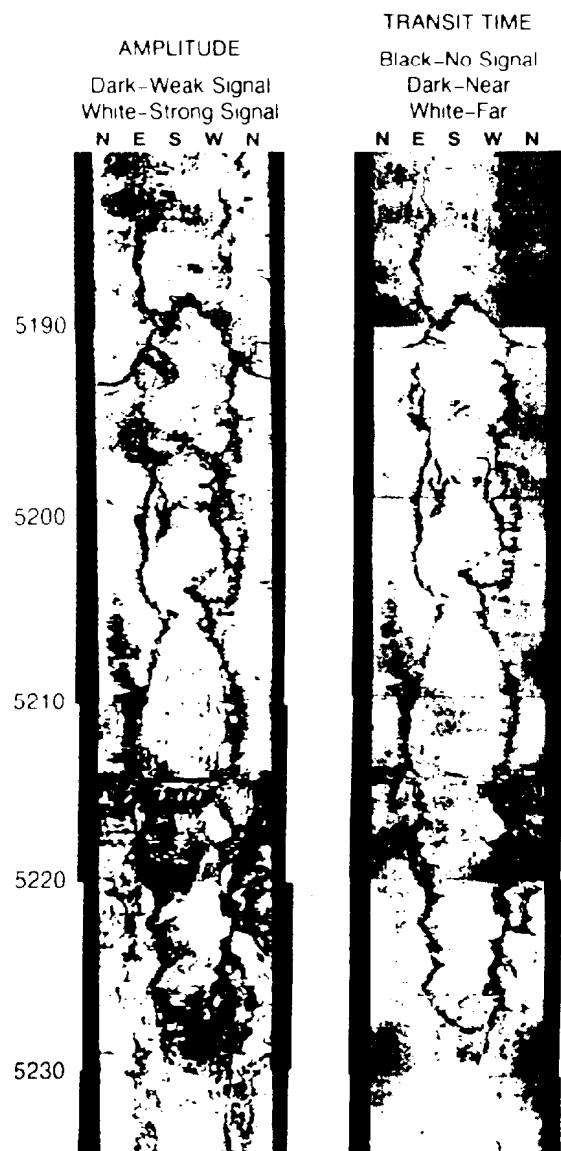


Fig. 51.99—Vertical fracture of the BHTV amplitude log on the left, confirmed to be open by the BHTV transit time log on the right.

and formation evaluation. Theoretical and experimental studies have significantly improved our understanding of the relationships between acoustic wave propagation and formation evaluation parameters, such as porosity, fluid saturation, and lithology. This, in turn, has prompted the development of new and improved borehole acoustic measurement technology and sophisticated digital signal processing technology to analyze the large amount of data. Even then, current applications often use only a small fraction of the information available in acoustic waveforms.

Advances in the understanding of acoustic wave propagation are interactively complementing improvements in downhole recording and transmission technology, and developments in signal processing. This should result not only in a broader and more quantitative use of the present applications, but also in the development of many new applications.

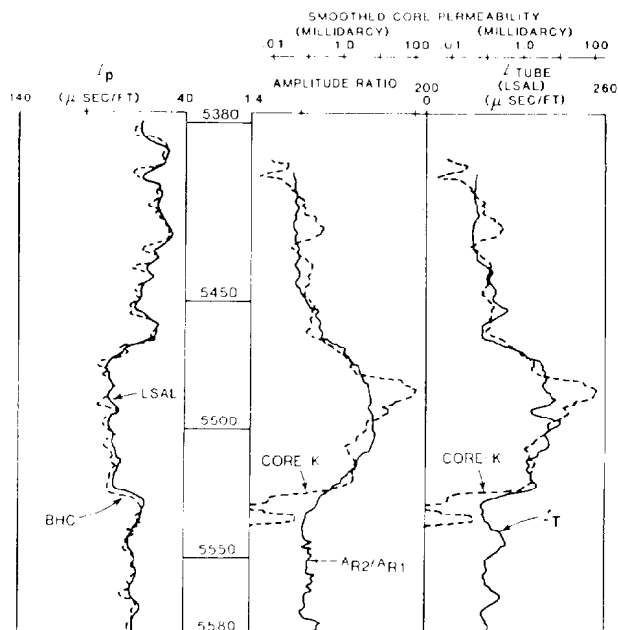


Fig. 51.100—Permeability correlation with tube wave data.

Nomenclature

- A = area; or signal amplitude
- A_o = signal amplitude at the source
- b = intercept defined by Eq. 13
- c = compressibility
- d = diameter
- D_i = depth of investigation
- E = Young's modulus
- f = frequency
- $f(K_f)$ = function of incompressibility of a fluid in pore spaces
- F = force
- F_{cp} = compaction correction factor
- F_q = quality factor
- G = shear modulus
- I = intensity
- I_o = acoustic intensity at the source
- K = bulk modulus
- L = length
- m = slope
- n = number
- p = pressure
- p_d = differential pressure
- p_f = internal (pore fluid) pressure
- p_f/D = pore fluid pressure gradient, psi/ft
- $(p_f/D)_n$ = normal hydrostatic pressure gradient (0.456 psi/ft for U.S. gulf coast)
- p_{fr} = fracture pressure
- p_o = external (overburden) pressure
- p_o/D = overburden stress gradient, psi/ft
- P_d = P-wave modulus for the rock frame (or the dry rock)

- r = borehole radius
 s = arbitrary point
 S = saturation
 t = travel time
 τ = transit time
 $\tau (=1/v_p)$ = transit time for the compressional waves for a liquid-saturated porous medium
 $\tau_L (=1/v_L)$ = transit time for saturant liquid
 τ_d = damaged zone transit time
 $\tau_m (=1/v_m)$ = transit time for rock matrix that forms the solid frame of a porous medium
 τ_n = transit time on the extrapolated normal curve at depth
 τ_{ob} = observed transit time at depth
 u = particle motion at s
 v = velocity
 v_f = compressional-wave velocity of drilling mud
 v_p = compressional-wave velocity
 v_r = pseudo-Rayleigh-wave velocity
 v_s = shear-wave velocity
 v_t = tube- or Stoneley-wave velocity
 α = coefficient of absorption; or attenuation coefficient
 δ = logarithmic decrement
 ϵ = strain
 ϵ_L = longitudinal strain
 ϵ_s = shearing strain
 ϵ_T = transverse strain
 θ_s = S-wave critical angle
 λ = wave length
 μ = Poisson's ratio
 ρ = density
 ϕ = porosity

Subscripts

- a = apparent
 c = corrected
 d = dry rock
 f = pore fluid
 g = gas
 hc = hydrocarbon
 L = liquid
 m = matrix
 N = neutron
 o = overburden or oil
 p = pore volume; or P-wave modulus
 s = S-wave modulus
 sh = shale
 w = water

Acknowledgments

I wish to thank A.A. Brown, G.S. De, and K.J. Dunn of Chevron Oil Field Research Co. and M.N. Toksöz of the Massachusetts Inst. of Technology for reviewing the manuscript, Debbie Ivey for typing, and, more importantly, the participants of the Chevron Formation Evaluation seminar during the past 20 years for many helpful suggestions toward the evolution of this chapter.

APPENDIX

Theory of Elastic Wave Propagation in Rocks

The first theoretical expression of elastic behavior of a saturated porous medium was given by Gassmann.⁴⁴ Later, Biot^{45,46} developed a more comprehensive theory of elastic wave propagation in a fluid-saturated, isotropic, porous solid over a wide frequency range. The predicted velocity dispersion by this theory is, in general, less than 3%⁴⁷; therefore, the low-frequency approximation should be useful for most applications.

Velocities predicted by this theory at the lower frequencies can be expressed simply by

$$v_p^2 = \frac{P_d + f(K_f)}{\rho_b} \quad \text{..... (A-1)}$$

and

$$v_s^2 = \frac{G}{\rho_b}, \quad \text{..... (A-2)}$$

where P_d is the P-wave modulus for the rock frame (or the dry rock), and $f(K_f)$ is the function of the incompressibility of the fluid in the pore spaces. The P-wave modulus for the dry rock can be expressed, in turn, by

$$P_d = K_d + \frac{4}{3}G_d; \quad \text{..... (A-3)}$$

and the function $f(K_f)$, by

$$f(K_f) = K_f \frac{(1 - K_d/K_m)^2}{(1 - K_f/K_m)\phi + (K_m - K_d)K_f/K_m^2}, \quad \text{.. (A-4)}$$

in which K is incompressibility (or bulk modulus), G is shear modulus, and the subscripts d , f , and m refer to the rock frame (or the dry rock), fluid, and rock matrix.

For rocks containing both water and hydrocarbons, the bulk density is expressed as

$$\rho_b = \phi\rho_f + (1 - \phi)\rho_m, \quad \text{..... (A-5)}$$

where

$$\rho_f = S_w\rho_w + (1 - S_w)\rho_{hc}, \quad \text{..... (A-6)}$$

and the fluid incompressibility, K_f , which is the inverse of compressibility, c_f , is given by

$$c_f = S_w c_w + (1 - S_w)c_{hc}, \quad \text{..... (A-7)}$$

where S denotes saturation, and the subscript hc refers to hydrocarbon.

Rock frame incompressibility, K_d , in Eq. A-3, which is the inverse of compressibility of dry rock, c_d , is related to PV compressibility, c_p , by

$$c_d = \phi c_p + c_m, \quad \text{..... (A-8)}$$

on the basis of Van der Knaap's⁵⁹ definitions. Substitution of this equation into Eq. A-1, after some manipulation, results in

$$\frac{3}{\rho_b v_p^2} \frac{1-\mu}{1+\mu} = \frac{\mu}{(c_f - c_m)^{-1} + c_p^{-1}} + c_m \quad \text{A-9}$$

Further substitutions into this equation for density from Eq. A-5 and rearranging yields a quadratic equation in μ . Neglecting terms involving μ^2 (since μ is a fraction) and assuming μ to be independent of porosity yields an equation expressing $1/v_p^2$ as a linear function of porosity. For lower porosities,

$$\frac{1}{v_p} = m\phi + b \quad \text{A-10}$$

If the Poisson ratios for the saturated rock and the rock matrix are assumed to be close in value, then b becomes approximately equal to $1/v_m$. The parameter m in Eq. A-10, however, is a strong function of c_p .

As the foregoing discussion indicates, Eq. A-10 is an approximation of Eq. A-9. Therefore, the commonly used time-average equation,^{18,19} which is of the same form as Eq. A-10,

$$\frac{1}{v_p} = \left(\frac{1}{v_f} - \frac{1}{v_m} \right) \phi + \frac{1}{v_m} \quad \text{A-11}$$

(where v_f is the velocity of saturant liquid) also may be considered to be an approximation of the more general theory.

References

- Leonardon, E.G.: "Logging, Sampling, and Testing," *History of Petroleum Engineering*, API, New York City (1961) 493-578.
- Geophysics* (Oct. 1944) 540.
- Mounce, W.D. et al.: "Seismic Velocity Logging," *Proc., Fifth Annual Midwestern Geophysical Meeting*, Dallas (Nov. 19-20, 1951).
- Summers, G.C. and Broding, R.A.: "Continuous Velocity Logging," *Geophysics* (1952) 27, 595.
- Vogel, C.B.: "A Seismic Velocity Logging Method," *Geophysics* (1952) 27, 586.
- Sears, F.W. and Zemansky, M.W.: *University Physics*, Addison-Wesley Publishing Co. Inc., Reading, MA (1955) 1031.
- Ewing, W.M., Jardetzky, W.S., and Press, F.: *Elastic Waves in Layered Media*, McGraw-Hill Book Co. Inc., New York City (1957) 380.
- White, J.E.: *Seismic Waves: Radiation, Transmission, and Attenuation*, McGraw-Hill Book Co. Inc., New York City (1965) 302.
- Goldman, R.: *Ultrasonic Technology*, Reinhold Publishing Corp., New York City (1962) 304.
- Krautkrämer, J. and Krautkrämer, H.: *Ultrasonic Testing of Materials*, Springer-Verlag, New York City (1969) 521.
- Guyod, H. and Shane, L.E.: *Geophysical Well Logging*, Hubert Guyod, Houston (1969) 1, 256.
- Timur, A.: "Rock Physics," *The Arabian J. for Science and Engineering Special Issue* (1978) 5-30.
- Jones, S.B., Thompson, D.D., and Timur, A.: "A Unified Investigation of Elastic Wave Propagation in Crustal Rocks," paper presented at the Rock Mechanics Conference, Vail, CO (1976).
- Toksöz, M.N., Cheng, C.H., and Timur, A.: "Velocities of Seismic Waves in Porous Rocks," *Geophysics* (1976) 41, 621-45.
- Toksöz, M.N., Johnston, D.H., and Timur, A.: "Attenuation of Seismic Waves in Dry and Saturated Rocks: Part I: Laboratory Measurements," *Geophysics* (1979) 44, 681-90.
- Johnston, D.H., Toksöz, M.N., and Timur, A.: "Attenuation of Seismic Waves in Dry and Saturated Rocks: Part II: Theoretical Models and Mechanisms," *Geophysics* (1979) 44, 691-711.
- Timur, A.: "Temperature Dependence of Compressional and Shear Wave Velocities in Rocks," *Geophysics* (1977) 42, 950-56.
- Wyllie, M.R.J., Gregory, A.R., and Gardner, G.H.F.: "Elastic Wave Velocities in Heterogeneous and Porous Media," *Geophysics* (1956) 21, 41-70.
- Wyllie, M.R.J., Gregory, A.R., and Gardner, G.H.F.: "An Experimental Investigation of Factors Affecting Elastic Wave Velocities in Porous Media," *Geophysics* (1958) 23, 459-93.
- Berry, J.E.: "Acoustic Velocity in Porous Media," *J. Pet. Tech.* (Oct. 1959) 262-70; *Trans., AIME*, 216.
- Tixier, M.P., Alger, R.P., and Doh, C.A.: "Sonic Logging," *J. Pet. Tech.* (May 1959) 106-14; *Trans., AIME* (1959) 216.
- Sarmiento, R.: "Geological Factors Influencing Porosity Estimate from Velocity Logs," *Bull., AAPG* (1961) 633-44.
- Wyllie, M.R.J.: *The Fundamentals of Well Log Interpretation*, Academic Press, New York City (1963).
- Wyllie, M.R.J., Gardner, G.H.F., and Gregory, A.R.: "Studies of Elastic Wave Attenuation in Porous Media," *Geophysics* (1962) 27, 269.
- Wyllie, M.R.J., Gardner, G.H.F., and Gregory, A.R.: "Some Phenomena Pertinent to Velocity Logging," *J. Pet. Tech.* (July 1961) 629-36.
- Gregory, A.R.: "Shear Wave Velocity Measurements of Sedimentary Rock Samples Under Compression," *Proc., Fifth Symposium on Rock Mechanics* (1963) 439.
- Pickett, G.R.: "Acoustic Character Logs and Their Applications in Formation Evaluation," *J. Pet. Tech.* (June 1963) 659-67; *Trans., AIME*, 228.
- Christensen, D.M.: "A Theoretical Analysis of Wave Propagation in Fluid Filled Drillholes for the Interpretation of the Three-Dimensional Velocity Log," *Trans. SPWLA* (1964) 5.
- Gardner, G.H.F., Gardner, L.W.R., and Gregory, A.R.: "Formation Velocity and Density—The Diagnostic Basics for Stratigraphic Traps," *Geophysics* (1974) 39, 770-80.
- Brandt, H.: "A Study of the Speed of Sound in Porous Granular Media," *J. Appl. Mech.* (1955) 22, 479.
- Hicks, W.G. and Berry, J.E.: "Application of Continuous Velocity Logs to Determining of Fluid Saturation of Reservoir Rocks," *Geophysics* (1956) 21, 739-54.
- Banthia, B.S., King, M.S., and Fatt, I.: "Ultrasonic Shear Wave Velocities in Rocks Subjected to Simulated Overburden Pressure and Internal Pore Pressure," *Geophysics* (1964) 30, 117-21.
- Gardner, G.H.F., Wyllie, M.R.J., and Droschak, D.M.: "Hysteresis in the Velocity-Pressure Characteristics of Rocks," *Geophysics* (1965) 30, 111-16.
- Hughes, D.S. and Cross, J.H.: "Elastic Wave Velocities in Rocks at High Pressures and Temperatures," *Geophysics* (Oct. 1951) 26, 557-93.
- Hughes, D.S. and Kelly, J.L.: "Variation of Elastic Wave Velocity with Saturation in Sandstone," *Geophysics* (1952) 17, 739-52.
- Hughes, D.S. and Maurette, C.: "Variation of Elastic Wave Velocities in Granites with Pressure and Temperature," *Geophysics* (1956) 21, No. 2, 277-84.
- Hughes, D.S. and Maurette, C.: "Variation of Elastic Wave Velocities in Basic Igneous Rocks with Pressure and Temperature," *Geophysics* (1957) 22, 23-31.
- Birch, F.: "Interpretation of Seismic Structure of the Crust in Light of Experimental Studies of Wave Velocities in Rocks," *Geophysics* (contribution in honor of Beno Gutenberg), Pergamon Press, Oxford (1958).
- Timur, A.: "Velocities of Compressional Waves in Porous Media at Permafrost Temperatures," *Geophysics* (1968) 33, 584-96.
- Collins, F.R.: "Test Wells, Umiat Area, Alaska, with Micropaleontologic Study of the Umiat Field, Northern Alaska, by H.R. Berquist," *U.S. Geol. Survey Prof.* (1958) 71, No. 206, paper 305-B.

41. Robinson, F.M.: "Test Wells, Simpson Area, Alaska, with a Section on Core Analysis, by S.T. Yuster," *U.S. Geol. Survey Prof.* (1959) 523-68, paper 305-J.
42. Barnes, D.F.: "Seismic Velocity Measurements, at the Ogotoruk Creek Chariot Site, Northwestern Alaska in Geological Investigations in Support of Project Chariot in the Vicinity of Cape Thompson, Northwest Alaska—Preliminary Report," U.S. Geol. Survey, TEI-735, issued by U.S. Atomic Energy Comm. Tech. Inf. Service, Oak Ridge, TN (1960) 62-78.
43. Müller, G.: "Geschwindigkeitsbestimmungen elastischer Wellen in gefrorenen Gesteinen und die Anwendung akustischer Messungen auf Untersuchungen des Frostmantels an Gefrierschächten," *Geophysical Prospecting* (1961) 9, No. 2, 276-95.
44. Gassmann, F.: "Ueber die Elastizität poröser Medien," *Vierteljahrsschrift der Naturforschenden Ges.*, Zürich (1951) 96, 1-23.
45. Biot, M.A.: "Theory of Propagation of Elastic Waves in Fluid-Saturated Porous Solid: I. Low Frequency Range," *J. Acoustical Soc. of America* (1956) 28, 168-78.
46. Biot, M.A.: "Theory of Propagation of Elastic Waves in a Fluid-Saturated Porous Solid: II. High Frequency Range," *J. Acoustical Soc. of America* (1956) 28, 179-91.
47. Geertsma, J.: "Velocity-Log Interpretation: The Effect of Rock Bulk Compressibility," *Soc. Pet. Eng. J.* (Dec. 1961) 235-48; *Trans.*, AIME, 222.
48. Brown, R.J.S. and Korringa, J.: "On the Dependence of the Elastic Properties of a Porous Rock on the Compressibility of the Pore Fluid," *Geophysics* (1975) 40, 608-16.
49. King, M.S.: "Wave Velocities in Rocks as a Function of Changes in Overburden Pressure and Pore Fluid Saturants," *Geophysics* (1966) 31, 50-73.
50. Gregory, A.R.: "Fluid Saturation Effects on Dynamic Elastic Properties of Sedimentary Rocks," *Geophysics* (1976) 41, 895-921.
51. Nur, A.M. and Simmons, G.: "The Effect of Saturation on Velocity in Low Porosity Rocks," *Earth Plan. Sci. Letters* (1969) 7, 183-93.
52. Voigt, W.: *Lehrbuch der Kristallphysik*, B.G. Teubner, Leipzig (1928).
53. Reuss, A.: "Berechnung der Fließgrenze von Mischkristallen auf Grund der Plastizitätsbedingung für Einkristalle," *Z. Angew. Math. Mech.* (1929) 9, 49-58.
54. Hill, R.: "The Elastic Behavior of a Crystalline Aggregate," *Proc. Phys. Soc.*, London (1952) 65, 349-54.
55. Hill, R.: "Elastic Properties of Reinforced Solids: Some Theoretical Principles," *J. Mech. Phys. Solids* (1963) 11, 357-72.
56. Timur, A., Hemphkins, W.B., and Weinbrandt, R.M.: "Scanning Electron Microscope Study of Pore Systems in Rocks," *J. Geophys. Res.* (1971) 76, No. 20, 4932-48.
57. Korringa, J. *et al.*: "Self-Consistent Imbedding and the Ellipsoidal Model for Porous Rocks," *J. Geophys. Res.* (1979) 84, 5591-98.
58. Hadley, K.: "Comparison of Calculated and Observed Crack Densities and Seismic Velocities in Westerly Granite," *J. Geophys. Res.* (1976) 81, 3484-94.
59. Van der Knaap, W.: "Nonlinear Behavior of Elastic Porous Media," *Trans.*, AIME (1959) 216, 179-87.
60. Biot, M.A.: "Propagation of Elastic Waves in a Cylindrical Bore Containing a Fluid," *J. Appl. Phys.* (Sept. 1952) 23, No. 9, 997-1005.
61. White, J.E.: "Elastic Waves Along a Cylindrical Bore," *Geophysics* (1962) 27, 327-33.
62. Christensen, D.M.: "A Theoretical Analysis of Wave Propagation in Fluid-Filled Drill Holes for the Interpretation of Three-Dimensional Velocity Log," *Trans.*, SPWLA (1964).
63. Geyer, R.L. and Myung, J.I.: "The 3-D Velocity Log: a Tool for In-Situ Determination of the Elastic Moduli of Rocks," *Dynamic Rock Mechanics, Proc.*, Twelfth Symposium on Rock Mechanics (1971) 71-107.
64. Rosenbaum, J.H.: "Synthetic Microseismogram Logging in Porous Formations," *Geophysics* (1974) 39, 14-32.
65. Tsang, L. and Rader, D.: "Numerical Evaluation of the Transient Acoustic Waveform Due to a Point Source in a Fluid-Filled Borehole," *Geophysics* (1979) 44, 1706-20.
66. Cheng, C.H. and Toksöz, M.N.: "Modeling of Full Wave Acoustic Logs," *Trans.*, SPWLA (1980) 21, paper J.
67. Cheng, C.H. and Toksöz, M.N.: "Elastic Wave Propagation in a Fluid-Filled Borehole and Synthetic Acoustic Logs," *Geophysics* (1981) 46, 1042-53.
68. Rader, D.: "Acoustic Logging: The Complete Waveform and its Interpretation," *Developments in Geophysical Exploration Methods—3*, A.A. Fitch (ed.), Applied Science Publishers (1982) 151-93.
69. Paillet, F. and White, J.E.: "Acoustic Models of Propagation in the Borehole and Their Relationship to Rock Properties," *Geophysics* (1982) 47, 1215-28.
70. Minear, J.W. and Fletcher, C.R.: "Full-Wave Acoustic Logging," *Trans.*, SPWLA (1983) paper EE.
71. Cheng, C.H. and Toksöz, M.N.: "Generation, Propagation and Analysis of Tube Waves in a Borehole," *Trans.*, SPWLA (1982) paper P.
72. Ingram, J.D.: "Method and Apparatus for Acoustic Logging of a Borehole," U.S. Patent No. 4,131,875 (1978).
73. Thomas, D.H.: "Seismic Applications of Sonic Logs," *The Log Analyst* (Jan.-Feb. 1977) 23-32.
74. Tixier, M.P., Alger, R.P., and Doh, C.A.: "Sonic Logging," *J. Pet. Tech.* (May 1959) 106-14; *Trans.*, AIME, 216.
75. Lynch, E.J.: *Formation Evaluation*, Harper and Row, New York City (1962) 422.
76. Kokesh, F.P. *et al.*: "A New Approach to Sonic Logging and Other Acoustic Measurements," *J. Pet. Tech.* (March 1965) 282-86.
77. Kimball, C.V. and Marzetta, T.L.: "Semblance Processing of Borehole Acoustic Array Data," *Geophysics* (1984) 49, 274-81.
78. Arditty, P.C., Ahrens, G., and Staron, Ph.: "EVA: A Long Spacing Sonic Tool for Evaluation of Velocities and Attenuation," paper presented at the 1981 SEG Annual Meeting, Los Angeles.
79. Ausburn, J.R.: "Well Log Editing in Support of Detailed Seismic Studies," *Trans.*, SPWLA (1977) paper F.
80. Jagcler, A.H.: "Improved Hydrocarbon Reservoir Evaluation Through Use of Borehole-Gravimeter Data," *J. Pet. Tech.* (June 1976) 709-18.
81. Hicks, W.G.: "Lateral Velocity Variations Near Boreholes," *Geophysics* (1959) 24, 451-64.
82. Goetz, J.F., Dupal, L., and Bowler, J.: "An Investigation into Discrepancies Between Sonic Log and Seismic Check Shot Velocities, Part I," *APEA J.* (1979) 19, 131-41.
83. Ransom, R.C.: "Methods Based on Density and Neutron Well-Logging Responses to Distinguish Characteristics of Shaly Sandstone Reservoir Rock," *The Log Analyst*, (May-June, 1977) 18, 47-62.
84. "The Long Spacing Sonic," Schlumberger technical pamphlet (1980).
85. Misk, A. *et al.*: "Effects of Hole Conditions on Log Measurements and Formation Evaluation," *SAID*, Third Annual Logging Symposium (June 1976).
86. "The Long Spacing Sonic," Schlumberger technical pamphlet (1982).
87. Spalding, J.S.: "Lithology Determination from the Micro-Seismogram," *The Log Analyst* (July-Aug. 1968).
88. Nations, J.F.: "Lithology and Porosity from Acoustic Shear and Compressional Wave Transit Time Relationships," *Trans.*, SPWLA 18th Annual Logging Symposium (June 1974).
89. Kowalski, J.: "Formation Strength Parameters from Well Logs," *Proc.*, Fifth Formation Evaluation Symposium, Canadian Well Logging Society, Calgary, Canada (1975).
90. Myung, John I.: "Fracture Investigation of the Devonian Shale Using Geophysical Well Logging Techniques," *Proc.*, Appalachian Petroleum Geology Symposium on Devonian Shales, West Virginia Geological and Economic Survey, Morgantown, WV (1976).
91. Koerperich, E.A.: "Shear Wave Velocities Determined From Long- and Short-Spaced Borehole Acoustic Devices," *Soc. Pet. Eng. J.* (Oct. 1980) 317-26.
92. Aron, J., Murray, J., and Seeman, B.: "Formation Compressional and Shear Interval-Transit-Time Logging by Means of Long Spacings and Digital Techniques," paper SPE 7446 presented at the 1978 Annual Technical Conference and Exhibition, Houston, Oct. 1-4.
93. Parks, T.W., McClellan, J.H., and Morris, C.F.: "Algorithms for Full-Waveform Sonic Logging," paper presented at the 1983 IEEE-ASSP Workshop on Spectral Estimation, Nov.
94. Ingram, J.D. *et al.*: "Direct Phase Determination of Shear Velocities from Acoustic Waveform Logs," paper presented at the 1981 SEG Meeting, Los Angeles, Oct.
95. Willis, M.E. and Toksöz, M.N.: "Automatic P and S Velocity Determination from Full Waveform Digital Acoustic Logs," *Geophysics* (1983) 48, 1631-44.

96. Zemanek, J. *et al.*: "The Borehole Televiwer—A New Logging Concept for Fracture Location and Other Types of Borehole Inspection," *J. Pet. Tech.* (June 1969) 762-74; *Trans., AIME*, **246**.
97. Wiley, R.: "Borehole Televiwer—Revisited," *Trans., SPWLA* (1980) **21**, paper HH.
98. "Seisviewer Logging," Birdwell, Div. of Seismograph Service Corp., technical pamphlet (1981).
99. Broding, R.A.: "Volumetric Scanning Well Logging," *Trans., SPWLA* (1981) **22**, paper B.
100. Taylor, T.J.: "Interpretation and Application of Borehole Televiwer Surveys," *Trans., SPWLA* (1983) **24**, paper QQ.
101. Pasternack, E.S. and Goodwill, W.P.: "Applications of Digital Borehole Televiwer Logging," *Trans., SPWLA* (1983) **24**, paper X.
102. Peterson, R.A., Fillipone, W.R., and Coker, F.B.: "The Synthesis of Seismograms from Well Log Data," *Geophysics* (July 1955) **20**, No. 3, 516-38.
103. Ausburn, B.E., Nath, A.K., and Wittick, T.R.: "Modern Seismic Methods—An Aid for the Petroleum Engineer," *J. Pet. Tech.* (Nov. 1978) 1519-30.
104. Ornes, G.: "Exploring with SH-Waves," paper presented at the 1978 CSEG Natl. Convention, Calgary, Canada, May.
105. "Log Interpretation Charts," Schlumberger (1979).
106. Clark, S.P.: "Handbook of Physical Constants," Geological Soc. of America, memoir 97 (1966) 587.
107. Simmons, G. and Wang, H.: *Single Crystal Elastic Constants and Calculated Aggregate Properties: A Handbook*, MIT Press, Cambridge, MA (1971) 370.
108. Wells, L.E., Sanyal, S.K., and Mathews, M.A.: "Matrix and Response Characteristics for Sonic, Density and Neutron," *Trans., SPWLA* (1979) **20**, paper Z.
109. Carmichael, R.S.: *Handbook of Physical Properties of Rocks*, CRC Press (1982) 2, 345.
110. "Evaluación de Formaciones en la Argentina," Schlumberger (1973) 94-95.
111. Raymer, L.L., Hunt, E.R., and Gardner, J.S.: "An Improved Sonic Transit Time-To-Porosity Transform," *Trans., SPWLA* (1980) paper P.
112. Hartley, K.B.: "Factors Affecting Sandstone Acoustic Compressional Velocities and An Examination of Empirical Correlations Between Velocities and Porosities," *Trans., SPWLA* (1981) paper PP.
113. Minear, J.W.: "Clay Models and Acoustic Velocities," paper SPE 11031 presented at the 1982 SPE Annual Technical Conference and Exhibition, New Orleans, Sept. 26-29.
114. Kuster, G.T. and Toksöz, M.N.: "Velocity and Attenuation of Seismic Waves in Two-Phase Media: Part 1: Theoretical Formulations," *Geophysics* (1974) **39**, 587-606.
115. Gardner, G.H.F. and Harris, M.H.: "Velocity and Attenuation of Elastic Waves in Sands," *Trans., SPWLA* (1968) **9**, paper M.
116. Domenico, S.N.: "Effect of Brine-Gas Mixture on Velocity in an Unconsolidated Sand Reservoir," *The Log Analyst* (1977) **18**, 38-46.
117. Kithas, B.A.: "Lithology, Gas Detection, and Rock Properties from Acoustic Logging Systems," *Trans., SPWLA* (1976) **17**, paper R.
118. Laws, W.R., Edwards, C.A.M., and Wichmann, P.A.: "A Study of the Acoustic and Density Changes Associated with High-Amplitude Events on Seismic Data," *Trans., SPWLA* (1974) **15**, paper D.
119. Hottman, C.E. and Johnson, R.K.: "Estimation of Formation Pressures from Log-Derived Shale Properties," *J. Pet. Tech.* (June 1965) 717-22; *Trans., AIME*, **234**.
120. Herring, E.A.: "North Sea Abnormal Pressures Determined from Logs," *Pet. Eng.* (1973) **45**, 72-84.
121. Fertl, W.H.: *Abnormal Formation Pressure*, Elsevier Scientific Publishing Co., New York City (1976) 382.
122. Eaton, B.A.: "The Equation for Geopressure Prediction from Well Logs," paper SPE 5544 presented at the 1975 SPE Annual Technical Conference and Exhibition, Dallas, Sept. 28-Oct. 1.
123. Grosmanin, M., Kokesh, F.P., and Majani, P.: "A Sonic Method for Analyzing the Quality of Cementation of Borehole Casings," *J. Pet. Tech.* (Feb. 1961) 165-71; *Trans., AIME*, **222**.
124. Walker, T.: "A Full-Wave Display of Acoustic Signal in Cased Holes," *J. Pet. Tech.* (Aug. 1968) 811-24.
125. Brown, H.D., Grijalva, V.E., and Raymer, L.L.: "New Developments in Sonic Wave Train Display and Analysis in Cased Holes," *Trans., SPWLA* (1970) **11**, paper F.
126. Pardue, G.H. *et al.*: "Cement Bond Log—A Study of Cement and Casing Variables," *J. Pet. Tech.* (May 1963) 545-55; *Trans., AIME*, **228**.
127. "Acoustic Cement Bond Log," Technical Pamphlet, Dresser Atlas (1979) 20.
128. "Cement Bond Evaluation in Cased Holes Through 3-D Velocity Logging," Technical Pamphlet, Birdwell (1978) 12.
129. Froelich, B., Pittman, D., and Seeman, B.: "Cement Evaluation Tool—A New Approach to Cement Evaluation," paper SPE 10207 presented at the 1981 SPE Annual Technical Conference and Exhibition, San Antonio, Oct. 4-7.
130. "Cement Evaluation Tool," Technical Pamphlet, Schlumberger (1983).
131. Fons, L.: "Acoustic Logging Through Casing," *Trans., CWLS Formation Evaluation Symposium* (1968) **2**, paper J.
132. Chang, S.K. and Everhart, A.H.: "A Study of Sonic Logging in a Cased Borehole," *J. Pet. Tech.* (Sept. 1983) 1745-50.
133. Simmons, G. and Brace, W.F.: "Comparison of Static and Dynamic Measurements of Compressibility of Rocks," *J. Geophys. Res.* (1965) **70**, 5649-56.
134. King, M.S.: "Static and Dynamic Elastic Moduli of Rocks Under Pressure," *Rock Mechanics—Theory and Practice, Proc., Eleventh Symposium on Rock Mechanics* (1970) 329-51.
135. Walsh, J.B.: "The Effect of Cracks on the Uniaxial Elastic Compression of Rocks," *J. Geophys. Res.* (1965) **70**, 399-411.
136. Myung, J.I. and Helander, D.P.: "Correlation of Elastic Moduli Dynamically Measured by In Situ and Laboratory Techniques," *The Log Analyst* (1972) **13**, 22-33.
137. McCann, D.M. and McCann, C.: "The Application of Borehole Acoustic Logging Techniques in Engineering Geology," *The Log Analyst* (1977) **18**, No. 3, 30-37.
138. Coates, G.R. and Denoo, S.A.: "Mechanical Properties Program Using Borehole Analysis and Mohr's Circle," *Trans., SPWLA* (1981) **22**, paper DD.
139. Anderson, T. and Walker, T.: "Log Derived Rock Properties for use in Well Stimulation," paper SPE 4095 presented at the 1972 SPE Annual Meeting, San Antonio, Oct. 8-11.
140. Hubbert, M.K. and Willis, D.G.: "Mechanics of Hydraulic Fracturing," *J. Pet. Tech.* (June 1957) 153-66; *Trans., AIME*, **210**.
141. Atkinson, A.: "Fracture Pressure Gradients from Acoustic and Density Log Data: An Updated Approach," *Trans., SPWLA* (1977) **18**, paper AA.
142. Walker, T.: "Acoustic Character of Unconsolidated Sands," Welx paper (1971).
143. Stein, N. and Hilchie, D.W.: "Estimating the Maximum Production Rate Possible from Friable Sandstones without Using Sand Control," *J. Pet. Tech.* (Sept. 1972) 1157-60; *Trans., AIME*, **253**.
144. Tixier, M.P., Loveless, G.W., and Anderson, R.A.: "Estimation of Formation Strength From the Mechanical Properties Log," *J. Pet. Tech.* (March 1975) 283-93.
145. Aguilera, A. and van Poollen, H.K.: "Current Status on the Study of Naturally Fractured Reservoirs," *The Log Analyst* (1977) **18**, 3-23.
146. Suau, J. and Gartner, J.: "Fracture Detection from the Logs," *Trans., Sixth European Formation Evaluation Symposium of the SPWLA London Chapter* (1979) paper L.
147. Aguilera, A.: *Naturally Fractured Reservoirs*, PennWell Publishing Co., Tulsa (1980) 703.
148. Walker, T.: "Progress Report on Acoustic Amplitude Logging for Formation Evaluation," paper SPE 451 presented at the 1962 SPE Annual Meeting, Los Angeles, Oct. 7-10.
149. Myung, J.I. and Baltosser, R.W.: "Fracture Evaluation by the Borehole Logging Method," *Stability Rock Slopes*, Thirteenth Symposium on Rock Mechanics (1972) 31-56.
150. Knopoff, L. and McDonald, G.H.F.: "Attenuation of Small Amplitude Stress Waves in Solids," *Geophysics* (1958) **34**.
151. Staal, J.J. and Robinson, J.D.: "Permeability Profiles from Acoustic Logging," paper SPE 6821 presented at the 1977 SPE Annual Technical Conference and Exhibition, Denver, Oct. 9-12.
152. Williams, D.M. *et al.*: "The Long Spacing Acoustic Logging Tool," *Trans., SPWLA* (1984) **25**, paper T.

Chapter 52

Mud Logging

Alun H. Whittaker, Exploration Logging Inc.*

Introduction

Conventional mud logging has been commercially available since 1939. The service involves extraction of gases from the returning mud stream and analysis of the gas for combustible hydrocarbons. Commonly, the resulting analyses are logged at drilled depth and plotted alongside a drill-time or rate of penetration log and a cuttings sample geological log. Although the mud log data cannot be related directly to undisturbed reservoir properties, they are important indicators of potentially productive horizons in the well. The conventional mud log continues to be the most important geological data source available before wireline logs are run.

The mud logging unit offers a useful location for the operation of other wellsite analyses and services. It provides a clean, well-lighted laboratory area with a stable electrical supply and is continuously operated by geologists or geologically trained technicians. Many mud logging contractors have made use of these assets to augment conventional mud logging with an extensive range of geological and engineering services. Often unrelated to the traditional gas analysis function of the unit, these services nevertheless generally are considered aspects of mud logging now in the same manner as sonic, density, and neutron logs often are grouped with "electric logs."

The earliest expansion of mud logging services began in the 1960's with the introduction of improved methods of geopressure detection. New techniques were added to the logging unit and it became common for a separate "pressure log" to be prepared alongside the mud log. The 24-hour activity of the mud logging unit allowed continuous operation of this service in which early detection was essential.

In the 1970's, the advent of rugged microelectronics allowed the introduction of more sophisticated and automated equipment into the logging unit. Most notably, the use of drilling rig data-acquisition systems

linked to minicomputers introduced a range of drilling optimization and control services. Unlike conventional mud logging and geopressure detection, these services are essentially nongeological. Generally, engineering personnel are added to the logging crew for these services.

In the 1980's three new aspects to mud logging services have been introduced. First, direct links between a wellsite minicomputer and an office data center allow centralized surveillance and control of several wells. The logging unit provides a wellsite access point to the central computer data base and analytical software.

Second, there is the increasing use of the mud logging unit as the surface receiving and control center for downhole measurement-while-drilling (MWD) services. The mud logging unit provides both a convenient working environment and support data (e.g., total depth measurement) for this service. Additionally, the ability to integrate mud logging and MWD data in a single computer adds economy and speed to the well evaluation process.

Third, the 1980's have brought the first fundamental changes in the methods of hydrocarbon and geological analysis, which continue to be the common denominator of all mud logging services. Improved sampling techniques, pyrolysis, chromatography, and other geochemical techniques have enhanced the diagnostic and quantitative value of mud logging. Wellsite geochemical screening for reservoir and source-bed type may now be performed in the mud logging unit.

Service Types

The number and range of mud logging contractors is possibly greater than that of any other oilfield service. The logging services offered by any single contractor may range from basic hydrocarbon logging, using equipment barely more sophisticated than that introduced 40 years ago, to complex chemical and physical analyses and a complete engineering surveillance and control center.

*The chapter on this topic in the 1962 edition was written by A.J. Pearson.

Similarly, logging personnel may be graduate geologists or engineers, or technicians of various levels of expertise. In specifying the mud log service for a well, the operator's engineer, geologist, and the logging contractor should define the objectives and problems anticipated and select those aspects of the service required.

Since extra service usually implies extra cost, economics must play a part in the decision. In engineering monitoring, it is relatively easy to compute the saving in drilling time or cost required to justify some addition to logging service day rate. This is discussed in detail at the end of this chapter.

Although overlaps occur, the services provided in mud logging may be grouped in line with the traditional oilfield disciplines: (1) *formation evaluation services*¹—hydrocarbon analysis, geological analysis, and geochemical analysis; (2) *petroleum engineering services*—geopressure evaluation and petrophysical measurements; (3) *drilling engineering services*—data acquisition and data analysis. This order is convenient for the following discussion of logging services since it closely parallels the historical development of mud logging and the level of sophistication of logging units used today.

Formation Evaluation Services

Gas Extraction Methods

Although the modern mud logging unit may perform many different services, probably its most critical one is the analysis of hydrocarbon gases.² Before this analysis can be performed, a sample of gas must be extracted from the drilling mud. This is performed by the gas trap (Fig. 52.1).

The gas trap is a square or cylindrical metal box immersed in the shale shaker ditch, preferably in a location

of maximum mud flow rate. Ports in the lower part of the trap allow mud to enter and leave the trap. An electric or pneumatic agitator motor provides both pumping and degassing of mud passing through the trap.

Gas evolved from the mud is mixed with ambient air in the upper part of the trap and drawn through a vacuum line to the logging unit for analysis. This device provides a relatively cheap and reliable method of obtaining a continuous gas sample. However, the efficiency of the device is somewhat affected by drilling practice. Pump rate and ditch mud level will influence mud flow rate through the trap; mud rheology will be a factor in the degassing efficiency of the trap; and mud and ambient air temperature around the trap and vacuum line will affect the relative efficiency with which light and heavy hydrocarbons are extracted and retained in the gas phase. This latter effect is most noticeable in areas of high diurnal temperature variation, where heavier alkane gases seen in daylight may condense and be lost in the cold of night.

An alternative to the conventional gas trap is the steam, or vacuum, mud still. In this device, a small sample of drilling mud is collected at the ditch, returned to the logging unit, and distilled under vacuum. The method provides a relatively high and uniform extraction efficiency for all hydrocarbons. It is, however, a time-consuming manual process. Analyses are noncontinuous and subject to human error; for example, light hydrocarbons can evaporate while the sample stands prior to analysis.

While a useful addition to the conventional gas trap at times, the mud still does not provide a real alternative. The development of a continuous gas trap with good and consistent efficiency of extraction is a high priority in the improvement of mud logging technology.

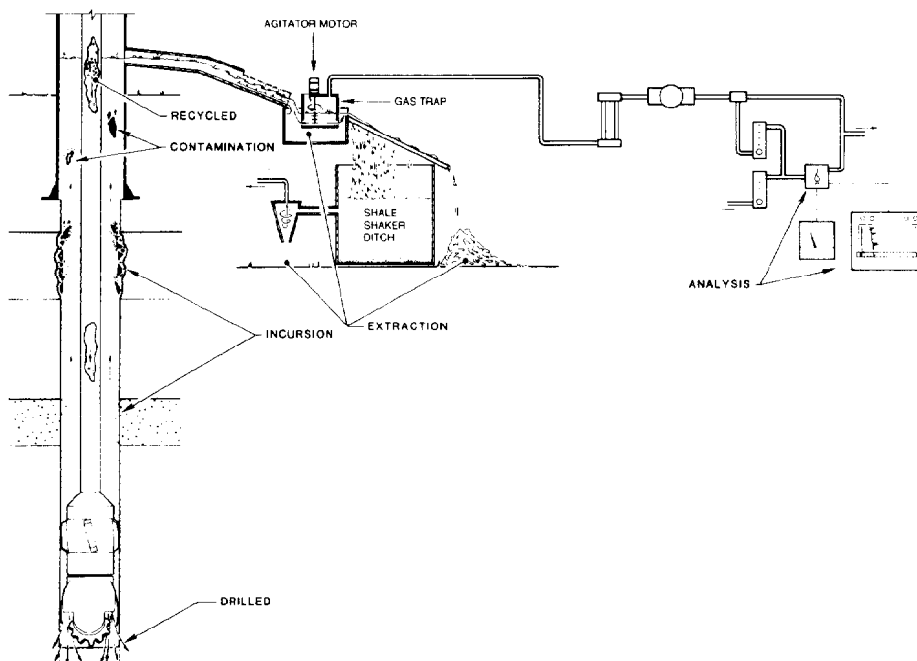


Fig. 52.1—Gas extraction at the ditch.

Hydrocarbon Analysis

The basic form of gas analysis involves the analysis by combustion of the bulk sample. Although commonly called "total gas analysis," it is, in reality, analysis for total *combustible* gases and primarily detects the low-molecular-weight alkanes (paraffins) such as methane, ethane, propane, butane, and pentane (with partial concentrations of hexane and heptane at higher ambient temperatures).

Catalytic Combustion Detector (CCD). After filtration and drying, the gas stream is injected at constant pressure and flowrate into a detector chamber (Fig. 52.2). The original type of mud logging gas detector, and probably still the most widely used, is the catalytic combustion, or "hot wire" detector (Fig. 52.3).

The hot wire detector is a Wheatstone bridge circuit consisting of four resistances: a fixed resistor, R_f ; a rheostat, R_v , used to trim or balance the bridge; and a matched pair of coiled platinum wire filaments, R_d and R_r . The two filaments are enclosed in an analysis cell with the detector filament, R_d , exposed to the flow of gas sample and the reference filament, R_r , isolated in pure air.

When a bridge voltage, V , is applied, the filaments become heated. A voltage between two and three volts is commonly selected to give a high enough filament temperature for hydrocarbon combustion at the filament surface (actual voltage used depends on the particular detector design). Combustion heat causes the temperature and hence resistance of the detector filament to rise relative to the reference filament. The bridge is unbalanced and current flows between the two sides of the bridge. Using a galvanometer of resistance R_m , this current, I_m , can be measured. Since combustion occurs at the filament surface only, the galvanometer current is quite sensitive and linear with changing gas concentration.

Obviously, detector response will depend on both the concentration and composition of the sample gas phase, since each hydrocarbon species will have its own particular heat of combustion. Table 52.1 shows these for the low-molecular-weight alkanes.

Since gas composition is unknown, the total gas detector cannot be calibrated for true compositional response. The detector is calibrated with a mixture of a single alkane, usually methane, in air. Detector response is then reported in percentage "equivalent methane in air" or EMA. Using a variable resistance, R_{vm} , in the bridge it is possible to adjust the bridge current, I_m , and graduate the galvanometer directly in percentage EMA. An older practice, which is now becoming obsolete, was to take the galvanometer reading in milliamps and relabel it as "gas units." Such units are obviously equipment specific although some company or regional standards have been enforced. Where this practice continues, confusion can be avoided by requiring the logging contractor to report calibration data on the mud log heading. For example, the contractor would report "100 total gas units = 2% EMA."

Fig. 52.4 shows the response of a typical CCD to commonly occurring combustible gases. Notice that a response of 1% EMA, or 50 total gas units, may indicate a concentration of 1% methane or a somewhat lower

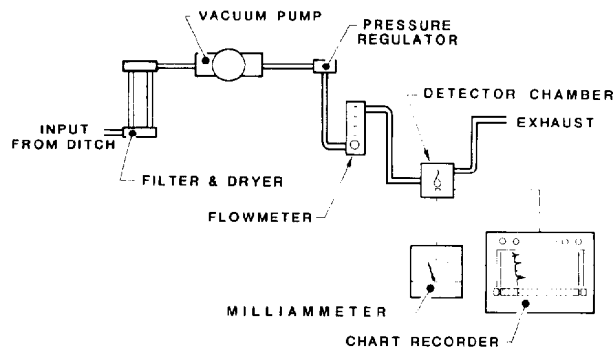


Fig. 52.2—Gas analysis system.

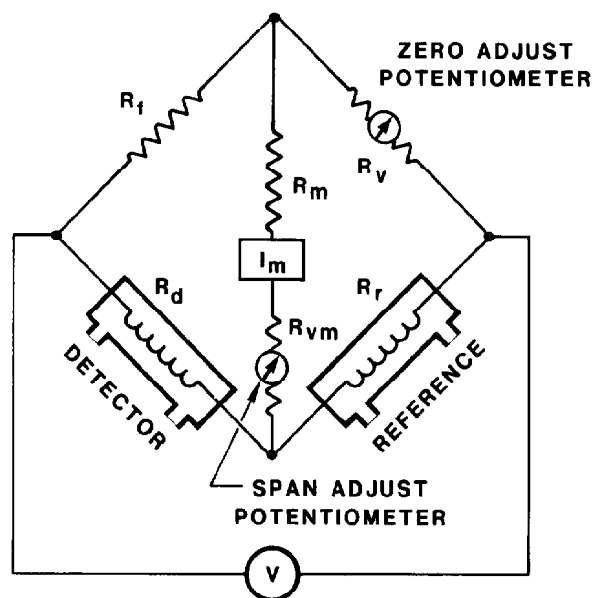
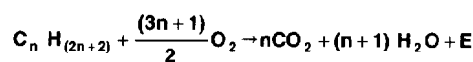


Fig. 52.3—Catalytic combustion detector.

TABLE 52.1—HEATS OF COMBUSTION OF THE SIMPLE ALKANES



	$n = 1$	Molecular Weight	E (kcal/mol)	kcal/gm	Structure
Methane	1	16	191	11.9	*
Ethane	2	30	342	11.4	**
Propane	3	44	493	11.2	***
Iso-butane	4	58	648	11.2	****
Butane	4	58	650	11.2	****

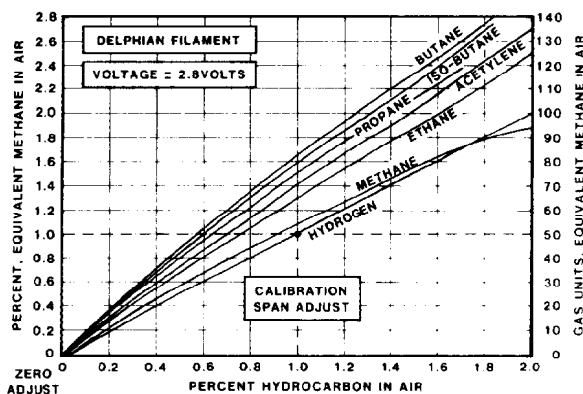


Fig. 52.4—Catalytic combustion detector response.

concentration of a mixture of methane and heavier alkanes. Total gas response may be thought of as a "gas richness indicator," increasing both with gas concentration and with addition of heavier fractions.

To assist in discriminating light alkanes from heavy ones, a second identical detector may be used. By setting a lower bridge voltage (1 to 1.4 V) and filament temperature, the detector is no longer capable of inducing combustion of methane. The resulting detector output, still reported in percentage EMA, is commonly labeled petroleum vapors, wet gas, or heavies, although only qualitative comparison of the two detector responses allows recognition of dry and oil-associated gas shows.

Response of the CCD can be maintained linearly up to the stoichiometric, or ideal, combustion composition of hydrocarbon in air. Above this composition, approximately 9.5% EMA, the detector "saturates," incomplete combustion occurs, and response becomes nonlinear. At higher concentrations, the sample must be diluted with air before it is introduced into the sample chamber to maintain a combustible gas mixture.

Theoretically, by using progressive sample dilution, a CCD can be maintained linearly up to concentrations of 100% EMA. In reality, each dilution stage requires a reduction in gas sample volume and an increasing mixing error. It is generally accepted that 40% EMA is the maximum limit of reliability of a CCD.

As an alternative to progressive dilution, where high gas concentrations are regularly expected, the detector can be reconfigured to operate as a thermal conductivity detector (TCD). Though the detector circuit remains essentially unchanged, it is operated at a lower voltage such that no gas combustion occurs. Bridge current now is reversed, responding to the cooling effect of the gas stream passing over the detector filament. Methane, which has a substantially greater thermal conductivity than air, will produce a large cooling effect, which may be linearly calibrated up to very high concentrations. The device is, however, poorly responsive to the heavier alkanes, CO_2 and hydrogen sulfide (H_2S), which have thermal conductivities close to that of air. The high conductivity gases, hydrogen and helium, will give responses even greater than that of methane.

The CCD is quite selective for hydrocarbons. Carbon dioxide (CO_2) and hydrogen sulfide (H_2S) will not burn at the detector filament. They will marginally reduce the

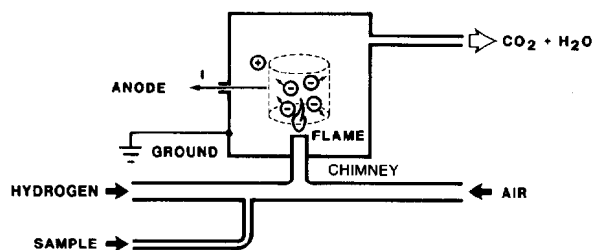


Fig. 52.5—Flame ionization detector.

thermal conductivity of the gas mixture and induce a small heating effect at the detector filament. This positive response is commonly so small as to be insignificant when compared with the greater hydrocarbon response. However, if the concentration of noncombustible gases becomes so high as to prevent complete combustion of hydrocarbon with air, a much larger negative response will occur.

Hydrogen will burn in the detector, even at low voltage, giving a concentration response similar to methane. Although free hydrogen does occur as an intermediate product of petroleum maturation, it is extremely reactive and diffusive. Occurrence of hydrogen in a petroleum gas show is therefore most uncommon. Significant concentrations of hydrogen have been shown to result from deep-seated structural movement, but the most common origin is from the corrosion of aluminum drillpipe or of steel drillpipe in extremely low pH drilling fluids.

A serious disadvantage of the CCD is the tendency of the catalyst surface to become poisoned by the accumulation of impurities and partial combustion products. This may result in a slow, progressive degradation of performance or a sudden, catastrophic loss, when, for example, silicon compounds are present in the mud. Regular detector calibration is essential to maintain reliable operation.

Flame Ionization Detector. The inherent limitations of the CCD resulted in a search for a more reliable detector technology. The most accepted and increasingly used is the flame ionization, or "hydrogen flame," detector (FID) (Fig. 52.5).

One important difference between the flame ionization and the catalytic combustion principles is that the flame ionization method involves complete combustion of the sample. A small quantity of sample is introduced into a hydrogen/oxygen mixture that is continuously burning in a combustion chamber. The heat generated by the hydrogen flame is sufficient to initiate complete combustion of all hydrocarbons in the sample. A large oxygen excess is maintained relative to the small sample volume and saturation never occurs. The heat output of the hydrogen flame is the sum of the heats of combustion of hydrogen and the sample hydrocarbons.

Unfortunately, most of the heat produced is from the large volume flow of pure hydrogen. The small, dilute flow of hydrocarbons produces such a small proportion of the total heat of combustion that it cannot be measured accurately. Combustion heat then cannot be used as a measure of hydrocarbon concentration. Detection of the hydrocarbons instead relies upon an unusual in-

intermediate stage in combustion that only occurs in hydrocarbons burning at high temperatures. This involves the creation of unstable electrically charged anions and cations. By placing a positive electrode, or anode, in the form of a cylindrical chimney above the hydrogen flame, the negative anions may be collected and the resultant electric current used to determine hydrocarbon concentration.

The ionization/combustion sequence is a complex one that involves many intermediate and alternate reaction steps. The number of ions created, and therefore the current flowing, is in direct proportion to the concentration of the alkanes and to the number of carbon atoms in the alkanes (Fig. 52.6). The FID response in percentage EMA is, therefore, like the CCD, a richness indicator showing increases with increasing concentration and increasing alkane molecular weight.

The FID is totally selective for compounds containing carbon-to-hydrogen (C-H) bonds. Other gases and impurities in the sample stream produce zero or negligible response and do not degrade detector performance.

Although the detector response is effectively linear throughout all concentrations, the electrometer used to monitor and amplify the detector current has performance limits of linearity. Since mud log gas shows may vary from tens of parts per million (ppm) to tens of percent, both electrical signal attenuation and sample splitting are required to ensure low-range sensitivity and high-range linearity of FID response. In most modern instruments this is handled automatically, ensuring a higher degree of accuracy than manual sample dilution.

Gas Chromatography. In addition to a total gas detector, most modern logging units will also contain a gas chromatograph. This device allows the separation of the individual alkanes and their separated detection, giving a gas analysis of composition and concentration. While this analysis is of greater value than the total gas response in EMA, the chromatograph does not provide a continuous analysis but processes batch samples separated by a number of minutes. In drilling terms, this translates into separate analyses several feet apart. The chromatograph does not replace the total gas recorder in showing the fine detail and progressive changes in a gas show.

In gas chromatography, a fixed volume gas sample is carried through a separating column by a carrier gas, usually air. The column contains liquid solvent surface or a fine molecular sieve solid. By difference in gas solubility or by differential diffusion, the gas mixture becomes separated into its components, the lightest traveling most quickly through the column and the heaviest most slowly.

Depending on the nature of the column, each component will pass through and exit the column in a characteristic time. From the column, the components pass in turn to a detector, which may be a CCD, TCD, or FID. The detector is calibrated with a gas mixture of known composition and concentrations. A separate calibration factor for each component can be used for detector response as the components occur in turn.

Since heavier components take longer to traverse the column, the time and depth interval between samples is governed by the number of components to be analyzed.

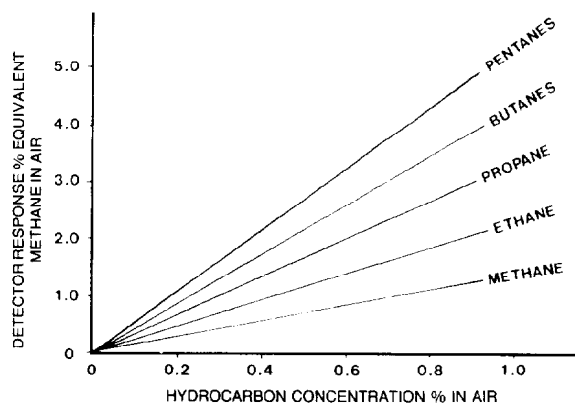


Fig. 52.6—Flame ionization detector response.

In routine logging, a chromatograph usually will be set to cycle through continuous automatic analyses for methane, ethane, propane, isobutane and n-butane. This requires approximately 3 to 5 minutes. If heavier alkanes (e.g., pentanes) need to be detected, the automatic control is disengaged and the analysis allowed to continue for a longer period of time.

Infrared Absorption Detector. The third, and least used, form of detector is the infrared absorption detector. This instrument uses the principle that any chemical bond will absorb infrared energy of a specific frequency governed by the chemical nature and geometry of that bond. For example, methane contains four identical carbon-to-hydrogen (C-H) bonds. If a gas sample is irradiated with infrared energy at a frequency characteristic of this bond, the energy absorbed by the sample will be in proportion to the number of C-H bonds and hence to the concentration of methane in the sample.

All other alkanes contain C-H and carbon-to-carbon (C-C) bonds. Although these bonds are chemically identical, they vary in geometry and hence characteristic infrared frequency, depending on their position within the alkane molecule. Theoretically it should be possible to pass the gas sample through a series of test cells, testing for infrared absorption at a series of characteristic infrared frequencies. Combination of the results would provide a continuous analysis of both alkane type and concentration—i.e., the equivalent of a continuous chromatograph.

Unfortunately, the C-H and C-C bonds show such a large number of minutely varying geometries that, instead of a series of discrete characteristic frequencies, a continuous band of overlapping absorptions occurs. At best, using a two-absorption cell system, it is possible to provide an estimate of methane concentration and total hydrocarbon concentration, in EMA. This result is comparable to the result obtainable from a dual CCD system and inferior to the results from an FID-equipped gas chromatograph.

Detection of Nonhydrocarbon Gases.¹ The most commonly occurring nonhydrocarbon gases in petroleum exploration are CO₂, H₂S, helium, nitrogen, and hydrogen. As discussed previously, the occurrence of naturally produced hydrogen is rare. Helium and nitrogen also tend to have regionally or geologically

specific occurrences. CO₂ and H₂S are common trace or significant components of natural gases and equipment for their detection should be used on any exploration well.

Chromatograph—Thermal Conductivity Detector.

The most versatile device for detection of nonhydrocarbons is a chromatograph equipped with a TCD. By selecting an appropriate column material and length, any single component or combination may be separated. The TCD will provide a response to any gas that has a thermal conductivity different from that of the carrier gas. This response will differ for each sample gas/carrier gas combination but, by using gas mixtures of known composition, calibration curves for each component can be developed.

Best response and sensitivity is achieved when the maximum difference exists between the thermal conductivities of the sample gas and the carrier gas. Thermal conductivity generally declines exponentially with increasing molecular weight. Thus the light gases (hydrogen and helium) may be readily detected by use of air as the carrier gas. For the heavier gases (nitrogen, CO₂, and H₂S) that have thermal conductivities closer to that of air, a lighter and higher thermal conductivity carrier gas must be used. Helium is a common choice but hydrogen also may be used if available.

An important consideration when assessing the reliability of analyses for nitrogen and CO₂ is their presence in the sample caused by the introduction of air into the gas trap and the aeration of drilling fluid.

Air of normal atmospheric composition, dissolved and entrained in drilling fluid, will be introduced continuously into the borehole. In the hot downhole environment, corrosion and other oxidation reactions will deplete oxygen from this air resulting in a relative increase in nitrogen and CO₂ concentration. Oxidation of carbonaceous material will further add to CO₂ enrichment. Alternatively, the presence of corrosion inhibitors in the mud may deplete both oxygen and CO₂. Regardless of the mechanism involved, oxygen depletion will increase with temperature and length of circulation time through the downhole system.

At the surface, this oxygen-depleted air and any gas recovered from the formation is mixed with ambient air at the gas trap. This air will vary in composition with the surrounding atmosphere—e.g., emissions from rig motors, vehicles, and others.

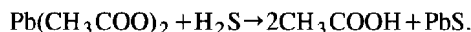
Any show of nitrogen or CO₂ from the formation must be recognized above background concentrations, which will show some random variation and a progressive increase as the hole is deepened and mud circulation becomes hotter and of longer duration. Regardless of the analytical method used, precision of the ppm level cannot be provided by the analysis. When only trace quantities of gas are expected or when a precise compositional analysis is required, mud logging analysis of CO₂ or nitrogen cannot be relied upon.

Of the nonhydrocarbon petroleum gases, H₂S and CO₂ are the most significant. They are the most commonly occurring gases in high concentrations and because of their polar nature pose serious problems of corrosion of drilling and production equipment. H₂S is

also toxic in relatively low concentrations. In many areas, detectors specific to these gases are considered standard mud logging equipment.

Infrared Absorption Detector. Continuous CO₂ detection is best handled with infrared absorption. An infrared analyzer is used that is responsive to the characteristic frequency of the carbon-to-oxygen (C-O) bond unique to CO₂. Correction of atmospheric CO₂ concentration is performed by alternately scanning two sample cells. One contains a sample from the gas trap and the other contains ambient air. Differential output provides a measure of CO₂ concentration above atmospheric.

Tube-Type Detector. Several types of H₂S detectors are used, all of which monitor a change resulting from the chemical oxidation of the gas. The simplest detector is the tube-type device in which the sample gas mixture is drawn at a controlled flow rate through a glass tube containing reactive lead acetate. The lead acetate, which is deposited on a substrate of high-surface-area silica gel granules, reacts with H₂S to produce lead sulfide and changes from white to dark brown or black in the process:



Since the amount of lead acetate in any unit length of tube is constant, the tube may be graduated in terms of concentration of H₂S in a fixed volume of sample.

The panel-mounted instrument has two tubes installed. Flow of sample from the ditch is constant through one of the tubes, and, if H₂S is present in the gas being evolved at the ditch, the lead acetate begins to discolor progressively from bottom to top (the direction of sample flow). Since the sample, and hence the discoloration, is continuous, this response is qualitative only. The discoloration indicates that H₂S is present in only trace or in enriched quantities, but no estimate of actual concentration can be made.

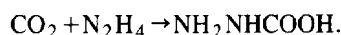
As soon as this discoloration is seen, a warning must be given since even trace quantities of gas can be dangerous. A quantitative analysis can be made by switching flow to the second tube and introducing a timed sample. In this case, a fixed amount of discoloration occurs and the scale allows reading of the H₂S concentration.

An alternative configuration for the tube indicator is in a small handbellows, often called a "puffer" or "sniffer," which can be used to sample the atmosphere in various locations around the rig.

Since the lead acetate reaction is not reversible, once the tube is used it must be replaced. The instrument cannot keep a continuous record of H₂S concentration but only a series of individual measurements. This is a drawback, but not a serious one since any quantity of H₂S in the atmosphere is both a health hazard and an indication that the mud system is totally saturated. Once H₂S is detected, mud treatment to remove it must begin. Gas measurement is required to ensure that it is removed and does not reappear.

The tube indicator may be used to detect CO₂ or any other gas for which a discoloring reactant is available. For CO₂, hydrazine is used in place of lead acetate.

Presence of CO_2 is indicated by a purple coloration of the chemical in the tube:



The tube method, however, is poorly suited to continuous monitoring since there will be a uniform rate of discoloration by atmospheric CO_2 .

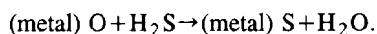
Paper-Tape-Type Detector. A more sophisticated version of this detection principle uses continuous paper tape, impregnated with lead acetate, to allow continuous analysis and a quantitative electrical output for chart recording and activation of alarms.

The detector mechanism is similar in appearance to an open-reel tape recorder. Its operation and operating components are analogous to that of tape recording. Paper tape, a porous filter paper coated with an even concentration of lead acetate, is wound from reel to reel at a constant speed. The tape passes through a sample chamber through which gas from the ditch passes continuously. The tape will be discolored by an amount proportional to the concentration of lead acetate on the tape, the speed at which the tape is moving (both of which are constant), and the concentration of H_2S in the sample. From the sample cell the tape passes to a detector where light from a collimated source is reflected from the tape to a photoelectric cell. The output of the photoelectric cell is readily calibrated in terms of H_2S concentrations by passing through the system test paper strips with zones of different color that correspond to a range of known concentrations.

The paper-tape-type detector may be used for the detection of CO_2 or other gases if a suitably impregnated paper tape is available. Unlike the tube indicator, it is possible to discriminate between a baseline of atmospheric discoloration and a true "show" above baseline.

Although the paper-tape-type is superior to the tube indicator, both suffer the disadvantage of requiring periodic replacement of the reactive material, lead acetate, and the possible degradation of the product in storage. Indicator tubes and rolls of paper tape are supplied in sealed, dated packages and should never be used if the seal is broken or the package is beyond its expiration date.

Solid-State Electrical Detector. The most modern H_2S analyzers involve use of a solid-state electrical detector. This device depends on the reversible reduction of metallic oxides by H_2S as its means of detection. A semiconductor sensor element is exposed to a flow of gas drawn from the ditch. The surface of this element consists of a proprietary metallic oxide layer. In the presence of H_2S , this layer will be partly reduced to metallic sulfides, and its electrical resistance will change:



This is an equilibrium reaction. If H_2S ceases to be present, the reaction reverses with the reoxidation of sulfides to oxides. At all times, the sulfide-to-oxide ratio (and

hence the electrical resistance) of the layer is a direct function of the concentration of H_2S in the sample present in the vicinity of the sensor.

Alternative configurations of this device involve multiple installations with either samples being drawn from, or sensor elements located in, various locations around the rig with centralized monitoring and alarm functions. Locating the sensor in a remote location may cause problems if the sensor is exposed to potential damage or mistreatment. It does, however, remove the risk of loss of response resulting from gas dissolving in condensation in long vacuum lines.

The device has high reliability and accuracy and is widely used in the industry. There are, however, two deficiencies that should always be considered. The first and most important is that if the sensor is operated for a period of time without any H_2S present, it tends to lose reaction speed. (It is important to note here that the sensor does not lose sensitivity! It will respond, within calibration, to the presence of H_2S , but will respond somewhat sluggishly to the first appearance.)

For safety reasons, the sensor must be reactivated regularly by using a sample of H_2S to maintain its reaction speed.

Second, the sensor will respond to certain organic sulfides that may be present in oil or result from mud additive decomposition. The response to these compounds is low but may result in a false H_2S show.

Soluble Sulfide Analyzer. One disadvantage common to all H_2S gas analyzers results from the high solubility of the gas in water. H_2S will not be liberated from the drilling fluid and will not be seen by a gas analyzer until a saturated solution of the gas exists. Since serious corrosion problems may be caused by low concentrations of the gas in mud and even a few ppm of the gas in air is a health hazard, it can be seen that by the time that H_2S gas is detected at the surface, a major problem already has developed.

Early detection of H_2S requires analysis of the drilling mud. This can be accomplished by regular sampling and wet chemical analysis, but the mud logging service can provide continuous soluble sulfide analysis by using a selective ion electrode measurement system.

With this device, a sensor probe, which is immersed in the drilling fluid, contains pH (hydrogen ion) and pS (sulfide ion) specific electrodes and a temperature sensor. When H_2S dissolves in water it will in part dissociate into bisulfide (HS^-) ions and sulfide (S^{--}) ions. The solubility of H_2S and the degree of dissociation are controlled by the pH and temperature of the solution. If these two parameters and the concentration of a single dissolved sulfide species are measured it is possible to deduce the concentration of all other species. In the soluble sulfide analyzer this is done automatically by a microprocessor. By using this device it is possible to detect H_2S and begin treatment to remove it from the mud without concentrations ever becoming high enough for gas detectors to be effective or for personnel to be placed at risk.

Geological Analysis

After gas analysis, the most important function of mud logging is the sampling and evaluation of drill cuttings.

Even when the mud logging unit operator is not a professional geologist, the minimum requirement is for identification and brief description of sample lithology, estimation of reservoir properties (amount and type of porosity and permeability), and description of oil staining.

Sample Lag Time. Hydrocarbon and geological analysis depend on the representative sampling of drill cuttings and gases liberated by the cutting action of the drillbit. In interpreting the analytical results, it is necessary to account for the lag time and physical effects of the gas and cuttings travel from the bottom of the hole to the surface.¹

Lagging of samples is essential so that results may be reported or logged at the depth from which the sample originated (at the time the sample arrives at surface, the depth, of course, will be somewhat greater). Lag time may be obtained simply by calculating the time necessary to displace the total annular volume of drilling fluid as given by

$$V_{an} = V_h - V_p, \dots\dots\dots (1)$$

$$v_{an} = \frac{q_p}{V_{an}}, \dots\dots\dots (2)$$

and

$$t_l = \frac{D}{v_{an}}, \dots\dots\dots (3)$$

where

- V_{an} = annular volume, m³/m,
- V_h = hole capacity, m³/m,
- V_p = pipe capacity and displacement, m³/m,
- v_{an} = annular velocity, m/s,
- q_p = pump output, m³/s,
- t_l = lag time, s, and
- D = depth, m.

Separate calculations must be performed for each annular section (drillpipe in casing, drillpipe in open hole, drill collars in open hole, etc.).

Calculated lag times are used when first drilling out of casing or in hard rock areas where an in-gauge hole is expected. However, a calculated lag time cannot take into account capacity variation in out-of-gauge holes or variation in pump rate or efficiency (for example, when the pump is stopped to make a connection).

Determining and using lag in terms of pump strokes has distinct advantages over lag determined on a time basis. The counters tracking the cuttings up the hole stop automatically when the pump is stopped. Clocks would continue to run, and some subtractive factor would have to be introduced. The most important advantage, however, lies in accuracy. A lag determined in terms of an interval of time is correct for only one speed of the circulating pump (that speed at which the lag determination was run), whereas the lag in pump cycles is accurate for any pump rate.

The lag can be determined by placing a tracer in the drillpipe at the surface when the kelly bushing is "broken off," allowing the tracer to be pumped through the hole and back to the surface, and counting the number of strokes required of the circulating pump to make this circulation. From this total pump stroke count, the number of strokes required to pump the tracer down through the pipe to the bottom of the hole is subtracted. This figure is calculated on the basis of the capacity of the drillpipe and the displacement of the circulating pump. The result is the "lag stroke."

Various materials (such as whole oats, barley, or strips of colored cellophane) may be used as tracers and picked up on the shaker screen for approximating the lag. Under ordinary circumstances, however, calcium carbide placed in the drillpipe will react with the mud to form acetylene. This gas will be picked up by the mud gas detector and is the most convenient and reliable method for determining the lag. Acetylene gas appears as wet gas on the gas detector and is easily distinguished from methane produced from the formation.

Representative Cuttings Samples. There is no substitute for representative cuttings samples accurately correlated to the depth from which they came. They are the required supportive data for the evaluation of any mud logging, geological, geophysical, or engineering data. Every rig has a shaker screen for separating the cuttings from the mud as they reach the surface. The shaker screen may or may not be a good place from which to take cuttings samples.³⁻⁵ If the shaker screen is used, a board or catching box should be placed at the foot of the screen for collecting composite samples. This becomes especially important where drill rate is low, to ensure that the sample collected is representative of the whole interval drilled and not just the final few inches.

Where a traditional "rhumba" shaker is used, differences in flow through the possum belly (ditch at the rear of the shale shaker) will result in density and size sortings of cuttings across the various screens. This sorting can be of assistance to the logging geologist in partially separating large cavings from the smaller bottomhole cuttings. However, great care must be taken to ensure that a representative sample is caught. Where a modern "doubledeck" shaker is used, cuttings on both the upper and lower screens should be sampled.

A sampling depth interval should be set that the mud logger can be expected to maintain while keeping up with other responsibilities. Sample intervals can be shortened as the hole is deepened and drill rate falls. The mud logger should never allow more than 15 minutes to pass between catching samples. For example, if the sample interval is 10 ft and the drill rate is 10 ft/hr, the mud logger should take four scoops of samples over the hour to fill the sample bag for the interval. Special samples should always be taken whenever background gas changes are seen or the lag time after drilling breaks occur. If a board or catcher box is used, it must be cleaned off after each sample is taken.

Samples should be taken from the desilter or desander outlets whenever these are running. In this way, the logging geologist can establish the quantity and appearance of sand and fine solids commonly contaminating the mud system. If an unconsolidated formation is penetrated,

sample from the desander will contain both formation sand and mud solids. The logging geologist must be able to discriminate between these.

Washing and preparing the cuttings to be examined are probably as important as the examination itself. In hard rock areas, the cuttings are usually quite easily cleaned, in which case washing is a matter of merely hosing the sample in a container of water to remove the mud film. Washing the cuttings in many areas, however, particularly areas and zones of tertiary sands and shales, is more difficult and requires several precautions. The clays and shales present are often soft and of a consistency which goes into solution and makes mud. Care must be taken to wash away as little of the shale as possible, and, in determining the sample composition, to take into account that which is washed away.

After washing the cuttings to remove the mud, they are washed through a 5-mm sieve unless doing so will further cause excessive loss of shale or clay. It is generally considered that the cuttings will pass through the 5-mm sieve, and that the material that does not is cavings and may be discarded. However, the material that does not pass through should be examined for sand cuttings. If they should be present, these afford an excellent opportunity for study of larger-than-normal cuttings chips.

Cuttings from wells drilled with oil-based or oil-emulsion muds are usually more representative of the drilled formation than cuttings drilled with water-based mud because the oil emulsion prevents sloughing and dispersion of clays and shales into the mud. At the same time, washing and handling cuttings drilled with this type mud poses somewhat of a problem; they cannot be cleaned by washing in water alone. It is usually necessary to wash the cuttings first in a detergent solution to remove the mud. Some of the liquid commercial detergents available may be used. In extreme cases, it may be necessary to wash the cuttings first with a nonfluorescent solvent such as naphtha, and then wash them in a detergent solution to remove the solvent. Use of a solvent is not advisable unless absolutely necessary because of the risk of removing any oil staining present.

An oven mounted on the wall of the logging unit can be used to dry a portion of the cuttings sample after it has been washed, but some of the washed cuttings are examined wet under the microscope. A sample of unwashed cuttings also is required for cuttings analysis in the blender. Although these cuttings should not be rigorously washed, a light rinsing to remove surface drilling mud film is advisable.

The logging geologist should extract a small amount of sample from each stage of the sample preparation process. From examination of all samples, an accurate estimate of sample composition can be produced.³ Once the percentages of the various constituents have been estimated, the sample description in logical order should contain (1) rock type, (2) color, (3) hardness (induration), (4) grain size, (5) grain shape, (6) sorting, (7) luster, (8) cementation or matrix, (9) structure, (10) porosity, (11) accessories, and (12) inclusions.

Only a visual sample examination usually is required at the wellsite in clastic (sand/shale) formations. In carbonates, other tests may be required to determine the chemical and physical nature of the rock. The simplest of these is to test cuttings with dilute hydrochloric acid; the

rate of reaction, which is rapid for calcite and slow for dolomite, provides a guide to relative composition.

This test can be made more quantitative by use of a calcimeter. In this device a weighed sample is treated with acid in a sealed reaction chamber. Reaction is monitored by measuring either the volume or pressure of evolved CO₂ over time until reaction is complete. Output is percentage of calcite and dolomite in the rock sample.

In more complex mixed carbonates and sulfates (e.g., anhydrite and gypsum), a chemical stain kit may be used. Small samples of washed drill cuttings are spot-tested with a series of chemical test solutions. Characteristic coloration of a test solution is indicative of the presence of a particular mineral in the sample.

Many excellent texts are available that discuss the geological aspects of mud logging. These include Low,⁶ Maher,⁷ and McNeal.⁸ Since this chapter deals primarily with the technology of mud logging, they are not discussed further here.

Hydrocarbon Content of Samples

In addition to a geological evaluation, cuttings samples must be tested for hydrocarbon content. A blender or cuttings gas analysis must be performed on every sample caught. This involves disintegration of a sample of cuttings in a blender, extraction of a sample of liberated gas, and injection into a total gas analyzer. This can be performed by manual extraction with syringe and injection into the unit's online gas analyzer. However, for speed and continuity of operation, modern logging units use automatic extraction and injection into an independent catalytic combustion cuttings gas analyzer.

As soon as a representative cuttings sample has been taken, a measured amount (100 cm³ in a measuring cup) of unwashed sample is placed in the blender jar and covered by 600 cm³ of water, then blended for 30 seconds and left to stand for another 30 seconds before taking a gas sample. If the hole is caving badly, the amount of cuttings may be increased but should be consistent—especially before and through a show. With hard carbonates, low-porosity sandstones, or similar reservoir rocks that cannot be efficiently pulverized by the cutter blades (40 to 60 seconds' blending is recommended), the blender jar should be allowed to stand for 2 or 3 minutes before taking any gas readings. After the gas analysis is performed, the water should be inspected for oil signs or petroleum odor. Any droplets can be skimmed off for examination. The crushed rock material also may be of value in clarifying lithological evaluation.

The blender is a good evaluation tool because it gives some indication of the quality of the reservoir with respect to the porosity and the GOR. A good porosity sandstone generally will be well-flushed by the time it reaches the surface, so the amount of cuttings gas obtained will increase proportionately to the decreasing porosity. This is also true with a sucrosic dolomite or high-porosity limestone such as chalk. However, if the reservoir is a fractured carbonate, etc., with all the oil and/or gas in the fractures, little or no cuttings gas will be recorded and the use of the blender as a porosity indicator is of limited value, because future production is

going to be more dependent on the complexity of the reservoir fracturing than the inherent porosity and permeability of the rock itself.

In oil reservoirs, gas is normally in solution with the oil, and the agitation of a covered sample provides an excellent index of the amount of gas with the oil, which is significant in view of the gas already recorded from the ditch. A high cuttings gas with an oil show should be treated as a very significant show and should be one of the more important factors to consider in the overall evaluation.

When large intervals of reservoir rock are cored, the blender readings obtained are not likely to be as informative as those obtained if the section had been drilled normally. Generally, the amount of sample is reduced because the center is still in the core barrel. With the often slower drill rate, the percentage of cavings may be increased. Also, if a diamond head is being used, the rock will be coming back in a very ground-up and often badly altered state. Thus, if the geologist is agreeable, representative 100-cm³ samples from the more broken-up parts of the recovered cores may be blended with water, and any readings can be used to supplement the readings obtained during the actual coring.

Inspection for liquid hydrocarbons should be made at the microscope (oil-stained cuttings), the blender jar (petroleum sheen and odor after blending), and in an ultraviolet light inspection box (fluorescent oil droplets on cuttings and diluted mud samples).

Visible oil stain and color is an important indication of oil presence and type as are ultraviolet fluorescence intensity and color, grading from dull brown for the heaviest (residual or wet) oil to bright blue-white for light oils and condensate. However, crosschecking of observations is essential to confirm the presence of oil. Many mud additives, contaminants, minerals, or rig floor debris will have an oily appearance or odor and may fluoresce under ultraviolet light. Only if visible stain and ultraviolet fluorescence yield the same conclusion is oil confirmed. For example, samples contaminated with pipe-dope will have a dark oily ap-

pearance suggesting heavy oil. However, the same cuttings examined under ultraviolet light will show a bright blue-white fluorescence characteristic of the highest gravity. This incompatibility allows the identification of a contaminant and avoids the logging of a false show. A good mud logger should examine all mud additives stocked at the wellsite and determine, before their use, their characteristic properties and appearance when mixed with drilling mud or cuttings.

If a true oil stain is identified, a single, representative cutting should be tested with an organic solvent. This is the "cut test." Solvent cut is valuable in assessing fluorescence and allows deductions to be made of oil mobility and permeability of the reservoir. By removing the oil from the colored background of the cutting, the solvent allows a better estimate of fluorescence. The way in which the solvent cut occurs (e.g., instantly for high-gravity oils, more slowly for more viscous lower-gravity oils, or irregularly streaming from limited permeability) also yields useful information. If no cut can be obtained from a washed cutting, the test should be repeated on a dried cutting, a crushed cutting, or after application of dilute hydrochloric acid. This will produce the required cut and yield further evidence on permeability or effective porosity. After the cut solvent has evaporated, a residue of oil remains in the cut dish, displaying the oil's natural color.

Finally, if sufficient oil is present, it may be possible to determine its refractive index. Just as oil stain color and fluorescence progressively change with oil type, refractive index correlates well with oil gravity. Portable refractometers that require only a small droplet of sample are available for use in the mud logging unit. By using a small quantity of oil (skimmed from the surface of the blender jar or a diluted mud sample), a very reliable estimate of oil gravity can be obtained.

Geochemical Analysis

More sophisticated analyses of hydrocarbon and hydrocarbon source material involve the principle of pyrolysis—thermal decomposition of a sample in an inert atmosphere. Three such devices are presently available: the Rock-Eval II™ (RE), the Oil Show Analyzer™ (OSA), and the Thermalytic Hydrocarbon Analyzer™ (THA). All these devices use variations of the Institut Français du Pétrole—Centre de Recherches du Groupe Petrofina (IFP-FINA) temperature-programmed pyroanalysis method developed by Espitalie.^{3,9} The process involves the heating of a weighed rock sample through an increasing temperature program in an inert helium stream. Since combustion cannot occur, the helium carries away from the sample hydrocarbons and CO₂ resulting from the thermal volatilization of petroleum and organic source material in the rock. These evolved gases may be analyzed by flame ionization and thermal conductivity detectors. The amount of gas expressed as milligrams per gram of rock, the evolved gas, and the time and temperature of evolution may be used to characterize the richness and type of a reservoir or source rock.

The differences between the three devices are shown in Fig. 52.7. The RE II uses a uniform temperature ramp of 25°C/min up to 550°C. The helium stream carrying evolved gases passes to a CO₂ trap and then to an FID.

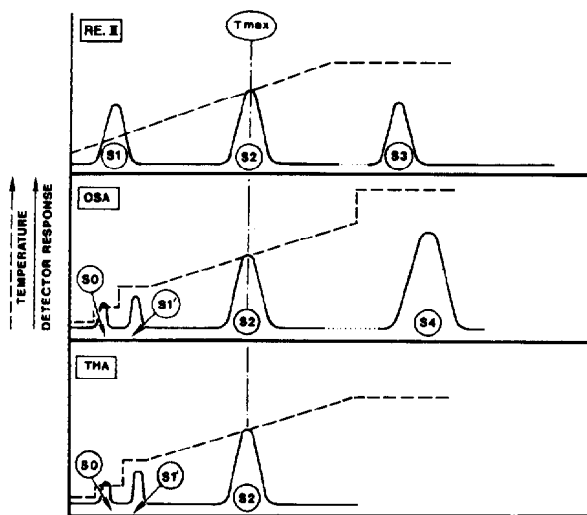


Fig. 52.7—Comparative results of REII, OSA, and THA.

On completion of the pyrolysis the trapped CO_2 is passed to a TCD. The output showing temperature, FID and TCD response is called a "pyrogram."

The RE II pyrogram characteristically shows two distinct peaks in FID response. The first, S1, represents true hydrocarbons, oil and gas, volatilized from the sample. The second, S2, represents hydrocarbons generated by the thermal cracking of hydrogen-rich organic source material, kerogen, in the sample. The temperature, T_{max} , at which the peak of S2 occurs is indicative of the maturity of the kerogen. Mature kerogen, capable of generating oil or gas, will have a T_{max} in the range of 435 to 470°C. A lower T_{max} indicates immature kerogen and a T_{max} above 470°C indicates postmature material that has already yielded the majority of its hydrocarbon product.

The TCD response, S3, represents the yield of CO_2 from the thermal cracking of oxygen-rich kerogen in the sample. A comparison of S2 and S3 provides the relative hydrogen/oxygen richness of the kerogen. This is useful in estimating source type. Hydrogen-rich kerogen is prone to rich oil yields, whereas oxygen richness gives more gas-prone and lower-yield kerogen.

The oil show analyzer (OSA) differs from the RE II in that it uses a nonuniform temperature consisting of two temperature steps followed by a temperature ramp. Following completion of pyrolysis the sample is further heated in an oxygen atmosphere causing the complete combustion of all remaining organic carbon in the sample.

The OSA pyrogram generally shows three characteristic peaks in FID response with S0 and S1 corresponding to the two temperature steps and representing the splitting of the RE II S1 peak into a lower-temperature (gas-indicating) peak and a higher-temperature (oil-indicating) peak. The S2 peak and T_{max} are the same as those seen in RE II. S4 represents CO_2 produced by pyrolysis (S3 equivalent) and by combustion. Combination of the pyrolysis and combustion gas products provides a measure of the total organic carbon content or the gross organic richness of the rock.

RE II has become widely used as a laboratory instrument and both it and the OSA have seen use in the mud logging unit in frontier exploration. The restriction on their wider implementation in mud logging has been the high complexity (and price) of these instruments, which has limited their use to the most advanced logging units and demanding exploration environments.

The THA, a much simpler device, is better suited to routine mud logging services. It uses only an FID and a temperature program similar to the OSA pyrolysis phase (without the final combustion phase). The THA pyrogram provides S0, S1, S2 and T_{max} . Neither CO_2 analysis, S3, nor S4 is available from the THA.

The Modern Mud Logging Unit

There are six basic requirements for a modern mud logging unit² based on the previous discussions.

1. A total combustible gas analyzer using catalytic combustion or flame ionization detector.
2. A gas sample dilution system, allowing maintenance of linear detector response at high gas concentrations or a backup thermal conductivity detector.
3. An automatic cycling chromatograph capable of

isolating and detecting methane, ethane, propane, butane, and isobutane or a second, low-voltage catalytic combustion detector, allowing discrimination of "total gas" from "petroleum vapors."

4. A separate cuttings gas analyzer, allowing gas analysis from blended cuttings samples.

5. A microscope and ultraviolet light inspection chamber for the identification and description of lithology and liquid hydrocarbons.

6. A pumpstroke counter, which, in conjunction with calcium carbide lag tests, allows gas readings and cuttings samples to be lagged back to correct drilled depth.

In addition, the unit requires a drilling depth and time recorder for the determination of sample depth and the calculation of rate of penetration, an important rock strength/porosity indicator. Ideally, this should be independent of the driller's depth recorder.

Since mud logging samples (gas, oil, and cuttings) are extracted from the mudstream, changes in mud chemistry and rheology must be considered when evaluating mud log results. The logging unit should be equipped to perform basic mud tests—e.g., mud balance, Marsh funnel, sand test kit, and filter press. Laboratory glassware and chemicals are required to perform chemical tests and titrations on cuttings and mud filtrate samples.

Although pressure control is not a *standard* function of mud logging (see Petroleum Engineering Services), the mud logger, by continuously monitoring mud gas content, should be aware of situations of potential drilling hazard. It is therefore usual for the mud logging unit to be equipped with a level monitor for the active mud pit. This allows the mud logger to be a second line of defense, after the driller, in detecting a well kick or loss of circulation.

The Mud Log

Format¹

Fig. 52.8 shows a typical modern mud log. There are currently no industry standards for mud logs, and presentation varies among operators. However, the track order commonly follows that shown in the example.

Track 1 is used for rate of penetration (ROP). Also included in this column are items of drilling data that may affect interpretation of the log (bit types, changes in drilling parameters, circulation breaks, etc.).

Track 2 is for depth notation and for symbolic representation of special evaluations (for example, cored or tested intervals).

Track 3 is a graphical representation of formations penetrated. Usually the column is subdivided into 10 equal columns and graphic symbols are used to represent 10% increments of lithology types seen in cuttings. Unlike other tracks on the log, the lithology track is not a calibrated physical measurement but a subjective assessment. Care should be taken to establish rules of drafting acceptable to the preparer and user of the log.

Even after removal of cavings and contaminants, a cuttings sample is not truly representative of a single depth interval. Variation in particle size and density cause differences in annular recovery rate and mixing of cuttings in the annulus. A true cuttings percentage will never show sharp formation boundaries as a result of this mixing. For example, a thin sandstone within a massive

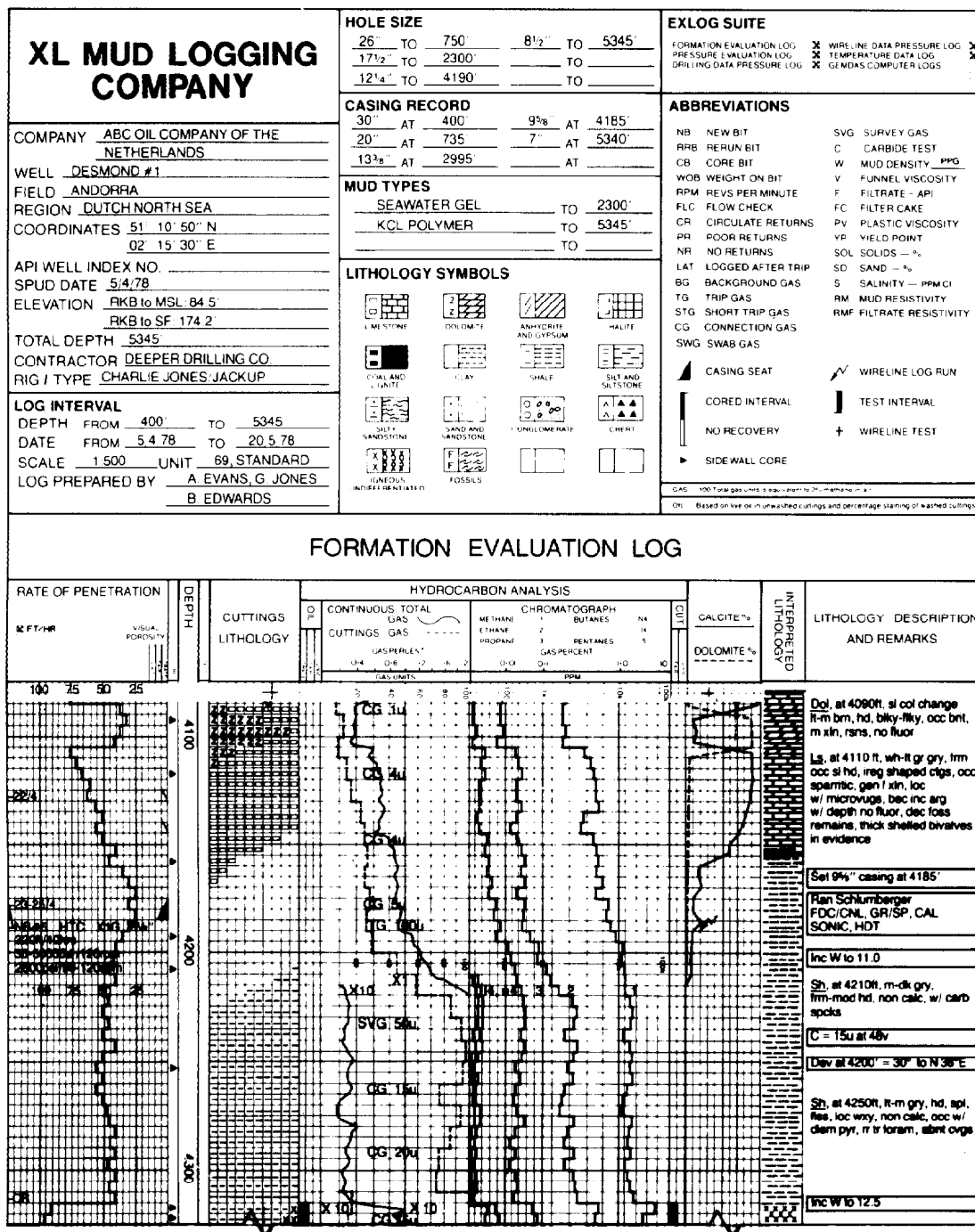


Fig. 52.8—Mud log format.

shale with sharp boundaries shown clearly by ROP and total gas analysis may appear from cuttings to be a sandy shale horizon of much greater vertical extent.

A geologist may use all available data to prepare an interpretive lithological log. That is, in the previous example, to sharply show the sandstone boundaries as indicated by ROP. Sometimes a mud logger will attempt to add some degree of interpretation to a cuttings log. Again, in the example the mud logger would show the presence of sand in all the cuttings samples but exaggerate the percent sand in the sample coinciding with the higher ROP.

This "semi-interpretation" may result in confusion when later sample examinations are compared with the mud log and, in my opinion, mud loggers should be instructed to prepare a true cuttings log representing the percentages of lithologies actually seen in the sample. If the mud logger is geologically qualified and the operator's geologist requires geological interpretation, then an interpretive lithological log should be prepared as an *additional* track on the mud log.

Track 4 presents the results of hydrocarbon analyses. It may consist of one single width track but most often is subdivided into two or more separate tracks, as in the example. Track 4 will include the results of total gas, cuttings gas, and chromatographic analyses and when oil shows occur, an estimate of oil show quality and oil cut will be added. Supplementary gas analyses (helium, hydrogen, CO₂, or H₂S) also may be added to this track or plotted on a supplementary log.

Track 5 primarily is used for brief sample descriptions. Also included in this track are mud test results, casing and cementation records, hole deviations, carbide test results, and many other operating data used in interpretation of the mud log. On wider format logs, Track 5 also may be subdivided to add an interpretive lithology and an extra data track to be used for the results of special analyses or calculations.

Interpretation

The object of logging drilling-mud gas shows is to identify potentially productive oil and gas horizons. While such zones often may be indicated by major events—e.g., large gas and fluorescence shows—more critical interpretation is required to avoid false alarms or missed opportunities.

Total Gas shows

The magnitude of a total gas show is not in itself a conclusive indication of show quality. Gas detected at the surface originates in three ways: (1) from the disintegration of a cylinder of rock by the drill bit as the hole is deepened, (2) from the influx of gas from previously drilled formations exposed in the borehole wall, and (3) from the drilling mud itself in the form of recycled oil and gas and decomposition of mud additives.

In extreme cases (for example, in long, geopressured shale sections or when using oil-based drilling fluids) influx or contamination may constitute the majority of gas seen at the surface. In such circumstances the magnitude of a gas show from a potential reservoir must be evaluated against the established background gas level from overlying sediments. Gas shows from relatively

thin horizons may be submerged in a high background and not identified from total gas alone (Fig. 52.9).

Even gas reliably identified as resulting from a drilled interval may be misleading as a show-quality indicator. Factors that affect the magnitude of a gas show include the volume of the rock cylinder crushed in the drilling process, controlled by bit diameter and ROP and dilution of liberated gas in mud (i.e., the flow rate of drilling mud passing bottom as the hole is cut). Thus, gas show magnitude will be expected to increase in larger diameter holes, at higher ROP's, or at reduced mud flow rate (Fig. 52.10).

A simple technique is available to remove these factors from evaluation by normalizing gas show magnitude to a standard or "normal" set of drilling conditions:

$$G_{pn} = G_{poB} \left(\frac{q_{oB}}{q_n} \right) \left[\frac{\pi \left(\frac{d_n}{2} \right)^2}{\pi \left(\frac{d_{oB}}{2} \right)^2} \right] \frac{R_n}{R_{oB}}, \dots (4)$$

where

- G_{poB} = observed total gas, %,
- G_{pn} = normalized total gas, %,
- q_{oB} = observed mud flow rate, m³/s,
- q_n = "normal" mud flow rate, m³/s,
- d_{oB} = observed bit diameter, m,
- d_n = "normal" bit diameter, m,
- R_{oB} = observed ROP, m/s, and
- R_n = "normal" ROP, m/s.

Once a "normal" set of conditions are selected, the equation can be readily simplified giving

$$G_{pn} = G_{poB} \left(\frac{q_{oB}}{0.050} \right) \left[\frac{\pi \left(\frac{0.251}{2} \right)^2}{\pi \left(\frac{d_{oB}}{2} \right)^2} \right] \frac{0.010}{R_{oB}}$$

and

$$G_{pn} = \frac{0.0126 G_{poB} q_{oB}}{(d_{oB})^2 R_{oB}}, \dots (5)$$

where

- $q_n = 0.050 \text{ m}^3/\text{s}$ (793 gal/min),
- $d_n = 0.251 \text{ m}$ (9.875 in.), and
- $R_n = 0.010 \text{ m/s}$ (118 ft/hr).

Normalization can be very useful in correlation of gas shows between wells drilled with very different programs. However, it should be remembered that normalization cannot remove the effect of influx and contamination; nor does it account for varying gas trap efficiency with ambient conditions.

Finally, remember that the gas produced by drilling is liberated by the crushing of material at the bottom of the hole and is representative of the fluid composition within the rock pore space at the time of impact. Remember that oil and gas flow from a producing well; they are *not* mined. The presence of a fluid within a rock is not

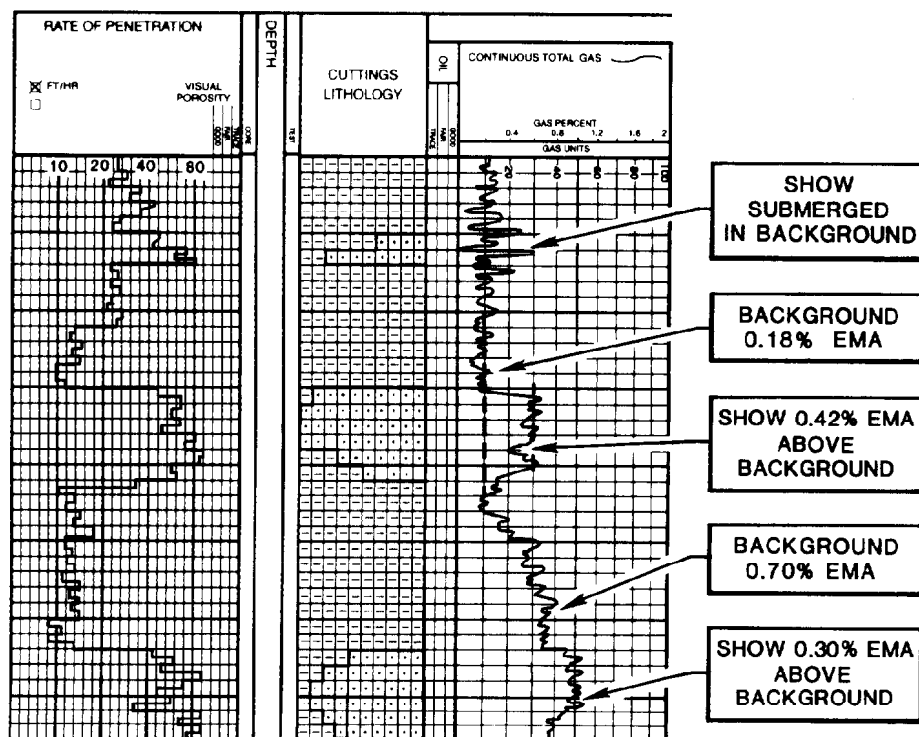


Fig. 52.9—Mud log total gas shows.

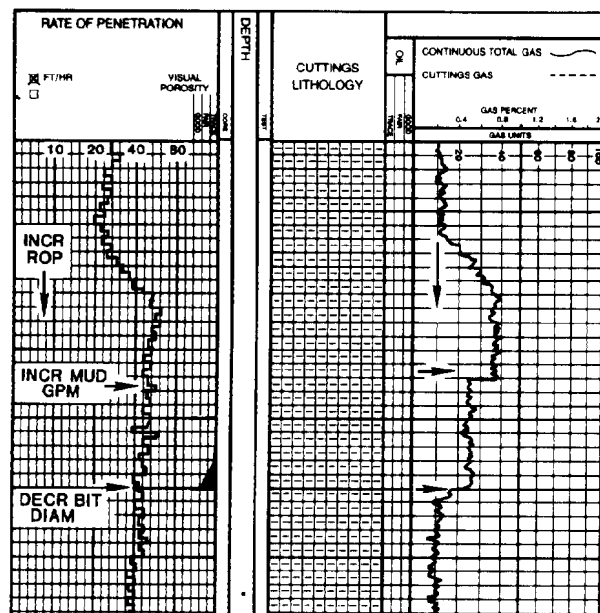


Fig. 52.10—Variation of total gas with drilling parameters.

necessarily indicative of productivity of that fluid *from that rock*. Comparison of total gas analyses from mud and cuttings and chromatography can yield useful clues as to the productivity of a hydrocarbon-containing formation.

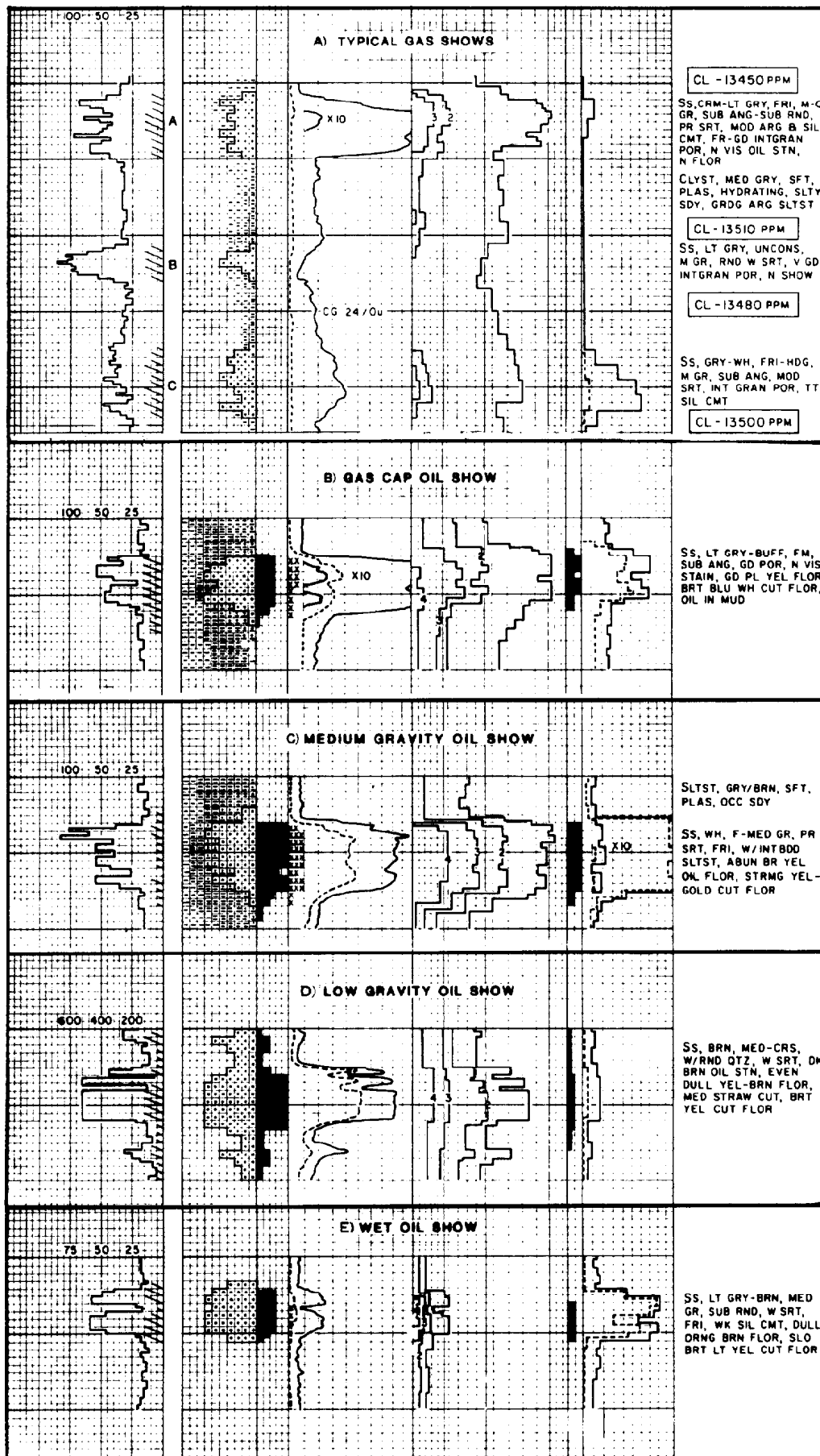
Total gas from the cuttings blender test is a good indicator of fluid mobility. As the crushed rock cuttings are carried to surface and relieved of formation

hydrostatic pressure, exsolution and expansion of gas should effectively flush the cuttings, leaving only a small volume of residual fluid at the surface. When higher cuttings total gas, relative to ditch total gas, is observed, this is an indication that this flushing has been impeded. An obvious explanation is that the rock lacks sufficient permeability to allow gas expansion and flushing. However, residual low-gravity oil or tar will have a similar effect in impeding gas exsolution and escape. Inspection of cuttings lithology, fluorescence, and the cut test should provide confirming evidence (Fig. 52.11). For example, strong cementation or shaliness in the cuttings would be indicative of low permeability, whereas dark or dull oil stain and fluorescence with a slow cut or absence of cut is more indicative of heavy oil.

At the opposite extreme of mobility, a formation may be so permeable that it is flushed effectively with mud filtrate even before being drilled. On recovery to surface neither mud nor cuttings will contain hydrocarbons. Indeed, no cuttings may be seen since such formations are commonly unconsolidated and disintegrate on recovery.

In this circumstance the first observations will be a sharp increase in rate of penetration followed, after the lag time, by a "negative" gas show; total gas declines below the original background. Testing the desander effluent or a mud sampling probably will show an increase in loose sand grains. The negative gas shows confirms only the excellent permeability, and for this reason alone the zone deserves closer inspection when a resistivity log is available. No evidence is available of the formation's fluid content from the mud log.

Most potential reservoirs fall between these two extremes: producing (1) a positive gas show and (2) cuttings blender gas, depending on permeability and oil



gravity. Color and fluorescence of the oil stain and results of the cut test are indicative of oil type. However, note again that presence of hydrocarbons in the rock and even presence of porosity and permeability are not conclusive evidence of hydrocarbon productivity.

Chromatogram Interpretation

The hydrocarbon chromatogram is often a useful guide to reservoir productivity. It is not the actual amount of any one alkane that is significant but the relative amounts of light and heavy components characteristic of the overall reservoir fluid. Such characteristics normally can be recognized on the mud log itself. An aid to this can be the calculation and plotting of the numerical ratios of the values of the various hydrocarbons (e.g., C_2/C_1 , C_3/C_1 , etc.). Such gas-ratio plots will often yield distinctive "character" or "events" not always immediately evident from the chromatogram itself. However, interpretation of the plots depends on the same logical procedures.

Most petroleum hydrocarbons originate from a similar organic source and proceed in their maturation by a similar temperature- and pressure-controlled physico-chemical process. For this reason, petroleum accumulations, although markedly different in composition, tend to show a spectral relationship to each other in terms of the type and amount of hydrocarbon species present. Therefore, although two crude oils of 30°API gravity may be extremely different in total composition, they will contain some similar components in similar compositional relationships to each other. Since petroleum maturation continues by the continuous "cracking" of complex branch molecules into simpler straight chain molecules, these significant relationships are readily seen in the petroleum gases methane through butane. Thus, study of chromatographic analysis of these gases often may lead to a gross estimate of the type and quality of the reservoir.

At low temperatures and shallow burial, biological and catalytic decomposition of organic debris results in a low-yield production of methane and CO_2 . Though the CO_2 will dissolve in and migrate with pore waters, the methane will accumulate in porous zones either as free gas or in solution in water. Such zones will yield impressive gas shows when drilled, but with few exceptions will produce only gas-cut water.

It is a reasonable general rule that a gas show containing methane as the only significant component is not commercially productive and is unworthy of further evaluation. However, it also should be remembered that exceptional cases do occur, including the southern North Sea nonassociated gas reservoirs that produce +94% methane.

At higher temperatures, organic material first polymerizes to form kerogen, which is then hydrogenated and cracked with increasing temperature to form bitumens, tars, and progressively higher-gravity oil and gas. Associated petroleum gases are fragments of this cracking process and as cracking continues, the proportion of light to heavy gases increases in a manner similar to the lightening of the liquid hydrocarbon. This fractionation of gases and liquids continues during the migration of the hydrocarbons from source to reservoir.

The end result of this process is reflected in a gas show chromatogram. A gas-productive interval will show predominantly methane and ethane with only traces of the heavier alkanes. Oil productivity is signaled by the enrichment of the heavier alkanes, especially propane. Decreasing oil gravity is reflected by progressively greater proportions of propane and the butanes. In lower-gravity oils, the concentration of these gases may exceed that of ethane. But all productive horizons will contain methane as the dominant alkane. Zones in which methane represents at least half of the total gas usually contain heavy residual oil from which the lighter gas and liquid fractions have migrated, leaving an immovable, nonproductive fluid.

These general rules of chromatograph evaluation can prove useful in reservoir evaluation but of course should not be used in isolation. Conclusions regarding oil gravity and mobility should be compared with the results of blender tests, cuttings examination, fluorescence, and cut tests. Furthermore, evaluation should proceed from the prior-show baseline values and throughout the show interval. Considering the variables inherent in the drilling, transportation, and extractions of samples, no conclusion may be drawn from a single sample or analysis.

Conventional Mud Log

The conventional mud log offers more drilling and formation evaluation data in a single form than any other data source. Many of these data are subject to uncontrolled variables in the measurement technology and by the very nature of borehole environment. As a result, no simple conclusive rules of quantitative log evaluation are available. However, integration of all the data on the log with geological and regional experience can make the conventional mud log a most powerful exploration tool.

Petroleum Engineering Services

Geopressure Evaluation

The petroleum engineering functions of mud logging developed from the introduction of a number of pressure evaluation techniques during the 1960's. These techniques are practiced conveniently in the logging unit and in some cases use data or equipment already available in the unit. Also, interpretation of the resultant data requires the same integrative approach, using drilling data and geological evaluation, as required in mud log interpretation. Unlike mud log evaluation, however, pressure evaluation techniques are able to provide reliable quantitative estimates of formation parameters, such as pressures and porosity.¹⁰

Drilling into a geopressured zone causes a change in a number of basic formation/drilling relationships. This change is usually a reversal of a gradual depth-related trend in a lithologically uniform formation.¹¹ Compaction increases uniformly with depth in a normal pressured clay rock. A geopressured zone may be poorly compacted relative to those zones overlying it. Porosity and water content decrease uniformly with depth in a normal pressured clay rock. A geopressured zone in which dewatering has been slowed will show a reversal in the trend, with increased water content and increased porosity. Other factors relating to fluid movement, such as ionic concentrations, hydrocarbon saturations, etc.,

may be different in geopressed zones. Differential pressure across bottom is the difference between the drilling mud hydrostatic pressure and the fluid pressure in pores of the undrilled formation at the bottom of the hole. Since drilling mud usually is denser than formation fluids, this difference will be positive and will increase with depth. In a geopressed zone, the formation pore pressure is abnormally high and the differential pressure across bottom will decline or even become negative.

Thus, any measureable parameter that reflects any or all of these factors may be used as a means of interpreting changes in formation pressure and eventually as a means of evaluating and obtaining quantitative estimates of formation pore pressures.

Gas Analysis. The incursion of formation fluids into the borehole may result from a number of causes, some but not all of which result from an underbalanced condition—either temporary or permanent.¹² If an underbalanced condition exists, there will be a natural tendency for fluid to flow from the formation into the borehole. With a formation having good porosity and permeability, this flow will be massive and a kick will occur. Such a kick will be indicated by the incursion of formation fluid downhole, causing the expulsion of mud from the borehole at surface. Were this to continue, a blowout would result. It is the logging geologist's responsibility (other duties permitting) to monitor the mud pit level and to report any unpredicted or unexplained level changes. A massive incursion of fluid resulting in a well kick is unlikely to be misinterpreted as a gas show. In fact, if the hole is full, the kick should be recognized by a rise in pit level long before the fluid causing it has time to appear at surface.

However, minor incursions caused by slight or temporary underbalance, or where insufficient permeability to provide a sustained kick exists, do occur and must be interpreted correctly.

When an underbalance sufficient to cause a kick exists but there is insufficient permeability to sustain a massive fluid influx, a steady fluid "feed-in" may result. If this minor flow is from a discrete formation already cut, it will be noticeable — producing a sustained minimum gas background even when circulating but not drilling. If this is the case, the logging geologist should make a note of this sustained circulating gas on the mud log.

If the feed-in is from the formation currently being drilled, then as a greater and greater area of formation in the borehole wall is exposed by drilling, increasing flow will take place. If this is the case, the mud gas will exhibit a sustained minimum when circulating but will consistently rise as drilling proceeds. Cuttings gas will inevitably be high relative to mud gas since it is only the lack of permeability that is preventing the feed-in from becoming a kick. Where permeability is effectively absent (e.g., in clays or shales) even a minor feed-in cannot take place. Fluid pressure in the rock will gain access to the borehole by the opening of pre-existent microfractures and partings in the rock. The result will be the caving or sloughing of rock fragments into the borehole, accompanied by a small amount of gas. A minimum gas background and, in this case,avings recovery exist when circulating without drilling.

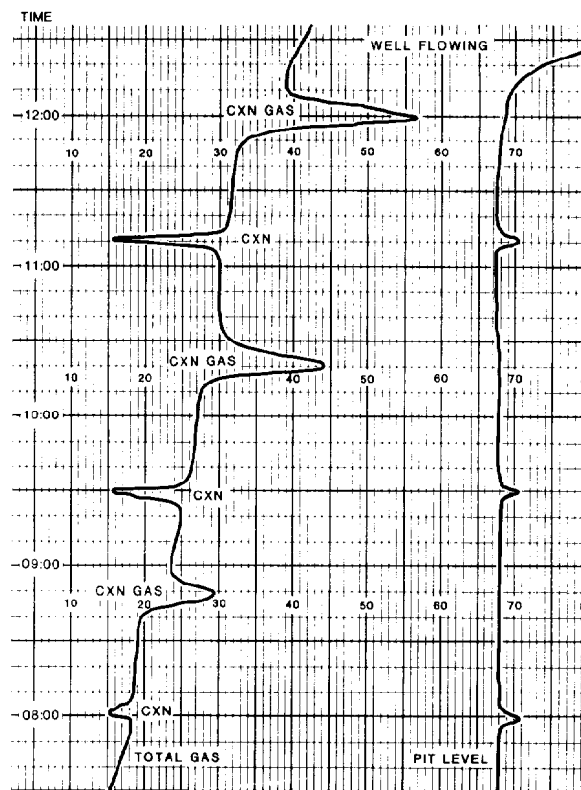


Fig. 52.12—Connection gas indicating underbalance.

Circulating bottomhole pressure is higher than when the mud is static. This is caused by annular pressure losses when circulating. It is therefore possible for a feed-in, caving, or even a kick to result because of a resultant underbalance when circulation is stopped. Furthermore, pressure is further reduced because of the swabbing effect when pipe is moved upward—e.g., when making a connection. The literal meaning of "swabbing" is the pulling of a full-gauge tool from the hole, acting like the plunger in a syringe and initiating fluid flow into the borehole. Swabbing by moving the drillstring does not work in this way. When pipe is pulled upward, the high-viscosity gelled mud will attempt to move with the pipe, thus reducing the effective hydrostatic pressure acting on the borehole wall. Pressure reduction is a function of pulling speed, mud rheology, and annular diameter. The important consideration is that pressure reduction takes place not just below the bit but at all points in the open hole.

Downtime gas or connection gas is a gas show resulting from the momentary underbalance caused by pump shutdown and/or pipe movement. It can be recognized by the occurrence of discrete gas show appearance at, or slightly less than, the lag time after circulation recommences. This is gas actually being produced by the formation and, while not being plotted on the mud log, the value should be reported on the log because it is indicative of formation permeability and fluid content. When a connection gas occurs, the logging geologist also should check a flowline mud sample for evidence of produced oil or salt water with the gas. The incidence of connection gas should be reported to the

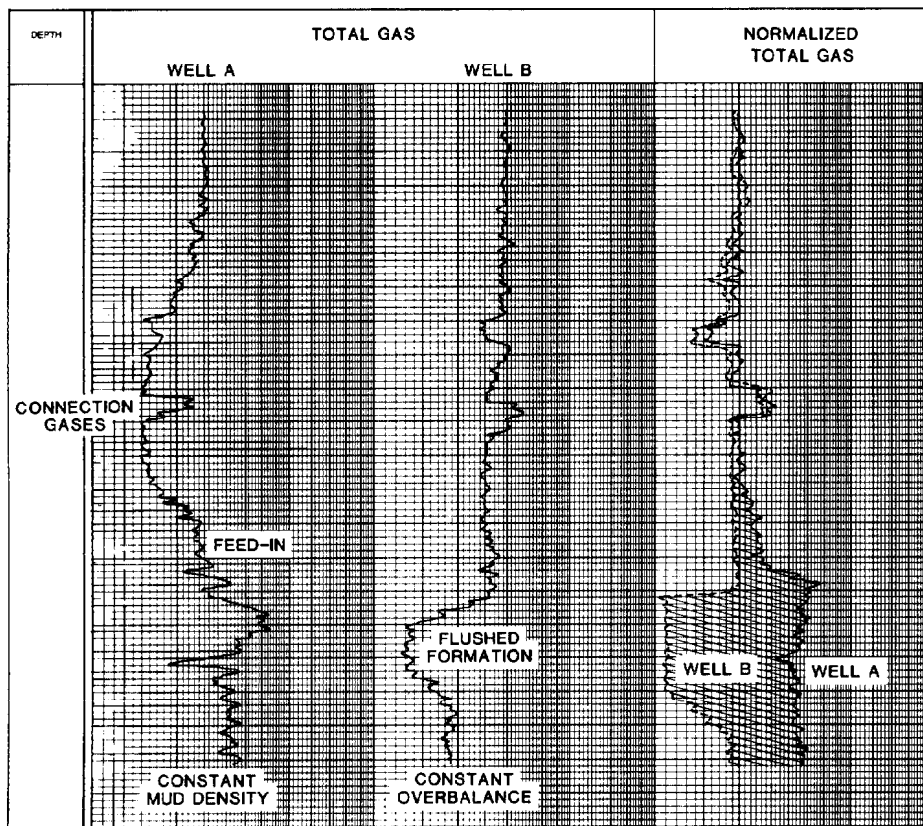


Fig. 52.13—Normalized total gas.

drilling supervisor, who may choose to increase mud density in response to the indicated underbalance.

It is important to remember that the entire openhole section will be underbalanced by swabbing. The connection gas may not come from the bottom of the hole but from some horizon above. In fact, two or even more connection gases may result from a connection. For this reason it is important that lag time and annular velocities should be identified accurately by the logging geologist so that connection gases can be identified with the producing formation and the mud log annotated accordingly.

Drilling into a permeable reservoir with an underbalance is potentially dangerous because a kick may result. Even if a kick does not occur immediately, the hazardous situation will be marked by an increasing feed-in as more formation is drilled, accompanied by progressively larger connection gases (Fig. 52.12). The condition should be reported by the logging geologist and noted on the mud log. If increases in mud density alleviate or remove the effect, this should also be noted on the mud log in explanation of the consequent reduction in gas.

Fig. 52.13 demonstrates the effect of varying differential pressure on gas show magnitude. The total gas curves for two wells drilled through a similar section are shown. The data for both wells have been normalized to reduce the effects of hole diameter, ROP, mud pump output, and surface extraction efficiency. Well A was

drilled with a constant mud density, whereas in Well B mud density was controlled to maintain a constant positive differential pressure (overbalance).

In the upper portion of the section, the two gas curves are similar and the normalized gas curves coincide almost exactly. In the lower portion a progressive deviation between the two wells is seen that is somewhat reduced but remains evident even in the normalized curves. We can interpret this as being caused by the penetration of a transition zone into a geopressured zone.

In Well A, maintaining a constant mud density results in a decreasing overbalance and eventually an underbalance or increasing negative differential pressure. Connection gases occur and become larger with deeper penetration. Additionally, feed-in of gas from the underbalanced borehole wall causes an increase in background gas that, since it is not a product of freshly cut formation, cannot be accounted for in the normalization calculation.

Well B, on which a constant overbalance was maintained by increases in mud density, did not show increases in gas background or connection gases. Indeed, if any zone showed good permeability, the overbalance may have resulted in flushing gas away from the borehole and a reduction in observed total gas.

By careful observation of these phenomena, a fairly accurate log of differential pressure (and hence pore pressure) may be obtained. This information should be used in conjunction with the other techniques described in the following paragraphs.

Cuttings Evaluation. During the normal mud-logging process, cuttings are sieved and graded to a size assumed to be representative of drilled cuttings. The larger fragments are cavings from the walls of the borehole and play no part in the compilation of a lithological log.

In geopressure evaluation, these cavings play a major role. The presence of cavings in the sample indicates that the borehole wall is unstable. The most noticeable and usually most predominant cavings are those of clay, shale, or calcareous lithologies. Coal, however, will cave as a matter of course, hence interpretations should not include coal cavings. The amount of cavings in the bulk sample is an indication of the degree of instability of the borehole walls. Simply watching the cuttings traverse the shaker screens will give a reasonable indication of the amount and size of the cavings in relation to the bulk sample.

Cavings are produced by underbalanced drilling and stress relief. Abrasion of the walls by the drillpipe will also cause cavings, but generally these will not be discernible from cuttings because of their small size.

If the pore pressure is higher than the hydrostatic pressure in the borehole, the hydrostatic pressure differential will cause the pore fluids to move toward the borehole. In an impermeable formation, the resultant pressure gradient adjacent to the borehole wall may become great enough to overcome the tensile strength of the rock. When this occurs, the rock fails in tension and cavings are formed.

All parts of the earth's crust contain stresses that change with depth, area, lithology, history, etc. Drilling a hole in the ground relieves some stresses other than those in the vertical plane, and the hole geometry in relation to some stresses acts to concentrate them. If the borehole wall is not supported sufficiently by the mud column, it may fail either (1) in compression from the vertical stress or (2) in tension from the horizontal stress, or both.

The drilling process causes the formation of microcracks and fractures, and these act as areas of stress concentration and potential initial failure points. Thus it is sometimes noticed that part of a borehole may cave copiously for a short time and then become stable. This is because of the removal of the damaged zone (i.e., cavings) adjacent to the bore/formation interface. Formation is exposed that is more coherent and lacks concentrations of stress, thus it absorbs the extra energy without failing.

Cavings produced by underbalanced drilling are typically long, splintery, concave, and delicate (Fig. 52.14a). Cavings produced by stress relief tend to be more blocky and can vary in size tremendously, depending on the formation characteristics. Examples are shown in Fig. 52.14b.

Remember that if the cavings are clays, they may react with the mud and lose their distinctive morphology. Interpretations based on reactive clays should be pursued with caution. The quantity and nature of cavings should be regularly reported on the mud log or on a supplementary data log if pressure evaluation services are being performed.

Shale Bulk Density. Shale density determination can be of great value since it provides information on the compaction of the shale. Under normal conditions, shale

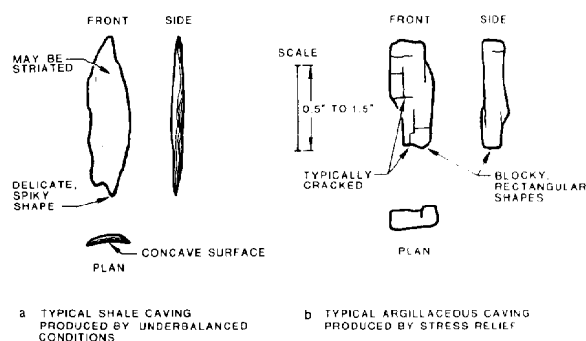


Fig. 52.14—Cavings resulting from underbalance and stress relief.

density should increase with depth. Any deviation from this consistent trend may indicate that geopressures exist. The magnitude of the bulk density change will vary with the type and magnitude of the geopressure. Often, the bulk density will decrease, but in other cases it may remain constant or continue to increase but at a lower rate than the previously established trend. Several methods are used for measurement of shale bulk density.

Pycnometer Method. By using a container with repeatable volume, this method involves measuring change of weight resulting from displacement of fluid by the sample. The most practical application of this method at the wellsite is to use a mud balance.

Place enough cuttings in the cup so that the balance indicates 8.34 lbm/gal (i.e., density of fresh water) with the cap on. Fill the cup with water and weigh again. The new reading is W_2 in the following equation.

$$\gamma_s = \frac{8.34}{16.68 - W_2}, \quad \dots \dots \dots (6)$$

where γ_s is the specific gravity of sample and W_2 is the "mud weight" of sample and water, lbm/gal.

Mercury Pump Method. The bulk volume of a known weight of sample is measured. The bulk weight of a prepared sample is first established using an accurate chemical balance. The bulk volume of selected cuttings is then determined using a high-pressure mercury pump by the Kobe system (Boyle's law principle) at a pressure of about 24 psi, which is recorded on the attached pressure gauge. Mercury is used to compress the air around the cuttings but does not contact the sample material.

The high accuracy of the instrument and large amount of sample used (approximately 25 g = 2,000 individual shale cuttings) give good consistency of results. Because of the accuracy and convenience in operation, this method should be used whenever possible; however, very careful and consistent sample handling is necessary for best results.

Buoyancy Method. The sample is weighed in air and in a liquid of known density. This is an alternative version of the pycnometer method. Theoretically, it should be a more accurate method if an accurate laboratory balance

is used. In practice, it is most inaccurate since the density of the liquid will vary with ambient temperature.

Density Comparison Methods. The simplest of these is the "float-and-sink" method. Shale cuttings are immersed in fluid mixtures of different densities in which they will either float or sink, depending on relative densities. This method is inexpensive and quick but is limited in sensitivity because of large difference in the densities of available fluids (approximately 0.1 to 0.05 g/cm³ and easy contamination of calibrated fluids.

Density Gradient Method. This consists of a fluid column in which density varies uniformly with depth. This is prepared by the partial mixing of a light fluid (neothene) and a heavy fluid (tetrabromoethane) in which beads of known density are suspended. A calibration curve of density vs. depth is prepared. Shale cuttings immersed in the column will sink to the level at which their density is the same as the fluid. Depth is recorded and density read off from the calibration curve.

Both of the heavy liquid methods (density comparison and density gradients), while being quick and simple, have the disadvantage of determining the density of individual cuttings. Special care must be taken to ensure that cuttings are true bottomhole cuttings, and several determinations should be made for each interval to avoid anomalous results. Six or eight cuttings should be chosen that are representative and free of dust or cracks that may

trap air and water and result in low apparent densities. In addition, the fluids used have unpleasant odors and some of them may be hazardous to health. Toxicity labels should be checked for specific mixtures but it is a good general rule to use these fluids in a fume hood or with a vapor extraction system.

It is commonly observed that shale density may decrease as much as 0.5 g/cm³ or more. If this reduction occurs over a significant depth interval, the calculated overburden gradient may reverse. The low-density zone also may change in lithologic character. Fissility, plasticity, carbonate content, color change, and other differences may not be apparent. Measurements from cuttings from water-based muds usually are too low, simply because of the adsorption characteristics of clays. Likewise, measurements taken from wireline logs can also give false indications. Specifically, the formation density log can be affected by a rugose hole and the shallow depth of investigation may not read beyond the hydrated zone. The result is erroneously low readings, causing excessive calculated porosities. The sonic log will be affected greatly by hydrated clays, resulting in very high transit times, high porosities, and too low densities.

Values may be successfully obtained from these logs when water-based muds are used, but caution should be exercised as errors may exist, as explained earlier.

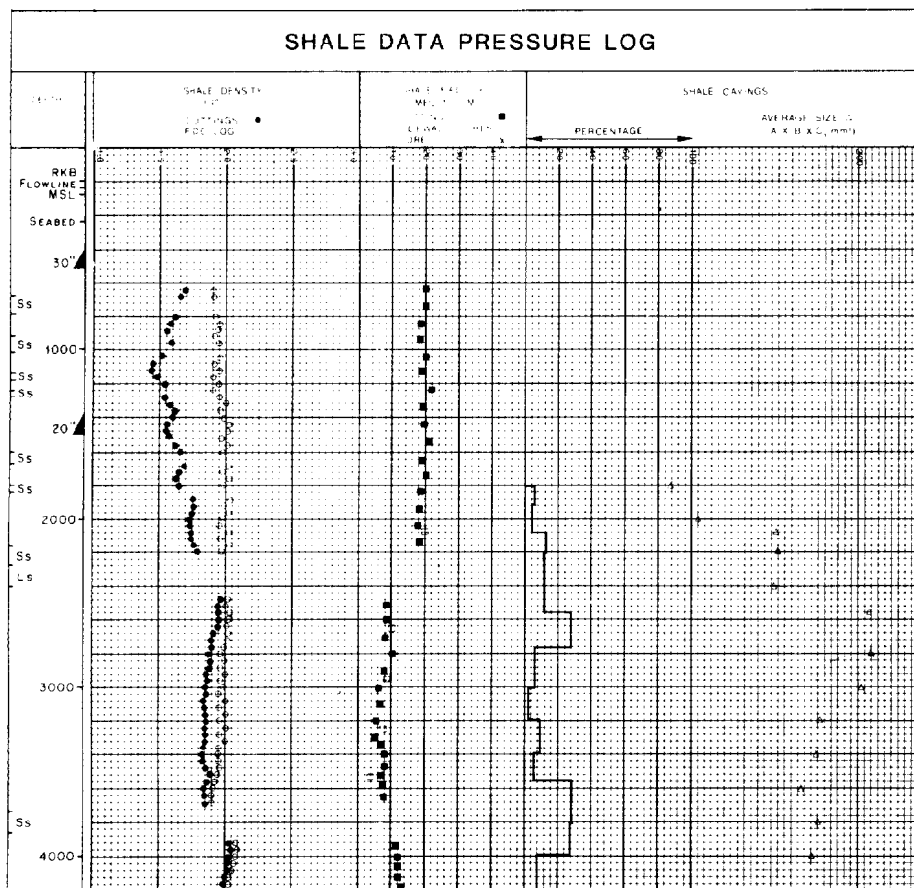


Fig. 52.15—Shale data log.

The best densities are those obtained from wells drilled with less reactive muds, such as oil- or potash-based fluids. Both actual cutting densities and log densities should be accurate because the clay remains in its virgin state.

Increases in density beyond the normal trend because of decreased porosity or calcification should be noted carefully since these may constitute caprocks above geopressures. Precipitation of pyrite or high iron concentration results in abnormally high bulk densities in clays and shales. It has been proposed that in some wells the occurrence of pyrite in shales masked the density reduction caused by porosity increase. Careful microscopic examination of clays may indicate the occurrence of very fine pyrite, and high iron concentration is indicated by a red/brown color cast. Pore pressure interpretations cannot be accomplished by using shale density if heavy minerals are present; however, since shale density is mainly used for qualitative purposes in geopressure evaluation, the role of the other geopressure indicators remains unchanged.

Any decrease in density (without change in clay character) may be recognized as a pressure transition zone.

Recognition of a normal bulk density trend line may be difficult because of degree of scatter in the rectangular coordinate plot. A semilog plot considerably reduces this scatter, but the normal bulk density range (approximately 1.6 to 2.7 g/cm³) results in a more distorted trend line and difficulty in recognizing deviations (Fig. 52.15).

Shale Factor. Ion-exchange reactions take place between an adsorbent solid and a solution. Ions bound to the solid surface are released into the solution and other ions from the solution become fixed at the surface. Ion exchange can proceed by the exchange of positive ions (cations) or negative ions (anions) but not both. The reactivity of a solid compound in ion exchange reactions is governed by its specific surface (surface area per unit volume) and by the surface density of ion exchange sites (points on the surface where ions may be bound). Reactivity is expressed as cation or anion exchange capacity (CEC or AEC) using units of milliequivalents (of a suitable ion) per hundred grams (of the compound).

Various clay types have different CEC's and consequently different adsorption capacities. A smectite-rich clay will undergo diagenesis to illite with increasing temperature and ionic exchange. For diagenesis to proceed, water must be flushed from the clays. If potassium exchange cations are not available, a montmorillonite clay will lose its water but will not convert to illite. Thus, if this type of clay is drilled with a water-based mud, the clay will immediately rehydrate and cause severe drilling problems.

Shale factor is a measure of clay CEC. CEC will decrease as clays convert from montmorillonite-rich to illite-rich with temperature (and thus with depth). Pure montmorillonite clays have a CEC of approximately 100 meq/100 g. Pure illites show no swelling characteristics, but their CEC is generally between 10 and 40 meq/100 g. Kaolinites have a CEC of approximately 10 meq/100 g. Of the most common clay types, it is only the smectite group (including montmorillonite) that has an affinity for water. Thus, any clay zone that contains montmorillonite

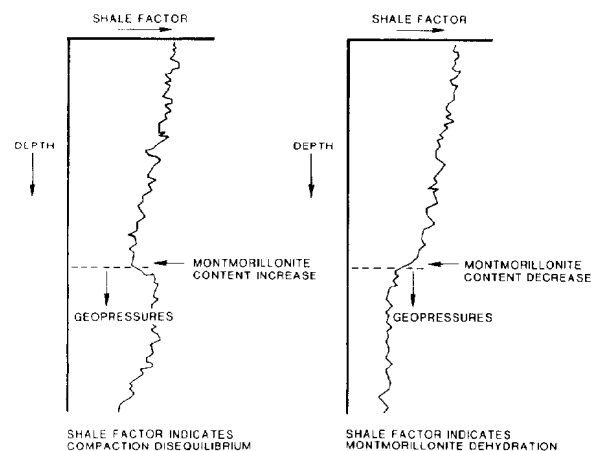


Fig. 52.16—Shale factor response.

will have an affinity for water in an amount proportional to the montmorillonite content, and this will be shown by a proportional value of shale factor. Note that the shale factor as measured at the wellsite will not give values corresponding to actual chemical CEC. This is because of impurities in the sample, methodology, experimental error, and the fact that the methylene blue dye (used in the titration) is a very large molecule and thus cannot be adsorbed in interlayer sites.

If the clay is calcareous, and calcimetry is also being performed, then the shale factor may be corrected for carbonate content as given by

$$F_{sht} = \frac{100}{100 - C_{carb}} \times F_{sha}, \dots\dots\dots (7)$$

where

F_{sht} = true shale factor, meq/100 g,

F_{sha} = apparent shale factor, meq/100 g, and

C_{carb} = carbonate content, %.

For example, a calcareous clay has a carbonate content of 37%, and an apparent shale factor of 16:

$$F_{sht} = \frac{100}{100 - 37} (16) = 25 \text{ meq/100 g.}$$

Theoretically, shale factor should indicate whether montmorillonite dehydration or compaction disequilibrium was the major mechanism in generating an apparent geopressure. Geopressures caused by compaction disequilibrium indicate that the pressured zone is immature with respect to shallower, normally pressured sediments. This implies that diagenesis has been restricted by the inefficiency of the dewatering mechanism, resulting in clays containing a larger proportion of montmorillonite within the geopressed zone. Shale factor would thus decrease to the top of the geopressed zone, increase within the zone, and then decrease as the pore pressure gradients decline (Fig. 52.16). Any overall increase in shale factor within a geopressed zone indicates that compaction disequilibrium has played a part in its formation.

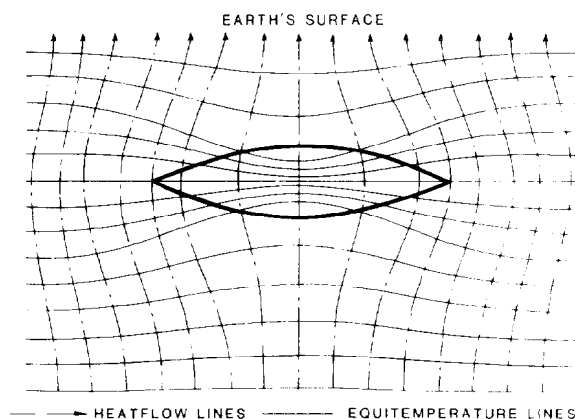


Fig. 52.17—Distortion of heat flow around an insulating geopressed zone.

If, however, a geopressed zone was caused by montmorillonite dehydration, then upon entering the interval a sharp decrease in montmorillonite content will be observed. Hence the geopressed zone will contain less montmorillonite, because it has been converted to illite, which releases to the pore spaces water that has been unable to escape fast enough and results in a pore pressure increase. Shale factor thus will decrease in the pressured zone (Fig. 52.16).

Shale factor cannot be a geopressure indicator. The differing responses described are not definitive, and geopressure has to be indicated from other sources before an interpretation by use of shale factor can be achieved. Geopressures caused by montmorillonite dehydration and compaction disequilibrium may cause no change in shale factor; also, if geopressures were caused by another process (e.g., aquathermal pressuring that results when trapped pore fluids are heated but are unable to expand and is therefore independent of matrix composition), a change may not be reflected in shale factor with depth.

In the past, the consensus was that shale factor should increase in geopressed zones and could thus act as an indicator. Re-evaluation of the various geopressure mechanisms show that this is not necessarily the case. However, shale factor should be capable of delineating between compaction disequilibrium and montmorillonite dehydration as the major geopressure mechanism.

Flowline Temperature. The geothermal gradient, the rate at which subsurface temperature increases with depth, can be calculated from

$$g_G = \frac{T_2 - T_1}{D_2 - D_1} (100), \dots \dots \dots (8)$$

where

g_G = geothermal gradient, °C/100 m,
 T_1 = temperature, °C (at depth D_1 , m), and
 T_2 = temperature, °C (at depth D_2 , m).

For any given area, the geothermal gradient is usually assumed constant. While the average gradient across

normally pressured formations may be constant, geopressed formations exhibit abnormally high geothermal gradients.¹³

Since a constant flow of heat occurs radially from the earth's core to the surface, the total flow of heat across any depth increment will be constant. However, the temperature differential across an increment depends on the thermal conductivity of the material. Since overall heat flow from the earth's surface is generally constant within any particular area, the heat flux through the various formations with depth is in equilibrium. The rate of change of temperature across a formation with a low thermal conductivity (caused mainly by high porosity) will be high; conversely, a low geothermal gradient is indicative of high thermal conductivity formations—i.e., lower porosity. Water and hydrocarbon migration to shallower depths may also affect the geothermal gradient. Pore fluids, as insulators, retain heat so that on migration these hot fluids modify the temperatures of the formations that they pass through and ultimately become trapped. Fowler¹⁴ cited examples from the Middle East, Canada, and U.S. oil fields of geothermal gradient bulges that indicated possible entrapment of hot fluids from greater depths. The mechanism also may be related to montmorillonite dehydration, because the huge volume of water squeezed from the clay provides the impetus for migration. "Dead" basins (i.e., no source rocks) have been shown to exhibit normal geothermal gradients, hence on initial exploration wells the geothermal gradient may indicate the potential of the whole area.

An insulating zone produces a distortion in the isothermal lines that normally run perpendicular to the lines of heat flow (Fig. 52.17; Ref. 15).

Because of the high geothermal gradient, these are more closely spaced in the insulating zone. In the zones above and below, the isothermal lines are more widely spaced in compensation and the zones exhibit a reduced geothermal gradient. The converse occurs in beds of high thermal conductivity (i.e., sands and some limestones).

Since water has a thermal conductivity of about one-third to one-sixth that of most rock matrix materials, it can be seen that thermal conductivity is directly related to the degree of compaction of a formation. The higher-than-normal water content of geopressed shales reduces the thermal conductivity. Therefore, the top of a geopressed zone is marked by a sharp increase in geothermal gradient. The temperature of the mud at the flowline may reflect the geotemperature, and recording of flowline temperature is a practical method to determine temperature gradient, provided variable factors such as pump rate, lag time, ambient temperature, lithology, and temperature changes at the surface that are caused by mud mixing and chemical treatments can be accounted for. In areas where large annual temperature variations occur, considerable differences may be noted in flowline temperatures; even diurnal temperature fluctuations may cause a 10°C variation in flowline temperature while drilling.

Prior to reaching a geopressed zone, a temperature transition zone will be encountered in which, because of distortion of the isothermal lines, there will be a reduction in geothermal gradient. In practice, this effect is

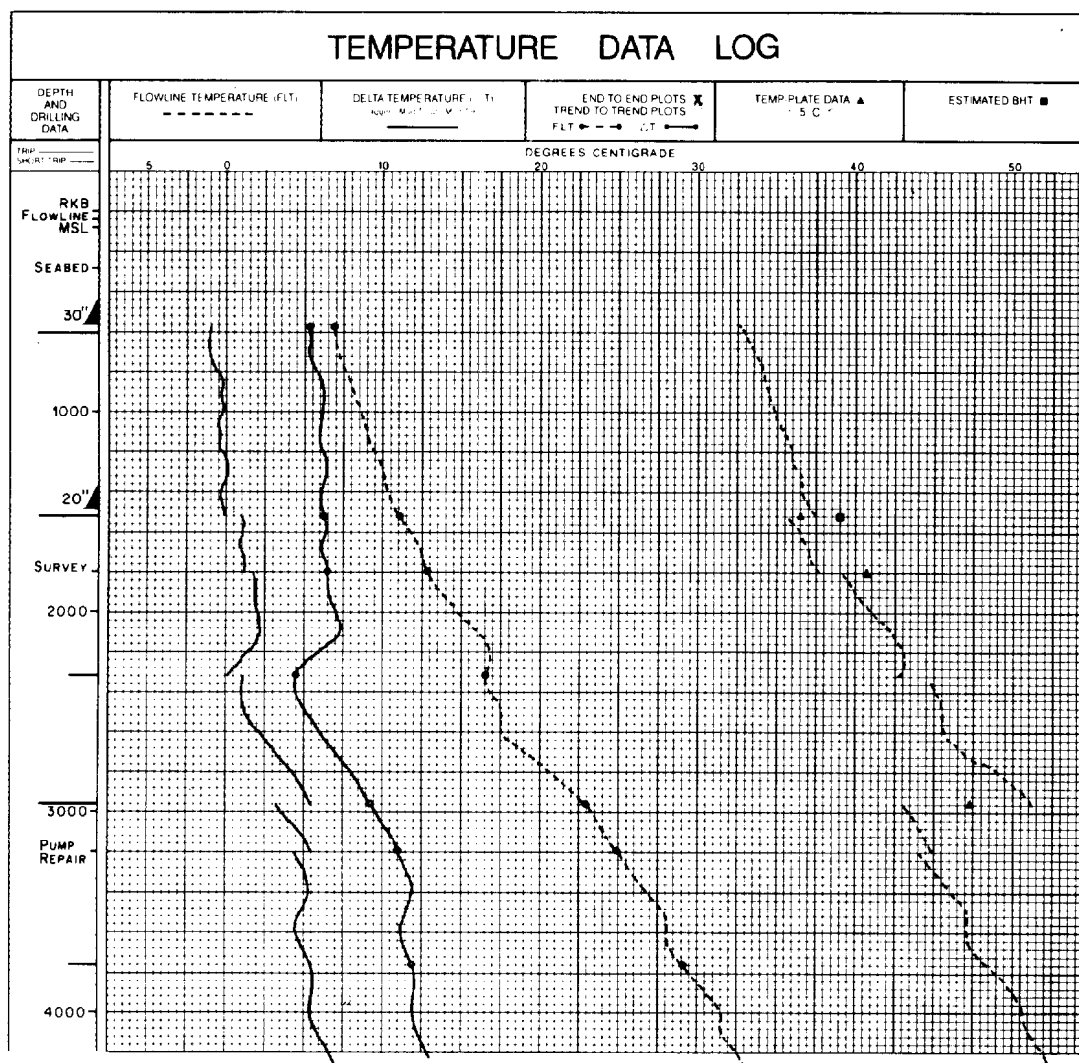


Fig. 52.18—Flowline temperature log.

reflected in the flowline temperature gradient, even to the extent of a fall in flowline temperature (i.e., a negative gradient), followed by an extremely large increase in flowline temperature as the geopressured zone is penetrated (Fig. 52.18).

A dual temperature probe system with sensors at the flowline and suction pit is effective in removing surface effect, if lagged differential temperature is plotted. It is normally sufficient for the points to be plotted at 30-ft intervals unless more frequent temperature variation is noticed, but points plotted at 10-ft intervals allow more accurate data and better resolution for improved interpretation. Circulations, mud additions, water additions, and other significant events should be noted.

It is found that the resultant temperature curve is broken when the bit is changed, or during short trips or other downtime, and a certain time is necessary for the mud system to re-establish a temperature equilibrium upon circulation. The rate at which this thermal equilibrium is re-established may be significant, as a more rapid re-establishment may indicate an increased geothermal gradient. Drilling variables that affect the

rate of re-establishment of equilibrium include total mud volume. The practice of reducing active pit volume to a minimum, dictated by hole size, aids in reducing the time required to attain equilibrium after tripping and reduces the circulation time needed to stabilize flowline temperature. A discontinuity in the plot also occurs at each casing depth and corresponds to a change in hole size. A higher annular velocity in open hole reduces the amount of heat gained from exposed formations, and a lower annular velocity in the marine riser increases the amount of heat lost to the sea. However, these factors only lead to a change in measured temperature; the rate of change of temperature should remain unchanged. Since pressure predictions can be based on temperature gradient rather than on temperature magnitude, each depth segment between discontinuities can be analyzed separately for gradient trends. It is also helpful to replot a smoothed curve of segments end to end without regard for absolute temperature values. In certain cases it has been found that, instead of plotting the individual segments as an end-to-end smoothed curve, end-to-end plotting of the individual segment trend lines may be of

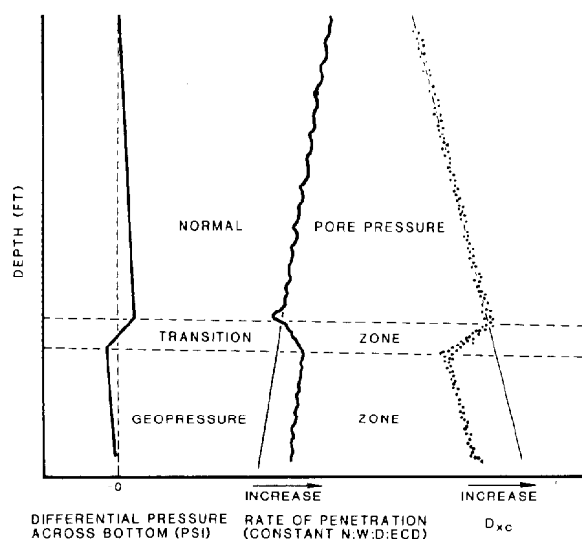


Fig. 52.19—Response of drilling rate to geopressure.

value. This trend-to-trend smoothed curve is merely a graphical method of removing irrelevant scatter from the plot.

The reduction in temperature gradient caused by distortion of isothermal lines may be noticed before the geopressured zone is encountered; that is, an advance warning of geopressure may be given. Thus a fall in flowline temperature gradient followed by a sharp rise when the geopressure transition zone is drilled provides a warning that even closer attention must be paid to other drilling parameters to achieve confirmation of possible geopressures. However, like other methods of pressure evaluation, flowline temperature reflects a varying physical parameter in an assumed constant rock type; therefore, changes in lithology must be closely monitored to avoid false indications.

Drilling Models. Bingham¹⁶ proposed that the relationship between ROP, weight on bit (WOB), rotary speed, and bit diameter may be expressed in the general form

$$\frac{R}{N} = K_D \left(\frac{W}{d_b} \right)^d, \quad \dots \dots \dots (9)$$

where

- R = ROP, ft/min,
- N = rotary speed, rev/min,
- d_b = bit diameter, ft,
- W = WOB, lbm,
- K_D = matrix strength constant (dimensionless),
- and
- d = formation "drillability" exponent (dimensionless).

Jorden and Shirley¹⁷ solved Eq. 9 for d , inserted constants to allow common oilfield units to be used and to produce values of d -exponent in a convenient workable range. Most important, however, they let K_D be unity,

removing the need to derive empirical matrix strength constants, but making d -exponent lithology-specific as in

$$d = \frac{\log \left(\frac{R}{60N} \right)}{\log \left(\frac{12W}{10^6 d_b} \right)}, \quad \dots \dots \dots (10)$$

where

- d = drilling exponent (dimensionless),
- R = ROP, ft/hr,
- N = rotary speed, rev/min,
- W = WOB, lbm, and
- d_b = bit diameter, in.

In a constant lithology, d -exponent will increase as the depth, compaction, and differential pressure across bottom increase. Upon penetration of a geopressured zone, compaction and differential pressure will decrease and be reflected by a decrease in d -exponent (Fig. 52.19).

Differential pressure is dependent on mud density as well as formation pore pressure. Therefore, any change in the mud density used promotes an unwanted change in d -exponent.

Rehm and McClendon¹⁸ proposed a "mud weight corrected" drilling exponent of the form

$$d_{xc} = \frac{\log \left(\frac{R}{60N} \right)}{\log \left(\frac{12W}{10^3 d_b} \right)} \left(\frac{g_{nfb}}{\rho_{ec}} \right), \quad \dots \dots \dots (11)$$

where

- d_{xc} = corrected d -exponent (dimensionless),
- R = ROP, ft/hr,
- N = rotary speed, rev/min,
- d_b = bit diameter, in.,
- g_{nfb} = normal formation balance gradient, lbm/gal,
- ρ_{ec} = effective circulating density, lbm/gal, and
- W = WOB, 1,000 lbm,

or in the metric form

$$d_{xc} = \frac{\log \left(\frac{R}{18.29N} \right)}{\log \left(\frac{W}{14.88 d_b} \right)} \left(\frac{g_{nfb}}{\rho_{ec}} \right), \quad \dots \dots \dots (12)$$

with R in m/hr, N in rpm, W in tonnes (1,000 kg), d_b in cm, and g_{nfb} and ρ_{ec} in g/cm³.

This correction was empirically derived but has been applied worldwide with much success. The use of actual mud density in place of effective circulating density (ECD) has been found to be acceptable within normal limits of accuracy. ECD should, however, be used when available.

Factors not considered by d -exponent in its basic form are drilling hydraulics, tooth efficiency, and matrix strength.

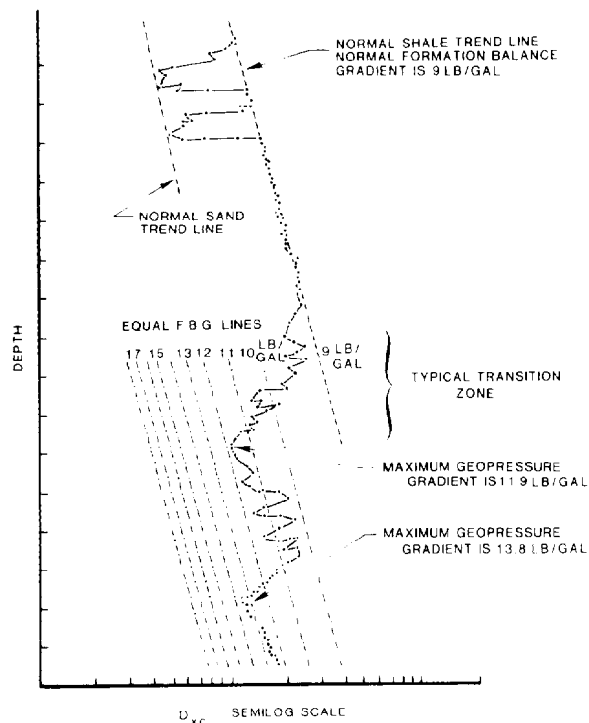


Fig. 52.20—Example of formation pore pressure gradients for d_{xc} plot.

Drilling hydraulics become important in large holes where efficient hole cleaning is impossible and in soft formation where jetting will make a large contribution to drilling.

Matrix strength controls both magnitude and rate of change of d -exponent with depth.

Tooth efficiency can affect d -exponent in two ways: (1) tooth wear will cause a gradual increase in d -exponent (i.e., decrease in ROP), and (2) a change of bit type may produce a change in d -exponent, especially if the change is a radical one (e.g., from milled-tooth bit to an insert or diamond bit).

If differential pressure becomes large, the simple ratio correction to the d -exponent will not eradicate the effect on ROP.

Furthermore, the relationships among force applied, W/d_b , rotary speed, N , differential pressure, g_{nh}/ρ_{ec} , and ROP, R , are more complex than the d -exponent formulation would imply. While working well within certain normal working ranges, radical changes in any of these parameters (for example, change in hole size after setting casing) may result in a shift in d -exponent trend.

When plotted on a logarithmic scale against depth, the d -exponent will exhibit an approximately linear increasing trend through "normal," hydrostatically pressured formations. Where geopressure, abnormally high formation fluid pressure is encountered, d -exponent values will fall consistently below the extrapolation of this normal trend. It has been shown empirically that d -exponent deviation may be related to formation pore pressure anomaly by the simple ratio

$$\frac{p_{pa}}{p_{pn}} = \frac{d_{xcn}}{d_{xco}}, \dots (13)$$

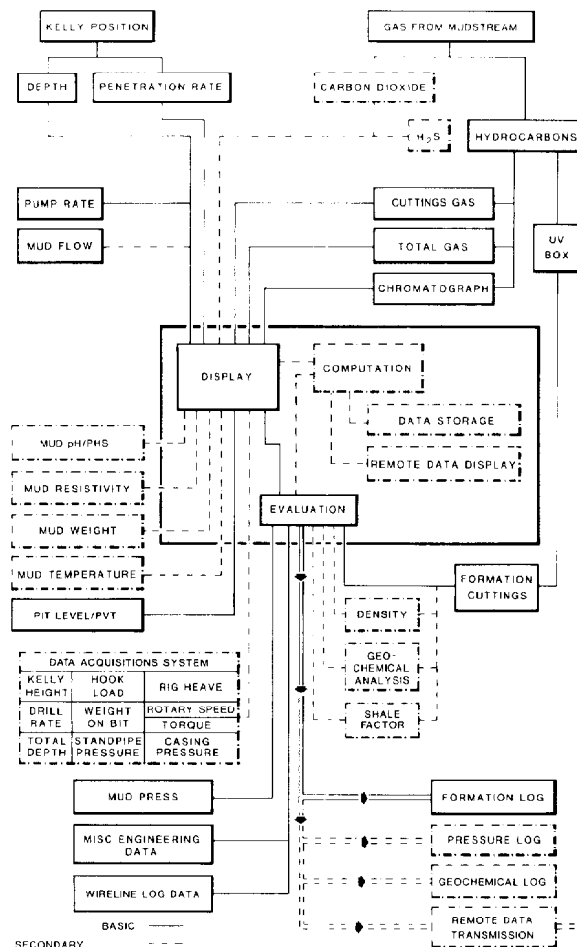


Fig. 52.21—Logging unit systems.

where

p_{pa} = actual pore pressure at depth of interest, psi, or formation balance gradient, lbm/gal equivalent mud density (EMD),

p_{pn} = normal pore pressure, psi, or formation balance gradient, lbm/gal (EMD),

d_{xco} = observed corrected d -exponent at depth of interest, and

d_{xcn} = expected corrected d -exponent on normal trend line at depth of interest.

Using this relationship, it is possible to calculate pore pressure or formation balance gradient (equivalent mud density to balance pore pressure) from d -exponent. Alternatively, the relationship may be used to prepare an overlay allowing direct reading of formation balance gradient from the d -exponent plot (Fig. 52.20).

Drilling exponents may be calculated from driller's data using a simple calculator and manual plotting and trend recognition. However, quality of the data is greatly improved when a data-acquisition system provides WOB, rotary speed, and mud density directly to the logging unit and a minicomputer is used to read these sensors automatically, to perform the calculations, and to print or plot the results. Computer-equipped mud log-

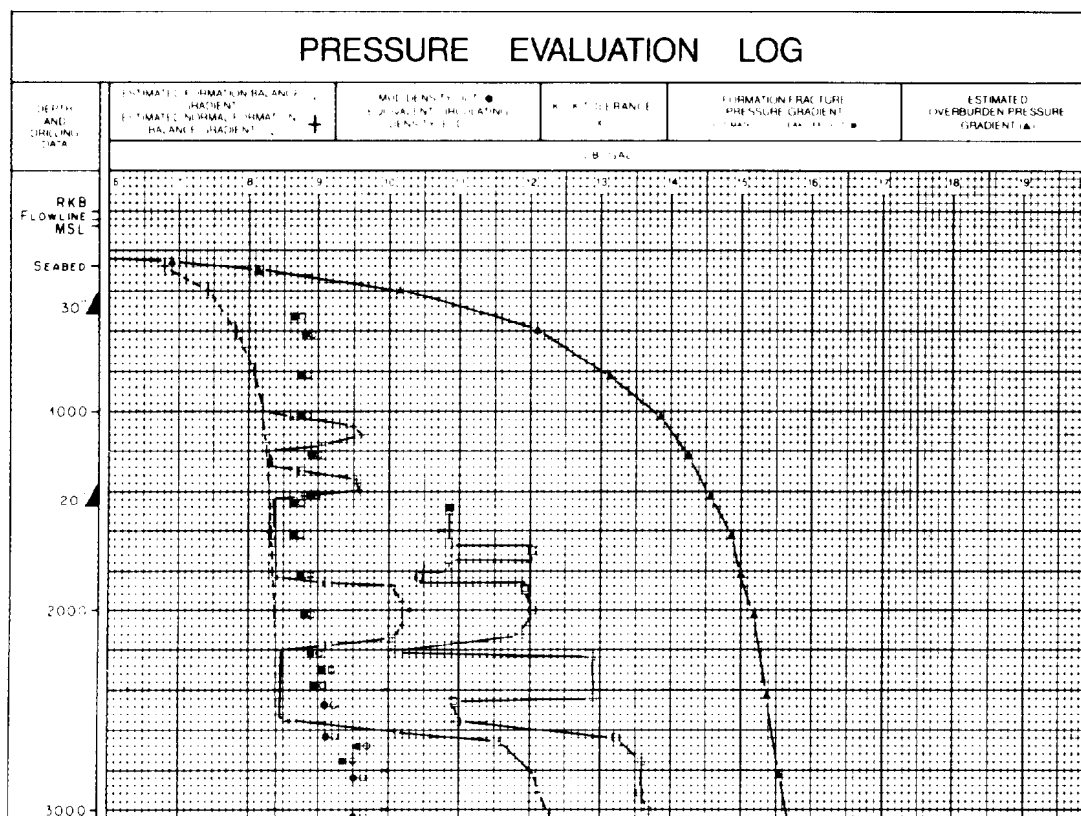


Fig. 52.22—Formation pressure log.

ging units were introduced to provide pressure evaluation services in areas of known geopressed problems (e.g., offshore U.S. gulf coast) and high-risk, hazardous exploration areas (e.g., the North Sea). Fig. 52.21 shows the available equipment configurations of a computerized logging unit. In addition to pore pressure, this type of unit commonly provides a pressure log including supplementary calculations of fracture pressure, overburden pressure, and kick tolerance (Fig. 52.22).

Petrophysical Measurements

Mud Log Data. As discussed previously, mud log data are qualitative in nature. It is not possible with conventional mud log measurements to obtain quantitative values of such parameters as porosity, permeability, hydrocarbon saturations, etc. However, the mud logging unit may provide special equipment or services, allowing more quantitative evaluations.

For example, while a mud log gas analysis cannot be truly representative of gas production composition, gas analysis of recovered fluids from a well test can be. Using conventional gas analyzers and chromatograph, a quantitative analysis of recovered natural gas may be obtained. For more complex fluids, special chromatographs, pyrolyzers, or analyzers can give complete analysis of oils or sour gas. The logging unit also may provide ionic analysis of recovered waters and, by use of tritium (^3H) or nitrate (NO_3^-) tracers, provide discrimination between recovery of mud filtrate and true formation water. These types of service can be of special

value in remote locations where logistics or distance prevent rapid transport of samples to an analytical laboratory.

Core Analysis. In addition to gas and fluid analysis, conventional core analyses¹⁹ (porosity, bulk density, permeability, and saturations) also may be performed in the logging unit when the drilling operation is remote from the laboratory. Wellsite core analysis offers the advantages of rapid evaluation and high-quality samples from fresh core but is rarely of the high quality to be expected from the specialized equipment and personnel in a core laboratory. A new technique, which is suitable to the logging unit, uses a pulsed nuclear magnetic resonance analyzer to determine fluid content, total and free-fluid porosity, and permeability. This device, working on a principle analogous to the nuclear magnetic logging tool (NML), provides accurate, repeatable data from minimal quantities of sample and without complex sample preparation. Samples may be obtained without causing core or sidewall core destruction and the test may be performed on cuttings.

Drilling Porosity

The d -exponent (Fig. 52.20) develops a consistent trend with depth controlled by increasing overburden loading and compaction. Changes in formation pore pressure gradient will result in major, consistent deviations from this trend. The d -exponent data also will exhibit minor,

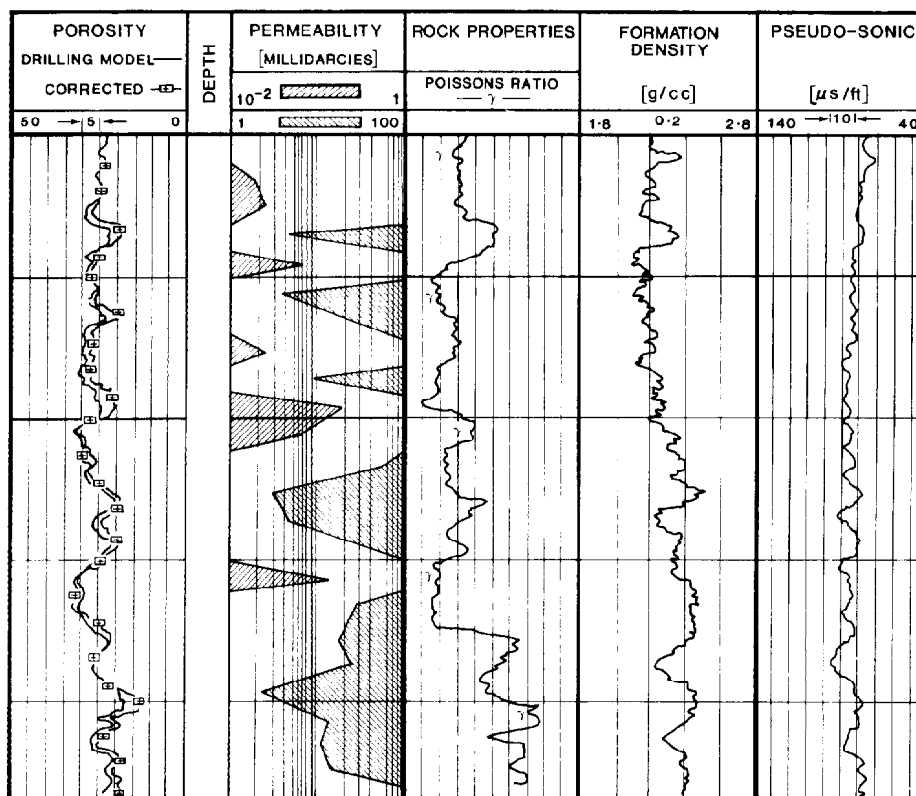


Fig. 52.23—Drilling porosity log.

inconsistent scatter about the prevailing trend, reflecting continuous variation in rock mineralogy, cohesion, and porosity.

More sophisticated, second-generation drilling exponents are able to isolate the major pore pressure and minor rock character variations. With this type of analysis it is possible to provide a continuous log of pore pressure and "drilling porosity." It is important to remember that drilling porosity, although scaled in percentage units, is not a true porosity measurement. It is primarily a rock strength indicator, reflecting both porosity and intergrain cohesion. As such, its response is very similar to that of the sonic log, and the two logs correlate extremely well (Fig. 52.23).

Unlike the *d*-exponent, the second generation drilling exponents require complex manipulations and iterations, limiting their use to logging units equipped with a computer. Also, unlike the *d*-exponent, they do not involve a widely published and used single method. Although based on similar drilling response models, all mud logging contractors offer drilling porosity logs involving their own unique mathematical methods that are commonly held as proprietary secrets. While understandable from a commercial view, this policy places the user in the position of being able to judge the value and reliability of a particular log only on the bases of his or her own experience and limited published results. It is hoped that, with the maturation of this type of service, wider publication and discussion of methods will begin.

Drilling Engineering Services

The mud logging unit can provide two levels of service of value to the drilling engineer—data acquisition and data analysis.

Data Acquisition

An automatic data acquisition system located in the logging unit will monitor sensors installed on equipment, flowline, mud pits, pumps, etc. Simple calculations are performed on the data (e.g., calculation of total depth and ROP, summation of pit volumes, comparison of current values with high- and low-alarm setpoints). Results then are displayed on TV monitors at various locations around the rig and may be recorded on a printer or magnetic tape. By use of a dedicated land line or satellite link, data can be transmitted to a remote location, allowing several rigs to be monitored from a single central control room.

This type of equipment was introduced by mud logging service companies as a means of obtaining drilling and mud data more reliably and rapidly than could be expected from standard rig instrumentation. While these data were required initially for pressure evaluation analyses, the data acquisition system provided an important secondary function as a rig monitoring service by supplying the drilling engineer accurate, up-to-date drilling information while away from the rig floor and a complete foot-by-foot record of drilling progress and performance on paper or magnetic tape.

Since that time, several conventional rig instrumentation manufacturers have upgraded their product lines to include similar data acquisition systems that operate in an unmanned, or "stand-alone," mode. While this offers the operator the advantage of flexibility in selecting services (i.e., the mud logging service best suited to the geologist and the data acquisition service best suited to the engineer), it does have drawbacks.

Reliability of a data acquisition system is primarily controlled by the operation of its sensors. In the rigorous environment of the rig this requires regular attention. The success of a stand-alone data acquisition system is related entirely to the training and motivation of the rig crew or the availability of manufacturer's service personnel.

The mud logging unit is manned at all times. Trained personnel are available at all times to calibrate, maintain, and service the data acquisition system and its sensors. Since these personnel are already at the wellsite as part of the mud logging service, this extra margin of reliability is achieved without extra cost beyond the similar cost of the data acquisition hardware.

Data Analysis

Beyond simple data acquisition, the mud logging service also may supply computers, software, and specialized wellsite personnel for drilling data analysis. The desirability of such services depends on the difficulty and cost of the drilling operation, availability of oil company expertise at the wellsite, and quality of communication with the exploration headquarters.

For example, infill drilling in an established domestic field using a well-developed drilling program, experienced wellsite supervisors, and close communication with home office requires data acquisition only as a means of monitoring optimal and safe adherence to the drilling program. On the other hand, on an offshore wildcat, the availability of data analysis and expertise at the wellsite can be very cost effective.²⁰ An increase in drilling efficiency or a decrease in downtime sufficient to save a single day of rig time can, in these circumstances, produce sufficient savings to pay for data analysis services for the whole well.

Data analysis services offered include: (1) bit optimization—selection of bit type and operating parameters to optimize bit ROP and bit life; (2) bit economics—cost per unit depth and breakeven calculation between bit types; (3) drilling hydraulics²¹—optimization of drillstring, nozzle, and annulus hydraulics; (4) directional analysis—determination of well path, bottomhole position, and intersection points for deviated wells; (5) trip monitoring—calculation of string weights, swab pressures and fillup requirements for tripping, monitoring of pit level deviations, and overpull (frictional drag in the borehole); (6) casing calculations—assembly of casing tally, calculation of cement volumes and mixing requirements, and monitoring of displacement; (7) pressure control—calculation of mud weight, volume and pressure requirements for safe well control¹⁰; and (8) logistics—usage and inventory control of well expandables, equipment maintenance scheduling, well progress data base, and report generation.

Selecting a Mud Logging Service

Mud logging contractors commonly offer three levels of standard service: (1) standard mud logging; (2) mud logging and data acquisition, and (3) mud logging and data analysis (including pressure evaluation). For the most basic level of mud logging, a single operator may be responsible for 24-hour operation. More sophisticated services and data acquisition usually require two geologists working 12-hour tours. Data analysis services require two people, a geologist and an engineer, on each tour.

Each of these services may be augmented with extra equipment such as sensors, special gas detectors, pyroanalyzers, more powerful computers or peripherals and specialist personnel at extra day rate as the drilling program demands.^{2,10}

At least two mud logging contractors now offer an additional, fourth level of service in which mud logging and data analysis are combined with an MWD service.

Very little of the information gathered by a mud logging unit is not obtainable from some other source. For example, stand-alone instrumentation can monitor gas, mud, and drilling parameters; rig crews can catch samples; porosity is available from wireline logs; and oil company geologists and engineers may perform geological evaluation and drilling data analysis. Why then is mud logging such a widely used service?

The advantage of mud logging service is that all these data may be derived from a single source, the mud logging unit, located at the wellsite and continuously manned with dedicated, specially trained personnel. Therefore the data are obtained more reliably, more quickly, and usually more economically than from any other combination of sources.

Reliability and speed therefore are the tests required in selecting a mud logging contractor. The equipment must be designed and maintained adequately to provide reliable and safe operation in the rigorous wellsite environment. The wellsite crew must be trained to operate, maintain, and troubleshoot the equipment and to understand its output. The contractor must maintain adequate service personnel and inventory to allow rapid repair or changeout in the event of major malfunctions. The logging crew must be trained in geological and engineering theory, be experienced in practical drilling operations, and have a thorough knowledge of the geological section, drilling program, and operational procedures of the particular well and operator.

Once a contractor is selected, economy becomes the prime consideration in choosing a level of service. In day-rate drilling, time and money may be directly equated. Any service that speeds well progress, reduces downtime, or promotes decision-making is potentially a cost saver. Even on footage drilling, personnel, communications, etc., are cost-generating factors which may be reduced by improved drilling efficiency. On rank wildcat exploration wells, the "bird in the hand" philosophy may be desirable to obtain data at the earliest possible time as a hedge against the risk of it being unavailable later. For example, to obtain porosity measurements from the mud logging unit while drilling is an investment against later borehole loss or damage that may prevent later wireline logging.

Quantification of cost saving is possible by using the same methods used to calculate drilling cost per foot. In its simplest form this is

$$C_d = \frac{C_{be} + C_r t_l}{D_t}, \dots\dots\dots (14)$$

where

C_d = drilling cost, \$/m,
 C_r = rig cost, \$/D,
 C_{be} = cost of bits and expendables, \$,
 t_l = time on location, days,
 D_t = total well depth, m.

For optimization of services and products this can be expanded to the form

$$C_d = [(C_{F1} + C_{F2} + \dots C_{Fn}) + (C_{dr1} + C_{dr2} \dots C_{drn}) \times (t_r + t_t + t_o + t_e + t_d)] \div D_t \dots\dots\dots (15)$$

and

$$C_d \times D_t = \Sigma(C_F)_n + \Sigma(C_{dr})_n \times \Sigma(t)_n, \dots\dots\dots (16)$$

where

C_F = individual fixed cost items or footage charges services, \$,
 C_{dr} = individual day rate services, rentals, salaries, etc., \$,
 t_r = rotating time, days,
 t_t = tripping time, days,
 t_o = off-bottom time (reaming, conditioning, well control, etc.), days,
 t_e = evaluation time (logging, testing, coring, etc.), days, and
 t_d = downtime (breakdowns, weather, decision making, etc.), days.

Using this formulation, it is possible to calculate the decrease in one cost category required to offset an increase in any other.

For example, consider the use of drilling optimization. Let us assume, conservatively, that regional statistics indicate that by upgrading a mud logging unit to include data acquisition equipment no overall ROP improvement is obtained but that a well can be completed using one less bit. Well cost as a result of this is given by

$$(C_d \times D_t)' = [\Sigma(C_F)_n - \Delta C_{Fb1}] + [\Sigma(C_{dr})_n + \Delta C_{xr}] [\Sigma(t_l)_n - \Delta t_{tl}], \dots (17)$$

where

ΔC_{Fb1} = cost of one bit saved, dollars,
 ΔC_{xr} = extra cost of mud logging, dollars/D,
 $(t_l)_n$ = total time on location, days
 Δt_{tl} = time for one trip saved, day, and
 $(C_d \times D_t)'$ = well cost, dollars.

For cost effectiveness (i.e., for the additional service to save its own cost or more), overall well cost must be unchanged or reduced. Thus,

$$\Delta(C_d \times D_t) = (C_d \times D_t)' - (C_d \times D_t) \leq 0, \dots\dots\dots (18)$$

$$\Delta(C_d \times D_t) = -\Delta C_{Fb1} - [\Sigma(C_{dr})_n \times \Delta t_{tl}] + \Delta C_{xr} \times [\Sigma(t_l)_n - \Delta t_{tl}], \dots\dots\dots (19)$$

and

$$\Delta C_{xr} \leq \frac{\Delta C_{Fb1} + [\Sigma(C_{dr})_n \times \Delta t_{tl}]}{[\Sigma(t_l)_n - \Delta t_{tl}]} \dots\dots\dots (20)$$

If this is evaluated as true, that the day rate for the extra equipment is in fact less than the evaluated expression, then the service is cost effective on the particular well. In this case, substituting some reasonable figures such as:

Onshore	Offshore
$\Delta C_{Fb1} = \$1,000$	$\Delta C_{Fb1} = \$1,000$
$\Sigma(C_{dr})_n = \$6,000/D$	$\Sigma(C_{dr})_n = \$19,000/D$
$\Delta t_{tl} = 12 \text{ hours} = 0.5 \text{ day}$	$\Delta t_{tl} = 12 \text{ hours} = 0.5 \text{ day}$
$\Sigma(t_l)_n = 30 \text{ days}$	$\Sigma(t_l)_n = 35 \text{ days}$

we obtain for onshore:

$$\Delta C_{xr} \leq \frac{1,000 + (6,000)(0.5)}{(30 - 0.5)} = \$135.59/D.$$

The extra equipment will result in an overall cost saving on the well so long as it does not increase the mud logging daily rate by more than \$135/D.

We obtain for offshore:

$$\Delta C_{xr} \leq \frac{1,000 + (19,000)(0.5)}{(35 - 0.5)} = \$304.35/D.$$

Using these same figures, let us now assume that, in addition to saving one bit, an overall decrease of 5% in drilling time is also achieved. If $t_r = 21$ days, saving in rotating time = $21 \times 5\% = 1.05$ days, then for onshore:

$$\Delta C_{xr} \leq \frac{1,000 + [6,000 (0.5 + 1.05)]}{(30 - 0.5 - 1.05)} = \$362.04/D.$$

For offshore:

$$\Delta C_{xr} \leq \frac{1,000 + [19,000 (0.5 + 1.05)]}{(35 - 0.5 - 1.05)} = \$910.31/D.$$

These cost justifications, or cost savings, refer only to the *extra* cost of data acquisition above that of standard mud logging and include only those benefits resulting from drilling optimization. Other cost savings resulting from better rig and mud monitoring and well control may also be quantifiable from a study of regional drilling statistics.

A cost benefit analysis of this type is a worthwhile approach to all aspects of drilling cost reduction. Cost saving resulting from advanced evaluation and monitoring commonly is appreciated in expensive offshore exploration. As the above examples show, such techniques may be equally successful in comparatively cheaper onshore development drilling, especially where problems such as geopressure or crooked holes occur.

Standards For and Status of Services

The terms "mud logging" covers a diverse range of services and qualities of service. It is regrettable that, in the U.S. especially, the whole industry is accorded a status reflecting its lowest level. Field employees of the higher quality and more reputable contractors commonly eschew the term "mud logger," preferring the title "logging geologist" or "logging engineer," depending on their educational background. The wide range of equipment and techniques used by such companies commonly results in their personnel being the best educated and trained service personnel present on any wellsite.

In 1980, the Soc. of Professional Well Log Analysts (SPWLA) established a Hydrocarbon Well Log Standards Committee comprising members of both the service company and exploration company sides of the field. The efforts of the committee have done much toward establishing standards and status representative of the best of the industry.^{22,23} I express my gratitude to this committee and its members for these efforts and for assistance in the development of this chapter.

Nomenclature

C_{be}	= cost of bits and expendables, dollars
C_{carb}	= carbonate content, %
C_d	= drilling cost, dollars/m
C_{dr}	= individual day rate services, rentals, salaries, etc., dollars
C_F	= individual fixed cost items or footage charges services, dollars
C_r	= rig cost, dollars/D
d	= formation "drillability" exponent (dimensionless)
d_b	= bit diameter, ft or in.
d_n	= "normal" bit diameter (m)
d_{oB}	= observed bit diameter (m)
d_{xc}	= corrected d -exponent (dimensionless)
d_{xcn}	= expected corrected d -exponent on normal trend line at depth of interest
d_{xco}	= observed corrected d -exponent at depth of interest
F_{sha}	= apparent shale factor, meq/100 g
F_{shf}	= true shale factor, meq/100 g
G_{pn}	= normalized total gas (%)
G_{poB}	= observed total gas (%)

g_G	= geothermal gradient, °C/100 m
g_{nfb}	= normal formation balance gradient, lbm/gal
K_D	= matrix strength constant (dimensionless)
N	= rotary-speed, rev/min
p_{pa}	= actual pore pressure at depth of interest, psi, or formation balance gradient, lbm/gal equivalent mud density (EMD)
p_{pn}	= normal pore pressure, psi, or formation balance gradient, lbm/gal (EMD)
q_n	= "normal" mud flow rate (m ³ /s)
q_{oB}	= observed mud flow rate (m ³ /s)
q_p	= pump output, m ³ /s)
R	= ROP, ft/min
R_n	= "normal" ROP (m/s)
R_{oB}	= observed ROP (m/s)
t_d	= downtime (breakdowns, weather, decision making, etc.), days
t_e	= evaluation time (logging, testing, coring, etc.), days
t_l	= lag time, seconds
$(t_l)_n$	= total time on location, days
t_o	= off-bottom time (reaming, conditioning, well control, etc.), days
t_r	= rotating time, days
t_t	= tripping time, days
V_{an}	= annular volume, m ³ /m
V_h	= hole capacity, m ³ /m
V_p	= pipe capacity and displacement, m ³ /m
v_{an}	= annular velocity, m/s
W	= WOB, lbm
$(C_d \times D_t)'$	= well cost, dollars
ΔC_{Fb1}	= cost of one bit saved, dollars
ΔC_{xr}	= extra cost of mud logging, dollars/D
Δt_{tl}	= time for one trip saved, day
ρ_{ec}	= effective circulating density, lbm/gal

References

1. "Field Geologists Training Guide," Exploration Logging Inc., Sacramento, CA (Jan. 1979).
2. "Mud Logging: Principles and Interpretation," Exploration Logging Inc., Sacramento, CA (Aug. 1979).
3. "Formation Evaluation—Part 1: Geological Procedures," Exploration Logging Inc., Sacramento, CA (Feb. 1981).
4. Hopkins, E.A.: "Factors Affecting Cuttings Removal During Rotary Drilling," *J. Pet. Tech.* (June 1967) 807-14; *Trans., AIME*, **240**.
5. Sifferman, T.R. *et al.*: "Drill Cutting Transport in Full Scale Vertical Annuli," *J. Pet. Tech.* (Nov. 1974) 1295-1302.
6. Low, J.W.: "Examination of Well Cuttings," *Quarterly of the Colorado School of Mines* (1951) **46**, No. 4, 1-48.
7. Maher, J.C.: *Guide book VIII: Logging Drill Cuttings*, Oklahoma Geological Survey, Norman (1959).
8. McNeal, R.P.: "Lithologic Analysis of Sedimentary Rocks," *Bull., AAPG* (April 1959) **43**, No. 4, 854-79.
9. Clementz, D.M., Demaison, G.J., and Daly, A.R.: "Wellsite Geochemistry by Programmed Pyrolysis," paper OTC 3410 presented at the 1979 Offshore Technology Conference, Houston, April 30-May 3.
10. "Theory and Evaluation of Formation Pressures: The Pressure Log Reference Manual," Exploration Logging Inc., Sacramento, CA (Sept. 1981).
11. Hottman, C.E. and Johnson, R.K.: "Estimation of Formation Pressures from Log-Derived Shale Properties," *J. Pet. Tech.* (June 1965) 717-22; *Trans., AIME*, **234**.

12. Goldsmith, R.G.: "Why Gas-Cut Mud is Not Always a Serious Problem," *World Oil* (Oct. 1972) **175**, No. 5, 51-54, 101.
13. Dowdle, W.L. and Cobb, W.M.: "Static Formation Temperature From Well Logs," *J. Pet. Tech.* (Nov. 1975) 1326-30.
14. Fowler, P.T.: "Telling Live Basins from Dead Ones by Temperature," *World Oil* (May 1980) **190**, No. 6, 107-22.
15. Lewis, C.R. and Rose, S.C.: "A Theory Relating High Temperature and Overpressures," *J. Pet. Tech.* (Jan. 1970) 11-16.
16. Bingham, M.G.: *A New Approach to Interpreting Rock Drillability*, Petroleum Publishing Co., Tulsa (1965).
17. Jorden, J.R. and Shirley, O.J.: "Application of Drilling Performance Data to Overpressure Detection," *J. Pet. Tech.* (Nov. 1966) 1387-94.
18. Rehm, B. and McClendon, R.: "Measurement of Formation Pressure From Drilling Data," *Drilling*, Reprint Series, SPE, Dallas (1973) **6a**, 49-60.
19. Anderson, G.: *Coring and Core Analysis Handbook*, Petroleum Publishing Co., Tulsa (1975).
20. Bellotti, P. and Giacca, D.: "Pressure Evaluation Improves Drilling Programs," *Oil and Gas J.* (Sept. 11, 1978) 76-85.
21. "Drilling Hydraulics Manual," Exploration Logging Inc., Sacramento, CA (July 1983) **8**, 1-8; **9**, 1-10; **10**, 1-7; **D**, 1-4.
22. "SPWLA Standard No. 1: Standard Hydrocarbon Well Log Form," SPWLA, Houston (June 1981).
23. "SPWLA Standard No. 2: Hydrocarbon Well Log Calibration Standards," SPWLA, Houston (June 1981).

General Reference

Jorden, J.R. and Campbell, F.L.: *Well Logging I—Rock Properties, Borehole Environment, Mud and Temperature Logging*, Monograph Series, SPE, Dallas (1984) **9**.

Chapter 53

Other Well Logs

Richard M. Bateman, Vizilog Inc.*

Introduction

Many well logs generally are not classified as electrical, nuclear, or acoustic logs. The most important of these are discussed in this chapter. Included as miscellaneous well logs are: (1) measurements taken while drilling (MWD), (2) directional surveys, (3) dipmeter logs, (4) caliper logs, and (5) casing inspection logs. All of these are used by the petroleum engineer on occasions. The logs are discussed in the order listed, which was selected for convenience only and is unrelated to the importance of the logs.

MWD

MWD plays an increasingly important role in modern drilling practices. It allows an operator almost immediate feedback on both the geometry of the hole being drilled and the characteristics of the formations penetrated. Without MWD this kind of information is available only from conventional sources such as deviation surveys and logs that, a priori, must be run after the drilling has taken place. Of particular benefit, MWD can be applied when drilling directional wells and/or when overpressured formations are of concern.

By having the kind of information MWD can supply more or less in real time, the driller may take appropriate action, such as changing the weight on bit (WOB), increasing the mud weight, or pulling out of the hole for a conventional logging run once the desired formation has been reached.

Many different MWD measuring systems are in commercial use today. However, they all have common characteristics: (1) a downhole sensor sub, (2) a power source, (3) a telemetry system, and (4) surface equipment. The downhole sensor subs may contain instrumentation capable of measuring parameters such as torque,

WOB, borehole pressure, borehole temperature, tool face angle, natural formation gamma ray activity, formation acoustic travel time, formation resistivity, hole deviation from vertical, and hole azimuth with respect to geographic coordinates. The sensors and the telemetry system can be activated by a surface power source, a downhole turbine, or downhole batteries. In the case of a surface power source it is necessary to make electrical connections between the surface and the downhole sensors, which, in turn, requires either special drillpipe or an electric cable. With a downhole turbine the circulating mud itself drives an electric generator located in the MWD drill collar. This, in turn, leads to an increase in the hydraulic horsepower required of the mud pumps to maintain circulation. In the case of batteries no special cabling or additional mud pumping is required, but the MWD system is limited by the life of the batteries used. Once they are discharged no further measurements can be made and the MWD sub must be retrieved and redressed with fresh batteries.

The telemetry system most commonly used is that of coded mud pressure pulses. The output from a specific sensor is converted from analog to a digital form and encoded as a series of pressure pulses, which are detected and decoded at the surface. The pressure pulses may be in the form of overpressure or underpressure anomalies introduced, respectively, by either a relief valve "shorting" the mud circulation or a check valve "choking" it.

However, coded mud pressure pulses are not the only means available for telemetry. Other methods, either in use or under experimentation, include: (1) electromagnetic e-mode (electric current) or h-mode (magnetic field); (2) acoustic telemetry through drillpipe and/or tubing in straight hole, or through the earth by seismic waves; (3) hardwire systems; (4) systems with self-energizing repeaters; and (5) hybrid systems that combine various transmission methods.¹

* Author of the original chapter on this topic, entitled "Miscellaneous Well Logs," in the 1962 edition was A.J. Pearson.

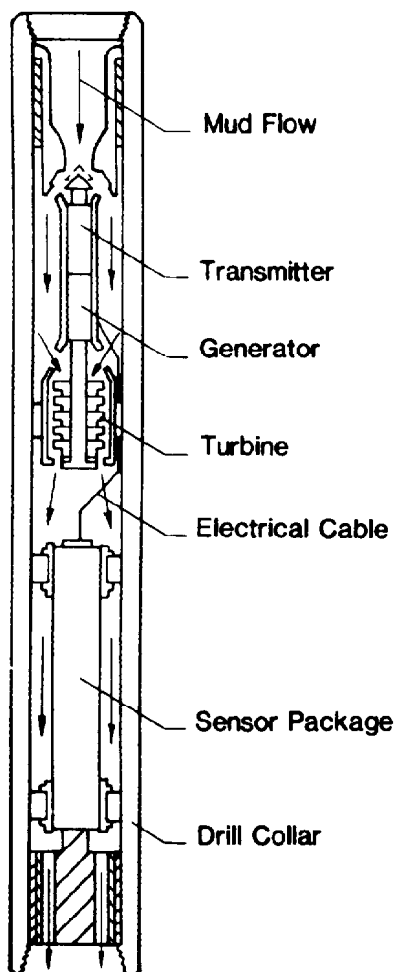


Fig. 53.1—Typical MWD downhole assembly.

The surface equipment consists of a decoder of the mud pulses (or other parameter, depending on the telemetry system in use) together with signal processing hardware and software that together produce the data that the drilling engineer needs. Output may be in the form of a visual display, either on the rig floor or at a remote site, or as a hard copy listing, or log, of the parameters recorded. Data also may be recorded on magnetic tape for future use.

In most systems, the transmission of data to the surface is selective. For example, a measurement of hole deviation and azimuth may require that the drilling process be suspended temporarily and the drillstring held motionless for a short period. Readings then are accumulated in a "buffer" and only transmitted to the surface when mud circulation recommences.

Fig. 53.1 illustrates an MWD downhole assembly with its mud pulse transmitter, turbine generator, and sensor sub.

Fig. 53.2 shows a data transmission schematic for MWD. Typically, each measurement or "word" is transmitted as part of a data frame, which in turn consists of a synchronization word and 15 measurement words. Some measurements are transmitted more than once in each frame. Current telemetry systems are capable of transmitting a complete frame in a matter of 1 or 2 minutes. The actual sampling rate in terms of measurements per unit of depth is inversely proportional to the rate of penetration (unit of depth/ unit of time).²

Fig. 53.3 shows a complete MWD logging system schematic and integrates surface and downhole sensors, the telemetry system, the surface hardware and software (for computer processing of the data), and the final product in the form of a log.³

Fig. 53.4 shows an MWD log on which is displayed gamma-ray, short normal resistivity, annular temperature, downhole WOB, surface WOB, and computed directional data (drift and azimuth).

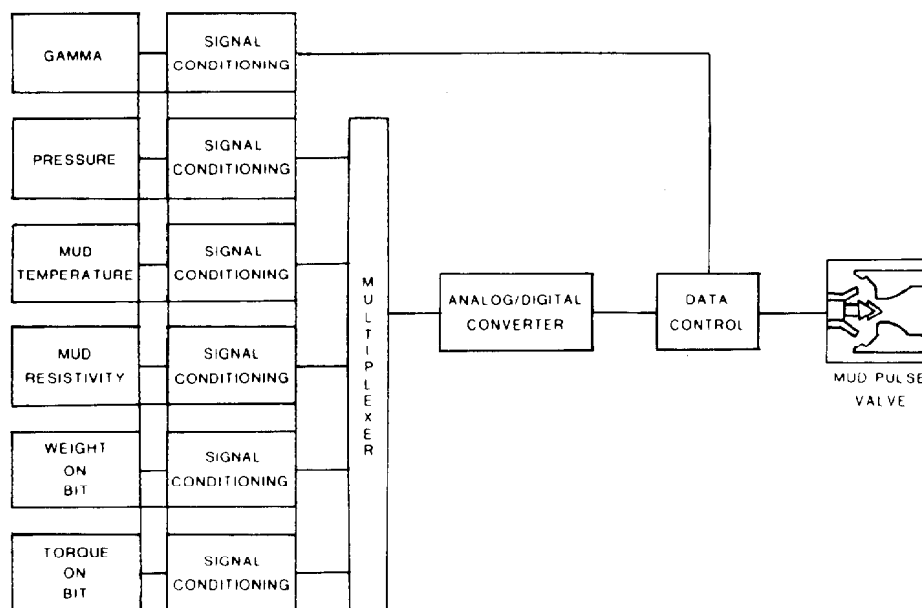


Fig. 53.2—MWD data transmission schematic.

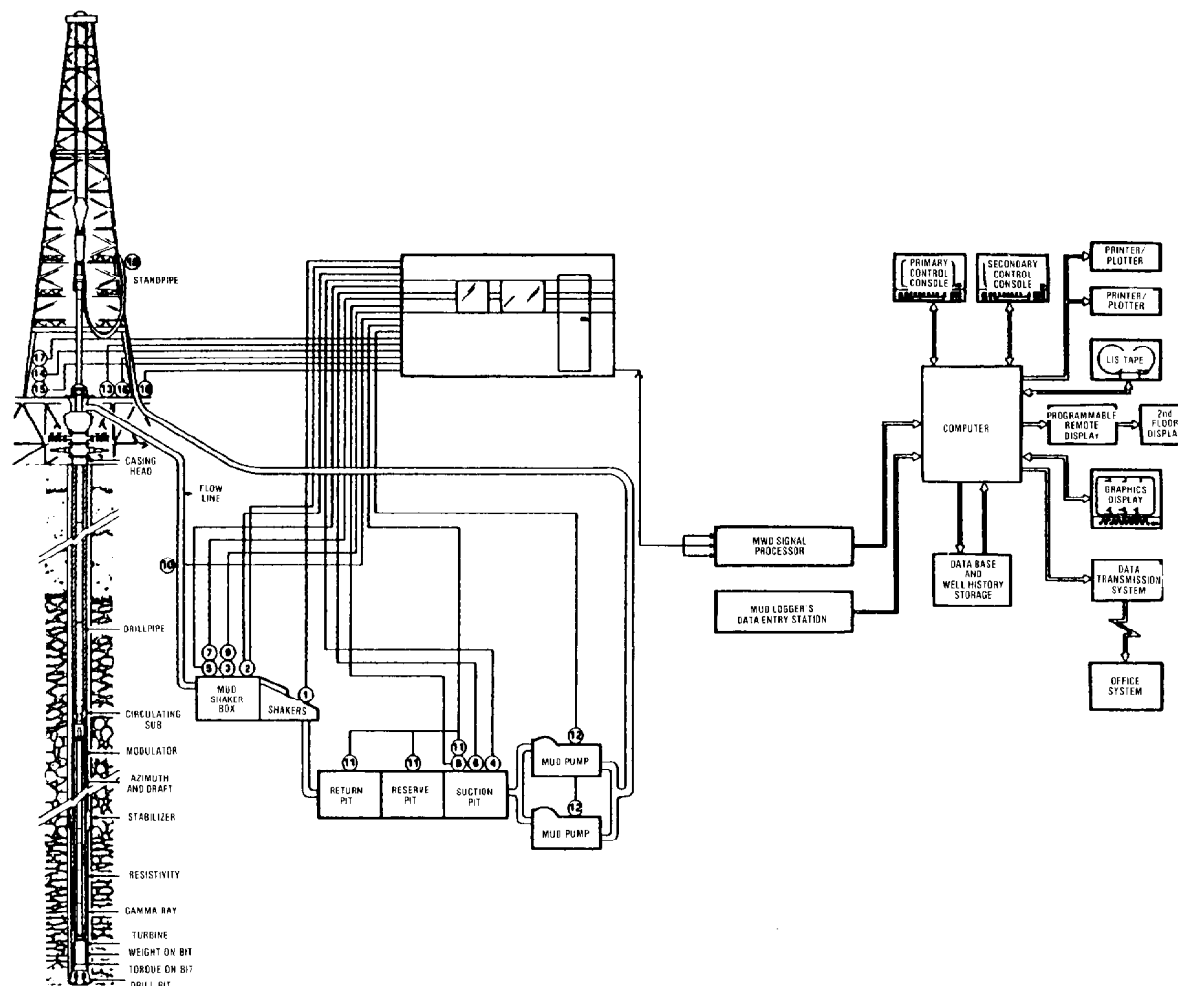


Fig. 53.3—MWD logging system schematic.

Fig. 53.5 shows a comparison between an MWD-generated computed directional survey and a multishot run in the same well. Table 53.1 illustrates a directional survey listing corresponding to the plan view shown in Fig. 53.5.

Directional Surveys

Directional surveys^{4,5} are used to determine the location of the hole path with respect to the surface location. This information is used (1) to prove legally that the bottomhole location is under the correct surface property, (2) to ascertain the bottomhole location in purposely deviated wells, (3) to determine the radius of curvature of the hole as it affects the ability to run casing or tools, and (4) to differentiate between measured depth and true vertical depth (TVD) when using formation elevations for structural mapping.

Available Tools

The two basic types of directional surveys are continuous surveys and station surveys. The station surveys can be either single shot or multishot. Single or multi refers to the number of stations recorded. Single shot surveys normally are recorded during the drilling operation and are

recorded at given depth or time intervals. These single-shot records are accumulated and used to plot the hole path. Multishot surveys are the result of several shots run at given depth intervals after the hole has been drilled. Continuous surveys are run after a portion of the hole has been drilled. These are recorded continuously over the selected interval. Although continuous, multishot, and single-shot instruments are all different, there is another classification of instruments that must be considered when choosing a survey.

Surveys run inside metal casing cannot use the magnetic compass for hole direction. Gyroscopes normally are used whenever a survey is needed inside casing. These gyroscopes must be aligned on the surface before proceeding with the survey. They also should have their alignment verified as part of the after-survey checks.

The openhole directional surveys normally use magnetic compass orientation to fix the hole direction. This requires the input of the deviation between magnetic and true north. All devices use a pendulum system for determining the angle of hole deviation.

All continuous dipmeter surveys measure data that can yield a directional survey. This directional survey is available either as part of the dipmeter or as a separate

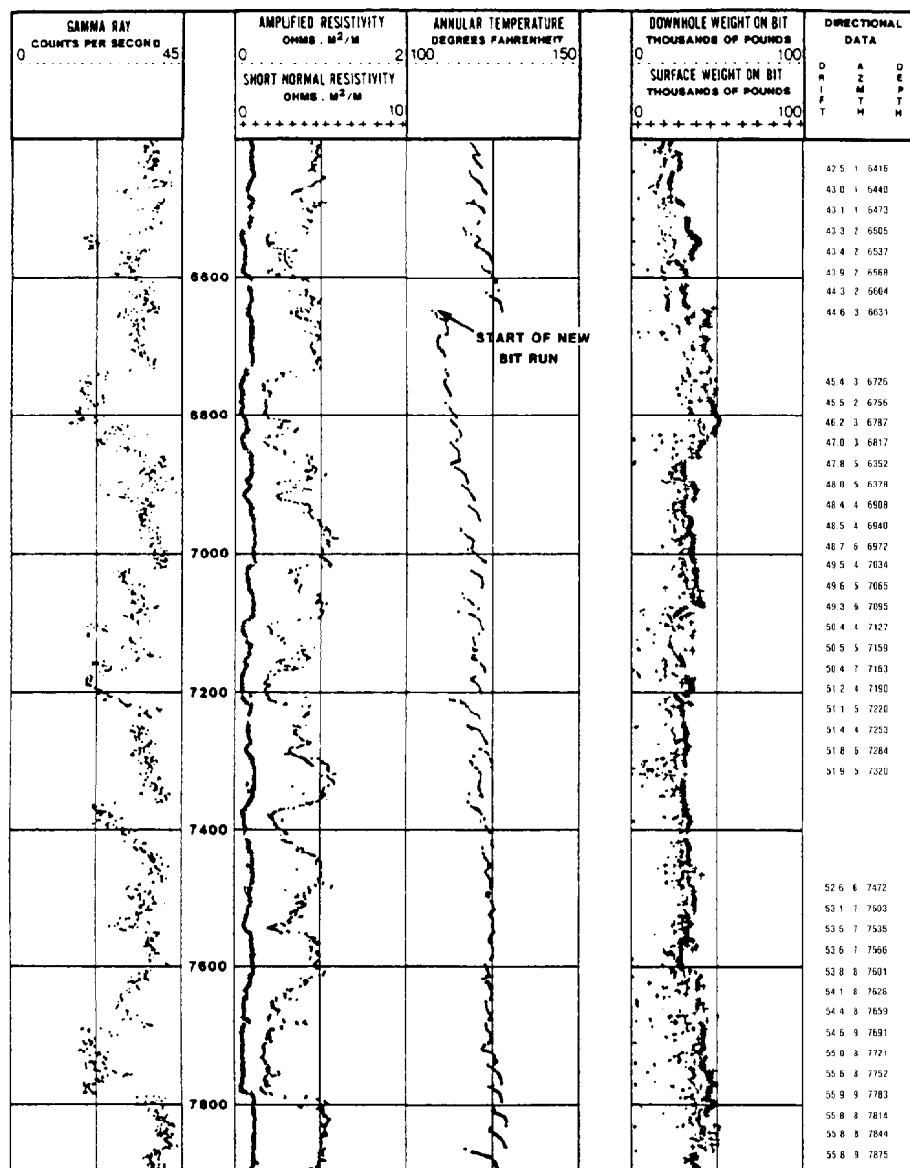


Fig. 53.4—An MWD rotary drilling log.

survey over portions of the hole where formation dips are not desired. At present, this instrument does not work in a cased hole, so the survey must be tied in to known coordinates at the bottom of the casing.

Any device that uses a magnetic compass to fix direction will be affected by metal in or near the borehole. This effect must be considered when a survey is run in an open hole that has been whipstocked past abandoned drillpipe or may be near a cased wellbore.

Fig. 53.6 illustrates a gyroscopic survey tool incorporating an accelerometer.

Legal Requirements

Each state has a separate definition of what constitutes a "legal" directional survey. These definitions may include specifications such as (1) length of downhole sensor, (2) whether or not such assembly is centered, (3)

method of calculating station-type surveys, (4) professional qualifications of person supervising or certifying the results, and (5) documentation, presentation, and distribution of results. These criteria must be considered when choosing a service company and a type of survey.

Computation of Results

Directional surveys are available in any area where directional drilling is done or where dipmeters are available. The field log may be a series of station readings or a continuous curve showing hole direction and deviation. The computed results will include a well plat that shows the vertical projection of the wellbore. Additional plots may show wellbore projections on a vertical plane passing through the surface location. A tabulated listing will show the wellbore coordinates and deviation angle.

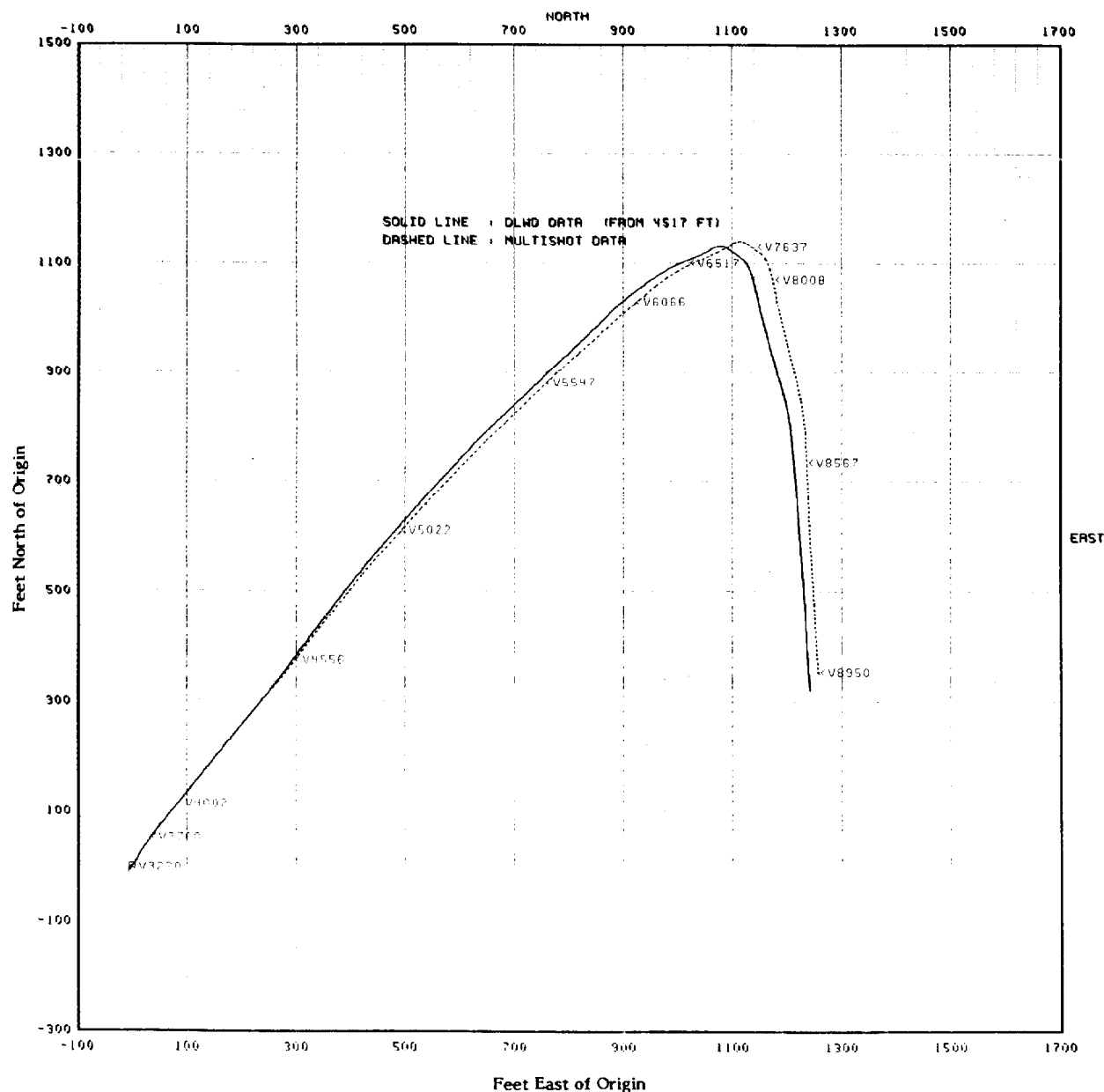


Fig. 53.5—Comparison of MWD directional with multishot directional.

Methods of Calculation. There are many methods of calculating directional surveys.⁶ Most companies use one of the following five basic methods.

1. Tangential Method. This method uses the inclination and azimuth angles at the bottom of each course length (distance between readings or stations). This is usually the most common and least accurate method. The error introduced increases with the inclination angle and the course length. This method is not recommended.

2. Balanced Tangential Method. This method uses the inclination and azimuth angles at both the top and bottom of each course length to tangentially balance the two sets of measurements over the course length. This method is more accurate than the tangential method but is still sensitive to the course length.

3. Angle Averaging Method. This method uses a simple mathematical average of the inclination and azimuth angles at the top and bottom of the course length to compute the survey using the tangential method. This is more accurate than the tangential method but still simple enough for hand calculations in the field. Course length should be kept as short as feasible.

4. Radius of Curvature Method. This method uses the inclination and azimuth angles at the top and bottom of the course length to generate a space curve representing the curve path. This space curve passes through the measured angles at the top and the bottom of the course length. This method usually is considered the most accurate but is still sensitive to course length.

TABLE 53.1—MWD DATA LISTING FOR DIRECTIONAL SURVEY

Survey Number	Readings				Analysis (confidence level = 99.0%)							
	Depth	Course Length (ft)	Inclined Angle (degrees)	Azimuth Angle (degrees)	Dogleg /100 ft	Vertical Depth (ft)	Position		Uncertainty Range			
							North	East	Vertical	Major	Minor	Axis
88	5,425.0	30.0	37.80	41.80	2.34	5,180.4	696	559	1.3	10.0	9.5	343
89	5,457.5	32.5	37.67	43.50	3.22	5,206.1	710	573	1.3	10.0	9.5	344
90	5,478.0	20.5	36.53	43.50	5.52	5,222.5	719	581	1.3	10.0	9.6	344
91	5,509.0	31.0	35.73	44.00	2.75	5,247.5	732	594	1.3	10.0	9.6	345
92	5,540.0	31.0	35.72	41.80	4.14	5,272.7	746	606	1.3	10.0	9.6	346
93	5,571.0	31.0	35.08	42.40	2.33	5,298.0	759	618	1.3	10.1	9.6	347
94	5,589.0	18.0	35.08	42.40	0.00	5,312.7	767	625	1.3	10.1	9.6	347
95	5,605.0	16.0	34.35	42.80	4.79	5,325.8	773	631	1.3	10.1	9.6	347
96	5,631.0	26.0	33.90	43.30	2.03	5,347.4	784	641	1.3	10.1	9.6	348
97	5,695.0	64.0	32.17	46.30	3.72	5,401.0	809	666	1.4	10.1	9.6	351
98	5,735.0	40.0	31.28	47.40	2.64	5,435.0	823	681	1.4	10.1	9.7	352
99	5,756.0	21.0	30.97	46.60	2.47	5,453.0	831	689	1.4	10.1	9.7	353
100	5,821.0	65.0	28.87	45.10	3.43	5,509.3	853	712	1.4	10.1	9.7	356
101	5,852.0	31.0	27.88	47.20	4.52	5,536.6	863	723	1.4	10.1	9.7	357
102	5,949.0	97.0	26.52	45.40	1.64	5,622.9	894	755	1.4	10.2	9.8	3
103	6,032.7	83.7	24.65	46.10	2.26	5,698.4	919	781	1.5	10.2	9.8	6
104	6,090.0	57.3	23.63	48.90	2.67	5,750.7	935	798	1.5	10.2	9.8	8
105	6,117.0	27.0	22.80	47.00	4.15	5,775.5	942	806	1.5	10.2	9.8	8
106	6,150.2	33.2	22.45	46.10	1.48	5,806.1	951	815	1.5	10.2	9.8	9
107	6,216.2	66.0	21.27	46.80	1.83	5,867.4	968	833	1.5	10.2	9.8	10
108	6,241.8	25.6	20.93	46.00	1.71	5,891.2	974	840	1.5	10.2	9.8	10
109	6,272.0	30.2	19.68	48.20	4.85	5,919.6	981	848	1.5	10.3	9.8	11
110	6,302.0	30.0	19.78	44.80	3.84	5,947.8	988	855	1.5	10.3	9.8	11
111	6,337.0	35.0	19.30	46.10	1.85	5,980.8	997	863	1.5	10.3	9.8	11
112	6,402.0	65.0	18.28	41.80	2.64	6,042.3	1,012	878	1.5	10.3	9.8	12
113	6,455.8	53.8	17.17	49.50	4.82	6,093.6	1,023	889	1.5	10.3	9.8	13
114	6,553.3	97.5	15.87	50.10	1.34	6,187.0	1,041	911	1.5	10.3	9.8	14
115	6,600.3	47.0	14.92	59.50	5.67	6,232.3	1,048	921	1.5	10.3	9.8	14
116	6,678.3	78.0	14.62	47.20	4.03	6,307.8	1,060	937	1.5	10.3	9.8	15
117	6,708.3	30.0	14.78	53.50	5.35	6,336.8	1,065	942	1.5	10.3	9.8	15
118	6,740.3	32.0	14.32	55.90	2.38	6,367.8	1,069	949	1.5	10.3	9.9	15
119	6,771.3	31.0	13.85	59.50	3.20	6,397.8	1,073	955	1.5	10.3	9.9	15
120	6,838.3	67.0	13.18	57.90	1.14	6,463.0	1,082	969	1.5	10.4	9.9	16
121	6,893.9	55.6	12.63	57.60	0.99	6,517.2	1,088	979	1.5	10.4	9.9	16
122	6,926.7	32.8	12.87	63.30	3.90	6,549.2	1,092	986	1.5	10.4	9.9	16
123	6,989.4	62.7	12.55	67.80	1.66	6,610.3	1,097	998	1.6	10.4	9.9	16
124	7,020.0	30.6	12.58	66.30	1.06	6,640.2	1,100	1,004	1.6	10.4	9.9	16
125	7,054.0	34.0	12.60	65.70	0.35	6,673.4	1,103	1,011	1.6	10.4	9.9	16
126	7,084.4	30.4	12.40	67.10	1.18	6,703.1	1,106	1,017	1.6	10.4	9.9	16
127	7,114.2	29.8	11.50	66.90	3.02	6,732.2	1,108	1,023	1.6	10.4	9.9	16
128	7,153.9	39.7	10.90	66.90	1.51	6,771.1	1,111	1,030	1.6	10.4	9.9	16
129	7,184.8	30.9	10.00	68.60	3.08	6,801.5	1,113	1,035	1.6	10.4	9.9	16
130	7,240.1	55.3	7.90	68.90	3.80	6,856.2	1,116	1,043	1.6	10.4	9.9	16
131	7,272.7	32.6	7.40	63.00	2.85	6,888.5	1,118	1,047	1.6	10.4	9.9	16
132	7,285.8	13.1	7.00	66.90	4.81	6,901.5	1,119	1,048	1.6	10.4	9.9	16
133	7,316.9	31.1	7.40	58.70	3.54	6,932.3	1,121	1,052	1.6	10.4	9.9	16
134	7,346.0	29.1	5.90	58.40	5.15	6,961.2	1,122	1,055	1.6	10.4	9.9	16

5. Mercury Methods. This method is used by the U.S. Government at the Mercury Test Site in Nevada. This is a combination of the tangential and balanced tangential methods. The portion of the course length defined by the length of the surveying instrument is treated by the tangential method. The remainder of the course length is treated by the balanced tangential method.

All these methods are critical to the course length or separation between stations. As the course length increases, their inaccuracies and deviations from each other increase. As the course length decreases, they all become more accurate. On very short course lengths (10 ft or less) there is very little to choose between the methods. For this reason, directionals computed from

continuously measuring devices, such as dipmeter tools, may be more accurate than station reading devices. Dipmeter devices normally compute every 1 or 2 ft although data listings may be accumulated and listed only every 50 ft.

Presentations. Directional data are normally presented both in well sketches and tabulated data. Well sketches include two elements.

1. Planar View. This is a vertical projection of the wellbore path on a horizontal plane. Such a projection shows the separation between the wellbore and the surface location. The wellbore path is marked with measured depths.

2. Vertical Sections. These are of two types. The first is a projection of the wellbore on a vertical plane through the surface location and aligned at various azimuths. The second is plot of depth against closure where closure is the horizontal distance of the wellbore from the surface location. The tabulated data listing will show the measured depth, vertical depth, hole azimuth, deviation angle, x and y distances, and closure distance.

Field Examples. Fig. 53.7 shows a number of presentations of deviation survey computations including: (A) plan view, (B) vertical section, and (C) depth vs. closure. The deviation survey listing is also shown in Table 53.2.

Dipmeter Logging

Introduction

The dipmeter tools are run to determine the direction and angle of formation dip from the survey of one borehole. This information is of obvious importance in the study of structural and stratigraphic problems.⁷

As illustrated in Fig. 53.8, the angle of formation dip is the angle between a horizontal plane and the bedding plane of the formation. The strike of a formation is the direction of the horizontal line formed by the intersection of these two planes. Although strike is a common geologic term (particularly in surface geology), it is more convenient to use "dip azimuth" in discussing the dipmeter. The direction of dip is perpendicular to the strike. In the remainder of this section dip azimuth will be used instead of strike.

Dipmeter tools are in a class by themselves. The technique, the purpose, and the interpretation of dipmeter logs are entirely different from those of other logging tools. The dipmeter's purpose is to measure the dips of formations. To do this, the tool must simultaneously and continuously do two separate jobs: first, it must orient itself in space, normally with respect to magnetic north and vertical, and second, it must react to formation bedding planes.

All present dipmeter tools go about this job in the same way. An inclinometer section supplies continuous measurements of deviation, both the amount and the direction, and of the orientations of the tool's electrode array, either with respect to the borehole direction or magnetic north (a few specialized tools for far north operations use gyroscopic orientation, nominally with true north). At the same time, an electrode array is maintained in contact with the borehole wall by pressured linkages. The electrodes respond to resistivity variations, while the expanding linkages activate a caliper recording.

These pads, normally numbering four, are identical, and so mounted as to remain in a plane normal to the tool axis. When an anomaly is detected by at least three pads, these deflections plus the caliper reading identify three points in what is assumed to be a plane, the plane of deposition of the formation. This identification is then referred to vertical and true north, giving the true dip of the formation.

Recording correct data with a dipmeter tool is a straightforward, more or less mechanical process, though the tools used to do it are some of the most sophisticated in the industry. Interpreting the data draws heavily on computer technology.

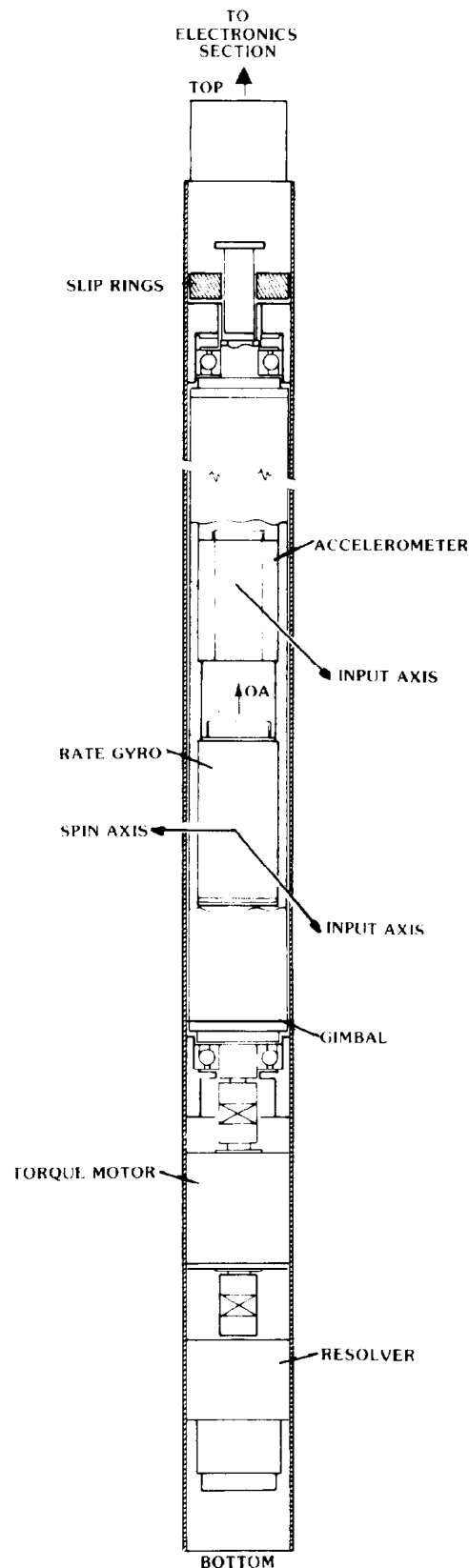


Fig. 53.6—Eastman Whipstock Seeker—1.

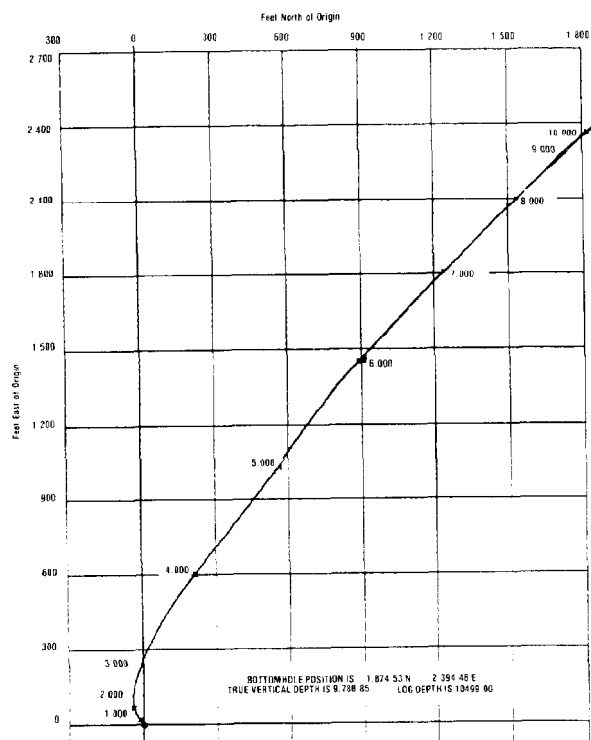


Fig. 53.7A—Deviation survey plan view.

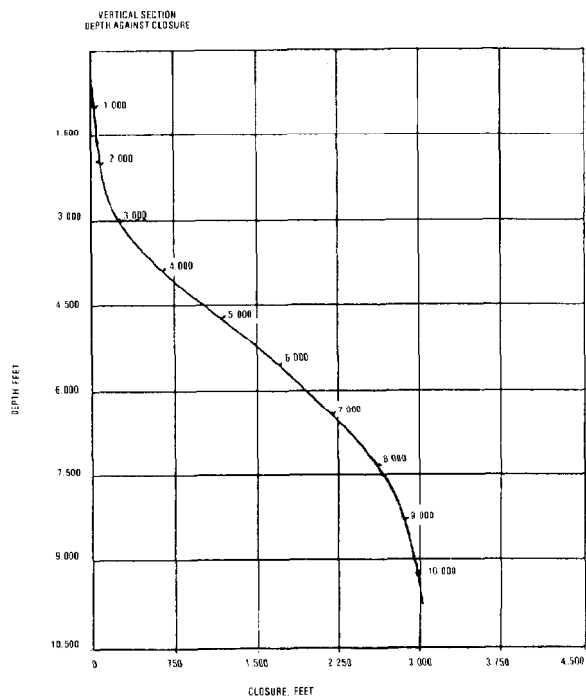


Fig. 53.7C—Deviation survey depth vs. closure.

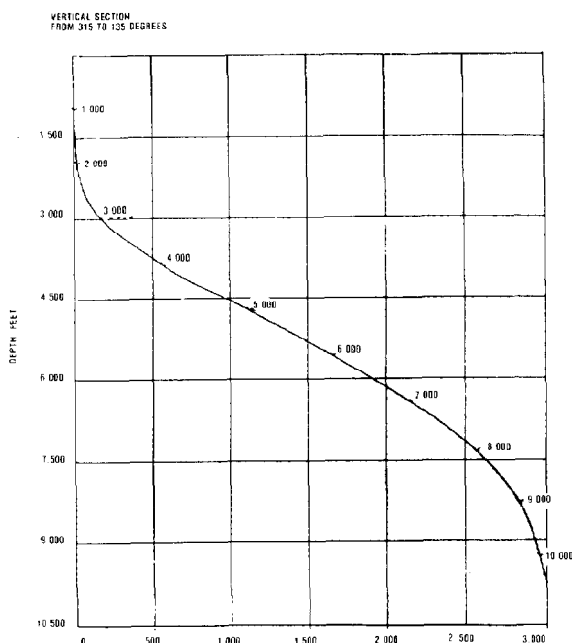


Fig. 53.7B—Deviation survey vertical section.

Tools Available. All major service companies use four-arm dipmeter tools. Fig. 53.9 shows a typical dipmeter tool's mechanical section with the four pads, the electrodes, and the caliper assembly visible. Most of these tools will operate to 20,000 psi and 350°F in holes between 6 and 16 in. in diameter. Different varieties of tools handle low- and high-deviation holes by using different methods of measuring hole deviation and hole azimuth angles. Fig. 53.10 illustrates a monitor log and a computer-answer log.

Calibration. The dipmeter is essentially a physical tool, and its calibration is physical. The inclinometer section is adjusted to read correctly in a special test jig. Special care is given to ensure that the deviation sensor registers zero with the tool held vertical. The operation of the inclinometer is checked before and after each log run, first by allowing the tool to hang vertical in the derrick, then by rotating the tool manually through at least one full revolution.

The calipers are checked as usual, by calibration jigs of known diameter. Four-arm dipmeters record a separate caliper with each opposing pair of pads, which can thus flex independently of each other while remaining in the same plane. Finally, the sensitivity of the electrodes is checked by shorting them out in sequence; this also verifies the correct wiring of the electrode array.

Oil-Base Muds. Dipmeters run in oil-base muds present a special problem. Because the oil-base mud will not connect the resistivity electrodes to the formation electrically it is necessary to use special knife-edge blade

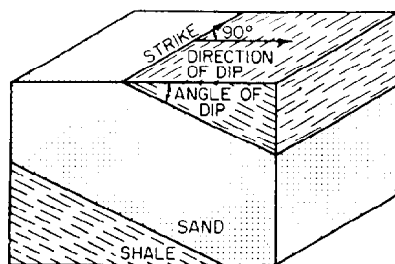


Fig. 53.8—Illustration of dip, strike, and dip azimuth.

electrodes. These blades mechanically cut into the formation and make contact with the water in the formation. This method does not give the quality of data that is obtained with the conventional system in water-base mud. The reason for this is the considerable amount of noise introduced into the resistivity recording caused by the knife blade sliding along the borehole wall. The better the contact made between the knife edge and the formation, the better the quality of the resistivity measurements. Two important things can be done to improve this contact.

1. Make sure that the knife-edge blade is sharp. Demanding new blades is the best way to ensure sharp edges. New blades are also less likely to have electrical insulation problems.

2. Have the logging company dress and adjust their dipmeter tool to apply the maximum arm pressure. This will force the knife edge electrodes into the formation mechanically. This adjustment may be made with different spring mechanisms or by applying greater pad pressure through a hydraulic linkage. Either way this is very important to obtain good resistivity data.

Because the oil-base mud dipmeter is a low-usage tool, the service company should be given maximum notice so they can prepare for the job. All special instructions and stipulations should be given at the same time.

When recording the log, it should be remembered that the final data can be expected to be only 10 to 20% as good as an ordinary dipmeter. Therefore, it is advisable to consider multiple repeats over critical zones. The data usually will be valid only for general structural use so particular attention should be paid to shale zones. All resistivity curves should have good character, although their similarity will not extend down to small details. A slow or dead curve usually indicates a faulty knife-edge electrode. The orientation curves are unchanged from an ordinary dipmeter so the same comments apply to both.

The Computed Dipmeter Log

The computation of dipmeter surveys⁸ requires sophisticated software and a substantial computer. The task requires that the anomalies recorded on the resistivity traces at bed boundaries be correlated and the displacement of each with respect to the others along the borehole be determined. Once this step has been taken then any two pairs of displacements are sufficient to define a plane. Where more than three resistivity curves are recorded, as with most modern dipmeter tools (4-, 6-, and 8-pad tools are in use), then multiple pairs of

TABLE 53.2—DEVIATION SURVEY LISTING*

Measured Depth (ft)	Vertical Depth (ft)	Hole Direction	Deviation Angle (degrees)	North Drift	East Drift	Closure
50.00	50.00	95	0.04	-0.00	0.02	0.02
100.00	100.00	95	0.08	-0.01	0.07	0.07
150.00	150.00	95	0.11	-0.01	0.15	0.15
200.00	200.00	95	0.15	-0.02	0.26	0.26
250.00	250.00	95	0.19	-0.04	0.41	0.41
300.00	300.00	95	0.23	-0.05	0.59	0.59
350.00	350.00	95	0.26	-0.07	0.81	0.81
400.00	400.00	95	0.30	-0.09	1.05	1.06
450.00	450.00	95	0.34	-0.12	1.33	1.34
500.00	500.00	95	0.38	-0.14	1.64	1.65
550.00	550.00	95	0.41	-0.17	1.99	1.99
600.00	599.99	95	0.45	-0.21	2.36	2.37
650.00	649.99	95	0.49	-0.24	2.77	2.78
700.00	699.99	95	0.53	-0.28	3.22	3.23
750.00	749.99	95	0.57	-0.32	3.69	3.71
800.00	799.99	95	0.60	-0.37	4.20	4.22
850.00	849.98	95	0.64	-0.41	4.74	4.76
900.00	899.98	95	0.68	-0.47	5.32	5.34
950.00	949.98	95	0.72	-0.52	5.92	5.95
1,000.00	999.97	95	0.75	-0.57	6.56	6.59
1,050.00	1,049.97	95	0.79	-0.63	7.23	7.26
1,100.00	1,099.96	95	0.83	-0.69	7.94	7.97
1,150.00	1,149.96	95	0.87	-0.76	8.68	8.71
1,200.00	1,199.95	95	0.90	-0.83	9.45	9.48
1,250.00	1,249.94	95	0.94	-0.90	10.25	10.29
1,300.00	1,299.94	95	0.98	-0.97	11.09	11.13
1,350.00	1,349.93	95	1.02	-1.05	11.96	12.00
1,400.00	1,399.92	95	1.06	-1.12	12.86	12.91
1,450.00	1,449.91	95	1.09	-1.21	13.79	13.84
1,500.00	1,499.90	95	1.13	-1.29	14.76	14.82
1,550.00	1,549.89	95	1.17	-1.38	15.76	15.82
1,600.00	1,599.88	95	1.21	-1.47	16.79	16.86
1,650.00	1,649.87	95	1.24	-1.56	17.86	17.93
1,700.00	1,699.86	95	1.28	-1.66	18.96	19.03
1,750.00	1,749.84	95	1.32	-1.76	20.09	20.16
1,800.00	1,799.83	95	1.36	-1.86	21.25	21.33
1,850.00	1,849.82	95	1.40	-1.96	22.45	22.53
1,900.00	1,899.80	95	1.43	-2.07	23.68	23.77
1,950.00	1,949.79	95	1.47	-2.18	24.94	25.03
2,000.00	1,999.77	95	1.51	-2.30	26.23	26.33
2,050.00	2,049.75	95	1.55	-2.41	27.56	27.67
2,100.00	2,099.73	95	1.58	-2.53	28.92	29.03
2,150.00	2,149.71	95	1.62	-2.65	30.32	30.43
2,200.00	2,199.69	95	1.66	-2.78	31.74	31.86
2,250.00	2,249.67	95	1.70	-2.90	33.20	33.33
2,300.00	2,299.65	95	1.73	-3.04	34.69	34.82
2,350.00	2,349.62	95	1.77	-3.17	36.22	36.35
2,400.00	2,399.60	95	1.81	-3.30	37.77	37.92
2,450.00	2,449.57	95	1.85	-3.44	39.36	39.51
2,500.00	2,499.55	95	1.89	-3.59	40.99	41.14
2,550.00	2,549.52	95	1.92	-3.73	42.64	42.80
2,600.00	2,599.49	95	1.96	-3.88	44.33	44.50
2,650.00	2,649.46	95	2.00	-4.03	46.05	46.23
2,700.00	2,699.43	95	2.04	-4.18	47.80	47.99
2,750.00	2,749.40	95	2.07	-4.34	49.59	49.78
2,800.00	2,799.37	95	2.11	-4.50	51.41	51.60
2,850.00	2,849.33	95	2.15	-4.66	53.26	53.46
2,900.00	2,899.29	95	2.19	-4.82	55.14	55.36
2,950.00	2,949.26	95	2.22	-4.99	57.06	57.28
3,000.00	2,999.22	95	2.26	-5.16	59.01	59.24
3,050.00	3,049.18	95	2.30	-5.34	60.99	61.23

*Referenced from RKB = 15 ft, MSL = 0 ft.
Magnetic declination 0.00 degrees west of north.

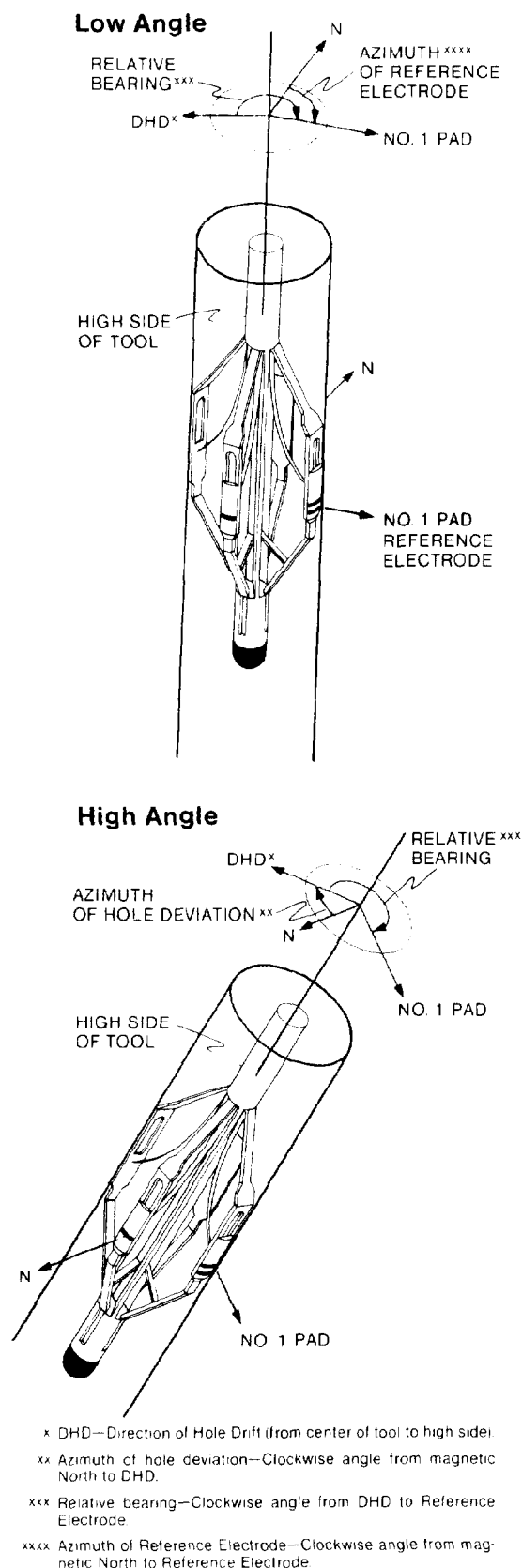


Fig. 53.9—Four-arm dipmeter tool.

displacements may be chosen and multiple apparent bedding planes defined. The correct choice of the most probable bedding plane is determined by the interpretation logic in the dipmeter program. The correlation of one resistivity curve to another is a more mechanical task and is controlled by the interpreter's choice of three parameters—the correlation length, the search angle, and the step length—as illustrated in Fig. 53.11. A short interval of one curve is correlated to a second curve at discrete steps throughout a depth range defined by the search angle. At each step a correlation function is evaluated.

When the value of the correlation function is determined at each step, then a correlogram can be built and a search made for a maximum value. This maximum indicates the displacement of the curve sector defined on the first curve by the correlation interval from a similar section on the second curve. Successive correlations are continued in the same correlation interval with other curves and then in the next correlation interval and so forth.

Once a plane at any point in the well has been defined its orientation relative to vertical and geographic north also must be computed. This requires that the position of the tool in the hole and the deviation and azimuth of the hole itself be known. These data are supplied from the orientation section of the tool.

The dipmeter log, as recorded, is not evaluated easily for quality, so an appraisal of the computed log should be included in dipmeter quality control. A computed dipmeter log may be available on location, if a computer logging unit is available, but it is normal to wait for days or even weeks for the results if processing is done at a central computer office.

Working with the computed log, look for two distinct defects: undetected problems with the recorded data and problems with the computation. A computed dipmeter should model real-life geology; if it seems not to do that, an investigation is in order. If the problem is in the computation, it normally can be solved by repeating the computation job. Even if the problem is with log measurements, the logging company's computer experts often can solve it by special handling.

Application of Dipmeter and Directional Data

Dipmeter Patterns. Once a dipmeter log has been run and computed then the results have to be interpreted in the light of known geological and geophysical facts. In general dipmeter results are used to find gross structural features, fine stratigraphic features, and true vertical and true stratigraphic thicknesses.

The most common method of representing computed dipmeter results is by an "arrow" or "tadpole" plot. A series of special characters is plotted as a function of depth with their origin indicating the dip magnitude and a short line indicating the dip azimuth, as illustrated in Fig. 53.12A. For the purpose of reference the uphole direction on the plot is considered north and the clockwise direction the short line points from its base is the dip azimuth angle. When viewed together as patterns, these dip vectors or "tadpoles" can be interpreted in terms of gross geological structure or sedimentary detail as illustrated in Fig. 53.12B.

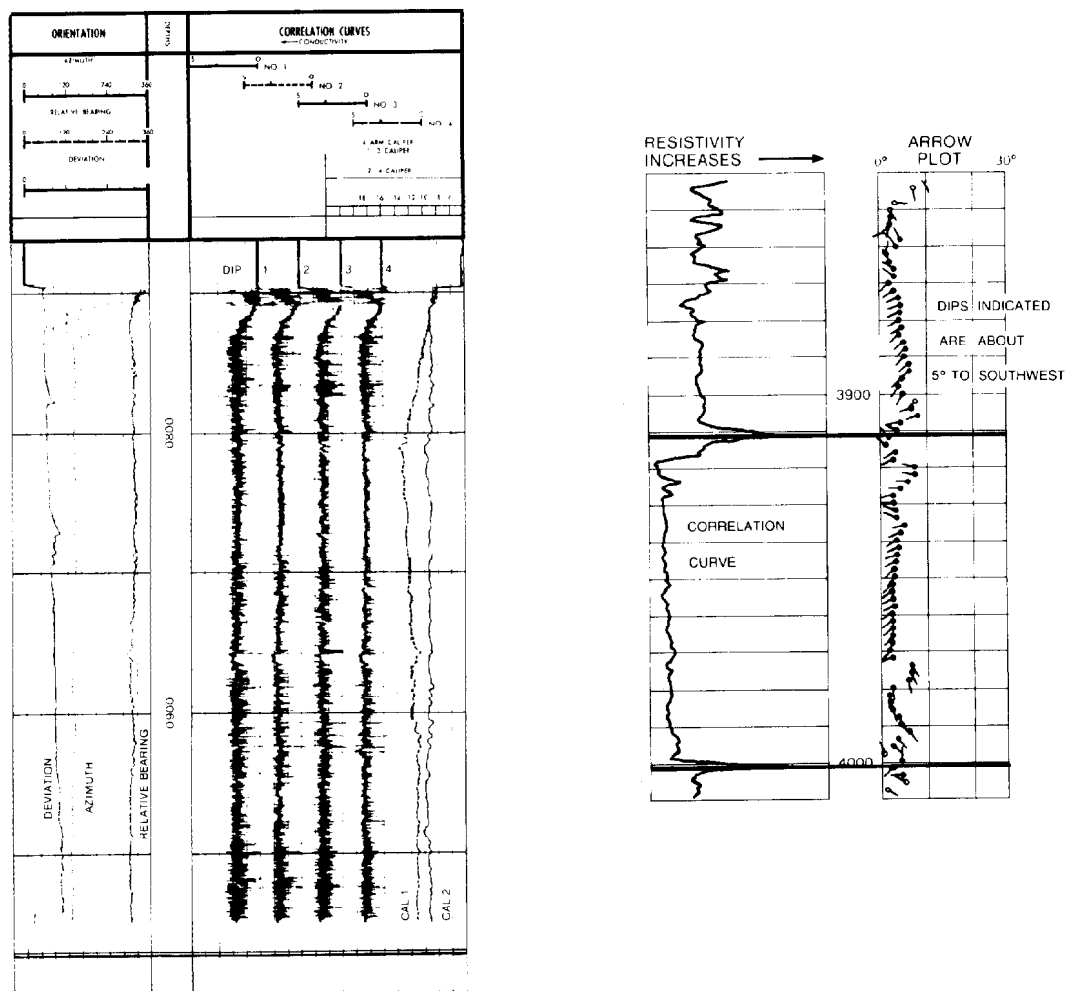


Fig. 53.10—Dipmeter monitor log and computed dipmeter log.

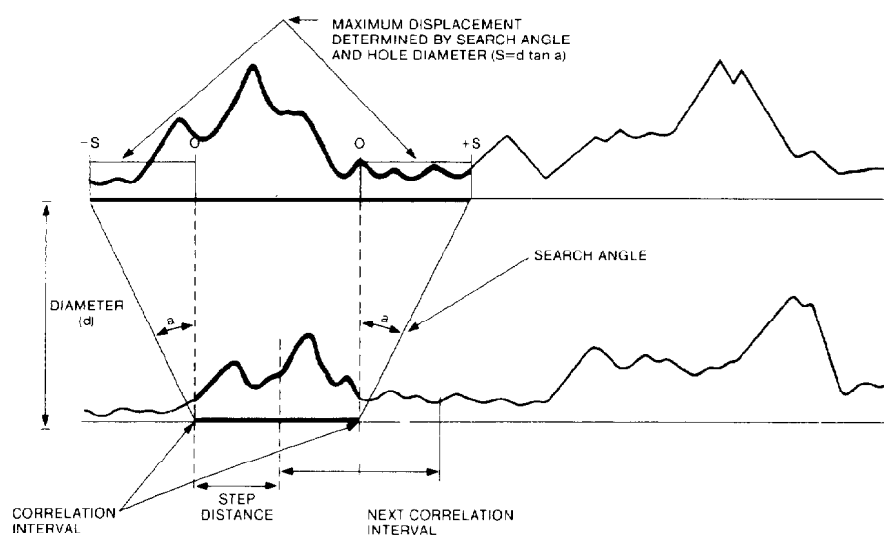


Fig. 53.11—Dipmeter computation terms "correlation interval," "step," and "search."

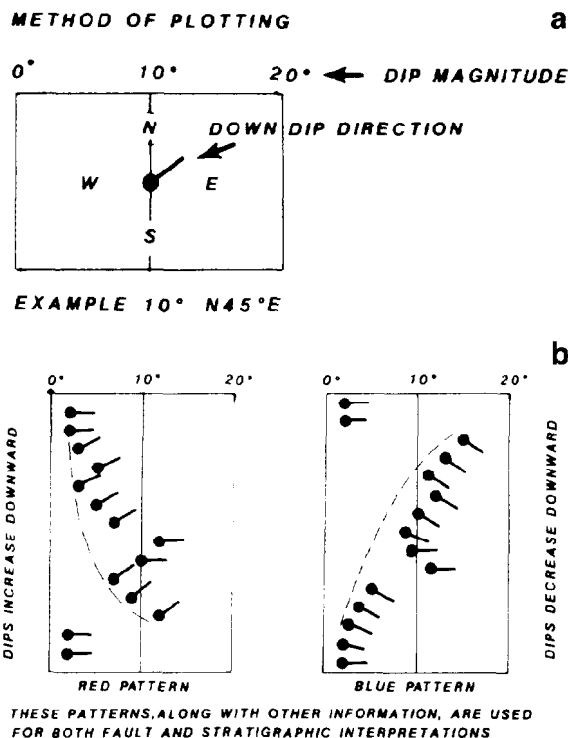


Fig. 53.12—Dipmeter interpretation rules showing (a) method of plotting dips and (b) patterns of dips.

Fig. 53.13 shows three common structures: a folded structure (anticline), an unconformity, and a normal fault. Fig. 53.14 shows three common sedimentary features: a channel cut and fill, a buried bar with shale drape, and current bedding.

Other complex patterns may develop, such as those related to: (1) missing and repeat sections (Fig. 53.15A), (2) stratigraphy of continental deposits (Fig. 53.15B), (3) stratigraphy of continental shelf deltas (Fig. 53.15C), (4) stratigraphy of continental shelf tide/wave-dominated deposits (Figs. 53.15D and E), and (5) continental slope and abyssal environments (Fig. 53.15F). Other forms of representing dip data are also used to good effect, such as polar and stereographic plots and azimuth frequency diagrams.

One of the main uses for dip data as far as the reservoir engineer is concerned is in computation of reservoir volumes, which require true vertical thickness measurements (TVT). For the geologist a related measure, the true stratigraphic thickness (TST) is of immediate concern.⁹⁻¹³

In the simple case where the wells are vertical and the bedding is horizontal, correlations can be made directly between logs of neighboring wells. Reservoir volume is calculated by multiplying reservoir thickness (directly derived from the logs) by reservoir area (delimited by other means).

However, this simple case is exceptional because (1) most reservoirs exist as the result of some structural event or accident, implying some formation dip at least at the reservoir periphery, and (2) most wells deviate to some extent from vertical, intentionally or not. As long

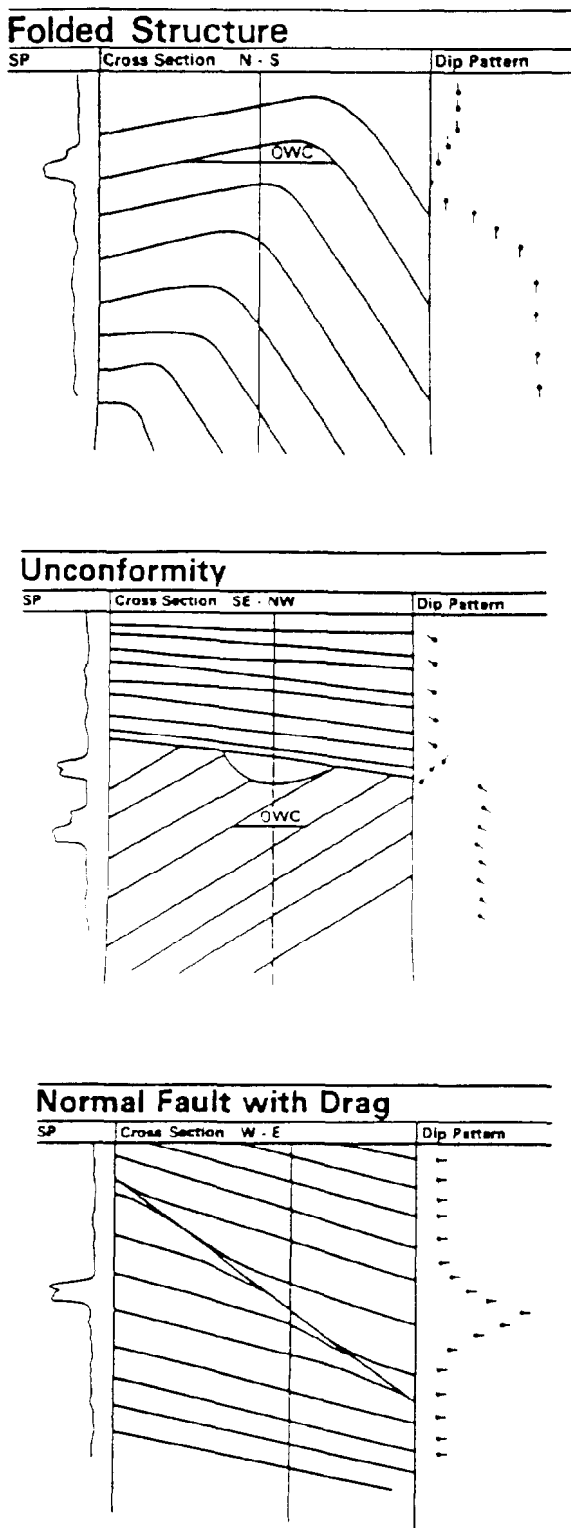


Fig. 53.13—Common geologic structures and corresponding dipmeter patterns.

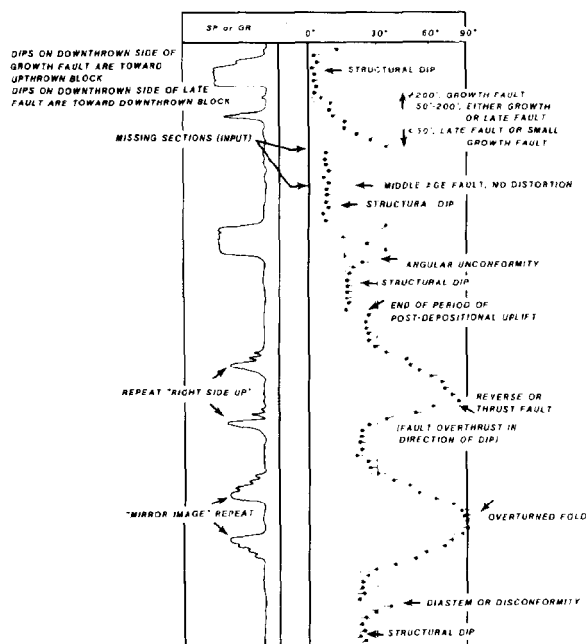
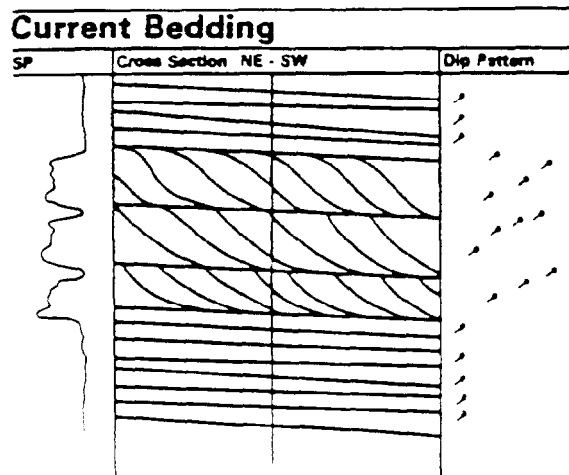
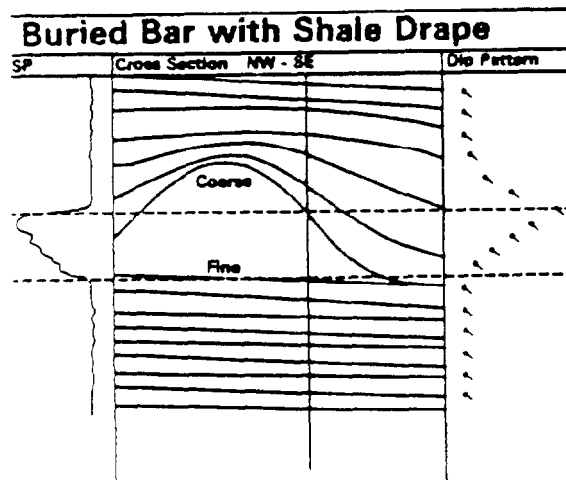
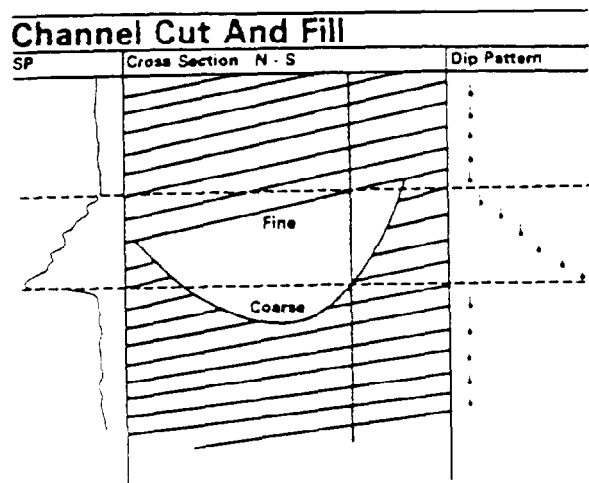


Fig. 53.15A—Missing and repeat sections.

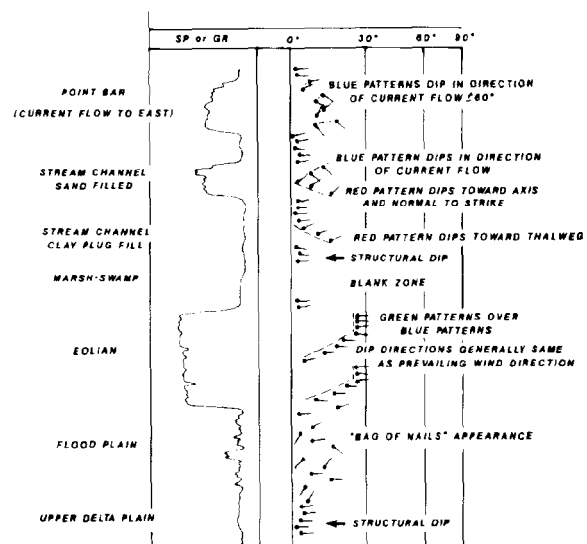


Fig. 53.15B—Stratigraphic interpretation, continental environment.

Fig. 53.14—Dipmeter patterns in sedimentary features.

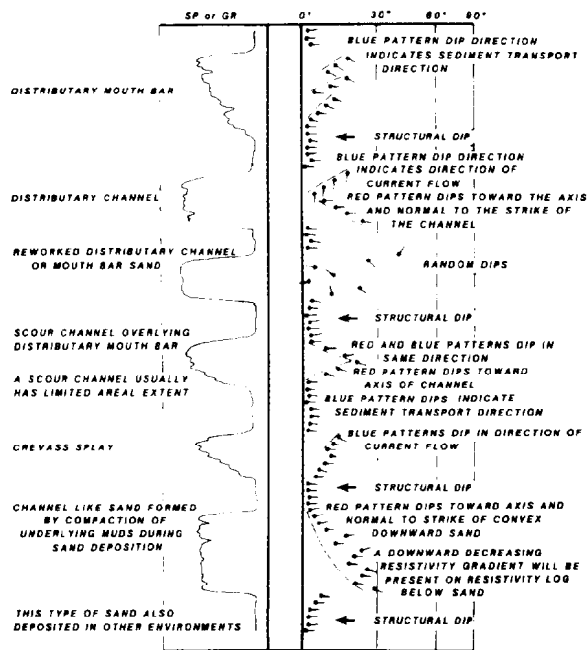


Fig. 53.15C—Stratigraphic interpretation, continental shelf, delta dominated.

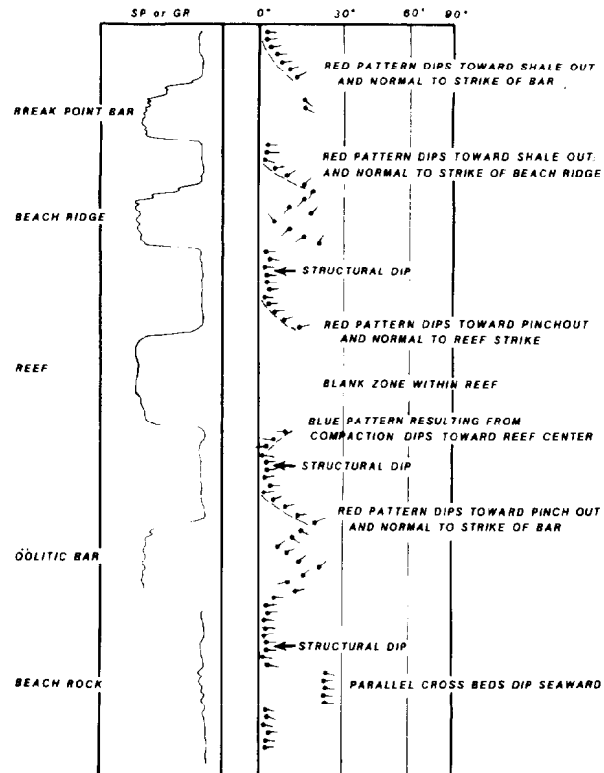


Fig. 53.15D—Stratigraphic interpretation, continental shelf, tidal wave dominated.

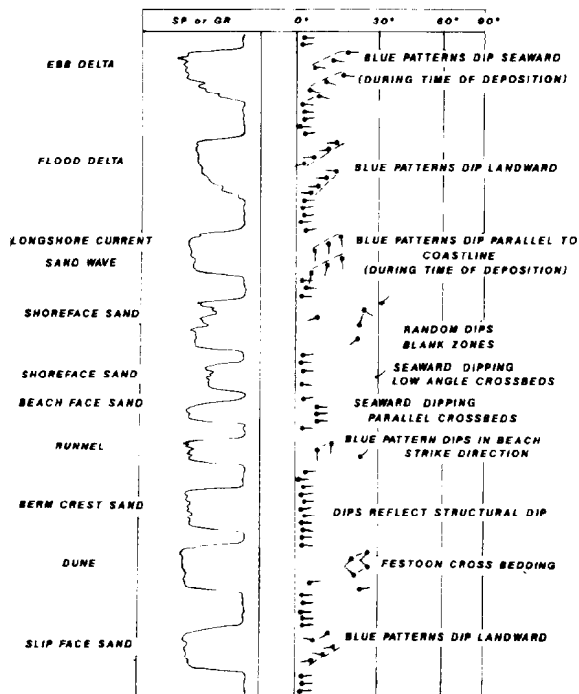


Fig. 53.15E—Stratigraphic interpretation, continental shelf, tidal wave dominated.

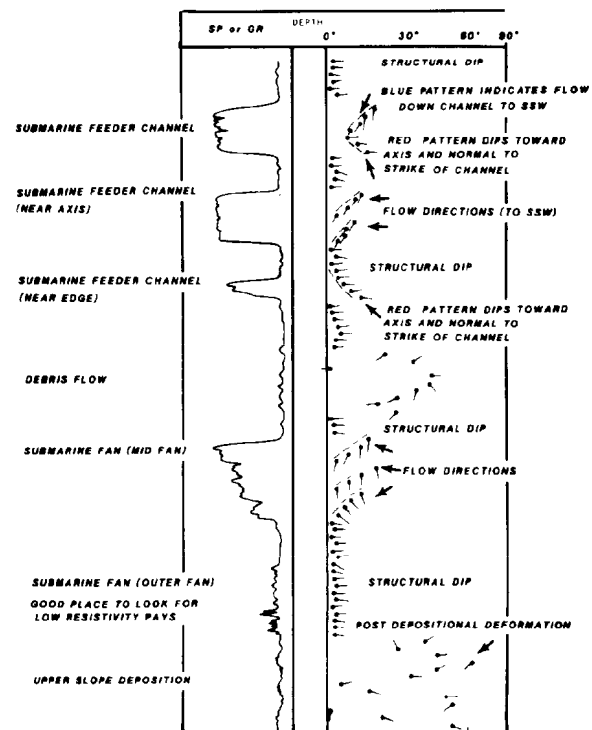


Fig. 53.15F—Continental slope and abyssal environments.

as dips and deviations do not exceed a few degrees, the simple vertical-horizontal case is approximated closely enough not to need corrections. But when deviations and dips exceed about 10 degrees, corrections are needed because apparent formation thicknesses measured on logs are greater than true stratigraphic thicknesses by different amounts in different wells. This adds to the difficulty of well-to-well log correlation. Also, if wells are deviated from vertical, and if formations have substantial dip, apparent thicknesses differ from the vertical thicknesses needed for reservoir volume calculation, and must be corrected.

To achieve these corrections in a convenient manner, modern data processing affords three different computed log products: the true vertical depth (TVD), TST, and TVT plots. Proper interpretation of these plots requires considerable caution and may be quite difficult.

Common Principles of TVD, TST, and TVT Plots.

Figs. 53.16 through 53.18 illustrate the principles of thickness transformations. Formation parameters recorded by logging tools are reproduced without alteration, but their depths are altered to suit respective purposes. Depths should be thought of as summations of overlying formation thicknesses.

Two methods exist for computation of altered depths: (1) *common surface point*, which assumes a hole drilled from the same surface point or formation top with a different course, and (2) *common subsurface point*, which assumes a hole drilled either vertically, or normal to the bed dip, from some point in the actual well course, such as a formation top, or a point of formation dip change. Depths may be reset arbitrarily at the common point. In this approach it is set to zero, thus representing only thickness as counted down from the common point.

TVD Plot. This plot ignores formation dip and corrects for well deviation only. Thus, it represents formations as they would look in a vertically drilled well, provided the formations had zero dip. It is useful in areas of directional drilling where dip is low, for well-to-well correlations, and for reservoir volume calculations. It usually is run only in the common surface point mode.

TST Plot. This plot accounts for formation dip, and requires knowledge of true well course, whether vertical or not. It displays formations as though the well had been drilled perpendicular to them. If a change of dip occurs, an equal and opposite change of deviation is assumed.

If only one dip is present, the plot represents the logs that would have been obtained if the well had been drilled at the same location perpendicular to that dip. If more than one dip is present, the interpretation becomes more complicated. At each dip change, some stratigraphic column must either disappear, or thin, or thicken, or even repeat itself.

TVT Plot. This plot is closely related to the TST, and as such accounts for both well deviation and formation dip. It shows formation thickness as though the well had been drilled vertically through the dipping beds. Evidently, a TVT in a vertical hole would be identical to the original log. The TVT is meant to be used for reservoir volume calculations from deviated hole logs.

Reductions in Special Cases. If the well is vertical and the formations are horizontal, all three transformed logs would be identical to the original log, and the processing

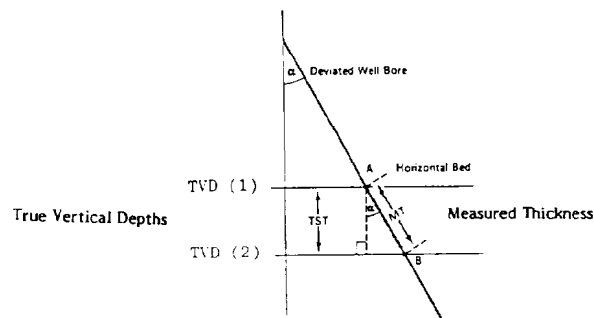


Fig. 53.16—Principle of true vertical depth (TVD).

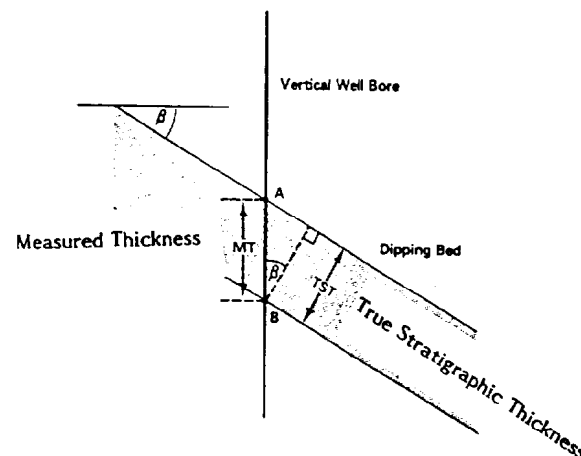


Fig. 53.17—Principle of true stratigraphic thickness (TST).

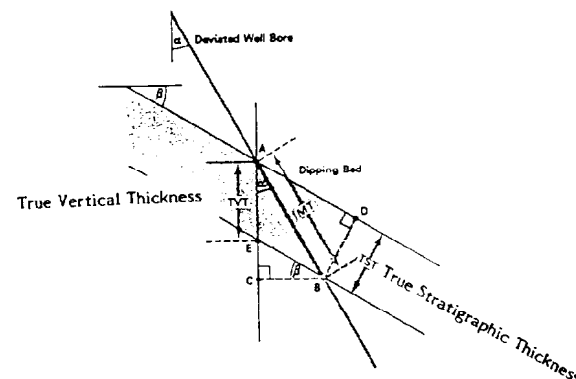


Fig. 53.18—Principle of true vertical thickness (TVT).

would be a waste of computer time. If the well is deviated and the formations are horizontal, the TST and the TVT are identical to the TVD, and running the latter is sufficient. If the well is vertical and the formations dip, the TVD and TVT plots would be wasted computer time, but the TST may be useful in well-to-well correlations. If the well is drilled perpendicular to the formation dip (as it often tends to be in hard rocks in particular) the TST would be a waste of computer time, but the TVT is needed for reservoir calculations, and the TVD may be of use if deviation is pronounced.

Algorithms. The algorithms used for computing the TVD, TST, and TVT have been covered well in the literature.¹⁴ Any implementation of these algorithms for computer applications should be approached with caution. Many programming languages differ in their treatment of trigonometric functions for angles exceeding 90°. Another area requiring care is in the matter of precision. When depth data are processed, a repetitive accumulation of depth increments is made. As many as 10⁴ or more additions must be made in a normal well. Thus the precision of each increment must be at least one part in 10⁶ or better. Depending on the computer used (16 bit, 32 bit, etc.) the programming of these algorithms should demand appropriate precision.

By way of summary, all three plots perform valuable functions, but all three may be misleading if not used with the proper caution, in particular with respect to absolute depths.

1. The TVD is incorrect in both formation thicknesses and in absolute depths if formations have appreciable dip.

2. The TST is always correct in formation thicknesses. It should be run in the common subsurface point mode. If changes of dips are present, it should reset the subsurface point at each change of dip and make independent plots through each dip zone. This resetting may be made automatically if the program allows it, and manually otherwise.

3. The TVT may produce apparent thicknesses greater than measured thicknesses. Such thicknesses may be fictitious when beds are truncated in their vertical extension by unconformities or faults. It should be run in independent sections for each change of dip, in the common subsurface point mode, as for the TST.

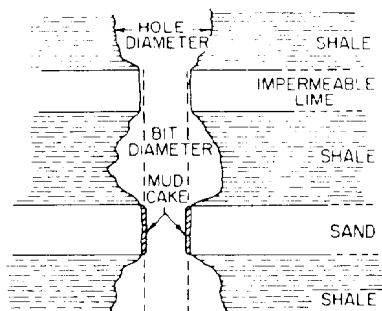


Fig. 53.19—A typical borehole.

Caliper Logs

Introduction

The caliper log measures the diameter of the borehole. The first caliper logs were developed to determine borehole size in holes shot with nitroglycerin. These early logs showed large variations in hole size even in the portions of the hole that had not been shot. This illustrated the need for the caliper log over the entire hole.

Methods of Recording

Several types of caliper are currently in use. One type consists of three or four spring-driven arms, which contact the wall of the borehole. The instrument is lowered to the total depth (TD), and the arms are released either mechanically or electrically. The spring tension against the arms centers the tool in the well. The arms move in and out with the change in wellbore diameter. The arm motion is transmitted to a rheostat so that change in the resistance of an electric circuit is proportional to the hole diameter. The borehole diameter is recorded at the surface by measuring the potential across this resistance.

Another instrument uses three flexible springs, which contact the wall of the borehole. These springs are connected to a plunger that moves up or down as the springs expand or contract with changes in borehole diameter. The plunger passes through two coils. When an alternating current is passed through one coil, an electromotive force (EMF) is induced in the other coil. The amount of this induced EMF is a function of the plunger position and is proportional to borehole diameter. Either of the preceding instruments may be adjusted so that they will record borehole area rather than hole diameter. If the caliper log is used to determine hole volume, area should be recorded on a linear scale. If the caliper log is used to determine hole configuration, the hole diameter is recorded on a linear scale.

A third type of caliper log is the microcaliper, which is discussed in connection with the electrical-log microdevices. This instrument uses two pads rather than arms or flexible springs. Hole diameter is determined by the movement of these pads, which are held against the borehole wall by springs.

Typical Borehole Configuration

A schematic of a typical borehole is shown in Fig. 53.19. As illustrated in this figure, some formations cave considerably, causing enlarged holes. Other formations do not cave, and because of the presence of mudcake, the hole size actually may be reduced to less than bit size. Although not illustrated in Fig. 53.19, some formations may swell, causing reduction in hole size.

The primary cause of formation caving is the action of the drilling fluid. Action of the bit and the drillpipe also have an effect. Most drilling muds are composed primarily of water. The chemical action of this water on shales (hydration of the shales) causes many shales to disintegrate and slough into the hole. The amount and rate of this sloughing depend on the nature of the mud and shale. Other shales (heaving shales) swell rather than disintegrate.

If a freshwater mud is used to drill a salt section, it will dissolve salt until the mud becomes salt-saturated. The drilling fluid does not react with formations such as

limestone, dolomite, and sandstone. However, if those formations are permeable, a mudcake will be formed, as illustrated in Fig. 53.19. This mudcake forms rapidly. The character (density and thickness) of the mudcake varies with the mud used to drill the well. Of course, thickness of the mudcake is limited by erosion of the drilling fluid while circulating.

In some areas the shallow portion of the hole is drilled with water. If loosely cemented sands are encountered, they may cave under this condition.

The action of the bit is probably not too important. But if a thin sand is surrounded by shales that have caved, the bit probably knocks off part of the sand ledge with each round trip.

Action of the drillpipe against the side of the hole causes some enlargement even in sandstones and limestone. Usually this enlargement is not great enough to affect hole volume appreciably, but it may cause the drillpipe to become differentially pressure stuck, necessitating a fishing job. Formation wear by the drillpipe will cause the hole to be noncylindrical, in which case a four-arm caliper will display the long and short axes of the hole.

Interpretation and Application of Caliper Logs

Caliper logs usually are recorded on vertical scales from 1 in.=100 ft to 5 in.=100 ft. The horizontal scale is selected to show a detail picture of hole diameter and is usually on the order of 1 in.=4 in. Because of the difference in scales, it is easy to get the impression from caliper logs that tremendous cavities are created. When plotted on the same horizontal and vertical scales, it is evident that the normal borehole is quite regular. This should be remembered when using the caliper log.

The primary uses of the caliper log are: (1) to compute hole volume to determine the amount of cement needed to fill up to a certain depth, (2) to determine hole diameter accurately for use in interpreting other logs, and (3) to locate permeable zones as evidenced by the presence of a filter cake. Other applications of the caliper log include proper location of casing centralizers, and packer seats for openhole drillstem tests.

Caliper logs are also available in conjunction with hole deviation and hole azimuth measurements, in which case the log is referred to as a borehole geometry log.

Fig. 53.20 is an example of a borehole geometry log using a standard three-track presentation. The borehole orientation is displayed in Track 1, while the two independent orthogonal caliper readings are recorded in Track 2 with a standard scaling. The caliper data are also available in Track 3 but with a reduced sensitivity. Together with the bit size and future casing size, this visual display, enhanced by the shading between the calipers and the bit size, quickly gives a clear impression of the borehole shape. Within the depth track the total hole volume integration is recorded along the edge of Track 1, and the cement volume (the difference between the total hole volume and the future casing volume) is presented along the edge of Track 2.

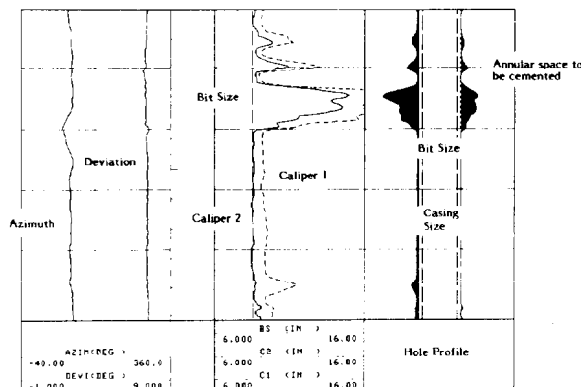


Fig. 53.20—Borehole geometry log.

Casing Inspection Logs

Introduction

Inspection of the mechanical state of the completion string is an important aspect of production logging. Many production (or injection) problems can be traced back to mechanical damage to, or corrosion of, the completion string. A number of casing inspection methods are available including: (1) multifingered caliper logs, (2) electrical potential logs, (3) electromagnetic inspection devices, and (4) borehole televewers or borehole TV. Of these the majority measure the extent to which corrosion has taken place. Only the electrical potential log may indicate where corrosion is currently occurring. With the exception of the caliper logs, all the devices require that the tubing be pulled before running the survey, since most are designed to inspect casing rather than tubing, and all are large-diameter tools.

Caliper Logs for Tubing and Casing Inspection

Various arrangements of caliper mechanisms are available to gauge the internal shape of a casing or tubing string. Fig. 53.21 illustrates three such tools. Table 53.3 lists the various sizes available, their respective number of feelers, and the appropriate casing size.

Tubing Profile Calipers. Tubing profile calipers will determine the extent of wear and corrosion, and will detect holes in the tubing string—all in a single run into the well. The large number of feelers on each size of caliper ensures detection of even very small irregularities in the tubing wall.

In pumping wells, the tubing caliper log may be run by one person and there is no need for a pulling unit crew to be present. A "pull sheet" showing the maximum percentage of wall loss of every joint of tubing in the well may be prepared. Before the well is pulled, a program of rearranging the tubing string can be provided. Moving partially worn joints nearer the surface and discarding thin-wall joints substantially prolongs the effective life of tubing strings and reduces pulling costs in pumping wells. In flowing or gas lift wells, the tubing profile caliper provides an economical method to check

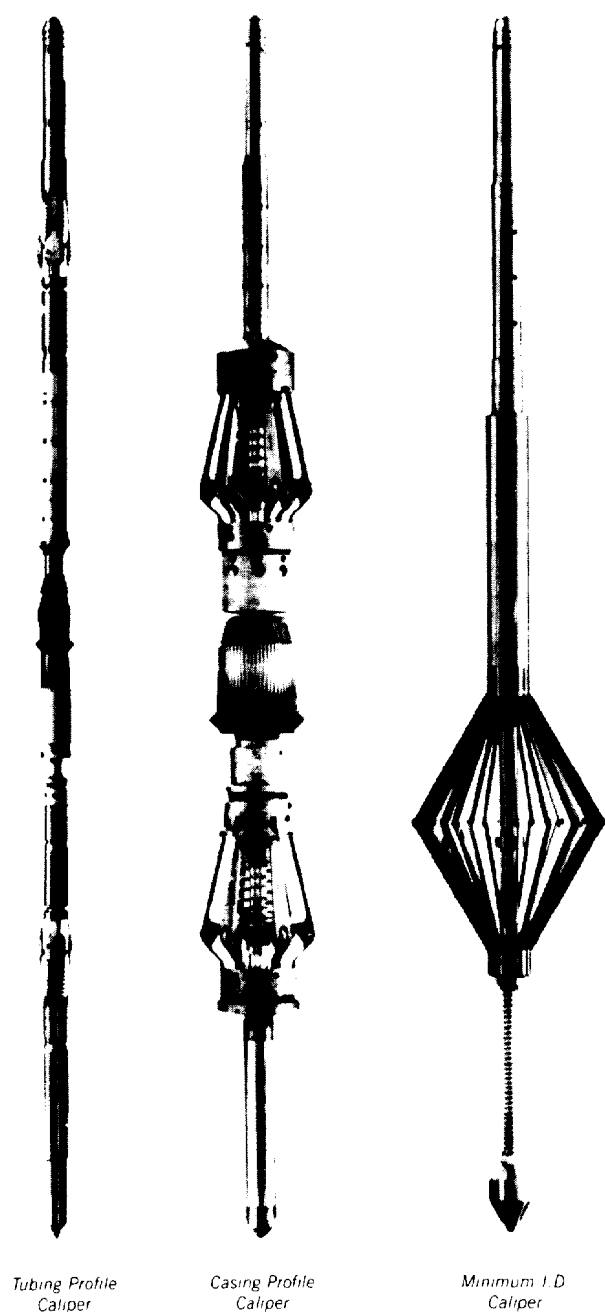


Fig. 53.21—Casing and tubing profile caliper tools.

TABLE 53.3—TUBING AND CASING PROFILE CALIPERS

Sizes of Tubing Profile Calipers

Tool Diameter (in.)	Number of Feelers	OD (in.)
1½	20	2
1½	20	2¼
1¾	26	2¾
2⅞	32	2⅞
2⅞	44	3½
3⅞	44	4

Sizes of Casing Profile Calipers

3⅞	40	4½ to 6
5⅞	64	6⅞ to 7⅞
7¼	64	8⅞ to 9
7¾	64	9⅞
8¼	64	10¾
9⅞	64	11¾
11⅞	64	13¾
13⅞	64	16
17⅞	64	20

periodically for corrosion damage, to monitor the effectiveness of a corrosion inhibitor program, or to detect and remove damaged tubing joints when working over a well.

Split Detector. This is an accessory tool that may be run in combination with the tubing profile caliper. This tool, functioning much like a magnetic collar locator, is designed to detect and log vertical splits or hairline cracks in the tubing that might be difficult to locate with the profile caliper. In practice, the split detector is used to log down the tubing, and the profile caliper to log up the tubing. This gives a complete inspection for wall thickness and splits in one run of the cable in the well.

Casing Profile Calipers. Casing profile calipers are available to log 4½-in.- through 20-in.-OD casing. The tool is especially valuable where drilling operations have been carried on for an extended period of time through a string of casing. The determination of casing wear is of great importance when deciding if a liner can be hung safely, or if a full production string is required. In producing wells, the casing profile caliper will locate holes or areas of corrosion that may require remedial work. The tool is also valuable when abandoning wells because it permits grading of casing to be salvaged before it is pulled.

Casing Minimum-ID Calipers. The minimum-ID caliper can pass through and accurately measure restrictions as small as 3⅞ in. in casing with a nominal ID up to 13¾ in. This log is of particular value in determining areas of collapsed or deformed casing, identifying casing-weight change intervals, or detecting parted casing.

Examples of these logs are given in Fig. 53.22.

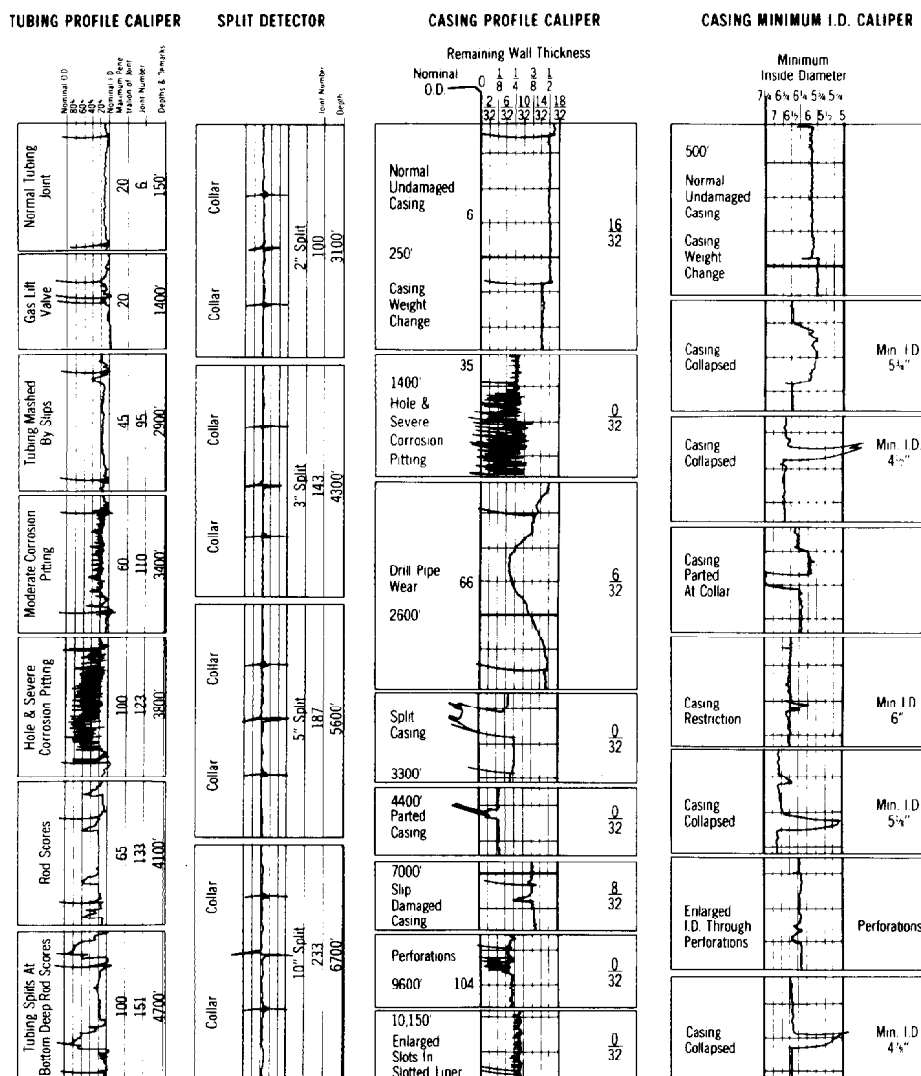


Fig. 53.22—Tubing and casing profile logs.

Electrical Potential Logs

An electrical potential log determines the galvanic current flow entering or leaving the casing. This will indicate not only where corrosion is taking place and the amount of iron being lost, but also where cathodic protection will be effective. The magnitude and direction of the current within and external to the casing is derived mathematically from electrical potential measurements made at fixed intervals throughout the casing string. To achieve reliable results from this kind of survey, the borehole fluid must be an electrical insulator (i.e., the hole must be either empty or filled with oil or gas). Mud or other aqueous solutions will provide a "short" that invalidates the measurements. The log itself is a recording vs. depth of the small galvanic voltages detected. Fig. 53.23 illustrates such a log with three different runs recorded, each with a differing level of cathodic protection applied to the casing.

Figs. 53.24 and 53.25 show an interpretation of casing potential profile logs run both with and without cathodic

protection. Note that in Fig. 53.25 the metal loss has been reduced to practically zero by the application of an appropriate cathodic protection.

Electromagnetic Devices

The most commonly used casing corrosion inspection tools are of the electromagnetic type. They come in two versions, those that attempt to measure the remaining metal thickness in a casing string¹⁵ and those that try to detect defects in the inner or outer wall of the casing.¹⁶ Although frequently run together, these tools will be discussed separately.

Electromagnetic Thickness Tools. The electromagnetic thickness tools are available under a variety of trade names such as ETT (Schlumberger), Magnelog (Dresser), and Electronic Casing Caliper Log (McCullough). They operate in a manner similar to openhole induction tools. Each consists of a transmitter coil and a receiver coil. An AC is sent through the transmitter coil.

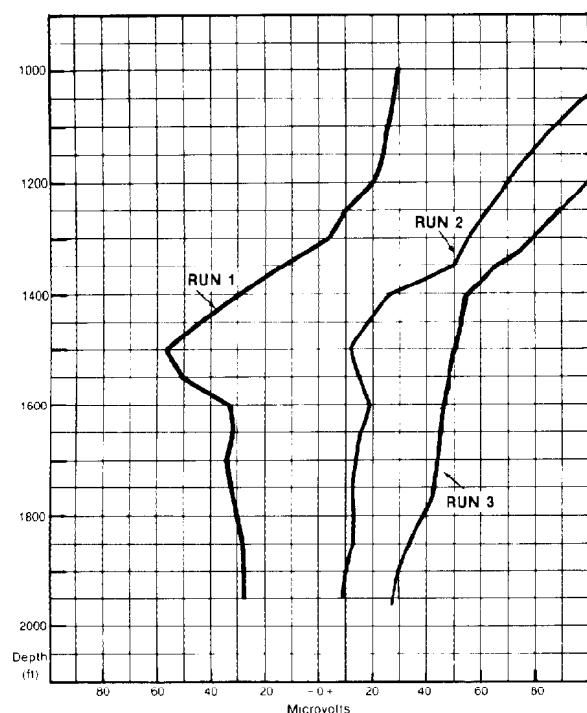


Fig. 53.23—Casing potential profile.

This sets up an alternating magnetic field, which interacts both with the casing and the receiver coil (see Fig. 53.26). The coils are spaced about three casing diameters apart to ensure that the flux lines sensed by the receiver coil are those that have passed through the casing.

The signal induced in the receiver coil will be out of phase with the transmitted signal. In general the phase difference is controlled by the thickness of the casing wall. Thus the raw log measurement is one of phase lag in degrees and the log is scaled in degrees. Fig. 53.27 illustrates an ETT log in severely corroded casing. Note that an increasing thickness corresponds to an increase in the phase shift angle and vice-versa. Some presentations of this log show a rescaling in terms of actual pipe thickness. This requires that the operator make some calibration readings in the type of casing present in the well. It is quite common to see quite large differences in thickness between adjacent stands resulting from a number of variables, such as the drift diameter of the pipe, the weight per foot, the magnetic relative permeability of the steel used, etc.

The ETT-type tool is good at finding vertical splits in pipe, since the magnetic flux lines pass perpendicular to the casing wall. A horizontal circumferential anomaly is less well defined.

Eddy Current and Flux leakage Tools (Pipe Analysis Log). Another closely related measurement uses a slightly different technique and forms the basis of the Pipe Analysis Log (PAL).¹⁶ Two electromagnetic measurements are of interest in the context of the pipe analysis tool—magnetic flux leakage and eddy current distortion.¹⁷

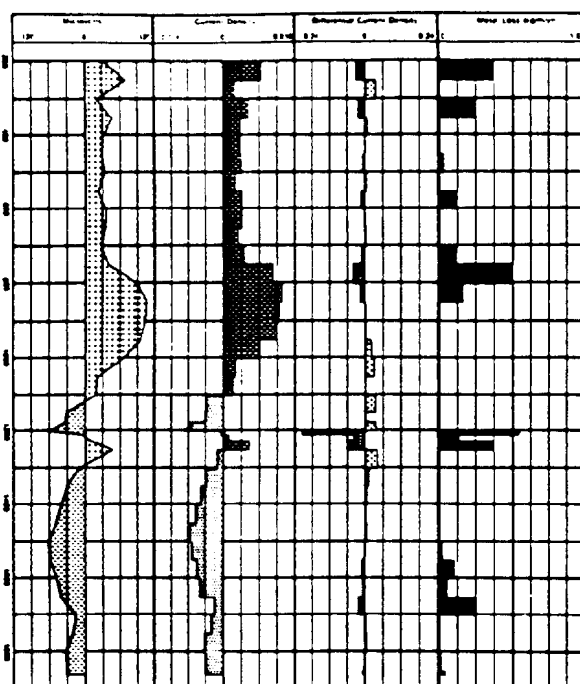


Fig. 53.24—Casing potential profile analysis—without cathodic protection.

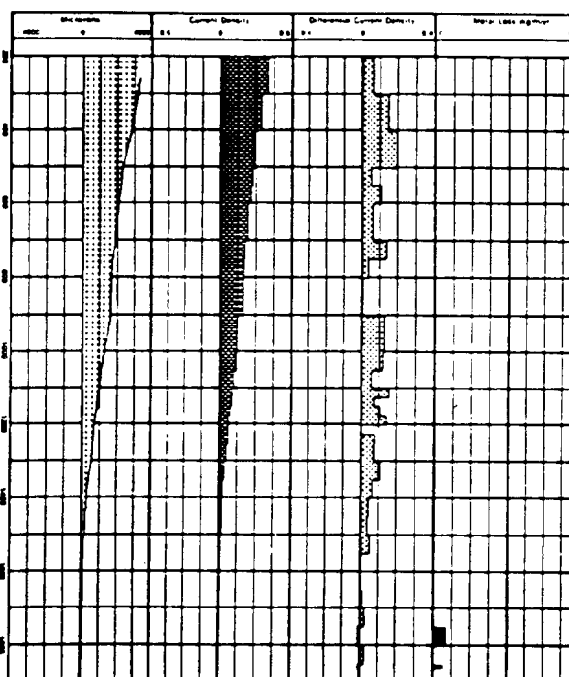


Fig. 53.25—Casing potential profile—with cathodic protection.

Flux leakage. If the poles of a magnet are positioned near a sheet of steel, magnetic flux will flow through the sheet (Fig. 53.28). So long as the metal has no flaws the flux lines will be parallel to the surface. However, at the location of a cavity either on the surface of the sheet or inside it, the uniform flux pattern will be distorted. The flux lines will move away from the surface of the steel at the location of the anomaly, an effect known as flux leakage. The amount of flux distortion will depend on the size of the defect. If a coil is moved at a constant speed along the direction of magnetic flux parallel to the metal sheet, a voltage will be induced in the coil as it passes through the area of flux leakage. The larger the anomaly, the greater the flux leakage and, therefore, the greater the voltage. The magnetic flux is distorted on both faces of the sheet, regardless of the location of the

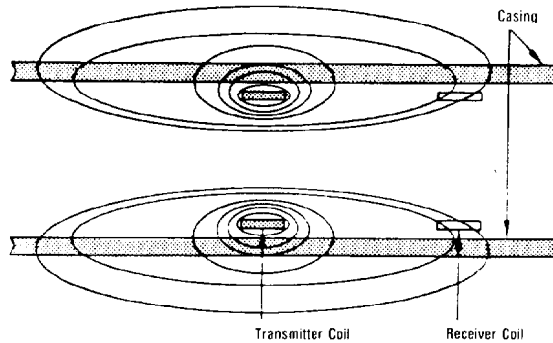


Fig. 53.26— Electromagnetic thickness tool.

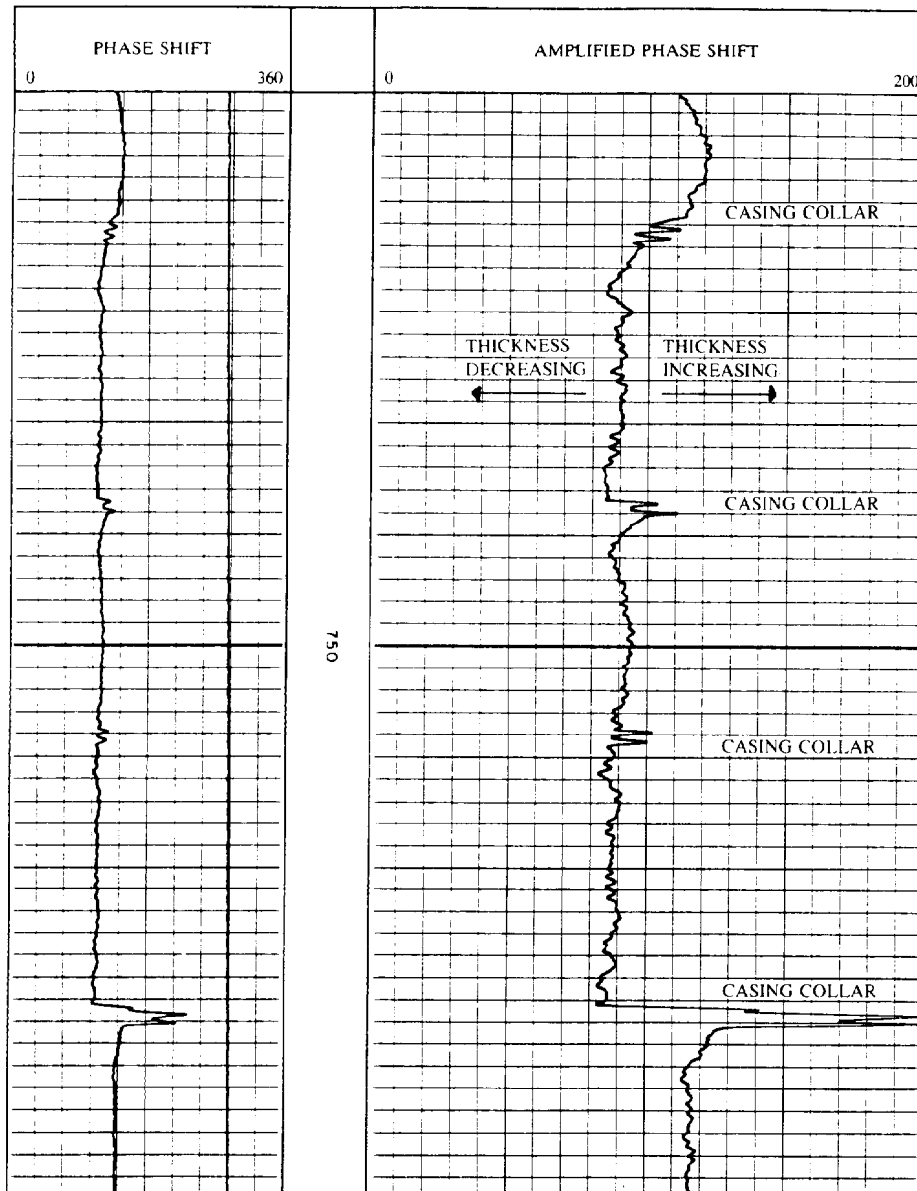


Fig. 53.27— Electromagnetic thickness log.

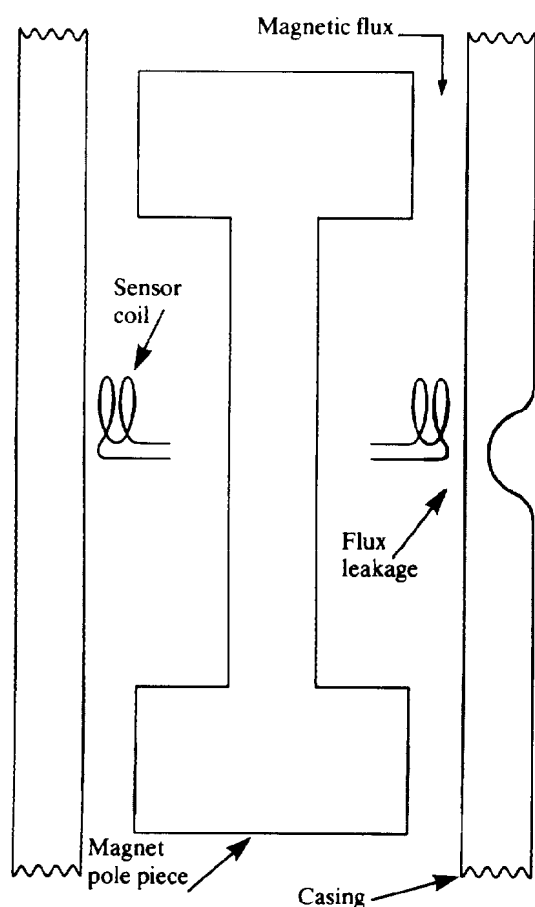


Fig. 53.28—Magnetic flux leakage principle.

defect, and therefore the coil needs to be moved along only one surface to survey the sheet completely. Since the coil must be moved through a changing magnetic flux to produce a voltage, no signal is generated when it is moved parallel to the surface of an undamaged sheet of steel.

Eddy Currents. When relatively high frequency AC is applied to a coil close to a sheet of steel, the resulting magnetic field induces eddy currents in the steel (Fig. 53.29). These eddy currents, in turn, produce a magnetic field that tends to cancel the original field, and the total magnetic field is the vector sum of the two fields. A measure voltage would be induced in a sensor (receiver) coil situated in the magnetic field. The generation of eddy currents is, at relatively high frequencies, a near-surface effect. Therefore, if the surface of the steel adjacent to the coil is damaged then the magnitude of the eddy currents will be reduced, and, consequently, the total magnetic field will be increased. This will result in a variation in the sensor coil voltage. A flaw in the sheet of metal on the surface away from the coils will not be detected and, depending on its distance from the surface, a cavity within the sheet will not influence the eddy currents either.

Tool Principle. The measuring sonde consists of an iron core with the pole pieces of an electromagnet at each end, and 12 sensor pads in two arrays between the pole pieces (Fig. 53.30). The two arrays are offset radially to ensure complete coverage of the inner surface of the casing. Each of the pads contains a transmitting coil (for the eddy current measurement) and two sensor coils wound in opposite directions (for both the flux leakage and eddy current measurements). The two sensor coils are wound in opposite directions so that for both measurements

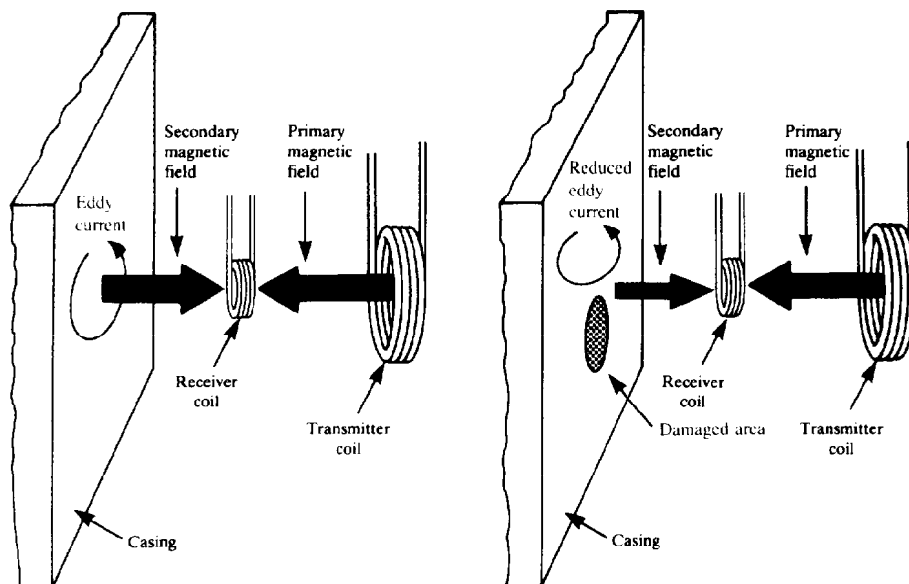


Fig. 53.29—Eddy current principle.

there is zero voltage as long as no anomaly exists, but a signal will be produced when the quality of the casing is different below the two coils. The same sensor coils can be used for both measurements since two distinct frequencies are involved. A frequency of 2 kHz is used for the eddy current measurement, giving a depth of investigation of about 1 mm. The sensor pads are mounted on springs so that they are held in contact with the casing, facilitated through centralization of the sonde. Various sizes of magnet pole pieces are available and are selected according to the casing ID to optimize the signal strength for the flux leakage measurement.

Six measurements of flux leakage and eddy current distortion are made on each array, and the maximum signal from each array is sent uphole to the surface instrumentation. Four signals, the eddy current and flux leakage data from the two arrays, are recorded.

The flux leakage data correspond to anomalies located anywhere in the casing, while eddy current distortion occurs only at the inside wall of the casing. The standard presentation of the measurements is as shown in Fig. 53.31, with the data from the two arrays displayed in Tracks 2 and 3. Enhanced data are displayed in Track 1, making any anomalies more obvious.

Interpretation. The measurements are generally suitable only for qualitative interpretation. This is because any voltages induced in the sensor coils depend not only on the size of any flaws in the casing, but also on the magnetic permeability of the casing, the logging speed, and the abruptness of a defect. The measurement, therefore, is used primarily to locate the presence of small defects in the casing, such as pits and holes. Defects such as gradual decreasing of the wall thickness cannot be detected. To get a complete picture of the state of the casing the electromagnetic thickness tool also should be used to measure the casing wall thickness, since the PAT device will give zero signal in the two extremes of no casing and perfect casing (except at the collars).

Two sets of data are recorded, one set influenced by defects occurring anywhere in the casing, and the other by faults on the inner surface. By examining the log, therefore, it can be inferred whether the casing is damaged on the inner or outer wall, assuming that there is no defect within the casing. Although the magnetic flux bulges away from both sides of the casing at the location of a defect, the effect is greater on the side of the flaw, hence for the flux leakage measurement, smaller defects can be detected on the inner surface than on the outer surface. Because of the overlapping configuration of the two-pad arrays all of the inner surface of the casing is surveyed, but there is a casing-diameter-dependent defect size below which the flaw will be seen by only one array, and above which it will be seen by both arrays.

The eddy current measurements are not able to detect flaws smaller than about 0.39-in. diameter, while the flux leakage limit is somewhat lower (0.25 in.). This means that if an anomaly of less than $\frac{3}{8}$ -in. diameter is present it cannot be determined whether it is on the inner or outer surface. If a deflection is noted on the eddy current measurement but not on the flux measurement it is

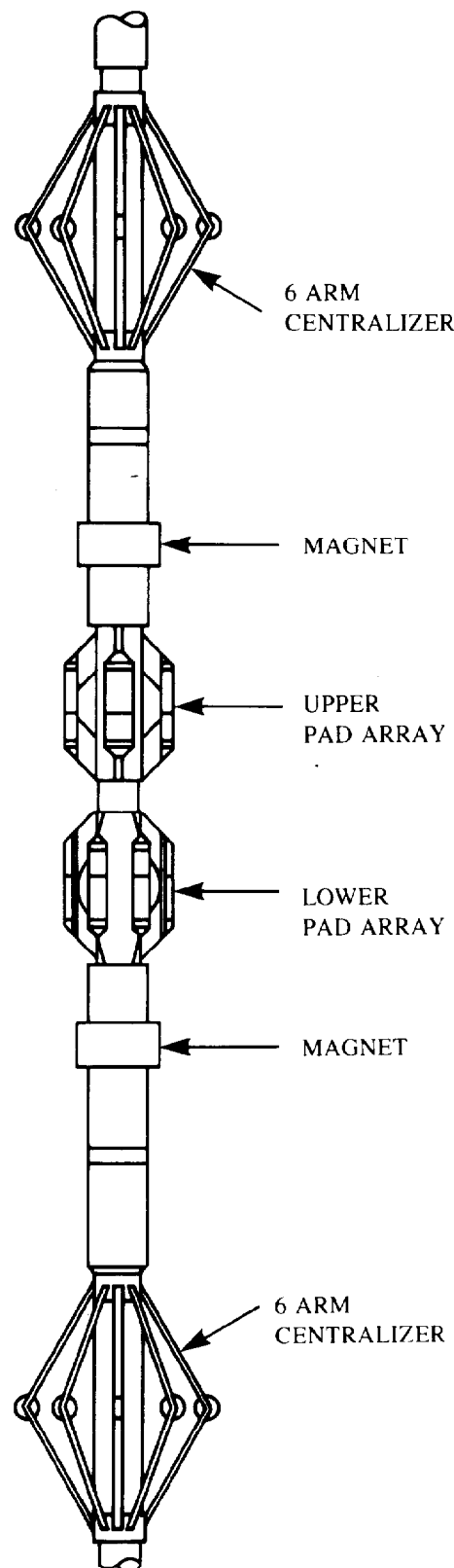


Fig. 53.30— The pipe analysis tool.

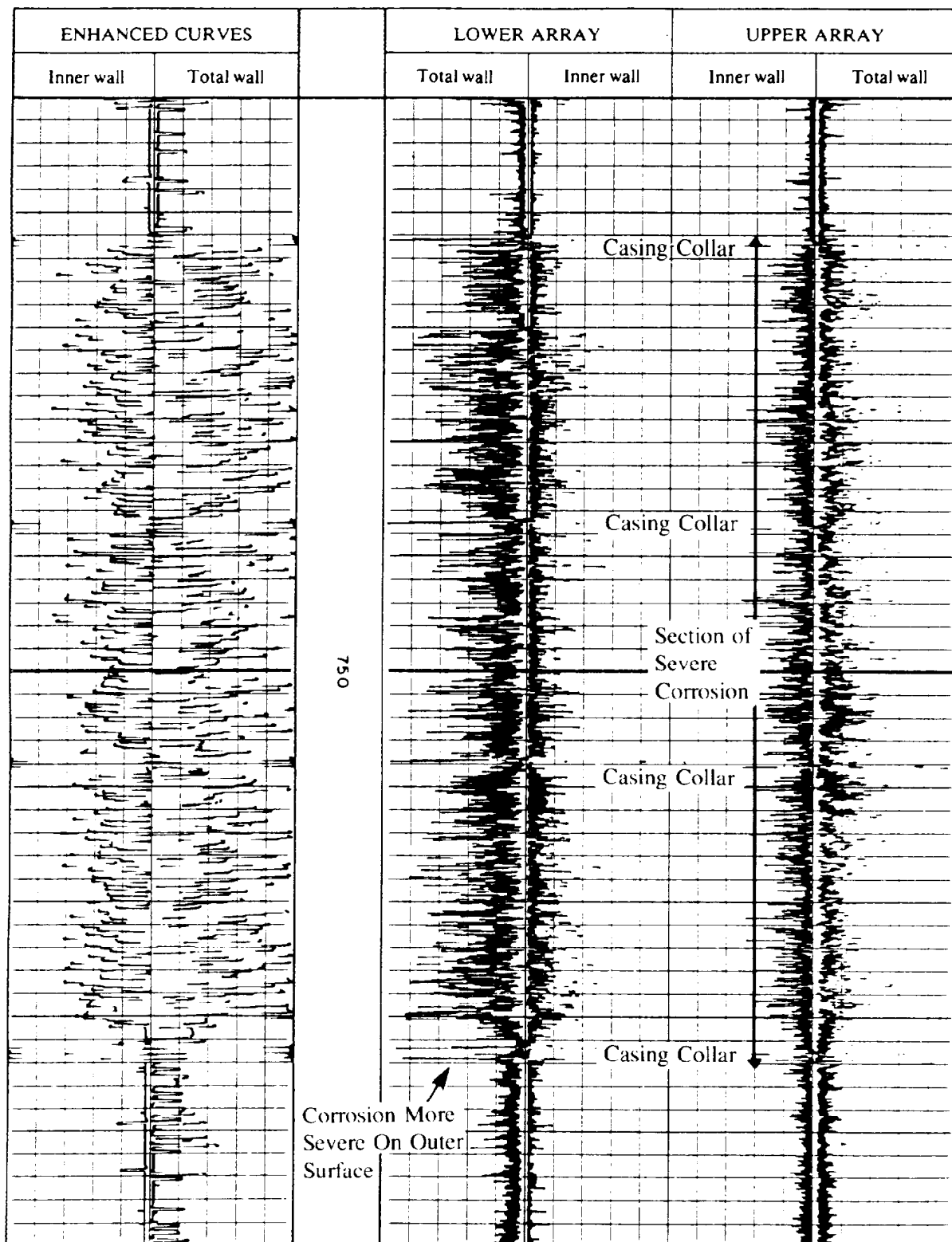


Fig. 53.31— The pipe analysis log in severely corroded casing.

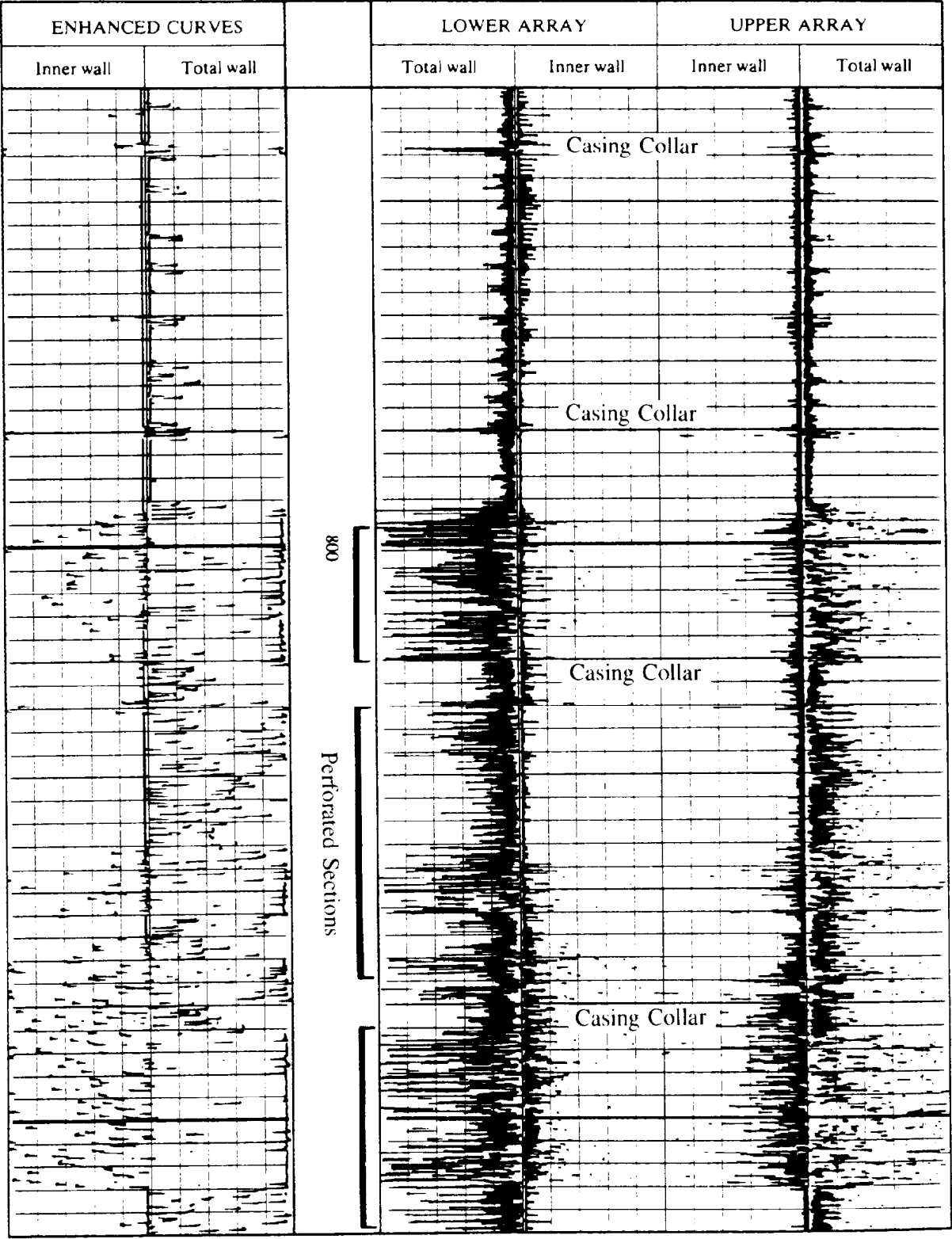


Fig. 53.32—Pipe analysis log over a perforated section of casing.

assumed that the defect on the inner wall is less than 1 mm deep, and also usually can be ignored. In addition, events can be seen on the flux leakage readings that are not caused by casing damage but are a result of the presence of localized magnetization in the casing. This is one reason why a reference PAT survey should be run in new casing, so that a time-lapse technique can be applied to determine the casing damage.

The example of Fig. 53.32 includes sections of perforated casing (798 to 805 m, 807 to 819 m and 821 to 830 m), and there is a clear indication of damaged and undamaged casing. The flux leakage measurement (total wall) is responding strongly through the perforated intervals, the eddy current curve less so. This is probably a result of the diameter of the perforations being fairly close to the detection limit of the eddy current measurement. In the upper section the tool response is much lower, indicating a certain amount of corrosion on both surfaces of the casing, but probably nothing major. The large deflections occurring on all the curves are caused by the casing collars.

Casing Collar-Locator Log

The collar locator is used to locate casing collars, usually in conjunction with another cased-hole service such as a nuclear log or a perforating gun. Perhaps its most common use is in precisely locating perforating points. To do this the collar locator is run with a nuclear log (either the gamma-ray or neutron log) after the casing is set. This survey accurately positions casing collar in reference to the nuclear log. By correlating the nuclear log with logs run in an open hole, casing collars can be positioned accurately with reference to the openhole logs. The collar locator is then run with the perforating gun. The collars adjacent to the desired perforating interval are located and the desired interval perforated using the casing collars as reference points. Use of the collar locator makes it possible to locate perforations within a few inches of the desired interval.

Various types of collar locators are now in use. Some of the collar locators are sensitive enough to locate old perforations in casing. The collar locator also can be used to locate the casing shoe in openhole completions.

References

1. Kamp, A.W.: "Downhole Telemetry From the User's Point of View," *J. Pet. Tech.* (Oct. 1983) 1792-96.
2. Grosso, D.S., Raynal, J.C., and Radar, D.: "Report on MWD Experimental Downhole Sensors," *J. Pet. Tech.* (May 1983) 899-904.
3. "Measurements While Drilling (M.W.D.) Technical Specifications," Schlumberger Well Services, Houston.
4. Hodgson, H. and Vernado, S.G.: "Computerized Well Planning for Directional Wells," paper SPE 12071 presented at the 1983 SPE Annual Technical Conference and Exhibition, San Francisco, Oct. 3-6.
5. Scott, A.C. and Wright, J.W.: "A New Generation Directional Survey System Using Continuous Gyrocompassing Techniques," paper SPE 11169 presented at the 1982 SPE Annual Technical Conference and Exhibition, New Orleans, Sept. 29-Oct. 2.
6. Walstrom, J.E., Harvey, R.P., and Eddy, H.D.: "A Comparison of Various Directional Survey Methods and an Approach to Model Error Analysis," *J. Pet. Tech.* (Aug. 1972) 935-43.
7. "Dipmeter Interpretation—Volume I—Fundamentals," Schlumberger Ltd., New York City (1981) 8, 10, 53.
8. Bateman, R.M. and Konen, C.E.: "The Log Analyst and the Programmable Pocket Calculator—Part III—Dipmeter Computation," *The Log Analyst* (Jan.-Feb. 1978) 19, No. 1, 3-11.
9. Bateman, R.M. and Hepp, V.R.: "Application of True Vertical Depth, True Stratigraphic Thickness and True Vertical Thickness Log Displays," paper presented at the 1981 SPWLA Annual Logging Symposium.
10. Pennbaker, P.E.: "Vertical Net Sandstone Determination for Isopach Mapping of Hydrocarbon Reservoirs," *Bull., AAPG* (Aug. 1972) 53, No. 8, 1520-29.
11. Hepp, V.R.: "Vertical Net Sandstone Determination for Isopach Mapping of Hydrocarbon Reservoirs—Discussion," *Bull., AAPG* (1973) 57, 1784-87.
12. Holt, O.R., Schoonovers, L.G., and Wichmann, P.A.: "True Vertical Depth, True Vertical Thickness, and True Stratigraphic Thickness Logs," *Trans., SPWLA Logging Symposium* (1977) paper Y.
13. Peveraro, R.: "Vertical Depth Correction Methods for Deviation Survey and Well Log Interpretation," *Trans., SPWLA European Symposium*, London (1979) paper P.
14. Bateman, R.M. and Konen, C.E.: "The Log Analyst and the Programmable Pocket Calculator—Part VI—Finding True Stratigraphic Thickness and True Vertical Thickness of Dipping Beds Cut by Directional Wells," *The Log Analyst* (March-April 1979).
15. Cuthbert, J.F. and Johnson, W.M. Jr.: "New Casing Inspection Log," paper SPE 5090 presented at the 1974 SPE Annual Meeting, Houston, Oct. 6-9.
16. Illiyan, I.S., Cotton, W.J. Jr., and Brown, G.A.: "Test Results of a Corrosion Logging Technique Using Electromagnetic Thickness and Pipe Analysis Logging Tools," *J. Pet. Tech.* (April 1983) 801-08.
17. "Well Evaluation Development—Continental Europe," Schlumberger Ltd., New York City (1982).

Chapter 54

Acidizing

A.W. Coulter Jr., Dowell-Schlumberger
A.R. Hendrickson, Dowell-Schlumberger
S.J. Martinez, U. of Tulsa *

Introduction

The use of acids to stimulate or to improve oil production from carbonate reservoirs was first attempted in 1895. Patents covering the use of both hydrochloric and sulfuric acids for this purpose were issued at that time. Although several "well treatments" were conducted, the process failed to arouse general interest because of severe corrosion of well casing and other metal equipment. The next attempts to use acid occurred between 1925 and 1930. These consisted of using hydrochloric acid (HCl) to dissolve scale in wells in the Glenpool field of Oklahoma and to increase production from the Jefferson Limestone (Devonian) in Kentucky. None of these efforts were successful and "acidizing" once again was abandoned.

The discovery of arsenic inhibitors, which allowed HCl to react with the formation rock without seriously damaging the metal well equipment, revived interest in oilwell acidizing in 1932. At that time, Pure Oil Co. and Dow Chemical Co. used these inhibitors with HCl to treat a well producing from a limestone formation in Isabella County, MI. Results of this treatment were outstanding. When similar treatments in neighboring wells produced even more spectacular results, the acidizing industry was born.

Throughout the years following those early treatments, the acidizing industry has grown to one using hundreds of millions of gallons of acid applied in tens of thousands of wells each year. Technology has developed with increasing rapidity, and many changes and innovations have been made to improve the effectiveness of acidizing treatments. Because of new techniques of application and development of additives to alter the characteristics of the acid itself, acidizing has become a highly skilled science. A knowledge of available materials, chemical reactions

at treating and well conditions, reservoir properties, and rock characteristics are required to design an effective and efficient acidizing treatment. Since it is beyond the scope of this text to cover all aspects of acidizing in detail, this discussion will be limited to a general description of materials, techniques, and design considerations. A bibliography is provided for those requiring a more detailed discussion of a particular subject. Also, the major well stimulation companies providing acidizing services offer literature and technical assistance for problem analysis and treatment design.

General Principles

The primary purpose of any acidizing treatment is to dissolve either the formation rock or materials, natural or induced, within the pore spaces of the rock. Originally, acidizing was applied to carbonate formations to dissolve the rock itself. Over a period of time, special acid formulations were developed for use in sandstone formations to remove damaging materials induced by drilling or completion fluids or by production practices.

There are two primary requirements that an acid must meet to be acceptable as a treating fluid: (1) it must react with carbonates or other minerals to form soluble products, and (2) it must be capable of being inhibited to prevent excessive reaction with metal goods in the well. Other important considerations are availability, cost, and safety in handling. While there are many formulations available, only four major types of acid have found extensive application in well treatments: hydrochloric, hydrofluoric, acetic, and formic acids.

Hydrochloric Acid (HCl)

An aqueous solution of HCl is most commonly used for acidizing treatments, for reasons of economy and because it leaves no insoluble reaction product. When HCl is

* Authors of the original chapter on this topic in the 1962 edition included this author (deceased), P.E. Fitzgerald, and Harold E. Staadt.

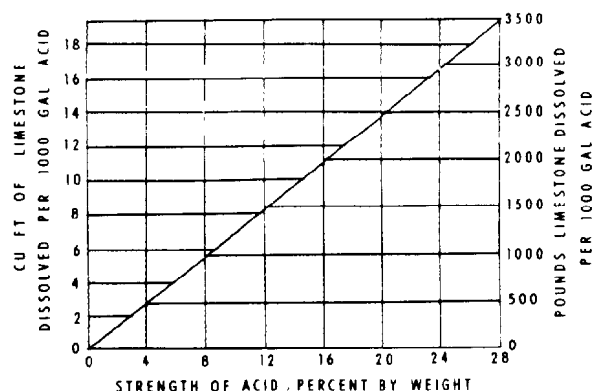


Fig. 54.1—Solution of limestone in acid.

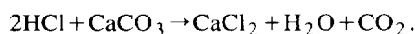
TABLE 54.1—HYDROCHLORIC ACID DENSITY AT 60°F

% HCl	Specific Gravity*	°Baumé**	lbm/gal	psi/ft depth
1.00	1.0048	0.7	8.377	0.4351
2.00	1.0097	1.4	8.418	0.4372
3.00	1.0147	2.1	8.460	0.4392
4.00	1.0197	2.8	8.501	0.4415
5.00	1.0248	3.5	8.544	0.4437
6.00	1.0299	4.2	8.586	0.4459
7.00	1.0350	4.9	8.629	0.4482
8.00	1.0402	5.6	8.672	0.4504
9.00	1.0447	6.2	8.710	0.4524
10.00	1.0500	6.9	8.754	0.4547
11.00	1.0550	7.6	8.796	0.4568
12.00	1.0600	8.2	8.837	0.4590
13.00	1.0646	8.8	8.876	0.4610
14.00	1.0702	9.5	8.922	0.4634
15.00	1.0749	10.1	8.962	0.4654
16.00	1.0801	10.8	9.006	0.4677
17.00	1.0849	11.4	9.045	0.4698
18.00	1.0902	12.0	9.089	0.4721
19.00	1.0952	12.6	9.132	0.4743
20.00	1.1002	13.2	9.171	0.4764
21.00	1.1057	13.9	9.218	0.4788
22.00	1.1108	14.5	9.261	0.4810
23.00	1.1159	15.1	9.303	0.4832
24.00	1.1214	15.7	9.349	0.4855
25.00	1.1261	16.3	9.385	0.4876
26.00	1.1310	16.9	9.433	0.4899
27.00	1.1368	17.5	9.478	0.4922
28.00	1.1422	18.0	9.523	0.4946
29.00	1.1471	18.6	9.563	0.4967
30.00	1.1526	19.2	9.609	0.4991
31.00	1.1577	19.8	9.663	0.5012
32.00	1.1628	20.3	9.694	0.5035
33.00	1.1680	20.9	9.738	0.5057
34.00	1.1727	21.4	9.777	0.5078
35.00	1.1779	21.9	9.820	0.5100
36.00	1.1827	22.4	9.860	0.5121
37.00	1.1880	22.9	9.924	0.5144
38.00	1.1924	23.4	9.941	0.5163
39.00	1.1963	23.8	9.974	0.5180
40.00	1.2008	24.3	10.011	0.5199
41.00	1.2053	24.7	10.049	0.5219

$$\text{*Specific gravity} = \frac{145}{145 - \text{°Baumé}}$$

$$\text{**°Baumé} = 145 - \frac{145}{\text{specific gravity}}$$

pumped into a limestone formation, a chemical reaction takes place, producing calcium chloride, CO_2 , and water. This reaction is represented by the following equation:



One thousand gallons of 15% HCl will dissolve approximately 10.8 cu ft (1,840 lbm) of limestone. It will liberate approximately 7,000 cu ft of CO_2 , measured at atmospheric conditions, and produce 2,042.4 lbm of calcium chloride. This salt is dissolved in the original water of the acid solution, plus 39.75 gal of water formed during the reaction. The specific gravity of this solution will be 1.181 (20.4% calcium chloride). While 15 wt% HCl has been the most commonly used, concentrations of 20 and 28% have become extremely popular over the past 2 decades. Regardless of the acid strength used, the reaction is the same and equivalent amounts of carbonate rock are dissolved. For example, 10,000 gal of 3% HCl solution will dissolve the same amount of rock as 1,000 gal of 28% HCl. Fig. 54.1 shows the effect of acid concentration on the amount of limestone dissolved. The main differences between the two solutions are their reaction rates (or spending times) and their physical volumes. Although lower concentrations of acid have greater equivalent volumes, their reaction times and depth of penetration into the reservoir, from the wellbore, are considerably less than those of the higher-strength solutions. Reaction rates and penetration will be discussed later.

Similar reactions occur when dolomite or impure limestone is treated with HCl. Dolomitic lime contains a large percentage of magnesium combined as calcium magnesium carbonate. Although it reacts more slowly, this mineral also dissolves in HCl, and the resulting magnesium chloride is soluble in the spent acid. Other impurities occurring in limestone and dolomite are often insoluble in acid, and if appreciable percentages of such components are present, special additives must be included in the acid solution to ensure their removal.

HCl ordinarily is manufactured in concentrations of 32 to 36 wt% HCl and is diluted at service company stations to 15, 20, or 28% for field use. The concentrated acid, the various chemical additives, and water are mixed in the tank truck used to haul the acid to the wellsite. Table 54.1 lists the weights of various concentrations of HCl. These data are useful in calculating mixing proportions for acid dilution, using the following equation:

$$V_{ca} = \frac{V_{da} C_{da} \gamma_{da}}{C_{ca(\text{HCl})} \gamma_{ca}}$$

where

V_{da} = final volume of dilute acid,

C_{da} = desired concentration of dilute acid,

γ_{da} = specific gravity of dilute acid,

V_{ca} = volume of concentrated acid required,

$C_{ca(\text{HCl})}$ = percent of HCl in concentrated acid, and

γ_{ca} = specific gravity of concentrated acid.

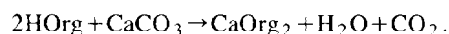
Approximate proportions of concentrated acid and water required for dilution are shown in Fig. 54.2.

Determination of acid strength can be estimated in the field using either a hydrometer or a field titration kit. The accuracy of hydrometer readings depends on the care and technique used by the field engineer. Both the hydrometer and the glass cylinder in which the test is made should be free from oil or dirt. The spindle should float freely in the acid, and all readings should be made at the lowest level of the acid meniscus. The temperature of the acid sample should be taken and the hydrometer reading corrected to 60°F.

Determination of acid strength by titration is simplified by the use of 0.59 *N* standard sodium hydroxide solution. If a 2-mL sample of the acid is titrated with this standard solution to a methyl orange end point, the burette reading (milliliters of sodium hydroxide used) will be equal to the acid strength (percent HCl).

Acetic and Formic Acids

Acetic acid (CH₃COOH) and formic acid (HCOOH) are weakly ionized, slowly reacting, organic acids. They are used much less frequently than HCl and are suitable primarily for wells with high bottomhole temperatures (BHT's above 250°F) or where prolonged reaction times are desired. The reaction of these acids with limestone is described by the following equation:

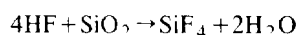


HAc is available in concentrations up to 100% as glacial HAc, while HCOOH is available in 70 to 90% concentrations. For field use, HAc solutions normally are diluted to 15% or less.

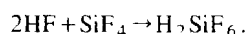
Above this concentration, one of the reaction products, calcium acetate, can precipitate from its "spent acid" solution because of its limited solubility. Similarly, the concentration of HCOOH normally is limited to 9 to 10% because of the limited solubility of calcium formate. At a 10% concentration, 1,000 gal HAc will dissolve 740 lbm of limestone, whereas 1,000 gal HCOOH dissolves 970 lbm. Where more dissolving power per gallon of acid is desired, HCl is sometimes mixed with HCOOH or HAc. Such blends still provide extended reaction times, when compared with HCl. HCOOH and HAc also may be blended together. Table 54.2 illustrates some of the more common acid strengths and blends.

Hydrofluoric Acid (HF)

HF is used in combination with HCl and has been referred to as "intensified acid" or "mud removal" acid, depending on the formulation and use. HF is used primarily to remove clay-particle damage in sandstone formations, to improve permeability of clay-containing formations, and to increase solubility of dolomitic formations. Its utility is based on the fact that some clays, silica, and other materials normally insoluble in HCl have some degree of solubility in HF. For example, 1,000 gal of an acid solution containing 3% HF and 12% HCl will dissolve 500 lbm of clay and up to 1,450 lbm of CaCO₃.



and



FORMULA FOR MIXING ACID IN ANY DESIRED CONCENTRATION:

$$\frac{\text{VOLUME OF STRONG} \times (\text{VOL OF WEAK}) \times (\% \text{WEAK}) \times (\text{SP. GR. OF WEAK})}{(\% \text{ OF STRONG}) \times (\text{SP. GR. OF STRONG})}$$

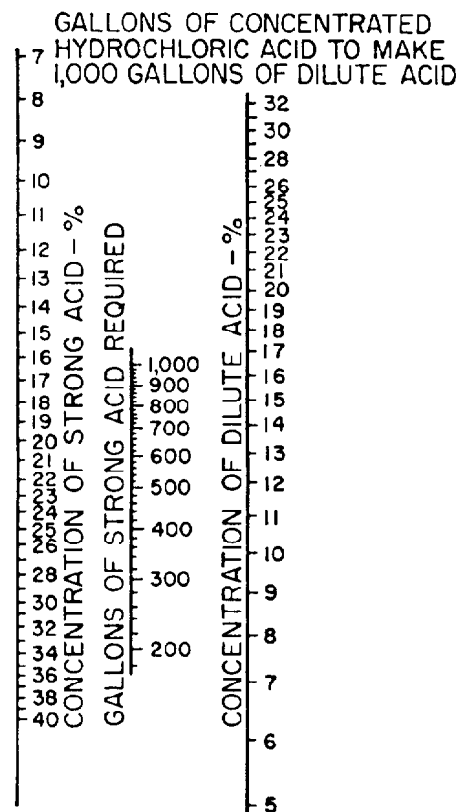


Fig. 54.2—Dilution of concentrated HCl.

TABLE 54.2—DIFFERENT ACIDIZING SOLUTIONS

Acid		CaCO ₃ Equivalent (lbm/1,000 gal acid)	Relative Reaction time*
Concentration (%)	Type		
7.5	HCl	890	0.7
15	HCl	1,840	1.0
28	HCl	3,670	6.0
36	HCl	4,860	12.0
10	Formic	910	5.0
10	Acetic	710	12.0
15	Acetic	1,065	18.0
7.5	Formic/ HCl mixture	2,420	6.0
14	Acetic/ HCl mixture	2,380	12.0
8	Formic/ Acetic mixture	1,700	18.0
14			

*Approximate time for acid reaction to be completed ("spent") to an equivalent strength of 2.5% HCl solution. Values are compared by using spending time of 15% HCl as 1.

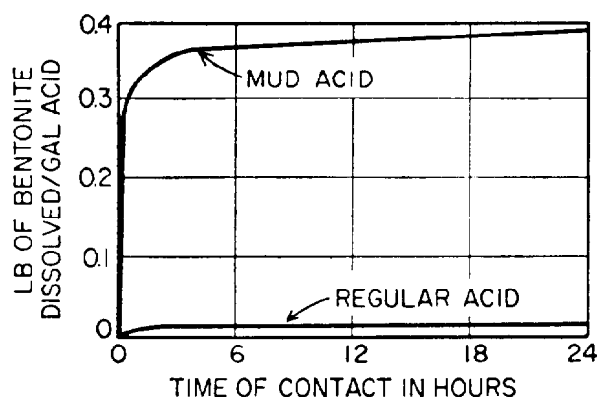


Fig. 54.3—Solubility of bentonite in mud removal acid.

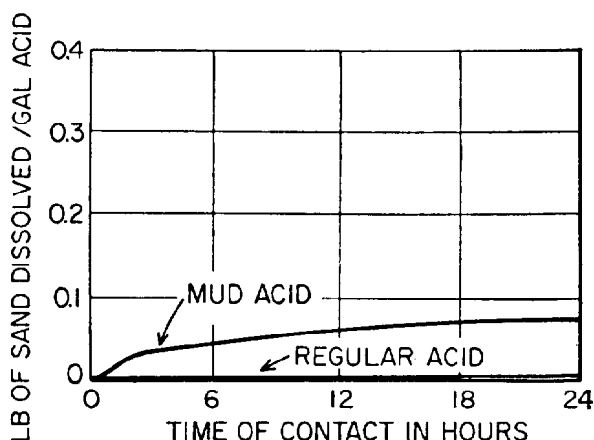


Fig. 54.4—Solubility of silica sand in mud removal acid.

Figs. 54.3 and 54.4 compare solubilities of bentonite and silica in HCl and HF acids.

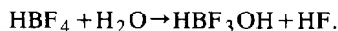
In carbonates, application of HF/HCl mixtures must be controlled carefully because of cost and possible precipitation of reaction products such as calcium fluorides or complex fluosilicates, which have a very limited solubility. For reaction with silicates, such as natural clays or clays in drilling fluids, the blends usually contain 2 to 10% HF and 5 to 26% HCl. The concentration of HCl used in the blend should be equal to or greater than that of the HF.

The so-called "intensified acids" used in dolomitic formations are mainly HCl containing small concentrations of HF, usually about 0.25%. Intercrystalline films of silica, insoluble in HCl, often occur in the crystal structure of dolomite. When such are present, they prevent the acid from contacting the soluble portions of the rock. The presence of fluoride intensifier in the acid will destroy such films, allowing the acid to react more completely with the soluble portions of the rock. Fig. 54.5 illustrates the comparative reaction rates of HCl and intensified acid on dolomite formations.

More recent developments of HF involve the use of delayed-action agents in sandstone acidizing. The first of these was a self-generating mud acid system, reported by Templeton *et al.*¹ The system provides slow generation of acid from the hydrolysis of methyl formate, yielding methyl alcohol and HCOOH acid. The acid then reacts with ammonium fluoride to yield HF in situ. They attribute the success of the system to getting the HF reaction away from the wellbore into areas that conventional HF solutions normally do not reach before spending. Equally important factors are the techniques of application and of returning the well to production following treatment. The treatment technique involves use of an aromatic solvent and mud acid preflush, along with the self-generating mud acid (SGMA). The wells are returned to production by opening the choke gradually over a 90-day period and never allowing an excessive drawdown. The process is available from most service companies as SGMA.

A significant development in this area of slow-reacting, HF-supplying, clay-dissolving acid has been the fluoboric acid system reported by Thomas and Crowe.² This acid

hydrolyzes to form hydroxyfluoboric acid and HF, which will dissolve clays.



This reaction provides a slow-release source of HF, which can penetrate deeply before spending. Perhaps more important, the slowly generated hydroxyfluoboric acid reacts with clays to form a nonswelling, nondispersing product that stabilizes fine clays and holds fine particles of silica in place.

Acid Reaction Rates

A knowledge of the factors affecting the reaction rate of acids is important for several reasons. First, these factors, correlated with reservoir and formation characteristics, form a guide for the selection of acid type and volume for a given treatment. Next, a study of these factors can furnish an understanding of what parameters govern spending time, which will determine how far a given formulation can penetrate into the formation before spending. Many factors govern the reaction rate of an acid, such as pressure, temperature, flow velocity, acid concentration, reaction products, viscosity, acid type, area/volume ratio, and formation composition (physical and chemical). These factors have been the subject of extensively reported research for many years. Details of such studies are available in published literature. Only a brief general discussion will be presented here.

Pressure

Fig. 54.6 shows the effect of pressure on the reaction rate of 15% HCl with limestone and dolomite at 80°F. Above 500 psi, pressure has little effect on reaction rate. At bottomhole treating pressures, there is only a small difference (a factor of 1.5 to 2) in the comparative reaction of acid with limestone and dolomite compared to the rather large difference (a factor of about 10) at atmospheric pressure.

Temperature

Acid reaction rate increases directly with temperature. At 140 to 150°F, the reaction rate of HCl and limestone is

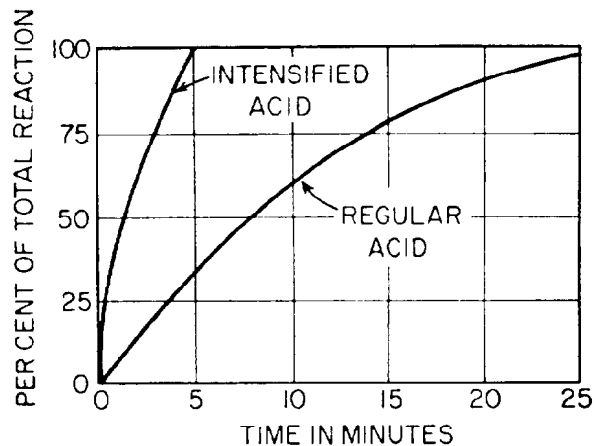


Fig. 54.5—Comparative reaction rates of conventional and intensified acids.

approximately twice that at 80°F. It must be recognized that the temperature controlling the reaction is affected by the injection temperature of the acid (a major factor), and by the heat liberated by the reaction itself (a minor factor). Computerized programs are used to estimate the bottomhole fluid temperature at various stages, allowing more effective acid treatment design.

Flow Velocity

Fig. 54.7 shows that increased flow velocity increases the reaction rate of 15% HCl with CaCO_3 . This velocity effect is more pronounced in narrower fractures. Reaction rate is a function of shear rate, $6v/b$, sec^{-1} as illustrated by the following equation:

$$R = [(28.5 v/b)^{0.8} + 184] \times 10^{-6}, \dots \dots \dots (1)$$

where R is the reaction rate in lbm/sq ft-sec , v is the flow velocity in fracture, ft/sec , and b is the fracture width, ft . (The reaction rate is for 15% HCl with marble at 80°F under 1,100 psi pressure.)

The flow velocity in fractures and channels depends on injection rate and actual geometry of the flow path.

$$v_{rf} = 0.18 i_{ac} / (r_f b) \quad (\text{radial fracture}), \dots \dots \dots (2a)$$

$$v_{lf} = 1.15 i_{ac} / (hb) \quad (\text{linear fracture}), \dots \dots \dots (2b)$$

$$v_{cc} = 17.2 i_{ac} / d^2 \quad (\text{cylindrical channel}), \dots \dots \dots (2c)$$

where

v = flow velocity in fractures and channels,
ft/sec,

i_{ac} = acid injection rate, bbl/min ,

r_f = fracture radius, ft ,

h = fracture height, ft ,

d = channel diameter, in. , and

b = fracture width, in.

Acid Concentration

Reaction rate increases with acid concentration up to 24 to 25% HCl, but not proportionally, as shown in Fig.

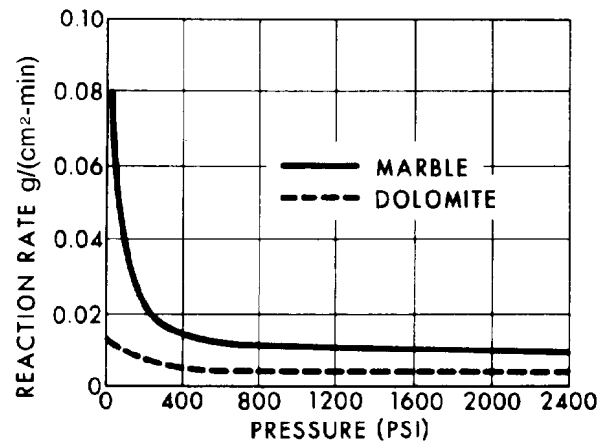


Fig. 54.6—Effect of pressure on reaction rate (15% HCl at 80°F).

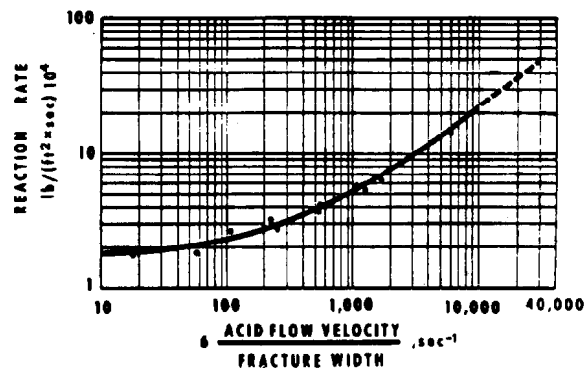


Fig. 54.7—Effect of flow on reaction rate (15% HCl with CaCO_3).

54.8. Above 25% HCl, the reaction rate actually decreases because of reduced acid activity. As acid spends, the reaction rate decreases as a result of reduced acid concentration and the retarding effect of dissolved reaction products, such as calcium or magnesium chloride.

Area/Volume Ratio

Area/volume (A/V) ratio is one of the major factors affecting reaction rate spending time, and may vary over a wide range. This ratio, the area in contact with a given volume of acid, is inversely proportional to pore radius or fracture width. Fig. 54.9 shows the time required for 15% HCl to spend on marble, at 80°F and 1,100 psi, for three different A/V ratios.

The term “spending time” has very little meaning or value by itself. It must be related to flow geometry and, thus, to the distance the acid penetrates before it is spent. In matrix acidizing, extremely high A/V ratios may be encountered. For example, a 10-md, 20%-porosity limestone may have an A/V ratio of 28,000 to 1. In such a formation, it would be very difficult to obtain significant penetration before spending. A natural fracture, 0.001 in. wide, has an A/V ratio of 3,200:1. A 0.1-in. fracture has an A/V ratio of 32:1. The smaller ratios in wider frac-

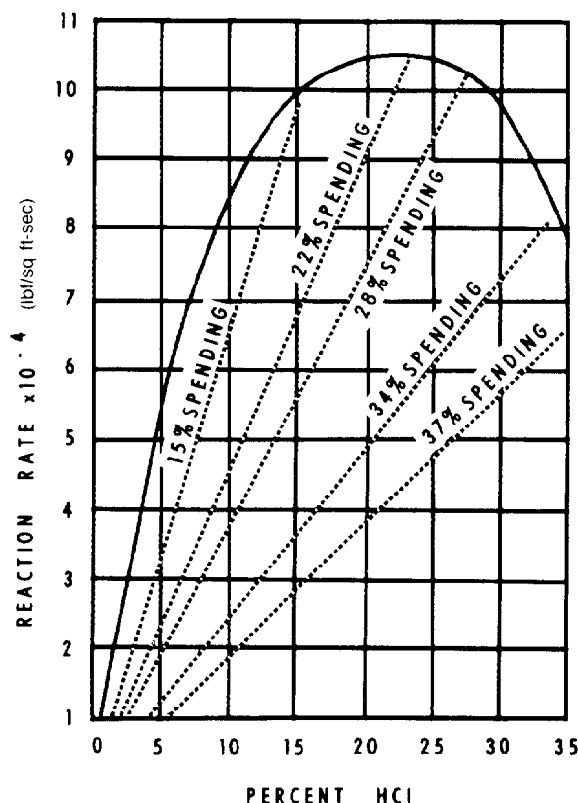


Fig. 54.8—Effect of concentration on reaction rate and spending rate.

TABLE 54.3—EFFECT OF TEMPERATURE ON ORGANIC INHIBITOR PROTECTION TIME

Concentration (%)	Temperature (°F)	Protection Time (hours)
0.6	175	24
1.0	250	6
2.0	300	6
2.0*	350	4

*With inhibitor acid.

tures allow greater penetration of the acid into the reservoir before spending is complete.

Formation Composition

Probably the most important factor that governs effectiveness of an acidizing treatment is the rock composition. Its chemical and physical characteristics determine how and where the acid will react with and dissolve the rock.

From the standpoint of chemical composition, there is little difference in the reaction rate of HCl on most limestones, all other factors remaining constant. The physical rock texture, however, can control pore size distribution, A/V ratio, pore geometry, and other properties. This, in turn, influences the type of flow channels created by acid reaction and is the key to acid response.

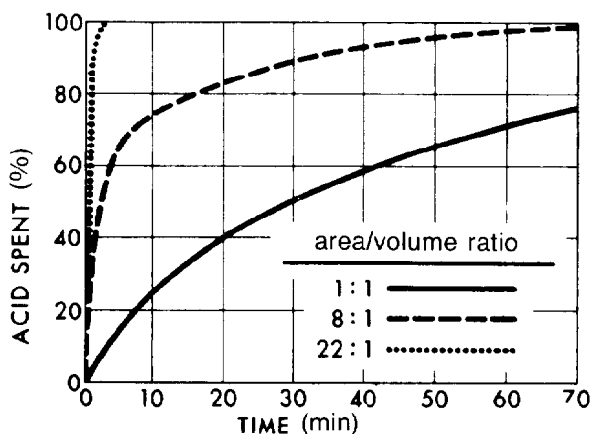


Fig. 54.9—Effect of A/V ratio on spending time (15% HCl, 80°F and 1,100 psi).

Two formations having the same acid solubility and permeability may respond differently to acid treatment because of variances in physical structure.

Acid Additives

The use of a corrosion inhibitor as an additive made possible the first commercially feasible acidizing treatments. Since that time, many auxiliary chemicals have been developed to modify acid solutions, influencing their application and recovery.

Corrosion Inhibitors

Inhibitors are chemical materials that, when dissolved in acid solutions, greatly retard the reaction rate of the acid with metals. They are used in acidizing to avoid damage to casing, tubing, pumps, valves, and other well equipment. Inhibitors cannot completely stop all reaction between the acid and metal; however, they do slow the reaction, eliminating 95 to 98% of the metal loss that would otherwise occur. Most inhibitors have practically no effect on the reaction rate of acid with limestone, dolomite, or acid-soluble scale deposits.

The length of time that an inhibitor is effective depends on the acid temperature, type of acid, acid concentration, type of steel, and the inhibitor concentration.

Organic inhibitors in HCl are effective up to 400°F, but above 200°F relatively large concentrations are required. The effect of temperature on corrosion inhibition is illustrated in Table 54.3.

Equations have been developed for estimating BHT's during acid treatments. By knowing these temperatures, adequate corrosion protection can be provided, even in wells with static BHT's up to 400°F.

Surfactants

Surfactants are chemicals used to lower the surface tension or interfacial tension of fresh acid or spent acid solutions. The use of a surfactant improves the treating efficiency in a number of ways.

The presence of a surfactant improves the penetrating ability of the acid solution entering a formation. This is extremely desirable in matrix acidizing treatments, be-

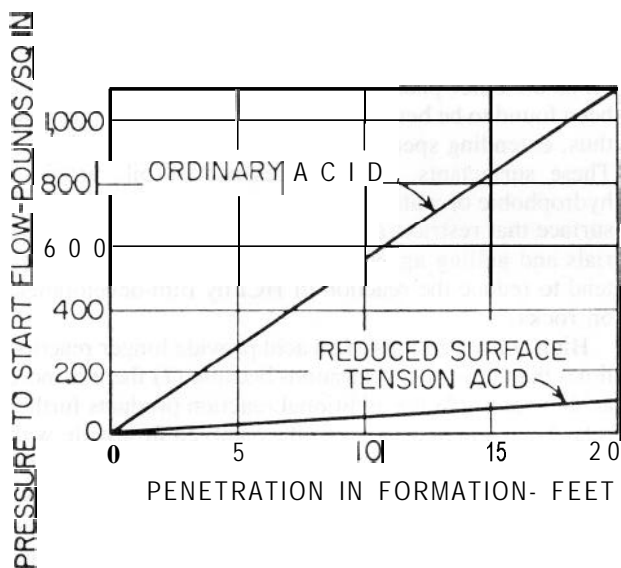


Fig. 54.10—Effect of surface-tension-reducing agent in facilitating return of spent acid.

cause it provides deeper penetration of acid into the formation. In addition, surfactants permit the acid to penetrate oily films clinging to the surface of the rock and lining the pores, so that the acid can come in contact with the rock and dissolve it.

The use of surfactants also facilitates the return of spent acid following the treatment (Fig. 54.10). Wetting of the formation is more nearly complete and there is less resistance to flow of the acid, so that the spent acid is readily returned through the treated section. This is especially important in low-pressure wells.

Another advantage in the use of surfactants in acid is the demulsifying action obtained. Many surfactants are capable of inhibiting the occurrence of emulsions or destroying those already formed.

Surfactants also promote dispersion and suspension of fine solids to provide better cleanup following treatment. These solids may be either mud solids or natural fines released from the formation. They are suspended and physically removed from the formation.

Special surfactants are used as antisludge agents. Some crudes form an insoluble sludge when in contact with acid. The sludge consists of asphaltenes, resin, paraffin, and other complex hydrocarbons. The acid reacts with the crude at the interface, forming an insoluble film. The coalescence of this film, which results on the sludge particles, can be avoided by use of proper additives. Ethylene glycol monobutyl ether is a mutual solvent surfactant used in matrix sandstone acidizing to water-wet the formation. This agent prevents particle migration and subsequent particle plugging. It improves cleanup by preventing the stabilization of emulsions by fine particles. Many different surfactants are used in acidizing. Type and concentration for a particular application should be selected on the basis of laboratory testing.

Silicate-Control Agents

Various silicate compounds, commonly known as clays and silts, usually are present in most limestones and dolo-

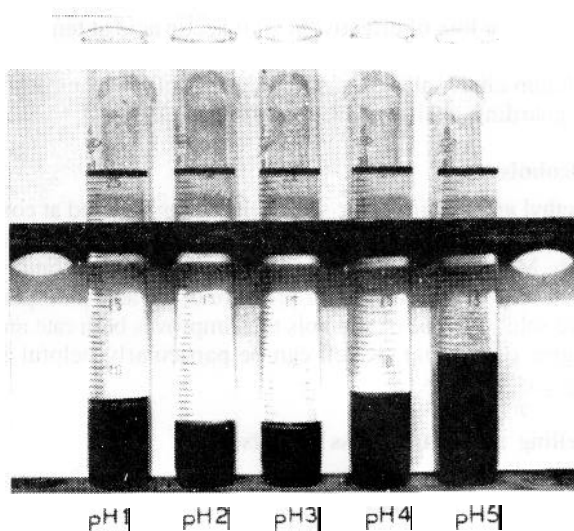


Fig. 54.11—Photograph showing effect of pH on the volume of silicate particles.

mites. One of the characteristics of these silicates is that they will swell in spent acid. Naturally, this is undesirable because swollen silicate particles may block formation flow channels, reducing well production.

Silicate-control additives are chemicals that prevent released silicate particles from adsorbing water. Some buffer the pH of the solution near the isoelectric point (where the volume of the swelled clays is at a minimum). Others cause shrinkage of the silicate particles by replacing the adsorbed water molecules with a water-repellent organic film. Thus, possible formation plugging is prevented, treating pressures are lowered, faster cleanup is provided, and the occurrence of particle-stabilized emulsions is minimized. This is illustrated in Fig. 54.11.

Iron-Control Agents

Iron control is approached two ways. The oldest and most common approach is to use sequestering agents, which act by complexing iron ions, thereby preventing precipitation when the acid spends. A second method is use of reducing agents that reduce any ferric ions (Fe^{3+}) to ferrous ions (Fe^{2+}), which do not precipitate as the hydroxide or hydrous oxide until the pH of the system is above 7. Since acids in contact with the formation rock will not spend to a pH that high, the hydroxide will not damage the well. Spent acid usually has a pH between 4.5 and 6.5, no higher.

Erythorbic acid is one of the most effective reducing agents that can be used for this purpose. The reduction of all the ferric iron to ferrous iron, however, does not prevent the precipitation of ferrous sulfide (FeS), which precipitates when the acid spends to a pH of 2, as it will readily in almost any formation. To protect fully against iron precipitation in a sour well, a complexing agent is needed. Citric, lactic, and acetic acids as well as EDTA or NTA are popular sequestrants. In some wells where H_2S can become mixed with the acid it also may be advisable to use both the reducing agent and the sequestering agents, since ferric iron can react with H_2S to

precipitate free sulfur, which itself can damage permeability. The loss of effectiveness of acetic acid at temperatures above 125°F and the possibility of precipitating calcium citrate also are factors that should be considered in guarding against iron precipitates.

Alcohols

Methyl and isopropyl alcohols sometimes are used at concentrations of 5 to 20 vol% of acid to reduce surface tension. Methyl alcohol is sometimes used at concentrations up to 66% to increase vapor pressure of the acid and spent acid solution. Use of alcohols thus improves both rate and degree of cleanup, which can be particularly helpful in dry gas wells.

Gelling and Fluid Loss Agents

Natural gums and synthetic polymers are added to acid to increase the viscosity of the acid solution.³ This reduces leakoff into large pore spaces and, to some extent, into natural hairline fractures. It also provides some degree of reaction rate retardation.

Other materials used to control leakoff are fine (100-mesh) sand⁴ and fine salt.⁵ These materials bridge in hairline fractures to reduce fluid flow out of the main fracture during fracture acidizing treatments.

Another successful fluid-loss control agent is a mixture of finely ground, oil-soluble resins.⁶ Originally designed as a diverting agent for use through gravel packs during sandstone matrix acidizing treatments, this agent was later shown to be effective as a fluid-loss agent in fracture acidizing, when used at higher concentrations.⁷

Liquefied Gases

Liquid nitrogen and liquid CO₂ sometimes are used in acid solutions to provide added energy for better well cleanup. Nitrogen also is used to make foamed acid, which provides excellent leakoff control in low permeability rock.^{8,9}

Retarded Acids

It is often desirable in acid fracturing treatments to retard the reaction rate of the acid to provide deeper penetration of active acid into the formation. Retardation may be accomplished by use of slower-reacting acids (HAc and HCOOH), by adding chemicals to reduce reaction rate, or by increasing concentration to extend spending time.

HAc and HCOOH are weakly ionized and sometimes are used to obtain longer reaction time. The additional cost of these acids may prohibit extensive use in certain formations. Deeper matrix penetration than would be obtained by HAc or HCOOH is obtained by the faster-reacting HCl because the channeling or wormhole effect produced by the HCl reduces the A/V ratio, thus prolonging reaction time. In fractures, the HAc and HCOOH would obtain deeper penetration than HCl; however, larger volumes would be required to dissolve an equivalent amount of rock.

Some chemicals, added to HCl, form a barrier on the rock surface, which interferes with its normal contact and "retards" the reaction rate of the acid. Acid-in-oil emulsions generally exhibit retarded reaction rates. The acid in the emulsion does not completely contact the rock sur-

face because of the presence of an interfering oil film. This is particularly true for emulsions with at least 20% oil as the outer phase. Certain surfactants recently have been found to be beneficial in reducing reaction rate and, thus, extending spending time and penetration distance. These surfactants, in the presence of oil, provide a hydrophobic or water-repellent, oil-like film on the rock surface that restricts acid/rock contact. Fluid-loss materials and gelling agents (acid-thickening additives) also tend to reduce the reaction of HCl by film development on rocks.

High concentrations of an acid provide longer reaction times than lower concentrations because (1) there is more acid to react, (2) the additional reaction products further retard reaction rates, and (3) the enlarged flow path, with reduced A/V ratio, extends the spending time and penetration of a high-concentration acid. For example, 28% HCl may take four to six times longer to react completely than does 15% HCl. In this case, the reaction time is extended in spite of the initially faster reaction rate of the 28% HCl.

Acidizing Techniques

There are three fundamental techniques used in acidizing treatments.

1. Wellbore Cleanup. This entails fill-up and soak of acid in the wellbore. Fluid movement is at a minimum, unless some mechanical means of agitation is used.

2. Matrix Acidizing. This is done by injecting acid into the matrix pore structure of the formation, below the hydraulic fracturing pressure. Flow pattern is essentially through the natural permeability structure.

3. Acid Fracturing. This is injection into the formation above hydraulic fracturing pressure. Flow pattern is essentially through hydraulic fractures; however, much of the fluid does leak off into the matrix along the fracture faces.

The technique selected will depend on what the operator wishes to accomplish with the treatment.

Matrix acidizing may be selected as a proper technique for one or more of the following reasons: (1) to remove either natural or induced formation damage, (2) to achieve low-pressure breakdown of the formation before fracturing, (3) to achieve uniform breakdown of all perforations, (4) to leave zone barriers intact, or (5) to achieve reduced treating costs.

The principal types of formation damage are mud invasion, cement, precipitates, saturation changes, and migration of fines. The effect of damage on injectivity or productivity is shown in Figs. 54.12 and 54.13. It can be seen that the greatest flow increase results from restoring the natural rock permeability. The magnitude of this primary flow increase depends on the extent (radius) of the damage. Further increase in pore size by matrix acidizing results in only a limited increase in flow (stimulation).

If the producing formation does not have enough natural permeability, then a hydraulic fracturing treatment should be considered. The primary purpose of fracturing is to achieve injectivity or productivity beyond the natural reservoir capability. An effective fracture may create a new permeability path, interconnect existing permeability streaks, or break into an untapped portion of the reservoir.

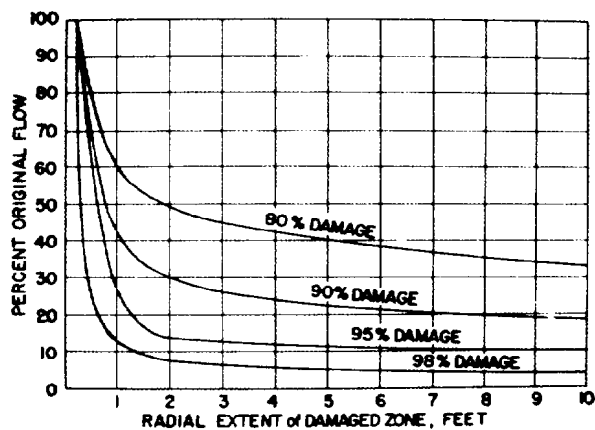


Fig. 54.12—Effect of damaged zone on flow.

The success of any fracturing treatment depends on two factors: fracture conductivity and effective penetration, as illustrated in Fig. 54.14. If enough etched fracture conductivity can be achieved, then increased penetration becomes important. For any given formation, there will be an optimum conductivity and penetration, which will be controlled by cost. In other words, there will be some point where production increase per dollar spent will be a maximum. This must be determined by pretreatment design.

Laboratory Testing

The physical and chemical characteristics of the formation rock often affect the results of an acidizing treatment. In some cases, the use of special additive chemicals will improve the action of the acid or avoid cleanup difficulties in returning the spent acid following the job. It is important, therefore, that samples of the formation rock (either cores or cuttings) and, if possible, samples of the crude oil and formation brine be subjected to laboratory testing before acidizing to design the most effective treatment.

Customarily, permeability, porosity, and oil- and water-saturation tests are run on formation core samples, using standardized core-analysis procedures. In addition, acid-solubility tests are run to determine to what extent the formation will respond to an acidizing treatment.

Formation solubility may be determined two different ways. In the first method, a weighed chunk of the rock is immersed in an excess of acid and maintained at formation temperature. After an hour, any insoluble residue is washed, dried, and weighed. With samples known to contain silicates, additional tests may be run in which the rock is exposed to the dissolving action of combined HCl and HF.

A more rapid test, suitable for samples known to consist largely of limestone or dolomite, entails dissolving a weighed sample of the rock in an excess of HCl and measuring the volume of CO₂ gas evolved during the reaction. A simple apparatus for conducting this test is shown in Fig. 54.15.

In addition to these tests of the formation rock, the emulsifying tendencies of the formation crude should be determined whenever possible. Samples of the crude are mixed

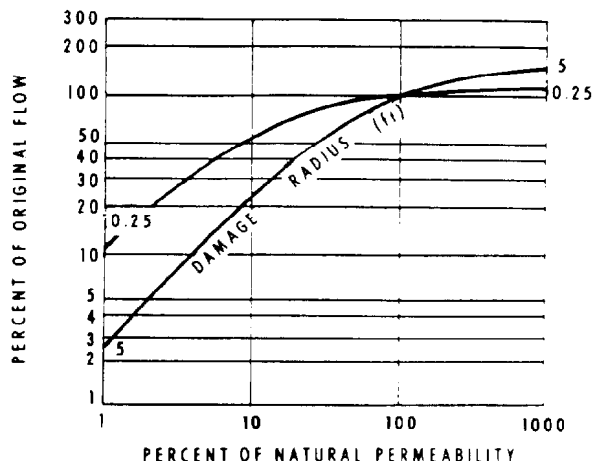


Fig. 54.13—Effect of permeability changes on radial flow.

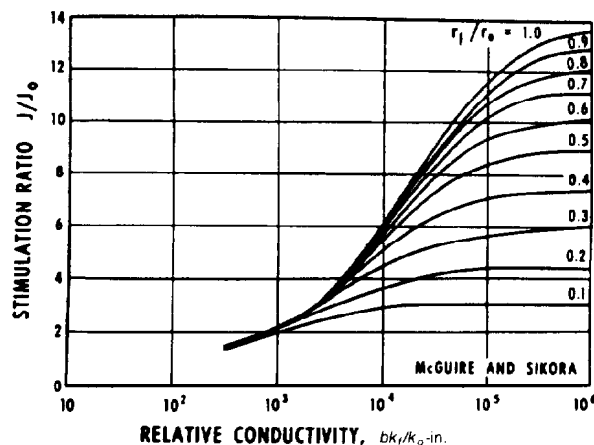


Fig. 54.14—Relationship of conductivity and penetration to productivity increase. J = productivity index of well after stimulation, J_0 = productivity index before stimulation, r_i = radius of fracture (ft), r_o = drainage radius (ft), k_f = permeability of fracture (md), k_o = permeability of formation (md), and b = fracture width (in.).

with the acid to be used in the acidizing treatment and then are shaken. The mixture is allowed to stand, and the time required for the oil and acid to separate is observed. Additional tests are run on mixtures of the crude oil with acid that has been spent completely on pulverized formation rock. If the formation crude shows a tendency to emulsify with either the fresh acid or the spent acid, the use of an appropriate surfactant is indicated.

Similar tests using a mixture of crude and acid are made to determine acid sludging tendencies. Sludge is identified by filtering the mixture through a small mesh screen. Appropriate surfactants that are added to the acid to prevent sludge formation are evaluated.

Other determinations of rock characteristics include tests for clay swelling tendencies and tests to determine rock composition (such as X-ray diffraction analysis) to indicate need for stabilizers, sequestering agents, or other acid additives.

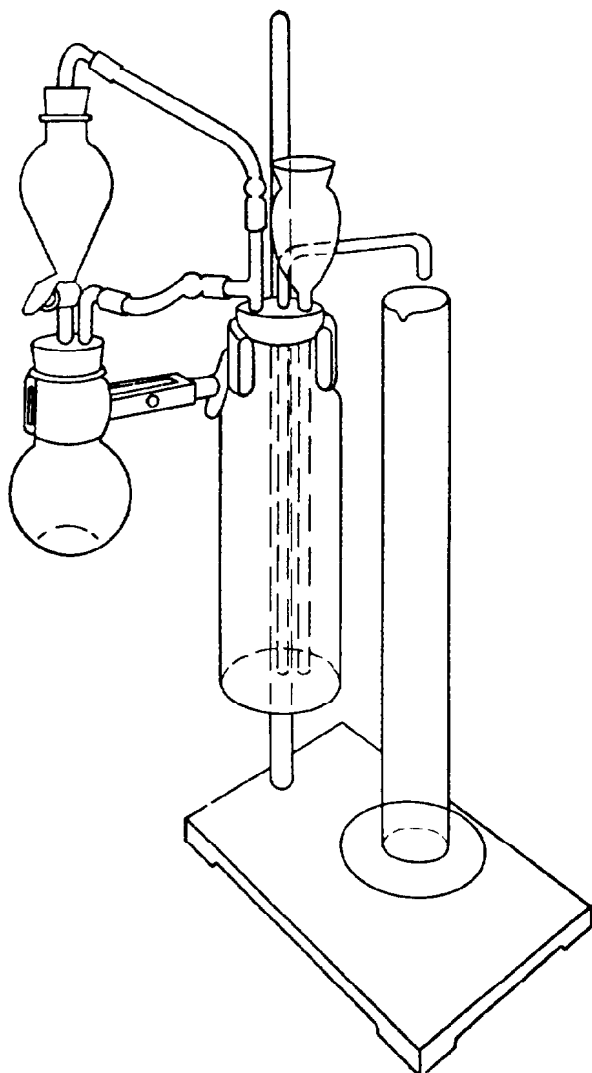


Fig. 54.15—Laboratory solubility tester (carbon dioxide evolution method).

Acid Treatment Design

Three techniques of acidizing have been described previously. Wellbore cleanup treatments normally do not require complicated design procedures. Matrix and fracture acidizing treatments, on the other hand, can involve extensive predesign laboratory testing and complicated design procedures and calculations.

Matrix Acidizing—Carbonate Formations

Matrix acidizing in carbonates normally is used to break down all perforations and to remove damage. Plugging materials can be removed and permeability restored in two ways: (1) by dissolving the damaging material itself or (2) by dissolving part of the rock in which the damage exists. In carbonate rocks with acid solubilities greater than 50%, the latter method is often most effective. The dislodged solid particles or liquids then can be removed physically by the return of the spent acids to the well.

HCl normally is used in matrix treatments of carbonates, but HAc and/or HCOOH should be considered

TABLE 54.4—FLOW THROUGH PORES OF VARIOUS SIZES

Diameter of Pore (μm)	Pore Volume (%)	Flow Through Pores (% of Total Flow)
< 1	60	10
1 to 2	25	15
2 to 5	12	30
5 and above	3	45

for wells with temperatures in excess of 250 to 300°F. Any acid solution should be modified by use of proper additives to meet special situations.

Acid inhibitor selection must be based primarily on treating temperature and, to some extent, on the type of acid formulation.

Surfactant type and concentration should be selected to minimize emulsion tendencies and, perhaps, to aid in dispersing fine undissolved solids. These may be drilling mud, cement solids, or natural clay particles released from the formation. Suspension and removal of these materials can play an important part in the overall treatment results.

Diverting agents may be used to promote uniform penetration in long sections. Acid-swellable synthetic polymers, controlled-solubility particulate solids, perforation ball sealers, gel slugs, etc., have been used successfully to provide more uniform injectivity. Assuring the distribution of acid into the entire interval is a critical part of carrying out a matrix treatment. Otherwise, large portions of the interval may get very little, if any, acid.

In matrix acidizing, injection rates should be controlled so that the formation is not fractured. The use of as high a rate as possible without exceeding the fracturing pressure is recommended. In certain cases, it may be necessary to create a fracture to open perforations, after which pressure can be reduced below fracturing pressure, thus providing a matrix flow pattern.

Controlling the injection pressure is the primary concern. Maintaining bottomhole pressures below hydraulic fracturing pressures may restrict injection rates to only fractional barrels per minute. An increasing rate may then be possible as the treatment progresses.

Because of differences in the size and shape of the pores, penetration of acid in a carbonate rock is far from uniform. Porosity anomalies may result from vugs, hairline fissures, or tortuous capillary-like pores. Because of these heterogeneities, a "channeling" or "wormholing" occurs with most acid formulations. The resultant effect is the attainment of much greater acid penetration of matrix than expected.

The wide distribution of flow in a rock of varying pore diameters (Table 54.4) is further accentuated by acidizing. As discussed in a preceding section, the fast-reacting HCl may provide greater penetration of the limestone matrix than the slow-reacting acetic acid, but not as great as with the emulsified or gelled acids. Evidently, the slow reaction of acetic acid does not change the flow distribution rapidly enough to "channel," but rather results in several small pore enlargements for short distances as opposed to a few large, long channels.

Since the formation damage normally does not exist for a great distance from the wellbore, the volume of acid needed is small. With a formation porosity of 10%, 60

gal of acid per foot of section will fill the porosity to a radius of 5 ft. Usually, matrix treatment volumes range from 50 to 250 gal per foot of section. If damage is deeper than 5 to 10 ft, then larger volumes of acid, a means of retarding the reaction rate, or, perhaps, fracturing techniques, may be required. Very little rock must be dissolved to result in a significant amount of damage repair or permeability increase. Removal of only 1% of limestone or dolomite rock for a distance of about 5 ft from the wellbore requires only 70 gal of 15% HCl/ft of vertical interval.

An overflush in the matrix acidizing treatment is recommended. This will ensure efficient displacement of the acid into the matrix. A minimum shut-in time is recommended before returning the spent acid to the well. Since the spending time of acid is short, a long shut-in time of several hours is not necessary, even for the so-called "retarded acid." The overflush fluid may be brine, water, oil, or a weak acid. Enough volume should be used to ensure maximum penetration of the last portion of the acid, before it is spent.

Matrix Acidizing—Sandstone Formations

The purpose of sandstone acidizing is to restore permeability by dissolving away formation-damaging clay-like minerals or other acid-soluble materials. The clay may be inherent in the formation or may be the result of drilling mud or workover fluid invasion.

The type of acid used most often in sandstones is a mixture of HF and HCl. These mixtures commonly are referred to as mud acids or mud removal acids. As previously discussed, fluoboric acid also has become popular in sandstone formations. Concentrations of 2 to 6% HF and 8 to 12% HCl normally are used. If a significant amount of calcium carbonate is present in the formation (5 to 10%), a spearhead of HCl should be used to react with it before the HF/HCl is injected. With carbonate content above 20%, HF acid probably is not needed, except to give entry through clay damage.

As in any matrix-type treatment, injection of the HF/HCl should be below fracturing pressure. The volume of acid required depends on the depth and severity of the damage. A total of 50 to 250 gal of acid per foot of interval is the normal treatment volume, if damage is not extensive. An acid solubility test may not be a realistic evaluation of acid requirements.

Results of a field study by Gidley *et al.*¹⁰ confirmed some earlier recommendations based on laboratory core flow studies. These results showed much greater success when more than 125 gal/ft acid was used.

The reported core flow test showed what response the formation will have to acid. This is illustrated in Fig. 54.16. Although some of these formations have approximately the same acid (HF/HCl) solubility, permeability, and porosity, the response to acid is quite different.

Initial reduction in permeability is a common occurrence observed with many formation core flow tests. It is attributed to sloughing particles (clays, silica, fines, etc.) that apparently bridge in the flow channels and restrict flow, before their further reaction with the acid. An inadequate acid volume treatment could lead to a restricted permeability in a formation, if the bridging is severe.

Since secondary reactions may occur, resulting in possible precipitation of damaging reaction products, mud

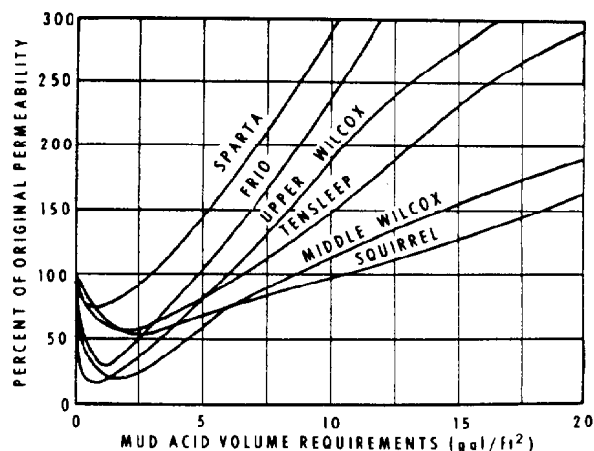


Fig. 54.16—Response of cores from producing formations to mud acid.

acid should be returned to the wellbore as soon as the initial spending time has elapsed. The spent HF/HCl acids should not be allowed to mix with formation brine, if at all possible because of the danger of precipitates.

Inhibitors, surfactants, and diverting methods should be selected just as in an HCl acid treatment. As in the case of matrix acid treatment in carbonates, an overflush is recommended. Suitable fluids include weak acid, oil, or water. Formation brine should not be used to overflush HF/HCl. Short shut-in times should be used—a few hours at the most.

Fracture Acidizing—Carbonate Formations

The primary purpose of an acid fracturing treatment of a carbonate formation is to achieve productivity or injectivity beyond the natural capabilities of the reservoir. It is most applicable in formations with a low and/or ineffective permeability structure. The effectiveness of an induced hydraulic fracture is a function of both its conductivity and the extent of penetration of the drainage radius of the well.

These factors will depend on well and reservoir properties, formation characteristics, injection rate, type and volume of acid used, and shape and orientation of the fracture. All these factors have been correlated by several companies into "guides" to acid fracture treatment design. Such guides provide mathematical relationships for determining the fracture area and conductivity achieved by different volumes of specific acid formulations at various injection formulations. These guides are programmed for computer calculation, so that rapid comparison of various treatment designs can be made for selection of best results per dollar of treatment cost. These guides are not sufficiently similar to get clear comparison between different companies but should be compared only with other calculations from the same system.

Critical Wells

In ultradeep, high-temperature wells, many factors must be considered in the stimulation treatment design. First, the high BHT can drastically affect reaction rate of acid, inhibition, and other properties of the acid formulation.

These effects can be partially offset by formation cool-down techniques. Basically, this consists of pumping a pad volume of fluid (generally gelled water) into the formation to cool the rock to a more normal treating temperature. Most companies have computer programs available to calculate pad volumes required for a given temperature reduction.

Another problem is created when fluids with temperatures lower than BHT's are used. This problem is mechanical and involves tubing movement. In ultradeep wells, such contraction can create stress in the tubing greater than tubing strength, resulting in a parted string. The solution to this problem is to slack off or to release tension at the top of the tubing string as the job progresses. Again, computer programs are available from most service companies to predict tubing movement under given conditions.

Summary

In summary, acidizing is a process that uses reactive materials to increase well production by dissolving either the reservoir rock or damaging materials blocking the pore spaces of the rock. Different kinds of acids and additives are available, so that treating fluids can be tailored to meet individual well needs. Acid formulations may be applied in either matrix- or fracture-type treatment, depending on the degree of stimulation or production increase desired. While acidizing, and acidizing treatment design, in detail are beyond the scope of this text, published literature offers answers and assistance in solving many of the problems encountered. The General References cover many of the recent technical developments in this field. In addition, most service companies providing acidizing service offer laboratory facilities, technical assistance, and computer programs for problem analyses and treatment design.

References

1. Templeton, C.C. *et al.*: "Self-Generating Mud Acid," *J. Pet. Tech.* (Oct. 1975) 1199-1203.
2. Thomas, R.L. and Crowe, C.W.: "Matrix Treatment Employs New Acid System for Stimulation and Control of Fines Migration in Sandstone Formations," paper SPE 7566 presented at the 1978 SPE Annual Technical Conference and Exhibition, Houston, Oct. 1-3.
3. Crowe, C.W., Martin, R.C., and Michaelis, A.M.: "Evaluation of Acid Gelling Agents for Use in Well Stimulation," paper SPE 9384 presented at the 1980 SPE Annual Technical Conference and Exhibition, Dallas, Sept. 21-24.
4. Miller, B.D. and Warembourg, P.A.: "Prepack Technique Using Fine Sand Improves Results of Fracturing and Fracture Acidizing Treatments," paper SPE 5643 presented at the 1975 SPE Annual Technical Conference and Exhibition, Dallas, Sept. 28-Oct. 1.
5. Schrieter, F.E. and Shaw, M.S.: "Use of Fine Salt as a Fluid Loss Material in Acid Fracturing Stimulation Treatments," paper SPE 7570 presented at the 1978 SPE Annual Technical Conference and Exhibition, Houston, Oct. 1-3.
6. Crowe, C.W.: "Evaluation of Oil-Soluble Resin Mixtures as Diverting Agents for Matrix Acidizing," paper SPE 3505 presented at the 1971 SPE Annual Meeting, New Orleans, Oct. 3-6.
7. Nierode, D.E. and Kruk, K.F.: "An Evaluation of Acid Fluid Loss Additives, Retarded Acids, and Acidized Fracture Conductivity," paper SPE 4549 presented at the 1973 SPE Annual Fall Meeting, Las Vegas, Sept. 30-Oct. 3.
8. King, G.E. and Hollingsworth, F.H.: "Evaluation of Diverting Agent Effectiveness and Clean-up Characteristics Using a Dynamic Laboratory Model—High Permeability Case," paper SPE 8400 presented at the 1979 SPE Annual Technical Conference and Exhibition, Las Vegas, Sept. 23-26.
9. Scherubel, G.A. and Crowe, C.W.: "Foamed Acid: A New Concept in Fracture Acidizing," paper SPE 7568 presented at the 1978 SPE Annual Technical Conference and Exhibition, Houston, Oct. 1-3.
10. Gidley, J.L., Ryan, J.C., and Mayhill, T.D.: "Study of Field Applications of Sandstone Acidizing," *J. Pet. Tech.* (Nov. 1976) 1289-94.

General References

- Abram, A. *et al.*: "The Development and Application of a High pH Acid Stimulation System for a Deep Mississippi Gas Well," paper SPE 7565 presented at the 1978 SPE Annual Technical Conference and Exhibition, Houston, Oct. 1-3.
- Barron, A.N., Hendrickson, A.R., and Wieland, D.R.: "The Effect of Flow on Acid Reactivity in a Carbonate Fracture," *J. Pet. Tech.* (April 1962) 409-15; *Trans., AIME*, 225.
- Black, H.N. and Stubbs, B.A.: "A Case History Study—Evaluation of San Andres Stimulation Results," paper SPE 5649 presented at the 1975 SPE Annual Technical Conference and Exhibition, Dallas, Sept. 29-Oct. 1.
- Broddus, E.C. and Knox, J.A.: "Influence of Acid Type and Quantity in Limestone Etching," paper API No. 851-39-1 presented at API Production Dev. Mid-Continent Dist., Wichita, March 31-April 2, 1965.
- Burkill, G.C.C. and Pierre, M.L.: "Successful Matrix Acidizing of Sandstones Requires a Reliable Estimate of Wellbore Damage," paper SPE 5590 presented at the 1975 SPE Annual Technical Conference and Exhibition, Dallas, Sept. 29-Oct. 1.
- Chatelain, J.C., Silberberg, I.H., and Schechter, R.S.: "Thermodynamic Limitations in Organic Acid-Carbonate Systems," *Soc. Pet. Eng. J.* (Aug. 1976) 189-95.
- Church, D.C., Quisenberry, J.L., and Fox, K.B.: "Field Evaluation of Gelled Acid for Carbonate Formations," *J. Pet. Tech.* (Dec. 1981) 2471-74.
- Clark, G.J., Wong, T.C.T., and Mungan, N.: "New Acid Systems for Sandstone Stimulation," *Proc., SPE Formation Damage Control Symposium*, Lafayette, LA (March 24-25, 1982) 187-97.
- Coppel, C.P.: "Factors Causing Emulsion Upsets in Surface Facilities Following Acid Stimulation," *J. Pet. Tech.* (Sept. 1975) 1060-66.
- Coulter, G.R. and Purvis, S.B.: "Successful Stimulation Practices—Offshore Holland," *J. Pet. Tech.* (June 1982) 1211-18.
- Coulter, A.W. Jr., Copeland, C.T., and Harrisberger, W.H.: "A Laboratory Study of Clay Stabilizers," *Soc. Pet. Eng. J.* (Oct. 1979) 267-69.
- Coulter, A.W. Jr. *et al.*: "Alternate Stages of Pad Fluid and Acid Provide Improved Leakoff Control for Fracture Acidizing," paper SPE 6124 presented at the 1976 SPE Annual Technical Conference and Exhibition, New Orleans, Oct. 3-6.
- Coulter, A.W. Jr. *et al.*: "Mathematical Model Simulates Actual Well Conditions In Fracture Acidizing Treatment Design," paper SPE 5004 presented at the 1974 SPE Annual Meeting, Houston, Oct. 6-9.
- Crawford, D.L., Coulter, A.W. Jr., and Osborn, F.E. III: "Removal of Wellbore Damage From Highly Permeable Formations and Naturally Fractured Reservoirs," paper SPE 8796 presented at the 1980 SPE Formation Damage Control Symposium, Bakersfield, CA, Jan. 28-29.
- Crenshaw, P.L., Flippen, F.F., and Pauley, P.O.: "Stimulation Treatment Design for the Delaware Basin Ellenburger," paper SPE 2375 presented at the 1968 SPE Annual Meeting, Houston, Sept. 29-Oct. 2.
- Crowe, C.W. and Minor, S.S.: "Effect of Acid Corrosion Inhibitors Upon Matrix Stimulation Results," paper SPE 11119 presented at the 1982 SPE Annual Technical Conference and Exhibition, New Orleans, Sept. 26-29.

- Davis, J.J., Mancillas, G., and Melnyk, J.D.: "Improved Acid Treatments by Use of the Spearhead Film Technique," paper SPE 1164 presented at the 1965 SPE Rocky Mountain Regional Meeting, Billings, MT, June 3-4.
- Deysarkar, A.K. *et al.*: "Crosslinked Fracture Acidizing Acid Gel," paper 82-33-16 presented at the 1982 CIM Annual Meeting, Calgary, June 6-9.
- Dill, W.R.: "Retarded Acidizing Fluids," U.S. Patent No. 4,322,306 (1982).
- Dill, W.R. and Keeney, B.R.: "Optimizing HCl-Formic Acid Mixtures for High Temperature Stimulation," paper SPE 7567 presented at the 1978 SPE Annual Technical Conference and Exhibition, Houston, Oct. 1-3.
- Dunlap, P.M. and Hegner, J.S.: "An Improved Acid for Calcium Sulfate Bearing Formations," *J. Pet. Tech.* (Jan. 1960) 67-70; *Trans.*, AIME, **219**.
- Ely, J., McDow, G., and Turner, J.: "Stimulation Techniques Used in the Austin Chalk," *Proc.*, 29th Annual Southwestern Pet. Assn. Short Course, Lubbock (1982) 110-21.
- Fogler, H.S., Lund, K., and McCune, C.C.: "Predicting the Flow and Reaction of HCl/HF Acid Mixtures in Porous Sandstone Cores," *Soc. Pet. Eng. J.* (Oct. 1976) 248-60; *Trans.*, AIME, **261**.
- Ford, W.G.F. and Roberts, L.D.: "The Effect of Foam on Surface Kinetics in Fracture Acidizing," *J. Pet. Tech.* (Jan. 1985) 89-97.
- Ford, W.G.F.: "Foamed Acid, An Effective Stimulation Fluid," paper SPE 9385 presented at the 1980 SPE Annual Technical Conference and Exhibition, Dallas, Sept. 21-24.
- Ford, W.G.F., Burkleca, L.F., and Squire, K.A.: "Foamed Acid Stimulation Success in the Illinois and Michigan Basins," paper SPE 9386 presented at the 1980 SPE Annual Technical Conference and Exhibition, Dallas, Sept. 21-24.
- Graham, J.W.: "Well Stimulation by Two-Phase Flow," U.S. Patent No. 4,174,753 (1979).
- Green, E.B., Lybarger, J.H., and Richardson, E.A.: "In-Situ Neutralization System Solves Facility Upset Problems," paper SPE 4796 presented at the 1974 SPE Annual Meeting, Houston, Oct. 6-9.
- Haafkens, R., Luque, R.F., and DeVries, W.: "Method for Forming Channels of High Fluid Conductivity in Formation Parts Around a Borehole," U.S. Patent No. 4,249,609 (1981).
- Hall, B.E.: "Methods and Compositions for Dissolving Silicates," U.S. Patent No. 4,304,676 (1981).
- Hall, B.E., Underwood, P.J., and Tinnemeyer, A.C.: "Stimulation of the North Coles Levee Field with a Retarded-HF-Acid," paper SPE 9934, presented at the 1981 SPE California Regional Meeting, Bakersfield, March 25-27.
- Hall, B.E. and Anderson, B.W.: "Field Results for a New Retarded Sandstone Acidizing System," paper SPE 6871 presented at the 1977 SPE Annual Technical Conference and Exhibition, Denver, Oct. 9-12.
- Harris, F.N.: "Application of Acetic Acid in Well Completion, Stimulation, and Reconditioning," *J. Pet. Tech.* (July 1961) 637-39.
- Harris, L.E.: "High Viscosity Acidic Treating Fluids and Methods of Foaming and Using the Same," U.S. Patent No. 4,324,668 (1982).
- Harris, O.E., Hendrickson, A.R., and Coulter, A.W. Jr.: "High Concentration Hydrochloric Acid Aids Stimulation Results in Carbonate Reservoirs," *J. Pet. Tech.* (Oct. 1966) 1291-96.
- Hendrickson, A.R. and Cameron, R.C.: "New Fracture Acid Technique Provides Efficient Stimulation of Massive Carbonate Sections," *J. Can. Pet. Tech.* (Jan.-March 1969) 1-5.
- Hendrickson, A.R., Roscne, R.B., and Wieland, D.R.: "The Role of Acid Reaction Rates in Planning Acidizing Treatments," *Trans.*, AIME, **222** (1961).
- Hendrickson, A.R., Hurst, R.E., and Wieland, D.R.: "Engineered Guide for Planning Acidizing Treatments Based on Specific Reservoir Characteristics," *J. Pet. Tech.* (Feb. 1960) 16-23; *Trans.*, AIME, **219**.
- Hill, D.G. and DeMott, D.N.: "Effect of Hydrogen Sulfide on Inhibition of Oil Field Tubing in Hydrochloric Acid," paper SPE 6660 presented at the 1977 SPE East Texas Section, Sour Gas Symposium, Tyler, Nov. 14-15.
- Holman, G.B.: "State-of-the-Art Well Stimulation," *J. Pet. Tech.* (Feb. 1982) 239-41.
- Horton, H.L., Hendrickson, A.R., and Crowe, C.W.: "Matrix Acidizing of Limestone Reservoirs," paper API-No. 906-10-F presented at the 1965 API Prod. Div. Southwest District Meeting, Dallas, March 10-12.
- Hudock, K. and Skelton, N.: "Fracture Acids Undergo Comparative Tests," *Northeast Oil Reporter* (Feb. 1982) 74-76, 78.
- Jennings, A.R.: "The Effect of Surfactant-Bearing Fluids on Permeability Behavior in Oil-Producing Formations," paper SPE 5635 presented at the 1975 SPE Annual Technical Conference and Exhibition, Dallas, Sept. 29-Oct. 1.
- Keeney, B.R. and Frost, J.G.: "Guidelines Regarding the Use of Alcohols in Acidic Stimulation Fluids," paper SPE 5158 presented at the 1974 SPE Annual Meeting, Houston, Oct. 6-9.
- Kincheloe, R.L.: "Matrix Acidizing Reduces Formation Damage," *Pet. Eng.* (Jan. 1967) 74-75, 78, 83.
- King, G.E.: "Foam Stimulation Fluids: What They Are, Where They Work," *Pet. Eng. Intl.* (July 1982) 52, 56, 58, 60.
- Knox, J.A., Lasater, R.M., and Dill, W.R.: "A New Concept in Acidizing Utilizing Chemical Retardation," paper SPE 975 presented at the 1964 SPE Annual Meeting, Houston, Oct. 11-14.
- Kunze, K.R. and Shaughnessy, C.M.: "Acidizing Sandstone Formations with Fluoboric Acid," paper SPE 9387 presented at the 1980 SPE Annual Technical Conference and Exhibition, Dallas, Sept. 21-24.
- Labrid, J.: "Acid Stimulation in Argillaceous Sandstone—Interpreting Acid Response Curves—Measuring Kinetic and Petrophysical Parameters," paper SPE 5156 presented at the 1974 SPE Annual Meeting, Houston, Oct. 6-9.
- Lee, M.H. and Roberts, L.D.: "The Effect of Heat of Reaction on Temperature Distribution and Acid Penetration in a Fracture," *Soc. Pet. Eng. J.* (Dec. 1980) 501-07.
- Leggett, B. *et al.*: "Use of a Novel Liquid Gelling Agent for Acidizing in the Levelland Field," paper SPE 11121 presented at the 1982 SPE Annual Technical Conference and Exhibition, New Orleans, Sept. 26-29.
- McBride, J.R., Rathbone, M.J., and Thomas, R.L.: "Evaluation of Fluoboric Acid Treatment in the Grand Isle Offshore Area Using Multiple-Rate Flow Test," paper SPE 8339 presented at the 1979 SPE Annual Technical Conference and Exhibition, Las Vegas, Sept. 23-26.
- McCune, C.C. *et al.*: "Acidization VI—A New Model of the Physical and Chemical Changes in Sandstone During Acidizing," paper SPE 5157 presented at the 1975 SPE Annual Technical Conference and Exhibition, Dallas, Sept. 29-Oct. 1.
- McLaughlin, W.A. and Berkshire, D.C.: "Acidizing Reservoirs While Chelating Iron with Sulfosalicylic Acid," Canada Patent No. 1,086,485 (1980).
- McLeod, H.O., Ledlow, L.B., and Till, M.V.: "The Planning, Execution and Evaluation of Acid Treatments in Sandstone Formations," paper SPE 11931 presented at the 1983 SPE Annual Technical Conference and Exhibition, San Francisco, Oct. 5-8.

- McLeod, H.O. and Coulter, A.W. Jr.: "The Use of Alcohol in Gas Well Stimulation," paper SPE 1663 presented at the 1966 SPE Eastern Regional Meeting, Columbus, OH, Nov. 10-11.
- McLeod, H.O., McGinty, J.E., and Smith, C.F.: "Deep Well Stimulation with Alcoholic Acid," paper SPE 1558 presented at the 1966 SPE Annual Meeting, Dallas, Oct. 2-5.
- Miller, B.D. and Bergstrom, J.M.: "Results of Acid-in-Oil Emulsion Stimulations of Carbonate Formations," paper SPE 5648 presented at the 1975 SPE Annual Technical Conference and Exhibition, Dallas, Sept. 28-Oct. 1.
- Moore, E.W., Crowe, C.W., and Hendrickson, A.R.: "Formation, Effect and Prevention of Asphaltene Sludges During Stimulation Treatment," *J. Pet. Tech.* (Sept. 1965) 1023-28.
- Muecke, T.W.: "Principles of Acid Stimulation," *Proc., SPE Intl. Petroleum Conference and Exhibition, Beijing, China* (1982) 2, 291-303.
- Norman, L.R., Conway, M.W., and Wilson, J.M.: "Temperature Stable Acid Gelling Polymers, Laboratory Evaluation and Field Results," paper SPE 10260 presented at the 1981 SPE Annual Technical Conference and Exhibition, San Antonio, Oct. 5-7.
- Norman, L.R.: "Aqueous Acid Solution Gelling Agents," Canada Patent No. 1,106,724 (1981).
- Novotny, E.J.: "Prediction of Stimulation from Acid Fracturing Treatments Using Finite Fracture Conductivity," *J. Pet. Tech.* (Sept. 1977) 1186-94; *Trans., AIME*, 263.
- Pabley, A.S., Ewing, B.C., and Callaway, R.E.: "Performance of Crosslinked Hydrochloric Acid in the Rocky Mountain Region," paper SPE 10877 presented at the 1982 SPE Rocky Mountain Regional Meeting, Billings, MT, May 19-21.
- Pollard, P.: "Evaluation of Acid Treatments From Pressure Buildup Analysis," *J. Pet. Tech.* (March 1959) 38-43; *Trans., AIME*, 216.
- Roberts, L.D. and Guin, J.A.: "A New Method for Predicting Acid Penetration Distances," *Soc. Pet. Eng. J.* (Aug. 1975) 277-85.
- Ross, W.M., Pierson, N.O., and Coulter, A.W.: "Matrix Acidizing Corrects Formation Damage in Sandstones," *Pet. Eng.* (Nov. 1968) 64-69.
- Rowan, G.: "Theory of Acid Treatments of Limestone Formations," *J. Inst. Pet.* (Nov. 1959) 321-32.
- Royle, R.A.: "Demulsifier for Inclusion in Injected Acidization Systems for Petroleum Formation Stimulation," U.S. Patent No. 4,290,901 (1981).
- Salathiel, W.M. and Shaughnessy, C.M.: "Method for Generating Hydrofluoric Acid in a Subterranean Formation," U.S. Patent No. 4,136,739 (1979).
- Scherubel, G.A.: "Method of Controlling Fluid Loss in Acidizing Treatment of a Subterranean Formation," U.S. Patent No. 4,237,974 (1980).
- Scherubel, G.A.: "Self-Breaking Retarded Acid Emulsion," Canada Patent No. 1,086,934 (1980).
- Shaughnessy, C.M. and Kunze, K.R.: "Understanding Sandstone Acidizing Leads to Improved Field Practices," paper SPE 9388 presented at the 1980 SPE Annual Technical Conference and Exhibition, Dallas, Sept. 21-24.
- Smith, C.F., Dollarhide, F.E., and Byth, N.J.: "Acid Corrosion Inhibitors—Are We Getting What We Need?" *J. Pet. Tech.* (May 1978) 737-46.
- Smith, C.F., Crowe, C.W., and Wieland, D.R.: "Fracture Acidizing in High Temperature Limestone," paper SPE 3008 presented at the 1970 SPE Annual Meeting, Houston, Oct. 4-7.
- Smith, C.F., Crowe, C.W., and Nolan, T.J. III: "Secondary Deposition of Iron Compounds Following Acid Treatments," *J. Pet. Tech.* (Sept. 1969) 1121-29.
- Smith, C.F., Nolan, T.J. III, and Crenshaw, P.L.: "Removal and Inhibition of Calcium Sulfate Scale In Waterflood Projects," *J. Pet. Tech.* (Nov. 1968) 1249-57.
- Smith, C.F., Ross, W.M., and Hendrickson, A.R.: "Hydrofluoric Acid Stimulation—Developments for Field Application," paper SPE 1284 presented at the 1965 SPE Annual Meeting, Denver, Oct. 3-6.
- Smith, C.F. and Hendrickson, A.R.: "Hydrofluoric Acid Stimulation of Sandstone Reservoirs," *J. Pet. Tech.* (Feb. 1965) 215-22; *Trans., AIME*, 234.
- Swanson, B.L.: "Well Acidizing Compositions," U.S. Patent No. 4,240,505 (1980).
- Vivian, T.A.: "Acidification of Subterranean Formations Employing Halogenated Hydrocarbons," U.S. Patent No. 4,320,014 (1982).
- Wade, R.P. and Aziz, K.: "Stimulating the Triassic Carbonates in the Foothills Gas Trend of Northeast British Columbia," paper 81-32-35 presented at the 1981 CIM Annual Meeting, Calgary, May 5-6.
- Walsh, M.P., Lake, L.W., and Schechter, R.S.: "A Description of Chemical Precipitation Mechanisms and Their Role in Formation Damage During Stimulation by Hydrofluoric Acid," *Proc., SPE Formation Damage Control Symposium, Lafayette, LA* (1982) 7-27.
- Watkins, D.R. and Roberts, G.I.: "On-Site Acidizing Fluid Analysis Shows HCl and HF Contents Often Varied Substantially From Specified Amounts," paper SPE 10770 presented at the 1982 SPE California Regional Meeting, San Francisco, March 24-26.
- Wiley, C.B.: "Success of a High Friction Diverting Gel in Acid Stimulation of a Carbonate Reservoir, Cornell Unit, Wasson San Andres Field," *J. Pet. Tech.* (Nov. 1981) 2196-2200; *Trans., AIME*, 271.
- Woodroof, R.A. Jr., Baker, J.R., and Jenkins, R.A. Jr.: "Corrosion Inhibition of Hydrochloric-Hydrofluoric Acid/Mutual Solvent Mixtures at Elevated Temperatures," paper SPE 5645 presented at the 1975 SPE Annual Technical Conference and Exhibition, Dallas, Sept. 29-Oct. 1.
- Young, P.J. and Romocki, J.M.E.: "Well Treating Compositions and Method," Great Britain Patent No. 2,047,305 (1980).

Chapter 55

Formation Fracturing

S.J. Martinez, U. of Tulsa *

R.E. Steanson, Dowell Schlumberger **

A.W. Coulter, Dowell Schlumberger **

Introduction

Fracturing techniques were developed in 1948 and the first commercial fracturing treatments were conducted in 1949. The process rapidly gained popularity because of its high success ratio, and within a very few years, thousands of wells per year were being stimulated by hydraulic fracturing treatments.

Early treatments consisted of pumping 1,000 to 3,000 gal of fracturing fluid, containing about 1 lbm of 20/40-mesh sand/gal, at rates of 1 to 2 bbl/min. Today, a single treatment can require several hundred thousand gallons of fluid and more than a million pounds of propping agent. Although injection rates have exceeded 300 bbl/min in some instances, rates of 20 to 60 bbl/min are about average. Materials, equipment, and techniques have become highly sophisticated. A bibliography is presented at the end of this chapter for those interested in a detailed discussion of particular technologies. This discussion is limited to a generalized description of fracturing theory, materials, techniques, equipment, and treatment planning and design.

Hydraulic Fracturing Theory

Oil and gas accumulations occur in the pore spaces or natural fractures of a subsurface rock where structural and/or stratigraphic features form a trap. When a well is drilled into an oil-bearing rock, the fluids must flow through the surrounding rock into the wellbore before they can be brought to the surface. If the pore spaces of the rock are interconnected so that channels exist through which the oil can flow, the rock is "permeable." The ease with which fluid can flow through a rock determines its degree of permeability. It has high permeability if oil, gas, or water can flow easily through existing channels and

low permeability if the connecting channels are very small and fluid flow is restricted.

In the case of high permeability, drilling fluids may enter the flow channels and later impair flow into the wellbore. In the case of low permeability, the flow channels may not permit enough flow into the wellbore. In either case, the well may not be commercial because fluid cannot flow into the wellbore fast enough. It then becomes necessary to create an artificial channel that will increase the ability of the reservoir rock to conduct fluid into the wellbore. Such channels often can be created by hydraulic fracturing.

During hydraulic fracturing treatments, what actually happens when a rock ruptures, or fractures, can be explained by basic rock mechanics. All subsurface rocks are stressed in three directions because of the weight of overlying formations and their horizontal reactions. Whether one of the horizontal stresses or the vertical stress is the greatest will depend on the additional stresses imposed on the rock by prior folding, faulting, or other geological movement in the area. These tectonic stresses will control the direction of the fracture and determine whether the fracture plane will be horizontal, vertical, or inclined.

Every formation rock has some measure of strength depending on its structure, compaction, and cementation. It has tensile strength in both vertical and horizontal directions. The forces tending to hold the rock together are the stresses on the rock and the strength of the rock itself. When a wellbore is filled with fluid and pressure is applied at the surface, the pressure of the fluid in a perforation or even in the pore spaces of the rock will increase. This hydraulic pressure is applied equally in all directions. If the pressure is increased, the forces applied by the fluid pressure in the rock will become equal to the forces tending to hold the rock together. Any additional pressure applied will cause the rock to split or fracture. The fracture will extend as long as sufficient pressure is applied by injection of additional fluids.

*Deceased; this author also wrote the original chapter on this topic with coauthor P.E. Fitzgerald.

**Retired

When the treatment is complete and flow is reversed to produce the well, pressure will gradually return (decline) to reservoir pressure. As this occurs, the forces tending to hold the rock together come into play again and the fracture will close or "heal." To prevent closure, some solid material must be placed in the fracture to hold it open. Such materials are called "propping agents." Since the permeability of these propping agents is much higher than that of the surrounding formation, the ability of the propped fracture to conduct fluids to the wellbore can result in good production increases. In fact, fracturing has made profitable production possible from many wells and fields that otherwise would not have been profitable.

Formations Fractured

Fracturing has been used successfully in all formations except those that are very soft. Fracturing has proved successful in sand, limestone, dolomitic limestone, dolomite, conglomerates, granite washes, hard or brittle shale, anhydrite, chert, and various silicates. The plastic nature of soft shales and clays makes them difficult to fracture.

Fracturing has helped wells producing from formations that have such a wide range of permeabilities that it is impossible to set upper and lower permeability limits of formations that might be helped by fracturing. Production increases have been obtained from zones having permeabilities ranging from less than 0.1 to as high as 900 md.

Fracture Planes

Analysis of pressures encountered on many thousands of fracturing treatments has shown that the bottomhole pressures (BHP) recorded during the injection of fracturing materials range from 0.40 to 1.80 psi/ft depth.¹ Only in a few treatments have fracturing pressure gradients been outside of this range. Those were almost all in shallow experimental treatments. The fracture gradient g_f is calculated from treatment data by Eq. 1:

$$g_f = \frac{p_h + p_s - p_f}{D}, \quad \dots \dots \dots (1)$$

where

- g_f = unit fracture gradient, psi/ft,
- p_h = total hydrostatic pressure, psi,
- p_s = total surface treating pressure, psi,
- p_f = total friction loss, psi, and
- D = depth of producing interval, ft.

Analysis of thousands of treatments plus experimental work in reservoirs with known fracture gradients indicate that horizontal fractures are produced in reservoirs having fracture gradients of 1.0 or higher. This is generally in shallow wells less than 2,000 ft deep. Vertical fractures are produced in reservoirs having fracture gradients of 0.7 or lower. Such gradients are normally encountered in wells deeper than 4,000 ft. Very few cases have been found where formations have gradients in the intermediate range between 0.7 and 1.0. Consequently, the use of fracture gradients to predict the general inclination of fractures should be useful in almost every case.

With few exceptions, wells in the same reservoir will have nearly identical fracture gradients. Thus, the gradient from one well generally will serve as a guide for the entire pool.

Fracture Area

In 1957, Howard and Fast² presented a mathematical equation to determine the surface area of a newly opened fracture. The equation, based on the quantity of fracturing materials used and the rate at which they are injected into the formation, takes into account the physical characteristics of the fracturing fluids and the specific reservoir conditions. This equation is:

$$A_t = \frac{ib}{4\pi K^2} \left[e^{x^2} \cdot \operatorname{erfc}(x) + \frac{2x}{\sqrt{\pi}} - 1 \right], \quad \dots \dots \dots (2)$$

where

$$x = \frac{2K\sqrt{\pi t}}{b},$$

and

- A_t = total area of one face of the fracture at any time during injection, sq ft,
- i = constant injection rate during fracture extension, cu ft/min,
- t = total pumping time, minutes,
- b = fracture width (breadth), ft,
- K = fluid coefficient, a constant that is a measure of the flow resistance of the fluid leaking off into the formation during fracture operations, and
- $\operatorname{erfc}(x)$ = complementary error function of x .

Essentially, during a fracturing treatment, only the volume of fracturing fluid that remains within the wall of the fracture is effective. The fluid that leaks off into the pores of the rock is lost insofar as added fracture extension is concerned.

When the width of a fracture is known or assumed (fracture width is normally calculated using either Perkins and Kern³ or Khristianovitch and Zheltov⁴ models), the volume of the fracture can be calculated. With these data, it is possible to plot the controllable variables of a fluid volume and injection rate against the fracture area produced for any particular fluid coefficient. Examples of such graphs, for various injection rates, are shown in Figs. 55.1 through 55.5.

The rate of fluid leakoff into the formation, as expressed by the fluid coefficient, is controlled by three variables: the viscosity and compressibility of the reservoir fluid, the viscosity of the fracturing fluid, and the fluid-loss characteristics of the fracturing fluid.

Reservoir-Controlled Fluids

This group includes those fracturing fluids having low viscosity and high fluid-loss characteristics, in which the rate of leakoff is controlled by the compressibility and viscosity of the reservoir fluid.

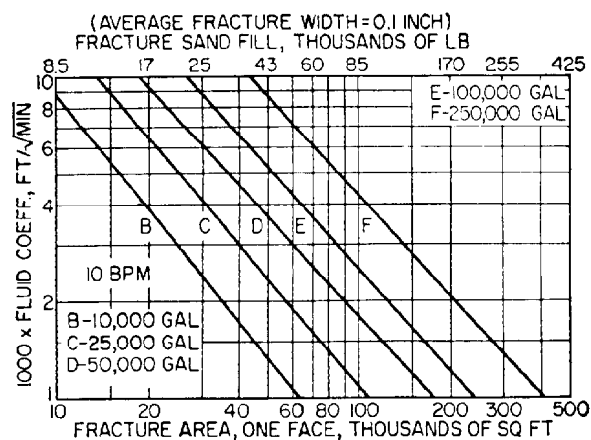


Fig. 55.1—Effect of fluid coefficient and volume on fracture area at constant injection rate of 10 bbl/min.

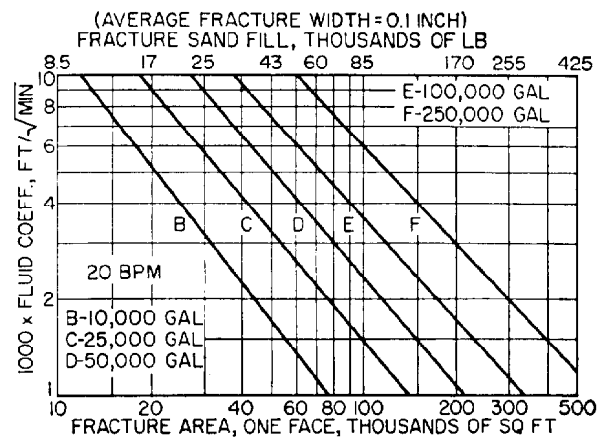


Fig. 55.2—Effect of fluid coefficient and volume on fracture area at constant injection rate of 20 bbl/min.

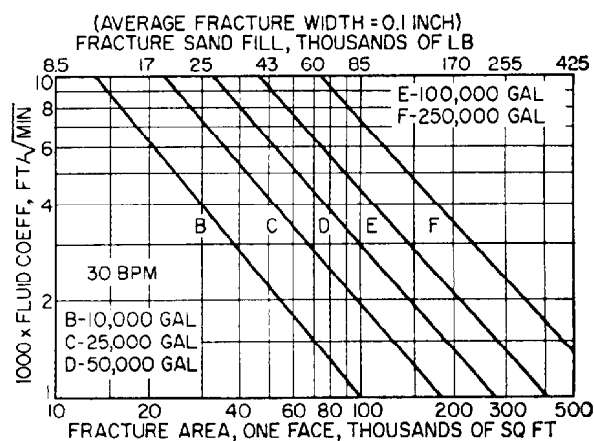


Fig. 55.3—Effect of fluid coefficient and volume on fracture area at constant injection rate of 30 bbl/min.

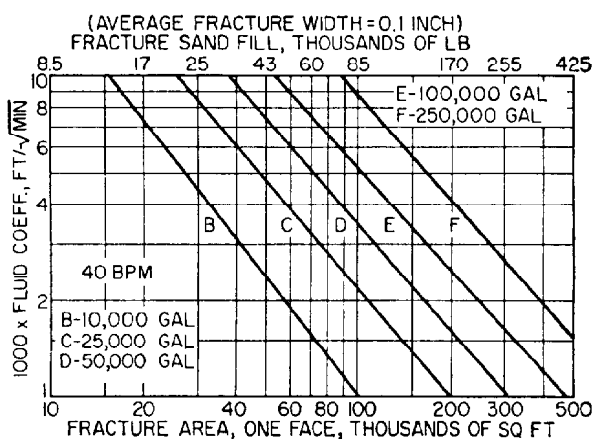


Fig. 55.4—Effect of fluid coefficient and volume on fracture area at constant injection rate of 40 bbl/min.

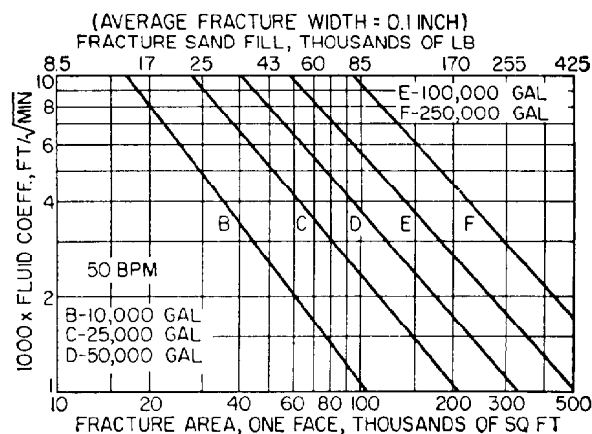


Fig. 55.5—Effect of fluid coefficient and volume on fracture area at constant injection rate of 50 bbl/min.

The coefficient for this type of fracturing fluid may be determined from Eq. 3.²

$$K_c = 0.0374 \Delta p \sqrt{\frac{k_e \phi_e c_R}{\mu_R}}, \quad \dots \dots \dots (3)$$

where

- K_c = fluid coefficient (compressibility-viscosity controlled), ft/min^{1/2},
- Δp = differential pressure, across the face of the fracture, psi,
- k_e = effective formation permeability, darcies,
- ϕ_e = effective formation porosity, %,
- c_R = isothermal coefficient of compressibility of the reservoir fluid, psi⁻¹, and
- μ_R = reservoir fluid viscosity, cp.

Compressibility considerations are generally found to be most applicable in high-pressure, low-volume-factor wells that have high saturations.

Viscosity-Controlled Fluids

This group includes those fracturing fluids in which the rate of leakoff is controlled by the viscosity of the fluid itself. The coefficient for this type of fracturing fluid is expressed by Eq. 4.²

$$K_v = 0.0469 \sqrt{\frac{k_e \Delta p \phi_e}{\mu_f}}, \quad \dots \dots \dots (4)$$

where

- K_v = fluid coefficient (viscosity controlled), ft/min^{1/2},
- k_e = effective formation permeability, darcies,
- Δp = differential pressure across the face of the fracture, psi—this is the product of the fracture gradient and depth, minus normal reservoir pressure, $(g_f \times D) - p_R$,
- ϕ_e = effective formation porosity, %, and
- μ_f = fracturing fluid viscosity, cp.

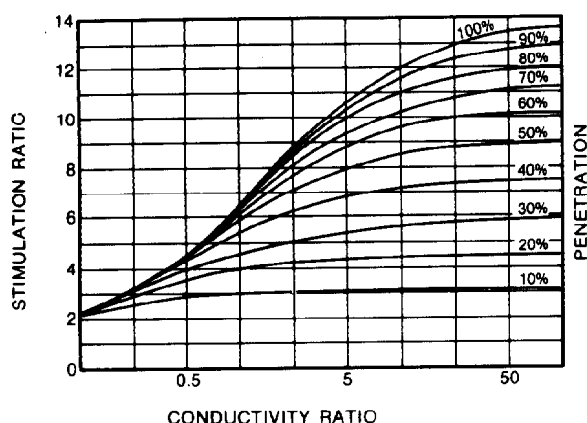


Fig. 55.6—Increased fracture penetration by containment of the fracture in the productive interval can provide much greater production increases.

The effective porosity represents the space in the matrix into which fracturing fluid will leak off. In figuring effective porosity, the effects of residual oil and water saturation should be considered. The permeability factor in the equation almost always will be the permeability of the water-wet formation, but it could be that of an oil-wet formation. The average md-ft of exposed section also is considered.

Fluid-Loss-Controlled Fluids

This group includes fracturing fluids containing special fluid-loss additives designed to reduce the loss of fluid taking place during a fracturing treatment.

The fluid coefficient for this type of fracturing fluid is based on Eq. 5.²

$$K_l = 0.0328 \frac{m}{2A}, \quad \dots \dots \dots (5)$$

where

- K_l = fluid coefficient, wall building (fluid-loss additive), ft/min^{1/2},
- m = the slope of the fluid-loss curve, plotting cumulative filtrate volume vs. the square root of flow time, mL/min^{1/2}, and
- A = cross-sectional area of test media through which flow takes place, cm².

In this case, the coefficient is obtained from an experimental test to determine the fluid loss resulting from the use of a particular fluid-loss additive in a particular fracturing fluid. The test must be performed at, or corrected to, bottomhole temperature (BHT) and pressure conditions. Spurt loss is the leakoff occurring while the fluid-retaining wall (filter cake) is being built up. It can be determined from this test by extrapolating the straight-line portion of the curve back to zero time on the ordinate. The value at this intercept is the spurt loss.

Stimulation Results

The increased production obtained following a fracturing treatment is the result of increased fracture penetration and conductivity. The greater penetration produces a larger drainage area from which reservoir fluids can be produced. Increased fracture conductivity results from the lowered resistance to flow through the fracture, permitting greater production of fluid under reservoir energy conditions.

Fig. 55.6⁵ shows the relationship between fracture penetration, fracture conductivity ratio, and production increase. These curves represent fracture penetration as a decimal fraction of the drainage radius. If a good conductivity ratio can be achieved, then a fracture penetrating 100% of the drainage radius can provide as much as a 13-fold increase in the production.

Fracture conductivity is controlled largely by propping agent permeability, size, and placement. Strength of the propping agent is also very important. The effect of these properties on fracture conductivity will be discussed later.

Fracture penetration is related directly to fracture-fluid efficiency and containment of the fracture within the production zone. A good fracturing fluid should be relatively low in cost and have low fluid loss, low friction loss,

good proppant transport characteristics, temperature stability, ability to thin for good cleanup, and compatibility with reservoir rock and fluids. Containment of the fracture within the productive interval is a function not only of fluid properties but also of technique.

Fracturing Materials

Fracturing Fluids

Fracturing fluids may be divided into three broad divisions: oil based, water based, and mix based. Classification depends primarily on the main constituent of the fracturing fluid. The aqueous-based fluids are either water or acid, and the mix-based fluids are emulsions.

Oil-Based Fluids. In the past, refined oils, crude oils and soap-type gels of crude, kerosene, or diesel oil were quite common. Because of safety considerations, lack of temperature stability, and cost of tailoring these materials to be efficient fluids, they are seldom used today. A new thickened and crosslinked hydrocarbon gel, made from either light refined oils or crude oil, is used extensively in hydraulic fracturing of oil- and gas-condensate wells producing from reservoirs adversely affected by water or brine. These gels exhibit all the characteristics of an efficient fracturing fluid.

Water-Based Fluids. Gels. Water-based fluids are natural or synthetic polymer gels of water or hydrochloric acid. They may be either linear or crosslinked gels. The water-based fluids are used almost exclusively except in those extremely water-sensitive reservoirs previously mentioned. The popularity of aqueous fluids is based on many factors, including these four: (1) they are safe to handle, (2) their cost is low in comparison to oil-based fluids, (3) they are, or can be formulated to be, compatible with nearly all reservoir fluids and conditions, and (4) they can be tailored to meet almost any treating requirements. Rheological properties, friction pressure, fluid loss, and break time can be closely controlled to provide an efficient fracturing fluid over a wide range of well and reservoir conditions. The primary disadvantage of aqueous fluids is that they may not be applicable in formations that are adversely affected by water.

Waterfrac services use linear (uncrosslinked) gels of fresh water, salt water, or produced brine as efficient and economical fracturing fluids. Guar and hydroxypropyl guar thickening agents are available to satisfy the requirements of a wide range of reservoir properties. They can be used in either batch- or continuous-mix techniques. A cellulose derivative thickener is available for applications in which fluids with extremely low residue are required.

The viscosity of fluids used in waterfrac services is controlled by thickening-agent concentration.

High-viscosity fracturing fluids have been developed that contribute directly to wider, better-propped, and more-conductive fractures. Fracture width is increased by increasing the viscosity of the fracturing fluid. Wider fractures permit use of larger proppant, which has greater permeability. These viscous fluids also have the proppant-transport properties required to carry higher concentrations of proppant deeper into the fracture. They achieve their high viscosity at gel concentrations in the same range as the traditional waterfrac fluids by using

special crosslinking systems and stabilizers. The high-viscosity gels are particularly useful in deep wells because of their temperature stability. They are able to create wide, deeply penetrating fractures at lower rates and can maintain their viscosity over the longer pumping times required in deeper wells. Fig. 55.7 shows the viscosity profile of one such fluid.

Two other characteristics of fracturing fluids normally are reported and are used in computer job design. These are the consistency index, I_c , and the behavior index, I_b . The power law model is used to calculate these characteristics. The consistency index is based on pipe flow geometry. The power law parameters are defined as follows:

I_b = behavior index; log slope of the shear stress vs. shear rate curve,
dimensionless, and

I_c = consistency index; shear stress at 1 sec^{-1} ,
 $\text{lbf-sec}^{-1}/\text{ft}^2$.

Apparent viscosity is related to the consistency index and behavior index as follows:

$$\mu_a = \frac{47,880 I_c}{\dot{\gamma}^{1-I_b}},$$

where

μ_a = apparent viscosity, cp, and
 $\dot{\gamma}$ = shear rate, sec^{-1}

Since shear history (shear rate and time at shear) adversely affects the rheology of some crosslinked gels, test methods have been developed that more accurately describe the fluids at the time they enter the fracture. Table 55.1 compares data developed by the API test method and shear history method.⁶ The data provided by the shear history method give more reliable prediction of friction losses while pumping. Such information is a requisite in job design to predict fracture geometry and reduce

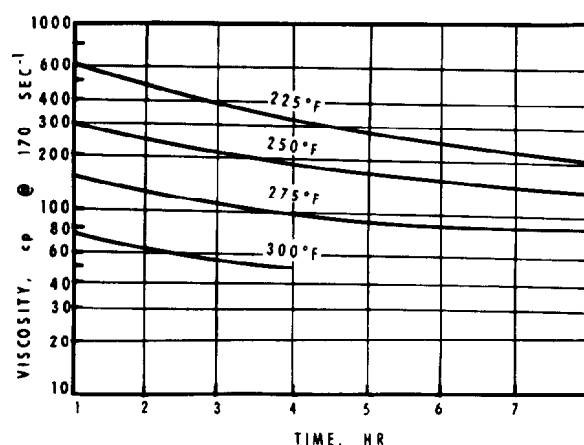


Fig. 55.7—Viscosity profile of high-viscosity, crosslinked, aqueous gel.

TABLE 55.1—COMPARISON OF RHEOLOGY DATA GENERATED BY API RP39M AND SHEAR HISTORY METHOD FOR CROSSLINKED AQUEOUS FLUID CONTAINING 30-lbm/1,000-gal THICKENER AND 10-lbm/100-gal STABILIZER

Temperature (°F)	Time (hours)	RP39M-XL"A"			SHSM*-XL"A"		
		I_b	I_c	cp at 170 sec ⁻¹	I_b	I_c	cp at 170 sec ⁻¹
225	0	—	—	—	0.7512	0.0017	23
	1	0.570	0.065	342	0.7709	0.0015	22
	2	0.588	0.045	259	0.7912	0.0013	20
	4	0.630	0.021	150	0.8309	0.0009	18
	6	0.672	0.011	98	0.8713	0.0007	17
	8	0.710	0.0058	63	0.9115	0.0005	15
250	0	—	—	—	0.7306	0.0021	25
	1	0.656	0.127	220	0.7743	0.0014	21
	2	0.674	0.019	170	0.8179	0.0009	17
	4	0.712	0.0095	103	0.9044	0.0004	11
	6	0.752	0.0046	62	0.9918	0.0002	7
	8	0.792	0.0024	39	—	—	—
275	0	—	—	—	0.7156	0.0020	22
	1	0.718	0.014	157	0.7371	0.0014	17
	4	0.740	0.010	126	0.7688	0.0009	13
	6	0.805	0.0048	84	—	—	—
	8	0.842	0.0037	79	—	—	—

*Shear history simulation method.

the possibility of premature screenout. Figs. 55.8 through 55.13 are examples of friction-loss data for various fluids.

In many of the high-viscosity fluids, shear history effects are minimized by using additives to delay crosslinking until the fluid reaches the bottom of the hole. This technique also reduces friction losses since high viscosity does not develop until after the fluid has passed through the tubulars.

Foams. During recent years, foams have become extremely popular as fracturing fluids. Normally classed as water-

based fluid, foam is a dispersion of a gas, usually nitrogen, within a liquid. A surfactant is used as a foaming agent to initiate the dispersion. Stabilizers are used where high temperatures or long pumping time occur. The volumetric ratio of the gas to the total volume of the foam, under downhole conditions, is called the quality of the foam. Quality is expressed as a number equal to the percentage. A 75-quality foam is 75% gas by volume at downhole temperature and pressure. In fracturing, foam quality usually ranges from 65 to 85 (compositions containing less than 52% gas are not normally stable foams).

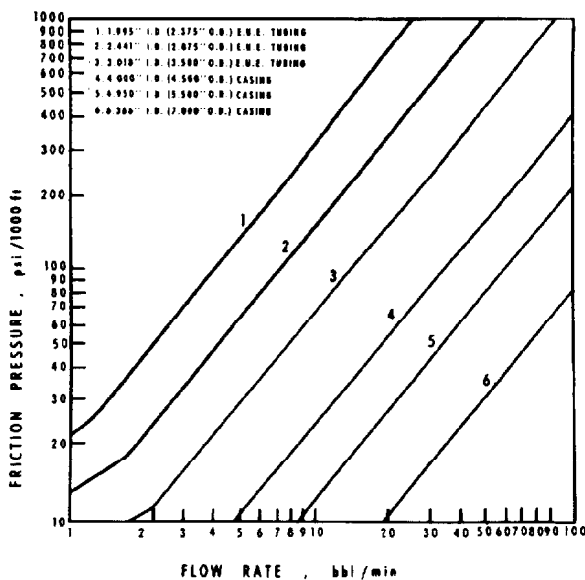


Fig. 55.8—Typical friction-loss curves for linear gel of fresh water or brine using guar or hydroxypropyl guar thickeners.

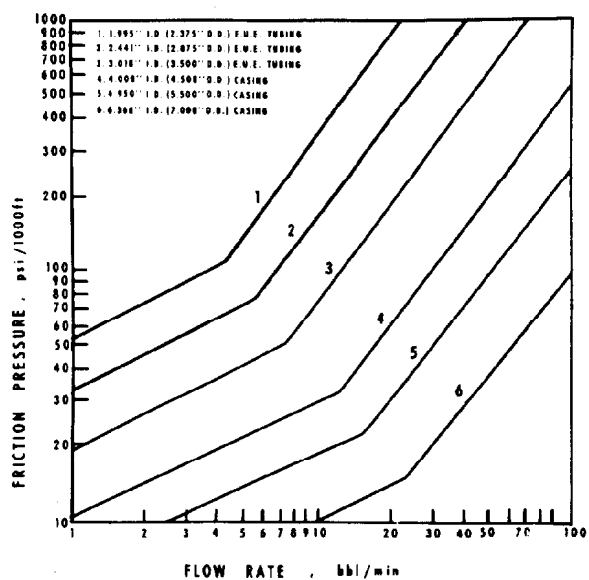


Fig. 55.9—Typical friction-loss curve of linear aqueous gel using cellulose thickener.

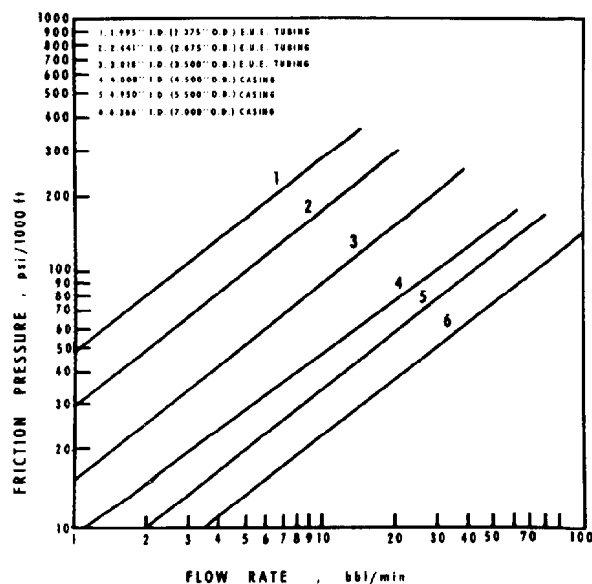


Fig. 55.10—Typical friction-loss curve for crosslinked aqueous gel using guar-based thickener.

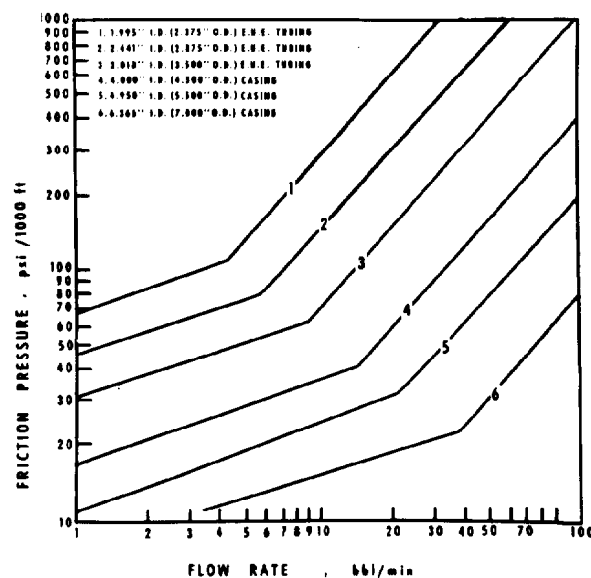


Fig. 55.11—Typical friction-loss curve for gelled oil fracturing fluid.

Foam is designed primarily for low-permeability or low-pressure gas wells. However, it may have equal advantages in low-pressure oil wells. In oil wells it may be necessary to use a different foaming agent that is compatible with reservoir fluids and reduces the possibility of emulsions.

Some advantages of foam are: (1) good proppant transport, (2) solids-free fluid-loss control, (3) low fluid loss, (4) minimum fluid retention owing to its low water content, (5) compatibility with reservoir fluids, and (6) low hydrostatic pressure of returned fluids, which gives rapid

cleanup and allows quicker well evaluation (gas in foam helps return liquids to the wellbore).

Some disadvantages of foam are: (1) more surface pressure is required because of low hydrostatic head; and (2) there is the added expense of gas, especially under high pressure where volume is reduced.

Mix-Based Fluids. Mix-based fluids are oil-in-water dispersions or emulsions that serve as highly efficient water-based fracturing fluids.

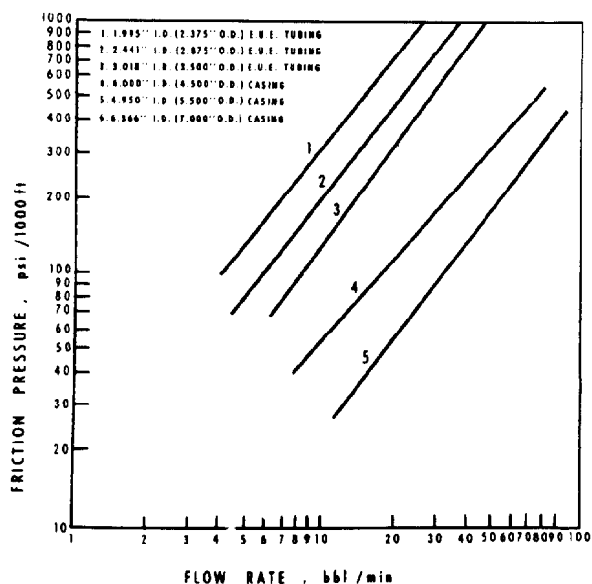


Fig. 55.12—Typical friction-loss curve for oil-in-water dispersion-type fracturing fluid.

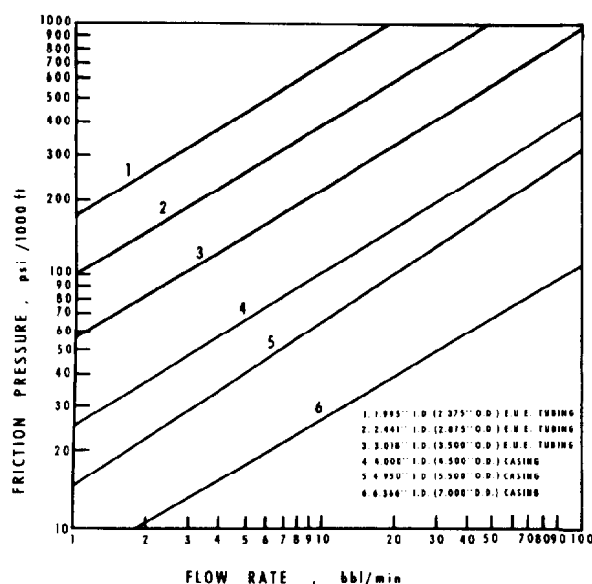


Fig. 55.13—Typical friction-loss curve for heavy oil-in-water emulsion-type fracturing fluid.

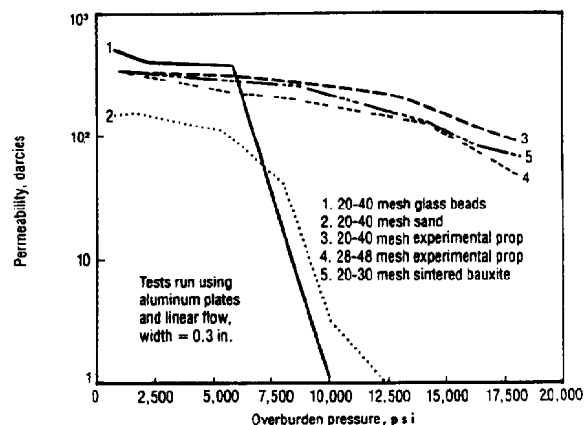


Fig. 55.14—Effect of closure stress on permeability of various propping agents.

The viscous emulsions are water-outside-phase emulsions containing two parts oil (crude or refined) and one part water or brine. These are commonly called "poly-emulsions" and are designed to provide high-viscosity fracturing fluids at temperatures up to 350°F. They are seldom used because of fire hazard and cost.

A crosslinked gel provides high viscosity in the water volume (95%), and a 5% oil phase is dispersed throughout the mixture to give excellent fluid-loss control properties without requiring the addition of solids. The leakoff control is the result of two-phase fluid flow that reduces the relative permeability of the formation more than conventional fracturing fluids do over a wide permeability range. The fluid is highly efficient even when compared to viscous-emulsion fracturing fluids. Normally, the 5% oil content is low enough to avoid significant effects on either friction pressure or hydrostatic head, even when used with the highly viscous water or brine gels.

Fracturing fluid composition is normally proprietary information of the service company supplying it. While competitive fluids are available from most of the service companies, rheological and friction-loss data will vary according to the fluid. Therefore, handbooks provided by the service companies should be used to obtain data for job design.

Propping Agents

Propping agents are used to maintain fracture-flow capacity after completion of a hydraulic fracturing treatment. The amount of proppant used, the manner in which it is placed in the fracture, and the properties of the material itself all play a vital role in maintaining productivity throughout the life of the well. The selection of the propping agent and scheduling of the proppant during the treatment are important parts of the overall completion and treatment design.

The six physical properties of propping agents that affect the resultant fracture conductivity are grain strength, grain size, grain size distribution, grain roundness factor, quality (amount of fines and impurities), and proppant density.

Grain Strength. While all these physical properties have a decided effect on fracture conductivity, quality standards

have been established so that the main considerations are grain strength and grain size. If a proppant is not strong enough to withstand closure stress of the fracture, it will crush, and permeability will be reduced greatly. Also, as reservoir pressure is reduced by fluid production, the closure stress will increase. Therefore, it is important that proppant strength be selected for the stress that will be present during the later life of the well. Fig. 55.14 shows the effect of closure stress on permeability of various propping agents when the formation is a hard, competent rock. Sand is an acceptable propping agent at closure stresses up to 6,000 psi. At stresses greater than this, high-strength proppants such as sintered bauxite particles or plastic-coated sand grains should be used.

In soft formations, the proppant will tend to embed into the formation under closure stress and reduce fracture width. This, in turn, reduces fracture flow capacity. In the past, deformable proppants such as rounded walnut shells and aluminum pellets have been used in an attempt to overcome this problem. By deforming or spreading out, these proppants presented a larger surface area to the face of the fracture and resisted embedment. The low density and malleability of these proppants caused both pumping and placement problems, and they were never widely accepted. There was also a corrosion or oxidation of the aluminum that resulted in loss of pack permeability.

A better solution to embedment is a wide, packed fracture. In such a fracture, width reduction resulting from embedment is a small percentage of total fracture width, and adequate flow capacity is maintained even after embedment occurs.

Grain Size. A large proppant grain size provides a more permeable pack under low closure stress conditions and can be used in shallow wells. However, dirty formations or those subject to significant fines migration are poor candidates for large-size proppants. The fines tend to invade the proppant pack, causing partial plugging and rapid reduction in permeability. In these cases, smaller sizes of proppant that resist invasion of fines are better.

Larger grain sizes are generally not considered for deeper wells because of greater susceptibility to crushing.

Proppant Placement. The manner in which a propping agent is placed in a fracture is also important. As previously stated, soft or high-permeability formations need a wide, fully packed fracture. In very-low-permeability formations, only a thin fracture may be necessary. However, fracture length becomes important in such formations because the greater the surface area of formation exposed to the propped fracture, the greater the volume of oil or gas that can drain into the fracture. Since fluid enters the fracture along its entire length, long fractures must be wider at the wellbore than at the tip to accommodate the increasing amount of fluid as the fracture nears the wellbore. To accomplish this fracture geometry, the proppant must be scheduled so that its concentration in the fracture fluid increases steadily as the treatment progresses.

Fracturing Techniques

Although fracturing treatments usually are performed by pumping materials down the casing or tubing at rates as high as well limitations and economics will permit, spe-

cial techniques sometimes are used to help control vertical fracture growth. Such control is directly related to fracturing efficiency. In the case of massive zones, adequate fracture height to cover the entire zone is desirable. With narrow zones, containment of the fracture within the productive zone improves efficiency and penetration and prevents fracture growth into undesirable zones.

While vertical growth can be controlled to some extent by controlling injection rate, more sophisticated techniques are required for optimum efficiency.

A Limited Entry® technique involves designing the number and size of perforations to match an economically feasible pump rate so that all perforations are forced to accept fluid during the treatment.

Another specialty technique to limit downward growth of a vertical fracture involves building an artificial lower barrier. This is done by using low injection rates and fluids with poor proppant transport characteristics at the beginning of the treatment. Propping agent can create a proppant pack at the bottom of the fracture. A pressure drop will exist across this pack and will divert the fluid that follows outward and upward, thus slowing or even stopping downward fracture growth.

Similarly, a buoyant propping agent can create an artificial upper barrier by floating to the top of the fracture and bridging to form a proppant pack. In this case also, the pressure drop across the pack will force subsequent fluids outward to increase fracture length.

Multiple-Zone Fracturing

Where multiple zones are open to the wellbore, mechanical devices such as packers or bridge plugs can be used to isolate zones so that each can be treated individually. Where it is desirable to fracture more than one zone in a single treatment, sized particulate materials or perforation ball sealers can be used. The particulate materials usually are suspended in a viscous fluid and filter out at the fracture entrance. After treatment, they generally flow back with produced fluids. They also can break down through chemical reaction. Ball sealers seat in perforations and divert fluid flow. They are unseated by reverse flow and either fall to the bottom or are produced along with the returning fluids. When ball sealers are used, a mechanical device to catch the balls should be used at the surface to prevent the balls from plugging valves or other surface equipment.

Fracturing Equipment

Hydraulic fracturing equipment consists of pumps and blenders, high-pressure manifolds and treating line, remotely controlled master valves, and tree savers.

Pumping equipment is the conventional triplex pump, quintuplex pump, or a pressure-multiplier type of pump. The latter employs an entirely different pumping concept from the triplex pump. It operates by using a low-pressure working fluid to push a large piston. This large piston is directly connected to a smaller piston, or ram, which handles the treating fluid. Because of a slow cycle speed, the pressure multipliers are capable of long pumping times at high pressures. Both the triplex and pressure multiplier are capable of high-pressure operation. Above 12,000-psi treating pressure, however, the multiplier is preferred. These units are capable of operating at pressures slightly in excess of 20,000 psi.

Individual pumping units are powered by engines ranging from less than 100 to more than 1,300 hp. For high horsepower requirements, multiple units are used.

Fluids used in hydraulic fracturing are mixed in blenders. They are either batch mixed before a job and stored in tanks on location or continuously mixed during the job. Blenders are capable of metering both dry and liquid additives into a fluid, mixing the fluid and additives, and metering and mixing propping agent into the fluids. After mixing and blending, the slurries are supplied by the blender to the suction on the high-pressure pumps under pressure. Blending units capable of handling volumes in excess of 100 bbl/min are available.

Liquid nitrogen is the gas normally used for foam or energized fluid. Special transport and pumping equipment is required to handle the nitrogen, which generally is metered into the treating line on the downstream (high-pressure) side of the triplex or multiplier pumps.

Another piece of equipment recently added to fracturing fleets is the treatment monitoring vehicle. This vehicle gathers data, uses a computer to analyze them, and presents the results as they occur, or in "real time." The data are presented by a printer, plotter, and on a CRT screen. Real-time analysis and presentation of data allow positive control of a treatment. Ample warning of problems normally is available so that changes can be made to permit successful completion of the job. Also, the equipment can be used to monitor a minifrac job before the main treatment. Analysis of the minifrac can either verify job design or indicate needed design changes before the main treatment.

Treatment Planning and Design

Success of a hydraulic fracturing treatment depends on creating a deeply penetrating, highly conductive fracture in the producing zone. Research, engineering studies, and experience have provided reliable planning or treatment design guides. Job calculations with these guides are based on reservoir conditions, laboratory tests, theoretical data, well information, and experience in a given area. Most service companies and many oil-producing companies have job-design calculations computerized to aid in rapid and accurate design comparisons. Special computer programs are available also to calculate tubing expansion and contraction, bottomhole cool-down (fluid temperature at the wellbore and in the fracture), proppant scheduling to provide best propped fracture geometry, and anticipated productivity increase.

Evaluating and selecting optimal treating conditions for any individual well includes several steps. First, accurate reservoir and well-completion data must be accumulated to provide a sound basis for engineered treatment preplanning. Next, the fracture area and the extent of formation penetration necessary to provide the desired productivity increase are calculated. The fracture conductivity, as related to the permeability of the matrix, is determined also.

After this, the comparative efficiency of various fracturing fluids, based on specific well conditions, is determined, as well as the volumes and injection rates necessary to provide the desired fracture extension. Horsepower requirements for each type of treatment then can be calculated; and fracturing materials and techniques can be selected that, theoretically, will most efficiently and eco-

nomically produce the desired productivity increase. Only when all these factors are considered collectively can a well-integrated fracturing treatment be carried out.

Nomenclature

- A = cross-sectional area of test media through which flow takes place, cm^2
 A_f = total area of one face of the fracture at any time during injection, sq ft
 b = fracture width (breadth), ft
 c_R = isothermal coefficient of compressibility of the reservoir fluid, psi^{-1}
 D = depth of producing interval, ft
 $\text{erfc}(x)$ = complementary error function of x
 g_f = unit fracture gradient, psi/ft
 i = constant injection rate during fracture extension, cu ft/min
 I_b = behavior index; log slope of the shear-stress vs. shear-rate curve, dimensionless
 I_c = consistency index: shear stress at 1 sec^{-1} , $\text{lbf-sec}^{-1}/\text{ft}^2$
 k_e = effective formation permeability, darcies
 K = fluid coefficient, a constant that is a measure of the flow resistance of the fluid leaking off into the formation during fracture operations
 K_c = fluid coefficient (compressibility-viscosity controlled), $\text{ft/min}^{1/2}$
 K_l = fluid coefficient, wall building (fluid-loss additive), $\text{ft/min}^{1/2}$
 K_v = fluid coefficient (viscosity controlled), $\text{ft/min}^{1/2}$
 m = slope of fluid-loss curve, plotting cumulative filtrate volume vs. square root of flow time, $\text{mL/min}^{1/2}$
 p_f = total friction loss, psi
 p_h = total hydrostatic pressure, psi
 p_R = normal reservoir pressure, psi
 p_s = total surface treating pressure, psi
 Δp = differential pressure across face of fracture, psi
 t = total pumping time, minutes
 γ = shear rate, sec^{-1}
 μ_a = apparent viscosity, cp
 μ_f = fracturing fluid viscosity, cp
 μ_R = reservoir fluid viscosity, cp
 ϕ_e = effective formation porosity, %

Key Equations in SI Metric Units

$$K_c = 1.9203 \times 10^{-4} \Delta p \sqrt{\frac{k_e \phi_e c_R}{\mu_R}}, \dots \dots \dots (3)$$

$$K_v = 2.41 \times 10^{-4} \sqrt{\frac{k_e \Delta p \phi_e}{\mu_f}}, \dots \dots \dots (4)$$

and

$$K_l = 0.001076 \frac{m}{2A}, \dots \dots \dots (5)$$

where

- K_c, K_v , and K_l are in $\text{m/s}^{1/2}$,
 Δp is in kPa ,
 k_e is in μm^2 ,
 ϕ_e is in percent,
 c_R is in kPa^{-1} ,
 μ_R is in $\text{Pa} \cdot \text{s}$,
 m is in $\text{mL/s}^{1/2}$, and
 A is in m^2 .

References

- Hurst, R.E., Franks, J.E., and Rollins, J.T.: "Horsepower Requirements for Well Stimulation," *Drill Bit* (Oct. 1958) 25.
- Howard, G.C. and Fast, C.R.: *Hydraulic Fracturing*, Monograph Series, SPE, Richardson, TX (1970) 2.
- Perkins, T.K. Jr. and Kern, L.R.: "Widths of Hydraulic Fractures," *J. Pet. Tech.* (Sept. 1961) 937-49; *Trans., AIME*, 222.
- Khristianovitch, S.A. and Zheltov, Y.P.: "Formation of Vertical Fracture by Means of Highly Viscous Fluids," *Proc., Fourth World Pet. Cong., Rome* (1955) 2, 579.
- McGuire, W.J. and Sikora, V.J.: "The Effect of Vertical Fractures on Well Productivity," *J. Pet. Tech.* (Oct. 1960) 72-74; *Trans., AIME*, 219.
- Craigie, L.J.: "A New Method for Determining the Rheology of Crosslinked Fracturing Fluids Using Shear History Simulation," paper SPE 11635 presented at the 1983 SPE/DOE Low-Permeability Gas Reservoirs Symposium, Denver, March 14-16.

General References

- Abou-Sayed, A.S.: "Laboratory Evaluation of In-Situ Stress Contrast in Deeply Buried Sediments," paper SPE 11069 presented at the 1982 SPE Annual Technical Conference and Exhibition, New Orleans, Sept. 26-29.
- Abou-Sayed, A.S., Ahmed, U., and Jones, A.: "Systematic Approach to Massive Hydraulic Fracturing Treatment Design," paper SPE 9877 presented at the 1981 SPE/DOE Low-Permeability Gas Reservoirs Symposium, Denver, May 27-29.
- Agarwal, R.G., Carter, R.D., and Pollock, C.B.: "Evaluation and Performance Prediction of Low-Permeability Gas Wells Stimulated by Massive Hydraulic Fracturing," *J. Pet. Tech.* (March 1979) 362-72.
- Ahmed, U., Strawn, J., and Schatz, J.: "Effect of Stress Distribution on Hydraulic Fracture Geometry: A Laboratory Simulation Study in One-Meter Cubic Blocks," paper SPE 11637 presented at the 1983 SPE/DOE Low-Permeability Gas Reservoirs Symposium, Denver, March 14-16.
- Ahmed, U. *et al.*: "State-of-the-Art Hydraulic Fracture Stimulation Treatment for a Western Tight Sand Reservoir," paper SPE 11184 presented at the 1982 SPE Annual Technical Conference and Exhibition, New Orleans, Sept. 26-29.
- Ainley, B.R. and Charles, G.J.: "Fracturing Using a Stabilized Foam Pad," paper SPE 10825 presented at the 1982 SPE/DOE Unconventional Gas Recovery Symposium, Pittsburgh, May 16-18.
- Almond, S.W.: "Factors Affecting Gelling-Agent Residue Under Low Temperature Conditions," paper SPE 10658 presented at the 1982 SPE Formation Damage Control Symposium, Lafayette, March 24-25.
- Aron, J. and Murray, J.: "Formation Compressional and Shear Interval Transit-Time Logging by Means of Long Spacings and Digital Techniques," paper SPE 7446 presented at the 1978 SPE Annual Technical Conference and Exhibition, Houston, Oct. 1-4.

- Baumgartner, S.A. *et al.*: "High-Efficiency Fracturing Fluids for High-Temperature, Low-Permeability Reservoirs," paper SPE 11615 presented at the 1983 SPE/DOE Low-Permeability Gas Reservoirs Symposium, Denver, March 14-16.
- Bennett, C.O., Reynolds, A.C., and Raghavan, R.: "Analysis of Finite Conductivity Fractures Intercepting Multilayer Reservoirs," paper SPE 11030 presented at the 1982 SPE Annual Technical Conference and Exhibition, New Orleans, Sept. 26-29.
- Bennett, C.O. *et al.*: "Performance of Finite Conductivity Vertically Fractured Wells in Single-Layer Reservoirs," paper SPE 11029 presented at the 1982 SPE Annual Technical Conference and Exhibition, New Orleans, Sept. 26-29.
- Callahan, M.J., McDaniel, R.R., and Lewis, P.E.: "Application of a New Second-Generation High-Strength Proppant in Tight Gas Reservoirs," paper SPE 11633 presented at the 1983 SPE/DOE Low-Permeability Gas Reservoirs Symposium, Denver, March 14-16.
- Cinco-Ley, H.: "Evaluation of Hydraulic Fracturing by Transient Pressure Analysis Methods," paper SPE 10043 presented at the 1982 SPE Intl. Petroleum Exhibition and Technical Symposium, Beijing, March 19-22.
- Cinco-Ley, H. and Samaniego-V., F.: "Transient Pressure Analysis for Fractured Wells," *J. Pet. Tech.* (Sept. 1981) 1749-66.
- Clark, J.A.: "The Prediction of Hydraulic Fracture Azimuth Through Geological, Core, and Analytical Studies," paper SPE 11611 presented at the 1983 SPE/DOE Low-Permeability Gas Reservoirs Symposium, Denver, March 14-16.
- Clark, P.E. and Quadir, J.A.: "Proppant Transport in Hydraulic Fractures: A Critical Review of Particle Settling Velocity Equations," paper SPE 9866 presented at the 1981 SPE/DOE Low-Permeability Gas Reservoirs Symposium, Denver, May 27-29.
- Clark, P.E. and Guler, N.: "Proppant Transport in Vertical Fractures: Settling Velocity Correlations," paper SPE 11636 presented at the 1983 SPE/DOE Low-Permeability Gas Reservoirs Symposium, Denver, March 14-16.
- Cleary, M.B.: "Analysis of Mechanisms and Procedures for Producing Favorable Shapes of Hydraulic Fractures," paper SPE 9260 presented at the 1983 SPE Annual Technical Conference and Exhibition, Dallas, Sept. 21-24.
- Cleary, M.P., Kavvasdas, M., and Lam, K.Y.: "A Fully Three-Dimensional Hydraulic Fracture Simulator," paper SPE 11631 presented at the 1983 SPE/DOE Low-Permeability Gas Reservoirs Symposium, Denver, March 14-16.
- Clifton, R.J. and Abou-Sayed, A.S.: "A Variational Approach to the Prediction of the Three-Dimensional Geometry of Hydraulic Fractures," paper SPE 9879 presented at the 1981 SPE/DOE Low-Permeability Gas Reservoirs Symposium, Denver, May 27-29.
- Cloud, J.E. and Clark, P.E.: "Stimulation Fluid Rheology III. Alternatives to the Power Law Fluid Model for Crosslinked Gels," paper SPE 9332 presented at the 1980 SPE Annual Technical Conference and Exhibition, Dallas, Sept. 21-24.
- Conway, M.W. and Harris, L.W.: "A Laboratory and Field Evaluation of a Technique for Hydraulic Fracturing Stimulation of Deep Wells," paper SPE 10964 presented at the 1982 SPE Annual Technical Conference and Exhibition, New Orleans, Sept. 26-29.
- Cooke, C.E. Jr.: "Effect of Fracturing Fluid on Fracture Conductivity," *J. Pet. Tech.* (Oct. 1975) 1273-82.
- Crawley, A.B., Northrup, D.A., and Sattler, A.R.: "The U.S. DOE Western Gas Sands Project Multiwell Experiment Updates," paper SPE 11183 presented at the 1982 SPE Annual Technical Conference and Exhibition, New Orleans, Sept. 26-29.
- Cutler, R.A. *et al.*: "New Proppants for Deep Gas Well Stimulation," paper SPE 9869 presented at the 1981 SPE/DOE Low-Permeability Gas Reservoirs Symposium, Denver, May 27-29.
- Cutler, R.A. *et al.*: "Comparison of the Fracture Conductivity of Commercially Available and Experimental Proppants at Intermediate and High Closure Stresses," *Soc. Pet. Eng. J.* (April 1985) 157-70.
- Daneshy, A.A.: "On the Design of Vertical Hydraulic Fractures," *J. Pet. Tech.* (Jan. 1973) 83-97; *Trans.*, AIME, 255.
- Daneshy, A.A.: "Numerical Solution of Sand Transport in Hydraulic Fracturing," *J. Pet. Tech.* (Jan. 1978) 132-40.
- Daneshy, A.A.: "Hydraulic Fracture Propagation in Layered Formations," *Soc. Pet. Eng. J.* (Feb. 1978) 33-41.
- Daneshy, A.A. *et al.*: "Effect of Treatment Parameters on the Geometry of a Hydraulic Fracture," paper SPE 3507 presented at the 1971 SPE Annual Meeting, New Orleans, Oct. 3-6.
- Dobkins, T.A.: "Improved Methods to Determine Hydraulic Fracture Height," *J. Pet. Tech.* (April 1981) 719-26.
- Elkins, L.E.: "Western Tight Sands Major Research Requirements," paper presented at the 1980 Intl. Gas Research Conference, Chicago, June 9-12.
- Fertl, W.H.: "Evaluation of Fractured Reservoir Rocks Using Geophysical Well Logs," paper SPE 8938 presented at the 1980 SPE/DOE Unconventional Gas Recovery Symposium, Pittsburgh, May 18-21.
- Gardner, D.C. and Eikerts, J.V.: "The Effects of Shear and Proppant on the Viscosity of Crosslinked Fracturing Fluids," paper SPE 11066 presented at the 1982 SPE Annual Technical Conference and Exhibition, New Orleans, Sept. 26-29.
- Geertsma, J. and de Klerk, F.: "A Rapid Method of Predicting Width and Extent of Hydraulically Induced Fractures," *J. Pet. Tech.* (Dec. 1969) 1571-81; *Trans.*, AIME, 246.
- Geertsma, J. and Haafkens, R.: "A Comparison of Theories for Predicting Width and Extent of Vertical Hydraulically Induced Fractures," *Trans.*, ASME (1979) 101, 8-19.
- Govier, G.W. and Aziz, K.: *The Flow of Complex Mixtures in Pipes*, Van Nostrand Reinhold Co., New York City (1972).
- Guppy, K.H., Cinco-Ley, H., and Ramey, H.J. Jr.: "Pressure Build-up Analysis of Fractured Wells Producing at High Flow Rates," *J. Pet. Tech.* (Nov. 1982) 2656-66.
- Hall, C.D. Jr. and Dollarhide, F.E.: "Performance of Fracturing Fluid Loss Agents Under Dynamic Conditions," *J. Pet. Tech.* (July 1968) 763-68; *Trans.*, AIME, 243.
- Hanson, J.M. and Owen, L.B.: "Fracture Orientation Analysis by the Solid Earth Tidal Strain Method," paper SPE 11070 presented at the 1982 SPE Annual Technical Conference and Exhibition, New Orleans, Sept. 26-29.
- Hanson, M.E. *et al.*: "Some Effects of Stress, Friction, and Fluid Flow on Hydraulic Fracturing," *Soc. Pet. Eng. J.* (June 1982) 321-32.
- Harrington, L.J., Hannah, R.R., and Beirute, R.: "Post-Fracturing Temperature Recovery and Its Implication for Stimulation Design," paper SPE 7560 presented at the 1978 SPE Annual Technical Conference and Exhibition, Houston, Oct. 1-4.
- Harrington, L.J., Hannah, R.R., and Williams, D.: "Dynamic Experiments and Proppant Settling in Crosslinked Fracturing Fluids," paper SPE 8342 presented at the 1979 SPE Annual Technical Conference and Exhibition, Las Vegas, Sept. 23-26.
- Harris, P.C.: "Dynamic Fluid-Loss Characteristics of Foam Fracturing Fluids," paper SPE 11065 presented at the 1982 SPE Annual Technical Conference and Exhibition, New Orleans, Sept. 26-29.
- Hurst, R.E.: "An Engineered Method for the Evaluation and Control of Fracturing Treatments," *Drill & Prod. Prac.*, API (1959) 168-76.
- King, G.E.: "Factors Affecting Dynamic Fluid Leakoff with Foam Fracturing Fluids," paper SPE 6817 presented at the 1977 SPE Annual Technical Conference and Exhibition, Denver, Oct. 9-12.

- Lee, W.J. and Holditch, S.A.: "Fracture Evaluation with Pressure Transient Testing in Low-Permeability Gas Reservoirs," *J. Pet. Tech.* (Sept. 1981) 1776-92.
- Lescarbouat, J.A., Sifferman, T.R., and Wahl, H.A.: "Evaluation of Fracturing Fluid Stability Using a Heated Pressurized Flow Loop," *Soc. Pet. Eng. J.* (June 1984) 249-55.
- McDaniel, R.R., Deysarkar, A.K., and Callanan, M.J.: "An Improved Method for Measuring Fluid Loss at Simulated Fracture Conditions," *Soc. Pet. Eng. J.* (Aug. 1985) 482-90.
- McLeod, H.O. Jr.: "A Simplified Approach to Design of Fracturing Treatments Using High-Viscosity Crosslinked Fluids," paper SPE 11614 presented at the 1983 SPE/DOE Low-Permeability Gas Reservoirs Symposium, Denver, March 14-16.
- Neal, E.A., Parnley, J.L., and Colpoys, P.J.: "Oxide Ceramic Proppants for Treatment of Deep Well Fractures," paper SPE 6816 presented at the 1977 SPE Annual Technical Conference and Exhibition, Denver, 9-12.
- Nolte, K.G.: "Determination of Fracturing Parameters from Fracturing Pressure Decline," paper SPE 8341 presented at the 1979 SPE Annual Technical Conference and Exhibition, Las Vegas, Sept. 23-26.
- Nolte, K.G.: "Fracture Design Considerations Based on Pressure Analysis," paper SPE 10911 presented at the 1982 SPE Cotton Valley Symposium, Tyler, TX, May 20.
- Nolte, K.G. and Smith, M.B.: "Interpretation of Fracturing Pressures," *J. Pet. Tech.* (Sept. 1981) 1767-75.
- Nordgren, R.P.: "Propagation of a Vertical Hydraulic Fracture," *Soc. Pet. Eng. J.* (Aug. 1972) 306-14.
- Palmer, I.D. and Carroll, H.B.: "Three-Dimensional Hydraulic Fracture Propagation in the Presence of Stress Variations," *Soc. Pet. Eng. J.* (Dec. 1983) 870-78.
- Palmer, I.D. and Carroll, H.B.: "Numerical Solution for Height of Elongated Hydraulic Fractures with Leakoff," paper SPE 11627 presented at the 1983 SPE/DOE Low-Permeability Gas Reservoirs Symposium, Denver, March 14-16.
- Penny, G.S.: "Nondamaging Fluid-Loss Additives for Use in Hydraulic Fracturing of Gas Wells," paper SPE 10659 presented at the 1982 SPE Formation Damage Control Symposium, Lafayette, March 24-25.
- Rogers, R.E., Veatch, R.W., and Nolte, K.G.: "Pipe Viscometer Study of Fracturing Fluid Rheology," *Soc. Pet. Eng. J.* (Oct. 1984) 575-81.
- Rosene, R.B. and Shumaker, E.G.: "Viscous Fluids Provide Improved Results from Hydraulic Fracturing Treatments," paper SPE 3347 presented at the 1971 SPE Rocky Mountain Regional Meeting, Billings, MT, June 2-4.
- Rosepiller, M.H.: "Determination of Principle Stresses and the Confinement of Hydraulic Fractures in Cotton Valley," paper SPE 8405 presented at the 1979 SPE Annual Technical Conference and Exhibition, Las Vegas, Sept. 23-26.
- Settari, A.: "Simulation of Hydraulic Fracturing Processes," *Soc. Pet. Eng. J.* (Dec. 1980) 487-500.
- Settari, A.: "Quantitative Analysis of Factors Controlling Vertical Fracture Growth (Containment)," paper SPE 11629 presented at the 1983 SPE/DOE Low-Permeability Gas Reservoirs Symposium, Denver, March 14-16.
- Settari, A.: "A New General Model of Fluid Loss in Hydraulic Fracturing," *Soc. Pet. Eng. J.* (Aug. 1985) 491-501.
- Sinclair, A.R.: "Heat Transfer Effects in Deep Well Fracturing," *J. Pet. Tech.* (Dec. 1971) 1484-92; *Trans., AIME*, **251**.
- Sinclair, A.R. and Graham, J.W.: "A New Proppant for Hydraulic Fracturing," paper presented at the 1978 ASME Energy Technology Conference, Houston, Nov. 5-9.
- Smith, M.B.: "Stimulation Design for Short, Precise Hydraulic Fractures—MHF," paper SPE 10313 presented at the 1981 SPE Annual Technical Conference and Exhibition, San Antonio, Oct. 4-7.
- Smith, M.B., Logan, J.M., and Wood, M.D.: "Fracture Azimuth—A Shallow Experiment," *Trans., ASME* (June 1980) **102**, 99-105.
- Smith, M.B., Rosenberg, R.J., and Bowen, J.F.: "Fracture Width: Design vs. Measurement," paper SPE 10965 presented at the 1982 SPE Annual Technical Conference and Exhibition, New Orleans, Sept. 26-29.
- Thomas, R.L. and Elbel, J.L.: "The Use of Viscosity Stabilizers in High Temperature Fracturing," paper SPE 8344 presented at the 1979 SPE Annual Technical Conference and Exhibition, Las Vegas, Sept. 23-26.
- Teufel, L.W.: "Determination of In-Situ Stresses from Anelastic Strain Recovery Measurements of Oriented Core: Applications to Hydraulic Fracturing Treatment Design," paper SPE 11649 presented at the 1983 SPE/DOE Low-Permeability Gas Reservoirs Symposium, Denver, March 14-16.
- Teufel, L.W. and Clark, J.A.: "Hydraulic Fracture Propagation in Layered Rock: Experimental Studies of Fracture Containment," *Soc. Pet. Eng. J.* (Feb. 1984) 19-32.
- Thiercelin, M. and Lemanczyk, R.: "The Effect of Stress Gradient on the Height of Vertical Hydraulic Fractures," paper SPE 11626 presented at the 1983 SPE/DOE Low-Permeability Gas Reservoirs Symposium, Denver, March 14-16.
- Tinsley, J.M. *et al.*: "Vertical Fracture Height—Its Effect on Steady-State Production Increase," *J. Pet. Tech.* (May 1969) 633-38; *Trans., AIME*, **246**.
- van Poolen, H.K., Tinsley, J.M., and Saunders, C.D.: "Hydraulic Fracturing—Fracture Flow Capacity vs. Well Productivity," *J. Pet. Tech.* (May 1958) 91-95; *Trans., AIME*, **213**.
- Veatch, R.W. Jr. and Crowell, R.F.: "Joint Research/Operations Programs Accelerate Massive Hydraulic Fracturing Technology," *J. Pet. Tech.* (Dec. 1982) 2763-75.
- Verbeek, C.M.J.: "Analysis of Production Tests of Hydraulically Fractured Wells in a Tight Solution Gas-Drive Reservoir," paper SPE 11084 presented at the 1982 SPE Annual Technical Conference and Exhibition, New Orleans, Sept. 26-29.
- Warpinski, N.R. *et al.*: "Laboratory Investigation on the Effect of In-Situ Stresses on Hydraulic Fracture Containment," *Soc. Pet. Eng. J.* (June 1982) 333-40.
- Waters, A.B.: "Hydraulic Fracturing—What Is It?" *J. Pet. Tech.* (Aug. 1981) 1416.
- Wendorff, C.L.: "Frac Sand Quality Control—A Must for Good Frac Treatments," paper presented at the 1978 ASME Petroleum Div. Annual Meeting, Houston, Nov. 5-9.
- Wheeler, J.A.: "Analytical Calculations of Heat Transfer from Fractures," paper SPE 2494 presented at the 1969 SPE Improved Oil Recovery Symposium, Tulsa, April 13-15.
- White, J.L. and Daniel, E.F.: "Key Factors in MHF Design," *J. Pet. Tech.* (Aug. 1981) 1501-12.
- Whitsitt, N.F. and Dysart, G.R.: "The Effect of Temperature on Stimulation Design," *J. Pet. Tech.* (April 1970) 493-502; *Trans., AIME*, **249**.
- Wood, M.D. *et al.*: "Fracture Proppant Mapping Using Surface Superconducting Magnetometers," paper SPE 11612 presented at the 1983 SPE/DOE Low-Permeability Gas Reservoirs Symposium, Denver, March 14-16.

Chapter 56

Remedial Cleanup, Sand Control, and Other Stimulation Treatments

A.W. Coulter Jr., Dowell Schlumberger*

S.J. Martinez, Information Services Div., U. of Tulsa*

K.F. Fischer, Dowell Schlumberger*

Introduction

Although fracturing and acidizing are the most common types of well stimulation used today, other types of stimulation treatments also are used. Some of these treatments use acid-type materials but are not generally classed as acidizing jobs. These treatments are specifically designed for the removal of a blocking agent such as gypsum (gyp), drilling mud, paraffin, formation silicate, particles, or other materials on the wellbore face and in the formation immediately adjacent.

The first stimulation treatments used in oil and gas wells involved explosives such as dynamite or nitroglycerin. This method was used for many decades before being discontinued for safety reasons. More recent attempts to stimulate with explosives involved displacement of explosive material into the producing formation in a fracture-type treatment. The material was then detonated. Because this method was hazardous, research involving explosives has been discontinued.

Reperforation

In some cases it is useful to reperforate a well in the same zone in which it was originally perforated. The detonation of the gun loosens blocking materials in the formation adjacent to the well and in the previous perforations, and simultaneously creates more drainage holes into the wellbore. Also, over a period of time, some of the original perforation tunnels might become totally blocked by migratory fines, scale, gyp, or paraffin. Reperforation in such cases could greatly increase drainage area into the wellbore.

Abrasive Jet Cleaning

Another method used to clean up shot holes or to remove gyp contaminating the formation near the wellbore makes

use of a jetting tool. One or more streams of sand-laden fluid are forced through a hardened, specially designed nozzle at pressures of 1,000 psi and up, to impinge against the wall of the borehole.

These jets, striking against the face of the open hole, loosen and break up gyp deposits, and may penetrate the formation. If the tool is moved up and down while jetting, the entire borehole can be cleaned. This same tool may be used for perforating pipe; the high-pressure jets of sand-laden fluid are able to cut through $\frac{1}{4}$ -in.-thick steel pipe in 15 to 30 seconds. They can then penetrate the formation to a depth of 12 or 15 in. in another 5 minutes or so, forming large unobstructed channels for the production of reservoir fluids.

Mud Removal

Several materials are used to remove drilling mud from the borehole and the adjacent formation. The most commonly used material is a mud-dissolving acid consisting of inhibited hydrochloric acid (HCl) with an added fluoride. This material dissolves part of the mud and loosens the remainder so that it may be flushed out. Mud-removal agents are often used ahead of fracturing, acid jobs, or cement, to clean the face of the pay, to allow a lower breakdown pressure, and to minimize mud contamination.

Acid cleanup solutions, containing special surfactants that increase penetration and provide special mud-dispersing properties, are also used when an infiltration of mud into the formation is suspected.

Other solutions, containing phosphates or other chemicals, may be used to loosen and disperse mud particles so they can be more easily flushed from their position in or adjacent to the wellbore.

Special blends of surfactants, iron chelating agents, and mud-dispersing agents also have been effective in removing mud from the formation.

*Authors of the original chapter on this topic in the 1982 edition were S.J. Martinez and P.E. Fitzgerald (both now deceased).

Water Blocks and Emulsions

Oil- and/or water-based solutions containing low-surface-tension, emulsion-breaking agents have been used successfully to remove water blocks or emulsions from a formation. More recently, solutions of special surfactants and alcohols have become popular. These materials are pumped into the formation to contact the water or emulsion block. By changing the blocking material's physical characteristics, the solution enables the blocking fluid to be produced. Treatments of this type usually consist of a specialized, commercially available product with an oil-carrying agent. If a large zone is to be treated, diverting agents, ball sealers, or packers should be used to ensure that the solution contacts the blocking fluids. Otherwise, the chemicals will probably enter the more permeable and nonblocked portions of the formation and miss the blockage completely.

Scale Deposits

When a well produces some water, gyp deposits may accumulate on the formation face and on downhole equipment and thereby reduce production. These deposits may have low solubility and be difficult to remove. Solutions of HCl and ethylenediaminetetraacetic acid (EDTA) can often be used to remove such scales. Soluble portions of the scale are dissolved by the HCl while the chelating action of EDTA breaks up and dissolves much of the remaining scale portions. When deposits contain hydrocarbons mixed with acid-soluble scales, a solvent-in-acid blend of aromatic solvents dispersed in HCl can be used to clean the wellbore, downhole equipment, and the first few inches of formation around the wellbore (critical area) through which all fluids must pass to enter the wellbore. These blends are designed as a single stage that provides the benefits of both an organic solvent and an acid solvent that contact the deposits continuously.

Paraffin Removal

Several good commercial paraffin solvents are on the market. These materials can be circulated past the affected parts of the wellbore or simply dumped into the borehole and allowed to soak opposite the trouble area for a period of time. Soaking, however, is much less effective because the solvent becomes saturated at the point of contact and stagnates.

In the past, many paraffin solvents have contained chlorinated materials having an organic chloride ion. Presumably such materials have been taken off the market because of problems encountered in refineries with poisoning of certain catalysts by organic chlorides. The nonorganic chloride ion from HCl is water soluble, and it can be readily extracted from the oil during refining processes. Therefore, the problem of catalyst poisoning does not arise when HCl is used in paraffin-removal formulations such as acid dispersions.

Hot-oil treatments also are commonly used to remove paraffin. In such a treatment, heated oil is pumped down the tubing and into the formation. The hot oil dissolves the paraffin deposits and carries them out of the wellbore when the well is produced. When this technique is used, hot-oil treatments are usually performed on a regularly scheduled basis.

Paraffin inhibitors are a recent development. These are designed to create a hydrophilic surface on the metal well

equipment. This in turn minimizes the adherence of paraffin accumulations to the treated surfaces.

Large-Volume Injection Treatments

A simple technique often used to free or to open blockages within the formation consists simply of pumping large volumes of crude oil, kerosene, or distillate into the formation. These treatments are especially effective when the formation is blocked by fine silicates or other solids. Pumping the oil into the formation may rearrange these fine particles so that flow channels to the wellbore are reopened. Sometimes it is helpful to add surface-active agents or emulsion-breaking agents to the oil.

Steam Injection

In some areas where low-gravity crude is produced, steam is used to heat and reduce the viscosity of the oil and thereby allow the oil to move more easily to the wellbore. Two types of steam injection are used. In some areas, steam is injected into a central injection well and the oil produced from adjacent or surrounding wells.

The other type of injection is often referred to as "huff 'n' puff." This consists of alternate steam-injection and oil-production cycles from the same well.

General Comments

In any case of production decline, it is important to have all available facts and to make the best possible analysis from these facts as to the factors contributing to the decline. If the problem is not analyzed as completely as possible before treatment, a great deal of money may be wasted in the use of an incorrect treatment. Also, whenever a fluid is to be pumped into a specific part of a zone, some chemical or mechanical method should be used to ensure that the fluid enters the proper zone.

Sand Control

Sand Formation Properties and Geology

Most oil and gas wells produce through sandstone formations that were deposited in a marine or detrital environment. Marine-deposited sands, where most of the hydrocarbons are found, are often cemented with calcareous or siliceous minerals and may be strongly consolidated. In contrast, Miocene and younger sands are often unconsolidated or only partially consolidated with soft clay or silt. These structurally weak formations may not restrain grain movement. When produced at high flow rates, they may produce sand along with the fluids.

Why Sand is Produced

Fluid movement through sandstone reservoirs creates stresses on the sand grains because of fluid pressure differences, fluid friction, and overburden pressures. If these stresses exceed the formation-restraining forces, then sand grains and fines can move and may be produced with the fluid. Rapid changes in fluid production rates and fluid phases cause unstable conditions that can result in increased sand production. When a well starts to produce water, it will often start to produce sand. Muecke¹ demonstrated that particle movement takes place in a multiphase system when the wetting phase starts to move.

Even consolidated sandstone can be mechanically and chemically damaged with time as the reservoir is produced. Overburden stress on sand grains increases as the

reservoir pressure decreases. Water movement can dissolve minerals that cement sand grains as well as change the carrying capacity of the formation fluids. Fines migration can reduce the permeability in the perforation tunnels. This can result in a higher pressure drop into the wellbore and a change in formation stresses. A calcite-cemented formation can be damaged by an improperly designed acid treatment, and increased sand production can result.

Consequences of Sand Production

Sand movement in unconsolidated formations and its ultimate production with oil and/or gas creates a number of costly and potentially dangerous problems. Most common among these problems are the following.^{2,3}

1. Production interruptions can be caused by sand plugging the casing, tubing, flowlines, or separator.
2. Casing collapse can be caused by changes in overburden pressure and stresses within the formation.
3. Downhole and surface equipment can be destroyed, resulting in downtime for equipment replacements, spills, cleanup or even an uncontrolled blowout.
4. Disposal of produced sands is costly because regulations require the disposed sands to be essentially oil-free.

Methods of Sand Control

Higher allowable production rates have increased the need for more effective and durable sand-control systems, which exhibit minimal permeability impairment. Experience indicates that sand control should be implemented before the formation is seriously disturbed by sand removal.⁴ Four general types of sand-control methods have been developed to reduce or to prevent the movement of formation sands with produced fluids.

1. In some cases, sand production can be prevented merely by restricting the production rate and thus reducing the drag forces on the sand grains.⁴ This simple approach is usually uneconomical. Increasing perforation size and density along with the use of clean, nondamaging completion fluids will help to decrease fluid velocity and drawdown pressure at higher production rates.
2. Gravel packing is the oldest, simplest, and most consistently reliable method of sand control. It has wide application both on land and offshore. Advances in gravel-pack technology, which use a viscous fluid to carry high gravel concentrations around a screen, have resulted in faster and more productive gravel packs. Improved completion tools and through-tubing tools that eliminate the need for costly workover rigs have expanded the application of gravel packing.
3. Sand consolidation plastic treatments inject resins into the producing interval, binding the formation sand grains together while leaving the pore spaces open. With use of special preflush systems and diverting agents, intervals up to 30 ft thick have been successfully consolidated and provided with the strength necessary to allow high production rates.
4. Resin-coated gravel packing places gravel coated with a resin both inside and outside the perforations and in the casing. As the resin cures, the sand grains are bound together. A strong, highly permeable, synthetic sandstone filter results. After curing, the excess resin-coated gravel is drilled from the casing, resulting in a full-open wellbore. This gravel pack can be used with or without a

screen, in primary or remedial work, and through coiled or concentric tubing.

The type of sand-control method selected will depend on the specific well conditions. Important variables such as grain-size distribution, clay content, interval length, bottomhole temperature, wellbore deviation, mechanical configuration, bottomhole pressure, anticipated production rates, and cost should be considered before deciding on the method of sand control best suited to the well.

Formation Sampling

The most important design parameter in sand control is the formation sand grain size. The success of gravel-pack methods relies upon formation particles being restrained by the larger pack gravel. Chances for a successful sand control job are highest when representative samples of the formation are available for sieve analysis. This enables selection of the proper size of gravel.

The most representative formation samples are obtained from rubber-sleeve core barrels. Sidewall cores, although they contain crushed grains and mud contamination, are the second choice. Bailed or separator samples are not representative since sand grains may have been segregated—the larger grains remaining in the hole and the smaller grains being produced with the well fluids.

Formation Analysis

Formation sand sieve analyses should be conducted to determine formation properties under bottomhole conditions. Treatment steps in acidizing, clay stabilization, and sand control can be determined. Typical sandstone analyses include permeability, porosity, response to acid, mineralogy, petrographic analysis, scanning electron microscope analysis, X-ray diffraction analysis, and optical emission spectrographic analysis.

Well Preparation

A successful sand-control installation is dependent on following the recommended procedures for all phases of the drilling and completion operations. Selection of the proper gravel size or resin, use of nondamaging drilling and completion fluids, perforation density and cleanliness, and gravel placement are among the important factors affecting well productivity. The following are some of the factors that should be considered before any sand control procedures are initiated.

Cleanliness. Clean Tubing. Steps must be taken to ensure that new or used tubing is as free as possible of rust, scale, mill varnish, and other contaminants or obstructions. Many of the contaminants can be removed chemically through the use of solvents or mechanically by "rabbeting" the joints before running.

Acidizing the tubing string after it has been run will remove rust and some of the pipe dope that accumulates (see next section) inside the tubing. The string can be acidized by pumping HCl down the string to within 100 to 200 ft of the bottom and then immediately reverse-circulating the acid out. Complexing or reducing agents should then be used. The acid should not be allowed to exit the tubing string nor to reach the perforations. Any iron present in the ferric state could precipitate as gelatinous ferric hydroxide (FeOH), which can be extremely damaging to the formation.

TABLE 56.1—PRESSURE DROP ACROSS A SAND-FILLED PERFORATION

Gravel	Flow Rate, q (BPD/perforation)	Δp (psi) With Perforation Diameter of			
		3/8 in.	1/2 in.	3/4 in.	1 in.
U.S. 10/20 mesh, 500 darcies	1	0.6	0.2	0.1	0.05
	10	24.0	8.0	2.3	1.00
	25	132.0	44.0	10.0	4.00
	50	495.0	175.0	37.0	13.00
	100	2,079.0	666.0	137.0	48.00
U.S. 20/40 mesh, 119 darcies	1	2.0	1.0	0.4	0.20
	10	55.0	21.0	6.0	3.00
	25	272.0	99.0	25.0	11.00
	50	983.0	357.0	81.0	31.00
	100	4,037.0	1,298.0	282.0	104.00
U.S. 40/60 mesh, 40 darcies	1	6.0	3.0	1.3	0.70
	10	177.0	67.0	20.0	9.00
	25	893.0	324.0	80.0	33.00
	50	3,250.0	1,178.0	260.0	98.00
	100	13,400.0	4,360.0	927.0	323.00
Formation sand, 1 darcy	1	450.0	190.0	64.0	32.00
	10	27,760.0	9,280.0	2,091.0	808.00

Pipe Dope. Pipe dope, when improperly applied, may be squeezed inside the tubing at the joints and can be transported into the formation by treatment fluids or become lodged in the screen or liner slots, resulting in decreased production. It is virtually impossible to remove the solids found in pipe dope from an oil or gas well chemically. Pipe dope should therefore be applied sparingly to the pin end of the tubing. It should not be used inside the collar where it can be squeezed into the tubing string when the joint is made up.

Filtering of Fluids. Significant reduction of oil and gas production can be caused by formation damage caused by solids in the fluids used in well completion or work-over operations. Clays, silt, or organic solids injected into a perforated interval can become trapped in the formation matrix or in the perforation tunnels where they can act as a low-permeability choke, reducing the productivity of the well.

Cement Bond. A good bond between the cement and the formation and between the cement and the casing is essential to isolate the producing zone. Primary cementing is one of the most critical phases in a successful well completion, and good cementing practices should be followed.

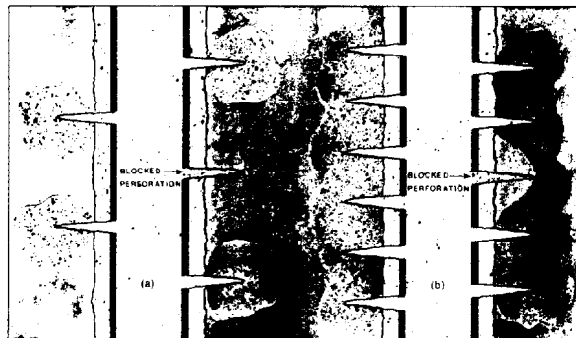


Fig. 56.1—Higher perforation density increases the success ratio for sand consolidation treatments.

An in-gauge borehole is important, and the string should be equipped with adequate centralizers, particularly in deviated holes. Spacer fluids and cement slurry properties must be controlled. The string should be equipped with scratchers through critical zones and either rotated or reciprocated during placement of the slurry. Turbulent flow is recommended.

If there is any indication of poor bonding, a squeeze cement job should be performed. Intervals to be treated separately should be effectively isolated by bonded cement to reduce the possibility of communication between zones.

Perforations. The success of sand-control treatments in cased holes, measured in terms of well productivity and treatment life, is greatly affected by perforation size and density and by perforating damage. Perforation tunnels must be open so they can be filled with pack gravel to prevent filling with formation sand. If perforations are plugged, gravel cannot be deposited in the tunnels (as carrier fluids flow into the formation) and formation consolidation chemicals cannot be injected.

If formation sand is lodged in the perforation tunnels, the pressure drop within the perforation can be excessive, even though the permeability of the formation sand is relatively high. Experimental results indicate that fluid flow can be turbulent in gravel-filled perforation tunnels with pressure drops far greater than those predicted by Darcy's linear flow equations. As shown in Table 56.1, pressure drop within a gravel-filled perforation tunnel can be quite significant.^{4,6}

The greater the perforation density, the less the drawdown through each perforation tunnel and the less the velocity through each effective perforation. Intervals perforated 4 shots/ft show cumulative production before sanding to be seven times greater than intervals perforated with only 1 shot/ft. Two perforations per foot show two-thirds the capacity of 4 shots/ft.⁷

In wells gravel-packed effectively, the lower fluid velocity resulting from high perforation density and large-diameter perforations reduces screen erosion and increases the life of the sand-control treatment. Pressure drop

through higher-density, large-diameter perforations also is reduced, resulting in higher wellhead pressure and greater oil or gas production.

For sand consolidation, closely spaced perforations (8 to 12 shots/ft) increase the likelihood of a uniform plastic pattern around the wellbore, even if some of the perforations are plugged. Fig. 56.1 illustrates what can happen when a perforation is plugged. Note that the sand is not consolidated behind the plugged perforation on the right side of Fig. 56.1(a), and that this is the spot where a failure is most apt to occur.

Perforation Cleaning. The high-pressure jet from a perforating gun pierces the casing and forms a hole by pulverizing cement and formation into compacted particles. Cement and material from the jet charge are mixed with the formation material in the compacted zone while loose debris fills the perforation tunnel. It is necessary to remove this debris from the perforation tunnel to increase the probability of success in sand consolidation or gravel packing. Fig. 56.2 shows the damage that can occur in the perforation and on the face of the formation during drilling and perforating.⁸

Perforation-cleaning methods include backflow, underbalanced perforating, backsurfing, washing, and acid stimulation, or combinations of these. These methods are discussed next.

Backflow. Flowing the well may not clean up more than a few perforations and, if enough differential is available to purge debris from the perforations, the well may sand up. Backflow must be done slowly and carefully.

Underbalance. Perforating with hydrostatic pressure less than formation pressure allows tunnel debris to be carried into the wellbore with the first surge of fluid from the formation.

Backsurfing. Backsurfing techniques dislodge gun debris and loose material from perforation tunnels by sudden exposure of a perforated zone to an open chamber at atmospheric pressure. The differential pressure created causes formation fluids to surge through the perforations into the casing, flushing the perforation tunnels. Backsurfing has proved to be very successful in improving productivity.

Perforation Washing. Washing is achieved by straddling a small increment of the perforated interval with a special tool and injecting nondamaging fluids into the perforations in the increment. The fluid circulates outside the casing and back through the perforations nearest the tool seals, removing debris and formation sand from the perforations and from behind the casing. The tool is moved in increments equal to the seal spacing until the entire perforated interval is washed.

After the perforations are washed or surged and debris is circulated out, a positive-depth indicator is placed in the well below the perforations to establish a reference point from which the string is accurately spaced out. This is especially important in multiple completions with closely spaced producing intervals.

Matrix Acid Stimulation. The purpose of matrix acidizing is to penetrate the formation at less than fracturing pressure and to remove damage from perforation tunnels and the critical area surrounding the wellbore. Mud filter cake, silt, and clay are typical damaging materials that may be removed by mud acid to restore a well's natural productivity.

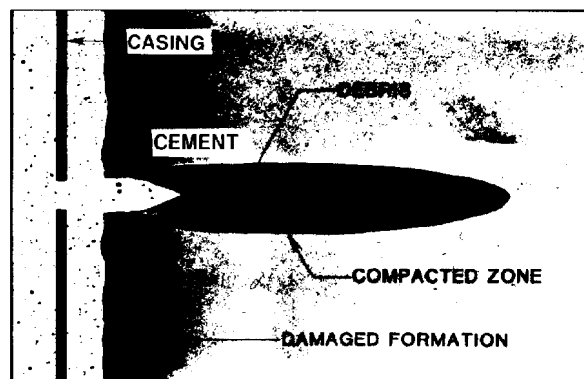


Fig. 56.2—Drawing of a perforation tunnel showing fluid invasion from the wellbore into the formation, and debris in the perforation and the compacted zone surrounding the perforation tunnel.

The formation solubility should be determined in both mud acid and HCl. If mud acid is used, a formation solubility at least 10% greater in mud acid than in HCl is preferred. Moreover, the formation solubility in HCl should be less than 20% to avoid calcium fluoride precipitation.

A typical three-step acid stimulation consists of an HCl preflush, matrix treatment with mud acid, and an HCl overflush.

HCl Preflush. A preflush of 50 to 100 gal/ft of perforations is advisable. The HCl is used to prevent contact of mud acid with calcareous materials or formation brine. This prevents or reduces the chances of precipitation of calcium fluoride and various fluosilicates.

Matrix Treatment With Acid. The proper volume of mud acid should be injected to remove damage near the wellbore. Usually 50 to 200 gal/ft of perforations is required. Success in matrix acidizing depends on acid contacting the entire production interval. This is achieved through the use of diverting agents.

A mutual solvent comprised of ethylene glycol monobutyl ether^{9,10} is sometimes needed to achieve good results. It is an effective water-wetting agent, demulsifier, and interfacial-tension reducer.

Overflush. Completion or workover brine should not be used as an overflush for mud acid because of the possible precipitation of sodium, potassium, or calcium fluosilicates. The use of dilute HCl, ammonium-chloride solution, light oil, or nitrogen as the overflush agent is recommended.

Clay Control

In many cases, formation permeability may be damaged by the various clay materials present. Many clays are water sensitive, and contact with foreign fluids may cause damage by two mechanisms. The first, and probably the more critical, mechanism is dispersion and migration of the clay particles. Dispersion may be caused by charge differences or by fluid movement. The dispersed clays are then free to move through the formation until they enter an opening too small to pass, thus lodging and reducing permeability. The second mechanism is expansion or swelling of the clay particles. Water absorbed between

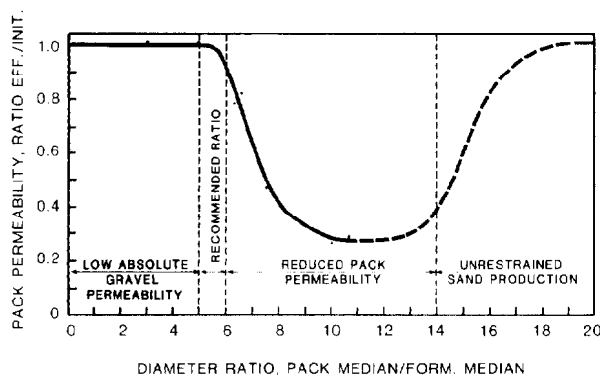


Fig. 56.3—Gravel-pack permeability impairment caused by formation sand invasion is illustrated by curve of change in ratio of increases. A ratio of 5 to 6 is the largest gravel that will stop all sand entry. Theoretical curve beyond 14 indicates sand flowing freely through gravel (after Ref. 12).

TABLE 56.2A—AVAILABLE GRAVEL SIZES

Gravel Size (in.)	U.S. Sieve Number	Approximate Median Diameter (in.)
0.006 to 0.017	40/100	0.012
0.008 to 0.017	40/70	0.013
0.010 to 0.017	40/60	0.014
0.012 to 0.023	30/50	0.017
0.017 to 0.033	20/40	0.025
0.023 to 0.047	16/30	0.035
0.033 to 0.066	12/20	0.050
0.033 to 0.079	10/20	0.056
0.047 to 0.079	10/16	0.063
0.066 to 0.094	8/12	0.080
0.079 to 0.132	6/10	0.106

TABLE 56.2B—FORMATION SAND SIEVE ANALYSIS

U.S. Sieve Number	Cumulative Wt% Retained	
	Sample A	Sample B
30	0.2	0.1
40	1.2	0.6
50	5.1	2.5
70	16.0	7.5
100	35.0	19.0
140	62.0	39.0
200	82.0	58.0
270	93.0	77.0
325	97.0	86.0
400	98.3	90.0
PAN	100.0	100.0

the clay particles causes the particles to expand, with a corresponding decrease in pore volume and the plugging of pore channels.

To avoid a production decrease, it is important to stabilize clays before or along with a sand-control treatment.

Gravel Selection

Gravel should be sized to prevent invasion of the pack by the finest formation sand.¹¹⁻¹³ For example, if 20% of a gravel pack is fine sands, the permeability will be 35% less than if no fines were present.^{13,14}

A gravel size should be selected that will restrict the movement of fine formation sand but will not reduce the flow of fluids to uneconomical rates. Saucier¹² suggests that the gravel size for controlling uniform sands should be five to six times the diameter of the mean (median) formation sand grain size. Degree of pack impairment is illustrated in Fig. 56.3, which shows the ratio of effective to initial pack permeability vs. the ratio of the pack median diameter to the formation median diameter.

Proper gravel size is determined by the following steps.

1. Obtain a representative formation sample; closely spaced samples from rubber-sleeve cores provide the best design bases.

2. Perform a sieve analysis.

3. Plot the sieve analysis data on either a cumulative logarithmic diagram (S-plot) or a logarithmic probability diagram.

4. Calculate the gravel median grain diameter using a five-to-six multiple of the 50-percentile formation grain diameter. When multiple cores from a single zone are provided, they should be analyzed and plotted separately. The samples should not be mixed. The sample with the smallest 50-percentile grain diameter is used to select the gravel. Tables 56.2A and 56.2B list some of the commercial gravel sizes available. Gravel should be screened and checked to verify size and distribution.

Sieve analysis data for two rubber-sleeve, core-barrel samples, taken from the same zone, are tabulated and are plotted in Figs. 56.4 and 56.5. Note that Sample A is from a portion of the zone that contains coarser sand than the portion from which Sample B was taken. If Sample A alone had been taken, a coarser gravel would have been selected, and a gravel-pack failure could have resulted.

In Fig. 56.6, produced, bailed, and core-barrel samples from the same well zone have been plotted. The core-barrel sample plots as a straight line (minor variations are typical, however). The dashed variation shown could indicate a sieving or weight problem. A bailed sample would typically rise on the left because finer formation grains would have been produced, leaving the larger grains in the wellbore. Conversely, a produced sample would rise on the right, indicating an excess of fines.

The same data are shown in an S-plot (Fig. 56.7). Each of the curves is typically S-shaped, and any curve plotted by itself would not readily be interpreted as varying from the norm. An error in gravel selection could result if the sample type were not known.

Gravel Quality. Studies have indicated that gravels containing fine particles outside the specified range will have lower permeability.¹⁴ Some supply sources furnish gravel with excessive amounts of particles smaller than specified. Angular gravels may be broken during shipping and

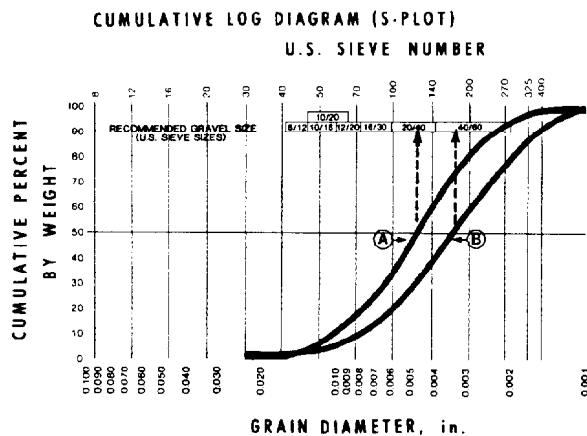


Fig. 56.4—Data from sieve analyses of Formation Sand Samples A and B, taken from the same zone, are plotted here. Note that using Plot A would result in the selection of 20/40-mesh gravel rather than the better choice of 40/60-mesh gravel for packing this zone, as indicated by Plot B.

handling, thereby creating fine particles that reduce the quality of the gravel. Rounded gravels provide tighter, more uniform compaction and somewhat higher permeability than angular gravels.

Screen Selection

Many types of wire-wrapped screens are available, including ribbed, all-welded, grooved, and wrapped-on-pipe. The all-welded screen has the wrapping wire resistance-welded to wire ribs at each point of contact. Spacer lugs, solder strips, and weld beads are not required and, therefore, the all-welded screen is stronger and more

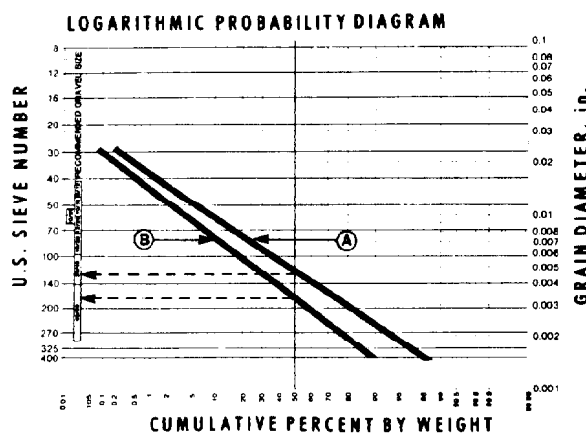


Fig. 56.5—Data for Samples A and B are again plotted here. Sieve-analysis data for sands with a normal grain-size distribution will plot as a straight line on a log probability grid. The logarithmic probability diagram has an advantage over the S-plot in that sampling errors are more readily detected. Variations from the straight-line plot could be caused by sieving and weighing errors, incorrect sample preparation, or by the sampling method itself.

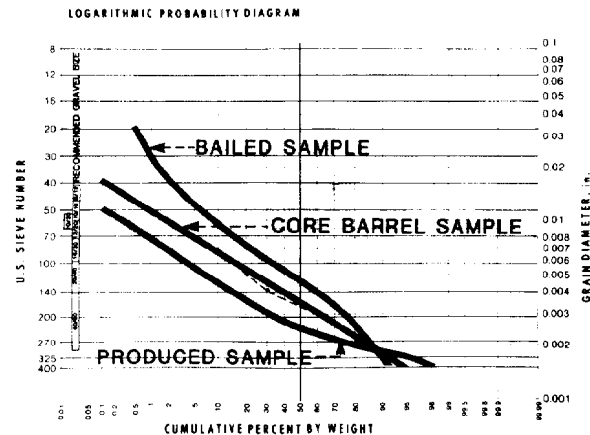


Fig. 56.6—Logarithmic probability diagram of produced, bailed, and core-barrel samples from the same well.

corrosion-resistant; it also has a lower pressure drop, and it will not unravel if the wire is eroded or broken.

The wrapping wire on these screens is usually made from 304 stainless steel while the pipe core is Pipe Grade S or K. Other wire and pipe materials are available.

The configuration of the openings in all screens is very important. If the sides of the slots are parallel, plugging may occur as the small sand grains bridge the slot. To reduce the chance of this occurring, the wire used to wrap the screen is wedge-shaped.

Fig. 56.8 shows the construction features of an all-welded screen.

For gravel packing, the gauge of the screen should be small enough to prevent the passage of the gravel-pack sand. Slot width is usually taken as one-half to two-thirds of the diameter of the smallest gravel-pack grains.

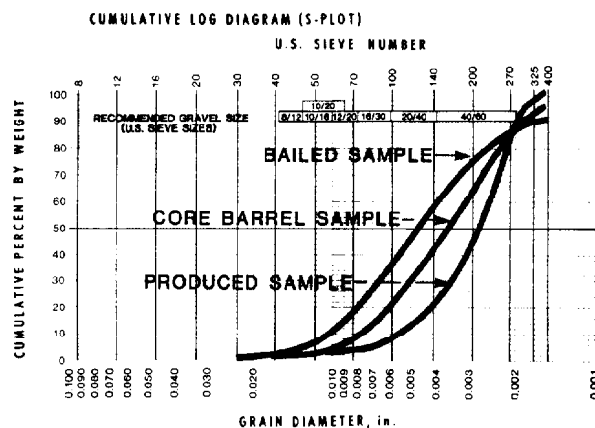


Fig. 56.7—Cumulative log diagrams (S-plot) of produced, bailed, and core-barrel samples from the same well. Note that a bailed sample would result in the selection of a coarser gravel.

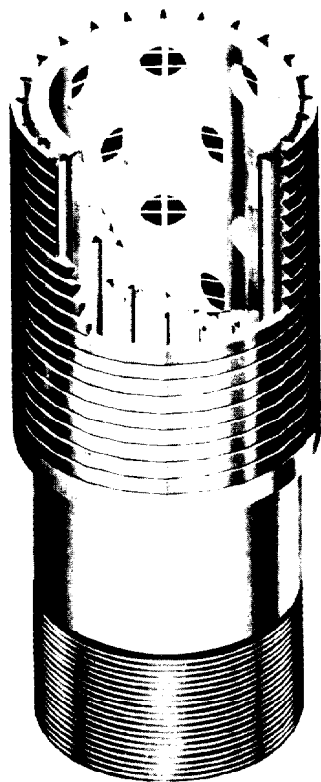


Fig. 56.8—All-welded screen.

The screen diameter should be as large as possible and yet leave adequate room for packing gravel. Table 56.3 shows the dimensions and inlet areas for several sizes of wire-wrapped screens. Screens are available with slot openings from 0.006 to 0.250 in. in 0.001-in. increments.

The screen length should overlap the perforated interval both above and below by 3 to 5 ft. Blank pipe should be run above the screen to provide a reservoir for extra gravel. Blank pipe length should be three to four times the screen length with a minimum length of 60 ft.

Gravel Packing

Methods. The term "gravel," as used here, refers to a uniform, graded, commercial silica sand that is placed in the wellbore and perforation tunnels for the purpose of mechanically retaining formation sands. These are described next.

Circulating gravel packs are done in two steps: an outside pack and an inside pack. The outside pack or pre-pack places gravel outside the perforations, where voids may exist in the formation surrounding the casing and in the perforations. An outside pack is, of course, not used in openhole completions. The outside pack is usually attained by pumping a gravel slurry through an open-ended workstring with the application of fluid pressure. To achieve good gravel placement, fluid must be lost to the formation.

The inside pack is achieved by pumping a slurry containing from $\frac{1}{4}$ to 15 lbm of gravel per gallon of fluid down the workstring and through a crossover tool into the annular space between the screen and the casing. The gravel is held in place by the screen while the carrier fluid

(brine, diesel oil, etc.) flows through the screen and crossover tool into the tubing/casing annulus and back to the surface.

A wash pipe extends from the crossover tool, inside the blank pipe and screen, to the bottom of the screen. Returns are taken through the wash pipe. It is recommended that the wash pipe outside diameter be 0.6 times the screen liner inside diameter and made up with flush joints. This ratio of wash pipe outside diameter to liner inside diameter optimizes gravel distribution along the screen in deviated holes.

The screen and blank pipe should be centralized every 15 ft, and the length of the screen should be such that it extends above and below the perforated interval by 3 to 5 ft. A calculated quantity of a high-density slurry at 15 lbm of gravel per gallon of fluid (density of 13.89 lbm/gal if fluid is water) is circulated into place. As the gravel settles out and packs in the hole outside the screen, injection pressure will increase. When the injection pressure has increased to between 750 and 1,500 psi above the originally established injection pressure, pumping is stopped. When the sandpack causes such a pressure increase, the condition is called a screenout.

The slurry remaining in the reservoir above the screen (established by the blank pipe) will settle out so that ample gravel exists above the top of the screen. Since about 60% of the slurry volume consists of gravel, 100 ft of slurry will result in 60 ft of settled gravel.

In gravel packing intervals with the circulating method and a high-density slurry, a lower tell-tale is recommended. The lower tell-tale is a short section of screen, not less than 5 ft long, located below the production screen. A seal sub, installed between the lower tell-tale and the production screen, seals the wash pipe. Returns are thus taken only through the lower tell-tale. By this method, gravel is placed at the bottom of the screen, and a denser pack can be achieved. After screenout of the tell-tale screen, the wash pipe is pulled up into the production screen to complete the gravel pack.

Squeeze gravel packing uses a gravel slurry consisting of 15 lbm of gravel added to a gallon of viscous carrier fluid. This gives a high-density (13.89 lbm/gal) slurry. The carrier fluid transports the gravel into place and is squeezed away into the formation. A viscosity breaker in the carrier fluid reduces the viscosity according to a preplanned schedule; this allows for fast well cleanup.

Reverse circulating gravel packing is a low-density method using $\frac{1}{4}$ to 2 lbm of gravel per gallon of carrier fluid. The slurry is circulated down the tubing/casing annulus. The gravel is retained on the outside of the screen while the carrier fluid flows through the screen and to the surface through the tubing. After the pack is completed and all the gravel in the annulus has settled, the tubing is pulled out of the hole, leaving the screen assembly with a polished nipple on top in the hole. A production packer with an overshot seal assembly is then run over the polished nipple. If the pack is done in perforated casing, a prepack is usually done first.

Several disadvantages associated with a reverse circulating gravel pack include (1) long rig time, (2) pack voids, (3) slurry pumped down the annulus scouring dirt and mill scale from the inside of the casing and the outside of the tubing, and (4) possible formation damage caused by large amounts of dirty fluid circulated and lost to the formation.

TABLE 56.3—COMMON SCREEN SPECIFICATIONS AND SIZES

Pipe Base						Screen				
OD (in.)	Weight (lbm/ft)	ID (in.)	Holes per ft	Hole Diam. (in.)	Total Hole Area (sq in./ft)	OD (in.)	Screen Surface Open Area in sq in./ft for slot opening (in.)			
							0.008	0.010	0.012	0.020
1.050	1.14	0.824	72	1/4	3.53	1.55	6.8	8.2	9.6	14.4
1.315	1.70	1.049	60	5/16	4.60	1.82	8.0	9.7	11.3	16.9
1.660	2.30	1.380	72	5/16	5.52	2.16	9.4	11.5	13.4	20.1
1.900	2.75	1.610	84	5/16	6.44	2.40	10.5	12.7	14.9	22.3
2.063	3.25	1.751	84	5/16	6.44	2.56	11.2	13.6	15.9	23.9
2.375	4.60	1.995	96	3/8	10.60	2.88	12.6	15.3	17.8	26.8
2.875	6.40	2.441	108	3/8	11.93	3.38	14.8	17.9	20.9	31.5
3.500	9.20	2.992	108	1/2	21.21	4.00	17.5	21.2	24.8	37.3
4.000	9.50	3.548	120	1/2	23.56	4.50	19.7	23.9	27.9	41.9
4.500	9.50	4.090	144	1/2	28.27	5.00	21.8	26.5	31.0	46.5
5.000	13.00	4.494	156	1/2	30.63	5.51	24.1	29.2	34.1	51.3
5.500	14.00	5.012	168	1/2	32.99	6.01	26.3	31.9	37.2	55.9
6.625	24.00	5.921	180	1/2	35.34	7.14	31.2	37.9	44.2	66.5
7.000	23.00	6.366	192	1/2	37.70	7.52	32.9	39.9	46.6	70.0
7.625	26.40	6.969	204	1/2	40.06	8.15	35.6	43.3	50.5	75.9
9.625	36.00	8.921	264	1/2	51.84	10.17	44.4	54.0	63.0	94.7

Cased Hole Completion

Casing (in.)	Screen Pipe Size (in.)
4 1/2	2 1/16
5	2 3/8
5 1/2	2 3/8
6 5/8	2 7/8
7	2 7/8 to 3 1/2
7 5/8	2 7/8 to 3 1/2
8 5/8	4
9 5/8	4 1/2 to 5 1/2
10 3/4	5 to 5 1/2

Openhole Completion

Casing (in.)	Openhole Diameter (in.)	Screen Pipe Size (in.)
5 1/2	12	2 7/8
6 5/8 to 7 3/4	14 to 16	4
7 5/8 to 8 5/8	14 to 18	5 1/2
9 5/8 to 10 3/4	16 to 20	7

Wash-down gravel packs are done by dumping the gravel down the casing, allowing it to settle, and then running a screen-and-wash pipe assembly with a wash-down set shoe into the hole. Circulation is established through the shoe, and the screen assembly is lowered as the gravel is washed up the annulus. When the shoe tags bottom, circulation is immediately stopped, and the gravel allowed to settle around the screen. The screen is then released, and a production packer with a seal sub is run into the hole to seal the production string.

References

- Muecke, T.W.: "Formation Fines and Factors Controlling Their Movements in Porous Media," *J. Pet. Tech.* (Feb. 1979) 144-50.
- Miles, L.H. and DaShanzer, W.A.: "An Evaluation of Plastic Sand Control Methods Used in the South Louisiana Area," paper SPE 4780 presented at the 1974 SPE Symposium on Formation Damage Control, New Orleans, Jan. 31-Feb. 1.
- Scheuerman, R.F. and Willard, R.O.: "Water-Base Viscous Gravel Pack System Results in High Productivity in Gulf Coast Completions," paper SPE 4774 presented at the 1974 SPE Symposium on Formation Damage Control, New Orleans, Jan. 31-Feb. 1.
- Suman, G.O. Jr.: "Sand Control," *World Oil*, Part 1 (Nov. 1974); Part 2 (Dec. 1974); Part 3 (Jan. 1975); Part 4 (Feb. 1975); Part 5 (March 1975); Part 6 (April 1975); Part 7 (May 1975).
- Bruist, E.H.: "Better Performance of Gulf Coast Wells," paper SPE 4777 presented at the 1974 SPE Symposium on Formation Damage Control, New Orleans, Jan. 31-Feb. 1.
- Gurley, D.G., Copeland, C.T., and Hendrick, J.O. Jr.: "Design, Plan, and Execute Gravel Pack Operations for Maximum Production," *J. Pet. Tech.* (Oct. 1977) 1259-66.
- Stein, N., Odeh, A.S., and Jones, L.G.: "Estimating Maximum Sand-Free Production Rates from Friable Sands for Different Well Completion Geometries," *J. Pet. Tech.* (Oct. 1974) 1156-58.
- Klotz, J.A., Krueger, R.F., and Pye, D.S.: "Maximum Well Productivity in Damaged Formations Requires Deep, Clean Perforations," paper SPE 4792 presented at the 1974 SPE Symposium on Formation Damage Control, New Orleans, Jan. 31-Feb. 1.
- Brooks, F.A.: "Evaluation of Preflushes for Sand Consolidation Plastics," *J. Pet. Tech.* (Oct. 1974) 1095-1102.
- Gidley, J.L.: "Stimulation of Sandstone Formations With the Acid-Mutual Solvent Method," *J. Pet. Tech.* (May 1971) 551-58.
- Gulati, M.S. and Maly, G.P.: "Thin-Section and Permeability Studies Call for Smaller Gravels in Gravel Packing," paper SPE 4773 presented at the 1974 SPE Symposium on Formation Damage Control, New Orleans, Jan. 31-Feb. 1.
- Saucier, R.J.: "Gravel Pack Design Considerations," *J. Pet. Tech.* (Feb. 1974) 205-12.
- Williams, B.B., Elliott, L.S., and Weaver, R.H.: "Productivity of Inside Casing Gravel Pack Completions," *J. Pet. Tech.* (April 1972) 419-25.
- Sparlin, D.D.: "Sand and Gravel—A Study of Their Permeabilities," paper SPE 4772 presented at the 1974 SPE Symposium on Formation Damage Control, New Orleans, Jan. 31-Feb. 1.

Chapter 57

Oil and Gas Leases

Joe B. Clarke Jr., Vermilion Oil and Gas Corp.*

The Landowner's Interest

Property

All property can be classified as either real or personal. Real property is land and that which is affixed or appurtenant to land. Personal property is every kind of property that is not real property. Oil and gas in place are considered to be a part of the land and are therefore a form of real property. When oil and gas are reduced to possession by being brought to the surface, they become personal property.

Ownership of property is the right to possess and use the property to the exclusion of others. Land cannot be without ownership. The rightful owners may be hard to determine, but ownership nevertheless exists. The extent of an owner's rights may vary. Absolute ownership is a superior status excluding participation by anyone else. The absolute owner is most frequently referred to as the fee owner and absolute ownership as fee ownership. There is a form of qualified ownership referring to a status establishing an equal right of participation in another person. For example, two parties are co-owners of a tract of land. Each party has certain rights to use and enjoy the land, but the rights of each party are qualified by the rights of the other party. Another form of ownership is limited ownership, which is a restricted right. The absolute owner who grants a 1-year grazing lease brings a form of limited ownership into being.

The absolute or fee owner is entitled to possession, which means the actual or physical occupancy of a thing. The party in possession of a thing is occasionally not the owner of that thing. Possession undoubtedly carries with it the intention to hold, but possession does not mean ownership.

The fee owner owns the surface of land and the minerals thereunder. The surface owner has no right to grant an oil and gas lease or mineral lease. However, the rights of mineral owners are often subject to the rights of

surface owners. The mineral owner has the right to grant mineral leases. A royalty owner has a right to receive royalty or a share of production as obtained but has no right to grant mineral leases or receive bonuses or rentals.

Ownership of Hydrocarbons in Place. Various ideas and theories have been suggested as to the nature of ownership of oil and gas in the reservoir prior to extraction. Two principal ideas have evolved: the absolute-ownership and the nonownership theories. In the absolute-ownership theory, hydrocarbons are considered a part of the land and absolute ownership of the land is absolute ownership of the oil and gas in place. This theory divests the absolute owner of the hydrocarbons in place when there is drainage across property lines. The nonownership theory requires the acceptance of oil and gas as fugitive minerals. Absolute ownership of the land will therefore carry with it only the exclusive right to drill on the land in an attempt to reduce the oil and gas to possession. Absolute ownership of the oil and gas is not attained until the oil and gas are reduced to actual possession.

Regardless of which theory of ownership each of the various states adheres to in its statutes, the courts are in agreement that oil and gas in place are minerals and a part of the land; when they are reduced to possession, they become personal property; a landowner has the right to drill a well on the property in an attempt to reduce the oil and gas to possession, and without liability for drainage from adjacent lands; these privileges and responsibilities can be transferred to others.

Rule of Capture

The theories of ownership provide for the migratory nature of oil and gas under certain conditions. The impossibility of determining liability for drainage where

*This author also wrote the original chapter on this topic in the 1962 edition.

landowners produce in a lawful manner from a well on their land is recognized. This freedom from liability for drainage is referred to as the "rule of capture." Since landowners cannot recover damages or enjoin the operator when their property is being drained by a well on adjacent lands, they must protect themselves as best they can. In short, they must drill, or have the lessee drill, a well on their own land as promptly as possible in order to prevent further drainage. This "offset drilling rule" is modified in these days of increased conservation legislation. Many states have statutes relating to well spacing, allocation of production, pooling, etc., which provide equitable relief for the landowners who are being drained by other means than the drilling of a well on their land, and which tend to prevent the drilling of unnecessary wells.

Mineral Severance

Severance of the minerals can occur in a number of ways. One of the most common ways is the conveyance of the land itself by a deed that provides for the reservation or exception of all or a part of the minerals to the grantor. Mineral severance is often accomplished by a deed conveying all or a part of the minerals themselves. A severance of oil and gas from the surface is recognized in all jurisdictions.

A lease or a conveyance using the term "minerals" will include oil and gas without otherwise describing them. A conveyance of a named mineral without the phrase "and other minerals" will convey only the mineral named. In some areas, "oil and gas" leases are obtained; in other areas, "oil, gas, and mineral" leases are obtained.

The owner of the mineral estate is entitled to the use of the surface as it may be necessary, subject to certain rights of the surface owner, for the exploration and recovery of the minerals. The foreclosure of a mortgage as to the surface estate is not effective as to the mineral estate, provided the execution of the mortgage is subsequent to the date of the mineral severance.

Adverse Possession. Adverse possession refers to the possession of real estate that is open, visible, continuous, and exclusive. The statutes of the various states establish the manner in which titles can be acquired by adverse possession. If such possession is continued for the time and in the manner prescribed by the statutes, the effect is to divest the owner of title and to vest in the adverse possessor a new title. If the minerals have not been severed, adverse possession of the surface is adverse possession of the minerals. Minerals severed from the surface prior to the commencement of adverse possession cannot be acquired by adverse possession. The years of occupancy, the construction and maintenance of fences, the construction and use of houses and outbuildings, the drilling of water wells, the grazing of cattle, the cutting of timber, the growing of crops, the payment of taxes, etc., are all important items to be considered by the title examiner in determining whether or not a basis exists for the establishment of an adverse title under the statutes of the state involved.

Partition. Partition is a division of real estate among co-owners whereby each acquires a separate tract. The ef-

fect of partition is to terminate the ownership of the undivided interests of the joint owners and to establish ownership in each co-owner as to the divided share. Partition is effected either voluntarily or involuntarily. The latter is called compulsory or judicial partition and consists of partition in kind or partition by sale and division of the proceeds. Partition in kind is, in general, the most equitable form of partition. Where such partition is impractical or unfair, partition by sale and division of the proceeds is resorted to.

A lessee who acquires an oil and gas lease from less than the entire group of cotenants is faced with certain problems, each of which has to be solved on its own merits under the applicable statutes. Partition of a tract subsequent to the granting of an oil and gas lease by the co-owners does not enlarge the obligations of the lessee. In such an instance, the lessee would not be required to drill an offset to prevent drainage in the event that the completed oil well is on one of the partitioned tracts.

Trespass. The landowner and his mineral lessee have several remedies for unauthorized entry and use of the surface and minerals. In determining the measure of damages for unauthorized intrusion it must first be determined whether the trespass was made in good faith or in bad faith. The measure of damages for unauthorized production in the case of good-faith trespassers is the value of the oil and gas at the surface less the reasonable costs of production; the measure of damages in the case of bad-faith trespassers is the value of the oil and gas at the surface.

Unauthorized penetration of the subsurface is a form of trespass. A lessee who commences a well on a tract of land and allows or causes the borehole to deviate from the vertical in such a manner so as to drill into the subsurface belonging to an owner who has not leased to the lessee is liable for trespass. In questions involving this type of trespass, a court order may be obtained for a well survey to determine whether or not a trespass has occurred. Should such a well produce, the measure of damages would be the value of the hydrocarbons removed. If the well results in a dry hole, the trespasser is liable to the landowner for damages for the destruction of the mineral value of the land.

Fee or absolute ownership carries with it the right of absolute control, including the right to grant oil and gas leases, to conduct exploratory operations on the land, to authorize others to so use the premises, etc. It therefore follows that a party who conducts exploratory operations without permission violates the rights of the landowner and is accordingly liable. In this type of trespass, damages may be recovered from the standpoint that such operation may have reduced or removed the marketability of an oil and gas lease on the land or reduced the leasing value of the land itself.

Correlative Rights. Despite the rule of capture, there has been much said and written, and some legislation, regarding correlative rights. Property owners overlying a common source of supply are restricted in their right to remove hydrocarbons by their duties to adjoining landowners. They are obligated not to injure the reservoir or dissipate the reservoir energy, and they cannot remove a disproportionate share of the hydrocarbons. In general,

owners may not use their land in such a manner as to injure the property of others. The principle of correlative rights is enforced by law in those states that have enacted comprehensive conservation legislation.

The Oil and Gas Lease

Background

A large number of printed lease forms are in use in the oil industry. The evolution of the oil-and-gas-lease contract has been a slow process. Present-day forms are quite lengthy when compared with the contracts made in the earlier years of the oil industry. The many refinements made since then have been based on the hard lessons learned through experience and on the many court decisions rendered as a result of the inevitable controversies which arose as the industry grew.

The courts have held, keeping in mind the fugitive nature of oil and gas, that the primary purpose of the oil and gas lease is development. Should the oil and gas lease not contain an express provision in this regard, the law will imply an obligation on the part of the lessee to explore and develop the leased premises.

An oil and gas lease is a conveyance or an interest or right. It is also a contract between the lessor and the lessee. Since an oil and gas lease conveys an interest in real estate, it must be in writing in accordance with the statute of frauds. A lease is sufficient if the names of the parties, the description of the property involved, and the terms of the agreement are set forth. It is not necessary that the lessee sign the lease to make it legally effective. Witnesses are not required in order to make the instrument effective between the parties. An acknowledgment is required only in connection with the recording of the instrument and does not affect the validity of the instrument between parties. Recording the lease is not necessary to the validity of the instrument between the parties, but is required to afford protection against bona fide purchasers.

The Lessor

A party owning a mineral interest and having the personal capacity to contract has the capacity to execute a valid oil and gas lease. Oil and gas leases from minors and insane persons are usually executed by guardians of such persons under the direction and approval of the court. The disabilities of minors may be removed in some states by judicial proceedings and leases obtained directly from such persons. Leases executed by minors are voidable at their election upon reaching majority. A lease executed by a person subsequently adjudged insane is voidable.

Landowners often leave a will devising certain real property to their children subject to a life estate or usufruct in the surviving widow, who is called the life tenant or usufructuary. The children are called the remaindermen or naked owners. Neither the life tenant nor the remainderman has the right to lease without the consent of the other. Both parties must join in the execution of an oil and gas lease for it to be valid. It is important that the rights of the lessors as to the bonus, delay rentals, and royalty payments be clearly set forth in the lease. Generally, the bonus and rental payments are payable to the life tenant, and royalty is payable to the remainderman.

A landowner can execute an oil and gas lease on lands that are subject to the qualified rights of others provided the lease does not interfere with such prior rights. The most common example is the landowner who grants a surface lease for grazing purposes and then at a subsequent date executes an oil and gas lease. The lessee in the oil and gas lease cannot be prevented from entering on the surface to exercise the rights granted in the lease, but at the same time the lessee is responsible to the tenant for damages to the extent that the tenant's rights are interfered with. A tenant's consent agreement is usually obtained prior to operations of any kind.

An administrator is one who is vested with the right of administration of an estate and is appointed by the court. An executor is a person appointed by a testator, or the party making a will, to execute his will. A trustee is a person holding property in trust for another party. Executors, administrators, and trustees have authority to execute oil and gas leases provided such specific authority is given by will, by the court, or by statutory provision. A power of attorney is an instrument authorizing one to act as the attorney or agent of the person granting it, and terminates upon the death of the grantor.

In the case of married persons, the husband may, in general, execute a lease without the joinder of his wife. Homestead statutes usually require that all instruments creating encumbrances upon the homestead be signed by both parties. The wife, in general, can execute a lease on her separate property. In community-property states the husband may or may not have the right to grant a lease on the community estate without joinder by his wife; however, most lessees will insist upon the joinder of the wife.

The law differs among the states as to whether or not a co-owner can execute a lease without the consent of the other cotenant. In most of the states, such a lease would be effective only as to the interest of the executing cotenant. Two or more lessees, each having leases on undivided interests in the same tract, are cotenants. Each is entitled to drill on any part of the leased premises but, if successful, must account to the other cotenant for his proportionate share of the production, less the cost of production.

Consideration, Date, Description, and Delivery

A valid oil and gas lease requires a consideration, a nominal cash payment or other consideration generally being sufficient. An undated lease takes effect upon execution and delivery. An exact description of the land to be leased is not necessary, provided the land can be identified with reasonable certainty. Delivery and acceptance of an oil and gas lease are required as with other conveyances: the intent of the lessor to make the instrument legally effective must be apparent.

The Granting Clause. This clause in an oil and gas lease is usually the first paragraph in the lease and is one of the most important paragraphs in the entire contract. The rights of the lessee are very broadly set forth. The remaining provisions of the contract modify or enlarge upon the provisions of this paragraph.

The granting of the lease is for the purpose of the development of the mineral estate. Accordingly, the lessee must have those exclusive rights that are necessary

to carry out the basic purpose of the lease. This includes the right to build pits and erect tanks and other equipment pertinent to the lessee's operations. The lessee has the right to construct, maintain, and use roads, pipelines, and/or canals on the leased premises. The lessee is not liable for operations on the leased premises unless the surface is used excessively, the operations are negligent, or any express provisions in the lease are violated. The lessee is required to restore the premises to their original condition, insofar as is practicable, when required by the lease. The lessee has the right to conduct exploratory operations on the leased premises and to conduct secondary-recovery operations and to dispose of salt water by reinjection into suitable formations.

The landowner is entitled to the use of the surface, less that required by the lessee, who has the responsibility of protecting this remaining surface for the benefit of the lessor. The lessee must exercise complete control over the surface storage of liquids and is responsible for damages in the event of leakage and injury to the adjoining surface.

The Habendum Clause. A simple form of this clause provides that "this lease shall be for a term of blank years from the date hereof, called primary term, and so long thereafter as oil or gas is produced." This clause fixes the ultimate duration of the lessee's interest. The lease may be terminated sooner, for example, by the failure of the lessee to pay delay rentals. The primary term will limit the life of the lease prior to the establishment of production from the leased premises. The primary term is one of the items that must be negotiated at the time of the purchase. The term most commonly used is either 3 or 5 years. It is usually difficult to acquire leases with terms longer than 5 years. In very active areas primary terms of 3 years and less are usual.

For the lease to be extended beyond its primary term, production must occur, subject to certain exceptions to be discussed subsequently. The fact that oil or gas may have been discovered on the leased premises will not in itself keep the lease in force unless specific provisions are made to the contrary. This is especially applicable to oil. In the case of gas, provision is frequently made in the lease to extend the lease past its primary term in the event the lessee is not able to market the gas for lack of transmission lines, lack of a gas market, etc. When such a provision appears in a lease, it is referred to as a shut-in gas clause. It usually provides for the payment of a sum of money on an annual basis in an amount that may be as high as the lessor would ordinarily receive as delay rentals.

The word "produced" in the habendum clause has been held to mean "produced in paying quantities." What constitutes production in paying quantities has been the subject of much dispute. In general, if a lease is past its primary term, and enough production is being obtained from the lease so that a profit is made, however small, in excess of the cost of operation, disregarding the drilling and completing costs, such lease is held by production in paying quantities.

While a lease may generally be maintained in force past its primary term only by production, there are other ways provided for in the lease to maintain the lease past the primary term. A lease can often be kept in force, in

the absence of production, through the date of expiration and after the primary term by the lessee's operations, which are conducted in a diligent manner looking toward the discovery and production of oil and gas. Most leases provide that the lease may be kept in force for an indefinite period of time in this manner provided that not more than 60 or perhaps 90 days elapse between the cessation of any such operations and the commencement of additional operations. Such additional operations might include reworking operations on any abandoned producer or deepening operations on a dry hole or possibly drilling operations for a new well at another location on the leased premises.

Drilling and Delay Rental Clause. A simplified drilling and delay rental clause might say that "the lease shall terminate on blank date unless on or before such date the lessee either commences operations for the drilling of a well on said land or pays to the lessor a rental of blank dollars per acre for all or that part of the land which lessee elects to continue to hold, which payment shall maintain lessee's rights in effect as to such land without drilling operations for 1 year from the above date." The lessee may continue to maintain such rights without drilling operations for successive 12-months periods by making similar payments to the lessor.

Early oil and gas leases usually provided for the commencement of a well. Changes were gradually made in the lease to allow the lessee to defer drilling operations by the payment of an annual sum called the delay rental. This alternative obligation to drill or pay a delay rental, when considered with the right of the lessee to surrender the lease at any time, is called an "or clause." Further changes were made. Wording was added to the lease to provide that, if no well was commenced before a certain time, usually 1 year from the date of the lease, the lease would terminate unless the lessee paid a delay rental. This further revised wording is known as the "unless clause."

Regardless of which clause is used, the lessee has the right either to commence a well within a specified time, pay a delay rental in lieu of commencing operations, or terminate the lease by the nonpayment of delay rentals. Almost all leases in use today are of the "unless" type.

Since the lessee is under no obligation either to pay delay rentals or commence operations for the drilling of a well, the practice has been to pay a substantial consideration, called the bonus, for the granting of the lease. The bonus may be any agreed-upon sum but is usually large when compared with the delay rental. The bonus is sufficient to keep the lease in force and effect until such time, usually 1 year, as a delay rental may be provided for. The bonus is subject to negotiation at the time of the purchase of the lease. The bonus may run from \$1 to many thousands of dollars per acre, depending on the size of the tract, the royalty, anticipated oil and gas reserves, the quality and quantity of geological and geophysical data available, etc.

Most leases provide for the commencement of "operations." The commencement of actual drilling is not necessary unless specifically provided for. Operations incident to the actual drilling are sufficient and include building roads, digging pits, building the derrick, etc. Such operations must be continuous, diligent, and in good faith.

The effect of the drilling of a dry hole during the primary term by the lessee may vary from one lease form to another. Most leases provide that, if a dry hole is completed on the leased premises within the primary term, the lease may be kept in force by the commencement of additional operations or by resuming the payment of delay rentals as provided for in the lease.

In the "unless" type of lease, there is no obligation to pay the delay rental and there is no liability for failure to pay. Unless otherwise specifically provided for in the lease, the entire amount of the delay rental must be paid. Most leases permit the lessee to surrender a portion of the leased premises and then pay delay rentals on the balance. Delay rentals in most states are not a matter for negotiation as is the bonus and are usually in the amount of \$1/acre/yr. Such is not the case in some areas, as in southern Louisiana. Here the delay rental is just as important as is the bonus as an item to be negotiated upon; it is the practice for rentals to be in an amount equal to at least one-third to one-half of the bonus consideration on a per-acre basis.

The lease provides that rentals may be made on or before the specified date, payable to the lessor or to the lessor's credit in a bank designated by the lessor. Most rentals are tendered by the lessee 3 to 6 weeks in advance of the due date to provide time for the lessee to receive a receipt from the lessor's depository bank evidencing deposit of the rentals to the lessor's credit. The lease also contains a proportionate-reduction clause or lesser-interest clause, which allows the lessee to reduce the amount of the delay rentals and royalty payments where the lessor does not own a full interest.

Royalty Clause. A simple royalty clause might provide that the royalties to be paid by the lessee are (1) on oil and liquid hydrocarbons, one-eighth of that produced and saved from the land; (2) on gas, one-eighth of the market value at the well of the gas used by the lessee in operations not connected with the land leased, the royalty on gas sold by the lessee to be one-eighth of the amount realized at the well from such sales; (3) one-eighth of the market value at the mouth of the well of gas used by the lessee in manufacturing gasoline.

The most common royalty is one-eighth, experience having shown this to be the most equitable fraction to be paid to the lessor in relatively unexplored areas. However, in known trends it is often difficult to purchase leases providing for a royalty of only one-eighth. Here again, the royalty is an item that must be negotiated in much the same manner as the bonus or delay rental. Royalties of one-sixth and more are now quite common in some areas.

The royalty interest created at the execution of the lease is payable to the lessor in the event of production. It does not refer to any additional royalties that may be created by the lessee out of the working interest and that are called overriding royalties. It does not refer to an advance royalty that can be deducted from any subsequently accruing royalties. It does not refer to a minimum royalty, which is a sum the lessee agrees to pay in the event of production regardless of whether or not it is equivalent to the lessor's share of gross production.

A failure to pay royalties does not in itself effect automatic termination of the lease. Failure to pay

royalties within a reasonable time could result in a forfeiture of the lease in a court action. Some delay, perhaps several months, in disbursing royalty is to be expected; title must be approved by the oil or gas purchaser and division orders circulated among those who will share in the production.

Oil royalties are payable to the lessor either in oil or to the lessor's credit in the pipeline, which is called payment in kind, or by payment in money based on the value of the royalty oil. Execution of a division order waives the lessor's right to receive royalty in kind. Royalty is computed as a share of the gross and not as a share of the net production, which means the royalty is not burdened with any production costs. However, the lessor is required to pay his proportionate share of the cost of transportation and gross production taxes.

Condensate or distillate is a liquid produced along with gas, but which originally was in the vapor phase in the reservoir. Casinghead gas is gas produced from an oil well. A gas well produces gas as distinguished from casinghead gas and may be defined in terms of gas/oil ratio by various regulatory bodies. The royalty payable on oil is also the royalty payable on condensate and other liquid hydrocarbons when separated on the leased premises. The royalties payable on gas are always payable in money and never in kind, and are subject to transportation costs. Royalty on gas is payable only on that gas which is sold or used off the leased premises. Royalty is not payable to the lessor on gas used by the lessee as a means of lifting the oil to the surface or that is injected into the reservoir for pressure-maintenance purposes.

A gasoline plant may be justified in areas where there are sufficient reserves of rich gas. A lessee will often enter into a contract with a processing plant whereby his gas wells are produced full-well stream to the plant for extraction of liquid hydrocarbons. The independently owned plant will retain a percentage of the value of the liquid hydrocarbons removed as a processing charge and credit the lessee with the value of the balance of the separated liquids as well as with all the residue gas. The lessee then disburses royalty to the lessor in accordance with the terms of the lease. If the lessee owns an interest in the plant, the lessee may be required to pay royalty on extracted liquids and residue gas less only the actual operating costs of the plant depending upon the terms of the lease.

The Pooling Clause. The pooling clause provides that the lessee, at its option, is given the right and power to pool or combine the land or mineral interest covered by the lease, or any portion thereof, with other land, lease or leases, and mineral interests in the immediate vicinity thereof, when in the lessee's judgment it is necessary or advisable to do so in order to develop or operate the leased premises properly to promote the conservation of oil and/or gas. The clause further states that "any unit or pool created for the production of oil shall not exceed 40 acres and that any unit for the production of gas shall not exceed blank acres." The number of acres inserted in the event of a gas well will vary from 160 to 640, depending on local practice.

The term "pooling" refers to the combining of small tracts for the purpose of forming a unit on which a well may be drilled. A lease form should be used that contains

an appropriate pooling clause. It may not be quite so important to obtain this right in certain areas where only oil is produced or in those states that provide for forced pooling and integration. The pooling right is related to development, and the owner of the working interest has the responsibility for such development.

The lessee must act in good faith in exercising the pooling privileges granted in the lease. When a lessee declares a unit and places the unit declaration of record in accordance with the lease, it is presumably done in the interest of proper development and conservation. Caution should be exercised in planning a unit to be declared so the unit will be in reasonable conformance to the subsurface and seismic data available. A lessee who declares a unit of an unusual shape for the obvious purpose of holding a lease past its expiration date, or that includes acreage most likely not productive, or that tends to disregard available geological control is probably not acting in good faith. Such a declared unit may be vulnerable to attack by the lessors.

When a lease contains a pooling clause, appropriate changes will appear elsewhere in the lease. The habendum clause may read, "this lease shall be for a term of blank years from the date hereof, called primary term, and so long thereafter as oil or gas is produced either on this land or on acreage pooled therewith, or with any part thereof." Operations for the drilling of a well or production from a well on a unit constitute operations or production from each of the tracts pooled.

Miscellaneous Clauses. Many miscellaneous clauses are found in leases for the benefit of the lessor or the lessee. The lessee is restricted in locating a well on the leased premises to the extent that no well may be drilled nearer than 200 ft to any house or barn. The lessee is required to lay pipelines at such a depth as not to interfere with plowing and cultivating operations. The lessee may be required to pay for all damages in connection with its operations on the land, although the damages are often restricted to timber and growing crops.

A paragraph is often found in leases that has as its purpose the inclusion of small strips of adjacent land owned by the lessor but not specifically described in the lease. The lessor usually intends to include such small parcels of land in the lease, but for various reasons a description of the strip may have been omitted. This paragraph is called the "Mother Hubbard clause." It is not intended that large tracts of land be subject to this clause but only strips or parcels of perhaps several acres in size. The lessee is given the right to use without cost gas, oil, and water produced on the leased premises for lessee's operations thereon. The lessee is given the right to remove machinery and fixtures from the leased premises, including casing, within a reasonable period of time after the lease has terminated.

The lease provides that the interests of the parties are assignable in whole or in part. No change in ownership of the land imposes any additional burden on the lessee until the lessee has been furnished with a certified copy of the recorded instrument evidencing the transfer. Since portions of many leases are eventually assigned, a clause is inserted to protect the lessee in the event of default in rental payments by the lessee's partial assignee. It provides that in the event of partial assignment a default in

the rental payment of the assignee shall not operate to defeat or affect the lease insofar as it covers that portion retained by the lessee.

The "warranty clause" provides that the lessor warrants and agrees to defend the title the land leased. If the covenant of general warranty is breached, the lessee can recover the consideration paid for the lease with interest and the expenses incurred in defending possession. The lessee is given the right to redeem for the lessor, by payment, any mortgages, taxes, or other liens on the leased premises and to apply to the repayment of the lessee any rentals and/or royalties accruing under the lease.

The Implied Covenant. It is important to keep in mind that the underlying purpose of the lease is to secure production. Most leases have very little to say about the manner in which wells will be drilled, or even if a well will be drilled at all. Little is ever said about the well density or the intervals at which development wells will be drilled. The lack of specific agreement between the lessor and lessee in these regards is intentional. Too much is unknown about the nature and characteristics of any reservoir present. The obligations of the lessee are the obligations of an ordinarily prudent operator under the same or similar circumstances, considering the lessor's interest as well as his own. The obligation to develop the leased premises as would a prudent operator arises only after discovery of oil or gas and continues for the life of the lease.

Assignments by the Landowner

Right to Transfer. Fee owners can dispose of their land in any way they see fit, either in whole or in part. They can convey the surface and reserve the minerals, or vice versa. They can sell all or a divided part or an undivided interest in the minerals. They can sell all or a part of their interest in the proceeds from the minerals. They can create a subordinate interest and transfer it to another party, as is done when a lease is granted.

Mineral Deeds and Interests. A mineral deed transfers the minerals or the right to obtain them as they exist in place. The owner of minerals has the right to go on the land, conduct exploratory operations, and produce oil and gas. If the minerals are subject to a lease at the time of the mineral conveyance, the mineral grantee may not exercise these rights until the lease terminates. The mineral owner has the right to execute a lease and to receive the bonus money therefrom. The mineral owner has the right to receive rentals and to share in the royalties if and when payable under any lease. Mineral interests are most often created by unqualified grants or reservations. However, many mineral conveyances are for a specified term of years, or for a specified term and so long thereafter as oil or gas is produced.

Royalty Deeds and Interests. Royalty is a share in production and, when applied to a lease, refers to the share of the oil and gas that is received by the lessor from production under the lease. This share is usually one-eighth of the whole, although it may be any other fraction agreed upon. Royalty also refers to an interest that is created by grant or reservation either before or after the

execution of a lease. The right to royalty is contingent on production and carries with it no right or interest in the minerals. The owner of a royalty interest receives no bonus and no delay rental payments. A royalty interest is an expense-free interest in the gross production and not in the net production. Royalties as well as minerals may be conveyed in fee or for a specified term of years, or for a specified term and as long thereafter as oil or gas is produced.

When referring to a conveyed royalty interest, it is customary to refer to the number of royalty acres conveyed, as well as to the fractional interest. If a landowner sold half of his one-eighth royalty in a tract of 80 acres, the royalty grantee is said to have purchased 40 royalty acres. If a royalty buyer purchased one-eighth of the same landowner's one-eighth royalty, the royalty purchaser would be entitled to one-sixty-fourth of all production and is said to own 10 royalty acres.

Assignments by the Lessee

Right to Transfer. The lessee is the owner of the lease, and the interest is usually seven-eighths of the production but may often be much less, depending on the amount of royalty. This interest is referred to as the working interest. A lessee may transfer his entire interest either in whole or part, or an undivided portion in the lease or a part thereof. The lessee has the right to convey overriding royalties, production payments, undivided interests, or an entire interest in a portion of the leased premises.

Assignments and Subleases. An assignment is a transfer of the assignor's entire interest in a lease either in its entirety or in a portion thereof. A sublease is a partial transfer in that the sublessor retains an interest in the lease in so far as it affects the property subleased. An instrument conveying the working interest but providing for the reservation of an overriding royalty is a sublease rather than an assignment.

Obligations undertaken by the lessee in the lease are called covenants. A contractual relationship exists between the lessor and the lessee, and there is said to be a privity of contract between the parties. The lessee has the right to assign the leasehold estate to a third party. The covenants contained in the lease are assumed by the third party and are said to be covenants running with the land. In the event of a true assignment, the lessee is usually relieved of his obligations to the lessor. In the event of a sublease, the lessee remains liable to the lessor because of the privity of contract between them.

Overriding Royalty. An overriding royalty interest is an interest carved out of the working interest and is not burdened with the cost of development or production. It is therefore a kind of royalty interest. An overriding royalty is usually created in a sublease, but may be created by grant. It in no way affects the royalty interest that is payable to the lessor. The overriding royalty owner generally cannot require the lessee to maintain the lease in force, to drill a well, or to develop the property, and shares in oil and gas only when, as, and if produced.

Production Payments. Oil payments, perhaps more correctly referred to as production payments, are related to overriding royalties in that they are usually carved out of the working interest and bear no cost of production. The overriding royalty differs from the production payment in that the former continues for the life of the lease and the latter terminates upon the payment of a specified sum of money from a stipulated percentage or fraction of the working interest. Production payments can be of practically any size and can be made payable out of any fraction or percentage of the working interest.

The production payment is occasionally used in negotiating a lease. A company may be willing to spend not more than \$100/acre as bonus for a lease but at the same time be willing to provide for a production payment of perhaps \$200/acre payable out of one-sixteenth of seven-eighths. A landowner can occasionally be shown the advantages of a production payment, with the result that a deal is made instead of lost.

The use of the production payment in the large-scale purchase of producing properties has become common. The task of how to purchase a producing property for a minimum cash outlay by the grantee with the grantor receiving the entire purchase price in cash and with the gain taxed at capital gains rates is often accomplished by an "ABC" transaction. A is the seller and the owner of the property. B is the purchaser of the property. C is the purchaser of the production payment and either has or can get the major part of the required cash. To illustrate, A owns a producing property that will sell for \$1,000,000. B wants to buy the property but has only \$200,000 for the purchase. A will convey the property to B for \$200,000, retaining a production payment of \$800,000 plus interest payable out of 85% of the production. A will then sell the production payment to C for \$800,000 cash. All parties to the transaction receive the maximum tax benefits allowed.

Unit Operations

Background

In recent years the objective has been to obtain the maximum ultimate recovery of oil and gas in place. In the early days of the industry a great number of unnecessary wells were drilled; only a fraction would have been required to obtain maximum efficient withdrawal. In time, limits were placed on the amount of production; well-spacing regulations came into existence; the establishment of drilling units and the pooling of small tracts of land followed. The advantages of cooperative development on a small scale became even more apparent when considered on the basis of the entire reservoir. Unit operation of a reservoir, whether for cooperative development, pressure maintenance, or secondary recovery, requires a knowledge of the hydrocarbons in place and an acceptance of the correlative rights of the owners; a fair distribution of the proceeds is best accomplished by contractual agreements among the royalty and working-interest owners.

The unit operation of an oil and gas reservoir is to be distinguished from pooling, which is the combination of small tracts to form a drilling unit or comply with spacing regulations. The term "unitization" is usually used interchangeably with unit operations. Unitization

therefore refers to the operation of all or a substantial part of the reservoir by a unit operator in accordance with the terms of a unitization contract. Unit operations may include two categories, depending on the manner in which they come into existence.

Voluntary Unit Operations. When the owners of the interests in a reservoir agree that all or a major portion of the reservoir is to be operated as a single unit regardless of property or lease lines, a voluntary unit operation comes into existence. The preparation of a unitization agreement acceptable to all the parties is a major undertaking. Two contracts are entered into, an operator's contract and a royalty owner's contract, sometimes called the unit contract. Many problems are involved regarding the operation of the reservoir and the drilling of additional wells that are best handled in a separate contract among the owners of the working interest. The royalty-unitization agreement must expressly provide for the consolidation of the interests of the lessors. Without such authority, lessors could demand that their tract be drilled to prevent drainage or be developed separately. The working out of a voluntary-unitization agreement requires a thorough knowledge of the conservation statutes. The voluntary-unitization agreement may provide that the contract will not become effective until approved by the appropriate regulatory body.

Compulsory Unit Operations. Compulsory unit operations come into being by order of a regulatory body in accordance with specific statutes. Early statutes provided that, if a certain percentage of the lessees in an area to be unitized petitioned the regulatory body to bestow jurisdiction to issue appropriate orders, it would do so. The laws of the states vary as to the percentage of ownership required. There must first be agreement among a majority of the lessees and royalty owners concerned regarding a unit plan. Here again a great deal of work and time are required. Numerous conferences are held among the working-interest owners and studies are made by various committees. Upon finalization of the plan, signatures are obtained from the working-interest and royalty-interest owners. A petition to the regulatory body is made and a hearing is held after proper notice has been given to all the interested parties. Upon issuance of the appropriate orders, accounting adjustments are made among the working-interest owners and the appointed unit operator assumes operations of the area.

Getting the Well Drilled

Lease Purchases. Oil and gas leases are purchased for a variety of reasons. Lease purchases are often of a trend nature, with no drillable prospect having been shown to exist. Such lease purchases could be in a sedimentary basin considered likely to contain accumulation of hydrocarbons, or as extensions to discovery wells. The owners of the leases might then plan to conduct seismic operations in an effort to isolate and define likely structures on large lease blocks or spreads of acreage. However, the owner of a geological idea or unleased prospect may have sufficient subsurface and/or seismic

data to justify the drilling of a well. In this instance, leases are acquired for the very definite purpose of drilling in the immediate future. Under such considerations, the amount of the rentals or the extent of the primary term becomes of secondary importance in negotiating the leases. A landman or lease broker will then be employed to review the records of the clerk of court to determine surface and mineral ownerships of all the tracts of land in the prospect including county roads, state and federal highways, rivers, school lands, canals, etc. Mineral leases will then be negotiated and acquired.

Capital to Drill the Well. Major oil companies have no real problem in raising the necessary capital to drill wells. Such funds are, to a large extent, available from earnings, and to a lesser extent, from borrowings. However, independents have been historically short of cash to drill wells. An "independent" is a small corporation or a partnership or perhaps an individual engaged in oil and gas exploration only. That is, an independent is not engaged in the transportation and refining of petroleum or in the marketing of petroleum products. Independents drill approximately 85% of all wells drilled in the U.S. and there are thousands of small companies and individuals engaged full time in oil and gas exploration.

In recent years, the limited partnership has been the primary source of venture capital for the independent. Investors buy units of a drilling fund and become limited partners. An experienced and successful independent becomes the general partner. Another significant source of venture capital for drilling wells has been the utility companies and end-users, such as the chemical industry. A typical independent may spend \$5 to \$15 million a year in drilling money, almost none of which belongs to the independent. The capital comes from investors and from persons who buy into drilling deals. Regardless of the source of the capital, the independent invariably promotes or lays off a part of his deal, usually on a third for a quarter basis. This means that the party being promoted or who buys into the deal will pay one-third of the cost of drilling the well for a one-quarter interest in the well. Variations of this type of promotion are endless; but by and large this type of promotion is standard between independents and investors as well.

Sources of Prospects. Major oil companies maintain large staffs of geologists, seismologists, paleontologists, and other supporting personnel engaged in development and exploration efforts. Major oil companies rarely participate in drilling on prospects not generated by them. On the other hand, most independents do not generate their own prospects but must buy them from geologists and others who generate geological prospects. The geologists, landmen, and others who can generate prospects and buy leases on them are then in a position, to a limited extent, to promote their prospect in dealing with an independent. Invariably, a nominal overriding royalty can be retained on the leases and occasionally a carried working interest to casing point. In this case it is difficult to obtain a carried working interest of as much as one-quarter because the independent taking the deal must

itself plan on laying off perhaps half of the deal and there must be some room left in the structuring of the deal to permit all concerned to realize some economic benefit.

Abstracts and Title Examination. Abstracts will be ordered on at least the proposed drillsite and offsetting tracts, and perhaps even on the entire prospect. The abstract will usually contain exact copies of all instruments of public record pertinent to the land from patent to date. Qualified oil and gas attorneys will review the abstracts and render a title opinion. There are usually numerous title deficiencies, most of which can be met by appropriate curative effort by the landman or title man. Supplemental title opinions will be obtained after the curative materials have been procured. Rarely can every requirement be met and the lessee may have to elect to waive such unmet remaining requirements and assume the business risk of proceeding with the drilling of the well.

Full-Interest Wells. When a lessee controls the entire acreage on all of the prospects it is fortunate indeed. The well can be drilled as the lessee pleases, being restricted only by appropriate regulations. Should the well result in being a producer the lessee will have control of the entire reservoir, assuming the lessee has more or less correctly anticipated the extent of the reservoir in the lease purchases. However, this situation is rarely found. Considerable work has yet to be done when a lessee is planning to drill a well and finds that all of the prospective acreage is not controlled.

Joint-Operating Agreements. Generally a lessee thinking of drilling a well will have at least some leases on the prospect. The remaining leases will be owned by one or more competitors, presumably people who are also interested in drilling wells and establishing production. Since the owners of the leases covering the prospect will all benefit in the event of production, it would seem equitable that each pay a proportionate part of a well or make a suitable contribution to the well.

However, it is not often that two or more lessees have the same data, or interpret the data in the same way. A lessee may elect to farm out its acreage, do nothing, or join in the drilling of a well. The other lessees will be contacted in an attempt to determine their interest in getting a well drilled. The other lessees may not have sufficient information to justify their joining in the drilling of a well. The party desiring to drill the well may find it desirable to make any information available to the adjacent lessees. This seismic or other control may represent a sizable investment, and the other lessees may be willing to pay for the data, exchange similar data of their own in another area, or negotiate almost any kind of agreement with the owner of the control. If all the lessees are eventually agreed that a joint well should be drilled, they will define a contract area that will be jointly owned. A joint-operating agreement will be entered into and the interests of the parties to the agreement determined on the basis of the surface acreage owned by each as compared with the total acres in the contract area. The joint-operating agreement will stipulate the interests of the participating parties, specify the operator, limit cer-

tain expenditures, establish liabilities, provide for the drilling of the first and subsequent wells, provide for nonconsent operations, etc. Certain operating costs are agreed on and an accounting procedure is attached to the joint-operating agreement.

The joint-operating agreement is a very useful tool in exploratory operations, particularly where the tracts of land are small or where it may be desirable to share the risk of an expensive exploratory well. Contract areas can be of practically any size but for exploratory purposes usually run from about 640 to several thousand acres in size. The joint-operating agreement is also used occasionally in development drilling. It finds frequent application in a unit or pool ordered by a regulatory body after a well has been completed as a producer.

Cash Contributions. A lessee may find it necessary to drill a well on a reduced-acreage basis with cash support from the adjacent lessees who might not be willing to farm out or enter into a joint operation. The most common type of cash contribution is the dry-hole contribution. It is usually a sum of money per foot drilled, determined by reservoir participation, discounted for lack of ownership in the well, etc. This type of contribution gets its name from the fact that no money is payable in the event the well is completed as a producer. The idea here is that the offset lessee is willing to make a cash contribution toward the drilling of a well that in all probability will be dry but which will at least partially evaluate the leases. In the unlikely event the well is completed as a producer it is thought that the rewards are sufficiently great for the owner of the well to make cash payment from the offset lessee unnecessary. A variation of the dry-hole contribution is the bottomhole contribution, which is payable upon reaching a specified depth regardless of whether or not the well is completed as a producer. Both types of cash contributions are used infrequently.

Farmouts. A transfer of the working interest with the obligation to drill a well is called a farmout. There are any number of ways in which a farmout can be negotiated. A farmout agreement provides for the drilling of a well, or the option to drill a well, at a mutually agreed location and to a mutually agreed depth on one of the leases owned by the party making the farmout. Upon completion of the well in accordance with the terms of the farmout agreement, the lessee will assign or sublease a portion of the leases and retain an interest, usually an overriding royalty. The amount of the overriding royalty will vary widely from area to area and will depend on a number of factors including the available geological and geophysical control, the amount of the working interest, the proximity of production, producing history in the area, lifting problems, suitable markets, size of the anticipated reservoir, the number of acres being farmed out, well costs, etc.

The operator that takes the farmout will be looking to the net revenue interest to recover costs. Gross income from the sale of production less royalty, overriding royalty, and any other burdens on the leases determines net revenue interest. Acceptable net revenue interests on farmouts vary widely: a net revenue interest in Oklahoma under a pooled section might be considered

unacceptable if less than 81.25%; in North Dakota in a wildcat well, 75%; in Louisiana in a low risk, close-in prospect, 68%.

A more complicated version of the farmout is found in the better producing areas. Such farmouts are often made on the basis of a portion of the working interest being retained by the party making the farmout. A typical arrangement might be the farmout of perhaps 2,000 acres on a 60/40 basis for a free well into the tanks to 12,000 ft. The party taking the farmout would agree to drill and complete a 12,000-ft test at the party's sole cost and risk and thereby earn an assignment of an undivided 60% interest in the 2,000-acre block. If the well is productive the party making the farmout owns 40% interest in the well and in the production, usually after the operator has recovered the costs to take full advantage of available tax deductions. The party taking the farmout will obtain payout from the proceeds of the sale of production from the earning well less any royalties and overriding royalties. Subsequent operations on the farmout block would be under the terms of a joint-operating agreement.

Variations of this type of deal are countless. The well could be a free well through the wellhead rather than into the tanks. This means the operator would pay for all completion costs through the well head but would share on a 60/40 basis in erecting tanks and treating equipment. Another variation is the free well to the sand. This means the operator would drill the well (at sole cost and risk) to the objective horizon, run an electrical log, and core and test as might be required to determine the possibility of production. If a decision is made to attempt a completion the operator will pay a negotiated fraction of the cost of running a production string of casing and setting subsurface production equipment, with the party making the farmout paying the remainder of the cost. Any interest may be negotiated; one-quarter and one-third interest deals are commonly made. Other variations might allow the operator to recover completion costs before the party making the farmout would be entitled to any share of the production. The party making the farmout might keep an overriding royalty during partial or complete payout and at the time of the payout would have the option to exchange the overriding royalty for a working interest.

Carried Interest. A carried-interest contract is an arrangement between co-owners of a working interest, whereby one agrees to advance all or some part of the development or operating costs on behalf of the others and to recover such advances from future production, if any, accruing to the other owners' shares of the working interest. The co-owner advancing such costs is referred to as the carrying party and the co-owners for whom costs are so advanced are referred to as the carried parties.

A carried interest usually comes into being in connection with a farmout. The carried-interest contract may apply not only to the first well but to subsequent wells. The party making the farmout may assign a portion of the working interest to an operator who will pay all the costs of drilling and equipping the first well, and possibly additional development wells. The grantee must look to the production, if any, attributable to the grantor's share of the working interest to recovery the gran-

tor's share of such costs. A carried interest is a share in the net and not the gross production.

Net-profits Interest. A net-profits interest is an interest in gross production measured by the net profits from the operation of an oil and gas property. A net-profits interest is similar to an overriding royalty in that it is created out of the working interest. The proceeds accruing to a net-profits interest are reducible by certain development and operating costs, which are specified in the net-profits contract. The net-profits interest is subject to such expenses to the extent of its share of the income. The owner of a net-profits interest is not required to pay out or advance money for development or operating costs, as in the case of the owner of a working interest, and is not liable for such costs. If no net profit is realized from the operation of the property the net-profits-interest owner receives no income but neither is the owner liable to the operator for a share of the loss. A net-profits interest can be regarded as a non-operating interest similar to an overriding royalty. The net-profits agreement finds its principal application in farmouts. Equitable as it may sound, this type of agreement is seldom used.

Lease Problems During Development

The lessor is often pleased and even overwhelmed by the discovery of hydrocarbons on the land and the sudden cash flow of royalty. Problems early in the development phase, such as the use of the surface for tank batteries, gathering lines, treating equipment, and roads are usually settled quickly. After a period of time, new problems arise of a subtle and sophisticated nature. As some lessors seek to maximize their royalty income, they turn to petroleum consultants and oil and gas attorneys for advice. From this effort come legal demands for additional development or release of undeveloped acreage. While development can occur both horizontally and vertically, lessor demands for development have generally been sustained by the courts in a horizontal sense only.

A more recent and more complex problem relates to the gas royalty clause and market value. The typical lease refers to the lessors' royalty as a fraction of market value. When a lessee discovers gas and enters into a long term contract for the sale of gas, the market value of gas and the contract price for gas are almost identical. However, the price of natural gas in recent years has risen dramatically. The lessee is sometimes contractually bound to a gas price with the purchaser and at the same time faces a demand from the lessor for gas prices at market value. The courts are not uniform from state to state on this issue. The U.S. Natural Gas Policy Act of 1978, with its price ceilings on categories of natural gas, may have been of some use in defending lessor suits for market value on royalty gas. Lessees now appear to be leaning to short-term gas contracts, provisions for frequent renegotiation of price, rewriting the gas royalty clause to provide for "price received" rather than market value, providing for in-kind royalty on gas, etc. Whether or not lessees will be successful in negotiating such gas contracts in periods of falling demand remains to be seen. Similarly, it can be expected that lessors and their attorneys will resist any changes in the lease form from the conventional wording on gas royalty. Resolution of this problem lies ahead.

Taxation*

The taxation of income related to oil and gas is a highly specialized field. The increasing complexity of tax laws and the very real effect that taxes have on the successful conduct of any business make it imperative that competent tax advice be sought out by any operator, however small his organization may be. The importance of tax planning can hardly be overestimated. Improper structuring of a drilling deal or a sale of a property from a tax standpoint can have the most serious of consequences. The larger organizations and major oil companies have tax departments comprised of specialists in the various subdivisions of taxation. Independents and small organizations must retain the services of tax consultants on a continuing basis.

Very briefly, all income less certain exclusions exempt from tax is gross income. Taxable income is gross income less deductions. Tax rates vary for individuals and corporations, as do long-term capital gains rates for individuals and corporations. Items of tax preference are deductions such as the excluded portion of capital gains, depletion, accelerated depreciation, and excess intangible drilling costs on productive property, all of which are subject to a minimum tax. Capital expenditures are not immediately deductible as are expenses, and must be recovered through depreciation or depletion. Some expenses, such as accelerated depreciation, are recaptured at sale, that is, become taxable at ordinary rates. The cost of tangible property used in business results in certain tax credits that are subtracted directly from the taxes due and are not a deduction.

Capital expenditures include the bonus costs of purchasing mineral leases, well and lease equipment, and most geological and geophysical exploration costs. Deductible expense items include overhead, lease rentals, abandoned leases, most intangible drilling costs, and geological and geophysical costs not resulting in lease acquisitions.

The enormous sums of money put into oil and gas exploration by private investors through limited partnerships deserve further comment. The private investor has taken advantage of the tax provisions in three principal areas: depletion, intangible drilling and development costs, and capital gains.

Depletion. A producing reservoir gradually suffers a reduction in the quantity and value of hydrocarbons in place. Depletion laws were enacted to provide for a return of capital because of mineral extraction. The taxpayer has a choice of two methods. Cost depletion provides for a reduction in basis as related to production and sale of minerals. Percentage depletion provides for a deduction of a percentage of the gross income from the property, which is limited to 50% of the net income from the property, and to 65% of net income from all sources. The U.S. Tax Reduction Act of 1975 effectively repealed percentage depletion, with certain exceptions. An exemption was allowed for independent producers and royalty owners as a percentage of qualified production, except as to transfers of producing property. For 1984

that percentage will be 15% of the first 1,000 BOPD produced, or 6 million cu ft/D gas.

Intangible Drilling and Development Costs. Taxpayers owning operating rights and incurring intangible costs may elect to expense or capitalize such costs. If the taxpayer elects to capitalize, the intangible drilling costs may be recovered through depreciation over 5 years, and are subject to an investment tax credit. Such capitalized costs do not represent a tax preference item. Since capitalization of such costs offers no real tax benefits, most taxpayers elect to expense such costs.

Intangible drilling costs may represent 80 to 90% of the cost of an exploratory well; the remaining portion representing tangible costs of equipment with salvage value. It is no surprise to note the enormous success of drilling funds through limited partnerships as such large deductions are made available to investors.

Capital Gains. A sale of a capital asset after a holding period set by law will subject the taxpayer to greatly reduced tax rates of a maximum of 20% of the profits of the sale. The sale of leases, either producing or non-producing, is subject to these favorable capital gains tax rates. The attraction of such favorable tax treatment in the event of future sales of properties has been a further inducement to investors in oil and gas exploration.

Offshore Leasing

Jurisdiction. Fifteenth and sixteenth century explorers claimed vast areas of waters, entire gulfs, seas, and oceans. However, these early claims, as a practical matter, were unenforceable. The extent of national sovereignty over the waters has not been resolved in international law. By presidential proclamation in 1945, the U.S. regards the natural resources of the Outer Continental Shelf (OCS) as a territory owned by the nation. The Submerged Lands Act of 1953 confirmed the jurisdiction and control of the U.S. over the natural resources of the seabed of the continental shelf seaward of the state boundaries.

Producing and Leasing History. The first commercial oil production in the Gulf of Mexico was discovered in 1947 on a Louisiana state lease. Drilling on federal lands under the OCS Lands Act began in 1954. Since 1956, the OCS (Atlantic, Pacific, Gulf of Mexico, and Alaska, comprising over more than 1 billion acres) has produced about 6 billion bbl of oil and about 55 Tcf gas. Leasing has proceeded at a snail's pace. For years, into the early 1970's, the abundance of oil and gas onshore and in world markets suppressed offshore leasing exploration with its high costs. As the search intensified, efforts to schedule lease sales met with great opposition from environmental groups. The time required for environmental assessment, state and local government comment, and so on, sometimes exceeded 3 years. The U.S. Dept. of Interior recently has moved to accelerate lease sales; almost the entire continental shelf will have been offered for lease at scheduled dates through 1987.

Leasing Procedure. The interior secretary prepares a proposed 5-year leasing program. In the preparation phase, the secretary invites and considers suggestions

*Written before the Tax Reform Act of 1986, which implements changes in alternative minimum tax, depletion, depreciation, investment tax credit, and deduction of losses.

from the governors of affected states, local government, industry, federal agencies, and all interested parties, including the general public. Time is provided for a response from the governors and others after preparation of a draft of a proposed program, and prior to publication in the *Federal Register*. Time is again provided for a response following publication and prior to submission to the president and congress for approval. The director of the Bureau of Land Management issues calls for nominations pursuant to an approved program, conferring with the governors where indicated. A list of tracts tentatively selected for leasing is drawn up. The director is free to make deletions or additions from the tentative selection of tracts. A selected tract will, in general, not exceed 5,760 acres. Upon approval by the secretary, the proposed notice of sale will be published in the *Federal Register*. The governors and local governments concerned again have an opportunity to comment. The secretary will make the final decision and will publish the notice of sale in the *Federal Register*. The sale itself will be held no sooner than 30 days after publication. Tracts are offered for lease by competitive sealed bidding. Leases are issued only to qualified bidders. Leases are issued for an initial period of 5 years, although longer times are provided for where unusually deep water or adverse conditions would discourage exploration and development. Annual rentals are due in advance to maintain the lease in the absence of production. Royalties bid are variable with one-eighth royalty being a minimum. Royalties on all leases in the Gulf of Mexico average about one-sixth.

After being awarded a lease, a lessee seeks to obtain the necessary permits. The lessee or operator will usually drill one or more test wells to determine whether hydrocarbons are present. If oil and/or gas is discovered, the operator, as a matter of common practice, will abandon the exploratory holes without attempting to complete

or produce from them. Exploratory wells are usually used to obtain information about potential oil and gas accumulation. Development or production wells are normally drilled from a production platform.

Economic Impact of Offshore Leasing. The interior secretary has stated that 85% of America's untapped oil wealth is on publicly owned lands, of which two-thirds is thought to be offshore. The economic implications for the future in exploring and developing such reserves are truly significant. The amount of capital required for such exploration and development is staggering. But consider the recent past: the OCS has produced about 6 billion bbl oil and 55 Tcf gas. There would appear to be little question about the ever-increasing significance of the leasing, exploration, and development of lands comprising the OCS.

General References

- Hardy, George W. III: *Louisiana Petroleum Land Operations*, Inst. for Energy Development Inc., Oklahoma City (1980).
- Kuntz, Eugene: *Kuntz Oil and Gas*, W.H. Anderson Co., Cincinnati, OH (1960).
- Mosburg, Lewis G. Jr.: *Petroleum Land Practices*, IED Exploration Inc., Tulsa (1978).
- Mosburg, Lewis G. Jr.: *Basics of Structuring Exploration Deals*, IED Exploration Inc., Tulsa (1979).
- "Outer Continental Shelf Mineral Leasing and Rights-of-Way Granting Programs," *Circular No. 2446*, U.S. Dept. of the Interior, Bureau of Land Management (1979).
- Prentice-Hall Federal Tax Handbook*, Prentice-Hall Inc., Englewood Cliffs, NJ (1986).
- Woodard, Robert G.: *Basic Land Management*, Inst. for Energy Development Inc., Oklahoma City (1982).

Chapter 58

The SI Metric System of Units and SPE Metric Standard

Society of Petroleum Engineers

Adopted for use as a voluntary standard by the SPE Board of Directors, June 1982.

Contents

Preface	58-2
<u>Part 1: SI—The International System of Units</u>	58-2
Introduction	58-2
SI Units and Unit Symbols	58-2
Application of the Metric System	58-3
Rules for Conversion and Rounding	58-5
Special Terms and Quantities Involving	
Mass and Amount of Substance	58-7
Mental Guides for Using Metric Units	58-8
Appendix A (Terminology)	58-8
Appendix B (SI Units)	58-9
Appendix C (Style Guide for Metric Usage)	58-11
Appendix D (General Conversion Factors)	58-14
Appendix E (Tables 1.8 and 1.9)	58-20
<u>Part 2: Discussion of Metric Unit Standards</u>	58-21
Introduction	58-21
Review of Selected Units	58-22
Unit Standards Under Discussion	58-24
Notes for Table 2.2	58-25
Notes for Table 2.3	58-25

Preface

The SPE Board in June 1982 endorsed revisions to "SPE Tentative Metric Standard" (Dec. 1977 *JPT*, Pages 1575-1611) and adopted it for implementation as this "SPE Metric Standard."

The following standard is the final product of 12 years' work by the Symbols and Metrication Committee. Members of the Metrication Subcommittee included John M. Campbell, chairman, John M. Campbell & Co.; Robert A. Campbell, Magnum Engineering Inc.; Robert E. Carlile, Texas Tech U.; J. Donald Clark, petroleum consultant; Hank Groeneveld, Mobil Oil Canada; Terry Pollard, retired, *ex-officio* member; and Howard B. Bradley, professional/technical training consultant.

With very few exceptions, the units shown are those

proposed and/or adopted by other groups involved in the metrication exercise, including those agencies charged with the responsibility (nationally and internationally) for establishing metric standards. These few exceptions, still to be decided, are summarized in the introduction to Part 2 of this report.

These standards include most of the units used commonly by SPE members. The subcommittee is aware that some will find the list incomplete for their area of specialty. Additions will continue to be made but too long a list can become cumbersome. The subcommittee believes that these standards provide a basis for metric practice beyond the units listed. So long as one maintains these standards a new unit can be "coined" that should prove acceptable.

Part 1: SI—The International System of Units*

Introduction

Worldwide scientific, engineering, industrial, and commercial groups are converting to SI metric units. Many in the U.S. are now active in such conversion, based on work accomplished by national¹ and international² authorities. Various U.S. associations, professional societies, and agencies are involved in this process, including, but not limited to, the American Soc. for Testing and Materials (ASTM),³ American Petroleum Inst. (API),^{4,5} American Natl. Standards Inst. (ANSI),^{3,6} American Soc. of Mechanical Engineers (ASME),⁷ and American Natl. Metric Council (ANMC).⁸ The Canadian Petroleum Assn. (CPA) and other Canadian groups have been especially active in conversion work.¹³ SPE intends to keep its worldwide membership informed on the conversion to and use of SI metric units.

The term "SI" is an abbreviation for *Le Système International d'Unités* or *The International System of Units*.

SI is not identical with any of the former cgs, mks, or mksA systems of metric units but is closely related to them and is an extension of and improvement over them. SI measurement symbols are identical in all languages. As in any other language, rules of spelling, punctuation, and pronunciation are essential to avoid errors in numerical work and to make the system easier to use and understand on a worldwide basis. These rules, together with decimal usage, units coherence, and a series of standard prefixes for multiples and submultiples of most SI units, provide a rational system with minimum difficulty of transition from English units or older systems of metric units. Refs. 1 through 4 of this paper are recommended to the reader wishing official information, development history, or more detail on SI; material from these and other references cited has been used freely in this report.

Appendix A provides definitions for some of the terms used.

SI Units and Unit Symbols³

The short-form designations of units (such as ft for feet, kg for kilograms, m for meters, mol for moles, etc.) have heretofore been called unit "abbreviations" in SPE terminology to avoid confusion with the term "symbols" applied to letter symbols used in mathematical equations. However, international and national standard practice is to call these unit designations "unit symbols"; the latter usage will be followed in this report.

SI Units

SI is based on seven well-defined "base units" that quantify seven *base quantities* that *by convention* are regarded as dimensionally independent. It is a matter of choice how many and which quantities are considered base quantities.⁹ SI has chosen the seven base quantities and base units listed in Table 1.1* as the basis of the International System. In addition, there are two "supplementary quantities" (Table 1.2).

Tables 1.1 and 1.2 show current practices for designating the dimensions of base and supplementary physical quantities, plus letter symbols for use in mathematical equations.

SI "derived units" are a third class, formed by combining, as needed, base units, supplementary units, and other derived units according to the algebraic relations linking the corresponding quantities. The symbols for derived units that do not have their own individual symbols are obtained by using the mathematical signs for multiplication and division, together with appropriate exponents (e.g., SI velocity, meter per second, m/s or $\text{m} \cdot \text{s}^{-1}$; SI angular velocity, radian per second, rad/s or $\text{rad} \cdot \text{s}^{-1}$).

Table 1.3 contains a number of SI derived units, including all the 19 approved units assigned special names and individual unit symbols.

Appendix B provides a more detailed explanation of the SI system of units, their definitions, and abbreviations.

*Prepared by T.A. Pollard for the subcommittee. Based on paper SPE 6212 presented by T.A. Pollard at the 1976 SPE Annual Technical Conference and Exhibition, New Orleans, Oct. 3-6.

*Table and figure numbers of the original SPE publication are used throughout this chapter.

SI Unit Prefixes⁸

The SI unit prefixes, multiplication factors, and SI prefix symbols are shown in Table 1.4. Some of the prefixes may seem strange at first, but there are enough familiar ones in the list to make it relatively easy for technical personnel to adjust to their use; kilo, mega, deci, centi, milli, and micro are known to most engineers and scientists.

One particular warning is required about the prefixes: in the SI system, k and M (kilo and mega) stand for 1000 and 1 000 000, respectively, whereas M and MM or m and mm have been used previously in the oil industry for designating thousands and millions of gas volumes. Note carefully, however, that there is no parallelism because SI prefixes are raised to the power of the unit employed, while the customary M and MM prefixes were not. Examples: km³ means cubic kilometers, *not* thousands of cubic meters; cm² means square centimeters, *not* one-hundredth of a square meter. The designation for 1000 cubic meters is 10³ m³ and for 1 million cubic meters is 10⁶ m³—*not* km³ and Mm³, respectively.

Appendix C gives examples of the vital importance of following the precise use of upper-case and lower-case letters for prefixes and for unit symbols.

Application of the Metric System

General

SI is the form of the metric system preferred for all applications. It is important that this modernized version be thoroughly understood and properly applied. This section, together with Appendix material, provides guidance and recommendations concerning style and usage of the SI form of the metric system.

Style and Usage

Take care to use unit symbols properly; the agreements in international and national standards provide uniform rules (summarized in Appendix C). It is essential that these rules be followed closely to provide maximum ease of communication and to avoid costly errors. Handling of unit names varies somewhat among different countries because of language differences, but using the rules in Appendix C should minimize most difficulties of communication.

Usage for Selected Quantities

Mass, Force, and Weight. The principal departure of SI from the gravimetric system of metric engineering units is the use of explicitly distinct units for mass and force. *In SI, kilogram is restricted to the unit of mass. The newton is the only SI unit of force*, defined as 1 (kg·m)/s², to be used wherever force is designated, including derived units that contain force—e.g., pressure or stress (N/m²=Pa), energy (N·m=J), and power [(N·m)/s=W].

There is confusion over the use of the term *weight* as a quantity to mean either *force* or *mass*. In science and technology, the term *weight of a body* usually means the force that, if applied to the body, would give it an acceleration equal to the local acceleration of free fall (*g*, when referring to the earth's surface). This acceleration varies in time and space; *weight*, if used to mean force, varies also. The term *force of gravity* (mass times acceleration of gravity) is more accurate than *weight* for this meaning.

In commercial and everyday use, on the other hand, the term *weight* nearly always means *mass*. Thus, when

TABLE 1.1 — SI BASE QUANTITIES AND UNITS*

Base Quantity or "Dimension"	SI Unit	SI Unit Symbol ("Abbreviation"), Use Roman (Upright) Type	SPE Letter Symbol for Mathematical Equations, Use Italic (Sloping) Type
length	meter	m	<i>L</i>
mass	kilogram	kg	<i>m</i>
time**	second	s	<i>t</i>
electric current**	ampere	A	<i>I</i>
thermodynamic temperature	kelvin	K	<i>T</i>
amount of substance	mole†	mol	<i>n</i>
luminous intensity	candela	cd	

*The seven base units, two supplementary units and other terms are defined in Appendixes A and B, Part 1.

**SPE heretofore has arbitrarily used charge *q*, the product of electric current and time, as a basic dimension. In unit symbols this would be A·s; in SPE mathematical symbols, *q*.

†When the mole is used, the elementary entities must be specified; they may be atoms, molecules, ions, electrons, other particles, or specified groups of such particles. In petroleum work, the terms "kilogram mole," "pound mole," etc., often are shortened erroneously to "mole."

TABLE 1.2 — SI SUPPLEMENTARY UNITS*

Supplementary Quantity or "Dimension"	SI Unit	SI Unit Symbol ("Abbreviation"), Use Roman (Upright) Type	SPE Letter Symbol for Mathematical Equations, Use Italic (Sloping) Type
plane angle**	radian	rad	<i>θ</i>
solid angle**	steradian	sr	<i>Ω</i>

*The seven base units, two supplementary units, and other terms are defined in Appendixes A and B, Part 1.

**ISO specifies these two angles as dimensionless with respect to the seven base quantities.

TABLE 1.3 — SOME COMMON SI DERIVED UNITS

Quantity	Unit	SI Unit Symbol ("Abbreviation"), Use Roman Type	Formula, Use Roman Type
absorbed dose	gray	Gy	J/kg
acceleration	meter per second squared	...	m/s ²
activity (of radionuclides)	becquerel	Bq	1/s
angular acceleration	radian per second squared	...	rad/s ²
angular velocity	radian per second	...	rad/s
area	square meter	...	m ²
Celsius temperature	degree Celsius	°C	K
density	kilogram per cubic meter	...	kg/m ³
dose equivalent	sievert	Sv	J/kg
electric capacitance	farad	F	A·s/V (= C/V)
electric charge	coulomb	C	A·s
electrical conductance	siemens	S	A/V
electric field strength	volt per meter	...	V/m
electric inductance	henry	H	V·s/A (= Wb/A)
electric potential	volt	V	W/A
electric resistance	ohm	Ω	V/A
electromotive force	volt	V	W/A
energy	joule	J	N·m
entropy	joule per kelvin	...	J/K
force	newton	N	kg·m/s ²
frequency	hertz	Hz	1/s
illuminance	lux	lx	lm/m ²
luminance	candela per square meter	...	cd/m ²
luminous flux	lumen	lm	cd·sr
magnetic field strength	ampere per meter	...	A/m
magnetic flux	weber	Wb	V·s
magnetic flux density	tesla	T	Wb/m ²
potential difference	volt	V	W/A
power	watt	W	J/s
pressure	pascal	Pa	N/m ²
quantity of electricity	coulomb	C	A·s
quantity of heat	joule	J	N·m
radiant flux	watt	W	J/s
radiant intensity	watt per steradian	...	W/sr
specific heat	joule per kilogram kelvin	...	J/(kg·K)
stress	pascal	Pa	N/m ²
thermal conductivity	watt per meter kelvin	...	W/(m·K)
velocity	meter per second	...	m/s
viscosity, dynamic	pascal second	...	Pa·s
viscosity, kinematic	square meter per second	...	m ² /s
voltage*	volt	V	W/A
volume*	cubic meter	...	m ³
wave number	1 per meter	...	1/m
work	joule	J	N·m

*In 1964, the General Conference on Weights and Measures adopted liter as a special name for the cubic decimeter but discouraged the use of liter for volume measurement of extreme precision (see Appendix B).

TABLE 1.4 — SI UNIT PREFIXES

Multiplication Factor	SI Prefix	SI Prefix Symbol, Use Roman Type	Pronunciation (U.S.)*	Meaning (U.S.)	Meaning In Other Countries
1 000 000 000 000 000 000 = 10 ¹⁸	exa**	E	ex' a (a as in a bout)	one quintillion times†	trillion
1 000 000 000 000 000 = 10 ¹⁵	peta**	P	as in p etal	one quadrillion times†	thousand billion
1 000 000 000 000 = 10 ¹²	tera	T	as in terra ce	one trillion times†	billion
1 000 000 000 = 10 ⁹	giga	G	jig' a (a as in a bout)	one billion times†	milliard
1 000 000 = 10 ⁶	mega	M	as in mega phone	one million times	
1 000 = 10 ³	kilo	k	as in kilo watt	one thousand times	
100 = 10 ²	hecto‡	h	heck' toe	one hundred times	
10 = 10	deka‡	da	deck' a (a as in a bout)	ten times	
0.1 = 10 ⁻¹	deci‡	d	as in deci mal	one tenth of	
0.01 = 10 ⁻²	centi‡	c	as in senti ment	one hundredth of	
0.001 = 10 ⁻³	milli	m	as in mili tary	one thousandth of	
0.000 001 = 10 ⁻⁶	micro	μ	as in micro phone	one millionth of	
0.000 000 001 = 10 ⁻⁹	nano	n	nan' oh (an as in an t)	one billionth of†	milliardth
0.000 000 000 001 = 10 ⁻¹²	pico	p	peek' oh	one trillionth of†	billionth
0.000 000 000 000 001 = 10 ⁻¹⁵	femto	f	fem' toe (fem as in fem inine)	one quadrillionth of†	thousand billionth
0.000 000 000 000 000 001 = 10 ⁻¹⁸	atto	a	as in anato my	one quintillionth of†	trillionth

*The first syllable of every prefix is accented to assure that the prefix will retain its identity. Therefore, the preferred pronunciation of kilometer places the accent on the first syllable, not the second.

**Approved by the 15th General Conference of Weights and Measures (CGPM), May-June 1975.

†These terms should be avoided in technical writing because the denominations above 1 million are different in most other countries, as indicated in the last column.

‡While hecto, deka, deci, and centi are SI prefixes, their use generally should be avoided except for the SI unit multiples for area, volume, moment, and nontechnical use of centimeter, as for body and clothing measurement.

one speaks of a person's weight, the quantity referred to is mass. Because of the dual use, the term weight should be avoided in technical practice except under circumstances in which its meaning is completely clear. When the term is used, it is important to know whether *mass* or *force* is intended and to use SI units properly as described above by using kilograms for mass and newtons for force.

Gravity is involved in determining mass with a balance or scale. When a standard mass is used to balance the measured mass, the effect of gravity on the two masses is canceled except for the indirect effect of air or fluid buoyancy. On a spring scale, mass is measured indirectly since the instrument responds to the force of gravity. Such scales may be calibrated in mass units if the variation in acceleration of gravity and buoyancy corrections are not significant in their use.

The use of the same name for units of force and mass causes confusion. When non-SI units are being converted to SI units, distinction should be made between *force* and *mass*—e.g., use lbf to denote force in gravimetric engineering units, and use lbm for mass.

Use of the metric ton, also called *tonne* (1.0 Mg), is common.

Linear Dimensions. Ref. 3 provides discussions of length units applied to linear dimensions and tolerances of materials and equipment, primarily of interest to engineers in that field.

Temperature. The SI temperature unit is the kelvin (not “degree Kelvin”); it is the preferred unit to express thermodynamic temperature. Degrees Celsius ($^{\circ}\text{C}$) is an SI derived unit used to express temperature and temperature intervals. The Celsius scale (formerly called centigrade) is related directly to the kelvin scale as follows: the temperature interval $1^{\circ}\text{C}=1\text{ K}$, exactly. Celsius temperature ($T_{^{\circ}\text{C}}$) is related to thermodynamic temperature (T_{K}) as follows: $T_{^{\circ}\text{C}}=T_{\text{K}}-T_0$ exactly, where $T_0=273.15\text{ K}$ by definition. Note that the SI unit symbol for the kelvin is K without the degree mark, whereas the older temperature units are known as degrees Fahrenheit, degrees Rankine, and degrees Celsius, with degree marks shown on the unit symbol ($^{\circ}\text{F}$, $^{\circ}\text{R}$, $^{\circ}\text{C}$).

Time. The SI unit for time is the second, and this is preferred, but use of the minute, hour, day, and year is permissible.

Angles. The SI unit for plane angle is the radian. The use of the arc degree and its decimal submultiples is permissible when the radian is not a convenient unit. Use of the minute and second is discouraged except possibly for cartography. Solid angles should be expressed in steradians.

Volume. The SI unit of volume is the cubic meter. This unit, or one of its regularly formed multiples, is preferred for all applications. The special name *liter* has been approved for the cubic decimeter (see Appendix B), but use of the liter is restricted to the measurement of liquids and gases.

Energy. The SI unit of energy, the joule, together with its multiples, is preferred for all applications. The kilowatt-hour is used widely as a measure of electric energy, but this unit should not be introduced into any new areas; eventually it should be replaced by the megajoule.

Torque and Bending Moment. The vector product of force and moment arm is expressed in newton meters ($\text{N}\cdot\text{m}$) by SPE as a convention when expressing torque energies.

Pressure and Stress. The SI unit for pressure and stress is the pascal (newton per square meter); with proper SI prefixes it is applicable to all such measurements. Use of the old metric gravitational units—kilogram-force per square centimeter, kilogram-force per square millimeter, torr, etc.—is to be discontinued. Use of the bar is discouraged by the standards organizations.

It has been recommended internationally that pressure units themselves should not be modified to indicate whether the pressure is “absolute” (above zero) or “gauge” (above atmospheric pressure). If the context leaves any doubt as to which is meant, the word “pressure” must be qualified appropriately: “...at a gauge pressure of 13 kPa,” or “...at an absolute pressure of 13 kPa,” etc.

Units and Names To Be Avoided or Abandoned

Tables 1.1 through 1.3 include all SI units identified by formal names, with their individual unit symbols. Virtually all other *named* metric units formerly in use (as well as nonmetric units) are to be avoided or abandoned. There is a long list of such units (e.g., dyne, stokes, “esu,” gauss, gilbert, abampere, statvolt, angstrom, fermi, micron, mho, candle, calorie, atmosphere, mm Hg, and metric horsepower). The reasons for abandoning the non-SI units are discussed in Appendix B. Two of the principal reasons are the relative simplicity and the coherence of the SI units.

Rules for Conversion and Rounding³

Conversion

Table 1.7, Appendix D, contains general conversion factors that give exact values or seven-digit accuracy for implementing these rules except where the nature of the dimension makes this impractical.

The conversion of quantities should be handled with careful regard to the implied correspondence between the accuracy of the data and the given number of digits. In all conversions, the number of significant digits retained should be such that accuracy is neither sacrificed nor exaggerated.

Proper conversion procedure is to multiply the specified quantity by the conversion factor exactly as given in Table 1.7 and then round to the appropriate number of significant digits. For example, to convert 11.4 ft to meters: $11.4 \times 0.3048 = 3.47472$, which rounds to 3.47 m.

Accuracy and Rounding

Do not round either the conversion factor or the quantity before performing the multiplication; this reduces ac-

curacy. Proper conversion procedure includes rounding the *converted* quantity to the proper number of significant digits commensurate with its intended precision. The practical aspects of measuring must be considered when using SI equivalents. If a scale divided into sixteenths of an inch was suitable for making the original measurements, a metric scale having divisions of 1 mm is obviously suitable for measuring in SI units, and the equivalents should not be reported closer than the nearest 1 mm. Similarly, a gauge or caliper graduated in divisions of 0.02 mm is comparable to one graduated in divisions of 0.001 in. Analogous situations exist for mass, force, and other measurements. A technique to determine the proper number of significant digits in rounding converted values is described here for general use.

General Conversion. This approach depends on first establishing the intended precision or accuracy of the quantity as a necessary guide to the number of digits to retain. The precision should relate to the number of digits in the original, but in many cases that is not a reliable indicator. A figure of 1.1875 may be a very accurate decimalization of a noncritical $1\frac{3}{8}$ that should have been expressed as 1.19. On the other hand, the value 2 may mean "about 2" or it may mean a very accurate value of 2, which should then have been written as 2.0000. It is therefore necessary to determine the intended precision of a quantity before converting. *This estimate of intended precision should never be smaller than the accuracy of measurement but usually should be smaller than one-tenth the tolerance if one exists.* After the precision of the dimension is estimated, the converted dimension should be rounded to a minimum number of significant digits (see section on Significant Digits) such that a unit of the last place is equal to or smaller than the converted precision.

Examples

1. A stirring rod 6 in. long: In this case, precision is estimated to be about $\frac{1}{2}$ in. ($\pm \frac{1}{4}$ in.). Converted, $\frac{1}{2}$ in. is 12.7 mm. The converted 6-in. dimension of 152.4 mm should be rounded to the nearest 10 mm, or 150 mm.

2. 50,000-psi tensile strength: In this case, precision is estimated to be about ± 200 psi (± 1.4 MPa) based on an accuracy of $\pm 0.25\%$ for the tension tester and other factors. Therefore, the converted dimension, 344.7379 MPa, should be rounded to the nearest whole unit, 345 MPa.

3. Test pressure 200 ± 15 psi: Since one-tenth of the tolerance is ± 1.5 psi (10.34 kPa), the converted dimension should be rounded to the nearest 10 kPa. Thus, 1378.9514 ± 103.421 kPa becomes 1380 ± 100 kPa.

Special Cases. Converted values should be rounded to the minimum number of significant digits that will maintain the required accuracy. In certain cases, deviation from this practice to use convenient or whole numbers may be feasible. In that case, the word "approximate" must be used following the conversion—e.g., $1\frac{1}{8}$ in. = 47.625 mm exact, 47.6 mm normal rounding, 47.5 mm (approximate) rounded to preferred or convenient half-millimeter, 48 mm (approximate) rounded to whole number.

A quantity stated as a limit, such as "not more than"

or "maximum," must be handled so that the stated limit is not violated. For example, a specimen "at least 4 in. wide" requires a width of at least 101.6 mm, or (rounded) at least 102 mm.

Significant Digits. Any digit that is necessary to define the specific value or quantity is said to be significant. For example, a distance measured to the nearest 1 m may have been recorded as 157 m; this number has three significant digits. If the measurement had been made to the nearest 0.1 m, the distance may have been 157.4 m—four significant digits. In each case, the value of the right-hand digit was determined by measuring the value of an additional digit and then rounding to the desired degree of accuracy. In other words, 157.4 was rounded to 157; in the second case, the measurement may have been 157.36, rounded to 157.4.

Importance of Zeros. Zeros may be used either to indicate a specific value, as does any other digit, or to indicate the magnitude of a number. The 1970 U.S. population figure rounded to thousands was 203 185 000. The six left-hand digits of this number are significant; each *measures* a value. The three right-hand digits are zeros that merely indicate the *magnitude* of the number rounded to the nearest thousand. To illustrate further, each of the following estimates and measurements is of different magnitude, but each is specified to have only one significant digit:

1 000
100
10
0.01
0.001
0.000 1.

It is also important to note that, for the first three numbers, the identification of significant digits is possible only through knowledge of the circumstances. For example, the number 1000 may have been rounded from about 965, or it may have been rounded from 999.7, in which case all three zeros are significant.

Data of Varying Precision. Occasionally, data required for an investigation must be drawn from a variety of sources where they have been recorded with varying degrees of refinement. Specific rules must be observed when such data are to be *added, subtracted, multiplied, or divided*.

The rule for addition and subtraction is that the *answer* shall contain no significant digits farther to the right than occurs in the least precise number. Consider the addition of three numbers drawn from three sources, the first of which reported data in millions, the second in thousands, and the third in units:

163 000 000
217 885 000
96 432 768
477 317 768

This total indicates a precision that is not valid. The numbers should *first* be rounded to *one significant digit*

farther to the right than that of the least precise number, and the sum taken as follows.

$$\begin{array}{r} 163\,000\,000 \\ 217\,900\,000 \\ \hline 96\,400\,000 \\ 477\,300\,000 \end{array}$$

Then, the total is rounded to 477 000 000 as called for by the rule. Note that if the second of the figures to be added had been 217 985 000, the rounding before addition would have produced 218 000 000, in which case the zero following 218 would have been a significant digit.

The rule for multiplication and division is that the *product* or *quotient* shall contain no more significant digits than are contained in the number with the *fewest significant digits* used in the multiplication or division. The difference between this rule and the rule for addition and subtraction should be noted; for addition and subtraction, the rule merely requires rounding digits to the right of the last significant digit in the least precise number. The following illustration highlights this difference.

Multiplication:	$113.2 \times 1.43 = 161.876$ rounded to 162.
Division:	$113.2 \div 1.43 = 79.16$ rounded to 79.2
Addition:	$113.2 + 1.43 = 114.63$ rounded to 114.6
Subtraction:	$113.2 - 1.43 = 111.77$ rounded to 111.8.

The above product and quotient are limited to three significant digits because 1.43 contains only three significant digits. In contrast, the rounded answers in the addition and subtraction examples contain four significant digits.

Numbers used in the illustration are all estimates or measurements. *Numbers that are exact counts (and conversion factors that are exact) are treated as though they consist of an infinite number of significant digits.* Stated more simply, when a *count* is used in computation with a measurement, the number of significant digits in the answer is the same as the number of significant digits in the measurement. If a count of 40 is multiplied by a measurement of 10.2, the product is 408. However, if 40 were an estimate accurate only to the nearest 10 and, hence, contained one significant digit, the product would be 400.

Rounding Values¹⁰

When a figure is to be rounded to fewer digits than the total number available, the procedure should be as follows.

When the First Digit Discarded is	The Last Digit Retained is
less than 5	unchanged
more than 5	increased by 1
5 followed only by zeros*	unchanged if even, increased by 1 if odd

*Unless a number of rounded values are to appear in a given problem, most roundings conform to the first two procedures — i.e., rounding upward when the first digit discarded is 5 or higher.

Examples:

4.463 25 if rounded to three places would be 4.463.
8.376 52 if rounded to three places would be 8.377.
4.365 00 if rounded to two places would be 4.36.
4.355 00 if rounded to two places would be 4.36.

Conversion of Linear Dimensions of Interchangeable Parts

Detailed discussions of this subject are provided by ASTM,³ API,⁴ and ASME⁷ publications and are recommended to the interested reader.

Other Units

Temperature. General guidance for converting tolerances from degrees Fahrenheit to kelvins or degrees Celsius is given in Table 1.5. Normally, temperatures expressed in a whole number of degrees Fahrenheit should be converted to the nearest 0.5 K (or 0.5°C). As with other quantities, the number of significant digits to retain will depend on implied accuracy of the original dimension; e.g.,*

$100 \pm 5^\circ\text{F}$ (tolerance); implied accuracy, estimated total 2°F (nearest 1°C) $37.7778 \pm 2.7778^\circ\text{C}$ rounds to $38 \pm 3^\circ\text{C}$.

$1,000 \pm 50^\circ\text{F}$ (tolerance); implied accuracy, estimated total 20°F (nearest 10°C) $537.7778 \pm 27.7778^\circ\text{C}$ rounds to $540 \pm 30^\circ\text{C}$.

Pressure or Stress. Pressure or stress values may be converted by the same principle used for other quantities. Values with an uncertainty of more than 2% may be converted without rounding by the approximate factor:

$$1 \text{ psi} = 7 \text{ kPa.}$$

For conversion factors see Table 1.7.

Special Length Unit—the Vara. Table 1.8, Appendix E, provides conversion factors and explanatory notes on the problems of converting the several kinds of vara units to meters.

Special Terms and Quantities Involving Mass and Amount of Substance

The Intl. Union of Pure and Applied Chemistry, the Intl. Union of Pure and Applied Physics, and the Intl.

*See Appendix A and prior paragraph on "General Conversion."

TABLE 1.5 — CONVERSION OF TEMPERATURE TOLERANCE REQUIREMENTS

Tolerance (°F)	Tolerance (K or °C)
± 1	± 0.5
± 2	± 1
± 5	± 3
± 10	± 5.5
± 15	± 8.5
± 20	± 11
± 25	± 14

Organization for Standardization provide clarifying usages for some of the terms involving the base quantities "mass" and "amount of substance." Two of these require modifying the terminology appearing previously in SPE's Symbols Standards.

Table 1.6 shows the old and the revised usages.

Mental Guides for Using Metric Units

Table 1.9, Appendix F, is offered as a "memory jogger" or guide to help locate the "metric ballpark" relative to customary units. Table 1.9 is *not* a conversion table. For accurate conversions, refer to Table 1.7, or to Tables 2.2 and 2.3 for petroleum-industry units, and round off the converted values to practical precision as described earlier.

References*

- "The International System of Units (SI)," NBS Special Publication 330, U.S. Dept. of Commerce, Natl. Bureau of Standards, Superintendent of Documents, U.S. Government Printing Office, Washington, D.C. (1981). (Order by SD Catalog No. C13.10:330/3.)
- "SI Units and Recommendations for the Use of Their Multiples and of Certain Other Units," second edition, 1981-02-15, Intl. Standard ISO 1000, Intl. Organization for Standardization, American Natl. Standards Inst. (ANSI), New York (1981).
- "Standard for Metric Practice," E 380-82, American Soc. for Testing and Materials, Philadelphia. (Similar material published in IEEE Std. 268-1982.)
- Metric Practice Guide—A Guide to the Use of SI—The International System of Units*, second edition, API Pub. 2563 (now being revised), American Petroleum Institute, Washington, D.C. (Jan. 1973). (This material is derived from ASTM E 380-72.)
- Conversion of Operational and Process Measurement Units to the Metric (SI) System*, first edition, API Pub. 2564, Washington, D.C. (March 1974).
- "A Bibliography of Metric Standards," ANSI, New York (June 1975). (Also see ANSI's annual catalog of national and international standards.)
- ASME Orientation and Guide for Use of SI (Metric) Units*, sixth edition, Guide SI-1, American Soc. of Mechanical Engineers (ASME), New York (May 1, 1975). (ASME also has published Guides SI-2, *Strength of Materials*; SI-3, *Dynamics*; SI-5, *Fluid Mechanics*; SI-6, *Kinematics*; SI-8, *Vibration*; and SI-10, *Steam Charts*.)
- Metric Editorial Guide*, third edition, American Natl. Metric Council (ANMC), Washington, D.C. (July 1981).
- "General Principles Concerning Quantities, Units and Symbols," *General Introduction to ISO 31*, second edition, Intl. Standard ISO 31/0, Intl. Organization for Standardization, ANSI, New York City (1981).
- "American National Standard Practice for Inch-Millimeter Conversion for Industrial Use," ANSI B48.1-1933 (R1947), ISO R370-1964, Intl. Organization for Standardization, ANSI, New York. (A later edition has been issued: "Toleranced Dimensions—Conversion From Inches to Millimeters and Vice Versa," ISO 370-1975.)
- "Factors for High-Precision Conversion," NBS LC1071 (July 1976).
- "Information Processing—Representations of SI and Other Units for Use in Systems With Limited Character Sets," Intl. Standard ISO 2955-1974, Intl. Organization for Standardization, ANSI, New York City. (Ref. 5 reproduces the 1973 edition of this standard in its entirety.)
- "Supplementary Metric Practice Guide for the Canadian Petroleum Industry," fourth edition, P.F. Moore (ed.), Canadian Petroleum Assn. (Oct. 1979).
- "Letter Symbols for Units of Measurement," ANSI/IEEE Std. 260-1978. Available from American Natl. Standards Inst., New York City.
- Mechtly, E.A.: "The International System of Units—Physical Constants and Conversion Factors," NASA SP-7012, Scientific and Technical Information Office, NASA, Washington, D.C. 1973 edition available from U.S. Government Printing Office, Washington, D.C.
- McElwee, P.G.: *The Texas Vara*. Available from Commissioner, General Land Office, State of Texas, Austin (April 30, 1940).

APPENDIX A³

Terminology

To ensure consistently reliable conversion and rounding practices, a clear understanding of the related nontechnical terms is prerequisite. Accordingly, certain terms used in this standard are defined as follows.

Accuracy (as distinguished from precision). The degree of conformity of a measured or calculated value to some recognized standard or specified value. This concept involves the systematic error of an operation, which is seldom negligible.

Approximate. A value that is nearly but not exactly correct or accurate.

Coherence. A characteristic of a coherent system of units, as described in Appendix B, such that the product or quotient of any two unit quantities is the unit of the

*For information on any of these references, contact the Book Order Dept. at SPE headquarters.

TABLE 1.6 — SPECIAL TERMS AND QUANTITIES INVOLVING MASS AND AMOUNT OF SUBSTANCE

Old Usage		Standardized Usage	
Term	Dimensions (ISO Symbols, See Table 1.1)	Term	SI Unit Symbol
atomic weight (SPE Symbols Standard)	M	mass of atom	kg
atomic weight (elsewhere)	*	relative atomic mass	*
equivalent	—	mole	mol
mass of molecule	M	molecular mass	kg
molar	—	molar (means, "divided by amount of substance")	1/mol
molarity	—	concentration	mol/m ³
molecular weight (SPE Symbols Standard)	M	molar mass	kg/mol
molecular weight (elsewhere)	*	relative molecular mass	*
normal — obsolete			

*Dimensionless

resulting quantity. The SI base units, supplementary units, and derived units form a coherent set.

Deviation. Variation from a specified dimension or design requirement, usually defining upper and lower limits (see also **Tolerance**).

Digit. One of the 10 Arabic numerals (0 to 9).

Dimension(s). Two meanings: (1) A group of fundamental (physical) quantities, arbitrarily selected, in terms of which all other quantities can be measured or identified.⁹ Dimensions identify the physical nature of, or the basic components making up, a physical quantity. They are the bases for the formation of useful dimensionless groups and dimensionless numbers and for the powerful tool of dimensional analysis. The dimensions for the arbitrarily selected base units of the SI are length, mass, time, electric current, thermodynamic temperature, amount of substance, and luminous intensity. SI has two supplementary quantities considered dimensionless—plane angle and solid angle. (2) A geometric element in a design, such as length and angle, or the magnitude of such a quantity.

Figure (numerical). An arithmetic value expressed by one or more digits or a fraction.

Nominal Value. A value assigned for the purpose of convenient designation; a value existing in name only.

Precision (as distinguished from accuracy). The degree of mutual agreement between individual measurements (repeatability and reproducibility).

Quantity. A concept used for qualitative and quantitative descriptions of a physical phenomenon.⁹

Significant Digit. Any digit that is necessary to define a value or quantity (see text discussion).

Tolerance. The total range of variation (usually bilateral) permitted for a size, position, or other required quantity; the upper and lower limits between which a dimension must be held.

U.S. Customary Units. Units based on the foot and the pound, commonly used in the U.S. and defined by the Natl. Bureau of Standards.¹¹ Some of these units have the same name as similar units in the U.K. (British, English, or U.K. units) but are not necessarily equal to them.

APPENDIX B³

SI Units

Advantages of SI Units

SI is a rationalized selection of units from the metric system that individually are not new. They include a unit of force (the newton), which was introduced in place of the kilogram-force to indicate by its name that it is a unit of force and not of mass. SI is a coherent system with seven base units for which names, symbols, and precise definitions have been established. Many derived units are defined in terms of the base units, with symbols

assigned to each; in some cases, special names and unit symbols are given—e.g., the newton (N).

One Unit per Quantity. The great advantage of SI is that there is one, and only one, unit for each physical quantity—the meter for length (L), kilogram (instead of gram) for mass (m), second for time (t), etc. From these elemental units, units for all other mechanical quantities are derived. These derived units are defined by simple equations among the quantities, such as $v=dL/dt$ (velocity), $a=dv/dt$ (acceleration), $F=ma$ (force), $W=FL$ (work or energy), and $P=W/t$ (power). Some of these units have only generic names, such as meter per second for velocity; others have special names and symbols, such as newton (N) for force, joule (J) for work or energy, and watt (W) for power. *The SI units for force, energy, and power are the same regardless of whether the process is mechanical, electrical, chemical, or nuclear.* A force of 1 N applied for a distance of 1 m can produce 1 J of heat, which is identical with what 1 W of electric power can produce in 1 second.

Unique Unit Symbols. Corresponding to the SI advantages of a unique unit for each physical quantity are the advantages resulting from the use of a unique and well-defined set of symbols. Such symbols eliminate the confusion that can arise from current practices in different disciplines, such as the use of “b” for both the *bar* (a unit of pressure) and *barn* (a unit of area).

Decimal Relation. Another advantage of SI is its retention of the decimal relation between multiples and sub-multiples of the base units for each physical quantity. Prefixes are established for designating multiple and sub-multiple units from “exa” (10^{18}) down to “atto” (10^{-18}) for convenience in writing and speaking.

Coherence. Another major advantage of SI is its coherence. This system of units has been chosen in such a way that the equations between numerical values, including the numerical factors, have the same form as the corresponding equations between the quantities: this constitutes a “coherent” system. Equations between units of a coherent unit system contain as numerical factors only the number 1. In a coherent system, the product or quotient of any two unit quantities is the unit of the resulting quantity. For example, in any coherent system, unit area results when unit length is multiplied by unit length ($1\text{ m} \times 1\text{ m} = 1\text{ m}^2$), unit force when unit mass* is multiplied by unit acceleration ($1\text{ kg} \times 1\text{ m/s}^2 = 1\text{ N}$), unit work when unit force is multiplied by unit length ($1\text{ N} \times 1\text{ m} = 1\text{ J}$), and unit power when unit work is divided by unit time ($1\text{ J} \div 1\text{ second} = 1\text{ W}$). Thus, in a coherent system in which the meter is the unit of length, the square meter is the unit of area, but the are** and hectare are not coherent. Much worse disparities occur in systems of “customary units” (both nonmetric and older metric) that require many numerical adjustment factors in equations.

Base Units. Whatever the system of units, whether it be coherent or noncoherent, particular samples of some

*Note that the kilogram (not the gram) is the coherent SI unit of mass.

**The are is an old metric unit.

physical quantities must be selected arbitrarily as units of those quantities. The remaining units are defined by appropriate experiments related to the theoretical interrelations of all the quantities. For convenience of analysis, units pertaining to *certain base quantities are by convention regarded as dimensionally independent; these units are called base units* (Table 1.1), and all others (derived units) can be expressed algebraically in terms of the base units. In SI, the unit of mass, the kilogram, is defined as the mass of a prototype kilogram preserved by the Intl. Bureau of Weights and Measures (BIPM) in Paris. All other base units are defined in terms of reproducible phenomena—e.g., the wave lengths and frequencies of specified atomic transitions.

Non-SI Metric Units

Various other units are associated with SI but are not a part thereof. They are related to units of the system by powers of 10 and are used in specialized branches of physics. An example is the bar, a unit of pressure, approximately equivalent to 1 atm and exactly equal to 100 kPa. The bar is used extensively by meteorologists. Another such unit is the gal, equal exactly to an acceleration of 0.01 m/s^2 . It is used in geodetic work. These, however, are not coherent units—i.e., equations involving both these units and SI units cannot be written without a factor of proportionality even though that factor may be a simple power of 10.

Originally (1795), the liter was intended to be identical to the cubic decimeter. The Third General Conference on Weights and Measures (CGPM) in 1901 defined the liter as the volume occupied by the mass of 1 kilogram of pure water at its maximum density under normal atmospheric pressure. Careful determinations subsequently established the liter so defined as equivalent to $1.000\,028 \text{ dm}^3$. In 1964, the CGPM withdrew this definition of the liter and declared that "liter" was a special name for the cubic decimeter. Thus, its use is permitted in SI but is discouraged because it creates two units for the same quantity and its use in precision measurements might conflict with measurements recorded under the old definition.

SI Base Unit Definitions

Authorized translations of the original French definitions of the seven base and two supplementary units of SI follow³ (parenthetical items added).

"Meter (m)—The meter is the length equal to $1\,650\,763.73$ wavelengths in vacuum of the radiation corresponding to the transition between the levels $2p_{10}$ and $5d_5$ of the krypton-86 atom." (Adopted by 11th CGPM 1960.)

"Kilogram (kg)—The kilogram is the unit of mass (and is the coherent SI unit); it is equal to the mass of the international prototype of the kilogram." (Adopted by First and Third CGPM 1889 and 1901.)

"Second (s)—The second is the duration of $9\,192\,631\,770$ periods of the radiation corresponding to the transition between the two hyperfine levels of the ground state of the cesium-133 atom.*" (Adopted by 13th CGPM 1967.)

"Ampere (A)—The ampere is that constant current which, if maintained in two straight parallel conductors of infinite length, of negligible circular cross-section,

and placed one meter apart in vacuum, would produce between these conductors a force equal to 2×10^{-7} newton per meter of length." (Adopted by Ninth CGPM 1948.)

"Kelvin (K)—The kelvin, unit of thermodynamic temperature, is the fraction $1/273.15$ of the thermodynamic temperature of the triple point of water."³ (Adopted by 13th CGPM 1967.)

"Mole (mol)—The mole is the amount of substance of a system which contains as many elementary entities as there are atoms in 0.012 kilograms of carbon-12." (Adopted by 14th CGPM 1971.)

"Note—When the mole is used, the elementary entities must be specified and may be atoms, molecules, ions, electrons, other particles, or specified groups of such particles."

"Candela (cd)—The candela is the luminous intensity in a given direction of a source that emits monochromatic radiation of frequency $540 (E + 12)$ hertz (Hz) and that has a radiant intensity in that direction of $1/683$ watt per steradian."

"Radian (rad)—The radian is the plane angle between two radii of a circle which cut off on the circumference an arc equal in length to the radius."

"Steradian (sr)—The steradian is the solid angle which, having its vertex at the center of a sphere, cuts off an area of the surface of the sphere equal to that of a square with sides of length equal to the radius of the sphere."

Definitions of SI Derived Units Having Special Names³

Physical Quantity	Unit and Definition
Absorbed dose	The <i>gray</i> (Gy) is the absorbed dose when the energy per unit mass imparted to matter by ionizing radiation is 1 J/kg .
Activity	The <i>becquerel</i> (Bq) is the activity of a radionuclide decaying at the rate of one spontaneous nuclear transition per second.
Celsius temperature	The <i>degree Celsius</i> ($^{\circ}\text{C}$) is equal to the kelvin and is used in place of the kelvin for expressing Celsius temperature (symbol $T_{^{\circ}\text{C}}$) defined by $T_{^{\circ}\text{C}} = T_K - T_0$, where T_K is the thermodynamic temperature and $T_0 = 273.15 \text{ K}$ by definition.
Dose equivalent	The <i>sievert</i> is the dose equivalent when the absorbed dose of ionizing radiation multiplied by the dimensionless factors Q (quality factor) and N (product of any other multiplying factors) stipulated by the Intl. Commission on Radiological Protection is 1 J/kg .
Electric capacitance	The <i>farad</i> (F) is the capacitance of a capacitor between the plates of which there appears a difference of potential of 1 V when it is charged by a quantity of electricity equal to 1 C .

* This definition supersedes the ephemeris second as the unit of time

Electric conductance	The <i>siemens</i> (S) is the electric conductance of a conductor in which a current of 1 A is produced by an electric potential difference of 1 V.
Electric inductance	The <i>henry</i> (H) is the inductance of a closed circuit in which an electromotive force of 1 V is produced when the electric current in the circuit varies uniformly at a rate of 1 A/s.
Electric potential difference, electromotive force	The <i>volt</i> (V) is the difference of electric potential between two points of a conductor carrying a constant current of 1 A when the power dissipated between these points is equal to 1 W.
Electric resistance	The <i>ohm</i> (Ω) is the electric resistance between two points of a conductor when a constant difference of potential of 1 V, applied between these two points, produces in this conductor a current of 1 A, this conductor not being the source of any electromotive force.
Energy	The <i>joule</i> (J) is the work done when the point of application of a force of 1 N is displaced a distance of 1 m in the direction of the force.
Force	The <i>newton</i> (N) is that force that, when applied to a body having a mass of 1 kg, gives it an acceleration of 1 m/s ² .
Frequency	The <i>hertz</i> (Hz) is the frequency of a periodic phenomenon of which the period is 1 second.
Illuminance	The <i>lux</i> (lx) is the illuminance produced by a luminous flux of 1 lm uniformly distributed over a surface of 1 m ² .
Luminous flux	The <i>lumen</i> (lm) is the luminous flux emitted in a solid angle of 1 sr by a point source having a uniform intensity of 1 cd.
Magnetic flux	The <i>weber</i> (Wb) is the magnetic flux that, linking a circuit of one turn, produces in it an electromotive force of 1 V as it is reduced to zero at a uniform rate in 1 s.
Magnetic flux density magnetic induction	The <i>tesla</i> (T) is the magnetic flux density of 1 Wb/m ² . In an alternative approach to defining the magnetic field quantities the <i>tesla</i> may also be defined as the magnetic flux density that produces on a 1-m length of wire carrying a current of 1 A, oriented normal to the flux density, a force of 1 N, magnetic flux density being defined as an axial vector quantity such that

the force exerted on an element of current is equal to the vector product of this element and the magnetic flux density.

Power The *watt* (W) is the power that represents a rate of energy transfer of 1 J/s.

Pressure or stress The *pascal* (Pa) is the pressure or stress of 1 N/m².

Electric charge, quantity of electricity *Electric charge* is the time integral of electric current; its unit, the *coulomb* (C), is equal to 1 A·s.

No other SI derived units have been assigned special names at this time.

APPENDIX C^{3,8*}

Style Guide for Metric Usage

Rules for Writing Metric Quantities

Capitals. Units—Unit names, including prefixes, are not capitalized except at the beginning of a sentence or in titles. Note that for “degree Celsius” the word “degree” is lower case; the modifier “Celsius” is always capitalized. The “degree centigrade” is now obsolete.

Symbols—The short forms for metric units are called unit symbols. They are lower case except that the first letter is upper case when the unit is named for a person. (An exception to this rule in the U.S. is the symbol L for liter.)

Examples:	Unit Name	Unit Symbol
	meter**	m
	gram	g
	newton	N
	pascal	Pa

Printed unit symbols should have Roman (upright) letters, because italic (sloping or slanted) letters are reserved for quantity symbols, such as *m* for mass and *L* for length.

Prefix Symbols—All prefix names, their symbols, and pronunciation are listed in Table 1.4. Notice that the top five are upper case and all the rest lower case.

The importance of following the precise use of upper-case and lower-case letters is shown by the following examples of prefixes and units.

G for giga; g for gram.

K for kelvin; k for kilo.

M for mega; m for milli.

N for newton; n for nano.

T for tera; t for tonne (metric ton).

Information Processing—Limited Character Sets—Prefixes and unit symbols retain their prescribed forms regardless of the surrounding typography, except for systems with limited character sets. ISO has provided a standard¹² for such systems; this standard is recommended.

Plurals and Fractions. Names of SI units form their plurals in the usual manner, except for lux, hertz, and siemens.

* Ref. 8 is primary source.

** The spellings “metre” and “litre” are preferred by ISO but “meter” and “liter” are official U.S. government spellings.

Values less than one take the singular form of the unit name; for example, 0.5 kilogram or $\frac{1}{2}$ kilogram. While decimal notation (0.5, 0.35, 6.87) is generally preferred, the most simple fractions are acceptable, such as those where the denominator is 2, 3, 4, or 5.

Symbols of units are the same in singular and plural—e.g., 1 m and 100 m.

Periods. A period is *not* used after a symbol, except at the end of a sentence. Examples: "A current of 15 mA is found..." "The field measured 350×125 m."

The Decimal Marker. ISO specifies the comma as the decimal marker⁹; in English-language documents a dot on the line is acceptable. In numbers less than one, a zero should be written before the decimal sign (to prevent the possibility that a faint decimal sign will be overlooked). Example: The oral expression "point seven five" is written 0.75 or 0,75.

Grouping of Numbers. Separate digits into groups of three, counting from the decimal marker. A comma should not be used between the groups of three⁹; instead, a space is left to avoid confusion, since the comma is the ISO standard for the decimal marker.

In a four-digit number, the space is not required unless the four-digit number is in a column with numbers of five digits or more:

For	4,720,525	write	4 720 525
For	0.52875	write	0.528 75
For	6,875	write	6875 or 6 875
For	0.6875	write	0.6875 or 0.687 5

Spacing. In symbols or names for units having prefixes, no space is left between letters making up the symbol or the name. Examples are kA, kiloampere; and mg, milligram.

When a symbol follows a number to which it refers, a space must be left between the number and the symbol, except when the symbol (such as °) appears in the superscript position. Examples: 455 kHz, 22 mg, 20 mm, 10^6 N, 30 K, 20°C.

When a quantity is used as an adjective, a hyphen should be used between the number and the symbol (except °C). Examples: It is a 35-mm film; the film width is 35 mm. I bought a 6-kg turkey; the turkey weighs 6 kg.

Leave a space on each side of signs for multiplication, division, addition, and subtraction, except within a compound symbol. Examples: 4 cm \times 3 m (not 4 cm \times 3 m); kg/m³; N·m.

Powers. For unit *names*, use the modifier *squared* or *cubed* after the unit name (except for area and volume)—e.g., meter per second squared. For area or volume, place a modifier before the unit name, including derived units:—e.g., cubic meter and watt per square meter.

For unit *symbols*, write the symbol for the unit followed by the power superscript—e.g., 14 m² and 26 cm³.

Compound Units. For a unit name (not a symbol) derived as a quotient (e.g., for kilometers per hour), it is preferable not to use a slash (/) as a substitute for "per" except where space is limited and a symbol might not be understood. Avoid other mixtures of words and symbols. Examples: Use meter per second, not m/s. Use only one "per" in any combination of units—e.g., meter per second squared, not meter per second per second.

For a unit symbol derived as a quotient do not, for example, write k.p.h. or kph for km/h because the first two are understood only in the English language, whereas km/h is used in all languages. The symbol km/h also can be written with a negative exponent—e.g., km·h⁻¹.

Never use more than one slash (/) in any combination of symbols unless parentheses are used to avoid ambiguity; examples are m/s², not m/s/s; W/(m·K), not W/m/K.

For a unit *name* derived as a product, a space or a hyphen is recommended but never a "product dot" (a period raised to a centered position)—e.g., write newton meter or newton-meter, not newton·meter. In the case of the watt hour, the space may be omitted—watt-hour.

For a unit *symbol* derived as a product, use a product dot—e.g., N·m. For computer printouts, automatic typewriter work, etc., a dot on the line may be used. Do not use the product dot as a multiplier symbol for calculations—e.g., use 6.2×5 , not $6.2 \cdot 5$.

Do not mix nonmetric units with metric units, except those for time, plane angle, or rotation—e.g., use kg/m³, not kg/ft³ or kg/gal.

A quantity that constitutes a ratio of two like quantities should be expressed as a fraction (either common or decimal) or as a percentage—e.g., the slope is 1/100 or 0.01 or 1%, not 10 mm/m or 10 m/km.

SI Prefix Usage. General—SI prefixes should be used to indicate orders of magnitude, thus eliminating non-significant digits and leading zeros in decimal fractions and providing a convenient alternative to the powers-of-10 notation preferred in computation. For example, 12 300 m (in computations) becomes 12.3 km (in non-computation situations); $0.0123 \mu\text{A}$ (12.3×10^{-9} A for computations) becomes 12.3 nA (in noncomputation situations).

Selection—When expressing a quantity by a numerical value and a unit, prefixes should be chosen so that the numerical value lies between 0.1 and 1000. Generally, prefixes representing steps of 1000 are recommended (avoiding hecto, deka, deci, and centi). However, some situations may justify deviation from the above:

1. In expressing units raised to powers (such as area, volume and moment) the prefixes hecto, deka, deci, and centi may be required—e.g., cubic centimeter for volume and cm⁴ for moment.

2. In tables of values of the same quantity, or in a discussion of such values within a given context, it generally is preferable to use the same unit multiple throughout.

3. For certain quantities in particular applications, one certain multiple is used customarily; an example is the millimeter in mechanical engineering drawings, even when the values lie far outside the range of 0.1 to 1000 mm.

Powers of Units—An exponent attached to a symbol

containing a prefix indicates that *the multiple or sub-multiple of the unit* (the unit with its prefix) *is raised to the power expressed by the exponent*. For example,

$$\begin{array}{lll} 1 \text{ cm}^3 & = (10^{-2} \text{ m})^3 & = 10^{-6} \text{ m}^3 \\ 1 \text{ ns}^{-1} & = (10^{-9} \text{ s})^{-1} & = 10^9 \text{ s}^{-1} \\ 1 \text{ mm}^2/\text{s} & = (10^{-3} \text{ m})^2/\text{s} & = 10^{-5} \text{ m}^2/\text{s} \end{array}$$

Double Prefixes—Double or multiple prefixes should not be used. For example,

use GW (gigawatt), not kMW;
use pm (picometer), not $\mu\mu\text{m}$;
use Gg (gigagram), not Mkg;
use 13.58 m, not 13 m 580 mm.

Prefix Mixtures—Do not use a mixture of prefixes unless the difference in size is extreme. For example, use 40 mm wide and 1500 mm long, not 40 mm wide and 1.5 m long; however, 1500 m of 2-mm-diameter wire is acceptable.

Compound Units—It is *preferable* that prefixes not be used in the denominators of complex units, except for kilogram (kg) which is a base unit. However, there are cases where the use of such prefixes is necessary to obtain a numerical value of convenient size. Examples of some of these rare exceptions are shown in the tables contained in these standards.

Prefixes may be applied to the numerator of a compound unit; thus, megagram per cubic meter (Mg/m^3), but *not* kilogram per cubic decimeter (kg/dm^3) *nor* gram per cubic centimeter (g/cm^3). Values required outside the range of the prefixes should be expressed by powers of 10 applied to the base unit.

Unit of Mass—Among the base units of SI, the kilogram is the only one whose name, for historical reasons, contains a prefix; it is also the coherent SI unit for mass (See Appendices A and B for discussions of coherence.) However, names of decimal multiples and submultiples of the unit of mass are formed by attaching prefixes to the word “gram.”

Prefixes Alone—Do not use a prefix without a unit—e.g., use kilogram, not kilo.

Calculations—Errors in calculations can be minimized if, instead of using prefixes, the *base* and the *coherent* derived SI units are used, expressing numerical values in powers-of-10 notation—e.g., $1 \text{ MJ} = 10^6 \text{ J}$.

Spelling of Vowel Pairs. There are three cases where the final vowel in a prefix is omitted: megohm, kilohm, and hectare. In all other cases, both vowels are retained and both are pronounced. No space or hyphen should be used.

Complicated Expressions. To avoid ambiguity in complicated expressions, symbols are preferred over words.

Attachment. Attachment of letters to a unit symbol for giving information about the nature of the quantity is incorrect: MWe for “megawatts electrical (power),” kPag for “kilopascals gauge (pressure),” Paa for “pascals absolute (pressure),” and Vac for “volts ac” are not acceptable. If the context is in doubt on any units used, supplementary descriptive phrases should be added to making the meanings clear.

Equations. When customary units appear in equations, the SI equivalents should be omitted. Instead of inserting the latter in parentheses, as in the case of text or small tables, the equations should be restated using SI unit symbols, or a sentence, paragraph, or note should be added stating the factor to be used to convert the calculated result in customary units to the preferred SI units.

Pronunciation of Metric Terms

The pronunciation of most of the unit names is well known and uniformly described in U.S. dictionaries, but four have been pronounced in various ways. The following pronunciations are recommended:

candela	— Accent on the second syllable and pronounce it like <i>dell</i> .
joule	— Pronounce it to rhyme with <i>pool</i> .
pascal	— The preferred pronunciation rhymes with <i>rascal</i> . An acceptable second choice puts the accent on the second syllable.
siemens	— Pronounce it like <i>seamen</i> 's.

For pronunciation of unit prefixes, see Table 1.4.

Typewriting Recommendations

Superscripts. The question arises of how numerical superscripts should be typed on a machine with a conventional keyboard. With an ordinary keyboard, numerals and the minus sign can be raised to the superscript position by rolling the platen half a space before typing the numeral, using care to avoid interference with the text in the line above.

Special Characters. For technical work, it is useful to have Greek letters available on the typewriter. If all SI symbols for units are to be typed properly, a key with the upright Greek lower-case μ (pronounced “mew,” not “moo”) is necessary, since this is the symbol for micro, meaning one millionth. The symbol can be approximated on a conventional machine by using a lower-case u and adding the tail by hand (μ). A third choice is to spell out the unit name in full.

For units of electricity, the Greek upper-case omega (Ω) for ohm also will be useful; when it is not available, the word “ohm” can be spelled out.

It is fortunate that, except for the more extensive use of the Greek μ for micro and Ω for ohm, the change to SI units causes no additional difficulty in manuscript preparation.

The Letter for Liter. On most U.S. typewriters, there is little difference between the lower-case “el” (“l”) and the numerical “one” (“1”). The European symbol for liter is a simple upright bar; the Canadians¹³ used a script *ℓ* but now have adopted the upright capital L; AN-SI now recommends the upright capital L.

Typewriter Modification. Where frequently used, the following symbols could be included on typewriters: superscripts ² and ³ for squared and cubed; Greek μ for micro; ° for degree; · for a product dot (not a period) for symbols derived as a product; and Greek Ω for ohm.

A special type-ball that contains all the superscripts, μ , Ω , and other characters used in technical reports is available for some typewriters. Some machines have replaceable character keys.

Longhand. To assure legibility of the symbols m, n, and μ , it is recommended that these three symbols be written to resemble printing. For example, write nm, not $n\mu$. The symbol μ should have a long distinct tail and should have the upright form (not sloping or italic).

Shorthand. Stenographers will find that the SI symbols generally are quicker to write than the shorthand forms for the unit names.

APPENDIX D

General Conversion Factors*

General

Table 1.7 is intended to serve two purposes:

1. To express the definitions of general units of measure as exact numerical multiples of coherent "metric" units. Relationships that are exact in terms of the fundamental SI unit are followed by an asterisk. Relationships that are not followed by an asterisk either are the result of physical measurements or are only approximate.

2. To provide multiplying factors for converting expressions of measurements given by numbers and general or miscellaneous units to corresponding new numbers and metric units.

Notation

Conversion factors are presented for ready adaptation to computer readout and electronic data transmission. The factors are written as a number equal to or greater than one and less than 10, with six or fewer decimal places (i.e., seven or fewer total digits). Each number is followed by the letter E (for exponent), a plus or minus symbol, and two digits that indicate the power of 10 by which the number must be multiplied to obtain the correct value. For example,

$$3.523\ 907\ (E-02) \text{ is } 3.523\ 907 \times 10^{-2}$$

or

$$0.035\ 239\ 07.$$

Similarly,

$$3.386\ 389\ (E+03) \text{ is } 3.386\ 389 \times 10^3$$

or

$$3\ 386.389.$$

An asterisk (*) after the numbers shown indicates that the conversion factor is exact and that all subsequent digits (for rounding purposes) are zero. All other conversion factors have been rounded to the figures given in accordance with procedures outlined in the preceding text.

Where fewer than six decimal places are shown, more precision is not warranted.

The following is a further example of the use of Table 1.7.

To Convert From	To	Multiply By
pound-force per square foot	Pa	4.788 026 E+01
pound-force per square inch	Pa	6.894 757 E+03
inch	m	2.540* E-02

These conversions mean that

1 lbf/ft² becomes 47.880 26 Pa,
 1 lbf/in.² becomes 6894.757 Pa or
 6.894 757 kPa, and
 1 inch becomes 0.0254 m (exactly).

The unit symbol for pound-force sometimes is written lbf and sometimes lb_f or lb_f; the form lbf is recommended.

Organization

The conversion factors generally are listed alphabetically by units having specific names and compound units derived from these specific units. A number of units starting with the pound symbol (lb) are located in the "p" section of the list.

Conversion factors classified by physical quantities are listed in Refs. 3 and 4.

The conversion factors for other compound units can be generated easily from numbers given in the alphabetical list by substitution of converted units. Two examples follow.

1. Find the conversion factor for productivity index, (B/D)/psi to (m³/d)/Pa. Convert 1 B/D to 1.589 873 (E-01) m³/d and 1 psi to 6.894 757 (E+03) Pa. Then, substitute

$$\begin{aligned} & [1.589\ 873\ (E-01)]/[6.894\ 757\ (E+03)] \\ & = 2.305\ 916\ (E-05)\ (m^3/d)/Pa. \end{aligned}$$

2. Find the conversion factor for tonf·mile/ft to MJ/m. Convert 1 tonf to 8.896 444 (E+03) N; 1 mile to 1.609 344* (E+03) m; and 1 ft to 3.048* (E-01) m. Then, substitute

$$\begin{aligned} & [8.896\ 444\ (E+03)] [1.609\ 344\ (E+03)] \\ & \div [3.048\ (E-01)] \\ & = 4.697\ 322\ (E+07)\ (N \cdot m)/m \text{ or } J/m \\ & = 4.697\ 322\ (E+01)\ MJ/m. \end{aligned}$$

When conversion factors for complex compound units are being calculated from Table 1.7, numerical uncertainties may be present in the seventh (or lesser last "significant") digit of the answer because of roundings already taken for the last digit of tabulated values. Mechtly¹⁵ provides conversion factors of more than seven digits for certain quantities.

*Based on ASTM Pub. E380-82 (Ref. 3), values of conversion factors tabulated herewith are identical with those in E380-82; generally similar material is found in Ref. 4. Conversion values in earlier editions of E 380 (for example, E 380-74) are based on Ref. 15, which has available some factors with more than seven digits.

TABLE 1.7—ALPHABETICAL LIST OF UNITS
(symbols of SI units given in parentheses)

To Convert From	To	Multiply By	
abampere	ampere (A)	1.0*	E + 01
abcoulomb	coulomb (C)	1.0*	E + 01
abfarad	farad (F)	1.0*	E + 09
abhenry	henry (H)	1.0*	E - 09
abmho	siemens (S)	1.0*	E + 09
abohm	ohm (Ω)	1.0*	E - 09
abvolt	volt (V)	1.0*	E - 08
acre-foot (U.S. survey) ⁽¹⁾	meter ³ (m ³)	1.233 489	E + 03
acre (U.S. survey) ⁽¹⁾	meter ² (m ²)	4.046 873	E + 03
ampere hour	coulomb (C)	3.6*	E + 03
are	meter ² (m ²)	1.0*	E + 02
angstrom	meter (m)	1.0*	E - 10
astronomical unit	meter (m)	1.495 979	E + 11
atmosphere (standard)	pascal (Pa)	1.013 250*	E + 05
atmosphere (technical = 1 kgf/cm ²)	pascal (Pa)	9.806 650*	E + 04
bar	pascal (Pa)	1.0*	E + 05
barn	meter ² (m ²)	1.0*	E - 28
barrel (for petroleum, 42 gal)	meter ³ (m ³)	1.589 873	E - 01
board foot	meter ³ (m ³)	2.359 737	E - 03
British thermal unit (International Table) ⁽²⁾	joule (J)	1.055 056	E + 03
British thermal unit (mean)	joule (J)	1.055 87	E + 03
British thermal unit (thermochemical)	joule (J)	1.054 350	E + 03
British thermal unit (39°F)	joule (J)	1.059 67	E + 03
British thermal unit (59°F)	joule (J)	1.054 80	E + 03
British thermal unit (60°F)	joule (J)	1.054 68	E + 03
Btu (International Table)-ft/(hr-ft ² -°F) (thermal conductivity)	watt per meter kelvin [W/(m·K)]	1.730 735	E + 00
Btu (thermochemical)-ft/(hr-ft ² -°F) (thermal conductivity)	watt per meter kelvin [W/(m·K)]	1.729 577	E + 00
Btu (International Table)-in./(hr-ft ² -°F) (thermal conductivity)	watt per meter kelvin [W/(m·K)]	1.442 279	E - 01
Btu (thermochemical)-in./(hr-ft ² -°F) (thermal conductivity)	watt per meter kelvin [W/(m·K)]	1.441 314	E - 01
Btu (International Table)-in./(s-ft ² -°F) (thermal conductivity)	watt per meter kelvin [W/(m·K)]	5.192 204	E + 02
Btu (thermochemical)-in./(s-ft ² -°F) (thermal conductivity)	watt per meter kelvin [W/(m·K)]	5.188 732	E + 02
Btu (International Table)/hr	watt (W)	2.930 711	E - 01
Btu (thermochemical)/hr	watt (W)	2.928 751	E - 01
Btu (thermochemical)/min	watt (W)	1.757 250	E + 01
Btu (thermochemical)/s	watt (W)	1.054 350	E + 03
Btu (International Table)/ft ²	joule per meter ² (J/m ²)	1.135 653	E + 04
Btu (thermochemical)/ft ²	joule per meter ² (J/m ²)	1.134 893	E + 04
Btu (thermochemical)/(ft ² -hr)	watt per meter ² (W/m ²)	3.152 481	E + 00
Btu (thermochemical)/(ft ² -min)	watt per meter ² (W/m ²)	1.891 489	E + 02
Btu (thermochemical)/(ft ² -s)	watt per meter ² (W/m ²)	1.134 893	E + 04
Btu (thermochemical)/(in. ² -s)	watt per meter ² (W/m ²)	1.634 246	E + 06
Btu (International Table)/(hr-ft ² -°F) (thermal conductance)	watt per meter ² kelvin [W/(m ² ·K)]	5.678 263	E + 00
Btu (thermochemical)/(hr-ft ² -°F) (thermal conductance)	watt per meter ² kelvin [W/(m ² ·K)]	5.674 466	E + 00
Btu (International Table)/(s-ft ² -°F)	watt per meter ² kelvin [W/(m ² ·K)]	2.044 175	E + 04
Btu (thermochemical)/(s-ft ² -°F)	watt per meter ² kelvin [W/(m ² ·K)]	2.042 808	E + 04
Btu (International Table)/lbm	joule per kilogram (J/kg)	2.326*	E + 03
Btu (thermochemical)/lbm	joule per kilogram (J/kg)	2.324 444	E + 03
Btu (International Table)/(lbm-°F) (heat capacity)	joule per kilogram kelvin [J/(kg·K)]	4.186 8*	E + 03
Btu (thermochemical)/(lbm-°F) (heat capacity)	joule per kilogram kelvin [J/(kg·K)]	4.184 000	E + 03

⁽¹⁾Since 1893 the U.S. basis of length measurement has been derived from metric standards. In 1959 a small refinement was made in the definition of the yard to resolve discrepancies both in this country and abroad, which changed its length from 3600/3937 m to 0.9144 m exactly. This resulted in the new value being shorter by two parts in a million. At the same time it was decided that any data in feet derived from and published as a result of geodetic surveys within the U.S. would remain with the old standard (1 ft = 1200/3937 m) until further decision. This foot is named the U.S. survey foot. As a result, all U.S. land measurements in U.S. customary units will relate to the meter by the old standard. All the conversion factors in these tables for units referenced to this footnote are based on the U.S. survey foot, rather than the international foot. Conversion factors for the land measure given below may be determined from the following relationships:

1 league = 3 miles (exactly)
 1 rod = 16 1/2 ft (exactly)
 1 chain = 66 ft (exactly)
 1 section = 1 sq mile
 1 township = 36 sq miles

⁽²⁾This value was adopted in 1956. Some of the older International Tables use the value 1.055 04 E + 03. The exact conversion factor is 1.055 055 852 62* E + 03.

TABLE 1.7—ALPHABETICAL LIST OF UNITS (continued)
(symbols of SI units given in parentheses)

To Convert From	To	Multiply By**
bushel (U.S.)	meter ³ (m ³)	3.523 907 E-02
caliber (inch)	meter (m)	2.54* E-02
calorie (International Table)	joule (J)	4.186 8* E+00
calorie (mean)	joule (J)	4.190 02 E+00
calorie (thermochemical)	joule (J)	4.184* E+00
calorie (15°C)	joule (J)	4.185 80 E+00
calorie (20°C)	joule (J)	4.181 90 E+00
calorie (kilogram, International Table)	joule (J)	4.186 8* E+03
calorie (kilogram, mean)	joule (J)	4.190 02 E+03
calorie (kilogram, thermochemical)	joule (J)	4.184* E+03
cal (thermochemical)/cm ²	joule per meter ² (J/m ²)	4.184* E+04
cal (International Table)/g	joule per kilogram (J/kg)	4.186* E+03
cal (thermochemical)/g	joule per kilogram (J/kg)	4.184* E+03
cal (International Table)/(g·°C)	joule per kilogram kelvin [J/(kg·K)]	4.186 8* E+03
cal (thermochemical)/(g·°C)	joule per kilogram kelvin [J/(kg·K)]	4.184* E+03
cal (thermochemical)/min	watt (W)	6.973 333 E-02
cal (thermochemical)/s	watt (W)	4.184* E+00
cal (thermochemical)/(cm ² ·min)	watt per meter ² (W/m ²)	6.973 333 E+02
cal (thermochemical)/(cm ² ·s)	watt per meter ² (W/m ²)	4.184* E+04
cal (thermochemical)/(cm·s·°C)	watt per meter kelvin [W/(m·K)]	4.184* E+02
capture unit (c.u. = 10 ⁻³ cm ⁻¹)	per meter (m ⁻¹)	1.0* E-01
carat (metric)	kilogram (kg)	2.0* E-04
centimeter of mercury (0°C)	pascal (Pa)	1.333 22 E+03
centimeter of water (4°C)	pascal (Pa)	9.806 38 E+01
centipoise	pascal second (Pa·s)	1.0* E-03
centistokes	meter ² per second (m ² /s)	1.0* E-06
circular mil	meter ² (m ²)	5.067 075 E-10
clo	kelvin meter ² per watt [(K·m ²)/W]	2.003 712 E-01
cup	meter ³ (m ³)	2.365 882 E-04
curie	becquerel (Bq)	3.7* E+10
cycle per second	hertz (Hz)	1.0* E+00
day (mean solar)	second (s)	8.640 000 E+04
day (sidereal)	second (s)	8.616 409 E+04
degree (angle)	radian (rad)	1.745 329 E-02
degree Celsius	kelvin (K)	$T_K = T_C + 273.15$
degree centigrade (see degree Celsius)		
degree Fahrenheit	degree Celsius	$T_C = (T_F - 32)/1.8$
degree Fahrenheit	kelvin (K)	$T_K = (T_F + 459.67)/1.8$
degree Rankine	kelvin (K)	$T_K = T_R/1.8$
°F·hr·ft ² /Btu (International Table)		
(thermal resistance)	kelvin meter ² per watt [(K·m ²)/W]	1.781 102 E-01
°F·hr·ft ² /Btu (thermochemical)		
(thermal resistance)	kelvin meter ² per watt [(K·m ²)/W]	1.762 250 E-01
denier	kilogram per meter (kg/m)	1.111 111 E-07
dyne	newton (N)	1.0* E-05
dyne·cm	newton meter (N·m)	1.0* E-07
dyne/cm ²	pascal (Pa)	1.0* E-01
electronvolt	joule (J)	1.602 19 E-19
EMU of capacitance	farad (F)	1.0* E+09
EMU of current	ampere (A)	1.0* E+01
EMU of electric potential	volt (V)	1.0* E-08
EMU of inductance	henry (H)	1.0* E-09
EMU of resistance	ohm (Ω)	1.0* E-09
ESU of capacitance	farad (F)	1.112 650 E-12
ESU of current	ampere (A)	3.335 6 E-10
ESU of electric potential	volt (V)	2.997 9 E+02
ESU of inductance	henry (H)	8.987 554 E+11
ESU of resistance	ohm (Ω)	8.987 554 E+11
erg	joule (J)	1.0* E-07
erg/cm ² ·s	watt per meter ² (W/m ²)	1.0* E-03
erg/s	watt (W)	1.0* E-07
faraday (based on carbon-12)	coulomb (C)	9.648 70 E+04
faraday (chemical)	coulomb (C)	9.649 57 E+04
faraday (physical)	coulomb (C)	9.652 19 E+04
fathom	meter (m)	1.828 8 E+00
fermi (femtometer)	meter (m)	1.0* E-15
fluid ounce (U.S.)	meter ³ (m ³)	2.957 353 E-05
foot	meter (m)	3.048* E-01
foot (U.S. survey) ⁽¹⁾	meter (m)	3.048 006 E-01

TABLE 1.7—ALPHABETICAL LIST OF UNITS (continued)
(symbols of SI units given in parentheses)

To Convert From	To	Multiply By**
foot of water (39.2°F)	pascal (Pa)	2.988 98 E + 03
sq ft	meter ² (m ²)	9.290 304* E - 02
ft ² /hr (thermal diffusivity)	meter ² per second (m ² /s)	2.580 640* E - 05
ft ² /s	meter ² per second (m ² /s)	9.290 304* E - 02
cu ft (volume; section modulus)	meter ³ (m ³)	2.831 685 E - 02
ft ³ /min	meter ³ per second (m ³ /s)	4.719 474 E - 04
ft ³ /s	meter ³ per second (m ³ /s)	2.831 685 E - 02
ft ⁴ (moment of section) ⁽³⁾	meter ⁴ (m ⁴)	8.630 975 E - 03
ft/hr	meter per second (m/s)	8.466 667 E - 05
ft/min	meter per second (m/s)	5.080* E - 03
ft/s	meter per second (m/s)	3.048* E - 01
ft/s ²	meter per second ² (m/s ²)	3.048* E - 01
footcandle	lux (lx)	1.076 391 E + 01
footlambert	candela per meter ² (cd/m ²)	3.426 259 E + 00
ft-lbf	joule (J)	1.355 818 E + 00
ft-lbf/hr	watt (W)	3.766 161 E - 04
ft-lbf/min	watt (W)	2.259 697 E - 02
ft-lbf/s	watt (W)	1.355 818 E + 00
ft-poundal	joule (J)	4.214 011 E - 02
free fall, standard (g)	meter per second ² (m/s ²)	9.806 650* E + 00
cm/s ²	meter per second ² (m/s ²)	1.0* E - 02
gallon (Canadian liquid)	meter ³ (m ³)	4.546 090 E - 03
gallon (U.K. liquid)	meter ³ (m ³)	4.546 092 E - 03
gallon (U.S. dry)	meter ³ (m ³)	4.404 884 E - 03
gallon (U.S. liquid)	meter ³ (m ³)	3.785 412 E - 03
gal (U.S. liquid)/day	meter ³ per second (m ³ /s)	4.381 264 E - 08
gal (U.S. liquid)/min	meter ³ per second (m ³ /s)	6.309 020 E - 05
gal (U.S. liquid)/hp-hr (SFC, specific fuel consumption)	meter ³ per joule (m ³ /J)	1.410 089 E - 09
gamma (magnetic field strength)	ampere per meter (A/m)	7.957 747 E - 04
gamma (magnetic flux density)	tesla (T)	1.0* E - 09
gauss	tesla (T)	1.0* E - 04
gilbert	ampere (A)	7.957 747 E - 01
gill (U.K.)	meter ³ (m ³)	1.420 654 E - 04
gill (U.S.)	meter ³ (m ³)	1.182 941 E - 04
grad	degree (angular)	9.0* E - 01
grad	radian (rad)	1.570 796 E - 02
grain (1/7000 lbm avoirdupois)	kilogram (kg)	6.479 891* E - 05
grain (lbm avoirdupois/7000)/gal (U.S. liquid)	kilogram per meter ³ (kg/m ³)	1.711 806 E - 02
gram	kilogram (kg)	1.0* E - 03
g/cm ³	kilogram per meter ³ (kg/m ³)	1.0* E + 03
gram-force/cm ²	pascal (Pa)	9.806 650* E + 01
hectare	meter ² (m ²)	1.0* E + 04
horsepower (550 ft-lbf/s)	watt (W)	7.456 999 E + 02
horsepower (boiler)	watt (W)	9.809 50 E + 03
horsepower (electric)	watt (W)	7.460* E + 02
horsepower (metric)	watt (W)	7.354 99 E + 02
horsepower (water)	watt (W)	7.460 43 E + 02
horsepower (U.K.)	watt (W)	7.457 0 E + 02
hour (mean solar)	second (s)	3.600 000 E + 03
hour (sidereal)	second (s)	3.590 170 E + 03
hundredweight (long)	kilogram (kg)	5.080 235 E + 01
hundredweight (short)	kilogram (kg)	4.535 924 E + 01
inch	meter (m)	2.54* E - 02
inch of mercury (32°F)	pascal (Pa)	3.386 38 E + 03
inch of mercury (60°F)	pascal (Pa)	3.376 85 E + 03
inch of water (39.2°F)	pascal (Pa)	2.490 82 E + 02
inch of water (60°F)	pascal (Pa)	2.488 4 E + 02
sq in.	meter ² (m ²)	6.451 6* E - 04
cu in. (volume; section modulus) ⁽⁴⁾	meter ³ (m ³)	1.638 706 E - 05
in. ³ /min	meter ³ per second (m ³ /s)	2.731 177 E - 07
in. ⁴ (moment of section) ⁽³⁾	meter ⁴ (m ⁴)	4.162 314 E - 07
in./s	meter per second (m/s)	2.54* E - 02
in./s ²	meter per second ² (m/s ²)	2.54* E - 02
kayser	1 per meter (1/m)	1.0* E + 02
kelvin	degree Celsius	$T_{°C} = T_K - 273.15$

⁽³⁾ This sometimes is called the moment of inertia of a plane section about a specified axis.⁽⁴⁾ The exact conversion factor is 1.638 706 4*E-05.

TABLE 1.7—ALPHABETICAL LIST OF UNITS (continued)
(symbols of SI units given in parentheses)

To Convert From	To	Multiply By**
kilocalorie (International Table)	joule (J)	4.186 8* E + 03
kilocalorie (mean)	joule (J)	4.190 02 E + 03
kilocalorie (thermochemical)	joule (J)	4.184* E + 03
kilocalorie (thermochemical)/min	watt (W)	6.973 333 E + 01
kilocalorie (thermochemical)/s	watt (W)	4.184* E + 03
kilogram-force (kgf)	newton (N)	9.806 65* E + 00
kgf·m	newton meter (N·m)	9.806 65* E + 00
kgf·s ² /m (mass)	kilogram (kg)	9.806 65* E + 00
kgf/cm ²	pascal (Pa)	9.806 65* E + 04
kgf/m ²	pascal (Pa)	9.806 65* E + 00
kgf/mm ²	pascal (Pa)	9.806 65* E + 06
km/h	meter per second (m/s)	2.777 778 E − 01
kilopond	newton (N)	9.806 65* E + 00
kilowatthour (kW·hr)	joule (J)	3.6* E + 06
kip (1000 lbf)	newton (N)	4.448 222 E + 03
kip/in. ² (ksi)	pascal (Pa)	6.894 757 E + 06
knot (international)	meter per second (m/s)	5.144 444 E − 01
lambert	candela per meter ² (cd/m ²)	1/π* E + 04
lambert	candela per meter ² (cd/m ²)	3.183 099 E + 03
langley	joule per meter ² (J/m ²)	4.184* E + 04
league	meter (m)	(see Footnote 1)
light year	meter (m)	9.460 55 E + 15
liter ⁽⁵⁾	meter ³ (m ³)	1.0* E − 03
maxwell	weber (Wb)	1.0* E − 08
mho	siemens (S)	1.0* E + 00
microinch	meter (m)	2.54* E − 08
microsecond/foot (μs/ft)	microsecond/meter (μs/m)	3.280 840 E + 00
micron	meter (m)	1.0* E − 06
mil	meter (m)	2.54* E − 05
mile (international)	meter (m)	1.609 344* E + 03
mile (statute)	meter (m)	1.609 3 E + 03
mile (U.S. survey) ⁽¹⁾	meter (m)	1.609 347 E + 03
mile (international nautical)	meter (m)	1.852* E + 03
mile (U.K. nautical)	meter (m)	1.853 184* E + 03
mile (U.S. nautical)	meter (m)	1.852* E + 03
sq mile (international)	meter ² (m ²)	2.589 988 E + 06
sq mile (U.S. survey) ⁽¹⁾	meter ² (m ²)	2.589 998 E + 06
mile/hr (international)	meter per second (m/s)	4.470 4* E − 01
mile/hr (international)	kilometer per hour (km/h)	1.609 344* E + 00
mile/min (international)	meter per second (m/s)	2.682 24* E + 01
mile/s (international)	meter per second (m/s)	1.609 344* E + 03
millibar	pascal (Pa)	1.0* E + 02
millimeter of mercury (0°C)	pascal (Pa)	1.333 22 E + 02
minute (angle)	radian (rad)	2.908 882 E − 04
minute (mean solar)	second (s)	6.0* E + 01
minute (sidereal)	second (s)	5.983 617 E + 01
month (mean calendar)	second (s)	2.628 000 E + 06
oersted	ampere per meter (A/m)	7.957 747 E + 01
ohm centimeter	ohm meter (Ω·m)	1.0* E − 02
ohm circular-mil per ft	ohm millimeter ² per meter [(Ω·mm ²)/m]	1.662 426 E − 03
ounce (avoirdupois)	kilogram (kg)	2.834 952 E − 02
ounce (troy or apothecary)	kilogram (kg)	3.110 348 E − 02
ounce (U.K. fluid)	meter ³ (m ³)	2.841 307 E − 05
ounce (U.S. fluid)	meter ³ (m ³)	2.957 353 E − 05
ounce-force	newton (N)	2.780 139 E − 01
ozf·in.	newton meter (N·m)	7.061 552 E − 03
oz (avoirdupois)/gal (U.K. liquid)	kilogram per meter ³ (kg/m ³)	6.236 021 E + 00
oz (avoirdupois)/gal (U.S. liquid)	kilogram per meter ³ (kg/m ³)	7.489 152 E + 00
oz (avoirdupois)/in. ³	kilogram per meter ³ (kg/m ³)	1.729 994 E + 03
oz (avoirdupois)/ft ²	kilogram per meter ² (kg/m ²)	3.051 517 E − 01
oz (avoirdupois)/yd ²	kilogram per meter ² (kg/m ²)	3.390 575 E − 02
parsec	meter (m)	3.085 678 E + 16
peck (U.S.)	meter ³ (m ³)	8.809 768 E − 03
pennyweight	kilogram (kg)	1.555 174 E − 03
perm (°C) ⁽⁶⁾	kilogram per pascal second meter ² [kg/(Pa·s·m ²)]	5.721 35 E − 11

⁽⁵⁾In 1964 the General Conference on Weights and Measures adopted the name liter as a special name for the cubic decimeter. Before this decision the liter differed slightly (previous value, 1.000 028 dm³) and in expression of precision volume measurement this fact must be kept in mind.

⁽⁶⁾Not the same as reservoir "perm."

TABLE 1.7—ALPHABETICAL LIST OF UNITS (continued)
(symbols of SI units given in parentheses)

To Convert From	To	Multiply By**
perm (23°C) ⁽⁶⁾	kilogram per pascal second meter ² [kg/(Pa·s·m ²)]	5.745 25 E − 11
perm-in. (0°C) ⁽⁷⁾	kilogram per pascal second meter [kg/(Pa·s·m)]	1.453 22 E − 12
perm-in. (23°C) ⁽⁷⁾	kilogram per pascal second meter [kg/(Pa·s·m)]	1.459 29 E − 12
phot	lumen per meter ² (lm/m ²)	1.0* E + 04
pica (printer's)	meter (m)	4.217 518 E − 03
pint (U.S. dry)	meter ³ (m ³)	5.506 105 E − 04
pint (U.S. liquid)	meter ³ (m ³)	4.731 765 E − 04
point (printer's)	meter (m)	3.514 598* E − 04
poise (absolute viscosity)	pascal second (Pa·s)	1.0* E − 01
pound (lbm avoirdupois) ⁽⁸⁾	kilogram (kg)	4.535 924 E − 01
pound (troy or apothecary)	kilogram (kg)	3.732 417 E − 01
lbm-ft ² (moment of inertia)	kilogram meter ² (kg·m ²)	4.214 011 E − 02
lbm-in. ² (moment of inertia)	kilogram meter ² (kg·m ²)	2.926 397 E − 04
lbm/ft-hr	pascal second (Pa·s)	4.133 789 E − 04
lbm/ft-s	pascal second (Pa·s)	1.488 164 E + 00
lbm/ft ²	kilogram per meter ² (kg/m ²)	4.882 428 E + 00
lbm/ft ³	kilogram per meter ³ (kg/m ³)	1.601 846 E + 01
lbm/gal (U.K. liquid)	kilogram per meter ³ (kg/m ³)	9.977 633 E + 01
lbm/gal (U.S. liquid)	kilogram per meter ³ (kg/m ³)	1.198 264 E + 02
lbm/hr	kilogram per second (kg/s)	1.259 979 E − 04
lbm/(hp · hr) (SFC, specific fuel consumption)	kilogram per joule (kg/J)	1.689 659 E − 07
lbm/in. ³	kilogram per meter ³ (kg/m ³)	2.767 990 E + 04
lbm/min	kilogram per second (kg/s)	7.559 873 E − 03
lbm/s	kilogram per second (kg/s)	4.535 924 E − 01
lbm/yd ³	kilogram per meter ³ (kg/m ³)	5.932 764 E − 01
poundal	newton (N)	1.382 550 E − 01
poundal/ft ²	pascal (Pa)	1.488 164 E + 00
poundal-s/ft ²	pascal second (Pa·s)	1.488 164 E + 00
pound-force (lbf) ⁽⁹⁾	newton (N)	4.448 222 E + 00
lbf-ft ⁽¹⁰⁾	newton meter (N·m)	1.355 818 E + 00
lbf-ft/in. ⁽¹¹⁾	newton meter per meter [(N·m)/m]	5.337 866 E + 01
lbf-in. ⁽¹¹⁾	newton meter (N·m)	1.129 848 E − 01
lbf-in./in. ⁽¹¹⁾	newton meter per meter [(N·m)/m]	4.448 222 E + 00
lbf-s/ft ²	pascal second (Pa·s)	4.788 026 E + 01
lbf/ft	newton per meter (N/m)	1.459 390 E + 01
lbf/ft ²	pascal (Pa)	4.788 026 E + 01
lbf/in.	newton per meter (N/m)	1.751 268 E + 02
lbf/in. ² (psi)	pascal (Pa)	6.894 757 E + 03
lbf/lbm (thrust/weight [mass] ratio)	newton per kilogram (N/kg)	9.806 650 E + 00
quart (U.S. dry)	meter ³ (m ³)	1.101 221 E − 03
quart (U.S. liquid)	meter ³ (m ³)	9.463 529 E − 04
rad (radiation dose absorbed)	gray (Gy)	1.0* E − 02
rhe	1 per pascal second [1/(Pa·s)]	1.0* E + 01
rod	meter (m)	(see Footnote 1)
roentgen	coulomb per kilogram (C/kg)	2.58 E − 04
second (angle)	radian (rad)	4.848 137 E − 06
second (sidereal)	second (s)	9.972 696 E − 01
section	meter ² (m ²)	(see Footnote 1)
shake	second (s)	1.000 000* E − 08
slug	kilogram (kg)	1.459 390 E + 01
slug/(ft·s)	pascal second (Pa·s)	4.788 026 E + 01
slug/ft ³	kilogram per meter ³ (kg/m ³)	5.153 788 E + 02
statampere	ampere (A)	3.335 640 E − 10
statcoulomb	coulomb (C)	3.335 640 E − 10
statfarad	farad (F)	1.112 650 E − 12
stathenry	henry (H)	8.987 554 E + 11
statmho	siemens (S)	1.112 650 E − 12
statohm	ohm (Ω)	8.987 554 E + 11
statvolt	volt (V)	2.997 925 E + 02
stere	meter ³ (m ³)	1.0* E + 00

⁽⁷⁾Not the same dimensions as "mildarcy-foot."⁽⁸⁾The exact conversion factor is 4.535 923 7·E − 01.⁽⁹⁾The exact conversion factor is 4.448 221 615 260 5·E + 00.⁽¹⁰⁾Torque unit; see text discussion of "Torque and Bending Moment."⁽¹¹⁾Torque divided by length; see text discussion of "Torque and Bending Moment."

TABLE 1.7—ALPHABETICAL LIST OF UNITS (continued)
(symbols of SI units given in parentheses)

To Convert From	To	Multiply By**	
stilb	candela per meter ² (cd/m ²)	1.0*	E + 04
stokes (kinematic viscosity)	meter ² per second (m ² /s)	1.0*	E - 04
tablespoon	meter ³ (m ³)	1.478 676	E - 05
teaspoon	meter ³ (m ³)	4.928 922	E - 06
tex	kilogram per meter (kg/m)	1.0*	E - 06
therm	joule (J)	1.055 056	E + 08
ton (assay)	kilogram (kg)	2.916 667	E - 02
ton (long, 2,240 lbm)	kilogram (kg)	1.016 047	E + 03
ton (metric)	kilogram (kg)	1.0*	E + 03
ton (nuclear equivalent of TNT)	joule (J)	4.184	E + 09 ⁽¹²⁾
ton (refrigeration)	watt (W)	3.516 800	E + 03
ton (register)	meter ³ (m ³)	2.831 685	E + 00
ton (short, 2000 lbm)	kilogram (kg)	9.071 847	E + 02
ton (long)/yd ³	kilogram per meter ³ (kg/m ³)	1.328 939	E + 03
ton (short)/hr	kilogram per second (kg/s)	2.519 958	E - 01
ton-force (2000 lbf)	newton (N)	8.896 444	E + 03
tonne	kilogram (kg)	1.0*	E + 03
torr (mm Hg, 0°C)	pascal (Pa)	1.333 22	E + 02
township	meter ² (m ²)	(see Footnote 1)	
unit pole	weber (Wb)	1.256 637	E - 07
watthour (W-hr)	joule (J)	3.60*	E + 03
W-s	joule (J)	1.0*	E + 00
W/cm ²	watt per meter ² (W/m ²)	1.0*	E + 04
W/in. ²	watt per meter ² (W/m ²)	1.550 003	E + 03
yard	meter (m)	9.144*	E - 01
yd ²	meter ² (m ²)	8.361 274	E - 01
yd ³	meter ³ (m ³)	7.645 549	E - 01
yd ³ /min	meter ³ per second (m ³ /s)	1.274 258	E - 02
year (calendar)	second (s)	3.153 600	E + 07
year (sidereal)	second (s)	3.155 815	E + 07
year (tropical)	second (s)	3.155 693	E + 07

⁽¹²⁾Defined (not measured) value.

APPENDIX E

TABLE 1.8 — CONVERSION FACTORS FOR THE VARA*

Location	Value of Vara in Inches	Conversion Factor, Varas to Meters		Source
Argentina, Paraguay	34.12	8.666	E - 01	Ref. 16
Cadiz, Chile, Peru	33.37	8.476	E - 01	Ref. 16
California,				
except San Francisco	33.3720	8.476 49	E - 01	Ref. 16
San Francisco	33.0	8.38	E - 01	Ref. 16
Central America	33.87	8.603	E - 01	Ref. 16
Colombia	31.5	8.00	E - 01	Ref. 16
Honduras	33.0	8.38	E - 01	Ref. 16
Mexico		8.380	E - 01	Refs. 16 and 17
Portugal, Brazil	43.0	1.09	E + 00	Ref. 16
Spain, Cuba, Venezuela, Philippine Islands	33.38**	8.479	E - 01	Ref. 17
Texas				
Jan. 26, 1801, to Jan. 27, 1838	32.8748	8.350 20	E - 01	Ref. 16
Jan. 27, 1838 to June 17, 1919, for surveys of state land made for Land Office	33-1/3	8.466 667	E - 01	Ref. 16
Jan. 27, 1838 to June 17, 1919, on private surveys (unless changed to 33-1/3 in. by custom arising to dignity of law and overcoming former law)	32.8748	8.350 20	E - 01	Ref. 16
June 17, 1919, to present	33-1/3	8.466 667	E - 01	Ref. 16

*It is evident from Ref. 16 that accurate defined lengths of the vara varied significantly, according to historical date and locality used. For work requiring accurate conversions, the user should check closely into the date and location of the surveys involved, with due regard to what local practice may have been at that time and place.

**This value quoted from Webster's New International Dictionary.

TABLE 1.9—“MEMORY JOGGER”—METRIC UNITS

Customary Unit	“BallPark” Metric Values; (Do Not Use As Conversion Factors)	
acre	{ 4000	square meters
	0.4	hectare
barrel	0.16	cubic meter
British thermal unit	1000	joules
British thermal unit per pound-mass	{ 2300	joules per kilogram
	2.3	kilojoules per kilogram
calorie	4	joules
centipoise	1*	millipascal-second
centistokes	1*	square millimeter per second
darcy	1	square micrometer
degree Fahrenheit (temperature difference)	0.5	kelvin
dyne per centimeter	1*	millinewton per meter
foot	{ 30	centimeters
	0.3	meter
cubic foot (cu ft)	0.03	cubic meter
cubic foot per pound-mass (ft ³ /lbm)	0.06	cubic meter per kilogram
square foot (sq ft)	0.1	square meter
foot per minute	{ 0.3	meter per minute
	5	millimeters per second
foot-pound-force	1.4	joules
foot-pound-force per minute	0.02	watt
foot-pound-force per second	1.4	watts
horsepower	750	watts (¾ kilowatt)
horsepower, boiler	10	kilowatts
inch	2.5	centimeters
kilowatthour	3.6*	megajoules
mile	1.6	kilometers
ounce (avoirdupois)	28	grams
ounce (fluid)	30	cubic centimeters
pound-force	4.5	newtons
pound-force per square inch (pressure, psi)	7	kilopascals
pound-mass	0.5	kilogram
pound-mass per cubic foot	16	kilograms per cubic meter
	{ 260	hectares
section	2.6	million square meters
	2.6	square kilometers
ton, long (2240 pounds-mass)	1000	kilograms
ton, metric (tonne)	1000*	kilograms
ton, short	900	kilograms

*Exact equivalents

APPENDIX F

Part 2: Discussion of Metric Unit Standards*

Introduction

The standards and conventions shown in Part 1 are part of the SPE tentative standards. Table 2.1 presents nomenclature for Tables 2.2 and 2.3. Table 2.2 is a modified form of a table in API 2564 reflecting SPE recommendations. Table 2.3 shows a few units commonly used in the petroleum industry that are not shown in Table 1.7 and 2.2. The columns in these tables are based on the following.

Quantity and SI Unit. The quantity and the base or derived SI unit that describes that quantity.

Customary Unit. The unit most commonly used in expressing the quantity in English units.

SPE Preferred. The base or derived SI unit plus the approved prefix, if any, that probably will be used most

commonly to achieve convenient unit size. Any approved prefix may be used in combination with an approved SI unit without violation of these standards except where otherwise noted.

Other Allowable. A small, selected list of non SI units that are approved *temporarily* for the convenience of the English-metric transition. Use of the allowable units may be discouraged but is not prohibited. Any traditional, non-SI unit not shown is prohibited under these standards.

Conversion Factor. For certain commonly used units, a conversion factor is shown. The primary purpose in these tables is to show how the *preferred metric unit* compares in size with the *traditional unit*. An effort has been made to keep the unit sizes comparable to minimize transition difficulties.

*Prepared by John M. Campbell for the subcommittee.

A detailed summary of general conversion factors is included as Table 1.7 in Part 1 of this report.

The notation for conversion factors in Tables 2.2 and 2.3 is explained in the introduction to Table 1.7.

Fig. 2.1 shows graphically how SI units are related in a very coherent manner. Although it may not be readily apparent, this internal coherence is a primary reason for adoption of the metric system of units.

The SPE Metrication Subcommittee is endeavoring to provide SPE members with all information needed on the International System of Units and to provide tentative standards (compatible with SI coherence, decimal, and other principles) for the application of the SI system to SPE fields of interest. The tentative SPE standards are intended to reflect reasonable input from many sources, and we solicit your positive input with the assurance that all ideas will receive careful consideration.

Review of Selected Units

Certain of the quantities and units shown in Tables 2.2 and 2.3 may require clarification of usage (see also the notes preceding Tables 2.2 and 2.3).

Time

Although second(s) is the base time unit, any unit of time may be used — minute (min), hour (h), day (d), and year

(a). Note that (a) is used as the abbreviation for year (annum) instead of (yr). The use of the minute as a time unit is discouraged because of abbreviation problems. It should be used only when another time unit is absolutely inappropriate.

Date and Time Designation

The Subcommittee proposes to recommend a standard date and time designation to the American Natl. Standards Inst., as shown below. This form already has been introduced in Canada.

76 — 10 — 03 — 16 : 24 : 14
year month day hour minute second
(76-10-03-16:24:14)

The sequence is orderly and easy to remember; only needed portions of the sequence would be used — most documents would use the first three. No recommendation has been made for distinguishing the century, such as 1976 vs. 1876 vs. 2076.

Area

The hectare (ha) is allowable but its use should be confined to large areas that describe the areal extent of a por-

TABLE 2.1—NOMENCLATURE FOR TABLES 2.2 AND 2.3

Unit Symbol	Name	Quantity	Type of Unit
A	ampere	electric current	base SI unit
a	annum (year)	time	allowable (not official SI) unit
Bq	becquerel	activity (of radionuclides)	derived SI unit = 1/s
bar	bar	pressure	allowable (not official SI) unit, = 10^5 Pa
C	coulomb	quantity of electricity	derived SI unit, = 1 A·s
cd	candela	luminous intensity	base SI unit
°C	degree Celsius	temperature	derived SI unit = 1.0 K
°	degree	plane angle	allowable (not official SI) unit
d	day	time	allowable (not official SI) unit, = 24 hours
F	farad	electric capacitance	derived SI unit, = 1 A·s/V
Gy	gray	absorbed dose	derived SI unit, = J/kg
g	gram	mass	allowable (not official SI) unit, = 10^{-3} kg
H	henry	inductance	derived SI unit, = 1 V·s/A
h	hour	time	allowable (not official SI) unit, = 3.6×10^3 s
Hz	hertz	frequency	derived SI unit, = 1 cycle/s
ha	hectare	area	allowable (not official SI) unit, = 10^4 m ²
J	joule	work, energy	derived SI unit, = 1 N·m
K	kelvin	temperature	base SI unit
kg	kilogram	mass	base SI unit
kn	knot	velocity	allowable (not official SI) unit, = $5.144\,444 \times 10^{-1}$ m/s = 1.852 km/h
L	liter	volume	allowable (not official SI) unit, = 1 dm ³
lm	lumen	luminous flux	derived SI unit, = 1 cd·sr
lx	lux	illuminance	derived SI unit, = 1 lm/m ²
m	meter	length	base SI unit
min	minute	time	allowable (not official SI) unit
'	minute	plane angle	Allowable cartography (not official SI) unit
N	newton	force	derived SI unit, = 1 kg·m/s ²
naut. mile	U.S. nautical mile	length	allowable (not official SI) unit, = 1.852×10^3 m
Ω	ohm	electric resistance	derived SI unit, = 1 V/A
Pa	pascal	pressure	derived SI unit, = 1 N/m ²
rad	radian	plane angle	supplementary SI unit
S	siemens	electrical conductance	derived SI unit, = 1 A/V
s	second	time	base SI unit
"	second	plane angle	allowable cartography (not official SI) unit
sr	steradian	solid angle	supplementary SI unit
T	tesla	magnetic flux density	derived SI unit, = 1 Wb/m ²
t	tonne	mass	allowable (not official SI) unit, = 10^3 kg = 1 Mg
V	volt	electric potential	derived SI unit, = 1 W/A
W	watt	power	derived SI unit, = 1 J/s
Wb	weber	magnetic flux	derived SI unit, = 1 V·s

tion of the earth's crust (normally replacing the acre or section).

Volume

The liter is an allowable unit for small volumes only. It should be used for volumes not exceeding 100 L. Above this volume (or volume rate), cubic meters should be used. The only two prefixes allowed with the liter are "milli" and "micro."

In the U.S., the "-er" ending for meter and liter is official. The official symbol for the liter is "L." In other countries the symbol may be written as "ℓ" and spelled out with the "-re" ending (metre, litre). Since SPE is international, it is expected that members will use local conventions.

Notice that "API barrel" or simply "barrel" disappears as an allowable volume term.

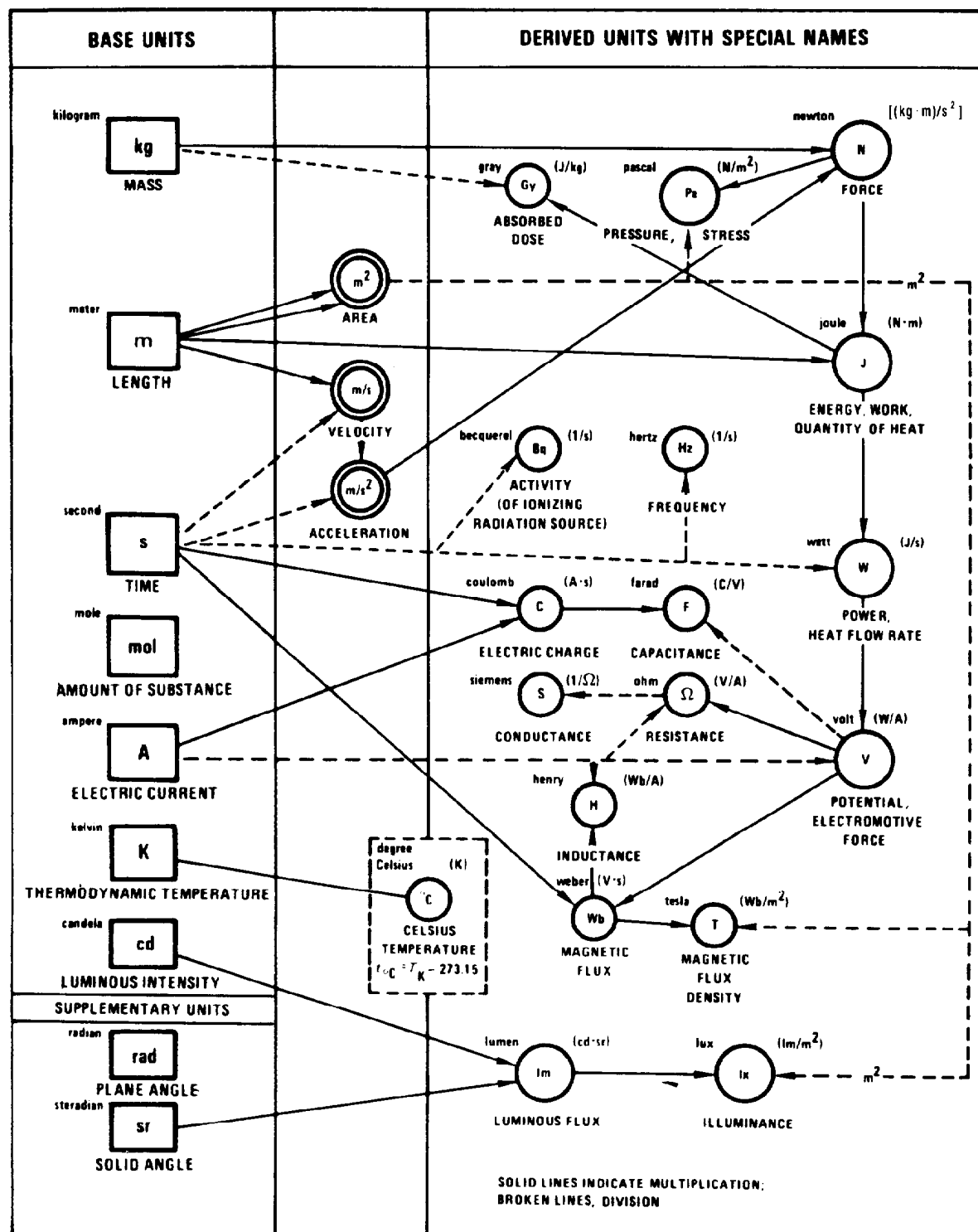


Fig. 2.1—Graphic relationships of SI units with names.

Force

Any force term will use the newton (N). Derived units involving force also require the newton. The expression of force using a mass term (like the kilogram) is absolutely forbidden under these standards.

Mass

The kilogram is the base unit, but the gram, alone or with any approved prefix, is an acceptable SI unit.

For large mass quantities the metric ton (t) may be used. Some call this "tonne." However, this spelling sometimes has been used historically to denote a regular short ton (2,000 lbm). A metric ton is also a megagram (Mg). The terms metric ton or Mg are preferred in text references.

Energy and Work

The joule (J) is the fundamental energy unit; kilojoules (kJ) or megajoules (MJ) will be used most commonly. The calorie (large or small) is no longer an acceptable unit under these standards. The kilowatthour is acceptable for a transition period but eventually should be replaced by the megajoule.

Power

The term horsepower disappears as an allowable unit. The kilowatt (kW) or megawatt (MW) will be the multiples of the fundamental watt unit used most commonly.

Pressure

The fundamental pressure unit is the pascal (Pa) but the kilopascal (kPa) is the most convenient unit. The bar (100 kPa) is an allowable unit. The pressure term kg/cm^2 is not allowable under these standards.

Viscosity

The terms poise, centipoise, stokes, and centistokes are no longer used under these standards. They are replaced by the metric units shown in Table 2.2.

Temperature

Although it is permissible to use $^{\circ}\text{C}$ in text references, it is recommended that "K" be used in graphical and tabular summaries of data.

Density

The fundamental SI unit for density is kg/m^3 . Use of this unit is encouraged. However, a unit like kg/L is permissible.

The traditional term "specific gravity" will not be used. It will be replaced by the term "relative density." API gravity disappears as a measure of relative density.

Relative Atomic Mass and Molecular Mass

The traditional terms "atomic weight" and "molecular weight" are replaced in the SI system of units by "relative atomic mass" and "relative molecular mass," respectively. See Table 1.6.

Unit Standards Under Discussion

There are some quantities for which the unit standards have not been clarified to the satisfaction of all parties and some controversy remains. These primary quantities are summarized below.

Permeability

The SPE-preferred permeability unit is the square micrometer (μm^2). One darcy (the traditional unit) equals $0.986\,923\,\mu\text{m}^2$.

The fundamental SI unit of permeability (in square meters) is defined as follows: "a permeability of one meter squared will permit a flow of $1\,\text{m}^3/\text{s}$ of fluid of $1\,\text{Pa}\cdot\text{s}$ viscosity through an area of $1\,\text{m}^2$ under a pressure gradient of $1\,\text{Pa/m}$."

The traditional terms of "darcy" and "millidarcy" have been approved as preferred units of permeability. Note 11 of Table 2.2 shows the relationships between traditional and SI units and points out that the units of the darcy and the square micrometer can be considered equivalent when high accuracy is not needed or implied.

Standard Temperature

Some reference temperature is necessary to show certain properties of materials, such as density, volume, viscosity, and energy level. Historically, the petroleum industry almost universally has used 60°F [15.56°C] as this reference temperature, and metric systems have used 0°C , 20°C , and 25°C most commonly, depending on the data and the area of specialty.

API has opted for 15°C because it is close to 60°F . ASME has used 20°C in some of its metric guides. The bulk of continental European data used for gas and oil correlations is at 0°C , although 15°C is used sometimes.

The SPE Subcommittee feels that the choice between 0°C and 15°C is arbitrary. Tentatively, a standard of 15°C has been adopted simply to conform to API standards. It may be desirable to have a flexible temperature standard for various applications.

Standard Pressure

To date, some groups have opted for a pressure reference of 101.325 kPa, which is the equivalent of 1 std atm. The Subcommittee considers this an unacceptable number. Its adoption possesses some short-term convenience advantages but condemns future generations to continual odd-number conversions to reflect the change of pressure on properties. It also violates the powers-of-10 aspect of the SI system, one of its primary advantages.

The current SPE standard is 100 kPa and should be used until further notice. It is our hope that reason will prevail and others will adopt this standard.

Gauge and Absolute Pressure

There is no provision for differentiating between gauge and absolute pressure, and actions by international bodies prohibit showing the difference by an addendum to the unit symbol. The Subcommittee recommends that gauge and absolute be shown using parentheses following p :

$$p=643\,\text{kPa}, \quad p(g)=543\,\text{kPa}$$

[p is found from $p(g)$ by adding actual barometric pressure. (100 kPa is suitable for most engineering calculations.)]

In custody transfer the standard pressure will be specified by contract. Unless there is a special reason not to do so, the standard pressure will be 100 kPa to preserve the "multiples of ten" principle of the metric system.

Standard pressure normally is defined and used as an absolute pressure. So, $p_{sc} = 100$ kPa is proper notation. Absolute pressure is implied if no (g) is added to denote gauge pressure specifically.

Standard Volumes

Cubic meters at standard reference conditions must be equated to a term with the standard "sc" subscript. For example, for a gas production rate of 1 200 000 m³/d, write

$$q_{gsc} = 1.2 \times 10^6 \text{ m}^3/\text{d} \text{ or } 1.2 \text{ (E+06) m}^3/\text{d} \\ \text{read as "1.2 million cubic meters per day."}$$

If the rate is 1200 cubic meters per day, write

$$q_{gsc} = 1.2 \times 10^3 \text{ m}^3/\text{d}.$$

For gas in place, one could write

$$G_{sc} = 11.0 \times 10^{12} \text{ m}^3.$$

Notes for Table 2.2

1. The cubem (cubic mile) is used in the measurement of very large volumes, such as the content of a sedimentary basin.
2. In surveying, navigation, etc., angles no doubt will continue to be measured with instruments that read out in degrees, minutes, and seconds and need not be converted into radians. But for calculations involving rotational energy, radians are preferred.
3. The unit of a million years is used in geochronology. The mega-annum is the preferred SI unit, but many prefer simply to use mathematical notation (i.e., $\times 10^6$).
4. This conversion factor is for an ideal gas.
5. Subsurface pressures can be measured in megapascals or as freshwater heads in meters. If the latter approach is adopted, the hydrostatic gradient becomes dimensionless.
6. Quantities listed under "Facility Throughput, Capacity" are to be used only for characterizing the size or capacity of a plant or piece of equipment. Quantities listed under "Flow Rate" are for use in design calculations.
7. This conversion factor is based on a density of 1.0 kg/dm³.
8. Seismic velocities will be expressed in km/s.
9. The interval transit time unit is used in sonic logging work.

10. See discussion of "Energy, Torque, and Bending Moment," Part 1.

11. The permeability conversions shown in Table 2.2 are for the traditional definitions of darcy and millidarcy.

In SI units, the square micrometer is the preferred unit of permeability in fluid flow through a porous medium, having the dimensions of viscosity times volume flow rate per unit area divided by pressure gradient, which simplifies to dimensions of length squared. (The *fundamental* SI unit is the square meter, defined by leaving out the factor of 10^{-12} in the equation below).

A permeability of 1 μm^2 will permit a flow of 1 m³/s of fluid of 1 Pa·s viscosity through an area of 1 m² under a pressure gradient of 10^{12} Pa/m (neglecting gravity effects):

$$1 \mu\text{m}^2 = 10^{-12} \text{ Pa} \cdot \text{s} [\text{m}^3/(\text{s} \cdot \text{m}^2)]/(\text{m}/\text{Pa}) \\ = 10^{-12} \text{ Pa} \cdot \text{s}(\text{m}/\text{s})/(\text{m}/\text{Pa}) \\ = 10^{-12} \text{ m}^2.$$

The range of values in petroleum work is best served by units of $10^{-3} \mu\text{m}^2$. The traditional millidarcy (md) is an informal name for $10^{-3} \mu\text{m}^2$, which may be used where high accuracy is not implied.

For virtually all engineering purposes, the familiar darcy and millidarcy units may be taken to be equal to 1 μm^2 and $10^{-3} \mu\text{m}^2$, respectively.

12. The ohm-meter is used in borehole geophysical devices.

13. As noted in Sec. 1, the mole is an amount of substance expressible in elementary entities as atoms, molecules, ions, electrons, and other particles or specified groups of such particles. Because the expression "kilogram mole" is inconsistent with other SI practices, we have used the abbreviation "kmol" to designate an amount of substance which contains as many kilograms (groups of molecules) as there are atoms in 0.012 kg of carbon 12 multiplied by the relative molecular mass of the substance involved. In effect, the "k" prefix is merely a convenient way to identify the type of entity and facilitate conversion from the traditional pound mole without violating SI conventions.

Notes for Table 2.3

1. The standard cubic foot (scf) and barrel (bbl) referred to are measured at 60°F and 14.696 psia; the cubic meter is measured at 15°C and 100 kPa (1 bar).
2. The kPa is the preferred SPE unit for pressure. But many are using the bar as a pressure measurement. The bar should be considered as a nonapproved name (or equivalent) for 100 kPa.
3. See discussion of "Torque and Bending Moment," Part 1.

TABLE 2.2—TABLES OF RECOMMENDED SI UNITS

Quantity and SI Unit	Customary Unit	Metric Unit		Conversion Factor* Multiply Customary Unit by Factor to Get Metric Unit		
		SPE Preferred	Other Allowable			
SPACE,** TIME						
Length	m	naut mile	km	1.852*	E + 00	
		mile	km	1.609 344*	E + 00	
		chain	m	2.011 68*	E + 01	
		link	m	2.011 68*	E - 01	
		fathom	m	1.828 8*	E + 00	
		m	m	1.0*	E + 00	
		yd	m	9.144*	E - 01	
		ft	m	3.048*	E - 01	
				cm	3.048*	E + 01
		in.	mm	2.54*	E + 01	
				cm	2.54*	E + 00
		cm	mm	1.0*	E + 01	
				cm	1.0*	E + 00
		mm	mm	1.0*	E + 00	
		mil	μm	2.54*	E + 01	
		micron (μ)	μm	1.0*	E + 00	
Length/length	m/m	ft/mi	m/km	1.893 939	E - 01	
Length/volume	m/m ³	ft/U.S. gal	m/m ³	8.051 964	E + 01	
		ft/ft ³	m/m ³	1.076 391	E + 01	
		ft/bbl	m/m ³	1.917 134	E + 00	
Length/temperature	m/K	see "Temperature, Pressure, Vacuum"				
Area	m ²	sq mile	km ²	2.589 988	E + 00	
		section	km ²	2.589 988	E + 00	
				ha	2.589 988	E + 02
		acre	m ²	4.046 856	E + 03	
				ha	4.046 856	E - 01
		ha	m ²	1.0*	E + 04	
		sq yd	m ²	8.361 274	E - 01	
		sq ft	m ²	9.290 304*	E - 02	
				cm ²	9.290 304*	E + 02
		sq in.	mm ²	6.451 6*	E + 02	
				cm ²	6.451 6*	E + 00
		cm ²	mm ²	1.0*	E + 02	
				cm ²	1.0*	E + 00
mm ²	mm ²	1.0*	E + 00			
Area/volume	m ² /m ³	ft ² /in. ³	m ² /cm ³	5.699 291	E - 03	
Area/mass	m ² /kg	cm ² /g	m ² /kg	1.0*	E - 01	
			m ² /g	1.0*	E - 04	
Volume, capacity	m ³	cubem	km ³	4.168 182	E + 00 ^{(1)†}	
		acre-ft	m ³	1.233 489	E + 03	
				ha·m	1.233 489	E - 01
		m ³	m ³	1.0*	E + 00	
		cu yd	m ³	7.645 549	E - 01	
		bbl (42 U.S. gal)	m ³	1.589 873	E - 01	
		cu ft	m ³	2.831 685	E - 02	
				dm ³	L	2.831 685
		U.K. gal	m ³	4.546 092	E - 03	
				dm ³	L	4.546 092
		U.S. gal	m ³	3.785 412	E - 03	
				dm ³	L	3.785 412
		liter	dm ³	L	1.0*	E + 00
		U.K. qt	dm ³	L	1.136 523	E + 00
		U.S. qt	dm ³	L	9.463 529	E - 01
		U.S. pt	dm ³	L	4.731 765	E - 01

*An asterisk indicates that the conversion factor is exact using the numbers shown; all subsequent numbers are zeros.

**Conversion factors for length, area, and volume (and related quantities) in Table 2.2 are based on the international foot. See Footnote 1 of Table 1.7, Part 1.

TABLE 2.2—TABLES OF RECOMMENDED SI UNITS (continued)

Quantity and SI Unit		Customary Unit	Metric Unit		Conversion Factor* Multiply Customary Unit by Factor to Get Metric Unit	
			SPE Preferred	Other Allowable		
SPACE,** TIME						
Volume, capacity	m³	U.K. fl oz	cm³		2.841 308	E + 01
		U.S. fl oz	cm³		2.957 353	E + 01
		cu in.	cm³		1.638 706	E + 01
		mL	cm³		1.0*	E + 00
Volume/length (linear displacement)	m³/m	bbl/in.	m³/m		6.259 342	E + 00
		bbl/ft	m³/m		5.216 119	E − 01
		ft³/ft	m³/m		9.290 304*	E − 02
		U.S. gal/ft	m³/m		1.241 933	E − 02
			dm³/m	L/m	1.241 933	E + 01
Volume/mass	m³/kg	see "Density, Specific Volume, Concentration, Dosage"				
Plane angle	rad	rad	rad		1.0*	E + 00
		deg (°)	rad	°	1.745 329	E − 02 ⁽²⁾
					1.0*	E + 00
		min (')	rad	'	2.908 882	E − 04 ⁽²⁾
					1.0*	E + 00
		sec (")	rad	"	4.848 137	E − 06 ⁽²⁾
					1.0*	E + 00
Solid angle	sr	sr	sr		1.0*	E + 00
Time	s	million years (MY)	Ma		1.0*	E + 00 ⁽³⁾
		yr	a		1.0*	E + 00
		wk	d		7.0*	E + 00
		d	d		1.0*	E + 00
		hr	h		1.0*	E + 00
				min	6.0*	E + 01
		min	s		6.0*	E + 01
				h	1.666 667	E − 02
				min	1.0*	E + 00
		s	s		1.0*	E + 00
millimicrosecond	ns		1.0*	E + 00		
MASS, AMOUNT OF SUBSTANCE						
Mass	kg	U.K. ton (long ton)	Mg	t	1.016 047	E + 00
		U.S. ton (short ton)	Mg	t	9.071 847	E − 01
		U.K. ton	kg		5.080 235	E + 01
		U.S. cwt	kg		4.535 924	E + 01
		kg	kg		1.0*	E + 00
		lbm	kg		4.535 924	E − 01
		oz (troy)	g		3.110 348	E + 01
		oz (av)	g		2.834 952	E + 01
		g	g		1.0*	E + 00
		grain	mg		6.479 891	E + 01
		mg	mg		1.0*	E + 00
		g	g		1.0*	E + 00
Mass/length	kg/m	see "Mechanics"				
Mass/area	kg/m²	see "Mechanics"				
Mass/volume	kg/m³	see "Density, Specific Volume, Concentration, Dosage"				
Mass/mass	kg/kg	see "Density, Specific Volume, Concentration, Dosage"				
Amount of substance	mol	lbm mol	kmol		4.535 924	E − 01
		g mol	kmol		1.0*	E − 03
		std m³ (0°C, 1 atm)	kmol		4.461 58	E − 02 ^(4 13)
		std m³ (15°C, 1 atm)	kmol		4.229 32	E − 02 ^(4 13)
		std ft³ (60°F, 1 atm)	kmol		1.195 3	E − 03 ^(4 13)

TABLE 2.2—TABLES OF RECOMMENDED SI UNITS (continued)

Quantity and SI Unit		Customary Unit	Metric Unit		Conversion Factor* Multiply Customary Unit by Factor to Get Metric Unit	
			SPE Preferred	Other Allowable		
CALORIFIC VALUE, HEAT, ENTROPY, HEAT CAPACITY						
Calorific value (mass basis)	J/kg	Btu/lbm	MJ/kg		2.326	E - 03
			kJ/kg	J/g	2.326	E + 00
				(kW·h)/kg	6.461 112	E - 04
		cal/g	kJ/kg	J/g	4.184*	E + 00
		cal/lbm	J/kg		9.224 141	E + 00
		kcal/g mol	kJ/kmol		4.184*	C + 03 ¹³
		Btu/lbm mol	MJ/kmol		2.326	E - 03 ¹³
			kJ/kmol		2.326	E + 00 ¹³
Calorific value (volume basis — solids and liquids)	J/m³	therm/U.K. gal	MJ/m³	kJ/dm³	2.320 80	E + 04
			kJ/m³		2.320 80	E + 07
				(kW·h)/dm³	6.446 660	E + 00
		Btu/U.S. gal	MJ/m³	kJ/dm³	2.787 163	E - 01
			kJ/m³		2.787 163	E + 02
				(kW·h)/m³	7.742 119	E - 02
		Btu/U.K. gal	MJ/m³	kJ/dm³	2.320 8	E - 01
			kJ/m³		2.320 8	E + 02
				(kW·h)/m³	6.446 660	E - 02
		Btu/ft³	MJ/m³	kJ/dm³	3.725 895	E - 02
			kJ/m³		3.725 895	E + 01
				(kW·h)/m³	1.034 971	E - 02
		kcal/m³	MJ/m³	kJ/dm³	4.184*	E - 03
			kJ/m³		4.184*	E + 00
		cal/mL	MJ/m³		4.184*	E + 00
		ft-lbf/U.S. gal	kJ/m³		3.581 692	E - 01
Calorific value (volume basis — gases)	J/m³	cal/mL	kJ/m³	J/dm³	4.184*	E + 03
		kcal/m³	kJ/m³	J/dm³	4.184*	E + 00
		Btu/ft³	kJ/m³	J/dm³	3.725 895	E + 01
				(kW·h)/m³	1.034 971	E - 02
Specific entropy	J/kg·K	Btu/(lbm·°R)	kJ/(kg·K)	J/(g·K)	4.186 8*	E + 00
		cal/(g·°K)	kJ/(kg·K)	J/(g·K)	4.184*	E + 00
		kcal/(kg·°C)	kJ/(kg·K)	J/(g·K)	4.184*	E + 00
Specific heat capacity (mass basis)	J/kg·K	kW·hr/(kg·°C)	kJ/(kg·K)	J/(g·K)	3.6*	E + 03
		Btu/(lbm·°F)	kJ/(kg·K)	J/(g·K)	4.186 8*	E + 00
		kcal/(kg·°C)	kJ/(kg·K)	J/(g·K)	4.184*	E + 00
Molar heat capacity	J/mol·K	Btu/(lbm mol·°F)	kJ/(kmol·K)		4.186 8*	E + 00 ¹³
		cal/(g mol·°C)	kJ/(kmol·K)		4.184*	E - 00 ¹³
TEMPERATURE, PRESSURE, VACUUM						
Temperature (absolute)	K	°R	K		5/9	
		°K	K		1.0*	E + 00
Temperature (traditional)	K	°F	°C		(°F - 32)/1.8	
		°C	°C		1.0*	E + 00
Temperature (difference)	K	°F	K	°C	5/9	E + 00
		°C	K	°C	1.0*	E + 00
Temperature/length (geothermal gradient)	K/m	°F/100 ft	mK/m		1.822 689	E + 01
Length/temperature (geothermal step)	m/K	ft/°F	m/K		5.486 4*	E - 01
Pressure	Pa	atm (760mm Hg at 0°C or 14.696 (lbf/in.²))	MPa		1.013 25*	E - 01
			kPa		1.013 25*	E + 02
				bar	1.013 25*	E + 00
		bar	MPa		1.0*	E - 01
			kPa		1.0*	E + 02
				bar	1.0*	E + 00
		at (technical atm., kgf/cm²)	MPa		9.806 65*	E - 02
			kPa		9.806 65*	E + 01
				bar	9.806 65*	E - 01

TABLE 2.2—TABLES OF RECOMMENDED SI UNITS (continued)

Quantity and SI Unit		Customary Unit	Metric Unit		Conversion Factor* Multiply Customary Unit by Factor to Get Metric Unit		
			SPE Preferred	Other Allowable			
TEMPERATURE, PRESSURE, VACUUM							
Pressure	Pa	lbf/in. ² (psi)	MPa		6.894 757	E - 03	
			kPa		6.894 757	E + 00	
				bar	6.894 757	E - 02	
				in. Hg (32°F)	kPa	3.386 38	E + 00
				in. Hg (60°F)	kPa	3.376 85	E + 00
				in. H ₂ O (39.2°F)	kPa	2.490 82	E - 01
				in. H ₂ O (60°F)	kPa	2.488 4	E - 01
				mm Hg (0°C) = torr	kPa	1.333 224	E - 01
				cm H ₂ O (4°C)	kPa	9.806 38	E - 02
				lbf/ft ² (psf)	kPa	4.788 026	E - 02
				μm Hg (0°C)	Pa	1.333 224	E - 01
				μbar	Pa	1.0*	E - 01
Vacuum, draft	Pa		dyne/cm ²	Pa	1.0*	E - 01	
			in. Hg (60°F)	kPa	3.376 85	E + 00	
			in. H ₂ O (39.2°F)	kPa	2.490 82	E - 01	
			in. H ₂ O (60°F)	kPa	2.488 4	E - 01	
			mm Hg (0°C) = torr	kPa	1.333 224	E - 01	
Liquid head	m		cm H ₂ O (4°C)	kPa	9.806 38	E - 02	
			ft	m	3.048*	E - 01	
Pressure drop/length	Pa/m		in.	mm	2.54*	E + 01	
				cm	2.54*	E + 00	
			psi/ft	kPa/m	2.262 059	E + 01	
		psi/100 ft	kPa/m	2.262 059	E - 01 ⁽⁵⁾		
DENSITY, SPECIFIC VOLUME, CONCENTRATION, DOSAGE							
Density (gases)	kg/m ³	lbm/ft ³	kg/m ³		1.601 846	E + 01	
			g/m ³		1.601 846	E + 04	
Density (liquids)	kg/m ³	lbm/U.S. gal	kg/m ³		1.198 264	E + 02	
				g/cm ³	1.198 264	E - 01	
		lbm/U.K. gal	kg/m ³		9.977 633	E + 01	
					kg/dm ³	9.977 633	E - 02
		lbm/ft ³	kg/m ³		1.601 846	E + 01	
					g/cm ³	1.601 846	E - 02
		g/cm ³	kg/m ³		1.0*	E + 03	
					kg/dm ³	1.0*	E + 00
Density (solids)	kg/m ³	°API	g/cm ³		141.5/(131.5 + °API)		
Specific volume (gases)	m ³ /kg	lbm/ft ³	kg/m ³		1.601 846	E + 01	
Specific volume (liquids)	m ³ /kg	ft ³ /lbm	m ³ /kg		6.242 796	E - 02	
			m ³ /g		6.242 796	E - 05	
		ft ³ /lbm	dm ³ /kg		6.242 796	E + 01	
Specific volume (mole basis)	m ³ /mol	U.K. gal/lbm	dm ³ /kg	cm ³ /g	1.002 242	E + 01	
		U.S. gal/lbm	dm ³ /kg	cm ³ /g	8.345 404	E + 00	
		L/g mol	m ³ /kmol		1.0*	E + 00 ¹³	
Specific volume (clay yield)	m ³ /kg	ft ³ /lbm mol	m ³ /kmol		6.242 796	E - 02 ¹³	
		bbl/U.S. ton	m ³ /t		1.752 535	E - 01	
Yield (shale distillation)	m ³ /kg	bbl/U.K. ton	m ³ /t		1.564 763	E - 01	
		bbl/U.S. ton	dm ³ /t	L/t	1.752 535	E + 02	
		bbl/U.K. ton	dm ³ /t	L/t	1.564 763	E + 02	
		U.S. gal/U.S. ton	dm ³ /t	L/t	4.172 702	E + 00	
Concentration (mass/mass)	kg/kg	U.S. gal/U.K. ton	dm ³ /t	L/t	3.725 627	E + 00	
		wt %	kg/kg		1.0*	E - 02	
			g/kg		1.0*	E + 01	
Concentration (mass/volume)	kg/m ³	wt ppm	mg/kg		1.0*	E + 00	
		lbm/bbl	kg/m ³	g/dm ³	2.853 010	E + 00	
		g/U.S. gal	kg/m ³		2.641 720	E - 01	
		g/U.K. gal	kg/m ³	g/L	2.199 692	E - 01	

TABLE 2.2—TABLES OF RECOMMENDED SI UNITS (continued)

Quantity and SI Unit	Customary Unit	Metric Unit		Conversion Factor* Multiply Customary Unit by Factor to Get Metric Unit		
		SPE Preferred	Other Allowable			
DENSITY, SPECIFIC VOLUME, CONCENTRATION, DOSAGE						
Concentration (mass/volume)	kg/m³	lbm/1000 U.S. gal	g/m³	mg/dm³	1.198 264 E + 02	
		lbm/1000 U.K. gal	g/m³	mg/dm³	9.977 633 E + 01	
		grains/U.S. gal	g/m³	mg/dm³	1.711 806 E + 01	
		grains/ft³	mg/m³		2.288 352 E + 03	
		lbm/1000 bbl	g/m³	mg/dm³	2.853 010 E + 00	
		mg/U.S. gal	g/m³	mg/dm³	2.641 720 E - 01	
		grains/100 ft³	mg/m³		2.288 352 E + 01	
Concentration (volume/volume)	m³/m³	bbl/bbl	m³/m³		1.0*	E + 00
		ft³/ft³	m³/m³		1.0*	E + 00
		bbl/acre-ft	m³/m³		1.288 923	E - 04
				m³/ha-m	1.288 923	E + 00
		vol %	m³/m³		1.0*	E - 02
		U.K. gal/ft³	dm³/m³	L/m³	1.605 437	E + 02
		U.S. gal/ft³	dm³/m³	L/m³	1.336 806	E + 02
		mL/U.S. gal	dm³/m³	L/m³	2.641 720	E - 01
		mL/U.K. gal	dm³/m³	L/m³	2.199 692	E - 01
		vol ppm	cm³/m³		1.0*	E + 00
			dm³/m³	L/m³	1.0*	E - 03
		U.K. gal/1000 bbl	cm³/m³		2.859 406	E + 01
		U.S. gal/1000 bbl	cm³/m³		2.380 952	E + 01
		U.K. pt/1000 bbl	cm³/m³		3.574 253	E + 00
Concentration (mole/volume)	mol/m³	lbm mol/U.S. gal	kmol/m³		1.198 264 E + 02	
		lbm mol/U.K. gal	kmol/m³		9.977 633 E + 01	
		lbm mol/ft³	kmol/m³		1.601 846 E + 01	
		std ft³ (60°F, 1 atm)/bbl	kmol/m³		7.518 18 E - 03	
Concentration (volume/mole)	m³/mol	U.S. gal/1000 std ft³ (60°F/60°F)	dm³/kmol	L/kmol	3.166 93 E + 00	
		bbl/million std ft³ (60°F/60°F)	dm³/kmol	L/kmol	1.330 11 E - 01	
FACILITY THROUGHPUT, CAPACITY						
Throughput (mass basis)	kg/s	million lbm/yr	t/a	Mg/a	4.535 924 E + 02	
		U.K. ton/yr	t/a	Mg/a	1.016 047 E + 00	
		U.S. ton/yr	t/a	Mg/a	9.071 847 E - 01	
		U.K. ton/D	t/d	Mg/d	1.016 047 E + 00	
				t/h, Mg/h	4.233 529 E - 02	
		U.S. ton/D	t/d		9.071 847 E - 01	
				t/h, Mg/h	3.779 936 E - 02	
		U.K. ton/hr	t/h	Mg/h	1.016 047 E + 00	
		U.S. ton/hr	t/h	Mg/h	9.071 847 E - 01	
		lbm/hr	kg/h		4.535 924 E - 01	
Throughput (volume basis)	m³/s	bbl/D	t/a		5.803 036 E + 01 (7)	
				m³/d	1.589 873 E - 01	
					6.624 471 E - 03	
		ft³/D	m³/h		1.179 869 E - 03	
				m³/d	2.831 685 E - 02	
		bbl/hr	m³/h		1.589 873 E - 01	
		ft³/h	m³/h		2.831 685 E - 02	
		U.K. gal/hr	m³/h		4.546 092 E - 03	
				L/s	1.262 803 E - 03	
		U.S. gal/hr	m³/h		3.785 412 E - 03	
				L/s	1.051 503 E - 03	
		U.K. gal/min	m³/h		2.727 655 E - 01	
				L/s	7.576 819 E - 02	
		U.S. gal/min	m³/h		2.271 247 E - 01	
				L/s	6.309 020 E - 02	

TABLE 2.2—TABLES OF RECOMMENDED SI UNITS (continued)

Quantity and SI Unit	Customary Unit	Metric Unit		Conversion Factor* Multiply Customary Unit by Factor to Get Metric Unit			
		SPE Preferred	Other Allowable				
FACILITY THROUGHPUT, CAPACITY							
Throughput (mole basis)	mol/s	lbm mol/hr	kmol/h	4.535 924	E – 01		
			kmol/s	1.259 979	E – 04		
FLOW RATE							
Pipeline capacity	m ³ /m	bbl/mile	m ³ /km	9.879 013	E – 02		
Flow rate (mass basis)	kg/s	U.K. ton/min	kg/s	1.693 412	E + 01		
		U.S. ton/min	kg/s	1.511 974	E + 01		
		U.K. ton/hr	kg/s	2.822 353	E – 01		
		U.S. ton/hr	kg/s	2.519 958	E – 01		
		U.K. ton/D	kg/s	1.175 980	E – 02		
		U.S. ton/D	kg/s	1.049 982	E – 02		
		million lbm/yr	kg/s	5.249 912	E + 00		
		U.K. ton/yr	kg/s	3.221 864	E – 05		
		U.S. ton/yr	kg/s	2.876 664	E – 05		
		lbm/s	kg/s	4.535 924	E – 01		
		lbm/min	kg/s	7.559 873	E – 03		
		lbm/hr	kg/s	1.259 979	E – 04		
Flow rate (volume basis)	m ³ /s	bbl/D	m ³ /d	1.589 873	E – 01		
			L/s	1.840 131	E – 03		
		ft ³ /D	m ³ /d	2.831 685	E – 02		
			L/s	3.277 413	E – 04		
		bbl/hr	m ³ /s	4.416 314	E – 05		
			L/s	4.416 314	E – 02		
		ft ³ /hr	m ³ /s	7.865 791	E – 06		
			L/s	7.865 791	E – 03		
		U.K. gal/hr	dm ³ /s	1.262 803	E – 03		
		U.S. gal/hr	dm ³ /s	1.051 503	E – 03		
		U.K. gal/min	dm ³ /s	7.576 820	E – 02		
		U.S. gal/min	dm ³ /s	6.309 020	E – 02		
		ft ³ /min	dm ³ /s	4.719 474	E – 01		
		ft ³ /s	dm ³ /s	2.831 685	E + 01		
		Flow rate (mole basis)	mol/s	lbm mol/s	kmol/s	4.535 924	E – 01 ¹³
				lbm mol/hr	kmol/s	1.259 979	E – 04 ¹³
million scf/D	kmol/s			1.383 449	E – 02 ¹³		
Flow rate/length (mass basis)	kg/s·m	lbm/(s·ft)	kg/(s·m)	1.488 164	E + 00		
		lbm/(hr·ft)	kg/(s·m)	4.133 789	E – 04		
Flow rate/length (volume basis)	m ² /s	U.K. gal/(min·ft)	m ² /s	m ³ /(s·m)	2.485 833	E – 04	
		U.S. gal/(min·ft)	m ² /s	m ³ /(s·m)	2.069 888	E – 04	
		U.K. gal/(hr·in.)	m ² /s	m ³ /(s·m)	4.971 667	E – 05	
		U.S. gal/(hr·in.)	m ² /s	m ³ /(s·m)	4.139 776	E – 05	
		U.K. gal/(hr·ft)	m ² /s	m ³ /(s·m)	4.143 055	E – 06	
		U.S. gal/(hr·ft)	m ² /s	m ³ /(s·m)	3.449 814	E – 06	
Flow rate/area (mass basis)	kg/s·m ²	lbm/(s·ft ²)	kg/s·m ²	4.882 428	E + 00		
		lbm/(hr·ft ²)	kg/s·m ²	1.356 230	E – 03		
Flow rate/area (volume basis)	m/s	ft ³ /(s·ft ²)	m/s	m ³ /(s·m ²)	3.048*	E – 01	
		ft ³ /(min·ft ²)	m/s	m ³ /(s·m ²)	5.08*	E – 03	
		U.K. gal/(hr·in. ²)	m/s	m ³ /(s·m ²)	1.957 349	E – 03	
		U.S. gal/(hr·in. ²)	m/s	m ³ /(s·m ²)	1.629 833	E – 03	
		U.K. gal/(min·ft ²)	m/s	m ³ /(s·m ²)	8.155 621	E – 04	
		U.S. gal/(min·ft ²)	m/s	m ³ /(s·m ²)	6.790 972	E – 04	
		U.K. gal/(hr·ft ²)	m/s	m ³ /(s·m ²)	1.359 270	E – 05	
		U.S. gal/(hr·ft ²)	m/s	m ³ /(s·m ²)	1.131 829	E – 05	
Flow rate/pressure drop (productivity index)	m ³ /s·Pa	bbl/(D·psi)	m ³ /(d·kPa)	2.305 916	E – 02		

TABLE 2.2—TABLES OF RECOMMENDED SI UNITS (continued)

Quantity and SI Unit		Customary Unit	Metric Unit		Conversion Factor* Multiply Customary Unit by Factor to Get Metric Unit
			SPE Preferred	Other Allowable	
ENERGY, WORK, POWER					
Energy, work	J	quad	MJ		1.055 056 E + 12
			TJ		1.055 056 E + 06
			EJ		1.055 056 E + 00
				MW-h	2.930 711 E + 08
				GW-h	2.930 711 E + 05
				TW-h	2.930 711 E + 02
		therm	MJ		1.055 056 E + 02
			kJ		1.055 056 E + 05
				kW-h	2.930 711 E + 01
		U.S. tonf-mile	MJ		1.431 744 E + 01
		hp-hr	MJ		2.684 520 E + 00
			kJ		2.684 520 E + 03
				kW-h	7.456 999 E - 01
		ch-hr or CV-hr	MJ		2.647 796 E + 00
			Kj		2.647 796 E + 03
				kW-h	7.354 99 E - 01
		kW-hr	MJ		3.6* E + 00
			kJ		3.6* E + 03
		Chu	kJ		1.899 101 E + 00
				kW-h	5.275 280 E - 04
Btu	kJ		1.055 056 E + 00		
			kW-h	2.930 711 E - 04	
kcal	kJ		4.184* E + 00		
cal	kJ		4.184* E - 03		
ft-lbf	kJ		1.355 818 E - 03		
lbf-ft	kJ		1.355 818 E - 03		
J	kJ		1.0* E - 03		
lbf-ft ² /s ²	kJ		4.214 011 E - 05		
erg	J		1.0* E - 07		
Impact energy	J	kgf-m	J	9.806 650* E + 00	
		lbf-ft	J	1.355 818 E + 00	
Work/length	J/m	U.S. tonf-mile/ft	MJ/m	4.697 322 E + 01	
Surface energy	J/m ²	erg/cm ²	mJ/m ²	1.0* E + 00	
Specific impact energy	J/m ²	kgf-m/cm ²	J/cm ²	9.806 650* E - 00	
		lbf-ft/in. ²	J/cm ²	2.101 522 E - 01	
Power	W	quad/yr	MJ/a		1.055 056 E + 12
			TJ/a		1.055 056 E + 06
			EJ/a		1.055 056 E + 00
				TW	3.170 979 E - 27
				GW	3.170 979 E - 24
		million Btu/hr	MW		2.930 711 E - 01
		ton of refrigeration	kW		3.516 853 E + 00
		Btu/s	kW		1.055 056 E + 00
		kW	kW		1.0* E + 00
		hydraulic horse-power — hhp	kW		7.460 43 E - 01
		hp (electric)	kW		7.46* E - 01
		hp (550 ft-lbf/s)	kW		7.456 999 E - 01
		ch or CV	kW		7.354 99 E - 01
		Btu/min	kW		1.758 427 E - 02
		ft-lbf/s	kW		1.355 818 E - 03
		kcal/hr	W		1.162 222 E + 00
		Btu/hr	W		2.930 711 E - 01
		ft-lbf/min	W		2.259 697 E - 02
Power/area	W/m ²	Btu/s-ft ²	kW/m ²	1.135 653 E + 01	
		cal/hr-cm ²	kW/m ²	1.162 222 E - 02	
		Btu/hr-ft ²	kW/m ²	3.154 591 E - 03	

TABLE 2.2—TABLES OF RECOMMENDED SI UNITS (continued)

Quantity and SI Unit		Customary Unit	Metric Unit		Conversion Factor* Multiply Customary Unit by Factor to Get Metric Unit	
			SPE Preferred	Other Allowable		
ENERGY, WORK, POWER						
Heat flow unit — hfu (geothermics)		μcal/s·cm²	mW/m²		4.184*	E + 01
Heat release rate, mixing power	W/m³	hp/ft³	kW/m³		2.633 414	E + 01
		cal/(hr·cm³)	kW/m³		1.162 222	E + 00
		Btu/(s·ft³)	kW/m³		3.725 895	E + 01
		Btu/(hr·ft³)	kW/m³		1.034 971	E − 02
Heat generation unit — hgu (radioactive rocks)		cal/(s·cm³)	μW/m³		4.184*	E + 12
Cooling duty (machinery)	W/W	Btu/(bhp·hr)	W/kW		3.930 148	E − 01
Specific fuel consumption (mass basis)	kg/J	lbm/(hp·hr)	mg/J	kg/MJ kg/(kW·h)	1.689 659	E − 01
					6.082 774	E − 01
Specific fuel consumption (volume basis)	m³/J	m³/(kW·hr)	dm³/MJ	mm³/J dm³/(kW·h)	2.777 778	E + 02
					1.0*	E + 03
		U.S. gal/(hp·hr)	dm³/MJ	mm³/J dm³/(kW·h)	1.410 089	E + 00
					5.076 321	E + 00
U.K. pt/(hp·hr)	dm³/MJ	mm³/J dm³/(kW·h)	2.116 809	E − 01		
			7.620 512	E − 01		
Fuel consumption (automotive)	m³/m	U.K. gal/mile	dm³/100 km	L/100 km	2.824 811	E + 02
		U.S. gal/mile	dm³/100 km	L/100 km	2.352 146	E + 02
		mile/U.S. gal	km/dm³	km/L	4.251 437	E − 01
		mile/U.K. gal	km/dm³	km/L	3.540 060	E − 01
MECHANICS						
Velocity (linear), speed	m/s	knot	km/h		1.852*	E + 00
		mile/hr	km/h		1.609 344*	E + 00
		m/s	m/s		1.0*	E + 00
		ft/s	m/s		3.048*	E − 01
				cm/s	3.048*	E + 01
				m/ms	3.048*	E − 04 ⁽⁸⁾
		ft/min	m/s		5.08*	E − 03
				cm/s	5.08*	E − 01
		ft/hr	mm/s		8.466 667	E − 02
				cm/s	8.466 667	E − 03
		ft/D	mm/s		3.527 778	E − 03
				m/d	3.048*	E − 01
		in./s	mm/s		2.54*	E + 01
				cm/s	2.54*	E + 00
in./min	mm/s		4.233 333	E − 01		
		cm/s	4.233 333	E − 02		
Velocity (angular)	rad/s	rev/min	rad/s		1.047 198	E − 01
		rev/s	rad/s		6.283 185	E + 00
		degree/min	rad/s		2.908 882	E − 04
Interval transit time	s/m	s/ft	s/m	μs/m	3.280 840	E + 00 ⁽⁹⁾
Corrosion rate	m/s	in./yr (ipy)	mm/a		2.54*	E + 01
		mil/yr	mm/a		2.54*	E − 02
Rotational frequency	rev/s	rev/s	rev/s		1.0*	E + 00
		rev/min	rev/s		1.666 667	E − 02
		rev/min	rad/s		1.047 198	E − 01
Acceleration (linear)	m/s²	ft/s²	m/s²		3.048*	E − 01
				cm/s²	3.048*	E + 01
		gal(cm/s²)	m/s²		1.0*	E − 02
Acceleration (rotational)	rad/s²	rad/s²	rad/s²		1.0*	E + 00
		rpm/s	rad/s²		1.047 198	E − 01
Momentum	kg·m/s	lbm·ft/s	kg·m/s		1.382 550	E − 01

TABLE 2.2—TABLES OF RECOMMENDED SI UNITS (continued)

Quantity and SI Unit	Customary Unit	Metric Unit		Conversion Factor* Multiply Customary Unit by Factor to Get Metric Unit	
		SPE Preferred	Other Allowable		
MECHANICS					
Force	N	U.K. tonf	kN	9.964 016	E + 00
		U.S. tonf	kN	8.896 443	E + 00
		kgf (kp)	N	9.806 650*	E + 00
		lbf	N	4.448 222	E + 00
		N	N	1.0*	E + 00
		pdl	mN	1.382 550	E + 02
		dyne	mN	1.0*	E - 02
Bending moment, torque	N·m	U.S. tonf·ft	kN·m	2.711 636	E + 00 ⁽¹⁰⁾
		kgf·m	N·m	9.806 650*	E + 00 ⁽¹⁰⁾
		lbf·ft	N·m	1.355 818	E + 00 ⁽¹⁰⁾
		lbf·in.	N·m	1.129 848	E - 01 ⁽¹⁰⁾
		pdl·ft	N·m	4.214 011	E - 02 ⁽¹⁰⁾
Bending moment/length	N·m/m	(lbf·ft)/in.	(N·m)/m	5.337 866	E + 01 ⁽¹⁰⁾
		(kgf·m)/m	(N·m)/m	9.806 650*	E + 00 ⁽¹⁰⁾
		(lbf·in.)/in.	(N·m)/m	4.448 222	E + 00 ⁽¹⁰⁾
Elastic moduli (Young's, Shear bulk)	Pa	lbf/in. ²	GPa	6.894 757	E - 06
Moment of inertia	kg·m ²	lbm·ft ²	kg·m ²	4.214 011	E - 02
Moment of section	m ⁴	in. ⁴	cm ⁴	4.162 314	E + 01
Section modulus	m ³	cu in.	cm ³	1.638 706	E + 01
		cu ft	cm ³	1.638 706	E + 04
			mm ³	2.831 685	E + 04
			m ³	2.831 685	E - 02
Stress	Pa	U.S. tonf/in. ²	MPa	N/mm ²	1.378 951 E + 01
		kgf/mm ²	MPa	N/mm ²	9.806 650* E + 00
		U.S. tonf/ft ²	MPa	N/mm ²	9.576 052 E - 02
		lbf/in. ² (psi)	MPa	N/mm ²	6.894 757 E - 03
		lbf/ft ² (psf)	kPa		4.788 026 E - 02
		dyne/cm ²	Pa		1.0* E - 01
Yield point, gel strength (drilling fluid)		lbf/100 ft ²	Pa	4.788 026	E - 01
Mass/length	kg/m	lbm/ft	kg/m	1.488 164	E + 00
Mass/area structural loading, bearing capacity (mass basis)	kg/m ²	U.S. ton/ft ²	Mg/m ²	9.764 855	E + 00
		lbm/ft ²	kg/m ²	4.882 428	E + 00
Coefficient of thermal expansion	m/(m·K)	in./(in.·°F)	mm/(mm·K)	5.555 556	E - 01
TRANSPORT PROPERTIES					
Diffusivity	m ² /s	ft ² /s	mm ² /s	9.290 304*	E + 04
		cm ² /s	mm ² /s	1.0*	E + 02
		ft ² /hr	mm ² /s	2.580 64*	E + 01
Thermal resistance	(k·m ²)/W	(°C·m ² ·hr)/kcal	(K·m ²)/kW	8.604 208	E + 02
		(°F·ft ² ·hr)/Btu	(K·m ²)/kW	1.761 102	E + 02
Heat flux	W/m ²	Btu/(hr·ft ²)	kW/m ²	3.154 591	E - 03
Thermal conductivity	W/(m·K)	(cal/s·cm ² ·°C)/cm	W/(m·K)	4.184*	E + 02
		Btu/(hr·ft ² ·°F/ft)	W/(m·K)	1.730 735	E + 00
			kJ·m/(h·m ² ·K)	6.230 646	E + 00
		kcal/(hr·m ² ·°C/cm)	W/(m·K)	1.162 222	E + 00
		Btu/(hr·ft ² ·°F/in.)	W/(m·K)	1.442 279	E - 01
		cal/(hr·cm ² ·°C/cm)	W/(m·K)	1.162 222	E - 01

TABLE 2.2—TABLES OF RECOMMENDED SI UNITS (continued)

Quantity and SI Unit		Customary Unit	Metric Unit		Conversion Factor* Multiply Customary Unit by Factor to Get Metric Unit	
			SPE Preferred	Other Allowable		
TRANSPORT PROPERTIES						
Heat transfer coefficient	W/(m²·K)	cal/(s·cm²·°C)	kW/(m²·K)		4.184*	E + 01
		Btu/(s·ft²·°F)	kW/(m²·K)		2.044 175	E + 01
		cal/(hr·cm²·°C)	kW/(m²·K)		1.162 222	E - 02
		Btu/(hr·ft²·°F)	kW/(m²·K)		5.678 263	E - 03
				kJ/(h·m²·K)	2.044 175	E + 01
		Btu/(hr·ft²·°R)	kW/(m²·K)		5.678 263	E - 03
Volumetric heat transfer coefficient	W/(m³·K)	kcal/(hr·m²·°C)	kW/(m²·K)		1.162 222	E - 03
		Btu/(s·ft³·°F)	kW/(m³·K)		6.706 611	E + 01
		Btu/(hr·ft³·°F)	kW/(m³·K)		1.862 947	E - 02
Surface tension	N/m	dyne/cm	mN/m		1.0*	E + 00
Viscosity (dynamic)	Pa·s	(lbf·s)/in.²	Pa·s	(N·s)/m²	6.894 757	E + 03
		(lbf·s)/ft²	Pa·s	(N·s)/m²	4.788 026	E + 01
		(kgf·s)/m²	Pa·s	(N·s)/m²	9.806 650*	E + 00
		lbm/(ft·s)	Pa·s	(N·s)/m²	1.488 164	E + 00
		(dyne·s)/cm²	Pa·s	(N·s)/m²	1.0*	E - 01
		cp	Pa·s	(N·s)/m²	1.0*	E - 03
		lbm/(ft·hr)	Pa·s	(N·s)/m²	4.133 789	E - 04
Viscosity (kinematic)	m²/s	ft²/s	mm²/s		9.290 304*	E + 04
		in.²/s	mm²/s		6.451 6*	E + 02
		m²/hr	mm²/s		2.777 778	E + 02
		cm²/s	mm²/s		1.0*	E + 02
		ft²/hr	mm²/s		2.580 64*	E + 01
		cSt	mm²/s		1.0*	E + 00
Permeability	m²	darcy	μm²		9.869 233	E - 01 ⁽¹¹⁾
		millidarcy	μm²		9.869 233	E - 04 ⁽¹¹⁾
				10 ⁻³ μm²	9.869 233	E - 01 ⁽¹¹⁾
ELECTRICITY, MAGNETISM						
Admittance	S	S	S		1.0*	E + 00
Capacitance	F	μF	μF		1.0*	E + 00
Capacity, storage battery	C	A·hr	kC		3.6*	E + 00
Charge density	C/m³	C/mm³	C/mm³		1.0*	E + 00
Conductance	S	S	S		1.0*	E + 00
		Ω (mho)	S		1.0*	E + 00
Conductivity	S/m	S/m	S/m		1.0*	E + 00
		Ω /m	S/m		1.0*	E + 00
		m Ω /m	mS/m		1.0*	E + 00
Current density	A/m²	A/mm²	A/mm²		1.0*	E + 00
Displacement	C/m²	C/cm²	C/cm²		1.0*	E + 00
Electric charge	C	C	C		1.0*	E + 00
Electric current	A	A	A		1.0*	E + 00
Electric dipole moment	C·m	C·m	C·m		1.0*	E + 00
Electric field strength	V/m	V/m	V/m		1.0*	E + 00
Electric flux	C	C	C		1.0*	E + 00
Electric polarization	C/m²	C/cm²	C/cm²		1.0*	E + 00
Electric potential	V	V	V		1.0*	E + 00
		mV	mV		1.0*	E + 00
Electromagnetic moment	A·m²	A·m²	A·m²		1.0*	E + 00
Electromotive force	V	V	V		1.0*	E + 00
Flux of displacement	C	C	C		1.0*	E + 00

TABLE 2.2—TABLES OF RECOMMENDED SI UNITS (continued)

Quantity and SI Unit	Customary Unit	Metric Unit		Conversion Factor* Multiply Customary Unit by Factor to Get Metric Unit	
		SPE Preferred	Other Allowable		
ELECTRICITY, MAGNETISM					
Frequency	Hz	cycles/s	Hz	1.0*	E + 00
Impedance	Ω	Ω	Ω	1.0*	E + 00
Interval transit time	s/m	μs/ft	μs/m	3.280 840	E + 00
Linear current density	A/m	A/mm	A/mm	1.0*	E + 00
Magnetic dipole moment	Wb·m	Wb·m	Wb·m	1.0*	E + 00
Magnetic field strength	A/m	A/mm	A/mm	1.0*	E + 00
		oersted	A/m	7.957 747	E + 01
		gamma	A/m	7.957 747	E − 04
Magnetic flux	Wb	mWb	mWb	1.0*	E + 00
Magnetic flux density	T	mT	mT	1.0*	E + 00
		gauss	T	1.0*	E − 04
Magnetic induction	T	mT	mT	1.0*	E + 00
Magnetic moment	A·m ²	A·m ²	A·m ²	1.0*	E + 00
Magnetic polarization	T	mT	mT	1.0*	E + 00
Magnetic potential difference	A	A	A	1.0*	E + 00
Magnetic vector potential	Wb/m	Wb/mm	Wb/mm	1	
Magnetization	A/m	A/mm	A/mm	1	
Modulus of admittance	S	S	S	1	
Modulus of impedance	Ω	Ω	Ω	1	
Mutual inductance	H	H	H	1	
Permeability	H/m	μH/m	μH/m	1	
Permeance	H	H	H	1	
Permittivity	F/m	μF/m	μF/m	1	
Potential difference	V	V	V	1	
Quantity of electricity	C	C	C	1	
Reactance	Ω	Ω	Ω	1	
Reluctance	H ^{−1}	H ^{−1}	H ^{−1}	1	
Resistance	Ω	Ω	Ω	1	
Resistivity	Ω·m	Ω·cm	Ω·cm	1	
		Ω·m	Ω·m	1	(12)
Self inductance	H	mH	mH	1	
Surface density of charge	C/m ²	mC/m ²	mC/m ²	1	
Susceptance	S	S	S	1	
Volume density of charge	C/m ³	C/mm ³	C/mm ³	1	
ACOUSTICS, LIGHT, RADIATION					
Absorbed dose	Gy	rad	Gy	1.0*	E − 02
Acoustical energy	J	J	J	1	
Acoustical intensity	W/m ²	W/cm ²	W/m ²	1.0*	E + 04
Acoustical power	W	W	W	1	
Sound pressure	N/m ²	N/m ²	N/m ²	1	
Illuminance	lx	footcandle	lx	1.076 391	E + 01
Illumination	lx	footcandle	lx	1.076 391	E + 01
Irradiance	W/m ²	W/m ²	W/m ²	1	
Light exposure	lx·s	footcandle·s	lx·s	1.076 391	E + 01
Luminance	cd/m ²	cd/m ²	cd/m ²	1	
Luminous efficacy	lm/W	lm/W	lm/W	1	

TABLE 2.2—TABLES OF RECOMMENDED SI UNITS (continued)

Quantity and SI Unit		Customary Unit	Metric Unit		Conversion Factor* Multiply Customary Unit by Factor to Get Metric Unit	
			SPE Preferred	Other Allowable		
ACOUSTICS, LIGHT, RADIATION						
Luminous exitance	lm/m ²	lm/m ²	lm/m ²		1	
Luminous flux	lm	lm	lm		1	
Luminous intensity	cd	cd	cd		1	
Quantity of light	l ^u ·m·s	talbot	l ^u ·m·s		1.0*	E + 00
Radiance	W/(m ² ·sr)	W/(m ² ·sr)	W/(m ² ·sr)		1	
Radiant energy	J	J	J		1	
Radiant flux	W	W	W		1	
Radiant intensity	W/sr	W/sr	W/sr		1	
Radiant power	W	W	W		1	
Wave length	m	Å	nm		1.0*	E - 01
Capture unit	m ⁻¹	10 ⁻³ cm ⁻¹	m ⁻¹		1.0*	E + 01
				10 ⁻³ cm ⁻¹	1	
Radioactivity	curie	m ⁻¹	m ⁻¹		1	
			Bq		3.7*	E + 10

TABLE 2.3—SOME ADDITIONAL APPLICATION STANDARDS

Quantity and SI Unit		Customary Unit	Metric Unit		Conversion Factor* Multiply Customary Unit by Factor to Get Metric Unit	
			SPE Preferred	Other Allowable		
Capillary pressure	Pa	ft (fluid)	m (fluid)		3.048*	E - 01
Compressibility of reservoir fluid	Pa ⁻¹	psi ⁻¹	Pa ⁻¹		1.450 377	E - 04
				kPa ⁻¹	1.450 377	E - 01
Corrosion allowance	m	in.	mm		2.54*	E + 01
Corrosion rate	m/s	mil/yr (mpy)	mm/a		2.54*	E - 02
Differential orifice pressure	Pa	in. H ₂ O (at 60°F)	kPa		2.488 4	E - 01
				cm H ₂ O	2.54*	E + 00
Gas-oil ratio	m ³ /m ³	scf/bbl	"standard" m ³ /m ³		1.801 175	E - 01 ^{(1)**}
Gas rate	m ³ /s	scf/D	"standard" m ³ /d		2.863 640	E - 02 ⁽¹⁾
Geologic time	s	yr	Ma			
Head (fluid mechanics)	m	ft	m		3.048*	E - 01
				cm	3.048*	E + 01
Heat exchange rate	W	Btu/hr	kW		2.930 711	E - 04
				kJ/h	1.055 056	E + 00
Mobility	m ² /Pa·s	d/cp	μm ² /mPa·s		9.869 233	E - 01
				μm ² /Pa·s	9.869 233	E + 02
Net pay thickness	m	ft	m		3.048*	E - 01
Oil rate	m ³ /s	bbl/D	m ³ /d		1.589 873	E - 01
		short ton/yr	Mg/a	t/a	9.071 847	E - 01
Particle size	m	micron	μm		1.0*	
Permeability-thickness	m ³	md-ft	md-m	μm ² ·m	3.008 142	E - 04
Pipe diameter (actual)	m	in.	cm		2.54*	E + 00
				mm	2.54*	E + 01
Pressure buildup per cycle	Pa	psi	kPa		6.894 757	E + 00 ⁽²⁾
Productivity index	m ³ /Pa·s	bbl/(psi-D)	m ³ /(kPa-d)		2.305 916	E - 02 ⁽²⁾
Pumping rate	m ³ /s	U.S. gal/min	m ³ /h		2.271 247	E - 01
				L/s	6.309 020	E - 02
Revolutions per minute	rad/s	rpm	rad/s		1.047 198	E - 01
				rad/m	6.283 185	E + 00
Recovery/unit volume (oil)	m ³ /m ³	bbl/(acre-ft)	m ³ /m ³		1.288 931	E - 04
				m ³ /ha·m	1.288 931	E + 00
Reservoir area	m ²	sq mile	km ²		2.589 988	E + 00
		acre		ha	4.046 856	E - 01
Reservoir volume	m ³	acre-ft	m ³		1.233 482	E + 03
				ha·m	1.233 482	E - 01
Specific productivity index	m ³ /Pa·s·m	bbl/(D-psi-ft)	m ³ /(kPa-d·m)		7.565 341	E - 02 ⁽²⁾
Surface or interfacial tension in reservoir capillaries	N/m	dyne/cm	mN/m		1.0*	E + 00
Torque	N·m	lbf-ft	N·m		1.355 818	E + 00 ⁽³⁾
Velocity (fluid flow)	m/s	ft/s	m/s		3.048*	E - 01
Vessel diameter	m	in.	cm		2.54*	E + 00
		ft	m		3.048*	E - 01

*An asterisk indicates the conversion factor is exact using the numbers shown; all subsequent numbers are zeros.

**See Notes 1 through 3 on page 58-25.

TABLE 2.4—FAHRENHEIT—CELSIUS TEMPERATURE CONVERSION CHART

-459.67 to -19		-18 to 53		54 to 350		360 to 1070		1080 to 1790		1800 to 3000	
(°C)	(°F)	(°C)	(°F)	(°C)	(°F)	(°C)	(°F)	(°C)	(°F)	(°C)	(°F)
-273.15	-459.67	-27.78	-18.0	12.2	54.0	187.2	360.0	582.2	1,080.0	982.2	1,800.0
-267.78	-450.0	-27.23	-17.1	12.8	55.0	187.8	370.0	587.8	1,090.0	987.8	1,810.0
-262.22	-440.0	-26.67	-16.2	13.3	56.0	193.3	380.0	593.3	1,100.0	993.3	1,820.0
-256.67	-430.0	-26.12	-15.3	13.9	57.0	198.9	390.0	598.9	1,110.0	998.9	1,830.0
-251.11	-420.0	-25.56	-14.4	14.4	58.0	204.4	400.0	604.4	1,120.0	1,004.4	1,840.0
-245.56	-410.0	-25.00	-13.5	15.0	59.0	210.0	410.0	610.0	1,130.0	1,010.0	1,850.0
-240.00	-400.0	-24.44	-12.6	15.6	60.0	215.6	420.0	615.6	1,140.0	1,015.6	1,860.0
-234.44	-390.0	-23.89	-11.7	16.1	61.0	221.1	430.0	621.1	1,150.0	1,021.1	1,870.0
-228.89	-380.0	-23.33	-10.8	16.7	62.0	226.7	440.0	626.7	1,160.0	1,026.7	1,880.0
-223.33	-370.0	-22.78	-9.9	17.2	63.0	232.2	450.0	632.2	1,170.0	1,032.2	1,890.0
-217.78	-360.0	-22.22	-8.9	17.8	64.0	237.8	460.0	637.8	1,180.0	1,037.8	1,900.0
-212.22	-350.0	-21.67	-7.9	18.3	65.0	243.3	470.0	643.3	1,190.0	1,043.3	1,910.0
-206.67	-340.0	-21.11	-6.9	18.9	66.0	248.9	480.0	648.9	1,200.0	1,048.9	1,920.0
-201.11	-330.0	-20.56	-5.9	19.4	67.0	254.4	490.0	654.4	1,210.0	1,054.4	1,930.0
-195.56	-320.0	-20.00	-4.9	20.0	68.0	260.0	500.0	660.0	1,220.0	1,060.0	1,940.0
-190.00	-310.0	-19.44	-3.9	20.6	69.0	265.6	510.0	665.6	1,230.0	1,065.6	1,950.0
-184.44	-300.0	-18.89	-2.9	21.1	70.0	271.1	520.0	671.1	1,240.0	1,071.1	1,960.0
-178.89	-290.0	-18.33	-1.9	21.7	71.0	276.7	530.0	676.7	1,250.0	1,076.7	1,970.0
-173.33	-280.0	-17.78	-0.9	22.2	72.0	282.2	540.0	682.2	1,260.0	1,082.2	1,980.0
-167.78	-270.0	-17.22	0.0	22.8	73.0	287.8	550.0	687.8	1,270.0	1,087.8	1,990.0
-162.22	-260.0	-16.67	1.0	23.3	74.0	293.3	560.0	693.3	1,280.0	1,093.3	2,000.0
-156.67	-250.0	-16.12	2.0	23.9	75.0	298.9	570.0	698.9	1,290.0	1,098.9	2,010.0
-151.11	-240.0	-15.56	3.0	24.4	76.0	304.4	580.0	704.4	1,300.0	1,104.4	2,020.0
-145.56	-230.0	-15.00	4.0	25.0	77.0	310.0	590.0	710.0	1,310.0	1,110.0	2,030.0
-140.00	-220.0	-14.44	5.0	25.6	78.0	315.6	600.0	715.6	1,320.0	1,115.6	2,040.0
-134.44	-210.0	-13.89	6.0	26.1	79.0	321.1	610.0	721.1	1,330.0	1,121.1	2,050.0
-128.89	-200.0	-13.33	7.0	26.7	80.0	326.7	620.0	726.7	1,340.0	1,126.7	2,060.0
-123.33	-190.0	-12.78	8.0	27.2	81.0	332.2	630.0	732.2	1,350.0	1,132.2	2,070.0
-117.78	-180.0	-12.22	9.0	27.8	82.0	337.8	640.0	737.8	1,360.0	1,137.8	2,080.0
-112.22	-170.0	-11.67	10.0	28.3	83.0	343.3	650.0	743.3	1,370.0	1,143.3	2,090.0
-106.67	-160.0	-11.11	11.0	28.9	84.0	348.9	660.0	748.9	1,380.0	1,148.9	2,100.0
-101.11	-150.0	-10.56	12.0	29.4	85.0	354.4	670.0	754.4	1,390.0	1,154.4	2,110.0
-95.56	-140.0	-10.00	13.0	30.0	86.0	360.0	680.0	760.0	1,400.0	1,160.0	2,120.0
-90.00	-130.0	-9.44	14.0	30.6	87.0	365.6	690.0	765.6	1,410.0	1,165.6	2,130.0
-84.44	-120.0	-8.89	15.0	31.1	88.0	371.1	700.0	771.1	1,420.0	1,171.1	2,140.0
-78.89	-110.0	-8.33	16.0	31.7	89.0	376.7	710.0	776.7	1,430.0	1,176.7	2,150.0
-73.33	-100.0	-7.78	17.0	32.2	90.0	382.2	720.0	782.2	1,440.0	1,182.2	2,160.0
-67.78	-90.0	-7.22	18.0	32.8	91.0	387.8	730.0	787.8	1,450.0	1,187.8	2,170.0
-62.22	-80.0	-6.67	19.0	33.3	92.0	393.3	740.0	793.3	1,460.0	1,193.3	2,180.0
-56.67	-70.0	-6.11	20.0	33.9	93.0	398.9	750.0	798.9	1,470.0	1,198.9	2,190.0
-51.11	-60.0	-5.56	21.0	34.4	94.0	404.4	760.0	804.4	1,480.0	1,204.4	2,200.0
-45.56	-50.0	-5.00	22.0	35.0	95.0	410.0	770.0	810.0	1,490.0	1,210.0	2,210.0
-40.00	-40.0	-4.44	23.0	35.6	96.0	415.6	780.0	815.6	1,500.0	1,215.6	2,220.0
-34.44	-30.0	-3.89	24.0	36.1	97.0	421.1	790.0	821.1	1,510.0	1,221.1	2,230.0
-28.89	-20.0	-3.33	25.0	36.7	98.0	426.7	800.0	826.7	1,520.0	1,226.7	2,240.0
-23.33	-10.0	-2.78	26.0	37.2	99.0	432.2	810.0	832.2	1,530.0	1,232.2	2,250.0
-17.78	0.0	-2.22	27.0	37.8	100.0	437.8	820.0	837.8	1,540.0	1,237.8	2,260.0
-12.22	10.0	-1.67	28.0	38.3	101.0	443.3	830.0	843.3	1,550.0	1,243.3	2,270.0
-6.67	20.0	-1.11	29.0	38.9	102.0	448.9	840.0	848.9	1,560.0	1,248.9	2,280.0
0.0	30.0	-0.56	30.0	39.4	103.0	454.4	850.0	854.4	1,570.0	1,254.4	2,290.0
4.44	40.0	0.0	31.0	40.0	104.0	460.0	860.0	860.0	1,580.0	1,260.0	2,300.0
8.89	50.0	0.56	32.0	40.6	105.0	465.6	870.0	865.6	1,590.0	1,265.6	2,310.0
13.33	60.0	1.11	33.0	41.1	106.0	471.1	880.0	871.1	1,600.0	1,271.1	2,320.0
17.78	70.0	1.67	34.0	41.7	107.0	476.7	890.0	876.7	1,610.0	1,276.7	2,330.0
22.22	80.0	2.22	35.0	42.2	108.0	482.2	900.0	882.2	1,620.0	1,282.2	2,340.0
26.67	90.0	2.78	36.0	42.8	109.0	487.8	910.0	887.8	1,630.0	1,287.8	2,350.0
31.11	100.0	3.33	37.0	43.3	110.0	493.3	920.0	893.3	1,640.0	1,293.3	2,360.0
35.56	110.0	3.89	38.0	43.9	111.0	498.9	930.0	898.9	1,650.0	1,298.9	2,370.0
40.00	120.0	4.44	39.0	44.4	112.0	504.4	940.0	904.4	1,660.0	1,304.4	2,380.0
44.44	130.0	5.00	40.0	45.0	113.0	510.0	950.0	910.0	1,670.0	1,310.0	2,390.0
48.89	140.0	5.56	41.0	45.6	114.0	515.6	960.0	915.6	1,680.0	1,315.6	2,400.0
53.33	150.0	6.11	42.0	46.1	115.0	521.1	970.0	921.1	1,690.0	1,321.1	2,410.0
57.78	160.0	6.67	43.0	46.7	116.0	526.7	980.0	926.7	1,700.0	1,326.7	2,420.0
62.22	170.0	7.22	44.0	47.2	117.0	532.2	990.0	932.2	1,710.0	1,332.2	2,430.0
66.67	180.0	7.78	45.0	47.8	118.0	537.8	1,000.0	937.8	1,720.0	1,337.8	2,440.0
71.11	190.0	8.33	46.0	48.3	119.0	543.3	1,010.0	943.3	1,730.0	1,343.3	2,450.0
75.56	200.0	8.89	47.0	48.9	120.0	548.9	1,020.0	948.9	1,740.0	1,348.9	2,460.0
80.00	210.0	9.44	48.0	49.4	121.0	554.4	1,030.0	954.4	1,750.0	1,354.4	2,470.0
84.44	220.0	10.00	49.0	50.0	122.0	560.0	1,040.0	960.0	1,760.0	1,360.0	2,480.0
88.89	230.0	10.56	50.0	50.6	123.0	565.6	1,050.0	965.6	1,770.0	1,365.6	2,490.0
93.33	240.0	11.11	51.0	51.1	124.0	571.1	1,060.0	971.1	1,780.0	1,371.1	2,500.0
97.78	250.0	11.67	52.0	51.7	125.0	576.7	1,070.0	976.7	1,790.0	1,376.7	2,510.0
102.22	260.0	12.22	53.0	52.2	126.0	582.2	1,080.0	982.2	1,800.0	1,382.2	2,520.0
106.67	270.0	12.78	54.0	52.8	127.0	587.8	1,090.0	987.8	1,810.0	1,387.8	2,530.0
111.11	280.0	13.33	55.0	53.3	128.0	593.3	1,100.0	993.3	1,820.0	1,393.3	2,540.0
115.56	290.0	13.89	56.0	53.9	129.0	598.9	1,110.0	998.9	1,830.0	1,398.9	2,550.0
120.00	300.0	14.44	57.0	54.4	130.0	604.4	1,120.0	1,004.4	1,840.0	1,404.4	2,560.0
124.44	310.0	15.00	58.0	55.0	131.0	610.0	1,130.0	1,010.0	1,850.0	1,410.0	2,570.0
128.89	320.0	15.56	59.0	55.6	132.0	615.6	1,140.0	1,015.6	1,860.0	1,415.6	2,580.0
133.33	330.0	16.12	60.0	56.1	133.0	621.1	1,150.0	1,021.1	1,870.0	1,421.1	2,590.0
137.78	340.0	16.67	61.0	56.7	134.0	626.7	1,160.0	1,026.7	1,880.0	1,426.7	2,600.0
142.22	350.0	17.22	62.0	57.2	135.0	632.2	1,170.0	1,032.2	1,890.0	1,432.2	2,610.0
146.67	360.0	17.78	63.0	57.8	136.0	637.8	1,180.0	1,037.8	1,900.0	1,437.8	2,620.0
151.11	370.0	18.33	64.0	58.3	137.0	643.3	1,190.0	1,043.3	1,910.0	1,443.3	2,630.0
155.56	380.0	18.89	65.0	58.9	138.0	648.9	1,200.0	1,048.9	1,920.0	1,448.9	2,640.0
160.00	390.0	19.44	66.0	59.4	139.0	654.4	1,210.0	1,054.4	1,930.0	1,454.4	2,650.0
164.44	400.0	20.00	67.0	60.0	140.0	660.0	1,220.0	1,060.0	1,940.0	1,460.0	2,660.0
168.89	410.0	20.56	68.0	60.6	141.0	665.6	1,230.0	1,065.6	1,950.0	1,465.6	2,670.0
173.33	420.0	21.11	69.0	61.1	142.0	671.1	1,240.0	1,071.1	1,960.0	1,471.1	2,680.0
177.78	430.0	21.67	70.0	61.7	143.0	676.7	1,250.0	1,076.7	1,970.0	1,476.7	2,690.0
182.22	440.0	22.22	71.0	62.2	144.0	682.2	1,260.0	1,082.2	1,980.0	1,482.2	2,700.0
186.67	450.0	22.78	72.0	62.8	145.0	687.8	1,270.0	1,087.8	1,990.0	1,487.8	2,710.0
191.11	460.0	23.33	73.0	63.3	146.0						

Chapter 59

SPE Letter and Computer Symbols Standard for Economics, Well Logging and Formation Evaluation, Natural Gas Engineering, and Petroleum Reservoir Engineering

Prepared by the Symbols Committee of the Society of Petroleum Engineers

Contents

<u>Symbols in Alphabetical Order</u>	59-2
<u>Quantities in Alphabetical Order</u>	59-18
<u>Subscript Definitions in Alphabetical Order</u>	59-52
<u>Subscript Symbols in Alphabetical Order</u>	59-63

Symbols in Alphabetical Order

Letter Symbol	Reserve SPE Letter Symbol	Computer Letter Symbol	Quantity	Dimensions
English				
A	S	ARA	area	L^2
A	F	HWF	Helmholtz function (work function)	mL^2/t^2
A		AMP	amplitude	various
A		AWT	atomic weight	m
A	S	ARA	cross section (area)	L^2
A_c		AMPC	amplitude, compressional wave	various
A_r		AMPR	amplitude, relative	various
A_s		AMPS	amplitude, shear wave	various
a		ACT	activity	
a	F_a	AIR	air requirement	various
a		DEC	decline factor, nominal	
a	L_a, L_1	DLW	distance between like wells (injection or production) in a row	L
a_E	F_{aE}	AIREX	air requirement, unit, in laboratory experimental run, volumes of air per unit mass of pack	L^3/m
a_R	F_{aR}	AIRR	air requirement, unit, in reservoir, volumes of air per unit bulk volume of reservoir rock	
B	C	COR	correction term or correction factor (either additive or multiplicative)	
B	F	FVF	formation volume factor, volume at reservoir conditions divided by volume at standard conditions	
B_g	F_g	FVFG	formation volume factor, gas	
B_{gb}	F_{gb}	FVFGB	bubblepoint formation volume factor, gas	
B_{gb}	F_{gb}	FVFGB	formation volume factor at bubblepoint conditions, gas	
B_o	F_o	FVFO	formation volume factor, oil	
B_{ob}	F_{ob}	FVFOB	bubblepoint formation volume factor, oil	
B_{ob}	F_{ob}	FVFOB	formation volume factor at bubblepoint conditions, oil	
B_t	F_t	FVFT	formation volume factor, total (two-phase)	
B_w	F_w	FVFW	formation volume factor, water	
b	w	WTH	breadth, width, or (primarily in fracturing) thickness	L
b	Y	ICP	intercept	various
b	f, F	RVF	reciprocal formation volume factor, volume at standard conditions divided by volume at reservoir conditions (shrinkage factor)	
b	w	WTH	width, breadth, or (primarily in fracturing) thickness	L
b_g	f_g, F_g	RVFG	reciprocal gas formation volume factor	
b_{gb}	f_{gb}, F_{gb}	RVFGB	reciprocal gas formation volume factor at bubblepoint conditions	
b_o	f_o, F_o	RVFO	reciprocal oil formation volume factor (shrinkage factor)	
C		ECQ	capacitance	q^2t^2/mL^2

Dimensions: L=length, m=mass, q=electrical charge, t=time, T=temperature, and M=money.

Letter Symbol	Reserve SPE Letter Symbol	Computer Letter Symbol	Quantity	Dimensions
C	C_i	INVT	capital investments, summation of all	M
C		CGW	coefficient of gas-well backpressure curve	$L^{3-2n}t^{4n}/m^{2n}$
C	n_C	NMBC	components, number of	
C	c, n	CNC	concentration	various
C	σ	ECN	conductivity (electrical logging)	tq^2/mL^3
C	K	CND	conductivity, other than electrical (with subscripts)	various
C	c, n	CNC	salinity	various
C	c	HSP	specific heat (always with phase or system subscripts)	L^2/t^2T
C		WDC	water-drive constant	L^4t^2/m
C_{C_1}	c_{C_1}	CNCC1	concentration, methane (concentration of other paraffin hydrocarbons would be indicated similarly, C_{C_2} , C_{C_3} , etc.)	various
C_L	c_L, n_L	CNTL	content, condensate or natural gas liquids	various
C_L		WDCL	water-drive constant, linear aquifer	L^4t^2/m
C_{O_2}	c_{O_2}	CNCO2	concentration, oxygen (concentration of other elements or compounds would be indicated similarly, C_{CO_2} , C_{N_2} , etc.)	various
C_a	σ_a	ECNA	conductivity, apparent	tq^2/mL^3
C_{fD}		CNDFQ	conductivity, fracture, dimensionless	
C_i		INVI	capital investment, initial	M
C_k		INVK	capital investment, subsequent, in year k	M
C_m	c_m, n_m	CNCFU	fuel concentration, unit (see symbol m)	various
C_{uk}		INVUK	unamortized investment over year k	
C_{wg}	c_{wg}, n_{wg}	CNTWG	content, wet-gas	various
c	k, κ	CMP	compressibility	Lt^2/m
c_f	k_f, κ_f	CMPF	compressibility, formation or rock	Lt^2/m
c_g	k_g, κ_g	CMPG	compressibility, gas	Lt^2/m
c_o	k_o, κ_o	CMPO	compressibility, oil	Lt^2/m
c_{pr}	k_{pr}, κ_{pr}	CMPPRD	compressibility, pseudo reduced	
c_w	k_w, κ_w	CMPW	compressibility, water	Lt^2/m
D		DLV	deliverability (gas well)	L^3/t
D	y, H	DPH	depth	L
D	μ, δ	DFN	diffusion coefficient	L^2/t
D		DSC	discount factor, general	
D_c		DSCC	discount factor, constant-income	
D_{sp}		DSCSP	discount factor, single-payment [$1/(1+i)^k$; or e^{-jk} , $j = \ln(1+i)$]	
D_{spc}		DSCSPC	discount factor, single-payment (constant annual rate) [$e^{-jk}(e^j - 1)/j$]	
d		DECE	decline factor, effective	
d	D	DIA	diameter	L
d	L_d, L_2	DUW	distance between adjacent rows of injection and production wells	L
\bar{d}_p	\bar{D}_p	DIAAVP	diameter, mean particle	L
d_h	d_H, D_h	DIAH	diameter, hole	L
d_i	d_I, D_i	DIAI	diameter, invaded zone (electrically equivalent)	L
E	η, e	EFF	efficiency	
E	V	EMF	electromotive force	mL^2/t^2q

Letter Symbol	Reserve SPE Letter Symbol	Computer Letter Symbol	Quantity	Dimensions
E	U	ENG	energy	mL^2/t^2
E	Y	ELMY	modulus of elasticity (Young's modulus)	m/Lt^2
E_A	η_A, e_A	EFFA	efficiency, areal (used in describing results of model studies only): area swept in a model divided by total model reservoir area (see E_P)	
E_D	η_D, e_D	EFFD	efficiency, displacement: volume of hydrocarbons (oil or gas) displaced from individual pores or small groups of pores divided by the volume of hydrocarbon in the same pores just prior to	
E_{Db}	η_{Db}, e_{Db}	EFFDB	efficiency, displacement, from burned portion of in-situ combustion pattern	
E_{Du}	η_{Du}, e_{Du}	EFFDU	efficiency, displacement, from unburned portion of in-situ combustion pattern	
E_I	η_I, e_I	EFFI	efficiency, invasion (vertical): hydrocarbon pore space invaded (affected, contacted) by the injection fluid or heat front divided by the hydrocarbon pore space enclosed in all layers behind the injected fluid or heat front	
E_π			Euler's number	
E_P	η_P, e_P	EFFP	efficiency, pattern sweep (developed from areal efficiency by proper weighting for variations in net pay thickness, porosity, and hydrocarbon saturation): hydrocarbon pore space enclosed behind the injected fluid or heat front divided by total hydrocarbon pore space of the reservoir or project	
E_R	η_R, e_R	EFFR	efficiency, overall reservoir recovery: volume of hydrocarbons recovered divided by volume of hydrocarbons in place at start of project ($E_R = E_P E_I E_D = E_V E_D$)	
E_{SP}	Φ_{SP}	EMFSP	SP (measured SP) (Self Potential)	$\text{mL}^2/\text{t}^2\text{q}$
E_{SSP}	Φ_{SSP}	EMFSSP	SSP (static SP)	$\text{mL}^2/\text{t}^2\text{q}$
E_V	η_V, e_V	EFFV	efficiency, volumetric: product of pattern sweep and invasion efficiencies	
E_{Vb}	η_{Vb}, e_{Vb}	EFFVB	efficiency, volumetric, for burned portion only, in-situ combustion pattern	
E_c	Φ_c	EMFC	electrochemical component of the SP	$\text{mL}^2/\text{t}^2\text{q}$
E_k	Φ_k	EMFK	electrokinetic component of the SP	$\text{mL}^2/\text{t}^2\text{q}$
E_k		ENGK	kinetic energy	mL^2/t^2
E_{pSP}	Φ_{SP}	EMFP	pseudo-SP	mL^2/qt^2
$-Ei(-x)$			exponential integral, $\int_x^\infty \frac{e^{-t}}{t} dt$, x positive	
$Ei(x)$			exponential integral, modified $\lim_{\epsilon \rightarrow 0} \left[\int_{-\infty}^{-\epsilon} \frac{e^t}{t} dt + \int_{\epsilon}^\infty \frac{e^t}{t} dt \right]$, x positive	
e	i	ENC	encroachment or influx rate	L^3/t
e_{O_2}	E_{O_2}	UTL02	oxygen utilization	

Letter Symbol	Reserve SPE Letter Symbol	Computer Letter Symbol	Quantity	Dimensions
e_g	i_g	ENCG	encroachment or influx rate, gas	L^3/t
e_o	i_o	ENCO	encroachment or influx rate, oil	L^3/t
e_w	i_w	ENCW	encroachment or influx rate, water	L^3/t
e^z	$exp\ z$	EXP	exponential function	
F		DGF	degrees of freedom	
F		FAC	factor in general, including ratios (always with identifying subscripts)	various
F	f	FLU	fluid (generalized)	various
F	Q	FCE	force, mechanical	mL/t^2
F		FAC	ratio or factor in general (always with identifying subscripts)	various
F_B		FACB	factor, turbulence	
F_R		FACHR	formation resistivity factor—equals R_o/R_w (a numerical subscript to F indicates the value R_w)	
F_{WV}	γ	WGTS	specific weight	mL^2/t^2
F_{aF}		FACAFU	air/fuel ratio	various
F_s	F_d	DMRS	damage ratio or condition ratio (conditions relative to formation conditions unaffected by well operations)	
F_{wF}		FACWFO	water/fuel ratio	various
F_{wo}		FACWO	water/oil ratio, producing, instantaneous	
F_{wop}		FACWOP	water/oil ratio, cumulative	
f	F	FRC	fraction (such as the fraction of a flow stream consisting of a particular phase)	
f	ν	FQN	frequency	$1/t$
f		FACF	friction factor	
f		FUG	fugacity	m/Lt^2
$f_{\phi sh}$	ϕ_{igfsh}	FIGSH	fraction of intergranular space ("porosity") occupied by all shales	
$f_{\phi shd}$	ϕ_{imfshd}	FIMSHD	fraction of intermatrix space ("porosity") occupied by nonstructural dispersed shale	
$f_{\phi w}$	ϕ_{igfw}	FIGW	fraction of intergranular space ("porosity") occupied by water	
f_L	F_L, f_L script l	FRCL	fraction liquid	
f_L	F_L, f_L script l	MFRTL	mole fraction liquid, $L/(L+V)$	
f_{Pk}		PRAPK	profit, annual, over year k , fraction of unamortized investment	
f_V	f_{Vb}, V_{bf}	FRCVB	fraction of bulk (total) volume	
f_g	F_g	FRCG	fraction gas	
f_g	F_g	MFRTV	mole fraction gas, $V/(L+V)$	
f_s	Q, x	QLTS	quality (usually of steam)	
G	F	GFE	free energy (Gibbs function)	mL^2/t^2
G	g	GASTI	gas in place in reservoir, total initial	L^3
G	g	GAS	gas(any gas, including air) always with identifying subscripts	various
G	f_G	GMF	geometrical factor (multiplier) (electrical logging)	
G	E_s	ELMS	shear modulus	m/Lt^2

Letter Symbol	Reserve SPE Letter Symbol	Computer Letter Symbol	Quantity	Dimensions
G_{Fi}	g_{Fi}	GASFI	free-gas volume, initial reservoir ($=mNB_{oi}$)	L^3
G_{Fp}	g_{Fp}	GASFP	free gas produced, cumulative	L^3
G_L	g_L	NGLTi	condensate liquids in place in reservoir, initial	L^3
G_{Lp}	g_{Lp}	NGLP	condensate liquids produced, cumulative	L^3
G_{an}	f_{Gan}	GMFAN	factor, geometrical (multiplier), annulus (electrical logging)	
G_{an}	f_{Gan}	GMFAN	geometrical factor (multiplier), annulus (electrical logging)	
G_e	g_e	GASE	gas influx (encroachment), cumulative	L^3
G_i	g_i	GASI	gas injected, cumulative	L^3
G_i	f_{Gi}	GMFI	geometrical factor (multiplier), invaded zoned (electrical logging)	
G_m	f_{Gm}	GMFM	geometrical factor (multiplier), mud (electrical logging)	
G_p	g_p	GASP	gas produced, cumulative	L^3
G_p	f_{Gp}	GMFP	geometrical factor (multiplier), pseudo (electrical logging)	
G_{pE}	g_{pE}	GASPEX	gas produced from experimental tube run	L^3
G_{pa}	g_{pa}	GASPUL	gas recovery, ultimate	L^3
G_t	f_{Gt}	GMFT	geometrical factor, (multiplier), true (noninvaded zone) (electrical logging)	
G_{wgp}	g_{wgp}	GASWGP	wet gas produced, cumulative	L^3
G_{xo}	f_{Gxo}	GMFXO	geometrical factor (multiplier), flushed zone (electrical logging)	
g		GRV	acceleration of gravity	L/t^2
g	γ	GRD	gradient	various
g_G	g_g	GRDGT	gradient, geothermal	T/L
g_T	g_h	GRDT	gradient, temperature	T/L
g_c		GRVC	conversion factor in Newton's Second Law of Motion	
H	I	HEN	enthalpy (always with phase or system subscripts)	mL^2/t^2
H_s	I_s	HENS	enthalpy (net) of steam or enthalpy above reservoir temperature	mL^2/t^2
h	d, e	THK	bed thickness, individual	L
h	i	HENS	enthalpy, specific	L^2/t^2
h	h_h, h_T	HTCC	heat-transfer coefficient, convective	m/t^3T
h	d, e	ZHT	height (other than elevation)	L
h		HPC	hyperbolic decline constant (from equation) $q = q_i / \left[1 + \frac{a_i t}{h} \right]^h$	
h	d, e	THK	thickness (general and individual bed)	L
h_{mc}	d_{mc}, e_{mc}	THKMC	thickness, mud cake	L
h_n	d_n, e_n	THKN	thickness, net pay	L
h_t	d_t, e_t	THKT	thickness, gross pay (total)	L
I		INC	cash income, operating	M
I	i script i, i	CUR	current, electric	q/t
I	i script i, i	CUR	electric current	q/t
I	I_T, I_θ	HTCI	heat transfer coefficient, radiation	m/t^3T
I	i	X	index (use subscripts as needed)	

Letter Symbol	Reserve SPE Letter Symbol	Computer Letter Symbol	Quantity	Dimensions
I	i	IJX	injectivity index	$L^4/t/m$
$g(z)$ script I			imaginary part of complex number z	
I_ϕ	i_ϕ	PRX	porosity index	
$I_{\phi 1}$	$i_{\phi 1}$	PRXPR	porosity index, primary	
$I_{\phi 2}$	$i_{\phi 2}$	PRXSE	porosity index, secondary	
I_{Ff}	i_{Ff}	FFX	free fluid index	
I_H	i_H	HYX	hydrogen index	
I_R	i_R	RSXH	hydrocarbon resistivity index R_t/R_0	
I_a		INCA	cash income, operating, after taxes	M
I_b		INCB	cash income, operating, before taxes	M
I_f	i_f, I_F, i_F	FRX	fracture index	
I_k		INCK	cash income, annual operating, over year k	M
I_s	i_s	IJXS	injectivity index, specific	$L^3/t/m$
I_{shGR}	i_{shGR}	SHXGR	shaliness gamma ray index, $(\gamma_{log} - \gamma_{cn})/(\gamma_{sh} - \gamma_{cn})$	
i		RTED	discount rate	
i		INJ	injection rate	L^3/t
i		IRCE	interest rate, effective compound (usually annual)	
i	k_i	RTE	rate: discount, effective profit, of return, reinvestment, etc; use symbol i with suitable subscripts	
i_M		IRPE	interest rate, effective, per period	
i_a		INJA	injection rate, air	L^3/t
i_g		INJG	injection rate, gas	L^3/t
i_r		RORI	rate of return (internal, true, or discounted cash flow) or earning power	
i_w		INJW	injection rate, water	L^3/t
J	j	PDX	productivity index	$L^4/t/m$
J_s	j_s	PDXS	productivity index, specific	$L^3/t/m$
j	r	IRA	interest rate, nominal annual	
j	ω		reciprocal permeability	$1/L^2$
K	K_b	BKM	bulk modulus	m/Lt^2
K		KSP	coefficient in the equation of the electro-chemical component of the SP (spontaneous electromotive force)	mL^2/t^2q
K	M	COE	coefficient or multiplier	various
K	d	DSP	dispersion coefficient	L^2/t
K	k, F_{eq}	EQR	equilibrium ratio (y/x)	
K	M	COE	multiplier or coefficient	various
K_R	M_R, a, C	COER	formation resistivity factor coefficient ($F_R \phi^m$)	
K_{ani}	M_{ani}	COEANI	anisotropy coefficient	
K_c	M_c, K_{ec}	COEC	electrochemical coefficient	mL^2/t^2q
k	κ	SUSM	magnetic susceptibility	mL/q^2
k	K	PRM	permeability, absolute (fluid flow)	L^2
k	r, j	RRC	reaction rate constant	L/t
k_g	K_g	PRMG	effective permeability to gas	L^2
k_g/k_o	K_g/K_o	PRMGO	gas/oil permability ratio	
k_h	λ	HCN	thermal conductivity (always with additional phase or system subscripts)	mL/t^3T
k_o	K_o	PRMO	effective permeability to oil	L^2

Letter Symbol	Reserve SPE Letter Symbol	Computer Letter Symbol	Quantity	Dimensions
k_{rg}	K_{rg}	PRMRG	relative permeability to gas	
k_{ro}	K_{ro}	PRMRO	relative permeability to oil	
k_{rw}	K_{rw}	PRMRW	relative permeability to water	
k_w	K_w	PRMW	effective permeability to water	L^2
k_w/k_o	K_w/K_o	PRMWO	water/oil permeability ratio	
$\mathcal{L}(y)$ script L			transform, Laplace of y , $\int_0^\infty y(t)e^{-st} dt$	
L	s, ℓ script l	LTH	distance, length, or length ⁰ of path	L
L	s, ℓ script l	LTH	length, path length, or distance	L
L	n_L	MOLL	liquid phase, moles of	
L	s, ℓ script l	LTH	path length, length, or distance	L
L_f	x_f	LTHFH	fracture half-length (specify "in the direction of" when using x_f)	L
L_s	s_s, ℓ_s script l	LENS	spacing (electrical logging)	L
L_v	λ_v	HLTV	heat of vaporization, latent	L^2/t^2
\ln			natural logarithm, base e	
\log			common logarithm, base 10	
\log_a			logarithm, base a	
M	I	MAG	magnetization	m/qt
M	F_λ	MBR	mobility ratio, general ($\lambda_{\text{displacing}}/\lambda_{\text{displaced}}$)	
M	F_λ	MBR	mobility ratio, sharp-front approximation (λ_D/λ_d)	
M		MWT	molecular weight	m
M	m	NMBCP	number of compounding periods (usually per year)	
M	$m_{\theta D}$	SAD	slope, interval transit time vs. density (absolute value)	tL^2/m
M		HSPV	volumetric heat capacity	m/Lt^2T
M_L		MWTAVL	molecular weight of produced liquids, mole-weighted average	m
$M_{\bar{S}}$	M_{Dd}, M_{su}	MBRSAV	mobility ratio, diffuse-front approximation $[(\lambda_D + \lambda_d)_{\text{swept}}/(\lambda_d)_{\text{unswept}}]$; D signifies displacing; d signifies displaced; mobilities are evaluated at average saturation conditions behind and ahead of front	
M_f		MAGF	magnetization, fraction	
M_t	$F_{\lambda t}$	MBRT	mobility ratio, total, $[(\lambda_t)_{\text{swept}}/(\lambda_t)_{\text{unswept}}]$; "swept" and "unswept" refer to invaded and uninvaded regions behind and ahead of leading edge of displacement front	
m		MPX	cementation (porosity) exponent (in an empirical relation between F_R and ϕ)	
m	F_F	FCM	fuel consumption	various
m		MAS	mass	m
m	F_{Fo}, F_{go}	MGO	ratio of initial reservoir free-gas volume to initial reservoir oil volume	
m	A	SLP	slope	various
m_E	F_{FE}	FCMEX	fuel consumption in experimental tube run	m/L^3
m_{Eg}	F_{FEg}	FCMEXG	fuel consumption in experimental tube run (mass of fuel per mole of produced gas)	m

Letter Symbol	Reserve SPE Letter Symbol	Computer Letter Symbol	Quantity	Dimensions
m_R	F_{FR}	FCMR	fuel consumption in reservoir	m/L^3
m_k		AMAK	amortization (annual write-off of unamortized investment at end of year k)	M
N	n, C	NMB	count rate (general)	1/t
N		NEU	neutron [usually with identifying subscript(s)]	various
N		NUMQ	number, dimensionless, in general (always with identifying subscripts)	
N	n	OIL	oil (always with identifying subscripts)	various
N	n	OILTI	oil in place in reservoir, initial	L^3
N	n	NMB	pump strokes, number of, cycles per unit of time	
N	$m_{\theta ND}$	SND	slope, neutron porosity vs. density (absolute value)	L^3/m
N_{GR}	N_{γ}, C_G	NGR	gamma-ray count rate	1/t
N_N	N_n, C_N	NEUN	neutron count rate	1/t
N_R	N_F	FUDR	fuel deposition rate	m/L^3t
N_{Re}		REYQ	Reynolds number (dimensionless number)	
N_e		OILE	oil influx (encroachment) cumulative	L^3
N_p	n_p	OILP	oil produced, cumulative	L^3
N_{pa}	n_{pa}	OILPUL	oil recovery, ultimate	L^3
n	N	NMB	density (indicating "number per unit volume")	$1/L^3$
n		NGW	exponent of backpressure curve, gas well	
n	μ	RFX	index of refraction	
n	N	NMB	number (of variables, or components, or steps, or increments, etc.)	
n	N	NMB	number (quantity)	
n		SXP	saturation exponent	
n_N		NMBN	density (number) of neutrons	$1/L^3$
n_j	N_j	MOLJ	moles of component j	
n_{pj}	N_{pj}	MOLPJ	moles of component j produced, cumulative	
n_t	N_t	NMBM	number of moles, total	
O		XPO	operating expense	various
O_u		XPOU	operating expense per unit produced	M/L^3
P		CFL	cash flow, undiscounted	M
P		NMBP	phases, number of	
P	P_t	PRFT	profit, total	M
P_{PV}		CFLPV	cash flow, discounted	M
P_c	P_C, p_C	PRSCP	capillary pressure	m/Lt^2
P_k		PRAK	profit, annual net, over year k	M
p	P	PRS	pressure	m/Lt^2
\bar{p}	\bar{P}	PRSAV	average pressure	m/Lt^2
\bar{p}	\bar{P}	PRSAV	pressure, average or mean	m/Lt^2
\bar{p}_R	\bar{P}_R	PRSAVR	pressure, reservoir average	m/Lt^2
p_D	P_D	PRSQ	pressure, dimensionless	
p_a	P_a	PRSA	pressure, atmospheric	m/Lt^2
p_b	p_s, P_s, P_b	PRSB	pressure, bubblepoint (saturation)	m/Lt^2
p_{bh}	P_{bh}	PRSBH	pressure, bottomhole	m/Lt^2
p_c	P_c	PRSC	pressure, critical	m/Lt^2
p_{cf}	P_{cf}	PRSCF	pressure, casing flowing	m/Lt^2
p_{cs}	P_{cs}	PRSCS	pressure, casing static	m/Lt^2
p_d	P_d	PRSD	pressure, dew point	m/Lt^2
p_e	P_e	PRSE	pressure, external boundary	m/Lt^2

Letter Symbol	Reserve SPE Letter Symbol	Computer Letter Symbol	Quantity	Dimensions
p_{ext}	P_{ext}	PRSXT	pressure, extrapolated	m/Lt ²
p_f	P_f	PRSF	pressure, front or interface	m/Lt ²
p_i	P_i	PRSI	pressure, initial	m/Lt ²
p_{iwf}	P_{iwf}	PRSIWF	pressure, bottomhole flowing, injection well	m/Lt ²
p_{iws}	P_{iws}	PRSIWS	pressure, bottomhole static, injection well	m/Lt ²
p_{pc}	P_{pc}	PRSPC	pressure, pseudocritical	m/Lt ²
p_{pc}	P_{pc}	PRSPC	pseudocritical pressure	m/Lt ²
p_{pr}	P_{pr}	PRSPRD	pressure, pseudoreduced	m/Lt ²
p_r	P_r	PRSRD	pressure, reduced	
p_{sc}	P_{sc}	PRSSC	pressure, standard conditions	m/Lt ²
p_{sp}	P_{sp}	PRSSP	pressure, separator	m/Lt ²
p_{lD}	P_{lD}	PRSTQQ	pressure function, dimensionless, at dimensionless time t_D	
p_{lf}	P_{lf}	PRSTF	pressure, tubing flowing	m/Lt ²
p_{ls}	P_{ls}	PRSTS	pressure, tubing static	m/Lt ²
p_w	P_w	PRSW	pressure, bottomhole general	m/Lt ²
p_{wf}	P_{wf}	PRSWF	pressure, bottomhole flowing	m/Lt ²
p_{ws}	P_{ws}	PRSWS	pressure, bottomhole static	m/Lt ²
p_{ws}	P_{ws}	PRSWS	pressure, bottomhole, at any time after shut-in	m/Lt ²
Q	q	CHG	charge	q
Q	q, Φ	HRT	heat flow rate	mL ² /t ³
Q_{lID}	Q_{lID} script l	ENCLTQQ	influx function, fluid, linear aquifer, dimensionless	
Q_V	Z_V	CEXV	cation exchange capacity per unit pore volume	
Q_i	q_i	FLUIQ	pore volumes of injected fluid, cumulative, dimensionless	
Q_p	Q_{lID} script l	FLUP	fluids, cumulative produced (where N_p and W_p are not applicable)	
Q_p		FLUP	produced fluids, cumulative (where N_p and W_p are not applicable)	L ³
Q_{tD}		ENCTQQ	fluid influx function, dimensionless, at dimensionless time t_D	
q	Q	RTE	production rate or flow rate	L ³ /t
\bar{q}	\bar{Q}	RTEAV	production rate or flow rate, average	L ³ /t
q_D	Q_D	RTEQ	production rate, dimensionless	
q_a	Q_a	RTEA	production rate at economic abandonment	L ³ /t
q_{dh}	q_{wf}, q_{DH}, Q_{dh}	RTEDH	volumetric flow rate downhole	L ³ /t
q_g	Q_g	RTEG	production rate, gas	L ³ /t
q_{gD}	Q_{gD}	RTEGQ	production rate, gas, dimensionless	
q_i	Q_i	RTEI	production rate at beginning of period	L ³ /t
q_o	Q_o	RTEO	production rate, oil	L ³ /t
q_{oD}	Q_{oD}	RTEOQ	production rate, oil, dimensionless	
$q_{\bar{p}}$	$Q_{\bar{p}}$	RTEPAV	production rate or flow rate at mean pressure	L ³ /t
q_s	Q_s	RTES	segregation rate (in gravity drainage)	L ³ /t
q_{sc}	q_{σ}, Q_{sc}	RTESC	surface production rate	L ³ /t
q_{sc}	q_{σ}, Q_{sc}	RTESC	volumetric flow rate, surface conditions	L ³ /t
q_w	Q_w	RTEW	production rate, water	L ³ /t
q_{wD}	Q_{wD}	RTEWQ	production rate, water, dimensionless	
R	ρ, r	RES	electrical resistivity (electrical logging)	mL ³ /tq ²

Letter Symbol	Reserve SPE Letter Symbol	Computer Letter Symbol	Quantity	Dimensions
R		RRR	gas constant, universal (per mole)	$\text{mL}^2/\text{t}^2\text{T}$
R	F_g, F_{go}	GOR	gas/oil ratio, producing	
R	N	MRF	molecular refraction	L^3
R		RRR	reaction rate	m/L^2
$\Re(z)$ script R			real part of complex number z	
R_0	ρ_0, r_0	RESZR	formation resistivity when 100% saturated with water of resistivity R_w	mL^3/tq^2
R_F	F_{gf}, F_{gof}	GORF	free gas/oil ratio, producing (free-gas volume/oil volume)	
R_a	ρ_a, r_a	RESA	apparent resistivity	mL^3/tq^2
R_i	ρ_i, r_i	RESI	invaded zone resistivity	mL^3/tq^2
R_m	ρ_m, r_m	RESM	mud resistivity	mL^3/tq^2
R_{mc}	ρ_{mc}, r_{mc}	RESMC	mudcake resistivity	mL^3/tq^2
R_{mf}	ρ_{mf}, r_{mf}	RESMF	mud-filtrate resistivity	mL^3/tq^2
R_p	F_{gp}, F_{gop}	GORP	cumulative gas/oil ratio	
R_s	F_{gs}, F_{gos}	GORS	solution gas/oil ratio (gas solubility in oil)	
R_{sb}	F_{gsb}	GORSB	solution gas/oil ratio at bubblepoint conditions	
R_{sh}	ρ_{sh}, r_{sh}	RESSH	shale resistivity	mL^3/tq^2
R_{si}	F_{gsi}	GORSI	solution gas/oil ratio, initial	
R_{sw}		GWRS	gas solubility in water	
R_t	ρ_t, r_t	REST	true formation resistivity	mL^3/tq^2
R_w	ρ_w, r_w	RESW	water resistivity	mL^3/tq^2
R_{xo}	ρ_{xo}, r_{xo}	RESXO	flushed-zone resistivity (that part of the invaded zone closest to the wall of the hole, where flushing has been maximum)	mL^3/tq^2
R_z	ρ_z, r_z	RESZ	apparent resistivity of the conductive fluids in	mL^3/tq^2
r	R	RAD	radius	L
r	R	RST	resistance	ML^2/tq^2
r_D	R_D	RADQ	radius, dimensionless	
r_H	R_H	RADHL	hydraulic radius	L
r_d	R_d	RADP	drainage radius	L
r_e	R_e	RADE	external boundary radius	L
r_s	R_s	RADS	radius of well damage or stimulation (skin)	L
r_w	R_w	RADW	well radius	L
r_{wa}	R_{wa}	RADWA	radius of wellbore, apparent or effective (includes effects of well damage or stimulation)	L
S	σ_t	HER	entropy, total	$\text{mL}^2/\text{t}^2\text{T}$
S	ρ, s	SAT	saturation	
S	s, σ	STO	storage or storage capacity	various
S_L	ρ_L, s_L	SATL	liquid saturation, combined total	
S_D	S_D	STOQ	dimensionless fractional storage capacity	
S_g	ρ_g, s_g	SATG	gas saturation	
S_{gc}	ρ_{gc}, s_{gc}	SATGC	gas saturation, critical	
S_{gr}	ρ_{gr}, s_{gr}	SATGR	gas saturation, residual	
S_h	ρ_h, s_h	SATH	saturation, hydrocarbon	
S_{hr}	ρ_{hr}, s_{hr}	SATHR	residual hydrocarbon saturation	
S_{iw}	ρ_{iw}, s_{iw}	SATIW	irreducible (interstitial or connate) water saturation	
S_o	ρ_o, s_o	SATO	oil saturation	
S_{og}	ρ_{og}, s_{og}	SATOG	gas-cap interstitial-oil saturation	
S_{or}	ρ_{or}, s_{or}	SATOR	residual oil saturation	
S_w	ρ_w, s_w	SATW	water saturation	
S_{wc}	ρ_{wc}, s_{wc}	SATWC	critical water saturation	

Letter Symbol	Reserve SPE Letter Symbol	Computer Letter Symbol	Quantity	Dimensions
S_{wg}	ρ_{wg}, S_{wg}	SATWG	interstitial-water saturation in gas cap	
S_{wi}	ρ_{wi}, S_{wi}	SATWI	initial water saturation	
S_{wo}	S_{wb}	SATWO	interstitial-water saturation in oil band	
S_{wr}	ρ_{wr}, S_{wr}	SATWR	residual water saturation	
s			Laplace transform variable	
s	L	DIS	displacement	L
s	σ	HERS	entropy, specific	L^2/t^2T
s	S, σ	SKN	skin effect	various
s		SDVES	standard deviation of a random variable, estimated	
s^2		VARES	variance of a random variable, estimated	
T	Θ	PER	period	t
T	T	TRM	transmissivity, transmissibility	various
T	θ	TEM	temperature	T
T_R	θ_R	TEMR	reservoir temperature	T
T_{bh}	θ_{BH}	TEMBH	bottomhole temperature	T
T_c	θ_c	TEMC	critical temperature	T
T_f	θ_f	TEMF	formation temperature	T
T_{pr}	θ_{pr}	TEMPRD	pseudoreduced temperature	T
T_r	θ_r	TEMRD	reduced temperature	
T_{sc}	θ_{sc}	TEMSC	temperature, standard conditions	T
t script t	Δt	TAC	interval transit time	t/L
t	τ	TIM	time	t
t_1	τ_1	TIMRP	relaxation time, proton thermal	t
$t_{1/2}$		TIMH	half life	t
t_2	τ_2	TIMAV	relaxation time, free-precession decay	t
t_D	τ_D	TIMQ	time, dimensionless	
t_{Dm}	τ_{Dm}	TIMMQ	time, dimensionless at condition m	
t_N	τ_N, t_n	NFL	neutron lifetime	1/t
t_d	τ_d	TIMD	time, delay	t
t_{dN}		TIMDN	decay time, neutron (neutron mean life)	t
t_p	τ_p	TIMP	time well was on production prior to shut-in, equivalent (pseudotime)	t
t_s	τ_s	TIMS	time for stabilization of a well	t
t_{sh} script t	Δt_{sh}	TACSH	shale interval transit time	t/L
U	U_T, U_θ	HTCU	heat transfer coefficient, over all	m/t^3T
u	ψ	FLX	flux	various
u	ψ	VELV	flux or flow rate, per unit area (volumetric velocity)	L/t
u	ψ	VELV	superficial phase velocity (flux rate of a particular fluid phase flowing in pipe; use appropriate phase subscripts)	L/t
V	R, V_i, R_i	GRRT	gross revenue ("value"), total	M
V	n_v	MDLV	moles of vapor phase	
V	U	VLV	potential difference (electric)	mL^2/qt^2
V	v	VOL	volume	L^3
V	f_V, F_V	VLF	volume fraction or ratio (as needed, use same subscripted symbols as for "volumes"; note that bulk volume fraction is unity and pore volume fractions are ϕ)	various

Letter Symbol	Reserve SPE Letter Symbol	Computer Letter Symbol	Quantity	Dimensions
V_M	v_m	VOLM	molal volume (volume per mole)	L^3
V_{Rb}		VOLRB	volume of reservoir rock burned	L^3
V_{Ru}		VOLRU	volume of reservoir rock unburned	L^3
V_b	v_b	VOLB	bulk volume	L^3
V_{bE}	v_{bE}	VOLBEX	bulk volume of pack burned in experimental tube run	L^3
V_{bp}	v_{bp}	VOLBP	volume at bubble point pressure	L^3
V_e	V_{pe}, v_e	VOLG	volume, effective pore	L^3
V_{gr}	v_{gr}	VOLGR	volume, grain (volume of all formation solids except shales)	L^3
V_{ig}	v_{ig}	VOLIG	volume, intergranular (volume between grains; consists of fluids and all shales) ($V_b - V_{gr}$)	L^3
V_{im}	v_{im}	VOLIM	volume, intermatrix (consists of fluids and dispersed shale) ($V_b - V_{ma}$)	L^3
V_{ma}	v_{ma}	VOLMA	matrix (framework) volume (volume of all formation solids except dispersed clay or shale)	L^3
V_{ma}	v_{ma}	VOLMA	volume, matrix (framework) (volume of all formation solids except dispersed shale)	
V_{ne}	V_{pne}, v_{ne}	VOLNE	volume, noneffective pore ($V_p - V_e$)	L^3
V_p	v_p	VOLP	pore volume ($V_b - V_s$)	L^3
V_{pD}	v_{pD}	VOLPQ	pore volume, dimensionless	
V_s	v_s	VOLS	volume, solid(s) (volume of all formation solids)	L^3
V_{sh}	v_{sh}	VOLSH	volume, shale(s) (volume of all shales: structural and dispersed)	L^3
V_{shd}	v_{shd}	VOLSHD	volume, shale, dispersed	L^3
V_{shs}	v_{shs}	VOLSHS	volume, shale, structural	L^3
V_u	R_u	GRRU	gross revenue ("value") per unit produced	M/L^3
v	V, u	VAC	acoustic velocity	L/t
v	v_s	SPV	specific volume	L^3/m
v	V, u	VEL	velocity	L/t
v_b	V_b, u_b	VELB	burning-zone advance rate (velocity of)	L/t
W	w	WTR	water (always with identifying subscripts)	various
W	w	WTRTI	water in place in reservoir, initial	L^3
W	w, G	WGT	weight (gravitational)	mL/t^2
W	w	WRK	work	mL^2/t^2
W_e	w_e	WTRE	water influx (encroachment), cumulative	L^3
W_i	w_i	WTRI	water injected, cumulative	L^3
W_p	w_p	WTRP	water produced, cumulative	L^3
w	z	ARR	Arrhenius reaction-rate velocity constant	L^3/m
w	m	MRT	mass flow rate	m/t
t_{ma} script t	Δt_{ma}	TACMA	matrix interval transit time	t/L
w	m	MRT	rate, mass flow	m/t
X		XEL	reactance	ML^2/tq^2
\bar{x}			tensor of x	
\bar{x}		MFRL	mole fraction of a component in liquid phase	
\vec{x}			vector of x	
$\bar{\bar{x}}$		MENES	mean value of a random variable, x , estimated	

Letter Symbol	Reserve SPE Letter Symbol	Computer Letter Symbol	Quantity	Dimensions
y	f	HOL	holdup (fraction of the pipe volume filled by a given fluid: y_o is oil holdup, y_w is water holdup, sum of all holdups at a given level is one)	
y		MFRV	mole fraction of a component in vapor phase	
Z		ANM	atomic number	
Z	D, h	ZEL	elevation referred to datum	L
Z	D, h	ZEL	height, or fluid head or elevation referred to a datum	L
Z		MPD	impedance	various
Z_a		MPDA	impedance, acoustic	m/L ² t
z	Z	ZED	gas compressibility factor (deviation factor) ($z = pV/nRT$)	
z		MFRM	mole fraction of a component in mixture	
z		VAL	valence	
$z_{\bar{p}}$	$Z_{\bar{p}}$	ZEDPAV	gas deviation factor (compressibility factor) at mean pressure	
Greek				
α	β, γ	ANG	angle	
α	M_α	COEA	attenuation coefficient	1/L
α	a, η_h	HTD	heat or thermal diffusivity	L ² /t
α		RED	reduction ratio or reduction term	
α	a, η_h	HTD	thermal or heat diffusivity	L ² /t
$\alpha_{SP_{sh}}$		REDSH	reduction ratio, SP, due to shaliness	
β	γ	BRGR	bearing, relative	
β	b	HEC	thermal cubic expansion coefficient	1/T
γ		GRY	gamma ray [usually with identifying subscript(s)]	various
γ	s, F_s	SPG	specific gravity (relative density)	
γ	k	HSPR	specific heat ratio	
γ	ϵ_s	STNS	strain, shear	
$\dot{\gamma}$	\dot{e}	SRT	shear rate	1/t
γ_g	s_g, F_{gs}	SPGG	specific gravity, gas	
γ_o	s_o, F_{os}	SPGO	specific gravity, oil	
γ_w	s_w, F_{ws}	SPGW	specific gravity, water	
Δ		DEL	difference or difference operator, finite ($\Delta x = x_2 - x_1$ or $x_1 - x_2$)	
ΔG_e	Δg_e	DELGASE	gas influx (encroachment) during an interval	L ³
ΔG_i	Δg_i	DELGASI	gas injected during an interval	L ³
ΔG_p	Δg_p	DELGASP	gas produced during an interval	L ³
ΔN_e	Δn_e	DELOILE	oil influx (encroachment) during an interval	L ³
ΔN_p	Δn_p	DELOILP	oil produced during an interval	L ³
ΔW_e	Δw_e	DELWTRE	water influx (encroachment) during an interval	L ³
ΔW_i	Δw_i	DELWTRI	water injected during an interval	L ³
ΔW_p	Δw_p	DELWTRP	water produced during an interval	L ³
Δr	ΔR	DELRAD	radial distance (increment along radius)	L
Δt_{wf}	$\Delta \tau_{wf}$	DELTIMWF	drawdown time (time after well is opened to production) (pressure drawdown)	t
Δt_{ws}	$\Delta \tau_{ws}$	DELTIMWS	buildup time; shut-in time (time after well is shut in) (pressure buildup, shut-in time)	t

Letter Symbol	Reserve SPE Letter Symbol	Computer Letter Symbol	Quantity	Dimensions
δ	Δ	DCR	decrement	various
δ		ANGH	deviation, hole (drift angle)	
δ	F_d	DPR	displacement ratio	
δ		ANGH	drift angle, hole (deviation)	
δ	r_s	SKD	skin depth (logging)	L
δ_{ob}	F_{dob}	DPROB	displacement ratio, oil from burned volume, volume per unit volume of burned reservoir rock	
δ_{ou}	F_{dou}	DPROU	displacement ratio, oil from unburned volume, volume per unit volume of unburned reservoir rock	
δ_{wb}	F_{dwb}	DPRWB	displacement ratio, water from burned volume, volume per unit volume of burned reservoir rock	
ϵ		DIC	dielectric constant	$q^2 t^2 / mL^3$
ϵ	e, ϵ_n	STN	strain, normal and general	
η		DFS	hydraulic diffusivity ($k/\phi c \mu$ or $\lambda/\phi c$)	L^2/t
Θ	α_d	ANGD	angle of dip	
Θ_a	α_{da}	ANGDA	dip, apparent angle of	
Θ_c	Γ_c, γ_c	ANGC	contact angle	
θ	β, γ	ANG	angle	
θ	θ_V	STNV	strain, volume	
λ	C	LAM	decay constant ($1/\tau_d$)	$1/t$
λ		MOB	mobility (k/μ)	$L^3 t/m$
λ		WVL	wave length ($1/\sigma$)	L
λ_g		MOBG	mobility, gas	$L^3 t/m$
λ_o		MOBO	mobility, oil	$L^3 t/m$
λ_t	Λ	MOBT	mobility, total, of all fluids in a particular region of the reservoir [e.g., $(\lambda_o + \lambda_g + \lambda_w)$]	$L^3 t/m$
λ_w		MOBW	mobility, water	$L^3 t/m$
μ	ν, σ	PSN	Poisson's ratio	
μ	M	RAZ	azimuth of reference on sonde	
μ	m	PRMM	magnetic permeability	mL/q^2
μ		MEN	mean value of a random variable	
μ	η	VIS	viscosity, dynamic	m/Lt
μ_a	η_a	VISA	viscosity, air	m/Lt
μ_g	η_g	VISG	viscosity, gas	m/Lt
μ_{ga}	η_{ga}	VISGA	viscosity, gas, at 1 atm	m/Lt
μ_o	η_o	VISO	viscosity, oil	m/Lt
$\mu_{\bar{p}}$	$\eta_{\bar{p}}$	VISPAV	viscosity at mean pressure	m/Lt
μ_w	η_w	VISW	viscosity, water	m/Lt
ν	N	VSK	kinematic viscosity	L^2/t
ν	N	VSK	viscosity, kinematic	L^2/t
ρ	D	DEN	density	m/L^3
ρ	R	RHO	electrical resistivity (other than logging)	mL^3/tq^2
$\bar{\rho}_L$	\bar{D}_L	DENAVL	density of produced liquid, weight-weighted average	m/L^3
ρ_F	D_F	DENFU	density, fuel	m/L^3
ρ_a	D_a	DENA	density, apparent	m/L^3
ρ_b	D_b	DENB	density, bulk	m/L^3
ρ_f	D_f	DENF	density, fluid	m/L^3
ρ_g	D_g	DENG	density, gas	m/L^3

Letter Symbol	Reserve SPE Letter Symbol	Computer Letter Symbol	Quantity	Dimensions
ρ_{ma}	D_{ma}	DENMA	density, matrix (solids, grain)	m/L ³
ρ_o	D_o	DENO	density, oil	m/L ³
ρ_{sE}	D_{sE}	DENSEX	density of solid particles making up experimental pack	m/L ³
ρ_t	D_t	DENT	density, true	m/L ³
ρ_w	D_w	DENW	density, water	m/L ³
ρ_{xo}	D_{xo}	DENXO	density, flushed zone	m/L ³
Σ	S	XSTMAC	cross section, macroscopic	1/L
Σ		SUM	summation (operator)	
σ	γ	SIG	conductivity, electrical (other than logging)	various
σ		XSTMIC	cross section, microscopic	1/L
σ	s	XLN	cross section of a nucleus, microscopic	L ²
σ	y, γ	SFT	interfacial, surface tension	m/t ²
σ		XSTMIC	microscopic cross section	L ²
σ		SDV	standard deviation of a random variable	
σ	s	STS	stress, normal and general	m/Lt ²
σ	y, γ	SFT	surface tension, interfacial	m/t ²
σ	$\bar{\nu}$	WVN	wave number (1/ λ)	1/L
σ^2		VAR	variance of a random variable	
τ	s_s	STSS	stress, shear	m/Lt ²
τ	τ_c	TIMC	time constant	t
$\bar{\tau}$	\bar{t}	TIMAV	lifetime, average (mean life)	t
τ_H		TORHL	hydraulic tortuosity	
τ_H		TORHL	tortuosity, hydraulic	
τ_d	t_d	TIMD	decay time (mean life) (1/ λ)	t
τ_d	t_d	TIMD	mean life (decay time) (1/ λ)	t
τ_e		TORE	tortuosity, electric	
Φ	β_d	DAZ	dip, azimuth of	
Φ	f	POT	potential or potential function	various
ϕ	f, ϵ	POR	porosity ($V_b - V_s$)/ V_b	
ϕ_E	f_E, ϵ_E	POREX	porosity of experimental pack	
ϕ_R	f_R, ϵ_R	PORR	porosity of reservoir or formation	
ϕ_a	f_a, ϵ_a	PORA	porosity, apparent	
ϕ_e	f_e, ϵ_e	PORE	porosity, effective (V_{pe}/V_b)	
ϕ_h	f_h, ϵ_h	PORH	porosity, hydrocarbon-filled, fraction or percent of rock bulk volume occupied by hydrocarbons	
ϕ_{ig}	f_{ig}, ϵ_{ig}	PORIG	"porosity" (space), intergranular ($V_b - V_{gr}$)/ V_b	
ϕ_{im}	f_{im}, ϵ_{im}	PORIM	"porosity" (space), intermatrix ($V_b - V_{ma}$)/ V_b	
ϕ_{ne}	f_{ne}, ϵ_{ne}	PORNE	porosity, noneffective (V_{pne}/V_b)	
ϕ_t	f_t, ϵ_t	PORT	porosity, total	
Ψ		STR	stream function	various
ψ		DSM	dispersion modulus (dispersion factor)	
ω			angular frequency	1/t
Math				
\propto			proportional to	
$\bar{}$		AV	average or mean (overbar)	
$<$		LT	smaller than	
\leq		LE	equal to or smaller than	
$>$		GT	larger than	
\geq		GE	equal to or larger than	

Letter Symbol	Reserve SPE Letter Symbol	Computer Letter Symbol	Quantity	Dimensions
\sim		ASYM	asymptotically equal to	
\approx		APPR	approximately equal to or is approximated by (usually with functions)	
∇		DEL	del (gradient operator)	
$\nabla \cdot$			divergence	
∇^2			Laplacian operator	
∇x			curl	
erf		ERF	error function	
$erfc$		ERFC	error function, complementary	
\lim		LM	limit	
b	γ	ICP	intercept	various
E_n			Euler's number	
$Ei(x)$			exponential integral, modified	
			$\lim_{\epsilon \rightarrow 0} \left[\int_{-\infty}^{-\epsilon} \frac{e^t}{t} dt + \int_{\epsilon}^{\infty} \frac{e^t}{t} dt \right], x \text{ positive}$	
$-Ei(-x)$			exponential integral, $\int_x^{\infty} \frac{e^{-t}}{t} dt, x \text{ positive}$	
e^z	$\exp z$	EXP	exponential function	
F		FAC	ratio	
f	F	FRC	fraction	
$\Im(z)$			imaginary part of complex number z	
$\mathcal{L}(y)$			Laplace transform of $y, \int_0^{\infty} y(t) e^{st} dt$	
\ln			logarithm, natural, base e	
\log			logarithm, common, base 10	
\log_a			logarithm, base a	
m	A	SLP	slope	various
N		NUMQ	number, dimensionless	
n		NMB	number (of variables, or steps, or increments, etc.)	
$\Re(z)$			real part of complex number z	
s			Laplace transform variable	
s		SDVES	standard deviation of a random variable, estimated	
s^2		VARES	variance of a random variable, estimated	
\bar{x}		MENES	mean value of a random variable, x , estimated	
\vec{x}			vector of x	
$\vec{\vec{x}}$			tensor of x	
α	β, γ	ANG	angle	
γ			Euler's constant=0.5772	
Δ			difference ($\Delta x = x_2 - x_1$ or $x_1 - x_2$)	
Δ			difference operator, finite	
μ		MEN	mean value of a random variable	
Φ	f	POT	potential or potential function	various
Ψ		STR	stream function	various
σ		SDV	standard deviation of a random variable	
σ^2		VAR	variance of a random variable	

Quantities in Alphabetical Order

Quantity	Letter Symbol	Reserve SPE Letter Symbol	Computer Letter Symbol	Dimensions
Arrhenius reaction-rate velocity constant	w	z	ARR	L^3/m
absolute permeability (fluid flow)	k	K	PRM	L^2
acceleration of gravity	g		GRV	L/t^2
acoustic impedance	Z_a		MPDA	m/L^2t
acoustic velocity	v	V, u	VAC	L/t
activity	a		ACT	
air/fuel ratio	F_{aF}		FACAFU	various
air injection rate	i_a		INJA	L^3/t
air requirement	a	F_a	AIR	various
air requirement, unit, in laboratory experimental run, volumes of air per unit mass of pack	a_E	F_{aE}	AIREX	L^3/m
air requirement, unit, in reservoir, volumes of air per unit bulk volume of reservoir rock	a_R	F_{aR}	AIRR	
air viscosity	μ_a	η_a	VISA	m/Lt
amortization (annual write-off of unamortized investment at end of year k)	m_k		AMAK	M
amplitude	A		AMP	various
amplitude, compressional wave	A_c		AMPC	various
amplitude, relative	A_r		AMPR	various
amplitude, shear wave	A_s		AMPS	various
angle	α	β, γ	ANG	
angle	θ	β, γ	ANG	
angle of dip	Θ	α_d	ANGD	
angle, contact	θ_c	Γ_c, γ_c	ANGC	
angular frequency	ω omega		FQNGANG	$1/t$
anisotropy coefficient	K_{ani}	M_{ani}	COEANI	
annual operating cash income, over year k	I_R		INCK	M
annulus geometrical factor (multiplier or fraction)	G_{an}	f_{Gan}	GMFAN	
apparent interval transit time	t_a script t	Δt	TACA	t/L
apparent conductivity	C_a	σ_a	ECNA	tq^2/mL^3
apparent density	ρ_a rho	D_a	DENA	m/L^3
apparent or effective wellbore radius (includes effects of well damage or stimulation)	r_{wa}	R_{wa}	RADWA	L
apparent porosity	ϕ_a	f_a, ϵ_a	PORA	
apparent resistivity	R_a	ρ_a, r_a	RESA	mL^3/tq^2
apparent resistivity of the conductive fluids in an invaded zone (due to fingering)	R_z	ρ_z, r_z	RESZ	mL^3/tq^2
approximately equal to or is approximated by (usually with functions)	\approx		APPR	
area	A	S	ARA	L^2
areal efficiency (used in describing results of model studies only); area swept in a model divided by total model reservoir area (see E_p)	E_A	η_A, e_A	EFFA	
asymptotically equal to	\sim		ASYM	

Dimensions: L=length, m=mass, q=electrical charge, t=time, T=temperature, and M=money.

Quantity	Letter Symbol	Reserve SPE Letter Symbol	Computer Letter Symbol	Dimensions
atmospheric pressure	p_a	P_a	PRSA	m/Lt ²
atomic number	Z		ANM	
atomic weight	A		AWT	m
attenuation coefficient	α	M_α	COEA	1/L
average flow rate or production rate	\bar{q}	\bar{Q}	RTEAV	L ³ /t
average or mean (overbar)	—		AV	
average pressure	\bar{p}	\bar{P}	PRSAV	m/Lt ²
average reservoir pressure	\bar{p}_R	\bar{P}	PRSAVR	m/Lt ²
azimuth of dip	Φ	β_d	DAZ	
azimuth of reference on sonde	μ	M	RAZ	
backpressure-curve exponent, gas well	n		NGW	
backpressure curve (gas well), coefficient of	C		CGW	L ³⁻²ⁿ t ⁴ⁿ /m ²ⁿ
backpressure curve (gas well), exponent of	n		NGW	
base a , logarithm	\log_a			
bearing, relative	β	γ	BRGR	
bed thickness, individual	h	d, e	THK	L
bottomhole flowing pressure	p_{wf}	P_{wf}	PRSWF	m/Lt ²
bottomhole pressure	p_{bh}	P_{BH}	PRSBH	m/Lt ²
bottomhole pressure flowing	p_{wf}	P_{wf}	PRSWF	m/Lt ²
bottomhole flowing pressure, injection well	p_{iwf}	P_{iwf}	PRSIWF	m/Lt ²
bottomhole static pressure, injection well	p_{iws}	P_{iws}	PRSIWS	m/Lt ²
bottomhole pressure at any time after shut-in	p_{ws}	P_{ws}	PRSWS	m/Lt ²
bottomhole pressure, general	p_w	P_w	PRSW	m/Lt ²
bottomhole pressure, static	p_{ws}	P_{ws}	PRSWS	m/Lt ²
bottomhole (well) pressure in water phase	p_{ww}	P_{ww}	PRSWW	m/Lt ²
bottomhole temperature	T_{bh}	θ_{BH}	TEMBH	T
breadth, width, or thickness (primarily in fracturing)	b	w	WTH	L
boundary pressure, external	p_e	P_e	PRSE	m/Lt ²
boundary radius, external	r_e	R_e	RADE	L
bubblepoint formation volume factor, gas	B_{gb}	F_{gb}	FVFGb	
bubblepoint formation volume factor, oil	B_{ob}	F_{ob}	FVFOB	
bubblepoint (saturation) pressure	p_b	p_s, P_s, P_b	PRSB	m/Lt ²
bubblepoint reciprocal gas formation volume factor at bubblepoint conditions	b_{gb}	f_{gb}, F_{gb}	RVFGb	
bubblepoint pressure, volume at	V_{bp}	v_{bp}	VOLBP	L ³
bubblepoint solution gas/oil ratio	R_{sb}	F_{gsb}	GORSB	
buildup time; shut-in time (time after well is shut in) (pressure buildup, shut-in time)	Δt_{ws}	$\Delta \tau_{ws}$	DELTIMWS	t
bulk density	ρ_b rho	D_b	DENB	m/L ³
bulk modulus	K	K_b	BKM	m/Lt ²
bulk volume	V_b	v_b	VOLB	L ³
bulk volume of pack burned in experimental tube run	V_{bE}	v_{bE}	VOLBEX	L ³
bulk (total) volume, fraction of	f_V	f_{Vb}, V_{bf}	FRCVB	
burned reservoir rock, volume of	V_{Rb}	v_{Rb}	VOLRB	L ³
burning-zone advance rate (velocity of)	v_b	V_b, u_b	VELB	L/t
capacitance	C		ECQ	q ² t ² /mL ²

Quantity	Letter Symbol	Reserve SPE Letter Symbol	Computer Letter Symbol	Dimensions
capacity, cation exchange, per unit pore volume	Q_V	Z_V	CEXV	
capacity, cation exchange, per unit pore volume, total	Q_{Vt}	Z_{Vt}	CEXUT	
capacity, storage	S	s, σ	STO	various
capacity, dimensionless fractional storage	S_{pD}	S_D	STOQ	
capillary pressure	P_c	P_C, p_C	PRSCP	m/Lt ²
capital investment, initial	C_i		INVI	M
capital investment, subsequent, in year k	C_k		INVK	M
capital investments, summation of all	C	C_i	INVT	M
cash flow, discounted (present value)	P_{PV}		CFLPV	M
cash flow, undiscounted	P		CFL	M
cash income, annual operating, over year k	I_k		INCK	M
cash income, operating	I		INC	M
cash income, operating, after taxes	I_a		INCA	M
cash income, operating, before taxes	I_b		INCB	M
casing pressure, flowing	p_{cf}	P_{cf}	PRSCF	m/Lt ²
casing pressure, static	p_{cs}	P_{cs}	RSCS	m/Lt ²
cation exchange capacity per unit pore volume	Q_V	Z_V	CEXV	
cation exchange capacity per unit pore volume, total	Q_{Vt}	Z_{Vt}	CEXUT	
cementation (porosity) exponent (in an empirical relation between F_R and ϕ)	m		MPX	
charge (current times time)	Q	q	CHG	q
coefficient, anisotropy	K_{ani}	M_{ani}	COEANI	
coefficient, attenuation	α	M_α	COEA	1/L
coefficient, convective heat transfer	h	h_h, h_T	HTCC	m/t ³ T
coefficient, diffusion	D	μ, δ	DFN	L ² /t
coefficient, electrochemical	K_c	M_c, K_{ec}	COEC	mL ² /t ² q
coefficient, formation resistivity factor ($F_R \phi^m$)	K_R	$M_R a, C$	COER	
coefficient in the equation of the electro- chemical component of the SP (spontaneous electromotive force)	K		KSP	mL ² /t ² q
coefficient of gas-well backpressure curve	C		CGW	L ³⁻²ⁿ t ⁴ⁿ /m ²ⁿ
coefficient heat transfer, overall	U	U_T, U_θ	HTCU	m/t ³ T
coefficient, heat transfer, radiation	I	I_T, I_θ	HTCI	m/t ³ T
coefficient, thermal cubic expansion	β	b	HEC	1/T
coefficient or multiplier	K	M	COE	various
combined total liquid saturation	S_L	ρ_L, S_L	SATL	
common logarithm, base 10	log			
component j , cumulative moles produced	n_{pj}	N_{pj}	MOLPJ	
component j , moles of	n_j	N_j	MOLJ	
component, mole fraction of, in liquid phase	x		MFRL	
component, mole fraction of, in mixture	z		MFRM	
component, mole fraction of, in vapor phase	y		MFRV	
components, number of	C	n_C	NMBC	
component of the SP, electrochemical	E_c	Φ_c	EMFC	mL ² /t ² q
component of the SP, electrokinetic	E_k	Φ_k	EMFK	mL ² /t ² q
compressibility	c	k, κ	CMP	Lt ² /m
compressibility factor (gas deviation factor, $z = pV/nRT$)	z	Z	ZED	

Quantity	Letter Symbol	Reserve SPE Letter Symbol	Computer Letter Symbol	Dimensions
compressibility factor or deviation factor for gas, at mean pressure	$z_{\bar{p}}$	$Z_{\bar{p}}$	ZEDPAV	
compressibility, formation or rock	c_f	k_f, κ_f	CMPF	Lt^2/m
compressibility, gas	c_g	k_g, κ_g	CMPG	Lt^2/m
compressibility, oil	c_o	k_o, κ_o	CMPO	Lt^2/m
compressibility, pseudoreduced	c_{pr}	k_{pr}, κ_{pr}	CMPPRD	
compressibility, water	c_w	k_w, κ_w	CMPW	Lt^2/m
compressional wave amplitude	A_c		AMPC	various
concentration	C	c, n	CNC	various
concentration, methane (concentration of other paraffin hydrocarbons would be indicated similarly, C_{C_2} , C_{C_3} , etc.)	C_{C_1}	c_{C_1}	CNCC1	various
concentration, oxygen (concentration of other elements or compounds would be indicated similarly, C_{CO_2} , C_{N_2} , etc.)	C_{O_2}	c_{O_2}	CNCO2	various
concentration, unit fuel (see symbol m)	C_m	c_m, n_m	CNCFU	various
condensate liquids in place in reservoir, initial	G_L	g_L	NGLTI	L^3
condensate liquids produced, cumulative	G_{Lp}	g_{Lp}	NGLP	L^3
condensate or natural gas liquids content	C_L	c_L, n_L	CNTL	various
conductivity, electrical (other than logging)	σ	γ	SIG	various
conductivity (electrical logging)	C	σ	ECN	tq^2/mL^3
conductivity (electrical), apparent	C_a	σ_a	ECNA	tq^2/mL^3
conductivity, fracture, dimensionless	C_{fD}	K_{fD}	CNDFQ	
conductivity, other than electrical (with subscripts)	C	K	CND	various
conductivity, thermal (always with additional phase or system subscripts)	k_h	λ	HCN	mL/t^3T
constant, Arrhenius reaction-rate velocity constant	w	z	ARR	L^3/m
constant, decay ($1/\tau_d$)	λ	C	LAM	$1/t$
constant, dielectric	ϵ epsilon		DIC	q^2t^2/mL^3
constant, Euler's = 0.5772	γ			
constant in general*				
constant-income discount factor	D_c		DSCC	
constant, hyperbolic decline, $q = q_i / \left[1 + \frac{a_i t}{h} \right]^h$	h		HPC	
constant, universal gas (per mole)	R		RRR	mL^2/t^2T
constant, waterdrive	C		WDC	L^4t^2/m
constant, waterdrive, linear aquifer	C_L		WDCL	L^4t^2/m
consumption, fuel	m	F_F	FCM	various
consumption of fuel in experimental tube run	m_E	F_{FE}	FCMEX	m/L^3
consumption of fuel in experimental tube run (mass of fuel per mole of produced gas)	m_{Eg}	F_{FEg}	FCMEXG	m
consumption of fuel in reservoir	m_R	F_{FR}	FCMR	m/L^3
contact angle	Θ_c	Γ_c, γ_c	ANGC	
content, condensate or natural gas liquids	C_L	c_L, n_L	CNTL	various
content, wet-gas	C_{wg}	c_{wg}, n_{wg}	CNTWG	various
convective heat-transfer coefficient	h	h_h, h_T	HTCC	m/t^3T

*Any suitable nonconflicting symbol defined in the text.

Quantity	Letter Symbol	Reserve SPE Letter Symbol	Computer Letter Symbol	Dimensions
conversion factor in Newton's Second Law of Motion	g_c		GRVC	
correction term or correction factor (either additive or multiplicative)	B	C	COR	
count rate (general)	N	n, C	NMB	1/t
count rate, neutron	N_N	N_n, C_N	NEUN	1/t
count rate, gamma ray	N_{GR}	N_γ, C_G	NGR	1/t
critical gas saturation	S_{gc}	ρ_{gc}, S_{gc}	SATGC	
critical pressure	P_c	P_c	PRSC	m/Lt ²
critical temperature	T_c	θ_c	TEMC	T
critical water saturation	S_{wc}	ρ_{wc}, S_{wc}	SATWC	
cross section (area)	A	S	ARA	L ²
cross section, macroscopic	Σ	S	XSTMAC	1/L
cross section, microscopic	σ		XSTMIC	1/L
cross section of a nucleus, microscopic	σ	s	XNL	L ²
cubic expansion coefficient, thermal	β	b	HEC	1/T
cumulative condensate liquids produced	G_{Lp}	g_{Lp}	NGLP	L ³
cumulative free gas produced	G_{Fp}	g_{Fp}	GASFP	L ³
cumulative gas influx (encroachment)	G_e	g_e	GASE	L ³
cumulative gas injected	G_i	g_i	GASI	L ³
cumulative gas/oil ratio	R_p	F_{gp}, F_{gop}	GORP	
cumulative gas produced	G_p	g_p	GASP	L ³
cumulative moles of component j produced	n_{pj}	N_{pj}	MOLPJ	
cumulative oil influx (encroachment)	N_e	n_e	OILE	L ³
cumulative oil produced	N_p	n_p	OILP	L ³
cumulative produced fluids (where N_p and W_p are not applicable)	Q_p		FLUP	
cumulative water influx (encroachment)	W_e	w_e	WTRE	L ³
cumulative water injected	W_i	w_i	WTRI	L ³
cumulative water/oil ratio	F_{wop}		FACWOP	mL/t ²
cumulative water produced	W_p	w_p	WTRP	L ³
cumulative wet gas produced	G_{wgp}	g_{wgp}	GASWGP	L ³
curl	$\nabla \times$			
current, electric	I	i script i, i	CUR	q/t
damage or stimulation radius of well (skin)	r_s	R_s	RADS	L
damage ratio or condition ratio (conditions relative to formation conditions unaffected by well operations)	F_s	F_d	DMRS	
datum, elevation referred to	Z	D, h	ZED	L
decay constant ($1/\tau_d$)	λ	C	LAM	1/t
decay time (mean life) ($1/\lambda$)	τ_d	t_d	TIMD	t
decay time, neutron (neutron mean life)	t_{dN}		TIMDN	t
decline constant, hyperbolic, from the equation $q = q_i / \left(1 + \frac{a_i t}{h} \right)^h$	h		HPC	
decline factor, effective	d		DECE	
decline factor, nominal	a		DEC	
decrement	δ	Δ	DCR	various
degrees of freedom	F		DGF	

Quantity	Letter Symbol	Reserve SPE Letter Symbol	Computer Letter Symbol	Dimensions
del (gradient operator)	∇		DEL	
delay time	t_d	τ_d	TIMDY	t
deliverability (gas well)	D		DLV	L ³ /t
density	ρ rho	D	DEN	m/L ³
density, apparent	ρ_a	D_a	DENA	m/L ³
density, bulk	ρ_b	D_b	DENB	m/L ³
density, fluid	ρ_f	D_f	DENF	m/L ³
density, flushed zone	ρ_{xo}	D_{xo}	DENXO	m/L ³
density (indicating "number per unit volume")	n	N	NMB	1/L ³
density, fuel	ρ_f	D_F	DENFU	m/L ³
density, gas	ρ_g	D_g	DENG	m/L ³
density, matrix (solids, grain)	ρ_{ma}	D_{ma}	DENMA	m/L ³
density (number) of neutrons	n_N		NMBN	1/L ³
density of produced liquid, weight-weighted average	$\bar{\rho}_L$	\bar{D}_L	DENAVL	m/L ³
density of solid particles making up experimental pack	ρ_{SE}	D_{SE}	DENSEX	m/L ³
density, oil	ρ_o	D_o	DENO	m/L ³
density, relative (specific gravity)	γ	s, F_s	SPG	
density, true	ρ_t	D_t	DENT	m/L ³
density, water	ρ_w	D_w	DENW	m/L ³
depletion	D_E		EDE	
deposition rate of fuel	N_R	N_F	FUDR	m/L ³ t
depreciation	D_P		EDP	
depth	D	y, H	DPH	L
depth, skin (logging)	δ	r_s	SKD	L
deviation factor (compressibility factor) for gas ($z = pV/nRT$)	z	Z	ZED	
deviation factor (compressibility factor) for gas, at mean pressure	$z_{\bar{p}}$	$Z_{\bar{p}}$	ZEDPAV	
deviation, hole (drift angle)	δ		ANGH	
dewpoint pressure	p_d	P_d	PRSD	m/Lt ²
diameter	d	D	DIA	L
diameter, hole	d_h	d_H, D_h	DIAH	L
diameter, invaded zone (electrically equivalent)	d_i	d_I, D_i	DIAI	L
diameter, mean particle	\bar{d}_p	\bar{D}_p	DIAAVP	L
dielectric constant	ϵ epsilon		DIC	q ² t ² /mL ³
difference or difference operator, finite ($\Delta x = x_2 - x_1$ or $x_1 - x_2$)	Δ		DEL	
diffusion coefficient	D	μ, δ	DFN	L ² /t
diffusivity, hydraulic ($k/\phi c \mu$ or $\lambda/\phi c$)	η		DFS	L ² /t
dimensionless fluid influx function, linear aquifer	Q_{LiD}	Q_{LiD} script l	ENCLTQQ	
dimensionless fluid influx function at dimensionless time t_D	Q_{iD}		ENCTQQ	
dimensionless fractional storage capacity	S_{fD}	S_D	STQQ	
dimensionless fracture conductivity	C_{fD}	K_{fD}	CNDFQ	
dimensionless gas production rate	q_{gD}	Q_{gD}	RTEGQ	
dimensionless number, in general (always with identifying subscripts) (Example: Reynolds number, N_{Re})	N		NUMQ	
dimensionless oil-production rate	q_{oD}	Q_{oD}	RTEOQ	
dimensionless pore volume	V_{pD}	v_{pD}	VOLPQ	

Quantity	Letter Symbol	Reserve SPE Letter Symbol	Computer Letter Symbol	Dimensions
dimensionless pressure	P_D	P_D	PRSQ	
dimensionless-pressure function at dimensionless time t_D	P_{tD}	P_{tD}	PRSTQQ	
dimensionless production rate	q_D	Q_D	RTEQ	
dimensionless quantity proportional to x	x_D			
dimensionless radius	r_D	R_D	RADQ	
dimensionless time	t_D	τ_D	TIMQ	
dimensionless time at condition m	t_{Dm}	τ_{Dm}	TIMMQ	
dimensionless water production rate	q_{wD}	Q_{wD}	RTEWQ	
dip, angle of	Θ	α_d	ANGD	
dip, apparent angle of	Θ_a	α_{da}	ANGDA	
dip, apparent azimuth of	Φ_a	β_{da}	DAZA	
dip, azimuth of	Φ	β_d	DAZ	
discount factor, constant-income	D_c		DSCC	
discount factor, general	D		DSC	
discount factor, single-payment [$1/(1+i)^k$; or e^{-jk} , $j = \ln(1+i)$]	D_{sp}		DSCSP	
discount factor, single-payment (constant annual rate) [$e^{-jk}(e^j - 1)/j$]	D_{spc}		DSCSPC	
discount rate	i		RTED	
discounted cash flow	P_{PV}		CFLPV	
dispersion coefficient	K	d	DSP	L^2/t
dispersion modulus (dispersion factor)	ψ		DSM	
displacement	s	L	DIS	L
displacement efficiency from burned portion of in-situ combustion pattern	E_{Db}	η_{Db}, e_{Db}	EFFDB	
displacement efficiency from unburned portion of in-situ combustion pattern	E_{Du}	η_{Du}, e_{Du}	EFFDU	
displacement efficiency: volume of hydrocarbons (oil or gas) displaced from individual pores or small groups of pores divided by the volume of hydrocarbons in the same pores just before displacement	E_D	η_D, e_D	EFFD	
displacement ratio	δ	F_d	DPR	
displacement ratio, oil from burned volume, volume per unit volume of burned reservoir rock	δ_{ob}	F_{dob}	DPROB	
displacement ratio, oil from unburned volume, volume per unit volume of unburned reservoir rock	δ_{ou}	F_{dou}	DPROU	
displacement ratio, water from burned volume, volume per unit volume of burned reservoir rock	δ_{wb}	F_{dwb}	DPRWB	
distance between adjacent rows of injection and production wells	d	L_d, L_2	DUW	L
distance between like wells (injection or production) in a row	a	L_a, L_1	DLW	L
distance, length, or length of path	L	s, ℓ script l	LTH	L
distance, radial (increment along radius)	Δr	ΔR	DELRAD	L

Quantity	Letter Symbol	Reserve SPE Letter Symbol	Computer Letter Symbol	Dimensions
divergence	∇			
drainage radius	r_d	R_d	RADD	L
drawdown time (time after well is opened to production) (pressure drawdown)	Δt_{wf}	$\Delta \tau_{wf}$	DELTIMWF	t
drift angle, hole (deviation)	δ		ANGH	
earning power or rate of return (internal, true, or discounted cash flow)	i_r		RORI	
effect, skin	s	S, σ	SKN	
effective decline factor	d		DECE	
effective or apparent wellbore radius (includes effects of well damage or stimulation)	r_{wa}	R_{wa}	RADWA	L
effective permeability to gas	k_g	K_g	PRMG	L ²
effective permeability to oil	k_o	K_o	PRMO	L ²
effective permeability to water	k_w	K_w	PRMW	L ²
effective porosity	ϕ_e	f_e, ϵ_e	PORE	
efficiency	E	η, e	EFF	
efficiency, areal (used in describing results of model studies only): area swept in a model divided by total model reservoir area (see E_p)	E_A	η_A, e_A	EFFA	
efficiency, displacement, from burned portion of in-situ combustion pattern	E_{Db}	η_{Db}, e_{Db}	EFFDB	
efficiency, displacement, from unburned portion of in-situ combustion pattern	E_{Du}	η_{Du}, e_{Du}	EFFDU	
efficiency, displacement: volume of hydrocarbons (oil or gas) displaced from individual pores or small groups of pores divided by the volume of hydrocarbon in the same pores just before displacement	E_D	η_D, e_D	EFFD	
efficiency, invasion (vertical): hydrocarbon pore space invaded (affected, contacted) by the injection fluid or heat front divided by the hydrocarbon pore space enclosed in all layers behind the injected fluid or heat front	E_I	η_I, e_I	EFFI	
efficiency, overall reservoir recovery: volume of hydrocarbons recovered divided by volume of hydrocarbons in place at start of project ($E_R = E_p E_I E_D = E_V E_D$)	E_R	η_R, e_R	EFFR	
efficiency, pattern sweep (developed from areal efficiency by proper weighting for variations in net pay thickness, porosity, and hydrocarbon saturation): hydrocarbon pore space enclosed behind the injected-fluid or heat front divided by total hydrocarbon pore space of the reservoir or project	E_P	η_P, e_P	EFFP	
efficiency, volumetric, for burned portion only, in-situ combustion pattern	E_{Vb}	η_{Vb}, e_{Vb}	EFFVB	
efficiency, volumetric: product of pattern sweep and invasion efficiencies	E_V	η_V, e_V	EFFV	
elasticity, modulus of (Young's modulus)	E	Y	ELMY	m/Lt ²

Quantity	Letter Symbol	Reserve SPE Letter Symbol	Computer Letter Symbol	Dimensions
electric current	I	<i>i script i, i</i>	CUR	q/t
electric impedance	Z_e	Z_E, η	MPDE	mL ² /tq ²
electrical conductivity (other than logging)	σ	γ	SIG	various
electrical resistivity (other than logging)	ρ rho	R	RHO	mL ³ /tq ²
electrical resistivity (electrical logging)	R	ρ, r	RES	mL ³ /tq ²
electrical tortuosity	τ_e		TORE	
electrically equivalent diameter of the invaded zone	d_i	d_I, D_i	DIAI	L
electrochemical coefficient	K_c	M_c, K_{ec}	COEC	mL ² /t ² q
electrochemical component of the SP	E_c	Φ_c	EMFC	mL ² /t ² q
electrokinetic component of the SP	E_k	Φ_k	EMFK	mL ² /t ² q
electromotive force	E	V	EMF	mL ² /t ² q
elevation referred to datum	Z	D, h	ZED	L
encroachment or influx, gas, cumulative	G_c	g_e	GASE	L ³
encroachment or influx, gas during an interval	ΔG_c	Δg_e	DELGASE	L ³
encroachment or influx, oil, cumulative	N_c	n_e	OILE	L ³
encroachment or influx, oil, during an interval	ΔN_c	Δn_e	DELOILE	L ³
encroachment or influx rate	e	i	ENC	L ³ /t
encroachment or influx rate, gas	e_g	i_g	ENCG	L ³ /t
encroachment or influx rate, oil	e_o	i_o	ENCO	L ³ /t
encroachment or influx rate, water	e_w	i_w	ENCW	L ³ /t
encroachment or influx, water, cumulative	W_e	w_e	WTRE	L ³
encroachment or influx, water, during an interval	ΔW_e	Δw_e	DELWTRE	L ³
energy	E	U	ENG	mL ² /t ²
enthalpy (always with phase or system subscripts)	H	I	HEN	mL ² /t ²
enthalpy (net) of steam or enthalpy above reservoir temperature	H_s	I_s	HENS	mL ² /t ²
enthalpy, specific	h	i	HENS	L ² /t ²
entropy, specific	s	σ	HERS	L ² /t ² T
entropy, total	S	σ_i	HER	mL ² /t ² T
equal to or larger than	\geq		GE	
equal to or smaller than	\leq		LE	
equilibrium ratio (y/x)	K	k, F_{eq}	EQR	
equivalent diameter (electrical) of the invaded zone	d_i	d_I, D_i	DIAI	L
equivalent time well was on production before shut-in (pseudotime)	t_p	τ_p	TIMP	t
equivalent water resistivity	R_{wc}		RWE	mL ³ /tq ²
error function	erf		ERF	
error function, complementary	$erfc$		ERFC	
Euler number	E_n			
Euler's constant = 0.5772	γ			
expansion coefficient, thermal cubic	β	b	HEC	1/T
experimental pack porosity	ϕ_E	f_E, ϵ_E	POREX	
exponent of backpressure curve, gas well	n		NGW	
exponent, porosity (cementation) (in an empirical relation between F_R and ϕ)	m		MXP	
exponent, saturation	n		SXP	
exponential function	e^z	$\exp z$	EXP	

Quantity	Letter Symbol	Reserve SPE Letter Symbol	Computer Letter Symbol	Dimensions
exponential integral $\int_x^\infty \frac{e^{-t}}{t} dt$, x positive	$-Ei(-x)$			
exponential integral, modified $\lim_{\epsilon \rightarrow 0} \left[\int_{-\infty}^\epsilon \frac{e^t}{t} dt + \int_\epsilon^\infty \frac{e^t}{t} dt \right]$, x positive	$Ei(x)$			
external boundary pressure	p_e	P_e	PRSE	m/Lt ²
external boundary radius	r_e	R_e	RADE	L
extrapolated pressure	p_{ext}	P_{ext}	PRSXT	m/Lt ²
factor, compressibility (gas deviation factor $z = pV/nRT$)	z	Z	ZED	
factor, discount	D		DSC	
factor, effective decline	d		DECE	
factor, nominal decline	a		DEC	
factor, conversion, in Newton's Second Law of Motion	g_c		GRVC	
factor, formation resistivity, equals R_0/R_w (a numerical subscript to F indicates the value of R_w)	F_R		FACHR	
factor, friction	f		FACF	
factor, geometrical (multiplier) (electrical logging)	G	f_G	GMF	
factor, geometrical (multiplier) annulus (electrical logging)	G_{an}	f_{Gan}	GMFAN	
factor, geometrical (multiplier) invaded zone (electrical logging)	G_i	f_{Gi}	GMFI	
factor, geometrical (multiplier) pseudo (electrical logging)	G_p	f_{Gp}	GMFP	
factor, geometrical (multiplier) flushed zone (electrical logging)	G_{xo}	f_{Gxo}	GMFXO	
factor, geometrical (multiplier) mud (electrical logging)	G_m	f_{Gm}	GMFM	
factor, geometrical (multiplier) true (noninvaded zone) (electrical logging)	G_t	f_{Gt}	GMFT	
factor in general, including ratios (always with identifying subscripts)	F	A, R, r	FAC	various
factor, turbulence	F_B		FACB	
flow rate, mass	w	m	MRT	m/t
flow rate, heat	Q	q, Φ	HRT	mL ² /t ³
flow rate or flux, per unit area (volumetric velocity)	u	ψ	VELV	L/t
flow rate or production rate	q	Q	RTE	L ³ /t
flow rate or production rate at mean pressure	$q_{\bar{p}}$	$Q_{\bar{p}}$	RTEPAV	L ³ /t
flow rate or production rate, average	\bar{q}	\bar{Q}	RTEAV	L ³ /t
flowing bottomhole pressure, injection well	p_{iwf}	P_{iwf}	PRSIWF	m/Lt ²
flowing pressure, bottomhole	p_{wf}	P_{wf}	PRSWF	m/Lt ²
flowing pressure, casing	p_{cf}	P_{cf}	PRSCF	m/Lt ²
flowing pressure, tubing	p_{tf}	P_{tf}	PRSTF	m/Lt ²

Quantity	Letter Symbol	Reserve SPE Letter Symbol	Computer Letter Symbol	Dimensions
flowing time after well is opened to production (pressure drawdown)	Δt_{wf}	$\Delta \tau_{wf}$	DELTIMWF	t
fluid (generalized)	F	f	FLU	various
fluid interval velocity	v_f	V_f, u_f	VACF	L/t
fluid head or height or elevation referred to a datum	Z	D, h	ZEL	L
fluid interval transit time	t_f <i>script t</i>	Δt_f	TACF	t/L
fluid density	ρ_f rho	D_f	DENF	m/L ³
fluid influx function, dimensionless, at dimensionless time t_D	Q_{tD}		ENCTQQ	
fluid influx function, linear aquifer, dimensionless	$Q_{L/D}$	Q_{tD} <i>script l</i>	ENCLTQQ	
fluids, cumulative produced (where N_p and W_p are not applicable)	Q_p	Q_{tD} <i>script l</i>	FLUP	
flushed-zone density	ρ_{xo} rho	D_{xo}	DENXO	m/L ³
flushed-zone resistivity (that part of the invaded zone closest to the wall of the hole, where flushing has been maximum)	R_{xo}	ρ_{xo}, r_{xo}	RESXO	mL ³ /tq ²
flushed-zone geometrical factor (fraction or multiplier)	G_{xo}	f_{Gxo}	GMFXO	
flux	u	ψ	FLX	various
flux or flow rate, per unit area (volumetric velocity)	u	ψ	VELV	L/t
force, mechanical	F	Q	FCE	mL/t ²
force, electromotive (voltage)	E	V	EMF	mL ² /t ² q
formation or reservoir porosity	ϕ_R	f_R, ϵ_R	PORR	
formation or rock compressibility	c_f	k_f, κ_f	CMPF	Lt ² /m
formation resistivity factor—equals R_o/R_w (a numerical subscript to F indicates the value R_w)	F_R		FACHR	
formation resistivity factor coefficient ($F_R \phi^n$)	K_R	M_R, a, C	COER	
formation resistivity, true	R_t	ρ_t, r_t	REST	mL ³ /tq ²
formation resistivity when 100% saturated with water of resistivity R_w	R_o	ρ_o, r_o	RESZR	mL ³ /tq ²
formation temperature	T_f	θ_f	TEMF	T
formation volume factor at bubblepoint conditions, gas	B_{gb}	F_{gb}	FVFGB	
formation volume factor at bubblepoint conditions, oil	B_{ob}	F_{ob}	FVFOB	
formation volume factor, gas	B_g	F_g	FVFG	
formation volume factor, oil	B_o	F_o	FVFO	
formation volume factor, total (two-phase)	B_t	F_t	FVFT	
formation volume factor, volume at reservoir conditions divided by volume at standard conditions	B	F	FVF	
formation volume factor, water	B_w	F_w	FVFW	
fraction (such as the fraction of a flow stream consisting of a particular phase)	f	F	FRC	
fraction gas	f_g	F_g	FRCG	

Quantity	Letter Symbol	Reserve SPE Letter Symbol	Computer Letter Symbol	Dimensions
fraction liquid	f_L	$F_{L,fl}$ script l	FRCL	
fraction of bulk (total) volume	f_V	f_{Vb}, V_{bf}	FRCVB	
fraction of intergranular space ("porosity") occupied by all shales	$f_{\phi sh}$	ϕ_{igfsh}	FIGSH	
fraction of intergranular space ("porosity") occupied by water	$f_{\phi w}$	ϕ_{igfw}	FIGW	
fraction of intermatrix space ("porosity") occupied by nonstructural dispersed shale	$f_{\phi shd}$	ϕ_{imfshd}	FIMSHD	
fracture conductivity, dimensionless	C_{fD}	K_{fD}	CNDFQ	
fracture half-length (specify "in the direction of" when using x_f)	L_f	x_f	LTHFH	L
fracture index	I_f	i_f, I_f, i_F	FRX	
free energy (Gibbs function)	G	F	GFE	mL^2/t^2
free fluid index	I_{Ff}	i_{Ff}	FFX	
free gas/oil ratio, producing (free-gas volume/oil volume)	R_F	F_{gF}, F_{goF}	GORF	
free gas produced, cumulative	G_{Fp}	g_{Fp}	GASFP	L^3
free-gas volume, initial reservoir ($=mNB_{oi}$)	G_{Fi}	g_{Fi}	GASFI	L^3
free producing gas/oil ratio (free-gas volume/ oil volume)	R_F	F_{gF}, F_{goF}	GORF	
frequency	f	ν	FQN	1/t
friction factor	f		FACF	
front or interface pressure	p_f	P_f	PRSF	m/Lt^2
fuel concentration, unit (see symbol m)	C_m	c_m, n_m	CNCFU	various
fuel consumption	m	F_F	FCM	various
fuel consumption in experimental tube run	m_E	F_{FE}	FCMEX	m/L^3
fuel consumption in experimental tube run (mass of fuel per mole of produced gas)	m_{Eg}	F_{FEg}	FCMEXG	m
fuel consumption in reservoir	m_R	F_{FR}	FCMR	m/L^3
fuel density	ρ_F rho	D_F	DENFU	m/L^3
fuel deposition rate	N_R	N_F	FUDR	m/L^3t
fugacity	f		FUG	m/Lt^2
gamma ray count rate	N_{GR}	N_γ, C_G	NGR	1/t
gamma ray [usually with identifying subscript(s)]	γ		GRY	various
gas(any gas, including air) always with identifying subscripts	G	g	GAS	various
gas-cap interstitial-oil saturation	S_{og}	ρ_{og}, S_{og}	SATOG	
gas-cap interstitial-water saturation	S_{wg}	ρ_{wg}, S_{wg}	SATWG	
gas compressibility	c_g	k_g, κ_g	CMPG	Lt^2/m
gas compressibility factor (deviation factor) ($z=pV/nRT$)	z	Z	ZED	
gas constant, universal (per mole)	R		RRR	mL^2/t^2T
gas density	ρ_g rho	D_g	DENG	m/L^3
gas deviation factor (compressibility factor) at mean pressure	$z_{\bar{p}}$	$Z_{\bar{p}}$	ZEDPAV	
gas deviation factor (compressibility factor, $z=pV/nRT$) (deviation factor)	z	Z	ZED	
gas, effective permeability to	k_g	K_g	PRMG	L^2
gas formation volume factor	B_g	F_g	FVFG	

Quantity	Letter Symbol	Reserve SPE Letter Symbol	Computer Letter Symbol	Dimensions
gas formation volume factor at bubblepoint conditions	B_{gb}	F_{gb}	FVFGB	
gas fraction	f_g	F_g	FRCG	
gas in place in reservoir, total initial	G	g	GASTI	L^3
gas influx (encroachment), cumulative	G_e	g_e	GASE	L^3
gas influx (encroachment) during an interval	ΔG_e	Δg_e	DELGASE	L^3
gas influx (encroachment) rate	e_g	i_g	ENCG	L^3/t
gas injected, cumulative	G_i	g_i	GASI	L^3
gas injected during an interval	ΔG_i	Δg_i	DELGASI	L^3
gas injection rate	i_g		INJG	L^3/t
gas liquids, natural, or condensate content	C_L	c_L, n_L	CNTL	various
gas mobility	λ_g		MOBG	$L^3 t/m$
gas, fraction	f_g	F_g	FRCG	
gas mole fraction $V/(L + V)$	f_g	F_g	MFRTV	
gas/oil permeability ratio	k_g/k_o	K_g/K_o	PRMG0	
gas/oil ratio, cumulative	R_p	F_{gp}, F_{gop}	GORP	
gas/oil ratio, free producing (free-gas volume/ oil volume)	R_f	F_{gf}, F_{gof}	GORF	
gas/oil ratio, producing	R	F_g, F_{go}	GOR	
gas/oil ratio, solution at bubblepoint conditions	R_{sb}	F_{gsb}	GORSB	
gas/oil ratio, solution (gas solubility in oil)	R_s	F_{gs}, F_{gos}	GORS	
gas/oil ratio, solution, initial	R_{si}	F_{gsi}	GORSI	
gas produced, cumulative	G_p	g_p	GASP	L^3
gas produced during an interval	ΔG_p	Δg_p	DELGASP	L^3
gas produced from experimental tube run	G_{pE}	g_{pE}	GASPEX	L^3
gas production rate	q_g	Q_g	RTEG	L^3/t
gas production rate, dimensionless	q_{gD}	Q_{gD}	RTEGQ	
gas reciprocal formation volume factor	b_g	f_g, F_g	RVFG	
gas reciprocal formation volume factor at bubblepoint conditions	b_{gb}	f_{gb}, F_{gb}	RVFGB	
gas recovery, ultimate	G_{pa}	g_{pa}	GASPUL	L^3
gas, relative permeability to	k_{rg}	K_{rg}	PRMRG	
gas saturation	S_g	ρ_g, S_g	SATG	
gas saturation, critical	S_{gc}	ρ_{gc}, S_{gc}	SATGC	
gas saturation, residual	S_{gr}	ρ_{gr}, S_{gr}	SATGR	
gas solubility in oil (solution gas/oil ratio)	R_s	F_{gs}, F_{gos}	GORS	
gas solubility in water	R_{sw}		GWRS	
gas specific gravity	γ_g	s_g, F_{gs}	SPGG	
gas viscosity	μ_g	η_g	VISG	m/Lt
gas viscosity at 1 atm	μ_{ga}	η_{ga}	VISGA	m/Lt
gas-well backpressure curve, coefficient of	C		CGW	$L^{3-2n} t^{4n}/m^{2n}$
gas-well backpressure curve, exponent of	n		NGW	
gas-well deliverability	D		DLV	L^3/t
gas, wet, produced, cumulative	G_{wgp}	g_{wgp}	GASWGP	L^3
general and individual bed thickness	h	d, e	THK	L
general dimensionless number (always with identifying subscripts)	N		NUMQ	
geometrical factor (multiplier) (electrical logging)	G	f_G	GMF	

Quantity	Letter Symbol	Reserve SPE Letter Symbol	Computer Letter Symbol	Dimensions
geometrical factor (multiplier), annulus (electrical logging)	G_{an}	f_{Gan}	GMFAN	
geometrical factor (multiplier), flushed zone (electrical logging)	G_{xo}	f_{Gxo}	GMFXO	
geometrical factor (multiplier), invaded zoned (electrical logging)	G_i	f_{Gi}	GMFI	
geometrical factor (multiplier), mud (electrical logging)	G_m	f_{Gm}	GMFM	
geometrical factor, (multiplier), true (noninvaded zone) (electrical logging)	G_t	f_{Gt}	GMFT	
geometrical factor (multiplier), pseudo (electrical logging)	G_p	f_{Gp}	GMFP	
geometrical factor (multiplier), true (electrical logging)	G_t	f_{Gt}	GMFT	
gradient	g	γ	GRD	various
gradient, geothermal	g_G	g_g	GRDGT	T/L
gradient operator	∇			
gradient, temperature	g_T	g_h	GRDT	T/L
grain (matrix, solids) density	ρ_{ma}	D_{ma}	DENMA	m/L ³
gravity, acceleration of	g		GRV	L/t ²
gravity, specific, relative density	γ	s, F_s	SPG	
gravity, specific, gas	γ_g	s_g, F_{gs}	SPGG	
gravity, specific, oil	γ_o	s_o, F_{os}	SPGO	
gravity, specific, water	γ_w	s_w, F_{ws}	SPGW	
gross (total) pay thickness	h_i	d_i, e_i	THKT	L
gross revenue ("value") per unit produced	V_u	R_u	GRRU	M/L ³
gross revenue ("value"), total	V	R, V_i, R_i	GRRT	M
half-life	$t_{1/2}$		TIMH	t
heat flow rate	Q	q, Φ	HRT	mL ² /t ³
heat of vaporization, latent	L_v	λ_v	HLTV	L ² /t ²
heat or thermal diffusivity	α	a, η_h	HTD	L ² /t
heat, specific (always with phase or system subscripts)	C	c	HSP	L ² /t ² T
heat transfer coefficient, convective	h	h_h, h_T	HTCC	m/t ³ T
heat transfer coefficient, overall	U	U_T, U_θ	HTCU	m/t ³ T
heat transfer coefficient, radiation	I	I_T, I_θ	HTCI	m/t ³ T
height, or fluid head, or elevation referred to a datum	Z	D, h	ZEL	L
height (other than elevation)	h	d, e	ZHT	L
Helmholtz function (work function)	A	F	HWF	mL ² /t ²
holdup (fraction of the pipe volume filled by a given fluid; y_o is oil holdup, y_w is water holdup, Σ of all holdups at a given level is one)	y	f	HOL	
hole deviation, drift angle	δ		ANGH	
hole diameter	d_h	d_H, D_h	DIAH	L
hydraulic diffusivity ($k/\phi c \mu$ or $\lambda/\phi c$)	η		DFS	L ² /t
hydraulic radius	r_H	R_H	RADHL	L
hydraulic tortuosity	τ_H		TORHL	

Quantity	Letter Symbol	Reserve SPE Letter Symbol	Computer Letter Symbol	Dimensions
hydrocarbon-filled porosity, fraction or percent of rock bulk volume occupied by hydrocarbons	ϕ_h	f_h, ϵ_h	PORH	
hydrocarbon resistivity index R_i/R_0	I_R	i_R	RSXH	
hydrocarbon saturation, residual	S_{hr}	ρ_{hr}, s_{hr}	SATHR	
hydrogen index	I_H	i_H	HYX	
hyperbolic decline constant (from equation) $q = q_i / \left(1 + \frac{a_i t}{h} \right)^h$	h		HPC	
imaginary part of complex number z	$\mathcal{I}(z)$ script I			
impedance	Z		MPD	various
impedance, acoustic	Z_a		MPDA	m/L ² t
impedance, electric	Z_e	Z_E, η	MPDE	mL ² /tq ²
index (use subscripts as needed)	I	i	$_X$	
index, fracture	I_f	i_f, I_F, i_F	FRX	
index, free fluid	I_{Ff}	i_{Ff}	FFX	
index, hydrogen	I_H	i_H	HYX	
index, injectivity	I	i	IJX	L ⁴ t/m
index of refraction	n	μ	RFX	
index, porosity	I_ϕ	i_ϕ	PRX	
index, primary porosity	$I_{\phi 1}$	$i_{\phi 1}$	PRXPR	
index, productivity	J	j	PDX	L ⁴ t/m
index, (hydrocarbon) resistivity R_i/R_0	I_R	i_R	RXSH	
index, secondary porosity	$I_{\phi 2}$	$i_{\phi 2}$	PRXSE	
index, shaliness gamma ray $(\gamma_{\log} - \gamma_{cn})/(\gamma_{sh} - \gamma_{cn})$	I_{shGR}	i_{shGR}	SHXGR	
index, specific injectivity	I_s	i_s	IJXS	L ³ t/m
index, specific productivity	J_s	j_s	PDXS	L ³ t/m
individual bed thickness	h	d, e	THK	L
influx (encroachment), cumulative, gas	G_e	g_e	GASE	L ³
influx (encroachment), cumulative, oil	N_e	n_e	OILE	L ³
influx (encroachment), cumulative, water	W_e	w_e	WTRE	L ³
influx (encroachment) during an interval, gas	ΔG_e	Δg_e	DELGASE	L ³
influx (encroachment) during and interval, oil	ΔN_e	Δn_e	DELOILE	L ³
influx (encroachment) during an interval, water	ΔW_e	Δw_e	DELWTRE	L ³
influx function, fluid, linear aquifer, dimensionless	Q_{LiD}	Q_{LiD} script l	ENCLTQQ	
influx function, fluid, dimensionless (at dimensionless time t_D)	Q_{iD}	Q_{iD} script l	ENCTQQ	
influx (encroachment) rate	e	i	ENC	L ³ /t
influx (encroachment) rate, gas	e_g	i_g	ENCG	L ³ /t
influx (encroachment) rate, oil	e_o	i_o	ENCO	L ³ /t
influx (encroachment) rate, water	e_w	i_w	ENCW	L ³ /t
initial condensate liquids in place in reservoir	G_L	g_L	NGLTI	L ³
initial capital investment	C_i		INVI	M
initial oil in place in reservoir	N	n	OILTl	L ³
initial pressure	P_i	P_i	PRSI	m/Lt ²

Quantity	Letter Symbol	Reserve SPE Letter Symbol	Computer Letter Symbol	Dimensions
initial reservoir free-gas volume ($=mNB_{oi}$)	G_{Fi}	g_{Fi}	GASFI	L^3
initial solution gas/oil ratio	R_{si}	F_{gsi}	GORSI	L/t^2
initial water in place in reservoir	W	w	WTRTI	L^3
initial water saturation	S_{wi}	ρ_{wi}, s_{wi}	SATWI	
injected gas, cumulative	G_i	g_i	GASI	L^3
injected gas during an interval	ΔG_i	Δg_i	DELGASI	L^3
injected water, cumulative	W_i	w_i	WTRI	L^3
injected water during an interval	ΔW_i	Δw_i	DELWTRI	L^3
injection rate	i		INJ	L^3/t
injection rate, air	i_a		INJA	L^3/t
injection rate, gas	i_g		INJG	L^3/t
injection rate, water	i_w		INJW	L^3/t
injection well bottomhole pressure, flowing	p_{iwf}	P_{iwf}	PRSIWF	m/Lt^2
injection well bottomhole pressure, static	p_{iws}	P_{iws}	PRSIWS	m/Lt^2
injectivity index	I	i	IJX	$L^4/t/m$
injectivity index, specific	I_s	i_s	IJXS	$L^3/t/m$
in-place condensate liquids in reservoir, initial	G_L	g_L	NGLTI	L^3
in-place gas in reservoir, total initial	G	g	GASTI	L^3
in-place oil in reservoir, initial	N	n	OILTI	L^3
in-place water in reservoir, initial	W	w	WTRTI	L^3
instantaneous producing water/oil ratio	F_{wo}		FACWO	
intercept	b	Y	ICP	various
interest rate, effective compound (usually annual)	i		IRCE	
interest rate, effective, per period	i_M		IRPE	
interest rate, nominal annual	j	r	IRA	
interface or front pressure	p_f	P_f	PRSF	m/Lt^2
interfacial, surface tension	σ	γ, γ	SFT	m/t^2
intergranular "porosity" (space) ($V_b - V_{gr}$)/ V_b	ϕ_{ig}	f_{ig}, ϵ_{ig}	PORIG	
integral, exponential $\int_x^\infty \frac{e^{-t}}{t} dt, x \text{ positive}$	$-Ei(-x)$			
integral, exponential, modified $\lim_{\epsilon \rightarrow 0} \left[\int_{-\infty}^{-\epsilon} \frac{e^t}{t} dt + \int_{\epsilon}^{\infty} \frac{e^t}{t} dt \right], x \text{ positive}$	$Ei(x)$			
intergranular space (porosity), fraction occupied by all shales	$f_{\phi sh}$	ϕ_{igfsh}	FIGSH	
intergranular space (porosity), fraction occupied by water	$f_{\phi w}$	ϕ_{igfw}	FIGW	
intermatrix space (porosity), fraction occupied by nonstructural dispersed shale	$f_{\phi shd}$	ϕ_{imfshd}	FIMSHD	
intermatrix "porosity" (space) ($V_b - V_{ma}$)/ V_b	ϕ_{im}	f_{im}, ϵ_{im}	PORIM	

Quantity	Letter Symbol	Reserve SPE Letter Symbol	Computer Letter Symbol	Dimensions
internal energy	U	E_i	INE	mL^2/t^2
interstitial-oil saturation in gas cap	S_{og}	ρ_{og}, S_{og}	SATOG	
interstitial-water saturation in gas cap	S_{wg}	ρ_{wg}, S_{wg}	SATWG	
interstitial-water saturation in oil band	S_{wo}	S_{wb}	SATWO	
interval transit time	t script t	Δt	TAC	t/L
interval transit time, apparent	t_a script t	Δt_a	TACA	t/L
interval transit time/density slope (absolute value)	M	$m_{\theta D}$	SAD	tL^2/m
interval transit time, fluid	t_f script t	Δt_f	TACF	t/L
interval transit time, matrix	t_{ma} script t	Δt_{ma}	TACMA	t/L
interval transit time, shale	t_{sh} script t	Δt_{sh}	TACSH	t/L
invaded-zone diameter, electrically equivalent	d_i	d_i, D_i	DIAI	L
invaded-zone geometrical factor (multiplier) (electrical logging)	G_i	f_{Gi}	GMFI	
invaded-zone resistivity	R_i	ρ_i, r_i	RESI	mL^3/tq^2
invasion (vertical) efficiency: hydrocarbon pore space invaded (affected, contacted) by the injected-fluid or heat front divided by the hydrocarbon pore space enclosed in all layers behind the injected-fluid or heat front	E_I	η_I, e_I	EFFI	
irreducible (or interstitial or connate) water saturation	S_{iw}	ρ_{iw}, S_{iw}	SATIW	
kinematic viscosity	ν nu	N	VSK	L^2/t
kinetic energy	E_k		ENGK	mL^2/t^2
Laplace transform of $y, \int_0^\infty y(t)e^{-st} dt$	$\mathcal{L}(y)$ script L			
Laplace transform variable	s			
Laplacian operator	∇^2			
larger than	$>$		GT	
latent heat of vaporization	L_v	λ_v	HLTV	L^2/t^2
length, path length, or distance	L	s, ℓ script l	LTH	L
lifetime, average (mean life)	$\bar{\tau}$	\bar{t}	TIMAV	t
limit	lim		LM	
linear aquifer waterdrive constant	C_L		WDCL	$\text{L}^4\text{t}^2/\text{m}$
liquid fraction	f_L	F_L, f_ℓ script l	FRCL	
liquid mole fraction $L/(L+V)$	f_L	F_L, f_ℓ script l	MFRTL	
liquid phase, mole fraction of component in	x		MFRL	
liquid phase, moles of	L	n_L	MOLL	
liquid saturation, combined total	S_L	ρ_L, S_L	SATL	
liquids, condensate, in place in reservoir, initial	G_L	g_L	NGLTI	
liquids, condensate, produced cumulative	G_{Lp}	g_{Lp}	NGLP	L^3
logarithm, base a	\log_a			
logarithm, common, base 10	\log			
logarithm, natural, base e	\ln			
macroscopic cross section	Σ	S	XSTMAC	$1/\text{L}$

Quantity	Letter Symbol	Reserve SPE Letter Symbol	Computer Letter Symbol	Dimensions
macroscopic cross section of a nucleus	σ	s	XNL	L^2
magnetic permeability	μ	m	PRMM	mL/q^2
magnetic susceptibility	k	κ	SUSM	mL/q^2
magnetization	M	I	MAG	m/qt
magnetization, fraction	M_f		MAGF	
mass	m		MAS	m
mass flow rate	w	m	MRT	m/t
matrix interval transit time	t_{ma} script t	Δt_{ma}	TACMA	t/L
matrix (solids, grain) density	ρ_{ma} rho	D_{ma}	DENMA	m/L^3
matrix (framework) volume (volume of all formation solids except dispersed clay or shale)	V_{ma}	v_{ma}	VOLMA	L^3
mean life (average lifetime)	$\bar{\tau}$	\bar{t}	TIMAV	t
mean life (decay time) $(1/\tau)$	τ_d	t_d	TIMD	t
mean or average pressure	\bar{p}	\bar{P}	PRSAV	m/Lt^2
mean or average (overbar)	—		AV	
mean value of a random variable	μ		MEN	
mean particle diameter	\bar{d}_p	\bar{D}_p	DIAAVP	L
mean value of a random variable, x , estimated	\bar{x}		MENES	
mechanical force	F	Q	FCE	mL/t^2
methane concentration (concentration of other paraffin hydrocarbons would be indicated similarly, C_{C_2} , C_{C_3} , etc.)	C_{C_1}	c_{C_1}	CNCC1	various
microscopic cross section	σ		XSTMIC	L^2
mixture, mole fraction of component	z		MFRM	
mobility (k/μ)	λ		MOB	L^3t/m
mobility, gas	λ_g		MOBG	L^3t/m
mobility, oil	λ_o		MOBO	L^3t/m
mobility ratio, general ($\lambda_{displacing}/\lambda_{displaced}$)	M	F_λ	MBR	
mobility ratio, diffuse-front approximation [$(\lambda_D + \lambda_d)_{swept}/(\lambda_d)_{unswept}$]; D signifies displacing; d signifies displaced; mobilities are evaluated at average saturation conditions behind and ahead of front	M_S	M_{Dd}, M_{su}	MBRSAV	
mobility ratio, sharp-front approximation (λ_D/λ_d)	M	F_λ	MBR	
mobility ratio, total, [$(\lambda_t)_{swept}/(\lambda_t)_{unswept}$]; "swept" and "unswept" refer to invaded and uninvaded regions behind and ahead of leading edge of displacement front	M_t	$F_{\lambda t}$	MBRT	
mobility, total, of all fluids in a particular region of the reservoir; e.g., $(\lambda_o + \lambda_g + \lambda_w)$	λ_t	Λ	MOBT	L^3t/m
mobility, water	λ_w		MOBW	L^3t/m
modulus, bulk	K	K_b	BKM	m/Lt^2
modulus, dispersion (dispersion factor)	ψ		DSM	
modulus, shear	G	E_s	ELMS	m/Lt^2
modulus of elasticity (Young's modulus)	E	Y	ELMY	m/Lt^2
molal volume (volume per mole)	V_M	v_m	VOLM	L^3

Quantity	Letter Symbol	Reserve SPE Letter Symbol	Computer Letter Symbol	Dimensions
mole fraction gas, $V/(L+V)$	f_g	F_g	MFRTV	
mole fraction liquid, $L/(L+V)$	f_L	F_L, f_{ℓ} script l	MFRTL	
mole fraction of a component in liquid phase	x		MFRL	
mole fraction of a component in mixture	z		MFRM	
mole fraction of a component in vapor phase	y		MFRV	
molecular refraction	R	N	MRF	L^3
molecular weight	M		MWT	m
molecular weight of produced liquids, mole-weighted average	M_L		MWTAVL	m
moles, number of	n	N	NMBM	
moles of component j	n_j	N_j	MOLJ	
moles of component j produced, cumulative	n_{pj}	N_{pj}	MOLPJ	
moles of liquid phase	L	n_L	MOLL	
moles of vapor phase	V	n_v	MOLV	
moles, number of, total	n_t	N_t	NMBMT	
mole-weighted average molecular weight of produced liquids	M_L		MWTAVL	m
mudcake resistivity	R_{mc}	ρ_{mc}, r_{mc}	RESMC	mL^3/tq^2
mudcake thickness	h_{mc}	d_{mc}, e_{mc}	THKMC	L
mud-filtrate resistivity	R_{mf}	ρ_{mf}, r_{mf}	RESMF	mL^3/tq^2
mud geometrical factor (multiplier) (electrical logging)	G_m	f_{Gm}	GMFM	
mud resistivity	R_m	ρ_m, r_m	RESM	mL^3/tq^2
multiplier (factor), geometrical (electrical logging)	G	f_G	GMF	
multiplier (factor), geometrical, annulus (electrical logging)	G_{an}	f_{Gan}	GMFAN	
multiplier (factor), geometrical, flushed zone (electrical logging)	G_{xo}	f_{Gxo}	GMFXO	
multiplier (factor), geometrical, invaded zone (electrical logging)	G_i	f_{Gi}	GMFI	
multiplier (factor), geometrical, mud (electrical logging)	G_m	f_{Gm}	GMFM	
multiplier (factor), geometrical, pseudo (electrical logging)	G_p	f_{Gp}	GMFP	
multiplier (factor), geometrical, true (electrical logging)	G_t	f_{Gt}	GMFT	
multiplier or coefficient	K	M	COE	various
natural gas liquids or condensate content	C_L	c_L, n_L	CNTL	various
natural logarithm, base e	\ln			
net pay thickness	h_n	d_n, e_n	THKN	L
neutron count rate	N_N	N_n, C_N	NEUN	1/t
neutrons, density (number) of	n_N		NMBN	
neutron lifetime	t_N	τ_N, t_n	NFL	1/t
neutron porosity/density slope (absolute value)	N	$m_{\phi ND}$	SND	L^3/m
neutron [usually with identifying subscript(s)]	N		NEU	various
Newton's Second Law of Motion, conversion factor in	g_c		GRVC	
nominal decline factor	a		DEC	

Quantity	Letter Symbol	Reserve SPE Letter Symbol	Computer Letter Symbol	Dimensions
nucleus cross section, microscopic	σ	s	XNL	L^2
number, atomic	Z		ANM	
number, dimensionless, in general (always with identifying subscripts)	N		NUMQ	
number of pump strokes, cycles per unit of time	N	n	NMBPS	
number (of variables, or components, or steps, or increments, etc.)	n	N	NMB	
number (quantity)	n	N	NMB	
number of compounding periods (usually per year)	M	m	NMBCP	
number of components	C	n_C	NMBC	
number of moles, total	n_t	N_t	NMBM	
number, Reynolds (dimensionless number)	N_{Re}		REYQ	
oil (always with identifying subscripts)	N	n	OIL	various
oil band interstitial-water saturation	S_{wo}	S_{wb}	SATWO	
oil compressibility	c_o	k_o, κ_o	CMPO	Lt^2/m
oil density	ρ_o rho	D_o	DENO	m/L^3
oil displaced from burned volume, volume per unit volume of burned reservoir rock	δ_{ob}	F_{dob}	DPROB	
oil displaced from unburned volume, volume per unit volume of unburned reservoir rock	δ_{ou}	F_{dou}	DPROU	
oil, effective permeability to	k_o	K_o	PRMO	L^2
oil formation volume factor	B_o	F_o	FVFO	
oil formation volume factor at bubblepoint conditions	B_{ob}	F_{ob}	FVFOB	
oil, gas solubility in (solution gas/oil ratio)	R_s	F_{gs}, F_{gos}	GORS	
oil in place in reservoir, initial	N	n	OILTI	L^3
oil influx (encroachment) cumulative	N_e		OILE	L^3
oil influx (encroachment) during an interval	ΔN_e	Δn_e	DELOILE	L^3
oil influx (encroachment) rate	e_o	i_o	ENCO	L^3/t
oil mobility	λ_o		MOBO	L^3t/m
oil produced, cumulative	N_p	n_p	OILP	L^3
oil produced during an interval	ΔN_p	Δn_p	DELOILP	L^3
oil production rate	q_o	Q_o	RTEO	L^3/t
oil production rate, dimensionless	q_{oD}	Q_{oD}	RTEOQ	
oil reciprocal formation volume factor (shrinkage factor)	b_o	f_o, F_o	RVFO	
oil recovery, ultimate	N_{pa}	n_{pa}	OILPUL	L^3
oil, relative permeability to	k_{ro}	K_{ro}	PRMRO	
oil saturation	S_o	ρ_o, s_o	SATO	
oil saturation in gas cap, interstitial	S_{og}	ρ_{og}, s_{og}	SATOG	
oil saturation, residual	S_{or}	ρ_{or}, s_{or}	SATOR	
oil specific gravity	γ_o	s_o, F_{os}	SPGO	
oil viscosity	μ_o	ν_o	VISO	m/Lt
operating cash income	I		INC	M
operating cash income, after taxes	I_a		INCA	M
operating cash income, before taxes	I		INCB	M
operating expense	O		XPO	various
operating expense per unit produced	O_v		XPOU	M/L^3
operator, Laplacian	∇^2			

Quantity	Letter Symbol	Reserve SPE Letter Symbol	Computer Letter Symbol	Dimensions
overall heat transfer coefficient	U	U_T, U_θ	HTCU	m/t^3T
overall reservoir recovery efficiency: volume of hydrocarbons recovered divided by volume of hydrocarbons in place at start of project ($E_R = E_P E_S E_O = E_V E_D$)	E_R	η_R, e_R	EFFR	
oxygen concentration (concentration of other elements or compounds would be indicated as C_{CO_2} , C_{N_2} , etc.)	C_{O_2}	c_{O_2}	CNCO2	various
oxygen utilization	e_{O_2}	E_{O_2}	UTLO2	
particle diameter, mean	\bar{d}_p	\bar{D}_p	DIAAVP	L
path length, length, or distance	L	$s, l \text{ script } l$	LTH	L
pattern sweep efficiency (developed from areal efficiency by proper weighting for variations in net pay thickness, porosity, and hydrocarbon saturation: hydrocarbon pore space enclosed behind the injected-fluid or heat front divided by total hydrocarbon pore space of the reservoir or project)	E_p	η_p, e_p	EFFP	
pay thickness, gross (total)	h_t	d_t, e_t	THKT	L
pay thickness, net	h_n	d_n, e_n	THKN	L
period	T	Θ	PER	t
permeability, absolute (fluid flow)	k	K	PRM	L^2
permeability, effective, to gas	k_g	K_g	PRMG	L^2
permeability, effective, to oil	k_o	K_o	PRMO	L^2
permeability, effective, to water	k_w	K_w	PRMW	L^2
permeability, magnetic	μ	m	PRMM	mL/q^2
permeability ratio, gas/oil	k_g/k_o	K_g/K_o	PRMGQ	
permeability ratio, water/oil	k_w/k_o	K_w/K_o	PRMWO	
permeability, relative, to gas	k_{rg}	K_{rg}	PRMRG	
permeability, relative, to oil	k_{ro}	K_{ro}	PRMRO	
permeability, relative, to water	k_{rw}	K_{rw}	PRMRW	
phases, number of	P		NMBP	
Poisson's ratio	μ	ν, σ	PSN	
pore volume $V_b - V_s$	V_p	ν_p	VOLP	L^3
pore volume, dimensionless	V_{pD}	ν_{pD}	VOLPQ	
pore volumes of injected fluid, cumulative	Q_i	q_i	FLUIQ	
porosity $(V_b - V_s)/V_b$	ϕ	f, ϵ	POR	
porosity, apparent	ϕ_a	f_a, ϵ_a	PORA	
porosity, effective (V_{pe}/V_b)	ϕ_e	f_e, ϵ_e	PORE	
porosity exponent (cementation) (in an empirical relation between F_R and ϕ)	m		MXP	
porosity, hydrocarbon-filled, fraction or percent of rock bulk volume occupied by hydrocarbons	ϕ_h	f_h, ϵ_h	PORH	
porosity index	I_ϕ	i_ϕ	PRX	
porosity index, primary	$I_{\phi 1}$	$i_{\phi 1}$	PRXP	
porosity index, secondary	$I_{\phi 2}$	$i_{\phi 2}$	PRXSE	
porosity, noneffective (V_{pne}/V_b)	ϕ_{ne}	f_{ne}, ϵ_{ne}	PORNE	

Quantity	Letter Symbol	Reserve SPE Letter Symbol	Computer Letter Symbol	Dimensions
"porosity" (space), intergranular ($V_b - V_{gr} / V_b$)	ϕ_{ig}	f_{ig}, ϵ_{ig}	PORIG	
"porosity" (space), intermatrix ($V_b - V_{ma} / V_b$)	ϕ_{im}	f_{im}, ϵ_{im}	PORIM	
porosity of experimental pack	ϕ_E	f_E, ϵ_E	POREX	
porosity of reservoir or formation	ϕ_R	f_R, ϵ_R	PORR	
porosity, total	ϕ_t	f_t, ϵ_t	PORT	
potential or potential function	Φ	f	POT	various
potential difference (electric)	V	U	VLT	mL ² /qt ²
potential energy	E_p		ENGP	mL ² /t ²
pressure, bottomhole	p_{bh}	P_{bh}	PRSBH	m/Lt ²
pressure	p	P	PRS	m/Lt ²
pressure, atmospheric	p_a	P_a	PRSA	m/Lt ²
pressure, average or mean	\bar{p}	\bar{P}	PRSAV	m/Lt ²
pressure, average, reservoir	\bar{p}_R	\bar{P}_R	PRSAVR	m/Lt ²
pressure, bottomhole, at any time after shut-in	p_{ws}	P_{ws}	PRSWs	m/Lt ²
pressure, bottomhole flowing	p_{wf}	P_{wf}	PRSWF	m/Lt ²
pressure, bottomhole flowing, injection well	p_{iwf}	P_{iwf}	PRSIWF	m/Lt ²
pressure, bottomhole general	p_w	P_w	PRSW	m/Lt ²
pressure, bottomhole static	p_{ws}	P_{ws}	PRSWs	m/Lt ²
pressure, bottomhole (well), in water phase	p_{ww}	P_{ww}	PRSWW	m/Lt ²
pressure, bottomhole static, injection well	p_{iws}	P_{iws}	PRSIWS	m/Lt ²
pressure, bubblepoint (saturation)	p_b	p_s, P_s, P_b	PRSB	m/Lt ²
pressure, capillary	P_c	P_C, p_C	PRSCP	m/Lt ²
pressure, casing flowing	p_{cf}	P_{cf}	PRSCF	m/Lt ²
pressure, casing static	p_{cs}	P_{cs}	PRSCS	m/Lt ²
pressure, critical	p_c	P_c	PRSC	m/Lt ²
pressure, dewpoint	p_d	P_d	PRSD	m/Lt ²
pressure, dimensionless	p_D	P_D	PRSQ	
pressure, external boundary	p_e	P_e	PRSE	m/Lt ²
pressure, extrapolated	p_{ext}	P_{ext}	PRSXT	m/Lt ²
pressure, flowing bottomhole	p_{wf}	P_{wf}	PRSWF	m/Lt ²
pressure, flowing casing	p_{cf}	P_{cf}	PRSCF	m/Lt ²
pressure, flowing tubing	p_{tf}	P_{tf}	PRSTF	m/Lt ²
pressure, front or interface	p_f	P_f	PRSF	m/Lt ²
pressure function, dimensionless, at dimensionless time t_D	p_{tD}	P_{tD}	PRSTQQ	
pressure, initial	p_i	P_i	PRSI	m/Lt ²
pressure, pseudocritical	p_{pc}	P_{pc}	PRSPC	m/Lt ²
pressure, pseudoreduced	p_{pr}	P_{pr}	PRSPRD	m/Lt ²
pressure, reduced	p_r	P_r	PRSRD	
pressure, reservoir average	\bar{p}_R	\bar{P}_R	PRSAVR	m/Lt ²
pressure, separator	p_{sp}	P_{sp}	PRSSP	m/Lt ²
pressure, standard conditions	p_{sc}	P_{sc}	PRSSC	m/Lt ²
pressure, static bottomhole	p_{ws}	P_{ws}	PRSWs	m/Lt ²
pressure, static casing	p_{cs}	P_{cs}	PRSCS	m/Lt ²
pressure, static tubing	p_{ts}	P_{ts}	PRSTS	m/Lt ²
pressure, tubing flowing	p_{tf}	P_{tf}	PRSTF	m/Lt ²
pressure, tubing static	p_{ts}	P_{ts}	PRSTS	m/Lt ²
primary porosity index	$I_{\phi 1}$	$i_{\phi 1}$	PRXPR	
produced condensate liquids, cumulative	G_{Lp}	g_{Lp}	NGLP	L ³

Quantity	Letter Symbol	Reserve SPE Letter Symbol	Computer Letter Symbol	Dimensions
produced fluids, cumulative (where N_p and W_p are not applicable)	Q_p		FLUP	L^3
produced free gas, cumulative	G_{Fp}	g_{Fp}	GASFP	L^3
produced gas, cumulative	G_p	g_p	GASP	L^3
produced gas during an interval	ΔG_p	Δg_p	DELGASP	L^3
produced gas from experimental tube run	G_{pE}	g_{pE}	GASPEX	L^3
produced gas, wet, cumulative	G_{wgp}	g_{wgp}	GASWGP	L^3
produced-liquid density, weight-weighted average	$\bar{\rho}_L$ rho	\bar{D}_L	DENAVL	m/ L^3
produced moles of component j , cumulative	n_{pj}	N_{pj}	MOLPJ	
produced oil, cumulative	N_p	n_p	OILP	L^3
produced oil during an interval	ΔN_p	Δn_p	DELOILP	L^3
produced water, cumulative	W_p	w_p	WTRP	L^3
produced water during an interval	ΔW_p	Δw_p	DELWTRP	L^3
produced wet gas, cumulative	G_{wgp}	g_{wgp}	GASWGP	L^3
producing gas/oil ratio	R	F_g, F_{gO}	GOR	
producing gas/oil ratio, free (free-gas volume/oil volume)	R_F	F_{gF}, F_{gOF}	GORF	
producing water/oil ratio, instantaneous	F_{wO}		FACWO	
production rate at beginning of period	q_i	Q_i	RTEI	L^3/t
production rate at economic abandonment	q_a	Q_a	RTEA	L^3/t
production rate, dimensionless	q_D	Q_D	RTEQ	
production rate, gas	q_g	Q_g	RTEG	L^3/t
production rate, gas, dimensionless	q_{gD}	Q_{gD}	RTEGQ	
production rate, oil	q_o	Q_o	RTEO	L^3/t
production rate, oil, dimensionless	q_{oD}	Q_{oD}	RTEOQ	
production rate or flow rate	q	Q	RTE	L^3/t
production rate or flow rate at mean pressure	$q_{\bar{p}}$	$Q_{\bar{p}}$	RTEPAV	L^3/t
production rate or flow rate, average	\bar{q}	\bar{Q}	RTEAV	L^3/t
production rate, water	q_w	Q_w	RTEW	L^3/t
production rate, water, dimensionless	q_{wD}	Q_{wD}	RTEWQ	
production time after well is opened to production (pressure drawdown)	Δt_{wf}	$\Delta \tau$	DELTIMWF	t
production time of well, equivalent, before shut-in (pseudotime)	t_p	τ_p	TIMP	t
productivity index	J	j	PDX	$L^4/t/m$
profit, annual net, over year k	P_k		PRAK	M
profit, annual, over year k , fraction of unamortized investment	f_{Pk}		PRAPK	
profit, total	P	P_t	PRFT	M
proportional to	\propto			
productivity index, specific	J_s	j_s	PDXS	$L^3 t/m$
pseudocritical temperature	T_{pc}	θ_{pc}	TEMPC	T
pseudocritical pressure	p_{pc}	P_{pc}	PRSPC	m/ Lt^2
pseudogeometrical factor (multiplier) (electrical logging)	G_p	f_{Gp}	GMFP	
pseudoreduced compressibility	c_{pr}	k_{pr}, κ_{pr}	CMPPRD	
pseudoreduced pressure	p_{pr}	P_{pr}	PRSPRD	
pseudo-SP	E_{pSP}	Φ_{SP}	EMFP	m L^2/qt^2

Quantity	Letter Symbol	Reserve SPE Letter Symbol	Computer Letter Symbol	Dimensions
pseudoreduced temperature	T_{pr}	θ_{pr}	TEMPRD	T
pseudotime (equivalent time well was on production before shut-in)	t_p	τ_p	TIMP	t
pump strokes, number of cycles per unit of time	N	n	NMBPS	
quality (usually of steam)	f_s	Q, x	QLTS	
radial distance (increment along radius)	Δr	ΔR	DELRAD	L
radiation heat transfer coefficient	I	I_T, I_θ	HCTI	m/t ³ T
radius	r	R	RAD	L
radius, apparent or effective, of wellbore (includes effects of well damage or stimulation)	r_{wa}	R_{wa}	RADWA	L
radius, dimensionless	r_D	R_D	RADQ	
radius, external boundary	r_e	R_e	RADE	L
radius, hydraulic	r_H	R_H	RADHL	L
radius of drainage	r_d	R_d	RADD	L
radius of wellbore, apparent or effective (includes effects of well damage or stimulation)	r_{wa}	R_{wa}	RADWA	L
radius of well damage or stimulation (skin)	r_s	R_s	RADS	L
radius, well	r_w	R_w	RADW	L
rate, air injection	i_a		INJA	L ³ /t
rate: discount, effective profit, of return, reinvestment, etc; use symbol i with suitable subscripts	i	k_i	RTE	
rate, flow or production	q	Q	RTE	L ³ /t
rate, gamma ray count	N_{GR}	N_γ, C_G	NGR	1/t
rate, gas influx (encroachment)	e_g	i_g	ENCG	L ³ /t
rate, gas injection	i_g		INJG	L ³ /t
rate, gas production	q_g	Q_g	RTEG	L ³ /t
rate, gas production, dimensionless	q_{gD}	Q_{gD}	RTEGQ	
rate, influx (encroachment)	e	i	ENC	L ³ /t
random variable, mean value of x , estimated	\bar{x}		MENES	
rate, injection	i		INJ	L ³ /t
rate, interest, effective compound (usually annual)	i		IRCE	
rate, interest, effective, per period	i_M		IRPE	
rate, interest, nominal annual	j	r	IRA	
rate, mass flow	w	m	MRT	m/t
rate of flow or flux, per unit area (volumetric velocity)	u	ψ	VELV	L/t
rate of heat flow	Q	q, Φ	HRT	mL ² /t ³
rate of return (internal, true, or discounted cash flow) or earning power	i_r		RORI	
rate, oil influx (encroachment)	e_o	i_o	ENCO	L ³ /t
rate, oil production	q_o	Q_o	RTEO	L ³ /t
rate per unit area, flow (volumetric velocity)	u	ψ	VELV	L/t
rate, oil production, dimensionless	q_{oD}	Q_{oD}	RTEOQ	
rate, production or flow	q	Q	RTE	L ³ /t
rate, production, at mean pressure	$q_{\bar{p}}$	$Q_{\bar{p}}$	RTEPAV	L ³ /t
rate, production, average	\bar{q}	\bar{Q}	RTEAV	L ³ /t
rate, production, dimensionless	q_D	Q_D	RTEQ	
rate, segregation (in gravity drainage)	q_s	Q_s	RTES	L ³ /t

Quantity	Letter Symbol	Reserve SPE Letter Symbol	Computer Letter Symbol	Dimensions
rate, shear	$\dot{\gamma}$	\dot{e}	SRT	1/t
rate (velocity) of burning-zone advance	v_b	V_b, u_b	VELB	L/t
rate, water influx (encroachment)	e_w	i_w	ENCW	L ³ /t
rate, water injection	i_w		INJW	L ³ /t
rate, water production	q_w	Q_w	RTEW	L ³ /t
rate, water production, dimensionless	q_{wD}	Q_{wD}	RTEWQ	
ratio, air/fuel	F_{aF}		FACAFU	various
ratio, damage ("skin" conditions relative to formation conditions unaffected by well operations)	F_s	F_d	DMRS	
ratio, displacement	δ	F_d	DPR	
ratio, displacement, oil from burned volume, volume per unit volume of burned reservoir rock	δ_{ob}	F_{dob}	DPROB	
ratio, displacement, oil from unburned volume, volume per unit volume of unburned reservoir rock	δ_{ou}	F_{dou}	DPROU	
ratio, displacement, water from burned volume, volume per unit volume of burned reservoir rock	δ_{wb}	F_{dwb}	DPRWB	
ratio, equilibrium (y/x)	K	k, F_{eq}	EQR	
ratio, free producing gas/oil (free-gas volume/oil volume)	R_F	F_{gF}, F_{goF}	GORF	
ratio, gas/oil, cumulative	R_p	F_{gp}, F_{gop}	GORP	
ratio, gas/oil, initial solution	R_{si}	F_{gsi}	GORSI	
ratio, gas/oil permeability	k_g/k_o	K_g/K_o	PRMGO	
ratio, gas/oil producing	R	F_g, F_{go}	GOR	
ratio, gas/oil, solution, at bubblepoint conditions	R_{sb}	F_{gsb}	GORSB	
ratio, gas/oil, solution (gas solubility in oil)	R_s	F_{gs}, F_{gos}	GORS	
ratio, mobility, general ($\lambda_{displacing}/\lambda_{displaced}$)	M	F_λ	MBR	
ratio, mobility, diffuse-front approximation [$(\lambda_D + \lambda_d)_{swept}/(\lambda_d)_{unswept}$]; D signifies displacing; d signifies displaced; mobilities are evaluated at average saturation conditions behind and ahead of front	$M_{\bar{S}}$	M_{Dd}, M_{su}	MBRSAV	
ratio, mobility, sharp-front approximation (λ_D/λ_d)	M	F_λ	MBR	
ratio, mobility, total [$(\lambda_t)_{swept}/(\lambda_t)_{unswept}$]; "swept" and "unswept" refer to invaded and uninvaded regions behind and ahead of leading edge of a displacement front	M_t	$F_{\lambda t}$	MBRT	
ratio of initial reservoir free-gas volume to initial reservoir oil volume	m	F_{Fo}, F_{go}	MGO	
ratio or factor in general (always with identifying subscripts)	F	A, R, r	FAC	various
ratio, permeability, gas/oil	k_g/k_o	K_g/K_o	PRMGO	
ratio, producing gas/oil	R	F_g, F_{go}	GOR	
ratio, permeability, water/oil	k_w/k_o	K_w/K_o	PRMWO	
ratio, solution gas/oil, at bubblepoint conditions	R_{sb}	F_{gsb}	GORSB	
ratio, solution gas/oil (gas solubility in oil)	R_s	F_{gs}, F_{gos}	GORS	

Quantity	Letter Symbol	Reserve SPE Letter Symbol	Computer Letter Symbol	Dimensions
ratio, solution gas/oil, initial	R_{si}	F_{gsi}	GORSI	
ratio, water/fuel	F_{wF}		FACWFU	
ratio, water/oil, cumulative	F_{wop}		FACWOP	
ratio, water/oil permeability	k_w/k_o	K_w/K_o	PRMWO	
ratio, water/oil, producing, instantaneous	F_{wo}		FACWO	
reactance	X		XEL	ML^2/tq^2
reaction rate	R		RRR	m/L^2
reaction rate constant	k	r, j	RRC	L/t
real part of complex number z	$\Re(z)$ <i>script R</i>			
reciprocal formation volume factor, volume at standard conditions divided by volume at reservoir conditions (shrinkage factor)	b	f, F	RVF	
reciprocal gas formation volume factor	b_g	f_g, F_g	RVFG	
reciprocal gas formation volume factor at bubblepoint conditions	b_{gb}	f_{gb}, F_{gb}	RVFGB	
reciprocal permeability	j	ω		$1/L^2$
reciprocal oil formation volume factor (shrinkage factor)	b_o	f_o, F_o	RVFO	
recovery efficiency, reservoir overall; volume of hydrocarbons recovered divided by volume of hydrocarbons in place at start of project. ($E_R = E_p E_i E_D = E_v E_D$)	E_R	η_R, e_R	EFFR	
recovery, ultimate gas	G_{pa}	g_{pa}	GASPUL	
reduced pressure	p_r	P_r	PRSRD	
reduced temperature	T_r	θ_r	TEMRD	
reduction ratio or reduction term	α		RED	
reduction, SP (general) due to shaliness	α_{SP}		REDSP	
refraction, molecular	R	N	MRF	
refraction index	n	μ	RFX	
reduction ratio, SP, due to shaliness	$\alpha_{SP, sh}$		REDSH	
relative amplitude	A_r		AMPR	
relative atomic mass (atomic weight)	A		AWT	
relative bearing	β	γ	BRGR	
relative density (specific gravity)	γ	s, F_s	SPG	
relative molecular mass (molecular weight)	M		MWT	
relative permeability to gas	k_{rg}	K_{rg}	PRMRG	
relative permeability to oil	k_{ro}	K_{ro}	PRMRO	
relative permeability to water	k_{rw}	K_{rw}	PRMRW	
relaxation time, free-precession decay	t_2	τ_2	TIMAV	t
relaxation time, proton thermal	t_1	τ_1	TIMRP	t
requirement, air	a	F_a	AIR	
requirement, unit air, in laboratory experimental run, volumes or air per unit mass of pack	a_E	F_{aE}	AIREX	L^3/m
requirement, unit air, in reservoir, volumes of air per unit bulk volume of reservoir rock	a_R	F_{aR}	AIRR	
reservoir initial free-gas volume ($=mNB_{oi}$)	G_{Fi}	g_{Fi}	GASFI	L^3
reservoir or formation porosity	ϕ_R	f_R, ϵ_R	PORR	
reservoir pressure, average	\bar{p}_R	\bar{P}_R	PRSAVR	m/Lt^2
reservoir recovery efficiency, overall; volume of hydrocarbons recovered divided	E_R	η_R, e_R	EFFR	

Quantity	Letter Symbol	Reserve SPE Letter Symbol	Computer Letter Symbol	Dimensions
by volume of hydrocarbons in place at start of project ($E_R = E_P E_I E_D = E_v E_D$)				
reservoir rock burned, volume of	V_{Rb}	v_{Rb}	VOLRB	L^3
reservoir rock unburned, volume of	V_{Ru}	v_{Ru}	VOLRU	L^3
reservoir temperature	T_R	θ_R	TEMR	T
residual gas saturation	S_{gr}	ρ_{gr}, S_{gr}	SATGR	
residual hydrocarbon saturation	S_{hr}	ρ_{hr}, S_{hr}	SATHR	
residual oil saturation	S_{or}	ρ_{or}, S_{or}	SATOR	
residual water saturation	S_{wr}	ρ_{wr}, S_{wr}	SATWR	
resistance	r	R	RST	ML^2/tq^2
resistivity, electrical (logging)	R	ρ, r	RES	mL^3/tq^2
resistivity, electrical (other than logging)	ρ	R	RHO	mL^3/tq^2
resistivity, annulus	R_{an}	ρ_{an}, r_{an}	RESAN	mL^3/tq^2
resistivity, apparent	R_a	ρ_a, r_a	RESA	mL^3/tq^2
resistivity, apparent, of the conductive fluids in an invaded zone (due to fingering)	R_z	ρ_z, r_z	RESZ	mL^3/tq^2
resistivity factor coefficient, formation ($F_R \phi^m$)	K_R	M_R, a, C	COER	mL^3/tq^2
resistivity factor, formation, equals R_0/R_w a numerical subscript to F indicates the R_w	F_R		FACHR	
resistivity flushed zone (that part of the invaded zone closest to the wall of the borehole, where flushing has been the maximum)	R_{xo}	ρ_{xo}, r_{xo}	RESXO	mL^3/tq^2
resistivity, formation 100% saturated with water of resistivity R_w	R_0	ρ_0, r_0	RESZR	mL^3/tq^2
resistivity, formation, true	R_t	ρ_t, r_t	REST	mL^3/tq^2
resistivity index (hydrocarbon) equals R_t/R_0	I_R	i_R	RSXH	
resistivity, invaded zone	R_i	ρ_i, r_i	RESI	mL^3/tq^2
resistivity, mud	R_m	ρ_m, r_m	RESM	mL^3/tq^2
resistivity, mudcake	R_{mc}	ρ_{mc}, r_{mc}	RESMC	mL^3/tq^2
resistivity, mud-filtrate	R_{mf}	ρ_{mf}, r_{mf}	RESMF	mL^3/tq^2
resistivity, shale	R_{sh}	ρ_{sh}, r_{sh}	RESSH	mL^3/tq^2
resistivity, surrounding formation	R_s	ρ_s, r_s	RESS	mL^3/tq^2
resistivity, water	R_w	ρ_w, r_w	RESW	mL^3/tq^2
revenue, gross ("value"), per unit produced	V_u	R_u	GRRU	M/L^3
revenue, gross ("value"), total	V	R, V_t, R_t	GRRT	M
Reynolds number (dimensionless number)	N_{Re}		REYQ	
rock or formation compressibility	c_f	k_f, κ_f	CMPF	Lt^2/m
salinity	C	c, n	CNC	various
saturation	S	ρ, s	SAT	
saturation exponent	n		SXP	
saturation, gas	S_g	ρ_g, S_g	SATG	
saturation, gas, critical	S_{gc}	ρ_{gc}, S_{gc}	SATGC	
saturation, gas, residual	S_{gr}	ρ_{gr}, S_{gr}	SATGR	
saturation, interstitial-oil, in gas cap	S_{og}	ρ_{og}, S_{og}	SATOG	
saturation, interstitial-water, in gas cap	S_{wg}	ρ_{wg}, S_{wg}	SATWG	
saturation, hydrocarbon	S_h	ρ_h, S_h	SATH	

Quantity	Letter Symbol	Reserve SPE Letter Symbol	Computer Letter Symbol	Dimensions
saturation, residual hydrocarbon	S_{hr}	ρ_{hr}, S_{hr}	SATHR	
saturation, oil	S_o	ρ_o, S_o	SATO	
saturation, oil, residual	S_{or}	ρ_{or}, S_{or}	SATOR	
saturation or bubblepoint pressure	p_b	p_s, P_s, P_b	PRSB	m/Lt ²
saturation, total (combined) liquid	S_L	ρ_L, S_L	SATL	
saturation, water	S_w	ρ_w, S_w	SATW	
saturation, water, critical	S_{wc}	ρ_{wc}, S_{wc}	SATWC	
saturation, water, initial	S_{wi}	ρ_{wi}, S_{wi}	SATWI	
saturation, water (irreducible, interstitial, or connate)	S_{iw}	ρ_{iw}, S_{iw}	SATIW	
saturation, water, residual	S_{wr}	ρ_{wr}, S_{wr}	SATWR	
secondary porosity index	$I_{\phi 2}$	$i_{\phi 2}$	PRXSE	
segregation rate (in gravity drainage)	q_s	Q_s	RTES	L ³ /t
separator pressure	p_{sp}	P_{sp}	PRSSP	m/Lt ²
shale interval transit time	t_{sh} script t	Δt_{sh}	TACSH	t/L
shale resistivity	R_{sh}	ρ_{sh}, r_{sh}	RESSH	mL ³ /tq ²
shaliness gamma ray index ($(\gamma_{log} - \gamma_{cn}) / (\gamma_{sh} - \gamma_{cn})$)	I_{shGR}	i_{shGR}	SHXGR	
shear modulus	G	E_s	ELMS	m/Lt ²
shear rate	$\dot{\gamma}$	\dot{e}	SRT	1/t
shear wave amplitude	A_s		AMPS	various
shrinkage factor (reciprocal oil formation volume factor)	b_o	f_o, F_o	RVFO	
shut-in bottomhole pressure, at any time	p_{ws}	P_{ws}	PRWS	m/Lt ²
shut-in time (time after well is shut in) (pressure buildup)	Δt_{ws}	$\Delta \tau_{ws}$	DELTIMWS	t
single-payment discount factor	D_{SP}		DSCSP	
single-payment discount factor (constant annual rate)	D_{SPC}		DSCSPC	
skin depth (logging)	δ	r_s	SKD	L
skin effect	s	S, σ	SKN	various
skin radius (radius of well damage or stimulation)	r_s	R_s	RADS	L
slope	m	A	SLP	various
slope, interval transit time vs. density (absolute value)	M	$m_{\theta D}$	SAD	tL ² /m
slope, neutron porosity vs. density (absolute value)	N	$m_{\theta ND}$	SND	L ³ /m
smaller than	<		LT	
solid particles density of experimental rock	ρ_{sE} rho	D_{sE}	DENSEX	m/L ³
solid(s) volume (volume of all formation solids)	V_s	v_s	VOLS	L ³
solids (matrix, grain) density	ρ_{ma} rho	D_{ma}	DENMA	m/L ³
solubility, gas in oil (solution gas/oil ratio)	R_s	F_{gs}, F_{gos}	GORS	
solubility, gas in water	R_{sw}		GWRS	
solution gas/oil ratio at bubblepoint conditions	R_{sb}	F_{gsb}	GORSB	
solution gas/oil ratio (gas solubility in oil)	R_s	F_{gs}, F_{gos}	GORS	
solution gas/oil ratio, initial	R_{si}	F_{gsi}	GORSI	
SP, electrochemical component of	E_c	Φ_c	EMFC	mL ² /t ² q
SP, electrokinetic component of	E_k	Φ_k	EMFK	mL ² /t ² q
SP (measured SP) (Self Potential)	E_{SP}	Φ_{SP}	EMFSP	mL ² /t ² q
SP, pseudo	E_{pSP}	Φ_{pSP}	EMFPSP	mL ² /t ² q

Quantity	Letter Symbol	Reserve SPE Letter Symbol	Computer Letter Symbol	Dimensions
SP, static (SSP)	E_{SSP}	Φ_{SSP}	EMFSSP	$\text{mL}^2/\text{t}^2\text{q}$
spacing (electrical logging)	L_s	s_s, ℓ_s <i>script l</i>	LENS	L
specific entropy	s	σ	HERS	$\text{L}^2/\text{t}^2\text{T}$
specific gravity (relative density)	γ	s, F_s	SPG	
specific gravity, gas	γ_g	s_g, F_{gs}	SPGG	
specific gravity, oil	γ_o	s_o, F_{os}	SPGO	
specific gravity, water	γ_w	s_w, F_{ws}	SPGW	
specific heat capacity (always with phase or system subscripts)	C	c	HSP	$\text{L}^2/\text{t}^2\text{T}$
specific heat capacity ratio	γ	k	HSPR	
specific injectivity index	I_s	i_s	IJXS	$\text{L}^3\text{t}/\text{m}$
specific productivity index	J_s	j_s	PDXS	$\text{L}^3\text{t}/\text{m}$
specific volume	v	v_s	SPV	L^3/m
specific weight	F_{wv}	γ	WGTS	mL^2/t^2
SSP (static SP)	E_{SSP}	Φ_{SSP}	EMFSSP	$\text{mL}^2/\text{t}^2\text{q}$
stabilization time of a well	t_s	τ_s	TIMS	t
standard deviation of a random variable	σ		SDV	
standard deviation of a random variable, estimated	s		SDVES	
static bottomhole pressure, injection well	p_{iws}	P_{iws}	PRSIWS	m/Lt^2
static pressure, bottomhole, at any time after shut-in	p_{ws}	P_{ws}	PRSWs	m/Lt^2
static pressure, casing	p_{cs}	P_{cs}	PRSCS	m/Lt^2
static pressure, tubing	p_{ts}	P_{ts}	PRSTS	m/Lt^2
stimulation or damage radius of well (skin)	r_s	R_s	RADS	L
storage or storage capacity	S	s, σ	STO	various
strain, normal and general	ϵ epsilon	e, ϵ_n	STN	
strain, shear	γ	ϵ_s	STNS	
strain, volume	θ	θ_V	STNV	
stream function	Ψ		STR	various
stress, normal and general	σ	s	STS	m/Lt^2
stress, shear	τ	s_s	STSS	m/Lt^2
summation (operator)	Σ		SUM	
superficial phase velocity (flux rate of a particular fluid phase flowing in pipe; use appropriate phase subscripts)	u	ψ	VELV	L/t
surface production rate	q_{sc}	q_σ, Q_{sc}	RTESC	L^3/t
surface tension, interfacial	σ	γ, γ	SFT	m/t^2
surrounding formation resistivity	R_s	ρ_s, r_s	RESS	mL^3/tq^2
susceptibility, magnetic	k	κ	SUSM	mL/q^2
temperature	T	θ	TEM	T
temperature, bottomhole	T_{bh}	θ_{BH}	TEMBH	T
temperature, critical	T_c	θ_c	TEMC	T
temperature, formation	T_f	θ_f	TEMF	T
temperature gradient	g_T	g_h	GRDT	T/L
temperature, pseudocritical	T_{pc}	θ_{pc}	TEMPC	T
temperature, pseudoreduced	T_{pr}	θ_{pr}	TEMPRD	T
temperature, reduced	T_r	θ_r	TEMRD	T
temperature, reservoir	T_R	θ_R	TEMR	T
temperature, standard conditions	T_{sc}	θ_{sc}	TEMSC	T
tension, surface (interfacial)	σ	γ, γ	SFT	m/t^2

Quantity	Letter Symbol	Reserve SPE Letter Symbol	Computer Letter Symbol	Dimensions
tensor of x	\bar{x}			
thermal conductivity (always with additional phase or system subscripts)	k_h	λ	HCN	mL/t ³ T
thermal cubic expansion coefficient	β	b	HEC	1/T
thermal or heat diffusivity	α	a, η_h	HTD	L ² /t
thickness (general and individual bed)	h	d, e	THK	L
thickness, gross pay (total)	h_i	d_i, e_i	THKT	L
thickness, mudcake	h_{mc}	d_{mc}, e_{mc}	THKMC	L
thickness, pay, gross (total)	h_i	d_i, e_i	THKT	L
thickness, net pay	h_n	d_n, e_n	THKN	L
time	t	τ	TIM	t
time after well is opened to production (pressure drawdown)	Δt_{wf}	$\delta \tau_{wf}$	DELTIMWF	t
time after well is shut in (pressure buildup)	Δt_{ws}	$\Delta \tau_{ws}$	DELTIMWS	t
time constant	τ	τ_c	TIMC	t
time, decay (mean life) (1/ λ)	τ_d	t_d	TIMD	t
time, delay	t_d	τ_d	TIMD	t
time difference (time period or interval, fixed length)	Δt	$\Delta \tau$	DELTIM	t
time, dimensionless	t_D	τ_D	TIMQ	
time, dimensionless at condition m	t_{Dm}	τ_{Dm}	TIMMQ	
time for stabilization of a well	t_s	τ_s	TIMS	t
time, interval transit	$t_{script} t$	Δt	TAC	t/L
time, interval transit, apparent	$t_a \text{ script } t$	Δt_a	TACA	t/L
time, interval transit, fluid	$t_f \text{ script } t$	Δt_f	TACF	t/L
time, interval transit, matrix	$t_{ma} \text{ script } t$	Δt_{ma}	TACMA	t/L
time, interval transit, shale	$t_{sh} \text{ script } t$	Δt_{sh}	TACSH	t/L
time, neutron decay (neutron mean life)	t_{dN}		TIMDN	t
time, payout (payoff, payback)	t_p	τ_p, t_{po}	TIMPO	t
time period or interval, fixed length	Δt	$\Delta \tau$	DELTIM	t
time well was on production before shut-in, equivalent (pseudotime)	t_p	τ_p	TIMP	t
tortuosity	τ		TOR	
tortuosity, electric	τ_e		TORE	
tortuosity, hydraulic	τ_H		TORHL	
total (combined) liquid saturation	S_L	ρ_L, s_L	SATL	
total entropy	s		HER	L ² /t ² T
total mobility of all fluids in a particular region of the reservoir; e.g., ($\lambda_o + \lambda_g + \lambda_w$)	λ_t	Λ	MOBT	L ³ t/m
total mobility ratio [(λ_t) _{swept} /(λ_t) _{unswept}]; "swept" and "unswept" refer to invaded and uninvaded regions behind and ahead of leading edge of a displacement front	M_t	$F_{\lambda t}$	MBRT	
total (gross) pay thickness	h_i	d_i, e_i	THKT	L
total gross revenue ("value")	V	R, V_t, R_t	GRRT	M
total initial gas in place in reservoir	G	g	GASTI	L ³
total moles	n	n_t, N_t	NMBM	
total porosity	ϕ_t	f_t, ϵ_t	PORT	
total (two-phase) formation volume factor	B_t	F_t	FVFT	

Quantity	Letter Symbol	Reserve SPE Letter Symbol	Computer Letter Symbol	Dimensions
transfer coefficient, convective heat	h	h_h, h_T	HTCC	m/t ³ T
transfer coefficient, heat, overall	U	U_T, U_θ	HTCU	m/t ³ T
transfer coefficient, heat, radiation	I	I_T, I_θ	HTCI	m/t ³ T
transit time, interval	$t \text{ script } t$	Δt	TAC	t/L
transit time, apparent, interval	$t_a \text{ script } t$	Δt_a	TACA	t/L
transit time, fluid interval	$t_f \text{ script } t$	Δt_f	TACF	t/L
transit time, matrix interval	$t_{ma} \text{ script } t$	Δt_{ma}	TACMA	t/L
transit time, shale interval	$t_{sh} \text{ script } t$	Δt_{sh}	TACSH	t/L
transform, Laplace of $y \int_0^\infty y(t) e^{-st} dt$	$\mathcal{L}(y) \text{ script } L$			
transform, Laplace, variable	s			
transmissivity, transmissibility	T	T	TRM	various
true density	ρ_t	D_t	DENT	m/L ³
true formation resistivity	R_t	ρ_t, r_t	REST	mL ³ /tq ²
true geometrical factor (multiplier) (noninvaded zone) (electrical logging)	G_t	f_{Gt}	GMFT	
tubing pressure, flowing	p_{tf}	P_{tf}	PRSTF	m/Lt ²
tubing pressure, static	p_{ts}	P_{ts}	PRSTS	m/Lt ²
turbulence factor	F_B		FACB	
two-phase or total formation volume factor	B_t	F_t	FVFT	
ultimate gas recovery	G_{pa}	g_{pa}	GASPUL	L ³
unamortized investment over year k	C_{uk}		INVUK	
undiscounted cash flow	P			M
unburned reservoir rock, volume of	V_{Ru}	v_{Ru}	VOLRU	L ³
unit air requirement in laboratory experimental run, volumes of air per unit mass of pack	a_E	F_{aE}	AIREX	L ³ /m
unit air requirement in reservoir, volumes of air per unit bulk volume of reservoir rock	a_R	F_{aR}	AIRR	
unit fuel concentration (see symbol m)	C_m	c_m, n_m	CNCFU	various
universal gas constant (per mole)	R		RRR	mL ² /t ² T
utilization, oxygen	e_{O_2}	E_{O_2}	UTLO2	
valence	z		VAL	
vapor phase, mole fraction of component	y		MFRV	
vapor phase, moles of	V		MOLV	
vaporization, latent heat of	L_v	λ_v	HLTV	L ² /t ²
variance of a random variable	σ^2		VAR	
variance of a random variable, estimated	s^2		VARES	
vector of x	\vec{x}			
velocity	v	V, u	VEL	L/t
velocity, acoustic	v	V, u	VAC	L/t
velocity, acoustic apparent (measured)	v_a	V_a, u_a	VACA	L/t
velocity, acoustic fluid	v_f	V_f, u_f	VACF	L/t
velocity, matrix acoustic	v_{ma}	V_{ma}, u_{ma}	VACMA	L/t
velocity, shale acoustic	v_{sh}	V_{sh}, u_{sh}	VACSH	L/t
velocity (rate) of burning-zone advance	v_b	V_b, u_b	VELB	L/t
vertical (invasion) efficiency: hydrocarbon pore space invaded (affected, contacted) by the injected-fluid or heat front divided by the	E_I	η_I, e_I	EFFI	

Quantity	Letter Symbol	Reserve SPE Letter Symbol	Computer Letter Symbol	Dimensions
hydrocarbon pore space enclosed in all layers behind the injected-fluid or heat front				
viscosity, air	μ_a	η_a	VISA	m/Lt
viscosity at mean pressure	$\mu_{\bar{p}}$	$\eta_{\bar{p}}$	VISPAV	m/Lt
viscosity, dynamic	μ	η	VIS	m/Lt
viscosity, gas	μ_g	η_g	VISG	m/Lt
viscosity, gas, at 1 atm	μ_{ga}	η_{ga}	VISGA	m/Lt
viscosity, kinematic	ν	N	VSK	L ² /t
viscosity, oil	μ_o	η_o	VISO	m/Lt
viscosity, water	μ_w	η_w	VISW	m/Lt
volume	V	v	VOL	L ³
volume at bubblepoint pressure	V_{bp}	v_{bp}	VOLBP	L ³
volume, bulk	V_b	v_b	VOLB	L ³
volume, bulk, of pack burned in experimental run	V_{bE}	v_{bE}	VOLBEX	L ³
volume, effective pore	V_e	V_{pe}, v_e	VOLG	L ³
volume fraction or ratio (as needed, use same subscripted symbols as for "volumes"; note that bulk volume fraction is unity and pore volume fractions are ϕ)	V	f_V, F_V	VLF	various
volume, free-gas, initial reservoir ($=mNb_{oi}$)	G_{Fi}	g_{Fi}	GASFI	L ³
volume, grain (volume of all formation solids except shales)	V_{gr}	v_{gr}	VOLGR	L ³
volume, intergranular (volume between grains; consists of fluids and all shales) ($V_b - V_{gr}$)	V_{ig}	v_{ig}	VOLIG	L ³
volume, intermatrix (consists of fluids and dispersed shale) ($V_b - V_{ma}$)	V_{im}	v_{im}	VOLIM	L ³
volume, matrix (framework) (volume of all formation solids except dispersed shale)	V_{ma}	v_{ma}	VOLMA	
volume, noneffective pore ($V_p - V_e$)	V_{ne}	V_{pne}, v_{ne}	VOLNE	L ³
volume of reservoir rock burned	V_{Rb}		VOLRB	L ³
volume of reservoir rock unburned	V_{Ru}		VOLRU	L ³
volume per mole (molal volume)	V_M		VOLM	L ³
volume, pore ($V_b - V_s$)	V_p	v_p	VOLP	L ³
volume, pore, dimensionless	V_{pD}	v_{pD}	VOLPQ	
volume, shale, dispersed	V_{shd}	v_{shd}	VOLSHD	L ³
volume, shale, laminated	V_{shl} <i>script l</i>	v_{shl} <i>script l</i>	VSHLAM	L ³
volume, shale, structural	V_{shs}	v_{shs}	VOLSHS	L ³
volume, shale(s) (volume of all shales: structural and dispersed)	V_{sh}	v_{sh}	VOLSH	L ³
volume, solid(s) (volume of all formation solids)	V_s	v_s	VOLS	L ³
volume, specific	v	v_s	SPV	L ³ /m
volumetric efficiency for burned portion only, in-situ combustion pattern	E_{Vb}	η_{Vb}, e_{Vb}	EFFVB	
volumetric efficiency: product of pattern sweep and invasion efficiencies	E_V	η_V, e_V	EFFV	

Quantity	Letter Symbol	Reserve SPE Letter Symbol	Computer Letter Symbol	Dimensions
volumetric flow rate	q	Q	RTE	L^3/t
volumetric flow rate downhole	q_{dh}	q_{wf}, q_{DH}, Q_{dh}	RTEDH	L^3/t
volumetric flow rate, surface conditions	q_{sc}	q_{σ}, Q_{sc}	RTESC	L^3/t
volumetric heat capacity	M		HSPV	m/Lt^2T
volumetric velocity (flow rate or flux, per unit area)	u	ψ	VELV	L/t
water (always with identifying subscripts)	W	w	WTR	various
water compressibility	c_w	k_w, κ_w	CMPW	Lt^2/m
water density	ρ_w rho	D_w	DENW	m/L^3
water displaced from burned volume, volume per unit volume of burned reservoir rock	δ_{wb}	F_{wb}	DPRWB	
waterdrive constant	C		WDC	L^4t^2/m
waterdrive constant, linear aquifer	C_L		WDCL	L^4t^2/m
water, effective permeability to	k_w	K_w	PRMW	L^2
water formation volume factor	B_w	F_w	FVFW	
water/fuel ratio	F_{wF}		FACWFU	various
water, gas solubility in	R_{sw}		GWRS	
water in place in reservoir, initial	W	w	WTRTI	L^3
water influx (encroachment), cumulative	W_e	w_e	WTRE	L^3
water influx (encroachment) during an interval	ΔW_e	Δw_e	DELWTRE	L^3
water influx (encroachment) rate	e_w	i_w	ENCW	L^3/t
water injected, cumulative	W_i	w_i	WTRI	L^3
water injected during an interval	ΔW_i	Δw_i	DELWTRI	L^3
water injection rate	i_w		INJW	L^3/t
water mobility	λ_w		MOBW	L^3t/m
water/oil permeability ratio	k_w/k_o	K_w/K_o	PRMWO	
water/oil ratio, cumulative	F_{wop}		FACWOP	
water/oil ratio, producing, instantaneous	F_{wo}		FACWO	
water produced, cumulative	W_p	w_p	WTRP	L^3
water produced during an interval	ΔW_p	Δw_p	DELWTRP	L^3
water production rate	q_w	Q_w	RTEW	L^3/t
water production rate, dimensionless	q_{wD}	Q_{wD}	RTEWQ	
water, relative permeability to	k_{rw}	K_{rw}	PRMRW	
water resistivity	R_w	ρ_w, r_w	RESW	mL^3/tq^2
water saturation	S_w	ρ_w, s_w	SATW	
water saturation, critical	S_{wc}	ρ_{wc}, s_{wc}	SATWC	
water saturation, initial	S_{wi}	ρ_{wi}, s_{wi}	SATWI	
water saturation (interstitial) in oil band	S_{wo}	S_{wb}	SATWO	
water saturation in gas cap, interstitial	S_{wg}	ρ_{wg}, s_{wg}	SATWG	
water saturation, interstitial, connate, or irreducible	S_{iw}	ρ_{iw}, s_{iw}	SATIW	
water saturation, residual	S_{wr}	ρ_{wr}, s_{wr}	SATWR	
water specific gravity	γ_w	s_w, F_{ws}	SPGW	
water viscosity	μ_w	η_w	VISW	m/Lt
wave length ($1/\sigma$)	λ		WVL	L
wave number ($1/\lambda$)	σ	$\tilde{\nu}$	WVN	$1/L$
weight (gravitational)	W	w, G	WGT	m/Lt^2
weight-weighted average density of produced liquid	$\bar{\rho}_L$ rho	\bar{D}_L	DENAVL	m/L^3
weight, atomic	A		AWT	m

Quantity	Letter Symbol	Reserve SPE Letter Symbol	Computer Letter Symbol	Dimensions
weight, molecular	M		MWT	m
well radius	r_w	R_w	RADW	L
well radius of damage or stimulation (skin)	r_s	R_s	RADS	L
well stabilization time	t_s	τ_s	TIMS	t
wellbore radius, effective or apparent (includes effects of well damage or stimulation)	r_{wa}	R_{wa}	RADWA	L
wet-gas content	C_{wg}	c_{wg}, n_{wg}	CNTWG	various
wet gas produced, cumulative	G_{wgp}	g_{wgp}	GASWGP	L ³
width, breadth, or thickness (primarily in fracturing)	b	w	WTH	L
work	W	w	WRK	mL ² /t ²
Young's modulus (modulus of elasticity)	E	Y	ELMY	m/Lt ²
zone diameter, invaded, electrically equivalent	d_i	d_I, D_i	DIAI	L
zone resistivity, invaded	R_i	ρ_i, r_i	RESI	mL ³ /tq ²

Subscript Definitions in Alphabetical Order

Subscript Definition	Letter Subscript	Reserve SPE Subscript	Computer Letter Subscript
abandonment	a	A	A
acoustic	a	A, α	A
activation log, neutron	NA	na	NA
active, activity, or acting	a		A
after taxes	a		A
air	a	A	A
air/fuel	aF		AFU
altered	a		A
amplitude log	A	a	A
angle, angular, or angular coordinate	θ		THE
anhydrite	anh		AH
anisotropic	ani		ANI
annulus apparent (from log readings; use tool description subscripts)	an	AN	AN
apparent (general)	a	ap	A
apparent wellbore (usually with wellbore radius r_{wa})	wa		WA
areal	A		A
atmosphere, atmospheric	a	A	A
average or mean pressure	\bar{p}		PAV
average or mean saturation	\bar{S}	$\bar{s}, \bar{\rho}$	SAV
band or oil band	b	B	B
bank or bank region	b		B
base	b	r, β	B
before taxes	b	B	B
bond log, cement	CB	cb	CB
borehole televiwer log	TV	tv	TV
bottomhole	bh	w, BH	BH
bottomhole, flowing (usually with pressure or time)	wf		WF
bottomhole, static (usually with pressure or time)	ws		WS
boundary conditions, external	e	o	E
breakthrough	BT	bt	BT
bubble	b		B
bubblepoint conditions, oil at (usually with formation volume factor, B_{ob})	ob		OB
bubblepoint conditions, solution at (usually with gas/oil ratio, R_{sb})	sb		SB
bubblepoint (saturation)	b	s, bp	BP
bubblepoint or saturation (usually with volume, V_{bp})	bp		BP
bulk (usually with volume, V_b)	b	B, t	B
burned in experimental tube run (usually with volume, V_{bE})	bE		BEX
burned or burning	b	B	B
burned portion of in-situ combustion pattern, displacement from (usually with efficiency, E_{Db})	Db		DB
burned portion of in-situ combustion pattern, volumetric of (usually with efficiency, E_{vb})	Vb		VB

Subscript Definition	Letter Subscript	Reserve SPE Subscript	Computer Letter Subscript
burned reservoir rock	<i>Rb</i>		RB
burned volume, oil from (usually with displacement ratio, δ_{ob})	<i>ob</i>		OB
burned volume, water from (usually with displacement ratio, δ_{wb})	<i>wb</i>		WB
calculated	<i>C</i>	<i>calc</i>	CA
caliper log	<i>C</i>	<i>c</i>	C
capillary (usually with capillary pressure, P_c)	<i>c</i>	<i>C</i>	CP
capture	<i>cap</i>		C
carbon dioxide	CO_2		CO2
carbon monoxide	CO		CO
casing or casinghead	<i>c</i>	<i>cg</i>	CS
casing, flowing (usually with pressure)	<i>cf</i>		CF
casing, static (usually with pressure)	<i>cs</i>		CS
cement bond log	<i>CB</i>	<i>cb</i>	CB
chemical	<i>c</i>		C
chlorine log	<i>CL</i>	<i>cl</i>	CL
clay	<i>cl</i>	<i>cla</i>	CL
clean	<i>cn</i>	<i>cln</i>	CN
coil	<i>C</i>	<i>c</i>	C
compaction	<i>cp</i>		CP
compensated density log	<i>CD</i>	<i>cd</i>	CD
compensated neutron log	<i>CN</i>	<i>cn</i>	CN
component(s)	<i>C</i>		C
component <i>j</i>	<i>j</i>		J
component <i>j</i> produced (usually with moles, n_{pj})	<i>pj</i>		PJ
compressional wave	<i>c</i>	<i>C</i>	C
conditions for infinite dimensions	∞	<i>INF</i>	INF
conductive liquids in invaded zone	<i>z</i>		Z
connate (interstitial, irreducible)	<i>i</i>	<i>ir</i> , <i>ι</i> <i>iota</i> , <i>i</i> script <i>i</i>	IR
constant	<i>c</i>	<i>C</i>	C
contact (usually with contact angle, θ_c)	<i>c</i>	<i>C</i>	C
contact log, microlog, minilog	<i>ML</i>	<i>ml</i> script <i>l</i>	ML
convective			C
conversion (usually with conversion factor in Newton's law of motion, g_c)	<i>c</i>		C
core	<i>c</i>	<i>C</i>	C
corrected	<i>cor</i>		COR
critical	<i>c</i>	<i>cr</i>	CR
cumulative influx (encroachment)	<i>e</i>	<i>i</i>	E
cumulative injected	<i>i</i>		I
cumulative produced	<i>p</i>		P
cumulative produced free value (usually with gas, G_{Fp})	F_p		FP
cumulative produced liquid (usually with condensate, G_{Lp})	L_p		LP
damage or damaged (includes "skin" conditions)	<i>s</i>	<i>d</i>	S
decay	<i>d</i>		D

Subscript Definition	Letter Subscript	Reserve SPE Subscript	Computer Letter Subscript
deep induction log	<i>ID</i>	<i>id</i>	ID
deep laterolog	<i>LLD</i>	<i>ll d script ll</i>	LLD
delay	<i>d</i>	δ	D
density	ρ		RHO
density log, compensated	<i>CD</i>	<i>cd</i>	CD
density log	<i>D</i>	<i>d</i>	D
depleted region, depletion	<i>d</i>	δ	D
dewpoint	<i>d</i>		D
differential separation	<i>d</i>		D
differential temperature log	<i>DT</i>	<i>dt</i>	DT
diffusivity	η		ETA
dimensionless pore value (usually with volume, V_{pD})	<i>pD</i>		PQ
dimensionless quantity	<i>D</i>		Q
dimensionless quantity at condition <i>m</i>	<i>Dm</i>		QM
dimensionless time	<i>tD</i>		TQ
dimensionless water	<i>wD</i>		WQ
dip (usually with angle, α_d)	<i>d</i>		D
diplog, dipmeter	<i>DM</i>	<i>dm</i>	DM
directional survey	<i>DR</i>	<i>dr</i>	DR
dirty (clayey, shaly)	<i>dy</i>	<i>dy</i>	DY
discounted value, present worth, or present value	<i>PV</i>	<i>pv</i>	PV
dispersed	<i>d</i>	<i>D</i>	D
dispersion	<i>K</i>	<i>d</i>	K
displaced	<i>d</i>	<i>s, D</i>	DD
displacement from burned portion of in-situ combustion pattern (usually with efficiency, E_{Db})	<i>Db</i>		DB
displacement from unburned portion of in-situ combustion pattern (usually with efficiency, E_{Du})	<i>Du</i>		DU
displacing or displacement (efficiency)	<i>D</i>	<i>s, \sigma</i>	DN
dolomite	<i>dol</i>		DL
downhole	<i>dh</i>	<i>DH</i>	DH
drainage (usually with drainage radius, r_d)	<i>d</i>		D
dual induction log	<i>DI</i>	<i>di</i>	DI
dual laterolog	<i>DLL</i>	<i>dl l script ll</i>	DLL
earth	<i>e</i>	<i>E</i>	E
effective (or equivalent)	<i>e</i>		E
electric, electrical	<i>e</i>	<i>E</i>	E
electrochemical	<i>c</i>	<i>ec</i>	C
electrode	<i>E</i>	<i>e</i>	E
electrokinetic	<i>k</i>	<i>ek</i>	K
electrolog, electrical log, electrical survey	<i>EL</i>	<i>el, ES</i>	EL
electromagnetic pipe inspection log	<i>EP</i>	<i>ep</i>	EP
electron	<i>el</i>	<i>e l script el</i>	E
empirical	<i>E</i>	<i>EM</i>	EM
encroachment (influx), cumulative	<i>e</i>	<i>i</i>	E

Subscript Definition	Letter Subscript	Reserve SPE Subscript	Computer Letter Subscript
entry	<i>e</i>	<i>E</i>	E
epithermal neutron log	<i>NE</i>	<i>ne</i>	NE
equivalent	<i>eq</i>	<i>EV</i>	EV
estimated	<i>E</i>	<i>est</i>	ES
ethane	<i>C₂</i>		C2
experimental	<i>E</i>	<i>EX</i>	EX
experimental value per mole of produced gas (usually with fuel consumption, m_{Eg})	<i>Eg</i>		EXG
external, outer boundary conditions	<i>e</i>	<i>o</i>	E
extrapolated	<i>ext</i>		XT
fast neutron log	<i>NF</i>	<i>nf</i>	NF
fill-up	<i>F</i>	<i>f</i>	F
finger or fingering	<i>f</i>	<i>F</i>	F
flash separation	<i>f</i>	<i>F</i>	F
flowing bottomhole (usually with pressure or time)	<i>wf</i>		WF
flowing casing (usually with pressure)	<i>cf</i>		CF
flowing conditions, injection well (usually with pressure, p_{iwf})	<i>iwf</i>		IWF
flowing conditions, well (usually with time)	<i>wf</i>	<i>f</i>	WF
flowing tubing (usually with pressure)	<i>tf</i>		TF
fluid	<i>f</i>	<i>fl</i>	F
fluids in an invaded zone, conductive	<i>z</i>		Z
flushed zone	<i>xo</i>		XO
formation 100% saturated with water (used in R_o only)	0 zero	<i>zr</i>	ZR
formation (rock)	<i>f</i>	<i>fm</i>	F
formation, surrounding	<i>s</i>		S
fraction or fractional	<i>f</i>	<i>r</i>	F
fracture, fractured, or fracturing	<i>f</i>	<i>F</i>	FR
free (usually with gas or gas/oil ratio quantities)	<i>F</i>	<i>f</i>	F
free fluid	<i>Ff</i>		FF
free value, cumulative produced, (usually with gas, G_{Fp})	<i>Fp</i>		FP
free value, initial (usually with gas, G_{Fi})	<i>Fi</i>		FI
front, front region, or interface	<i>f</i>	<i>F</i>	F
fuel, mass of (usually with fuel concentration, C_m)	<i>m</i>		FU
fuel (usually with fuel properties, such as ρ_f)	<i>F</i>		FU
gamma-gamma ray log	<i>GG</i>	<i>gg</i>	GG
gamma ray log	<i>GR</i>	<i>gr</i>	GR
gas	<i>g</i>	<i>G</i>	G
gas at atmospheric conditions	<i>ga</i>		GA
gas at bubblepoint conditions	<i>gb</i>		GB
gas cap, oil in (usually with saturation, S_{og})	<i>og</i>		OG
gas cap, water in (usually with saturation, S_{wg})	<i>wg</i>		WG
gas, dimensionless	<i>gD</i>		GQ
gas/oil, solution (usually with gas/oil ratios)	<i>s</i>		S
gas/water, solution (usually with gas solubility in water, R_{sw})	<i>sw</i>		SW
geometrical	<i>G</i>		G

Subscript Definition	Letter Subscript	Reserve SPE Subscript	Computer Letter Subscript
geothermal	G	T	GT
grain	gr		GR
grain (matrix, solids)	ma		MA
gravity meter log	GM	gm	GM
gross (total)	t	T	T
guard log	G	g	G
gypsum	gyp		GY
half	$1/2$		H
heat or thermal	h	T, θ	HT
heavy phase	HP	hp	HP
hole	h	H	H
horizontal	H	h	H
hydraulic	H		HL
hydrocarbon	h	H	H
hydrogen nuclei or atoms	H		HY
hydrocarbon, residual	hr		HR
hydrogen sulfide	H_2S		H2S
imbibition	I	$i, \text{script } i$	I
induction log, deep investigation	ID	id	ID
induction log	I	i	I
induction log, dual	DI	di	DI
induction log, medium investigation	IM	im	IM
infinite dimensions, conditions for	∞		INF
influx (encroachment), cumulative	e	i	E
initial conditions or value	i		I
initial free value (usually with gas, G_{Fi})	Fi		FI
initial solution (usually with gas/oil ratio, R_{si})	si		SI
injected, cumulative	i	I	I
injection, injected, or injecting	i	inj	I
injection well, flowing conditions (usually with pressure, p_{iwf})	iwf		IWF
injection well, static conditions (usually with pressure, p_{iws})	iws		IWS
inner, interior, or internal	i	$i, \text{script } i$	I
interface, front region, or front	f	F	F
interference	I	$i, \text{script } i$	I
intergranular	ig		IG
intermatrix	im		IM
internal	i	$i, \text{script } i$	I
interstitial	i	$i, \text{script } i$	I
intrinsic	int		I
invaded	i	I	I
invaded zone	i	I	I
invaded zone, conductive liquids in an	z		Z
invasion (usually with invasion efficiency, E_I)	I	i	I
irreducible, interstitial, or connate	i	$ir, i, \text{script } i$	IR
j th component	j		J
j th component, produced (usually with moles, n_{pj})	pj		PJ
junction	j		J

Subscript Definition	Letter Subscript	Reserve SPE Subscript	Computer Letter Subscript
laminar	ℓ script <i>l</i>	<i>L</i>	LAM
laminated, lamination	ℓ script <i>l</i>	<i>L</i>	LAM
lateral (resistivity) log	<i>L</i>	ℓ script <i>l</i>	L
laterolog (add further tool configuration subscripts as needed)	<i>LL</i>	$\ell\ell$ script <i>ll</i>	LL
laterolog, dual	<i>DLL</i>	$d\ell\ell$ script <i>ll</i>	DLL
lifetime log, neutron, TDT	<i>NL</i>	$n\ell$ script <i>l</i>	NL
light phase	<i>LP</i>	ℓp script <i>l</i>	LP
limestone	<i>ls</i>	<i>lst</i>	LS
limiting value	<i>lim</i>		LM
linear, lineal	<i>L</i>	ℓ script <i>l</i>	L
liquid or liquid phase	<i>L</i>	ℓ script <i>l</i>	L
liquids, conductive, invaded zone	<i>z</i>		Z
liquid produced, cumulative (usually with condensate, G_{Lp})	<i>Lp</i>		LP
location subscripts, usage is secondary to that for representing times or time periods	1, 2, 3, etc.		
log	log	log	L
lower	ℓ script <i>l</i>	<i>L</i>	L
magnetism log, nuclear	<i>NM</i>	<i>nm</i>	NM
mass of fuel (usually with fuel concentration, C_m)	<i>m</i>		FU
matrix (solids, grain)	<i>ma</i>		MA
matrix [solids except (nonstructural) clay or shale]	<i>ma</i>		MA
maximum	max		MX
mean or average pressure	\bar{p}		PAV
mean or average saturation	\bar{S}	$\bar{s}, \bar{\rho}$	SAV
medium investigation induction log	<i>IM</i>	<i>im</i>	IM
methane	C_1		C1
microlaterolog	<i>MLL</i>	$m\ell\ell$ script <i>ll</i>	MLL
microlog, minilog, contact log	<i>ML</i>	$m\ell$ script <i>l</i>	ML
microseismogram log, signature log, variable density log	<i>VD</i>	<i>vd</i>	VD
minimum	min		MN
mixture	<i>M</i>	<i>z,m</i>	M
mobility	λ	<i>M</i>	LAM
molal (usually with volume, V_M)	<i>M</i>		M
<i>M</i> th period or interval	<i>M</i>	<i>m</i>	M
mud	<i>m</i>		M
mudcake	<i>mc</i>		MC
mud filtrate	<i>mf</i>		MF
net	<i>n</i>		N
neutron	<i>N</i>	<i>n</i>	N
neutron activation log	<i>NA</i>	<i>na</i>	NA
neutron lifetime log, TDT	<i>NL</i>	$n\ell$ script <i>l</i>	NL
neutron log, compensated	<i>CN</i>	<i>cn</i>	CN
neutron log	<i>N</i>	<i>n</i>	N
neutron log, epithermal	<i>NE</i>	<i>ne</i>	NE

Subscript Definition	Letter Subscript	Reserve SPE Subscript	Computer Letter Subscript
neutron log, fast	NF	nf	NF
neutron log, sidewall	SN	sn	SN
neutron log, thermal	NT	nt	NT
nitrogen	N_2		N2
noneffective	ne		NE
nonwetting	nw	NW	NW
normal	n		N
normal (resistivity) log (add numerical spacing to subscript to N ; e.g., $N16$)	N	n	N
normalized (fractional or relative)	n	r, R	N
n th year, period, income, payment, or unit	n	N	N
nuclear magnetism log	NM	nm	NM
numerical subscripts (intended primarily to represent times or time periods; available secondarily as location subscripts or for other purposes)	1,2,3, etc.		
observed	OB		OB
oil at bubblepoint conditions (usually with formation volume factor, B_{ob})	ob		OB
oil, dimensionless	oD		OQ
oil (except when used with resistivity)	o	N	O
oil from burned volume (usually with displacement ratio, δ_{ob})	ob		OB
oil from unburned volume (usually with displacement ratio, δ_{ou})	ou		OU
oil in gas cap (usually with saturation, S_{og})	og		OG
outer (external) boundary conditions	e	o	E
oxygen	O_2		O2
particle (usually with diameter, d_p)	p		P
particular period, element, or interval	k	K	K
pattern (usually with pattern efficiency, E_p)	P		P
payout, payoff, or payback	p	po	PO
permeability	k		K
phase or phases	P		P
pipe inspection log, electromagnetic	EP	ep	EP
pore (usually with volume, V_p)	p	P	P
pore value, dimensionless (usually with volume, V_{pD})	pD		PQ
porosity	ϕ	f, ϵ	PHI
porosity data	ϕ	f, ϵ	P
pressure, mean or average	\bar{p}		PAV
primary	1 one	p, pri	PR
produced	p	P	P
produced component j (usually with moles, n_{pj})	pj		PJ
produced, cumulative	p		P
produced free value, cumulative (usually with gas, G_{fp})	F_p		FP
produced in experiment	pE		PEX
produced liquid, cumulative (usually with condensate, G_{Lp})	Lp		LP

Subscript Definition	Letter Subscript	Reserve SPE Subscript	Computer Letter Subscript
produced water/oil (cumulative) (usually with cumulative water/oil ratio, F_{wop})	wop		WOP
production period (usually with time, t_p)	p	P	P
profit — unamortized investment	Pk		PK
proximity log	P	p	P
pseudo	p		P
pseudocritical	pc		PC
pseudodimensionless	pD		PQ
pseudoreduced	pr		PRD
pseudo-SP	pSP		PSP
radius, radial, or radial distance	r	R	R
rate	R		
rate of return	r	R	R
ratio	R		
recovery (usually with recovery efficiency, E_R)	R		R
reduced	r		RD
reference	r	b, ρ	R
relative	r	R	R
reservoir	R	r	R
reservoir rock, burned	Rb		RB
reservoir rock, unburned	Ru		RU
residual	r	R	R
residual hydrocarbon	hr		HR
resistivity	R		R
resistivity log	R	r, ρ	R
Reynolds (used with Reynolds number only, N_{Re})	Re		
rock (formation)	f	fm	F
sand	sd	sa	SD
sandstone	ss	sst	SS
saturation, mean or average	\bar{S}	$\bar{s}, \bar{\rho}$	SAV
saturation or bubblepoint	b	s, bp	BP
saturation or bubblepoint (usually with volume, V_{bp})	bp		BP
scattered, scattering	sc		SC
secondary	2	s, sec	SE
segregation (usually with segregation rate, q_s)	s	S, σ	S
separator conditions	sp		SP
shale	sh	sha	SH
shallow laterolog	LLS	$lls \text{ script ll}$	LLS
shear	s	τ	S
shear wave	s	τ	S
sidewall	S	SW	SW
sidewall neutron log	SN	sn	SN
signature log, microseismogram log, variable density log	VD	vd	VD
silt	sl	slt	SL
single payment	sp		SP

Subscript Definition	Letter Subscript	Reserve SPE Subscript	Computer Letter Subscript
skin (stimulation or damage)	s	S	S
slip or slippage	s	σ	S
slurry ("mixture")	M	z, m	M
solid(s) (all formation solids)	s	σ	S
solids in experiment	sE		SEX
solids (matrix, grain)	ma		MA
solution at bubblepoint conditions (usually with gas/oil ratio, R_{sb})	sb		SB
solution in water (usually with gas solubility in water, R_{sw})	sw		SW
solution, initial (usually with gas/oil ratio, R_{si})	si		SI
solution (usually with gas/oil ratios)	s		S
sonde, tool	T	t	T
sonic velocity log	SV	sv	SV
SP	SP	sp	SP
spacing	s		L
specific (usually with J and I)	s		S
SSP	SSP		SSP
stabilization (usually with time)	s	S	S
standard conditions	sc	σ	SC
static bottomhole (usually with pressure or time)	ws		WS
static casing (usually with pressure)	cs		CS
static conditions, injection well (usually with pressure)	iws		IWS
static or shut-in conditions (usually with time)	ws	s	WS
static tubing (usually with pressure)	ts		TS
static well conditions (usually with time)	ws	s	WS
steam or steam zone	s	S	S
stimulation (includes "skin" conditions)	s	S	S
stock-tank conditions	st		ST
storage or storage capacity	S	s, σ	S
strain	ϵ	e	EPS
structural	st	s	ST
surface	s	σ	S
surrounding formation	s		S
swept or swept region	s	S, σ	S
system	s	σ	S
TDT log, neutron lifetime log	NL	$nl \text{ script } l$	NL
televiewer log, borehole	TV	tv	TV
temperature	T	h, θ	T
temperature log	T	t, h	T
temperature log, differential	DT	dt	DT
thermal (heat)	h	T, θ	HT
thermal decay time (TDT) log	NL	$nl \text{ script } l$	NL
thermal neutron log	NT	nt	NT
time, dimensionless	tD		TQ
times or time periods	1, 2, 3, etc.		
tool-description subscripts: see individual entries such as "amplitude log," "neutron log," etc.			

Subscript Definition	Letter Subscript	Reserve SPE Subscript	Computer Letter Subscript
tool, sonde	T	t	T
total initial in place in reservoir	ti		TI
total (gross)	t	T	T
total, total system	t	T	T
transmissibility	T	t	T
treatment or treating	t	τ	T
true (opposed to apparent) (electrical logging)	t	tr	T
tubing flowing (usually with pressure)	tf		TF
tubing or tubinghead	t	tg	T
tubing, static (usually with pressure)	ts		TS
turbulence (used with F only, F_B)	B		B
ultimate	ul	a	UL
unamortized	u	U	U
unburned	u		U
unburned portion of in-situ combustion pattern	Du		DU
displacement from (usually with efficiency, E_{Du})			
unburned reservoir rock	Ru		RU
unburned volume, oil from (usually with displacement ratio, δ_{ou})	ou		OU
unit	u	U	U
unswept or unswept region	u	U	U
upper	u	U	U
vaporization, vapor, or vapor phase	v	V	V
variable density log, microseismogram log, signature log	VD	vd	VD
velocity	v	V	V
velocity, sonic or acoustic log	SV	sv	SV
vertical	V	v	V
volumetric of burned portion of in-situ combustion pattern (usually with efficiency, E_{vb})	Vb		VB
volume or volumetric	V	v	V
water	w	W	W
water, dimensionless	wD		WQ
water from burned volume (usually with displacement ratio, δ_{wb})	wb		WB
water/fuel	wF		WFU
water in gas cap (usually with saturation, S_{wg})	wg		WG
water/oil (usually with instantaneous producing water/oil ratio, F_{wo})	wo		WO
water/oil, produced (cumulative) (usually with cumulative water/oil ratio, F_{wop})	wop		WOP
water, solution in (usually with gas solubility in water, R_{sw})	sw		SW
water-saturated formation, 100%	0 zero	zr	ZR
weight	W	w	W
well conditions	w		W
well, flowing conditions (usually with time)	wf	f	WF
well, injection, flowing conditions (usually with pressure, p_{iwf})	iwf		IWF

Subscript Definition	Letter Subscript	Reserve SPE Subscript	Computer Letter Subscript
well, injection, static conditions (usually with pressure, p_{iws})	<i>iws</i>		IWS
well, static conditions (usually with time)	<i>ws</i>	<i>s</i>	WS
wellbore, apparent (usually with wellbore radius, r_{wa})	<i>wa</i>		WA
wellhead	<i>wh</i>	<i>th</i>	WH
wet gas (usually with composition or content, C_{wg})	<i>wg</i>		WG
wet gas produced	<i>wgp</i>		WGP
wetting	<i>w</i>	<i>W</i>	W
Young's modulus, refers to	<i>Y</i>		Y
zero hydrocarbon saturation	0 <i>zero</i>	<i>zr</i>	ZR
zone, conductive fluids in an invaded	<i>z</i>		Z
zone, flushed	<i>xo</i>		XO
zone, invaded	<i>i</i>	<i>I</i>	I

Subscript Symbols in Alphabetical Order

Letter Subscript	Reserve SPE Subscript	Computer Letter Subscript	Subscript Definition
Greek and Numerical			
ϵ	e	EPS	strain
η		ETA	diffusivity
θ		THE	angle, angular, or angular coordinate
λ	M	LAM	mobility
ρ		RHO	density
ϕ	f, ϵ	PHI	porosity
ϕ	f, ϵ	P	porosity data, derived from tool-description subscripts: see individual entries such as "amplitude log," "neutron log," etc.
0 zero	zr	ZR	formation 100% saturated with water (used in R_0 only)
1	p, pri	PR	primary
1,2,3,etc.			location subscripts, usage is secondary to that for representing times or time periods
1,2,3,etc.			numerical subscripts (intended primarily to represent times or time periods; available secondarily as location subscripts or for other purposes)
1,2,3,etc.			times or time periods
1/2		H	half
2	s, sec	SE	secondary
∞		INF	conditions for infinite dimensions
English			
A	a	A	amplitude log
A		A	areal
a	A	A	abandonment
a	A, α	A	acoustic
a		A	active, activity, or acting
a		A	after taxes
a	A	A	air
a		A	altered
a	ap	A	apparent (general)
a	A	A	atmosphere, atmospheric
aF		AFU	air/fuel
an	AN	AN	annulus apparent (from log readings: use tool description subscripts)
anh		AH	anhydrite
ani		ANI	anisropic
B		B	turbulence (used with F only, F_B)
BT	bt	BT	breakthrough
b	B	B	band or oil band
b		B	bank or bank region
b	r, β	B	base

Letter Subscript	Reserve SPE Subscript	Computer Letter Subscript	Subscript Definition
<i>b</i>	<i>B</i>	B	before taxes
<i>b</i>		B	bubble
<i>b</i>	<i>s, bp</i>	B	bubblepoint (saturation)
<i>b</i>	<i>B, t</i>	B	bulk (usually with volume, V_b)
<i>b</i>	<i>B</i>	B	burned or burning
<i>bE</i>		BEX	burned in experimental tube run (usually with volume, V_{bE})
<i>bh</i>	<i>w, BH</i>	BH	bottomhole
<i>bp</i>		BP	bubblepoint or saturation (usually with volume, V_{bp})
<i>C</i>	<i>calc</i>	CA	calculated
<i>C</i>	<i>c</i>	C	caliper log
<i>C</i>	<i>c</i>	C	coil
<i>C</i>		C	component(s)
<i>C</i>		C	convective
<i>C₁</i>		C1	methane
<i>C₂</i>		C2	ethane
<i>CB</i>	<i>cb</i>	CB	bond log, cement
<i>CD</i>	<i>cd</i>	CD	compensated density log
<i>CL</i>	<i>cl</i>	CL	chlorine log
<i>CN</i>	<i>cn</i>	CN	compensated neutron log
<i>CO</i>		CO	carbon monoxide
<i>CO₂</i>		CO2	carbon dioxide
<i>c</i>	<i>C</i>	CP	capillary (usually with capillary pressure, P_c)
<i>c</i>	<i>cg</i>	CS	casing or casinghead
<i>c</i>		C	chemical
<i>c</i>	<i>C</i>	C	compressional wave
<i>c</i>	<i>C</i>	C	constant
<i>c</i>	<i>C</i>	C	contact (usually with contact angle, θ_c)
<i>c</i>		C	conversion (usually with conversion factor in Newton's law of Motion, g_c)
<i>c</i>	<i>C</i>	C	core
<i>c</i>	<i>cr</i>	CR	critical
<i>c</i>	<i>ec</i>	C	electrochemical
<i>cap</i>		C	capture
<i>cb</i>	<i>CB</i>	CB	cement bond log
<i>cf</i>		CF	casing, flowing (usually with pressure)
<i>cl</i>	<i>cla</i>	CL	clay
<i>cn</i>	<i>cin</i>	CN	clean
<i>cor</i>		COR	corrected
<i>cp</i>		CP	compaction
<i>cs</i>		CS	casing, static (usually with pressure)
<i>D</i>	<i>d</i>	D	density log
<i>D</i>		D	dimensionless quantity
<i>D</i>	<i>s, σ</i>	DN	displacing or displacement (efficiency)
<i>DI</i>	<i>di</i>	DI	dual induction log
<i>DLL</i>	<i>dll script II</i>	DLL	dual laterolog
<i>DM</i>	<i>dm</i>	DM	diplog, dipmeter
<i>DR</i>	<i>dr</i>	DR	directional survey

Letter Subscript	Reserve SPE Subscript	Computer Letter Subscript	Subscript Definition
<i>DT</i>	<i>dt</i>	DT	differential temperature log
<i>Db</i>		DB	displacement from burned portion of in-situ combustion pattern (usually with efficiency, E_{Db})
<i>Dm</i>		QM	dimensionless quantity at condition m
<i>Du</i>		DU	displacement from unburned portion of in-situ combustion pattern (usually with efficiency, E_{Du})
<i>d</i>		D	decay
<i>d</i>	δ	D	delay
<i>d</i>	δ	D	depleted region, depletion
<i>d</i>		D	dewpoint
<i>d</i>		D	differential separation
<i>d</i>		D	dip (usually with angle, α_d)
<i>d</i>	<i>D</i>	D	dispersed
<i>d</i>	<i>s,D</i>	D	displaced
<i>d</i>		D	drainage (usually with drainage radius, r_d)
<i>dh</i>	<i>DH</i>	DH	downhole
<i>dol</i>		DL	dolomite
<i>dy</i>	<i>dy</i>	DY	dirty (clayey, shaly)
<i>E</i>	<i>e</i>	E	electrode
<i>E</i>	<i>EM</i>	EM	empirical
<i>E</i>	<i>est</i>	ES	estimated
<i>E</i>	<i>EX</i>	EX	experimental
<i>Eg</i>		EXG	experimental value per mole of produced gas (usually with fuel consumption, m_{Eg})
<i>EL</i>	<i>el,ES</i>	EL	electrolog, electrical log, electrical survey
<i>EP</i>	<i>ep</i>	EP	electromagnetic pipe inspection log
<i>c</i>	<i>ec</i>	C	electrochemical
<i>e</i>	<i>o</i>	E	boundary conditions, external
<i>e</i>	<i>i</i>	E	cumulative influx (encroachment)
<i>e</i>	<i>E</i>	E	earth
<i>e</i>		E	effective (or equivalent)
<i>e</i>	<i>E</i>	E	electric, electrical
<i>e</i>	<i>E</i>	E	entry
<i>e</i>	<i>o</i>	E	external or outer boundary conditions
<i>el</i>	<i>el script el</i>	E	electron
<i>eq</i>	<i>EV</i>	EV	equivalent
<i>ext</i>		XT	extrapolated
<i>F</i>	<i>f</i>	F	fill-up
<i>F</i>	<i>f</i>	F	free (usually with gas or gas/oil ratio quantities)
<i>F</i>		FU	fuel (usually with fuel properties, such as ρ_F)
<i>Fp</i>		FP	cumulative produced free value (usually with gas, G_{Fp})
<i>Ff</i>		FF	free fluid
<i>Fi</i>		FI	free value, initial (usually with gas, G_{Fi})
<i>f</i>	<i>F</i>	F	finger or fingering
<i>f</i>	<i>F</i>	F	flash separation
<i>f</i>	<i>fl</i>	F	fluid
<i>f</i>	<i>fm</i>	F	formation (rock)
<i>f</i>	<i>r</i>	F	fraction or fractional
<i>f</i>	<i>F</i>	FR	fracture, fractured, or fracturing

Letter Subscript	Reserve SPE Subscript	Computer Letter Subscript	Subscript Definition
<i>f</i>	<i>F</i>	F	front, front region, or interface
<i>f</i>	<i>fm</i>	F	rock (formation)
<i>G</i>		G	geometrical
<i>G</i>	<i>T</i>	GT	geothermal
<i>G</i>	<i>g</i>	G	guard log
<i>GG</i>	<i>gg</i>	GG	gamma-gamma ray log
<i>GM</i>	<i>gm</i>	GM	gravity meter log
<i>GR</i>	<i>gr</i>	GR	gamma ray log
<i>g</i>	<i>G</i>	G	gas
<i>gD</i>		GQ	gas, dimensionless
<i>ga</i>		GA	gas at atmospheric conditions
<i>gb</i>		GB	gas at bubblepoint conditions
<i>gr</i>		GR	grain
<i>gyp</i>		GY	gypsum
<i>H</i>	<i>h</i>	H	horizontal
<i>H</i>		HL	hydraulic
<i>H</i>		HY	hydrogen nuclei or atoms
<i>H₂S</i>		H2S	hydrogen sulfide
<i>HP</i>	<i>hp</i>	HP	heavy phase
<i>h</i>	<i>T, θ</i>	HT	heat or thermal
<i>h</i>	<i>H</i>	H	hole
<i>h</i>	<i>H</i>	H	hydrocarbon
<i>h</i>	<i>T, θ</i>	HT	thermal (heat)
<i>hr</i>		HR	hydrocarbon, residual
<i>I</i>	<i>i script i</i>	I	imbibition
<i>I</i>	<i>i</i>	I	induction log
<i>I</i>	<i>i, i script i</i>	I	interference
<i>I</i>	<i>i</i>	I	invasion (usually with invasion efficiency, E_I)
<i>ID</i>	<i>id</i>	ID	induction log, deep investigation
<i>IM</i>	<i>im</i>	IM	induction log, medium investigation
<i>i</i>		I	cumulative injected
<i>i</i>		I	initial conditions or value
<i>i</i>	<i>inj</i>	I	injection, injected, or injecting
<i>i</i>	<i>i, i script i</i>	I	inner, interior, or internal
<i>i</i>	<i>I</i>	I	invaded
<i>i</i>	<i>I</i>	I	invaded zone
<i>i</i>	<i>ir, i, i script i</i>	IR	irreducible, interstitial, or connate
<i>ig</i>		IG	intergranular
<i>im</i>		IM	intermatrix
<i>int</i>		I	intrinsic
<i>iwf</i>		IWF	injection well, flowing conditions (usually with pressure, p_{iwf})
<i>iws</i>		IWS	injection well, static conditions (usually with pressure, p_{iws})
<i>ws</i>	<i>s</i>	WS	well, static conditions (usually with time)
<i>j</i>		J	<i>j</i> th component
<i>j</i>		J	junction
<i>K</i>	<i>d</i>	K	dispersion
<i>k</i>	<i>ek</i>	K	electrokinetic
<i>k</i>	<i>K</i>	K	particular period, element, or interval

Letter Subscript	Reserve SPE Subscript	Computer Letter Subscript	Subscript Definition
<i>k</i>		K	permeability
<i>ℓ</i> script <i>l</i>	<i>L</i>	LAM	laminar
<i>ℓ</i> script <i>l</i>	<i>L</i>	LAM	laminated, lamination
<i>L</i>	<i>ℓ</i> script <i>l</i>	L	lateral (resistivity log)
<i>L</i>	<i>ℓ</i> script <i>l</i>	L	linear, lineal
<i>L</i>	<i>ℓ</i> script <i>l</i>	L	liquid or liquid phase
<i>ℓ</i> script <i>l</i>	<i>L</i>	L	lower
<i>L_p</i>		LP	cumulative produced liquid (usually with condensate, <i>G_{Lp}</i>)
<i>LL</i>	<i>ℓℓ</i> script <i>ll</i>	LL	laterolog (add further tool configuration subscripts as needed)
<i>LLD</i>	<i>ℓℓd</i> script <i>ll</i>	LLD	deep laterolog
<i>LLS</i>	<i>ℓℓs</i> script <i>ll</i>	LLS	shallow laterolog
LOG	<i>log</i>	L	log
<i>LP</i>	<i>ℓp</i> script <i>l</i>	LP	light phase
<i>Lp</i>		LP	liquid produced, cumulative (usually with condensate, <i>G_{Lp}</i>)
<i>lim</i>		LM	limiting value
<i>ls</i>	<i>lst</i>	LS	limestone
<i>M</i>	<i>m</i>	M	<i>M</i> th period or interval
<i>M</i>	<i>z,m</i>	M	mixture
<i>M</i>		M	molal (usually with volume, <i>V_M</i>)
<i>m</i>		M	mud
<i>M</i>	<i>z,m</i>	M	slurry ("mixture")
<i>ML</i>	<i>mℓ</i> script <i>l</i>	ML	contact log, microlog, minilog
<i>MLL</i>	<i>mℓℓ</i> script <i>ll</i>	MLL	microlaterolog
<i>m</i>		FU	mass of fuel (usually with fuel concentration, <i>C_m</i>)
<i>m</i>		M	mud
<i>ma</i>		MA	grain (matrix, solids)
<i>ma</i>		MA	matrix [solids except (nonstructural) clay or shale]
max		MX	maximum
<i>mc</i>		MC	mudcake
<i>mf</i>		MF	mud filtrate
min		MN	minimum
<i>N</i>	<i>n</i>	N	neutron
<i>N</i>	<i>n</i>	N	neutron log
<i>N</i>	<i>n</i>	N	normal (resistivity) log (add numerical spacing to subscript N; e.g., N16)
<i>N₂</i>		N2	nitrogen
<i>NA</i>	<i>na</i>	NA	neutron activation log
<i>NE</i>	<i>ne</i>	NE	neutron log, epithermal
<i>NF</i>	<i>nf</i>	NF	neutron log, fast
<i>NL</i>	<i>nℓ</i> script <i>l</i>	NL	neutron lifetime log, TDT
<i>NM</i>	<i>nm</i>	NM	nuclear magnetism log
<i>NT</i>	<i>nt</i>	NT	neutron log, thermal
<i>n</i>		N	net
<i>n</i>		N	normal
<i>n</i>	<i>r,R</i>	N	normalized (fractional or relative)
<i>n</i>	<i>N</i>	N	<i>n</i> th year, period, income, payment, or unit
<i>ne</i>		NE	noneffective
<i>nw</i>	<i>NW</i>	NW	nonwetting
<i>O₂</i>		O2	oxygen

Letter Subscript	Reserve SPE Subscript	Computer Letter Subscript	Subscript Definition
<i>OB</i>		OB	observed
<i>o</i>	<i>N</i>	O	oil (except when used with resistivity)
<i>ob</i>		OB	oil at bubblepoint conditions (usually with formation volume factor, B_{ob})
<i>ob</i>		OB	oil from burned volume (usually with displacement ratio, δ_{ob})
<i>oD</i>		OD	oil, dimensionless
<i>og</i>		OG	oil in gas cap (usually with saturation, S_{og})
<i>ou</i>		OU	oil from unburned volume (usually with displacement ratio, δ_{ou})
<i>P</i>		P	phase or phases
<i>P</i>	<i>p</i>	P	proximity log
<i>NL</i>	<i>nl script l</i>	NL	neutron lifetime log, TDT
<i>PV</i>	<i>pv</i>	PV	discounted value, present worth, or present value
<i>Pk</i>		PK	profit—unamortized investment
<i>p</i>		P	particle (usually with diameter, d_p)
<i>P</i>		P	pattern (usually with pattern efficiency, E_p)
<i>p</i>	<i>po</i>	PO	payout, payoff, or payback
<i>p</i>	<i>P</i>	P	pore (usually with volume, V_p)
\bar{p}		PAV	pressure, mean or average
<i>p</i>	<i>P</i>	P	produced
<i>p</i>		P	produced, cumulative
<i>p</i>	<i>P</i>	P	production period (usually with time, t_p)
<i>p</i>		P	pseudo
<i>pD</i>		PQ	pore value, dimensionless (usually with volume, V_{pD})
<i>pD</i>		PQ	pseudodimensionless
<i>pE</i>		PEX	produced in experiment
<i>pSP</i>		PSP	pseudo-SP
<i>pc</i>		PC	pseudocritical
<i>pj</i>		PJ	produced component j (usually with moles, n_{pj})
<i>pr</i>		PRD	pseudoreduced
<i>R</i>			rate
<i>R</i>			ratio
<i>R</i>		R	recovery (usually with recovery efficiency, E_R)
<i>R</i>	<i>r</i>	R	reservoir
<i>R</i>		R	resistivity
<i>R</i>		R	resistivity log
<i>Rb</i>	<i>r, \rho</i>	RB	reservoir rock, burned
<i>Ru</i>		RU	reservoir rock, unburned
<i>Re</i>			Reynolds (used with Reynolds number only, N_{Re})
<i>r</i>	<i>R</i>	R	radius, radial, or radial distance
<i>r</i>	<i>R</i>	R	rate of return
<i>r</i>		RD	reduced
<i>r</i>	<i>b, \rho</i>	R	reference
<i>r</i>	<i>R</i>	R	relative

Letter Subscript	Reserve SPE Subscript	Computer Letter Subscript	Subscript Definition
r	R	R	residual
\bar{S}	$\bar{s}, \bar{\rho}$	SAV	saturation, mean or average
S	SW	SW	sidewall
\bar{S}	s, σ	S	storage or storage capacity
\bar{S}	$\bar{s}, \bar{\rho}$	SAV	average or mean saturation
SN	sn	SN	neutron log, sidewall
SP	sp	SP	SP
SSP		SSP	SSP
SV	sv	SV	sonic, velocity or acoustic log
SWN	swn	SWN	sidewall neutron log
s	d	S	damage or damaged (includes "skin" conditions)
s		S	formation, surrounding
s		S	gas/oil ratio, solution
s	$S\sigma$	S	segregation (usually with segregation rate, q_s)
s	τ	S	shear
s	τ	S	shear wave
s	S	S	skin (stimulation or damage)
s	σ	S	slip or slippage
s	σ	S	solid (usually with volume or density)
s		S	solution (usually with gas/oil ratios)
s		L	spacing
s		S	specific (usually with J and I)
s	S	S	stabilization (usually with time)
s	S	S	steam or steam zone
s	S	S	stimulation (includes "skin" conditions)
s	σ	S	surface
s		S	surrounding formation
s	S, σ	S	swept or swept region
s	σ	S	system
sE		SEX	solids in experiment
sb		SB	solution at bubblepoint conditions (usually with gas/oil ratio, R_{sb})
sc		SC	scattered, scattering
sc	σ	SC	standard conditions
sd	sa	SD	sand
sh	sha	SH	shale
si		SI	solution, initial (usually with gas/oil ratio, R_{si})
sl	slt	SL	silt
sp		SP	separator conditions
sp		SP	single payment
ss	sst	SS	sandstone
st		ST	stock-tank conditions
st	s	ST	structural
sw		SW	solution in water (usually with gas solubility in water, R_{sw})
gyp		GY	gypsum
T	h, θ	T	temperature
T	t, h	T	temperature log
T	t	T	tool, sonde
T	t	T	transmissibility
TV	tv	TV	televviewer log, borehole

Letter Subscript	Reserve SPE Subscript	Computer Letter Subscript	Subscript Definition
t	T	T	gross (total)
t	T	T	total, total system
t	τ	T	treatment or treating
t	tr	T	true (electrical logging) (opposed to apparent)
t	tg	T	tubing or tubinghead
tD		TQ	time, dimensionless
tf		TF	tubing flowing (usually with pressure)
ti		TI	total initial in place in reservoir
ts		TS	tubing, static (usually with pressure)
u	U	U	unamortized
u		U	unburned
u	U	U	unit
u	U	U	unswept or unswept region
u	U	U	upper
ul	a	UL	ultimate
V	v	V	vertical
V	v	V	volume or volumetric
VD	vd	VD	microseismogram log, signature log, variable density log
Vb		VB	volumetric or burned portion of in-situ combustion pattern (usually with efficiency, E_{Vb})
v	V	V	vaporization, vapor, or vapor phase
v	V	V	velocity
v	W	W	water
W	w	W	weight
w		W	well conditions
w	W	W	wetting
wD		WQ	water, dimensionless
wF		WFU	water/fuel
wa		WA	wellbore, apparent (usually with wellbore radius, r_{wa})
wb		WB	water from burned volume (usually with displacement ratio, δ_{wb})
wf		WF	bottomhole, flowing (usually with pressure or time)
wf	f	WF	well, flowing conditions (usually with time)
wg		WG	water in gas cap (usually with saturation, S_{wg})
wg		WG	wet gas (usually with composition or content, C_{wg})
wgp		WGP	wet gas produced
wh	th	WH	wellhead
wo		WO	water/oil (usually with instantaneous producing water/oil ratio, F_{wo})
wop		WOP	water/oil, produced (cumulative) (usually with cumulative water/oil ratio, F_{wop})
ws		WS	static bottomhole (usually with pressure or time)
ws	s	WS	well, static, or shut-in conditions (usually with time)
xo		XO	flushed zone
Y		Y	Young's modulus, refers to
z		Z	conductive liquids in invaded zone
z			zone, conductive invaded

Author Index

A

- Abbott, W.A., v, 4-11
 Abernathy, B.F., 44-31, 44-51
 Abou El-Nour, F., 25-24
 Abou-Kassem, J.H., 48-11, 48-19
 Abou-Sayed, A.S., 55-10, 55-11
 Abram, A., 54-12
 Ache, P.S., 44-29, 44-50
 ACS Industries Inc., vi, 12-43
 Addington, D.V., 48-20
 Adeney, W.E., 25-22
 Aepelbaum, V.A., 25-22
 Afanas'eva, N.L., 25-25
 Afoju, B.I., 46-45
 Agarwal, R.G., 55-10
 Aguilera, A., 51-45, 51-52
 Aguilera, R., 29-9
 Ahmed, U., 55-10
 Aho, G.E., 47-26
 Ahrens, G., xii, 51-51
 Ainley, B.R., 55-10
 Air Products and Chemical Inc., 39-28
 Ajitsaria, N.K., 20-9, 20-18
 Akbar, A.M., 48-20
 Akstinat, M.H., xi, 47-25
 Alaska Oil & Gas Conservation Commission, viii
 Alberta Energy Resources Conservation Board, 48-18
 Alcauska, J.B., 25-21
 Alder, S.B., viii, 25-23
 Alexander, J.D., 46-13, 46-43
 Alger, R.P., 49-41, 49-42, 51-50, 51-51
 Al-Hussainy, R., 35-10, 35-21
 Aliev, S.N., 12-43
 Allen, D.R., 46-45
 Allen, F.H., 23-13, 39-13, 39-28
 Allen, L.S., 50-38
 Almond, S.W., 55-10
 Al-Saadoon, F.T., 37-21, 37-27
 Althouse, W.H., 4-11
 American Assn. of Petroleum Geologists (AAPG), 24-22, 29-9, 40-2, 40-37
 American Bureau of Shipping, 18-21, 18-52
 American Gas Assn. (AGA), vi, 13-8, 13-59, 33-13, 33-23, 40-38
 American Gear Manufacturer's Assn. (AGMA), 10-12
 American Hot Dip Galvanizers Assn., vi, 11-14
 American Inst. of Mining, Metallurgical and Petroleum Engineers (AIME), 12-43
 American Meter Co., vi, 13-41, 13-59
 American Natl. Metric Council (ANMC), 58-2, 58-8
 American Natl. Standards Inst. (ANSI), 58-2, 58-8, 58-22
 ANSI B16.5, 15-11, 15-34
 ANSI B26.5, vii
 ANSI B31.1, 15-11, 15-34
 ANSI B31.8, 15-11, 15-34
 ANSI B48.1, 58-8
 ANSI/API 2530, vi, 13-3, 13-59
 ANSI/ASME B31.3 & 31.4, 15-11, 15-34
 ANSI/ASME SPPE-1 & 1b, 3-34, 3-39, 3-40
 ANSI/IEEE Std. 260, 58-8
 American Petroleum Inst. (API), 24-3, 39-27, 40-2, 40-37, 40-38, 41-37, 58-2, 58-7
 API Bull. D-14, 40-37, 40-38
 API Bull. 2N, 18-52
 API Bull. 5C2, 2-46, 2-60, 2-74, 3-1, 3-40
 API Bull. 5C3, 2-74
 API Bull. 5C4, 2-74
 API Bull. 11L3, 9-3, 9-4, 9-14
 API Circ. PS-1360, 2-46, 2-74
 API Circ. PS-1398, 2-74
 API Code 25, 17-1
 API Code 27, 26-10, 26-11, 26-33
 API Committee on Standardization of Steel Tanks for Oil Storage, 11-3
 API Committee on Standardization of Valves and Wellhead Equipment, 3-3
 API Fundamental Research on Occurrence and Recovery of Petroleum, 39-27
 API Manual 14BM, 6-21, 6-72
 API Manual of Petroleum Measurement Standards, ix, 16-16, 17-1, 17-3, 17-8, 19-6, 19-34, 32-16
 API Manual on Disposal of Refinery Wastes, vii, 15-19, 15-24, 15-34
 API Petroleum Safety Data 2210, 11-9
 API Pub. 2563 and 2564, 58-8
 API RP 2A, 18-25, 18-27
 API RP 2K, 18-17, 18-52
 API RP 2P, 18-16, 18-52
 API RP 2Q, 18-17, 18-52
 API RP 5C1, 3-1, 3-40
 API RP 5C2, v
 API RP 5C3, v
 API RP 6F, 3-38, 3-40
 API RP 7C-11F, 10-19, 10-37
 API RP 10E, 15-10, 15-34
 API RP 11AR, 8-10
 API RP 11BR, vi, 9-14
 API RP 11ER, 10-12, 10-37
 API RP 11G, vi, 10-7, 10-12, 10-13, 10-37
 API RP 11L, vi, 8-10, 9-2, 9-3, 9-14, 10-7, 10-37
 API RP 11R, 7-17
 API RP 11S, 7-17
 API RP 11U, v
 API RP 12L, 19-7
 API RP 12RI, 11-14
 API RP 14B, 3-40
 API RP 14C, 3-40, 12-43, 18-46, 18-52, 19-28, 19-34
 API RP 14E, vii, 12-43, 15-7, 15-33, 19-34
 API RP 14F, 3-34, 3-40, 18-44, 18-46, 18-52
 API RP 14H, 3-40
 API RP 36, 32-3, 32-16
 API RP 38, 44-44, 44-51
 API RP 39M, 55-6
 API RP 44, 39-5, 39-27
 API RP 45, 19-34, 24-5, 24-22, 44-51
 API RP 49, 18-20, 18-52
 API RP 53, 18-12, 18-20, 18-52
 API RP 66, 6-72
 API RP 500B, vi, 10-37, 18-46, 18-52
 API RP 520, 11-7
 API Spec. 5A, v, 2-74, 3-2, 3-14, 3-40
 API Spec. 5B, v, 2-64, 2-74
 API Spec. 5AC, 2-74
 API Spec. 5AQ, 2-74
 API Spec. 5AX, 2-74
 API Spec. 5L, v, 2-74, 3-2, 3-40, 15-10, 15-34
 API Spec. 5LE, 15-10, 15-33
 API Spec. 5LP, 15-10, 15-33
 API Spec. 5LR, 15-10, 15-34
 API Spec. 5LX, 15-12
 API Spec. 6A, v, 3-1, 3-5, 3-18, 3-36, 3-38, 3-40, 15-13, 15-34
 API Spec. 7B-11C, 10-17, 10-37
 API Spec. 11AX, v, 8-2, 8-6, 8-10
 API Spec. 11B, vi, 9-1, 9-14
 API Spec. 11C, vi, 9-14
 API Spec. 11E, 10-1, 10-4, 10-5, 10-7, 10-37
 API Spec. 11N, 16-16
 API Spec. 12B, vi
 API Spec. 12D, 11-2, 11-14
 API Spec. 12F, 11-1, 11-14
 API Spec. 12J, 12-44
 API Spec. 12K, 19-34
 API Spec. 12L, 19-34
 API Spec. 14A, 3-34, 3-40
 API Spec. 14D, 3-34, 3-39, 3-40
 API Standardization Conference, 2-46, 2-60, 2-63, 2-74
 API Standing Subcommittee on Secondary Recovery Methods, 39-28
 API Std. 5B, 2-57
 API Std. 12B, 11-3, 11-14
 API Std. 510, 12-43
 API Std. 620, 11-7, 11-14
 API Std. 650, 11-2, 11-7, 11-9, 11-14
 API Std. 1101, ix, 16-6, 16-16, 17-4, 17-7, 32-16
 API Std. 1104, 12-44, 19-34
 API Std. 2000, vi, 11-6, 11-14
 API Std. 2500, 17-1
 API Std. 2531 & 2533, 17-4
 API Std. 2534, 17-4, 17-7
 API Std. 2543, 17-5, 17-8
 API Std. 2545, 17-3, 17-8
 API Std. 2550 to 2556, 17-3
 API Technical Data Book, 21-3, 21-20
 API Vocational Training Series, v, 5-57
 American Soc. of Mechanical Engineers, (ASME) 46-45, 58-2, 58-7, 58-8
 ASME Code for Boilers and Pressure Vessels, vi, 12-38 to 12-41, 12-43
 ASME B31, 15-11, 15-33
 American Soc. for Testing and Materials, (ASTM) 1-80, 24-3, 24-5, 24-22, 58-2, 58-7
 ASTM A 123, 11-14
 ASTM D 1250, 17-5, 17-6
 ASTM D 1298, 17-5
 ASTM D 2887, 21-1, 21-20
 ASTM D 4051, 17-5
 ASTM E 380-82, 58-8, 58-14
 ASTM Standards on Petroleum Products and Lubricants, vii
 ASTM Steam Tables, x
 Amero, R.C., 25-27
 Amirjafari, B., 25-26
 Amyx, J.W., 24-23, 26-1
 Anders, E.L. Jr., 43-19
 Anderson, A.E., 49-41
 Anderson, B.W., 54-13
 Anderson, D.F., 47-25
 Anderson, G., 52-31
 Anderson, G.L., 16-16
 Anderson, M.A., 26-33
 Anderson, R.A., 51-52
 Anderson, T., 51-44, 51-52
 Andresen, K.H., 44-51
 Angier, J.D., 6-72
 Angino, E.E., 24-19, 24-23
 Anthony, R.G., 25-26, 25-27
 Antoine, C., 20-13, 20-17, 20-18
 Aoyagi, K., 25-12, 25-23
 Apache Santa Fe Intl. Corp., vii
 Archer, D.L., 28-11, 28-15, 47-20, 47-26
 Archie, G.E., 26-28, 26-29, 26-31, 49-4, 49-5, 49-41
 Arditty, P.C., xii, 51-51
 Arnold, D.M., xi, 50-32, 50-38
 Arnold, K.E., 15-1, 19-1, 19-33
 Arnold, M.D., 48-20
 Arnold, R.B., 4-11
 Aron, J., 51-51, 55-10

Aronofsky, J.S., 44-19, 44-20, 44-29, 44-34, 44-49, 44-50
 Arps, J.J., 30-9, 30-15, 30-16, 37-14, 37-15, 37-27, 40-1, 40-19, 40-32, 40-37, 40-38, 41-1, 41-5, 41-23, 41-37, 44-50, 44-51
 Arrow Specialty Co., vi
 Arthur, M.G., 39-26, 39-28
 Aruna, M., 36-10
 Aseltine, R.J., 46-44
 Ashby, W.H. Jr., 24-14, 24-23
 Ashford, F.E., ix, 28-11, 28-15
 Asymyan, K.D., 25-26
 Atkinson, A., 51-44, 51-52
 Atkinson, H., 44-40, 44-51
 Atkinson, M.H., 16-16
 Attra, H.D., 43-4, 43-16, 43-19
 Au, A.D.K., 48-19
 Ausburn, B.E., 29-1, 51-52
 Ausburn, J.R., xii, 51-51
 Auvenshine, W.L., 39-16, 39-28
 Azarnoosh, A., 25-25
 Aziz, K., vii, 20-5, 20-9, 20-15, 20-18, 45-14, 48-11, 48-16 to 48-19, 54-14, 55-11

B

Babson, E.C., 34-55, 40-9, 40-38
 Bagley, J.W. Jr., 36-10
 Bailey, N.J.L., 24-22
 Baiton, N., 45-15
 Baker, J.R., 54-14
 Baker, O., viii, 22-17, 22-22
 Baker Oil Tool Div., v, 4-11
 Baker Performance Chemicals Inc., vii
 Baldwin, J., 50-38
 Bálint, A.M., 28-15
 Ballard, D., 25-23
 Baltosser, R.W., xii, 51-52
 Bansal, P.P., 48-20
 Bansback, P.L., 19-33
 Banthia, B.S., 51-6, 51-50
 Barakat, Y., 47-25
 Barb, C.F., 24-22
 Barber, A.H. Jr., 36-10
 Barbrow, L.E., 1-1, 1-68
 Bardgette, J.J., 18-52
 Bardon, C., 28-11, 28-15
 Barduhn, A.J., 25-26, 25-27
 Barfield, E.C., 44-17, 44-49
 Barham, R.H., 38-20
 Barker, C., 24-22
 Barlyaev, E.V., 25-25
 Barnes, D.F., 51-51
 Barnes, K.B., 44-51
 Barnes, V.E., 24-22
 Barrett, M.L. Jr., 16-16
 Barrett, R., 12-43
 Barron, A.N., 54-12
 Barry, A.F., 12-43
 Barstow, W.F., 39-28
 Bartell, F.E., 44-2, 44-49
 Bartholome, E., 25-21
 Bartlesville Energy Technology Center, vii
 Bartlett, E.P., 25-22
 Barton, J.R., 25-21
 Barton, W.C. Jr., 43-16
 Bass, D.M. Jr., 24-23, 26-1
 Basset, J., 25-22
 Bassiouni, Z., 28-12, 28-16
 Bateman, R.M., xi, 53-1, 53-26
 Bates, G.O., 39-28
 Bates, R.L., 29-9
 Battino, R., 25-23
 Batycky, J.P., 28-12, 28-15
 Baucum, A.W., 40-16, 40-38
 Baugh, E.G., 45-15
 Baumgaertner, M., 25-16, 25-17, 25-23
 Baumgartner, S.A., 55-11
 Bavy, D., 48-18
 Baxendall, P.B., 34-37, 34-55
 Bayless, C.R., 16-16
 Beach, F.W., 16-16
 Beal, C., 22-14 to 22-16, 22-22, 46-45
 Bear, J., 28-15
 Beardon, P.L., 38-20
 Beaty, J.W., 44-51
 Bebout, D.G., 29-9
 Becher, P., 19-34
 Beck, R.L., ix, 34-46, 34-55
 Becker, H.G., 25-22
 Beebe, W.B., 29-9
 Beeler, H.S., 24-22
 Beeson, C.M., 26-33
 Beestecher, E., 24-22
 Beggs, H.D., 5-57, 7-9, 7-17, 22-1, 22-7 to 22-12, 22-15, 22-16, 22-22, 34-55, 46-7, 46-43, 46-45
 Behie, A., 48-20
 Beider, S.Y., 25-26
 Beirute, R., 55-11
 Belknap, W.B., 50-38
 Bell, C.A., 6-34, 6-72
 Bell, C.R., vii
 Bell, W.E., 44-51
 Bellotti, P., 52-31
 Benedict, M., 20-7, 20-18
 Benham, A.L., 34-55, 46-16, 46-45
 Ben-Naim, A., 25-21, 25-24
 Benner, F.C., 44-2, 44-49
 Bennett, C.O., 55-11
 Bennett, E.N., 39-16, 39-28
 Bennett, E.O., 39-26, 39-28
 Bennett, K.E., 47-25
 Bennion, D.W., 48-18
 Benson, B.B., 25-22
 Berg, R.A., 36-10
 Berg, R.R., 36-10
 Berger, W.R., 24-22
 Bergman, J.C., ix, 30-16
 Bergstrom, J.M., 54-14
 Berkshire, D.C., 54-13
 Bernard, G.G., 45-14, 47-25
 Bernard, H.A., 36-3, 36-10
 Bernard, W.J., 44-51
 Berry, D.W., 48-10, 48-19
 Berry, F.A.F., 24-23
 Berry, J.E., 51-6, 51-50
 Berry, J.F., 28-16
 Berry, P., 36-10
 Berry, V.J. Jr., 37-23, 37-25, 37-27, 40-38, 43-4, 43-16, 43-19, 46-43
 Berryman, J.E., 39-15, 39-28
 Bertiger, W.I., 48-19
 Bertozzi, W., 50-38
 Bertuzzi, A.F., 34-1, 34-55
 Bertuzzi, W., xi
 Beson, J., 3-1
 Bessler, D.U., 19-33, 19-34
 Best, D.L., xi, 49-41
 Biggs, W.P., 49-42
 Bijl, A., 25-21
 Bilhartz, H.L., 44-51
 Billett, F., 25-21
 Billings, G.K., 24-23
 Billingsley, R.H., 46-44
 Billitzer, J., 25-24
 Bily, C., 25-18, 25-24
 Binckley, C.W., 33-1, 33-23, 34-27, 34-29, 34-55
 Binder, G.G. Jr., 45-14, 46-43
 Bingham, M.G., 52-24, 52-31
 Biot, M.A., 51-8, 51-11, 51-36, 51-47, 51-49, 51-51
 Birch, F., 51-50
 Bird, R.B., 47-24
 Birdwell Div. of Seismograph Service Corp., xii, 51-52
 Birdwell Technical Pamphlet, xii
 Bissey, L.T., 25-26
 Black, C., 25-25, 25-26
 Black, C.J.J., 28-16
 Black, H.N., 54-12
 Black, W., 19-34
 Blackwell, R.J., 28-2, 28-4, 28-15, 45-14
 Blair, C.M., 19-34
 Blair, E.A., 43-16
 Blair, P.M., 44-29, 44-50, 48-14, 48-20
 Blanton, J.R., 45-15
 Blaskovich, F.T., 48-5, 48-18
 Bleakley, W.B., 4-1, 6-34, 6-72, 45-15, 46-44
 Blevins, T.R., 46-44
 Bloomquist, C.W., 48-18
 Boatright, B.B., 39-26, 39-28
 Bobek, J.E., 44-49
 Boberg, T.C., 46-9, 46-11, 46-13, 46-43, 48-19
 Bobrowski, F.P., 37-27, 40-38
 Bockmeulen, H., 24-22
 Bodine, J.A., 18-1
 Bodvarsson, G.S., 48-20
 Bogdanov, M.I., 25-25
 Bogdanov, V.S., 28-11, 28-15
 Bohr, C., 25-21
 Boley, D.W., 44-50
 Boling, D.R., 11-1
 Bondareva, M.M., 25-27
 Bone, M.P., 36-10
 Boone, D.M., 6-72
 Borden, G. Jr., 22-22
 Borger, H.D., 24-22
 Boston, J.F., 25-24
 Botset, H.G., 28-2, 44-49
 Bouma, H., 29-9
 Bourrel, M., 47-25
 Bowen, J.F., 55-12
 Bowler, J., xii, 51-51
 Bowman, R.W., 46-44, 46-45, 47-24
 Boyd, W.L., x, 41-31, 41-37
 Boyd, W.S., 25-21
 Boyle, W.G., 3-1, 3-40
 Bozeman, J.F., 39-28
 Brace, W.F., 51-43, 51-52
 Bradbury, E.J., 25-24
 Bradley, H.B., iii, 24-12, 39-1, 44-20, 44-50, 58-2
 Bradstreet, E.B., 25-21
 Bragg, J.R., 47-25
 Brainerd, H.A., 16-16
 Brandt, H., 51-6, 51-50
 Brannan, G., 45-15
 Braun, E.M., 28-2, 28-4, 28-15
 Braun, P.H., x, 44-49, 45-13
 Braunstein, J., 29-9
 Breeding, C.W., 41-37
 Breitenbach, E.A., 48-14, 48-16, 48-18, 48-20
 Brewer, S.W., 46-45
 Brian Watt Assocs., vii
 Brigham, W.E., 45-15, 46-45
 Bright, J., 24-22
 Brill, J.P., 34-37, 34-55
 Brill, T.P., 46-7, 46-43
 Brinkley, T.W., 37-27, 39-20, 39-23, 39-28
 Brinkman, F.H., 40-38
 Briscoe, C.F., 25-21
 Bristol Co., The, vi
 Britt, H.I., 25-24
 Britton, M.W., 46-45
 Broddus, E.C., 54-12
 Broding, R.A., xii, 51-50, 51-52
 Brons, F., 35-16, 35-21, 40-38, 41-37
 Brooks, F.A., 56-9
 Brooks, R.H., 28-12, 28-15, 46-31, 46-34, 46-45
 Brooks, W.B., 25-26

- Broussard, W.F., 12-43
 Brown, A.A., 51-49
 Brown, A.R., 36-10
 Brown, F.B., 6-1, 6-36, 6-66, 6-69, 6-72
 Brown, G.A., 53-26
 Brown, G.G., vii, ix, x, 20-5, 20-18, 34-55, 40-38, 45-13
 Brown, H.D., 51-52
 Brown, H.W., 26-24, 26-25, 26-33
 Brown, J.N., 44-51
 Brown, K., 6-28, 6-34, 6-37, 6-38, 6-72
 Brown, K.E., 7-17, 34-37, 34-55
 Brown, R.B., 36-11
 Brown, R.J.S., 51-8, 51-51
 Brownlow, 47-26
 Browncombe, E.R., 25-23, 30-16, 38-9, 38-20
 Bruce, W.A., 26-33
 Bruist, E.H., 56-9
 Brunsmann, J.J., 15-34
 Bryan, G.M., 25-24
 Buchanan, R.D., 39-28
 Buckley, S.E., 24-22, 28-3, 28-6, 28-7, 28-15, 39-15, 39-28, 40-13, 40-16 to 40-18, 40-38, 43-3, 43-4, 43-16, 43-19, 44-7, 44-10, 44-11, 44-26, 44-29, 44-49, 47-2, 47-24, 48-1, 48-18
 Buckwald, R.W. Jr., 46-45
 Buehner, L.O., 6-72
 Bull, A.D., 46-45
 Bunge, A.L., 47-21, 47-26
 Bunting, E.N., 26-4 to 26-6, 26-33
 Burcik, E.J., viii, 39-2, 39-27
 Burger, J.G., 46-43
 Burke, B.G., 18-52
 Burke, R.E., 46-45
 Burkill, G.C.C., 54-12
 Burkleca, L.F., 54-13
 Burnett, E.S., 20-4, 20-18
 Burns, G.E., 18-1
 Burrell, G.R., 16-1
 Burrows, D.B., 20-15, 20-18, 39-27
 Bursell, C.G., 46-44
 Burt, R.A. Jr., 45-15
 Burton, M.B., 44-18, 44-20, 44-21, 44-49
 Busch, D.A., 29-9
 Bush, D.C., 50-38
 Bush, J., 47-26
 Buthod, P., 21-1
 Buxton, T.S., 46-44
 Byk, S.S., 25-23, 25-28
 Byth, N.J., 54-14
- C**
- Cady, G.H., 25-3, 25-21
 Cady, G.V., 46-43, 46-45
 Cairns, R.J., 19-34
 Calahan, D.A., 48-20
 Calder, J.A., 25-27
 Calhoun, J.C. Jr., ix, 32-16, 39-28, 40-38, 44-29, 44-50, 45-14
 California Dept. of Natural Resources, 29-9
 California Research Corp., vii, viii
 Calingcart, G., 20-13, 20-17, 20-18
 Callahan, M.J., 55-11, 55-12
 Callanan, J.E., 25-27
 Callaway, F.H., 38-20, 44-51
 Callaway, R.E., 54-14
 Calver, J.C., xi
 Camacho, C.A., 34-40, 34-55
 Camco Inc., v
 Cameron, R.C., 54-13
 Camilleri, D., 47-25
 Campbell, A.W., 45-15
 Campbell, F.L., 49-42, 52-31
 Campbell, J.B., 45-15
 Campbell, J.L.P., 50-1
 Campbell, J.M., vi, 12-43, 12-44, 13-1, 13-59, 14-6, 14-22, 25-23, 25-26, 41-37, 58-2, 58-21
 Campbell, R.A., 58-2
 Campbell, W.P., 24-22
 Canadian Petroleum Assn. (CPA), 58-2, 58-8
 CanOcean Resources Ltd., vii
 Capell, R.G., 25-27
 Caraway, W.H., 26-33
 Cardwell, W.T. Jr., 39-28, 40-38
 Carlile, R.E., 58-2
 Carll, J.F., 44-1, 44-49
 Carlson, F.M., 28-12, 28-15
 Carmichael, L.T., 25-27
 Carmichael, R.S., 51-30, 51-52
 Carothers, W.W., 24-22
 Carpenter, C.W., 44-50, 44-52
 Carpenter, P.G., ix, 34-37, 34-55
 Carr, A.H., 48-19
 Carr, N.L., 20-9, 20-10, 20-15, 20-16, 20-18, 39-4, 39-13, 39-27
 Carraway, P.M., 46-45
 Carroll, H.B., 55-12
 Carson, D.B., 25-5, 25-23, 25-28
 Carter, R.D., 38-2, 38-3, 38-20, 55-10
 Casale, C., 25-21
 Case, C.H., 43-16
 Case, C.R., 50-38
 Case, R.C., 16-16
 Cassé, F.J., 46-45
 Cassingham, R.W., 43-17, 45-15
 Cato, R.W., 46-44
 Caudle, B.H., 43-10, 43-19, 44-17, 44-19, 44-20, 44-29, 44-34, 44-37, 44-49 to 44-51, 45-14, 46-17, 46-45, 47-24
 Cayias, J.L., 47-25
 CBI Industries Inc., vi
 C-E Natco, vi, vii
 Chaddock, R.E., 25-25
 Chambers, A., 26-33
 Chan, A.F., 47-24
 Chan, S.A., 41-37
 Chancey, D.G., 17-1
 Chang, S.K., 51-52
 Chappellear, J.E., 48-20
 Charles, G.J., 55-10
 Chase, C.A., 48-18
 Chastain, J., 10-37
 Chatas, A.T., 38-20
 Chatelain, J.C., 54-12
 Cheek, R.E., 44-20, 44-49
 Chemineer-Kenics, vii
 Chen, C.-C., 25-18, 25-24
 Chen, W.H., 46-43, 48-18
 Chenault, R.L., 8-1
 Cheng, C.H., xi, xii, 51-50, 51-51
 Chepkasov, V.M., 12-43
 Cherskii, N.V., 25-24
 Chew, J., 6-72, 7-12, 7-17, 22-14 to 22-16, 22-22, 39-4, 39-27, 46-45
 Chierci, G.L., 28-12, 28-15, 34-55
 Chilingar, G.V., 46-45
 Chilton, C.H., vii, 20-18, 25-15
 Chou, J.C.S., 24-13, 24-14, 24-23
 Christ, F.C., 6-34, 6-38, 6-72
 Christensen, D.M., 51-50, 51-51
 Christian, L.D., 45-15
 Christie, M.A., 48-19
 Chu, C., 46-1, 46-13 to 46-19, 46-21, 46-43 to 46-46
 Church, D.C., 54-12
 Cinco-Ley, H., 55-11
 Ciucci, G.M., 34-55
 Clappitt, R.L., 47-24
 Clapeyron, B.P.E., 20-11 to 20-13, 20-16, 20-17
 Claridge, E.L., 45-14, 47-24
 Clark, C.R., 6-72
 Clark, G.A., 46-44
 Clark, G.J., 54-12
 Clark, J.A., 55-11, 55-12
 Clark, J.B. Jr., 57-1
 Clark, J.D., 58-2
 Clark, K.M., 6-34, 6-72
 Clark, N.J., 45-13, 45-14
 Clark, P.E., 55-11
 Clark, S.P., 51-30, 51-52
 Clausius, R., 20-12, 20-16, 20-17
 Claussen, W.F., 25-21
 Clavier, C., 49-41
 Clayton, J.M., 44-51
 Clayton, R.N., 24-23
 Cleary, M.B., 55-11
 Clementz, D.M., 52-30
 Clifton, R.J., 55-11
 Clinedinst, W.O., 2-1, 2-60, 2-74
 Clinkenbeard, P., 39-25, 39-28
 Closman, P.J., 38-20
 Cloud, J.E., 55-11
 Coan, C.R., 25-21
 Coates, G.R., xi, 49-41, 51-52
 Coats, K.H., 39-22, 39-28, 43-17, 45-14, 46-11, 46-12, 46-43, 46-45, 48-1, 48-16, 48-18 to 48-20
 Coberly, C.J., 6-1, 6-66, 6-69, 6-72
 Cobb, T.R., 44-50
 Cobb, W.M., 31-7, 48-18, 52-31
 Coffin, C.R., 24-22
 Coker, F.B., 51-52
 Colegrove, G.T., 48-19
 Coleman, C.F., 25-26
 Coleman, H.J., 21-20
 Coleman, J.M., 29-9
 Coll, R., 25-25
 Collie, B., 19-34
 Collins, A.G., viii, 24-1, 24-22
 Collins, F.A., 38-9, 38-20
 Collins, F.R., 51-50
 Collins, R.E., 44-50
 Colpoys, P.J., 55-12
 Combaz, A., 50-38
 Combs, G.D., 43-16
 Concus, P., 48-20
 Conley, F.R., 47-26
 Conlon, D.R., 30-16
 Connally, C.A. Jr., 6-72, 7-12, 7-17, 22-14 to 22-16, 22-22, 39-4, 39-27, 46-45
 Connell, J.G., 49-42
 Connolly, J.F., 25-26
 Conway, M.W., 54-14, 55-11
 Cook, A.B., 37-23, 37-27, 39-12, 39-28, 40-38
 Cook, G.W., 48-20
 Cook, H.L., 5-57
 Cook, R.E., 43-17, 48-19
 Cooke, C.E. Jr., 31-7, 44-51, 47-20, 47-26, 55-11
 Cooper, F.E., 12-43
 Cooper, H.E. Jr., 44-49
 Cooper, R.J., 44-51
 Copeland, C.T., 54-12, 56-9
 Coppel, C.P., 19-34, 54-12
 Cordell, J.C., 37-25, 37-27
 Core Laboratories Inc., viii, x, 26-5, 26-33
 Corey, A.T., 28-8, 28-12, 28-15, 46-34, 46-45
 Cornelissen, J., 15-34
 Cornell, D., 26-28, 26-33, 34-9, 34-10 to 34-22, 34-24, 34-55
 Correia, R.J., 24-23
 Corteville, J., 48-19
 Cosgrove, J.J., 44-29, 44-51
 Cotter, W.H., 43-16
 Cotton, W.J. Jr., 53-26
 Coulter, A.W. Jr., 54-1, 54-12 to 54-14, 55-1, 56-1
 Coulter, G.R., 54-12

Counihan, T.M., 46-44
 Courand, G., 36-10
 Cox, E.R., 20-12, 20-13, 20-17, 20-18
 Cozzolino, J.M., 41-37
 Craft, B.C., x, 37-27, 39-27, 43-16, 43-17, 43-19, 44-6, 44-16, 44-17, 44-49, 48-18
 Craig, F.F. Jr., 43-16, 43-17, 43-19, 44-9, 44-11, 44-19, 44-20, 44-27 to 44-32, 44-34, 44-49 to 44-51, 45-13, 46-43, 46-44, 47-24
 Craigie, L.J., 55-10
 Crane Co., 15-33
 Crawford, D.L., 54-12
 Crawford, J.G., 24-22
 Crawford, P.B., 35-21, 44-18, 44-20, 44-21, 44-25, 44-49, 44-50, 46-46
 Crawley, A.B., 55-11
 Craze, R.C., 36-1, 40-16, 40-17, 40-38
 Crenshaw, P.L., 54-12, 54-14
 Crichlow, H.G., 48-17
 Crichton, J.A., 40-38
 Crocker, F., 6-34, 6-72
 Croft, H.O., 26-33
 Cronquist, C., x, 37-22, 37-23, 37-27
 Crookston, H.B., 48-18
 Crookston, R.B., 46-12, 46-43
 Crosby, C.C., 44-51
 Cross, J.H., 51-50
 Crowe, C.W., 54-4, 54-12, 54-14
 Crowell, D.C., 28-10, 28-15
 Crowell, R.F., 55-12
 Crozier, T.E., 25-21
 Crump, J.S., 39-28, 45-13
 Culberson, O.L., 25-17, 25-21, 25-24
 Culham, W.E., 46-43, 48-18
 Cullender, M.H., 5-37, 5-38, 5-57, 33-4, 33-6, 33-10, 33-15, 33-23, 34-24, 34-25, 34-27, 34-29, 34-55
 Culver, R.B., 50-38
 Cunningham, R.G., 6-36, 6-38, 6-72
 Curtis, S., 10-14
 Cuthbert, J.F., 53-26
 Cutler, R.A., 55-11
 Cutler, W.W. Jr., 40-29, 40-38
 Cyca, L.G., 45-15

D

Dahm, C.G., ix, 36-11
 Dake, L.P., 32-16, 35-21, 37-3, 37-27
 Dalati, R.N., 32-1
 Dalton, R.L., 44-51, 48-20
 Daly, A.R., 52-30
 Daneshy, A.A., 55-11
 Daniel, E.F., 55-12
 Daniel Industries Inc., vii
 Danniell, A., 25-24, 25-26
 Dardaganian, S.G., 43-16, 43-19
 DaShanzer, W.A., 56-9
 Daugherty, R.L., 15-33
 Davidson, C.D., 45-15
 Davidson, D.W., 25-4, 25-9, 25-23, 25-27
 Davidson, J.F., 34-55
 Davidson, R.D., 39-28
 Davies, E.E., 12-43
 Davis, D.H., 26-33
 Davis, D.S., 20-13, 20-17, 20-18
 Davis, G.J., ix, 34-55
 Davis, H.T., 47-25
 Davis, J.B., 24-22
 Davis, J.E., 25-21, 25-24
 Davis, J.J., 54-13
 Davis, R.E., 41-37
 Day, J.H. Jr., 10-1
 De, G.S., 51-49
 Dean, M.R., 25-25
 Dean, P.C., 44-49
 Deaton, W.M., viii, 25-2, 25-5, 25-10, 25-14, 25-20, 25-23

DeFord, R.K., 24-22
 DeGolyer, E.L., 41-7, 41-37
 deHaan, M.J., 46-45
 Deibert, A.D., 46-44
 DeKiss, A.V., 25-21
 deKlerk, F., 55-11
 DeLoos, T.W., 25-25
 Delshad, M., 28-11, 28-15
 Demaison, G.J., 52-30
 DeMott, D.N., 54-13
 Dempsey, J.R., 48-19
 Denekas, M.O., 44-49
 Denoo, S.A., 51-52
 Deppe, J.C., 44-29, 44-33, 44-34, 44-50
 Derr, R.B., 25-27
 Desbrandes, R., 50-38
 DesBrisay, C.L., 45-15
 DeSitter, L.U., 24-20, 24-23
 DeVerter, P.L., 16-16
 deVries, D.A., 22-22
 DeVries, W., 54-13
 Dew, J.N., 46-43
 deWitte, A.J., 26-30, 26-31, 26-33, 49-41
 DeWitte, L., 49-41
 Deysarkar, A.K., 54-13, 55-12
 deZabala, E.F., 47-26, 48-19
 Dharmawardhana, P.B., viii, 25-9, 25-11, 25-23, 25-27
 Dia-Log Co., The, xiii
 Dias-Couto, L.E., 37-21, 37-27
 Dick, J.W.L., 25-18, 25-24
 Dickey, P.A., 24-21, 24-22, 44-49, 44-51
 Diepen, G.A.M., 25-24, 25-25, 25-27
 Dietz, D.N., 35-6, 35-21, 46-43, 47-24
 diFranco, R., 48-20
 Dill, W.R., 54-13
 Dingman, R.J., 24-23
 Dixon, P.C., 12-43, 39-26, 39-28
 Dixon, T.N., 48-18
 Dobkins, T.A., 55-11
 Doble, P.A.C., 16-16
 Dodds, W.S., 25-21
 Dode, M., 25-22
 Dodson, C.R., viii, 22-22, 25-17, 25-21, 37-27, 39-2, 39-27, 41-38
 Doh, C.A., 51-50, 51-51
 Doherty, W.T., 10-37
 Dolan, J.P., 30-13, 30-17
 Doll, H.G., 49-1, 49-41
 Dollarhide, F.E., 54-14, 55-11
 Domenico, S.N., xii, 51-52
 Dominguez, J.G., 47-24
 Donaldson, A.B., 46-45
 Donaldson, E.C., 47-26
 Donaruma, L.G., x, 47-24
 Donohoe, C.W., 39-1, 39-28
 Donohue, D.A.T., 43-17, 45-14
 Dorsey, N.E., 24-13, 24-23
 Doscher, T.M., 46-9, 46-43
 Dotson, B.J., iii, 26-33
 Dotson, C.R., 24-13, 24-23, 41-5, 41-7
 Dotterweich, F.H., 5-57, 12-43
 Douglas, E., 25-22
 Douglas, J. Jr., 44-29, 44-31, 44-50, 44-51, 48-14, 48-16, 48-18, 48-20
 Dow Chemical Co., viii, 25-24
 Dowdle, W.L., 31-7, 52-31
 Dowell Schlumberger, xiii
 Downie, J., 45-14
 Drake, E., 18-1
 Draper, A.L., 45-14
 Dresser-Atlas, xii, xiii, 49-41, 50-38, 51-52
 Dresser Industries, v, vi
 Driscoll, V.J., 36-10, 48-6, 48-18
 Droschak, D.M., 51-50
 Dubrevil, L.R., 44-51
 Duda, J.L., 47-24
 Duerksen, J.H., 46-45, 48-18

Duffy, J.R., 25-21
 Duggan, J.O., 34-46, 34-55
 Dukler, A.E., 34-55
 Dumanoir, J.L., xi, 49-41
 Dumitrescu, D.T., 34-38, 34-55
 Dumoré, J.M., 37-27
 Dunham, C.L., 16-16
 Dunlap, H.F., 49-41
 Dunlap, P.M., 54-13
 Dunn, K.J., 51-49
 Dunning, H.N., 39-16, 39-28, 45-51
 Duns, H. Jr., 34-36, 34-37, 34-40, 34-55
 Dupal, L., xii, 51-51
 DuPont Co., 14-9
 Dyes, A.B., 30-17, 35-15, 35-21, 43-8, 43-19, 44-20, 44-25, 44-49, 44-50, 45-14, 47-24
 Dykstra, H., 40-18, 40-19, 40-38, 44-7 to 44-9, 44-26, 44-29, 44-30, 44-32, 44-49, 45-14, 47-17, 47-24
 Dysart, G.R., 55-12

E

Eakins, J.L., 39-16, 39-28
 Earlougher, R.C. Jr., x, 30-17, 32-16, 35-19, 35-21, 36-10, 44-29 to 44-31, 44-51, 46-6, 46-43, 46-44
 Eaton, B.A., 51-39, 51-52
 Eaton, J.R., 6-72
 Ebert, C.K., 37-25, 37-27
 Eckles, W.W., 39-28
 Eddy, H.D., 53-26
 Edmondson, T.A., 44-51
 Edmundson, H., xi, 50-32, 50-38
 Edwards, A.T.W., 25-22
 Edwards, C.A.M., xii, 51-52
 Eganhouse, R.P., 25-27
 Eggleston, W.S., 41-37
 Ehrlich, R., 44-51, 46-43, 47-26
 Eichenberg, R., v
 Eichmeier, J.R., 4-11
 Eikerts, J.V., 55-11
 Eilers, H., 15-34
 Eilerts, C.K., x, 39-2, 39-4, 39-5, 39-27
 Einarsen, C.A., 30-17
 Elbel, J.L., 55-12
 Elfrink, E.B., 37-27, 40-38
 El-Hattab, M.I., 44-51
 El-Khatib, N.A.F., 37-27
 Elkins, L.E., 55-11
 Ellenberger, A.R., 44-51
 Elliott Co. Bull. P-11, 14-9
 Elliott, F.B. Jr., 10-1
 Elliott, L.S., 56-9
 Ellis, A.J., 25-21
 Ellis, D.V., xi, 50-1, 50-38
 Ellis Engineering Inc., vi, 12-43
 Ellis, G.O., 12-27, 12-43
 Ellison, W.F., 15-1
 Elworthy, R.T., 24-22
 Ely, J., 54-13
 Emanuel, A.S., 48-19, 48-20
 Emery, L.W., 44-51
 EnDean, H.J., 16-16
 Energy Resources and Conservation Board, 27-9, 34-55, 35-21
 Engineering Specialties Inc., vii
 Engle, D.D., 18-52
 Enick, R.M., 40-38, 47-24
 Enns, T., 25-21
 Enright, R.J., 44-51
 Erbar, J.H., 14-22, 25-16, 25-24
 Erickson, D.D., 25-9, 25-23, 43-19
 Erickson, J.W., 6-72
 Erickson, R.A., 43-10, 44-49, 45-14, 47-24
 Ersoy, D., 4-11
 Espanol, J.H., 34-37, 34-55

Essley, P.L. Jr., 40-38
 Eubank, P.T., 25-21
 Eucken, A., 25-21
 European Continental Shelf Guide, 27-9
 Evans, H.J., 13-59
 Evans, J.G., 46-43
 Evans, L.B., 25-24
 Evans, R.D., xi, 50-38
 Everett, J.P., 45-14
 Everhart, A.H., 51-52
 Evinger, H.H., 32-4, 32-16, 34-31, 34-55, 37-19, 37-27
 Ewing, B.C., 54-14
 Ewing, J., 25-24
 Ewing, R.E., 48-19
 Ewing, W.M., 51-50
 EXLOG, xiii
 Exploration Logging Inc., xii, 52-30, 52-31

F

Fagin, K.M., 41-5, 41-37
 Fagin, R.G., 48-14, 48-18
 Falabella, B.J., 25-23
 Fan, S.K., 47-24
 Fancher, G.H. Jr., 34-55
 Farhi, L.E., 25-22
 Farkas, E.J., 25-26
 Farouq Ali, S.M., x, 46-7, 46-13, 46-14, 46-43, 46-46
 Farshad, F.F., 35-13, 35-21, 40-38
 Fash, R.H., 24-22
 Fassih, M.R., 46-37, 46-45
 Fast, C.R., 55-2, 55-10
 Fatt, I., 26-7, 26-33, 28-10, 28-15, 51-50
 Faulkner, B.L., 45-14
 Fay, C.H., 44-20, 44-49
 Fayers, F.J., 48-18
 Feillolay, A., 25-21
 Fekete, L.A., 12-43
 Felsenthal, M., 44-29, 44-50
 Feldman, W., 6-72
 Fenix & Scisson Inc., vi, 11-13
 Fenninger, W.D., 25-21
 Ferrero, E.P., 21-20
 Ferrier, J.J., 46-45
 Fertl, W.H., 50-38, 51-52, 55-11
 Fetkovich, M.J., 34-1, 34-31, 34-33, 34-55, 38-8, 38-20
 Fettke, C.R., 24-1, 24-21
 Fillipone, W.R., 51-52
 Finch, E.M., 44-51
 Firoozabadi, A., 48-19
 Fischer, F., 25-21
 Fischer Governor Co., vi
 Fischer, K.F., 56-1
 Fischer, M.J., 44-25, 44-50
 Fisher Controls Co., vi
 Fiske, L.E., 41-2, 41-37
 Fiskin, J.M., viii, 23-13
 Fitzgerald, P.E., 54-1, 55-1, 56-1
 Flaum, C., 50-38
 Fleming, P.D. III, 48-18
 Fletcher, C.R., xii, 51-51
 Flid, R.M., 25-24
 Flippen, F.F., 54-12
 Flock, D.L., 44-20, 44-50
 Fluor Subsea Services, vii
 Fogler, H.S., 54-13
 Fomina, V.I., 25-23, 25-28
 Fong, D.K., 48-18
 Fons, L., 51-52
 Fontaine, E.T., 19-34
 Ford, G., 1-69
 Ford, W.G.F., 54-13
 Forsyth, P.A., 48-20
 Foster, H.P. Jr., 48-19
 Foster, J.H., 3-1

Foster, K.W., 16-16
 Foster, V., 41-37
 Fowler, E.D., 3-40
 Fowler, F.C., 34-4, 34-55
 Fowler, P.T., 52-22, 52-31
 Fox, C.J.J., 25-22
 Fox, K.B., 54-12
 Fox, R.L., 46-45
 Frailing, W.G., 40-38
 Franck, E.U., 25-21, 25-22, 25-24
 Franklin, P., 1-1, 1-68
 Franks, J.E., 55-10
 Fraser, H.J., viii, 26-33
 Frauenthal, J.C., 48-11, 48-20
 French, W.S., 36-11
 Frick, T.C., iii, 46-45
 Fried, A.N., 45-14, 47-25
 Friedman, R.L., 25-18, 25-24
 Fritsch, D.R., 16-16
 Friz, H., 25-21
 Frnka, W.A., 46-44
 Froelich, B., 51-52
 Frolich, P.K., 25-21
 From, K.T., 45-15
 Froning, H.R., 25-27, 47-25
 Frost, E., 50-38
 Frost, E.M., viii, 25-2, 25-5, 25-10, 25-14, 25-20, 25-23
 Frost, J.B., 54-13
 Fuhner, H., 25-26
 Fulcher, R.A., 28-12, 28-16
 Fuller, K.L., 48-18
 Fulton, K., 36-10
 Funkhouser, H.J., 24-22
 Fussell, D.D., 48-18, 48-19
 Fussell, L.T., 48-18

G

Gaddy, V.L., 25-15, 25-17, 25-22, 25-23
 Gabelle, C.P., 46-45
 Gainar, I., 25-22
 Galbraith, M., 36-11
 Gale, R.P., 25-26
 Gall, J.W., 47-24
 Galley, J.E., 29-9
 Galloway, J.R., 46-44
 Galloway, T.J., viii, 25-2, 25-20, 29-9
 Garb, F.A., 40-1, 40-37, 41-1, 41-5, 41-37
 Garder, A.O. Jr., 37-21, 37-27, 48-14, 48-18
 Gardner, D.C., 55-11
 Gardner, F.H., 25-22
 Gardner, G.H.F., xi, xii, 26-28, 26-33, 36-11, 45-14, 45-15, 51-7, 51-47, 51-50, 51-52
 Gardner, J.S., xi, xii, 49-41, 50-38, 51-35, 51-52
 Gardner, L.W.R., xi, 51-50
 Garms, K.M., 43-1
 Garon, A.M., 46-43
 Garrison, A.D., 24-2, 24-22
 Garthwaite, D.L., 43-16
 Gartner, J., 51-45, 51-52
 Gas Processors Suppliers Assn. (GPSA) vi, vii, viii, 12-43, 13-59, 14-17, 14-22, 20-18, 23-11, 23-13, 39-12, 39-27
 Gash, B.H., 47-24
 Gaskell, M.H., 45-14
 Gaskell, T.F., 12-43
 Gassmann, F., 51-8, 51-11, 51-36, 51-49, 51-51
 Gates, C.F., 46-15 to 46-17, 46-19, 46-44, 46-45
 Gates, G.L., 26-33, 44-51
 Gatlin, C., 45-13
 Gearhart, 49-41
 Geertsma, J., 26-7, 26-33, 51-8, 51-51, 55-11
 Geffen, T.M., 39-15, 39-28, 43-17, 43-19, 44-29, 44-50, 45-13, 46-13, 46-14, 46-43
 General Conference of Weights and Measures (CGPM), 58-4, 58-10, 58-18
 Gentry, R.W., 41-37
 Geophysics, 51-50
 George, C.J., 36-10
 George, R.A., 44-51
 Geotimes, 25-24
 Gernet, J.M., 45-15
 Gester, G.C., 25-26
 Geyer, R.L., xii, 51-51
 Ghassemi, F., 46-9, 46-43
 Ghauri, W.K., 44-51
 Giacca, D., 52-31
 Gibbs, G.B., 25-26
 Gibbs, J.W., 25-1, 25-20
 Gibbs, S.G., 10-37
 Gidley, J.L., 54-11, 54-12, 56-9
 Gilbert, W.E., 34-45, 34-46, 34-55
 Gilchrist, W.A. Jr., 50-38
 Gillespie, P.C., 25-15, 25-21
 Gilliland, H.E., 47-26
 Gillund, G.N., 45-15
 Gilman, J.R., 48-5, 48-18
 Giussani, A., 25-27
 Giusti, L.E., 46-43
 Gjaldback, J.C., 25-21, 25-25
 Gladfelter, R.E., 38-20
 Glaister, R.P., 24-22
 Glasser, S.R., 45-15
 Glew, D.N., 25-23
 Glinsmann, G.R., 47-25
 Glover, C.J., 47-25
 Goetz, J.F., xii, 51-20, 51-51
 Gogarty, W.B., 45-13, 47-25, 48-18
 Golan, M., 37-21, 37-27
 Golding, B.H., 21-10, 21-11, 21-13, 21-15, 21-16, 21-20
 Golding, R.M., 25-21
 Goldman, R., 51-50
 Goldsmith, R.G., 52-31
 Goldup, A., 25-26
 Golub, G.H., 48-20
 Golynets, Y.F., 25-24
 Gornaa, E.E., 46-17, 46-18, 46-45, 48-6, 48-18
 Gondouin, M., 49-40
 Gooch, F.W. Jr., 45-14
 Goodman, J.B., 25-22
 Goodman, M.A., 18-52
 Goodwill, D., 22-22
 Goodwill, W.P., 51-52
 Gordon, W.C., 24-2, 24-22
 Gosline, J.E., 6-36, 6-37, 6-72, 22-22, 34-55
 Gottfried, B.S., 48-18
 Goudouin, M., 49-41
 Gould, T.L., 34-40, 34-55, 34-56
 Govier, G.W., 40-38, 55-11
 Goyal, A., 47-26
 Grabowski, J.W., 46-12, 46-43
 Graciaa, A., 47-25
 Graebner, R.J., ix, 36-10, 36-11
 Graham, D.E., 19-34
 Graham, J.W., 54-13, 55-12
 Granberry, R.J., 50-38
 Grant, A.A., 6-72
 Grant, B.R., 46-43
 Graton, L.C., viii, 26-33
 Graue, D.J., 23-13, 44-51, 47-26, 48-6, 48-18
 Graves, R.M., 26-9, 26-33
 Gravis, C.K., 12-43
 Gray, K.E., 30-17
 Greaser, G.R., 46-44
 Greco, G., 25-21
 Green, E.B., 54-13
 Greenberger, M.H., 40-38, 44-29, 44-32, 44-51

Greenkorn, R.A., 36-10
 Greenwalt, W.A., 41-37
 Gregory, A.R., xi, xii, 26-33, 51-8, 51-36, 51-50, 51-51
 Grever, J., 25-21
 Griffith, B.L., 45-14
 Griffin, F.D., 10-1
 Griffith, J.D., 45-15, 48-19
 Griffith, P., ix, 34-37 to 34-39, 34-55
 Griffith, T.D., 47-24
 Grigoriou, G.C., 25-28
 Grijalva, V.E., 51-52
 Grim, R.E., 47-26
 Griswold, J., 25-27
 Griswold, W.T., 24-1, 24-21
 Groeneveld, H., 44-51, 58-2
 Groschuff, E., 25-27
 Grosmaning, M., 51-52
 Grossling, B.F., 41-37
 Grosso, D.S., 53-26
 Grove, M.L., 39-28
 Grovenburg, W.W., 16-17
 Gruy, H.J., 40-38, 41-5, 41-37
 Gubbins, K.E., 25-21
 Guckert, L.G., 44-21, 44-50
 Guerrero, E.T., x, 12-43, 37-15, 37-27, 44-29 to 44-31, 44-51
 Guimard, A., ix, 30-16
 Guin, J.A., 54-14
 Gulati, M.S., 56-9
 Guler, N., 55-11
 Guppy, K.H., 55-11
 Gurley, D.G., 56-9
 Gustavson, F.G., 48-20
 Gusto, B.V., vii
 Guthrie, R.K., 40-38, 44-29, 44-32, 44-51
 Guyod, H., xii, 49-41, 51-50

H

Haafkens, R., 54-13, 55-11
 Haas, N.C., 25-22
 Habermann, B., 44-20, 44-50, 45-14
 Hachmuth, K.H., 25-25
 Hadley, K., 51-11, 51-51
 Haehnel, O., 25-21
 Hafemann, D.R., 25-25, 25-27
 Hagedorn, A.R., 34-37, 34-55
 Hageman, P.S., 30-16
 Hagenar, D.S., ix
 Hagoort, J., 28-11, 28-15, 47-24
 Halbouty, M.T., 29-9
 Hall, A.H., 16-17
 Hall, A.L., 46-44
 Hall, B.E., 54-13
 Hall, C.D. Jr., 55-11
 Hall, H.N., 26-7 to 26-9, 26-33, 45-13
 Hall, K.R., 20-8, 20-9, 20-18, 25-21, 33-18, 33-23
 Hamilton Bros. Oil Co., vii
 Hammerlindl, D.J., 4-11, 26-8, 26-33
 Hammerschmidt, E.G., 25-23
 Hancock, G.L. Jr., 40-38
 Hand, J.H., 25-24, 25-28
 Handy, L.L., 37-27
 Hanna, M.A., 29-9
 Hannah, R.R., 55-11
 Hansen, D.N., vii
 Hansen, P.W., 45-15
 Hanson, J.M., 55-11
 Hanson, M.E., 55-11
 Hanzlik, E.J., 48-6, 48-18
 Harbert, L.W., 28-12, 28-16
 Harder, A.H., 25-21
 Harder, M.L., 32-3, 32-16
 Hardy, G.W. III, 57-12
 Hardy, J.H., 45-15
 Hardy, W.C., 46-44, 46-45
 Harouaka, A., 44-51
 Harpole, K.J., 48-10, 48-19
 Harrington, L.J., 55-11
 Harris, C.D., 48-18
 Harris, D.G., 36-10
 Harris, F.N., 54-13
 Harris, L.E., 54-13
 Harris, L.W., 55-11
 Harris, M.H., xii, 51-35, 51-47, 51-52
 Harris, O.E., 54-13
 Harris, P.C., 55-11
 Harris, W.E., 24-22
 Harrisberger, W.H., 54-12
 Harrison, N.H., 39-28
 Harting, P., 25-24
 Hartley, K.B., xii, 51-34, 51-52
 Hartman, J.A., 36-10
 Hartsock, J.H., 44-50
 Harvey, A.H., 48-20
 Harvey, M.T., 45-15
 Harvey, R.P., 53-26
 Harwell, J.H., xi, 47-25
 Hasiba, H.H., 47-26
 Hassan, M., 50-38
 Hassler, G.L., 28-2, 28-3, 28-5 to 28-7, 28-15
 Hatch, M.J., x, 47-24
 Hauber, W.C., 44-29, 44-50
 Haughn, J.E., 25-25
 Havlena, D., 37-2, 37-3, 37-6, 37-7, 37-27, 38-12, 38-20
 Hawes, R.I., 48-18
 Hawkins, M.F. Jr., x, 23-1, 24-14, 24-23, 37-27, 39-27, 40-38, 43-16, 43-17, 43-19, 44-6, 44-16, 44-17, 44-49, 48-18
 Hawthorne, H.R., 49-41
 Hayduk, W., 25-22
 Hazebrook, P., 35-16, 35-21, 44-35, 44-51
 Heald, K.C., 31-7
 Healy, R.N., xi, 47-13, 47-25
 Hearn, C.L., 46-44, 47-24, 48-8, 48-10, 48-19
 Heaviside, J., 28-12, 28-16
 Hebard, G.G., 16-16
 Hegner, J.S., 54-13
 Heiba, A.A., 28-12, 28-16
 Heinemann, Z.E., 48-19
 Heins, C., 25-23
 Helander, D.P., 51-43, 51-52
 Helfferich, F., 47-25
 Heller, J.P., 44-50
 Hellums, L.J., 48-19
 Hemphins, W.B., xi, 51-51
 Henderson, J.H., 46-19, 48-6, 48-18
 Hendrick, J.O. Jr., 56-9
 Hendrickson, A.R., 54-1, 54-12 to 54-14
 Hendrickson, G.E., 44-28, 44-29, 44-50
 Hendrix, J.R., 8-1
 Henley, D.H., 44-49
 Henry, J.R., 34-46, 34-55
 Henshaw, T.L., 6-72
 Henson, W.L., 38-20
 Hepp, V.R., 53-26
 Herald, F.A., ix, 29-9
 Herbeck, E.F., 45-15, 48-18
 Hermanson, D.E., 9-1
 Herrera, A.J., 46-44
 Herrera, J.Q., 48-6, 48-18
 Herring, E.A., xii, 51-52
 Herron, E.H. Jr., 48-18
 Herron, M.M., 50-38
 Herschel, W.H., 22-22
 Hertzberg, G., 25-21
 Hertzberg, R.H., 46-45
 Hertzog, R.C., xi, 50-38
 Herzfeld, J.R., 41-37
 Hestenes, M.R., 48-20
 Heuer, G.J., 44-50
 Hewitt, C.H., 36-10, 46-44
 Hewlett-Packard, 22-17, 22-22
 Hiatt, W.N., 44-29, 44-51
 Hickman, B.M., 44-50, 46-45
 Hicks, A.L., 38-3, 38-20
 Hicks, W.G., 51-6, 51-19, 51-50, 51-51
 Higgins, R.V., x, 40-38, 44-28 to 44-30, 44-32, 44-50, 45-17
 Highland Pump Co. Inc., v
 Hilchie, D.W., 50-38, 51-52
 Hildebrand, M.A., 25-28
 Hildebrand, S.M., 16-17
 Hill, D.G., 54-13
 Hill, G.A., 30-17
 Hill, H.G., 41-37
 Hill, H.J., 26-30, 26-31, 26-33, 47-26, 49-41
 Hill, K.E., 41-37
 Hill, R., 51-51
 Hill, R.W., 16-16
 Hillestad, J.G., 48-20
 Hilterman, F.J., 36-11
 Hiltz, R.G., 43-17
 Hinds, R.F., 37-23, 37-27, 40-38, 45-1
 Hiraoka, H., 25-24
 Hirasaki, G.J., 47-5, 47-9, 47-24, 47-25, 48-20
 Hitchon, B., 24-22, 24-23
 Hobson, G.D., 40-38
 Hock, R.L., 39-28
 Hockaday, D., 44-51
 Hocott, C.R., 24-22, 39-28
 Hodgson, H., 53-26
 Hoenmans, P.J., 44-51
 Hoffman, A.E., 39-12, 39-28
 Hoffman, S.J., 46-45
 Hoke, S.H., 24-22
 Holbren, J.H., 44-51
 Holbrook, S.T., 47-25
 Holden, W.R., 25-21
 Holden, W.W., 39-28
 Holder, G.D., 25-18, 25-24, 25-28
 Holditch, S.A., 55-12
 Hollingsworth, F.H., 54-12
 Hollway, C.C., 48-19
 Hollrah, V.M., 45-14
 Holm, L.W., 45-1, 45-13, 45-14, 45-15, 47-9, 47-25
 Holman, G.B., 54-13
 Holmes, B.G., 46-19, 46-45
 Holmes, C.S., 34-55
 Holmgren, C.R., 44-49
 Holste, J.C., 25-21
 Holt, O.R., 53-26
 Honna, T., 25-22
 Hon, M.S., 20-7, 20-18
 Honarpour, M., 28-16
 Hood, J.T., 10-1
 Hopkins, E.A., 52-30
 Hopkinson, E.C., 50-38
 Horn, A.B., 25-21
 Horne, A.L., 45-15
 Horner, D.R., 30-9, 30-10, 30-17, 35-15, 35-16, 35-19, 35-21
 Hoskold, H.D., 41-16, 41-18, 41-20 to 41-22, 41-37
 Hoss, R.L., 43-17
 Hossin, A., 50-38
 Hottman, C.E., 51-39, 51-52, 52-30
 Houghton, G., 25-22
 Houston Geological Society, ix, 29-9
 Howard, D.S. Jr., 38-20
 Howard, G.C., 55-2, 55-10
 Howard, J.V., 46-45
 Howe, L.S., 25-23
 Howell, J.C., 46-42
 Howell, J.V., 24-21
 Howell, R.G., 36-10
 Hoyer, W.A., 50-38
 Hoyt, W.V., ix, 29-1

Hsiao, L., 44-51
 Hsu, C.C., 25-21
 Hsu, W., 47-25
 Huang, W., 46-43
 Hubbard, M.G., 34-55
 Hubbard, R.A., 41-37
 Hubbert, M.K., 26-33, 29-9, 51-44, 51-52
 Hubby, L.M., 16-16
 Hudock, K., 54-13
 Hughes, D.S., 51-50
 Huh, C., 47-13, 47-25
 Hung, J.H., 25-21
 Hunt, E.R., xii, 51-52
 Hunt, J.M., 23-13
 Huntington, R.L., 25-27, 40-38
 Hurd, C.O., vii
 Hurdle, J.M., 43-17, 45-15
 Hurford, G.T., 45-15
 Hurst, R.E., 55-10, 55-11
 Hurst, W., 30-10, 30-14, 30-17, 35-1, 35-21, 38-1, 38-8, 38-20, 39-20, 39-28, 40-37, 44-17, 44-20, 44-29, 44-49, 45-15
 Hutchinson, C.A. Jr., x, 30-17, 35-15, 35-21, 44-25, 44-50, 45-13, 45-14
 Hutchinson, T.S., 38-20
 Hutton, J.M., 25-28
 Huygen, H.H.A., 46-43
 Huzarevich, J.E., 43-17
 Hvizdos, L.J., 46-45
 Hwang, M.K., 48-18
 Hydraulic Inst., 6-50, 6-72
 Hydrocarbon Research Inc., vii

I

Illiyen, I.S., 53-26
 Imai, S., 25-25
 Independent Petroleum Assn. of America (IPAA), 41-37
 Inga, R.F., 25-25
 Ingersoll, A.C., 15-33
 Ingram, J.D., 51-51
 Inks, C.G., 44-51
 Inst. Français du Pétrole, 28-7, 28-15
 Inst. of Electrical and Electronic Engineers (IEEE):
 IEEE Std. 117, 10-37
 IEEE Std. 260, 58-8
 IEEE Std. 268, 58-8
 Interscience Encyclopedia Inc., vii
 Interstate Oil Compact Commission, 33-13, 33-23, 39-27
 Intl. Bureau of Weights and Measures (BIPM), 58-10
 Intl. Organization for Standardization (ISO), 12-43, 58-3, 58-11, 58-12
 ISO 31/0, 58-8
 ISO 1000, 58-8
 ISO R370, 58-8
 ISO 2955, 58-8
 KWIC Index of Intl. Stds., vi
 Intl. Union of Pure and Applied Chemistry, 58-7
 Intl. Union of Pure and Applied Physics, 58-7
 IPAA, 41-37
 Irick, J.T., 18-52
 Eisenhower, W.M., 18-52
 Ivey, D., 51-49
 Iyoho, A.W., 46-13, 46-14, 46-43
 Izabakarov, M. 25-21

J

Jacks, H.H., 48-19
 Jackson, J.A., 29-9
 Jacobs, W.L., 47-25
 Jacoby, R.H. 20-8, 20-18, 25-27, 37-23 to 37-25, 37-27, 40-38, 43-4, 43-16, 43-17, 43-19, 45-14, 48-19

Jacuzzi, R., 6-34, 6-72
 Jageler, A.H., 51-51
 Janzen, H.B., 44-19, 44-20, 44-34, 44-49
 Jaragua S.A. Industrias Mecanicas, vi
 Jardtetzky, W.S., 51-50
 Jardine, D., 36-5, 36-10
 Jea, N.C., 48-20
 Jeffries-Harris, M.J., 44-51
 Jenkins, R.A. Jr., 54-14
 Jenkins, R.E., 27-1, 50-38
 Jenks, L.H., 45-15
 Jennings, A.R., 54-13
 Jennings, H.Y. Jr., 47-19, 47-20, 47-26
 Jennings, R.R., 47-24
 Jensen, C.M., 23-13
 Jensen, J., 24-22
 Jessen, F.W., 24-22
 Jhaveri, I., 25-28
 Jines, W.R., 48-18
 Joffe, J., 20-7, 20-18, 48-18
 Johansen, R.T., 44-51
 John, V.T., 25-28
 Johnson, C.E. Jr., 40-19, 40-38, 44-9, 44-32, 44-49, 44-51, 45-14, 47-24, 47-26, 48-18
 Johnson, C.R., 36-10
 Johnson, D.H., xi, 51-50
 Johnson, E.F., 45-14
 Johnson, G.A., 48-6, 48-18
 Johnson, H.M., 49-42
 Johnson, J.P., 36-10, 44-29, 44-50
 Johnson, L.A., Jr., 46-3, 46-43, 46-45
 Johnson, O.C., 45-14
 Johnson, R.K., 51-39, 51-52, 52-30
 Johnson, W.M., Jr., 53-26
 Johnston, N., 26-33
 Jones, A., 55-10
 Jones, K.E., 40-38
 Jones, L.G., 56-9
 Jones, R.G., viii, 26-33
 Jones, S.B., xi, 51-50
 Jones, S.C., 28-15
 Jones, T.J., 19-34
 Jordan, C.A., 44-37, 44-51
 Jordan, D., 25-26
 Jordan, J.K., 44-51
 Jorden, J.R., 49-42, 52-24, 52-31
 Joris, G.G., 25-25
 Jorjue, M.A., 44-51
 Josendal, V.A., 45-14
 Joseph, C., 46-45
 Jossi, J.A., 20-18
 J. Cdn. Pet. Tech., 46-45
 Judson, L.V., 1-1, 1-68
 Jung, K.D., 46-44
 Justen, J.J., 44-51, 45-14
 Justus, J.B., 43-16
 Justus, W.W., 6-63, 6-72

K

Kamp, A.W., 53-26
 Kandarpa, V., 44-51
 Kane, A.V., 45-15
 Kansas State Corp. Commission, 39-27
 Kasarnovskii, J.S., 25-17, 25-24
 Kasch, J.E., 25-27
 Kasic, M.J. Jr., 48-20
 Katz, D.L., vii, 12-43, 20-5, 20-9, 20-10, 20-18, 22-4, 22-17, 22-21, 22-22, 25-2, 25-3, 25-5, 25-10, 25-11, 25-16 to 25-18, 25-20, 25-21, 25-23, 25-24, 25-28, 26-28, 26-33, 34-55, 34-56, 39-1, 39-27, 40-15, 40-38, 45-14, 48-18, 48-19
 Kavvadas, M., 55-11
 Kay, W.B., 20-5, 20-10
 Kazaryan, T.S., 25-25, 25-26

Kazemi, H., 48-5, 48-18, 48-19
 Keeney, B.R., 54-13
 Keese, J.A., 46-45
 Kehn, D.M., 45-14
 Keleman, S., 25-22
 Keller, G.V., 49-42
 Kelley, H.S., 16-16
 Kelley, L., 6-72
 Kelly, J.L., 51-50
 Kelly, P., 43-17
 Kelm, C.H., 45-15
 Kelton, F.C., 26-7, 26-33
 Kemp, C.E., 38-20, 44-50
 Kempton, E.A., 6-72
 Kendall, H.A., 45-14
 Kennedy, G.C. 25-22
 Kennedy, H.T., viii, 26-21, 26-33, 39-13, 39-28
 Kennedy, S.L., 43-17
 Kern, L.R., 43-4, 43-16, 43-19, 55-2, 55-10
 Kersch, K.M., 30-17
 Kershaw, D.S., 48-20
 Kerver, J.K., 49-42
 Kesler, M.G., 20-13, 20-17, 20-18
 Kestin, J., 24-16, 24-23
 Khalifa, H.E., 24-23
 Khan, S.A., x, 47-25
 Kharaka, Y.K., 24-23
 Khitarov, N.I., 25-22
 Khoury, F., 25-20
 Khristianovitch, S.A., 55-2, 55-10
 Khurana, A.K., 48-20
 Kieschnick, W.F. Jr., 45-14
 Killian, J.W., 44-25, 44-50
 Killough, J.E., 48-19, 48-20
 Kilmer, J.W., 39-28
 Kim, J.J., 25-24
 Kimball, C.V., 51-51
 Kimbler, O.K., 44-21, 44-49
 Kimmel, J.D., 32-1
 Kimmell, G.O., vi, 12-43
 Kincheloe, R.L., 54-13
 King, A.D. Jr., 25-21
 King, G.E., 54-12, 54-13, 55-11
 King, M.S., xi, 51-8, 51-9, 51-50 to 51-52
 King, R.E., 29-9
 King, W.R., v, 5-12
 Kinra, R.K., 18-52
 Kirby, J.E. Jr., 43-16
 Kircher, C.E. Jr., 21-10, 21-20, 22-22
 Kirk, R.S., 46-44
 Kirkpatrick, C.V., v, 5-1, 5-37
 Kithas, B.A., xii, 51-52
 Klaus, E.E., 47-24
 Klausutis, N.A., 25-25
 Kleppinger, K.B., 16-17
 Klinkenberg, L.J., viii, 26-18, 26-33, 28-13
 Kloepter, C.V., 45-15
 Kloth, T.L., 46-45
 Klots, C.E., 25-22
 Klotz, J.A., 56-9
 Klovian, J.E., 24-23
 Knapp, H., 25-18, 25-24
 Knezek, R.B., 43-16
 Knopoff, L., 51-46, 51-52
 Knox, J.A., 54-12, 54-13
 Kobayashi, R., viii, 20-15, 20-18, 25-1 to 25-3, 25-5, 25-10, 25-11, 25-15, 25-17, 25-18, 25-20, 25-21, 25-23, 25-24, 25-28, 39-27
 Kobe, Inc., v, 26-6
 Kobe, K.A., 25-22, 25-24
 Koch, H.A. Jr., x, 43-19, 45-13, 45-14
 Koch, R.L., 46-43, 46-45
 Koeller, R.C., 40-38
 Koepf, E.H., 27-1
 Koerperich, E.A., 51-24, 51-25, 51-51
 Kokes, F.P., 51-51, 51-25, 51-51

Kokesh, F.P., 51-51, 51-52
 Kolodzie, P.A., 44-51, 47-26
 Konen, C.E., 53-26
 Koppers Co. Inc., 11-14
 Kornfeld, J.A., 44-51
 Korringa, J., 51-8, 51-51
 Kortekaas, T.F.M., 28-12, 28-15
 Koshelev, V.S., 25-28
 Kotcher, J.S., 36-11
 Krase, N.W., 25-22
 Krause, D.J., 25-22
 Krautkrämer, H., xi, 51-50
 Krautkrämer, J., xi, 51-50
 Krebill, F.K., 43-16
 Krebs, H.J., 44-51
 Kreft, A., 50-38
 Krejci-Graf, K., 24-22
 Kresheck, G.C., 25-26
 Krichevskii, I.R., 25-17, 25-22, 25-24
 Krishnan, C.V., 25-18, 25-24
 Krueger, R.F., 56-9
 Krueger, W.C. Jr., 36-10
 Krug, J.A., 26-9, 26-33
 Kruk, K.F., 54-12, 54-14
 Krumbein, W.C., viii, 26-7, 26-33
 Krutter, H., 44-21, 44-50
 Krynine, P.D., 29-9
 Kuba, D.W., 48-20
 Kufus, H.B., 44-29, 44-50
 Kuhn, C.S., 46-43
 Kunerth, W., 25-22
 Kunkel, G.C., 36-10
 Kuntz, E., 57-12
 Kunz, K., 49-41
 Kunze, K.R., 54-13, 54-14
 Kurovskaya, N.A., 25-24
 Kuster, G.T., 51-34, 51-52
 Kvenvolden, K.A., 25-18, 25-24
 Kwan, T.V., 48-20
 Kwong, J.N.S., 20-7, 20-8, 20-18, 23-12, 23-13, 39-28
 Kyte, J.R., 44-49, 48-10, 48-19

L

Labrid, J., 54-13
 Lacey, J.W., 45-14
 Lacey, W.N., x, 21-10, 21-20, 22-22, 23-13, 25-20, 39-2, 39-27, 45-14
 Lachance, D.P., 26-9, 26-33
 Lackland, S.D., 45-15
 Lagers, G.H.C., vii
 Lahring, R.I., 44-51
 Lajtai, I., 25-21
 Lake, L.W., xi, 28-15, 47-1, 47-24 to 47-26, 54-14
 Lam, K.Y., 55-11
 Lamborn, R.E., 24-22
 Lamont, N., 49-41
 Lampe, H.W., 48-20
 Land, C.S., 28-12, 28-15, 44-49
 Landrum, B.L., 44-25, 44-50
 Lane, A.C., 24-2, 24-22
 Lane, L.C., 45-15
 Langenheim, R.N., 46-7 to 46-9, 46-43
 Langston, E.P., 44-36, 44-51
 Langton, J.R., 43-17
 Lannung, A., 25-21
 Lantz, R.B., 46-9, 46-11, 46-43, 48-10, 48-19
 Larson, R.G., 47-25
 Larson, S., 25-23
 Larson, T.A., 41-1
 Lasater, J.A., 7-9, 7-17, 22-5 to 22-10, 22-22
 Lasater, R.H., 15-1
 Lasater, R.M., 54-13
 Last, G.J., 43-17

Laulhere, B.M., 25-21
 Laumbach, D.D., 46-43
 Law, J., 39-28
 Lawrence, L.L., 12-44
 Laws, W.R., xii, 51-52
 Lawson, J.B., 47-9, 47-25, 47-26
 Lawson, J.D., 34-37, 34-55
 Lea, J.F., 5-52, 5-57
 Leach, R.O., 44-40, 44-51, 47-26
 Leas, W.J., 44-50
 Lease, W.O., 28-7, 28-12, 28-15
 LeBlanc, R.J., 36-3, 36-10
 LeBreton, J.G., 25-26
 Ledbetter, R.L., 38-20
 Ledlow, L.B., 54-13
 Lee, B.D., 44-17, 44-49
 Lee, B.I., 20-13, 20-17, 20-18
 Lee, J., 35-12, 35-21
 Lee, M.H., 54-13
 Lee, S.T., 46-37, 46-45
 Lee, W.J., 55-12
 Lefebvre du Prey, E.J., 28-10, 28-15
 Lefkowitz, H.C., 40-38
 Leggett, B., 54-13
 Leibrock, R.M., 43-17
 Leighton, A.J., x, 44-28 to 44-30, 44-32, 44-50, 45-14
 Leland, T.W. Jr., 25-24
 Lemanczyk, R., 55-12
 Lents, M.R., x, 39-19, 39-20, 39-23, 39-28
 Lentz, H., 25-24, 25-25
 Leonardon, E.G., 31-7, 51-50
 Lerner, B.J., 12-43
 Lescarbours, J.A., 55-12
 Lessem, L.B., 39-25, 39-28
 Lester, G.W., 44-35, 44-51
 Letkeman, J.P., 48-20
 LeVelle, J.A., 16-16
 Leverett, M.C., 26-24, 26-33, 28-2, 28-3, 28-6, 28-7, 28-15, 40-13, 40-17, 40-18, 40-38, 43-3, 43-4, 43-16, 43-19, 44-4, 44-7, 44-9 to 44-11, 44-26, 44-29, 44-49, 47-2, 47-24, 48-1, 48-18
 Levesque, J.M., 48-20
 Levine, J.S., 37-21, 37-22, 37-27
 Levorsen, A.I., 29-9
 Lewin and Assocs. Inc., 46-4, 46-13, 46-14, 46-43
 Lewis, C.R., 52-31
 Lewis, J.O., 40-15, 40-38, 44-49
 Lewis, P.E., 55-11
 Lewis, W.B., 44-4, 44-49
 Lewis, W.K., 22-22
 Lewis, W.M., 37-27
 Li, C.C., 25-25
 Liabastre, A.A., 25-26
 Lien, C., 48-19
 Lin, C., ix, 28-12, 28-15
 Lindbad, E.N., 39-27, 45-15
 Lindsey, W.C., 18-52
 Lipson, L.B., 49-42
 Lisbon, T.N., 34-46, 34-55
 Little, L.A., 10-1
 Little, T.P., 46-44
 Lockhart, R.W., 34-37, 34-55
 Log Analyst, The, xiii
 Logan, J.L., 4-11
 Logan, J.M., 55-12
 Lohec, R.E., 43-17
 Loncaric, I.G., 44-20, 44-37, 44-50
 Lone Star Steel, 2-46, 2-74
 Longeron, D.G., 28-11, 28-15
 Longstaff, W.J., 48-19
 Loomis, A.G., 28-10, 28-15
 Loprest, F.J., 25-22
 Lorenz, P.B., 47-26
 Lotter, Y.G., 25-26
 Loveless, G.W., 51-52

Lovell, F.P., 25-25
 Low, J.W., 52-9, 52-30
 Lowe, R.M., 38-20
 Loy, M.E., 49-41
 Lubinski, A., 4-11
 Lubojacky, R.W., 36-10
 Lucas, M., 25-21
 Lufkin Industries Inc., vi
 Lumpkin, W.B., 43-17
 Lund, K., 54-13
 Luque, R.F., 54-13
 Lybarger, J.H., 54-13
 Lynch, E.J., xii, 44-29, 44-50, 51-51

M

Maas, O., 25-22
 MacDonald, R.C., 48-14, 48-20
 Mace, C., x, 46-44
 MacLean, M.A., 46-44
 MacNaughton, L.W., 41-37
 Macon, R.S., 45-15
 Macrygeorgos, C.A., 40-38
 Maddox, R.N., 14-1, 14-22
 Maerker, J.M., 47-6, 47-24
 Maharij, D.M., 25-27
 Maher, J.C., 52-9, 52-30
 Maini, B.B., 28-12, 28-15
 Majani, P., 51-52
 Makogon, Y.F., 25-18, 25-23, 25-24
 Malesinska, B., 25-22
 Malik, V.K., 25-22
 Malinin, S.D., 25-22, 25-24
 Maly, G.P., 56-9
 Mancillas, G., 54-13
 Mandl, G., 46-8, 46-9, 46-15, 46-43
 Maney, E., 47-26
 Mann, L.D., 48-6, 48-18
 Manning, R.K., xi, 47-6, 47-24
 Mansurov, R.I., 19-34
 Mapes, G.J., 12-43
 Markham, A.E., 25-22
 Markhasin, I.L., 28-11, 28-15
 Marrs, D.G., 45-15
 Marshall, D.L., x, 39-20, 39-21, 39-28
 Marshall, D.R., viii, 25-2, 25-5, 25-20, 25-24
 Marshall, P.W., 18-52
 Martin, F.D., x, 47-22, 47-24, 47-26
 Martin, J.C., 35-2, 35-21, 43-16, 44-50
 Martin, J.J., 20-8, 20-18, 39-28, 48-18
 Martin, J.W., 7-17
 Martin, M., 49-1, 49-41
 Martin, R.C., 54-12
 Martin, W.A., 40-38
 Martin, W.L., 46-43, 46-45
 Martinelli, R.C., 34-37, 34-55
 Martinez, S.J., 54-1, 55-1, 56-1
 Marx, J.W., 46-7 to 46-9, 46-43
 Marzetta, T.L., 51-51
 Maslennikova, V.Y., 25-22, 25-23, 25-26
 Matheny, S.L. Jr., 16-16
 Mathews, J.D., 48-18
 Mathews, M.A., 51-52
 Matous, J., 25-22
 Mattax, C.C., 44-49, 48-19, 48-20
 Matthews, C.S., 35-16, 35-21, 40-38, 44-25, 44-50, 44-51
 Matthews, T.A., vii, 20-9, 20-10, 20-18
 Matthes, E.P., 36-10
 Maurer, O., 25-18, 25-24
 Maurette, C., 51-50
 Mayer, C., 49-42
 Mayer, E.H., iii, 22-22, 47-26
 Mayhill, T.D., 54-12
 Mayland, B.J., x, 46-37, 46-45
 Mayorga, G., 25-24
 Mazzullo, S.J., 29-9

- McAdams, W.H., 46-43
 McAuliffe, C.D., 24-23, 25-21, 47-20, 47-26
 McBain, J.W., 25-25
 McBean, W.N., 46-44
 McBride, J.R., 54-13
 McCaffery, F.G., 28-11, 28-15
 McCann, C., 51-52
 McCann, D.M., 51-52
 McCarter, E.D., 48-18
 McCarty, D.G., 44-17, 44-49
 McCarty, E.L., 25-21
 McCarty, G.M., 44-17, 44-49
 McCaskill, N., 45-15
 McCay, R.C., 25-22
 McClaffin, G.G., 6-72, 19-34
 McClellan, J.H., xii, 51-51
 McClendon, R., 52-54, 52-31
 McCormick, G.W., viii
 McCord, D.R., 43-16
 McCracken, T.A., 48-11, 48-19
 McCray, A.W., 41-37
 McCrossan, R.G., 24-22
 McCulloch, R.C., 43-17
 McCune, C.C., 44-37, 44-51, 54-13
 McCurdy, R.C., 26-33
 McDaniel, R.R., 55-11, 55-12
 McDonald, A.E., 48-20
 McDonald, G.H.F., 51-46, 51-52
 McDonald, J.A., 36-11
 McDow, G., 54-13
 McElwee, P.G., 58-8
 McEvoy Co., v
 McFarlane, R.C., 43-17
 McGarry, M.W. Jr., 40-37, 41-38
 McGhee, E., 16-16, 19-34
 McGinty, J.E., 54-14
 McGrain, P., 24-22
 McGraw, J.H., 43-17
 McGuire, W.J., 54-9, 55-10
 McKelvey, J.G., 24-23
 McKetta, J.J., 25-1, 25-16, 25-17, 25-21, 25-23, 25-24, 25-25, 25-26, 25-27
 McKinley, D.C., 16-16
 McKinney, O.B., 24-22
 McKoy, V., 25-5, 25-23
 McLaughlin, W.A., 54-13
 McLean, A.M., 25-22
 McLeod, H.D. Jr., 25-23
 McLeod, H.O., 54-13, 54-14
 McLeod, H.O. Jr., 55-12
 McMahon, J.J., 37-27, 38-9, 38-11, 38-20
 McMahon, W.F., 6-34, 6-72
 McMenamin, M.A., 25-18, 25-24
 McNeal, R.P., 52-9, 52-30
 McNeil, J.S., x, 46-14, 46-19, 46-43 to 46-45
 McNellis, J.M., 24-19, 24-23
 Meabon, H.P., 47-25
 Mead, H.N., 7-17
 Meads, R., 28-16
 Mechem, O.E., 26-33
 Mechtly, E.A., 58-8, 58-14
 Meckel, L.D., 36-10
 Meents, W.F., 24-22
 Megyesy, E.F., vi, 12-43
 Mehta, B.R., 25-28
 Meijerink, J.A., 48-14, 48-20
 Melcher, A.F., 26-3
 Meldau, R.F., 46-45, 46-46, 48-6, 48-18
 Melnyk, J.D., 54-13
 Melrose, J.C., 24-16, 44-51
 Meltzer, B.D., 43-17, 45-15
 Mennie, J.H., 25-22
 Mennon, V.B., 19-34
 Menten, P.D., 25-27
 Menzie, D.E., 44-20, 44-49
 Merrill, L.S., 48-19
 Messer, P.H., 34-55
 Messner, E.S., 26-24
 Metcalfe, R.S., 20-1, 23-9, 23-13, 45-10, 45-14
 Meter, D.M., 47-4, 47-24
 Meyers, D.C., 16-16
 Michaelis, A.M., 54-12
 Michels, A., 25-21
 Mid-Continent Dist. Study Commission, 24-22
 Mid-Continent Oil and Gas Assn., 41-37
 Mikesha, F.J., 16-16
 Milburn, J.D., 26-30, 26-31, 26-33
 Miles, L.H., 56-9
 Miller, B., 25-27
 Miller, B.D., 54-12, 54-14
 Miller, C.C., 30-9, 30-12, 30-17, 35-15, 35-21
 Miller, F.G., 43-17
 Miller, M.A., 28-12, 28-16
 Miller, M.G., x, 39-19, 39-20, 39-23, 39-28
 Miller, S.L., 25-25, 25-27
 Millican, M.L., 49-42
 Millikan, C.V., 30-1, 30-16, 31-1
 Mills, F. van A., 24-1, 24-22
 Milne, J.H., 24-23
 Milton, H.W. Jr., 47-25
 Minear, J.W., xii, 51-34, 51-51, 51-52
 Minnich, B.H., 25-22
 Minor, H.F., 24-22
 Minor, S.S., 54-12
 Minssieux, L., xi, 47-26
 Mintz, F., 41-37
 Misk, A., xii, 51-22, 51-51
 Mitchell, R.W., 44-51
 Modine, A.D., 48-20
 Modular Production Equipment Inc., vii
 Mohanty, K.K., 28-12, 28-15, 28-16, 47-25
 Moilliet, J.L., 19-34
 Molokowu, F.W., 36-10
 Monroe, R.R., 22-22
 Montadert, L., 36-10
 Moody, L.F., ix, 34-38, 34-52, 34-55
 Moore, C.H., 29-9
 Moore, E.W., 54-14
 Moore, G.T., 29-9
 Moore, J.C., 25-21
 Moore, J.L., 45-1
 Moore, J.W., 25-27
 Moore, T.V., 32-3, 32-16, 34-37
 Moore, W.D., 38-20
 Moorwood, R.A.S., 25-23
 Moran, J., 49-41
 Moranville, M.B., 48-18
 Morel-Seytoux, H.J., 44-29, 44-51, 47-24
 Moreland, E.E., 33-23
 Morgan, C.O., 24-19, 24-23
 Morgan, J.T., 46-44
 Morkill, D.B., 41-16, 41-19, 41-22, 41-37
 Morris, C.F., xii, 51-51
 Morris, F.C., 26-33
 Morris, J.K., 12-43
 Morris, R.L., 49-42
 Morrissey, N.S., 41-37
 Morrison, J.B., 44-51
 Morrison, T.J., 25-21
 Morse, R.A., 43-17, 44-29, 44-49, 45-13
 Mortada, M., 38-1, 38-20, 44-25, 44-50
 Mosburg, L.G. Jr., 57-12
 Moscrip, R. III, 43-16
 Moseley, N.F., 4-10, 4-11
 Moses, P.L., 39-1, 39-16, 39-28
 Moshfeghian, M., 25-16, 25-18, 25-24
 Moss, J.T., x, 44-20, 44-50 46-43, 46-44
 Moughamian, J.M., 48-6, 48-18
 Mounce, W.D., 49-41, 51-50
 Mower, L.N., 5-57
 Mrosovsky, I., 40-38, 48-17, 48-20
 Muecke, T.W., 54-14, 56-2, 56-9
 Mueller, T.D., 38-20, 43-17
 Mulac, A.J., 46-45
 Müller, G., 51-51
 Müller, H.G., 25-5, 25-23
 Mullins, L.D., 37-27, 40-38
 Mungan, N., x, 44-51, 48-19, 54-12
 Munjal, P.K., 25-22
 Munn, M.J., 24-1, 24-21
 Murphy, G.B., 21-20, 39-27
 Murray, C.N., 25-22
 Murray, J., 51-51, 55-10
 Murzin, V.I., 25-25
 Muskat, M., 6-37, 6-39, 6-72, 28-2, 28-5, 28-15, 30-9, 30-11, 30-16, 30-17, 32-4, 32-16, 34-31, 34-55, 37-7, 37-10, 37-13, 37-14, 37-19, 37-27, 39-19, 39-20, 39-27, 39-28, 40-9, 40-10, 40-18, 40-38, 43-17, 43-19, 44-13, 44-14, 44-16, 44-17, 44-20, 44-21, 44-26, 44-29, 44-33, 44-49, 44-50, 45-14, 45-15, 48-17, 48-18
 Myhill, N.A., 46-9, 46-15, 46-43
 Myung, J.I., xii, 51-43, 51-51, 51-52
- N**
- Naar, J., 28-15
 Nabor, G.W., 38-20, 44-25, 44-50
 Nagata, I., 25-5, 25-23
 Nagy, B., 25-21, 25-22
 Nalco Chemical Co. CTS-V3, 19-34
 Namiot, A.Y., 25-21, 25-26, 25-27
 Nath, A.K., 51-52
 Nations, L.F., xii, 51-35, 51-51
 Natl. Aeronautical and Space Admin. (NASA): NASA SP-7012, 58-8
 Natl. Assn. of Corrosion Engineers (NACE), 12-43, 19-34, NACE Std. MR-01-75, 3-36, 3-37, 3-40, 9-14, NACE Std. RP-01-75, 11-14, NACE Std. RP-03-72, 11-14, NACE Std. RP-05-75, 11-14, 19-34, NACE Std. TM-01-73, 44-51, NACE Std. TPC-5, 19-34
 Natl. Bureau of Standards (See U.S. Natl. Bureau of Standards)
 Natl. Electrical Code (NEC), 3-34, 3-40, 10-26, 18-44, 18-46, 18-52
 Natl. Electrical Manufacturers Assn. (NEMA), vi, 10-17 through 10-20, 10-24, 10-25, 10-27, 10-37
 Natl. Fire Protection Assn. Bull. 496, 18-46, 18-52
 Natl. Oilwell, v
 Natl. Petroleum Council, 18-52
 Natl. Production Systems, 6-72
 Natural Gas Assn. of America (NGAA), 39-12, 39-27
 Natural Gas Supply Mens Assn. (NGSMA), vi
 Navone, R., 25-21
 Neal, E.A., 55-12
 Needham, R.B., 47-24
 Negri, G., 25-21
 Neilsen, R.F., 35-1
 Neilson, I.D.R., 44-20, 44-50
 Neinast, G.S., 46-42
 Nelson, C.C., 6-34, 6-72
 Nelson, D.E., 44-51
 Nelson, E.F., 21-20, 39-27
 Nelson, R.C., 23-13, 47-20, 47-25, 47-26, 48-18
 Nelson, T.W., 46-14, 46-19, 46-45
 Nelson, W.L., vii, 21-9, 21-20, 22-22
 Nemeth, L.K., 39-13, 39-28
 Neuman, C.H., 46-9, 46-43

Neustadter, E.L., 19-34
 Newburg, A.H., 16-16
 Newendorp, P.D., 41-37
 Newman, G.H., 26-8, 26-33
 Newman, S.A., 25-18, 25-24
 New Mexico Oil Conservation Commission, 39-27
 Nezdoininoga, N.A., 25-22
 Ng, H.J., 25-5, 25-9, 25-11, 25-20, 25-23, 25-24, 25-28
 Nghiem, L.X., 48-18
 Nichols, D.T., 21-20
 Nichols, E.A., 31-7
 Nicholson, R.W., 44-51
 Nicklin, D.J., 34-39, 34-55
 Niebrugge, T.W., 6-72
 Nielson, R.F., 25-26
 Niemann, H., 25-25
 Nierode, D.E., 54-12, 54-14
 Nikolaev, N.A., 12-43
 Ninth Oil Recovery Conference, 39-28
 Nisle, R.G., ix, 34-28, 34-55
 Noad, D.F., 24-22
 Noaker, L.J., 25-5, 25-23
 Nobles, M.A., 44-19, 44-20, 44-34, 44-49
 Nolan, T.J. III, 54-14
 Nolen, J.S., 48-20
 Nolte, K.G., 55-12
 Nordgren, R.P., 55-12
 Norman, L.R., 54-14
 Northern, T.P., 16-16
 Northrup, D.A., 55-11
 Norton, A.E., 22-22
 Nosov, E.F., 25-25
 November, M.H., 13-59
 Novotny, E.J., 54-14
 Nowak, T.J., 44-35, 44-51
 Nur, A.M., 51-51
 Nute, A.J., 45-15
 Nutting, P.G., 26-3, 26-33, 44-40, 44-51

O

O'Brien, L.J., 45-15
 O'Brien, M.P., 6-36, 6-37, 6-72
 O'Connor, J.J., 25-25
 OCS Order No. 5, U.S. Dept. of the Interior, 3-34, 3-40
 Odeh, A.S., 28-15, 32-16, 33-23, 37-2, 37-3, 37-6, 37-7, 37-19, 37-27, 38-12, 38-20, 48-2, 48-18, 56-9
 O'Dell, P.M., 48-18, 48-19
 Offeringa, J., 45-14
 Offshore Services and Technology, 12-43
 Oglesby, K.D., 46-44
 Oil and Gas J., vii, x, 16-16, 16-17, 19-34, 21-21, 40-38, 46-3, 46-43 to 46-45
 Oilfield Publications Ltd., viii
 Oilwell Div. of U.S. Steel Corp., v
 Oilwell Research, 26-6
 Olds, R.H., 21-10, 21-11, 21-20, 23-13, 25-2, 25-11, 25-20
 Oleinikova, A.L., 25-25
 Oliver, D.W., 50-38
 Oliver, F.L., 29-1
 Oliver, L.R., x, 39-20, 39-21, 39-28
 O'Meara, D.J. Jr., 28-7, 28-12, 28-15
 Omnes, G., 51-52
 O'Neil, R.K., 7-17
 Organick, E.I., 21-10, 21-11, 21-13, 21-15, 21-16, 21-20, 39-4, 39-27
 Orkiszewski, J., 7-12, 7-17, 34-37 to 34-40, 34-55
 Orr, F.M. Jr., 23-1, 23-13, 45-14, 48-9, 48-19
 Osborn, F.E. III, 54-12
 Osif, T.L., 24-13, 24-23
 Osoba, J.S., 28-15
 Ostroff, A.G., 24-22, 44-51
 O'Sullivan, T.D., 25-21
 Otis Engineering Corp., v
 Otsuka, E., 25-24
 Otto, F.D., 25-23, 25-28
 Ovchinnikov, A.A., 12-43
 Overbeck, J.Th.G., x, 47-25
 Overton, H.L., 49-42
 Owen, J.D., 26-33
 Owen, L.B., 55-11
 Owen, W.W., 28-11, 28-15
 Owens, W.W., 45-13, 47-20, 47-26

P

Paasch, R.D., 41-37
 Pabley, A.S., 54-14
 Pacific Energy Assn., 13-59
 Packard, H.C., 16-16
 Padmanabhan, L., 48-19
 Paillet, F., 51-13, 51-51
 Paine, P., 41-37
 Palmer, F.S., 45-15
 Palmer, I.D., 55-12
 Palmour, H.H., 6-72
 Pankov, A.G., 25-25
 Panteleev, V.G., ix, 28-15
 Panvelker, S.B., 40-38, 47-24
 Paragon Engineering Services Inc., vii
 Paratella, A.A., 25-22
 Pardue, G.H., 51-52
 Parent, C.F., 44-51
 Parker, P.D.M., 25-22
 Parks, A.S., 12-43
 Parks, T.W., xii, 51-51
 Parmley, J.L., 55-12
 Parrish, D.R., 46-40, 46-43, 46-44
 Parrish, W.R., 25-2, 25-5, 25-8, 25-20, 25-27
 Parsons, R.L., 39-28, 40-18, 40-19, 40-38, 44-7 to 44-9, 44-26, 44-29, 44-30, 44-32, 44-49, 45-14, 45-15
 Parsons, R.W., 46-44
 Pasternack, E.S., 51-52
 Patel, C., 45-15
 Patnode, H.W., 49-41
 Patterson, D.R., 16-1, 16-16
 Patton, C.C., 24-22, 44-51
 Patton, E.C. Jr., 39-28, 43-9, 43-17, 43-19
 Patton, J.T., 47-8, 47-25, 48-19
 Patton, L.D., v, 4-1, 4-11
 Paul, G.W., 47-25, 47-26
 Pauley, P.O., 54-12
 Paulsell, B.L., 44-20, 44-50
 Pavlova, S.P., 25-26
 Paynter, D.D., 36-10
 Payton, E., 29-9
 Peaceman, D.W., 44-51, 45-14, 48-16 to 48-20
 Pearson, A.J., 52-1, 53-1
 Peerless Manufacturing Co., vi, 12-43
 Peery, J.H., 48-18
 Peng, D.Y., ix, 20-7, 20-8, 20-18, 23-13, 25-8, 25-16, 25-17, 25-23, 39-28, 48-18
 Penick, D.P., 12-43
 Pennbaker, P.E., 53-26
 Penny, G.S., 55-12
 Perkins, T.K., 44-49, 45-14, 46-43
 Perkins, T.K. Jr., x, 55-2, 55-10
 Perry, C.W., 25-25, 46-45
 Perry Equipment Co., vii
 Perry, J.H., 20-18, 22-22
 Perry, R.H., vii, 25-15
 Pet. Engr., 16-16
 Pet. Equipment, 16-16
 Peters, B.A., 12-43
 Peterson, A.V., 39-16, 39-28
 Peterson, M.E., 46-44
 Peterson, R.A., 51-52
 Peterson, R.E., 25-22
 Peterson, R.L., 45-15
 Petrie, H., 6-1, 6-34, 6-72
 Petrie, T.A., 41-37
 Petroleum de Venezuela S.A., 27-9
 Petroleum Publishing Co., 18-52
 Petrov, A.N., 19-34, 25-25
 Petrunia, J.P., 25-28
 Peveraro, R., 53-26
 Pickett, G.R., 51-50
 Pierce, H.R., 30-8, 30-16
 Pierre, M.L., 54-12
 Pierson, N.O., 54-14
 Pierson, R.G., 48-18, 48-19
 Pinson, J., 44-50
 Piper, A.M., 24-19, 24-23
 Pirie, G., 50-38
 Piros, J.J., 16-16
 Pirson, S.J., ix, 29-9, 39-28, 40-17, 40-38, 43-16, 43-17, 44-49, 49-42
 Pittman, D., 51-52
 Pittman, G.M., 46-44
 Pittman, R.W., 34-55
 Pitzer, K.S., 20-13, 24-15, 24-23, 25-24
 Plasek, R.E., xi, 50-38
 Platt, C.R., 37-27
 Platteeuw, J.C., 25-2, 25-5, 25-6, 25-10, 25-20, 25-23
 Plenty Metrol Ltd., vi, 12-43
 Plisga, G.J., 30-1, 31-1
 Plummer, F.B., 24-22
 Poettmann, F.H., ix, x, 25-25, 34-1, 34-4, 34-9, 34-28, 34-37, 34-46, 34-55, 34-56, 39-28, 46-13, 46-14, 46-16, 46-37, 46-44, 46-45
 Polglase, M.F., 25-21
 Pollak, A., 12-43
 Pollard, P., 54-14
 Pollard, T.A., 39-1, 40-38, 58-2
 Pollitzer, F., 25-22
 Pollock, C.B., 46-44, 55-10
 Pontious, S.B., 45-15
 Pontius, P.E., 1-71
 Pope, G.A., xi, 23-13, 47-5, 47-24 to 47-26, 48-18
 Pope, S.H., 16-16
 Porta-Test Systems Ltd., vi, 12-43
 Postgate, J.R., 24-22
 Poston, S.W., 36-1, 36-10, 46-37, 46-45
 Pottier, J., 45-15
 Poupon, A., 49-41
 Powers, W.J., 7-1
 Pozzi, A.L., 45-14
 Prats, M., 37-20 to 37-22, 44-20, 44-25, 44-28 to 44-32, 44-34, 44-49, 44-50, 46-43, 46-45, 46-46
 Prausnitz, J.M., 20-18, 23-13, 25-2, 25-5, 25-8, 25-14, 25-20, 25-21
 Pray, H.A., 25-22
 Prehn, W.L. Jr., 26-33
 Prentice-Hall Inc., 57-12
 Press, F., 51-50
 Price, H.S., 43-17, 45-14, 48-16, 48-20
 Price, P., 24-22
 Prince, L.C., 24-23
 Prokop, C.L., 49-42
 Province of Manitoba, 24-22
 Province of Saskatchewan, 24-22
 Pruess, K., 48-11, 48-20
 Pryor, J.A., 46-45
 Pryor, W.A., 36-10, 46-42
 Puerto, M.C., 47-25
 Pujol, L., 46-13, 46-43
 Pursley, S.A., 46-43
 Purvis, S.B., 54-12
 Pusch, W.H., 46-45
 Pushkar, P., 24-22
 Pye, D.S., 56-9
 Pyndus, G.T., 45-14

Q

Quadir, J.A., 55-11
 Quirein, J.A., 50-38
 Quisenberry, J.L., 54-12

R

Rachford, H.H. Jr., 38-20, 44-51, 45-14, 48-16, 48-18, 48-20
 Rachinskii, M.A., 25-21
 Radar, D., 51-51, 53-26
 Radke, C.J., 47-21, 47-26
 Raghavan, R., 34-9, 34-55, 55-11
 Rahme, H.D., 44-29, 44-50
 Railroad Commission of Texas, ix, 34-55
 Raimondi, P., 47-26
 Rainbow, H., 44-51
 Rall, C., 24-22
 Ramagost, B.P., 35-13, 35-21, 40-38
 Ramakrishnan, T.S., 47-26
 Ramesh, A.B., 48-19
 Ramey, H.J. Jr., 4-11, 28-12, 28-16, 30-17, 33-23, 34-9, 34-55, 35-10, 35-21, 36-8, 36-10, 43-16, 44-20, 44-29, 44-34, 44-50, 46-5, 46-6, 46-8, 46-15 to 46-17, 46-19, 46-43 to 46-45, 55-11
 Ransom, R.C., xii, 51-51
 Rapoport, L.A., 44-29, 44-50, 44-52
 Rathbone, M.J., 54-13
 Rathmell, J.J., 44-49
 Rau, R., xi
 Rawlins, E.L., ix, 30-8, 30-16, 33-3, 33-5, 33-13, 33-23, 34-45, 34-55
 Raymer, L.L., xi, xii, 49-42, 50-38, 51-33, 51-34, 51-52
 Raynal, J.C., 53-26
 Rayne, J.R., 45-14
 Reader, P.J., 43-17
 Reading, H.G., 36-10
 Reamer, H.H., viii, 23-13, 25-24, 25-26, 25-27, 25-28
 Records, J.R., 25-10, 25-12, 25-23
 Redlich, O., 20-7, 20-8, 20-18, 23-12, 23-13, 39-28
 Reed, C.D., 25-26
 Reed, G.A., 16-16
 Reed, R.L., xi, 47-13, 47-25
 Reeds, C.B., 18-1
 Reese, C.P., 16-16
 Regier, S., 39-28
 Reheis, G.M., 43-17
 Rehkopf, B.L., 46-44
 Rehm, B., 52-24, 52-31
 Reid, L.S., 25-21, 25-27
 Reid, R.C., 20-18, 23-13
 Reid, T.B., 47-24
 Reid, W., 33-1, 33-23
 Reineck, H.E., 36-10
 Reistle, C.E., 24-19, 24-23
 Renon, H., 25-18, 25-24
 Republic Bank of Dallas, x
 Resen, L., 16-17
 Reudelhuber, F.O., 37-23, 37-27, 40-38
 Reuss, A., 51-51
 Reynolds, A.C., 55-11
 Reynolds, F.S., 41-7, 41-37
 Reznik, A.A., 40-19, 40-38, 47-24
 Rhodes, A.E., 3-40
 Rice, J.D., 38-20
 Rice, P.A., 25-26
 Rich, J.L., 24-2, 24-22
 Richards, L.A., 28-2, 28-6, 28-15
 Richards, W.L., 25-27
 Richardson, E.A., 54-13
 Ridings, R.L., 37-13, 37-21, 37-27, 48-20
 Rigby, M., 25-14, 25-21
 Riley, J.P., 25-22
 Rintoul, B., 18-52
 Ripmeester, J.A., 25-27
 Ritchie, P.D., 25-22
 Ritterbusch, W.H. Jr., 9-1
 Rittenhouse, G., 24-22
 Roberts, G.I., 54-14
 Roberts, G.W., 46-45
 Roberts, L.D., 54-13, 54-14
 Roberts, O.L., 25-23
 Roberts, S.J., 48-20
 Roberts, T.G., 37-14, 37-15, 37-27, 40-38, 44-29, 44-50
 Robinson, D.B., viii, 20-7, 20-8, 20-18, 23-13, 25-5, 25-8, 25-9, 25-11, 25-16, 25-17, 25-20, 25-23, 25-24, 25-28, 39-28, 40-38, 48-17
 Robinson, F.M., 51-51
 Robinson, G.E., 48-19
 Robinson, J., 12-43
 Robinson, J.D., 51-47, 51-52
 Robinson, J.R., 22-15, 22-16, 22-22, 46-31, 46-45
 Robinson, R.L. Jr., 20-8, 20-18
 Roddy, J.W., 25-26
 Rodgers, J.K., 39-15, 39-28
 Roe, R.P., 23-13, 39-13, 39-15, 39-28
 Roebuck, I.F. Jr., 43-1
 Roger, P.S.Z., 24-15, 24-23
 Rogers, G.S., 24-22
 Rogers, H.D., 24-21
 Rogers, J.H., 47-24
 Rogers, R.E., 55-12
 Rogers, W.B., 24-21
 Roland, C.H., vii, 20-18
 Rollins, J.T., 55-10
 Rolshausen, F.W., 24-22
 Romero-Juarez, A., 31-7
 Romocki, J.M.E., 54-14
 Ronk Electrical Industries Inc., vi
 Roof, W.E., 11-1
 Ros, N.C.J., 34-36, 34-37, 34-40, 34-46, 34-55, 34-56
 Rosbaco, J.A., 37-21, 37-27
 Rose, S.C., 52-31
 Rose, W., ix, 28-1, 28-3, 28-5, 28-15
 Rosenbaum, J.H., 51-47, 51-51
 Rosenbaum, M.J.F., 44-51
 Rosenberg, R.J., 55-12
 Rosene, R.B., 54-13, 55-12
 Rosepiller, M.H., 55-12
 Rosman, A., 45-14, 48-19
 Ross, J.S., 24-22
 Ross, W.M., 54-14
 Roszelle, W.O., 28-15
 Rouher, O.S., 25-27
 Rowan, G., 54-14
 Rowe, A.M. Jr., 24-13, 24-14, 24-23
 Royle, R.A., 54-14
 Rubin, L.C., 20-7, 20-18
 Ruble, D.B., 44-36, 44-51
 Rushing, M.D., 45-14
 Russel, W.L., 29-9
 Russell, D.G., 35-21
 Russell, G.B., 25-21
 Russell, G.F., 25-27
 Russell, J.T., 25-28
 Russell, T.F., 48-19
 Russell, W.L., 26-3, 26-4, 26-33
 Rust, C.F., 26-33
 Rust, W.M. Jr., 49-41
 Ryabtsev, N.I., 25-25, 25-26
 Ryan, J.C., 54-12
 Rzasa, M.J., 22-22, 34-55, 39-1, 39-27, 45-14

S

Sage, B.H., viii, x, 21-10, 21-11, 21-20, 23-13, 25-20, 25-27, 45-14
 Sage, W.H., 22-22, 39-2, 39-27
 Sagramora, G., 25-22
 Sahuquet, B.C., 46-43, 46-45
 Saito, S., viii, 25-2, 25-5, 25-20, 25-23, 25-24
 Salter, S.J., 28-12, 28-15, 28-16, 47-25
 Salthiel, W.M., 54-14
 Samaniego-V., F., 55-11
 Sams, H., ix, 29-9
 Sanchez, M., 25-24, 25-25
 Sandberg, C.R., 40-38
 Sander, W., 25-22
 Sandiford, B.B., 44-39, 44-51
 Sandler, S., 25-18, 25-24
 Sandmeyer, D.J., 4-11
 Sanyal, S.K., 51-52
 Saref, D.N., 28-10, 28-15
 Sarem, A.M., 28-10, 28-15
 Sargent, E.C., 24-22
 Sargent Oil Well Equipment Co., vi
 Sarmiento, R., 51-50
 Sass, L.C., 24-22
 Satman, A., 46-14, 46-45
 Satter, A., 46-6, 46-43
 Sattler, A.R., 55-11
 Saucier, R.J., 56-6, 56-9
 Saunders, C.D., 55-12
 Sauve, E.R., 18-1
 Savel'eva, N.I., 25-22
 Savins, J.G., 47-24
 Sawabini, C.T., 46-37, 46-45
 Saye, H.A., 16-17
 Scala, C., 49-41
 Scarborough, R.M., 46-45
 Scauzillo, F.R., viii, 12-44, 25-24
 Schaaf, D., 24-22
 Schatz, J., 55-10
 Schauer, P.E., 44-29, 44-51
 Schechter, R.S., 47-24, 47-25, 54-12, 54-14
 Scheffer, F.E.C., 25-24, 25-27
 Scheidegger, 28-5, 28-7, 28-15
 Schellhardt, M.A., ix, 33-23
 Schenk, L., 46-45
 Scheraga, H.A., 25-25
 Scherubel, G.A., 54-4, 54-12
 Scheuerman, R.F., 56-9
 Schilling, J.R., 12-43
 Schilthuis, R.I., 22-22, 24-2, 24-22, 34-37, 37-5, 37-27, 38-8, 38-20, 40-37
 Schlumberger, xii, xiii, 50-38, 51-51, 51-52
 Schlumberger Ltd., 53-26
 Schlumberger Offshore Services, xiii
 Schlumberger Well Services, xi, 49-41, 49-42, 53-26
 Schlumberger Well Surveying Corp., 49-41
 Schmalz, J.P., 44-29, 44-50
 Schneider, F.N., 28-11, 28-15
 Schneider, H., 25-25
 Schneider, R.D., 44-51
 Schnitz, L.B., 43-16
 Schoewe, W.H., 24-22
 Scholander, P.F., 25-21
 Scholle, P.A., 29-9, 36-10
 Schoonovers, L.G., 53-26
 Schrider, L.A., 44-29, 44-50
 Schrieter, F.E., 54-12
 Schroeder, W., 25-21
 Schroeter, J.P., 25-28
 Schueler, S., 33-23
 Schuetze, H., 25-24
 Schultz, H.E., 7-17
 Schultz, W.P., 42-1, 45-14
 Schulze, R.P., xi, 49-41
 Schweickent, C.E., 25-22
 Sclocchi, G., 34-55
 Scott, A.C., 53-26

- Scott, J.O., 16-17
 Scott, V.B., 16-17
 Seovill, W.E., 16-16
 Scriven, L.E., 47-25
 Sears, F.W., xi, 51-50
 Seely, D.H. Jr., 25-10, 25-12, 25-22, 25-23
 Seeman, B., 51-51, 51-52
 Segesman, F., 49-1, 49-41, 50-15, 50-38
 Seinfeld, J.H., 48-19
 Selleck, F.T., 25-27
 Selley, R.C., 36-10
 Sells, R.L., 50-38
 Selly, R.C., 36-10
 Seright, R.S., 47-24
 Serra, O., 50-38
 Sessions, R.E., 45-15
 Settari, A., 45-14, 48-16, 48-17, 48-20, 55-12
 Shah, P.C., 48-19
 Shane, L.E., xii, 51-50
 Shank, G.D., 48-18
 Shariot, A., 25-16, 25-24
 Shatto, H.L., 16-17
 Shaughnessy, C.M., 54-13, 54-14
 Shaw, J.K., 44-51
 Shaw, M.S., 54-12
 Shaw, S.F., 34-55
 Shearin, H.M., 42-1, 45-14
 Sheffield, M., 48-18
 Sheffield, R., 18-52
 Shehabi, J.A.N., 43-17
 Sheil, A.G., 6-72
 Sheldon, J.W., 48-14, 48-18
 Sheldon, W.C., 39-28, 45-15
 Shell Development Co., vii
 Shell Oil Co., 36-10
 Shelton, J.L., 45-14, 45-15, 48-19
 Shen, J., 44-51
 Sherwood, T.K., 20-18, 23-13
 Shiba, F.F., 45-10
 Shipley, R.G., 46-45, 48-18
 Shirer, J.A., 44-51
 Shirley, H.T., 39-28
 Shirley, O.J., 52-24, 52-31
 Shiu, K.S., 5-57
 Shoor, S.K., 25-21
 Shore, R.A., 46-44, 46-45
 Showalter, E., 10-14
 Showalter, W.E., 46-13, 46-16, 46-17, 46-43, 46-44
 Shreir, L.L., 19-34
 Shreve, D.R., 43-4, 43-16, 43-19
 Shtof, I.K., 19-34
 Shumaker, E.G., 55-12
 Shupe, R.D., 47-24
 Shutler, N.D., 48-18
 Sibbit, A., 49-42
 Sibbitt, W.L., 25-22
 Sifferman, T.R., 52-30, 55-12, 6-72
 Sigmund, P.M., 28-11, 28-15
 Sikora, V.J., 38-1, 38-20
 Sikora, V.J., 37-1, 37-14, 37-23, 37-27, 54-9, 54-10
 Silberberg, I.H., 44-50, 46-45, 54-12
 Silcox, W.H., 18-1, 18-52
 Silva, M.K., 45-14, 48-19
 Simandoux, P., 48-19
 Simard, G.L., 49-41
 Simmons, G., 51-30, 51-43, 51-51, 51-52
 Simmons, J., 44-50
 Simon, R., 45-14, 48-19
 Simpson, L.B., 25-25
 Sims, W.P., 40-38
 Simulation Sciences Inc., vi, 12-33, 12-43
 Sinaiskii, E.G., 12-44
 Sinanoglu, O., 25-5, 25-23
 Sinclair, A.R., 55-12
 Singh, D., x, 37-15, 37-27
 Singh, I.B., 36-10
 Singhai, A.K., 46-43
 Skelton, N., 54-13
 Skiba, F.F., 45-14
 Skinner, W. Jr., 25-12, 25-23
 Skirvin, R.T., 29-1
 Sklar, I., 46-44
 Skripka, V.G., 25-21, 25-26
 Slattery, J.C., ix, 28-12, 28-15
 Sleinikova, A.L., 25-25
 Slider, H.C., 44-30, 44-32, 44-50
 Sloan, E.D., viii, 25-1, 25-2, 25-4, 25-9, 25-10, 25-20, 25-23, 25-27
 Sloan, J.P., 39-1, 39-27
 Sloat, B., 44-51, 47-26
 Slobod, R.L., x, 26-25, 26-33, 43-19, 44-17, 44-19, 44-20, 44-49, 45-13, 45-14
 Slonneger, J.C., 10-18, 10-37
 Sloss, L.L., viii, 26-7, 26-33
 Smart, E.E., 6-72
 Smart, G.T., 48-19
 Smeaton, R.W., vi
 Smith, A.E., 30-9, 30-16
 Smith, C.F., 54-14
 Smith, F.W., 46-43
 Smith, G.L., 40-1
 Smith, H.D. Jr., xi, 50-38
 Smith, H.V., 12-1, 19-1
 Smith, M.B., 55-12
 Smith, N.A., 25-21
 Smith, N.O., 25-21, 25-22
 Smith, O.E., 48-19
 Smith, R.C., 31-7
 Smith, R.H., 40-15, 40-38
 Smith, R.L., 21-11, 21-20
 Smith, R.S., 12-43
 Smith, R.V., 5-37, 5-38, 5-57, 33-1, 33-15, 33-18, 33-23, 34-24 to 34-27, 34-29, 34-46, 34-55, 34-56, 46-44
 Smith, R.W., x
 Smith, S.S., v, 5-57, 25-27
 Smits, L.J.M., 49-41
 Snider, R.M., 36-6, 36-10
 Snell, L.E., 25-23
 Snyder, L.J., 48-18
 Snyder, R.W., 43-16, 44-29, 44-50
 Soave, G., 20-7, 20-8, 20-18, 23-13, 48-18
 Soc. of Automotive Engineers Inc., 10-12
 Soc. of Petroleum Engineers (SPE), 12-42, 23-13, 35-21, 39-27, 40-2, 40-37, 41-37, 45-14, 46-44, 46-45
 Board of Directors, 58-1
 Metrication Subcommittee, 58-22
 Metric Standard, 17-7
 Symbols Committee, 59-1
 Soc. of Professional Well Logging Analysts (SPWLA), 52-3
 Soldate, A.M., 25-25
 Sollami, B.J., 25-21
 Somasundaran, M.C., 47-26
 Somerton, W.H., 46-37, 46-45, 47-26
 Song, K.Y., viii, 25-1, 25-10, 25-15, 25-23
 Spalding, J.S., 51-51
 Spangler, M.B., 26-33
 Sparlin, D.D., 56-9
 Spearing, D., 36-10
 Spence, K., 48-19
 Spencer, C.F., viii, 25-23
 Spencer, G.B., 37-27, 39-28, 40-38
 Spillette, A.G., 48-14, 48-20
 Spisak, C.D., 6-34, 6-72
 Spivak, A., 43-17
 Squire, K.A., 54-13
 Squires, F., 44-40, 44-51
 Squires, L., 22-22
 Staadt, H.E., 54-1
 Staal, J.J., 51-47, 51-52
 Staggs, H.M., 48-18
 Stahl, C.D., 44-17, 44-49
 Stahl, R.F., 40-38
 Stalkup, F.I. Jr., 23-13, 45-14
 Stamm, H.E. III, 43-16
 Standing, M.B., vii, viii, 6-21, 6-38, 6-39, 6-72, 7-9, 7-12, 7-17, 20-5, 20-9, 20-18, 21-9, 21-16, 21-18 to 21-20, 22-1, 22-5, 22-6, 22-8 to 22-11, 22-13, 22-14, 22-21, 22-22, 23-13, 24-13, 24-23, 25-17, 25-21, 34-34, 34-35, 34-55, 37-19 to 37-21, 37-27, 39-2, 39-11 to 39-13, 39-15, 39-19, 39-27, 39-28, 40-38, 45-15
 Starling, K.E., 20-7, 20-18
 Staron, Ph., xii, 51-51
 State of Kansas, 33-13, 33-23
 Steanson, R.E., 55-1
 Steel, G., 36-10
 Steffensen, R.J., 31-7, 37-1, 45-15
 Stegemeier, G.L., 46-9, 46-13, 46-15, 46-43, 47-25
 Stein, N., 51-52, 56-9
 Steinle, P., 40-16, 40-38
 Stelzer, R.B., x, 39-20 to 39-22, 39-28
 Stenmark, D.G., 47-25
 Stephenson, E.A., 41-37
 Stephenson, R.E., 48-18
 Stevens, A.B., viii, 26-4 to 26-6
 Stewart, C.H. Jr., 48-14, 48-18
 Stewart, F.M., 38-20, 43-16
 Stewart, M., 19-33
 Stewart, P.B., 25-22
 Stiefel, E., 48-20
 Stiel, L.I., vii, 20-18
 Stiff, H.A. Jr., 24-19, 24-23
 Stiles, L.H., 36-7, 36-10
 Stiles, W.E., 36-6, 36-10, 40-18, 40-19, 40-20, 40-38, 43-7, 43-19, 44-7 to 44-9, 44-26, 44-28 to 44-32, 44-39, 44-49, 44-51, 45-14
 Stock, L.G., 47-26
 Stockwell, A., 19-34
 Stokes, D.D., 46-43, 46-44
 Stoll, R.D., 25-18, 25-24
 Stone, H.L., ix, 28-8, 28-15, 37-21, 37-27, 45-13, 48-14, 48-16, 48-18, 48-20
 Stormont, D.H., 16-17
 Stosur, J.J., 46-45
 Stout, W., 24-22
 Stovall, S.L., 46-43
 Strange, L.K., 46-20, 46-45
 Strawn, J., 55-10
 Strebel, E., 25-22
 Strickland, R.F., 43-17
 Strickler, W.R., 44-50
 Stright, D.H. Jr., 48-18
 Strong, E.R. Jr., 25-27
 Stubbs, B.A., 54-12
 Stutz, R.M., 16-16
 Stutzman, L.F., 25-21, 43-16
 Suau, J., 51-45, 51-52
 Suciu, S.N., 25-22
 Suder, F.E., 44-29, 44-50, 45-14
 Sufi, A.H., 28-12, 28-15
 Sukkar, Y.K., 34-9, 34-10 to 34-22, 34-24, 34-55
 Sultanov, R.G., 25-21, 25-26
 Suman, G.O. Jr., 56-9
 Summers, G.C., 51-50
 Sunwall, M.T., 24-22
 Surface, R.A., 46-44
 Sustek, A.J., 46-44
 Suter, H.H., 24-22
 Swan Wooster Engineering Ltd., vii
 Swanson, B.L., 54-14
 Swearingen, J.W., 44-17, 44-49
 Swendenborg, E.A., 24-22
 Swerdlhoff, W., viii, 22-17, 22-22

Swetnam, J.C., 7-17
 Sydansk, R.D., 47-26
 Symbols Committee of SPE, 59-1
 Szasz, S.E., 46-43

T

Taber, J.J., 23-1, 44-51, 47-22, 47-26
 Taggart, M.S. Jr., 24-22
 Takahashi, S., 25-23
 Takenouchi, S., 25-22
 Tan, T.B.S., 48-20
 Tanguy, D.R., 49-41
 Tannahill, C.A., 18-52
 Tarner, J., x, 37-7, 37-10, 37-27, 40-9, 40-10, 40-38
 Taylor, D.M., 16-17
 Taylor, H.S., 25-25
 Taylor, M.O., 37-10, 37-13, 37-14, 37-27, 40-38
 Taylor, T.J., xii, 51-52
 Tek, M.R., 34-50, 34-55, 34-56
 Templeton, C.C., 54-4, 54-12
 Terry, L.F., 41-37
 Terry, W.M., 45-14
 Terwilliger, P.L., 40-38, 46-45
 Teubner, W.G., 45-15
 Teufel, L.W., 55-12
 Texas Railroad Commission, 36-10, 39-27
 Thakur, G.C., 48-6, 48-18
 Tham, M.J., 45-15
 Thiercelin, M., 55-12
 Thijssen, H.A.C., 22-22
 Thodos, G., vii, 20-9, 20-10, 20-15, 20-16, 20-18, 43-16
 Thomas, C.P., 48-18
 Thomas, D.H., xii, 51-17, 51-51
 Thomas, E.C., 49-41
 Thomas, G.B., 30-10, 30-17
 Thomas, G.R., 24-22
 Thomas, G.W., 48-14, 48-17, 48-20
 Thomas, J.F., 48-6, 48-18
 Thomas, L.K., 34-1, 43-17, 48-5, 48-18, 48-19
 Thomas, R., 34-55
 Thomas, R.D., 47-26
 Thomas, R.L., 54-4, 54-12, 54-13, 55-12
 Thompson, D.D., xi, 51-50
 Thomson, E.S., 25-25
 Thomson, J., 6-72
 Thornhill-Craver, 5-8
 Thrash, J.C., 45-15
 Thrasher, W.B., 12-43
 Threlkeld, C.B., 47-24
 Throop, W.H., xi, 49-41
 Thurnau, D.H., 48-14, 48-18, 48-20
 Thury, G., 25-21
 Tickell, F.G., 24-19, 24-23, 26-2, 26-33
 Tidman, J., xi
 Tiffin, D.L., 45-14
 Till, M.V., 54-13
 Timmerman, E.H., 37-27, 38-9, 38-11, 38-20, 40-37, 44-28, 44-51
 Timur, A., xi, xii, 51-1, 51-4, 51-50, 51-51
 Tinker, C.N., 36-10
 Tinker, G.E., 47-24
 Tinnemeyer, A.C., 54-13
 Tinsley, J.M., 55-12
 Tittle, R.M., 45-15
 Tixier, M.P., 26-29, 26-33, 49-1, 49-41, 49-42, 51-50 to 51-52
 Todd, M., 16-17
 Todd, M.R., 48-11, 48-18, 48-19
 Todheide, K., 25-21, 25-22, 25-24
 Toksöz, M.N., xi, xii, 51-35, 51-50 to 51-52
 Torcaso, M.A., 40-38
 Torp, S.B., 48-19
 Torrey, P.D., 24-1, 24-21, 24-22, 44-49, 44-52

Tosch, W.D., 45-13
 Towler, B.F., 48-20
 Tracy, G.W., 30-17, 37-7 to 37-10, 37-21, 37-27, 38-2, 38-3, 38-20, 43-17
 Trainer, R.R., 22-22
 Trantham, J.C., 46-43
 Traverse, E.F., 46-44
 Travis, R.H., 16-17
 Trebin, F.A., 25-23
 Tretolite Div.-Petrolite Corp., 19-34
 Trico Industries, v
 Trimble, A.E., 46-18, 46-45
 Trimble, R.H., 48-20
 Tripp, H.A., 9-14
 Trofimuk, A.A., 25-18, 25-24
 Trostel, E.G., 46-35
 Trube, A.S., 20-11, 20-16, 20-18, 22-11, 22-12, 22-22
 Trushenski, S.P., 47-25
 TRW Energy Product Group, Reba Pump Div., v
 Tsang, L., 51-51
 Tsarev, V.P., 25-24
 Tsaturyants, A.B., 25-21
 Tsauro, K., 47-24
 Tsiklis, D.S., 25-22, 25-23, 25-26
 Turner, J., 54-13
 Turner, R.G., 34-46, 34-55
 Tyler, J.C., 48-18

U

Udell, K.S., 46-45
 Underwood, P.J., 54-13
 Underwriters' Laboratories Inc., 10-27
 University of Texas, 11-14, 12-43, 19-34
 University of Tulsa, 24-22
 Unruh, C.H., 25-5, 25-23
 U.S. Bureau of Mines (USBM), 1-80, 13-45, 19-34, 24-21, 24-23, 30-8, 30-16
 U.S. Bureau of Standards, 14-9
 USCG Regulation 30CFR, 18-52
 USCG Regulation 33CFR, 18-52
 USCG Regulation 46CFR, 18-44, 18-52
 U.S. Dept. of Commerce, 25-15
 U.S. Dept. of Energy (DOE), x, 40-38, 46-21, 46-45, 48-18
 U.S. Dept. of Interior, 12-43, 18-52, 57-11, 57-12
 U.S. Filter, Fluid System Corp., vii
 U.S. Geological Survey (USGS), 3-39
 U.S. Natl. Bureau of Standards (NBS), 1-68, 1-69, 1-71, 1-80, 58-9
 NBS LC 1071, 58-8
 NBS Special Pub. 330, 58-8
 U.S. Securities and Exchange Comm., 40-38
 U.S. Steel Corp., Bull USS, v
 U.S. Weather Bureau, ix

V

Valleroy, V.V., 46-44
 van Cleeff, A., 25-23, 25-24, 25-27
 Van der Knapp, W., 26-8, 26-33, 51-50, 51-51
 van der Poel, C., 44-25, 44-50, 45-19
 van der Waals, J.D., 20-17, 20-18, 23-12, 25-2, 25-5, 25-6, 25-10, 25-20, 25-23
 Van Der Worst, H.A., 48-20
 Vanderzee, C.E., 25-22
 VanDijk, W.J.D., 32-13
 van Dijk, C., 46-44
 van Domselaar, H.R., 47-25
 van Everdingen, A.F., 30-14, 30-15, 32-5, 32-16, 35-1, 35-21, 37-5, 37-27, 38-1, 38-9, 38-11, 38-20, 39-28, 40-37, 40-38
 Van-Guy, N., 48-19
 VanMeter, O.E., viii, 26-33
 Van Orstrand, C.E., 31-7

Vanpee, M., 25-23
 Van Poollen, H.K., 48-18, 48-20, 51-45, 51-52, 55-12
 van Wingen, N., 43-16
 van Wijk, W.R., 22-22
 Varga, R.S., 48-16, 48-20
 Varrien, J.P., 36-6, 36-10
 Vasquez, M., 7-9, 7-17, 22-7 to 22-12, 22-16, 22-22
 Vatalaro, F.J., 7-17
 Vdovina, N.A., 25-22
 Veatch, R.W., 55-12
 Verbeek, C.M.J., 55-12
 Verma, V.K., 25-18, 25-24, 25-28
 Vernado, S.G., 53-26
 Verrien, J.P., 36-6, 36-10
 Vestal, C.R., 48-18
 Vetter, O.J., 44-51
 Vilcu, R., 25-22
 Villard, P., 25-2, 25-20
 Villarreal, J.F., 25-26
 Vine, J.D., 24-23
 Vink, D.J., 21-16, 21-20, 22-22
 Vinsome, P.K.W., 48-19, 48-20
 Vispatch, 19-34
 Vivian, T.A., 54-14
 Vizilog Inc., xiii
 Vogel, C.B., 51-50
 Vogel, J.V., 7-9, 7-17, 34-31, 34-32, 34-34, 34-35, 34-55, 37-19, 37-21, 37-27, 46-9, 46-43
 Voigt, W., 51-51
 Volck, C.W., 46-8, 46-9, 46-15, 46-43, 46-45
 Vondy, D., 12-31, 12-43
 von Rosenberg, D.V., 45-14
 von Stackelberg, M., viii, 25-5, 25-23
 Vortec Inc., 12-43

W

Wachter, A., 25-27
 Wade, R.P., 54-14
 Wade, W.H., 47-25
 Wagner, O.R., 44-40, 44-51, 46-21, 46-45, 47-26
 Wagner, R.J., 44-29, 44-50
 Wahl, H.A., 55-12
 Wahl, J.S., xi, 50-38
 Wahl, W.L., 37-27, 40-38
 Walker, C.J., 39-28
 Walker, R.D., 25-21
 Walker, T., xii, 51-44, 51-52
 Walkley, J., 25-27
 Wallace, W.E., 24-22
 Wallis, G.B., vii, 34-37 to 34-39, 34-55
 Wallis, J.R., 48-20
 Walsh, J.B., 51-43, 51-52
 Walsh, M.P., 54-14
 Walstrom, J.E., 53-26
 Walters, J.D., 44-51
 Walton, D.L., 38-1
 Wang, H., 51-30, 51-52
 Ward, D., 10-37
 Warembourg, P.A., 54-12, 54-14
 Warner, B.J., 12-44
 Warner, H.R. Jr., 45-15
 Warpinski, N.R., 55-12
 Warren, F.H., 16-17
 Warren, J.E., 44-29, 44-51, 45-14, 49-41
 Washburn, E.W., 26-4 to 26-6, 26-33
 Wasicek, J.J., 16-17
 Wason, C.B., 36-10
 Wassan, D.T., 19-34, 47-26
 Wasserman, M.L., 48-19
 Wasson, J.A., 44-29, 44-50
 Waters, A.B., 55-12
 Watkins, D.R., 54-14
 Watkins, J.W., 24-1, 24-22

- Weaver, E.G., 16-17
 Weaver, R.H., 56-9
 Webb, G.B., 20-7, 20-18
 Weber, A.G., 38-20
 Weber, K.J., 36-6, 36-7, 36-10
 Webster's New International Dictionary, 58-20
 Weeks, L.G., 29-9
 Wegner, R.E., 44-50
 Wehe, A.H., 25-1, 25-21, 25-25
 Weidner, C.R., ix, 34-55
 Weidner, R.T., vii, 50-38
 Weijdemans, J., 46-43
 Weiler, B.E., 25-9, 25-23
 Weinaug, C.F., 20-1, 40-38, 48-14, 48-20
 Weinbrandt, R.M., xi, 46-37, 46-45, 51-51
 Weinstein, H.G., 48-16, 48-18, 48-20
 Weiss, R.F., 25-22
 Welch, L.W. Jr., 43-4, 43-16, 43-19
 Welchon, J.K., 34-1, 34-55
 Welx Inc., 49-41
 Welge, H.J., 26-24, 26-33, 40-14, 40-17, 40-38, 43-4, 43-16, 43-19, 44-7, 44-11, 44-32, 44-49, 45-14, 48-18
 Weller, W.T., 37-19, 37-22, 37-27
 Wellington, S.L., 47-24
 Wells, L.E., xi, 51-30, 51-52
 Wen, W.-Y., 25-21
 Wendorff, C.L., 55-12
 Wenzel, H., 25-16, 25-23
 West, R.C.C., 46-11, 46-43
 West, T.J., 47-24
 Westaway, M.T., 25-26
 Westaway, P., 50-38
 Wetlaufer, D.B., 25-26
 Wharton, J.B. Jr., 40-37
 Wharton, R.P., 49-41
 Wheeler, D., 44-51
 Wheeler, J.A., 48-18, 55-12
 Wheeler, M.F., 48-19
 Whinery, K.F., 12-44
 Whitaker, A.H., 52-1
 Whitaker, S., 28-16
 White, D.E., 24-1, 24-22
 White, J.E., 51-13, 51-50, 51-51
 White, J.L., 55-12
 White, P.D., 46-44
 White, P.E., 44-50
 White, V.C., 24-22
 Whiting, R.L., 24-23
 Whitsitt, N.F., 55-12
 Whitson, C.H., 39-11, 39-27, 48-19
 Whittingham, K.P., 19-34
 Whittington, H.M. Jr., 45-15
 Whorton, L.P., 45-14
 Wichert, E., vii, 20-5, 20-9, 20-15, 20-18
 Wichmann, P.A., xii, 51-52, 53-26
 Wiebe, R., 25-15, 25-17, 25-22, 25-23
 Wieland, D.R., 54-12 to 54-14
 Wiggins, W.R., 22-22
 Wijen, A.J.M., 25-25
 Wilcock, R.J., 25-23
 Wilcox, W.I., 25-5, 25-23
 Wilde, H.D. Jr., 34-37
 Wiley, C.B., 54-14
 Wiley, R., xii, 51-52
 Wilf, J., 25-21
 Wilhelm, O., 29-9
 Wilkes, J.O., 34-55
 Willard, R.O., 56-9
 Willhite, G.P., 46-6, 46-43, 47-24
 Williams, B.B., 56-9
 Williams, D., 55-11
 Williams, D.M., xii, 51-47, 51-52
 Williams, H.L., 18-1
 Williams, R.E., 44-51, 47-26
 Williams, R.L., 48-6, 48-18
 Willis, D.G., 51-44, 51-52
 Willis, M.E., 51-51
 Willits, K.L., vii, 18-52
 Willman, B.T., 46-4, 46-12, 46-43
 Willmore, C.B., 25-27
 Wilson, D.L., 18-1
 Wilson, G.M., 25-15, 25-18, 25-21, 25-24
 Wilson, J.F., 45-14
 Wilson, J.M., 54-14
 Wilson, K., 39-16, 39-28
 Wilson, P., 6-72
 Wilson, P.M., 6-28, 6-34, 6-72
 Wilson, W.W., x, 41-31, 41-37
 Winkler, H.W., v, 5-1, 5-57
 Winkler, L.W., 25-21, 25-23
 Winsauer, W.O., 26-29, 26-33, 49-4, 49-41
 Winsor, P.A., 47-11, 47-12, 47-25
 Winter, W.K., 48-18
 Witherspoon, P.A., 38-20
 Witte, M.D., 44-29, 44-34, 44-50
 Wittick, T.R., 51-52
 Wong, J.Y., 48-20
 Wong, T.C.T., 54-12
 Woo, P.T., 46-45, 48-16, 48-19, 48-20
 Wood, J.W., 41-37
 Wood, M.D., 55-12
 Wood, P.M., 12-43
 Woodard, R.G., 57-12
 Woody, L.D. Jr., 26-33, 38-20, 43-16
 Woodland, A.W., 29-9
 Woodroof, R.A. Jr., 54-14
 Woods, E.G., 36-10, 48-18, 48-20
 Woods, R.W., 37-27, 40-13, 40-38
 Woodward, P.J., 21-20
 Wooley, G.R., 31-7
 Work, L.T., 12-43
 Worley, S.M., 12-44
 Wright, F.F., 44-51
 Wright, H.T. Jr., 26-33
 Wright, J., 24-22
 Wright, J.W., 53-26
 Wrightman, L.S., 16-17
 Wroblewski, S., 25-22
 Wu, B.-J., 25-23
 Wycoff, R.D., 30-11, 30-15, 30-17, 44-14, 44-16, 44-17, 44-19 to 44-21, 44-49
 Wygal, R.J. Jr., 46-43
 Wyllic, M.R.J., xi, xii, 24-23, 26-20, 26-28, 26-30, 26-31, 26-33, 28-1, 28-8, 28-10, 28-15, 40-38, 49-41, 49-42, 51-6, 51-29, 51-47, 51-50
 Wyrick, J., 11-13
- Y**
- Yaacobi, M., 25-21, 25-24
 Yamamoto, S., 25-21
 Yanosik, J.L., 48-11, 48-19
 Yarborough, L., 20-7 to 20-9, 20-18, 23-9, 23-13, 33-18, 33-23, 45-14, 48-19
 Yashida, F., 25-24
 Yasunishi, A., 25-24
 Yeh, S.-Y., 25-22
 Yellig, W.F., 45-14
 Yen, T.F., 50-38
 Yoelin, S.D., 46-45
 Yokoyama, Y., 28-11, 28-15
 Youmans, A.H., 50-38
 Young, A., 29-9
 Young, D.M., 48-16, 48-20
 Young, E.C., 14-1
 Young, L.C., 48-18
 Young, P.J., 54-14
 Youngren, G.K., 46-12, 46-43, 48-18
 Yuster, S.T., 28-15, 39-16, 39-28, 44-29, 44-50
- Z**
- Zaba, J., 10-37
 Zana, E.T., 23-13, 45-14, 48-6, 48-19
 Zanker, K.J., 19-34
 Zapata, V.J., 47-24
 Zarrella, W.M., 24-22
 Zawisza, A., 25-22
 Zeito, G.A., 36-6, 36-10
 Zel'evskii, Y.D., 25-22
 Zemanek, J., 51-52
 Zemansky, M.W., xi, 51-50
 Zerbe, C., 25-21
 Zerpa, C., 25-25
 Zhavoronkov, N.M., 25-22
 Zheltov, Y.P., 55-2, 55-10
 Zinc Institute, vi, 11-14
 Zlomke, D., 47-26
 Zublin, J.A., 6-34, 6-72
 Zudkevitch, D., 20-7, 20-18, 48-18

Subject Index

A

- Abandonment pressure, 39-8, 39-10, 39-11, 39-14, 39-16, 39-23, 40-8, 40-10, 40-16, 40-24, 40-33, 40-34
- Abandonment time, 41-21 to 41-23, 41-27
- ABC transaction, 41-8, 57-7
- Abrasion-resistant coatings, 11-6
- Abrasive jet cleaning, 56-1
- Abrasive well fluids, 6-34
- Absolute open flow, 33-6 to 33-10, 34-33, 34-35
- Absolute ownership,
 - control, 57-2
 - definition, 57-1
 - theory, 57-1
- Absolute permeability, effect of temperature on, 46-37, 46-38
- Absolute pipe roughness, 15-4, 34-2, 34-24, 34-27
- Absolute viscosity, definition, 22-13
- Absolute zero, definition, 20-1
- Absorbed dose, unit and definition, 58-10, 58-23, 58-36
- Absorption, 26-11, 39-27
- Absorptive interactions, 50-9
- Abstract of API manual, 17-3 to 17-8
- Abstracts examination, 57-9
- Acceleration head, 6-50, 6-51
- Accelerometer, 53-4
- Accessory equipment for liquid hydrocarbon metering systems, 17-4
- Accounting method of valuation, 41-16, 41-17, 41-19, 41-22 to 41-24
- Accumulator, 18-13 to 18-15, 18-50, 18-51
- Accuracy and rounding of numbers, 58-5, 58-6
- Accuracy, of bubblepoint pressure
 - correlations, 22-8, 22-9
 - of Organick-Golding correlation, 21-15
 - vs. precision, 58-8, 58-9
- Acentric factor, 20-13
- Acetic acid (HAc), as sequestering agent, 54-7
 - in acidizing, 54-3, 54-8, 54-10
- Acetylene water system, 25-24
- Acid,
 - concentration, effect on limestone dissolved, 54-2
 - emulsions, 54-8
 - major types for acidizing, 54-1
 - primary requirements for acidizing, 54-1
 - solubility test, 54-11
 - solution of limestone in, 54-2
 - strength, estimated in field, 54-3
 - treatment design, 54-9 to 54-11
- Acid additives,
 - alcohols, 54-8
 - corrosion inhibitors, 54-6
 - gelling and fluid-loss agents, 54-8
 - iron-control agents, 54-7, 54-8
 - liquefied gases, 54-8
 - retarded acids, 54-8
 - sequestering agents, 54-7
 - silicate-control agent, 54-7
 - surfactants, 54-6, 54-7
 - thickeners, 54-8
- Acid concentration, effect on acid reaction rate, 54-5
- Acid fracturing, 54-8, 54-9
- Acid gases removal, 14-21, 14-22
- Acid-in-oil emulsion, 54-8
- Acid inhibitor, 54-10
- Acid number, 47-19, 47-23
- Acid penetration of matrix, 54-10
- Acid reaction rates, factors affecting,
 - acid concentration, 54-5
 - area/volume ratio, 54-5
 - flow velocity, 54-5
 - formation composition, 54-6
 - pressure and temperature, 54-4, 54-5
- Acid solubility, 54-6
- Acid solubility tests, 54-9
- Acid-soluble scales, 54-6, 56-2
- Acid solvent, 56-2
- Acid strength, 54-2
- Acid-swallowable synthetic polymers, 54-10
- Acid-thickening additives, 54-8
- Acid treatment design,
 - fracture acidizing—carbonate formations, 54-11
 - matrix acidizing—carbonate formations, 54-10, 54-11
 - matrix acidizing—sandstone formations, 54-11
- Acids used in acidizing, 54-1 to 54-4
- Acidizing,
 - acid reaction rates, 54-4 to 54-6
 - additives, 54-6 to 54-8
 - critical wells, 54-11, 54-12
 - general principles, 54-1 to 54-4
 - general references, 54-12 to 54-14
 - introduction, 54-1
 - laboratory testing, 54-9
 - references, 54-12
 - solutions, 54-3
 - summary, 54-12
 - techniques, 54-8, 54-9
 - treatment design, 54-9 to 54-11
 - well treatment, 6-3, 35-4, 56-3
- Acme thread profiles, 2-1, 2-38
- Acoustic array logging, 51-25
- Acoustic array sonde, 51-27, 51-28
- Acoustic backup system, 18-15, 18-16
- Acoustic beacons, 18-21
- Acoustic energy, 51-1, 51-11, 51-20, 51-24, 51-41
- Acoustic impedance, 51-46, 51-47
- Acoustic intensity, 51-3
- Acoustic log correlation, 51-30
- Acoustic log vs. core analysis porosity, 51-32
- Acoustic logging,
 - acoustic wave propagation in rocks, 51-4 to 51-11
 - acoustic wave propagation methods, 51-11 to 51-14
 - applications, 51-28
 - conclusions, 51-47, 51-48
 - elasticity, 51-1 to 51-4
 - introduction, 51-1
 - methods of recording acoustic data, 51-14 to 51-28
 - nomenclature, 51-48
 - references, 51-50 to 51-52
 - theory of elastic wave propagation in rocks, 51-49, 51-50
- Acoustic logs, 41-8, 51-30 to 51-33, 51-37, 51-38
- Acoustic positioning beacons, 18-10
- Acoustic properties of rock, 51-4, 51-5
- Acoustic signal transmission system, 18-3
- Acoustic telemetry, 53-1
- Acoustic transit (travel) time, 51-16 to 51-33, 51-35, 51-39, 51-40, 51-45, 51-47, 53-1
- Acoustic velocities, 34-45, 34-46, 51-29, 51-31, 51-43
- Acoustic velocity log, 51-5
- Acoustic wave propagation in rock,
 - acoustic properties, 51-4, 51-5, 51-43
 - borehole modeling, 51-25
 - fluid composition, 51-7, 51-8
 - introduction to, 51-4
 - porosity, 51-5
 - rock composition, 51-5
 - stress, 51-6, 51-7
 - studies, 51-34
 - summary of, 51-11
 - temperature, 51-7
 - texture, 51-8 to 51-11
 - understanding of, 51-48
- Acoustic wave propagation logging, 51-27
- Acoustic wave propagation methods,
 - in fluid-filled borehole, 51-12
 - introduction to, 51-11
 - reflection, 51-2
 - transmission, 51-2
- Acoustic wave propagation properties, 51-1
- Acoustic wave train analysis, 27-1
- Acoustic waveform, 51-12, 51-14, 51-18, 51-24, 51-26, 51-27, 51-40 to 51-43, 51-45, 51-47, 51-48
- Acoustic waves,
 - characteristics, 51-3
 - compressional, 51-2
 - information contained in, 51-18
 - shear, 51-2
 - transit time of, 51-29, 51-30
- Acoustical survey, 5-40, 49-1
- Acoustical well sounder, 30-7
- Acoustics, units and conversions, 58-36
- Acquisition and acquisition costs, 41-13, 41-15
- Acre-feet diagram, 40-4
- Acrylamide polymer, 44-39
- Activated aluminas, 14-21
- Activation energy, 46-12
- Activation gamma ray, 50-3
- Activity coefficient of water, 25-3
- Activity coefficient plot, 25-4
- Activity of radionuclide, unit and definition, 58-10, 58-23
- Actuator ratio, 3-27
- Actuator specifications, 3-27
- Ad valorem taxes, 39-27, 41-1, 41-4, 41-7, 41-9, 41-12
- Adapter, 3-9, 3-39
- Adapter flange, 3-8, 3-9, 3-13
- Adaptive implicit formulation, 48-14
- Adiabatic horsepower, 34-42, 34-44, 34-45
- Adjustable choke, 5-54, 14-3
- Adjustment factors, critical flow prover, 33-13 to 33-15
- Administration and supervision costs, 41-12
- Administrator of an estate, definition, 57-3
- Adsorption approach, statistical mechanics for, 25-5
- Adsorption cycle, 14-10
- Adsorption dehydration unit, 14-20
- Adsorption ion exchange, 48-5
- Adsorption rate of an emulsion, 19-5
- Adsorption reaction, Darcy's law, 26-11

- Advanced Ocean Drilling Program, 18-15
- Advantages, of batch-type meters, 32-10, 32-11
- of gas lift, 5-1, 5-2
- of positive-displacement meters, 32-11, 32-12
- of SI units, 58-9
- Adverse mobility ratio waterfloods, 48-11
- Adverse possession, 57-2
- Aeolian dune sandstones, 36-4
- Aerobic bacteria, 24-16, 24-17
- After breakthrough performance, 44-20 to 44-25
- Afterflow, 30-9, 30-10, 31-6
- Agglomerator, 12-12
- Agitation, in crude oil emulsions, 19-6 to 19-9, 19-12, 19-13, 19-27
- in foaming oils, 12-7
- in removing nonsolution gas, 12-13
- in separation of water from oil, 12-27
- Agitation of stored product, evaporation loss, 11-12
- Air-balanced pumping units, 10-1 to 10-3, 10-8, 10-9
- Air buoyancy, effect of, 1-70, 1-71
- effect on mass, 1-70
- Air-buoyancy risers, 18-15
- Air circuit breaker, 10-28
- Air compressors, 46-20
- Air counterbalance diagram, 10-3
- Air flotation process, 15-27
- Air injection, fireflood, 46-28, 46-29, 46-31, 46-32
- Air injection rate, fireflood, 46-19, 46-28, 46-33
- Air motor engine starters, 10-19
- Air/oil ratio, 46-17, 46-19, 46-28 to 46-30
- Air Products-Greenwich, 46-31
- Air requirements, firefloods, 46-13, 46-16, 46-19
- Air-steam injection, 46-23
- Air/steam ratio, 46-23
- Air/water ratio, 46-33
- Airy phase, 51-12, 51-13
- Alabama, 24-20, 44-36
- Alarm-signal loops, 16-9
- Alaska, 18-3, 18-38, 18-41, 18-42, 24-20, 24-21, 27-9, 27-19, 51-8, 57-11
- Alberta, characteristics of produced waters, table, 24-8, 24-12
- pilot project, 44-40
- Redwater D-3 reef reservoirs, 40-2, 40-20
- reservoirs, water-oil displacements, 48-6
- sedimentary strata in, 24-19
- Alcohols, in acidizing, 54-8
- in hydrate inhibiting, 14-6
- in phase environment shifts, 47-13
- in removing water blocks, 56-2
- Algae, 44-42, 44-44
- Algorithms, for applicability in jet pump performance, 6-46, 6-47
- for computing dipmeter plots, 53-16
- for computing relative permeability, 28-14
- for screening of micellar/polymer flooding, 48-6
- Alkaline flooding, 48-5, 48-7
- Alkaline processes, 47-1
- Alkaline water breakthrough, 44-40
- Alkalinity, 44-44
- Alkanolamine condensates, 19-10
- Allowable depletion, 41-13, 41-14
- Allowable gas velocity, 12-22
- Allowable loading, 9-4
- Allowable stress, 9-4, 9-8, 9-13, 12-38, 12-41
- Allowable working pressure, maximum, 12-40
- Allowable working pressures for piping, 15-11
- Allowables,
- discovery, 32-2, 32-3, 32-15
- history of, 41-9
- production rate, 32-1, 43-2, 43-10
- Texas rule, 32-1
- yardstick schedule, 32-3
- Allowance factor, 39-24
- All-welded screens, 56-7, 56-8
- Alpha emitter, 50-6
- Alpha radiation, 50-2
- Alternative minimum tax, 41-14, 41-15
- Alternative subsea control systems, 18-49, 18-50
- Alternating-direction iterative methods (ADI), 48-16
- Aluminum, 12-41, 24-9, 50-3, 50-4, 50-8, 50-18, 50-23, 50-34, 50-35
- Aluminum bolted tanks, 11-9
- Aluminum pellets, 55-8
- Alundum, 26-6
- Amagat's law, 20-4
- Amerada gauge temperature element, 31-1
- Amerada pressure gauges, 30-1, 30-2, 30-4, 32-6
- American Assn. of Petroleum Geologists (AAPG), 40-2
- American Gear Manufacturers' Assn., 10-12, 10-13
- American Natl. Standard Inst. (ANSI), piping pressure ratings, 15-14
- American Petroleum Inst. (API),
- API analysis of oilfield waters, 24-5, 44-43
- API barrel, 58-23
- API casing and tubing threads, 6-2
- API casing hangers, 3-29
- API circumferential displacement values, 9-9
- API committee, gamma ray calibration standards, 50-20
- API committee, standardization of steel tanks for oil storage, 11-3
- API committee, statistical study of recovery efficiency, 44-32
- API estimation of oil and gas reserves, 40-12
- API flanged or clamped wellhead equipment, adapters, 3-9
- backpressure valves, 3-8
- bottomhole test adapter, 3-13
- casing hangers, 3-5, 3-6
- casinghead and tubing-head flanges, 3-4
- Christmas-tree fittings, 3-13
- clamp-type connectors, 3-5
- crossover flange, 3-9
- flange data, 3-18 to 3-25, 3-27
- intermediate casing hangers, 3-8
- intermediate casing heads, 3-6 to 3-8
- joint gaskets, 3-28 to 3-32
- lowermost casing heads, 3-2 to 3-5
- multiple-completion equipment, 3-13 to 3-18
- physical properties, 3-2 to 3-4
- thread limitations, 3-1
- tubing hangers, 3-8, 3-9
- tubing-head adapter flange, 3-9 to 3-11
- tubing heads, 3-8
- valves, 3-11 to 3-15
- wellhead assembly, 3-2
- working and test pressure terminology, 3-1, 3-2
- working pressure ratings, 3-2
- API flanges, 3-39
- API gravity, 58-24
- API gravity, correction of observed value, 17-5, 17-6
- API gravity of crude petroleum, 17-5
- API gravity of fluid columns, 6-22, 6-23, 6-26
- API gravity of light hydrocarbons, 17-5
- API gravity of liquid petroleum products, 17-5
- API gravity scale hydrometer test method, 17-1
- API horsepower rating curves, 10-17
- API independently screwed wellhead equipment, 3-39
- API joint committee, proved reserve definition, 40-2
- API magnetic tape standard, 49-37
- API maximum working pressure ratings, casinghead and tubing-head flanges, 3-4
- flanged-end connection, 3-4
- valves, 3-11
- wellhead assembly, 3-3
- wellhead equipment, 3-3
- API Midwest Research Inst., 10-7
- API modified Goodman diagram, 9-4, 9-5, 9-8, 9-9
- API oil-water separator, 15-25
- API pin thread, 9-12
- API piping pressure rating, 15-14
- API preferred metric units, 17-7
- API pump barrel tolerance, 8-5
- API pump designation, 8-2
- API recommended practice for design calculations for sucker rod pumping systems, 8-10, 9-2, 9-3
- API Research Project 25, 31-1
- API rod grades, 9-5, 9-8
- API safety and pollution prevention equipment (SPPE), 3-39
- API scale, relative density, 1-80
- API separators, 15-23, 15-24
- API spec. for bolted production tanks, 11-1
- API spec. for pumping units, 10-4
- API spec. for reinforced plastic sucker rods, 9-11
- API spec. for shop-welded tanks for storage of production liquids, 11-1
- API spec. for sucker rods, 9-1
- API spec. for wellhead and Christmas-tree equipment, 3-36
- API std. for hydraulic pumps, 6-21
- API study on well spacing, 40-16
- API Subcommittee on Recovery Efficiency, 40-12, 40-17
- API subsurface pump bores, 8-1
- API subsurface pump classification, 8-3, 8-4
- API subsurface pumps and fittings, 8-2, 8-3, 8-6
- API sucker rod pins, 9-10
- API sucker rod pumping system design book, 9-4
- API task force on performance properties, 2-54
- API test method, 55-5
- API threading data, 2-64 to 2-72
- API torque rating, 10-5
- API unit of radioactivity, 50-15, 50-20, 50-24
- API valve rods, 8-2
- American Soc. of Mechanical Engineers (ASME),
- ASME code for unfired pressure vessels, 12-38
- ASME qualification as SPPE certificate holder, 3-39

- American Soc. for Testing Materials (ASTM).
 ASTM, API scale approved, 1-80
 ASTM, Committee D-19 standardizes methods of analyzing oilfield waters, 24-5
 ASTM distillation method, 26-22
 ASTM RVP technique, 14-13
 ASTM std. viscosity/temperature charts, 19-8
 ASTM viscosity charts, 6-67
 ASTM wood-back or corrosion-resistant metal cup case, 17-1
 American Standards Assn., valves, 3-11
 American wire gauge, 7-5
 Amine gas desulfurizer, 14-21
 Ammeter chart record, 7-6
 Ammeter spikes, 7-14
 Ammonia, 14-8, 14-9
 Ammonium fluoride, 54-4
 Amoco, 16-13, 46-14, 46-15, 46-18, 46-30, 46-33, 47-22
 Amortization, 41-5, 41-7, 41-16 to 41-18, 41-20, 41-21, 41-23, 41-24
 Amount of substance, 58-7, 58-8, 58-23, 58-27
 Amphoterics, 47-7
 Amplitude attenuation, 51-14
 Amplitude log, 51-45 to 51-48
 Amplitude/time recording, 51-18
 Anaerobic digestion, 25-18
 Analog computer, 9-2
 Analog methods for areal sweep efficiency, 44-17
 Analog model, 39-22, 44-18
 Analogies, single-phase value to multiphase equivalent, 35-2
 Analogy technique for reserve estimation, 40-1
 Analysis methods, for oilfield waters, 24-5
 for water drive reservoirs, 38-4 to 38-9
 Analysis, of a reservoir, 42-3
 of condensate liquid and gas, 21-8
 Analytic models for pump performance, 7-12
 Analytical-appraisal method for fair market value, 41-2
 Analyzing crude oil emulsions, 19-6
 Anchor line tension, 18-10
 Angle-averaging method of calculating directional surveys, 53-5
 Angles of incidence, 51-12
 Angles, SI units for, 58-5
 Angular velocities, conversion of, table, 1-76
 Anhydrite, 50-34, 50-35, 51-31
 Aniline point, 21-3 to 21-5, 21-9
 Anion exchange capacity (AEC), 52-21
 Anionic repulsion, 47-3
 Anionics, 47-7, 47-8, 47-21
 Anions, 24-9, 24-12, 24-17, 44-45
 Anions conversions, 49-4
 Anisotropy of strata, 49-5
 Annual deferment factors, 41-27, 41-30
 Annuity, tables,
 amount of, 1-63
 amounting to a given sum (sinking fund), 1-65
 present worth of an, 1-66
 provided for by a given capital, 1-66
 Annular preventers, 18-11, 18-12, 18-15
 Annular temperature, 53-2, 53-4
 Annular velocities, 52-18
 Annulus, effect on induction log, 49-17
 Antelope field, Texas, 16-12
 Anticlinal folds, 29-2
 Antisludge agents, 54-7
 Antoine equation, 20-13, 20-17
 Appalachian area, 24-1, 24-6, 24-7
 Appalachian oil fields, 44-44
 Apparent convergence pressure, 39-11
 Apparent formation resistivity factor, 26-30, 26-31
 Apparent formation thickness, 53-15, 53-16
 Apparent limestone porosity, 50-21, 50-28, 50-30
 Apparent liquid density, definition, 22-20
 of natural gases, 22-4
 Apparent mole weight, 20-14
 Apparent molecular weight of gas mixtures, 20-4
 Apparent viscosity, 47-5, 55-5
 Apparent water-filled porosity, 49-34
 Application and selection, of gas scrubbers, 12-35, 12-38
 of separators, 12-35
 Application of acoustic logging,
 cased-hole evaluation, 51-42, 51-43
 cement bond quality, 51-40
 fracture evaluation, 51-45 to 51-47
 geopressure detection, 51-39, 51-40
 hydrocarbon content, 51-35 to 51-38
 introduction to, 51-28
 lithology, 51-35
 mechanical properties, 51-43 to 51-45
 permeability, 51-47
 porosity, 51-29 to 51-35
 seismic and geological interpretation, 51-28, 51-29
 Application of metric system,
 general, 58-3
 style and usage, 58-3
 units and names to be avoided, 58-5
 usage for selected quantities, 58-3 to 58-5
 Applications, of BHP, 30-8 to 30-15
 of caliper logs, 53-17
 of dipmeter and directional data, 53-10 to 53-16
 of ESP system, 7-1, 7-2
 of fiberglass sucker rods, 9-12
 of floating production facilities, 18-34, 18-35
 of gas lift, 5-1
 of range of jet pumps, 6-46, 6-47
 of sizing of jet pump, 6-41, 6-42
 of sucker rods, steel, 9-2
 of wellhead equipment, 3-36 to 3-39
 Appraisal equations, oil and gas reserves, 41-17, 41-18
 Appraisal value: methods for computation,
 intermediate interest rate, 41-8
 safe interest rate, 41-3, 41-5, 41-6
 speculative interest rate, 41-6 to 41-8
 Approach factor, 13-2, 13-3
 Approximate methods for water drive behavior, 38-8, 38-9
 Appurtenances, 11-6
 Aquathermal pressuring, 52-22
 Aqueous phase relative permeability, 47-9
 Aqueous/volatile gas systems, 25-3
 Aquifer conductivity, 38-9
 Aquifer geometry, 38-1, 38-4, 38-5, 38-8
 Aquifer material balance, 38-8
 Aquifer permeability, 38-9
 Arabian Gulf, 18-2
 Aramid fiber, 6-50
 Archie equation, 26-31, 49-5
 Arctic,
 discovery, commercial, 18-3
 environmental conditions, 18-38 to 18-40
 production structures, 18-40 to 18-42
 special considerations, 18-43
 transportation systems, 18-42, 18-43
 Arctic Marine Hydrocarbon Production project, 18-3
 Arctic mobile drilling structure, 18-42
 Arctic Ocean, 18-38, 18-43
 Arctic oil fields, 18-43
 Arctic Pilot Project, 18-3
 Arctic pipelines, 18-43
 Arctic polar pack, 18-39
 Area equivalents, table, 1-73
 Area ratio, jet pump, 6-36 to 6-43, 6-46
 Area units, SI metric system, 58-22, 58-23
 Area/volume ratio, effect on acid reaction rate, 54-5
 Areal coverage, 44-39
 Areal coverage factor, 44-7, 44-8
 Areal cusping, 48-10
 Areal pattern efficiency, 44-5, 44-12 to 44-25
 Areal sweep, 46-14, 46-21, 46-30, 46-31
 Areal sweep efficiency, 39-15, 39-17, 39-18, 39-22, 39-23, 43-3, 43-7 to 43-9, 44-2, 44-28, 46-24, 47-2
 Areal sweep efficiency,
 at breakthrough, 44-20, 44-25
 by analog investigations, 44-17
 by mathematical analysis, 44-13 to 44-17
 by numerical models, 44-17
 directional permeability effects, 44-25
 methods of determining, 44-13 to 44-25
 mobility ratio effects, 44-17 to 44-24
 reservoir dip effect, 44-25
 reservoir fractures effect, 44-25, 44-26
 Areas of circles by eighths, table, 1-28, 1-29
 Areas of circles by hundredths, table, 1-26, 1-27
 Areas of circles, sq ft, table, 1-30
 Argentina, 51-33, 58-20
 Arithmetic average temperature, 34-8
 Arkansas, 21-4, 21-7, 24-8, 24-21, 27-2, 27-3, 46-3, 46-15, 46-24 to 46-26
 Arkose sediments, 29-7, 29-8
 Aromatic solvents, 56-2
 Arrhenius equation, 46-12
 Arrhenius reaction rate, 48-5
 Arrow plot, 53-10, 53-11
 Arsenic, in emulsion-treating chemicals, 19-10
 Arsenic inhibitors, 54-1
 Articulated loading tower, 18-30
 Articulated tower, 18-34, 18-35
 Artificial ignition devices, 46-20
 Artificial islands, 18-40
 Artificial lift, 5-1, 5-28, 6-1, 6-6, 6-7, 6-60, 6-69, 18-44, 39-16, 40-4
 Artificial lift system, 36-2
 Artificial lifting, 30-8, 30-14, 30-15
 Artificial lifting equipment, 41-3
 Artificial radiation, 50-6
 Asbestos-cement pipe, 15-7, 15-10
 Asphalt quality, 21-7
 Asphalt Ridge field, Utah, 46-16, 46-30, 46-31, 46-33, 46-34
 Asphalt seals, 29-5
 Asphaltene buildup, 46-22
 Asphaltenes, 19-10, 19-30
 Asphaltic-based oils, 19-5
 Asphaltic crudes, 6-67
 Asphaltic oils, 24-18
 Asphalts, 39-1
 Assignments by landowner, 57-6
 Assignments by lessee, 57-7
 Associated/dissolved gas, 40-3
 Associated gas, 40-3
 Asymmetrical anticlines, 29-2
 Athabasca tar sand, 46-34
 Atlantic Refining Co., 38-4

Atomic C/O density ratio, 50-2, 50-35
 Atomic densities, 50-35
 Atomic H/C ratio, 46-16
 Atomic number, 50-2, 50-3, 50-7
 Attenuation, 51-3, 51-4, 51-11, 51-12, 51-38, 51-47
 Attenuation curve, 49-34, 49-35
 Attenuation factor, 49-33, 49-34
 Attenuation rate, 49-32
 Attic oil, 43-1, 43-2
 Austin chalk, 36-1
 Australia, 12-39, 27-9, 27-19
 Austria, 12-39
 Authority for expenditure (AFE), 15-31
 Automated water jets, 19-29
 Automatic backwash, 16-14
 Automatic casing hanger, 3-6
 Automatic control, installations, 16-10
 of dry-desiccant-type gas dehydrators, 16-15
 of injection-pumping rate, 16-15
 of water-supply wells, 16-15
 valves, 16-4, 16-11, 16-12, 16-15
 Automatic controller, 13-50
 Automatic controls,
 for rod-pumped wells, 16-11
 of gas-lift well, 16-11
 Automatic custody transfer (ACT), 12-3, 16-2, 16-5, 16-6, 16-13
 Automatic cycling of desiccant beds, 16-15
 Automatic lease process control, 16-14
 Automatic positive choke, 13-57
 Automatic production-control equipment, 16-2 to 16-4
 Automatic production programmers, 16-3
 Automatic quantitative liquid measurement, 16-5
 Automatic safety shut-in system, 18-47, 18-48
 Automatic sampler, 16-7
 Automatic tank battery, 32-14
 Automatic water-treating plant, 16-14
 Automatic well manifolds, 16-11, 16-12
 Automatic well testing, 16-12
 Automatic wellhead controls, 16-10
 Automatic wellhead safety controls, 16-10
 Automatic well-testing system, 16-12
 Automatically controlled valves and accessories, 16-2, 16-3
 Automation of lease equipment,
 BS&W monitor, 16-7
 control installations, 16-10 to 16-12
 gas measurement, 16-6, 16-7
 general references, 16-16
 introduction, 16-1, 16-2
 net-oil computer, 16-7, 16-8
 production control equipment, 16-2 to 16-4
 production safety controls, 16-4, 16-5
 quantitative measurements, 16-5, 16-6
 references, 16-16
 sampler, 16-7
 supervisory control and data transfer (SCADA) systems, 16-8 to 16-10
 temperature measurement, 16-7
 well testing, 16-12 to 16-16
 Autotransformer converter, 10-35, 10-36
 Average annual ROR method, 41-17, 41-19, 41-21, 41-23, 41-24
 Average book method of valuation, 41-22
 Average deferment factor, 41-25, 41-29, 41-31
 Average GOR, 32-15
 Average reservoir pressure, 30-8, 30-9
 Average reservoir pressure, determination, 35-16
 Avogadro's number, 50-6, 50-35

Avogadro's principle, 5-11
 Axial-flow pump, 6-1, 15-15
 Axial-flow turbine meter, 13-48
 Axial load(s) or loading, 2-2, 2-20 to 2-28, 2-34, 2-35, 18-6, 18-17, 18-22, 18-24
 Axial stress, 2-3, 2-34, 2-35, 2-46, 2-55, 2-56, 9-9
 Axial stress on casing, 2-20 to 2-28, 2-32, 2-35
 Azimuth,
 of hole, 53-1, 53-2, 53-7, 53-10, 53-17
 of hole deviation, 53-10
 of reference electrode, 53-10
 Azimuth angle, 53-5, 53-6, 53-8
 Azimuth frequency diagrams, 53-12

B

Bachaquero field, Venezuela, 24-13
 Backflow, 44-35
 Backflow method, 56-5
 Backpressure controller, 13-51, 13-58
 Backpressure curve, 34-3, 34-31 to 34-34, 34-46
 Backpressure equations, 33-5, 34-30 to 34-35
 Backpressure regulation, 13-54
 Backpressure test data, 39-23
 Backpressure testing, 33-3 to 33-6, 33-10, 33-20
 Backpressure valve mandrel, 3-9
 Backpressure valves, 3-8, 3-9, 11-10, 13-56
 Backsurging method, 56-5
 Backup control systems offshore, 18-15
 Backwash cycle, 16-14
 Backwashing, 39-26, 44-43, 44-47
 Bacteria, 18-30, 44-46
 Bacteria control equipment, 24-2
 Bactericide, 44-41 to 44-44
 Baffle plates, 19-12, 19-13
 Baffling, 12-7, 12-13
 Bahama Islands, 29-8
 Balance line valve, 3-27
 Balanced tangential method of calculating directional surveys, 53-5, 53-6
 Balanced-type gas lift valves, 5-39
 Ball bearings, 13-48
 Ball joint angle, 18-17
 Ball sealers, 55-9
 Ball valve seat, 5-14, 5-15
 Ballasting systems, 18-7
 Ballooning effect of tubing string, 4-9, 4-10
 Baltic Sea, 24-19
 Bankline-Owen field, Texas, 40-33
 Barge-launched jacket, 18-25
 Barge-mounted deck, 18-23
 Barges, measurement and calibration, 17-3
 Barium, 24-9, 44-44, 44-45, 50-16 to 50-18
 Barn, definition, 50-6
 Barrier bar, 36-4
 Barrier-island sandstones, 36-4
 Bartlesville Energy Technology Center (BETC), 21-9 to 21-11
 Bartlesville sand, 44-1, 44-4
 Base conditions for natural gas fluids, 17-7
 Base of crude oil, 21-1, 21-3
 Base pressure, 32-14
 Base units, SI metric system, 1-69, 58-3, 58-9, 58-10, 58-21
 Basic data required, solution-gas-drive reservoirs,
 OIP, 37-3
 pseudorelative permeability, 37-4, 37-5
 PVT, 37-3
 relative permeability, 37-3
 saturation, initial fluid, 37-3
 Basic energy equation, 34-2, 34-9
 Basic orifice factors, 33-13
 Basic orifice flow factor, 13-3 to 13-11
 Basic sediments and water (BS&W), 16-2, 16-7, 16-13, 17-2, 19-1, 19-6, 19-10, 19-15, 19-31, 32-6, 32-7, 32-10
 BS&W monitor, 12-16
 Batch treatment method, 19-11
 Batch-type meters, 32-6, 32-9 to 32-11
 Bathymetry, 18-16, 18-39
 Batturum No. 1 field, Saskatchewan, 46-4
 Baumé scale, relative density, 1-80
 Bauxite, sintered particles, 55-8
 Bay Marchand field, Louisiana, 44-37, 44-38
 Beal's correlation for dead-oil viscosity, 22-14
 Beam-balanced pumping units, 10-1 to 10-3
 Beam-type pumping unit, 10-16, 10-23
 Bean, 34-45
 Bearings in turbine meters, 13-48
 Bed detection and definition of well logs, 49-25 to 49-36
 Bed thickness, effect on acoustic velocity logging device, 51-16
 Beggs and Brill correlation, 46-7
 Beggs and Robinson correlation, 22-15, 22-16
 Behavior index, 55-5
 Bell Creek MP flood, Montana, 47-16
 Bellamy field, Missouri, 46-3
 Bellevue field, Louisiana, 46-4, 46-15, 46-18, 46-19, 46-34
 Bellows-assembly load rate, 5-16, 5-17, 5-37
 Bellows BHP element, 30-1, 30-6, 30-7
 Bellows-charge pressure, 5-16, 5-17, 5-33
 Bellows-charged dome pressure, 5-3, 5-6, 5-7, 5-18, 5-19, 5-46, 5-49
 Bellows-charged gas lift valves, 5-6, 5-12, 5-16, 5-17, 5-20, 5-21, 5-23, 5-37, 5-39, 5-42
 Bellows guide tube, 5-12
 Bellows meter, 13-36, 13-37
 Bellows PD meter, 32-12
 Bellows protection, 5-16
 Bellows-type chart recorder, 16-6
 Bending failure, 18-39
 Bending load fracture strength of casing, 2-61
 Bending moment, SI unit for, 58-5, 58-34
 Bending stress, 18-13, 18-17
 Benedict-Webb-Rubin EOS, 20-7
 Benzene, 24-4, 24-18
 Berea cores, 47-8
 Berea sandstone, 28-8, 28-9, 28-11, 51-6, 51-8
 Bering Sea, 18-42
 Berl saddles, 12-10
 Bernoulli's theorem, 15-1, 15-2
 Beryllium, 50-6
 Bessel factor, 1-61
 Beta radiation, 50-2
 Bid shopping, 15-31
 Bimetallic corrosion, 3-36
 Binary liquid/vapor system, 23-3
 Binary phase diagrams, 23-2 to 23-6
 Binomial coefficients, table, 1-37
 Binomial distribution, 50-5
 Biocides, 47-5, 47-10
 Biofouling, 18-51
 Biogenesis, 25-18
 Bioherm reefs, 36-5, 36-6
 Bioherms, 29-4, 29-8
 Biological degradation, 47-5
 Biological surveys, 18-5
 Biopolymers, 47-4
 Biostrome reefs, 36-5, 36-6

- Biostromes, 29-4, 29-8
 Biot theory, 51-8
 Birdwell, 51-18, 51-27
 Bi-rotor PD meter, 32-11, 32-12
 Bit guide, 3-6 to 3-8
 Bittern, 24-20
 Bitumen, 19-30, 46-31
 Black iron sulfide scale, 9-8
 Black-oil material balance, 37-25, 37-26
 Black-oil model, 48-4 to 48-7, 48-9, 48-14
 Black-oil reservoirs, 48-2, 48-8
 Black-oil rings, 39-5, 39-22
 Black-oil simulator, 36-10, 45-13
 Black oils, 37-22, 37-23, 37-25, 37-26, 39-17, 39-26, 40-13
 Black Sea, 24-19
 Blank runs, 26-21
 Blanking tool, 6-48
 Bleed-type sensors, 3-34
 Blender jar, 52-9, 52-10
 Blenders, 55-9
 Blind and test flanges, 3-25
 Blind-shear ram, 18-11, 18-20
 Blind zone on lateral curves, 49-13, 49-14
 Block-and-bleed-type sensors, 3-34
 Block diagram, 15-30, 51-28
 Blocking agent, 56-1
 Blocking fluids, 56-2
 Bloomer field, Kansas, 16-12
 Blotter model, 39-21, 44-17
 Blowdowns, 11-6
 Blowout, 18-11, 56-3
 Blowout preventer (BOP), 3-2, 3-6, 3-9, 3-38, 3-39, 7-13, 18-4, 18-6, 18-9, 18-11 to 18-21, 18-34
 Blowout preventers,
 annular, 18-11, 18-12
 hydraulic connectors, 18-12
 kill and choke (K&C) valves, 18-12
 ram, 18-11
 unitized stack, 18-12
 Blowout preventer stack, 18-11 to 18-19, 18-31, 18-34
 Bluff body, 16-6
 Boberg and Lantz method, 46-9
 Boberg and West correlation, 46-11
 Bodcau field, Louisiana, 46-21
 Boiling point,
 cubic average, 21-12, 21-15
 definition of types of, 21-11, 21-12
 mean average, 21-11, 21-15
 molal average, 21-6, 21-11, 21-13 to 21-15, 21-17
 molar distribution of SCN groups, 39-11
 of hydrocarbons, 19-7
 of six refrigerants, 14-10
 volumetric average, 21-11, 21-12
 vs. K-value, 39-12
 Boise sandstone, 51-8, 51-9
 Boll-weevil casing hanger, 3-6
 Boll-weevil tubing hanger, 3-9
 Bolted steel tanks, 11-1 to 11-3, 11-6, 11-9, 11-11
 Bonding conditions, cement, 51-40 to 51-42
 Bonus, oil and gas lease, 57-4, 57-7
 Booster application, ESP, 7-2, 7-3
 Booster pump, 15-17, 44-47
 Borehole acoustic measurements, 51-28, 51-29, 51-44, 51-45, 51-47, 51-48
 Borehole-compensated (BHC) acoustic log, 51-15
 Borehole-compensated device, 50-15
 Borehole-compensated sonde, 51-15
 Borehole-compensated sonic log, 49-15, 51-16, 51-17, 51-24, 51-26, 51-30, 51-32, 51-37
 Borehole-compensated sonic tool, 49-32
 Borehole-compensated sonic travel time, 51-22
 Borehole-compensated transit time, 51-21
 Borehole configuration, 53-16, 53-17
 Borehole corrections, IL, 49-18
 Borehole, fluid-filled, acoustic wave propagation in, 51-12 to 51-14
 Borehole geometry, 51-19, 51-28
 Borehole geometry log, 53-17
 Borehole geophysical devices, 58-25
 Borehole measurement of transit times, 51-26
 Borehole reflection method, 51-46
 Borehole size effects, 51-19
 Borehole televiewer, 51-27 to 51-29, 51-41, 51-46, 53-17
 Borehole televiewer log, 51-46 to 51-48
 Boron, 24-4, 24-5, 24-12, 50-6, 50-11, 50-12, 50-14, 50-32, 50-36
 Borosilicate glass, 24-4
 Boscan field, Venezuela, 6-24, 10-18
 Bottle tests, 19-10, 19-15
 Bottom discharge application, ESP, 7-2, 7-3
 Bottom gas lift valve, selecting, 5-26
 Bottom intake application, ESP, 7-2, 7-3
 Bottom-seating holddown, 8-3
 Bottom-seating stationary-barrel rod pumps, 8-8
 Bottom-unloading gas lift valve, 5-51
 Bottomhole assembly (BHA), 6-3 to 6-6, 6-31, 6-39
 Bottomhole bumper spring, 5-52, 5-53
 Bottomhole collar lock, 5-52
 Bottomhole GOR, 37-23, 37-24
 Bottomhole pressure (BHP):
 gas wells, 34-3 to 34-27
 gas-condensate wells, 34-27, 34-28
 gas injection wells, 34-28 to 34-30
 liquid injection wells, 34-28
 Bottomhole pressure buildup analysis, 40-27
 Bottomhole pressure calculations,
 by Cullender-Smith method, 34-25, 34-26
 by Sukkar-Cornell method, 34-9 to 34-24
 flowing gas wells, 34-23, 34-24
 gas-condensate wells, 34-27
 static gas well, 34-8, 34-9
 Bottomhole pressure gauge, 31-1
 Bottomhole pressure instruments, 30-1 to 30-6, 30-15
 Bottomhole pressure, steamflood, 46-17
 Bottomhole pressures, 30-1 to 30-15
 Bottomhole test adapter, 3-13
 Bottomhole valve temperature, 5-46
 Bottom-water, 24-2
 Bottomwater drive, 40-15, 41-10, 48-4
 Bounded reservoirs, shape factors, 35-5
 Bounding additive, 46-19
 Bourdon tube, 13-38, 13-56, 16-4, 16-7, 30-1, 30-2, 30-4, 30-6, 30-7, 31-1
 Box and pin entrance threads, extreme-line casing joint, 2-64, 2-69, 2-70
 Box and pin subcoupling, 9-4
 Boyle's law, 20-1, 20-2, 26-6, 26-7, 27-1, 30-8
 Boyle's-law-type porosimeter, 26-4, 26-6
 Bradford field, Pennsylvania, 24-1, 24-2, 44-1, 44-4, 47-22
 Brake horsepower, 10-9, 10-17, 10-19
 Brazil, 12-2, 12-21, 46-3, 46-4, 58-20
 Brea field, California, 46-16, 46-18, 46-24, 46-25
 Brea-Olinda field, California, 46-15, 47-22
 Breakdown pressures, 44-3, 44-46, 56-1
 Breakthrough of free gas, 40-10
 Breakthrough of gas, 40-14
 Breakthrough of inert gas, 39-17
 Breakthrough of polymer, 44-40
 Breakthrough of water, 40-18, 40-19, 44-4, 44-7, 44-9, 44-11, 44-12, 44-14, 44-15, 44-34
 Breakthrough sweep efficiency, 44-15, 44-16, 44-25
 Breast mooring system, 18-2
 Breathing losses in tanks, 11-12, 11-13
 Breccia, 29-8
 Bridge plugs, 55-9
 Bridging in flow channels, 54-11
 Brightness of emulsions, 19-5
 Brine displacement of product method of solution mining, 11-13, 11-14
 Brine/oil ratios, 47-14
 Brine salinity, 47-3 to 47-5, 47-10, 47-11, 47-13, 47-21
 Brinnell hardness, 2-2, 2-37, 9-5
 British Commonwealth countries, 1-69
 British imperial gallon, 1-69, 1-70
 British system of weights and measures, 1-69, 1-70
 Bromide, 19-10, 24-9, 24-12, 24-18, 24-20
 Bromine, 24-5, 24-20, 24-21
 Brownscombe-Collins method of water-drive predictions, 38-9
 Bubble flow, 34-36 to 34-39
 Bubble Reynolds number, 34-38, 34-39
 Bubble rise coefficient, 34-38, 34-39
 Bubble rise velocity, 34-38, 34-39
 Bubble size range of foams, 47-8
 Bubblepoint curve, 20-2
 Bubblepoint equation, constants for, 22-8
 Bubblepoint liquid, definition, 22-21
 Bubblepoint of a system, definition, 22-20
 Bubblepoint of crude, 6-21
 Bubblepoint pressure, 6-39, 22-1, 22-5 to 22-9, 22-11, 22-12, 22-21, 23-3, 23-11, 24-12, 24-14, 24-15, 34-31, 34-33, 34-34, 35-2, 37-1, 37-3, 37-5, 37-6, 37-8 to 37-10, 37-15, 37-22, 39-6, 40-6, 40-7, 40-10 to 40-13, 40-19, 44-5
 Bubblepoint pressure correlations,
 accuracy, 22-8
 empirical, 21-9, 21-10
 Lasater, 22-5 to 22-7
 Standing, 22-5
 Vasquez and Beggs, 22-7, 22-8
 Bubblepoint pressure factor, 22-7
 Bubblepoint viscosity, 22-16
 Buckley-Leverett calculations, 48-1
 Buckley-Leverett equation, 28-3
 Buckley-Leverett frontal-drive method, 40-13
 Buckling,
 of ice, 18-39
 of pipe, 18-37
 of tubing string, 4-9, 4-10
 Buildup curve, 30-9 to 30-13, 30-15
 Buildup test, 35-4, 35-14 to 35-16, 35-19
 Bulk density, 50-1 to 50-4, 50-7, 50-8, 50-17, 50-26 to 50-28, 50-30, 50-33, 51-14, 51-37
 Bulk modulus, 6-55, 51-1, 51-2, 51-4, 51-14, 51-43, 51-44, 51-49
 Bulk pore compressibilities, 51-43
 Bulk volume (BV), 26-1 to 26-7, 26-22, 27-1, 37-11
 Bumper subs, 18-13, 18-14, 18-18
 Bundle of capillary tubes model, 28-12
 Buoyancy effect, 2-2, 13-51, 18-2, 18-15 to 18-17, 18-24, 18-25, 18-29, 18-37, 18-49, 24-2
 Buoyancy, effect on water-drive recovery, 40-20
 Buoyancy method of gravity measurements, 52-19, 52-20
 Burbank unit, Oklahoma, 44-41

Bureau of Land Management, 57-12
 Buried bar with shale drape, 53-12, 53-13
 Burners for emulsion-treating equipment, 19-28
 Butane as IC engine fuel, 10-16
 Butterfly charts, 49-28
 Butterfly diagram, 24-19
 Butterfly valve, 13-58
 Buttress-thread casing and coupling, 2-1, 2-5, 2-7, 2-9, 2-11, 2-13, 2-15, 2-17, 2-19, 2-29 to 2-31, 2-57 to 2-61, 2-63, 2-64
 Buttress thread profile, 2-38
 Bypass valve, 13-59

C

Cabimas field, Venezuela, 24-13
 Cable junction box, 7-13
 Cable-tool cores, 26-20, 26-21
 Cable tray, 18-46
 Cabled transmission system, 17-4
 Cabling systems for SCADA, 16-9
 Caddo Lake field, Louisiana, 18-1
 Cadiz, 58-20
 Cadmium, 50-15
 Caisson-retained production island, 18-40
 Caisson units, 18-41
 CAL wellsite analysis, 49-37
 Calcinometer, 52-9, 52-21
 Calcite, 19-5, 51-5, 51-6
 Calcium acetate, 54-3
 Calcium aluminate cement, 46-19
 Calcium carbide lag tests, 52-11
 Calcium carbonate, 19-4, 24-2, 44-44, 44-45
 Calcium chloride, 8-9, 54-2
 Calcium citrate precipitation, 54-7
 Calcium fluorides, 54-4, 56-5
 Calcium formate, 54-3
 Calcium magnesium carbonate, 54-2
 Calcium scale, 44-44
 Calcium sulfate, 44-44, 44-45
 Calculated bottomhole pressure, 30-7, 30-8
 Calculation methods, directional surveys, 53-5 to 53-7
 Calculation of relative permeability, automated centrifuge technique, 28-7
 Institut Français du Pétrole method, 28-7
 Calculation procedure, Jacoby and Berry method, 37-23 to 37-26
 Calculation sequence and supplemental equations, jet pump, power-fluid flow through nozzle, 6-42
 programming considerations, 6-46
 pump performance and return flow, 6-42, 6-43, 6-46
 sizing considerations, 6-46
 worksheets, 6-44, 6-45
 Calculations for sizing prime movers, 10-17 to 10-19
 Calculations for sucker rods, 9-2 to 9-4
 Calculations: see also example problems
 Calculator programs, for HP-41C, 22-17
 Calibrate tails, 49-18
 Calibration, of barges, 17-3
 of bellows meter, 13-36
 of bottomhole gauges, 30-2, 30-3, 30-5
 of capacity standard, 1-71
 of conventional acoustic logs, 51-17
 of dipmeter tool, 53-8
 of gas measurement equipment, 13-1
 of horizontal tanks, 17-3
 of induction log, 49-18
 of spheres and spheroids, 17-3
 of standard of mass, 1-70

of tank cars, 17-3
 of tanks, liquid method, 17-3
 of upright cylindrical tanks, 17-3
 standards, 50-20, 50-29
 California, 6-5, 6-24, 6-59, 17-2, 18-1 to 18-3, 19-2, 19-5, 21-2, 21-4, 21-7, 24-7, 24-8, 24-20, 26-19, 26-23, 26-30, 27-4, 27-5, 29-2, 29-8, 34-41, 34-45, 40-15, 40-22, 40-23, 41-5, 44-37, 44-39, 44-40, 46-3, 46-4, 46-14 to 46-16, 46-18, 46-19, 46-22 to 46-25, 46-35, 47-22, 58-20
 California condensate systems, 21-12
 California oil systems, 22-5
 Califormium, 50-35
 Calingart and Davis equation, 20-13, 20-17
 Caliper curve and surveys, 49-1, 49-34, 49-35, 49-38, 49-39
 Caliper log, 51-16, 51-19, 51-23, 51-24, 51-26, 51-33, 51-38, 51-45, 51-46
 Caliper logs, borehole configuration, 53-16, 53-17
 for casing and tubing inspection, 53-17, 53-18
 interpretation and application, 53-17
 introduction, 53-1, 53-16
 methods of recording, 53-16
 types, 53-16 to 53-18
 Calorific value, 58-28
 Caltex, 46-4
 Calvin field, Illinois, 40-33
 Canada, 1-70, 12-10, 12-39, 18-2, 18-3, 18-38, 18-39, 19-2, 24-6, 24-8, 24-11, 24-19, 24-20, 27-9, 27-20, 33-5, 44-40, 46-3, 46-4, 46-18, 46-21, 51-1, 52-12, 58-22
 Canadian Arctic Islands, 18-3
 Canadian Beaufort Sea, 18-3
 Cap rock, 29-6, 29-7
 Capacitance kilovars, 10-35
 Capacitance of a process, 13-50
 Capacitance probes, 16-2, 16-7, 16-8, 16-12, 19-31
 Capacities of orifice well testers, 13-38 to 13-44
 Capacities of separators, 12-21 to 12-25
 Capacities of spherical separators, 12-30 to 12-32
 Capacitive reactance, 10-34
 Capacitive transducer, 30-5, 30-6
 Capacitor converter, 10-35
 Capacitors, 10-25, 10-32 to 10-35
 Capacity curves for separators, 12-27 to 12-32
 Capacity distribution, 45-10, 45-12
 Capacity-distribution curve, 44-8
 Capacity equivalents, table, 1-73
 Capacity, of a process, 13-51
 of API bolted steel tanks, 11-3
 of API shop-welded tanks, 11-5
 of equipment, 58-25, 58-30, 58-31
 venting requirement, 11-7
 Capacity, standard of, 1-71
 Capillary desaturation curve (CDC), 47-9, 47-10
 Capillary discontinuity, 28-3
 Capillary forces, 37-11, 44-31, 46-13, 47-9
 Capillary imbibition, 48-4
 Capillary number, 47-9, 47-17
 Capillary pressure, as threshold pressure, 28-6
 averaging of data, 26-25 to 26-27
 converting to reservoir conditions, 26-25
 curves, 26-24, 26-26, 28-5
 definition, 26-23, 26-27, 28-3
 effect on unit displacement efficiency, 43-6
 end effect, 28-7
 forces, 22-16, 22-17, 40-14
 gradient, 40-17, 44-10
 laboratory measurements, 26-24 to 26-27
 relative permeability calculation based on, 28-8
 saturation data, 26-26
 standards, 58-38
 tests, 44-4
 water saturation from, 26-22, 26-25, 27-8, 44-6
 Capillary tube concepts, 47-5
 Capillary tubes, bundle of, 26-10, 26-20
 Capillary tubes for flow network, 26-19, 26-20
 Capital expenditure, 57-11
 Capital gains, definition, 57-11
 Capital to drill a well, 57-8
 Capture cross section, 50-11, 50-22
 Capture gamma rays, 50-3, 50-4, 50-22
 Carbon dioxide (CO₂), 3-35 to 3-37, 4-4, 4-5, 6-4, 6-62, 8-9, 9-5, 9-8, 9-9, 10-16, 12-3, 12-8, 14-3, 14-13, 14-17, 14-20 to 14-22, 15-29, 19-29, 19-31, 20-5, 20-6, 22-5, 22-17, 23-7, 23-12, 23-13, 24-4, 24-5, 24-16, 24-17, 26-18, 28-10, 37-24, 39-2, 39-5, 39-6, 39-14, 39-16, 40-22, 42-2, 43-2, 44-42, 44-43, 45-1, 45-4 to 45-6, 45-9, 46-12, 46-22, 46-28, 48-5 to 48-11, 52-4 to 52-7, 52-9 to 52-11, 52-13, 52-16
 CO₂ analyzer, 19-28
 CO₂ content, 25-5, 25-8, 25-13 to 25-15, 25-20
 CO₂/crude oil systems, 23-10
 CO₂/decane system, 23-9
 CO₂ floods, 19-28
 CO₂ in acidizing, 54-8 to 54-10
 CO₂ injection, 48-2, 48-7, 48-8
 CO₂/methane/decane system, 23-13
 CO₂/propane system, 23-9
 CO₂/C₄/C₁₀ system, 23-9
 CO₂ density required for miscible displacement, 45-6
 CO₂ miscible process, 45-5, 45-6
 CO₂/water system, 25-3, 25-14, 25-15
 Carbon/oxygen ratio: see C/O ratio
 Carbon steel pipe, 11-2, 15-10, 15-12
 Carbon steel, properties of materials, 12-41
 Carbon-to-hydrogen ratio, 21-3, 21-5
 Carbonate banks or shoals, 36-5, 36-6
 Carbonate reservoirs, bioherm reefs, 36-5
 biostrome reefs, 36-5
 nearshelf deposits, 36-6
 shelf carbonates, 36-6
 steamflood, 46-27
 types, 29-8
 Carbonate rocks, laboratory measurement of porosity, 26-6, 26-7
 Carbonic acid, 9-8
 Carbonylsulfide (COS), 14-22
 Carboxymethylhydroxyethyl cellulose (CMHEC), 47-3
 Carnot cycle, 14-10
 Carr-Kobayashi-Burrows method for natural gas viscosity, 20-9, 20-10, 20-15, 20-16
 Carried interest, 41-1, 41-2, 57-10
 Carrier fluid, 56-8
 Carthage field, Texas, 39-3
 Cartography, 58-5
 Cartridge filters, 15-20, 44-47
 Carved-out production payment, 41-1
 Case cup thermometer, 17-1
 Case histories of gravity drainage, Lakeview pool, 40-15
 Oklahoma City Wilcox reservoir, 40-15

- Case histories, thermal recovery.
- Fireflood projects,
 - Asphalt Ridge, 46-30, 46-31, 46-33, 46-34
 - combination reverse/forward combustion, 46-30, 46-31, 46-33, 46-34
 - deepest, 46-28 to 46-30
 - Forest Hill, 46-31, 46-34
 - Gloriana, 46-29 to 46-32
 - largest, 46-28, 46-29
 - oxygen-enriched air, 46-31, 46-34
 - Sloss, 46-30, 46-33
 - Suplacu de Barcau, 46-15, 46-28, 46-29
 - thinnest producing reservoir, 46-29 to 46-31
 - West Heidelberg, 46-28 to 46-30
 - wet combustion, tertiary recovery, 46-30, 46-33
 - Steamflood projects,
 - Brea, 46-24, 46-25
 - carbonate reservoir, 46-27 to 46-29
 - distillation drive, 46-24, 46-25
 - fracture-assisted, 46-26 to 46-28
 - gas-cap reservoir, 46-24 to 46-26
 - Kern River, 46-23, 46-24
 - Lacq Supérieur, 46-27 to 46-29
 - largest, 46-23, 46-24
 - Slocum, 46-26, 46-27
 - Smackover, 46-24 to 46-26
 - Street Ranch, 46-26 to 46-28
 - watersand reservoir, 46-26, 46-27
- Cased-hole completions, 56-9
- Cased-hole evaluation, 51-42, 51-43
- Cased-hole logging, 50-1
- Cash contributions to drilling well, 57-9
- Cash flow, multiwell template effect on, 18-32
- Cash-flow projection preparation, 41-3, 41-4
- Casing anchor, 8-9
- Casing and tubing inspection by caliper logs, 53-17, 53-18
- Casing and tubing leaks, 33-21, 33-22
- Casing,
 - API liners, 2-1, 2-2
 - API types, 2-1
 - axial stress on, 2-20 to 2-28, 2-32, 2-35
 - centralizers, location of, 53-17
 - collapse, 53-18, 56-3
 - collapse pressure, 2-1 to 2-3, 2-20 to 2-28, 2-32, 2-34, 2-35, 2-46, 2-55, 2-56, 18-20
 - collapse pressure under axial-tension stress, 2-55
 - collapse resistance, 2-1 to 2-4, 2-6, 2-8, 2-10, 2-12, 2-14, 2-16, 2-18, 2-29, 2-32, 2-46, 2-55, 2-56
 - collapse resistance under axial load, 2-20 to 2-28, 2-34, 2-35
 - collar-locator log, 53-26
 - combination strings, 2-2 to 2-4
 - design of strings, 2-1, 2-2
 - dimensions, 2-28, 2-29, 2-57 to 2-59, 2-63, 2-64, 2-66
 - elongation, 2-2
 - equations for calculating performance properties, 2-46, 2-54 to 2-56
 - extreme-line, 2-1, 2-4, 2-6, 2-8, 2-10, 2-12, 2-14, 2-16, 2-18, 2-29 to 2-31, 2-62 to 2-64, 2-67, 2-68
 - extreme-line joint, 2-5, 2-7, 2-9, 2-11, 2-13, 2-15, 2-17, 2-19, 2-60, 2-63, 2-67 to 2-72
 - flow (annular) installation design, 5-37, 5-38
 - gross linear footage from net footage, 2-29, 2-31
 - hanger, 3-5, 3-6, 3-8, 3-11, 3-37, 33-39
 - hanger bowl, 3-2, 3-6, 3-8
 - hanger-seal assembly, 18-20
 - injection-gas pressure, 5-54
 - internal pressure leak resistance, 2-5, 2-7, 2-9, 2-11, 2-13, 2-15, 2-17, 2-19, 2-57 to 2-59, 2-64
 - internal pressure resistance, 2-5, 2-7, 2-9, 2-11, 2-13, 2-15, 2-17, 2-19
 - joint strength, 2-2, 2-5, 2-7, 2-9, 2-11, 2-13, 2-15, 2-17, 2-19, 2-60, 2-61
 - leak, 31-5, 31-6
 - long thread, 2-5, 2-7, 2-9, 2-11, 2-13, 2-15, 2-17, 2-19, 2-31, 2-58, 2-64
 - minimum-ID calipers, 53-18, 53-19
 - multiplication factor, 2-29, 2-31
 - non-API steel grade, 2-5, 2-7, 2-9, 2-11, 2-13, 2-15, 2-17, 2-19
 - non-API weight and grades, 2-4, 2-6, 2-8, 2-10
 - performance properties, 2-4 to 2-19
 - plain-end liner, 2-32
 - potential profile, 53-20
 - profile calipers, 53-18, 53-19
 - range lengths, 2-3
 - round-thread, 2-1, 2-5, 2-7, 2-9, 2-11, 2-13, 2-15, 2-17, 2-19, 2-28, 2-30, 2-57, 2-58, 2-61, 2-64
 - round-thread height dimensions, 2-66
 - safety factors, 2-1 to 2-3, 2-34, 2-35
 - short-thread, 2-5, 2-7, 2-9, 2-11, 2-13, 2-15, 2-17, 2-19, 2-29, 2-57, 2-64
 - single-weight string suspended in rotary mud, 2-37
 - sizes, F , values for, 34-25
 - special joints, 2-1
 - stress in, 2-36
 - stretch in, 2-35 to 2-37
 - tensile strength, 2-2
 - threads, 3-2
 - tolerance, 2-28, 2-29
 - travel time, 51-41
 - weight, 2-28, 2-29
 - with helical strokes, 18-21
 - yield strength, 2-2
- Casing heads, 3-2 to 3-6, 3-8, 3-11, 3-13, 3-37, 3-39
- Casing inspection logs,
 - caliper logs for, 53-17
 - electrical potential logs, 53-19
 - electromagnetic devices, 53-19, 53-20
 - introduction, 53-1, 53-17
- Casing/tubing annulus, 3-8
- Casinghead bowl, 3-5 to 3-7
- Casinghead flange, 3-5, 3-6, 3-8
- Casinghead gas, definition, 40-3, 57-5
- Cast-iron pipe, 15-10
- Cat Canyon field, California, 46-34
- Catalyst poisoning, 56-2
- Catalyst selection, guidelines, 15-30
- Catalysts, 24-5
- Catalytic combustion detector (CCD), 52-3 to 52-5, 52-11
- Catalytic converters, 15-16
- Catalytic ignition systems, 46-20
- Catenary mooring configuration, 18-10, 18-16
- Cathodic protection, 3-36, 11-6, 15-10, 18-29, 18-33, 18-34, 53-19, 53-20
- Cation exchange, 24-20, 47-20, 47-21
- Cation exchange capacity (CEC), 50-15, 52-21
- Cationics, 47-7
- Cations, 24-9, 24-19, 44-45
- Cations conversions, 49-4
- Caustic flooding, 19-28, 44-40, 48-5, 48-7
- Caustic soda, 14-22
- Cavern storage application, ESP, 7-1, 7-2
- Cavings, 33-21
- Cavitation, 6-32 to 6-36, 6-41 to 6-43, 6-45, 6-46, 6-50, 6-60
- Cavitation area, 6-37
- Cavitation correction, 6-38
- Cavity pumps, 19-5
- Cellophane diaphragm, 26-24
- Cellulose derivative thickener, 55-5, 55-6
- Celsius scale, 58-5, 58-39
- Celsius temperature, unit and definition, 58-7, 58-10
- Cement bond, 35-4, 56-4
- Cement bond logging, 51-40
- Cement bond quality;
 - bond to casing and to high velocity formation, 51-40, 51-41
 - bonding conditions summary, 51-42
 - free pipe, 51-40
 - good bond to casing and formation, 51-40
 - partial bonding, 51-41
- Cement evaluation log, 51-42
- Cement Evaluation Tool, 51-41
- Cement lining for steel pipe, 15-10
- Cement sheath, 51-40, 51-41
- Cement slurry, 56-4
- Cementation, 26-2, 40-8, 40-11, 55-1
- Cementation factor, 26-29
- Central America, 25-18, 58-20
- Central battery systems, 6-60, 6-62, 32-7
- Centralized control room, 18-46
- Centrifugal compressor, 14-8
- Centrifugal compressor efficiencies, 14-9
- Centrifugal force, 6-63, 12-7, 12-8, 12-10, 12-13, 12-14, 12-19, 12-20, 13-45, 14-3, 19-6, 19-15
- Centrifugal gas scrubbers, 12-20, 12-21
- Centrifugal (elbow) meters, 13-45, 13-49
- Centrifugal pump, 6-1, 6-34, 6-49, 6-51, 6-62, 7-2, 7-3, 15-15, 15-17, 19-5, 44-42, 44-47
- Centrifugal separator, 12-20
- Centrifuge extraction method, 26-22
- Centrifuge method for determining water and sediment in oil, 17-1, 17-5
- Centrifuge method of capillary pressure measurement, 26-24, 26-25
- Centrifuge technique for determining relative permeability, 28-7, 28-11, 28-12
- Centrifuges, 15-20, 19-6, 26-22
- Centripetal flow, 12-20
- Cerveza platform, 18-2, 18-23
- Chain drives, 10-12
- Chain rule for derivatives, 37-13
- Chaining, 19-13
- Chamber installations, gas lift, 5-19, 5-50 to 5-52
- Chamber length equation, 5-51, 5-52
- Chamber operating gas lift valves, 5-51
- Channel cut and fill, 53-12, 53-13
- Channeling, in acidizing, 54-8, 54-10
- in cement bonding, 51-41
 - in emulsion treater, 19-23
 - in glass wool packing, 19-14
 - of injection water, 44-3
- Channels, permeability of, 26-15, 26-16
- Chanslor-Western Oil and Development Co., 46-15, 46-19
- Chapel Hill field, Texas, 39-3, 39-20 to 39-22
- Characteristics of well fluids, 12-3, 12-21
- Characterization factor, 21-3 to 21-11, 21-13, 21-14, 21-21, 39-11
- Characterization of the reservoir,
 - engineering, 36-6 to 36-8
 - geology, 36-3 to 36-6
 - geophysics, 36-8, 36-9

- Charge pump, 6-62
 Charged particle accelerators, 50-6
 Charles' law, 20-1, 20-2
 Charpy impact values, 18-21
 Charpy tests, 12-41
 Charpy V-notch impact requirements, 3-38
 Chart Rcor-1, 49-21
 Chart Rcor-2, 49-21, 49-24
 Chart Rcor-4, 49-18
 Charts used in BHP gauges, 30-2
 Chase water, 47-2, 47-11
 Chatter condition, 5-16
 Cheater bars, 9-10
 Checklist, deck and subsea BOP testing, 18-12
 Chelating agents, 44-45
 Chemical absorption, 48-2
 Chemical alteration of formation, 51-20
 Chemical analyses, interpretation of, 24-18
 Chemical analyses of produced waters, 24-2
 Chemical analysis, 21-1, 21-2
 Chemical and mechanical properties of plastic sucker rods, 9-11
 Chemical corrosion inhibitor, 8-9
 Chemical degradation, 47-5, 47-22, 48-2
 Chemical demulsifiers, 19-9 to 19-12, 19-32
 Chemical destabilization, 19-7, 19-8
 Chemical diffusion, 28-13
 Chemical distributor for flowlines, 19-11
 Chemical flood model, 48-4, 48-5, 48-7
 Chemical flooding, chemical agent numerical dispersion, 48-10
 high-pH processes, 47-18 to 47-22
 improved (enhanced) recovery, 40-4, 48-2
 introduction, 47-1
 low-IFT processes, 47-9 to 47-18
 mobility control processes, 47-1 to 47-9
 production, 46-3
 references, 47-24 to 47-26
 summary, 47-22, 47-23
 Chemical inhibitors, 3-35, 6-55, 44-42
 Chemical injection valves, 3-35
 Chemical kinetics, 46-12, 46-13, 46-37
 Chemical potential, 25-6, 25-9
 Chemical potential sink, 47-15
 Chemical properties of oilfield waters, 24-5
 Chemical reaction kinetics, 46-11, 46-12
 Chemical reservoirs, 29-6, 29-8
 Chemical scavengers, 15-29
 Chemical stain kit, 52-9
 Chemical stoichiometry, 46-12
 Chemicals in oil and gas separation, 12-7, 12-13
 Chevron, 46-14, 46-15, 46-18, 47-22
 Chevron Oil Field Research Co., 51-49
 Chevron packing, 18-15
 Chew and Connally method, 22-14, 22-15
 Chile, 58-20
 Chiller, 14-8 to 14-10
 China, People's Republic of, 12-39
 Chloride stress cracking, 3-35, 3-36
 Chloride test, 27-1
 Chlorides, 24-9, 24-18, 44-44
 Chlorine, 44-43, 46-20, 50-3, 50-4, 50-11, 50-12, 50-18, 50-21, 50-34
 Choke capacity chart, 5-8
 Choke-control operation, 5-41 to 5-44
 Choke nipple, 13-56
 Choke performance curve, 34-46, 34-50
 Christmas-tree assembly, 3-8 to 3-11, 3-13, 3-17, 3-39
 Christmas-tree fittings, 3-13
 Christmas trees, offshore, 18-3, 18-28, 18-31, 18-32, 18-34, 18-37, 18-38
 Chromatogram interpretation, 52-16
 Chromatograph/thermal conductivity detector, 52-6
 Chromatography, 39-6
 Chromic acid, 11-6
 Chromium, 9-5
 Circuit breakers, 10-28, 10-30
 Circular conduits, fluid flow in, 26-10
 Circular drainage area, 35-6
 Circular flotation chamber, 15-27
 Circumferences of circles by eighths, table, 1-28, 1-29
 Circumferences of circles by hundredths, table, 1-24, 1-25
 Circumferential bond image, 51-42
 Circumferential displacement, 9-9, 9-10
 Cities Service, 46-14, 46-15, 46-18, 46-20, 46-21
 Citric acid as sequestering agent, 44-45, 54-7
 Clamp-type connectors, 3-2, 3-5
 Clamp-type permeameter, 26-18
 Clamp-type riser coupling, 18-15
 Clapeyron equation, 20-12, 20-13
 Clarification of water produced with emulsions, 19-28
 Classification of oil and gas separators by, application, 12-17 to 12-19
 configuration, 12-16
 function, 12-16
 operating pressure, 12-16, 12-17
 principle used to accomplish primary separation, 12-19, 12-20
 Classifications, of hazardous areas, 10-36, 10-37
 of insulation for motors, 10-26
 of material balance equation, 40-7
 of NEMA, for control enclosures, 10-27
 of production packers, 4-1
 of reservoir rocks, 29-6 to 29-8
 of surfactants, 47-7
 Clastic porosity, 29-8
 Clastic reservoirs, 36-3, 36-4
 Clastic rocks, 29-7
 Clastic sedimentary deposits, 29-4
 Clastic sediments, 36-3
 Clathrates, 14-2
 Clausius-Clapeyron equation, 20-12, 20-16, 20-17, 46-13
 Clay control, 56-5, 56-6
 Clay hydration, 51-19
 Clay minerals, 44-2, 50-37
 Clay stabilization, 56-3
 Clay types, identification and quantification, 50-2
 Clay yield, 58-29
 Clean-sand points, 50-34
 Cleaning vessels, 12-42, 19-28, 19-29
 Cleanup, remedial, abrasive jet cleaning, 56-1
 large-volume injection treatments, 56-2
 mud removal, 56-1
 paraffin removal, 56-2
 reperforation, 56-1
 scale deposits, 56-2
 steam injection, 56-2
 water blocks and emulsions, 56-2
 Clearance volume, definition of, 6-21
 Climatological data, 31-2, 31-3
 Closed gas lift installation, 5-2, 5-3
 Closed linear system, 38-9
 Closed-loop control, 16-2
 Closed power-fluid system, 6-4, 6-5, 6-25 to 6-28, 6-30, 6-55, 6-59, 6-60, 6-63
 Closed radial system, 38-9
 Closed regeneration system, 14-11, 14-12
 Closed, rotative, gas-lift system, 5-1 to 5-3, 5-11, 5-24, 5-38
 Closure, 29-3, 29-8
 Closure stress, 55-8
 CLUSTER log analysis, 49-37
 CO₂/CO ratio in produced gas, 46-16
 Coal caving, 52-19
 Coal tar coating, 11-5
 Coal tar epoxy internal coatings, 6-62
 Coal-tar-epoxy system, 15-10
 Coalescence, 12-8, 12-10, 12-11, 12-19, 12-35, 15-22, 15-23, 19-1, 19-3 to 19-7, 19-9, 19-12 to 19-15, 19-17, 19-19, 19-21, 19-23, 19-25, 19-26, 19-28
 Coalescing material, 19-14
 Coalescing packs, 12-10
 Coalescing-type mist extractor, 12-8, 12-11
 Coanda effect, 12-20
 Coastal interdeltaic environment, 36-3
 Coatings, corrosion prevention, 18-29, 18-33, 18-34
 Coatings for bolted tanks, 11-1
 Coatings, protective, 3-36
 Code authorities for various countries, 12-39
 Code vectorization, 48-17
 Codes and regulatory authorities, 18-44
 Coefficient, of adsorption, 51-4
 of compressional wave attenuation, 51-4
 of expansion, 26-20
 of isothermal compressibility, 20-11, 20-16
 of shear wave attenuation, 51-4
 of thermal expansion, 58-34
 Coefficients, for choke nipple, 34-45
 interaction, 28-3
 transport, 28-1, 28-3
 COFCAW pilot or process, 46-2, 46-14, 46-33
 Cogeneration of steam and electricity, 46-19
 Cognac platform, 18-2, 18-23
 Coherence, definition and usage SI metric, 58-8, 58-9, 58-22
 Co-injection of gas and steam, 46-22, 46-23
 Coke, 19-29, 46-12, 46-21
 Cold drawn steel, 9-2
 Cold electric grid, 19-25
 Cold environment, 18-21
 Cold Lake field, Alberta, Canada, 46-4, 46-34
 Cold oil productivity, 46-10, 46-11
 Cold-separation unit, 12-1
 Collapse equation factors, 2-54 to 2-56
 Collapse pressure equations, 2-46
 Collapse pressure, of casing, 2-1 to 2-3, 2-20 to 2-28, 2-32, 2-34, 2-35, 2-46, 2-55, 2-56
 of line pipe, 2-48, 2-49
 of tubing, 2-39, 2-41, 2-43, 2-46
 Collapse pressure under axial load, 2-32
 Collapse pressure under axial-tension stress, 2-55
 Collapse resistance, of casing, 2-1 to 2-4, 2-6, 2-8, 2-10, 2-12, 2-14, 2-16, 2-18, 2-32, 2-46, 2-55, 2-56
 of line pipe, 2-48
 of tubing, 2-39, 2-41, 2-43, 2-46
 Collapse resistance under axial load, casing, 2-20 to 2-28, 2-34, 2-35
 Collapse safety factor, 2-1 to 2-3, 2-32, 2-34, 2-35, 2-39, 2-45, 2-46
 Collar locator, 53-26
 Colombia, 21-2, 46-3, 58-20
 Color of emulsions, 19-5, 19-6
 Colorado, 24-8, 24-11, 24-20, 40-23
 Colorado School of Mines, 25-9, 25-11
 Column-stabilized drilling vessel, 18-2
 Combination casing strings, safety factors, collapse, 2-2, 2-3, 2-34

- internal yield, 2-32, 2-34
- joint strength, 2-32, 2-34
- pipe-body yield strength, 2-32, 2-34
- Combination drive reservoirs, 43-16, 45-8
- Combination recovery procedures, 39-24
- Combination reverse/forward combustion, 46-30, 46-31, 46-33, 46-34
- Combination thermal and epithermal neutron device, 50-37
- Combination traps, 29-5
- Combination valve operators, 16-3
- Combustible-gas detectors, 18-47
- Combustion efficiency, 19-28
- Combustion, in-situ,
 - dry forward, 46-1, 46-2
 - production by, 46-4
 - reverse, 46-2
 - wet, 46-2, 46-3
- Combustion of coke, 46-12
- Combustion tubes, 46-13, 46-15, 46-19
- Comolith log analysis, 49-37
- Common fractions of an in. to mm, table, 1-72
- Common logarithms, table, 1-38 to 1-41
- Common subsurface point, 53-15
- Common surface point, 53-15, 53-16
- Communication adapter, 16-8 to 16-10
- Communication facilities for SCADA, 16-9, 16-10
- Compaction, 55-1
- Compaction correction factor, 51-33
- Compaction disequilibrium, 52-21, 52-22
- Compaction, effect on porosity, 26-7
- Compaction of porous rocks, 26-7 to 26-10
- Comparison of fluid saturation measurement methods,
 - averaging capillary-pressure data, 26-25 to 26-27
 - converting laboratory data, 26-25
 - introduction, 26-24, 26-25
 - water saturation from capillary-pressure data, 26-25
- Comparison of predicted vs. actual reservoir performance, 37-25, 37-26
- Comparison of project execution formats, 15-32
- Comparison of separators, 12-21
- Comparison of Turner's and Tracy's method, 37-10
- Compatibility of coatings, 11-4
- Compatibility tests, 19-10
- Compensated density device, 50-17
- Compensated Formation Density (FDC™), 49-23, 49-24, 49-36, 49-38
- Compensated formation density log, 46-21
- Compensated Neutron Log (CNL™), 49-36, 49-38, 50-29
- Complementary error function, 46-8
- Complementary metal-oxide silicon (CMOS), 16-9
- Completion costs, 41-9
- Completion factor, 40-27
- Completion flow efficiency, 37-21
- Completion intervals in firefloods and steamfloods, 46-17
- Completion string inspection, 53-17
- Completion/workover system controls, 18-48
- Complex propagation factor, 49-33
- Complexing agent, 56-3
- Component parts of a pumping unit, 10-4, 10-5
- Composite reservoir, 35-7
- Composition of oilfield waters,
 - Appalachian area, 24-6, 24-7
 - California, 24-7, 24-8
 - Canada, 24-8, 24-12
 - Illinois basin, 24-7, 24-9
 - midcontinent area, 24-8 to 24-10
 - Rocky Mountain area, 24-8, 24-11
 - U.S. Gulf Coast, 24-7, 24-8
 - Venezuela, 24-9, 24-13
- Composition of produced stream, GC system, 39-14
- Composition ranges, GC systems, 39-2
- Compositional analysis, 17-7
- Compositional-balance equation, 43-6
- Compositional material balance, 39-8
- Compositional model, 43-2, 48-4, 48-6, 48-7, 48-9, 48-14
- Compositional simulator, 36-10, 45-10, 45-13
- Compound interest, 41-25
- Compound interest factor, 41-17
- Compound interest, table, 1-62, 1-63
- Compound units, SI metric system, 58-12 to 58-14
- Compressed air, 3-31
- Compressed vapor recovery unit, 11-13
- Compressibility factor,
 - of ethylene, 17-7
 - of gas, 20-4, 20-7, 20-8, 20-10, 20-11, 20-14, 34-28, 40-22
 - of injected dry gas, 39-24
 - of natural gas, 5-4, 20-5, 20-6, 40-21
 - of nitrogen, 39-16
 - of pure compounds, 20-5
- Compressibility factor charts, 20-5, 20-6, 40-21
- Compressibility of CO₂, 45-5
- Compressibility of formation, 40-7
- Compressibility of formation water, 24-12, 24-15
- Compressibility of gas, 51-37
- Compressibility of hydrocarbon liquids, 22-3, 22-5
- Compressibility of natural gas mixtures, 17-7
- Compressibility of oil, 40-7
- Compressibility of pore fluid, 51-30, 51-31, 51-37
- Compressibility of porous rocks, 26-7 to 26-10
- Compressibility of reservoir fluid, 58-38
- Compressibility tests, 51-44
- Compressibility, total, 35-2
- Compression, 39-27
- Compression loading, 9-13
- Compression packer, 4-2 to 4-4, 4-8
- Compression plant, 39-17, 39-24
- Compression ratio, 6-10, 6-21, 8-9, 8-10, 10-15, 18-14, 39-24
- Compression refrigeration system, 14-9
- Compression stress in pipe, 2-35
- Compression stroke, 10-14
- Compression system, 11-13
- Compression-type seal, 3-6
- Compressional energy, 34-28, 34-29, 39-40
- Compressional forces, 29-2, 29-3
- Compressional transit time curves, 51-29
- Compressional-wave attenuations, 51-2, 51-6
- Compressional-wave transit time, 51-19, 51-24 to 51-27, 51-29 to 51-31, 51-35 to 51-37, 51-39, 51-43
- Compressional-wave velocities, 51-1, 51-2, 51-4 to 51-9, 51-12, 51-15, 51-20, 51-24, 51-25, 51-30, 51-34, 51-35, 51-37, 51-38, 51-43
- Compressional-wave velocity log, 51-28
- Compressional waves, 51-2, 51-3, 51-12 to 51-15, 51-25, 51-27, 51-28, 51-30, 51-35, 51-46
- Compressive load, 18-22
- Compressive strength of cement, 51-40, 51-42
- Compressor, field booster, 13-57
- Compressor fuel consumption, 39-24
- Compressor-oil carry-over, 39-24
- Compressor suction pressure, 13-58
- Compton scattering, 50-6 to 50-8, 50-12 to 50-14, 50-16
- Compton tail, 50-13, 50-14
- Compulsory unit operations, 57-8
- Comslog analysis, 49-37
- Concentration, definitions of, 48-5
- Concentration, units and conversions, 58-29, 58-30
- Conceptual studies, 15-30
- Concrete dust, 11-5
- Concrete (gravity) structures, 18-1, 18-2, 18-23, 18-25
- Condensable vapors, 12-3, 12-8
- Condensate content, 39-23
- Condensate (distillate) liquids, 22-20, 39-23
- Condensate-liquids recovery, 39-6
- Condensate properties and correlations, 21-8, 21-10 to 21-16
- Condensate well fluids, 20-7, 34-4
- Condensates, 11-12, 12-3, 12-32, 14-1, 14-3, 14-5 to 14-8, 14-11, 14-14, 18-28, 39-10, 39-11, 40-3, 57-5
- Condensing-gas drive, 45-1 to 45-4, 45-11, 45-12
- Conductance ratio, 44-34
- Conduction, 46-25
- Conductive cloth model, 44-20
- Conductive solids, effect on electrical properties of rock, 26-30, 26-31
- Conductivity, 44-33 to 44-35
- Conductivity log, 51-38
- Conductivity units, 49-1
- Conductor casing, 18-18, 18-19
- Conductor strings, 3-3
- Cone-bottom tanks, 11-2, 11-3
- Configurations of separators, 12-16, 12-22, 12-31, 12-35
- Confining pressure, 51-7
- Conformance efficiency, 39-9, 43-3, 43-5 to 43-7, 43-9, 44-9, 44-32, 45-6, 45-7, 45-10, 45-13
- Conformance factor, 39-18
- Conformity of flood, 44-46
- Congo, 46-3
- Conjugate gradient, 48-17
- Connate water: see also interstitial water
- Connate water, 24-2, 24-16, 24-18, 24-19
- Connection gas indicating underbalance, 52-17, 52-18
- Conoco Inc., 46-15, 46-26
- Conservation, 43-1
- Conservation commission, 30-8
- Conservation commission completion, 41-8
- Conservation equations, steam injection model, energy balance, 46-12
 - mass balance of coke, 46-12
 - mass balance of H₂O, 46-12
 - mass balance of hydrocarbons, 46-12
 - mass balance of inert gases, 46-12
 - mass balance of oxygen, 46-12
- Conservation laws, 39-16
- Conservation of mass, 34-1
- Consistency index, 55-5
- Consolidated rocks, porosity of, 51-29 to 51-31
- Constant-composition expansion, 39-7
- Constant-enthalpy expansion, 14-1, 14-2
- Constant-enthalpy expansion system, 14-3 to 14-8
- Constant-flow control valve, 6-51, 6-54, 6-56
- Constant percentage decline, 40-28 to 40-32, 41-9, 41-10, 41-12, 41-17

- Constant-percentage-decline deferment factor, 41-24, 41-27, 41-28
- Constant-pressure controller, 6-51, 6-54
- Constant-pressure cycling, 39-23, 39-24
- Constant-rate case for DCF-ROR, 41-18, 41-22, 41-23
- Constant-rate deferment factor, 41-24, 41-25, 41-27 to 41-29
- Constant-rate income, 41-18, 41-21
- Constant-rate production, 41-5, 41-11, 41-12
- Constant ratio of net profit, 41-20
- Constant surface closing, gas-lift valve, 5-44
- Constant-terminal-pressure case, 38-1 to 38-3
- Constant-terminal-rate case, 38-1, 38-2
- Constant valve surface closing pressure, 5-46, 5-47
- Constant-volume gas reservoirs, 40-34
- Constraint equations, 48-4
- Construction codes for separators,
 - ASME code for unfired pressure vessels, 12-38
 - ASME design equations for separators, 12-38
 - materials of construction for separators, 12-38
- Construction design factor, 15-11, 15-13
- Construction materials for separator, 12-38, 12-39, 12-41
- Construction of meters, 13-37
- Construction types for underground storage, 11-13
- Contact angle, 28-10
- Contact log, 44-3
- Contact resistivity devices, 26-31
- Containers for samples, 24-4
- Containment of fracture, 55-5
- Contaminants of water, 18-30
- Continental sediments, 36-3
- Continental shelf, 29-7, 53-12, 53-14
- Continental slope and abyssal environments, 53-12, 53-14
- Continuity of reservoir rock, 44-3
- Continuity principles, 37-2
- Continuous compounding, 41-26, 41-28, 41-30, 41-35
- Continuous dipmeter surveys, 53-3
- Continuous-flow gas lift,
 - bottom valve, selecting, 5-26
 - casing (annular) flow installation design, 5-37
 - depth of top valve, 5-24, 5-25
 - design procedures, 34-40 to 34-45
 - flowing pressure gradient curves, 5-25, 5-26
 - flowing temperature at depth, 5-26
 - installation design, 5-22, 5-26 to 5-35
 - introduction, 5-21, 5-22
 - multiphase-flow correlations, 5-25, 5-26
 - operations, 5-24, 5-41
 - orifice-check valve for the operating gas-lift valve, 5-23, 5-24
 - production pressure (fluid)-operated valves, 5-35 to 5-37
 - safety factors in simplified installation, 5-22, 5-23
 - slope of static load fluid traverse, 5-25
 - uses gas energy fully, 5-1
- Continuous-flow installations, 5-21 to 5-26, 5-30, 5-31, 5-34, 5-35, 5-37, 5-43
- Contraction of pipe, lateral, 2-35
- Control agent, gas regulation, 13-50
- Control circuit logic, 3-27
- Control curves, gas regulation, 13-52, 13-53
- Control Data Corp., 48-17
- Control enclosures for motors, 10-26, 10-27
- Control fluids, subsea control systems, 18-49
- Control for oilfield motors, 10-27 to 10-29
- Control fuses for oilfield motors, 10-29
- Control-head compression packer, 4-2, 4-3, 4-9
- Control-head tension packer, 4-2, 4-9
- Control lines in subsea completions, 18-33, 18-34
- Control manifolds, 6-54
- Control of field compressors, 13-57
- Control of subsea production facilities, 18-48
- Control system, 3-31, 3-33, 3-34
- Control systems offshore,
 - alternate approaches, 18-49, 18-50
 - control fluids, 18-49
 - direct hydraulic control, 18-50
 - discrete-piloted hydraulic, 18-51
 - drilling, 18-15, 18-16
 - introduction, 18-43 to 18-48
 - multiplexed electrohydraulic, 18-52
 - operational considerations, 18-49
 - redundancy, 18-48, 18-49
 - reliability/maintainability, 18-48
 - safety systems, 18-47
 - sequential-piloted hydraulic, 18-51, 18-52
 - subsea production facilities, 18-48
 - umbilicals, 18-49
- Control-valve travel, 13-55
- Controlled-solubility particulate solids, 54-10
- Controller types, 16-3 to 16-5
- Controlling injection-pumping rate, 16-14
- Controls nomenclature, 13-49, 13-50
- Convection, 46-4, 46-12, 46-25
- Convection heat-transfer coefficient, 46-5
- Conventional acoustic logging,
 - calibration, 51-17, 51-18
 - curves recorded, 51-16
 - cycle skipping and triggering on the noise, 51-16, 51-17
 - log presentation, 51-16
 - tool characteristics, 51-15, 51-16
 - tool span, 51-16
- Conventional acoustic logs, 51-19, 51-20, 51-22 to 51-25, 51-35
- Conventional coring procedures, 27-9
- Conventional crank-balanced pumping units, 10-1 to 10-4, 10-8, 10-9
- Conventional gas-lift equipment, 5-2
- Conventional lay barges, 18-37, 18-38, 18-43
- Conventional (black-oil) material balance, 37-25, 37-26
- Conventional mooring system, 18-4
- Conventional mud logging, 52-1, 52-16
- Conventional resistivity devices, 49-12, 49-25
- Conventional resistivity logs, application, 49-14
- Conventional steel pipe, 18-36, 18-37
- Conventional tubing mandrel, 5-12
- Conventional wireline cores, 27-9
- Conventionally mined caverns, 11-13
- Convergence pressure, 23-11
- Conversion factors, for density units,
 - table, 1-79
 - for permeability, 26-14, 58-35
- Conversion factors, SI units,
 - for vara, 58-20
 - general, 58-14, 58-22
 - memory joggers, 58-21
 - notation, 58-14
 - organization, 58-14
 - tables of, 58-15 to 58-21
- Conversion of temperature-tolerance requirements, 58-7
- Conversion of units in Darcy's law,
 - gases at base pressure and average flowing temperature, 26-13, 26-14
 - linear-flow liquids, 26-13
 - permeability conversion factors, 26-14, 26-15
 - radial-flow liquids, 26-13
- Conversion rules, 58-5 to 58-7
- Conversion, tables of,
 - angular velocity, 1-76
 - areas, 1-74
 - capacities, 1-74
 - density, 1-79
 - energy, 1-78
 - heat, 1-78
 - heat flow, 1-79
 - lengths, 1-71
 - linear velocity, 1-76
 - masses, 1-75
 - power, 1-78
 - pressures, 1-76
 - relative densities, 1-80
 - thermal conductance, 1-79
 - thermal conductivity, 1-79
 - volumes, 1-74
 - work, 1-78
- Conveyances, tax consequences related to, 41-15, 41-16
- Convolutions, 5-16
- Cook Inlet, Alaska, 18-3
- Cooling, creates hydrates, 14-3
 - cycles, 14-11
 - gas to condense hydrocarbon vapor, 14-5
 - in condensate removal, 14-1, 14-2
 - in gas-to-gas heat exchangers, 14-11
 - load, 14-10
 - with refrigerants, 14-9
- Copper electrodes, 39-21
- Coquinas, 29-4, 29-8
- C/O ratio, 50-1 to 50-4, 50-9, 50-22, 50-24, 50-35, 50-36
- Core analysis and core analysis data, 24-1, 26-1, 26-7, 26-22, 26-23, 36-3, 37-3, 39-18, 40-1, 40-3, 40-5, 40-12, 40-16, 40-19, 40-25, 41-8, 42-4, 44-6, 46-21, 50-26, 50-35 to 50-37, 51-31, 51-32, 52-26
- Core analysis, average values,
 - gravity, 27-5, 27-7, 27-11, 27-13, 27-15, 27-17, 27-19
 - interstitial water saturation, 27-3, 27-5, 27-7, 27-11, 27-13, 27-15, 27-17, 27-19, 27-20
 - oil saturation, 27-3, 27-5, 27-7, 27-9, 27-11, 27-13, 27-15, 27-17, 27-19, 27-20
 - permeability, 27-3 to 27-6, 27-8, 27-10 to 27-17, 27-19, 27-20
 - permeability, 27-3 to 27-6, 27-8, 27-10 to 27-17, 27-19, 27-20
 - porosity, 27-3, 27-5, 27-7, 27-8, 27-11, 27-13, 27-15, 27-17, 27-19, 27-20
 - total water saturation, 27-5, 27-7, 27-11, 27-13, 27-15, 27-17
 - water saturation, reservoir, 27-20
- Core analysis of different formations,
 - data from non-U.S. areas, 27-8
 - data from U.S. areas, 27-9
 - liquid saturations, 27-8
 - percussion sidewall core data, 27-9
 - permeability, 27-1
 - porosity, 27-1
- Core-barrel sample, 56-7
- Core barrels, rubber-sleeve, 56-3, 56-6
- Core-sample resistivity cell, 26-28
- CORIBAND log analysis, 49-37
- Coring data, 41-8
- Coring program,
 - core analyses, 46-21
 - during and after project, 46-20
 - log analyses, 46-21
 - microscopic studies, 46-21
 - mineral analyses of cores, 46-21
 - photographic and visual examination, 46-21
 - tracers, 46-21
- Corner well producing cuts, 44-24, 44-25

- Correction,
 of observed API gravity to API gravity at 60°F, 17-5, 17-6
 of observed density to density at 15°C, 17-6
 of observed relative density to relative density at 60/60°F, 17-5, 17-6
 of volume to 15°C against API gravity at 60°F, 17-6
 of volume to 15°C against density at 15°C, 17-6
 of volume to 60°F against relative density at 60/60°F, 17-5, 17-6
 of volume to 15°C against thermal expansion coefficients at 15°C, 17-6
 of volume to 60°F against thermal expansion coefficients at 60°F, 17-6
- Correction factor,
 for dead-end oil IFT, 22-17
 for gas flow, 33-2
 for gas mixtures, 20-6
- Correlation index, 21-9, 21-11
- Correlation length, dipmeter, 53-10, 53-11
- Correlation(s),
 accuracy of, 22-89, 22-9
 acoustic log, 51-30
 Baker and Swerdloff, 22-17
 Beal, 22-14 to 22-16
 Beggs and Brill, 46-7
 Beggs and Robinson, 22-15, 22-16
 between AOR and WAR, 46-19
 between diaphragm and dynamic capillary pressure methods, 26-25
 between interstitial water and log of permeability, 26-23
 between maximum friction pressure and maximum total flow rate, 6-19
 between oil recovery and pore volume burned, 46-17
 Boberg and West, 46-11
 bubblepoint pressure, 21-9, 21-10, 22-5 to 22-9
 carbon/oxygen, 50-1 to 50-4, 50-9, 50-22, 50-24, 50-35, 50-36
 Carr-Kobayashi-Burrows, 20-9, 20-10, 20-15, 20-16
 chart, 40-22
 Chew and Connolly, 22-14 to 22-16, 39-4
 Cullender and Smith, 5-37
 dead-oil viscosity, 22-14
 dewpoint pressure, 21-10 to 21-15
 Dykstra-Parsons, 44-9
 empirical, of electrical properties, 26-29 to 26-31
 empirical, ultimate recovery, 40-13
 equilibrium ratios, 39-15
 flow temperature gradient, 5-26, 5-27
 fluid flow, 44-20, 44-21
 for approximating true vapor pressure, 14-13
 for liquid and gas properties, 6-47
 formation resistivity factor, 26-29
 formation volume, 21-15 to 21-20
 gamma ray log, well-to-well, 50-2
 gas-plus-liquid FVF, empirical, 6-38
 Gates and Ramey, 46-15
 geological, 51-29, 51-30
 Hall, 26-8, 26-9
 Hammerlindl's, 26-8
 K-value, 39-12
 Lasater, 22-5 to 22-7, 22-9, 22-10
 multiphase flow, 5-22, 5-25, 5-26, 5-38, 5-40, 34-37 to 34-40
 Muskat's, 39-20
 of capillary pressure data, 26-26
 of solubility ratios with IFT, 47-14
 of steam stimulation results, 46-11
 of water saturation with permeability, 26-27
 of well logs, 49-25, 49-26
- oil formation volume factor, 22-10 to 22-13
 oil systems, 22-1 to 22-21
 oil viscosity, 22-13 to 22-16
 Organick and Golding, 21-11 to 21-15
 Orkiszewski, 34-37 to 34-40
 permeability with tube wave data, 51-48
 petrophysical, 28-13
 Poettmann and Carpenter, 34-37
 porosity compressibility with depth, 26-8
 predicts cavitation damage, 6-36
 productivity index—permeability, 32-4
 recovery factor from statistical data, 40-16
 relating fuel content to API gravity, 46-16
 resistivity index vs. saturation, 26-3
 Sage and Old, 21-11
 sand-by-sand, 36-7
 Showalter, 46-16
 sour water stripper, 25-17, 25-18
 Standing, 22-5, 22-8 to 22-11, 22-13, 22-14
 Thodos, 20-11, 20-16
 total formation volume, 21-15 to 21-20
 transit time/pressure, 51-40
 Trube, 20-11, 20-16
 undersaturated systems, oil viscosity, 22-16
 Van der Knapp, 26-8
 vapor/liquid equilibrium, GC systems, 39-11 to 39-13
 Vasquez and Beggs, 22-7 to 22-13
 velocity/porosity, 51-34
 vertical multiphase flowing gradient, 6-43, 6-45
 viscosity of gas, 20-9
 water-saturated rock conductivity vs. water conductivity, 26-30
 waterflood recovery, 44-8, 44-32
- Correlative right, 57-2
- Correlogram, dipmeter, 53-10
- Corrosion, attacks, 9-1
 by iron sulfide deposits, 11-10
 cathodic protection, 19-31
 caused by microbiological growth, 44-44
 cell, 9-2
 control procedures, 39-26
 electrochemical, 3-36
 in casing, tubing and cement jobs, 39-24
 in dry desiccant dehydration, 14-21
 in ethanolamine sweetening units, 14-22
 in oil and gas separators, 12-3, 12-8, 12-40
 in pipe, 14-17
 in power oil plunger pumps, 6-33
 in reverse flow systems, 6-5
 in subsurface sucker-rod pumps, 8-9
 in surface system and injection wells, 44-43
 in water-injection systems, 24-2
 increased with CO₂ increase, 44-42
 minimized by internal coatings, 19-31
 minimized by use of plastics, 44-47
 on tank bottoms, 11-2
 oxygen exclusion, 19-30
 pits, 9-5, 9-8 to 9-10
 problems, 6-55, 46-22
 products, 6-48, 6-59
 products carryover, 39-24
 protection, 11-1, 11-3
 resistant alloys, 3-36
 special metallurgy, 19-31
- Corrosion of wellhead equipment, 3-35
 electrochemical, 3-36
 external, 3-36
 internal, 3-36
 material selection, 3-36
 oxygen, 3-36
 weight loss, 3-36
 wellhead aspects, 3-35, 3-36
- Corrosion inhibitors, 3-36, 6-5, 6-55, 9-1, 9-5, 9-8, 9-10, 9-13, 19-30, 19-32, 44-45, 44-46, 53-18, 54-6
- Corrosion rates, 44-41, 44-42, 58-38
 Corrosive fluids in separator, 12-40
 Corrosive well fluids, 4-4, 4-5
 Corrugated plate interceptor (CPI), 15-24 to 15-26
 Cost accounting system, 19-32
 Cost and profit margin relationship, 36-2
 Cost/benefit analysis, 52-30
 Cost comparison, production packers, 4-6
 Cost-depletion allowance, 41-5, 41-13, 41-14
 Cost justification, 52-29, 52-30
 Cost of emulsion treating, 19-33
 Cost of engine equipment, 10-16, 10-17
 Cost-plus format, 15-32
 Cosurfactants, 47-5, 47-11, 47-13
 Cotton Valley Bodcaw reservoir, Texas, 39-19, 39-23
 Cottonwood Creek field, Wyoming, 24-18
 Coulter counter, 44-45
 Counterbalance, 10-1 to 10-3, 10-6, 10-7, 10-9
 Counterflow imbibition, 28-13
 Counterweight, 9-2
 Counting rate, gamma ray, 50-15, 50-16, 50-19, 50-20, 50-28
 Coupling failures, 9-9
 Couplings and subcouplings, sucker rods, 9-3, 9-4
 Coverage, 40-18, 44-9
 Cox chart, 20-12, 20-13, 20-17
 Cracked-gas/water system, 25-26
 Cracking, 46-3
 Crank-balanced units, 10-4, 10-6
 Cray-IS computer, 48-17
 Creep compaction, 28-13
 Crestal-gas injection, 40-14, 43-3
 Cricondenbar, 39-3
 Cricondentherm, 23-6, 39-3, 45-2, 45-4
 Criterion of reservoir performance, 32-15
 Critical breakthrough pressure, 44-36
 Critical constants of hydrocarbons, 20-2, 20-3
 Critical constants of solvent gases, 45-5
 Critical-flow conditions, 13-53, 34-45 to 34-49
 Critical-flow prover, 13-37, 13-45, 33-6, 33-7, 33-13
 Critical gas mixture, 45-4
 Critical gas saturation, 28-9, 34-31, 37-1, 37-3, 37-4, 48-13
 Critical hydrate formation loci, 25-3
 Critical locus, 23-3, 23-4, 45-3
 Critical micelle concentration (CMC), 47-10, 47-11, 47-15
 Critical point, 14-2, 20-2, 23-1, 23-2, 25-1, 39-2, 39-3, 39-15
 Critical pressure, 20-2, 20-3, 20-5, 40-21, 44-3
 Critical ratio for flow prover, 13-37
 Critical saturation, 49-30
 Critical state, definition, 22-20
 Critical temperature, 20-2, 20-3, 20-5, 22-20, 39-1, 39-4, 40-21, 45-5
 Critical thickness, 49-13
 Critical volume, 20-3
 Critical wells in acidizing, 54-11, 54-12
 Critique of unsteady-state k_f methods, 28-7
 Cross imbibition, 48-13
 Cross plot of photoelectric factor vs. density, 50-33
 Cross rails, motor mounts, 10-19
 Cross section of interaction, 50-6
 Cross sections, 41-8
 Cross yoke, 10-2
 Cross-yoke bearing, 10-3, 10-4
 Crossbedding, 44-3
 flow, 44-29
 Crossflow, 39-19, 39-20, 44-7, 44-8, 48-10
 Crossflow devices, 15-25, 15-26
 Crosshead, 10-14
 Crosslinked aqueous fluid, 55-6

- Crosslinked gels, 55-5, 55-7, 55-8
 Crossover flange, 3-7 to 3-9
 Crossover seat, 5-16, 5-37
 Crossover tool, 56-8
 CRT screen display of fracturing data, 55-9
 Crude-oil analysis, 21-7 to 21-9
 Crude Oil Analysis System (COASYS), 21-9
 Crude oil, API gravity loss vs. temperature, 19-9
 Crude oil as semidiesel fuel, 10-16
 Crude oil, definition, 12-3, 40-3
 Crude oil, differences between natural gas, 36-2
 Crude-oil disposal, 18-29, 18-30
 Crude-oil emulsions,
 description of treatment equipment, 19-16 to 19-28
 economics of treating, 19-32
 general references, 19-33, 19-34
 introduction, 19-1
 methods used in treating, 19-6 to 19-15
 operational considerations for treating equipment, 19-28 to 19-32
 sampling and analyzing, 19-6
 theories of, 19-1 to 19-6
 treating equipment and systems, 19-15, 19-16
 Crude oil, measuring, sampling, and testing, 17-1 to 17-8
 Crude-oil properties, 21-1 to 21-10
 base, 21-1, 21-3
 evaluation, 21-1, 21-2, 21-4
 Crude-oil reservoirs, 39-1, 39-2
 Crude oil, viscosity/temperature relationships, 19-7, 19-8
 Crude oil, volume loss vs. temperature, 19-9
 Crude-oil/water emulsion, 19-6
 Crude oils, temperature corrections for, 17-5, 17-6
 Crude price, gross, 41-9
 Crude stabilization, 40-13
 Crude viscosity, effect of solution gas, 6-68
 Crystalline porosity, 29-8
 Crystallization temperatures, 25-19
 Cuba, 58-20
 Cube roots of certain fractions, table, 1-18
 Cube roots of whole numbers, table, 1-7, 1-14 to 1-18
 Cubes of numbers, table, 1-7 to 1-10
 Cubic average boiling point, 21-12, 21-15
 Cubic packing of spheres, 26-1, 26-2
 Cullender and Smith correlation, 5-37
 Cullender and Smith method of determining BHP in gas wells, 34-24 to 34-26
 Cumulative-gas/cumulative-oil curve, 40-32
 Cumulative logarithmic diagram (S-plot), 56-6, 56-7
 Cumulative oil production vs. GOR, 37-25
 Cup-type plunger, 8-6
 Current bedding, 53-12, 53-13
 Current status of thermal recovery,
 geographical distribution of projects, 46-3
 major projects, 46-3
 potential for incremental recovery, 46-3
 production mechanisms, 46-4
 reservoirs amenable to, 46-3
 U.S. oil production by EOR, 46-3
 Curve shapes, 49-12, 49-13
 Custody transfer, 13-48
 Customary units (English), 17-7, 58-21, 58-26 to 58-38
 Cutoffs on engine installations, 10-19
 Cut-out rams, 7-12
 Cut test, 52-10, 52-14, 52-16
 Cuttings evaluation, 52-19
 Cuttings gas, 52-17
 Cuttings gas analyzer, 52-11
 Cuttings, representative sample, 52-8, 52-9, 52-11
 Cuttings sample geological log, 52-1
 Cyberdip log analysis, 49-37
 Cyberlook, pass one log, 49-37, 49-38
 pass two log, 43-39
 Cycle efficiency of refrigerants, 14-10
 Cycle frequency, maximum, 5-40
 Cycle skipping, 51-16, 51-17, 51-24, 51-45
 Cycles of steam stimulation, 46-9
 Cyclic load,
 derating factor, 10-18
 of oilwell pumping unit, 10-25
 Cyclic load factor, 10-25
 Cyclic steam injection, 46-21
 Cyclic steam stimulation, 46-22, 48-46
 Cycling operations, 39-4, 39-6, 39-15 to 39-24, 39-27
 Cycling operations prediction with model studies, 39-20 to 39-22
 Cycling performance, GC reservoir,
 areal sweep efficiency, 39-17
 displacement efficiency, 39-18
 effectiveness, 39-17
 invasion efficiency, 39-17, 39-18
 pattern ($h\phi S$ -weighted) efficiency, 39-17
 permeability distribution, 39-18 to 39-20
 reservoir efficiency, 39-17
 Cycling to improve recovery, 40-4
 Cyclohexane/water system, 25-26
 Cyclone separator (desander), 6-60 to 6-63, 12-20, 15-19
 Cyclonic flow, 12-19
 Cyclopropane/water system, 25-25, 25-27
 Cylindrical shell equations, 12-38
 Cylindrical tanks, 11-2
- D**
- Daily production rate, continuous-flow gas lift, 5-54
 Daily production rates, prediction of, 5-40
 Dalton's law, 20-4, 23-11
 Damage,
 by fluid jet, 8-7
 ratio, 30-13
 Damaged casing, 51-29
 Damköhler number, 47-21
 Darcy head loss, 15-1
 Darcy's law or equation, 26-10, 26-11, 26-13, 26-15, 26-16, 26-18, 26-19, 28-1, 28-2, 32-4, 35-10, 37-11, 39-20, 43-3, 44-9, 44-13, 44-17, 45-13, 48-2, 48-3, 56-4
 Data acquisition system, 52-25, 52-27, 52-28
 Data gathering and handling, 42-3
 Data of varying precision, 58-6, 58-7
 Data required to estimate recovery from injection operations, 42-2
 Data requirements for engineering analysis of gas-injection operations, 43-17
 Data requirements for GC cycling study, 39-22, 39-23
 Data transmission schematic for MWD, 53-2
 Date designation SI metric system, 58-22
 Dead basins, 52-22
 Dead-end oil IFT, 22-17
 Dead-oil viscosity, 22-14, 22-15, 40-12
 Dead oils, 45-5
 Dead Sea, 24-19
 Dead space of separator, 12-26, 12-30
 Dead time of a process, 13-50
 Dead-weight gauge, 33-6
 Dead-weight regulator, 13-54
 Dead-weight tester, 5-53, 13-37, 30-2
 Dean-Stark extraction, 46-21
 Debris or solids in well, ESP, 7-16, 7-17
 Decay constant, exponential, 50-22
 Decay times, 50-22
 Decimal equivalents, table, 1-67
 Decimal relation in SI metric system, 58-9, 58-22
 Decimals of an in. to mm, table, 1-72
 Deck drainage, skim pile sizing, 15-26
 Decline-curve analysis, 40-27
 Decline tables for constant-percentage decline, 40-28 to 40-32
 Decline-trend analyses, 40-1
 Decreasing-injection-gas-pressure installation design method, 5-22
 Deep dual laterolog (LLD), 49-19, 49-20
 Deep marine sediments, 36-3
 Deep Sea Drilling Project, 25-18
 Deep-seated domes, 29-5, 29-6
 Deepwater drilling, 18-10, 18-20, 18-21
 Deerfield field, Missouri, 46-14
 De-ethanizer, 14-8
 Deferment-factor (weighted-average) charts, 41-23
 Deferment factors, 41-5 to 41-8, 41-20, 41-21, 41-24 to 41-35
 Definitions, for valuation of oil and gas reserves, 40-3, 40-4
 of fluid properties, 22-1
 of gas/oil ratio terms, 32-14
 of petroleum reserves, 40-2, 40-3
 of pump parts, 8-2
 of water-drive oil reservoir terms, 38-1
 Defoaming plates, 12-6
 Deformations of acoustic waves, 51-2
 Degasser boot, 19-22
 Degassing, 19-18
 Degassing efficiency, 52-2
 Degassing elements, 12-22
 Degradation of an oil accumulation, 24-17
 Degrees and minutes expressed in radians, table, 1-42
 Degrees of freedom, 25-1, 25-2
 Dehydration by adsorption, 14-20, 14-21
 Dehydration efficiency, 14-19
 Dehydration, storage tank used for, 19-18
 Dehydration units, 14-17, 14-19
 Dehydration with organic liquid desiccants, 14-17 to 14-20
 Dehydrator, 14-10, 14-13, 14-18
 Dehydrator pots, 13-53
 Delaware-Childers field, Oklahoma, 46-3
 Delaware effect, 49-11, 49-22
 Delay rentals, 41-1, 41-13, 57-4, 57-5, 57-7
 Deliverability of gas-lift well, 5-40
 Deliverability of gas to compressor plant, 13-58
 Deliverability of gas wells, 34-3, 34-9
 Deliverability plot approach, 35-12
 Deliverability testing, 35-10
 Delta-bar sediments, 36-3
 Delta-delta transformer, 10-30, 10-31
 Delta-wye transformer, 10-30
 Deltaic bar deposits, 36-4
 Deltaic channel deposits, 36-4
 Deltaic environment, 36-3
 Demand-pressure regulator, 3-33
 Demethanizer, 14-8
 Demulsifiers, 17-2, 19-9 to 19-13, 56-5
 Dendritic fingers, 45-7
 Density, apparent liquid, definition of, 22-20
 Density comparison method, 52-20
 Density, definition of, 1-80
 Density difference (gravity separation), 12-8, 12-9, 12-19
 Density equivalents, table, 1-79
 Density gradient method, 52-20
 Density in SI metric system, 58-24, 58-29
 Density log, 44-3, 49-25, 49-26, 49-34, 49-38, 50-24, 51-14, 51-19, 51-31, 51-33, 51-43

- Density meters, installing and proving, 17-7
 Density/neutron crossplot, 51-36
 Density of crude petroleum, 17-5
 Density of formation water, 24-14
 Density of gaseous hydrocarbons, 20-3
 Density of light hydrocarbons, 17-5
 Density of liquid petroleum products, 17-5
 Density of NaCl solutions, 24-14
 Density of natural gas, 20-14, 20-15
 Density porosity, 50-31, 50-33
 Density/pressure relationship, 26-12
 Density, pseudoliquid, 22-2 to 22-4
 Denton field, New Mexico, 6-24
 Deoxygenating control equipment, 24-2
 Dept. of Commerce, 1-69
 Dept. of Energy (DOE), 40-2, 46-16, 46-30, 46-31, 46-33, 46-34
 Dept. of the Treasury, 41-15
 Dept. of Transportation, 15-13
 Departure curves, 49-7, 49-27
 Depletion, 41-13, 41-16, 41-17, 47-21 to 47-24, 57-11
 Depletion allowance, 41-13 to 41-15
 Depletion-drive calculation, 43-13, 43-14, 43-16
 Depletion-drive performance, 37-16 to 37-18
 Depletion-drive process, 42-5
 Depletion-drive recoveries, 37-24
 Depletion equation, 37-10
 Depletion mechanism, 40-8, 40-10, 40-12, 40-13, 40-15
 Depletion performance, volatile oil reservoirs, 37-22, 37-23
 Depletion-recovery factors, 40-10, 40-11
 Depletion technique,
 dry gas reservoir, example problem, 36-3
 gas reservoirs, 36-2, 36-3
 oil reservoirs, 36-2
 Depletion-type gas wells, 41-10
 Depletion-type reservoir, 29-8, 40-8 to 40-12, 40-16, 40-32, 40-33
 Depositional environment, 36-3 to 36-7
 Depreciation, 41-11, 41-13, 41-21, 41-22, 57-11
 Depression of metastable dewpoint, 25-12, 25-14
 Depth micrometer, 5-16
 Depth of top gas-lift valve, 5-24
 Depthograph, 30-7
 Derating factors of motor, 10-24, 10-25, 10-31
 Derivation of an orifice equation, 13-2, 13-3
 Derivative response, 13-50, 13-52, 13-53
 Derived units, SI metric system, 1-69, 1-71, 58-2, 58-4, 58-10, 58-11, 58-21
 Derrick barges, 18-26
 Desalting crude oil, 19-26, 19-27
 Description needed for oilfield water sample, 24-5
 Design engineering, 15-31
 Design features,
 common to steamfloods and firefloods, 46-17
 pertaining to firefloods only, 46-18, 46-19
 pertaining to steamfloods only, 46-18
 Design methods, intermittent gas lift, 5-42
 Design of casing strings,
 oil, water, and mud-weight factors, 2-1
 safety factor, 2-1 to 2-3, 2-34, 2-35
 single-weight and -grade casing string, 2-1, 2-2
 Design of gas-lift installation, 5-32 to 5-35
 Design of hydraulic fracturing treatment, 55-9, 55-10
 Design operating gas-lift valve depth, 5-54
 Design properties for piping, 15-11
 Design safety factors for casing, 2-1 to 2-3, 2-32, 2-34, 2-35
 Design slip of motor, 10-24
 Design standards of electric motors, 10-19, 10-20
 Destabilization of emulsions, 19-6, 19-7
 Desulfurization unit, 14-21, 14-22
 Det norske Veritas, 18-44
 Detail engineering, 15-31
 Detection efficiency, 50-12 to 50-14
 Detection of nonhydrocarbon gases, 52-5 to 52-7
 Detector resolution, 50-14
 Deterministic analysis, 18-27, 18-28
 Detrital, 29-6, 29-8
 Detrital environment, 56-2
 Detrital porosity, 29-8
 Detrital reservoirs, 29-7, 29-8
 Deuterium ion, 50-6
 Development costs,
 tangible and intangible, 41-11
 well spacing, 41-11
 Development drilling, 36-2, 36-3, 36-6, 40-1
 Development, historical, thermal recovery, 46-3
 Development of waterflooding, 44-1
 Development plan for oil and gas reservoirs, characterization of the reservoir, 36-3 to 36-9
 introduction, 36-1, 36-2
 oil and gas differences, 36-2, 36-3
 prediction of performance, 36-9, 36-10
 references, 36-10, 36-11
 Development wells, 41-11
 Developments in wellbore heat losses, 46-7
 Deviation angle, 53-7
 Deviation, definition, 58-9
 Deviation factor, 39-7, 39-8, 39-10, 39-14, 39-23
 Deviation of hole, 53-2, 53-3, 53-10, 53-17
 Deviation survey computations, 53-7
 Deviation surveys, 49-1, 53-1, 53-7 to 53-9
 Dewatering of gas wells, 6-34, 39-15, 39-16
 Dewpoint boundary, 39-3
 Dewpoint chart, 25-11
 Dewpoint curve, 14-1, 20-2
 Dewpoint cycling, above or below, 48-7
 Dewpoint depression, 12-20, 14-17, 14-18, 14-20
 Dewpoint of a system, definition, 22-20
 Dewpoint pressure, 22-20, 22-21, 23-3, 23-12, 39-5, 39-7 to 39-11, 39-13, 39-14, 39-16, 39-18, 39-23
 Dewpoint pressure correlations, 21-10 to 21-15
 Dewpoint reservoirs, 23-7
 Dewpoint temperature, 14-1
 Dewpoint water content chart, 25-12
 Dextran, 47-3
 Diagenesis, 24-2, 24-20, 52-21
 Diagenetic alteration, 50-37
 Diagenetic history, 36-3
 Diagenetic water, definition, 24-18
 Dia-Log caliper tools, 53-18
 Diamond cores, 27-9
 Diaphragm BHP element, 30-6, 30-7
 Diaphragm control valve, 16-4, 16-11
 Diaphragm gas-engine starters, 10-19
 Diaphragm motor oil-control valves, 12-6, 12-7
 Diaphragm motor valve, 13-49, 13-53
 Diaphragm operators, 16-3
 Diaphragm pressure, 13-54, 13-56
 Diaphragm pump, 15-15
 Diaphragm-type weight-loaded valve, 13-55
 Diatomaceous earth filters, 15-20, 15-22, 44-47
 Diatomic gases, 13-37
 Dielectric constants, 16-7
 Dielectric measurements, 51-19
 Dielectric permittivity, 49-32
 Dielectric strength, 7-3
 Diesel engines, 6-1, 10-15, 10-16, 18-45
 Diesel fuel, 10-15
 Diesel index, 21-7
 Diethanolamine (DEA), 14-21, 14-22
 Diethylene glycol (DEG), 14-7, 14-18, 14-19, 25-19, 25-20
 Differential compaction, 29-3 to 29-6
 Differential gas liberation, definition, 22-20
 Differential gas separation, 37-1
 Differential head loss, 13-3
 Differential liberation, 40-6
 Differential-opening pressure valve, 5-13, 5-14, 5-43
 Differential-pressure control valve, 6-63
 Differential-pressure gradients, 34-42
 Differential-pressure taps, 13-3, 13-8
 Differential-pressure transducers, 16-6, 46-21
 Differential process, definition, 22-20
 Differential separation (vaporization), 12-32, 37-3, 45-8
 Diffuser, 6-32, 6-35, 6-36, 7-3
 Diffusion baffle, 19-24
 Diffusion length, 50-11, 50-20, 50-21
 Diffusion theory, 50-17
 Diffusivity, 38-9, 58-34
 Diffusivity equation, 35-1, 35-2, 35-10, 36-8, 38-1
 Digit, definition, 58-9
 Digital age, 49-36 to 49-39
 Digital computer program, 14-16
 Digital computer systems, 16-10
 Digital computers, 40-10, 40-13
 Digital signal-processing technology, 51-48
 Digital sonic logs comparison, 51-43
 Diglycolamine (DGA), 14-21, 14-22
 Dikes, 11-11
 Dilution caused by weighted-average permeability profile, 39-19
 Dilution plane, 23-10
 Dimensionless pressure values, 38-4
 Dimensionless pressures for aquifer systems, 38-4 to 38-6, 38-12 to 38-19
 Dimensionless water-influx values, 38-4
 Dimensions,
 definition, 58-9
 of buttress-thread casing and coupling, 2-29, 2-59, 2-64
 of casing long thread, 2-58
 of casing round-thread height, 2-66
 of casing short thread, 2-57
 of chemical, electrical, and physical quantities, 59-2 to 59-51
 of external-upset tubing coupling, 2-43, 2-66
 of extra-strong threaded line pipe, 2-50
 of extreme-line casing threading and machining, 2-63
 of integral-joint tubing thread, 2-65
 of integral-joint tubing upset, 2-45
 of line-pipe lengths, 2-47
 of line-pipe thread, 2-47, 2-58, 2-62, 2-65
 of line-pipe thread height, 2-62
 of nonupset tubing coupling, 2-42, 2-66
 of plain-end line pipe, 2-50 to 2-53
 of round-thread casing coupling, 2-28, 2-58
 of round-thread tubing coupling, 2-58
 of threaded line pipe, 2-47, 2-58
 of tubing round-thread height, 2-66
 Dip azimuth, 53-7, 53-9, 53-10
 Dip vectors, 53-10, 53-12
 Dipmeter, 49-25, 49-36, 49-37
 Dipmeter logging,
 application of dipmeter and directional data, 53-10 to 53-16
 calibration, 53-8
 computed dipmeter log, 53-9, 53-10
 device, 53-6
 interpretation rules, 53-12
 introduction, 53-1, 53-7
 oil-based muds, 53-8, 53-9

- principles of TVD, TST, and TVT plots, 53-15, 53-16
- survey computations, 53-9
- tools available, 53-8
- Dipmeter patterns, 53-10, 53-12 to 53-15
- Dipmeter surveys, 49-1
- Direct-acting spring-loaded regulator, 13-55
- Direct-acting weight regulator, 13-55
- Direct costs (expenses), 41-11 to 41-14
- Direct-current (DC) motor, 10-21
- Direct-fired heater, 19-21
- Direct hydraulic subsea control, 18-50
- Direct lifting costs, 41-3
- Direct line drive, 44-13 to 44-16, 44-22, 44-33
- Direct phase determination, 51-25
- Direction of dip, 53-7
- Direction of hole drift, 53-10
- Directional drilling, 18-30
- Directional permeability effect, 44-25
- Directional permeability test, 27-1
- Directional surveys,
 - available tools, 53-3, 53-4
 - computation of results, 53-4 to 53-7
 - introduction, 53-1
 - legal requirements, 53-4
 - MWD-data listing, 53-6
- Directional well survey, 41-8
- Directional wells, 53-1
- Disadvantages,
 - of batch-type meters, 32-10, 32-11
 - of positive-displacement meters, 32-11, 32-12
- Discharge coefficient, 13-8
- Discharge (return) gradient, 6-26, 6-29
- Discharge piping, 15-17
- Discharge pressure, 39-24
- Discounted cash flow (DCF) method, 41-3, 41-17 to 41-22
- Discounted future net cash income, 41-5
- Discounted present worth, 44-5
- Discovery allowable, 32-2, 32-3, 32-15
- Discrete-piloted hydraulic control, subsea, 18-50 to 18-52
- Discrete remote control, subsea, 18-50, 18-51
- Dispersed-gas drive, 37-1
- Dispersed-gas injection, 43-2, 43-8 to 43-15, 43-17
- Dispersed-gas units, 15-27, 15-28
- Dispersion, 15-22, 19-1, 45-6, 45-7
- Dispersion curves, 51-13, 51-14
- Dispersion of clay particles, 56-5
- Displacement calculation procedures,
 - Dykstra-Parsons, 44-8, 44-9
 - frontal advance, 44-9 to 44-11
 - Stiles, 44-7, 44-8
 - Welge, 44-11, 44-12
- Displacement efficiency, 39-9, 39-15, 39-17, 39-18, 39-22, 39-23, 40-34, 43-3, 43-5, 43-6, 43-9, 44-39, 45-6 to 45-10, 47-1, 47-2, 47-17
- Displacement equations, 43-4 to 43-6, 43-8 to 43-10
- Displacement fronts for different mobility ratios, 45-7
- Displacement mechanisms, 36-10, 47-19, 47-20
- Displacement meter systems, 17-4
- Displacement of downhole pumps, 6-21, 6-24
- Displacement process, 28-6, 28-7
- Displacement-type controller, 13-51, 13-53
- Displacement-type liquid-level controls, 13-53
- Displacement volumes, 44-23, 44-24, 44-28
- Displacement volumes injected, 43-3, 43-7, 43-8
- Disposal water, 24-5
- Dissociation of water, 47-18
- Dissolved acid gases, 44-47
- Dissolved gas(es), 22-1, 22-20, 24-17, 40-3, 44-43
- Dissolved-gas drive, 22-20, 44-2, 44-4
- Dissolved-gas effect on oil viscosity, 22-14, 22-15
- Dissolved-gas removal, 15-28, 15-29
- Dissolved-gas systems, 21-18
- Dissolved-gas units, 15-27
- Dissolved salt, 24-7, 24-8
- Dissolved solids, 19-1, 24-3, 24-15, 24-16, 24-18 to 24-20, 44-45
- Dissolved-solids removal, 15-29
- Distillates, 11-12, 12-32, 57-5
- Distillation method, for water in crude oil, 17-5
- Distillation, removing water from crude oil emulsions, 19-15
- Distributary channel sediments, 36-3
- Distributary channels, 36-4, 36-6
- Distributing piping specs., 15-12
- Distribution of fluids in permeable formations invaded by mud filtrate, 49-5 to 49-7
- Distribution system, 12-10, 12-11
- Distribution transformers, types of, 10-30, 10-31
- Divalent cations, 47-13, 47-15, 47-21
- Divalent/hydroxide compounds, 47-20
- Diverging vortex separator, 12-14, 12-20
- Diverless subsea tree and running tools, 18-32
- Diverting agents, 54-8, 54-10, 56-2, 56-3, 56-5
- Division-order interest, 41-2
- Dixon plates, 12-25
- Dog-and-groove riser coupling, 18-15
- Dogleg, 7-1, 7-9, 10-3, 10-6, 53-6
- Dolomite,
 - acid reaction rate, pressure effect, 54-4
 - clays and silts in, 54-7
 - effect of corrosion inhibitor on acid reaction rate, 54-6
 - laboratory tests for acidizing, 54-9
 - silica in crystal structure of, 54-4
 - treated with HCL, 54-2
- Dolomitization, 24-18, 24-20, 26-2
- Dosage, units and conversions, 58-30
- Dose equivalent, unit and definition, 58-10
- Double-acting downhole unit, 6-9, 6-20
- Double-acting pump, 6-8, 6-9, 6-16, 6-18
- Double-deck shaker, 52-8
- Double-flanged head, 3-8
- Double-port diaphragm motor valve, 13-57
- Double-ported valves, 13-55, 13-58
- Double-studded adapter, 3-9
- Double-studded crossover flange, 3-9
- Double-valve arrangements, 8-7
- Double-welded butt joints, 12-40
- Doughnut tubing hanger, 3-39
- Douleb oil field, Tunisia, 24-18
- Dow Chemical Co., 54-1
- Downcomer pipes, 11-13
- Downcomer/spreader, 19-19
- Downdip gas flow, 43-11
- Downflow filters, 15-20
- Downhole assembly, MWD, 53-2
- Downhole digitizer, 51-27
- Downhole jet pump accessories,
 - dummy pumps, 6-48
 - pressure recorders, 6-48
 - safety valves, 6-48, 6-49
 - screens and filters, 6-48
 - standing valves, 6-48
 - swab cups (noses), 6-47, 6-48
- Downhole pumps,
 - closed power-fluid systems, 6-4, 6-5
 - displacement of, 6-21, 6-24, 6-25
 - handling of formation-fluid volumes, 6-67
 - installation, 6-2
 - jet free completions, 6-34
- P/E ratio, 6-27
- pressure recorders, 6-48
- pressures and force balance in, 6-16 to 6-19
- reciprocating, 6-51, 6-55
- reverse-flow systems, 6-5
- TFL installations, 6-6
- types of installations, 6-2 to 6-4
- with wireline-retrievable safety valve, 6-49
- Downhole sensor, 53-4
- Downhole sensor sub, 53-1
- Downhole steam generators, 46-4, 46-19
- Downhole temperature profiles, 46-21
- Downkicking, 6-31
- Downstream taps, 13-30 to 13-34, 13-37
- Downtime analysis, 18-7, 18-8
- Downtime gas, 52-17
- Drag-body flowmeter, 32-13
- Drain cylinders, 12-12
- Drainage area, 35-1, 35-5, 35-6, 35-13, 35-16 to 35-18, 36-8, 55-4, 56-1
- Drainage-area shape, 37-21
- Drainage channels for tanks, 11-11
- Drainage channels, mist extractor, 12-11, 12-12
- Drainage curve, 28-5, 28-9, 28-11, 28-12
- Drainage relative-permeability data, 28-14
- Drainage shapes, 35-4, 35-5, 35-16
- Drainage tests, 26-24
- Drawdown effects 39-25
- Drawdown pressure, 30-10 to 30-13
- Drawdown tests, 35-3, 35-4, 35-14, 35-15, 44-41
- Dresser Atlas, 49-2, 49-36, 49-37, 51-18
- Drift, 13-50
- Drift diameter, 3-12 to 3-14
- Drill-time log, 52-1
- Drilling clause, 57-4, 57-5
- Drilling contractor, 18-16
- Drilling data analysis, 52-28
- Drilling efficiency, 52-28
- Drilling engineer, 18-4
- Drilling engineering services, 52-2, 52-27, 52-28
- Drilling-equipment considerations offshore,
 - backup control systems, 18-15, 18-16
 - BOP, 18-11, 18-12
 - control systems, 18-15
 - extended water-depth capability, 18-16
 - flex joints, 18-12, 18-13
 - K&C systems, 18-15
 - marine riser, 18-14, 18-15
 - motion compensator, 18-13, 18-14
 - re-entry systems, 18-14
 - riser tensioner, 18-13
 - slip joints, 18-13
- Drilling fluid, offshore, 18-12 to 18-14, 18-18, 18-41
- Drilling funds, 57-11
- Drilling, high-current, 18-21, 18-22
- Drilling models, 52-24 to 52-26
- Drilling motion compensator, 18-14
- Drilling mud, acoustic velocity in, 51-31
- Drilling offshore,
 - mooring and riser analyses, 18-16, 18-17
 - operating manual and emergency procedures, 18-16
 - planning and preparations, 18-3 to 18-5
 - rig selection, 18-5 to 18-16
- Drilling operations, 18-28, 18-29, 18-31, 18-32, 18-39, 18-40
- Drilling optimization, 52-29, 52-30
- Drilling porosity, 52-26
- Drilling riser, 18-16, 18-18, 18-34
- Drilling vessels: see specific type
- Drilling wells, estimation of BHT, 31-6
- Drillships, 18-3, 18-4, 18-7, 18-14, 18-15, 18-20

Drillstem test or testing, 6-34, 18-20, 18-34, 24-3, 27-8, 30-8, 30-11, 30-13, 30-15, 41-8, 42-4, 48-8, 49-31

Drillstem tests, openhole, 53-17

Drillstring motion compensators, 18-13

Drip pots, 13-37, 13-53

Drip-proof motor, 10-26

Drips, 39-26

Drive mechanism, effects on recovery, 36-3

Drop method, surface-tension measurement, 24-16

Droplet size distribution, 15-23

Drowned gas wells, 39-16

Dry chambers for subsea completions, 18-31

Dry-desiccant dehydration, 14-20, 14-21

Dry-desiccant dehydrators, 13-56, 14-10, 16-15

Dry forward combustion, 46-1 to 46-3, 46-14, 46-18, 46-19

Dry gas, 10-16, 39-1, 39-16, 39-18 to 39-20, 39-23, 39-24

Dry-gas breakthrough, 39-17 to 39-20, 39-22

Dry-gas front, 39-17, 39-18, 39-21 to 39-23

Dry-gas injection, 39-16, 39-21, 39-25, 39-26

Dry-gas reservoir, 35-3, 36-3, 39-1, 40-24, 40-25

Dry-gas/wet-gas cycling operation, 39-23

Dry-gas/wet-gas interfaces, 39-21, 39-22

Dry reverse combustion, 46-2

Dry vs. wet combustion, 46-18, 46-19

Dual-detector compensated-neutron device, 50-20

Dual-detector thermal device, 50-30, 50-32

Dual-element fuses, 10-28

Dual-fuel engines, 10-16

Dual induction-laterolog 8 (DIL), 49-15 to 49-20, 49-28

Dual induction-laterolog log, 46-21

Dual intermittent gas-lift installations, 5-40, 5-45

Dual laterolog, 49-11, 49-20, 49-23, 49-24, 49-28

Dual laterolog/gamma ray tools, 49-20

Dual-parallel-string installations, 3-11, 3-13

Dual-tube separator, 12-9, 12-10, 12-16, 12-18

Dual-vessel system, 6-63

Dual-water model, 49-38

Dual wells or zones, 6-7, 6-8

Dual-wing well manifold, 16-11, 16-12

Dummy pumps, 6-48

Dummy valve, 3-35

Dump cycles, 19-30

Dump valves, 18-50, 19-20, 19-22, 19-23

Dun and Ros method, 34-37, 34-40

Duplex pumps, 15-14

Dura Rod, 9-13

Duri field, Indonesia, 46-4

Dykstra-Parsons calculation, 44-8, 44-9

Dykstra-Parsons coefficient, 47-17

Dykstra-Parsons method, 40-19, 44-7, 44-9

Dynamic amplification factor, 18-26, 18-27

Dynamic-capillary-pressure method, 26-24, 26-25

Dynamic elastic constants, 51-4

Dynamic lag, 13-51

Dynamic miscibility, 45-1, 45-2, 45-4, 45-5, 48-5

Dynamic positioning, 18-2, 18-10, 18-14, 18-20, 18-21

Dynamic stresses, 18-17

Dynamic viscosity, 24-16, 58-35

Dynamite, 56-1

Dynamometer card analysis, 10-5, 10-6

Dynamometer cards, 10-6

Dynamometer test, 40-27

E

E-core transformer, 30-6

Early-time region (ETR), 35-3, 35-4, 35-6, 35-8, 35-15

Earth resistivities, 49-1

East Coalinga field, California, 46-18

East Texas area, 27-2, 27-3

East Texas field, 29-5, 29-6, 40-2, 40-34, 41-5

East Venezuela field, 46-16

Eccentric orifices, 13-45, 13-48

Eccentricity, 6-69, 6-72

Echometer, 30-7, 32-6

Economic analyses, 39-10, 39-15, 44-32

Economic balance, 19-15

Economic considerations of stage separation, 12-33

Economic evaluation, 24-21, 44-7, 45-10

Economic justification of automation, 16-2

Economic limit, 40-12, 40-19, 40-20, 40-27, 40-32, 41-10, 41-11

Economic-limit rate, 40-25, 40-27

Economics, impact of offshore leasing, 57-12

Economics, letter and computer symbols, 59-2 to 59-51

Economics of GC reservoir operations, 39-26

Economics of injection operations, 42-6

Economics of treating crude-oil emulsions, 19-32, 19-33

Eddy currents, 13-2, 13-36, 13-48, 19-12, 53-20, 53-22, 53-26

Edge water, 24-2

Edgewater drive, 40-15

Edgewater encroachment, 28-4

EDTA, sequestering agent, 54-7

Effective annual interest rate, 41-25, 41-26

Effective decline rates, 40-27, 41-27

Effective formation permeability, 55-4

Effective gas permeability, 39-25

Effective grain volume, 26-4, 26-6

Effective hydrocarbon porosity, 40-25

Effective interest rate, 41-17, 41-20, 41-21, 41-26, 41-27

Effective isopermeability map, 39-22

Effective mobility ratio, 47-18

Effective molecular weight, 22-7

Effective permeability, 26-15, 28-1 to 28-4, 28-6, 28-8, 28-13, 39-17, 44-32, 44-33, 46-21

Effective porosity, 26-2 to 26-6, 28-2, 40-5, 55-4

Effective salinity, 47-13

Effective shear rate, 47-5

Effective stress, 51-30, 51-31, 51-35, 51-43

Effectiveness of cycling, 39-17

Efficiency factor in orifice equation, 13-3

Efficiency of cycling, 39-17

Efficiency of ESP system, 7-1

Efficiency of gas lift, 30-14, 30-15

Efficiency of motor, 10-25

Efficiency of permeability variation, 44-8

Efficiency of separation, 12-21

Effluent fluids quality, 12-16

Effluent oil from separator, 12-15

Effluent water from separator, 12-15

El Dorado field, Kansas, 46-14

Elastic collapse-pressure equation, 2-55

Elastic limit, 51-1, 51-2

Elastic limit of material, 2-46

Elastic moduli, 51-1 to 51-3, 51-12, 51-30, 51-31, 51-43, 51-44, 58-34

Elastic parameters, relationships among, 51-2

Elastic properties, 51-44

Elastic scattering, 50-9, 50-10

Elastic transition zone, 2-55

Elastic wave propagation, 51-6, 51-8, 51-12, 51-14, 51-29, 51-49

Elastic wave velocities, 51-7

Elasticity, characteristics of acoustic waves, 51-2, 51-3 introduction, 51-1, 51-2

Elastomeric hoses, 18-49

Elastomeric joints, 18-13

Electric charge, unit and definition, 58-11, 58-23

Electric conductance, unit and definition, 58-11, 58-23, 58-35

Electric dipole moment, 49-32

Electric generating systems, 10-21

Electric inductance, unit and definition, 58-11, 58-23

Electric-log analysis, 26-22, 26-25

Electric-motor valve operators, 16-3

Electric motors for oilwell pumping, design standards, 10-19, 10-20 direct current (DC), 10-21 generating systems, 10-21 horsepower ratings of, 10-20 multiple-horsepower rated, 10-20 multiple-size rated, 10-21 performance factors of, 10-23 selecting size of, 10-21 single-phase type, 10-21 ultrahigh-slip, 10-22 voltage frequency of, 10-21, 10-23

Electric porosimeter, 26-4

Electric potential difference, unit and definition, 58-11

Electric power supply, ESP, 7-9 to 7-12

Electric pressure control, 12-39

Electric resistance, unit and definition, 58-11, 58-23, 58-36

Electric-solenoid valves, 16-3

Electric-starter motors, 10-19

Electric submersible pumps (ESP), application, 7-1, 7-2 general references, 7-17 handling, installation, and operation, 7-12 to 7-14 installation, 7-1, 7-2 performance curves, 6-35 references, 7-17 selection data and methods, 7-9 to 7-12 system, 7-1, 7-2 system components, 7-3 to 7-9 troubleshooting, 7-14 to 7-17

Electric submersibles, 18-44

Electrical capacitance in electronic interface controllers, 19-31

Electrical capacitance, unit and definition, 58-10, 58-23, 58-35

Electrical conductivity in electronic interface controllers, 19-31

Electrical conductivity of fluid-saturated rocks, fundamental concepts, 26-28, 26-29 introduction, 26-27, 26-28 resistivity measurement of rocks, 26-29

Electrical conductivity, units and conversions, 58-35

Electrical distribution system, grounding of, 10-31, 10-32 open delta transformer, 10-30, 10-31 phase converters, types of, 10-35, 10-36 power factor and use of capacitors, 10-33 to 10-35 primary system and voltage, 10-29 secondary system, 10-29, 10-30 transformers, 10-30 voltage drop in, 10-32

Electrical logging, electromagnetic propagation tool, 49-32 to 49-36 focused-electrode logs, 49-18 to 49-22 fundamentals, 49-1 to 49-7

- general references, 49-41, 49-42
- induction logging, 49-14 to 49-18
- microresistivity devices, 49-22 to 49-25
- nomenclature, 49-39 to 49-41
- references, 49-41
- resistivity logging devices, 49-11 to 49-14
- SP log, 49-7 to 49-11
- the digital age, 49-36 to 49-39
- typical log, 49-3
- uses and interpretation of well logs, 49-25 to 49-32
- Electrical one-line diagram, 18-45
- Electrical parameters used in characterizing porous media, 26-31
- Electrical potential logs, 53-17, 53-19
- Electrical properties of reservoir rocks, empirical correlations, conductive-solids effect, 26-30, 26-31
- introduction, 26-29
- parameters used in characterizing, 26-31, 26-32
- resistivity of partially water-saturated rocks, 26-31
- Electrical resistivity measurement of rocks, 26-29
- Electrical survey (ES), 49-11, 49-19
- Electrical systems offshore, code and regulatory authorities, 18-44
- distribution system, 18-45, 18-46
- equipment enclosures, 18-46
- hazardous areas, 18-46
- introduction, 18-43, 18-44
- layout of facilities, 18-44
- platform loads, 18-44
- primary electric power, 18-44, 18-45
- secondary/back-up power, 18-45
- wiring methods, 18-46
- Electrically controlled valves, 16-3
- Electrically equivalent diameter of invasion, 49-6
- Electricity, units and conversions, 58-35, 58-36
- Electrochemical corrosion, 3-36
- Electrochemical potential, 49-8 to 49-10
- Electrode array, 53-7
- Electrofiltration potential, 49-10
- Electrohydraulic control system, 18-11
- Electrohydraulic subsea controls, 18-49
- Electrohydraulic systems, 3-31
- Electrokinetic effects, 28-1
- Electrolytic conduction, 26-28
- Electrolytic corrosion, 12-40
- Electrolytic model, 39-20, 39-21, 44-17, 44-18, 44-20, 44-21
- Electromagnetic e-mode telemetry, 53-1
- Electromagnetic force (EMF), 53-16
- Electromagnetic inspection devices, 53-17, 53-19
- Electromagnetic propagation log, 49-1, 49-2
- Electromagnetic propagation tool (EPT)TM, 49-32 to 49-36
- Electromagnetic radiation, 50-3
- Electromagnetic thickness log, 53-21
- Electromagnetic thickness tools, 53-19 to 53-21, 53-23
- Electro-mechanical timers, 16-4
- Electromotive force, 58-11, 58-23, 58-35
- Electron density, 50-16, 50-17
- Electron-density index, 50-7, 50-26 to 50-28
- Electron microscopy, 27-1
- Electronic casing caliper log, 53-19
- Electronic chart scanners, 30-2
- Electronic computers, 40-9
- Electronic (solid-state) controller, 16-4
- Electronic interface controllers, 19-31
- Electronic model, 39-20
- Electronic timers, 5-55
- Electropneumatic operators, 16-3
- Electrostatic coalescing, 19-13
- Electrostatic coalescing treaters, 19-25, 19-26
- Electrostatic emulsion treaters, 19-2, 19-10, 19-13, 19-25 to 19-27, 19-31
- Elemental models, 46-11 to 46-13
- Elevated separator, 12-17 to 12-19
- Elf Aquitaine, 46-27, 51-25
- Elk Basin field, Wyoming, 26-23, 39-16
- Ellipsoidal head equations, 12-38
- Elongation, of API body and bonnet members, 3-2, 3-3
- of API casing and liner casing, 2-2
- of API tubing, 2-37
- of line pipe, 2-46
- of sucker-rod types, 9-5
- Embayments, 29-7
- Embedment, 55-8
- Emergency disconnect conditions, 18-21
- Emergency power, 18-45
- Emergency procedures offshore, 18-16
- Emergency shutdown system (ESD), 3-33, 3-34, 18-47, 18-48
- Emergency venting of storage tanks, 11-7 to 11-9
- Empirical correlation factor, 27-8
- Empirical equations, ice movement rate and shape, 18-39
- Emulsification of oil, 10-13
- Emulsified water, 19-3
- Emulsifying agent, 19-2 to 19-5, 19-9, 19-14
- Emulsion breakers, 19-10, 46-22
- Emulsion-breaking agents, 56-2
- Emulsion conditions, ESP chart, 7-16
- Emulsion, definition of, 19-1
- Emulsion, effect on oil viscosity, 6-27
- Emulsion flood, 47-21
- Emulsion formation, 47-19
- Emulsion plugging, 6-56
- Emulsion treater, 11-12, 12-3, 12-4, 12-13
- Emulsion-treating equipment, 19-15, 19-16, 19-21, 19-27 to 19-32
- Emulsion treating, overall system performance, 19-33
- Emulsion-treating system, 19-6, 19-7, 19-9, 19-11, 19-13, 19-15, 19-16, 19-30, 19-32
- Emulsion viscosity, 6-67
- Emulsions, as mixed-base fracturing fluids, 55-5, 55-7
- chances of forming, 8-6
- decreases injection cycles/day, 5-40
- effect of silicate control agents, 54-7
- effect of surfactants, 54-7
- gas lift can intensify, 5-2
- in firefloods and steamfloods, 46-21, 46-22
- prevents application of gradient curves, 5-25
- Emulsions, methods used in treating, agitation, 19-12, 19-13
- centrifugation, 19-15
- chemical demulsifier, 19-9 to 19-12
- distillation, 19-15
- electrostatic coalescing, 19-13
- fibrous packing, 19-14
- filtering, 19-14
- gravity settling, 19-14, 19-15
- heating, 19-7 to 19-9
- water washing, 19-13
- Emulsions theories: See Theories of emulsions
- Enclosed motor, totally, 10-26
- Enclosures for motors, 10-26, 10-27
- End effects, 28-3, 28-5, 28-7
- End-to-end flowline valves, 3-12 to 3-14
- Endicott development, 18-3
- Endogenous subsurface water, definition, 24-19
- Endpoint displacement data, 28-8
- Endpoint mobility ratio, 47-1
- Endurance limit, 9-11
- Energy balance, 13-1, 34-36, 46-12
- Energy-balance equation, 34-1, 34-2, 34-9
- Energy, definition, 22-21
- Energy equivalents, table, 1-77
- Energy loss, 13-2, 13-3
- Energy relationships for flowing fluid, 34-1, 34-2
- Energy, SI unit for, 58-5, 58-11, 58-23, 58-24, 58-32
- Engine displacement, 6-30
- Engine efficiency, 6-31
- Engine selection, calculations for, 10-17 to 10-19
- equipment life and cost, 10-16, 10-17
- fuel availability, 10-16
- horsepower, 10-17
- installation, 10-19
- safety controls, 10-17
- Engineering, analysis, 42-3
- appraisal method, 41-2, 41-3
- computer simulation methods, 36-7
- in developing oil and gas reservoirs, 36-1, 36-6 to 36-8
- interference testing, 36-7, 36-8
- material-balance studies, 36-7
- net-pay/net-connected-pay ratio, 36-7
- England, 18-25
- Enhanced oil recovery (EOR), 23-1, 23-7, 24-16, 25-1, 25-14, 46-3, 47-1, 47-2, 47-6, 47-7, 47-18, 47-22, 48-2, 48-4, 48-6, 48-8
- Enhanced-oil-recovery (EOR) projects, 19-28
- Enhanced-recovery methods, 40-4
- Enhanced-recovery operation, 51-42
- Enos Creek field, Wyoming, 24-18
- Enriched-gas drive, 45-2, 45-3, 45-5
- Environment, 11-4, 13-1
- Environmental conditions (forces), 11-6, 18-1, 18-3, 18-4, 18-7 to 18-10, 18-17, 18-21, 18-25, 18-31, 18-36, 18-44, 18-47
- Environmental conditions, ice characteristics, 18-38, 18-39
- ice loading, 18-39
- permafrost, 18-39
- waves, 18-39
- Environmental corrections, gas effect, 50-30, 50-31
- matrix effect, 50-28 to 50-30
- shale effect, 50-31 to 50-33
- Environmental criteria, 18-26
- Environmental factor, 11-8
- Environmental impact, 24-9
- Environmental load predictions, 18-22
- Environmental regulations, 44-41
- Environments, wellhead equipment, 3-36 to 3-39
- Epigenetic interstitial water, definition, 24-18
- EPILOG log analysis, 49-37
- Epipressure contours, 44-15, 44-16
- Epithermal counting rate, 50-20, 50-29
- Epithermal detector, 50-19, 50-20, 50-21
- Epithermal diffusion coefficient, 50-19
- Epithermal matrix effect, 50-30
- Epithermal neutron flux, 50-15, 50-20
- Epithermal neutrons, 50-8, 50-9, 50-14, 50-17, 50-19, 50-30
- Epithermal porosity device, 50-28, 50-32
- Epoxy resin coating, 11-6
- Epoxy thermoset resin, 9-12
- Equal-payment-series present-worth factor, 41-25
- Equalizer for tank battery, 11-9
- Equalizing valves, 3-29
- Equation factors for collapse pressure equations, 2-54 to 2-56

- Equation, general for critical-flow prover, 13-45
- Equations for computing subsurface pressures, 33-15
- Equations for jet pumps, 6-36, 6-37
- Equations for oil and gas separator, gas capacity, 12-23
sizing for gas capacity, 12-23 to 12-25
- Equations for valuation methods, 41-18, 41-19
- Equations for water-drive reservoirs, 38-1 to 38-4
- Equations in SI metric system, 58-13
- Equations of state (EOS), 14-16, 20-4, 20-6 to 20-8, 23-10, 23-12, 23-13, 25-8, 25-16, 39-16, 48-4, 48-5, 48-9
- Equilibrium behavior, GC systems, 39-2 to 39-4
- Equilibrium constants, 14-16, 23-11, 37-23
- Equilibrium data sources, 25-1 to 25-4
- Equilibrium dewpoint, 14-18
- Equilibrium dewpoint locus, 25-1, 25-2
- Equilibrium dewpoint water content, 25-2
- Equilibrium flash calculations, 12-33, 12-34, 14-16
- Equilibrium flash separation, 14-16
- Equilibrium gas, 39-7, 39-8, 39-14
- Equilibrium gas saturation, 40-11, 40-12, 43-11
- Equilibrium phase diagrams, 23-1, 45-2
- Equilibrium ratios, 21-11, 21-16, 23-11, 25-5, 39-6, 39-9, 39-11 to 39-13, 39-15
- Equilibrium vaporization constants, 46-12, 46-37, 46-39
- Equilibrium vaporization ratios, 37-23
- Equilibrium water dewpoint, 14-18
- Equipment coordination, surface/downhole, 4-4
- Equipment enclosures offshore, 18-46
- Equipment for control of oilfield motors, hand-off-auto switch, 10-27
line disconnect switch, 10-27
local remote switch, 10-27
motor starter contactor, 10-28
programmer, 10-27, 10-28
sequence-restart timer, 10-27
- Equipment selection, reciprocating pumps, 6-28
- Equipment used in emulsion treating, clarification of water produced, 19-28
desalting crude oil, 19-26, 19-27
electrostatic coalescing treaters, 19-25, 19-26
EOR projects, 19-28
free-water knockouts, 19-17, 19-18
horizontal treaters, 19-23 to 19-25
reverse emulsions, 19-27
settling tanks, 19-18 to 19-22
storage tanks, 19-18
vertical treaters, 19-22, 19-23
- Equivalent circular pipe, 34-27
- Equivalent conductivity, 49-34
- Equivalent formation-water resistivity, 49-11
- Equivalent hydraulic gradient, 26-11
- Equivalent length of valves and fittings, 15-4
- Equivalent limestone porosity, 50-28, 50-30
- Equivalent linear permeability, 26-18
- Equivalent liquid permeability, 26-18, 27-1, 27-8
- Equivalent methane in air (EMA), 52-3 to 52-5
- Equivalent molecular weights, modified weight average, 21-12 to 21-15
- Equivalent mud density (EMD), 52-25
- Equivalent proton masses (EPM), 24-19
- Equivalent slowing-down length, 50-29
- Equivalent water conductivity, 49-39
- Equivalent wellbore radius, 35-4
- Equivalents, tables, areas, 1-73
capacity, 1-73
density, 1-79
energy, 1-77
length, 1-71
mass, 1-75
power, 1-78
pressure, 1-77
velocity, 1-76
volume, 1-73
work, 1-77
- Erection of pumping units, 10-7, 10-12
- Erosion, pump cavitation damage, 6-36
- Error analysis, 50-28
- Errors in basic data, 38-7, 38-8
- Erythorbic acid, reducing agent, 54-7
- Escalation clauses, 41-3, 41-9
- Esso, 46-4, 46-14
- Estimating reserves, 40-1
- Ethane/water system, 25-17, 25-18, 25-24, 25-27
- Ethanolamine, 14-21
- Ethylene density, 17-6
- Ethylene glycol (EG), 14-7, 14-18, 14-19
- Ethylene glycol, hydrate inhibition, 25-19, 25-20
- Ethylene glycol monobutyl ether, 54-7, 56-5
- Ethylene/water system, 25-24, 25-27
- Ethylenediaminetetraacetic acid (EDTA), 56-2
- European countries, concrete gravity structures, 18-23
- Evaluation of fracturing prospects, 51-45
- Evaporation method of capillary-pressure measurement, 26-24
- Evaporation, preventing, 11-12, 11-13
- Evaporites, 49-25
- Evinger-Muskat equation, 34-31
- Example problems:
casing, tubing, and line pipe, 2-36, 2-37, 2-55, 2-56
crude-oil properties and condensate properties and correlations, 21-15 to 21-20
electric submersible pumps, 7-17
estimation of oil and gas reserves, 40-8, 40-9, 40-12 to 40-14, 40-16, 40-17, 40-31
gas-condensate reservoirs, 39-10, 39-11, 39-23, 39-24
gas lift, 5-4 to 5-8, 5-10 to 5-12, 5-15, 5-20, 5-25, 5-26, 5-29 to 5-37, 5-46, 5-47, 5-49, 5-50, 5-52
gas measurement and regulation, 13-8
gas properties and correlations, 20-13 to 20-17
hydraulic pumping, 6-20, 6-21, 6-24, 6-29, 6-30, 6-44 to 6-46
miscible displacement, 45-10 to 45-13
mud logging, 52-29
phase behavior of water/hydrocarbon systems, 25-13, 25-14
properties of reservoir rocks, 26-3, 26-5, 26-6, 26-14, 26-15, 26-17, 26-26, 26-27
pumping units and prime movers for pumping unit, 10-8 to 10-11, 10-18, 10-19, 10-21 to 10-24, 10-31
solution-gas-drive oil reservoirs, 37-24, 37-25
subsurface sucker-rod pumps, 8-5
sucker rods, 9-4
water-drive oil reservoirs, 38-5 to 38-7
well-performance equations, 35-7 to 35-9, 35-13, 35-14, 35-19, 35-20
wellbore hydraulics, 34-8, 34-9, 34-23 to 34-26, 34-30, 34-32 to 34-35, 34-41 to 34-45
- Excelsior packs, 19-23, 19-31, 19-32
- Excess-flow valves, 3-29
- Excitation, BHP gauges, 30-5, 30-6
- Executor, definition, 57-3
- Exhaust-gas turbocharger, 15-16
- Exhaust power fluid, 6-25
- Exogenous subsurface water, definition, 24-19
- Exothermic reaction, 31-6
- Exotic metals for pipe, 15-11
- Expander, 14-8
- Expansion-drive gas reservoirs, 40-26
- Expansion factor, 13-2, 13-8, 13-26 to 13-34
- Expansion separator or vessel, 12-1
- Expansivity, 24-15
- Experimental procedure, steady-state k , methods, 28-3 to 28-7
unsteady-state k , methods, 28-7
- Exploration geologists, 18-3
- Exploration hazards, 46-22
- Exploratory well, 41-11
- Explosion proof, 3-34
- Explosion-proof motors, 10-27, 10-36, 18-46
- Exponent of backpressure curve, 33-5 to 33-13
- Exponential-integral solution, 35-3, 35-4
- Exponentials, table, 1-55
- Extended flanged outlets, 3-3
- Extended flanges, 3-8
- Extended water-depth capability, 18-16
- Extension nipple, 8-1, 8-4
- Extensive properties, definition, 22-21
- External boundary conditions, definitions, 38-1
- External coatings, 11-6
- External corrosion, 3-36, 18-33
- External gas-injection pressure maintenance, 43-16
- External-upset tubing, 2-38 to 2-45, 2-64, 2-66
- Externally adjustable secondary seal, 3-6
- Extra-strong threaded line pipe, 2-46, 2-50
- Extracting-liquid drive, 45-5, 45-6
- Extraction method for determining sediment in oil, 17-5
- Extraction methods for determining water saturation, 26-22
- Extraction of minerals, 24-20
- Extraneous materials in well fluids, 12-3
- Extreme-line casing, 2-1, 2-4, 2-6, 2-8, 2-10, 2-12, 2-14, 2-16, 2-18, 2-29 to 2-31, 2-62 to 2-64, 2-67, 2-68
- Extreme-line casing joint, 2-5, 2-7, 2-9, 2-11, 2-13, 2-15, 2-17, 2-19, 2-60, 2-63, 2-67 to 2-72
- Extruded-plastic system, 15-10
- Exxon Co. U.S.A., 16-13, 47-22
- Exxon Corp., 20-8

F

- "F" Pairs log analysis
- Facies, 29-5, 29-8
- Facilities, for fireflood, 46-20
for steamflood, 46-19, 46-20
- Facility throughput, 58-25, 58-30, 58-31
- Factor analysis, 24-20
- Factor, gas-pressure-at-depth, 5-5, 5-6
- Factors affecting oil viscosity, 22-14
- Factors affecting permeability measurements, gas slippage, 26-18
overburden pressure, 26-19
reactive fluids, 26-18, 26-19
- Factors contributing to vapor and gravity losses in tanks, agitation, 11-12
breathing, 11-12
filling, 11-12
storage size, 11-12
surface area, 11-12
tank pressures, 11-12

- temperature, 11-12
- vapor pressure, 11-12
- Factors for test-pressure equations, 2-63
- Factors in design of injection operations, 42-2
- Factors in evaluation of permeability from other parameters, 26-19, 26-20
- Factory-baked coatings, 11-1
- Fail-safe hydraulic actuators, 18-3
- Fail-safe valves, 3-18
- Failure diagram, 9-4
- Failures of sucker rods, 9-8, 9-9, 9-13
- Fair market value, 40-1
- Fair-market-value determination, 41-2, 41-3, 41-5, 41-8
- Fanning friction factor, 34-24
- Fanning's equation, 26-10
- Farmouts, 57-9, 57-10
- Fathometer, 18-5
- Fatigue analysis, 18-27
- Fatigue cracks or cracking, 9-1, 18-16
- Fatigue damage, 18-27
- Fatigue failure, 9-9, 18-21
- Fatigue life, 9-11
- Fatty amine compounds, 44-45
- Fault traps, 29-3
- Feasibility analysis, 39-17
- FED DDL wellsite analysis, 49-37
- Federal excise taxes, 41-1, 41-3, 41-4, 41-9, 41-12
- Federal income taxes, 41-5, 41-6, 41-8, 41-12
- Federal Power Commission (FPC) approval certificates, 41-9
- Federal Register, 57-12
- Federal taxes, 41-5, 41-7, 41-12 to 41-16, 44-5
- Fcc ownership, control, 57-2
- definition, 57-1
- Fcc simple interest, 41-1
- Fence diagram, 45-8, 45-9
- Ferric hydroxide, 56-3
- Ferrous sulfide precipitation, 54-7
- 6FF28 IES tool, 49-15
- 6FF40 IES logs and tool, 49-15, 49-17, 49-18
- Fiber-reinforced plastic pipe, 15-10
- Fiberglass casing and tubing, 44-46
- Fiberglass filaments, 12-12
- Fiberglass-lined steel tanks, 19-31
- Fiberglass-reinforced polyesters (FRP's), 11-9
- Fiberglass/steel rod string, 9-12
- Fiberglass sucker rods, application, 9-12, 9-13
- body, 9-12
- care, handling, and storage, 9-13, 9-14
- chemical and mechanical properties, 9-11
- end-fitting grades, 9-12
- expected life, 9-13
- failures, 9-13
- general dimensions, 9-11
- introduction, 9-10
- manufacture of, 9-12
- physical dimensions, 9-11
- rod-body-to-steel connector-joint design, 9-12
- stress-range diagram, 9-13
- Fibrous filters, 39-26
- Fibrous packing, 19-14
- Fibrous-type mist extractors, 12-12
- Field behavior vs. predicted performance, waterflooding, 44-31
- Field capillary number, 47-17
- Field compressors, control of, 13-57
- Field development, 36-1, 46-11
- Field development plan offshore, 18-25, 18-26
- Field engineers, 39-1
- Field examples, deviation survey, 53-7, 53-8
- Field facilities, fireflood, air compressors, 46-20
- ignition devices, 46-20
- steamflood, generation and injection, 46-19
- water treatment, 46-20
- Field-filtered sample, 24-4
- Field filtering equipment, 24-4
- Field instrumentation for SCADA, 16-9
- Field operations offshore, drillstem testing, 18-20
- introduction, 18-17
- location, establishing, 18-18
- plug and abandonment, 18-20
- running BOP, 18-18 to 18-20
- running 20-in. casing, 18-18
- running 30-in. casing, 18-18
- spudding the well, 18-18
- Field performance, 48-6, 48-7
- Field-performance data, 37-7
- Field pilot tests, 48-13
- Field pilots, 46-11
- Field projects, thermal recovery, dry vs. wet combustion, 46-18, 46-19
- reservoir performance, 46-14 to 46-17
- screening guides, 46-13
- Field response, MP flooding, 47-16
- Field results, chemical flooding, 47-21, 47-22
- foam injection, 47-9
- high-pH processes, 47-21, 47-22
- polymer floods, 47-6
- Field sampling, GC reservoir, 39-5
- Field separation conditions, optimum, 39-5
- Field titration kit, 54-3
- Field-welded tanks, 11-2, 11-9
- Filing losses, storage tanks, 11-11 to 11-13
- Fill-up, 44-9, 44-34, 44-39, 44-41, 44-46
- Film thickness of coatings, 11-4
- Filter/separator, 12-1, 12-2
- Filter-type mist extractor, 12-11
- Filtering, 12-8, 12-11, 19-7, 19-14, 19-28
- Filters, 15-20, 15-21
- Filtration, 15-20
- Finger in gas displacement, 43-7
- Fingering of miscible slug, 45-6
- Finite-closed aquifer, 38-5, 38-6, 38-8, 38-13, 38-18
- Finite-closed boundary, 38-1
- Finite-difference equations, 48-1, 48-2, 48-13
- Finite-difference method, 43-13 to 43-15
- Finite-difference simulator, 45-10
- Finite-element simulator, 45-10
- Finite linear aquifers, 38-2
- Finite-outcropping aquifer, 38-5, 38-8, 38-10, 38-11, 38-14 to 38-19
- Finite-outcropping boundary, definition, 38-1
- Fire detectors and detection systems, 18-47
- Fire hazard, 18-46
- Fire tests for valves, 3-38
- Fire tubes, 19-28
- Fireflood, 46-1, 46-3, 46-4, 46-13 to 46-28
- Fireflood pots, 46-13
- Firewall, 11-9, 11-11
- First-contact miscible flooding, 45-1, 45-2, 45-5
- First law of thermodynamics, 34-1
- First-stage separator gas, 39-6, 39-10
- Fishing characteristics of packers, 4-6
- Fissility, 52-20
- Fitting factor, 38-7
- Five-point difference scheme, 48-11
- Five-spot pattern, 43-2, 43-8, 44-1, 44-8, 44-13 to 44-20, 44-22, 44-23, 44-25, 44-26 to 44-29, 44-33, 44-34, 44-37, 44-38, 44-40, 45-7, 46-13, 46-17, 46-18, 46-23, 46-25, 46-26, 46-28, 46-30, 47-10
- Five valve manifold, 13-37
- Fixed choke, 5-54
- Fixed drilling platforms, 18-2, 18-24
- Fixed-pad Kingsbury thrust bearing, 7-3
- Fixed platform drilling, 3-38, 3-39
- Fixed pump installation, 6-2, 6-3
- Fixed-roof tanks, 11-2
- Flagging the bottom valve, gas lift, 5-44
- Flame arresters, 11-6, 11-8 to 11-10, 19-28
- Flame ionization detector (FID), 52-4, 52-5, 52-10, 52-11
- Flammable gases, 10-36
- Flammable liquids, 10-36
- Flange data, 3-16 to 3-25, 3-27
- Flange taps, 13-3 to 13-8, 13-14 to 13-19, 13-26, 13-27, 13-30, 13-31, 13-33, 13-34
- Flank waterflood, 48-13
- Flare boom, 18-20
- Flash calculations for separators, 12-33, 12-36, 12-37
- Flash calculations, multicomponent, 40-13
- Flash chamber, trap or vessel, 12-1
- Flash distillation system, 19-15, 19-16
- Flash gas liberation, definition, 22-20
- Flash gas separation, 37-1
- Flash liberation process, 32-7
- Flash point, 11-7 to 11-9
- Flash process, definition, 22-20
- Flash separation (vaporization), 12-32, 21-4, 37-3, 45-8
- Flat-bottom tanks, 11-2
- Flat-plate orifice, 13-2
- Flat-sided tanks (non-API), 11-2
- Flex joints, 18-12, 18-13, 18-19, 18-25
- Flexible pipe, 18-36, 18-37
- Flexural failure, 18-39
- Float-actuated pilot-operated valve, 13-53
- Float-and-sink (density) method, 52-20
- Float cages, 13-54
- Float-operated controller, 13-54
- Float-operated controls, 12-18
- Float-operated mechanical oil valves, 13-53
- Float-operated pilot, 12-5, 12-39
- Float-operated trap, 13-58
- Float traps, 13-53, 13-54
- Floating barges, 18-34
- Floating drilling operation or system, 18-3, 18-11, 18-14, 18-16
- Floating drilling rigs or vessels, 18-2, 18-6, 18-10, 18-13, 18-17, 18-20, 18-31, 18-34
- Floating drilling, subsea systems, 18-19
- Floating platforms, 3-38
- Floating drilling vessels, 3-39
- Floating production facilities (FPF), applications, 18-34, 18-35
- disposal of oil, gas, and water, 18-36
- semisubmersibles vs. tankers, 18-35, 18-36
- under Coast Guard jurisdiction, 18-44
- Floating-roof tanks, 11-2, 11-6
- Floatless level controller, 13-53
- Floatless level controls, 13-54
- Flocculation, 19-9, 19-10, 19-28, 44-46
- Flood coverage, 39-18, 44-18
- Flood efficiency, 39-18, 44-46
- Flood fronts, 44-16
- Flood pot tests, 40-16, 40-17
- Florida, 24-20, 24-21, 29-7, 29-8, 44-36
- Flotation, 15-20, 19-28
- Flow-after-flow, 33-4
- Flow channels, 26-10, 55-1
- Flow coefficient, 34-31
- Flow computer, 5-53
- Flow conductivity, 28-2
- Flow-control devices, safety shut-in systems, control systems, 3-31, 3-33, 3-34
- introduction, 3-18
- production platform, 3-19

- regulations, 3-34
- sensors, 3-34
- subsurface safety valves, 3-26, 3-27, 3-29, 3-31
- surface safety valves, 3-21
- with hydraulic and pneumatic valves, 3-20
- Flow-control valve, 16-11
- Flow-direction change to remove oil from gas, 12-9
- Flow in annulus, 41-42
- Flow in tubing, gas, 34-9 to 34-27
- Flow-measurement pulsed-data transmission systems, 17-4
- Flow nozzle flowmeter, 32-13
- Flow provers, 32-14
- Flow rate, equivalent total, 35-2
- Flow rate, units and conversions, 58-31
- Flow regimes, 34-36 to 34-38, 34-40
- Flow-string sizes, table, 34-23
- Flow-string weights, table, 34-23
- Flow surges, 12-20
- Flow systems of combinations of beds, 26-14, 26-15
- Flow systems of simple geometry, horizontal flow, 26-11, 26-12
- radial flow, 26-13
- vertical flow, 26-12, 26-13
- Flow-temperature gradient correlation, 5-26, 5-27
- Flow-test data on a well, 30-11 to 30-13
- Flow through chokes, 34-45, 34-46
- Flow through pores of various sizes, 54-10
- Flow velocities for pumps, 15-17
- Flow velocity change to remove oil from gas, 12-9
- Flow velocity, effect on acid reaction rate, 54-5
- Flowing BHP, gas, calculation of, 34-9 to 34-27
- Flowing gas column, 34-9
- Flowing gas wells, 34-23, 34-29
- Flowing-pressure-at-depth traverse, 5-23, 5-26
- Flowing pressure gradient, 5-1, 5-32, 5-43, 44-33
- Flowing pressure gradient curves, 5-25, 5-26, 5-30, 5-43
- Flowing pressure surveys, 5-43
- Flowing pressure traverses, 5-21, 5-23
- Flowing production pressure at depth, 5-45
- Flowing production pressure, gas-lift valve, 5-17 to 5-19, 5-21, 5-23, 5-24, 5-26 to 5-28, 5-30 to 5-33, 5-35, 5-36, 5-41 to 5-43, 5-45, 5-46, 5-48
- Flowing production transfer pressure, 5-33, 5-34, 5-36
- Flowing temperature adjustment factor, 33-15
- Flowing temperature factor, 13-3, 13-13
- Flowing wellhead backpressure, 5-54
- Flowing wellhead production pressure, 5-53
- Flowline backpressure, 6-25
- Flowline breaks, 16-11
- Flowline choke, 5-53, 5-54
- Flowline headers, 3-21
- Flowline pressure, 6-25, 6-43
- Flowline-pressure term, 6-28
- Flowline sampling, 24-3, 24-4
- Flowline temperature, 52-22 to 52-24
- Flowlines in subsea completions, 18-33, 18-34, 18-36 to 18-38
- Flowmeters, 32-6, 32-10, 32-13
- Flue gas, 45-1, 45-4, 45-6, 46-21
- Fluid channel gradient, 31-5
- Fluid coefficient, 55-2 to 55-4
- Fluid columns, specific gravities and unit pressure of, 6-22, 6-23
- Fluid composition, 51-7, 51-8
- Fluid conductivity, 26-10, 26-28
- Fluid-content investigation, 49-26, 49-27
- Fluid-controlled valves, 16-3, 16-4
- Fluid controls, 6-51
- Fluid data, ESP, 7-9
- Fluid distributions, 44-2 to 44-4, 44-11
- Fluid-electric-controlled valves, 16-3
- Fluid-flow effects on waterflooding, 44-29
- Fluid-flow model, 44-20, 44-21
- Fluid/fluid interstitial configurations, 28-3
- Fluid friction in hydraulic pumps, 6-19, 6-20
- Fluid friction in sandstone reservoirs, 56-2
- Fluid friction in tubular and annular flow passages, 6-26
- Fluid-friction losses, 6-5, 6-25, 6-47, 6-49 to 6-51, 6-67, 6-69
- Fluid-gradient calculations, 6-26
- Fluid identification, 50-2, 50-3
- Fluid incompressibility, 51-49
- Fluid-inventory equations, 43-9
- Fluid jet, 8-7
- Fluid level in well, 30-7, 30-8, 30-15
- Fluid-loss additives, 55-4
- Fluid-loss agents, 54-8
- Fluid-loss characteristics of fracturing fluids, 55-2, 55-7, 55-8
- Fluid-loss-controlled fluids, 55-4
- Fluid mapper, 44-20
- Fluid mobility, 39-20, 44-7, 51-47, 52-14
- Fluid pound, 10-5, 10-6
- Fluid power, 6-15
- Fluid pressure differences, 56-2
- Fluid pressure regulator, 13-54
- Fluid properties, data, 37-16
- gas and liquid FVF, 6-67 to 6-69
- gravity, 6-67
- introduction, 6-66
- oil systems, 22-1
- viscosity, 6-67
- Fluid pumpoff chart, ESP, 7-15
- Fluid sample analysis, 41-8
- Fluid saturation configurations, 28-2
- Fluid saturation distributions, 28-2, 46-2
- Fluid saturations, comparison of methods of measurement, 26-24 to 26-27
- determination from rock samples, 26-21, 26-22
- interstitial water, 26-22 to 26-24
- laboratory measurement of capillary pressure, 26-24
- of cores, factors affecting, 26-20, 26-21
- of reservoir for waterflooding, 46-3, 46-4
- Fluid viscosity, 6-27
- Fluids in motion, energy relationships, 34-1, 34-2
- irreversibility losses, 34-2, 34-3
- Flume pipe, 19-21
- Fluoboric acid system, 54-4, 54-11
- Fluorescence X-ray, 50-7
- Fluoride, 19-10, 56-1
- Fluoride intensifier, 54-4
- Fluosilicates, 54-4, 56-4
- Flushing agent, 10-13
- Flushing efficiency, 39-18
- Flux-gate magnetometer, 51-28
- Flux leakage, 53-20 to 53-23, 53-26
- Flywheel, 10-15, 10-19
- Foam, 18-47, 19-23, 32-7, 45-8
- Foam flooding, 47-1, 47-6 to 47-9
- Foam quality, 55-6
- Foam separator, 12-18
- Foam stability, 47-7
- Foaming agents, 39-16, 55-6
- Foaming in desulfurizer, 14-22
- Foaming oil, 12-3, 12-6, 12-7, 12-13, 12-17, 12-19 to 12-22, 12-32, 12-35
- Foams as fracturing fluids, 55-6, 55-7, 55-9
- Focused electrical-resistivity devices, 26-31
- Focused-electrode devices, 49-11, 49-18
- Focused-electrode logs, 49-18 to 49-22
- Folded structure, 53-12
- Force balance equations, 5-13
- Force balance in downhole pumps, 6-16 to 6-19
- Force of gravity, 58-3
- Force summing devices, 30-1, 30-2, 30-6
- Force, unit and definition, 58-11, 58-23, 58-24, 58-34
- Forced-circulation heating, 19-22
- Forced-draft burners, 19-28
- Forchheimer equation, 35-11
- Fordoch field, Louisiana, 39-16
- Forecast of future rate of production, constant percentage decline, 41-9, 41-10
- declining production, 41-9
- harmonic decline, 41-10
- hyperbolic decline, 41-10
- part constant rate-part declining production, 41-10, 41-11
- produced product prices, 41-11
- proration of market curtailment, 41-11
- Foreign objects in flow string, 33-20, 33-22
- Forest Hill field, Texas, 46-31, 46-34
- Formation, analysis, in sand control, 56-3
- damage, 56-4, 56-8
- properties, in sand control, 56-2
- sampling, in sand control, 56-3
- Formation alteration, effect on log measurements, 51-20 to 51-23
- Formation balance gradient, 52-25, 52-26
- Formation compaction, 26-8
- Formation composition, effect on acid reaction rate, 54-6
- Formation compressibility, 40-34
- Formation compressibility vs. depth, 26-7
- Formation conductivity, 54-8, 54-9
- Formation damage, 4-9, 30-8, 35-4, 39-25, 51-21, 54-8 to 54-10
- Formation density log, 52-20
- Formation drillability exponent, 52-24
- Formation evaluation, 51-1, 51-48
- Formation evaluation letter and computer symbols, 59-2 to 59-51
- Formation evaluation services, 52-2 to 52-11
- Formation factor, dependence on porosity and lithology, 49-4
- evaluation, 49-14, 49-26, 49-30
- Formation fluid pressure, 51-39
- Formation fracturing, fluid-loss-controlled fluids, 55-4
- formations fractured, 55-2
- fracture area, 55-2, 55-3
- fracture planes, 55-2
- fracturing equipment, 55-9
- fracturing materials, 55-5 to 55-8
- fracturing techniques, 55-8, 55-9
- general references, 55-10 to 55-12
- hydraulic fracturing theory, 55-1, 55-2
- introduction, 55-1
- multiple-zone fracturing, 55-9
- operations, 8-8
- references, 55-10
- reservoir-controlled fluids, 55-2, 55-4
- stimulation results, 55-4, 55-5
- treatment planning, 55-9, 55-10
- viscosity-controlled fluids, 55-4
- Formation of an emulsion, 19-2, 19-3
- Formation permeability, 50-2
- Formation pore pressure, 52-17
- Formation pressure gradient, 51-39
- Formation resistivity factor, 26-28 to 26-31, 49-4
- Formation shear-wave velocity, 51-25
- Formation tests, 40-3

- Formation transit time, 51-19, 51-20
- Formation volume.
- of gas plus liquid phases, 21-19
 - of well production at reservoir conditions, 21-20
 - total, gas-condensate system, 21-16, 21-18
 - total by Standing's correlation, 21-19
- Formation volume correlations, 21-15 to 21-20
- Formation volume factor (FVF) of gas, 6-67, 20-11, 20-16, 22-13, 22-20, 37-16, 39-14, 39-23, 40-5, 40-7, 40-9, 40-22 to 40-24
- FVF of gas plus liquid phase, 6-47
- FVF of oil, 6-67, 22-1, 22-10 to 22-13, 22-20, 37-16, 40-6, 40-8, 40-9, 40-11, 40-16
- FVF of water, 24-15, 24-16
- FVF, total (two-phase), 6-47, 6-68, 22-1, 22-13, 22-14, 22-20
- FVF's vs. pressure, 37-16
- Formation water, definition, 24-18
- Formation water density, 24-14
- Formation water resistivity, 24-14, 24-16, 49-4
- Formation water sample, 24-3
- Formation water viscosity, 24-16, 24-17
- Formations fractured, 55-2
- Formazin polymer, 44-44
- Formazin turbidity units (FTU), 44-44
- Formic acid (HCOOH) in acidizing, 54-3, 54-8, 54-10
- Forms of meter, 13-2
- Formulation sequential, 48-14
- FORTAN IV, 17-6, 17-7
- FORTAN card deck, 17-5
- FORTAN source code listing, 9-3
- Fossil water, 24-2
- Foster field, Texas, 44-30
- Foundations for pump and prime mover, 15-18
- Foundations of pumping units, 10-7
- Four-arm caliper, 53-17
- Four-arm dipmeter tools, 53-8, 53-10
- Four-cycle engine, 10-14 to 10-16, 10-19
- Four-stage separation, 12-34
- Four-way engine valves, 6-9
- Fourier heat equation, 26-16
- F_r values for various annuli, 33-17
- F_r values for various flow strings, 33-16
- Fractional analyses, 39-2
- Fractional-flow curve, 40-14, 43-10, 43-11, 44-12
- Fractional-flow equation, 40-17, 43-3, 43-5, 43-10, 44-4, 44-9, 44-10
- Fractional flow of gas, 40-14, 43-6, 43-8
- Fractional horsepower motors, 18-46
- Fractional oil recovery, 44-9
- Fractional water cut, 44-8
- Fractionation, 39-27
- Fractionation equipment, 39-5
- Fracture acidizing, 54-9, 54-11
- Fracture area, 55-2, 55-3
- Fracture-assisted steamflood, 46-26
- Fracture conductivity, 54-8, 54-9, 55-4, 55-8, 55-9
- Fracture conductivity ratio, 55-4
- Fracture evaluation, 51-45 to 51-47
- Fracture flow capacity, 55-8
- Fracture-fluid efficiency, 55-4
- Fracture geometry, 55-5, 55-9
- Fracture gradient, 55-2
- Fracture of pipe, 2-60
- Fracture penetration, 55-4, 55-9
- Fracture planes, 55-2
- Fracture porosity, 44-2
- Fracture pressures, 44-3, 44-46, 51-44
- Fracture strength of casing, 2-61
- Fractured-matrix imbibition, 48-9
- Fractured matrix model, 48-5
- Fractured porosity, 29-8
- Fractures, permeability of, 26-16
- Fracturing: See Formation fracturing
- Fracturing, 26-2, 40-23, 40-24, 51-44, 56-1
- Fracturing efficiency, 55-9
- Fracturing equipment, 55-9
- Fracturing fluids, comparative efficiency, 55-9
- early treatments with, 55-1
 - effective volume of, 55-2
 - foams, 55-6, 55-7
 - gelled-oil, 55-7
 - heavy oil-in-water emulsions, 55-7
 - high-viscosity, 55-8
 - leakoff, 55-4
 - mixed-base, 55-7
 - oil-base, 55-5
 - oil-in-water dispersion, 55-7
 - rate of leakoff controlled by viscosity, 55-4
 - viscosity of, 55-2
 - viscous emulsion, 55-8
 - volume of, 55-3
 - water-base, 55-5 to 55-7
- Fracturing materials, fluids, 55-5 to 55-8
- propping agents, 55-8
- selection, 55-9
- Fracturing pressure, 54-10, 54-11, 56-5
- Fracturing pressure gradients, 55-2
- Fracturing techniques, 55-8, 55-9
- France, 1-68, 12-39, 46-3, 46-27 to 46-29
- Frangible-roof tanks, 11-2
- Frax log analysis, 49-37
- Free condensate, 14-5
- Free gas, 6-2, 6-38, 6-39, 6-47, 6-50, 6-57, 6-62, 8-10, 12-3, 22-1, 22-9, 37-1, 37-2, 37-5, 40-5, 40-8, 40-13, 40-22 to 40-24, 40-33, 44-4
- Free-gas cap, 40-6 to 40-8, 40-10
- Free-gas production, 37-2
- Free-gas production rate, 37-11
- Free-gas saturation, 37-22, 40-19, 44-4, 44-5
- Free pump cycle, 6-3, 6-6
- Free pump installations, 6-3, 6-4
- Free-standing risers, 18-15
- Free-stretch factor of casing, 2-35
- Free water, 14-3, 14-5, 14-6, 14-17, 14-20, 19-9, 19-17, 19-24, 19-25
- Free water knockout (FWKO), 12-3, 12-4, 12-13, 15-21, 18-28, 19-9, 19-17 to 19-19, 19-22, 19-32
- Freezing point, 14-2, 14-6, 14-10, 14-19, 21-19, 25-19
- Freezing problem, 13-53
- French design, concrete structures, 18-23
- French Natl. Assembly, 1-68
- Freon 12, 14-9
- Frequency of wave, 51-14
- Frequency response, 30-5, 30-6
- Frequency, unit and definition, 58-11, 58-23, 58-36
- Fresh core techniques, 44-5
- Fresh mud, 49-20, 49-25, 49-27
- Fresh water, 44-41, 44-42
- Freshwater buffer, MP flooding, 47-10
- Freshwater recharge, 24-20
- Friction coefficient, 9-9
- Friction factor, 15-1 to 15-3, 15-5 to 15-7, 15-10, 34-2, 34-3, 34-24, 34-38, 34-39, 39-25
- Friction in downhole pumps, 6-21
- Friction loss, 13-2
- Friction loss curves, 55-6, 55-7
- Friction loss gradient, 34-36, 34-38 to 34-40
- Friction losses, 46-29
- Friction pressure, 55-5, 55-6
- Friction pressure-drop curves, 6-26, 6-70, 6-71
- Friction relationships.
- annular sections—flow between tubing and casing, 6-69 to 6-72
 - circular sections—tubing, 6-69
 - pressure drop in tubing annular flow, 6-70, 6-71
- Friction wheel engine starters, 10-19
- Frictional horsepower, 10-18, 10-19
- Frictional pressure drop or loss, 6-1, 6-18 to 6-20, 6-25, 6-35, 46-7
- Fritted glass, 26-6, 26-24
- Front displacement models.
- Mandl-Volek's refinement of Marx-Langenheim method, 46-8
 - Marx-Langenheim method, 46-7, 46-8
 - Ramey's generalization of Marx-Langenheim method, 46-8
- Frontal-advance applications, 43-16
- Frontal-advance calculation, 43-12, 44-9 to 44-11
- Frontal-advance equation, 40-14, 40-17, 40-18, 44-10
- Frontal-advance performance, 43-12
- Frontal advance theory, 44-7
- Frontal-drive method, for oil reservoir with gas-cap drive, 40-13, 40-14
- for oil reservoir with water drive, 40-17, 40-18
- Frost heaving, 18-41
- Frost point, 25-5
- Fry pool, Texas, 44-1
- Fuel availability for engines, 10-16
- Fuel consumption, 10-17, 58-33
- Fuel content as performance indicator, firefloods, 46-16
- Fuel-gas scrubbers, 19-28
- Fugacity coefficient, 25-11
- Fugacity of hydrate, 25-11
- Full-bore flowline valves, 3-12 to 3-14
- Full-capacity relief valves, 12-40
- Full-diameter core analysis, 27-1, 27-8
- Full-diameter core method, 26-17
- Full diesels, 10-15
- Full-interest wells, 57-9
- Full-line injection-gas pressure, 5-53
- Full-load rating of motor, 10-26, 10-28, 10-30
- Full-load slip, 10-24
- Fullerton-Clearfork unit, California, 36-7
- Fully implicit formulation, 48-14
- Fungi, 44-43, 44-44
- Funicular distribution, 26-24
- Fuses for motors, 10-28
- Fusible plugs for fire detection, 18-47
- Future inflow performance, 34-34, 34-35
- Future net cash income, 41-5, 41-6
- Future performance calculations, 43-10 to 43-16
- Future performance, water-drive reservoirs.
- pressure gradient between new and original front positions, 38-13, 38-14
 - reservoir above bubblepoint pressure, 38-14
 - reservoir below bubblepoint pressure, 38-14 to 38-16
 - reservoir simulation models, 38-16

G

- Galling, 6-50
- Galvanic anodes, 19-31
- Galvanic corrosion, 3-36
- Galvanized coating, 11-6
- Galvanized wire armor, 18-49
- Gamma-gamma density devices, 50-7, 50-15 to 50-17, 50-26 to 50-28, 50-37
- Gamma probability function, 39-11
- Gamma radiation, 50-3

- Gamma ray absorption, 50-2, 50-13
 Gamma ray attenuation, 50-2, 50-4
 Gamma ray curve and log, 36-4, 46-27,
 49-15, 49-19, 49-20, 49-25, 49-38,
 49-39, 50-15, 50-24 to 50-27, 51-16,
 51-17, 51-19, 51-23, 51-26, 51-27,
 51-33, 51-38, 51-45, 53-2, 53-4, 53-26
 Gamma ray detection, 50-14, 50-23
 Gamma ray devices, 50-15, 50-16
 Gamma ray emission spectra, 50-15, 50-17
 Gamma ray energy, 50-7, 50-13, 50-15
 Gamma ray flux, geometry for, 50-16
 Gamma ray index, 50-24
 Gamma ray interactions, 50-6 to 50-8,
 50-12, 50-14
 Gamma ray measurements, 50-24 to 50-26
 Gamma ray spectroscopy, 50-2, 50-3,
 50-12, 50-13, 50-22, 50-24, 50-35
 Garden Banks platform, 18-2
 Gas analysis, 52-17, 52-18
 Gas analysis system, 52-3
 Gas anchors, 8-9, 8-10
 Gas and oil differences, 36-2
 Gas backpressure valve, 12-4, 12-5, 12-9
 Gas boot, 6-33, 6-57 to 6-59, 19-13, 19-18,
 19-21
 Gas break-out, 16-14
 Gas breakthrough, 43-3, 43-5, 43-8, 43-9
 Gas cap, 37-2, 37-3, 37-5 to 37-8, 37-13 to
 37-17, 39-5, 40-5
 Gas-cap drive, 36-2, 37-1, 40-8, 40-13, 40-14
 Gas-cap-drive reservoirs, 43-9, 42-5
 Gas-cap encroachment, 36-2
 Gas-cap expansion, 43-12, 43-15, 43-16
 Gas-cap gas expansion, 37-5
 Gas-cap gas production, 37-5
 Gas cap in vessel, 6-62
 Gas-cap injection, 43-3
 Gas cap/oil production, 37-10
 Gas-cap reservoir, 46-24 to 46-26
 Gas capacity chart, 5-8
 Gas capacity of separators, 12-23 to 12-25,
 12-27 to 12-29, 12-31, 12-32
 Gas chromatography, 27-1, 52-5
 Gas compressibility, 36-2
 Gas compressibility factor, 5-8, 5-11,
 12-22, 12-23, 12-25, 12-26, 12-29,
 12-30, 20-4, 20-7, 20-8, 20-10, 20-11,
 20-14, 22-13, 46-45
 Gas/condensate ratio, 39-5
 Gas-condensate recovery, 39-13
 Gas-condensate reservoirs,
 economics of operation, 39-26, 39-27
 formation and fluid data for, 39-11
 general operating problems, 39-24 to
 39-26
 introduction, 39-1
 nomenclature, 39-27
 operation by pressure depletion, 39-10 to
 39-15
 operation by pressure maintenance or
 cycling, 39-15 to 39-24
 properties and behavior, 39-1 to 39-4
 references, 39-27, 39-28
 sample collection and evaluation, 39-6 to
 39-10
 well tests and sampling, 39-4 to 39-6
 Gas condensate systems, 20-4, 21-16 to
 21-20, 22-1
 Gas-condensate wells, 3-36, 3-37, 33-4,
 34-37, 34-28, 34-36
 Gas condensates, 20-11, 40-13, 40-24
 Gas coning, 32-3, 37-2, 37-13, 48-6
 Gas cushion, 19-17, 19-18
 Gas cutting, 18-47
 Gas cycling, 34-28, 45-13, 45-14
 Gas cyclone, 12-20
 Gas deliverability approach, 35-12
 Gas-depletion drive, 29-7
 Gas deviation factor, definition, 22-20
 Gas-discharge counters, 50-12
 Gas discharge radiation detector, 50-12
 Gas displacement, 43-3 to 43-6, 43-8, 43-16
 Gas disposal, 18-30
 Gas distribution system, 12-38
 Gas drive, 46-3, 46-5
 Gas effect, on acoustic log, 51-37
 on velocity ratio, 51-38
 Gas effect on neutron porosity, 50-30,
 50-31
 Gas eliminators, 15-14
 Gas evolution, 37-22, 37-23
 Gas expansion, 37-6
 Gas expansion factor, 39-11, 40-7
 Gas-expansion method of determining
 porosity, 26-6
 Gas-expansion porosimeter, 26-6
 Gas exsolution, 52-14
 Gas extraction methods, 52-2
 Gas filter, 12-1, 12-2
 Gas-fired crude oil heating unit, 19-28
 Gas flaring, 18-30
 Gas flotation units, 15-27
 Gas-flow computers, 16-6, 16-12
 Gas flow, Weymouth formula, chart, 15-8,
 15-9
 Gas formation volume factor (FVF), 6-67,
 20-11, 20-16, 22-13, 22-20, 37-16,
 39-14, 39-23, 40-5, 40-7, 40-9, 40-22 to
 40-24
 Gas-free hydraulic loop, 18-34
 Gas-free viscosity, 22-14, 22-15
 Gas fuel consumption, 39-24
 Gas fundamentals as applied to gas lift,
 gas pressure at depth, 5-3 to 5-6
 gas volume stored in conduit, 5-11, 5-12
 introduction, 5-3
 temperature effect on confined bellows-
 charged dome pressure, 5-6 to 5-8
 volumetric gas throughput of a choke or
 gas lift valve port, 5-8 to 5-10
 Gas/gas interface, 39-21
 Gas-gathering facilities, 5-53
 Gas-gathering system, 12-10, 12-11, 12-33
 Gas gravities of natural gases, table, 25-6
 Gas-gravity/condensate-gas ratio, 34-28
 Gas gravity, definition, 22-20
 Gas handling, approximation for, 6-38, 6-39
 Gas-hydrate equilibrium locus, 25-2
 Gas hydrate region, oil and gas reservoirs
 that exist in, 25-18, 25-19
 Gas in effluent oil, 12-15, 12-16
 Gas in place,
 by material balance, 40-6, 40-7
 by volumetric method, 40-5, 40-6
 in reservoir containing nonassociated gas
 and interstitial water but no residual oil,
 40-23
 Gas injection, 42-5, 43-16
 Gas injection, BHP calculation, 34-28 to
 34-30
 Gas injection data, 39-23
 Gas-injection operations, 43-2, 43-3, 43-7,
 43-9, 43-17
 Gas-injection performance, 43-5, 43-16
 Gas injection pressure maintenance in oil
 reservoirs,
 calculation of performance, 43-8 to 43-10
 efficiencies of oil recovery by gas
 displacement, 43-3
 example calculations of future
 performance, 43-10 to 43-16
 introduction, 43-1, 43-2
 methods of evaluating areal sweep
 efficiency, 43-7, 43-8
 methods of evaluating conformance
 efficiency, 43-6, 43-7
 methods of evaluating displacement
 efficiency, 43-3 to 43-6
 nomenclature, 43-18
 optimal time to initiate, 43-3
 references, 43-16, 43-17, 43-19
 types of gas-injection operations, 43-2, 43-3
 Gas interference, 6-21, 6-22, 6-24
 Gas law constants, 20-2
 Gas liberation, 37-3
 Gas lift, charts, 6-43
 continuous flow, 5-21 to 5-38, 34-40 to 34-45
 design procedures, 34-40, 34-41
 designing installations, 34-28
 gas fundamentals as applied to, 5-3 to 5-12
 intermittent flow, 5-38 to 5-53
 introduction, 5-1 to 5-3
 nomenclature, 5-55
 operations, description of, 5-1
 performance, 34-44
 references, 5-57
 unloading procedures and proper
 adjustment of injection gas, 5-53 to 5-55
 valve mechanics, 5-12 to 5-21
 valves, 6-2, 6-6, 18-28, 18-34
 well control, 16-11
 wells, energy losses, 34-37
 wells, tubing profile caliper, 53-17
 Gas-lifting methods, 44-42
 Gas/liquid/hydrate equilibrium, 25-5
 Gas/liquid ratio (GLR), 5-23, 5-25, 5-26,
 5-34, 5-36, 5-38, 5-43, 6-27, 6-29,
 6-30, 6-35, 6-41, 6-42, 6-44, 12-21,
 12-22, 39-2 to 39-6, 39-10
 Gas/liquid relative permeability data, 39-7
 Gas lock, 7-4, 7-6, 7-10, 7-15, 7-16
 Gas lock breakers, 6-21
 Gas lock chart, ESP, 7-15
 Gas locking, 6-10, 6-21, 8-9
 Gas measurement, automatic, of lease
 equipment, 16-6, 16-7
 flow nipple and pitot tube for, 33-2
 general references, 13-59
 instruments, 33-13
 introduction, 13-1
 metering systems, 13-37
 orifice constants, 13-3 to 13-35
 physical setup of system for, 13-36, 13-37
 references, 13-59
 velocity meters, 13-1 to 13-3
 Gas mobility, 37-3, 39-25, 43-7
 Gas motor engine starters, 10-19
 Gas/oil contact, 26-25, 40-4, 40-14, 40-15,
 41-9, 46-26
 Gas/oil flow through chokes, 34-47 to 34-49
 Gas/oil interface, 18-47, 50-36
 Gas/oil interfacial tension (IFT), 22-16, 22-17
 Gas/oil ratio (GOR), 5-25, 5-26, 6-24,
 6-25, 6-29, 6-30, 6-38, 6-39, 6-44,
 6-47, 12-35, 22-20, 34-41 to 34-43,
 34-47 to 34-49, 38-16, 39-1, 39-2,
 40-33, 41-8, 44-39, 58-38
 Gas/oil relative permeability, 28-9
 Gas/oil relative permeability ratio, 37-1,
 37-2, 39-13
 Gas/oil separator, 22-20
 Gas override, 48-12
 Gas passage charts, 5-8 to 5-10
 Gas payment, definition, 41-1
 Gas permeability, 39-13, 39-25, 47-9
 Gas-plus-liquid FVF, 6-38
 Gas pressure at depth,
 charts, 5-3, 5-6
 factors for approximating, 5-5, 5-6, 5-11

- injection curves, 5-5
 - static injection calculations, 5-3 to 5-6
 - Gas-pressure-at-depth factor, 5-5, 5-6, 5-49
 - Gas pressure function, 37-8 to 37-10
 - Gas pressure-maintenance performance, 43-8 to 43-10
 - Gas price, gross, 41-9
 - Gas processing plants, 40-3
 - Gas Processors Assn. (GPA), 20-8, 25-9
 - Gas Processors Suppliers Assn. (GPSA), 20-8
 - Gas-producing intervals, location of, 31-4, 31-6
 - Gas properties and correlations,
 - Amagat's law, 20-4
 - Calingeart and Davis equation, 20-13
 - coefficient of isothermal compressibility, 20-11
 - Cox chart, 20-12, 20-13
 - critical temperature and pressure, 20-2, 20-3
 - Dalton's law, 20-4
 - equations of state, 20-6, 20-7
 - example problems, 20-13 to 20-17
 - formation volume factor, 20-11
 - ideal gas, 20-1, 20-2
 - Lee-Kessler equation, 20-13
 - mole fraction and apparent MW of gas mixtures, 20-4
 - molecular weight, 20-1, 20-3
 - natural gasoline content of gas, 20-10, 20-11
 - principles of corresponding states, 20-4
 - real gases, 20-4 to 20-6
 - references, 20-18
 - van der Waals' equation, 20-7 to 20-9
 - specific gravity (relative density), 20-4
 - specific gravity of gas mixtures, 20-4
 - vapor pressure, 20-3, 20-11, 20-12
 - viscosity, 20-9
 - viscosity correlations, 20-9, 20-10
 - Gas properties, effect on gas well performance, 35-10
 - Gas property ownership, 41-1, 41-2
 - Gas-purchase contracts, 41-3, 41-9
 - Gas quality from scrubbers, 12-15
 - Gas recoveries by natural water drive or gas injection, 39-16
 - Gas regulation,
 - definitions, 13-49, 13-50
 - field compressors, control of, 13-57 to 13-59
 - high-pressure service, 13-55, 13-56
 - liquid-level control, 13-53, 13-54
 - low-pressure service, 13-55
 - principles of control, 13-49
 - process characteristics, 13-50 to 13-53
 - references, 13-59
 - regulators, types of, 13-54 to 13-57
 - Gas regulator, 10-19
 - Gas relative permeability, 28-8 to 28-12, 40-25, 40-26
 - Gas relative permeability vs. total wetting-fluid saturation, 28-8
 - Gas reserves: See also Reserves
 - Gas reservoir,
 - development plan for, 36-1 to 36-11
 - infinite acting, 35-11, 35-12
 - Gas reservoirs, depletion technique, 36-2, 36-3
 - free gas in, 40-5
 - in gas hydrate region, 25-18, 25-19
 - nonassociated, material balance recovery estimates, 40-33, 40-34
 - nonassociated, volumetric recovery estimates, 40-21 to 40-26
 - with water drive, 40-7, 40-26
 - without water drive, 40-24, 40-25, 40-33
- Gas richness indicator, 52-4
- Gas sales contract, 12-33, 14-1
- Gas sales line, 3-19
- Gas-saturated crude oil, 22-15
- Gas scrubbers, 12-1, 12-10, 12-11, 12-20 to 12-22, 12-35, 12-38, 18-28
- Gas separator to remedy gas locking, 7-16
- Gas shows, total, 52-13 to 52-16, 52-18
- Gas sizing of separator, 12-30
- Gas slippage, effect on permeability measurements, 26-18, 26-19
- Gas-slippage effects, study required, 28-13
- Gas solubility, 40-9
- Gas solubility in oil, 22-21
- Gas stripping, 15-29
- Gas sweeteners, 12-35
- Gas throughput performance, 5-22
- Gas-to-gas heat exchanger, 14-5 to 14-8, 14-11, 14-14, 14-15, 14-20
- Gas-transmission-line pressure, 14-15
- Gas transmission lines, 12-38
- Gas transmission piping specs., 15-12
- Gas trap, 52-2
- Gas-treating systems, 14-17 to 14-22
- Gas turbine meters, 16-6
- Gas turbines, 15-16, 15-17, 46-19
- Gas-vent string, 6-4
- Gas venting passage, 6-2, 6-5
- Gas viscosity, 40-9, 44-6
- Gas volume stored, in casing annulus, within a conduit, 5-11, 5-12,
- Gas/water contact, 39-21
- Gas/water flow, 34-27
- Gas/water interface, 39-21, 39-22
- Gas well inflow equation, 33-5 to 33-7
- Gas well performance,
 - deterioration causes, 33-20 to 33-22
 - gas properties, effect of, 35-10
 - infinite-acting gas reservoir, 35-11, 35-12
 - long-term forecast, 35-12
 - non-Darcy flow, 35-10, 35-11
 - pseudosteady-state solutions, 35-12
- Gas wells,
 - flow through tubing-casing annulus, 34-27
 - flowing BHP calculation, 34-9 to 34-27
 - not suitable for TFL service, 18-34
 - openflow, 33-1 to 33-23
 - static BHP calculation, 34-3 to 34-9
- Gasoline as four-cycle engine fuel, 10-15
- Gasoline content, 39-1, 39-5
- Gasoline-driven engine starters, 10-19
- Gasoline-plant recovery efficiency, 45-12 to 45-15
- Gasoline plants, 11-13, 40-13, 41-3, 57-5
- Gasoline/water system, 25-27
- Gassmann-Biot theory, 51-36
- Gassmann's theory, 51-8
- Gassy conditions, ESP chart, 7-16
- Gassy fluid, 6-21
- Gassy wells, 6-28, 6-34
- Gate valves, 3-11 to 3-13, 3-21
- Gathering systems, 11-13, 40-1
- Gauge cocks, 12-42
- Gauge glasses, 12-42
- Gauge location factor, 13-8, 13-35
- Gauge tables, correcting for incrustation, 17-3
- Gauging petroleum and petroleum products, 17-3
- Gaussian elimination, 48-16
- Gear pump, 19-5
- Gear reducer, 10-2 to 10-6, 10-12, 10-13
- Gear reduction units, 6-50
- Gearhart, 49-2, 49-36, 49-37
- Geiger-Müller tube, 50-16
- Gel or gelatin model, 39-21, 44-17, 44-18, 44-20, 44-21
- Gel slugs, 54-10
- Gel strength, 58-34
- Gelled-oil fracturing fluid, 55-7
- Gelled water in acidizing, 54-12
- Gelling agents, 54-8
- Gels as fracturing fluids, 55-5, 55-6
- General Conference on Weights and Measures, 1-69
- General crude, 46-16, 46-18, 46-21
- General flow equations, 13-1
- General overhead (GO), 41-14
- General Petroleum Co., 46-14 to 46-15
- General principles of acidizing,
 - acetic and formic acids, 54-3
 - hydrochloric acid, 54-1 to 54-3
 - hydrofluoric acid, 54-3, 54-4
- General references: See also References,
 - acidizing, 54-12 to 54-14
 - automation of lease equipment, 16-16, 16-17
 - crude oil emulsions, 19-33, 19-34
 - electric submersible pumps, 7-17
 - electrical logging, 49-41, 49-42
 - estimation of oil and gas reserves, 40-38
 - formation fracturing, 55-10 to 55-12
 - gas-injection pressure maintenance in oil reservoirs, 43-16, 43-17
 - gas measurement and regulation, 13-59
 - hydrate/volatile-gas systems, 25-27, 25-28
 - miscible displacement, 45-15
 - mud logging, 52-30
 - oil and gas leases, 57-12
 - petroleum reservoir traps, 29-9
 - phase behavior of water/hydrocarbon systems, 25-24 to 25-28
 - relative permeability, 28-16
 - reservoir simulation, 48-20
 - sucker rods, 9-14
 - temperature in wells, 31-7
 - thermal recovery, 46-45, 46-46
 - valuation of oil and gas reserves, 41-37
 - water-drive oil reservoirs, 38-20
 - water-injection pressure maintenance and waterflood processes, 44-52
 - water/volatile-gas systems, 25-24 to 25-27
 - wellhead equipment and flow-control devices, 3-40
- Generator voltage, 10-21
- Geochemical analysis, 52-1, 52-2
- Geochemical model, 24-20
- Geochemical parameters, 50-37
- Geochemical water analyses, 24-5
- Geochemistry, 50-36, 50-37
- Geochronology, 58-25
- Geodetic surveys, 1-69
- GEODIP log analysis, 49-37
- Geographical distribution of thermal recovery projects, 46-3
- Geological analysis, 52-2, 52-7 to 52-9, 52-28
- Geological correlation, 51-29, 51-30
- Geological interpretation, 51-28, 51-29
- Geological map, 40-4
- Geologists, 57-8
- Geology, in oil and gas reservoirs development,
 - carbonate reservoirs, 36-5, 36-6
 - clastic reservoirs, 36-3, 36-4
 - paleo-environments, interpretation of, 36-3
 - shale stringers, extent of, 36-6
- Geology in sand control, 56-2
- Geometric-mean air permeabilities, 44-37
- Geometric progression, 6-39
- Geometric series, 40-30
- Geometric spread of energy, 51-3
- Geometric spreading, 51-12, 51-13
- Geometrical factor, 49-16 to 49-18, 49-22
- Geometrical spreading factor, 51-13
- Geometrical spreading loss, 49-34
- Geophysics, in characterizing reservoirs, 36-8, 36-9

- Geopressure detection, 51-39
 Geopressure evaluation, 52-2, 52-16 to 52-26
 Geopressure gradient, 52-25
 Geopressure transition zone, 52-24
 Geopressured shales, 52-22
 Geopressured zone, 52-22 to 52-24
 Geotechnical analysis, 18-41
 Geothermal gradient,
 assumed to estimate BHT, 31-6
 basis for pressure-at-depth curves, 5-5
 definition of, 52-22
 in sedimentary basins, 31-2
 in southwest U.S., 31-3
 increased, 5-23
 linear, 46-5
 temperature profile, 4-6
 Geothermal temperature, 5-26
 Geothermal temperature gradient, 5-6
 Geothermics, 58-33
 Germanium (Ge) detector, 50-14, 50-23
 Germany, 12-39, 46-3
 Getting the well drilled, 57-8
 Getty Oil Co., 46-4, 46-14, 46-15, 46-18, 46-20, 46-23, 46-24
 Gibbs theory, 47-8, 47-11
 Gilbert's equation, 34-45, 34-46
 Gippsland basin, Australia, 27-19
 Glass wool, 19-14
 Glauconite, 46-21
 Glen Hummel field, Texas, 46-15, 46-18
 Glenpool field, Oklahoma, 54-1
 GLOBAL log analysis, 49-37
 Gloriana field, Texas, 46-15, 46-29 to 46-32
 Glossary of terms, reserves estimation,
 crude oil, 40-3
 improved recovery, 40-4
 natural gas, 40-3
 natural gas liquids, 40-3
 possible reserves, 40-4
 probable reserves, 40-4
 reservoir, 40-3
 Glossary of terms, petroleum reservoir traps, 29-8, 29-9
 Glossary of terms, reservoir engineering phase behavior, 22-20, 22-21
 Glucan, 47-3
 Gluconic acid, 44-45
 Glycol absorbers, 13-54, 14-18
 Glycol-condensate separator, 14-7
 Glycol dehydrators, 12-35, 14-18
 Glycol foaming, 14-20
 Glycol injection LTS system, 14-6 to 14-8, 14-14, 14-15
 Glycol reboiler, 14-6, 14-7, 14-15
 Glycol/water mixture, 39-5
 Glycols, 12-35, 13-36, 14-6 to 14-8, 14-15, 14-18 to 14-20
 Government authorities or agencies, 12-39, 18-44
 Governmental regulations, 3-34
 Governors, 10-14
 Graben, 29-3, 29-8
 Gradient curves, 5-25, 5-36, 5-37
 Gradient fluid flow, 31-4
 Gradient gas flow, 31-4
 Gradient of power fluid, 6-25, 6-26, 6-29, 6-43, 6-44
 Gradient of return fluid, 6-43
 Gradient of well servicing fluid, 4-7
 Grain density, 50-28, 50-33
 Grain density test, 27-1
 Grain roundness factor, 55-8
 Grain-size distribution, 56-3, 56-7
 Grain size of proppants, 55-8
 Grain size test, 27-1
 Grain volume: See Sand grain volume
 Granting clause, 57-3, 57-4
 Graphic plots,
 introduction, 24-18
 Reistle diagram, 24-19
 Stiff diagram, 24-19
 Tickell diagram, 24-19
 Graphic relationships for SI units, 58-23
 Graphical correlations, 22-5, 22-7, 22-8
 Graphite, 12-41
 Graphite impregnated cloth model, 39-21
 Gravel-flow pack, 46-19
 Gravel-pack completions, 47-6
 Gravel-pack failure, 56-6
 Gravel-pack permeability improvement, 56-6
 Gravel packing, 56-3, 56-5 to 56-9
 Gravel quality, 56-6, 56-7
 Gravel selection, 56-6, 56-7
 Gravel sizes available, 56-6
 Gravimetric determination of BV, 26-3
 Gravimetric system, 58-3
 Gravitational forces, 26-12, 26-24, 29-3
 Gravitational units, 58-5
 Gravity conservation with storage tanks, 11-12 to 11-14
 Gravity drainage, 28-11, 29-7, 37-1, 37-2, 37-5, 37-7, 37-17, 40-14, 40-15, 40-29, 41-11, 43-1 to 43-3, 43-5 to 43-7, 43-16, 44-36, 44-39, 47-8, 48-4, 48-12
 Gravity dump piping, 6-62
 Gravity faults, 29-3
 Gravity forces, 37-11, 44-31
 Gravity losses, preventing, 11-12, 11-13
 Gravity platform construction, 18-23, 18-24
 Gravity segregation, 12-3, 37-2, 37-4, 40-8, 43-5, 43-7, 43-16, 45-7, 45-8, 48-8
 Gravity separation, 6-56 to 6-59, 12-8, 12-19, 12-21, 12-23, 15-21, 19-6, 19-7, 19-13
 Gravity separation devices, 15-23
 Gravity settling, 15-18, 19-14, 19-15, 19-28
 Gravity stabilization, 45-8
 Gravity structures, 18-2, 18-3, 18-23, 18-41, 18-42
 Gravity systems in piping design, 15-14, 15-15
 Graywacke sediments, 29-7
 Great Britain, 1-70
 Great Lakes, 18-1
 Great Salt Lake, 24-19
 Grid network, 44-17
 Grid orientation effects, 48-10 to 48-13
 Grid spacings, 48-8
 Gridblocks, 37-2, 48-2 to 48-8, 48-10 to 48-12, 48-14, 48-15, 48-17
 Gridded multiphase reservoir simulators, 37-11, 37-13, 37-14
 Gridded reservoir models, 37-2, 37-5
 Gridded simulator equations, 37-11, 37-22
 Gridded simulator studies, 37-2
 Groningen gas field, Netherlands, 51-47
 Grooved pin-end plunger, 8-4
 Grounding of electrical system, 10-31, 10-32
 Guar as thickening agent, 55-5 to 55-7
 Guard-electrode device, 49-20
 Guarding of pumping units, 10-12
 Guatemala, 25-18
 Guide posts, 18-19, 18-32
 Guide, to number of digits to retain, 58-6 to style for metric usage, 58-11
 Guidebase, ocean floor, 18-18, 18-19
 Guidecones, 18-14
 Guided wave, 51-13
 Guideline tensioning systems, 18-11, 18-13
 Guidelineless drilling systems, 3-39
 Guidelineless re-entry systems, 18-14
 Guidelines,
 for marine cargo inspection, 17-8
 for offshore structure selection, 18-25
 for running down BOP stack, 18-16
 for selection of storage tanks, 11-1
 for use of SI units, 17-7
 for wire-rope, spudding offshore wells, 18-18
 subsea system, 18-19
 to BOP testing procedures, 18-12
 to surveys to be performed and analyzed for offshore drilling permit, 18-5
 Guides for using metric units, 58-8
 Guides to acid fracture treatment design, 54-11
 Gulf BHP gauge, 30-1
 Gulf coast, 18-2, 24-7, 24-8, 29-3, 33-21, 41-5, 47-3, 51-38, 51-39
 Gulf of Mexico, 18-2, 18-3, 18-7, 18-24, 19-5, 19-15, 25-18, 29-7, 51-34, 57-11, 57-12
 Gulf of Thailand, 36-9
 Gulf Oil Corp., 16-12, 46-15, 46-16, 46-18, 46-28 to 46-30
 Gunbarrel tank, 19-20 to 19-22
 Gunbarrels, 19-7, 19-18, 19-32
 Guyed towers, 18-2, 18-3, 18-24, 18-25
 Guyline system, 18-24, 18-25
 Gypsum (gyp), 56-1, 56-2
 Gyroscopes for directional surveys, 53-3
 Gyroscopic orientation, 53-7
- ## H
- h-mode telemetry, 53-1
 Habendum clause, 57-4
 Halite, 24-20
 Hall-Yarborough equation, 20-8
 Hammer lugs, 3-39
 Hand-held calculator, 20-7, 20-9, 20-13, 40-30
 Hand-off-auto switch, 10-27
 Handling ESP equipment, 7-12
 Hard-wired logic, 16-1, 16-8
 Hardness, 44-44, 47-5, 47-10, 47-11, 47-13
 Harmonic decline, 40-29, 40-31, 40-32, 41-11, 41-12
 Harmonic-decline deferment factor, 41-29, 41-31, 41-35
 Harmonic voltages, 10-30, 10-32
 Harrisburg field, Nebraska, 44-40, 47-22
 Hassler method, 28-3, 28-5 to 28-7
 Hastalloy®, 7-3
 Havlena and Odeh's method for OIP, 37-3, 38-12
 Hazardous area classification, 10-36, 10-37
 Hazardous areas, electrical systems offshore, 18-46
 Hazen-Williams equation, 15-2
 HCl: See Hydrochloric acid
 Head, definition, 34-2
 Head loss due to friction, 15-1
 Head meters, 13-2
 Heading, in separators, 12-22, 12-31, 12-35
 Heading conditions, 5-22, 5-24, 5-25, 6-60
 Heading of wells, 34-46, 34-50
 Heads of well fluids, 12-1, 12-32
 Heal of fracture, 55-2
 Healing, 47-8
 Heat capacity,
 of rock, 46-7
 of steam, 46-5
 of water, 46-2
 SI units, 58-28
 volumetric, 46-7, 46-10
 Heat conduction, 46-4, 46-12, 48-5
 Heat conduction, transient, 46-6
 Heat content, of petroleum fractions, 21-6 of natural gas, 14-17
 Heat exchange rate, 58-38
 Heat exchangers, 11-12, 11-13, 12-13, 14-5 to 14-8, 14-11, 14-14, 14-18, 14-21, 14-22, 19-8, 19-21, 19-23, 19-28

- Heat flow, conversion of units, table, 1-79
 Heat flow distortion, 52-22
 Heat flow rate, 58-23
 Heat in oil and gas separation, 12-7, 12-13
 Heat injection rate, 46-8
 Heat losses, factor in pattern selection, 46-17
 higher steam rate required in steamfloods, 48-18
 surface lines, 46-4
 wellbore, 46-5, 46-19
 with thermal stresses, 46-19
 Heat of reaction, 46-12
 Heat of vaporization, 14-21
 Heat transfer, 9-1, 14-1, 14-3, 14-20, 28-13
 Heat transfer coefficient, 58-35
 Heat treating, 9-1, 9-2
 Heated gunbarrel emulsion treater, 19-22
 Heat treater, 15-21, 16-3 to 16-5, 16-12
 Heating capacity, 19-29
 Heating efficiency, 19-28
 Heating in treating emulsions, 19-7, 19-11
 Heating value, gross, of natural gas mixtures, 17-7
 Heats of combustion, 52-3
 Heavy oil-in-water emulsion-type fracturing fluid, 55-7
 Heavy viscous oil, 12-17
 Heidelberg field, Mississippi, 46-15, 46-18
 Helical spring BHP element, 30-1
 Helium, 14-17, 50-14, 52-5, 52-6, 52-10, 52-13
 Hemispherical head equations, 12-38
 Hempel distillation, 21-3
 Hencky-von Mises theory of yielding, 2-55
 Henry's law constants, 25-17
 Hercules wellhead, 7-7
 Heterogeneity effects on waterflooding, 44-29
 Heterogeneous system, definition, 22-21
 Hewitt field, Oklahoma, 44-35, 44-36
 Hewlett Packard BHP gauge, 30-4, 30-7
 HF: See Hydrofluoric acid
 Hibernia development, 18-3
 Higgins-Leighton method, 44-28, 44-30, 44-31
 High-capacity operation of separator, 12-42
 High-frequency phase analysis, 27-1
 High injection-gas cycle frequency, 5-51
 High-liquid-level control, 12-39
 High-pH chemistry in chemical flooding, 47-18, 47-19
 High-pH field tests, 47-21 to 47-23
 High-pH processes,
 consumption, 47-22
 displacement mechanisms, 47-19, 47-20
 high-pH chemistry, 47-18, 47-19
 rock/fluid interactions, 47-20, 47-21
 High porosity presentation, 49-40
 High-pressure gas engine starters, 10-19
 High-pressure gas injection, 45-4, 45-11, 45-12
 High-pressure gas wells, 33-4
 High-pressure models, 46-13
 High-pressure seals, 3-36
 High-pressure service regulators, 13-55
 High-pressure steamfloods, 25-4
 High-resolution spectroscopy, 50-4, 50-35, 50-37
 High-slip motors, 9-3
 High-speed engines, 10-14 to 10-19
 High-voltage megger, 7-13
 High yield strength pipe, 15-12
 Hiras-Lawson theory, 47-9
 Histogram of acid numbers, 47-19
 Historical background of relative permeability, 28-2
 Historical performance of reservoir, 36-10
 Historical review of offshore operations, 18-1 to 18-3
 History matching, 48-9, 48-13
 History of reservoir simulation, 48-1
 Holddown, 8-2, 8-3
 Hole azimuth, 53-1, 53-2, 53-7, 53-8, 53-10, 53-17
 Hole casing programs, 18-41
 Hole deviation, 52-13, 53-2, 53-4, 53-10, 53-17
 Hole deviation, angle of, 53-3
 Hole direction, 53-4
 Hole enlargement, effect on acoustic velocity logging tools response, 51-15
 Hole rugosity, 51-19
 Homestead statutes, 57-3
 Homogeneous system, definition, 22-21
 Hondo platform, 18-2, 18-23
 Honduras, 58-20
 Hooke's law, 51-1, 51-2
 Horizontal emulsion treater, 19-21, 19-23, 19-25, 19-26
 Horizontal flow system, 26-11, 26-12
 Horizontal force vs. displacement curve, 18-10
 Horizontal fractures, 44-26, 44-28, 55-2
 Horizontal FWKO, 19-18
 Horizontal gas flow, 43-10, 43-11
 Horizontal permeability, 39-17 to 39-19
 Horizontal pressure vessel sizing, 15-24
 Horizontal scrubber, 12-38
 Horizontal separator, 12-1, 12-6, 12-7, 12-10, 12-16 to 12-18, 12-20 to 12-31, 12-35, 12-40, 16-15, 18-28
 Horizontal separator sizing, 12-30
 Horizontal stresses, 55-1
 Horizontal three-phase separator, 19-17
 Horizontal three-phase oil/gas/water separator, 12-4
 Horizontal vessels, 13-53
 Horner plot, 30-9, 35-15, 35-16, 35-19
 Horner-type analysis of static BHT, 31-6
 Horsehead, 10-2 to 10-4, 10-12
 Horsepower at prime mover, 10-18
 Horsepower, definition, 6-14, 58-24
 Horsepower of engines, 10-17 to 10-19, 10-32, 10-33, 10-35
 Horsepower of pumping unit, 9-11
 Horsepower-rated motors, 10-21
 Horsepower rating of motors, 10-17, 10-19, 10-20
 Horsepower requirements, 34-41, 34-42, 34-44, 34-45
 Horsepower vs. injection pressure, 34-44
 Horst, 29-3, 29-8
 Hoskold method, 41-16, 41-18, 41-20 to 41-22
 Hot-dip process, 11-1, 11-6
 "Hot" dolomites, 50-16
 Hot electric grid, 19-25
 Hot oil production, 46-9, 46-10
 Hot oil productivity, 46-11
 Hot oil treatments, 46-21, 56-2
 Hot-rolled steel, 9-1
 Hot spots, 7-1
 Hot water, cooling of, 46-6
 Hot-water injection, 46-1
 Hot-water stimulation, 48-2
 Hot waterflood, 46-4, 46-5, 46-13, 46-23, 46-24
 Hot-wire detector, 52-3
 Huff'n'puff method, 46-1, 47-10, 56-2
 Hugoton field, Texas, 33-1, 33-7, 33-9, 33-22, 34-46
 Humble formula (relation), 26-29, 26-31, 49-4, 49-32
 Humble gauge temperature element, 31-1
 Humble pressure gauge, 30-1
 Huntington Beach field, California, 19-5, 46-22, 46-23
 Husky Oil Co., 46-22, 46-23
 Hutton platform, 18-24
 Hydrate depression, 25-19
 Hydrate dissociation model, 25-9
 Hydrate dissociation predictions, 25-5 to 25-9
 Hydrate dissociation pressure, 25-6
 Hydrate formation, 12-3, 14-1, 14-2, 14-4 to 14-7, 14-17
 Hydrate formation, condition of methanol propane mixture, 25-20
 conditions, effect of GOR, 25-19
 conditions for paraffin hydrocarbons, 25-4
 on expansion of gas, 25-11
 pressure, procedure for determining, 25-8, 25-9
 temperature, 12-40
 Hydrate inhibition, 25-19, 25-20
 Hydrate inhibitors, 14-3, 14-5 to 14-8, 14-17
 Hydrate problem, 13-53
 Hydrate stability conditions, 25-4 to 25-9
 Hydrate temperature, 14-2, 14-3, 14-5 to 14-7, 14-17
 Hydrate/volatile-gas systems, 25-3
 Hydrated iron oxide, 14-22
 Hydrates, 5-12, 5-24, 14-2, 14-3, 14-5, 14-6, 33-20, 33-21, 39-24, 39-25
 Hydration of cementation material, 26-18
 Hydraulic actuators, 3-21, 18-28
 Hydraulic BOP control system, 18-21
 Hydraulic connectors, 18-12, 18-18, 18-34
 Hydraulic control circuit, 3-33
 Hydraulic control system, 18-11, 18-15
 Hydraulic currents, 24-2
 Hydraulic forces, 44-46
 Hydraulic fracturing theory, 55-1, 55-2
 Hydraulic head, 26-10, 26-12
 Hydraulic horsepower, 6-45, 10-17, 10-18
 Hydraulic installations, system pressures and losses,
 in calculation of fluid gradients, 6-26
 in closed power-fluid system, 6-26
 in fluid friction in tubular and annular flow passages, 6-26, 6-27
 in open power-fluid system, 6-25
 Hydraulic power transmission, 6-1, 6-15
 Hydraulic pressure, 55-1
 Hydraulic-pumped-well control, 16-11
 Hydraulic pumping,
 downhole pumps, 6-2 to 6-7
 fluid properties, 6-66 to 6-69
 frictional relationships, 6-69 to 6-72
 introduction, 6-1, 6-2
 jet pumps, 6-34 to 6-49
 principles of operation—reciprocating pumps, 6-8 to 6-33
 references, 6-72
 surface equipment, 6-49 to 6-63
 Hydraulic PV compressibility method, 26-8
 Hydraulic radius, 34-27, 34-39
 Hydraulic-set packer, 4-3, 4-5, 4-6
 Hydraulic subsea controls, 18-49
 Hydraulic surface safety valves, 3-20, 3-21
 Hydraulic transformer, 6-19
 Hydraulic transformer process, 6-16
 Hydraulic transmission system, 18-3
 Hydraulic turbine, 6-1
 Hydrocarbon analyses, crude oil and gas condensates, 39-2
 formation evaluation service, 52-2 to 52-7, 52-13
 of produced well stream, 39-7
 of separator products and calculated well stream, 39-7
 used in pressure depletion predictions, 39-10, 39-11

- Hydrocarbon chromatogram, 52-16
 Hydrocarbon content of samples, 52-9, 52-10
 Hydrocarbon content from logs, 51-35 to 51-38
 Hydrocarbon gas viscosity, 15-6
 Hydrocarbon/liquid condensation, 39-13
 Hydrocarbon liquid recovery, 37-22, 37-23
 Hydrocarbon liquid recovery calculations, 14-16
 Hydrocarbon liquid recovery system, 14-8
 Hydrocarbon liquid saturations, 39-10
 Hydrocarbon mixtures, 39-2, 39-4, 39-12
 Hydrocarbon pore space, 39-8, 39-9, 39-11, 39-18
 Hydrocarbon recovery systems, lease-operated,
 gas treating for removal of water vapor, CO₂ and H₂S, 14-17 to 14-22
 low-temperature separation (LTS), 14-1 to 14-17
 references, 14-22
 Hydrocarbon recovery unit, 14-10, 14-11
 Hydrocarbon reservoir, definition, 39-1
 Hydrocarbon-rich phase at three-phase critical conditions, 25-5
 Hydrocarbon saturation, 49-27, 50-2
 Hydrocarbon stabilization, 14-13 to 14-17
 Hydrocarbon/water phase diagrams, 25-1 to 25-4
 Hydrocarbon/water systems, 25-3, 25-27
 Hydrocarbon Well Log Standards Committee, 52-30
 Hydrocarbons in place, ownership of, 57-1
 Hydrocarbons presence detection, 50-1, 50-3
 Hydrocarbons, removing from solids, 15-30
 Hydrocarbons, treating from water, 15-21
 Hydrochloric acid (HCL),
 acidizing treatments, 54-1, 54-2
 as synthetic polymer gel, 55-5
 channeling and wormhole effect, 54-8
 combined with HF, dissolving action, 54-9
 density at 60°F, 54-2
 dissolution of concentrated, 54-3
 dissolving limestone, 54-2
 in acidizing, 54-1 to 54-3
 in matrix acid stimulation, 56-5
 inhibited, as mud-dissolving acid, 56-1
 inhibitors used with, 54-1, 54-6
 matrix treatment of carbonates, 54-10
 organic inhibitors in, 54-6
 reaction rate, effect of,
 acid concentration, 54-5
 area/volume ratio, 54-5
 flow velocity, 54-5
 formation composition, 54-6
 pressure, 54-4
 retardation of, 54-8
 rubber lining protection from, 11-6
 temperature, 54-4, 54-5
 to acidize pH, 24-4
 to clean tubing, 56-3
 to dissolve corrosion products, 39-26
 to remove scale, 56-2
 used in combination with HF, 54-3, 54-9
 Hydrocyclone, 6-62
 Hydrocyclone operation, 15-19, 15-30
 Hydrodynamic forces, 18-17, 18-25
 Hydroelectric valve operators, 16-3
 Hydrofluoric acid (HF) in acidizing, 54-3, 54-4, 54-9, 54-11
 Hydrofluoric/hydrochloric acid (HF/HCl) mixtures in acidizing, 54-11
 Hydrogen, 1-80, 26-18, 50-1, 50-3, 50-4, 50-9, 50-13, 50-17, 50-18, 50-20, 50-26, 50-31, 50-34, 51-31
 Hydrogen density, 50-32
 Hydrogen embrittlement, 3-36
 Hydrogen flame detector, 52-4
 Hydrogen sulfide (H₂S), 3-36, 3-37, 4-4, 4-5, 6-4, 6-54, 7-11, 7-14, 8-9, 9-1, 9-5, 9-8, 11-6, 12-3, 12-8, 14-3, 14-13, 14-17, 14-20 to 14-22, 15-28, 15-29, 18-20, 18-47, 20-5, 20-6, 22-5, 24-5, 24-17, 39-5, 39-6, 40-22, 44-36, 44-42 to 44-44, 45-5, 52-4 to 52-7, 52-13, 54-7
 Hydrogen sulfide content, 25-5, 25-8, 25-13, 25-20
 Hydrogen sulfide fumes, 10-13
 Hydrogen sulfide gas detectors, 18-47
 Hydrogen sulfide/water system, 25-27
 Hydrolysis of methyl formate, 54-4
 Hydrolyzed polyacrylamide (HPAM), 47-3 to 47-6
 Hydrometer, 1-80, 54-3
 Hydrometer test method, 17-5
 Hydrophile, 47-7
 Hydrophobe/hydrophile balance, 19-10
 Hydrophobic surface, 47-8
 Hydro pneumatic tensioning units, 18-13, 18-14
 Hydrostatic equilibrium, 26-11
 Hydrostatic gradient, 58-25
 Hydrostatic head, 6-25, 6-28, 6-51, 55-7, 55-8
 Hydrostatic pressure, 3-29, 3-31, 18-17, 29-1, 51-39, 51-44
 Hydrostatic PV compressibility technique, 26-8, 26-9
 Hydrostatic test pressure, 2-62, 3-1, 3-2, 3-13
 Hydroxyethyl cellulose (HEC), 47-3
 Hydroxyfluoboric acid, 54-4
 Hydroxyl reactions, 47-21
 Hydroxypropyl guar as thickening agent, 55-5, 55-6
 Hyperbolic cosines, table, 1-59
 Hyperbolic decline, 40-28, 40-29, 40-31, 40-32, 41-10, 41-11, 41-29
 Hyperbolic-decline deferment factor, 41-29 to 41-31
 Hyperbolic sines, table, 1-58
 Hyperbolic tangents, table, 1-60
 Hyperclean™ technique, 46-21
 Hysteresis, 28-2, 28-3, 28-6, 28-10, 28-13, 30-3, 30-6, 30-7, 33-6
- I**
- I-wire, 7-5
 Ice characteristics, 18-38
 Ice-class rigs, 18-21
 Ice impact, 18-43
 Ice islands, 18-39
 Ice loading, 18-39
 Ice management, 18-43
 Ice point, 25-1 to 25-3, 25-5
 Icebergs, 18-39
 Icebreaker assistance vessels, 18-43
 Ideal equilibrium ratios, 23-11
 Ideal gas, 20-1 to 20-3, 26-12
 Ideal-gas law, 13-8, 20-2, 20-4, 20-6, 20-7, 39-8, 40-21, 47-13
 Ideal productivity index (PI), 32-3
 Ideal solution principles, density from, 22-2, 22-5
 Idealized pore models, 26-28
 IFP-ICPP, 46-4, 46-15, 46-18, 46-28, 46-29
 Igneous rock, 29-3, 29-8
 Ignition devices, 46-20
 Illinois, 40-16, 40-32, 40-33, 44-41, 44-42, 46-3, 46-4, 46-15
 Illinois basin, 24-6, 24-7, 24-9, 44-44
 Illite, 46-21, 50-21, 50-32, 50-34, 50-37, 52-21
 Illuminance, unit and definition, 58-11, 58-23, 58-36
 Imbibition curves, 26-24, 28-5, 28-9 to 28-12
 Imbibition effect, 40-20
 Imbibition of water, 40-20
 Imbibition without relative permeability data, 28-4
 Immiscibility of methane gas and oil, 45-2
 Immiscible displacement, 42-2
 Immiscible displacement fluid, 40-4
 Immiscible fluids, 28-2, 28-12, 28-13
 Immiscible gas drive, 45-4
 Immiscible gas injection, 43-1, 43-2
 Immiscible liquids, 19-1, 19-2, 19-14
 Immiscible processes, 39-18
 Impact energy, 58-32
 Impact kinetic energy, 13-1
 Impact loading or loads, 3-1, 18-5
 Impact pressure, 13-45 to 13-48, 33-1 to 33-4
 Impact requirement, wellhead equipment, 3-38
 Impedances, 10-30
 Impingement, 12-8 to 12-11, 12-13, 12-19
 Implicit-pressure/explicit-saturation formulation (IMPES), 48-14, 48-15
 Implied covenant, 57-6
 Impressed-current system, 11-6
 Improved recovery reserves, 40-3, 40-34
 Impurities in well fluids, 12-3
 In-transit deck-load capability, 18-8
 Inaccessible pore volume (IPV), 47-5
 Inbreathing (vacuum relief) of storage tanks, 11-6, 11-7
 Incident flux, 50-5 to 50-7
 Incident gamma ray, 50-7, 50-12, 50-13
 Inclination angle, 53-5, 53-6
 Inclinator, 53-8
 Inclinator section, 53-7
 Inconel®, 7-3, 15-21
 Incremental gas production, 37-10
 Incremental oil production, 37-9, 37-17
 Incremental oil recovery (IOR), 47-6, 47-21 to 47-23
 Incremental recovery, potential for, 46-3
 Incrustation, 17-3
 Independent oil company, 57-8
 Independent screwed wellhead, 3-39
 Indian Petroleum Corp., 18-1
 Indiana, 24-7
 Indirect heater, 14-3, 14-5, 14-6
 Indirect-fired heaters, 19-21
 Indonesia, 12-39, 46-3, 46-4
 Induced-gamma-ray spectroscopy, 50-4, 50-34, 50-35, 50-37
 Induced hydraulic fractures, 54-11
 Induced porosity, 26-1, 26-2
 Induced radiation, 50-6
 Induction conductivity curve, 49-15
 Induction device, deep-reading (ID), 49-15, 49-17, 49-20
 Induction device, medium-reading (IM), 49-15, 49-17, 49-18
 Induction-electrical log (IEL), 49-27, 49-29 to 49-31
 Induction-electrical surveys (IES), 49-11, 49-15
 Induction log (IL), 49-1, 49-2, 49-5, 49-6, 49-14 to 49-18, 49-25 to 49-27, 49-29, 49-30
 Induction log resistivity, 51-17, 51-26, 51-37, 51-38, 51-46
 Induction motors, 10-19 to 10-21, 10-23 to 10-25, 10-30, 10-32, 10-36
 Induction motor poles vs. synchronous speeds, 10-23
 Induction spherically focused log (ISF), 49-15, 49-16, 49-19, 49-20, 49-34, 49-36
 Inductive couplers, 18-52
 Inelastic gamma-ray spectroscopy, 50-35
 Inelastic neutron reactions, 50-13
 Inelastic scattering, 50-9, 50-23

- Inelastic spectrometry, 50-22
- Inert-gas injection, 39-16
- Inertial effects, 35-10
- Inertial forces, 35-11
- Industrial multitube boilers, 46-19
- Inferential meters, 16-5
- Infiltration by permeation, 24-18
- Infinite-acting pressure solution, 35-3, 35-4, 35-7, 35-12, 35-14
- Infinite aquifer, 38-3, 38-6, 38-9
- Infinite boundary, definition, 38-1
- Infinite linear aquifers, 38-2, 38-8
- Infinite radial aquifer, 38-3, 38-5 to 38-8
- Inflation factor, 41-15
- Inflow performance relationship (IPR), 6-4, 6-25, 6-41 to 6-43, 6-46, 6-47, 34-30 to 34-35, 34-46, 34-50, 37-17 to 37-21
- Inflow well performance, 5-22
- Influence-function curves, 38-3
- Infrared (IR) absorbance, 12-16
- Infrared absorption detector, 52-5 to 52-7
- Infrared absorption method, 46-21
- Infrared detectors, 3-34
- Infrared fire sensors, 18-47
- Inglewood field, California, 46-14
- Initial fluid saturations, 37-3
- Initial gas saturation, 44-6, 44-38
- Initial hydrate formation conditions, 25-1, 25-2, 25-5, 25-6, 25-11, 25-12, 25-15, 25-19
- Initial hydrate formation, estimating, 25-5
- Initial oil saturation, 44-4
- Initial saturation conditions, 43-5
- Initial saturations, effect of, 44-6
- Initial water distribution, 44-11, 44-37
- Injection application, ESP, 7-2
- Injection, BHP calculation, 34-28 to 34-30
- Injection fluids, 42-2, 42-5
- Injection-gas breakthrough, 5-52
- Injection gas cycle, 5-12, 5-43, 5-48, 5-52
- Injection-gas-cycle frequency, 5-55
- Injection-gas cycles per day, 5-40 to 5-42, 5-54, 5-55
- Injection gas-line pressure, 5-48, 5-54, 5-55
- Injection-gas/oil ratio (GOR), 34-41 to 34-43
- Injection-gas opening pressure, 5-18 to 5-20, 5-26, 5-28, 5-29, 5-33, 5-39, 5-40, 5-51
- Injection-gas operating pressure, 5-48, 5-53
- Injection-gas pressure, 5-20, 5-21, 5-24, 5-26, 5-28, 5-31, 5-32, 5-35, 5-37, 5-39 to 5-41, 5-44, 5-46, 5-48 to 5-54
- Injection-gas-pressure-at-depth curves, 5-5
- Injection-gas-pressure-at-depth traverse, 5-36
- Injection-gas rate, proper adjustment, 5-53 to 5-55
- Injection-gas requirement for intermittent lift, 5-40 to 5-42
- Injection-gas throughput, maximum, 5-36, 5-43
- Injection-gas volume per cycle, 5-51
- Injection-gas volumetric rate, 5-3, 5-54
- Injection-gas volumetric throughput, 5-37, 5-40
- Injection-gas volumetric throughput profiles, 5-20
- Injection operations, 42-1 to 42-6
- Injection pressure effect on horsepower, 34-42
- Injection-pressure-operated gas lift valve, 5-13, 5-14, 5-16 to 5-24, 5-27, 5-32, 5-33, 5-36, 5-40, 5-54
- Injection profile, foam, 47-9
- Injection profiles, 4-6 to 4-8
- Injection-pumping rate, controlling, 16-14
- Injection quill, 19-11
- Injection treatments, large-volume, 56-2
- Injection water, 24-5
- Injection well plugging, 39-26
- Injection wells,
 - gas, 34-28 to 34-30
 - liquid, 34-28
- Injectivity, 44-29, 44-33 to 44-35, 44-43, 46-22
- Injectivity, effect of damage on, 54-8, 54-9
- Injectivity index, 44-34, 44-35
- Injectivity/productivity ratio, 46-17
- Injectivity profile, of water-injection well, 31-4
- Injectivity testing, 39-25, 39-26, 44-46
- Inner-valve assembly, 13-49
- Inorganic constituents,
 - anions, 24-9, 24-12
 - cations, 24-9
- Inorganic solids, 19-5
- Input safety valves (ISV's), 3-35
- Insert pump, 8-1
- In-situ analyses, 18-26
- In-situ combustion, 19-28, 48-2, 48-5 to 48-7
- In-situ combustion models, 46-12
- In-situ combustion processes,
 - chemical reactions, 46-37
 - dry forward combustion, 46-1, 46-2
 - production by, 46-4
 - reverse combustion, 46-2
 - wet combustion, 46-2, 46-3
- In-situ "static" analysis, 18-27
- Insoluble reaction products, 54-1
- Inspection of tubing and casing by caliper logs, 53-17, 53-18
- Installation design calculations, gas lift, 5-29 to 5-32
- Installation design considerations, gas lift, 5-22
- Installation design, continuous flow gas lift,
 - calculation of test rack-set opening pressure, 5-29, 5-33
 - determination of valve depths, 5-28, 5-29, 5-32, 5-33
 - example calculations, 5-29 to 5-35
 - selection of port size, 5-28
- Installation design, intermittent gas lift,
 - calculation of test rack set opening pressure, 5-46, 5-49
 - determination of valve depths, 5-45, 5-46, 5-48, 5-49
 - example calculations, 5-46, 5-47, 5-49, 5-50, 5-52
 - lift chamber application, 5-50 to 5-52
 - percent tubing load, 5-48
 - selection of port size, 5-44
- Installation design methods, gas lift, 5-22
- Installation/maintenance system controls, 18-48
- Installation of ESP equipment, 7-12 to 7-14
- Installation of prime mover, 10-19
- Installation of pumping units, 10-7, 10-12
- Installation of safety devices, 12-40
- Institut Français du Pétrole method, 28-7
- Instrument-adjustment factor, 13-52
- Instrumentation for liquid hydrocarbon metering systems, 17-4
- Instrumentation systems offshore, 18-43 to 18-47
- Insulating additive, 46-19
- Insulation classification, 10-26
- Insulation for oilwell pumping motors,
 - classification of, 10-26
 - winding materials for, 10-26
- Insulation materials, winding of, 10-26
- Intangible drilling costs, 57-11
- Intangibles and intangible cost, 41-11, 41-13, 41-14, 41-15
- Integral flange, 3-16, 3-22, 3-24
- Integral joint tubing, 2-38 to 2-45, 2-64, 2-65
- Integral values, tabulated, 34-5 to 34-7, 34-10 to 34-22
- Intensified acid, 54-3, 54-5
- Intensity/time recording, 51-18
- Intensive properties, 22-21, 39-2
- Interaction coefficient, 28-3
- Interest,
 - carried, 57-10
 - landowner's, 57-1, 57-2
 - mineral, 57-6
 - net profits, 57-10
 - royalty, 57-5 to 57-8
 - working, 57-5, 57-7, 57-9, 57-10
- Interest tables, 41-25 to 41-34
- Interface level controller, 19-23
- Interfacial buildup, 19-30
- Interfacial sludge, 19-32
- Interfacial tension (IFT)
 - dead-end oil, 22-17
 - definition, 22-1, 24-16
 - effects on relative permeability, 28-10, 28-11
 - gas/oil, 45-4, 45-6
 - liquid/gas, 22-16
 - of acid solutions, 54-6
 - of condensate and water, 34-50
 - oil/water, 47-1, 47-9, 48-5
 - reduced by surface-active agents, 44-39
 - results in spherical form of water droplets, 19-1
 - units and conversion factors, 58-38
- Interfacial tension reducer, 56-5
- Interfacial tension reduction, 44-40, 48-2
- Interference, 44-33
- Interference effects, 38-1, 38-3
- Interference tests and testing, 30-8, 36-7, 36-8, 42-4
- Intergranular porosity, 26-1, 26-3, 51-31
- Intermediate domes, 29-5, 29-6
- Intermediate packers, 4-11
- Intermittent controller, 16-4
- Intermittent flow, skim pile, 15-26
- Intermittent gas lift,
 - comparison of time cycle to choke control of injection gas, 5-41, 5-42
 - cycle of operation, 5-38
 - daily production rates, 5-40
 - disadvantages of, 5-38, 5-39
 - gas-lift valves, 5-42, 5-43
 - heads or slugs in, 12-32, 12-35
 - injection gas requirement, 5-40, 5-41
 - installation design methods, 5-39, 5-42, 5-44 to 5-50
 - introduction, 5-38
 - lift chamber application and installation design, 5-50 to 5-52
 - operation, 5-1, 5-3, 5-11, 5-13, 5-19, 5-37 to 5-53
 - percent tubing load installation designs, 5-48
 - plunger applications, 5-52
 - pressure-gradient spacing factors, 5-43, 5-44
 - surface closing pressure of valves, 5-44
 - types of installations, 5-39, 5-40
 - unloading injection-gas pressure, effect of installation design methods, 5-39
 - valve port size, 5-44
- Intermittent pressure gradient spacing factor, 5-42, 5-43
- Intermittent spacing factor, 5-45
- Intermittent spacing factor gradient, 5-44, 5-45, 5-47
- Intermittent spacing factor traverse, 5-46, 5-47
- Internal coatings, 11-4, 11-5
- Internal-combustion-engine driven generators, 18-45
- Internal-combustion engines,
 - diesel, 10-15, 10-16
 - four-stroke cycle, 10-15

- in inert gas injection, 39-16
- installation, 10-19
- multiplex pumps analogous, 6-49
- oil engine, 10-15, 10-16
- selection of, 10-16 to 10-19
- two-stroke cycle, 10-14, 10-15
- Internal corrosion, 3-36
- Internal energy, 13-1
- Internal floating roofs, 11-2, 11-6
- Internal flushing efficiency, 39-18
- Internal gas drive, 37-1, 40-8
- Internal gas-driven reservoir, 32-15, 32-16
- Internal injection, 43-2
- Internal pressure leak resistance, of casing, 2-5, 2-7, 2-9, 2-11, 2-13, 2-15, 2-17, 2-19, 2-57, 2-58, 2-64
- Internal pressure, of casing, 2-1, 2-61 of pipe, 2-59
- of line pipe, 2-56, 2-63
- Internal pressure resistance of, casing, 2-5, 2-7, 2-9, 2-11, 2-13, 2-15, 2-17, 2-19
- line pipe, 2-56
- tubing, 2-46
- Internal rate of return (ROR) method, 41-17
- Internal Revenue Code, 41-14, 41-15
- Internal Revenue Service, 41-2
- Internal spiral element, 12-19
- Internal water weir, 12-35
- Internal yield pressure of pipe and couplings, 2-5, 2-7, 2-9, 2-11, 2-13, 2-15, 2-17, 2-19, 2-32, 2-56, 2-57, 2-63, 3-1
- Internal yield pressure safety factor, 2-2, 2-32, 2-34, 2-35, 2-45, 2-46
- Internally coated pipe, 39-26
- Internally plastic-lined tubing, 44-46
- International atomic weight table, 20-1
- Intl. Bureau of Weight and Measures, 1-69 to 1-71
- Intl. Commission on Radiological Protection, 58-10
- International foot, 1-69
- Intl. Metric Convention, 1-68, 1-69
- Intl. prototype kilogram, 1-69, 1-70
- Intl. Standards Organization (ISO), 10-12
- Intl. system of units, guidelines for use, 17-7
- Interpretation, chart for Rocky Mountain method, 49-31, 49-32
- chart for R_{co}/R_f and shaly sand method, 49-28
- IEL method, 49-30, 49-31
- of caliper logs, 53-17
- of casing inspection log, 53-23 to 53-26
- of chemical analyses, 24-18, 24-19
- of EPT log, 49-34 to 49-36
- of microlog, 49-23
- of paleo-environments, 36-3
- of pipe analysis log, 53-13 to 53-26
- of rules of dipmeter, 53-10, 53-12
- of well logs, 49-25 to 49-36
- quantitative, of hydrocarbon saturation, 49-27
- stratigraphic, 53-13, 53-14
- Interpretation of nuclear logs, gamma ray measurements, 50-24 to 50-26
- introduction, 50-23, 50-24
- lithology determination, 50-33 to 50-35
- porosity determination, 50-26 to 50-33
- saturation determination, 50-35 to 50-37
- Interstate Oil Compact Commission, 33-15
- Interstitial clay, effect on formation resistivity factors, 26-30
- Interstitial water, 24-2, 24-3, 24-16, 24-18, 26-20, 27-8, 40-8, 40-10, 40-13, 40-16, 40-19, 40-23
- Interstitial water content, 39-17, 39-18, 39-21 to 39-23, 40-12
- Interstitial water saturation, 26-26, 28-4, 28-14, 37-3, 37-4, 37-15, 37-17, 39-10, 40-5 to 40-10, 40-12, 40-15, 40-16, 40-19, 40-24, 42-4, 43-5, 44-4, 44-6, 44-9, 44-36
- Interstitial water saturations, capillary pressure, 26-23, 26-24
- oil-based mud, 26-22, 26-23
- Interval transit (travel) time, 51-15, 51-17, 51-19, 51-23, 51-24, 51-27, 51-43, 58-25, 58-33, 58-36
- Interzonal hydrostatic head, 7-2
- Intrawell continuity, 36-1, 36-6, 36-7
- Invaded-zone correction, 49-22
- Invariant point, 47-12
- Invasion effects on IL, 49-17
- Invasion efficiency, 39-15, 39-17, 39-18, 39-22, 39-23, 40-34, 47-1
- Inverse emulsion, 19-1
- Inverse lever rule, 23-3, 23-8
- Inverse simulation, 48-9
- Inverted bucket traps, 13-53
- Inverted nine-spot well pattern, 45-10, 46-17, 46-18, 46-28
- Investors method, 41-17
- Involute element, 12-19
- Iodide, 19-10, 24-9
- Iodine, 24-5, 24-20, 24-21
- Ion diffusion, 24-19
- Ion exchange, 24-19, 24-20
- Ion-exchange conduction, 49-4
- Ion-exchange reactions, 52-21
- Ion-exchange resins, 15-29
- Ionization, 50-3
- Ionized-gas counter, 50-12
- Iran, 29-6
- Iron bacteria, 44-43
- Iron chelating agents, 56-1
- Iron-control agents, 54-7, 54-8
- Iron sponge sweetening, 14-22
- Iron sulfide, 14-22, 19-4, 19-9, 44-44
- Iron sulfide deposits, 11-10
- Irreducible saturation, 28-5, 28-8
- Irreducible water saturation, 44-6, 44-11, 44-12, 46-34, 46-37, 46-38, 47-9
- Irreversibility losses, 34-2
- Isobaric contour maps, 39-23
- Isobutane/water system, 25-25, 25-27
- Isochronal backpressure test, 34-31
- Isochronal test data, 39-25
- Isochronal testing, 33-4 to 33-6, 33-10 to 33-13
- Isoelectric point, 54-7
- Isolation packer, 4-2, 4-3
- Isometric of fractures, 51-28, 51-29
- Isopachous maps, 39-21, 40-5, 41-8, 46-30, 46-31
- Isopentane/water system, 25-26
- Isoporosity map, 39-22
- Isoporosity maps, 44-3
- Isopotential lines, 44-15 to 44-17
- Isopropyl alcohol in acidizing, 54-8
- Isothalic thermoset resin, 9-12
- Isothermal coefficient of compressibility, 55-4
- Isothermal compositional model, 48-5
- Isothermal model, 48-4
- Isovol map, 39-17
- Italy, 12-39
- Iterative method or solution, 37-8, 37-9, 37-11, 48-1, 48-13
- J**
- J-function, definition, 26-25, 26-26
- J-lay first-end connection, 18-38
- Jackson candle units (JCU), 44-44
- Jackup rig, 3-38
- Jackups, 18-2 to 18-6
- Japan, 12-39
- Jay/Little Escambia Creek field, 44-36, 44-37
- Jefferson limestone, Kentucky, 54-1
- Jet pump, 6-1, 6-2, 6-4, 6-7
 - application range, 6-46, 6-47
 - application sizing, 6-41, 6-42
 - approximation for handling gas, 6-38, 6-39
 - calculation sequence and supplemental equations, 6-42
 - cavitation in, 6-35, 6-36
 - downhole pump accessories, 6-47 to 6-49
 - hydraulic, 6-6
 - installation, 6-43
 - mathematical presentation, 6-36 to 6-38
 - nomenclature, 6-35
 - nozzle and throat annulus area, 6-41
 - nozzle and throat size, 6-39, 6-41
 - performance characteristics, 6-34 to 6-37
 - production unit performance, 6-42
 - ratios and throat annulus areas, 6-40
 - reverse-flow casing type, 6-5
 - single seal, 6-35
 - subsurface, 6-32, 6-47
 - worksheet and summary of equations, 6-44, 6-45
- Jetting wells, 32-15
- Joho field, 46-4
- Johnson pressure gauge, 30-2
- Johnston-Macco/Schlumberger BHP gauges, 30-4
- Joint efficiency, 12-38, 12-40
- Joint-interest owner, 41-2
- Joint-operating agreements, 57-9
- Joint strength of, casing, 2-2, 2-5, 2-7, 2-9, 2-11, 2-13, 2-15, 2-17, 2-19, 2-60, 2-61
- line pipe, 2-48, 2-61 to 2-64
- tubing, 2-39, 2-41, 2-43, 2-61
- Joint strength safety factor, 2-2, 2-32, 2-34, 2-35, 2-45, 2-46
- Jostling decrement, 51-47
- Joule-Thomson effect, 12-17, 14-2
- Jug heater, 19-21
- Jumpout load of casing, 2-61
- Junction box, ESP, 7-7, 7-8
- Jurassic, 36-2
- Juvenile water, 24-2
- K**
- K&C systems, 18-15
- K-Monel®, 4-4, 4-5, 7-3, 7-6
- K-value correlation, 39-12
- K-values, 23-10, 23-11, 25-5, 39-12, 48-4, 48-5
- Kalman filtering, 50-5
- Kalrez®, 4-5
- Kansas, 16-12, 16-13, 19-3, 21-2, 24-8, 24-9, 27-8, 27-10 to 27-13, 33-1, 39-25, 40-23, 44-42, 46-4, 46-14
- Kansas Corp. Commission, 33-15
- Kaolinite, 46-21, 50-21, 50-32, 50-34, 50-37
- Karman vortex trail, 13-49
- Kay's rule, 20-5
- Kentucky, 24-6, 24-7, 41-11, 46-16, 54-1
- Kern River field, California, 46-4, 46-14, 46-15, 46-18, 46-20, 46-23, 46-24, 46-34, 46-39
- Kerogen, 52-16
- Kerosene, 19-4
- Kerosene/water system, 25-27
- Kettleman Hills field, California, 6-24, 29-2

Kick-off injection-gas pressure, 5-24, 5-25, 5-28, 5-33
 Kickover tool, 5-2
 Kihara potential, 25-5, 25-8, 25-9
 Kill and choke (K&C) valves, 18-12
 Kill fluid, 5-24, 18-33
 Killed steel, 12-41
 Kilogram, definition of, 1-69
 Kilogram of the Archives, 1-69
 Kilovoltamp reactive (kVAR), 10-31, 10-33 to 10-35
 Kilovoltamps (kVA) rating of transformers, 10-30 to 10-35
 Kinematic viscosity, 6-67, 6-69, 19-8, 22-13, 24-16, 58-35
 Kinetic energy, 6-34, 13-1, 13-45, 20-1, 20-2, 34-9, 34-29, 34-36, 50-3, 50-8, 50-13
 Kinetic mixer, 19-11, 19-12
 Klinkenberg corrections, 27-1
 Knife-edge blade electrodes, 53-8, 53-9
 Knitted-wire-mesh coalescing pack, 12-10, 12-11
 Knitted-wire-mesh fibrous packs, 12-12
 Knitted-wire-mesh mist extractor, 12-7, 12-8, 12-10
 Knocking, 6-33, 6-50
 Knockout drum, trap or vessel, 12-1, 12-4
 Kobe porosimeter, 26-4, 26-6
 Kozeny equation, 26-20
 Krypton-85, 46-21
 Krypton-86, 1-69, 1-70
 Kuparuk field, Alaska, 18-3
 Kuster pressure gauges, 30-2
 Kyrock field, Kentucky, 46-16

L

La Concepción field, Venezuela, 24-13
 La Paz field, Venezuela, 24-13
 Laboratory coreflood, 47-17, 47-21
 Laboratory curves,
 for lateral sonde, 49-13
 for normal sonde, 49-12
 Laboratory depletion recovery, 39-14
 Laboratory-derived data, 39-10, 39-11
 Laboratory displacement tests, 44-40
 Laboratory experimentation,
 elemental models, 46-12, 46-13
 fuel content, firefloods, 46-16
 of AOR and WAR, 46-17
 partially scaled models, 46-13
 use of water in firefloods, 46-18, 46-19
 Laboratory layout for performing routine core analysis, 26-22
 Laboratory-measured relative-permeability data, 37-4
 Laboratory measurement of capillary pressure,
 centrifuge method, 26-24
 dynamic method, 26-24
 evaporation method, 26-24
 mercury-injection method, 26-24
 porous-diaphragm method, 26-24
 Laboratory measurement of porosity,
 bulk volume, 26-3
 carbonate rocks, 26-6, 26-7
 pore volume, 26-5, 26-6
 precision of measurement, 26-6
 sand-grain volume, 26-3 to 26-5
 Laboratory measurement of transit times, 51-26
 Laboratory pressure-depletion study, 39-13
 Laboratory PVT analysis, 39-13
 Laboratory PVT data, 37-3
 Laboratory restored-state floods, 44-4
 Laboratory solubility tester, 54-10
 Laboratory testing of formation rock for acidizing, 54-9
 Labyrinth path design, 7-4
 Labyrinth path protector, 7-4, 7-5, 7-11
 Lacq Supérieur field, France, 46-27 to 46-29
 LACT systems or units, 11-13, 15-14, 17-4
 Lactic acid as sequestering agent, 54-7
 Lag, 13-50
 Lag stroke, 52-8
 Lag time, 52-8, 52-14, 52-18, 52-22
 Lagoonal clays, 36-4
 Lagoven, 46-14
 Lagunillas field, Venezuela, 24-13, 46-4
 Lake Maracaibo field, Venezuela, 18-1
 Lakeview pool, California, 40-15
 Laminar-flow regime, 28-13
 Laminar-flow region, 34-3
 Landman, 57-8
 Landowner's interest, 57-1, 57-2
 Landowner's royalty, 41-1
 Langmuir constants, 25-9
 Laplacian interblock flow terms, 48-15
 LaSalle anticline, 24-7
 Lasater correlation, 22-5 to 22-7, 22-9, 22-10
 Laser liquid particle spectrometer, 12-15, 12-16
 Last-chance hydraulic stab system, 18-15, 18-16
 Last-stroke method, hydraulic pumping, 6-28
 Latched packers, 4-3
 Late-time region (LTR), 35-3, 35-6 to 35-8, 35-11, 35-12
 Latent heat, factor in refrigeration cooling load, 14-10
 Latent heat from sensible heat, 19-15
 Latent heat of steam, 46-5
 Latent heat of vaporization, 46-2
 Lateral device, 49-12, 49-19, 49-31
 Lateral loading or loads, 18-5, 18-6
 Lateral-sweep factor, 40-16, 40-17
 Lateral wave loading or loads, 18-23, 18-26
 Laterals in hard formations, 49-13
 Laterolog™ (LL), 49-1, 49-5, 49-6, 49-11, 49-18, 49-21, 49-23, 49-25, 49-27
 Laterolog 3 (LL3), 49-18 to 49-22
 Laterolog 7 (LL7), 49-18 to 49-22
 Laterolog 8 (LL8), 49-15, 49-17, 49-20, 49-27
 Layout drawings, 15-30
 Layout of electrical offshore facilities, 18-44
 Leaching, 24-20, 26-2
 Lead acetate, 52-6
 Leak resistance, casing joints, 2-1
 Leak resistance limit, 2-59
 Leakage,
 fluid, 6-21
 fluid-seal plunger, 6-33
 in downhole unit, 6-55
 in pump plungers, 8-4, 8-5
 of field gas-condensate samples, 39-5
 of pump, 6-24
 of tubing pressure, 6-3
 pressure-relief valve, 6-33
 Leakoff of fluids, 54-8, 55-2, 55-4, 55-8
 Leaky modes of acoustic waveforms, 51-12, 51-13
 Leap-frog formulations, 48-14
 Lease, and assignment provisions, 41-9
 automatic custody transfer (LACT), 16-1, 16-7, 16-12, 16-13
 bonus, 41-1, 41-13
 broker, 57-8
 facilities, 41-9
 location data, 41-8
 problems, 57-10
 purchases, 57-8
 tank battery installation, 11-10
 Lease-operated hydrocarbon-recovery systems,
 gas treating for removal of water vapor, CO₂, and H₂S, 14-17 to 14-22
 low-temperature separation (LTS), 14-1 to 14-17
 references, 14-22
 Leasehold costs, capitalized, 41-13
 Leases, oil and gas, 57-1 to 57-12
 Least-squares fit, 38-10
 Lee-Kesler equation, 20-13, 20-17
 Legal requirements, directional surveys, 53-4
 Lena platform, 18-24
 Length equivalents, table, 1-71
 Length, standard of, 1-70
 Lenticular deposits, 49-25
 Lessor, in the oil and gas lease, 57-3
 LETC field site, Utah, 46-33
 Letter subscripts, SPE std., 59-52 to 59-70
 Letter symbols for mathematical equations, 58-3
 Letter symbols in alphabetical order, SPE std., 59-2 to 59-17
 Leutert pressure gauge, 30-2
 Level controllers and gauges, 19-31
 Lever-operated dump valves, 19-22
 Lever rule, 23-5
 Lever-type valve, 12-6, 12-18
 Leverage, 41-8
 Life of engine equipment, 10-16, 10-17
 Lift equipment, effectiveness of, 40-27, 41-9
 value of BHP measurements, 30-14
 Lifting potential concept, 34-50
 Lifting surface flowmeter, 32-13
 Light, units and conversions, 58-36
 Lightning arresters, 10-28 to 10-32
 Lignites, 49-25
 Liguera platform, 18-2
 Limestone sonde, 49-14, 49-26, 49-27
 Limit switches, 16-3, 16-13
 Limitations of gas lift, 5-1, 5-2
 Limited character sets, 58-11
 Limited Entry® technique, 55-9
 Limiting tie line, 45-3 to 45-5
 Line disconnect switch, 10-27
 Line drive pattern, 44-1, 44-20, 44-25, 46-17, 46-18
 Line pipe,
 and coupling, schematic, 2-54
 axial stress, 2-48, 2-49
 collapse pressure, 2-48, 2-49
 collapse pressure under axial-tension stress, 2-55
 collapse resistance, 2-48
 collapse resistance under axial load, 2-48, 2-49
 dimensions, 2-47, 2-50 to 2-53
 elongation, 2-46
 equations for calculating performance, 2-46, 2-54 to 2-56
 hydrostatic test pressure, 2-62, 2-63
 internal-pressure leak resistance, 2-57 to 2-59
 internal-pressure resistance, 2-56
 internal yield pressure, 2-56
 joint strength, 2-48
 plain-end, 2-50 to 2-53
 safety factors, 2-32
 tensile strength, 2-46
 test pressure, 2-47, 2-50 to 2-53, 2-62
 thread dimensions, 2-58, 2-65
 thread form, 2-62

- thread height dimensions, 2-62
 threaded or threads, 2-47, 2-48, 3-2
 tolerance on lengths, 2-47
 weight, 2-47, 2-50
 yield strength, 2-46
 Line scale, 12-2
 Line sink, 39-20
 Line source, 39-20
 Line-source solution, 35-4
 Line tension, maximum, 18-10
 Linear-absorption coefficient, 50-7
 Linear aquifers, 38-2, 38-4, 38-18
 Linear diffraction analysis, 18-39
 Linear dimensions, conversion of, 58-7
 units applied to, 58-5
 Linear-flow system, 26-13 to 26-15
 Linear frontal advance, 38-13
 Linear gels, 55-5, 55-6
 Linear geometry, definition, 38-1
 Linear parabolic difference equations, 48-15
 Linear partial differential equation, 35-1, 35-10
 Linear variable differential transformer, 51-5
 Linear velocities, conversion of, table, 1-76
 Lined pipe, 39-26
 Liners in steel pipe, 15-10
 Lipophiles, 47-7, 47-11, 47-19
 Liquefaction, 12-3
 Liquefied gases in acidizing, 54-8
 Liquefied petroleum gas (LPG), as
 injection fluid, 42-2, 45-1 to 45-3, 45-6 to 45-9, 45-12, 45-13
 Liquefied petroleum products, density of, 17-5
 Liquid block or blocking, 39-26, 46-1, 46-3
 Liquid (oil) capacity of separators, 12-28, 12-29, 12-31
 Liquid carryover, from compressor, 39-26
 in mist extractor, 12-40
 in separator, 12-42
 Liquid contents of GC systems, 39-4
 Liquid desiccants, 14-17
 Liquid-discharge control valves, 12-42
 Liquid-distribution coefficient, 34-39, 34-40
 Liquid entrainment, 34-36
 Liquid fallback, 5-40, 5-43, 5-44, 5-48, 5-52
 Liquid/gas ratio, 12-35, 39-2, 39-5
 Liquid holdup, 34-36, 34-37, 34-46
 Liquid hydrocarbon, 12-33, 12-35
 Liquid-hydrocarbon content, 12-15
 Liquid-hydrocarbon recovery, 11-13
 Liquid injection, BHP calculation, 34-28
 Liquid knockout, 12-1
 Liquid-level control, 3-19, 13-51, 13-53, 13-54
 Liquid-level controller, 12-2, 12-5 to 12-7, 12-9, 12-18, 12-35, 12-39, 14-3, 14-14, 14-18, 19-17 to 19-20, 19-31, 32-7
 Liquid-level controls, 16-4, 16-5
 Liquid/liquid equilibria, 23-1
 Liquid loading in wells, 34-46, 34-50
 Liquid measurement, 16-5
 Liquid mist, 12-8 to 12-12, 12-20, 12-22
 Liquid natural gas (LNG), 17-4, 17-7
 Liquid petroleum, calculation of quantities measured by turbine or displacement meters, 17-7
 Liquid petroleum (LP) gas, 10-15, 10-16, 17-4
 Liquid-phase distribution, 39-25
 Liquid-phase shrinkage, 39-4
 Liquid production per cycle, 5-52
 Liquid recovery, maximum, 5-51, 12-32
 Liquid recovery per cycle, 5-40
 Liquid-saturation data, 27-8
 Liquid saturations, 27-8
 Liquid seal in separator, 12-5
 Liquid slug process, 45-1
 Liquid slugs, 5-1, 5-11, 5-19, 5-38 to 5-44, 5-51, 5-52, 5-54
 Liquid-storage facilities, 12-33
 Liquid surges, 12-2, 12-20
 Liquid turbine meters, 13-48
 Liquid/vapor equilibrium, 23-1, 23-5
 Liter, definition of, 1-69
 Lithium, 24-9, 24-20, 24-21, 50-6, 50-14
 Lithological log, 52-14, 52-19
 Lithology determination,
 direct measurement, 50-37
 induced-gamma-ray spectrometry, 50-34, 50-35
 introduction, 50-2
 neutron/density combination, 50-33
 photoelectric factor, 50-33, 50-34
 Lithology, effect on formation factor, 49-4
 effect on water-injection efficiency, 44-2
 estimation from logs, 51-35
 parameters, 50-18
 Lithostatic pressure, 26-8
 Lloydminster field, Canada, 46-34
 Lloyds of London, 18-44
 Load analyses, offshore facilities, 18-44
 Load capacity, ultrahigh-slip motor, 10-22
 Load fluid gradient, 5-25, 5-28, 5-33, 5-45, 5-46
 Load fluid production rate, 5-53
 Load fluid traverse, 5-25
 Load production pressure, 5-49
 Loading or load up of wells, 32-15, 34-46, 34-50, 39-16
 Loan payout calculation factors, 41-32 to 41-35
 Loan payout, calculation of, 41-31 to 41-36
 Local control loops, 18-47
 Local remote switch, 10-27
 Location surveys offshore, 18-5
 Lock screws, 3-3, 3-5, 3-6, 3-8, 3-9
 Lockout cap, 3-27
 Log analyses, company computer centers, 49-37
 in coring program, thermal recovery, 46-21
 Log-linear grid, 49-15
 Log mean temperature, 34-8, 34-9
 Log-normal permeability distribution, 44-8
 Log presentation, acoustic logging, 51-16
 Log (electric) presentation and scales, 49-15, 49-16, 49-22, 49-23
 Log-probability graph paper, 40-18
 Logarithmic decrement, 51-4, 51-47
 Logarithmic energy decrement, average, 50-10, 50-11, 50-22
 Logarithmic probability diagram, 56-6, 56-7
 Logarithmic sensitivity scale, 49-27
 Logarithms of equivalents, 1-73, 1-75, 1-77
 Logging engineer, 52-30
 Logging geologist, 52-9, 52-18, 52-30
 Logging-system schematic, MWD, 53-2, 53-3
 Logging unit systems, 52-25, 52-26
 Logistics considerations offshore, 18-4, 18-5
 Long Beach crude oil, 47-20
 Long, gross, or shipper's ton, 1-70
 Long-range planning, 42-1
 Long-spaced acoustic logging,
 borehole-size effects, 51-19, 51-20
 formation-alteration effect, 51-20, 51-21
 introduction to, 51-19
 summary of, 51-23, 51-24
 tool, 51-21 to 51-23, 51-47
 Long-spaced acoustic logs, 51-22
 Long Spacing Sonic™ tool, 51-21
 Long-term forecast, gas-well performance, 35-13
 Long-thread casing, 2-5, 2-7, 2-9, 2-11, 2-13, 2-15, 2-17, 2-19, 2-31, 2-58, 2-64
 Longitudinal capillary imbibition, 28-12
 Longitudinal dispersion, 45-6
 Longitudinal waves, 51-2
 Looped networks in gathering and distribution systems, 15-14
 Lorenz coefficient, 44-36
 Los Angeles, 46-24
 Loss-free propagation time, 49-32 to 49-34
 Loss-ratio method, 40-32
 Louisiana, 18-1, 18-2, 21-4, 24-7, 24-8, 24-20, 26-7, 26-23, 27-6 to 27-8, 29-3, 32-1, 36-4, 37-25, 39-16, 40-23, 41-1, 44-37, 46-3, 46-4, 46-15, 46-18, 46-19, 49-29, 57-4, 57-10, 57-11
 Louisiana Dept. of Conservation, 32-1
 Louisiana gulf coast, 27-6 to 27-8, 44-37, 51-22, 51-23
 Louvered baffles, 19-23
 Low-alloy steel, 12-41
 Low-interfacial-tension (IFT) processes,
 lowering ROS, 47-9, 47-10
 MP flooding, 47-10 to 47-18
 Low-liquid-level control, 12-39
 Low-pressure service regulators, 13-55
 Low-pressure waterflooding, 42-2
 Low-temperature fractional distillation, 39-6
 Low-temperature operation of separator, 12-40
 Low-temperature separation (LTS),
 temperature, 14-17
 with hydrate inhibitor, 14-6 to 14-8
 without hydrate inhibitor, 14-3 to 14-6
 Low-temperature separation (LTS) systems,
 compression refrigeration, 14-9, 14-10
 constant-enthalpy expansion, 14-3 to 14-8
 cooling, 14-1, 14-2
 hydrate formation, 14-2, 14-3
 hydrocarbon stabilization, 14-13 to 14-17
 mechanical refrigeration, 14-8, 14-9
 retrograde condensation, 14-1
 selective absorption, 14-10 to 14-13
 theoretical considerations, 14-1 to 14-3
 turbine expansion, 14-8
 Low-temperature separation (LTS) unit, 12-1, 13-57, 18-46
 Low-temperature separator, 12-17, 14-5
 Low-temperature stabilization, 14-7
 Low-tension ignition, 10-17
 Lower explosive limit (LEL), 18-47
 Lower marine riser package (LMRP), 18-12, 18-15, 18-17, 18-19
 Lubricating oils, temperature correction for, 17-6
 Lubrication of pumping units, 10-12
 Lubricator, 6-48, 6-54, 6-57
 Luminous flux, unit and definition, 58-11, 58-23, 58-37
 Lump-sum deferment factors, 41-20, 41-21, 41-24, 41-25
 Lump-sum payment, 41-25
 Lynes BHP gauges, 30-4
- ## M
- Machining details, extreme-line casing joint, 2-64, 2-67, 2-68
 Macrodevices, 49-7, 49-14
 Macroresistivity curves, 49-26
 Macroscopic anisotropy, 49-5
 Macroscopic convective dispersion, 45-6
 Macroscopic cross section, 50-10, 50-21, 50-23, 50-36
 Macroscopic fluid velocity, 35-10

- Macroscopic photoelectric cross section, 50-17, 50-33, 50-34
- Macroscopic thermal absorption cross section, 50-10 to 50-12, 50-21, 50-30, 50-33
- Magnetlog, 53-19
- Magnesium, 24-5, 24-6, 24-8 to 24-13, 24-18, 24-20, 24-21, 44-44, 44-45, 47-13
- Magnesium chloride, 8-9, 19-29, 54-1
- Magnetic collar locator, 53-18
- Magnetic compass for hole deviation, 53-3, 53-4
- Magnetic flux, 53-21 to 53-23
- Magnetic flux density, unit and definition, 58-11, 58-23, 58-36
- Magnetic flux, unit and definition, 58-11, 58-23, 58-36
- Magnetic induction, unit and definition, 58-11, 58-36
- Magnetic permeability, 49-33, 53-23
- Magnetic relative permeability, 53-20
- Magnetic sensor, 13-48
- Magnetic tape recordings, 49-36, 49-37
- Magnetic trip capability of circuit breakers, 10-28
- Magnetic valve operators, 16-3
- Magnetism, units and conversions, 58-36
- Magnetometer, 18-5
- Magnetos, 10-17
- Magnolia Petroleum Co., 46-14, 46-16
- Main Reservoir field, Louisiana, 37-25
- Maintenance and operation of tank batteries, 11-10, 11-11
- Maintenance cost, emulsion treating, 19-33
- Major thermal recovery projects, 46-3, 46-4
- Makeup gas, 39-23, 39-24, 44-41
- Mandl-Volek model, 46-15
- Mandl-Volek refinement of Marx-Langenheim method, 46-8, 46-9
- Mandrel and boll-weevil tubing hangers, 3-16
- Mandrel hanger, 3-39
- Manganese, 3-3, 24-4, 24-5, 24-9, 44-44, 50-12, 50-18, 50-35
- Manifolds, high-pressure, 55-9
- Manifolds in subsea completions, 18-32
- Manitoba, Canada, 24-8
- Manometer factor, 13-8, 13-35
- Manual adjustable positive choke, 13-57
- Manual casing hanger, 3-6
- Manual emergency shut-down valve, 3-19
- Manufacture, of fiberglass sucker rods, 9-12 of steel sucker rods, 9-1, 9-2
- Manufacturer's field representative, 7-13
- Manufacturers' pumps, multiplex-plunger type, 6-52 to 6-55 nozzle and throat sizes, 6-39 nozzle vs. throat annulus area, 6-41 throat annulus areas and area ratios, 6-40 types of, 6-10 to 6-17
- Manufacturers' rated capacities for separators, 12-32
- Manways, 11-6, 12-42
- Marathon Oil Co., 46-15
- Maraven, 46-4, 46-15
- Marginal well tests, 12-17
- Maricopa field, California, 6-24
- Marine bulk carriers, metering systems for loading and unloading, 17-4
- Marine cargo inspection, guidelines for, 17-8
- Marine environment, 56-2
- Marine measurement, 17-8
- Marine pipelines, 18-43
- Marine risers, 18-14 to 18-16, 18-19
- Marine terminals, 18-43
- Marine water, 24-19, 24-20
- Mark II crank-balanced pumping units, 10-1 to 10-4, 10-6, 10-8, 10-9
- Market capacity, 32-1
- Market value, 41-3, 41-5, 41-6
- Market-value yardstick, 41-5
- Marx-Langenheim method, 46-7 to 46-9
- Mass-absorption coefficient, 50-8
- Mass-balance equations, 48-3
- Mass balance of hydrocarbons, 46-11
- Mass balance of oxygen, 46-12
- Mass balance of water, 46-11
- Mass-conservation equation, 48-3, 48-5
- Mass equivalents, table, 1-75
- Mass flowmeter, 32-13
- Mass flow ratio, 6-36 to 6-38, 6-45
- Mass or force as weight quantity, 58-3, 58-5
- Mass, special terms and quantities involving, 58-7, 58-8
- Mass spectrometry, 27-1
- Mass, standard of, 1-70
- Mass, unit and definition, 58-3, 58-5, 58-23, 58-27
- Mass vs. weight, 1-70
- Massachusetts Inst. of Technology, 51-49
- Material balance, 14-16, 38-4, 38-5
- Material-balance calculations, 22-13, 28-11, 35-16, 37-13, 40-1, 40-13, 40-24, 42-3, 43-12, 43-16, 48-1, 48-14
- Material-balance equation, 35-8, 37-2, 37-5 to 37-7, 37-10, 37-13 to 37-17, 38-4, 38-8, 38-9, 38-12 to 38-14, 40-6, 40-7, 40-9, 40-10, 40-12, 40-33, 40-44, 43-4, 43-6, 43-8, 43-12, 43-13
- Material-balance method, for average reservoir pressure, 35-3 for nonassociated gas reservoirs, 40-33 for oil in place, 40-2, 40-6 to 40-8
- Material-balance studies, 36-7
- Materials of construction for separators, 12-38, 12-39
- Materials of construction for storage tanks, 11-9
- Mathematical analysis of areal pattern efficiency, 44-13 to 44-17
- Mathematical analysis, water-drive oil reservoirs, 38-1 to 38-17
- Mathematical modeling, 28-7, 28-10
- Mathematical models, 9-3, 36-10, 39-17, 39-18, 48-1
- Mathematical reservoir simulation, 39-24, 45-10
- Mathematical reservoir simulators, 39-22
- Mathematical-simulation models, 38-16
- Mathematical simulators, 39-17, 45-13
- Mathematical tables, 1-2 to 1-67
- Matrix acid stimulation, 56-5
- Matrix acidizing, A/V ratio high, 54-5 carbonate formations, 54-10, 54-11 definition of, 54-8 overflush, 54-11 sandstone formations, 54-11 with surfactants, 54-6
- Matrix blocks, 48-5
- Matrix compaction, 26-7
- Matrix correction chart, 50-29
- Matrix, definition, 26-2
- Matrix density, 50-1, 50-27, 50-28
- Matrix effect on neutron porosity, 50-28 to 50-30
- Matrix identification chart, 50-19
- Matrix permeability, 26-15, 27-18
- Matrix porosity, 26-7, 44-2
- Matrix steam injection, 46-27, 46-28
- Matrix transit time, 51-30, 51-35
- Matrix treatment with acid, 56-5
- Maximum efficient rate (MER), 32-2, 41-9
- Maximum-indicating pressure gauge, 30-4
- Maximum present worth, 42-2
- Maximum producible oil index, 49-28
- Maximum theoretical valve spread, 5-42
- Maximum transfer pressure, 5-32
- Maxwell's equation, 49-33
- May Libby field, Louisiana, 46-15
- Mean average boiling point, 21-11, 21-12, 21-15
- Mean free path, 50-10, 50-22
- Mean hydraulic radius, 26-31
- Means field, Texas, 36-5, 36-7
- Measured phase compositions, 23-12
- Measurement, of barges, 17-3 of horizontal tanks, 17-3 of liquid hydrocarbons by displacement meter systems, 17-4 of petroleum by weight, 17-7, 17-8 of petroleum liquid hydrocarbons by positive-displacement meter, 17-4, 17-5 of spheres and spheroids, 17-3 of tank cars, 17-3 of upright cylindrical tanks, 17-3
- Measurement control charts, 17-7
- Measurement methodologies of relative permeability, calculation methods, 28-7 capillary-pressure and endpoint-displacement method, 28-8 critique of methods, 28-7 stationary-fluids methods, 28-8 steady-state methods, 28-3 to 28-7 unsteady-state methods, 28-7
- Measurement tickets, 17-7
- Measurement-while-drilling (MWD), data listing for, 53-6 data-transmission schematic, 53-2 directional vs. multishot directional, 53-5 downhole assembly, 53-2 log, 53-2, 53-4 logging system, 53-3 measuring systems, 53-1 rotary-drilling log, 53-4 services, 52-1, 52-28
- Measuring crude oil, 17-1 to 17-8
- Measuring natural-gas fluids, 17-7
- Measuring quality of separated fluids, 12-15, 12-16
- Measuring temperature of petroleum and petroleum products, 17-5 to 17-7
- Mechanical damage, 51-20
- Mechanical data, electric submersible pump (ESP), 7-9
- Mechanical degradation, 47-5
- Mechanical energy, 22-21, 51-2, 51-3
- Mechanical-energy gradients, 28-13, 28-14
- Mechanical failure, 39-25
- Mechanical flow sheets, 15-31
- Mechanical lock holddown, 8-8
- Mechanical losses in hydraulic pumps, 6-19, 6-20, 6-21
- Mechanical power, 6-15
- Mechanical pressure control, 12-39
- Mechanical properties, elastic moduli, 51-43 fracturing, 51-44 sand control, 51-45
- Mechanical recording BHP gauges, 30-2
- Mechanical refrigeration, 11-13
- Mechanical-refrigeration systems, 14-8 to 14-10
- Mechanical timers, 16-4
- Mechanical wave propagation, 51-2
- Mechanically operated valve, 13-53

- Mechanically set packer, 4-3, 4-4, 4-6
 Mechanics, units and conversions, 58-33, 58-34
 Mediterranean Sea, 24-19
 Medium-slip motors, 9-3
 Melcher-Nutting grain-volume method, 26-3
 Melting curve, 23-1, 23-2
 Membrane-filterability tests, 44-43
 Membrane filtration, 24-18 to 24-20
 Memory jogger, metric units, 58-21
 Mene Grande field, 24-13
 Mene Grande Oil Co., 46-16
 Mene Grande tar sand, Venezuela, 46-3
 Mercaptans, 14-17
 Mercury, 26-3, 26-4, 26-24, 39-8
 Mercury-injection method of capillary-pressure measurement, 26-24, 26-25
 Mercury manometers, 13-3, 13-36
 Mercury method of calculating directional surveys, 53-6
 Mercury porosimeter, 26-22
 Mercury-pump method, 52-19
 Mercury-pump porosimeter, 26-6
 Mercury test site, Nevada, 53-5
 Mercury-type meters, 13-8, 13-35 to 13-37
 Mercury valve switch, 16-3
 Metal on-metal seal ring, 18-18
 Metal spray coupling, 9-9
 Metal-to-metal plungers, 8-4
 Metallic storage tanks, 11-9
 Metamorphosed rock, 29-3, 29-8
 Metastable dewpoint locus, 25-1, 25-2
 Metastable equilibrium, 14-4
 Metastable-equilibrium locus, 25-2
 Metastable liquid water, 25-10
 Meteoric water, 24-2
 Meter, definition, 1-69
 Meter factor or multipliers, 32-10, 32-12, 32-13
 Meter loops, 6-54
 Meter model, 47-4
 Meter proving, 16-6, 16-14, 17-4
 Meter-tank-type LACT system, 16-12, 16-13
 Meter tube, 5-53
 Metering and metering assemblies, 17-4, 17-5
 Metering separator, 12-17 to 12-19, 32-13, 32-14
 Metering systems, critical flow provers, 13-37, 13-45
 orifice well tester, 13-37
 pitot tube, 13-2, 13-45
 velocity, other meters using, 13-45, 13-48, 13-49
 Metering trim, 13-53
 Meters using velocity, centrifugal (elbow) meters, 13-45
 eccentric orifices, 13-45
 rotameter, 13-45
 segmental orifices, 13-45
 sonic meters, 13-48
 turbine meters, 13-45
 vortex shedding meter, 13-48
 Methane/butane/decane system, 23-5
 Methane/butane system, 23-6
 Methane/decane system, 23-6
 Methane hydrates, 25-10
 Methane/propane hydrates, 25-10
 Methane/propane system, 25-9
 Methane/propane/water system, 25-10
 Methane-rich gas, 25-13
 Methane/water system, 25-1, 25-2, 25-17, 25-18
 Methanol, as hydrate inhibitor, 25-19, 25-20
 for freezing and corrosion protection, 3-35
 Method of least squares, 26-31, 40-6
 Methyl alcohol, in acidizing, 54-8
 in in-situ formation of hydrofluoric acid, 54-4
 Methyl orange end point, 54-3
 Methyldiethanolamine (MDEA), 14-21, 14-22
 Metric Conversion Act of 1975, 1-69
 Metric standard for orifice equations and constants, 13-3
 Metric system, definition, origin, and development, 1-68, 1-69
 Intl. Bureau of Weights and Measures, 1-69
 present status in U.S., 1-69
 units and standards of, 1-69
 Metric ton, 1-70
 Mexico, 12-39, 21-2, 58-20
 Micellar floods, 19-28, 48-5, 48-7
 Micellar fluids, 28-11
 Micellar/polymer (MP) flooding, 47-1, 47-9 to 47-22, 48-6
 formulation, 47-13, 47-15
 phase behavior, 47-11, 47-13, 47-20
 slug, 47-10, 47-15 to 47-17
 surfactants, 47-7, 47-17
 Micelles, 47-10, 47-11
 Microannulus, 51-41
 Microbiological growth, 44-44
 Microcaliper curve, 49-1, 49-11, 49-22, 49-25, 49-26, 49-29, 49-31
 Microcaliper log, 53-16
 Microcomputers, 16-1, 16-6, 16-8
 Microdevices, 49-7, 49-14
 Microemulsion, 28-11, 45-1
 Microemulsion flooding, 47-10
 Microemulsion phase, 47-11 to 47-14
 Microfiche, 17-5
 Microfilm, 17-5
 Microinverse, 49-23
 Microlaterolog (MLL), 49-22, 49-24 to 49-26, 49-28
 Microlog (ML), 26-31, 44-3, 49-22 to 49-29, 49-31, 49-32
 Microlog shaly-sand method, 49-28
 Micrometer screw, 26-3, 26-4
 Micronormal, 49-23
 Microprocessor-based instrument system, 18-47
 Microprocessors, 16-1
 Microresistivity, 51-19
 Microresistivity devices, 49-1, 49-22 to 49-25, 49-26
 Microresistivity survey, 49-11
 Microscopic anisotropy, 49-5
 Microscopic convective dispersion, 45-6
 Microscopic cross section, 50-6
 Microscopic displacement of fluids, 39-18
 Microscopic efficiency, 40-34
 Microscopic pore volumes, 39-17
 Microscopic studies, 46-21
 Microscopic sweep efficiency, 47-2
 Microseismogram, 51-24, 51-35, 51-45, 51-46
 Micro-Seismogram Log™, 51-18
 MICROSLF (MSFL), 49-20, 49-22, 49-24, 49-25
 Microswitch valve switch, 16-3
 Mid-American trench, 25-18
 Mid-Continent, 21-4, 21-6, 24-8 to 24-10, 29-3, 40-19, 41-5, 44-4
 Middle East, 27-9, 27-20, 52-22
 Middle-time region (MTR), 35-3, 35-4, 35-6, 35-8, 35-10 to 35-12, 35-14, 35-15
 Midway field, California, 29-2
 Midway Sunset field, California, 46-14, 46-15, 46-18, 46-19
 Midwest Research Inst., 8-10
 Midyear compound-interest factor, 41-17
 Midyear lump-sum deferment factor, 41-6 to 41-8, 41-27 to 41-29
 Miga field, Venezuela, 46-15, 46-18
 Migration length, 50-12, 50-20, 50-21, 50-29, 50-30, 50-32
 Migration of clay particles, 56-5
 Migration of oil and gas, 24-1
 Migration of oil, 24-17
 of water, 24-18
 Mile Six Pool, Peru, 40-14
 Mill scale, 11-5
 Mill varnish, 51-41, 56-3
 Miller-Dyes-Hutchinson (MDH) plot, 35-15, 35-17 to 35-20
 Millipore™ filter test, 44-45
 Mineral, analyses of cores, 46-21
 deeds, 57-6
 dissolution, 47-20
 interests, 41-1, 41-15, 57-6
 owner, 57-1, 57-6
 severance, 57-2
 Mineral Management Service, 3-34
 Mineralogy, 56-3
 Minerals, in water, 44-44, 44-45
 in a lease or a conveyance, definition, 57-2
 recovery from brines, 24-20, 24-21
 Miner's rule, 18-27
 Minicomputer, 51-4
 Minifrac job, 55-9
 Minimum hydrodynamic potential, 29-3, 29-8
 Minimum miscibility pressure (MMP), 45-6, 45-8, 45-9
 Minimum pump intake pressure, 7-10
 Minor isostatic adjustment, 29-7, 29-8
 Miscibility, definition, 45-1, 45-6
 development, 45-4, 45-5
 maintaining, 45-7
 of methane gas and propane liquid, 45-2
 of propane liquid and oil, 45-2
 of refrigerants with water, 14-10
 pressure, 22-17
 providing to improve recovery, 39-15
 Miscible displacement, engineering examples, 45-10 to 45-13
 engineering study, 45-8 to 45-10
 factors affecting displacement efficiency, 45-6 to 45-8
 fluids, 40-4
 general references, 45-15
 introduction, 45-1
 methods, 44-19
 nomenclature, 45-13
 numerical dispersion effect in, 48-10
 processes, 23-7
 references, 40-13 to 40-15
 theoretical aspects, 45-1 to 45-6
 Miscible-drive projects, 42-5
 Miscible flood, 39-23, 48-2, 48-10
 Miscible-fluid displacement, 43-7
 Miscible-phase displacement, 39-16
 Miscible processes, 39-18
 Miscible slug process, 42-2, 45-1 to 45-3, 45-6 to 45-9, 45-12, 45-13
 Mississippi, 24-20, 24-21, 26-19, 40-23, 46-3, 46-4, 46-15, 46-18, 46-28 to 46-30, 54-1
 Mississippi River, 36-4
 Missouri, 24-8, 46-3, 46-14
 Mist eliminators, 12-12, 39-26

- Mist extractors, 12-1 to 12-5, 12-7 to 12-9, 12-11, 12-12, 12-15, 12-19, 12-21, 12-23 to 12-26, 12-31, 12-40, 19-22, 19-24, 19-25, 39-26
- Mist flow, 34-27, 34-36, 34-37, 34-40
- Mix-based fracturing fluids, 55-7, 55-8
- Mixed-lithology rocks, 51-35
- Mixing efficiency, 19-27
- mm to decimals of an in., table, 1-72
- Mobil Corp., 46-4, 46-15, 46-18
- Mobile analyzer, 24-4
- Mobility, 58-38
- Mobility-buffer drives, 47-1
- Mobility buffer, MP flooding, 47-10, 47-17
- Mobility-buffer salinity, 47-15
- Mobility-control processes, effect of low mobility on oil recovery, 47-1, 47-2
- foam flooding, 47-6 to 47-9
- polymer flooding, 47-2 to 47-6
- Mobility improvement, 44-39, 44-40
- Mobility of displacing fluid, 44-17
- Mobility of foams, 47-8, 47-9
- Mobility ratio, 39-15, 39-18, 39-21, 40-18, 40-19, 43-7, 43-8, 44-4, 44-8 to 44-10, 44-15, 44-17 to 44-25, 44-27, 44-29, 44-33 to 44-40, 45-4, 45-7, 45-9, 45-11, 47-1, 47-2, 47-20
- Mobility-ratio effects, 44-17 to 44-24, 44-34, 44-36
- Mobility, total, 35-2
- Model assumptions, 48-9
- Model basin, 18-7
- Model formulation, 48-14 to 48-16
- Model grid selection, 48-7
- Model input data, 48-6
- Model, radial flow, 35-6
- Model(s), analog, 39-22, 44-18
- analytical for pump performance, 7-12
- analytical for steam injection, 46-7 to 46-11
- assumptions, 48-9
- black oil, 48-4 to 48-7, 48-9, 48-14
- blotter, 44-17
- bundle of capillary tubes, 28-12
- chemical flood, 48-4, 48-5, 48-7
- compositional, 43-2, 48-4, 48-6, 48-7, 48-9, 48-14
- computer, 39-4, 44-38
- conductive cloth, 44-20
- dispersed clay, 51-34
- drilling, 52-24 to 52-26
- dual-water, 49-38
- electrolytic, 39-20, 39-21, 44-17, 44-18, 44-20, 44-21
- electronic, 39-20
- elemental, 46-11 to 46-13
- fluid flow, 44-20, 44-21
- fluid mapper, 44-20
- fractured matrix, 48-5
- framewood structural, 51-34
- frontal displacement, 46-7 to 46-9
- future interpretation, 50-36
- gel or gelatin, 39-2, 44-17, 44-18, 44-20, 44-21
- geochemical, 24-20
- grain boundary structural, 51-34
- graphical, 22-5, 22-7, 22-8
- graphite-impregnated cloth, 39-21
- gridded reservoir, 37-2, 37-5, 37-11
- high-pressure, 46-13
- hydrate dissociation, 25-9
- idealized pore, 26-28
- in-situ combustion, 46-12
- isothermal, 48-4
- Kuster-Toksöz, 51-34
- laminated, 51-34
- Lasater, 22-5 to 22-7, 22-9, 22-10
- Mandl-Volek, 46-15
- mathematical, 9-3, 36-10, 39-17, 39-18, 48-1, 48-16, 48-17
- mathematical simulation, 38-16
- meter, 47-4
- numerical, 44-17, 44-20, 46-11, 46-20
- numerical simulation, 40-2
- partially scaled, 46-11 to 46-13
- perforation prediction, 37-19
- physical, 46-11 to 46-13
- porous reservoir, 44-17
- positive seal double-bag, 7-11
- potentiometric, 39-21, 39-22, 44-17, 44-19, 44-34
- power law, 47-4, 55-5
- process, 28-3
- randomized network, 28-12
- reservoir simulation, 38-16, 40-34, 43-2, 43-17, 48-1 to 48-6
- resistance network, 44-20
- rock flow, 44-20
- sand, for fluid flow, 26-11 to 26-13
- scaled physical, 45-10
- scaled porous, 44-17, 44-34
- shaly sand, 51-34
- simple two-mineral, 50-33
- simulation, 44-31, 44-32, 48-7 to 48-9
- steam chest, 46-9
- steam injection, 46-11, 46-12
- streamtube, 45-10
- tandem labyrinth path, 7-11
- tank-type, 37-2, 37-4, 37-5, 37-11, 37-14, 37-17
- theoretical, 51-8
- thermal, 48-4 to 48-7, 48-14
- thermal numerical, 46-12
- vacuum, 46-13
- Modems, 16-10
- Modified black-oil simulator, 45-10
- Modified Griffith and Wallis method, 34-37
- Modified Stiles permeability-block method, 40-20
- Modified turnkey format, 15-32
- Modulus of elasticity, 9-3, 9-11, 9-12
- Moisture-resistant coatings, 11-6
- Molal average boiling point, 21-6, 21-11, 21-13 to 21-15
- Mole, definition, 22-21
- Mole fraction gas mixtures, 20-4
- Mole, unit and definition, 58-25
- Molecular diffusion, 45-6
- Molecular sieves, 14-21
- Molecular weight, 20-1, 20-3, 20-4, 20-9, 20-10
- Molecular weight, effect on water content in vapor phase, 25-16
- Molybdenum, 9-5
- Moment of inertia, 58-34
- Monatomic gases, 13-37
- Monel®, 3-36, 7-5, 15-21, 30-4
- Monel bellows, 5-16, 5-17
- Monitor log, 53-8, 53-11
- Monitoring programs, thermal recovery, 46-20, 46-21
- Monoethanolamine (MEA), 14-21, 14-22
- Monotube separator, 12-16, 12-21, 12-22
- Monovalent cation, 47-15
- Monovalent/divalent ratios, 47-13
- Montana, 24-8, 24-11, 24-20, 40-23
- Montmorillonite, 44-2, 47-21, 52-21, 52-22
- Moody diagram, 15-2, 15-3, 15-7
- Moody friction factor, 34-24, 34-38
- Moonpool, 18-2, 18-23, 18-42
- Moored buoy, 18-30
- Moored positioning, 18-2, 18-9
- Mooring analysis, 18-9, 18-16, 18-17, 18-21
- Mooring systems, 18-4, 18-8 to 18-10, 18-16, 18-18, 18-21, 18-24
- Morkill method, 41-16, 41-19, 41-22
- Mother Hubbard clause, 57-6
- Motion characteristics, drilling vessels, 18-7
- Motion compensators, 18-2
- Motion-response curves, 18-7
- Motor control centers (MCC's), 18-44, 18-46
- Motor, control for, 10-27 to 10-29
- cyclic load factor of, 10-25
- derating factors for, 10-25
- direct current, 10-21
- drip-proof, 10-26, 18-46
- efficiency of, 10-25
- electric, for oilwell pumping, 10-19 to 10-37
- enclosures for, 10-26
- explosion-proof, 10-27, 18-46
- fractional horsepower, 18-46
- fuses for, 10-28
- horsepower ratings of, 10-20
- induction, 10-19 to 10-21, 10-23 to 10-25
- insulation for, 10-26
- multiple horsepower rated, 10-20
- multiple-size rated, 10-21
- oilfield, control for and protection of, 10-27 to 10-29
- performance factors of, 10-23 to 10-26
- power factor of, 10-25
- power triangle for, 10-33
- rated voltage, 10-21
- selecting size of, 10-21
- service factor of, 10-25, 10-26
- single-phase, 10-21
- slip of, 10-23, 10-24
- speed variations of, 10-24, 10-25
- splash-proof, 10-26
- starter contactor for, 10-28
- temperature rise of, 10-26
- torque of, 10-25
- totally enclosed, 10-26, 18-46
- ultra-slip, 10-24
- voltage frequency of, 10-21, 10-23
- winding temperature sensors, 10-29
- Motor flat cable, ESP, 7-5
- Motor horsepower, 10-36
- Motor load transducers, 46-21
- Motor rated voltage, 10-21
- Motor torque, 10-24
- Motor valve diaphragm pressure, 13-54
- Motor winding temperature sensor, 10-29
- Motor windings, 10-26
- Mount Poso field, California, 46-4, 46-15, 46-18
- Movable oil, 46-8
- Mud acid, 56-5
- Mud acid preflush, 54-4
- Mud acid system, 54-4, 54-11
- Mud contamination, 56-1, 56-3
- Mud damage, 35-4
- Mud-dispersing agents, 56-1
- Mud log, 49-23
- Mud-log data, 52-26
- Mud-log format, 52-11 to 52-16
- Mud-log services, 52-1, 52-2
- Mud logger, 52-30
- Mud logging, 52-1 to 52-30
- Mud logging contractor services, 52-28
- Mud removal, 56-1
- Mud-removal acid, 54-3, 54-4, 54-11
- Mud transit time, 51-20, 51-23
- Mud weight, 30-15
- Mud-weight factors, 2-1, 2-3, 2-33, 2-38

- Multicomponent flash method, 37-23 to 37-26
- Multicylinder diesel engines, 10-17
- Multicylinder gas engine, 6-1
- Multicylinder pump, 44-47
- Multifingered caliper logs, 53-17
- Multilayer prediction method, 44-31
- Multiphase displacement experiments, 28-3
- Multiphase flow, Buckley-Leverett description of, 28-6
- continuous-flow gas-lift design, 34-40 to 34-45, 34-50
- correlations, 5-22, 5-25, 5-26, 5-38, 5-40, 34-37, 37-40
- gas plus liquid, hydraulic pumping, 6-27
- immiscible fluids, no gravity forces, 28-2
- in heterogeneous porous media, 48-1, 48-2
- introduction, 34-35, 34-36
- modeling of, 28-12
- pseudosteady-state behavior, 35-6
- theoretical considerations, 34-36, 34-37
- well-performance equation, 35-2
- Multiphase flowing gradient calculations, 6-72
- Multiphase flowing pressure-gradient curves, 5-21
- Multiphase inflow performance relationship (IPR) equation, 34-32
- Multiphase pressure-drop correlations, 34-37
- Multipiece structure, 18-23
- Multiple-bore mandrel tubing hanger, 3-14, 3-16
- Multiple-bore riser, 18-35
- Multiple-completion equipment, 3-13
- Multiple completions, 56-5
- Multiple-contact miscibility, 39-16, 45-1, 45-5, 45-6, 48-5, 48-10
- Multiple-cylinder engines, 10-15
- Multiple-horsepower-rated motors, 10-20
- Multiple-motor installation, 10-36
- Multiple-parallel tubing strings, 3-14
- Multiple-regression equation, 2-60
- Multiple-seal pumps, 6-39
- Multiple-segment tubing hanger, 3-16
- Multiple-size-rated motors, 10-21
- Multiple-stage separation, 12-16, 12-32, 12-33
- Multiple thrusters, 18-10
- Multiple tubing strings, 3-8
- Multiple-zone fracturing, 55-9
- Multiples of 0.4343, table, 1-60
- Multiples of 2.3026, table, 1-60
- Multiplex BOP control system, 18-21
- Multiplex pumps, 6-28, 6-49 to 6-55, 6-57 to 6-59, 6-62
- Multiplex transmission systems, 18-3
- Multiplexed electrohydraulic control, subsea, 18-52
- Multiplication factor, for casing joint length, 2-29, 2-31 for tubing joint length, 2-45
- Multipoint backpressure test, 34-31
- Multipoint gas injection, 5-32, 5-36
- Multipoint testing, 33-4 to 33-13, 33-22
- Multipool aquifers, 38-16
- Multishot survey, 53-3
- Multistage centrifugal pumps, 6-1
- Multistage emulsion, 19-2, 19-3
- Multiwell templates, 18-32
- Multiyear ice, 18-39
- Muskat material balance, 37-13
- Muskat method, 37-10 to 37-13, 37-21
- Muskat's correlations, 39-20
- Muskat's method, 40-9
- N**
- n-Butane/water system, 25-26
- n-Decane/water system, 25-26
- n-Hexane/water system, 25-26
- n-Pentane/water system, 25-26
- Naphtha, 26-22
- Naphtha/water system, 25-26
- Naphthenic base, 19-27
- Napierian logarithms, 1-56, 1-57
- Natl. Assn. of Corrosion Engineers (NACE), 4-4
- Natl. Bureau of Standards (NBS), 1-68 to 1-71, 17-4
- Natl. Conference of Weights and Measures, 17-7, 17-8
- Natl. Electric Code (NEC), 10-26
- Natl. Electrical Code, 18-46
- Natl. Electrical Manufacturers Assn. (NEMA), classification for control enclosures, 7-5, 7-6, 10-27
- D-electric motors, 10-17, 10-18
- rated motors, 10-24
- specifications for motors, 10-20
- Natl. Science Foundation, 18-15
- Natural cosecants, table, 1-48, 1-49
- Natural cosines, table, 1-44, 1-45, 1-50 to 1-54
- Natural cotangents, table, 1-46, 1-47, 1-50 to 1-54
- Natural gamma ray activity, 50-2, 50-15
- Natural-gas container, 36-2
- Natural-gas, definition, 12-3, 40-3
- Natural-gas engineering letter and computer symbols, 59-2 to 59-51
- Natural-gas engines, 15-16
- Natural-gas fluids measurement, 17-7
- Natural-gas fuel, 10-15
- Natural-gas liquids (NGL), 40-3, 40-4
- Natural-gas mixtures, 17-7
- Natural Gas Policy Act, 43-2
- Natural-gas/water system, 25-3
- Natural gases, compositions and gas gravities, 25-6
- Natural gasoline, 40-3
- Natural gasoline content of gas, 20-10, 20-11
- Natural gasoline plants, 41-11
- Natural gums in acidizing, 54-8
- Natural logarithms, table, 1-56, 1-57
- Natural secants, table, 1-48, 1-49
- Natural sines, table, 1-44, 1-45, 1-50 to 1-54
- Natural tangents, table, 1-46, 1-47, 1-50 to 1-54
- Natural water drive, 39-15 to 39-17, 39-26, 44-2
- Nearshore carbonate deposits, 36-6
- Nebraska, 24-8, 24-20, 40-23, 44-40, 46-14, 46-15, 46-18, 46-21, 46-30, 46-33, 47-22
- Nederlandse Oil Co., 46-14
- Negative gas show, 52-14
- Negotiated turnkey format, 15-32
- Neopentane/water system, 25-26
- Neothene, 52-20
- Nephelometer, 44-44
- Nephelometric turbidity units (NTU), 44-44
- Net cash flow, 41-3, 41-5 to 41-8
- Net-oil computers, 16-2, 16-7, 16-8, 16-12
- Net-pay/net-connected-pay ratio, 36-7
- Net positive suction head (NPSH), 15-17
- Net-profit/initial-investment ratio, 41-22
- Net-profit/unreturned-investment-balance ratio, 41-22
- Net-profits interest, 41-1, 41-2, 57-10
- Netherlands, 12-39, 46-3, 46-14, 51-47
- Neuquen basin, Argentina, 51-33
- Neutron absorption, 50-2
- Neutron cross section, total, 50-9
- Neutron/density combination, 50-30, 50-31, 50-33
- Neutron-density crossplot, 50-30, 50-33
- Neutron detectors, 50-14, 50-15
- Neutron energy, 50-8 to 50-10, 50-23
- Neutron/gamma-ray tool, 49-19
- Neutron interactions, 50-8 to 50-12
- Neutron log, 44-3, 49-26, 49-34, 49-38, 51-31, 51-33
- Neutron porosity, 50-24, 50-31, 51-20, 51-33
- Neutron-porosity devices, 50-17 to 50-21, 50-28 to 50-33
- Neutron-slowness-down properties, 50-2, 50-4, 50-11
- Nevada, 24-21, 53-6
- New England, 29-7
- New Hampshire, 51-45
- New Mexico, 6-24, 21-4, 24-8, 24-20, 27-16, 27-17, 36-8, 39-25, 40-23, 44-40
- New Mexico Conservation Commission, 33-15
- New York, 24-1, 44-1
- Newton-Raphson iteration procedure, 23-11, 48-14, 48-15
- Newtonian fluid, 22-13
- NEXUS log analysis, 49-37
- Ni-Resist, 7-3
- Ni-Span C[®], 30-3
- Nickel, 9-5
- Nigeria, 50-26
- Nigerian reservoirs, offshore, 48-6
- Nikurodse friction-factor equation, 34-24
- Nine-point difference scheme, 48-11
- Nine-spot grids, 48-11, 48-12
- Nine-spot pattern or network, 43-2, 44-13, 44-14, 44-21, 44-23 to 44-25, 44-34, 46-17, 46-25, 46-28
- Nipple-up operations, 3-6
- Niralloy, 7-3
- Nitric acid (HNO₃), 24-4
- Nitrile[®], 4-5
- Nitrogen (N₂) 1-70, 5-6, 5-7, 12-3, 14-13, 14-17, 16-3, 20-5, 22-5, 22-17, 23-7, 25-14, 26-18, 37-24, 39-2, 39-6, 39-14, 39-16, 40-22, 43-2, 45-1, 45-4, 45-6, 45-12, 48-5, 48-6, 48-9, 52-6, 55-6, 55-9, 56-5
- Nitrogen-charged dome pressure, 5-7
- Nitrogen-charged gas-lift valves, 5-16, 5-17, 5-26
- Nitrogen in acidizing, 54-8
- Nitrogen/water system, 25-3
- Nitroglycerin, 24-1, 56-1
- Nitrox solution, 46-22
- Nominal decline rate, 40-27 to 40-29
- Nominal interest rate, 41-25 to 41-35
- Nominal rate-of-return (ROR), 41-18
- Nominal value, definition, 58-9
- Nomograph, 22-5, 22-6, 22-10, 22-13
- Non-API, pumps, 8-9
- steel-grade casing, 2-5, 2-7, 2-9, 2-11, 2-13, 2-15, 2-17, 2-19
- weights and grades of casing, 2-4, 2-6, 2-8, 2-10, 2-12, 2-14, 2-16, 2-18
- Non-Darcy flow, 34-31, 34-32, 34-34, 35-10, 35-11
- Non-Darcy flow factor, 33-5
- Non-Newtonian effects, polymers, 47-4
- Non-Newtonian rheology, 28-13
- Non-SI metric units, 58-10, 58-21
- Non-upset tubing, 2-38 to 2-44, 2-64, 2-66
- Non-U.S. areas, core analysis data from, 27-9

- Nonassociated dry gas reservoir, 40-24
 Nonassociated gas, 40-3, 40-23, 40-33, 40-34
 Noncircular drainage area, 32-5
 Noncollinear flow, 28-12
 Nonequilibrium gas displacement, 43-16
 Nonideal effects, micellar/polymer (MP) flooding, 47-13
 Noninjection gas requirements in cycling, 39-23
 Noninteractive scattering theory, 51-8, 51-9
 Nonionics, 47-7, 47-8
 Nonlinear partial differential equation, 35-2
 Nonmetallic storage tanks, 11-9
 Nonmetric units, 58-5
 Nonownership theory, 57-1
 Nonsymmetrical aquifers, 38-3
 Nonsymmetrical geometry, definition, 38-1
 Nonwetting immiscible fluids, 28-3, 28-5, 28-6
 Nonwetting phase, 26-24, 40-26, 47-9
 Normal ammeter chart, electric submersible pump (ESP), 7-14, 7-16
 Normal boiling point, 20-11
 Normal brass standards, 1-71
 Normal compaction trend line, 51-39
 Normal device, 49-12, 49-19, 49-20
 Normal fault with drag, 53-12
 Normal faults, 29-3, 29-8
 Normal-flow installations, 6-6
 Normal startup chart, electric submersible pump (ESP), 7-14
 Normal venting capacity of tanks, 11-7
 Normalized total gas, 52-18
 Normals in hard formations, 49-13
 North America, 24-6, 29-3
 North Anderson Ranch field, New Mexico, 36-8
 North Atlantic, 18-38
 North Burbank unit, Oklahoma, 47-6
 North Dakota, 24-20, 57-10
 North Louisiana area, 27-4, 27-5
 North Sea, 18-2, 18-3, 18-18, 18-23 to 18-26, 18-36, 18-41, 18-44, 27-9, 27-20, 36-2, 44-37, 44-46, 50-24, 50-25, 51-39, 51-40, 52-16, 52-26
 North Slope, 18-3
 North Tisdale field, Wyoming, 46-15
 Northward-Estes field, Texas, 47-22
 Northwest Atkinson field, Texas, 29-4
 Norway, 12-39, 18-25, 21-9
 Norwegian fields, 18-23
 Nozzle flow gradient, 6-37
 Nozzle of jet pump, 6-32, 6-34 to 6-39, 6-41, 6-42, 6-46, 6-62, 6-63
 Nozzle loss coefficient, 6-37
 Nozzle size, jet pumps, 6-35 to 6-39, 6-43, 6-44
 Nozzle/throat-area ratio, jet pumps, 6-35
 Nuclear counting rates, 50-5
 Nuclear log, 53-26
 Nuclear logging techniques, interpretation of nuclear logs, 50-23 to 50-37
 introduction, 50-1 to 50-3
 nomenclature, 50-37, 50-38
 nuclear physics for logging applications, 50-3 to 50-15
 nuclear radiation logging devices, 50-15 to 50-23
 references, 50-38
 Nuclear magnetic logging (NML), 52-26
 Nuclear magnetic relaxation analysis, 27-1
 Nuclear magnetic resonance (NMR), 28-10, 50-2
 Nuclear measurements, 50-24
 Nuclear physics for logging applications, fundamentals of gamma ray interactions, 50-6 to 50-8
 fundamentals of neutron interactions, 50-8 to 50-12
 nuclear radiation, 50-3 to 50-6
 nuclear radiation detectors, 50-12 to 50-15
 Nuclear radiation, in wireline logging, 50-1
 introduction, 50-2 to 50-5
 nuclear reactions, 50-6
 particle reactions, 50-5, 50-6
 Nuclear-radiation detectors, gamma ray, 50-12 to 50-14
 neutron, 50-14, 50-15
 Nuclear-radiation logging devices, gamma-gamma density, 50-16, 50-17
 gamma ray, 50-15, 50-16
 inelastic and capture gamma ray spectrometry, 50-22, 50-23
 neutron porosity, 50-17 to 50-21
 pulsed-neutron logging, 50-21, 50-22
 Nuclear reactions, 50-6
 Nuclear spectrometry, 49-1
 Nucleonic densitometer, 12-16
 Number groupings, SI metric system, 58-12
 Numerical dispersion, 48-10 to 48-12
 Numerical models, 44-17, 44-20
 Numerical simulation, in-situ combustion models, 46-12
 models, 40-2
 of chemical flood performance, 48-6
 of thermal recovery processes, 46-11, 46-12
 steam injection models, 46-11, 46-12
 Numerical simulators, 3D and 3-phase, 46-7, 46-11
 Nutating disk positive displacement (PD) meter, 32-11, 32-12
 NuTri™, 46-22
- ## O
- Obigbo field, Nigeria, 36-7, 36-8
 Obsidian, 19-5
 Obstruction in tubing, 33-21
 Occurrence, origin, and evolution of oilfield waters, introduction, 24-19, 24-20
 membrane filtration, 24-20
 quantities of produced water, 24-20
 shale compaction, 24-20
 Ocean engineers, 18-3
 Ocean saltwater, 44-42
 Oceanographer, 18-4, 18-26
 Octane number, 21-4, 21-7
 Off-lap deposition, 29-8
 Offset, 41-11, 41-15
 Offset-drilling rule, 57-2
 Offset of controller, 13-52
 Offshore bars, 36-3
 Offshore field operations, drillstem testing, 18-20
 establishing location, 18-18
 introduction, 18-17
 plug and abandonment, 18-20
 running 20-in. casing, 18-18
 30-in. casing, 18-18
 BOP, 18-18 to 18-20
 spudding well, 18-18
 Offshore installations, 6-5 to 6-7, 11-6
 Offshore leasing, economic impact, 57-12
 jurisdiction, 57-11
 procedure, 57-11
 producing history, 57-11
 Offshore operations, arctic, 18-38 to 18-43
 drilling, 18-3 to 18-17
 electrical, instrumentation, and control systems, 18-43 to 18-52
 field, 18-17 to 18-20
 historical review, 18-1 to 18-3
 introduction, 18-1
 production, 18-27 to 18-38
 references, 18-52
 special considerations, 18-20 to 18-22
 structures, 18-22 to 18-27
 Offshore pipelines, expensive element, 18-29
 flowlines for subsea wells, 18-36 to 18-38
 larger lines, 18-38
 Offshore platforms, rigs, or structures, 5-2, 6-55, 6-59, 6-63, 7-1, 7-2, 12-16, 12-18, 12-20, 12-21, 12-35, 12-39, 18-1 to 18-7, 18-22 to 18-25, 18-28 to 18-30, 18-40 to 18-42, 18-44
 Offshore production operations, floating production facilities, 18-34 to 18-36
 introduction, 18-27
 pipelines, 18-36 to 18-38
 platform production, 18-28 to 18-30
 subsea completions, 18-30 to 18-34
 Offshore, special considerations, cold environment, 18-21
 deepwater drilling, 18-20, 18-21
 high-current drilling, 18-21, 18-22
 Offshore structure classification, concrete gravity, 18-23
 gravity platform construction, 18-23, 18-24
 template/jacket, 18-22
 template/jacket construction, 18-22, 18-23
 Offshore Technology Conference, 18-38
 Oficina field, Venezuela, 24-13
 Ohio, 24-6, 24-7, 26-23, 43-1
 Ohmic potential drop, 49-13
 Ohm's law, 26-16, 26-29, 39-20, 44-17, 49-14
 Oil and gas differences, best depletion techniques, 36-2, 36-3
 sales method, 36-2
 Oil and Gas Inst., 41-7
 Oil and gas leases, 57-1 to 57-12
 Oil and gas separators, accessories, 12-39, 12-40
 capacity curves, 12-27 to 12-32
 centrifugal gas scrubbers, 12-20, 12-21
 centrifugal separators, 12-20, 12-21
 classification, 12-16 to 12-20
 comparison of horizontal, spherical, and vertical types, 12-21
 computer sizing, 12-25 to 12-27
 construction codes, 12-38, 12-39, 12-41
 controls, 12-39, 12-40
 estimated quality of separated fluids, 12-13 to 12-16
 estimating sizes and capacities, 12-21 to 12-25
 general references, 12-43
 illustrations of, 12-21
 introduction, 12-1 to 12-3
 measuring quality of separated fluids, 12-15, 12-16
 methods used to remove gas from oil, 12-13
 methods used to remove oil from gas, 12-8 to 12-11
 mist extractors for, 12-11, 12-12
 nomenclature, 12-42, 12-43
 operation and maintenance considerations, 12-40

- practical consideration in sizing, 12-32
- primary functions of, 12-3, 12-4
- references, 12-43
- safety features, 12-39, 12-40
- secondary functions of, 12-4, 12-5
- selection and application of separators and scrubbers, 12-35 to 12-38
- special problems in, 12-6 to 12-8
- stabilization of separated liquid hydrocarbons, 12-33, 12-35
- stage separation of oil and gas, 12-32 to 12-35
- summary, 12-1
- valves, 12-39, 12-40
- well fluids and their characteristics, 12-3
- Oil bank, 44-11, 44-33
- Oil-base (based) muds, 26-21 to 26-23, 40-19, 44-4, 53-8, 53-9
- Oil-based fluids, 18-49, 18-52
- Oil-based fracturing fluids, 55-5
- Oil-bucket construction, 12-35
- Oil carrying agent, 56-2
- Oil changing in pumping units, 10-13
- Oil collectors, 19-20
- Oil coning, 48-9
- Oil cut, 47-18
- Oil density, definition, 22-1
- Oil-density determination from ideal-solution principles,
 - composition known, 22-2 to 22-4
 - composition unknown, 22-4, 22-5
- Oil-discharge control valve, 12-5, 12-6, 12-9, 12-39
- Oil-displacement efficiencies, 44-39
- Oil-displacement rate, 46-8
- Oil engines, 10-15
- Oil equivalent volumes, 41-13
- Oil-external microemulsion, 47-12, 47-15
- Oil foam, 12-6
- Oil formation volume factor (FVF) 6-67,
 - 22-1, 22-10 to 22-13, 22-20, 37-16, 40-6, 40-8, 40-9, 40-11, 40-16
- Oil FVF, constants for, 22-11
- Oil FVF correlations,
 - saturated systems, 22-10
 - Standing, 22-10
 - undersaturated systems, 22-11 to 22-13
 - Vasquez and Beggs, 22-10, 22-11
- Oil/gas/water separator, 12-4, 12-5, 12-21
- Oil gravity,
 - effect on air requirements, 46-16, 46-17
 - effect on fuel content, 46-16, 46-17
 - test, 27-1
- Oil in effluent gas, 12-15, 12-16
- Oil in effluent water, 12-15, 12-16
- Oil-in-place (OIP), 37-2 to 37-4, 37-6, 40-5 to 40-8
- Oil-in-water dispersion-type fracturing fluid, 55-7
- Oil-in-water emulsions, 6-27, 19-1 to 19-3, 19-11, 19-27, 24-2, 55-7
- Oil isoperms, 28-7
- Oil isothermal compressibility,
 - Trube method, 22-11, 22-12
 - Vasquez and Beggs method, 22-12, 22-13
- Oil mist, 12-19, 44-4
- Oil mobility, 43-7
- Oil mobilization, 28-12, 48-4
- Oil payments, 41-1, 44-5
- Oil power fluid, 6-27, 6-29, 6-44, 6-47, 6-55, 6-56, 6-60, 6-61, 6-63
- Oil pressure function, 37-8 to 37-10
- Oil production above bubble point, 37-6
- Oil production, time required for, 37-21
- Oil property changes, steamfloods, 46-15
- Oil property ownership, 41-1, 41-2
- Oil-rate-vs.-time plot, calculation of, 47-17
- Oil recovery,
 - by chemical flooding, 47-13, 47-16, 47-17, 47-19, 47-20
 - by gas displacement, 43-3
 - by solution-gas drive, 37-2, 37-5, 37-6, 37-10, 37-11, 37-13 to 37-15, 37-17, 37-19, 37-21, 40-18, 40-20, 44-4
 - by water injection, predicting,
 - areal sweep and pattern efficiency, 44-12 to 44-25
 - displacement calculation procedures, 44-7 to 44-12
 - reservoir fractures, effect of, 44-25, 44-26
 - waterflood performance method selection, 44-31, 44-32
 - waterflood performance prediction methods, 44-26 to 44-31
 - by waterflood, 44-5, 44-8
 - effect of low mobility, 47-1, 47-2
 - efficiency, 44-30, 44-32, 47-16
 - estimation, 48-1
 - process, 48-3, 48-4, 48-12
 - thermal, 46-14, 46-15
 - vs. volume of fuel burned, 46-15
- Oil relative permeability, 28-6, 28-8 to 28-13, 44-12, 46-37, 46-38
- Oil-removal efficiency, 15-28
- Oil reserves: see reserves
- Oil reservoir, development plan for, 36-1 to 36-11
- Oil reservoir volume factor, 37-10
- Oil reservoir with gas cap, 40-7
- Oil reservoirs, depletion technique, 36-2
- Oil reservoirs in gas-hydrate region, 25-18, 25-19
- Oil reservoirs under gravity drainage,
 - case histories after pressure depletion, 40-15
 - occurrence of, 40-14, 40-15
- Oil reservoirs with gas-cap drive, 40-13, 40-14
- Oil reservoirs with water drive,
 - average recovery factor, 40-16, 40-17
 - buoyancy and inhibition effect, 40-20
 - general discussion, 40-15, 40-16
 - permeability distribution effect, 40-18 to 40-20
 - recovery-efficiency factor, 40-16
 - unit recovery computed by frontal-drive method, 40-17, 40-18
 - unit-recovery equation, 40-16
- Oil retention time, separator, 12-3, 12-15, 12-25 to 12-30
- Oil saturation, 26-22, 37-9, 37-10
- Oil Show Analyzer™ (OSA), 52-10, 52-11
- Oil shrinkage, 37-1, 37-6, 37-22, 37-23, 40-8
- Oil sizing of separator, 12-30
- Oil-soluble coating, 9-10
- Oil-soluble paint, 9-2
- Oil-soluble resins, 54-8
- Oil specific gravity, 6-67
- Oil staining, 52-9, 52-10
- Oil/steam ratio, 46-9, 46-15, 46-23
- Oil storage,
 - appurtenances, 11-6
 - capacity, 18-30, 18-36
 - general references, 11-14
 - gravity conservation, 11-12, 11-13
 - gravity structure, 18-41
 - materials of construction, 11-9
 - production equipment, 11-9 to 11-11
 - references, 11-14
 - tank corrosion protection, 11-4 to 11-6
 - tank types, 11-1 to 11-4
 - tanks, 11-6, 11-7, 18-43
 - temporary, 18-2
 - underground storage, 11-13, 11-14
 - vapor control, 11-12, 11-13
 - vapor losses, 11-11, 11-12
 - vapor-recovery system, 11-12, 11-13
 - venting atmospheric and low-pressure storage tanks, 11-6 to 11-9
- Oil surge chamber, 19-23, 19-24
- Oil system correlations,
 - bubblepoint pressure, 22-5 to 22-9
 - density determination, 22-2 to 22-5
 - empirical, 22-7
 - FVF, 22-10 to 22-13
 - gas/oil IFT, 22-16, 22-17
 - general references, 22-22
 - glossary, 22-20, 22-21
 - graphical, 22-5, 22-7, 22-8
 - introduction, 22-1
 - pseudoliquid density, 22-2
 - references, 22-21, 22-22
 - oil FVF, 22-10 to 22-13
 - solution GOR for saturated oils, 22-9, 22-10
 - total FVF's, 22-13
 - viscosity, 22-13 to 22-16
- Oil viscosities, 22-1, 22-13 to 22-16, 37-12, 37-16, 40-9, 40-17, 40-32, 46-31, 46-34, 46-35
- Oil-viscosity correlations,
 - factors affecting, 22-14
 - introduction, 22-13
 - saturated systems, 22-14 to 22-16
 - undersaturated systems, 22-16
- Oil/water capillary pressure, 26-29
- Oil/water contact (OWC), 41-9, 44-39
- Oil/water interface, 12-39, 18-47, 19-4, 19-5, 19-9, 19-11, 19-18 to 19-20, 19-22, 19-23, 19-30, 19-31, 40-15
- Oil/water interfacial tension, 44-40, 47-9
- Oil/water mobility ratio, 48-5
- Oil/water relative-permeability curve, 47-18
- Oil/water separator, 24-3
- Oil/water system, 25-27, 25-28, 39-20
- Oil/water viscosity ratio, 40-19, 44-6, 44-9
- Oil-weight factors, 2-1, 2-33, 2-38
- Oil wells,
 - computing inflow rates, 34-32
 - future inflow performance, 34-34, 34-35
 - inflow performance, 34-30 to 34-33
 - single- and two-phase IPR equation, 34-33, 34-34
- Oil-wet, 19-9, 44-6
- Oilfield brines, 24-5
- Oilfield motors,
 - equipment for control of, 10-27, 10-28
 - protection equipment for, 10-28, 10-29
- Oilfield steam generators, 46-19
- Oilfield waters,
 - analysis methods, 24-5
 - chemical properties, 24-5 to 24-13
 - composition, 24-6
 - definition, 24-18
 - evolution, 24-19, 24-20
 - occurrence, 24-19, 24-20
 - origin, 24-19, 24-20
 - pH, 24-16
 - physical properties, 24-12 to 24-18
 - sample description, 24-5
- Oilwell performance,
 - infinite-acting pressure solution, 35-3, 35-4
 - production rate variation (superposition), 35-8, 35-9
 - pseudosteady-state behavior, 35-6 to 35-8
 - skin effect, 35-4
 - superposition, example problem, 35-9

- transient and pseudosteady state, example problem, 35-7, 35-8
- well pressure performance—closed reservoir, 35-2, 35-3
- wellbore storage effect, 35-4 to 35-6
- Oilwell production-meter installation, 32-13
- Oilwell Research porosimeter, 26-6
- Oklahoma, 6-24, 16-13, 21-2, 21-4, 21-10, 24-8, 24-10, 24-21, 27-8, 27-9 to 27-12, 33-1, 33-7, 33-9, 33-12, 40-15, 40-23, 44-1, 44-4, 44-36, 44-41, 44-44, 46-3, 46-14, 46-16, 47-6, 57-10
- Oklahoma City field, 6-24, 40-2
- Oklahoma City Wilcox reservoir, 40-15
- Oleic phase, 47-11, 47-15
- Olympic pool, Oklahoma, 44-41
- On-lap deposition, 29-8
- Oolicast, 29-9
- Oolitic porosity, 29-8, 29-9
- Oolith, 29-9
- Oolitic porosity, 26-1
- Open-cycle selective hydrocarbon adsorption system, 14-12
- Open delta transformer, 10-30, 10-31
- Open-flow capacity, 30-10, 33-3
- Open flow of gas wells, 33-1 to 33-23
- Open-flow potential, 33-5 to 33-8, 33-10, 33-11
- Open-flow testing of gas wells, 13-45
- Open-flow tests, 33-3, 41-9
- Open gas-lift installation, 5-2, 5-3
- Open-loop control, 16-2
- Open power-fluid system, 6-17, 6-18, 6-25 to 6-28, 6-30, 6-57 to 6-59, 6-63
- Open regeneration system, 14-11, 14-12
- Openhole completions, 47-6, 56-8, 56-9
- Openhole logging, 50-1
- Operating agreements, 41-9
- Operating costs, emulsion treating, 19-33
- Operating downtime offshore, 18-8
- Operating equipment, BHP gauges, 30-3, 30-4
- Operating expenses,
 - ad valorem taxes, 41-12
 - average cost per barrel, 41-11, 41-12
 - breakeven, 40-32
 - check list item for evaluation, 41-9
 - cost per well-month, 41-11
 - direct, 41-11
 - direct lifting, 41-11
 - field or district, 41-12
 - range of, 41-12
 - recompletion, 41-12
 - stimulation, 41-12
 - trucking charges, 41-12
- Operating gas-lift valve, 5-39 to 5-42, 5-44, 5-51 to 5-53, 5-55
- Operating injection-gas pressure, 5-23, 5-26 to 5-28, 5-30, 5-32, 5-35, 5-36, 5-38, 5-39, 5-44, 5-48, 5-49, 5-53, 5-54
- Operating interest, 41-2, 41-13
- Operating limits,
 - drilling vessels, table, 18-8
 - riser, table, 18-18
- Operating manuals, offshore, 18-16
- Operating pressures, of separators, 12-16 of wellhead equipment, 3-1
- Operating problems, gas condensate (GC) reservoir,
 - number of wells required, 39-26
 - well injectivity, 39-25, 39-26
 - well productivity and testing, 39-24, 39-25
- Operation and maintenance considerations for separators,
 - cleaning of vessels, 12-42
 - corrosive fluids, 12-40
 - gauge cocks and glasses, 12-42
 - high-capacity operation, 12-42
 - insulation of safety devices, 12-40
 - low temperatures, 12-40
 - mist extractors, 12-40
 - paraffin, 12-42
 - periodic inspection, 12-40
 - pressure gauges, 12-42
 - pressure shock loads, 12-42
 - safety heads (rupture disks), 12-40
 - throttling discharge of liquid, 12-40
- Operation factor, 12-22
- Operation of ESP equipment, 7-12
- Operational considerations for emulsion treating equipment,
 - burners and fire tubes, 19-28
 - cleaning vessels, 19-28, 19-29
 - corrosion, 19-30, 19-31
 - excelsior packs, changing of, 19-31, 19-32
 - interfacial buildup, 19-30
 - level controllers and gauges, 19-31
 - removing sand and other settled solids, 19-29, 19-30
 - safety features for electrostatic treaters, 19-31
 - water-in-oil detectors (BS&W monitors), 19-31
- Operational considerations, subsea control systems, 18-49
- Operational problems and remedies, problems common to steam and firefloods,
 - emulsions, 46-21, 46-22
 - sanding, 46-21
 - well productivity, 46-21
- problems plaguing firefloods only,
 - corrosion, 46-22
 - exploration hazards, 46-22
 - poor injectivity, 46-22
- problems plaguing steamfloods only,
 - steam placement, 46-22
 - steam splitting, 46-22
- Operational well modes, 4-6 to 4-8
- Optical emission spectrographic analysis, 56-3
- Optimal conditions, generating for micellar/polymer (MP) flood, 47-14, 47-15
- Optimal economic recovery, 42-1, 42-2
- Optimal time to waterflood, 44-5
- Optimization, of injection operations, 42-1, 42-3
- Optimization studies, 48-7
- Optimum efficiency of fracturing, 55-9
- Optimum pressure on separator, 12-4
- Orcutt Hill field, California, 47-22
- Organic constituents of oilfield water, 24-17, 24-18
- Organic inhibitors, 54-6
- Organic liquid desiccants, 14-17 to 14-20
- Organic phosphates, 44-45
- Organic solvents, 56-2
- Organick and Golding correlation, 21-11 to 21-15
- Organisms, 44-43
- Orientation curves, 53-9
- Orifice check valve, 5-10, 5-22 to 5-24, 5-26, 5-28, 5-31, 5-35, 5-36
- Orifice coefficient for provers, 13-45
- Orifice constants,
 - basic orifice factor, 13-3
 - expansion factor, 13-8
 - flowing-temperature factor, 13-3
 - gauge-location factor, 13-8
 - manometer factor, 13-8
 - pressure-base factor, 13-3
 - Reynolds-number factor, 13-8
 - specific-gravity factor, 13-3
 - supercompressibility factor, 13-8
 - temperature-base factor, 13-3
 - thermal-expansion factor, 13-8
- Orifice equations, 13-3
- Orifice location, 13-36
- Orifice meter, 5-53, 13-8, 13-36, 13-45, 13-48, 16-6, 16-8, 33-6, 33-13
- Orifice metering of natural gas, 17-7
- Orifice-plate flowmeter, 32-13
- Orifice plates, 14-2, 17-7
- Orifice well tester, 13-37 to 13-44, 32-6, 32-14
- Original oil in place (OOIP), 38-9 to 38-13
- Orkiszewski correlation, 34-37 to 34-40
- Orogenic movements, 29-7
- Orthogonal-wave equation migrations, 36-8
- Orthomin technique, 48-17
- Oscillating piston PD meter, 32-11
- Oscilloscope, 51-3, 51-12
- Osmotic effects, 24-19
- Ossum field, Louisiana, 26-7
- Otto cycle, 10-15
- Outbreathing (pressure relief) of storage tanks, 11-6, 11-7
- Outer continental shelf (OCS), 3-34, 57-11, 57-12
- Oval gear positive displacement (PD) meter, 32-11
- Overall displacement efficiency, 39-18
- Overall economic analysis, 39-27
- Overall efficiency of miscible displacement, 45-7
- Overall efficiency of pumping system, 10-25
- Overall heat-transfer coefficient, 46-4 to 46-7
- Overall instantaneous cycling efficiency, 39-18
- Overall oil recovery, 46-14
- Overall particle-removal efficiency, 15-27
- Overall recovery efficiency, 43-3, 45-8
- Overall recovery factor, 40-23
- Overall reservoir recovery efficiency, 40-34
- Overbalance condition, 52-18
- Overburden heat loss, 48-5
- Overburden pressure, 26-9, 26-19, 51-4 to 51-7, 51-25, 51-44, 51-47, 52-26, 55-8, 56-2, 56-3
- Overburden stress, 28-4, 28-13, 51-4, 51-30, 51-43
- Overflow connections for tank, 11-9
- Overflush agent, 56-5
- Overflush in acidizing, 54-11
- Overhead, 41-12, 41-13
- Overhead allocation, 41-9
- Overhead costs, 36-2
- Overload shutdown conditions, ESP chart, 7-16, 7-17
- Overloading separators with liquid, 12-10
- Overpressure, of storage tanks, 11-4
- Overpressured formations, 35-1
- Overpressured gas reservoir, 40-34
- Overpressuring of separator, 13-58
- Overriding royalty interest, definition, 41-1 to 41-3
- Overtemperature lockout circuit, 10-29
- Overtensioning of pipe, 18-37
- Overtorquing, 9-9
- Overtravel of fiberglass rods, 9-11, 9-12
- Overturned anticlines, 29-2
- Ownership maps, 41-8
- Ownership of hydrocarbons in place, 57-1
- Oxidation potential, 24-16
- Oxyalkylated phenols, 19-10

Oxygen (O₂), 6-55, 9-8, 14-3, 14-17, 14-20, 14-22, 15-28, 15-29, 19-30, 19-31, 24-4, 24-5, 24-16, 24-17, 24-20, 39-16, 44-42, 44-43, 44-47, 46-12, 46-22, 46-34, 48-5, 50-1, 50-13, 50-18, 50-35
 Oxygen analyzer, 19-28
 Oxygen corrosion, 3-36
 Oxygen-enriched air fireflood, 46-31, 46-34
 Oxygen injection, 42-6
 Oxygen scavengers, 15-29, 47-5, 47-10
 Oxygen utilization efficiency, 46-15, 46-21

P

p-x diagrams for mixtures of CO₂, 23-10
 P-wave critical angle, 51-12
 P-wave modulus for dry rock, 51-49
 P-wave modulus for rock frame, 51-49
 P-wave velocity, 51-11, 51-37
 P-waves, 51-2 to 51-5, 51-11, 51-36, 51-47
 Pack gravel, 56-4
 Packer mechanics, 4-4
 Packer operations, modes of, 4-1
 Packer seats, location of, 53-17
 Packer selection, considerations for, corrosive well fluids, 4-4 fishing characteristics, 4-6 packer mechanics, 4-4 purchase price, 4-6 retrievability, 4-5 sealing elements, 4-5 surface/downhole equipment coordination, 4-4 through-tubing operations, 4-6
 Packer utilization, 4-1 to 4-3, 4-6 permanent packers, 4-3 retrievable packers, 4-2, 4-3 success, 4-6
 Packing of uniform spheres, 26-1
 Packoff element, 3-6
 Painter field, Wyoming, 39-16
 Pair production, 50-6 to 50-8, 50-13, 50-14, 50-16
 Paleo-environments, interpretation of, 36-3, 36-7
 Paleontologists, 57-8
 Paloma field, California, 26-30
 Paluxy gas-condensate reservoir, Texas, 39-20, 39-21
 Pan American/Casper Oil Co., 46-14, 46-18
 Panama Canal, 18-7
 Panhandle equation, 15-7
 Panhandle field, Texas, 44-30
 Paper-tape-type H₂S detector, 52-7
 Parachor, definition, 22-16
 Parachors, for hydrocarbons, 22-18 for pure substances, 22-17
 Paraffin, 5-25, 5-52, 5-53, 6-31 to 6-33, 7-13, 11-13, 12-3, 12-7, 12-8, 12-10, 12-11, 12-40, 12-42, 19-4, 19-5, 19-9, 19-10, 19-30, 26-3, 32-11, 44-4
 Paraffin hydrocarbons, 20-13, 39-2
 Paraffin inhibitors, 56-2
 Paraffin problem, 3-27
 Paraffin removal, 56-1, 56-2
 Paraffin scrapers, 18-33
 Paraffinic hydrocarbon series, 20-5
 Paraffinic oils, 6-67, 24-18
 Paraguay, 58-20
 Parallel-bore valves, 3-15
 Parallel-plate interceptor (PPI), 15-24, 15-25
 Paris Academy of Science, 1-68
 Paris Valley field, California, 46-22, 46-23
 Paroscientific digiquartz, 30-7
 Parrish and Prausnitz development, 25-5 to 25-9
 Partial buildup curve, 30-9

Partial cement bonding, 51-41, 51-42
 Partial differential equations, 48-2
 Partial penetration, 35-4
 Partial pressure maintenance, 42-3, 43-9 to 43-17
 Partial pressure of gas, 20-4
 Partial water drive, 39-24
 Partial water-drive reservoir, 40-6
 Partially scaled models, high-pressure, 46-13 physical types, 46-11, 46-12 vacuum, 46-13
 Particle reactions, 50-5, 50-6
 Particle-size distribution, 26-2, 44-45
 Partition, 57-2
 Past performance analysis, gas pressure maintenance, 43-9
 Pattern effects on waterflooding, 44-29
 Pattern efficiency, 44-15, 44-18, 45-6, 45-8 to 45-10
 Pattern ($h\phi S$ -weighted) efficiency, 39-15, 39-17, 39-18, 39-20 to 39-23, 39-26
 Pattern floods, 46-1
 Pattern injection, 43-2
 Pattern selection, thermal recovery, 46-17
 Pattern types in firefloods and steamfloods, 46-18
 Payout, 41-3, 41-35, 41-36
 Payout schedule, 41-31
 Peace River field, 46-34
 Peak crank torque, 9-2, 9-3
 Peak polished-rod load, 9-2
 Peak torque, 10-26
 Pendular rings, 26-24
 Penetration of acid, 54-8
 Peng-Robinson equation, 20-8, 23-13
 Penn State arrangement, 28-5
 Pennsylvania, 18-1, 21-2, 24-1, 24-2, 24-6, 24-7, 44-1, 44-4, 47-22
 Pennsylvania Oil Producers, 17-1
 Penultimate layer, 36-4
 Percent factor, assigned spacing design line, 5-33
 Percent-load design method, 5-42
 Percent-load intermittent-gas-lift installation designs, 5-44
 Percent-load production pressure, 5-48
 Percent-tubing-load installation design, 5-48
 Percentage depletion, 57-11
 Percentage-depletion allowance, 41-5, 41-13, 41-14
 Percentage factor, gas lift, 5-32
 Percentage-time controller, 16-4
 Percentage timer, 10-28
 Percussion-sampling techniques, 27-9
 Percussion sidewall core data, 27-9
 Perforated-interval completion, 5-51
 Perforating gun, 53-26
 Perforating operations, 51-40
 Perforating pipe, 56-1
 Perforation ball sealers, 54-10
 Perforation cleaning methods, backflow, 56-5 backsurging, 56-5 HCl preflush, 56-5 matrix acid stimulation, 56-5 matrix treatment with acid, 56-5 overflush, 56-5 perforation washing, 56-5 underbalance, 56-5
 Perforation, sand control, 56-4, 56-5
 Perforation tunnels, 56-1, 56-4, 56-5, 56-8
 Perforation washing, 56-5
 Perforations, locating, 53-26
 Performance calculations, reciprocating pumps, 6-28 to 6-30
 Performance characteristics, jet pumps, 6-34

Performance coefficient, of backpressure equation, 33-5 to 33-10, 33-12
 of refrigerants, 14-11
 Performance curves, abandonment contour vs. cumulative oil, 40-34 cumulative gas vs. cumulative oil, 40-32, 40-33 improved recovery reserves, 40-34 material balance method for nonassociated gas reservoirs, 40-33, 40-34 of jet pump, 6-35, 6-36, 6-38, 6-41 to 6-43, 6-46, 6-47 of tubing and choke, 34-5 oil percentage in total fluid vs. cumulative oil, 40-32 water/oil contact (WOC), 40-34
 Performance evaluation of rigs, 18-7, 18-8
 Performance factors for motors, cyclic load, 10-25 efficiency, 10-25 power, 10-25 service, 10-25, 10-26 slip, 10-23, 10-24 speed variation, 10-24, 10-25 temperature rise, 10-26 torque, 10-25
 Performance indicators, common to both steamfloods and firefloods, changes in oil property, 46-15 oil recovery, 46-14, 46-15 sweep efficiency, 46-14 pertaining to firefloods only, air/oil ratio (AOR), 46-17 air requirements, 46-16 fuel content, 46-16 pertaining to steamfloods only, steam/oil ratio (SOR), 46-15
 Performance of solution-gas-drive reservoirs, 37-1, 37-2
 Performance predictions, models, 37-19 of micellar-polymer flooding, 47-17 of oil and gas reservoirs, 36-9, 36-10 of solution-gas drive, 37-14 to 39-18 of volatile oil reservoir, 37-22 to 37-26
 Performance profiles, 5-20, 5-21
 Performance properties, of casing, 2-1, 2-4 to 2-19, 2-32 of pipe, 2-46, 2-54 to 2-56 of tubing, 2-38 to 2-43
 Performance technique for reserve estimation, 40-1
 Performance-time predictions, 43-9, 43-10
 Performax plate pack, 19-13
 Periodic inspection of separators, 12-40
 Periodic production tests, 12-17
 Peripheral flood, 44-2, 44-13, 44-17, 44-36
 Permafrost, 18-38, 18-39, 18-41 to 18-43
 Permafrost cement, 18-41
 Permafrost problem, 3-27
 Permanent packers, 4-1 to 4-6, 4-8
 Permeability-block method, 40-19, 40-20, 40-24, 40-26
 Permeability, calculations, 26-16 changes, effect on radial flow, 54-9 consideration in waterflooding, 44-2 conversion of units in Darcy's law, 26-13 to 26-15 correlation with tube-wave data, 51-48 damage, 30-13, 30-14 definition of, 27-1, 28-1, 55-1 distribution, 26-26, 36-3, 36-7, 39-16, 39-18 to 39-20, 40-12, 40-18 to 40-20, 40-24, 40-25, 44-8, 44-15, 45-11, 45-12 distribution factor, 40-16, 40-17

- effective, 26-15, 28-1 to 28-4, 28-6, 28-8, 28-13, 39-17, 44-32, 44-33, 46-21
- factors affecting measurement, 26-18, 26-19
- factors in evaluation of, 26-19, 26-20
- flow systems of simple geometry, 26-11 to 26-13
- from pressure-buildup curve, 30-12
- in acoustic logging, 51-47
- interstitial-water relationships, 26-23
- introductory theory, 26-10, 26-11
- limits of formations, 55-2
- measurement of, 26-17, 26-18
- net thickness product, 39-21
- of channels and fractures, 26-15, 26-16
- of matrix, 55-9
- of pack, 55-8
- of propping agents, 55-2, 55-8
- of reservoir rocks, 30-11, 39-13, 44-3
- physical analogies to Darcy's law, 26-16
- pinchout, 44-39
- prediction, 50-2
- profile, 31-4, 36-4, 39-19, 44-3, 45-10, 51-47
- ratio, 37-14, 37-15
- reduction, 47-3 to 47-5, 55-8
- reduction factor, 35-5
- relative, 28-1 to 28-3, 28-6, 28-8 to 28-14, 28-16, 30-11, 39-13, 44-2, 44-4, 44-5, 44-9, 55-8
- SPE preferred unit, 58-24, 58-25
- stratification, 39-18, 39-20
- transforms, 50-37
- unit in SI metric system, 58-24, 58-35, 58-36
- variation, 39-19, 39-20, 39-23, 39-26, 40-18, 40-19, 44-3, 44-8 to 44-10, 44-36, 45-7
- viscosity ratio, 47-8
- Perm-plug method of permeability measurement, 26-17
- Permeameter, 26-17, 26-18
- Permian Basin, 49-11
- Persian Gulf, 44-37
- Personal computer, 39-11, 39-12
- Personal property, definition, 57-1
- Personnel protection at wellsite, 10-31
- Peru, 40-14, 58-20
- Peters factor, 1-61
- Petrographic analysis, 56-3
- Petroleum engineering services, 52-2, 52-16 to 52-27
- Petroleum engineers, 22-1, 22-14
- Petroleum Engineers Club of Dallas, 41-5
- Petroleum liquid, acoustic velocity in, 51-31
- Petroleum measurement subsidiary, 17-6
- Petroleum reserves—definitions and nomenclature, possible, 40-2 probable, 40-2 proved, 40-2, 40-3 proved developed, 40-3 proved undeveloped, 40-3
- Petroleum reservoir engineering, 42-1
- Petroleum reservoir engineering letter and computer symbols, 59-2 to 59-51
- Petroleum reservoir traps, 29-1 to 29-9
- Petroleum sulfonates, 47-7
- Petrophysical and physical parameters, relationship to nuclear logging, clay types, 50-2 fluid identification, 50-2 hydrocarbon saturation, 50-2 lithology, 50-2 permeability, 50-2 porosity, 50-1, 50-2 presence of hydrocarbons, 50-1
- Petrophysical correlations, 28-12
- Petrophysical descriptors, 50-2, 50-3
- Petrophysical measurements, 52-2, 52-26, 52-27
- Petrophysical properties, 28-8, 47-20
- Petrophysical work, 48-8, 48-9
- pH, 24-4, 24-5, 24-16, 24-17, 44-44
- pH control, 44-40, 44-42
- Phase analysis, high-frequency, 27-1
- Phase behavior, and interfacial tension, 47-14, 47-15 definition, 22-21, 23-1 of $\text{CO}_2/\text{C}_4/\text{C}_{10}$ mixture, 23-9 of gas/condensate system, 39-2 to 39-4, 39-12, 39-13 of pure component, 23-2 of surfactant/brine/oil system, 47-11 to 47-13 of water/hydrocarbon systems, 25-1 to 25-28
- Phase-boundary curves, 45-3, 45-4
- Phase compositions, calculation of, 23-10 to 23-13
- Phase converters, types of, 10-35
- Phase diagrams, by measuring liquid volumes at several temperatures, 39-7 of Eilert's fluids, 39-3 of gas condensate fluids, 39-4 of reservoir-fluid systems, 23-6, 23-7 of single component, 23-1, 23-2 of surfactant/brine/oil system, 47-11, 47-12 ternary, 23-5, 23-6 types of, 23-2 to 23-10
- Phase equilibrium, 12-21
- Phase equilibrium calculations, 20-10
- Phase lag, 53-20
- Phase loss relay, 10-28
- Phase rotation, 7-13
- Phase rule, 23-2, 23-8, 25-1
- Phase shift angle, 53-20
- Phenolic-resin gravel packing, 46-21
- Philippine Islands, 58-20
- Phillips Petroleum Co., 16-13, 45-15, 46-24, 46-26
- Phosphoric acid, 11-6
- Photoelectric absorption, 50-4, 50-7, 50-12 to 50-14, 50-17
- Photoelectric absorption factor, 50-7, 50-17, 50-24, 50-33, 50-34
- Photoelectric effect, 50-6 to 50-8
- Photographic history of injection-fluid fronts, 44-18
- Photographs and visual examination of cores, 46-21
- Photometry, 1-69
- Photomicrographs, 19-2 to 19-5
- Photomultiplier, 50-12 to 50-14
- Physical analogies to Darcy's law, 26-16, 26-17
- Physical dimension of fiberglass sucker rods, 9-11
- Physical models, 46-11 to 46-13
- Physical parameters and nuclear radiation, 50-2, 50-3
- Physical-properties data of liquid hydrocarbons, 17-5
- Physical properties of foams, 47-8, 47-9
- Physical properties of oil, 21-3 to 21-8
- Physical properties of oil systems, 22-1
- Physical properties of produced waters, compressibility, 24-12 to 24-14 density, 24-14, 24-15 dissolved gas, 24-17 formation volume factor (FVF), 24-15, 24-16 organic constituents, 24-17, 24-18
- pH, 24-16
- redox potential (Eh), 24-16, 24-17
- resistivity, 24-16
- surface (interfacial) tension, 24-16
- viscosity, 24-16
- Physical properties of wellhead equipment, 3-2, 3-3
- Physical setup of metering system, orifice location, 13-36 recorder, 13-36 size of orifice and metering run, 13-36 straightening vanes, 13-36
- Physico-chemical changes, 46-12, 46-13
- Piercement domes, 29-5, 29-7
- Piezoelectric element, 51-3
- Piezoelectric transducer, 30-5, 30-6
- Pig launcher, 15-14
- Pig trap, 15-14, 15-16
- Pigging, 18-29
- Pile hammers, 18-23
- Pile jacking, 18-41
- Piled structures, 18-42, 18-43
- Pilings, 3-3
- Pilot floods, 44-37 to 44-39
- Pilot-gas-control manifold, 16-15, 16-16
- Pilot-loaded regulators, 13-55
- Pilot-loaded valves, 13-55
- Pilot LPG flood, 45-14
- Pilot-operated control valve, 13-53
- Pilot-operated diaphragm motor valve, 13-55
- Pilot-operated dump valves, 16-5
- Pilot-operated gas-lift valve, 5-13, 5-43, 5-44, 5-51
- Pilot-operated relief valve, 11-8, 12-40
- Pilot operation, 45-10, 42-6
- Pilot plug, 13-54
- Pilot project, 40-3
- Pilot relay, 13-50
- Pilot valve, 3-34
- Pilot valve diaphragm failure, 11-8
- Piloted union-type rise coupling, 18-15
- Pin-and-socket connectors, 18-52
- Pinchouts, 29-8
- Pinnacle reefs, 36-5
- Pipe analysis log (PAL), 53-20, 53-24, 53-25
- Pipe analysis tool, 53-23
- Pipe body safety factor, 2-2, 2-32, 2-34, 2-35
- Pipe-body yield strength, 2-2, 2-4, 2-6, 2-8, 2-10, 2-12, 2-14, 2-16, 2-18, 2-32, 2-56
- Pipe coils, 19-21
- Pipe diameters, choosing in gas lines, 15-7 choosing in liquid lines, 15-2
- Pipe dope as formation contaminant, 56-3, 56-4
- Pipe-laying reels, 18-37
- Pipe rams, 18-11, 18-15, 18-20
- Pipe storage, 11-2, 11-4
- Pipe taps, 13-3, 13-8 to 13-11, 13-20 to 13-25, 13-28, 13-29, 13-32
- Pipe-wall thickness, 15-11
- Pipeline, gas, 36-2
- Pipeline metering systems, 17-4
- Pipeline run statements, 41-9
- Pipeline trunk lines, 16-2
- Pipeline valve, 11-11
- Pipeline valve switches, 16-3
- Piper diagram, 24-19
- Piping, design considerations, 15-13 drawings, 15-31 on offshore platforms, 15-11 pressure breaks, 15-13 pressure rating classes, 15-13

- pressure/temperature ratings, 15-13
- system design, 15-1 to 15-14
- system materials, 15-7 to 15-11
- Pisolith, 29-9
- Pisolitic limestone, 29-8
- Piston-and-valve assembly, 6-51
- Piston BHP element, 30-1
- Piston effect of tubing string, 4-9, 4-10
- Piston gauge, 33-6
- Piston-like displacement, 44-7, 44-9
- Piston pneumatic/hydraulic pump ratio, 3-33
- Piston/stem area ratio, 3-21
- Piston-type actuators, 3-21
- Pitcher nipple, 18-14, 18-15
- Pitman side members, 10-3, 10-4, 10-12
- Pitot tube, 13-2, 13-37, 13-45 to 13-48, 32-13, 32-14, 33-1 to 33-4
- Plain-end, liner casing, 2-32
- line pipe, 2-46, 2-50 to 2-53
- Plait point, 23-5, 23-8 to 23-10, 47-11 to 47-13
- Planar view, directional data presentation, 53-6
- Planning and preparations offshore, 18-3 to 18-5
- Plant costs, 39-1
- Plant products, 39-9 to 39-11, 39-23
- Plastic blanket, 9-14
- Plastic-coated sand grains, 55-8
- Plastic-collapse pressure equation, 2-54, 2-55
- Plastic lining for steel pipe, 15-10
- Plastic-packed secondary seal, 3-6
- Plastic-packed-type seal, 3-9
- Plastic pipe, 15-10
- Plasticity, 52-20
- Plate coalescers, 15-23 to 15-26
- Plate-count method, 44-44
- Plate heat exchanger, 19-23
- Plate-type heating elements, 19-21
- Platform deck layout for process facilities, 18-30
- Platform jacket, 18-28, 18-34
- Platform loads, 18-44
- Platform production,
 - crude oil disposal, 18-29, 18-30
 - gas disposal, 18-30
 - process equipment, 18-28
 - water disposal, 18-30
 - well completion, 18-28
 - well servicing, 18-28, 18-29
 - well workovers, 18-28, 18-29
- Platform rigs, 36-2
- Platform vibration, 12-23
- Platform well bay, 18-29
- Platinum-iridium standard, 1-70
- Plot of buildup with afterflow, 30-10
- Plot of water FVF vs. pressure, 24-15
- Plow steel, 30-4
- Plug and abandonment of well, 18-20
- Plug valves, 3-11 to 3-14
- Plugback operations, 33-21
- Plugging, 5-16, 5-23, 5-53, 14-2, 19-15, 19-30, 24-2, 39-25, 39-26, 44-36, 44-42 to 44-45, 56-6
- Plugging agents, 29-5, 39-26
- Plugging materials, 54-10
- Plunger application for intermittent gas lift, 5-52, 5-53
- Plunger-arrival detector, 5-52
- Plunger clearances, 8-6
- Plunger/engine (P/E) area ratio, 6-11 to 6-13, 6-15, 6-16, 6-18, 6-27, 6-28, 6-30
- Plunger lift, 5-38
- Plunger overtravel, 10-25
- Plunger pumps, 6-50, 6-52 to 6-55, 8-5
- Plunger stroke, 9-2
- Pneumatic actuators, 3-21, 3-27, 18-28
- Pneumatic control valves, 16-3
- Pneumatic controls, 13-49
- Pneumatic/hydraulic relay, 3-33
- Pneumatic pilots, 13-56
- Pneumatic/pneumatic relay, 3-33
- Pneumatic pressure control, 12-39
- Pneumatic surface safety valve, 3-20, 3-21
- Poettmann and Carpenter correlation, 34-37
- Poettmann's method, 34-9
- Point bars, 36-6
- Poisuille's equation, 26-10, 26-15, 26-19, 26-20
- Poisonous-gas sensors, 18-47
- Poisson distribution, 50-5
- Poisson's ratio, 51-2, 51-4, 51-13, 51-37, 51-43, 51-44, 51-50
- Polar packs, 18-39
- Polar plots, 53-12
- Polished-joint tubing hanger, 3-9
- Polished rod, 8-10, 9-1, 10-1, 10-2, 10-5, 10-7
- Polished-rod coupling, 9-4
- Polished-rod horsepower, 9-2, 9-3, 10-18
- Polished-rod velocities and acceleration, 10-7
- Polished-sealbore packer, 4-3, 4-8, 4-9
- Polyacrylamide (PAM), 47-3
- Polyacrylamide polymer, 44-39, 44-40
- Polyamine derivatives, 19-10
- Polyemulsions, 55-8
- Polyethylene, 11-9, 24-4, 24-5
- Polyethylene bedding jacket, 18-49
- Polyethylene line pipe, 15-10
- Polyethyleneoxide (PEO), 47-3
- Polyglycol esters, 19-10
- Polymer-driven flood, 47-21
- Polymer-flood statistics, 47-6
- Polymer flooding, 19-28, 47-1 to 47-6, 47-10, 47-18, 47-22, 48-7
- Polymer gels, 55-5
- Polymer properties,
 - biological degradation, 47-5
 - chemical degradation, 47-5
 - mechanical degradation, 47-5, 47-6
 - non-Newtonian effects, 47-4, 47-5
 - permeability reduction, 47-5
 - polymer retention, 47-5
 - viscosity relations, 47-4, 47-5
- Polymer retention, 47-5
- Polymer-solution viscosity, 47-4
- Polymer/surfactant incompatibility, 47-13
- Polymer types, 47-3
- Polymer waterflooding, 48-5
- Polymerized oils, 19-10
- Polyphosphates, 44-45
- Polypropylene, 11-9, 12-12
- Polysaccharides, 47-3
- Polyvinyl alcohol (PA), 47-3
- Polyvinyl chloride, 11-9
- Polyvinyl chloride (PVC) plastic, 18-46
- Pony rods, 9-1, 9-3, 9-11
- Pooling clause, 57-5, 57-6
- Poorly consolidated rocks, 51-33, 51-34
- Pop-off safety release valve, 5-53
- Pop-off valve, 13-59
- Porcelain diaphragm, 26-24
- Pore aspect ratio, 51-9, 51-12
- Pore compressibility, 26-7
- Pore configuration, 26-2
- Pore-fluid compressibility, 51-4
- Pore-fluid pressure, 28-4, 51-4, 51-5, 51-7, 51-8, 51-25, 51-30, 51-39, 51-44
- Pore geometry, 28-2, 54-6
- Pore liquid saturation, 27-9
- Pore pressure, 52-18, 52-21, 52-22, 52-24 to 52-27
- Pore-size distribution, 26-19, 26-24, 44-27, 47-5, 47-10, 51-30, 54-6
- Pore structure of rock, 26-10
- Pore-throat-blocking effect, 47-9
- Pore throats, 47-21
- Pore volume (PV), 26-1 to 26-7, 26-22
- Pore-volume compressibility, 26-7 to 26-10, 47-37, 47-38
- Pore volume, laboratory measurement, 26-5 to 26-7
- Porosimeter, 26-4 to 26-6
- Porosity,
 - apparent water filled, 49-34
 - balance check, 49-30
 - by density log, 49-26, 49-34, 49-36, 49-38
 - by electromagnetic-propagation tool, 49-36
 - by neutron log, 49-26, 49-34, 49-36, 49-38
 - by sonic log, 49-26, 49-27
 - compaction and compressibility of porous rock, 26-7 to 26-10
 - compressibility, 26-8
 - definition of, 27-1
 - distribution, carbonate reservoirs, 36-6
 - effect on formation factor, 49-4
 - estimating, 51-5, 51-33
 - evaluation from acoustic log, 51-30
 - factor to consider in waterflooding, 44-2, 44-3
 - index, 49-38
 - introduction, 26-1, 26-2
 - investigation, 49-26
 - laboratory measurement of, 26-3 to 26-7
 - logs, 49-11, 51-29, 51-31, 51-32
 - measurement comparisons, 26-6
 - methods of determining, 26-4, 26-5
 - of consolidated rocks, 51-29 to 51-32
 - of poorly consolidated rocks, 51-33, 51-34
 - of secondary porosity, 51-31, 51-33
 - of shaly sand, 51-34, 51-35
 - profile, 36-4
 - Rocky Mountain method, 49-31, 49-32
 - velocity relationship, 51-5
- Porosity determination,
 - bulk-density measurement, 50-1, 50-2
 - gamma-gamma density devices, 50-26 to 50-28
 - neutron-porosity devices, 50-28 to 50-33
- Porous-diaphragm method of capillary-pressure measurement, 26-24, 26-25
- Porous diaphragm or membrane, 26-24
- Porous reservoir models, 44-17
- Port configurations, gas-lift valve, 5-15
- Port size, selection for gas-lift valves, 5-28
- Port-to-bellows area ratio, 5-15
- Portable well testers, 32-6 to 32-8
- Portland cement, 46-19
- Portugal, 58-20
- Position-sensing valve switch, 16-3
- Positive-depth indicator, 56-5
- Positive-displacement meter, 12-6, 12-18, 12-19, 16-2, 16-5 to 16-7, 16-12, 17-4 to 17-6, 32-6 to 32-8, 32-10 to 32-12
- Positive-displacement meter, measurement of petroleum liquid hydrocarbons by, 17-4
- Positive-displacement-meter prover tanks, tables, 17-6
- Positive-displacement-meter-type LACT system, 16-13
- Positive-displacement pumps, 6-1, 6-34, 6-49 to 6-51, 6-62, 13-54, 15-14, 15-17, 28-4, 44-47
- Positive-seal double-bag model, 7-11
- Positive-seal protector, 7-4, 7-5

- Positive-volume dump meters, 16-13
 Positive-volume meters, 16-2, 16-5, 16-7
 Possible reserves, definition, 40-4
 Posted barges, 18-2
 Potassium, 24-5, 24-9, 24-18, 24-20, 50-2 to 50-4, 50-16, 50-18, 50-24 to 50-27, 50-34, 50-35
 Potassium chloride for control of clay swelling, 46-20
 Potential distribution, 39-20
 Potential energy, 6-1, 6-34, 13-1, 13-2, 34-28, 34-29, 34-36
 Potential function, 26-11
 Potential gradient, 26-11, 39-21
 Potential of a process, 13-50
 Potential tests, 12-17, 41-19
 Potential tests of oil wells, 32-1 to 32-16
 Potentiometric model, 39-21, 39-22, 44-17, 44-19, 44-34
 Potentiometric model studies, 39-20, 39-21
 Potentiometric transducer, 30-5, 30-6
 Poth "A" sand, 46-29 to 46-32
 Pothead, 7-5
 Pounding, 6-33, 6-34
 Pour point, 21-7, 21-9, 21-10, 46-27, 46-31, 46-33
 Power cable, ESP, 7-5, 7-6
 Power control manifold module, 6-54, 6-56
 Power, definition of, 6-14
 Power-distribution system, offshore, 18-45
 Power equivalents, table, 1-78
 Power-factor correction, 10-35
 Power factor of motor, 10-25, 10-33 to 10-35
 Power fluctuations, ESP, 7-14
 Power fluid, 6-1 to 6-5, 6-9, 6-10, 6-20, 6-21, 6-24 to 6-30, 6-34, 6-37, 6-38, 6-41, 6-42, 6-48, 6-51, 6-60, 6-62
 Power-fluid discharge-pressure friction, 6-27
 Power-fluid flow through nozzle, 6-42
 Power-fluid friction, 6-30
 Power-fluid friction pressure, 6-27
 Power-fluid gradient, 6-25, 6-26, 6-29, 6-30
 Power-fluid pressure, 6-7, 6-9, 6-16 to 6-18, 6-25, 6-27, 6-28, 6-41 to 6-43
 Power-fluid systems, 6-54 to 6-57
 Power-fluid tubing friction pressure, 6-42
 Power-fluid tubing string, 6-2, 6-3
 Power-law coefficient, 47-4, 47-9
 Power-law model, 47-4, 55-5
 Power method for parameter determination, 48-16
 Power-oil emulsion, 6-31
 Power-oil plunger pumps, 6-33
 Power-oil tank and accessories, closed system, 6-59
 open system, 6-57 to 6-59
 Power stroke, 10-14
 Power supplies, uninterruptible (UPS's), 18-45
 Power triangle of motor, 10-33 to 10-35
 Power, unit and definition, 58-11, 58-23, 58-24, 58-32
 Powers of numbers, three-halves table, 1-19, 1-20
 Powers of numbers, two-thirds table, 1-20
 Powers of SI units, 58-12
 Pozzolan, 46-19
 Precision of gas meter, 13-1
 Precision vs. accuracy, 58-8, 58-9
 Predicted reservoir performance, 42-5, 42-6
 Pre-exponential factor, 46-12
 Preferred metric unit, 58-21, 58-26 to 58-38
 Preflush, hydrochloric acid, 56-5
 micellar-polymer flooding, 47-10, 47-16
 systems, 56-3
 PREOS, 25-8, 25-9, 25-16
 Preparation of well for testing, 33-6
 Present value or present worth, 41-3 to 41-8, 41-12, 41-16, 41-17, 41-23, 41-25, 41-27, 41-29, 42-6
 Present-worth factor, 41-25
 Present worth of an annuity, table, 1-66
 Pressure and force in static plunger and cylinder assembly, 6-18
 Pressure, average drainage-region, 35-19, 35-20
 Pressure-balanced valves, 13-55
 Pressure-base factor, 13-3, 13-12
 Pressure behavior, constant rate in closed reservoir, 35-2, 35-3
 Pressure bombs, 30-4
 Pressure-buildup analysis, 39-18, 39-19
 Pressure-buildup behavior, 30-14
 Pressure-buildup data, 6-48
 Pressure-buildup tests, 42-3, 42-4, 48-8
 Pressure changes in wellbore, calculations including, 46-6
 Pressure-composition phase diagram, 23-2, 23-3, 23-6, 23-8, 23-9
 Pressure control for high-pressure well, 13-56
 Pressure controls, separators, 12-39
 Pressure conversions, 58-7, 58-28, 58-29
 Pressure correction for gas viscosities, 20-9
 Pressure decline, rapid, 37-1, 37-2
 Pressure dependence, of compressional- and shear-wave attenuation, 51-6
 of compressional- and shear-wave velocities, 51-5
 of porosity, 51-6
 Pressure depletion, 26-21, 39-7 to 39-16, 39-23, 39-24, 39-26, 44-1
 Pressure-depletion behavior, 39-4
 Pressure-depletion operation of GC reservoir, hydrocarbon/liquid-condensation effect, 39-13
 prediction with laboratory-derived data and hydrocarbon analysis, 39-10, 39-11
 prediction with vapor/liquid equilibrium calculation and correlation, 39-11 to 39-13
 pressure drawdown at wells, effect on productivity and recovery, 39-13
 relative merits of measured vs. calculated behavior, 39-13, 39-15
 Pressure-depth diagram, 5-21
 Pressure distribution, 35-6, 44-17, 44-30
 Pressure drawdown, 6-48, 34-31, 34-34, 35-6, 37-2, 37-19 to 37-21, 48-10
 Pressure drop, across sand-filled perforations, 56-4
 in flowing gas column, 34-9
 in gas lines, 15-5, 15-7
 in liquid lines, 15-2, 15-3
 in tubing, 6-70, 6-71
 Pressure, effect on acid-reaction rate, 54-4, 54-5
 effect on gas-saturated crude oils, 22-16
 effect on tubing string, 4-9
 Pressure equivalents, table, 1-77
 Pressure evaluation, 52-26 to 52-28
 Pressure filters, 44-47
 Pressure for hydrate formation, 25-8
 Pressure, force and flow in dynamic plunger and cylinder assembly, 6-18
 Pressure function, 34-35, 37-8
 Pressure gauges, 12-42
 Pressure gradient, 2-39, 34-29, 38-13, 39-21, 41-3, 41-6, 41-16
 Pressure-gradient curves, 34-36
 Pressure-gradient traverse, 5-25
 Pressure-hydrometer test method, 17-5
 Pressure hysteresis, 48-10
 Pressure-loaded balanced diaphragm valve, 13-56
 Pressure log, 52-1, 52-26
 Pressure maintenance, 23-1, 40-4, 40-14, 43-11 to 43-16, 48-2, 48-4
 Pressure-maintenance operations, 18-44, 34-28, 43-1 to 43-3, 43-8
 Pressure maintenance or cycling of GC reservoirs, choosing between, 39-26
 combination recovery procedures, 39-24
 reservoir cycling, gas injection, 39-16 to 39-24
 water drive and water injection, 39-15, 39-16
 Pressure-multiplier pump, 55-9
 Pressure-operated gas-lift valve, 5-24
 Pressure, optimum of separator, 12-4
 Pressure/permeability data, 44-3
 Pressure pilot, 13-56
 Pressure/production history, 37-3, 37-6
 Pressure profiles, 4-6, 35-4
 Pressure pulses, 53-1
 Pressure radius, 44-33
 Pressure range, GC reservoirs, 39-2
 Pressure rating classes of fittings, 15-13
 Pressure ratings for steel pipe, 15-11
 Pressure ratio, 6-36, 6-37, 6-45
 Pressure recorders, 6-48
 Pressure-recording charts, two-pen, 5-18, 5-23, 5-39, 5-41
 Pressure-reducing regulator, 5-13, 12-39
 Pressure-reducing valve, 13-55
 Pressure reduction in gas analysis, 52-17
 Pressure-reduction regulation, 13-54
 Pressure regulators, 13-54
 Pressure relationships used to estimate producing BHP, 6-28
 Pressure relief of storage tanks, 11-7
 Pressure-relief valve, 6-51, 11-8, 11-9, 12-39, 19-28
 Pressure ridges, 18-39
 Pressure-sensing instrument (PSI), 7-7, 7-8
 Pressure shock loads, 12-42
 Pressure, SI unit for, 58-5, 58-11, 58-23 to 58-25, 58-28, 58-29
 Pressure storage of products, 11-12
 Pressure, surface closing, gas lift valves, 5-44 to 5-46
 Pressure surveys, 5-2
 Pressure switches, 16-4
 Pressure/temperature diagram, 14-2
 Pressure/temperature phase diagram, 23-6
 Pressure/temperature rating of steel, 3-38
 Pressure-transducer technology, 30-6 to 30-8
 Pressure transducers, 46-21
 Pressure-transient behavior, 35-4
 Pressure-transient tests, 5-3
 Pressure transition zone, 52-21
 Pressure traverses, 34-36, 34-41 to 34-44, 41-41 to 41-44
 Pressure/vacuum relieving system, 11-13
 Pressure/vacuum valves, 11-8, 11-9
 Pressure/volume (PV), compressibility, 51-49
 diagram for pure components, 20-2
 equilibrium cell, 20-4
 method for waterflood water requirements, 44-41
 relation, 20-2, 20-6, 39-7
 Pressure-volume-temperature (PVT), analysis, 22-1, 22-2, 22-10, 22-12, 10-21
 cell, 39-13

- data, 7-9, 37-3, 37-22, 40-6
- properties, 44-37, 48-2, 48-13
- Pressure waves, 51-2
- Pressures and forces in reciprocating pumps, 6-10, 6-14 to 6-16
- Pressures and losses,
 - in closed power-fluid installation, 6-26
 - in open power-fluid installation, 6-25
- Pressures, forces and flows in hydraulic transformer, 6-19
- Pressures in downhole pumps, 6-16 to 6-19
- Pressurized ball joints, 18-12, 18-13
- Prevention of emulsions, 19-5
- Primary cementing, 56-4
- Primary depletion, 37-1, 42-2
- Primary drainage, 28-12
- Primary electric power, 18-44, 18-45
- Primary electrical system, 10-29
- Primary functions of oil and gas separators,
 - removal of gas from oil, 12-3
 - removal of oil from gas, 12-3
 - separation of water from oil, 12-3, 12-4
- Primary oil recovery, 24-3, 40-33
- Primary performance, injection operations, 42-3, 42-4
- Primary-performance predictions, volatile oil reservoirs, 37-23
- Primary porosity, 26-1, 29-3, 36-6
- Primary production, 41-12
- Primary recovery, 42-1, 45-9
- Primary-recovery methods and operations, 44-1, 44-2, 44-5, 44-36
- Primary separation in separator, 12-19, 12-20
- Primary separator gas, 39-6, 39-9, 39-10, 39-14
- Primary stratigraphic traps, 29-4, 29-5
- Primary term, habendum clause, 57-4, 57-5
- Primary waves, 51-2
- Prime movers for pumping units,
 - electric motors, 10-19 to 10-37
 - internal-combustion engines, 10-14 to 10-19
- Principal amounting to a given sum, table, 1-64, 1-65
- Principle of additive volume, 20-11
- Principle of corresponding states, 20-4, 20-5, 20-9, 20-13
- Principle of flux-leakage tool, 53-22, 53-23
- Principle of operation, reciprocating pumps, 6-8 to 6-32
- Principle of superposition, 38-1 to 38-3
- Principles of regulation control,
 - derivative response, 13-52, 13-53
 - nomenclature of process controls, 13-49, 13-50
 - process characteristics, 13-50
 - proportional control, 13-51, 13-52
 - reset, 13-52
- Principles of TVD, TST, and TVT plots, 53-15, 53-16
- Prism diagram, 47-12, 47-13
- Probability theory, 26-28
- Probable error, factors for computing, table, 1-61
- Probable reserves, 40-4
- Problem examples: see Example problems
- Problems,
 - common to steamfloods and firefloods, 46-21, 46-22
 - plaguing firefloods only, 46-22
 - plaguing steamfloods only, 46-22
- Problems, special in oil and gas separators,
 - corrosion, 12-8
 - paraffin, 12-7, 12-8
 - sand, silt, mud, salt, etc. 12-8
 - separating foaming crude oil, 12-6, 12-7
- Process characteristics, 13-50 to 13-53
- Process control computer, 16-10
- Process equipment and facilities offshore, 18-28, 18-30, 18-32, 18-42
- Process flow for expansion process, 14-8
- Process flow sheets, 15-31
- Process model, 28-3
- Process selection, 15-30 to 15-32
- Processing plant, 11-13
- Procurement, an engineering effort, 15-31
- Pro-Dip log and wellsite analysis, 49-37
- Produced-fluid gradient, 6-25, 6-26, 6-29, 6-44
- Produced-product prices, 41-11
- Produced water, 12-3, 24-5
- Producer BHP, steamfloods, 46-17
- Producibility of well, 39-5, 39-6
- Producing efficiency, 30-15
- Producing gas/oil ratio (GOR), 6-27, 37-1 to 37-3, 37-5, 37-7, 37-9 to 37-14, 37-22, 37-23, 37-26, 39-2
- Producing properties, check list of data required for oil and gas, 41-8, 41-9
- Producing wells,
 - gas, 34-3 to 34-27
 - gas-condensate, 34-27, 34-28
 - gas/water flow, 34-27
- Product thread form, extreme-line casing joint, 2-64, 2-71, 2-72
- Production casing string, 3-8
- Production data, ESP, 7-9
- Production decline, 41-9 to 41-11
- Production decline curves, constant-percentage, 40-28 to 40-32
 - decline tables for constant-percentage decline, 40-30 to 40-32
 - economic limit, 40-27
 - general principles, 40-26, 40-27
 - harmonic, 40-29, 41-10
 - hyperbolic, 40-28
 - loss-ratio method, 40-32
 - nominal and effective decline, 40-27
 - relationship between effective and nominal decline, 40-29
 - reserves and decline relationship, 40-32
 - straightening curves, 40-31
 - to evaluate pilot flood performance, 44-39
 - types of, 40-28, 40-29
 - types of plots, 40-31
- Production discharge friction pressure, 6-27
- Production equipment,
 - tank battery, 11-9 to 11-11
 - tank grades, 11-11
- Production fluid gradient, 5-40
- Production history, 41-9
- Production loans, 44-5
- Production logging, 53-17
- Production mechanisms, 46-4
- Production packers,
 - classification and objectives, 4-1
 - combination tubing/packer systems, 4-11
 - considerations for packer selection, 4-4 to 4-6
 - in production packing, 56-8, 56-9
 - references, 4-11
 - tubing/packer forces on intermediate packers, 4-11
 - tubing/packer systems, 4-6 to 4-9
 - tubing response characteristics, 4-8 to 4-11
 - tubing-to-packer connections, 4-1
 - utilization and constraints, 4-1 to 4-3
- Production payments, 41-1, 41-2, 41-8, 41-9, 41-15, 57-7
- Production-pressure effect, 5-18, 5-30
- Production-pressure factors, 5-14, 5-17 to 5-22, 5-24, 5-26, 5-27, 5-32, 5-33, 5-35, 5-39, 5-40, 5-42, 5-44, 5-48, 5-54
- Production-pressure-operated gas-lift valve, 5-13, 5-16, 5-17, 5-21, 5-32, 5-33, 5-35 to 5-37, 5-40, 5-54
- Production profile, 40-1
- Production-rate allowables, 32-1, 43-2, 43-10
- Production-rate and time calculations,
 - solution-gas-drive, introduction, 37-17
 - rates based on IPR, 37-19 to 37-21
 - rates based on PI, 37-19
 - time required for oil production, 37-21, 37-22
- Production rate of gas wells, 33-20
- Production rate variation (superposition), 35-8, 35-9
- Production response from high-pH flood, 47-22
- Production safety controls, 16-4
- Production separator, 12-17
- Production string, 3-39
- Production structures offshore,
 - artificial islands, 18-40, 18-41
 - gravity type, 18-41, 18-42
 - piled, 18-42
- Production taxes, 41-1, 41-3, 41-4, 41-12
- Production tests, 18-34
- Production-transfer-pressure traverse, 5-36
- Productive stringer, 36-7
- Productivity, decline or loss, 39-25
- Productivity, effect of damage on, 54-8, 54-9
- Productivity, from drawdown tests, 44-42
- Productivity index (PI), 5-38, 5-39, 5-45, 6-41, 6-46, 30-10 to 30-13, 30-15, 32-2 to 32-6, 34-30 to 34-36, 35-6, 35-10, 37-19 to 37-21, 40-27, 42-4, 46-10, 58-14, 58-38
- Productivity index for different GOR's, 32-5
- Productivity-index/permeability correlation, 32-4
- Productivity ratio, 30-13, 30-14
- Productivity test, 24-1, 39-25
- Products of crude oils, temperature correction for, 17-5, 17-6
- Profile calipers, 53-17, 53-18
- Profile of a gravity system, 15-15
- Profiles, injection-gas volumetric throughput, 5-20
- Profit margin, 41-6
- Profit margin and cost relationship, 36-2
- Profit-to-investment ratio, 41-7
- Profitability, 39-17
- Programmable calculators, 6-34, 6-38, 6-41, 6-46, 20-7, 20-9
- Programmable controllers, 16-4, 18-47
- Programmable logic controllers, 19-29
- Programmer for oilfield motors, 10-27
- Project control, 15-32, 15-33
- Project definition, 15-30
- Project design, thermal recovery,
 - features common to both steamfloods and firefloods,
 - completion intervals, 46-17
 - pattern selection, 46-17
 - producer BHP, 46-17
 - features pertaining to firefloods only,
 - air injection rate, 46-19
 - dry vs. wet gas combustion, 46-18
 - WAR, 46-19
 - features pertaining to steamfloods only,
 - steam injection rate, 46-18
 - steam quality, 46-18
- Project execution format, 15-31, 15-32
- Project inspection and expediting, 15-31
- Project management, 15-30 to 15-32
- Projected oil recovery, 42-2, 42-3

- Prolog wellsite analysis, 49-37
- Pronunciation of metric terms, 58-13
- Propagation time, 49-32, 49-34
- Propane as IC engine fuel, 10-16
- Propane as refrigerant, 14-9
- Propane compressibility table, 17-7
- Propane critical pressure, 25-3
- Propane/water system, 25-2, 25-3, 25-17, 25-25, 25-27
- Properties and behavior of gas condensate fluids,
composition ranges, 39-2
gas/liquid ratios, 39-4
introduction, 39-1
liquid contents, 39-4
phase and equilibrium behavior, 39-2 to 39-4
pressure and temperature ranges, 39-2
properties of separated phases, 39-4
viscosities, 39-4
- Properties of construction materials for pressure vessels, 12-41
- Properties of crude oils and gas condensates, 39-2
- Properties of produced waters,
analysis methods for oilfield water, 24-5
chemical properties of oilfield waters, 24-5 to 24-13
inorganic constituents, 24-9, 24-12
interpretation of chemical analyses, 24-18, 24-19
introduction and history, 24-1 to 24-3
nomenclature, 24-20
occurrence, origin, and evolution of oilfield waters, 24-19, 24-20
physical properties of oilfield waters, 24-12 to 24-18
recovery of minerals from brines, 24-20, 24-21
references, 24-21, 24-22
sampling, 24-3 to 24-5
- Properties of separated phases, GC streams, 39-4
- Properties of ternary diagrams, 23-4
- Proportional action of controller, 13-52
- Proportional control, 13-49, 13-51 to 13-53, 13-56
- Proportional counter, 50-14
- Proportional pilot for pneumatic service, 13-56
- Proportional/reset controller, 13-52
- Proportionality constant for rock, 26-11
- Proppant,
density, 55-8
grain roundness factor, 55-8
grain size, 55-8
grain-size distribution, 55-8
grain strength, 55-8
permeability, 55-8
placement, 55-8
quality, 55-8
transport, 55-7, 55-9
- Proppant-transport properties, 55-5
- Propping agent,
amounts used, 55-1
definition of, 55-2
grain size of, 55-8
grain strength of, 55-8
permeability, 55-4
placement of, 55-8
- Propylene, 14-9
- Propylene compressibility table, 17-7
- Propylene/water system, 25-25
- Propyne/water system, 25-25
- Proration, 41-3, 41-10, 41-11
- Proration records, 13-3
- Protected-slope production island, 18-40
- Protection equipment for oilfield motors,
air circuit breaker, 10-28
control fuses, 10-29
lightning arresters, 10-28
motor fuses, 10-28
motor-winding temperature sensors, 10-29
over-temperature lockout circuit, 10-29
phase loss relay, 10-28, 10-29
pumping-unit vibration switch, 10-29
thermal-overload relay, 10-29
under-voltage relay, 10-28
- Protective coatings, 9-10
- Proved developed reserves, definition, 40-3
- Proved reserves definitions, 40-2
- Proved undeveloped reserves, definition, 40-3
- Proving systems, 17-4
- Proximity log (PL), 49-22 to 49-25, 49-27
- Prudhoe Bay field, Alaska, 18-3, 18-39, 18-41, 48-17
- Pseudo-Rayleigh waves, 51-12 to 51-14, 51-25, 51-27
- Pseudobinary diagram, 23-9
- Pseudocomponents, 47-11
- Pseudocritical calculations,
from gas analysis, 40-21
from specific gravity, 40-22
- Pseudocritical constants, corrected, 20-5
- Pseudocritical density, 20-10, 20-15
- Pseudocritical pressure, 20-5, 20-7, 20-10, 20-16, 22-12, 40-21, 40-22
- Pseudocritical properties, 22-21, 34-4
- Pseudocritical properties of C_{7+} , 20-10
- Pseudocritical temperature, 20-5, 20-7, 20-10, 20-16, 22-12, 40-20, 40-21
- Pseudocritical-temperature gradient factor, 20-7
- Pseudocriticals, for heptanes and heavier, 21-17
of gases and condensate well fluids, 21-19
- Pseudogeometrical factors, 49-22, 49-25
- Pseudoliquid density, 22-2 to 22-4
- Pseudophase theory, 47-13
- Pseudoreduced compressibility, 20-11, 20-12, 22-12, 22-13
- Pseudoreduced pressure, 20-5, 20-9, 20-11, 20-12, 22-13, 22-21, 40-21
- Pseudoreduced properties, 22-21, 34-5 to 34-7, 34-10 to 34-22, 34-24
- Pseudoreduced temperature, 20-5, 20-9, 20-11, 20-12, 22-13, 40-21
- Pseudorelative-permeability curves, 37-4, 48-8 to 48-10, 48-12
- Pseudorelative-permeability data, 37-4, 37-5
- Pseudostatic SP, 49-9, 49-10, 49-28
- Pseudosteady state, 35-2, 35-3, 35-7, 35-8, 35-10, 35-12 to 35-14, 35-16
- Pseudosteady-state aquifer productivity index, 38-8
- Pseudosteady-state behavior, 35-6 to 35-8, 35-15
- Pseudosteady-state flow, 5-25, 32-3 to 32-6, 33-5 to 33-7, 34-30, 34-31, 37-19, 37-21
- Pseudoternary diagram, 45-2, 45-3, 45-5
- Public Law 93-380, Aug. 21, 1974, 1-69
- Public Law 94-168, Dec. 23, 1975, 1-69
- Puffer, 52-6
- Pull bar, 7-12
- Pull curves, casing-hanger, 3-6, 3-7
- Pull-in procedure, 18-37
- Pull sheet, 53-17
- Pull tube, 8-4
- Pulling and running sucker rods, 9-10
- Pullout strength of line-pipe joint, 2-62
- Pulsation dampers, 6-50, 6-51, 6-61, 15-17
- Pulse testing or tests, 36-7, 36-8, 48-8
- Pulsed-data transmission systems, 17-4
- Pulsed nuclear magnetic resonance analyzer, 52-26
- Pulsed-neutron logging, 50-36
- Pulsed-neutron logging devices, 50-21, 50-22
- Pultrusion process, 9-12
- Pump discharge pressure, 6-17, 6-25 to 6-27, 6-28, 6-41 to 6-43, 6-47, 6-49, 6-51
- Pump displacement, 6-11 to 6-13, 6-15, 6-16, 6-21, 6-24, 6-29, 6-30, 6-52 to 6-55, 8-5, 8-9, 9-2
- Pump drivers, 15-15, 15-16
- Pump efficiency, 6-24, 6-31, 6-37, 6-38, 6-49, 46-21
- Pump-efficiency equations, 6-68
- Pump-end volumetric efficiency, 6-21, 6-22
- Pump intake, 7-4, 7-5
- Pump-out method of solution mining, 11-13, 11-14
- Pump performance curve, 7-10, 7-11
- Pump piping and installation, 15-17
- Pump-protector motor unit, 7-2
- Pump selection, 8-2 to 8-4
- Pump-selection table, 7-10
- Pump speed, maximum rated, 6-11 to 6-13, 6-15, 6-16, 6-21
- Pump submergence, 6-25, 6-26
- Pump suction gradient, 6-42, 6-44
- Pump-suction (intake) pressure, 6-4, 6-17, 6-25, 6-26, 6-38, 6-43, 6-47
- Pump terminology, 8-2, 8-6 to 8-9
- Pumpdown pressure recorders, 6-34
- Pumped-off well, definition of, 10-27
- Pumping equipment for fracturing, 55-9
- Pumping speed factor, 10-6
- Pumping speed, maximum practical, 9-4, 9-5
- Pumping-unit bearings, 10-5
- Pumping-unit design calculations, 10-8 to 10-11
- Pumping-unit geometry, 9-2, 10-2
- Pumping-unit loading, 10-5
- Pumping units, 10-1 to 10-13
- Pumpoff, 7-6, 7-10, 7-16
- Pumpoff controls, 10-27
- Pumpstroke counter, 52-11
- Pure Oil Co., 54-1
- Purging offshore distribution system, 18-46
- Pycnometer, 26-3
- Pycnometer method, 52-19
- Pyrod-type thermocouple, 16-7
- Pyramidal rule, 40-5
- Pyrenees Mts., 46-27
- Pyroanalyzers, 52-28
- Pyrolysis, 52-1

Q

- Quadruple point, 25-15
- Quality control, 12-38
- Quality factor, 51-4
- Quality of foams, 47-8
- Quality of separated fluids, 12-13, 12-15
- Quality power oil, 6-55
- Quantities (chemical, electrical, and physical) in alphabetical order, 59-18 to 59-51
- Quantity, definition, 58-9
- Quartzose sediments, 29-7
- Quaternary compounds, 44-45
- Quaternary diagrams, 24-19
- Quench water, 46-21, 46-22
- Quick-cycle units, 14-10, 14-13
- Quintaplex pump, 55-9
- Quintiplex positive-displacement pump, 6-1, 6-49, 6-51

R

- Rabbiting, 56-3
 Radial aquifers, 38-2 to 38-4, 38-8 to 38-19
 Radial differential temperature log, 31-7
 Radial-flow equation, 30-12
 Radial-flow pumps, 15-15
 Radial-flow system, 26-13 to 26-15
 Radial frontal advance, 38-13
 Radial geometry, definition, 38-1
 Radial gridded simulator, 37-21
 Radial pseudogeometrical factors, 49-20
 Radians expressed in degrees, table, 1-43
 Radiation, 46-4
 Radiation detector, 50-14
 Radiation heat-transfer coefficient, 46-5
 Radiation log, 49-25
 Radiation, units and conversions, 58-37
 Radio frequency, 19-31
 Radio-frequency preheater, 9-12
 Radio triangulation systems, 18-18
 Radioactive capture, 50-9
 Radioactive decay, 50-4, 50-6, 50-21
 Radioactive isotopes, 50-15
 Radioactive rocks, 58-33
 Radioactive tracers, 28-4, 46-21
 Radioactivity logging and logs, 41-8, 51-42
 Radioactivity surveys, 49-1
 Radiograph, of areal sweepout efficiency, 44-18
 of welded pipe, 12-41
 Radioisotopes, 46-21
 Radionuclide, 58-10
 Radium, 50-4, 50-6, 50-15
 Radius of circumscribed circle, equation, 1-36
 Radius of curvature method of calculating directional surveys, 53-5
 Radius of inscribed circle, equation, 1-36
 Ram preventers, 18-11, 18-12, 18-15
 Ramey's equation for wellbore heat transmission, 46-5, 46-6
 Ramey's generalization of Marx-Langenheim method, 46-8
 Random flood pattern or network, 44-13, 44-14, 44-17
 Randomized network model, 28-12
 Range lengths, API casing and liner casing, 2-3
 API tubing, 2-37
 line pipe, 2-47
 Rangeability of gas meter, 13-1, 13-45, 13-48
 Rangely field, Colorado, 23-9, 23-10, 26-23, 48-6
 Raoult's law, 23-11
 Rarefactions, 51-2
 Rasching rings, 12-10
 Rate/cumulative curve or relationship, 40-25, 40-27 to 40-29, 40-31, 40-32
 Rate-dependent skin factor, 35-10
 Rate of frontal advance, 39-17
 Rate-of-penetration (ROP), 52-11, 52-13, 52-18, 52-24, 52-25, 52-27 to 52-29
 Rate-of-penetration log, 52-1
 Rate of return (ROR), 41-6 to 41-8, 41-16 to 41-24, 44-2
 Rate/pressure curves, 44-36
 Rate/time curve or relationship, 40-27 to 40-29, 40-31, 40-32, 41-10
 Ratio(s),
 air/water, 46-33
 compression, 6-10, 6-21, 8-9, 8-10, 10-15, 18-14, 39-24
 conductance, 44-34
 damage, 30-13
 equilibrium, 21-11, 21-16, 23-11, 25-5, 39-6, 39-9, 39-11 to 39-13, 39-15
 equilibrium vaporization, 37-23
 gas-gravity/condensate-gas, 34-28
 gas/oil, 5-25, 5-26, 6-24, 6-25, 6-29, 6-30, 6-38, 6-39, 6-44, 6-47, 12-35, 22-20, 34-41 to 34-43, 34-47 to 34-49, 38-16, 39-1, 39-2, 40-33, 41-8, 44-39, 58-38
 injectivity/productivity, 46-17
 liquid/gas, 12-35, 39-2, 39-5
 methods, 49-28
 net-pay/net-connected-pay, 36-17
 net-profit/initial-investment, 41-22
 net-profit/unreturned-investment balance, 41-22
 of differential pressure to absolute pressure, 13-8
 of epithermal counting rates, 50-20, 50-29
 of gas-cap/oil-zone volume, 37-5, 37-6, 37-13, 37-14
 of net profit, constant, 41-20
 of nozzle area to throat area, 6-34
 of orifice to pipe diameter, 13-36
 of pump displacement to engine displacement, 6-18
 oil/steam, 46-9, 46-15, 46-23
 permeability, 37-14, 37-15
 permeability/viscosity, 47-8
 piston/engine (P/E), 6-11 to 6-13, 6-15, 6-16, 6-18, 6-27, 6-28, 6-30
 piston pneumatic/hydraulic pump, 3-33
 pore aspect, 51-9, 51-12
 pressure, 6-36, 6-37, 6-45
 producing gas/oil, 6-27, 37-1 to 37-3, 37-5, 37-7, 37-9 to 37-14, 37-22, 37-23, 37-26, 39-2
 productivity, 30-13, 30-14
 profit-to-investment, 41-7
 sand, 36-4
 solubilization, 47-13, 47-14, 47-20
 stage compression, 39-24
 stage pressure, 12-33
 steam/oil, 46-8, 46-14, 46-15, 46-23, 46-24, 46-27
 steam/tar, 46-27, 46-28
 sulfur/oxide, 52-7
 surface-gas-gravity/well-fluid-gravity, 21-17
 tube amplitude, 51-47, 51-48
 velocity, 51-38
 viscosity, 43-5, 43-6, 45-7, 45-11
 viscosity vs. pseudoreduced temperature, 20-9
 viscous/gravity forces, 44-25
 volumetric, 55-6
 water/oil, 19-17, 24-20, 28-5, 34-41, 40-18 to 40-20, 44-7, 44-9, 44-11, 44-31, 44-32, 44-39, 46-33
 water/oil mobility, 44-7, 44-8, 47-6
 water/oil viscosity, 40-18, 44-10
 Reaction kinetics, 48-2
 Reaction-rate equation, 46-12
 Reaction rate of acids, factors affecting,
 acid concentration, 54-5
 area/volume ratio, 54-5
 corrosion inhibitors, 54-6
 flow velocity, 54-5
 formation composition, 54-6
 pressure, 54-4
 temperature, 54-4, 54-5
 Reactive fluids, effect on permeability measurements, 26-18, 26-19
 Reactive power rating of transformers (kVAR), 10-31, 10-33 to 10-35
 Real-gas law, 20-4, 20-11
 Real-gas pseudopressure, 35-10
 Real gases, 20-4
 Real property, definition, 57-1
 Receipt and delivery tickets, 17-7
 Receiver of sonic meter, 13-49
 Reciprocal gas formation volume factor, 40-22, 40-23, 40-33, 40-34
 Reciprocal mobility ratio, 44-19, 44-22, 44-23
 Reciprocal of numbers, table, 1-21 to 1-23
 Reciprocated induction curve, 49-15
 Reciprocating oilwell pumps, 8-1
 Reciprocating piston positive-displacement meter, 32-11
 Reciprocating pump,
 displacement of downhole pumps, 6-21, 6-24
 equipment selection and performance calculations, 6-28
 fluid friction and mechanical losses in hydraulic pumps, 6-19 to 6-21
 for waterfloods, 15-14, 15-15, 15-17, 15-18
 gas/liquid ratio in vented systems, 6-27
 in closed power-fluid systems, 6-4
 in reverse-flow systems, 6-5
 manufacturer specifications, 6-11 to 6-13, 6-15, 6-16
 multiphase flow and pump discharge pressure, 6-27
 pressure and force balance in downhole pumps, 6-16 to 6-19
 pressure and forces in, 6-10, 6-14 to 6-16
 pressure relationships used to estimate producing BHP, 6-28
 principle of operation, 6-8 to 6-10
 subsurface troubleshooting guide, 6-31
 system pressures and losses in hydraulic installations, 6-24 to 6-27
 turbulence in, 19-5
 worksheets and summary of equations, 6-29, 6-30
 Recoil electron ejection, 50-12
 Recombined separator samples, 39-5
 Recommended practices before unloading, 5-53
 Recompletion costs, 41-9, 41-12
 Recompletions, 41-9, 44-7
 Recorder for metering system, 13-36, 13-37
 Recording acoustic data, methods of,
 acoustic-array logging, 51-25 to 51-27
 amplitude/time recording, 51-18
 conventional acoustic logging, 51-15 to 51-18
 intensity/time recording, 51-18
 introduction, 51-14
 long-spaced acoustic logging, 51-19 to 51-24
 reflection, 51-27, 51-28
 shear-wave logging, 51-24, 51-25
 Recording ammeter, 7-14
 Recording caliper logs, 53-16
 Recoverable gas reserves, 40-24, 40-27
 Recoverable gasoline content, 20-11
 Recoverable hydrocarbon reserves, 41-3
 Recoverable hydrocarbons, 39-26
 Recoverable oil, 40-27, 44-32, 44-37, 44-38
 Recovery by miscible displacement, 45-9, 45-10
 Recovery by pressure maintenance, 39-9
 Recovery efficiency, 39-11, 39-15, 42-5, 43-2, 43-6, 43-9, 44-3, 45-8, 45-12, 45-13, 46-14, 46-27, 47-16, 47-17
 Recovery-efficiency factor, 40-16, 40-17
 Recovery estimates, 40-1
 Recovery factor, 40-1, 40-11, 40-19, 40-20, 40-23, 40-25 to 40-27

- Recovery factor, average from correlation of statistical data, 40-16, 40-17
- Recovery factor vs. reservoir pressure, 37-14, 37-15
- Recovery from gas reservoirs with water drive, 40-26, 40-27
- Recovery of LPG products, 45-12
- Rectangular tanks, 11-2
- Rectilinear flow of compressible fluids, 26-11
- Red Sea, 24-19
- Redalerm™ motor controller, 7-6, 7-16
- Redlich and Kwong equation, 20-7, 20-8, 23-12, 23-13
- Redox potential (Eh), 24-4, 24-5, 24-9, 24-16, 24-17
- Reduced properties, definition, 22-21
- Reduced-state relationships, 22-21
- Reduced vapor pressure, 20-13
- Reducing agents, 54-7, 56-3
- Reduction factor or ratio, 6-50, 49-9
- Redundancy, subsea production facilities, 18-48
- Redwater D-3 pool, Alberta, Canada, 40-20
- Redwater field, Alberta, Canada, 40-2
- Reel barges, 18-37, 18-38
- Re-entry systems, 18-14
- References (see also General References), acidizing, 54-12
- acoustic well logging, 51-50 to 51-52
 - automation of lease equipment, 16-16
 - bottomhole pressures, 30-16, 30-17
 - casing, tubing, and line pipe, 2-74
 - chemical flooding, 47-24 to 47-26
 - crude-oil properties and condensate properties and correlations, 21-20
 - development planning for oil wells, 36-10, 36-11
 - electric submersible pumps, 7-17
 - electrical logging, 49-41
 - estimation of oil and gas reservoirs, 40-37, 40-38
 - formation fracturing, 55-10
 - gas-condensate reservoirs, 39-27, 39-28
 - gas-injection pressure maintenance in oil reservoirs, 43-19
 - gas lift, 5-57
 - gas measurement and regulation, 13-59
 - gas properties and correlations, 20-18
 - hydraulic pumping, 6-72
 - lease-operated hydrocarbon-recovery systems, 14-22
 - measuring, sampling and testing crude oil, 17-8
 - miscible displacement, 45-13 to 45-15
 - mud logging, 52-30
 - nuclear logging techniques, 50-38
 - offshore operations, 18-52
 - oil and gas separators, 12-43
 - oil storage, 11-14
 - oil-system correlations, 22-21, 22-22
 - open flow of oil wells, 33-23
 - other well logs, 53-26
 - petroleum reservoir traps, 29-9
 - phase behavior of water-hydrocarbon systems, 25-20 to 25-24
 - phase diagrams, 23-13
 - potential tests of oil wells, 32-16
 - production packers, 4-11
 - properties of produced water, 24-21 to 24-23
 - properties of reservoir rocks, 26-33
 - pumping units and prime movers for pumping units, 10-37
 - relative permeability, 28-15, 28-16
 - remedial cleanup and other stimulation treatments, 56-9
 - reservoir simulation, 48-17 to 48-20
 - solution-gas-drive oil reservoirs, 37-27
 - subsurface sucker-rod pumps, 8-10
 - sucker rods, 9-14
 - surface facilities for waterflooding and saltwater disposal, 15-33, 15-34
 - temperature in wells, 31-7
 - thermal recovery, 46-43 to 46-45
 - typical core analysis of different formations, 27-9
 - valuation of oil and gas reserves, 41-37
 - water-drive oil reservoirs, 38-20
 - water-injection pressure maintenance and waterflood processes, 44-49 to 44-52
 - well-performance equations, 35-21
 - wellbore hydraulics, 34-55, 34-56
 - wellhead equipment and flow-control devices, 3-40
- Reflected conical wave, 51-12
- Reflection method, acoustic-wave-propagation logging, 51-11, 51-27, 51-28
- Reflection peak, 49-13
- Refrigerants, comparison of common types, 14-9
- Refrigerants, properties of six types, 14-10
- Refrigerated storage, 11-12
- Refrigeration process, 14-9
- Regeneration cycle, 14-10
- Regeneration gas, 14-11 to 14-14, 14-20, 14-21
- Regeneration-rate controller, 16-15
- Regeneration system, 14-6, 14-7, 14-11, 14-12
- Regression equations, 46-15 to 46-17
- Regular polygons, table, 1-36
- Regulator types, 13-54 to 13-57
- Regulatory agencies, 16-1, 16-2, 18-12, 19-28, 32-1, 32-2, 32-15, 33-5, 40-1, 40-3, 40-4, 41-3, 43-2
- Regulatory agency form, 32-2
- Regulatory codes, 18-44
- Reid vapor pressure (RVP), 12-33, 14-13, 17-3, 21-19
- Reistel diagram, 24-19
- Relationship,
 - between bending and curvature radius of casing, 2-61
 - between total and external load of casing, 2-61
- Relative atomic mass, 58-24
- Relative bearing, dipmeter, 53-10
- Relative density, correction of observed value, 17-5, 17-6
- definition of, 1-80, 58-24
 - hydrometer test method, 17-5
 - of C₇₊ fraction, 20-10
 - of crude petroleum, 17-5
 - of liquid petroleum products, 17-5
 - of natural gas, 20-13
- Relative dielectric permittivity, 49-32
- Relative molecular mass, 58-24
- Relative oil volume, definition, 22-21
- Relative permeability,
 - calculating cumulative gas production, 37-10
 - conclusions, 28-13, 28-14
 - critique of recent work, 28-10 to 28-12
 - curves, 28-6, 28-8 to 28-13
 - definition, 28-1
 - effect of GOR or WOR changes, 30-11
 - factor in waterflooding, 44-2
 - framework ideas, 28-2, 28-3
 - general references, 28-16
 - historical background, 28-2
 - in determining mobility in a layer, 44-9
 - in two-phase fluid flow, 55-8
 - introduction, 28-1, 28-2
 - measurement methodologies, 28-3 to 28-9
 - nomenclature, 28-14
 - of reservoir rock, 44-4, 44-5
 - ramifications needing attention, 28-12, 28-13
 - recent literature, 28-9, 28-10
 - references, 28-15, 28-16
- Relative-permeability characteristics, 37-2, 37-19, 44-27
- Relative-permeability curves, 28-6, 28-8 to 28-13, 34-31, 39-13, 44-6, 46-13, 46-34, 46-37
- Relative-permeability data, 37-3, 37-4, 37-10, 39-9, 40-13, 43-11, 46-12
- Relative-permeability-ratio data, 37-23
- Relative-permeability ratios, 40-8 to 40-12, 40-14, 43-5 to 43-7, 43-12
- Relative pipe roughness, 15-2, 15-3, 15-7
- Relative-roughness factor, 34-2, 34-3, 34-38, 34-40
- Relaxation pressure, 40-34
- Relays for motors, 10-28
- Reliability/maintainability, subsea production facilities, 18-48
- Reliability of gas meter, 13-1
- Reliability of sensors, 3-31
- Remedial operations, 4-9, 33-22
- Remedial work, 41-8
- Remedial workover operations, 39-24
- Remote, closed-loop controls, 18-46
- Remote control of subsea equipment, 18-48
- Remote-control valves, 18-3
- Remote-controlled SSV system, 3-34
- Remote terminal unit (RTU), 16-4, 16-6, 16-8 to 16-11
- Removal of acid gases, 14-21, 14-22
- Removal of CO₂, 14-17, 14-21, 14-22
- Removal of gas from oil, 12-3
- Removal of gas from oil in separators,
 - methods used,
 - agitation, 12-13
 - bafling, 12-13
 - centrifugal force, 12-13
 - chemicals, 12-13
 - heat, 12-13
 - settling, 12-13
- Removal of H₂S, 14-17, 14-21, 14-22
- Removal of oil from gas, 12-3
- Removal of oil from gas in separators,
 - methods used,
 - centrifugal force, 12-9, 12-10
 - coalescence, 12-10, 12-11
 - density difference (gravity separation), 12-8
 - filtering, 12-11
 - flow-direction change, 12-9
 - flow-velocity change, 12-9
 - impingement, 12-9
- Removal of water vapor, 14-17 to 14-21
- Repeatability of BHP gauges, 30-4, 30-6
- Repeatability of meters, 13-48
- Reperforation, 56-1
- Representative-element simulation, 48-7
- Reproducibility, 13-50
- Reserve SPE letter symbols, 59-2 to 59-51
- Reserve SPE subscripts, 59-52 to 59-70
- Reserved production payment, 41-1
- Reserves,
 - and decline relationship, 40-32
 - cost of developing, 42-1, 42-2
 - possible, 36-1, 40-4
 - probable, 36-1, 40-4
 - proved, 36-1, 40-2, 40-3
 - proved developed, 40-3
 - proved undeveloped, 40-3
 - ultimate depletion of, 42-2

- Reserves, oil and gas,
 definition and nomenclature, 40-2, 40-3
 estimating, 40-1, 40-2, 40-12
 general references, 40-38
 glossary of terms, 40-3, 40-4
 nomenclature, 40-35 to 40-37
 nonassociated-gas reservoirs, 40-21 to 40-26
 oil- or gas-in-place computation, 40-5 to 40-8
 oil reservoirs under gravity drainage, 40-14, 40-15
 oil reservoirs with gas-cap drive, 40-13, 40-14
 oil reservoirs with water drive, 40-15 to 40-21
 performance curves, 40-32
 production-decline curves, 40-26 to 40-32
 references, 40-37, 40-38
 reservoir-volume computation, 40-4, 40-5
 saturated depletion-type oil reservoirs, 40-8 to 40-12
 undersaturated oil reservoirs without water drive, 40-12
 volatile oil reservoirs, 40-13
- Reservoir above bubblepoint pressure, 38-13
 Reservoir anisotropy, 36-8
 Reservoir below bubblepoint pressure, 38-13
 Reservoir continuity, 36-6 to 36-8
 Reservoir-controlled fluids, 55-2, 55-4
 Reservoir coverage, 39-18
 Reservoir cycling efficiency, 39-17, 39-18, 39-22, 39-23
 Reservoir cycling, gas injection,
 calculation of cycling performance, 39-17 to 39-20
 dry-gas injection, 39-16
 inert-gas injection, 39-16, 39-17
 noninjection-gas requirements, 39-23, 39-24
 prediction of operations with mathematical reservoir simulator, 39-22, 39-23
 prediction of operations with model studies, 39-20 to 39-22
 ultimate recovery, 39-23
 Reservoir cycling operations, efficiency terms, 39-18
 Reservoir, definition, 40-3
 Reservoir deliverability, 5-23
 Reservoir depth, 44-2, 44-3
 Reservoir description, uncertain data, 48-12
 Reservoir-dip effect, 44-25
 Reservoir discontinuities, 36-4, 36-5
 Reservoir engineer, 22-10, 26-7, 36-10, 39-3, 39-24, 44-7, 44-31
 Reservoir-fluid characteristics, 36-1, 36-2, 42-4, 42-5
 Reservoir-fluid compositions, 37-24
 Reservoir-fluid properties, 43-10
 Reservoir-fluid recovery, 39-23
 Reservoir-fluid samples, 42-4
 Reservoir-fluid systems, phase diagrams, 23-6, 23-7
 Reservoir-fracture effect, 44-25, 44-26
 Reservoir geometry, 44-2
 Reservoir-geometry factor, 38-13
 Reservoir heterogeneities, 28-11, 30-14
 Reservoir identification from mud log, 52-15
 Reservoir interference, 38-3, 38-4
 Reservoir limit tests, 32-5
 Reservoir performance, calculating under steam stimulation, 46-9
 indicator pertaining to steamfloods, 46-15
 indicators common to both steamfloods and firefloods, 46-14, 46-15
 indicators pertaining to firefloods, 46-16
 prediction of, 36-9, 36-10
 Reservoir performance data, 37-7
 Reservoir productivity guide, 52-16
 Reservoir-rock characteristics, 36-1, 36-2, 42-4, 42-5
 Reservoir-rock heterogeneity, 28-11
 Reservoir-rock properties,
 continuity of, factor in waterflooding, 44-2, 44-3
 electrical conductivity of fluid-saturated rocks, 26-27 to 26-29
 empirical correlation of electrical properties, 26-29 to 26-32
 fluid saturations, 26-20 to 26-27
 nomenclature, 26-32
 permeability, 26-10 to 26-20
 porosity, 26-1 to 26-10
 references, 26-33
 Reservoir simulation, as extension of material-balance technique, 36-7
 general references, 48-20
 history of, 48-1, 48-2
 introduction, 48-1
 mathematical models for, 43-17
 models, 38-16, 40-34, 43-2, 43-17, 48-1 to 48-9
 nomenclature, 48-17
 purpose of, 48-6, 48-7
 references, 48-17 to 48-20
 studies of gas-condensate reservoirs, 39-22
 technology, 48-13 to 48-17
 validity of results, 48-9 to 48-13
 Reservoir-simulation models, 38-16, 40-34, 43-2, 43-17, 48-1 to 48-9
 Reservoir simulators, 28-14, 36-7, 36-10, 46-11
 Reservoir traps, 29-1 to 29-9
 Reservoir volume, computation of, 40-4, 40-5
 Reservoir-volume estimation, 38-9, 38-11
 Reservoir with watersand, 46-26
 Reservoirs amenable to thermal recovery, 46-3, 46-4
 Reset, 13-50, 13-52, 13-53
 Residual free-gas saturation, 40-8
 Residual gas saturation, 36-3, 40-16, 44-25, 49-26
 Residual hydrocarbon saturation, 44-6
 Residual liquids, definition, 27-8
 Residual oil after waterflooding,
 effect of initial saturations, 44-6
 fresh-core techniques, 44-5
 influence of wettability, 44-6, 44-7
 interpretation of conventional core-analysis data, 44-5
 relative-permeability curves, 44-6
 restored-state technique, 44-5, 44-6
 Residual oil, definition, 22-21
 Residual oil saturation (ROS), 28-5, 28-8, 28-11, 37-4, 40-16, 40-17, 40-19, 42-2, 42-4, 44-2, 44-4 to 44-6, 44-9, 44-11, 44-32, 44-46, 46-21, 46-37, 47-1, 47-9, 47-10, 47-17, 49-26, 49-27, 49-36
 Residual-resistance factor, 35-5
 Residual-viscosity function, 20-9
 Residual wellbore storage, 35-19
 Residue gas, 10-16, 39-16
 Resilient-type seal, 3-9
 Resin-coated gravel packing, 56-3
 Resin derivatives, 19-10
 Resistance factor, 47-5
 Resistance function, 38-4
 Resistance-network model, 44-20
 Resistance networks, 44-34
 Resistance of a process, 13-50
 Resistance thermal detector (RTD), 16-7
 Resistivity,
 annulus region, 49-6, 49-7
 apparent, 49-7
 devices, requirements for and types, 49-7
 formation factor, 49-4
 formation, relation to saturation, 49-5
 formation waters, 49-4, 49-26
 in permeable formations invaded by mud filtrate, 49-5 to 49-7
 index, 49-5, 49-26
 invaded zone 49-6, 49-7
 logging devices, 49-11 to 49-14
 mud, 49-4
 mud-filtrate, 49-4
 mudcake, 49-4
 ranges of, 49-5
 scales, 49-21
 true, determination of, 49-27
 uncontaminated zone, 49-27
 units, 49-2
 versus NaCl concentration, 49-3
 water,
 dependence on salinity and temperature, 49-3
 relation to formation resistivity, 49-5
 Resistivity index, 26-28, 26-29, 26-31, 44-6
 Resistivity log, 51-33
 Resistivity of a material, definition, 26-28
 Resistivity of formation water, 24-14, 24-16
 Resistivity of partially water-saturated rocks, 26-31, 26-32
 Resolution of BHP gauge, 30-2, 30-4, 30-6, 30-7
 Response time, subsea valves, 18-49 to 18-51
 Responses of normals and laterals in hard formations, 49-13
 Restored pressure measurement, 51-31
 Restored-state capillary-pressure method, 26-24, 26-25, 28-4, 28-10
 Restored-state technique, 44-5, 44-6
 Restoring forces, 18-9, 18-10, 18-16
 Retarded acids, 54-8, 54-11
 Retention time for coalescence, 19-9, 19-15, 19-18, 19-22, 19-23
 Retort method, 26-21
 Retorting, 27-8
 Retrievability, of packers, 4-4, 4-5
 Retrievable gas-lift valve, 5-2, 5-34
 Retrievable packers,
 all latched, 4-3
 control-head compression, 4-2
 control-head tension, 4-2
 hydraulic set, 4-3
 isolation, 4-2
 mechanically set, 4-3
 removal of, 4-5, 4-6
 solid-head compression, 4-2
 solid-head tension, 4-2
 weight-set tension type, 4-4
 Retrievable-valve mandrel, 5-2, 5-22
 Retrograde-condensate gas, 43-1
 Retrograde condensation, 14-1, 23-4, 39-3, 39-8, 39-9, 39-16, 48-7
 Retrograde dewpoint pressure, 21-12
 Retrograde liquid, 39-7 to 39-10, 39-14, 39-16
 Retrograde vaporization, 23-4
 Return-flow equations, jet pump, 6-46
 Return-flow fluid gradient, 6-42
 Return on investment, 36-1
 Return water saltwater, 44-42, 44-43
 Revenue-interest fraction (RI), 41-2
 Revenue interests, 41-3, 41-4, 41-9
 Reverse ballooning of tubing strings, 4-10
 Reverse-circulating gravel pack, 56-8

- Reverse combustion, 46-2, 46-3, 46-14, 46-31
- Reverse emulsions, 19-1, 19-2, 19-28
- Reverse fault, 29-3
- Reverse flow, check valve, 5-12, 5-23, 5-37
free-pump cycle, 6-6
installation, 6-6, 6-8
jet-pump casing type, 6-5
systems, 6-5 to 6-7
tubing arrangement, 6-7
- Reversionary interest, definition, 41-1
- Reynolds number, 6-36, 6-56, 6-57, 15-1 to 15-3, 15-5, 15-24, 17-7, 19-2, 34-2, 34-3, 34-27, 34-38, 34-39
- Reynolds-number factor, 13-8, 13-14 to 13-25
- Rheological properties, 55-5, 55-6, 55-8
- Rheology, 18-29, 18-36
- Rhombohedral packing of spheres, 26-1, 26-2
- Rhumba shaker, 52-8
- Rice University, 25-20
- Rig-selection considerations offshore, criteria, 18-4
drilling equipment, 18-10 to 18-16
mooring system (stationkeeping), 18-8 to 18-10
motion characteristics, 18-7
performance evaluation, 18-7, 18-8
types of rigs, 18-5 to 18-7
- Rig types for offshore operations, 18-6 to 18-8
- Right to transfer, by landowner, 57-6
by lessee, 57-7
- Ring-joint gasket, 3-28 to 3-32
- Ring-type plunger, 8-6
- Ring-type tester, 5-16, 5-17
- Riser analysis, ball-joint angle, 18-17
introduction, 18-16, 18-17
pipe collapse, 18-17
pipe stress, 18-17
sheave friction, 18-17
tensioner-line angle, 18-17
top angle, 18-17
top tension, 18-17
- Riser angle, 18-13
- Riser pipe, 3-38, 3-39
- Riser-pipe collapse, 18-17
- Riser-pipe stress, 18-17
- Riser tensioner, 18-11, 18-13 to 18-15
- Riser-tensioner systems, 18-17
- Riser-top angle, 18-17
- Riser-top tensions, 18-4, 18-16 to 18-18
- Risk factor, 41-3
- RMS efficiency of motor, 10-25
- Robinson field, Illinois, 46-15
- Robots, 3-36
- Rock bulk compressibility, 26-7
- Rock compaction, 26-7
- Rock composition, 51-5
- Rock compressibility, 26-7, 26-9, 37-2, 37-3, 37-6, 37-10
- Rock Creek field, Texas, 41-4
- Rock-Eval IITM (RE), 52-10, 52-11
- Rock flow model, 44-20
- Rock/fluid interactions, 47-20, 47-21
- Rock-frame compressibility, 51-4
- Rock-frame incompressibility, 51-49
- Rock-grain compressibility, 51-4
- Rock matrix, 51-39, 51-49
- Rock-matrix compressibility, 26-7
- Rock-matrix density, 50-26
- Rock mechanics, 55-1
- Rock properties, 39-1, 43-7
- Rock quality designation (RQD), 51-43, 51-44
- Rock tortuosity, 26-28
- Rock wettability alteration, 44-39, 44-40
- Rocking a well, 5-54
- Rockwell C scale, 9-1
- Rockwell hardness, 2-2, 2-37
- Rocky Mountain area, 24-8, 27-14, 27-15, 28-11, 28-18, 41-1, 47-3
- Rocky Mountain method, 49-27, 49-31, 49-32
- Rod-and-plunger system, 6-10, 6-16
- Rod and pump data, 9-6, 9-7
- Rod grades, 9-5
- Rod-pumped-well control, 16-11
- Rod pumps, 8-1 to 8-4, 8-8
- Rod stress, 9-2
- Rod string design, 9-5
- Rollover fault closures, 29-3
- Romania, 46-3, 46-4, 46-15, 46-18, 46-28, 46-29
- Rose equation, 28-3
- Rosin, 44-45
- Rotameter, 13-45, 13-48
- Rotary converter, 10-36
- Rotary cores, 26-20, 26-21
- Rotary floating drilling vessel, 18-2
- Rotary gas meter, 16-6
- Rotary gas separator, 7-5, 7-6
- Rotary inducer-centrifuge, 7-5
- Rotary pumps, 15-15
- Rotary-vane positive-displacement meter, 32-11
- Roughness factors for new pipe, 15-2, 15-3
- Round-thread casing and coupling, 2-1, 2-5, 2-7, 2-9, 2-11, 2-13, 2-15, 2-17, 2-19, 2-28, 2-30, 2-57, 2-58, 2-61, 2-64
- Round-thread tubing form, 2-64
- Rounding rules, 58-5 to 58-7
- Royalties, definition, 41-1
- Royalty, acres, 57-7
clause, 57-5, 57-10
deeds, 57-6, 57-7
gas, 57-10
interest, 57-5 to 57-8
oil, 57-5
overriding, 57-5, 57-7 to 57-10
- Royalty interests, definition, 41-1 to 41-3
- Rubber lining coating, 11-6
- Rubble pile, 18-39
- "Rubin," computer subordinate routine, 17-6
- Rugosity, 51-33
- Rule of capture, 57-1, 57-2
- Rules for writing metric quantities, 58-11
- Rules of thumb, for critical-flow-pressure ratio, 13-37
for liquid recovery, LTS system, 14-5
for regulators, 13-55
for sizing transformers, 10-31
for sucker-rod length and cycle strokes, 9-3
of performance history required, 37-3
of water-handling equipment, 44-46
of when gas-condensate system exists, 39-2
- Run tickets, 17-7
- Running, and pulling sucker rods, 9-10
BOP, 18-18 to 18-20
20-in. casing, 18-18
30-in. casing, 18-18
- Rupture disk, 12-39, 12-40
- Ruska universal permeameter, 26-17
- Russell grain-volume method, 26-3, 26-4
- R_w/R_o method for water saturation, 49-28
- Rylon®, 4-5
- Ryton, 7-3
- S
- S. El Mene field, Venezuela, 24-13
- S-plot (cumulative logarithmic diagram), 56-6
- S-wave critical angle, 51-12
- S-wave velocity, 51-11, 51-37
- S-wave velocity ratio vs. porosity, 51-9
- S-waves, 51-2, 51-3, 51-5, 51-11, 51-36, 51-44, 51-47
- Saccharoidal, 29-8, 29-9
- Sacrificial anodes, 11-6
- SAE 20 lubricating oil, 25-4
- Safe nominal interest rate, 41-21, 41-22, 41-24
- Safety and pollution prevention equipment (SPPE) certificate holder, 3-39
- Safety controls of engines, 10-17
- Safety factor of Goodman diagram, 9-9
- Safety factor of motor temperature, 10-26
- Safety factors for casing strings, collapse strength, 2-1 to 2-3, 2-32, 2-34, 2-35
internal yield pressure, 2-1, 2-2, 2-32, 2-34, 2-35
joint strength, 2-1, 2-2, 2-32, 2-34, 2-35
pipe-body yield strength, 2-1, 2-2, 2-34, 2-35
- Safety factors, gas lift, 5-3, 5-24, 5-27
- Safety factors in continuous-flow gas-lift installation design, 5-22
- Safety factors, manufacturers', 3-1
- Safety features for oil and gas separators, 12-39
- Safety head, 12-39, 12-40
- Safety relief valves, 12-40
- Safety shut-in system, 3-19
- Safety shut-in valves, 16-3, 16-4, 16-11
- Safety shutdown system, 13-58, 18-43, 18-44
- Safety systems offshore, 18-47, 18-48
- Safety valves, 6-48, 6-49, 18-28, 18-34
- Sage and Olds correlation, 21-11
- Salem unit, Illinois, 44-41
- Sales contracts, 40-1
- Sales gas, 14-6 to 14-8, 14-12, 14-14
- Sales-gas line, 14-5, 14-11, 14-15, 14-18, 14-20, 14-21
- Sales-gas pressure, 14-3
- Sales-gas volumes, 39-10
- Sales method of oil and gas, 36-2
- Salient gradient floods, 47-15
- Salinity, definition, 47-2
effect on IFT, 47-20
from representative oilfield brines, 47-3
general, 47-14
of brine, 19-26, 47-3 to 47-5, 47-10, 47-11, 47-13, 47-21
of ice, 18-39
of injection water, 44-2, 47-22
of oilfield waters, 24-13, 24-20
- Salt-bath heater, 14-14, 14-15
- Salt content, 19-26, 24-14
- Salt deposition in flow string, 33-20, 33-21
- Salt domes, 24-7
- Salt intrusions, 29-5
- Salt plugs, 29-5 to 29-7
- Saltwater disposal projects, 24-3
- Saltwater sources, 44-41 to 44-43
- Salty muds, 49-20, 49-25, 49-27
- Salvage value, 41-3, 41-11, 41-13
- Sample collection and evaluation, gas-condensate reservoirs, dewpoint and P/V relations, 39-7
recombination of separator samples, 39-6
simulated pressure depletion, 39-7 to 39-10

- Sample containers, 24-4
- Sample, Control and Alarm Network (SCAN), 46-20
- Sample description tabulation, 24-5
- Sample lag time, 52-8
- Sample logs, 41-8
- Sample procedure, oilfield waters, containers, 24-4, 24-5
- field-filtered sample, 24-4
- for determining unstable properties or species, 24-4
- for sample containing dissolved gas, 24-3
- for sampling at wellhead, 24-3, 24-4
- for stable-isotope analysis, 24-4
- for tabulation of sample description, 24-5
- sampling at flowline, 24-3
- Sampling crude oil, 17-1 to 17-8
- Sampling crude-oil emulsions, 19-6
- Sampling natural-gas fluids, 17-7
- Sampling of petroleum and petroleum products, 17-5
- Sampling of produced waters, drillstem test, 24-3
- procedure for, 24-3 to 24-5
- Sampling of water, 44-43
- Samson post, 10-3, 10-4
- San Ardo field, California, 46-4, 46-15, 46-18
- San Joaquin Valley, California, 46-23
- San Miguel-4 tar sand, Texas, 46-26
- Sand bridging, gas lift, 5-38
- Sand-by-sand correlation, 36-7
- Sand consolidation treatments, 56-3 to 56-5
- Sand control, an acoustic log use, 51-45, 51-46
- clay control, 56-5, 56-6
- consequences of sand production, 56-3
- formation analysis, 56-3
- formation properties, 56-2
- formation sampling, 56-3
- geology of sand formation, 56-2
- gravel packing, 56-8, 56-9
- gravel selection, 56-6, 56-7
- methods of, 56-3
- properties of sand formation, 56-2
- screen selection, 56-6, 56-7
- well preparation, 56-3 to 56-5
- why sand is produced, 56-2, 56-3
- Sand counts, 49-22, 49-25
- Sand filters, 15-20, 15-21, 16-14
- Sand formation properties and geology, 56-2
- Sand-grain volume (GV), 26-3 to 26-5, 26-7
- Sand-grain volume, laboratory measurement, 26-3 to 26-5
- Sand-jetting and drain systems, 19-20
- Sand line, 49-10
- Sand model, for radial flow, 26-13
- for rectilinear flow, 26-11
- for vertical flow, 26-12
- Sand pans, 19-29, 19-30
- Sand pressure filters, 44-47
- Sand production, consequences of, 56-3
- Sand removal, 19-29
- Sandblasting, 46-21
- Sandface plugging, 39-25
- Sandface pressure, 34-28
- Sandia Laboratories, 30-7
- Sanding, 46-21
- Sandpacks, 26-11, 26-12
- Sandstone acidizing, 54-4
- Sansinena field, California, 6-24
- Santa Barbara Channel, California, 18-1, 18-2
- Santa Fe Springs field, California, 29-2
- SARABAND log analysis, 49-37
- Saskatchewan, Canada, 24-8, 24-12, 51-32
- Satellite navigation (SAT NAV) systems, 18-18
- Satter's equation, 46-6
- Saturated depletion-type oil reservoirs, 40-8 to 40-12
- Saturated liquid, definition, 22-21
- Saturated-oil viscosity, 22-15
- Saturated steam, 46-5, 46-6, 46-40
- Saturated systems, oil formation volume factor for, 22-10, 22-11
- Saturated systems, oil-viscosity correlations, Beal's for dead oil, 22-14
- Beggs and Robinson, 22-15, 22-16
- Chew and Connally, 22-14, 22-15
- Saturated water content of natural gas, 25-11 to 25-15
- Saturation change with frontal advance, 38-15
- Saturation curves, 23-1, 23-2
- Saturation exponent, 26-31
- Saturation gradient, 28-3
- Saturation measurements, 28-4 to 28-7
- Saturation method of determining porosity, 26-6
- Saturation pressure, 14-10, 21-11, 21-13 to 21-15, 22-1, 22-5, 22-21
- Saturation vapor pressure, 17-7
- Saudi Arabia, 12-39
- Saunders-type valve bodies, 16-3
- Saybolt seconds furol (SSF), 22-13, 22-14
- Saybolt seconds universal (SSU), 22-13
- Scale or scaling, 5-25, 5-53, 6-48, 6-55, 9-2, 11-13, 19-1, 19-2, 19-26, 19-29, 19-32, 56-1
- Scale deposits, 44-43, 56-2
- Scale trap, 13-59
- Scaled physical models, 45-10
- Scaled porous models, 44-17, 44-34
- Scales, resistivity, 49-21
- Scaling laws, 46-13
- Scanning electron micrographs (SEM), 51-8 to 51-11
- Scanning electron microscope, 46-21
- Scanning-electron-microscope analysis, 56-3
- Scattered neutron, 50-9, 50-10
- Schilthuis equation, 37-5
- Schlumberger, 49-2, 49-36, 49-37, 51-18, 51-21, 51-24, 51-25, 51-41
- Schlumberger Borehole Compensated Sonic log, 51-24
- Schlumberger Ltd., 53-19
- Schlumberger neutron porosity (SNP), 50-29
- Scholem Alechem field, Oklahoma, 6-24
- Schoonebeek field, Netherlands, 46-3, 46-14
- Scintillation detector, 50-12, 50-13
- Scoring, 6-50
- Screen-factor devices, 47-5
- Screen selection, 56-7, 56-8
- Screen specifications and sizes, 56-9
- Screening guides and parameters, 47-1, 47-22
- Screening guides, thermal recovery, 46-13, 46-14
- Screening thermal prospects, 46-12 to 46-14
- Screenout, 56-8
- Screens and filters, jet pumps, 6-48
- Scrubbers, 6-33, 12-1, 12-2, 12-10, 12-13, 13-58, 39-26
- Scurry field, Texas, 29-4
- Sea ice, 18-38, 18-39
- Seafloor manifold, 18-33, 18-35
- Seal Beach field, California, 6-24
- Sealing bores, 6-3, 6-4
- Sealing element of packers, 4-5
- Search angle, dipmeter, 53-10, 53-11
- Seating nipple, 5-3
- Seating shoe, 6-3
- Seawater, 24-17, 24-18, 24-20, 24-21
- Seawater-injection projects, 44-37
- Second-stage separator gas, 39-9, 39-10, 39-14
- Secondary/backup power, 18-45
- Secondary drainage, 28-12
- Secondary electrical systems, 10-29, 10-30, 10-32
- Secondary functions of oil and gas separators, maintain liquid seal, 12-5
- maintain optimum pressure, 12-4
- Secondary imbibition, 28-12
- Secondary porosity, 26-1, 29-3, 36-6, 51-31, 51-33
- Secondary recovery, 16-2, 18-44, 24-2, 24-3, 29-7, 40-4, 41-9, 43-1, 44-45, 45-9
- Secondary-recovery methods, 44-1 to 44-3
- Secondary-seal assembly, 3-6 to 3-8
- Secondary separation in separator, 12-19
- Secondary skin-effect correction, 49-16, 49-17
- Secondary stratigraphic traps, 29-5
- Secondary voltage, 10-29
- Section gauge log, 49-25
- Securities and Exchange Commission (SEC), 40-1, 40-2, 41-3
- Sediment in crude oil by centrifuge method, 17-5
- Sediment in crude oils by extraction method, 17-5
- Sediment in fuel oils by extraction method, 17-5
- Sedimentary features, dipmeter patterns in, 53-13
- Sedimentary rock porosity, 26-7
- Sedimentation flume capacity, 15-18, 15-19
- Seeligson field, Texas, 39-3
- Segmental orifices, 13-45, 13-48
- Segments of circles, table, 1-31, 1-32
- Segments of spheres, table, 1-33
- Segregation, complete, 37-14, 37-15
- Segregation, in gas-injection performance predictions, 43-16
- Seismic analyses, 18-27
- Seismic compressional surveys, 51-28
- Seismic exploration, 51-10
- Seismic interpretation, 51-28, 51-29
- Seismic mapping, 18-18
- Seismic studies, 18-5
- Seismic velocities, 58-25
- Seismograph Service Corp., 51-1
- Seismologists, 57-8
- Seisviewer®, 51-27
- Selecting appropriate P/E ratio, 6-28
- Selecting motor size, 10-21
- Selecting mud-logging service, 52-28 to 52-30
- Selecting pumps and drivers, 15-14 to 15-18
- Selection, of backpressure valves, 3-8
- of casing hangers, 3-6
- of gas-lift installation and equipment, 5-3
- of gas-lift port size, 5-28
- of independently screwed wellhead equipment, 3-39
- of intermediate casing heads, 3-7
- of lowermost casing heads, 3-2 to 3-5
- of materials for wellhead service, 3-36, 3-37
- of multiple-completion tubing hangers, 3-16, 3-17
- of storage-tank location, 11-11
- of subsurface safety valves, 3-27, 3-29, 3-31

- of surface closing pressure, gas-lift valves, 5-44
- of surface safety valves, 3-27
- of tubing hangers, 3-9
- of waterflood plants, 44-45
- Selection and application of gas scrubbers, 12-35
- Selection and application of separators,
 - horizontal, 12-35
 - spherical, 12-35
 - vertical, 12-35
- Selection data and methods, electric submersible pumps (ESP), 7-9 to 7-12
- Selective adsorption systems, 14-10 to 14-13, 14-15, 14-17
- Self-contained pressure gauges, 30-1 to 30-3
- Self-contained thermometers, 31-1, 31-2
- Self-generating mud acid (SGMA), 54-4
- Self-operated controller, 13-50
- Semblance, 51-25
- Semiconductor sensor element, 52-7
- Semidiesels, 10-15, 10-16
- Semilog straight-line solution, 35-4, 35-8, 35-16
- Semipermanent packers, 4-1, 4-3, 4-6
- Semiquartzitic sandstone, 26-6
- Semisteady state, 37-21, 37-22
- Semisubmersible rig, 3-38, 18-2 to 18-7, 18-13, 18-21, 18-25, 18-34 to 18-36
- Sensible heat, 14-5, 14-10, 14-21
- Sensitivity analysis, 39-17
- Sensitivity of material-balance results, 37-13 to 37-17
- Sensitivity of regulators, 13-54, 13-55
- Sensitivity of variable, 13-50
- Sensitivity studies, 37-16 to 37-18, 48-14
- Sensitivity to shock, BHP gauges, 30-5, 30-7
- Sensitivity to vibration, BHP gauges, 30-5 to 30-7
- Sensor coils, 53-22, 53-23
- Sensor sub, 53-2
- Sensors, 3-18, 3-19, 3-31, 3-33, 3-34
- Separated fluids, estimated quality of,
 - crude oils, 12-13
 - gas, 12-15
 - gas from scrubber, 12-15
 - measuring, 12-15, 12-16
 - water, 12-15
- Separating foaming crude oil, 12-6, 12-7
- Separation of water from oil, 12-3, 12-4
- Separator, design, 12-21 to 12-32, 23-1
- Separator high-level float control, 16-9
- Separator pressure, 12-16, 12-17, 12-22, 12-23, 12-25 to 12-34, 12-36 to 12-39, 39-9
- Separator temperature, 12-17, 12-22, 12-23, 12-25, 12-26, 12-28 to 12-30, 12-36, 12-37, 12-40, 12-41
- Separators: see oil and gas separators
- Sequence-restart timer, 10-27
- Sequential-piloted hydraulic control, subsea, 18-51, 18-52
- Sequestering agents, 44-45, 54-7, 54-9
- Service company nomenclature (table), 49-2
- Service facilities, 39-24
- Service factor, of motor, 10-25, 10-26
- Service factor, of steel sucker rods, 9-4, 9-5
- Settled solids removal, 19-29
- Settling, in breaking foaming oil, 12-7
 - in water treating, 44-46
 - to remove gas from oil in separators, 12-13
- Settling space, in emulsion treating, 19-8
- Settling tanks, 6-59, 19-18 to 19-21
- Settling time, 11-13, 12-3, 19-9, 19-15
- Seven-point, hexagonal-gridblock scheme, 48-11
- Seven-spot pattern, 43-2, 44-13, 44-14, 44-16, 44-17, 44-21, 44-23, 44-34, 46-17, 46-18, 46-26
- Severance of minerals, 57-2
- Severance tax, 39-27, 41-9, 41-12, 41-15
- Shaker screen, 52-8, 52-19
- Shale baseline, 49-10
- Shale bulk density, 52-19
- Shale compaction, 24-20
- Shale-data log, 52-20
- Shale distillation, yield, 58-29
- Shale effect on neutron porosity, 50-31 to 50-33
- Shale effects on compressional and shear velocities, 51-34
- Shale factor, 52-21, 52-22
- Shale index, 49-38, 49-39
- Shale intercalations, 36-6
- Shale-outs, 44-2, 44-39
- Shale point, 50-24, 50-34
- Shale/sand ratio, 36-4
- Shale stringers, extent of, 36-6
- Shale transit time, 51-39
- Shallow dual laterolog (LLS), 49-19
- Shallow-hazard surveys, 18-5
- Shallow laterolog (LLS), 49-20
- Shallow MICROSL (MSFL), 49-20, 49-22, 49-28
- Shaly (dirty) formations, 49-4
- Shaly sand, 26-31, 50-34, 51-34, 51-35
- Shannon Pool field, Wyoming, 46-14
- Shape factor, 6-57, 26-18, 35-4, 35-5, 35-7, 35-12, 35-16, 37-19, 37-20
- Shape functions, 32-5
- Sharing arrangements, 41-15
- Sharp-edged orifice plates, 13-36, 13-37, 13-45
- Sharp-edged valve seat, 5-14, 5-15, 5-20, 5-35, 5-40
- Shear bulk modulus, 58-34
- Shear-history method, for friction losses in fluids, 55-5, 55-6
- Shear modulus, 51-1, 51-4, 51-37, 51-43, 51-44, 51-49
- Shear rams, 18-15
- Shear rate, in fluids, 55-5
- Shear rate, in oilfield emulsions, 19-6
- Shear-rate/viscosity relations, 47-4
- Shear-thinning fluid, 47-4, 47-9
- Shear-wave amplitude, 51-46
- Shear-wave attenuations, 51-2, 51-6
- Shear-wave logging, 51-24
- Shear-wave transit (travel) times, 51-5, 51-15, 51-24, 51-25 to 51-27, 51-30, 51-31, 51-35, 51-43
- Shear-wave velocities, 51-2, 51-4 to 51-9, 51-12 to 51-14, 51-24, 51-25, 51-28, 51-30, 51-34, 51-35, 51-37, 51-38, 51-43
- Shear waves, 51-2, 51-3, 51-12 to 51-14, 51-24, 51-25, 51-27, 51-30, 51-35, 51-44
- Shearing stress, 22-1, 22-13
- Sheave friction, 18-17
- Shedding, 13-48
- Shelf carbonates, 36-6
- Shell breccia, 29-8, 29-9
- Shell group, 46-13
- Shell Oil Co., 16-12, 46-4, 46-15, 46-16, 46-18, 46-24, 46-25
- Shipper's ton, 1-70
- Ships and ship-shaped vessels, 18-5, 18-7, 18-13, 18-21, 18-34, 18-36
- Shock load, 10-28
- Shock mobility ratio, 47-1
- Shoestring sands, 29-4, 29-9
- Shop-welded tanks, 11-1, 11-5, 11-9
- Shoreline sandstone, 36-4
- Short or net ton, 1-70
- Short-cycle units, 14-10, 14-13, 14-17
- Short-duration cycling, electric submersible pump (ESP), 7-15
- Short lateral, 49-11
- Short normal, 49-11, 49-14, 49-26, 49-27, 49-29 to 49-31
- Short-normal resistivity, 53-2, 53-4
- Short-normal resistivity log, 51-26, 51-46
- Short-spaced acoustic logs, 51-24
- Short-thread casing, 2-5, 2-7, 2-9, 2-11, 2-13, 2-15, 2-17, 2-19, 2-29, 2-57, 2-64
- Shoulder-bed corrections, 49-11, 49-21
- Shrinkage,
 - by liquid recovery, 39-23
 - definition, 22-21
 - factors, 22-20, 44-3
 - of liquid, 32-10, 32-15, 33-14
 - of oils, 19-7, 37-1, 37-6, 37-22, 37-23, 43-1
 - test, 39-6
- Shrouded configuration application, electric submersible pump (ESP), 7-1 to 7-3
- Shuttle ball, 13-48
- Shuttle tankers, 18-36
- SI,
 - angle unit, 58-5
 - base quantities and units, 58-3, 58-9, 58-10, 58-21, 58-23
 - bending moment, 58-5, 58-34
 - derived units, 58-2, 58-4, 58-10, 58-11, 58-21, 58-23
 - energy unit, 58-5, 58-11, 58-23, 58-24, 58-32
 - international system of units, 58-2 to 58-20
 - metric system of units, 17-7, 58-1 to 58-20
 - non-SI metric units, 58-10
 - prefixes, 58-4, 58-12, 58-13 to 58-20
 - pressure unit, 58-5, 58-11, 58-23 to 58-25, 58-28, 58-29
 - stress unit, 58-5, 58-11, 58-23, 58-34
 - supplemental units, 58-2, 58-3
 - temperature units, 58-5, 58-23, 58-24, 58-28
 - time units, 58-5, 58-22, 58-23, 58-27
 - torque units, 58-5, 58-34, 58-38
 - unit prefixes, 58-3
 - unit symbols, 58-3, 58-4, 58-15 to 58-20, 58-22
 - units, 58-9 to 58-11, 58-26 to 58-38
 - volume units, 58-5, 58-23
- Side-pocket mandrel, 3-35, 5-2, 5-53
- Side-scan sonar, 18-5
- Side-static method of gas metering, 13-37
- Side-well producing cuts, 44-24, 44-25
- Sidewall cores, 26-20, 26-21
- Sidewall epithermal neutron device, 50-20
- Sidewall neutron logs, 51-33
- Sidewall neutron porosity, 51-19
- Sidewall-pad tool, 49-22
- Sidewall vs. conventional core analysis,
 - comparative data, 27-8
- Sidum steam-injection pilot, Arkansas, 46-26
- Sieve analysis, 56-3, 56-6, 56-7
- Siggins field, Illinois, 47-9
- Signal Oil Co., 46-22, 46-23
- Significant digits, 58-6, 58-9
- Silica, 19-5, 24-4
- Silica flour, 46-19
- Silica gel beads, 14-21
- Silicate-control agents, 54-7

- Silicon-controlled rectifiers (SCR's), 18-45
 Silicone, as surface tension reducer, 12-13
 Silicone-controlled rectifier relays, 7-6
 Silver, 50-12
 Silverdale field, Alberta, Canada, 46-18, 46-21
 Simple harmonic motion, 51-2, 51-3
 Simple interest, 41-25
 Simpson's rule, 34-24, 34-26, 40-4, 40-5
 Simulated pressure depletion, 39-7 to 39-10
 Simulation and simulator studies, 37-21, 37-22, 40-1
 Simulation models, consideration in applications, fluid- and rock-description data, 48-8, 48-9
 history matching, 48-9
 model grid selection, 48-7, 48-8
 of complex reservoir, 44-31, 44-32
 type selection, 48-7
 Simulation steps, 36-10
 Simulation technology, 48-13 to 48-17
 Simultaneous formulations, 48-14
 Sinclair, 47-22
 Singapore, 12-39
 Single-acting downhole unit, 6-10, 6-20
 Single-acting pump, 6-8 to 6-10, 6-18 to 6-20
 Single- and two-phase inflow-performance-relationship (IPR) equation, 34-33, 34-34
 Single-carbon-number (SCN) groups, 39-11
 Single-component phase diagrams, 23-1, 23-2
 Single-contact miscibility, 48-5 to 48-7
 Single-control line valve, 3-27, 3-29
 Single-cylinder engines, 10-15
 Single-element fuses, 10-28
 Single-element simulation, 48-7
 Single-element unbalanced gas-lift valve, 5-12 to 5-15
 Single-horsepower rating, 10-25
 Single-pattern simulation studies, 48-8
 Single-payment present-worth factor, 41-25
 Single-phase flow, 28-2, 34-2, 34-3, 34-31, 34-33, 34-36, 34-38, 34-45
 Single-phase fluid, constant compressibility, 35-3
 Single-phase motors, 10-21
 Single-phase transformer, 7-6, 7-7, 10-30, 19-25
 Single-phase turbulent flow, 34-37
 Single-piece jacket, 18-23
 Single-point mooring (SPM), 18-2, 18-34
 Single-ported valves, 13-55, 13-57
 Single satellite wells, 18-31, 18-32
 Single-seal pumps, 6-39
 Single-seated valve, 13-55
 Single-shot surveys, 53-3
 Single-stage desalting, 19-26
 Single-tubing-string completions, 3-13
 Single-welded butt joints, 12-40
 Single-well coning studies, 48-14
 Single-well depletion reservoir, 35-1
 Single-well power unit, 6-60, 6-61
 Single-well systems, 6-60 to 6-63
 Single-wing well manifold, 16-11, 16-12
 Singleton field, Nebraska, 44-40, 47-22
 Sinking fund, 41-16, 41-21, 41-22
 Sinking fund, table, 1-65
 Sinusoidal alternating-current field, 19-13
 Siphon breaker, 6-62
 Siphon strings, 33-21
 Site conditions and considerations offshore, expected environment, 18-4
 introduction, 18-3
 logistics, 18-4, 18-5
 seismic and other location studies, 18-5
 water depth, 18-4
 Site survey offshore, 18-5
 Six-pole induction motor, 10-23
 Six-spot pattern, 46-17
 Sizes, of casing hanger, 3-6
 of casing head, 3-7
 of meter and meter run, 13-36
 of separator, estimating, 12-21 to 12-25
 of tubing hanger, 3-9
 of tubing heads, 3-8
 Sizing and capacities of separators, capacities of spherical separators, 12-30, 12-31
 capacity curves for vertical and horizontal separators, 12-27 to 12-29
 computer sizing of separators, 12-25 to 12-27
 equation for gas capacity, 12-23
 equation for sizing, 12-23 to 12-25
 gas velocity, maximum, 12-22
 horizontal separator sizing, 12-30
 vertical separator sizing, 12-29
 Sizing, curves, 13-53
 equations for plate coalescers, 15-24
 instructions, ultrahigh-slip motor, 10-22
 of waterflood plants, 44-45
 oil and gas separators, 12-25 to 12-27, 12-32
 pumping units, 10-7
 Skewness, definition, 26-2
 Skim piles, 15-23, 15-26, 15-27, 15-30
 Skim tanks and vessels, 15-23, 19-28
 Skimming, 19-23
 Skin-effect correction, 1L, 49-17
 Skin effects, 30-10, 30-14, 32-5, 35-4, 35-7, 35-11, 35-14, 35-15, 35-19, 40-27, 49-16
 Skin factor, 33-11, 37-20
 Skirt piles, 18-3, 18-22, 18-23
 Sleeve bearings, 13-48
 Slide-rail motor mounts, 10-19
 Sliding-sleeve valve, 3-35
 Slim-hole coupling, 9-5
 Slim-hole-coupling derating factor, 9-5, 9-8
 Slim-tube displacement tests, 39-16
 Slim-tube displacements, 48-9
 Slip joints, 18-13, 18-20
 Slip of motor, 10-23, 10-24
 Slip-on socket connection, 3-3
 Slip-type tubing hanger, 3-39
 Slip velocity, 34-27, 34-38
 Slip-weld casing hanger, 3-6
 Slipform methods, of gravity platform construction, 18-23
 Slippage effect on energy losses, gas-lift wells, 34-37
 Slippage-loss equation, 8-5
 Slippage, past pump plunger, 8-4 to 8-6
 Slocum field, Texas, 46-15, 46-18, 46-26, 46-27
 Slope of backpressure curve, 33-5
 Slope of buildup curve, 30-10, 30-12
 Sloping-sided structure, 18-42
 Sloss field MP pilot, Nebraska, 47-18
 Sloss field, Nebraska, 46-14, 46-15, 46-18, 46-21, 46-30, 46-33
 Slow-speed engines, 10-14 to 10-19
 Slowing-down length, 50-11, 50-19 to 50-21, 50-29 to 50-32
 Slowness time coherence, 51-25
 Sludge, 19-11, 19-12, 19-32
 Sludge tank, 44-47
 Sludging of oil, 10-13
 Slug flow, 34-36 to 34-40
 Slug-mist transition flow, 34-36, 34-37, 34-40
 Slug-size retention ratio, 47-17
 Slugging, 12-23, 12-35, 12-38, 39-26
 Slugs of well fluids, 12-1, 12-20, 12-32
 Smackover field, Arkansas, 46-15, 46-24 to 46-26
 "Smart" end devices, 16-2
 Smectite-rich clay, 52-21
 Smoke point, 21-7, 21-9
 Snap action, control mode, 13-49, 13-51 to 13-53, 13-56
 Snell's law, 51-3, 51-12
 Sniffer, 52-6
 Soaking, in steam stimulation, 46-9
 Soap-type gels, 55-5
 Soave modification of Redlich-Kwong equation, 20-8, 23-13
 Soc. of Automotive Engineers (SAE), 10-12
 Soc. of Petroleum Engineers (SPE), joint committee member on reserve definitions, 40-2
 SPE letter and computer symbols std., 59-2 to 59-70
 SPE metric unit standards, 58-21 to 58-39
 SPE papers on relative permeability, 28-12
 SPE-preferred metric unit, 58-21, 58-24 to 58-38
 SPE Reprint Series, 44-36
 Soc. of Professional Well Log Analysts (SPWLA), 52-30
 Soda ash, 14-22
 Sodium aluminate sand-consolidation technique, 46-21
 Sodium chloride (NaCl), as water contaminant, 24-16
 Sodium chloride conversion chart, 49-3
 Sodium dodecyl sulfate, 47-7
 Sodium hydroxide, 44-40, 44-42, 47-18, 54-3
 Sodium iodide (NaI), detector, 50-12 to 50-16, 50-23, 50-35
 Soft-packed plungers, 8-6
 Soft-start capability, 7-9
 Solid-desiccant dehydration unit, 14-20, 14-22
 Solid-head compression packer, 4-2, 4-8
 Solid-head tension packer, 4-2, 4-8
 Solid hydrates, 25-1, 25-3, 25-19
 Solid-propellant gas generators, 18-16
 Solid-state detector, gamma rays, 50-12, 50-14, 50-23, 50-35
 Solid-state electrical detector, 52-7
 Solid-state electronic components, 16-9
 Solid-state electronics, 16-1
 Solid-state switchboards, 7-6
 Solids in brine, 14-4
 Solids wetting, 19-9, 19-10
 Soluble-sulfide analyzer, 52-7
 Solubility, definition, 45-1
 of bentonite in mud-removal acid, 54-4
 of CO₂ in water, 25-15
 of methane in water, 25-16
 of natural gas in water, 25-17
 of propane in water, 25-17
 of silica in mud-removal acid, 54-4
 of water in refrigerants, 14-10
 of water in various hydrocarbons, 25-16
 Solubilization parameter or ratio, 47-13, 47-14, 47-20
 Solutes concentration in aqueous phase, 25-16
 Solution cavities, 26-6
 Solution gas, definition, 12-3
 in oil reservoirs, 40-6, 40-13
 increases as temperature decreases, 22-10
 release of, 22-21
 Solution-gas drive, definition, 22-20, 40-8
 Solution-gas-drive process, 42-5

- Solution-gas-drive reservoirs,
 basic data required, 37-3 to 37-5
 calculation of reservoir pressure, 35-8
 comparison of Turner's and Tracy's methods, 37-10
 definitions, 37-1
 insights from simulator studies, 37-22
 introduction, 37-1
 material-balance calculations using Muskat and Taylor's method, 37-10 to 37-13
 material-balance calculations using Tracy's method, 37-7 to 37-10
 material-balance equation, 37-5, 37-6
 material-balance equation as a straight line, 37-6, 37-7
 models, types used, 37-2
 nomenclature, 37-26, 37-27
 nonideal behavior of, 35-3
 performances, 37-1, 37-2
 production rate and time calculations, 37-17 to 37-21
 references, 37-27
 sensitivity of material-balance results, 37-13 to 37-17
 single empirical IPR equation for, 34-31
 tank-type material balance, basic assumptions of, 37-2, 37-3
 volatile-oil-reservoir performance predictions, 37-22 to 37-26
- Solution-gas production rate, 37-11
- Solution GOR, definition, 22-1, 22-21, 37-14 to 37-18, 37-21, 37-22, 40-6, 40-8, 40-9, 40-13, 46-34, 46-36
- Solution GOR for saturated oils,
 Lasater correlation, 22-9
 Standing correlation, 22-9
 Vasquez and Beggs correlation, 22-9
- Solution-mined caverns, 11-13
- Solution porosity, 29-8
- Solution techniques for math models, 48-16, 48-17
- Solvent breakthrough, 45-7
- Solvent extraction, 12-16
- Solvent extraction and distillation, 27-8
- Solvent-extraction effect, 46-4, 46-5
- Solvent override, 48-12
- Solvent slug, 45-2
- Sondes, 49-1
- Sonic fluid-level tests, 40-27
- Sonic level control, 16-5
- Sonic log and logging, 44-3, 49-15, 49-16, 49-25 to 49-27, 52-20, 52-27, 58-25
- Sonic meters, 13-49, 13-50
- Sonolog, 32-6
- Sonoloy, 30-7
- Sour corrosion, 3-36, 4-4
- Sour crude, 11-10
- Sour-crude tanks, 11-6
- Sour gas, 5-2, 10-16, 14-7, 14-21, 18-47
- Sour-water stripper correlations, 25-17, 25-18
- Sour-water systems, 25-16
- Source of hydrocarbon prospects, 57-8
- Source rock, definition, 24-19
- South America, 18-7
- South Belridge fireflood, California, 46-14, to 46-16, 46-18
- South Oklahoma field, 46-15, 46-16
- South Pass 27 field, Louisiana, 36-4
- South Sunshine field, Wyoming, 24-18
- Southeast Texas field, 47-22
- S.P. PacksTM, 19-12, 19-19
- Space, SI units for, 58-26, 58-27
- Spacer fluids, 56-4
- Spacing, definition, 49-12
- Spacing-factor gradient, 5-45
- Spacing factor, intermittent pressure gradient, 5-42, 5-43
- Spacing-load design, 5-48
- Spacing pressure differential, 5-29
- Spain, 58-20
- Sparker, 18-5
- Spatial gradient, 48-10
- Spatial truncation error, 48-7, 48-9 to 48-12
- Special alloy rods, 9-8
- Special-service structures, 18-25
- Specific conductivity, 39-20
- Specific entropy, 58-28
- Specific fuel consumption, 58-33
- Specific gravities of fluid columns, 6-22, 6-23
- Specific gravity (relative density), 20-4, 20-10
- Specific-gravity factor, 13-3, 33-14
- Specific gravity, increase with pressure, saltwater, 24-15
 of gas mixtures, 20-4
 of natural-gas mixtures, 17-7
 of salt solutions, 24-14
 vs. temperature for crude oils, 19-8
- Specific heat capacity, 58-28
- Specific heat ratio, 13-8, 13-13, 14-10, 39-24
- Specific heats, of mid-continent liquid oils, 21-6
- Specific-isopermeability map, 39-22
- Specific permeability, 28-1, 28-2, 28-13, 43-3, 43-5
- Specific productivity index (PI), 30-11, 32-4, 58-38
- Specific volume, gas-condensate system, 21-16, 21-17
 of oil, 22-4, 22-5
 of total fluids, 46-7
 units and conversions, 58-29
 vs. molality, 24-15
- Specification of reservoir rock and fluid description data, 48-8
- Specifications of coatings, 11-4
- Specifications of diesel fuel, 10-16
- Spectral fatigue analysis, 18-27, 18-28
- Spectral gamma ray device, 50-15, 50-16, 50-24
- Spectral gamma ray log, 50-25
- Spectrographic technique, qualitative emission, 24-5
- Spectroscopic gamma ray detection, 50-12
- Spectroscopic-quality gamma ray detectors, 50-15
- Speculative interest rate, 41-17, 41-21, 41-24
- Speculative nominal interest rate, 41-22
- Speculative nominal rate of return, 41-18, 41-22, 41-24
- Speculative rate of return, 41-21
- Speed factor, ultrahigh-slip motor, 10-22
- Speed reducer, 10-5
- Speed/torque curves, 10-24
- Speed variation of engines, 10-14, 10-17, 10-22
- Speed variation of motor, 10-24
- Spending time of acids, 54-4, 54-5, 54-8, 54-11
- Spent acid, 54-3 to 54-7, 54-9, 54-11
- Sperry Sun BHP gauge, 30-4
- Spheres and spheroids, measurement and calibration, 17-3
- Spherical-cell model, 25-8
- Spherical separator, 12-1, 12-16 to 12-18, 12-21, 12-30 to 12-32
- Spherical-shell equations, 12-38
- Spherical three-phase oil/gas/water separator, 12-5
- Spherically focused log (SFL), 49-15, 49-18, 49-20, 49-27
- Spiking, 51-24
- Spindletop dome, Texas, 18-1, 24-7
- Splash-proof motor, 10-26
- Splash zone, 3-36
- Split detector, 53-18, 53-19
- Spontaneous ignition, 46-2, 46-19, 46-20
- Spontaneous potential (SP), 49-1
 baseline shift, 49-10
 current path, 49-8
 curve, 46-26, 49-11, 49-15, 49-19, 49-25, 49-38, 49-39, 51-16, 51-17, 51-22 to 51-24, 51-32, 51-46
 deflections, factors influencing shape and amplitude, 49-9
 effect of interstitial shales, 49-8
 effect of invasion, 49-8, 49-10
 geometric effect, 49-9
 in hard formations, 49-10
 in soft formations, 49-10
 influence of mud resistivity and hole diameter, 49-9
 origin, 49-7
 phenomena in highly resistive formations, 49-10
 pseudostatic, 49-9, 49-10, 49-28 to 49-30
 R_w determination from, 49-8
 static, 49-9 to 49-11, 49-28 to 49-30
- Spool adapter flange, 3-9
- Spraberry field, Texas, 40-2
- Spray zone, 3-36
- Spread-mooring patterns or system, 18-9
- Spreader or spreader plate, 6-58, 19-13, 19-18 to 19-20, 19-23 to 19-25, 19-29
- Spreader bar, 7-12
- Spring compression regulator, 13-54
- Spring-loaded gas-lift valves, 5-17, 5-19 to 5-21, 5-42
- Spring-loaded regulator, 13-54, 13-55, 13-57
- Spring-loaded valves, 6-49, 6-50, 13-55 to 13-57
- Spring-return fail-safe actuators, 18-15
- Spudding the well, 18-18
- Spurt loss, 55-4
- Square roots of certain fractions, table, 1-13
- Square roots of numbers, table, 1-2, 1-11 to 1-13
- Squares of numbers, table, 1-1 to 1-6
- Squeeze cement job, 56-4
- Squeeze cementing, 51-40
- Squeeze gravel packing, 56-8
- Squirrel-cage rotor, 7-3
- Stability analyses, 48-1
- Stability of BHP gauges, 30-5 to 30-7
- Stabilization of separated fluids, 12-21, 12-33, 12-35
- Stabilization period of wells, 32-15
- Stabilization process and unit, 12-33, 12-35, 12-42, 14-14, 14-15, 39-27
- Stabilized PI, 34-30 to 34-35
- Stabilizer, 14-5, 14-7, 14-8, 14-11, 14-14, 14-15, 14-17, 54-9, 55-6
- Stable emulsions, 19-2, 19-4 to 19-6
- Stable isotopes, sample for analysis, 26-4
- Stage-compression ratio, 39-24
- Stage-pressure ratio, 12-33
- Stage separation, 12-32 to 12-35, 14-14, 14-15
- Stage separator, 12-1, 12-17, 12-19
- Staggered line drive, 44-13 to 44-16, 44-22, 44-34, 44-36
- Stainless steel, 30-4, 56-7
- Stainless-steel filaments, 12-12
- Stainless-steel pipe, 15-11

- Standard conditions, definition, 22-21, 58-24, 58-25
- Standard deviation, 50-5
- Standard distribution of residuals, table, 1-61
- Standard lateral, 49-11
- Standard of weights and measures, definition of, 1-68
- Standards for mud logging, 52-30
- Standing and Katz charts, 20-9
- Standing correlations, 22-5, 22-8 to 22-11, 22-13, 22-14
- Standing valve, 5-50 to 5-53, 6-3, 6-31, 6-32, 6-48, 6-49, 6-51, 19-28
- Standing valve puller, 8-2, 8-4
- Standing's equations, 37-21
- Star diagram, 24-19
- Starter contactor for motors, 10-28
- Starters for engines, 10-19
- Startup of a project, 15-31
- Startup spike, electric submersible pump (ESP), 7-14
- Startup-spikes chart, ESP, 7-15
- Static-body test pressure, 3-1
- Static BHP, calculation of, 34-3 to 34-9
- Static drainage-area pressure, 30-9
- Static elastic constants, 51-4
- Static electricity, 11-13
- Static error, 13-50
- Static-fluid level, 5-25, 5-28, 5-37, 5-45, 5-46, 5-48
- Static fluids, 34-3
- Static-force balance equations, 5-17 to 5-19, 5-23
- Static geothermal surface temperature, 5-23
- Static injection-gas pressure, 5-37
- Static injection-gas pressure at depth, 5-3 to 5-6
- Static-load fluid gradient, 5-23, 5-25, 5-33, 5-48
- Static-load fluid gradient traverse, 5-45, 5-46, 5-49
- Static-load fluid traverse, 5-25, 5-28, 5-29, 5-33, 5-45
- Static pressure, downstream taps, 13-30 to 13-32
- Static pressure from partial buildup, 30-9, 30-10
- Static pressure, mean of up-and down stream taps, 13-33, 13-34
- Static pressure, upstream taps, 13-26 to 13-29
- Static self potential (SP), definition, 49-9
- determination of, 49-10, 49-28
- determination of R_{sp} , 49-10, 49-11
- Static stress, 18-17
- Static-type gas separator, 7-4, 7-5
- Static voltage level, 10-29
- Station-keeping systems, 18-2, 18-8 to 18-11, 18-16, 18-21, 18-24, 18-43
- Stationary-barrel rod pump, 8-3, 8-4, 8-8, 8-10
- Stationary-fluid methods, 28-8
- Stationary metering installation, 32-13
- Statistical mechanical theory, 25-2
- Statistical mechanics for adsorption approach, 25-5
- Steady-state analog techniques, 39-21
- Steady-state conductivity, 44-33
- Steady-state electrical model, 39-20
- Steady-state flow, 32-4, 32-5, 43-3, 43-4
- Steady-state injectivity, 44-33, 44-34
- Steady-state methods of relative-permeability measurement, 28-3 to 28-7, 28-14
- Steady-state radial flow, 34-31
- Steady-state relative-permeability apparatus, 28-4
- Steady-state relative-permeability methods, experimental procedure, 28-3, 28-4
- saturation measurements, 28-4 to 28-7
- Steam-breakthrough times, 48-12
- Steam-chest models, 46-9
- Steam displacement, 46-1, 46-23, 46-24
- Steam distillation, 46-4, 46-5, 46-15
- Steam-distillation drive, 46-24
- Steam flooding or floods, 19-28, 48-2, 48-5 to 48-8, 48-10, 48-11, 48-13, 48-17
- Steam generation and injection, 46-19
- Steam-generation water, 24-5
- Steam generators, 46-19, 46-20
- Steam injection, 42-6, 56-2
- Steam-injection model, 46-11, 46-12
- Steam-injection rate, steamfloods, 46-18
- Steam/oil ratio (SOR), 46-8, 46-14, 46-15, 46-23, 46-24, 46-27
- Steam placement, 46-22
- Steam properties (table), 46-40
- Steam quality, 46-5, 46-7, 46-13, 46-18, 46-22
- Steam recovery, mechanisms contributing to, 46-5
- Steam splitting, 46-22
- Steam stimulation, 46-1, 46-3, 46-4, 46-22
- Steam-stimulation operations, coinjection of gas and steam, 46-22
- Huntington Beach, 46-22
- Paris Valley, 46-22, 46-23
- Steam/tar ratio, 46-27, 46-28
- Steam/water equilibrium, 46-12
- Steamdrive, 46-1
- Steamflood, 46-1 to 46-4, 46-12 to 46-28
- Steamflood front in nine-spot pattern, 48-12
- Steamflood projects, 46-23 to 46-28
- Steamflooding operations, 25-1
- Steaming, 6-48
- Steel gravity oil-storage structure, 18-2
- Steel gravity structure, 18-2
- Steel island, 18-1
- Steel jackets, 18-2, 18-26
- Steel-laminated elastomers, 18-13
- Steel sucker rods, allowable loading, 9-4
- application, 9-2
- care and handling, 9-10
- coupling connections, 9-2
- failures, 9-8, 9-9
- manufacture of, 9-1
- predictive calculations, 9-2 to 9-4
- rod grades, 9-5, 9-8
- rod storage, 9-10
- running and pulling, 9-10
- service factor, 9-5
- unloading and loading, 9-10
- Steel template, 18-2
- Steelman field, Saskatchewan, Canada, 51-32
- Stem travel, 5-15, 5-19, 5-28
- Step length, dipmeter, 53-10, 53-11
- Step profile transit time, 51-20
- Stepdown transformer, 10-21
- Stereographic plots, 53-12
- Stevens porosimeter, 26-4 to 26-6
- Stiff diagram, 24-19
- Stiffness analysis, 18-26 to 18-28
- Stiles calculation, 44-7, 44-8
- Stiles method, 40-19, 40-20, 44-7
- Stimulation costs, 41-12
- Stimulation ratio, 55-4
- Stimulation results, fracturing, 55-4, 55-5
- Stock-tank gas, 39-9, 39-14
- Stock-tank measurement, 32-6, 32-7
- Stock-tank oil, definition, 22-21
- Stock-tank oil in place per acre-ft, 40-6, 40-8
- Stokes' law, 6-56, 6-57, 12-22, 15-18, 15-21, 15-26, 19-14, 19-15
- Stoneley waves, 51-12 to 51-14, 51-25, 51-27, 51-47
- Stopcock controller, 16-4
- Stopcocked wells, 32-15
- Storage capacity offshore, 18-7
- Storage facilities, 6-60
- Storage of sucker rods, 9-10, 9-13, 9-14
- Storage pressure of products, 11-12
- Storage size, evaporation losses, 11-12
- Storage-tank types, bolted-steel, 11-1, 11-3
- cone-bottom, 11-2
- field-welded, 11-2
- fixed-roof, 11-2
- flat-sided (non-API), 11-2
- floating, 11-2
- pipe, 11-2, 11-4
- welded-steel, 11-1
- Storm chokes, 13-57
- Straight-line extrapolation, 40-31, 40-32
- Straight-line relationship, 39-25
- Straightening vanes, 12-22, 12-25, 13-36
- Strain-gauge transducers, 30-5, 30-7
- Strain-sensitive resistor, 30-7
- Strand line, 29-4, 29-5, 29-9
- Stratification, 36-5, 42-3, 45-7 to 45-10, 45-12, 45-13
- Stratification ratio, 39-19
- Stratified reservoirs, 44-7, 44-29
- Stratigraphy, 44-2
- Stratigraphy from dipmeter patterns, 53-10, 53-12, 53-14
- Stratigraphic traps, 29-3 to 29-5, 29-8, 44-2
- Streamlines, 44-15, 44-16
- Streamtube models, 45-10
- Street Ranch field, Texas, 46-26 to 46-28
- Stress analyses, 18-25, 18-27
- Stress-concentration effect, 9-8
- Stress-concentration factor, 9-5
- Stress conversions, 58-7
- Stress, in acoustic-wave propagation in rocks, 51-6, 51-7
- Stress, in suspended casing strings, 2-36
- Stress-range diagram, 9-11, 9-13
- Stress ranges recommended for riser pipe, 18-17
- Stress relaxation, 28-13
- Stress, SI unit for, 58-5, 58-11, 58-23, 58-34
- Stress/strain diagram, 51-2
- Stretch factor, 10-6
- Stretch, in casing, 2-35 to 2-37
- in tubing, 2-46
- Strike of a formation, 53-7
- Strike-slip faults, 29-3, 29-9
- Stripper hanger, 3-39
- Stripper rubber, 3-9
- Stripper wells, 8-6
- Strongly implicit procedure (SIP), 48-16
- Strontium, 24-9, 24-18, 44-44, 44-45
- Structural bearings, 10-4, 10-5, 10-12
- Structural casing, 18-18, 18-19
- Structural closure, 29-1, 29-5, 29-6
- Structural contours, 39-22
- Structural-design process, offshore, environmental criteria, 18-25
- fatigue analysis, 18-27
- field-development plan, 18-25, 18-26
- in-situ analysis, 18-26
- transportation and launch, 18-26, 18-27
- Structural drawings, 15-31
- Structural engineer, 18-22
- Structural-frame analysis, 18-22

- Structural maps, 41-8
- Structural nose, 29-3, 29-4
- Structural pinchouts, 44-39
- Structural traps, 29-1 to 29-3
- Structure map, 44-38
- Structure map, West Heidelberg field, 46-28, 46-30
- Structure, principal factor in gravitational segregation, 44-2
- Structure selection offshore,
 - concrete gravity, 18-25
 - guyed towers, 18-25
 - template/jackets, 18-25
 - tension-leg platform, 18-25
- Structures, offshore,
 - background and philosophy, 18-22
 - classification of, 18-22 to 18-24
 - design process of, 18-25 to 18-27
 - guyed towers, 18-24
 - selection of, 18-25
 - special services, 18-25
 - tension-leg platform, 18-24, 18-25
- Strudel scour, 18-43
- Studded adapter flange, 3-9
- Studded flanged outlets, 3-3
- Studded flanges, 3-8
- Stymie condition, 5-54
- Sub-bottom profiler, 18-5
- Subleases, 41-15, 57-7
- Sublimation curves, 23-1, 23-2
- Submarine cables, 18-44, 18-45
- Submarines, 3-38
- Submerged Lands Act of 1953, 57-11
- Submerged zone, 3-36
- Submersible electric motor, 7-1, 7-3, 7-4
- Submersible electrically driven pumps, 11-14
- Submersible pumps, 7-1 to 7-17, 44-42
- Submersible rig, 18-2, 18-5, 18-6
- Subordinate phase, 44-6
- Subscript symbols in alphabetical order, 59-63 to 59-70
- Subsea applications,
 - fixed platform drilling, 3-38
 - floating drilling vessels, 3-39
 - SPPE/OCS equipment, 3-39
- Subsea completion system, 18-3
- Subsea drilling system, 18-10
- Subsea hydraulic power unit, 18-52
- Subsea (seafloor) pipelines, 18-29, 18-30, 18-35, 18-36
- Subsea satellite wells, 18-33
- Subsea tree, 18-31, 18-32
- Subsea valve actuator, 18-50, 18-51
- Subsea well completions,
 - control lines, 18-33, 18-34
 - flowlines, 18-33, 18-34
 - introduction, 18-30, 18-31
 - manifolds, 18-32
 - multiple templates, 18-32
 - single satellite wells, 18-31
 - well servicing, 18-34
 - well workovers, 18-34
 - wet vs. dry, 18-31
- Subsea wellhead installation, 6-6, 6-7
- Subsea wells, 18-3, 18-14, 18-31, 18-34 to 18-38, 18-48
- Subsurface completions, 3-26
- Subsurface-controlled subsurface safety valves (SSCSV's), 3-29
- Subsurface flowing pressure, calculation, 33-18
- Subsurface mapping, 40-1
- Subsurface-pressure surveys, 42-4
- Subsurface pressures, calculation, 33-13
- Subsurface pump, 9-1, 9-13
- Subsurface-pump bores, 8-1
- Subsurface-pump stroke length, 9-12
- Subsurface safety valves (SSSV's), 3-26, 3-27, 3-31, 3-33, 3-34, 6-48
- Subsurface saltwater, 44-42
- Subsurface shut-in pressure, calculation, 33-19
- Subsurface sucker-rod pumps, 8-1 to 8-10
- Subsurface waters, 24-3, 24-19
- Successive overrelaxation (SOR), 48-16
- Sucker-rod failure, 10-29
- Sucker-rod life, 10-17
- Sucker Rod Pumping Research Inc., 8-10
- Sucker-rod pumps, 6-8, 8-1, 8-10
- Sucker-rod string, 8-8, 8-10, 10-1, 10-5, 10-6
- Sucker rods,
 - allowable stress and range of stress, 9-8
 - chemical and mechanical properties, 9-4
 - chemistries of, 9-5
 - couplings and subcouplings, 9-3, 9-4
 - fiberglass, 9-10 to 9-14
 - general dimension, 9-2, 9-3
 - introduction, 9-1
 - joint circumferential displacement values, 9-10
 - mechanical properties, 9-5
 - pin failures, 9-9
 - references, 9-14
 - rod and pump data, 9-6, 9-7
 - steel, 9-1 to 9-10
 - storage, 9-10
 - tolerances, 9-3
- Suction gradient, 6-29
- Suction piping, 15-17
- Sukkar and Cornell's method, 34-9 to 34-24
- Sukkar-Cornell integral for BHP calculation, 34-10 to 34-22
- Sulfate-reducing bacteria (SRB), 44-41, 44-43, 44-44
- Sulfide stress cracking, 3-35, 3-36
- Sulfonates, 19-10, 47-16
- Sulfur, 3-3, 10-16, 19-28, 24-16, 46-22
- Sulfur dioxide, 14-17, 14-22
- Sulfur oil, 11-6
- Sulfur/oxide ratio, 52-7
- Sulfuric acid, 11-6
- Summation-of-fluids method, porosity, 27-1
- Sun Oil Co., 46-15, 46-18, 46-29 to 46-32
- Supercompressibility factor, 13-8, 22-20, 33-13
- Supercritical CO₂, 45-5
- Supercritical-fluid drive, 45-5, 45-6
- Superficial velocity of gas, 34-46
- Superheated steam, 46-5
- Superposition, 35-8, 35-9, 40-12
- Supervisory control and data acquisition (SCADA), 16-1, 16-2, 16-6 to 16-10, 16-12
- Suplacu de Barcau field, Romania, 46-4, 46-15, 46-18, 46-28, 46-29
- Surface-active agents,
 - adding to oil, 56-2
 - in controlling stability of emulsions, 19-1
 - in drilling fluids, 44-5
- Surface-active agents in waterflooding,
 - interfacial-tension reduction, 44-40
 - mobility improvement, 44-39, 44-40
 - rock-wettability alteration, 44-40
- Surface-active chemicals, 24-2
- Surface area of crude, evaporation from, 11-12
- Surface area of fracture, 55-2, 55-8
- Surface area, specific, 28-8
- Surface casing, 3-3
- Surface closing pressure, gas-lift valves, 5-44 to 5-47
- Surface control valve, 18-50
- Surface-controlled subsurface safety valves (SCSSV's), 3-29, 18-47, 18-48
- Surface-driven pumps, 44-42
- Surface environment, 36-2
- Surface equipment, hydraulic pumping, control manifolds, 6-54
- fluid controls, 6-51
- lubricators, 6-54
- power-fluid systems, 6-54 to 6-57
- power-oil tank and accessories, 6-57 to 6-59
- pumps, 6-49 to 6-54
- single-well systems, 6-60 to 6-63
- Surface extraction efficiency, 52-18
- Surface facilities, design and operating program for, 39-23
- for closed power-fluid system, 6-59
- for open power-fluid system, 6-58
- for saltwater disposal and waterflooding, 15-1 to 15-33
- formulating policy for, 40-1
- Surface-flowline backpressure, 5-54
- Surface-gas gravity to well-fluid gravity ratio, 21-17
- Surface geothermal temperature, 5-48
- Surface injection-gas pressure, 5-44
- Surface kick-off injection-gas pressure, 5-46, 5-48
- Surface-line heat losses, 46-4
- Surface opening pressures, gas-lift valve, 5-39
- Surface preparation for coatings, 11-5
- Surface production equipment, 12-2
- Surface production facilities, 36-2
- Surface pumping unit, 9-1, 9-3, 9-13
- Surface pumps, 6-49 to 6-51
- Surface-recording BHP gauges, 30-4, 30-5
- Surface safety valves (SSV's), 3-19 to 3-21, 3-27, 3-31, 3-33, 3-34, 3-39, 18-47, 18-48
- Surface seismic shear surveys, 51-28
- Surface separation equipment, 40-24
- Surface steam generators, 46-4, 46-19
- Surface tension, 19-14, 22-16, 22-17, 22-19, 22-21, 24-16, 47-8, 54-6 to 54-8, 58-35, 58-38
- Surface transfer pumps, 19-28
- Surface unloading flowing wellhead temperature, 5-46, 5-48
- Surfactant absorption on metal oxide surface, 47-15
- Surfactant as foaming agent, 55-6
- Surfactant breakthrough times, 47-17
- Surfactant/brine/oil phase behavior, 47-11 to 47-13
- Surfactant chemistry, 47-7
- Surfactant/divalent complexes, 47-15
- Surfactant flooding, 48-7
- Surfactant/polymer processes, 23-7
- Surfactant retention, 47-10, 47-15 to 47-17
- Surfactant slug, 48-5
- Surfactant systems, 23-8
- Surfactants, adsorption of, 47-8
 - chemistry of, 47-7
 - classification of, 47-7
 - definition of, 54-6
 - in interfacial-tension reduction, 44-40
 - in mud removal, 56-1
 - in water blocks and emulsion removal, 56-2
 - micellar/polymer, 47-7
 - molecular structures, 47-7
 - reducing acid reaction rate, 54-8
 - solutions, 47-11
 - surface tension of, 47-8
 - to avoid emulsification, 54-9, 54-10
- Surge tank, 24-3, 44-47
- Surging, applicability of horizontal separator, 12-35
- in gas-lift installations, 5-1, 5-22, 5-24, 5-38
- in rod pumps, 8-4

Surging flow, 13-52, 13-53
 Suspended solids, 15-18, 19-15, 24-5, 44-36, 44-45
 Swab cups or noses, 6-47
 Swabbing, 52-17, 52-18
 Sweden, 12-39
 Sweep after breakthrough, 44-29
 Sweep efficiency, 39-18, 46-14
 Sweep efficiency at breakthrough, 44-19, 44-20
 Sweepout-pattern efficiency, 44-23 to 44-25, 44-28
 Sweet corrosion, 3-35, 4-4, 4-5, 9-8
 Sweet gas, 11-10, 14-21, 14-22
 Sweet natural-gas systems method, for estimating initial hydrate formation, 25-5
 Sweetening by ethanolamines, 14-21, 14-22
 Swelling clays, 26-18
 Swelling tests, 48-9
 Switchboard, electric submersible pump (ESP), 7-5 to 7-7, 7-12
 Switchboard-motor controller, 7-8
 Switches for control of oilfield motors, 10-27
 Switching valves, 13-56
 Switzerland, 12-39
 Symbol subscript definitions in alphabetical order, 59-52 to 59-62
 Symbol subscripts in alphabetical order, 59-63 to 59-70
 Symbols in alphabetical order, SPE standard, 59-2 to 59-17
 Symmetrical folds, 29-2
 Syngenetic interstitial water, definition, 24-18
 Syntactic foam, 18-15
 Synthetic polymers in acidizing, 54-8
 System, definition, 22-21
 Système International d'Unités, 58-2

T

Tadpole plot, 53-10, 53-12
 Tadpole symbol or structure, 47-7
 Tailgate booster, 7-2
 Tailing, 9-10
 "Taint," computer subordinate routine, 17-6
 Tandem labyrinth path model, 7-11
 Tandem pumps, 6-7, 6-8
 Tangential method of calculating directional surveys, 53-5, 53-6
 Tangible cost, 41-11, 41-13
 Tangible property, 57-11
 Tank battery, connections, 11-9
 consolidation, 16-1, 16-2
 for hydrogen-sulfide crude storage, 11-10
 installation and hookup, 11-9
 maintenance and operation, 11-10, 11-11
 Tank bottoms, 19-32
 Tank calibration, 17-3
 Tank cars, measurement and calibration, 17-3
 Tank corrosion protection, cathodic protection, 11-6
 coatings specifications, 11-4 to 11-6
 Tank dimensions, 11-4, 11-5
 Tank gauging, 17-3, 17-4
 Tank grades, 11-11
 Tank pressures, evaporation loss from, 11-12
 Tank-type depletion performance, 37-10
 Tank-type material balance, 37-2, 37-4, 37-19, 37-21
 Tank-type models, 37-2, 37-4, 37-5, 37-11, 37-14, 37-17
 Tanker loading operations, 18-36
 Tanker mooring devices, 18-2
 Tanker mooring systems, 18-43
 Tankers, 18-43
 Tankers vs. semisubmersibles, 18-35, 18-36
 Tanks, aboveground, nonrefrigerated, emergency venting capacity, 11-7, 11-8
 means of venting, 11-8, 11-9
 normal venting capacity, 11-7
 venting requirements, determination of, 11-6
 Tanks, measurement and calibration, 17-3
 Tapered valve seat, 5-15
 Tar production history, 46-28
 Tar sands, 46-3, 46-31
 Tar Springs sand reservoir, Illinois, 40-32, 40-33
 Tarner method, 37-10, 40-9, 40-10
 Tax consequences related to conveyances, 41-15, 41-16
 Taxation, 57-11
 Taylor method, 37-10 to 37-13
 Taylor series expansions, 48-10
 Tectonic stresses, 55-1
 Teflon® seal rings, 2-1, 2-38, 4-5
 Telemetry, 3-18, 3-27, 18-45, 51-27
 Telemetry system, 53-1, 53-2
 Tell-tale screen, 56-8
 Temperature, actual, 31-2 to 31-4
 average annual, U.S., 31-3
 gradient, effect of cement behind casing, 31-6
 ideal curves of fluid migrating through casing hole, 31-5
 in wells, 31-1 to 31-7
 logs, 31-1
 mean surface, 31-3
 radial differential log, 31-7
 static bottomhole, 31-6
 surveys, 31-1 to 31-7, 42-4
 Temperature-base factor, 13-3, 13-12
 Temperature controls, 12-40
 Temperature conversion chart, 58-39
 Temperature conversion tolerance requirements, 58-7
 Temperature correction factor (coefficient), 5-6, 5-7, 30-2, 30-3
 Temperature data log, 52-23
 Temperature dependence of compressional- and shear-wave velocities, 51-8
 Temperature distribution, in annular completion, 46-6
 in Marx-Langenheim model, 46-7
 Temperature effect of tubing string, 4-9, 4-10
 Temperature, effect on acid reaction rate, 54-4
 effect on BHP gauges, 30-2, 30-3, 30-5
 effect on corrosion inhibition, 54-6
 effect on confined bellows-charged dome pressure, 5-6 to 5-8
 effect on elastic-wave velocities, 51-7
 Temperature gradient, 33-18, 58-28
 Temperature log, 46-26, 49-25
 Temperature measurement, 16-7
 Temperature, method of measuring of petroleum and petroleum products, 17-5
 Temperature of crude, evaporation loss, 11-12
 Temperature, of liquid hydrocarbons, 17-5
 Temperature profiles, 4-6, 4-7
 Temperature ranges, of gas-condensate reservoirs, 39-2
 Temperature rating of insulations, 10-26
 Temperature rise of motor, 10-25
 Temperature sensors, 10-29
 Temperature, SI unit for, 58-5, 58-23, 58-24, 58-28
 Temperature transition zone, 52-22
 Temperature vs. pressure drop, 14-2
 Template/jacket, 18-22, 18-23, 18-25
 Ten Section field, California, 34-35
 Tendon system, 18-25
 Tenneco Oil Co., 46-14, 46-18
 Tensile load, 18-22
 Tensile strength, 3-3, 9-4, 9-5, 9-8, 9-12, 11-9, 18-49, 30-4, 55-1
 Tensile strength, API casing and liner casing, 2-2
 API tubing, 2-37
 line pipe, 2-46
 of construction materials, 12-41
 Tensiometer, 24-16
 Tension-leg platform (TLP), 18-2, 18-3, 18-24, 18-25, 18-44
 Tension packer, 4-2, 4-3
 Tension tests of round-thread casing joints, 2-60
 Tension-type tubing hanger, 3-16
 Tensional forces, 29-2, 29-3
 Tensioner-line angle, 18-17
 Tensioning unit, 18-13
 Tensleep sand reservoir, Wyoming, 40-19
 Terminology in conversion and rounding practices, 58-8, 58-9
 Ternary-phase diagrams, 23-4 to 23-6, 23-8, 23-13, 47-11
 Tertiary oil recovery, 24-2, 24-3
 Tertiary polymer floods, 47-6, 47-10
 Tertiary recovery, wet combustion, 46-30, 46-33
 Test pressures, extra-strong threaded line pipe, 2-50
 extreme-line casing, 2-62
 internal-joint tubing, 2-62
 plain-end line pipe, 2-50 to 2-53, 2-62
 threaded line pipe, 2-47, 2-62, 2-63
 wellhead equipment, 3-1, 3-2
 Test procedures, gas-condensate reservoir, 39-5
 Test-rack closing pressure, 5-6, 5-17, 5-18, 5-20
 Test-rack opening pressure, 5-6 to 5-8, 5-16 to 5-18, 5-21, 5-22, 5-29, 5-31 to 5-37, 5-46, 5-47, 5-49 to 5-51
 Test separator, 12-17, 32-6
 Tester setting temperature, 5-46, 5-49
 Testing crude oil, 17-1 to 17-8
 Testing natural gas fluids, 17-7
 Tetrabromoethane, 52-20
 Tetraethylene glycols (TRG), 14-18
 Texaco, 46-4, 46-15, 46-18
 Texas, 16-12, 16-13, 18-2, 19-15, 21-2, 21-4, 21-8, 24-3, 24-7, 24-8, 24-10, 24-20, 24-21, 26-7, 29-3, 29-4, 29-7, 29-8, 32-1, 32-2, 33-1, 33-21, 36-1, 36-2, 36-6, 39-3, 39-20 to 39-22, 39-25, 40-19, 40-23, 40-33, 40-34, 41-4, 44-14, 44-36, 44-37, 44-40, 44-42, 44-46, 46-3, 46-4, 46-15, 46-18, 46-26 to 46-32, 47-3, 47-7, 47-22, 49-11, 49-31, 58-20
 Texas allowable rule, 32-1
 Texas gulf coast, 27-6 to 27-8
 Texas Railroad Commission, 32-1, 32-2, 32-15, 33-15
 Texture of foams, 47-8
 Texture of rock, 51-8 to 51-11
 Thallium, 50-13
 Thaw settlements, 18-41
 Theoretical considerations of multiphase flow, 34-36, 34-37
 Theoretical considerations of thermal recovery, surface-line heat losses, 46-4
 wellbore heat losses, 46-5
 Theoretical models, 51-8
 Theoretical productivity index, 32-4

- Theories of emulsions,
 color, 19-5
 definition of an emulsion, 19-1, 19-2
 effect on viscosity of fluids, 19-6
 emulsifying agents, 19-3 to 19-5
 how emulsions form, 19-2, 19-3
 prevention of, 19-5
 stability of, 19-5, 19-6
- Theory of elastic-wave propagation in rocks,
 51-49, 51-50
- Theory of elasticity,
 bulk modulus, 51-1, 51-2
 elastic parameters, relationships among,
 51-2
 Poisson's ratio, 51-2
 shear modulus, 51-1
 Young's modulus, 51-1
- Thermal-absorption cross section, 50-10,
 50-22
- Thermal ammeter, 10-33
- Thermal analysis, 18-41
- Thermal breathing, 11-6
- Thermal conductance, conversion of units,
 table, 1-79
- Thermal conductivity, conversion of units,
 table, 1-79
- Thermal detector (TCD), 52-4 to 52-6, 52-11
 of a gas, 31-2
 of a material over a depth increment,
 52-22
 of adjacent formation, 31-7
 of cement, 46-6
 of common sediments, 31-4
 of geological strata, 31-2
 of insulating materials, 46-4
 of Kern River oil sands, 46-39
 of mineral oils in motors, 7-3
 of refrigerants, 14-11
 overburden, 46-7
 units and conversion factors, 58-34
 variation with brine saturation, 46-37
- Thermal contraction of liquid, 22-21
- Thermal cracking, 46-12, 46-15, 46-16
- Thermal detectors, 50-20, 50-21
- Thermal-diffusion coefficient, 50-11
- Thermal diffusivity, 46-5, 46-7, 46-10
- Thermal efficiency, 46-8, 46-9, 46-14
- Thermal energy neutron, 50-11, 50-17,
 50-36
- Thermal-expansion coefficients, 17-5, 17-6
- Thermal-expansion factor, 13-8
- Thermal expansion of hydrocarbon liquids,
 22-3, 22-5
- Thermal flooding, 40-4
- Thermal inbreathing, 11-6, 11-7
- Thermal lag, 31-1, 31-2
- Thermal model, 48-4 to 48-7, 48-14
- Thermal neutron absorption, 50-4, 50-21
- Thermal neutron detectors, 50-15
- Thermal neutron porosity device, 50-12,
 50-20, 50-30, 50-32
- Thermal overload relay, 10-29
- Thermal packers, 46-19
- Thermal porosity device, 50-21, 50-28,
 50-32
- Thermal properties,
 chemical kinetics, 46-37
 oil viscosities, 46-31, 46-34, 46-35
 pore-volume compressibility, 46-37
 relative-permeability curve, 46-34, 46-37
 steam properties, 46-40
 thermal conductivity, 46-37
 vaporization equilibrium, 46-37
- Thermal recovery,
 analytical models for steam injection, 46-7
 to 46-11
 case histories, 46-22 to 46-31
 current status, 46-3, 46-4
 field facilities, 46-19, 46-20
 field projects, 46-13 to 46-17
 general references, 46-45, 46-46
 geographical distribution of projects, 46-3
 historical development, 46-3
 in-situ combustion, three forms of, 46-1
 to 46-3
 introduction to, 46-1
 laboratory experimentation, 46-12, 46-13
 monitoring and coring programs, 46-20,
 46-21
 nomenclature, 46-40, 46-41
 numerical simulation, 46-11, 46-12
 oil recovery, 46-14, 46-15
 operational problems and remedies, 46-21,
 46-22
 project design, 46-17 to 46-19
 references, 46-43 to 46-45
 reservoirs amenable to, 46-3, 46-4
 steam injection processes, two forms of,
 46-1
 theoretical considerations, 46-4 to 46-7
 thermal properties, 46-31 to 46-40
 well completion, 46-19
- Thermal resistance, 58-34
- Thermal strength stabilizing agent, 46-19
- Thermal stress, 46-19
- Thermal trip capability of circuit breakers,
 10-28
- Thermal venting capacity of tanks, 11-7
- Thermalization, 50-22
- Thermalytic Hydrocarbon Analyzer (THA),
 52-10, 52-11
- Thermistor, 16-7, 31-2
- Thermocouple-amplifier transducers, 46-21
- Thermocouples, 16-7, 31-2, 51-5
- Thermodynamic equilibrium, 23-12
- Thermodynamic temperature, 58-10, 58-23
- Thermogenic hydrates, 25-18
- Thermometers,
 differential, 31-2, 31-5
 electrical surface-recording, 31-2, 31-5
 in gas, 31-2
 self-contained, 31-1, 31-2
 time response, 31-2
- Thermometry, 1-68, 1-69, 31-2 to 31-7
- Thermoplastic line pipe, 15-10
- Thermoset resins, 9-12
- Thermosetting resin line pipe, 15-10
- Thermosiphon, 19-21
- Thickening agents, 55-5
- Thief hatch, 11-9, 11-11, 11-13
- Thief sampler, 17-1, 17-2
- Thin-bed corrections, induction log, 49-17
- Thin-film epoxy system, 15-10
- Thin-film strain-gauge transducer, 30-7
- Thinnest reservoir, fireflood, 46-29
- Thiosulfates, 14-22
- "Third for a quarter" transaction, 41-15
- 13-spot pattern, 46-17, 47-18, 46-26
- Thodos gas-viscosity method, 20-9, 20-15
- Thorium, 50-2 to 50-4, 50-15, 50-16, 50-24
 to 50-27, 50-34, 50-35
- Thread galling, 9-9
- Thread limitations, wellhead equipment,
 3-1, 3-2
- Thread pressure rating for casing, line pipe,
 and tubing, 3-3, 3-4
- Threaded adapter flange, 3-9, 3-11
- Threaded flanges, 3-8, 3-17
- Threaded line pipe, 2-46 to 2-49
- Threading and machining dimensions, 2-63,
 2-64, 2-67, 2-68
- Threading data, API, 2-64 to 2-72
- 3-D Log™, 51-18
- 3D seismic techniques, 36-1, 36-8, 36-9
- 3D simulator, 36-10
- 3D velocity log, 51-44
- 3D vertical migration, 36-9
- Three-phase autotransformer, 7-6
- Three-phase critical point, 25-15
- Three-phase flow, 28-9
- Three-phase induction motors, 10-20, 10-31,
 10-35
- Three-phase numerical simulators, 46-7
- Three-phase relative mobility, 28-9
- Three-phase relative permeability, 28-12
- Three-phase saturation conditions, 28-8,
 28-9
- Three-phase saturation trajectory, 28-7
- Three-phase separator, 12-4, 12-5, 12-14,
 12-15, 12-19, 12-21, 15-21, 16-7, 16-8
- Three-phase standard transformer, 7-6
- Three-phase transformer, 10-30
- Three-phase voltage, 10-23
- Three-phase well tester, horizontal skid-
 mounted, 12-4, 12-21
 with batch-type meters, 32-9
 with oil-volume meter and PD meter,
 32-8
 with PD meters, 32-7
- Three-point rule, 41-10
- Three-stage separation, 12-33, 12-34
- Three-tube pump, 8-8, 8-9
- Three-way bypass valve, 14-5, 14-6
- Three-way engine valves, 6-9
- Threshold energy, 50-7, 50-9
- Threshold pressure, 28-6
- Throat annulus, jet pump, 6-38, 6-40, 6-41,
 6-46
- Throat-diffuser loss coefficient, 6-37
- Throat of jet pump, 6-32, 6-34 to 6-37,
 6-39 to 6-42, 6-46, 6-47
- Throttling discharge of liquid, 12-42
- Through-flowline (TFL) completions, 5-2
- Through-flowline (TFL) installations, 6-2,
 6-6, 6-7, 6-34
- Through-flowline (TFL) well servicing,
 18-34
- Thrust fault, 29-3
- Tia Juana Este field, Venezuela, 46-4,
 46-15, 46-18
- Tickell diagram, 24-19
- Tie lines, 23-5, 23-9, 23-10, 45-5
- Tier and rate structure, windfall profit tax,
 41-15
- Time-average equation, 51-30, 51-33 to
 51-35, 51-50
- Time-clock tab, 10-28
- Time-cycle control, 5-41 to 5-44, 5-54
- Time-cycle controller, 5-38, 5-40, 5-48,
 5-53, 5-55, 14-11, 14-20, 16-3, 16-4,
 16-11
- Time-cycle-operated controller, adjustment
 of, 5-55
- Time designation, SI metric system, 58-22
- Time lag of a process, 13-52, 13-53
- Time-lapse technique, 50-36
- Time of injection operations, 42-2
- Time-rate performance, 45-12
- Time, SI units for, 58-5, 58-22, 58-23,
 58-27
- Time truncation error, 48-10
- Time value of money, 41-3
- Title examination, 57-9
- Titled polar scan displays, 51-28
- Tixier relation, 26-29
- Tolerance, definition, 58-9
- Tolerances,
 of buttress-thread casing coupling, 2-29
 of external-upset tubing coupling, 2-43
 of integral-joint tubing upset, 2-45
 of line-pipe lengths, 2-47
 of nonupset tubing coupling, 2-42
 of ring-joint gaskets, 3-28, 3-30, 3-32
 of round-thread casing coupling, 2-28
 of sucker and pony rods, 9-3, 9-11
- Toluene, 17-2, 17-5, 24-18, 26-22
- Ton as a unit, 1-70

- Tool characteristics, acoustic logging, 51-15
 Tool-face angle, 53-1
 Tool for long-spacing acoustic logging, 51-21 to 51-23
 Tool span, conventional acoustic logging, 51-16
 Tools available for directional surveys, 53-3, 53-4
 Tooth efficiency, 52-25
 Top-seating holddown, 8-3
 Topworks (motor), 13-49
 Torispherical head equations, 12-38
 Tornado charts, 49-28
 Torpeda sandstone, 28-10, 46-5
 Torque, engine, 10-17
 Torque factors, 10-6, 10-7
 Torque mode of motors, 10-20 to 10-22, 10-25, 10-31, 10-32
 Torque of motor, 10-25
 Torque reductions, 10-24
 Torque, SI unit for, 58-5, 58-34, 58-38
 Torsion, 29-2, 29-9
 Torsion modulus, 51-1
 Torsional waves, 51-2
 Tortuosity, 26-28, 26-29, 26-31, 28-6
 Total dissolved solids (TDS), 15-29, 24-5, 24-7 to 24-13, 24-20, 44-44, 47-2, 47-3
 Total dynamic head (TDH), 7-10
 Total (two-phase) FVF, 6-47, 6-48, 22-1, 22-13, 22-14, 22-20
 Total-gas analysis, 52-3
 Total-gas analyzer, 52-9
 Total-gas detector, 52-5
 Total liquid saturation, 40-10
 Total porosity, 26-2, 26-3, 26-7
 Total solids, 44-45
 Total water, definition of, 27-8
 Totally enclosed fan cooled (TEFC) motor, 10-26
 Totally enclosed nonventilated (TENV) motor, 10-26
 Tow and launch analysis procedure, 18-27
 Toxic concentration of refrigerants, 14-10
 Toxic decomposition products of refrigerants, 14-11
 Toxicity, 52-20
 Trace-element absorption factor, 50-34
 Tracer studies, 15-23
 Tracers, 26-21, 46-21, 52-26
 Tracy's method, 37-7 to 37-10, 37-21
 Trans-Alaska Pipeline System, 18-3
 Transducer assembly of sonic meter, 13-49
 Transducer criteria, 30-5
 Transducers, 30-6, 30-7, 46-21
 Transfer pressure line, 5-48
 Transformer voltage drop, 10-33
 Transformers, 7-6, 7-11, 10-29 to 10-31, 10-35, 19-31
 Transient backpressure, 44-35
 Transient period, 30-11 to 30-13
 Transient-pressure test, 36-7
 Transient testing, 35-11
 Transient well-test analysis, buildup testing, 35-15, 35-16
 determination of p_R , 35-16
 drawdown test, 35-14, 35-15
 Transit time, 51-15
 Transit-time integration curves, 51-22
 Transit-time log, 51-47, 51-48
 Transit-time measurement, 51-14
 Transit-time/pressure correlation, 51-40
 Transition collapse-pressure equation, 2-54, 2-55
 Transition flow (slug-mist), 34-36, 34-37, 34-40
 Transition zones, 27-8
 Transitional sediments, 36-3
 Transmissibility, 39-19, 48-3, 48-14 to 48-16
 Transmission method, 51-11, 51-12, 51-27
 Transmission oil, 10-12
 Transmission system, 12-10, 12-11
 Transmitter of sonic meter, 13-49
 Transport coefficient, 28-1, 28-3
 Transport energy, 34-46
 Transport equations, 28-13, 28-14
 Transport properties, units and conversions, 58-34, 58-35
 Transportation and launch offshore, 18-26
 Transportation fatigue, 18-27
 Transportation systems offshore, marine terminals, 18-43
 pipeline, 18-42, 18-43
 tankers, 18-43
 Transverse capillary imbibition, 28-12
 Transverse dispersion, 28-12, 45-6
 Trap, 12-1
 Trap classification, 29-1 to 29-6
 Trapezoidal integration, 34-24
 Trapezoidal rule, 33-17, 40-15
 Travel time, 51-15
 Travel-time measurement, borehole-compensated (BHC) log, 51-16
 Traveling-barrel rod pump, 8-4, 8-10
 Traveling valve, 19-28
 Traverse waves, 51-2
 Treating crude-oil emulsions, 19-6 to 19-15
 Treating emulsions produced from EOR projects, 19-28
 Treatment planning, hydraulic fracturing, 55-9
 Treatment plant, 39-24
 Tree savers, 55-9
 Trespass, 57-2
 Triangular diagram, 23-4, 23-5, 23-8, 23-13, 45-2 to 45-7
 Triaxial PV-compressibility technique, 26-8, 26-9
 Triethylene glycol (TEG), 14-7, 14-18 to 14-20, 25-19
 Triethylene-glycol/water mixtures, 39-5
 Triggering, 51-16, 51-17
 Trigonometric functions, table, 1-50 to 1-54
 Trinidad, 36-9, 46-3
 Triple point, 23-1, 23-2
 Triplex pumps, 6-1, 6-30, 6-33, 6-45, 6-46, 6-49 to 6-51, 6-60, 6-61, 15-14, 16-11, 55-9
 Tripolite, 51-5, 51-6
 Tritium, 46-21
 Tritium ion, 50-6
 Trix-Liz field, Texas, 46-18
 Troubleshooting electrical submersible pump (ESP), 7-1, 7-14 to 7-17
 Troubleshooting guide, 6-28, 6-31 to 6-33, 6-47, 6-51
 Troy granite, 51-8 to 51-10
 Trube correlation, 20-11, 20-16
 Trube method, 22-11, 22-12
 Trucking charges, 41-12
 True boiling point, 21-7 to 21-9
 True equilibrium state, 25-3
 True mass, definition of, 1-70
 True porosity, 50-20, 50-28 to 50-30
 True stratigraphic thickness (TST), 53-10, 53-12, 53-15, 53-16
 True vapor pressure, 11-12, 14-13
 True vertical depth (TVD), 5-4, 5-6, 18-41, 49-37, 53-3, 53-15, 53-16
 True vertical thickness (TVT), 53-10, 53-12, 53-15, 53-16
 Truncation, 29-4, 29-5, 29-9
 Trustee, definition, 57-3
 Tube amplitude ratio, 51-47, 51-48
 Tube-type H₂S detector, 52-6, 52-7
 Tube wave, 51-12, 51-47, 51-48
 Tubing, collapse pressure, 2-46
 collapse resistance, 2-39, 2-41, 2-43
 design factors, 2-38
 design safety factors, 2-38, 2-39, 2-45, 2-46
 dimensions, 2-42, 2-43, 2-45, 2-58, 2-65, 2-66
 elongation, 2-37
 equation for calculating performance properties, 2-46, 2-54 to 2-56
 external upset, 2-38 to 2-45
 gross linear footage from net footage, 2-45
 hydrostatic test pressure, 2-62
 integral joint, 2-38 to 2-45
 internal yield, 2-39, 2-41, 2-43, 2-46
 joint strength, 2-61
 joint yield strength, 2-39, 2-41, 2-43, 2-46
 multiplication factors, 2-45
 nonupset coupling, 2-38 to 2-44
 performance properties, 2-38 to 2-43
 range lengths, 2-37, 2-38
 round-thread and form, 2-58, 2-64
 round-thread height dimensions, 2-66
 safety factors, 2-38, 2-39, 2-54 to 2-56
 selection of weight and grade, 2-39
 special joints, 2-38
 stretch when freely suspended, 2-46
 string of single weight and grade, 2-38
 tensile requirements, 2-37, 2-38
 thread dimensions, 2-65, 2-66
 tolerance, 2-42, 2-43, 2-45
 weight, 2-42, 2-43, 2-45
 yield strength, 2-37
 Tubing/casing annulus, 6-2, 6-4, 6-5, 18-33, 34-27
 Tubing cleanliness, 56-3
 Tubing constants, 4-10
 Tubing hanger bowl, 3-8, 3-13
 Tubing hangers, 3-8, 3-11, 3-14, 3-16, 3-26, 3-37, 3-39
 Tubing-head adapter flange, 3-9, 3-11
 Tubing-head bowl, 3-8, 3-9, 3-39
 Tubing heads, 3-8, 3-11, 3-14, 3-37, 3-39
 Tubing installation, 33-21
 Tubing/packer system, advantages, 4-6
 combination, 4-11
 illustration, 4-9
 in completion or workover, 4-10
 operational well modes, 4-6 to 4-8
 where packers are used, 4-6
 Tubing performance curve, 34-50
 Tubing plug, 3-35
 Tubing-profile calipers, 53-17 to 53-19
 Tubing pump, 8-1, 8-4
 Tubing response characteristics, ballooning and reverse ballooning, 4-10
 buckling effects, 4-10, 4-11
 introduction, 4-8, 4-9
 piston effect, 4-9
 temperature effect, 4-9
 Tubing-retrievable subsurface safety valves (SSSV's), 3-27, 3-33
 Tubing size vs. constant B , 6-20
 Tubing sizes, F_p values for, 34-25
 Tubing support, electrical submersible pump (ESP), 7-6
 Tubing threads, wellhead equipment, 3-2
 Tubing-to-packer connections, 4-1
 Tubular goods sizes, 3-5
 Tungsten carbide, 6-34
 Tunisia, 24-18
 Turbidity, 44-44
 Turbine expansion systems, 14-8
 Turbine meters, 13-45, 13-49, 16-6, 16-7, 16-12, 17-4, 17-7, 32-6, 32-12
 Turbine-powered propulsion systems, 18-43
 Turbine prime mover, 18-45

Turbo-expander process, 14-8
 Turbocharged engine, 15-16
 Turbopumps, 6-67
 Turbulence, 14-2, 14-3
 Turbulence and short-circuiting factor, 15-19
 Turbulence, energy loss due to, 13-2, 13-3
 permanent pressure loss from, 13-2
 Turbulent flow regime, 28-13
 Turnkey format, 15-32
 Two-cycle engines, 10-14 to 10-16, 10-19
 Two-dimensional (2D) relief maps, 51-28
 2- and 3D seismic surveys, comparison, 36-9
 2D simulator, 36-10
 Two-phase compressibility factor, 39-7, 39-8, 39-10, 39-14
 Two-phase flow, 34-33, 34-34, 34-37
 Two-phase (total) formation volume factor (FVF), 6-47, 6-48, 22-1, 22-13, 22-14, 22-20
 Two-phase separators, 12-9, 12-10, 12-17 to 12-19, 12-21, 12-25
 Two-phase vertical-flow model, 7-12
 Two-phase waterflooding, 47-1
 Two-phase well tester,
 with positive displacement (PD) meter, 32-8
 with volume meters, 32-9
 Two-receiver system, acoustic logging, 51-15, 51-16
 Two-stage desalting, 19-26, 19-27
 Two-stage separation, 12-33, 12-34, 22-7
 Type curve, 35-6
 Type II(–) phase, 23-8
 Types of injection, 42-4
 Typewriting recommendations, SI metric system, 58-13

U

Ultimate chemical analysis, 21-1, 21-2
 Ultimate depletion, 42-2
 Ultimate gas recovery, 40-24, 40-34
 Ultimate oil recovery, 44-37, 47-20
 Ultimate recovery, 30-11, 36-3, 37-3, 37-21, 37-25, 39-10, 39-13, 39-17, 39-20, 39-23, 39-24, 40-1, 40-2, 40-4, 40-8, 40-11, 40-13, 40-15, 40-16, 40-24, 40-26, 40-32, 40-33, 40-37, 40-39, 41-10, 41-11, 42-2, 42-6, 44-2 to 44-4, 44-7, 44-31
 Ultimate recovery efficiency, 43-3
 Ultimate water requirements, 44-41
 Ultrahigh-slip motors, 10-19 to 10-24, 10-31, 10-32
 Ultrasonic level device, 16-5
 Ultrasonic tests, 19-30
 Ultrasonic thickness indicators, 12-40
 Ultraviolet absorption unit, 12-16
 Ultraviolet detectors, 3-34
 Ultraviolet light, 52-10, 52-11
 Ultraviolet photographs, 46-21
 Ultraviolet radiation, 11-9
 Ultraviolet (UV) sensors, 18-47
 Umbilicals in subsea control systems, 18-49
 Umbrella effect, 43-7
 Unbalanced backpressure regulator, 5-13
 Unbalanced gas-lift valves, 5-39
 Unbalanced pressure regulator, 5-12
 Unbalanced, single-element gas-lift valves, 5-12, 5-14, 5-17, 5-19 to 5-22, 5-41 to 5-44
 Unconformity, 29-5, 29-8, 29-9, 49-25, 53-12
 Uncrosslinked gels, 55-5
 Underbalance method, 56-5
 Underbalanced condition, 52-17 to 52-19
 Undercurrent loading, 7-15

Underflow slurry, 15-19
 Underground storage, 11-13, 11-14
 Undersaturated carbonate reservoir, 44-36
 Undersaturated oil, 37-10
 Undersaturated oil reservoirs, 40-7, 40-12
 Undersaturated reservoir, 37-5, 37-6, 37-9
 Undersaturated system, definition, 22-21
 Undersaturated systems, oil FVF for,
 Trube method, 22-11, 22-12
 Vasquez and Beggs method, 22-12, 22-13
 Undersaturated systems, oil-viscosity correlations, 22-16
 Undervoltage relay, 10-28
 Underwriters' Laboratories Inc., 10-27
 Undiscounted future net cash flow, 41-5
 Unfavorable mobility ratio, 28-7
 Uniboom, 18-5
 Union of Soviet Socialist Republics (USSR), 12-39, 21-2
 Union Oil Co., 46-15, 47-22
 Unit displacement, 43-10, 43-11
 Unit displacement efficiency, 42-3, 43-3, 43-5, 43-6, 43-8, 43-9
 Unit-of-production basis, 41-16, 41-17, 41-23
 Unit of weights and measures, definition of, 1-68
 Unit operations, 57-7, 57-8
 Unit pressure of fluid columns, 6-22, 6-23
 Unit-recovery equation,
 depletion recovery factors, 40-10 to 40-12
 depletion-type reservoir, 40-8
 dry-gas reservoir, 40-25
 Muskat's method, 40-9
 Tarnier's method, 40-9, 40-10
 water-drive reservoir, 40-16
 Unit-recovery factor, 40-16, 40-18, 40-19, 40-24
 Unit recovery for gas reservoir without water drive, 40-24
 Unit response function, 35-8, 35-9
 United Geophysical, 51-1
 United States (U.S.), 1-68 to 1-71, 9-8, 12-38, 12-39, 17-4, 18-3, 18-18, 18-20, 18-23, 18-25, 18-46, 24-1, 24-2, 24-6, 24-21, 36-2, 39-16, 40-16, 41-12, 44-1, 44-4, 51-1, 52-22, 52-26, 52-30
 U.S. areas, core-analysis data from, 27-9
 U.S. Beaufort Sea, 18-3
 U.S. Bureau of Mines (USBM), 1-80, 33-1, 33-3
 USBM BHP gauge, 30-1
 U.S. Bureau of Standards, 21-8
 U.S. bushel, 1-69, 1-70
 U.S. Coast Guard jurisdiction, 18-44
 U.S. customary units, 58-9
 U.S. Dept. of Interior, 57-11
 U.S. DOE, 21-9, 45-1
 U.S. gallon, 1-69, 1-70
 United States Geological Survey (USGS), 3-39, 41-9
 U.S. Government, 53-5
 U.S. gulf coast area, 24-7, 24-8, 24-17
 U.S. Metric Board, 1-69
 U.S. Mineral Management Service, 18-5
 U.S. Natural Gas Policy Act of 1978, 57-10
 U.S. Navy, 18-4
 U.S. oil production by EOR, 46-3
 U.S. OCS Orders, 18-46, 18-47
 U.S. Prototype Kilogram No. 20, 1-69, 1-70
 U.S. sieve number, 56-6, 56-7
 U.S. survey foot, 1-69
 U.S. system of weights and measures, 1-69, 1-70
 U.S. Tax Reduction Act of 1975, 57-11
 U.S. Weather Bureau, 31-2
 Unitization agreements, 41-9, 57-8
 Unitization, definition of, 57-7

Unitization of tank batteries, 32-7
 Unitized BOP stack, 18-12
 Unitized pressure-energized secondary seal, 3-6
 Uitorque geometry, 10-4
 Units and names to be avoided, 58-5
 Units and systems of weights and measures,
 British and U.S. systems, 1-69, 1-70
 relative density and density, 1-80
 standards of, 1-70, 1-71
 subdivision of units, 1-70
 tables of, 1-71 to 1-80
 the metric system, 1-68, 1-69
 unit and standard definitions, 1-68
 Universal rails, motor mounts, 10-19
 U. of Houston, 50-15
 Unloading and loading sucker rods, 9-10
 Unloading daily production rate, 5-23
 Unloading flowing-pressure traverse, 5-28, 5-32
 Unloading flowing-temperature-at-depth traverse, 5-32
 Unloading gas-lift valve, 5-55
 Unloading gas-lift valve depths, 5-51
 Unloading gas-lift valve temperature, 5-46, 5-48
 Unloading intermittent-spacing-factor traverse, 5-45, 5-46
 Unloading procedure, gas lift, 5-53 to 5-55
 Unloading temperature traverse, 5-46
 Unrecoverable oil, 44-11
 Unsegregated reservoir, 37-5
 Unstable properties, sample for determining, 24-4
 Unsteady-state methods of relative-permeability measurement, 28-3, 28-10, 28-12, 28-14
 Upflow filters, 15-20
 Upkicking, 6-31
 Upset configuration, 9-2
 Upstream taps, 13-26 to 13-29, 13-33, 13-34, 13-37
 Uranium, 24-16, 50-2 to 50-4, 50-15, 50-16, 50-23 to 50-27, 50-34, 50-35
 Urethane jacket, 18-49
 Utah, 24-8, 24-20, 24-21, 46-16, 46-30, 46-31, 46-33, 46-34

V

V-belt drive, 10-5, 10-12
 Vacuum-breaker holes, 11-13
 Vacuum deaeration, 15-29
 Vacuum distillation, 27-8
 Vacuum-line system, 11-13
 Vacuum models, 46-13
 Vacuum relief of storage tanks, 11-7
 Vacuum units and conversions, 58-29
 Validity of simulation results,
 model assumptions, 48-9, 48-10
 spatial truncation errors, 48-10, 48-12
 uncertain reservoir-description data, 48-12, 48-13
 Valuation,
 analytical methods for computation of appraisal value, 41-3 to 41-8
 cash-flow projection preparation, 41-3
 check list of data required for evaluation, 41-8, 41-9
 fair-market-value determination, 41-2, 41-3
 Valuation concepts,
 accounting method, 41-16, 41-17, 41-22, 41-23
 average annual ROR method, 41-23, 41-24
 DCF method, 41-17 to 41-20
 Hoskold's method, 41-16, 41-20 to 41-22

- Morkill's method, 41-16, 41-22
- Valuation methods, equations, 41-17, 41-18
- Valuation of oil and gas reserves, concepts of, 41-16 to 41-24
- development and operating costs, 41-11, 41-12
- federal taxes, 41-12 to 41-16
- forecast of future production rate, 41-9 to 41-11
- general references, 41-37
- interest tables and deferment factors, 41-25 to 41-36
- nomenclature, 41-36
- references, 41-37
- types of oil and gas property ownership, 41-1, 41-2
- valuation, 41-2 to 41-9
- Valve depths, continuous-flow gas-lift installation, 5-32 to 5-35
- Valve depths, gas lift, 5-28
- Valve mechanics, gas lift, bellows-assembly load rate, 5-16, 5-17
- bellows protection, 5-16
- constant closing pressure, 5-13
- crossover seat, 5-16
- injection-gas volumetric throughput profiles, 5-20, 5-21
- introduction, 5-12
- opening and closing pressures, 5-19
- pilot and differential opening injection-pressure-operated valves, 5-13, 5-14
- port configurations, 5-15
- production-pressure factor and valve spread, 5-19, 5-20
- purposes of valves, 5-12
- specifications and stem travel, 5-14, 5-15
- static-force balance equations, 5-17 to 5-19
- unbalanced single-element valves, 5-12, 5-13
- Valve port area, 5-36
- Valve port size, gas lift, 5-44
- Valve-spacing transfer production pressures, 5-48
- Valve specifications and stem travel, 5-14, 5-15
- Valve spread, 5-19
- Valve surface closing pressure, 5-47
- Valve switches, 16-3
- Valve-travel increment, 13-54
- Valve types, 16-3, 16-4
- Valves at wellhead, 3-11 to 3-13
- Valves, gas-lift, crossover seats, 5-15
- for intermittent lift, 5-42, 5-43
- injection-pressure operated, 5-12 to 5-14
- mechanics, 5-12 to 5-21
- nitrogen-charged, 5-16, 5-17
- pilot-operated, 5-13
- port configuration, 5-15
- production-pressure-operated, 5-13
- purpose of, 5-12
- unbalanced, single-element, 5-12, 5-13
- wireline-retrievable, 5-2
- van der Waals' equation, 20-7 to 20-9, 23-12
- van der Waals forces, 47-8
- Van Everdingen, Timmerman, and McMahon method, 38-9 to 38-11
- Vanadium, 50-23, 50-35
- Vane-type compressor, 11-13
- Vane-type mist extractor, 12-8, 12-9, 12-11
- Vapor control in storage tanks, 11-12 to 11-14
- Vapor equivalent of stock-tank liquid, 39-10
- Vapor/liquid equilibrium (VLE) constant, 14-16
- Vapor/liquid equilibrium ratio, 39-11, 39-12, 39-15
- Vapor/liquid/hydrate formation conditions, 25-13
- Vapor losses, 11-11, 11-12
- Vapor pressure, 6-36, 11-11, 11-12, 19-8, 20-3, 20-11 to 20-13, 20-16, 20-17
- Vapor-pressure curves, for binary mixtures, 23-4
- for light hydrocarbons, 23-4
- Vapor pressure, empty hydrate, 25-11
- of water, 25-15
- temperature curves, 14-13
- temperature plot, 20-12
- Vapor recovery, equipment, 19-32
- line valve, 11-11
- system, 11-12, 11-13
- unit, 15-27
- Vapor/solid equilibrium constants, 25-7, 25-8
- Vapor-solids equilibrium ratio method, 25-5
- Vaporization/condensation phenomenon, 46-11 to 46-13
- Vaporization (vapor-pressure) curve, 23-1, 23-2
- Vaporization equilibrium, of an oil fraction, 46-37
- of hydrocarbons, 46-12
- Vaporization losses, storage tanks, 11-12
- Vaporizing gas drive, 45-1, 45-2, 45-4, 45-5, 45-13
- Vaporizing gas drive simulator, 45-14
- Vara as length unit, 58-7, 58-21
- Variable-bore rams, 18-11
- Variable deck load, 18-7
- Variable deck-load capacity, 18-7
- Variable Density Log™ (VDL), 51-18, 51-35, 51-41, 51-42, 51-45, 51-46
- Variable-density presentation, 51-24, 51-25
- Variable flowing pressure-gradient method, 5-22
- Variable-gradient design, 5-22
- Variable-gradient valve spacing, 5-32 to 5-37
- Variable-inductance transducer, 30-6
- Variable-reluctance transducer, 30-5
- Variable-speed drive, 7-7 to 7-9, 7-12, 7-16
- Variables that affect sucker-rod string and pumping-unit loading, 10-5
- Variance, 38-9
- Vasquez and Beggs correlations, 22-7 to 22-13
- Velocity, equivalents (table), 1-76
- in gas lines, 15-7
- in liquid lines, 15-2, 15-5
- of propagation, 51-2
- porosity correlations, 51-34
- porosity laboratory data, 51-6
- ratio, compressional to shear wave, 51-35 to 51-38
- Velocity meters, derivation of an orifice equation, 13-2, 13-3
- energy balance, 13-1, 13-2
- forms of meter, 13-2
- Vena contracta, 13-3
- Venango fields, Pennsylvania, 44-4
- Venezuela, 6-24, 10-18, 12-39, 18-1, 19-2, 21-4, 24-6, 24-9, 24-13, 27-9, 27-20, 46-3, 46-4, 46-15, 46-16, 46-18, 58-20
- Vent discharge for tanks, 11-9
- Venting atmospheric and low-pressure storage tanks, 11-6 to 11-9
- Venting capacity of tanks, 11-7
- Venting requirements for storage tanks, 11-6
- Ventura Avenue field, California, 40-12
- Ventura field, California, 6-24
- Venture capital, 57-8
- Venturi plug valves, 3-12
- Venturi tube, 13-2
- Venturi-tube flowmeter, 32-13
- Versentates™, 44-45
- Vertical communication, 48-10, 48-12
- Vertical conformance, 44-5
- Vertical coverage, 44-39
- Vertical cylindrical vessel, 15-24
- Vertical electric grids, 19-26
- Vertical emulsion treaters, 19-7, 19-21 to 19-23
- Vertical flow downward, 34-28
- Vertical-flow system, 26-12, 26-13
- Vertical fractures, 44-25, 44-28, 51-28, 51-46 to 51-48, 55-2, 55-9
- Vertical free-water knockout, 19-17
- Vertical hydraulic fracture, 35-4
- Vertical multiphase flowing-gradient correlation, 6-27, 6-28, 6-30, 6-43, 6-45
- Vertical multistage pumps, 11-14
- Vertical permeability, 37-5, 48-8
- Vertical recycling separator, 12-14
- Vertical reservoir continuity, 36-4
- Vertical saturation distribution, 37-4
- Vertical scrubber, 12-38
- Vertical sections, directional-data presentation, 53-7
- Vertical segregation, 37-1
- Vertical separator, 12-1, 12-7 to 12-9, 12-14, 12-16 to 12-25, 12-27 to 12-30, 12-35, 12-40, 18-28
- Vertical-separator sizing, 12-29, 12-30
- Vertical settling tank, 19-21
- Vertical-sided structures, 18-42
- Vertical splits of pipe, 53-18, 53-20
- Vertical stratification, 39-18
- Vertical stresses, 55-1
- Vertical sweep, 46-14, 46-21, 46-30, 46-31
- Vertical sweep efficiency, 39-17, 39-18, 47-1, 47-2
- Vertical three-phase oil/gas/water separator, 12-4
- Vertical three-phase separator, 19-17
- Vertical vessels, 13-53
- Vertically fractured reservoirs, 35-4
- Vertically fractured reservoirs, shape factors, 35-5
- Vessel-motion terminology, 18-7
- Vessel response to motion, 18-8
- Vibrating crystal (quartz) transducer, 30-6, 30-7
- Vibrating wire transducer, 30-5 to 30-7
- Vibration, dampening, 16-5
- fatigue, 18-34
- lacking in jet pumps, 6-34
- of casing in high-current drilling, 18-21
- problems in instrumentation for gas measurement, 13-1
- stresses, 3-1
- surface pumps with oil power fluid, 6-55
- switch for pumping unit, 10-29
- vortex shedding, 18-21, 18-22
- Vinyl ester, 9-12
- Viscosities of gas-condensate (GC) systems, 39-4
- Viscosity breaker, 56-8
- Viscosity-controlled fluids, 55-4
- Viscosity corrections, 6-20
- Viscosity correlations, gas, 20-9
- Viscosity factor, 20-15, 20-16
- Viscosity gradients, 6-69
- Viscosity in SI metric system, 58-24, 58-35
- Viscosity index, 21-7
- Viscosity number, 10-12, 10-13
- Viscosity, of brine, 24-16
- of dead and live oils, 46-31, 46-35, 46-36
- of fluids, effect of emulsion on, 19-6
- of formation water, 24-16, 24-17
- of gas, 20-9, 20-15
- of gas-free crude, 6-68, 46-35

- of hydrocarbon gas, 15-6
 - of oil vs. specific gravity, 6-67
 - of oils, 6-24
 - of pure compounds, 20-8
 - of refrigerants, 14-11
 - of sodium chloride (NaCl) solutions, 24-17
 - of water, 6-24, 6-67
 - profile, 55-5
 - ratio vs. pseudoreduced temperature, 20-9
 - ratios, 43-5, 43-6, 45-7, 45-11
 - recommendations for gear and chain reducers, 10-12
 - relations, polymers, 47-4
 - temperature relationships, 19-7, 19-8, 46-31, 46-34, 46-35
 - Viscous emulsions, 55-8
 - Viscous fingering or fingers, 28-13, 45-7, 45-8, 47-2, 48-13
 - Viscous forces, 35-11, 44-31, 47-9
 - Viscous hydrocarbons, metering, 17-4
 - Visual cell, 39-7
 - Viton[®], 4-5
 - Vocabulary of petroleum measurement standard, 17-3
 - Vogel method, for thermal efficiency, 46-9
 - Vogel's inflow-performance relationship (IPR), 34-31 to 34-35, 37-21
 - Void volume, definition of, 27-1
 - Volan[™], 49-37, 49-38
 - Volatile-oil reservoir,
 - comparison of predicted vs. actual reservoir performance, 37-25, 37-26
 - material balance, 37-25, 37-26
 - multicomponent-flash method, 37-23 to 37-26
 - Muskat-method applicability, 40-9
 - performance predictions, 37-2, 37-25, 37-26
 - volumetric methods, 40-13
 - Volatile solvents, 39-26
 - Voltage drop for overhead and buried cable, 10-33
 - Voltage drop in electrical systems, 10-32
 - Voltage frequency, 10-21, 10-23
 - Voltage gradient, 19-25
 - Volume correction factors, 17-5, 17-6
 - Volume correction to 15°C, 17-6
 - Volume correction to 60°F, 17-5, 17-6
 - Volume equivalents, table, 1-73
 - Volume-limit switches, 16-13
 - Volume loss vs. temperature for crude oil, 19-9
 - Volume meters, 32-8, 32-9, 32-11
 - Volume of spheres by hundredths, table, 1-34, 1-35
 - Volume, SI unit for, 58-5, 58-23
 - Volume tank for engine installations, 10-19
 - Volumeters, 26-3
 - Volumetric analysis, 40-1
 - Volumetric-average boiling point, 21-11, 21-12
 - Volumetric-average density, 34-27
 - Volumetric balance, 40-10, 44-38
 - Volumetric behavior,
 - of a binary mixture, 23-3
 - of a pure component, 23-2
 - Volumetric calculations, 37-3
 - Volumetric efficiency, 6-10, 6-24, 6-25, 6-38, 6-67, 8-4, 10-9, 43-3, 45-8, 45-9
 - Volumetric flow rates, 28-3, 34-27
 - Volumetric gas throughput, 5-3, 5-8 to 5-10, 5-15, 5-16
 - Volumetric heat capacity, 46-7, 46-10
 - Volumetric heat-transfer coefficient, 58-35
 - Volumetric liquid-settling capacity, 12-29
 - Volumetric material balance, 40-13
 - Volumetric material-balance equation, 48-2
 - Volumetric metering vessels, 12-6
 - Volumetric meters, 13-1
 - Volumetric methods,
 - free gas in gas reservoir of gas cap, 40-5
 - nonassociated-gas reservoirs, 40-21 to 40-26
 - oil-in-place, 40-5, 4-6
 - oil in reservoir, 40-5, 40-6
 - oil reservoirs with gas-cap drive, 40-13, 40-14
 - oil reservoirs with water drive, 40-15 to 40-20
 - saturated depletion-type oil reservoirs, 40-8 to 40-12
 - solution gas in oil reservoir, 40-6, 40-13
 - undersaturated oil reservoirs, 40-12
 - volatile-oil reservoirs, 40-13
 - Volumetric pump efficiency, 40-27
 - Volumetric ratio, 55-6
 - Volumetric recovery estimates for
 - nonassociated-gas reservoirs, compressibility factor, 40-21, 40-22
 - gas FVF, 40-22, 40-23
 - gas in place, 40-23, 40-24
 - permeability distribution effect, 40-24 to 40-26
 - recovery with water drive, 40-26
 - unit recovery without water drive, 40-24
 - Volumetric reserves, 36-7
 - Volumetric reservoir, 36-3, 37-6, 37-10
 - Volumetric solubility of methane in water, 25-16, 25-17
 - Volumetric sweep, 46-14, 46-19, 46-30, 46-31
 - Volumetric-sweep efficiency, 39-17, 39-18, 47-1, 47-2, 47-17
 - Volumetric technique for reserve estimation, 40-1
 - Volumetric unit recovery, 40-13
 - Voluntary unit operations, 57-8
 - Vortex breaker, 11-2, 19-18
 - Vortex chamber, 12-20, 12-21
 - Vortex core, 6-62, 6-63
 - Vortex finder, 6-62, 6-63, 12-20
 - Vortex-finder tube, 12-20, 12-21
 - Vortex flow pattern, 13-49
 - Vortex meter, 16-6, 16-7
 - Vortex retainer, 12-13
 - Vortex shedding, 18-21, 18-22
 - Vortex-shedding meter, 13-48
 - Vortices, jet pumps, 6-36
 - Vugs, 26-1, 26-6
 - Vugular pore openings, 26-2
- W**
- W. Guara field, Venezuela, 24-13
 - Wabasca tar sand, 46-34
 - WAG (water-alternating-gas), 45-8, 48-6
 - Walking beam, 10-2 to 10-4
 - Wall-resistivity devices, 49-7
 - Walnut shells, 55-8
 - Warranty clause, 57-6
 - Wash-down gravel pack, 56-9
 - Wash pipe, 56-8
 - Wash tank, 19-20
 - Washburn-Bunting porosimeter, 26-4 to 26-6
 - Washouts, 51-33
 - Wasson field, Texas, 16-12, 23-10
 - Waste disposal, 41-9, 41-12
 - Watch-dog timer, 16-8
 - Water/air ratio (WAR), 46-2, 46-16, 46-17, 46-19, 46-28, 46-30
 - Water-alternating-gas (WAG), 45-8, 48-6
 - Water analyses, 24-18, 24-19
 - Water-based fluids, 18-49
 - Water-based fracturing fluids,
 - foams, 55-6, 55-7
 - gels, 55-5, 55-6
 - Water-based muds, 26-21, 40-19, 44-5, 53-9
 - Water block, 56-2
 - Water breakthrough, 39-16, 44-4, 44-7, 44-9, 44-11, 44-12, 44-14, 44-15, 44-34
 - Water channeling, 31-5
 - Water compressibility, 24-12, 24-13, 37-3, 37-6, 37-10, 40-7, 40-34
 - Water coning, 32-3, 48-6, 48-9
 - Water content,
 - dewpoint chart, 25-11, 25-12
 - equations, 25-13
 - equilibrium, 25-12
 - for natural gas in equilibrium with brines, 25-14
 - in light-hydrocarbon systems, 25-16
 - in vapor phase, effects of molecular weight, 25-16
 - metastable, 25-12, 25-13
 - of CO₂, 25-14, 25-15
 - of CO₂-rich fluid phases, 25-15
 - of effluent oil, 12-13
 - of gas in equilibrium with hydrates, 25-10, 25-11
 - of gases in vapor/hydrate region, 25-12
 - of hydrocarbon-rich liquid, 25-10, 25-11
 - of natural gases, 14-4, 25-11 to 25-15
 - of nitrogen in equilibrium with hydrates, 25-14
 - of propane liquid and vapor phase, 25-18
 - of separated crude oil, 12-13
 - of untreated oil, 19-1
 - of vapor in equilibrium with hydrates, 25-12, 25-13
 - of vapor in vapor/hydrate region, 25-13 to 25-15
 - of volume occupied by various gases, 25-14
 - saturated, of natural gas in equilibrium with aqueous phase, 25-11 to 25-15
 - suppression, 25-13
 - Water cut, 5-12, 6-24, 6-25, 6-27, 6-29, 6-30, 6-36, 6-42, 6-44, 6-47, 6-56, 40-19, 44-7, 44-9, 44-25, 44-28, 44-32, 44-39
 - Water-cut oil, 11-2
 - Water-cut recovery calculation, 45-10
 - Water-cut recovery curve, 44-8
 - Water depth, offshore operations, 18-4
 - Water dewpoint of natural gas, 14-4
 - Water dewpoint temperature, 14-17
 - Water-discharge control valves, 12-39, 19-29
 - Water displacement, 28-10
 - Water disposal, 18-30
 - Water drive, 36-2, 36-3, 39-15, 39-16, 39-24, 40-6, 40-7, 40-12, 40-14, 40-18, 40-24, 40-34, 44-10, 44-25
 - Water-drive behavior, 38-8
 - Water-drive constant, 40-6
 - Water-drive equations, 38-12, 38-13, 38-16
 - Water-drive oil reservoirs,
 - general references, 38-20
 - introduction, 38-1
 - mathematical analysis, 38-1 to 38-16
 - nomenclature, 38-17, 38-18
 - recovery efficiency of, 40-16
 - references, 38-20
 - shape factor, 35-5
 - Water-drive sand fields, 40-17
 - Water-drive unit recovery, 40-16 to 40-18
 - Water-dump valve, 19-20, 19-30
 - Water-external microemulsion, 47-11
 - Water films, 11-8
 - Water formation volume factor, definition, 22-20
 - Water fractional flow, 44-12, 44-13
 - Water/gas contact (WGC), 38-1
 - Water/gas relative permeability, 28-10

- Water gradient, 6-29, 6-44
- Water-hammer problems, 15-2
- Water/hydrocarbon systems, behavior of, 25-1 to 25-28
- Water in crude oil by centrifuge method, 17-5
- Water in crude oil by distillation method, 17-5
- Water in effluent oil, 12-15, 12-16
- Water-in-oil detectors, 19-31
- Water-in-oil emulsions, 6-27, 19-1, 19-2, 19-4, 19-7, 19-10, 19-11, 19-13, 19-28, 44-40
- Water in propane-rich fluid phases, 25-4
- Water influx, 37-1, 37-3, 37-5 to 37-7, 38-2, 38-3, 40-6, 40-7, 40-15, 40-24, 40-26
- Water influx rates, 38-2, 38-4 to 38-6, 38-8, 38-10, 38-14, 40-18
- Water-injection case histories, 44-36, 44-37
- Water injection, gas-condensate reservoirs, 39-15, 39-16, 39-18, 39-23, 39-24
- Water-injection gradient, 31-5
- Water-injection oil-recovery performance, areal sweep and pattern efficiency, 44-12 to 44-25
- displacement calculation procedures, 44-7 to 44-12
- reservoir fractures, effect of, 44-25, 44-26
- waterflood performance-method selection, 44-31, 44-32
- waterflood performance-prediction methods, 44-26 to 44-31
- Water-injection pressure maintenance, case histories, 44-36, 44-37
- factors in, 44-2 to 44-5
- introduction, 44-1
- nomenclature, 44-47, 44-48
- oil-recovery performance predictions, 44-7 to 44-32
- pilot floods, 44-37 to 44-39
- references, 44-49 to 44-52
- residual oil determination, 44-5 to 44-7
- selection and sizing of waterflood plants, 44-45 to 44-47
- surface-active agents in, 44-39 to 44-43
- water treating, 44-43 to 44-45
- well behavior, 44-32 to 44-36
- Water-injection rate, 44-32, 44-41
- Water-injection requirements, 18-44
- Water-injection operations, 42-5, 42-6, 43-1
- Water-injection systems, 6-1
- Water-injection well behavior, 44-32 to 44-36
- Water jets or jetting, 19-29, 19-30
- Water knockout, 12-1, 12-2
- Water legs, 19-20
- Water manometer, 13-37
- Water of crystallization, 26-21
- Water/oil contact (WOC), 38-1, 38-5, 38-9, 40-4, 40-5, 40-15, 40-34
- Water/oil mobility ratio, 44-7, 44-8, 47-6
- Water/oil ratio (WOR), 19-27, 24-20, 28-5, 34-41, 40-18 to 40-20, 44-7, 44-9, 44-11, 44-31, 44-32, 44-39, 46-33
- Water/oil viscosity ratio, 40-18, 44-10
- Water permeability, 47-8
- Water power fluid, 6-27, 6-29, 6-44, 6-55, 6-56, 6-60, 6-62, 6-63
- Water-pressure function, 37-8, 37-10
- Water-producing intervals, location of, 31-4, 31-6
- Water relative permeability, 28-6, 28-10, 28-13, 40-18, 40-26, 44-12, 44-40, 46-37, 46-38
- Water resistivity, 26-31
- Water retention time, 12-15
- Water salinity, 24-3, 24-17, 24-18, 26-18, 26-19, 44-40, 50-3, 50-36
- Water/sand discharge, 19-30
- Water-saturation data, 39-9
- Water saturation, determining, 26-22
- Water-saturation distributions, 44-11
- Water saturation from capillary-pressure data, 26-25
- Water-saturation profile, 44-11
- Water sheds, 35-16
- Water slugs, 14-21
- Water source, 44-41 to 44-43
- Water specific gravity, 6-67
- Water-supply wells, 16-14
- Water surge tanks, 44-47
- Water table, 44-41
- Water-temperature bypass control, 13-59
- Water treating, dissolved gas, 44-43
- microbiological growth, 44-44
- minerals, 44-44
- sampling, 44-43
- Water treatment for steam generation, 46-20
- Water-treatment plant, 16-14
- Water types, condensate water, 24-18
- connate water, 24-18
- diagenetic water, 24-18
- formation water, 24-18
- interstitial water, 24-18
- juvenile water, 24-18
- meteoric water, 24-18
- seawater, 24-18
- Water underrun, 48-12
- Water-vapor content, 14-3
- Water-vapor removal, 14-17 to 14-21
- Water viscosity, 44-6, 44-32, 44-33
- Water/volatile-gas systems, 25-24 to 25-27
- Water wash or washing, 19-7, 19-13, 19-15, 19-18 to 19-22, 19-27
- Water-weight factors, 2-1, 2-33, 2-38
- Water-wet, 19-9, 44-6
- Water-wetting agent, 56-5
- Watered-out, 39-15
- Waterflood applications, 3-37
- Waterflood displacement performance, 44-13
- Waterflood oil-recovery predictions, 44-6
- Waterflood performance-prediction methods, 44-26 to 44-31
- Waterflood plant facilities, 44-47
- Waterflood plants, selection and sizing, 44-45 to 44-47
- Waterflood prediction methods, table, 44-29
- selection of, 44-31
- Waterflood processes, case histories, 44-36, 44-37
- factors in, 44-2 to 44-5
- introduction, 44-1
- nomenclature, 44-47, 44-48
- oil-recovery performance predictions, 44-7 to 44-32
- pilot floods, 44-37 to 44-39
- references, 44-49 to 44-52
- residual oil determination, 44-5 to 44-7
- selection and sizing of waterflood plants, 44-45 to 44-47
- surface-active agents in, 44-39 to 44-43
- water treating, 44-43 to 44-45
- well behavior, 44-32 to 44-36
- Waterflood recovery process, 28-8
- Waterflood requirements, daily water-injection rates, 44-41
- fresh waters, 44-41, 44-42
- makeup water, 44-41
- salt waters, 44-42, 44-43
- ultimate water, 44-41
- water sources, 44-41
- Waterflood susceptibility data, 45-8
- Waterflood sweep efficiencies, 44-39
- Waterflooding, an imbibition process, 28-14
- complete, 40-16
- factor in, 44-2 to 44-5
- history and development, 44-1
- injection wells, 34-28
- of dissolved-gas reservoirs, 25-19
- reservoir simulation of, 48-4, 48-7, 48-10, 48-13
- tests, 44-8
- volume of produced water, 24-2
- Waterfloods, in chemical flooding, 47-9, 47-10, 47-21
- Waterfrac services, 55-5
- Waters produced from, Appalachian area, 24-6, 24-7
- California fields, 24-8
- Canadian fields, 24-12
- gulf coast fields, 24-8
- Illinois fields, 24-9
- mid-continent fields, 24-9, 24-10
- Rocky Mountain fields, 24-11
- Venezuela fields, 24-13
- Wave baffle, 19-17, 19-18
- Wave equation, 9-3
- Wave forces, 18-24
- Wave propagation, 51-2, 51-3, 51-12, 51-46
- Wave scatter diagrams, 18-26, 18-27
- Waves in Arctic, 18-39
- Waxes, 39-1
- Waxing, 6-56
- Waxy-based hydrocarbon liquids or heavy ends, 14-6, 14-7
- Waxy distillates, 14-5
- Weather-related downtime, 18-8
- Weight, definition of, 1-70
- Weight-loaded regulator, 13-54, 13-55
- Weight-loss corrosion, 3-36
- Weight of a body, 58-3
- Weight on bit (WOB), 18-13, 18-14, 53-1, 53-2, 53-4
- Weighted-average deferment factor, 41-21, 41-23, 41-24
- Weighted loaded valves, 13-55
- Weights and measures, definition of, 1-68
- of buttress-thread casing coupling, 2-29
- of concentrations of HCl, 54-2
- of external-upset tubing coupling, 2-43
- of extra-strong threaded line pipe, 2-50
- of integral-joint tubing upset, 2-45
- of nonupset tubing coupling, 2-42
- of plain-end line pipe, 2-50 to 2-53
- of round-thread casing coupling, 2-28
- of threaded line pipe, 2-47
- Weir or weir box, 19-19, 19-20, 19-23
- Weir-tank-type LACT system, 16-13
- Welch field, Texas, 44-30
- Weld-neck line-pipe flange, 3-17, 3-19, 3-23, 3-24
- Welded-steel tanks, 11-1, 11-2, 11-9, 11-11
- Welded-type seal, 3-9
- Welding slag, 5-53
- Welex, 49-2, 49-36, 49-37, 51-18
- Wedge calculations, 44-11, 44-12
- Well completions, consideration in pilot waterflooding, 44-39
- offshore, 18-28
- steam and firefloods, 46-19, 46-20
- Well conditioning, gas-condensate reservoir, 39-5
- Well costs and spacing, 39-1
- Well deliverability, 5-12, 39-1
- Well-effluent composition, 21-16
- Well fluids and their characteristics, condensate, 12-3
- crude oil, 12-3
- impurities and extraneous materials, 12-3
- natural gas, 12-3
- physical and chemical, 12-21
- water, 12-3

- Well injectivity, 39-5, 39-6, 39-23 to 39-26, 46-17
- Well kick, 18-11
- Well killing, 39-25
- Well-log analysis, 37-3
- Well logging, letter and computer symbols, 59-2 to 59-51
- Well logs,
 caliper, 53-1
 casing collar-locator, 53-26
 casing inspection, 53-1
 dipmeter, 53-1
 directional surveys, 53-1
 in interpretation of paleoenvironments, 36-3
 measurement while drilling (MWD), 53-1 to 53-3
 references, 53-26
- Well-pattern geometry, 39-1
- Well-performance equations,
 diffusivity, 35-1, 35-2
 gas well, 35-9 to 35-14
 multiphase flow, 35-2
 nomenclature, 35-20
 oil well, 35-2 to 35-9
 references, 35-21
 transient well-test analysis, 35-14 to 35-20
- Well preparation for sand control,
 cement bond, 56-4
 cleanliness, 56-3, 56-4
 perforation cleaning, 56-5
 perforations, 56-4, 56-5
- Well-pressure performance, closed reservoir, 35-2
- Well productivity, 39-5, 39-6, 39-13, 39-23 to 39-26, 46-17, 46-21, 56-3, 56-4
- Well re-entry workover, 18-33
- Well servicing, 18-28, 18-29, 18-34
- Well spacing, 39-13, 41-11
- Well stimulation, 7-16, 56-1
- Well-test control logic, 16-12
- Well tester, 32-7 to 32-10
- Well testing, 39-24, 39-25
- Well-testing procedures, 32-15
- Well tests and sampling gas-condensate (GC) reservoirs,
 field sampling and test procedures, 39-5, 39-6
 well conditioning, 39-5
- Well-workover equipment, 18-28
- Well workovers, 18-28, 18-29, 18-34, 44-39
- Wellbore cleanup by acidizing, 54-8
- Wellbore deviation, 56-3
- Wellbore fluid expansion, 35-6
- Wellbore heat losses,
 calculations including pressure changes, 46-6, 46-7
 hot water, 46-6
 model treating, 46-7
 overall heat-transfer coefficient, 46-6
 recent developments, 46-7
 saturated steam, 46-5, 46-6
 superheated steam, 46-5
- Wellbore hydraulics,
 flow through chokes, 34-45 to 34-49
 injection wells, 34-28 to 34-30
 liquid loading in wells, 34-46, 34-50
 metric conversion for key equations, 34-51 to 34-55
 multiphase flow, 34-35 to 34-45
 nomenclature, 34-50, 34-51
 oil wells, inflow performance, 34-30 to 34-35
 producing gas wells, 34-3 to 34-28
 references, 34-55, 34-56
 theoretical basis, 34-1 to 34-3
- Wellbore problems, 34-3
- Wellbore-storage effect, 30-14, 35-4, 35-6, 35-7, 35-12, 35-15
- Wellbore variables, influence on focused electrode logs, 49-21, 49-22
- Wellhead assembly, 3-2, 3-3
- Wellhead choke, 34-45
- Wellhead control valve, 6-51, 6-59
- Wellhead corrosion aspects, 3-35
- Wellhead corrosion protection methods, 3-36
- Wellhead equipment and flow-control devices,
 API flanged or clamped types, 3-1 to 3-18
 corrosion, 3-35, 3-36
 general references, 3-40
 independent screwed wellhead, 3-39
 introduction, 3-1
 other control devices, 3-34, 3-35
 references, 3-40
 safety shut-in systems, 3-18 to 3-34
 special application, 3-36 to 3-39
- Wellhead sampling, 24-3, 24-4
- Wellhead support, electrical submersible pump (ESP), 7-6
- Well's inflow performance, 7-8 to 7-10, 7-12
- Wells required, gas-condensate (GC) reservoirs, 39-26
- Wellsite data-acquisition system, 51-25
- Wellsite log analysis, in real time, 49-36
 in replay time, 49-37, 49-38
- West Edmond field, 40-2
- West Heidelberg field, Mississippi, 46-28, 46-30
- West Newport field, California, 46-16, 46-18
- West Panhandle field, Texas, 34-46
- West Texas area, 27-16, 27-17
- West Virginia, 21-2, 24-6, 24-7
- Wet combustion, 46-2, 46-3, 46-14, 46-17 to 46-19, 46-22, 46-30, 46-33
 reverse, 46-31
- Wet gas, 5-2, 10-16, 39-1, 39-10, 39-11, 39-13, 39-18 to 39-20, 39-23, 39-24
- Wet vs. dry subsea completions, 18-31
- Wettability, 28-10 to 28-13, 44-5, 44-6, 44-27, 44-39
- Wettability reversal, 47-19
- Wetting agents, 42-2
- Wetting immiscible fluids, 28-3, 28-5, 28-6
- Wetting phase, 47-9
- Wetting-phase relative permeability, 28-12
- Wetting-phase saturation, 26-27, 28-6
- Weyburn field, Saskatchewan, Canada, 51-32
- Weymouth equation, 15-7 to 15-9
- Wheatstone bridge circuit, 52-3
- Whittier field, California, 44-40, 47-21, 47-22
- Whole-core analysis, 27-1, 27-8
- Whole-core measurement of permeability, 26-17, 26-18
- Whole cores, 26-2, 26-7
- Wichert and Aziz's chart, 20-15
- Wilmington field, California, 6-24, 44-39
- Windfall Profits Tax (WPT), 41-1, 41-4, 41-12, 41-15
- Winding-insulation materials, 10-26
- Winkelman Dome field, Wyoming, 46-15, 46-18
- Winsor microemulsion systems, 47-12
- Wire-mesh filters, 39-26
- Wire rope guidelines, 18-14
- Wire-wrapped screens, 56-7, 56-8
- Wireline cores, 26-2
- Wireline equipment, 49-1
- Wireline formation tester, 49-1
- Wireline logging, 50-1
- Wireline logging operations (schematic), 49-2
- Wireline lubricator, 18-34
- Wireline operations, 6-2, 6-48
- Wireline-retrievable gas-lift equipment, 5-2, 5-16, 5-26, 5-50, 5-53
- Wireline-retrievable standing valve, 6-3, 6-48
- Wireline-retrievable subsurface safety valves (SSSV's), 3-27, 3-33, 6-48, 6-49
- Wireline tensile strengths, 30-4
- Wireline unit, 18-28
- Wireline well servicing, 18-34
- Wiring methods offshore, 18-46
- Woodson Shallow field, Texas, 44-4
- Woodson field, Texas, 46-3
- Work equivalents, table, 1-77
- Work, unit in SI metric system, 58-23, 58-24, 58-32
- Working barrel, 10-1
- Working fluid level, 5-51
- Working interest, 41-1 to 41-4, 41-9, 41-13, 41-15, 41-35, 57-5, 57-7, 57-9, 57-10
- Working-interest fraction (WI), 41-2
- Working pressure, wellhead equipment, 3-1 to 3-5, 3-7, 3-8, 3-12 to 3-25, 3-27, 3-38
- Workover fluid, 5-2
- Workover-fluid invasion, 54-11
- Workover operations, 8-8, 30-8, 39-24 to 39-26, 56-4
- Workover rigs, 56-3
- Wormhole effect in acidizing, 54-8, 54-10
- Woven wire mesh, 19-14
- Wrap-around tubing hanger, 3-8
- Wye-delta transformer, 10-30
- Wye-wye transformer, 10-30
- Wyllie time-average equation, 51-29
- Wyllie's equation, 26-20
- Wyoming, 21-4, 23-7, 24-8, 24-11, 24-18, 24-20, 39-16, 40-19, 40-23, 44-42, 46-3, 46-14, 46-15, 46-18

X

- X-plot wellsite analysis, 49-37
- X-ray absorbers, 28-4
- X-ray crystallography, 25-5
- X-ray diffraction, 25-6, 51-5
- X-ray-diffraction analysis, 54-9, 56-3
- X-ray shadowgraph, 44-17, 44-19 to 44-21, 44-25, 44-34
- X-Y recording mode, 51-18
- Xanthan gum, 47-3

Y

- Y method, adjustment procedure for material-balance equation, 40-6
- Yardsticks, 32-1, 32-3, 42-6
- Yates field, Texas, 40-2
- Year-end compound-interest factors, 41-20 to 41-22
- Yield point, 58-34
- Yield-point collapse pressure, 2-54
- Yield point of construction materials, 12-41
- Yield strength, collapse-pressure equation, 2-54
 of API body and bonnet members, 3-3
 of API casing and liner casing, 2-2
 of API tubing, 2-37, 2-61
 of elastic material, 58-2
 of line pipe, 2-46, 2-56, 2-63
 of pipe body, 2-2, 2-4, 2-6, 2-8, 2-10, 2-12, 2-14, 2-16, 2-18, 2-32
 of pipe material, 18-17
 of sucker rods, 9-5
- Yorba Linda field, California, 46-3, 46-18
- Young's modulus of elasticity, 2-35, 51-1, 51-43, 51-44, 58-34

Z

- Zeolite ion exchange, 46-20
- Zeros, importance of, 58-6
- Zinc acetate, 44-42